Efficient iterative schemes forab initiototal-energy calc set

Physical Review B

54, 11169-11186

DOI: 10.1103/physrevb.54.11169

Citation Report

#	Article	IF	Citations
3	Molecular Precursors in the Dissociative Adsorption ofO2on Pt(111). Physical Review Letters, 1997, 79, 4481-4484.	2.9	309
4	Role of silicon vacancies in yttrium-disilicide compounds from ab initio calculations. Physical Review B, 1997, 55, 13479-13484.	1.1	30
5	An Introduction toAb-InitioMolecular Dynamics Schemes. Molecular Simulation, 1997, 20, 63-77.	0.9	7
6	Application of Ab Initio Methods to Secondary Lithium Batteries. Materials Research Society Symposia Proceedings, 1997, 496, 65.	0.1	3
7	Transitory Metastable Phases in Refractory Metals-Based Systems Solidified by Drop-Tube Processing: A First-Principles Approach. Materials Research Society Symposia Proceedings, 1997, 481, 27.	0.1	0
8	Ab INITIO CALCULATION OF THE LixCoO2 PHASE DIAGRAM. Materials Research Society Symposia Proceedings, 1997, 496, 121.	0.1	5
9	First principles calculations on crystalline and liquid iron at Earth's core conditions. Faraday Discussions, 1997, 106, 205-218.	1.6	106
10	Ab initio simulation of molecular processes on oxide surfaces. Faraday Discussions, 1997, 106, 135-154.	1.6	69
11	Ab initiodensity functional studies of transition-metal sulphides: II. Electronic structure. Journal of Physics Condensed Matter, 1997, 9, 11107-11140.	0.7	109
12	Ab initiodensity functional studies of transition-metal sulphides: I. Crystal structure and cohesive properties. Journal of Physics Condensed Matter, 1997, 9, 11085-11106.	0.7	118
13	H2dissociative adsorption on Pd(111). Physical Review B, 1997, 56, 15396-15403.	1.1	151
14	Ab initio simulation of the metal/nonmetal transition in expanded fluid mercury. Physical Review B, 1997, 55, 7539-7548.	1.1	131
15	A systematic study of the surface energetics and structure of TiO2(110) by first-principles calculations. Surface Science, 1997, 385, 386-394.	0.8	224
16	Ensemble Density-Functional Theory forAb InitioMolecular Dynamics of Metals and Finite-Temperature Insulators. Physical Review Letters, 1997, 79, 1337-1340.	2.9	345
17	First-principles calculations of the radial breathing mode of single-wall carbon nanotubes. Physical Review B, 1998, 58, R8869-R8872.	1.1	294
18	Length-scale ill conditioning in linear-scaling DFT. Computer Physics Communications, 1998, 112, 103-111.	3.0	23
19	Model of the epitaxial growth of SiC-polytypes under surface-stabilized conditons. Journal of Electronic Materials, 1998, 27, 848-852.	1.0	26
20	The electrochemical stability of lithium-metal oxides against metal reduction. Solid State Ionics, 1998, 109, 151-157.	1.3	17

#	Article	IF	Citations
21	A Synthesis of Isocryptolepine. Journal of Chemical Research Synopses, 1998, , 377-377.	0.3	16
22	Ab initiomolecular-dynamics studies of the graphitization of flat and stepped diamond (111) surfaces. Physical Review B, 1998, 58, 13167-13175.	1.1	52
23	Structural and electronic properties of the MoS2(101Ì„0) edge-surface. Surface Science, 1998, 407, 237-250.	0.8	108
24	The adsorption and dissociation of ROH molecules on TiO2(110). Surface Science, 1998, 409, 336-349.	0.8	192
25	Ab initio study of the dissociative adsorption of H2 on the Pd(110) surface. Surface Science, 1998, 412-413, 518-526.	0.8	44
26	Adsorption of thiophene onRuS2: Anab initiodensity-functional study. Physical Review B, 1998, 58, R1782-R1785.	1.1	14
27	Phonon dispersion relation in rhodium:Ab initiocalculations and neutron- scattering investigations. Physical Review B, 1998, 57, 324-333.	1.1	39
28	Noncollinear magnetism in rough ultrathin Î³-Fe films. Physical Review B, 1998, 58, 5197-5200.	1.1	17
29	On the Nature of Water Interacting with BrÃ¸nsted Acidic Sites. Ab Initio Molecular Dynamics Study of Hydrated HSAPO-34. Journal of Physical Chemistry B, 1998, 102, 7307-7310.	1.2	56
30	BrÃ¸nsted Acid Sites in HSAPO-34 and Chabazite:â€‰ An Ab Initio Structural Study. Journal of Physical Chemistry B, 1998, 102, 5573-5580.	1.2	166
31	Theoretical investigation of edge dislocations in AlN. Applied Physics Letters, 1998, 72, 3467-3469.	1.5	42
32	Peierls barriers and stresses for edge dislocations in Pd and Al calculated from first principles. Physical Review B, 1998, 58, 2487-2496.	1.1	162
33	Adsorption of Thiophene on the Catalytically Active Surface ofMoS2: AnAb InitioLocal-Density-Functional Study. Physical Review Letters, 1998, 80, 1481-1484.	2.9	128
34	First-principles investigation of phase stability inLixCoO2. Physical Review B, 1998, 58, 2975-2987.	1.1	632
35	First-order phase transitions by first-principles free-energy calculations: The melting of Al. Physical Review B, 1998, 57, 8223-8234.	1.1	124
36	Ab initiocalculation of the lithium-tin voltage profile. Physical Review B, 1998, 58, 15583-15588.	1.1	254
37	First-principles simulations of liquid Fe-S under Earthâ€™s core conditions. Physical Review B, 1998, 58, 8248-8256.	1.1	84
38	Adsorption of Methanol on TiO2(110):Â A First-Principles Investigation. Journal of Physical Chemistry B, 1998, 102, 2017-2026.	1.2	127

#	Article	IF	Citations
39	Relaxations of nonpolar zinc blende (110) surface of GaN, AlN, and BN. Journal of Applied Physics, 1998, 84, 1977-1980.	1.1	6
40	Acetylene structure and dynamics on Pd(111). Physical Review B, 1998, 57, R12705-R12708.	1.1	66
41	Structure and dynamics of liquid selenium. Physical Review B, 1998, 57, 10482-10495.	1.1	78
42	Si-richSiC(111)/(0001)3Ã—3and3Ã—3surfaces: A Mott-Hubbard picture. Physical Review B, 1998, 58, 13712-13716.	1.1	73
43	Ab initiocalculations of the structural properties of theYSi2(0001) surface. Physical Review B, 1998, 58, 10857-10859.	1.1	11
44	Interlayer Self-Diffusion on Stepped Pt(111). Physical Review Letters, 1998, 81, 168-171.	2.9	115
45	Reversed spin polarization at the Co(001)-HfO2(001) interface. Physical Review B, 1998, 58, 15422-15425.	1.1	15
46	Ab initiostudies of the (111) and (1Â¯ 1Â¯ 1Â¯) surfaces of cubic BN: Structure and energetics. Physical Review B, 1998, 58, 15636-15646.	1.1	25
47	First-Principles Computation of the Vibrational Entropy of Ordered and DisorderedNi3Al. Physical Review Letters, 1998, 80, 4911-4914.	2.9	111
48	Supersoft Transition Metal Silicides. Physical Review Letters, 1998, 81, 1969-1972.	2.9	19
49	Anomalous Isostructural Transformation in Ice VIII. Physical Review Letters, 1998, 81, 2466-2469.	2.9	25
50	Ab initiostudies of the (100), (110), and (111) surfaces ofCoSi2. Physical Review B, 1998, 57, 4088-4098.	1.1	27
51	Bond-rotation versus bond-contraction relaxation of (110) surfaces of group-III nitrides. Physical Review B, 1998, 58, R1722-R1725.	1.1	67
52	Adsorption of CO on Pd(100): Steering into less favored adsorption sites. Physical Review B, 1998, 57, 10110-10114.	1.1	43
53	Relaxations ofTiO2- and SrO-terminatedSrTiO3(001) surfaces. Physical Review B, 1998, 58, 8075-8078.	1.1	61
54	Novel Reconstruction Mechanism for Dangling-Bond Minimization: Combined Method Surface Structure Determination ofSiC(111)-(3Ã—3). Physical Review Letters, 1998, 80, 758-761.	2.9	170
55	High Pressure Polymorphism in Silica. Physical Review Letters, 1998, 80, 2145-2148.	2.9	205
56	First-Principles Calculation of Transport Coefficients. Physical Review Letters, 1998, 81, 5161-5164.	2.9	170

#	Article	IF	Citations
57	Vibrations of O on stepped Pt(111). Physical Review B, 1998, 58, 2179-2184.	1.1	34
58	Carbon vacancy in SiC: A negative- U system. Europhysics Letters, 1998, 44, 309-314.	0.7	17
59	Defect Generation and Diffusion Mechanisms in Al and Al-Cu. Materials Research Society Symposia Proceedings, 1998, 516, 189.	0.1	3
60	Exploring the Excited States of Vacancy Defects in Silica. Materials Research Society Symposia Proceedings, 1998, 540, 379.	0.1	3
61	Ab initio Simulation of Vacancy Processes in Ni3Al. Materials Research Society Symposia Proceedings, 1998, 552, 1.	0.1	6
62	Coulomb potential inside a large finite crystal. Journal of Physics Condensed Matter, 1999, 11, 6159-6168.	0.7	25
63	First-principles molecular dynamics studies of liquid selenium close to the critical point. Journal of Physics Condensed Matter, 1999, 11, 10211-10218.	0.7	3
64	Electronic structure of the (111) and(1Â¯1Â¯1Â¯)surfaces of cubic BN: A local-density-functionalab initiostudy. Physical Review B, 1999, 60, 8719-8726.	1.1	9
65	Electrochemical properties of spinelLixCoO2:A first-principles investigation. Physical Review B, 1999, 59, 742-749.	1.1	60
66	Reaction channels for the catalytic oxidation of CO on Pt(111). Physical Review B, 1999, 59, 5960-5967.	1.1	100
67	Structural stability of lithium manganese oxides. Physical Review B, 1999, 59, 6120-6130.	1.1	227
68	Variations in the Nature of Metal Adsorption on Ultrathin Al2O3Films. Physical Review Letters, 1999, 82, 4050-4053.	2.9	175
69	Adsorption of ammonia on the rhodium (111), (100), and stepped (100) surfaces: An ab initio and experimental study. Journal of Chemical Physics, 1999, 111, 8124-8130.	1.2	45
70	Anomalous behavior of the semiconducting gap inWO3from first-principles calculations. Physical Review B, 1999, 59, 2684-2693.	1.1	121
71	First-principles step- and kink-formation energies on Cu(111). Physical Review B, 1999, 60, 11118-11122.	1.1	35
72	Model of noncontact scanning force microscopy on ionic surfaces. Physical Review B, 1999, 59, 2436-2448.	1.1	134
73	Dissociation of water on the surface of galena (PbS): A comparison of periodic and cluster models. Journal of Chemical Physics, 1999, 111, 6942-6946.	1.2	25
74	Adsorption-induced lattice relaxation and diffusion by concerted substitution. Physical Review B, 1999, 59, 5892-5897.	1.1	34

#	Article	IF	Citations
75	Interpretation of O binding-site preferences on close-packed group-VIII metal surfaces. Physical Review B, 1999, 59, 2327-2331.	1.1	12
76	Band-gap and k.p. parameters for GaAlN and GaInN alloys. Journal of Applied Physics, 1999, 86, 3768-3772.	1.1	47
77	Elimination of the long-range dipole interaction in calculations with periodic boundary conditions. Physical Review B, 1999, 60, 15476-15479.	1.1	119
78	First-principles investigation of the Zr (0001) surface structure. Physical Review B, 1999, 60, 15624-15627.	1.1	25
79	Ab initiostudy of theCoSi2(111)/Si(111)interface. Physical Review B, 1999, 60, 17112-17122.	1.1	17
80	Atomic structure of thec(2Ã—2)Si/Cu(110) surface alloy fromab initiocalculation. Physical Review B, 1999, 60, 6034-6038.	1.1	6
81	Extrapolative approaches to Brillouin-zone integration. Physical Review B, 1999, 59, 4685-4693.	1.1	54
82	Correcting overbinding in local-density-approximation calculations. Physical Review B, 1999, 59, 14992-15001.	1.1	103
83	Polyanionic and octet phases in the K-Sb system. I. Crystalline intermetallic compounds. Physical Review B, 1999, 59, 829-842.	1.1	17
84	Influence of crystal structure on the lattice sites and formation energies of hydrogen in wurtzite and zinc-blende GaN. Physical Review B, 1999, 60, R5101-R5104.	1.1	39
85	Large Fermi Density Waves on the Reconstructed Pt(100) Surface. Physical Review Letters, 1999, 83, 2604-2607.	2.9	12
86	Defect generation and diffusion mechanisms in Al and Alâ€“Cu. Applied Physics Letters, 1999, 74, 34-36.	1.5	36
87	Dislocation Structures of Submonolayer Films near the Commensurate-Incommensurate Phase Transition: Ag on Pt(111). Physical Review Letters, 1999, 82, 4488-4491.	2.9	26
88	Ab InitioMolecular Dynamics Studies of Off-Center Displacements in CuCl. Physical Review Letters, 1999, 83, 568-571.	2.9	18
89	Simulations of fluid hydrogen: Comparison of a dissociation model with tight-binding molecular dynamics. Physical Review E, 1999, 60, 1665-1673.	0.8	19
90	Metal-on-Metal Bonding and Rebonding Revisited. Physical Review Letters, 1999, 82, 5301-5304.	2.9	24
91	Trends in the chemical reactivity of surfaces studied byab initioquantum-dynamics calculations. Physical Review B, 1999, 59, 13297-13300.	1.1	67
92	Defects in liquid selenium. Physical Review B, 1999, 59, 3501-3513.	1.1	36

#	Article	IF	Citations
93	Ab initiostudy of phonons in hexagonal GaN. Physical Review B, 1999, 60, 15511-15514.	1.1	43
94	Modeling STM tips by single absorbed atoms on W(100) films: 5d transition metal atoms. Solid State Communications, 1999, 113, 245-250.	0.9	49
95	An order(N) tight-binding molecular dynamics study of intrinsic defect diffusion in silicon. Chemical Engineering Journal, 1999, 74, 67-75.	6.6	8
96	Transition metal defect behavior and Si density of states in the processing temperature regime. Physica B: Condensed Matter, 1999, 273-274, 358-362.	1.3	2
97	Monovacancies in 3C and 4H SiC. Materials Science and Engineering B: Solid-State Materials for Advanced Technology, 1999, 61-62, 244-247.	1.7	7
98	STM experiment and atomistic modelling hand in hand: individual molecules on semiconductor surfaces. Surface Science Reports, 1999, 33, 1-81.	3.8	71
99	Investigating the effects of silicon tip contamination in noncontact scanning force microscopy (SFM). Applied Surface Science, 1999, 144-145, 608-612.	3.1	24
100	Crystal structure, compressibility and possible phase transitions in oldvarepsilon-FeSi studied by first-principles pseudopotential calculations. Acta Crystallographica Section B: Structural Science, 1999, 55, 484-493.	1.8	107
101	A new investigation of copper's role in enhancing Alâ€“Cu interconnect electromigration resistance from an atomistic view. Acta Materialia, 1999, 47, 3227-3231.	3.8	51
102	Soft X-ray fluorescence spectra of photoluminescent layered polysilanes. Chemical Physics Letters, 1999, 301, 474-480.	1.2	1
103	Rotational effects in the dissociation of H2 on metal surfaces studied by ab initio quantum-dynamics calculations. Chemical Physics Letters, 1999, 311, 1-7.	1.2	32
104	Ab initio pseudopotentials for electronic structure calculations of poly-atomic systems using density-functional theory. Computer Physics Communications, 1999, 119, 67-98.	3.0	1,313
105	Pairing in dense lithium. Nature, 1999, 400, 141-144.	13.7	375
106	The melting curve of iron at the pressures of the Earth's core from ab initio calculations. Nature, 1999, 401, 462-464.	13.7	270
107	Ab initio molecular dynamics, a simple algorithm for charge extrapolation. Computer Physics Communications, 1999, 118, 31-33.	3.0	98
108	Catalysis of the reaction HCl+HOCl†'H2O+Cl2 on an ice surface. Chemical Physics Letters, 1999, 309, 335-343.	1.2	26
109	Ab initio molecular dynamics study on the hydrolysis of molecular chlorine. Chemical Physics Letters, 1999, 311, 93-101.	1.2	15
110	A theoretical study of CHx chemisorption on the Ru(0001) surface. Chemical Physics Letters, 1999, 311, 185-192.	1.2	87

#	Article	IF	Citations
111	Ab initio molecular dynamics study on the thermal dissociation of acetic acid. Chemical Physics Letters, 1999, 314, 317-325.	1.2	19
112	Vacancies in SiC: Influence of Jahn-Teller distortions, spin effects, and crystal structure. Physical Review B, 1999, 59, 15166-15180.	1.1	225
113	Cohesive, structural, and electronic properties of Fe-Si compounds. Physical Review B, 1999, 59, 12860-12871.	1.1	215
114	Mg clusters on MgO surfaces: characterization by MIES and electronic structure ab initio calculations. Nuclear Instruments & Methods in Physics Research B, 1999, 157, 162-166.	0.6	10
115	Determination of Band Structure Parameters in Nitride Alloys for Use in Quantum Well Calculations. Physica Status Solidi (B): Basic Research, 1999, 216, 351-354.	0.7	0
116	Ab initiocalculation of the lattice dynamics and phase diagram of boron nitride. Physical Review B, 1999, 59, 8551-8559.	1.1	359
117	Structure and electronic properties of amorphousWO3. Physical Review B, 1999, 60, 16463-16474.	1.1	88
118	WhyPb(B,Bâ€²)O3perovskites disorder at lower temperatures thanBa(B,Bâ€²)O3perovskites. Physical Review B, 1999, 60, R12542-R12545.	1.1	83
119	Linear scaling electronic structure methods. Reviews of Modern Physics, 1999, 71, 1085-1123.	16.4	1,247
120	Mechanism of Boron Diffusion in Silicon: AnAb Initioand Kinetic Monte Carlo Study. Physical Review Letters, 1999, 83, 4341-4344.	2.9	175
121	Theoretical study of two expanded phases of crystalline germanium: clathrate-I and clathrate-II. Journal of Physics Condensed Matter, 1999, 11, 6129-6145.	0.7	74
122	From ultrasoft pseudopotentials to the projector augmented-wave method. Physical Review B, 1999, 59, 1758-1775.	1.1	61,625
123	Thermally Activated Reorientation of Di-interstitial Defects in Silicon. Physical Review Letters, 1999, 83, 1990-1993.	2.9	61
124	First-principles calculations to describe zirconia pseudopolymorphs. Physical Review B, 1999, 59, 4044-4052.	1.1	162
125	Retardation of O diffusion through polycrystalline Pt by Be doping. Physical Review B, 1999, 59, 16047-16052.	1.1	12
126	First-Principles Study of Boron Diffusion in Silicon. Physical Review Letters, 1999, 83, 4345-4348.	2.9	206
127	Resolving discrepancies between LEED and STM throughab initiocalculations: Surface and bonding of sulfur on Mo(110). Physical Review B, 1999, 60, 11783-11788.	1.1	16
128	Why clathrates are good thermoelectrics: A theoretical study of Sr8Ga16Ge30. Journal of Chemical Physics, 1999, 111, 3133-3144.	1.2	123

#	Article	IF	Citations
129	Spectroscopy of low-coordinated surface sites:â€,Theoretical study of MgO. Physical Review B, 1999, 59, 2417-2430.	1.1	164
130	Mg clusters on MgO surfaces: study of the nucleation mechanism with MIES and ab initio calculations. Faraday Discussions, 1999, 114, 173-194.	1.6	77
131	Geometry and electronic structure of magic iron oxide clusters. Physical Review B, 1999, 59, 12672-12677.	1.1	51
132	Reaction channels for the catalytic oxidation of CO on Pt(111). Surface Science, 1999, 433-435, 58-62.	0.8	47
133	Oxygen adsorption on Pt(110)-(1Ã—2): new high-coverage structures. Surface Science, 1999, 430, L533-L539.	0.8	37
134	Hydrogen, sulphur and chlorine coadsorption on Pd(111): a theoretical study of poisoning and promotion. Surface Science, 1999, 430, 176-191.	0.8	70
135	Ethylene, sulphur, and chlorine coadsorption on Pd(111): a theoretical study of poisoning and promotion. Surface Science, 1999, 430, 192-198.	0.8	24
136	Molecular precursors in the dissociative adsorption of O2 on Ni(111). Surface Science, 1999, 433-435, 756-760.	0.8	40
137	SiCl4 desorption in chlorine etching of Si(100) â€" a first principles study. Surface Science, 1999, 432, 125-138.	0.8	5
138	Density functional study of the structural and electronic properties of RuS2(111). Surface Science, 1999, 439, 163-172.	0.8	16
139	Primary slip system of Îµ-iron and anisotropy of the Earth's inner core. Physics of the Earth and Planetary Interiors, 1999, 110, 147-156.	0.7	40
140	Oxygen in the Earth's core: a first-principles study. Physics of the Earth and Planetary Interiors, 1999, 110, 191-210.	0.7	51
141	Transport coefficients of liquids from first principles. Journal of Non-Crystalline Solids, 1999, 250-252, 82-90.	1.5	11
142	Band structure ofInxGa1â^'xAs1â^'yNyalloys and effects of pressure. Physical Review B, 1999, 60, 4430-4433.	1.1	172
143	Magnetism and magneto-structural effects in transition-metal sulphides. Journal of Physics Condensed Matter, 1999, 11, 8197-8222.	0.7	60
144	Polymorphism in silica studied in the local density and generalized-gradient approximations. Journal of Physics Condensed Matter, 1999, 11, 3833-3874.	0.7	174
145	Electronic structure calculations on nitride semiconductors. Semiconductor Science and Technology, 1999, 14, 23-31.	1.0	153
146	Role of surface vacancies and water products in metal nucleation: Pt/MgO(100). Surface Science, 1999, 437, L741-L747.	0.8	95

#	Article	IF	Citations
147	Self-diffusion along step bottoms on Pt(111). Physical Review B, 1999, 60, 4972-4981.	1.1	45
148	Ab initiocalculation of the origin of the distortion of Î±-PbO. Physical Review B, 1999, 59, 8481-8486.	1.1	160
149	Ab-initio energy profiles for thiophene HDS on the MoS2 (1010) edge-surface. Studies in Surface Science and Catalysis, 1999, 127, 309-317.	1.5	21
150	Origin of the Lone Pair of Î±-PbO from Density Functional Theory Calculations. Journal of Physical Chemistry B, 1999, 103, 1258-1262.	1.2	157
151	The structure of iron under the conditions of the Earth's inner core. Geophysical Research Letters, 1999, 26, 1231-1234.	1.5	47
152	An introduction to â€œComputational Crystallographyâ€• Zeitschrift Fur Kristallographie - Crystalline Materials, 1999, 214, 506-527.	0.4	27
153	First principles calculations on the high-pressure behavior of magnesite. American Mineralogist, 1999, 84, 1627-1631.	0.9	14
154	Estimation of The Critical Radius for The Nucleation of the C54 Phase in C49 TiSi2: Role of The Difference in Density. Materials Research Society Symposia Proceedings, 1999, 580, 129.	0.1	2
155	Dynamics of Silicon Oxidation. Materials Research Society Symposia Proceedings, 1999, 592, 30.	0.1	4
156	Stress Effects on Al and Al(Cu) Thin Film Grain-Boundary Diffusion. Materials Research Society Symposia Proceedings, 1999, 594, 451.	0.1	0
157	Theoretische Chemie 1998. Nachrichten Aus Der Chemie, 1999, 47, 186-195.	0.0	3
158	Atomic Structure of Pd-Intercalated Graphite by High-Resolution Electron Microscopy and First Principles Calculations. Materials Transactions, JIM, 1999, 40, 1213-1218.	0.9	3
159	Acceleration of Self-Consistent Electronic-Structure Calculations: Storage-Saving and Multiple-Secant Implementation of the Broyden Method. Materials Transactions, JIM, 1999, 40, 1186-1192.	0.9	7
160	Effect of Lattice Coherency on Solution Energies of Impurities: Stability of an Epitaxial InAs Monolayer Deposited on GaAs. Materials Transactions, JIM, 1999, 40, 1295-1300.	0.9	0
161	First-Principles Calculation on Dissociation of Hydrogen Molecule in Nickel. Materials Transactions, JIM, 2000, 41, 1114-1117.	0.9	5
162	Ab Initio Studies of AlSb (001) Adatom Behavior and Reconstruction. Materials Research Society Symposia Proceedings, 2000, 618, 11.	0.1	0
163	Fundamental Cluster and Hydrogen Sites in Ti-Zr-Ni Quasicrystals. Materials Research Society Symposia Proceedings, 2000, 643, 521.	0.1	0
164	Grain boundary structure in B2 Fe-Al ordered alloys: an atomic-scale simulation. Materials Research Society Symposia Proceedings, 2000, 652, 1.	0.1	0

#	Article	IF	Citations
165	Atomic Scale Simulation of the Effect of Hydrogen on Dislocations in Zr. Materials Research Society Symposia Proceedings, 2000, 653, 1.	0.1	0
166	Hybrid Electronic-density-functional/molecular-dynamics Simulation on Parallel Computers: Oxidation of Si Surface. Materials Research Society Symposia Proceedings, 2000, 653, .	0.1	0
167	Practical methods for ab initio calculations on thousands of atoms. International Journal of Quantum Chemistry, 2000, 77, 831-842.	1.0	25
168	Recent developments in ab initio thermodynamics. , 2000, 77, 871-879.		26
169	Electronic structure, properties, and phase stability of inorganic crystals: A pseudopotential plane-wave study. International Journal of Quantum Chemistry, 2000, 77, 895-910.	1.0	1,566
170	Why are Clathrates Good Candidates for Thermoelectric Materials?. Journal of Solid State Chemistry, 2000, 149, 455-458.	1.4	129
172	What are the possible structures for CNx compounds? The example of C3N. Chemical Physics Letters, 2000, 325, 53-60.	1.2	45
173	Dissociative chemisorption of molecular chlorine on Si(100) â€“ a first principles study. Chemical Physics Letters, 2000, 318, 15-21.	1.2	4
174	The adsorption of aromatics on sp-metals: benzene on Al(111). Chemical Physics Letters, 2000, 318, 43-48.	1.2	65
175	Structures and physical properties of âˆ-FeSi-type and CsCl-type RuSi studied by first-principles pseudopotential calculations. Acta Crystallographica Section B: Structural Science, 2000, 56, 369-376.	1.8	16
176	Defect study on Ce3+ in LiBaF3. Journal of Luminescence, 2000, 87-89, 1023-1025.	1.5	6
177	The roles of charged and neutral oxidising species in silicon oxidation from ab initio calculations. Microelectronics Reliability, 2000, 40, 567-570.	0.9	17
178	Structural modelling of the Tiâ€“Zrâ€“Ni quasicrystal. Materials Science & Engineering A: Structural Materials: Properties, Microstructure and Processing, 2000, 294-296, 361-365.	2.6	27
179	An ab initio based structure model of i(Alâ€“Pdâ€“Mn). Materials Science & Engineering A: Structural Materials: Properties, Microstructure and Processing, 2000, 294-296, 351-354.	2.6	1
180	Development of glue-type potentials for the Alâ€“Pb system: phase diagram calculation. Acta Materialia, 2000, 48, 1753-1761.	3.8	77
181	Atomic-scale computational materials science. Acta Materialia, 2000, 48, 71-92.	3.8	163
182	Calculation of the energy profile for the fluorination of dichloromethane over an Î±-alumina catalyst. Applied Catalysis A: General, 2000, 200, 263-274.	2.2	10
183	A scalable molecular-dynamics algorithm suite for materials simulations: design-space diagram on 1024 Cray T3E processors. Future Generation Computer Systems, 2000, 17, 279-291.	4.9	33

#	Article	IF	Citations
184	Computational chemistry on Fujitsu vectorâ€“parallel processors: Development and performance of applications software. Parallel Computing, 2000, 26, 887-911.	1.3	7
185	Co-deposition of In and Sn on the Si(100) 2Ã—1 surface: growth of a one-dimensional alloy?. Applied Surface Science, 2000, 162-163, 638-643.	3.1	8
186	Structure and bandgap closure in dense hydrogen. Nature, 2000, 403, 632-635.	13.7	178
187	Constraints on the composition of the Earth's core from ab initio calculations. Nature, 2000, 405, 172-175.	13.7	100
188	Six-dimensional classical dynamics of H2 dissociative adsorption on Pd(111). Chemical Physics Letters, 2000, 320, 328-334.	1.2	55
189	Spontaneous proton transfer between O-sites in zeolites. Chemical Physics Letters, 2000, 324, 373-380.	1.2	36
190	Spontaneous proton transfer in Na zeolites. Chemical Physics Letters, 2000, 330, 457-462.	1.2	8
191	Why Pb(B1/3Bâ€²2/3)O3 perovskites disorder more easily than Ba(B1/3Bâ€²2/3)O3 perovskites and the thermodynamics of 1:1-type short-range order in PMN. Journal of Physics and Chemistry of Solids, 2000, 61, 327-333.	1.9	31
192	Atomistic modelling of radiation effects: Towards dynamics of exciton relaxation. Nuclear Instruments & Methods in Physics Research B, 2000, 166-167, 1-12.	0.6	18
193	Self-trapped excitons in quartz. Nuclear Instruments & Methods in Physics Research B, 2000, 166-167, 451-458.	0.6	20
194	Quantum study of the active sites of the Î³-alumina surface: chemisorption and adsorption of water, hydrogen sulfide and carbon monoxide on aluminum and oxygen sites. Computational and Theoretical Chemistry, 2000, 505, 81-94.	1.5	48
195	Ab Initio Study of the H2â€“H2S/MoS2 Gasâ€“Solid Interface: The Nature of the Catalytically Active Sites. Journal of Catalysis, 2000, 189, 129-146.	3.1	350
196	Structure, Energetics, and Electronic Properties of the Surface of a Promoted MoS2 Catalyst: An ab Initio Local Density Functional Study. Journal of Catalysis, 2000, 190, 128-143.	3.1	321
197	Growth and structure of ultrathin vanadium oxide layers on Pd(111). Physical Review B, 2000, 61, 13945-13954.	1.1	124
198	Phase stability and structure of spinel-based transition aluminas. Physical Review B, 2000, 63, .	1.1	228
199	Boron diffusion and activation in the presence of other species. , 0, , .		6
200	Structure and dynamics of liquid iron under Earthâ€™s core conditions. Physical Review B, 2000, 61, 132-142.	1.1	245
201	Dielectric and lattice-dynamical properties of III-nitrides. Journal of Electronic Materials, 2000, 29, 281-284.	1.0	4

#	Article	IF	Citations
202	High-pressure phases in the Al 2 SiO 5 system and the problem of aluminous phase in the Earth's lower mantle: ab initio calculations. Physics and Chemistry of Minerals, 2000, 27, 430-439.	0.3	48
203	First-principles Investigation of B-site Ordering in Ba(MgxTa1-x)O3Microwave Dielectrics with the Complex Perovskite Structure. Japanese Journal of Applied Physics, 2000, 39, 1241-1248.	0.8	18
204	Vibrational thermodynamics: coupling of chemical order and size effects. Modelling and Simulation in Materials Science and Engineering, 2000, 8, 295-309.	0.8	16
205	Interface assisted formation of a metastable hcp phase by ion mixing in an immiscible Ag-Ni system. Journal of Physics Condensed Matter, 2000, 12, 9231-9235.	0.7	6
206	Strain-induced tetragonal distortions in epitaxial Ni-films grown on Cu(001). Journal of Physics Condensed Matter, 2000, 12, L139-L146.	0.7	16
207	Ordering of self-diffusion barrier energies on Pt(110)-(1Ã—2). Physical Review B, 2000, 61, R2452-R2455.	1.1	26
208	Cation-vacancy ordering in dehydrated Na6[AlSiO4]6. Journal of Chemical Physics, 2000, 113, 10215-10225.	1.2	14
209	Adsorbate-induced vacancy formation and substrate relaxation on Cr(100). Physical Review B, 2000, 62, 5163-5167.	1.1	25
210	Density-functional calculation of the Hugoniot of shocked liquid deuterium. Physical Review B, 2000, 61, 1-4.	1.1	167
211	C incorporation in epitaxialGe1â^'yCylayers grown on Ge(001):â€ƒAnab initiostudy. Physical Review B, 2000, 62, R7723-R7726.	1.1	20
212	Atom-by-atom and concerted hopping of adatom pairs on an open metal surface. Physical Review B, 2000, 61, R2456-R2459.	1.1	12
213	High-pressure bct to fcc structural transformation in Ga. Physical Review B, 2000, 62, 9900-9902.	1.1	18
214	Boron diffusion in silicon in the presence of other species. Applied Physics Letters, 2000, 77, 2683-2685.	1.5	10
215	Stability of Si-Interstitial Defects: From Point to Extended Defects. Physical Review Letters, 2000, 84, 503-506.	2.9	156
216	Complex reconstruction ofÎ³-iron multilayers on Cu(100):Ab initiolocal-spin-density investigations. Physical Review B, 2000, 61, 16129-16136.	1.1	33
217	Possible metastable states in the Ni-W system predicted byab initiocalculations. Physical Review B, 2000, 62, 11277-11279.	1.1	14
218	Electronic Properties of theSi/SiO2Interface from First Principles. Physical Review Letters, 2000, 85, 1298-1301.	2.9	111
219	Energetics and diffusion of hydrogen inSiO2. Physical Review B, 2000, 61, 4417-4420.	1.1	60

#	Article	IF	Citations
220	Density-functional calculation of the Hugoniot of shocked liquid nitrogen. Physical Review B, 2000, 63, .	1.1	47
221	Excitonic Effects in Core-Excitation Spectra of Semiconductors. Physical Review Letters, 2000, 85, 2168-2171.	2.9	76
222	First-principles calculations of the thermodynamic and structural properties of strainedInxGa1â^'xNandAlxGa1â^'xNalloys. Physical Review B, 2000, 62, 2475-2485.	1.1	187
223	Structure and magnetism of Î³-Fe overlayers on face-centered-cubic Co(001) substrates. Physical Review B, 2000, 62, 9575-9585.	1.1	14
224	Dissociation and sticking ofH2on the Ni(111), (100), and (110) substrate. Physical Review B, 2000, 62, 8295-8305.	1.1	191
225	Intravacancy transition energies in3Câ^'and4Hâ^'SiC. Physical Review B, 2000, 61, 13655-13658.	1.1	15
226	Ab initiobased modeling ofi-AlPdMn. Physical Review B, 2000, 61, 9336-9344.	1.1	29
227	First-principles estimate of the orderâ€"disorder transition in Ba(ZnxNb1â^'x)O3 microwave dielectrics. Journal of Materials Research, 2000, 15, 2061-2064.	1.2	5
228	Lithium trapping by excess oxygen inWO3:A first-principles study. Physical Review B, 2000, 62, 1508-1511.	1.1	6
229	Nature of Metal-Ceramic Adhesion: Computational Experiments with Co on TiC. Physical Review Letters, 2000, 85, 1898-1901.	2.9	77
230	Structures of magic Ba clusters and magic Ba suboxide clusters. Physical Review A, 2000, 62, .	1.0	16
231	Interface energy and electron structure for Fe/VN. Physical Review B, 2000, 61, 2221-2229.	1.1	77
232	Structure, optical absorption, and luminescence energy calculations ofCe3+defects inLiBaF3. Physical Review B, 2000, 61, 16477-16490.	1.1	49
233	Band-gap modifications ofÎ²â^'FeSi2with lattice distortions corresponding to the epitaxial relationships on Si(111). Physical Review B, 2000, 62, 11063-11070.	1.1	73
234	Photoluminescence-linewidth-derived reduced exciton mass forInyGa1â^'yAs1â^'xNxalloys. Physical Review B, 2000, 62, 7144-7149.	1.1	27
235	Ab initiostudies of theCoSi2(100)/Si(100)interface. Physical Review B, 2000, 62, 2209-2219.	1.1	14
236	First-principles studies on the intrinsic stability of the magicFe13O8cluster. Physical Review B, 2000, 61, 5781-5785.	1.1	25
237	Investigation of chemisorbed molecular states for oxygen on rhodium (111). Journal of Chemical Physics, 2000, 113, 4388-4391.	1.2	9

#	Article	IF	Citations
238	Structure of III-Sb(001) Growth Surfaces: The Role of Heterodimers. Physical Review Letters, 2000, 84, 4649-4652.	2.9	67
239	Formation and Diffusion of S-Decorated Cu Clusters on Cu(111). Physical Review Letters, 2000, 85, 606-609.	2.9	84
240	Phonon Anomaly in High-Pressure Zn. Physical Review Letters, 2000, 85, 5130-5133.	2.9	42
241	Nature, Strength, and Consequences of Indirect Adsorbate Interactions on Metals. Physical Review Letters, 2000, 85, 1910-1913.	2.9	175
242	Local-spin-density-approximation molecular-dynamics simulations of dense deuterium. Physical Review E, 2000, 63, 015301.	0.8	36
243	Ab initio energetics of boron-interstitial clusters in crystalline Si. Applied Physics Letters, 2000, 77, 1834.	1.5	64
244	Spin state of vacancies: From magnetic Jahn-Teller distortions to multiplets. Physical Review B, 2000, 62, 6854-6857.	1.1	63
245	Extreme softening of Vanderbilt pseudopotentials: General rules and case studies of first-row andd-electron elements. Physical Review B, 2000, 61, 4576-4587.	1.1	102
246	Band offsets and stability of BeTe/ZnSe (100) heterojunctions. Physical Review B, 2000, 62, R16302-R16305.	1.1	14
247	Transferable atomic-type orbital basis sets for solids. Physical Review B, 2000, 62, 4899-4905.	1.1	121
248	NMR second-moment study of hydrogen sites in icosahedralTi45Zr38Ni17quasicrystals. Physical Review B, 2000, 62, 11444-11449.	1.1	16
249	First-principles computation of the vibrational entropy of ordered and disorderedPd3V. Physical Review B, 2000, 61, 5972-5978.	1.1	114
250	Ab initiostep and kink formation energies on Pb(111). Physical Review B, 2000, 62, 17020-17025.	1.1	33
251	Silicon-doped icosahedral, cuboctahedral, and decahedral clusters of aluminum. Physical Review B, 2000, 61, 8541-8547.	1.1	80
252	Structural, electronic, and magnetic properties of thin Mn/Cu(100) films. Physical Review B, 2000, 61, 11492-11505.	1.1	64
253	Elastic properties of potential superhard phases ofRuO2. Physical Review B, 2000, 61, 10029-10034.	1.1	72
254	Geometry and electronic structures of magic transition-metal oxide clustersM9O6(M=Fe,Co, and Ni). Physical Review B, 2000, 62, 8500-8507.	1.1	43
255	Adsorption energetics and bonding from femtomole calorimetry and from first principles theory. Advances in Catalysis, 2000, 45, 207-259.	0.1	43

#	Article	IF	Citations
256	Highly optimized empirical potential model of silicon. Modelling and Simulation in Materials Science and Engineering, 2000, 8, 825-841.	0.8	151
257	Fully unconstrained noncollinear magnetism within the projector augmented-wave method. Physical Review B, 2000, 62, 11556-11570.	1.1	707
258	Dissociation pathways of oxygen on copper (110) surface: a first principles study. Computational Materials Science, 2000, 17, 133-140.	1.4	23
259	First principles calculations on the diffusivity and viscosity of liquid Feâ€“S at experimentally accessible conditions. Physics of the Earth and Planetary Interiors, 2000, 120, 145-152.	0.7	58
260	Ab initio free energy calculations on the polymorphs of iron at core conditions. Physics of the Earth and Planetary Interiors, 2000, 117, 123-137.	0.7	89
261	Adsorption of group III atoms on SiC(111) surfaces. Surface Science, 2000, 454-456, 127-130.	0.8	1
262	Adsorption and energetics of isolated CO molecules on Pd(111). Surface Science, 2000, 453, 25-31.	0.8	68
263	Atomic and electronic structure of the (111) surface of cubic BN: an LDF ab initio study. Surface Science, 2000, 454-456, 494-497.	0.8	8
264	Density functional theory calculations of adsorption of water at calcium oxide and calcium fluoride surfaces. Surface Science, 2000, 452, 9-19.	0.8	83
265	Ï€ adsorption of ethene on to the {111} surface of copper. Surface Science, 2000, 459, 93-103.	0.8	18
266	Pathways to dissociation of O2 on Cu (110) surface: first principles simulations. Surface Science, 2000, 459, 104-114.	0.8	46
267	First-principles study of the adsorption of atomic H on Ni (111), (100) and (110). Surface Science, 2000, 459, 287-302.	0.8	294
268	Ultrathin aluminum oxide films: Al-sublattice structure and the effect of substrate on ad-metal adhesion. Surface Science, 2000, 464, 108-116.	0.8	59
269	Energetics and structure of stoichiometric SnO2 surfaces studied by first-principles calculations. Surface Science, 2000, 463, 93-101.	0.8	269
270	Step- versus kink-formation energies on Pt(111). Surface Science, 2000, 463, L661-L665.	0.8	20
271	Surface and subsurface alloy formation of vanadium on Pd(111). Surface Science, 2000, 463, 199-210.	0.8	45
272	Structural and dynamical behavior of Al trimer on Al(111) surface. Surface Science, 2000, 465, 65-75.	0.8	15
273	Surface reconstructions on the (100) CoSi2 surface. Surface Science, 2000, 465, 259-265.	0.8	5

#	Article	IF	Citations
274	Cu interactions with Î±-Al2O3(0001): effects of surface hydroxyl groups versus dehydroxylation by Ar-ion sputtering. Surface Science, 2000, 465, 163-176.	0.8	96
275	The energetics and structure of oxygen vacancies on the SnO2(110) surface. Surface Science, 2000, 467, 35-48.	0.8	87
276	Limits of perturbation theory: first principles simulations of scanning tunneling microscopy scans on Fe(100). Surface Science, 2000, 466, L795-L801.	0.8	29
277	Electron-stimulated bond rearrangements on the H/Si(100)-3Ã—1 surface. Surface Science, 2000, 446, 211-218.	0.8	19
278	Phonons and static dielectric constant inCaTiO3from first principles. Physical Review B, 2000, 62, 3735-3743.	1.1	172
279	Real-space mesh techniques in density-functional theory. Reviews of Modern Physics, 2000, 72, 1041-1080.	16.4	432
280	Theory of Adsorption on Metal Substrates. Handbook of Surface Science, 2000, , 285-356.	0.3	37
281	Electronic Structure and Bonding at the Al-terminated Al(111)/Î±-Al₂O₃(0001) Interface: A First Principles Study. Materials Research Society Symposia Proceedings, 2000, 654, 421.	0.1	5
282	Dynamics and polarization of group-III nitride lattices:â€,A first-principles study. Physical Review B, 2000, 62, 8003-8011.	1.1	108
283	Long-range versus short-range interactions and the configurational energies of Ba(B,B')O3and Pb(B,B')O3perovskites. Modelling and Simulation in Materials Science and Engineering, 2000, 8, 211-219.	0.8	6
284	Ab initiostudies on the vibrational and thermal properties ofAl3Li. Physical Review B, 2000, 61, 14531-14536.	1.1	49
285	Compact surface-cluster diffusion by concerted rotation and translation. Physical Review B, 2000, 61, R5125-R5128.	1.1	24
286	Critical size and anomalous lattice expansion in nanocrystallineBaTiO3particles. Physical Review B, 2000, 62, 3065-3070.	1.1	124
287	Ab initiocalculations of phonons inLiNbO3. Physical Review B, 2000, 61, 272-278.	1.1	101
288	Diffusion of Ge below the Si(100) Surface: Theory and Experiment. Physical Review Letters, 2000, 84, 2441-2444.	2.9	78
289	Efficient real-space solution of the Kohnâ€“Sham equations with multiscale techniques. Journal of Chemical Physics, 2000, 112, 9223-9228.	1.2	36
290	Ab initio simulation of the interaction of hydrogen with the {111} surfaces of platinum, palladium and nickel. A possible explanation for their difference in hydrogenation activity. Chemical Communications, 2000, , 705-706.	2.2	33
291	First-Principles Studies on Pd Intercalated Graphite. Molecular Crystals and Liquid Crystals, 2000, 340, 283-288.	0.3	1

#	Article	IF	Citations
292	Stability and electronic property investigations of the graphitic C3N4 system showing an orthorhombic unit cell. Journal of Materials Chemistry, 2000, 10, 709-713.	6.7	51
293	Bond Scission in a Perfect Polyethylene Chain and the Consequences for the Ultimate Strength. Macromolecules, 2000, 33, 9098-9108.	2.2	32
294	Precursor-mediated adsorption of oxygen on the (111) surfaces of platinum-group metals. Physical Review B, 2000, 62, 4744-4755.	1.1	319
295	First-principles Investigation of the Phase Stability for Ba(B1/3â€²2+B2/3â€²â€²5+)O3Microwave Dielectrics with the Complex Perovskite Structure. Japanese Journal of Applied Physics, 2000, 39, 5637-5641.	0.8	30
296	O/N Ordering in Y2Si3O3N4 with the Melilite-type Structure from First-Principles Calculations. Chemistry of Materials, 2000, 12, 1071-1075.	3.2	27
297	Theoretical Study of the Adsorption of Acetylene on the Si(001) Surface. Journal of Physical Chemistry B, 2000, 104, 8259-8267.	1.2	106
298	CO Adsorption on Molybdenum Nitride's Î³-Mo2N(100) Surface:â€‰ Formation of NCO Species? A Density Functional Study. Journal of Physical Chemistry B, 2000, 104, 11972-11976.	1.2	29
299	Direct calculation ofkâ‹…pparameters for wurtzite AlN, GaN, and InN. Physical Review B, 2000, 61, 12933-12938.	1.1	69
300	Oxametallacycle Intermediates on Clean and Cs-Promoted Ag(111) Surfaces. Journal of Physical Chemistry B, 2000, 104, 8685-8691.	1.2	28
301	Density Functional Theory Calculations on the Interaction of Ethene with the {111} Surface of Platinum. Journal of Physical Chemistry B, 2000, 104, 6439-6446.	1.2	49
302	Integrated Experimental and Computational Methods for Structure Determination and Characterization of a New, Highly Stable Cesium Silicotitanate Phase, Cs2TiSi6O15(SNL-A). Chemistry of Materials, 2000, 12, 3449-3458.	3.2	50
303	Thermodynamic Stability of Fe/O Solid Solution at Inner-Core Conditions. Geophysical Research Letters, 2000, 27, 2417-2420.	1.5	17
304	A DFT Study of Transition States for Câ^'H Activation on the Ru(0001) Surfaceâ€. Journal of Physical Chemistry B, 2000, 104, 3364-3369.	1.2	162
305	First-principles molecular dynamics studies of liquid tellurium. Journal of Physics Condensed Matter, 2000, 12, 6053-6061.	0.7	24
306	Dissociation of O2 on the reduced SnO2 (110) surface. Chemical Communications, 2000, , 1235-1236.	2.2	37
307	Ab initiostudy of transitory metastable phases solidified by drop-tube processing. Modelling and Simulation in Materials Science and Engineering, 2000, 8, 233-237.	0.8	3
308	THEORETICALSTUDIES OFATOMIC-SCALEPROCESSESRELEVANT TOCRYSTALGROWTH. Annual Review of Physical Chemistry, 2000, 51, 623-653.	4.8	121
309	Chemical trends of the rattling phonon modes in alloyed germanium clathrates. Journal of Applied Physics, 2000, 87, 7726-7734.	1.1	95

#	Article	IF	Citations
310	Band structure and optical parameters of theSnO2(110)surface. Physical Review B, 2001, 64, .	1.1	115
311	Chemisorption of Hydrogen Molecules on Carbon Nanotubes under High Pressure. Physical Review Letters, 2001, 87, 205502.	2.9	134
312	Coexistence of Atomic and Molecular Chemisorption States:H2/Pd(210). Physical Review Letters, 2001, 87, 096103.	2.9	70
313	Structural and electronic properties of tin clathrate materials. Physical Review B, 2001, 64, .	1.1	61
314	Nonlinear macroscopic polarization in III-V nitride alloys. Physical Review B, 2001, 64, .	1.1	272
315	Search for ultra-hard materials: theoretical characterisation of novel orthorhombic BC2N crystals. Solid State Sciences, 2001, 3, 943-957.	0.8	66
316	Structural stability and lattice defects in copper:Ab initio, tight-binding, and embedded-atom calculations. Physical Review B, 2001, 63, .	1.1	1,756
317	Theoretical Study of Oxygen Adsorption on Graphite and the (8,0) Single-walled Carbon Nanotube. Journal of Physical Chemistry B, 2001, 105, 11227-11232.	1.2	258
318	Small clusters of tin: Atomic structures, energetics, and fragmentation behavior. Physical Review B, 2001, 64, .	1.1	82
319	Energetics of native defects in ZnO. Journal of Applied Physics, 2001, 90, 824-828.	1.1	360
320	Density Functional Theory Calculations of Hydrogen-Containing Defects in Forsterite, Periclase, and Î±-Quartz. Journal of Physical Chemistry B, 2001, 105, 9747-9754.	1.2	53
321	Tetragonal Y-doped zirconia: Structure and ion conductivity. Physical Review B, 2001, 64, .	1.1	145
322	Phase stability and electronic structure of theHfAl3compound. Physical Review B, 2001, 64, .	1.1	26
323	Atomic-scale characterization of boron diffusion in silicon. Physical Review B, 2001, 64, .	1.1	43
324	Metal-Encapsulated Fullerenelike and Cubic Caged Clusters of Silicon. Physical Review Letters, 2001, 87, 045503.	2.9	371
325	Atomic and ionic processes of silicon oxidation. Physical Review B, 2001, 63, .	1.1	70
326	Computational challenges in structural and functional genomics. IBM Systems Journal, 2001, 40, 265-296.	3.1	20
327	Concerted Use of Slab and Cluster Models in an ab Initio Study of Hydrogen Desorption from the Si(100) Surface. Journal of Physical Chemistry B, 2001, 105, 4031-4038.	1.2	42

#	Article	IF	Citations
328	Classical and Quantum-Mechanical Studies of Crystalline FOX-7 (1,1-Diamino-2,2-dinitroethylene). Journal of Physical Chemistry A, 2001, 105, 5010-5021.	1.1	121
329	Modeling STM tips by single absorbed atoms on W(100) films:3dand4dtransition-metal atoms. Physical Review B, 2001, 64, .	1.1	44
330	Ab initiocalculations on etching of graphite and diamond surfaces by atomic hydrogen. Physical Review B, 2001, 63, .	1.1	32
331	Role of disorder in incorporation energies of oxygen atoms in amorphous silica. Physical Review B, 2001, 63, .	1.1	56
332	Upper Limit of the Oâ˜'HÂ·Â·Â·O Hydrogen Bond. Ab Initio Study of the Kaolinite Structure. Journal of Physical Chemistry B, 2001, 105, 10812-10817.	1.2	109
333	Accurate calculation of polarization-related quantities in semiconductors. Physical Review B, 2001, 63, .	1.1	168
334	Ab initiostudy of the vibrational and electronic properties of CdGa2S4and CdGa2Se4under pressure. Journal of Physics Condensed Matter, 2001, 13, 10117-10124.	0.7	23
335	Proof of the Thermodynamical Stability of theEâ€²Center inSiO2. Physical Review Letters, 2001, 86, 3064-3067.	2.9	46
336	Ab initiocalculations of defects in Fe and dilute Fe-Cu alloys. Physical Review B, 2001, 65, .	1.1	376
337	Defect ordering in aliovalently doped cubic zirconia from first principles. Physical Review B, 2001, 64, .	1.1	152
338	Ab initiomolecular-dynamics study of highly nonideal structural and thermodynamic properties of liquid Ni-Al alloys. Physical Review B, 2001, 64, .	1.1	23
339	The origin of the electron distribution in SnO. Journal of Chemical Physics, 2001, 114, 758.	1.2	96
340	Layered-to-Spinel Phase Transition in Li[sub x]MnO[sub 2]. Electrochemical and Solid-State Letters, 2001, 4, A78.	2.2	298
341	Lattice dynamics and elasticity of silver thiogallate (AgGaS2) from ab initio calculations. Journal of Chemical Physics, 2001, 114, 6734-6738.	1.2	17
342	First-principles studies on pure and doped C32clusters. Journal of Physics Condensed Matter, 2001, 13, 1931-1938.	0.7	16
343	The vibrational spectrum of crystalline benzoic acid: Inelastic neutron scattering and density functional theory calculations. Journal of Chemical Physics, 2001, 115, 3241-3248.	1.2	70
344	First-principles theory of ionic diffusion with nondilute carriers. Physical Review B, 2001, 64, .	1.1	405
345	Stability of Chiral Domains Produced by Adsorption of Tartaric Acid Isomers on the Cu(110) Surface:â€‰ A Periodic Density Functional Theory Study. Journal of the American Chemical Society, 2001, 123, 6639-6648.	6.6	110

#	Article	IF	Citations
346	Optical properties of semiconductors using projector-augmented waves. Physical Review B, 2001, 63, .	1.1	259
347	Ab initio molecular dynamics simulation of liquid water and waterâ€“vapor interface. Journal of Chemical Physics, 2001, 115, 9815-9820.	1.2	71
348	Phonon Density of States of Iron up to 153 Gigapascals. Science, 2001, 292, 914-916.	6.0	284
349	Hundâ€™s rule in metal clusters: Prediction of high magnetic moment state ofAl12Cufrom first-principles calculations. Physical Review B, 2001, 64, .	1.1	38
350	Origin of the Different Reconstructions of Diamond, Si, and Ge(111) Surfaces. Physical Review Letters, 2001, 87, 016103.	2.9	64
351	Eleyâ€“Rideal and hot atom reactions between hydrogen atoms on Ni(100): Electronic structure and quasiclassical studies. Journal of Chemical Physics, 2001, 115, 9018-9027.	1.2	39
352	Modeling disorder in amorphous silica with embedded clusters:â€ƒThe peroxy bridge defect center. Physical Review B, 2001, 64, .	1.1	39
353	Long time scale kinetic Monte Carlo simulations without lattice approximation and predefined event table. Journal of Chemical Physics, 2001, 115, 9657-9666.	1.2	398
354	Spin-dependent tunneling conductance ofFe|MgO|Fesandwiches. Physical Review B, 2001, 63, .	1.1	1,791
355	Theoretical structure determination ofÎ³â€˜Al2O3. Physical Review B, 2001, 65, .	1.1	213
356	Structure and bonding in crystalline and molten Li-Sn alloys: A first-principles density-functional study. Physical Review B, 2001, 63, .	1.1	23
357	Adsorption of linear hydrocarbons in zeolites: A density-functional investigation. Journal of Chemical Physics, 2001, 114, 6327-6334.	1.2	38
358	Effect of Particle Size on the Adsorption of O and S Atoms on Pt:Â A Density-Functional Theory Study. Journal of Physical Chemistry B, 2001, 105, 7739-7747.	1.2	65
359	A Comparison of the Adsorption and Diffusion of Hydrogen on the {111} Surfaces of Ni, Pd, and Pt from Density Functional Theory Calculations. Journal of Physical Chemistry B, 2001, 105, 4889-4894.	1.2	184
360	Molecular Dynamics Simulations of Pd Deposition on the Î±-Al2O3(0001) Surface. Journal of Physical Chemistry B, 2001, 105, 12111-12117.	1.2	30
361	First Principles Theory of Mantle and Core Phases. Reviews in Mineralogy and Geochemistry, 2001, 42, 319-343.	2.2	6
362	Phase stability and electronic structure in ZrAl3 compound. Journal of Alloys and Compounds, 2001, 319, 154-161.	2.8	52
363	Dynamical properties of pnictide ZnSnP2 from ab initio calculations. Journal of Alloys and Compounds, 2001, 328, 162-165.	2.8	8

#	Article	IF	Citations
364	First-principles characterisation of new ternary heterodiamond BC2N phases. Computational Materials Science, 2001, 20, 107-119.	1.4	68
365	Energetics and diffusivity of atomic boron in silicon by density-functional-based tight-binding simulations. Computational Materials Science, 2001, 22, 44-48.	1.4	10
366	Cation polarizability from first-principles: Sn2+. Computational Materials Science, 2001, 22, 94-98.	1.4	20
367	Ab initio modeling study of boron diffusion in silicon. Computational Materials Science, 2001, 21, 496-504.	1.4	11
368	Structure and reactivity of amorphous silicon nitride investigated with density-functional methods. Journal of Non-Crystalline Solids, 2001, 293-295, 238-243.	1.5	33
369	Atomic networks and clustering in liquid Te and Kâ€“Te alloys. Journal of Non-Crystalline Solids, 2001, 293-295, 193-198.	1.5	15
370	Cu, Ag, and Au atoms adsorbed on TiO2(110): cluster and periodic calculations. Surface Science, 2001, 471, 21-31.	0.8	131
371	STM-induced void formation at the Al2O3/Ni3Al(111) interface. Surface Science, 2001, 472, L157-L163.	0.8	14
372	Adsorption sites and STM images of C2H2 on Si(100): a first-principles study. Surface Science, 2001, 475, 83-88.	0.8	38
373	Quenching surface states with the tip: STM scans on Fe(100). Surface Science, 2001, 482-485, 1113-1118.	0.8	8
374	Stability, electronic properties and chemical reactivity of palladiumâ€“vanadium(1 1 1) surface alloys. Surface Science, 2001, 482-485, 712-717.	0.8	12
375	Benzene on silicon: combining STM experiments with first principles studies. Surface Science, 2001, 482-485, 1181-1185.	0.8	23
376	Accelerated mound decay at adjacent kinks on Cu(111). Surface Science, 2001, 478, L349-L354.	0.8	12
377	The structure of the oxygen induced (1Ã—5) reconstruction of V(100). Surface Science, 2001, 480, 11-24.	0.8	39
378	The first-principle study of the iodine-modified silver surfaces. Surface Science, 2001, 487, 77-86.	0.8	21
379	Physisorption of water on salt surfaces. Surface Science, 2001, 488, 177-192.	0.8	42
380	Structure and energetics of Cu(100) vicinal surfaces. Surface Science, 2001, 489, 151-160.	0.8	22
381	Density-functional bridge between surfaces and interfaces. Surface Science, 2001, 493, 253-270.	0.8	31

#	Article	IF	Citations
382	Structural and electronic properties of silver surfaces: ab initio pseudopotential density functional study. Surface Science, 2001, 490, 125-132.	0.8	48
383	A first principles survey of stoichiometric (1Ã—2) reconstructions on the rutile surface. Surface Science, 2001, 495, 211-233.	0.8	23
384	First-principles study of the interaction of oxygen with the SnO2(110) surface. Surface Science, 2001, 490, 221-236.	0.8	98
385	Investigation of vinyl phosphonic acid/hydroxylated Î±-Al2O3() reaction enthalpies. Surface Science, 2001, 494, 1-20.	0.8	48
386	First-principles calculations for VxOy grown on Pd(111). Surface Science, 2001, 492, 329-344.	0.8	66
387	Pt-dimer dissociation on Pt(111). Surface Science, 2001, 492, L723-L728.	0.8	15
388	Structure of an ultrathin TiOx film, formed by the strong metal support interaction (SMSI), on Pt nanocrystals on TiO2(110). Surface Science, 2001, 492, L677-L687.	0.8	72
389	Application of Ab Initio Molecular Dynamics for A Priori Elucidation of the Mechanism in Unimolecular Decomposition:Â The Case of 5-Nitro-2,4-dihydro-3H-1,2,4-triazol-3-one (NTO). Journal of the American Chemical Society, 2001, 123, 2243-2250.	6.6	54
390	First-principles studies of the stability of Zintl ions in alkali-tin alloys: I. Crystalline intermetallic compounds. Journal of Physics Condensed Matter, 2001, 13, 959-980.	0.7	10
391	Breaking the NO bond on Rh, Pd, and Pd3Mn alloy (100) surfaces: A quantum chemical comparison of reaction paths. Journal of Chemical Physics, 2001, 115, 8101-8111.	1.2	61
392	Electron standing-wave observation in the Pd overlayer on Au(111) and Cu(111) surfaces by scanning tunneling microscopy. Physical Review B, 2001, 64, .	1.1	19
393	The electronic structure of tantalum (oxy)nitrides TaON and Ta3N5. Journal of Materials Chemistry, 2001, 11, 1248-1252.	6.7	178
394	Parallel FP-LAPW for distributed-memory machines. Computing in Science and Engineering, 2001, 3, 18-29.	1.2	5
395	Ab initiostudy of the electronic and structural properties of the ferroelectric transition inKH2PO4. Physical Review B, 2001, 65, .	1.1	65
396	Local ordering of hydroxy groups in hydroxyapatite. Chemical Communications, 2001, , 1646-1647.	2.2	84
397	CO Adsorption on Ptâ^'Ru Surface Alloys and on the Surface of Ptâ^'Ru Bulk Alloy. Journal of Physical Chemistry B, 2001, 105, 9533-9536.	1.2	90
398	Structure and Energetics of Iron Pentacarbonyl Formation at an Fe(100) Surface. Journal of Physical Chemistry B, 2001, 105, 12547-12552.	1.2	37
399	Adsorption of benzene on Si(100)-(2Ã—1):â€ƒAdsorption energies and STM image analysis byab initiomethods. Physical Review B, 2001, 63, .	1.1	91

#	Article	IF	Citations
400	Periodic density functional plane wave calculations of triplet exciton in NaCl. Radiation Effects and Defects in Solids, 2001, 155, 311-315.	0.4	1
401	First-principles studies of the stability of Zintl ions in alkali-tin alloys: II. Liquid alloys. Journal of Physics Condensed Matter, 2001, 13, 981-1021.	0.7	14
402	A Periodic DFT Study of Intramolecular Isomerization Reactions of Toluene and Xylenes Catalyzed by Acidic Mordenite. Journal of the American Chemical Society, 2001, 123, 7655-7667.	6.6	116
403	Stability of Zn(II) Cations in Chabazite Studied by Periodical Density Functional Theory. Journal of the American Chemical Society, 2001, 123, 4530-4540.	6.6	41
404	The Chemical Nature of Surface Point Defects on MoO3(010):Â Adsorption of Hydrogen and Methyl. Journal of the American Chemical Society, 2001, 123, 2224-2230.	6.6	58
405	Density of constitutional and thermal point defects inL12Al3Sc. Physical Review B, 2001, 63, .	1.1	60
406	Ab initiostudy of deuterium in the dissociating regime: Sound speed and transport properties. Physical Review E, 2001, 64, 066406.	0.8	27
407	Dynamical and optical properties of warm dense hydrogen. Physical Review B, 2001, 63, .	1.1	135
408	A Theoretical Study of the Alkylation Reaction of Toluene with Methanol Catalyzed by Acidic Mordenite. Journal of the American Chemical Society, 2001, 123, 2799-2809.	6.6	177
409	Density functional theory calculations of proton-containing defects in forsterite. Radiation Effects and Defects in Solids, 2001, 154, 255-259.	0.4	3
410	The Water Molecule in Na6[AlSiO4]6 Sodalite. Journal of Physical Chemistry B, 2001, 105, 3813-3822.	1.2	8
411	The CO/Pt(111) Puzzle. Journal of Physical Chemistry B, 2001, 105, 4018-4025.	1.2	642
412	First-principles density-functional study of metal-carbonitride interface adhesion: Co/TiC(001) and Co/TiN(001). Physical Review B, 2001, 64, .	1.1	112
413	First-principles investigation of the cooperative Jahn-Teller effect for octahedrally coordinated transition-metal ions. Physical Review B, 2001, 63, .	1.1	89
414	Ab initiostudy of hydrogen adsorption to single-walled carbon nanotubes. Physical Review B, 2001, 63, .	1.1	161
415	Theoretical study of the ordered-vacancy semiconducting compound CdAl2Se4. Journal of Physics Condensed Matter, 2001, 13, 1669-1684.	0.7	26
416	Ab-initiosimulation of isolated screw dislocations in bcc Mo and Ta. Philosophical Magazine A: Physics of Condensed Matter, Structure, Defects and Mechanical Properties, 2001, 81, 1305-1316.	0.8	115
417	The Cs/K Exchange in Muscovite Interlayers: An Ab Initio Treatment. Clays and Clay Minerals, 2001, 49, 500-513.	0.6	34

#	Article	IF	Citations
418	Modeling Boron and Indium Electrical Activities in Silicon in the Presence of Nitrogen. Materials Research Society Symposia Proceedings, 2001, 669, 1.	0.1	0
419	Stoichiometry and Adhesion of Al/WC. Materials Research Society Symposia Proceedings, 2001, 677, 4251.	0.1	1
420	Screening Beneficial Dopants to Cu Interconnect by Modeling. Materials Research Society Symposia Proceedings, 2001, 677, 7131.	0.1	1
421	Simulations of long time scale dynamics using the dimer method. Materials Research Society Symposia Proceedings, 2001, 677, 811.	0.1	4
422	Influence of magnetic interaction on lattice dynamics of FeBO 3. Europhysics Letters, 2001, 56, 275-281.	0.7	21
423	Structure and elasticity of wadsleyite at high pressures. American Mineralogist, 2001, 86, 1387-1395.	0.9	49
424	Bonding Character of Hydrogen in Aluminum Clusters. Materials Transactions, 2001, 42, 2175-2179.	0.4	8
425	From DFT Calculations to Dynamic Monte Carlo Simulations. The reactivity of CHX on the Ru(0001) Surface. Studies in Surface Science and Catalysis, 2001, , 221-228.	1.5	4
426	Solving large nonlinear generalized eigenvalue problems from Density Functional Theory calculations in parallel. Applied Numerical Mathematics, 2001, 37, 189-199.	1.2	15
427	Photocatalytic TiO2 thin film deposited onto glass by DC magnetron sputtering. Thin Solid Films, 2001, 392, 338-344.	0.8	318
428	Nonmetalâ€“metal transition in Ban clusters. Solid State Communications, 2001, 117, 635-639.	0.9	1
429	The different roles of charged and neutral atomic and molecular oxidising species in silicon oxidation from ab initio calculations. Solid-State Electronics, 2001, 45, 1233-1240.	0.8	21
430	Electron and atom dynamics at solid surfaces and relation to epitaxy. Journal of Physics and Chemistry of Solids, 2001, 62, 1689-1730.	1.9	10
431	On the nature of RuS2 HDS active sites: insight from ab initio theory. Journal of Molecular Catalysis A, 2001, 174, 239-244.	4.8	8
432	Parallel between infrared characterisation and ab initio calculations of CO adsorption on sulphided Mo catalysts. Catalysis Today, 2001, 70, 255-269.	2.2	111
433	Ab initio vs literature stiffness values for Ga: a caveat about crystal settings. Physica B: Condensed Matter, 2001, 307, 191-196.	1.3	6
434	Ab initio search of carbon nitrides, isoelectronic with diamond, likely to lead to new ultra hard materials. Comptes Rendus De L'Academie Des Sciences - Series IIc: Chemistry, 2001, 4, 255-272.	0.1	6
435	Ab initio molecular dynamics simulation of hydration and ion-exchange processes in low Al-zeolites. Microporous and Mesoporous Materials, 2001, 42, 1-19.	2.2	14

#	Article	IF	Citations
436	Adhesion, lubrication and wear on the atomic scale. Surface and Interface Analysis, 2001, 31, 619-626.	0.8	46
437	Theoretical Study of Possible Iridium Ditelluride Phases Attainable under High Pressure. Journal of Solid State Chemistry, 2001, 162, 63-68.	1.4	11
439	TlF and PbO under High Pressure: Unexpected Persistence of the Stereochemically Active Electron Pair. Angewandte Chemie - International Edition, 2001, 40, 4624-4629.	7.2	29
440	Modeling and Simulation for Microelectronic Materials Research. Physica Status Solidi (B): Basic Research, 2001, 226, 47-56.	0.7	2
441	Post-Spinel Phases of Silicon Nitride. Physica Status Solidi (B): Basic Research, 2001, 226, R6-R7.	0.7	30
442	HARES: an efficient method for first-principles electronic structure calculations of complex systems. Computer Physics Communications, 2001, 137, 341-360.	3.0	37
443	Hybrid finite-element/molecular-dynamics/electronic-density-functional approach to materials simulations on parallel computers. Computer Physics Communications, 2001, 138, 143-154.	3.0	136
444	Linear-scaling density-functional-theory calculations of electronic structure based on real-space grids: design, analysis, and scalability test of parallel algorithms. Computer Physics Communications, 2001, 140, 303-314.	3.0	126
445	Amorphous WO3: a first-principles approach. Electrochimica Acta, 2001, 46, 1989-1993.	2.6	52
446	There is a true precursor for hydrogen adsorption after all: the system H2/Pd(1 1 1) + subsurface V. Chemical Physics Letters, 2001, 342, 473-478.	1.2	39
447	NO reduction over Pt(1 0 0): reaction rates from first principles. Chemical Physics Letters, 2001, 343, 383-389.	1.2	32
448	Influence of composition fluctuations and strain on gap bowing inInxGa1â^'xN. Physical Review B, 2001, 63, .	1.1	35
449	Thermodynamics of hexagonal-close-packed iron under Earthâ€™s core conditions. Physical Review B, 2001, 64, .	1.1	252
450	Structure and electrical levels of point defects in monoclinic zirconia. Physical Review B, 2001, 64, .	1.1	307
451	Pdâ€“Mn Silica-Supported Catalysts. Journal of Catalysis, 2001, 198, 243-255.	3.1	7
452	Morphology and Surface Properties of Boehmite (Î³-AlOOH): A Density Functional Theory Study. Journal of Catalysis, 2001, 201, 236-246.	3.1	218
453	The phase diagram and electronic structure of Pd-V alloys:ab initiodensity functional calculations. Journal of Physics Condensed Matter, 2001, 13, 3545-3572.	0.7	22
454	First-principles prediction of structure, energetics, formation enthalpy, elastic constants, polarization, and piezoelectric constants of AlN, GaN, and InN: Comparison of local and gradient-corrected density-functional theory. Physical Review B, 2001, 64, .	1.1	421

#	Article	IF	Citations
455	Structural, vibrational, and thermodynamic properties of Al-Sc alloys and intermetallic compounds. Physical Review B, 2001, 64, .	1.1	87
456	Crystal structure and stability of complex precipitate phases in Alâ€“Cuâ€“Mgâ€“(Si) and Alâ€“Znâ€“Mg alloys. Acta Materialia, 2001, 49, 3129-3142.	3.8	394
457	Ab initio density functional theory applied to the structure and proton dynamics of clays. Chemical Physics Letters, 2001, 333, 479-484.	1.2	45
458	Optimally localized Wannier functions within the Vanderbilt ultrasoft pseudo-potential formalism. Computational and Theoretical Chemistry, 2001, 544, 49-60.	1.5	12
459	Determination of solid-state sulfidation mechanisms in ion-implanted copper. Nuclear Instruments & Methods in Physics Research B, 2001, 175-177, 382-387.	0.6	12
460	Icosahedral growth and non-metal-metal transition in strontium clusters. Scripta Materialia, 2001, 44, 1949-1953.	2.6	2
461	Capacitance of magic Ba n clusters. Scripta Materialia, 2001, 44, 1959-1962.	2.6	3
462	Ab initio local-spin-density study of the structural and magnetic properties of La1â^'xCaxMnO3 systems. Journal of Magnetism and Magnetic Materials, 2001, 226-230, 889-891.	1.0	5
463	Complex reconstructions and interdiffusion in Î³-iron films on Cu(100) â€" ab-initio study. Journal of Magnetism and Magnetic Materials, 2001, 226-230, 1600-1601.	1.0	1
464	Self-diffusion of adatoms on Ni(100) surfaces. Journal of Physics Condensed Matter, 2001, 13, L321-L328.	0.7	18
465	First Principles Study on Li Deintercalation Effect in Orthorhombic LiMnO2. Japanese Journal of Applied Physics, 2001, 40, 6878-6883.	0.8	1
466	Orientation of OH groups in kaolinite and dickite: Ab initio molecular dynamics study. American Mineralogist, 2001, 86, 1057-1065.	0.9	98
467	Determining the range of forces in empirical many-body potentials using first-principles calculations. Philosophical Magazine A: Physics of Condensed Matter, Structure, Defects and Mechanical Properties, 2001, 81, 991-1008.	0.8	26
468	Restricting Dislocation Movement in Transition Metal Carbides by Phase Stability Tuning. Science, 2001, 293, 2434-2437.	6.0	110
469	MgB2under pressure: phonon calculations, Raman spectroscopy, and optical reflectance. Journal of Physics Condensed Matter, 2001, 13, 9945-9962.	0.7	68
470	Car-Parrinello methods in chemical engineering: Their scope and potential. Advances in Chemical Engineering, 2001, 28, 353-397.	0.5	4
471	Near-Edge X-ray Absorption Spectra of Carbon-Nitride Molecules and Solids. Physica Scripta, 2001, 63, 70-86.	1.2	18
472	Ordering effects in the Reâ€“W and Reâ€“Ta sigma phases. Journal of Physics Condensed Matter, 2001, 13, 9433-9443.	0.7	14

#	Article	IF	Citations
473	Phonon band structures and resonant scattering in Na 8 Si 46 and Cs 8 Sn 44 clathrates. Europhysics Letters, 2001, 56, 261-267.	0.7	32
474	Ab InitioFermi Surface Calculation for Charge-Density Wave Instability in Transition Metal Oxide Bronzes. Physical Review Letters, 2001, 86, 5100-5103.	2.9	30
475	Origins of Nonstoichiometry and Vacancy Ordering inSc1â^'xâ–¡xS. Physical Review Letters, 2001, 87, 275508.	2.9	27
476	Site occupancy in the Re-W sigma phase. Physical Review B, 2001, 64, .	1.1	46
477	Vibrational modes in epitaxialTi1â^'xScxN(001)layers: Anab initiocalculation and Raman spectroscopy study. Physical Review B, 2001, 64, .	1.1	50
478	Atomic structures and energetics ofLaNi5â^'Hsolid solution and hydrides. Physical Review B, 2001, 64, .	1.1	54
479	Diffusion Kinetics in thePd/Cu(001)Surface Alloy. Physical Review Letters, 2001, 86, 4588-4591.	2.9	77
480	Initial stages of oxidation of (100) and (110) surfaces of iron caused by water. Physical Review B, 2001, 64, .	1.1	98
481	Density-functional calculation of van der Waals forces for free-electron-like surfaces. Physical Review B, 2001, 64, .	1.1	49
482	Density-functional theory calculations of the interaction of protons and water with low-coordinated surface sites of calcium oxide. Physical Review B, 2001, 63, .	1.1	37
483	Native defects and complexes in SiC. Journal of Physics Condensed Matter, 2001, 13, 9027-9037.	0.7	18
484	First principles investigation of scaling trends of zirconium silicate interface band offsets. Journal of Applied Physics, 2001, 90, 1333-1341.	1.1	35
485	First-principles study of solute-dislocation interaction in aluminum-rich alloys. Physical Review B, 2001, 64, .	1.1	35
486	Electronic structure, bonding nature, and charge transfer in Ba@Si20 and Si20 clusters: An ab initio study. Physical Review B, 2001, 64, .	1.1	27
487	Stability of a nonequilibrium phase in an immiscible Ag-Ni system studied byab initiocalculations and ion-beam-mixing experiment. Physical Review B, 2001, 63, .	1.1	26
488	Density-functional calculations for prototype metal-boron nanotubes. Physical Review B, 2001, 64, .	1.1	60
489	Structure and magnetism in thin films and multilayers of hexagonal ruthenium and iron. Physical Review B, 2001, 63, .	1.1	13
490	Transition-metal interactions in aluminum-rich intermetallics. Physical Review B, 2001, 64, .	1.1	25

#	Article	IF	Citations
491	Migration of O vacancies in Î±-quartz: The effect of excitons and electron holes. Physical Review B, 2001, 64, .	1.1	39
492	Patterning of Si(001) with halogens: Surface structure as a function of the halogen chemical potential. Physical Review B, 2001, 64, .	1.1	23
493	Adsorbate-induced demagnetization and restructuring of ultrathin magnetic films: CO chemisorbed onÎ³-Fe/Cu(100). Physical Review B, 2001, 64, .	1.1	18
494	Electronic structure and magnetic interactions in Mn doped semiconductors. Journal of Applied Physics, 2001, 89, 7021-7023.	1.1	50
495	Ab initio study of hexagonal Fe/Ru multilayers. Journal of Applied Physics, 2001, 89, 7080-7082.	1.1	2
496	Adhesion of ultrathin ZrO2(111) films on Ni(111) from first principles. Journal of Chemical Physics, 2001, 114, 5816-5831.	1.2	112
497	Comparative dielectric response in CaTiO3 and CaAl1/2Nb1/2O3 from first principles. Journal of Applied Physics, 2001, 90, 1459-1468.	1.1	27
498	Structure and stability of the clathrates Ba8Ga16Ge30, Sr8Ga16Ge30, Ba8Ga16Si30, and Ba8In16Sn30. Journal of Chemical Physics, 2001, 114, 10063-10074.	1.2	136
499	Multiscale modeling of stress-mediated diffusion in silicon: Ab initio to continuum. Applied Physics Letters, 2001, 78, 201-203.	1.5	33
500	Parametrization of modified embedded-atom-method potentials for Rh, Pd, Ir, and Pt based on density functional theory calculations, with applications to surface properties. Physical Review B, 2001, 63, .	1.1	34
501	Jahn-Teller mediated ordering in layeredLixMO2compounds. Physical Review B, 2001, 63, .	1.1	63
502	Thermal and lattice dynamical properties ofNa8Si46clathrate. Physical Review B, 2001, 64, .	1.1	31
503	Multigrid method for electronic structure calculations. Physical Review B, 2001, 63, .	1.1	152
504	Magic behavior and bonding nature in hydrogenated aluminum clusters. Physical Review B, 2001, 65, .	1.1	81
505	Towards 100% spin-polarized charge-injection: The half-metallic NiMnSb/CdS interface. Physical Review B, 2001, 64, .	1.1	184
506	Ab initio simulation of ammonia monohydrate (NH3â‹…H2O) and ammonium hydroxide (NH4OH). Journal of Chemical Physics, 2001, 115, 7006-7014.	1.2	44
507	Mask-function real-space implementations of nonlocal pseudopotentials. Physical Review B, 2001, 64, .	1.1	19
508	Stability, reconstruction, and surface electronic states of group-III atoms on SiC(111). Physical Review B, 2001, 64, .	1.1	12

#	Article	IF	Citations
509	Irradiation and interface induced formation of a nonequilibriumAg3Cophase predicted byab initiocalculation. Physical Review B, 2001, 64, .	1.1	23
510	CO adsorption on hydrogen saturated Ru(0001). Journal of Chemical Physics, 2001, 115, 5244-5251.	1.2	23
511	The competition between chemical bonding and magnetism in the adsorption of atomic Ni on MgO(100). Journal of Chemical Physics, 2001, 115, 8172-8177.	1.2	50
512	Determination of buried dislocation structures by scanning tunneling microscopy. Physical Review B, 2001, 63, .	1.1	24
513	Calculation of a Deuterium Double Shock Hugoniot fromAb InitioSimulations. Physical Review Letters, 2001, 87, 275502.	2.9	89
514	Quantum size effects in metal films:â€ƒEnergies and charge densities of Pb(111) grown on Cu(111). Physical Review B, 2001, 63, .	1.1	43
515	Ab initiostudies of high-pressure transformations inGeO2. Physical Review B, 2001, 63, .	1.1	56
516	Hydrogen in jellium: First-principles pair interactions. Physical Review B, 2001, 64, .	1.1	22
517	Growth of face-centered-cubic Fe films on Cu(100): Interdiffusion, surfactant effects, and island formation. Physical Review B, 2001, 64, .	1.1	29
518	Novel Interface-Mediated Metastable Oxide Phases: Vanadium Oxides on Pd(111). Physical Review Letters, 2001, 87, 086102.	2.9	112
519	Thermodynamics of uniaxial phase transition:Ab initiostudy of the diamond-to-Î²-tin transition in Si and Ge. Physical Review B, 2001, 63, .	1.1	23
520	Neglected adsorbate interactions behind diffusion prefactor anomalies on metals. Physical Review B, 2001, 64, .	1.1	68
521	An experimental and theoretical investigation of the thiophene/aluminum interface. Journal of Chemical Physics, 2001, 114, 935.	1.2	30
522	On the Constitution of Sodium at Higher Densities. Physical Review Letters, 2001, 86, 2830-2833.	2.9	145
523	Role of Stress in Thin Film Alloy Thermodynamics: Competition between Alloying and Dislocation Formation. Physical Review Letters, 2001, 86, 660-663.	2.9	51
524	Surface Relaxations, Current Enhancements, and Absolute Distances in High Resolution Scanning Tunneling Microscopy. Physical Review Letters, 2001, 87, 236104.	2.9	134
525	Structure of the Ba-InducedSi(111)-(3Ã—2)Reconstruction. Physical Review Letters, 2001, 87, 056104.	2.9	64
526	Adsorption Sites and Ligand Effect for CO on an Alloy Surface: A Direct View. Physical Review Letters, 2001, 87, 036103.	2.9	129

#	Article	IF	Citations
527	Surface-diffusion mechanism versus electric field:â€ƒPt/Pt(001). Physical Review B, 2001, 64, .	1.1	103
528	Mechanism of Interstitial Oxygen Diffusion in Hafnia. Physical Review Letters, 2002, 89, 225901.	2.9	146
529	The Role of the Nanoscale in Surface Reactions:CO2on CdSe. Physical Review Letters, 2002, 89, 075506.	2.9	22
530	Vibrational Recognition of Hydrogen-Bonded Water Networks on a Metal Surface. Physical Review Letters, 2002, 89, 176104.	2.9	229
531	Two-Dimensional Oxide on Pd(111). Physical Review Letters, 2002, 88, 246103.	2.9	267
532	Ab initio density functional investigation of the (001) surface of mordenite. Journal of Chemical Physics, 2002, 117, 7295-7305.	1.2	48
533	Belonoshko, Ahuja, and Johansson Reply:. Physical Review Letters, 2002, 89, .	2.9	5
534	Effects of morphology on the electronic and transport properties of Sn-based clathrates. Journal of Chemical Physics, 2002, 117, 1302-1312.	1.2	34
535	Comprehensiveab initioThermodynamic Treatment of Impurities in Ordered Alloys: Application to Boron inB2Fe-Al. Physical Review Letters, 2002, 89, 225502.	2.9	16
536	Theoretical and experimental investigation of boron diffusion in polycrystalline HfO2 films. Applied Physics Letters, 2002, 81, 1441-1443.	1.5	18
537	Surface model and exchange-correlation functional effects on the description of Pd/Î±-Al2O3(0001). Journal of Chemical Physics, 2002, 116, 1684-1691.	1.2	51
538	Energetics of hydrogen impurities in aluminum and their effect on mechanical properties. Physical Review B, 2002, 65, .	1.1	75
539	Energetics of transition-metal ions in low-coordination environments. Physical Review B, 2002, 66, .	1.1	2
540	First-principles investigations forYH3(YD3):â€ƒEnergetics, electric-field gradients, and optical properties. Physical Review B, 2002, 66, .	1.1	19
541	Ab initio GWquasiparticle calculation of small alkali-metal clusters. Physical Review B, 2002, 65, .	1.1	46
542	Atomistic potential for adsorbate/surface systems: CO on Pt. Physical Review B, 2002, 66, .	1.1	20
543	Structural characterization of the hydrogen-covered C(100) surface by density functional theory calculations. Physical Review B, 2002, 66, .	1.1	38
544	Screening beneficial dopants to Cu interconnects by modeling. Applied Physics Letters, 2002, 80, 763-765.	1.5	9

#	Article	IF	Citations
545	Stability of Ge-related point defects and complexes in Ge-dopedSiO2. Physical Review B, 2002, 66, .	1.1	16
546	First-principles calculation of the phonon spectrum ofMgAl2O4spinel. Physical Review B, 2002, 65, .	1.1	66
547	Crystal structure and lattice dynamics ofAlB2under pressure and implications forMgB2. Physical Review B, 2002, 66, .	1.1	71
548	Shear instability in fcc Fe and thin Fe-Cu[001] films. IEEE Transactions on Magnetics, 2002, 38, 2646-2648.	1.2	1
549	Shear instability in ultrathin Fe/Cu(100) films. , 0, , .		0
550	Ab initiocalculations for bromine adlayers on the Ag(100) and Au(100) surfaces: Thec(2Ã—2)structure. Physical Review B, 2002, 65, .	1.1	26
551	Hydrogen adsorption on an open metal surface:H2/Pd(210). Physical Review B, 2002, 65, .	1.1	86
552	First-Principles Investigations of Precursor Molecules for Microclusters. Phase Transitions, 2002, 75, 31-39.	0.6	0
553	Vibrational properties of tin clathrate materials. Physical Review B, 2002, 65, .	1.1	33
554	Atomistic and electronic structure calculation of defects at the surfaces of oxides. Radiation Effects and Defects in Solids, 2002, 157, 773-781.	0.4	12
555	Interaction of Pd withÎ±â^'Al2O3(0001):â€ƒA case study of modeling the metal-oxide interface on complex substrates. Physical Review B, 2002, 65, .	1.1	55
556	First-principles calculations of the adsorption, diffusion, and dissociation of a CO molecule on the Fe(100) surface. Physical Review B, 2002, 66, .	1.1	121
557	Hydrogen defects in Forsterite: A test case for the embedded cluster method. Journal of Chemical Physics, 2002, 116, 2628-2635.	1.2	38
558	Efficient Eley-Rideal Reactions of H Atoms with Single Cl Adsorbates on Au(111). Physical Review Letters, 2002, 89, 268302.	2.9	32
559	Stability of elongated and compact types of structures inSiO2nanoparticles. Physical Review B, 2002, 65, .	1.1	37
560	Self-Diffusion Rates in Al from Combined First-Principles and Model-Potential Calculations. Physical Review Letters, 2002, 89, 065901.	2.9	67
561	Elastic interaction of oxygen atoms on a graphite surface. Physical Review B, 2002, 66, .	1.1	6
562	Initial Stage of Carbon Incorporation into Si(001) and One-Dimensional Ordering of Embedded Carbon. Physical Review Letters, 2002, 89, 106102.	2.9	30

#	Article	IF	Citations
563	Linking Surface Stress to Surface Structure: Measurement of Atomic Strain in a Surface Alloy using Scanning Tunneling Microscopy. Physical Review Letters, 2002, 89, 036101.	2.9	34
564	Formation energy of Cr/Al vacancies in spinelMgCr2O4andMgAl2O4by first-principles calculations. Physical Review B, 2002, 65, .	1.1	21
565	Nonconstant electronic density of states tunneling inversion for A15 superconductors:Nb3Sn. Physical Review B, 2002, 65, .	1.1	17
566	Instability of metallicInâ"Sndimer lines on Si(100)2Ã—1surface. Physical Review B, 2002, 65, .	1.1	12
567	Electronic states of prototype supertetrahedral framework materials. Physical Review B, 2002, 66, .	1.1	3
568	First principles study of Pt adhesion and growth on SrO- and TiO2-terminated SrTiO3(100). Journal of Chemical Physics, 2002, 116, 9914-9925.	1.2	74
569	SrTiO3/MgO(001)andMgO/SrTiO3(001)systems:â€ƒEnergetics and stresses. Physical Review B, 2002, 66, .	1.1	15
570	Substitutional carbon in group-III nitrides:Ab initiodescription of shallow and deep levels. Physical Review B, 2002, 66, .	1.1	38
571	Raman scattering study of stoichiometric Si and Ge type II clathrates. Journal of Applied Physics, 2002, 92, 7225-7230.	1.1	58
572	Dynamics of self-interstitial cluster formation in silicon. Physical Review B, 2002, 66, .	1.1	13
573	Theoretical Evaluation of Zirconia and Hafnia as Gate Oxides for Si Microelectronics. Physical Review Letters, 2002, 89, 266101.	2.9	167
574	Hydrogen Vibration Modes in GaP:N: The Pivotal Role of Nitrogen in Stabilizing theH2*Complex. Physical Review Letters, 2002, 88, 125506.	2.9	42
575	Atomistic Modeling of Diffusion in Aluminum. Phase Transitions, 2002, 75, 265-272.	0.6	9
576	Adaptive nudged elastic band approach for transition state calculation. Journal of Chemical Physics, 2002, 117, 4651-4658.	1.2	148
577	Classical dynamics of dissociative adsorption for a nonactivated system: The role of zero point energy. Journal of Chemical Physics, 2002, 116, 9005-9013.	1.2	86
578	Connecting atomistic and experimental estimates of ideal strength. Physical Review B, 2002, 65, .	1.1	127
579	Structure and bonding of propyne on Cu(111) from density functional periodic and cluster models. Journal of Chemical Physics, 2002, 116, 1165-1170.	1.2	20
580	Atomistic modeling of solid-state amorphization in an immiscible Cu-Ta system. Physical Review B, 2002, 66, .	1.1	56

#	Article	IF	Citations
581	Density-functional theory investigation of hardness, stability, and electron-energy-loss spectra of carbon nitrides withC11N4stoichiometry. Physical Review B, 2002, 65, .	1.1	95
582	Self-interstitial trapping by carbon complexes in crystalline silicon. Physical Review B, 2002, 66, .	1.1	45
583	Pt80Fe20surface from first principles: Electronic structure and adsorption of CO and atomic H. Physical Review B, 2002, 66, .	1.1	29
584	Self-diffusion on fcc (100) metal surfaces: Comparison of different approximations. Physical Review B, 2002, 65, .	1.1	17
585	Comment on â€œMagnetism of the V(001) surface: Contradictory results from pseudopotential and linearized augmented plane-wave calculationsâ€• Physical Review B, 2002, 66, .	1.1	23
586	First-principles calculations of grain boundary theoretical shear strength using transition state finding to determine generalized gamma surface cross sections. Physical Review B, 2002, 65, .	1.1	29
587	Assigning the(1Ã—2)surface reconstruction on reduced rutile by first-principles energetics. Physical Review B, 2002, 65, .	1.1	18
588	GW self-energy calculations for systems with huge supercells. Physical Review B, 2002, 66, .	1.1	54
589	Electronic structure of the molecule-based magnetMn[N(CN)2]2from theory and experiment. Physical Review B, 2002, 66, .	1.1	21
590	Structure and dynamics of atomic hydrogen on NiAl(110). Physical Review B, 2002, 65, .	1.1	7
591	Structural and superconducting transitions inMg1â^'xAlxB2. Physical Review B, 2002, 66, .	1.1	19
592	Spontaneous magnetization of aluminum nanowires deposited on the NaCl(100) surface. Physical Review B, 2002, 66, .	1.1	31
593	Optical Absorption of Large Band-Gap SbxBi1-xI3 Alloys. Materials Research Society Symposia Proceedings, 2002, 744, 1.	0.1	1
594	Comparative Hartree-Fock and density-functional theory study of cubic and hexagonal diamond. The Philosophical Magazine: Physics of Condensed Matter B, Statistical Mechanics, Electronic, Optical and Magnetic Properties, 2002, 82, 1767-1776.	0.6	28
595	Properties of interfaces between cubic and hexagonal polytypes of silicon carbide. Journal of Physics Condensed Matter, 2002, 14, 12725-12731.	0.7	12
596	Laminar Growth of Ultrathin Metal Films on Metal Oxides: Co on Hydroxylated alpha -Al2O3(0001). Science, 2002, 297, 827-831.	6.0	132
597	Structure of Hydrated Microporous Aluminophosphates:â€‰ Static and Molecular Dynamics Approaches of AlPO4-34 from First Principles Calculations. Journal of Physical Chemistry B, 2002, 106, 8599-8608.	1.2	34
598	Activation of group III combinations in silicon and modifications introduced by nitrogen. Journal of Vacuum Science & Technology an Official Journal of the American Vacuum Society B, Microelectronics Processing and Phenomena, 2002, 20, 230.	1.6	8

#	Article	IF	Citations
599	Covalent bonding and bandgap formation in transition-metal aluminides: di-aluminides of group VIII transition metals. Journal of Physics Condensed Matter, 2002, 14, 5755-5783.	0.7	48
600	Spontaneous assembly of perfectly ordered identical-size nanocluster arrays. Nanotechnology, 2002, 13, 736-740.	1.3	6
601	Magnetic properties of 3d impurities substituted in GaAs. Journal of Physics Condensed Matter, 2002, 14, 3295-3302.	0.7	13
602	Covalent bonding and band-gap formation in ternary transition-metal di-aluminides: Al4MnCo and related compounds. Journal of Physics Condensed Matter, 2002, 14, 7201-7219.	0.7	20
603	Novel Bismuth Nanotubes. Chinese Physics Letters, 2002, 19, 1785-1787.	1.3	4
604	Ab initioprediction of the structure of glide set dislocation cores in GaAs. Journal of Physics Condensed Matter, 2002, 14, 12673-12680.	0.7	18
605	Phase stability and pressure-induced semiconductor to metal transition in crystalline GeSe2. Journal of Physics Condensed Matter, 2002, 14, 9589-9600.	0.7	13
606	Prediction of Possible Metastable Alloy Phases in an Equilibrium Immiscible Yâ€“Mo System by ab initio Calculation. Journal of Materials Research, 2002, 17, 528-531.	1.2	3
607	Comparative study of nonequilibrium phase of A3B and AB3 types in the Niâ€“Mo system by first principles and thermodynamic calculations. Journal of Materials Research, 2002, 17, 2720-2726.	1.2	2
608	Modeling Copper Diffusion in Silicon Oxide, Nitride, and Carbide. Materials Research Society Symposia Proceedings, 2002, 716, 841.	0.1	5
609	First-principles calculation of the effect of strain on the diffusion of Ge adatoms on Si and Ge (001) surfaces. Materials Research Society Symposia Proceedings, 2002, 749, 1.	0.1	0
610	Exohedral Bonding Nature of Si Atom on the Ba@Si₂₈ Cluster; <I>Ab Initio</I> Study. Materials Transactions, 2002, 43, 704-707.	0.4	3
611	Surface alloying and de-alloying of Pb on single-crystal Cu surfaces. Chemical Physics of Solid Surfaces, 2002, 10, 152-183.	0.3	5
612	Ab initio Calculation to Predict Possible Non-Equilibrium Solid Phases in an Immiscible Yâ€“Nb System. Journal of the Physical Society of Japan, 2002, 71, 141-143.	0.7	14
613	Low Temperature Photoluminescence Studies of Narrow Bandgap Gaassbn Quantum Wells on GaAs. Materials Research Society Symposia Proceedings, 2002, 744, 1.	0.1	0
614	Atomic Structure of Ultrathin Iron Silicide Films on Si(111): Metastable Phases and a New Template Structure. Materials Research Society Symposia Proceedings, 2002, 749, 1.	0.1	0
615	Interface Structure and Energy Calculations for Carbide Precipitates in Î³-TiAl. Materials Research Society Symposia Proceedings, 2002, 753, 1.	0.1	0
616	A DFT-Study of Structure and Properties of Amorphous SiCN. Materials Research Society Symposia Proceedings, 2002, 731, 321.	0.1	1

#	Article	IF	Citations
617	First-Principles Simulation of Hydrogen Interaction in Amorphous Silicon Nitride. Materials Research Society Symposia Proceedings, 2002, 719, 8371.	0.1	1
618	Si nanostructures embedded in SiO 2 : electronic and optical properties. , 2002, 4808, 73.		3
619	Ab initio calculation of the stability of one-dimensional long-period structures in the Cu₃Pd compound. The Philosophical Magazine: Physics of Condensed Matter B, Statistical Mechanics, Electronic, Optical and Magnetic Properties, 2002, 82, 1067-1087.	0.6	2
620	A Theoretical Study of the Electronic and Optical Properties of the Graphite Intercalation Compound K(NH3)4C24. Journal of Physical Chemistry B, 2002, 106, 12916-12928.	1.2	1
621	Periodic Density Functional Theory Study of the Dissociative Adsorption of Molecular Oxygen over La2O3. Journal of Physical Chemistry B, 2002, 106, 6543-6547.	1.2	46
622	Ab Initio Studies on the Thermal Dissociation Channels ofcis- andtrans-Azomethane. Journal of Physical Chemistry A, 2002, 106, 6792-6801.	1.1	10
623	Chemisorption of Trichloroethene on the PdCu Alloy (110) Surface:Â A Periodical Density Functional Study. Langmuir, 2002, 18, 2625-2635.	1.6	19
624	Dimensional changes as a function of charge injection for trans-polyacetylene: A density functional theory study. Journal of Chemical Physics, 2002, 117, 7691-7697.	1.2	19
625	Fe nanowires on vicinal Cu surfaces:Ab initiostudy. Physical Review B, 2002, 65, .	1.1	78
626	A First Principles Study of Carbonâ^'Carbon Coupling over the {0001} Surfaces of Co and Ru. Journal of Physical Chemistry B, 2002, 106, 2826-2829.	1.2	67
627	Density Functional Theory Calculations of Solid Solutions of Fluor- and Chlorapatites. Chemistry of Materials, 2002, 14, 435-441.	3.2	23
628	First Principles Calculations of the Adsorption Properties of CO and NO on the Defective TiO2(110) Surface. Journal of Physical Chemistry B, 2002, 106, 6184-6199.	1.2	66
629	A DFT Study of CHxChemisorption and Transition States for Câ^'H Activation on the Ru(112Ì„0) Surface. Journal of Physical Chemistry B, 2002, 106, 6200-6205.	1.2	68
630	Phonon Softening in Metallic Nanotubes by a Peierls-like Mechanism. Physical Review Letters, 2002, 88, 235506.	2.9	180
631	Ab Initio Studies on Al+(H2O)n, HAlOH+(H2O)n-1, and the Size-Dependent H2 Elimination Reaction. Journal of the American Chemical Society, 2002, 124, 10846-10860.	6.6	36
632	Adhesion, atomic structure, and bonding at theAl(111)/Î±â^'Al2O3(0001)interface: A first principles study. Physical Review B, 2002, 65, .	1.1	212
633	Dimensional Changes as a Function of Charge Injection in Single-Walled Carbon Nanotubes. Journal of the American Chemical Society, 2002, 124, 15076-15080.	6.6	87
634	From Local Adsorption Stresses to Chiral Surfaces:â€‰ (R,R)-Tartaric Acid on Ni(110). Journal of the American Chemical Society, 2002, 124, 503-510.	6.6	193

#	Article	IF	Citations
635	Shear Instability ofÎ³-Fe in Bulk and in Ultrathin Films. Physical Review Letters, 2002, 88, 056101.	2.9	47
636	First-principles calculations of lithium ordering and phase stability onLixNiO2. Physical Review B, 2002, 66, .	1.1	122
637	O/Ag(100) Surface:â€‰ A Density Functional Study with Slab Model. Journal of Physical Chemistry B, 2002, 106, 3662-3667.	1.2	30
638	Assembling Phenomena of Calix[4]hydroquinone Nanotube Bundles by One-Dimensional Short Hydrogen Bonding and Displaced Ï€â^'Ï€ Stacking. Journal of the American Chemical Society, 2002, 124, 14268-14279.	6.6	106
639	Structural Stability and Phase Transitions inK8Si46Clathrate under High Pressure. Physical Review Letters, 2002, 89, 195507.	2.9	71
640	Dissociation of CH3I on the Al(111) Surface â^' An STM and Density Functional Theory Study. Journal of the American Chemical Society, 2002, 124, 14202-14209.	6.6	13
641	Temperature dependence of infrared-active phonons inCaTiO3:A combined spectroscopic and first-principles study. Physical Review B, 2002, 66, .	1.1	54
642	Ideal Pure Shear Strength of Aluminum and Copper. Science, 2002, 298, 807-811.	6.0	686
643	Cluster Assembled Metal Encapsulated Thin Nanotubes of Silicon. Nano Letters, 2002, 2, 1243-1248.	4.5	96
644	Bismuth nanotubes: potential semiconducting nanomaterials. Nanotechnology, 2002, 13, 746-749.	1.3	40
645	Elasticity of (Mg,Fe)SiO3-Perovskite at high pressures. Geophysical Research Letters, 2002, 29, 34-1.	1.5	85
646	The ab initio simulation of the Earth's core. Philosophical Transactions Series A, Mathematical, Physical, and Engineering Sciences, 2002, 360, 1227-1244.	1.6	31
647	Ab initio determination of the (001) antiphase-boundary energy in the D022 Ni3V compound. The Philosophical Magazine: Physics of Condensed Matter B, Statistical Mechanics, Electronic, Optical and Magnetic Properties, 2002, 82, 1715-1729.	0.6	3
648	Broken symmetries in the crystalline and magnetic structures ofÎ³-iron. Physical Review B, 2002, 66, .	1.1	136
649	FIRST PRINCIPLES MOLECULAR DYNAMICS INVOLVING EXCITED STATES AND NONADIABATIC TRANSITIONS. Journal of Theoretical and Computational Chemistry, 2002, 01, 319-349.	1.8	136
650	First-principles study of the structure and lattice dielectric response ofCaCu3Ti4O12. Physical Review B, 2002, 65, .	1.1	317
651	Role of carbon in GaN. Journal of Applied Physics, 2002, 92, 6553-6560.	1.1	227
652	Electrical conductivity for warm, dense aluminum plasmas and liquids. Physical Review E, 2002, 66, 025401.	0.8	426

#	Article	IF	Citations
653	First-principles simulations of metal-ceramic interface adhesion: Co/WC versus Co/TiC. Physical Review B, 2002, 65, .	1.1	160
654	Atomic-layer-resolved quantum oscillations in the work function:â€ƒ Theory and experiment for Ag/Fe(100). Physical Review B, 2002, 66, .	1.1	89
655	Amorphous structures of Cu, Ag, and Au nanoclusters from first principles calculations. Journal of Chemical Physics, 2002, 117, 9548-9551.	1.2	122
656	The effect of misfit on heterophase interface energies. Journal of Physics Condensed Matter, 2002, 14, 2877-2900.	0.7	54
657	Talc under tension and compression: Spinodal instability, elasticity, and structure. Journal of Geophysical Research, 2002, 107, ECV 2-1-ECV 2-10.	3.3	40
658	Room-Temperature Ferromagnetism in Mn-Doped SemiconductingCdGeP2. Physical Review Letters, 2002, 88, 047205.	2.9	85
659	Theory of quantum size effects in thin Pb(111) films. Physical Review B, 2002, 66, .	1.1	253
660	Thermal effects in the ultrafast photoinduced electron transfer from a molecular donor anchored to a semiconductor acceptor. Israel Journal of Chemistry, 2002, 42, 213-224.	1.0	45
661	Complementary approaches to the ab initio calculation of melting properties. Journal of Chemical Physics, 2002, 116, 6170-6177.	1.2	88
662	Bcc and Fcc Transition Metals and Alloys:â€‰ A Central Role for the Jahnâ^'Teller Effect in Explaining Their Ideal and Distorted Structures. Journal of the American Chemical Society, 2002, 124, 4811-4823.	6.6	33
663	Optical properties of Ge and Si nanocrystallites fromab initiocalculations. II. Hydrogenated nanocrystallites. Physical Review B, 2002, 65, .	1.1	94
664	Gap bowing and Stokes shift in InxGa1â^'xN alloys: First-principles studies. Applied Physics Letters, 2002, 80, 1394-1396.	1.5	45
665	Molecular dynamics study of phase transitions in Xe. Journal of Chemical Physics, 2002, 117, 7233-7244.	1.2	33
666	Band structure, Born effective charges, and lattice dynamics of CuInS2 fromab initiocalculations. Journal of Chemical Physics, 2002, 117, 2726-2731.	1.2	47
667	Adsorption of hydrogen and deuterium atoms on the (0001) graphite surface. Journal of Chemical Physics, 2002, 117, 8486-8492.	1.2	249
668	Quantum studies of Eleyâ€“Rideal reactions between H atoms on a graphite surface. Journal of Chemical Physics, 2002, 116, 7158-7169.	1.2	136
669	The Effects of Lattice Motion on Eley-Rideal and Hot Atom Reactions:Â Quasiclassical Studies of Hydrogen Recombination on Ni(100)â€. Journal of Physical Chemistry B, 2002, 106, 8342-8348.	1.2	30
670	Electronic Structure of Chemically-Delithiated LiCoO2 Studied by Electron Energy-Loss Spectrometry. Journal of Physical Chemistry B, 2002, 106, 1286-1289.	1.2	91

#	Article	IF	Citations
671	Theoretical Calculations of Voltage-Dependent STM Images of Acetylene on the Si(001) Surface. Journal of Physical Chemistry B, 2002, 106, 1316-1321.	1.2	24
672	Fragmentation of small tin cluster ions (Snx+: x=4â€“20) in the low-energy collisions with a highly oriented pyrolytic graphite surface. Journal of Chemical Physics, 2002, 117, 4317-4322.	1.2	29
673	A Periodic Density Functional Theory Study of Intermolecular Isomerization of Toluene and Benzene Catalyzed by Acidic Mordenite Zeolite:Â Effect of the Zeolite Steric Constraints. Journal of Physical Chemistry B, 2002, 106, 4652-4657.	1.2	25
674	Density functional theory calculations of local ordering of hydroxy groups and fluoride ions in hydroxyapatite. Physical Chemistry Chemical Physics, 2002, 4, 3865-3871.	1.3	59
675	Nonadiabatic Molecular Dynamics Simulation of Light-Induced Electron Transfer from an Anchored Molecular Electron Donor to a Semiconductor Acceptorâ€. Journal of Physical Chemistry B, 2002, 106, 8047-8054.	1.2	180
676	The sâ^'p Bonded Representatives of the Prominent BaAl4Structure Type:Â A Case Study on Structural Stability of Polar Intermetallic Network Structures. Journal of the American Chemical Society, 2002, 124, 4371-4383.	6.6	81
677	Screened Coulomb interactions in metallic alloys. â€,â€,II.â€ƒScreening beyond the single-site and atomic-sphere approximations. Physical Review B, 2002, 66, .	1.1	121
678	Quantum transport through one-dimensional aluminum wires. Journal of Vacuum Science & Technology an Official Journal of the American Vacuum Society B, Microelectronics Processing and Phenomena, 2002, 20, 812.	1.6	6
679	First Principles Study of Cu Atoms Deposited on the Î±-Al2O3(0001) Surface. Journal of Physical Chemistry B, 2002, 106, 11495-11500.	1.2	34
680	Structural stability of one-dimensional long-period structures in the TiAl3 compound. Journal of Physics Condensed Matter, 2002, 14, 6713-6727.	0.7	15
681	Properties of hexagonal polytypes of group-IV elements from first-principles calculations. Physical Review B, 2002, 66, .	1.1	134
682	Hydrogen Stabilization of {111} Nanodiamond. Materials Research Society Symposia Proceedings, 2002, 740, 1.	0.1	2
683	Artificial nanocluster crystal: Lattice of identical Al clusters. Applied Physics Letters, 2002, 80, 3186-3188.	1.5	112
684	Icosahedral growth, magnetic behavior, and adsorbate-induced metal-nonmetal transition in palladium clusters. Physical Review B, 2002, 66, .	1.1	146
685	Density functional study of the adsorption of CO on Fe(). Surface Science, 2002, 507-510, 99-102.	0.8	62
686	Self-Compensation in Manganese-Doped Ferromagnetic Semiconductors. Physical Review Letters, 2002, 89, 227201.	2.9	156
687	A First-Principles Study of 11-Cis-Retinal: Modelling the Chromophore-Protein Interaction In Rhodopsin. Phase Transitions, 2002, 75, 11-17.	0.6	10
688	Binary nitrides Î±-M3N2(M = Be, Mg, Ca): a theoretical study. Journal of Materials Chemistry, 2002, 12, 2475-2479.	6.7	48

#	Article	IF	Citations
689	Halide adsorption on single-crystal silver substrates: dynamic simulations and ab initio density functional theory. Faraday Discussions, 2002, 121, 53-69.	1.6	20
690	Modeling and simulation design of advanced Cu alloy interconnects. Journal of Applied Physics, 2002, 91, 6089-6094.	1.1	1
691	Composition and temperature of the Earthâ€™s core constrained by combining ab initio calculations and seismic data. Earth and Planetary Science Letters, 2002, 195, 91-98.	1.8	257
692	The effect of ferromagnetism on the equation of state of Fe 3 C studied by first-principles calculations. Earth and Planetary Science Letters, 2002, 203, 567-575.	1.8	108
693	First-principles study of the structural and energetic properties of H atoms on a graphite () surface. Surface Science, 2002, 496, 318-330.	0.8	301
694	Effects of Co magnetism on Co/TiC() interface adhesion: a first-principles study. Surface Science, 2002, 497, 171-182.	0.8	27
695	Superstructures of carbon on V(). Surface Science, 2002, 497, 294-304.	0.8	10
696	First-principles study of Pdâ€“V surface alloys I. Electronic structure of clean surfaces. Surface Science, 2002, 498, 21-36.	0.8	23
697	First-principles study of Pdâ€“V surface alloys. Surface Science, 2002, 498, 37-52.	0.8	17
698	Tip effects in scanning tunneling microscopy of atomic-scale magnetic structures. Surface Science, 2002, 498, L65-L70.	0.8	11
699	First-principles study of metallic iron interfaces. Surface Science, 2002, 501, 261-269.	0.8	64
700	CO oxidation on transition metal surfaces: reaction rates from first principles. Surface Science, 2002, 498, 314-320.	0.8	157
701	Adhesion, stability, and bonding at metal/metal-carbide interfaces: Al/WC. Surface Science, 2002, 498, 321-336.	0.8	224
702	Vibrational identification of the surface reaction intermediates for the dehalogenation of trichloroethene on PdCu(110) alloy. Surface Science, 2002, 505, 153-162.	0.8	22
703	NO pairing and transformation to N2O on Cu() and Pt() from first principles. Surface Science, 2002, 506, L237-L242.	0.8	59
704	Modelling of point defects in monoclinic zirconia. Journal of Non-Crystalline Solids, 2002, 303, 101-107.	1.5	48
705	Ab initio molecular dynamics: recent progresses and limitations. Journal of Non-Crystalline Solids, 2002, 312-314, 52-59.	1.5	26
706	Isothiazoles (1,2-thiazoles): synthesis, properties and applications. Russian Chemical Reviews, 2002, 71, 673-694.	2.5	50

#	Article	IF	Citations
707	Iron under Earthâ€™s core conditions: Liquid-state thermodynamics and high-pressure melting curve fromab initiocalculations. Physical Review B, 2002, 65, .	1.1	277
708	Ab InitioStudy of Field Emission from Graphitic Ribbons. Physical Review Letters, 2002, 88, 127601.	2.9	114
709	Absorption and diffusion of hydrogen in palladium-silver alloys by density functional theory. Physical Review B, 2002, 66, .	1.1	57
710	Theoretical approach of phase selection in refractory metals and alloys. Journal of Alloys and Compounds, 2002, 334, 27-33.	2.8	14
711	Electronic structures of perovskite-type ScRh3Bx (0â‰¤xâ‰¤1): X-ray photoelectron and nuclear magnetic resonance spectroscopies and ab initio band calculation. Journal of Alloys and Compounds, 2002, 339, 317-326.	2.8	17
712	Theoretical and experimental investigation of the electronic structure of Tiâ€“Zrâ€“Ni and Tiâ€“Zrâ€“Ni:H alloys. Journal of Alloys and Compounds, 2002, 342, 337-342.	2.8	16
713	Density-functional study of impurity-related DX centers in CdF2. Computational Materials Science, 2002, 25, 404-412.	1.4	1
714	Phase stability of the Hf-Nb system: From first-principles to CALPHAD. Calphad: Computer Coupling of Phase Diagrams and Thermochemistry, 2002, 26, 491-511.	0.7	35
715	The alloy theoretic automated toolkit: A user guide. Calphad: Computer Coupling of Phase Diagrams and Thermochemistry, 2002, 26, 539-553.	0.7	1,193
716	Theoretical calculation of the phase diagram between one-dimensional long-period structures in the quasi binary sections: Pd3xRh3(1â^'x)V, Pt3xRh3(1â^'x)V, and Pt3VxTi(1â^'x). Calphad: Computer Coupling of Phase Diagrams and Thermochemistry, 2002, 26, 563-571.	0.7	3
717	Phonon spectrum ofZnAl2O4spinel from inelastic neutron scattering and first-principles calculations. Physical Review B, 2002, 66, .	1.1	60
718	A facile route to poly[1-(2,4,6-trichlorophenyl)-1H-1,2,4-triazol-5-yl]alkane derivatives. Journal of the Chemical Society, Perkin Transactions 1, 2002, , 991-995.	1.3	2
719	Partial Dissociation of Water on Ru(0001). Science, 2002, 295, 99-102.	6.0	464
720	Absolute surface energies of group-IV semiconductors: Dependence on orientation and reconstruction. Physical Review B, 2002, 65, .	1.1	366
721	Optical properties of Ge and Si nanocrystallites fromab initiocalculations. I. Embedded nanocrystallites. Physical Review B, 2002, 65, .	1.1	57
722	Direct space representation of metallicity and structural stability in SiO solids. Journal of Physics Condensed Matter, 2002, 14, 10251-10263.	0.7	30
723	Thermoelastic Properties of (Mg,Fe)SiO3 Perovskite. Materials Research Society Symposia Proceedings, 2002, 718, 1.	0.1	0
724	Nitrogen-Stabilized H2* Defects in GaP:N. Materials Research Society Symposia Proceedings, 2002, 719, 631.	0.1	0

#	Article	IF	Citations
725	Structural, Electronic and Optical Properties of Ru2Si3, Ru2Ge3, Os2Si3 and Os2Ge3. Physica Status Solidi (B): Basic Research, 2002, 231, 171-180.	0.7	38
726	Carbon-Based Defects in GaN: Doping Behaviour. Physica Status Solidi (B): Basic Research, 2002, 234, 864-867.	0.7	9
727	FeGa3 and RuGa3: Semiconducting Intermetallic Compounds. Journal of Solid State Chemistry, 2002, 165, 94-99.	1.4	105
728	Polymorphism of IrSn4. Journal of Solid State Chemistry, 2002, 168, 34-40.	1.4	23
729	First-principles investigation of perfect and diffuse antiphase boundaries in HCP-based Ti-Al alloys. Metallurgical and Materials Transactions A: Physical Metallurgy and Materials Science, 2002, 33, 735-741.	1.1	40
730	A mapping of the electron localization function for the silica polymorphs: evidence for domains of electron pairs and sites of potential electrophilic attack. Physics and Chemistry of Minerals, 2002, 29, 307-318.	0.3	19
731	Incorporating first-principles energetics in computational thermodynamics approaches. Acta Materialia, 2002, 50, 2187-2197.	3.8	91
732	Structure and stability of hcp bulk and nano-precipitated Ag2Al. Acta Materialia, 2002, 50, 2443-2459.	3.8	31
733	The connection between ab initio calculations and interface adhesion measurements on metal/oxide systems: Ni/Al2O3 and Cu/Al2O3. Acta Materialia, 2002, 50, 3803-3816.	3.8	213
734	Modeling of alloy steels. Materials Today, 2002, 5, 14-23.	8.3	10
735	Field emission of carbon nanotubes and electronic structure of carbon nanopeapods. Current Applied Physics, 2002, 2, 57-60.	1.1	4
736	Klockmannite, CuSe: structure, properties and phase stability from ab initio modeling. Acta Crystallographica Section B: Structural Science, 2002, 58, 437-447.	1.8	40
737	Quantitative modelling in scanning force microscopy on insulators. Applied Surface Science, 2002, 188, 306-318.	3.1	20
738	Lithium reactions with intermetallic-compound electrodes. Journal of Power Sources, 2002, 110, 406-411.	4.0	115
739	Modelling molecular vibrations in extended hydrogen-bonded networks â€“ crystalline bases of RNA and DNA and the nucleosides. Chemical Physics, 2002, 280, 53-70.	0.9	32
740	Molecular deformations of halogeno-mesitylenes in the crystal: structure, methyl group rotational tunneling, and numerical modeling. Chemical Physics, 2002, 285, 299-308.	0.9	12
741	Electronic structure and prediction of magnetism in metallic nanowires. Journal of Magnetism and Magnetic Materials, 2002, 249, 193-199.	1.0	16
742	Liquid metal embrittlement of the martensitic steel 91: influence of the chemical composition of the liquid metal.. Journal of Nuclear Materials, 2002, 301, 70-76.	1.3	65

#	Article	IF	Citations
743	Metastable states in an equilibrium immiscible Niâ€“Ru system studied by ab initio calculation and ion mixing experiment. Solid State Communications, 2002, 121, 375-379.	0.9	2
744	High pressure elastic properties of solid argon from first-principles density functional and quasi-harmonic lattice dynamic calculations. Solid State Communications, 2002, 122, 557-560.	0.9	7
745	Adsorption and reaction of thiophene on Î±-Mo 2 C(0001). Surface Science, 2002, 511, 294-302.	0.8	46
746	Full-coverage adsorption of water on SnO2(): the stabilisation of the molecular species. Surface Science, 2002, 512, 29-36.	0.8	27
747	Surface relaxation and surface stress of Au(111). Surface Science, 2002, 513, 263-271.	0.8	60
748	First principles calculations for electronic band structure of single-walled carbon nanotube under uniaxial strain. Surface Science, 2002, 514, 222-226.	0.8	41
749	Acetylene molecules on the Si() surface: room-temperature adsorption and structural modification upon annealing. Surface Science, 2002, 514, 376-382.	0.8	24
750	The structure of the oxygen-induced c(6Ã—2) reconstruction of V(110). Surface Science, 2002, 512, 16-28.	0.8	14
751	Reconstructions of strongly reduced SnO2(110) studied by first-principles methods. Surface Science, 2002, 513, 26-36.	0.8	52
752	Density-functional theory studies of pyrite FeS2() and () surfaces. Surface Science, 2002, 513, 511-524.	0.8	144
753	A first principles study of sub-monolayer Ge on Si(). Surface Science, 2002, 515, 483-490.	0.8	23
754	Structure determination of Cu()â€“O using X-ray diffraction and DFT calculations. Surface Science, 2002, 516, 16-32.	0.8	25
755	Finite temperature studies of Te adsorption on. Surface Science, 2002, 519, 79-89.	0.8	18
756	Computing accurate surface energies and the importance of electron self-energy in metal/metal-oxide adhesion. Surface Science, 2002, 520, L611-L618.	0.8	90
757	Theoretical study of the structure of propene adsorbed on Pt(). Surface Science, 2002, 519, 250-258.	0.8	31
758	Density-functional theory studies of pyrite FeS2 () and () surfaces. Surface Science, 2002, 520, 111-119.	0.8	82
759	A tool for the interactive 3D visualization of electronic structure in molecules and solids. Computers & Chemistry, 2002, 26, 313-319.	1.2	47
760	The structure and chemistry of the TiO2-rich surface of SrTiO3 (001). Nature, 2002, 419, 55-58.	13.7	342

#	Article	IF	Citations
761	First-principles study of illiteâ€“smectite and implications for clay mineral systems. Nature, 2002, 420, 165-168.	13.7	95
762	Fullerene C60 formation in partially ionized carbon vapor. JETP Letters, 2002, 76, 522-526.	0.4	4
763	First-principles study of metalâ€“carbide/nitride adhesion: Al/VC vs. Al/VN. Acta Materialia, 2002, 50, 619-631.	3.8	127
764	Atomic-scale Ab-initio study of the Zr-H system: I. Bulk properties. Acta Materialia, 2002, 50, 3513-3526.	3.8	156
765	Thin Ta films: growth, stability, and diffusion studied by molecular-dynamics simulations. Thin Solid Films, 2002, 413, 110-120.	0.8	24
766	Hybrid quantum mechanical/molecular dynamics simulation on parallel computers: density functional theory on real-space multigrids. Computer Physics Communications, 2002, 149, 30-38.	3.0	56
767	Do we know the fundamental energy gap of InN?. Journal of Crystal Growth, 2002, 246, 315-319.	0.7	117
768	The mechanisms of the thermal decomposition of 5-nitro-1-hydrogen-tetrazole: ab initio MD and quantum chemistry studies. Chemical Physics Letters, 2002, 351, 459-468.	1.2	6
769	Tuning in on single molecular states: adsorption sites and STM images of maleic anhydride on Si(100). Chemical Physics Letters, 2002, 355, 347-354.	1.2	22
770	Ab initio and transition state theory studies of the energetics of H atom resurfacing on Ni(111). Chemical Physics Letters, 2002, 357, 389-396.	1.2	20
771	Ab initio molecular dynamics of hydroxylâ€“water coadsorption on Rh(111). Chemical Physics Letters, 2002, 359, 337-342.	1.2	38
772	The adsorption of molecular oxygen on neutral and negative Aun clusters (n=2â€“5). Chemical Physics Letters, 2002, 359, 493-499.	1.2	202
773	M@Si16, M=Ti, Zr, Hf: Ï€ conjugation, ionization potentials and electron affinities. Chemical Physics Letters, 2002, 363, 319-322.	1.2	67
774	Dispersion of vibrational modes in benzoic acid crystals. Chemical Physics Letters, 2002, 364, 34-38.	1.2	38
775	Electronic structure and STM images of self-assembled styrene lines on a Si(100) surface. Chemical Physics Letters, 2002, 365, 129-134.	1.2	34
776	Linear Hydrocarbons Adsorbed in the Acid Zeolite Gmelinite at 700 K ab Initio Molecular Dynamics Simulation of Hexane and Hexene. Journal of Catalysis, 2002, 205, 147-156.	3.1	21
777	A Periodic DFT Study of the Isomerization of Thiophenic Derivatives Catalyzed by Acidic Mordenite. Journal of Catalysis, 2002, 205, 388-397.	3.1	18
778	Trichloroethene Dechlorination Reactions on the PdCu(110) Alloy Surface: A Periodical Density Functional Theory Study of the Mechanism. Journal of Catalysis, 2002, 207, 127-138.	3.1	24

#	Article	IF	Citations
779	Extraframework Aluminum Species in Zeolites: Ab Initio Molecular Dynamics Simulation of Gmelinite. Journal of Catalysis, 2002, 209, 480-488.	3.1	42
780	Periodic Density Functional Theory Study of Methane Activation over La2O3:Â Activity of O2-, O-, O22-, Oxygen Point Defect, and Sr2+-Doped Surface Sites. Journal of the American Chemical Society, 2002, 124, 8452-8461.	6.6	202
781	Synthesis and energetics of yellow TaON. Solid State Sciences, 2002, 4, 1071-1076.	1.5	79
782	Ab initiomelting curve of the fcc phase of aluminum. Physical Review B, 2002, 65, .	1.1	124
783	Binding energies and electronic structures of adsorbed titanium chains on carbon nanotubes. Physical Review B, 2002, 66, .	1.1	103
784	Crystal Shape of a Nickel Particle Related to Carbon Nanotube Growth. Japanese Journal of Applied Physics, 2002, 41, 6142-6144.	0.8	41
785	Abnormally high melting temperature of theSn10cluster. Physical Review B, 2002, 66, .	1.1	71
786	Structure of the (001) surface of Î³ alumina. Journal of Chemical Physics, 2002, 117, 4509-4516.	1.2	31
787	Metal-Encapsulated Caged Clusters of Germanium with Large Gaps and Different Growth Behavior than Silicon. Physical Review Letters, 2002, 88, 235504.	2.9	112
788	First-principles calculations of gap bowing inInxGa1â^'xNandInxAl1â^'xNalloys: Relation to structural and thermodynamic properties. Physical Review B, 2002, 65, .	1.1	172
789	Computational studies of grain boundaries in covalent materials. Modelling and Simulation in Materials Science and Engineering, 2002, 10, R31-R59.	0.8	88
790	Dynamical simulation of field emission in nanostructures. Physical Review B, 2002, 65, .	1.1	67
791	Vacancy and interstitial defects in hafnia. Physical Review B, 2002, 65, .	1.1	560
792	First-principles simulation: ideas, illustrations and the CASTEP code. Journal of Physics Condensed Matter, 2002, 14, 2717-2744.	0.7	8,382
793	Collective and single particle diffusion on surfaces. Advances in Physics, 2002, 51, 949-1078.	35.9	487
794	Automating first-principles phase diagram calculations. Journal of Phase Equilibria and Diffusion, 2002, 23, 348-359.	0.3	768
795	Spin-polarization in half-metals (invited). Journal of Applied Physics, 2002, 91, 8340.	1.1	201
796	Structural relaxation and relative stability of nanodiamond morphologies. Diamond and Related Materials, 2003, 12, 1867-1872.	1.8	107

#	Article	IF	Citations
797	Ab initio modelling of the stability of nanocrystalline diamond morphologies. Philosophical Magazine Letters, 2003, 83, 39-45.	0.5	65
798	Lattice dynamics of CuAu-orderedCuInSe2. Physical Review B, 2003, 68, .	1.1	31
799	Ab initiomodelling of band states in doped diamond. Philosophical Magazine, 2003, 83, 1163-1174.	0.7	27
800	Elucidation by computer simulations of the CUS regeneration mechanism during HDS over MoS2 in combination with 35S experiments. Research on Chemical Intermediates, 2003, 29, 589-607.	1.3	15
801	Accurate density functional calculations for the phonon dispersion relations of graphite layer and carbon nanotubes. Physical Review B, 2003, 67, .	1.1	310
802	Stress-induced defects inSb2Te3. Physical Review B, 2003, 68, .	1.1	77
803	Intermolecular Interactions in Bithiophene as a Model for Polythiophene. Journal of Physical Chemistry A, 2003, 107, 8980-8984.	1.1	44
804	Lattice-dynamical and ground-state properties ofCaF2studied by inelastic neutron scattering and density-functional methods. Physical Review B, 2003, 68, .	1.1	60
805	Coexistence of bucky diamond with nanodiamond and fullerene carbon phases. Physical Review B, 2003, 68, .	1.1	104
806	Collapsing Cristobalitelike Structures in Silica Analogues at High Pressure. Physical Review Letters, 2003, 91, 015503.	2.9	58
807	Electronic structure and origin of ferromagnetism in Ga1â^'xMnxAs semiconductors. Physica B: Condensed Matter, 2003, 340-342, 874-877.	1.3	9
808	Methanol at the waterâ€“platinum interface studied by ab initio molecular dynamics. Surface Science, 2003, 544, L697-L702.	0.8	30
809	Density functional theory studies of sulfur binding on Pd, Cu and Ag and their alloys. Surface Science, 2003, 546, 12-26.	0.8	104
810	Function of subsurface boron on Si(001)-2Ã—1: water adsorption. Surface Science, 2003, 547, L882-L886.	0.8	6
811	Hydrogen bonding in mixed ligand copper organophosphonates. Chemical Physics Letters, 2003, 378, 400-405.	1.2	4
812	Phase equilibria in prototype Nb-Pd-Hf-Al alloys. Metallurgical and Materials Transactions A: Physical Metallurgy and Materials Science, 2003, 34, 1771-1782.	1.1	6
813	First-principles-based calculations of the CaCO 3 -MgCO 3 and CdCO 3 -MgCO 3 subsolidus phase diagrams. Physics and Chemistry of Minerals, 2003, 30, 88-97.	0.3	42
814	The electron localization function: a tool for locating favorable proton docking sites in the silica polymorphs. Physics and Chemistry of Minerals, 2003, 30, 305-316.	0.3	70

#	Article	IF	Citations
815	Chemical pressure and hydrogen insertion effects in CeNiIn. Solid State Sciences, 2003, 5, 1385-1393.	1.5	18
816	The influence of triaxial stress on the ideal tensile strength of iron. Scripta Materialia, 2003, 49, 1007-1011.	2.6	52
817	Structure sensitivity for NO dissociation on palladium and rhodium surfaces. Journal of Catalysis, 2003, 213, 211-225.	3.1	113
818	Perspectives on the first principles elucidation and the design of active sites. Journal of Catalysis, 2003, 216, 73-88.	3.1	157
819	A periodic density functional theory study of thiophenic derivative cracking catalyzed by mordenite. Journal of Catalysis, 2003, 215, 20-29.	3.1	29
820	Adsorption of unsaturated aldehydes on the (111) surface of a Ptâ€“Fe alloy catalyst from first principles. Journal of Catalysis, 2003, 217, 354-366.	3.1	73
821	The connection between the electronic structure and the properties of binderless tungsten carbides. International Journal of Refractory Metals and Hard Materials, 2003, 21, 55-61.	1.7	27
822	A flexible nudged elastic band program for optimization of minimum energy pathways usingab initio electronic structure methods. Journal of Computational Chemistry, 2003, 24, 990-996.	1.5	34
823	High-pressure metastable phase transitions in ?-Ge3N4 studied by Raman spectroscopy. Journal of Raman Spectroscopy, 2003, 34, 567-577.	1.2	15
824	Zur Rolle von Thrâ€‰94 und Wat2b bei der Protonierung des Retinalchromophors in Rhodopsin. Angewandte Chemie, 2003, 115, 3365-3367.	1.6	1
825	Thrâ€‰94 and Wat2b Effect Protonation of the Retinal Chromophore in Rhodopsin. Angewandte Chemie - International Edition, 2003, 42, 3245-3247.	7.2	20
826	A comparative study of precipitation behavior of Heusler phase (Ni2TiAl) from B2-TiNi in Niâ€“Tiâ€“Al and Niâ€“Tiâ€“Alâ€“X (X=Hf, Pd, Pt, Zr) alloys. Acta Materialia, 2003, 51, 6341-6357.	3.8	57
827	Surface diffusion of Xe on Nb(110). Chemical Physics Letters, 2003, 381, 376-380.	1.2	9
828	Ab initio study of energy-level alignments in polymer-dye blends. Chemical Physics Letters, 2003, 381, 392-396.	1.2	10
829	Thermal excitation of COâ€“Pt on the (2Ã—1) Pt {110} surface: a theoretical simulation of a variable-temperature STM contrast. Chemical Physics Letters, 2003, 382, 41-47.	1.2	0
830	Surface energy anisotropy of iron surfaces by carbon adsorption. Current Applied Physics, 2003, 3, 457-460.	1.1	26
831	Influence of electron concentration and temperature on fullerene formation in a carbon plasma. Carbon, 2003, 41, 173-178.	5.4	25
832	Structures and thermodynamic phase transitions for oxygen and silver oxide phases on Ag{1 1 1}. Chemical Physics Letters, 2003, 367, 344-350.	1.2	113

#	Article	IF	Citations
833	Defect structure for proton transport in a triflic acid monohydrate solid. Chemical Physics Letters, 2003, 368, 108-114.	1.2	89
834	Quasi-chemical study of Be2+(aq) speciation. Chemical Physics Letters, 2003, 371, 613-619.	1.2	57
835	Weak bonding of carbon atoms at corner sites in titanium-carbide nanocrystals. Chemical Physics Letters, 2003, 372, 836-841.	1.2	8
836	Structure and electronic properties of new model dinitride systems: a density-functional study of CN2, SiN2, and GeN2. Chemical Physics Letters, 2003, 373, 636-641.	1.2	44
837	Collective mode formulation of the response algorithm for solving Kohnâ€“Sham equations. Computer Physics Communications, 2003, 151, 265-271.	3.0	7
838	The structure, ordering and equation of state of ammonia dihydrate (nh3 Â· 2h2o). Icarus, 2003, 162, 59-73.	1.1	30
839	Local reactivity of thin Pd overlayers on Au single crystals. Journal of Electroanalytical Chemistry, 2003, 548, 121-130.	1.9	129
840	Adsorption of water molecules on the CdTe surface. Surface Science, 2003, 545, 34-40.	0.8	5
841	High-resolution electron spectroscopy of different adsorption states of ethylene on Pd(111). Surface Science, 2003, 545, 122-136.	0.8	56
842	Scattering of atomic nitrogen on W(100). Surface Science, 2003, 544, 329-338.	0.8	16
843	Structure of Fe() studied by quantitative LEED analysis and pseudopotential DFT calculations. Surface Science, 2003, 546, L808-L812.	0.8	4
844	Electron-induced attachment of chlorinated benzenes to Si(100)2Ã—1. Surface Science, 2003, 547, 324-334.	0.8	26
845	Re-evaluation of the adsorption mode of ethene on the {111} surface of palladium using density functional theory. Surface Science, 2003, 547, L853-L858.	0.8	6
846	A DFT periodic study of the vanadyl pyrophosphate (100) surface. Surface Science, 2003, 547, 438-451.	0.8	11
847	Prediction of XPS spectra of silicon self-interstitials with the all-electron mixed-basis method. Physica B: Condensed Matter, 2003, 340-342, 570-574.	1.3	5
848	Dislocation cores and their electronic states: partial dislocations in GaAs. Physica B: Condensed Matter, 2003, 340-342, 1001-1004.	1.3	12
849	A first principles analysis of CO oxidation over Pt and Pt66.7%Ru33.3% (111) surfaces. Electrochimica Acta, 2003, 48, 3759-3773.	2.6	114
850	Epitaxially stabilized AgGaSe2 for high-efficiency spin-polarized electron source. Journal of Physics and Chemistry of Solids, 2003, 64, 1881-1885.	1.9	1

#	Article	IF	Citations
851	Defect-induced nonpolar-to-polar transition at the surface of CuInSe2. Journal of Physics and Chemistry of Solids, 2003, 64, 1547-1552.	1.9	19
852	Tinâ€“magnesium substitution in Ir3Sn7â€”structure and chemical bonding in Mgxlr3Sn7â€“x (x=0â€“1.67). Journal of Solid State Chemistry, 2003, 173, 418-424.	1.4	27
853	NaPdPS4 and RbPdPS4: systems with infinite straight [PdPS4]â^' chains soluble in polar solvents and the structure of cubic RbPdPS4{Rb0.33P0.4S2.23Ox}. Journal of Solid State Chemistry, 2003, 175, 133-145.	1.4	14
854	Pathways to metastable nitride structures. Journal of Solid State Chemistry, 2003, 176, 530-537.	1.4	65
855	Metalâ€“ligand bonding and rutile- versus CdI2-type structural preference in platinum dioxide and titanium dioxide. Journal of Solid State Chemistry, 2003, 175, 353-358.	1.4	13
856	Synergetic theoretical and experimental structure determination of nanocrystalline materials: study of LiMoS2. Journal of Solid State Chemistry, 2003, 175, 380-383.	1.4	12
857	A DFT study of lithium battery materials: application to the Î²-VOXO4 systems (X=P, As, S). Journal of Solid State Chemistry, 2003, 176, 556-566.	1.4	19
858	Vibrational spectroscopy using ab initio density-functional techniques. Journal of Molecular Structure, 2003, 651-653, 3-17.	1.8	27
859	A density functional study of Br on Cu() at low coverages. Surface Science, 2003, 524, 141-147.	0.8	10
860	Dissociative adsorption of hydrogen on strained Cu surfaces. Surface Science, 2003, 525, 107-118.	0.8	147
861	CO adsorption on Niâ€“â€“a density functional theory study. Surface Science, 2003, 526, 332-340.	0.8	74
862	Characteristics of S adsorption on Pd vicinal surfaces. Surface Science, 2003, 532-535, 154-159.	0.8	5
863	First principle calculations of benzotriazole adsorption onto clean Cu(1 1 1). Surface Science, 2003, 529, 428-442.	0.8	68
864	Hydrogen recombination on a mixed adsorption layer at saturation on a metal surface: Hâ†'(D+H)sat+Ni(). Surface Science, 2003, 529, 11-22.	0.8	11
865	Structure and reactivity of Pd doped Ag surfaces. Surface Science, 2003, 529, 403-409.	0.8	8
866	Surface core level shift observed on NiAl(1 1 0). Surface Science, 2003, 529, L263-L268.	0.8	16
867	A combined ab initio and atomistic simulation study of the surface and interfacial structures and energies of hydrated scheelite: introducing a CaWO4 potential model. Surface Science, 2003, 531, 159-176.	0.8	58
868	Adsorption and diffusion of a Si adatom on the H/Si() surface: comparison with the H/Si() surface. Surface Science, 2003, 530, 155-160.	0.8	13

#	Article	IF	Citations
869	Interplay between gas adsorption and dislocation structure on a metal surface. Surface Science, 2003, 531, 29-38.	0.8	14
870	Calculation of magnetic and structural properties of small Coâ€“Rh clusters. Surface Science, 2003, 532-535, 334-340.	0.8	37
871	Ab initio density functional study of O on the Ag(001) surface. Surface Science, 2003, 531, 272-286.	0.8	56
872	Electric field effects on surface dynamics: Si ad-dimer diffusion and rotation on Si(). Surface Science, 2003, 536, 121-129.	0.8	22
873	Thin Pt films on the polar SrTiO3(111) surface: an experimental and theoretical study. Surface Science, 2003, 537, 134-152.	0.8	60
874	A comparative study of CO chemisorption on flat and stepped Ni surfaces using density functional theory. Surface Science, 2003, 537, 217-227.	0.8	51
875	Surface structure of cubic diamond nanowires. Surface Science, 2003, 538, 204-210.	0.8	22
876	A density functional study of adsorption of sodium-chloride overlayers on a stepped and a flat copper surface. Surface Science, 2003, 540, 172-184.	0.8	41
877	Dimer binding energies on fcc() metal surfaces. Surface Science, 2003, 539, L560-L566.	0.8	28
878	Adsorption of Au atoms on stoichiometric and reduced TiO2(110) rutile surfaces: a first principles study. Surface Science, 2003, 542, 72-80.	0.8	87
879	Relaxation of the surface in binary Sc, Ti and V nitrides: a first principles density functional study. Surface Science, 2003, 541, 217-224.	0.8	15
880	Mixed PbSi dimer chains on Si(100): a first-principles study. Surface Science, 2003, 542, L649-L654.	0.8	4
881	Performance of the Vienna ab initio simulation package (VASP) in chemical applications. Computational and Theoretical Chemistry, 2003, 624, 37-45.	1.5	275
882	Non-adiabatic molecular dynamics simulation of ultrafast solar cell electron transfer. Computational and Theoretical Chemistry, 2003, 630, 33-43.	1.5	26
883	A new three-layer hybrid method (LSCF/MM/Madelung) devoted to the study of chemical reactivity in zeolites. Preliminary results. Computational and Theoretical Chemistry, 2003, 632, 83-90.	1.5	14
884	The surface science of titanium dioxide. Surface Science Reports, 2003, 48, 53-229.	3.8	6,917
885	Proton tunnelling in the hydrogen bonds of halogen-substituted derivatives of benzoic acid studied by NMR relaxometry: the case of large energy asymmetry. Chemical Physics, 2003, 291, 41-52.	0.9	34
886	Hydration of krypton and consideration of clathrate models of hydrophobic effects from the perspective of quasi-chemical theory. Biophysical Chemistry, 2003, 105, 323-338.	1.5	45

#	Article	IF	Citations
887	Comparison of simulation methods for electronic structure calculations with experimental electron energy-loss spectra. Micron, 2003, 34, 255-260.	1.1	9
888	The ideal strength of iron in tension and shear. Acta Materialia, 2003, 51, 2271-2283.	3.8	196
889	First-principles calculations of the dielectric properties of perovskite-type materials. Journal of the European Ceramic Society, 2003, 23, 2375-2379.	2.8	18
890	Rattling guest atoms in Si, Ge, and Sn-based type-II clathrate materials. Physica Status Solidi (B): Basic Research, 2003, 239, 26-34.	0.7	29
891	Electronic and vibrational properties of group-III nitrides:Ab initio studies. Physica Status Solidi C: Current Topics in Solid State Physics, 2003, 0, 1732-1749.	0.8	8
892	Optimized structures of Si28 and Ba@Si28 clusters: Ab initio study. International Journal of Quantum Chemistry, 2003, 91, 328-332.	1.0	2
893	First principles calculations of the formation energy of Cr/Al vacancies in spinel-type MgCr2O4 and MgAl2O4. International Journal of Quantum Chemistry, 2003, 91, 208-210.	1.0	3
894	Ferromagnetic instabilities in atomically thin lithium and sodium wires. International Journal of Quantum Chemistry, 2003, 91, 239-244.	1.0	19
895	Association simulation by a metallic Car-Parrinello dynamics. International Journal of Quantum Chemistry, 2003, 91, 165-170.	1.0	0
896	Interface structures of III-V semiconductor heterostructures. International Journal of Quantum Chemistry, 2003, 95, 561-571.	1.0	5
897	Theoretical Investigation of the Solid State Reaction of Silicon Nitride and Silicon Dioxide forming Silicon Oxynitride (Si2N2O) under Pressure. Zeitschrift Fur Anorganische Und Allgemeine Chemie, 2003, 629, 1737-1750.	0.6	48
898	Chemical Reactivity of Tetrasulfur Tetranitride: Synthesis, Physical Properties, and Structural Characterization of the Amorphous Phase Cu7S4N4. Zeitschrift Fur Anorganische Und Allgemeine Chemie, 2003, 629, 1751-1759.	0.6	1
899	First-Principles Calculations of Microdomain Models for Î²-Sialon Si5AlON7. Journal of the American Ceramic Society, 2003, 86, 1956-1958.	1.9	10
900	Possible thermal and chemical stabilization of body-centred-cubic iron in the Earth's core. Nature, 2003, 424, 536-539.	13.7	249
901	Synthesis and properties of plasma-deposited carbon condensates. Technical Physics Letters, 2003, 29, 933-935.	0.2	1
902	Crystal structures and shape-memory behaviour of NiTi. Nature Materials, 2003, 2, 307-311.	13.3	320
903	Ferromagnetism above room temperature in bulk and transparent thin films of Mn-doped ZnO. Nature Materials, 2003, 2, 673-677.	13.3	1,687
904	Local structure and electronic properties of BaTaO2N with perovskite-type structure. Journal of Physics and Chemistry of Solids, 2003, 64, 281-286.	1.9	67

#	Article	IF	Citations
905	In search of new candidates for ultra-hard materials: the ternary BC3N3 stoichiometry. Journal of Physics and Chemistry of Solids, 2003, 64, 1539-1545.	1.9	15
906	Ab initio calculation of intrinsic point defects in CuInSe2. Journal of Physics and Chemistry of Solids, 2003, 64, 1657-1663.	1.9	52
907	Hopping and optical absorption of electrons in nano-porous crystal 12CaOÂ·7Al2O3. Thin Solid Films, 2003, 445, 161-167.	0.8	64
908	Challenges and errors: interpreting high resolution images in scanning tunneling microscopy. Progress in Surface Science, 2003, 71, 147-183.	3.8	154
909	Oxygen vacancy defects in tantalum pentoxide: a density functional study. Microelectronic Engineering, 2003, 69, 190-194.	1.1	15
910	Influence of electron concentration and temperature on endohedral metallofullerene Me@C84 formation in a carbon plasma. Chemical Physics, 2003, 293, 253-261.	0.9	8
911	Lattice dielectric response ofCdCu3Ti4O12andCaCu3Ti4O12from first principles. Physical Review B, 2003, 67, .	1.1	93
912	Interactions between nitrogen, hydrogen, and gallium vacancies inGaAs1â^'xNxalloys. Physical Review B, 2003, 67, .	1.1	99
913	Molecular alligator clips: a theoretical study of adsorption of S, Se and Sâ€“H on Au(111). Nanotechnology, 2003, 14, 849-858.	1.3	25
914	Thermodynamics from first principles: temperature and composition of the Earthâ€™s core. Mineralogical Magazine, 2003, 67, 113-123.	0.6	34
915	Magnetic Properties and Diffusion of Adatoms on a Graphene Sheet. Physical Review Letters, 2003, 91, 017202.	2.9	419
916	Dynamic structure factor of liquid and amorphous Ge fromab initiosimulations. Physical Review B, 2003, 67, .	1.1	37
917	Initial stages in the oxidation and reduction of the4Ã—4surface oxide phase on Ag{111}: A combined density-functional theory and STM simulation study. Physical Review B, 2003, 68, .	1.1	17
918	Comparison between plane-wave and linear-scaling localized basis sets for structural calculations of microporous molecular sieves. Physical Review B, 2003, 68, .	1.1	12
919	New Mechanism for theÎ±toÏ‰Martensitic Transformation in Pure Titanium. Physical Review Letters, 2003, 91, 025701.	2.9	156
920	Local reactivity of metal overlayers: Density functional theory calculations of Pd on Au. Physical Review B, 2003, 67, .	1.1	130
921	The geometry and the radial breathing mode of carbon nanotubes: beyond the ideal behaviour. New Journal of Physics, 2003, 5, 125-125.	1.2	154
922	Surface Coverage Effects on the Formation of Molecular Hydrogen on a Graphite Surface via an Eleyâ^'Rideal Mechanism. Journal of Physical Chemistry A, 2003, 107, 10862-10871.	1.1	20

#	Article	IF	Citations
923	Ferromagnetism in Mn-doped GaAs due to substitutional-interstitial complexes. Physical Review B, 2003, 68, .	1.1	119
924	Surface Structures of SrTiO3(001):Â A TiO2-rich Reconstruction with a c(4 Ã— 2) Unit Cell. Journal of the American Chemical Society, 2003, 125, 10050-10056.	6.6	134
925	Size dependent phase stability of carbon nanoparticles: Nanodiamond versus fullerenes. Journal of Chemical Physics, 2003, 118, 5094-5097.	1.2	91
926	Pt and Pt2 on MgO(100) and BaO(100): structure, bonding, and chemical properties. Journal of Chemical Physics, 2003, 119, 3896-3904.	1.2	41
927	Adatoms, dimers, and interstitials on group-IV(113) surfaces:â€ƒFirst-principles studies of energetical, structural, and electronic properties. Physical Review B, 2003, 67, .	1.1	26
928	Structural and Electronic Properties of the Layered LiNi0.5Mn0.5O2Lithium Battery Material. Chemistry of Materials, 2003, 15, 4280-4286.	3.2	84
929	Adsorption of gold on stoichiometric and reduced rutile TiO2â€‚(110) surfaces. Journal of Chemical Physics, 2003, 118, 6536-6551.	1.2	202
930	Structure of the P vacancy on the InP(110) surface from first principles. Physical Review B, 2003, 67, .	1.1	8
931	Ab initio simulation of the ice II structure. Journal of Chemical Physics, 2003, 119, 4567-4572.	1.2	28
932	Ab initiocalculation of the ideal tensile and shear strength of cubic silicon nitride. Physical Review B, 2003, 67, .	1.1	41
933	Modelling inorganic solids and their interfaces: A combined approach of atomistic and electronic structure simulation techniques. Faraday Discussions, 2003, 124, 155.	1.6	29
934	CubicHf3N4andZr3N4:A class of hard materials. Physical Review B, 2003, 68, .	1.1	294
935	Magnetism of Transition-Metal/Carbon-Nanotube Hybrid Structures. Physical Review Letters, 2003, 90, 257203.	2.9	198
936	Structure of the icosahedral Ti-Zr-Ni quasicrystal. Physical Review B, 2003, 67, .	1.1	46
937	First-principles calculations of intrinsic defects inAl2O3. Physical Review B, 2003, 68, .	1.1	270
938	Spontaneous Cross Linking of Small-Diameter Single-Walled Carbon Nanotubes. Nano Letters, 2003, 3, 585-587.	4.5	30
939	Specific Ethene Surface Activation on Silver Oxide Covered Ag{111} from the Interplay of STM Experiment and Theory. Journal of the American Chemical Society, 2003, 125, 3119-3125.	6.6	61
940	A theoretical study of the energetics and IR frequencies of hydroxyl defects in forsterite. Journal of Geophysical Research, 2003, 108, .	3.3	47

#	Article	IF	Citations
941	Carbon Monoxide Dissociation on Planar and Stepped Ru(0001) Surfaces. Journal of Physical Chemistry B, 2003, 107, 3808-3812.	1.2	156
942	Metal-Nonmetal Transition in the Boron Group Elements. Physical Review Letters, 2003, 90, 065701.	2.9	111
943	Free energy of liquid water on the basis of quasichemical theory andab initiomolecular dynamics. Physical Review E, 2003, 68, 041505.	0.8	133
944	First-principles investigations of homogeneous lattice-distortive strain and shuffles in Ni2MnGa. Journal of Physics Condensed Matter, 2003, 15, 159-164.	0.7	80
945	First-principles simulations of direct coexistence of solid and liquid aluminum. Physical Review B, 2003, 68, .	1.1	93
946	Modelling and simulation of amorphous silicon oxycarbide. Journal of Materials Chemistry, 2003, 13, 1657.	6.7	50
947	Surface Strain versus Substrate Interaction in Heteroepitaxial Metal Layers: Pt on Ru(0001). Physical Review Letters, 2003, 91, 016101.	2.9	316
948	Influence of Zeolite Framework Geometry Structure on the Stability of the [ZnOZn]2+Cluster by Periodical Density Functional Theory. Journal of Physical Chemistry B, 2003, 107, 4532-4536.	1.2	25
949	Physisorption and Chemisorption of Somen-Hydrocarbons at the BrÃ¸nsted Acid Site in Zeolites 12-Membered Ring Main Channels:Â Ab Initio Study of the Gmelinite Structure. Journal of Physical Chemistry B, 2003, 107, 9756-9762.	1.2	46
950	Study of the Activation of Câ^'H and Hâ^'H Chemical Bonds by the [ZnOZn]2+Oxycation:Â Influence of the Zeolite Framework Geometry. Journal of Physical Chemistry B, 2003, 107, 14342-14349.	1.2	28
951	Adsorption and Coadsorption of CO and H on Ruthenium Surfaces. Journal of Physical Chemistry B, 2003, 107, 164-172.	1.2	65
952	A Periodic DFT Study of Isobutene Chemisorption in Proton-Exchanged Zeolites:Â Dependence of Reactivity on the Zeolite Framework Structure. Journal of Physical Chemistry B, 2003, 107, 1309-1315.	1.2	129
953	Theory of dopants and defects in Co-dopedTiO2anatase. Physical Review B, 2003, 67, .	1.1	76
954	Adsorption Structures of Phenylacetylene and 1-Phenyl-1-propyne on a Si(100)-(2 Ã— 1) Surface. Journal of Physical Chemistry B, 2003, 107, 11987-11995.	1.2	19
955	Structural, electronic, and magnetic properties of a ferromagnetic semiconductor: Co-dopedTiO2rutile. Physical Review B, 2003, 68, .	1.1	75
956	Adsorption of HCl on Single-Crystal Î±-Al2O3(0001) Surface:Â A DFT Study. Journal of Physical Chemistry B, 2003, 107, 186-195.	1.2	36
957	Adsorption and Desorption of Methanol on Pd (111) and on a Pd/V Surface Alloy. Journal of Physical Chemistry B, 2003, 107, 2552-2558.	1.2	68
958	Weakening of a Polyethylene Chain by Methyl Side Groups. Soft Materials, 2003, 1, 223-233.	0.8	3

#	Article	IF	Citations
959	Crystal Structures of (Pyrene)10(I3-)4(I2)10and [1,3,6,8-Tetrakis(methylthio)pyrene]3(I3-)3(I2)7:Â Structural Trends in Fused Aromatic Polyiodides. Chemistry of Materials, 2003, 15, 1420-1433.	3.2	26
960	The layering effect of water on the structure of scheelite. Physical Chemistry Chemical Physics, 2003, 5, 433-436.	1.3	10
961	First-Principle Study of the Intercalation Process in the LixV2O5 System. Chemistry of Materials, 2003, 15, 1812-1819.	3.2	55
962	Alloying effects on elastic properties of TiN-based nitrides. Journal Physics D: Applied Physics, 2003, 36, 2725-2729.	1.3	130
963	Structure and Energetics of Single-Walled Armchair and Zigzag Silicon Nanotubes. Journal of Physical Chemistry B, 2003, 107, 7577-7581.	1.2	85
964	Carbon Monoxide Adsorption on Molybdenum Phosphides:Â Fourier Transform Infrared Spectroscopic and Density Functional Theory Studies. Journal of Physical Chemistry B, 2003, 107, 13698-13702.	1.2	26
965	Atomistic Simulation of the Dissociative Adsorption of Water on Calcite Surfaces. Journal of Physical Chemistry B, 2003, 107, 7676-7682.	1.2	141
966	Density Functional Theory Studies of Chemisorption and Diffusion Properties of Ni and Niâ^'Thiophene Complexes on the MoS2 Basal Plane. Journal of Physical Chemistry B, 2003, 107, 1988-2000.	1.2	16
967	Spin Crossover of Spiro-Biphenalenyl Neutral Radical Molecular Conductors. Journal of the American Chemical Society, 2003, 125, 13334-13335.	6.6	42
968	All-electron and pseudopotential study of MgO: Equation of state, anharmonicity, and stability. Physical Review B, 2003, 67, .	1.1	151
969	Chemisorption of NO2on Carbon Nanotubes. Journal of Physical Chemistry B, 2003, 107, 9363-9369.	1.2	104
970	Electronic correlation effects in transition-metal sulfides. Journal of Physics Condensed Matter, 2003, 15, 979-996.	0.7	231
971	First-Principles Calculations of the Adsorption of Nitromethane and 1,1-Diamino-2,2-dinitroethylene (FOX-7) Molecules on the Al(111) Surface. Journal of Physical Chemistry B, 2003, 107, 8953-8964.	1.2	40
972	The properties of iron under core conditions from first principles calculations. Physics of the Earth and Planetary Interiors, 2003, 140, 101-125.	0.7	138
973	The particle-in-cell model for ab initio thermodynamics: implications for the elastic anisotropy of the Earthâ€™s inner core. Physics of the Earth and Planetary Interiors, 2003, 139, 243-253.	0.7	36
974	Ab initio investigations in magnetic oxides. Progress in Solid State Chemistry, 2003, 31, 239-299.	3.9	62
975	Epitaxial BiFeO3 Multiferroic Thin Film Heterostructures. Science, 2003, 299, 1719-1722.	6.0	5,548
976	Carbon dissolution and diffusion in ferrite and austenite from first principles. Physical Review B, 2003, 67, .	1.1	398

#	Article	IF	Citations
977	An ab initio study of the ideal tensile and shear strength of single-crystal Î²â€“Si₃N₄. Journal of Materials Research, 2003, 18, 1168-1172.	1.2	25
978	Novel Stabilization Mechanism on Polar Surfaces: ZnO(0001)-Zn. Physical Review Letters, 2003, 90, 016102.	2.9	493
979	Cluster expansion method for adsorption: Application to hydrogen chemisorption on graphene. Physical Review B, 2003, 68, .	1.1	256
980	Intermolecular potential and the equation of state of solid C60. Journal of Chemical Physics, 2003, 119, 1386-1396.	1.2	17
981	First-principles study of the structural energetics of PdTi and PtTi. Physical Review B, 2003, 67, .	1.1	37
982	Quantum Dynamics Simulations of Interfacial Electron Transfer in Sensitized TiO2Semiconductors. Journal of the American Chemical Society, 2003, 125, 7989-7997.	6.6	368
983	Theoretical study about adsorption of atomic oxygen on unmodified and I-modified Ag(100) surface. Journal of Chemical Physics, 2003, 118, 11210-11216.	1.2	6
984	Charge State Dependent Jahn-Teller Distortions of theE-Center Defect in Crystalline Si. Physical Review Letters, 2003, 91, 235503.	2.9	20
985	Adsorption energy and spin state of first-row transition metals adsorbed on MgO(100). Physical Review B, 2003, 67, .	1.1	67
986	Structure effects on the energetic, electronic, and magnetic properties of palladium nanoparticles. Journal of Chemical Physics, 2003, 118, 5793-5801.	1.2	74
987	Ab-initio calculation of enthalpies of formation of intermetallic compounds and enthalpies of mixing of solid solutions. Intermetallics, 2003, 11, 1095-1102.	1.8	47
988	Proximity effects on semiconducting mineral surfaces II:. Geochimica Et Cosmochimica Acta, 2003, 67, 941-953.	1.6	39
989	Anisotropy of the mobility of pentacene from frustration. Synthetic Metals, 2003, 139, 109-114.	2.1	125
990	Magnetism of ultrathin wires suspended in free space and adsorbed on vicinal surfaces. Physical Review B, 2003, 67, .	1.1	47
991	Oxygen adsorption on Au clusters and a rough Au(111) surface: The role of surface flatness, electron confinement, excess electrons, and band gap. Journal of Chemical Physics, 2003, 118, 4198-4205.	1.2	257
992	Hydrogenated Silicon Fullerenes: Effects of H on the Stability of Metal-Encapsulated Silicon Clusters. Physical Review Letters, 2003, 90, 055502.	2.9	152
993	Identification of new adsorption sites of H and D on rhodium(100). Journal of Chemical Physics, 2003, 119, 5253-5266.	1.2	21
994	Catalytic conversion of hydrocarbons over zeolites from first principles. Computational Materials Science, 2003, 27, 87-95.	1.4	8

#	Article	IF	Citations
995	Magnetism of monoatomic wires on vicinal surfaces. Computational Materials Science, 2003, 27, 138-150.	1.4	11
996	Electronic structure of perovskite-type YBRh3: X-ray photoelectron spectroscopy and ab initio band calculations. Journal of Alloys and Compounds, 2003, 349, 206-210.	2.8	3
997	Lattice dynamics of YCu2. Journal of Alloys and Compounds, 2003, 349, 28-36.	2.8	3
998	Ab initio calculation of the crystal structure of the lanthanide Ln2O3 sesquioxides. Journal of Alloys and Compounds, 2003, 351, 31-34.	2.8	137
999	Electronic structure calculations for LaNi5 and LaNi5H7: energetics and elastic properties. Journal of Alloys and Compounds, 2003, 353, 74-85.	2.8	103
1000	Energetics, electric-field gradients and optical properties of YH3 (YD3) by first-principles calculations. Journal of Alloys and Compounds, 2003, 356-357, 73-79.	2.8	12
1001	First principles study of sodiumâ€“aluminumâ€“hydrogen phases. Journal of Alloys and Compounds, 2003, 356-357, 486-489.	2.8	41
1002	Effects of the iron-oxide layer in Fe-FeO-MgO-Fe tunneling junctions. Physical Review B, 2003, 68, .	1.1	213
1003	Theory of the effects of substitutions on the phase stabilities of Ti1âˆ’xAlxN. Journal of Applied Physics, 2003, 93, 4505-4511.	1.1	75
1004	Phonon spectrum and thermal properties of cubic Si3N4 from first-principles calculations. Journal of Applied Physics, 2003, 93, 5175-5180.	1.1	50
1005	Co-phase penetration ofWC(101Â¯0)/WC(101Â¯0)grain boundaries from first principles. Physical Review B, 2003, 67, .	1.1	85
1006	First-principles calculation of the effect of strain on the diffusion of Ge adatoms on Si and Ge(001) surfaces. Physical Review B, 2003, 67, .	1.1	45
1007	Density-functional calculations of the liquid deuterium Hugoniot, reshock, and reverberation timing. Physical Review B, 2003, 68, .	1.1	166
1008	First-principles study of small-radius single-walled BN nanotubes. Physical Review B, 2003, 68, .	1.1	176
1009	Relationship between surface dipole, work function and charge transfer:â€,â€,Some exceptions to an established rule. Physical Review B, 2003, 68, .	1.1	344
1010	Variations of the Geometries and Band Gaps of Single-Walled Carbon Nanotubes and the Effect of Charge Injection. Journal of Physical Chemistry B, 2003, 107, 6924-6931.	1.2	88
1011	Ordering tendencies in octahedral MgO-ZnO alloys. Physical Review B, 2003, 68, .	1.1	69
1012	Electronic band gaps of diamond nanowires. Physical Review B, 2003, 68, .	1.1	39

#	Article	IF	Citations
1013	Enhancement of electronic conductivity ofLiFePO4by Cr doping and its identification by first-principles calculations. Physical Review B, 2003, 68, .	1.1	249
1014	First-principles study of adhesion atCu/SiO2interfaces. Physical Review B, 2003, 68, .	1.1	81
1015	Vacancy concentration in Al from combined first-principles and model potential calculations. Physical Review B, 2003, 67, .	1.1	73
1016	Self-Doping of Gold Chains on Silicon: A New Structural Model forSi(111)-(5Ã—2)-Au. Physical Review Letters, 2003, 91, 206101.	2.9	88
1017	Scanning tunneling microscopy and spectroscopy of gallium oxide deposition and oxidation on GaAs(001)-c(2Ã—8)/(2Ã—4). Journal of Chemical Physics, 2003, 119, 6719-6728.	1.2	139
1018	Equation of state and phonon frequency calculations of diamond at high pressures. Physical Review B, 2003, 68, .	1.1	82
1019	Melem (2,5,8-Triamino-tri-s-triazine), an Important Intermediate during Condensation of Melamine Rings to Graphitic Carbon Nitride:Â Synthesis, Structure Determination by X-ray Powder Diffractometry, Solid-State NMR, and Theoretical Studies. Journal of the American Chemical Society, 2003, 125, 10288-10300.	6.6	954
1020	Understanding the complex metallic element Mn. I.â€,Crystalline and noncollinear magnetic structure of Î±-Mn. Physical Review B, 2003, 68, .	1.1	236
1021	Cation distribution and magnetic ordering in FeSbO4. Journal of Materials Chemistry, 2003, 13, 2848.	6.7	42
1022	Mg Segregation atAl/Al3ScHeterophase Interfaces on an Atomic Scale: Experiments and Computations. Physical Review Letters, 2003, 91, 036101.	2.9	93
1023	Steric Effects on the Adsorption of Alkylthiolate Self-Assembled Monolayers on Au (111)â€. Journal of Physical Chemistry B, 2003, 107, 3803-3807.	1.2	78
1024	CO adsorption on the CO-precovered Pt(111) surface characterized by density-functional theory. Physical Review B, 2003, 68, .	1.1	34
1025	Magnetism in Transition-Metal-Doped Silicon Nanotubes. Physical Review Letters, 2003, 91, 146802.	2.9	175
1026	First-principles calculations of the adsorption of nitromethane and 1,1-diamino 2,2-dinitroethylene (FOX-7) molecules on the Al[111]surface. , 0, , .		1
1027	Nucleation of Single-Walled Carbon Nanotubes. Physical Review Letters, 2003, 90, 145501.	2.9	127
1028	Measuring electronic structure of wurtzite InN using electron energy loss spectroscopy. Applied Physics Letters, 2003, 82, 1407-1409.	1.5	27
1029	Ab initio modeling of B and N in C29 and C29H24 nanodiamond. Journal of Chemical Physics, 2003, 118, 10725-10728.	1.2	23
1030	First-principles study of oxygen-vacancy pinning of domain walls inPbTiO3. Physical Review B, 2003, 68, .	1.1	248

#	Article	IF	Citations
1031	Computational chemistry models leading to mediation of gun tube erosion. , 0, , .		0
1032	Cross-sectional scanning tunneling microscopy of Mn-doped GaAs:â€,â€,Theory and experiment. Physical Review B, 2003, 68, .	1.1	43
1033	Site preferences in Î²-sialon from first-principles calculations. Journal of Materials Chemistry, 2003, 13, 335-337.	6.7	13
1034	Novel Method for the Activation of Acceptor Dopant in AlN Introducing Localized Band by Isoelectronic Dopant. Materials Research Society Symposia Proceedings, 2003, 798, 164.	0.1	0
1035	Modeling the Polymorphism of Pentacene. Journal of the American Chemical Society, 2003, 125, 6323-6330.	6.6	214
1036	Influence of Stress on Thermoelectric Properties of Antimony Telluride. Materials Research Society Symposia Proceedings, 2003, 793, 38.	0.1	0
1037	Local Structural Variations in Al72Ni20Co8 Decagonal Quasicrystals. Materials Research Society Symposia Proceedings, 2003, 805, 248.	0.1	0
1038	Order-disorder transition in the Cd-Ca cubic approximant. Materials Research Society Symposia Proceedings, 2003, 805, 50.	0.1	4
1039	Ab-initio Study of the Diffusion Coefficients in Fe-based Liquids. Materials Research Society Symposia Proceedings, 2003, 806, 155.	0.1	1
1040	Semiconducting Aluminum Transition-Metal Quasicrystals. Materials Research Society Symposia Proceedings, 2003, 805, 138.	0.1	0
1041	<I>Ab initio</I> determination of edge surface structures for dioctahedral 2:1 phyllosilicates: implications for acid-base for reactivity. Clays and Clay Minerals, 2003, 51, 359-371.	0.6	135
1042	Quantum dots as dynamical systems. Philosophical Transactions Series A, Mathematical, Physical, and Engineering Sciences, 2003, 361, 275-290.	1.6	13
1043	Cohesive Properties of PuGa Alloys. Materials Research Society Symposia Proceedings, 2003, 802, 203.	0.1	0
1044	Quasicrystal approximants with novel compositions and structures. Materials Research Society Symposia Proceedings, 2003, 805, 112.	0.1	3
1045	Electronic versus geometric contrast in cross-sectional STM images of III-V semiconductor heterostructures. Physical Review B, 2003, 67, .	1.1	19
1046	Initial and final state effects in the x-ray absorption process ofLa1â^'xSrxMnO3. Physical Review B, 2003, 68, .	1.1	21
1047	Structure, bonding, and adhesion at the TiC(100)/Fe(110) interface from first principles. Journal of Chemical Physics, 2003, 118, 8982-8996.	1.2	183
1048	Atomic and electronic structure of theSi/SrTiO3interface. Physical Review B, 2003, 68, .	1.1	129

#	Article	IF	Citations
1049	Stability of gold nanowires at large Au-Au separations. Physical Review B, 2003, 67, .	1.1	72
1050	Bi incorporation in GaN andAlxGa1â^'xNalloys. Physical Review B, 2003, 68, .	1.1	5
1051	Energetics and structural relaxation of constitutional defects in CoAl and CoTi from first principles. Physical Review B, 2003, 68, .	1.1	11
1052	Energetics of Li atom displacements inK1â^'xLixTaO3:First-principles calculations. Physical Review B, 2003, 68, .	1.1	39
1053	Density-functional theory studies of xanthate adsorption on the pyrite FeS2(110) and (111) surfaces. Journal of Chemical Physics, 2003, 118, 6022-6029.	1.2	42
1054	Site occupation in the Ni-NbÎ¼phase. Physical Review B, 2003, 67, .	1.1	30
1055	First-principles study of point-defect structures inC15ZrCo2andZrCr2andB2ZrCo. Physical Review B, 2003, 68, .	1.1	18
1056	Manipulation of fullerene-induced impurity states in carbon peapods. Physical Review B, 2003, 68, .	1.1	25
1057	First-principles studies of cation-doped spinelLiMn2O4for lithium ion batteries. Physical Review B, 2003, 67, .	1.1	51
1058	Divalent-dopant criterion for the suppression of Jahn-Teller distortion in Mn oxides: First-principles calculations and x-ray absorption spectroscopy measurements for Co inLiMnO2. Physical Review B, 2003, 68, .	1.1	31
1059	Toward one-band superconductivity inMgB2. Physical Review B, 2003, 68, .	1.1	83
1060	Ab initiovalence band offsets between Si(100) andSiO2from microscopic models. Physical Review B, 2003, 67, .	1.1	26
1061	Optical consequences of long-range order in wurtziteAlxGa1â^'xNalloys. Physical Review B, 2003, 68, .	1.1	14
1062	Covalent and Reversible Short-Range Electrostatic Imaging in Noncontact Atomic Force Microscopy. Physical Review Letters, 2003, 91, 216401.	2.9	25
1063	Signature of a Chemical Bond in the Conductance between Two Metal Surfaces. Physical Review Letters, 2003, 91, 036803.	2.9	70
1064	Oxidation of Carbon Nanotubes by SingletO2. Physical Review Letters, 2003, 90, 086403.	2.9	120
1065	The crystalline surfaces of Î²-PdH{111}: Ideal surface terminations of a stoichiometric bulk compound relevant to heterogeneous catalysis. Journal of Chemical Physics, 2003, 118, 5623-5634.	1.2	21
1066	Nearest-Neighbor Configuration in (GaIn)(NAs) Probed by X-Ray Absorption Spectroscopy. Physical Review Letters, 2003, 90, 145505.	2.9	116

#	Article	IF	Citations
1067	Hafnium Nitride with Thorium Phosphide Structure: Physical Properties and an Assessment of the Hf-N, Zr-N, and Ti-N Phase Diagrams at High Pressures and Temperatures. Physical Review Letters, 2003, 90, 125501.	2.9	167
1068	Eleyâ€“Rideal reactions of H atoms with Cl adsorbed on Au(111): Quantum and quasiclassical studies. Journal of Chemical Physics, 2003, 118, 2357-2366.	1.2	27
1069	SnGe superstructure materials for Si-based infrared optoelectronics. Applied Physics Letters, 2003, 83, 3489-3491.	1.5	42
1070	Adaptive Crystal Structures: CuAu and NiPt. Physical Review Letters, 2003, 90, 045502.	2.9	50
1071	Theories of scanning probe microscopes at the atomic scale. Reviews of Modern Physics, 2003, 75, 1287-1331.	16.4	432
1072	Surface structure and dynamics ofKTaO3(001). Physical Review B, 2003, 68, .	1.1	11
1073	First-principles investigation of phonon softenings and lattice instabilities in the shape-memory systemNi2MnGa. Physical Review B, 2003, 68, .	1.1	109
1074	Surface structure and stability of PdZn and PtZn alloys:â€ƒDensity-functional slab model studies. Physical Review B, 2003, 68, .	1.1	108
1075	3Ã—2reconstruction of the Sm/Si(111) interface. Physical Review B, 2003, 67, .	1.1	26
1076	Semiconducting Alâ€“transition-metal quasicrystals. Physical Review B, 2003, 68, .	1.1	26
1077	Dimensional change as a function of charge injection in graphite intercalation compounds: â€ƒA density functional theory study. Physical Review B, 2003, 68, .	1.1	24
1078	Validity of effective-medium theory for optical properties of embedded nanocrystallites fromab initiosupercell calculations. Physical Review B, 2003, 67, .	1.1	55
1079	Prediction of dopant ionization energies in silicon: The importance of strain. Physical Review B, 2003, 68, .	1.1	16
1080	Prediction of insulating quasicrystalline approximants usingab initioelectronic structure calculations. Physical Review B, 2003, 67, .	1.1	9
1081	Bulk and surface ordering phenomena in binary metal alloys. Journal of Physics Condensed Matter, 2003, 15, R1429-R1500.	0.7	98
1082	Thermodynamics of tin clusters. Physical Review B, 2003, 67, .	1.1	52
1083	Vanadium surface oxides on Pd(111):â€,â€,A structural analysis. Physical Review B, 2003, 68, .	1.1	34
1084	Predicted hcp Ag-Al metastable phase diagram, equilibrium ground states, and precipitate structure. Physical Review B, 2003, 67, .	1.1	45

#	Article	IF	Citations
1085	Atomic clusters of magnetic oxides: Structure and phonons. Journal of Applied Physics, 2003, 93, 7379-7381.	1.1	13
1086	Using bond-length-dependent transferable force constants to predict vibrational entropies in Au-Cu, Au-Pd, and Cu-Pd alloys. Physical Review B, 2003, 67, .	1.1	55
1087	Multilayer relaxation of Cu(210) studied by layer-doubling LEED analysis and pseudopotential density functional theory calculations. Physical Review B, 2003, 68, .	1.1	18
1088	Tetramers on diamond, Si, and Ge(113) surfaces:Ab initiostudies. Physical Review B, 2003, 68, .	1.1	16
1089	Ordered versus disordered growth of copper quantum wires on Mo and W vicinal surfaces. Physical Review B, 2003, 67, .	1.1	3
1090	Ab initiostudy of Al-ceramic interfacial adhesion. Physical Review B, 2003, 67, .	1.1	127
1091	Lattice dynamics of HgSe: Neutron scattering measurements andab initiostudies. Physical Review B, 2003, 67, .	1.1	21
1092	Predicted absence of ferromagnetism in manganese-doped diamond. Physical Review B, 2003, 68, .	1.1	32
1093	First-principles study on the energetics and vibrational properties of theS2â^'impurity in alkali-halide crystals. Physical Review B, 2003, 68, .	1.1	6
1094	First-principles study of the solubility, diffusion, and clustering of C in Ni. Physical Review B, 2003, 68, .	1.1	71
1095	Carbon nanotube bundles under high pressure:â€ƒTransformation to low-symmetry structures. Physical Review B, 2003, 68, .	1.1	69
1096	Absolute In coverage and bias-dependent STM images of the Si(111)4Ã—1-In surface. Physical Review B, 2003, 67, .	1.1	32
1097	Ab initiostudies of stepped Pd surfaces with and without S. Physical Review B, 2003, 67, .	1.1	22
1098	Structural relaxation in Si and Ge nanocrystallites: Influence on the electronic and optical properties. Physical Review B, 2003, 67, .	1.1	59
1099	Vibrational properties of the quasi-one-dimensionalIn/Si(111)â^'(4Ã—1)system. Physical Review B, 2003, 68, .	1.1	12
1100	Exchange-correlation energy and the phase diagram of Si. Physical Review B, 2003, 68, .	1.1	38
1101	Vibrations of a water adlayer on Ru(0001). Physical Review B, 2003, 67, .	1.1	56
1102	Interactions and structure of poly(dimethylsiloxane) at silicon dioxide surfaces: Electronic structure and molecular dynamics studies. Journal of Chemical Physics, 2003, 118, 5132-5142.	1.2	60

#	Article	IF	Citations
1103	Theory of polarization enhancement in epitaxial BaTiO3/SrTiO3 superlattices. Applied Physics Letters, 2003, 82, 1586-1588.	1.5	316
1104	Hydrogen bonding in solid ammonia fromab initiocalculations. Journal of Chemical Physics, 2003, 118, 5987-5994.	1.2	47
1105	Effect of composition on vacancy mediated diffusion in random binary alloys: First principles study of the Si1â^'xGex system. Journal of Applied Physics, 2003, 94, 174-185.	1.1	40
1106	Combining density-functional calculations with kinetic models: NO/Rh(111). Journal of Chemical Physics, 2003, 118, 7081-7089.	1.2	47
1107	Tile Hamiltonian for decagonal AlCoCu derived from first principles. Physical Review B, 2003, 67, .	1.1	11
1108	Distance Dependence of the Interaction between Single Atoms: Gold Dimers on NiAl(110). Physical Review Letters, 2003, 90, 196103.	2.9	81
1109	Quantum molecular-dynamics study of the electrical and optical properties of shocked liquid nitrogen. Physical Review B, 2003, 67, .	1.1	30
1110	A computational study of the surface structure and reactivity of calcium fluoride. Journal of Materials Chemistry, 2003, 13, 93-101.	6.7	96
1111	Cyclic and linear polymeric structures ofAlnH3n(n=3â€“7) molecules. Physical Review A, 2003, 67, .	1.0	36
1112	Theoretical study of laser characteristics of InPAsN/GaInAsP/InP laser diode using first-principles method. , 0, , .		0
1113	When Scanning Tunneling Microscopy Gets the Wrong Adsorption Site: H on Rh(100). Physical Review Letters, 2003, 90, 176101.	2.9	21
1114	Alternating Layer and Island Growth of Pb on Si by Spontaneous Quantum Phase Separation. Physical Review Letters, 2003, 90, 076104.	2.9	84
1115	Modeling oxide-metal interfaces from density-functional theory: Platinum adsorption on tetragonal zirconia. Physical Review B, 2003, 68, .	1.1	16
1116	Layer Spacings in Coherently Strained Epitaxial Metal Films. Physical Review Letters, 2003, 90, 216105.	2.9	35
1117	Comparative study of structural, electronic and optical properties ofCa2Si,Ca2Ge,Ca2Sn,andCa2Pb. Physical Review B, 2003, 67, .	1.1	72
1118	Linear monatomic wires stabilized by alloying:Ab initiodensity functional calculations. Physical Review B, 2003, 67, .	1.1	34
1119	Density-functional theory simulation of large quantum dots. Physical Review B, 2003, 68, .	1.1	30
1120	Significance of single-electron energies for the description of CO on Pt(111). Physical Review B, 2003, 68, .	1.1	225

#	Article	IF	Citations
1121	Strong correlation effects in the electronic structure ofSr2FeMoO6. Physical Review B, 2003, 67, .	1.1	23
1122	Modeling charge self-trapping in wide-gap dielectrics: Localization problem in local density functionals. Physical Review B, 2003, 67, .	1.1	87
1123	Effects of the substrate on quantum well states: A first-principles study for Ag/Fe(100). Physical Review B, 2003, 68, .	1.1	35
1124	Excitation Energies and Radiative Lifetimes ofGe1â^'xSixNanocrystals: Alloying Versus Confinement Effects. Physical Review Letters, 2003, 90, 085501.	2.9	35
1125	Why Do Grain Boundaries Exhibit Finite Facet Lengths?. Physical Review Letters, 2003, 90, 246102.	2.9	34
1126	Changing the Diffusion Mechanism of Ge-Si Dimers on Si(001) using an Electric Field. Physical Review Letters, 2003, 91, 206104.	2.9	16
1127	Competing stabilization mechanism for the polar ZnO(0001)-Zn surface. Physical Review B, 2003, 68, .	1.1	335
1128	Uniaxial phase transition in Si:Ab initiocalculations. Physical Review B, 2003, 67, .	1.1	16
1129	Assignment of the(1Ã—2)surface of rutileTiO2(110)from first principles. Physical Review B, 2003, 67, .	1.1	23
1130	First-principles study of magnetism in spinelMnO2. Physical Review B, 2003, 67, .	1.1	25
1131	Local lattice relaxations in random metallic alloys: Effective tetrahedron model and supercell approach. Physical Review B, 2003, 67, .	1.1	97
1132	Ab initiostudies of the passive film formed on iron. Physical Review B, 2003, 67, .	1.1	24
1133	Embedded-atom-method tantalum potential developed by the force-matching method. Physical Review B, 2003, 67, .	1.1	93
1134	Ab initiostudy of elastic properties of Ir and Ir3X compounds. Journal of Applied Physics, 2003, 93, 2414-2417.	1.1	128
1135	Role of dynamic trapping in H2 dissociation and reflection on Pd surfaces. Journal of Chemical Physics, 2003, 118, 11226-11234.	1.2	64
1136	Magnetization of the unsegregated and segregated (100) surface of MoV binary alloys. Physical Review B, 2003, 68, .	1.1	5
1137	Nonenhancement of magnetic moments on transition metal impurities by alkali metal hosts. Physical Review B, 2003, 67, .	1.1	6
1138	Vacancies below the (111) surface of Pd. Physical Review B, 2003, 67, .	1.1	19

#	Article	IF	Citations
1139	Reactive Wetting:H2O/Rh(111). Physical Review Letters, 2003, 90, 186103.	2.9	41
1140	Modified conjugate gradient method for diagonalizing large matrices. Physical Review E, 2003, 68, 056706.	0.8	7
1141	Comment on â€œVibrational Recognition of Hydrogen-Bonded Water Networks on a Metal Surfaceâ€: Physical Review Letters, 2003, 91, 059601; author reply 059602.	2.9	41
1142	Observation of Spin-Polarized Surface States on Ultrathin bct Mn(001) Films by Spin-Polarized Scanning Tunneling Spectroscopy. Physical Review Letters, 2003, 90, 056803.	2.9	97
1143	Vacancy-Mediated and Exchange Diffusion in aPb/Cu(111)Surface Alloy: Concurrent Diffusion on Two Length Scales. Physical Review Letters, 2003, 90, 126102.	2.9	43
1144	Theoretical analysis of clock-reconstructed PdCu surface alloy. Physical Review B, 2003, 67, .	1.1	10
1145	Defect sites at the (001) surface of mordenite:â€‚Anab initiostudy. Journal of Chemical Physics, 2003, 118, 8437-8445.	1.2	22
1146	Ab initiodensity functional studies of stepped TaC surfaces. Physical Review B, 2003, 67, .	1.1	5
1147	Six low-strain zinc-blende half metals:â€ƒAnab initioinvestigation. Physical Review B, 2003, 67, .	1.1	176
1148	Coexistence of ferromagnetic and antiferromagnetic order in Mn-dopedNi2MnGa. Physical Review B, 2003, 67, .	1.1	208
1149	Magnetic properties of Co and Co-Ag alloys in equilibrium/nonequilibrium structures studied byab initiocalculations. Physical Review B, 2003, 68, .	1.1	26
1150	Formation of clean dimers during gas-source growth of Si(001). Physical Review B, 2003, 67, .	1.1	12
1151	First Principles Investigations of Diamond Ultrananocrystals. International Journal of Modern Physics B, 2003, 17, 3865-3879.	1.0	25
1152	Interactions of model organic species and explosives with clay minerals. Theoretical and Computational Chemistry, 2003, 12, 341-388.	0.2	1
1153	Hydrogenation of Nanodiamond Surfaces: Structure and Effects on Crystalline Stability. Surface Review and Letters, 2003, 10, 233-239.	0.5	26
1154	Ab initio modelling of boron and nitrogen in diamond nanowires. Philosophical Magazine, 2003, 83, 2301-2309.	0.7	7
1155	Interface structure and stabilization of metastable B2-FeSi/Si(111) studied with low-energy electron diffraction and density functional theory. Journal of Physics Condensed Matter, 2003, 15, 5207-5221.	0.7	22
1156	Quantum transport properties of ultrathin silver nanowires. Nanotechnology, 2003, 14, 501-504.	1.3	75

#	Article	IF	Citations
1157	Semiconductivity in aluminumâ€“transition-metal quasicrystalline alloys induced by ordering in six dimensions. Europhysics Letters, 2003, 63, 63-68.	0.7	3
1158	Structural relaxations, vibrational dynamics and thermodynamics of vicinal surfaces. Journal of Physics Condensed Matter, 2003, 15, S3197-S3226.	0.7	27
1159	Anab initiostudy of WO3under pressure up to 30 GPa. Journal of Physics Condensed Matter, 2003, 15, 3121-3133.	0.7	12
1160	Comparison of density functional theory methods as applied to compound semiconductor-oxide interfaces: Slab versus cluster models. Journal of Vacuum Science & Technology an Official Journal of the American Vacuum Society B, Microelectronics Processing and Phenomena, 2003, 21, 1908.	1.6	10
1161	Vibrational modes of three-membered self-interstitial clusters in silicon. Journal of Physics Condensed Matter, 2003, 15, 7851-7857.	0.7	7
1162	Construction of an N-Body Cuâ€“Ta Potential and Study of Interfacial Behavior between Immiscible Cu and Ta through Molecular Dynamics Simulation. Journal of the Physical Society of Japan, 2003, 72, 5-8.	0.7	5
1163	Electrical and Optical Properties of Ultra-small Carbon Nanotubes Arrayed in Channels of Zeolite Single Crystals. Materials Transactions, 2003, 44, 2066-2069.	0.4	4
1164	Eleyâ€“Rideal and hot atom reactions between H atoms on metal and graphite surfaces. Chemical Physics of Solid Surfaces, 2003, , 51-77.	0.3	5
1165	Isotope velocity differentiation in thin carbon nanotubes through quantum diffusion. Europhysics Letters, 2003, 63, 254-260.	0.7	3
1166	Reaction Mechanisms in Zeolite Catalysis. , 2003, , .		1
1167	Construction of an Embedded-Atom Potential for an Immiscible Cuâ€“V System. Journal of the Physical Society of Japan, 2003, 72, 464-467.	0.7	3
1168	Structure of Dislocation Cores in GaAs. Materials Research Society Symposia Proceedings, 2003, 779, 321.	0.1	0
1169	Models of defects in wide-gap oxides. , 2003, , 151-222.		17
1170	Structural Stability and the Correlation of Lattice Constant versus Tantalum Concentration of the Ag-Based Fcc Solid Solutions Studied by Molecular Dynamics Simulation. Japanese Journal of Applied Physics, 2004, 43, 2589-2593.	0.8	3
1171	Ab initiomolecular dynamics simulation on temperature-dependent properties of Alâ€“Si liquid alloy. Journal of Physics Condensed Matter, 2004, 16, 2507-2514.	0.7	23
1172	Ab initiotheory of magnetic interactions at surfaces. Journal of Physics Condensed Matter, 2004, 16, S2557-S2574.	0.7	11
1173	First-principles study of binary transition-metal clusters and alloys. Journal of Physics Condensed Matter, 2004, 16, S2263-S2272.	0.7	24
1174	Theoretical Investigation of a Single Molecule Device: Geometrical Configurations and Electronic Properties. Chinese Physics Letters, 2004, 21, 568-571.	1.3	2

#	Article	IF	Citations
1175	Ab initiomolecular dynamics study on the formation process of Al layers on Si(001) surface. Modelling and Simulation in Materials Science and Engineering, 2004, 12, 1147-1157.	0.8	2
1176	Ab initio calculations of spin polarization at Co2CrAl/GaAs interfaces. Journal of Physics Condensed Matter, 2004, 16, S5725-S5728.	0.7	24
1177	Lattice vibrations and thermal properties of carbon nitride with defect ZnS structure from first-principles calculations. Journal of Physics Condensed Matter, 2004, 16, 3027-3034.	0.7	7
1178	Nitrogen Adatom Diffusion on a Ga-Rich GaN (0001) Surface. Chinese Physics Letters, 2004, 21, 527-529.	1.3	3
1179	The interstitial CiOi defect in bulk Si and Si1ÂxGex. Journal of Physics Condensed Matter, 2004, 16, 8545-8555.	0.7	5
1180	MPI parallelization of the first-principles pseudopotential method program with respect to each band. Modelling and Simulation in Materials Science and Engineering, 2004, 12, 945-957.	0.8	18
1181	Atomic and Electronic Structures of Zr Atomic Chains. Chinese Physics Letters, 2004, 21, 1791-1794.	1.3	8
1182	The pressure induced phase transition of confined water from ab initio molecular dynamics simulation. Journal of Physics Condensed Matter, 2004, 16, 8851-8859.	0.7	4
1183	Reversible short-range electrostatic imaging in frequency modulation atomic force microscopy on metallic surfaces. Nanotechnology, 2004, 15, S55-S59.	1.3	6
1184	Ab initiomelting curve of copper by the phase coexistence approach. Journal of Chemical Physics, 2004, 120, 2872-2878.	1.2	68
1185	An ab initio study of the relative stabilities and equations of state of Fe3S polymorphs. Mineralogical Magazine, 2004, 68, 813-817.	0.6	6
1186	Conduction Switching of Photochromic Molecules. Physical Review Letters, 2004, 93, 248302.	2.9	124
1187	Electron-phonon coupling ofÎ±â^'Gaboron. Physical Review B, 2004, 70, .	1.1	54
1188	Charge-induced structural changes inAl12Cclusters. Physical Review B, 2004, 70, .	1.1	33
1189	Quantum motion of hydrogen onCu(001)using first-principles calculations. Physical Review B, 2004, 70, .	1.1	37
1190	Stabilization of substitutional Mn in silicon-based semiconductors. Physical Review B, 2004, 70, .	1.1	38
1191	Stability of reducedV2O5(001)surfaces. Physical Review B, 2004, 70, .	1.1	119
1192	First-principles calculations for the surface termination of pure and yttria-doped zirconia surfaces. Physical Review B, 2004, 69, .	1.1	73

#	Article	IF	Citations
1193	Hybridization of Cr3dâ€“N2pâ€“Ga4sin the wide band-gap diluted magnetic semiconductorGa1âˆ’xCrxN. Physical Review B, 2004, 70, .	1.1	18
1194	Atomistic mechanisms for the (1Ã—1)â‡Œhex surface phase transformations of Pt(100). Journal of Chemical Physics, 2004, 121, 2317-2325.	1.2	17
1195	Ab initiocalculation of optical second harmonic generation at the rutileTiO2(110)surface. Physical Review B, 2004, 70, .	1.1	10
1196	Electronic structures of rocksalt, litharge, and herzenbergite SnO by density functional theory. Physical Review B, 2004, 70, .	1.1	114
1197	HonPt(110): An atypical chemisorption site at low coverages. Physical Review B, 2004, 70, .	1.1	22
1198	Carrier-mediated ferromagnetism in N codoped (Zn,Mn)O(101Â¯0)thin films. Physical Review B, 2004, 70, .	1.1	112
1199	Tunable variation of the electron effective mass and exciton radius in hydrogenatedGaAs1âˆ’xNx. Physical Review B, 2004, 69, .	1.1	40
1200	Electronic structure of crystalline binary and ternaryCdâˆ’Teâˆ’Ocompounds. Physical Review B, 2004, 70, .	1.1	37
1201	Vibrational properties of the high-pressureCmcmphase ofZnTe. Physical Review B, 2004, 70, .	1.1	13
1202	Complexes, clustering, and native-defect-assisted diffusion of aluminum in silicon. Physical Review B, 2004, 70, .	1.1	10
1203	(3Ã—1)-Br/Pt(110) structure and the charge-density-wave-assistedc(2Ã—2)to(3Ã—1)phase transition. Physical Review B, 2004, 69, .	1.1	23
1204	Structure of ultrathin crystallineSiO2films on Mo(112). Physical Review B, 2004, 69, .	1.1	29
1205	Magnetism ofFeâˆ’Conanostructures on flat and steppedW(110)surfaces: Effects of dimensionality and substrate. Physical Review B, 2004, 70, .	1.1	22
1206	Relationship between domain-boundary free energy and the temperature dependence of stress-domain patterns of Pb on Cu(111). Physical Review B, 2004, 70, .	1.1	18
1207	Adsorption and dissociation of NO on stepped Pt (533). Journal of Chemical Physics, 2004, 121, 7946.	1.2	44
1208	Surface energetics and structure of the Ge wetting layer on Si(100). Physical Review B, 2004, 70, .	1.1	58
1209	Self-trapping and diffusion of hydrogen in Nb and Ta from first principles. Physical Review B, 2004, 70, .	1.1	45
1210	CubicTiO2as a potential light absorber in solar-energy conversion. Physical Review B, 2004, 70, .	1.1	66

#	Article	IF	Citations
1211	Atomic and electronic structure of theKâ^•Si(111)3Ã—3R30Â°â^'Bchemisorption system. Physical Review B, 2004, 70, .	1.1	18
1212	Entropy ofLiintercalation inLixCoO2. Physical Review B, 2004, 70, .	1.1	103
1213	Migration, incorporation, and passivation reactions of molecular hydrogen at theSiâ€ŠSiO2interface. Physical Review B, 2004, 70, .	1.1	48
1214	Lattice constant, effective mass, and gap recovery in hydrogenatedGaAs1â^'xNx. Physical Review B, 2004, 69, .	1.1	11
1215	Coordination-dependence of hyperfine interactions at impurities on fcc metal surfaces. II. Magnetic hyperfine field. Physical Review B, 2004, 70, .	1.1	16
1216	Charge-Orbital Ordering and Verwey Transition in Magnetite. Physical Review Letters, 2004, 93, 156403.	2.9	249
1217	Molecular Chemisorption as the Theoretically Preferred Pathway for Water Adsorption on Ideal RutileTiO2(110). Physical Review Letters, 2004, 93, 086105.	2.9	156
1218	Rule for Structures of Open Metal Surfaces. Physical Review Letters, 2004, 93, 136102.	2.9	17
1219	Self-Assembly via Adsorbate-Driven Dislocation Reactions. Physical Review Letters, 2004, 92, 106101.	2.9	19
1220	Changes in the Lattice Constants of Thin-Film LiCoO[sub 2] Cathodes at the 4.2 V Charged State. Journal of the Electrochemical Society, 2004, 151, A1063.	1.3	30
1221	Boron diffusion in strained Si:â€ƒA first-principles study. Journal of Applied Physics, 2004, 96, 5543-5547.	1.1	8
1222	Ab initio study on structural and electronic properties of BanOm clusters. Journal of Chemical Physics, 2004, 120, 8020-8024.	1.2	12
1223	Energetic stability and magnetic properties of Mn dimers in silicon. Applied Physics Letters, 2004, 84, 2289-2291.	1.5	52
1224	Long-Range Surface Reconstruction:Si(110)â^'(16Ã—2). Physical Review Letters, 2004, 93, 136104.	2.9	65
1225	Phosphine Dissociation on the Si(001) Surface. Physical Review Letters, 2004, 93, 226102.	2.9	65
1226	Antiferromagnetic Coupling Driven by Bond Length Contraction near theGa1â^'xMnxNFilm Surface. Physical Review Letters, 2004, 93, 155501.	2.9	56
1227	Experimental Evidence for a Partially Dissociated Water Bilayer on Ru{0001}. Physical Review Letters, 2004, 93, 196102.	2.9	130
1228	Atomic force algorithms in density functional theory electronic-structure techniques based on local orbitals. Journal of Chemical Physics, 2004, 121, 6186-6194.	1.2	39

#	Article	IF	Citations
1229	New spintronic superlattices composed of half-metallic compounds with zinc-blende structure. Journal of Physics Condensed Matter, 2004, 16, S5669-S5676.	0.7	10
1230	A first-principles potential energy surface and vibrational states for hydrogen on Cu(100). Journal of Chemical Physics, 2004, 121, 7434-7439.	1.2	15
1231	Nanotubular boron-carbon heterojunctions. Journal of Chemical Physics, 2004, 121, 10680-10686.	1.2	18
1232	N vacancy diffusion and trapping in Mg-doped wurtzite GaN. Journal of Applied Physics, 2004, 96, 2015-2022.	1.1	22
1233	Conjugate-gradient optimization method for orbital-free density functional calculations. Journal of Chemical Physics, 2004, 121, 2030-2036.	1.2	38
1234	Localization of the Cu(111) Surface State by Single Cu Adatoms. Physical Review Letters, 2004, 93, 206803.	2.9	100
1235	New Pseudophase Structure forÎ±â^'Pu. Physical Review Letters, 2004, 92, 095503.	2.9	27
1236	Adatom Ascending at Step Edges and Faceting on fcc Metal (110) Surfaces. Physical Review Letters, 2004, 92, 106102.	2.9	52
1237	Structure and Mobility of Defects Formed from Collision Cascades in MgO. Physical Review Letters, 2004, 92, 115505.	2.9	96
1238	Coexistence of localized magnetic moment and opposite-spin itinerant electrons in MnC. Physical Review B, 2004, 70, .	1.1	23
1239	Interaction of neutral vacancies and interstitials with theSi(001)surface. Physical Review B, 2004, 70, .	1.1	13
1240	Stable fcc cage of III-IV mixed clusters with large energy gaps: Predictions based onab initiomolecular dynamics simulations. Physical Review B, 2004, 70, .	1.1	5
1241	Computational study of electron states in Au chains on NiAl(110). Physical Review B, 2004, 70, .	1.1	22
1242	Crystal structure and properties ofYSiO2N. Physical Review B, 2004, 69, .	1.1	17
1243	Magnetic structure of free iron clusters compared to iron crystal surfaces. Physical Review B, 2004, 70, .	1.1	58
1244	Eâ€²center in Ge-dopedSiO2glass. Physical Review B, 2004, 70, .	1.1	8
1245	Diffusion of Fe atoms on W surfaces andFeâ•Wfilms and along surface steps. Physical Review B, 2004, 70, .	1.1	41
1246	Energetics ofSradatom interactions on theMo(112)surface. Physical Review B, 2004, 69, .	1.1	22

#	Article	IF	Citations
1247	Intermixing tendencies in garnets:â€ƒPyrope and grossular. Physical Review B, 2004, 70, .	1.1	19
1248	Atomic scale study of superlow friction between hydrogenated diamond surfaces. Physical Review B, 2004, 70, .	1.1	77
1249	First-principles study of noncommutative band offsets atÎ±â^'Cr2O3/Î±â^'Fe2O3(0001)interfaces. Physical Review B, 2004, 69, .	1.1	32
1250	Electronic structure of the transition-metal dicyanamidesM[N(CN)2]2(M=Mn,Fe,Co,Ni,Cu). Physical Review B, 2004, 69, .	1.1	10
1251	Initial stages of Ge and Si growth nearSBmonoatomic steps on Si(100). Physical Review B, 2004, 70, .	1.1	3
1252	Density functional theory study of H and H2 interacting with NiAl(110). Journal of Chemical Physics, 2004, 121, 751-760.	1.2	44
1253	First-principles calculations for the adsorption of water molecules on theCu(100)surface. Physical Review B, 2004, 70, .	1.1	39
1254	Ferromagnetism and piezomagnetic behavior in Mn-doped germanium nanotubes. Physical Review B, 2004, 69, .	1.1	22
1255	Nonmetallic nature ofIn-induced nanoclusters onSi(100). Physical Review B, 2004, 70, .	1.1	8
1256	Mixed-basis cluster expansion for thermodynamics of bcc alloys. Physical Review B, 2004, 70, .	1.1	95
1257	Effects of next-nearest-neighbor interactions on the orientation dependence of step stiffness:â€ƒReconciling theory with experiment for Cu(001). Physical Review B, 2004, 70, .	1.1	28
1258	First-stage Mn adsorption on clean Ge(111). Physical Review B, 2004, 70, .	1.1	8
1259	Water adsorption on Ti-doped silicon clusters. Physical Review B, 2004, 70, .	1.1	18
1260	Epitaxial growth of the diluted magnetic semiconductors CryGe1â^'y and CryMnxGe1â^'xâ^'y. Applied Physics Letters, 2004, 84, 1725-1727.	1.5	27
1261	Structure, energetics, and extrinsic levels of small self-interstitial clusters in silicon. Physical Review B, 2004, 69, .	1.1	48
1262	Elastic anomaly forSrTiO3thin films grown on Si(001). Physical Review B, 2004, 70, .	1.1	35
1263	Sulfur point defects in crystalline and amorphous silicon. Physical Review B, 2004, 70, .	1.1	44
1264	Electronic states of linear Au clusters supported on metal surfaces: Why are they like those of a particle in a box?. Journal of Chemical Physics, 2004, 120, 7738-7740.	1.2	9

#	Article	IF	Citations
1265	Effect of backbond oxidation on silicon nanocrystallites. Physical Review B, 2004, 70, .	1.1	56
1266	Oxygen adsorption on Cu(100):â€ƒFirst-principles pseudopotential calculations. Physical Review B, 2004, 70, .	1.1	52
1267	Chemical short-range-order effects on stability in Î´-Puâ€“Ga alloys. Philosophical Magazine, 2004, 84, 1877-1888.	0.7	8
1268	Contrast Reversal and Shape Changes of Atomic Adsorbates Measured with Scanning Tunneling Microscopy. Physical Review Letters, 2004, 92, 206101.	2.9	66
1269	Complexity of Small Silicon Self-Interstitial Defects. Physical Review Letters, 2004, 92, 045501.	2.9	69
1270	First principles calculation of Ga-N codoped wurtzite ZnO. , 2004, , .		0
1271	First-principles study of magnetism in (112Ì„0)â€‰Zn1â^'xMnxO thin film. Applied Physics Letters, 2004, 84, 4170-4172.	1.5	27
1272	Decay and dephasing of the Cu(100) image states induced by Cu adatoms. Physical Review B, 2004, 70, .	1.1	24
1273	Calculation of a Î²-cyclodextrin-binaphthyl inclusion complex using density functional theory. Phase Transitions, 2004, 77, 53-61.	0.6	6
1274	STM observation of Ga -dimers on a GaAs(001)-c(8Ã—2)-Ga surface. Physical Review B, 2004, 70, .	1.1	15
1275	Reliable First-Principles Alloy Thermodynamics via Truncated Cluster Expansions. Physical Review Letters, 2004, 92, 255702.	2.9	115
1276	Theoretical study of strain-induced ordering in cubicInxGa1â^'xNepitaxial layers. Physical Review B, 2004, 69, .	1.1	13
1277	Density-functional perturbational theory for dielectric tensors in the ultrasoft pseudopotential scheme. Physical Review B, 2004, 69, .	1.1	23
1278	Novel Water Overlayer Growth on Pd(111) Characterized with Scanning Tunneling Microscopy and Density Functional Theory. Physical Review Letters, 2004, 93, 116101.	2.9	173
1279	Structure, electronic density of states and electric field gradients of icosahedral AlCuFe: Anab initiostudy of the original and a modified Cockayne model. Physical Review B, 2004, 69, .	1.1	15
1280	Electronic structure and bonding in the Y-Si-O-N quaternary crystals. Physical Review B, 2004, 70, .	1.1	33
1281	Structure- and spin-dependent excitation energies and lifetimes of Si and Ge nanocrystals fromab initiocalculations. Physical Review B, 2004, 69, .	1.1	65
1282	Finite-Size Effects on the Structure of Grain Boundaries. Physical Review Letters, 2004, 93, 156101.	2.9	29

#	Article	IF	Citations
1283	Role of Spin-Orbit Splitting and Dynamical Fluctuations in the Si(557)-Au Surface. Physical Review Letters, 2004, 93, 146803.	2.9	89
1284	Molecular adsorption on the surface of strongly correlated transition-metal oxides: A case study for CO/NiO(100). Physical Review B, 2004, 69, .	1.1	216
1285	Initial growth of Ba on Si(001). Physical Review B, 2004, 69, .	1.1	12
1286	Doping-dependent changes in nitrogen2pstates in the diluted magnetic semiconductorGa1âˆ'xCrxN. Physical Review B, 2004, 70, .	1.1	16
1287	AbÂInitioCalculations to Model Anomalous Fluorine Behavior. Physical Review Letters, 2004, 93, 245901.	2.9	42
1288	Structure and diffusion of interstitial boron pairs in silicon. Physical Review B, 2004, 69, .	1.1	3
1289	Induced Ge spin polarization at theFeâ•Geinterface. Physical Review B, 2004, 70, .	1.1	18
1290	Quantum molecular dynamics simulations of shocked nitrogen oxide. Physical Review B, 2004, 69, .	1.1	16
1291	Contrasting Growth Modes of Mn on Ge(100) and Ge(111) Surfaces: Subsurface Segregation versus Intermixing. Physical Review Letters, 2004, 93, 126102.	2.9	60
1292	The effect of Cr doping on Li ion diffusion in LiFePO4from first principles investigations and Monte Carlo simulations. Journal of Physics Condensed Matter, 2004, 16, 2265-2272.	0.7	79
1293	Conductance investigations of stretched molecules. , 0, , .		0
1294	Activation Energies for Quantum Diffusion of Hydrogen in Metals and on Metal Surfaces using Delocalized Nuclei within the Density-Functional Theory. Physical Review Letters, 2004, 92, 155901.	2.9	44
1295	Local modes of Fe and Co atoms in NiAl intermetallics. Physical Review B, 2004, 70, .	1.1	18
1296	Dipole moment of a Pb-O vacancy pair inPbTiO3. Physical Review B, 2004, 69, .	1.1	62
1297	Irreversibility of the pressure-induced phase transition of quartz and the relation between three hypothetical post-quartz phases. Physical Review B, 2004, 70, .	1.1	20
1298	Optical phonon softening in strained SrTiO3 thin film: First-principles study. Applied Physics Letters, 2004, 85, 5649-5651.	1.5	10
1299	Energetics of transient enhanced diffusion of boron in Ge and SiGe. Physical Review B, 2004, 69, .	1.1	34
1300	Electronic and superconducting properties of oxygen-orderedMgB2compounds of the formMg2B3Ox. Physical Review B, 2004, 70, .	1.1	6

#	Article	IF	Citations
1301	Density functional study of CO on Rh(111). Physical Review B, 2004, 70, .	1.1	337
1302	Evidence from first principles calculations for a bent CO2 intermediate in the oxidation of carbon monoxide on the Cu (110) surface. Journal of Chemical Physics, 2004, 121, 4339-4345.	1.2	8
1303	Wetting of TiC and TiN by metals. Physical Review B, 2004, 69, .	1.1	98
1304	First-principles calculations of steering forces in epitaxial growth. Physical Review B, 2004, 69, .	1.1	12
1305	Neutral boron-interstitial clusters in crystalline silicon. Physical Review B, 2004, 69, .	1.1	19
1306	Semiconductivity in Aluminumâ€"Transition-Metal Quasicrystals Induced by Ordering in Six Dimensions. Ferroelectrics, 2004, 305, 189-192.	0.3	0
1307	Role of electronic correlations on the ground-state properties and on the pressure-induced metal-insulator transition inBaVS3. Physical Review B, 2004, 70, .	1.1	8
1308	Thermodynamics fromab initiocomputations. Physical Review B, 2004, 70, .	1.1	53
1309	First-principles calculation of the structure and magnetic phases of hematite. Physical Review B, 2004, 69, .	1.1	402
1310	First-principles study of C adsorption, O adsorption, and CO dissociation on flat and stepped Ni surfaces. Journal of Chemical Physics, 2004, 121, 10241-10249.	1.2	44
1311	Dynamics of oxygen species on reducedTiO2(110)rutile. Physical Review B, 2004, 70, .	1.1	60
1312	Phonon spectrum and soft-mode behavior ofMgCNi3. Physical Review B, 2004, 69, .	1.1	33
1313	Impact on electronic correlations on the structural stability, magnetism, and voltage ofLiCoPO4battery. Physical Review B, 2004, 69, .	1.1	59
1314	Coordination dependence of hyperfine interactions at impurities on fcc metal surfaces. I. Electric-field gradient. Physical Review B, 2004, 70, .	1.1	27
1315	Structural elements on reconstructed Si andGe(110)surfaces. Physical Review B, 2004, 70, .	1.1	55
1316	Theoretical study ofGa-based nanowires and the interaction ofGawith single-wall carbon nanotubes. Physical Review B, 2004, 70, .	1.1	12
1317	Periodic density functional theory study of the crystal morphology ofFeZn13. Physical Review B, 2004, 70, .	1.1	9
1318	Defect-induced perturbation onSi(111)4Ã—1â^'In: Period-doubling modulation and its origin. Physical Review B, 2004, 70, .	1.1	39

#	Article	IF	Citations
1319	Correlation of magnetic moment versus spacing distance of metastable fcc structured iron. Applied Physics Letters, 2004, 84, 3627-3629.	1.5	46
1320	Resistivity of hydrogen-loaded Fe/V and Mo/V (100) superlattices: The role of vanadium expansion. Physical Review B, 2004, 69, .	1.1	12
1321	Calculations of electronic structure ofGe44Mn2Ba8andGe42Mn4Ba8clathrates. Physical Review B, 2004, 70, .	1.1	5
1322	Defect structure ofGa1â^'xMnxAs: A cross-sectional scanning tunneling microscopy study. Physical Review B, 2004, 70, .	1.1	20
1323	Quasiparticle band structures and optical spectra ofÎ²-cristobaliteSiO2. Physical Review B, 2004, 69, .	1.1	38
1324	Spin driving reconstructions on the GaAs(001):Mn surface. Physical Review B, 2004, 69, .	1.1	17
1325	Structure and stability of rare-earth and transition-metal oxides. Physical Review B, 2004, 69, .	1.1	114
1326	Ab initiocalculations of zinc-blende CrAs/GaAs superlattices. Journal of Applied Physics, 2004, 95, 6518-6520.	1.1	25
1327	Ab initiostructural characterization of a hydrogen-covered diamond (001) surface. Physical Review B, 2004, 70, .	1.1	26
1328	Structure of the cobalt-filled missing-row reconstruction of Pt(110). Physical Review B, 2004, 70, .	1.1	3
1329	First-principles study of adsorption of methanethiol onCo(0001). Physical Review B, 2004, 70, .	1.1	19
1330	Density-functional theory calculations of the adsorption of Cl at perfect and defective Ag(111) surfaces. Physical Review B, 2004, 69, .	1.1	25
1331	Pressure effects on the structure and vibrations ofÎ²- andÎ³â^'C3N4. Physical Review B, 2004, 70, .	1.1	15
1332	Optical and structural properties of SixSnyGe1â^'xâ^'y alloys. Applied Physics Letters, 2004, 84, 888-890.	1.5	81
1333	A first principles study on the solvation and structure of SO[sub 4][sup 2â^'](H[sub 2]O)[sub n], n=6â€“12. Journal of Chemical Physics, 2004, 121, 8299.	1.2	53
1334	Mechanical properties of graphite oxides:Ab initiosimulations and continuum theory. Physical Review B, 2004, 70, .	1.1	29
1335	The influence of bond flexibility and molecular size on the chemically selective bonding of In2O and Ga2O on GaAs(001)-c(2Ã—8)/(2Ã—4). Journal of Chemical Physics, 2004, 120, 5745-5754.	1.2	16
1336	Low coverage spontaneous etching and hyperthermal desorption of aluminum chlorides from Cl2/Al(111). Journal of Chemical Physics, 2004, 121, 9018-9030.	1.2	4

#	Article	IF	Citations
1337	The nonmetallicity of molybdenum clusters. Journal of Chemical Physics, 2004, 121, 7717.	1.2	48
1338	Interaction between interstitials and arsenic-vacancy complexes in crystalline silicon. Applied Physics Letters, 2004, 85, 4935-4937.	1.5	15
1339	Low work function of the (1000) Ca2N surface. Journal of Applied Physics, 2004, 96, 1751-1753.	1.1	21
1340	Adsorption and vibrational spectroscopy of ammonia at mordenite: Ab initio study. Journal of Chemical Physics, 2004, 120, 10263-10277.	1.2	39
1341	9. Molecular Dynamics Simulations in Biology, Chemistry and Physics. Lecture Notes in Physics, 0, , 177-206.	0.3	4
1342	â€œMigration energyâ€•for impurity diffusion in crystalline solids: A closer look. Journal of Applied Physics, 2004, 96, 7095-7107.	1.1	10
1343	Ab initio calculation of point defect energies and atom migration profiles in varying surroundings in L12-ordered intermetallic compounds. Materials Research Society Symposia Proceedings, 2004, 842, 297.	0.1	1
1344	Positron Annihilation Study of Formation of Mg Vacancy in MgO. Materials Science Forum, 2004, 445-446, 153-155.	0.3	10
1345	Carrier capture cross-section of nonradiative recombination centres introduced by proton implantation in GaAs. Semiconductor Science and Technology, 2004, 19, 1325-1328.	1.0	1
1346	From The Cover: Hydration and mobility of HO-(aq). Proceedings of the National Academy of Sciences of the United States of America, 2004, 101, 7229-7233.	3.3	145
1347	Density-of-states of crystalline 2,-bithiophene:ab initioanalysis and comparison with inelastic neutron scattering response. Journal of Physics Condensed Matter, 2004, 16, 7385-7396.	0.7	16
1348	Stability and Structural Transition of Gold Nanowires under Their Own Surface Stresses. Materials Research Society Symposia Proceedings, 2004, 854, U5.7.1.	0.1	0
1349	Hydrogen-Nitrogen Tailors Semiconductor Optoelectronics: The Case of Dilute Nitride III-V Alloys. Materials Research Society Symposia Proceedings, 2004, 813, 521.	0.1	0
1350	Ab Initio Simulation of Lewis Sites in Mordenite and Comparative Study of the Strength of Active Sites via CO Adsorption. Journal of Physical Chemistry B, 2004, 108, 13656-13666.	1.2	57
1351	The computational design of zinc-blende half-metals and their nanostructures. Journal of Physics Condensed Matter, 2004, 16, S5525-S5531.	0.7	15
1352	Ab Initio Calculations and Structural Stability of Boron-Doped Sodium Manganese Oxide. Journal of the Electrochemical Society, 2004, 151, J8.	1.3	7
1353	Theory for the Potential Shift for OH[sub ads] Formation on the Pt Skin on Pt[sub 3]Cr(111) in Acid. Journal of the Electrochemical Society, 2004, 151, E85.	1.3	57
1354	Pressure dependence of elastic constants in wurtzite and zinc-blende nitrides and their influence on the optical pressure coefficients in nitride heterostructures. Materials Research Society Symposia Proceedings, 2004, 831, 120.	0.1	0

#	Article	IF	Citations
1355	Interface States in Abrupt SiO₂/4H- and 6HSiC(0001) from First-Principles: Effects of Si Dangling Bonds, C Dangling Bonds and C Clusters. Materials Science Forum, 2004, 457-460, 1297-1300.	0.3	11
1356	Electronic Structure and Hydrogen Desorption in NaAlH₄. Materials Research Society Symposia Proceedings, 2004, 837, 31.	0.1	1
1357	Assessment of the Hfâ€“N, Zrâ€“N and Tiâ€“N phase diagrams at high pressures and temperatures: balancing between MN and M3N4(M = Hf, Zr, Ti). Journal of Physics Condensed Matter, 2004, 16, S1235-S1244.	0.7	42
1358	First-principles Calculation of Electron Mobilities in Ultrathin SOI MOSFETs. Materials Research Society Symposia Proceedings, 2004, 829, 326.	0.1	0
1359	Controlling the Charge State of Individual Gold Adatoms. Science, 2004, 305, 493-495.	6.0	393
1360	Chemical bonding at the Al-terminated stoichiometric Î±-Al2O3(0001)/Cu(111) interface. Philosophical Magazine Letters, 2004, 84, 425-434.	0.5	37
1361	Hardness, elasticity, and fracture toughness of polycrystalline spinel germanium nitride and tin nitride. Journal of Materials Research, 2004, 19, 1392-1399.	1.2	28
1362	Classical versus ab initio structural relaxation: electronic excitations and optical properties of Ge nanocrystals embedded in a SiC matrix. Materials Research Society Symposia Proceedings, 2004, 832, 313.	0.1	0
1363	Enthalpy of Formation of Various Phases and Formation Energy of Point Defects in Perovskite-Type NaNbO3by First-Principles Calculation. Japanese Journal of Applied Physics, 2004, 43, 6793-6798.	0.8	65
1364	First-principles design of ferromagnetic nanostructures based on group-IV semiconductors. Journal of Physics Condensed Matter, 2004, 16, S5735-S5738.	0.7	8
1365	Electrode Potential-Dependent Stages in OH[sub ads] Formation on the Pt[sub 3]Cr Alloy (111) Surface. Journal of the Electrochemical Society, 2004, 151, E340.	1.3	35
1366	Structure and stability of possible new alanates. Europhysics Letters, 2004, 67, 607-613.	0.7	41
1367	Ab initio molecular-dynamics studies on Li x Mn 2 O 4 as cathode material for lithium secondary batteries. Europhysics Letters, 2004, 67, 28-34.	0.7	56
1368	Determination of melting of water clusters using density functional theory. Phase Transitions, 2004, 77, 63-79.	0.6	11
1369	Interaction of atomic hydrogen with silane molecules. Phase Transitions, 2004, 77, 139-147.	0.6	1
1370	Ab initio, tight-binding and QM/MM calculations of the rhodopsin chromophore in its binding pocket. Phase Transitions, 2004, 77, 31-45.	0.6	10
1371	Ab-initioElectron Transport Calculations of Carbon Based String Structures. Physical Review Letters, 2004, 93, 136404.	2.9	151
1372	CO adsorption on close-packed transition and noble metal surfaces: trends fromab initiocalculations. Journal of Physics Condensed Matter, 2004, 16, 1141-1164.	0.7	366

#	Article	IF	Citations
1373	Twinning pathway in BCC molybdenum. Europhysics Letters, 2004, 68, 405-411.	0.7	26
1374	A Monte Carlo Study of Surface Reconstruction in (100) and (111) Diamond Surfaces and Nanodiamond. Molecular Simulation, 2004, 30, 1-8.	0.9	5
1375	Theoretical analysis of field emission from metallic nanostructures on Si(100) surfaces. Journal of Physics Condensed Matter, 2004, 16, 4685-4696.	0.7	11
1376	First-principles calculations of the atomistic behaviors in Ni/Al [001] and Al/Ni [001] system. , 2004, , .		0
1377	Phase stability of Â-Pu alloys: a key role of chemical short range order. Modelling and Simulation in Materials Science and Engineering, 2004, 12, 693-707.	0.8	11
1378	Ultra-stable nanoparticles of CdSe revealed from mass spectrometry. Nature Materials, 2004, 3, 99-102.	13.3	469
1379	Tailoring ferromagnetic chalcopyrites. Nature Materials, 2004, 3, 410-414.	13.3	151
1380	A first-order Mott transition in LixCoO2. Nature Materials, 2004, 3, 627-631.	13.3	164
1381	Bismuth-induced embrittlement of copper grain boundaries. Nature Materials, 2004, 3, 621-626.	13.3	242
1382	Bismuth embrittlement of copper is an atomic size effect. Nature, 2004, 432, 1008-1011.	13.7	174
1383	Density and thermodynamics of hydrogen adsorbed inside narrow carbon nanotubes. Physics of the Solid State, 2004, 46, 584-589.	0.2	5
1384	Effect of vanadium doping on the structure of TiAl: Ab initio calculations. Physics of the Solid State, 2004, 46, 1383-1385.	0.2	5
1385	Structural relationships, phase stability and bonding of compounds PdSnn (n=2, 3, 4). Solid State Sciences, 2004, 6, 147-155.	1.5	101
1386	First principles search of hard materials within the Siî—¸Cî—¸N ternary system. Solid State Sciences, 2004, 6, 315-323.	1.5	18
1387	Ferromagnetism of 3d-impurities substituted in Ge. Journal of Magnetism and Magnetic Materials, 2004, 284, 253-259.	1.0	8
1388	Hydrogenation of ethylene and formaldehyde on Pt (111) and Pt80Fe20 (111): a density-functional study. Journal of Catalysis, 2004, 226, 273-282.	3.1	43
1389	Energetics of native point defects in cubic silicon carbide. European Physical Journal B, 2004, 38, 437-444.	0.6	22
1390	Spin Splitting ofsandpStates in Single Atoms and Magnetic Coupling in Dimers on a Surface. Physical Review Letters, 2004, 92, 186802.	2.9	47

#	Article	IF	Citations
1391	Ab initiostudy of incorporation ofO2molecules intoSi(001)surfaces: Oxidation bySiejection. Physical Review B, 2004, 70, .	1.1	23
1392	Initial stages of Mn adsorption on Ge(111). Physical Review B, 2004, 70, .	1.1	56
1393	Oxidation of Zigzag Carbon Nanotubes by Singlet O2:â€‰ Dependence on the Tube Diameter and the Electronic Structure. Journal of Physical Chemistry B, 2004, 108, 11435-11441.	1.2	58
1394	Comparative energies of Zn(II) cation localization as a function of the distance between two forming cation position aluminium ions in high-silica zeolites. Research on Chemical Intermediates, 2004, 30, 99-103.	1.3	13
1395	Copper Segregation to the Â5 (310)/[001] Symmetric Tilt Grain Boundary in Aluminum. Journal of Materials Science, 2004, 12, 165-174.	1.2	19
1396	Density Functional Study of the Aluminumâ€”Graphite Interface. Journal of Computational Electronics, 2004, 3, 51-56.	1.3	5
1397	Kohn-Shamab initiomolecular dynamics study of liquidAlnear melting. Physical Review B, 2004, 70, .	1.1	48
1398	Hydrogen in aluminum: First-principles calculations of structure and thermodynamics. Physical Review B, 2004, 69, .	1.1	300
1399	First Principles Analysis of the Stability and Diffusion of Oxygen Vacancies in Metal Oxides. Physical Review Letters, 2004, 93, 225502.	2.9	158
1400	Crystal structure and thermodynamic stability of the lithium alanatesLiAlH4andLi3AlH6. Physical Review B, 2004, 69, .	1.1	114
1401	Chiral Single-Wall Gold Nanotubes. Physical Review Letters, 2004, 93, 196807.	2.9	89
1402	Theoretical study of the single-walled gold (5,3) nanotube. Applied Physics Letters, 2004, 85, 2923-2925.	1.5	32
1403	Ideal shear strain of metals and ceramics. Physical Review B, 2004, 70, .	1.1	334
1404	Effects of additives in Î±- and Î¸-alumina: an ab initio study. Journal of Physics Condensed Matter, 2004, 16, 8971-8980.	0.7	32
1405	Active Sites for the Vapor Phase Beckmann Rearrangement over Mordenite:Â An ab Initio Study. Journal of Physical Chemistry A, 2004, 108, 11388-11397.	1.1	46
1406	Adsorption and migration of carbon adatoms on carbon nanotubes: Density-functionalab initioand tight-binding studies. Physical Review B, 2004, 69, .	1.1	111
1407	A comparative theoretical study of Au, Ag and Cu adsorption on TiO2 (110) rutile surfaces. Korean Journal of Chemical Engineering, 2004, 21, 537-547.	1.2	20
1408	The simple cubic structure of Ir clusters and the element effect on cluster structures. Chemical Physics Letters, 2004, 383, 67-71.	1.2	72

#	Article	IF	Citations
1409	Competitive CN and N2 formation on Rh(1 1 1): a case of entropic stabilization. Chemical Physics Letters, 2004, 385, 52-54.	1.2	16
1410	Potential new candidates for hard materials within the ternary XC3N3 (XÂ=ÂB, Al, Ga) stoichiometry. Comptes Rendus Chimie, 2004, 7, 529-535.	0.2	6
1411	Nucleation and growth of epitaxial ZrB2(0001) on Si(111). Journal of Crystal Growth, 2004, 267, 554-563.	0.7	30
1412	Adsorption and migration of carbon adatoms on zigzag carbon nanotubes. Carbon, 2004, 42, 1021-1025.	5.4	52
1413	GIBBS: isothermal-isobaric thermodynamics of solids from energy curves using a quasi-harmonic Debye model. Computer Physics Communications, 2004, 158, 57-72.	3.0	1,598
1414	Tuning of the electron effective mass and exciton wavefunction size in GaAs1âˆ’xNx. Physica E: Low-Dimensional Systems and Nanostructures, 2004, 21, 747-751.	1.3	1
1415	Ab initio study of the tensile behavior of single polyimide molecular chain. Polymer, 2004, 45, 9023-9028.	1.8	5
1416	Interplay of local structure and magnetism in Co-doped TiO2 anatase. Solid State Communications, 2004, 129, 741-746.	0.9	44
1417	First-principles calculations of positron lifetimes of lattice defects induced by hydrogen absorption. Solid State Ionics, 2004, 172, 149-153.	1.3	3
1418	Phase stability of BaCo1?yFeyO3?? by first principles calculations. Solid State Ionics, 2004, 172, 159-163.	1.3	20
1419	Carbon induced ()R30Â° reconstruction on Si(111) surface: a theoretical study. Surface Science, 2004, 548, 51-58.	0.8	10
1420	Theoretical study of segregation of Zn and Pd in Pdâ€“Zn alloys. Surface Science, 2004, 548, 291-300.	0.8	54
1421	FS+ and FS+(OHâˆ’) defect centers at the MgO(100) surface: cluster and periodic calculations. Surface Science, 2004, 549, 294-304.	0.8	24
1422	A combined density functional theory and interatomic potential-based simulation study of the hydration of nano-particulate silicate surfaces. Surface Science, 2004, 554, 193-210.	0.8	63
1423	Modeling of the carbon-rich c(4Ã—4) reconstruction on Si(100). Surface Science, 2004, 554, 90-102.	0.8	5
1424	A DFT investigation of the adsorption of methyl on Rh(111). Surface Science, 2004, 558, 15-22.	0.8	20
1425	Atomic and electronic structure of the Si(001)2Ã—1â€“K surface. Surface Science, 2004, 561, 215-226.	0.8	6
1426	The adsorption of CO on Au(111) at elevated pressures studied by STM, RAIRS and DFT calculations. Surface Science, 2004, 566-568, 995-1000.	0.8	96

#	Article	IF	Citations
1427	Effect of the electronic structure on CO oxidation on Pd doped Ag(111). Surface Science, 2004, 566-568, 1063-1066.	0.8	8
1428	Theoretical study of hydrogenated 3Câ€“SiC(001)-(2Ã—1) surface. Surface Science, 2004, 571, 21-30.	0.8	4
1429	Pt thin films on stepped SrTiO3 surfaces: SrTiO3(620) and SrTiO3(622). Journal of Molecular Catalysis A, 2004, 216, 233-245.	4.8	11
1430	An integrated framework for multi-scale materials simulation and design. Journal of Computer-Aided Materials Design, 2004, 11, 183-199.	0.7	46
1431	Modelling the Deposition of High-k Dielectric Films by First Principles. Journal of Electroceramics, 2004, 13, 117-120.	0.8	20
1432	A modeling of the structure and favorable H-docking sites and defects for the high-pressure silica polymorph stishovite. Physics and Chemistry of Minerals, 2004, 31, 232-239.	0.3	22
1433	Experimental and theoretical evidence for carbon-vacancy binding in austenite. Metallurgical and Materials Transactions A: Physical Metallurgy and Materials Science, 2004, 35, 2239-2245.	1.1	24
1434	Concentrations of native and gold defects in HgCdTe from first principles calculations. Journal of Electronic Materials, 2004, 33, 737-741.	1.0	11
1435	Interplay of Electronic Structure and Bulk Properties in 2D and 3D Ternary Carbonitrides from First Principles. Zeitschrift Fur Anorganische Und Allgemeine Chemie, 2004, 630, 2587-2598.	0.6	9
1436	Phase separation, effects of biaxial strain, and ordered phase formations in cubic nitride alloys. Microelectronics Journal, 2004, 35, 53-57.	1.1	4
1437	Structural and magnetic properties of Fe-Ni clusters. Physica Status Solidi A, 2004, 201, 3263-3270.	1.7	22
1438	Investigations of conductance of photochromic switching molecules. Physica Status Solidi (B): Basic Research, 2004, 241, 2326-2330.	0.7	15
1439	Surface chemistry effects on vacancy and interstitial annihilation on Si(001). Physica Status Solidi (B): Basic Research, 2004, 241, 2303-2312.	0.7	9
1440	Hole carrier transfer by apical oxygen in YBCO. Physica Status Solidi C: Current Topics in Solid State Physics, 2004, 1, 1863-1866.	0.8	3
1441	Possibility of superconductivity in intercalation compound related to MgB2. International Journal of Quantum Chemistry, 2004, 96, 457-462.	1.0	5
1442	Long-range interactions in embedded ionic cluster calculations. International Journal of Quantum Chemistry, 2004, 96, 483-491.	1.0	11
1443	First-principles calculation of formation energy of neutral point defects in perovskite-type BaTiO3. International Journal of Quantum Chemistry, 2004, 99, 824-827.	1.0	35
1444	First-principles calculations as a tool for structure validation in electron crystallography. Acta Crystallographica Section A: Foundations and Advances, 2004, 60, 75-81.	0.3	6

#	Article	IF	Citations
1445	Quantum-Chemical Studies on the Geometric and Electronic Structures of Bertholloide Cobalt Oxynitrides. Advanced Functional Materials, 2004, 14, 371-376.	7.8	5
1446	Models for the treatment of crystalline solids and surfaces. Journal of Computational Chemistry, 2004, 25, 1551-1567.	1.5	56
1447	Vegard's law deviation in lattice constant and band gap bowing parameter of zincblende InxGa1â^'xN. Optics Communications, 2004, 237, 363-369.	1.0	91
1448	The Li intercalation potential of LiMPO4 and LiMSiO4 olivines with M=Fe, Mn, Co, Ni. Electrochemistry Communications, 2004, 6, 1144-1148.	2.3	390
1449	Reactivity of Pd doped Ag surfaces. Vacuum, 2004, 74, 169-172.	1.6	1
1450	Calculation of surface properties of bcc iron. Vacuum, 2004, 74, 179-183.	1.6	69
1451	Atomistic simulations of Cu deposition on the Î±-Al2O3 (0001) surface. Computational and Theoretical Chemistry, 2004, 709, 79-85.	1.5	1
1452	Electronic properties of semiconducting silicides: fundamentals and recent predictions. Thin Solid Films, 2004, 461, 141-147.	0.8	63
1453	Stabilization of monoatomic gold wires by carbon impurities. Solid State Communications, 2004, 130, 755-757.	0.9	14
1454	Pressure dependence of elastic constants in zinc-blende GaN and InN and their influence on the pressure coefficients of the light emission in cubic InGaN/GaN quantum wells. Solid State Communications, 2004, 131, 763-767.	0.9	28
1455	Proton transfer mechanism in solid CsHSO4 by first-principles study. Solid State Ionics, 2004, 172, 145-148.	1.3	7
1456	Ab initio study on geometrical structures of the TTTA molecular crystal. Science and Technology of Advanced Materials, 2004, 5, 689-692.	2.8	8
1457	Revisit to the Ising model for orderâ€“disorder phase transition on Si(001). Surface Science, 2004, 554, 150-158.	0.8	7
1458	Assessment of competing mechanisms of the abstraction of hydrogen from CH4 on Li/MgO(001). Surface Science, 2004, 549, 217-226.	0.8	18
1459	Assessment of heterochiral and homochiral glycine adlayers on Cu(110) using density functional theory. Surface Science, 2004, 548, 301-308.	0.8	99
1460	Multilayer relaxations of (311), (331) and (210) fcc transition metal surfaces studied by pseudopotential DFT calculations. Surface Science, 2004, 548, 309-316.	0.8	18
1461	The geometric and electronic properties of the PbS, PbSe and PbTe (001) surfaces. Surface Science, 2004, 551, 91-98.	0.8	36
1462	Conveying chirality onto the electronic structure of achiral metals: (R,R)-tartaric acid on nickel. Surface Science, 2004, 554, 141-149.	0.8	51

#	Article	IF	Citations
1463	Strain-induced formation of arrays of catalytically active sites at the metalâ€“oxide interface. Surface Science, 2004, 554, L120-L126.	0.8	70
1464	Sum frequency generation and density functional studies of COâ€“H interaction and hydrogen bulk dissolution on Pd(111). Surface Science, 2004, 554, 43-59.	0.8	72
1465	V2O3(0001) surface terminations: a density functional study. Surface Science, 2004, 555, 118-134.	0.8	64
1466	Surface properties of alkaline earth metal oxides. Surface Science, 2004, 554, 262-271.	0.8	90
1467	Mechanisms of monovacancy annihilation and type-A defect creation on Si(001)â€“2Ã—1. Surface Science, 2004, 555, 187-192.	0.8	7
1468	Dissociative adsorption of N2 on the W(100) surface. Surface Science, 2004, 556, 129-144.	0.8	38
1469	Electronic and elastic contributions in the enhanced stability of Ge() under compressive strain. Surface Science, 2004, 556, 121-128.	0.8	73
1470	New structural model of the high-index Si2Ã—1 surface. Surface Science, 2004, 557, 183-189.	0.8	34
1471	On the geometric structure of the (0001) hematite surface. Surface Science, 2004, 558, 4-14.	0.8	48
1472	Local reactivity of supported metal clusters: Pd n on Au(1 1 1). Surface Science, 2004, 559, L180-L186.	0.8	75
1473	Adsorption of Mn atoms on the Si(100) surface. Surface Science, 2004, 566-568, 688-692.	0.8	9
1474	STM, LEED, and DFT characterization of epitaxial ZrO2 films on Pt(111). Surface Science, 2004, 562, 204-218.	0.8	44
1475	DFT plane-wave calculations of the Rh/MgO(001) interface. Surface Science, 2004, 566-568, 977-982.	0.8	10
1476	S and O adsorption on pure and Ge doped Ag(111). Surface Science, 2004, 566-568, 1067-1070.	0.8	1
1477	Influence of structural relaxation on the optical and electronic properties of embedded Ge nanocrystals. Surface Science, 2004, 566-568, 961-964.	0.8	2
1478	Adsorption and dissociation of CO on Fe(110) from first principles. Surface Science, 2004, 570, 167-177.	0.8	118
1479	Stress relief from missing dimers on Bi/Si(001). Surface Science, 2004, 569, 176-184.	0.8	5
1480	CO and hydrogen adsorption on Pd(210). Surface Science, 2004, 570, 227-236.	0.8	27

#	Article	IF	Citations
1481	The adsorption structure on Co{0001}: a combined Tensor LEED and DFT study. Surface Science, 2004, 572, 1-10.	0.8	13
1482	First-principles study of indium on silicon (100)â€"the structure, defects and interdiffusion. Surface Science, 2004, 572, 77-83.	0.8	15
1483	TiO2-rich reconstructions of SrTiO3(001): a theoretical study of structural patterns. Surface Science, 2004, 573, 446-456.	0.8	56
1484	On the graphical analysis of the electronic structure of ferromagnetic clusters of medium size. Journal of Molecular Graphics and Modelling, 2004, 23, 291-295.	1.3	4
1485	Ab initio investigations of surface magnetism in Vâ€"Mo. Journal of Magnetism and Magnetic Materials, 2004, 272-276, 1198-1200.	1.0	2
1486	First-principles studies of the electronic structure and magnetism in fayalites: M2SiO4 (M=Fe and Co). Journal of Magnetism and Magnetic Materials, 2004, 282, 287-290.	1.0	5
1487	Defect energetics of Î²-SiC using a new tight-binding molecular dynamics model. Journal of Nuclear Materials, 2004, 329-333, 1219-1222.	1.3	18
1488	High potential positive materials for lithium-ion batteries: transition metal phosphates. Journal of Physics and Chemistry of Solids, 2004, 65, 229-233.	1.9	85
1489	The melting curve of iron from quantum mechanics calculations. Journal of Physics and Chemistry of Solids, 2004, 65, 1573-1580.	1.9	28
1490	Chemical kinetics and design of gas inlets for IIIâ€"V growth by MOVPE in a quartz showerhead reactor. Journal of Crystal Growth, 2004, 272, 47-51.	0.7	3
1491	Elastic properties of platinum Rh and Rh3X compounds. Physics Letters, Section A: General, Atomic and Solid State Physics, 2004, 331, 400-403.	0.9	59
1492	Role of shuffles and atomic disorder in Niâ€"Mnâ€"Ga. Materials Science & Engineering A: Structural Materials: Properties, Microstructure and Processing, 2004, 378, 419-423.	2.6	42
1493	Effects of N on the electronic structures of H defects in IIIâ€"V semiconductors. Optical Materials, 2004, 25, 261-269.	1.7	4
1494	On the ordering in new low gap semiconductors: PtSnS, PtSnSe, PtSnTe. Experimental and DFT studies. Journal of Solid State Chemistry, 2004, 177, 2591-2599.	1.4	18
1495	Investigation of the relative stabilities of various allotropic phases of elemental tellurium under pressure and their interconversion paths by electronic structure calculations and crystal structure analyses. Journal of Solid State Chemistry, 2004, 177, 4724-4731.	1.4	7
1496	A comparative ab initio study of the â€˜idealâ€™ strength of single crystal Î±- and Î²-Si3N4. Acta Materialia, 2004, 52, 233-238.	3.8	67
1497	Atomic-scale ab initio study of the Zrâ€"H system: II. Interaction of H with plane defects and mechanical properties. Acta Materialia, 2004, 52, 1495-1502.	3.8	80
1498	Effects of cobalt intergranular segregation on interface energetics in WCâ€"Co. Acta Materialia, 2004, 52, 2199-2207.	3.8	91

#	Article	IF	Citations
1499	A combined CALPHAD/first-principles remodeling of the thermodynamics of Alâ€“Sr: unsuspected ground state energies by â€œrounding up the (un)usual suspectsâ€• Acta Materialia, 2004, 52, 2739-2754.	3.8	72
1500	First-principles study of crystal structure and stability of Al?Mg?Si?(Cu) precipitates. Acta Materialia, 2004, 52, 4213-4227.	3.8	317
1501	First principles assessment of ideal fracture energies of materials with mobile impurities: implications for hydrogen embrittlement of metals. Acta Materialia, 2004, 52, 4801-4807.	3.8	191
1502	Molecular dynamics simulation of silicon sputtering: sensitivity to the choice of potential. Applied Surface Science, 2004, 231-232, 29-38.	3.1	22
1503	First principles simulations of Cu and Au deposition on Î±-Al2O3 (0001) surface. Applied Surface Science, 2004, 238, 228-232.	3.1	19
1504	Atomic geometry and theoretical scanning tunneling microscopy images of K chains on InAs(110). Applied Surface Science, 2004, 237, 200-205.	3.1	0
1505	What the stretch frequency spectrum of D2O/Ru(0001) does and does not mean. Chemical Physics Letters, 2004, 389, 92-95.	1.2	26
1506	Intermolecular transfer integrals for organic molecular materials: can basis set convergence be achieved?. Chemical Physics Letters, 2004, 390, 110-115.	1.2	137
1507	From planar to three-dimensional structural transition in gold clusters and the spinâ€“orbit coupling effect. Chemical Physics Letters, 2004, 392, 452-455.	1.2	180
1508	Surface energetics of hydroxyapatite: a DFT study. Chemical Physics Letters, 2004, 396, 38-42.	1.2	62
1509	The role of surface elasticity in giant corrugations observed by scanning tunneling microscopes. Chemical Physics Letters, 2004, 397, 354-359.	1.2	28
1510	A reexamination of the chemisorption and desorption of ozone on the exterior of a (5,5) single-walled carbon nanotube. Chemical Physics Letters, 2004, 398, 297-303.	1.2	64
1511	Electronic structures of InTaO4, a promising photocatalyst. Chemical Physics Letters, 2004, 398, 449-452.	1.2	40
1512	Theoretical evidence for fast H-divacancy rotation on H/Pd(111). Chemical Physics Letters, 2004, 400, 163-168.	1.2	3
1513	Effect of external stress on the patterning of nanostructures: a kinetic Monte Carlo simulation of Ta deposited on anistropically compressed Ta(100) surfaces. Chemical Physics Letters, 2004, 400, 74-77.	1.2	1
1514	Individualities and average behavior in the physical properties of small diameter single-walled carbon nanotubes. Carbon, 2004, 42, 971-978.	5.4	32
1515	Electronic structure of the extended vanadyl pyrophosphate (1 0 0) surface. Catalysis Today, 2004, 91-92, 177-180.	2.2	9
1516	Adsorption of Pd atoms on Î³-Al2O3: a density functional study of metalâ€“support interactions. Applied Surface Science, 2004, 238, 82-85.	3.1	23

#	Article	IF	Citations
1517	Elastic polarizable environment cluster embedding approach for water adsorption on the Î±-Al2O3(0001) surface. A density functional study. Physical Chemistry Chemical Physics, 2004, 6, 4505-4513.	1.3	16
1518	Density functional study of methoxide decomposition on PdZn(100). Physical Chemistry Chemical Physics, 2004, 6, 4499-4504.	1.3	29
1519	Effects of Ag and Ni Additives on Zn Diffusion in Steel Hot-Dip Galvanizing:Â An ab Initio Molecular Dynamics Simulation. Chemistry of Materials, 2004, 16, 5567-5573.	3.2	7
1520	Effects of metal buffer layer on the morphology of the ZnO columns. , 2004, , .		0
1521	Inner shell definition and absolute hydration free energy of K+(aq) on the basis of quasi-chemical theory and ab initio molecular dynamics. Physical Chemistry Chemical Physics, 2004, 6, 1966-1969.	1.3	88
1522	Quantifying lateral adsorbate interactions by kinetic Monte-Carlo simulations and density-functional theory: NO dissociation on Rh(100). Physical Chemistry Chemical Physics, 2004, 6, 1830.	1.3	30
1523	The interdependence of defects, electronic structure and surface chemistry. Dalton Transactions, 2004, , 3076.	1.6	22
1524	Dynamical properties of Ni2MnGa determined from density functional calculations. Phase Transitions, 2004, 77, 253-259.	0.6	5
1525	Optical Spectra, Properties and First Principles Computations of Ba(Fe, Nb)O3and Pb(Fe, Nb)O3. Ferroelectrics, 2004, 302, 279-283.	0.3	10
1526	Structural, electronic and optical properties of semiconducting rhenium silicide. Journal of Physics Condensed Matter, 2004, 16, 303-312.	0.7	8
1527	Detection and visualization of anomalous structures in molecular dynamics simulation data. , 0, , .		15
1528	Energetics of segregation and embrittling potency for non-transition elements in the Ni Â5 (012) symmetrical tilt grain boundary: a first-principles study. Journal of Physics Condensed Matter, 2004, 16, 3933-3956.	0.7	74
1529	Nitrogen doping and chirality of carbon nanotubes. Physical Review B, 2004, 70, .	1.1	103
1530	Phase stability of nanocarbon in one dimension: Nanotubes versus diamond nanowires. Journal of Chemical Physics, 2004, 120, 3817-3821.	1.2	52
1531	Electron correlation effects on SiC(111) and SiC(0001) surfaces. Journal of Physics Condensed Matter, 2004, 16, S1721-S1732.	0.7	28
1532	Evidence for interstitial hydrogen as the dominant electronic defect in nanometer alumina films. Physical Review B, 2004, 69, .	1.1	48
1533	Density Functional Theory Study of Silica Zeolite Structures:Â Stabilities and Mechanical Properties of SOD, LTA, CHA, MOR, and MFI. Journal of Physical Chemistry B, 2004, 108, 9208-9215.	1.2	89
1534	Electron-Deficient Bonding in â§« Rhomboid Rings. Journal of the American Chemical Society, 2004, 126, 13119-13131.	6.6	45

#	Article	IF	Citations
1535	Oxygen vacancies on TiO2 (110) from first principles calculations. Journal of Chemical Physics, 2004, 121, 7427-7433.	1.2	75
1536	Proposed Definition of Microchemical Inhomogeneity and Application To Characterize Some Selected Miscible/Immiscible Binary Metal Systems. Journal of Physical Chemistry B, 2004, 108, 16071-16076.	1.2	20
1537	Reduced SnO2 surfaces by first-principles calculations. Applied Physics Letters, 2004, 84, 909-911.	1.5	88
1538	First principles calculations of the chemisorption properties of nitro-containing molecules on the Al/sub 2/O/sub 3/(0001) surface. , 2004, , .		0
1539	Density-Functional Based Modeling of the Intermediate in the Water Production Reaction on Pt(111). Physical Review Letters, 2004, 92, 136103.	2.9	70
1540	Semiempirical approach to the energetics of interlayer binding in graphite. Physical Review B, 2004, 70, .	1.1	173
1541	Density functional calculations forC60peapods. Physical Review B, 2004, 70, .	1.1	46
1542	The influence of electronic structure on hydrogen absorption in palladium alloys. Journal of Physics Condensed Matter, 2004, 16, 6267-6277.	0.7	75
1543	Solute Diffusion in Metals: Larger Atoms Can Move Faster. Physical Review Letters, 2004, 92, 085901.	2.9	208
1544	Importance of Shear in the bcc-to-hcp Transformation in Iron. Physical Review Letters, 2004, 93, 115501.	2.9	133
1545	Nonicosahedral growth and magnetic behavior of rhodium clusters. Physical Review B, 2004, 70, .	1.1	99
1546	Phonon Density of States and Compression Behavior in Iron Sulfide under Pressure. Physical Review Letters, 2004, 93, 195503.	2.9	30
1547	Nature of One-Dimensional Short Hydrogen Bonding:â€‰ Bond Distances, Bond Energies, and Solvent Effects. Journal of the American Chemical Society, 2004, 126, 2186-2193.	6.6	86
1548	Adhesion and adhesive transfer at aluminum/diamond interfaces:â€‚A first-principles study. Physical Review B, 2004, 69, .	1.1	118
1549	Distribution of Cations in FeSbO4: A Computer Modeling Study. Chemistry of Materials, 2004, 16, 1954-1960.	3.2	37
1550	Effect of strain on atomic ordering and action of surfactants in ternary alloy thin films. Physical Review B, 2004, 70, .	1.1	5
1551	Theoretical study of bulk and surface oxygen and aluminum vacancies inÎ±â^'Al2O3. Physical Review B, 2004, 69, .	1.1	84
1552	Structures of Carbon Nanocrystals. Chemistry of Materials, 2004, 16, 4905-4911.	3.2	27

#	Article	IF	Citations
1553	Simulating the atomic layer deposition of alumina from first principles. Journal of Materials Chemistry, 2004, 14, 3246.	6.7	134
1554	Energetics and electronic structure of stacking faults in ZnO. Physical Review B, 2004, 70, .	1.1	85
1555	Density-functional band-structure calculations for La-, Y-, and Sc-filledCoP3-based skutterudite structures. Physical Review B, 2004, 70, .	1.1	27
1556	Computational Study of Benzene-to-Phenol Oxidation Catalyzed by N2O on Iron-Exchanged Ferrierite. Journal of Physical Chemistry B, 2004, 108, 5944-5950.	1.2	46
1557	First Principles Calculation of Defect Formation Energies in Sr- and Mg-Doped LaGaO3. Journal of Physical Chemistry B, 2004, 108, 9168-9172.	1.2	38
1558	Structural and electronic properties of oxygen vacancies in cubic and antiferrodistortive phases ofSrTiO3. Physical Review B, 2004, 69, .	1.1	101
1559	The Nature of the Complex Counterion of the Chromophore in Rhodopsin. Journal of Physical Chemistry B, 2004, 108, 3673-3680.	1.2	30
1560	The Simple Cubic Structure of Ruthenium Clusters. Journal of Physical Chemistry B, 2004, 108, 2140-2147.	1.2	70
1561	CH3O Decomposition on PdZn(111), Pd(111), and Cu(111). A Theoretical Study. Langmuir, 2004, 20, 8068-8077.	1.6	133
1562	A First Principles Analysis of the Location and Affinity of Protons in the Secondary Structure of Phosphotungstic Acid. Journal of Physical Chemistry B, 2004, 108, 12292-12300.	1.2	36
1563	Vibrational behavior of adsorbed CO2 on single-walled carbon nanotubes. Journal of Chemical Physics, 2004, 120, 5377-5386.	1.2	73
1564	Ice Tessellation on a Hydroxylated Silica Surface. Physical Review Letters, 2004, 92, 146102.	2.9	87
1565	Impurity-doped Si10 cluster: Understanding the structural and electronic properties from first-principles calculations. Physical Review B, 2004, 70, .	1.1	43
1566	Characterization of Water Clusters in Organic Molecular Hosts from Density Functional Theory Calculations. Journal of Physical Chemistry B, 2004, 108, 3431-3436.	1.2	6
1567	Atomic and Electronic Structure of Pyridine on Ge(100). Journal of Physical Chemistry B, 2004, 108, 15229-15232.	1.2	30
1568	Phase separation inLixFePO4induced by correlation effects. Physical Review B, 2004, 69, .	1.1	159
1569	Electronic structure ofPbFe1/2Ta1/2O3:Crystallographic ordering and magnetic properties. Physical Review B, 2004, 69, .	1.1	64
1570	Scanning Tunneling Microscopy and Theoretical Study of Competitive Reactions in the Dissociative Chemisorption of CCl4on Iron Oxide Surfaces. Journal of Physical Chemistry B, 2004, 108, 16753-16760.	1.2	21

#	Article	IF	Citations
1571	Effect of Sulfur Impurity on Fe(110) Adhesion:Â A DFT Study. Journal of Physical Chemistry B, 2004, 108, 10965-10972.	1.2	13
1572	Chains of gold atoms with tailored electronic states. Physical Review B, 2004, 69, .	1.1	252
1573	Atomistic mechanism of proton conduction in solidCsHSO4by a first-principles study. Physical Review B, 2004, 69, .	1.1	22
1574	First-principles-based kinetic Monte Carlo simulation of nitric oxide decomposition over Pt and Rh surfaces under lean-burn conditions. Molecular Physics, 2004, 102, 361-369.	0.8	50
1575	Experimental and Theoretical Investigation on the Relative Stability of the PdS2- and Pyrite-Type Structures of PdSe2. Inorganic Chemistry, 2004, 43, 1943-1949.	1.9	100
1576	Dielectric Permittivity Study of KTaO3Weakly Doped by6Li Isotope. Ferroelectrics, 2004, 302, 203-206.	0.3	1
1577	Density Functional Theory Study of Co, Rh, and Ir Atoms Deposited on the Î±-Al2O3(0001) Surface. Journal of Physical Chemistry B, 2004, 108, 15671-15678.	1.2	30
1578	Ethylene Decomposition on Rh(100):Â Theory and Experimentâ€. Journal of Physical Chemistry B, 2004, 108, 14541-14548.	1.2	23
1579	Structural and Spectroelectrochemical Study of Carbonate and Bicarbonate Adsorbed on Pt(111) and Pd/Pt(111) Electrodes. Journal of Physical Chemistry B, 2004, 108, 17928-17939.	1.2	39
1580	Effects of Subsurface Boron and Phosphorus on Surface Reactivity of Si(001):Â Water and Ammonia Adsorption. Journal of Physical Chemistry B, 2004, 108, 16147-16153.	1.2	3
1581	Ab initioInvestigation of the Early Stage of Nano-scale Thin Film Growth: Al and Co Adatoms on Co (111) Surface. Japanese Journal of Applied Physics, 2004, 43, 3815-3817.	0.8	6
1582	Ab Initio Molecular Dynamics Study of Formate Ion Hydration. Journal of the American Chemical Society, 2004, 126, 344-351.	6.6	73
1583	Molecular Simulations of Anhydrous Na6[Al6Si6O24] Sodalite. Chemistry of Materials, 2004, 16, 2121-2133.	3.2	28
1584	How the Counterion Affects Ground- and Excited-State Properties of the Rhodopsin Chromophore. Journal of Physical Chemistry B, 2004, 108, 20419-20426.	1.2	44
1585	Density Functional Theory Studies of the Interaction of H, S, Niâ^'H, and Niâ^'S Complexes with the MoS2Basal Plane. Journal of Physical Chemistry B, 2004, 108, 239-249.	1.2	29
1586	The Properties of Methylene- and Amine-Substituted Zeolites from First Principles. Journal of the American Chemical Society, 2004, 126, 1843-1848.	6.6	53
1587	A note on temperature-dependent band narrowing in oligo-acene crystals. Journal of Physics Condensed Matter, 2004, 16, 2023-2032.	0.7	18
1588	Coverage Dependent Adsorption of Acrolein on Pt(111) from a Combination of First Principle Theory and HREELS Study. Journal of Physical Chemistry B, 2004, 108, 9085-9093.	1.2	75

#	Article	IF	Citations
1589	Effect of electron correlations on the electronic and magnetic structure of Ti-dopedÎ±-hematite. Physical Review B, 2004, 69, .	1.1	67
1590	Influence of hydrogen on the stability of iron phases under pressure. Geophysical Research Letters, 2004, 31, .	1.5	14
1591	Ab-initiohigh-pressure alloying of iron and potassium: Implications for the Earth's core. Geophysical Research Letters, 2004, 31, n/a-n/a.	1.5	33
1592	Dual role of fluorine at the Siâ€“SiO2 interface. Applied Physics Letters, 2004, 85, 4950-4952.	1.5	22
1593	The Location of Adsorbed Hydrogen in Graphite Nanostructures. Journal of the American Chemical Society, 2004, 126, 13095-13099.	6.6	45
1594	Irradiation-Induced Magnetism in Graphite: A Density Functional Study. Physical Review Letters, 2004, 93, 187202.	2.9	612
1595	Structural and electronic properties ofYBa2Cu3O7andYSr2Cu3O7under mechanical and strontium chemical pressures. Physical Review B, 2004, 70, .	1.1	17
1596	Theoretical study of crossed and parallel carbon nanotube junctions and three-dimensional grid structures. Physical Review B, 2004, 70, .	1.1	34
1597	Ab initiostudy of the (0001) surfaces of hematite and chromia: Influence of strong electronic correlations. Physical Review B, 2004, 70, .	1.1	357
1598	Binding of propene on small gold clusters and on Au(111): Simple rules for binding sites and relative binding energies. Journal of Chemical Physics, 2004, 121, 3756-3766.	1.2	94
1599	Prediction of the local structure of liquid and supercooled tantalum. Physical Review B, 2004, 70, .	1.1	69
1600	Ab InitioMolecular-Dynamics Simulations of Short-Range Order in LiquidAl80Mn20andAl80Ni20Alloys. Physical Review Letters, 2004, 93, 207801.	2.9	55
1601	Ab initio molecular dynamics simulations of local structure of supercooled Ni. Journal of Chemical Physics, 2004, 120, 6124-6127.	1.2	108
1602	Surface Structure of Hydroxylated and Sulfated Zirconia. A Periodic Density-Functional Studyâ€. Journal of Physical Chemistry B, 2004, 108, 14652-14662.	1.2	82
1603	Adsorption of C60on the Si(001) surface calculated within the generalized gradient approximation. Nanotechnology, 2004, 15, S1-S4.	1.3	26
1604	Interstitial oxygen in Si andSi1â^'xGex. Physical Review B, 2004, 69, .	1.1	25
1605	Structural, bonding, and dynamical properties of liquid Fe-Si alloys: â€ƒAn ab initio molecular-dynamics simulation. Physical Review B, 2004, 70, .	1.1	16
1606	Oxygen neutral defects in silica: Origin of the distribution of the formation energies. Europhysics Letters, 2004, 66, 680-686.	0.7	19

#	Article	IF	Citations
1607	Predicting the Energetics, Phase Stability, and Morphology Evolution of Faceted and Spherical Anatase Nanocrystals. Journal of Physical Chemistry B, 2004, 108, 18435-18440.	1.2	115
1608	Adsorption of a carbon atom on theNi38magic cluster and three low-index nickel surfaces: A comparative first-principles study. Physical Review B, 2004, 69, .	1.1	40
1609	Energetics and diffusivity of indium-related defects in silicon. Physical Review B, 2004, 69, .	1.1	20
1610	Ab initiostudy of structural and electronic properties of planar defects in Si and SiC. Physical Review B, 2004, 70, .	1.1	10
1611	Ab initiomolecular dynamics simulations of liquid structure change with temperature for a GaSb alloy. Physical Review B, 2004, 70, .	1.1	15
1612	Structure Dependence of NO Adsorption and Dissociation on Platinum Surfaces. Journal of the American Chemical Society, 2004, 126, 1551-1559.	6.6	112
1613	Theoretical prediction of electronic structures of fully Ï€-conjugated zinc oligoporphyrins with curved surface structures. Journal of Chemical Physics, 2004, 120, 7963-7970.	1.2	24
1614	Structures of Platinum Clusters:Â Planar or Spherical?â€. Journal of Physical Chemistry A, 2004, 108, 8605-8614.	1.1	254
1615	Ideal tensile strength ofB2transition-metal aluminides. Physical Review B, 2004, 70, .	1.1	52
1616	Trends in ferromagnetism, hole localization, and acceptor level depth for Mn substitution in GaN, GaP, GaAs, and GaSb. Applied Physics Letters, 2004, 85, 2860-2862.	1.5	69
1617	Structure and magnetic properties of adatoms on carbon nanotubes. Physical Review B, 2004, 69, .	1.1	82
1618	Local structural distortions and Mn random distributions in (Ga,Mn)As: A first-principles study. Physical Review B, 2004, 69, .	1.1	12
1619	Why Do Gallium Clusters Have a Higher Melting Point than the Bulk?. Physical Review Letters, 2004, 92, 135506.	2.9	111
1620	Experimental Evidence for a High-Pressure Isostructural Phase Transition in Osmium. Physical Review Letters, 2004, 93, 095502.	2.9	119
1621	Early chemistry in hot and dense nitromethane: Molecular dynamics simulations. Journal of Chemical Physics, 2004, 120, 10146-10153.	1.2	103
1622	Lattice dynamics inPbMg1âˆ•3Nb2âˆ•3O3. Physical Review B, 2004, 70, .	1.1	102
1623	Atomic and magnetic configurational energetics by the generalized perturbation method. Physical Review B, 2004, 70, .	1.1	128
1624	Water adsorption on metal surfaces: A general picture from density functional theory studies. Physical Review B, 2004, 69, .	1.1	448

#	Article	IF	Citations
1625	First-principles study of binary bcc alloys using special quasirandom structures. Physical Review B, 2004, 69, .	1.1	266
1626	Ab initiomorphology and surface thermodynamics ofÎ±â˜Al2O3. Physical Review B, 2004, 69, .	1.1	117
1627	Density functional study of the adsorption of propene on silver clusters, Agmq (m=1â€“5; q=0, +1). Journal of Chemical Physics, 2004, 121, 9925-9930.	1.2	41
1628	Ab initiocalculations of ideal tensile strength and mechanical stability in copper. Journal of Physics Condensed Matter, 2004, 16, 1045-1052.	0.7	61
1629	Bonding and compressibility in molecular and polymeric phases of solid CO2. Journal of Physics Condensed Matter, 2004, 16, S1263-S1270.	0.7	8
1630	The Interaction of Water with the Pt(533) Surface. Journal of Physical Chemistry B, 2004, 108, 12575-12582.	1.2	59
1631	Ab initiostudy ofÎ³â˜Al2O3surfaces. Physical Review B, 2004, 70, .	1.1	197
1632	The Nowotny Chimney Ladder Phases:Â Following thecpseudoClue toward an Explanation of the 14 Electron Rule. Inorganic Chemistry, 2004, 43, 6151-6158.	1.9	79
1633	The Nowotny Chimney Ladder Phases:Â Whence the 14 Electron Rule?. Inorganic Chemistry, 2004, 43, 6159-6167.	1.9	98
1634	Nonequilibrium electron transport in two-dimensional nanostructures modeled using Greenâ€™s functions and the finite-element method. Physical Review B, 2004, 69, .	1.1	36
1635	First-principles calculations for the electronic band structures of small diameter single-wall carbon nanotubes. Physical Review B, 2004, 70, .	1.1	136
1636	Complete Spin Polarization for a Carbon Nanotube with an Adsorbed Atomic Transition-Metal Chain. Nano Letters, 2004, 4, 561-563.	4.5	75
1637	First-principles investigation of the assumptions underlying model-Hamiltonian approaches to ferromagnetism of3dimpurities in III-V semiconductors. Physical Review B, 2004, 69, .	1.1	133
1638	Site preference for Mn substitution in spintronicCuMIIIX2VIchalcopyrite semiconductors. Physical Review B, 2004, 69, .	1.1	45
1639	Metal encapsulated nanotubes of silicon and germanium. Journal of Materials Chemistry, 2004, 14, 555.	6.7	49
1640	Ab initiothermodynamics of oxide surfaces:O2onFe2O3(0001). Physical Review B, 2004, 69, .	1.1	147
1641	Diffusion of interstitial hydrogen into and through bcc Fe from first principles. Physical Review B, 2004, 70, .	1.1	406
1642	First-principles calculation of defect-formation energies in theY2(Ti,Sn,Zr)2O7pyrochlore. Physical Review B, 2004, 70, .	1.1	139

#	Article	IF	Citations
1643	Transport in Proton Conductors for Fuel-Cell Applications:â€‰ Simulations, Elementary Reactions, and Phenomenology. Chemical Reviews, 2004, 104, 4637-4678.	23.0	1,952
1644	First-principles prediction of redox potentials in transition-metal compounds withLDA+U. Physical Review B, 2004, 70, .	1.1	871
1645	Adsorption, Diffusion, and Dissociation of H2S on Fe(100) from First Principles. Journal of Physical Chemistry B, 2004, 108, 19140-19145.	1.2	101
1646	A computer modelling study of the uptake and segregation of fluoride ions at the hydrated hydroxyapatite (0001) surface: introducing a Ca10(PO4)6(OH)2potential model. Physical Chemistry Chemical Physics, 2004, 6, 1860-1866.	1.3	94
1647	First-principles exploration of alternative gate dielectrics:â€ƒElectronic structure ofZrO2/SiandZrSiO4/Siinterfaces. Physical Review B, 2004, 69, .	1.1	116
1648	Origin of electron accumulation at wurtzite InN surfaces. Physical Review B, 2004, 69, .	1.1	205
1649	Implications of the B20 crystal structure for the magnetoelectronic structure ofMnSi. Physical Review B, 2004, 70, .	1.1	78
1650	Anomalous energetics and defect-assisted diffusion of Ga in silicon. Applied Physics Letters, 2004, 85, 4902-4904.	1.5	18
1651	Intrinsic hole localization mechanism in magnetic semiconductors. Journal of Physics Condensed Matter, 2004, 16, L457-L462.	0.7	64
1652	Electronic and Magnetic Properties of 3 d Transition-Metal-Doped IIIâ€“V Magnetic Semiconductor. Chinese Physics Letters, 2004, 21, 1632-1635.	1.3	12
1653	Charge transfer complexes between tetranitrofluorenone and polyaromatic compounds from gasoil: a combined DFT and experimental study. Physical Chemistry Chemical Physics, 2004, 6, 1169.	1.3	24
1654	Symmetry breaking and structural distortions in chargedXH4(X=C,Si, Ge, Sn, and Pb) molecules. Physical Review A, 2004, 69, .	1.0	5
1655	Unusual Directional Dependence of Exchange Energies in GaAs Diluted with Mn: Is the RKKY Description Relevant?. Physical Review Letters, 2004, 93, 177201.	2.9	141
1656	Density functional study of the adsorption of propene on mixed gold-silver clusters, AunAgm: Propensity rules for binding. Journal of Chemical Physics, 2004, 121, 9931-9937.	1.2	58
1657	Theoretical study of structural and electronic properties ofÎ²â^'Ta2O5andÎ´â^'Ta2O5. Physical Review B, 2004, 69, .	1.1	68
1658	First-principles study of hydrogen diffusion inÎ±â^'Al2O3and liquid alumina. Physical Review B, 2004, 69, .	1.1	71
1659	Magnetism and energetics ofMn-DopedZnO(101Â¯0)thin films. Physical Review B, 2004, 69, .	1.1	56
1660	Evolution of theGeâ^•Si(001)wetting layer during Si overgrowth and crossover between thermodynamic and kinetic behavior. Physical Review B, 2004, 69, .	1.1	26

#	Article	IF	Citations
1661	Structural, electronic, and optical properties ofÎ²â^'(Fe1â^'xCox)Si2. Physical Review B, 2004, 69, .	1.1	2
1662	Ab initiomolecular dynamics of metal surfaces. Journal of Physics Condensed Matter, 2004, 16, S2575-S2596.	0.7	18
1663	Ab initiostudy of the phase diagram of epitaxialBaTiO3. Physical Review B, 2004, 69, .	1.1	217
1664	High-Pressure Melting of Molybdenum. Physical Review Letters, 2004, 92, 195701.	2.9	86
1665	Ab initiomolecular dynamics simulation of liquidAlxGe1â^'xalloys. Physical Review B, 2004, 70, .	1.1	5
1666	Free Energy of Adsorption of Water and Metal Ions on the {101Ì„4} Calcite Surface. Journal of the American Chemical Society, 2004, 126, 10152-10161.	6.6	276
1667	Ab initiocharacterization of magneticCuFeS2. Physical Review B, 2004, 70, .	1.1	24
1668	Electronic properties of rutileTiO2ultrathin films: Odd-even oscillations with the number of layers. Physical Review B, 2004, 70, .	1.1	144
1669	High-coverage stable structures of potassium adsorbed on single-walled carbon nanotubes. Physical Review B, 2004, 69, .	1.1	16
1670	Monovacancy and divacancy formation and migration in copper: A first-principles theory. Physical Review B, 2004, 70, .	1.1	38
1671	First principles study of the ferromagnetism in Ga1ÂxMnxAs semiconductors. Journal of Physics Condensed Matter, 2004, 16, 8243-8250.	0.7	15
1672	The Formation and Stability of Adsorbed Formyl as a Possible Intermediate in Fischerâ^'Tropsch Chemistry on Ruthenium. Journal of Physical Chemistry B, 2004, 108, 3614-3624.	1.2	49
1673	Atomic strings of group IV, IIIâ€"V, and IIâ€"VI elements. Applied Physics Letters, 2004, 85, 6179-6181.	1.5	30
1674	Density functional study of the adsorption of aC60monolayer on Ag(111) and Au(111) surfaces. Physical Review B, 2004, 69, .	1.1	160
1675	Stable geometries and magnetic properties of single-walled carbon nanotubes doped with3dtransition metals:â€ƒA first-principles study. Physical Review B, 2004, 69, .	1.1	236
1676	Formation of Chiral Domains for Tartaric Acid on Cu(110):Â A Combined DFT and Kinetic Monte Carlo Study. Journal of Physical Chemistry B, 2004, 108, 11035-11043.	1.2	66
1677	Electronic and magnetic properties of zinc blende half-metal superlattices. Applied Physics Letters, 2004, 84, 239-241.	1.5	43
1678	First-principles elastic constants and phonons ofÎ´â€Pu. Physical Review B, 2004, 70, .	1.1	36

#	Article	IF	Citations
1679	First-principles study of Li ion diffusion inLiFePO4. Physical Review B, 2004, 69, .	1.1	250
1680	Ab initio Monte Carlo simulations for finite-temperature properties: application to lithium clusters and bulk liquid lithium. Computational Materials Science, 2004, 29, 145-151.	1.4	16
1681	Ab initio study on the lattice instability of silicon and aluminum under [001] tension. Computational Materials Science, 2004, 29, 397-406.	1.4	15
1682	Elastic tensor of the forsterite (Mg2SiO4) under pressure. Computational Materials Science, 2004, 29, 414-418.	1.4	30
1683	Metallicâ€“semiconducting transition of single-walled carbon nanotubes under high axial strain. Computational Materials Science, 2004, 31, 33-41.	1.4	18
1684	Overcoming the doping bottleneck in semiconductors. Computational Materials Science, 2004, 30, 337-348.	1.4	462
1685	Electronic structure of bulk and (001) surface layers of pyrite FeS2. Computational Materials Science, 2004, 30, 358-363.	1.4	38
1686	Classification of amorphous-silicon microstructures by structural parameters: molecular dynamics study. Computational Materials Science, 2004, 31, 258-268.	1.4	14
1687	Predictions of novel nanostructures of silicon by metal encapsulation. Computational Materials Science, 2004, 30, 260-268.	1.4	45
1688	Bond-valence methods for pKa prediction: critical reanalysis and a new approach. Geochimica Et Cosmochimica Acta, 2004, 68, 2025-2042.	1.6	118
1689	First-principles calculation on free energy of precipitate nucleation. Calphad: Computer Coupling of Phase Diagrams and Thermochemistry, 2004, 28, 173-176.	0.7	42
1690	Bandgap calculations for conjugated polymers. Synthetic Metals, 2004, 141, 171-177.	2.1	154
1691	Thermodynamic assessment of the Zrâ€“N system. Journal of Alloys and Compounds, 2004, 373, 194-201.	2.8	28
1692	Electronic structure and Rietveld refinement parameters of Ti-doped sodium alanates. Journal of Alloys and Compounds, 2004, 375, 1-10.	2.8	81
1693	A theoretical search for intermetallic compounds and solution phases in the binary system Sn/Zn. Journal of Alloys and Compounds, 2004, 379, 110-116.	2.8	9
1694	Density functional study of structural and phase stabilities for RMn2 Laves phases (R = Sc, Y, Lu, Ti, Zr,) Tj ETQq1 1 0.784314 rgBT /Ov	2.8	18
1695	Characterization of the electronic properties of YB4 and YB6 using 11B NMR and first-principles calculations. Journal of Alloys and Compounds, 2004, 383, 232-238.	2.8	57
1696	Covalent bonding and semiconducting bandgap formation in Alâ€“transition-metal quasicrystalline approximants. Journal of Non-Crystalline Solids, 2004, 334-335, 342-346.	1.5	6

#	Article	IF	Citations
1697	Tiâ€“Zrâ€“Ni and Tiâ€“Hfâ€“Ni quasicrystals and approximants as hydrogen storage alloys. Journal of Non-Crystalline Solids, 2004, 334-335, 461-465.	1.5	16
1698	A DFT study of the compressibility of amorphous silicon oxynitride. Journal of Non-Crystalline Solids, 2004, 345-346, 720-723.	1.5	6
1699	Direct Observation of Charge Transfer at a MgO(111) Surface. Physical Review Letters, 2004, 92, 026101.	2.9	36
1700	Magnetic properties of vacancies in graphene and single-walled carbon nanotubes. New Journal of Physics, 2004, 6, 68-68.	1.2	370
1701	Electronic Structure and Bonding of Au on aSiO2Cluster: A Nanobullet for Tumors. Physical Review Letters, 2004, 93, 186803.	2.9	51
1702	Atomic and electronic structure of theSi(001)2Ã—2â˜Lichemisorption system at 0.5 monolayer coverage. Physical Review B, 2004, 69, .	1.1	10
1703	Melting curve of materials: theory versus experiments. Journal of Physics Condensed Matter, 2004, 16, S973-S982.	0.7	59
1704	Theoretical analysis of electron transport through organic molecules. Journal of Chemical Physics, 2004, 120, 1542-1554.	1.2	178
1705	First principles investigations of complex hydrides AMH4 and A3MH6 (A=Li, Na, K, M=B, Al, Ga) as hydrogen storage systems. Journal of Alloys and Compounds, 2004, 364, 6-12.	2.8	90
1706	Structural phase transitions in the Cu-based Cuâ€“V solid solutions studied by molecular dynamics simulation. Journal of Alloys and Compounds, 2004, 366, 205-212.	2.8	6
1707	Hydrogen incorporation in stishovite at high pressure and symmetric hydrogen bonding in Î´-AlOOH. Earth and Planetary Science Letters, 2004, 221, 421-431.	1.8	83
1708	Role of Hybridization inNaxCoO2and the Effect of Hydration. Physical Review Letters, 2004, 92, 196405.	2.9	73
1709	An ab initio study of structural properties and single vacancy defects in Wurtzite AlN. Journal of Chemical Physics, 2004, 120, 4890-4896.	1.2	31
1710	Molecular-dynamics study of the local symmetry changes in metallic liquids. Phase Transitions, 2004, 77, 89-100.	0.6	0
1711	Quasiharmonic approach to a second-order phase transition. Physical Review B, 2004, 70, .	1.1	17
1712	Effects of particle morphology and surface hydrogenation on the phase stability ofTiO2. Physical Review B, 2004, 70, .	1.1	200
1713	Ab initiocalculations of cohesive energies ofFe-based glass-forming alloys. Physical Review B, 2004, 70, .	1.1	75
1714	Ab initiostudy of foreign interstitial atom (C, N) interactions with intrinsic point defects inÎ±-Fe. Physical Review B, 2004, 69, .	1.1	351

#	Article	IF	Citations
1715	Surface properties ofCeO2from first principles. Physical Review B, 2004, 69, .	1.1	299
1716	Diamond under pressure: Ab-initio calculations of the equation of state and optical phonon frequency revisited. High Pressure Research, 2004, 24, 101-110.	0.4	17
1717	Modelling, refinement and analysis of the â€œType IIIâ€•Î´-Bi2O3-related superstructure in the Bi2O3â€“Nb2O5 system. Journal of Solid State Chemistry, 2004, 177, 1838-1846.	1.4	60
1718	The Earth's core: An approach from first principles. Geophysical Monograph Series, 2004, , 1-12.	0.1	4
1719	High Temperature Thermistor Material Design of Spinel Type MgCr2O4 by First Principles Calculations and Experiments. Funtai Oyobi Fummatsu Yakin/Journal of the Japan Society of Powder and Powder Metallurgy, 2004, 51, 487-491.	0.1	0
1720	Using diverse theoretical approaches to study electron transport through organic molecules. , 2004, 5352, 44.		0
1721	A new polymorphic material? Structural degeneracy of ZrMn 2. Europhysics Letters, 2004, 67, 807-813.	0.7	17
1722	Theory of elastic and inelastic tunnelling microscopy and spectroscopy: CO on Cu revisited. Philosophical Transactions Series A, Mathematical, Physical, and Engineering Sciences, 2004, 362, 1173-1183.	1.6	33
1723	Structural Stability of the Metastable Solid Solution in the Equilibrium Immiscible Agâ€“Mo System Predicted by anab InitioDerived Potential. Journal of the Physical Society of Japan, 2004, 73, 1222-1227.	0.7	5
1724	Atomistic Modeling of Metastable Phase Selection of a Highly Immiscible Agâ€“W System. Journal of the Physical Society of Japan, 2004, 73, 2023-2027.	0.7	6
1725	Periodic solids and electron bands. , 2004, , 73-99.		1
1726	The Kohnâ€“Sham auxiliary system. , 2004, , 135-151.		1
1727	Functionals for exchange and correlation. , 2004, , 152-171.		3
1728	Plane waves and grids: basics. , 2004, , 236-253.		0
1729	Localized orbitals: tight-binding. , 2004, , 272-297.		0
1730	Localized orbitals: full calculations. , 2004, , 298-312.		0
1731	Augmented functions: APW, KKR, MTO. , 2004, , 313-344.		0
1732	Quantum molecular dynamics (QMD). , 2004, , 371-386.		0

#	Article	IF	Citations
1733	Excitation spectra and optical properties. , 2004, , 406-417.		0
1739	Augmented functions: linear methods. , 2004, , 345-368.		0
1742	A Second-Variational Prediction Operator for Fast Convergence in Self-Consistent Electronic-Structure Calculations. Materials Transactions, 2004, 45, 1422-1428.	0.4	8
1743	Free-Energy Calculation of Precipitate Nucleation in an Fe-Cu-Ni Alloy. Materials Transactions, 2004, 45, 1978-1981.	0.4	32
1744	Chemical Bonding and Electronic States in .ALPHA.-PbO: Analysis by an ab initio Band Calculation. Journal of the Ceramic Society of Japan, 2004, 112, 50-56.	1.3	5
1745	First Principles Calculation of Free Energy on Precipitate Nucleation. Nippon Kinzoku Gakkaishi/Journal of the Japan Institute of Metals, 2004, 68, 973-976.	0.2	2
1746	Interaction between Substitutional and Interstitial Elements in .ALPHA.-Fe Studied by First-Principles Calculation. Nippon Kinzoku Gakkaishi/Journal of the Japan Institute of Metals, 2004, 68, 977-982.	0.2	8
1747	Stability of Copper Atoms Embedded in Sodium-Chloride Crystals. Materials Transactions, 2004, 45, 1450-1451.	0.4	3
1748	First-Principles Characterization of Atomic Structure of Al₂O₃(0001)/Cu Nano-Hetero Interface. Materials Transactions, 2004, 45, 1973-1977.	0.4	34
1749	Ab initio Modeling of the Stress-Strain Response of SiAlON (Si_{6-z}Al_zO_zN_{8-z},) Tj ETQq1 1 0.784314 rgBT /Ove		
1750	Vibrational Contribution on Nucleation Free Energy of Cu Precipitates in Fe-Cu System. Materials Transactions, 2004, 45, 1473-1477.	0.4	7
1751	Density functional theory: foundations. , 2004, , 119-134.		6
1752	A DFT study of the adsorption of butane in MOR and activation on the Lewis center. Studies in Surface Science and Catalysis, 2005, 158, 939-946.	1.5	0
1753	Vacancy Ordering and Non-Stoichiometry in TiC1â^'x â–¡x and TiN1â^'x â–¡x. , 2005, , 99-109.		2
1754	Methylchloride Adsorption on Si(001) â€" Electronic Properties. , 2005, , 115-127.		0
1755	First Principles Calculation of Defect Structure in Non-stoichiometric CoAl and CoTi. Materials Transactions, 2005, 46, 1112-1116.	0.4	5
1756	Interaction between Substitutional and Interstitial Elements in α iron Studied by First-principles Calculation. Materials Transactions, 2005, 46, 1140-1147.	0.4	13
1757	High-Pressure Elasticity and Auxetic Property of α-Cristobalite. Materials Transactions, 2005, 46, 1161-1166.	0.4	18

#	Article	IF	Citations
1758	Atomic Structures and Magnetic Behavior of Small Ruthenium Clusters. Materials Transactions, 2005, 46, 159-162.	0.4	17
1759	Density-functional Calculation of Structural Properties in Ionic and Semiconductor Crystals. , 2005, , 319-328.		1
1760	Atomic structure of Si-rich6Hâ€SiC(0001Â¯)â€2Ã—2surface. Physical Review B, 2005, 71, .	1.1	7
1761	Reactive Co magic cluster formation onSi(111)â^'(7Ã—7). Physical Review B, 2005, 72, .	1.1	45
1762	Interfaces in nanostructured thin films and their influence on hardness. International Journal of Materials Research, 2005, 96, 468-480.	0.8	26
1763	Surface diffusion and incorporation of adatom in Co/Al (001) system. Journal of Solid State Chemistry, 2005, 178, 47-51.	1.4	6
1764	Transition metal intermetallics: Structure maps based on quantum mechanical stability. Journal of Solid State Chemistry, 2005, 178, 1269-1283.	1.4	21
1765	Origin of visible-light-driven photocatalysis: A comparative study on N/F-doped and Nâ€“F-codoped TiO2 powders by means of experimental characterizations and theoretical calculations. Journal of Solid State Chemistry, 2005, 178, 3293-3302.	1.4	327
1766	Hydrides with the perovskite structure: General bonding and stability considerations and the new representative CaNiH3. Journal of Solid State Chemistry, 2005, 178, 3381-3388.	1.4	52
1767	Structural and magnetic properties of clean and methylthiolate-adsorbed Co(0001) surfaces: a first-principles study. Journal of Magnetism and Magnetic Materials, 2005, 286, 119-123.	1.0	7
1768	A critical discussion of calculated modulated structures, Fermi surface nesting and phonon softening in magnetic shape memory alloys Ni2Mn(Ga, Ge, Al) and Co2Mn(Ga, Ge). Journal of Magnetism and Magnetic Materials, 2005, 290-291, 874-877.	1.0	32
1769	Clustering of Mn in (Ga,Mn)As. Journal of Magnetism and Magnetic Materials, 2005, 290-291, 1398-1401.	1.0	14
1770	Ab initio study of phonons in the rutile structure of TiO2. Journal of Physics and Chemistry of Solids, 2005, 66, 1069-1073.	1.9	60
1771	Calculation of valence electron momentum densities using the projector augmented-wave method. Journal of Physics and Chemistry of Solids, 2005, 66, 1128-1135.	1.9	47
1772	Structure instability of A2Al2B2O7 (A=K, Na) crystals. Journal of Physics and Chemistry of Solids, 2005, 66, 1655-1659.	1.9	18
1773	First-principles calculation of defect formation energy in chalcopyrite-type CuInSe2, CuGaSe2 and CuAlSe2. Journal of Physics and Chemistry of Solids, 2005, 66, 1924-1927.	1.9	47
1774	Modelling polymer-derived ceramics. Journal of the European Ceramic Society, 2005, 25, 163-174.	2.8	43
1775	A theoretical investigation of 4fâ†'5d transition of trivalent rare earth ions in fluorides and complex oxides. Journal of Luminescence, 2005, 114, 255-266.	1.5	30

#	Article	IF	Citations
1776	Silicon potentials under (ion) attack: towards a new MEAM model. Nuclear Instruments & Methods in Physics Research B, 2005, 228, 198-211.	0.6	22
1777	Annealing of vacancy complexes in P-doped silicon. Nuclear Instruments & Methods in Physics Research B, 2005, 228, 218-225.	0.6	25
1778	Developing pair potentials for simulating radiation damage in complex oxides. Nuclear Instruments & Methods in Physics Research B, 2005, 228, 288-292.	0.6	45
1779	Epitaxial film growth of zirconium diboride on Si(001). Journal of Crystal Growth, 2005, 277, 364-371.	0.7	15
1780	Properties of charge and magnetic impurities in a spin-polarized electron gas: A semiclassical approach. Physica E: Low-Dimensional Systems and Nanostructures, 2005, 28, 313-322.	1.3	1
1781	Metallization of the semiconducting carbon nanotube by encapsulated bromine molecules. Physica E: Low-Dimensional Systems and Nanostructures, 2005, 29, 693-697.	1.3	14
1782	Structural stabilities and electronic structures of Ti atomic chains. Physica E: Low-Dimensional Systems and Nanostructures, 2005, 30, 138-142.	1.3	14
1783	First principles study of wurtzite and zinc blende GaN: a comparison of the electronic and optical properties. Physics Letters, Section A: General, Atomic and Solid State Physics, 2005, 336, 145-151.	0.9	30
1784	Ab initio investigation of the surface properties of Cu(111) and Li diffusion in Cu thin film. Physics Letters, Section A: General, Atomic and Solid State Physics, 2005, 337, 247-255.	0.9	45
1785	The role of the hydrogen bonding network for the shear modulus of PIPD. Polymer, 2005, 46, 9144-9154.	1.8	18
1786	Orientation of ethoxy, mono-, di-, and tri-fluoroethoxy on Cu(111): a DFT study. Journal of Molecular Catalysis A, 2005, 228, 77-82.	4.8	16
1787	Theory and experiments on the structure of 7Ã... alumina films grown on Ni3Al. Journal of Molecular Catalysis A, 2005, 228, 83-87.	4.8	9
1788	On the heat capacity of Ti3GeC2. Materials Science and Engineering B: Solid-State Materials for Advanced Technology, 2005, 119, 159-163.	1.7	28
1789	Ab initio study of the effect of hydrogen and point defects on arsenic segregation at Si (100)/SiO2 interfaces. Materials Science and Engineering B: Solid-State Materials for Advanced Technology, 2005, 124-125, 359-362.	1.7	0
1790	Ab initio study of the elastic properties of TiSi2. Materials Science in Semiconductor Processing, 2005, 8, 540-544.	1.9	2
1791	Multiscale approach for the analysis of channeling profile measurements of ion implantation damage. Nuclear Instruments & Methods in Physics Research B, 2005, 228, 360-363.	0.6	7
1792	Threshold displacement energies in rutile TiO2: A molecular dynamics simulation study. Nuclear Instruments & Methods in Physics Research B, 2005, 239, 191-201.	0.6	53
1793	First-principles calculation for bowing parameter of wurtzite InxGa1â^'xN. Optics Communications, 2005, 249, 217-223.	1.0	33

#	Article	IF	Citations
1794	Ab initio derivation of the electronic structure properties across the Cuâ€“Cu2O interface. Electrochimica Acta, 2005, 50, 4297-4307.	2.6	5
1795	First-principles calculations on the surface electronic and reactive properties of M/SnO2 (M=Ge, Mn) (110). Computational and Theoretical Chemistry, 2005, 714, 221-233.	1.5	17
1796	Quantum mechanics calculations on the diastereomeric salts of cyclic phosphoric acids with ephedrine. Computational and Theoretical Chemistry, 2005, 717, 205-214.	1.5	0
1797	Strain effect on dielectric property of SrTiO3 lattice: first-principles study. Thin Solid Films, 2005, 475, 97-101.	0.8	12
1798	Structural and dielectric properties of crystalline and amorphous ZrO2. Thin Solid Films, 2005, 486, 125-128.	0.8	160
1799	A kinetic Monte Carlo study of proton diffusion in disordered perovskite structured lattices based on first-principles calculations. Solid State Ionics, 2005, 176, 3035-3040.	1.3	78
1800	Magnetic and structural properties of isolated and assembled clusters. Surface Science Reports, 2005, 56, 189-275.	3.8	384
1801	Hydrogen adsorption energies on bimetallic overlayer systems at the solidâ€“vacuum and the solidâ€“liquid interface. Surface Science, 2005, 597, 42-50.	0.8	50
1802	Ab initio studies of the cubic boron nitride (110) surface. Surface Science, 2005, 574, 269-286.	0.8	33
1803	Atomic and electronic structure of the Si(001)2Ã—1â€“Li chemisorption system at 1.0 monolayer coverage. Surface Science, 2005, 574, 233-243.	0.8	4
1804	Oscillatory interaction between O impurities and Al adatoms on Al(111) and its effect on nucleation and growth. Surface Science, 2005, 575, 89-102.	0.8	9
1805	Cu, Ag and Au atoms deposited on the Î±-Al2O3(0001) surface: a comparative density functional study. Surface Science, 2005, 575, 189-196.	0.8	63
1806	Pd nanoclusters at the MgO(100) surface. Surface Science, 2005, 575, 197-209.	0.8	40
1807	Dynamical properties and the proton transfer mechanism in the wetting water layer on Pt(111). Surface Science, 2005, 575, 300-306.	0.8	34
1808	Molecular precursor-mediated methanol dissociation on Si(111)7Ã—7: ab initio study. Surface Science, 2005, 577, 15-21.	0.8	5
1809	Density functional theory studies of the structure and electronic structure of pure and defective low index surfaces of ceria. Surface Science, 2005, 576, 217-229.	0.8	683
1810	Tuning electronic properties of novel metal oxide nanocrystals using interface interactions: MoO3 monolayers on Au(111). Surface Science, 2005, 577, L71-L77.	0.8	36
1811	Adsorption and reaction of N2H4 on Si(100)-2Ã—1: A computational study with single- and double-dimer cluster models. Surface Science, 2005, 579, 197-214.	0.8	8

#	Article	IF	Citations
1812	DFT study of Pt adsorption on low index SrTiO3 surfaces: SrTiO3(100), SrTiO3(111) and SrTiO3(110). Surface Science, 2005, 581, 66-87.	0.8	41
1813	Cobalt concentration effect in Pt1â^'xCox on the reversible potential for forming OHads from H2Oads in acid solution. Surface Science, 2005, 581, 105-117.	0.8	41
1814	A first principles study of adhesion and adhesive transfer at Al(111)/graphite(0001). Surface Science, 2005, 581, 155-168.	0.8	47
1815	On-surface and sub-surface oxygen on ideal and reconstructed Cu(100). Surface Science, 2005, 584, 62-69.	0.8	36
1816	Interface stabilization of Fe/Al(001) films by Ti interlayersâ€"an ab-initio DFT study. Surface Science, 2005, 582, 69-78.	0.8	14
1817	First principles study of H2S adsorption and dissociation on Fe(110). Surface Science, 2005, 583, 60-68.	0.8	75
1818	Surface segregation in palladium based alloys from density-functional calculations. Surface Science, 2005, 583, 100-106.	0.8	113
1819	The first-principle study on chlorine-modified silver surfaces. Surface Science, 2005, 584, 187-198.	0.8	23
1820	Structure and vibrational spectra of crystalline SiO2 ultra-thin films on Mo(112). Surface Science, 2005, 584, 225-236.	0.8	65
1821	Phase transition at finite temperature in one dimension: Adsorbate ordering in Ba/Si(111)3Ã—2. Surface Science, 2005, 585, L171-L176.	0.8	7
1822	CO adsorption on Cu(111) and Cu(001) surfaces: Improving site preference in DFT calculations. Surface Science, 2005, 590, 117-126.	0.8	116
1823	Band structure and electron gas of In chains on Si(111). Surface Science, 2005, 589, 77-90.	0.8	12
1824	Effect of S contamination on properties of Fe(100) surfaces. Surface Science, 2005, 590, 63-75.	0.8	20
1825	An ab initio study of C60 adsorption on the Si(001) surface. Surface Science, 2005, 591, 45-55.	0.8	60
1826	Hydrogen tunneling on a metal surface: A density-functional study of H and D atoms on Cu(001). Surface Science, 2005, 593, 102-109.	0.8	22
1827	A simple chemical view of relaxations at stoichiometric (110) surfaces of rutile-structure type oxides: A first-principles study of stishovite, SiO2. Surface Science, 2005, 594, 70-82.	0.8	10
1828	First-principles study of adsorption of methyl, coadsorption of methyl and hydrogen, and methane dissociation on Ni(100). Surface Science, 2005, 594, 83-92.	0.8	22
1829	Surface sites and unrelaxed surface energies of tetrahedral silica polymorphs and silicate. Surface Science, 2005, 595, 6-19.	0.8	31

#	Article	IF	Citations
1830	Group V dimers on Si(001): Can they act as Lewis bases?. Surface Science, 2005, 595, 233-238.	0.8	2
1831	CO adsorption on monometallic Pd, Rh, Cu and bimetallic PdCu and RhCu monolayers supported on Ru(0001). Surface Science, 2005, 598, 144-155.	0.8	34
1832	Atomic structure of the 6Hâ€“SiC(0001) nanomesh. Surface Science, 2005, 596, 176-186.	0.8	179
1833	Evolution of Fermi level position and Schottky barrier height at Ni/MgO(001) interface. Surface Science, 2005, 599, 255-261.	0.8	15
1834	Effects of hydrogen on electronic properties of doped diamond. Carbon, 2005, 43, 1009-1014.	5.4	16
1835	Adsorption of atomic and molecular oxygen on Cu(100). Catalysis Today, 2005, 100, 403-406.	2.2	30
1836	First principles calculations of the adsorption and diffusion of hydrogen on Fe(100) surface and in the bulk. Catalysis Today, 2005, 105, 44-65.	2.2	90
1837	A density functional theory study of the adsorption of acetone to the (111) surface of Pt: Implications for hydrogenation catalysis. Catalysis Today, 2005, 105, 85-92.	2.2	43
1838	Nucleation and growth of 1B metal clusters on rutile TiO2(110): Atomic level understanding from first principles studies. Catalysis Today, 2005, 105, 78-84.	2.2	22
1839	Computational study of carbon segregation and diffusion within a nickel grain boundary. Acta Materialia, 2005, 53, 87-96.	3.8	36
1840	Ab initio theoretical tensile test on Y-doped Î£=3 grain boundary in Î±-Al2O3. Acta Materialia, 2005, 53, 403-410.	3.8	40
1841	A combined first-principles and experimental study of the lattice site preference of Pt in B2 NiAl. Acta Materialia, 2005, 53, 2101-2109.	3.8	71
1842	First-principles study of constitutional point defects in B2 NiAl using special quasirandom structures. Acta Materialia, 2005, 53, 2643-2652.	3.8	42
1843	Grain boundary impurities in iron. Acta Materialia, 2005, 53, 2715-2726.	3.8	86
1844	First-principles calculation of structural energetics of Alâ€“TM (TM=Ti, Zr, Hf) intermetallics. Acta Materialia, 2005, 53, 3225-3252.	3.8	202
1845	Predicting yield-stress anomalies in L12 alloys: Ni3Geâ€“Fe3Ge pseudo-binaries. Acta Materialia, 2005, 53, 3601-3612.	3.8	28
1846	Kinetic Monte Carlo study of Alâ€“Mg precipitation. Acta Materialia, 2005, 53, 3721-3728.	3.8	21
1847	Prediction of strong adhesion at the MoSi2/Fe interface. Acta Materialia, 2005, 53, 4489-4496.	3.8	29

#	Article	IF	Citations
1848	Probing vibrational excitations in molecular crystals by inelastic scattering: From neutrons to X-rays. Chemical Physics, 2005, 317, 153-158.	0.9	9
1849	The role of water in the initial steps of methanol oxidation on Pt(111). Chemical Physics, 2005, 319, 185-191.	0.9	68
1850	Lattice modes of hexamethylbenzene studied by inelastic neutron scattering. Chemical Physics, 2005, 317, 143-152.	0.9	8
1851	Constricted boron nanotubes. Chemical Physics Letters, 2005, 402, 21-26.	1.2	47
1852	Role of surface geometry and electronic structure in STM images of O/Ru(0001). Chemical Physics Letters, 2005, 405, 131-135.	1.2	21
1853	Structural and electronic properties of liquid InSb alloy: An ab initio molecular-dynamics simulation. Chemical Physics Letters, 2005, 408, 348-353.	1.2	10
1854	Water bilayer on the Pd/Au(111) overlayer system: Coadsorption and electric field effects. Chemical Physics Letters, 2005, 409, 157-162.	1.2	110
1855	A wetting layer breaks the ice rules. Chemical Physics Letters, 2005, 410, 120-124.	1.2	19
1856	First principles calculations of thermodynamics for semiconductor alloys. Chemical Physics Letters, 2005, 412, 92-96.	1.2	0
1857	Interactions of uranium atom with tetraketone complexes. Chemical Physics Letters, 2005, 415, 243-245.	1.2	4
1858	Description of coordinatively unsaturated sites regeneration over MoS2-based HDS catalysts using 35S experiments combined with computer simulations. Applied Catalysis A: General, 2005, 289, 51-58.	2.2	30
1859	A periodic density functional theory study of gallium-exchanged mordenite. Comptes Rendus Chimie, 2005, 8, 509-520.	0.2	12
1860	Quantum dynamics of the dissociation of H2 on Rh(111). European Physical Journal B, 2005, 45, 425-432.	0.6	9
1861	Metal encapsulated nanotubes of germanium with metal dependent electronic properties. European Physical Journal D, 2005, 34, 295-298.	0.6	11
1862	Hydrogen Embrittlement of Aluminum: The Crucial Role of Vacancies. Physical Review Letters, 2005, 94, 155501.	2.9	234
1863	Electronic properties of single-walled silicon nanotubes compared to carbon nanotubes. Physical Review B, 2005, 72, .	1.1	145
1864	Adsorption of Ar atoms on the relaxed defect-freeTiO2(110)surface. Physical Review B, 2005, 71, .	1.1	17
1865	Ab initioTi-Zr-Ni phase diagram predicts stability of icosahedral TiZrNi quasicrystals. Physical Review B, 2005, 71, .	1.1	29

#	Article	IF	Citations
1866	Adsorption and Vibrational Spectroscopy of CO on Mordenite:Â Ab initio Density-Functional Study. Journal of Physical Chemistry B, 2005, 109, 7345-7357.	1.2	32
1867	Physics of thin-film ferroelectric oxides. Reviews of Modern Physics, 2005, 77, 1083-1130.	16.4	1,932
1868	Application of Density Functional Theory to the Modeling of the Mixed Ionic and Electronic Conductor La2NiO4+Î´:â€‰ Lattice Relaxation, Oxygen Mobility, and Energetics of Frenkel Defects. Chemistry of Materials, 2005, 17, 6538-6544.	3.2	80
1869	Prediction of ordered structures in the bcc binary systems of Mo, Nb, Ta, and W from first-principles search of approximately 3,000,000 possible configurations. Physical Review B, 2005, 72, .	1.1	53
1870	Uniform Catalytic Site in Sn-Î²-Zeolite Determined Using X-ray Absorption Fine Structure. Journal of the American Chemical Society, 2005, 127, 12924-12932.	6.6	147
1871	Electronic structure calculations of physisorption and chemisorption on oxide glass surfaces. Physical Review B, 2005, 72, .	1.1	44
1872	Clustering of Ti on a C60Surface and Its Effect on Hydrogen Storage. Journal of the American Chemical Society, 2005, 127, 14582-14583.	6.6	675
1873	Crystal structure ofCa(AlH4)2predicted from density-functional band-structure calculations. Physical Review B, 2005, 71, .	1.1	58
1874	Energy landscape of deformation twinning in bcc and fcc metals. Physical Review B, 2005, 71, .	1.1	215
1875	Band Structure and the Magnetic and Elastic Properties of SrFeO[sub 3] and LaFeO[sub 3] Perovskites. Physics of the Solid State, 2005, 47, 2082.	0.2	74
1876	Comparative Analysis of the Phonon Modes in AgNbO[sub 3] and NaNbO[sub 3]. Physics of the Solid State, 2005, 47, 2130.	0.2	10
1877	Optimization of the Calculations of the Electronic Structure of Carbon Nanotubes. Physics of the Solid State, 2005, 47, 2196.	0.2	3
1878	Impurities block the Î± to Ï‰ martensitic transformation in titanium. Nature Materials, 2005, 4, 129-133.	13.3	207
1879	Trans-interface diffusion-controlled coarsening. Nature Materials, 2005, 4, 309-316.	13.3	230
1880	Enhanced current transport at grain boundaries in high-Tc superconductors. Nature, 2005, 435, 475-478.	13.7	177
1881	Doping semiconductor nanocrystals. Nature, 2005, 436, 91-94.	13.7	1,491
1882	Highly controlled acetylene accommodation in a metalâ€“organic microporous material. Nature, 2005, 436, 238-241.	13.7	1,386
1883	Anisotropy of Earth's Dâ€³ layer and stacking faults in the MgSiO3 post-perovskite phase. Nature, 2005, 438, 1142-1144.	13.7	219

#	Article	IF	Citations
1884	Visible Light-Sensitive InTaO4-Based Photocatalysts for Organic Decomposition. Journal of the American Ceramic Society, 2005, 88, 3137-3142.	1.9	22
1885	Density functional theory study of the partial oxidation of methanol on copper surfaces. Journal of Catalysis, 2005, 231, 420-429.	3.1	102
1886	Magnetoresistance and Hall effect measurements of Ni to 6GPa. Journal of Magnetism and Magnetic Materials, 2005, 294, 347-358.	1.0	3
1887	First principles calculations on Ni impurities in Cu clusters. Journal of Magnetism and Magnetic Materials, 2005, 294, 122-126.	1.0	6
1888	A computational search for ductilizing additives to Mo. Scripta Materialia, 2005, 52, 205-210.	2.6	24
1889	Age hardening of PACVD TiBN thin films. Scripta Materialia, 2005, 53, 241-245.	2.6	71
1890	Theory of tunneling magnetoresistance for epitaxial systems. IEEE Transactions on Magnetics, 2005, 41, 2645-2648.	1.2	28
1891	Accuracy and efficiency of atomic basis set methods versus plane wave calculations with ultrasoft pseudopotentials for DNA base molecules. Journal of Computational Chemistry, 2005, 26, 599-605.	1.5	15
1892	A theoretical study on the structures and energetics of hypothetical TiM(NCN)3compounds of the 3dtransition metals. Journal of Computational Chemistry, 2005, 26, 1180-1188.	1.5	0
1893	Testing the Pairwise Additive Potential Approximation Using DFT: Coadsorption of CO and N on Rh(100). ChemPhysChem, 2005, 6, 473-480.	1.0	14
1894	The Influence of Promoters and Poisons on Carbon Monoxide Adsorption on Rh(100): A DFT Study. ChemPhysChem, 2005, 6, 1293-1298.	1.0	15
1895	Phase Stability and Broken-Symmetry Transition of Elemental Lithium up to 140 GPa. ChemPhysChem, 2005, 6, 1703-1706.	1.0	39
1896	Boron Nanotubes. ChemPhysChem, 2005, 6, 2001-2008.	1.0	120
1897	Density functional calculations of the reflectivity of shocked xenon with ionization based gap corrections. Contributions To Plasma Physics, 2005, 45, 300-304.	0.5	40
1898	SrSi6N8-A Reduced Nitridosilicate with a Sïï£¿Si Bond. Angewandte Chemie - International Edition, 2005, 44, 567-570.	7.2	42
1899	Prediction of Novel Phases of Tantalum(V) Nitride and Tungsten(VI) Nitride That Can Be Synthesized under High Pressure and High Temperature. Angewandte Chemie - International Edition, 2005, 44, 4249-4254.	7.2	83
1900	SrAlSiH: A Polyanionic Semiconductor Hydride. Angewandte Chemie - International Edition, 2005, 44, 7269-7273.	7.2	46
1901	Experimental and Theoretical Investigation of the Electronic and Geometrical Structures of the Au32 Cluster. Angewandte Chemie - International Edition, 2005, 44, 7119-7123.	7.2	129

#	Article	IF	Citations
1902	SrSi6N8-A Reduced Nitridosilicate with a Sïï£¿Si Bond. Angewandte Chemie, 2005, 117, 573-576.	1.6	26
1906	Self-Organized Nanostructures in Hard Ceramic Coatings. Advanced Engineering Materials, 2005, 7, 1071-1082.	1.6	58
1907	On local structural changes in lizardite-1T: {Si4+/Al3+}, {Si4+/Fe3+}, [Mg2+/Al3+], [Mg2+/Fe3+] substitutions. Physics and Chemistry of Minerals, 2005, 32, 362-373.	0.3	9
1908	Pressure sensitivity of olivine slip systems: first-principle calculations of generalised stacking faults. Physics and Chemistry of Minerals, 2005, 32, 646-654.	0.3	58
1909	Ab initio study of the high-pressure behavior of CaSiO3 perovskite. Physics and Chemistry of Minerals, 2005, 32, 146-153.	0.3	65
1910	A mapping of the electron localization function for earth materials. Physics and Chemistry of Minerals, 2005, 32, 208-221.	0.3	19
1911	Electron density distribution and bond critical point properties for forsterite, Mg2 SiO4, determined with synchrotron single crystal X-ray diffraction data. Physics and Chemistry of Minerals, 2005, 32, 301-313.	0.3	64
1912	Vegardâ€™s law deviation in band gap and bowing parameter of AlxIn1-xN. Applied Physics A: Materials Science and Processing, 2005, 81, 651-655.	1.1	48
1913	First-principles calculation for bowing parameter of wurtzite AlxGa1-xN. Applied Physics A: Materials Science and Processing, 2005, 81, 1459-1463.	1.1	20
1914	Computer simulations in the study of gold nanowires: the effect of impurities. Applied Physics A: Materials Science and Processing, 2005, 81, 1551-1558.	1.1	15
1915	NO adsorption on the stoichiometric and reduced SnO2(110) surface. Theoretical Chemistry Accounts, 2005, 114, 52-59.	0.5	10
1916	Atomistic behaviors of Co adatom on Al (001) surface: first-principle approach. Journal of Magnetism and Magnetic Materials, 2005, 286, 399-404.	1.0	6
1917	Electronic structure and magnetism of diluted magnetic semiconductorsâ€”a first principles study. Journal of Magnetism and Magnetic Materials, 2005, 290-291, 1408-1411.	1.0	12
1918	Ab initio investigation of potential indium and gallium free chalcopyrite compounds for photovoltaic application. Journal of Physics and Chemistry of Solids, 2005, 66, 2019-2023.	1.9	85
1919	Ab initio assisted process modeling for Si-based nanoelectronic devices. Materials Science and Engineering B: Solid-State Materials for Advanced Technology, 2005, 124-125, 62-71.	1.7	1
1920	The relationship between adsorption and solid acidity of heteropolyacids. Catalysis Today, 2005, 105, 134-143.	2.2	34
1921	Structure of enantiopure and racemic alanine adlayers on Cu(110). Surface Science, 2005, 574, L1-L8.	0.8	99
1922	Anatase and rutile surfaces with adsorbates representative of acidic and basic conditions. Surface Science, 2005, 582, 173-188.	0.8	107

#	Article	IF	Citations
1923	First-principles calculations of step formation energies and step interactions on TiN(001). Surface Science, 2005, 582, 145-150.	0.8	15
1924	Energy scaling and surface patterning of halogen-terminated Si(001) surfaces. Surface Science, 2005, 591, L292-L298.	0.8	8
1925	First-principles study of sulfur overlayers on Pd(111) surface. Surface Science, 2005, 596, 229-241.	0.8	38
1926	Surface atomic structure and energetics of tantalum. Surface Science, 2005, 598, 276-284.	0.8	29
1927	LEED and DFT investigation on the (2Ã—2)-S overlayer on Co(0001). Surface Science, 2005, 599, 113-121.	0.8	22
1928	Adsorption of atomic oxygen on the Cu(100) surface. Surface Science, 2005, 599, 160-172.	0.8	14
1929	Reassessment of Al-Ce and Al-Nd binary systems supported by critical experiments and first-principles energy calculations. Metallurgical and Materials Transactions A: Physical Metallurgy and Materials Science, 2005, 36, 3269-3279.	1.1	95
1930	Linking first-principles energetics to CALPHAD: An application to thermodynamic modeling of the Al-Ca binary system. Metallurgical and Materials Transactions A: Physical Metallurgy and Materials Science, 2005, 36, 5-13.	1.1	41
1931	Diffusion of gold and native defects in mercury cadmium telluride. Journal of Electronic Materials, 2005, 34, 868-872.	1.0	5
1932	Density functional theory study of alloy element interstitials in Al. Journal of Computer-Aided Materials Design, 2005, 10, 155-162.	0.7	8
1933	Electronic structure of Î±-Al2O3 in the bulk and on the surface. Russian Physics Journal, 2005, 48, 1127-1133.	0.2	4
1934	Crystal Structure, Electronic Structure, and Luminescence of Cs2KYF6:Pr3+. Zeitschrift Fur Anorganische Und Allgemeine Chemie, 2005, 631, 3046-3052.	0.6	22
1935	A First Principles Study of Hydrogen Storage in NaAlH4-Related Complex Hydrides. Zeitschrift Fur Anorganische Und Allgemeine Chemie, 2005, 631, 1982-1984.	0.6	6
1936	Density functional theory calculations on microscopic aspects of oxygen diffusion in ceria-based materials. International Journal of Quantum Chemistry, 2005, 101, 826-839.	1.0	40
1937	Adsorption of 1-propanol on the Si(100) surface. International Journal of Quantum Chemistry, 2005, 105, 359-367.	1.0	8
1938	DFT LCAO and plane wave calculations of SrZrO3. Physica Status Solidi (B): Basic Research, 2005, 242, R11-R13.	0.7	29
1939	Structural, electronic and optical properties of a new binary phase - ruthenium disilicide. Physica Status Solidi (B): Basic Research, 2005, 242, 2864-2871.	0.7	9
1940	Li2O at high pressures: structural properties, phase-transition, and phonons. Physica Status Solidi (B): Basic Research, 2005, 242, 1857-1863.	0.7	44

#	Article	IF	Citations
1941	Spin polarization and electronic structure of ferromagnetic Mn5Ge3 epilayers. Physica Status Solidi (B): Basic Research, 2005, 242, R67-R69.	0.7	66
1942	Density Functional Electronic Structure Calculations of Lithium Ion Adsorption on Defective Carbon Nanotubes. E-Journal of Surface Science and Nanotechnology, 2005, 3, 358-361.	0.1	14
1943	Lateral Interactions in O/Pt(111): Density-Functional Theory and Kinetic Monte Carlo. Lecture Notes in Computer Science, 2005, , 1020-1029.	1.0	5
1944	Atomistic Computer Simulation of Diffusion. , 2005, , 113-171.		9
1945	Ab initioinvestigation of the lattice dynamics of fluoride scheelite LiYF4. Journal of Physics Condensed Matter, 2005, 17, 4953-4962.	0.7	10
1946	Ab initiostudy of the structure and dynamical properties of crystalline ice. Phase Transitions, 2005, 78, 179-196.	0.6	6
1947	Ab Initio Molecular Dynamics Simulations on Structural Properties of Liquid In 20 Sn 80. Chinese Physics Letters, 2005, 22, 1987-1990.	1.3	2
1948	Fundamentals of Cu/Barrier-Layer Adhesion in Microelectronic Processing. Materials Research Society Symposia Proceedings, 2005, 863, B9.2-1.	0.1	7
1949	Evaluations of Phases and Vacancy Formation Energies in KNbO3by First-Principles Calculation. Japanese Journal of Applied Physics, 2005, 44, 8048-8054.	0.8	51
1950	Stability of the MgCO3 structures under lower mantle conditions. American Mineralogist, 2005, 90, 1008-1011.	0.9	44
1951	Comment on "Grain Boundary Decohesion by Impurity Segregation in a Nickel-Sulfur System". Science, 2005, 309, 1677c-1677c.	6.0	20
1952	Formation of Vacancies and Divacancies in Plane-Stressed Silicon. Solid State Phenomena, 2005, 108-109, 433-438.	0.3	3
1953	Experimental and theoretical studies of plasma resonance and the electronic structure of binary skutterudites. Materials Research Society Symposia Proceedings, 2005, 886, 1.	0.1	0
1954	Mechanisms of Diffusion and Dissociation of E-Centers in Silicon. Defect and Diffusion Forum, 2005, 237-240, 1129-1134.	0.4	0
1955	Ab Initio Study of Phase Stability for (Mg1-_xAl_x)₂Sn Alloys. Materials Science Forum, 2005, 488-489, 253-256.	0.3	0
1956	Grain Boundary Decohesion by Impurity Segregation in a Nickel-Sulfur System. Science, 2005, 307, 393-397.	6.0	303
1957	Electronic Structure of AgPbmSbTem+2 Compounds â€“ Implications on Thermoelectric Properties. Materials Research Society Symposia Proceedings, 2005, 886, 1.	0.1	1
1958	Stability and Structures of Constitutional Defects in Nonstoichiometric Intermetallic Compounds by First-Principles Calculations. Materials Science Forum, 2005, 475-479, 3111-3114.	0.3	0

#	Article	IF	Citations
1959	First-Principles Investigation of Laves Phases in Mg-Al-Ca System. Materials Science Forum, 2005, 488-489, 169-176.	0.3	13
1960	Solving large-scale eigenvalue problems in SciDAC applications. Journal of Physics: Conference Series, 2005, 16, 425-434.	0.3	10
1961	Identification of Mg Vacancy in MgO by Positron Lifetime Measurements and First-Principles Calculations. Defect and Diffusion Forum, 2005, 242-244, 1-8.	0.4	1
1962	First-principles Studies of Phase Stability and the Neutral Atomic Vacancies in LiNbO3, NaNbO3 and KNbO3. Materials Research Society Symposia Proceedings, 2005, 902, 1.	0.1	2
1963	Barrier to Migration of the Intrinsic Defects in Silicon in Different Charged System Using First-principles Calculations. Materials Research Society Symposia Proceedings, 2005, 864, 9171.	0.1	2
1964	Orientation and Composition Dependences of the Surface Energy and Work Function Observed by First-Principles Calculation for the Moâ€“Hf System. Journal of the Physical Society of Japan, 2005, 74, 1766-1771.	0.7	9
1965	Chemical-pressureâ€“induced modifications on the magnetic and electronic properties of Ba 1 â˜' x Sr x VS 3. Europhysics Letters, 2005, 71, 952-958.	0.7	3
1966	Ab InitioCalculation of Work Functions of ZrO/W(100) and YO/W(100) Surfaces. Japanese Journal of Applied Physics, 2005, 44, 7518-7520.	0.8	3
1967	First-Principles Calculations of Atomistic Behaviors in Ni/Al (001) and Al/Ni (001) System. Japanese Journal of Applied Physics, 2005, 44, 5700-5702.	0.8	14
1968	Materials Design and Molecular-Beam Epitaxy of Half-Metallic Zinc-Blende CrAs and the Heterostructures. , 0, , 293-311.		0
1969	Combined theoretical and experimental study of the site-specificity of vibrational dynamics of CO adsorbed on monovalent metal cations in zeolites. Studies in Surface Science and Catalysis, 2005, , 625-632.	1.5	9
1970	27Al NMR chemical shifts do not correlate with average T-O-T angles: Theoretical study of MCM-58 zeolite. Studies in Surface Science and Catalysis, 2005, 158, 917-924.	1.5	2
1971	First-Principles Study of Structural and Magnetic Properties for Ultrathin Cr Films on W(100) and W(110). Chinese Physics Letters, 2005, 22, 1232-1235.	1.3	5
1972	Ultrathin antiferromagnetic films on a ferromagnetic substrate: a first-principles study of Mn on Fe(001). Journal of Physics Condensed Matter, 2005, 17, 3269-3283.	0.7	10
1973	Nonlinear algorithm for the solution of the Kohnâ€“Sham equations in solids. Journal of Physics Condensed Matter, 2005, 17, 3701-3715.	0.7	6
1974	Classical versus ab initio structural relaxation: electronic excitations and optical properties of Ge nanocrystals embedded in an SiC matrix. Journal of Physics Condensed Matter, 2005, 17, 643-651.	0.7	1
1975	Atomic and electronic structure of carbon strings. Journal of Physics Condensed Matter, 2005, 17, 3823-3836.	0.7	30
1976	Chirality Dependence of Mechanical Properties of Single-Walled Carbon Nanotubes under Axial Tensile Strain. Japanese Journal of Applied Physics, 2005, 44, L1307-L1309.	0.8	30

#	Article	IF	Citations
1977	Structural and magnetic properties of ultrathin bcc Fe films on Ge(001). Journal Physics D: Applied Physics, 2005, 38, 1055-1060.	1.3	1
1978	Layered growth modelling of epitaxial growth processes for SiC polytypes. Journal of Physics Condensed Matter, 2005, 17, 5355-5366.	0.7	7
1979	Origin of transition metal clustering tendencies in GaAs based dilute magnetic semiconductors. Applied Physics Letters, 2005, 86, 172504.	1.5	42
1980	Generalized stacking fault energies, ductilities, and twinnabilities of Ni and selected Ni alloys. Applied Physics Letters, 2005, 87, 121901.	1.5	167
1981	Hydrogenationâˆ•deuteration of the Siâ€“SiO2 interface: Atomic-scale mechanisms and limitations. Applied Physics Letters, 2005, 86, 112107.	1.5	9
1982	Doping a C60 molecule with potassium atoms: A theoretical study. Journal of Applied Physics, 2005, 98, 116103.	1.1	0
1983	First-principles calculation of free Si(100) surface impurity enrichment. Applied Physics Letters, 2005, 87, 232101.	1.5	7
1984	Molecular dissociation of group-V hydrides onSi(001). Physical Review B, 2005, 72, .	1.1	16
1985	Coverage and strain dependent magnetization of titanium-coated carbon nanotubes. Physical Review B, 2005, 71, .	1.1	14
1986	First principles calculations of melting temperatures for free Na clusters. Physical Review B, 2005, 71, .	1.1	55
1987	Ab initiostudy of disorder broadening of core photoemission spectra in randomCuâˆ’PdandAgâˆ’Pdalloys. Physical Review B, 2005, 72, .	1.1	25
1988	Electronic structure and transport properties ofLa0.7Ce0.3MnO3. Physical Review B, 2005, 72, .	1.1	18
1989	Polar phonons and intrinsic dielectric response of the ferromagnetic insulating spinelCdCr2S4from first principles. Physical Review B, 2005, 72, .	1.1	55
1990	Magnetic coupling between Cr atoms doped at bulk and surface sites of ZnO. Applied Physics Letters, 2005, 87, 162509.	1.5	57
1991	Thermal decomposition mechanisms of hafnium and zirconium silicates at the atomic scale. Journal of Applied Physics, 2005, 97, 114911.	1.1	22
1992	Normal mode approach for predicting the mechanical properties of solids from first principles: Application to compressibility and thermal expansion of zeolites. Physical Review B, 2005, 71, .	1.1	21
1993	Shock wave propagation in dissociating low-Z liquids: D2. Journal of Chemical Physics, 2005, 122, 124503.	1.2	11
1994	MgO addimer diffusion on MgO(100): A comparison ofab initioand empirical models. Physical Review B, 2005, 72, .	1.1	64

#	Article	IF	Citations
1995	Encapsulation of atomic-scale Bi wires in epitaxial silicon without loss of structure. Physical Review B, 2005, 72, .	1.1	22
1996	A first-principles study of Group IV dimer chains on Si(100). Physical Review B, 2005, 72, .	1.1	21
1997	Monte Carlo simulation of equilibrium L10 ordering in FePt nanoparticles. Journal of Applied Physics, 2005, 97, 10J311.	1.1	26
1998	Phase separation and charge localization in UHV-lithiated anataseTiO2nanoparticles. Physical Review B, 2005, 71, .	1.1	15
1999	Irregular stacking sequence in the initial growth of ultrathin Rh films on Ru(0001). Physical Review B, 2005, 72, .	1.1	5
2000	Lifting the Pt{100} surface reconstruction through oxygen adsorption: A density functional theory analysis. Journal of Chemical Physics, 2005, 122, 184709.	1.2	35
2001	Ab initiocharacterization of the mechanical and electronic properties ofÎ²-SiAlON (Si6âˆ'zAlzOzN8âˆ'z;z=0â€“5). Physical Review B, 2005, 71, .	1.1	16
2002	Temperature and particle-size dependence of the equilibrium order parameter of FePt alloys. Physical Review B, 2005, 72, .	1.1	97
2003	First-principles investigation of a monolayer ofC60onhâˆ'BNâˆ•Ni(111). Physical Review B, 2005, 72, .	1.1	18
2004	Hydrogen-induced magnetism in carbon nanotubes. Physical Review B, 2005, 72, .	1.1	53
2005	Ab initiotight-binding LMTO method for nonequilibrium electron transport in nanosystems. Physical Review B, 2005, 71, .	1.1	81
2006	Real-space investigation of the metal-insulator transition ofSi(557)âˆ'Au. Physical Review B, 2005, 72, .	1.1	47
2007	Electronic structure and bonding of intergranular glassy films in polycrystallineSi3N4:Ab initiostudies and classical molecular dynamics simulations. Physical Review B, 2005, 71, .	1.1	36
2008	Chemical characterization of a zirconia-supported Pt cluster. Physical Review B, 2005, 71, .	1.1	19
2009	Atomic vibrational density of states of crystallineÎ²âˆ'FeSi2and amorphousFeSi2thin films. Physical Review B, 2005, 71, .	1.1	21
2010	Origin of nonlocal interactions in adsorption of polar molecules on Si(001)-2Ã—1. Journal of Chemical Physics, 2005, 122, 164706.	1.2	26
2011	First-principles determination of exchange interactions in delafossiteYCuO2.5. Physical Review B, 2005, 71, .	1.1	25
2012	Partitioning of solutes in multiphaseTiâ€“Alalloys. Physical Review B, 2005, 71, .	1.1	39

#	Article	IF	Citations
2013	Theoretical study of B diffusion with charged defects in strained Si. Physical Review B, 2005, 72, .	1.1	28
2014	[11Â¯00]âˆ•(1102)twin boundaries in wurtziteZnOand group-III-nitrides. Physical Review B, 2005, 71, .	1.1	26
2015	Isomers of smallPbnclusters(n=2â€“15): Geometric and electronic structures based onab initiomolecular dynamics simulations. Physical Review B, 2005, 72, .	1.1	59
2016	In siturevelation of a zinc-blende InN wetting layer during Stranski-Krastanov growth on GaN(0001) by molecular-beam epitaxy. Physical Review B, 2005, 71, .	1.1	2
2017	Length dependence of the electronic and structural properties of monoatomic gold wires. Physical Review B, 2005, 72, .	1.1	26
2018	Fluorine in Si: Native-defect complexes and the suppression of impurity diffusion. Physical Review B, 2005, 72, .	1.1	53
2019	Density functional calculations of the influence of hydrogen adsorption on the surface relaxation of Ti (0001). Physical Review B, 2005, 71, .	1.1	29
2020	Annealing process in quenched Al-Sn alloys:â€ƒA positron annihilation study. Physical Review B, 2005, 71, .	1.1	21
2021	Gallium stabilization ofÎ´â€™Pu: Density-functional calculations. Physical Review B, 2005, 72, .	1.1	50
2022	Cooperative versus dispersion effects: What is more important in an associated liquid such as water?. Journal of Chemical Physics, 2005, 123, 204116.	1.2	62
2023	Spinel-type gallium oxynitrides attainable at high pressure and high temperature. Physical Review B, 2005, 72, .	1.1	24
2024	First-order Raman spectra ofAB1âˆ•2â€²B1âˆ•2â€³O3double perovskites. Physical Review B, 2005, 71, .	1.1	95
2025	Dissolution dynamics of NaCl nanocrystal in liquid water. Physical Review E, 2005, 72, 012602.	0.8	29
2026	Atom Transfer and Single-Adatom Contacts. Physical Review Letters, 2005, 94, 126102.	2.9	191
2027	Vacancy-assisted arsenic diffusion and time-dependent clustering effects in silicon. Physical Review B, 2005, 71, .	1.1	6
2028	Observation of substitutional and interstitial phosphorus on cleanSi(100)â€“(2Ã—1)with scanning tunneling microscopy. Physical Review B, 2005, 72, .	1.1	11
2029	Atomic and electronic structure of theSi(001)â€“Rbchemisorption system at 0.5 and 1.0 monolayer coverage. Physical Review B, 2005, 71, .	1.1	0
2030	Quasiparticle bands and optical spectra of highly ionic crystals: AlN and NaCl. Physical Review B, 2005, 72, .	1.1	65

#	Article	IF	Citations
2031	Using Ar adsorption to estimate the van der Waals contribution to the wetting of Ru(0001). Physical Review B, 2005, 72, .	1.1	20
2032	Structural, thermal, and electronic properties ofFe2VSi1âˆ'xAlx. Physical Review B, 2005, 71, .	1.1	22
2033	Physical mechanisms of negative-bias temperature instability. Applied Physics Letters, 2005, 86, 142103.	1.5	113
2034	Chemically resolved scanning tunneling microscopy imaging of Al on p-type Al0.1Ga0.9As(001)â€¢(2Ã—8)âˆ•(2Ã—4). Journal of Chemical Physics, 2005, 122, 124702.	1.2	1
2035	On the convergence of isolated neutral oxygen vacancy and divacancy properties in metal oxides using supercell models. Journal of Chemical Physics, 2005, 122, 224705.	1.2	27
2036	First-principles study of the interfacial adhesion betweenSiO2andMoSi2. Physical Review B, 2005, 72, .	1.1	36
2037	Ab initio study of the effect of hydrogen and point defects on arsenic segregation at Si(100)âˆ•SiO2 interfaces. Applied Physics Letters, 2005, 86, 152106.	1.5	10
2038	Ab initiostudy of the adsorption of Fe atoms on a defective MgO(001) surface: Blind adsorption. Physical Review B, 2005, 71, .	1.1	15
2039	Origin of modulated structures inYBa2Cu3O6.63: A first-principles approach. Physical Review B, 2005, 71, .	1.1	15
2040	Surface electronic structure of Cr(001): Experiment and theory. Physical Review B, 2005, 72, .	1.1	31
2041	Structure, stability, and electronic properties of thei-AlPdMn quasicrystalline surface. Physical Review B, 2005, 71, .	1.1	58
2042	Ideal torsional strengths and stiffnesses of carbon nanotubes. Physical Review B, 2005, 72, .	1.1	27
2043	Design of a very thin direct-band-gap semiconductor nanotube of germanium with metal encapsulation. Physical Review B, 2005, 71, .	1.1	18
2044	Decomposition reactions forNaAlH4,Na3AlH6, and NaH: First-principles study. Physical Review B, 2005, 71, .	1.1	97
2045	Effect of alkali-metal adsorption on the conductance of a molecular device. Physical Review B, 2005, 72, .	1.1	7
2046	CO adsorption on a Cu(211) surface: First-principle calculation and STM study. Physical Review B, 2005, 71, .	1.1	27
2047	First-principles modeling of electronic transport in Ï€-stacked molecular junctions. Journal of Applied Physics, 2005, 98, 033712.	1.1	8
2048	First-principles study of the effect of lattice vibrations on Cu nucleation free energy in Fe-Cu alloys. Physical Review B, 2005, 72, .	1.1	32

#	Article	IF	Citations
2049	Hplacement inCr(Mo,Fe)âˆ•Vsupercells: The origin of the dead layers. Physical Review B, 2005, 71, .	1.1	9
2050	Pressure induced complexity in a lithium monolayer:Ab initiocalculations. Physical Review B, 2005, 72, .	1.1	23
2051	B and N ion implantation into carbon nanotubes: Insight from atomistic simulations. Physical Review B, 2005, 71, .	1.1	88
2052	Effect of hydrogen on the surface relaxation of Pd(100), Rh(100), and Ag(100). Physical Review B, 2005, 72, .	1.1	24
2053	Polarons in semiconducting polymers: Study within an extended Holstein model. Physical Review B, 2005, 71, .	1.1	37
2054	Atomic Structure of a Thin Silica Film on a Mo(112) Substrate: A Two-Dimensional Network ofSiO4Tetrahedra. Physical Review Letters, 2005, 95, 076103.	2.9	201
2055	Ab initio study of the structural stability of TiSi2 compounds. Applied Physics Letters, 2005, 87, 041910.	1.5	26
2056	An interaction model for OH+H2O-mixed and pure H2O overlayers adsorbed on Pt(111). Journal of Chemical Physics, 2005, 122, 194705.	1.2	53
2057	Raman modes of the deformed single-wall carbon nanotubes. Physical Review B, 2005, 72, .	1.1	51
2058	First-principles study of symmetry lowering and polarization inBaTiO3âˆ•SrTiO3superlattices with in-plane expansion. Physical Review B, 2005, 71, .	1.1	127
2059	Density functional calculations of Ti-enhancedNaAlH4. Physical Review B, 2005, 71, .	1.1	107
2060	A density-functional study of the structural, electronic, magnetic, and vibrational properties of Ti8C12 metallocarbohedrynes. Journal of Chemical Physics, 2005, 123, 154106.	1.2	23
2061	Ab initio studies of a water layer at transition metal surfaces. Journal of Chemical Physics, 2005, 122, 054701.	1.2	89
2062	Photoinduced Hydrophilic and Electrochemical Properties of Nitrogen-Doped TiO[sub 2] Films. Journal of the Electrochemical Society, 2005, 152, E351.	1.3	72
2063	First-principles study of ferromagnetic coupling in Zn1âˆ’xCrxTe thin film. Journal of Applied Physics, 2005, 97, 043904.	1.1	16
2064	Valence-band structure of InN from x-ray photoemission spectroscopy. Physical Review B, 2005, 72, .	1.1	57
2065	Initial Stages of Ti Growth on Diamond (100) Surfaces: From Single Adatom Diffusion to Quantum Wire Formation. Physical Review Letters, 2005, 94, 086101.	2.9	20
2066	Melting Curve of MgO from First-Principles Simulations. Physical Review Letters, 2005, 94, 235701.	2.9	158

#	Article	IF	Citations
2067	Surface and Interface Studies of GaN Epitaxy on Si(111) viaZrB2Buffer Layers. Physical Review Letters, 2005, 95, 266105.	2.9	53
2068	General Rule for Displacive Phase Transitions in Perovskite Compounds Revisited by First Principles Calculations. Physical Review Letters, 2005, 94, 035502.	2.9	43
2069	Role of Strain-Dependent Surface Energies inGe/Si(100)Island Formation. Physical Review Letters, 2005, 94, 176102.	2.9	77
2070	Comparison between experimental and theoretical determination of the local structure of theGaAs1âˆ’yNydilute nitride alloy. Physical Review B, 2005, 71, .	1.1	11
2071	Effect of external electric field on the surface energetics ofAgâˆ•Si(111). Physical Review B, 2005, 71, .	1.1	15
2072	First-principles study of Siâ€“SiO2 interface and the impact on mobility. Applied Physics Letters, 2005, 86, 082104.	1.5	8
2073	Ferromagnetism of an all-carbon composite composed of a carbon nanowire inside a single-walled carbon nanotube. Applied Physics Letters, 2005, 86, 163105.	1.5	22
2074	AbÂInitioTheory of Dynamical Core-Hole Screening in Graphite from X-Ray Absorption Spectra. Physical Review Letters, 2005, 94, 167401.	2.9	51
2075	Distortion and Segregation in a Dislocation Core Region at Atomic Resolution. Physical Review Letters, 2005, 95, 145501.	2.9	50
2076	Low-Temperature Resistance Anomaly atSrTiO3Grain Boundaries: Evidence for an Interface-Induced Phase Transition. Physical Review Letters, 2005, 95, 197601.	2.9	23
2077	Two-Dimensional Carbon Incorporation into Si(001): C Amount and Structure ofSi(001)âˆ’c(4Ã—4). Physical Review Letters, 2005, 94, 076102.	2.9	28
2078	Unusual Behavior of the Ferroelectric Polarization inPbTiO3/SrTiO3Superlattices. Physical Review Letters, 2005, 95, 177601.	2.9	226
2079	First-principles study of phonon modes inPuCoGa5superconductor. Physical Review B, 2005, 72, .	1.1	39
2080	First-principles calculations of the isosteric Bain path of cobalt. Physical Review B, 2005, 72, .	1.1	4
2081	Structure determination of indium-inducedSi(111)âˆ’Inâˆ’4Ã—1surface by LEED Patterson inversion. Physical Review B, 2005, 72, .	1.1	18
2082	Spin-polarized ballistic transport in a thin superlattice of zinc blende half-metallic compounds. Physical Review B, 2005, 71, .	1.1	16
2083	First-principles study of phase stability in pseudobinary(Ni1âˆ’xPtx)3Alalloys. Physical Review B, 2005, 72, .	1.1	38
2084	First-principles investigation of ferroelectricity in epitaxially strainedPb2TiO4. Physical Review B, 2005, 71, .	1.1	20

#	Article	IF	Citations
2085	Atomic and electronic structure of the(4Ã—1)and(8Ã—2)Inâ•Si(111)surfaces. Physical Review B, 2005, 71, .	1.1	25
2086	Cubic and orthorhombic structures of aluminum hydrideAlH3predicted by a first-principles study. Physical Review B, 2005, 71, .	1.1	67
2087	Pressure-induced structural phase transition inNaBH4. Physical Review B, 2005, 72, .	1.1	38
2088	Structure and dynamics of the diarsenic complex in crystalline silicon. Physical Review B, 2005, 72, .	1.1	9
2089	Metallic atomic wires on patterned dihydrogenated Si(001). Physical Review B, 2005, 71, .	1.1	7
2090	On fitting a gold embedded atom method potential using the force matching method. Journal of Chemical Physics, 2005, 123, 204719.	1.2	227
2091	Top-gated field-effect transistor and rectifying diode operation of core-shell structured GaP nanowire devices. Physical Review B, 2005, 71, .	1.1	39
2092	Structure and phonons ofZnGeN2. Physical Review B, 2005, 72, .	1.1	38
2093	First-principles calculation of intrinsic defect formation volumes in silicon. Physical Review B, 2005, 72, .	1.1	76
2094	Vacancy-mediated hydrogen desorption inNaAlH4. Physical Review B, 2005, 72, .	1.1	81
2095	Interaction of doping impurities with the 30Â° partial dislocations in SiC: Anab initioinvestigation. Physical Review B, 2005, 72, .	1.1	16
2096	Interaction of oxygen with ZrC(001) and VC(001): Photoemission and first-principles studies. Physical Review B, 2005, 72, .	1.1	50
2097	Crystal structures of Ni2MnGa from density functional calculations. Phase Transitions, 2005, 78, 259-266.	0.6	22
2098	First-principles studies on the reactions of O2 with silicon clusters. Journal of Chemical Physics, 2005, 122, 174311.	1.2	20
2099	Electronic structure and vibrational properties ofBa8Si46,Ba8AgnSi46â^'n, andBa8AunSi46â^'n. Physical Review B, 2005, 72, .	1.1	41
2100	Magnetic doping of4dtransition-metal surfaces: A first-principles study. Physical Review B, 2005, 71, .	1.1	19
2101	Interrupted chain-assisted Al atomic wires on Si(211): Density functional calculations. Physical Review B, 2005, 72, .	1.1	1
2102	Ab initiostudy of ferromagnetism inGa1â^'xCrxNthin films. Physical Review B, 2005, 72, .	1.1	21

#	Article	IF	Citations
2103	Electronic structure of identical metal cluster arrays onSi(111)â˜7Ã—7surfaces. Physical Review B, 2005, 72, .	1.1	27
2104	Ab initiocalculation of impurity effects in copper oxide materials. Physical Review B, 2005, 72, .	1.1	25
2105	Neutral self-defects in a silica model: A first-principles study. Physical Review B, 2005, 71, .	1.1	55
2106	Violation of the symmetry rule for the[2+2]addition in the chemisorption ofC2H4on Si(100). Physical Review B, 2005, 72, .	1.1	32
2107	Ab initiostudy of quasiperiodic monolayers on a fivefoldiâ˜AlPdMnsurface. Physical Review B, 2005, 71, .	1.1	40
2108	Hydrogen pairs and local vibrational frequencies in H-irradiatedGaAs1â˜yNy. Physical Review B, 2005, 72, .	1.1	33
2109	Systematic pathway generation and sorting in martensitic transformations: TitaniumÎ±toï‰. Physical Review B, 2005, 72, .	1.1	27
2110	Ab initio molecular dynamics study of glycine intramolecular proton transfer in water. Journal of Chemical Physics, 2005, 122, 184506.	1.2	104
2111	Ab initioinvestigation of the magnetism of tetragonal Mn: Bulk, surface, ultrathin films, and multilayers. Physical Review B, 2005, 72, .	1.1	69
2112	Crossover energetics for halogenated Si(100): Vacancy line defects, dimer vacancy lines, and atom vacancy lines. Physical Review B, 2005, 71, .	1.1	12
2113	Free-energy calculations for the cubic ZrO2 crystal as an example of a system with a soft mode. Journal of Chemical Physics, 2005, 123, 204708.	1.2	30
2114	First-principles study of Sn and Ca doping inCuInO2. Physical Review B, 2005, 72, .	1.1	21
2115	Atomic and electronic structures of N interstitials in GaAs. Physical Review B, 2005, 72, .	1.1	27
2116	Zinc-blende half-metallic ferromagnets are rarely stabilized by coherent epitaxy. Physical Review B, 2005, 71, .	1.1	68
2117	Density-functional studies of tungsten trioxide, tungsten bronzes, and related systems. Physical Review B, 2005, 72, .	1.1	97
2118	Influence of oxygen on optical properties of Si nanocrystallites. Applied Physics Letters, 2005, 87, 143113.	1.5	25
2119	Ab initiostudies on the stability and electronic structure ofLiCoO2(003) surfaces. Physical Review B, 2005, 71, .	1.1	29
2120	Transition from ferromagnetism to antiferromagnetism in Ga1â˜xMnxN. Journal of Applied Physics, 2005, 98, 083905.	1.1	18

#	Article	IF	Citations
2121	Computational study of stacking faults in sapphire using total energy methods. Physical Review B, 2005, 71, .	1.1	25
2122	Structure of GaSb digitally doped with Mn. Physical Review B, 2005, 71, .	1.1	10
2123	Surface energy anisotropy of FePt nanoparticles. Journal of Applied Physics, 2005, 97, 084315.	1.1	23
2124	Differential tunneling spectroscopy simulations:â€ƒImaging surface states. Physical Review B, 2005, 71, .	1.1	32
2125	Ab initiostudy ofMg(AlH4)2. Physical Review B, 2005, 72, .	1.1	49
2126	Surface restructuring under gas pressure from first principles: A mechanism for CO-induced removal of theAu(110)â^'(1Â—2)reconstruction. Physical Review B, 2005, 71, .	1.1	21
2127	First-principles study ofZrO2â^•Siinterfaces: Energetics and band offsets. Physical Review B, 2005, 72, .	1.1	58
2128	Growth of Te on As-exposed Si(211): Electronic structure calculations. Physical Review B, 2005, 71, .	1.1	12
2129	High-pressure structural study of the scheelite tungstatesCaWO4andSrWO4. Physical Review B, 2005, 72, .	1.1	159
2130	Nonmetal ordering inTiC1â^'xNx: Ground-state structure and the effects of finite temperature. Physical Review B, 2005, 72, .	1.1	17
2131	Adsorption-induced constraint on delocalization of electron states in an Au chain on NiAl(110). Physical Review B, 2005, 72, .	1.1	4
2132	First-principles study of ultrathin magnetic Mn films on W surfaces. II. Surface diffusion. Physical Review B, 2005, 72, .	1.1	5
2133	Reduction of amplitude and wavelength of Friedel oscillation on Na(111) surface. Physical Review B, 2005, 72, .	1.1	6
2134	Radial-breathing-like phonon modes of double-walled carbon nanotubes. Physical Review B, 2005, 72, .	1.1	8
2135	First-principles studies of GaN(0001) heteroepitaxy onZrB2(0001). Physical Review B, 2005, 72, .	1.1	34
2136	Ab initio molecular dynamics and quasichemical study of H+(aq). Proceedings of the National Academy of Sciences of the United States of America, 2005, 102, 6704-6708.	3.3	94
2137	Effects of fluorination on electronic and excited states of fused zinc oligoporphyrins. Journal of Chemical Physics, 2005, 122, 184702.	1.2	15
2138	Electromechanical responses of single-walled carbon nanotubes: Interplay between the strain-induced energy-gap opening and the pinning of the Fermi level. Journal of Applied Physics, 2005, 98, 044311.	1.1	11

#	Article	IF	Citations
2139	Applications of quantum chemical methods in zeolite science. Studies in Surface Science and Catalysis, 2005, , 243-262.	1.5	7
2140	Structure of the thinnest most stable semiconducting and insulating nanotubes ofSiOx(x=1,2). Physical Review B, 2005, 72, .	1.1	17
2141	Role of Elastic Scattering in Electron Dynamics at Ordered Alkali Overlayers on Cu(111). Physical Review Letters, 2005, 95, 176802.	2.9	71
2142	Experimental and Theoretical Investigation of Single Cu, Ag, and Au Atoms Adsorbed onSi(111)â˜'(7Ã—7). Physical Review Letters, 2005, 94, 176104.	2.9	76
2143	Density-functional band-structure calculations of magnesium alanateMg(AlH4)2. Physical Review B, 2005, 72, .	1.1	27
2144	Charging mechanism for the bond elongation observed in suspended chains of gold atoms. Physical Review B, 2005, 72, .	1.1	17
2145	Fast diffusion mechanism of silicon tri-interstitial defects. Physical Review B, 2005, 72, .	1.1	11
2146	Quantum confinement in Si- and Ge-capped nanocrystallites. Physical Review B, 2005, 72, .	1.1	49
2147	Crystallographic investigation of temperature-induced phase transition of the tetrathiafulvalene-p-bromanil, TTF-BA charge transfer complex. Physical Review B, 2005, 72, .	1.1	37
2148	First-principles study of the atomic and electronic structure of theSi(111)â˜'(5Ã—2)â˜'Ausurface reconstruction. Physical Review B, 2005, 71, .	1.1	43
2149	AbÂInitioIdentification of the Nitrogen Diffusion Mechanism in Silicon. Physical Review Letters, 2005, 95, 025901.	2.9	28
2150	Excitation of Frustrated Translation and Nonadiabatic Adatom Hopping Induced by Inelastic Tunneling. Physical Review Letters, 2005, 95, 226102.	2.9	36
2151	Effect of the Mn clustering in (GaMn)N on the magnetic transition temperature. Physical Review B, 2005, 71, .	1.1	24
2152	Vacancy-Impurity Complexes in Highly Sb-Doped Si Grown by Molecular Beam Epitaxy. Physical Review Letters, 2005, 94, 165501.	2.9	36
2153	Schottky defect formation energy in MgO calculated by diffusion Monte Carlo. Physical Review B, 2005, 71, .	1.1	69
2154	Oxygen-vacancy mediated adsorption and reactions of molecular oxygen on theZnO(101Â¯0)surface. Physical Review B, 2005, 72, .	1.1	78
2155	First-principles study of ultrathin magnetic Mn films on W surfaces.. Physical Review B, 2005, 72, .	1.1	19
2156	Vanishing Magnetic Interactions in Ferromagnetic Thin Films. Physical Review Letters, 2005, 94, 217202.	2.9	12

#	Article	IF	Citations
2157	The effect of octahedral tilting on proton binding sites and transition states in pseudo-cubic perovskite oxides. Journal of Chemical Physics, 2005, 123, 094703.	1.2	89
2158	Charging of Metal Atoms on UltrathinMgO/Mo(100)Films. Physical Review Letters, 2005, 94, 226104.	2.9	338
2159	How adiabatic is activated adsorption/associative desorption?. Journal of Chemical Physics, 2005, 123, 074704.	1.2	117
2160	Scanning tunneling microscopy and spectroscopy of NaCl overlayers on the stepped Cu(311) surface:â€ƒExperimental and theoretical study. Physical Review B, 2005, 71, .	1.1	50
2161	First-principles study of strain stabilization of Ge(105) facet on Si(001). Physical Review B, 2005, 72, .	1.1	94
2162	Ab initiostudy of ground-state properties of the Laves-phase compoundZrMn2. Physical Review B, 2005, 72, .	1.1	40
2163	Water adsorption at metal surfaces: A first-principles study of thep(3Ã—3)R30Â°H2Obilayer on Ru(0001). Physical Review B, 2005, 71, .	1.1	60
2164	Adsorption of TripletO2on Si(100): The Crucial Step in the Initial Oxidation of a Silicon Surface. Physical Review Letters, 2005, 94, 016101.	2.9	55
2165	Diffusion of Ag adatom on the H-terminated and clean Si(111) surfaces: A first-principles study. Physical Review B, 2005, 71, .	1.1	14
2166	Random conductivity of Î´-Bi2O3 films. Applied Physics Letters, 2005, 86, 241910.	1.5	30
2167	FERROMAGNETISM IN Co-DOPED TiO2 ANATASE DUE TO THE COBALT CLUSTERING. International Journal of Modern Physics B, 2005, 19, 2520-2525.	1.0	0
2168	STUDY OF THE ELECTRONIC STRUCTURE AND PHYSICAL PROPERTIES OF THE IRIDIUM BASED INTERMETALLIC COMPOUNDS UNDER PRESSURE. International Journal of Modern Physics B, 2005, 19, 4587-4604.	1.0	12
2169	AB INITIO STUDY OF INDIUM QUANTUM WIRE FORMATION ON FLAT AND STEPPED Si(100) SURFACES. Surface Review and Letters, 2005, 12, 483-487.	0.5	3
2170	Surface Bonding and Dynamical Behavior of the CH3SH Molecule on Au(111). Journal of Physical Chemistry B, 2005, 109, 22463-22468.	1.2	82
2171	High-pressure characteristics of Î±-Fe2O3using DFT+U. Phase Transitions, 2005, 78, 251-258.	0.6	24
2172	Effects of vibrational entropy on the Alâ€“Si phase diagram. Journal of Physics Condensed Matter, 2005, 17, 2197-2210.	0.7	37
2173	Conformational dependence of a protein kinase phosphate transfer reaction. Proceedings of the National Academy of Sciences of the United States of America, 2005, 102, 15347-15351.	3.3	24
2174	Ab initio quantum chemistry: Methodology and applications. Proceedings of the National Academy of Sciences of the United States of America, 2005, 102, 6648-6653.	3.3	279

#	Article	IF	Citations
2175	Effect of clustering on ferromagnetism in (Ga,Mn)As. , 2005, , .		0
2176	Study on the Filling Fraction Limit of Impurities in CoSb3. Materials Research Society Symposia Proceedings, 2005, 886, 1.	0.1	0
2177	Oxygen-induced p-type doping of a long individual single-walled carbon nanotube. Nanotechnology, 2005, 16, 1048-1052.	1.3	122
2178	In Search of Metallic Nanowires on Si(001). Materials Research Society Symposia Proceedings, 2005, 872, 1.	0.1	0
2179	Interface States in SiO₂/4H-SiC(0001) Interfaces from First-Principles: Effects of Si-Si Bonds and of Nitrogen Atom Termination. Materials Science Forum, 2005, 483-485, 573-576.	0.3	4
2180	Vegard's law deviation in band gaps and bowing parameters of the wurtzite III-nitride ternary alloys. , 2005, 5628, 296.		14
2181	Pt 3 Cr (111) Alloy Effect on the Reversible Potential of OOH(ads) Formation from O2(ads) relative to Pt(111). Journal of Fuel Cell Science and Technology, 2005, 2, 86-93.	0.8	24
2182	Tetragonal Phase Transformation in Gold Nanowires. Journal of Engineering Materials and Technology, Transactions of the ASME, 2005, 127, 417-422.	0.8	44
2183	Lattice vibrations in cubic, tetragonal, and monoclinic phases of ZrO2. Journal of Chemical Physics, 2005, 122, 064707.	1.2	57
2184	Small Pd Clusters, up to the Tetramer At Least, Are Highly Mobile on the MgO(100) Surface. Physical Review Letters, 2005, 95, 146103.	2.9	87
2185	First Principles Based Design and Experimental Evidence for a ZnO-Based Ferromagnet at Room Temperature. Physical Review Letters, 2005, 94, 187204.	2.9	439
2186	Systematic treatment of displacements, strains, and electric fields in density-functional perturbation theory. Physical Review B, 2005, 72, .	1.1	675
2187	The Effect of Film Thickness on the C40 TiSi[sub 2] to C54 TiSi[sub 2] Transition Temperature. Journal of the Electrochemical Society, 2005, 152, G754.	1.3	4
2188	Atomistic Modeling of Cation Transport in the Passive Film on Iron and Implications for Models of Growth Kinetics. Journal of the Electrochemical Society, 2005, 152, B271.	1.3	27
2189	Stability of Fe-Based Alloys With Structure Type C6Cr23. Journal of Materials Research, 2005, 20, 237-242.	1.2	31
2190	Nitrogen incorporation into GaInNAs lattice-matched to GaAs: The effects of growth temperature and thermal annealing. Journal of Applied Physics, 2005, 98, 083524.	1.1	34
2191	Role of titanium in hydrogen desorption in crystalline sodium alanate. Applied Physics Letters, 2005, 86, 251913.	1.5	69
2192	Bond-length alternation and charge transfer in a linear carbon chain encapsulated within a single-walled carbon nanotube. Physical Review B, 2005, 72, .	1.1	83

#	Article	IF	Citations
2193	Ab initiolattice dynamics and phase transformations ofZrO2. Physical Review B, 2005, 71, .	1.1	109
2194	Atomistic simulation of Ag thin films on MgO(100) substrate: A template substrate for heterogeneous adsorption. Physical Review B, 2005, 72, .	1.1	27
2195	Fe-dopedCuInSe2: Anab initiostudy of magnetic defects in a photovoltaic material. Physical Review B, 2005, 71, .	1.1	28
2196	Stability of carbon nanotubes under electron irradiation: Role of tube diameter and chirality. Physical Review B, 2005, 72, .	1.1	146
2197	Influence of the Anion on Lone Pair Formation in Sn(II) Monochalcogenides:â€‰ A DFT Study. Journal of Physical Chemistry B, 2005, 109, 18868-18875.	1.2	182
2198	Ab initio calculation of Ni50â^'xFexTi50. Journal of Physics and Chemistry of Solids, 2005, 66, 1748-1754.	1.9	2
2199	The origin of the stereochemically active Pb(II) lone pair: DFT calculations on PbO and PbS. Journal of Solid State Chemistry, 2005, 178, 1422-1428.	1.4	243
2200	Surface energy, stress and structure of well-relaxed amorphous silicon: A combination approach of ab initio and classical molecular dynamics. Surface Science, 2005, 585, 17-24.	0.8	60
2201	Adsorption and diffusion of Pt and Au on the stoichiometric and reducedTiO2rutile (110) surfaces. Physical Review B, 2005, 72, .	1.1	92
2202	High-resolution valence-band XPS spectra of the nonconductors quartz and olivine. Physical Review B, 2005, 72, .	1.1	71
2203	Ab initioinvestigation of the nitrofluoride SiNF. Physical Review B, 2005, 72, .	1.1	7
2204	Quantum Theory of Reactive Scattering and Adsorption at Surfaces. , 2005, , 1713-1733.		3
2205	Band structures and optical spectra of InN polymorphs: Influence of quasiparticle and excitonic effects. Physical Review B, 2005, 72, .	1.1	108
2206	Chemical and icosahedral short-range orders in liquid and undercooled Al80Mn20 and Al80Ni20 alloys: A first-principles-based approach. Journal of Chemical Physics, 2005, 123, 104508.	1.2	29
2207	Theoretical Investigation of CO Interaction with Copper Sites in Zeolites:Â Periodic DFT and Hybrid Quantum Mechanical/Interatomic Potential Function Study. Journal of Physical Chemistry B, 2005, 109, 9631-9638.	1.2	77
2208	Vacancy formation in Î´-plutonium: A density-functional study in the generalized gradient approximation. Europhysics Letters, 2005, 71, 412-417.	0.7	21
2209	Photoinduced cation interstitial diffusion in IIâ€“VI semiconductors. Physical Review B, 2005, 72, .	1.1	14
2210	The Role of Ti as a Catalyst for the Dissociation of Hydrogen on a Mg(0001) Surface. Journal of Physical Chemistry B, 2005, 109, 18037-18041.	1.2	113

#	Article	IF	Citations
2211	Ab initiomolecular dynamics simulation of self-interstitial diffusion in silicon. Physical Review B, 2005, 72, .	1.1	21
2212	Electronic and magnetic structure of transition-metal-dopedÎ±-hematite. Physical Review B, 2005, 71, .	1.1	89
2213	Adsorption structures of benzene on a Si(5512)-2Ã—1 surface: A combined scanning tunneling microscopy and theoretical study. Journal of Chemical Physics, 2005, 123, 244702.	1.2	14
2214	Calculation of ferromagnetic states in metastable bcc and hcp Ni by projector-augmented wave method. Journal of Applied Physics, 2005, 97, 106107.	1.1	27
2215	Atomic-scale mechanisms of selective adsorption and dimerization of pentacene on Si surfaces. Applied Physics Letters, 2005, 87, 233109.	1.5	23
2216	Impact of interface structure on Schottky-barrier height for Niâ•ZrO2(001) interfaces. Applied Physics Letters, 2005, 86, 132103.	1.5	43
2217	Pinning mass-selected Agn clusters on the TiO2(110)â˜1Ã—1 surface via deposition at high kinetic energy. Journal of Chemical Physics, 2005, 123, 204701.	1.2	28
2218	The high-pressure phase of alumina and implications for Earth's D'' layer. Proceedings of the National Academy of Sciences of the United States of America, 2005, 102, 10828-10831.	3.3	110
2219	Model study of coherent quantum dynamics of hole states in functionalized semiconductor nanostructures. Journal of Chemical Physics, 2005, 122, 154709.	1.2	43
2220	Structure and energetics of water adsorbed on theZnO(101Â¯0)surface. Physical Review B, 2005, 72, .	1.1	64
2221	The role of nitrogen-related defects in high-k dielectric oxides: Density-functional studies. Journal of Applied Physics, 2005, 97, 053704.	1.1	138
2222	Structure, stability, and diffusion of arsenic-silicon interstitial pairs. Applied Physics Letters, 2005, 87, 231905.	1.5	26
2223	Comprehensive Global Energy Minimum Modeling of the Sarinâ˜Serine Adduct. Journal of Physical Chemistry B, 2005, 109, 1006-1014.	1.2	18
2224	The interaction of CO2 with sodium-promoted W(011). Physical Chemistry Chemical Physics, 2005, 7, 3866.	1.3	17
2225	Filling Fraction Limit for Intrinsic Voids in Crystals: Doping in Skutterudites. Physical Review Letters, 2005, 95, 185503.	2.9	177
2226	Storage of Molecular Hydrogen in Bâ˜N Cage:â€‰ Energetics and Thermal Stability. Nano Letters, 2005, 5, 1273-1277.	4.5	106
2227	Ferromagnetism in Mn-Doped GaN Nanowires. Physical Review Letters, 2005, 95, 167202.	2.9	96
2228	First-principles investigation of transition-metal-doped group-IV semiconductors:RxY1â˜x(R=Cr,Mn,Fe;Y=Si,Ge). Physical Review B, 2005, 71, .	1.1	58

#	Article	IF	Citations
2229	The Chemistry of Deformation: How Solutes Soften Pure Metals. Science, 2005, 310, 1665-1667.	6.0	206
2230	Influence of dipole interactions on the lattice dynamics of crystalline ice. Phase Transitions, 2005, 78, 799-810.	0.6	1
2231	Investigation of the humidity effect on the electrical properties of single-walled carbon nanotube transistors. Applied Physics Letters, 2005, 87, 093101.	1.5	120
2232	Reaction mechanisms for size-dependent H loss in Mg+(H2O)n: solvation controlled electron transfer. Physical Chemistry Chemical Physics, 2005, 7, 1005.	1.3	31
2233	First-Principles Study on the Elastic Properties of Platinum Nitride. Chinese Physics Letters, 2005, 22, 2637-2638.	1.3	26
2234	Vibrational behavior of theMn+1AXnphases from first-order Raman scattering(M=Ti,V,Cr,A=Si,X=C,N). Physical Review B, 2005, 71, .	1.1	139
2235	Atomic and electronic structures of neutral and cationSnn(n=2â€“20)clusters: A comparative theoretical study with different exchange-correlation functionals. Physical Review B, 2005, 71, .	1.1	40
2236	First-principles calculation of cluster geometries and magnetization of pure Ni and Feâ€“Ni clusters. Phase Transitions, 2005, 78, 723-731.	0.6	8
2237	Gold Atoms and Dimers on Amorphous SiO2:Â Calculation of Optical Properties and Cavity Ringdown Spectroscopy Measurements. Journal of Physical Chemistry B, 2005, 109, 19876-19884.	1.2	47
2238	Simulations of Tetra-Tethered Organic/Inorganic Nanocubeâ^'Polymer Assemblies. Macromolecules, 2005, 38, 6168-6180.	2.2	69
2239	Theoretical Study of CO and NO Chemisorption on RhCu(111) Surfaces. Journal of Physical Chemistry B, 2005, 109, 4654-4661.	1.2	21
2240	Pristine Semiconducting [110] Silicon Nanowires. Nano Letters, 2005, 5, 2302-2305.	4.5	40
2241	Polymorphism of Crystalline Î±-Quaterthiophene and Î±-Sexithiophene:Â Ab Initio Analysis and Comparison with Inelastic Neutron Scattering Response. Journal of Physical Chemistry A, 2005, 109, 4202-4207.	1.1	36
2242	Structural and electronic properties of the (100) surface and bulk of alkaline-earth metal oxides. Physical Review B, 2005, 72, .	1.1	65
2243	Bundling up Carbon Nanotubes through Wigner Defects. Nano Letters, 2005, 5, 1045-1049.	4.5	32
2244	Charge-Doped and Heteroatom-Substituted Polysilane, Poly(vinylenedisilanylene), and Poly(butadienylenedisilanylene):Â Electronic Structures and Band Gaps. Journal of Physical Chemistry B, 2005, 109, 13499-13509.	1.2	20
2245	Ab Initio and Microcalorimetric Investigations of Alkene Adsorption on Phosphotungstic Acid. Langmuir, 2005, 21, 4738-4745.	1.6	25
2246	Molecular adsorption of NO on NiO(100): DFT andDFT+Ucalculations. Physical Review B, 2005, 71, .	1.1	61

#	Article	IF	Citations
2247	Neutron Vibrational Spectroscopy Gives New Insights into the Structure of Poly(p-phenylene) Tj ETQq0 0 0 rgBT /Overlock 10 Tf 50 742	6.6	21
2248	Electronic Structures and Charge Transport Properties of the Organic Semiconductor Bis[1,2,5]thiadiazolo-p-quinobis(1,3-dithiole), BTQBT, and Its Derivatives. Journal of Physical Chemistry B, 2005, 109, 12891-12898.	1.2	23
2249	Mismatched Heteroepitaxy of Tetrahedral Semiconductors with Si via ZrB2Templates. Chemistry of Materials, 2005, 17, 4647-4652.	3.2	15
2250	First Principles Study on the Solvation and Structure of C2O42-(H2O)n,n= 6â^'12. Journal of Physical Chemistry A, 2005, 109, 9104-9111.	1.1	12
2251	Effects of Alloying on the Chemistry of CO and H2S on Fe Surfaces. Journal of Physical Chemistry B, 2005, 109, 20469-20478.	1.2	24
2252	Reduction of the (001) Surface of Î³-V2O5Compared to Î±-V2O5. Journal of Physical Chemistry B, 2005, 109, 374-380.	1.2	19
2253	First-principles investigation of the structural, magnetic, and electronic properties of olivineLiFePO4. Physical Review B, 2005, 71, .	1.1	57
2254	Low-temperature polymorphs ofZrO2andHfO2: A density-functional theory study. Physical Review B, 2005, 72, .	1.1	194
2255	Dimensional Effects on the LOâ^'TO Splitting in CF4:Â First-Principles and Infrared Absorption Studies. Journal of the American Chemical Society, 2005, 127, 3198-3206.	6.6	12
2256	Vibrational properties of protons in hydratedBaInxZr1â^'xO3â^'xâ•2. Physical Review B, 2005, 72, .	1.1	71
2257	First-Principles Modeling of Dopants in C29 and C29H24 Nanodiamonds. Journal of Physical Chemistry B, 2005, 109, 11991-11995.	1.2	11
2258	Adsorption and dissociation of hydrogen molecules on bare and functionalized carbon nanotubes. Physical Review B, 2005, 72, .	1.1	255
2259	A Density Functional Theory Study of Molecular and Dissociative Adsorption of H2on Active Sites in Mordenite. Journal of Physical Chemistry B, 2005, 109, 22491-22501.	1.2	45
2260	Reactions of Hydrazoic Acid on TiO2 Nanoparticles:â€‰ an Experimental and Computational Study. Journal of Physical Chemistry B, 2005, 109, 5133-5142.	1.2	14
2261	Effect of Sulfur Coverage on Fe(110) Adhesion:Â A DFT Study. Journal of Physical Chemistry B, 2005, 109, 10204-10212.	1.2	7
2262	Conductance Investigations of Stretched Molecules. IEEE Nanotechnology Magazine, 2005, 4, 403-405.	1.1	5
2263	Vanadium Oxides on Aluminum Oxide Supports. 2. Structure, Vibrational Properties, and Reducibility of V2O5 Clusters on Î±-Al2O3(0001). Journal of Physical Chemistry B, 2005, 109, 23532-23542.	1.2	27
2264	Periodic DFT Calculations of the Stability of Al/Si Substitutions and Extraframework Zn2+Cations in Mordenite and Reaction Pathway for the Dissociation of H2and CH4. Journal of Physical Chemistry B, 2005, 109, 20361-20369.	1.2	56

#	Article	IF	Citations
2265	Double Dative Bond Configuration:Â Pyrimidine on Ge(100). Journal of Physical Chemistry B, 2005, 109, 348-351.	1.2	40
2266	Coverage-Dependent Adsorption of Atomic Sulfur on Fe(110):Â A DFT Study. Journal of Physical Chemistry B, 2005, 109, 9604-9612.	1.2	25
2267	Vanadium Oxides on Aluminum Oxide Supports. 1. Surface Termination and Reducibility of Vanadia Films on Î±-Al2O3(0001). Journal of Physical Chemistry B, 2005, 109, 23523-23531.	1.2	42
2268	Screening by Kinetic Monte Carlo Simulation of Ptâ"Au(100) Surfaces for the Steady-State Decomposition of Nitric Oxide in Excess Dioxygenâ€. Journal of Physical Chemistry B, 2005, 109, 2234-2244.	1.2	49
2269	First-Principles Calculations of the Adsorption of Nitromethane and 1,1-Diamino-2,2-dinitroethylene (FOX-7) Molecules on the Î±-Al2O3(0001) Surface. Journal of Physical Chemistry B, 2005, 109, 1451-1463.	1.2	48
2270	Modeling the Morphology and Phase Stability of TiO2 Nanocrystals in Water. Journal of Chemical Theory and Computation, 2005, 1, 107-116.	2.3	191
2271	Coexistence of ionic and metallic bonding in noble-metal oxides. Physical Review B, 2005, 72, .	1.1	64
2272	Dopant Sources Choice for Formation of p-Type ZnO:â€‰ Phosphorus Compound Sources. Chemistry of Materials, 2005, 17, 852-855.	3.2	39
2273	Equilibrium Morphology of Face-Centered Cubic Gold Nanoparticles >3 nm and the Shape Changes Induced by Temperature. Journal of Physical Chemistry B, 2005, 109, 24465-24472.	1.2	138
2274	Location, Acid Strength, and Mobility of the Acidic Protons in Keggin 12-H3PW12O40:â€‰ A Combined Solid-State NMR Spectroscopy and DFT Quantum Chemical Calculation Study. Journal of the American Chemical Society, 2005, 127, 18274-18280.	6.6	130
2275	Reactions of Trimethylindium on TiO2Nanoparticles:Â Experimental and Computational Study. Journal of Physical Chemistry B, 2005, 109, 20858-20867.	1.2	15
2276	A Periodic Density Functional Theory Study of Cumene Formation Catalyzed by H-Mordeniteâ€. Journal of Physical Chemistry B, 2005, 109, 2203-2211.	1.2	39
2277	Ab initiostudy ofAgâˆ•Al2O3andAuâˆ•Al2O3interfaces. Physical Review B, 2005, 72, .	1.1	73
2278	Potential Shift for OH(ads) Formation on the Pt Skin on Pt[sub 3]Co(111) Electrodes in Acid. Journal of the Electrochemical Society, 2005, 152, E193.	1.3	58
2279	First-principles study of the optical transitions ofFcenters in the bulk and on the (0001) surface ofÎ±â"Al2O3. Physical Review B, 2005, 72, .	1.1	29
2280	Far- and Mid-Infrared of Crystalline 2,2â€˜-Bithiophene:â€‰ Ab Initio Analysis and Comparison with Infrared Response. Journal of Physical Chemistry A, 2005, 109, 1684-1691.	1.1	33
2281	Oxidative Activation ofn-Butane on Sulfated Zirconia. Journal of the American Chemical Society, 2005, 127, 16159-16166.	6.6	86
2282	Reduced influence of defects on oxidized Si nanocrystallites. Physical Review B, 2005, 71, .	1.1	28

#	Article	IF	Citations
2283	Anionogenic Ferromagnets. Journal of the American Chemical Society, 2005, 127, 16325-16328.	6.6	62
2284	Effect of Steps on the Decomposition of CH3O at PdZn Alloy Surfaces. Journal of Physical Chemistry B, 2005, 109, 4568-4574.	1.2	48
2285	Oxygen vacancies and ferromagnetism in CoxTi1â^'xO2â^'xâ^'y. Journal of Applied Physics, 2005, 97, 073908.	1.1	116
2286	Unpaired Spin Populations and Spin-Pairing Tendencies of the Nonequivalent Vanadium Sites of the Magnetic Metal NaV6O11Investigated by Electronic Band Structure Calculations and Spin Dimer Analysis. Chemistry of Materials, 2005, 17, 4344-4349.	3.2	4
2287	Ab initiomolecular dynamics studies of the structure and dynamics of moltenSexTe1â^'xalloys. Physical Review B, 2005, 72, .	1.1	7
2288	Multiple scattering in a vacuum barrier obtained from real-space wavefunctions. Journal of Physics Condensed Matter, 2005, 17, 2705-2713.	0.7	92
2289	Phenanthrenequinone Adsorbed on Si(001):Â Geometries, Electronic Properties, and Optical Response. Journal of Physical Chemistry B, 2005, 109, 7928-7933.	1.2	24
2290	First-Principles Study of CO Adsorption and Vibration on Au Surfaces. Journal of Physical Chemistry B, 2005, 109, 9596-9603.	1.2	28
2291	Theoretical study of the structure and optical properties of carbon-doped rutile and anatase titanium oxides. Journal of Chemical Physics, 2005, 123, 084704.	1.2	140
2292	A systematic density functional theory study of the electronic structure of bulk and (001) surface of transition-metals carbides. Journal of Chemical Physics, 2005, 122, 174709.	1.2	180
2293	Structural and Electronic Factors Controlling the Refractive Indices of the Chalcogenides ZnQ and CdQ (Q = O, S, Se, Te). Inorganic Chemistry, 2005, 44, 3594-3598.	1.9	7
2294	Calculated pressure dependence of the localized vibrational mode of nitrogen inGaNxAs1â^'x. Physical Review B, 2005, 72, .	1.1	20
2295	Structures of Glycine, Enantiopure Alanine, and Racemic Alanine Adlayers on Cu(110) and Cu(100) Surfaces. Journal of Physical Chemistry B, 2005, 109, 16764-16773.	1.2	101
2296	N2O Decomposition on TiO2 (110) from Dynamic First-Principles Calculations. Journal of Physical Chemistry B, 2005, 109, 16223-16226.	1.2	38
2297	Density Functional Study of Lithiumâ^'Aromatic Sandwich Compounds and Their Crystals. Journal of Physical Chemistry A, 2005, 109, 478-483.	1.1	25
2298	Comparison of the Electron Localization Function and Deformation Electron Density Maps for Selected Earth Materials. Journal of Physical Chemistry A, 2005, 109, 10022-10027.	1.1	20
2299	Removing Critical Errors for DFT Applications to Transition-Metal Nanoclusters:â€‰ Correct Ground-State Structures of Ru Clusters. Journal of Physical Chemistry B, 2005, 109, 23113-23117.	1.2	43
2300	Ferromagnetic GaNâ^'Cr Nanowires. Nano Letters, 2005, 5, 1587-1590.	4.5	49

#	Article	IF	Citations
2301	Anhydrous and Water-Assisted Proton Mobility in Phosphotungstic Acid. Journal of the American Chemical Society, 2005, 127, 5238-5245.	6.6	99
2302	Magnetic Couplings in Vanadium Aromatic Sandwich Complexes and Their Crystals by Using DFT Methods. Journal of Physical Chemistry A, 2005, 109, 9292-9298.	1.1	20
2303	Crystal Structure and Vibrational Spectra of AlVO4. A DFT Study. Journal of Physical Chemistry B, 2005, 109, 394-400.	1.2	39
2304	A Combined Experimental and Theoretical Evaluation of the Structure of Hydrated Microporous Aluminophosphate AlPO4-18. Journal of Physical Chemistry B, 2005, 109, 22939-22946.	1.2	22
2305	Atomistic Modeling of Crystal-to-Amorphous Transition and Associated Kinetics in the Niâ^'Nb System by Molecular Dynamics Simulations. Journal of Physical Chemistry B, 2005, 109, 4717-4725.	1.2	12
2306	Simulations of the optical properties of warm dense aluminum. Physical Review E, 2005, 71, 016409.	0.8	145
2307	Modeling alkali alanates for hydrogen storage by density-functional band-structure calculations. Journal of Materials Research, 2005, 20, 3199-3213.	1.2	41
2308	Ab initiocalculations on the effects of additives on alumina phase stability. Physical Review B, 2005, 71, .	1.1	25
2309	Atomic chains of group-IV elements and III-V and II-VI binary compounds studied by a first-principles pseudopotential method. Physical Review B, 2005, 72, .	1.1	70
2310	Geometrical and electronic structures of the (5, 3) single-walled gold nanotube from first-principles calculations. Physical Review B, 2005, 71, .	1.1	21
2311	Silica glass structure generation forab initiocalculations using small samples of amorphous silica. Physical Review B, 2005, 71, .	1.1	134
2312	Ferroelectric transition inYMnO3from first principles. Physical Review B, 2005, 72, .	1.1	351
2313	Strength, elasticity, and equation of state of the nanocrystalline cubic silicon nitrideÎ³â^'Si3N4to68GPa. Physical Review B, 2005, 72, .	1.1	43
2314	Structure and bonding properties of(Bi2Se3)m(Bi2)nstacks by first-principles density functional theory. Physical Review B, 2005, 72, .	1.1	103
2315	Studies of Iridium Nanoparticles Using Density Functional Theory Calculations. Journal of Physical Chemistry B, 2005, 109, 20817-20823.	1.2	87
2316	Real-space grid implementation of the projector augmented wave method. Physical Review B, 2005, 71, .	1.1	1,606
2317	Water adsorption on hydroxylated silica surfaces studied using the density functional theory. Physical Review B, 2005, 71, .	1.1	105
2318	Modeling the â€˜free carbonâ€™ phase in amorphous silicon oxycarbide. Journal of Non-Crystalline Solids, 2005, 351, 1121-1126.	1.5	35

#	Article	IF	Citations
2319	A DFT study of amorphous silicon oxynitride. Journal of Non-Crystalline Solids, 2005, 351, 1127-1132.	1.5	20
2320	Structural information on ball milled magnesium hydride from vibrational spectroscopy and ab-initio calculations. Journal of Alloys and Compounds, 2005, 393, 1-4.	2.8	65
2321	Crystal structures and electronic structures of alkali aluminohexahydrides from density functional calculations. Journal of Alloys and Compounds, 2005, 404-406, 757-761.	2.8	16
2322	Hydrogen diffusion in magnesium metal (phase) studied by ab initio computer simulations. Journal of Alloys and Compounds, 2005, 404-406, 235-237.	2.8	41
2323	Some thermodynamic aspects of metal hydrogen systems. Journal of Alloys and Compounds, 2005, 404-406, 16-23.	2.8	26
2324	Atom relaxations around hydrogen defects in lanthanum hydride. Journal of Alloys and Compounds, 2005, 404-406, 55-59.	2.8	16
2325	First principle study of neutral and charged self-defects in amorphous SiO2. Journal of Non-Crystalline Solids, 2005, 351, 1825-1829.	1.5	36
2326	O interstitial energetics in Ti from ab initio calculations. Computational Materials Science, 2005, 32, 13-19.	1.4	3
2327	First principles study of the stability of SiNF. Computational Materials Science, 2005, 34, 22-34.	1.4	4
2328	A fast configuration space method for solving local Kohnâ€“Sham equations. Computational Materials Science, 2005, 34, 188-212.	1.4	31
2329	Density functional theory investigation of molecular oxygen interacting with Si(100)-(2Ã—1). Computational Materials Science, 2005, 33, 26-30.	1.4	13
2330	Predictive process design: a theoretical model of atomic layer deposition. Computational Materials Science, 2005, 33, 20-25.	1.4	29
2331	A DFT study of the perovskite and hexagonal phases of BaTiO3. Computational Materials Science, 2005, 34, 157-165.	1.4	41
2332	The effect of temperature on the seismic anisotropy of the perovskite and post-perovskite polymorphs of MgSiO3. Earth and Planetary Science Letters, 2005, 230, 1-10.	1.8	137
2333	In situ observations of phase transition between perovskite and CaIrO-type phase in MgSiO and pyrolitic mantle composition. Earth and Planetary Science Letters, 2005, 236, 914-932.	1.8	138
2334	The axial ratio of hcp iron at the conditions of the Earthâ€™s inner core. Physics of the Earth and Planetary Interiors, 2005, 152, 67-77.	0.7	63
2335	First-principles study of spontaneous polarization in multiferroicBiFeO3. Physical Review B, 2005, 71, .	1.1	1,225
2336	Influence of strain and oxygen vacancies on the magnetoelectric properties of multiferroic bismuth ferrite. Physical Review B, 2005, 71, .	1.1	339

#	Article	IF	Citations
2337	Bonding of Pd, Ag, and Au atoms on MgO(100) surfaces andMgOâˆ•Mo(100)ultra-thin films: A comparative DFT study. Physical Review B, 2005, 72, .	1.1	82
2338	Simulation of Screw Dislocation Motion in Iron by Molecular Dynamics Simulations. Physical Review Letters, 2005, 95, 215506.	2.9	203
2339	Influence of crystal chemistry on ideal plastic shear anisotropy in forsterite: First principle calculations. American Mineralogist, 2005, 90, 1072-1077.	0.9	36
2340	Transition metal-doped TiO2and ZnOâ€"present status of the field. Journal of Physics Condensed Matter, 2005, 17, R657-R689.	0.7	492
2341	Validation of intermolecular transfer integral and bandwidth calculations for organic molecular materials. Journal of Chemical Physics, 2005, 122, 234707.	1.2	76
2342	Nonadiabatic Molecular Dynamics Study of Electron Transfer from Alizarin to the Hydrated Ti4+ Ion. Journal of Physical Chemistry B, 2005, 109, 17998-18002.	1.2	48
2343	Designing meaningful density functional theory calculations in materials scienceâ€"a primer. Modelling and Simulation in Materials Science and Engineering, 2005, 13, R1-R31.	0.8	342
2344	Weak ferromagnetism and magnetoelectric coupling in bismuth ferrite. Physical Review B, 2005, 71, .	1.1	1,235
2345	First principles methods using CASTEP. Zeitschrift Fur Kristallographie - Crystalline Materials, 2005, 220, .	0.4	9,458
2346	Diffusion of phosphorus inÎ±â^'Fe: Anab initiostudy. Physical Review B, 2005, 71, .	1.1	81
2347	Structural and electronic properties of epitaxial core-shell nanowire heterostructures. Physical Review B, 2005, 71, .	1.1	88
2348	First-principles study of LiMPO4compounds (M=Mn, Fe, Co, Ni) as electrode material for lithium batteries. Philosophical Magazine, 2005, 85, 1747-1754.	0.7	23
2349	A density functional theory study of adsorbate-induced work function change and binding energy: Olefins on Ag(111). Molecular Physics, 2005, 103, 883-890.	0.8	39
2350	Monte Carlo simulations applied toAlxGayIn1â^'xâ^'yXquaternary alloys(X=As,P,N): A comparative study. Physical Review B, 2005, 71, .	1.1	4
2351	Quantum studies of H atom trapping on a graphite surface. Journal of Chemical Physics, 2005, 122, 014709.	1.2	56
2352	Atomistic Computer Simulation of Diffusion. , 2005, , 113-171.		1
2353	Ab initiomolecular-dynamics simulations of liquid GaSb and InSb. Physical Review B, 2005, 71, .	1.1	21
2354	Chiral discrimination of 2,2â€²-dihydro-1,1â€²-binaphthyl byÎ²-cyclodextrin: a first-principles study. Phase Transitions, 2005, 78, 677-687.	0.6	1

#	Article	IF	Citations
2355	Models and modeling schemes for binary IV-VI glasses. Physical Review B, 2005, 71, .	1.1	53
2356	Lattice dynamics ofNaAlH4from high-temperature single-crystal Raman scattering andab initiocalculations:â€ƒEvidence of highly stableAlH4â^’anions. Physical Review B, 2005, 71, .	1.1	71
2357	Predicting ionic conductivity of solid oxide fuel cell electrolyte from first principles. Journal of Applied Physics, 2005, 98, 103513.	1.1	162
2358	Oxygen vacancies in ZnO. Applied Physics Letters, 2005, 87, 122102.	1.5	1,015
2359	n-type doping ofCuInSe2andCuGaSe2. Physical Review B, 2005, 72, .	1.1	429
2360	Electronic structure calculations of metal-nanotube contacts with or without oxygen adsorption. Physical Review B, 2005, 72, .	1.1	39
2361	The Perdewâ€“Burkeâ€“Ernzerhof exchange-correlation functional applied to the G2-1 test set using a plane-wave basis set. Journal of Chemical Physics, 2005, 122, 234102.	1.2	754
2362	High temperature elastic anisotropy of the perovskite and post-perovskite polymorphs of Al2O3. Geophysical Research Letters, 2005, 32, .	1.5	37
2363	Effect of Al on the sharpness of the MgSiO3perovskite to post-perovskite phase transition. Geophysical Research Letters, 2005, 32, n/a-n/a.	1.5	71
2364	Formation of spinel-type gallium oxynitrides: a density-functional study of binary and ternary phases in the system Gaâ€“Oâ€“N. Journal of Materials Chemistry, 2005, 15, 3296.	6.7	56
2365	Surfactant-favored disorder in (001)-oriented CuPt-orderedAIII(BV,CV)alloy thin films: Action of Sb and Bi. Physical Review B, 2005, 72, .	1.1	2
2366	Phase Stability, Phase Transformations, and Elastic Properties of Cu6Sn5: Ab initio Calculations and Experimental Results. Journal of Materials Research, 2005, 20, 3102-3117.	1.2	129
2367	First-Principles Analysis of the Effects of Alloying Pd with Ag for the Catalytic Hydrogenation of Acetyleneâ^’Ethylene Mixtures. Journal of Physical Chemistry B, 2005, 109, 12449-12466.	1.2	172
2368	Molecular electronic excitations calculated from a solid-state approach: Methodology and numerics. Physical Review B, 2005, 72, .	1.1	64
2369	Spinel-Structured Gallium Oxynitride (Ga3O3N) Synthesis and Characterization:â€‰ An Experimental and Theoretical Study. Chemistry of Materials, 2005, 17, 5465-5472.	3.2	73
2370	Trajectory Surface Hopping in the Time-Dependent Kohn-Sham Approach for Electron-Nuclear Dynamics. Physical Review Letters, 2005, 95, 163001.	2.9	611
2371	Effect of pressure on the structural properties and Raman modes ofLiCoO2. Physical Review B, 2005, 72, .	1.1	48
2372	Geometrical, electronic, and magnetic properties ofNa0.5CoO2from first principles. Physical Review B, 2005, 71, .	1.1	18

#	Article	IF	Citations
2373	Structure and magnetic properties of theFe3O4(001)surface:â€ƒAb initiostudies. Physical Review B, 2005, 71, .	1.1	47
2374	Quasiclassical study of Eleyâ€“Rideal and hot atom reactions of H atoms with Cl adsorbed on a Au(111) surface. Journal of Chemical Physics, 2005, 122, 074705.	1.2	24
2375	Theoretical Prediction of New High-Performance Lead-Free Piezoelectrics. Chemistry of Materials, 2005, 17, 1376-1380.	3.2	333
2376	Electronic and magnetic properties of substitutional Mn clusters in (Ga,Mn)As. Physical Review B, 2005, 72, .	1.1	57
2377	From Nanodiamond to Nanowires. , 2005, , 25-38.		5
2378	Theoretical Study of Main-Group Metalâ^'Borazine Sandwich Complexes. Journal of Physical Chemistry A, 2005, 109, 1458-1467.	1.1	21
2379	Scanning Tunneling Spectroscopy of Cl Vacancies in NaCl Films: Strong Electron-Phonon Coupling in Double-Barrier Tunneling Junctions. Physical Review Letters, 2005, 95, 225503.	2.9	147
2380	Magnetic Interactions Influence the Properties of Helium Defects in Iron. Physical Review Letters, 2005, 94, 046403.	2.9	163
2381	Charging of Au Atoms on TiO2Thin Films from CO Vibrational Spectroscopy and DFT Calculations. Journal of Physical Chemistry B, 2005, 109, 18418-18426.	1.2	126
2382	Adsorption of Atomic Oxygen and Nitrogen at Î²-Cristobalite (100):Â A Density Functional Theory Study. Journal of Physical Chemistry B, 2005, 109, 14954-14964.	1.2	49
2383	Structural, electronic, and dielectric properties of amorphousZrO2fromab initiomolecular dynamics. Physical Review B, 2005, 71, .	1.1	135
2384	Theoretical study of the adsorption ofH2on (3,3) carbon nanotubes. Physical Review B, 2005, 72, .	1.1	40
2385	Pressure-induced phase transition in ZnO andZnOâ^'MgOpseudobinary system: A first-principles lattice dynamics study. Physical Review B, 2005, 72, .	1.1	98
2386	DFT Studies of Pt/Au Bimetallic Clusters and Their Interactions with the CO Molecule. Journal of Physical Chemistry B, 2005, 109, 22341-22350.	1.2	128
2387	First-Principles Mobility Calculations and Atomic-Scale Interface Roughness in Nanoscale Structures. Physical Review Letters, 2005, 95, 106802.	2.9	61
2388	Thermodynamics of structural vacancies in titanium monoxide from first-principles calculations. Physical Review B, 2005, 71, .	1.1	44
2389	Role of vacancies in the structural stability ofÎ±â^'TiO: A first-principles study based on density-functional calculations. Physical Review B, 2005, 72, .	1.1	50
2390	Anomalous vibrational effects in nonmagnetic and magnetic Heusler alloys. Physical Review B, 2005, 72, .	1.1	132

#	Article	IF	Citations
2391	Theoretical Study of Binding of Metal-Doped Graphene Sheet and Carbon Nanotubes with Dioxin. Journal of the American Chemical Society, 2005, 127, 9839-9843.	6.6	91
2392	Nonlinear elasticity in III-N compounds:Ab initiocalculations. Physical Review B, 2005, 72, .	1.1	130
2393	Magnetoresistance and Hall-effect measurements of Ni thin films. Journal of Applied Physics, 2005, 97, 083902.	1.1	3
2394	Size-dependent charge-separation reaction for hydrated sulfate dianion cluster, SO42â^'(H2O)n, with n=3â€“7. Journal of Chemical Physics, 2005, 123, 224302.	1.2	28
2395	Quantum stability and reentrant bilayer-by-bilayer growth of atomically smooth Pb films on semiconductor substrates. Physical Review B, 2005, 72, .	1.1	68
2396	Ab initiostudy of the surface properties and ideal strength of (100) silicon thin films. Physical Review B, 2005, 72, .	1.1	59
2397	Impact of oxygen on the work functions of Mo in vacuum and on ZrO2. Journal of Applied Physics, 2005, 97, 064911.	1.1	32
2398	Local Electronic Structure of Layered LixNi0.5Mn0.5O2 and LixNi1/3Mn1/3Co1/3O2. Journal of Physical Chemistry B, 2005, 109, 23473-23479.	1.2	26
2399	Iron-oxygen vacancy defect centers inPbTiO3: Newman superposition model analysis and density functional calculations. Physical Review B, 2005, 71, .	1.1	146
2400	First-principles studies of Au(100)-hex reconstruction in an electrochemical environment. Physical Review B, 2005, 72, .	1.1	28
2401	Substitutional and interstitial oxygen in wurtzite GaN. Journal of Applied Physics, 2005, 98, 103531.	1.1	71
2402	Ab initio prediction of a multiferroic with large polarization and magnetization. Applied Physics Letters, 2005, 86, 012505.	1.5	207
2403	Structural stability of silica at high pressures and temperatures. Physical Review B, 2005, 71, .	1.1	146
2404	Energetics of lithium ion adsorption on defective carbon nanotubes. Physical Review B, 2005, 71, .	1.1	116
2405	Kinetic Pathway for the Formation of Fe Nanowires on Stepped Cu(111) Surfaces. Physical Review Letters, 2005, 94, 155503.	2.9	46
2406	Negative-U property of oxygen vacancy in cubic HfO2. Applied Physics Letters, 2005, 87, 062105.	1.5	48
2407	Electronic properties of bulkÎ³â^'Al2O3. Physical Review B, 2005, 72, .	1.1	103
2408	Carbon atom adsorption on and diffusion into Fe(110) and Fe(100) from first principles. Physical Review B, 2005, 71, .	1.1	136

#	Article	IF	Citations
2409	Influence of Thermal Fluctuations on Interfacial Electron Transfer in Functionalized TiO2 Semiconductors. Journal of the American Chemical Society, 2005, 127, 18234-18242.	6.6	196
2410	Ab Initio Surface Phase Diagram of the {101Ì„4} Calcite Surface. Journal of Physical Chemistry B, 2005, 109, 18211-18213.	1.2	34
2411	Modeling Proton Transfer in Zeolites:Â Convergence Behavior of Embedded and Constrained Cluster Calculations. Journal of Chemical Theory and Computation, 2005, 1, 1232-1239.	2.3	58
2412	Low-temperature orientation dependence of step stiffness on {111} surfaces. Physical Review B, 2005, 71, .	1.1	29
2413	Analysis of the Refractive Indices of TiO2, TiOF2, and TiF4:â€‰ Concept of Optical Channel as a Guide To Understand and Design Optical Materials. Inorganic Chemistry, 2005, 44, 3589-3593.	1.9	38
2414	Half-metallic properties of atomic chains of carbonâ€“transition-metal compounds. Physical Review B, 2005, 72, .	1.1	35
2415	Characterization of cathodic arc deposited titanium aluminium nitride films prepared using plasma immersion ion implantation. Journal of Physics Condensed Matter, 2005, 17, 2791-2800.	0.7	6
2416	Structural and magnetic isomers of small Pd and Rh clusters: anab initiodensity functional study. Journal of Physics Condensed Matter, 2005, 17, 5927-5963.	0.7	108
2417	Cubic magic clusters of rhodium stabilized with eight-center bonding: Magnetism and growth. Physical Review B, 2005, 72, .	1.1	71
2418	Ab initiostudy of ground-state properties of the Laves phase compoundsTiCr2,ZrCr2, andHfCr2. Physical Review B, 2005, 71, .	1.1	64
2419	Chemical, magnetic and charge ordering in the system hematiteâ€“ilmenite, Fe2O3â€“FeTiO3. Phase Transitions, 2005, 78, 239-249.	0.6	8
2420	Ab-Initio Simulations of the Optical Properties of Warm Dense Gold. Physical Review Letters, 2005, 95, 085002.	2.9	64
2421	Quantitative Analysis of WC Grain Shape in Sintered WC-Co Cemented Carbides. Physical Review Letters, 2005, 94, 066105.	2.9	48
2422	Dopant-induced stabilization of rhombohedralLiMnO2against Jahn-Teller distortion. Physical Review B, 2005, 71, .	1.1	40
2423	Cleavage and Recovery of Molecular Water in Silica. Journal of Physical Chemistry B, 2005, 109, 10936-10945.	1.2	18
2424	Theoretical Study of Complexes of Extended Cyclopentadienyl Ligands with Zinc and Cadmium. Journal of Physical Chemistry A, 2005, 109, 4342-4351.	1.1	44
2425	Energy Ranking of Molecular Crystals Using Density Functional Theory Calculations and an Empirical van der Waals Correction. Journal of Physical Chemistry B, 2005, 109, 15531-15541.	1.2	266
2426	Electronic structure and properties of isoreticular metal-organic frameworks: The case of M-IRMOF1 (M=Zn, Cd, Be, Mg, and Ca). Journal of Chemical Physics, 2005, 123, 124713.	1.2	147

#	Article	IF	Citations
2427	Carbon string structures: First-principles calculations of quantum conductance. Physical Review B, 2005, 71, .	1.1	17
2428	Nitrogen in graphite and carbon nanotubes: Magnetism and mobility. Physical Review B, 2005, 72, .	1.1	117
2429	Silicon and III-V compound nanotubes: Structural and electronic properties. Physical Review B, 2005, 72, .	1.1	250
2430	First-Principles Studies of SnS2Nanotubes: A Potential Semiconductor Nanowire. Journal of Physical Chemistry B, 2005, 109, 30-32.	1.2	59
2431	Registry-dependent interlayer potential for graphitic systems. Physical Review B, 2005, 71, .	1.1	413
2432	Angle-resolved photoemission spectroscopy of the metallic sodium tungsten bronzesNaxWO3. Physical Review B, 2005, 72, .	1.1	20
2433	Dielectric functions and electronic band structure of lead zirconate titanate thin films. Journal of Applied Physics, 2005, 98, 094108.	1.1	62
2434	DXcenters in GaAs and GaSb. Physical Review B, 2005, 72, .	1.1	25
2435	First-principles study on the tensile strength and fracture of the Al-terminated stoichiometric Î±-Al2O3(0001)/Cu(111) interface. Philosophical Magazine, 2005, 85, 2961-2976.	0.7	41
2436	Common origin for enhanced low-dose-rate sensitivity and bias temperature instability under negative bias. IEEE Transactions on Nuclear Science, 2005, 52, 2265-2271.	1.2	65
2437	Diffusion, Coalescence, and Reconstruction of Vacancy Defects in Graphene Layers. Physical Review Letters, 2005, 95, 205501.	2.9	472
2438	Density Functional Study of H-Induced Defects as Nucleation Sites in Hybrid Carbon Nanomaterials. Chemistry of Materials, 2005, 17, 527-535.	3.2	31
2439	Simulating nano-carbon materials. Molecular Simulation, 2005, 31, 495-504.	0.9	5
2440	Electronic structure calculations of potassium-intercalated single-walled carbon nanotubes. Physical Review B, 2005, 72, .	1.1	11
2441	AbInitioNonadiabatic Molecular Dynamics of the Ultrafast Electron Injection across the Alizarinâ^'TiO2Interface. Journal of the American Chemical Society, 2005, 127, 7941-7951.	6.6	261
2442	Nonequivalence of the generalized gradient approximations PBE and PW91. Physical Review B, 2006, 73, .	1.1	129
2443	Two-Dimensional Ir Cluster Lattice on a Graphene MoirÃ© on Ir(111). Physical Review Letters, 2006, 97, 215501.	2.9	533
2444	Universal Behavior of Nearly Free Electron States in Carbon Nanotubes. Physical Review Letters, 2006, 96, 196803.	2.9	63

#	Article	IF	Citations
2445	Spintronic properties of carbon-based one-dimensional molecular structures. Physical Review B, 2006, 74, .	1.1	21
2446	Structure, Metastability, and Electron Density of Al Lattices in Light of the Model of Anions in Metallic Matrices. Journal of Physical Chemistry B, 2006, 110, 18609-18618.	1.2	11
2447	Interface Energetics and Level Alignment at Covalent Metal-Molecule Junctions: Ï€-Conjugated Thiols on Gold. Physical Review Letters, 2006, 96, 196806.	2.9	258
2448	Segregation and ordering in binary transition metal clusters. Phase Transitions, 2006, 79, 693-700.	0.6	18
2449	Ab initiothermodynamic properties of point defects and O-vacancy diffusion in Mg spinels. Physical Review B, 2006, 74, .	1.1	16
2450	Electronic Structure of Intercalation Compounds of CoxNbS2. Chemistry of Materials, 2006, 18, 4996-5001.	3.2	16
2451	Atomic Structure and Bonding of Water Overlayer on Cu(110):Â The Borderline for Intact and Dissociative Adsorption. Journal of the American Chemical Society, 2006, 128, 9282-9283.	6.6	90
2452	First-principles calculations of impurity diffusion activation energies in Al. Physical Review B, 2006, 73, .	1.1	37
2453	Ionic Polarizability of Conductive Metal Oxides and Critical Thickness for Ferroelectricity inBaTiO3. Physical Review Letters, 2006, 96, 107603.	2.9	215
2454	Structure and properties of liquid InSb alloy below and above the melting point:ab initiomolecular dynamics simulations. Journal of Physics Condensed Matter, 2006, 18, 4471-4480.	0.7	6
2455	Selective Nontemplated Adsorption of Organic Molecules on Nanofacets and the Role of Bonding Patterns. Physical Review Letters, 2006, 97, 156105.	2.9	65
2456	First-principles study of the adhesive and mechanical properties of the O-terminatedÎ±-Al2O3(0001)/Cu(111) interfaces. Philosophical Magazine, 2006, 86, 5123-5135.	0.7	23
2457	First principles reaction modeling of the electrochemical interface: Consideration and calculation of a tunable surface potential from atomic and electronic structure. Physical Review B, 2006, 73, .	1.1	394
2458	CO Adsorption on CoMo and NiMo Sulfide Catalysts:â€‰ A Combined IR and DFT Study. Journal of Physical Chemistry B, 2006, 110, 1261-1270.	1.2	135
2459	Methanethiolate Adsorption Site on Au(111):Â A Combined STM/DFT Study at the Single-Molecule Level. Journal of Physical Chemistry B, 2006, 110, 21161-21167.	1.2	75
2460	Realistic Modeling of Nanostructures Using Density Functional Theory. MRS Bulletin, 2006, 31, 681-687.	1.7	24
2461	First-principles study of the atomic and electronic structures of Pb on Si(001). Journal of Applied Physics, 2006, 100, 083703.	1.1	4
2462	Genuine converging solution of self-consistent field equations for extended many-electron systems. Journal of Physics: Conference Series, 2006, 35, 163-174.	0.3	3

#	Article	IF	Citations
2463	Reduction of NO2on Ceria Surfaces. Journal of Physical Chemistry B, 2006, 110, 2256-2262.	1.2	117
2464	Energetic and magnetic properties of transition-metal nanowire encapsulated BxCyNz composite nanotubes. Applied Physics Letters, 2006, 88, 193117.	1.5	17
2465	Grain-Boundary Physics in PolycrystallineCuInSe2Revisited: Experiment and Theory. Physical Review Letters, 2006, 96, 205501.	2.9	106
2466	Relation between the magnetic properties and the crystal and electronic structures of manganese spinels LiNi0.5Mn1.5O4 and LiCu0.5Mn1.5O4â˜Î´ (0<Î´<0.125). Journal of Applied Physics, 2006, 100, 093908.	1.1	26
2467	Theoretical prediction and experimental realization of transition metal doped rutiles as diluted magnetic semiconductors. Rare Metals, 2006, 25, 420-426.	3.6	2
2468	A model study for the breaking of cyanogen out of CNx within DFT. Diamond and Related Materials, 2006, 15, 1609-1613.	1.8	9
2469	Ab initiostudy of ultrathinMgOfilms onFe(001): Influence of interfacial structures. Physical Review B, 2006, 73, .	1.1	57
2470	Hardness of nanocrystalline diamonds. Physical Review B, 2006, 73, .	1.1	51
2471	Theoretical assessment of the elastic constants and hydrogen storage capacity of some metal-organic framework materials. Journal of Chemical Physics, 2006, 125, 084714.	1.2	94
2472	Schottky barrier formation at a carbon nanotubeâ€"metal junction. Applied Physics Letters, 2006, 89, 243107.	1.5	41
2473	Electronic band structure, electron-phonon interaction, and superconductivity of (5,5), (10,10), and (5,0) carbon nanotubes. Physical Review B, 2006, 73, .	1.1	24
2474	Atoms in Dense Plasmas. , 2006, , 1303-1318.		2
2475	Adsorption trends for water, hydroxyl, oxygen, and hydrogen on transition-metal and platinum-skin surfaces. Physical Review B, 2006, 74, .	1.1	106
2476	Density-functional calculation of methane adsorption on graphite (0001). Physical Review B, 2006, 73, .	1.1	39
2477	Prediction of ground-state structures and order-disorder phase transitions in II-III spinel oxides: A combined cluster-expansion method and first-principles study. Physical Review B, 2006, 73, .	1.1	91
2478	Structural and electronic properties ofAun(n=2â€"10)clusters and their interactions with single S atoms:Ab initiomolecular dynamics simulations. Physical Review B, 2006, 73, .	1.1	73
2479	Ab initiostudy of the migration of small polarons in olivineLixFePO4and their association with lithium ions and vacancies. Physical Review B, 2006, 73, .	1.1	317
2480	Adsorption of oxygen molecules on individual single-wall carbon nanotubes. Journal of Applied Physics, 2006, 99, 034306.	1.1	48

#	Article	IF	Citations
2481	Ab Initio and Molecular Dynamics Studies of Crystalline TNAD (trans-1,4,5,8-Tetranitro-1,4,5,8-tetraazadecalin). Journal of Physical Chemistry B, 2006, 110, 10651-10661.	1.2	52
2482	Structural properties of hexagonal boron nitride. Modelling and Simulation in Materials Science and Engineering, 2006, 14, 515-535.	0.8	75
2483	Encapsulation of Floating Carbon Nanotubes inSiO2. Physical Review Letters, 2006, 97, 266805.	2.9	30
2484	Circuit elements at optical frequencies from first principles: A synthesis of electronic structure and circuit theories. Journal of Applied Physics, 2006, 100, 034305.	1.1	2
2485	Synthesis and Characterization of the Nitrides of Platinum and Iridium. Science, 2006, 311, 1275-1278.	6.0	486
2486	Extended Finnisâ€“Sinclair potential for bcc and fcc metals and alloys. Journal of Physics Condensed Matter, 2006, 18, 4527-4542.	0.7	119
2487	The atomic and electronic structure of dislocations in Ga-based nitride semiconductors. Philosophical Magazine, 2006, 86, 2241-2269.	0.7	22
2488	Pressure-Induced Internal Redox Reaction of Cs2[PdI4]Â·I2, Cs2[PdBr4]Â·I2, and Cs2[PdCl4]Â·I2. Inorganic Chemistry, 2006, 45, 9818-9825.	1.9	18
2489	Ferromagnetism in Cu-doped ZnO from first-principles theory. Physical Review B, 2006, 74, .	1.1	166
2490	Transition between Icosahedral and Cuboctahedral Nanoclusters of Lead. Journal of Physical Chemistry B, 2006, 110, 24642-24645.	1.2	10
2491	Statistical model applied toAxByC1âˆ’xâˆ’yDquaternary alloys: Bond lengths and energy gaps ofAlxGayIn1âˆ’xâˆ’yX(X=As, P, or N) systems. Physical Review B, 2006, 73, .	1.1	16
2492	Correlation between Electronic Properties and Hydrodesulfurization Activity of 4d-Transition-Metal Sulfides. Journal of Physical Chemistry B, 2006, 110, 7951-7966.	1.2	25
2493	Effect of pressure on the first-order Raman intensity in semiconductors. Physical Review B, 2006, 73, .	1.1	22
2494	Probing the Electronic Properties of Self-Organized Poly(3-dodecylthiophene) Monolayers by Two-Dimensional Scanning Tunneling Spectroscopy Imaging at the Single Chain Scale. Nano Letters, 2006, 6, 1711-1718.	4.5	55
2495	Forecast of Piezoelectric Properties of Crystalline Materials from First Principles Calculation. Journal of Physics: Conference Series, 2006, 29, 61-64.	0.3	6
2496	Density functional investigation of the adsorption of a methane monolayer on an MgO(100) surface. Physical Review B, 2006, 73, .	1.1	16
2497	Variational density-functional perturbation theory for dielectrics and lattice dynamics. Physical Review B, 2006, 73, .	1.1	735
2498	Density-functional electronic structure calculations for native defects and Cu impurities in CdS. Physical Review B, 2006, 74, .	1.1	58

#	Article	IF	Citations
2499	Magnetic and Electric Phase Control in EpitaxialEuTiO3from First Principles. Physical Review Letters, 2006, 97, 267602.	2.9	337
2500	Structure, dynamics, and electronic properties of lithium disilicate melt and glass. Journal of Chemical Physics, 2006, 125, 114702.	1.2	73
2501	Vacancy defects and the formation of local haeckelite structures in graphene from tight-binding molecular dynamics. Physical Review B, 2006, 74, .	1.1	81
2502	WhyN2Molecules with Thermal Energy Abundantly Dissociate on W(100) and Not on W(110). Physical Review Letters, 2006, 97, 056102.	2.9	75
2503	Systematic Method to New Phases of Polymeric Nitrogen under High Pressure. Physical Review Letters, 2006, 97, 155503.	2.9	59
2504	Hydrogen adsorption and dissociation on small platinum clusters: An electronic structure density functional study. Physical Review B, 2006, 74, .	1.1	26
2505	First principles phase diagram calculations for the wurtzite-structure systems AlNâ€“GaN, GaNâ€“InN, and AlNâ€“InN. Journal of Applied Physics, 2006, 100, 113528.	1.1	54
2506	Youngâ€™s moduli of ZnO nanoplates: Ab initio determinations. Applied Physics Letters, 2006, 89, 183111.	1.5	86
2507	Direct evidence of impurity decoration of Ga vacancies inGaNfrom positron annihilation spectroscopy. Physical Review B, 2006, 73, .	1.1	94
2508	Structural studies of phosphorus induced dimers on Si(001). Physical Review B, 2006, 73, .	1.1	11
2509	Molecular studies of the structural properties of hydrogen gas in bulk water. Molecular Simulation, 2006, 32, 269-278.	0.9	23
2510	Structure, spectroscopic and electronic properties of a well defined silica supported olefin metathesis catalyst, [(î€,SiO)Re(î€,CR)(î€CHR)(CH2R)], through DFT periodic calculations: silica is just a large siloxy ligand. New Journal of Chemistry, 2006, 30, 842-850.	1.4	77
2511	Extension of molecular electronic structure methods to the solid state: computation of the cohesive energy of lithium hydride. Physical Chemistry Chemical Physics, 2006, 8, 5178.	1.3	70
2512	A structural analysis of lead hydroxyvanadinite. Physical Chemistry Chemical Physics, 2006, 8, 1845.	1.3	16
2513	Prediction of thermodynamic stability and electronic structure of novel ternary lanthanide hydrides. Journal of Materials Chemistry, 2006, 16, 1154.	6.7	10
2514	The influence of carbon on the adsorption of CO on a Rh(100) single crystal. Physical Chemistry Chemical Physics, 2006, 8, 624-632.	1.3	23
2515	Theoretical properties of the N vacancy in p-type GaN(Mg,H) at elevated temperatures. Journal of Applied Physics, 2006, 99, 113506.	1.1	15
2516	First-principles study of lattice instabilities in ferromagnetic L12 Fe3Ni: direct force constants method versus linear response. Phase Transitions, 2006, 79, 853-861.	0.6	4

#	Article	IF	Citations
2517	First-principles structural stability in the strontiumâ€“titaniumâ€“oxygen system. Philosophical Magazine, 2006, 86, 2283-2292.	0.7	24
2518	Ab initio based tight-binding molecular dynamics simulation of the sticking and scattering of O2â^•Pt(111). Journal of Chemical Physics, 2006, 124, 174713.	1.2	29
2519	Experimental and theoretical study of annealed Ni-Pt alloys. Physical Review B, 2006, 74, .	1.1	16
2520	First principles investigation of electronic structure, magnetic properties and spin polarized conductance of self assembled molecular monolayers (SAMs) on Ni. , 2006, , .		0
2521	Thermal donor formation processes in silicon and the catalytic role of hydrogen. Applied Physics Letters, 2006, 88, 051916.	1.5	35
2522	Canonical cell model of cadmium-based icosahedral alloys. Philosophical Magazine, 2006, 86, 519-527.	0.7	23
2523	Magnetism of close packed Fe147 clusters. Phase Transitions, 2006, 79, 701-707.	0.6	4
2524	Pulse electrodeposition of 2.4 T Co/sub 37/Fe/sub 63/ alloys at nanoscale for magnetic recording application. IEEE Transactions on Magnetics, 2006, 42, 132-139.	1.2	30
2525	High-pressure chemistry of nitride-based materials. Chemical Society Reviews, 2006, 35, 987.	18.7	200
2526	Ab initio rigid water: Effect on water structure, ion hydration, and thermodynamics. Physical Chemistry Chemical Physics, 2006, 8, 2153.	1.3	33
2527	Possible one-dimensional structures obtained from transition metal atom doped silicon nanoclusters. Phase Transitions, 2006, 79, 709-716.	0.6	3
2528	Pressure-induced phase transformations in theBa8Si46clathrate. Physical Review B, 2006, 74, .	1.1	24
2529	Gold as intermolecular glue: a predicted planar triaurotriazine, C3Au3N3, isomer of gold cyanide. Chemical Communications, 2006, , 2890.	2.2	14
2530	The effect of cation coordination on the properties of oxygen vacancies in FeSbO4. Journal of Materials Chemistry, 2006, 16, 1943.	6.7	19
2531	On the site-specificity of polycarbonyl complexes in Cu/zeolites: combined experimental and DFT study. Physical Chemistry Chemical Physics, 2006, 8, 5535-5542.	1.3	35
2532	How Phonons Govern the Behavior of Short, Strong Hydrogen Bonds in Ureaâ^'Phosphoric Acid. Journal of the American Chemical Society, 2006, 128, 2963-2969.	6.6	38
2533	Role of Pr Segregation in Acceptor-State Formation at ZnO Grain Boundaries. Physical Review Letters, 2006, 97, 106802.	2.9	109
2534	Theoretical Study of Endohedral C36and Its Dimers. Journal of Physical Chemistry A, 2006, 110, 4780-4786.	1.1	18

#	Article	IF	Citations
2535	FTIR spectroscopic and computational studies on hydrogen adsorption on the zeolite Liâ€“FER. Physical Chemistry Chemical Physics, 2006, 8, 2286-2292.	1.3	57
2536	Interaction of SO3 with c-ZrO2(111) films on Pt(111). Physical Chemistry Chemical Physics, 2006, 8, 1593.	1.3	12
2537	Chemisorption of HCl to the MgO(001) surface: A DFT study. Physical Chemistry Chemical Physics, 2006, 8, 4359.	1.3	15
2538	Nature of Point Defects on SiO2/Mo(112) Thin Films and Their Interaction with Au Atoms. Journal of Physical Chemistry B, 2006, 110, 17015-17023.	1.2	28
2539	Charge transfers at metal/oxide interfaces: a DFT study of formation of KÎ´+and AuÎ´â^'species on MgO/Ag(100) ultra-thin films from deposition of neutral atoms. Physical Chemistry Chemical Physics, 2006, 8, 3335-3341.	1.3	82
2540	Advanced Modeling and Simulation for Microelectronic Materials. , 2006, , .		0
2541	First-Principles Calculations for Co-Doped LiMn[sub 1.5]Ni[sub 0.5]O[sub 4] and LiMn[sub 2]O[sub 4] Battery Electrodes. Electrochemical and Solid-State Letters, 2006, 9, A289.	2.2	5
2542	Role of hydrogen atoms in the photoinduced formation of stable electron centers in H-doped12CaOâ^™7Al2O3. Physical Review B, 2006, 73, .	1.1	39
2543	Effect of spin-orbit coupling on small platinum nanoclusters. Physical Review A, 2006, 73, .	1.0	83
2544	Evaluation of27Al and51V Electric Field Gradients and the Crystal Structure for Aluminum Orthovanadate (AlVO4) by Density Functional Theory Calculations. Journal of Physical Chemistry B, 2006, 110, 5975-5983.	1.2	34
2545	Radial deformation and stability of single-wall carbon nanotubes under hydrostatic pressure. Physical Review B, 2006, 74, .	1.1	77
2546	Effects of Water on the Aging and Radiation Response of MOS Devices. IEEE Transactions on Nuclear Science, 2006, 53, 3629-3635.	1.2	25
2547	Phase stability and structural distortion of NiO under high pressure. Transactions of Nonferrous Metals Society of China, 2006, 16, s52-s58.	1.7	2
2548	Adsorption of atomic S and C on Mg(0001) surface. Transactions of Nonferrous Metals Society of China, 2006, 16, s253-s256.	1.7	1
2549	Transition pressures and enthalpy barriers for the cubic diamondâ†'Î²-tin transition in Si and Ge under nonhydrostatic conditions. Physical Review B, 2006, 73, .	1.1	26
2550	Vibrational and electron paramagnetic resonance properties of free and MgO supported AuCO complexes. Journal of Chemical Physics, 2006, 124, 174709.	1.2	25
2551	Dynamical core-hole screening in the x-ray absorption spectra of graphite,C60, and carbon nanotubes: A first-principles electronic structure study. Physical Review B, 2006, 73, .	1.1	28
2552	Electronic structure of theÎ±andÎ´phases ofBi2O3: A combinedab initioand x-ray spectroscopy study. Physical Review B, 2006, 73, .	1.1	187

#	Article	IF	Citations
2553	A theoretical and experimental study of lead substitution in calcium hydroxyapatite. Physical Chemistry Chemical Physics, 2006, 8, 967.	1.3	73
2554	Crystal structure prediction usingab initioevolutionary techniques: Principles and applications. Journal of Chemical Physics, 2006, 124, 244704.	1.2	2,044
2555	Au and Pd atoms adsorbed on pure and Ti-doped SiO2âˆ•Mo(112) films. Journal of Chemical Physics, 2006, 124, 034701.	1.2	41
2556	First-principles study of bulk ordering and surface segregation in Pt-Rh binary alloys. Physical Review B, 2006, 74, .	1.1	67
2557	Structure and magnetism in bcc-based iron-cobalt alloys. Physical Review B, 2006, 73, .	1.1	87
2558	Influence of the Hydroxylation of Î³-Al2O3Surfaces on the Stability and Diffusion of Single Pd Atoms:Â A DFT Study. Journal of Physical Chemistry B, 2006, 110, 1759-1767.	1.2	103
2559	Semiempirical van der Waals correction to the density functional description of solids and molecular structures. Physical Review B, 2006, 73, .	1.1	707
2560	Phase Diagram and Electrical Conductivity of High Energy-Density Water from Density Functional Theory. Physical Review Letters, 2006, 97, 017801.	2.9	123
2561	Ab Initio Study of Energetic Solids:Â Cupric Azide, Mercuric Azide, and Lead Azide. Journal of Physical Chemistry B, 2006, 110, 18196-18203.	1.2	56
2562	Structure of neutral aluminum clustersAln(2â©½nâ©½23): Genetic algorithm tight-binding calculations. Physical Review B, 2006, 73, .	1.1	113
2563	Dimensional Dependence of Electronic Structure of Fullerene Polymers. Journal of Physical Chemistry B, 2006, 110, 22374-22381.	1.2	19
2564	Static ionic displacements in Feâ€“Ni alloys from first principles. Journal of Applied Physics, 2006, 99, 08P906.	1.1	7
2565	Water adsorption on hydroxylatedÎ±-quartz (0001) surfaces: From monomer to flat bilayer. Physical Review B, 2006, 73, .	1.1	117
2566	Structural study of gold clusters. Journal of Chemical Physics, 2006, 124, 114309.	1.2	220
2567	Hydrated Arrays of Acidic Surface Groups as Model Systems for Interfacial Structure and Mechanisms in PEMs. Journal of Physical Chemistry B, 2006, 110, 20469-20477.	1.2	49
2568	Surface Dipoles and Work Functions of Alkylthiolates and Fluorinated Alkylthiolates on Au(111). Journal of Physical Chemistry B, 2006, 110, 22628-22634.	1.2	161
2569	Mechanism of the increase in bulk modulus of perovskiteScRh3Bxby vacancies. Physical Review B, 2006, 73, .	1.1	17
2570	Electric-field-switchable magnets: The case ofBaNiF4. Physical Review B, 2006, 74, .	1.1	56

#	Article	IF	Citations
2571	First-principles study of ground- and excited-state properties ofMgO,ZnO, andCdOpolymorphs. Physical Review B, 2006, 73, .	1.1	361
2572	Convergence of the formation energies of intrinsic point defects in wurtzite ZnO: first-principles study by projector augmented wave method. Journal of Physics Condensed Matter, 2006, 18, 1495-1508.	0.7	56
2573	Tuning the chemical functionality of a gas sensitive material: Water adsorption on SnO2(101). Surface Science, 2006, 600, 29-32.	0.8	45
2574	Structure and bonding ofAu5M(M=Na, Mg, Al, Si, P, and S) clusters. Physical Review B, 2006, 74, .	1.1	113
2575	Chemical Control of Electronic Structure and Superconductivity in Layered Borides and Borocarbides:Â Understanding the Absence of Superconductivity in LixBC. Journal of the American Chemical Society, 2006, 128, 10043-10053.	6.6	49
2576	Water adsorption on a NaCl (001) surface: A density functional theory study. Physical Review B, 2006, 74, .	1.1	43
2577	Energetics, structure, and long-range interaction of vacancy-type defects in carbon nanotubes: Atomistic simulations. Physical Review B, 2006, 74, .	1.1	202
2578	Stable structural and magnetic isomers of small transition-metal clusters from the Ni group: anab initiodensity-functional study. Journal of Physics Condensed Matter, 2006, 18, 9703-9748.	0.7	67
2579	Nitrogen-doped carbon nanotubes under electron irradiation simulated with a tight-binding model. Physical Review B, 2006, 74, .	1.1	17
2580	Formation of monatomic Fe chains on vicinalCu(111)surfaces: An atomistic view. Physical Review B, 2006, 73, .	1.1	25
2581	Diffusion of zinc vacancies and interstitials in zinc oxide. Applied Physics Letters, 2006, 88, 201918.	1.5	202
2582	First-Principle Study of Adsorption of Hydrogen on Ti-Doped Mg(0001) Surface. Journal of Physical Chemistry B, 2006, 110, 21747-21750.	1.2	52
2583	Ab initio energetic study of oxide ceramics with rare-earth elements. Rare Metals, 2006, 25, 549-555.	3.6	12
2584	Elastic anisotropy of FeSiO3end-members of the perovskite and post-perovskite phases. Geophysical Research Letters, 2006, 33, n/a-n/a.	1.5	59
2585	Ab initio study of the phase separation of argon in molten iron at high pressures. Geophysical Research Letters, 2006, 33, .	1.5	8
2586	Electronic spin transitions and the seismic properties of ferrous iron-bearing MgSiO3post-perovskite. Geophysical Research Letters, 2006, 33, .	1.5	50
2587	High-pressure alloying of iron and xenon: â€œMissingâ€•Xe in the Earth's core?. Journal of Geophysical Research, 2006, 111, n/a-n/a.	3.3	25
2588	Ab initiostudy of the composition dependence of the pressure-induced spin transition in the (Mg1â^'x,Fex)O system. Geophysical Research Letters, 2006, 33, .	1.5	76

#	Article	IF	Citations
2589	Bulk and surface oxygen vacancy formation and diffusion in single crystals, ultrathin films, and metal grown oxide structures. Journal of Chemical Physics, 2006, 125, 074711.	1.2	61
2590	Intermolecular interactions in solid benzene. Journal of Chemical Physics, 2006, 124, 044514.	1.2	43
2591	First-principles study of intrinsic point defects in ZnO: Role of band structure, volume relaxation, and finite-size effects. Physical Review B, 2006, 73, .	1.1	463
2592	Thermodynamics of doping and vacancy formation inBaZrO3perovskite oxide from density functional calculations. Physical Review B, 2006, 73, .	1.1	139
2593	NaTaO3 photocatalysts of different crystalline structures for water splitting into H2 and O2. Applied Physics Letters, 2006, 89, 211904.	1.5	131
2594	Experimental determination of the local geometry around In and Inâ€“C complexes in Si. Applied Physics Letters, 2006, 88, 212102.	1.5	8
2595	Phonon driven proton transfer in crystals with short strong hydrogen bonds. Journal of Chemical Physics, 2006, 124, 234503.	1.2	30
2596	Empirical tight-binding model for titanium phase transformations. Physical Review B, 2006, 73, .	1.1	30
2597	Ab initiocalculation of structural phase transitions in AlN crystal. Physical Review B, 2006, 74, .	1.1	125
2598	Compressibility of boron-doped diamond. High Pressure Research, 2006, 26, 79-85.	0.4	5
2599	Salt Permeation and Exclusion in Hydroxylated and Functionalized Silica Pores. Physical Review Letters, 2006, 96, 095504.	2.9	79
2600	Structural and chemical embrittlement of grain boundaries by impurities: A general theory and first-principles calculations for copper. Physical Review B, 2006, 74, .	1.1	127
2601	Thermal stability, atomic vibrational dynamics, and superheating of confined interfacial Sn layers inSnâˆ•Simultilayers. Physical Review B, 2006, 73, .	1.1	8
2602	Levitation apparatus for neutron diffraction investigations on high temperature liquids. Review of Scientific Instruments, 2006, 77, 053903.	0.6	70
2603	Ab initiostudies of the electronic structure of defects in PbTe. Physical Review B, 2006, 74, .	1.1	123
2604	Nitrogen Vacancies as Major Point Defects in Gallium Nitride. Physical Review Letters, 2006, 96, 196402.	2.9	141
2605	Intrinsic and Rashba spin-orbit interactions in graphene sheets. Physical Review B, 2006, 74, .	1.1	960
2606	Orbital Ordering and Jahn-Teller Distortion in Perovskite RuthenateSrRuO3. Physical Review Letters, 2006, 97, 067002.	2.9	84

#	Article	IF	Citations
2607	Density Functional Theory and DFT+U Study of Transition Metal Porphines Adsorbed on Au(111) Surfaces and Effects of Applied Electric Fields. Journal of the American Chemical Society, 2006, 128, 3659-3668.	6.6	100
2608	Modeling Adsorption of the Uranyl Dication on the Hydroxylated Î±-Al2O3(0001) Surface in an Aqueous Medium. Density Functional Study. Langmuir, 2006, 22, 2141-2145.	1.6	49
2609	Classical Studies of H Atom Trapping on a Graphite Surfaceâ€. Journal of Physical Chemistry B, 2006, 110, 18811-18817.	1.2	28
2610	Determination of the high-pressure crystal structure ofBaWO4andPbWO4. Physical Review B, 2006, 73, .	1.1	95
2611	Signature of nearly icosahedral structures in liquid and supercooled liquid copper. Physical Review B, 2006, 74, .	1.1	127
2612	LSDA+Ustudy of cupric oxide: Electronic structure and native point defects. Physical Review B, 2006, 73, .	1.1	213
2613	Origin of Bulklike Structure and Bond Length Disorder of Pt37and Pt6Ru31Clusters on Carbon:Â Comparison of Theory and Experiment. Journal of the American Chemical Society, 2006, 128, 131-142.	6.6	55
2614	Volume-dependent exchange interactions and noncollinear magnetism in zinc-blende MnAs. Physical Review B, 2006, 74, .	1.1	11
2615	Development of a bond-order type interatomic potential for Siâ€“B systems. Modelling and Simulation in Materials Science and Engineering, 2006, 14, S29-S37.	0.8	8
2616	Thermodynamics of mixing in pyrope-grossular, Mg3Al2Si3O12-Ca3Al2Si3O12, solid solution from lattice dynamics calculations and Monte Carlo simulations. American Mineralogist, 2006, 91, 1815-1830.	0.9	35
2617	TIN-BASED GROUP IV SEMICONDUCTORS: New Platforms for Opto- and Microelectronics on Silicon. Annual Review of Materials Research, 2006, 36, 497-554.	4.3	231
2618	Finite-temperature behavior of small silicon and tin clusters: Anab initiomolecular dynamics study. Physical Review B, 2006, 73, .	1.1	35
2619	Calculated Phase Diagrams for the Electrochemical Oxidation and Reduction of Water over Pt(111). Journal of Physical Chemistry B, 2006, 110, 21833-21839.	1.2	388
2620	Co9S8as a Catalyst for Electroreduction of O2:Â Quantum Chemistry Predictions. Journal of Physical Chemistry B, 2006, 110, 936-941.	1.2	177
2621	Catalytic Effects of Subsurface Carbon in the Chemisorption of Hydrogen on a Mg(0001) Surface:Â an Ab-initio Study. Journal of Physical Chemistry B, 2006, 110, 1814-1819.	1.2	55
2622	Chemoâ^'Regioselectivity in Heterogeneous Catalysis:Â Competitive Routes for CO and CC Hydrogenations from a Theoretical Approach. Journal of the American Chemical Society, 2006, 128, 1316-1323.	6.6	122
2623	Ab initiocalculations of the alloy resistivities of lattice-matched and lattice-mismatched metal pairs: Influence of local-impurity-induced distortions. Physical Review B, 2006, 74, .	1.1	7
2624	First-principles study of interaction of cluster Au32 with CO, H2, and O2. Journal of Chemical Physics, 2006, 125, 124703.	1.2	60

#	Article	IF	Citations
2625	Ab initiostudy of the critical thickness for ferroelectricity in ultrathinPtâˆ•PbTiO3âˆ•Ptfilms. Physical Review B, 2006, 74, .	1.1	66
2626	Modeling the structure and electronic properties ofTiO2nanoparticles. Physical Review B, 2006, 73, .	1.1	53
2627	Olefin Adsorption on Silica-Supported Silver Salts â˜ A DFT Study. Langmuir, 2006, 22, 5716-5722.	1.6	21
2628	Thermal properties ofSi136: Theoretical and experimental study of the type-II clathrate polymorph of Si. Physical Review B, 2006, 74, .	1.1	42
2629	From electrons to finite elements: A concurrent multiscale approach for metals. Physical Review B, 2006, 73, .	1.1	103
2630	Dielectric properties of BaTiO3âˆ•SrTiO3 ferroelectric thin film artificial lattice. Journal of Applied Physics, 2006, 100, 051613.	1.1	18
2631	Structural, electronic and magnetic properties of Gd investigated by DFT+Umethods: bulk, clean and H-covered (0001) surfaces. Journal of Physics Condensed Matter, 2006, 18, 7021-7043.	0.7	64
2632	Location and energy of interstitial hydrogen in the1âˆ•1approximantW-TiZrNiof the icosahedralTiZrNiquasicrystal: Rietveld refinement of x-ray and neutron diffraction data and density-functional calculations. Physical Review B, 2006, 73, .	1.1	7
2633	Interlayer exchange coupling in Feâˆ•MgOâˆ•Fe magnetic tunnel junctions. Applied Physics Letters, 2006, 89, 112503.	1.5	123
2634	Factors that affect Li mobility in layered lithium transition metal oxides. Physical Review B, 2006, 74, .	1.1	431
2635	Effect of Au coating on the magnetic and structural properties of Fe nanoclusters for use in biomedical applications: A density-functional theory study. Physical Review B, 2006, 73, .	1.1	49
2636	Migration Energy of He in W Revisited byAbÂInitioCalculations. Physical Review Letters, 2006, 97, 196402.	2.9	283
2637	Derivation of Force Field Parameters for SnO2â˜H2O Surface Systems from Plane-Wave Density Functional Theory Calculations. Journal of Physical Chemistry B, 2006, 110, 8386-8397.	1.2	53
2638	Ozone-Based Atomic Layer Deposition of Alumina from TMA:Â Growth, Morphology, and Reaction Mechanism. Chemistry of Materials, 2006, 18, 3764-3773.	3.2	161
2639	Coulomb correlation effects in zinc monochalcogenides. Journal of Applied Physics, 2006, 100, 043709.	1.1	86
2640	A Well-Defined, Silica-Supported Tungsten Imido Alkylidene Olefin Metathesis Catalyst. Organometallics, 2006, 25, 3554-3557.	1.1	152
2641	Ultrafast Vibrationally-Induced Dephasing of Electronic Excitations in PbSe Quantum Dots. Nano Letters, 2006, 6, 2295-2300.	4.5	88
2642	Comparative First-Principles Study of Structural and Optical Properties of Alkali Metal Azides. Journal of Physical Chemistry B, 2006, 110, 9856-9862.	1.2	48

#	Article	IF	Citations
2643	A First-Principles Analysis of Hydrogen Interaction in Ti-Doped NaAlH4Surfaces:Â Structure and Energetics. Journal of Physical Chemistry B, 2006, 110, 25863-25868.	1.2	45
2644	One-Dimensional Metallic Conducting Pathway of Cyclohexyl-Substituted Spiro-Biphenalenyl Neutral Radical Molecular Crystal. Journal of the American Chemical Society, 2006, 128, 1418-1419.	6.6	28
2645	One-Dimensional Transition Metalâ^'Benzene Sandwich Polymers:Â Possible Ideal Conductors for Spin Transport. Journal of the American Chemical Society, 2006, 128, 2310-2314.	6.6	202
2646	Suppressing Aggregation in a Large Polycyclic Aromatic Hydrocarbon. Journal of the American Chemical Society, 2006, 128, 1334-1339.	6.6	141
2647	Multinuclear High-Resolution NMR Study of Compounds from the Ternary System NaFâ^'CaF2â^'AlF3:â€‰ from Determination to Modeling of NMR Parameters. Inorganic Chemistry, 2006, 45, 10215-10223.	1.9	30
2648	Dissociative Adsorption of Carbon Monoxide on Mo(110):Â First-Principles Theory. Journal of Physical Chemistry B, 2006, 110, 18363-18367.	1.2	15
2649	Formation and Structural Anomaly of the Metastable Phases in an Immiscible Agâ^'Mo System Studied by Ion Beam Mixing and Molecular Dynamics Simulation. Journal of Physical Chemistry B, 2006, 110, 595-606.	1.2	22
2650	First-Principles Calculations of Migration Energy of Lithium Ions in Halides and Chalcogenides. Journal of Physical Chemistry B, 2006, 110, 8258-8262.	1.2	26
2651	Density functional calculations of the formation and migration enthalpies of monovacancies in Ni: Comparison of local and nonlocal approaches. Physical Review B, 2006, 74, .	1.1	45
2652	Electronic structure and bonding in hexagonal boron nitride. Journal of Physics Condensed Matter, 2006, 18, 97-115.	0.7	137
2653	Theoretical Evidence of PtSn Alloy Efficiency for CO Oxidation. Journal of the American Chemical Society, 2006, 128, 9129-9136.	6.6	147
2654	Magnetic excitations and phonons in the spin-chain compoundNaCu2O2. Physical Review B, 2006, 73, .	1.1	14
2655	Unravelling the Origin of the High-Catalytic Activity of Supported Au:Â A Density-Functional Theory-Based Interpretation. Journal of the American Chemical Society, 2006, 128, 15600-15601.	6.6	65
2656	Structure, electronic properties, and magnetic transition in manganese clusters. Physical Review B, 2006, 73, .	1.1	98
2657	Structural Model of Eumelanin. Physical Review Letters, 2006, 97, 218102.	2.9	170
2658	Electron Correlation Effects in the Fe Dimer. Journal of Physical Chemistry A, 2006, 110, 10799-10804.	1.1	18
2659	First-Principles Calculations within Periodic Boundary Conditions of the NMR Shielding Tensor for a Transition Metal Nucleus in a Solid State System:Â The Example of51V in AlVO4. Journal of Physical Chemistry B, 2006, 110, 21403-21407.	1.2	27
2660	Growth of Ultrathin Films of Amorphous Rutheniumâ^'Phosphorus Alloys Using a Single Source CVD Precursor. Journal of the American Chemical Society, 2006, 128, 16510-16511.	6.6	25

#	Article	IF	Citations
2661	First-principles study on the adhesion nature of the Î±-Al2O3(0001)/Ni(111) interface. Modelling and Simulation in Materials Science and Engineering, 2006, 14, S21-S28.	0.8	15
2662	In Search for Structure of Active Site in Iron-Based Oxygen Reduction Electrocatalysts. Journal of Physical Chemistry B, 2006, 110, 4179-4185.	1.2	28
2663	Reactions of Hydrazoic Acid and Trimethylindium on TiO2Rutile (110) Surface:Â A Computational Study on the Formation of the First Monolayer InN. Journal of Physical Chemistry B, 2006, 110, 2263-2270.	1.2	13
2664	Structure and Bonding between an Aryl Group and Metal Surfaces. Journal of the American Chemical Society, 2006, 128, 6030-6031.	6.6	131
2665	On the Performance of Au(111) for Ethylene Epoxidation:â€‰ A Density Functional Study. Journal of Physical Chemistry B, 2006, 110, 13310-13313.	1.2	48
2666	Comment on â€œCombinatorial Search for Optimal Hydrogen-Storage Nanomaterials Based on Polymersâ€• Physical Review Letters, 2006, 97, 209601.	2.9	69
2667	Electronic structure ofNiOâˆ•Ag(100)thin films fromDFT+Uand hybrid functional DFT approaches. Physical Review B, 2006, 74, .	1.1	68
2668	Formation of a Regular Fullerene Nanochain Lattice. Journal of Physical Chemistry B, 2006, 110, 21394-21398.	1.2	87
2669	First-Principles Study of K and Cs Adsorbed on Pd(111). Journal of Physical Chemistry B, 2006, 110, 23904-23910.	1.2	10
2670	Molecular Understanding of Alumina Supported Single-Site Catalysts by a Combination of Experiment and Theory. Journal of the American Chemical Society, 2006, 128, 9157-9169.	6.6	125
2671	Water Adsorption and Diffusion on NaCl(100). Journal of Physical Chemistry B, 2006, 110, 24559-24564.	1.2	24
2672	Debye temperature and stiffness of carbon and boron nitride polymorphs from first principles calculations. Physical Review B, 2006, 73, .	1.1	218
2673	Polyanionic Hydrides from Polar Intermetallics AeE2(Ae = Ca, Sr, Ba; E = Al, Ga, In). Journal of the American Chemical Society, 2006, 128, 817-824.	6.6	33
2674	Density Functional Study of Chemical Stability and Nitrogen Encapsulation of C48N12 and C58N12. Journal of Physical Chemistry A, 2006, 110, 12241-12248.	1.1	3
2675	Native point defects in yttria and relevance to its use as a high-dielectric-constant gate oxide material: First-principles study. Physical Review B, 2006, 73, .	1.1	84
2676	Simulating Temperature Programmed Desorption of Water on Hydrated Î³-Alumina from First-Principles Calculations. Journal of Physical Chemistry B, 2006, 110, 7392-7395.	1.2	27
2677	Theoretical Study of Boron Nitride Nanotubes with Defects in Nitrogen-Rich Synthesis. Journal of Physical Chemistry B, 2006, 110, 4621-4628.	1.2	58
2678	First Principles Study of Adsorption and Dissociation of CO on W(111). Journal of Physical Chemistry B, 2006, 110, 1344-1349.	1.2	21

#	Article	IF	Citations
2679	Magnetism and thermodynamics of defect-free Fe-Cr alloys. Physical Review B, 2006, 74, .	1.1	174
2680	Electronic and magnetic properties of V-doped anataseTiO2from first principles. Physical Review B, 2006, 74, .	1.1	80
2681	Stability of the body-centered-tetragonal phase of Fe at high pressure: Ground-state energies, phonon spectra, and molecular dynamics simulations. Physical Review B, 2006, 74, .	1.1	21
2682	Periodic Density Functional Theory Investigation of the Uranyl Ion Sorption on the TiO2Rutile (110) Face. Inorganic Chemistry, 2006, 45, 6568-6570.	1.9	29
2683	Point Defect Concentrations in Metastable Fe-C Alloys. Physical Review Letters, 2006, 96, 175501.	2.9	113
2684	How Do Aryl Groups Attach to a Graphene Sheet?. Journal of Physical Chemistry B, 2006, 110, 23628-23632.	1.2	191
2685	Effect of Particle Size on the Oxidizability of Platinum Clusters. Journal of Physical Chemistry A, 2006, 110, 5839-5846.	1.1	75
2686	Structure and stability ofZrSiO4under hydrostatic pressure. Physical Review B, 2006, 74, .	1.1	40
2687	Visible Light Sensitive Photocatalyst, Delafossite Structured Î±-AgGaO2. Journal of Physical Chemistry B, 2006, 110, 23274-23278.	1.2	152
2688	Organometallic Benzene-Vanadium Wire: A One-Dimensional Half-Metallic Ferromagnet. Physical Review Letters, 2006, 97, 097201.	2.9	202
2689	Interactions of Hydrogen with Pd and Pd/Ni Alloy Chain-Functionalized Single Walled Carbon Nanotubes from Density Functional Theory. Journal of Physical Chemistry B, 2006, 110, 22415-22425.	1.2	23
2690	V@Au12-:Â An Improved Novel Catalyst for CO Oxidation?. Journal of Physical Chemistry B, 2006, 110, 11600-11603.	1.2	61
2691	Structural, electronic, and magnetic properties ofSrRuO3under epitaxial strain. Physical Review B, 2006, 74, .	1.1	162
2692	Bistability-Mediated Carrier Recombination at Light-Induced Boron-Oxygen Complexes in Silicon. Physical Review Letters, 2006, 97, 256602.	2.9	35
2693	Changes in Electronic Structure upon Li Insertion Reaction of Monoclinic Li3Fe2(PO4)3. Journal of Physical Chemistry B, 2006, 110, 17743-17750.	1.2	23
2694	A density-functional theory study of the adsorption of CO molecules on Au/Ni(111). Journal of Physics Condensed Matter, 2006, 18, 10825-10835.	0.7	8
2695	Ba Adsorption on the Stoichiometric and Defective TiO2 (110) Surface from First-Principles Calculations. Journal of Physical Chemistry B, 2006, 110, 19552-19556.	1.2	5
2696	Effect of Adsorption Site, Size, and Composition of Pt/Au Bimetallic Clusters on the CO Frequency:Â A Density Functional Theory Study. Journal of Physical Chemistry A, 2006, 110, 14036-14042.	1.1	46

#	Article	IF	Citations
2697	Thermodynamic Equilibrium Compositions, Structures, and Reaction Energies of PtxOy(x= 1â^'3) Clusters Predicted from First Principles. Journal of Physical Chemistry B, 2006, 110, 16591-16599.	1.2	51
2698	Small-radius clean and metal-doped boron carbide nanotubes: A density functional study. Physical Review B, 2006, 74, .	1.1	18
2699	eâ^•a dependence of the lattice instability of cubic Heusler alloys from first principles. Applied Physics Letters, 2006, 88, 111903.	1.5	78
2700	Electronic Switching of Single Silicon Atoms by Molecular Field Effects. Journal of the American Chemical Society, 2006, 128, 16791-16797.	6.6	40
2701	Effects of Morphology and Doping on the Electronic and Structural Properties of Hydrogenated Silicon Nanowires. Nano Letters, 2006, 6, 920-925.	4.5	78
2702	Theoretical Calculation of the Dehydrogenation of Ethanol on a Rh/CeO2(111) Surface. Journal of Physical Chemistry B, 2006, 110, 14816-14823.	1.2	55
2703	Theoretical prediction of low-energy crystal structures and hydrogen storage energetics inLi2NH. Physical Review B, 2006, 73, .	1.1	67
2704	A theoretical and experimental study of the distorted pyrochlore Bi2Sn2O7. Journal of Materials Chemistry, 2006, 16, 3452.	6.7	30
2705	Identification of Destabilized Metal Hydrides for Hydrogen Storage Using First Principles Calculations. Journal of Physical Chemistry B, 2006, 110, 8769-8776.	1.2	273
2706	How Large Is the [FeIII(Protoporphyrin IX)]+Ion (Hemin+) in the Gas Phase?. Journal of Physical Chemistry B, 2006, 110, 24207-24211.	1.2	15
2707	The Crystal Structure and Surface Energy of NaAlH4:Â A Comparison of DFT Methodologies. Journal of Physical Chemistry B, 2006, 110, 622-630.	1.2	43
2708	Role of Kinetics in the Selective Surface Oxidations of Transition Metal Carbides. Journal of Physical Chemistry B, 2006, 110, 15454-15458.	1.2	31
2709	Single and Dual Cation Sites in Zeolites:Â Theoretical Calculations and FTIR Spectroscopic Studies on CO Adsorption on K-FER. Journal of Physical Chemistry B, 2006, 110, 22542-22550.	1.2	79
2710	First Crystal Structure Studies of CaAlH5. Inorganic Chemistry, 2006, 45, 3849-3851.	1.9	46
2711	Carbon Nanotubes Functionalized by NO2:Â Coexistence of Charge Transfer and Radical Transfer. Journal of Physical Chemistry B, 2006, 110, 22462-22470.	1.2	28
2712	Combined Theoretical and FTIR Spectroscopic Studies on Hydrogen Adsorption on the Zeolites Naâ^'FER and Kâ^'FER. Journal of Physical Chemistry B, 2006, 110, 395-402.	1.2	72
2713	Atomic Structures of Benzene and Pyridine on Si(5 5 12)-2 Ã— 1. Journal of Physical Chemistry B, 2006, 110, 15912-15919.	1.2	14
2714	Surface Structure of (101Ì„0) and (112Ì„0) Surfaces of ZnO with Density Functional Theory and Atomistic Simulation. Journal of Physical Chemistry B, 2006, 110, 7985-7991.	1.2	71

#	Article	IF	Citations
2715	Filling fraction limits for rare-earth atoms inCoSb3: Anab initioapproach. Physical Review B, 2006, 74, .	1.1	53
2716	Ab initiodensity-functional theory study ofNHxdehydrogenation and reverse reactions on the Rh(111) surface. Physical Review B, 2006, 74, .	1.1	41
2717	Mechanistic Study of the Electrochemical Oxygen Reduction Reaction on Pt(111) Using Density Functional Theory. Journal of Physical Chemistry B, 2006, 110, 15338-15344.	1.2	91
2718	Effect of S Arrangement on Fe(110) Properties at 1/3 Monolayer Coverage:Â A DFT Study. Journal of Physical Chemistry B, 2006, 110, 956-962.	1.2	18
2719	A Quantum Chemical Study of the Decomposition of Keggin-Structured Heteropolyacids. Journal of Physical Chemistry B, 2006, 110, 4170-4178.	1.2	37
2720	Ab initiostudies of Al, O, andO2adsorption onÎ±â^'Al2O3(0001)surfaces. Physical Review B, 2006, 74, .	1.1	42
2721	Structural properties ofPbTeâ^•CdTeinterfaces from first principles. Physical Review B, 2006, 74, .	1.1	51
2722	Do Methanethiol Adsorbates on the Au(111) Surface Dissociate?. Physical Review Letters, 2006, 97, 045505.	2.9	57
2723	Theory of Overlithiation Reaction in LiMO2Battery Electrodes. Chemistry of Materials, 2006, 18, 1296-1302.	3.2	18
2724	Structures of Dense Glycine and Alanine Adlayers on Chiral Cu(3,1,17) Surfaces. Langmuir, 2006, 22, 8096-8103.	1.6	38
2725	Perturbation of Adsorbed CO by Amine Derivatives Coadsorbed on the Î³-Al2O3Surface:Â FTIR and First Principles Studies. Journal of Physical Chemistry B, 2006, 110, 4742-4750.	1.2	13
2726	Chemical Structure and Orientation of Ethylene on Si(114)â^'(2Ã—1)/c(2Ã—2). Journal of Physical Chemistry B, 2006, 110, 6841-6847.	1.2	6
2727	Comparative Theoretical Study of Formaldehyde Decomposition on PdZn, Cu, and Pd Surfaces. Journal of Physical Chemistry B, 2006, 110, 14890-14897.	1.2	96
2728	Rebonding at coherent interfaces between rocksalt-PbTe/zinc-blende-CdTe. New Journal of Physics, 2006, 8, 317-317.	1.2	32
2729	Hydrogen adsorption and diffusion on Pt {111} and PtSn {111}. Journal of Materials Chemistry, 2006, 16, 1989.	6.7	43
2730	Phase Diagram of Mg Insertion into Chevrel Phases, MgxMo6T8 (T = S, Se). 1. Crystal Structure of the Sulfides. Chemistry of Materials, 2006, 18, 5492-5503.	3.2	116
2731	Atomic Hydrogen Diffusion in Novel Magnesium Nanostructures: The Impact of Incorporated Subsurface Carbon Atoms. Journal of Physics: Conference Series, 2006, 29, 167-172.	0.3	9
2732	Electronic structure of Si(111)-bound alkyl monolayers: Theory and experiment. Physical Review B, 2006, 74, .	1.1	103

#	Article	IF	Citations
2733	The Nature of Contact between Pd Leads and Semiconducting Carbon Nanotubes. Nano Letters, 2006, 6, 1415-1419.	4.5	48
2734	High-pressure phases of CaCO3: Crystal structure prediction and experiment. Earth and Planetary Science Letters, 2006, 241, 95-103.	1.8	318
2735	An ab initio study of nickel substitution into iron. Earth and Planetary Science Letters, 2006, 248, 147-152.	1.8	18
2736	Al2O3 incorporation in MgSiO3 perovskite and ilmenite. Earth and Planetary Science Letters, 2006, 252, 152-161.	1.8	39
2737	Arsenite sorption and co-precipitation with calcite. Chemical Geology, 2006, 233, 328-336.	1.4	140
2738	Competing structural and magnetic effects in small iron clusters. Computational Materials Science, 2006, 35, 275-278.	1.4	90
2739	Structural properties of small copper clusters with a nickel impurity. Computational Materials Science, 2006, 35, 311-315.	1.4	8
2740	Recent theoretical progress on electronic and structural properties of clusters: Permanent electric dipoles, magnetism, novel caged structures, and their assemblies. Computational Materials Science, 2006, 35, 375-381.	1.4	22
2741	Modeling interatomic interactions across Cu/Î±â€“Al2O3 interface. Computational Materials Science, 2006, 36, 281-291.	1.4	19
2742	Total energy calculations for systems with magnetic and chemical disorder. Computational Materials Science, 2006, 35, 1-5.	1.4	44
2743	A density functional theory study of CO adsorption on Ptâ€“Au nanoparticles. Computational Materials Science, 2006, 35, 247-253.	1.4	56
2744	A first principles study of the elastic properties in perovskite-type RRh3B and RRh3C with R=Sc, Y and La. Computational Materials Science, 2006, 36, 12-16.	1.4	23
2745	Ring structures of small ZnO clusters. Computational Materials Science, 2006, 36, 258-262.	1.4	61
2746	Comparison of simulations of liquid metals by classical and ab initio molecular dynamics. Computational Materials Science, 2006, 36, 189-193.	1.4	11
2747	An atomistic approach to the initiation mechanism of galling. Computational Materials Science, 2006, 37, 193-197.	1.4	31
2748	Structure of hydrated Zn2+ at the rutile TiO2 (110)-aqueous solution interface: Comparison of X-ray standing wave, X-ray absorption spectroscopy, and density functional theory results. Geochimica Et Cosmochimica Acta, 2006, 70, 4039-4056.	1.6	52
2749	Assessment of the thermodynamic properties and phase diagram of the Biâ€“Pd system. Calphad: Computer Coupling of Phase Diagrams and Thermochemistry, 2006, 30, 14-17.	0.7	7
2750	First-principles calculation of lattice stability of C15â€“M2R and their hypothetical C15 variants (M=Al,) Tj ETQq1 1 0.784314 rgBT /O 341-348.	0.7	21

#	Article	IF	Citations
2751	Miedemaâ€™s model revisited: The parameter for Ti, Zr, and Hf. Calphad: Computer Coupling of Phase Diagrams and Thermochemistry, 2006, 30, 266-269.	0.7	43
2752	Ab initio lattice stabilities of some elemental complex structures. Calphad: Computer Coupling of Phase Diagrams and Thermochemistry, 2006, 30, 357-366.	0.7	76
2753	Multiscale modeling and related hybrid approaches. Current Opinion in Solid State and Materials Science, 2006, 10, 2-14.	5.6	14
2754	Unusual Hydrogen Bonding in Water-Filled Carbon Nanotubes. Journal of the American Chemical Society, 2006, 128, 12090-12097.	6.6	261
2755	First principles study of electronic and mechanical properties of molybdenum selenide type nanowires. Physical Review B, 2006, 74, .	1.1	26
2756	Mechanism of the Verwey transition in magnetite: Jahnâ€“Teller distortion and charge ordering patterns. Journal of Physics Condensed Matter, 2006, 18, 10427-10436.	0.7	53
2757	First-principles modelling of Earth and planetary materials at high pressures and temperatures. Reports on Progress in Physics, 2006, 69, 2365-2441.	8.1	152
2758	First-principles aluminum database: Energetics of binary Al alloys and compounds. Physical Review B, 2006, 73, .	1.1	110
2759	Magnetic instability within the seriesTCu3N(T=Pd, Rh, and Ru): A first-principles study. Physical Review B, 2006, 74, .	1.1	32
2760	Prediction of a Highly Activated State of CO Adsorbed on an Al/Fe(100) Bimetallic Surfaceâ€. Journal of Physical Chemistry B, 2006, 110, 22213-22219.	1.2	15
2761	Screened hybrid density functionals applied to solids. Journal of Chemical Physics, 2006, 124, 154709.	1.2	1,915
2762	Optical properties and electronic structures of(4CuInSe2)y(CuIn5Se8)1âˆ’y. Physical Review B, 2006, 74, .	1.1	34
2763	Origin of ferromagnetism of (Co,Al)-codoped ZnO from first-principles calculations. Applied Physics Letters, 2006, 89, 172502.	1.5	40
2764	Density Functional Theory Based Ab Initio Molecular Dynamics Using the Car-Parrinello Approach. , 2006, , 223-285.		9
2765	Spin-dependent tunneling in FMâˆ£semiconductorâˆ£FM structures. Journal of Applied Physics, 2006, 99, 08K302.	1.1	3
2766	Ab initiomolecular-dynamics simulations of the structural properties of liquidIn20Sn80in the temperature range798â€“1193K. Physical Review B, 2006, 73, .	1.1	16
2767	Synthesis, boron-nonstoichiometry and hardness of perovskite-type rare earth rhodium borides RRh3Bx (R=La, Gd, Lu and Sc). Journal of Alloys and Compounds, 2006, 408-412, 379-383.	2.8	11
2768	Hardness and oxidation resistance of the perovskite-type RRh3BxC1âˆ’x (R=Y, Sc). Journal of Alloys and Compounds, 2006, 408-412, 375-378.	2.8	14

#	Article	IF	Citations
2769	Distinct magnetic states of metastable fcc structured Fe and Feâ€“Cu alloys studied by ab initio calculations. Journal of Alloys and Compounds, 2006, 414, 36-41.	2.8	25
2770	Ab-initio calculations of titanium solubility in NaAlH4 and Na3AlH6. Journal of Alloys and Compounds, 2006, 416, 245-249.	2.8	20
2771	Thermodynamics modeling of the Mgâ€“Sr and Caâ€“Mgâ€“Sr systems. Journal of Alloys and Compounds, 2006, 421, 172-178.	2.8	41
2772	Theoretical calculation of thermodynamic data for gold-rare earth alloys with the embedded-atom method. Journal of Alloys and Compounds, 2006, 420, 83-93.	2.8	31
2773	Contribution of first-principles energetics to the Caâ€“Mg thermodynamic modeling. Journal of Alloys and Compounds, 2006, 420, 98-106.	2.8	36
2774	First-principles study of constitutional and thermal point defects in B2 PdIn. Intermetallics, 2006, 14, 248-254.	1.8	10
2775	Lattice stability of Ca, Sr and Yb disilicides. Intermetallics, 2006, 14, 1472-1486.	1.8	34
2776	Characterization of exciton self-trapping in amorphous silica. Journal of Non-Crystalline Solids, 2006, 352, 2589-2595.	1.5	29
2777	Ab initio molecular dynamics simulations of oxygen-deficient centers in pure and Ge-doped silica glasses: Structure and optical properties. Journal of Non-Crystalline Solids, 2006, 352, 2596-2600.	1.5	10
2778	Elasticity of CaSiO3 perovskite at high pressure and high temperature. Physics of the Earth and Planetary Interiors, 2006, 155, 249-259.	0.7	84
2779	Phase stability of CaSiO3 perovskite at high pressure and temperature: Insights from ab initio molecular dynamics. Physics of the Earth and Planetary Interiors, 2006, 155, 260-268.	0.7	46
2780	Elasticity of Mg2SiO4 ringwoodite at mantle conditions. Physics of the Earth and Planetary Interiors, 2006, 157, 181-187.	0.7	34
2781	Structural geomimetism: A conceptual framework for devising new materials from first principlesâ˜†. Progress in Solid State Chemistry, 2006, 34, 21-66.	3.9	8
2782	Dynamical charge tensors and infrared spectra of the crystalline Î±-quaterthiophene polymorph phases from first-principles calculations. Synthetic Metals, 2006, 156, 519-524.	2.1	9
2783	Growth of intact water ice onRu(0001)between 140 and160K: Experiment and density-functional theory calculations. Physical Review B, 2006, 73, .	1.1	125
2784	The Magnetic Nature of Intrinsic and Irradiation-induced Defects in Carbon Systems. , 2006, , 371-396.		5
2785	Defect Structure of Nonstoichiometric Plutonium Oxide. Journal of the Physical Society of Japan, 2006, 75, 143-145.	0.7	2
2786	Slip systems and plastic shear anisotropy in Mg2SiO4 ringwoodite: insights from numerical modelling. European Journal of Mineralogy, 2006, 18, 149-160.	0.4	49

#	Article	IF	Citations
2787	The thermoelastic properties of MgSO47D2O (epsomite) from powder neutron diffraction and ab initio calculation. European Journal of Mineralogy, 2006, 18, 449-462.	0.4	50
2788	Compton Profiles of Hydrated Na+and F-Ions. Zeitschrift Fur Physikalische Chemie, 2006, 220, 849-857.	1.4	0
2789	Electronic structure calculations for substitutional copper and monovacancies in silicon. Physica Scripta, 2006, T126, 61-64.	1.2	6
2790	AN X-RAY- AND NEUTRON-DIFFRACTION STUDY OF SYNTHETIC FERRICOPIAPITE, Fe14/3(SO4)6(OD,OH)2(D2O,H2O)20, AND AB INITIO CALCULATIONS ON THE STRUCTURE OF MAGNESIOCOPIAPITE, MgFe4(SO4)6(OH)2(H2O)20. Canadian Mineralogist, 2006, 44, 1227-1237.	0.3	12
2791	Grain Boundary Decohesion by Sulfur Segregation in Ferromagnetic Iron and Nickel —A First-Principles Study—. Materials Transactions, 2006, 47, 2682-2689.	0.4	68
2792	Influence of Interface Structure on Schottky Barrier Heights of α-Al₂O₃(0001)/Ni(111) interfaces: A First-Principles Study. Materials Transactions, 2006, 47, 2696-2700.	0.4	16
2793	Ab-Initio Lattice Instability Analysis on Ni and Ni3Al Single Crystals. JSME International Journal Series A-Solid Mechanics and Material Engineering, 2006, 49, 100-106.	0.4	6
2794	First-Principles Calculation of Point Defects in Uranium Dioxide. Materials Transactions, 2006, 47, 2651-2657.	0.4	104
2795	First-Principles Study of Molecule/Al Interfaces. Materials Transactions, 2006, 47, 2701-2705.	0.4	2
2796	First-Principles Calculations of Schottky Barrier Heights of Monolayer Metal/6<I>H</I>-SiC{0001} Interfaces. Materials Transactions, 2006, 47, 2690-2695.	0.4	9
2797	Anions in metallic matrices model: application to the aluminium crystal chemistry. Acta Crystallographica Section B: Structural Science, 2006, 62, 220-227.	1.8	29
2798	Structural characterization of Ni2Si pseudoepitaxial transrotational structures on [001] Si. Acta Crystallographica Section B: Structural Science, 2006, 62, 729-736.	1.8	14
2799	The crystal structure of Zr2NiD4.5. Acta Crystallographica Section B: Structural Science, 2006, 62, 972-978.	1.8	2
2800	Density functional theory meets statistical physics: from the atomistic to the mesoscopic properties of alloys. Surface and Interface Analysis, 2006, 38, 1158-1163.	0.8	14
2801	Room-Temperature Ferromagnetism in Doped Face-Centered Cubic Fe Nanoparticles. Small, 2006, 2, 804-809.	5.2	41
2802	First-principles studies of various crystallographic phases and neutral atomic vacancies in KNbO3 and KTaO3. Physica Status Solidi C: Current Topics in Solid State Physics, 2006, 3, 2862-2866.	0.8	10
2803	The exchange interaction in (Ga,Cr)N doped with oxygen impurities. Physica Status Solidi C: Current Topics in Solid State Physics, 2006, 3, 4147-4150.	0.8	1
2804	DFT study of a singleF center in cubic SrTiO3 perovskite. International Journal of Quantum Chemistry, 2006, 106, 2173-2183.	1.0	30

#	Article	IF	Citations
2805	First principles calculation of isolated intermediate bands formation in a transition metal-doped chalcopyrite-type semiconductor. Physica Status Solidi (A) Applications and Materials Science, 2006, 203, 1395-1401.	0.8	77
2806	Systematic studies on electronic structures of CuInSe2and the other chalcopyrite related compounds by first principles calculations. Physica Status Solidi (A) Applications and Materials Science, 2006, 203, 2634-2638.	0.8	57
2807	Three real-space discretization techniques in electronic structure calculations. Physica Status Solidi (B): Basic Research, 2006, 243, 1016-1053.	0.7	93
2808	Carâ€"Parrinello molecular dynamics using real space wavefunctions. Physica Status Solidi (B): Basic Research, 2006, 243, 1001-1015.	0.7	15
2809	First-principles study of carrier-mediated ferromagnetism in ZnTe-based thin film. Physica Status Solidi (B): Basic Research, 2006, 243, 1375-1382.	0.7	5
2810	Dissociation of VGaâ€"ON complexes in HVPE GaN by high pressure and high temperature annealing. Physica Status Solidi (B): Basic Research, 2006, 243, 1436-1440.	0.7	10
2811	Shell-like structure of valence band orbitals of silicon nanocrystals in silica glass. Physica Status Solidi (B): Basic Research, 2006, 243, R47-R49.	0.7	27
2812	Core-level shifts in complex metallic systems from first principle. Physica Status Solidi (B): Basic Research, 2006, 243, 2447-2464.	0.7	42
2813	Spin-polarized electronic structure of Mnâ€"IVâ€"V2 chalcopyrites. Physica Status Solidi (B): Basic Research, 2006, 243, 2159-2163.	0.7	7
2814	Structure and energy of the partial dislocation cores in GaAs. Physica Status Solidi (B): Basic Research, 2006, 243, 2122-2132.	0.7	8
2815	Carrier-mediated stabilization of ferromagnetism in semiconductors: holes and electrons. Physica Status Solidi (B): Basic Research, 2006, 243, 2170-2187.	0.7	46
2816	Electronic structure of Pd-covered (10,0) carbon nanotube. Physica Status Solidi (B): Basic Research, 2006, 243, 2164-2169.	0.7	6
2817	Theory of spintronic materials. Physica Status Solidi (B): Basic Research, 2006, 243, 2133-2150.	0.7	12
2818	First-principles studies of the electronic structure of cyclopentene on Si(001): density functional theory and GW calculations. Physica Status Solidi (B): Basic Research, 2006, 243, 2048-2053.	0.7	12
2819	Semiconductor-to-metal transition of double walled carbon nanotubes induced by inter-shell interaction. Physica Status Solidi (B): Basic Research, 2006, 243, 3476-3479.	0.7	30
2820	Tubeâ€"tube interaction in double-wall carbon nanotubes. Physica Status Solidi (B): Basic Research, 2006, 243, 3268-3272.	0.7	28
2821	Effects of Doping on Magnetic Properties of YCo5-x Fex and YCo5-x Agx â€" First Principles Calculation. Journal of Rare Earths, 2006, 24, 293-297.	2.5	3
2822	Interstitial Oxygen in Tin-Doped Indium Oxide Transparent Conductors. Journal of the American Ceramic Society, 2006, 89, 616-619.	1.9	30

#	Article	IF	Citations
2823	Local density of states effects at the metal-molecule interfaces in a molecular device. Nature Materials, 2006, 5, 394-399.	13.3	98
2824	First-principles studies of doped InTaO4 for photocatalytic applications. Comptes Rendus Chimie, 2006, 9, 841-845.	0.2	7
2825	Density functional study of graphite bulk and surface properties. Carbon, 2006, 44, 231-242.	5.4	192
2826	Pressure induced reactivity change on the side-wall of a carbon nanotube: A case study on the addition of singlet O2. Carbon, 2006, 44, 928-938.	5.4	10
2827	Composition evolution of nanoscale AlSc precipitates in an Alâ€“Mgâ€“Sc alloy: Experiments and computations. Acta Materialia, 2006, 54, 119-130.	3.8	103
2828	Site preference of ternary alloying elements in Ni3Al: A first-principles study. Acta Materialia, 2006, 54, 1147-1154.	3.8	130
2829	Origin of the modified orientation relationship for S(Sâ€³)-phase in Alâ€“Mgâ€“Cu alloys. Acta Materialia, 2006, 54, 1731-1740.	3.8	61
2830	Effects of Pt on the elastic properties of B2 NiAl: A combined first-principles and experimental study. Acta Materialia, 2006, 54, 2361-2369.	3.8	30
2831	Finite-temperature thermodynamic and vibrational properties of Alâ€“Niâ€“Y compounds via first-principles calculations. Acta Materialia, 2006, 54, 2291-2304.	3.8	34
2832	Hyperfine interactions in hexagonal Îµ-Fe6Ny phase investigated by MÃ¶ssbauer spectroscopy and ab initio calculations. Acta Materialia, 2006, 54, 2407-2417.	3.8	21
2833	Phase stability and structural relations of nanometer-sized, matrix-embedded precipitate phases in Alâ€“Mgâ€“Si alloys in the late stages of evolution. Acta Materialia, 2006, 54, 2945-2955.	3.8	136
2834	Effect of nitrogen on generalized stacking fault energy and stacking fault widths in high nitrogen steels. Acta Materialia, 2006, 54, 2991-3001.	3.8	153
2835	Structure stability and magnetic properties of the Niâ€“Ru system studied by ab initio and molecular dynamics calculations together with ion beam mixing. Acta Materialia, 2006, 54, 3375-3381.	3.8	22
2836	A combined first-principles/CALPHAD modeling of the Alâ€“Ir system. Acta Materialia, 2006, 54, 4101-4110.	3.8	21
2837	Phase stability and cohesive properties of Tiâ€“Zn intermetallics: First-principles calculations and experimental results. Acta Materialia, 2006, 54, 4977-4997.	3.8	91
2838	Vacancyâ€“solute complexes in aluminum. Applied Surface Science, 2006, 252, 3285-3289.	3.1	12
2839	Vacancy-solute complexes and their clusters in iron. Applied Surface Science, 2006, 252, 3303-3308.	3.1	32
2840	Theoretical calculations on atomistic behaviors in transition metals (Fe, Co, Ni)â€“Al multilayer system: ab initio approach. Applied Surface Science, 2006, 252, 8380-8383.	3.1	8

#	Article	IF	Citations
2841	Theoretical study of Ti and Fe surface alloys on Al(001) substrate. Applied Surface Science, 2006, 252, 5376-5378.	3.1	3
2842	A quantum chemical study of tertiary carbenium ions in acid catalyzed hydrocarbon conversions over phosphotungstic acid. Catalysis Today, 2006, 116, 90-98.	2.2	16
2843	USPEXâ€"Evolutionary crystal structure prediction. Computer Physics Communications, 2006, 175, 713-720.	3.0	946
2844	Direct observation of molecularly-aligned molecules in the second physisorbed layer-CO/Ag(110). Chemical Physics Letters, 2006, 418, 90-95.	1.2	4
2845	First-principles study of the stability and electronic properties of sheets and nanotubes of elemental boron. Chemical Physics Letters, 2006, 418, 549-554.	1.2	65
2846	Bending the rules: Contrasting vacancy energetics and migration in graphite and carbon nanotubes. Chemical Physics Letters, 2006, 418, 132-136.	1.2	302
2847	Dynamics of hydration water in CaCl2 complexes. Chemical Physics Letters, 2006, 419, 111-114.	1.2	10
2848	Adsorption of acrolein on single-crystal surfaces of silver: Density functional studies. Chemical Physics Letters, 2006, 420, 60-64.	1.2	25
2849	Electron scattering in scanning probe microscopy experiments. Chemical Physics Letters, 2006, 420, 177-182.	1.2	23
2850	A novel photoluminescence transition influenced by O implantation in ZnO bulk. Chemical Physics Letters, 2006, 421, 309-311.	1.2	2
2851	A mechanistic study of H2S decomposition on Ni- and Cu-based anode surfaces in a solid oxide fuel cell. Chemical Physics Letters, 2006, 421, 179-183.	1.2	67
2852	Density functional theory study of the structural and optical properties of lithium azide. Chemical Physics Letters, 2006, 422, 117-121.	1.2	39
2853	Adsorption and oxidation of NO on Au(111) surface: Density functional studies. Chemical Physics Letters, 2006, 422, 412-416.	1.2	45
2854	The Hâ€"D isotope effect in the stability of lithium alanate. Chemical Physics Letters, 2006, 423, 102-105.	1.2	21
2855	Interplay between theory and experiment in the quest for silica with reduced dimensionality grown on a Mo(112) surface. Chemical Physics Letters, 2006, 424, 115-119.	1.2	27
2856	Self-catalyzed hydrogenation and dihydrogen adsorption on titanium carbide nanoparticles. Chemical Physics Letters, 2006, 425, 273-277.	1.2	60
2857	OsB2 and RuB2, ultra-incompressible, hard materials: First-principles electronic structure calculations. Chemical Physics Letters, 2006, 425, 311-314.	1.2	93
2858	Oxygen atoms on the (111) surface of coinage metals: On the chemical state of the adsorbate. Chemical Physics Letters, 2006, 429, 86-90.	1.2	30

#	Article	IF	Citations
2859	Energy level reordering and stability of MPb12 clusters: An interplay between geometry and electronic structure. Chemical Physics Letters, 2006, 430, 101-107.	1.2	23
2860	Density functional theory study of single-wall platinum nanotubes. Chemical Physics Letters, 2006, 430, 319-322.	1.2	9
2861	Structures of undecagold clusters: Ligand effect. Chemical Physics Letters, 2006, 432, 163-166.	1.2	36
2862	3D-magnetic ordering of Co4+ dimers in a new Co3+,4+ oxychloride: Neutron diffraction analysis and DFT calculations. Chemical Physics Letters, 2006, 432, 88-93.	1.2	14
2863	The electronic structure of the dizincocene core. Chemical Physics, 2006, 327, 283-290.	0.9	38
2864	An ab initio study of the Li-ion battery cathode material Li2FeSiO4. Electrochemistry Communications, 2006, 8, 797-800.	2.3	102
2865	Prospects on Mn-doped ZnGeP2 for spintronics. Microelectronics Reliability, 2006, 46, 1747-1749.	0.9	12
2866	Effect of â^2 grain boundaries on plastic deformation of WCâ€“Co cemented carbides. Materials Science & Engineering A: Structural Materials: Properties, Microstructure and Processing, 2006, 416, 119-125.	2.6	26
2867	Multi-scale modelling of defect behavior in bcc transition metals and iron alloys for future fusion power plants. Materials Science & Engineering A: Structural Materials: Properties, Microstructure and Processing, 2006, 423, 74-78.	2.6	14
2868	Ion relaxation and hydrogen LVM in H-irradiated GaAsN. Physica B: Condensed Matter, 2006, 376-377, 583-586.	1.3	2
2869	Effects of Mn clustering on ferromagnetism in (Ga,Mn)As. Physica B: Condensed Matter, 2006, 376-377, 643-646.	1.3	4
2870	Phonons in UCoGa5. Physica B: Condensed Matter, 2006, 378-380, 1003-1004.	1.3	11
2871	Effect of boron on the stability of monoclinic NaMnO2: Theoretical and experimental studies. Materials Science and Engineering B: Solid-State Materials for Advanced Technology, 2006, 128, 115-124.	1.7	20
2872	Stress induced anisotropy of vacancy interaction and clustering in uniaxially loaded Si monocrystal. Materials Science and Engineering B: Solid-State Materials for Advanced Technology, 2006, 134, 244-248.	1.7	6
2873	Ab initio studies of intrinsic point defects, interstitial oxygen and vacancy or oxygen clustering in germanium crystals. Materials Science in Semiconductor Processing, 2006, 9, 494-497.	1.9	32
2874	The effect of compressive biaxial stress on vacancy clustering in thin Siâ€“Ge layers. Materials Science in Semiconductor Processing, 2006, 9, 507-513.	1.9	2
2875	Investigation of the impact of defect models on Monte Carlo simulations of RBS/C spectra. Nuclear Instruments & Methods in Physics Research B, 2006, 249, 776-779.	0.6	2
2876	Ab initio comparative study of C54 and C49 TiSi2 surfaces. Applied Surface Science, 2006, 252, 4943-4950.	3.1	15

#	Article	IF	Citations
2877	Highly luminescent nanocrystal quantum dots fabricated by lattice-type mismatched epitaxy. Physica E: Low-Dimensional Systems and Nanostructures, 2006, 35, 241-245.	1.3	8
2878	First-principles studies on the adsorption of molecular oxygen on Ba(110) surface. Physics Letters, Section A: General, Atomic and Solid State Physics, 2006, 352, 526-530.	0.9	8
2879	Microstructural design of hard coatings. Progress in Materials Science, 2006, 51, 1032-1114.	16.0	793
2880	Quantum mechanics based multiscale modeling of stress-induced phase transformations in iron. Journal of the Mechanics and Physics of Solids, 2006, 54, 1276-1303.	2.3	30
2881	Calculation of helium defect clustering properties in iron using a multi-scale approach. Journal of Nuclear Materials, 2006, 351, 109-118.	1.3	83
2882	Ab initio modelling of defect properties with substitutional and interstitials elements in steels and Zr alloys. Journal of Nuclear Materials, 2006, 351, 1-19.	1.3	95
2883	Elastic properties and high-pressure behavior of from ab initio calculations. Journal of Physics and Chemistry of Solids, 2006, 67, 1477-1483.	1.9	44
2884	Theoretical and experimental study of CaWO4 and SrWO4 under pressure. Journal of Physics and Chemistry of Solids, 2006, 67, 2164-2171.	1.9	24
2885	Pressure induced metallization of Germane. Journal of Physics and Chemistry of Solids, 2006, 67, 2095-2099.	1.9	59
2886	A density-functional and molecular-dynamics study on the physical properties of yttrium-doped tantalum oxynitride. Journal of Solid State Chemistry, 2006, 179, 2265-2270.	1.4	14
2887	Mn5Si3-type host-interstitial boron rare-earth metal silicide compounds RE5Si3: Crystal structures, physical properties and theoretical considerations. Journal of Solid State Chemistry, 2006, 179, 2310-2328.	1.4	33
2888	New insights into the role of native point defects in ZnO. Journal of Crystal Growth, 2006, 287, 58-65.	0.7	315
2889	Lattice dynamics and electrical properties of wurtzite ZnO determined by a density functional theory method. Journal of Crystal Growth, 2006, 287, 199-203.	0.7	37
2890	Nonparabolicity and excitons in optical absorption of InN. Journal of Crystal Growth, 2006, 288, 294-297.	0.7	5
2891	A combined first-principles calculation and thermodynamic modeling of the Fâ€“Kâ€“Na system. Materials Science & Engineering A: Structural Materials: Properties, Microstructure and Processing, 2006, 418, 161-171.	2.6	13
2892	Electronic and structural properties of cementite-type M3X (M=Fe, Co, Ni; X=C or B) by first principles calculations. Physica B: Condensed Matter, 2006, 371, 126-132.	1.3	130
2893	Formation of and in p-type GaN(Mg,H). Physica B: Condensed Matter, 2006, 376-377, 477-481.	1.3	1
2894	Influence of local Coulomb interactions on lattice dynamics in superconductor. Physica B: Condensed Matter, 2006, 378-380, 1029-1030.	1.3	0

#	Article	IF	Citations
2895	Electronic structure and optical absorption spectra of CdSe covered with ZnSe and ZnS epilayers. Solid State Communications, 2006, 137, 332-337.	0.9	9
2896	Phenomenological band structure model of magnetic coupling in semiconductors. Solid State Communications, 2006, 138, 353-358.	0.9	134
2897	Density functional studies on the ferromagnetic properties of (Zn,Cr)Te. Solid State Communications, 2006, 138, 275-278.	0.9	5
2898	Strong Coulomb correlation effects in ZnO. Solid State Communications, 2006, 139, 391-396.	0.9	15
2899	Magnetic coupling in the cluster Fe2Mn4 : A fully unconstrained density-functional study. Solid State Communications, 2006, 140, 480-482.	0.9	3
2900	Oxygen reduction reactions in the SOFC cathode of Ag/CeO2. Solid State Ionics, 2006, 177, 939-947.	1.3	101
2901	Ab initio density functional study on changes in local structure in perovskite compound, LixLa1/3NbO3. Solid State Ionics, 2006, 177, 1259-1266.	1.3	12
2902	Growth and decay of the Pd(111)â€“Pd5O4 surface oxide: Pressure-dependent kinetics and structural aspects. Surface Science, 2006, 600, 205-218.	0.8	57
2903	A new structural model for the SiC(0001)(3Ã—3) surface derived from first principles studies. Surface Science, 2006, 600, 298-304.	0.8	10
2904	Combined STM, LEED and DFT study of Ag(100) exposed to oxygen near atmospheric pressures. Surface Science, 2006, 600, 617-624.	0.8	29
2905	Using Î²-hydride elimination to test propositions for characterizing surface catalyzed reactions. Surface Science, 2006, 600, L25-L28.	0.8	12
2906	Adsorption dynamics of O2 on Cu(100). Surface Science, 2006, 600, 1574-1578.	0.8	22
2907	Self-assembled molecular corrals on a semiconductor surface. Surface Science, 2006, 600, 43-47.	0.8	26
2908	Metallization of Ge(001)-p(2Ã—1) surface as result of thermal fluctuations. Surface Science, 2006, 600, 1654-1658.	0.8	1
2909	Adsorption and reactions of HN3 on Si(100)-2Ã—1: A computational study. Surface Science, 2006, 600, 1113-1124.	0.8	3
2910	Ammonia activation on platinum {111}: A density functional theory study. Surface Science, 2006, 600, 1714-1734.	0.8	117
2911	Theoretical STM images of alkaline-earth metal adsorbed Si(111)3Ã—2 surfaces. Surface Science, 2006, 600, 3606-3609.	0.8	7
2912	Oxygen induced segregation of copper to Ag/Cu(100) surface. Surface Science, 2006, 600, 4103-4107.	0.8	9

#	Article	IF	Citations
2913	Ab initio studies of hydrogen desorption from low index magnesium hydride surface. Surface Science, 2006, 600, 1854-1859.	0.8	67
2914	The effect of embedded Pb on Cu diffusion on Pb/Cu(111) surface alloys. Surface Science, 2006, 600, 1901-1908.	0.8	13
2915	Comparison of S, Pt, and Hf adsorption on NiAl(110). Surface Science, 2006, 600, 2079-2090.	0.8	26
2916	Atomic and electronic structure of Sr/Si(001)-(2Ã—2). Surface Science, 2006, 600, 3614-3618.	0.8	5
2917	First-principles studies on initial growth of Ni on MgO(001) surface. Surface Science, 2006, 600, 2154-2162.	0.8	18
2918	Scattering of Cu(100) image state electrons from single Cu adatoms and vacancies: A comparative study. Surface Science, 2006, 600, 2184-2194.	0.8	9
2919	Formation of one-dimensional crystalline silica on a metal substrate. Surface Science, 2006, 600, L164-L168.	0.8	19
2920	Observation of a (â^š3Ã—â^š3)-R30Â° reconstruction on GaN(0001) by RHEED and LEED. Surface Science, 2006, 600, 169-174.	0.8	12
2921	Experimental and theoretical studies of adsorption of on Î±-Fe2O3 (0001) surfaces. Surface Science, 2006, 600, 2874-2885.	0.8	17
2922	Density functional theory study of hydrogen sulfide dissociation on bi-metallic Niâ€“Mo catalysts. Surface Science, 2006, 600, 3202-3216.	0.8	28
2923	Kinetic Monte Carlo simulations of the partial oxidation of methanol on oxygen-covered Cu(110). Surface Science, 2006, 600, 3258-3265.	0.8	32
2924	Theoretical studies on the adsorption and decomposition of H2O on Pd(111) surface. Surface Science, 2006, 600, 4572-4583.	0.8	85
2925	Initial incorporation of sulfur into the Pd(111) surface: A theoretical study. Surface Science, 2006, 600, 4508-4516.	0.8	13
2926	The chemisorption of pentacene on Si(001)-2Ã—1. Surface Science, 2006, 600, 5092-5103.	0.8	25
2927	Site-specific electronic structure analysis by channeling EELS and first-principles calculations. Ultramicroscopy, 2006, 106, 1019-1023.	0.8	18
2928	Partial oxidation of methanol on Cu(110): Energetics and kinetics. Computational and Theoretical Chemistry, 2006, 771, 117-122.	1.5	22
2929	Ba adsorption on the TiO2 (110) surface. A density functional study. Computational and Theoretical Chemistry, 2006, 769, 237-242.	1.5	4
2930	Electronic structure of dimetallocene molecules: Dizincocene Zn2(Î·5-C5Me5)2. Computational and Theoretical Chemistry, 2006, 773, 43-52.	1.5	20

#	Article	IF	Citations
2931	Evolution of the dizincocene metalâ€“metal bond in the series Zn2L2 where L=H, CH3, F, Î·5-C5H5. Computational and Theoretical Chemistry, 2006, 776, 113-123.	1.5	17
2932	First-Principles Study of Hydrogen Storage on Li12C60. Journal of the American Chemical Society, 2006, 128, 9741-9745.	6.6	533
2933	Effect of Ti and metal vacancies on the electronic structure, stability, and dehydrogenation ofNa3AlH6: Supercell band-structure formalism and gradient-corrected density-functional theory. Physical Review B, 2006, 73, .	1.1	35
2934	Magnetic interactions in transition-metal-doped ZnO: Anab initiostudy. Physical Review B, 2006, 74, .	1.1	291
2935	Hydrogen storage capacity of titanium met-cars. Journal of Physics Condensed Matter, 2006, 18, 9509-9517.	0.7	32
2936	Self-interstitial atom defects in bcc transition metals: Group-specific trends. Physical Review B, 2006, 73, .	1.1	360
2937	Design of shallow acceptors inZnO: First-principles band-structure calculations. Physical Review B, 2006, 74, .	1.1	198
2938	Atomistic Models of OH Defects in Nominally Anhydrous Minerals. Reviews in Mineralogy and Geochemistry, 2006, 62, 67-83.	2.2	23
2939	Magnetic properties ofFeâ•Co(001)superlattices from first-principles theory. Physical Review B, 2006, 74, .	1.1	6
2940	Structural and electronic properties of4Ã…carbon nanotubes onSi(001)surfaces. Physical Review B, 2006, 74, .	1.1	23
2941	Quasiharmonic approximation applied toLiBH4and its decomposition products. Physical Review B, 2006, 73, .	1.1	51
2942	Oxidation energies of transition metal oxides within theGGA+Uframework. Physical Review B, 2006, 73, .	1.1	1,991
2943	Heterolytic Splitting of H2and CH4on Î³-Alumina as a Structural Probe for Defect Sites. Journal of Physical Chemistry B, 2006, 110, 23944-23950.	1.2	141
2944	Effects of cationdstates on the structural and electronic properties of III-nitride and II-oxide wide-band-gap semiconductors. Physical Review B, 2006, 74, .	1.1	318
2945	Modelling the phase diagram of magnetic shape memory Heusler alloys. Journal Physics D: Applied Physics, 2006, 39, 865-889.	1.3	306
2946	Ab initiocalculation of the phase stability in Au-Pd and Ag-Pt alloys. Physical Review B, 2006, 73, .	1.1	116
2947	Dielectric Properties of Rare-Earth Oxides: General Trends from Theory. , 0, , 225-246.		2
2948	Room temperature ferromagnetism in Mn-doped Î³-Ga2O3 with spinel structure. Applied Physics Letters, 2006, 89, 181903.	1.5	97

#	Article	IF	Citations
2949	Effects of atomic relaxation and the electronic structure of niobium (100) and (110) surfaces. Physics of Metals and Metallography, 2006, 102, 604-610.	0.3	14
2950	Structure and properties of BeO nanotubes. Physics of the Solid State, 2006, 48, 398-401.	0.2	72
2951	Charge state and diffusion of hydrogen in the TiZrNi icosahedral alloy. Physics of the Solid State, 2006, 48, 1625-1628.	0.2	6
2952	Energy and electronic properties of non-carbon nanotubes based on silicon dioxide. Physics of the Solid State, 2006, 48, 2021-2027.	0.2	8
2953	Geometry and electronic properties of single vacancies in achiral carbon nanotubes. European Physical Journal B, 2006, 54, 243-247.	0.6	13
2954	An embedded-atom potential for the Cuâ€“Ag system. Modelling and Simulation in Materials Science and Engineering, 2006, 14, 817-833.	0.8	444
2955	Ab initiothermodynamics and phase diagram of solid magnesium: A comparison of the LDA and GGA. Journal of Chemical Physics, 2006, 125, 194507.	1.2	38
2956	Comment on â€œMagnetism in Atomic-Size Palladium Contacts and Nanowiresâ€• Physical Review Letters, 2006, 96, 079701; author reply 079702.	2.9	32
2958	Acid-based Catalysis in Zeolites Investigated by Density-Functional Methods. Topics in Catalysis, 2006, 37, 41-54.	1.3	46
2959	Reactivity of Bimetallic Systems Studied from First Principles. Topics in Catalysis, 2006, 37, 29-39.	1.3	189
2960	Density Functional Study of the CO Oxidation on a Doped Rutile TiO2(110): Effect of Ionic Au in Catalysis. Catalysis Letters, 2006, 107, 143-147.	1.4	107
2961	Structural relaxation and magnetic anisotropy: Co wire at the Pt(111) step edge. European Physical Journal D, 2006, 56, 51-59.	0.4	5
2962	Theoretical study of the structural properties of SiC(001)â€”Si-terminated surface and the formation of its STM images. European Physical Journal D, 2006, 56, 85-92.	0.4	2
2963	Properties of ferroelectric ultrathin films from first principles. Journal of Materials Science, 2006, 41, 137-145.	1.7	37
2964	Structure and stability of binary alloy surfaces: Segregation, relaxation, and ordering from first-principles calculations. Applied Physics A: Materials Science and Processing, 2006, 82, 415-419.	1.1	40
2965	Equation of state of MgGeO3 perovskite to 65ÂGPa: comparison with the post-perovskite phase. Physics and Chemistry of Minerals, 2006, 33, 699-709.	0.3	43
2966	Real-space density-functional calculations for Si divacancies with large size supercell models. Physica B: Condensed Matter, 2006, 376-377, 196-199.	1.3	4
2967	First-principles calculation of positron states and annihilation at defects in semiconductors. Physica B: Condensed Matter, 2006, 376-377, 971-974.	1.3	8

#	Article	IF	Citations
2968	Adhesion at metalâ€“ZrO2 interfaces. Surface Science Reports, 2006, 61, 303-344.	3.8	173
2969	Methylthiolate adsorption on Au(111): Energetics, vibrational modes and STM imaging. Surface Science, 2006, 600, 4039-4043.	0.8	11
2970	Surface electronic structure of O(2Ã—1)/Cu(110): Role of the surface state at the zone boundary -point in STS. Surface Science, 2006, 600, 4310-4314.	0.8	7
2971	Low temperature adsorption of oxygen on reduced V2O3(0001) surfaces. Surface Science, 2006, 600, 1497-1503.	0.8	55
2972	Extended embedded-atom method for platinum nanoparticles. Surface Science, 2006, 600, 1982-1990.	0.8	17
2973	Energetics of the growth mode transition in InAs/GaAs(001) small quantum dot formation: A first-principles study. Surface Science, 2006, 600, 2007-2010.	0.8	9
2974	Theoretical insight of adsorption thermodynamics of multifunctional molecules on metal surfaces. Surface Science, 2006, 600, 2103-2112.	0.8	76
2975	Active role of buried ultrathin oxide layers in adsorption of O2 on Au films. Surface Science, 2006, 600, 3388-3393.	0.8	14
2976	Organic/metal interfaces in self-assembled monolayers of conjugated thiols: A first-principles benchmark study. Surface Science, 2006, 600, 4548-4562.	0.8	128
2977	Theoretical investigation of site-specific characteristics of CO adsorption complexes in the Li+-FER zeolite. Applied Catalysis A: General, 2006, 307, 118-127.	2.2	43
2978	Ab initio molecular dynamics study of the hydration of the formohydroxamate anion. Biophysical Chemistry, 2006, 124, 222-228.	1.5	9
2979	Lamellar reaction phenomena: from intercalation to nanomaterials formation. Journal of Physics and Chemistry of Solids, 2006, 67, 888-895.	1.9	11
2980	Azine bridged silver coordination polymers: Powder X-ray diffraction route to crystal structure determination of silver benzotriazole. Journal of Solid State Chemistry, 2006, 179, 1053-1059.	1.4	30
2981	Computational study of cation substitutions in apatites. Journal of Solid State Chemistry, 2006, 179, 1581-1587.	1.4	49
2982	Density functional study of the stability and electronic properties of TaxNy compounds used as copper diffusion barriers. Microelectronic Engineering, 2006, 83, 2077-2081.	1.1	22
2983	Investigation of metal/carbon-related materials for fuel cell applications by electronic structure calculations. Materials Science and Engineering C, 2006, 26, 1207-1210.	3.8	89
2984	A constrained optimization algorithm for total energy minimization in electronic structure calculations. Journal of Computational Physics, 2006, 217, 709-721.	1.9	44
2985	Self-consistent-field calculations using Chebyshev-filtered subspace iteration. Journal of Computational Physics, 2006, 219, 172-184.	1.9	152

#	Article	IF	Citations
2986	Adsorption on the carbon nanotubes. Frontiers of Physics in China, 2006, 1, 317-322.	1.0	9
2987	Polarization, piezoelectric constants, and elastic constants of ZnO, MgO, and CdO. Journal of Electronic Materials, 2006, 35, 538-542.	1.0	136
2988	Gold nanowires and the effect of impurities. Nanoscale Research Letters, 2006, 1, 91-98.	3.1	17
2989	Mechanisms of plastic deformation of WCâ€“Co and Ti(C, N)â€“WCâ€“Co. International Journal of Refractory Metals and Hard Materials, 2006, 24, 135-144.	1.7	93
2990	Strength and reinforcement of interfaces in cemented carbides. International Journal of Refractory Metals and Hard Materials, 2006, 24, 80-88.	1.7	30
2991	Promoter and poisoning effects on NO-catalyzed dissociation on bimetallic RhCu(111) surfaces. Journal of Catalysis, 2006, 239, 431-440.	3.1	45
2992	First-principles-based kinetic Monte Carlo simulation of the selective hydrogenation of acetylene over Pd(111). Journal of Catalysis, 2006, 242, 1-15.	3.1	178
2993	Energetics of methane dissociative adsorption on Rh{111} from DFT calculations. Journal of Catalysis, 2006, 242, 309-318.	3.1	90
2994	A theoretical study of coverage effects for ethylene epoxidation on Cu(111) under low oxygen pressure. Journal of Catalysis, 2006, 243, 404-409.	3.1	41
2995	A density functional theory study of the alkylation of isobutane with butene over phosphotungstic acid. Journal of Catalysis, 2006, 244, 65-77.	3.1	51
2996	First-Principles Study on Atomistic Behaviors and Magnetism of Physisorpted Co and Fe Atoms on MgO. IEEE Transactions on Magnetics, 2006, 42, 3174-3176.	1.2	5
2997	Phase stability of Ti3SiC2 at elevated temperatures. Scripta Materialia, 2006, 54, 105-107.	2.6	43
2998	A first-principles study of the site preference of Cr in B2 NiAl. Scripta Materialia, 2006, 54, 405-410.	2.6	25
2999	Al2(Mg,Ca) phases in Mgâ€“Alâ€“Ca ternary system: First-principles prediction and experimental identification. Scripta Materialia, 2006, 55, 573-576.	2.6	53
3000	The strength and hardness of cubic spinel SiAlON (c-Si6â^'zAlzOzN8â^'z, z=1). Scripta Materialia, 2006, 55, 391-394.	2.6	3
3001	Structural stability of intermetallic phases in the Zrâ€“Sn system. Scripta Materialia, 2006, 55, 485-488.	2.6	34
3002	Site preference of transition metal elements in Ni3Al. Scripta Materialia, 2006, 55, 433-436.	2.6	133
3003	Effects of Cr on the elastic properties of B2 NiAl: A first-principles study. Scripta Materialia, 2006, 55, 759-762.	2.6	18

#	Article	IF	Citations
3004	Ab Initio Molecular Dynamics Studies of Ionic Dissolution and Precipitation of Sodium Chloride and Silver Chloride in Water Clusters, NaCl(H2O)n and AgCl(H2O)n,n = 6, 10, and 14. Chemistry - A European Journal, 2006, 12, 6382-6392.	1.7	31
3005	Some Experimental Evidence that Zn4O(BO3)2 is Zn6O(OH)(BO3)3. Angewandte Chemie - International Edition, 2006, 45, 4060-4062.	7.2	8
3006	When the Reporter Induces the Effect: Unusual IR spectra of CO on Au1/MgO(001)/Mo(001). Angewandte Chemie - International Edition, 2006, 45, 2633-2635.	7.2	101
3007	Mysterious Platinum Nitride. Angewandte Chemie - International Edition, 2006, 45, 4365-4368.	7.2	56
3008	Synthesis and Structure of Ultrathin Aluminosilicate Films. Angewandte Chemie - International Edition, 2006, 45, 7636-7639.	7.2	45
3009	Thermodynamic Modeling of Hydrogen Adsorption on Carbon Nanotubes During CVD Growth. Chemical Vapor Deposition, 2006, 12, 388-394.	1.4	4
3010	Migration of Carbon into Subsurface Layers of Rh(100): A DFT Study. ChemPhysChem, 2006, 7, 1022-1025.	1.0	10
3011	Acetylene Decomposition on Rh(100): Theory and Experiment. ChemPhysChem, 2006, 7, 1068-1074.	1.0	6
3012	Atomâ€“Molecule Interactions on Transition Metal Surfaces: A DFT Study of CO and Several Atoms on Rh(100), Pd(100) and Ir(100). ChemPhysChem, 2006, 7, 1075-1080.	1.0	7
3013	Predicting the Shape and Structure of Face-Centered Cubic Gold Nanocrystals Smaller than 3 nm. ChemPhysChem, 2006, 7, 1544-1553.	1.0	74
3014	Asymmetry Induction by Cooperative Intermolecular Hydrogen Bonds in Surface-Anchored Layers of Achiral Molecules. ChemPhysChem, 2006, 7, 2197-2204.	1.0	46
3015	Characterization of O2â€“CeO2 Interactions Using In Situ Raman Spectroscopy and First-Principle Calculations. ChemPhysChem, 2006, 7, 1957-1963.	1.0	184
3016	Surface Composition of Materials Used as Catalysts for Methanol Steam Reforming: A Theoretical Study. ChemPhysChem, 2006, 7, 1802-1812.	1.0	26
3020	CdIn2S4 Nanotubes and â€œMarigoldâ€•Nanostructures: A Visible-Light Photocatalyst. Advanced Functional Materials, 2006, 16, 1349-1354.	7.8	345
3021	Defect Formation Energies in Chalcopyrite-Type AgInSe2 and the Rerated Chalcopyrite Compounds by First Principles Calculations. , 2006, , .		4
3022	Reconstruction and structural transition at metal/diamond interfaces. International Journal of Materials Research, 2006, 97, 768-771.	0.1	0
3023	Polarity Control of ZnO on N-Terminated GaN(000ar1) Surfaces. Japanese Journal of Applied Physics, 2006, 45, 8578-8580.	0.8	4
3024	Diâ€“Ïƒ and Dative Binding of Benzene and Pyridine on a Si(5,5,12)-2 Ã—1. Japanese Journal of Applied Physics, 2006, 45, 2175-2179.	0.8	10

#	Article	IF	Citations
3025	Dilute Ga Dopant in TiO2by X-ray Absorption Near-Edge Structure. Japanese Journal of Applied Physics, 2006, 45, 7028-7031.	0.8	14
3026	The structural models for the reconstructions of 3C-SiC(111) and 6H-SiC(0001) surfaces. Journal of Physics Condensed Matter, 2006, 18, 6953-6963.	0.7	1
3027	TiNi Monatomic Chains Stabilized by Alloying: a First-Principles Study. Chinese Physics Letters, 2006, 23, 182-185.	1.3	6
3028	Theoretical Investigation of the Band Alignment at the LaAlO3/SrTiO3 Interface. Materials Research Society Symposia Proceedings, 2006, 966, 1.	0.1	1
3029	Spin-Polarized Electronic Structure. , 2006, , 13-39.		1
3030	Thermodynamic modeling of the sodium alanates and the Naâ€“Alâ€“H system. International Journal of Materials Research, 2006, 97, 1484-1494.	0.1	26
3031	Possiblegraphitic-boron-nitride-based metal-free molecular magnets from first principles study. Journal of Physics Condensed Matter, 2006, 18, 569-575.	0.7	23
3032	A New Period-Doubled Modulation on the In/Si(111)4 Ã—1 Surface Induced by Defects. Japanese Journal of Applied Physics, 2006, 45, 2087-2090.	0.8	2
3033	Complexities in modeling the metal to molecule interface. Journal of Vacuum Science & Technology B, 2006, 24, 1987.	1.3	2
3034	Vibrational properties and superconductivity in Ba 24 Si 100. Europhysics Letters, 2006, 75, 153-159.	0.7	8
3035	A multiscale study of ferromagnetism in clustered (Ga,Mn)N. Journal of Physics Condensed Matter, 2006, 18, 1561-1567.	0.7	12
3036	Localized magnetism in liquid Al 80 Mn 20 alloys: A first-principles investigation. Europhysics Letters, 2006, 74, 275-280.	0.7	3
3037	Nucleation of cobalt silicide islands on Si(111)-7 Ã— 7. Journal of Physics Condensed Matter, 2006, 18, 6987-6995.	0.7	24
3038	First-Principles Study of the Step Oxidation at Vicinal Si(001) Surfaces. Japanese Journal of Applied Physics, 2006, 45, 2144-2147.	0.8	4
3039	Nanospintronic properties of carbon-cobalt atomic chains. Europhysics Letters, 2006, 73, 642-648.	0.7	18
3040	Apparent diameter of carbon nanotubes in scanning tunnelling microscopy measurements. Journal of Physics Condensed Matter, 2006, 18, 5793-5805.	0.7	11
3041	First principles study of Asâ€“vacancy interaction and the ring mechanism of diffusion in the presence of Ge in Si. Journal of Physics Condensed Matter, 2006, 18, 4879-4886.	0.7	7
3042	A density functional study of the pressure induced phase transition in LiYF4. Journal of Physics Condensed Matter, 2006, 18, 2429-2441.	0.7	12

#	Article	IF	Citations
3043	Characterization of the electronic properties of YB12, ZrB12, and LuB12using11B NMR and first-principles calculations. Journal of Physics Condensed Matter, 2006, 18, 2525-2535.	0.7	42
3044	Calculations of effect of anisotropic stress/strain on dopant diffusion in silicon under equilibrium and nonequilibrium conditions. Journal of Vacuum Science & Technology B, 2006, 24, 456.	1.3	21
3045	First principles calculations of dopant solubility based on strain compensation and direct binding between dopants and group IV impurities. Journal of Vacuum Science & Technology B, 2006, 24, 700.	1.3	12
3046	First-principles studies of chiral step reconstructions of Cu(100) by adsorbed glycine and alanine. Journal of Chemical Physics, 2006, 124, 074703.	1.2	44
3047	The chemisorption of coronene on Si(001)-2Ã—1. Journal of Chemical Physics, 2006, 124, 054701.	1.2	19
3048	Vibrational lifetimes of molecular adsorbates on metal surfaces. Journal of Chemical Physics, 2006, 125, 054706.	1.2	89
3049	Coverage dependence and hydroperoxyl-mediated pathway of catalytic water formation on Pt (111) surface. Journal of Chemical Physics, 2006, 125, 054701.	1.2	61
3050	Structure change of liquid GaSb under pressure: An ab initio molecular-dynamics simulation. Journal of Chemical Physics, 2006, 125, 094506.	1.2	1
3051	Size-dependent alternation of magnetoresistive properties in atomic chains. Journal of Chemical Physics, 2006, 125, 121102.	1.2	11
3052	Self-diffusion constants in silicon: Ab initio calculations in combination with classical rate theory. Journal of Chemical Physics, 2006, 125, 226101.	1.2	8
3053	Orbital-corrected orbital-free density functional theory. Journal of Chemical Physics, 2006, 124, 081107.	1.2	20
3054	Femtosecond laser induced associative desorption of H2 from Ru(0001): Comparison of â€œfirst principlesâ€•theory with experiment. Journal of Chemical Physics, 2006, 124, 244702.	1.2	71
3055	Constrained dynamics and extraction of normal modes fromab initiomolecular dynamics: Application to ammonia. Journal of Chemical Physics, 2006, 125, 064707.	1.2	7
3056	Initial oxidation of the Rh(110) surface: Ordered adsorption and surface oxide structures. Journal of Chemical Physics, 2006, 125, 094701.	1.2	57
3057	Low sticking probability in the nonactivated dissociation of N2 molecules on W(110). Journal of Chemical Physics, 2006, 125, 144705.	1.2	42
3058	Thiol and thiolate bond formation of ferrocene-1,1-dithiol to a Ag(111) surface. Journal of Chemical Physics, 2006, 125, 194705.	1.2	7
3059	Structural and electronic properties of diazonium functionalized (4, 4) single walled carbon nanotube: anab initiostudy. Molecular Simulation, 2006, 32, 1213-1217.	0.9	4
3060	First Principles Study on Na x Li 1â^' x FePO 4 As Cathode Material for Rechargeable Lithium Batteries. Chinese Physics Letters, 2006, 23, 61-64.	1.3	49

#	Article	IF	Citations
3061	No evidence of metallic methane at high pressure. High Pressure Research, 2006, 26, 369-375.	0.4	21
3062	Modelling of the energetics and kinetics of Al deposition on 5-fold Al-rich quasicrystal surfaces. Philosophical Magazine, 2006, 86, 831-840.	0.7	13
3063	Energies of conservative and non-conservative antiphase boundaries in Ti3Al: a first principles study. Philosophical Magazine, 2006, 86, 1243-1259.	0.7	17
3064	Using EELS to observe composition and electronic structure variations at dislocation cores in GaN. Philosophical Magazine, 2006, 86, 4727-4746.	0.7	15
3065	X-ray diffraction study and theoretical calculations on the X-phase, Al9(Co,â€‰Ni)4. Philosophical Magazine, 2006, 86, 451-456.	0.7	7
3066	The Role of Phase Stability in Ductile, Ordered B2 Intermetallics. Materials Research Society Symposia Proceedings, 2006, 980, 10.	0.1	5
3067	First-Principles Calculations of the Electrochemical Reactions of Water at an Immersed Ni(111)âˆ•H[sub 2]O Interface. Journal of the Electrochemical Society, 2006, 153, E207.	1.3	66
3068	Applications of Density Functional Theory in the Geosciences. MRS Bulletin, 2006, 31, 675-680.	1.7	13
3069	Scanning tunneling spectroscopy simulations of poly(3-dodecylthiophene) chains adsorbed on highly oriented pyrolytic graphite. Journal of Chemical Physics, 2006, 125, 034708.	1.2	11
3070	Molecular dynamics simulation of aluminium diffusion in decagonal quasicrystals. Philosophical Magazine, 2006, 86, 1051-1057.	0.7	8
3071	Restructuring of Nuclear Oxide Fuel under High Burnup Irradiation. Advances in Science and Technology, 2006, 45, 1952-1960.	0.2	1
3072	Effects of Segregated Ga on an Al Grain Boundary: A First-Principles Computational Tensile Test. Materials Transactions, 2006, 47, 2678-2681.	0.4	23
3073	Interstitial-Mediated Arsenic Clustering in Ultrashallow Junction Formation. Electrochemical and Solid-State Letters, 2006, 9, G354.	2.2	21
3074	Ideal strength of a Cu multi-shell nano-wire. Modelling and Simulation in Materials Science and Engineering, 2006, 14, 1031-1039.	0.8	8
3075	Structure Models of Massively Transformed High Niobium Containing TiAl Alloys. Materials Research Society Symposia Proceedings, 2006, 980, 1.	0.1	5
3076	Reaction Energy for LiMn[sub 2]O[sub 4] Spinel Dissolution in Acid. Electrochemical and Solid-State Letters, 2006, 9, A265.	2.2	76
3077	The Role of Metallic Bonding in the Crystallographic Pitting of Magnesium. Journal of the Electrochemical Society, 2006, 153, B358.	1.3	39
3078	Phase Stability of Carbides and Nitrides in Steel. Materials Research Society Symposia Proceedings, 2006, 979, 1.	0.1	4

#	Article	IF	Citations
3079	Mechanisms for Interstitial-Mediated Transient Enhanced Diffusion of N-type Dopants. Materials Research Society Symposia Proceedings, 2006, 912, 1.	0.1	0
3080	Theoretical investigation of Pt monosilicide and several germanides: electronic structure, surface energetics, and work functions. Materials Research Society Symposia Proceedings, 2006, 980, 43.	0.1	0
3081	Synthesis and Characterization of Nitrides of Iridium and Palladium. Materials Research Society Symposia Proceedings, 2006, 987, 1.	0.1	0
3082	Theoretical first step towards an understanding of the uranyl ion sorption on the rutile TiO2(110) face: A DFT periodic and cluster study. Radiochimica Acta, 2006, 94, 601-607.	0.5	19
3083	First Principles Calculation of Defect and Magnetic Structures in FeCo. Materials Transactions, 2006, 47, 2646-2650.	0.4	7
3084	H Adsorption On Rh (110) Surface. Materials Research Society Symposia Proceedings, 2006, 927, 1.	0.1	0
3085	Experimental and theoretical characterization of Al3Sc precipitates in Alâ€“Mgâ€“Siâ€“Cuâ€“Scâ€“Zr alloys. International Journal of Materials Research, 2006, 97, 321-324.	0.8	3
3086	First-principles study of the effects of segregated Ga on an Al grain boundary. Journal of Physics Condensed Matter, 2006, 18, 5121-5128.	0.7	34
3087	Stability and electronic structure of InN nanotubes from first-principles study. Chinese Physics B, 2006, 15, 798-801.	1.3	6
3088	Modeling of Defect Evolution and TED under Stress based on DFT Calculations. , 2006, , .		3
3089	Structural transformations and improved ductility in ordered FeCo and ZrCo intermetallics. Materials Research Society Symposia Proceedings, 2006, 980, 3.	0.1	0
3090	First Principles Study of the Aluminumâ€“Cubic Boron Nitride Interface. Journal of Adhesion, 2006, 82, 779-803.	1.8	5
3091	Fermi surface deformation in lithium under high pressure. High Pressure Research, 2006, 26, 461-465.	0.4	3
3092	The energetics of oxide surfaces by quantum Monte Carlo. Journal of Physics Condensed Matter, 2006, 18, L435-L440.	0.7	37
3093	Spin transitions in theFexMn1âˆ'xS2system. Physical Review B, 2006, 73, .	1.1	22
3094	Local Electronic Structure ofBi2Sr2CaCu2O8near Oxygen Dopants: A Window on the High-TcPairing Mechanism. Physical Review Letters, 2006, 96, 197002.	2.9	45
3095	Lattice Relaxation in Oxide Heterostructures:LaTiO3/SrTiO3Superlattices. Physical Review Letters, 2006, 97, 056802.	2.9	237
3096	Could the relaxed and the O-deficient CrO2(100) surface retain half-metallicity?. Applied Physics Letters, 2006, 88, 121903.	1.5	9

#	Article	IF	Citations
3097	Anomalous lattice expansion of coherently strainedSrTiO3thin films grown onSi(001)by kinetically controlled sequential deposition. Physical Review B, 2006, 73, .	1.1	60
3098	Half-Metallic Digital Ferromagnetic Heterostructure Composed of aî´-Doped Layer of Mn in Si. Physical Review Letters, 2006, 96, 027211.	2.9	56
3099	Defects in virgin andN+-implanted ZnO single crystals studied by positron annihilation, Hall effect, and deep-level transient spectroscopy. Physical Review B, 2006, 74, .	1.1	135
3100	Ab initiostudy of the ideal shear strength and elastic deformation behaviors of B2FeAlandNiAl. Physical Review B, 2006, 73, .	1.1	20
3101	Role of Lateral Alkyl Chains in Modulation of Molecular Structures on Metal Surfaces. Physical Review Letters, 2006, 96, 226101.	2.9	51
3102	Suitability ofp-type conditions for ferromagnetism inGaN:Mn. Physical Review B, 2006, 73, .	1.1	39
3103	Strain-Free Polarization Superlattice in Silicon Carbide: A Theoretical Investigation. Physical Review Letters, 2006, 96, 236803.	2.9	17
3104	Prediction of unusual stable ordered structures of Au-Pd alloys via a first-principles cluster expansion. Physical Review B, 2006, 74, .	1.1	71
3105	Preferential growth of Pt on rutileTiO2. Physical Review B, 2006, 73, .	1.1	32
3106	Orientational Defects in Ice Ih: An Interpretation of Electrical Conductivity Measurements. Physical Review Letters, 2006, 96, 075501.	2.9	35
3107	Prediction of different crystal structure phases in metal borides: A lithium monoboride analog toMgB2. Physical Review B, 2006, 73, .	1.1	77
3108	Magnetically Induced Phonon Anisotropy inZnCr2O4from First Principles. Physical Review Letters, 2006, 96, 205505.	2.9	109
3109	Electronic structure and equation of state data of warm dense gold. Physical Review E, 2006, 73, 056403.	0.8	28
3110	Ferromagnetism and its evolution during long-term annealing in (Ga,Mn)As. Physical Review B, 2006, 74, .	1.1	10
3111	Parallel self-consistent-field calculations via Chebyshev-filtered subspace acceleration. Physical Review E, 2006, 74, 066704.	0.8	145
3112	Electron Core-Hole Interaction and Its Induced Ionic Structural Relaxation in Molecular Systems under X-Ray Irradiation. Physical Review Letters, 2006, 97, 246101.	2.9	40
3113	Atomistic lattice-gas modeling of CO oxidation on Pd(100): Temperature-programed spectroscopy and steady-state behavior. Journal of Chemical Physics, 2006, 124, 154705.	1.2	49
3114	Mastering the Molecular Dynamics of a Bistable Molecule by Single Atom Manipulation. Physical Review Letters, 2006, 97, 216103.	2.9	42

#	Article	IF	Citations
3115	First-principles calculations of the adsorption and hydrogenation reactions ofCHx(x=0,4)species on aFe(100)surface. Physical Review B, 2006, 73, .	1.1	88
3116	Evidence for the Formation of Different Energetically Similar Atomic Structures inAg(111)â˜'(7Ã—7)â˜'R19.1Â°â˜'CH3S. Physical Review Letters, 2006, 97, 226103.	2.9	37
3117	Neutral and negatively chargedAl12X(X=Si, Ge, Sn, Pb) clusters studied from first principles. Physical Review B, 2006, 74, .	1.1	43
3118	Solute/defect-mediated pathway for rapid nanoprecipitation in solid solutions:Î³surface analysis in fcc Al-Ag. Physical Review B, 2006, 73, .	1.1	46
3119	Single-walled carbon nanotube bundle under hydrostatic pressure studied by first-principles calculations. Physical Review B, 2006, 73, .	1.1	26
3120	Magnetism of two-dimensional defects in Pd: Stacking faults, twin boundaries, and surfaces. Physical Review B, 2006, 74, .	1.1	43
3121	Angle-Resolved Photoemission Spectroscopy of the InsulatingNaxWO3: Anderson Localization, Polaron Formation, and Remnant Fermi Surface. Physical Review Letters, 2006, 96, 147603.	2.9	37
3122	Size-sensitive melting characteristics of gallium clusters: Comparison of experiment and theory forGa17+andGa20+. Physical Review B, 2006, 73, .	1.1	38
3123	Magnetic properties ofGaNâ•MnxGa1â˜'xNdigital heterostructures: First-principles and Monte Carlo calculations. Physical Review B, 2006, 73, .	1.1	15
3124	Vibrations of adsorbates on metal surfaces from geometry optimizations. Physical Review E, 2006, 74, 066705.	0.8	3
3125	Role of charge in destabilizingAlH4andBH4complex anions for hydrogen storage applications:Ab initiodensity functional calculations. Physical Review B, 2006, 74, .	1.1	45
3126	Predication of an ultrahigh filling fraction for K in CoSb3. Applied Physics Letters, 2006, 89, 112105.	1.5	29
3127	Ab initio prediction of half-metallic properties for the ferromagnetic Heusler alloys Co[sub 2]MSi (M=Ti,V,Cr). Journal of Applied Physics, 2006, 100, 113901.	1.1	180
3128	Ab initiostudy of biphenyl chemisorption on Si(001): Configurational stability. Physical Review B, 2006, 73, .	1.1	25
3129	First-principles calculation of the thermodynamics ofInxGa1â˜'xNalloys: Effect of lattice vibrations. Physical Review B, 2006, 73, .	1.1	83
3130	Coverage dependence of the 1-propanol adsorption on theSi(001)surface and fragmentation dynamics. Physical Review B, 2006, 73, .	1.1	14
3131	Perpendicular Magnetocrystalline Anisotropy in Tetragonally Distorted Fe-Co Alloys. Physical Review Letters, 2006, 96, 037205.	2.9	118
3132	Two-Dimensional Roughening of Adsorbate Islands in Thermodynamic Equilibrium. Physical Review Letters, 2006, 96, 166102.	2.9	7

#	Article	IF	Citations
3133	Quantum Size Effect on the Diffusion Barriers and Growth Morphology ofPb/Si(111). Physical Review Letters, 2006, 96, 226102.	2.9	68
3134	Effects of different hydrogen distributions on the magnetic properties of hydrogenated single-walled carbon nanotubes. Physical Review B, 2006, 73, .	1.1	25
3135	Adsorption, diffusion, and site exchange for Ge ad-dimers on Sb-coveredSi(001)from first-principles total-energy calculations. Physical Review B, 2006, 74, .	1.1	7
3136	Ab initiostudy of quasiperiodic Bi monolayers on a tenfolddâˆ'Alâˆ'Coâˆ'Nisurface. Physical Review B, 2006, 73, .	1.1	14
3137	Understanding and controlling the weakly interacting interface inperyleneâˆ•Ag(110). Physical Review B, 2006, 73, .	1.1	29
3138	Modeling the momentum distributions of annihilating electron-positron pairs in solids. Physical Review B, 2006, 73, .	1.1	113
3139	Charge centers inCaF2:Ab initiocalculation of elementary physical properties. Physical Review B, 2006, 74, .	1.1	16
3140	Bonding Trends and Dimensionality Crossover of Gold Nanoclusters on Metal-Supported MgO Thin Films. Physical Review Letters, 2006, 97, 036106.	2.9	268
3141	AbÂInitioStudy of Deep Defect States in Narrow Band-Gap Semiconductors: Group III Impurities in PbTe. Physical Review Letters, 2006, 96, 056403.	2.9	125
3142	Spontaneous symmetry breaking of theIr(100)âˆ'(5Ã—1)âˆ'hexsurface induced by hydrogen adsorption. Physical Review B, 2006, 74, .	1.1	13
3143	Chemical tuning of band alignments for metal gate/high-Îºoxide interfaces. Physical Review B, 2006, 73, .	1.1	40
3144	Interaction of manganese with single-wallB2Onanotubes: Anab initiostudy. Physical Review B, 2006, 73, .	1.1	2
3145	Electronic structure and magnetic properties of cubic and hexagonalSrMnO3. Physical Review B, 2006, 74, .	1.1	152
3146	Influence of interface structure on electronic properties and Schottky barriers inFeâˆ•GaAsmagnetic junctions. Physical Review B, 2006, 73, .	1.1	33
3147	Reconstruction of quasi-one-dimensionalInâˆ•Si(111)systems: Charge- and spin-density waves versus bonding. Physical Review B, 2006, 73, .	1.1	34
3148	First-principles calculations of Ag-Sb nanodot formation in thermoelectricAgPbmSbTe2+m(m=6,14,30). Physical Review B, 2006, 73, .	1.1	37
3149	Ab initiomolecular dynamics study ofCaSiO3perovskite atPâˆ'Tconditions of Earthâ€™s lower mantle. Physical Review B, 2006, 73, .	1.1	47
3150	Ferromagnetism inHfO2induced by hole doping: First-principles calculations. Physical Review B, 2006, 73, .	1.1	32

#	Article	IF	Citations
3151	Ab initiostudy on stability of half-metallic Co-based full-Heusler alloys. Journal of Applied Physics, 2006, 99, 08J112.	1.1	97
3152	Hydrogen-Mediated Nitrogen Clustering in Dilute III-V Nitrides. Physical Review Letters, 2006, 97, 075503.	2.9	13
3153	Ab initio calculations for properties of MAX phases Ti2TlC, Zr2TlC, and Hf2TlC. Applied Physics Letters, 2006, 88, 101911.	1.5	43
3154	First-principles investigation of the WCâ•HfO2 interface properties. Journal of Applied Physics, 2006, 99, 084104.	1.1	11
3155	Vacancy-enhanced ferromagnetism in Fe-doped rutileTiO2. Physical Review B, 2006, 74, .	1.1	61
3156	Density functional study of the effect of pressure on the ferroelectricGeTe. Physical Review B, 2006, 73, .	1.1	37
3157	Adsorption and diffusion of Co on the Si(001) surface. Physical Review B, 2006, 74, .	1.1	16
3158	Adsorption of water on chlorine-terminated Si(111) from first principles: Substrate-induced ordering versus intermolecular interactions. Physical Review B, 2006, 73, .	1.1	5
3159	Dehydrogenation mechanism in catalyst-activatedMgH2. Physical Review B, 2006, 74, .	1.1	46
3160	First-principles study of structural and electronic properties of group IV arsenides with 3:4 stoichiometry. Physical Review B, 2006, 74, .	1.1	6
3161	Electron scattering due to threading edge dislocations in n-type wurtzite GaN. Journal of Applied Physics, 2006, 99, 033706.	1.1	53
3162	Coherent control of tunnelling dynamics in functionalized semiconductor nanostructures: a quantum-control scenario based on stochastic unitary pulses. Journal of Modern Optics, 2006, 53, 2519-2532.	0.6	13
3163	Epitaxial semimetallic HfxZr1â^'xB2 templates for optoelectronic integration on silicon. Applied Physics Letters, 2006, 89, 242110.	1.5	11
3164	Ab initiocalculations of the stability of a vacancy in Na clusters and correlation with melting. Physical Review B, 2006, 73, .	1.1	14
3165	Dimer rotation on the carbon-inducedSi(001)â^'c(4Ã—4)structure. Physical Review B, 2006, 74, .	1.1	5
3166	Initial stages of the adsorption of Ge atoms on theSi(111)â^'(7Ã—7)surface. Physical Review B, 2006, 74, .	1.1	8
3167	Spin-polarized electron transport of a self-assembled organic monolayer on a Ni(111) substrate: An organic spin switch. Physical Review B, 2006, 73, .	1.1	35
3168	Energetics ofCOon stepped and kinked Cu surfaces: A comparative theoretical study. Physical Review B, 2006, 74, .	1.1	29

#	Article	IF	Citations
3169	Theoretical study of metal borides stability. Physical Review B, 2006, 74, .	1.1	79
3170	Atomic dynamics of In nanoclusters onSi(100). Physical Review B, 2006, 74, .	1.1	4
3171	Electronic structure and magnetic coupling inFeSbO4: A DFT study using hybrid functionals andGGA+Umethods. Physical Review B, 2006, 73, .	1.1	43
3172	Detection of a Fermi-level crossing in Si(557)-Au with inverse photoemission. Physical Review B, 2006, 73, .	1.1	10
3173	Work functions of self-assembled monolayers on metal surfaces by first-principles calculations. Physical Review B, 2006, 74, .	1.1	120
3174	Vacancy At Si-SiO2 Interface: Ab-Initio Study. , 2006, , .		0
3175	Synthesis and thermoelectric properties of Sr-filled skutterudite SryCo4Sb12. Journal of Applied Physics, 2006, 99, 053711.	1.1	165
3176	Segregation trends of the metal alloys Moâ€“Re and Moâ€“Pt on HfO2: A first-principles study. Journal of Applied Physics, 2006, 100, 013506.	1.1	3
3177	Enhancement of ferromagnetic coupling in Mnâˆ•GaAs digital ferromagnetic heterostructure by free-hole injection. Journal of Applied Physics, 2006, 99, 08D517.	1.1	9
3178	Generalized planar fault energies and twinning in Cuâ€“Al alloys. Applied Physics Letters, 2006, 89, 191911.	1.5	91
3179	Low temperature chemical vapor deposition of Si-based compounds via SiH3SiH2SiH3: Metastable SiSnâˆ•GeSnâˆ•Si(100) heteroepitaxial structures. Applied Physics Letters, 2006, 89, 231924.	1.5	75
3180	The influence of the additional confining potentials on ferromagnetism in IIIâ€“V digital ferromagnetic heterostructures. Journal of Applied Physics, 2006, 99, 113903.	1.1	6
3181	Ab initio Study of Boron Pile-up at the Si(001)/SiO2 Interface. , 2006, , .		0
3182	Theoretical prediction of ferromagnetic MnN layers embedded in wurtzite GaN. Applied Physics Letters, 2006, 88, 022507.	1.5	6
3183	Impurity-induced phase stabilization of semiconductors. Applied Physics Letters, 2006, 89, 011907.	1.5	20
3184	Ab initio studies on the reaction of O2 with Ban (n=2,5) clusters. Journal of Chemical Physics, 2006, 124, 224711.	1.2	6
3185	Revisiting the (110) surface structure ofTiO2: A theoretical analysis. Physical Review B, 2006, 73, .	1.1	75
3186	Structural and electronic transitions in potassium-doped pentacene. Physical Review B, 2006, 73, .	1.1	17

#	Article	IF	Citations
3187	Extended lattice gas interactions of Cu on Cu(111) and Cu(001):Ab initioevaluation and implications. Physical Review B, 2006, 73, .	1.1	34
3188	Nanocables made of a transition metal wire and boron nitride sheath: Density functional calculations. Physical Review B, 2006, 74, .	1.1	24
3189	Surface and interface structures of epitaxialZrO2films onPt(111): Experiment and density-functional theory calculations. Physical Review B, 2006, 74, .	1.1	24
3190	Femâ^•Aunmultilayers from first principles. Physical Review B, 2006, 74, .	1.1	12
3191	Theoretical analysis of highly spin-polarized transport in the iron nitrideFe4N. Physical Review B, 2006, 73, .	1.1	186
3192	General trend of the mechanical properties of the ternary carbidesM3SiC2(M=transitionmetal). Physical Review B, 2006, 74, .	1.1	48
3193	Strain-engineered photoluminescence of silicon nanoclusters. Physical Review B, 2006, 74, .	1.1	64
3194	Origin of ferroelectricity in the multiferroic barium fluoridesBaMF4: A first principles study. Physical Review B, 2006, 74, .	1.1	98
3195	Ab initiocalculations of surface phonons from a direct method with a filling slab approach: MgO(001) andLiâ^•MgO(001)surfaces. Physical Review B, 2006, 74, .	1.1	14
3196	Electron energy-loss spectra calculations and experiments as a tool for the identification of a lamellarC3N4compound. Physical Review B, 2006, 73, .	1.1	41
3197	Ordering tendencies in the binary alloys of Rh, Pd, Ir, and Pt: Density functional calculations. Physical Review B, 2006, 74, .	1.1	31
3198	Interaction between a single Pt atom and a carbon nanotube studied by density functional theory. Physical Review B, 2006, 73, .	1.1	38
3199	Adsorbate vibration and resonance lifetime broadening of a cobalt adatom on a Cu(111) surface. Physical Review B, 2006, 74, .	1.1	10
3200	Mechanical stability of possible structures of PtN investigated using first-principles calculations. Physical Review B, 2006, 73, .	1.1	168
3201	Effects of Al addition on the native defects in hafnia. Applied Physics Letters, 2006, 88, 182903.	1.5	24
3202	First-principles study of wurtzite InN (0001) and(0001Â¯)surfaces. Physical Review B, 2006, 74, .	1.1	45
3203	Spin-dependent electronic structure of transition-metal atomic chains adsorbed on single-wall carbon nanotubes. Physical Review B, 2006, 74, .	1.1	41
3204	Diffusion mechanisms for silicon di-interstitials. Physical Review B, 2006, 73, .	1.1	9

#	Article	IF	Citations
3205	Imaging Bond Formation Between a Gold Atom and Pentacene on an Insulating Surface. Science, 2006, 312, 1196-1199.	6.0	299
3206	Density functional theory investigation of surface-stress-induced phase transformations in fcc metal nanowires. Physical Review B, 2006, 74, .	1.1	43
3207	Improved hybrid algorithm with Gaussian basis sets and plane waves: First-principles calculations of ethylene adsorption onÎ²â^'SiC(001)â^'(3Ã—2). Physical Review B, 2006, 74, .	1.1	27
3208	Large magnetic moments and anomalous exchange coupling in As-doped Mn clusters. Physical Review B, 2006, 73, .	1.1	10
3209	Band-gap unification of partially Si-substituted single-wall carbon nanotubes. Physical Review B, 2006, 74, .	1.1	13
3210	First-principles potential energy surfaces and vibrational states of Hâ^•Rh(111) at 0.25 and 1 monolayer coverages. Journal of Applied Physics, 2006, 99, 113704.	1.1	5
3211	Origin of intergranular embrittlement of Al alloys induced by Na and Ca segregation: Grain boundary weakening. Physical Review B, 2006, 73, .	1.1	122
3212	Role of Ti in the reversible dehydrogenation of Ti-doped sodium alanate. Applied Physics Letters, 2006, 89, 201904.	1.5	15
3213	Quantum size effect in core-shell structured silicon-germanium nanowires. Physical Review B, 2006, 74, .	1.1	71
3214	Segregation of H as a surfactant during the formation of an Ag cluster on H-terminated Si(111): First-principles total-energy calculations. Physical Review B, 2006, 73, .	1.1	10
3215	Effect of coadsorption and Ru alloying on the adsorption of CO on Pt. Physical Review B, 2006, 74, .	1.1	38
3216	Electronic and magnetic properties of Mn-doped InP nanowires from first principles. Physical Review B, 2006, 73, .	1.1	30
3217	Comparison of the full-potential and frozen-core approximation approaches to density-functional calculations of surfaces. Physical Review B, 2006, 73, .	1.1	80
3218	Influence of complex point defects in ordered alloys: An ab initio study of B2 Fe-Al-B. Physical Review B, 2006, 74, .	1.1	20
3219	First-principles study of migration mechanisms and diffusion of oxygen in zinc oxide. Physical Review B, 2006, 73, .	1.1	133
3220	Electronic structure calculations of the phenalenyl-based neutral radical conductor bis(9-cyclohexylimino-1-phenalenyl) boron. Physical Review B, 2006, 74, .	1.1	16
3221	Time-dependent density functional theory with ultrasoft pseudopotentials: Real-time electron propagation across a molecular junction. Physical Review B, 2006, 73, .	1.1	74
3222	Theory of hypothetical ferroelectric superlattices incorporating head-to-head and tail-to-tail 180Â° domain walls. Physical Review B, 2006, 73, .	1.1	49

#	Article	IF	Citations
3223	Reactions of excess hydrogen at aSi(111)surface with H termination: First-principles calculations. Physical Review B, 2006, 74, .	1.1	10
3224	Prediction of the anomalous fluorine-silicon interstitial pair diffusion in crystalline silicon. Physical Review B, 2006, 74, .	1.1	13
3225	Half-metallicity at the (110) interface between a full Heusler alloy andGaAs. Physical Review B, 2006, 73, .	1.1	64
3226	Complexity and Fermi surface deformation in compressed lithium. Physical Review B, 2006, 74, .	1.1	43
3227	Calculations of hydrogen coverage on single-walled carbon nanotubes: Dependence on nanotube size, temperature, and pressure. Physical Review B, 2006, 74, .	1.1	28
3228	Comparative study of Ag, Au, Pd, and Pt adsorption on Mo andTa(112)surfaces. Physical Review B, 2006, 74, .	1.1	10
3229	Broad boron sheets and boron nanotubes: Anab initiostudy of structural, electronic, and mechanical properties. Physical Review B, 2006, 74, .	1.1	224
3230	Structure and magnetism of ultrathin epitaxial Fe on Ag(100). Physical Review B, 2006, 73, .	1.1	15
3231	Influence of local electron interactions on phonon spectrum in iron. Physical Review B, 2006, 74, .	1.1	13
3232	An Experimental and Computational Study of the Electrode Material Olivine-LiCoAsO[sub 4]. Journal of the Electrochemical Society, 2006, 153, A673.	1.3	18
3233	Structural evidence for enhanced polarization in a commensurate short-period BaTiO3â•SrTiO3 superlattice. Applied Physics Letters, 2006, 89, 092905.	1.5	80
3234	Comparison of screened hybrid density functional theory to diffusion Monte Carlo in calculations of total energies of silicon phases and defects. Physical Review B, 2006, 74, .	1.1	131
3235	Relaxations and bonding mechanism inHg1â^'xCdxTewith mercury vacancy defect: First-principles study. Physical Review B, 2006, 73, .	1.1	18
3236	First-principles study of lattice dynamics and diffusion inDO3-typeFe3Si. Physical Review B, 2006, 73, .	1.1	34
3237	Transition metal impurities in Ge: Chemical trends and codoping studied by electronic structure calculations. Physical Review B, 2006, 73, .	1.1	52
3238	Origin and temperature dependence of the electric dipole moment in niobium clusters. Physical Review B, 2006, 73, .	1.1	20
3239	Adsorption, desorption, and dissociation of benzene onTiO2(110)andPdâ•TiO2(110): Experimental characterization and first-principles calculations. Physical Review B, 2006, 74, .	1.1	20
3240	Experimental and theoretical evidence for substitutional molybdenum atoms in theTiO2(110)subsurface. Physical Review B, 2006, 73, .	1.1	20

#	Article	IF	Citations
3241	Stability of conductance oscillations in monatomic sodium wires. Physical Review B, 2006, 74, .	1.1	17
3242	Energy gradients with respect to atomic positions and cell parameters for the Kohn-Sham density-functional theory at the Î“ point. Journal of Chemical Physics, 2006, 124, 224107.	1.2	2
3243	Charge-induced effects on the structure and properties of silane and disilane derivatives. Physical Review B, 2006, 73, .	1.1	3
3244	Acetone on Si(001) - an adsorption study for siliconbased molecular electronics. , 2006, , .		0
3245	N doping of TiO2(110): Photoemission and density-functional studies. Journal of Chemical Physics, 2006, 125, 094706.	1.2	127
3246	Ferroelectricity in the Dion-Jacobson CsBiNb2O7 from first principles. Applied Physics Letters, 2006, 88, 262902.	1.5	25
3247	Atomic-Scale Mechanisms for Low-NIEL Dopant-Type Dependent Damage in Si. IEEE Transactions on Nuclear Science, 2006, 53, 3621-3628.	1.2	14
3248	Anomalous electrical performance of nanoscaled interfacial oxides for bonded n-GaAs wafers. Applied Physics Letters, 2006, 88, 112112.	1.5	2
3249	The energetics and structure of rutile TiO2(110). Journal of Physics Condensed Matter, 2006, 18, 4207-4217.	0.7	69
3250	Large fluorine-vacancy clusters in Si and their capture efficiency for self-interstitials. Applied Physics Letters, 2006, 89, 092113.	1.5	14
3251	Kinetic-Anisotropy-Induced Ordering-Orientation Transition in Epitaxial Growth: A Method to Synthesize Ordering-Orientation Superlattices. Physical Review Letters, 2006, 97, 126105.	2.9	5
3252	Oxidation of Step Edges onSi(001)â^'c(4Ã—2). Physical Review Letters, 2006, 97, 036103.	2.9	19
3253	The chemisorption of dibenzo[a,j]coronene on Si(001)-2Ã—1. Journal of Chemical Physics, 2006, 124, 224708.	1.2	10
3254	Oxygen Migration, Agglomeration, and Trapping: Key Factors for the Morphology of theSiâ^'SiO2Interface. Physical Review Letters, 2006, 97, 116101.	2.9	42
3255	Density-functional-theory calculations for the silicon vacancy. Physical Review B, 2006, 74, .	1.1	63
3256	Vacancy clustering and diffusion in silicon: Kinetic lattice Monte Carlo simulations. Physical Review B, 2006, 74, .	1.1	14
3257	Diffusion and clustering of substitutional Mn in (Ga,Mn)As. Applied Physics Letters, 2006, 89, 012505.	1.5	25
3258	High Curie temperatures in (Ga,Mn)N from Mn clustering. Applied Physics Letters, 2006, 88, 122501.	1.5	37

#	Article	IF	Citations
3259	Ab-Initio Molecular Dynamics Simulations of Molten Ni-Based Superalloys. , 2006, , .		0
3260	Structural Stabilities and Electronic Structures of Ga Atomic Chains. Chinese Journal of Chemical Physics, 2006, 19, 219-222.	0.6	2
3261	Transition metal doping and clustering in Ge. Applied Physics Letters, 2006, 89, 202510.	1.5	20
3262	Computational study of Ge and Sn doping of CdTe. Journal of Applied Physics, 2006, 99, 033704.	1.1	10
3263	Electronic and magnetic properties of Mnâˆ•Ge digital ferromagnetic heterostructures: An ab initio investigation. Journal of Applied Physics, 2006, 99, 08D705.	1.1	9
3264	Selective Analysis of Molecular States by Functionalized Scanning Tunneling Microscopy Tips. Physical Review Letters, 2006, 96, 156102.	2.9	44
3265	â€œMagic Meltersâ€•Have Geometrical Origin. Physical Review Letters, 2006, 96, 135703.	2.9	53
3266	Ab initiodensity-functional study of NO on close-packed transition and noble metal surfaces: I. Molecular adsorption. Journal of Physics Condensed Matter, 2006, 18, 13-40.	0.7	85
3267	Comment on â€œStructural Stability of Complex Hydrides:LiBH4Revisitedâ€• Physical Review Letters, 2006, 97, 119601; author reply 119602.	2.9	16
3268	Magic Numbers of Atoms in Surface-Supported Planar Clusters. Physical Review Letters, 2006, 97, 165504.	2.9	36
3269	Low Photoemission Intensity nearEFInduced by the Surface Relaxed Structure ofCrO2(001). Physical Review Letters, 2006, 96, 167206.	2.9	10
3270	Nanoscaled interfacial oxide layers of bonded n- and p-type GaAs wafers. Applied Physics Letters, 2006, 88, 172104.	1.5	2
3271	Surface Reconstructions ofTiO2(110)Driven by Suboxides. Physical Review Letters, 2006, 96, 226105.	2.9	53
3272	Interfaces BetweenAl2O3andÎ²â^'Ni1â^'xAlxAlloys: Complex Structures andAbÂInitioThermodynamics. Physical Review Letters, 2006, 97, 246102.	2.9	10
3273	Ab initiostudy of the surface of a decagonal Al-Co-Ni quasicrystal. Physical Review B, 2006, 73, .	1.1	37
3274	Clustering of Cr in GaN nanotubes and the onset of ferrimagnetic order. Physical Review B, 2006, 73, .	1.1	30
3275	Formation kinetics of the Mo(100)-Agc(2Ã—2)surface alloy. Physical Review B, 2006, 74, .	1.1	7
3276	Evolution of magnetism of Cr nanoclusters on Au(111): First-principles electronic structure calculations. Physical Review B, 2006, 73, .	1.1	19

#	Article	IF	Citations
3277	Density functional study ofÎ±â^'CrCl2: Structural, electronic, and magnetic properties. Physical Review B, 2006, 74, .	1.1	14
3278	Interstitial-mediated mechanisms of As and P diffusion in Si: Gradient-corrected density-functional calculations. Physical Review B, 2006, 74, .	1.1	13
3279	Comparison of theoretical and experimental dielectric functions: Electron energy-loss spectroscopy and density-functional calculations on skutterudites. Physical Review B, 2006, 74, .	1.1	28
3280	Understanding mixed valent materials: Effects of dynamical core-hole screening in high-pressure x-ray spectroscopy. Physical Review B, 2006, 74, .	1.1	16
3281	Pt thin films on the polarLaAlO3(100)surface: A first-principles study. Physical Review B, 2006, 73, .	1.1	22
3282	Magneto-optical properties of La0.7Sr0.3MnO3 thin films with perpendicular magnetic anisotropy. Journal of Applied Physics, 2006, 99, 043908.	1.1	22
3283	Ferromagnetism inAl1â^'xCrxNthin films by density functional calculations. Physical Review B, 2006, 73, .	1.1	25
3284	Descriptions of surface chemical reactions using a neural network representation of the potential-energy surface. Physical Review B, 2006, 73, .	1.1	113
3285	First-principles calculations for the structural stabilities of orderedNb4clusters on theCu(111)surface. Physical Review B, 2006, 73, .	1.1	16
3286	Tuning the surface metal work function by deposition of ultrathin oxide films: Density functional calculations. Physical Review B, 2006, 73, .	1.1	231
3287	Multiple adsorption configurations ofNH3molecules on the Si(001) surface. Physical Review B, 2006, 73, .	1.1	33
3288	Surface vacancies at the fivefold icosahedral Al-Pd-Mn quasicrystal surface: A comparison ofab initiocalculated and experimental STM images. Physical Review B, 2006, 73, .	1.1	49
3289	Stability of Ti in NaAlH4. Applied Physics Letters, 2006, 88, 161917.	1.5	32
3290	Possible lowest-reactivity structure of the silicon clusterSi45. Physical Review B, 2006, 73, .	1.1	10
3291	Structural, magnetic, and chemical properties of thin Fe films grown on Rh(100) surfaces investigated with density functional theory. Physical Review B, 2006, 73, .	1.1	16
3292	h-BNmonolayer adsorption on theNi(111)surface: A density functional study. Physical Review B, 2006, 74, .	1.1	61
3293	Quantum size effects in Pb films from first principles: The role of the substrate. Physical Review B, 2006, 74, .	1.1	72
3294	Ab initiomolecular dynamics simulations on structural change of liquid eutectic alloyGe15Te85from573to1073K. Physical Review B, 2006, 74, .	1.1	11

#	Article	IF	Citations
3295	Broken parity and a chiral ground state in the frustrated magnetCdCr2O4. Physical Review B, 2006, 74, .	1.1	46
3296	Atomic structure of a thin silica film on aMo(112)substrate: A combined experimental and theoretical study. Physical Review B, 2006, 73, .	1.1	61
3297	Comparative NMR study of hybridization effect and structural stability inD022-typeNbAl3andNbGa3. Physical Review B, 2006, 74, .	1.1	31
3298	Tile decoration model of the W-(Alâ€“Coâ€“Ni) approximant. Philosophical Magazine, 2006, 86, 557-565.	0.7	8
3299	Vibrational assignments and line shapes in inelastic tunneling spectroscopy: H onCu(100). Physical Review B, 2006, 74, .	1.1	8
3300	Electronic and thermodynamic properties of Î²-Ga2O3. Applied Physics Letters, 2006, 88, 261904.	1.5	125
3301	Ga1âˆ’xAlxNsystem, Madelung, and strain energies: A study on the quality of cluster expansions. Physical Review B, 2006, 74, .	1.1	5
3302	Resonant inelastic soft x-ray scattering at double core excitations in solid LiCl. Physical Review B, 2006, 73, .	1.1	5
3303	Electronic structure and optical properties of layered perovskitesSr2MO4(M=Ti, V, Cr, and Mn): Anab initiostudy. Physical Review B, 2006, 74, .	1.1	32
3304	Ab initiodensity functional theory study of strain effects on ferroelectricity atPbTiO3surfaces. Physical Review B, 2006, 74, .	1.1	42
3305	Compositional dependence of the local structure ofSexTe1âˆ’xalloys: Electron energy-loss spectra, real-space multiple-scattering calculations, and first-principles molecular dynamics. Physical Review B, 2006, 73, .	1.1	2
3306	Inversion of defect interactions due to ordering inSr1âˆ’3xâ€¢2LaxTiO3perovskites: An atomistic simulation study. Physical Review B, 2006, 74, .	1.1	12
3307	Theoretical investigation ofPtSisurface energies and work functions. Physical Review B, 2006, 73, .	1.1	41
3308	Nanoscale pressure effects in individual double-wall carbon nanotubes. Physical Review B, 2006, 73, .	1.1	32
3309	Probing theSi(001)surface with a Si tip: Anab initiostudy. Physical Review B, 2006, 73, .	1.1	38
3310	Undissociated screw dislocation in Si: Glide or shuffle set?. Applied Physics Letters, 2006, 89, 051910.	1.5	33
3311	Effect of pressure on the Raman modes of antimony. Physical Review B, 2006, 74, .	1.1	79
3312	Unusual adsorption site of hydrogen on the unreconstructed Ir(100) surface. Physical Review B, 2006, 73, .	1.1	67

#	Article	IF	Citations
3313	Effective interactions between theNâ^'Hbond orientations in lithium imide and a proposed ground-state structure. Physical Review B, 2006, 74, .	1.1	60
3314	Analytic bond-order potential for the gallium arsenide system. Physical Review B, 2006, 73, .	1.1	56
3315	NO structures adsorbed on Rh(111): Theoretical approach to high-coverage STM images. Physical Review B, 2006, 73, .	1.1	20
3316	Ab initiocalculation of the electronic structure and spectroscopic properties of spinelÎ³â^'Sn3N4. Physical Review B, 2006, 73, .	1.1	49
3317	Structural transformations of double-walled carbon nanotube bundle under hydrostatic pressure. Applied Physics Letters, 2006, 89, 113101.	1.5	41
3318	Complex adsorbate-substrate interplay of H onIr(100)â^'(5Ã—1)-hex: Density functional calculations. Physical Review B, 2006, 74, .	1.1	10
3319	Stable cubic metal-semiconductor alloy clusters:X4Y4(X=Cu,Ag,Au,Ti;Y=C,Si). Physical Review B, 2006, 73, .	1.1	18
3320	Fcc breathing instability inBaBiO3from first principles. Physical Review B, 2006, 73, .	1.1	31
3321	Ab initiocalculations of magnetic structure and lattice dynamics inFeâ^•FeSimultilayers. Physical Review B, 2006, 73, .	1.1	5
3322	Importance of charging in atomic resolution scanning tunneling microscopy: Study of a single phosphorus atom in aSi(001)surface. Physical Review B, 2006, 74, .	1.1	14
3323	Effect of indium-nitrogen bonding on the localized vibrational mode inInyGa1â^'yNxAs1â^'x. Physical Review B, 2006, 73, .	1.1	18
3324	Electron-mediated ferromagnetism and negativesâ^'dexchange splitting in semiconductors. Physical Review B, 2006, 73, .	1.1	23
3325	Interface reconstruction ofMSi2â^•Si(001)(M=Co,Ni)from first principles. Physical Review B, 2006, 74, .	1.1	10
3326	Ab initio study of the effect of water adsorption on the carbon nanotube field-effect transistor. Applied Physics Letters, 2006, 89, 243110.	1.5	63
3327	Charge-orbital ordering in low-temperature structures of magnetite:GGA+Uinvestigations. Physical Review B, 2006, 74, .	1.1	80
3328	First-principles study of cation disordering inMgAl2O4spinel with cluster expansion and Monte Carlo simulation. Physical Review B, 2006, 73, .	1.1	47
3329	Tight-binding calculations of the elastic constants and phonons of hcp Zr: Complications due to anisotropic stress and long-range forces. Physical Review B, 2006, 74, .	1.1	20
3330	Robust half-metallic antiferromagnetsLaAVOsO6andLaAMoYO6(A=Ca,Sr,Ba;Y=Re,Tc) from first-principles calculations. Physical Review B, 2006, 73, .	1.1	64

#	Article	IF	Citations
3331	Effective potentials for quasicrystals fromab-initiodata. Philosophical Magazine, 2006, 86, 753-758.	0.7	92
3332	Structure of expanded fluid Rb and Cs: a quantum molecular dynamics study. Journal of Physics Condensed Matter, 2006, 18, 5597-5605.	0.7	13
3333	Ab initio study of molecular adsorption on hydrogenated diamond (001) surfaces. Journal of Physics: Conference Series, 2006, 29, 145-149.	0.3	14
3334	Optimization of ionic conductivity in doped ceria. Proceedings of the National Academy of Sciences of the United States of America, 2006, 103, 3518-3521.	3.3	464
3335	Absolute rate of thermal desorption from first-principles simulation. Journal of Physics Condensed Matter, 2006, 18, L451-L457.	0.7	15
3336	Atomic Pillar-Based Nanoprecipitates Strengthen AlMgSi Alloys. Science, 2006, 312, 416-419.	6.0	283
3337	Modulation of band structure in wurtzite ZnO via site-selective Gaâ€“N codoping. Journal of Physics Condensed Matter, 2006, 18, 6281-6287.	0.7	2
3338	Theoretical Investigation of Intercalated Water Molecules and Hydroxyl Groups in BAM (BaMgAl[sub) Tj ETQq1 1 0.784314 rgBT /Ove Electrochemical Society, 2006, 153, H202.	1.3	5
3339	On the theory underlying the Car-Parrinello method and the role of the fictitious mass parameter. Journal of Chemical Physics, 2006, 124, 044111.	1.2	58
3340	AB-Initio Modeling of Intermediate Band Materials Based on Metal-Doped Chalcopyrite Compounds. , 2006, , .		1
3341	Structural distortion and electronic properties of NiO under high pressure: anab initioGGA+Ustudy. Journal of Physics Condensed Matter, 2006, 18, 9691-9701.	0.7	8
3342	The role of self-purification and the electronic structure of magnetically doped semiconductor nanocrystals. Phase Transitions, 2006, 79, 739-753.	0.6	6
3343	Designing New Structural Materials Using Density Functional Theory: The Example of Gum Metal^{TM}. MRS Bulletin, 2006, 31, 688-692.	1.7	32
3344	Ab initiodensity-functional study of NO adsorption on close-packed transition and noble metal surfaces: II. Dissociative adsorption. Journal of Physics Condensed Matter, 2006, 18, 41-54.	0.7	47
3345	DIRECT DYNAMICS INVESTIGATION ON MECHANISM OF REACTION BETWEEN TRICHLORIDE AND H RADICAL. Journal of Theoretical and Computational Chemistry, 2006, 05, 51-57.	1.8	5
3346	Effect of a Si Additive on an Al Grain Boundary: A First-Principles Investigation. Materials Science Forum, 2007, 546-549, 829-832.	0.3	4
3347	A DFT INVESTIGATION OF SULFUR ADSORPTION ON Ir(100). Journal of Theoretical and Computational Chemistry, 2007, 06, 177-185.	1.8	2
3348	FIRST-PRINCIPLES STUDY OF ADSORPTION OF CN ON Cu(111). Journal of Theoretical and Computational Chemistry, 2007, 06, 523-529.	1.8	3

#	Article	IF	Citations
3349	Density functional analysis of the structural evolution of Gan (n=30â€“55) clusters and its influence on the melting characteristics. Journal of Chemical Physics, 2007, 127, 054308.	1.2	20
3350	Efficient evaluation of analytic vibrational frequencies in Hartree-Fock and density functional theory for periodic nonconducting systems. Journal of Chemical Physics, 2007, 127, 144106.	1.2	28
3351	Simulating adsorption of complex molecules using the linearity between interaction energies and tunnelling currents: the case of hexabenzocoronene on a Ag/Pt dislocation network. New Journal of Physics, 2007, 9, 393-393.	1.2	2
3352	Theoretical analysis on the structure and properties of thiourea dioxide crystal. Molecular Simulation, 2007, 33, 975-978.	0.9	1
3353	On the Existence of Voids Within Precursorâ€derived Amorphous Siâ€Câ€N Ceramics. Soft Materials, 2007, 4, 187-205.	0.8	5
3354	An improved QM/MM approach for metals. Modelling and Simulation in Materials Science and Engineering, 2007, 15, 275-284.	0.8	52
3355	Polynitrogen/Nanoaluminum Surface Interactions. , 2007, , .		0
3356	Peierlsâ€“Nabarro model for dislocations in MgSiO₃post-perovskite calculated at 120â€‰GPa from first principles. Philosophical Magazine, 2007, 87, 3229-3247.	0.7	57
3357	Interatomic bonds and the tensile anisotropy of trialuminides in the elastic limit: a density functional study for Al3(Sc,â€‰Ti,â€‰V,â€‰Cr). Philosophical Magazine, 2007, 87, 1769-1794.	0.7	24
3358	Structure, energetics, and bonding of amorphous Auâ€“Si alloys. Journal of Chemical Physics, 2007, 127, 224710.	1.2	27
3359	Ab intio total energy calculations for a brittle versus ductile behavior of Î±-Fe. Radiation Effects and Defects in Solids, 2007, 162, 367-372.	0.4	1
3360	Prediction of MAX phases, VN+1SiCN (N=1,2), from first-principles theory. Journal of Applied Physics, 2007, 101, 013511.	1.1	16
3361	Structures and stabilities of small lead oxide clusters PbmOn (m=1â€“4,n=1â€“2m). Journal of Chemical Physics, 2007, 126, 134705.	1.2	19
3362	Isotope quantum effects in the electron momentum density of water. Journal of Chemical Physics, 2007, 126, 154508.	1.2	25
3363	Comparison of proton conduction in KTaO3 and SrZrO3. Journal of Chemical Physics, 2007, 126, 194701.	1.2	21
3364	On the structure of the first hydration layer on NaCl(100): Role of hydrogen bonding. Journal of Chemical Physics, 2007, 126, 214707.	1.2	14
3365	Interaction of oxygen with TiN(001):Nâ†”O exchange and oxidation process. Journal of Chemical Physics, 2007, 126, 244713.	1.2	51
3366	Oxygen adsorption on Mo(112) surface studied by ab initio genetic algorithm and experiment. Journal of Chemical Physics, 2007, 126, 234710.	1.2	37

#	Article	IF	Citations
3367	Ab initio statistical mechanics of surface adsorption and desorption. I. H2O on MgO (001) at low coverage. Journal of Chemical Physics, 2007, 127, 114709.	1.2	20
3368	Microscopic structure and dynamics of molten Se50Te50 alloys. Journal of Chemical Physics, 2007, 127, 144707.	1.2	3
3369	Vibrational lifetimes of cyanide and carbon monoxide on noble and transition metal surfaces. Journal of Chemical Physics, 2007, 127, 154303.	1.2	37
3370	Biatomic substrates for bulk-molecule interfaces: The PtCo-oxygen interface. Journal of Chemical Physics, 2007, 127, 244706.	1.2	15
3371	Methane dissociation on Ni(111): The effects of lattice motion and relaxation on reactivity. Journal of Chemical Physics, 2007, 127, 224702.	1.2	62
3372	Infrared spectroscopy of physisorbed and chemisorbed N2 in the Pt(111)(3Ã—3)N2 structure. Journal of Chemical Physics, 2007, 127, 194708.	1.2	7
3373	Hierarchical geometric frustration in La3Cu2VO9. Journal of Physics Condensed Matter, 2007, 19, 145280.	0.7	1
3374	Onset of Microplasticity in Copper Crystal during Nanoindentation. Key Engineering Materials, 2007, 348-349, 801-804.	0.4	2
3375	Estimates of Thermodynamic Stability of Ironâ€“Chromium Spinels in Aqueous Solution Based on First-Principles Calculations. Electrochemical and Solid-State Letters, 2007, 10, C57.	2.2	10
3376	Role of Water in the Ion Selectivity of Niobate-Based Octahedral Molecular Sieves. Journal of Physical Chemistry C, 2007, 111, 13212-13221.	1.5	13
3377	Chapter 9 Integrated Approach to Dielectric Film Growth Modeling: Growth Mechanisms and Kinetics. Thin Films and Nanostructures, 2007, 34, 467-522.	0.1	0
3378	The location of Ti atom in sodium alanate: an ab initio spin-polarised study. International Journal of Nanotechnology, 2007, 4, 564.	0.1	2
3379	Chapter 4 Aun and Agn (n=1â€“8) nanocluster catalysts: gas-phase reactivity to deposited structures. Chemical Physics of Solid Surfaces, 2007, , 151-199.	0.3	16
3380	Characterization by Ab Initio Calculations of an Intermediate Band Material Based on Chalcopyrite Semiconductors Substituted by Several Transition Metals. Journal of Solar Energy Engineering, Transactions of the ASME, 2007, 129, 314.	1.1	22
3381	Electronic structure and ferromagnetism of Cu-doped ZnO. Physica Scripta, 2007, T129, 358-361.	1.2	9
3382	Atomic and electronic structures of neutral and charged Pbn clusters (n=2â€“15): Theoretical investigation based on density functional theory. Journal of Chemical Physics, 2007, 126, 244704.	1.2	40
3383	Direct and indirect causes of Fermi level pinning at the SiOâˆ•GaAs interface. Journal of Chemical Physics, 2007, 126, 084703.	1.2	25
3384	Ionization induced relaxation in solvation structure: A comparison between Na(H2O)n and Na(NH3)n. Journal of Chemical Physics, 2007, 126, 084501.	1.2	41

#	Article	IF	Citations
3385	A study on the stability of O2 on oxometalloporphyrins by the first principles calculations. Journal of Chemical Physics, 2007, 126, 194303.	1.2	3
3386	Self-assembly of semifluorinated n-alkanethiols on {111}-oriented Au investigated with scanning tunneling microscopy experiment and theory. Journal of Chemical Physics, 2007, 127, 024702.	1.2	11
3387	Density functional theory study of Î²-hydride elimination of ethyl on flat and stepped Cu surfaces. Journal of Chemical Physics, 2007, 127, 144710.	1.2	10
3388	Observable consequences of formation of Au anions from deposition of Au atoms on ultrathin oxide films. Journal of Chemical Physics, 2007, 127, 144713.	1.2	29
3389	A density functional theory study on the binding of NO onto FePc films. Journal of Chemical Physics, 2007, 127, 214701.	1.2	29
3390	Oscillatory exchange coupling in magnetic molecules. Journal of Physics Condensed Matter, 2007, 19, 216205.	0.7	3
3391	Theoretical investigations of Ge nanowires grown along the [110] and [111] directions. Nanotechnology, 2007, 18, 295706.	1.3	31
3392	CO adsorption on a Au/Ni(111) surface alloyâ€"a DFT study. Journal of Physics Condensed Matter, 2007, 19, 246219.	0.7	10
3393	Structural features and electronic properties of group-III-, group-IV-, and group-V-doped Si nanocrystallites. Journal of Physics Condensed Matter, 2007, 19, 466211.	0.7	37
3394	Metastable phase formation in the immiscible Cuâ€"Co system studied by thermodynamic, molecular dynamics andab initiocalculations together with ion beam mixing. Journal of Physics Condensed Matter, 2007, 19, 026219.	0.7	8
3395	The computational materials design of (Ga, Cr)N: effects of co-doping on exchange interactions. Journal of Physics Condensed Matter, 2007, 19, 365238.	0.7	0
3396	Tailoring the character of the band-gap in langle 011angle -, langle 111angle - and langle 112angle -oriented silicon nanowires. Nanotechnology, 2007, 18, 375703.	1.3	12
3397	Effect of electronic correlation on the Na ordering of NaxCoO2. Journal of Physics Condensed Matter, 2007, 19, 086203.	0.7	7
3398	Detection of spin-states in Mn-doped gallium arsenide films. Nanotechnology, 2007, 18, 044006.	1.3	1
3399	Structural Stabilities of Ordered Nb 4 Clusters on the Cu(111) and Cu(100) Surfaces. Chinese Physics Letters, 2007, 24, 172-175.	1.3	2
3400	Density-functional investigation of Na₁₆A₈Ge₁₃₆(A = Rb,Cs) clathrates. Journal of Physics Condensed Matter, 2007, 19, 466206.	0.7	6
3401	First-principles study of Ï‰-phase formation in the Ti₃Al₂V system. Journal of Physics Condensed Matter, 2007, 19, 386221.	0.7	5
3402	Theoretical Study of the Stability of X@B6and X@B12Clusters: X=Hâ€"Br in Crystalline Silicon. Japanese Journal of Applied Physics, 2007, 46, 467-473.	0.8	2

#	Article	IF	Citations
3403	Electronic Structure of Si 1â^' x IV x /Si Superlattices on Si (001). Chinese Physics Letters, 2007, 24, 811-813.	1.3	1
3404	First-principles investigations of the pressure-induced structural transitions in Mg(AlH4)2. Journal of Physics Condensed Matter, 2007, 19, 176205.	0.7	11
3405	First-principles study of defect equilibria in lithium zinc nitride. Journal of Physics Condensed Matter, 2007, 19, 046201.	0.7	6
3406	First-principles computational tensile test on a Na-segregated Al grain boundary with an Si additive and an intergranular embrittlement suppression mechanism. Journal of Physics Condensed Matter, 2007, 19, 456225.	0.7	27
3407	Ab initiocalculations of elastic properties of isotropic and oriented Ti1â^'xAlxN hard coatings. Journal Physics D: Applied Physics, 2007, 40, 4021-4026.	1.3	15
3408	Anomalous magnetic behavior of<mml:math xmlns:mml="http://www.w3.org/1998/Math/MathML" display="inline"><mml:mrow><mml:mi>Mn</mml:mi><mml:mtext>â^'</mml:mtext><mml:mi>Mn</mml:mi></mml:mrow></mml:math> in the dilute magnetic semiconductor<mml:math xmlns:mml="http://www.w3.org/1998/Math/MathML" display="inline"><mml:mrow><mml:mrow><mml:mo>(</mml:mo><mml:mi>Ga</mml:mi><mml:mo>,</mml:mo><mml:mi>Mn</mml:mi><mml:mi mathvariant="normal">N</mml:mi></mml:mrow></mml:mrow></mml:math>. Physical Review B, 2007, 76, .	1.1	10
3409	Influence of oxygen on the interfacial stability of Cu onCo(0001)thin films. Physical Review B, 2007, 75, .	1.1	4
3410	Mechanism of the electro-optic effect in the perovskite-type ferroelectric KNbO3 and LiNbO3. Journal of Applied Physics, 2007, 101, 103506.	1.1	17
3411	Inhomogeneity ofC13isotope distribution in isotope engineered carbon nanotubes: Experiment and theory. Physical Review B, 2007, 75, .	1.1	21
3412	Distinct atomic structures of the Ni-Nb metallic glasses formed by ion beam mixing. Journal of Applied Physics, 2007, 102, .	1.1	9
3413	Magnetic needles encapsulated inside (BN)36 cage: Prediction of atomic, electronic, and magnetic structure from first principle calculations. Applied Physics Letters, 2007, 91, 223112.	1.5	12
3414	Ab initioand classical molecular dynamics of neon melting at high pressure. Physical Review B, 2007, 75, .	1.1	17
3415	Crystal structure of<mml:math xmlns:mml="http://www.w3.org/1998/Math/MathML" display="inline"><mml:mrow><mml:mi mathvariant="normal">Si</mml:mi><mml:msub><mml:mi mathvariant="normal">H</mml:mi><mml:mn>4</mml:mn></mml:msub></mml:mrow></mml:math>at high pressure. Physical Review B, 2007, 76, .	1.1	63
3416	Spin-polarization study ofCOmolecules adsorbed onFe(110)using metastable-atom deexcitation spectroscopy and first-principles calculations. Physical Review B, 2007, 75, .	1.1	15
3417	Determining the site preference of trivalent dopants in bixbyite sesquioxides by atomic-scale simulations. Physical Review B, 2007, 75, .	1.1	61
3418	Adsorption and diffusion of a molybdenum atom on the<mml:math xmlns:mml="http://www.w3.org/1998/Math/MathML" display="inline"><mml:mrow><mml:mi mathvariant="normal">Ti</mml:mi><mml:msub><mml:mi mathvariant="normal">O</mml:mi><mml:mn>2</mml:mn></mml:msub><mml:mrow><mml:mo>(</mml:mo><mml:mn>110</mml:mn></mml:math> A first-principles study. Physical Review B, 2007, 76, .	1.1	12
3419	Comparative study of passivation mechanism of oxygen vacancy with fluorine in HfO2 and HfSiO4. Applied Physics Letters, 2007, 90, 142904.	1.5	11
3420	Structure of the hydrogen double vacancy on Pd(111). Physical Review B, 2007, 76, .	1.1	2

#	Article	IF	Citations
3421	Polymer adhesion: First-principles calculations of the adsorption of organic molecules onto Si surfaces. Physical Review B, 2007, 76, .	1.1	21
3422	Dehydrogenation from 3d-transition-metal-doped NaAlH4: Prediction of catalysts. Applied Physics Letters, 2007, 90, 141904.	1.5	26
3423	Morphology and magnetism of<mml:math xmlns:mml="http://www.w3.org/1998/Math/MathML" display="inline"><mml:msub><mml:mi mathvariant="normal">Fe</mml:mi><mml:mi>n</mml:mi></mml:msub></mml:math>clusters<mml:math xmlns:mml="http://www.w3.org/1998/Math/MathML" display="inline"><mml:mrow><mml:mo>(</mml:mo><mml:mi>n</mml:mi><mml:mo>=</mml:mo><mml:mn>1</mml:mn><mml:mo>â€	1.1	11
3424	on a Pd(001) substrate. Physical Review B, 2007, 76, . First-principles calculations of cohesive energies in theAlâ^'Cobinary alloy system. Physical Review B, 2007, 75, .	1.1	47
3425	Pressure-induced amorphization of<mml:math xmlns:mml="http://www.w3.org/1998/Math/MathML" display="inline"><mml:mrow><mml:mi mathvariant="normal">Cu</mml:mi><mml:mi mathvariant="normal">Fe</mml:mi><mml:msub><mml:mi mathvariant="normal">S</mml:mi><mml:mn>2</mml:mn></mml:msub></mml:mrow></mml:math>studied by<mml:math xmlns:mml="http://www.w3.org/1998/Math/MathML" display="inline"><mml:mmultiscripts><mml:mi mathvariant="normal">Fe</mml:mi><mml:mprescripts />	1.1	10
3426	Structural, magnetic, and electronic properties of the Co-Fe-Al oxide spinel system: Density-functional theory calculations. Physical Review B, 2007, 76, .	1.1	168
3427	Filled Ir<inf>x</inf>Co<inf>1-x</inf>Sb<inf>3</inf>-based skutterudite solid solutions. , 2007, , .		0
3428	Electronic structure of InN studied using soft x-ray emission, soft x-ray absorption, and quasiparticle band structure calculations. Physical Review B, 2007, 76, .	1.1	18
3429	Embedded Green-function calculation of the conductance of oxygen-incorporated Au and Ag monatomic wires. Physical Review B, 2007, 75, .	1.1	23
3430	Total energy evaluation in the Strutinsky shell correction method. Journal of Chemical Physics, 2007, 127, 064101.	1.2	4
3431	Spin dependence of interfacial reflection phase-shift at the Cu-Co interface. Physical Review B, 2007, 76, .	1.1	3
3432	Geometric and electronic structure of aC60monolayer on Ag(100). Physical Review B, 2007, 75, .	1.1	42
3433	Polygonization and anomalous graphene interlayer spacing of multi-walled carbon nanofibers. Physical Review B, 2007, 75, .	1.1	26
3434	First-principles study of magnetic properties in V-doped ZnO. Applied Physics Letters, 2007, 91, 063116.	1.5	38
3435	Evolution-operator method for density functional theory. Physical Review B, 2007, 75, .	1.1	18
3436	On Raman scattering from selected M2AC compounds. Journal of Materials Research, 2007, 22, 2651-2654.	1.2	47
3437	Effects of chlorine residue in atomic layer deposition hafnium oxide: A density-functional-theory study. Applied Physics Letters, 2007, 91, 022901.	1.5	10
3438	First-principles prediction of phase-segregating alloy phase diagrams and a rapid design estimate of their transition temperatures. Physical Review B, 2007, 75, .	1.1	95

#	Article	IF	Citations
3439	Density functional study of multiferroic<mml:math xmlns:mml="http://www.w3.org/1998/Math/MathML" display="inline"><mml:mrow><mml:msub><mml:mi mathvariant="normal">Bi</mml:mi><mml:mn>2</mml:mn></mml:msub><mml:mi mathvariant="normal">Ni</mml:mi><mml:mi mathvariant="normal">Mn</mml:mi><mml:msub><mml:mi mathvariant="normal">O</mml:mi><mml:mn>6</mml:mn></mml:msub></mml:mrow></mml:math>. Physical Review B, 2007, 76, .	1.1	40
3440	Theoretical study of dopedTl2Mn2O7andTl2Mn2O7under pressure. Physical Review B, 2007, 75, .	1.1	1
3441	Headgroup dimerization in methanethiol monolayers on the Au(111) surface: A density functional theory study. Physical Review B, 2007, 76, .	1.1	11
3442	Reconstruction energies of partial dislocations in cubic semiconductors. Physical Review B, 2007, 76, .	1.1	13
3443	Ferromagnetic to ferrimagnetic crossover in Cr-doped GaN nanohole arrays. Physical Review B, 2007, 75, .	1.1	11
3444	Structures and defects of atomic wires on Si(553)-Au: An STM and theoretical study. Physical Review B, 2007, 76, .	1.1	32
3445	X-ray absorption near-edge structures of disordered<mml:math xmlns:mml="http://www.w3.org/1998/Math/MathML" display="inline"><mml:mrow><mml:msub><mml:mi mathvariant="normal">Mg</mml:mi><mml:mrow><mml:mn>1</mml:mn><mml:mo>â^’</mml:mo><mml:mi>x</mml:mi></mml:mrow><mml:mi mathvariant="normal">Zn</mml:mi><mml:mi>x</mml:mi></mml:msub><mml:mi mathvariant="normal">O</mml:mi></mml:mrow></mml:math>solid solutions. Physical Review B, 2007, 76, .	1.1	15
3446	Electronic structure, elastic properties, surface energies, and work functions ofNiGeandPtGewithin the framework of density-functional theory for various surface terminations. Physical Review B, 2007, 75, .	1.1	23
3447	Nanotwin formation in copper thin films by stress/strain relaxation in pulse electrodeposition. Applied Physics Letters, 2007, 91, .	1.5	80
3448	First-principles study of the tensile strength and failure of<mml:math xmlns:mml="http://www.w3.org/1998/Math/MathML" display="inline"><mml:mrow><mml:mi>Î±</mml:mi><mml:mtext>â^’</mml:mtext><mml:msub><mml:mi mathvariant="normal">Al</mml:mi><mml:mn>2</mml:mn></mml:msub><mml:msub><mml:mi mathvariant="normal">O</mml:mi><mml:mn>3</mml:mn></mml:msub><mml:mrow><mml:mo>(</mml:mo><mml:mn>0001</mml:mn>		

#	Article	IF	Citations
3457	General-stacking-fault energies in highly strained metallic environments:Ab initiocalculations. Physical Review B, 2007, 76, .	1.1	79
3458	Phonons of (100) and (110) iron surfaces from first-principles calculations. Physical Review B, 2007, 75, .	1.1	18
3459	Ab initiostudy of small vacancy complexes in beryllium. Physical Review B, 2007, 75, .	1.1	31
3460	Thermodynamics of carbon-doped Al and Ga clusters:Ab initiomolecular dynamics simulations. Physical Review B, 2007, 76, .	1.1	38
3461	Calculations of codoping effects between combinations of donors (P/As/Sb) and acceptors (B/Ga/In) in Si. Journal of Applied Physics, 2007, 102, 123709.	1.1	3
3462	Ab initiostudies of structural, vibrational, and electronic properties of durene crystals and molecules. Physical Review B, 2007, 75, .	1.1	23
3463	Interplay between structural, magnetic, and electronic properties in a<mml:math xmlns:mml="http://www.w3.org/1998/Math/MathML" display="inline"><mml:mrow><mml:mi mathvariant="normal">Fe</mml:mi><mml:mi mathvariant="normal">O</mml:mi><mml:mo>âˆ•</mml:mo><mml:mi mathvariant="normal">Pt</mml:mi><mml:mrow><mml:mo>(</mml:mo><mml:mn>111</mml:mn><mml:mo>)</mml:mo></mml:mrow></mml:mrow> film. Physical Review B, 2007, 76, .	1.1	129
3464	Effects of strain and defects on the electron conductance of metallic carbon nanotubes. Physical Review B, 2007, 75, .	1.1	36
3465	Local zero-bias anomaly in tunneling spectra of a transition-metal oxide thin film. Physical Review B, 2007, 75, .	1.1	20
3466	Response of trialuminides to [110] uniaxial loading: Anab initiostudy for<mml:math xmlns:mml="http://www.w3.org/1998/Math/MathML" display="inline"><mml:mrow><mml:msub><mml:mi mathvariant="normal">Al</mml:mi><mml:mn>3</mml:mn></mml:msub><mml:mrow><mml:mo>(</mml:mo><mml:mi) Tj ETQq1 1 0	1.1	22
3467	Hydrogen adsorption by tungsten carbide nanotube. Applied Physics Letters, 2007, 90, 223104.	1.5	34
3468	Surface influence on stability and structure of hexagon-shaped III-V semiconductor nanorods. Journal of Applied Physics, 2007, 102, 063528.	1.1	66
3469	Theoretical and experimental investigation of valence band offsets for direct silicon bond hybrid orientation technology. Applied Physics Letters, 2007, 90, 043503.	1.5	6
3470	Oxygen pressure dependence of HfO2 stoichiometry: An ab initio investigation. Applied Physics Letters, 2007, 91, 022904.	1.5	9
3471	Band alignment at the ZrO2âˆ•Si(100) interface studied by photoelectron and x-ray absorption spectroscopy. Journal of Applied Physics, 2007, 101, 104120.	1.1	7
3472	Direct Dynamics Simulation of Reaction Between F2 and Ethylene. Chinese Journal of Chemical Physics, 2007, 20, 109-112.	0.6	6
3473	Ab-initio Atomic Scale Study of Nearly Frictionless Surfaces. , 2007, , 57-77.		2
3474	Dual-frequency resonant phonon scattering in BaxRyCo4Sb12 (R=La, Ce, and Sr). Applied Physics Letters, 2007, 90, 192111.	1.5	213

#	Article	IF	Citations
3475	Mechanical strengths of silicon nitrides studied by ab initio calculations. Applied Physics Letters, 2007, 90, 191903.	1.5	54
3476	Single hydrogen atoms on the Si(001) surface. Physical Review B, 2007, 76, .	1.1	28
3477	Ripening of monolayer vacancy pits on metal surfaces: Pathways, energetics, and size-scaling for Ag(111) versus Ag(100). Physical Review B, 2007, 75, .	1.1	14
3478	Surface core-level shifts ofGaAs(100)(2Ã—4)from first principles. Physical Review B, 2007, 76, .	1.1	22
3479	Rotation possibility of a molecule adsorbed on the<mml:math xmlns:mml="http://www.w3.org/1998/Math/MathML" display="inline"><mml:mrow><mml:mi>Si</mml:mi><mml:mo>(</mml:mo><mml:mn>001</mml:mn><mml:mo>)</mml:mo></mml:mrow></mml:math>initiostudy. Physical Review B, 2007, 76, .	1.1	5
3480	Quantum Mechanical Description of Displacement Damage Formation. IEEE Transactions on Nuclear Science, 2007, 54, 1906-1912.	1.2	18
3481	Structural and magnetic properties of (Ga,Mn)N from first principles. Physical Review B, 2007, 75, .	1.1	29
3482	Dimer-breaking-assisted exchange mechanism in surfactant-mediated epitaxial growth of Ge on Si(001):Ab initiototal energy calculations. Physical Review B, 2007, 76, .	1.1	3
3483	Ab initiostudy ofWâ^'Alâ^'Coâ^'Ni: An approximant of the decagonalAlâ^'Coâ^'Niquasicrystal. Physical Review B, 2007, 75, .	1.1	8
3484	Pb-Pu Superlattices: An Example of Nanostructured Actinide Materials. Physical Review Letters, 2007, 98, 116401.	2.9	6
3485	Ab initiostudy of the oxidation on vicinal Si(001) surfaces: The step-selective oxidation. Physical Review B, 2007, 76, .	1.1	6
3486	How Pb-Overlayer Islands Move Fast Enough to Self-Assemble on Pb-Cu Surface Alloys. Physical Review Letters, 2007, 98, 096106.	2.9	19
3487	Ab initiostudy of electronic and structural properties of gold nanowires with light-element impurities. Physical Review B, 2007, 75, .	1.1	28
3488	Surface Metal-Insulator Transition on a Vanadium Pentoxide (001) Single Crystal. Physical Review Letters, 2007, 99, 226103.	2.9	113
3489	Electronic band gap of Si/SiO2 quantum wells: Comparison ofab initiocalculations and photoluminescence measurements. Journal of Vacuum Science and Technology A: Vacuum, Surfaces and Films, 2007, 25, 1500-1504.	0.9	19
3490	Theoretical study of the chemical gap tuning in silicon nanowires. Physical Review B, 2007, 76, .	1.1	65
3491	Formation of carbon nanotube semiconductor-metal intramolecular junctions by self-assembly of vacancy defects. Physical Review B, 2007, 76, .	1.1	32
3492	Modeling the structural, dynamical, and magnetic properties of liquidAl1â^'xMnx(x=0.14, 0.2, and 0.4): A first-principles investigation. Physical Review B, 2007, 76, .	1.1	11

#	Article	IF	Citations
3493	Electronic structures and atomic surface diffusion in Cr/Fe(001) and Fe/Cr(001) systems: First-principles study. , 2007, , .		0
3494	Influence of miscibility on the energy-gap dispersion inAlxGa1âˆ’xNalloys: First-principles calculations. Physical Review B, 2007, 75, .	1.1	23
3495	First-principles study of grain boundary sliding inÎ±âˆ’Al2O3. Physical Review B, 2007, 75, .	1.1	32
3496	Complete set of elastic constants ofÎ±-quartz at high pressure: A first-principles study. Physical Review B, 2007, 75, .	1.1	59
3497	Negative Differential Resistance in Transport through Organic Molecules on Silicon. Physical Review Letters, 2007, 98, 066807.	2.9	54
3498	Anchoring phthalocyanine molecules on the 6H-SiC(0001)3Ã—3 surface. Applied Physics Letters, 2007, 91, .	1.5	26
3499	Hydrogen shuttling near Hf-defect complexes in Siâˆ•SiO2âˆ•HfO2 structures. Applied Physics Letters, 2007, 91, .	1.5	30
3500	Cyclic Voltammograms for H on Pt(111) and Pt(100) from First Principles. Physical Review Letters, 2007, 99, 126101.	2.9	189
3501	Coaxial nanocable: Carbon nanotube core sheathed with boron nitride nanotube. Applied Physics Letters, 2007, 90, 133103.	1.5	29
3502	Structural stability and characteristics of the metastable Agâ€“W phases studied by ab initio and molecular dynamics calculations. Journal of Applied Physics, 2007, 101, 063512.	1.1	9
3503	Methane Dissociation on Ni(111): The Role of Lattice Reconstruction. Physical Review Letters, 2007, 98, 173003.	2.9	122
3504	How Can We Make Stable Linear Monoatomic Chains? Gold-Cesium Binary Subnanowires as an Example of a Charge-Transfer-Driven Approach to Alloying. Physical Review Letters, 2007, 98, 076101.	2.9	24
3505	Theoretical study of deep-defect states in bulk PbTe and in thin films. Physical Review B, 2007, 76, .	1.1	57
3506	Theoretical investigation of a Mn-dopedSiâˆ•Geheterostructure. Physical Review B, 2007, 75, .	1.1	9
3507	Surface modification of oxides by electron-stimulated desorption for growth-mode control of metal films: Experiment and density-functional calculations. Physical Review B, 2007, 76, .	1.1	21
3508	Oxygen-ion arrangements and concerted motion inÎ²âˆ’La2Mo2O9. Physical Review B, 2007, 76, .	1.1	25
3509	Diffusion of O vacancies nearSi:HfO2interfaces: Anab initioinvestigation. Physical Review B, 2007, 76, .	1.1	48
3510	First-principles calculations for the elastic properties of nanostructured superhard TiNâˆ•SixNy superlattices. Applied Physics Letters, 2007, 91, 081916.	1.5	26

#	Article	IF	Citations
3511	First-principles study of indium-stabilized {103} facets in Ge quantum dots. Physical Review B, 2007, 75, .	1.1	7
3512	Ab initiostudies of magnetic properties of cobalt and tetracobalt nitrideCo4N. Physical Review B, 2007, 75, .	1.1	65
3513	Heat capacity and lattice dynamics of cubic and hexagonalSrMnO3: Calorimetry and density functional theory simulations. Physical Review B, 2007, 75, .	1.1	29
3514	Electronic properties and chemical trends of the arsenicin situimpurities in<mml:math xmlns:mml="http://www.w3.org/1998/Math/MathML" display="inline"><mml:mrow><mml:msub><mml:mi mathvariant="normal">Hg</mml:mi><mml:mrow><mml:mn>1</mml:mn><mml:mo>â^'</mml:mo><mml:mi>x</mml:mi></mml:mrow></mml:msub><mml:mi mathvariant="normal">Cd</mml:mi><mml:mi>x</mml:mi></mml:msub><mml:mi mathvariant="normal">Te</mml:mi></mml:mrow></mml:math>: First-principles study. Physical Review B, 2007, 76, .	1.1	15
3515	Limits of the scaled shift correction to levels of interstitial defects in semiconductors. Physical Review B, 2007, 75, .	1.1	16
3516	Electronic and vibrational properties of framework-substituted type-II silicon clathrates. Physical Review B, 2007, 75, .	1.1	42
3517	Structural and electronic properties of fluorinated double-walled boron nitride nanotubes: Effect of interwall interaction. Physical Review B, 2007, 75, .	1.1	22
3518	Structure and stability of the low-index surfaces ofFe3Si:Ab initiodensity functional investigations. Physical Review B, 2007, 75, .	1.1	22
3519	Interactions between Al atoms on Al(110) from first-principles calculations. Physical Review B, 2007, 75, .	1.1	15
3520	Association of oxygen vacancies with impurity metal ions in lead titanate. Physical Review B, 2007, 76, .	1.1	94
3521	Suppressed Dependence of Polarization on Epitaxial Strain in Highly Polar Ferroelectrics. Physical Review Letters, 2007, 98, 217602.	2.9	146
3522	Conductance and Kondo Effect in a Controlled Single-Atom Contact. Physical Review Letters, 2007, 98, 016801.	2.9	161
3523	Multistate modified embedded atom method. Physical Review B, 2007, 75, .	1.1	52
3524	First-principles study of pressure-induced metal-insulator transition in BiNiO3. Applied Physics Letters, 2007, 91, 101901.	1.5	29
3525	First-principles study of contact between Ti surface and semiconducting carbon nanotube. Journal of Applied Physics, 2007, 102, 013709.	1.1	24
3526	Atomic arrangement and impurity bonding at aÎ²â^'Al2O3(001)â^•Al(771)interface: First-principles calculations. Physical Review B, 2007, 76, .	1.1	2
3527	Surface segregation energy in bcc Fe-rich Fe-Cr alloys. Physical Review B, 2007, 75, .	1.1	36
3528	Modified mean-field potential approach to thermodynamic properties of a low-symmetry crystal: Beryllium as a prototype. Physical Review B, 2007, 75, .	1.1	18

#	Article	IF	Citations
3529	Influence of superimposed biaxial stress on the tensile strength of perfect crystals from first principles. Physical Review B, 2007, 76, .	1.1	46
3530	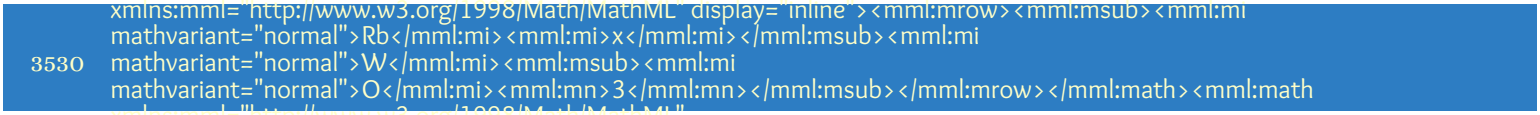		

#	Article	IF	Citations
3547	Ordered arrays of identicalNb4clusters on the GaN(0001) surface studied with first-principles calculations. Physical Review B, 2007, 75, .	1.1	9
3548	Water adsorption onO(2Ã—2)â^•Ru(0001): STM experiments and first-principles calculations. Physical Review B, 2007, 76, .	1.1	22
3549	Immersion structures of monovalent metal adatoms on<mml:math xmlns:mml="http://www.w3.org/1998/Math/MathML" display="inline"><mml:mrow><mml:mi mathvariant="normal">Ag</mml:mi><mml:mo>â^•</mml:mo><mml:mi mathvariant="normal">Si</mml:mi><mml:mrow><mml:mo>(</mml:mo><mml:mn>111</mml:mn><mml:mo>)</mml:mo></mml:mrow> Physical Review B, 2007, 76, .	1.1	15
3550	Confined states in multiple quantum well structures of<mml:math xmlns:mml="http://www.w3.org/1998/Math/MathML" display="inline"><mml:mrow><mml:msub><mml:mi mathvariant="normal">Si</mml:mi><mml:mi>n</mml:mi></mml:msub><mml:msub><mml:mi mathvariant="normal">Ge</mml:mi><mml:mi>n</mml:mi></mml:msub></mml:mrow></mml:math>nanowire superlattices. Physical Review B, 2007, 76, .	1.1	18
3551	Efficient multiscale algorithms for solution of self-consistent eigenvalue problems in real space. Physical Review B, 2007, 75, .	1.1	11
3552	Interstitial Fe in Si and its interactions with hydrogen and shallow dopants. Physical Review B, 2007, 76, .	1.1	50
3553	Energy decomposition analysis of metal silicide nanowires from first principles. Physical Review B, 2007, 75, .	1.1	12
3554	Adsorption and diffusion dynamics of atomic and molecular oxygen on reconstructed Cu(100). Physical Review B, 2007, 75, .	1.1	31
3555	Global space-group optimization problem: Finding the stablest crystal structure without constraints. Physical Review B, 2007, 75, .	1.1	148
3556	Interstitials in FeCr alloys studied by density functional theory. Physical Review B, 2007, 76, .	1.1	44
3557	Reoxidation ofTiO2(110)via Ti interstitials and line defects. Physical Review B, 2007, 75, .	1.1	67
3558	Energetics of interlayer binding in graphite: The semiempirical approach revisited. Physical Review B, 2007, 76, .	1.1	63
3559	Electron transport through<mml:math xmlns:mml="http://www.w3.org/1998/Math/MathML" display="inline"><mml:mi>Ï€</mml:mi></mml:math>-stacked molecular multilayers: Metal-semiconductor transition. Physical Review B, 2007, 76, .	1.1	1
3560	Effect of Si adsorption on the atomic and electronic structure ofAunclusters(n=1â€“8)and the Au (111) surface: First-principles calculations. Physical Review B, 2007, 75, .	1.1	45
3561	Theory of genus reduction in alkali-induced graphitization of nanoporous carbon. Physical Review B, 2007, 76, .	1.1	14
3562	Localization of oxygen donor states in gallium nitride from first-principles calculations. Physical Review B, 2007, 76, .	1.1	25
3563	Intercalation of oxygen and water molecules in pentacene crystals: First-principles calculations. Physical Review B, 2007, 75, .	1.1	66
3564	Atomic-scale modeling of next-layer nucleation and step flow at the Ge(105) rebonded-step surface. Physical Review B, 2007, 75, .	1.1	9

#	Article	IF	Citations
3565	Building blocks of amorphous<mml:math xmlns:mml="http://www.w3.org/1998/Math/MathML" display="inline"><mml:mrow><mml:msub><mml:mi mathvariant="normal">Ge</mml:mi><mml:mn>2</mml:mn></mml:msub><mml:msub><mml:mi mathvariant="normal">Sb</mml:mi><mml:mn>2</mml:mn></mml:msub><mml:msub><mml:mi mathvariant="normal">Te</mml:mi><mml:mn>5</mml:mn></mml:msub></mml:mrow></mml:math>. Physical Review B, 2007, 76, .	1.1	35
3566	Electronic structure of sodium tungsten bronzesNaxWO3by high-resolution angle-resolved photoemission spectroscopy. Physical Review B, 2007, 75, .	1.1	48
3567	First-principles simulations of Si vacancy diffusion in erbium silicide. Physical Review B, 2007, 76, .	1.1	1
3568	Thermodynamics of ordered and disordered phases in the binary Mo-Ru system. Physical Review B, 2007, 75, .	1.1	14
3569	Including the probe tip in theoretical models of inelastic scanning tunneling spectroscopy: CO on Cu(100). Physical Review B, 2007, 76, .	1.1	27
3570	Density-functional calculation of the shock Hugoniot for diamond. Physical Review B, 2007, 76, .	1.1	24
3571	Order-disorder phase transition of the Cu(001) surface under equilibrium oxygen pressure. Physical Review B, 2007, 76, .	1.1	32
3572	Anomalous strain dependent effective masses in (111) Si nanowires. Applied Physics Letters, 2007, 91, 083116.	1.5	11
3573	Comment on â€œSymmetry and Stability ofÎ´Plutonium: The Influence of Electronic Structureâ€• Physical Review Letters, 2007, 99, 019703; discussion 019704.	2.9	4
3574	Superconductivity and Magnetic Order inCeRhIn5: Spectra of Coexistence. Physical Review Letters, 2007, 98, 126406.	2.9	8
3575	Effect of oxygen vacancies on spin-dependent tunneling in Feâ•MgOâ•Fe magnetic tunnel junctions. Applied Physics Letters, 2007, 90, 072502.	1.5	76
3576	Nonvolatile Memory Elements Based on the Intercalation of Organic Molecules Inside Carbon Nanotubes. Physical Review Letters, 2007, 98, 056401.	2.9	24
3577	Influence of Temperature on the Interaction between Pd Clusters and the<mml:math xmlns:mml="http://www.w3.org/1998/Math/MathML" display="inline"><mml:msub><mml:mi>TiO</mml:mi><mml:mn>2</mml:mn></mml:msub></mml:math>(110) Surface. Physical Review Letters, 2007, 99, 066102.	2.9	11
3578	Reciprocal Space Constraints Create Real-Space Anomalies in Doped Carbon Nanotubes. Physical Review Letters, 2007, 99, 196803.	2.9	6
3579	Density functional study of the interaction between small Au clusters, Aunâ€(n=1â€“7) and the rutile TiO2 surface. II. Adsorption on a partially reduced surface. Journal of Chemical Physics, 2007, 127, 244708.	1.2	52
3580	Surface Reconstruction with a Fractional Hole:(5Ã—5)R26.6Â°LaAlO3(001). Physical Review Letters, 2007, 98, 086102.	2.9	45
3581	Formation of polybromine anions and concurrent heavy hole doping in carbon nanotubes. Applied Physics Letters, 2007, 90, 093502.	1.5	17
3582	Stability and electronic structures of CuxTe. Applied Physics Letters, 2007, 91, .	1.5	61

#	Article	IF	Citations
3583	Marcasite osmium nitride with high bulk modulus: First-principles calculations. Applied Physics Letters, 2007, 90, 061922.	1.5	50
3584	Phonons at the Fe(110) Surface. Physical Review Letters, 2007, 99, 066103.	2.9	46
3585	Identification ofGe/SiIntermixing Processes at theBi/Ge/Si(111)Surface. Physical Review Letters, 2007, 98, 166104.	2.9	21
3586	Structural stability in the Alâ€“Liâ€“Si system. Applied Physics Letters, 2007, 90, 251902.	1.5	7
3587	Prediction of Uncompensated Polarity in Ultrathin Films. Physical Review Letters, 2007, 98, 205701.	2.9	94
3588	Energetics of positron states trapped at vacancies in solids. Physical Review B, 2007, 76, .	1.1	38
3589	First principles studies of ideal strength and bonding nature of AlN polymorphs in comparison to TiN. Applied Physics Letters, 2007, 91, .	1.5	66
3590	AgRaman modes and ion-position dependence of the electronic structures ofYBa2Cu3O7andYBa2Cu4O8from first principles. Physical Review B, 2007, 76, .	1.1	1
3591	Nonlinear response theories and effective pair potentials. Physical Review B, 2007, 76, .	1.1	14
3592	Band offset and magnetic property engineering for epitaxial interfaces: A monolayer ofM2O3(M=Al,Ga,Sc,Ti,Ni)at theÎ±â^'Fe2O3â^•Î±â^'Cr2O3(0001) interface. Physical Review B, 2007, 75, .	1.1	6
3593	Lattice relaxation study of the<mml:math xmlns:mml="http://www.w3.org/1998/Math/MathML" display="inline"><mml:mrow><mml:mn>4</mml:mn><mml:mi>f</mml:mi><mml:mtext>â^'</mml:mtext><mml:mn>5</mml:mn><mml:m of<mml:math xmlns:mml="http://www.w3.org/1998/Math/MathML" display="inline"><mml:msup><mml:mi mathvariant="normal">Ce</mml:mi><mml:mrow><mml:mn>3</mml:mn><mml:mo>+</mml:mo></mml:mrow></mml:msup></mml:mat xmlns:mml="http://www.w3.org/1998/Math/MathML". Physical Review B, 2007, 76, .	1.1	48
3594	Structures and magnetic properties of (Mn, N)-codoped ZnO thin films. Applied Physics Letters, 2007, 90, 242509.	1.5	55
3595	Bonding characteristics and site occupancies of alloying elements in differentNb5Si3phases from first principles. Physical Review B, 2007, 76, .	1.1	39
3596	Valence electronic structure of cross-linkedC60polymers:In situhigh-resolution photoelectron spectroscopic and density-functional studies. Physical Review B, 2007, 75, .	1.1	27
3597	Density functional study ofGe1â^'xMnxTe. Physical Review B, 2007, 75, .	1.1	15
3598	Pseudomorphic quasiperiodic alkali metal monolayers on aniâ^'Alâ^'Pdâ^'Mnsurface. Physical Review B, 2007, 75, .	1.1	20
3599	Chemical bonding effect of Ge atoms on B diffusion in Si. Physical Review B, 2007, 76, .	1.1	10
3600	Polarization enhancement in short period superlattices via interfacial intermixing. Physical Review B, 2007, 76, .	1.1	39

#	Article	IF	Citations
3601	Comparison of chain versus sheet crystal structures for the cyanidesMCN(M=Cuî—¸Au)and dicarbidesMC2(M=Beî—¸Ba,Znî—¸Hg). Physical Review B, 2007, 76, .	1.1	28
3602	Mechanisms of silicon diffusion in erbium silicide. Physical Review B, 2007, 75, .	1.1	4
3603	Kadowaki-Woods ratio for strongly coupled Fermi liquids. Physical Review B, 2007, 76, .	1.1	1
3604	Calculating carbon nanotubeâ€“catalyst adhesion strengths. Physical Review B, 2007, 75, .	1.1	39
3605	<mml:math xmlns:mml="http://www.w3.org/1998/Math/MathML" display="inline"><mml:mrow><mml:mi mathvariant="normal">N</mml:mi><mml:msub><mml:mi mathvariant="normal">H</mml:mi><mml:mn>2</mml:mn></mml:msub></mml:mrow></mml:math>and NH bonding sites determined by STM-induced activation on the<mml:math xmlns:mml="http://www.w3.org/1998/Math/MathML" display="inline"><mml:mrow><mml:mi mathvariant="normal">N</mml:mi><mml:msub><mml:mi mathvariant="normal">H</mml:mi><mml:mn>3</mml:mn></mml:msub></mml:mrow></mml:math>	1.1	7
3606	â€‡Dynamics of phononic dissipation at the atomic scale: Dependence on internal degrees of freedom. Physical Review B, 2007, 76, .	1.1	11
3607	Long-range empirical potential for the bcc structured transition metals. Physical Review B, 2007, 75, .	1.1	43
3608	Emergence of noncollinear magnetic ordering in small magnetic clusters:<mml:math xmlns:mml="http://www.w3.org/1998/Math/MathML" display="inline"><mml:msub><mml:mi mathvariant="normal">Mn</mml:mi><mml:mi>n</mml:mi></mml:msub></mml:math>and<mml:math xmlns:mml="http://www.w3.org/1998/Math/MathML" display="inline"><mml:mrow><mml:mi mathvariant="normal">As</mml:mi><mml:mi>@</mml:mi><mml:msub><mml:mi mathvariant="normal">Mn</mml:mi><mml:mi>n</mml:mi></mml:msub></mml:mrow></mml:math>clusters. Phys	1.1	39
3609	Tuning the ferromagnetism of one-dimensionalFeâˆ•Ptâˆ•Femultilayer barcode nanowires via the barcode layer effect. Physical Review B, 2007, 76, .	1.1	18
3610	Ab initiostudy of thallium nanoclusters on<mml:math xmlns:mml="http://www.w3.org/1998/Math/MathML" display="inline"><mml:mrow><mml:mi mathvariant="normal">Si</mml:mi><mml:mrow><mml:mo>(</mml:mo><mml:mn>111</mml:mn><mml:mo>)</mml:mo></mml:mrow></mml:mrow></mml:math> Physical Review B, 2007, 76, .	1.1	19
3611	Ab initiostudies of possible magnetism in a<mml:math xmlns:mml="http://www.w3.org/1998/Math/MathML" display="inline"><mml:mrow><mml:mi>BN</mml:mi></mml:mrow></mml:math>sheet by nonmagnetic impurities and vacancies. Physical Review B, 2007, 76, .	1.1	120
3612	Analysis of electron-positron momentum spectra of metallic alloys as supported by first-principles calculations. Physical Review B, 2007, 75, .	1.1	41
3613	Structure of AlSb(001) and GaSb(001) surfaces under extreme Sb-rich conditions. Physical Review B, 2007, 76, .	1.1	19
3614	Atomic and electronic structures of doped silicon nanowires: A first-principles study. Physical Review B, 2007, 76, .	1.1	39
3615	Nonlinear elasticity effect in group III-nitride quantum heterostructures:Ab initiocalculations. Physical Review B, 2007, 75, .	1.1	48
3616	Magnetic endohedral metallofullerenes with floppy interiors. Physical Review B, 2007, 75, .	1.1	19
3617	Lattice dynamics and anomalous bonding in rhombohedral As: First-principles supercell method. Physical Review B, 2007, 76, .	1.1	31
3618	Proposed power-functionN-body potential for the fcc structured metals Ag, Au, Cu, Ni, Pd, and Pt. Physical Review B, 2007, 76, .	1.1	11

#	Article	IF	Citations
3619	First-principles studies of the interlayer exchange coupling in fine-layeredFeâ•Aumultilayers. Physical Review B, 2007, 75, .	1.1	6
3620	Theoretical study of stability and electronic structure of Li(Mg,Zn)N alloys: A candidate for solid state lighting. Physical Review B, 2007, 76, .	1.1	20
3621	Corner- versus face-sharing octahedra inAMnO3perovskites (A=Ca, Sr, and Ba). Physical Review B, 2007, 75, .	1.1	76
3622	Atomic-scale structure of the<mml:math xmlns:mml="http://www.w3.org/1998/Math/MathML" display="inline"><mml:mrow><mml:mi mathvariant="normal">Sr</mml:mi><mml:mi mathvariant="normal">Ti</mml:mi><mml:msub><mml:mi mathvariant="normal">O</mml:mi><mml:mn>3</mml:mn></mml:msub><mml:mrow><mml:mo>(</mml:mo><mml:mn>001</mml:mn> Physical Review B, 2007, 76, .	1.1	55
3623	Atomic structure determination of the3C-SiC(001)c(4Ã—2)surface reconstruction: Experiment and theory. Physical Review B, 2007, 75, .	1.1	14
3624	First-principles study of a single-molecule magnetMn12monolayer on the Au(111) surface. Physical Review B, 2007, 76, .	1.1	39
3625	Electronic-structure calculations for polar lattice-structure-mismatched interfaces:<mml:math xmlns:mml="http://www.w3.org/1998/Math/MathML" display="inline"><mml:mrow><mml:mi mathvariant="normal">Pb</mml:mi><mml:mi mathvariant="normal">Te</mml:mi><mml:mo>â•</mml:mo><mml:mi mathvariant="normal">Cd</mml:mi><mml:mi mathvariant="normal">Te</mml:mi></mml:mrow></mml:math>	1.1	22
3626	<mml:math xmlns:mml="http://www.w3.org/1998/Math/MathML" display="inline"><mml:mrow><mml:msub><mml:mi mathvariant="normal">Ti</mml:mi><mml:mrow><mml:mn>1</mml:mn><mml:mo>â^’</mml:mo><mml:mi>x</mml:mi></mml:mrow></mml:msub><mml:msub><mml:mi mathvariant="normal">Si</mml:mi><mml:mi>x</mml:mi></mml:msub><mml:mi mathvariant="normal">N</mml:mi></mml:mrow></mml:math>solid solution and the stability of fcc SiN studied by combined ab initio density functional theory and therm. Physical Review B, 2007, 75, .	1.1	23
3627	Effect of intramolecular disorder and intermolecular electronic interactions on the electronic structure of poly-p-phenylene vinylene. Physical Review B, 2007, 76, .	1.1	28
3628	Adsorption and electronic excitation of biphenyl onSi(100): A theoretical STM analysis. Physical Review B, 2007, 75, .	1.1	11
3629	Ab initiostudy of hydrogen interaction with pure and nitrogen-doped carbon nanotubes. Physical Review B, 2007, 75, .	1.1	60
3630	Interplay between indirect interaction and charge-density wave in Pb-adsorbedIn(4Ã—1)â^’Si(111). Physical Review B, 2007, 76, .	1.1	9
3631	Restored quantum size effects of Pb overlayers at high coverages. Physical Review B, 2007, 75, .	1.1	19
3632	Hydrogenated caged clusters of Si, Ge, and Sn and their endohedral doping with atoms:Ab initiocalculations. Physical Review B, 2007, 75, .	1.1	50
3633	Substitutional NaCl hydration in ice. Physical Review B, 2007, 75, .	1.1	9
3634	Reaction energetics and crystal structure ofLi4BN3H10from first principles. Physical Review B, 2007, 75, .	1.1	70
3635	Symmetrizing evolution of dimer structures on tensile-strainedSi(001)surfaces: First-principles density-functional calculations. Physical Review B, 2007, 75, .	1.1	9
3636	Ab initio study of the effects of transition metal doping of <mml:math xmlns:mml="http://www.w3.org/1998/Math/MathML" display="inline"><mml:mrow><mml:msub><mml:mi mathvariant="normal">Mg</mml:mi><mml:mn>2</mml:mn></mml:msub><mml:mi mathvariant="normal">Ni</mml:mi><mml:msub><mml:mi mathvariant="normal">H</mml:mi><mml:mn>4</mml:mn></mml:msub></mml:mrow></mml:math>. Physical Review B, 2007, 76, .	1.1	61

#	Article	IF	Citations
3637	Concurrent substitutional and displacive phase transformations in Al-Mg-Si nanoclusters. Physical Review B, 2007, 76, .	1.1	14
3638	Short-range order of low-coverage Tiâ•Al(111): Implications for hydrogen storage in complex metal hydrides. Applied Physics Letters, 2007, 90, 151917.	1.5	15
3639	Quantum mechanics/molecular mechanics methodology for metals based on orbital-free density functional theory. Physical Review B, 2007, 76, .	1.1	26
3640	Theoretical investigation of bulk ordering and surface segregation in Ag-Pd and other isoelectornic alloys. Physical Review B, 2007, 75, .	1.1	26
3641	Structural and electronic properties ofRunclusters(n=2â€“14)studied by first-principles calculations. Physical Review B, 2007, 76, .	1.1	50
3642	Theoretical calculations of mobility enhancement in strained silicon. Physical Review B, 2007, 75, .	1.1	21
3643	Surface oxides on Pd(111): STM and density functional calculations. Physical Review B, 2007, 76, .	1.1	69
3644	Ab initiostudy of structural, magnetic, vibrational, and thermodynamic properties of the Laves-phase compoundHfMn2. Physical Review B, 2007, 76, .	1.1	11
3645	Ordering and segregation of aCu75Pt25(111)surface: A first-principles cluster expansion study. Physical Review B, 2007, 76, .	1.1	31
3646	Ferroelectric distortion inSrTiO3thin films onSi(001)by x-ray absorption fine structure spectroscopy: Experiment and first-principles calculations. Physical Review B, 2007, 75, .	1.1	62
3647	Surface effects on metallic nanowires and the stability of material properties. , 2007, , .		0
3648	First-principles study of electronic properties of La2Hf2O7 and Gd2Hf2O7. Journal of Applied Physics, 2007, 102, 063704.	1.1	42
3649	Initial interactions between water molecules and Ti-adsorbed carbon nanotubes. Applied Physics Letters, 2007, 91, 161906.	1.5	11
3650	Cationic and anionic vacancies on the NiO(100) surface: DFT+U and hybrid functional density functional theory calculations. Journal of Chemical Physics, 2007, 127, 174711.	1.2	93
3651	First-principles analysis of interfacial nanoscaled oxide layers of bonded N- and P-type GaAs wafers. Journal of Applied Physics, 2007, 102, 013710.	1.1	5
3652	First-principles investigation on the geometry and electronic structure of the three-dimensional cuboidal C60 polymer. Journal of Chemical Physics, 2007, 127, 134906.	1.2	16
3653	Experimental and theoretical study of reactivity trends for methanol on Coâ•Pt(111) and Niâ•Pt(111) bimetallic surfaces. Journal of Chemical Physics, 2007, 127, 114707.	1.2	69
3654	First Principles Study of Al(100) Twisted Interfaces. Solid State Phenomena, 2007, 129, 131-136.	0.3	1

#	Article	IF	Citations
3655	Elastic constants and thermodynamic properties of Mgâ€“Pr, Mgâ€“Dy, Mgâ€“Y intermetallics with atomistic simulations. Journal Physics D: Applied Physics, 2007, 40, 7584-7592.	1.3	30
3656	Theoretical Tensile Deformation of Î£13 Pyramidal Twin Grain Boundary in Alumina. Key Engineering Materials, 2007, 352, 21-24.	0.4	0
3657	Tensile Strength of Perfect Cubic Crystals under Superimposed Transverse Plain Stress. Materials Science Forum, 2008, 567-568, 73-76.	0.3	6
3658	Determination of symmetry reduced structures by a soft-phonon analysis in Ni₂MnGa. Materials Research Society Symposia Proceedings, 2007, 1050, 1.	0.1	3
3659	Energies of ions in water and nanopores within density functional theory. Journal of Chemical Physics, 2007, 127, 154722.	1.2	25
3660	Ab initiomelting curve of molybdenum by the phase coexistence method. Journal of Chemical Physics, 2007, 126, 194502.	1.2	89
3661	Free Energy Calculations of Precipitate Nucleation. Materials Science Forum, 2007, 539-543, 2395-2400.	0.3	1
3662	First-Principles Study of Structural and Electronic Property of Pyrochlore Dy₂Sn₂O₇. Advanced Materials Research, 2007, 26-28, 933-936.	0.3	1
3663	First-principles Calculations on the Zn1-xMgxO Window Layer Material for CIS Thin Film Solar Cells. Materials Research Society Symposia Proceedings, 2007, 1012, 1.	0.1	2
3664	COKING MECHANISM AND PROMOTER DESIGN FOR Ni-BASED CATALYSTS: A FIRST PRINCIPLES STUDY. International Journal of Nanoscience, 2007, 06, 131-135.	0.4	4
3665	Density functional study of the charge on Aun clusters (n=1â€“7) supported on a partially reduced rutile TiO2(110): Are all clusters negatively charged?. Journal of Chemical Physics, 2007, 126, 104701.	1.2	72
3666	A First-Principles Analysis for Sulfur Tolerance of CeO₂in Solid Oxide Fuel Cells. Journal of Physical Chemistry C, 2007, 111, 11117-11122.	1.5	63
3667	Dynamical Simulation of SiO₂/4H-SiC(0001) Interface Oxidation Process: from First-Principles. Materials Science Forum, 2007, 556-557, 615-620.	0.3	9
3668	New Metal Nitride Compounds: Can they be Synthesized at High-Pressures?. Materials Research Society Symposia Proceedings, 2007, 1040, 1.	0.1	0
3669	Electronic properties of adsorbates on GaAs(001)-c(2Ã—8)âˆ•(2Ã—4). Journal of Chemical Physics, 2007, 127, 134705.	1.2	41
3670	First Principles Study on Ideal Strength of Cu Multi-Shell Nano-Wire. Key Engineering Materials, 2007, 345-346, 919-924.	0.4	0
3671	Fundamental Interactions of Fe in Silicon: First-Principles Theory. Solid State Phenomena, 2008, 131-133, 233-240.	0.3	8
3672	Structure, Composition, and Electronic Properties of TiOx/Mo(112) Thin Films. Journal of Physical Chemistry C, 2007, 111, 7437-7445.	1.5	11

#	Article	IF	Citations
3673	Chapter 14 Theory of magnetic clusters and nanostructures at surfaces. Chemical Physics of Solid Surfaces, 2007, , 535-588.	0.3	0
3674	First principles calculations of relationship between the Cu surface states and relaxations. Chinese Physics B, 2007, 16, 1429-1433.	1.3	3
3675	Phase Transitions in Silicon-Carbon-Nitride Compounds. Materials Research Society Symposia Proceedings, 2007, 1040, 1.	0.1	0
3676	Negative or Zero Thermal Expansion in Silicon Dicarbodiimide, Si(NCN)2. Materials Research Society Symposia Proceedings, 2007, 1040, 1.	0.1	0
3677	FunctionalizingÎ»-AlOOH Surface with Silanol -- an Ab-initio Study. Materials Research Society Symposia Proceedings, 2007, 1000, 1.	0.1	0
3678	Effect of cation ordering and pressure on spinel elasticity by ab initio simulation. American Mineralogist, 2007, 92, 174-178.	0.9	27
3679	Molecular dynamics simulations of stretched gold nanowires: The relative utility of different semiempirical potentials. Journal of Chemical Physics, 2007, 126, 144707.	1.2	57
3680	A theoretical study of half-metallic antiferromagnetic diluted magnetic semiconductors. Journal of Physics Condensed Matter, 2007, 19, 216220.	0.7	27
3681	An approach to control the radius and the chirality of nanotubes. Nanotechnology, 2007, 18, 155703.	1.3	26
3682	Site-Selective Electronic Structure of Aluminum in Oxide Ceramics Obtained by TEM-EELS Analysis Using the Electron Standing-Wave Method. Materials Transactions, 2007, 48, 2590-2594.	0.4	15
3683	Development of Interatomic Potential for Zr-Ni Amorphous Systems. Materials Transactions, 2007, 48, 1313-1321.	0.4	9
3684	First-Principles Calculation on the Stable Structure and Adhesive Strength of Ni/Fe(100) or Cu/Fe(100) Interfaces. Nippon Kinzoku Gakkaishi/Journal of the Japan Institute of Metals, 2007, 71, 1024-1031.	0.2	5
3685	Theoretical Studies of the Atomic and Electronic Structure of Nano-Hetero Metal/Inorganic Material Interfaces in Collaboration with Electron Microscopy Observations. Materials Transactions, 2007, 48, 675-683.	0.4	13
3686	Metal Sandwich Molecules: Planar Metal Atom Arrays between Aromatic Hydrocarbons. Materials Transactions, 2007, 48, 693-699.	0.4	6
3687	CO oxidation reaction on Pt(111) studied by the dynamic Monte Carlo method including lateral interactions of adsorbates. Journal of Chemical Physics, 2007, 126, 044704.	1.2	44
3688	Formation of Atomistic Island in Al Film Growth by Kinetic Monte Carlo. Nihon Kikai Gakkai Ronbunshu, A Hen/Transactions of the Japan Society of Mechanical Engineers, Part A, 2007, 73, 490-497.	0.2	4
3689	Structural and electronic properties of Al12X+ (X=C, Si, Ge, Sn, and Pb) clusters. Journal of Chemical Physics, 2007, 126, 014703.	1.2	14
3690	Computer simuations for the nano-scale. Acta Physica Slovaca, 2007, 57, 1-176.	1.4	9

#	Article	IF	Citations
3691	One-dimensional Au on TiO2. Journal of Physics Condensed Matter, 2007, 19, 082202.	0.7	22
3692	First-principles investigation on the atomic structure and stability of a Pt monolayer on Fe(001). Journal of Physics Condensed Matter, 2007, 19, 482002.	0.7	4
3693	Electronic and electron-transport properties of peanut-shaped C60polymers. Journal of Physics: Conference Series, 2007, 61, 899-903.	0.3	13
3694	Field emission of metal nanowires studied by first-principles methods. Nanotechnology, 2007, 18, 475706.	1.3	17
3695	HR-TEM Studies of FePt Nanoparticles by Exit Wave Reconstruction. Materials Research Society Symposia Proceedings, 2007, 998, 1.	0.1	5
3696	The perovskite to post-perovskite transition in CaIrO3: Clapeyron slope and changes in bulk and shear moduli by density functional theory. Physics of the Earth and Planetary Interiors, 2007, 164, 50-62.	0.7	23
3697	First principles determination of dislocations properties of MgSiO3 perovskite at 30GPa based on the Peierlsâ€“Nabarro model. Physics of the Earth and Planetary Interiors, 2007, 163, 283-291.	0.7	35
3698	Ab initio calculations of the elastic properties of ferropericlase Mg1â^'xFexO (). Physics of the Earth and Planetary Interiors, 2007, 164, 177-185.	0.7	11
3699	Structure, ordering, and bonding of half antiperovskites: PbNi3/2S and BiPd3/2S. Progress in Solid State Chemistry, 2007, 35, 309-327.	3.9	47
3700	Transport properties of liquid nickel near the melting point: An ab initio molecular dynamics study. Journal of Chemical Physics, 2007, 126, 234508.	1.2	47
3701	Ab initio molecular dynamics study of manganese porphine hydration and interaction with nitric oxide. Journal of Chemical Physics, 2007, 126, 024501.	1.2	12
3702	Short-Range Order in Liquid Aluminum Chloride:Â Ab Initio Molecular Dynamics Simulations and Quantum-Chemical Calculations. Journal of Physical Chemistry B, 2007, 111, 5316-5321.	1.2	11
3703	DFT Studies on the Four Polymorphs of Crystalline CL-20 and the Influences of Hydrostatic Pressure on Îµ-CL-20 Crystal. Journal of Physical Chemistry B, 2007, 111, 2090-2097.	1.2	147
3704	Crystal Growth, Structure, and Electronic Band Structure of Tetraceneâ^'TCNQ. Journal of Physical Chemistry C, 2007, 111, 3486-3489.	1.5	38
3705	Modification of electronic, optical, and magnetic properties of titanate nanotubes by metal intercalation. Physical Review B, 2007, 75, .	1.1	33
3706	Structural transition of PETN-I to ferroelastic orthorhombic phase PETN-III at elevated pressures. Journal of Chemical Physics, 2007, 127, 094502.	1.2	18
3707	The Samson phase, Î²-Mg2Al3, revisited. Zeitschrift FÃ¼r Kristallographie, 2007, 222, .	1.1	118
3708	Electronic structure and optical properties ofZnX(X=O,S, Se, Te): A density functional study. Physical Review B, 2007, 75, .	1.1	225

#	Article	IF	Citations
3709	Substrate-induced band gap in graphene on hexagonal boron nitride:Ab initiodensity functional calculations. Physical Review B, 2007, 76, .	1.1	1,292
3710	Stability of nanoscale co-precipitates in a superalloy: A combined first-principles and atom probe tomography study. Physical Review B, 2007, 76, .	1.1	38
3711	Crystal and electronic structure of Li15Si4. Journal of Applied Physics, 2007, 102, .	1.1	93
3712	First-Principles Simulations on the Nature of the Melting Line of Sodium. Physical Review Letters, 2007, 98, 055501.	2.9	35
3713	Ab initio calculations of the elasticity of iron and iron alloys at inner core conditions: Evidence for a partially molten inner core?. Earth and Planetary Science Letters, 2007, 254, 227-232.	1.8	119
3714	Electronic spin transitions in iron-bearing MgSiO3 perovskite. Earth and Planetary Science Letters, 2007, 253, 282-290.	1.8	93
3715	The 10ÂÃ... phase at high pressure by first principles calculations and implications for the petrology of subduction zones. Earth and Planetary Science Letters, 2007, 260, 212-226.	1.8	28
3716	Development of bond-order potentials that can reproduce the elastic constants and melting point of silicon for classical molecular dynamics simulation. Computational Materials Science, 2007, 39, 457-464.	1.4	151
3717	Atomistic modeling of an Fe system with a small concentration of C. Computational Materials Science, 2007, 40, 119-129.	1.4	165
3718	Ab initio calculations of mechanical and thermodynamic properties for the B2-based AlRE. Computational Materials Science, 2007, 40, 226-233.	1.4	38
3719	Ab initio simulations of clustering and precipitation in Alâ€“Mgâ€“Si alloys. Computational Materials Science, 2007, 40, 309-318.	1.4	17
3720	First-principles study of structural stabilities and electronic characteristics of Mgâ€“La intermetallic compounds. Computational Materials Science, 2007, 41, 78-85.	1.4	42
3721	Thermodynamic modelling of the Bâ€“Ca, Bâ€“Sr and Bâ€“Ba systems. Calphad: Computer Coupling of Phase Diagrams and Thermochemistry, 2007, 31, 286-291.	0.7	17
3722	Ab initiomodeling of Li-B-H boron-chain alloys for hydrogen storage applications. Physical Review B, 2007, 76, .	1.1	13
3723	Control of the Charge State of Metal Atoms on Thin MgO Films. Physical Review Letters, 2007, 98, 096107.	2.9	310
3724	Structural and electronic properties of lead chalcogenides from first principles. Physical Review B, 2007, 75, .	1.1	182
3725	Model GW band structure ofInAsandGaAsin the wurtzite phase. Physical Review B, 2007, 75, .	1.1	136
3726	Structural, electronic, and magnetic properties of Mn-doped Ge nanowires byab initiocalculations. Physical Review B, 2007, 75, .	1.1	16

#	Article	IF	Citations
3727	Multi-scale modeling of oxygen molecule adsorption on a Si(100)-p(2Ã—2) surface. Journal of Non-Crystalline Solids, 2007, 353, 594-598.	1.5	12
3728	Structure of chalcogenide glasses by neutron diffraction. Journal of Non-Crystalline Solids, 2007, 353, 729-732.	1.5	18
3729	First principles molecular dynamics of silicate oxynitride melt doped with scandium, yttrium and lanthanum. Journal of Non-Crystalline Solids, 2007, 353, 2025-2028.	1.5	3
3730	Ab-initio molecular dynamics simulations of the structure of liquid aluminates. Journal of Non-Crystalline Solids, 2007, 353, 1789-1792.	1.5	24
3731	First-principle molecular dynamics study of the structural and electronic properties of liquid and amorphous Niâ€“Al alloys. Journal of Non-Crystalline Solids, 2007, 353, 2638-2645.	1.5	21
3732	Short-range order of liquid and undercooled metals: Ab initio molecular dynamics study. Journal of Non-Crystalline Solids, 2007, 353, 3684-3688.	1.5	25
3733	Ab initio analysis of sulfur tolerance of Ni, Cu, and Niâ€“Cu alloys for solid oxide fuel cells. Journal of Alloys and Compounds, 2007, 427, 25-29.	2.8	56
3734	Ab initio studies of the electronic structure of the quaternary system LiBC4N4. Journal of Alloys and Compounds, 2007, 427, 61-66.	2.8	6
3735	On the ternary Laves phases {Sc,Ti}2M3Si (M=Cr, Mn, Fe, Co, Ni) with MgZn2-type. Journal of Alloys and Compounds, 2007, 429, 10-18.	2.8	18
3736	Thermodynamic modeling of the Baâ€“Niâ€“Ti system. Journal of Alloys and Compounds, 2007, 430, 188-193.	2.8	9
3737	Two polymorphs of Ba3Sn2P4: Single crystal and electronic structures. Journal of Alloys and Compounds, 2007, 430, 54-59.	2.8	7
3738	Structural phase transition in the Hfâ€“Ni system studied by ab initio calculation and ion beam mixing. Journal of Alloys and Compounds, 2007, 430, 142-148.	2.8	1
3739	First principles screening of destabilized metal hydrides for high capacity H2 storage using scandium. Journal of Alloys and Compounds, 2007, 446-447, 23-27.	2.8	33
3740	Hydrogen-related defects in sodium alanate. Journal of Alloys and Compounds, 2007, 446-447, 459-461.	2.8	10
3741	Experimental and theoretical investigation of the cycle durability against CO and degradation mechanism of the LaNi5 hydrogen storage alloy. Journal of Alloys and Compounds, 2007, 446-447, 208-211.	2.8	18
3742	The importance of vibrations in modelling complex metal hydrides. Journal of Alloys and Compounds, 2007, 446-447, 455-458.	2.8	16
3743	Models and simulations of nuclear fuel materials properties. Journal of Alloys and Compounds, 2007, 444-445, 415-423.	2.8	42
3744	Point defect structures of YAl2 and ZrCo2 Laves phase compounds by first-principles calculations. Intermetallics, 2007, 15, 20-25.	1.8	11

#	Article	IF	Citations
3745	Stability and elastic properties of L12-(Al,Cu)3(Ti,Zr) phases: Ab initio calculations and experiments. Intermetallics, 2007, 15, 44-54.	1.8	75
3746	Moisture-induced embrittlement mechanism for (Ni,Fe)Ti alloys. Intermetallics, 2007, 15, 288-293.	1.8	3
3747	Solid solution mechanism and thermodynamic properties of Tiâ€“Re alloy system: Experiment and theory. Intermetallics, 2007, 15, 1116-1121.	1.8	4
3748	Reassessment of the Ceâ€“Ni binary system supported by key experiments and ab initio calculations. Intermetallics, 2007, 15, 1401-1408.	1.8	24
3749	The establishment of the statistical-thermodynamic model of D81-structure and its application to Î±-Nb5Si3. Intermetallics, 2007, 15, 1558-1563.	1.8	12
3750	Shear-induced chemical disordering in Ni3Al at different temperatures. Intermetallics, 2007, 15, 1568-1572.	1.8	1
3751	Structural distortion of -structured MnO and FeO. Solid State Communications, 2007, 142, 6-9.	0.9	19
3752	Quasiparticle band structure and optical spectrum ofCaF2. Physical Review B, 2007, 75, .	1.1	29
3753	Stability analysis of doped materials for reversible hydrogen storage in destabilized metal hydrides. Physical Review B, 2007, 76, .	1.1	26
3754	Theoretical Studies of Photoinduced Electron Transfer in Dye-Sensitized TiO2. Annual Review of Physical Chemistry, 2007, 58, 143-184.	4.8	534
3755	Band structure of indium oxide: Indirect versus direct band gap. Physical Review B, 2007, 75, .	1.1	180
3756	A density functional theory study of atomic oxygen and nitrogen adsorption over Î±-alumina (0001). Physical Chemistry Chemical Physics, 2007, 9, 5112.	1.3	21
3757	Multiple Charge States of Ag Atoms on Ultrathin NaCl Films. Physical Review Letters, 2007, 98, .	2.9	105
3758	Li2MnO3-stabilized LiMO2 (M = Mn, Ni, Co) electrodes for lithium-ion batteries. Journal of Materials Chemistry, 2007, 17, 3112.	6.7	1,817
3759	Ensemble effects on ethylene dehydrogenation on PdAu(001) surfaces investigated with first-principles calculations and nudged-elastic-band simulations. Physical Review B, 2007, 75, .	1.1	38
3760	First-principles elastic constants of Î±- and Î¸-Al2O3. Applied Physics Letters, 2007, 90, 101909.	1.5	238
3761	Atomistic mechanism of interfacial reaction and asymmetric growth kinetics in an immiscibleCuâ”Rusystem at equilibrium. Physical Review B, 2007, 75, .	1.1	22
3762	Na-Induced Correlations inNaxCoO2. Physical Review Letters, 2007, 98, .	2.9	62

#	Article	IF	Citations
3763	First-principles calculations of reconstructed [0001] ZnO nanowires. Physical Review B, 2007, 76, .	1.1	58
3764	Mechanical properties of cubic zinc carboxylate IRMOF-1 metal-organic framework crystals. Physical Review B, 2007, 76, .	1.1	124
3765	Adsorption of Pd Atoms and Dimers on the TiO2(110) Surface:â€‰ A First Principles Study. Journal of Physical Chemistry C, 2007, 111, 3949-3955.	1.5	51
3766	Effects of the wave function localization in AlInGaN quaternary alloys. Applied Physics Letters, 2007, 91, 061125.	1.5	38
3767	Composition dependence of structural and electronic properties of<mml:math xmlns:mml="http://www.w3.org/1998/Math/MathML" display="inline"><mml:mrow><mml:msub><mml:mi mathvariant="normal">Ga</mml:mi><mml:mi>m</mml:mi></mml:msub><mml:msub><mml:mi mathvariant="normal">As</mml:mi><mml:mi>n</mml:mi></mml:msub></mml:mrow></mml:math>clusters from first principles. Physical Review B, 2007, 76, .	1.1	21
3768	Molecular Dynamics Simulations of Alkanethiol Monolayers with Azobenzene Molecules on the Au(111) Surface. Journal of Physical Chemistry C, 2007, 111, 14743-14752.	1.5	14
3769	Nucleation ofPdn(n=1â€“5)clusters and wetting of Pd particles onÎ³âˆ’Al2O3surfaces: A density functional theory study. Physical Review B, 2007, 75, .	1.1	84
3770	First Row Transition Metal Atom Adsorption on Defect-Free MgO(100) Surface. Journal of Physical Chemistry C, 2007, 111, 6781-6788.	1.5	20
3771	Electronic and structural properties of oligophenylene ethynylenes on Au(111) surfaces. Journal of Chemical Physics, 2007, 126, 184706.	1.2	8
3772	Shellwise Mackay Transformation in Iron Nanoclusters. Physical Review Letters, 2007, 99, 083402.	2.9	80
3773	A direct first principles study on the structure and electronic properties of BexZn1âˆ’xO. Applied Physics Letters, 2007, 91, 121121.	1.5	64
3774	Structure and Stability of Small Boron and Boron Oxide Clusters. Journal of Physical Chemistry A, 2007, 111, 6539-6551.	1.1	65
3775	Modelling of morphology and proton transport in PFSA membranes. Physical Chemistry Chemical Physics, 2007, 9, 2602.	1.3	209
3776	Hybrid functionals applied to rare-earth oxides: The example of ceria. Physical Review B, 2007, 75, .	1.1	502
3777	First-principles study of thePtâˆ•CeO2(111)interface. Physical Review B, 2007, 76, .	1.1	82
3778	A Trust Region Direct Constrained Minimization Algorithm for the Kohnâ€“Sham Equation. SIAM Journal of Scientific Computing, 2007, 29, 1854-1875.	1.3	57
3779	Ferroelectricity in Asymmetric Metal-Ferroelectric-Metal Heterostructures: A Combined First-Principlesâ€“Phenomenological Approach. Physical Review Letters, 2007, 98, 207601.	2.9	93
3780	Adsorption of molecular hydrogen and hydrogen sulfide on Au clusters. Journal of Chemical Physics, 2007, 126, 244705.	1.2	54

#	Article	IF	Citations
3781	Absorption of Atomic Oxygen into Subsurfaces of Pt(100) and Pt(111):â€‰ Density Functional Theory Study. Journal of Physical Chemistry C, 2007, 111, 9877-9883.	1.5	95
3782	Chemical Environment Effects on the Atomic Oxygen Absorption into Pt(111) Subsurfaces. Journal of Physical Chemistry C, 2007, 111, 17388-17396.	1.5	50
3783	Theoretical Study on Gold-Coated Iron Oxide Nanostructure:â€‰ Magnetism and Bioselectivity for Amino Acids. Journal of Physical Chemistry C, 2007, 111, 4159-4163.	1.5	30
3784	First-principles study of surface properties of<mml:math xmlns:mml="http://www.w3.org/1998/Math/MathML" display="inline"><mml:mrow><mml:mi mathvariant="normal">Li</mml:mi><mml:mi mathvariant="normal">Fe</mml:mi><mml:mi mathvariant="normal">P</mml:mi><mml:msub><mml:mi mathvariant="normal">O</mml:mi><mml:mn>4</mml:mn></mml:msub></mml:mrow></mml:math>: Surface energy, structure, Wulff shape, and surface redox potential. Physical Review B, 2007, 76, .	1.1	223
3785	Theory of electron transport through single molecules of polyaniline. Journal of Physics Condensed Matter, 2007, 19, 215204.	0.7	17
3786	Tuning the Electron Affinity and Secondary Electron Emission of Diamond (100) Surfaces by Dielsâ"Alder Reaction. Langmuir, 2007, 23, 9722-9727.	1.6	17
3787	Single P and As dopants in the Si(001) surface. Journal of Chemical Physics, 2007, 127, 184706.	1.2	8
3788	Electronic structure, bonding, charge distribution, and x-ray absorption spectra of the (001) surfaces of fluorapatite and hydroxyapatite from first principles. Physical Review B, 2007, 76, .	1.1	70
3789	Oxygen Reduction on LaMnO3-Based Cathode Materials in Solid Oxide Fuel Cells. Chemistry of Materials, 2007, 19, 1690-1699.	3.2	126
3790	First-principles calculation of charge transfer at surfaces: The case of core-excited<mml:math xmlns:mml="http://www.w3.org/1998/Math/MathML" display="inline"><mml:mrow><mml:msup><mml:mi		

#	Article	IF	Citations
3799	Observing Spin Polarization of Individual Magnetic Adatoms. Physical Review Letters, 2007, 99, 067202.	2.9	76
3800	Structure of SiAu16: Can a silicon atom be stabilized in a gold cage?. Journal of Chemical Physics, 2007, 127, 214706.	1.2	52
3801	Impact of Bidirectional Charge Transfer and Molecular Distortions on the Electronic Structure of a Metal-Organic Interface. Physical Review Letters, 2007, 99, 256801.	2.9	206
3802	Selective Hydrogenation of the CO Bond in Acrolein through the Architecture of Bimetallic Surface Structures. Journal of the American Chemical Society, 2007, 129, 7101-7105.	6.6	109
3803	Surface Energy of In-Doped ZnO Studied by PAW+U Method. Materials Science Forum, 2007, 561-565, 1861-1864.	0.3	7
3804	Effect of an Electric Field on the Adsorption of Metal Clusters on Boron-Doped Carbon Surfaces. Journal of Physical Chemistry C, 2007, 111, 14804-14812.	1.5	27
3805	Volume and pressure dependence of ground-state and lattice-dynamical properties ofBaF2from density-functional methods. Physical Review B, 2007, 75, .	1.1	20
3806	A computational investigation of stoichiometric and calcium-deficient oxy- and hydroxy-apatites. Faraday Discussions, 2007, 134, 195-214.	1.6	65
3807	Coupling of magnetic ordering and vibrational properties: a density functional theory study of magnetic and structural phase transitions. Phase Transitions, 2007, 80, 445-468.	0.6	1
3808	Ab initiostudy of oxygen interstitial diffusion nearSi:HfO2interfaces. Physical Review B, 2007, 75, .	1.1	19
3809	Structure and bonding in boron carbide: The invincibility of imperfections. New Journal of Chemistry, 2007, 31, 473.	1.4	118
3810	s-Electron Ferromagnetism in Gold and Silver Nanoclusters. Nano Letters, 2007, 7, 3134-3137.	4.5	73
3811	Hydrogen Storage in Organometallic Structures Grafted on Silsesquioxanes. Chemistry of Materials, 2007, 19, 3074-3078.	3.2	22
3812	Synthesis, Characterization, and Catalytic Properties of Î³-Al2O3-Supported Zirconium Hydrides through a Combined Use of Surface Organometallic Chemistry and Periodic Calculations. Organometallics, 2007, 26, 3329-3335.	1.1	33
3813	Nitrogen-Mediated Carbon Nanotube Growth: Diameter Reduction, Metallicity, Bundle Dispersability, and Bamboo-like Structure Formation. ACS Nano, 2007, 1, 369-375.	7.3	207
3814	Lattice dynamics of CoO from first principles. Physical Review B, 2007, 75, .	1.1	65
3815	Thiol density-dependent classical potential for methyl thiol on a Au(111) surface. Physical Review B, 2007, 76, .	1.1	9
3816	Quantum chemical and vibrational investigation of sodium exchanged Î³-alumina surfaces. Physical Chemistry Chemical Physics, 2007, 9, 2577-2582.	1.3	26

#	Article	IF	Citations
3817	New Forcefields for Modeling Biomineralization Processes. Journal of Physical Chemistry C, 2007, 111, 11943-11951.	1.5	119
3818	Ground state structure of sodium ions in<mml:math xmlns:mml="http://www.w3.org/1998/Math/MathML" display="inline"><mml:mrow><mml:msub><mml:mi mathvariant="normal">Na</mml:mi><mml:mi>x</mml:mi></mml:msub><mml:mi mathvariant="normal">Co</mml:mi><mml:msub><mml:mi mathvariant="normal">O</mml:mi><mml:mn>2</mml:mn></mml:msub></mml:mrow></mml:math>: A combined Monte Carlo and first-principles approach. Physical Review B, 2007, 76, .	1.1	25
3819	Structural transformation of ZnO nanostructures. Applied Physics Letters, 2007, 90, 023115.	1.5	68
3820	Ab Initio Study of the Structural and Electronic Properties of the Graphene/SiC{0001} Interface. Materials Science Forum, 0, 556-557, 693-696.	0.3	7
3821	Theoretical Analysis of the Nature of Hydrogen at the Electrochemical Interface Between Water and a Ni(111) Single-Crystal Electrode. Journal of the Electrochemical Society, 2007, 154, F55.	1.3	41
3822	Massless fermions in multilayer graphitic systems with misoriented layers:Ab initiocalculations and experimental fingerprints. Physical Review B, 2007, 76, .	1.1	295
3823	Density-functional calculations of prefactors and activation energies for H diffusion in<mml:math xmlns:mml="http://www.w3.org/1998/Math/MathML" display="inline"><mml:mrow><mml:mi mathvariant="normal">Ba</mml:mi><mml:mi mathvariant="normal">Zr</mml:mi><mml:msub><mml:mi mathvariant="normal">O</mml:mi><mml:mn>3</mml:mn></mml:msub></mml:mrow></mml:math>. Physical Review B, 2007, 76, .	1.1	98
3824	The mechanism of chemical disordering in Cu3Au nanometre-sized systems. Nanotechnology, 2007, 18, 235706.	1.3	19
3825	Ab initiocalculations of third-order elastic constants and related properties for selected semiconductors. Physical Review B, 2007, 76, .	1.1	109
3826	Liquid-Liquid Phase Transformation in Silicon: Evidence from First-Principles Molecular Dynamics Simulations. Physical Review Letters, 2007, 99, 205702.	2.9	97
3827	Clean and metal-doped bundles of boron-carbide nanotubes: A density functional study. Physical Review B, 2007, 76, .	1.1	4
3828	Bending of MgO tubes: Mechanically induced hexagonal phase of magnesium oxide. Physical Review B, 2007, 75, .	1.1	14
3829	Search for highTcin layered structures: The case of LiB. Physical Review B, 2007, 75, .	1.1	35
3830	Hydrogen Cycle on CeO₂ (111) Surfaces:â€‰ Density Functional Theory Calculations. Journal of Physical Chemistry C, 2007, 111, 15337-15341.	1.5	131
3831	Strain influence on valence-band ordering and excitons in ZnO: Anab initiostudy. Applied Physics Letters, 2007, 91, 241915.	1.5	55
3832	Phase stability, electronic structure, and optical properties of indium oxide polytypes. Physical Review B, 2007, 76, .	1.1	194
3833	Theoretical study of new superhard materials: B4C3. Journal of Applied Physics, 2007, 102, 084311.	1.1	16
3834	Electronic and vibrational properties of nickel sulfides from first principles. Journal of Chemical Physics, 2007, 127, 214705.	1.2	98

#	Article	IF	Citations
3835	First-principles study of the structural, electronic, and elastic properties of<mml:math xmlns:mml="http://www.w3.org/1998/Math/MathML" display="inline"><mml:mrow><mml:mi>R</mml:mi><mml:msub><mml:mi mathvariant="normal">Rh</mml:mi><mml:mn>3</mml:mn></mml:msub><mml:msub><mml:mi mathvariant="normal">B</mml:mi><mml:mi>x</mml:mi></mml:msub><mml:msub><mml:mi		

#	Article	IF	Citations
3853	An ab Initio and Classical Molecular Dynamics Investigation of the Structural and Vibrational Properties of Talc and Pyrophyllite. Journal of Physical Chemistry C, 2007, 111, 12752-12759.	1.5	73
3854	First-principles calculations of phonon and thermodynamic properties in the boron-alkaline earth metal binary systems: B-Ca, B-Sr, and B-Ba. Physical Review B, 2007, 75, .	1.1	72
3855	First principles phase diagram calculations for the system NaNbO3â€“KNbO3: Can spinodal decomposition generate relaxor ferroelectricity?. Applied Physics Letters, 2007, 91, 092907.	1.5	12
3856	Lattice and local-mode vibrations in anhydrous and protonized LiMn2O4 spinels from first-principles theory. Journal of Materials Chemistry, 2007, 17, 4908.	6.7	15
3857	First-Principles Study of Defect-Induced Magnetism in Carbon. Physical Review Letters, 2007, 99, 107201.	2.9	170
3858	Formation ofsp3Hybridized Bonds and Stability ofCaCO3at Very High Pressure. Physical Review Letters, 2007, 98, 268501.	2.9	32
3859	Electron transport via polaron hopping in bulkTiO2: A density functional theory characterization. Physical Review B, 2007, 75, .	1.1	394
3860	ZnO Films Grown on Si Substrates with Au Nanocrystallites as Nuclei. Crystal Growth and Design, 2007, 7, 564-568.	1.4	7
3861	Lattice stability of aluminum-rare earth binary systems: A first-principles approach. Physical Review B, 2007, 75, .	1.1	59
3862	Electronic and magnetic structure of cuprous oxideCu2Odoped with Mn, Fe, Co, and Ni: A density-functional theory study. Physical Review B, 2007, 75, .	1.1	55
3863	Impurity Clustering and Ferromagnetic Interactions that are not Carrier Induced in Dilute Magnetic Semiconductors: The Case ofCu2Oâˆ¶Co. Physical Review Letters, 2007, 99, 167203.	2.9	43
3864	Synthesis, Growth Mechanism, and Work Function at Highly Oriented {001} Surfaces of Bismuth Sulfide Microbelts. Journal of Physical Chemistry C, 2007, 111, 12145-12148.	1.5	34
3865	Theoretical study of the insulator/insulator interface: Band alignment at theSiO2â•HfO2junction. Physical Review B, 2007, 75, .	1.1	99
3866	Au34-:â€‰ A Fluxional Coreâ“Shell Cluster. Journal of Physical Chemistry C, 2007, 111, 8228-8232.	1.5	103
3867	Correlation effects and energetics of point defects in uranium dioxide: a first principle investigation. Philosophical Magazine, 2007, 87, 2561-2569.	0.7	104
3868	Anab initiostudy of adsorption of alanine on the chiral calcite surface. Molecular Simulation, 2007, 33, 343-351.	0.9	33
3869	Effect of structure, surface passivation, and doping on the electronic properties of Ge nanowires: A first-principles study. Physical Review B, 2007, 76, .	1.1	40
3870	Orbital-Occupancy versus Charge Ordering and the Strength of Electron Correlations in Electron-Doped<mml:math xmlns:mml="http://www.w3.org/1998/Math/MathML" display="inline"><mml:msub><mml:mi>CaMnO</mml:mi><mml:mn>3</mml:mn></mml:msub></mml:math>. Physical Review Letters, 2007, 99, 036402.	2.9	66

#	Article	IF	Citations
3871	Structural transition ofLi2BeH4under high pressure: A first-principles study. Physical Review B, 2007, 75, .	1.1	9
3872	Decohesion of iron grain boundaries by sulfur or phosphorous segregation: First-principles calculations. Physical Review B, 2007, 76, .	1.1	79
3873	Hydrogen storage in calcium alanate: First-principles thermodynamics and crystal structures. Physical Review B, 2007, 75, .	1.1	93
3874	Phonon Density of States of Metallic Sn at High Pressure. Physical Review Letters, 2007, 98, 245502.	2.9	23
3875	Ordering and correlation of cluster orientations in CaCd ₆. Philosophical Magazine, 2007, 87, 2671-2677.	0.7	9
3876	Graphite and Graphene as Perfect Spin Filters. Physical Review Letters, 2007, 99, 176602.	2.9	415
3877	Electronic structure of chromia aerogels from soft x-ray absorption spectroscopy. Journal of Applied Physics, 2007, 101, 124315.	1.1	19
3878	Thermodynamics of mono- and di-vacancies in barium titanate. Journal of Applied Physics, 2007, 102, .	1.1	129
3879	Weak ferromagnetism in Cu-doped GaN. Applied Physics Letters, 2007, 91, .	1.5	38
3880	Redox properties of CeO2â€“MO2 (M=Ti, Zr, Hf, or Th) solid solutions from first principles calculations. Applied Physics Letters, 2007, 90, 031909.	1.5	87
3881	Charging and discharging of oxide defects in reliability issues. , 2007, , .		6
3882	Energy pathways and directionality in deformation twinning. Applied Physics Letters, 2007, 91, .	1.5	58
3883	Trilayer superlattices: A route to magnetoelectric multiferroics?. Applied Physics Letters, 2007, 90, 242916.	1.5	30
3884	Vacancy mediated desorption of hydrogen from a sodium alanate surface: An ab initio spin-polarized study. Applied Physics Letters, 2007, 90, 143119.	1.5	12
3885	Phase diagram and adsorption-desorption kinetics of CO on Ru(0001) from first principles. Journal of Chemical Physics, 2007, 126, 094701.	1.2	38
3886	Zn vacancy induced room-temperature ferromagnetism in Mn-doped ZnO. Applied Physics Letters, 2007, 91, .	1.5	160
3887	The effect of Ga vacancies on the defect and magnetic properties of Mn-doped GaN. Journal of Applied Physics, 2007, 102, 083910.	1.1	14
3888	Solvation and electronic structures of M+Ln, with M+â€,=â€,Mg+ and Ca+, Lâ€,=â€,H2O, CH3OH, and NH3, and nâ€,=â€,1â€“6. Canadian Journal of Chemistry, 2007, 85, 873-884.	0.6	3

#	Article	IF	Citations
3889	First Principles Calculations of the Formation Energy of the Neutral Vacancy in Germanium. Solid State Phenomena, 0, 131-133, 241-246.	0.3	9
3890	Theoretical and spectroscopic study of the reaction of diethylhydroxylamine on silicon(100)-2Ã—1. Physical Chemistry Chemical Physics, 2007, 9, 1629-1634.	1.3	10
3891	Slab model studies of water adsorption and decomposition on clean and X- (X = C, N and O) contaminated Pd(111) surfaces. Physical Chemistry Chemical Physics, 2007, 9, 739-746.	1.3	64
3892	Gold as intermolecular glue: a theoretical study of nanostrips based on quinoline-type monomers. Physical Chemistry Chemical Physics, 2007, 9, 3025.	1.3	11
3893	Functional anion concept: effect of fluorine anion on hydrogen storage of sodium alanate. Physical Chemistry Chemical Physics, 2007, 9, 1499-1502.	1.3	83
3894	Microscopic models of PdZn alloy catalysts: structure and reactivity in methanol decomposition. Physical Chemistry Chemical Physics, 2007, 9, 3470-3482.	1.3	96
3895	First-principles investigation of strain effects on the energy gaps in silicon nanoclusters. Journal of Physics Condensed Matter, 2007, 19, 266212.	0.7	27
3896	Density Functional Theory Study of CO Adsorption and Dissociation on Molybdenum(100). Journal of Physical Chemistry C, 2007, 111, 13473-13480.	1.5	16
3897	Melting curve of tantalum from first principles. Physical Review B, 2007, 75, .	1.1	99
3898	REAu₂In₄ (RE = La, Ce, Pr, Nd):â€‰ Polyindides from Liquid Indium. Inorganic Chemistry, 2007, 46, 6933-6941.	1.9	24
3899	Growth Pathway of Pt Clusters on Î±-Al₂O₃(0001) Surface. Journal of Physical Chemistry C, 2007, 111, 13786-13793.	1.5	35
3900	New semiconducting silicide Ca3Si4. Journal of Physics Condensed Matter, 2007, 19, 346207.	0.7	20
3901	Role of Lithium Vacancies in Accelerating the Dehydrogenation Kinetics on a LiBH₄(010) Surface:â€‰ An Ab Initio Study. Journal of Physical Chemistry C, 2007, 111, 12124-12128.	1.5	10
3902	Surface Energy Estimation of Catalytically Relevant fcc Transition Metals Using DFT Calculations on Nanorods. Journal of Physical Chemistry C, 2007, 111, 4998-5005.	1.5	36
3903	Role of charged defects and impurities in kinetics of hydrogen storage materials: A first-principles study. Physical Review B, 2007, 76, .	1.1	92
3904	Catalytic ammonia oxidation on platinum: mechanism and catalyst restructuring at high and low pressure. Physical Chemistry Chemical Physics, 2007, 9, 3522-3540.	1.3	101
3905	Energetics driving the short-range order in CuxPd1â€“x/Ru(0001) monolayer surface alloys. Physical Chemistry Chemical Physics, 2007, 9, 5127.	1.3	22
3906	A computational study of H2dissociation on silver surfaces: The effect of oxygen in the added row structure of Ag(110). Physical Chemistry Chemical Physics, 2007, 9, 1247-1254.	1.3	43

#	Article	IF	Citations
3907	ab Initio Molecular Dynamics Simulations of Molten Ni-Based Superalloys. , 2007, , .		0
3908	The role of water in the radiation response of wet and dry oxides. , 2007, , .		1
3909	Ab initiocalculations of strain fields and failure patterns in silicon nitride intergranular glassy films. Philosophical Magazine, 2007, 87, 3839-3852.	0.7	19
3910	Atomic configurations of Pd atoms in PdAu(111) bimetallic surfaces investigated using the first-principles pseudopotential plane wave approach. Physical Review B, 2007, 75, .	1.1	72
3911	Chapter 11 Ab initio simulations of photoinduced molecule-semiconductor electron transfer. Theoretical and Computational Chemistry, 2007, , 275-300.	0.2	3
3912	Local order and phase selection in undercooled transition metal based systems: ab initio molecular dynamics study. Phase Transitions, 2007, 80, 369-384.	0.6	8
3913	Carbon monoxide adsorption on low-silica zeolitesâ€"from single to dual and to multiple cation sites. Physical Chemistry Chemical Physics, 2007, 9, 4657.	1.3	44
3914	Structure and thermodynamic stability of hydrogen interstitials in BaZrO3perovskite oxide from density functional calculations. Faraday Discussions, 2007, 134, 247-265.	1.6	116
3915	Superconductivity in high-pressure SiH 4. Europhysics Letters, 2007, 78, 37003.	0.7	89
3916	Similarities and differences on the molecular mechanism of CO oxidation on Rh(111) and bimetallic RhCu(111) surfaces. Physical Chemistry Chemical Physics, 2007, 9, 2877-2885.	1.3	11
3917	Theoretical and experimental determination of the electronic structure of V2O5, reduced V2O5â^'xand sodium intercalated NaV2O5. Physical Chemistry Chemical Physics, 2007, 9, 2564-2576.	1.3	67
3918	First-Principle Studies of the Formation and Diffusion of Hydrogen Vacancies in Magnesium Hydride. Journal of Physical Chemistry C, 2007, 111, 8360-8365.	1.5	61
3919	Ab Initio Molecular Dynamical Investigation of the Finite Temperature Behavior of the Tetrahedral Au₁₉ and Au₂₀ Clusters. Journal of Physical Chemistry A, 2007, 111, 10769-10775.	1.1	36
3920	Density Functional Theory and Kinetic Studies of Methanation on Iron Surface. Journal of Physical Chemistry C, 2007, 111, 11012-11025.	1.5	50
3921	Density-Functional Theory Study of NHxOxidation and Reverse Reactions on the Rh(111) Surface. Journal of Physical Chemistry C, 2007, 111, 9839-9852.	1.5	26
3922	Computational and Experimental Investigation of the Transformation of V₂O₅ Under Pressure. Chemistry of Materials, 2007, 19, 5262-5271.	3.2	45
3923	Dipole Formation at Interfaces of Alkanethiolate Self-assembled Monolayers and Ag(111). Journal of Physical Chemistry C, 2007, 111, 14448-14456.	1.5	55
3924	First-Principles Investigation of Adsorption and Dissociation of Hydrogen on Mg2Si Surfaces. Journal of Physical Chemistry C, 2007, 111, 6910-6916.	1.5	21

#	Article	IF	Citations
3925	Studying Reduction in Solid Oxide Fuel Cell Activity with Density Functional Theoryâ˜ Effects of Hydrogen Sulfide Adsorption on Nickel Anode Surface. Journal of Physical Chemistry C, 2007, 111, 14457-14468.	1.5	30
3926	Vibrational Properties of Polyanionic Hydrides SrAl₂H₂ and SrAlSiH:â€‰ New Insights into Alâ˜H Bonding Interactions. Inorganic Chemistry, 2007, 46, 6987-6991.	1.9	20
3927	Crystal Structure and Electron Density of Tantalum Oxynitride, a Visible Light Responsive Photocatalyst. Chemistry of Materials, 2007, 19, 588-593.	3.2	90
3928	Ab Initio Study of Clean and Hydrogen-Saturated Unreconstructed SiC{0001} Surfaces. Materials Science Forum, 0, 556-557, 493-496.	0.3	3
3929	Model for the Formation Energies of Alanates and Boranates. Journal of Physical Chemistry C, 2007, 111, 9592-9594.	1.5	9
3930	Theoretical Study of NO Dissociation on Stepped Rh(221) and RhCu(221) Surfaces. Journal of Physical Chemistry C, 2007, 111, 11376-11383.	1.5	27
3931	Structure of Active Sites in Pd-Exchanged Mordenite:â€‰ A Density Functional Investigation. Journal of Physical Chemistry C, 2007, 111, 6454-6464.	1.5	17
3932	Vibrational Study of CO Chemisorption on the Pt3Sn(111)-(2 Ã— 2) Surface. Journal of Physical Chemistry C, 2007, 111, 8524-8531.	1.5	18
3933	Theoretical study of the filling fraction limits for impurities inCoSb3. Physical Review B, 2007, 75, .	1.1	57
3934	Nature of adsorption on TiC(111) investigated with density-functional calculations. Physical Review B, 2007, 75, .	1.1	59
3935	Three Novel Phases in the Smâ˜Coâ˜Ga System. Syntheses, Crystal and Electronic Structures, and Electrical and Magnetic Properties. Inorganic Chemistry, 2007, 46, 4177-4186.	1.9	16
3936	TUNABLE ELECTRIC CONDUCTIVITIES OF Au-DOPED BORON NITRIDE NANOTUBES. Nano, 2007, 02, 367-372.	0.5	3
3937	X-ray Photoelectron Spectroscopy and First Principles Calculation of BCN Nanotubes. Journal of the American Chemical Society, 2007, 129, 1705-1716.	6.6	198
3938	Hydrogen Dissociation Dynamics on Precovered Pd Surfaces: Langmuir is Still Right. Physical Review Letters, 2007, 98, 206107.	2.9	105
3939	ZnO nanoparticle growth on single-walled carbon nanotubes by atomic layer deposition and a consequent lifetime elongation of nanotube field emission. Applied Physics Letters, 2007, 90, 263104.	1.5	46
3940	Electronic structures of CuPc on a Ag(110) surface. Journal of Physics Condensed Matter, 2007, 19, 136002.	0.7	21
3941	Spontaneous Emergence of Cl-Anions from NaCl(100) at Low Relative Humidity. Journal of Physical Chemistry C, 2007, 111, 8000-8004.	1.5	17
3942	Dislocation transmission across the Cu/Ni interface: a hybrid atomisticâ€“continuum study. Philosophical Magazine, 2007, 87, 1513-1529.	0.7	28

#	Article	IF	Citations
3943	Importance of cluster distortions in the tetrahedral cluster compounds<mml:math xmlns:mml="http://www.w3.org/1998/Math/MathML" display="inline"><mml:mrow><mml:mi		

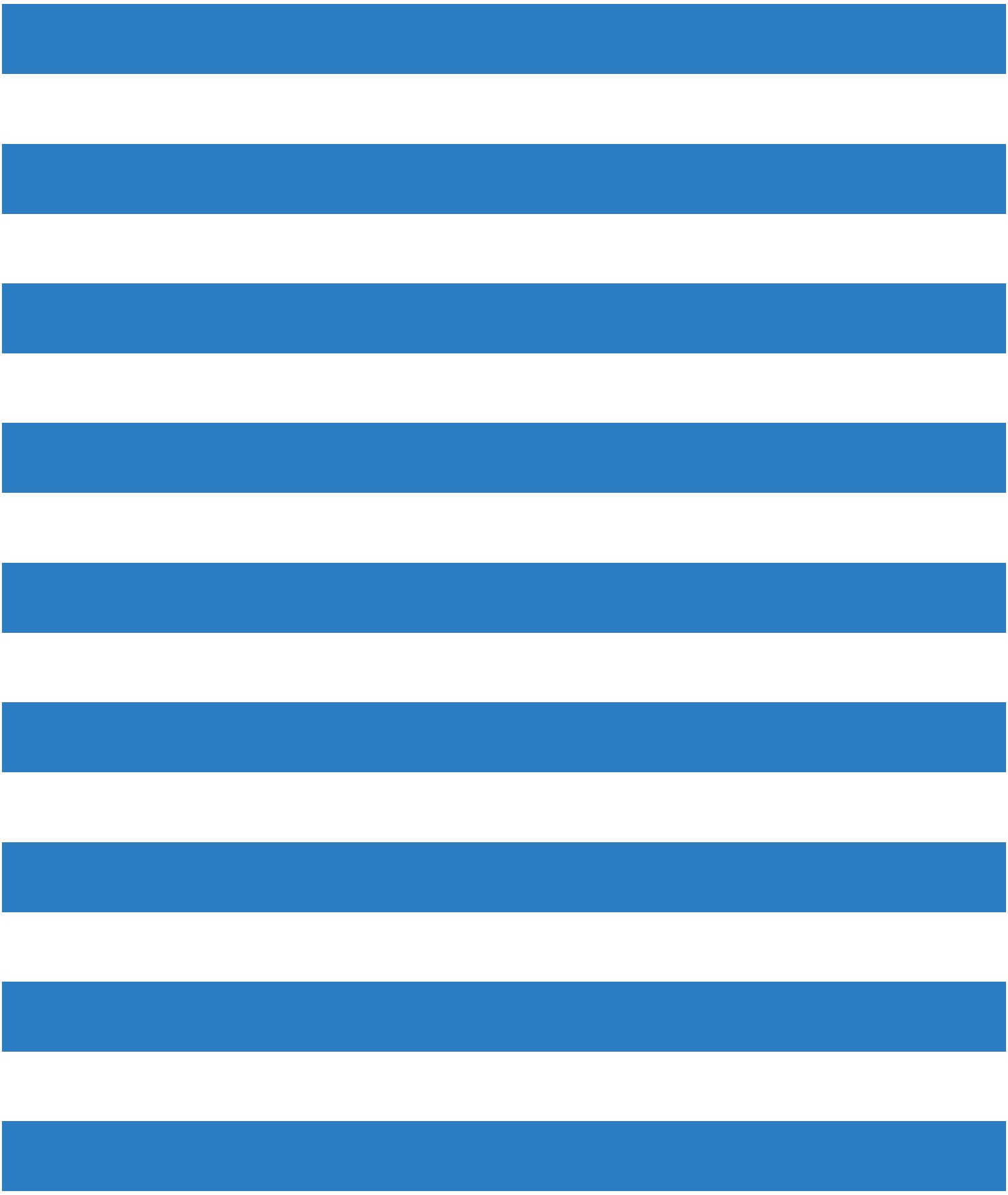

#	Article	IF	Citations
3961	Structure and dynamics oflâ˜'Ge: Neutron scattering experiments andab initiomolecular dynamics simulations. Physical Review B, 2007, 75, .	1.1	21
3962	First-Principles Calculation of Solution Energy of Alkaline-Earth Metal Elements to BaTiO3. Japanese Journal of Applied Physics, 2007, 46, 7136-7140.	0.8	26
3963	First-principles calculations of Cs adsorbed on Cu(001): Quantum size effect in surface energetics and surface chemical reactivities. Physical Review B, 2007, 75, .	1.1	17
3964	Structural distortions and model Hamiltonian parameters: From LSDA to a tight-binding description ofLaMnO3. Physical Review B, 2007, 76, .	1.1	29
3965	Crystal Structure and Electron Density of Î±-Silicon Nitride:â€‰ Experimental and Theoretical Evidence for the Covalent Bonding and Charge Transfer. Journal of Physical Chemistry B, 2007, 111, 3609-3613.	1.2	33
3966	Theoretical Study of Aqueous Solvation of K⁺ Comparing ab Initio, Polarizable, and Fixed-Charge Models. Journal of Chemical Theory and Computation, 2007, 3, 2068-2082.	2.3	87
3967	The Activation of H2by Zeolitic Zn(II) Cations. Journal of Physical Chemistry C, 2007, 111, 8337-8348.	1.5	29
3968	Ab Initio Molecular Dynamics Study of H₂S Dissociation on the Fe(110) Surface. Journal of Physical Chemistry C, 2007, 111, 16372-16378.	1.5	24
3969	CO Oxidation on Rh(100):â€‰ Multisite Atomistic Lattice-Gas Modeling. Journal of Physical Chemistry C, 2007, 111, 14698-14706.	1.5	57
3970	First-Principles Study of C Adsorption and Diffusion on the Surfaces and in the Subsurfaces of Nonreconstructed and Reconstructed Ni(100). Journal of Physical Chemistry C, 2007, 111, 3447-3453.	1.5	14
3971	Integrated Experimentalâ˜'Theoretical Investigation of the Naâ˜'Liâ˜'Alâ˜'H System. Inorganic Chemistry, 2007, 46, 1401-1409.	1.9	16
3972	Structural distortions inAlF3: A test for density-functional methods. Physical Review B, 2007, 75, .	1.1	3
3973	Nonmetal Doping at Octahedral Vacancy Sites in Rutile:â€‰ A Quantum Mechanical Study. Journal of Physical Chemistry C, 2007, 111, 10915-10922.	1.5	17
3974	Electrochemical Data Transferability within LiyVOXO4(X = Si, Ge0.5Si0.5, Ge, Si0.5As0.5, Si0.5P0.5, As, P) Polyoxyanionic Compounds. Chemistry of Materials, 2007, 19, 2411-2422.	3.2	24
3975	Characterization of the Chemisorption of Methylsilane on a Au(1,1,1) Surface from the Silicon K- and L-Edge Spectra:â€‰ A Theoretical Study Using the Four-Component Static Exchange Approximation. Journal of Physical Chemistry C, 2007, 111, 13846-13850.	1.5	9
3976	Density Functional Study of the Adsorption of Atomic Oxygen on the (001) Surface of Early Transition-Metal Carbides. Journal of Physical Chemistry C, 2007, 111, 1307-1314.	1.5	66
3977	Organic Bonding to Silicon via a Carbonyl Group:Â New Insights from Atomic-Scale Images. Journal of the American Chemical Society, 2007, 129, 11402-11407.	6.6	26
3978	Electronic Properties of DNA Base Molecules Adsorbed on a Metallic Surface. Journal of Physical Chemistry C, 2007, 111, 14541-14551.	1.5	56

#	Article	IF	Citations
3979	Multiple Adsorption of NO on Fe2+Cations in the Î±- and Î²-Positions of Ferrierite:â€‰ An Experimental and Density Functional Study. Journal of Physical Chemistry C, 2007, 111, 9393-9402.	1.5	41
3980	Predicting Reaction Equilibria for Destabilized Metal Hydride Decomposition Reactions for Reversible Hydrogen Storage. Journal of Physical Chemistry C, 2007, 111, 1584-1591.	1.5	84
3981	On the Trapping of Bjerrum Defects in Ice I_h:â€‰ The Case of the Molecular Vacancy. Journal of Physical Chemistry B, 2007, 111, 12537-12542.	1.2	17
3982	Melting of Aluminum Cluster Cations with 31â^'48 Atoms:â€‰ Experiment and Theory. Journal of Physical Chemistry C, 2007, 111, 17788-17794.	1.5	30
3983	Detection and Determination of the {Fe(NO)2} Core Vibrational Features in Dinitrosylâ^'Iron Complexes from Experiment, Normal Coordinate Analysis, and Density Functional Theory:Â An Avenue for Probing the Nitric Oxide Oxidation State. Journal of Physical Chemistry B, 2007, 111, 2335-2346.	1.2	25
3984	First-principles study of cation and hydrogen arrangements in the Li-Mg-N-H hydrogen storage system. Physical Review B, 2007, 76, .	1.1	23
3985	Atomic-scale study of diffusion in A15Nb3Sn. Physical Review B, 2007, 75, .	1.1	41
3986	Precursor Ï€-Complex in the Addition of Vinyl Bromide on Si(100). Journal of Physical Chemistry C, 2007, 111, 6365-6371.	1.5	7
3987	Molecular Dynamics Simulations of the Coalescence of Iridium Clusters. Journal of Physical Chemistry C, 2007, 111, 6713-6719.	1.5	14
3988	Theoretical Studies of the Formation and Reactivity of C2Hydrocarbon Species on the Fe(100) Surface. Journal of Physical Chemistry C, 2007, 111, 13149-13162.	1.5	41
3989	A Systematic Density Functional Study of Molecular Oxygen Adsorption and Dissociation on the (001) Surface of Group IVâ^'VI Transition Metal Carbides. Journal of Physical Chemistry C, 2007, 111, 16982-16989.	1.5	60
3990	Influence of Anatase Support on Geometrical Structure of Vanadium Oxide at Varying Temperatures and Pressures. Periodic DFT Study. Journal of Physical Chemistry C, 2007, 111, 4216-4225.	1.5	18
3991	Weakening of an aluminum grain boundary induced by sulfur segregation: A first-principles computational tensile test. Physical Review B, 2007, 75, .	1.1	88
3992	First-Principles Prediction of Equilibrium Potentials for Water Activation by a Series of Metals. Journal of the Electrochemical Society, 2007, 154, F217.	1.3	30
3993	Methane Activation on Pt and Pt4:Â A Density Functional Theory Study. Journal of Physical Chemistry B, 2007, 111, 1657-1663.	1.2	70
3994	Binding Formation of 12-Hydroxydodecanoic Acid on Si(001)-(2 Ã— 2). Journal of Physical Chemistry C, 2007, 111, 4375-4378.	1.5	3
3995	Ab initio investigation of ammonia-borane complexes for hydrogen storage. Journal of Chemical Physics, 2007, 126, 184703.	1.2	116
3996	Charge Order and the Origin of Giant Magnetocapacitance inLuFe2O4. Physical Review Letters, 2007, 98, 246403.	2.9	149

#	Article	IF	Citations
3997	Methanol Adsorption and Dissociation on TiO2(110) from First Principles Calculations. Journal of Physical Chemistry C, 2007, 111, 10023-10028.	1.5	106
3998	Hydrogen-Related Instabilities in MOS Devices Under Bias Temperature Stress. IEEE Transactions on Device and Materials Reliability, 2007, 7, 502-508.	1.5	40
3999	The Structure of Ultrathin H-Passivated [112] Silicon Nanowires. Journal of Physical Chemistry C, 2007, 111, 7933-7937.	1.5	27
4000	Methanol Adsorption on the Clean CeO2(111) Surface:â€‰ A Density Functional Theory Study. Journal of Physical Chemistry C, 2007, 111, 10514-10522.	1.5	56
4001	Polymorphism in Bismuth Stannate:â€‰ A First-Principles Study. Chemistry of Materials, 2007, 19, 5158-5164.	3.2	48
4002	Ammonia Dissociation on Pt{100}, Pt{111}, and Pt{211}:â€‰ A Comparative Density Functional Theory Study. Journal of Physical Chemistry C, 2007, 111, 17551-17557.	1.5	72
4003	Adsorption and Dissociation of H₂O on a W(111) Surface:â€‰ A Computational Study. Journal of Physical Chemistry C, 2007, 111, 17333-17339.	1.5	29
4004	First-Principles Study of the Oxygenation of Carbon Nanotubes and Boron Nitride Nanotubes. Chemistry of Materials, 2007, 19, 3767-3772.	3.2	11
4005	Adsorption of Al, O, Hf, Y, Pt, and S Atoms on Î±-Al2O3(0001). Journal of Physical Chemistry C, 2007, 111, 7105-7126.	1.5	101
4006	Kinetics of NH Formation and Dissociation on Pt(111). Journal of Physical Chemistry C, 2007, 111, 7127-7136.	1.5	17
4007	Chemisorption of 3-Aminopropyltrimethoxysilane on Si(001)-(2 Ã— 2). Journal of Physical Chemistry C, 2007, 111, 15020-15025.	1.5	10
4008	Infrared Spectroscopy of Small Sodium-Doped Water Clusters:â€‰ Interaction with the Solvated Electron. Journal of Physical Chemistry A, 2007, 111, 12355-12362.	1.1	28
4009	First Principles and Thermodynamic Modeling of CdS Surfaces and Nanorods. Journal of Physical Chemistry C, 2007, 111, 18112-18117.	1.5	41
4010	Shape and Thermodynamic Stability of Pyrite FeS₂ Nanocrystals and Nanorods. Journal of Physical Chemistry C, 2007, 111, 11742-11746.	1.5	52
4011	Influence of oxygen vacancies on the dielectric properties of hafnia: First-principles calculations. Physical Review B, 2007, 75, .	1.1	44
4012	Theoretical study of<mml:math xmlns:mml="http://www.w3.org/1998/Math/MathML" display="inline"><mml:mrow><mml:mi mathvariant="normal">Ce</mml:mi><mml:msub><mml:mi mathvariant="normal">O</mml:mi><mml:mn>2</mml:mn></mml:msub></mml:mrow></mml:math>doped with tetravalent ions. Physical Review B, 2007, 76, .	1.1	61
4013	Tuning the electronic structure of graphene nanoribbons through chemical edge modification: A theoretical study. Physical Review B, 2007, 75, .	1.1	156
4014	Computational Study of Hydrogen Storage Characteristics of Covalent-Bonded Graphenes. Journal of the American Chemical Society, 2007, 129, 8999-9003.	6.6	161

#	Article	IF	Citations
4015	Shear Instabilities in Metallic Nanoparticles:Â Hydrogen-Stabilized Structure of Pt37on Carbon. Journal of the American Chemical Society, 2007, 129, 3658-3664.	6.6	66
4016	First-Principle Study of Sulfur Adsorption on Ir(100) Surface. Materials Science Forum, 2007, 561-565, 2435-2438.	0.3	1
4017	Band-structure anomalies of the chalcopyrite semiconductorsCuGaX2versusAgGaX2(X=Sand Se) and their alloys. Physical Review B, 2007, 75, .	1.1	132
4018	Electrochemical Reduction of Oxygen on Gold Surfaces:â€‰ A Density Functional Theory Study of Intermediates and Reaction Paths. Journal of Physical Chemistry C, 2007, 111, 2607-2613.	1.5	79
4019	First-principles study on the spin polarization of benzene adsorbed on Fe(100) surface. Journal of Applied Physics, 2007, 101, 09G526.	1.1	6
4020	Modification of the Oxidative Power of ZnO(101Ì„0) Surface by Substituting Some Surface Zn Atoms with Other Metals. Journal of Physical Chemistry C, 2007, 111, 8617-8622.	1.5	61
4021	Electronic structure of biphenyl on Si(100). Physical Review B, 2007, 76, .	1.1	13
4022	On the structural and energetic properties of the hydrogen absorber Li2Mg(NH)2. Applied Physics Letters, 2007, 91, 091924.	1.5	14
4023	Ab initiocalculations of structural and electronic properties of CdTe clusters. Physical Review B, 2007, 75, .	1.1	46
4024	Integration of first-principles calculations, calphad modeling, and phase-field simulations. , 2007, , 171-213.		4
4025	Adsorption Configurations and Energetics of BClx(x= 0â^'3) on TiO2Anatase (101) and Rutile (110) Surfacesâ€. Journal of Physical Chemistry A, 2007, 111, 6746-6754.	1.1	23
4026	Chemisorption of Sulfur and Sulfur-Based Simple Molecules on Au(111). Journal of Physical Chemistry C, 2007, 111, 12383-12390.	1.5	20
4027	Predicted Oxidation of CO Catalyzed by Au Nanoclusters on a Thin Defect-Free MgO Film Supported on a Mo(100) Surface. Journal of the American Chemical Society, 2007, 129, 2228-2229.	6.6	167
4028	Ferroelectricity Driven by the Noncentrosymmetric Magnetic Ordering in Multiferroic<mml:math xmlns:mml="http://www.w3.org/1998/Math/MathML" display="inline"><mml:msub><mml:mi>TbMn</mml:mi><mml:mn>2</mml:mn></mml:msub><mml:msub><mml:mi mathvariant="normal">O</mml:mi><mml:mn>5</mml:mn></mml:msub></mml:math>: A First-Principles Study. Physical Review Letters, 2007, 99, 177203.	7.9	91
4029	Temperature-dependent elastic properties of<mml:math xmlns:mml="http://www.w3.org/1998/Math/MathML" display="inline"><mml:mi>Î±</mml:mi></mml:math>-beryllium from first principles. Physical Review B, 2007, 76, .	1.1	30
4030	Time-Domainab InitioStudy of Charge Relaxation and Recombination in Dye-Sensitized TiO2. Journal of the American Chemical Society, 2007, 129, 8528-8543.	6.6	207
4031	Synthesis and Thermoelectric Properties of Polycarbazole, Polyindolocarbazole, and Polydiindolocarbazole Derivatives. Chemistry of Materials, 2007, 19, 2128-2138.	3.2	119
4032	Existence of the Naâ^'HÎ´-Â·Â·Â·HÎ´â€˜+â^'O Dihydrogen Bond in the Hydrogenation Process by Na2O:â€‰ A First-Principles Identification. Journal of Physical Chemistry C, 2007, 111, 5064-5068.	1.5	5

#	Article	IF	Citations
4033	First-Principles Study of the Four Polymorphs of Crystalline Octahydro-1,3,5,7-tetranitro-1,3,5,7-tetrazocine. Journal of Physical Chemistry B, 2007, 111, 12715-12722.	1.2	108
4034	Dissociative Adsorption of Water at Vacancy Defects in Graphite. Journal of Physical Chemistry C, 2007, 111, 18258-18263.	1.5	86
4035	Carâ€“Parrinello Molecular Dynamics Simulations and Biological Systems. , 2006, , 133-171.		20
4036	Electronic Structure Investigation of Surfaceâˆ'Adsorbate and Adsorbateâˆ'Adsorbate Interactions in Multilayers of CH4on MgO(100). Journal of Physical Chemistry C, 2007, 111, 966-976.	1.5	14
4037	Theoretical Analysis of Intermolecular Covalent Ï€âˆ'Ï€ Bonding and Magnetic Properties of Phenalenyl and spiro-Biphenalenyl Radical Ï€-Dimers. Journal of Physical Chemistry A, 2007, 111, 6304-6315.	1.1	39
4038	Effect of Molecular and Electronic Structure on the Light-Harvesting Properties of Dye Sensitizers. Journal of Physical Chemistry C, 2007, 111, 7539-7547.	1.5	22
4039	Site-Specific Kondo Effect at Ambient Temperatures in Iron-Based Molecules. Physical Review Letters, 2007, 99, 106402.	2.9	242
4040	Accurate single-particle determination of the band gap in silicon nanowires. Physical Review B, 2007, 76, .	1.1	39
4041	Site- and Orientation-Selective Anchoring of a Prototypical Molecular Building Block. Journal of the American Chemical Society, 2007, 129, 5007-5011.	6.6	23
4042	Bonding Analyses, Formation Energies, and Vibrational Properties of Mâˆ'R₂dtc Complexes (M = Ag(I), Ni(II), Cu(II), or Zn(II)). Journal of Physical Chemistry A, 2007, 111, 13075-13087.	1.1	31
4043	Geometries and stabilities of Ag-doped Sin (n=1â€“13) clusters: A first-principles study. Journal of Chemical Physics, 2007, 127, 144313.	1.2	46
4044	Ab initiostudy of monoclinic iridium nitride as a high bulk modulus compound. Physical Review B, 2007, 75, .	1.1	50
4045	Electrically Benign Behavior of Grain Boundaries in Polycrystalline<mml:math xmlns:mml="http://www.w3.org/1998/Math/MathML" display="inline"><mml:msub><mml:mi>CuInSe</mml:mi><mml:mn>2</mml:mn></mml:msub></mml:math>Films. Physical Review Letters, 2007, 99, 235504.	2.9	192
4046	Spintronic materials based on main-group elements. Journal of Physics Condensed Matter, 2007, 19, 165203.	0.7	26
4047	Equation of state and optical properties of warm dense helium. Physical Review B, 2007, 76, .	1.1	62
4048	Structure, bonding, and magnetism of cobalt clusters from first-principles calculations. Physical Review B, 2007, 76, .	1.1	143
4049	Total Oxidation of Methanol on Cu(110):Â A Density Functional Theory Study. Journal of Physical Chemistry A, 2007, 111, 8814-8822.	1.1	74
4050	Formation of lithium clusters and their effects on conductivity in diamond: A density functional theory study. Diamond and Related Materials, 2007, 16, 840-844.	1.8	5

#	Article	IF	Citations
4051	Structure of molten yttrium aluminates: a neutron diffraction study. Journal of Physics Condensed Matter, 2007, 19, 415105.	0.7	5
4052	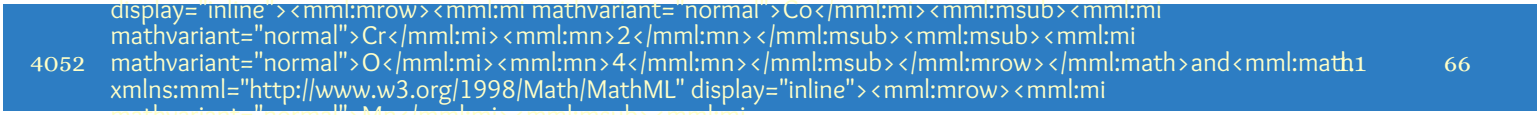	1.1	66
4053	Anomalous Thermal Expansion in<mml:math xmlns:mml="http://www.w3.org/1998/Math/MathML" display="inline"><mml:mi>Î±</mml:mi></mml:math>-Titanium. Physical Review Letters, 2007, 99, 015901.	2.9	37
4054	Surface segregation in CuPt alloys by means of an improved modified embedded atom method. Physical Review B, 2007, 76, .	1.1	15
4055	Electronic structure and properties of the Fermi surface of the superconductor LaOFeP. Physical Review B, 2007, 75, .	1.1	249
4056	Symmetry-adapted configurational modelling of fractional site occupancy in solids. Journal of Physics Condensed Matter, 2007, 19, 256201.	0.7	182
4057	AbÂInitioStudy of Graphene on SiC. Physical Review Letters, 2007, 99, 076802.	2.9	465
4058	Analytic bond-order potential for bcc and fcc ironâ€”comparison with established embedded-atom method potentials. Journal of Physics Condensed Matter, 2007, 19, 326220.	0.7	124
4059	Competition between magnetic structures in the Fe rich fcc FeNi alloys. Physical Review B, 2007, 76, .	1.1	119
4060	First-principlesLDA+UandGGA+Ustudy of cerium oxides: Dependence on the effective U parameter. Physical Review B, 2007, 75, .	1.1	634
4061	Dual Nature of Improper Ferroelectricity in a Magnetoelectric Multiferroic. Physical Review Letters, 2007, 99, 227201.	2.9	282
4062	Understanding Ceria Nanoparticles from First-Principles Calculations. Journal of Physical Chemistry C, 2007, 111, 10142-10145.	1.5	99
4063	On the activation of molecular hydrogen by gold: a theoretical approximation to the nature of potential active sites. Chemical Communications, 2007, , 3371.	2.2	146
4064	First-principles study of vacancy formation in hydroxyapatite. Physical Review B, 2007, 75, .	1.1	119
4065	Ab initiostudy of the thermodynamic properties of nonmagnetic elementary fcc metals: Exchange-correlation-related error bars and chemical trends. Physical Review B, 2007, 76, .	1.1	218
4066	First-principles calculations of the diamond (110) surface: A Mott insulator. Physical Review B, 2007, 75, .	1.1	5
4067	Bond-order potential for silicon. Physical Review B, 2007, 75, .	1.1	32
4068	Density-Functional Characterization of the Multiferroicity in Spin Spiral Chain Cuprates. Physical Review Letters, 2007, 99, 257203.	2.9	86

#	Article	IF	Citations
4069	Ab initiostudy of Cr interactions with point defects in bcc Fe. Physical Review B, 2007, 75, .	1.1	269
4070	Experimental and Theoretical Study of Cobalt Selenide as a Catalyst for O2Electroreduction. Journal of Physical Chemistry C, 2007, 111, 10508-10513.	1.5	88
4071	Accurate Thermochemical Properties for Energetic Materials Applications. II. Heats of Formation of Imidazolium-, 1,2,4-Triazolium-, and Tetrazolium-Based Energetic Salts from Isodesmic and Lattice Energy Calculationsâ€. Journal of Physical Chemistry B, 2007, 111, 4788-4800.	1.2	139
4072	Effect of acceptor dopants on the proton mobility in<mml:math xmlns:mml="http://www.w3.org/1998/Math/MathML" display="inline"><mml:mrow><mml:mi mathvariant="normal">Ba</mml:mi><mml:mi mathvariant="normal">Zr</mml:mi><mml:msub><mml:mi mathvariant="normal">O</mml:mi><mml:mn>3</mml:mn></mml:msub></mml:mrow></mml:math>: A density functional investigation. Physical Review B, 2007, 76, .	1.1	148
4073	Density Functional Theory Study of ZnO Nanostructures for NO and NO2 Sensing. , 2007, , .		4
4074	Formation of Single-Walled Carbon Nanotube via the Interaction of Graphene Nanoribbons:â€‰Ab Initio Density Functional Calculations. Nano Letters, 2007, 7, 3349-3354.	4.5	24
4075	First-principles investigations of the structure and stability of oxygen adsorption and surface oxide formation at Au(111). Physical Review B, 2007, 76, .	1.1	119
4076	Predicting Anisotropic Electrical Conductivities of a Magnetic Insulator on the Basis of Its Magnetic Properties. Chemistry of Materials, 2007, 19, 4393-4395.	3.2	3
4077	Properties of the gold oxidesAu2O3andAu2O: First-principles investigation. Physical Review B, 2007, 75, .	1.1	101
4078	Structural behavior of uranium dioxide under pressure byLSDA+Ucalculations. Physical Review B, 2007, 75, .	1.1	97
4079	Processing, Structure, Properties, and Applications of PZT Thin Films. Critical Reviews in Solid State and Materials Sciences, 2007, 32, 111-202.	6.8	375
4080	Elastic and electronic properties of TcB2 and superhard ReB2: First-principles calculations. Applied Physics Letters, 2007, 91, .	1.5	118
4081	Stability of the<mml:math xmlns:mml="http://www.w3.org/1998/Math/MathML" display="inline"><mml:mrow><mml:msub><mml:mi mathvariant="normal">Ce</mml:mi><mml:mn>2</mml:mn></mml:msub><mml:msub><mml:mi mathvariant="normal">O</mml:mi><mml:mn>3</mml:mn></mml:msub></mml:mrow></mml:math>phases: A<mml:math xmlns:mml="http://www.w3.org/1998/Math/MathML" display="inline"><mml:mrow><mml:mi>DFT</mml:mi><mml:mo>+</mml:mo><mml:mi>U</mml:mi></mml:mrow></mml:math>investig	1.1	77
4082	Origin of quasi-constant pre-exponential factors for adatom diffusion on Cu and Ag surfaces. Physical Review B, 2007, 76, .	1.1	24
4083	Vibrational dynamics and stability of the high-pressure chain and ring phases in S and Se. Journal of Chemical Physics, 2007, 126, 084503.	1.2	42
4084	Apparent bipolarity and Seebeck sign inversion in a layered semiconductor: LaZnOP. Physical Review B, 2007, 76, .	1.1	28
4085	Adsorption Behavior of Iron Phthalocyanine on Au(111) Surface at Submonolayer Coverage. Journal of Physical Chemistry C, 2007, 111, 9240-9244.	1.5	140
4086	Ab initioDFT simulation of ideal shear deformation of SiC polytypes. Modelling and Simulation in Materials Science and Engineering, 2007, 15, 27-37.	0.8	31

#	Article	IF	Citations
4087	First principles study of magnetism in nanographenes. Journal of Chemical Physics, 2007, 127, 124703.	1.2	191
4088	Theory of tunnel magnetoresistance and spin filter effect in magnetic tunnel junctions. Journal Physics D: Applied Physics, 2007, 40, 1228-1233.	1.3	11
4089	Local Electronic Structure of Olivine Phases of LixFePO4. Journal of Physical Chemistry A, 2007, 111, 4242-4247.	1.1	37
4090	Ag+- and Pb2+-Doped SrTiO3Photocatalysts. A Correlation Between Band Structure and Photocatalytic Activity. Journal of Physical Chemistry C, 2007, 111, 1847-1852.	1.5	126
4091	Why does the B3LYP hybrid functional fail for metals?. Journal of Chemical Physics, 2007, 127, 024103.	1.2	481
4092	Anti-Polarity in Ideal BiMnO3. Journal of the American Chemical Society, 2007, 129, 9854-9855.	6.6	115
4093	Conservation of dielectric constant upon amorphization in perovskite oxides. Physical Review B, 2007, 76, .	1.1	10
4094	Structural phase transition inCaH2at high pressures. Physical Review B, 2007, 75, .	1.1	47
4095	Density functional study of the interaction between small Au clusters, Aun (n=1â€“7) and the rutile TiO2 surface. I. Adsorption on the stoichiometric surface. Journal of Chemical Physics, 2007, 127, 084704.	1.2	55
4096	AbInitioMolecular Dynamics Study of Carbon Dioxide and Bicarbonate Hydration and the Nucleophilic Attack of Hydroxide on CO2. Journal of Physical Chemistry B, 2007, 111, 4453-4459.	1.2	87
4097	Sublimation of Ammonium Salts:â€‰ A Mechanism Revealed by a First-Principles Study of the NH₄Cl System. Journal of Physical Chemistry C, 2007, 111, 13831-13838.	1.5	38
4098	Bonding differences between single iron atoms versus iron chains with carbon nanotubes: First-principles calculations. Physical Review B, 2007, 76, .	1.1	22
4099	Diffusion mechanisms of native point defects in rutileTiO2:Ab initiototal-energy calculations. Physical Review B, 2007, 75, .	1.1	107
4100	Reduced Band Gap Hybrid Perovskites Resulting from Combined Hydrogen and Halogen Bonding at the Organicâ”Inorganic Interface. Chemistry of Materials, 2007, 19, 600-607.	3.2	227
4101	Structural Requirements and Reaction Pathways in Dimethyl Ether Combustion Catalyzed by Supported Pt Clusters. Journal of the American Chemical Society, 2007, 129, 13201-13212.	6.6	49
4102	Ammonia Dehydrogenation over Platinum-Group Metal Surfaces. Structure, Stability, and Reactivity of Adsorbed NHxSpecies. Journal of Physical Chemistry C, 2007, 111, 860-868.	1.5	118
4103	Toward Control of the Metalâ”Organic Interfacial Electronic Structure in Molecular Electronics:Â A First-Principles Study on Self-Assembled Monolayers of Ï€-Conjugated Molecules on Noble Metals. Nano Letters, 2007, 7, 932-940.	4.5	257
4104	Optimizing performance of half-metals at finite temperature. Journal of Physics Condensed Matter, 2007, 19, 315212.	0.7	20

#	Article	IF	Citations
4105	Geometry and electronic and magnetic properties of<mml:math xmlns:mml="http://www.w3.org/1998/Math/MathML" display="inline"><mml:mrow><mml:mi>M</mml:mi><mml:msub><mml:mi mathvariant="normal">Pd</mml:mi><mml:mn>12</mml:mn></mml:msub></mml:mrow></mml:math>clusters		

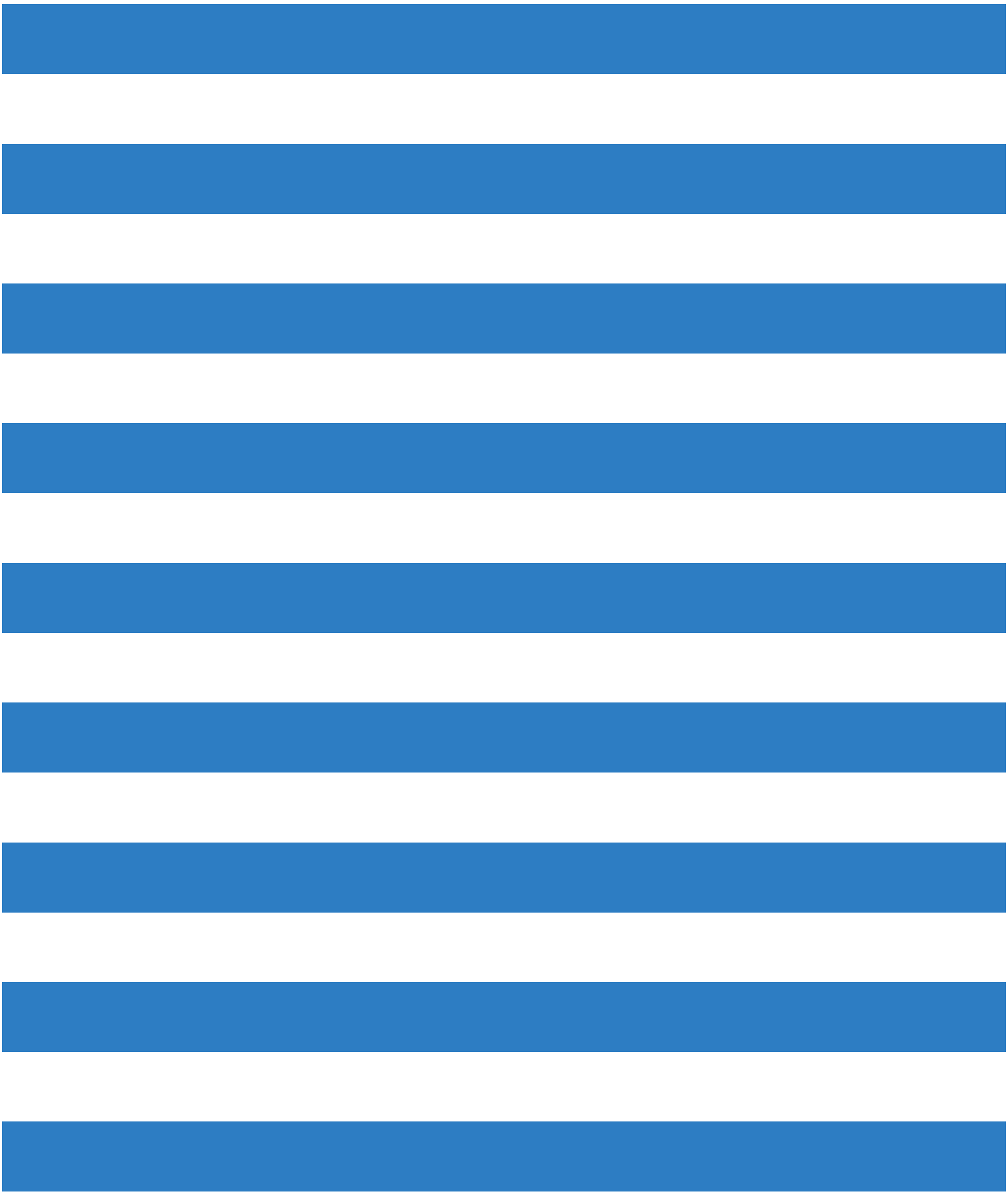

#	Article	IF	Citations
4123	Roles of inter- and intramolecular vibrations and band-hopping crossover in the charge transport in naphthalene crystal. Journal of Chemical Physics, 2007, 127, 044506.	1.2	97
4124	Size dependency of the elastic modulus of ZnO nanowires: Surface stress effect. Applied Physics Letters, 2007, 91, .	1.5	63
4125	Origins of the<mml:math xmlns:mml="http://www.w3.org/1998/Math/MathML" display="inline"><mml:mi>p</mml:mi></mml:math>-type nature and cation deficiency in<mml:math xmlns:mml="http://www.w3.org/1998/Math/MathML" display="inline"><mml:mrow><mml:msub><mml:mi mathvariant="normal">Cu</mml:mi><mml:mn>2</mml:mn></mml:msub><mml:mi mathvariant="normal">O</mml:mi></mml:mrow></mml:math>and related materials. Physical Review B, 2007, 76, .	1.1	456
4126	Thermodynamics of<mml:math xmlns:mml="http://www.w3.org/1998/Math/MathML" display="inline"><mml:mrow><mml:mi>L</mml:mi><mml:msub><mml:mn>1</mml:mn><mml:mn>0</mml:mn></mml:msub></mml:mr in FePt nanoparticles studied by Monte Carlo simulations based on an analytic bond-order potential. Physical Review B, 2007, 76, .	1.1	67
4127	Pt Monolayer on Fe(001) Catalyst for O2 Reduction: A First Principles Study. E-Journal of Surface Science and Nanotechnology, 2007, 5, 117-121.	0.1	6
4128	Catalysis by Design - Theoretical and Experimental Studies of Model Catalysts. , 2007, , .		2
4129	An ab initio investigation on the endohedral metallofullerene Gd3Nâ€“C80. Journal of Applied Physics, 2007, 101, 09E105.	1.1	9
4130	Ab-Initio Modeling of Defects in Germanium. , 2007, , 187-210.		1
4131	Combined DFT/Spectroscopic Studies of ĐœĐ¾Đž Species Interacting with TiO2 Support. Studies in Surface Science and Catalysis, 2007, , 377-380.	1.5	1
4132	Pd0.213Cd0.787 and Pd0.235Cd0.765 Structures: Their Longc Axis and Composite Crystals, Chemical Twinning, and Atomic Site Preferences. Chemistry - A European Journal, 2007, 13, 1394-1410.	1.7	34
4133	Supramolecular Self-Assembly Initiated by Solidâ€“Solid Wetting. Chemistry - A European Journal, 2007, 13, 7785-7790.	1.7	27
4134	A Quantum Mechanically Guided View of Mg₄₄Rh₇. Chemistry - A European Journal, 2007, 13, 7852-7863.	1.7	20
4135	Interpenetrating Polar and Nonpolar Sublattices in Intermetallics: The NaCd2 Structure. Angewandte Chemie - International Edition, 2007, 46, 1958-1976.	7.2	70
4136	High-Pressure Synthesis of Crystalline Carbon Nitride Imide, C2N2(NH). Angewandte Chemie - International Edition, 2007, 46, 1476-1480.	7.2	82
4137	Î³-TaON: A Metastable Polymorph of Tantalum Oxynitride. Angewandte Chemie - International Edition, 2007, 46, 2931-2934.	7.2	61
4138	Computational Study on the Catalytic Mechanism of Oxygen Reduction on La_{0.5}Sr_{0.5}MnO₃ in Solid Oxide Fuel Cells. Angewandte Chemie - International Edition, 2007, 46, 7214-7219.	7.2	101
4139	Catalytic Consequences of Composition in Polyoxometalate Clusters with Keggin Structure. Angewandte Chemie - International Edition, 2007, 46, 7864-7868.	7.2	108
4140	Structural and Electronic Properties of Pristine and Baâ€Doped Clathrateâ€Like Carbon Fullerenes. Angewandte Chemie - International Edition, 2007, 46, 6275-6277.	7.2	9

#	Article	IF	Citations
4141	On the Mechanism of Formation of Metal Nanowires by Selfâ€Assembly. Angewandte Chemie - International Edition, 2007, 46, 7094-7097.	7.2	53
4142	Direct Visualization of Enantiospecific Substitution of Chiral Guest Molecules into Heterochiral Molecular Assemblies at Surfaces. Angewandte Chemie - International Edition, 2007, 46, 7613-7616.	7.2	40
4143	A Stable Roomâ€Temperature Molecular Assembly of Zwitterionic Organic Dipoles Guided by a Si(111)â€7Ã—7 Template Effect. Angewandte Chemie - International Edition, 2007, 46, 9287-9290.	7.2	32
4144	Combined Experimental and Theoretical Study on the Nature and the Metastable Decay Pathways of the Amino Acid Ion Fragment [Mâ^'H]^{â^'}. Angewandte Chemie - International Edition, 2007, 46, 8057-8059.	7.2	47
4152	On the Mechanism of Formation of Metal Nanowires by Selfâ€Assembly. Angewandte Chemie, 2007, 119, 7224-7227.	1.6	7
4156	Design of Nanocomposite Low-Friction Coatings. Advanced Functional Materials, 2007, 17, 1611-1616.	7.8	84
4157	Density Functional Theoretical Studies on Polyaniline/HNb₃O₈ Layered Nanocomposites. Advanced Functional Materials, 2007, 17, 3521-3529.	7.8	18
4158	Firstâ€Principles Determination of Multicomponent Hydride Phase Diagrams: Application to the Liâ€Mgâ€Nâ€H System. Advanced Materials, 2007, 19, 3233-3239.	11.1	217
4159	A theoretical study of fullereneâ€“ferrocene hybrids. Journal of Computational Chemistry, 2007, 28, 594-600.	1.5	13
4160	A DFT study on the dimerization of C62 , H2 ï£¿C62 , and F2 ï£¿C62. Journal of Computational Chemistry, 2007, 28, 1417-1426.	1.5	4
4161	DFT studies using supercells and projector-augmented waves for structure, energetics, and dynamics of glycine, alanine, and cysteine. Journal of Computational Chemistry, 2007, 28, 1817-1833.	1.5	45
4162	Properties of Dense Fluid Hydrogen and Helium in Giant Gas Planets. Contributions To Plasma Physics, 2007, 47, 375-380.	0.5	19
4163	Conformational Analysis of One-Dimensional Coordination Polymers Based on [Cp2Cr2(CO)4(Î¼,Î·2-P2)] by Solid-State Multinuclear NMR Spectroscopy and Density Functional Calculations. European Journal of Inorganic Chemistry, 2007, 2007, 2775-2782.	1.0	35
4164	A Theoretical Study of Surface Reduction Mechanisms of CeO2(111) and (110) by H2. ChemPhysChem, 2007, 8, 849-855.	1.0	142
4165	Pitfalls in Interpreting Temperature Programmed Desorption Spectra of Alloys: The CO/CoPt Puzzle. ChemPhysChem, 2007, 8, 654-656.	1.0	12
4166	Dehydrogenation Reaction for Naï£¿Oï£¿H System: A Firstâ€Principles Study. ChemPhysChem, 2007, 8, 1979-1987.	1.0	2
4167	High-pressure Raman and infrared study of ZrV 2O7. Solid State Communications, 2007, 141, 680-684.	0.9	34
4168	First-principles and Monte Carlo combinational study on Zn1â^'xCoxO diluted magnetic semiconductor. Solid State Communications, 2007, 142, 242-246.	0.9	31

#	Article	IF	Citations
4169	Adsorption and diffusion of OH on Mo modified Pt(111) surface: First-principles theory. Solid State Communications, 2007, 142, 148-153.	0.9	10
4170	Ab initio study on the structural and elastic properties of MAlSi (M=Ca, Sr, and Ba). Solid State Communications, 2007, 143, 425-428.	0.9	63
4171	First-principles study of electron doping and disorder effects on electronic and magnetic properties in Sr2â˜xNdxFeMoO6 double perovskites. Solid State Communications, 2007, 144, 230-235.	0.9	19
4172	Energetics of oxygen vacancies at rutile TiO2(110) surface. Solid State Communications, 2007, 144, 324-328.	0.9	32
4173	Electrochemical impedance analysis of solid oxide fuel cell electrolyte using kinetic Monte Carlo technique. Solid State Ionics, 2007, 178, 195-205.	1.3	48
4174	Chemical routes to ultra thin films for copper barriers and liners. Surface and Coatings Technology, 2007, 201, 9256-9259.	2.2	16
4175	Segregation of Pt at clean surfaces of (Pt, Ni)3Al. Surface Science, 2007, 601, 376-380.	0.8	14
4176	Combined investigation of water sorption on TiO2 rutile (110) single crystal face: XPS vs. periodic DFT. Surface Science, 2007, 601, 518-527.	0.8	150
4177	Structure, magnetism, and adhesion at Cr/Fe interfaces from density functional theory. Surface Science, 2007, 601, 699-705.	0.8	31
4178	Ab initio study of S dynamics on iron surfaces. Surface Science, 2007, 601, 665-671.	0.8	19
4179	Density functional slab model studies of water adsorption on flat and stepped Cu surfaces. Surface Science, 2007, 601, 954-964.	0.8	89
4180	Surface segregation in Pt25Rh75 alloys studied by Monte Carlo simulations and the modified embedded atom method. Surface Science, 2007, 601, 1668-1676.	0.8	13
4181	Water adsorption and dissociation on BeO(001) and (100) surfaces. Surface Science, 2007, 601, 1608-1614.	0.8	10
4182	Active oxidation: Silicon etching and oxide decomposition basic mechanisms using density functional theory. Surface Science, 2007, 601, 2082-2088.	0.8	15
4183	Diffusion of oxygen atom in the topmost layer of the Si(100) surface: Structures and oxidation kinetics. Surface Science, 2007, 601, 2339-2343.	0.8	29
4184	Ab-initio calculations and STM observations on tetrapyridyl and Fe(II)-tetrapyridyl-porphyrin molecules on Ag(111). Surface Science, 2007, 601, 2409-2414.	0.8	46
4185	Study of Si(001)4Ã—2-Ga structure by scanning tunneling microscopy and ab initio calculation. Surface Science, 2007, 601, 2415-2419.	0.8	4
4186	Dissociative adsorption of N2 on W(110): Theoretical study of the dependence on the incidence angle. Surface Science, 2007, 601, 3726-3730.	0.8	13

#	Article	IF	Citations
4187	An ab initio study of 3-aminopropyltrimethoxysilane molecule on Si(111)-() surface. Surface Science, 2007, 601, 3740-3744.	0.8	10
4188	Initial stages of H2O adsorption and hydroxylation of Fe-terminated Î±-Fe2O3(0001) surface. Surface Science, 2007, 601, 2426-2437.	0.8	93
4189	The effects of exchange and correlation on the computed equilibrium shapes of wet MgO crystallites. Surface Science, 2007, 601, 4144-4148.	0.8	24
4190	Formation and stabilization of Fe-induced magic clusters on Si(111)-(7Ã—7) template. Surface Science, 2007, 601, 2486-2490.	0.8	15
4191	Spin-flop structure at an antiferromagnetic/ferromagnetic interface: Mn/Fe(100). Surface Science, 2007, 601, 4348-4351.	0.8	5
4192	Construction of modified embedded atom method potentials for Cu, Pt and Cuâ€“Pt and modelling surface segregation in Cu3Pt alloys. Surface Science, 2007, 601, 2952-2961.	0.8	13
4193	NH3 on Si(001): Can Gaussian cluster and planewave slab models agree on energetics?. Surface Science, 2007, 601, 3020-3033.	0.8	14
4194	Adsorption of V on a hematite (0001) surface and its oxidation: Submonolayer coverage. Surface Science, 2007, 601, 3082-3098.	0.8	27
4195	Structural evolution at the initial growth stage of perylene on Au(111). Surface Science, 2007, 601, 3179-3185.	0.8	17
4196	Comparison of the adsorption of N2 on Ru(109) and Ru(001) â€“ A detailed look at the role of atomic step and terrace sites. Surface Science, 2007, 601, 3533-3547.	0.8	9
4197	Vibrational entropy-driven dealloying of Mo(100) and W(100) surface alloys. Surface Science, 2007, 601, L95-L101.	0.8	9
4198	The structure of a stoichiometric TiO2 nanophase on Pt(1 1 1). Surface Science, 2007, 601, 3488-3496.	0.8	40
4199	Nano-faceting of fcc(1 1 0) surfaces controlled by adsorbates and atom deposition or removal. Surface Science, 2007, 601, L115-L119.	0.8	5
4200	Theoretical analysis of reactivity on Pt(111) and Ptâ€“Pd(111) alloys. Surface Science, 2007, 601, 4786-4792.	0.8	45
4201	First-principles studies of the structure of sulfur on the Pd(111) surface. Surface Science, 2007, 601, 4899-4909.	0.8	12
4202	Segregation at the surface of an Au/Pd alloy exposed to CO. Surface Science, 2007, 601, 5332-5339.	0.8	84
4203	A DFT+U description of oxygen vacancies at the TiO2 rutile (110) surface. Surface Science, 2007, 601, 5034-5041.	0.8	475
4204	Chemical vapor deposition of amorphous rutheniumâ€“phosphorus alloy films. Thin Solid Films, 2007, 515, 5298-5307.	0.8	40

#	Article	IF	Citations
4205	Influence of structural features on the photocatalytic activity of NaTaO3 powders from different synthesis methods. Applied Catalysis A: General, 2007, 331, 44-50.	2.2	163
4206	Atomic structure and electronic properties of Ta(1â€‰1â€‰2) and W(1â€‰1â€‰2) surfaces. Applied Surface Science, 2007, 253, 3803-3813.	3.1	5
4207	First-principles study of oxygenated diamond (001) surfaces with and without hydrogen. Applied Surface Science, 2007, 253, 4260-4266.	3.1	11
4208	Adsorption structure of germanium on the Ru(0001) surface. Applied Surface Science, 2007, 254, 431-435.	3.1	3
4209	Effects of temperature and oxygen pressure on binary oxide growth using aperture-controlled combinatorial pulsed-laser deposition. Applied Surface Science, 2007, 254, 785-788.	3.1	17
4210	Structural and electronic properties of PbTe (rocksalt)/CdTe (zinc-blende) interfaces. Applied Surface Science, 2007, 254, 397-400.	3.1	7
4211	Algorithms for the evolution of electronic properties in nanocrystals. Computer Physics Communications, 2007, 177, 1-5.	3.0	8
4212	Modelling STM images of TiO2(110) from first-principles: Defects, water adsorption and dissociation products. Chemical Physics Letters, 2007, 437, 73-78.	1.2	52
4213	Adsorption of S on Ir(100) surface from first-principles calculations. Chemical Physics Letters, 2007, 441, 53-57.	1.2	8
4214	Computational evidence for the possible existence of the open heterofullerenes C56X2Y (X=N,P; Y=O,S) and C60â˜6kN4k. Chemical Physics Letters, 2007, 441, 300-304.	1.2	11
4215	Pd, Rh, Ir and Pt adsorption on gold: A theoretical study of different surfaces. Chemical Physics Letters, 2007, 442, 105-109.	1.2	6
4216	CO adsorbs upside-down on small PtmAun clusters. Chemical Physics Letters, 2007, 443, 304-308.	1.2	10
4217	Ti in GaN: Ordering ferromagnetically from first-principles study. Chemical Physics Letters, 2007, 443, 92-94.	1.2	22
4218	Vibrational properties of TiHn complexes adsorbed on carbon nanostructures. Chemical Physics Letters, 2007, 444, 140-144.	1.2	15
4219	Terahertz spectroscopy of the crystalline Î±-quaterthiophene: A combined experimental and density functional theory study. Chemical Physics Letters, 2007, 445, 47-50.	1.2	14
4220	Confinement effects on site-preferences for cycloadditions into carbon nanotubes. Chemical Physics Letters, 2007, 444, 155-160.	1.2	34
4221	Modeling metal adsorption at amorphous silica: Gold atoms and dimers as example. Chemical Physics Letters, 2007, 444, 280-286.	1.2	22
4222	Growth pattern and bonding trends in Pt (n= 2â€“13) clusters: Theoretical investigation based on first principle calculations. Chemical Physics Letters, 2007, 446, 374-379.	1.2	77

#	Article	IF	Citations
4223	First-principle studies of electronic structure and C-doping effect in boron nitride nanoribbon. Chemical Physics Letters, 2007, 447, 181-186.	1.2	180
4224	An ab initio analysis of adsorption and diffusion of silver atoms on partially hydroxylated Î±-Al2O3(0001) surfaces. Chemical Physics Letters, 2007, 449, 155-159.	1.2	12
4225	The catalytic role of an isolated-Ti atom in the hydrogenation of Ti-doped Al(001) surface: An ab initio density functional theory calculation. Chemical Physics Letters, 2007, 450, 80-85.	1.2	29
4226	Structural and electronic properties of the Li-ion battery cathode material LixCoSiO4. Current Applied Physics, 2007, 7, 611-616.	1.1	37
4227	First-principles study of carbon diffusion in bulk nickel during the growth of fishbone-type carbon nanofibers. Carbon, 2007, 45, 21-27.	5.4	45
4228	Density functional calculation of hydrogen-filled C60 molecules. Carbon, 2007, 45, 2451-2453.	5.4	10
4229	Computational study of sulfurâ€“nickel interactions: A new Sâ€“Ni phase diagram. Electrochemistry Communications, 2007, 9, 2212-2217.	2.3	121
4230	First principles study of the coking resistance and the activity of a boron promoted Ni catalyst. Chemical Engineering Science, 2007, 62, 5039-5041.	1.9	27
4231	Ab initio study of the change from Î·5- to Î·1-coordination in group 12 dimetallocenes MMâ€²(C5H5)2 with M, Mâ€²=Zn, Cd, Hg. Chemical Physics, 2007, 333, 201-207.	0.9	20
4232	A DFT study of the heterofullerenes Sc3N@C79B, Sc3N@C79N, and Sc3N@C78BN. Chemical Physics, 2007, 334, 29-35.	0.9	6
4233	Chemical bonding in metal sandwich molecules MnR2 with R=pyrene C16H10 and tetracene C18H12. Chemical Physics, 2007, 337, 55-67.	0.9	12
4234	Enhanced photocatalytic activities of Ta, N co-doped TiO2 thin films under visible light. Chemical Physics, 2007, 339, 124-132.	0.9	112
4235	Bonding and magnetism in transition metal sandwich structures with the aromatic hydrocarbon coronene C24H12 outer layers. Chemical Physics, 2007, 342, 223-235.	0.9	15
4236	Calculations of thermophysical properties of cubic carbides and nitrides using the Debyeâ€“GrÃ¼neisen model. Acta Materialia, 2007, 55, 1215-1226.	3.8	155
4237	Morphology of WC grains in WCâ€“Co alloys: Theoretical determination of grain shape. Acta Materialia, 2007, 55, 1515-1521.	3.8	82
4238	Site preference of early transition metal elements in C15 NbCr2. Acta Materialia, 2007, 55, 1599-1605.	3.8	47
4239	Surface segregation of Pt in Î³â€²-Ni3Al: A first-principles study. Acta Materialia, 2007, 55, 1641-1647.	3.8	20
4240	Phase stability and structural features of matrix-embedded hardening precipitates in Alâ€“Mgâ€“Si alloys in the early stages of evolution. Acta Materialia, 2007, 55, 2183-2199.	3.8	114

#	Article	IF	Citations
4241	Effects of segregating elements on the adhesive strength and structure of the Î±-Al2O3/Î²-NiAl interface. Acta Materialia, 2007, 55, 2791-2803.	3.8	100
4242	Integrated design of Nb-based superalloys: Ab initio calculations, computational thermodynamics and kinetics, and experimental results. Acta Materialia, 2007, 55, 3281-3303.	3.8	78
4243	First-principles calculations of structural energetics of Cuâ€“TM (TM=Ti, Zr, Hf) intermetallics. Acta Materialia, 2007, 55, 3347-3374.	3.8	109
4244	Lattice stability prediction of elemental tetrahedrally close-packed structures. Acta Materialia, 2007, 55, 3707-3718.	3.8	20
4245	The crystal structure of the Î²â€² phase in Alâ€“Mgâ€“Si alloys. Acta Materialia, 2007, 55, 3815-3823.	3.8	364
4246	Theory-guided bottom-up design of Î²-titanium alloys as biomaterials based on first principles calculations: Theory and experiments. Acta Materialia, 2007, 55, 4475-4487.	3.8	220
4247	Phase stabilities and spinodal decomposition in the Cr1âˆ’xAlxN system studied by ab initio LDA and thermodynamic modeling: Comparison with the Ti1âˆ’xAlxN and TiN/Si3N4 systems. Acta Materialia, 2007, 55, 4615-4624.	3.8	76
4248	Defect structures and ternary lattice site preference of the B2 phase in the Alâ€“Niâ€“Ru system. Acta Materialia, 2007, 55, 4781-4787.	3.8	14
4249	Site preference of transition-metal elements in B2 NiAl: A comprehensive study. Acta Materialia, 2007, 55, 4799-4806.	3.8	78
4250	Effect of partitioning of Mn and Si on the growth kinetics of cementite in tempered Feâ€“0.6 mass% C martensite. Acta Materialia, 2007, 55, 5027-5038.	3.8	186
4251	Soluteâ€“vacancy binding in aluminum. Acta Materialia, 2007, 55, 5867-5872.	3.8	326
4252	First-principles calculations of Î²â€³-Mg5Si6/Î±-Al interfaces. Acta Materialia, 2007, 55, 5934-5947.	3.8	88
4253	Elastic anisotropy of Î³â€²-Fe4N and elastic grain interaction in Î³â€²-Fe4N1âˆ’y layers on Î±-Fe: First-principles calculations and diffraction stress measurements. Acta Materialia, 2007, 55, 5833-5843.	3.8	78
4254	Theoretical and experimental studies of devitrification pathways in the Zr2Cu1âˆ’xPdx metallic glass system. Acta Materialia, 2007, 55, 5901-5909.	3.8	13
4255	Structure and chemical analysis of aluminum wear debris: Experiments and ab initio simulations. Acta Materialia, 2007, 55, 6489-6498.	3.8	15
4256	Predicting twinning stress in fcc metals: Linking twin-energy pathways to twin nucleation. Acta Materialia, 2007, 55, 6843-6851.	3.8	370
4257	Comparative study of H2 adsorption on W(100)-c(2Ã—2)Cu and W(100): Surface alloying effects. Applied Surface Science, 2007, 254, 82-86.	3.1	4
4258	Dynamics at the nanoscale. Materials Science and Engineering C, 2007, 27, 972-980.	3.8	5

#	Article	IF	Citations
4259	Defects and threshold displacement energies in SrTiO3 perovskite using atomistic computer simulations. Nuclear Instruments & Methods in Physics Research B, 2007, 254, 211-218.	0.6	69
4260	Inelastic neutron scattering and DFT study of 2-amino-3-hydroxymethyl-1,3-propane diol (TRIS). Chemical Physics, 2007, 340, 245-259.	0.9	2
4261	The role of water in the initial steps of methanol oxidation on Pt(2â€‰1â€‰1). Electrochimica Acta, 2007, 52, 2236-2243.	2.6	37
4262	A first principles analysis of the electro-oxidation of CO over Pt(111). Electrochimica Acta, 2007, 52, 5517-5528.	2.6	61
4263	Electronic structure of insulator-confined ultra-thin Si channels. Microelectronic Engineering, 2007, 84, 2043-2046.	1.1	12
4264	First-principles calculations of CH4 dissociation on Ni(100) surface along different reaction pathways. Journal of Molecular Catalysis A, 2007, 264, 299-308.	4.8	33
4265	Metastable phases and spinodal decomposition in Ti1âˆ'xAlxN system studied by ab initio and thermodynamic modeling, a comparison with the TiNâ€“Si3N4 system. Materials Science & Engineering A: Structural Materials: Properties, Microstructure and Processing, 2007, 448, 111-119.	2.6	91
4266	Electronic structure, structural and optical properties of thermally evaporated CdTe thin films. Physica B: Condensed Matter, 2007, 387, 227-238.	1.3	108
4267	First-principles calculation of Mg(0001) thin films: Quantum size effect and adsorption of atomic hydrogen. Physica B: Condensed Matter, 2007, 390, 225-230.	1.3	16
4268	Electronic and magnetic properties of beryllium oxide with 3d impurities from first-principles calculations. Physica B: Condensed Matter, 2007, 400, 47-52.	1.3	13
4269	Understanding the defect physics in polycrystalline photovoltaic materials. Physica B: Condensed Matter, 2007, 401-402, 25-32.	1.3	51
4270	First-principles study of iron and iron pairs in Si. Physica B: Condensed Matter, 2007, 401-402, 105-108.	1.3	7
4271	Retardation of boron diffusion in SiGe alloy. Physica B: Condensed Matter, 2007, 401-402, 196-199.	1.3	1
4272	Ab initio calculation of the formation energy of charged vacancies in germanium. Physica B: Condensed Matter, 2007, 401-402, 205-209.	1.3	21
4273	Deep defect states in narrow band-gap semiconductors. Physica B: Condensed Matter, 2007, 401-402, 291-295.	1.3	29
4274	Theoretical and experimental studies on oxygen vacancy in p-type ZnO. Physica B: Condensed Matter, 2007, 401-402, 417-420.	1.3	11
4275	Algorithms for defects in nanostructures. Physica B: Condensed Matter, 2007, 401-402, 531-536.	1.3	0
4276	Hydrogen effects in MOS devices. Microelectronic Engineering, 2007, 84, 2344-2349.	1.1	34

#	Article	IF	Citations
4277	Surface reconstructions on Sb-irradiated GaAs(001) formed by molecular beam epitaxy. Microelectronics Journal, 2007, 38, 620-624.	1.1	9
4278	Periodic density functional and FTIR spectroscopic studies on CO adsorption on the zeolite Na-FER. Microporous and Mesoporous Materials, 2007, 106, 162-173.	2.2	44
4279	Density functional theory of high-k dielectric gate stacks. Microelectronics Reliability, 2007, 47, 686-693.	0.9	7
4280	Ab initio calculations about intrinsic point defects and He in W. Nuclear Instruments & Methods in Physics Research B, 2007, 255, 23-26.	0.6	197
4281	Electron, hole and exciton self-trapping in germanium doped silica glass from DFT calculations with self-interaction correction. Nuclear Instruments & Methods in Physics Research B, 2007, 255, 188-194.	0.6	14
4282	Calculation of the thermodynamic properties of B2 AlRE (RE=Sc, Y, La, Ceâ€“Lu). Physica B: Condensed Matter, 2007, 399, 27-32.	1.3	43
4283	Investigation of electrically active defects of silicon carbide using atomistic scale modeling and simulation. Physica B: Condensed Matter, 2007, 401-402, 81-84.	1.3	7
4284	NixCu6â^'xSn5 alloys as negative electrode materials for rechargeable lithium batteries. Journal of Power Sources, 2007, 167, 171-177.	4.0	19
4285	Synthesis and electrochemistry of Li3MnO4: Mn in the +5 oxidation state. Journal of Power Sources, 2007, 172, 189-197.	4.0	35
4286	Chemical bonding in EuTGe (T=Ni, Pd, Pt) and physical properties of EuPdGe. Journal of Solid State Chemistry, 2007, 180, 533-540.	1.4	11
4287	Titanium vacancy defects in solâ€“gel prepared anatase. Journal of Solid State Chemistry, 2007, 180, 670-678.	1.4	87
4288	Crystal chemistry of the G-phases in the {Ti, Zr, Hf}â€“Niâ€“Si systems. Journal of Solid State Chemistry, 2007, 180, 733-741.	1.4	12
4289	Structural arrangements of the ternary metal boride carbide compounds MB2C4 (M=Mg, Ca, La and Ce) from first-principles theory. Journal of Solid State Chemistry, 2007, 180, 2465-2470.	1.4	8
4290	Ab initio study on structure and phase transition of A- and B-type rare-earth sesquioxides Ln2O3 (Ln=Laâ€“Lu, Y, and Sc) based on density function theory. Journal of Solid State Chemistry, 2007, 180, 3280-3287.	1.4	109
4291	Ba2In2O4(OH)2: Proton sites, disorder and vibrational properties. Journal of Solid State Chemistry, 2007, 180, 3388-3392.	1.4	20
4292	Correlation effects in PuCoGa5 superconductor. Physica C: Superconductivity and Its Applications, 2007, 460-462, 655-656.	0.6	1
4293	Theory of interface structure, energetics, and electronic properties of embedded Si/a-SiO2 nanocrystals. Physica E: Low-Dimensional Systems and Nanostructures, 2007, 38, 99-105.	1.3	39
4294	Structures and magnetic moments of Nin () clusters. Physics Letters, Section A: General, Atomic and Solid State Physics, 2007, 360, 629-631.	0.9	26

#	Article	IF	Citations
4295	DFT study on the structures and properties of 3-nitro-1,2,4-triazol-5-one crystals at high pressure. Journal of Molecular Graphics and Modelling, 2007, 26, 415-419.	1.3	9
4296	Ab initio modeling of martensitic transformations (MT) in magnetic shape memory alloys. Journal of Magnetism and Magnetic Materials, 2007, 310, 2761-2763.	1.0	9
4297	Ab-initio study of giant moment reduction of Fe impurity in dilute. Journal of Magnetism and Magnetic Materials, 2007, 310, e541-e543.	1.0	1
4298	Interfacial electronic structure and oxygen vacancy states in Fe/MgO/Fe tunneling junctions. Journal of Magnetism and Magnetic Materials, 2007, 310, e644-e645.	1.0	12
4299	Electronic structure and spin-filter effect of ferromagnetic insulators with double perovskite structure. Journal of Magnetism and Magnetic Materials, 2007, 310, 1994-1996.	1.0	14
4300	Transition metal doping in Ge. Journal of Magnetism and Magnetic Materials, 2007, 310, 2147-2149.	1.0	4
4301	Theoretical studies on the influence of oxygen impurity upon magnetic properties of (Ga,Cr)N. Journal of Magnetism and Magnetic Materials, 2007, 310, 2155-2157.	1.0	1
4302	Systematic group-specific trends for point defects in bcc transition metals: An ab initio study. Journal of Nuclear Materials, 2007, 367-370, 257-262.	1.3	35
4303	Ab initio structural and energetic study of (, Ga) perovskites. Journal of Physics and Chemistry of Solids, 2007, 68, 570-575.	1.9	34
4304	First-principles study on the formation energies of intrinsic defects in LiNbO3. Journal of Physics and Chemistry of Solids, 2007, 68, 1336-1340.	1.9	35
4305	Electronic structure and optical properties of crystalline strontium azide and barium azide by ab initio pseudopotential plane-wave calculations. Journal of Physics and Chemistry of Solids, 2007, 68, 1762-1769.	1.9	14
4306	Elastic properties, thermal expansion coefficients and electronic structures of Ti0.75X0.25C carbides. Journal of Physics and Chemistry of Solids, 2007, 68, 1805-1811.	1.9	48
4307	Ab initio study of exciton transfer dynamics from a coreâ€“shell semiconductor quantum dot to a porphyrin-sensitizer. Journal of Photochemistry and Photobiology A: Chemistry, 2007, 190, 342-351.	2.0	67
4308	Structureâ€“reactivity relationship for bimetallic electrodes: Pt overlayers and PtAu surface alloys on Au(111). Journal of Electroanalytical Chemistry, 2007, 607, 47-53.	1.9	41
4309	Adsorption of formic acid on Pt(111) in the presence of water. Journal of Electroanalytical Chemistry, 2007, 607, 133-139.	1.9	44
4310	Alkane metathesis by a tungsten carbyne complex grafted on gamma alumina: Is there a direct chemical role of the support?. Journal of Catalysis, 2007, 251, 507-513.	3.1	27
4311	Structure of GaSb/GaAs(001) surface using the first principles calculation. Journal of Crystal Growth, 2007, 301-302, 880-883.	0.7	1
4312	Chloridobis[(2-oxoazocan-1-yl)methyl]germanium(IV) trifluoromethanesulfonate. Acta Crystallographica Section C: Crystal Structure Communications, 2007, 63, m144-m146.	0.4	7

#	Article	IF	Citations
4313	IrIn 7 GeO 8 = [IrIn 6](GeO 4)(InO 4) und Verbindungen der Mischkristallreihe [IrIn 6](Ge 1+x In 1â^'4x/3) Tj ETQq0 0 0 rgBT /Overlock Chemie, 2007, 633, 1464-1471.	0.6	8
4314	Stuffed Graphiteâ€like vs. Stuffed Diamondâ€like Structures of the 18 Valence Electron Compounds REAuSn (RE = Sc, Y, Laâ€Nd, Sm, Gdâ€Lu). Zeitschrift Fur Anorganische Und Allgemeine Chemie, 2007, 633, 2631-2634.	0.6	9
4315	Energy gap and bond lengths of AlxGayIn1â€“x â€“yN, AlxGayIn1â€“x â€“yP and AlxGayIn1â€“x â€“yAs quaternary alloys. Physica Status Solidi C: Current Topics in Solid State Physics, 2007, 4, 229-233.	0.8	0
4316	Cluster expansion failings when applied to semiconductor superlattices. Physica Status Solidi C: Current Topics in Solid State Physics, 2007, 4, 427-429.	0.8	1
4317	Defects in N+ion-implanted ZnO single crystals studied by positron annihilation and Hall effect. Physica Status Solidi C: Current Topics in Solid State Physics, 2007, 4, 3642-3645.	0.8	2
4318	Positron studies of surfaces, structure and electronic properties of nanocrystals. Physica Status Solidi C: Current Topics in Solid State Physics, 2007, 4, 3883-3888.	0.8	7
4319	Identification of lattice defects in Cu thin films by positron annihilation spectroscopy. Physica Status Solidi C: Current Topics in Solid State Physics, 2007, 4, 3550-3553.	0.8	4
4320	Model computations for Cd adsorption on the (001) surface of CdTe. Physica Status Solidi C: Current Topics in Solid State Physics, 2007, 4, 3191-3203.	0.8	3
4321	Investigation of the nanoscale self-assembly of donor-Ïƒ-acceptor molecules. International Journal of Quantum Chemistry, 2007, 107, 2233-2242.	1.0	7
4322	Semiconducting Cyanideâ€“Transition-Metal Nanotubes. Small, 2007, 3, 1253-1258.	5.2	5
4323	Largeâ€Scale Synthesis of Titanate and Anatase Tubular Hierarchitectures. Small, 2007, 3, 1518-1522.	5.2	69
4324	The influence of ionic liquid's nature on free radical polymerization of vinyl monomers and ionic conductivity of the obtained polymeric materials. Polymers for Advanced Technologies, 2007, 18, 50-63.	1.6	92
4325	Ab-initio modeling of spintronic materials. Physica Status Solidi (A) Applications and Materials Science, 2007, 204, 33-43.	0.8	2
4326	Hydride electronics. Physica Status Solidi (A) Applications and Materials Science, 2007, 204, 3538-3544.	0.8	17
4327	Influence of the lattice discreteness on magnetic ordering in nanostructures and nanoarrays. Physica Status Solidi (B): Basic Research, 2007, 244, 1133-1165.	0.7	15
4328	Atomistic characterization of structural and elastic properties of auxetic crystalline SiO2. Physica Status Solidi (B): Basic Research, 2007, 244, 900-909.	0.7	30
4329	Electronic structure and magnetic properties of Fe3C with 3d and 4d impurities. Physica Status Solidi (B): Basic Research, 2007, 244, 1971-1981.	0.7	23
4330	Structural properties of ZnO polymorphs. Physica Status Solidi (B): Basic Research, 2007, 244, 1538-1543.	0.7	19

#	Article	IF	Citations
4331	Electronic structure and stability of thorium carbonitrides. Physica Status Solidi (B): Basic Research, 2007, 244, 3198-3205.	0.7	13
4332	Ab initio study of elastic, thermal physical properties and electronic structure of Feâ€“Ga alloys. Physica Status Solidi (B): Basic Research, 2007, 244, 3583-3592.	0.7	8
4333	New principle of hydrogen adsorption inside nanotubes. Physica Status Solidi (B): Basic Research, 2007, 244, 4327-4330.	0.7	0
4334	Magnetism of linear Fe, Co, and Ni nanowires encapsulated in zigzag (n,0) carbon nanotubes (CNT) with n = 5 to 9: A firstâ€principles study. Physica Status Solidi (B): Basic Research, 2007, 244, 4407-4410.	0.7	8
4335	Effects of spinâ€flip tunneling on temperature and voltage dependence of TMR. Physica Status Solidi (B): Basic Research, 2007, 244, 4452-4455.	0.7	1
4336	Synthesis, crystal structure, and electronic properties of double orthovanadate Sr2Bi2/3 (VO4)2. Doklady Physical Chemistry, 2007, 415, 186-189.	0.2	3
4337	Magnetization of beryllium oxide in the presence of nonmagnetic impurities: Boron, carbon, and nitrogen. JETP Letters, 2007, 85, 246-250.	0.4	16
4338	Hydrogen multicentre bonds. Nature Materials, 2007, 6, 44-47.	13.3	658
4339	Substrate-induced magnetic ordering and switching of iron porphyrin molecules. Nature Materials, 2007, 6, 516-520.	13.3	396
4340	Lattice dynamics of the Znâ€“Mgâ€“Sc icosahedral quasicrystal and its Znâ€“Sc periodic 1/1 approximant. Nature Materials, 2007, 6, 977-984.	13.3	52
4341	Nano-architectures by covalent assembly of molecular building blocks. Nature Nanotechnology, 2007, 2, 687-691.	15.6	1,187
4342	Implications for plastic flow in the deep mantle from modelling dislocations in MgSiO3 minerals. Nature, 2007, 446, 68-70.	13.7	84
4343	Sulphate adsorption at the Fe (hydr)oxide?H2O interface: comparison of cluster and periodic slab DFT predictions. European Journal of Soil Science, 2007, 58, 978-988.	1.8	49
4344	Atomic Structures and Electrical Properties of ZnO Grain Boundaries. Journal of the American Ceramic Society, 2007, 90, 337-357.	1.9	96
4345	First-Principles Investigation of the Atomic and Electronic Structures of ?-Al2O3(0001)/Ni(111) Interfaces. Journal of the American Ceramic Society, 2007, 90, 2429-2440.	1.9	27
4346	Catalysis by doped oxides: CO oxidation by AuxCe1â^'xO2. Journal of Catalysis, 2007, 245, 205-214.	3.1	325
4347	A density functional theory study of HCN hydrogenation to methylamine on Ni(111). Journal of Catalysis, 2007, 245, 436-445.	3.1	27
4348	Interplay between molecular adsorption and metalâ€“support interaction for small supported metal clusters: CO and C2H4 adsorption on Pd4/Î³Pd4/Î³-Al2O3. Journal of Catalysis, 2007, 247, 339-355.	3.1	80

#	Article	IF	Citations
4349	A computer modeling study of redox processes on the FeSbO4 (100) surface. Journal of Catalysis, 2007, 248, 77-88.	3.1	17
4350	A Pd-doped perovskite catalyst, BaCe1â^'xPdxO3â^'Î´BaCe1â^'xPdxO3â^'Î´, for CO oxidation. Journal of Catalysis, 2007, 249, 349-358.	3.1	91
4351	Dependence of structural properties of ZnO on high pressure. Materials Chemistry and Physics, 2007, 106, 11-15.	2.0	28
4352	Single adatom site exchange during the Ge growth on group V element covered Si(001). Scripta Materialia, 2007, 56, 113-116.	2.6	1
4353	Lattice and elastic constants of titaniumâ€“niobium monoborides containing aluminum and vanadium. Scripta Materialia, 2007, 56, 273-276.	2.6	14
4354	Formation of amorphous phases in an immiscible Cuâ€“Nb system studied by molecular dynamics simulation and ion beam mixing. Scripta Materialia, 2007, 57, 157-160.	2.6	24
4355	Positive correlation between the magnetic moment of Fe and atomic volume in the binary Feâ€“(Cu, Ag,) Tj ETQq0 0 0 rgBT /Overlock 10	2.6	8
4356	Concept of optical channel as a guide for tuning the optical properties of insulating materials. Solid State Sciences, 2007, 9, 600-603.	1.5	13
4357	Magnetism and transport of CuCr2Se4 thin films. Journal of Magnetism and Magnetic Materials, 2007, 318, 65-73.	1.0	30
4358	Electronic structure and magnetocrystalline anisotropy in Feâ€“Coâ€“Ni binary alloy monolayers on Cu(001). Journal of Magnetism and Magnetic Materials, 2007, 317, 46-52.	1.0	8
4359	Ab Initio Studies of Magnetic Properties of CoFePd Alloys and Multilayers. IEEE Transactions on Magnetics, 2007, 43, 2199-2201.	1.2	2
4360	Defect-Mediated Properties of Magnetic Tunnel Junctions. IEEE Transactions on Magnetics, 2007, 43, 2770-2775.	1.2	10
4361	Exchange Interactions in Bcc Co: Implications for Temperature Dependence of TMR. IEEE Transactions on Magnetics, 2007, 43, 2794-2796.	1.2	2
4362	Firstâ€principles study of the electronic structure and the associated magnetism of carbonâ€doped TiO₂. Physica Status Solidi - Rapid Research Letters, 2007, 1, 217-219.	1.2	19
4363	Charge state and hydrogen diffusion in Ti-based alloys. Crystallography Reports, 2007, 52, 975-979.	0.1	3
4364	Synthesis and study of manganese-containing endohedral fullerenes. Physics of the Solid State, 2007, 49, 599-602.	0.2	1
4365	Ab initio calculations of the stability and structural defects of the B2 CuxFe1â^'x Al phases. Physics of the Solid State, 2007, 49, 1253-1258.	0.2	12
4366	Exploring the molecular mechanisms of reactions at surfaces. Russian Journal of Physical Chemistry B, 2007, 1, 292-306.	0.2	6

#	Article	IF	Citations
4367	Ab initioheat capacity and atomic temperature factors of chalcopyrites. Physical Review B, 2007, 75, .	1.1	17
4368	Formation of the cerium orthovanadateCeVO4:DFT+Ustudy. Physical Review B, 2007, 76, .	1.1	61
4369	Thermodynamic functions and pressure-temperature phase diagram of lithium alanates byab initiocalculations. Physical Review B, 2007, 76, .	1.1	34
4370	First-Principles Studies of Ferroelectric Oxides. , 2007, , 117-174.		57
4371	Structure of Feâ€“Co/Pt(001) superlattices: a realization of tetragonal Feâ€“Co alloys. Journal of Physics Condensed Matter, 2007, 19, 016008.	0.7	13
4372	Structures and energetics of Ga₂O₃polymorphs. Journal of Physics Condensed Matter, 2007, 19, 346211.	0.7	253
4373	First-principles investigation of metal-hydride phase stability: The Ti-H system. Physical Review B, 2007, 76, .	1.1	71
4374	Pressure-Induced Cubic to Monoclinic Phase Transformation in Erbium Sesquioxide Er2O3. Inorganic Chemistry, 2007, 46, 6164-6169.	1.9	71
4375	Creation of paired electron states in the gap of semiconducting carbon nanotubes by correlated hydrogen adsorption. New Journal of Physics, 2007, 9, 275-275.	1.2	33
4376	First-principles study of native point defects in hafnia and zirconia. Physical Review B, 2007, 75, .	1.1	203
4377	Density-functional theory study of the electronic structure of thinSiâˆ•SiO2quantum nanodots and nanowires. Physical Review B, 2007, 75, .	1.1	17
4378	Thermodynamics of reversible gas adsorption on alkali-metal exchanged zeolitesâ€”the interplay of infrared spectroscopy and theoretical calculations. Physical Chemistry Chemical Physics, 2007, 9, 1421-1437.	1.3	96
4379	Effect of Spin State on the Dihydrogen Binding Strength to Transition Metal Centers in Metal-Organic Frameworks. Journal of the American Chemical Society, 2007, 129, 12606-12607.	6.6	82
4380	Using first principles calculations to identify new destabilized metal hydride reactions for reversible hydrogen storage. Physical Chemistry Chemical Physics, 2007, 9, 1438.	1.3	173
4381	Structural investigation and electronic properties of the nickel ferrite NiFe2O4: a periodic density functional theory approach. Journal of Physics Condensed Matter, 2007, 19, 346219.	0.7	85
4382	First-principles calculations of the diffusion of atomic oxygen in nickel: thermal expansion contribution. Journal of Physics Condensed Matter, 2007, 19, 296201.	0.7	20
4383	Thermodynamic guidelines for the prediction of hydrogen storage reactions and their application to destabilized hydride mixtures. Physical Review B, 2007, 76, .	1.1	127
4384	A New Class of Supramolecular Wires. Journal of Physical Chemistry C, 2007, 111, 18912-18916.	1.5	12

#	Article	IF	Citations
4385	Density functional theory analysis of the structural and electronic properties of TiO2 rutile and anatase polytypes: Performances of different exchange-correlation functionals. Journal of Chemical Physics, 2007, 126, 154703.	1.2	307
4386	Native point defects in ZnO. Physical Review B, 2007, 76, .	1.1	2,051
4387	Crystal Chemistry and Electronic Structure of the Metallic Lithium Ion Conductor, LiNiN. Journal of the American Chemical Society, 2007, 129, 1912-1920.	6.6	21
4388	Structural and thermodynamic properties of hexagonal BeO at high pressures and temperatures. Journal of Physics Condensed Matter, 2007, 19, 456209.	0.7	11
4389	Theoretical study of the thermal behavior of free and alumina-supported Fe-C nanoparticles. Physical Review B, 2007, 75, .	1.1	73
4390	Modified embedded-atom method interatomic potentials for theMgâ^'Alalloy system. Physical Review B, 2007, 75, .	1.1	60
4391	Charged Fullerenes as High-Capacity Hydrogen Storage Media. Nano Letters, 2007, 7, 2578-2583.	4.5	220
4392	Hydrogen storage capacity of Ti-doped boron-nitride and<mml:math xmlns:mml="http://www.w3.org/1998/Math/MathML" display="inline"><mml:mrow><mml:mi mathvariant="normal">B</mml:mi><mml:mo>â^•</mml:mo><mml:mi mathvariant="normal">Be</mml:mi></mml:mrow></mml:math>-substituted carbon nanotubes. Physical Review B, 2007, 76, .	1.1	86
4393	Quantum Molecular Dynamics Simulations for the Nonmetal-to-Metal Transition in Fluid Helium. Physical Review Letters, 2007, 98, 190602.	2.9	63
4394	Oxidation of the Ptâ^•HfO2 interface: The role of the oxygen chemical potential. Journal of Applied Physics, 2007, 101, 014310.	1.1	15
4395	Mechanism of the<mml:math xmlns:mml="http://www.w3.org/1998/Math/MathML" display="inline"><mml:mrow><mml:mi>B</mml:mi><mml:mn>3</mml:mn></mml:mrow></mml:math>to<mml:math xmlns:mml="http://www.w3.org/1998/Math/MathML" display="inline"><mml:mrow><mml:mi>B</mml:mi><mml:mn>1</mml:mn></mml:mrow></mml:math>transformation in cubic AlN under uniaxial stress. Physical Review B, 2007, 76, .	1.1	26
4396	Li-decorated metalâ€“organic framework 5: A route to achieving a suitable hydrogen storage medium. Proceedings of the National Academy of Sciences of the United States of America, 2007, 104, 20173-20176.	3.3	232
4397	Simulation of interstitial diffusion in graphite. Physical Review B, 2007, 76, .	1.1	40
4398	Cooperative Behaviors in Carbene Additions through Local Modifications of Nanotube Surfaces. Chemistry of Materials, 2007, 19, 1028-1034.	3.2	32
4399	Multiscale modeling of crowdion and vacancy defects in body-centered-cubic transition metals. Physical Review B, 2007, 76, .	1.1	396
4400	Difficulty for oxygen to incorporate into the silicon network during initial O2 oxidation of Si(100)-(2Ã—1). Journal of Chemical Physics, 2007, 126, 114707.	1.2	32
4401	Crystal Structures of and Displacive Transitions in OsN2, IrN2, RuN2, and RhN2. Angewandte Chemie - International Edition, 2007, 46, 1136-1140.	7.2	116
4402	Molecular dynamics simulations of thermodynamics, elastic constants and solid solution strengths for Mg-Gd alloys. European Physical Journal B, 2007, 57, 305-312.	0.6	21

#	Article	IF	Citations
4403	From compact point defects to extended structures in silicon. European Physical Journal B, 2007, 57, 229-234.	0.6	15
4404	Elastic and brittle properties of the B2-MgRE (RE = Sc, Y, Ce, Pr, Nd, Gd, Tb, Dy, Ho,ÂEr) intermetallics. European Physical Journal B, 2007, 60, 75-81.	0.6	92
4405	Catalyst poisoning in the conversion of CO and N 2O to CO 2 and N 2 on Pt 4 - in the gas phase. European Physical Journal D, 2007, 43, 189-192.	0.6	48
4406	Embedding atom-jellium model for metal surface. European Physical Journal D, 2007, 43, 247-250.	0.6	1
4407	Hydrogen Spillover Mechanism on a Pd-Doped Mg Surface as Revealed by ab initio Density Functional Calculation. Journal of the American Chemical Society, 2007, 129, 10201-10204.	6.6	105
4408	Correlation between local structure of melts and glass forming ability for Al-based alloys: A first-principles study. Applied Physics Letters, 2007, 91, .	1.5	22
4409	Role of the nanoscale in catalytic CO oxidation by supported Au and Pt nanostructures. Physical Review B, 2007, 76, .	1.1	122
4410	Optimisation of accurate rutile TiO2 (110), (100), (101) and (001) surface models from periodic DFT calculations. Theoretical Chemistry Accounts, 2007, 117, 565-574.	0.5	213
4411	Chemistry at surfaces: from ab initio structures to quantum dynamics. Theoretical Chemistry Accounts, 2007, 117, 805-825.	0.5	28
4412	Potential routes to carbon inclusion in apatite minerals: a DFT study. Physics and Chemistry of Minerals, 2007, 34, 495-506.	0.3	16
4413	Factors in gold nanocatalysis: oxidation of CO in the non-scalable size regime. Topics in Catalysis, 2007, 44, 145-158.	1.3	190
4414	Chemisorption of hydrogen on the missing-row Pt(110)-(1 Ã— 2) surface. Topics in Catalysis, 2007, 46, 161-167.	1.3	22
4415	First Principles Analysis of the Electrocatalytic Oxidation of Methanol and Carbon Monoxide. Topics in Catalysis, 2007, 46, 306-319.	1.3	66
4416	Continuum and Quantum-Chemical Modeling of Oxygen Reduction on the Cathode in a Solid Oxide Fuel Cell. Topics in Catalysis, 2007, 46, 386-401.	1.3	30
4417	Synthesis and structures of tris(pentafluorophenyl)silylamines. Russian Chemical Bulletin, 2007, 56, 1394-1401.	0.4	5
4418	Magnetic origin of nano-clustering and point defect interaction in Feâ€“Cr alloys: an ab-initio study. Journal of Computer-Aided Materials Design, 2007, 14, 159-169.	0.7	39
4419	Engineering model of a biased metalâ€“moleculeâ€“metal junction. Journal of Computational Electronics, 2007, 6, 425-430.	1.3	1
4421	Multiscale model of electronic behavior and localization in stretched dry DNA. Journal of Materials Science, 2007, 42, 8894-8903.	1.7	5

#	Article	IF	Citations
4422	Ab initio study on fracture toughness of Ti0.75X0.25C ceramics. Journal of Materials Science, 2007, 42, 9713-9716.	1.7	13
4423	Vacancy-induced magnetism of beryllium monoxide. Journal of Structural Chemistry, 2007, 48, 1145-1147.	0.3	4
4424	Towards superconductivity in hydrides: computational studies of two hypothetical ternary compounds, % MathType!Translator!2!1!AMS LaTeX.tdl!TeX -- AMS-LaTeX! % MathType!MTEF!2!1!+- % feaaeaart1ev0aaatCvAUfeBSjuyZL2yd9gzLbvyNv2CaerbbjxAHX % garmWu51MyVXgatuuDJXwAK1uy0HwmaeHbfv3ySLgzG0uy0Hgip5wz % aebbnrfifHhDYfgasaacH8qrps0lbbf9q8WrFfeuY-Hhbbf9v8qqaq % Fr0xc9pk0xbba9q8WqFfea0-yr0RYxir-Jbba9q8aq0-yq-He9q8qq % Qlf5Fe9Fqt85f0 ...	0.8	6
4425	Glass Formation, Phase Equilibria, and Thermodynamic Assessment of the Al-Ce-Co System Assisted by First-Principles Energy Calculations. Metallurgical and Materials Transactions A: Physical Metallurgy and Materials Science, 2007, 38, 2540-2551.	1.1	20
4426	First-Principles Phase Stability Calculations of Pseudobinary Alloys of (Al,Zn)3Ti with L12, D022, and D023 Structures. Journal of Phase Equilibria and Diffusion, 2007, 28, 9-22.	0.5	21
4427	Asymmetric-dimerâ€“symmetric-dimer mixed phase on tensile-strained Si(001) surface. Computer Physics Communications, 2007, 177, 42.	3.0	0
4428	Tuning catalytic properties of bimetallic surfaces: Oxygen adsorption on pseudomorphic Pt/Ru overlayers. Electrochimica Acta, 2007, 52, 2219-2228.	2.6	93
4429	Nitrogen complex species and its chemical nature in TiO2 for visible-light sensitized photocatalysis. Chemical Physics, 2007, 339, 57-63.	0.9	214
4430	Structural features of silicon clusters (). Physics Letters, Section A: General, Atomic and Solid State Physics, 2007, 368, 396-401.	0.9	19
4431	Analytic bond-order potentials for modelling the growth of semiconductor thin films. Progress in Materials Science, 2007, 52, 196-229.	16.0	29
4432	An ab initio analysis of adsorption and diffusion of silver atoms on alumina surfaces. Surface Science, 2007, 601, 134-145.	0.8	55
4433	Surface structure of K/Pd(100) and the effect of H coadsorption: Density functional theory calculations. Surface Science, 2007, 601, 852-857.	0.8	3
4434	Correlations between magnetic properties and bond formation in Rhâ€“MgO(001). Surface Science, 2007, 601, 1218-1230.	0.8	4
4435	Effect of hydrogenation on P/Si(001)-(1Ã—2). Surface Science, 2007, 601, 1489-1493.	0.8	3
4436	A multi-scale Monte Carlo study of oxide structures on the Cu(100) surface. Surface Science, 2007, 601, 1813-1821.	0.8	6
4437	Structural properties of oxygen on InN(0001) surface. Surface Science, 2007, 601, 2161-2165.	0.8	11
4438	Effect of hydrogenation on B/Si(001)-(1Ã—2). Surface Science, 2007, 601, 3711-3716.	0.8	2
4439	Local reactivity of ultrathin platinum overlayers and surface alloys on a gold surface. Surface Science, 2007, 601, 3702-3706.	0.8	23

#	Article	IF	Citations
4440	Towards hybrid silicon-organic molecular electronics: The stability of acetone on the Si(001) surface. Surface Science, 2007, 601, 5757-5761.	0.8	6
4441	The growth of epitaxial VN(111) nanolayer surfaces. Surface Science, 2007, 601, 4817-4823.	0.8	21
4442	The surface stress of the (110) and (100) surfaces of rutile and the effect of water adsorbents. Surface Science, 2007, 601, 4824-4836.	0.8	36
4443	A density functional theory study of formaldehyde adsorption on ceria. Surface Science, 2007, 601, 4993-5001.	0.8	44
4444	Theoretical modelling of intermediate band solar cell materials based on metal-doped chalcopyrite compounds. Thin Solid Films, 2007, 515, 6280-6284.	0.8	96
4445	Structures and crystal chemistry of the double perovskites Ba2LnBâ€²O6 (Ln=lanthanide Bâ€²=Nb5+ and) Tj ETQq1 1 0.784314 rgBT /O Journal of Solid State Chemistry, 2007, 180, 2991-3000.	1.4	50
4446	First-principles study of structural and vibrational properties of crystalline silver azide under high pressure. Journal of Solid State Chemistry, 2007, 180, 3521-3528.	1.4	37
4447	Determination of vibrational energy levels and transition dipole moments of CO2 molecules by density functional theory. Journal of Molecular Spectroscopy, 2008, 252, 108-114.	0.4	5
4448	Quantum mechanical calculations of uranium phases and niobium defects in Î³-uranium. Journal of Nuclear Materials, 2008, 375, 113-119.	1.3	38
4449	Atomic diffusion mechanism of Xe in UO2. Journal of Nuclear Materials, 2008, 378, 40-44.	1.3	74
4450	Multiscale modelling of radiation damage and phase transformations: The challenge of FeCr alloys. Journal of Nuclear Materials, 2008, 382, 112-125.	1.3	127
4451	Formation of stable sessile interstitial complexes in reactions between glissile dislocation loops in bcc Fe. Journal of Nuclear Materials, 2008, 382, 126-133.	1.3	36
4452	Free standing double walled boron nanotubes. Journal of Physics and Chemistry of Solids, 2008, 69, 2004-2012.	1.9	16
4453	On the mechanism of the zircon-reidite pressure induced transformation. Journal of Physics and Chemistry of Solids, 2008, 69, 2277-2280.	1.9	28
4454	High pressure study and bonding analysis of. Journal of Solid State Chemistry, 2008, 181, 2058-2064.	1.4	2
4455	Electron charge distribution of CaAl2â^'xZnx: Maximum entropy method combined with Rietveld analysis of high-resolution-synchrotron X-ray powder diffraction data. Journal of Solid State Chemistry, 2008, 181, 1998-2005.	1.4	7
4456	High-pressure modifications of CaZn2, SrZn2, SrAl2, and BaAl2: Implications for Laves phase structural trends. Journal of Solid State Chemistry, 2008, 181, 3016-3023.	1.4	22
4457	Probing the nano-scale with first-principles calculations. Materials Science and Engineering B: Solid-State Materials for Advanced Technology, 2008, 152, 109-113.	1.7	3

#	Article	IF	Citations
4458	ECR plasma assisted deposition of zinc nanowires. Nuclear Instruments & Methods in Physics Research B, 2008, 266, 4980-4986.	0.6	7
4459	Adsorption of chlorophenol on the Cu(111) surface: A first-principles density functional theory study. Applied Surface Science, 2008, 254, 4218-4224.	3.1	27
4460	Initial stages of hydration and Zn substitution/occupation on hydroxyapatite (0001) surfaces. Biomaterials, 2008, 29, 257-265.	5.7	73
4461	GGA+U modeling of structural, electronic, and magnetic properties of iron porphyrin-type molecules. Chemical Physics, 2008, 343, 47-60.	0.9	96
4462	Density-functional calculation of the adsorption and reaction of CO and H2O molecules over a 4Rh/CeO2(111) surface. Chemical Physics, 2008, 348, 161-168.	0.9	22
4463	Molecular and all-solid DFT studies of the magnetic and chemical bonding properties within KM[Cr(CN)6] (M=V, Ni) complexes. Chemical Physics, 2008, 352, 85-91.	0.9	5
4464	Rapid iterative method for electronic-structure eigenproblems using localised basis functions. Computer Physics Communications, 2008, 178, 128-134.	3.0	143
4465	Introducing PROFESS: A new program for orbital-free density functional theory calculations. Computer Physics Communications, 2008, 179, 839-854.	3.0	90
4466	Ab initio study of interfacial correlations in polymer electrolyte membranes for fuel cells at low hydration. Electrochimica Acta, 2008, 53, 6920-6927.	2.6	19
4467	Ab initio study on the Li deintercalation in ternary lithium nitridocuprate Li2.5Cu0.5N. Electrochimica Acta, 2008, 53, 7915-7920.	2.6	4
4468	First-principles study of MgB2 film on the MgO(111) polar surface. Physics Letters, Section A: General, Atomic and Solid State Physics, 2008, 372, 1671-1675.	0.9	9
4469	Distribution and magnetization of Co near the rutile TiO2 (110) surface: A first-principles study. Physics Letters, Section A: General, Atomic and Solid State Physics, 2008, 372, 2098-2102.	0.9	6
4470	Short-to-medium-range order in Mg65Cu25Y10 metallic glass. Physics Letters, Section A: General, Atomic and Solid State Physics, 2008, 372, 3078-3084.	0.9	28
4471	First-principle study of extrinsic defects in CuScO2 and CuYO2. Physics Letters, Section A: General, Atomic and Solid State Physics, 2008, 372, 3759-3762.	0.9	14
4472	Protonic defects in pure and doped La2Zr2O7 pyrochlore oxide. Solid State Ionics, 2008, 178, 1642-1647.	1.3	53
4473	Defect migration in fluorite-type tantalum oxynitrides: A first-principles study. Solid State Ionics, 2008, 179, 816-818.	1.3	10
4474	Monolayer bimetallic surfaces: Experimental and theoretical studies of trends in electronic and chemical properties. Surface Science Reports, 2008, 63, 201-254.	3.8	472
4475	Elucidation of the low coverage chiral adsorption assembly of l-lysine on Cu(110) surface: A theoretical study. Surface Science, 2008, 602, 1032-1039.	0.8	29

#	Article	IF	Citations
4476	Selective thermal reduction of single-layer MoO3 nanostructures on Au(111). Surface Science, 2008, 602, 1166-1174.	0.8	52
4477	Peierls instability in Pt chains on Ge(001). Surface Science, 2008, 602, 1731-1735.	0.8	53
4478	H2S dissociation on the Fe(100) surface: An ab initio molecular dynamics study. Surface Science, 2008, 602, 1547-1553.	0.8	32
4479	2-Chlorophenol adsorption on Cu(100): First-principles density functional study. Surface Science, 2008, 602, 1554-1562.	0.8	14
4480	DFT characterization of adsorption and diffusion mechanisms of H, As, S, and Se on the zinc orthotitanate(010) surface. Surface Science, 2008, 602, 1877-1882.	0.8	2
4481	First-principles study of a single C60 cluster adsorbed on KBr(100). Surface Science, 2008, 602, 1916-1920.	0.8	3
4482	Effect of hydrocarbon chain length and cyclization on the adsorption strength of unsaturated hydrocarbons on Pt/3d bimetallic surfaces. Surface Science, 2008, 602, 2513-2523.	0.8	18
4483	First-principles studies of H2S adsorption and dissociation on metal surfaces. Surface Science, 2008, 602, 2758-2768.	0.8	161
4484	Reversed surface segregation in palladium-silver alloys due to hydrogen adsorption. Surface Science, 2008, 602, 2840-2844.	0.8	75
4485	Investigation of submonolayer SiOX species formed from oxidation of silane on Pt(111). Surface Science, 2008, 602, 3225-3231.	0.8	7
4486	Surface termination effects on metal atom adsorption on Î±-alumina. Surface Science, 2008, 602, 3445-3453.	0.8	31
4487	Interaction of acetone with the Si(001) surface. Surface Science, 2008, 602, 3484-3498.	0.8	11
4488	CO oxidation with Pt(111) supported on pure and boron-doped carbon: A DFT investigation. Surface Science, 2008, 602, 3595-3602.	0.8	35
4489	Density functional theory studies of submonolayer oxidized silicon structures on Pd(111) and Pt(111). Surface Science, 2008, 602, 3603-3610.	0.8	4
4490	A test of empirical correction to site preference: DFT calculations for CO adsorption on Co(0001) surface. Computational and Theoretical Chemistry, 2008, 864, 68-71.	1.5	7
4491	Effect of chlorine doping on electrical and optical properties of ZnO thin films. Thin Solid Films, 2008, 516, 8146-8149.	0.8	55
4492	Synthesis and specific features of the structure of the mixed anionic six-coordinate silicon complexes with the (O,O)-dianionic and (C,O)-monoanionic chelate ligands. Russian Chemical Bulletin, 2008, 57, 2093-2100.	0.4	8
4493	Ab initio DFT study of ideal shear strength of polytypes of silicon carbide. Strength of Materials, 2008, 40, 2-6.	0.2	7

#	Article	IF	Citations
4494	Gamma-alumina: An Active Support to Obtain Immobilized Electron Poor Zr Complexes. Topics in Catalysis, 2008, 48, 114-119.	1.3	11
4495	Hydrocarbon Selective Oxidation on Vanadium Phosphorus Oxide Catalysts: Insights from Electronic Structure Calculations. Topics in Catalysis, 2008, 50, 116-123.	1.3	7
4496	Ferroelectric distortion and electronic structure in Bi4Ti3O12. Journal of Electroceramics, 2008, 21, 49-54.	0.8	17
4497	Ab initio investigation of twin boundary motion in the magnetic shape memory Heusler alloy Ni2MnGa. Journal of Materials Science, 2008, 43, 3825-3831.	1.7	41
4498	Atomistic study of the effect of B addition in the FeAl compound. Journal of Materials Science, 2008, 43, 3867-3872.	1.7	19
4499	Electronic structures of ZnO(0001)-Zn and (000â¯1)-O polar surfaces. Journal of Materials Science: Materials in Electronics, 2008, 19, 229-233.	1.1	13
4500	Adsorption of transition metal atoms on the NiO(100) surface and on NiO/Ag(100) thin films. Theoretical Chemistry Accounts, 2008, 120, 575-582.	0.5	15
4501	Zn7Cu6: a magic cluster of brass?. Theoretical Chemistry Accounts, 2008, 120, 583-589.	0.5	9
4502	Density functional studies of coinage metal nanoparticles: scalability of their properties to bulk. Theoretical Chemistry Accounts, 2008, 120, 565-573.	0.5	61
4503	A model study of dickite intercalated with formamide and N-methylformamide. Physics and Chemistry of Minerals, 2008, 35, 299-309.	0.3	22
4504	First-principles simulation of high-pressure polymorphs in MgAl2O4. Physics and Chemistry of Minerals, 2008, 35, 381-386.	0.3	32
4505	The mechanism of Li, N dual-acceptor co-doped p-type ZnO. Applied Physics A: Materials Science and Processing, 2008, 91, 467-472.	1.1	39
4506	Theoretical study of adsorption and dissociation of NH3 on the Ir{110}(1Ã—2) surface. Science Bulletin, 2008, 53, 3169-3172.	4.3	5
4507	Structural, magnetic and redox properties of a new cathode material for Li-ion batteries: the iron-based metal organic framework. Ionics, 2008, 14, 279-283.	1.2	34
4508	Redox mechanism in the NiP2 electrode for Li-ion batteries: A DFT study coupled with local chemical bond analyses. Ionics, 2008, 14, 197-202.	1.2	8
4509	The first-principles design of ductile refractory alloys. Jom, 2008, 60, 61-65.	0.9	51
4510	The Mechanism of Zr and Hf in Reducing Radiation-Induced Segregation in 316 Stainless Steel. Metallurgical and Materials Transactions A: Physical Metallurgy and Materials Science, 2008, 39, 218-224.	1.1	13
4511	Phase Stability and Transformations in the Zr2Ni x Cu1â¯x Amorphous System. Metallurgical and Materials Transactions A: Physical Metallurgy and Materials Science, 2008, 39, 1847-1856.	1.1	16

#	Article	IF	Citations
4512	Phase stability in ferroelectric bismuth titanate: a first-principles study. Acta Crystallographica Section A: Foundations and Advances, 2008, 64, 368-375.	0.3	33
4513	Structures of 6H perovskites Ba₃CaSb₂O₉ and Ba₃SrSb₂O₉ determined by synchrotron X-ray diffraction, neutron powder diffraction and ab initio calculations. Acta Crystallographica Section B: Structural Science, 2008, 64, 154-159.	1.8	8
4514	Structure and electron density of oxysulfide Sm₂Ti₂S₂O_{4.9}, a visible-light-responsive photocatalyst. Acta Crystallographica Section B: Structural Science, 2008, 64, 291-298.	1.8	32
4515	Periodic density functional theory calculations of bulk and the (010) surface of goethite. Geochemical Transactions, 2008, 9, 4.	1.8	72
4516	A cyberenvironment for crystallography and materials science and an integrated user interface to the Crystallography Open Database and Predicted Crystallography Open Database. Journal of Applied Crystallography, 2008, 41, 471-475.	1.9	2
4517	VESTA: a three-dimensional visualization system for electronic and structural analysis. Journal of Applied Crystallography, 2008, 41, 653-658.	1.9	4,545
4518	Understanding the properties of interfaces between organic selfâ€assembled monolayers and noble metalsâ€”a theoretical perspective. Surface and Interface Analysis, 2008, 40, 371-378.	0.8	41
4519	DFT study on the adsorption of NO on iron tapeâ€porphyrin. Surface and Interface Analysis, 2008, 40, 1082-1084.	0.8	9
4520	Firstâ€principles study of the (001) surface of cubic PbTiO₃. Surface and Interface Analysis, 2008, 40, 1382-1387.	0.8	18
4521	Unstable Singleâ€Layered Colloidal TiS₂ Nanodisks. Small, 2008, 4, 945-950.	5.2	85
4522	New Insight into Carbonâ€Nanotube Electronicâ€Structure Selectivity. Small, 2008, 4, 2035-2042.	5.2	21
4523	Filling the green gap: A firstâ€principles study of the LiMg_{1â€x}Zn_xN alloy. Physica Status Solidi C: Current Topics in Solid State Physics, 2008, 5, 2326-2328.	0.8	1
4524	DFT study for the anisotropic epitaxial growth of a-face ZnO(1120). Physica Status Solidi C: Current Topics in Solid State Physics, 2008, 5, 2726-2728.	0.8	4
4525	Electronic structure of oxygen deficient amorphous oxide semiconductor aâ€InGaZnO_{4â€“x}: Optical analyses and firstâ€principle calculations. Physica Status Solidi C: Current Topics in Solid State Physics, 2008, 5, 3098-3100.	0.8	214
4526	First principle MD study on the structural and electronic properties of liquid and amorphous NI₈₁B₁₉ and NI₈₀P₂₀ alloy. International Journal of Quantum Chemistry, 2008, 108, 370-377.	1.0	1
4527	Twistâ€dependent stacking energy of baseâ€pair steps in Bâ€DNA geometry: A density functional theory approach. International Journal of Quantum Chemistry, 2008, 108, 1173-1180.	1.0	12
4528	Ab initio modeling of noncontact atomic force microscopy imaging of benzene on Cu(110) surface. International Journal of Quantum Chemistry, 2008, 108, 2803-2812.	1.0	4
4529	Ab initio simulations of diluted magnetic semiconductors: cobaltâ€doped zinc oxide. Physica Status Solidi (A) Applications and Materials Science, 2008, 205, 1839-1846.	0.8	10

#	Article	IF	Citations
4530	DFT studies on structure, mechanics and phase behavior of magnetic shape memory alloys: Ni₂MnGa. Physica Status Solidi (A) Applications and Materials Science, 2008, 205, 1026-1035.	0.8	79
4531	Siâ€“SiO₂ interface bandâ€gap transition â€“ effects on MOS inversion layer. Physica Status Solidi (A) Applications and Materials Science, 2008, 205, 1290-1295.	0.8	29
4532	Interface electronic structures of zinc oxide and metals: Firstâ€principle study. Physica Status Solidi (A) Applications and Materials Science, 2008, 205, 1929-1933.	0.8	22
4533	Structure and energetics for an additional H absorbed into superionic phase of CsHSO₄ by a firstâ€principles study. Physica Status Solidi (B): Basic Research, 2008, 245, 657-665.	0.7	3
4534	Theoretical study of the CsMgH₃, Cs₂MgH₄ and Cs₄Mg₃H₁₀ complex hydrides from firstâ€principles. Physica Status Solidi (B): Basic Research, 2008, 245, 2749-2755.	0.7	3
4535	Electronic properties of durene crystals: Implications for charge transport. Physica Status Solidi (B): Basic Research, 2008, 245, 825-829.	0.7	4
4536	Density functional study of graphene overlayers on SiC. Physica Status Solidi (B): Basic Research, 2008, 245, 1425-1435.	0.7	48
4537	Firstâ€principles study of the (001) surface of cubic Ba_{0.5}Sr_{0.5}TiO₃. Physica Status Solidi (B): Basic Research, 2008, 245, 1147-1151.	0.7	1
4538	Ab initio study of hydrogen chemical adsorption on platinum surface/carbon nanotube join system. Physica Status Solidi (B): Basic Research, 2008, 245, 1546-1551.	0.7	7
4539	A comparison of polycrystalline elastic properties computed by analytic homogenization schemes and FEM. Physica Status Solidi (B): Basic Research, 2008, 245, 2630-2635.	0.7	23
4540	Multiscale simulation of polycrystal mechanics of textured Î²â€Ti alloys using ab initio and crystalâ€based finite element methods. Physica Status Solidi (B): Basic Research, 2008, 245, 2642-2648.	0.7	26
4541	Error propagation in multiscale approaches to the elasticity of polycrystals. Physica Status Solidi (B): Basic Research, 2008, 245, 2636-2641.	0.7	15
4542	Boron doped graphene nanostructures. Physica Status Solidi (B): Basic Research, 2008, 245, 2077-2081.	0.7	15
4543	The electronic band structure of fullereneâ€cubane cocrystals. Physica Status Solidi (B): Basic Research, 2008, 245, 2018-2021.	0.7	3
4544	Phonon dispersion of small diameter semiconducting chiral carbon nanotubes â€“ a theoretical study. Physica Status Solidi (B): Basic Research, 2008, 245, 2137-2140.	0.7	8
4545	Theoretical study of the electronic structure and the totally symmetric vibrations of selected CoMoCat carbon nanotubes. Physica Status Solidi (B): Basic Research, 2008, 245, 2141-2144.	0.7	2
4546	Red Ionic Waterâ€Soluble Imidazoliumâ€Containing Polydiacetylene. Macromolecular Rapid Communications, 2008, 29, 580-586.	2.0	7
4547	The Energetics of Large Deformations of a Single Polyimide Molecular Chain: DFT and MO Calculations. Macromolecular Theory and Simulations, 2008, 17, 488-495.	0.6	1

#	Article	IF	Citations
4548	The Elusive Structure of CrCl₂â€"A Combined Computational and Gasâ€Phase Electronâ€Diffraction Study. Chemistry - A European Journal, 2008, 14, 5130-5143.	1.7	20
4549	HPâ€Ca₂Si₅N₈â€"A New Highâ€Pressure Nitridosilicate: Synthesis, Structure, Luminescence, and DFT Calculations. Chemistry - A European Journal, 2008, 14, 7892-7902.	1.7	35
4550	DFT Study of Effects of Potassium Doping on Band Structure of Crystalline Cuprous Azide. Chinese Journal of Chemistry, 2008, 26, 2145-2149.	2.6	15
4551	Spiral Adsorbate Structures on Monoatomic Nanowire Electrodes. ChemPhysChem, 2008, 9, 1371-1374.	1.0	6
4552	Density Functional Investigations of Electronic Structure and Dehydrogenation Reactions of Alâ€•and Siâ€Substituted Magnesium Hydride. ChemPhysChem, 2008, 9, 928-934.	1.0	32
4553	CO Adsorption on a LaNi₅ Hydrogen Storage Alloy Surface: A Theoretical Investigation. ChemPhysChem, 2008, 9, 1564-1569.	1.0	5
4554	Spatial Effect of Cï£¿H Dipoles on the Electron Affinity of Diamondâ€‰(100)â€2Ã—1 Adsorbed with Organic Molecules. ChemPhysChem, 2008, 9, 1338-1344.	1.0	3
4555	Roomâ€Temperature Electronic Template Effect of the SmSi(111)â€8Ã—2 Interface for Selfâ€Alignment of Organic Molecules. ChemPhysChem, 2008, 9, 1437-1441.	1.0	20
4556	Evidence for a Sizeâ€Selective Adsorption Mechanism on Oxide Surfaces: Pd and Au atoms on SiO₂/Mo(112). ChemPhysChem, 2008, 9, 1367-1370.	1.0	31
4557	Ab initio study of electronic structure and optical properties of heavy-metal azides: TlN3, AgN3, and CuN3. Journal of Computational Chemistry, 2008, 29, 176-184.	1.5	74
4558	Electronic structure, chemical bonding, and geometry of pure and Srâ€doped CaCO₃. Journal of Computational Chemistry, 2008, 29, 343-349.	1.5	12
4559	Atomsâ€inâ€molecules analysis for planewave DFT calculationsâ€"A numerical approach on a successively interpolated charge density grid. Journal of Computational Chemistry, 2008, 29, 1306-1315.	1.5	11
4560	Firstâ€principles and molecularâ€dynamics study of structure and bonding in perovskiteâ€type oxynitrides ABO₂N (A = Ca, Sr, Ba; B = Ta, Nb). Journal of Computational Chemistry, 2008, 29, 2260-2267.	1.5	68
4561	Adsorption of benzene, fluorobenzene and metaâ€diâ€fluorobenzene on Cu(110): A computational study. Journal of Computational Chemistry, 2008, 29, 1589-1595.	1.5	17
4562	Analysis of electronic structures and chemical bonding of metalâ€rich compounds. I. Density functional study of Pt metal, LiPt₂, LiPt, and Li₂Pt. Journal of Computational Chemistry, 2008, 29, 2154-2160.	1.5	11
4563	A firstâ€principles DFT study of UN bulk and (001) surface: Comparative LCAO and PW calculations. Journal of Computational Chemistry, 2008, 29, 2079-2087.	1.5	40
4564	DFT calculations of quadrupolar solidâ€state NMR properties: Some examples in solidâ€state inorganic chemistry. Journal of Computational Chemistry, 2008, 29, 2279-2287.	1.5	52
4565	Highâ€precision calculation of Hartreeâ€Fock energy of crystals. Journal of Computational Chemistry, 2008, 29, 2098-2106.	1.5	25

#	Article	IF	Citations
4566	Abâ€initiosimulations of materials using VASP: Densityâ€functional theory and beyond. Journal of Computational Chemistry, 2008, 29, 2044-2078.	1.5	2,717
4567	Application of semiempirical longâ€range dispersion corrections to periodic systems in density functional theory. Journal of Computational Chemistry, 2008, 29, 2088-2097.	1.5	294
4568	A Major Advance in Crystal Structure Prediction. Angewandte Chemie - International Edition, 2008, 47, 2427-2430.	7.2	283
4569	An Atomistic Branching Mechanism for Carbon Nanotubes: Sulfur as the Triggering Agent. Angewandte Chemie - International Edition, 2008, 47, 2948-2953.	7.2	76
4570	Lattice Widening in Niobiumâ€Doped TiO₂ Nanotubes: Efficient Ion Intercalation and Swift Electrochromic Contrast. Angewandte Chemie - International Edition, 2008, 47, 7934-7937.	7.2	101
4571	Evaluation of Halfâ€Heusler Compounds as Thermoelectric Materials Based on the Calculated Electrical Transport Properties. Advanced Functional Materials, 2008, 18, 2880-2888.	7.8	486
4572	Transition Metal Borides: Superhard versus Ultraâ€incompressible. Advanced Materials, 2008, 20, 3620-3626.	11.1	467
4573	Tunable Magnetism in Carbonâ€ionâ€implanted Highly Oriented Pyrolytic Graphite. Advanced Materials, 2008, 20, 4679-4683.	11.1	103
4577	Atomic models of non-stoichiometric layered diborides M1â^'xB2 (M=Mg, Al, Zr and Nb) from first principles. Physica C: Superconductivity and Its Applications, 2008, 468, 2224-2228.	0.6	9
4578	First-principles investigations of Cr doping effects on electronic structure and magnetic properties in Sr2FeReO6. Physics Letters, Section A: General, Atomic and Solid State Physics, 2008, 372, 2911-2916.	0.9	6
4579	First-principles calculations for magnetic properties of Mn-doped GaN nanotubes. Physics Letters, Section A: General, Atomic and Solid State Physics, 2008, 372, 2688-2691.	0.9	14
4580	Structural evolution of Cu during rapid quenching by ab initio molecular dynamics. Physics Letters, Section A: General, Atomic and Solid State Physics, 2008, 372, 5831-5837.	0.9	26
4581	p-type doping of GaInNAs quaternary alloys. Physics Letters, Section A: General, Atomic and Solid State Physics, 2008, 373, 165-168.	0.9	6
4582	Interatomic potentials of the binary transition metal systems and some applications in materials physics. Physics Reports, 2008, 455, 1-134.	10.3	112
4583	Nanotwin formation and its physical properties and effect on reliability of copper interconnects. Microelectronic Engineering, 2008, 85, 2155-2158.	1.1	27
4584	Towards atomic-scale design: A theoretical investigation of magnetic nanoparticles and ultrathin films. Microelectronics Journal, 2008, 39, 184-189.	1.1	1
4585	Inelastic neutron scattering and DFT study of 1,6-anhydro-Î²-d-glucopyranose (levoglucosan). Journal of Molecular Structure, 2008, 874, 108-120.	1.8	9
4586	Ab initio calculations of phosphorus and arsenic clustering parameters for the improvement of process simulation models. Materials Science and Engineering B: Solid-State Materials for Advanced Technology, 2008, 154-155, 193-197.	1.7	11

#	Article	IF	Citations
4587	Ab-initio simulation of self-interstitial in germanium. Materials Science in Semiconductor Processing, 2008, 11, 328-331.	1.9	17
4588	Theoretical prediction of electronic structures and optical properties of Y-doped Î³-Si3N4. Physica B: Condensed Matter, 2008, 403, 2515-2520.	1.3	11
4589	Ab initio molecular-dynamics simulation of liquid alloys. Physica B: Condensed Matter, 2008, 403, 3302-3306.	1.3	6
4590	Surface regeneration of sulfur-poisoned Ni surfaces under SOFC operation conditions predicted by first-principles-based thermodynamic calculations. Journal of Power Sources, 2008, 176, 23-30.	4.0	67
4591	First-principles investigation of R2O3(ZnO)3 (R=Al, Ga, and In) in homologous series of compounds. Journal of Solid State Chemistry, 2008, 181, 137-142.	1.4	14
4592	On the correct spin lattice for the spin-gapped magnetic solid NH4CuPO4Â·H2O. Journal of Solid State Chemistry, 2008, 181, 276-281.	1.4	13
4593	A density-functional study on the stability of anatase-type phases in the system Mgâ€“Taâ€“Oâ€“N. Journal of Solid State Chemistry, 2008, 181, 2684-2689.	1.4	10
4594	Crystal structure and high-pressure studies of WAl2, an aluminide crystallizing with the CrSi2 structure type. Journal of Solid State Chemistry, 2008, 181, 2719-2724.	1.4	8
4595	An ab initio study of possible pathways in the thermal decomposition of NaAlH4. Journal of Solid State Chemistry, 2008, 181, 3037-3043.	1.4	10
4596	The effect of uniaxial stress on band structure and electron mobility of silicon. Mathematics and Computers in Simulation, 2008, 79, 1071-1077.	2.4	9
4597	Complexation of tris(pentafluorophenyl)silanes with neutral Lewis bases. Journal of Organometallic Chemistry, 2008, 693, 1005-1019.	0.8	19
4598	Alkali-metal lithium on graphite monolayer surface: Theoretical study. Journal of Physics and Chemistry of Solids, 2008, 69, 1158-1161.	1.9	6
4599	First-principles calculations for structural phase transition of LixFeS2. Journal of Physics and Chemistry of Solids, 2008, 69, 1353-1355.	1.9	3
4600	CoO under pressure from first principles. Journal of Physics and Chemistry of Solids, 2008, 69, 1698-1703.	1.9	18
4601	Electronic structure, phase stability, and hardness of the osmium borides, carbides, nitrides, and oxides: First-principles calculations. Journal of Physics and Chemistry of Solids, 2008, 69, 2096-2102.	1.9	54
4602	The effect of silicon impurities on the phase diagram of iron and possible implications for the Earth's core structure. Journal of Physics and Chemistry of Solids, 2008, 69, 2177-2181.	1.9	26
4603	The Na-adsorbed Ge(001) surface: Structure and STM image simulations. Applied Surface Science, 2008, 254, 4279-4285.	3.1	3
4604	A theoretical study of structural and electronic properties of a missing dimer defect on Si- and C-terminated SiC(0â€‰0â€‰1). Applied Surface Science, 2008, 254, 4357-4364.	3.1	0

#	Article	IF	Citations
4605	The adsorption of Be on the surface of (0001) InN. Applied Surface Science, 2008, 255, 2533-2537.	3.1	17
4606	Enhancement of optical second harmonic generation by nitrogen adsorption on Cu(001). Applied Surface Science, 2008, 255, 3289-3293.	3.1	1
4607	The electronic and reduction properties of Ce0.75Zr0.25O2(110). Chemical Physics Letters, 2008, 450, 286-291.	1.2	27
4608	Thermodynamically tuning LiBH4 by fluorine anion doping for hydrogen storage: A density functional study. Chemical Physics Letters, 2008, 450, 318-321.	1.2	101
4609	Field-assisted oxidation of rhodium. Chemical Physics Letters, 2008, 452, 133-138.	1.2	26
4610	Spin polarization study of benzene on Fe(100) at the initial stages of multilayer growth. Chemical Physics Letters, 2008, 452, 156-161.	1.2	5
4611	The adsorption with chiral structure of fluorene-1-carboxylic acid molecules on Cu(110) surface. Chemical Physics Letters, 2008, 452, 275-280.	1.2	6
4612	Evidence for spontaneous CO2 activation on cobalt surfaces. Chemical Physics Letters, 2008, 454, 262-268.	1.2	76
4613	First principles studies of adsorption of Pd, Ag, Pt, and Au on yttrium disilicide nanowires. Chemical Physics Letters, 2008, 454, 327-331.	1.2	3
4614	Surface segregation of core atoms in coreâ€“shell structures. Chemical Physics Letters, 2008, 456, 64-67.	1.2	43
4615	Magnetism in germanium-doped boron-nitride nanotubes. Chemical Physics Letters, 2008, 457, 169-173.	1.2	22
4616	Shape-controlled synthesis of silver nanoparticles: Ab initio study of preferential surface coordination with citric acid. Chemical Physics Letters, 2008, 458, 113-116.	1.2	199
4617	Local atomic structure and chemical bonding in liquid Te: An ab initio molecular-dynamics simulation. Chemical Physics Letters, 2008, 458, 101-107.	1.2	2
4618	Effect of pressure and temperature on structural stability of potential hydrogen storage compound Li3AlH6. Chemical Physics Letters, 2008, 460, 442-446.	1.2	8
4619	CH2I2 adsorption and dissociation on Ag(111) surface using density functional theory study. Chemical Physics Letters, 2008, 461, 47-52.	1.2	6
4620	Atomic modeling of surface photovoltage: Application to Si(1 1 1):H. Chemical Physics Letters, 2008, 461, 266-270.	1.2	23
4621	C60 as a chemical Faraday cage for three ferromagnetic Fe atoms. Chemical Physics Letters, 2008, 462, 72-74.	1.2	8
4622	First-principles theoretical analysis of dopant adsorption and diffusion on surfaces of ZnSe nanocrystals. Chemical Physics Letters, 2008, 462, 265-268.	1.2	3

#	Article	IF	Citations
4623	Clusters of hafnium, Hfn= 2â€“8. Chemical Physics Letters, 2008, 462, 183-187.	1.2	9
4624	Adsorption of the first row of transition metals on the perfect and defective MgO(100) surface. Chemical Physics Letters, 2008, 463, 106-111.	1.2	17
4625	Towards size-converged properties of model ceria nanoparticles: Monitoring by adsorbed CO using DFT +U approach. Chemical Physics Letters, 2008, 465, 106-109.	1.2	31
4626	Circumacenes versus periacenes: HOMOâ€“LUMO gap and transition from nonmagnetic to magnetic ground state with size. Chemical Physics Letters, 2008, 466, 72-75.	1.2	103
4627	An atomistic view of structural and electronic properties of rare earth ensembles on Si(001) substrates. Chemical Physics Letters, 2008, 466, 159-164.	1.2	8
4628	Ab initio study of magnetic properties of bimetallic Co1Mn and Co1V clusters. Chemical Physics Letters, 2008, 467, 114-119.	1.2	25
4629	A first-principles study on the bond characteristics in carbon containing Mo, Ag, or Al impurity atoms. Carbon, 2008, 46, 185-188.	5.4	31
4630	Ductility improvement of amorphous steels: Roles of shear modulus and electronic structure. Acta Materialia, 2008, 56, 88-94.	3.8	188
4631	The influence of interstitial distribution on phase stability and properties of hexagonal Îµ-Fe6Cx, Îµ-Fe6Ny and Îµ-Fe6CxNy phases: A first-principles calculation. Acta Materialia, 2008, 56, 719-725.	3.8	21
4632	Phase stabilities and thermal decomposition in the Zr1â^'Al N system studied by ab initio calculation and thermodynamic modeling. Acta Materialia, 2008, 56, 968-976.	3.8	77
4633	Thermodynamic analysis of the filling fraction limits for impurities in CoSb3 based on ab initio calculations. Acta Materialia, 2008, 56, 1733-1740.	3.8	38
4634	A critique of rhenium clustering in Niâ€“Re alloys using extended X-ray absorption spectroscopy. Acta Materialia, 2008, 56, 2669-2675.	3.8	65
4635	Cubic MgH2 stabilized by alloying with transition metals: A density functional theory study. Acta Materialia, 2008, 56, 2948-2954.	3.8	41
4636	First-principles calculations of the structural and thermodynamic properties of bcc, fcc and hcp solid solutions in the Alâ€“TM (TM=Ti, Zr and Hf) systems: A comparison of cluster expansion and supercell methods. Acta Materialia, 2008, 56, 3202-3221.	3.8	132
4637	Point defect thermodynamics and diffusion in Fe3C: A first-principles study. Acta Materialia, 2008, 56, 3236-3244.	3.8	26
4638	Theoretical investigation of typical fcc precipitates in Mg-based alloys. Acta Materialia, 2008, 56, 3353-3357.	3.8	43
4639	Effects of solute concentrations on kinetic pathways in Niâ€“Alâ€“Cr alloys. Acta Materialia, 2008, 56, 3422-3438.	3.8	71
4640	The effect of platinum on defect formation energies in Î²-NiAl. Acta Materialia, 2008, 56, 3502-3510.	3.8	37

#	Article	IF	Citations
4641	Atomic mobilities, diffusivities and simulation of diffusion growth in the Coâ€“Si system. Acta Materialia, 2008, 56, 3940-3950.	3.8	69
4642	Thermodynamic reassessment of the Niâ€“Ru system and assessment of the Alâ€“Niâ€“Ru system at 1273â€“1523 K using ab initio calculations. Acta Materialia, 2008, 56, 4062-4069.	3.8	17
4643	Mechanical instabilities and structural phase transitions: The cubic to tetragonal transformation. Acta Materialia, 2008, 56, 4226-4232.	3.8	38
4644	Influence of Pb segregation on the deformation of nanocrystalline Al: Insights from molecular simulations. Acta Materialia, 2008, 56, 4750-4761.	3.8	33
4645	GPB zones and composite GPB/GPBII zones in Alâ€“Cuâ€“Mg alloys. Acta Materialia, 2008, 56, 4804-4815.	3.8	131
4646	Lattice stability, elastic constants and macroscopic moduli of NiTi martensites from first principles. Acta Materialia, 2008, 56, 6232-6245.	3.8	200
4647	First-principles study of site occupancy of dilute 3d, 4d and 5d transition metal solutes in L10 TiAl. Acta Materialia, 2008, 56, 6224-6231.	3.8	49
4648	Mixed sites and promoter segregation: A DFT study of the manifestation of Le Chatelier's principle for the Co(Ni)MoS active phase in reaction conditions. Catalysis Today, 2008, 130, 160-169.	2.2	147
4649	Aging of Co(Ni)MoP/Al2O3 catalysts in working state. Catalysis Today, 2008, 130, 97-108.	2.2	78
4650	A DFT study of pseudomorphic monolayer Pt and Pd catalysts for NOx storage reduction applications. Catalysis Today, 2008, 136, 76-83.	2.2	24
4651	Transition metal sandwich molecules with large (Cn, nâ©¾24) zigzag poly aromatic hydrocarbons. Chemical Physics, 2008, 348, 69-82.	0.9	10
4652	Geometry, bonding and magnetism in planar triangulene graphene molecules with D3h symmetry: Zigzag (m=2,â€¦,15). Chemical Physics, 2008, 354, 1-15.	0.9	47
4653	First-principles study of the pressure-induced rutileâ€“CaCl2 phase transition in MgF2. Solid State Communications, 2008, 145, 283-287.	0.9	23
4654	Phase transformation in Sm2O3 at high pressure: In situ synchrotron X-ray diffraction study and ab initio DFT calculation. Solid State Communications, 2008, 145, 250-254.	0.9	59
4655	Electronic structures, lattice dynamics, and electronâ€“phonon coupling of simple cubic Ca under pressure. Solid State Communications, 2008, 146, 181-185.	0.9	41
4656	First-principles phase transition and equation of state of titanium. Solid State Communications, 2008, 146, 105-109.	0.9	25
4657	The elastic behavior in Ni monocrystal: Nonlinear effects. Solid State Communications, 2008, 146, 253-257.	0.9	10
4658	Chemical synthesis, structural elucidation and quantum-chemical modeling of a doped gallium oxynitride prepared by precursor nitridation. Solid State Communications, 2008, 147, 41-45.	0.9	16

#	Article	IF	Citations
4659	CO adsorption on magnetic Co(0001) surface: A study of density functional theory. Solid State Communications, 2008, 147, 152-156.	0.9	9
4660	Interaction of cholesterol with carbon nanotubes: A density functional theory study. Solid State Communications, 2008, 147, 146-151.	0.9	10
4661	Pushing p-type conductivity in ZnO by (Zr, N) codoping: A first-principles study. Solid State Communications, 2008, 147, 194-197.	0.9	32
4662	Energetic and electronic properties of hydrogen passivated ZnO nanowires. Solid State Communications, 2008, 148, 101-104.	0.9	10
4663	Hydrogen adsorption on hexagonal silicon nanotubes. Solid State Communications, 2008, 148, 469-471.	0.9	20
4664	Studies of the mechanism of electrical conduction in As-doped ZnO by structural and chemical-bonding analyses and first principle calculations. Solid State Communications, 2008, 148, 301-304.	0.9	15
4665	Elastic constants of B2-MgRE (REÂ= ÂSc, Y, Laâ€“Lu) calculated with first-principles. Solid State Communications, 2008, 148, 314-318.	0.9	54
4666	Interfacial fracture toughness of transition metal nitrides. Surface and Coatings Technology, 2008, 203, 598-601.	2.2	69
4667	Pt surface segregation in bimetallic Pt3M alloys: A density functional theory study. Surface Science, 2008, 602, 107-113.	0.8	202
4668	Adsorbate induced reconstruction of cobalt surfaces. Surface Science, 2008, 602, 17-27.	0.8	97
4669	Theory of quasicrystal surfaces: Probing the chemical reactivity by atomic and molecular adsorption. Surface Science, 2008, 602, 182-197.	0.8	7
4670	Adsorption and dissociation of methanol on the fully oxidized and partially reduced (111) cerium oxide surface: Dependence on the configuration of the cerium 4f electrons. Surface Science, 2008, 602, 162-175.	0.8	61
4671	SO2 and its fragments on a Cu(110) surface. Surface Science, 2008, 602, 321-344.	0.8	6
4672	DFT study of the Au(321) surface reconstruction by consecutive deposition of oxygen atoms. Surface Science, 2008, 602, 424-435.	0.8	22
4673	Density functional study of surface properties of chromium. Surface Science, 2008, 602, 517-524.	0.8	27
4674	Ab initio study of element segregation and oxygen adsorption on PtPd and CoCr binary alloy surfaces. Surface Science, 2008, 602, 876-884.	0.8	31
4675	A systematic density functional study of ordered sulfur overlayers on Cu(111) and Ag(111): Influence of the adsorbate coverage. Surface Science, 2008, 602, 906-913.	0.8	29
4676	Classical dynamics study of atomic oxygen sticking on the Î²-cristobalite (1 0 0) surface. Surface Science, 2008, 602, 975-985.	0.8	19

#	Article	IF	Citations
4677	Ab initio study of pentacene on the Fe(100) surface. Surface Science, 2008, 602, 1191-1198.	0.8	10
4678	Sensitivity of short-range trio interactions to lateral relaxation of adatoms: Challenges for detailed lattice-gas modeling. Surface Science, 2008, 602, 1243-1249.	0.8	11
4679	First-principles study of decomposition of NH3 on Ir(100). Surface Science, 2008, 602, 1288-1294.	0.8	50
4680	Atomic and electronic structures of Tl/Si(111)-. Surface Science, 2008, 602, 1376-1380.	0.8	12
4681	Self-assembly of adenine-dimer chains on Cu(110): Driving forces from first-principles calculations. Surface Science, 2008, 602, 1643-1649.	0.8	17
4682	H2O adsorption and dissociation on defective hematite (0001) surfaces: A DFT study. Surface Science, 2008, 602, 2047-2054.	0.8	55
4683	Formation mechanisms of polar and non-polar amorphous oxideâ€“semiconductor interfaces. Surface Science, 2008, 602, L74-L78.	0.8	10
4684	Oxygen adsorption on Zr(0001) surfaces: Density functional calculations and a multiple-layer adsorption model. Surface Science, 2008, 602, 2212-2216.	0.8	23
4685	Density functional theory study of NO on the Rh(100) surface. Surface Science, 2008, 602, 2189-2196.	0.8	21
4686	An atomic view of Fermi level pinning of Ge(100) by O2. Surface Science, 2008, 602, 2373-2381.	0.8	28
4687	First principles calculations of methylamine and methanol adsorption on hydroxylated quartz (0001). Surface Science, 2008, 602, 2478-2485.	0.8	25
4688	Lateral electronic confinement in unidimensional noble metal (Au, Pt) nanowires. Surface Science, 2008, 602, L104-L107.	0.8	4
4689	Adsorption of an organic zwitterion on a Si(111)-7Ã—7 surface at room temperature. Surface Science, 2008, 602, 2719-2723.	0.8	14
4690	The chemistry of chlorine on Ag(1 1 1) over the sub-monolayer range: A density functional theory investigation. Surface Science, 2008, 602, 2639-2642.	0.8	9
4691	Atomic structure and electronic properties of Ni3Al(001) surface. Surface Science, 2008, 602, 2994-2999.	0.8	4
4692	DFT study of reconstructed Cu(100) surface with high oxygen coverages. Surface Science, 2008, 602, 3239-3245.	0.8	22
4693	Origin of chemoselective behavior of S-covered Cu(111) towards catalytic hydrogenation of unsaturated aldehydes. Surface Science, 2008, 602, 3284-3290.	0.8	20
4694	Formation of one-dimensional molybdenum oxide on Mo(112). Surface Science, 2008, 602, 3338-3342.	0.8	23

#	Article	IF	Citations
4695	Bonding of Pt/Fe overlayer and its effects on atomic oxygen chemisorption from density functional theory study. Surface Science, 2008, 602, 3415-3423.	0.8	15
4696	Oxygen adsorption and surface segregation in (211) surfaces of Pt(shell)/M(core) and Pt3M (M=Co, Ir) alloys. Surface Science, 2008, 602, 3531-3539.	0.8	37
4697	The role of preadsorbed sulphur and oxygen in O2 dissociation on Pd(100). Surface Science, 2008, 602, 3660-3666.	0.8	3
4698	Ethanol and ethylene glycol on Ni/Pt(111) bimetallic surfaces: A DFT and HREELS study. Surface Science, 2008, 602, 3578-3587.	0.8	81
4699	Analysis of defects on BN nano-structures using high-resolution electron microscopy and density-functional calculations. Ultramicroscopy, 2008, 108, 1484-1489.	0.8	4
4700	Enhancement of visible light-induced hydrophilicity on nitrogen and sulfur-codoped TiO2 thin films. Vacuum, 2008, 83, 683-687.	1.6	41
4701	Phase stabilities of self-organized nc-TiN/a-Si3N4 nanocomposites and of Ti1â^'xSixNy solid solutions studied by ab initio calculation and thermodynamic modeling. Thin Solid Films, 2008, 516, 2264-2275.	0.8	73
4702	Surface alloying in the Sn/Ni(111) system studied by synchrotron radiation photoelectron valence band spectroscopy and ab-initio density of states calculations. Thin Solid Films, 2008, 516, 2962-2965.	0.8	0
4703	Optical properties of chalcopyrite-type intermediate transition metal band materials from first principles. Thin Solid Films, 2008, 516, 7055-7059.	0.8	47
4704	Defects in Cu2O, CuAlO2 and SrCu2O2 transparent conducting oxides. Thin Solid Films, 2008, 516, 8130-8135.	0.8	54
4705	Super hard cubic phases of period VI transition metal nitrides: First principles investigation. Thin Solid Films, 2008, 517, 824-827.	0.8	72
4706	Role of hydrogen at germanium/dielectric interfaces. Thin Solid Films, 2008, 517, 144-147.	0.8	14
4707	Simulations of iodine adsorbed Ge(001) surface and its STM images. Applied Surface Science, 2008, 254, 4380-4385.	3.1	3
4708	Theoretical study of structural, optical and electrical properties of zirconium-doped zinc oxide. Applied Surface Science, 2008, 254, 6983-6986.	3.1	23
4709	Electronic structures and optical properties of Î³-Si3N4 doped with La. Physica B: Condensed Matter, 2008, 403, 2200-2206.	1.3	18
4710	First-principles study of structural stabilities and electronic properties of Mgâ€“Nd intermetallic compounds. Physica B: Condensed Matter, 2008, 403, 2344-2348.	1.3	19
4711	First-principles calculation of the elastic constants, the electronic density of states and the ductility mechanism of the intermetallic compounds: YAg, YCu and YRh. Physica B: Condensed Matter, 2008, 403, 3792-3797.	1.3	38
4712	Electronic structure and magnetic state of. Physica B: Condensed Matter, 2008, 403, 4232-4235.	1.3	11

#	Article	IF	Citations
4713	Ab initio investigation of perovskite and post-perovskite CaPtO3. Chemical Physics, 2008, 352, 92-96.	0.9	6
4714	Vibrational Stark tuning rates from periodic DFT calculations: CO/Pt(111). Electrochimica Acta, 2008, 53, 2897-2906.	2.6	13
4715	Multiscale modelling of nanoindentation test in copper crystal. Engineering Fracture Mechanics, 2008, 75, 3755-3762.	2.0	9
4716	Charge of self-interstitials and boron-interstitial pairs as a function of doping concentration. Materials Science and Engineering B: Solid-State Materials for Advanced Technology, 2008, 154-155, 198-201.	1.7	1
4717	Computer simulation study of defect formation and migration energy in calcium fluoride. Nuclear Instruments & Methods in Physics Research B, 2008, 266, 2698-2701.	0.6	8
4718	A first principles study of positively charged oxygen vacancies migration in pure and Ge-doped amorphous silica. Nuclear Instruments & Methods in Physics Research B, 2008, 266, 2719-2722.	0.6	0
4719	A new layer perovskites Pb2Ga2Nb2O10 and RbPb2Nb2O7: An efficient visible light driven photocatalysts to hydrogen generation. International Journal of Hydrogen Energy, 2008, 33, 6904-6912.	3.8	29
4720	Density Functional Theory studies of dehydrogenated and zwitterionic glycine and alanine on Pd and Cu surfaces. Journal of Molecular Catalysis A, 2008, 281, 44-48.	4.8	21
4721	Modeling extra framework aluminum (EFAL) formation in the zeolite ZSM-5 using parametric quantum and DFT methods. Journal of Molecular Catalysis A, 2008, 294, 93-101.	4.8	28
4722	The structural peculiarities and chemical bonding in three organogermanes Cl3GeCH2OC(O)R with rigid coordination centre. Journal of Molecular Structure, 2008, 875, 135-142.	1.8	15
4723	Ab initio study of the diffusion mechanisms of gallium in a silicon matrix. European Physical Journal B, 2008, 64, 165-172.	0.6	11
4724	Interplay of negative pressure and hydrogen chemical effects in CeRhSn from first principles. European Physical Journal B, 2008, 65, 491-498.	0.6	5
4725	Development of a ReaxFF description for gold. European Physical Journal B, 2008, 66, 75-79.	0.6	58
4726	Band-gap bowing and p-type doping of (Zn, Mg, Be)O wide-gap semiconductor alloys: a first-principles study. European Physical Journal B, 2008, 66, 439-444.	0.6	63
4727	Improved endohedral fullerenelike structures of silicon clusters Si31â€“Si39 by density functional calculations. European Physical Journal D, 2008, 47, 367-372.	0.6	4
4728	First principle study of free and surface terminated CdTe nanoparticles. European Physical Journal D, 2008, 48, 355-364.	0.6	28
4729	Influence of magnetism on the structural stability of cubic L21Ni2MnGa. European Physical Journal: Special Topics, 2008, 158, 193-198.	1.2	16
4730	Origin of Negative Differential Resistance in a Strongly Coupled Single Molecule-Metal Junction Device. Physical Review Letters, 2008, 100, 246801.	2.9	82

#	Article	IF	Citations
4731	Doping Graphene with Metal Contacts. Physical Review Letters, 2008, 101, 026803.	2.9	2,247
4732	Equation of state for diamond in wide ranges of pressure and temperature. Journal of Applied Physics, 2008, 104, .	1.1	17
4733	Superlattice structures of graphene-based armchair nanoribbons. Physical Review B, 2008, 78, .	1.1	148
4734	The Theory and Interpretation of Electron Energy Loss Near-Edge Fine Structure. Annual Review of Materials Research, 2008, 38, 535-558.	4.3	46
4735	Hydrogen spillover in the context of hydrogen storage using solid-state materials. Energy and Environmental Science, 2008, 1, 338.	15.6	133
4736	Structural properties and enthalpy of formation of magnesium hydride from quantum Monte Carlo calculations. Physical Review B, 2008, 77, .	1.1	72
4737	Hydrogen vacancies facilitate hydrogen transport kinetics in sodium hydride nanocrystallites. Physical Review B, 2008, 78, .	1.1	26
4738	A first-principles study of molecular oxygen dissociation at an electrode surface: a comparison of potential variation and coadsorption effects. Physical Chemistry Chemical Physics, 2008, 10, 3613.	1.3	76
4739	Atomic dynamics of i-ScZnMg and its 1/1 approximant phase: Experiment and simulation. Philosophical Magazine, 2008, 88, 2311-2318.	0.7	8
4740	Functionalization of carbon-based nanostructures with light transition-metal atoms for hydrogen storage. Physical Review B, 2008, 77, .	1.1	315
4741	The Importance of Strong Carbonâ^'Metal Adhesion for Catalytic Nucleation of Single-Walled Carbon Nanotubes. Nano Letters, 2008, 8, 463-468.	4.5	269
4742	Microscopic mechanisms for improper ferroelectricity in multiferroic perovskites: a theoretical review. Journal of Physics Condensed Matter, 2008, 20, 434208.	0.7	52
4743	First-principles study of metal adatom adsorption on graphene. Physical Review B, 2008, 77, .	1.1	1,245
4744	Work function changes induced by deposition of ultrathin dielectric films on metals: A theoretical analysis. Physical Review B, 2008, 78, .	1.1	180
4745	First-principles calculations of carbon nanotubes adsorbed on diamond (100) surfaces. Journal of Physics Condensed Matter, 2008, 20, 225016.	0.7	7
4746	Thermal stability of graphene edge structure and graphene nanoflakes. Journal of Chemical Physics, 2008, 128, 094707.	1.2	82
4747	Glass-transition behavior of Ni: Calculation, prediction, and experiment. Journal of Applied Physics, 2008, 104, .	1.1	32
4748	Spin-orbit interaction in Au structures of various dimensionalities. Applied Physics Letters, 2008, 92, 023115.	1.5	12

#	Article	IF	Citations
4749	Density functional study of<mml:math xmlns:mml="http://www.w3.org/1998/Math/MathML" display="inline"><mml:mrow><mml:mrow><mml:mo>âŸ¨</mml:mo><mml:mrow><mml:mn>110</mml:mn></mml:mrow><mml:mo>âŸ© thin silicon nanowires. Physical Review B, 2008, 77, .	1.1	27
4750	Modeling the interplay of inter- and intramolecular hydrogen bonding in conformational polymorphs. Journal of Chemical Physics, 2008, 128, 244708.	1.2	83
4751	Configurational thermodynamics of alloys from first principles: effective cluster interactions. Reports on Progress in Physics, 2008, 71, 046501.	8.1	264
4752	Chromium Aromatic Hydrocarbon Sandwich Molecules and the Eighteen-Electron Rule. Journal of Physical Chemistry A, 2008, 112, 2034-2042.	1.1	12
4753	Firstâ€principles study on the concentrations of native point defects in highâ€dielectricâ€constant binary oxide materials. Physica Status Solidi - Rapid Research Letters, 2008, 2, 227-229.	1.2	14
4754	A first-principles studies on TlX (X=P, As). Open Physics, 2008, 6, .	0.8	13
4755	A theoretical study of the dissociative chemisorption of hydrogen on carbon nanotubes. Russian Journal of Physical Chemistry A, 2008, 82, 2117-2121.	0.1	6
4756	A DFT study of hydrogen chemisorption on V (100) surfaces. Russian Journal of Physical Chemistry A, 2008, 82, 2354-2361.	0.1	11
4757	Analysis of hydrogen adsorption in the bulk and on the surface of magnesium nanoparticles. Journal of Experimental and Theoretical Physics, 2008, 107, 126-132.	0.2	8
4758	Tight-binding Hamiltonian from first-principles calculations. Scientific Modeling and Simulation SMNS, 2008, 15, 81-95.	0.8	9
4759	Characterization of Bulk Structure in Zinc Orthotitanate: A Density Functional Theory and EXAFS Investigation. Journal of the American Ceramic Society, 2008, 91, 584-590.	1.9	17
4760	Thermochemical and Mechanical Stabilities of the Oxide Scale of ZrB₂+SiC and Oxygen Transport Mechanisms. Journal of the American Ceramic Society, 2008, 91, 1475-1480.	1.9	83
4761	Vacancyâ€Ordered Structure of Cubic Bismuth Oxide from Simulation and Crystallographic Analysis. Journal of the American Ceramic Society, 2008, 91, 2349-2356.	1.9	45
4762	Hydrous silicate melt at high pressure. Nature, 2008, 452, 983-986.	13.7	127
4763	Anatase TiO2 single crystals with a large percentage of reactive facets. Nature, 2008, 453, 638-641.	13.7	3,753
4764	Charge self-regulation upon changing the oxidation state of transition metals in insulators. Nature, 2008, 453, 763-766.	13.7	241
4765	New boron barrelenes and tubulenes. JETP Letters, 2008, 87, 489-493.	0.4	13
4766	Orientation-dependent ionization energies and interface dipoles in ordered molecular assemblies. Nature Materials, 2008, 7, 326-332.	13.3	564

#	Article	IF	Citations
4767	A complete representation of structureâ€“property relationships in crystals. Nature Materials, 2008, 7, 455-458.	13.3	99
4768	Dipole-directed assembly of lines of 1,5-dichloropentane on silicon substrates by displacement of surface charge. Nature Nanotechnology, 2008, 3, 222-228.	15.6	57
4769	Probing warm dense lithium by inelastic X-ray scattering. Nature Physics, 2008, 4, 940-944.	6.5	148
4770	A Fully Three-Dimensional Atomistic Quantum Mechanical Study on Random Dopant-Induced Effects in 25-nm MOSFETs. IEEE Transactions on Electron Devices, 2008, 55, 1720-1726.	1.6	8
4771	Selective promotion of different modes of methanol adsorption via the cation substitutional doping of a ZnO(101Â¯0) surface. Journal of Catalysis, 2008, 254, 325-331.	3.1	38
4772	Promoting O2 activation on noble metal surfaces. Journal of Catalysis, 2008, 254, 349-354.	3.1	23
4773	Mechanism of HCl oxidation (Deacon process) over RuO2. Journal of Catalysis, 2008, 255, 29-39.	3.1	169
4774	Active sites of olefin metathesis on molybdena-alumina system: A periodic DFT study. Journal of Catalysis, 2008, 256, 1-14.	3.1	53
4775	Non-localized charge compensation in zeolites: A periodic DFT study of cationic gallium-oxide clusters in mordenite. Journal of Catalysis, 2008, 255, 139-143.	3.1	34
4776	Correlating hydrogenation activity with binding energies of hydrogen and cyclohexene on M/Pt(111) (M = Fe, Co, Ni, Cu) bimetallic surfaces. Journal of Catalysis, 2008, 257, 297-306.	3.1	91
4777	Dimer saddle point searches to determine the reactivity of formate on Cu(111). Journal of Catalysis, 2008, 258, 44-51.	3.1	51
4778	The mechanism of propene oxidation to acrolein on iron antimony oxide. Journal of Catalysis, 2008, 259, 17-25.	3.1	14
4779	Catalyst size matters: Tuning the molecular mechanism of the waterâ€“gas shift reaction on titanium carbide based compounds. Journal of Catalysis, 2008, 260, 103-112.	3.1	81
4780	A DFT study of the origin of the HDS/HydO selectivity on Co(Ni)MoS active phases. Journal of Catalysis, 2008, 260, 276-287.	3.1	66
4781	A computational method to identify interstitial sites in complex materials. Scripta Materialia, 2008, 58, 739-742.	2.6	22
4782	Microstructure investigation of the 6H-type long-period stacking order phase in Mg97Y2Zn1 alloy. Scripta Materialia, 2008, 58, 807-810.	2.6	14
4783	Studies of magnetic interactions in Mn-doped Î²-Ga2O3 from first-principles calculations. Scripta Materialia, 2008, 58, 943-946.	2.6	30
4784	Formation of nonequilibrium phases and associated structural transitions in the Rhâ€“Ta system induced by ion beam mixing. Scripta Materialia, 2008, 59, 3-6.	2.6	10

#	Article	IF	Citations
4785	First-principles study of Co3(Al,W) alloys using special quasi-random structures. Scripta Materialia, 2008, 59, 1075-1078.	2.6	85
4786	The first-principles study on the LaN. Materials Chemistry and Physics, 2008, 108, 120-123.	2.0	95
4787	B3â€“B1 phase transition and pressure dependence of elastic properties of ZnS. Materials Chemistry and Physics, 2008, 111, 559-564.	2.0	30
4788	Synthesis, crystal and electronic structure of Li13Ag5Si6, a potential anode for Li-ion batteries. Solid State Sciences, 2008, 10, 5-11.	1.5	21
4789	Two novel Zintl compounds Na12Ge8Sn and Na15Ge8SnP: Single crystal and electronic structures. Solid State Sciences, 2008, 10, 525-532.	1.5	1
4790	Effects of Cu, N, and Li intercalation on the structural stability and electronic structure of cubic Cu3N. Solid State Sciences, 2008, 10, 1651-1657.	1.5	32
4791	Long-range antiferromagnetic interactions in<mml:math xmlns:mml="http://www.w3.org/1998/Math/MathML" display="inline"><mml:mrow><mml:msub><mml:mrow><mml:mtext>ZnFe</mml:mtext></mml:mrow><mml:mn>2</mml:mn></mml:m xmlns:mml="http://www.w3.org/1998/Math/MathML" display="inline"><mml:mrow><mml:msub><mml:mrow><mml:mtext>CdFe</mml:mtext></mml:mrow><mml:mn>2</mml:mn></mml:m Physical Review B, 2008, 78, .	1.1	46
4792	Marcasite vs. arsenopyrite structural choice in MN2 (M = Ir, Os and Rh) transition metal nitrides. Journal of Materials Chemistry, 2008, 18, 2090.	6.7	21
4793	Template Effects in Vinyl Acetate Synthesis on PdAu Surface Alloys: A Density Functional Theory Study. Journal of the American Chemical Society, 2008, 130, 14406-14407.	6.6	44
4794	Characterizing the Interaction of Pt and PtRu Clusters with Boron-Doped, Nitrogen-Doped, and Activated Carbon: Density Functional Theory Calculations and Parameterization. Journal of Physical Chemistry C, 2008, 112, 13607-13622.	1.5	60
4795	Location of Mg Cations in Mordenite Zeolite Studied by IR Spectroscopy and Density Functional Theory Simulations with a CO Adsorption Probe. Journal of Physical Chemistry A, 2008, 112, 1352-1358.	1.1	14
4796	First-principles supercell studies of the substitutional carbon in c-BN. Diamond and Related Materials, 2008, 17, 2025-2028.	1.8	3
4797	Electron Transport in a Ï€-Stacking Molecular Chain. Journal of Physical Chemistry B, 2008, 112, 2795-2800.	1.2	21
4798	Density functional theory studies of hydrostatic compression of crystalline ammonium perchlorate. Physical Chemistry Chemical Physics, 2008, 10, 7318.	1.3	33
4799	Spatial Carrier Confinement in Coreâ^'Shell and Multishell Nanowire Heterostructures. Nano Letters, 2008, 8, 3341-3344.	4.5	65
4800	Electronic and Magnetic Properties of Metal Phthalocyanines on Au(111) Surface: A First-Principles Study. Journal of Physical Chemistry C, 2008, 112, 13650-13655.	1.5	81
4801	O 2 evolution on a clean partially reduced rutile TiO2(110) surface and on the same surface precovered with Au1 and Au2: The importance of spin conservation. Journal of Chemical Physics, 2008, 129, 074705.	1.2	113
4802	Relativistic Effects and the Unique Low-Symmetry Structures of Gold Nanoclusters. ACS Nano, 2008, 2, 897-904.	7.3	128

#	Article	IF	Citations
4803	Bridging the temperature and pressure gaps: close-packed transition metal surfaces in an oxygen environment. Journal of Physics Condensed Matter, 2008, 20, 184021.	0.7	27
4804	Effective metal dispersion in pyridinelike nitrogen doped graphenes for hydrogen storage. Applied Physics Letters, 2008, 92, .	1.5	72
4805	Volume dependent magnetism in zinc-blende MnXâ€ˆ(X=N,P,As,Sb,Bi) compounds. Journal of Applied Physics, 2008, 103, .	1.1	5
4806	Chemisorption and Reactivity of CH_x (x = 0â€“4) on Feâ€“Co Alloy Surfaces. Journal of Physical Chemistry C, 2008, 112, 13642-13649.	1.5	13
4807	Plane-Wave DFT Investigations of the Adsorption, Diffusion, and Activation of CO on Kinked Fe(710) and Fe(310) Surfaces. Journal of Physical Chemistry C, 2008, 112, 10472-10489.	1.5	48
4808	Enhanced adsorption energy of Au1 and O2 on the stoichiometric TiO2(110) surface by coadsorption with other molecules. Journal of Chemical Physics, 2008, 128, 044714.	1.2	54
4809	Surfactant and Hydrocarbon Aggregates on Defective Graphite Surface: Structure and Dynamics. Journal of Physical Chemistry B, 2008, 112, 12954-12961.	1.2	31
4810	Computational Studies of the Adsorption and Diffusion of Hydrogen on Feâ€“Co Alloy Surfaces. Journal of Physical Chemistry C, 2008, 112, 3667-3678.	1.5	8
4811	Adsorption and Dissociation of CO on a Feâ€“Co Alloy (110) Surface:â€‰ A Theoretical Study. Journal of Physical Chemistry C, 2008, 112, 3679-3691.	1.5	13
4812	Atomic Scale Insights on Chlorinated Î³-Alumina Surfaces. Journal of the American Chemical Society, 2008, 130, 11030-11039.	6.6	61
4813	Hydrogen Activation on Silver:â€‰ A Computational Study on Surface and Subsurface Oxygen Species. Journal of Physical Chemistry C, 2008, 112, 1628-1635.	1.5	44
4814	Study of the Mechanism of Carbonization of Template in Silicon-Substituted Aluminophosphate Zeolite Crystals. Journal of Physical Chemistry C, 2008, 112, 11702-11706.	1.5	10
4815	Liâ€“Feâ€“Pâ€“O₂ Phase Diagram from First Principles Calculations. Chemistry of Materials, 2008, 20, 1798-1807.	3.2	621
4816	No Cage, No Tube: Relative Stabilities of Nanostructures. Journal of Physical Chemistry C, 2008, 112, 13200-13203.	1.5	11
4817	Enhanced Hydrogen Uptake and the Electronic Structure of Lithium-Doped Metalâ€“Organic Frameworks. Journal of Physical Chemistry C, 2008, 112, 9278-9284.	1.5	74
4818	Nonadiabaticity in the iron bcc to hcp phase transformation. Journal of Chemical Physics, 2008, 128, 104703.	1.2	25
4819	The AM05 density functional applied to solids. Journal of Chemical Physics, 2008, 128, 084714.	1.2	220
4820	Stoneâ€“Wales Defects in Single-Walled Boron Nitride Nanotubes:â€‰ Formation Energies, Electronic Structures, and Reactivity. Journal of Physical Chemistry C, 2008, 112, 1365-1370.	1.5	105

#	Article	IF	Citations
4821	Spin States of Zigzag-Edged MÃ¶bius Graphene Nanoribbons from First Principles. Journal of Physical Chemistry C, 2008, 112, 5348-5351.	1.5	27
4822	Ab initiocalculations of free-energy reaction barriers. Journal of Physics Condensed Matter, 2008, 20, 064211.	0.7	54
4823	Ab initio study of substitutional impurity atoms in 4H-SiC. Journal of Applied Physics, 2008, 104, .	1.1	15
4824	Lattice dynamics and Raman scattering from GaN:Mn crystals. Physical Review B, 2008, 77, .	1.1	11
4825	Enhanced Ferromagnetic Stability in Cu Doped Passivated GaN Nanowires. Nano Letters, 2008, 8, 1825-1829.	4.5	54
4826	Electronic transport properties of quantum-well states in ultrathin Pb (111) films. Physical Review B, 2008, 78, .	1.1	30
4827	Non-planar Dislocation Cores: A Ubiquitous Phenomenon Affecting Mechanical Properties of Crystalline Materials. Dislocations in Solids, 2008, , 439-514.	1.6	69
4828	Synthesis and characterization of nitrides of iridium and palladium. Journal of Materials Research, 2008, 23, 1-5.	1.2	141
4829	Quantum studies of light particle trapping, sticking, and desorption on metal and graphite surfaces. Journal of Chemical Physics, 2008, 128, 114704.	1.2	24
4830	Systematic investigation of the structure of the Si(553)-Au surface from first principles. Physical Review B, 2008, 77, .	1.1	27
4831	Nanoporous Si as an Efficient Thermoelectric Material. Nano Letters, 2008, 8, 3750-3754.	4.5	259
4832	Computational Study of BrÃ¸nsted Acidity of Faujasite. Effect of the Al Content on the Infrared OH Stretching Frequencies. Journal of Physical Chemistry C, 2008, 112, 19293-19301.	1.5	30
4833	Structural Understanding of Selfâ€Assembled Rare Earth Disilicide Nanostructures Via Scanning Probe Microscopy and First Principles Studies. Israel Journal of Chemistry, 2008, 48, 73-79.	1.0	3
4834	Magnetically induced ferroelectricity in orthorhombic manganites: Microscopic origin and chemical trends. Physical Review B, 2008, 78, .	1.1	96
4835	Electronic structure and magnetism of EuX (X = O, S, Se and Te): A first-principles investigation. Europhysics Letters, 2008, 83, 69001.	0.7	17
4836	Density functional studies of model cerium oxide nanoparticles. Physical Chemistry Chemical Physics, 2008, 10, 5730.	1.3	125
4837	Atomic and Electronic Structure of Cerium Oxide Stepped Model Surfaces. Journal of Physical Chemistry C, 2008, 112, 17643-17651.	1.5	40
4838	Phase transition and elastic constants of zirconium from first-principles calculations. Journal of Physics Condensed Matter, 2008, 20, 235230.	0.7	35

#	Article	IF	Citations
4839	Ab initiosupercell calculations on nitrogen-vacancy center in diamond: Electronic structure and hyperfine tensors. Physical Review B, 2008, 77, .	1.1	238
4840	Ferromagnetism induced by defect complex in Co-doped ZnO. Applied Physics Letters, 2008, 93, 132506.	1.5	51
4841	Ab initiostudy of a charged vacancy in yttrium aluminum garnet (Y₃Al₅O₁₂). Journal of Physics Condensed Matter, 2008, 20, 325212.	0.7	35
4842	Imaging the Phase Separation in Atomically Thin Buried<mml:math xmlns:mml="http://www.w3.org/1998/Math/MathML" display="inline"><mml:msub><mml:mi>SrTiO</mml:mi><mml:mn>3</mml:mn></mml:msub></mml:math>Layers by Electron Channeling. Physical Review Letters, 2008, 100, 036101.	2.9	32
4843	Origin of incommensurate modulations in the high-pressure phosphorus IV phase. Physical Review B, 2008, 78, .	1.1	24
4844	Defect energetics in ZnO: A hybrid Hartree-Fock density functional study. Physical Review B, 2008, 77, .	1.1	655
4845	Proximity of antiferromagnetism and superconductivity in<mml:math xmlns:mml="http://www.w3.org/1998/Math/MathML" display="inline"><mml:mrow><mml:msub><mml:mrow><mml:mtext>LaFeAsO</mml:mtext></mml:mrow><mml:mrow><mml:mn>1</mml:m Effective Hamiltonian fromab initiostudies. Physical Review B, 2008, 77, .	1.1	245
4846	Stability of MgO(111) Polar Surface:â€‰ Effect of the Environment. Journal of Physical Chemistry C, 2008, 112, 3327-3333.	1.5	26
4847	First-Principle Calculations of the Adsorption, Dissociation and Diffusion of Hydrogen on the Mg(0001) Surface. Acta Physico-chimica Sinica, 2008, 24, 55-60.	0.6	34
4848	The optical phonon spectrum of SmFeAsO. Europhysics Letters, 2008, 84, 67013.	0.7	27
4849	Phase Diagrams for Systems with Low Free Energy Variation:â€‰ A Coupled Theory/Experiments Method Applied to Li-Graphite. Journal of Physical Chemistry C, 2008, 112, 3982-3988.	1.5	37
4850	Scattering potentials at Si-Ge and Sn-Ge impurity dimers on Ge(001) studied by scanning tunneling microscopy andab initiocalculations. Physical Review B, 2008, 78, .	1.1	3
4851	Evolutionary crystal structure prediction as a tool in materials design. Journal of Physics Condensed Matter, 2008, 20, 064210.	0.7	89
4852	Effect of packing on the cohesive and electronic properties of methanofullerene crystals. Physical Review B, 2008, 78, .	1.1	38
4853	Nondilute diffusion from first principles: Li diffusion in<mml:math xmlns:mml="http://www.w3.org/1998/Math/MathML" display="inline"><mml:mrow><mml:msub><mml:mrow><mml:mtext>Li</mml:mtext></mml:mrow><mml:mi>x</mml:mi></mml:msub> Physical Review B, 2008, 78, .	1.1	224
4854	Entropy Driven Stabilization of Energetically Unstable Crystal Structures Explained from First Principles Theory. Physical Review Letters, 2008, 100, 095901.	2.9	331
4855	Problems with reconciling density functional theory calculations with experiment in ferropnictides. Physical Review B, 2008, 78, .	1.1	352
4856	Analysis of the Spin Lattice Model for the Spin-Gapped Layered Compounds Na3Cu2SbO6 and Na2Cu2TeO6 on the Basis of Electronic Structure Calculations. Inorganic Chemistry, 2008, 47, 128-133.	1.9	50

#	Article	IF	Citations
4857	Electrochemical Materials for PEM Fuel Cells: Insights from Physical Theory and Simulation. Modern Aspects of Electrochemistry, 2008, , 1-79.	0.2	3
4858	Large-scale density-functional calculations on silicon divacancies. Physical Review B, 2008, 77, .	1.1	44
4859	Electronic, Energetic, and Chemical Effects of Intrinsic Defects and Fe-Doping of CoAl₂O₄: A DFT+UStudy. Journal of Physical Chemistry C, 2008, 112, 12044-12050.	1.5	75
4860	Electric Field Control of Structure, Dimensionality, and Reactivity of Gold Nanoclusters on Metal-Supported MgO Films. Physical Review Letters, 2008, 100, 056102.	2.9	58
4861	Electronic Nature of Step-Edge Barriers against Adatom Descent on Transition-Metal Surfaces. Physical Review Letters, 2008, 101, 216101.	2.9	27
4862	Magnetic phase transition in two-phase multiferroics predicted from first principles. Physical Review B, 2008, 78, .	1.1	126
4863	Magnetoelectric effect at the<mml:math xmlns:mml="http://www.w3.org/1998/Math/MathML" display="inline"><mml:mrow><mml:msub><mml:mrow><mml:mtext>Fe</mml:mtext></mml:mrow><mml:mn>3</mml:mn> interface: A first-principles study. Physical Review B, 2008, 78, .	1.1	155
4864	A Computational Study on Adsorption Configurations and Dissociative Reactions of the HN3 Molecule on the TiO2 Anatase (101) Surface. Journal of Physical Chemistry C, 2008, 112, 18017-18027.	1.5	7
4865	Chromium and tantalum site substitution patterns in Ni3Al(L12)â€Î³â€²-precipitates. Applied Physics Letters, 2008, 93, .	1.5	86
4866	Bi₅FeTi₃O₁₅ Hierarchical Microflowers: Hydrothermal Synthesis, Growth Mechanism, and Associated Visible-Light-Driven Photocatalysis. Journal of Physical Chemistry C, 2008, 112, 17835-17843.	1.5	85
4867	Determination of the structure of the high-pressure phase of AuAl₂with the help of first-principles calculations. Journal of Physics Condensed Matter, 2008, 20, 325215.	0.7	5
4868	First principles calculations of the formation energy and deep levels associated with the neutral and charged vacancy in germanium. Journal of Applied Physics, 2008, 103, .	1.1	25
4869	Calcium as the Superior Coating Metal in Functionalization of Carbon Fullerenes for High-Capacity Hydrogen Storage. Physical Review Letters, 2008, 100, 206806.	2.9	391
4870	Point defects and clustering in uranium dioxide by<mml:math xmlns:mml="http://www.w3.org/1998/Math/MathML" display="inline"><mml:mrow><mml:mi>LSDA</mml:mi><mml:mo>+</mml:mo><mml:mi mathvariant="normal">U</mml:mi></mml:mrow></mml:math>calculations. Physical Review B, 2008, 77,	1.1	100
4871	Stability of Hydroxylated (1ì„11) and (1ì„01) Surfaces of Monoclinic Zirconia:â€‰ A Combined Study by DFT and Infrared Spectroscopy. Journal of Physical Chemistry C, 2008, 112, 6469-6476.	1.5	68
4872	Electrocatalytic Properties of PtBi and PtPb Intermetallic Line Compounds via DFT: CO and H Adsorption. Journal of Physical Chemistry C, 2008, 112, 8266-8275.	1.5	31
4873	Magnetic properties of carbon doped CdS: A first-principles and Monte Carlo study. Physical Review B, 2008, 77, .	1.1	147
4874	Theoretical prediction of perfect spin filtering at interfaces between close-packed surfaces of Ni or Co and graphite or graphene. Physical Review B, 2008, 78, .	1.1	186

#	Article	IF	Citations
4875	Optical absorption spectra of doped and codoped Si nanocrystallites. Physical Review B, 2008, 78, .	1.1	31
4876	Tight-binding Hamiltonian from first-principles calculations. Lecture Notes in Computational Science and Engineering, 2008, , 81-95.	0.1	1
4877	Sources of Electrical Conductivity in<mml:math xmlns:mml="http://www.w3.org/1998/Math/MathML" display="inline"><mml:msub><mml:mi>SnO</mml:mi><mml:mn>2</mml:mn></mml:msub></mml:math>. Physical Review Letters, 2008, 101, 055502.	2.9	352
4878	Origins of band-gap renormalization in degenerately doped semiconductors. Physical Review B, 2008, 78, .	1.1	282
4879	Hydrides as materials for semiconductor electronics. Philosophical Magazine, 2008, 88, 2461-2476.	0.7	33
4880	Boron-Based Organometallic Nanostructures:â€‰ Hydrogen Storage Properties and Structure Stability. Nano Letters, 2008, 8, 157-161.	4.5	88
4881	A Periodic DFT Study of N₂O₄ Disproportionation on Alkali-Exchanged Zeolites X. Journal of Physical Chemistry C, 2008, 112, 5510-5519.	1.5	37
4882	Lotus Effect in Engineered Zirconia. Nano Letters, 2008, 8, 988-996.	4.5	64
4883	The sticking of H and D atoms on a graphite (0001) surface: The effects of coverage and energy dissipation. Journal of Chemical Physics, 2008, 128, 084702.	1.2	56
4884	Dynamics of Hydrogen Spillover on Carbon-Based Materials. Journal of Physical Chemistry C, 2008, 112, 17465-17470.	1.5	62
4885	Universal band gap modulation by radial deformation in semiconductor single-walled carbon nanotubes. Physical Review B, 2008, 78, .	1.1	27
4886	Stability of dislocation defect with two pentagon-heptagon pairs in graphene. Physical Review B, 2008, 78, .	1.1	101
4887	Magnetism and clustering in Cu doped ZnO. Applied Physics Letters, 2008, 92, 182509.	1.5	67
4888	Crystallographic phase transition and high-T_csuperconductivity in LaFeAsO:F. Superconductor Science and Technology, 2008, 21, 125028.	1.8	230
4889	F and F⁺ Centers on MgO/Ag(100) or MgO/Mo(100) Ultrathin Films:â€‰ Are They Stable?. Journal of Physical Chemistry C, 2008, 112, 3857-3865.	1.5	31
4890	Ab initiomolecular dynamics simulations on structure change of liquid Te from normal- to supercooled-state. Journal of Physics Condensed Matter, 2008, 20, 335102.	0.7	2
4891	Phase stability and cohesive properties of Auâ€“Sn intermetallics: A first-principles study. Journal of Materials Research, 2008, 23, 1398-1416.	1.2	15
4892	Methane Activation and Oxygen Vacancy Formation over CeO₂ and Zr, Pd Substituted CeO₂ Surfaces. Journal of Physical Chemistry C, 2008, 112, 14955-14964.	1.5	180

#	Article	IF	Citations
4893	Pt(100)-Catalyzed Ammonia Oxidation Studied by DFT: Mechanism and Microkinetics. Journal of Physical Chemistry C, 2008, 112, 13554-13562.	1.5	107
4894	First-Principles Calculation of Self-Diffusion Coefficients. Physical Review Letters, 2008, 100, 215901.	2.9	231
4895	First Principles Study of Improper Ferroelectricity in<mml:math xmlns:mml="http://www.w3.org/1998/Math/MathML" display="inline"><mml:msub><mml:mi>TbMnO</mml:mi><mml:mn>3</mml:mn></mml:msub></mml:math>. Physical Review Letters, 2008, 101, 037210.	2.9	166
4896	Spin-Orbit Coupling and Ion Displacements in Multiferroic<mml:math xmlns:mml="http://www.w3.org/1998/Math/MathML" display="inline"><mml:msub><mml:mi>TbMnO</mml:mi><mml:mn>3</mml:mn></mml:msub></mml:math>. Physical Review Letters, 2008, 101, 037209.	2.9	171
4897	Migration of Ag in low-temperature Ag2S from first principles. Journal of Chemical Physics, 2008, 128, 014704.	1.2	26
4898	First-principles study of the geometric and electronic structure of<mml:math xmlns:mml="http://www.w3.org/1998/Math/MathML" display="inline"><mml:msub><mml:mi mathvariant="normal">Au</mml:mi><mml:mn>13</mml:mn></mml:msub></mml:math>clusters: Importance of the prism motif. Physical Review B, 2008, 77, .	1.1	43
4899	Structural Characterization and Thermoelectric Transport Properties of Uniform Single-Crystalline Lead Telluride Nanowires. Journal of Physical Chemistry C, 2008, 112, 11314-11318.	1.5	108
4900	Electronic structure of graphene and doping effect on<mml:math xmlns:mml="http://www.w3.org/1998/Math/MathML" display="inline"><mml:mrow><mml:msub><mml:mrow><mml:mtext>SiO</mml:mtext></mml:mrow><mml:mn>2</mml:mn></mml:msub></mml:mrow></mml:math>. Physical Review B, 2008, 78, .	1.1	138
4901	Light elements in the core: Effects of impurities on the phase diagram of iron. Geophysical Research Letters, 2008, 35, .	1.5	38
4902	Structural stability ofFe5Si3andNi2Sistudied by high-pressure x-ray diffraction andab initiototal-energy calculations. Physical Review B, 2008, 77, .	1.1	51
4903	Investigation of band inversion in (Pb,Sn)Te alloys usingab initiocalculations. Physical Review B, 2008, 77, .	1.1	47
4904	Water-Induced Negative Electron Affinity on Diamond (100). Journal of Physical Chemistry C, 2008, 112, 2487-2491.	1.5	35
4905	A peculiar bonding of sulphur at the Nb(001) surface. Europhysics Letters, 2008, 83, 26001.	0.7	8
4906	Molecular-Based Synthetic Approach to New Group IV Materials for High-Efficiency, Low-Cost Solar Cells and Si-Based Optoelectronics. Journal of the American Chemical Society, 2008, 130, 16095-16102.	6.6	79
4907	Boron nitride and carbon double-wall hetero-nanotubes: first-principles calculation of electronic properties. Nanotechnology, 2008, 19, 095707.	1.3	12
4908	Adsorption of diatomic molecules on iron tape-porphyrin: A comparative study. Physical Review B, 2008, 77, .	1.1	26
4909	First-principles study of native defects and lanthanum impurities in<mml:math xmlns:mml="http://www.w3.org/1998/Math/MathML" display="inline"><mml:mrow><mml:msub><mml:mrow><mml:mtext>NaTaO</mml:mtext></mml:mrow><mml:mn>3</mml:mn></mml:msub></mml:mrow></mml:math>. Physical Review B, 2008, 78, .	1.1	58
4910	Quantum Confinement and Electronic Properties of Rutile TiO₂ Nanowires. Journal of Physical Chemistry C, 2008, 112, 20241-20245.	1.5	50

#	Article	IF	Citations
4911	Density Functional Study of Surface Passivation of Nonpolar Wurtzite CdSe Surfaces. Journal of Physical Chemistry C, 2008, 112, 20413-20417.	1.5	20
4912	Surface Properties and Dissolution Trends of Pt₃M Alloys in the Presence of Adsorbates. Journal of Physical Chemistry C, 2008, 112, 14520-14528.	1.5	99
4913	Optimization of metal dispersion in doped graphitic materials for hydrogen storage. Physical Review B, 2008, 78, .	1.1	111
4914	Electronic and magnetic properties of<mml:math xmlns:mml="http://www.w3.org/1998/Math/MathML" display="inline"><mml:mrow><mml:mn>3</mml:mn><mml:mi>d</mml:mi></mml:mrow></mml:math>transition-metal atom adsorbed graphene and graphene nanoribbons. Physical Review B, 2008, 77, .	1.1	452
4915	THEORETICAL ADVANCES IN THE ELECTRONIC AND ATOMIC STRUCTURES OF SILICON NANOTUBES AND NANOWIRES. , 2008, , 217-257.		2
4916	Thermodynamic stabilities of ternary metal borides: Anab initioguide for synthesizing layered superconductors. Physical Review B, 2008, 78, .	1.1	29
4917	Thermodynamics of the Formation of Ti- and Cr-doped CuGaS₂ Intermediate-band Photovoltaic Materials. Journal of Physical Chemistry C, 2008, 112, 9525-9529.	1.5	50
4918	Role of oxygen defects in diluted Mn:Ge. Physical Review B, 2008, 78, .	1.1	10
4919	Theoretical Description of Carrier Mediated Magnetism in Cobalt Doped ZnO. Physical Review Letters, 2008, 100, 256401.	2.9	261
4920	Molecular engineering of hybrid sensitizers incorporating an organic antenna into ruthenium complex and their application in solar cells. New Journal of Chemistry, 2008, 32, 2233.	1.4	39
4921	Spin-orbit split two-dimensional electron gas with tunable Rashba and Fermi energy. Physical Review B, 2008, 77, .	1.1	99
4922	N2O decomposition on iron exchanged ferrierite. A combined periodic DFT and static IN-SITU FTIR study. Studies in Surface Science and Catalysis, 2008, , 713-716.	1.5	0
4923	First Principles Calculation of Localized Surface Phonons and Electron-Phonon Interaction at Pb(111) Thin Films. Physical Review Letters, 2008, 100, 205501.	2.9	34
4924	Evaluation of first-principles techniques for obtaining materials parameters of<mml:math xmlns:mml="http://www.w3.org/1998/Math/MathML" display="inline"><mml:mi>Î±</mml:mi></mml:math>-uranium and the (001)<mml:math xmlns:mml="http://www.w3.org/1998/Math/MathML" display="inline"><mml:mi>Î±</mml:mi></mml:math>-uranium surface. Physical Review B, 2008, 77, .	1.1	93
4925	Energy-gap modulation of BN ribbons by transverse electric fields: First-principles calculations. Physical Review B, 2008, 77, .	1.1	272
4926	Effects of Hydrogen on the Radiation Response of Bipolar Transistors: Experiment and Modeling. IEEE Transactions on Nuclear Science, 2008, 55, 3039-3045.	1.2	18
4927	Adsorption of NO on Cu-SAPO-34 and Co-SAPO-34:â€‰ A Periodic DFT Study. Journal of Physical Chemistry C, 2008, 112, 2632-2639.	1.5	17
4928	Magneto-mechanical coupling behavior of defective single-walled carbon nanotubes. Nanotechnology, 2008, 19, 325701.	1.3	5

#	Article	IF	Citations
4929	Theoretical Insight into Faceted ZnS Nanowires and Nanotubes from Interatomic Potential and First-Principles Calculations. Journal of Physical Chemistry C, 2008, 112, 3509-3514.	1.5	37
4930	Manipulation and Control of Hydrogen Bond Dynamics in Absorbed Ice Nanoclusters. Physical Review Letters, 2008, 101, 136102.	2.9	64
4931	Hydroxyl Chain Formation on the Cu(110) Surface: Watching Water Dissociation. Journal of Physical Chemistry C, 2008, 112, 17672-17677.	1.5	52
4932	Wetting of mixed OHâˆ•H2O layers on Pt(111). Journal of Chemical Physics, 2008, 128, 074701.	1.2	37
4933	Agâˆ•PbTe(111) interface behavior studied by photoemission spectroscopy. Applied Physics Letters, 2008, 92, 122112.	1.5	10
4934	Tailor-Made Force Fields for Crystal-Structure Prediction. Journal of Physical Chemistry B, 2008, 112, 9810-9829.	1.2	129
4935	Effect of dopants on grain boundary decohesion of Ni: A first-principles study. Applied Physics Letters, 2008, 93, .	1.5	48
4936	Short-range and long-range contributions to the size effect in metal-ferroelectric-metal heterostructures. Physical Review B, 2008, 77, .	1.1	108
4937	Observation of Rotated-Oriented Attachment during the Growth of Ag₂S Nanorods under Mediation of Protein. Journal of Physical Chemistry B, 2008, 112, 9795-9801.	1.2	23
4938	Modeling doped and defective oxides in catalysis with density functional theory methods: Room for improvements. Journal of Chemical Physics, 2008, 128, 182505.	1.2	221
4939	Thermal Stability of Graphene and Nanotube Covalent Functionalization. Nano Letters, 2008, 8, 3315-3319.	4.5	91
4940	Design of Janus Nanoparticles with Atomic Precision: Tungsten-Doped Gold Nanostructures. ACS Nano, 2008, 2, 341-347.	7.3	37
4941	First-principles study of Schottky barrier formation of a semiconducting carbon nanotube-metal contact. , 2008, , .		0
4942	Chain metallicity and competition between paramagnetism and antiferromagnetism in underdoped<mml:math xmlns:mml="http://www.w3.org/1998/Math/MathML" display="inline"><mml:mrow><mml:msub><mml:mrow><mml:mtext>YBa</mml:mtext></mml:mrow><mml:mn>2</mml:mn></mml:ms A first principles de. Physical Review B, 2008, 78, .	1.1	13
4943	Substitution of Bi for Sb and its Role in the Thermoelectric Properties and Nanostructuring in Ag_{1â^'x}Pb₁₈MTe₂₀ (M = Bi, Sb) (x = 0, 0.14, 0.3). Chemistry of Materials, 2008, 20, 3512-3520.	3.2	76
4944	Multiple valley couplings in nanometer Si metalâ€“oxideâ€“semiconductor field-effect transistors. Journal of Applied Physics, 2008, 103, 124507.	1.1	4
4945	Honeycomb chain structure of theAuâˆ•Si(111)â^'(5Ã—2)surface reconstruction: A first-principles study. Physical Review B, 2008, 77, .	1.1	20
4946	First-principles study of a hybrid carbon material: Imperfect fullerenes covalently bonded to defective single-walled carbon nanotubes. Physical Review B, 2008, 77, .	1.1	22

#	Article	IF	Citations
4947	Polymorphism and hydrogen bonding in cinchomeronic acid: a variable temperature experimental and computational study. CrystEngComm, 2008, 10, 1404.	1.3	9
4948	Metal Ion Induced FRET OFFâ"ON in Tren/Dansyl-Appended Rhodamine. Organic Letters, 2008, 10, 213-216.	2.4	236
4949	Adsorption of 4-Mercaptopyridine on Au(111): A Periodic DFT Study. Langmuir, 2008, 24, 13985-13992.	1.6	50
4950	First-principles investigations of multimetallic transition metal clusters. Philosophical Magazine, 2008, 88, 2725-2738.	0.7	27
4951	Ab initiotheoretical study of magnetization and phase stability of the<mml:math xmlns:mml="http://www.w3.org/1998/Math/MathML" display="inline"><mml:mrow><mml:msub><mml:mrow><mml:mrow><mml:mo>(</mml:mo><mml:mrow><mml:mtext>Fe</mml:mtext> Physical Review B, 2008, 78, .	1.1	62
4952	Mechanics of silicon nanowires: size-dependent elasticity from first principles. Molecular Simulation, 2008, 34, 1-8.	0.9	37
4953	Native defects and oxygen and hydrogen-related defect complexes in CdTe: Density functional calculations. Journal of Applied Physics, 2008, 104, 093521.	1.1	50
4954	First-principles study of silicon nitride nanotubes. Physical Review B, 2008, 78, .	1.1	9
4955	On the origin of ferromagnetism in CeO2 nanocubes. Applied Physics Letters, 2008, 93, .	1.5	131
4956	Carbon diffusion around the edge region of nickel nanoparticles. Applied Physics Letters, 2008, 92, 043103.	1.5	22
4957	Hydrogen adsorption, dissociation and diffusion on the Î±-U(001) surface. Journal of Physics Condensed Matter, 2008, 20, 445001.	0.7	13
4958	Band structure engineering of graphene by strain: First-principles calculations. Physical Review B, 2008, 78, .	1.1	537
4959	Anomalous compressive behavior in CeO₂nanocubes under high pressure. New Journal of Physics, 2008, 10, 123016.	1.2	19
4960	Microscopic Description of Light Induced Defects in Amorphous Silicon Solar Cells. Physical Review Letters, 2008, 101, 265501.	2.9	38
4961	CO Oxidation by Rutile TiO₂(110) Doped with V, W, Cr, Mo, and Mn. Journal of Physical Chemistry C, 2008, 112, 12398-12408.	1.5	115
4962	Unique Activity of Platinum Adislands in the CO Electrooxidation Reaction. Journal of the American Chemical Society, 2008, 130, 15332-15339.	6.6	142
4963	Lattice Dynamics To Trigger Low Temperature Oxygen Mobility in Solid Oxide Ion Conductors. Journal of the American Chemical Society, 2008, 130, 16080-16085.	6.6	104
4964	Strain relaxation and band-gap tunability in ternary<mml:math xmlns:mml="http://www.w3.org/1998/Math/MathML" display="inline"><mml:mrow><mml:msub><mml:mrow><mml:mtext>In</mml:mtext></mml:mrow><mml:mi>x</mml:mi></mml:msu Physical Review B, 2008, 78, .	1.1	69

#	Article	IF	Citations
4965	<mml:math xmlns:mml="http://www.w3.org/1998/Math/MathML" display="inline"><mml:mrow><mml:msub><mml:mrow><mml:mtext>SrTiO</mml:mtext></mml:mrow><mml:mn>3</mml:mn></mml:m xmlns:mml="http://www.w3.org/1998/Math/MathML" display="inline"><mml:mrow><mml:msub><mml:mrow><mml:mtext>BaTiO</mml:mtext></mml:mrow><mml:mn>3</mml:mn></mml:m using the projector augmented wave method: Performance of hybrid and semilocal functionals. Physical Review B, 2008, 78, .	1.1	219
4966	Interplay of strain and magnetism inLa1âˆ'xSrxMnO3from first principles. Physical Review B, 2008, 78, .	1.1	36
4967	Decomposition of lanthanum hafnate at high pressures. Physical Review B, 2008, 77, .	1.1	40
4968	Stability of intrinsic defects and defect clusters in<mml:math xmlns:mml="http://www.w3.org/1998/Math/MathML" display="inline"><mml:mrow><mml:mi mathvariant="normal">Li</mml:mi><mml:mi mathvariant="normal">Nb</mml:mi><mml:msub><mml:mi mathvariant="normal">O</mml:mi><mml:mn>3</mml:mn></mml:msub></mml:mrow></mml:math>from density functional theory calculations. Physical Review B, 2008, 78, .	1.1	109
4969	First-principles solution to the problem of Mo lattice stability. Physical Review B, 2008, 77, .	1.1	58
4970	The formation and electronic structures of 3d transition-metal atoms doped in silicon nanowires. Journal of Applied Physics, 2008, 104, 084307.	1.1	12
4971	Tuning the Transparency of Cu₂O with Substitutional Cation Doping. Chemistry of Materials, 2008, 20, 5522-5531.	3.2	67
4972	Structure and Stability of a Homologous Series of Tin Oxides. Physical Review Letters, 2008, 100, 045702.	2.9	146
4973	Multiply Twinned Morphologies of FePt and CoPt Nanoparticles. Physical Review Letters, 2008, 100, 087203.	2.9	147
4974	Structural and electronic properties of [0001] AlN nanowires: A first-principles study. Journal of Applied Physics, 2008, 104, 084313.	1.1	20
4975	Vacancy-induced magnetism in ZnO thin films and nanowires. Physical Review B, 2008, 77, .	1.1	409
4976	Electronic Band Structure of Tetraceneâ^'TCNQ and Peryleneâ^'TCNQ Compounds. Journal of Physical Chemistry A, 2008, 112, 2497-2502.	1.1	46
4977	Free Energy for Protonation Reaction in Lithium-Ion Battery Cathode Materials. Chemistry of Materials, 2008, 20, 5485-5490.	3.2	58
4978	First-principles calculations of the electronic structure and pressure-induced magnetic transition in siderite<mml:math xmlns:mml="http://www.w3.org/1998/Math/MathML" display="inline"><mml:mrow><mml:msub><mml:mrow><mml:mtext>FeCO</mml:mtext></mml:mrow><mml:mn>3</mml:mn></mml:m Physical Review B, 2008, 78, .	1.1	42
4979	H₂ Chemisorption on W(100) and W(110) Surfaces. Journal of Physical Chemistry C, 2008, 112, 5579-5588.	1.5	41
4980	DFT Study of Dissociative Adsorption of Hydrogen Sulfide on Cu(111) and Au(111). Langmuir, 2008, 24, 14022-14026.	1.6	56
4981	Evolution of atomic and electronic structure of Pt clusters: Planar, layered, pyramidal, cage, cubic, and octahedral growth. Physical Review B, 2008, 77, .	1.1	160
4982	Changes in single-walled carbon nanotube chirality during growth and regrowth. Journal of Chemical Physics, 2008, 128, 124708.	1.2	12

#	Article	IF	Citations
4983	Adsorption and Protonation of CO₂ on Partially Hydroxylated Î³-Al₂O₃ Surfaces: A Density Functional Theory Study. Langmuir, 2008, 24, 12410-12419.	1.6	120
4984	Electron Propagation along Cu Nanowires Supported on a Cu(111) Surface. Nano Letters, 2008, 8, 2712-2717.	4.5	18
4985	Effects of oxygen, fluorine, and hydroxyl passivation on electronic properties of âŸ¨001âŸ©-oriented silicon nanowires. Journal of Applied Physics, 2008, 104, 024314.	1.1	13
4986	Atomic and electronic structures of thallium-basedIII-V-VI2ternary chalcogenides:Ab initiocalculations. Physical Review B, 2008, 77, .	1.1	27
4987	On the prediction of the crystal and electronic structure of mixed-valence materials by periodic density functional calculations: The case of Prussian Blue. Journal of Chemical Physics, 2008, 128, 044713.	1.2	35
4988	Adiabatic Electron-Phonon Interaction and High-Temperature Thermodynamics of<mml:math xmlns:mml="http://www.w3.org/1998/Math/MathML" display="inline"><mml:mi>A</mml:mi><mml:mn>15</mml:mn></mml:math>Compounds. Physical Review Letters, 2008, 101, 105504.	2.9	39
4989	Twinned structure for shape memory: First-principles calculations. Physical Review B, 2008, 78, .	1.1	23
4990	Connector model for describing many-body interactions at surfaces. Physical Review B, 2008, 78, .	1.1	13
4991	Network structure and dynamics of hydrogenated amorphous silicon. Journal of Non-Crystalline Solids, 2008, 354, 2149-2154.	1.5	12
4992	Lattice stability of intermediate phases of the Srâ€“Si system. Journal of Alloys and Compounds, 2008, 457, 29-35.	2.8	16
4993	Molecular dynamics study on planar clustering of xenon in UO2. Journal of Alloys and Compounds, 2008, 457, 465-471.	2.8	54
4994	Electronic structure of LiSi. Journal of Alloys and Compounds, 2008, 458, 151-157.	2.8	39
4995	Structure and optical properties of - and -cerium sesquisulfide. Journal of Alloys and Compounds, 2008, 459, 438-446.	2.8	16
4996	First-principles study of Alâ€“Niâ€“Y ternary compounds for crystal structure validation. Journal of Alloys and Compounds, 2008, 462, 262-266.	2.8	15
4997	Thermodynamic modeling of Mgâ€“Caâ€“Ce system by combining first-principles and CALPHAD method. Journal of Alloys and Compounds, 2008, 463, 294-301.	2.8	21
4998	On the ternary Laves phases Ti(Mn1â^'xAlx)2 with MgZn2-type. Intermetallics, 2008, 16, 16-26.	1.8	27
4999	Prediction of the ordering behaviours of the orthorhombic phase based on Ti2AlNb alloys by combining thermodynamic model with ab initio calculation. Intermetallics, 2008, 16, 42-51.	1.8	37
5000	First-principles calculations of the elastic constants of Feâ€“Pt alloys. Intermetallics, 2008, 16, 113-118.	1.8	34

#	Article	IF	Citations
5001	Crystal structure, phase stability and elastic properties of the Laves phase ZrTiCu2. Intermetallics, 2008, 16, 651-657.	1.8	19
5002	Constitutional and thermal defects in D019-SnTi3. Intermetallics, 2008, 16, 923-932.	1.8	15
5003	Local structure and electronicâ€“spin transition of Fe-bearing MgSiO3 perovskite under conditions of the Earth's lower mantle. Physics of the Earth and Planetary Interiors, 2008, 166, 77-82.	0.7	6
5004	Experimental constraints on the temperature profile in the lower mantle. Physics of the Earth and Planetary Interiors, 2008, 170, 267-273.	0.7	45
5005	Elastic properties of the post-perovskite phase of Fe2O3 and implications for ultra-low velocity zones. Physics of the Earth and Planetary Interiors, 2008, 170, 260-266.	0.7	15
5006	The stability of bcc-Fe at high pressures and temperatures with respect to tetragonal strain. Physics of the Earth and Planetary Interiors, 2008, 170, 52-59.	0.7	34
5007	Hydrogen insertion effects on the magnetic properties and chemical bonding within C14 Laves phases. Progress in Solid State Chemistry, 2008, 36, 192-212.	3.9	7
5008	A First-Principle Study of Chain Propagation Steps in the Fischerâ˜Tropsch Synthesis on Fe(100). Journal of Physical Chemistry C, 2008, 112, 13681-13691.	1.5	17
5009	First-principles calculations of the crystal structure, electronic structure, and thermodynamic stability of<mml:math xmlns:mml="http://www.w3.org/1998/Math/MathML" display="inline"><mml:mrow><mml:mtext>Be</mml:mtext><mml:msub><mml:mrow><mml:mrow><mml:mo>(</mml:mo><mml:mrow> Physical Review B, 2008, 77, .	1.1	31
5010	A Density Functional Study of Î±-Mg(BH4)2. Chemistry of Materials, 2008, 20, 4952-4956.	3.2	76
5011	Ferroelectrically Induced Weak Ferromagnetism by Design. Physical Review Letters, 2008, 100, 167203.	2.9	185
5012	Predicting Enthalpies of Molecular Substances: Application to<mml:math xmlns:mml="http://www.w3.org/1998/Math/MathML" display="inline"><mml:msub><mml:mi>LiBH</mml:mi><mml:mn>4</mml:mn></mml:msub></mml:math>. Physical Review Letters, 2008, 100, 040602.	2.9	40
5013	Ni-induced destabilization dynamics of crystalline zinc borohydride. Applied Physics Letters, 2008, 92, 134101.	1.5	8
5014	Adsorption and Dissociation of the HCl and Cl₂Molecules on W(111) Surface: A Computational Study. Journal of Physical Chemistry C, 2008, 112, 12342-12348.	1.5	10
5015	Adsorption and Dissociation of CO_x (x = 1, 2) on W(111) Surface :â€‰A Computational Study. Journal of Physical Chemistry C, 2008, 112, 3341-3348.	1.5	21
5016	Combined powder diffraction and solid-state DFT study of [Cu (2,6-dimethoxynicotinate)2(Î¼-ronicol)2]n complex. Zeitschrift Fur Kristallographie - Crystalline Materials, 2008, 223, .	0.4	5
5017	Thermodynamic Stability of Novel Boron Sheet Configurations. Journal of Physical Chemistry B, 2008, 112, 10217-10220.	1.2	41
5018	Density Functional Characterization of the Band Edges, the Band Gap States, and the Preferred Doping Sites of Halogen-Doped TiO₂. Chemistry of Materials, 2008, 20, 6528-6534.	3.2	165

#	Article	IF	Citations
5019	Multivalency Iodine Doped TiO₂:â€‰ Preparation, Characterization, Theoretical Studies, and Visible-Light Photocatalysis. Langmuir, 2008, 24, 3422-3428.	1.6	192
5020	First-Principles Investigation of the Liâ^'Feâ^'F Phase Diagram and Equilibrium and Nonequilibrium Conversion Reactions of Iron Fluorides with Lithium. Chemistry of Materials, 2008, 20, 5274-5283.	3.2	219
5021	Density-functional theory study of the effects of atomic impurity on the band edges of monoclinic<mml:math xmlns:mml="http://www.w3.org/1998/Math/MathML" display="inline"><mml:mrow><mml:msub><mml:mrow><mml:mtext>WO</mml:mtext></mml:mrow><mml:mn>3</mml:mn></mml:ms Physical Review B, 2008, 77, .	1.1	93
5022	Hydrogen dissociation and diffusion on Ni- and Ti-doped Mg(0001) surfaces. Journal of Chemical Physics, 2008, 128, 094703.	1.2	65
5023	Ab initiocalculations of the phonon spectra and the thermal expansion coefficients of the<mml:math xmlns:mml="http://www.w3.org/1998/Math/MathML" display="inline"><mml:mrow><mml:mn>4</mml:mn><mml:mi>d</mml:mi></mml:mrow></mml:math>metals. Physical Review B, 2008, 77, .	1.1	39
5024	Effect of the local environment on the mobility of dislocations in refractory bcc metals: Concurrent multiscale approach. Physical Review B, 2008, 78, .	1.1	4
5025	First-principles study of the H2 interaction with transition metal (Ti, V, Ni) doped Mg(0001) surface: Implications for H-storage materials. Journal of Chemical Physics, 2008, 129, 174703.	1.2	34
5026	Structural, electronic, and magnetic properties of<mml:math xmlns:mml="http://www.w3.org/1998/Math/MathML" display="inline"><mml:mrow><mml:mn>3</mml:mn><mml:mi>d</mml:mi></mml:mrow></mml:math>transition metal monatomic chains: First-principles calculations. Physical Review B, 2008, 77, .	1.1	63
5027	Temperature-dependent diffusion coefficients fromab initiocomputations: Hydrogen, deuterium, and tritium in nickel. Physical Review B, 2008, 77, .	1.1	186
5028	A modified embedded-atom method interatomic potential for indium. Calphad: Computer Coupling of Phase Diagrams and Thermochemistry, 2008, 32, 82-88.	0.7	19
5029	A modified embedded-atom method interatomic potential for Germanium. Calphad: Computer Coupling of Phase Diagrams and Thermochemistry, 2008, 32, 34-42.	0.7	18
5030	A Calphad assessment of Alâ€“Câ€“Fe system with the carbide modelled as an ordered form of the fcc phase. Calphad: Computer Coupling of Phase Diagrams and Thermochemistry, 2008, 32, 361-370.	0.7	60
5031	First-principles based calculation of binary and multicomponent phase diagrams for titanium carbonitride. Calphad: Computer Coupling of Phase Diagrams and Thermochemistry, 2008, 32, 543-565.	0.7	31
5032	Thermodynamic description of the Mgâ€“Eu binary system. Calphad: Computer Coupling of Phase Diagrams and Thermochemistry, 2008, 32, 462-465.	0.7	8
5033	Combined ab-initio and experimental assessment of mixed carbides. Calphad: Computer Coupling of Phase Diagrams and Thermochemistry, 2008, 32, 615-623.	0.7	29
5034	Thermodynamic re-assessment of the Alâ€“Ir system. Calphad: Computer Coupling of Phase Diagrams and Thermochemistry, 2008, 32, 686-692.	0.7	16
5035	Ab-initio study of the effects of pressure and chemistry on the electron-capture radioactive decay constants of 7Be, 22Na and 40K. Earth and Planetary Science Letters, 2008, 267, 628-636.	1.8	21
5036	Ab initio calculations on the free energy and high Pâ€“T elasticity of face-centred-cubic iron. Earth and Planetary Science Letters, 2008, 268, 444-449.	1.8	31

#	Article	IF	Citations
5037	High-pressure phase transformations of FeS: Novel phases at conditions of planetary cores. Earth and Planetary Science Letters, 2008, 272, 481-487.	1.8	50
5038	Novel high-pressure structures of MgCO3, CaCO3 and CO2 and their role in Earth's lower mantle. Earth and Planetary Science Letters, 2008, 273, 38-47.	1.8	211
5039	Initial stage of Ag deposition on regular MgO(001) surface: A DFT study. Computational Materials Science, 2008, 42, 43-49.	1.4	15
5040	DFT evaluation of thermomechanical properties of scheelite type MLiF4 (M=La, Ce, Pr, Nd, Pm, Sm, Gd,) Tj ETQq1 1 0.784314 rgBT /Ov	1.4	6
5041	Large-scale ab initio calculations based on three levels of parallelization. Computational Materials Science, 2008, 42, 329-336.	1.4	156
5042	First principles calculations of thermal equations of state and thermodynamical properties of MgH2 at finite temperatures. Computational Materials Science, 2008, 42, 510-516.	1.4	22
5043	Structural and bonding properties of stannate pyrochlores: A density functional theory investigation. Computational Materials Science, 2008, 42, 653-658.	1.4	44
5044	Stability and magnetic properties of Mn-substituted ScN semiconductor from first principles. Computational Materials Science, 2008, 43, 392-398.	1.4	15
5045	Studies of magnetic interactions in Ni-doped ZnO from first-principles calculations. Computational Materials Science, 2008, 43, 489-494.	1.4	26
5046	Theoretical study of linear monoatomic nanowires, dimer and bulk of Cu, Ag, Au, Ni, Pd and Pt. Computational Materials Science, 2008, 43, 522-530.	1.4	51
5047	Influence of superimposed normal stress on the <mml:math xmlns:mml="http://www.w3.org/1998/Math/MathML" altimg="si17.gif" overflow="scroll"><mml:mrow><mml:mo stretchy="false">ã€ˆ</mml:mo><mml:mn>1</mml:mn><mml:mspace width="0.12em" /><mml:mn>1</mml:mn><mml:mspace width="0.12em" /><mml:mn>2</mml:mn><mml:mo stretchy="false">ã€‰</mml:mo><mml:mo stretchy="false">{</mml:mo><mml:mn>1</mml:mn><mml:mspace	1.4	14
5048	Electronic structures of wurtzite ZnO, BeO, MgO and p-type doping in Zn1âˆ’xYxO (Y=Mg, Be). Computational Materials Science, 2008, 44, 72-78.	1.4	25
5049	A density functional theory study of oxygen diffusion in LaAlO3 and SrTiO3. Computational Materials Science, 2008, 44, 53-60.	1.4	29
5050	Structural and electronic properties of cubic HfO2 surfaces. Computational Materials Science, 2008, 44, 46-52.	1.4	61
5051	Electronic calculation of Mn3AlN with anti-perovskite structure. Computational Materials Science, 2008, 44, 97-101.	1.4	5
5052	Interactions between transition metals and defective carbon nanotubes. Computational Materials Science, 2008, 43, 823-828.	1.4	64
5053	Ab initio molecular dynamics simulation for structural transition of Zr during rapid quenching processes. Computational Materials Science, 2008, 43, 1123-1129.	1.4	34
5054	Ab initio calculation of the total energy and elastic properties of Laves phase C15 Al2RE (RE=Sc, Y, La,) Tj ETQq1 1 0.784314 rgBT /Ov	1.4	48

#	Article	IF	Citations
5055	The impact of system restriction in molecular dynamics applied to the melting of Ne at high pressure. Computational Materials Science, 2008, 44, 605-610.	1.4	1
5056	Structural characterization of Mg65Cu25Y10 metallic glass from ab initio molecular dynamics. Computational Materials Science, 2008, 44, 802-806.	1.4	31
5057	Mantleâ€wide sequestration of carbon in silicates and the structure of magnesite II. Geophysical Research Letters, 2008, 35, .	1.5	31
5058	Cation disorder in ringwoodite and its effects on wave speeds in the Earth's transition zone. Journal of Geophysical Research, 2008, 113, .	3.3	17
5059	Carrier Multiplication in Semiconductor Nanocrystals: Theoretical Screening of Candidate Materials Based on Band-Structure Effects. Nano Letters, 2008, 8, 3174-3181.	4.5	80
5060	Spontaneously Formed Sulfur Adlayers on Gold in Electrolyte Solutions: Adsorbed Sulfur or Gold Sulfide?. Journal of Physical Chemistry C, 2008, 112, 11394-11402.	1.5	87
5061	Ab initioequation of state for the body-centered-cubic phase of iron at high pressure and temperature. Physical Review B, 2008, 78, .	1.1	34
5062	Diffusion of Interstitial Mn in the Dilute Magnetic Semiconductor (Ga,Mn)As: The Effect of a Charge State. Physical Review Letters, 2008, 101, 177204.	2.9	15
5063	Effect of atomic scale plasticity on hydrogen diffusion in iron: Quantum mechanically informed and on-the-fly kinetic Monte Carlo simulations. Journal of Materials Research, 2008, 23, 2757-2773.	1.2	50
5064	Effects of ferroelectricity and magnetism on electron and spin transport in Feâˆ•BaTiO3âˆ•Fe multiferroic tunnel junctions. Journal of Applied Physics, 2008, 103, 07A701.	1.1	32
5065	Nature of the Band Gap of<mml:math xmlns:mml="http://www.w3.org/1998/Math/MathML" display="inline"><mml:msub><mml:mi>In</mml:mi><mml:mn>2</mml:mn></mml:msub><mml:msub><mml:mi mathvariant="normal">O</mml:mi><mml:mn>3</mml:mn></mml:msub></mml:math>Revealed by First-Principles Calculations and X-Ray Spectroscopy. Physical Review Letters, 2008, 100, 167402.	2.9	576
5066	Transverse vibrations driven negative thermal expansion in a metallic compound GdPd3B0.25C0.75. Applied Physics Letters, 2008, 92, .	1.5	20
5067	Density-functional theory study of vibrational relaxation of CO stretching excitation on Si(100). Journal of Chemical Physics, 2008, 129, 174702.	1.2	27
5068	Elastic and thermodynamic properties of OsSi, OsSi2 and Os2Si3. Computational Materials Science, 2008, 43, 812-817.	1.4	22
5069	Acetylacetonate Anchors for Robust Functionalization of TiO₂Nanoparticles with Mn(II)â^'Terpyridine Complexes. Journal of the American Chemical Society, 2008, 130, 14329-14338.	6.6	151
5070	Shock-Wave Exploration of the High-Pressure Phases of Carbon. Science, 2008, 322, 1822-1825.	6.0	224
5071	n-Type Behavior of Graphene Supported on Si/SiO₂ Substrates. ACS Nano, 2008, 2, 2037-2044.	7.3	241
5072	Ab initiocalculations of the thermodynamics and phase diagram of zirconium. Physical Review B, 2008, 78, .	1.1	25

#	Article	IF	Citations
5073	Surface Protonation at the Rutile (110) Interface: Explicit Incorporation of Solvation Structure within the Refined MUSIC Model Framework. Langmuir, 2008, 24, 12331-12339.	1.6	88
5074	Hydrogen Storage in Carbon Nanotubes through the Formation of Stable Câ˜H Bonds. Nano Letters, 2008, 8, 162-167.	4.5	186
5075	Computation of Large Invariant Subspaces Using Polynomial Filtered Lanczos Iterations with Applications in Density Functional Theory. SIAM Journal on Matrix Analysis and Applications, 2008, 30, 397-418.	0.7	25
5076	Negative temperature coefficient of resistance in a crystalline compound. Europhysics Letters, 2008, 84, 47007.	0.7	15
5077	Estimation of Dissociation Energy in Donorâ˜Acceptor Complex AuClÂ·PPh₃ via Topological Analysis of the Experimental Electron Density Distribution Function. Journal of Physical Chemistry A, 2008, 112, 11519-11522.	1.1	97
5078	Fermi surface nesting and the origin of charge density waves in metals. Physical Review B, 2008, 77, .	1.1	478
5079	Modelling of bitumen fragment adsorption on Cu+ and Ag+ exchanged zeolite nanoparticles. Molecular Simulation, 2008, 34, 943-951.	0.9	15
5080	Computational studies of conductivity in wide-band-gap semiconductors and oxides. Journal of Physics Condensed Matter, 2008, 20, 064230.	0.7	22
5081	Electronic structure of ZnO:GaN compounds: Asymmetric bandgap engineering. Physical Review B, 2008, 78, .	1.1	93
5082	Symmetry Breaking Induced Bandgap in Epitaxial Graphene Layers on SiC. Nano Letters, 2008, 8, 4464-4468.	4.5	154
5083	Au Dimers on Thin MgO(001) Films: Flat and Charged or Upright and Neutral?. Journal of the American Chemical Society, 2008, 130, 7814-7815.	6.6	62
5084	Charge-induced formation of linear Au clusters on thin MgO films: Scanning tunneling microscopy and density-functional theory study. Physical Review B, 2008, 78, .	1.1	64
5085	Phonon spectra of the high-frequency modes in dilute nitride randomGaNxAs1â˜xalloy. Physical Review B, 2008, 77, .	1.1	6
5086	Nanoscale control of an interfacial metalâ€“insulator transition at room temperature. Nature Materials, 2008, 7, 298-302.	13.3	525
5087	Uniaxial Strain on Graphene: Raman Spectroscopy Study and Band-Gap Opening. ACS Nano, 2008, 2, 2301-2305.	7.3	1,409
5088	Bonded interactions and the crystal chemistry of minerals: a review. Zeitschrift Fur Kristallographie - Crystalline Materials, 2008, 223, 01-40.	0.4	43
5089	First-principles approach to monitoring the band gap and magnetic state of a graphene nanoribbon via its vacancies. Physical Review B, 2008, 78, .	1.1	120
5090	Dissociative dynamics of spin-triplet and spin-singlet O2 on Ag(100). Journal of Chemical Physics, 2008, 129, 224702.	1.2	39

#	Article	IF	Citations
5091	Low Dimensional Nanomaterials for Spintronics. , 2008, , 247-271.		0
5092	Phase stability of cation-doped LiMnO₂within the GGA+U approximation. Modelling and Simulation in Materials Science and Engineering, 2008, 16, 055008.	0.8	9
5093	Fine tuning the charge transfer in carbon nanotubes via the interconversion of encapsulated molecules. Physical Review B, 2008, 77, .	1.1	79
5094	Implementation of a Density Functional Theory-Based Method for the Calculation of the Hyperfine A-tensor in Periodic Systems with the Use of Numerical and Slater Type Atomic Orbitals: Application to Paramagnetic Defects. Journal of Physical Chemistry A, 2008, 112, 4521-4526.	1.1	10
5095	Quantum confinement effect in Si/Ge core-shell nanowires: First-principles calculations. Physical Review B, 2008, 77, .	1.1	69
5096	Possible thermodynamic stability and superconductivity of antifluorite<mml:math xmlns:mml="http://www.w3.org/1998/Math/MathML" display="inline"><mml:mrow><mml:msub><mml:mrow><mml:mtext>Be</mml:mtext></mml:mrow><mml:mn>2</mml:mn></mml:msu Physical Review B, 2008, 78, .	1.1	10
5097	Spin and band-gap engineering in doped graphene nanoribbons. Physical Review B, 2008, 78, .	1.1	128
5098	Atomistically Informed Electrostatic Model of an Edge Dislocation in a Complex Crystalline Material. Mathematics and Mechanics of Solids, 2008, 13, 267-291.	1.5	5
5099	Modeling of Nanoscale Morphology of Regioregular Poly(3-hexylthiophene) on a ZnO (101Ì…0) Surface. Nano Letters, 2008, 8, 4185-4190.	4.5	33
5100	Syntheses, Structures, Physical Properties, and Electronic Properties of Some AMUQ₃ Compounds (A = Alkali Metal, M = Cu or Ag, Q = S or Se). Inorganic Chemistry, 2008, 47, 6873-6879.	1.9	30
5101	Structural, magnetic, and optical properties of<mml:math xmlns:mml="http://www.w3.org/1998/Math/MathML" display="inline"><mml:mrow><mml:msub><mml:mrow><mml:mtext>BiFeO</mml:mtext></mml:mrow><mml:mn>3</mml:mn></mml:m xmlns:mml="http://www.w3.org/1998/Math/MathML" display="inline"><mml:mrow><mml:msub><mml:mrow><mml:mtext>Bi</mml:mtext></mml:mrow><mml:mn>2</mml:mn></mml:msub Physical Review B, 2008, 78, .	1.1	158
5102	Comparative DFT Study of Crystalline Ammonium Perchlorate and Ammonium Dinitramide. Journal of Physical Chemistry A, 2008, 112, 4688-4693.	1.1	37
5103	Optical properties in conjugated polymers. Journal of Physics Condensed Matter, 2008, 20, 064231.	0.7	15
5104	Semiconducting hydrides. Europhysics Letters, 2008, 82, 17006.	0.7	23
5105	Hybrid functionals applied to extended systems. Journal of Physics Condensed Matter, 2008, 20, 064201.	0.7	500
5106	Theoretical investigation of the defect formation mechanism relevant to nonstoichiometry in hydroxyapatite. Physical Review B, 2008, 77, .	1.1	41
5107	Theoretical trend of ion exchange ability with divalent cations in hydroxyapatite. Physical Review B, 2008, 78, .	1.1	34
5108	Adsorption of Thiols on the Pd(111) Surface: A First Principles Study. Langmuir, 2008, 24, 10838-10842.	1.6	18

#	Article	IF	Citations
5109	Electronic structure of C60 semiconductors under controlled doping with B, N, and Co atoms. Diamond and Related Materials, 2008, 17, 749-752.	1.8	4
5110	Stable nanoporous alkali halide polymorphs: a first principles bottom-up study. Journal of Materials Chemistry, 2008, 18, 5871.	6.7	30
5111	A first-principles study of K adsorption on Pb(111). Physical Chemistry Chemical Physics, 2008, 10, 1669.	1.3	5
5112	Stability and structure of atomic chains on Si(111). Physical Review B, 2008, 78, .	1.1	16
5113	Lattice match in density functional calculations: ice Ih vs. Î²-AgI. Physical Chemistry Chemical Physics, 2008, 10, 4688.	1.3	55
5114	Direct observation of space charge induced hydrogen ion insertion in nanoscale anatase TiO2. Chemical Communications, 2008, , 6342.	2.2	11
5115	Coadsorbed H and CO interaction on platinum. Physical Chemistry Chemical Physics, 2008, 10, 6052.	1.3	11
5116	Polynitrogen/Nanoaluminum Surface Interactions. , 2008, , .		0
5117	Electronic Band Structure of Transparent Conductor: Nb-Doped Anatase TiO2. Applied Physics Express, 2008, 1, 111203.	1.1	134
5118	Charging and Discharging of Oxide Defects in Reliability Issues. IEEE Transactions on Device and Materials Reliability, 2008, 8, 491-500.	1.5	19
5119	Kinetic-anisotropy-induced ordering-orientation transitions calculated in CoPt alloys under various epitaxial growth conditions. Physical Review B, 2008, 77, .	1.1	2
5120	Opening space for<mml:math xmlns:mml="http://www.w3.org/1998/Math/MathML" display="inline"><mml:mrow><mml:msub><mml:mtext>H</mml:mtext><mml:mn>2</mml:mn></mml:msub></mml:mrow></mml:math Cointercalation of graphite with lithium and small organic molecules. Physical Review B, 2008, 78, .	1.1	24
5121	Classical potential describes martensitic phase transformations between the<mml:math xmlns:mml="http://www.w3.org/1998/Math/MathML" display="inline"><mml:mi>Î±</mml:mi></mml:math>,<mml:math xmlns:mml="http://www.w3.org/1998/Math/MathML" display="inline"><mml:mi>Î²</mml:mi></mml:math>, and<mml:math xmlns:mml="http://www.w3.org/1998/Math/MathML" display="inline"><mml:mi>Î³</mml:mi></mml:math>titanium phases. Physical Review B, 2008, 78, .	1.1	173
5122	A first-principle analysis on the phase stabilities, chemical bonds and band gaps of wurtzite structure A_xZn_{1â^'x}O alloys (A = Ca, Cd, Mg). Journal of Physics Condensed Matter, 2008, 20, 235221.	0.7	67
5123	GaSb/GaAs Quantum Nanostructures by Molecular Beam Epitaxy. , 2008, , 271-292.		4
5124	Towards an ab-initio characterization of novel intermediate band photovoltaic materials. Optoelectronic and Microelectronic Materials and Devices (COMMAD), Conference on, 2008, , .	0.0	0
5125	Modeling Electrostatic and Quantum Detection of Molecules. IEEE Sensors Journal, 2008, 8, 857-862.	2.4	12
5126	Modeling of a carbon nanotube junction with ab-initio software VASP. , 2008, , .		0

#	Article	IF	Citations
5127	Magnetic properties of one-dimensional Ni/Cu and Ni/Al multilayered nanowires: Role of nonmagnetic spacers. Physical Review B, 2008, 77, .	1.1	14
5128	Prediction of Dislocation Cores in Aluminum from Density Functional Theory. Physical Review Letters, 2008, 100, 045507.	2.9	152
5129	P-V equation of state for Fe2P and pressure-induced phase transition in Fe3P. High Pressure Research, 2008, 28, 375-384.	0.4	16
5130	From nanostrips to nanorings: the elastic properties of gold-glued polyauronaphthyridines and polyacenes. Physical Chemistry Chemical Physics, 2008, 10, 114-120.	1.3	13
5131	Ab-initio Molecular Dynamics Simulations of Molten Ni-Based Superalloys. , 2008, , .		3
5132	Electron transport through carbon nanotube intramolecular heterojunctions with peptide linkages. Physical Chemistry Chemical Physics, 2008, 10, 5225.	1.3	16
5133	Elasticity theory of topological defects in carbon nanotubes and graphene. Philosophical Magazine Letters, 2008, 88, 159-167.	0.5	8
5134	Electronic structure of Co doped ZnO: Theory and experiment. Journal of Applied Physics, 2008, 103, .	1.1	11
5135	Inhomogeneity in Co doped ZnO diluted magnetic semiconductor. Journal of Applied Physics, 2008, 103, .	1.1	26
5136	Structure and Stability of Formates and Carbonates on Monoclinic Zirconia: A Combined Study by Density Functional Theory and Infrared Spectroscopy. Journal of Physical Chemistry C, 2008, 112, 16096-16102.	1.5	62
5137	Electronic Structure of Self-Assembled Amorphous Polyfluorenes. ACS Nano, 2008, 2, 1381-1388.	7.3	65
5138	Hydrogen-Bonded Helices for Anion Binding and Separation. Crystal Growth and Design, 2008, 8, 1909-1915.	1.4	50
5139	On the possibility of ferromagnetism in carbon-doped anatase TiO2. Applied Physics Letters, 2008, 93, 132507.	1.5	125
5140	Alkali-metal-filled<mml:math xmlns:mml="http://www.w3.org/1998/Math/MathML" display="inline"><mml:mrow><mml:mi mathvariant="normal">Co</mml:mi><mml:msub><mml:mi mathvariant="normal">Sb</mml:mi><mml:mn>3</mml:mn></mml:msub></mml:mrow></mml:math>skutterudites as thermoelectric materials: Theoretical study. Physical Review B, 2008, 77, .	1.1	52
5141	Theoretical Investigation of the Uranyl Ion Sorption on the Rutile TiO₂(110) Face. Inorganic Chemistry, 2008, 47, 10991-10997.	1.9	35
5142	Electron Emission Originated from Free-Electron-like States of Alkali-Doped Boronâ^'Nitride Nanotubes. Journal of the American Chemical Society, 2008, 130, 17012-17015.	6.6	20
5143	Coadsorption of Gold with Hydrogen or Potassium on TiO2(110) Surface. Journal of Physical Chemistry C, 2008, 112, 14010-14014.	1.5	13
5144	First-Principles Study of Structural Stability and Electronic Structure of CdS Nanoclusters. Journal of Physical Chemistry C, 2008, 112, 8206-8214.	1.5	31

#	Article	IF	Citations
5145	Physisorption and Chemisorption of Hydrocarbons in H-FAU Using QM-Pot(MP2//B3LYP) Calculations. Journal of Physical Chemistry C, 2008, 112, 11796-11812.	1.5	55
5146	Electronic Characterization of Si(100)-Bound Alkyl Monolayers Using Kelvin Probe Force Microscopy. Journal of Physical Chemistry C, 2008, 112, 7145-7150.	1.5	28
5147	NH₃ Oxidation on Oxygen-Precovered Au(111):â€‰ A Density Functional Theory Study on Selectivity. Journal of Physical Chemistry C, 2008, 112, 247-252.	1.5	32
5148	Phase diagram studies on iron and nickel silicides: high-pressure experiments andab initiocalculations. Journal of Physics: Conference Series, 2008, 121, 022013.	0.3	2
5149	Thermophysical properties of warm dense hydrogen using quantum molecular dynamics simulations. Physical Review B, 2008, 77, .	1.1	204
5150	Melting curve and Hugoniot of molybdenum up to 400 GPa byab initiosimulations. Journal of Physics: Conference Series, 2008, 121, 012009.	0.3	11
5151	A Combined Density-Functional and IRAS Study on the Interaction of NO with Pd Nanoparticles: Identifying New Adsorption Sites with Novel Properties. Journal of Physical Chemistry C, 2008, 112, 16539-16549.	1.5	41
5152	First-principles study of cubic Bi pyrochlores. Physical Review B, 2008, 77, .	1.1	61
5153	Molecular Dynamics of Localized Reaction, Experiment and Theory: Methyl Bromide on Si(111)-7Ã—7. ACS Nano, 2008, 2, 699-706.	7.3	26
5154	Overview of Electrons and Orbitals in a Nearly One-Dimensional Co³⁺/Co⁴⁺ System. Chemistry of Materials, 2008, 20, 1741-1749.	3.2	13
5155	Adsorption and Decomposition of CO on Stepped Fe(310) Surfaces. Journal of Physical Chemistry C, 2008, 112, 3692-3700.	1.5	17
5156	Three-Dimensional Self-Assembly of Ag Nanodisks in Crystallography Orientations by Modified Electrochemical Deposition. Journal of Physical Chemistry C, 2008, 112, 8545-8547.	1.5	10
5157	Nitrogen/Hydrogen Codoping of Anatase: A DFT Study. Journal of Physical Chemistry C, 2008, 112, 7653-7664.	1.5	28
5158	Site-Specific Chemistry of Ethylene on Si(114)-(2 Ã— 1). Journal of Physical Chemistry C, 2008, 112, 3349-3357.	1.5	1
5159	Computational and Fourier Transform Infrared Spectroscopic Studies on Carbon Monoxide Adsorption on the Zeolites Na-ZSM-5 and K-ZSM-5:â€‰ Evidence of Dual-Cation Sites. Journal of Physical Chemistry C, 2008, 112, 4658-4666.	1.5	63
5160	First-principles study of the phase and electronic structure of<mml:math xmlns:mml="http://www.w3.org/1998/Math/MathML" display="inline"><mml:mrow><mml:mi mathvariant="normal">Tb</mml:mi><mml:msub><mml:mi mathvariant="normal">Mn</mml:mi><mml:mn>2</mml:mn></mml:msub><mml:msub><mml:mi mathvariant="normal">O</mml:mi><mml:mn>5</mml:mn></mml:msub></mml:mrow></mml:math>. Physical Review B, 2008, 77, .	1.1	59
5161	Asymmetric Spin Gap Opening of Graphene on Cubic Boron Nitride (111) Substrate. Journal of Physical Chemistry C, 2008, 112, 12683-12686.	1.5	23
5163	How Electron Localization Function Quantifies and Pictures Chemical Changes in a Solid: The B3 â†’ B1 Pressure Induced Phase Transition in BeO. Journal of Physical Chemistry B, 2008, 112, 9787-9794.	1.2	26

#	Article	IF	Citations
5164	Gold Nanostructures on TiOx/Mo(112) Thin Films. Journal of Physical Chemistry C, 2008, 112, 191-200.	1.5	15
5165	Origin of the OH Vibrational Blue Shift in the LiOH Crystal. Journal of Physical Chemistry A, 2008, 112, 13487-13494.	1.1	9
5166	Azomethane Decomposition Catalyzed by Pt(111):â€‰ An Example of Anti-BrÃ¶nstedâ^'Evansâ^'Polanyi Behavior. Journal of Physical Chemistry C, 2008, 112, 1072-1080.	1.5	6
5167	Point Defect Configurations of Supersaturated Au Atoms Inside Si Nanowires. Nano Letters, 2008, 8, 1016-1019.	4.5	119
5168	Structure of Iron-Containing Nitrogenated Carbon. Journal of Physical Chemistry C, 2008, 112, 9777-9782.	1.5	5
5169	The â€œStapleâ€•Motif:â€‰ A Key to Stability of Thiolate-Protected Gold Nanoclusters. Journal of the American Chemical Society, 2008, 130, 2777-2779.	6.6	231
5170	Formation of Dopant-Pair Defects and Doping Efficiency in B- and P-Doped Silicon Nanowires. Nano Letters, 2008, 8, 3086-3091.	4.5	33
5171	Effect of particle size and surface structure on adsorption of O and OH on platinum nanoparticles: A first-principles study. Physical Review B, 2008, 77, .	1.1	173
5172	Arsenate Incorporation in Gypsum Probed by Neutron, X-ray Scattering and Density Functional Theory Modeling. Journal of Physical Chemistry A, 2008, 112, 5159-5166.	1.1	47
5173	Vibrational Property Study of SrGa2H2 and BaGa2H2 by Inelastic Neutron Scattering and First Principles Calculations. Inorganic Chemistry, 2008, 47, 1496-1501.	1.9	13
5174	Predicting Youngâ€™s modulus of nanowires from first-principles calculations on their surface and bulk materials. Journal of Applied Physics, 2008, 104, .	1.1	60
5175	Density Functional Theory Study of Methanol Decomposition on the CeO2(110) Surface. Journal of Physical Chemistry C, 2008, 112, 4257-4266.	1.5	42
5176	17O Solid-State NMR and First-Principles Calculations of Sodium Trimetaphosphate (Na3P3O9), Tripolyphosphate (Na5P3O10), and Pyrophosphate (Na4P2O7). Inorganic Chemistry, 2008, 47, 7327-7337.	1.9	23
5177	The Reaction Pathways for HSCH₃Adsorption on Au(111):â€‰ A Density Functional Theory Study. Langmuir, 2008, 24, 3274-3279.	1.6	38
5178	Enhanced Ferromagnetism and Tunable Saturation Magnetization of Mn/C-Codoped GaN Nanostructures Synthesized by Carbothermal Nitridation. Journal of the American Chemical Society, 2008, 130, 16366-16373.	6.6	36
5179	Adsorption and Formation of BaO Overlayers on Î³-Al₂O₃ Surfaces. Journal of Physical Chemistry C, 2008, 112, 18050-18060.	1.5	29
5180	Electronic properties of bulk and thin film<mml:math xmlns:mml="http://www.w3.org/1998/Math/MathML" display="inline"><mml:mrow><mml:msub><mml:mrow><mml:mtext>SrRuO</mml:mtext></mml:mrow><mml:mn>3</mml:mn></mml:m Search for the metal-insulator transition. Physical Review B, 2008, 78, .	1.1	143
5181	Influence of Surface Reactions on Complex Hydride Reversibility. Journal of Physical Chemistry C, 2008, 112, 18270-18279.	1.5	4

#	Article	IF	Citations
5182	Orbital Interpretation of Kinetic Energy Density and a Direct Space Comparison of Chemical Bonding in Tetrahedral Network Solids. Journal of Physical Chemistry A, 2008, 112, 7705-7716.	1.1	4
5183	A Density Functional Study on Transition-Metal-Coated Single-Walled Carbon Nanotubes. Journal of Physical Chemistry C, 2008, 112, 9128-9132.	1.5	15
5184	Adsorption of Water on O(2 Ã— 2)/Ru(0001): Thermal Stability and Inhibition of Dissociation. Journal of Physical Chemistry C, 2008, 112, 14052-14057.	1.5	12
5185	First-principles study of TMNa_n(TM = Cr, Mn, Fe, Co, Ni;n= 4â€“7) clusters. Journal of Physics Condensed Matter, 2008, 20, 255243.	0.7	11
5186	Magnetic â€œDeadâ€•Layer at a Complex Oxide Interface. Physical Review Letters, 2008, 101, 247204.	2.9	43
5187	Ab initioprediction of stable boron sheets and boron nanotubes: Structure, stability, and electronic properties. Physical Review B, 2008, 77, .	1.1	315
5188	The structural properties of wurtzite and rocksalt Mg_xZn_{1â^’}_xO. Semiconductor Science and Technology, 2008, 23, 025008.	1.0	30
5189	Development of an electron-temperature-dependent interatomic potential for molecular dynamics simulation of tungsten under electronic excitation. Physical Review B, 2008, 78, .	1.1	68
5190	Effect of the surface polarization in polar perovskites studied from first principles. Physical Review B, 2008, 77, .	1.1	77
5191	First-Principles Study of the Structural Stability and Electronic Properties of ZnS Nanowires. Journal of Physical Chemistry C, 2008, 112, 20291-20294.	1.5	11
5192	Combined Density Functional Theory and Interatomic Potential Study of the Bulk and Surface Structures and Properties of the Iron Sulfide Mackinawite (FeS). Journal of Physical Chemistry C, 2008, 112, 10960-10967.	1.5	70
5193	On the Thermodynamic Stability of (â^š3 Ã— â^š3)R30Â° Methanethiolate Lattice on Reconstructed Au(111) Surface Models. Journal of Physical Chemistry C, 2008, 112, 19121-19124.	1.5	20
5194	Thermodynamic Properties of Trialkali (Li, Na, K) Hexa-alanates: A Combined DFT and Experimental Study. Journal of Physical Chemistry C, 2008, 112, 18598-18607.	1.5	15
5195	Superconducting High Pressure Phase of Germane. Physical Review Letters, 2008, 101, 107002.	2.9	224
5196	Effect of Ag Adatoms on High-Coverage Alkanethiolate Adsorption on Au(111). Journal of Physical Chemistry C, 2008, 112, 4557-4563.	1.5	8
5197	Theoretical strength and charge redistribution of fcc Ni in tension and shear. Journal of Physics Condensed Matter, 2008, 20, 335216.	0.7	36
5198	Framework Fe Ions in Fe-ZSM-5 Zeolite Studied by UV Resonance Raman Spectroscopy and Density Functional Theory Calculations. Journal of Physical Chemistry C, 2008, 112, 16036-16041.	1.5	64
5199	Density Functional Theory Calculations of Pressure Effects on the Vibrational Structure of Î±-RDX. Journal of Physical Chemistry A, 2008, 112, 12228-12234.	1.1	31

#	Article	IF	Citations
5200	Characterization of the Magnetic and Structural Properties of Copper Carbodiimide, CuNCN, by Neutron Diffraction and First-Principles Evaluations of Its Spin Exchange Interactions. Journal of Physical Chemistry C, 2008, 112, 11013-11017.	1.5	41
5201	First Row Transition Metal Atom Adsorption On-Top of FÂ°_s Defects of a MgO(100) Surface. Journal of Physical Chemistry C, 2008, 112, 16491-16496.	1.5	13
5202	Density Functional Calculations of Pd Nanoparticles Using a Plane-Wave Method. Journal of Physical Chemistry A, 2008, 112, 8911-8915.	1.1	41
5203	Oddâ^'Even Effects in Self-Assembled Monolayers of Ï‰-(Biphenyl-4-yl)alkanethiols:â€‰ A First-Principles Study. Langmuir, 2008, 24, 474-482.	1.6	75
5204	CO Oxidation by BNâ^'Fullerene Cage: Effect of Impurity on the Chemical Reactivity. ACS Nano, 2008, 2, 1422-1428.	7.3	56
5205	Adsorption and Cluster Growth of Vanadium on TiO₂(110) Studied by Density Functional Theory. Journal of Physical Chemistry C, 2008, 112, 4622-4625.	1.5	23
5206	Adsorption of 3d Transition Elements on a TiO₂(110) Surface. Journal of Physical Chemistry C, 2008, 112, 19616-19619.	1.5	14
5207	Comparative Theoretical Study of O- and S-Containing Hydrogen-Bonded Supramolecular Structures. Journal of Physical Chemistry C, 2008, 112, 17340-17350.	1.5	8
5208	First Principles Study of NO and NNO Chemisorption on Silicon Carbide Nanotubes and Other Nanotubes. Journal of Chemical Theory and Computation, 2008, 4, 1690-1697.	2.3	70
5209	Chemisorption of hydrogen molecules on carbon nanotubes: charging effect from first-principles calculations. Nanotechnology, 2008, 19, 075707.	1.3	15
5210	DFT Study of the CO Oxidation on the Au(321) Surface. Journal of Physical Chemistry C, 2008, 112, 17291-17302.	1.5	65
5211	Guanine Crystals:â€‰ A First Principles Study. Journal of Physical Chemistry B, 2008, 112, 1540-1548.	1.2	34
5212	Energetics of Mg and B adsorption on polar zinc oxide surfaces from first principles. Physical Review B, 2008, 77, .	1.1	43
5213	Comparisons of Multilayer H₂O Adsorption onto the (110) Surfaces of Î±-TiO₂ and SnO₂ as Calculated with Density Functional Theory. Journal of Physical Chemistry B, 2008, 112, 11616-11624.	1.2	81
5214	Electronic Correlations Decimate the Ferroelectric Polarization of Multiferroic<mml:math xmlns:mml="http://www.w3.org/1998/Math/MathML" display="inline"><mml:msub><mml:mi>HoMn</mml:mi><mml:mn>2</mml:mn></mml:msub><mml:msub><mml:mi mathvariant="normal">O</mml:mi><mml:mn>5</mml:mn></mml:msub></mml:math>. Physical Review Letters, 2008, 100, 227603.	7.9	71
5215	Adsorption, Desorption, and Dissociation of CO on Tungsten(100), a DFT Study. Journal of Physical Chemistry C, 2008, 112, 7436-7444.	1.5	10
5216	Adsorption Configurations and Reactions of Boric Acid on a TiO₂ Anatase (101) Surface. Journal of Physical Chemistry C, 2008, 112, 8276-8287.	1.5	44
5217	Formation of Methyl Isocyanide from Dimethylamine on Pt(111). Journal of Physical Chemistry C, 2008, 112, 3794-3799.	1.5	4

#	Article	IF	Citations
5218	Can Undoped Calcium Tetraborides Exist? An Answer from the Comparison of Its Density Functional Theory Electronic Structure with that of Rare-Earth Metal Tetraboride. Inorganic Chemistry, 2008, 47, 6137-6143.	1.9	12
5219	Thermal Decomposition of Trimethylgallium Ga(CH₃)₃: A Shock-Tube Study and First-Principles Calculations. Journal of Physical Chemistry A, 2008, 112, 6330-6337.	1.1	17
5220	Mechanism and Kinetics for Ammonium Perchlorate Sublimation: A First-principles Study. Journal of Physical Chemistry C, 2008, 112, 14481-14485.	1.5	27
5221	Origin of High Activity and Selectivity of PdAu(001) Bimetallic Surfaces toward Vinyl Acetate Synthesis. Journal of Physical Chemistry C, 2008, 112, 1539-1543.	1.5	43
5222	Ab initiostudy of atomic structure and Schottky barrier height at the<mml:math xmlns:mml="http://www.w3.org/1998/Math/MathML" display="inline"><mml:mrow><mml:mtext>GaAs</mml:mtext><mml:mo>/</mml:mo><mml:msub><mml:mrow><mml:mtext>Ni</mml:mtext></mml:mrow> Physical Review B, 2008, 77, .	1.1	11
5223	Theoretical Study of the Stable Radicals Galvinoxyl, Azagalvinoxyl and Wurstera€™s Blue Perchlorate in the Solid State. Journal of Physical Chemistry A, 2008, 112, 7734-7738.	1.1	15
5224	First-Principles Study of Experimental and Hypothetical Mg(BH₄)₂ Crystal Structures. Journal of Physical Chemistry C, 2008, 112, 4391-4395.	1.5	61
5225	The Mechanism of Propane Oxidation over Iron Antimony Oxide. Journal of Physical Chemistry C, 2008, 112, 9783-9797.	1.5	4
5226	Redox Behavior of the Model Catalyst Pd/CeO2â^'x/Pt(111). Journal of Physical Chemistry C, 2008, 112, 10918-10922.	1.5	62
5227	Free energy of bcc iron: Integratedab initioderivation of vibrational, electronic, and magnetic contributions. Physical Review B, 2008, 78, .	1.1	188
5228	A first-principles investigation of the effect of Pt cluster size on CO and NO oxidation intermediates and energetics. Physical Chemistry Chemical Physics, 2008, 10, 6009.	1.3	45
5229	Manipulating magnetic properties of<mml:math xmlns:mml="http://www.w3.org/1998/Math/MathML" display="inline"><mml:mrow><mml:msub><mml:mrow><mml:mtext>SrRuO</mml:mtext></mml:mrow><mml:mn>3</mml:mn></mml: xmlns:mml="http://www.w3.org/1998/Math/MathML" display="inline"><mml:mrow><mml:msub><mml:mrow><mml:mtext>CaRuO</mml:mtext></mml:mrow><mml:mn>3</mml:mn></mml: epitaxial and uniaxial strains. Physical Review B, 2008, 77, .	1.1	98
5230	Structure of Isolated Molybdenum(VI) Oxide Species on Î³-Alumina: A Periodic Density Functional Theory Study. Journal of Physical Chemistry C, 2008, 112, 14456-14463.	1.5	41
5231	New Data on the Structure of Uranium Monocarbide. Chemistry of Materials, 2008, 20, 3199-3204.	3.2	25
5232	Interaction of Dioxygen with Al Clusters and Al(111):â€‰ A Comparative Theoretical Study. Journal of Physical Chemistry C, 2008, 112, 6924-6932.	1.5	41
5233	Determination of the Spinâ^'Lattice Relevant for the Quaternary Magnetic Oxide Bi₄Cu₃V₂O₁₄ on the Basis of Tight-Binding and Density Functional Calculations. Inorganic Chemistry, 2008, 47, 4779-4784.	1.9	41
5234	Direct Correlation between the ³¹P MAS NMR Response and the Electronic Structure of Some Transition Metal Phosphides. Journal of Physical Chemistry C, 2008, 112, 20481-20490.	1.5	47
5235	Adsorption of Au and Pd Atoms on Thin SiO₂ Films:â€‰ the Role of Atomic Structure. Journal of Physical Chemistry C, 2008, 112, 3405-3409.	1.5	29

#	Article	IF	Citations
5236	Origins of Superstructure Ordering and Incommensurability in Stuffed CoSn-Type Phases. Journal of the American Chemical Society, 2008, 130, 8195-8214.	6.6	28
5237	Polyanionic Gallium Hydrides from AlB2-Type Precursors AeGaE (Ae = Ca, Sr, Ba; E = Si, Ge, Sn). Journal of the American Chemical Society, 2008, 130, 12139-12147.	6.6	36
5238	Bismuth-induced deep levels and carrier compensation in CdTe. Physical Review B, 2008, 78, .	1.1	13
5239	The Oxidation of H₂ and CH₄ on an Oxygen-Enriched Yttria-Stabilized Zirconia Surface: A Theoretical Study Based on Density Functional Theory. Journal of Physical Chemistry C, 2008, 112, 19662-19669.	1.5	65
5240	Adsorption of NO on Pd-Exchanged Mordenite: Ab Initio DFT Modeling. Journal of Physical Chemistry C, 2008, 112, 12349-12362.	1.5	13
5241	First-principles study of vacancy formation in LaNi₅. Journal of Physics Condensed Matter, 2008, 20, 275232.	0.7	4
5242	Methane Dissociation on the Ceria (111) Surface. Journal of Physical Chemistry C, 2008, 112, 17311-17318.	1.5	62
5243	Adsorption and Reaction of Surface Carbon Species on Fe₅C₂(001). Journal of Physical Chemistry C, 2008, 112, 14883-14890.	1.5	22
5244	Ab initio molecular dynamics simulations for thermal equation of state of B2-type NaCl. Journal of Applied Physics, 2008, 103, 023510.	1.1	24
5245	DFT Study of the Thermodynamic Stability of Pdâ^'Pt Bulk Oxide Phases. Journal of Physical Chemistry C, 2008, 112, 13623-13628.	1.5	28
5246	Ab initiostudy of stress-induced domain switching in<mml:math xmlns:mml="http://www.w3.org/1998/Math/MathML" display="inline"><mml:mrow><mml:mi mathvariant="normal">Pb</mml:mi><mml:mi mathvariant="normal">Ti</mml:mi><mml:msub><mml:mi mathvariant="normal">O</mml:mi><mml:mn>3</mml:mn></mml:msub></mml:mrow></mml:math>. Physical Review B, 2008, 77, .	1.1	50
5247	Crystal structures classifier for an evolutionary algorithm structure predictor. , 2008, , .		8
5248	Design of Mold Materials with Excellent Releasability for IC Encapsulation using Epoxy Compounds. , 2008, , .		0
5249	First Principles Study of the Stability and the Formation Kinetics of Subsurface and Bulk Carbon on a Ni Catalyst. Journal of Physical Chemistry C, 2008, 112, 9679-9685.	1.5	37
5250	First-principles study of microscopic properties of the Nb antisite in<mml:math xmlns:mml="http://www.w3.org/1998/Math/MathML" display="inline"><mml:mrow><mml:msub><mml:mrow><mml:mtext>LiNbO</mml:mtext></mml:mrow><mml:mn>3</mml:mn></mml:r Comparison to phenomenological polaron theory. Physical Review B, 2008, 78, .	1.1	69
5251	Role of Electrostatic Interactions on Engineering Reaction Barriers: The Case of CO Dissociation on Supported Cobalt Particles. Journal of Chemical Theory and Computation, 2008, 4, 1709-1717.	2.3	4
5252	Theoretical Study of Early Steps in Corrosion of Pt and Pt/Co Alloy Electrodes. Journal of Physical Chemistry C, 2008, 112, 18566-18571.	1.5	22
5253	Buried<mml:math xmlns:mml="http://www.w3.org/1998/Math/MathML" display="inline"><mml:mi>Ni</mml:mi><mml:mo>/</mml:mo><mml:mi>Cu</mml:mi><mml:mo stretchy="false">(</mml:mo><mml:mn>001</mml:mn><mml:mo) Tj ETQq1 1 0.784314 rgBT /Overlock 10 Tf 50 52 Td (stretchy="false" 100, 146101.	2.9	15

#	Article	IF	Citations
5254	Au â†" N Synergy and N-Doping of Metal Oxide-Based Photocatalysts. Journal of the American Chemical Society, 2008, 130, 12056-12063.	6.6	115
5255	Investigation of the Vanadyl Bond Ordering and Analysis of the Spin Exchange Interactions in Pb2V3O9 and Pb2As2VO9. Chemistry of Materials, 2008, 20, 6929-6938.	3.2	12
5256	Interaction of Metallic Nanoparticles with a Biologically Active Molecule, Dopamine. Journal of Physical Chemistry B, 2008, 112, 15256-15259.	1.2	22
5257	Intermediates in the Formation of Graphitic Carbon on a Flat FCC-Co(111) Surface. Journal of Physical Chemistry C, 2008, 112, 12899-12904.	1.5	48
5258	First-Principles Study on the Effects of Zr Dopant on the CO Adsorption on Ceria. Journal of Physical Chemistry C, 2008, 112, 15341-15347.	1.5	27
5259	Electronic Ground State of Higher Acenes. Journal of Physical Chemistry A, 2008, 112, 332-335.	1.1	236
5260	The Mechanism Responsible for Extraordinary Cs Ion Selectivity in Crystalline Silicotitanate. Journal of the American Chemical Society, 2008, 130, 11689-11694.	6.6	132
5261	Theoretical Study of Work Function Modification by Organic Molecule-Derived Linear Nanostructure on Hâ^'Silicon(100)-2 Â— 1. Journal of Physical Chemistry C, 2008, 112, 3780-3784.	1.5	42
5262	In Search of a Structural Model for a Thiolate-protected Au₃₈ Cluster. Journal of Physical Chemistry C, 2008, 112, 13905-13910.	1.5	62
5263	Lattice dynamics and thermodynamical properties of silicon nitride polymorphs. Physical Review B, 2008, 78, .	1.1	79
5264	Endohedral BN Metallofullerene M@B₃₆N₃₆ Complex As Promising Hydrogen Storage Materials. Journal of Physical Chemistry C, 2008, 112, 12195-12200.	1.5	41
5265	Small-Angle Rotation in Individual Colloidal CdSe Quantum Rods. ACS Nano, 2008, 2, 1179-1188.	7.3	19
5266	Electronic-structureâ€"induced reconstruction and magnetic ordering at the LaAlO ₃ |SrTiO ₃ interface. Europhysics Letters, 2008, 84, 27001.	0.7	74
5267	Discovery of novel hydrogen storage materials: an atomic scale computational approach. Journal of Physics Condensed Matter, 2008, 20, 064228.	0.7	75
5268	<mml:math xmlns:mml="http://www.w3.org/1998/Math/MathML" display="inline"><mml:mrow><mml:mtext>DFT</mml:mtext><mml:mo>+</mml:mo><mml:mi>U</mml:mi></mml:mrow></mml:math>s for the energy minimum among eight collinear and noncollinear magnetic structures of<mml:math xmlns:mml="http://www.w3.org/1998/Math/MathML" display="inline"><mml:mrow><mml:msub><mml:mrow><mml:mtext>GdB</mml:mtext></mml:mrow><mml:mn>4</mml:mn></mml:ms Physical Review B, 2008, 78, .	1.1	12
5269	Dynamics of Silica-Supported Catalysts Determined by Combining Solid-State NMR Spectroscopy and DFT Calculations. Journal of the American Chemical Society, 2008, 130, 5886-5900.	6.6	98
5270	Thermodynamic analysis of hydrogen sorption reactions in Liâ€"Mgâ€"Nâ€"H systems. Applied Physics Letters, 2008, 92, 021907.	1.5	22
5271	Electronic properties and stabilities of bulk and low-index surfaces of SnO in comparison with<mml:math xmlns:mml="http://www.w3.org/1998/Math/MathML" display="inline"><mml:mrow><mml:mi mathvariant="normal">Sn</mml:mi><mml:msub><mml:mi mathvariant="normal">O</mml:mi><mml:mn>2</mml:mn></mml:msub></mml:mrow></mml:math>: A first-principles density functional approach with an empirical correction of van der Waals interactions. Physical Review B, 2008, 77, .	1.1	115

#	Article	IF	Citations
5272	Structure and Electric Properties of Sn_N Clusters (N = 6â˜’20) from Combined Electric Deflection Experiments and Quantum Theoretical Studies. Journal of Physical Chemistry A, 2008, 112, 12312-12319.	1.1	72
5273	Kinetic Model of Surface Segregation in Pt-Based Alloys. Journal of Chemical Theory and Computation, 2008, 4, 1991-1995.	2.3	14
5274	Reducing the Metal Work Function beyond Pauli Pushback: A Computational Investigation of Tetrathiafulvalene and Viologen on Coinage Metal Surfaces. Journal of Physical Chemistry C, 2008, 112, 20357-20365.	1.5	43
5275	First Principles Molecular Dynamics Simulation of a Task-Specific Ionic Liquid Based on Silverâ˜’Olefin Complex: Atomistic Insights into a Separation Process. Journal of Physical Chemistry B, 2008, 112, 10202-10206.	1.2	27
5276	Structure and Optoelectronics of Electrodeposited Cadmium Ditelluride (CdTe₂). Chemistry of Materials, 2008, 20, 6550-6555.	3.2	15
5277	Trapped-Dopant Model of Doping in Semiconductor Nanocrystals. Nano Letters, 2008, 8, 2878-2882.	4.5	69
5278	Two-Dimensional Pentacene:3,4,9,10-Perylenetetracarboxylic Dianhydride Supramolecular Chiral Networks on Ag(111). Journal of the American Chemical Society, 2008, 130, 12285-12289.	6.6	61
5279	Novel Self-Organized Structure of a Agâ˜’S Complex on the Ag(111) Surface below Room Temperature. Journal of Physical Chemistry C, 2008, 112, 4281-4290.	1.5	24
5280	Electronic, optical, and surface properties of PtSi thin films. Physical Review B, 2008, 78, .	1.1	33
5281	Reversible Catalytic Reactions and the Stability of Ti Surface Defects in NaAlH4. Chemistry of Materials, 2008, 20, 7539-7544.	3.2	6
5282	First-principles investigation of anisotropic constitutive relationships in pentaerythritol tetranitrate. Physical Review B, 2008, 77, .	1.1	46
5283	First-principles local density approximation+U and generalized gradient approximation+U study of plutonium oxides. Journal of Chemical Physics, 2008, 128, 084705.	1.2	106
5284	Periodic trends in the geometric structures of 13-atom metal clusters. Physical Review B, 2008, 77, .	1.1	80
5285	Theoretical Studies of Solid Bicyclo-HMX:â€‰ Effects of Hydrostatic Pressure and Temperature. Journal of Physical Chemistry B, 2008, 112, 3882-3893.	1.2	40
5286	Size- and charge-dependent geometric and electronic structures of Binâ€ˆ(Binâ˜’) clusters (n=2â€“13) by first-principles simulations. Journal of Chemical Physics, 2008, 128, 194304.	1.2	34
5287	The local electronic structure of Î±-Li3N. Journal of Chemical Physics, 2008, 129, 044702.	1.2	27
5288	Crystal structure of the pressure-induced metallic phase of SiH4 from ab initio theory. Proceedings of the National Academy of Sciences of the United States of America, 2008, 105, 16454-16459.	3.3	63
5289	First-principles calculations for titanium monoxide clusters Ti n O (n = 1â€“9). Chinese Physics B, 2008, 17, 3336-3342.	0.7	7

#	Article	IF	Citations
5290	Structural phase transitions in vanadium under high pressure. Europhysics Letters, 2008, 81, 37003.	0.7	28
5291	Origin of bcc to fcc phase transition under pressure in alkali metals. New Journal of Physics, 2008, 10, 063022.	1.2	26
5292	A theoretical view on self-assembled monolayers in organic electronic devices. Proceedings of SPIE, 2008, , .	0.8	10
5293	Role of Ge Switch in Phase Transition: Approach using Atomically Controlled GeTe/Sb₂Te₃ Superlattice. Japanese Journal of Applied Physics, 2008, 47, 5763.	0.8	68
5294	Effect of the stoichiometry on the electronic structure of the Ni(111)/Î±-Al 2 O 3 (0001) interface: a first-principles investigation. Chinese Physics B, 2008, 17, 2655-2661.	0.7	0
5295	First-principle study of native defects in CuScO ₂ and CuYO ₂. Chinese Physics B, 2008, 17, 4279-4284.	0.7	13
5296	First-Principles Study of Defects in CuGaO 2. Chinese Physics Letters, 2008, 25, 2997-3000.	1.3	16
5297	First-principles study of Co-doped single-walled silicon nanotubes. Nanotechnology, 2008, 19, 205707.	1.3	12
5298	First-principles investigations of disorder effects on electronic structure and magnetic properties in Sr2CrMoO6. Journal of Physics Condensed Matter, 2008, 20, 255230.	0.7	11
5299	Finding the lowest-energy crystal structure starting from randomly selected lattice vectors and atomic positions: first-principles evolutionary study of the Auâ€“Pd, Cdâ€“Pt, Alâ€“Sc, Cuâ€“Pd, Pdâ€“Ti, and Irâ€“N binary systems. Journal of Physics Condensed Matter, 2008, 20, 295212.	0.7	26
5300	Ab INITIO COMPUTATIONAL MODELS IN MATERIALS SCIENCE: A COMMON PLAYGROUND FOR SURFACE CHEMISTRY AND SOLID-STATE PHYSICS. Chemical Engineering Communications, 2008, 195, 1465-1476.	1.5	1
5301	Calculations for displacive Ï‰-phase transformations in Tiâ€“Al alloys with Nb additions at finite temperature. Journal of Physics Condensed Matter, 2008, 20, 465206.	0.7	7
5302	Atomistic Modeling of {311} Defects and Dislocation Ribbons. Materials Research Society Symposia Proceedings, 2008, 1070, 1.	0.1	1
5303	Possible structural polymorphism in Al-bearing magnesiumsilicate post-perovskite. American Mineralogist, 2008, 93, 533-539.	0.9	18
5304	First-Principles Study on Phase Stability in Li[sub x]CuSb with Heusler-type Structure. Journal of the Electrochemical Society, 2008, 155, A505.	1.3	9
5305	Modeling of Effect of Stress on C Diffusion/Clustering in Si. Materials Research Society Symposia Proceedings, 2008, 1070, 1.	0.1	1
5306	Pd Segregation at (001) B2-NiSi/Si Epitaxial Interface Studied by Density Functional Theory. Materials Research Society Symposia Proceedings, 2008, 1079, 1.	0.1	0
5307	Shell model potential for PbTiO3and its applicability to surfaces and domain walls. Journal of Physics Condensed Matter, 2008, 20, 325225.	0.7	44

#	Article	IF	Citations
5308	Pressure Response of Novel Superconducting {Sr,Ba}Pt4Ge12. Journal of the Physical Society of Japan, 2008, 77, 350-352.	0.7	5
5309	Characterization of siloxane adsorbates covalently attached to TiO 2. Proceedings of SPIE, 2008, , .	0.8	10
5310	Energetics and kinetics of Ti clustering on neutral and charged C60 surfaces. Journal of Chemical Physics, 2008, 129, 134707.	1.2	34
5311	Interaction of nanomaterials with biological molecules: Manganese and dopamine. , 2008, , .		0
5312	THE IMPACT OF ACCEPTOR DOPANT MAGNESIUM AND OXYGEN VACANCY DEFECTS ON THE LATTICE OF BARIUM STRONTIUM TITANATE. Integrated Ferroelectrics, 2008, 101, 142-151.	0.3	8
5313	Origin of the flat-band voltage (V<inf>fb</inf>) roll-off phenomenon in metal/high-k gate stacks. , 2008, , .		2
5314	2D calculation of anharmonic OH vibrations in a layered hydroxide crystal. Journal of Chemical Physics, 2008, 129, 064502.	1.2	4
5315	Atomic chains on surfaces. Journal of Physics Condensed Matter, 2008, 20, 393001.	0.7	32
5316	Design of water gas shift catalysts for hydrogen production in fuel processors. Journal of Physics Condensed Matter, 2008, 20, 064237.	0.7	13
5317	First-Principles Investigation of the Fundamental Corrosion Properties of a Model Cu[sub 38] Nanoparticle and the (111), (113) Surfaces. Journal of the Electrochemical Society, 2008, 155, C407.	1.3	68
5318	Heterogeneous oxidation catalysis on ruthenium: bridging the pressure and materials gaps and beyond. Journal of Physics Condensed Matter, 2008, 20, 184017.	0.7	57
5319	MAGNETIZATION OF BERYLLIUM MONOXIDE (BeO) WITHOUT MAGNETIC IMPURITIES: A FIRST-PRINCIPLES STUDY. International Journal of Modern Physics B, 2008, 22, 4987-4992.	1.0	14
5320	Electronic and structural investigations of gold clusters doped with copper: Aunâ^'1Cuâ^' (n=13â€“19). Journal of Chemical Physics, 2008, 128, 184314.	1.2	33
5321	Ferrocene-1,1â€²-dithiol as molecular wire between Ag electrodes: The role of surface defects. Journal of Chemical Physics, 2008, 128, 064704.	1.2	11
5322	First-principles local density approximation (LDA) +Uand generalized gradient approximation (GGA) +Ustudies of plutonium oxides. Chinese Physics B, 2008, 17, 1364-1370.	0.7	26
5323	Structural Analysis and First-Principles Calculation of Lithium Vanadium Oxide for Advanced Li-Ion Batteries. Advances in Quantum Chemistry, 2008, , 23-33.	0.4	13
5324	Polarity in oxide ultrathin films. Journal of Physics Condensed Matter, 2008, 20, 264003.	0.7	44
5325	Decomposition pathways of methanol on the PtAu(111) bimetallic surface: A first-principles study. Journal of Chemical Physics, 2008, 128, 064706.	1.2	39

#	Article	IF	Citations
5326	Theoretical characterization of titanyl phthalocyanine as a p-type organic semiconductor: Short intermolecular Ï€-Ï€ interactions yield large electronic couplings and hole transport bandwidths. Journal of Chemical Physics, 2008, 128, 034701.	1.2	92
5327	New insight brought by density functional theory on the chemical state of alaninol on Cu(100): Energetics and interpretation of x-ray photoelectron spectroscopy data. Journal of Chemical Physics, 2008, 128, 114709.	1.2	14
5328	Origin of unexpected magnetism in Cu-doped TIO ₂. Europhysics Letters, 2008, 81, 17004.	0.7	10
5329	First-principles study of the electronic and magnetic properties of Sr2Fe1+xMo1â^'xO6. Journal of Physics Condensed Matter, 2008, 20, 075218.	0.7	4
5330	Teraflops Sustained Performance With Real World Applications. International Journal of High Performance Computing Applications, 2008, 22, 131-148.	2.4	1
5331	Free Energies for Acid Attack Reactions of Lithium Cobaltate. Journal of the Electrochemical Society, 2008, 155, A711.	1.3	16
5332	First-principles calculations of the thermodynamic and elastic properties of the L1₂-based Al₃RE (RE = Sc, Y, Laâ€“Lu). International Journal of Materials Research, 2008, 99, 582-588.	0.1	35
5333	Vacancy-mediated dehydrogenation of sodium alanate. Proceedings of the National Academy of Sciences of the United States of America, 2008, 105, 3673-3677.	3.3	101
5334	Adhesive metal transfer at the Al(1â€‰1â€‰1)/Î±-Fe₂O₃(0â€‰0â€‰0â€‰1) interface: a study withab initiomolecular dynamics. Modelling and Simulation in Materials Science and Engineering, 2008, 16, 085001.	0.8	6
5335	Ab-initiostudy on indium diffusion in silicon substrate under hydrostatic stress. Molecular Simulation, 2008, 34, 47-50.	0.9	0
5336	New filled P-based skutteruditesâ€”promising materials for thermoelectricity?. New Journal of Physics, 2008, 10, 053004.	1.2	8
5337	Structure and electronic properties of PbnM (M=C, Al, In, Mg, Sr, Ba, and Pb; n=8, 10, 12, and 14) clusters: Theoretical investigations based on first principles calculations. Journal of Chemical Physics, 2008, 128, 024308.	1.2	31
5338	Magnetic molecules made of nitrogen or boron-doped fullerenes. Applied Physics Letters, 2008, 92, 033103.	1.5	12
5339	The effects of electronic structure and charged state on thermodynamic properties: An ab initio molecular dynamics investigations on neutral and charged clusters of Na39, Na40, and Na41. Journal of Chemical Physics, 2008, 128, 104701.	1.2	19
5340	Binding characteristics of pyridine on Ag(110). Journal of Chemical Physics, 2008, 128, 134707.	1.2	16
5341	Characterization of enantiospecific chemisorption on chiral Cu surfaces vicinal to Cu(111) and Cu(100) using density functional theory. Journal of Chemical Physics, 2008, 128, 144709.	1.2	22
5342	First principles studies for formation mechanism and properties of ethylene molecule adsorbing on diamond (100) surface. Journal of Chemical Physics, 2008, 128, 114710.	1.2	2
5343	The role of exchange-correlation functionals in the potential energy surface and dynamics of N2 dissociation on W surfaces. Journal of Chemical Physics, 2008, 128, 154704.	1.2	48

#	Article	IF	Citations
5344	Thermodynamics and kinetics of oxygen-induced segregation of 3d metals in Ptâ€“3dâ€“Pt(111) and Ptâ€“3dâ€“Pt(100) bimetallic structures. Journal of Chemical Physics, 2008, 128, 164703.	1.2	85
5345	A first principles study on organic molecule encapsulated boron nitride nanotubes. Journal of Chemical Physics, 2008, 128, 164701.	1.2	26
5346	The adsorption of O2 on Pb films and the effect of quantum modulation: A first-principles prediction. Journal of Chemical Physics, 2008, 128, 164705.	1.2	19
5347	Î“ -point lattice free energy estimates from O(1) force calculations. Journal of Chemical Physics, 2008, 128, 184708.	1.2	1
5348	Low-lying isomers of Sin+ and Sinâ¯ (n=31â€“50) clusters. Journal of Chemical Physics, 2008, 128, 234302.	1.2	18
5349	Ca (Al H 4) 2 , CaAlH5, and CaH2+6LiBH4: Calculated dehydrogenation enthalpy, including zero point energy, and the structure of the phonon spectra. Journal of Chemical Physics, 2008, 128, 234505.	1.2	9
5350	Stability of suspended gold and silver alloy monatomic chains. Journal of Chemical Physics, 2008, 128, 244703.	1.2	15
5351	First-principles study of substitutional magnesium and zinc in hydroxyapatite and octacalcium phosphate. Journal of Chemical Physics, 2008, 128, 245101.	1.2	101
5352	Theoretical simulations of the tip-induced configuration changes of the 4,4â€²-diacetyl-p-terphenyl molecule chemisorbed on Si(001). Journal of Chemical Physics, 2008, 128, 244710.	1.2	5
5353	Electronic structures of organic molecule encapsulated BN nanotubes under transverse electric field. Journal of Chemical Physics, 2008, 129, 024710.	1.2	17
5354	Structure versus electron effects in the growth mode of pentacene on metal-induced Si(111)-3Ã—3 surfaces. Journal of Chemical Physics, 2008, 129, 034703.	1.2	4
5355	The competition of double-, four-, and three-ring tubular B3nâ€¯(n=8â€“32) nanoclusters. Journal of Chemical Physics, 2008, 129, 024903.	1.2	36
5356	Interaction of gas molecules with Ti-benzene complexes. Journal of Chemical Physics, 2008, 129, 074305.	1.2	19
5357	Quasiparticle energy spectra of alkali-metal clusters: All-electron first-principles calculations. Journal of Chemical Physics, 2008, 129, 104104.	1.2	22
5358	Nonuniform temperature dependence of the reactivity of disordered VOx/Î²-Al2O3(001) surfaces: A density functional theory based Monte Carlo study. Journal of Chemical Physics, 2008, 129, 224710.	1.2	5
5359	Reduction in charged defects associated with oxygen vacancies in hafnia by magnesium incorporation: First-principles study. Applied Physics Letters, 2008, 93, .	1.5	25
5360	Predictions of melting, crystallization, and local atomic arrangements of aluminum clusters using a reactive force field. Journal of Chemical Physics, 2008, 129, 244506.	1.2	47
5361	Bonding in the Ïµ-phase of high pressure oxygen. Journal of Physics: Conference Series, 2008, 121, 012006.	0.3	5

#	Article	IF	Citations
5362	Self-trapping nature of Tl nanoclusters on the Si(111)-7Ã—7 surface. New Journal of Physics, 2008, 10, 053013.	1.2	2
5363	Crystallographic phase stabilities and electronic structures in AgNbO3by first-principles calculation. Molecular Simulation, 2008, 34, 1105-1114.	0.9	20
5364	X-ray diffraction line-profile analysis of hexagonalÏµ-iron nitride compound layers: compositionâ€“and stressâ€“depth profiles. Philosophical Magazine, 2008, 88, 145-169.	0.7	21
5365	On the surface relaxation of transition metals. Philosophical Magazine, 2008, 88, 2709-2714.	0.7	6
5366	Ab-Initio Study on the Magnetic Structures in the Ordered Mn$_{3}$Pt Alloy. IEEE Transactions on Magnetics, 2008, 44, 3131-3133.	1.2	12
5367	Defect formation in graphene nanosheets by acid treatment: an x-ray absorption spectroscopy and density functional theory study. Journal Physics D: Applied Physics, 2008, 41, 062001.	1.3	112
5368	Electronic origin of anomalously high shear modulus and intrinsic brittleness of fcc Ir. Journal of Physics Condensed Matter, 2008, 20, 085221.	0.7	17
5369	Alkaline-earth metal monolayers on 5-fold i-Alâ€“Pdâ€“Mn surface: Influence of adatom size on quasiperiodic ordering. Philosophical Magazine, 2008, 88, 2117-2122.	0.7	1
5370	First principles calculations of the structural, electronic and vibrational properties of the clathrates Ba8Al16Ge30and Ba8Al16Si30. Journal of Physics Condensed Matter, 2008, 20, 415214.	0.7	14
5371	Interface structure and magnetism of Fe3Si/GaAs(110) multilayers: Anab-initiostudy. Philosophical Magazine, 2008, 88, 2699-2707.	0.7	5
5372	Coupling of surface relaxation and polarization in PbTiO₃from atomistic simulation. Journal of Physics Condensed Matter, 2008, 20, 395004.	0.7	12
5373	Chemisorption of Hydrogen Molecule on Axially Strained (8, 0) Carbon Nanotube. Journal of Physical Chemistry C, 2008, 112, 18516-18520.	1.5	5
5374	Effect of M²⁺ (M = Zn and Cu) Dopants on the Electronic Structure and Photocatalytic Activity of In(OH)_yS_z Solid Solution. Journal of Physical Chemistry C, 2008, 112, 16046-16051.	1.5	35
5375	Efficient Channels of Energy Transfer in High Light Yield LuI3:Ce Scintillator. Materials Research Society Symposia Proceedings, 2008, 1111, 1.	0.1	0
5376	Ab Initio Alloying of Mg for Hydrogen Storage. Materials Research Society Symposia Proceedings, 2008, 1098, 1.	0.1	1
5377	Dissociation of H2O molecule adsorbed on Si (001) 2Ã—1 surface: a theoretical study. Materials Research Society Symposia Proceedings, 2008, 1145, 1.	0.1	0
5378	Ab Initio Equation of State Data for Hydrogen, Helium, and Water and the Internal Structure of Jupiter. Astrophysical Journal, 2008, 683, 1217-1228.	1.6	222
5379	Prediction of incommensurate crystal structure in Ca at high pressure. Proceedings of the National Academy of Sciences of the United States of America, 2008, 105, 20627-20630.	3.3	45

#	Article	IF	Citations
5380	Ab Initio DFT Study of Ideal Strength of Crystal and Surfaces in Covalent Systems. Materials Research Society Symposia Proceedings, 2008, 1086, 1.	0.1	1
5381	Computer simulation of electronic and magnetic properties of ternary chalcopyrites doped with transition metals. Proceedings of SPIE, 2008, , .	0.8	5
5382	Molecular Dynamics Simulations of Liquid Phosphorus at High Temperature and Pressure. Communications in Theoretical Physics, 2008, 49, 1323-1332.	1.1	3
5383	Crystal Structure of Î²-La ₂ Mo ₂ O ₉ from First Principles Calculation. Chinese Physics Letters, 2008, 25, 3342-3345.	1.3	12
5384	Structural and electronic properties of NM-doped ceria (NM = Pt, Rh): a first-principles study. Journal of Physics Condensed Matter, 2008, 20, 035210.	0.7	39
5385	Ultrahigh-Pressure Equation of State for Copper at 0 K. Chinese Physics Letters, 2008, 25, 3350-3352.	1.3	1
5386	Simulation of mechanical properties and residual stress of nanostructural coatings based on transition metals nitrides. Proceedings of SPIE, 2008, , .	0.8	0
5387	Ab Initio Study of Elastic Properties in Fe3Al-based Alloys. Materials Research Society Symposia Proceedings, 2008, 1128, 20401.	0.1	4
5388	Advances in Computation of Temperature-Pressure Phase Diagrams of High-Pressure Nitrides. Key Engineering Materials, 0, 403, 77-80.	0.4	7
5389	First-principles local density approximation (generalized gradient approximation) +U study of catalytic CenOm clusters: U value differs from bulk. Journal of Chemical Physics, 2008, 128, 164718.	1.2	21
5390	Structural instability of epitaxial zinc-blende vanadium pnictides and chalcogenides for half-metallic ferromagnets. Journal of Applied Physics, 2008, 104, 053709.	1.1	16
5391	Phosphorus diffusion and activation in silicon: Process simulation based on ab initio calculations. Materials Research Society Symposia Proceedings, 2008, 1070, 1.	0.1	1
5392	Fluid helium at conditions of giant planetary interiors. Proceedings of the National Academy of Sciences of the United States of America, 2008, 105, 11071-11075.	3.3	46
5393	The structure and properties of small Pd clusters. Nanotechnology, 2008, 19, 205701.	1.3	17
5394	Density functional characterization of B doping at rutile TiO₂(1â€‰1â€‰0) surface. Journal Physics D: Applied Physics, 2008, 41, 195411.	1.3	12
5395	Structural and mechanical properties of Mg₁₇Al₁₂and Mg₂₄Y₅from first-principles calculations. Journal Physics D: Applied Physics, 2008, 41, 195408.	1.3	65
5396	Band offset determination of the GaAs/GaAsN interface using the density functional theory method. Journal of Physics Condensed Matter, 2008, 20, 315004.	0.7	17
5397	Modelling the structure of GaAs and InAs nanowires. Journal of Physics Condensed Matter, 2008, 20, 454226.	0.7	59

#	Article	IF	Citations
5398	First principles calculations for modern ceramic science and engineering. Journal of Physics Condensed Matter, 2008, 20, 064215.	0.7	4
5399	Materials design and development of functional materials for industry. Journal of Physics Condensed Matter, 2008, 20, 064227.	0.7	15
5400	Density functional theory and beyondâ€"opportunities for quantum methods in materials modeling semiconductor technology. Journal of Physics Condensed Matter, 2008, 20, 064232.	0.7	13
5401	Functionalizing graphene by embedded boron clusters. Nanotechnology, 2008, 19, 335707.	1.3	19
5402	Diffusion of an Extra Ga Atom in GaAs(001)(2 4) Rich-As Surface. Chinese Journal of Chemical Physics, 2008, 21, 69-75.	0.6	1
5403	Theoretical study of the localization of excess electrons at the surface of ice. Journal of Physics Condensed Matter, 2008, 20, 225003.	0.7	7
5404	TDAE chemisorbed on gold. Journal of Physics Condensed Matter, 2008, 20, 315008.	0.7	2
5405	First-principles studies for structural transitions in ordered phase of cubic approximant Cd₆Ca. Journal of Physics Condensed Matter, 2008, 20, 315206.	0.7	13
5406	Modeling the reactive ion etching process for the CoO(001) surfaceviafirst principles calculations. Journal of Physics Condensed Matter, 2008, 20, 355006.	0.7	4
5407	Formation of Ga dimer linear chains on Si(001): a first-principles study. Journal of Physics Condensed Matter, 2008, 20, 445002.	0.7	3
5408	Phase transitions of BaCO₃ at high pressures. Mineralogical Magazine, 2008, 72, 659-665.	0.6	20
5409	Ab-initio melting curve and principal Hugoniot of tantalum. Journal of Physics: Conference Series, 2008, 121, 012010.	0.3	4
5410	A density-functional study of the possibility of noncollinear magnetism in small Mn clusters using SIESTA and the generalized gradient approximation to exchange and correlation. Journal of Chemical Physics, 2008, 128, 114315.	1.2	21
5411	Electric-field-gradient tensor and charge densities in LaB6: B11 nuclear-magnetic-resonance single-crystal investigations and first-principles calculations. Journal of Applied Physics, 2008, 103, 083534.	1.1	13
5412	Effect of ionic substitutions on the structure and dielectric properties of hafnia: A first principles study. Journal of Applied Physics, 2008, 103, 084103.	1.1	23
5413	Tuning the work function of ultrathin oxide films on metals by adsorption of alkali atoms. Journal of Chemical Physics, 2008, 128, 164707.	1.2	44
5414	Dynamic aspects of the liquid-liquid phase transformation in silicon. Journal of Chemical Physics, 2008, 129, 104503.	1.2	27
5415	Lattice parameters, deviations from Vegardâ€™s rule, and E2 phonons in InAlN. Applied Physics Letters, 2008, 93, .	1.5	44

#	Article	IF	Citations
5416	Coverage dependence of the structure of tetracene on Ag(110). Journal of Physics Condensed Matter, 2008, 20, 315010.	0.7	9
5417	Pathways of nitric oxide dissociation on Si(001) and subsequent atomistic processes: a first-principles molecular dynamics study. New Journal of Physics, 2008, 10, 093029.	1.2	5
5418	Elastic Constants of Co/Pt Superlattice Studied by Acoustic Measurements andAb initioCalculations. Japanese Journal of Applied Physics, 2008, 47, 3847-3850.	0.8	15
5419	Accuracy of order-Ndensity-functional theory calculations on DNA systems using CONQUEST. Journal of Physics Condensed Matter, 2008, 20, 294201.	0.7	25
5420	Effects of pressure and temperature on the carrier transports in organic crystal: A first-principles study. Journal of Chemical Physics, 2008, 128, 194706.	1.2	43
5421	First-principles simulation of supercooled liquid alloys. Journal of Physics Condensed Matter, 2008, 20, 114114.	0.7	6
5422	Reliable lateral and vertical manipulations of a single Cu adatom on a Cu(111) surface with multi-atom apex tip: semiempirical and first-principles simulations. Nanotechnology, 2008, 19, 335710.	1.3	12
5423	Thermodynamic properties and elastic constants of Ndâ€“Mg intermetallics: a molecular dynamics study. International Journal of Materials Research, 2008, 99, 42-49.	0.1	1
5424	First-Principles Study on Piezoresistance Effect in Silicon Nanowires. Japanese Journal of Applied Physics, 2008, 47, 5132-5138.	0.8	40
5425	Structural phase transitions in IrO2at high pressures. Journal of Physics Condensed Matter, 2008, 20, 045202.	0.7	8
5426	The study of structural, electronic and optical properties of double-walled carbon nanotube bundles under hydrostatic pressure. Europhysics Letters, 2008, 81, 47003.	0.7	6
5427	Predicting the hydrogen pressure to achieve ultralow friction at diamond and diamondlike carbon surfaces from first principles. Applied Physics Letters, 2008, 92, .	1.5	29
5428	First-principles calculations of elastic constants of DO₃-Mg₃RE (RE = Sc, Y, La,) Tj ETQq0 0 0 rgBT /Overlock 1	1.2	13
5429	Theoretical investigation of hydrogen storage in metal-intercalated graphitic materials. Journal of Physics Condensed Matter, 2008, 20, 285212.	0.7	14
5430	Structural, electronic and magnetic properties of the surfaces of tetragonal and cubic HfO₂. New Journal of Physics, 2008, 10, 063031.	1.2	34
5431	Al-induced reduction of the oxygen diffusion in HfO₂: anab initiostudy. Journal of Physics Condensed Matter, 2008, 20, 135206.	0.7	7
5432	Resistance of copper nanowires and comparison with carbon nanotube bundles for interconnect applications using first principles calculations. Journal of Physics Condensed Matter, 2008, 20, 095209.	0.7	56
5433	The power of joint application of LEED and DFT in quantitative surface structure determination. Journal of Physics Condensed Matter, 2008, 20, 304204.	0.7	5

#	Article	IF	Citations
5434	Role of hydroxyl groups in the formation of defect configurations in silicon devices. Journal Physics D: Applied Physics, 2008, 41, 245407.	1.3	2
5435	Carrier-induced enhancement and suppression of ferromagnetism in Zn_{1-x}Cr_xTe and Ga_{1-x}Cr_xAs: origin of the spinodal decomposition. New Journal of Physics, 2008, 10, 113007.	1.2	8
5436	Morphology transformation of patterned, uniform and faceted GaN microcrystals. Journal Physics D: Applied Physics, 2008, 41, 015406.	1.3	6
5437	Antiferromagnetism and segregation in cuboctahedral FePt nanoparticles. Journal Physics D: Applied Physics, 2008, 41, 134015.	1.3	19
5438	Atomic and electronic structure of Bi/GaAs(001)-Î±2(2 Ã— 4). Journal of Physics Condensed Matter, 2008, 20, 265003.	0.7	6
5439	Density functional theory calculations of the surface structure of the inverse spinel zinc orthotitanate. Journal of Physics Condensed Matter, 2008, 20, 095001.	0.7	3
5440	Atomic structure of misfit dislocations at InAs/GaAs(110). Journal of Physics Condensed Matter, 2008, 20, 235227.	0.7	11
5441	The partitioning and site preference of rhenium or ruthenium in model nickel-based superalloys: An atom-probe tomographic and first-principles study. Applied Physics Letters, 2008, 93, .	1.5	71
5442	The origins of high mobility and low operation voltage of amorphous oxide channel TFTs. , 2008, , .		0
5443	Bond-Counting Rule for Carbon and its Application to the Roughness of Diamond (001). Physical Review Letters, 2008, 100, 026101.	2.9	8
5444	Ferromagnetism of Cu doped ZnO: First-principles calculation and Monte Carlo simulation. , 2008, , .		2
5445	On the heat capacities of Ta2AlC, Ti2SC, and Cr2GeC. Journal of Applied Physics, 2008, 104, .	1.1	21
5446	Structures and magnetic properties of (Fe, Li)-codoped NiO thin films. Applied Physics Letters, 2008, 92, .	1.5	22
5447	Charge carrier induced lattice strain and stress effects on As activation in Si. Applied Physics Letters, 2008, 93, .	1.5	10
5448	Structural effect of junction interface on magnetic properties in a Co/MgO/Co system: First-principles calculations. Journal of Applied Physics, 2008, 103, .	1.1	8
5449	Mutual Passivation of Electrically Active and Isovalent Impurities in Dilute Nitrides. Physical Review Letters, 2008, 100, 045505.	2.9	20
5450	Ferromagnetic states in<mml:math xmlns:mml="http://www.w3.org/1998/Math/MathML" display="inline"><mml:mrow><mml:mi>Fe</mml:mi><mml:mtext>â^'</mml:mtext><mml:mi>Ru</mml:mi></mml:mrow></mml:math>sy studied byab initiocalculation and ion-beam mixing. Physical Review B, 2008, 77, .	1.1	4
5451	Electronic and vibronic interactions at weakly bound organic interfaces: The case of pentacene on graphite. Physical Review B, 2008, 78, .	1.1	30

#	Article	IF	Citations
5452	Bridge structure for the graphene/Ni(111) system: A first principles study. Physical Review B, 2008, 77, .	1.1	158
5453	Large impurity effects in rubrene crystals: First-principles calculations. Physical Review B, 2008, 78, .	1.1	37
5454	Nature of boron solution and diffusion in<mml:math xmlns:mml="http://www.w3.org/1998/Math/MathML" display="inline"><mml:mi>Î±</mml:mi></mml:math>-iron. Physical Review B, 2008, 77, .	1.1	44
5455	Electronic and vibrational properties ofÎ³âˆ’AlH3. Physical Review B, 2008, 77, .	1.1	25
5456	First-principles theory of the coherency strain, defect energetics, and solvus boundaries in thePbTe-AgSbTe2system. Physical Review B, 2008, 78, .	1.1	26
5457	High-pressure phases of calcium and their finite-temperature phase boundaries. Physical Review B, 2008, 78, .	1.1	41
5458	Disorder-Recrystallization Effects in Low-Energy Beam-Solid Interactions. Physical Review Letters, 2008, 100, 185502.	2.9	20
5459	Geometric Structure ofTiO2(011)(2Ã—1). Physical Review Letters, 2008, 101, 185501.	2.9	87
5460	Detailed scanning probe microscopy tip models determined from simultaneous atom-resolved AFM and STM studies of the<mml:math xmlns:mml="http://www.w3.org/1998/Math/MathML" display="inline"><mml:mrow><mml:msub><mml:mrow><mml:mtext>TiO</mml:mtext></mml:mrow><mml:mn>2</mml:mn></mml:msu Physical Review B, 2008, 78, .	1.1	81
5461	Pressure-induced Bardeen-Schrieffer-type superconducting behavior in the electride<mml:math xmlns:mml="http://www.w3.org/1998/Math/MathML"		

#	Article	IF	Citations
5470	Quantum molecular dynamics simulations of warm dense lithium hydride: Examination of mixing rules. Physical Review B, 2008, 77, .	1.1	35
5471	Structure and Local-Equilibrium Thermodynamics of thec(2Ã—2)Reconstruction of RutileTiO2(100). Physical Review Letters, 2008, 100, 086102.	2.9	25
5472	Topology of the Spin-Polarized Charge Density in bcc and fcc Iron. Physical Review Letters, 2008, 100, 017208.	2.9	32
5473	Atomic and electronic structures of<mml:math xmlns:mml="http://www.w3.org/1998/Math/MathML" display="inline"><mml:mrow><mml:mtext>Ag</mml:mtext><mml:mo>/</mml:mo><mml:mtext>Si</mml:mtext><mml:mrow><mml:mo A first-principles study. Physical Review B, 2008, 78, .	1.1	8
5474	Equation of state for transition metals. Physical Review B, 2008, 77, .	1.1	10
5475	Monodisperse Microisland Formation on<mml:math xmlns:mml="http://www.w3.org/1998/Math/MathML" display="inline"><mml:mi>Ni</mml:mi><mml:mo>/</mml:mo><mml:mi>Ru</mml:mi><mml:mo stretchy="false">(</mml:mo><mml:mn>0001</mml:mn><mml:mo) Tj ETQq1 1 0.784314 rgBT /Overlock 10 Tf 50 527 Td (stretchy="fal	2.9	5
5476	Direct evidence for hidden one-dimensional Fermi surface of hexagonalK0.25WO3. Physical Review B, 2008, 77, .	1.1	13
5477	Adsorption and bonding mechanism of a<mml:math xmlns:mml="http://www.w3.org/1998/Math/MathML" display="inline"><mml:mrow><mml:mtext>N</mml:mtext><mml:mo>,</mml:mo><mml:msup><mml:mtext>N</mml:mtext><mml:mo> ...on corrections. Physical Review B, 2008, 78, .	1.1	3
5478	Structural and electronic properties of<mml:math xmlns:mml="http://www.w3.org/1998/Math/MathML" display="inline"><mml:mrow><mml:msub><mml:mrow><mml:mtext>SrFeO</mml:mtext></mml:mrow><mml:mn>2</mml:mn></mml:r first principles. Physical Review B, 2008, 78, .	1.1	68
5479	First-principles characterization of Ni diffusion kinetics in<mml:math xmlns:mml="http://www.w3.org/1998/Math/MathML" display="inline"><mml:mi>Î²</mml:mi></mml:math>-NiAl. Physical Review B, 2008, 78, .	1.1	32
5480	Impurity segregation and ordering in<mml:math xmlns:mml="http://www.w3.org/1998/Math/MathML" display="inline"><mml:mrow><mml:mtext>Si</mml:mtext><mml:mo>/</mml:mo><mml:msub><mml:mrow><mml:mtext>SiO</mml:mt Physical Review B, 2008, 77, .	1.1	13
5481	Binding-energy relations and equations of state for the<mml:math xmlns:mml="http://www.w3.org/1998/Math/MathML" display="inline"><mml:mrow><mml:mn>4</mml:mn><mml:mi>d</mml:mi></mml:mrow></mml:math>and<mml:math xmlns:mml="http://www.w3.org/1998/Math/MathML" display="inline"><mml:mrow><mml:mn>5</mml:mn><mml:mi>d</mml:mi></mml:mrow></mml:math>transition metals. Physical Review B, 2008, 78, .	1.1	17
5482	Symmetry-broken crystal structure of elemental boron at low temperature. Physical Review B, 2008, 77, .	1.1	97
5483	Pinning of graphene to Ir(111) by flat Ir dots. Physical Review B, 2008, 77, .	1.1	126
5484	Surface structure and water adsorption on<mml:math xmlns:mml="http://www.w3.org/1998/Math/MathML" display="inline"><mml:mrow><mml:msub><mml:mi mathvariant="normal">Fe</mml:mi><mml:mn>3</mml:mn></mml:msub><mml:msub><mml:mi mathvariant="normal">O</mml:mi><mml:mn>4</mml:mn></mml:msub><mml:mrow><mml:mo>(</mml:mo><mml:mn>111</mml:mn> ... Physical Review B, 2008, 77, .	1.1	96
5485	Modeling dislocation cores in<mml:math xmlns:mml="http://www.w3.org/1998/Math/MathML" display="inline"><mml:mrow><mml:mi mathvariant="normal">Sr</mml:mi><mml:mi mathvariant="normal">Ti</mml:mi><mml:msub><mml:mi mathvariant="normal">O</mml:mi><mml:mn>3</mml:mn></mml:msub></mml:mrow></mml:math>using the Peierls-Nabarro model. Physical Review B, 2008, 77, .	1.1	62
5486	Iron in silicon: Interactions with radiation defects, carbon, and oxygen. Physical Review B, 2008, 77, .	1.1	58
5487	Highly destabilized Mg-Ti-Ni-H system investigated by density functional theory and hydrogenography. Physical Review B, 2008, 77, .	1.1	39

#	Article	IF	Citations
5488	Model calculation of the electron-phonon coupling in Cs/Cu(111). Physical Review B, 2008, 78, .	1.1	8
5489	Magnetism and chemical ordering in binary transition metal clusters. Physical Review B, 2008, 78, .	1.1	29
5490	Structural, electronic, and energetic properties ofSiC[111]âˆ•ZrB2[0001]heterojunctions: A first-principles density functional theory study. Physical Review B, 2008, 77, .	1.1	11
5491	Peculiar distribution of Pd on Au nanoclusters: First-principles studies. Physical Review B, 2008, 78, .	1.1	62
5492	DX centers in CdTe: A density functional study. Applied Physics Letters, 2008, 92, 181908.	1.5	10
5493	Method to extract anharmonic force constants from first principles calculations. Physical Review B, 2008, 77, .	1.1	295
5494	Origin of ferromagnetism in ZnO codoped with Ga and Co: Experiment and theory. Physical Review B, 2008, 78, .	1.1	65
5495	Dielectric properties and excitons for extended systems from hybrid functionals. Physical Review B, 2008, 78, .	1.1	303
5496	Manipulation of benzene on Cu(110) by dynamic force microscopy: Anab initiostudy. Physical Review B, 2008, 77, .	1.1	23
5497	Resolving the Optical Spectrum of Water: Coordination and Electrostatic Effects. Physical Review Letters, 2008, 100, 207403.	2.9	62
5498	Dynamic structure in supported Pt nanoclusters: Real-time density functional theory and x-ray spectroscopy simulations. Physical Review B, 2008, 78, .	1.1	77
5499	Unoccupied states of individual silver clusters and chains on Ag(111). Physical Review B, 2008, 77, .	1.1	35
5500	Effect of on-site Coulomb repulsion term<mml:math xmlns:mml="http://www.w3.org/1998/Math/MathML" display="inline"><mml:mi>U</mml:mi></mml:math>on the band-gap states of the reduced rutile (110)<mml:math xmlns:mml="http://www.w3.org/1998/Math/MathML" display="inline"><mml:mrow><mml:mi mathvariant="normal">Ti</mml:mi><mml:msub><mml:mi mathvariant="normal">O</mml:mi><mml:mn>2</mml:mn></mml:msub></mml:mrow></mml:math>surface.	1.1	165
5501	display="inline"><mml:mi>In</mml:mi><mml:mi>M</mml:mi><mml:msub><mml:mi mathvariant="normal">O</mml:mi><mml:mn>3</mml:mn></mml:msub><mml:mo stretchy="false">(</mml:mo><mml:mi>ZnO</mml:mi><mml:msub><mml:mo) Tj ETQq1 1 0.784314 rgBT /Overlock 10 Tf 50 207 Td (st	2.9	63
5502	Atomic Nanowires on the<mml:math xmlns:mml="http://www.w3.org/1998/Math/MathML" display="inline"><mml:mi>Pt</mml:mi><mml:mo>/</mml:mo><mml:mi>Ge</mml:mi><mml:mo stretchy="false">(</mml:mo><mml:mn>001</mml:mn><mml:mo) Tj ETQq0 0 0 rgBT /Overlock 10 Tf 50 177 Td (stretchy="false")</mml	2.9	44
5503	Lattice dynamics of ferromagnetic<mml:math xmlns:mml="http://www.w3.org/1998/Math/MathML" display="inline"><mml:mrow><mml:mi mathvariant="normal">Co</mml:mi><mml:msub><mml:mi mathvariant="normal">Sb</mml:mi><mml:mn>3</mml:mn></mml:msub></mml:mrow></mml:math>: Inelastic x-ray scattering on . Physical Review B, 2008, 77, .	1.1	41
5504	Magnetism and chemical ordering in icosahedral Al-Pd-Mn quasicrystal. Physical Review B, 2008, 78, .	1.1	7
5505	Atomic Scale Design and Control of Cation Distribution in Hexagonal Ferrites. Physical Review Letters, 2008, 101, 067201.	2.9	31

#	Article	IF	Citations
5506	Electronic Structure of the<mml:math xmlns:mml="http://www.w3.org/1998/Math/MathML" display="inline"><mml:msub><mml:mi>Na</mml:mi><mml:mi>x</mml:mi></mml:msub><mml:msub><mml:mi>Co</mml:mi><mml:m Physical Review Letters, 2008, 101, 246808.	2.9	11
5507	Density functional calculations of the electronic structure and optical properties of the ternary carbides<mml:math xmlns:mml="http://www.w3.org/1998/Math/MathML" display="inline"><mml:mrow><mml:msub><mml:mrow><mml:mtext>Al</mml:mtext></mml:mrow><mml:mn>4</mml:mn></mml:msu xmlns:mml="http://www.w3.org/1998/Math/MathML" display="inline"><mml:mrow><mml:msub><mml:mrow><mml:mtext>Al</mml:mte. Physical Review B, 2008, 78, .	1.1	24
5508	Superconductivity and spin fluctuations in{Th,U}Pt4Ge12skutterudites. Physical Review B, 2008, 78, .	1.1	38
5509	<i>Ab initio</i>study of the band structures of different phases of higher manganese silicides. Physical Review B, 2008, 77, .	1.1	103
5510	Magnetism enhanced layer-like structure of small cobalt clusters. Physical Review B, 2008, 78, .	1.1	47
5511	Insights into the structure of the stable and metastable<mml:math xmlns:mml="http://www.w3.org/1998/Math/MathML"		

#	Article	IF	Citations
5524	First-principles study of In, Ga, and N adsorption on<mml:math xmlns:mml="http://www.w3.org/1998/Math/MathML" display="inline"><mml:mrow><mml:msub><mml:mrow><mml:mtext>In</mml:mtext></mml:mrow><mml:mi>x</mml:mi></mml:msub> and<mml:math xmlns:mml="http://www.w3.org/1998/Math/MathML" display="inline"><mml:mrow><mml:mro. Physical Review B, 2008, 77, .	1.1	8
5525	First-principles LDA+U studies of the In-doped ZnO transparent conductive oxide. Journal of Applied Physics, 2008, 104, 063703.	1.1	41
5526	Electronic origin of void formation in fcc metals. Physical Review B, 2008, 77, .	1.1	17
5527	Atomic gold chain on hydrogen terminated<mml:math xmlns:mml="http://www.w3.org/1998/Math/MathML" display="inline"><mml:mrow><mml:mtext>Si</mml:mtext><mml:mrow><mml:mo>(</mml:mo><mml:mrow><mml:mn>001</mml:m A density functional theory study. Physical Review B, 2008, 77, .	1.1	4
5528	Anomalies in transition metal conductivity: Strong evidence for Fermi-velocity dominance. Physical Review B, 2008, 77, .	1.1	0
5529	A study of Hf vacancies at Si:HfO2 heterojunctions. Applied Physics Letters, 2008, 92, 152911.	1.5	4
5530	Ab initioprediction of ordered ground-state structures in<mml:math xmlns:mml="http://www.w3.org/1998/Math/MathML" display="inline"><mml:mrow><mml:msub><mml:mrow><mml:mtext>ZrO</mml:mtext></mml:mrow><mml:mn>2</mml:mn></mml:ms Physical Review B, 2008, 77, .	1.1	76
5531	Physical Review B, 2008, 77, . the layered crystals<mml:math xmlns:mml="http://www.w3.org/1998/Math/MathML" display="inline"><mml:mrow><mml:mtext>LaCoO</mml:mtext><mml:mi>X</mml:mi><mml:mspace width="0.3em" /><mml:mrow><mml:mo>(</mml:mo><mml:mrow><mml:mi>X</mml:mi><mml:mo>=</mml:mo><mml:mtext>P</mml:mtext><mml:mn	1.1	138
5532	Physical Review B, 2008, 77, . Adatom-induced variations of the atomic and electronic structures ofSi(111)3Ã—3â^'Ag: A first-principles study. Physical Review B, 2008, 77, .	1.1	18
5533	Effect of adsorbed hydrogen on the stability of titanium atoms on aluminum surfaces. Physical Review B, 2008, 77, .	1.1	14
5534	Atomic scale study of the degradation mechanism of boron contaminated hafnium oxide. Applied Physics Letters, 2008, 92, 052907.	1.5	1
5535	Indium-oxide polymorphs from first principles: Quasiparticle electronic states. Physical Review B, 2008, 77, .	1.1	219
5536	Theoretical study of electron confinement in Cu corrals on a Cu(111) surface. Physical Review B, 2008, 77, .	1.1	10
5537	Effects of Y doping on the structural stability and defect properties of cubic HfO2. Journal of Applied Physics, 2008, 104, .	1.1	31
5538	Air-stable n-type operation of Gd-contacted carbon nanotube field effect transistors. Applied Physics Letters, 2008, 93, .	1.5	16
5539	Ballistic conductance of oxygen and sulfur-incorporated zigzag Au atomic wires. Physical Review B, 2008, 77, .	1.1	12
5540	Fivefold<mml:math xmlns:mml="http://www.w3.org/1998/Math/MathML" display="inline"><mml:mrow><mml:mi>i</mml:mi><mml:mtext>â^'</mml:mtext><mml:mi mathvariant="normal">Al</mml:mi><mml:mtext>â^'</mml:mtext><mml:mi mathvariant="normal">Pd</mml:mi><mml:mtext>â^'</mml:mtext><mml:mi mathvariant="normal">Mn</mml:mi></mml:mrow></mml:math>surface as template for growing monatomic quasiperiodic layers: First-principles simulations for adatoms from groups one to three. P	1.1	14
5541	Crystallographic phase transition and island height selection in In/Si(111) growth. Physical Review B, 2008, 77, .	1.1	30

#	Article	IF	Citations
5542	Theoretical study of the surface reactivity of alkaline earth oxides: Local density of states evaluation of the local softness. Journal of Chemical Physics, 2008, 128, 034708.	1.2	31
5543	Low-energy antiphase boundaries, degenerate superstructures, and phase stability in frustrated fcc Ising model and Ag-Au alloys. Physical Review B, 2008, 77, .	1.1	32
5544	Modeling the sorption dynamics of NaH using a reactive force field. Journal of Chemical Physics, 2008, 128, 164714.	1.2	29
5545	First-principles calculation of defect formation energies and electronic properties in stannate pyrochlores. Journal of Applied Physics, 2008, 104, .	1.1	23
5546	The formation of pentagon-heptagon pair defect by the reconstruction of vacancy defects in carbon nanotube. Applied Physics Letters, 2008, 92, 043104.	1.5	33
5547	First-principles study for transport properties of armchair carbon nanotubes with a double vacancy under strain. Journal of Applied Physics, 2008, 103, 113714.	1.1	5
5548	Ab initio investigation on oxygen defect clusters in UO2+x. Applied Physics Letters, 2008, 93, 201903.	1.5	36
5549	Density functional theory calculations of anisotropic constitutive relationships in alpha-cyclotrimethylenetrinitramine. Journal of Applied Physics, 2008, 104, .	1.1	17
5550	The interaction between a monolayer of single-molecule magnets and a metal surface. Journal of Applied Physics, 2008, 103, 07B907.	1.1	14
5551	First-principles study of structural and energetic properties of A2Hf2O7 (A=Dy, Ho, Er) compounds. Journal of Applied Physics, 2008, 104, .	1.1	17
5552	Atomic size mismatch strain induced surface reconstructions. Applied Physics Letters, 2008, 92, 062104.	1.5	9
5553	Freestanding (3,0) boron nitride nanotube: Expected to be stable well over room temperature. Applied Physics Letters, 2008, 93, 223108.	1.5	20
5554	First principles study of Geâ^•Si exchange mechanisms at the Si(001) surface. Applied Physics Letters, 2008, 92, 191908.	1.5	21
5555	Heteroepitaxial growth and optoelectronic properties of layered iron oxyarsenide, LaFeAsO. Applied Physics Letters, 2008, 93, 162504.	1.5	91
5556	Are there stable long-range ordered Fe1â^'xCrx compounds?. Applied Physics Letters, 2008, 92, .	1.5	37
5557	Sources of unintentional conductivity in InN. Applied Physics Letters, 2008, 92, 032104.	1.5	85
5558	Metastable phase formation and magnetic properties of the Feâ€“Nb system studied by atomistic modeling and ion beam mixing. Journal of Applied Physics, 2008, 104, 014914.	1.1	7
5559	Optical properties of (GeTe, Sb2Te3) pseudobinary thin films studied with spectroscopic ellipsometry. Applied Physics Letters, 2008, 93, .	1.5	53

#	Article	IF	Citations
5560	Effect of chlorine residue on electrical performance of atomic layer deposited hafnium silicate. Journal of Applied Physics, 2008, 103, 114102.	1.1	10
5561	First-principles calculations on solid nitrogen: A comparative study of high-pressure phases. Physical Review B, 2008, 77, .	1.1	45
5562	Enhancement in middle-ultraviolet emission in a surface-plasmon-assisted coaxial nanocavity. Applied Physics Letters, 2008, 93, 091902.	1.5	4
5563	Intershell interaction in double walled carbon nanotubes: Charge transfer and orbital mixing. Physical Review B, 2008, 77, .	1.1	61
5564	First-principles-based investigation of kinetic mechanism of SiC(0001) dry oxidation including defect generation and passivation. Journal of Applied Physics, 2008, 104, 093508.	1.1	54
5565	Anode Material of CoMnSb for Rechargeable Li-Ion Battery. Journal of the Electrochemical Society, 2008, 155, A61.	1.3	9
5566	Stability mechanism of cuboctahedral clusters in<mml:math xmlns:mml="http://www.w3.org/1998/Math/MathML" display="inline"><mml:mrow><mml:mi mathvariant="normal">U</mml:mi><mml:msub><mml:mi mathvariant="normal">O</mml:mi><mml:mrow><mml:mn>2</mml:mn><mml:mo>+</mml:mo><mml:mi>x</mml:mi></mml:mrow></m First-principles calculations. Physical Review B, 2008, 77, .	1.1	47
5567	xmlns:mml="http://www.w3.org/1998/Math/MathML" display="inline"><mml:mrow><mml:mrow><mml:mo>(</mml:mo><mml:mrow><mml:mn>2</mml:mn><mml:mover) Tj ETQq1 1 0.784	1.1	43
5568	Electronic structure and Fermi surface character of LaNiPO from first principles. Physical Review B, 2008, 77, .	1.1	19
5569	First-principles theory of nanoscale pattern formation in ultrathin alloy films: A comparative study of Fe-Ag on Ru(0001) and Mo(110) substrates. Physical Review B, 2008, 77, .	1.1	13
5570	Ab initio determination of Ehrlichâ€“Schwoebel barriers on Cu{111}. Applied Physics Letters, 2008, 92, .	1.5	35
5571	Effect of strain on the band gap and effective mass of zigzag single-wall carbon nanotubes: First-principles density-functional calculations. Physical Review B, 2008, 77, .	1.1	42
5572	First-principles study of the spin-lattice coupling in spin frustrated<mml:math xmlns:mml="http://www.w3.org/1998/Math/MathML" display="inline"><mml:mrow><mml:msub><mml:mrow><mml:mtext>DyMn</mml:mtext></mml:mrow><mml:mn>2</mml:mn></mml:m Physical Review B, 2008, 78, .	1.1	16
5573	Calculation of surface core-level shifts within complete screening: Problems with pseudohydrogenated slabs. Physical Review B, 2008, 77, .	1.1	17
5574	Hydrogen-induced magnetization and tunable hydrogen storage in graphitic structures. Physical Review B, 2008, 77, .	1.1	33
5575	Ab initiostudies of structural and electronic properties of the crystalline<mml:math xmlns:mml="http://www.w3.org/1998/Math/MathML" display="inline"><mml:mrow><mml:msub><mml:mrow><mml:mtext>Ge</mml:mtext></mml:mrow><mml:mn>2</mml:mn></mml:msu Physical Review B, 2008, 77, .	1.1	30
5576	Melting of Na at high pressure fromab initiocalculations. Physical Review B, 2008, 77, .	1.1	31
5577	Electrical, thermal, and elastic properties of theMAX-phase Ti2SC. Journal of Applied Physics, 2008, 104, .	1.1	69

#	Article	IF	Citations
5578	Surface Modification of Ni-YSZ Using Niobium Oxide for Sulfur-Tolerant Anodes in Solid Oxide Fuel Cells. Journal of the Electrochemical Society, 2008, 155, B449.	1.3	45
5579	Pt-induced nanowires on Ge(001):Ab initiostudy. Physical Review B, 2008, 78, .	1.1	22
5580	Oxygen defect accumulation at Si:HfO2 interfaces. Applied Physics Letters, 2008, 92, .	1.5	40
5581	Defect-mediated ferromagnetism in insulating Co-doped anatase<mml:math xmlns:mml="http://www.w3.org/1998/Math/MathML" display="inline"><mml:mrow><mml:msub><mml:mrow><mml:mtext>TiO</mml:mtext></mml:mrow><mml:mn>2</mml:mn></mml:msub></mml:mrow></mml:math>films. Physical Review B, 2008, 78, .	1.1	59
5582	Calculation of dopant segregation ratios at semiconductor interfaces. Physical Review B, 2008, 78, .	1.1	8
5583	Theory of the excitation of the vibrational mode of an adatom-substrate system under a resonant laser field. Physical Review B, 2008, 78, .	1.1	2
5584	Peierls Potential for Crowdions in the bcc Transition Metals. Physical Review Letters, 2008, 101, 115504.	2.9	48
5585	Defect-Dipole Formation in Copper-Doped<mml:math xmlns:mml="http://www.w3.org/1998/Math/MathML" display="inline"><mml:msub><mml:mi>PbTiO</mml:mi><mml:mn>3</mml:mn></mml:msub></mml:math>Ferroelectrics. Physical Review Letters, 2008, 100, 095504.	2.9	118
5586	Icosahedral ordering in Zr41Ti14Cu12.5Ni10Be22.5 bulk metallic glass. Applied Physics Letters, 2008, 92, 201913.	1.5	33
5587	Transport properties of single vacancies in nanotubes. Physical Review B, 2008, 77, .	1.1	35
5588	Tunable bandgap structures of two-dimensional boron nitride. Journal of Applied Physics, 2008, 104, .	1.1	59
5589	Electronic structure of Cu3N films studied by soft x-ray spectroscopy. Journal of Physics Condensed Matter, 2008, 20, 235212.	0.7	12
5590	Density functional theory study of mercury adsorption on metal surfaces. Physical Review B, 2008, 77, .	1.1	65
5591	<mml:math xmlns:mml="http://www.w3.org/1998/Math/MathML" display="inline"><mml:mrow><mml:msub><mml:mtext>H</mml:mtext><mml:mn>2</mml:mn></mml:msub></mml:mrow></mml:math>on strained pseudomorphic monolayers of Cu and Pd on Ru(0001). Physical Review B, 2008, 77, .	1.1	34
5592	First principles calculations of the structural and electronic properties of the type-I semiconductor clathrate alloysBa8Ga16SixGe30â^'xandSr8Ga16SixGe30â^'x. Physical Review B, 2008, 77, .	1.1	23
5593	Density functional theory prediction of a hysteretic phase transition in InPu crystals. Physical Review B, 2008, 77, .	1.1	1
5594	Divide-and-conquer density functional theory on hierarchical real-space grids: Parallel implementation and applications. Physical Review B, 2008, 77, .	1.1	63
5595	Local atomic and electronic structures around Mg and Al dopants in<mml:math xmlns:mml="http://www.w3.org/1998/Math/MathML" display="inline"><mml:mrow><mml:msub><mml:mrow><mml:mtext>LiNiO</mml:mtext></mml:mrow><mml:mn>2</mml:mn></mml:msub></mml:mrow></mml:math>studied by XANES and ELNES and first-principles calculations. Physical Review B, 2008, 78, .	1.1	38

#	Article	IF	Citations
5596	Strain relief through stair-rod dislocations in ultrathin epitaxial metal films: Defect geometry and energetics. Physical Review B, 2008, 78, .	1.1	7
5597	Mg acceptor energy levels in<mml:math xmlns:mml="http://www.w3.org/1998/Math/MathML" display="inline"><mml:mrow><mml:msub><mml:mi mathvariant="normal">Al</mml:mi><mml:mi>x</mml:mi></mml:msub><mml:msub><mml:mi mathvariant="normal">In</mml:mi><mml:mi>y</mml:mi></mml:msub><mml:msub><mml:mi mathvariant="normal">Ga</mml:mi><mml:mrow><mml:mn>1</mml:mn><mml:mo>â^'</mml:mo><mml:mi>x</mml:mi><mml:mo>â^'	1.1	15
5598	Dynamical stabilization of cubic<mml:math xmlns:mml="http://www.w3.org/1998/Math/MathML" display="inline"><mml:mrow><mml:msub><mml:mrow><mml:mtext>ZrO</mml:mtext></mml:mrow><mml:mn>2</mml:mn></mml:msub></mml:mrow></mml:math> phonon-phonon interactions:Ab initiocalculations. Physical Review B, 2008, 78, .	1.1	26
5599	Hydrogen dissociation on Mg(0001) studied via quantum Monte Carlo calculations. Physical Review B, 2008, 78, .	1.1	40
5600	Quasigraphite: Density functional theory based predictions of a structure and its properties. Physical Review B, 2008, 78, .	1.1	3
5601	Bayesian approach to the calculation of lateral interactions: NO/Rh(111). Physical Review B, 2008, 78, .	1.1	20
5602	Probing and modifying the empty-state threshold of anataseTiO2: Experiments andab initiotheory. Physical Review B, 2008, 78, .	1.1	17
5603	Time-resolved optical spectroscopy measurements of shocked liquid deuterium. Physical Review B, 2008, 78, .	1.1	43
5604	Atomic-scale study of low-temperature equilibria in iron-rich Al-C-Fe. Physical Review B, 2008, 78, .	1.1	11
5605	Comment on â€œHuge Excitonic Effects in Layered Hexagonal Boron Nitrideâ€. Physical Review Letters, 2008, 100, 189701; discussion 189702.	2.9	64
5606	Density functional study of single-wall and double-wall platinum nanotubes. Physical Review B, 2008, 78, .	1.1	18
5607	Size dependence of lattice constants of semiconductor nanocrystals. Applied Physics Letters, 2008, 92, 043130.	1.5	13
5608	Lubricant effect of copper nanoclusters on the dislocation core inÎ±â^'Fe. Physical Review B, 2008, 77, .	1.1	12
5609	Near Neutrality of an Oxygen Molecule Adsorbed on a Pt(111) Surface. Physical Review Letters, 2008, 101, 146101.	2.9	51
5610	Carrier compensation in semi-insulating CdTe: First-principles calculations. Physical Review B, 2008, 77, .	1.1	59
5611	Enhanced mechanical strength and ductility of metal-repaired defective carbon nanotubes: A density functional study. Applied Physics Letters, 2008, 92, .	1.5	1
5612	Quantum Electron Transport through Ultrathin Si Films: Effects of Interface Passivation on Fermi-Level Pinning. Physical Review Letters, 2008, 101, 166801.	2.9	5
5613	First-principles study of water on copper and noble metal (110) surfaces. Physical Review B, 2008, 77, .	1.1	99

#	Article	IF	Citations
5614	Elastically induced coexistence of surface reconstructions. Physical Review B, 2008, 77, .	1.1	15
5615	Spin Tunneling in Junctions with Disordered Ferromagnets. Physical Review Letters, 2008, 100, 057205.	2.9	31
5616	Ground-state structure of coherent lattice-mismatched zinc-blendeA1â^'xBxCsemiconductor alloys (x=0.25and 0.75). Physical Review B, 2008, 77, .	1.1	10
5617	Electronic structure and orbital ordering of<mml:math xmlns:mml="http://www.w3.org/1998/Math/MathML" display="inline"><mml:mrow><mml:mi mathvariant="normal">Sr</mml:mi><mml:msub><mml:mi mathvariant="normal">Ru</mml:mi><mml:mrow><mml:mn>1</mml:mn><mml:mo>â^'</mml:mo><mml:mi>x</mml:mi></mml:mrow><mml:mi mathvariant="normal">Ti</mml:mi><mml:mi>x</mml:mi></mml:msub><mml:msub><mml:mi mathvariant="normal">O</mml:mi><mml:mn>3</mml:mn></mml:msub></mml:mrow></mml:math>:<mml:math	1.1	17
5618	Structural, electronic, and magnetic properties of 13-, 55-, and 147-atom clusters of Fe, Co, and Ni: A spin-polarized density functional study. Physical Review B, 2008, 78, .	1.1	70
5619	Short- and medium-range order in a<mml:math xmlns:mml="http://www.w3.org/1998/Math/MathML" display="inline"><mml:mrow><mml:msub><mml:mrow><mml:mtext>Zr</mml:mtext></mml:mrow><mml:mrow><mml:mn>43</mml:mn></mml:mrow></mml:msub></mml:mrow></mml:math> Experimental and simulation studies. Physical Review B, 2008, 78, .	1.1	73
5620	Constructing an Array of Anchored Single-Molecule Rotors on Gold Surfaces. Physical Review Letters, 2008, 101, 197209.	2.9	127
5621	Work function anisotropy and surface stability of half-metallicCrO2. Physical Review B, 2008, 77, .	1.1	18
5622	High pressure structural phase transitions in Sr fromab initiocalculations. Physical Review B, 2008, 77, .	1.1	13
5623	Unique magnetic coupling between Mn doped stannaspherenes Mn@Sn12. Applied Physics Letters, 2008, 92, .	1.5	25
5624	Formation of Pt-induced Ge atomic nanowires on Pt/Ge(001): A density functional theory study. Physical Review B, 2008, 77, .	1.1	130
5625	Magnetic coupling properties of Mn-doped ZnO nanowires: First-principles calculations. Journal of Applied Physics, 2008, 103, 073903.	1.1	22
5626	Spin confinement in the superlattices of graphene ribbons. Applied Physics Letters, 2008, 92, .	1.5	79
5627	Electronic structure of Ga-, In-, and Tl-doped PbTe: A supercell study of the impurity bands. Physical Review B, 2008, 78, .	1.1	62
5628	Ab initioelectronic structure and correlations in pristine and potassium-doped molecular crystals of copper phthalocyanine. Physical Review B, 2008, 77, .	1.1	50
5629	Density functional study of a ferromagnetic ferroelectric<mml:math xmlns:mml="http://www.w3.org/1998/Math/MathML" display="inline"><mml:mrow><mml:mi mathvariant="normal">La</mml:mi><mml:mi mathvariant="normal">Mn</mml:mi><mml:msub><mml:mi mathvariant="normal">O</mml:mi><mml:mn>3</mml:mn></mml:msub><mml:mo>â•</mml:mo><mml:mi mathvariant="normal">Ba</mml:mi><mml:mi mathvariant="normal">Ti</mml:mi><mml:msub><mml:mi mathvariant="normal">O</mml:mi><mml:mn>3</mml:mn></mml:msub></mml:mrow></mml:math>superlattice.	1.1	13
5630	Carbon impurity dissolution and migration in bcc Fe-Cr: First-principles calculations. Physical Review B, 2008, 78, .	1.1	35
5631	Preconditioning of self-consistent-field cycles in density-functional theory: The extrapolar method. Physical Review B, 2008, 78, .	1.1	29

#	Article	IF	Citations
5632	Effect of normal stress on the ideal shear strength in covalent crystals. Physical Review B, 2008, 77, .	1.1	52
5633	Using molecular fragments to estimate electron-phonon coupling and possible superconductivity in covalent materials. Physical Review B, 2008, 78, .	1.1	13
5634	Combined experimental and theoretical study of thin hafnia films. Physical Review B, 2008, 78, .	1.1	32
5635	Growth of Co nanostructures on Cu(110): Atomic-scale simulations. Physical Review B, 2008, 78, .	1.1	21
5636	Chemical pressure effect on the transport and electronic band structure of<mml:math xmlns:mml="http://www.w3.org/1998/Math/MathML" display="inline"><mml:mrow><mml:msub><mml:mrow><mml:mtext>Fe</mml:mtext></mml:mrow><mml:mn>2</mml:mn></mml:msub	1.1	20
5637	Physical Review B, 2008, 78, . Structure of 38Ak<mml:math xmlns:mml="http://www.w3.org/1998/Math/MathML" display="inline"><mml:msub><mml:mi>T</mml:mi><mml:mi>c</mml:mi></mml:msub></mml:math><mml:math xmlns:mml="http://www.w3.org/1998/Math/MathML" display="inline"><mml:msub><mml:mi>Cs</mml:mi><mml:mn>3</mml:mn></mml:msub><mml:msub><mml:mi	2.9	22
5638	First-Principles Theory of Competing Order Types, Phase Separation, and Phonon Spectra in Thermoelectric<mml:math xmlns:mml="http://www.w3.org/1998/Math/MathML" display="inline"><mml:msub><mml:mi>AgPb</mml:mi><mml:mi>m</mml:mi></mml:msub><mml:msub><mml:mi>SbTe</mml:mi><mm Physical Review Letters, 2008, 101, 155704.	2.9	82
5639	Ab initiostudy ofEMIM-BF4molecule adsorption on Li surfaces as a model for ionic liquid/Li interfaces in Li-ion batteries. Physical Review B, 2008, 78, .	1.1	38
5640	High temperature ferromagnetism in single crystalline dilute Fe-doped<mml:math xmlns:mml="http://www.w3.org/1998/Math/MathML" display="inline"><mml:mrow><mml:mi mathvariant="normal">Ba</mml:mi><mml:mi mathvariant="normal">Ti</mml:mi><mml:msub><mml:mi mathvariant="normal">O</mml:mi><mml:mn>3</mml:mn></mml:msub></mml:mrow></mml:math>. Physical Review B, 2008, 77, .	1.1	104
5641	Boron in copper: A perfect misfit in the bulk and cohesion enhancer at a grain boundary. Physical Review B, 2008, 77, .	1.1	65
5642	Mechanical properties, glass transition temperature, and bond enthalpy trends of high metalloid Fe-based bulk metallic glasses. Applied Physics Letters, 2008, 92, .	1.5	46
5643	Energetic stability, electronic structure, and magnetism in Mn-doped silicon dilute magnetic semiconductors. Physical Review B, 2008, 77, .	1.1	25
5644	Resonant Raman-active localized vibrational modes inAlyGa1âˆ'yNxAs1âˆ'xalloys: Experiment and first-principles calculations. Physical Review B, 2008, 77, .	1.1	7
5645	Electronic structure of a potential optical crystal YBa3B9O18: Experiment and theory. Applied Physics Letters, 2008, 92, 171903.	1.5	7
5646	First-principles effective Hamiltonian for ferroelectric polarization inBaTiO3/SrTiO3 superlattices. Journal of Applied Physics, 2008, 103, 124106.	1.1	15
5647	Li- and B-decorated cis-polyacetylene: A computational study. Physical Review B, 2008, 77, .	1.1	14
5648	Identification of a stable phase for the high-capacity hydrogen-storage material<mml:math xmlns:mml="http://www.w3.org/1998/Math/MathML" display="inline"><mml:mrow><mml:mtext>Zn</mml:mtext><mml:msub><mml:mrow><mml:mrow><mml:mo>(</mml:mo><mml:mrow density functional theory and lattice dynamics. Physical Review B, 2008, 77, .	1.1	18
5649	First principles assessment of metal/oxide interface adhesion. Applied Physics Letters, 2008, 92, .	1.5	62

#	Article	IF	Citations
5650	Electronic structure analysis of self-consistent embedding theory for quantum/molecular mechanics simulations. Physical Review B, 2008, 78, .	1.1	14
5651	Computational study of (111) epitaxially strained ferroelectric perovskites<mml:math xmlns:mml="http://www.w3.org/1998/Math/MathML" display="inline"><mml:mrow><mml:msub><mml:mrow><mml:mtext>BaTiO</mml:mtext></mml:mrow><mml:mn>3</mml:mn></mml:msub></mml:mrow></mml:math>/<mml:math xmlns:mml="http://www.w3.org/1998/Math/MathML" display="inline"><mml:mrow><mml:msub><mml:mrow><mml:mtext>PbTiO</mml:mtext></mml:mrow><mml:mn>3</mml:mn></mml:msub></mml:mrow></mml:math> superlattices. Physical Review B, 2008, 78, .	1.1	33
5652	Anomalous surface relaxation in hcp transition metals. Physical Review B, 2008, 78, .	1.1	10
5653	Optical spectra of Si nanocrystallites: Bethe-Salpeter approach versus time-dependent density-functional theory. Physical Review B, 2008, 78, .	1.1	64
5654	High-pressure phases of lithiaLi2O: First-principles calculations. Physical Review B, 2008, 77, .	1.1	26
5655	Origin of<mml:math xmlns:mml="http://www.w3.org/1998/Math/MathML" display="inline"><mml:mrow><mml:msub><mml:mi>a</mml:mi><mml:mrow><mml:mn>1</mml:mn><mml:mi>g</mml:mi></mml:mrow></mml:msub></mml:mrow></mml:math> surface state in<mml:math xmlns:mml="http://www.w3.org/1998/Math/MathML" display="inline"><mml:mrow><mml:msubsup><mml:mi>e</mml:mi><mml:mi>g</mml:mi><mml:mo>â€²</mml:mo></mml:msubsup></mml:mrow></mml:math> surface state influenced by the surface lattice structure in<mml:math xmlns:mml="http://www.w3.org/1998/Math/MathML" display="inline"><mml:mrow><mml:mi mathvariant="normal">Be</mml:mi><mml:mrow><mml:mo>(</mml:mo><mml:mn>10</mml:mn><mml:mover) Tj ETQq0 0 0 rgBT /Over	1.1	13
5656	Physical Review B, 2008, 77, .	1.1	10
5657	Interplay of shape, interface structure, and electrostatic fields of ionic nanodots embedded in a polar semiconductor matrix. Physical Review B, 2008, 78, .	1.1	12
5658	Yb-induced(2Ã—3)and(2Ã—4)reconstructions on Si(100) studied by first-principles calculations and high-resolution core-level photoelectron spectroscopy. Physical Review B, 2008, 78, .	1.1	8
5659	Electronic structure and chemical and magnetic interactions in ZnO doped with Co and Al: Experiments andab initiodensity-functional calculations. Physical Review B, 2008, 78, .	1.1	47
5660	First-principles theory of the energetics of He defects in bcc transition metals. Physical Review B, 2008, 78, .	1.1	130
5661	Lattice dynamics of cobalt-deficient CoO from first principles. Physical Review B, 2008, 78, .	1.1	25
5662	Structural phase transitions of cubic<mml:math xmlns:mml="http://www.w3.org/1998/Math/MathML" display="inline"><mml:mrow><mml:msub><mml:mrow><mml:mtext>Gd</mml:mtext></mml:mrow><mml:mn>2</mml:mn></mml:msub></mml:mrow></mml:math> at high pressures. Physical Review B, 2008, 78, .	1.1	107
5663	Optimizing optical absorption of TiO2 by alloying with TiS2. Applied Physics Letters, 2008, 92, .	1.5	24
5664	Studies of the periodic faceting of epitaxial molybdenum oxide grown on Mo(110). Physical Review B, 2008, 77, .	1.1	15
5665	Atomic oxygen adsorption and incipient oxidation of the Pb(111) surface: A density-functional theory study. Physical Review B, 2008, 78, .	1.1	25
5666	Effective Hamiltonian for FeAs-based superconductors. Physical Review B, 2008, 78, .	1.1	27
5667	Role of diatomic hydrogen in the electronic structure of ZnO. Physical Review B, 2008, 78, .	1.1	16

#	Article	IF	Citations
5668	Mechanism of phase transitions and electronic density of states in<mml:math xmlns:mml="http://www.w3.org/1998/Math/MathML" display="inline"><mml:mrow><mml:msub><mml:mrow><mml:mtext>LaFeAsO</mml:mtext></mml:mrow><mml:mrow><mml:mn>1</m xmlns:mml="http://www.w3.org/1998/Math/MathML" display="inline"><mml:mrow><mml:msub><mml:mrow><mml:mtext>SmFeAsO</mml. Physical Review B, 2008, 78, .	1.1	12
5669	Self-consistent calculations of strain-induced band gap changes in semiconducting<mml:math xmlns:mml="http://www.w3.org/1998/Math/MathML" display="inline"><mml:mrow><mml:mrow><mml:mo>(</mml:mo><mml:mrow><mml:mi>n</mml:mi><mml:mo>,</mml:mo><mml:m nanotubes. Physical Review B, 2008, 78, .	1.1	32
5670	Quasiatomic orbitals forab initiotight-binding analysis. Physical Review B, 2008, 78, .	1.1	90
5671	Crystal structure, electronic structure, and vibrational properties of<mml:math xmlns:mml="http://www.w3.org/1998/Math/MathML" display="inline"><mml:mrow><mml:mi>M</mml:mi><mml:mtext>AlSiH</mml:mtext></mml:mrow></mml:math><mml:math xmlns:mml="http://www.w3.org/1998/Math/MathML" display="inline"><mml:mrow><mml:mo>(</mml:mo><mml:mrow><mml:mi>M</mml:mi><mml:mo>=</mml:mo><mml:mtext>Ca</m Physical Review B, 2008, 78, .	1.1	24
5672	Formation of collective spins in frustrated clusters. Physical Review B, 2008, 77, .	1.1	7
5673	Functionalization of silicon nanowires with transition metal atoms. Physical Review B, 2008, 78, .	1.1	26
5674	Thermodynamic Ground States of Platinum Metal Nitrides. Physical Review Letters, 2008, 100, 095501.	2.9	68
5675	Dihydride dimer structures on the Si(100):H surface studied by low-temperature scanning tunneling microscopy. Physical Review B, 2008, 78, .	1.1	25
5676	Segregation of Cr impurities at bcc iron surfaces: First-principles calculations. Physical Review B, 2008, 78, .	1.1	44
5677	Role of Hydrogen in Giant Spin Polarization Observed on Magnetic Nanostructures. Physical Review Letters, 2008, 100, 026806.	2.9	24
5678	Shape and surface structure of gold nanoparticles under oxidizing conditions. Physical Review B, 2008, 77, .	1.1	49
5679	Extrinsic Nature of Point Defects on the Si(001) Surface: Dissociated Water Molecules. Physical Review Letters, 2008, 100, 036107.	2.9	53
5680	Dopant-Assisted Concentration Enhancement of Substitutional Mn in Si and Ge. Physical Review Letters, 2008, 100, 027205.	2.9	48
5681	<mml:math xmlns:mml="http://www.w3.org/1998/Math/MathML" display="inline"><mml:mrow><mml:mi mathvariant="normal">C</mml:mi><mml:msub><mml:mi mathvariant="normal">H</mml:mi><mml:mn>3</mml:mn></mml:msub><mml:mi mathvariant="normal">S</mml:mi><mml:mi mathvariant="normal">H</mml:mi></mml:mrow></mml:math>molecules deposited on Cu(111) and	1.1	8
5682	Charging of Metal Adatoms on Ultrathin Oxide Films: Au and Pd on<mml:math xmlns:mml="http://www.w3.org/1998/Math/MathML" display="inline"><mml:mi>FeO</mml:mi><mml:mo>/</mml:mo><mml:mi>Pt</mml:mi><mml:mo stretchy="false">(</mml:mo><mml:mn>111</mml:mn><mml:mo) Tj ETQq0 0 0 rgBT /Overlock 10 Tf 50 167 Td (stretchy="false">)</mm	2.9	109
5683	Self-Trapped Interstitial-Type Defects in Iron. Physical Review Letters, 2008, 100, 145503.	2.9	94
5684	Nondestructive Room-Temperature Adsorption of2,4,6-tri(2â€²-thienyl)âˆ’1,3,5-triazineon a Si-B Interface: High-Resolution STM Imaging and Molecular Modeling. Physical Review Letters, 2008, 100, 076405.	2.9	30
5685	Charge origin and localization at the<mml:math xmlns:mml="http://www.w3.org/1998/Math/MathML" display="inline"><mml:mi>n</mml:mi></mml:math>-type<mml:math xmlns:mml="http://www.w3.org/1998/Math/MathML" display="inline"><mml:mrow><mml:msub><mml:mrow><mml:mtext>SrTiO</mml:mtext></mml:mrow><mml:mn>3</mml:mn></mml:mrow></mm Physical Review B, 2008, 78, .	1.1	189

#	Article	IF	Citations
5686	Hydrogen in ZnO revisited: Bond center versus antibonding site. Physical Review B, 2008, 78, .	1.1	35
5687	First-principles study of magnetism at grain boundaries in iron and nickel. Physical Review B, 2008, 78, .	1.1	73
5688	First-Principles Approach to Lattice-Mediated Magnetoelectric Effects. Physical Review Letters, 2008, 101, 117201.	2.9	91
5689	Two FeH pairs in<mml:math xmlns:mml="http://www.w3.org/1998/Math/MathML" display="inline"><mml:mi>n</mml:mi></mml:math>-type Si and their implications: A theoretical study. Physical Review B, 2008, 78, .	1.1	8
5690	Origin of the Structural and Magnetic Anomalies of the Layered Compound<mml:math xmlns:mml="http://www.w3.org/1998/Math/MathML" display="inline"><mml:msub><mml:mi>SrFeO</mml:mi><mml:mn>2</mml:mn></mml:msub></mml:math>: A Density Functional Investigation. Physical Review Letters, 2008, 100, 167207.	2.9	148
5691	Electronic structure and properties of Li-insertion materials:<mml:math xmlns:mml="http://www.w3.org/1998/Math/MathML" display="inline"><mml:mi>Si</mml:mi><mml:mo stretchy="false">(</mml:mo><mml:mn>111</mml:mn><mml:mo stretchy="false">)</mml:mo><mml:mtext mathvariant="normal">â^'</mml:mtext><mml:mo stretchy="false">(</mml:mo><mml:mn>7</mml:mn><mml:mo>Ã—</mml:mo><mml:mn>7</mml:mn><mml:mo	2.9	29
5692	First-principles-based phase diagram of the cubic BNC ternary system. Physical Review B, 2008, 77, .	1.1	36
5693	Electronic structure and properties of Li-insertion materials:<mml:math xmlns:mml="http://www.w3.org/1998/Math/MathML" display="inline"><mml:mrow><mml:msub><mml:mi mathvariant="normal">Li</mml:mi><mml:mn>2</mml:mn></mml:msub><mml:mi mathvariant="normal">Ru</mml:mi><mml:msub><mml:mi mathvariant="normal">O</mml:mi><mml:mn>3</mml:mn></mml:msub></mml:mrow></mml:math>and<mml:math xmlns:mml="http://www.w3.org/1998/Math/MathML" display="inline"><mml:mrow><mml:mi mathvariant	1.1	31
5694	Significance of third-order elasticity for determination of the pressure coefficient of the light emission in strained quantum wells. Physical Review B, 2008, 78, .	1.1	10
5695	Density functional study of surface-supported planar magic Ag nanoclusters. Physical Review B, 2008, 78, .	1.1	11
5696	The Role of Water in the Radiation Response of Wet and Dry Oxides. IEEE Transactions on Nuclear Science, 2008, 55, 2085-2089.	1.2	7
5697	Structure of gold atoms on stoichiometric and defective ceria surfaces. Journal of Chemical Physics, 2008, 129, 194708.	1.2	103
5698	Ab Initio Study of the Surface Properties and Nanoscale Effects of LiMnPO[sub 4]. Electrochemical and Solid-State Letters, 2008, 11, A94.	2.2	73
5699	Engineering the magnetic structure of Fe clusters by Mn alloying. Nanotechnology, 2008, 19, 245701.	1.3	13
5700	Giant strain in lead-free (Bi0.5Na0.5)TiO3-based single crystals. Applied Physics Letters, 2008, 92, .	1.5	129
5701	Intrinsic point defects in aluminum antimonide. Physical Review B, 2008, 77, .	1.1	40
5702	Density Functional Model Studies of Uranyl Adsorption on (001) Surfaces of Kaolinite. Langmuir, 2008, 24, 9515-9524.	1.6	90
5703	Real-space pseudopotential method for first principles calculations of general periodic and partially periodic systems. Physical Review B, 2008, 78, .	1.1	79

#	Article	IF	Citations
5704	Theoretical study of kinks on screw dislocation in silicon. Physical Review B, 2008, 77, .	1.1	49
5705	Fe-induced spin-polarized electronic states in a realistic semiconductor tunnel barrier. Physical Review B, 2008, 77, .	1.1	5
5706	Electronic properties of<mml:math xmlns:mml="http://www.w3.org/1998/Math/MathML" display="inline"><mml:mrow><mml:msub><mml:mi mathvariant="normal">Sc</mml:mi><mml:mn>5</mml:mn></mml:msub><mml:msub><mml:mi>M</mml:mi><mml:mn>4</mml:mn></ mathvariant="normal">Si</mml:mi><mml:mn>10</mml:mn></mml:msub></mml:mrow></mml:math><mml:math xmlns:mml="http://www.w3.org/1998/Math/MathML"		

#	Article	IF	Citations
5722	Intrinsic ferromagnetism due to cation vacancies in Gd-doped GaN: First-principles calculations. Physical Review B, 2008, 78, .	1.1	82
5723	Observation of a metallic ground state of<mml:math xmlns:mml="http://www.w3.org/1998/Math/MathML" display="inline"><mml:mrow><mml:mtext>Sn</mml:mtext><mml:mo>/</mml:mo><mml:mtext>Ge</mml:mtext><mml:mrow><mml:mo> 4 K. Physical Review B, 2008, 78, .	1.1	10
5724	Concentration dependence of self-interstitial and boron diffusion in silicon. Applied Physics Letters, 2008, 92, .	1.5	6
5725	Electrical activity of hydrogen impurities in GaSb: First-principles calculations. Physical Review B, 2008, 78, .	1.1	16
5726	Bismuth-stabilized<mml:math xmlns:mml="http://www.w3.org/1998/Math/MathML" display="inline"><mml:mrow><mml:mrow><mml:mo>(</mml:mo><mml:mrow><mml:mn>2</mml:mn><mml:mo>Ã—</mml:mo><mml:m xmlns:mml="http://www.w3.org/1998/Math/MathML" display="inline"><mml:mrow><mml:mrow><mml:mo>(</mml:mo><mml:mrow><mml:mn>2</mml:mn><mml:mo>Ã—</mml:mo><mml:m Physical Review B, 2008, 78, .	1.1	36
5727	on<mml:math xmlns:mml="http://www.w3.org/1998/Math/MathML" display="inline"><mml:mrow><mml:mi mathvariant="normal">Au</mml:mi><mml:mo>â^•</mml:mo><mml:mi mathvariant="normal">Pd</mml:mi><mml:mrow><mml:mo>(</mml:mo><mml:mn>111</mml:mn><mml:mo>)</mml:mo></mml:mrow></mml:mro Physical Review B, 2008, 77, .	1.1	52
5728	High-pressure structures of lithium, potassium, and rubidium predicted by anab initioevolutionary algorithm. Physical Review B, 2008, 78, .	1.1	132
5729	Adsorbate cluster expansion for an arbitrary number of inequivalent sites. Physical Review B, 2008, 78, .	1.1	39
5730	On the Adsorption of Chiral Propylene Oxide onto Pd(111): A DFT Study. Adsorption Science and Technology, 2008, 26, 415-422.	1.5	0
5731	Structure of and ion segregation to an alumina grain boundary: Implications for growth and creep. Journal of Materials Research, 2008, 23, 1494-1508.	1.2	25
5732	Ferrite transformation from oxideâ€“steel interface in HAZ-simulated Câ€“Mn steel. International Journal of Materials Research, 2008, 99, 347-351.	0.1	15
5733	Atomic and electronic structures of the group-IV elements on Si(111)-(âˆš3 Ã— âˆš3) surface. Journal of Physics: Conference Series, 2008, 100, 072025.	0.3	2
5734	Comparative creation of surface Schottky defects on SnO₂(110) and TiO₂(110). Journal of Physics: Conference Series, 2008, 117, 012021.	0.3	2
5735	Ab initioand classical molecular dynamics calculations of the high-pressure melting of Ne. Journal of Physics: Conference Series, 2008, 121, 012005.	0.3	3
5736	Atomic, electronic, and transport properties of quasi-one-dimensional nanostructures. , 2008, , .		0
5737	Chapter 9 Ab-initio studies of quasicrystalline surfaces. Handbook of Metal Physics, 2008, 3, 313-355.	0.0	0
5738	Atomic and Electronic Structures of Boron Clusters in Crystalline Silicon: The Case of X@B6 and X@B12, X=Hâ€“Br. Advances in Quantum Chemistry, 2008, , 89-102.	0.4	0
5739	First-principles study of p-type transparent conductive oxides CuXO2 (X=Y, Sc, and Al). Journal of Applied Physics, 2008, 104, .	1.1	34

#	Article	IF	Citations
5740	Electronic and magnetic properties of endohedrally doped fullerene Mn@C60: A total energy study. Journal of Chemical Physics, 2008, 128, 074304.	1.2	16
5741	Ab Initio Study of Ideal Strength of Covalent Crystals: Effect of Multiaxial Stress and Structure. Journal of Solid Mechanics and Materials Engineering, 2008, 2, 1360-1368.	0.5	0
5742	Magnetic Properties of Mn Doped Armchair Graphene Nanoribbon. Materials Transactions, 2008, 49, 2445-2447.	0.4	10
5743	First Principles Calculation of CO and H₂ Adsorption on Strained Pt Surface. Materials Transactions, 2008, 49, 2484-2490.	0.4	6
5744	Bonding and Magnetism in High Symmetry Nano-Sized Graphene Molecules: Linear Acenes C_{4<I>m</I>+2}H_{2<I>m</I>+4} (<I>m</I>=2,…25); Zigzag Hexangulenes C_{6<I>m</I>^{**}2}H_{6<I>m</I>} (<I>m</I>=2,…10); Crenelated Hexangulenes C_{6(3<I>m</I>^{**}2−3<I>m</I>+1)}H_{6(2<I>m</I>−1)} (<I>m</I>=2,…6); Zigzag Triangulenes C_{<I>m</I>^{**}2+4<I>m</I>+1}H<SUB>	0.4	23
5745	<I>Ab Initio</I> Electronic Structure Study of α-Zirconium and Hydrogen. Materials Transactions, 2008, 49, 2765-2769.	0.4	5
5746	First-Principles Calculations of the Grain-Boundary Cohesive Energy. Nippon Kinzoku Gakkaishi/Journal of the Japan Institute of Metals, 2008, 72, 657-666.	0.2	33
5747	First-Principles Calculation of Photoabsorption Spectra of Cadmium Selenide Clusters. Materials Transactions, 2008, 49, 2420-2423.	0.4	6
5748	Structural, Electronic and Optical Properties of the Al₂O₃ Doped SiO₂: First Principles Calculations. Materials Transactions, 2008, 49, 2474-2479.	0.4	7
5749	High-quality single crystal growth of Bi-based perovskite ferroelectrics based on defect chemistry. Journal of the Ceramic Society of Japan, 2008, 116, 994-1001.	0.5	26
5750	Dependence of Magnetism on Doping Concentration in V-Doped Bulk ZnO. Materials Transactions, 2008, 49, 2469-2473.	0.4	6
5751	First-principles Study of the Bulk Properties for LiMPO4 Compounds (M=Mn, Fe, Co, Ni) as Cathode Materials for Lithium Ion Battery. Electrochemistry, 2008, 76, 752-762.	0.6	8
5752	Half-metallic L21 structures with (001) planar insertions. Journal of Applied Physics, 2008, 103, .	1.1	9
5753	Superconductivity and Magnetism in MPt₄Ge₁₂, M = Ca, Ba, Sr, Eu. Journal of the Physical Society of Japan, 2008, 77, 121-127.	0.7	17
5754	Rietveld structure refinement of MgGeO3 post-perovskite phase to 1 Mbar. American Mineralogist, 2008, 93, 965-976.	0.9	32
5755	Effect of applied stress on vacancy segregation near the grain boundary in nickel. Journal of Applied Physics, 2008, 104, 053519.	1.1	8
5756	Atomic structures of supersaturated ZnOâ€“Al2O3 solid solutions. Journal of Applied Physics, 2008, 103, 014309.	1.1	68
5757	Structural, energetic, and electronic properties of hydrogenated titanium clusters. Journal of Chemical Physics, 2008, 128, 194714.	1.2	22

#	Article	IF	Citations
5758	Ferromagnetic and half-metallic behaviors of fullerene-cobalt polymer chains. Journal of Chemical Physics, 2008, 128, 074707.	1.2	8
5759	Free energy calculation of the reaction path of the N2O decomposition over Fe(II)-ferrierite. Studies in Surface Science and Catalysis, 2008, , 689-694.	1.5	1
5760	Strain-induced modulation of band structure of silicon. Journal of Applied Physics, 2008, 104, .	1.1	20
5761	Charge transfer and adhesion in Rh/MgO(001). Journal of Physics: Conference Series, 2008, 100, 082027.	0.3	3
5762	Simulations of the fragmentation of the [V-H]^{â˜'}anions as formed upon DEA to L-valine. Journal of Physics: Conference Series, 2008, 115, 012014.	0.3	2
5763	Ferromagnetism in (Mn,Li) co-doped CdSe. Europhysics Letters, 2008, 84, 57012.	0.7	4
5764	Anomalous static electronic screening in compressed lithium. Journal of Physics: Conference Series, 2008, 121, 012007.	0.3	1
5765	Quantum-Chemical Calculations of the Equilibrium Constants of a Fission Product Mixture in a Steam-Hydrogen Carrier Gas in Severe Accident Conditions. Nuclear Technology, 2008, 163, 245-251.	0.7	0
5766	Investigations of dopants introduction in hafnia: Electronic properties, diffusion, and their role on the gate leakage current. Journal of Applied Physics, 2008, 104, 033709.	1.1	4
5767	Coexistence of superconductivity and antiferromagnetism in CeRhIn₅; model Hamiltonian and ab-initio calculations. Journal of Physics: Conference Series, 2008, 121, 052008.	0.3	0
5768	Similarity of electronic structure and optical properties of Mg ₂ NiH ₄ and Si. Europhysics Letters, 2008, 82, 48004.	0.7	11
5769	Atomistic study on electronic properties of nanoscale SOI channels. Journal of Physics: Conference Series, 2008, 109, 012012.	0.3	8
5770	⁷³Ge-NMR study andab initiocalculations on clathrate compound Ba₂₄Ge₁₀₀. Journal of Physics: Conference Series, 2008, 121, 052011.	0.3	2
5771	Computational challenges of large-scale, long-time, first-principles molecular dynamics. Journal of Physics: Conference Series, 2008, 125, 012058.	0.3	19
5772	Ti-induced destabilization of NaBH₄ from first-principles theory. Journal of Physics Condensed Matter, 2008, 20, 122202.	0.7	6
5773	The nature of highly anisotropic free-electron-like states in a glycinate monolayer on Cu(100). Journal of Physics Condensed Matter, 2008, 20, 312002.	0.7	6
5774	Oxygen vacancy migration in CSZ using density functional theory. Materials Research Society Symposia Proceedings, 2008, 1122, 8.	0.1	0
5775	Thermal properties of guest-free Si136 and Ge136 clathrates: A first-principles study. Journal of Applied Physics, 2008, 104, 033535.	1.1	16

#	Article	IF	Citations
5776	Nucleation and growth of cobalt disilicide precipitates during in situ transmission electron microscopy implantation. Journal of Applied Physics, 2008, 104, 033527.	1.1	10
5777	Local reactivity of O2 with Pt3 on Co3Pt and related backgrounds. Journal of Chemical Physics, 2008, 128, 204701.	1.2	7
5778	Electronic Structure and Formation Enthalpy of Hydroaluminates and Hydroborates. , 2008, , 1-6.		2
5779	Ab initio studies on orientational ordering in cubic Znâ€“Sc. Zeitschrift FÃ¼r Kristallographie, 2008, 223, 830-832.	1.1	8
5781	Testing Interatomic Potentials for QM/MM Embedded-Cluster Calculations on Ceria Surfaces. E-Journal of Surface Science and Nanotechnology, 2009, 7, 413-420.	0.1	8
5782	Interfacial electronic states of tetracene deposited on Si(111). Journal of Chemical Physics, 2009, 130, 174712.	1.2	7
5783	Electronic Structure of a Collapsed Armchair Single-Walled Carbon Nanotube. E-Journal of Surface Science and Nanotechnology, 2009, 7, 541-545.	0.1	7
5784	Mutual deactivation of electrically active F interstitials and O vacancies into fluorine-oxygen-vacancy complexes inSiO2. Physical Review B, 2009, 79, .	1.1	0
5785	Static and dynamic properties of hydrogenated amorphous silicon with voids. Physical Review B, 2009, 79, .	1.1	22
5786	Incommensurate spin correlation driven by frustration inBiCu2PO6. Physical Review B, 2009, 80, .	1.1	36
5787	Equation of state and phase diagram of water at ultrahigh pressures as in planetary interiors. Physical Review B, 2009, 79, .	1.1	212
5788	Absence of temperature dependence of the valence-band spectrum of<mml:math xmlns:mml="http://www.w3.org/1998/Math/MathML" display="inline"><mml:mrow><mml:msub><mml:mrow><mml:mtext>Co</mml:mtext></mml:mrow><mml:mn>2</mml:mn></mml:msu Physical Review B, 2009, 79, .	1.1	36
5789	Properties of multiferroic<mml:math xmlns:mml="http://www.w3.org/1998/Math/MathML" display="inline"><mml:mrow><mml:msub><mml:mrow><mml:mtext>BiFeO</mml:mtext></mml:mrow><mml:mn>3</mml:mn></mml:msub></mml:n high magnetic fields from first principles. Physical Review B, 2009, 79, .	1.1	42
5790	Magnetism at surfaces and defects in icosahedral Al-Pd-Mn quasicrystals. Physical Review B, 2009, 80, .	1.1	8
5791	Ab initiostudy of ferroelectricity in edgedPbTiO3nanowires under axial tension. Physical Review B, 2009, 79, .	1.1	53
5792	Biaxial strain effects on the structure and stability of self-interstitial clusters in silicon. Physical Review B, 2009, 79, .	1.1	9
5793	Adsorption of CO on Ni/Cu(110) bimetallic surfaces. Physical Review B, 2009, 80, .	1.1	23
5794	Modifying the electronic structure of semiconducting single-walled carbon nanotubes byAr+ion irradiation. Physical Review B, 2009, 79, .	1.1	42

#	Article	IF	Citations
5795	Structure and stability of Au rods on<mml:math xmlns:mml="http://www.w3.org/1998/Math/MathML" display="inline"><mml:mrow><mml:msub><mml:mrow><mml:mtext>TiO</mml:mtext></mml:mrow><mml:mn>2</mml:mn></mml:msu by first-principles calculations. Physical Review B, 2009, 80, .	1.1	25
5796	Density functional study of the overdoped iron chalcogenide<mml:math xmlns:mml="http://www.w3.org/1998/Math/MathML" display="inline"><mml:mrow><mml:msub><mml:mrow><mml:mtext>TlFe</mml:mtext></mml:mrow><mml:mn>2</mml:mn></mml:ms xmlns:mml="http://www.w3.org/1998/Math/MathML" display="inline"><mml:mrow><mml:msub><mml:mrow><mml:mtext>ThCr</mml:mtext></mml:mrow><mml:mn>2</mml:mn></mml:m	1.1	36
5797	Probing the dynamical properties of the metastable bcc<mml:math xmlns:mml="http://www.w3.org/1998/Math/MathML" display="inline"><mml:mrow><mml:msub><mml:mrow><mml:mtext>Fe</mml:mtext></mml:mrow><mml:mi>x</mml:mi></mml:msub> Physical Review B, 2009, 79, .	1.1	4
5798	High-pressure behavior of<mml:math xmlns:mml="http://www.w3.org/1998/Math/MathML" display="inline"><mml:mrow><mml:msub><mml:mrow><mml:mtext>TiO</mml:mtext></mml:mrow><mml:mn>2</mml:mn></mml:ms determined by experiment and theory. Physical Review B, 2009, 79, .	1.1	86
5799	First-principles prediction of a metastable crystalline phase of Ga with<mml:math xmlns:mml="http://www.w3.org/1998/Math/MathML" display="inline"><mml:mrow><mml:mi>C</mml:mi><mml:mi>m</mml:mi><mml:mi>c</mml:mi><mml:mi>m</mml:mi></mml:mrow></ Physical Review B, 2009, 80, .	1.1	10
5800	Interplay between Jahn-Teller instability, uniaxial magnetism, and ferroelectricity inCa3CoMnO6. Physical Review B, 2009, 79, .	1.1	67
5801	First-principles prediction of low-energy structures for<mml:math xmlns:mml="http://www.w3.org/1998/Math/MathML" display="inline"><mml:mrow><mml:msub><mml:mrow><mml:mtext>AlH</mml:mtext></mml:mrow><mml:mn>3</mml:mn></mml:msu Physical Review B, 2009, 79, .	1.1	9
5802	Onset of three-dimensional Ir islands on a graphene/Ir(111) template. Physical Review B, 2009, 80, .	1.1	36
5803	Role of di-interstitial clusters in oxygen transport in<mml:math xmlns:mml="http://www.w3.org/1998/Math/MathML" display="inline"><mml:mrow><mml:msub><mml:mrow><mml:mtext>UO</mml:mtext></mml:mrow><mml:mrow><mml:mn>2</mml:m first principles. Physical Review B, 2009, 80, .	1.1	49
5804	Zero-bias conductance anomaly of a FeO-bound Au atom triggered by CO adsorption. Physical Review B, 2009, 79, .	1.1	6
5805	Energetics and fragmentation of single-doped tin and lead clusters. Physical Review B, 2009, 79, .	1.1	7
5806	13-atom metallic clusters studied by density functional theory: Dependence on exchange-correlation approximations and pseudopotentials. Physical Review B, 2009, 80, .	1.1	42
5807	<i>Ab initio</i>determination of ion traps and the dynamics of silver in silver-doped chalcogenide glass. Physical Review B, 2009, 79, .	1.1	15
5808	Surface atomic order of compound III-V semiconductor alloys at finite temperature. Physical Review B, 2009, 80, .	1.1	10
5809	Microscopic mechanism of templated self-assembly: Indium metallic atomic wires on Si(553)-Au. Physical Review B, 2009, 79, .	1.1	20
5810	Large anisotropic adatom kinetics on nonpolar GaN surfaces: Consequences for surface morphologies and nanowire growth. Physical Review B, 2009, 79, .	1.1	172
5811	Confinement of electrons in size-modulated silicon nanowires. Physical Review B, 2009, 80, .	1.1	11
5812	Hexagonal-based ordered phases in H-Zr. Physical Review B, 2009, 80, .	1.1	32

#	Article	IF	Citations
5813	First-principles study of silicon bulk and nanowire (111) surfaces terminated with trihydrides: Symmetric, rotated, and tilted. Physical Review B, 2009, 80, .	1.1	1
5814	Superconducting high-pressure phase of cesium iodide. Physical Review B, 2009, 79, .	1.1	27
5815	Cooperativity among defect sites in<mml:math xmlns:mml="http://www.w3.org/1998/Math/MathML" display="inline"><mml:mrow><mml:mi>A</mml:mi><mml:msub><mml:mtext>O</mml:mtext><mml:mrow><mml:mn>2</mml:mn><mm xmlns:mml="http://www.w3.org/1998/Math/MathML" display="inline"><mml:mrow><mml:msub><mml:mi>A</mml:mi><mml:mn>4</mml:mn></mml:msub><mml:msub><mml:mtext>O</mml:mtext><mm Physical Review B, 2009, 79, .	1.1	142
5816	Adsorption structure of pyrazine on Si(100): Density-functional calculations. Physical Review B, 2009, 80, .	1.1	13
5817	Diffusion barriers for Ag and Cu adatoms on the terraces and step edges on Cu(100) and Ag(100): Anab initiostudy. Physical Review B, 2009, 80, .	1.1	51
5818	Atomic-resolution three-dimensional imaging of germanium self-interstitials near a surface: Aberration-corrected transmission electron microscopy. Physical Review B, 2009, 80, .	1.1	32
5819	Density-gradient-corrected embedded atom method. Physical Review B, 2009, 79, .	1.1	9
5820	Quantitative prediction of twinning stress in fcc alloys: Application to Cu-Al. Physical Review B, 2009, 79, .	1.1	72
5821	Electronic structure and thermoelectric properties of layered<mml:math xmlns:mml="http://www.w3.org/1998/Math/MathML" display="inline"><mml:mrow><mml:msub><mml:mrow><mml:mtext>PbSe-WSe</mml:mtext></mml:mrow><mml:mn>2</mml:mn></m Physical Review B, 2009, 80, .	1.1	57
5822	Two-dimensional metal-organic coordination networks of Mn-7,7,8,8-tetracyanoquinodimethane assembled on Cu(100): Structural, electronic, and magnetic properties. Physical Review B, 2009, 80, .	1.1	41
5823	Magnetic anisotropy of transition-metal dimers: Density functional calculations. Physical Review B, 2009, 79, .	1.1	114
5824	Water-induced superconductivity inSrFe2As2. Physical Review B, 2009, 80, .	1.1	69
5825	Optimal site-centered electronic structure basis set from a displaced-center expansion: Improved results viaa prioriestimates of saddle points in the density. Physical Review B, 2009, 80, .	1.1	25
5826	Optical properties of zinc selenide clusters from first-principles calculations. Physical Review B, 2009, 80, .	1.1	26
5827	Electronic, vibrational, and thermodynamic properties of metacinnabar<mml:math xmlns:mml="http://www.w3.org/1998/Math/MathML" display="inline"><mml:mrow><mml:mi>Î²</mml:mi><mml:mtext>-HgS</mml:mtext></mml:mrow></mml:math>, HgSe, and HgTe. Physical Review B, 2009, 80, .	1.1	80
5828	Properties of helium defects in bcc and fcc metals investigated with density functional theory. Physical Review B, 2009, 80, .	1.1	134
5829	First-principles study of the formation and migration of native defects in<mml:math xmlns:mml="http://www.w3.org/1998/Math/MathML" display="inline"><mml:mrow><mml:msub><mml:mrow><mml:mtext>NaAlH</mml:mtext></mml:mrow><mml:mn>4</mml:mn></mml:m Physical Review B, 2009, 80, .	1.1	54
5830	Density functional theory study of the initial oxidation of the Pt(111) surface. Physical Review B, 2009, 79, .	1.1	96

#	Article	IF	Citations
5831	Atomic-scale segregation behavior of Pr at a ZnO [0001]<mml:math xmlns:mml="http://www.w3.org/1998/Math/MathML" display="inline"><mml:mrow><mml:mi>Î£</mml:mi><mml:mn>49</mml:mn></mml:mrow></mml:math>tilt grain boundary. Physical Review B, 2009, 80, .	1.1	23
5832	Time-dependent density-functional study of field emission from tipped carbon nanotubes. Physical Review B, 2009, 80, .	1.1	13
5833	Crucial role of surface in stability and mobility of vacancy clusters in metals. Physical Review B, 2009, 79, .	1.1	14
5834	Dye adsorbates BrPDI, BrGly, and BrAsp on anataseTiO2(001)for dye-sensitized solar cell applications. Physical Review B, 2009, 80, .	1.1	25
5835	First-principles study of the optical properties of<mml:math xmlns:mml="http://www.w3.org/1998/Math/MathML" display="inline"><mml:mrow><mml:msub><mml:mrow><mml:mtext>Mg</mml:mtext></mml:mrow><mml:mi>x</mml:mi></mml:msub> Physical Review B, 2009, 79, .	1.1	20
5836	Ordered ground state wurtzite alloys from zinc-blende parent compounds. Physical Review B, 2009, 80, .	1.1	3
5837	Adsorption of metal adatoms on FeO(111) and MgO(111) monolayers: Effects of charge state of adsorbate on rumpling of supported oxide film. Physical Review B, 2009, 80, .	1.1	49
5838	Robust room-temperature magnetism of (110)<mml:math xmlns:mml="http://www.w3.org/1998/Math/MathML" display="inline"><mml:mrow><mml:msub><mml:mrow><mml:mtext>CrO</mml:mtext></mml:mrow><mml:mn>2</mml:mn></mml:ms films. Physical Review B, 2009, 80, .	1.1	12
5839	Transport properties of lithium hydride from quantum molecular dynamics and orbital-free molecular dynamics. Physical Review B, 2009, 80, .	1.1	51
5840	Density functional theory study of the iron-based porphyrin haem(b) on the Si(111):H surface. Physical Review B, 2009, 79, .	1.1	18
5841	Flattening-induced electronic changes in zigzag single- and multi-walled boron nitride nanotubes: A first-principles DFT study. Physical Review B, 2009, 80, .	1.1	12
5842	Suppression of disorder broadening of core-level photoelectron lines in CuAu alloys by inhomogeneous lattice distortion. Physical Review B, 2009, 79, .	1.1	12
5843	Ultra-incompressible phases of tungsten dinitride predicted from first principles. Physical Review B, 2009, 79, .	1.1	58
5844	Comparative study of CO adsorption on flat, stepped, and kinked Au surfaces using density functional theory. Physical Review B, 2009, 79, .	1.1	50
5845	First-principles calculations of the magnetic properties of (Cd,Mn)Te nanocrystals. Physical Review B, 2009, 79, .	1.1	17
5846	First-principles simulation of the elastic properties of multicomponent amorphous steels. Physical Review B, 2009, 80, .	1.1	14
5847	Stopping of energetic cobalt clusters and formation of radiation damage in graphite. Physical Review B, 2009, 80, .	1.1	31
5848	Interstitials in tetrahedrally close-packed phases: C, N, O, and F in<mml:math xmlns:mml="http://www.w3.org/1998/Math/MathML" display="inline"><mml:mi>Î²</mml:mi></mml:math>-tungsten from first principles. Physical Review B, 2009, 80, .	1.1	16

#	Article	IF	Citations
5849	Polarization and rumpling in oxide monolayers deposited on metallic substrates. Physical Review B, 2009, 79, .	1.1	81
5850	Ab initiocalculations of ferroelectric instability in<mml:math xmlns:mml="http://www.w3.org/1998/Math/MathML" display="inline"><mml:mrow><mml:msub><mml:mrow><mml:mtext>PbTiO</mml:mtext></mml:mrow><mml:mn>3</mml:mn></mml:msub></mml:mrow></mml:math>with symmetric and asymmetric electrode layers. Physical Review B, 2009, 80, .	1.1	35
5851	Ab initiostudy of atomic ordering and spin-glass transition in dilute CuMn alloys. Physical Review B, 2009, 79, .	1.1	15
5852	Greenâ€™s function method for elimination of the spurious multipole interaction in the surface/interface slab model. Physical Review B, 2009, 80, .	1.1	72
5853	Excited electron dynamics in Cu nanowires supported on a Cu(111) surface. Physical Review B, 2009, 79, .	1.1	9
5854	Indium on Cu(100) from first principles: Energetics, complex formation, and diffusion of adsorbates and vacancies on terraces and at steps. Physical Review B, 2009, 79, .	1.1	2
5855	<mml:math xmlns:mml="http://www.w3.org/1998/Math/MathML" display="inline"><mml:mrow><mml:mn>3</mml:mn><mml:mi>d</mml:mi></mml:mrow></mml:math>transition metal impurities in aluminum: A first-principles study. Physical Review B, 2009, 80, .	1.1	62
5856	Structural and electronic properties of Ge-Si, Sn-Si, and Pb-Si dimers on Si(001) from density-functional calculations. Physical Review B, 2009, 79, .	1.1	1
5857	Chemisorption of small fullerenes<mml:math xmlns:mml="http://www.w3.org/1998/Math/MathML" display="inline"><mml:mrow><mml:msub><mml:mtext>C</mml:mtext><mml:mi>n</mml:mi></mml:msub></mml:mrow></mml:math> xmlns:mml="http://www.w3.org/1998/Math/MathML"		

#	Article	IF	Citations
5867	Electronic structure, stability, and mechanism of the decohesion and shear of interfaces in superhard nanocomposites and heterostructures. Physical Review B, 2009, 79, .	1.1	69
5868	Formation of Y-Ti-O nanoclusters in nanostructured ferritic alloys: A first-principles study. Physical Review B, 2009, 79, .	1.1	87
5869	Formation and electronic states of In nanoclusters on the<mml:math xmlns:mml="http://www.w3.org/1998/Math/MathML" display="inline"><mml:mrow><mml:mtext>Si</mml:mtext><mml:mrow><mml:mo>(</mml:mo><mml:mrow><mml:mn>111</mml:mn> Physical Review B, 2009, 79, .	1.1	16
5870	Role of K/Bi disorder in the electronic structure of<mml:math xmlns:mml="http://www.w3.org/1998/Math/MathML" display="inline"><mml:mrow><mml:mi>Î²</mml:mi><mml:msub><mml:mrow><mml:mtext>-K</mml:mtext></mml:mrow><mml:mn> Physical Review B, 2009, 80, .	1.1	12
5871	Shear deformation, ideal strength, and stacking fault formation of fcc metals: A density-functional study of Al and Cu. Physical Review B, 2009, 79, .	1.1	135
5872	First-principles modeling of hardness in transition-metal diborides. Physical Review B, 2009, 80, .	1.1	52
5873	Formation and migration of charged native point defects in<mml:math xmlns:mml="http://www.w3.org/1998/Math/MathML" display="inline"><mml:mrow><mml:msub><mml:mrow><mml:mtext>MgH</mml:mtext></mml:mrow><mml:mn>2</mml:mn></mml:ms First-principles calculations. Physical Review B, 2009, 80, .	1.1	48
5874	Multimorphism in molecular monolayers: Pentacene on Cu(110). Physical Review B, 2009, 79, .	1.1	51
5875	Extended Frenkel pairs and band alignment at metal-oxide interfaces. Physical Review B, 2009, 79, .	1.1	31
5876	Strain-driven magnetism inLaCoO3thin films. Physical Review B, 2009, 79, .	1.1	32
5877	First-principles study of defect-induced potentials in<mml:math xmlns:mml="http://www.w3.org/1998/Math/MathML" display="inline"><mml:mrow><mml:msub><mml:mrow><mml:mtext>Ca</mml:mtext></mml:mrow><mml:mn>2</mml:mn></mml:msu Physical Review B, 2009, 80, .	1.1	5
5878	Calculation of properties of crystalline lithium hydride using correlated wave function theory. Physical Review B, 2009, 80, .	1.1	66
5879	Origin of the magnetism in<mml:math xmlns:mml="http://www.w3.org/1998/Math/MathML" display="inline"><mml:mrow><mml:msub><mml:mrow><mml:mtext>CaB</mml:mtext></mml:mrow><mml:mn>6</mml:mn></mml:msub></mml:ms A first-principles study. Physical Review B, 2009, 79, .	1.1	13
5880	Ab initioatomistic thermodynamics study on the selective oxidation mechanism of the surfaces of intermetallic compounds. Physical Review B, 2009, 80, .	1.1	29
5881	Assessment through first-principles calculations of an intermediate-band photovoltaic material based on Ti-implanted silicon: Interstitial versus substitutional origin. Physical Review B, 2009, 79, .	1.1	81
5882	Mechanism of alkane dehydrogenation catalyzed by acidic zeolites: Ab initio transition path sampling. Journal of Chemical Physics, 2009, 131, 214508.	1.2	55
5883	Piezoresistive effect in silicon nanowires — A comprehensive analysis based on first-principles calculations. , 2009, , .		6
5884	Exploring Ce3+/Ce4+ cation ordering in reduced ceria nanoparticles using interionic-potential and density-functional calculations. Journal of Chemical Physics, 2009, 131, 064701.	1.2	50

#	Article	IF	Citations
5885	Prediction of a Switchable Two-Dimensional Electron Gas at Ferroelectric Oxide Interfaces. Physical Review Letters, 2009, 103, 016804.	2.9	115
5886	The effect of impurities on hydrogen bonding site and local vibrational frequency in ZnO. Journal of Applied Physics, 2009, 106, 053522.	1.1	7
5887	Wurtzite-Type CoO Nanocrystals in Ultrathin ZnCoO Films. Physical Review Letters, 2009, 102, 156102.	2.9	22
5888	Ab initio study of EMIM-BF4 crystal interaction with a Li (100) surface as a model for ionic liquid/Li interfaces in Li-ion batteries. Journal of Chemical Physics, 2009, 131, 244705.	1.2	40
5889	Understanding the Clean Interface between Covalent Si and Ionic<mml:math xmlns:mml="http://www.w3.org/1998/Math/MathML" display="inline"><mml:msub><mml:mi>Al</mml:mi><mml:mn>2</mml:mn></mml:msub><mml:msub><mml:mi mathvariant="normal">O</mml:mi><mml:mn>3</mml:mn></mml:msub></mml:math>. Physical Review Letters, 2009, 103, 116101.	2.9	20
5890	Chemical Identification of Ions in Doped NaCl by Scanning Force Microscopy. Physical Review Letters, 2009, 102, 256103.	2.9	21
5891	Energetics and electronic structure of aluminum point defects in HfO2: A first-principles study. Journal of Applied Physics, 2009, 106, 014104.	1.1	21
5892	Efficient First-Principles Simulation of Noncontact Atomic Force Microscopy for Structural Analysis. Physical Review Letters, 2009, 102, 176101.	2.9	18
5893	Calculation of Cu/Ta interface electron transmission and effect on conductivity in nanoscale interconnect technology. Applied Physics Letters, 2009, 95, .	1.5	26
5894	Strain effects on work functions of pristine and potassium-decorated carbon nanotubes. Journal of Chemical Physics, 2009, 131, 224701.	1.2	34
5895	Magnetoelastic Coupling through the Antiferromagnet-to-Ferromagnet Transition of Quasi-Two-Dimensional[Cu(HF2)(pyz)2]BF4Using Infrared Spectroscopy. Physical Review Letters, 2009, 103, 157401.	2.9	28
5896	Mg-doped GaN nanostructures: Energetics, magnetism, and H2 adsorption. Applied Physics Letters, 2009, 94, 013108.	1.5	17
5897	Local Vibrational Excitation through Extended Electronic States at a Germanium Surface. Physical Review Letters, 2009, 103, 266102.	2.9	12
5898	Electron spectroscopy study of the initial stages of iron phthalocyanine growth on highly oriented pyrolitic graphite. Journal of Chemical Physics, 2009, 131, 214709.	1.2	29
5899	The importance of anharmonic effects in models that interconnect point defect parameters with bulk properties in solids. Journal of Applied Physics, 2009, 105, 083524.	1.1	15
5900	Magnetic Anisotropy and Magnetization Dynamics of Individual Atoms and Clusters of Fe and Co on Pt(111). Physical Review Letters, 2009, 102, 257203.	2.9	143
5901	Improving thermoelectric performance of caged compounds through light-element filling. Applied Physics Letters, 2009, 95, .	1.5	167
5902	Origin of the phase transition of AlN, GaN, and ZnO nanowires. Applied Physics Letters, 2009, 94, .	1.5	18

#	Article	IF	Citations
5903	Defects in Compound Semiconductors Caused by Molecular Nitrogen. Physical Review Letters, 2009, 103, 145501.	2.9	24
5904	Switching a Single Spin on Metal Surfaces by a STM Tip:AbÂInitioStudies. Physical Review Letters, 2009, 103, 057202.	2.9	60
5905	Polarization Vortices in Germanium Telluride Nanoplatelets: A Theoretical Study. Physical Review Letters, 2009, 103, 247601.	2.9	16
5906	Stabilizing a 22 karat nanogolden cage. Journal of Chemical Physics, 2009, 131, 204501.	1.2	3
5907	Enhanced reactivity of nanoenergetic materials: A first-principles molecular dynamics study based on divide-and-conquer density functional theory. Applied Physics Letters, 2009, 95, .	1.5	36
5908	Half-metallic properties of perovskite BaCrO3 and BaCr0.5Ti0.5O3 superlattice: LSDA+U calculations. Journal of Applied Physics, 2009, 106, .	1.1	40
5909	Comparative analysis of electronic structure and optical properties of crystalline and amorphous silicon nitrides. Journal of Applied Physics, 2009, 106, .	1.1	13
5910	Temperature Stabilized Surface Reconstructions at Polar ZnO(0001). Physical Review Letters, 2009, 103, 065502.	2.9	118
5911	Diffusion of hydrogen vacancy in Na3AlH6. Applied Physics Letters, 2009, 95, 111910.	1.5	10
5912	Density functional calculations on atomic and electronic structures of amorphous HfO2/Si(001) interface. Applied Physics Letters, 2009, 95, .	1.5	13
5913	An energetic stability predictor of hydrogen-terminated Si nanostructures. Applied Physics Letters, 2009, 95, .	1.5	14
5914	Electronic structures of BC3 nanoribbons. Applied Physics Letters, 2009, 94, .	1.5	58
5915	The effects of local disorder on the electronic structures of amorphous semiconductor GaAs. , 2009, , .		0
5916	Theoretical prediction on the structural, electronic, and polarization properties of tetragonal Bi2ZnTiO6. Journal of Applied Physics, 2009, 105, .	1.1	20
5917	The chemisorption of tetracene on Si(100)-2Ã—1 surface. Journal of Chemical Physics, 2009, 131, 044703.	1.2	8
5918	Broadband dielectric spectroscopy of Ruddlesdenâ€“Popper Srn+1TinO3n+1 (n=1,2,3) thin films. Applied Physics Letters, 2009, 94, 042908.	1.5	27
5919	First-principles study of ionic oxygen mobility of Sr-containing LaAlO₃perovskite. Journal of Physics Condensed Matter, 2009, 21, 305502.	0.7	2
5920	Ab initiostudy of subsurface diffusion of Cu on the H-passivated Si(001) surface. Physical Review B, 2009, 80, .	1.1	8

#	Article	IF	Citations
5921	Structure and energetics of Er defects in<mml:math xmlns:mml="http://www.w3.org/1998/Math/MathML" display="inline"><mml:mrow><mml:msub><mml:mrow><mml:mtext>LiNbO</mml:mtext></mml:mrow><mml:mn>3</mml:mn></mml:r first-principles and thermodynamic calculations. Physical Review B, 2009, 80, .	1.1	35
5922	Origin of the anatase to rutile conversion of metal-doped<mml:math xmlns:mml="http://www.w3.org/1998/Math/MathML" display="inline"><mml:mrow><mml:msub><mml:mrow><mml:mtext>TiO</mml:mtext></mml:mrow><mml:mn>2</mml:mn></mml:ms Physical Review B, 2009, 79, .	1.1	28
5923	Absence of superconductivity in the high-pressure polymorph of<mml:math xmlns:mml="http://www.w3.org/1998/Math/MathML" display="inline"><mml:mrow><mml:msub><mml:mrow><mml:mtext>MgB</mml:mtext></mml:mrow><mml:mn>2</mml:mn></mml:ms Physical Review B, 2009, 79, .	1.1	43
5924	Soft-phonon instability in zincblende HgSe and HgTe under moderate pressure:Ab initiopseudopotential calculations. Physical Review B, 2009, 80, .	1.1	10
5925	Ohmic contacts on silicon carbide: The first monolayer and its electronic effect. Physical Review B, 2009, 80, .	1.1	63
5926	Density-functional study of the pressure-induced phase transitions in Ti at zero Kelvin. Physical Review B, 2009, 79, .	1.1	34
5927	Growth of Dome-Shaped Carbon Nanoislands on Ir(111): The Intermediate between Carbidic Clusters and Quasi-Free-Standing Graphene. Physical Review Letters, 2009, 103, 166101.	2.9	178
5928	Electric-field effects on the diffusion of Si and Ge adatoms on Si(001) studied by density functional simulations. Physical Review B, 2009, 79, .	1.1	3
5929	Mechanical and electronic properties of<mml:math xmlns:mml="http://www.w3.org/1998/Math/MathML" display="inline"><mml:mrow><mml:msub><mml:mrow><mml:mtext>CeO</mml:mtext></mml:mrow><mml:mn>2</mml:mn></mml:ms xmlns:mml="http://www.w3.org/1998/Math/MathML" display="inline"><mml:mrow><mml:msub><mml:mrow><mml:mtext>ThO</mml:mtext></mml:mrow><mml:mn>2</mml:mn></mml:ms and<mml:math xmlns:mml="http://www.w3.org/1998/Math/MathML" display="inline"><mml:mrow. Physi	1.1	72
5930	First-principles determination of low-temperature order and ground states of Fe-Ni, Fe-Pd, and Fe-Pt. Physical Review B, 2009, 80, .	1.1	53
5931	First-principles study of thin<mml:math xmlns:mml="http://www.w3.org/1998/Math/MathML" display="inline"><mml:mrow><mml:msub><mml:mrow><mml:mtext>TiO</mml:mtext></mml:mrow><mml:mi>x</mml:mi><mml:msub bulklike rutile nanowires. Physical Review B, 2009, 80, .	1.1	21
5932	Role of Si and Ge as impurities in ZnO. Physical Review B, 2009, 80, .	1.1	84
5933	First-principles studies of a two-dimensional electron gas at the interface in ferroelectric oxide heterostructures. Physical Review B, 2009, 80, .	1.1	34
5934	Coherent {001} interfaces between rocksalt and zinc-blende crystal structures. Physical Review B, 2009, 79, .	1.1	21
5935	Stability and structure of rare-earth metal and Ba-induced reconstructions on a Si(100) surface. Physical Review B, 2009, 80, .	1.1	9
5936	Dependence of electronic polarization on octahedral rotations in<mml:math xmlns:mml="http://www.w3.org/1998/Math/MathML" display="inline"><mml:mrow><mml:msub><mml:mrow><mml:mtext>TbMnO</mml:mtext></mml:mrow><mml:mn>3</mml:mn></mml:m First-principles thermodynamic framework for the evaluation of thermochemical<mml:math	1.1	24
5937	xmlns:mml="http://www.w3.org/1998/Math/MathML" display="inline"><mml:mrow><mml:msub><mml:mtext>H</mml:mtext><mml:mn>2</mml:mn></mml:msub><mml:mtext>O</mml:mte or<mml:math xmlns:mml="http://www.w3.org/1998/Math/MathML" display="inline"><mml:mrow><mml:msub><mml:mrow><mml:mtext>CO</mml:mtext></mml:mrow><mml:mn>2</mml:mn></mml:msu materials. Physical Review B, 2009, 80, .	1.1	104
5938	Quantum wells in polar-nonpolar oxide heterojunction systems. Physical Review B, 2009, 79, .	1.1	2

#	Article	IF	Citations
5939	Dynamic decomposition of aliphatic molecules on Al(111) fromab initiomolecular dynamics. Physical Review B, 2009, 79, .	1.1	9
5940	Fundamental interaction process between pure edge dislocation and energetically stable grain boundary. Physical Review B, 2009, 79, .	1.1	33
5941	Spin injection across the Fe/GaAs interface: Role of interfacial ordering. Physical Review B, 2009, 80, .	1.1	40
5942	Genetic algorithm and first-principles DFT study of the high-pressure molecularÎ¶phase of nitrogen. Physical Review B, 2009, 80, .	1.1	13
5943	F4TCNQ on Cu, Ag, and Au as prototypical example for a strong organic acceptor on coinage metals. Physical Review B, 2009, 79, .	1.1	116
5944	Electronic properties of the<mml:math xmlns:mml="http://www.w3.org/1998/Math/MathML" display="inline"><mml:mi>n</mml:mi></mml:math>-doped hydrogenated silicon (100) surface and dehydrogenated structures at 5 K. Physical Review B, 2009, 80, .	1.1	39
5945	Atomic and electronic properties of the Pb/Mo(110) adsorption system. Physical Review B, 2009, 80, .	1.1	10
5946	Modeling charge-imbalanced<mml:math xmlns:mml="http://www.w3.org/1998/Math/MathML" display="inline"><mml:mrow><mml:msub><mml:mrow><mml:mtext>NaNbO</mml:mtext></mml:mrow><mml:mn>3</mml:mn></mml:msub></mml:mrow></mml:math>: Lattice relaxation and metallicity. Physical Review B, 2009, 80, .	1.1	12
5947	Analysis of diamond nanocrystal formation from multiwalled carbon nanotubes. Physical Review B, 2009, 80, .	1.1	18
5948	Hydrogen-vacancy complexes in electron-irradiated niobium. Physical Review B, 2009, 79, .	1.1	25
5949	Theoretical characterization of silicon self-interstitial clusters in uniform strain fields. Physical Review B, 2009, 80, .	1.1	8
5950	First-principles molecular dynamics study of the structure and dynamic behavior of liquid<mml:math xmlns:mml="http://www.w3.org/1998/Math/MathML" display="inline"><mml:mrow><mml:msub><mml:mrow><mml:mtext>Li</mml:mtext></mml:mrow><mml:mn>4</mml:mn></mml:msub></mml:mrow></mml:math>: Physical Review B, 2009, 80, .	1.1	15
5951	Band structures and native defects of ammonia borane. Physical Review B, 2009, 80, .	1.1	20
5952	Defects in AlSb: A density functional study. Physical Review B, 2009, 79, .	1.1	11
5953	Computational study of boron nitride nanotube synthesis: How catalyst morphology stabilizes the boron nitride bond. Physical Review B, 2009, 80, .	1.1	16
5954	Non-<mml:math xmlns:mml="http://www.w3.org/1998/Math/MathML" display="inline"><mml:mrow><mml:msup><mml:mi>d</mml:mi><mml:mn>0</mml:mn></mml:msup></mml:mrow></mml:math>Mn ferroelectricity in antiferromagnetic<mml:math xmlns:mml="http://www.w3.org/1998/Math/MathML" display="inline"><mml:mrow><mml:msub><mml:mrow><mml:mtext>BaMnO</mml:mtext></mml:mrow><mml:mn>3</mml:mn></mml:msub></mml:mrow></mml:math> Physical Review B, 2009, 79, .	1.1	162
5955	First-principles study of back-contact effects on CdTe thin-film solar cells. Physical Review B, 2009, 80, .	1.1	13
5956	Activated molecular adsorption of CO on the Be(0001) surface: A density-functional theory study. Physical Review B, 2009, 80, .	1.1	7

#	Article	IF	Citations
5957	Edge versus interior in the chemical bonding of graphene materials. Physical Review B, 2009, 79, .	1.1	11
5958	Diffusion pathways of phosphorus atoms on silicon (001). Physical Review B, 2009, 79, .	1.1	19
5959	First-principles prediction of disordering tendencies in pyrochlore oxides. Physical Review B, 2009, 79, .	1.1	140
5960	Density functional theory studies of the hydrogenation properties of Mg and Ti. Physical Review B, 2009, 79, .	1.1	35
5961	Chemical versus van der Waals Interaction: The Role of the Heteroatom in the Flat Absorption of Aromatic Molecules<mml:math xmlns:mml="http://www.w3.org/1998/Math/MathML" display="inline"><mml:msub><mml:mi mathvariant="bold">C</mml:mi><mml:mn>6</mml:mn></mml:msub><mml:msub><mml:mi mathvariant="bold">H</mml:mi><mml:mn>6</mml:mn></mml:msub></mml:math>,<mml:math xmlns:mml="http://www.w3.org/1998/Math/MathML" display="inline"><mml:msub><mml:mi mathvariant	2.9	132
5962	Structure and dynamics of NiAl(110) studied by high-resolution ion scattering combined with density functional calculations. Physical Review B, 2009, 80, .	1.1	4
5963	Adsorbate-induced restructuring of Pb mesas grown on vicinal Si(111) in the quantum regime. Physical Review B, 2009, 80, .	1.1	8
5964	Controlling interlayer exchange coupling in one-dimensional Fe/Pt multilayered nanowire. Physical Review B, 2009, 79, .	1.1	2
5965	Sublayer Si atoms as reactive centers in the chemisorption on Si(100): Adsorption of<mml:math xmlns:mml="http://www.w3.org/1998/Math/MathML" display="inline"><mml:mrow><mml:msub><mml:mtext>C</mml:mtext><mml:mn>2</mml:mn></mml:msub><mml:msub><mml:mtext	1.1	21
5966	<mml:math xmlns:mml="http://www.w3.org/1998/Math/MathML" display="inline"><mml:mrow><mml:msub><mml:mtext>C</mml:mtext><mml:mn>2</mml:mn></mml:msub><mml:msub><mml:mtext Physical Review B, 2009, 79, . Convergence acceleration and stabilization of dynamical mean-field theory calculations. Physical Review B, 2009, 80, .	1.1	22
5967	Group-IIIA versus IIIB delafossites: Electronic structure study. Physical Review B, 2009, 80, .	1.1	69
5968	Magnetism in hybrid carbon nanostructures: Nanobuds. Physical Review B, 2009, 79, .	1.1	31
5969	Relative stability of extended interstitial defects in silicon: First-principles calculations. Physical Review B, 2009, 79, .	1.1	8
5970	Mesoscopic theory of shear banding and crack propagation in metallic glasses. Physical Review B, 2009, 80, .	1.1	25
5971	Substrate-induced antiferromagnetism of a Fe monolayer on the Ir(001) surface. Physical Review B, 2009, 80, .	1.1	33
5972	Bonding and magnetism in nanosized graphene molecules: Singlet states of zigzag edged hexangulenes C6m2H6m(m=2,3,â€¦,10). Journal of Chemical Physics, 2009, 131, 214706.	1.2	21
5973	Atomic structure of the Ag/Ge(111)-(3Ã—3) surface: From scanning tunneling microscopy observation to theoretical study. Journal of Chemical Physics, 2009, 131, 224705.	1.2	12
5974	Role of hybridization on the Schottky barrier height of carbon nanotube field effect transistors. Physical Review B, 2009, 79, .	1.1	7

#	Article	IF	Citations
5975	Vibrational mode shifts as a measure of local strain in the dilute nitride semiconductor alloyGaNxAs1â^'x. Physical Review B, 2009, 79, .	1.1	3
5976	Density functional theory examination of Pd(111) and Pd(100) under NO oxidation conditions. Physical Review B, 2009, 79, .	1.1	11
5977	Ab initiostudy of surface self-segregation effect on the adsorption of oxygen on the<mml:math xmlns:mml="http://www.w3.org/1998/Math/MathML" display="inline"><mml:mrow><mml:mi>Î³</mml:mi><mml:mtext>-TiAl</mml:mtext><mml:mrow><mml:mo>(</mml:mo><mml:mrow><mml:mi></mml:mi></mml:mrow></mml:mrow></mml:mrow></mml:math>Physical Review B, 2009, 79, .	1.1	41
5978	Density functional study of the electronic structure and magnetism of LaFeAsO alloyed with Zn. Physical Review B, 2009, 80, .	1.1	24
5979	Ab initiothermodynamic study of the structure and chemical bonding of aÎ²-Ni1â^'xAlx/Î±-Al2O3interface. Physical Review B, 2009, 80, .	1.1	10
5980	Density functional theory study of the energetics, electronic structure, and core-level shifts of NO adsorption on the Pt(111) surface. Physical Review B, 2009, 79, .	1.1	45
5981	Trends in ferromagnetism in Mn-doped dilute III-V alloys from a density functional perspective. Physical Review B, 2009, 79, .	1.1	0
5982	Evidence for the formation of a Mott state in potassium-intercalated pentacene. Physical Review B, 2009, 79, .	1.1	38
5983	Ferromagnetism in nitrogen-doped MgO: Density-functional calculations. Physical Review B, 2009, 80, .	1.1	42
5984	Half-metallic antiferromagnetic nature ofLa2VTcO6andLa2VCuO6fromab initiocalculations. Physical Review B, 2009, 80, .	1.1	38
5985	Stability and work function of<mml:math xmlns:mml="http://www.w3.org/1998/Math/MathML" display="inline"><mml:mrow><mml:msub><mml:mrow><mml:mtext>TiC</mml:mtext></mml:mrow><mml:mi>x</mml:mi></mml:msub>surfaces: Density functional theory calculations. Physical Review B, 2009, 80, .	1.1	19
5986	Magnetism and spin-polarized transport in carbon atomic wires. Physical Review B, 2009, 80, .	1.1	25
5987	Key role of the wetting layer in revealing the hidden path of Ge/Si(001) Stranski-Krastanow growth onset. Physical Review B, 2009, 80, .	1.1	96
5988	Origin of the Ising ferrimagnetism and spin-charge coupling in<mml:math xmlns:mml="http://www.w3.org/1998/Math/MathML" display="inline"><mml:mrow><mml:msub><mml:mrow><mml:mtext>LuFe</mml:mtext></mml:mrow><mml:mn>2</mml:mn></mml:msub></mml:mrow></mml:math>Physical Review B, 2009, 80, .	1.1	32
5989	Observation of theoP8crystal structure in potassium at high pressure. Physical Review B, 2009, 80, .	1.1	43
5990	Chemical bonding and diffusion of B dopants in C-predoped Si. Physical Review B, 2009, 80, .	1.1	2
5991	Universal optical response of Si-Si bonds and its evolution from nanoparticles to bulk crystals. Physical Review B, 2009, 79, .	1.1	11
5992	Lack of support for adaptive superstructureNiPt7: Experiment and first-principles calculations. Physical Review B, 2009, 79, .	1.1	15

#	Article	IF	Citations
5993	First-principles study on energetics of intrinsic point defects inLaAlO3. Physical Review B, 2009, 80, .	1.1	67
5994	Quantifying the anomalous self-diffusion in molybdenum with first-principles simulations. Physical Review B, 2009, 80, .	1.1	28
5995	Stress effects on impurity solubility in crystalline materials: A general model and density-functional calculations for dopants in silicon. Physical Review B, 2009, 79, .	1.1	26
5996	Dipole-active optical phonons in<mml:math xmlns:mml="http://www.w3.org/1998/Math/MathML" display="inline"><mml:mrow><mml:msub><mml:mrow><mml:mtext>YTiO</mml:mtext></mml:mrow><mml:mn>3</mml:mn></mml:msub></mml:mrow></mml:math>: Ellipsometry study and lattice-dynamics calculations. Physical Review B, 2009, 79, .	1.1	17
5997	Hydrogen-related defects and the role of metal additives in the kinetics of complex hydrides: A first-principles study. Physical Review B, 2009, 80, .	1.1	35
5998	Charge and spin states of metal atoms adsorbed on ultrathin MgO/Fe(001) films. Physical Review B, 2009, 79, .	1.1	20
5999	Atomic scale high-angle annular dark field STEM analysis of the N configuration in dilute nitrides of GaAs. Physical Review B, 2009, 80, .	1.1	22
6000	Predicted structure and stability of<mml:math xmlns:mml="http://www.w3.org/1998/Math/MathML" display="inline"><mml:mrow><mml:msub><mml:mi>A</mml:mi><mml:mn>4</mml:mn></mml:msub><mml:msub><mml:mi>B</mml:mi> xmlns:mml="http://www.w3.org/1998/Math/MathML"	1.1	54
6001	High-pressure phases, vibrational properties, and electronic structure of<mml:math xmlns:mml="http://www.w3.org/1998/Math/MathML" display="inline"><mml:mrow><mml:mtext>Ne</mml:mtext><mml:msub><mml:mrow><mml:mrow><mml:mo>(</mml:mo><mml:mrow xmlns:mml="http://www.w3.org/1998/Math/MathML" display="inline"><mml:mrow><mml:mtext>Ar</mml:mtext><mml:msub><mml:mrow><mml:mrow><mml:mm. Physical Review B, 2009, 80, .	1.1	59
6002	Local structure of the Ag(100) surface reacting with molecular iodine: Experimental and theoretical study. Physical Review B, 2009, 80, .	1.1	22
6003	Unconventional spin topology in surface alloys with Rashba-type spin splitting. Physical Review B, 2009, 79, .	1.1	62
6004	Role of Ti Antisitelike Defects in<mml:math xmlns:mml="http://www.w3.org/1998/Math/MathML" display="inline"><mml:msub><mml:mi>SrTiO</mml:mi><mml:mn>3</mml:mn></mml:msub></mml:math>. Physical Review Letters, 2009, 103, 185502.	2.9	109
6005	Predicted High-Temperature Superconducting State in the Hydrogen-Dense Transition-Metal Hydride<mml:math xmlns:mml="http://www.w3.org/1998/Math/MathML" display="inline"><mml:msub><mml:mi>YH</mml:mi><mml:mn>3</mml:mn></mml:msub></mml:math>at 40ÂK and 17.7ÂGPa. Physical Review Letters, 2009, 103, 077002.	2.9	79
6007	Comment on â€œAbÂInitioElectronic and Optical Properties of theNâ^'Vâ^'Center in Diamondâ€• Physical Review Letters, 2009, 102, 149703; discussion 149704.	2.9	3
6008	A comparative study on the LDA + U and hybrid functional methods on the description of the electronic structure of YTiO3 under high pressure. Canadian Journal of Chemistry, 2009, 87, 1374-1382.	0.6	3
6009	Density functional theory study of 13-atom metal clusters<mml:math xmlns:mml="http://www.w3.org/1998/Math/MathML" display="inline"><mml:mrow><mml:msub><mml:mi>M</mml:mi><mml:mrow><mml:mn>13</mml:mn></mml:mrow></mml:msub> xmlns:mml="http://www.w3.org/1998/Math/MathML" display="inline"><mml:mrow><mml:mi>M</mml:mi><mml:mo>=</mml:mo><mml:mtext>Ta</mml:mtext><mml:mo>â€“</mml:mo> Physical Review A, 2009, 79, .	1.0	50
6010	Implementation of a Morse potential to model hydroxyl behavior in phyllosilicates. Journal of Chemical Physics, 2009, 130, 134713.	1.2	45
6011	Effect of oxidation of the ultrathin Fe electrode material on the strength of magnetoelectric coupling in composite multiferroics. Physical Review B, 2009, 80, .	1.1	22

#	Article	IF	Citations
6012	Theory of Spin-Conserving Excitation of the<mml:math xmlns:mml="http://www.w3.org/1998/Math/MathML" display="inline"><mml:mi>N</mml:mi><mml:mo>â^'</mml:mo><mml:msup><mml:mi>V</mml:mi><mml:mo>â^'</mml:mo></mml:msup in Diamond. Physical Review Letters, 2009, 103, 186404.	2.9	206
6013	Atomic-resolution imaging of lithium in<mml:math xmlns:mml="http://www.w3.org/1998/Math/MathML" display="inline"><mml:mrow><mml:msub><mml:mrow><mml:mtext>Al</mml:mtext></mml:mrow><mml:mn>3</mml:mn></mml:ms Physical Review B, 2009, 80, .	1.1	40
6014	Magnetic doping of a thiolated-gold superatom: First-principles density functional theory calculations. Physical Review B, 2009, 80, .	1.1	64
6015	Electronic structure of amorphous indium oxide transparent conductors. Physical Review B, 2009, 80, .	1.1	49
6016	Competition between strain and chemistry effects on adhesion of Si and SiC. Physical Review B, 2009, 79, .	1.1	7
6017	Spontaneous Formation and Growth of a New Polytype on SiC(0001). Physical Review Letters, 2009, 103, 256101.	2.9	8
6018	Superhard Semiconducting Optically Transparent High Pressure Phase of Boron. Physical Review Letters, 2009, 102, 185501.	2.9	139
6019	Atomistic origins of the phase transition mechanism in Ge2Sb2Te5. Journal of Applied Physics, 2009, 106, .	1.1	29
6020	Determination of the Structural Parameters of an Incommensurate Phase from First Principles: The Case of Sc-II. Physical Review Letters, 2009, 102, 085701.	2.9	15
6021	AbÂInitioStudy of Fluorine in Silicon: Large Clusters and the Dominant Mobile Defect. Physical Review Letters, 2009, 103, 075503.	2.9	3
6022	Modifying the Adsorption Characteristic of Inert Silica Films by Inserting Anchoring Sites. Physical Review Letters, 2009, 102, 016102.	2.9	21
6023	Structure and energetics of<mml:math xmlns:mml="http://www.w3.org/1998/Math/MathML" display="inline"><mml:mrow><mml:mtext>Si</mml:mtext><mml:mrow><mml:mo>(</mml:mo><mml:mrow><mml:mn>111</mml:mn></mml:m Physical Review B, 2009, 80, .	1.1	62
6024	Hydrogen adsorption and etching on the Si-rich 3C-SiC(001)3Ã—2surface: First-principles molecular dynamics calculations. Physical Review B, 2009, 79, .	1.1	14
6025	Structural properties and superconductivity in the ternary intermetallic compoundsMAB(M=Ca, Sr,) Tj ETQq1 1 0.784314 rgBT /Overl	1.1	56
6026	Surface relaxation phenomena at electrified interfaces: Revealing adsorbate, potential, and solvent effects by combined x-ray diffraction, STM and DFT studies. Physical Review B, 2009, 79, .	1.1	37
6027	Microscopic picture of Co clustering in ZnO. Physical Review B, 2009, 79, .	1.1	24
6028	First-principles model study of the phase stabilities of dilute Fe-Cu alloys: Role of vibrational free energy. Physical Review B, 2009, 80, .	1.1	23
6029	Spin-polarized electronic structure for the layered two-dimensional[FeII(TCNE)(NCMe)2][FeIIICl4]organic-based magnet. Physical Review B, 2009, 80, .	1.1	7

#	Article	IF	Citations
6030	First-Principles Modeling of Multiferroic<mml:math xmlns:mml="http://www.w3.org/1998/Math/MathML" display="inline"><mml:mi>R</mml:mi><mml:msub><mml:mi>Mn</mml:mi><mml:mn>2</mml:mn></mml:msub><mml:mi mathvariant="bold">O</mml:mi><mml:mn>5</mml:mn></mml:msub></mml:math>. Physical Review Letters, 2009, 103, 257201.	7.9	40
6031	Real space calculation of optical constants from optical to x-ray frequencies. Physical Review B, 2009, 80, .	1.1	31
6032	Self-assembly of methanethiol on the reconstructed Au(111) surface. Physical Review B, 2009, 80, .	1.1	36
6033	Identification of Zn-vacancyâ€“hydrogen complexes in ZnO single crystals: A challenge to positron annihilation spectroscopy. Physical Review B, 2009, 79, .	1.1	117
6034	Strain-modulated electronic properties of Ge nanowires: A first-principles study. Physical Review B, 2009, 80, .	1.1	71
6035	Hexagon-on-cube versus cube-on-cube epitaxy: The case of ZnSe(111) onSrTiO3(001). Physical Review B, 2009, 79, .	1.1	10
6036	Enhancing piezoelectricity through polarization-strain coupling in ferroelectric superlattices. Physical Review B, 2009, 79, .	1.1	30
6037	Electron energy loss spectroscopy of theL2,3edge of phosphorus skutterudites and electronic structure calculations. Physical Review B, 2009, 80, .	1.1	9
6038	Theoretical study of pressure effect on the dislocation core properties in semiconductors. Physical Review B, 2009, 79, .	1.1	39
6039	Surface electronic band structure and temperature dependence of the surface state atAÂ¯onMg(101Â¯0)surface. Physical Review B, 2009, 80, .	1.1	3
6040	Three-dimensional band structure of highly metallic<mml:math xmlns:mml="http://www.w3.org/1998/Math/MathML" display="inline"><mml:mrow><mml:msub><mml:mrow><mml:mtext>Na</mml:mtext></mml:mrow><mml:mrow><mml:mn>0.8</mml:mn></mml:mrow> angle-resolved photoemission spectroscopy. Physical Review B, 2009, 79, .	1.1	4
6041	Complex metallic surface phases in the Al/Cu(111) system: An experimental and computational study. Physical Review B, 2009, 80, .	1.1	16
6042	Fermi-surface pockets in<mml:math xmlns:mml="http://www.w3.org/1998/Math/MathML" display="inline"><mml:mrow><mml:msub><mml:mrow><mml:mtext>YBa</mml:mtext></mml:mrow><mml:mn>2</mml:mn> Comparison ofab initiotechniques. Physical Review B, 2009, 79, .	1.1	11
6043	Roles of Cu codoping and oxygen vacancies on ferromagnetism in<mml:math xmlns:mml="http://www.w3.org/1998/Math/MathML" display="inline"><mml:mrow><mml:msub><mml:mrow><mml:mtext>In</mml:mtext></mml:mrow><mml:mn>2</mml:mn> Physical Review B, 2009, 79, .	1.1	31
6044	Evolution of the electronic structure of a ferromagnetic metal: Case ofSrRuO3. Physical Review B, 2009, 80, .	1.1	59
6045	Stability of a planar defect structure of the wurtzite AlN<mml:math xmlns:mml="http://www.w3.org/1998/Math/MathML" display="inline"><mml:mrow><mml:mrow><mml:mo>(</mml:mo><mml:mrow><mml:mn>10</mml:mn><mml:mover>	1.1	12
6046	Structural effects on the spin-state transition in epitaxially strained<mml:math xmlns:mml="http://www.w3.org/1998/Math/MathML" display="inline"><mml:mrow><mml:msub><mml:mrow><mml:mtext>LaCoO</mml:mtext></mml:mrow><mml:mn>3</mml:mn> Physical Review B, 2009, 79, .	1.1	89
6047	Ab initiostudy of early stages of III-V epitaxy on high-index surfaces of group-IV semiconductors: In adsorption on Si(112). Physical Review B, 2009, 80, .	1.1	5

#	Article	IF	Citations
6048	Predicting from first principles the chemical evolution of crystalline compounds due to radioactive decay: The case of the transformation of CsCl to BaCl. Physical Review B, 2009, 79, .	1.1	25
6049	First-principles calculations of the effect of pressure on the iron-based superconductor LaFeAsO. Physical Review B, 2009, 80, .	1.1	6
6050	Ferrimagnetic Fe-doped GaN: An unusual magnetic phase in dilute magnetic semiconductors. Physical Review B, 2009, 79, .	1.1	27
6051	First-principles study of Au nanostructures on rutile<mml:math xmlns:mml="http://www.w3.org/1998/Math/MathML" display="inline"><mml:mrow><mml:msub><mml:mrow><mml:mtext>TiO</mml:mtext></mml:mrow><mml:mn>2</mml:mn></mml:msub></mml:mrow></mml:math> Physical Review B, 2009, 79, .	1.1	32
6052	Electronic structure and optical properties of ZnSiO3 and Zn2SiO4. Journal of Applied Physics, 2009, 106, .	1.1	75
6053	Individual charge-trapping dislocations in an ionic insulator. Applied Physics Letters, 2009, 95, .	1.5	7
6054	Effects of barium incorporation into HfO2 gate dielectrics on reduction in charged defects: First-principles study. Applied Physics Letters, 2009, 94, 022903.	1.5	12
6055	Magnetic properties of some metastable Coâ€“Ru alloys studied by ion beam mixing and ab initio calculation. Applied Physics Letters, 2009, 94, 131903.	1.5	6
6056	First-principles study of native point defects in crystalline indium gallium zinc oxide. Journal of Applied Physics, 2009, 105, .	1.1	72
6057	Ab initio study of Alâ€“Ni bilayers on SiO2: Implications to effective work function modulation in gate stacks. Journal of Applied Physics, 2009, 105, .	1.1	16
6058	Diffusivity calculation on noble gas silica systems using first-principles molecular simulations. Molecular Simulation, 2009, 35, 942-952.	0.9	3
6059	Hydrogen complexes in Zn deficient ZnO. Journal of Applied Physics, 2009, 105, .	1.1	32
6060	First-principles prediction of mechanical properties of gamma-boron. Applied Physics Letters, 2009, 94, 191906.	1.5	40
6061	Schottky barrier formation at metal electrodes and semiconducting carbon nanotubes. Applied Physics Letters, 2009, 94, 093107.	1.5	26
6062	Origin of reduced polarizations in short-period BaTiO3/SrTiO3 ferroelectric superlattices. Journal of Applied Physics, 2009, 105, .	1.1	17
6063	Symmetry-breaking-induced enhancement of visible light absorption in delafossite alloys. Applied Physics Letters, 2009, 94, 251907.	1.5	20
6064	Oxygen vacancy effect on room-temperature ferromagnetism of rutile Co:TiO2 thin films. Applied Physics Letters, 2009, 94, .	1.5	57
6065	Low-field and high-field electron transport in zinc blende InN. Applied Physics Letters, 2009, 94, 022102.	1.5	38

#	Article	IF	Citations
6066	Influence of the electronic states anisotropy on the band gap pressure coefficient of InxGa1â^'xN alloys. Journal of Applied Physics, 2009, 106, 113511.	1.1	1
6067	Structural properties of wurtzitelike ScGaN films grown by NH3-molecular beam epitaxy. Journal of Applied Physics, 2009, 106, 113533.	1.1	25
6068	Controlling transistor threshold voltages using molecular dipoles. Journal of Applied Physics, 2009, 105, .	1.1	13
6069	Prediction of the formation of stable periodic self-interstitial cluster chains [(I4)m,m=1â€“4] in Si under biaxial strain. Applied Physics Letters, 2009, 94, 264101.	1.5	8
6070	Surface adsorption phase diagram of O/Ni(110) system: An ab initio atomistic thermodynamics investigation. Applied Physics Letters, 2009, 94, 091901.	1.5	4
6071	Modeling the environmental stability of FeS₂nanorods, using lessons from biomineralization. Nanotechnology, 2009, 20, 115702.	1.3	6
6072	On the interplay between tungsten and tantalum atoms in Ni-based superalloys: An atom-probe tomographic and first-principles study. Applied Physics Letters, 2009, 94, .	1.5	63
6073	The origin of p-type conduction in (P, N) codoped ZnO. Journal of Applied Physics, 2009, 106, 043707.	1.1	36
6074	Fundamental mechanisms of oxygen plasma-induced damage of ultralow-k organosilicate materials: The role of thermal P3 atomic oxygen. Applied Physics Letters, 2009, 94, 204102.	1.5	43
6075	Local Investigation of Femtosecond Laser Induced Dynamics of Water Nanoclusters on Cu(111). Physical Review Letters, 2009, 103, 026101.	2.9	37
6076	Interaction between silver nanowires and CO on a stepped platinum surface. Journal of Chemical Physics, 2009, 131, 064702.	1.2	10
6077	Phase partitioning and site-preference of hafnium in the Î³â€²(L12)âˆ•Î³(fcc) system in Ni-based superalloys: An atom-probe tomographic and first-principles study. Applied Physics Letters, 2009, 95, .	1.5	34
6078	Liquid-Liquid Transition in Supercooled Silicon Determined by First-Principles Simulation. Physical Review Letters, 2009, 102, 075701.	2.9	116
6079	Hydrogen-Vacancy Interactions in Fe-C Alloys. Physical Review Letters, 2009, 103, 085501.	2.9	44
6080	Kondo Decoherence: Finding the Right Spin Model for Iron Impurities in Gold and Silver. Physical Review Letters, 2009, 102, 056802.	2.9	77
6081	Atomic hydrogen adsorption and incipient hydrogenation of the Mg(0001) surface: A density-functional theory study. Journal of Chemical Physics, 2009, 131, 034706.	1.2	17
6082	Tailoring the Nature of Magnetic Coupling of Fe-Porphyrin Molecules to Ferromagnetic Substrates. Physical Review Letters, 2009, 102, 047202.	2.9	188
6083	Thermal expansion of select Mn+1AXn (M=earlytransitionmetal, A=Agroupelement, X=C or N) phases measured by high temperature x-ray diffraction and dilatometry. Journal of Applied Physics, 2009, 105, .	1.1	107

#	Article	IF	Citations
6084	Magnetism of semiconductor-based magnetic tunnel junctions under electric field from first principles. Applied Physics Letters, 2009, 94, .	1.5	2
6085	Benchmarking DFT surface energies with quantum Monte Carlo. Molecular Simulation, 2009, 35, 609-612.	0.9	11
6086	A body-centered-cubic polymorph of the Ge2Sb2Te5 phase change alloy. Applied Physics Letters, 2009, 95, .	1.5	18
6087	Origins of Distinctly Different Behaviors of Pd and Pt Contacts on Graphene. Physical Review Letters, 2009, 103, 066802.	2.9	100
6088	Absence of Critical Thickness in an Ultrathin Improper Ferroelectric Film. Physical Review Letters, 2009, 102, 107601.	2.9	70
6089	Solid-State Materials for Clean Energy: Insights from Atomic-Scale Modeling. MRS Bulletin, 2009, 34, 935-941.	1.7	27
6090	First-Principles Analysis of the Initial Electroreduction Steps of Oxygen over Pt(111). Journal of the Electrochemical Society, 2009, 156, B126.	1.3	207
6091	The Formation of Self-Assembled Nanowire Arrays on Ge(001): a DFT Study of Pt Induced Nanowire Arrays. Materials Research Society Symposia Proceedings, 2009, 1177, 19.	0.1	2
6092	Ab Initio Study on Structural and Magnetic Properties of Ni-Pd and Ni-Pt Linear and Zigzag Nanowires. Communications in Theoretical Physics, 2009, 52, 123-127.	1.1	4
6093	Molecular adsorption and metal-support interaction for transition-metal clusters in zeolites: NO adsorption on Pdnâ€ˆ(n=1â€“6) clusters in mordenite. Journal of Chemical Physics, 2009, 130, 104503.	1.2	26
6094	Element Lines: Bonding in the Ternary Gold Polyphosphides, Au2MP2 with M = Pb, Tl, or Hg. Journal of the American Chemical Society, 2009, 131, 2199-2207.	6.6	22
6095	Atomistic modeling of IIIâ€“V nitrides: modified embedded-atom method interatomic potentials for GaN, InN and Ga_{1â^'x}In_xN. Journal of Physics Condensed Matter, 2009, 21, 325801.	0.7	22
6096	Ion beam-induced amorphous-to-tetragonal phase transformation and grain growth of nanocrystalline zirconia. Nanotechnology, 2009, 20, 245303.	1.3	49
6097	Investigating the effects of a Ga layer on an Al grain boundary by a first-principles computational tensile test. Modelling and Simulation in Materials Science and Engineering, 2009, 17, 015003.	0.8	7
6098	Polarization effects on quantum levels in InN/GaN quantum wells. Nanotechnology, 2009, 20, 485204.	1.3	3
6099	The elastic stability, bifurcation and ideal strength of gold under hydrostatic stress: anab initiocalculation. Journal of Physics Condensed Matter, 2009, 21, 455401.	0.7	15
6100	Stability and electronic properties of small boron nitride nanotubes. Journal of Applied Physics, 2009, 105, 084312.	1.1	69
6101	Bonding characteristics in NiAl intermetallics with O impurity: a first-principles computational tensile test. Journal of Physics Condensed Matter, 2009, 21, 025402.	0.7	12

#	Article	IF	Citations
6102	Effects of cation distribution in ZnFe₂O₄and CdFe₂O₄:ab initiostudies. Journal of Physics: Conference Series, 2009, 145, 012028.	0.3	14
6103	Ab initio molecular dynamics calculations of ion hydration free energies. Journal of Chemical Physics, 2009, 130, 204507.	1.2	111
6104	Ab initiocalculations of the wolframite MnWO₄under high pressure. High Pressure Research, 2009, 29, 578-581.	0.4	11
6105	First-principles study of methane dehydrogenation on a bimetallic Cu/Ni(111) surface. Journal of Chemical Physics, 2009, 131, 174702.	1.2	94
6106	From molecular to polymeric CO2: bonding transformations under pressure. High Pressure Research, 2009, 29, 113-117.	0.4	1
6107	Substitutional alloy of Ce and Al. Proceedings of the National Academy of Sciences of the United States of America, 2009, 106, 2515-2518.	3.3	43
6108	Structure and bonding properties of Y doped Î£37 grain boundary in alumina. Chinese Physics B, 2009, 18, 1181-1187.	0.7	4
6109	Kinetic Monte Carlo Simulations of Solid Oxide Fuel Cell. Journal of the Electrochemical Society, 2009, 156, B1406.	1.3	15
6110	Methane dissociation on Ni(111) and Pt(111): Energetic and dynamical studies. Journal of Chemical Physics, 2009, 130, 054701.	1.2	124
6111	Low-temperature Î±-alumina thin film growth:ab initiostudies of Al adatom surface migration. Journal Physics D: Applied Physics, 2009, 42, 125302.	1.3	11
6112	Atomic and electronic structure of the YBa2Cu3O7/SrTiO3 interface from first principles. Journal of Applied Physics, 2009, 106, 093714.	1.1	13
6113	UNCLE: a code for constructing cluster expansions for arbitrary lattices with minimal user-input. Modelling and Simulation in Materials Science and Engineering, 2009, 17, 055003.	0.8	109
6114	Helium cluster dissolution in molybdenum. Journal of Physics Condensed Matter, 2009, 21, 335401.	0.7	13
6115	Electrostatic condition for the termination of the opposite face of the slab in density functional theory simulations of semiconductor surfaces. Journal of Applied Physics, 2009, 105, .	1.1	46
6116	Effect of the exchange-correlation potential and of surface relaxation on the description of the H2O dissociation on Cu(111). Journal of Chemical Physics, 2009, 130, 224702.	1.2	84
6117	General trend for adsorbate-induced segregation of subsurface metal atoms in bimetallic surfaces. Journal of Chemical Physics, 2009, 130, 174709.	1.2	108
6118	Atomic and electronic structures of montmorillonite in soft rock. Chinese Physics B, 2009, 18, 2933-2937.	0.7	20
6119	Dislocation modeling in calcium silicate perovskite based on the Peierls-Nabarro model. American Mineralogist, 2009, 94, 135-142.	0.9	20

#	Article	IF	Citations
6120	SPIN-POLARIZED DENSITY FUNCTIONAL STUDY ON HETEROFULLERENE AND METALLOFULLERENE CLUSTERS. International Journal of Modern Physics B, 2009, 23, 5119-5130.	1.0	9
6121	AB INITIO STUDY OF SIZE AND STRAIN EFFECTS ON THE ELECTRONIC PROPERTIES OF Si NANOWIRES. International Journal of Applied Mechanics, 2009, 01, 483-499.	1.3	32
6122	Insights into electron tunneling across hydrogen-bonded base-pairs in complete molecular circuits for single-stranded DNA sequencing. Journal of Physics Condensed Matter, 2009, 21, 035110.	0.7	7
6123	High-pressure phases and transitions of the layered alkaline earth nitridosilicates SrSiN₂and BaSiN₂. Journal of Physics Condensed Matter, 2009, 21, 275408.	0.7	12
6124	First-principles study of phase equilibria in Cuâ€“Ptâ€“Rh disordered alloys. Journal of Physics Condensed Matter, 2009, 21, 415401.	0.7	6
6125	Effect of nucleated Cu phase on magnetic properties and electronic structures in bcc Fe: Ab initio study. Journal of Applied Physics, 2009, 106, 083910.	1.1	9
6126	Local electronic structure analysis by site-selective ELNES using electron channeling and first-principles calculations. Journal of Physics Condensed Matter, 2009, 21, 104213.	0.7	17
6127	Role of Ag-doping in small transition metal clusters from first-principles simulations. Journal of Chemical Physics, 2009, 131, 184301.	1.2	13
6128	Design and control of electron transport properties of single molecules. Proceedings of the National Academy of Sciences of the United States of America, 2009, 106, 15259-15263.	3.3	88
6129	Mechanical Properties of Nanostructured Hard Coating of ZrO2. Materials Research Society Symposia Proceedings, 2009, 1224, 1.	0.1	1
6130	Adsorption and Organization of the Organic Radical 3-Carboxyproxyl on a Cu(110) Surface: A Combined STM, RAIRS, and DFT Study. Journal of Physical Chemistry C, 2009, 113, 13223-13230.	1.5	11
6131	Fundamental Aspects of Magnetic Shape Memory Alloys: Insights from <i>Ab Initio</i> and Monte Carlo Studies. Materials Science Forum, 0, 635, 3-12.	0.3	41
6132	Electronic structure studies of Niâ€“X (X: B, S, P) alloys using x-ray photoelectron spectroscopy, x-ray induced Auger electron spectroscopy and density functional theory calculations. Journal of Physics Condensed Matter, 2009, 21, 245503.	0.7	15
6133	Surface relaxation and stress for 5d transition metals. Journal of Physics Condensed Matter, 2009, 21, 095007.	0.7	26
6134	First-principles study of structrural and corrected band properties of wurtzite Zn _{1-x} Cd _x O and Zn _{1-x} Mg _x O systems. Chinese Physics B, 2009, 18, 2992-2997.	0.7	16
6135	X-ray absorption near edge structure/electron energy loss near edge structure calculation using the supercell orthogonalized linear combination of atomic orbitals method. Journal of Physics Condensed Matter, 2009, 21, 104202.	0.7	22
6136	Theoretical Studies on Defects of Kaolinite in Clays. Chinese Physics Letters, 2009, 26, 059101.	1.3	11
6137	A Possible Structure of the Al ₃₆ Cluster: Coexistence of Icosahedral and fcc -Like Structures. Chinese Physics Letters, 2009, 26, 087103.	1.3	0

#	Article	IF	Citations
6138	Elastic stability and electronic structure of low energy tetragonal and monoclinic PdN₂and PtN₂. Chinese Physics B, 2009, 18, 3934-3939.	0.7	11
6139	Structure and Stability of Multivalent Metal Tetraborohydrides. Materials Research Society Symposia Proceedings, 2009, 1216, 1.	0.1	0
6140	Estimating the quantum effects from molecular vibrations of water under high pressures and temperatures. Journal of Physics Condensed Matter, 2009, 21, 375101.	0.7	27
6141	Effect of strain on geometric and electronic structures of graphene on a Ru(0001) surface. Chinese Physics B, 2009, 18, 3008-3013.	0.7	19
6142	Schottky Barrier Formation at a Carbon Nanotubeâ€“Scandium Junction. Chinese Physics Letters, 2009, 26, 027302.	1.3	6
6143	Li- Site and Metal-Site Ion Doping in Phosphate-Olivine LiCoPO 4 by First-Principles Calculation. Chinese Physics Letters, 2009, 26, 038202.	1.3	11
6144	A first-principles density functional study of chlorophenol adsorption on Cu2O(110):CuO. Journal of Chemical Physics, 2009, 130, 184505.	1.2	30
6145	First-principles study of defects and carrier compensation in semiconductor radiation detector materials. Materials Research Society Symposia Proceedings, 2009, 1164, 1.	0.1	3
6146	Electronic structure and phase stability of In-free photovoltaic semiconductors, Cu₂ZnSnSe₄ and Cu₂ZnSnS₄ by first-principles calculation. Materials Research Society Symposia Proceedings, 2009, 1165, 1.	0.1	43
6147	Amorphous Semiconductors Studied by First-principles Simulations: Structure and Electronic Properties. Materials Research Society Symposia Proceedings, 2009, 1153, 1.	0.1	1
6148	First-principles energetics and structural relaxation of antigorite. American Mineralogist, 2009, 94, 1271-1278.	0.9	14
6149	Electronic structure of pyrochlore Cd₂Re₂O₇. Journal of Physics Condensed Matter, 2009, 21, 195602.	0.7	15
6150	Studies of LaSn[sub 3] as a Negative Electrode for Lithium-Ion Batteries. Journal of the Electrochemical Society, 2009, 156, A536.	1.3	17
6151	Hafnia surface and high-k gate stacks. Materials Research Society Symposia Proceedings, 2009, 1155, 1.	0.1	0
6152	First-principles study of ferromagnetic Ni2CoGa(Zn) alloys in the Heusler and the inverse Heusler structure. Materials Research Society Symposia Proceedings, 2009, 1200, 50.	0.1	3
6153	Semi-Empirical Potential Methods for Atomistic Simulations of Metals and Their Construction Procedures. Journal of Engineering Materials and Technology, Transactions of the ASME, 2009, 131, .	0.8	16
6154	Halogen-Induced Corrosion of Platinum. Journal of the American Chemical Society, 2009, 131, 2827-2829.	6.6	25
6155	Spin-Polarized Density Functional Theory Study of Reactivity of Diatomic Molecule on Bimetallic System: The Case of O₂ Dissociative Adsorption on Pt Monolayer on Fe(001). Journal of Physical Chemistry A, 2009, 113, 14302-14307.	1.1	22

#	Article	IF	Citations
6156	The elastic constants for Fe₃AlX (X=B, C and N) with anti-perovskite structure. Physica Scripta, 2009, 80, 055603.	1.2	7
6157	First-principles study of the magnetization of oxygen-depleted In₂O₃(001) surfaces. Journal of Physics Condensed Matter, 2009, 21, 272202.	0.7	22
6158	The Adsorption of NO on Various Metal Tape-Porphyrins: A First-Principles Study. Journal of the Physical Society of Japan, 2009, 78, 014706.	0.7	10
6159	Simulation of inelastic electronic tunneling spectra of adsorbates from first principles. Journal of Chemical Physics, 2009, 130, 134707.	1.2	12
6160	Isotope effects in the vibrational lifetime of hydrogen on germanium(100): Theory and experiment. Journal of Chemical Physics, 2009, 131, 124502.	1.2	13
6161	Structural and electronic properties of identical-sized Zn nanoclusters grown on Si(111)-(7Ã—7) surfaces. Journal of Chemical Physics, 2009, 130, 024701.	1.2	10
6162	Tunable coupling in CrO2 via RuO2 layers. Journal of Applied Physics, 2009, 105, 07C922.	1.1	2
6163	Calculated electronic and magnetic structure of rutile phase V1â^'xCrxO2. Journal of Applied Physics, 2009, 105, 07E510.	1.1	16
6164	Density functional theory study of multiply ionized weakly bound fullerene dimers. Journal of Chemical Physics, 2009, 130, 224302.	1.2	14
6165	Comprehensive study of sodium, copper, and silver clusters over a wide range of sizes 2â‰¤Nâ‰¤75. Journal of Chemical Physics, 2009, 131, 174510.	1.2	87
6166	On the structure and dynamics of secondary n-alkyl cations. Journal of Chemical Physics, 2009, 131, 104314.	1.2	14
6167	First-principles calculations of adsorption and dehydrogenation of trans-2-butene molecule on Pd(110) surface. Journal of Chemical Physics, 2009, 131, 154703.	1.2	2
6168	Model Hamiltonian for the interaction of NO with the Au(111) surface. Journal of Chemical Physics, 2009, 130, 174716.	1.2	64
6169	Substantial stabilization of ferromagnetism in ZnO:Mn induced by N codoping. Journal of Physics Condensed Matter, 2009, 21, 185503.	0.7	12
6170	Surface segregation of Si and its effect on oxygen adsorption on a Î³-TiAl(111) surface from first principles. Journal of Physics Condensed Matter, 2009, 21, 225005.	0.7	33
6171	CoAl(001) surface structures: a kinetic Monte Carlo simulation. Journal of Physics Condensed Matter, 2009, 21, 445005.	0.7	2
6172	How does an external electrical field affect adsorption patterns of thiol and thiolate on the gold substrate?. Journal of Physics Condensed Matter, 2009, 21, 055008.	0.7	5
6173	Direct observation of atomic scale surface relaxation in ortho twin structures in GaAs by XSTM. Journal of Physics Condensed Matter, 2009, 21, 055404.	0.7	9

#	Article	IF	Citations
6174	Half-metallic interface between a Heusler alloy and Si. Journal of Physics Condensed Matter, 2009, 21, 064244.	0.7	3
6175	First Principles Study on FeAs Single Layers. Chinese Journal of Chemical Physics, 2009, 22, 139-142.	0.6	2
6176	Ab initiocalculations of structural and magnetic properties of Fe(0â€‰0â€‰1)/MgO(0â€‰0â€‰1)/Fe(0â€‰0â€‰1) magnetic tunnel junction with interfacial Mg vacancy. Journal Physics D: Applied Physics, 2009, 42, 015003.	1.3	2
6177	First principles calculation of the effects of solute atom on electromigration resistance of Al interconnects. Journal Physics D: Applied Physics, 2009, 42, 125501.	1.3	5
6178	First-principles calculation of oxygen K-electron energy loss near edge structure of HfO₂. Journal of Physics Condensed Matter, 2009, 21, 104212.	0.7	17
6179	Modelling the relative stability of carbon nanotubes exposed to environmental adsorbates and air. Journal of Physics Condensed Matter, 2009, 21, 144205.	0.7	4
6180	Adsorption of benzene, phenol, propane and carbonic acid molecules on oxidized Al(111) and Î±-Al₂O₃(0001) surfaces: a first-principles study. Journal of Physics Condensed Matter, 2009, 21, 225001.	0.7	13
6181	Study of the electronic structure at the interface between fluorene-1-carboxylic acid molecules and Cu(110). Journal of Physics Condensed Matter, 2009, 21, 355005.	0.7	1
6182	First-principles super-cell investigation of the rattling effect in Li-doped KCl. Journal of Physics Condensed Matter, 2009, 21, 045401.	0.7	1
6183	Diversity driven unbiased search of minimum energy cluster configurations. Journal of Physics Condensed Matter, 2009, 21, 084209.	0.7	9
6184	Accelerated molecular dynamics simulation of thin-film growth with the bond-boost method. Journal of Physics Condensed Matter, 2009, 21, 084212.	0.7	26
6185	Systematic study on the spacer-dependent magnetic properties of Mn Î´-doped GaAs/(Ga, Mn)As ferromagnetic heterostructures: from first principles. Journal Physics D: Applied Physics, 2009, 42, 025002.	1.3	2
6186	Ab initiophase diagram of oxygen adsorption on W(110). Journal of Physics Condensed Matter, 2009, 21, 134017.	0.7	18
6187	Formation of Planar Magic Ag Nanostructures. Japanese Journal of Applied Physics, 2009, 48, 06FF11.	0.8	0
6188	Dynamical stabilization of the body centered cubic phase in lanthanum and thorium by phononâ€“phonon interaction. Journal of Physics Condensed Matter, 2009, 21, 175402.	0.7	12
6189	Ab initiomolecular-dynamics simulation of liquid AsxTe1â^'xalloys. Journal of Physics Condensed Matter, 2009, 21, 275602.	0.7	3
6190	High-pressure polymorphs of Li2BeH4predicted by first-principles calculations. Journal of Physics Condensed Matter, 2009, 21, 385405.	0.7	3
6191	Consequences of the intrachain dimerâ€“monomer spin frustration and the interchain dimerâ€“monomer spin exchange in the diamond-chain compound azurite Cu₃(CO₃)₂(OH)₂. Journal of Physics Condensed Matter, 2009, 21, 392201.	0.7	38

#	Article	IF	Citations
6192	Instability of CaLi ₂ at high pressure: Theoretical prediction and experimental results. Europhysics Letters, 2009, 86, 56001.	0.7	13
6193	Correlations in hot dense helium. Journal of Physics A: Mathematical and Theoretical, 2009, 42, 214001.	0.7	11
6194	Nanorod Calculations on Body-Centered Cubic Iron: A Method for Estimation of Size-Dependent Surface Energies of Metal Nanocrystals. Journal of Physical Chemistry C, 2009, 113, 644-649.	1.5	5
6195	Electronic structure and magnetic couplings in anatase TiO2:V codoped with N, F, Cl. Journal of Physics Condensed Matter, 2009, 21, 125502.	0.7	9
6196	Point defects in the NiAl(100) surface. Journal of Physics Condensed Matter, 2009, 21, 134007.	0.7	1
6197	A kinetic Monte Carlo study on the role of defects and detachment in the formation and growth of In chains on Si(100). Journal of Physics Condensed Matter, 2009, 21, 405002.	0.7	13
6198	Effect of iron additions on intergranular cohesion in chromium. Journal of Physics Condensed Matter, 2009, 21, 485002.	0.7	12
6199	Ideal strengths, structure transitions, and bonding properties of a ZnO single crystal under tension. Journal of Physics Condensed Matter, 2009, 21, 495402.	0.7	5
6200	Electronic Structures of 4H-SiC with Group I and VII Elements: First-Principles Study of Possible p-Type Doping. Japanese Journal of Applied Physics, 2009, 48, 041301.	0.8	6
6201	Crystallographic and electronic contribution to the apparent step height in nanometer-thin Pb(111) films grown on Cu(111). New Journal of Physics, 2009, 11, 123003.	1.2	12
6202	Pressure-induced structural phase transitions on Na0.5CoO2: a first principles study. Journal of Physics Condensed Matter, 2009, 21, 155401.	0.7	0
6203	Evolution of unoccupied resonance during the synthesis of a silver dimer on Ag(111). New Journal of Physics, 2009, 11, 063020.	1.2	24
6204	First-principles investigation of the structural, magnetic and electronic properties of perovskite SrRu_{1â^'x}Mn_xO₃. Journal of Physics Condensed Matter, 2009, 21, 495501.	0.7	2
6205	The role of steps in the dissociation of H₂on Mg(0001). Journal of Physics Condensed Matter, 2009, 21, 095004.	0.7	17
6206	First-Principles Simulation on Orientation Dependence of Piezoresistance Properties in Silicon Nanowires. Japanese Journal of Applied Physics, 2009, 48, 06FG09.	0.8	15
6207	Structural evolution due to Zn and Te adsorption on As-exposed Si(211): density functional calculation. Journal of Physics Condensed Matter, 2009, 21, 375502.	0.7	0
6208	Unexpected Coulomb binding between Ca and H[sup +] in ZnO. Journal of Vacuum Science & Technology B, 2009, 27, 1601.	1.3	0
6209	Effective radii of noble gas atoms in silicates from first-principles molecular simulation. American Mineralogist, 2009, 94, 600-608.	0.9	10

#	Article	IF	Citations
6210	First-Principles Molecular Dynamics Calculations of the Equation of State for Tantalum. International Journal of Molecular Sciences, 2009, 10, 4342-4351.	1.8	22
6211	Periodic trends governing the interactions between impurity atoms [Hâ€“Ar] and Î±-U. Philosophical Magazine, 2009, 89, 465-487.	0.7	8
6212	Negative compressibility of selenium chains confined in the channels of AlPO₄-5 single crystals. New Journal of Physics, 2009, 11, 103014.	1.2	16
6213	Co-doped rutile TiO_{2-Î´}thin films studied by XANES and first principles calculations. Journal of Physics: Conference Series, 2009, 190, 012107.	0.3	1
6214	Review of Stress Effects on Dopant Solubility in Silicon and Silicon-Germanium Layers. Solid State Phenomena, 0, 156-158, 173-180.	0.3	1
6215	Anharmonic OH vibrations in brucite: Small pressure-induced redshift in the range 0-22 GPa. American Mineralogist, 2009, 94, 1687-1697.	0.9	19
6216	Spin-filtering effect in the transport through a single-molecule magnet Mn12 bridged between metallic electrodes. Journal of Applied Physics, 2009, 105, .	1.1	26
6217	Restructuring of the Pt3Sn(111) surfaces induced by atomic and molecular oxygen from first principles. Journal of Chemical Physics, 2009, 130, 124716.	1.2	8
6218	Interplay between magnetic, electronic, and vibrational effects in monolayer Mn3O4 grown on Pd(100). Journal of Chemical Physics, 2009, 130, 124707.	1.2	32
6219	Energetics, relative stabilities, and size-dependent properties of nanosized carbon clusters of different families: Fullerenes, bucky-diamond, icosahedral, and bulk-truncated structures. Journal of Chemical Physics, 2009, 130, 184708.	1.2	23
6220	Shape prediction of two-dimensional adatom islands on crystal surfaces during homoepitaxial growth. Applied Physics Letters, 2009, 94, 183107.	1.5	13
6221	The role of morphology in stability of Si nanowires. Journal of Applied Physics, 2009, 105, .	1.1	15
6222	Enhanced magnetic moments of Fe clusters supported on MgO/Fe(001) ultrathin films. Journal of Chemical Physics, 2009, 130, 184711.	1.2	7
6223	The preserved aromaticity of aniline molecules adsorbed on a Si(5â€,5â€,12)â˜2Ã—1 surface. Journal of Chemical Physics, 2009, 130, 234703.	1.2	6
6224	Thermal stability and formation barrier of a high-energetic material N8 polymer nitrogen encapsulated in (5,5) carbon nanotube. Applied Physics Letters, 2009, 95, 021904.	1.5	30
6225	Reversible atomic modification of nanostructures on surfaces using direction-depended tip-surface interaction with a trimer-apex tip. Applied Physics Letters, 2009, 95, 073105.	1.5	7
6226	A charge-passivated codoping approach for enhancing ferromagnetism and electron transport on rutile TiO2(110) surface. Applied Physics Letters, 2009, 95, 052508.	1.5	4
6227	Carbonyl mediated attachment to silicon: Acetaldehyde on Si(001). Journal of Chemical Physics, 2009, 131, 104707.	1.2	8

#	Article	IF	Citations
6228	Efficient organometallic spin filter based on Europium-cyclooctatetraene wire. Journal of Chemical Physics, 2009, 131, .	1.2	43
6229	Diffusion and clustering of Au adatoms on H-terminated Si(111)-(1Ã—1): A first principles study. Journal of Chemical Physics, 2009, 131, 144702.	1.2	3
6230	Formation of atomic gold chain on hydrogen terminated Si(001):3Ã—1 surface: A density functional study. Journal of Applied Physics, 2009, 106, 093712.	1.1	1
6231	Transition state analysis of solid-solid transformations in nanocrystals. Journal of Chemical Physics, 2009, 131, 164116.	1.2	20
6232	Determination of Co spin state in rutile Co:TiO2. Journal of Applied Physics, 2009, 106, 123918.	1.1	2
6233	Interaction potential for indium phosphide: a molecular dynamics and first-principles study of the elastic constants, generalized stacking fault and surface energies. Journal of Physics Condensed Matter, 2009, 21, 095002.	0.7	25
6234	The role of tip size and orientation, tipâ€“surface relaxations and surface impurities in simultaneous AFM and STM studies on the TiO2(110) surface. Nanotechnology, 2009, 20, 264020.	1.3	21
6235	Gold-induced surface reconstruction on GaAs(111)Bsurface. Molecular Simulation, 2009, 35, 258-261.	0.9	1
6236	Rescaled potentials for transition metal solutes in Î±-iron. Philosophical Magazine, 2009, 89, 3393-3411.	0.7	8
6237	Ag-Conducting Chalcogenide Glasses: Applications In Programmable Metallization Cells. NATO Science for Peace and Security Series B: Physics and Biophysics, 2009, , 435-443.	0.2	0
6238	High pressure investigations on hydrous magnesium silicate-phase A using first principles calculations: H---H repulsion and changes in hydrogen bond geometry with compression. High Pressure Research, 2009, 29, 405-413.	0.4	4
6239	Periodic Density Functional Theory Investigation of the Uranyl Ion Sorption on Three Mineral Surfaces: A Comparative Study. International Journal of Molecular Sciences, 2009, 10, 2633-2661.	1.8	32
6240	Seebeck coefficient and thermal conductivity in doped C60. Journal of Renewable and Sustainable Energy, 2009, 1, 023104.	0.8	9
6241	Lattice dynamics of Fe-doped CoO from first principles. Journal of Physics Condensed Matter, 2009, 21, 125601.	0.7	13
6242	Hydroxyl vacancies in single-walled aluminosilicate and aluminogermanate nanotubes. Journal of Physics Condensed Matter, 2009, 21, 195301.	0.7	20
6243	Oxygen Reduction on Pt(111) Cathode of Fuel Cells. Journal of the Physical Society of Japan, 2009, 78, 114601.	0.7	7
6244	Phase stabilities and mechanical properties of two new carbon crystals. Europhysics Letters, 2009, 87, 56003.	0.7	33
6245	First-principles study of static displacements in Fe-Pd magnetic shape-memory alloys. Materials Research Society Symposia Proceedings, 2009, 1200, 57.	0.1	2

#	Article	IF	Citations
6246	Theoretical and Experimental Study of Tip Electronic Structure in Scanning Tunneling Microscope. Materials Research Society Symposia Proceedings, 2009, 1177, 1.	0.1	1
6247	Halogen-Assisted Copper Atom Abstraction: A Computational Perspective. Japanese Journal of Applied Physics, 2009, 48, 095501.	0.8	2
6248	First-principles Investigation of Edged Ferroelectric PbTiO3 Nanowires and the Role of Axial Strain. Materials Research Society Symposia Proceedings, 2009, 1199, 147.	0.1	0
6249	Dehydriding process of Î±-AlH3 observed by transmission electron microscopy and electron energy-loss spectroscopy. Journal of Applied Physics, 2009, 105, .	1.1	40
6250	Materials modeling by design: applications to amorphous solids. Journal of Physics Condensed Matter, 2009, 21, 084207.	0.7	28
6251	Energetics and electronic structure of a single copper atomic chain wrapped in a carbon nanotube: a first-principles study. Chinese Physics B, 2009, 18, 5468-5473.	0.7	5
6252	Study of the theoretical tensile strength of Fe by a first-principles computational tensile test. Chinese Physics B, 2009, 18, 1923-1930.	0.7	32
6253	First-Principles Studies on Properties of Boron-Related Impurities in c-BN. Chinese Physics Letters, 2009, 26, 037105.	1.3	1
6254	Assessing nanoparticle size effects on metal hydride thermodynamics using the Wulff construction. Nanotechnology, 2009, 20, 204001.	1.3	127
6255	First-principles investigation of the electronic structure and magnetism of eskolaite. Chinese Physics B, 2009, 18, 2551-2556.	0.7	3
6256	Structural Stabilities of Ordered Arrays of Nb 4 Clusters on NaCl(100) Surface. Chinese Physics Letters, 2009, 26, 016802.	1.3	2
6257	Structural and electronic properties of lutecia from first principles. Journal of Physics Condensed Matter, 2009, 21, 455601.	0.7	12
6258	First-Principles study of HfO2/:GaAs interface passivation by Si and Ge. Materials Research Society Symposia Proceedings, 2009, 1155, 1.	0.1	0
6259	First Principles Calculations of Complex Intermediate Band Materials for Photovoltaic Devices. Materials Research Society Symposia Proceedings, 2009, 1211, 1.	0.1	0
6260	Adsorption and Reaction Behaviors of Hf Precursor with Two Hydroxyls on Si(100): First Principles Study. Materials Research Society Symposia Proceedings, 2009, 1155, 1.	0.1	1
6261	Theoretical studies of defect states in GaTe. Journal of Physics Condensed Matter, 2009, 21, 015504.	0.7	14
6262	Glass-forming region of the Niâ€“Nbâ€“Ta ternary metal system determined directly from n-body potential through molecular dynamics simulations. Journal of Materials Research, 2009, 24, 1815-1819.	1.2	11
6263	Interaction of Hf Precursor with H2O-terminated Si(001): First Principles Study. Materials Research Society Symposia Proceedings, 2009, 1155, 1.	0.1	0

#	Article	IF	Citations
6264	Reversible ferromagnetic spin ordering governed by hydrogen in Co-doped ZnO semiconductor. Applied Physics Letters, 2009, 95, 172514.	1.5	50
6265	Ground-state phase diagram of Na_xCoO₂: correlation of Na ordering with CoO₂stacking sequences. Journal of Physics Condensed Matter, 2009, 21, 035401.	0.7	15
6266	Elastic anisotropy of Ni4Ti3 from first principles. Scripta Materialia, 2009, 60, 207-210.	2.6	61
6267	Influence of shear strain on the hydrogen trapped in bcc-Fe: A first-principles-based study. Scripta Materialia, 2009, 60, 555-558.	2.6	43
6268	Role of the alloying element in suppressing the negative effect of O in NiAl: Cr as an example. Scripta Materialia, 2009, 61, 189-192.	2.6	11
6269	First-principles study of the diffusion of Ga via interstitial-mediated mechanisms in ZnO. Scripta Materialia, 2009, 61, 324-326.	2.6	5
6270	Electronic structure and magnetic interactions in Ni-doped Î²-Ga2O3 from first-principles calculations. Scripta Materialia, 2009, 61, 477-480.	2.6	16
6271	Nucleation of a (1Â¯012) twin in hexagonal close-packed crystals. Scripta Materialia, 2009, 61, 903-906.	2.6	181
6272	Theoretical study on the stability and electronic property of Ag2SnO3. Solid State Sciences, 2009, 11, 259-264.	1.5	34
6273	Elastic properties and electronic structures of CdCNi3: A comparative study with MgCNi3. Solid State Sciences, 2009, 11, 251-258.	1.5	36
6274	High-pressure synthesis and characterization of the alkaline earth borate Î²-BaB4O7. Solid State Sciences, 2009, 11, 336-342.	1.5	21
6275	First-principle study of hydrogen stability within TiCo3. Solid State Sciences, 2009, 11, 894-899.	1.5	4
6276	Investigation of changes in crystal and electronic structures by hydrogen within LaNi5 from first-principles. Solid State Sciences, 2009, 11, 1098-1106.	1.5	17
6277	Electronic structure and chemical bonding properties of UO2F2 from first principles. Solid State Sciences, 2009, 11, 1380-1385.	1.5	5
6278	First-principles investigation of the binary AB2 type Laves phase in Mgâ€“Alâ€“Ca alloy: Electronic structure and elastic properties. Solid State Sciences, 2009, 11, 1400-1407.	1.5	100
6279	Structural and electronic properties of lithium ion battery anode material LiMN (M=Ni, Co, Cu). Solid State Sciences, 2009, 11, 1898-1902.	1.5	3
6280	Structural and dynamic properties of the polyanionic hydrides SrAlGeH and BaAlGeH. Solid State Sciences, 2009, 11, 1847-1853.	1.5	14
6281	Structural, elastic and electronic properties of Î²â€² phase precipitate in Mgâ€“Gd alloy system investigated via first-principles calculation. Solid State Sciences, 2009, 11, 2156-2161.	1.5	37

#	Article	IF	Citations
6282	Magnetism of a free-standing W monoatomic sheet. Solid State Sciences, 2009, 11, 2142-2148.	1.5	2
6283	Preparation of gallium oxynitride in the presence of iron through a citrate route. Materials Research Bulletin, 2009, 44, 1656-1659.	2.7	13
6284	Electronic Structure and Magnetic Properties of Spinel ${hbox {LiCr}}_{2}{hbox {O}}_{4}$: A ${hbox {GGA}}+$ U Study. IEEE Transactions on Magnetics, 2009, 45, 3985-3988.	1.2	3
6285	Suitability of Fe/GaAs and (Co,Ni)Mn(Ga,Ge) for Spintronics Applications: An Ab Initio Study. IEEE Transactions on Magnetics, 2009, 45, 3965-3968.	1.2	4
6286	Strain Effects on Electronic Bandstructures in Nanoscaled Silicon: From Bulk to Nanowire. IEEE Transactions on Electron Devices, 2009, 56, 553-559.	1.6	50
6287	Understanding the nature of surface nitrates in BaO/Î³-Al2O3 NOx storage materials: A combined experimental and theoretical study. Journal of Catalysis, 2009, 261, 17-22.	3.1	79
6288	Mechanism of ammonia oxidation over PGM (Pt, Pd, Rh) wires by temporal analysis of products and density functional theory. Journal of Catalysis, 2009, 261, 217-223.	3.1	47
6289	A DFT study on the removal of adsorbed sulfur from a nickel(111) surface: Reducing anode poisoning. Journal of Catalysis, 2009, 263, 380-389.	3.1	41
6290	Theoretical elucidation of the selectivity changes for the hydrogenation of unsaturated aldehydes on Pt(111). Journal of Catalysis, 2009, 265, 35-42.	3.1	41
6291	Edge sites as a gate for subsurface carbon in palladium nanoparticles. Journal of Catalysis, 2009, 266, 59-63.	3.1	71
6292	CO oxidation by Ti- and Al-doped ZnO: Oxygen activation by adsorption on the dopant. Journal of Catalysis, 2009, 266, 50-58.	3.1	58
6293	Temperature-programed reduction of unpromoted MoS2-based hydrodesulfurization catalysts: Experiments and kinetic modeling from first principles. Journal of Catalysis, 2009, 267, 67-77.	3.1	35
6294	Hydrogenation of acetyleneâ€“ethylene mixtures over Pd and Pdâ€“Ag alloys: First-principles-based kinetic Monte Carlo simulations. Journal of Catalysis, 2009, 268, 181-195.	3.1	256
6295	Influence of step sites in the molecular mechanism of the water gas shift reaction catalyzed by copper. Journal of Catalysis, 2009, 268, 131-141.	3.1	96
6296	First-Principles Simulation of the Active Sites and Reaction Environment in Electrocatalysis. , 0, , 93-128.		2
6297	Intrinsic Surface Dipoles Control the Energy Levels of Conjugated Polymers. Advanced Functional Materials, 2009, 19, 3874-3879.	7.8	64
6298	Electronic Structure of Selfâ€Assembled Monolayers on Au(111) Surfaces: The Impact of Backbone Polarizability. Advanced Functional Materials, 2009, 19, 3766-3775.	7.8	37
6299	Highly Ordered, Millimeterâ€Scale, Continuous, Singleâ€Crystalline Graphene Monolayer Formed on Ru (0001). Advanced Materials, 2009, 21, 2777-2780.	11.1	389

#	Article	IF	Citations
6300	Chemical Interactions at Metal/Molecule Interfaces in Molecular Junctionsâ€"A Pathway Towards Molecular Recognition. Advanced Materials, 2009, 21, 320-324.	11.1	27
6301	Electronic Manifestation of Cationâ€Vacancyâ€Induced Magnetic Moments in a Transparent Oxide Semiconductor: Anatase Nb:TiO₂. Advanced Materials, 2009, 21, 2282-2287.	11.1	97
6302	Modification of the Surface Properties of Indium Tin Oxide with Benzylphosphonic Acids: A Joint Experimental and Theoretical Study. Advanced Materials, 2009, 21, 4496-4501.	11.1	152
6303	Interface Atomicâ€Scale Structure and its Impact on Quantum Electron Transport. Advanced Materials, 2009, 21, 4966-4969.	11.1	23
6304	Ferroelectric Switching in Multiferroic Magnetite (Fe₃O₄) Thin Films. Advanced Materials, 2009, 21, 4452-4455.	11.1	148
6305	Research on Advanced Materials for Liâ€ion Batteries. Advanced Materials, 2009, 21, 4593-4607.	11.1	1,633
6307	Group 12 Dihalides: Structural Predilections from Gases to Solids. Chemistry - A European Journal, 2009, 15, 158-177.	1.7	45
6308	Effect of Doped Transition Metal on Reversible Hydrogen Release/Uptake from NaAlH₄. Chemistry - A European Journal, 2009, 15, 1685-1695.	1.7	36
6309	Theoretical Study on the Role of Surface Basicity and Lewis Acidity on the Etherification of Glycerol over Alkaline Earth Metal Oxides. Chemistry - A European Journal, 2009, 15, 10864-10870.	1.7	62
6310	ESIMS Studies and Calculations on Alkaliâ€Metal Adduct Ions of Ruthenium Olefin Metathesis Catalysts and Their Catalytic Activity in Metathesis Reactions. Chemistry - A European Journal, 2009, 15, 10948-10959.	1.7	37
6311	The Effect of Platinum on Diffusion Kinetics in Î²â€NiAl: Implications for Thermal Barrier Coating Lifetimes. ChemPhysChem, 2009, 10, 226-235.	1.0	12
6312	Critical Size for O₂ Dissociation by Au Nanoparticles. ChemPhysChem, 2009, 10, 348-351.	1.0	108
6313	Density Functional Characterization of the Electronic Structure and Visibleâ€Light Absorption of Crâ€Doped Anatase TiO₂. ChemPhysChem, 2009, 10, 2327-2333.	1.0	60
6314	STM and DFT Investigations of Isolated Porphyrin on a Siliconâ€Based Semiconductor at Room Temperature. ChemPhysChem, 2009, 10, 3190-3193.	1.0	13
6315	Where does Hydrogen Adsorb on Ru Nanoparticles? A Powerful Joint ²H MASâ€NMR/DFT Approach. ChemPhysChem, 2009, 10, 2939-2942.	1.0	30
6316	A New Class of Boron Nanotube. ChemPhysChem, 2009, 10, 3119-3121.	1.0	19
6317	Review: GaN growth by ammonia based methods â€" density functional theory study. Crystal Research and Technology, 2009, 44, 1038-1046.	0.6	15
6318	Highâ€Pressureâ€"Highâ€Temperature Behavior of Î¶â€Fe₂N and Phase Transition to Ïµâ€Fe₃N_{1.5}. European Journal of Inorganic Chemistry, 2009, 2009, 1634-1639.	1.0	30

#	Article	IF	Citations
6319	A theoretical study on fullereneâ€dizincocene hybrids. Journal of Computational Chemistry, 2009, 30, 978-982.	1.5	6
6320	A combinatorial study of full Heusler alloys by firstâ€principles computational methods. Journal of Computational Chemistry, 2009, 30, 1290-1299.	1.5	101
6321	Interaction of NO molecules with Pd clusters: Ab initio densityâ€“functional study. Journal of Computational Chemistry, 2009, 30, 1910-1922.	1.5	20
6322	Performance of planeâ€waveâ€based LDA+U and GGA+U approaches to describe magnetic coupling in molecular systems. Journal of Computational Chemistry, 2009, 30, 2316-2326.	1.5	35
6323	First principles investigation on the ultraâ€incompressible and hard TaN. Journal of Computational Chemistry, 2009, 30, 2358-2363.	1.5	33
6324	Identifying the O₂ diffusion and reduction mechanisms on CeO₂ electrolyte in solid oxide fuel cells: A DFT + U study. Journal of Computational Chemistry, 2009, 30, 2433-2442.	1.5	57
6325	A combinatorial study of inverse Heusler alloys by firstâ€principles computational methods. Journal of Computational Chemistry, 2010, 31, 612-619.	1.5	93
6326	Electronic properties for small tin clusters Sn_n (n â‰ 20) from density functional theory and the convergence toward the solid state. Journal of Computational Chemistry, 2010, 31, 929-937.	1.5	47
6327	Selective oxidation of styrene on an oxygenâ€adsorbed Cu(111): A comparison with Au(111). Journal of Computational Chemistry, 2010, 31, 1618-1624.	1.5	5
6329	Potassiumâ€Modified Mg(NH₂)₂/2â€‰LiH System for Hydrogen Storage. Angewandte Chemie - International Edition, 2009, 48, 5828-5832.	7.2	181
6330	Highâ€Yield Synthesis of Ultrathin Metal Nanowires in Carbon Nanotubes. Angewandte Chemie - International Edition, 2009, 48, 8298-8302.	7.2	89
6331	Structureâ€sensitivity of CH₃ dissociation on Ni(100)from firstâ€principles calculations. Asia-Pacific Journal of Chemical Engineering, 2009, 4, 511-517.	0.8	3
6332	Preconditioned gradient flows for nonlinear eigenvalue problems and application to the Hartreeâ€Fock functional. Numerical Methods for Partial Differential Equations, 2009, 25, 380-400.	2.0	7
6333	First principles calculations on the influence of water-filled cavities on the electronic structure of Prussian Blue. Journal of Molecular Modeling, 2009, 15, 567-572.	0.8	18
6334	First-principle electronic structure calculations for magnetic moment in iron-based superconductors: An LSDA+negative U study. Physica C: Superconductivity and Its Applications, 2009, 469, 908-911.	0.6	26
6335	First-principle calculation for the phonon structure on iron-based superconductors. Physica C: Superconductivity and Its Applications, 2009, 469, 1024-1026.	0.6	8
6336	First-principles study of narrow single-walled GaN nanotubes. Physics Letters, Section A: General, Atomic and Solid State Physics, 2009, 373, 367-370.	0.9	23
6337	Structural stability and magnetic properties of Co-doped or adsorbed polar-ZnO surface. Physics Letters, Section A: General, Atomic and Solid State Physics, 2009, 373, 391-395.	0.9	12

#	Article	IF	Citations
6338	Atomic structure for Mg on InN(0001) surface. Physics Letters, Section A: General, Atomic and Solid State Physics, 2009, 373, 1796-1799.	0.9	9
6339	Ferromagnetism in carbon-doped ZnO films from first-principle study. Physics Letters, Section A: General, Atomic and Solid State Physics, 2009, 373, 3091-3096.	0.9	27
6340	Electronic and magnetic properties of zigzag edge graphene nanoribbons with Stoneâ€“Wales defects. Physics Letters, Section A: General, Atomic and Solid State Physics, 2009, 373, 3354-3358.	0.9	41
6341	Density functional theory description of the mechanism of ferromagnetism in nitrogen-doped SnO2. Physics Letters, Section A: General, Atomic and Solid State Physics, 2009, 374, 319-322.	0.9	36
6342	Ab initio investigation of the CdTe (001) surface. Superlattices and Microstructures, 2009, 46, 733-744.	1.4	7
6343	First principle study of structural, phase stabilization and oxygen-ion diffusion properties of Î²-La2â^'xLxMo2O9 (L=Gd, Sm, Nd and Bi) and Î²-La2Mo2â^'yMyO9 (M=Cr, W). Solid State Ionics, 2009, 180, 946-951.	1.3	12
6344	Scanning tunneling microscopy and ab initio studies of precursor states of Ga-induced cluster on Si(001) surface. Surface Science, 2009, 603, 183-189.	0.8	2
6345	Reactions of vinyl groups on a model chromia surface: Vinyl chloride on stoichiometric Î±-Cr2O3. Surface Science, 2009, 603, 265-272.	0.8	3
6346	Density functional and dynamics study of the dissociative adsorption of hydrogen on Mg (0001) surface. Surface Science, 2009, 603, 304-310.	0.8	29
6347	STM simulation of molecules on ultrathin insulating overlayers using tight-binding: Auâ€“pentacene on NaCl bilayer on Cu. Surface Science, 2009, 603, 437-444.	0.8	8
6348	Surface segregation in bimetallic Pt3M (M=Fe, Co, Ni) alloys with adsorbed oxygen. Surface Science, 2009, 603, 349-353.	0.8	46
6349	Relating the coverage dependence of oxygen adsorption on Au and Pt fcc(111) surfaces through adsorbate-induced surface electronic structure effects. Surface Science, 2009, 603, 794-801.	0.8	97
6350	Surface atomic distribution and water adsorption on Ptâ€“Co alloys. Surface Science, 2009, 603, 912-920.	0.8	20
6351	First-principles studies of the oxygen adsorption on unreconstructed and reconstructed Ni(110) surfaces. Surface Science, 2009, 603, 1002-1009.	0.8	12
6352	STM study of Si(113) 3Ã—2-Ga surface. Surface Science, 2009, 603, 1197-1202.	0.8	4
6353	Effect of hydrogenation on the electronic structure of the P/Si(0 0 1)-(1 Ã— 2) surface. Surface Science, 2009, 603, 2271-2275.	0.8	1
6354	Stabilization of the (110) tetragonal zirconia surface by hydroxyl chemical transformation. Surface Science, 2009, 603, 2526-2531.	0.8	21
6355	Theoretical studies of Sm/Si(111)â€“nÃ—1 (n=5, 7) and Sm/Si(111)â€“(8Ã—2) structures. Surface Science, 2009, 603, 2771-2776.	0.8	2

#	Article	IF	Citations
6356	Electrostatic field effect on molecular structures at metal surfaces. Surface Science, 2009, 603, 2815-2819.	0.8	13
6357	Probing the properties of the (111) and (100) surfaces of LaB6 through infrared spectroscopy of adsorbed CO. Surface Science, 2009, 603, 3011-3020.	0.8	14
6358	CO2 dissociation on Ni(211). Surface Science, 2009, 603, 2991-2998.	0.8	47
6359	Molecular dynamics simulation comparison of atomic scale intermixing at the amorphous Al2O3/semiconductor interface for a-Al2O3/Ge, a-Al2O3/InGaAs, and a-Al2O3/InAlAs/InGaAs. Surface Science, 2009, 603, 3191-3200.	0.8	33
6360	DFT study on H2O activation by stepped and planar Rh surfaces. Surface Science, 2009, 603, 3275-3281.	0.8	31
6361	Adsorption of NO and NO2 on the ZnO() surface: A DFT study. Surface Science, 2009, 603, 3389-3399.	0.8	49
6362	Structure and reducibility of titania-supported monomeric and dimeric molybdenum oxide entities studied by DFT calculations. Computational and Theoretical Chemistry, 2009, 903, 73-82.	1.5	17
6363	Molybdenum thin film growth on a TiO2 (110) substrate. Computational and Theoretical Chemistry, 2009, 903, 67-72.	1.5	1
6364	Density functional theory (DFT) study of the interaction of ammonia with pure and tungstenâ€“doped ceria. Computational and Theoretical Chemistry, 2009, 912, 73-81.	1.5	27
6365	Transition states for hydride-water (Hâ€“)(H2O)n clusters, n=2â€“6, 20. Computational and Theoretical Chemistry, 2009, 916, 61-71.	1.5	5
6366	Crystal structure re-investigation in wide band gap CIGSe compounds. Thin Solid Films, 2009, 517, 2145-2148.	0.8	13
6367	Ab-initio valence band spectra of Al, In doped ZnO. Thin Solid Films, 2009, 517, 2448-2451.	0.8	41
6368	A nucleation mechanism of deformation twins in pure aluminum. Acta Materialia, 2009, 57, 4500-4507.	3.8	68
6369	First-principles study of ternary bcc alloys using special quasi-random structures. Acta Materialia, 2009, 57, 4716-4726.	3.8	66
6370	Density functional theory study of hydrogenation mechanism in Fe-doped Mg(0001) surface. Applied Surface Science, 2009, 255, 6338-6344.	3.1	17
6371	Structural, electronic properties and stability of the (1Ã—1) PbTiO3 (111) polar surfaces by first-principles calculations. Applied Surface Science, 2009, 255, 8145-8152.	3.1	20
6372	Adsorption of gold on hydrogen terminated Si(001): Formation of chain structure. Applied Surface Science, 2009, 256, 495-498.	3.1	0
6373	The effect of defects on the hydrogenation in Mg (0001) surface. Applied Surface Science, 2009, 256, 46-51.	3.1	30

#	Article	IF	Citations
6374	First principles studies of SnTiO3 perovskite as potential environmentally benign ferroelectric material. Chemical Physics, 2009, 355, 43-49.	0.9	74
6375	Collagen and component polypeptides: Low frequency and amide vibrations. Chemical Physics, 2009, 355, 141-148.	0.9	22
6376	Geometry and bonding in the ground and lowest triplet state of D6h symmetric crenellated edged C6[3m(mâˆ'1)+1]H6(2mâˆ'1) (m=2,â€¦,6) graphene hydrocarbon molecules. Chemical Physics, 2009, 358, 85-95.	0.9	15
6377	Surface structure for Au on (001) SrTiO3. Chemical Physics, 2009, 360, 79-84.	0.9	4
6378	Is the CO frequency shift a reliable indicator of coumarin binding to metal ions through the carbonyl oxygen?. Chemical Physics, 2009, 365, 69-79.	0.9	17
6379	Calculations of thermodynamic properties of PuO2 by the first-principles and lattice vibration. Journal of Nuclear Materials, 2009, 385, 18-20.	1.3	34
6380	Ab initio study of solution energy and diffusion of caesium in uranium dioxide. Journal of Nuclear Materials, 2009, 385, 368-371.	1.3	36
6381	First-principles theory for helium and xenon diffusion in uranium dioxide. Journal of Nuclear Materials, 2009, 385, 364-367.	1.3	45
6382	Modeling solute-vacancy trapping at oversized solutes and its effect on radiation-induced segregation in Feâ€“Crâ€“Ni alloys. Journal of Nuclear Materials, 2009, 389, 279-287.	1.3	25
6383	Point defect properties in hcp and bcc Zr with trace solute Nb revealed by ab initio calculations. Journal of Nuclear Materials, 2009, 393, 197-202.	1.3	25
6384	First-principles investigation on dissolution and diffusion of oxygen in tungsten. Journal of Nuclear Materials, 2009, 393, 508-512.	1.3	28
6385	Suppression of Jahnâ€“Teller distortion by chromium and magnesium doping in spinel LiMn2O4: A first-principles study using GGA and GGA+U. Journal of Physics and Chemistry of Solids, 2009, 70, 1200-1206.	1.9	35
6386	Vibrational properties of the gallium monohydrides SrGaGeH, BaGaSiH, BaGaGeH, and BaGaSnH. Journal of Solid State Chemistry, 2009, 182, 2068-2073.	1.4	14
6387	Electronic structure and photoluminescence properties of Eu2+-activated Ca2BN2F. Journal of Solid State Chemistry, 2009, 182, 3299-3304.	1.4	8
6388	Determination of phases in the system chromiumâ€“platinum (Crâ€“Pt) and thermodynamic calculations. Materials Science & Engineering A: Structural Materials: Properties, Microstructure and Processing, 2009, 510-511, 322-327.	2.6	9
6389	First principles study of point defects in titanium oxycarbide. Materials Science and Engineering B: Solid-State Materials for Advanced Technology, 2009, 165, 194-197.	1.7	18
6390	Probing coupling between â€˜rattlingâ€™ and extended lattice modes using time-of-flight neutron scattering combined with ab-initio calculationsâ€”introducing the PALD method. Nuclear Instruments and Methods in Physics Research, Section A: Accelerators, Spectrometers, Detectors and Associated Equipment, 2009, 600, 226-228.	0.7	8
6391	First-principle calculations on color center in Yâ€“Alâ€“O system. Nuclear Instruments & Methods in Physics Research B, 2009, 267, 3028-3031.	0.6	8

#	Article	IF	Citations
6392	The effect of vacancy created by ion irradiation on the ordering of FePt: A first-principle study. Nuclear Instruments & Methods in Physics Research B, 2009, 267, 3271-3273.	0.6	6
6393	First-principles study of helium effect in a ferromagnetic iron grain boundary: Energetics, site preference and segregation. Nuclear Instruments & Methods in Physics Research B, 2009, 267, 3200-3203.	0.6	28
6394	PHON: A program to calculate phonons using the small displacement method. Computer Physics Communications, 2009, 180, 2622-2633.	3.0	664
6395	Quantum confinement and phase transition in PbS nanowire: A first principles study. Chemical Physics Letters, 2009, 479, 244-247.	1.2	7
6396	Cathode catalysts for fuel cell development: A theoretical study based on band structure calculations for tungsten nitride and cobalt tungsten nitrides. Electrochimica Acta, 2009, 54, 6732-6739.	2.6	21
6397	Modeling of modern MOSFETs with strain. Journal of Computational Electronics, 2009, 8, 192-208.	1.3	7
6398	Pt effects in Î³-Ni(Al)/Î±-Al2O3 adhesion. Journal of Materials Science, 2009, 44, 1734-1740.	1.7	23
6399	Effect of dopants on alumina grain boundary sliding: implications for creep inhibition. Journal of Materials Science, 2009, 44, 1741-1749.	1.7	12
6400	Ab initio study of antiferroelectric PbZrO3 (001) surfaces. Journal of Materials Science, 2009, 44, 5249-5255.	1.7	19
6401	Charge compensation in an irradiation-induced phase of Î´-Sc4Zr3O12. Journal of Materials Science, 2009, 44, 4754-4757.	1.7	9
6402	Heat capacity and phonon spectra of A IIIN. Journal of Thermal Analysis and Calorimetry, 2009, 95, 403-407.	2.0	16
6403	Density Functional Study of the Effects of Strains on the Adsorption of Methoxide and its Decomposed Intermediates on Cu(100) Surface. Catalysis Letters, 2009, 127, 113-118.	1.4	11
6404	Adsorption of Formic Acid and its Decomposed Intermediates on (100) Surfaces of Pt and Pd: A Density Functional Study. Catalysis Letters, 2009, 128, 221-226.	1.4	29
6405	Steam Reforming of Formaldehyde on Cu(100) Surface: A Density Functional Study. Catalysis Letters, 2009, 129, 444-448.	1.4	27
6406	Theoretical Study of the Stability of Carbene Intermediates Formed During the Hydrodechlorination Reaction of the CF x Cl4â^'x Family on the Pd(110) Surface. Catalysis Letters, 2009, 133, 243-255.	1.4	2
6407	Mars-van Krevelen-like Mechanism of CO Hydrogenation on an Iron Carbide Surface. Catalysis Letters, 2009, 133, 257-261.	1.4	116
6408	Chemical bonding in the crystal structure of 1-hydrosilatrane. Russian Chemical Bulletin, 2009, 58, 25-30.	0.4	17
6409	Insights into the Geometry, Stability and Vibrational Properties of OH Groups on Î³-Al2O3, TiO2-Anatase and MgO from DFT Calculations. Topics in Catalysis, 2009, 52, 1005-1016.	1.3	34

#	Article	IF	Citations
6410	H/D Exchange on Silica-Grafted Tantalum(V) Imido Amido [(â‰¡SiO)2Ta(V)(NH)(NH2)] Synthesized from Either Ammonia or Dinitrogen: IR and DFT Evidence for Heterolytic Splitting of D2. Topics in Catalysis, 2009, 52, 1482-1491.	1.3	14
6411	Molecular and crystal structure of two phases of 1-fluorosilatrane. Specific features of the electron density distribution. Journal of Structural Chemistry, 2009, 50, 873-879.	0.3	7
6412	The role of acoustic phonon scattering in charge transport in organic semiconductors: a first-principles deformation-potential study. Science in China Series B: Chemistry, 2009, 52, 1646-1652.	0.8	67
6413	Structural stability and magnetism of metastable Ni-Pt intermetallic compounds studied by ab initio calculation. Science in China Series D: Earth Sciences, 2009, 52, 2681-2687.	0.9	7
6414	Structural and magnetic properties of bimetallic Co n â^' 1Cr clusters with density functional theory. Frontiers of Physics in China, 2009, 4, 408-414.	1.0	4
6415	A first-principles study on the electronic structure of one-dimensional [TM(Bz)]â^ž polymer (TM= Y, Zr,) Tj ETQq1 1 0.784314 rgBT /Ov	1.0	3
6416	Exploring at nanoscale from first principles. Frontiers of Physics in China, 2009, 4, 256-268.	1.0	1
6417	First-Principles Calculation of Phase Stability and Cohesive Properties of Ni-Sn Intermetallics. Metallurgical and Materials Transactions A: Physical Metallurgy and Materials Science, 2009, 40, 4-23.	1.1	41
6418	Elastic Properties, Thermal Expansion Coefficients, and Electronic Structures of Mg and Mg-Based Alloys. Metallurgical and Materials Transactions A: Physical Metallurgy and Materials Science, 2009, 40, 2751-2760.	1.1	37
6419	AbÂInitio Studies of Hydrogen Defects in CdTe. Journal of Electronic Materials, 2009, 38, 1539-1547.	1.0	11
6420	Thermodynamic Assessment of the Au-Co-Sn Ternary System. Journal of Electronic Materials, 2009, 38, 2158-2169.	1.0	17
6421	First-Principle Calculation Assisted Thermodynamic Assessment of the Pt-Pb System. Journal of Phase Equilibria and Diffusion, 2009, 30, 318-322.	0.5	7
6422	First-Principles Study of Magnetic Properties of 3d Transition Metals Doped in ZnO Nanowires. Nanoscale Research Letters, 2009, 4, 480-484.	3.1	43
6423	Density functional theory and tight binding-based dynamical studies of carbon metal systems of relevance to carbon nanotube growth. Nano Research, 2009, 2, 774-782.	5.8	7
6424	A local-MP2 approach to the ab initio study of electron correlation in crystals and to the simulation of vibrational spectra: the case of Ice XI. Theoretical Chemistry Accounts, 2009, 123, 327-335.	0.5	13
6425	Influence of the exchangeâ€“correlation potential on the description of the molecular mechanism of oxygen dissociation by Au nanoparticles. Theoretical Chemistry Accounts, 2009, 123, 119-126.	0.5	47
6426	DFT studies of pressure effects on structural and vibrational properties of crystalline octahydro-1,3,5,7-tetranitro-1,3,5,7-tetrazocine. Theoretical Chemistry Accounts, 2009, 124, 179-186.	0.5	54
6427	Peierls dislocation modelling in perovskite (CaTiO3): comparison with tausonite (SrTiO3) and MgSiO3 perovskite. Physics and Chemistry of Minerals, 2009, 36, 233-239.	0.3	20

#	Article	IF	Citations
6428	Spontaneous Phosphorusâ€Halogen Bond Cleavage in Nâ€Heterocyclic Halogenophosphanes Revisited: The Case of Pâ€“Br and Pâ€“I Bonds. Zeitschrift Fur Anorganische Und Allgemeine Chemie, 2009, 635, 245-252.	0.6	27
6429	New Ternary Silicide LiRh₂Si₂ â€“ Structure and Bonding Peculiarities. Zeitschrift Fur Anorganische Und Allgemeine Chemie, 2009, 635, 1894-1903.	0.6	15
6430	Synthesis, Crystal and Electronic Structure of a Samarium Carbochromate(III), Sm2[Cr2C3]. Zeitschrift Fur Anorganische Und Allgemeine Chemie, 2009, 635, 1741-1745.	0.6	3
6431	Highâ€pressure Phase Transition and Properties of Cu₃N: An Experimental and Theoretical StudyÂ. Zeitschrift Fur Anorganische Und Allgemeine Chemie, 2009, 635, 1959-1968.	0.6	20
6432	A First-Principle Study on Size-Dependent Thermodynamic Properties of Small TiO2 Nanoclusters. Chinese Journal of Catalysis, 2009, 30, 384-390.	6.9	7
6433	Electronic structure of the amorphous oxide semiconductor aâ€InGaZnO_{4â€“x}: Taucâ€“Lorentz optical model and origins of subgap states. Physica Status Solidi (A) Applications and Materials Science, 2009, 206, 860-867.	0.8	207
6434	Tin monoxide as an sâ€orbitalâ€based pâ€type oxide semiconductor: Electronic structures and TFT application. Physica Status Solidi (A) Applications and Materials Science, 2009, 206, 2187-2191.	0.8	213
6435	Theoretical description of timeâ€resolved pump/probe photoemission in TaS₂: a singleâ€band DFT+DMFT(NRG) study within the quasiequilibrium approximation. Physica Status Solidi (B): Basic Research, 2009, 246, 948-954.	0.7	26
6436	Group II element nitrides M₃N₂ under pressure: a comparative density functional study. Physica Status Solidi (B): Basic Research, 2009, 246, 1604-1613.	0.7	25
6437	Lattice dynamics and thermal properties of SrHfO₃ by firstâ€principles calculations. Physica Status Solidi (B): Basic Research, 2009, 246, 1628-1633.	0.7	11
6438	Abâ€initio theory of semiconductor band structures: New developments and progress. Physica Status Solidi (B): Basic Research, 2009, 246, 1877-1892.	0.7	120
6439	Competing stoichiometric phases and the intermediate phase in Ge_xSe_{1â^’x} glasses. Physica Status Solidi (B): Basic Research, 2009, 246, 1849-1853.	0.7	18
6440	Abâ€initio investigation of thermoactivated directional transport of hydrogen molecules inside narrow carbon nanotubes. Physica Status Solidi (B): Basic Research, 2009, 246, 2598-2601.	0.7	1
6441	Singleâ€wall carbon nanotubes: spintronics in the Luttinger liquid phase. Physica Status Solidi (B): Basic Research, 2009, 246, 2744-2749.	0.7	0
6442	Junctions of leftâ€and rightâ€handed chiral carbon nanotubes â€“ nanobamboo. Physica Status Solidi (B): Basic Research, 2009, 246, 2671-2674.	0.7	3
6443	Two component doping of fullereneâ€“cubane cocrystals. Physica Status Solidi (B): Basic Research, 2009, 246, 2618-2621.	0.7	1
6444	Pt adsorption on the PbTiO₃(110) polar surface: a density functional theory study. Surface and Interface Analysis, 2009, 41, 785-793.	0.8	0
6445	Convergence of the binding energy of oxygen on Cu(100): A cautionary tale for computational chemists using periodic bound conditions. International Journal of Quantum Chemistry, 2009, 109, 357-361.	1.0	0

#	Article	IF	Citations
6446	A theoretical and experimental study on manipulating the structure and properties of carbon nanotubes using substitutional dopants. International Journal of Quantum Chemistry, 2009, 109, 97-118.	1.0	70
6447	Periodic DFT investigation on the structure and properties of TNAD crystal. International Journal of Quantum Chemistry, 2009, 109, 1598-1608.	1.0	1
6448	Investigation of lattice defects in LaNi ₅ by positron annihilation spectroscopy and firstâ€principles calculations. International Journal of Quantum Chemistry, 2009, 109, 2758-2763.	1.0	1
6449	Light emission due to the quantum confinement of carriers in siliconâ€based nanostructures. International Journal of Quantum Chemistry, 2009, 109, 2764-2772.	1.0	3
6450	Optical properties of the Si(111):H surface with adsorbed Ag clusters. International Journal of Quantum Chemistry, 2009, 109, 3694-3704.	1.0	19
6451	The topologies of the charge densities in Zr and Ru. Acta Crystallographica Section A: Foundations and Advances, 2009, 65, 141-144.	0.3	11
6452	Significant progress in predicting the crystal structures of small organic molecules â€“ a report on the fourth blind test. Acta Crystallographica Section B: Structural Science, 2009, 65, 107-125.	1.8	371
6453	Transparent dense sodium. Nature, 2009, 458, 182-185.	13.7	710
6454	Designer magnetic superatoms. Nature Chemistry, 2009, 1, 310-315.	6.6	223
6455	The role of non-covalent interactions in electrocatalytic fuel-cell reactions on platinum. Nature Chemistry, 2009, 1, 466-472.	6.6	535
6456	Cooperative molecular dynamics in surface reactions. Nature Chemistry, 2009, 1, 716-721.	6.6	42
6457	Conduction at domain walls in oxide multiferroics. Nature Materials, 2009, 8, 229-234.	13.3	1,212
6458	A one-dimensional ice structure built from pentagons. Nature Materials, 2009, 8, 427-431.	13.3	212
6459	New Ga-enriched reconstructions on the GaAs(001) surface. JETP Letters, 2009, 89, 185-190.	0.4	3
6460	Diamond-like C2H nanolayer, diamane: Simulation of the structure and properties. JETP Letters, 2009, 90, 134-138.	0.4	169
6461	Density functional theory study of first-layer adsorption of ZrO2 and HfO2 on Ge(100). Microelectronic Engineering, 2009, 86, 249-258.	1.1	6
6462	Isopropanol adsorption on Î³-Al2O3 surfaces: A computational study. Journal of Molecular Catalysis A, 2009, 304, 58-64.	4.8	51
6463	Vacancies and E-centers in silicon as multi-symmetry defects. Materials Science and Engineering B: Solid-State Materials for Advanced Technology, 2009, 159-160, 107-111.	1.7	14

#	Article	IF	Citations
6464	Modelling the scattering of X-rays in warm dense matter. Nuclear Instruments and Methods in Physics Research, Section A: Accelerators, Spectrometers, Detectors and Associated Equipment, 2009, 606, 142-145.	0.7	2
6465	Eu2+-doped Ba2CsI5, a new high-performance scintillator. Nuclear Instruments and Methods in Physics Research, Section A: Accelerators, Spectrometers, Detectors and Associated Equipment, 2009, 612, 138-142.	0.7	109
6466	Recovery and restructuring induced by fission energy ions in high burnup nuclear fuel. Nuclear Instruments & Methods in Physics Research B, 2009, 267, 960-963.	0.6	30
6467	First-principles approach to the properties of point defects and small helium-vacancy clusters in palladium. Nuclear Instruments & Methods in Physics Research B, 2009, 267, 3037-3040.	0.6	12
6468	Effect of He on the structure and bonding properties of W: A first-principles computational tensile test. Nuclear Instruments & Methods in Physics Research B, 2009, 267, 3193-3196.	0.6	26
6469	First-principles investigation of energetics and site preference of He in a W grain boundary. Nuclear Instruments & Methods in Physics Research B, 2009, 267, 3189-3192.	0.6	52
6470	First-principles study of hydrogen in perfect tungsten crystal. Nuclear Instruments & Methods in Physics Research B, 2009, 267, 3170-3174.	0.6	29
6471	The ideal tensile strength and deformation behavior of a tungsten single crystal. Nuclear Instruments & Methods in Physics Research B, 2009, 267, 3282-3285.	0.6	38
6472	Vibrational contributions to the stability of point defects in bcc iron: A first-principles study. Nuclear Instruments & Methods in Physics Research B, 2009, 267, 3009-3012.	0.6	50
6473	Electronic structure of the pentaceneâ€“gold interface: A density-functional theory study. Organic Electronics, 2009, 10, 1571-1578.	1.4	25
6474	Electronic properties of the Au impurity in : First-principles study. Physica B: Condensed Matter, 2009, 404, 131-137.	1.3	6
6475	Atomic and electronic structure of hydrogen-related centers in hydrogen storage materials. Physica B: Condensed Matter, 2009, 404, 793-797.	1.3	4
6476	Layered growth model and epitaxial growth structures for SiCAlN alloys. Physica B: Condensed Matter, 2009, 404, 1840-1846.	1.3	0
6477	Investigation of the electronic structure of Me/Al2O3(0001) interfaces. Physica B: Condensed Matter, 2009, 404, 2065-2071.	1.3	27
6478	Energetics and electronic properties of Mg7TMH16 (TM=Sc, Ti, V, Y, Zr, Nb): An ab initio study. Physica B: Condensed Matter, 2009, 404, 2234-2240.	1.3	42
6479	The adsorption of In on the surface of (001) CdTe. Physica B: Condensed Matter, 2009, 404, 3530-3533.	1.3	2
6480	Search of hydrogen transition states on Î±-Fe: The monomer adapted to first principles calculations. Physica B: Condensed Matter, 2009, 404, 2880-2882.	1.3	8
6481	First-principles molecular dynamics simulations of the structure of germanium dioxide under pressures. Physica B: Condensed Matter, 2009, 404, 4178-4184.	1.3	14

#	Article	IF	Citations
6482	First-principles study of palladium atom adsorption on the boron- or nitrogen-doped carbon nanotubes. Physica B: Condensed Matter, 2009, 404, 4173-4177.	1.3	20
6483	The electronic properties of the interface structure between ZnO and amorphous HfO2. Physica B: Condensed Matter, 2009, 404, 4823-4826.	1.3	7
6484	Freeâ€“free opacity in warm dense aluminum. High Energy Density Physics, 2009, 5, 124-131.	0.4	32
6485	Aluminum hydride coated single-walled carbon nanotube as a hydrogen storage medium. International Journal of Hydrogen Energy, 2009, 34, 370-375.	3.8	64
6486	Hydrogen dissociation and diffusion on transition metal (=Ti, Zr, V, Fe, Ru, Co, Rh, Ni, Pd, Cu, Ag)-doped Mg(0001) surfaces. International Journal of Hydrogen Energy, 2009, 34, 1922-1930.	3.8	331
6487	Bulk modulus and thermal expansion coefficient of mechano-chemically synthesized Mg2FeH6 from high temperature and high pressure studies. International Journal of Hydrogen Energy, 2009, 34, 3410-3416.	3.8	16
6488	Density functional theory study of structural, vibrational, and thermodynamic properties of crystalline 2,4-dinitrophenol, 2,4-dinitroresorcinol, and 4,6-dinitroresorcinol. Computational and Theoretical Chemistry, 2009, 895, 131-137.	1.5	12
6489	First-principles study of crystalline mono-amino-2,4,6-trinitrobenzene, 1,3-diamino-2,4,6-trinitrobenzene, and 1,3,5-triamino-2,4,6-trinitrobenzene. Computational and Theoretical Chemistry, 2009, 900, 84-89.	1.5	33
6490	Density functional theory study of high-pressure behavior of crystalline hexanitrostilbene. Computational and Theoretical Chemistry, 2009, 910, 148-153.	1.5	24
6491	Structural and electronic properties of Pt monolayer adsorption on PbTiO3(100) surface. Thin Solid Films, 2009, 517, 6817-6823.	0.8	1
6492	Theoretical and spectroscopic investigations on the structure and bonding in Bâ€“Câ€“N thin films. Thin Solid Films, 2009, 518, 1459-1464.	0.8	18
6493	A first-principles study of dual acceptors behaviors in Mn -doped digital ferromagnetic heterostructures. Solid State Communications, 2009, 149, 163-167.	0.9	1
6494	First-principles study of diffusion of zinc vacancies and interstitials in ZnO. Solid State Communications, 2009, 149, 199-204.	0.9	48
6495	Ab initio studies on the structural and magnetic properties of RhH. Solid State Communications, 2009, 149, 322-324.	0.9	10
6496	Synthesis, crystal and electronic structures of La3Cr2N6. Solid State Communications, 2009, 149, 273-276.	0.9	8
6497	First-principles investigations on elastic properties of - and - Ta4AlC3. Solid State Communications, 2009, 149, 441-444.	0.9	23
6498	Optical properties of amorphous IIIâ€“V compound semiconductors from first principles study. Solid State Communications, 2009, 149, 638-640.	0.9	7
6499	Density functional investigation of the magnetic properties of PbMBO4 (M=Cr, Mn, Fe). Solid State Communications, 2009, 149, 602-604.	0.9	15

#	Article	IF	Citations
6500	The new antiferromagnetic semiconductor : Predicting from first-principle theory. Solid State Communications, 2009, 149, 888-892.	0.9	0
6501	Phase-transition mechanism of h-BN w-BN from first principles. Solid State Communications, 2009, 149, 843-846.	0.9	15
6502	Two-leg spin ladder model for Ag2VOP2O7 from mapping analysis based on first principles density functional calculations. Solid State Communications, 2009, 149, 847-851.	0.9	1
6503	High-density strontium hydride: An experimental and theoretical study. Solid State Communications, 2009, 149, 830-834.	0.9	31
6504	Structural and electronic properties of Zn on a CdTe(001) surface. Solid State Communications, 2009, 149, 982-985.	0.9	9
6505	On the compression behavior of Ti2InC, (Ti0.5, Zr0.5)2InC, and M2SnC (, Nb, Hf) to quasi-hydrostatic pressures up to 50 GPa. Solid State Communications, 2009, 149, 1978-1983.	0.9	27
6506	Relaxation and electronic states of Au(100), (110) and (111) surfaces. Solid State Communications, 2009, 149, 1561-1564.	0.9	14
6507	The geometric structure influence on the ferromagnetism in Carbon-doped anatase : First-principles study. Solid State Communications, 2009, 149, 1717-1721.	0.9	15
6508	Role of Coulomb interactions in semicore levels Ga d levels of GaX semiconductors: Implication on band offsets. Solid State Communications, 2009, 149, 1810-1813.	0.9	4
6509	Joint experiment and theory to study the band structure of SrZrO3 in orthorhombic phase. Solid State Communications, 2009, 149, 2250-2253.	0.9	8
6510	Lattice dynamics and phase transition of NiTi alloy. Solid State Communications, 2009, 149, 2164-2168.	0.9	12
6511	Oxygen ion conduction in 12CaOÂ·7Al2O3: O2â˜' conduction mechanism and possibility of Oâ˜' fast conductionâ˜†. Solid State Ionics, 2009, 180, 550-555.	1.3	57
6512	Crystal structure and lattice vibration of proton dissolved BaZr0.8Sc0.2O2.9. Solid State Ionics, 2009, 180, 560-562.	1.3	6
6513	Properties of oxide thin films and their adsorption behavior studied by scanning tunneling microscopy and conductance spectroscopy. Surface Science Reports, 2009, 64, 595-659.	3.8	213
6514	Correlating STM contrast and atomic-scale structure by chemical modification: Vacancy dislocation loops on FeO/Pt(111). Surface Science, 2009, 603, L15-L18.	0.8	53
6515	(6Ã—2) Reconstruction of the Ag/Si(111) surface at 77K. Surface Science, 2009, 603, 311-314.	0.8	4
6516	Growth mode and novel structure of ultra-thin KCl layers on the Si(100)-2Ã—1 surface. Surface Science, 2009, 603, 419-424.	0.8	7
6517	Reactivity of the Cu2O(1 0 0) surface: Insights from first principles calculations. Surface Science, 2009, 603, 1637-1645.	0.8	70

#	Article	IF	Citations
6518	DFT studies of Cr(VI) complex adsorption on hydroxylated hematite () surfaces. Surface Science, 2009, 603, 736-746.	0.8	56
6519	Flip motion of heterogeneous buckled dimers on Ge(001) by electron injection from STM tip. Surface Science, 2009, 603, 781-787.	0.8	2
6520	Band offsets at the epitaxial anatase TiO2/n-SrTiO3(001) interface. Surface Science, 2009, 603, 771-780.	0.8	50
6521	Coverage-dependent absorption of atomic hydrogen into the sub-surface of Cu(111) studied by density-functional-theory calculations. Surface Science, 2009, 603, 1081-1086.	0.8	9
6522	Realization of an atomic sieve: Silica on Mo(112). Surface Science, 2009, 603, 1145-1149.	0.8	25
6523	Structure and adhesion of MoSi2/Ni interfaces: Evaluation of MoSi2 as an alternative bond coat alloy. Surface Science, 2009, 603, 1276-1283.	0.8	3
6524	Atomic and electronic structures of thin NaCl films grown on a Ge(001) surface. Surface Science, 2009, 603, 2102-2107.	0.8	8
6525	Ab-initio investigation of Ni(Fe)/ZrO2(001) and Niâ€“Fe/ZrO2(001) interfaces. Surface Science, 2009, 603, 2218-2225.	0.8	21
6526	Ab-initio calculations of interactions between Cu adatoms on Cu(110): Sensitivity of strong multi-site interactions to adatom relaxations. Surface Science, 2009, 603, 2387-2392.	0.8	12
6527	Structural and electronic properties of the Ti/W(111) adsorption system. Surface Science, 2009, 603, 2507-2519.	0.8	8
6528	Atomic and electronic structure of group-IV adsorbates on the GaAs(001)-(1Ã—2) surface. Surface Science, 2009, 603, 2683-2687.	0.8	3
6529	Core-level shifts of InP(100)(2Ã—4) surface: Theory and experiment. Surface Science, 2009, 603, 2664-2668.	0.8	5
6530	Eleyâ€“Rideal reaction dynamics between O atoms on Î²-cristobalite (100) surface: A new interpolated potential energy surface and classical trajectory study. Surface Science, 2009, 603, 2742-2751.	0.8	20
6531	Adsorption and diffusion of a single Pt atom on Î³-Al2O3 surfaces. Surface Science, 2009, 603, 2793-2807.	0.8	39
6532	Structural properties of Cu clusters on Si(111):Cu2Si magic family. Surface Science, 2009, 603, 2874-2878.	0.8	14
6533	Stable hydroxyl network on diamond (001) via first-principles and MD investigation. Surface Science, 2009, 603, 3035-3040.	0.8	1
6534	Nanoclusters of TiO2 wetted with gold. Surface Science, 2009, 603, 3131-3135.	0.8	8
6535	Effects of water and electric field on atomic oxygen adsorption on Ptâ€“Co alloys. Surface Science, 2009, 603, 3239-3248.	0.8	22

#	Article	IF	Citations
6536	Origin of the contrast inversion in the STM image of CO on Cu(1 1 1). Surface Science, 2009, 603, 3286-3291.	0.8	9
6537	Anomalous hybridization in the In-rich InAs(001) reconstruction. Surface Science, 2009, 603, 3321-3328.	0.8	28
6538	Energetics of oxygen embedment into unreconstructed and reconstructed Cu(1 0 0) surfaces: Density functional theory calculations. Surface Science, 2009, 603, 3404-3409.	0.8	26
6539	Ab initio study of hydrogen binding on Ca-inserted porphyrin. Vacuum, 2009, 84, 537-539.	1.6	5
6540	Theoretical investigations on the high light yield of the LuI3:Ce scintillator. Journal of Luminescence, 2009, 129, 1555-1559.	1.5	16
6541	Point defects in Al2O3 and their impact on gate stacks. Microelectronic Engineering, 2009, 86, 1756-1759.	1.1	38
6542	Modeling complexity of a complex gate oxide. Microelectronic Engineering, 2009, 86, 1763-1766.	1.1	3
6543	Stability of Si impurity in high-Î¹ oxides. Microelectronic Engineering, 2009, 86, 1780-1781.	1.1	0
6544	Electronic properties of defects in polycrystalline dielectric materials. Microelectronic Engineering, 2009, 86, 1751-1755.	1.1	25
6545	CO hydrogenation reaction on sulfided molybdenum catalysts. Journal of Molecular Catalysis A, 2009, 312, 7-17.	4.8	53
6546	The Z-phase in 9â€“12% Cr ferritic steels: A phase stability analysis. Materials Science & Engineering A: Structural Materials: Properties, Microstructure and Processing, 2009, 505, 1-5.	2.6	31
6547	Modification of the electronic properties of rubrene crystals by water and oxygen-related species. Organic Electronics, 2009, 10, 333-340.	1.4	21
6548	Heats of formation of Zirconium binary transition metal alloys. Physics Procedia, 2009, 2, 927-932.	1.2	3
6549	Exploring tin tantalates and niobates as prospective catalyst supports for water electrolysis. Physica B: Condensed Matter, 2009, 404, 1737-1745.	1.3	14
6550	First-principles calculations of elastic and thermo-physical properties of Al, Mg and rare earth lanthanide elements. Physica B: Condensed Matter, 2009, 404, 2299-2304.	1.3	11
6551	Model study on sorption of polycyclic aromatic hydrocarbons to goethite. Journal of Colloid and Interface Science, 2009, 330, 244-249.	5.0	37
6552	Design and epitaxy of structural III-nitrides. Journal of Crystal Growth, 2009, 311, 478-481.	0.7	5
6553	Expansion ratio dependence of lattice vibration of GaN using ab initio molecular dynamics calculations. Journal of Crystal Growth, 2009, 311, 3100-3102.	0.7	1

#	Article	IF	Citations
6554	Preferential orientation of Te particles in melt-grown CZT. Journal of Crystal Growth, 2009, 311, 2641-2647.	0.7	16
6555	Functionalization of single-walled carbon nanotube with borane for hydrogen storage. Physica E: Low-Dimensional Systems and Nanostructures, 2009, 41, 1340-1346.	1.3	31
6556	First-principles study of cobalt silicide nanosheet and nanotubes: Stability and electronic properties. Physica E: Low-Dimensional Systems and Nanostructures, 2009, 41, 1795-1799.	1.3	5
6557	A self-consistent and environment-dependent Hamiltonian for large-scale simulations of complex nanostructures. Physica E: Low-Dimensional Systems and Nanostructures, 2009, 42, 1-16.	1.3	17
6558	Binding energy of hydrogenâ€“Cd vacancy complex in CdTe. Physics Letters, Section A: General, Atomic and Solid State Physics, 2009, 373, 791-794.	0.9	5
6559	New template for metal decoration and hydrogen adsorption on graphene-like C3N4. Physics Letters, Section A: General, Atomic and Solid State Physics, 2009, 373, 2778-2781.	0.9	47
6560	Determination of preferential rare earth adatom adsorption geometries on Si(001). Physics Letters, Section A: General, Atomic and Solid State Physics, 2009, 373, 3459-3463.	0.9	4
6561	First-principles study of lattice dynamics of LiFePO4. Physics Letters, Section A: General, Atomic and Solid State Physics, 2009, 373, 4096-4100.	0.9	48
6562	Microtwinning and other shearing mechanisms at intermediate temperatures in Ni-based superalloys. Progress in Materials Science, 2009, 54, 839-873.	16.0	305
6563	Structure and magnetism of near-stoichiometric FePd nanoparticles. Journal of Magnetism and Magnetic Materials, 2009, 321, 861-864.	1.0	13
6564	Electronic and magnetic behavior of ultrathin Ti nanowires. Journal of Magnetism and Magnetic Materials, 2009, 321, 1856-1862.	1.0	8
6565	Magnetism in strained pseudomorphic ultrathin films of fcc 3d-transition metals (Cr, Mn, Fe, Co and) Tj ETQq1 1 0.784314 rgBT /Over 321, 2827-2832.	1.0	9
6566	Theoretical study of the magnetic interaction of Cr-doped ZnO with and without vacancies. Journal of Magnetism and Magnetic Materials, 2009, 321, 3067-3070.	1.0	34
6567	Effects of hydrogen absorption on physical properties of. Journal of Magnetism and Magnetic Materials, 2009, 321, 3422-3425.	1.0	3
6568	H-impurity induced high-temperature ferromagnetism in Co-doped ZnO. Journal of Magnetism and Magnetic Materials, 2009, 321, 3507-3510.	1.0	11
6569	Energetics of intrinsic point defects in uranium dioxide from electronic-structure calculations. Journal of Nuclear Materials, 2009, 384, 61-69.	1.3	127
6570	First-principles modeling of He-clusters in UO2. Journal of Nuclear Materials, 2009, 385, 72-74.	1.3	16
6571	Numerical prediction of thermodynamic properties of ironâ€“chromium alloys using semi-empirical cohesive models: The state of the art. Journal of Nuclear Materials, 2009, 385, 268-277.	1.3	67

#	Article	IF	Citations
6572	Magnetic cluster expansion simulations of FeCr alloys. Journal of Nuclear Materials, 2009, 386-388, 22-25.	1.3	43
6573	Vacancies, interstitials and gas atoms in beryllium. Journal of Nuclear Materials, 2009, 386-388, 79-81.	1.3	38
6574	Ab initio study of interstitial migration in Feâ€“Cr alloys. Journal of Nuclear Materials, 2009, 386-388, 86-89.	1.3	55
6575	Multiscale modeling of point defect interactions in Feâ€“Cr alloys. Journal of Nuclear Materials, 2009, 386-388, 227-230.	1.3	25
6576	Theory of He trapping, diffusion, and clustering in UO2. Journal of Nuclear Materials, 2009, 385, 510-516.	1.3	40
6577	Structure, stability and diffusion of hydrogen in tungsten: A first-principles study. Journal of Nuclear Materials, 2009, 390-391, 1032-1034.	1.3	116
6578	Radiation damage effects in the uranium-bearing Î´-phase oxide Y6U1O12. Journal of Nuclear Materials, 2009, 389, 497-499.	1.3	7
6579	First-principles study of structural, elastic and electronic properties of thorium dicarbide (ThC2) polymorphs. Journal of Nuclear Materials, 2009, 393, 192-196.	1.3	13
6580	First-principles study on cerium ion behavior in irradiated cerium dioxide. Journal of Nuclear Materials, 2009, 393, 321-327.	1.3	23
6581	Atomic and dislocation dynamics simulations of plastic deformation in reactor pressure vessel steel. Journal of Nuclear Materials, 2009, 394, 174-181.	1.3	12
6582	Helium atoms in chromium-rich Feâ€“Cr alloys â€“ Ab initio results. Journal of Nuclear Materials, 2009, 395, 45-49.	1.3	5
6583	Si-Fluoro substituted quasisilatranes (Nâ†’Si) FYSi(OCH2CH2)2NR. Journal of Organometallic Chemistry, 2009, 694, 607-615.	0.8	26
6584	An unexpected cluster opening upon the formation of electronically unsaturated Î·3-(cyclooctenyl)metallacarboranes of rhodium(III) and iridium(III) with sterically reduced [(PhCH2)2C2B9H9]2â¯ ligand. Journal of Organometallic Chemistry, 2009, 694, 1727-1735.	0.8	23
6585	Coordination chemistry of mercury-containing anticrowns. Synthesis and structures of the complexes of cyclic trimeric perfluoro-o-phenylenemercury with ethanol, THF and bis-2,2â€²-tetrahydrofuryl peroxide. Journal of Organometallic Chemistry, 2009, 694, 2604-2610.	0.8	27
6586	Electronic structure of substitutional defects and vacancies in GaSe. Journal of Physics and Chemistry of Solids, 2009, 70, 344-355.	1.9	32
6587	Bonding mechanism and relaxation energy of (): First-principles study. Journal of Physics and Chemistry of Solids, 2009, 70, 707-712.	1.9	8
6588	Intrinsic magnetism induced by vacancy in GaN. Journal of Physics and Chemistry of Solids, 2009, 70, 1223-1225.	1.9	12
6589	First-principles study on lithium removal from Li2MnO3. Journal of Power Sources, 2009, 189, 798-801.	4.0	158

#	Article	IF	Citations
6590	First-principles investigation of the bonding, optical and lattice dynamical properties of CeO2. Journal of Power Sources, 2009, 194, 830-834.	4.0	54
6591	The effect of oxygen vacancies on the structure and electrochemistry of LiTi2(PO4)3 for lithium-ion batteries: A combined experimental and theoretical study. Journal of Power Sources, 2009, 194, 1075-1080.	4.0	107
6592	Crystal, electronic structures and photoluminescence properties of rare-earth doped LiSi2N3. Journal of Solid State Chemistry, 2009, 182, 301-311.	1.4	60
6593	A new triclinic modification of the pyrochlore-type KOs2O6 superconductor. Journal of Solid State Chemistry, 2009, 182, 428-434.	1.4	7
6594	Structure of Î´-Bi2O3 from density functional theory: A systematic crystallographic analysis. Journal of Solid State Chemistry, 2009, 182, 1222-1228.	1.4	17
6595	Structure and crystal chemistry of fluorite-related Bi38Mo7O78 from single crystal X-ray diffraction and ab initio calculations. Journal of Solid State Chemistry, 2009, 182, 1312-1318.	1.4	13
6596	Structureâ€“composition sensitivity in â€œMetallicâ€•Zintl phases: A study of Eu(Ga1â^'xTtx)2 (Tt=Si, Ge,) Tj ETQq0 0 0 rgBT /Overlock	1.4	14
6597	Electronic band structure of from first principles. Journal of Solid State Chemistry, 2009, 182, 2678-2684.	1.4	11
6598	Structural, mechanical, and electronic properties of <mml:math xmlns:mml="http://www.w3.org/1998/Math/MathML" altimg="si0104.gif" overflow="scroll"><mml:msub><mml:mrow><mml:mi>TaB</mml:mi></mml:mrow><mml:mrow><mml:mn>2</mml:mn></mml:mrow><mml:TaB, <mml:math xmlns:mml="http://www.w3.org/1998/Math/MathML" altimg="si0105.gif" overflow="scroll"><mml:msub><mml:mrow><mml:mi>IrB</mml:mi></mml:mrow><mml:mrow><mml:mn>2</mml:mn></mml:mrow></m and IrB: First-principle calculation. Journal of Solid State Chemistry, 2009, 182, 2880-2886.	1.4	47
6599	A new material for hydrogen storage; ScAl0.8Mg0.2. Journal of Solid State Chemistry, 2009, 182, 3113-3117.	1.4	19
6600	Nanostructure formation on Ir(100). Progress in Surface Science, 2009, 84, 2-17.	3.8	20
6601	Nature of the magnetic interaction between Fe-porphyrin molecules and ferromagnetic surfaces. Progress in Surface Science, 2009, 84, 18-29.	3.8	43
6602	Catalytic activity of supported metal particles for sulfuric acid decomposition reaction. Catalysis Today, 2009, 139, 291-298.	2.2	47
6603	Hydrogen adsorption on model tungsten carbide surfaces. Catalysis Today, 2009, 146, 223-229.	2.2	29
6604	Surface anion vacancies on ceria: Quantum modelling of mutual interactions and oxygen adsorption. Catalysis Today, 2009, 143, 315-325.	2.2	60
6605	Ethanol oxidation on metal oxide-supported platinum catalysts. Catalysis Today, 2009, 147, 107-114.	2.2	43
6606	DFT studies of dry reforming of methane on Ni catalyst. Catalysis Today, 2009, 148, 260-267.	2.2	320
6607	A first principles study of NO2 chemisorption on silicon carbide nanotubes. Chemical Physics, 2009, 355, 50-54.	0.9	49

#	Article	IF	Citations
6608	Vibrational spectra of crystalline formic and acetic acid isotopologues by inelastic neutron scattering and numerical simulations. Chemical Physics, 2009, 355, 118-122.	0.9	9
6609	Ab initio molecular simulations with numeric atom-centered orbitals. Computer Physics Communications, 2009, 180, 2175-2196.	3.0	2,170
6610	Atomic configurations of Pd atoms in PdAu(111) and PdAu(100) surface alloys: Ab initio density functional calculations. Chemical Physics Letters, 2009, 468, 162-165.	1.2	23
6611	First-principles study of the relaxation and energy of bcc-Fe, fcc-Fe and AISI-304 stainless steel surfaces. Applied Surface Science, 2009, 255, 9032-9039.	3.1	120
6612	Half metallicity in a zigzag double-walled nanotube nanodot: An ab initio prediction. Chemical Physics Letters, 2009, 468, 257-259.	1.2	3
6613	The transition from metalâ€“metal bonding to metalâ€“solvent interactions during a dissolution event as assessed from electronic structure. Chemical Physics Letters, 2009, 469, 99-103.	1.2	32
6614	First principle studies of zigzag AlN nanoribbon. Chemical Physics Letters, 2009, 469, 183-185.	1.2	86
6615	Ti 3p electrons: Core or valence?. Chemical Physics Letters, 2009, 471, 75-79.	1.2	9
6616	Long-range interactions between polar molecules and metallic surfaces: A comparison of classical and density functional theory based models. Chemical Physics Letters, 2009, 471, 239-243.	1.2	33
6617	First principles studies of ZrNi and ZrNiH3. Chemical Physics Letters, 2009, 473, 61-65.	1.2	24
6618	Helical and linear [K(As11)]2â^' chains: Role of solvent on the conformation of chains formed by Zintl anions. Chemical Physics Letters, 2009, 473, 305-311.	1.2	11
6619	First-principles theoretical analysis of pure and hydrogenated crystalline carbon phases and nanostructures. Chemical Physics Letters, 2009, 474, 168-174.	1.2	11
6620	Accurate simulations of metals at the mesoscale: Explicit treatment of 1 million atoms with quantum mechanics. Chemical Physics Letters, 2009, 475, 163-170.	1.2	96
6621	Increased CO adsorption on supported VIB and IB metals. Chemical Physics Letters, 2009, 475, 215-219.	1.2	2
6622	Electronic structure and lattice anisotropy of <mml:math xmlns:mml="http://www.w3.org/1998/Math/MathML" altimg="si18.gif" display="inline" overflow="scroll"><mml:mrow><mml:mtext>Cd</mml:mtext><mml:mo stretchy="false">(</mml:mo><mml:msub><mml:mrow><mml:mtext>UO</mml:mtext></mml:mrow><mml:mrow><mml:mn>2</mml:m	1.2	3
6623	Chemical Physics Letters, 2009, 476, 213-217. Au adatom-linked CH3Sâ€“Auâ€“SCH3 complexes on Au(1 1 1). Chemical Physics Letters, 2009, 477, 90-94.	1.2	11
6624	Investigation of the catalytic activity for ozonation on the surface of NiO nanoparticles. Chemical Physics Letters, 2009, 479, 310-315.	1.2	28
6625	Density functional studies of the magnetic properties in nitrogen doped TiO2. Chemical Physics Letters, 2009, 481, 99-102.	1.2	58

#	Article	IF	Citations
6626	An NMR investigation on the adducted hydrogen in weak ferromagnetic rhombohedral C60 polymers. Chemical Physics Letters, 2009, 482, 66-71.	1.2	4
6627	Growth mechanism of cross-like SnO structure synthesized by thermal decomposition. Chemical Physics Letters, 2009, 482, 287-290.	1.2	29
6628	Gate field induced electronic current modulation in a single wall boron nitride nanotube: Molecular scale field effect transistor. Chemical Physics Letters, 2009, 482, 312-315.	1.2	4
6629	From trans-polyacetylene to zigzag-edged graphene nanoribbons. Chemical Physics Letters, 2009, 483, 120-123.	1.2	24
6630	Electronic structure of self-assembled (fluoro)methylthiol monolayers on the Au(111) surface: Impact of fluorination and coverage density. Journal of Electron Spectroscopy and Related Phenomena, 2009, 174, 70-77.	0.8	12
6631	First principles study of the structure and stability of carbynes. Carbon, 2009, 47, 367-383.	5.4	39
6632	Adatom complexes and self-healing mechanisms on graphene and single-wall carbon nanotubes. Carbon, 2009, 47, 901-908.	5.4	78
6633	Correlation between the vacancy defects and ferromagnetism in graphite. Carbon, 2009, 47, 1399-1406.	5.4	94
6634	Electronic and magnetic properties of deformed and defective single wall carbon nanotubes. Carbon, 2009, 47, 3252-3262.	5.4	35
6635	Using ab initio calculations in designing bcc Mgâ€“Li alloys for ultra-lightweight applications. Acta Materialia, 2009, 57, 69-76.	3.8	135
6636	First-principles study of vacancy formation and migration in clean and Re-doped Î³â€²-Ni3Al. Acta Materialia, 2009, 57, 224-231.	3.8	27
6637	Modified embedded-atom method interatomic potentials for pure Mn and the Feâ€“Mn system. Acta Materialia, 2009, 57, 474-482.	3.8	67
6638	Energy landscape for martensitic phase transformation in shape memory NiTi. Acta Materialia, 2009, 57, 1624-1629.	3.8	62
6639	Defect energetics and Xe diffusion in UO2 and ThO2. Acta Materialia, 2009, 57, 1655-1659.	3.8	60
6640	Variable-charge method applied to study coupled grain boundary migration in the presence of oxygen. Acta Materialia, 2009, 57, 1988-2001.	3.8	45
6641	Microstructural evolution during multiaxial deformation of pseudoelastic NiTi studied by first-principles-based micromechanical modeling. Acta Materialia, 2009, 57, 3856-3867.	3.8	28
6642	Effect of alloying elements on the elastic properties of Mg from first-principles calculations. Acta Materialia, 2009, 57, 3876-3884.	3.8	177
6643	First principles impurity diffusion coefficients. Acta Materialia, 2009, 57, 4102-4108.	3.8	213

#	Article	IF	Citations
6644	Ab-initio calculations of the hydrogenâ€“uranium system: Surface phenomena, absorption, transport and trapping. Acta Materialia, 2009, 57, 4707-4715.	3.8	43
6645		3.8	325
6646	Influence of the electronic structure on the ductile behavior of B2 CsCl-type AB intermetallics. Acta Materialia, 2009, 57, 5876-5881.	3.8	90
6647	Energetics of charged point defects in rutile TiO2 by density functional theory. Acta Materialia, 2009, 57, 5882-5891.	3.8	32
6648	The effect of alloying elements on the dislocation climbing velocity in Ni: A first-principles study. Acta Materialia, 2009, 57, 5914-5920.	3.8	81
6649	First-principles calculations of vacancyâ€“solute element interactions in body-centered cubic iron. Acta Materialia, 2009, 57, 5947-5955.	3.8	120
6650	Solvothermal preparation, electronic structure and photocatalytic properties of PbMoO4 and SrMoO4. Applied Catalysis B: Environmental, 2009, 91, 135-143.	10.8	149
6651	Fabrication and characterization of brookite-rich, visible light-active TiO2 films for water splitting. Applied Catalysis B: Environmental, 2009, 93, 90-95.	10.8	54
6652	Optical properties of titanium oxycarbide thin films. Applied Surface Science, 2009, 255, 5615-5619.	3.1	9
6653	Electronic structure of superconducting galliumâ€doped germanium from abâ€initio calculations. Physica Status Solidi - Rapid Research Letters, 2009, 3, 224-226.	1.2	8
6654	A hard semiconductor OsN₄ with high elastic constant c₄₄. Physica Status Solidi - Rapid Research Letters, 2009, 3, 272-274.	1.2	9
6655	Band gap engineering of (N,Ta)-codoped TiO2: A first-principles calculation. Chemical Physics Letters, 2009, 478, 175-179.	1.2	95
6656	On the existence of Siâ€“C double bonded graphene-like layers. Chemical Physics Letters, 2009, 479, 255-258.	1.2	39
6657	Al-centered icosahedral ordering in Cu46Zr46Al8 bulk metallic glass. Applied Physics Letters, 2009, 94, 091904.	1.5	61
6658	Fundamental steps towards interface amorphization during silicon oxidation: Density functional theory calculations. Physical Review B, 2009, 79, .	1.1	18
6659	Activated dissociation ofO2on Pb(111) surfaces by Pb adatoms. Physical Review B, 2009, 80, .	1.1	7
6660	Adsorption and dissociation of<mml:math xmlns:mml="http://www.w3.org/1998/Math/MathML" display="inline"><mml:mrow><mml:msub><mml:mtext>O</mml:mtext><mml:mn>2</mml:mn></mml:msub></mml:mrow></mml:math Be(0001): First-principles prediction of an energy barrier on the adiabatic potential energy surface. Physical Review B, 2009, 79, .	1.1	16
6661	First-principles simulations on bulk Ta2O5 and Cu/Ta2O5/Pt heterojunction: Electronic structures and transport properties. Journal of Applied Physics, 2009, 106, .	1.1	51

#	Article	IF	Citations
6662	Superhard Monoclinic Polymorph of Carbon. Physical Review Letters, 2009, 102, 175506.	2.9	480
6663	Intermixing-driven scenario for the growth of nanowires on (110) metal surfaces. Physical Review B, 2009, 79, .	1.1	16
6664	High Waterâ^'Gas Shift Activity in TiO₂(110) Supported Cu and Au Nanoparticles: Role of the Oxide and Metal Particle Size. Journal of Physical Chemistry C, 2009, 113, 7364-7370.	1.5	223
6665	Combined Experimental and Theoretical Investigation of Nanosized Effects of Pt Catalyst on Their Underlying Methanol Electro-Oxidation Activity. Journal of Physical Chemistry C, 2009, 113, 9197-9205.	1.5	16
6666	First-principles study on defect chemistry and migration of oxide ions in ceria doped with rare-earth cations. Physical Chemistry Chemical Physics, 2009, 11, 3241.	1.3	224
6667	Interatomic potentials for the Beâ€“Câ€“H system. Journal of Physics Condensed Matter, 2009, 21, 445002.	0.7	56
6668	Topics in the theory of amorphous materials. European Physical Journal B, 2009, 68, 1-21.	0.6	114
6669	AbÂinitio study of structural, electronic, and elastic properties of M2SbP (MÂ=ÂTi, Zr, and Hf). European Physical Journal B, 2009, 68, 193-196.	0.6	5
6670	GGA+U study of the incorporation of iodine in uranium dioxide. European Physical Journal B, 2009, 69, 203-209.	0.6	61
6671	Thermoactivated transport of molecules H2 in narrow single-wall carbon nanotubes. European Physical Journal B, 2009, 69, 363-368.	0.6	5
6672	First-principles study for transport properties of defective carbon nanotubes with oxygen adsorption. European Physical Journal B, 2009, 69, 375-382.	0.6	10
6673	Magnetic couplings vs. stress and strain in epitaxial (La, Sr)MnO3. European Physical Journal B, 2009, 70, 343-346.	0.6	4
6674	Strain effects on the electric polarization of BiMnO3. European Physical Journal B, 2009, 71, 435-437.	0.6	19
6675	First-principle study on energetics and electronic structure of a single copper atomic chain bound in carbon nanotube. European Physical Journal B, 2009, 72, 119-126.	0.6	17
6676	A systematic investigation of stacking faults in magnesium via first-principles calculation. European Physical Journal B, 2009, 72, 397-403.	0.6	74
6677	Structural and electronic properties of Snn-1Pb and Pbn-1Sn clusters: a theoretical investigation through first principles calculations. European Physical Journal D, 2009, 55, 613-625.	0.6	4
6678	Accelerated coarsening of Ag adatom islands on Ag(111) due to trace amounts of S: Mass-transport mediated by Agâ€“S complexes. Journal of Chemical Physics, 2009, 130, 094701.	1.2	26
6679	<mml:math xmlns:mml="http://www.w3.org/1998/Math/MathML" display="inline"><mml:mrow><mml:msub><mml:mrow><mml:mtext>Cu</mml:mtext></mml:mrow><mml:mn>2</mml:mn></mml:msu a potential photovoltaic material: A hybrid Hartree-Fock density functional theory study. Physical Review B, 2009, 79, .	1.1	402

#	Article	IF	Citations
6680	Hydrogen and oxygen adsorption on ZnO nanowires: A first-principles study. Physical Review B, 2009, 79, .	1.1	51
6681	Anab initiostudy of energetic stability and electronic confinement for different structural phases of ZnO nanowires. Nanotechnology, 2009, 20, 215202.	1.3	13
6682	Magnetic and electronic properties of 3d transition-metal-doped In ₂ O ₃ : An ab initio study. Europhysics Letters, 2009, 87, 27013.	0.7	24
6683	Pressure-induced structural, electronic, and magnetic effects in<mml:math xmlns:mml="http://www.w3.org/1998/Math/MathML" display="inline"><mml:mrow><mml:msub><mml:mrow><mml:mtext>BiFeO</mml:mtext></mml:mrow><mml:mn>3</mml:mn></mml:mrow> Physical Review B, 2009, 79, .	1.1	53
6684	Nanosize confinement induced enhancement of spontaneous polarization in a ferroelectric nanowire. Applied Physics Letters, 2009, 95, 232901.	1.5	49
6685	Electronic structure and stability of quaternary chalcogenide semiconductors derived from cation cross-substitution of II-VI and<mml:math xmlns:mml="http://www.w3.org/1998/Math/MathML" display="inline"><mml:mrow><mml:msub><mml:mrow><mml:mtext>I-III-VI</mml:mtext></mml:mrow><mml:mn>2</mml:mn></mml:mrow> Physical Review B, 2009, 79, .	1.1	413
6686	Intrinsic Hole Migration Rates in TiO₂from Density Functional Theory. Journal of Physical Chemistry C, 2009, 113, 346-358.	1.5	166
6687	Ab initioenergetics of<mml:math xmlns:mml="http://www.w3.org/1998/Math/MathML"		

#	Article	IF	Citations
6698	Identifying Optimal Inorganic Nanomaterials for Hybrid Solar Cells. Journal of Physical Chemistry C, 2009, 113, 18968-18972.	1.5	34
6699	Dots versus Antidots: Computational Exploration of Structure, Magnetism, and Half-Metallicity in Boronâ^'Nitride Nanostructures. Journal of the American Chemical Society, 2009, 131, 17354-17359.	6.6	174
6700	Porous Graphene as the Ultimate Membrane for Gas Separation. Nano Letters, 2009, 9, 4019-4024.	4.5	850
6701	Interface Characterization of Cobalt Contacts on Bismuth Selenium Telluride for Thermoelectric Devices. Electrochemical and Solid-State Letters, 2009, 12, H395.	2.2	27
6702	Tuning the Electronic Structure of Graphene by an Organic Molecule. Journal of Physical Chemistry B, 2009, 113, 2-5.	1.2	219
6703	Influence of water on elementary reaction steps in electrocatalysis. Faraday Discussions, 2008, 140, 233-244.	1.6	78
6704	Monolayer honeycomb structures of group-IV elements and III-V binary compounds: First-principles calculations. Physical Review B, 2009, 80, .	1.1	1,769
6705	First-principles study of hydrogenated amorphous silicon. Physical Review B, 2009, 79, .	1.1	61
6706	Lithium Insertion and Transport in the TiO₂â^'B Anode Material: A Computational Study. Chemistry of Materials, 2009, 21, 4778-4783.	3.2	169
6707	Ab initiostudy of high-pressure structural properties of the LuVO₄and ScVO₄zircon-type orthovanadates. High Pressure Research, 2009, 29, 582-586.	0.4	12
6708	Evidence of kinetic-energy-driven antiferromagnetism in double perovskites: A first-principles study of La-doped<mml:math xmlns:mml="http://www.w3.org/1998/Math/MathML" display="inline"><mml:mrow><mml:msub><mml:mrow><mml:mtext>Sr</mml:mtext></mml:mrow><mml:mn>2</mml:mn></mml:msub> Physical Review B, 2009, 80, .	1.1	47
6709	Symmetry-Dependent Strong Reduction of the Spin Exchange Interactions in Cs₂CuCl₄ by the 6p Orbitals of Cs⁺ Ions. Inorganic Chemistry, 2009, 48, 4165-4170.	1.9	3
6710	Density-functional study of the thermodynamic properties and the pressureâ€“temperature phase diagram of Ti. Physical Review B, 2009, 80, .	1.1	94
6711	First-Principles Prediction of Thermodynamically Reversible Hydrogen Storage Reactions in the Li-Mg-Ca-B-H System. Journal of the American Chemical Society, 2009, 131, 230-237.	6.6	256
6712	Experimental and theoretical screening of nanoscale oxide reactivity with LiBH₄. Nanotechnology, 2009, 20, 204024.	1.3	15
6713	Potential of AlN Nanostructures as Hydrogen Storage Materials. ACS Nano, 2009, 3, 621-626.	7.3	201
6714	Theoretical Study of Hydrogen Storage in Ca-Coated Fullerenes. Journal of Chemical Theory and Computation, 2009, 5, 374-379.	2.3	130
6715	Electronics and Magnetism of Patterned Graphene Nanoroads. Nano Letters, 2009, 9, 1540-1543.	4.5	235

#	Article	IF	Citations
6716	Molecular simulation as a scientific base of nanotechnologies in power engineering. Journal of Engineering Thermophysics, 2009, 18, 197-226.	0.6	4
6717	Calculation of the energy of binding of titanium and scandium complexes to the surface of carbon nanotubes. Russian Journal of Physical Chemistry B, 2009, 3, 679-683.	0.2	5
6718	Bromine adsorption on Ge(001) surface: comparative study for coverages of 0.25, 0.5, 0.75 and 1 monolayer. Open Physics, 2009, 7, .	0.8	3
6719	Modeling and calculations of the physicochemical parameters of diffusion of atomic hydrogen on the surface of differently sized nanotubes with different chiralities. Russian Journal of Physical Chemistry A, 2009, 83, 649-653.	0.1	1
6720	Vibrational modes of hydrogen in (NH4)H5(PO4)2 (Neutron scattering and simulation). Crystallography Reports, 2009, 54, 477-482.	0.1	1
6721	Nanomechanical properties and phase transitions in a double-walled (5,5)@(10,10) carbon nanotube: ab initio calculations. Journal of Experimental and Theoretical Physics, 2009, 108, 621-628.	0.2	24
6722	Electronic structure and spin polarization at the NiMnSb/GaAs(110) interface. Journal of Experimental and Theoretical Physics, 2009, 109, 339-344.	0.2	1
6723	Hydrogen adsorption on low-index surfaces of B2 titanium alloys. Physics of the Solid State, 2009, 51, 1281-1289.	0.2	18
6724	Theoretical study of hydrogen absorption near symmetric tilt grain boundaries in Pd and TiFe. Technical Physics, 2009, 54, 1204-1209.	0.2	1
6725	Structural and Dynamic Properties of BaInGeH: A Rare Solid-State Indium Hydride. Inorganic Chemistry, 2009, 48, 5602-5604.	1.9	13
6726	Electronic States in Zinc Magnesium Oxide Alloy Semiconductors: Hard X-ray Photoemission Spectroscopy and Density Functional Theory Calculations. Chemistry of Materials, 2009, 21, 144-150.	3.2	15
6727	Synthesis and Fundamental Properties of Stable Ph3SnSiH3 and Ph3SnGeH3 Hydrides: Model Compounds for the Design of Siâ^'Geâ^'Sn Photonic Alloys. Inorganic Chemistry, 2009, 48, 6314-6320.	1.9	10
6728	Energetic and Electronic Properties of P Doping at the Rutile TiO₂ (110) Surface from First Principles. Journal of Physical Chemistry C, 2009, 113, 9423-9430.	1.5	18
6729	First-Principles Study of the Relaxed Structures and Electronic Properties of Au Nanowires. Journal of Physical Chemistry C, 2009, 113, 17678-17684.	1.5	3
6730	Characteristic Energies and Shifts in Optical Spectra of Colloidal IVâ^'VI Semiconductor Nanocrystals. ACS Nano, 2009, 3, 3505-3512.	7.3	37
6731	Structural and Electronic Properties of a W₃O₉Cluster Supported on the TiO₂(110) Surface. Journal of Physical Chemistry C, 2009, 113, 17509-17517.	1.5	34
6732	Plane-Wave Density Functional Theory Investigations of the Adsorption and Activation of CO on Fe₅C₂Surfaces. Journal of Physical Chemistry C, 2009, 113, 9256-9274.	1.5	58
6733	Effects of Confinement on Oxygen Adsorbed between Pt(111) Surfaces. Journal of Physical Chemistry C, 2009, 113, 7851-7856.	1.5	14

#	Article	IF	Citations
6734	Optimized many body potential for fcc metals. Philosophical Magazine Letters, 2009, 89, 136-144.	0.5	22
6735	Model for Self-Assembly of Carbon Nanotubes from Acetylene Based on Real-Time Studies of Vertically Aligned Growth Kinetics. Journal of Physical Chemistry C, 2009, 113, 15484-15491.	1.5	59
6736	Effect of Ligands on the Geometric and Electronic Structure of Au13 Clusters. Journal of Physical Chemistry C, 2009, 113, 12072-12078.	1.5	99
6737	Enantiospecific Adsorption of Amino Acids on Hydroxylated Quartz (0001). Langmuir, 2009, 25, 10737-10745.	1.6	29
6738	Ab initio Structure Determination of Mg₁₀Ir₁₉B₁₆. Chemistry of Materials, 2009, 21, 2499-2507.	3.2	6
6739	Structure investigation of the (100) surface of the orthorhombic<mml:math xmlns:mml="http://www.w3.org/1998/Math/MathML" display="inline"><mml:mrow><mml:msub><mml:mrow><mml:mtext>Al</mml:mtext></mml:mrow><mml:mrow><mml:mn>13</mml:mn> Physical Review B, 2009, 80, .	1.1	43
6740	Active Alloying of Au with Pt in Nanoclusters Supported on a Thin Film of Al2O3/NiAl(100). Journal of Physical Chemistry C, 2009, 113, 21054-21062.	1.5	30
6741	Density Functional Studies of the Adsorption and Dissociation of NO_x (x = 1,) Tj ETQq1 1 0.784314 rgBT /Ov	1.5	10
6742	Structural Versatility of the Îµ-SmGax Phase: X-Ray, Electron Diffraction, and DFT Studies. Inorganic Chemistry, 2009, 48, 2399-2406.	1.9	5
6743	Growth and properties of Au nanowires. Molecular Simulation, 2009, 35, 1051-1056.	0.9	4
6744	Magnetism of O-Terminated ZnO(0001) with Adsorbates. Journal of Physical Chemistry C, 2009, 113, 16116-16120.	1.5	36
6745	Complex Rare-Earth Aluminum Hydrides: Mechanochemical Preparation, Crystal Structure and Potential for Hydrogen Storage. Journal of the American Chemical Society, 2009, 131, 16735-16743.	6.6	39
6746	Prediction of O2 Dissociation Kinetics on LaMnO3-Based Cathode Materials for Solid Oxide Fuel Cells. Journal of Physical Chemistry C, 2009, 113, 7290-7297.	1.5	57
6747	Modeling Hydrogen Sulfide Adsorption on Mo-Edge MoS2 Surfaces under Solid Oxide Fuel Cell Conditions. Journal of Physical Chemistry C, 2009, 113, 193-203.	1.5	25
6748	Tuning Electronic Properties of Hydro-Boronâ^'Carbon Compounds by Hydrogen and Boron Contents: A First Principles Study. Journal of Physical Chemistry C, 2009, 113, 18468-18472.	1.5	39
6749	Alternating the Crystalline Structural Transition of Coronene Molecular Overlayers on Ag(110) through Temperature Increase. Journal of Physical Chemistry C, 2009, 113, 17643-17647.	1.5	9
6750	Effect of Preadsorbed S on the Adsorption of CO on Co(0001). Journal of Physical Chemistry C, 2009, 113, 16210-16215.	1.5	7
6751	Hydrogen Absorption and Diffusion in Bulk Î±-MoO₃. Journal of Physical Chemistry C, 2009, 113, 11399-11407.	1.5	126

#	Article	IF	Citations
6752	First Principle Study on the Adsorption of Styrene on Si(100)2 Ã— 1. Journal of Physical Chemistry C, 2009, 113, 5263-5273.	1.5	11
6753	Enhancement of Adsorption Inside Single-Walled Carbon Nanotubes: Li Doping Effect on n-Heptane van der Waals Bonding. Journal of Physical Chemistry C, 2009, 113, 4829-4838.	1.5	13
6754	Magnetism of 3d-Transition Metal (Fe, Co, and Ni) Nanowires on w-BN (0001). Journal of Physical Chemistry C, 2009, 113, 14615-14622.	1.5	10
6755	Work Function Measurements of Thin Oxide Films on Metalsâ€"MgO on Ag(001). Journal of Physical Chemistry C, 2009, 113, 11301-11305.	1.5	102
6756	First-principles phase diagram calculations for the HfCâ€“TiC, ZrCâ€“TiC, and HfCâ€“ZrC solid solutions. Physical Review B, 2009, 80, .	1.1	65
6757	Dehydrogenation of Ethanol on a 2Ru/ZrO₂(111) Surface: Density Functional Computations. Journal of Physical Chemistry C, 2009, 113, 6132-6139.	1.5	9
6758	Tungsten-Doped Titanium Dioxide in the Rutile Structure: Theoretical Considerations. Chemistry of Materials, 2009, 21, 1627-1635.	3.2	32
6759	Vanadium Oxides Supported on a Thin Silica Film Grown on Mo(112): Insights from Density Functional Theory. Journal of Physical Chemistry C, 2009, 113, 8336-8342.	1.5	17
6760	Density Functional Theory Study of the Oxidation of Ammonia on RuO₂(110) Surface. Journal of Physical Chemistry C, 2009, 113, 17411-17417.	1.5	26
6761	DFT Study of NHx (x = 1â^'3) Adsorption on RuO2(110) Surfaces. Journal of Physical Chemistry C, 2009, 113, 2816-2821.	1.5	26
6762	A Dominant Dissociation Mode of cis-Dichloroethylene on Si(100)2 Ã— 1: Adjacent Si Dimer Double Dechlorination. Journal of Physical Chemistry C, 2009, 113, 21797-21804.	1.5	3
6763	THE CO-ADSORPTION OF BENZENE ANDCOONCo(0001). Surface Review and Letters, 2009, 16, 749-755.	0.5	5
6764	First-principles investigation of pentagonal and hexagonal core-shell silicon nanowires with various core compositions. Physical Review B, 2009, 80, .	1.1	22
6765	Dynamics of Open-Shell Species at Metal Surfaces. Journal of Physical Chemistry C, 2009, 113, 16311-16320.	1.5	18
6766	Topological Analysis of the Interactions between Organic Molecules and Co(Ni)MoS Catalytic Active Phases. Journal of Chemical Theory and Computation, 2009, 5, 580-593.	2.3	11
6767	Revisiting the Blind Tests in Crystal Structure Prediction: Accurate Energy Ranking of Molecular Crystals. Journal of Physical Chemistry B, 2009, 113, 16303-16313.	1.2	71
6768	First-Principles Study of Electronic, Absorption, and Thermodynamic Properties of Crystalline Styphnic Acid and Its Metal Salts. Journal of Physical Chemistry B, 2009, 113, 10315-10321.	1.2	30
6769	Surface energies of stoichiometric FePt and CoPt alloys and their implications for nanoparticle morphologies. Physical Review B, 2009, 80, .	1.1	121

#	Article	IF	Citations
6770	Phases of Solid Methanol. Journal of Physical Chemistry A, 2009, 113, 3321-3329.	1.1	34
6771	Building Clusters Atom-by-Atom: From Local Order to Global Order. Journal of Physical Chemistry A, 2009, 113, 2659-2662.	1.1	26
6772	Work Function Pinning at Metalâ^'Organic Interfaces. Journal of Physical Chemistry C, 2009, 113, 9974-9977.	1.5	49
6773	Anchoring Sites for Initial Au Nucleation on CeO₂{111}: O Vacancy versus Ce Vacancy. Journal of Physical Chemistry C, 2009, 113, 6411-6417.	1.5	79
6774	Classification of hydrides according to features of band structure. Philosophical Magazine, 2009, 89, 1111-1120.	0.7	9
6775	Theoretical Investigation of Formamide Adsorption on Ag(111) Surfaces. Journal of Physical Chemistry C, 2009, 113, 10541-10547.	1.5	31
6776	Effect of the Support on the Electronic Structure of Au Nanoparticles Supported on Transition Metal Carbides: Choice of the Best Substrate for Au Activation. Journal of Physical Chemistry C, 2009, 113, 19994-20001.	1.5	28
6777	Moâ^'Sâ^'I Nanowires: A Promising Anode Material for Lithium-Ion Batteries. A First-Principles Study. Journal of Physical Chemistry C, 2009, 113, 18436-18440.	1.5	14
6778	Shape Control of Al Nanoclusters by Ligand Size. Journal of the American Chemical Society, 2009, 131, 8522-8526.	6.6	21
6779	Molybdenum Clusters on a TiO2(110) Substrate Studied by Density Functional Theory. Journal of Physical Chemistry C, 2009, 113, 5308-5312.	1.5	2
6780	High-Pressure, High-Temperature Single-Crystal Growth, Ab initio Electronic Structure Calculations, and Equation of State of Îµ-Fe₃N_{1+x}. Chemistry of Materials, 2009, 21, 392-398.	3.2	63
6781	Aminoxyl Radicals on the Silicon (001) Surface. Journal of Physical Chemistry C, 2009, 113, 1020-1027.	1.5	2
6782	Influence of metal work function on the position of the Dirac point of graphene field-effect transistors. Applied Physics Letters, 2009, 95, 243105.	1.5	17
6783	Room-temperature ferromagnetism and ferroelectricity in Fe-doped<mml:math xmlns:mml="http://www.w3.org/1998/Math/MathML" display="inline"><mml:mrow><mml:msub><mml:mrow><mml:mtext>BaTiO</mml:mtext></mml:mrow><mml:mn>3</mml:mn></mml:msub></mml:mrow></mml:math>. Physical Review B, 2009, 79, .	1.1	154
6784	Quantum Chemical Modeling of Zeolite-Catalyzed Methylation Reactions: Toward Chemical Accuracy for Barriers. Journal of the American Chemical Society, 2009, 131, 816-825.	6.6	288
6785	Theoretical Interpretation of the Structural Variations along the Eu(Zn1â^'xGex)2 (0 â‰¤ x â‰¤ 1) Series. Inorganic Chemistry, 2009, 48, 6391-6401.	1.9	12
6786	Quantum Nature of Two-Dimensional Electron Gas Confinement at<mml:math xmlns:mml="http://www.w3.org/1998/Math/MathML" display="inline"><mml:msub><mml:mi>LaAlO</mml:mi><mml:mn>3</mml:mn></mml:msub><mml:mo>/</mml:mo><mml:msub><mml:mi>SrTiO</mml:mi><mml:mn>3</mml:mn></mml:msub></mml:math> Physical Review Letters, 2009, 102, 106803.	7.9	108
6787	Density Functional Theory Calculations of the Interaction of Hydrazine with Low-Index Copper Surfaces. Journal of Physical Chemistry C, 2009, 113, 15714-15722.	1.5	40

#	Article	IF	Citations
6788	Ca Deposition on TiO₂(110) Surfaces: Insights from Quantum Calculations. Journal of Physical Chemistry C, 2009, 113, 3740-3745.	1.5	7
6789	Hydrogen Bonds and Vibrations of Water on (110) Rutile. Journal of Physical Chemistry C, 2009, 113, 13732-13740.	1.5	74
6790	Prediction of a spin-polarized two-dimensional electron gas at theLaAlO3/EuO(001)interface. Physical Review B, 2009, 79, .	1.1	44
6791	Interplay between Order and Disorder in the High Performance of Amorphous Transparent Conducting Oxides. Chemistry of Materials, 2009, 21, 5119-5124.	3.2	90
6792	Modeling and Investigation of Interfacial Interaction between PLA and One Type of Deficient Hydroxyapatite. Journal of Physical Chemistry A, 2009, 113, 7112-7123.	1.1	6
6793	Chemical Fingerprints of Large Organic Molecules in Scanning Tunneling Microscopy: Imaging Adsorbateâ˜Substrate Coupling of Metalloporphyrins. Journal of Physical Chemistry C, 2009, 113, 16450-16457.	1.5	61
6794	First Principles Study of the Effect of Carbon and Boron on the Activity of a Ni Catalyst. Journal of Physical Chemistry C, 2009, 113, 4099-4106.	1.5	39
6795	Norbornadiene-Based Molecules for Functionalizing The Si(001) Surface. Journal of Physical Chemistry C, 2009, 113, 16094-16103.	1.5	4
6796	IR Spectroscopic Measurement of Diffusion Kinetics of Chemisorbed Pyridine through Nanocrystalline MgO Particles. The Involvement of Surface Defect Sites in Slow Diffusion. Journal of Physical Chemistry C, 2009, 113, 2219-2227.	1.5	19
6797	On the Dissociative Chemisorption of Tris(dimethylamino)silane on Hydroxylated SiO₂(001) Surface. Journal of Physical Chemistry C, 2009, 113, 9731-9736.	1.5	42
6798	First-Principles Studies of the Dynamics of [2]Rotaxane Molecular Switches. Nano Letters, 2009, 9, 3225-3229.	4.5	20
6799	Adsorbate-Induced Defect Formation and Annihilation on Graphene and Single-Walled Carbon Nanotubes. Journal of Physical Chemistry B, 2009, 113, 941-944.	1.2	34
6800	Growth of N,Nâ€²-Bis(1-ethylpropyl)perylene-3,4,9,10-tetracarboxdiimide Films on Ag (111). Journal of Physical Chemistry C, 2009, 113, 17866-17875.	1.5	29
6801	Carbon Adsorption and Absorption in the (111) L12 Fe3Al Surface. Journal of Physical Chemistry C, 2009, 113, 18321-18330.	1.5	2
6802	Morphological Stability of Pyrite FeS₂ Nanocrystals in Water. Journal of Physical Chemistry C, 2009, 113, 5376-5380.	1.5	19
6803	Adsorption and Diffusion of Light Gases in ZIF-68 and ZIF-70: A Simulation Study. Journal of Physical Chemistry C, 2009, 113, 16906-16914.	1.5	126
6804	Understanding the Electronic Structure of Metal/SAM/Organicâ˜Semiconductor Heterojunctions. ACS Nano, 2009, 3, 3513-3520.	7.3	48
6805	Effect of Magnetic Dipoleâ˜Dipole Interactions on the Spin Orientation and Magnetic Ordering of the Spin-Ladder Compound Sr₃Fe₂O₅. Inorganic Chemistry, 2009, 48, 9051-9053.	1.9	49

#	Article	IF	Citations
6806	Surfaces and Clusters of Mg(NH2)2 Studied by Density Functional Theory Calculations. Journal of Physical Chemistry C, 2009, 113, 21648-21656.	1.5	4
6807	Tuning the Magnetic Interaction between Manganese Porphyrins and Ferromagnetic Co Substrate through Dedicated Control of the Adsorption. Journal of Physical Chemistry C, 2009, 113, 14381-14383.	1.5	56
6808	Adsorption Configurations and Decomposition Pathways of Boric Acid on TiO2 Rutile (110) Surface: A Computational Study. Journal of Physical Chemistry C, 2009, 113, 3751-3762.	1.5	11
6809	Influence of vanadium spin-polarization on the dissolution of hydrogen in vanadium. Physical Review B, 2009, 79, .	1.1	2
6810	Nanoconfined Water in Magnesium-Rich 2:1 Phyllosilicates. Journal of the American Chemical Society, 2009, 131, 8155-8162.	6.6	55
6811	Formation of the Calcium/Poly(3-Hexylthiophene) Interface: Structure and Energetics. Journal of the American Chemical Society, 2009, 131, 13498-13507.	6.6	41
6812	Theoretical Studies on Structural, Magnetic, and Spintronic Characteristics of Sandwiched Eu_nCOT_{n+1} (n = 1â^'4) Clusters. ACS Nano, 2009, 3, 2515-2522.	7.3	51
6813	SiC(0001) 3 Ã— 3 Heterochirality Revealed by Single-Molecule STM Imaging. Journal of the American Chemical Society, 2009, 131, 3210-3215.	6.6	16
6814	Inaccuracy of Density Functional Theory Calculations for Dihydrogen Binding Energetics onto Ca Cation Centers. Physical Review Letters, 2009, 103, 216102.	2.9	34
6815	Melting of Fe and<mml:math xmlns:mml="http://www.w3.org/1998/Math/MathML" display="inline"><mml:mrow><mml:msub><mml:mrow><mml:mtext>Fe</mml:mtext></mml:mrow><mml:mrow><mml:mn>0.9375</mml:mn></mml:mrow></mml:msub></mml:mrow></mml:math> Earthâ€™s core pressures studied usingab initiomolecular dynamics. Physical Review B, 2009, 79, .	1.1	29
6816	Adsorption Configuration and Dissociative Reaction of NH₃ on Anatase (101) Surface with and without Hydroxyl Groups. Journal of Physical Chemistry C, 2009, 113, 6663-6672.	1.5	20
6817	Ca-Decorated Graphene-Based Three-Dimensional Structures for High-Capacity Hydrogen Storage. Journal of Physical Chemistry C, 2009, 113, 20499-20503.	1.5	50
6818	Adsorption and Dissociation of CO on Body-Centered Cubic Transition Metals and Alloys: Effect of Coverage and Scaling Relations. Journal of Physical Chemistry C, 2009, 113, 11041-11049.	1.5	33
6819	Nonlocal Chemical Reactivity at Organicâ^'Metal Interfaces. ACS Nano, 2009, 3, 3684-3690.	7.3	48
6820	Control and Manipulation of Gold Nanocatalysis: Effects of Metal Oxide Support Thickness and Composition. Journal of the American Chemical Society, 2009, 131, 538-548.	6.6	203
6821	Band Engineering in Strained GaN/ultrathin InN/GaN Quantum Wells. Crystal Growth and Design, 2009, 9, 1698-1701.	1.4	12
6822	Ferromagnetism in armchair graphene nanoribbons. Physical Review B, 2009, 79, .	1.1	43
6823	Insight into CH₄ Formation in Iron-Catalyzed Fischerâ^'Tropsch Synthesis. Journal of the American Chemical Society, 2009, 131, 14713-14721.	6.6	213

#	Article	IF	Citations
6824	Surface magnetism in amine-capped ZnO nanoparticles. Nanotechnology, 2009, 20, 165702.	1.3	29
6825	Influence of Deoxyribose Group on Self-Assembly of Thymidine on Au(111). Journal of Physical Chemistry C, 2009, 113, 17590-17594.	1.5	10
6826	Borohydride Oxidation over Au(111): A First-Principles Mechanistic Study Relevant to Direct Borohydride Fuel Cells. Journal of the Electrochemical Society, 2009, 156, B86.	1.3	70
6827	X-ray Photoemission Study of the Charge State of Au Nanoparticles on Thin MgO/Fe(001) Films. Journal of Physical Chemistry C, 2009, 113, 19957-19965.	1.5	27
6828	Pentacene Binds Strongly to Hydrogen-Terminated Silicon Surfaces Via Dispersion Interactions. Journal of Physical Chemistry C, 2009, 113, 9969-9973.	1.5	12
6829	Hydrogen Interaction in Ti-Doped LiBH₄ for Hydrogen Storage: A Density Functional Analysis. Journal of Chemical Theory and Computation, 2009, 5, 3079-3087.	2.3	20
6830	Uncertainty and figure selection for DFT based cluster expansions for oxygen adsorption on Au and Pt (111) surfaces. Molecular Simulation, 2009, 35, 920-927.	0.9	35
6831	Ferromagnetism and Electronic Structures of Nonstoichiometric Heusler-Alloy<mml:math xmlns:mml="http://www.w3.org/1998/Math/MathML" display="inline"><mml:msub><mml:mi>Fe</mml:mi><mml:mrow><mml:mn>3</mml:mn><mml:mo>â^'</mml:mo><mml:mi>x</mml:mi></mml:mrow></mml:msub></mml:math> Grown on Ge(111). Physical Review Letters, 2009, 102, 137204.	2.9	94
6832	Vanadia and Water Coadsorption on Tetragonal Zirconia Surfaces. Journal of Physical Chemistry C, 2009, 113, 18191-18203.	1.5	17
6833	First-Principles Study of the Liâ^'Mgâ^'Nâ^'H System: Compound Structures and Hydrogen-Storage Properties. Journal of Physical Chemistry C, 2009, 113, 14551-14558.	1.5	27
6834	Surface Raman Spectroscopy of trans-Stilbene on Ag/Ge(111): Surface-Induced Effects. Journal of Physical Chemistry C, 2009, 113, 208-212.	1.5	10
6835	Adsorption of Water on a PdO(101) Thin Film: Evidence of an Adsorbed HOâ^'H2O Complex. Journal of Physical Chemistry C, 2009, 113, 1495-1506.	1.5	59
6836	Novel Amphiphilic Ruthenium Sensitizer with Hydrophobic Thiophene or Thieno(3,2-b)thiophene-Substituted 2,2â€²-Dipyridylamine Ligands for Effective Nanocrystalline Dye Sensitized Solar Cells. Chemistry of Materials, 2009, 21, 5719-5726.	3.2	51
6837	First Principles Study of the Liâ€“Biâ€“F Phase Diagram and Bismuth Fluoride Conversion Reactions with Lithium. Electrochemical and Solid-State Letters, 2009, 12, A125.	2.2	20
6838	Direct Spectroscopic Observation of the Role of Humidity in Surface Diffusion through an Ionic Adsorbent Powder. The Behavior of Adsorbed Pyridine on Nanocrystalline MgO. Journal of Physical Chemistry C, 2009, 113, 2228-2234.	1.5	19
6839	Density Functional Theory Calculations of Solid Nitromethane under Hydrostatic and Uniaxial Compressions with Empirical van der Waals Correction. Journal of Physical Chemistry A, 2009, 113, 3610-3614.	1.1	38
6840	Indirect Detection via Spin-1/2 Nuclei in Solid State NMR Spectroscopy: Application to the Observation of Proximities between Protons and Quadrupolar Nuclei. Journal of Physical Chemistry A, 2009, 113, 12864-12878.	1.1	81
6842	Influence of Dopants Ti and Ni on Dehydrogenation Properties of NaAlH₄: Electronic Structure Mechanisms. Journal of Physical Chemistry C, 2009, 113, 10215-10221.	1.5	17

#	Article	IF	Citations
6843	Structures, Phase Transitions, Hydration, and Ionic Conductivity of Ba₄Nb₂O₉. Chemistry of Materials, 2009, 21, 3853-3864.	3.2	38
6844	Transition-Metal Strings Templated on Boron-Doped Carbon Nanotubes: A DFT Investigation. Journal of Physical Chemistry C, 2009, 113, 15346-15354.	1.5	12
6845	Optimization of Mn doping in group-IV-based dilute magnetic semiconductors by electronic codopants. Physical Review B, 2009, 79, .	1.1	39
6846	Diffusion of the Linear CH₃Sâ^'Auâ^'SCH₃ Complex on Au(111) from First Principles. Journal of Physical Chemistry C, 2009, 113, 3763-3766.	1.5	22
6847	A Density Functional Study of Initial Steps in the Oxidation of Early Transition Metal Nitrides, MN (M =) Tj ETQq0 0 0 rgBT /Overlock 10 T	1.5	12
6848	Adsorption of CO₂ on Sodium-Exchanged Ferrierites: The Bridged CO₂ Complexes Formed between Two Extraframework Cations. Journal of Physical Chemistry C, 2009, 113, 2928-2935.	1.5	75
6849	Pressure-Induced Invar Behavior in<mml:math xmlns:mml="http://www.w3.org/1998/Math/MathML" display="inline"><mml:msub><mml:mi>Pd</mml:mi><mml:mn>3</mml:mn></mml:msub><mml:mi>Fe</mml:mi></mml:math>. Physical Review Letters, 2009, 102, 237202.	7.9	73
6850	Itinerant Flat-Band Magnetism in Hydrogenated Carbon Nanotubes. ACS Nano, 2009, 3, 1646-1650.	7.3	17
6851	Cu-Adatom-Mediated Bonding in Close-Packed Benzoate/Cu(110)-Systems. Langmuir, 2009, 25, 856-864.	1.6	28
6852	Obtaining correct orbital ground states in<mml:math xmlns:mml="http://www.w3.org/1998/Math/MathML" display="inline"><mml:mi>f</mml:mi></mml:math>-electron systems using a nonspherical self-interaction-corrected<mml:math xmlns:mml="http://www.w3.org/1998/Math/MathML" display="inline"><mml:mrow><mml:mtext>LDA</mml:mtext><mml:mo>+</mml:mo><mml:mi>U</mml:mi></mml:mrow></mml:math> Physical Review B, 2009, 80, .	1.1	37
6853	First-Principles Investigation of Surface and Subsurface H Adsorption on Ir(111). Journal of Physical Chemistry C, 2009, 113, 21361-21367.	1.5	42
6854	First-Principles Study for the Anisotropy of Iron-Based Superconductors toward Power and Device Applications. Journal of the Physical Society of Japan, 2009, 78, 123712.	0.7	45
6855	Chemisorption of Transition-Metal Atoms on Boron- and Nitrogen-Doped Carbon Nanotubes: Energetics and Geometric and Electronic Structures. Journal of Physical Chemistry C, 2009, 113, 7069-7078.	1.5	71
6856	Roles of Conformational Restrictions of a Bismalonate in the Interactions with a Carbon Nanotube. Journal of Physical Chemistry C, 2009, 113, 14184-14194.	1.5	16
6857	KSSOLVâ€"a MATLAB toolbox for solving the Kohn-Sham equations. ACM Transactions on Mathematical Software, 2009, 36, 1-35.	1.6	79
6858	Modeling of the Phase Evolution in Mg1â^'xAlxB2 (0 < x < 0.5) and Its Experimental Signatures. Journal of Physical Chemistry B, 2009, 113, 11965-11976.	1.2	5
6859	A Density Functional Theory + U Study of Oxygen Vacancy Formation at the (110), (100), (101), and (001) Surfaces of Rutile TiO₂. Journal of Physical Chemistry C, 2009, 113, 7322-7328.	1.5	223
6860	Infrared and Computational Studies on Interactions of Carbon Dioxide and Titania Nanoparticles with Acetate Groups. Journal of Physical Chemistry C, 2009, 113, 21022-21028.	1.5	27

#	Article	IF	Citations
6861	Catalytic Fe-xN Sites in Carbon Nanotubes. Journal of Physical Chemistry C, 2009, 113, 21629-21634.	1.5	83
6862	Reconstruction and alignment of vacancies in carbon nanotubes. Physical Review B, 2009, 79, .	1.1	16
6863	Adsorption and diffusion of Au atoms on the (001) surface of Ti, Zr, Hf, V, Nb, Ta, and Mo carbides. Journal of Chemical Physics, 2009, 130, 244706.	1.2	17
6864	Phonon-Induced Dephasing of Excitons in Semiconductor Quantum Dots: Multiple Exciton Generation, Fission, and Luminescence. ACS Nano, 2009, 3, 2487-2494.	7.3	115
6865	Investigation in the Binary System Ybâ^'Ga: Crystal Structure of the Ga-Rich Compound YbGa3.34. Inorganic Chemistry, 2009, 48, 9250-9257.	1.9	3
6866	Carbon on Platinum Substrates: From Carbidic to Graphitic Phases on the (111) Surface and on Nanoparticles. Journal of Physical Chemistry A, 2009, 113, 11963-11973.	1.1	44
6867	Probing Conformers and Adsorption Footprints at the Single-Molecule Level in a Highly Organized Amino Acid Assembly of (S)-Proline on Cu(110). Journal of the American Chemical Society, 2009, 131, 10173-10181.	6.6	67
6868	Mechanism of CH2 Steam Reforming on a Rh/ZrO2(111) Surface: A Computational Study. Journal of Physical Chemistry C, 2009, 113, 20139-20142.	1.5	3
6869	Superexchange-Driven Magnetoelectricity in Magnetic Vortices. Physical Review Letters, 2009, 102, 157203.	2.9	55
6870	Structure and Decomposition Pathways of Vinyl Acetate on Clean and Oxygen-Covered Pd(100). Journal of Physical Chemistry C, 2009, 113, 971-978.	1.5	16
6871	Ab Initio Study on Thermal and Chemical Stabilities of Silicon Monoxide Clusters. Journal of Physical Chemistry C, 2009, 113, 12736-12741.	1.5	13
6872	AM05 Density Functional Applied to the Water Molecule, Dimer, and Bulk Liquid. Journal of Chemical Theory and Computation, 2009, 5, 887-894.	2.3	30
6873	Ozone Oxidation of Single Walled Carbon Nanotubes from Density Functional Theory. Journal of Physical Chemistry C, 2009, 113, 17636-17642.	1.5	45
6874	<mml:math xmlns:mml="http://www.w3.org/1998/Math/MathML" display="inline"><mml:mrow><mml:msub><mml:mrow><mml:mtext>BaPtSi</mml:mtext></mml:mrow><mml:mn>3</mml:mn></mml:msub></mml:mrow></mml:math> A noncentrosymmetric BCS-like superconductor. Physical Review B, 2009, 80, .	3.1	105
6875	Structure of Aqueous Solutions of Monosodium Glutamate. Journal of Physical Chemistry B, 2009, 113, 7687-7700.	1.2	21
6876	Surface magnetization in non-doped ZnO nanostructures. Applied Physics Letters, 2009, 94, .	1.5	74
6877	Theoretical Investigations of the Relaxation and Reconstruction of the Î³-AlO(OH) Boehmite (101) Surface and Boehmite Nanorods. Journal of Physical Chemistry C, 2009, 113, 5228-5237.	1.5	23
6878	Dissociative Adsorption of Methane on Surface Oxide Structures of Pdâ^'Pt Alloys. Journal of Physical Chemistry C, 2009, 113, 21097-21105.	1.5	18

#	Article	IF	Citations
6879	Growth of Carbon Structures on Stepped (211)Co Surfaces. Journal of Physical Chemistry C, 2009, 113, 15658-15666.	1.5	19
6880	Bonding and Adhesion at the SiC/Fe Interface. Journal of Physical Chemistry A, 2009, 113, 4367-4373.	1.1	22
6881	On the Reversibility of Hydrogen-Storage Reactions in Ca(BH₄)₂: Characterization via Experiment and Theory. Journal of Physical Chemistry C, 2009, 113, 20088-20096.	1.5	59
6882	DFT Study of Planar Boron Sheets: A New Template for Hydrogen Storage. Journal of Physical Chemistry C, 2009, 113, 18962-18967.	1.5	130
6883	Constructing Goldâ^'Thiolate Oligomers and Polymers on Au(111) Based on the Linear Sâ^'Auâ^'S Geometry. Journal of Physical Chemistry C, 2009, 113, 7838-7842.	1.5	18
6884	Potential Energy Surface of Methanol Decomposition on Cu(110). Journal of Physical Chemistry C, 2009, 113, 4522-4537.	1.5	105
6885	Energy Gaps in Supramolecular Functionalized Graphene Nanoribbons. ACS Nano, 2009, 3, 1995-1999.	7.3	49
6886	Density Functional Theory Study of Ferrihydrite and Related Fe-Oxyhydroxides. Chemistry of Materials, 2009, 21, 5727-5742.	3.2	81
6887	Manganese Borohydride As a Hydrogen-Storage Candidate: First-Principles Crystal Structure and Thermodynamic Properties. Journal of Physical Chemistry C, 2009, 113, 13416-13424.	1.5	19
6888	Vacancy trapping mechanism for hydrogen bubble formation in metal. Physical Review B, 2009, 79, .	1.1	268
6889	Optical and Vibrational Properties of Boron Nitride Nanotubes. , 2009, , 105-148.		12
6890	Size Independence and Doping Dependence of Bending Modulus in ZnO Nanowires. Crystal Growth and Design, 2009, 9, 1640-1642.	1.4	11
6891	Structureâ^'Reactivity Relationship for Catalytic Activity of Gallium Oxide and Sulfide Clusters in Zeolite. Journal of Physical Chemistry C, 2009, 113, 4246-4249.	1.5	32
6892	Combined DFT/CC and IR spectroscopic studies on carbon dioxide adsorption on the zeolite H-FER. Energy and Environmental Science, 2009, 2, 1187.	15.6	75
6893	Surface Photovoltage at Nanostructures on Si Surfaces: Ab Initio Results. Journal of Physical Chemistry C, 2009, 113, 3530-3542.	1.5	51
6894	Activity and Reactivity of Fe2+ Cations in the Zeolite. Ab Initio Free-Energy MD Calculation of the N2O Dissociation over Iron-Exchanged Ferrierite. Journal of Physical Chemistry C, 2009, 113, 18807-18816.	1.5	9
6895	Structural Characterization of a Nanocrystalline Inorganicâ^'Organic Hybrid with Fiberlike Morphology and One-Dimensional Antiferromagnetic Properties. Chemistry of Materials, 2009, 21, 3356-3369.	3.2	36
6896	The making of ferromagnetic Fe doped ZnO nanoclusters. Applied Physics Letters, 2009, 94, .	1.5	45

#	Article	IF	Citations
6897	Mechanism of Selective Hydrogenation of Î±,Î²-Unsaturated Aldehydes on Silver Catalysts: A Density Functional Study. Journal of Physical Chemistry C, 2009, 113, 13231-13240.	1.5	47
6898	Application of Hybrid Functionals to the Modeling of NO Adsorption on Cuâ^'SAPO-34 and Coâ^'SAPO-34: A Periodic DFT Study. Journal of Physical Chemistry C, 2009, 113, 5274-5291.	1.5	22
6899	SiC/Ti3SiC2interface: Atomic structure, energetics, and bonding. Physical Review B, 2009, 79, .	1.1	53
6900	Density Functional Theory Study of the Adsorption and Reaction of H₂S on TiO₂ Rutile (110) and Anatase (101) Surfaces. Journal of Physical Chemistry C, 2009, 113, 20411-20420.	1.5	61
6901	Periodic density functional theory study of spin crossover in the cesium iron hexacyanochromate prussian blue analog. Journal of Chemical Physics, 2009, 130, 014702.	1.2	13
6902	Structural Phase Transformations of Mg₃N₂ at High Pressure: Experimental and Theoretical Studies. Inorganic Chemistry, 2009, 48, 9737-9741.	1.9	23
6903	Tailoring the Interaction Strength between Gold Particles and Silica Thin Films via Work Function Control. Physical Review Letters, 2009, 103, 056801.	2.9	37
6904	Phase stability and physical properties of<mml:math xmlns:mml="http://www.w3.org/1998/Math/MathML" display="inline"><mml:mrow><mml:msub><mml:mrow><mml:mtext>Ta</mml:mtext></mml:mrow><mml:mn>5</mml:mn></mml:m from first-principles calculations. Physical Review B, 2009, 80, .	1.1	77
6905	Adsorption of hydrogen on boron-doped graphene: A first-principles prediction. Journal of Applied Physics, 2009, 105, .	1.1	96
6906	A theoretical study of thermal stability and electronic properties of wurtzite and zincblende ZnO_xS_{1â^'x}. New Journal of Physics, 2009, 11, 093008.	1.2	42
6907	Oxidative Dehydrogenation of Methanol to Formaldehyde by Isolated Vanadium, Molybdenum, and Chromium Oxide Clusters Supported on Rutile TiO2(110). Journal of Physical Chemistry C, 2009, 113, 16083-16093.	1.5	38
6908	Adsorption of Late Transition Metal Atoms on MgO/Mo(100) and MgO/Ag(100) Ultrathin Films: A Comparative DFT Study. Journal of Physical Chemistry C, 2009, 113, 16694-16701.	1.5	37
6909	Fast determination of phases in LixFePO4 using low losses in electron energy-loss spectroscopy. Applied Physics Letters, 2009, 94, .	1.5	35
6910	Re-modeling of Laves phases in the Crâ€“Nb and Crâ€“Ta systems using first-principles results. Calphad: Computer Coupling of Phase Diagrams and Thermochemistry, 2009, 33, 179-186.	0.7	38
6911	Calphad-type assessment of the Feâ€“Nbâ€“Ni ternary system. Calphad: Computer Coupling of Phase Diagrams and Thermochemistry, 2009, 33, 136-161.	0.7	39
6912	Construction of modified embedded atom method potentials for the study of the bulk phase behaviour in binary Ptâ€“Rh, Ptâ€“Pd, Pdâ€“Rh and ternary Ptâ€“Pdâ€“Rh alloys. Calphad: Computer Coupling of Phase Diagrams and Thermochemistry, 2009, 33, 370-376.	0.7	28
6913	Stability of Laves phases in the Crâ€“Zr system. Calphad: Computer Coupling of Phase Diagrams and Thermochemistry, 2009, 33, 382-387.	0.7	30
6914	Multicomponent multisublattice alloys, nonconfigurational entropy and other additions to the Alloy Theoretic Automated Toolkit. Calphad: Computer Coupling of Phase Diagrams and Thermochemistry, 2009, 33, 266-278.	0.7	638

#	Article	IF	Citations
6915	Thermodynamic investigation of the galvanizing systems, I: Refinement of the thermodynamic description for the Feâ€“Zn system. Calphad: Computer Coupling of Phase Diagrams and Thermochemistry, 2009, 33, 433-440.	0.7	44
6916	First-principles study of ground-state properties and phase stability of vanadium nitrides. Calphad: Computer Coupling of Phase Diagrams and Thermochemistry, 2009, 33, 469-477.	0.7	19
6917	Thermodynamic modeling of the Snâ€“V binary system. Calphad: Computer Coupling of Phase Diagrams and Thermochemistry, 2009, 33, 539-544.	0.7	12
6918	Thermodynamic and ab initio investigation of the Cuâ€“Dy system. Calphad: Computer Coupling of Phase Diagrams and Thermochemistry, 2009, 33, 511-516.	0.7	8
6919	Thermodynamic modeling of the Mgâ€“Si system with the Kaptay equation for the excess Gibbs energy of the liquid phase. Calphad: Computer Coupling of Phase Diagrams and Thermochemistry, 2009, 33, 673-678.	0.7	42
6920	A thermodynamic description of the Geâ€“Sr system acquired via a hybrid approach of CALPHAD and first-principles calculations. Calphad: Computer Coupling of Phase Diagrams and Thermochemistry, 2009, 33, 719-722.	0.7	7
6921	First-principles study of binary special quasirandom structures for the Alâ€“Cu, Alâ€“Si, Cuâ€“Si, and Mgâ€“Si systems. Calphad: Computer Coupling of Phase Diagrams and Thermochemistry, 2009, 33, 769-773.	0.7	17
6922	Thermodynamics of silicate liquids in the deep Earth. Earth and Planetary Science Letters, 2009, 278, 226-232.	1.8	191
6923	Structure and elasticity of serpentine at high-pressure. Earth and Planetary Science Letters, 2009, 279, 11-19.	1.8	86
6924	Detecting deeply subducted crust from the elasticity of hollandite. Earth and Planetary Science Letters, 2009, 288, 349-358.	1.8	41
6925	Ab initio calculations of the elasticity of hcp-Fe as a function of temperature at inner-core pressure. Earth and Planetary Science Letters, 2009, 288, 534-538.	1.8	97
6926	The self-consistent ab initio lattice dynamical method. Computational Materials Science, 2009, 44, 888-894.	1.4	108
6927	DFT studies of sulfur induced stress corrosion cracking in nickel. Computational Materials Science, 2009, 44, 1236-1242.	1.4	35
6928	Structural stabilities, electronic structures and lithium deintercalation in LixMSiO4 (M=Mn, Fe, Co,) Tj ETQq1 1 0.784314 rgBT /Overlock	1.4	106
6929	First-principles study of the (110) polar surface of cubic PbTiO3. Computational Materials Science, 2009, 44, 1360-1365.	1.4	18
6930	First-principles study on the structural, elastic, and electronic properties of Î³-LiAlO2. Computational Materials Science, 2009, 46, 221-224.	1.4	26
6931	Mobility of small clusters of self-interstitial atoms in dilute Feâ€“Cr alloy studied by means of atomistic calculations. Computational Materials Science, 2009, 46, 1178-1186.	1.4	11
6932	Rare earth elements in Î±-Ti: A first-principles investigation. Computational Materials Science, 2009, 46, 1187-1191.	1.4	11

#	Article	IF	Citations
6933	NO adsorption effects on various functional molecular nanowires. Computational Materials Science, 2009, 47, 111-120.	1.4	8
6934	Effects of alloying elements on elastic properties of Ni by first-principles calculations. Computational Materials Science, 2009, 47, 254-260.	1.4	78
6935	First-principles calculations of mechanical and thermodynamic properties of the Laves C15-Mg2RE (RE=La, Ce, Pr, Nd, Pm, Sm, Gd). Computational Materials Science, 2009, 47, 297-301.	1.4	23
6936	Comparison of interaction between Cu precipitate and vacancy in Fe using first-principle calculations and empirical N-body potential calculations. Computational Materials Science, 2009, 47, 521-525.	1.4	6
6937	Cu/Ag EAM potential optimized for heteroepitaxial diffusion from ab initio data. Computational Materials Science, 2009, 47, 577-583.	1.4	54
6938	First principles study of structural phase stability of wide-gap semiconductors MgTe, MgS and MgSe. Computational Materials Science, 2009, 47, 593-598.	1.4	71
6939	Zinc surface complexes on birnessite: A density functional theory study. Geochimica Et Cosmochimica Acta, 2009, 73, 1273-1284.	1.6	63
6940	On the role of Mn(IV) vacancies in the photoreductive dissolution of hexagonal birnessite. Geochimica Et Cosmochimica Acta, 2009, 73, 4142-4150.	1.6	87
6941	Numerical modelling of dislocations and deformation mechanisms in CaIrO3 and MgGeO3 post-perovskitesâ€"Comparison with MgSiO3 post-perovskite. Physics of the Earth and Planetary Interiors, 2009, 174, 165-173.	0.7	33
6942	Ab initio predictions of potassium partitioning between Fe and Al-bearing MgSiO3 perovskite and post-perovskite. Physics of the Earth and Planetary Interiors, 2009, 174, 247-253.	0.7	7
6943	Pressure dependence of harmonic and anharmonic lattice dynamics in MgO: A first-principles calculation and implications for lattice thermal conductivity. Physics of the Earth and Planetary Interiors, 2009, 174, 33-38.	0.7	33
6944	Ab initio molecular dynamics study of elasticity of akimotoite MgSiO3 at mantle conditions. Physics of the Earth and Planetary Interiors, 2009, 173, 115-120.	0.7	14
6945	Oxide nitrides: From oxides to solids with mobile nitrogen ions. Progress in Solid State Chemistry, 2009, 37, 81-131.	3.9	66
6946	Theory and computer simulation of perfect and defective solids. Progress in Solid State Chemistry, 2009, 37, 70-80.	3.9	4
6947	Elastic constants of binary Mg compounds from first-principles calculations. Intermetallics, 2009, 17, 313-318.	1.8	212
6948	First-principles investigation of migration barriers and point defect complexes in B2â€"NiAl. Intermetallics, 2009, 17, 319-329.	1.8	35
6949	Effect of O impurity on structure and mechanical properties of NiAl intermetallics: A first-principles study. Intermetallics, 2009, 17, 358-364.	1.8	36
6950	Constitutional and thermal defects in B82â€"SnTi2. Intermetallics, 2009, 17, 291-304.	1.8	12

#	Article	IF	Citations
6951	First-principles calculations on the electronic structure and cohesive properties of titanium stannides. Intermetallics, 2009, 17, 768-773.	1.8	20
6952	Enthalpies of formation of magnesium compounds from first-principles calculations. Intermetallics, 2009, 17, 878-885.	1.8	159
6953	Structure and dynamics of liquid Al1â^'xSix alloys by ab initio molecular dynamics simulations. Journal of Non-Crystalline Solids, 2009, 355, 340-347.	1.5	18
6954	Structural change of liquid Si15Te85 and Si20Te80 with temperature: Ab initio molecular dynamics simulations. Journal of Non-Crystalline Solids, 2009, 355, 1687-1692.	1.5	2
6955	Metastability and crystal structure of the bialkali complex metal borohydride NaK(BH4)2. Journal of Alloys and Compounds, 2009, 476, 446-450.	2.8	45
6956	Electronic and magnetic properties of Al adsorption on Î±-uranium (001) surface: Ab initio calculations. Journal of Alloys and Compounds, 2009, 476, 675-682.	2.8	15
6957	High-pressure high-temperature phase transition of Î³â€²-Fe4N. Journal of Alloys and Compounds, 2009, 480, 76-80.	2.8	40
6958	A first-principles study of the Laâ€“H system. Journal of Alloys and Compounds, 2009, 480, 111-113.	2.8	10
6959	On the enthalpy of formation of aluminum diboride, AlB2. Journal of Alloys and Compounds, 2009, 477, L11-L12.	2.8	15
6960	First-principles investigation of sodium and lithium alloyed alanates. Journal of Alloys and Compounds, 2009, 479, 678-683.	2.8	9
6961	Adsorption and dissociation of hydrogen on MgO surface: A first-principles study. Journal of Alloys and Compounds, 2009, 480, 788-793.	2.8	61
6962	A quantum chemical study on magnesium(Mg)/magnesiumâ€“hydrogen(Mgâ€“H) nanowires. Journal of Alloys and Compounds, 2009, 484, 308-313.	2.8	33
6963	First-principles investigations of F and Cl impurities in NaAlH4. Journal of Alloys and Compounds, 2009, 484, 347-351.	2.8	6
6964	Elastic properties and pressure induced transitions of ZnO polymorphs from first-principle calculations. Journal of Alloys and Compounds, 2009, 484, 431-438.	2.8	85
6965	Crystal, electronic structures, optical and magnetic properties of Tb4Al2O9. Journal of Alloys and Compounds, 2009, 484, 943-948.	2.8	14
6966	Influence of oxygen on the structure and devitrification pathways in Zr66.7Ni33.3 and Zr66.7Cu33.3 amorphous systems. Journal of Alloys and Compounds, 2009, 484, 914-919.	2.8	13
6967	Thermodynamics, lattice stability and defect structure of strontium silicides via first-principles calculations. Journal of Alloys and Compounds, 2009, 484, 822-831.	2.8	11
6968	Microstructure and electronic characteristics of the 6H-type ABACAB LPSO structure in Mg97Zn1Y2 alloy. Journal of Alloys and Compounds, 2009, 485, 672-676.	2.8	24

#	Article	IF	Citations
6969	Lithium incorporation into a silica thin film: Scanning tunneling microscopy and density functional theory. Physical Review B, 2009, 80, .	1.1	21
6970	Oxygen Reduction on Well-Defined Coreâ^'Shell Nanocatalysts: Particle Size, Facet, and Pt Shell Thickness Effects. Journal of the American Chemical Society, 2009, 131, 17298-17302.	6.6	688
6971	Tunable hydrogen storage in magnesiumâ€“transition metal compounds: First-principles calculations. Physical Review B, 2009, 79, .	1.1	48
6972	Electronic structure and phase stability of MgTe, ZnTe, CdTe, and their alloys in theB3,B4, andB8 structures. Physical Review B, 2009, 79, .	1.1	55
6973	Experimental andab initiostructural studies of liquid<mml:math xmlns:mml="http://www.w3.org/1998/Math/MathML" display="inline"><mml:mrow><mml:msub><mml:mrow><mml:mtext>Zr</mml:mtext></mml:mrow><mml:mn>2</mml:mn></mml:msub> Physical Review B, 2009, 79, .	1.1	35
6974	First-principles study of two- and one-dimensional honeycomb structures of boron nitride. Physical Review B, 2009, 79, .	1.1	580
6975	High-pressure structures and vibrational spectra of barium fluoride: Results obtained under nearly hydrostatic conditions. Physical Review B, 2009, 79, .	1.1	13
6976	Understanding the Phase Transitions of the<mml:math xmlns:mml="http://www.w3.org/1998/Math/MathML" display="inline"><mml:msub><mml:mi>Ni</mml:mi><mml:mn>2</mml:mn></mml:msub><mml:mi>MnGa</mml:mi></mml:math>Ma Shape Memory System from First Principles. Physical Review Letters, 2009, 102, 035702.	2.9	138
6977	Liquid boron: X-ray measurements andab initiomolecular dynamics simulations. Physical Review B, 2009, 79, .	1.1	15
6978	First principles studies of multiferroic materials. Journal of Physics Condensed Matter, 2009, 21, 303201.	0.7	164
6979	Intrinsic<mml:math xmlns:mml="http://www.w3.org/1998/Math/MathML" display="inline"><mml:mi>n</mml:mi></mml:math>-Type Behavior in Transparent Conducting Oxides: A Comparative Hybrid-Functional Study of<mml:math xmlns:mml="http://www.w3.org/1998/Math/MathML" display="inline"><mml:msub><mml:mi>In</mml:mi><mml:mn>2</mml:mn></mml:msub><mml:msub><mml:mi mathvariant="bold">O</mml:mi><mml:mn>3</mml:mn></mml:msub></mml:math>,<mml:math xmlns:mml	2.9	295
6980	Quantum electron transport through SrTiO3: Effects of dopants on conductance channel. Applied Physics Letters, 2009, 94, .	1.5	7
6981	Two- and One-Dimensional Honeycomb Structures of Silicon and Germanium. Physical Review Letters, 2009, 102, 236804.	2.9	2,837
6982	Electronic properties of graphene nanoribbons embedded in boron nitride sheets. Applied Physics Letters, 2009, 95, .	1.5	123
6983	First-principles investigation of mechanical and electronic properties of MNNi3 (M=Zn, Mg, or Cd). Journal of Applied Physics, 2009, 105, 123921.	1.1	26
6984	First-principles investigation of atomic structures and stability of proton-exchanged layered sodium titanate. Physical Review B, 2009, 79, .	1.1	24
6985	Vinyl Acetate Synthesis on Homogeneous and Heterogeneous Pd-Based Catalysts: A Theoretical Analysis on the Reaction Mechanisms. Journal of Physical Chemistry A, 2009, 113, 11758-11762.	1.1	13
6986	Density functional theory for transition metals and transition metal chemistry. Physical Chemistry Chemical Physics, 2009, 11, 10757.	1.3	1,431

#	Article	IF	Citations
6987	Changes in the crystal and electronic structure of LiCoO2 and LiNiO2 upon Li intercalation and de-intercalation. Physical Chemistry Chemical Physics, 2009, 11, 3278.	1.3	164
6988	Selective Facet Reactivity during Cation Exchange in Cadmium Sulfide Nanorods. Journal of the American Chemical Society, 2009, 131, 5285-5293.	6.6	372
6989	Effect of vacancy defects in graphene on metal anchoring and hydrogen adsorption. Applied Physics Letters, 2009, 94, .	1.5	111
6990	Effect of Surface Ligands on Optical and Electronic Spectra of Semiconductor Nanoclusters. Journal of the American Chemical Society, 2009, 131, 7717-7726.	6.6	245
6991	Calculations of ZnO properties using the Heyd-Scuseria-Ernzerhof screened hybrid density functional. Physical Review B, 2009, 80, .	1.1	101
6992	Magnetoelectric coupling and electric control of magnetization in ferromagnet/ferroelectric/normal-metal superlattices. Physical Review B, 2009, 80, .	1.1	92
6993	Thiolated Gold Nanowires: Metallic versus Semiconducting. ACS Nano, 2009, 3, 2351-2357.	7.3	57
6994	Hydrogen in beryllium: Solubility, transport, and trapping. Physical Review B, 2009, 79, .	1.1	51
6995	New Views of the Earthâ€™s Inner Core from Computational Mineral Physics. , 2009, , 397-412.		1
6996	Site occupation in the Cr-Ru and Cr-Os<mml:math xmlns:mml="http://www.w3.org/1998/Math/MathML" display="inline"><mml:mi>Ïƒ</mml:mi></mml:math>phases. Physical Review B, 2009, 80, .	1.1	19
6997	Density-functional theory of the magnetic anisotropy of nanostructures: an assessment of different approximations. Journal of Physics Condensed Matter, 2009, 21, 426001.	0.7	53
6998	Ab initiomolecular dynamics simulations of properties of a-Al2O3 /vacuum and a-ZrO2 /vacuum vs a-Al2O3âˆ•Ge(100)(2Ã—1) and a-ZrO2âˆ•Ge(100)(2Ã—1) interfaces. Journal of Chemical Physics, 2009, 130, 124717.	1.2	28
6999	Atomically abrupt and unpinned Al2O3/In0.53Ga0.47As interfaces: Experiment and simulation. Journal of Applied Physics, 2009, 106, .	1.1	81
7000	â€œNarrowâ€•Graphene Nanoribbons Made Easier by Partial Hydrogenation. Nano Letters, 2009, 9, 4025-4030.	4.5	120
7001	First-principles study on ferromagnetism in nitrogen-doped In2O3. Applied Physics Letters, 2009, 95, 012509.	1.5	59
7002	A Quantum Chemical Interpretation of Compressibility in Solids. Journal of Chemical Theory and Computation, 2009, 5, 2108-2114.	2.3	30
7003	Comparison of Electronic and Magnetic Properties of Fe, Co, and Ni Nanowires Encapsulated in Boron Nitride Nanotubes. Journal of Physical Chemistry C, 2009, 113, 17745-17750.	1.5	23
7004	Catalyzed Î² scission of a carbenium ion IIIÂâ€” Scission observed in ab initio molecular dynamics simulations. Canadian Journal of Chemistry, 2009, 87, 1512-1520.	0.6	4

#	Article	IF	Citations
7005	Interaction of graphene with FCCâ€“Co(111). Physical Chemistry Chemical Physics, 2009, 11, 803-807.	1.3	53
7006	Magnetic properties of first-row element-doped ZnS semiconductors: A density functional theory investigation. Physical Review B, 2009, 80, .	1.1	79
7007	Density Functional Investigation of the Antiferromagnetic Ordering, Spin Orientation, and Ferroelectric Polarization of Rare-Earth Iron Borate TbFe₃(BO₃)₄. Chemistry of Materials, 2009, 21, 2534-2539.	3.2	7
7008	First-principles study for vacancy-induced magnetism in nonmagnetic ferroelectric BaTiO3. Physical Chemistry Chemical Physics, 2009, 11, 10934.	1.3	67
7009	Density Functional Studies of Methanol Decomposition on Subnanometer Pd Clusters. Journal of Physical Chemistry C, 2009, 113, 21789-21796.	1.5	33
7010	The importance of chargeâ€“quadrupole interactions for H2adsorption and diffusion in CuBTC. Molecular Simulation, 2009, 35, 60-69.	0.9	39
7011	Theory of Scanning Tunneling Microscopy and Applications in Catalysis. , 0, , 97-118.		1
7012	First principles study of C3N4 carbon nitride nanotubes. Journal of Materials Chemistry, 2009, 19, 3020.	6.7	57
7013	C-BN Single-Walled Nanotubes from Hybrid Connection of BN/C Nanoribbons: Prediction by ab initio Density Functional Calculations. Journal of the American Chemical Society, 2009, 131, 1682-1683.	6.6	106
7014	Structural, electronic and magnetic properties of V2O5â^'x: An ab initio study. Journal of Chemical Physics, 2009, 130, 214704.	1.2	36
7015	A pathway to p-type wide-band-gap semiconductors. Applied Physics Letters, 2009, 95, .	1.5	37
7016	bcc-to-hcp transformation pathways for iron versus hydrostatic pressure: Coupled shuffle and shear modes. Physical Review B, 2009, 79, .	1.1	44
7017	(Cu₂S₂)(Sr₃Sc₂O₅)â^'A Layered, Direct Band Gap, p-Type Transparent Conducting Oxychalcogenide: A Theoretical Analysis.. Chemistry of Materials, 2009, 21, 5435-5442.	3.2	78
7018	Origin of electronic and optical trends in ternary<mml:math xmlns:mml="http://www.w3.org/1998/Math/MathML" display="inline"><mml:mrow><mml:msub><mml:mrow><mml:mtext>In</mml:mtext></mml:mrow><mml:mn>2</mml:mn></mml:ms conducting oxides<mml:math xmlns. Physical Review B, 2009, 79, .	1.1	74
7019	Unraveling the Jahn-Teller effect in Mn-doped GaN using the Heyd-Scuseria-Ernzerhof hybrid functional. Physical Review B, 2009, 79, .	1.1	122
7020	Ab initio Study on the Structural Stability and Magnetism of Metastable A3B Phases in Niâ€“Au (Cu, Zn,) Tj ETQq1 1 0.784314 rgBT /O	0.7	1
7021	Electronic structure of two-dimensional crystals fromab initiotheory. Physical Review B, 2009, 79, .	1.1	941
7022	Polyol-Mediated Synthesis of Ultrafine TiO2 Nanocrystals and Tailored Physiochemical Properties by Ni Doping. Journal of Physical Chemistry C, 2009, 113, 9210-9217.	1.5	46

#	Article	IF	Citations
7023	Substrate-induced magnetism in epitaxial graphene buffer layers. Nanotechnology, 2009, 20, 275705.	1.3	22
7024	A Methanol-Tolerant Carbon-Supported Ptâ^'Au Alloy Cathode Catalyst for Direct Methanol Fuel Cells and Its Evaluation by DFT. Journal of Physical Chemistry C, 2009, 113, 7461-7468.	1.5	140
7025	STM topography and manipulation of single Au atoms on Si(100). Physical Review B, 2009, 79, .	1.1	12
7026	THEORETICAL STUDIES ON THE EXTRINSIC DEFECTS OF MONTMORILLONITE IN SOFT ROCK. Modern Physics Letters B, 2009, 23, 2933-2941.	1.0	11
7027	Anomalous Dual-Element Filling in Partially Filled Skutterudites. Journal of the American Chemical Society, 2009, 131, 5560-5563.	6.6	24
7028	Graphene Oxide as an Ideal Substrate for Hydrogen Storage. ACS Nano, 2009, 3, 2995-3000.	7.3	342
7029	First-principles study of diffusion of oxygen vacancies and interstitials in ZnO. Journal of Physics Condensed Matter, 2009, 21, 195403.	0.7	29
7030	Visible Light-Induced Photocatalytic Oxidation of Phenol and Aqueous Ammonia in Flowerlike Bi₂Fe₄O₉ Suspensions. Journal of Physical Chemistry C, 2009, 113, 12826-12831.	1.5	131
7031	Electronic structures of zigzag graphene nanoribbons with edge hydrogenation and oxidation. Physical Review B, 2009, 79, .	1.1	239
7032	Enhanced magnetic moment in Fe-doped Pd_nclusters (n= 1â€“13): a density functional study. Journal of Physics Condensed Matter, 2009, 21, 396001.	0.7	9
7033	Full-Zone Spin Splitting for Electrons and Holes in Bulk GaAs and GaSb. Physical Review Letters, 2009, 102, 056405.	2.9	47
7034	Computational Studies of Metalâ^'Carbon Nanotube Interfaces for Regrowth and Electronic Transport. Nano Letters, 2009, 9, 1117-1120.	4.5	31
7035	Identification of a Frenkel-pair defect in electron-irradiated 3<mml:math xmlns:mml="http://www.w3.org/1998/Math/MathML" display="inline"><mml:mrow><mml:mi>C</mml:mi></mml:mrow></mml:math>SiC. Physical Review B, 2009, 80, .	1.1	10
7036	Point defects in CaF2 and CeO2 investigated by the periodic electrostatic embedded cluster method. Journal of Chemical Physics, 2009, 130, 174710.	1.2	88
7037	Predicted Trends of Coreâ^'Shell Preferences for 132 Late Transition-Metal Binary-Alloy Nanoparticles. Journal of the American Chemical Society, 2009, 131, 14023-14029.	6.6	233
7038	Hydrogen multicenter bonds and reversible hydrogen storage. Journal of Chemical Physics, 2009, 130, 114301.	1.2	23
7039	Carbon Doping of the TiO₂ (110) Rutile Surface. A Theoretical Study Based on DFT. Chemistry of Materials, 2009, 21, 1431-1438.	3.2	39
7040	Redox properties of gold-substituted zirconia surfaces. Journal of Materials Chemistry, 2009, 19, 710-717.	6.7	12

#	Article	IF	Citations
7041	A Single-Component Molecular Metal Based on a Thiazole Dithiolate Gold Complex. Journal of the American Chemical Society, 2009, 131, 16961-16967.	6.6	102
7042	First-Principles Analysis of NO_x Adsorption on Anhydrous Î³-Al₂O₃ Surfaces. Journal of Physical Chemistry C, 2009, 113, 7779-7789.	1.5	28
7043	Monte Carlo Theory Analysis of Thermal Programmed Desorption of Chiral Propylene Oxide from Pd(111) Surfaces. Journal of Physical Chemistry C, 2009, 113, 3254-3258.	1.5	11
7044	What Is the Structure of Kaolinite? Reconciling Theory and Experiment. Journal of Physical Chemistry B, 2009, 113, 6756-6765.	1.2	63
7045	Energy Minimization of Single-Walled Titanium Oxide Nanotubes. ACS Nano, 2009, 3, 3401-3412.	7.3	19
7046	First-Principles Calculations of Rare-Earth Dopants in BaTiO3. Japanese Journal of Applied Physics, 2009, 48, 09KC03.	0.8	22
7047	First-principles calculation of nitrogen-tungsten codoping effects on the band structure of anatase-titania. Applied Physics Letters, 2009, 94, .	1.5	113
7048	Elasticity of phaseâ€X at high pressure. Geophysical Research Letters, 2009, 36, .	1.5	20
7049	MÃ¶ssbauer modeling to interpret the spin state of iron in (Mg,Fe)SiO₃ perovskite. Geophysical Research Letters, 2009, 36, .	1.5	64
7050	Partitioning of Si and O between liquid iron and silicate melt: A twoâ€phase abâ€initio molecular dynamics study. Geophysical Research Letters, 2009, 36, .	1.5	9
7051	High CO tolerance of Pt/Ru nanocatalyst: Insight from first principles calculations. Journal of Chemical Physics, 2009, 130, 124714.	1.2	27
7052	Application of density functional theory to CO tolerance in fuel cells: a brief review. Journal of Physics Condensed Matter, 2009, 21, 474226.	0.7	8
7053	Temperature of the inner-core boundary of the Earth: Melting of iron at high pressure from first-principles coexistence simulations. Physical Review B, 2009, 79, .	1.1	136
7054	Synthesis, Thermal Stability and Properties of ZnO₂ Nanoparticles. Journal of Physical Chemistry C, 2009, 113, 1320-1324.	1.5	79
7055	Antiferromagnetic bipolar semiconductor LaMnPO with ZrCuSiAs-type structure. Journal of Applied Physics, 2009, 105, 093916.	1.1	47
7056	Intrinsic Half-Metallicity in Modified Graphene Nanoribbons. Physical Review Letters, 2009, 102, 096601.	2.9	398
7057	Ab Initio Study of Hydrogen Adsorption in MOF-5. Journal of the American Chemical Society, 2009, 131, 4143-4150.	6.6	225
7058	Surface vs. bulk electronic structure of silver determined by photoemission. Europhysics Letters, 2009, 88, 67004.	0.7	17

#	Article	IF	Citations
7059	Interface and transport properties of Fe/V/MgO/Fe and Fe/V/Fe/MgO/Fe magnetic tunneling junctions. Physical Review B, 2009, 79, .	1.1	20
7060	Simulating functional magnetic materials on supercomputers. Journal of Physics Condensed Matter, 2009, 21, 293201.	0.7	33
7061	Algorithms for the electronic and vibrational properties of nanocrystals. Journal of Physics Condensed Matter, 2009, 21, 064207.	0.7	9
7062	Density functional theory studies of the structural, electronic, and phonon properties of<mml:math xmlns:mml="http://www.w3.org/1998/Math/MathML" display="inline"><mml:mrow><mml:msub><mml:mrow><mml:mtext>Li</mml:mtext></mml:mrow><mml:mn>2</mml:mn></mml:ms<mml:math xmlns:mml="http://www.w3.org/1998/Math/MathML" display="inline"><mml:mrow><mml:msub><mml:mrow><mml:mtext>Li</mml:mtext></mml:mrow><mml:mn>2</mml:mn></mml:ms Physical Review B, 2009, 79, .	1.1	92
7063	Electronic Structure Modulations of Radially Deformed Single Wall Carbon Nanotubes under Transverse External Electric Fields. Journal of Physical Chemistry C, 2009, 113, 4792-4796.	1.5	34
7064	Ferroelectricity in multiferroic magnetite<mml:math xmlns:mml="http://www.w3.org/1998/Math/MathML" display="inline"><mml:mrow><mml:msub><mml:mrow><mml:mtext>Fe</mml:mtext></mml:mrow><mml:mn>3</mml:mn></mml:m by noncentrosymmetric<mml:math xmlns:mml="http://www.w3.org/1998/Math/MathML" display="inline"><mml:mrow><mml:msub><mml:mrow><mml:mtext>Fe</mml:mtext></mml:mrow><mml:mrow><mml:mn>2</mml:mn> Physical Review B, 2009, 79, .	1.1	89
7065	Density Functional Theory Study of the Adsorption of Au Atom on Cerium Oxide: Effect of Low-Coordinated Surface Sites. Journal of Physical Chemistry C, 2009, 113, 4948-4954.	1.5	54
7066	Multiferroicity in TTF-CA Organic Molecular Crystals Predicted throughAbÂInitioCalculations. Physical Review Letters, 2009, 103, 266401.	2.9	94
7067	Magnetically Induced Electronic Ferroelectricity in Half-Doped Manganites. Physical Review Letters, 2009, 103, 037601.	2.9	57
7068	Multiferroicity in Rare-Earth Nickelates<mml:math xmlns:mml="http://www.w3.org/1998/Math/MathML" display="inline"><mml:mi>R</mml:mi><mml:msub><mml:mi>NiO</mml:mi><mml:mn>3</mml:mn></mml:msub></mml:math>. Physical Review Letters, 2009, 103, 156401.	2.9	103
7069	Density-functional analysis of spin exchange and ferroelectric polarization in<mml:math xmlns:mml="http://www.w3.org/1998/Math/MathML" display="inline"><mml:mrow><mml:msub><mml:mrow><mml:mtext>AgCrO</mml:mtext></mml:mrow><mml:mn>2</mml:mn></mml:<mml:math xmlns:mml="http://www.w3.org/1998/Math/MathML" display="inline"><mml:mrow><mml:msub><mml:mrow><mml:mtext>AgCrO</mml:mtext></mml:mrow><mml:mn>2</mml:mn></mml: Physical Review B, 2009, 80, .	1.1	28
7070	IR and X-ray Study of Polymorphism in 1-Alkyl-3-methylimidazolium Bis(trifluoromethanesulfonyl)imides. Journal of Physical Chemistry B, 2009, 113, 9538-9546.	1.2	82
7071	Electronic properties of zigzag graphene nanoribbons on Si(001). Applied Physics Letters, 2009, 95, 023107.	1.5	27
7072	Band Edge Electronic Structure of BiVO₄: Elucidating the Role of the Bi s and V d Orbitals. Chemistry of Materials, 2009, 21, 547-551.	3.2	624
7073	Effect of magnetic state on the<mml:math xmlns:mml="http://www.w3.org/1998/Math/MathML" display="inline"><mml:mrow><mml:mi>Î³</mml:mi><mml:mtext>â^'</mml:mtext><mml:mi>Î±</mml:mi></mml:mrow></mml:math>tra in iron: First-principles calculations of the Bain transformation path. Physical Review B, 2009, 79, .	1.1	61
7074	Experimental and Theoretical Investigation of the Catalytic Ozonation on the Surface of NiOâ^'CuO Nanoparticles. Langmuir, 2009, 25, 8001-8011.	1.6	26
7075	The non-degenerate core structure of a Â½âŸ¨111âŸ© screw dislocation in bcc transition metals modelled using Finnisâ€“Sinclair potentials: The necessary and sufficient conditions. Philosophical Magazine, 2009, 89, 3235-3243.	0.7	27
7076	Quantum transport in alkane molecular wires: Effects of binding modes and anchoring groups. Journal of Chemical Physics, 2009, 131, 244712.	1.2	29

#	Article	IF	Citations
7077	Cluster expansion method for multicomponent systems based on optimal selection of structures for density-functional theory calculations. Physical Review B, 2009, 80, .	1.1	116
7078	CO Adsorption on One-, Two-, and Three-Dimensional Au Clusters Supported on MgO/Ag(001) Ultrathin Films. Journal of Physical Chemistry C, 2009, 113, 10256-10263.	1.5	29
7079	Ab initio thermodynamic evaluation of Pd atom interaction with CeO2 surfaces. Journal of Chemical Physics, 2009, 131, 084701.	1.2	51
7080	Electronic Structure of Si-Doped BN Nanotubes Using X-ray Photoelectron Spectroscopy and First-Principles Calculation. Chemistry of Materials, 2009, 21, 136-143.	3.2	56
7081	Î±- to Î²-(dmes)BiI₅ (dmes = Dimethyl(2-ethylammonium)sulfonium Dication): Umbrella Reversal of Sulfonium in the Solid State and Short IÂ·Â·Â·I Interchain Contactsâ€”Crystal Structures, Optical Properties, and Theoretical Investigations of 1D Iodobismuthates. Inorganic Chemistry, 2009, 48, 879-888.	1.9	77
7082	Studies on the Hydrogen Storage of Magnesium Nanowires by Density Functional Theory. Journal of Physical Chemistry C, 2009, 113, 3007-3013.	1.5	55
7083	Density functional theory study of graphite oxide for different oxidation levels. Physical Review B, 2009, 79, .	1.1	224
7084	Ozone Adsorption on Graphene: Ab Initio Study and Experimental Validation. Journal of Physical Chemistry C, 2009, 113, 14225-14229.	1.5	170
7085	Adsorption and Reactivity of CO₂ on Defective Graphene Sheets. Journal of Physical Chemistry A, 2009, 113, 493-498.	1.1	110
7086	Magnetoelectric Response of Multiferroic<mml:math xmlns:mml="http://www.w3.org/1998/Math/MathML" display="inline"><mml:msub><mml:mi>BiFeO</mml:mi><mml:mn>3</mml:mn></mml:msub></mml:math>and Related Materials from First-Principles Calculations. Physical Review Letters, 2009, 103, 267205.	2.9	87
7087	Basal and prism dislocation cores in magnesium: comparison of first-principles and embedded-atom-potential methods predictions. Modelling and Simulation in Materials Science and Engineering, 2009, 17, 055012.	0.8	153
7088	Edge effects on quantum thermal transport in graphene nanoribbons: Tight-binding calculations. Physical Review B, 2009, 79, .	1.1	110
7089	Heyd-Scuseria-Ernzerhof hybrid functional for calculating the lattice dynamics of semiconductors. Physical Review B, 2009, 80, .	1.1	164
7090	Electronic and magnetic structure of<mml:math xmlns:mml="http://www.w3.org/1998/Math/MathML" display="inline"><mml:mrow><mml:msub><mml:mrow><mml:mtext>Fe</mml:mtext></mml:mrow><mml:mn>3</mml:mn></mml:msub></mml:mrow></mml:math>from<mml:math xmlns:mml="http://www.w3.org/1998/Math/MathML" display="inline"><mml:mrow><mml:mtext>GGA</mml:mtext><mml:mo>+</mml:mo><mml:mtext>U</mml:mtext></mml:mrow></mml:math>Physical Review B, 2009, 79, .	1.1	61
7091	Small polarons in Nb- and Ta-doped rutile and anatase TiO2. Journal of Materials Chemistry, 2009, 19, 5175.	6.7	154
7092	Molecular Dynamics Simulations of Au Penetration through Alkanethiol Monolayers on the Au(111) Surface. Journal of Physical Chemistry C, 2009, 113, 6360-6366.	1.5	7
7093	Atomistic Origins of Molecular Memristors. Journal of Physical Chemistry C, 2009, 113, 20713-20718.	1.5	20
7094	Comparative study of single Cu, Ag, Au, and K atoms adsorbed on<mml:math xmlns:mml="http://www.w3.org/1998/Math/MathML" display="inline"><mml:mrow><mml:mtext>Si</mml:mtext><mml:mrow><mml:mo>(</mml:mo><mml:mrow><mml:mn>111</mml:mn></mml:mrow></mml:math>Physical Review B, 2009, 79, .	1.1	15

#	Article	IF	Citations
7095	Why nitrogen cannot lead to p-type conductivity in ZnO. Applied Physics Letters, 2009, 95, .	1.5	364
7096	Interatomic potentials for hydrogen in<mml:math xmlns:mml="http://www.w3.org/1998/Math/MathML" display="inline"><mml:mi>Î±</mml:mi></mml:math>â€“iron based on density functional theory. Physical Review B, 2009, 79, .	1.1	166
7097	Understanding the p-Type Conduction Properties of the Transparent Conducting Oxide CuBO₂: A Density Functional Theory Analysis. Chemistry of Materials, 2009, 21, 4568-4576.	3.2	100
7098	Electronic structure and band-gap modulation of graphene via substrate surface chemistry. Applied Physics Letters, 2009, 94, .	1.5	158
7099	Can crystal structure prediction guide experimentalists to a new polymorph of paracetamol?. CrystEngComm, 2009, 11, 2475.	1.3	39
7100	Parametrization of a reactive many-body potential for Moâ€“S systems. Physical Review B, 2009, 79, .	1.1	241
7101	Molecular dynamics simulation of the effect of pH on the adsorption of rhodamine laser dyes on TiO₂hydroxylated surfaces. Molecular Simulation, 2009, 35, 1140-1151.	0.9	15
7102	Interactions between hydrogen impurities and vacancies in Mg and Al: A comparative analysis based on density functional theory. Physical Review B, 2009, 80, .	1.1	109
7103	Hybrid functional study of prototypical multiferroic bismuth ferrite. Physical Review B, 2009, 79, .	1.1	63
7104	Understanding adsorption of hydrogen atoms on graphene. Journal of Chemical Physics, 2009, 130, 054704.	1.2	303
7105	Chair and Twist-Boat Membranes in Hydrogenated Graphene. ACS Nano, 2009, 3, 4017-4022.	7.3	89
7106	Electronic Structure Engineering via On-Plane Chemical Functionalization: A Comparison Study on Two-Dimensional Polysilane and Graphane. Journal of Physical Chemistry C, 2009, 113, 16741-16746.	1.5	133
7107	Molecular adsorption in graphene with divacancy defects. Physical Review B, 2009, 79, .	1.1	155
7108	Geometry, electronic structure and thermodynamic stability of intrinsic point defects in indium oxide. Journal of Physics Condensed Matter, 2009, 21, 455801.	0.7	71
7109	Formation entropies of intrinsic point defects in cubic In2O3 from first-principles density functional theory calculations. Physical Chemistry Chemical Physics, 2009, 11, 3226.	1.3	41
7110	First-principles approaches to intrinsic strength and deformation of materials: perfect crystals, nano-structures, surfaces and interfaces. Modelling and Simulation in Materials Science and Engineering, 2009, 17, 013001.	0.8	106
7111	Surface Concavityâ^'Convexity Sensitive Oxidation Dynamics of Carbon Nanotubes. Journal of Physical Chemistry C, 2009, 113, 3569-3573.	1.5	4
7112	Oxygen vacancy clusters on ceria: Decisive role of cerium<mml:math xmlns:mml="http://www.w3.org/1998/Math/MathML" display="inline"><mml:mi>f</mml:mi></mml:math>electrons. Physical Review B, 2009, 79, .	1.1	103

#	Article	IF	Citations
7113	Li12Si60H60 Fullerene Composite: A Promising Hydrogen Storage Medium. ACS Nano, 2009, 3, 3294-3300.	7.3	45
7114	Tailoring the Morphology of LiCoO₂: A First Principles Study. Chemistry of Materials, 2009, 21, 3799-3809.	3.2	243
7115	Strong Electron Correlations Determine Energetic Stability and Electronic Properties of Er-Doped Goldberg-Type Silicon Quantum Dots. Journal of Physical Chemistry C, 2009, 113, 15964-15968.	1.5	3
7116	Theory of the neutral nitrogen-vacancy center in diamond and its application to the realization of a qubit. Physical Review B, 2009, 79, .	1.1	82
7117	Identification of individual<mml:math xmlns:mml="http://www.w3.org/1998/Math/MathML" display="inline"><mml:mrow><mml:mmultiscripts><mml:mtext>C</mml:mtext><mml:mprescripts /><mml:none /><mml:mrow><mml:mn>13</mml:mn></mml:mrow></mml:mmultiscripts></mml:mrow></mml:math>isotopes of nitrogen-vacancy center in diamond by combining the polarization studies of nuclear spins and first-principles calculations. Physical Review B, 2009, 80, .	1.1	49
7118	Magnetism in graphene due to single-atom defects: dependence on the concentration and packing geometry of defects. Journal of Physics Condensed Matter, 2009, 21, 196002.	0.7	96
7119	First-principles study of elastic and phonon properties of the heavy fermion compound CeMg. Journal of Physics Condensed Matter, 2009, 21, 246001.	0.7	24
7120	Quantum-mechanical calculations of zircon to scheelite transition pathways inZrSiO4. Physical Review B, 2009, 79, .	1.1	27
7121	Multiple adsorption of NO on cobalt-exchanged chabazite, mordenite, and ferrierite zeolites: A periodic density functional theory study. Journal of Chemical Physics, 2009, 131, 054101.	1.2	8
7122	Effects of Coulomb interaction on the electronic structure and lattice dynamics of the Mott insulator<mml:math xmlns:mml="http://www.w3.org/1998/Math/MathML" display="inline"><mml:mrow><mml:msub><mml:mrow><mml:mtext>Fe</mml:mtext></mml:mrow><mml:mn>2</mml:mn></mml:msub> Physical Review B, 2009, 79, .	1.1	16
7123	Promotion of CO Oxidation on Bimetallic Auâ^'Ag(110) Surfaces: A Combined Microscopic and Theoretical Study. Journal of Physical Chemistry C, 2009, 113, 13151-13159.	1.5	28
7124	Effects of vacancies on phonon entropy of<mml:math xmlns:mml="http://www.w3.org/1998/Math/MathML" display="inline"><mml:mrow><mml:mi>B</mml:mi><mml:mn>2</mml:mn></mml:mrow></mml:math>FeAl. Physical Review B, 2009, 80, .	1.1	7
7125	Ab initiostudy of generalized collective excitations in molten NaI. Physical Review B, 2009, 79, .	1.1	15
7126	Ion structure in warm dense matter: Benchmarking solutions of hypernetted-chain equations by first-principle simulations. Physical Review E, 2009, 79, 010201.	0.8	94
7127	Density functional study on ferromagnetism in nitrogen-doped anatase TiO2. Applied Physics Letters, 2009, 95, 062505.	1.5	85
7128	Wall thickness of single-walled carbon nanotubes and its Young's modulus. Physica Scripta, 2009, 79, 025702.	1.2	27
7129	Characterization of surface and bulk nitrates of Î³-Al2O3â€“supported alkaline earth oxides using density functional theory. Physical Chemistry Chemical Physics, 2009, 11, 3380.	1.3	10
7130	Synergistic Effects of Bi/S Codoping on Visible Light-Activated Anatase TiO₂ Photocatalysts from First Principles. Journal of Physical Chemistry C, 2009, 113, 8373-8377.	1.5	49

#	Article	IF	Citations
7131	Adsorption of selected ions on the anatase TiO₂(101) surface: a density-functional study. Molecular Simulation, 2009, 35, 567-576.	0.9	10
7132	Hydrogen in anion vacancies of semiconductors. Physical Review B, 2009, 79, .	1.1	15
7133	The phase diagram of halogens on Pt(110): structure of the (4 Ã— 1)-Br/Pt(110) phase. Journal of Physics Condensed Matter, 2009, 21, 134003.	0.7	9
7134	AbÂInitioMolecular Dynamics Study of Hot Atom Dynamics after Dissociative Adsorption of<mml:math xmlns:mml="http://www.w3.org/1998/Math/MathML" display="inline"><mml:msub><mml:mi mathvariant="bold">H</mml:mi><mml:mn>2</mml:mn></mml:msub></mml:math>on Pd(100). Physical Review Letters, 2009, 103, 246101.	2.9	52
7135	Suppression of the structural phase transition and lattice softening in slightly underdopedBa1âˆ’xKxFe2As2with electronic phase separation. Physical Review B, 2009, 79, .	1.1	37
7136	Ab initiostudy of the interface properties of Fe/GaAs(110). Physical Review B, 2009, 80, .	1.1	7
7137	Ab initio study of noncovalent sidewall functionalization of carbon nanotubes. Applied Physics Letters, 2009, 95, 243110.	1.5	12
7138	Assessment of thermoelectric performance of Cu2ZnSnX4, X=S, Se, and Te. Applied Physics Letters, 2009, 95, .	1.5	75
7139	Monte Carlo simulations of diluted magnetic semiconductors usingab initioexchange parameters. Journal of Physics Condensed Matter, 2009, 21, 064238.	0.7	25
7140	Impurity diffusion activation energies in Al from first principles. Physical Review B, 2009, 79, .	1.1	126
7141	Non-transition-metal doped diluted magnetic semiconductors. Applied Physics Letters, 2009, 94, .	1.5	64
7142	How Graphene Is Cut upon Oxidation?. Journal of the American Chemical Society, 2009, 131, 6320-6321.	6.6	323
7143	The structure of strontium-doped hydroxyapatite: an experimental and theoretical study. Physical Chemistry Chemical Physics, 2009, 11, 568-577.	1.3	185
7144	Phase-Dependent Photocatalytic Ability of TiO₂: A First-Principles Study. Journal of Chemical Theory and Computation, 2009, 5, 3074-3078.	2.3	68
7145	First-principles calculation of the 6.1 Ã... family bowing parameters and band offsets. Journal of Applied Physics, 2009, 105, .	1.1	6
7146	Magnetic coupling properties of rare-earth metals (Gd, Nd) doped ZnO: First-principles calculations. Journal of Applied Physics, 2009, 106, .	1.1	76
7147	Modelling of electron and hole trapping in oxides. Modelling and Simulation in Materials Science and Engineering, 2009, 17, 084004.	0.8	51
7148	Implementation of a DFT-Based Method for the Calculation of the Zeeman g-Tensor in Periodic Systems with the Use of Numerical and Slater-Type Atomic Orbitals. Journal of Physical Chemistry A, 2009, 113, 1327-1334.	1.1	14

#	Article	IF	Citations
7149	Hydrogen Dissociation on Pd4S Surfaces. Journal of Physical Chemistry C, 2009, 113, 18800-18806.	1.5	34
7150	First principles study of the graphene/Ru(0001) interface. Journal of Chemical Physics, 2009, 130, 074705.	1.2	111
7151	Enhanced Stability of Thiolate Self-Assembled Monolayers (SAMs) on Nanostructured Gold Substrates. Langmuir, 2009, 25, 5661-5666.	1.6	70
7152	Tailoring Bicomponent Supramolecular Nanoporous Networks: Phase Segregation, Polymorphism, and Glasses at the Solidâ^'Liquid Interface. Journal of the American Chemical Society, 2009, 131, 13062-13071.	6.6	134
7153	Mechanism for phase transitions and vacancy island formation in alkylthiol/Au(111) self-assembled monolayers based on adatom and vacancy-induced reconstructions. Physical Review B, 2009, 79, .	1.1	37
7154	Ab initioexamination of ductility features of fcc metals. Physical Review B, 2009, 79, .	1.1	91
7155	Stable calcium adsorbates on carbon nanostructures: Applications for high-capacity hydrogen storage. Physical Review B, 2009, 79, .	1.1	74
7156	Shock Compression of Quartz to 1.6 TPa: Redefining a Pressure Standard. Physical Review Letters, 2009, 103, 225501.	2.9	190
7157	First-principles study of the (001) surface of cubic PbHfO₃and BaHfO₃. Chinese Physics B, 2009, 18, 1194-1200.	0.7	7
7158	Ab initiocalculations for point defect clusters with P, As, and Sb in Si. Physical Review B, 2009, 80, .	1.1	19
7159	Electronic structure models of oxygen adsorption at the solvated, electrified Pt(111) interface. Physical Chemistry Chemical Physics, 2009, 11, 10108.	1.3	35
7160	Magnetically induced ferroelectricity in TbMnO₃: inverse Goodenoughâ€"Kanamori interaction. Journal of Physics Condensed Matter, 2009, 21, 064203.	0.7	12
7161	Local bonding effect on the defect states of oxygen vacancy in amorphous HfSiO4. Applied Physics Letters, 2009, 95, 082905.	1.5	4
7162	Ab Initio Study of Molecular Hydrogen Adsorption in Covalent Organic Framework-1. Journal of Physical Chemistry C, 2009, 113, 8498-8504.	1.5	32
7163	Electronic and Magnetic Properties of Partially Open Carbon Nanotubes. Journal of the American Chemical Society, 2009, 131, 17919-17925.	6.6	47
7164	Electronic and magnetic properties of Mn-doped BeSiAs₂and BeGeAs₂compounds. Journal of Physics Condensed Matter, 2009, 21, 045507.	0.7	21
7165	Magnetoelectric effect at the SrRuO3/BaTiO3 (001) interface: An ab initio study. Applied Physics Letters, 2009, 95, .	1.5	119
7166	<mml:math xmlns:mml="http://www.w3.org/1998/Math/MathML" display="inline"><mml:mrow><mml:mtext>DFT</mml:mtext><mml:mo>+</mml:mo><mml:mtext>U</mml:mtext></mml:mrow></mml:math>study of the ground state and metastable states of uranium dioxide. Physical Review B, 2009, 79, .	1.1	306

#	Article	IF	Citations
7167	Band Gap Narrowing of Titanium Oxide Semiconductors by Noncompensated Anion-Cation Codoping for Enhanced Visible-Light Photoactivity. Physical Review Letters, 2009, 103, 226401.	2.9	347
7168	Novel Structures and Superconductivity of Silane under Pressure. Physical Review Letters, 2009, 102, 087005.	2.9	146
7169	Density matrix treatment of combined instantaneous and delayed dissipation for an electronically excited adsorbate on a solid surface. Journal of Chemical Physics, 2009, 131, 144106.	1.2	17
7170	Immobilization of Alkali Metal Ions in a 3D Lanthanide-Organic Framework: Selective Sorption and H2 Storage Characteristics. Chemistry of Materials, 2009, 21, 5406-5412.	3.2	53
7171	Thermodynamics of fission products in UO_{2 Â±x}. Journal of Physics Condensed Matter, 2009, 21, 435602.	0.7	52
7172	Phonons in the cubic phase of<mml:math xmlns:mml="http://www.w3.org/1998/Math/MathML"		

#	Article	IF	Citations
7185	Prediction of half-metallic conductivity in Prussian Blue derivatives. Journal of Materials Chemistry, 2009, 19, 2032.	6.7	41
7186	A first principles comparison of the mechanism and site requirements for the electrocatalytic oxidation of methanol and formic acid over Pt. Faraday Discussions, 2008, 140, 363-378.	1.6	400
7187	Direct enumeration studies of band-gap properties of AlxGayIn1â^'xâ^'yP alloys. Journal of Applied Physics, 2009, 105, 123531.	1.1	5
7188	Nitrogen-Treated Graphite and Oxygen Electroreduction on Pyridinic Edge Sites. Journal of Physical Chemistry C, 2009, 113, 6730-6734.	1.5	199
7189	Ferromagnetism in Semihydrogenated Graphene Sheet. Nano Letters, 2009, 9, 3867-3870.	4.5	771
7190	CaFeO₂: A New Type of Layered Structure with Iron in a Distorted Square Planar Coordination. Journal of the American Chemical Society, 2009, 131, 221-229.	6.6	89
7191	Microscopic origin of magnetism and magnetic interactions in ferropnictides. Physical Review B, 2009, 79, .	1.1	155
7192	Ab initioconstruction of interatomic potentials for uranium dioxide across all interatomic distances. Physical Review B, 2009, 80, .	1.1	19
7193	First-principles calculations of defects near a grain boundary in MgO. Physical Review B, 2009, 79, .	1.1	86
7194	Impact of Stoichiometry on the Hydrogen Storage Properties of LiNH₂â^'LiBH₄â^'MgH₂ Ternary Composites. Journal of Physical Chemistry C, 2009, 113, 2004-2013.	1.5	20
7195	Phase stability and pressure-induced structural transitions at zero temperature in ZnSiO₃and Zn₂SiO₄. Journal of Physics Condensed Matter, 2009, 21, 485801.	0.7	20
7196	Short-range order and Fe clustering in<mml:math xmlns:mml="http://www.w3.org/1998/Math/MathML" display="inline"><mml:mrow><mml:msub><mml:mrow><mml:mtext>Mg</mml:mtext></mml:mrow><mml:mrow><mml:mn>1-x</mml:mn></mml:mrow></mml:msub><mml:msub><mml:mrow><mml:mtext>Fe</mml:mtext></mml:mrow><mml:mrow><mml:mi>x</mml:mi></mml:mrow></mml:msub><mml:msub><mml:mrow><mml:mtext>SiO</mml:mtext></mml:mrow><mml:mrow><mml:mn>3</mml:mn></mml:mrow></mml:msub></mml:mrow></mml:math>at high pressure. Physical Review B, 2009, 80, .	1.1	44
7197	Strain-induced ferroelectricity in orthorhombic<mml:math xmlns:mml="http://www.w3.org/1998/Math/MathML" display="inline"><mml:mrow><mml:msub><mml:mrow><mml:mtext>CaTiO</mml:mtext></mml:mrow><mml:mrow><mml:mn>3</mml:mn></mml:mrow></mml:msub></mml:mrow></mml:math>from first principles. Physical Review B, 2009, 79, .	1.1	87
7198	Effect of In-Adlayer on AlN (0001) and (000â^'1) Polar Surfaces. Journal of Physical Chemistry C, 2009, 113, 10185-10188.	1.5	6
7199	Connections between the energy functional and interaction potentials for materials simulations. Physical Review B, 2009, 80, .	1.1	12
7200	Nonlinear elastic behavior of graphene:Ab initiocalculations to continuum description. Physical Review B, 2009, 80, .	1.1	364
7201	Monoclinic to tetragonal transformations in hafnia and zirconia: A combined calorimetric and density functional study. Physical Review B, 2009, 80, .	1.1	109
7202	Structure and diffusion of intrinsic defects, adsorbed hydrogen, and water molecules at the surface of alkali-earth fluorides calculated using density functional theory. Physical Review B, 2009, 80, .	1.1	32

#	Article	IF	Citations
7203	N-doped ZnO thin films and nanowires: energetics, impurity distribution and magnetism. New Journal of Physics, 2009, 11, 063035.	1.2	25
7204	First-principles study of defects and phase transition in UO₂. Journal of Physics Condensed Matter, 2009, 21, 435401.	0.7	71
7205	From bare Ge nanowire to Ge/Si core/shell nanowires: A first-principles study. Physical Review B, 2009, 80, .	1.1	39
7206	Ab initiolattice dynamics of MnO. Journal of Physics Condensed Matter, 2009, 21, 275402.	0.7	17
7207	LiSc(BH₄)₄ as a Hydrogen Storage Material: Multinuclear High-Resolution Solid-State NMR and First-Principles Density Functional Theory Studies. Journal of Physical Chemistry C, 2009, 113, 9956-9968.	1.5	71
7208	Noncollinear magnetism in manganese nanostructures. Physical Review B, 2009, 80, .	1.1	32
7209	Ab initiocalculations of second-, third-, and fourth-order elastic constants for single crystals. Physical Review B, 2009, 79, .	1.1	117
7210	The delicate electronic and magnetic structure of the LaFePnO system (Pnâ€‰=â€‰pnicogen). New Journal of Physics, 2009, 11, 025004.	1.2	47
7211	Unravelling the Nature of Gold Surface Sites by Combining IR Spectroscopy and DFT Calculations. Implications in Catalysis. Journal of Physical Chemistry C, 2009, 113, 16772-16784.	1.5	136
7212	Large-scaleab initiosimulations of binary transition metal clusters for storage media materials. Journal of Physics Condensed Matter, 2009, 21, 064228.	0.7	26
7213	Growth of boehmite particles in the presence of xylitol: morphology oriented by the nest effect of hydrogen bonding. Physical Chemistry Chemical Physics, 2009, 11, 11310.	1.3	53
7214	The structure, energetics and thermal evolution of SiGe nanotubes. Nanotechnology, 2009, 20, 315705.	1.3	20
7215	Density Functional Theory Comparison of Water Dissociation Steps on Cu, Au, Ni, Pd, and Pt. Journal of Physical Chemistry C, 2009, 113, 7269-7276.	1.5	257
7216	Adsorption Isotherm and Orientation of Alcohols on Hydrophilic SiO₂ under Ambient Conditions. Journal of Physical Chemistry C, 2009, 113, 10632-10641.	1.5	49
7217	Magnetism in undoped MgO studied by density functional theory. Physical Review B, 2009, 80, .	1.1	106
7218	Theoretical investigation of dinitrosyl complexes in Cu-zeolites as intermediates in deNOx process. Physical Chemistry Chemical Physics, 2009, 11, 1447.	1.3	29
7219	Concluding remarks. Faraday Discussions, 2009, 141, 467-475.	1.6	9
7220	Order and disorder in the wetting layer on Ru(0001). Faraday Discussions, 2009, 141, 231-249.	1.6	39

#	Article	IF	Citations
7221	Layered Titanium Oxide Nanosheet and Ultrathin Nanotubes: A First-Principles Prediction. Journal of Physical Chemistry C, 2009, 113, 13610-13615.	1.5	41
7222	Properties of metalâ€“water interfaces studied from first principles. New Journal of Physics, 2009, 11, 125003.	1.2	284
7223	Effect of lateral contraction and magnetism on the energy release upon fracture in metals: First-principles computational tensile tests. Physical Review B, 2009, 79, .	1.1	51
7224	Active Sites for H₂Adsorption and Activation in Au/TiO₂and the Role of the Support. Journal of Physical Chemistry A, 2009, 113, 3750-3757.	1.1	142
7225	Crystal, spin, and electronic structure of the superconductor LiFeAs. Physical Review B, 2009, 80, .	1.1	21
7226	Density functional study of excess Fe in<mml:math xmlns:mml="http://www.w3.org/1998/Math/MathML" display="inline"><mml:mrow><mml:msub><mml:mrow><mml:mtext>Fe</mml:mtext></mml:mrow><mml:mrow><mml:mn>1</mml:mn> Magnetism and doping. Physical Review B, 2009, 79, .	1.1	156
7227	First-principles determination of crystal structures, phase stability, and reaction thermodynamics in the Li-Mg-Al-H hydrogen storage system. Physical Review B, 2009, 79, .	1.1	50
7228	The interaction of oxygen vacancies with grain boundaries in monoclinic HfO2. Applied Physics Letters, 2009, 95, .	1.5	178
7229	Effects of pressure on the electronic and structural properties of LaOFeAs. Journal of Applied Physics, 2009, 106, 073910.	1.1	9
7230	Hydrogen interactions with acceptor impurities in<mml:math xmlns:mml="http://www.w3.org/1998/Math/MathML" display="inline"><mml:mrow><mml:msub><mml:mrow><mml:mtext>SnO</mml:mtext></mml:mrow><mml:mrow><mml:mn>2</mml:mn></mml: First-principles calculations. Physical Review B, 2009, 79, .	1.1	63
7231	Ternary cobalt spinel oxides for solar driven hydrogen production: Theory and experiment. Energy and Environmental Science, 2009, 2, 774.	15.6	60
7232	Comparative Studies on the Phase Stability, Electronic Structure, and Topology of the Charge Density in the Li3XO4 (X = P, As, V) Lithium Orthosalt Polymorphs. Chemistry of Materials, 2009, 21, 1861-1874.	3.2	18
7233	Role of Coverage and Surface Oxidation Degree in the Adsorption of Acetone on TiO₂(110). A Density Functional Study. Journal of Physical Chemistry C, 2009, 113, 19973-19980.	1.5	24
7234	Conductance of Conjugated Molecular Wires: Length Dependence, Anchoring Groups, and Band Alignment. Journal of Physical Chemistry C, 2009, 113, 20967-20973.	1.5	52
7235	Molecular models and simulations of layered materials. Journal of Materials Chemistry, 2009, 19, 2470.	6.7	244
7236	New Metallic Carbon Crystal. Physical Review Letters, 2009, 102, 055703.	2.9	119
7237	Tunable Ferromagnetic Spin Ordering in Boron Nitride Nanotubes with Topological Fluorine Adsorption. Journal of the American Chemical Society, 2009, 131, 6874-6879.	6.6	85
7238	Structures and Stabilities of Pb_n (n â‰ 20) Clusters. Journal of Physical Chemistry A, 2009, 113, 6217-6221.	1.1	37

#	Article	IF	Citations
7239	Theoretical study of PTCDA adsorbed on the coinage metal surfaces, Ag(111), Au(111) and Cu(111). New Journal of Physics, 2009, 11, 053010.	1.2	182
7240	Finite-temperature Anisotropic Elastic Properties of Ni-Mn-In Magnetic Shape Memory Alloy. Materials Research Society Symposia Proceedings, 2009, 1200, 63.	0.1	0
7241	First-principles computational discovery of materials for hydrogen storage. Journal of Physics: Conference Series, 2009, 180, 012076.	0.3	11
7242	Elucidating the Bimodal Acidâ^'Base Behavior of the Waterâ^'Silica Interface from First Principles. Journal of the American Chemical Society, 2009, 131, 18358-18365.	6.6	214
7243	Screened hybrid density functionals for solid-state chemistry and physics. Physical Chemistry Chemical Physics, 2009, 11, 443-454.	1.3	384
7244	Dynamics of liquid and undercooled silicon: Anab initiomolecular dynamics study. Physical Review B, 2009, 79, .	1.1	30
7245	First-principles investigation on bonding formation and electronic structure of metal-graphene contacts. Applied Physics Letters, 2009, 94, .	1.5	99
7246	Adsorption and diffusion ofSCH3radicals andAu(SCH3)2complexes on the unreconstructed Au(111) surface in the submonolayer coverage regime. Physical Review B, 2009, 79, .	1.1	18
7247	Effects of hydrogen chemisorption on the structure and deformation of single-walled carbon nanotubes. Applied Physics Letters, 2009, 94, .	1.5	25
7248	Double Metallocene Nanowires. Journal of the American Chemical Society, 2009, 131, 14246-14248.	6.6	61
7249	Magnetic properties of transition-metal-doped<mml:math xmlns:mml="http://www.w3.org/1998/Math/MathML"		

#	Article	IF	Citations
7257	Neutral and Anionic Gold Decamers: Planar Structure with Unusual Spatial Charge-Spin Separation. Journal of Chemical Theory and Computation, 2009, 5, 1216-1223.	2.3	32
7258	Parametrization of a reactive force field for aluminum hydride. Journal of Chemical Physics, 2009, 131, 044501.	1.2	35
7259	Electronic Structure and Reactivity of Boron Nitride Nanoribbons with Stone-Wales Defects. Journal of Chemical Theory and Computation, 2009, 5, 3088-3095.	2.3	127
7260	Doping Effect on High-Pressure Structural Stability of ZnO Nanowires. Journal of Physical Chemistry C, 2009, 113, 1164-1167.	1.5	22
7261	First-principles study of diffusion of Li, Na, K and Ag in ZnO. Journal of Physics Condensed Matter, 2009, 21, 345802.	0.7	45
7262	Visible Light-Induced Efficient Contaminant Removal by Bi₅O₇I. Environmental Science & Technology, 2009, 43, 2005-2010.	4.6	233
7263	First-principles study of zinc oxide honeycomb structures. Physical Review B, 2009, 80, .	1.1	298
7264	Ab initiodensity functional calculations of ferromagnetism in low-dimensional nanostructures: From nanowires to nanorods. Physical Review B, 2009, 79, .	1.1	24
7265	Implementing and testing the AM05 spin density functional. Physical Review B, 2009, 79, .	1.1	108
7266	Magnetization of graphane by dehydrogenation. Applied Physics Letters, 2009, 95, .	1.5	110
7267	First principles study of the photo-oxidation of water on tungsten trioxide (WO3). Journal of Chemical Physics, 2009, 130, 114701.	1.2	105
7268	Interfacial Electron Transfer in TiO₂ Surfaces Sensitized with Ru(II)â^'Polypyridine Complexes. Journal of Physical Chemistry A, 2009, 113, 12532-12540.	1.1	80
7269	Structural Properties of Tetra-tert-butyl Zinc(II) Phthalocyanine Isomers on a Au(111) Surface. Journal of Physical Chemistry C, 2009, 113, 11223-11227.	1.5	18
7270	Ab-initio simulation of the tensile strength of silicon nanofilms. International Journal of Materials Research, 2009, 100, 822-825.	0.1	0
7271	Thermodynamic and Mechanical Stabilities of Tantalum Nitride. Physical Review Letters, 2009, 103, 185501.	2.9	68
7272	Electrostatic Potential Derived Atomic Charges for Periodic Systems Using a Modified Error Functional. Journal of Chemical Theory and Computation, 2009, 5, 2866-2878.	2.3	281
7273	Structure and stability of high pressure synthesized Mgâ€“TM hydrides (TM = Ti, Zr, Hf, V, Nb and Ta) as possible new hydrogen rich hydrides for hydrogen storage. Journal of Materials Chemistry, 2009, 19, 8150.	6.7	77
7274	On the difficulties of present theoretical models to predict the oxidation state of atomic Au adsorbed on regular sites of CeO[sub 2](111). Journal of Chemical Physics, 2009, 131, 094702.	1.2	64

#	Article	IF	Citations
7275	Realistic adsorption geometries and binding affinities of metal nanoparticles onto the surface of carbon nanotubes. Applied Physics Letters, 2009, 94, .	1.5	27
7276	Functionalized heterofullerenes for hydrogen storage. Applied Physics Letters, 2009, 94, .	1.5	89
7277	Proton diffusion pathways and rates in Y-doped BaZrO3 solid oxide electrolyte from quantum mechanics. Journal of Chemical Physics, 2009, 130, 194707.	1.2	75
7278	Optical spin control in nanocrystalline magnetic nanoswitches. Applied Physics Letters, 2009, 95, 043111.	1.5	8
7279	Crossover between multipole Coulomb and Kubas interactions in hydrogen adsorption on metal-graphene complexes. Physical Review B, 2009, 79, .	1.1	92
7280	Strain effects in group-III nitrides: Deformation potentials for AlN, GaN, and InN. Applied Physics Letters, 2009, 95, .	1.5	151
7281	Density Functional Characterization of the Visible-Light Absorption in Substitutional C-Anion- and C-Cation-Doped TiO₂. Journal of Physical Chemistry C, 2009, 113, 2624-2629.	1.5	166
7282	Magnetic ordering in the frustrated Heisenberg chain system cupric chloride<mml:math xmlns:mml="http://www.w3.org/1998/Math/MathML" display="inline"><mml:mrow><mml:msub><mml:mrow><mml:mtext>CuCl</mml:mtext></mml:mrow><mml:mn>2</mml:mn></mml	1.1	102
7283	The use of nanometer-sized hydrographene species for support material for fuel cell electrode catalysts: a theoretical proposal. Physical Chemistry Chemical Physics, 2009, 11, 8275.	1.3	76
7284	Ultrathin oxide films and heterojunctions: CaO layers on BaO and SrO. Physical Chemistry Chemical Physics, 2009, 11, 3217.	1.3	4
7285	Chemical Bonding and Schottky Barrier for Metal-Carbon Nanotube Contacts. , 2009, , .		1
7286	Synthesis, characterization and computational simulation of visible-light irradiated fluorine-doped titanium oxide thin films. Journal of Materials Chemistry, 2009, 19, 6907.	6.7	38
7287	Electronic charge transfer between ceria surfaces and gold adatoms: a GGA+U investigation. Physical Chemistry Chemical Physics, 2009, 11, 5246.	1.3	83
7288	Thickness Dependence of the Effective Masses in a Strained Thin Silicon Film. , 2009, , .		3
7289	Î±-CrCl₂ under Pressure: Prediction of a Metallic Phase Transition. Journal of Physical Chemistry A, 2009, 113, 12022-12027.	1.1	1
7290	DFT Investigation of Intermediate Steps in the Hydrolysis of Î±-Al₂O₃(0001). Journal of Physical Chemistry C, 2009, 113, 2149-2158.	1.5	81
7291	First-Principles Study of S Doping at the Rutile TiO₂ (110) Surface. Journal of Physical Chemistry C, 2009, 113, 17464-17470.	1.5	19
7292	First-principles study of the structural, electronic, vibrational, and elastic properties of orthorhombic NiSi. Physical Review B, 2009, 79, .	1.1	202

#	Article	IF	Citations
7293	Strontium Substitution in Bioactive Calcium Phosphates: A First-Principles Study. Journal of Physical Chemistry B, 2009, 113, 3584-3589.	1.2	52
7294	Effect of Cr substitution on the electronic structure of<mml:math xmlns:mml="http://www.w3.org/1998/Math/MathML" display="inline"><mml:mrow><mml:msub><mml:mrow><mml:mtext>CuAl</mml:mtext></mml:mrow><mml:mrow><mml:mn>1</mml:mn> Physical Review B, 2009, 79, .	1.1	116
7295	Investigation of the Interaction of Water with the Calcite (10.4) Surface Using Ab Initio Simulation. Journal of Physical Chemistry C, 2009, 113, 7207-7212.	1.5	83
7296	Gold nanoparticles under gas pressure. Physical Chemistry Chemical Physics, 2009, 11, 4145.	1.3	23
7297	First-Principles Study of the Potential Step in Metal/Graphene Contact. , 2009, , .		0
7298	Covalent-adsorption induced magnetism in graphene. Journal of Materials Chemistry, 2009, 19, 9274.	6.7	58
7299	Direct minimization technique for metals in density functional theory. Physical Review B, 2009, 79, .	1.1	47
7300	Optical properties of pseudobinary GeTe,<mml:math xmlns:mml="http://www.w3.org/1998/Math/MathML" display="inline"><mml:mrow><mml:msub><mml:mrow><mml:mtext>Ge</mml:mtext></mml:mrow><mml:mrow><mml:mn>2</mml:mn></mml:mrow><mml:mi></mml:mi></mml:msub></mml:mrow></mml:math><mml:math xmlns:mml="http://www.w3.org/1998/Math/MathML" display="inline"><mml:mrow><mml:msub><mml:mrow><mml:mn></mml:mn> Physical Review B, 2009, 80, .	1.1	128
7301	Vibrational properties of MgZn2. Zeitschrift Fur Kristallographie - Crystalline Materials, 2009, 224, .	0.4	6
7302	The Linear Combination of Bulk Bands-Method for Electron and Hole Subband Calculations in Strained Silicon Films and Surface Layers. , 2009, , .		2
7303	Polynitrogen/Nanoaluminum Surface Interactions. , 2009, , .		0
7304	Heterojunctions between metals and carbon nanotubes as ultimate nanocontacts. Proceedings of the National Academy of Sciences of the United States of America, 2009, 106, 4591-4595.	3.3	110
7305	A new phase in the decomposition of Mg(BH4)2: first-principles simulated annealing. Journal of Materials Chemistry, 2009, 19, 7081.	6.7	27
7306	Theoretical investigation of atomic and electronic structures of<mml:math xmlns:mml="http://www.w3.org/1998/Math/MathML" display="inline"><mml:mrow><mml:msub><mml:mrow><mml:mtext>Ga</mml:mtext></mml:mrow><mml:mrow><mml:mn>2</mml:mn></mml:mrow></mml:msub></mml:mrow></mml:math> Physical Review B, 2009, 80, .	1.1	27
7307	Bis(terpyridine)-based surface template structures on graphite: a force field and DFT study. Physical Chemistry Chemical Physics, 2009, 11, 8867.	1.3	29
7308	Corrugated layered heptazine-based carbon nitride: the lowest energy modifications of C3N4 ground state. Journal of Materials Chemistry, 2009, 19, 3013.	6.7	122
7309	Cisâ€“trans conversion of the CH3Sâ€“Auâ€“SCH3 complex on Au(111). Physical Chemistry Chemical Physics, 2009, 11, 8601.	1.3	20
7310	Nanoporous In-MOF with multiple one-dimensional pores. Chemical Communications, 2009, , 4953.	2.2	53

#	Article	IF	Citations
7311	Acetone on silicon (001): ambiphilic molecule meets ambiphilic surface. Physical Chemistry Chemical Physics, 2009, 11, 2747.	1.3	20
7312	A computational study of electronic structure, thermodynamics and kinetics of hydrogen desorption from Al- and Si-doped Î±-, Î³-, and Î²-MgH2. Journal of Materials Chemistry, 2009, 19, 4348.	6.7	32
7313	The electronic structure and ionic diffusion of nanoscale LiTiO2 anatase. Physical Chemistry Chemical Physics, 2009, 11, 5742.	1.3	130
7314	Computational identification of a metal organic framework for high selectivity membrane-based CO2/CH4 separations: Cu(hfipbb)(H2hfipbb)0.5. Physical Chemistry Chemical Physics, 2009, 11, 11389.	1.3	83
7315	Structural transformation of grains and grain boundaries with introducing boron atoms into CoPtCr magnetic layer investigated by ultrasoft pseudopotential calculation and transmission electron microscopy analysis. Journal of Applied Physics, 2009, 105, 063530.	1.1	0
7316	Local condensation around oxygen vacancies in t-LaNbO4 from first principles calculations. Physical Chemistry Chemical Physics, 2009, 11, 5550.	1.3	24
7317	Modelling nanoscale FeS2 formation in sulfur rich conditions. Journal of Materials Chemistry, 2009, 19, 3389.	6.7	37
7318	Ferromagnetism of undoped GaN mediated by through-bond spin polarization between nitrogen dangling bonds. Applied Physics Letters, 2009, 94, 162505.	1.5	112
7319	Oxidation of Al doped Au clusters: A first principles study. Journal of Chemical Physics, 2009, 130, 234309.	1.2	20
7320	A density functional study of the high-pressure chemistry of MSiN₂(M = Be, Mg, Ca): prediction of high-pressure phases and examination of pressure-induced decomposition. Journal of Physics Condensed Matter, 2009, 21, 275407.	0.7	19
7321	Site preference of Eu2+ dopants in the (Ba,Sr)13â^'xAl22â^'2xSi10+2xO66 phosphor and its effect on the luminescence properties: a density functional investigation. Journal of Materials Chemistry, 2009, 19, 9170.	6.7	13
7322	The interplay of van der Waals and weak chemical forces in the adsorption of salicylic acid on NaCl(001). Physical Chemistry Chemical Physics, 2009, 11, 9337.	1.3	10
7323	Multinuclear gallium-oxide cations in high-silica zeolites. Physical Chemistry Chemical Physics, 2009, 11, 2893.	1.3	50
7324	Metal fragment isomerisation upon grafting a d2 ML4 perhydrocarbyl Os complex on a silica surface: origin and consequence. Dalton Transactions, 2009, , 5879.	1.6	16
7325	Theoretical study of hydrogen dissociative adsorption on strained pseudomorphic monolayers of Cu and Pd deposited onto a Ru(0001) substrate. Physical Chemistry Chemical Physics, 2009, 11, 7303.	1.3	27
7326	KAgF3, K2AgF4 and K3Ag2F7: important steps towards a layered antiferromagnetic fluoroargentate(II),. CrystEngComm, 2009, 11, 1702.	1.3	38
7327	Beryllium doping of GaAs and GaAsN studied from first principles. Physical Review B, 2009, 79, .	1.1	27
7328	Interaction between hydrogen molecules and metallofullerenes. Journal of Chemical Physics, 2009, 131, 064707.	1.2	22

#	Article	IF	Citations
7329	Anharmonic OH vibrations in Mg(OH)2 (brucite): Two-dimensional calculations and crystal-induced blueshift. Journal of Chemical Physics, 2009, 131, 244517.	1.2	17
7330	Influence of nitrogen doping on the radial breathing mode in carbon nanotubes. Physical Review B, 2009, 79, .	1.1	22
7331	Structure, reactivity, and electronic properties of V-doped Co clusters. Physical Review B, 2009, 80, .	1.1	33
7333	Environmental Fate and Transport of Energetic Materials. , 2009, , .		0
7334	First-principles investigation of organic semiconductors for thermoelectric applications. Journal of Chemical Physics, 2009, 131, 224704.	1.2	68
7335	Theoretical investigations ofLaOFePn(Pn=P, As and Sb). Physica B: Condensed Matter, 2009, 404, 3242-3245.	1.3	1
7336	Thermodynamic properties of PbTe, PbSe, and PbS: First-principles study. Physical Review B, 2009, 80, .	1.1	231
7337	H-Spillover through the Catalyst Saturation: An Ab Initio Thermodynamics Study. ACS Nano, 2009, 3, 1657-1662.	7.3	127
7338	Hydrogen storage in Alâ€“N cage based nanostructures. Applied Physics Letters, 2009, 94, .	1.5	20
7339	Electronic Structure of Few-Layer Epitaxial Graphene on Ru(0001). Nano Letters, 2009, 9, 2654-2660.	4.5	219
7340	Magnetoelectric Effect in Graphene Nanoribbons on Substrates via Electric Bias Control of Exchange Splitting. Physical Review Letters, 2009, 103, 187204.	2.9	71
7341	Ab initiostudy of the high-pressure phases and dynamical properties of ZnAl₂O₄and ZnGa₂O₄. High Pressure Research, 2009, 29, 573-577.	0.4	9
7342	A theoretical study on the interaction of aromatic amino acids with graphene and single walled carbon nanotube. Journal of Chemical Physics, 2009, 130, 124911.	1.2	251
7343	Theory of doping properties of Ag acceptors in ZnO. Physical Review B, 2009, 80, .	1.1	84
7344	Electronic and crystal-field effects in the fine structure of electron energy-loss spectra of manganites. Physical Review B, 2009, 79, .	1.1	32
7345	Density Functional Theory Study of Finite Carbon Chains. ACS Nano, 2009, 3, 3788-3794.	7.3	56
7346	R₅Pn₃-type Phases of the Heavier Trivalent Rare-Earth-Metal Pnictides (Pn = Sb,) Tj ETQq0 0 0 rgBT /Overlock Inorganic Chemistry, 2009, 48, 4362-4371.	1.9	11
7347	Formation of a coplanar Oâ€“Al bonding cluster: the effect of O impurity on a Î£ = 5 NiAl grain boundary from first-principles. Journal of Physics Condensed Matter, 2009, 21, 015002.	0.7	10

#	Article	IF	Citations
7348	Changing the physical and chemical properties of titanium oxynitrides<mml:math xmlns:mml="http://www.w3.org/1998/Math/MathML" display="inline"><mml:mrow><mml:msub><mml:mrow><mml:mtext>TiN</mml:mtext></mml:mrow><mml:mrow><mml:mn>1</mml:m changing the composition. Physical Review B, 2009, 80, .	1.1	48
7349	Interactions between co-adsorbed CO and H on a Rh(100) single crystal surface. Physical Chemistry Chemical Physics, 2009, 11, 10009.	1.3	21
7350	First-principles study of the interaction and charge transfer between graphene and metals. Physical Review B, 2009, 79, .	1.1	1,064
7351	Electronic and elastic properties of CaF₂under high pressure fromab initiocalculations. Journal of Physics Condensed Matter, 2009, 21, 415501.	0.7	23
7352	Development of empirical bond-order-type interatomic potential for amorphous carbon structures. Journal of Applied Physics, 2009, 105, 064310.	1.1	19
7353	Tight-Binding Molecular Dynamics for Carbon and Applications to Nanostructure Formation. , 2009, , 9137-9158.		0
7354	Magnetism of chromia from first-principles calculations. Physical Review B, 2009, 79, .	1.1	74
7355	Vacancy-assisted diffusion mechanism of group-III elements in ZnO: An ab initio study. Journal of Applied Physics, 2009, 105, 073504.	1.1	18
7356	Magnetic structure and ferroelectric polarization of<mml:math xmlns:mml="http://www.w3.org/1998/Math/MathML" display="inline"><mml:mrow><mml:msub><mml:mrow><mml:mtext>MnWO</mml:mtext></mml:mrow><mml:mn>4</mml:mn></mml by density functional calculations and classical spin analysis. Physical Review B, 2009, 80, .	1.1	34
7357	Effects of Na-substitution on structural and electronic properties of Li2CoSiO4 cathode material. Transactions of Nonferrous Metals Society of China, 2009, 19, 182-186.	1.7	24
7358	Density functional theory study on hydrogenation mechanism in catalyst-activated Mg(0001) surface. Transactions of Nonferrous Metals Society of China, 2009, 19, 383-388.	1.7	14
7359	First-principles study for surface tension and depolarizing effect on ferroelectric properties of BaTiO3 nanowires. Transactions of Nonferrous Metals Society of China, 2009, 19, 1634-1638.	1.7	4
7360	First-Principles Study of Electron Transport through the Single-Molecule Magnet<mml:math xmlns:mml="http://www.w3.org/1998/Math/MathML" display="inline"><mml:msub><mml:mi>Mn</mml:mi><mml:mn>12</mml:mn></mml:msub></mml:math>. Physical Review Letters, 2009, 102, 246801.	2.9	77
7361	Ab initioup to the melting point: Anharmonicity and vacancies in aluminum. Physical Review B, 2009, 79, .	1.1	232
7362	Site preference of Fe atoms in<mml:math xmlns:mml="http://www.w3.org/1998/Math/MathML" display="inline"><mml:mrow><mml:msub><mml:mrow><mml:mtext>FeMgSiO</mml:mtext></mml:mrow><mml:mn>4</mml:mn></mml:mr xmlns:mml="http://www.w3.org/1998/Math/MathML" display="inline"><mml:mrow><mml:mtext>FeMg</mml:mtext><mml:msub><mml:mrow><mml:mrow><mml:mo>(</mml:mo><mml:mr Physical Review B, 2009, 79, .	1.1	21
7363	Silicon Surface with Giant Spin Splitting. Physical Review Letters, 2009, 103, 046803.	2.9	196
7364	Phase stability of the rare-earth sesquioxides under pressure. Physical Review B, 2009, 80, .	1.1	32
7365	Epitaxial film growth and optoelectrical properties of layered semiconductors, LaMnXO (X=P, As, and) Tj ETQq1 1 0.784314 rgBT /Ove	1.1	33

#	Article	IF	Citations
7366	A Strain-Driven Morphotropic Phase Boundary in BiFeO ₃. Science, 2009, 326, 977-980.	6.0	1,065
7367	Scintillation properties of Eu²⁺-activated barium fluoroiodide. , 2009, , .		2
7368	Mechanism for tautomerization induced conductance switching of naphthalocyanin molecule. Applied Physics Letters, 2009, 95, 182103.	1.5	21
7369	Kinetic Monte Carlo simulations of surface growth during plasma deposition of silicon thin films. Journal of Chemical Physics, 2009, 131, 034503.	1.2	18
7370	Non-self-consistent Density-Functional Theory Exchange-Correlation Forces for GGA Functionals. Journal of Chemical Theory and Computation, 2009, 5, 1499-1505.	2.3	12
7371	Oxygen-vacancy-induced ferromagnetism in<mml:math xmlns:mml="http://www.w3.org/1998/Math/MathML" display="inline"><mml:mrow><mml:msub><mml:mrow><mml:mtext>CeO</mml:mtext></mml:mrow><mml:mn>2</mml:mn></mml:msub></mml:mrow></mml:math>: first principles. Physical Review B, 2009, 79, .	1.1	105
7372	Design of quaternary chalcogenide photovoltaic absorbers through cation mutation. , 2009, , .		7
7373	A Computational Study on the Adsorption Configurations and Reactions of Phosphorous Acid on TiO₂ Anatase (101) and Rutile (110) Surfaces. Journal of Physical Chemistry C, 2009, 113, 8394-8406.	1.5	12
7374	Correlating Acid Properties and Catalytic Function: A First-Principles Analysis of Alcohol Dehydration Pathways on Polyoxometalates. Journal of Physical Chemistry C, 2009, 113, 1872-1885.	1.5	110
7375	Iron substitution in CdSe nanoparticles: Magnetic and optical properties. Physical Review B, 2009, 80, .	1.1	56
7376	Origin of Nanoscale Phase Stability Reversals in Titanium Oxide Polymorphs. Journal of Physical Chemistry C, 2009, 113, 4240-4245.	1.5	62
7377	Deriving Carbon Atomic Chains from Graphene. Physical Review Letters, 2009, 102, 205501.	2.9	571
7378	Structure and electronic properties of iron oxide clusters: A first-principles study. Physical Review B, 2009, 80, .	1.1	40
7379	Ca-Coated Boron Fullerenes and Nanotubes as Superior Hydrogen Storage Materials. Nano Letters, 2009, 9, 1944-1948.	4.5	165
7380	Pressure dependence of the Curie temperature in bcc iron studied byab initiosimulations. Physical Review B, 2009, 79, .	1.1	49
7381	Dissociation and Diffusion of Hydrogen on the Mg(0001) Surface: Catalytic Effect of V and Ni Double Substitution. Journal of Physical Chemistry C, 2009, 113, 10574-10579.	1.5	26
7382	Twofold Coordinated Ground-State and Eightfold High-Pressure Phases of Heavy Transition Metal Nitrides MN₂ (M = Os, Ir, Ru, and Rh). Inorganic Chemistry, 2009, 48, 9904-9909.	1.9	47
7383	Density Functional Study of Calcium Nitride: Refined Geometries and Prediction of High-Pressure Phases. Journal of Physical Chemistry C, 2009, 113, 2943-2949.	1.5	13

#	Article	IF	Citations
7384	Density Functional Investigations of Defect-Induced Mid-Gap States in Graphane. Journal of Physical Chemistry C, 2009, 113, 21063-21067.	1.5	40
7385	Hydrogen Bonding and Vibrational Spectra in Kaolinite-Dimethylsulfoxide and -Dimethylselenoxide Intercalatesâ€“A Solid-State Computational Study. Clays and Clay Minerals, 2009, 57, 54-71.	0.6	20
7386	Anab initiostudy of the interaction between an iron atom and graphene containing a single Stoneâ€“Wales defect. Journal of Physics Condensed Matter, 2009, 21, 485506.	0.7	16
7387	Topological description of the Stone-Wales defect formation energy in carbon nanotubes and graphene. Physical Review B, 2009, 79, .	1.1	83
7388	Origin of p-Type Doping in Zinc Oxide Nanowires Induced by Phosphorus Doping: A First Principles Study. Journal of Physical Chemistry C, 2009, 113, 9541-9545.	1.5	26
7389	Adsorption of atomic nitrogen and oxygen on mathrm {ZnO(2ar {1} ar {1}0)} surface: a density functional theory study. Journal of Physics Condensed Matter, 2009, 21, 144208.	0.7	13
7390	Stabilization of Square Planar Silicon: A New Building Block for Conjugated Si-Containing Systems. Journal of Physical Chemistry A, 2009, 113, 707-712.	1.1	14
7391	Ab initio ab initio investigation of phase stability of <mml:math xmlns:mml="http://www.w3.org/1998/Math/MathML" display="inline"><mml:mrow><mml:msub><mml:mtext>Y</mml:mtext><mml:mn>2</mml:mn></mml:msub><mml:msub><mml:mrow> xmlns:mml="http://www.w3.org/1998/Math/MathML" display="inline"><mml:mrow><mml:msub><mml:mtext>Y</mml:mtext><mml:mn>2</mml:mn></mml:msub><mml:msub><mml:mrow> Physical Review B, 2009, 80, .	1.1	48
7392	Growth of Semiconducting Graphene on Palladium. Nano Letters, 2009, 9, 3985-3990.	4.5	307
7393	Electromagnetic properties of undoped LaFePnO (Pn= P, As). Journal of Physics: Conference Series, 2009, 150, 052090.	0.3	3
7394	Vacancy trapping by solute atoms during quenching in Cu-based dilute alloys studied by positron annihilation spectroscopy. Journal of Physics: Conference Series, 2009, 191, 012019.	0.3	4
7395	Another way of looking at bonding on bimetallic surfaces: the role of spin polarization of surface metal d states. Journal of Physics Condensed Matter, 2009, 21, 492201.	0.7	9
7397	First-principles studies on organic electronic materials. EPJ Applied Physics, 2009, 46, 12511.	0.3	8
7398	First Principles Calculations of Vacancy Formation Energies in Σ13 Pyramidal Twin Grain Boundary of α-Al₂O₃. Materials Transactions, 2009, 50, 1019-1022.	0.4	19
7399	Local Electronic and Atomic Structure of Ce³⁺-Containing Fluoride/Oxide Determined by TEM-EELS and First-Principles Calculations. Materials Transactions, 2009, 50, 952-958.	0.4	7
7400	First Principles Calculations of Vibrational Free Energy Estimated by the Quasi-Harmonic Approximation. Nippon Kinzoku Gakkaishi/Journal of the Japan Institute of Metals, 2009, 73, 566-570.	0.2	2
7401	Formation Energies of Substitutional Sodium and Potassium in Hydroxyapatite. Materials Transactions, 2009, 50, 1041-1045.	0.4	25
7402	Formation of Atomistic Island in Al Film Growth by Kinetic Monte Carlo. Journal of Computational Science and Technology, 2009, 3, 148-158.	0.4	0

#	Article	IF	Citations
7403	First Principles Calculations on Electron Conduction Paths in Solid Electrolytes: Toward an Understanding of the Working Mechanism of Atomic Switches. Nippon Kinzoku Gakkaishi/Journal of the Japan Institute of Metals, 2009, 73, 577-582.	0.2	0
7404	Dislocation Properties and Peierls Stress of BCC Iron Based on Generalized-Stacking-Fault Energy Surface by Using First Principles Calculations. Nippon Kinzoku Gakkaishi/Journal of the Japan Institute of Metals, 2009, 73, 595-600.	0.2	8
7405	Conduction-Band Structures of Wurtzite ZnO Solid Solutions by First Principles Calculations. Materials Transactions, 2009, 50, 1067-1070.	0.4	6
7406	First Principles Lattice Dynamics Calculations of Ag⁺ Doped KX (X=Cl, Br and I). Materials Transactions, 2009, 50, 999-1003.	0.4	0
7407	A density functional theory study of the correlation between analyte basicity, ZnPc adsorption strength, and sensor response. Journal of Chemical Physics, 2009, 130, 204307.	1.2	20
7408	Crystal structure determination of N,Nâ€²-1,4-phenylene-bis(3-oxobutanamide) from laboratory powder diffraction data. Zeitschrift FÃ¼r Kristallographie, 2009, 224, 593-597.	1.1	1
7409	AUTOCATALYTIC DECOMPOSITION AT SHEAR-STRAIN INTERFACES. , 2009, , .		0
7410	Effect of hydrogen on stability of vacancy in LaNi₅. Journal of Physics: Conference Series, 2009, 165, 012043.	0.3	2
7411	Theoretical Reinvestigation of the Electronic Structure of CuNCN: the Influence of Packing on the Magnetic Properties. Journal of Physical Chemistry C, 2009, 113, 18891-18896.	1.5	22
7412	Influence of Hydrogen on Growth of Carbon Nanotubes. Materials Research Society Symposia Proceedings, 2009, 1204, 1.	0.1	0
7413	Effects of charged surface states on Sb ad-dimer rotation on Si(001). Europhysics Letters, 2009, 86, 36003.	0.7	1
7414	Stable structure and effects of the substrate Ti pre-treatment on the epitaxial growth of SrTiO ₃ on GaAs. Europhysics Letters, 2009, 86, 46008.	0.7	15
7415	Arrangement of La and vacancies in La2/3TiO3 predicted by first-principles density functional calculation with cluster expansion and Monte Carlo simulation. Journal of the Ceramic Society of Japan, 2009, 117, 911-916.	0.5	17
7416	Density-Functional-Theory-Based Finite-Element Analysis of Diamond Single Crystal. Journal of Solid Mechanics and Materials Engineering, 2009, 3, 541-551.	0.5	3
7417	The Role of Ferromagnetic Substrate in the Reactivity of Pt/Fe Overlayer: A Density Functional Theory Study. Journal of the Physical Society of Japan, 2009, 78, 064603.	0.7	12
7418	Physical and Chemical Properties of Oxygen at Vanadium and Molybdenum Oxide Surfaces: Theoretical Case Studies. , 0, , 375-415.		0
7419	SIMULATING STRUCTURE AND PHYSICAL PROPERTIES OF COMPLEX METALLIC ALLOYS. Book Series on Complex Metallic Alloys, 2009, , 291-329.	0.1	1
7420	Stability of Three-Hydrogen Clusters on Graphene. Journal of the Physical Society of Japan, 2009, 78, 035002.	0.7	13

#	Article	IF	Citations
7421	EFFECT OF DEFECTS ON INITIATION OF CHEMISTRY IN HMX. , 2009, , .		0
7422	Structural stability and decomposition of Mg(BH₄)₂isomorphsâ€"anab initiofree energy study. Journal of Physics Condensed Matter, 2009, 21, 012203.	0.7	57
7423	Electronic confinement effects and optical properties of multilayer slabs of silicon: numerical model studies. , 2009, , .		2
7424	Structure and electrical properties of [0001] GaN nanowires. Proceedings of SPIE, 2009, , .	0.8	2
7425	Photoinduced Conductivity of a Porphyrinâ^'Gold Composite Nanowire. Journal of Physical Chemistry A, 2009, 113, 4549-4556.	1.1	37
7426	Making Mn Substitutional Impurities in InAs using a Scanning Tunneling Microscope. Nano Letters, 2009, 9, 4333-4337.	4.5	11
7427	The equation of state of B2-type NaCl. Journal of Physics: Conference Series, 2010, 215, 012196.	0.3	15
7428	Modelling of the microstructure and properties in the length scales varying from nano- to macroscopic. Bulletin of the Polish Academy of Sciences: Technical Sciences, 2010, 58, .	0.8	2
7429	Electronic structures and stability of Ag-In-Ca surfaces. Journal of Physics: Conference Series, 2010, 226, 012030.	0.3	5
7430	Mn doping in model amorphous Si and Ge: A theoretical investigation. Journal of Physics: Conference Series, 2010, 200, 032014.	0.3	2
7431	Alternating layers of plutonium and lead or indium as surrogate for plutonium. IOP Conference Series: Materials Science and Engineering, 2010, 9, 012098.	0.3	0
7432	Structural model of quasiperiodic Pb monolayer deposited on fivefold i-Al-Pd-Mn surface. Journal of Physics: Conference Series, 2010, 226, 012005.	0.3	3
7433	Possible formation of crystalline sodium carbene carbonate Na₂(CO)CO₃at high pressure. Journal of Physics: Conference Series, 2010, 215, 012129.	0.3	0
7434	Ab Initio Calculations of Crystalline and Amorphous In2Se3 Compounds for Chalcogenide Phase Change Memory. Materials Research Society Symposia Proceedings, 2010, 1251, 34.	0.1	0
7435	First-principles Study of Back Contact Effects on CdTe Thin Film Solar Cells. Materials Research Society Symposia Proceedings, 2010, 1268, 1.	0.1	0
7436	Modeling giant planets and brown dwarfs. Proceedings of the International Astronomical Union, 2010, 6, 473-474.	0.0	1
7437	Electronic work function of the Cu (100) surface under different strain states. Europhysics Letters, 2010, 89, 66004.	0.7	19
7438	Interactions of Defects and Domain Walls in LiNbO₃â€" Insights from Simulations. IOP Conference Series: Materials Science and Engineering, 2010, 15, 012003.	0.3	3

#	Article	IF	Citations
7439	First-principles study for effect of lattice defects on the crystal structure of the Zn-Sc cubic crystalline approximant. Journal of Physics: Conference Series, 2010, 226, 012031.	0.3	1
7440	Tuning the spin state of iron phthalocyanine by ligand adsorption. Journal of Physics Condensed Matter, 2010, 22, 472002.	0.7	59
7441	Magnetoelectric coupling at biferroic interface studied from first principles. Journal of Physics: Conference Series, 2010, 200, 072027.	0.3	4
7442	Thermodynamic instability at the stoichiometric LaAlO₃/SrTiO₃(001) interface. Journal of Physics Condensed Matter, 2010, 22, 312201.	0.7	77
7443	First-principles study of the structural stability of L1₁order in Pt-based alloys. Journal of Physics: Conference Series, 2010, 200, 072021.	0.3	9
7444	Phonons in iron monolayers. Journal of Physics: Conference Series, 2010, 217, 012144.	0.3	6
7445	Delafossite-alloy photoelectrodes for PEC hydrogen production: a density functional theory study. Proceedings of SPIE, 2010, , .	0.8	4
7446	A comparative study of (Fe, Fe₃Si)/GaAs and Heusler/MgO for spintronics applications. Journal of Physics: Conference Series, 2010, 200, 072038.	0.3	1
7447	X-ray powder diffraction, solid-state NMR and dispersion-corrected DFT calculations to investigate the solid state structure of 2-ammonio-5-chloro-4-methylbenzenesulfonate. Zeitschrift FÃ¼r Kristallographie, 2010, 225, 382-387.	1.1	16
7448	Band alignment at Cu2O/La0.7Sr0.3MnO3 interface: A combined experimental-theoretical determination. Applied Physics Letters, 2010, 97, .	1.5	11
7449	Impact of substitutional and interstitial carbon defects on lattice parameters in MgB2. Journal of Applied Physics, 2010, 107, 023902.	1.1	13
7450	Energy-gap opening and quenching in graphene under periodic external potentials. Journal of Chemical Physics, 2010, 133, 224705.	1.2	8
7451	First-principles calculations of the elastic properties of hydroxyapatite doped with divalent ions. Journal of the Ceramic Society of Japan, 2010, 118, 548-549.	0.5	9
7452	Minimum Energy Motion and Core Structure of Pure Edge and Screw Dislocations in Aluminum. Journal of Computational Science and Technology, 2010, 4, 185-193.	0.4	5
7453	First-Principles Study on Stability and Electronic Structures of Pt-Rh Bimetallic Nanoparticles. Materials Transactions, 2010, 51, 321-324.	0.4	12
7454	Diagnostic Structures for Interatomic Potentials. Materials Transactions, 2010, 51, 675-678.	0.4	3
7455	Thermoelectric Properties of Si₂Ti-Type Al-Mn-Si Alloys. Materials Transactions, 2010, 51, 1127-1135.	0.4	20
7456	Local Atomic Configuration of Dislocation-Accumulated Grain Boundary and Energetics of Gradual Transition from Low Angle to High Angle Grain Boundary in Pure Aluminum by First-Principles Calculations. Materials Transactions, 2010, 51, 51-57.	0.4	7

#	Article	IF	Citations
7457	Effect of Zn on the adsorption of CO on Pd(111). Journal of Chemical Physics, 2010, 133, 214702.	1.2	12
7458	Communication: Emergence of localized magnetic moment at adsorbed beryllium dimer on graphene. Journal of Chemical Physics, 2010, 133, 231104.	1.2	9
7459	Theoretical studies on electronic and magnetic properties of ultrathin Mo nanowires. Journal of Applied Physics, 2010, 107, 024307.	1.1	3
7460	Ab initio study on pressure-induced change of effective Coulomb interaction in superconducting yttrium. Applied Physics Letters, 2010, 96, .	1.5	5
7461	First-Principles Calculations of the Specific Heats of Cubic Carbides and Nitrides. Materials Transactions, 2010, 51, 574-577.	0.4	28
7462	First Principles Investigation for H2 Dissociative Adsorption on Ni and Cr-Decorated Ni Surfaces - An Application to Alkaline Polymer Electrolyte Fuel Cell. E-Journal of Surface Science and Nanotechnology, 2010, 8, 325-330.	0.1	6
7463	First Principles Calculation on the Surface Energy of Metal Nitride with NaCl Structure. Hyomen Gijutsu/Journal of the Surface Finishing Society of Japan, 2010, 61, 535-540.	0.1	6
7464	Influence of gallium (and aluminum) substituted in monoclinic Î± plutonium: A possible structural change induced with increasing content of alloying element. IOP Conference Series: Materials Science and Engineering, 2010, 9, 012085.	0.3	2
7467	Stabilization Mechanism of Vacancies in Group-III Nitrides: Exchange Splitting and Electron Transfer. Journal of the Physical Society of Japan, 2010, 79, 083705.	0.7	9
7468	Electronic Structures of Tungsten and Molybdenum Carbides as a Fuel Cell Anode Catalyst. Bulletin of the Chemical Society of Japan, 2010, 83, 1501-1503.	2.0	9
7469	Study of H:Si(113)2×2 Structure by Scanning Tunneling Microscopy and Ab Initio Calculation. E-Journal of Surface Science and Nanotechnology, 2010, 8, 261-265.	0.1	2
7470	Ab initio investigation of the clustering of carbon adatoms on Fe(001) and Fe(111) surfaces. Journal of Experimental and Theoretical Physics, 2010, 110, 81-87.	0.2	1
7471	Electronic structure of the NiMnSb-semiconductor (110) interface. Physics of the Solid State, 2010, 52, 105-111.	0.2	1
7472	Digital magnetic heterostructures based on Si and Fe. Physics of the Solid State, 2010, 52, 1680-1687.	0.2	5
7473	Effect of electron correlations on the electronic structure and magnetic properties of the perovskite-like high-pressure phase ErCu3V4O12. Physics of the Solid State, 2010, 52, 1709-1713.	0.2	8
7474	Dependence of the intrinsic line width of surface states on the wave vector: The Cu(111) and Ag(111) surfaces. Physics of the Solid State, 2010, 52, 1768-1773.	0.2	11
7475	Electronic structure and adhesion on metal-aluminum-oxide interfaces. Physics of the Solid State, 2010, 52, 2589-2595.	0.2	16
7476	Towards the theory of hardness of materials. Journal of Superhard Materials, 2010, 32, 143-147.	0.5	70

#	Article	IF	Citations
7477	First-principles investigation of the structure and electronic properties of CdS/CdSe/CdS and CdS/CdTe/CdS quantum wells using a slab approximation. Nanotechnologies in Russia, 2010, 5, 191-197.	0.7	8
7478	First-principles study of Sr adsorption on InN (0001). European Physical Journal B, 2010, 73, 75-78.	0.6	4
7479	Stability of FeAl(110) alloy surface structures: a first-principles study. European Physical Journal B, 2010, 73, 367-373.	0.6	8
7480	Comparison of the structural, electronic and magnetic properties of Fe, Co and Ni nanowires encapsulated into silicon carbide nanotube. European Physical Journal B, 2010, 73, 555-561.	0.6	16
7481	Electronically driven phase transitions in a quasi-one-dimensional adsorbate system. European Physical Journal B, 2010, 75, 15-22.	0.6	6
7482	Mechanical and chemical bonding properties of ground state BeH2. European Physical Journal B, 2010, 74, 303-308.	0.6	25
7483	First-principle study of the electronic structures and ferroelectric properties in BaZnF4. European Physical Journal B, 2010, 74, 447-450.	0.6	10
7484	Structural and electronic properties of carbon adsorbed on Fe(100). European Physical Journal B, 2010, 74, 555-564.	0.6	9
7485	Density functional study of K and Na adsorbed on Co(0001). European Physical Journal B, 2010, 75, 469-474.	0.6	5
7486	Atomic and electronic properties of tert-butanol on the Si(001)-(2Ã—1) surface. European Physical Journal B, 2010, 76, 359-363.	0.6	2
7487	Structural, electronic and magnetic properties of the 3d transition metal atoms adsorbed on boron nitride nanotubes. European Physical Journal B, 2010, 76, 289-299.	0.6	19
7488	Electronic structure and magnetic coupling properties of Gd-doped AlN: first-principles calculations. European Physical Journal B, 2010, 77, 345-349.	0.6	7
7489	The main factors influencing the O vacancy formation on the Ir doped ceria surface: A DFT+U study. European Physical Journal B, 2010, 77, 373-380.	0.6	20
7490	First principles calculations of the relaxed structural and electronic properties of Cu nanobelts. European Physical Journal B, 2010, 78, 87-93.	0.6	0
7491	Special electronic structures of inverse spinels LiMVO4(M = Ni and Cu): a first-principles study. European Physical Journal B, 2010, 78, 299-304.	0.6	4
7492	Comparison of the dynamics of MIL-53(Cr) and MIL-47(V) frameworks using neutron scattering and DFT methods. European Physical Journal: Special Topics, 2010, 189, 263-271.	1.2	31
7493	Diffusion of the Cu monomer and dimer on Ag(111): Molecular dynamics simulations and density functional theory calculations. Physical Review B, 2010, 82, .	1.1	28
7494	Tuning Electronic Structures of ZnO Nanowires by Surface Functionalization: A First-Principles Study. Journal of Physical Chemistry C, 2010, 114, 8861-8866.	1.5	34

#	Article	IF	Citations
7495	Heterogeneous nucleation of solid Al from the melt by<mml:math xmlns:mml="http://www.w3.org/1998/Math/MathML" display="inline"><mml:mrow><mml:msub><mml:mrow><mml:mtext>Al</mml:mtext></mml:mrow><mml:mn>3</mml:mn></mml:msub> Molecular dynamics simulations. Physical Review B, 2010, 82, .	1.1	39
7496	TAMkin: A Versatile Package for Vibrational Analysis and Chemical Kinetics. Journal of Chemical Information and Modeling, 2010, 50, 1736-1750.	2.5	155
7497	Crystal structure prediction via particle-swarm optimization. Physical Review B, 2010, 82, .	1.1	1,870
7498	Wurtzite-derived polytypes of kesterite and stannite quaternary chalcogenide semiconductors. Physical Review B, 2010, 82, .	1.1	259
7499	Structural, magnetic, and defect properties of Co-Pt-type magnetic-storage alloys: Density-functional theory study of thermal processing effects. Physical Review B, 2010, 82, .	1.1	54
7500	ScVO₄: Explorations of Novel Crystalline Inorganic Optical Materials in Rare-Earth Orthovanadate Systems. Crystal Growth and Design, 2010, 10, 4389-4400.	1.4	39
7501	Adsorption of Aromatic and Anti-Aromatic Systems on Graphene through Ï€âˆ'Ï€ Stacking. Journal of Physical Chemistry Letters, 2010, 1, 3407-3412.	2.1	344
7502	Controlling Band Gap Energies in Cluster-Assembled Ionic Solids through Internal Electric Fields. ACS Nano, 2010, 4, 5813-5818.	7.3	72
7503	Metallacarboranes: Toward Promising Hydrogen Storage Metal Organic Frameworks. Journal of the American Chemical Society, 2010, 132, 14126-14129.	6.6	55
7504	Gate-Controlled Donor Activation in Silicon Nanowires. Nano Letters, 2010, 10, 3791-3795.	4.5	5
7505	Electronic correlation effects in reduced rutile<mml:math xmlns:mml="http://www.w3.org/1998/Math/MathML" display="inline"><mml:mrow><mml:msub><mml:mrow><mml:mtext>TiO</mml:mtext></mml:mrow><mml:mn>2</mml:mn></mml:msub> the<mml:math xmlns:mml="http://www.w3.org/1998/Math/MathML" display="inline"><mml:mrow><mml:mtext>LDA</mml:mtext><mml:mo>+</mml:mo><mml:mi>U</mml:mi></mml:mrow></mml:math> Physical Review B, 2010, 82, .	1.1	193
7506	Defect formation energy and magnetic structure of shape memory alloys Niâ€“Xâ€“Ga (X=Mn, Fe, Co) by first principle calculation. Journal of Applied Physics, 2010, 108, .	1.1	36
7507	First-principles modelling of scanning tunneling microscopy using non-equilibrium Greenâ€™s functions. Frontiers of Physics in China, 2010, 5, 369-379.	1.0	13
7508	Impacts of fluorine on GaN high electron mobility transistors: Theoretical study. Physica Status Solidi - Rapid Research Letters, 2010, 4, 332-334.	1.2	10
7509	Mechanical and lattice dynamical properties of the Re₂C compound. Physica Status Solidi - Rapid Research Letters, 2010, 4, 347-349.	1.2	22
7510	First-order liquid-liquid phase transition in dense hydrogen. Physical Review B, 2010, 82, .	1.1	121
7511	Crystal and Electronic Structure of FeSe at High Pressure and Low Temperature. Journal of Physical Chemistry B, 2010, 114, 12597-12606.	1.2	79
7512	Statistical model of defects in Al-H system. Physical Review B, 2010, 81, .	1.1	35

#	Article	IF	Citations
7513	Vacancy Clusters in Graphane as Quantum Dots. ACS Nano, 2010, 4, 3510-3514.	7.3	119
7514	Morphological and phase stability of zinc blende, amorphous and mixed coreâ€“shell ZnS nanoparticles. Nanoscale, 2010, 2, 2294.	2.8	31
7515	Efficient low-order scaling method for large-scale electronic structure calculations with localized basis functions. Physical Review B, 2010, 82, .	1.1	26
7516	The structure of tavorite LiFePO4(OH) from diffraction and GGA + U studies and its preliminary electrochemical characterization. Dalton Transactions, 2010, 39, 5108.	1.6	66
7517	On the Structure of a Thiolated Gold Cluster: Au₄₄(SR)₂₈^{2â^'}. Journal of Physical Chemistry C, 2010, 114, 15883-15889.	1.5	54
7518	Structures and energetics of<mml:math xmlns:mml="http://www.w3.org/1998/Math/MathML" display="inline"><mml:mrow><mml:msub><mml:mrow><mml:mtext>Bi</mml:mtext></mml:mrow><mml:mn>2</mml:mn></mml:msub> in a defective fluorite family derived by systematic first-principles lattice dynamics calculations. Physical Review B, 2010, 81, .	1.1	33
7519	A systematic study of electronic structure from graphene tographane. Journal of Physics Condensed Matter, 2010, 22, 465502.	0.7	56
7520	First-Principles Calculations of Complex Metal-Oxide Materials. Annual Review of Condensed Matter Physics, 2010, 1, 211-235.	5.2	31
7521	The Role of Surface Oxides in NO_x Storage Reduction Catalysts. ChemCatChem, 2010, 2, 658-660.	1.8	13
7522	Revisiting the Structure of Methyltrioxorhenium Chemisorbed on Alumina. ChemCatChem, 2010, 2, 812-815.	1.8	19
7523	Aqueousâ€Phase Hydrogenation of Acetic Acid over Transition Metal Catalysts. ChemCatChem, 2010, 2, 1420-1424.	1.8	123
7524	Atomistic models of hydrogenated amorphous silicon nitride from first principles. Physical Review B, 2010, 82, .	1.1	22
7525	Chemical trends in structure and magnetism of bimetallic nanoparticles from atomistic calculations. Journal Physics D: Applied Physics, 2010, 43, 474008.	1.3	17
7526	Modelling of nanoparticles: approaches to morphology and evolution. Reports on Progress in Physics, 2010, 73, 086502.	8.1	166
7527	First principles study of lithium insertion in bulk silicon. Journal of Physics Condensed Matter, 2010, 22, 415501.	0.7	145
7528	Mediating distribution of magnetic Co ions by Cr-codoping in (Co,Cr): ZnO thin films. Applied Physics Letters, 2010, 97, 042504.	1.5	15
7529	Fast diffusion of a graphene flake on a graphene layer. Physical Review B, 2010, 82, .	1.1	85
7530	Submonolayers of carbon on<mml:math xmlns:mml="http://www.w3.org/1998/Math/MathML" display="inline"><mml:mrow><mml:mi>Î±</mml:mi><mml:mtext>-Fe</mml:mtext></mml:mrow></mml:math>facets: Anab initiostudy. Physical Review B, 2010, 82, .	1.1	17

#	Article	IF	Citations
7531	Plasticity in carbon nanotubes: Cooperative conservative dislocation motion. Physical Review B, 2010, 81, .	1.1	18
7532	First principles calculations of vacancyâ€“vacancy interactions in nickel: thermal expansion effects. Journal of Physics Condensed Matter, 2010, 22, 485502.	0.7	18
7533	Crystal Structures and Thermodynamic Investigations of LiK(BH₄)₂, KBH₄, and NaBH₄ from First-Principles Calculations. Journal of Physical Chemistry C, 2010, 114, 678-686.	1.5	56
7534	First principles calculations for defects in U. Journal of Physics Condensed Matter, 2010, 22, 505703.	0.7	47
7535	Defect studies of nanocrystalline zirconia powders and sintered ceramics. Physical Review B, 2010, 81, .	1.1	68
7536	Novel Computational Methods for Nanostructure Electronic Structure Calculations. Annual Review of Physical Chemistry, 2010, 61, 19-39.	4.8	20
7537	Electronic, vibrational, and thermodynamic properties of ZnS with zinc-blende and rocksalt structure. Physical Review B, 2010, 81, .	1.1	33
7538	Epitaxial-Strain-Induced Multiferroicity in<mml:math xmlns:mml="http://www.w3.org/1998/Math/MathML" display="inline"><mml:msub><mml:mi>SrMnO</mml:mi><mml:mn>3</mml:mn></mml:msub></mml:math>from First Principles. Physical Review Letters, 2010, 104, 207204.	2.9	297
7539	Low-Temperature CO Oxidation on Ni(111) and on a Au/Ni(111) Surface Alloy. ACS Nano, 2010, 4, 4380-4387.	7.3	80
7540	Atomistic cluster alignment method for local order mining in liquids and glasses. Physical Review B, 2010, 82, .	1.1	120
7541	Competing structural ordering tendencies in Heusler-type alloys with high Curie temperatures:<mml:math xmlns:mml="http://www.w3.org/1998/Math/MathML" display="inline"><mml:mrow><mml:msub><mml:mrow><mml:mtext>Fe</mml:mtext></mml:mrow><mml:mn>2</mml:mn></mml:msub></mml:mrow></mml:math>Physical Review B, 2010, 82, .	1.1	27
7542	Experimental Realization of a Three-Dimensional Topological Insulator Phase in Ternary Chalcogenide<mml:math xmlns:mml="http://www.w3.org/1998/Math/MathML" display="inline"><mml:msub><mml:mi>TlBiSe</mml:mi><mml:mn>2</mml:mn></mml:msub></mml:math>. Physical Review Letters, 2010, 105, 146801.	2.9	219
7543	Intrinsic n-type Defect Formation in TiO₂: A Comparison of Rutile and Anatase from GGA+U Calculations. Journal of Physical Chemistry C, 2010, 114, 2321-2328.	1.5	367
7544	Interaction of gold nanotubes with the Si(211) surface: A density functional study. Physical Review B, 2010, 82, .	1.1	1
7545	Intermetallic hydrides: A review with ab initio aspects. Progress in Solid State Chemistry, 2010, 38, 1-37.	3.9	80
7546	Long-range interactions in carbon atomic chains. Physical Review B, 2010, 82, .	1.1	86
7547	Thermodynamically stable single-side hydrogenated graphene. Physical Review B, 2010, 82, .	1.1	47
7548	Deformation and transfer doping of a single-walled carbon nanotube adsorbed on metallic substrates. Physical Review B, 2010, 81, .	1.1	13

#	Article	IF	Citations
7549	Equation of state and pressure-induced structural changes in mirabilite (Na2SO4Â·10H2O) determined from ab initio density functional theory calculations. Physics and Chemistry of Minerals, 2010, 37, 265-282.	0.3	17
7550	The combined inelastic neutron scattering and solid state DFT study of hydrogen atoms dynamics in a highly ordered kaolinite. Physics and Chemistry of Minerals, 2010, 37, 571-579.	0.3	33
7551	Peierlsâ€“Nabarro modelling of dislocations in diopside. Physics and Chemistry of Minerals, 2010, 37, 711-720.	0.3	4
7552	Structure and bonding of ethoxy species adsorbed on transition metal surfaces. Theoretical Chemistry Accounts, 2010, 126, 223-229.	0.5	8
7553	DFT study of the electronic, vibrational, and optical properties of SnO2. Theoretical Chemistry Accounts, 2010, 126, 39-44.	0.5	100
7554	Charge state of metal atoms on oxide supports: a systematic study based on simulated infrared spectroscopy and density functional theory. Theoretical Chemistry Accounts, 2010, 126, 265-273.	0.5	17
7555	Adsorption of tetralin and hydrogenated intermediates and products on the (100) surfaces of Ir, Pt and Pd: a DFT study. Theoretical Chemistry Accounts, 2010, 127, 401-409.	0.5	11
7556	Modulation of the work function of silicon nanowire by chemical surface passivation: a DFT study. Theoretical Chemistry Accounts, 2010, 127, 689-695.	0.5	25
7557	Studies of high-temperature electronâ€“phonon interactions withÂinelastic neutron scattering and first-principles computations. Applied Physics A: Materials Science and Processing, 2010, 99, 523-529.	1.1	2
7558	A critical consideration of magnetism and composition ofÂ(bcc)ÂCuÂprecipitates in (bcc) Fe. Applied Physics A: Materials Science and Processing, 2010, 99, 697-704.	1.1	32
7559	Very large scale wavefunction orthogonalization in Density Functional Theory electronic structure calculations. Computer Physics Communications, 2010, 181, 1057-1068.	3.0	13
7560	Effects of carbon on the weak ferromagnetism in doped GaN. Chemical Physics Letters, 2010, 487, 251-255.	1.2	24
7561	Spin and band-gap engineering in copper-doped BN sheet. Chemical Physics Letters, 2010, 491, 203-207.	1.2	28
7562	Oxygen interstitial structures in close-packed metal oxides. Chemical Physics Letters, 2010, 492, 44-48.	1.2	48
7563	The influence of electron correlation and spinâ€“orbit coupling on the half metallic properties of LaSrMoReO6, LaSrMoTcO6 and LaSrVOsO6. Chemical Physics Letters, 2010, 492, 241-245.	1.2	1
7564	Investigation of ferromagnetism in Al-doped 4Hâ€“SiC by density functional theory. Chemical Physics Letters, 2010, 496, 276-279.	1.2	29
7565	Prediction of diamond-like, metallic boron structures. Chemical Physics Letters, 2010, 496, 280-283.	1.2	3
7566	Evolution of a Pt (111) surface at high oxygen coverage in acid medium. Chemical Physics Letters, 2010, 498, 328-333.	1.2	15

#	Article	IF	Citations
7567	Electronic properties of F/Zr co-doped anatase TiO2 photocatalysts from GGA +U calculations. Chemical Physics Letters, 2010, 498, 338-344.	1.2	23
7568	First principles mechanistic study of borohydride oxidation over the Pt(111) surface. Electrochimica Acta, 2010, 55, 1175-1183.	2.6	66
7569	Static ion structure factor for dense plasmas: Semi-classical and ab initio calculations. High Energy Density Physics, 2010, 6, 305-310.	0.4	8
7570	Hydrogenography of Mg Ni1â^'H gradient thin films: Interplay between the thermodynamics and kinetics of hydrogenation. Acta Materialia, 2010, 58, 658-668.	3.8	29
7571	The theoretical shear strength of fcc crystals under superimposed triaxial stress. Acta Materialia, 2010, 58, 3117-3123.	3.8	19
7572	Atomistic study of edge and screw â€^c+aã€‰ dislocations in magnesium. Acta Materialia, 2010, 58, 4332-4343.	3.8	117
7573	Investigation of the structural stability of Co2NiGa shape memory alloys via ab initio methods. Acta Materialia, 2010, 58, 5220-5231.	3.8	28
7574	Identification of MnCr2O4 nano-octahedron in catalysing pitting corrosion of austenitic stainless steels. Acta Materialia, 2010, 58, 5070-5085.	3.8	122
7575	Interactions between carbon solutes and dislocations in bcc iron. Acta Materialia, 2010, 58, 5481-5490.	3.8	36
7576	Mechanical properties, electronic structure and bonding of Î±- and Î²-tricalcium phosphates with surface characterization. Acta Biomaterialia, 2010, 6, 3763-3771.	4.1	83
7577	Electronic structure of Co-phthalocyanine calculated by GGA+U and hybrid functional methods. Chemical Physics, 2010, 377, 96-99.	0.9	22
7578	YNi and its hydrides: Phase stabilities, electronic structures and chemical bonding properties from first principles. Chemical Physics, 2010, 377, 109-114.	0.9	4
7579	Two-dimensionality of electronic structure and strong Fermi surface nesting in highly anisotropic iron-based superconductors. Physica C: Superconductivity and Its Applications, 2010, 470, 1002-1006.	0.6	4
7580	Ferromagnetism in phosphorus-doped ZnO: First-principles calculation. Physics Letters, Section A: General, Atomic and Solid State Physics, 2010, 374, 628-631.	0.9	14
7581	First-principles study on ferromagnetism in C-doped AlN. Physics Letters, Section A: General, Atomic and Solid State Physics, 2010, 374, 3671-3675.	0.9	28
7582	Ab-initio investigations of the electronic properties of bulk wurtzite Beryllia and its derived nanofilms. Physics Letters, Section A: General, Atomic and Solid State Physics, 2010, 374, 3977-3981.	0.9	5
7583	Dissociation of H2 molecule on the Î²-Ga2O3 (100)B surface: The critical role of oxygen vacancy. Physics Letters, Section A: General, Atomic and Solid State Physics, 2010, 374, 4169-4173.	0.9	27
7584	First-principles calculations on the role of Ni-doping in Cu clusters: From geometric and electronic structures to chemical activities towards CO2. Physics Letters, Section A: General, Atomic and Solid State Physics, 2010, 374, 4324-4330.	0.9	24

#	Article	IF	Citations
7585	Possible room temperature ferromagnetism of Li-doped anatase TiO2: A first-principles study. Physics Letters, Section A: General, Atomic and Solid State Physics, 2010, 374, 4451-4454.	0.9	18
7586	Indium distribution and light emission in wurtzite InGaN alloys: Several-atom In-N clusters. Physics Letters, Section A: General, Atomic and Solid State Physics, 2010, 374, 4767-4773.	0.9	13
7587	Dopings in the transition-metal aluminides OsAl2 to obtain materials with high spin polarization: A first-principles study. Physics Letters, Section A: General, Atomic and Solid State Physics, 2010, 374, 4909-4914.	0.9	5
7588	Improving the sensitivity of carbon nanotube sensors by benzene functionalization. Sensors and Actuators B: Chemical, 2010, 147, 316-321.	4.0	26
7589	Deoxygenation of IrO2(110) surface: Core-level spectroscopy and density functional theory calculation. Surface Science, 2010, 604, 118-124.	0.8	21
7590	First-principles calculations of C diffusion through the surface and subsurface of Ag/Ni(100) and reconstructed Ag/Ni(100). Surface Science, 2010, 604, 186-195.	0.8	8
7591	Peculiarities of Al magic cluster self-assembly on Si(1 0 0) surface. Surface Science, 2010, 604, 674-678.	0.8	0
7592	Dehydration of goethite to hematite from molecular dynamics simulation. Computational and Theoretical Chemistry, 2010, 950, 20-26.	1.5	19
7593	First-principles study of hydrogen interaction with carbon-doped GaN nanotube. Computational and Theoretical Chemistry, 2010, 956, 77-82.	1.5	8
7594	Surface electronic structure of Ti-covered W(111) by photofield emission. Ultramicroscopy, 2010, 111, 5-10.	0.8	0
7595	Ab-initio calculations and phase diagram assessments of Anâ€“Al systems (An= U, Np, Pu). Journal of Nuclear Materials, 2010, 397, 1-7.	1.3	25
7596	An atomistic approach to self-diffusion in uranium dioxide. Journal of Nuclear Materials, 2010, 400, 103-106.	1.3	26
7597	Structural, mechanical, thermodynamic, and electronic properties of thorium hydrides from first-principles. Journal of Nuclear Materials, 2010, 401, 124-129.	1.3	24
7598	Comparison of empirical interatomic potentials for iron applied to radiation damage studies. Journal of Nuclear Materials, 2010, 406, 19-38.	1.3	217
7599	Ab initio interionic potentials for UN by multiple lattice inversion. Journal of Nuclear Materials, 2010, 404, 6-8.	1.3	7
7600	Effect of impurity and alloying elements on Zr grain boundary strength from first-principles computations. Journal of Nuclear Materials, 2010, 404, 121-127.	1.3	45
7601	Development of a pair potential for Feâ€“He by lattice inversion. Journal of Nuclear Materials, 2010, 405, 156-159.	1.3	21
7602	Structural, electronic, and thermodynamic properties of UN: Systematic density functional calculations. Journal of Nuclear Materials, 2010, 406, 218-222.	1.3	34

#	Article	IF	Citations
7603	First principles study of intrinsic defects in hexagonal tungsten carbide. Journal of Nuclear Materials, 2010, 406, 323-329.	1.3	22
7604	Vacancy formation and solid solubility in the Uâ€“Zrâ€“N system. Journal of Nuclear Materials, 2010, 406, 351-355.	1.3	9
7605	First-principles investigation of the surface structures of Cu(n, nâˆ'1, 0) (n=2, 3 and 4) stepped surfaces. Journal of Physics and Chemistry of Solids, 2010, 71, 764-769.	1.9	5
7606	Oxidation fracturing of the graphitic BN sheet. Journal of Physics and Chemistry of Solids, 2010, 71, 1221-1224.	1.9	8
7607	Optical properties of revealed by ab initio calculations. Journal of Physics and Chemistry of Solids, 2010, 71, 1690-1693.	1.9	5
7608	Interactions of Ba2YCu3O6+y with the Gd3NbO7 buffer layer in coated conductors. Journal of Solid State Chemistry, 2010, 183, 649-657.	1.4	2
7609	Pressure induced structural phase transition of OsB2: First-principles calculations. Journal of Solid State Chemistry, 2010, 183, 915-919.	1.4	12
7610	Coupled anion and cation ordering in Sr3RFe4O10.5 (R=Y, Ho, Dy) anion-deficientperovskites. Journal of Solid State Chemistry, 2010, 183, 2845-2854.	1.4	14
7611	Inelastic neutron scattering and DFT study of potassium hydrogen phthalate. Journal of Molecular Structure, 2010, 967, 89-93.	1.8	2
7612	Electronic structure analysis of Sb-doped BaSnO3. Materials Science and Engineering B: Solid-State Materials for Advanced Technology, 2010, 173, 33-36.	1.7	12
7613	Density functional study of oxygen vacancy formation and spin density distribution in octahedral ceria nanoparticles. Journal of Molecular Modeling, 2010, 16, 1617-1623.	0.8	22
7614	Graphene-like bilayer hexagonal silicon polymorph. Nano Research, 2010, 3, 694-700.	5.8	46
7615	Ab initio molecular dynamics simulation of the atom packing and density of Al-Ni amorphous alloys. Science China Technological Sciences, 2010, 53, 3175-3182.	2.0	11
7616	Density functional study of ferromagnetism in alkali metal thin films. Pramana - Journal of Physics, 2010, 74, 653-659.	0.9	2
7617	First-principle investigation on electronic structures and elastic properties of Al-doped MoSi2. Central South University, 2010, 17, 888-894.	0.5	9
7618	A multi-stage hierarchical approach to alloy design. Jom, 2010, 62, 25-29.	0.9	14
7619	Electronic Structures and Transport Properties of Single-Filled CoSb3. Journal of Electronic Materials, 2010, 39, 1832-1836.	1.0	16
7620	A First-Principles Study of the Role of Na Vacancies in the Thermoelectricity of Na x CoO2. Journal of Electronic Materials, 2010, 39, 1681-1686.	1.0	12

#	Article	IF	Citations
7621	Study of Electronic Structure and Defect Formation in Ti1â^'x Ni1+x Sn Half-Heusler Alloys. Journal of Electronic Materials, 2010, 39, 1549-1553.	1.0	10
7622	Theoretical Investigations into Self-Organized Ordered Metallic Semi-Clusters Arrays on Metallic Substrate. Nanoscale Research Letters, 2010, 5, 1020-1026.	3.1	2
7623	Effect of Li and Na impurities on the electronic and magnetic properties of beryllium oxide. Journal of Structural Chemistry, 2010, 51, 960-963.	0.3	1
7624	Doped C60 Study from First Principles Simulation. Journal of Superconductivity and Novel Magnetism, 2010, 23, 877-880.	0.8	4
7625	Bonding in the â€œ111â€•Type Ferropnictide Superconductor LiFeAs. Journal of Superconductivity and Novel Magnetism, 2010, 23, 579-581.	0.8	0
7626	An advanced description of oxide traps in MOS transistors andÂitsÂrelation to DFT. Journal of Computational Electronics, 2010, 9, 135-140.	1.3	14
7627	A first principles investigation of isotactic polypropylene. Journal of Materials Science, 2010, 45, 443-447.	1.7	19
7628	First-principles study on electronic properties of SiC nanoribbon. Journal of Materials Science, 2010, 45, 3259-3265.	1.7	56
7629	Core-level shift analysis of amorphous CdTeO x materials. Journal of Materials Science, 2010, 45, 5071-5076.	1.7	6
7630	Computer simulation study of amorphous compounds: structural and vibrational properties. Journal of Materials Science, 2010, 45, 5124-5134.	1.7	14
7631	Chemical vapor synthesis of fluorine-doped SnO2 (FTO) nanoparticles. Journal of Nanoparticle Research, 2010, 12, 2579-2588.	0.8	33
7632	Theoretical study of small clusters of manganese-doped gallium oxide: Mn(GaO) n and Mn2(GaO) n with nÂ=Â1â^'7. Journal of Nanoparticle Research, 2010, 12, 727-736.	0.8	2
7633	The Interior Structure, Composition, and Evolution ofÂGiant Planets. Space Science Reviews, 2010, 152, 423-447.	3.7	279
7634	First-principles study of electronic structure, absorption spectra, and thermodynamic properties of crystalline 1H-tetrazole and its substituted derivatives. Structural Chemistry, 2010, 21, 847-854.	1.0	16
7635	Theoretical Prediction and Experimental Verification of Stability of Ptâ€“3dâ€“Pt Subsurface Bimetallic Structures: From Single Crystal Surfaces to Polycrystalline Films. Topics in Catalysis, 2010, 53, 338-347.	1.3	19
7636	Desulfurization Reactions on Surfaces of Metal Carbides: Photoemission and Densityâ€“Functional Studies. Topics in Catalysis, 2010, 53, 393-402.	1.3	27
7637	Effects of Ring Structure on the Reaction Pathways of Cyclic Esters and Ethers on Pd(111). Topics in Catalysis, 2010, 53, 1179-1184.	1.3	7
7638	Mechanical Response and Energy-Dissipation Processes in Oligothiophene Monolayers Studied with First-Principles Simulations. Tribology Letters, 2010, 39, 295-309.	1.2	7

#	Article	IF	Citations
7639	Theoretical investigations of the (110) interface between the full Heusler alloys and GaAs. Russian Physics Journal, 2010, 53, 225-230.	0.2	1
7640	Enhanced ozonation of dichloroacetic acid in aqueous solution using nanometer ZnO powders. Journal of Environmental Sciences, 2010, 22, 1527-1533.	3.2	55
7641	Comparisons of Performance Potentials of Silicon Nanowire and Graphene Nanoribbon MOSFETs Considering First-Principles Bandstructure Effects. IEEE Transactions on Electron Devices, 2010, 57, 406-414.	1.6	31
7642	Origin of the Flatband-Voltage Roll-Off Phenomenon in Metal/High- k Gate Stacks. IEEE Transactions on Electron Devices, 2010, 57, 2047-2056.	1.6	39
7643	Density functional theory modelling of and surfaces: Structure, properties and adsorption of N2O. Materials Chemistry and Physics, 2010, 119, 505-514.	2.0	34
7644	High-pressure meta-stable phase of BeO: A first principle study. Materials Chemistry and Physics, 2010, 124, 768-772.	2.0	7
7645	Adsorption of Ge nanowire with 3d transition metals: A density-functional theory study. Materials Chemistry and Physics, 2010, 124, 1113-1120.	2.0	7
7646	A new synthesis of hexadecylamine-capped Mn-doped wurtzite CdSe nanoparticles. Materials Letters, 2010, 64, 1513-1516.	1.3	19
7647	Pressure-dependent stability of cubic and wurtzite phases within the TiNâ€“AlN and CrNâ€“AlN systems. Scripta Materialia, 2010, 62, 349-352.	2.6	70
7648	First-principles density functional calculations for Mg alloys: A tool to aid in alloy development. Scripta Materialia, 2010, 63, 680-685.	2.6	48
7649	First-principles calculations of twin-boundary and stacking-fault energies in magnesium. Scripta Materialia, 2010, 62, 646-649.	2.6	141
7650	Layered atomic structures of double oxides for low shear strength at high temperatures. Scripta Materialia, 2010, 62, 735-738.	2.6	130
7651	First-principles understanding of environmental embrittlement of the Ni/Ni3Al interface. Scripta Materialia, 2010, 63, 391-394.	2.6	27
7652	Modelling thermal activation of <110>{110} slip at low temperature in SrTiO3. Scripta Materialia, 2010, 63, 434-437.	2.6	13
7653	First principles prediction of vanadium and niobium nitrides with M2N3 stoichiometry. Scripta Materialia, 2010, 63, 532-535.	2.6	20
7654	A pathway to p-type conductivity in (nN, B)-codoped ZnO. Scripta Materialia, 2010, 63, 1069-1072.	2.6	8
7655	Cooperative Jahnâ€“Teller distortion leading to the spin-1/2 uniform antiferromagnetic chains in triclinic perovskites AgCuF3 and NaCuF3. Solid State Sciences, 2010, 12, 680-684.	1.5	20
7656	Spin dimer and mapping analyses of the magnetic properties of VO(CH3CO2)2 and VO(OCH2CH2O). Solid State Sciences, 2010, 12, 685-690.	1.5	7

#	Article	IF	Citations
7657	DFT study of hydrogen instability and magnetovolume effects in CeNi. Solid State Sciences, 2010, 12, 59-64.	1.5	9
7658	DFT study of electronic and magnetic structure of perovskite and post-perovskite CaRhO3. Solid State Sciences, 2010, 12, 373-378.	1.5	15
7659	Potential existence of anti-postperovskite iron nitride Fe4N. Solid State Sciences, 2010, 12, 1131-1135.	1.5	2
7660	Ab initio study on the structural and electronic properties of Li3GaP2 compared with Li3GaN2. Solid State Sciences, 2010, 12, 1080-1083.	1.5	1
7661	First-principles study of high pressure structure phase transition and elastic properties of titanium. Solid State Sciences, 2010, 12, 1473-1479.	1.5	37
7662	AMoO4 (AÂ=ÂMg, Ni) molybdates: Phase stabilities, electronic structures and chemical bonding properties from first principles. Solid State Sciences, 2010, 12, 1779-1785.	1.5	37
7663	Effects of Ta content on the phase stability and elastic properties of Î² Tiâ€“Ta alloys from first-principles calculations. Solid State Sciences, 2010, 12, 2120-2124.	1.5	25
7664	DFT study of nitrided zeolites: Mechanism of nitrogen substitution in HY and silicalite. Journal of Catalysis, 2010, 269, 53-63.	3.1	27
7665	A density functional theory study of water gas shift over pseudomorphic monolayer alloy catalysts: Comparison with NO oxidation. Journal of Catalysis, 2010, 272, 151-157.	3.1	8
7666	Effect of surface hydroxyls on selective CO2 hydrogenation over Ni4/Î³-Al2O3: A density functional theory study. Journal of Catalysis, 2010, 272, 227-234.	3.1	159
7667	N2O decomposition over Fe-zeolites: Structure of the active sites and the origin of the distinct reactivity of Fe-ferrierite, Fe-ZSM-5, and Fe-beta. A combined periodic DFT and multispectral study. Journal of Catalysis, 2010, 272, 262-274.	3.1	119
7668	Methane complete and partial oxidation catalyzed by Pt-doped CeO2. Journal of Catalysis, 2010, 273, 125-137.	3.1	186
7669	Mediatory role of tin in the catalytic performance of tailored platinumâ€“tin alloy surfaces for carbon monoxide oxidation. Journal of Catalysis, 2010, 273, 211-220.	3.1	15
7670	Modulation of catalyst particle structure upon support hydroxylation: Ab initio insights into Pd13 and Pt13/Î³-Al2O3. Journal of Catalysis, 2010, 274, 99-110.	3.1	137
7671	Temperature-programmed reduction of unpromoted MoS2-based hydrodesulfurization catalysts: First-principles kinetic Monte Carlo simulations and comparison with experiments. Journal of Catalysis, 2010, 275, 117-128.	3.1	20
7672	Descriptors controlling the catalytic activity of metallic surfaces toward water splitting. Journal of Catalysis, 2010, 276, 92-100.	3.1	86
7673	Mechanism of Charging of Au Atoms and Nanoclusters on Li Doped SiO₂/Mo(112) Films. ChemPhysChem, 2010, 11, 412-418.	1.0	14
7674	Ab Initio Molecular Dynamics Simulations of the Adsorption of H₂ on Palladium Surfaces. ChemPhysChem, 2010, 11, 1374-1381.	1.0	48

#	Article	IF	Citations
7675	Adsorption of Proline and Glycine on the TiO₂(110) Surface: A Density Functional Theory Study. ChemPhysChem, 2010, 11, 1053-1061.	1.0	59
7676	Interactions between Oxygen Atoms on Pt(100): Implications for Ordering during Chemisorption and Catalysis. ChemPhysChem, 2010, 11, 2174-2181.	1.0	17
7677	Photostimulated Reduction Processes in a Titania Hybrid Metalâ€“Organic Framework. ChemPhysChem, 2010, 11, 2341-2344.	1.0	48
7678	Firstâ€principles calculation of electronic structure of Vâ€doped anatase TiO₂. ChemPhysChem, 2010, 11, 2606-2611.	1.0	28
7679	A firstâ€principles study on the existence and structures of the lighter alkalineâ€earth pernitrides. Journal of Computational Chemistry, 2010, 31, 1613-1617.	1.5	8
7680	Thermal dissociation of tripropylamine as the first step in the growth of carbon nanotubes inside AlPO₄â€5 channels. Journal of Computational Chemistry, 2010, 31, 1681-1688.	1.5	3
7681	Phase stability and mechanical properties of rhenium borides by firstâ€principles calculations. Journal of Computational Chemistry, 2010, 31, 1904-1910.	1.5	29
7682	Implementation of an algorithm based on the Rungeâ€Kuttaâ€Fehlberg technique and the potential energy as a reaction coordinate to locate intrinsic reaction paths. Journal of Computational Chemistry, 2010, 31, 2510-2525.	1.5	11
7683	A densityâ€functional study of the phase diagram of cementiteâ€type (Fe,Mn)₃C at absolute zero temperature. Journal of Computational Chemistry, 2010, 31, 2620-2627.	1.5	10
7684	Structural stability and phase transition in OsC and RuC. Journal of Computational Chemistry, 2010, 31, 2883-2888.	1.5	17
7685	Progress in the Theory of Dense Strongly Coupled Plasmas. Contributions To Plasma Physics, 2010, 50, 970-985.	0.5	39
7686	Stability of LiF Crystal in the Warm Dense Matter State. Contributions To Plasma Physics, 2010, 50, 31-34.	0.5	38
7687	Polymorphism of Fluoroargentates(II): Facile Collapse of a Layered Network of Î±â€K₂AgF₄ Due to the Insufficient Size of the Potassium Cation. European Journal of Inorganic Chemistry, 2010, 2010, 2919-2925.	1.0	16
7688	Using Ab Initio Calculations in Designing bcc Mgâ€“X Alloys for Ultraâ€Lightweight Applications. Advanced Engineering Materials, 2010, 12, 1198-1205.	1.6	20
7689	On the Design of Highâ€Efficiency Thermoelectric Clathrates through a Systematic Crossâ€Substitution of Framework Elements. Advanced Functional Materials, 2010, 20, 755-763.	7.8	195
7690	Universal Behavior and Electricâ€Fieldâ€Induced Structural Transition in Rareâ€Earthâ€Substituted BiFeO₃. Advanced Functional Materials, 2010, 20, 1108-1115.	7.8	364
7691	Graphite Oxide as a Photocatalyst for Hydrogen Production from Water. Advanced Functional Materials, 2010, 20, 2255-2262.	7.8	746
7692	Large Spaceâ€Charge Effects in a Nanostructured Proton Conductor. Advanced Functional Materials, 2010, 20, 4107-4116.	7.8	18

#	Article	IF	Citations
7693	Revealing the Design Principles of Highâ€Performance Biological Composites Using Ab initio and Multiscale Simulations: The Example of Lobster Cuticle. Advanced Materials, 2010, 22, 519-526.	11.1	285
7694	Efficient Spin Injection Through Exchange Coupling at Organic Semiconductor/Ferromagnet Heterojunctions. Advanced Materials, 2010, 22, 1626-1630.	11.1	74
7696	Ab Initio Guided Design of bcc Ternary Mgâ€“Liâ€“X (Xâ€‰=â€‰Ca, Al, Si, Zn, Cu) Alloys for Ultraâ€Lightweight Applications. Advanced Engineering Materials, 2010, 12, 572-576.	1.6	21
7697	Aggregation and Contingent Metal/Surface Reactivity of 1,3,8,10â€Tetraazaperopyrene (TAPP) on Cu(111). Chemistry - A European Journal, 2010, 16, 2079-2091.	1.7	89
7698	Dynamic Supramolecular Polymers Based on Benzeneâ€1,3,5â€tricarboxamides: The Influence of Amide Connectivity on Aggregate Stability and Amplification of Chirality. Chemistry - A European Journal, 2010, 16, 810-821.	1.7	93
7699	Crystal Structure Prediction and Isostructurality of Three Small Molecules. Chemistry - A European Journal, 2010, 16, 12701-12709.	1.7	15
7700	Phenakiteâ€Type BeP₂N₄â€”A Possible Precursor for a New Hard Spinelâ€Type Material. Chemistry - A European Journal, 2010, 16, 7208-7214.	1.7	34
7701	Methane Activation by Platinum: Critical Role of Edge and Corner Sites of Metal Nanoparticles. Chemistry - A European Journal, 2010, 16, 6530-6539.	1.7	126
7702	Gold Sulfide Nanoclusters: A Unique Coreâ€inâ€Cage Structure. Chemistry - A European Journal, 2010, 16, 4999-5003.	1.7	34
7703	Modular, Homochiral, Porous Coordination Polymers: Rational Design, Enantioselective Guest Exchange Sorption and Ab Initio Calculations of Hostâ€“Guest Interactions. Chemistry - A European Journal, 2010, 16, 10348-10356.	1.7	67
7704	A Radical Polymer as a Twoâ€Dimensional Organic Half Metal. Chemistry - A European Journal, 2010, 16, 12141-12146.	1.7	25
7705	Detection of Carbocationic Species in Zeolites: Large Crystals Pave the Way. Chemistry - A European Journal, 2010, 16, 9340-9348.	1.7	26
7706	Surface Passivationâ€Induced Strong Ferromagnetism of Zinc Oxide Nanowires. Chemistry - A European Journal, 2010, 16, 13072-13076.	1.7	7
7707	Unexpected Deformations Induced by Surface Interaction and Chiral Selfâ€Assembly of Co^{II}â€Tetraphenylporphyrin (Coâ€TPP) Adsorbed on Cu(110): A Combined STM and Periodic DFT Study. Chemistry - A European Journal, 2010, 16, 11641-11652.	1.7	48
7708	A Neutral Zwitterionic Molecular Solid. Chemistry - A European Journal, 2010, 16, 14051-14059.	1.7	36
7720	Local Vibrational Mechanism for Negative Thermal Expansion: A Combined Neutron Scattering and Firstâ€Principles Study. Angewandte Chemie - International Edition, 2010, 49, 585-588.	7.2	87
7721	Hydrogen Diffusion into Palladium Nanoparticles: Pivotal Promotion by Carbon. Angewandte Chemie - International Edition, 2010, 49, 4743-4746.	7.2	91
7722	2D Random Organization of Racemic Amino Acid Monolayers Driven by Nanoscale Adsorption Footprints: Proline on Cu(110). Angewandte Chemie - International Edition, 2010, 49, 2344-2348.	7.2	46

#	Article	IF	Citations
7723	A Molecular Double Decker: Extending the Limits of Current Metalâ€“Molecule Hybrid Structures. Angewandte Chemie - International Edition, 2010, 49, 341-345.	7.2	28
7724	Carbon Monoxide as a Promoter for its own Oxidation on a Gold Electrode. Angewandte Chemie - International Edition, 2010, 49, 1241-1243.	7.2	77
7725	Scandiumâ€Doped AlN 1D Hexagonal Nanoprisms: A Class of Roomâ€Temperature Ferromagnetic Materials. Angewandte Chemie - International Edition, 2010, 49, 173-176.	7.2	36
7726	Ab Initio Thermochemistry of Solidâ€State Materials. Angewandte Chemie - International Edition, 2010, 49, 5242-5266.	7.2	158
7727	A Ferromagnetic Carbodiimide: Cr₂(NCN)₃. Angewandte Chemie - International Edition, 2010, 49, 4738-4742.	7.2	67
7728	The Interplay between Structure and CO Oxidation Catalysis on Metalâ€Supported Ultrathin Oxide Films. Angewandte Chemie - International Edition, 2010, 49, 4418-4421.	7.2	191
7729	Planar Fe₆ Cluster Units in the Crystal Structure of RE₁₅Fe₈C₂₅ (RE=Y, Dy, Ho, Er). Angewandte Chemie - International Edition, 2010, 49, 5688-5692.	7.2	19
7730	Coreâ€Protected Platinum Monolayer Shell Highâ€Stability Electrocatalysts for Fuelâ€Cell Cathodes. Angewandte Chemie - International Edition, 2010, 49, 8602-8607.	7.2	554
7731	First-principles calculation of parameters of electron paramagnetic resonance spectroscopy in solids. Magnetic Resonance in Chemistry, 2010, 48, S2-S10.	1.1	6
7732	First-principles calculations of NMR parameters for phosphate materials. Magnetic Resonance in Chemistry, 2010, 48, S142-S150.	1.1	28
7733	GaN/LiNbO3 (0001) interface formation calculated from first-principles. Applied Surface Science, 2010, 256, 5740-5743.	3.1	9
7734	Ab initio calculations of generalized-stacking-fault energy surfaces and surface energies for FCC metals. Applied Surface Science, 2010, 256, 6345-6349.	3.1	89
7735	Spatial and electronic structure of the Ni3P surface. Applied Surface Science, 2010, 256, 7692-7695.	3.1	11
7736	Preparation, electronic structure, and photocatalytic properties of Bi2O2CO3 nanosheet. Applied Surface Science, 2010, 257, 172-175.	3.1	171
7737	Synergy between theory and experiment in structure resolution of low-dimensional oxides. Progress in Surface Science, 2010, 85, 398-434.	3.8	90
7738	Metalâ€“organic interaction probed by First Principles STM simulations. Progress in Surface Science, 2010, 85, 435-459.	3.8	16
7739	Iterative diagonalization in augmented plane wave based methods in electronic structure calculations. Journal of Computational Physics, 2010, 229, 453-460.	1.9	21
7740	A massively-parallel electronic-structure calculations based on real-space density functional theory. Journal of Computational Physics, 2010, 229, 2339-2363.	1.9	114

#	Article	IF	Citations
7741	Platinum-monolayer electrocatalysts: Palladium interlayer on IrCo alloy core improves activity in oxygen-reduction reaction. Journal of Electroanalytical Chemistry, 2010, 649, 232-237.	1.9	45
7742	The influence of Mg on the C adsorption on Ni(100): A DFT study. Journal of Molecular Catalysis A, 2010, 315, 171-177.	4.8	7
7743	Investigation the active site of methane dissociation on Ni-based catalysts: A first-principles analysis. Journal of Molecular Catalysis A, 2010, 315, 187-196.	4.8	29
7744	Mechanistic aspect of ethanol synthesis from methanol under CO hydrogenation condition on MoSx cluster model catalysts. Journal of Molecular Catalysis A, 2010, 329, 77-85.	4.8	14
7745	Structural ordering tendencies in the new ferromagnetic Niâ€“Coâ€“Feâ€“Gaâ€“Zn Heusler alloys. Physics Procedia, 2010, 10, 144-148.	1.2	2
7746	Ab initio molecular dynamics simulations on the structural change of liquid eutectic alloy Si15Te85 from 673 to 1373k. Physica B: Condensed Matter, 2010, 405, 785-792.	1.3	7
7747	Adsorption geometry of tetracene on SiO2/Si (111) substrate with the balance of moleculeâ€“substrate and intermolecular interaction. Physica B: Condensed Matter, 2010, 405, 990-995.	1.3	5
7748	Structural, electronic and magnetic properties of Fe nanowires encapsulated in boron nitride nanotubes. Physica B: Condensed Matter, 2010, 405, 1035-1039.	1.3	17
7749	Structural and electronic properties of amorphous InSb from first principles study. Physica B: Condensed Matter, 2010, 405, 2481-2484.	1.3	5
7750	Elastic properties of cubic perovskite BaRuO3 from first-principles calculations. Physica B: Condensed Matter, 2010, 405, 3117-3119.	1.3	14
7751	Hydrogen desorption energies of Aluminum hydride (AlnH3n) clusters. Physica B: Condensed Matter, 2010, 405, 3075-3081.	1.3	15
7752	First principles study on the new sp3 bonded metallic carbon crystal. Physica B: Condensed Matter, 2010, 405, 3324-3327.	1.3	4
7753	Ab initio molecular dynamics simulations of structural change in liquid Se30Te70 from low- to high-density phases. Physica B: Condensed Matter, 2010, 405, 3342-3349.	1.3	3
7754	First-principles study of the perfect and vacancy defect AlN nanoribbon. Physica B: Condensed Matter, 2010, 405, 3775-3781.	1.3	65
7755	Adsorption of S, O, and H on the NiAl(110)-(2Ã—2) surface. Physica B: Condensed Matter, 2010, 405, 4059-4063.	1.3	12
7756	Structural, elastic, electronic, and thermodynamic properties of PrN from first principles calculations. Physica B: Condensed Matter, 2010, 405, 4139-4144.	1.3	15
7757	Electronic structure and optical properties of from ab initio calculations. Physica B: Condensed Matter, 2010, 405, 4578-4581.	1.3	6
7758	First-principles study on the electronic properties of BaCu2S2. Physica B: Condensed Matter, 2010, 405, 4582-4585.	1.3	11

#	Article	IF	Citations
7759	Rational design of novel cathode materials in solid oxide fuel cells using first-principles simulations. Journal of Power Sources, 2010, 195, 1441-1445.	4.0	77
7760	Regenerating Ptâ€“3dâ€“Pt model electrocatalysts through oxidationâ€“reduction cycles monitored at atmospheric pressure. Journal of Power Sources, 2010, 195, 3140-3144.	4.0	57
7761	Factors affecting Li mobility in spinel LiMn2O4â€”A first-principles study by GGA and GGA+U methods. Journal of Power Sources, 2010, 195, 4971-4976.	4.0	138
7762	Elastic softening of amorphous and crystalline Liâ€“Si Phases with increasing Li concentration: A first-principles study. Journal of Power Sources, 2010, 195, 6825-6830.	4.0	367
7763	Neutron powder diffraction and first-principles computational studies of CuLixMg2â^'x (xâ‰…0.08), CuMg2, and Cu2Mg. Journal of Solid State Chemistry, 2010, 183, 10-19.	1.4	12
7764	UTa2O(S2)3Cl6: A ribbon structure containing a heterobimetallic 5dâ€“5f M3 cluster. Journal of Solid State Chemistry, 2010, 183, 285-290.	1.4	11
7765	The influence of sulfur substitution on the atomic displacement in Bi2Ti2O7. Journal of Solid State Chemistry, 2010, 183, 262-269.	1.4	3
7766	Order-to-disorder phase transformation in ion irradiated uranium-bearing delta-phase oxides RE6U1O12 (RE=Y, Gd, Ho, Yb, and Lu). Journal of Solid State Chemistry, 2010, 183, 844-848.	1.4	23
7767	Potential existence of post-perovskite nitrides; DFT studies of ThTaN3. Journal of Solid State Chemistry, 2010, 183, 994-999.	1.4	14
7768	Synthesis of Li2PtH6 using high pressure: Completion of the homologous series A2PtH6 (A=alkali) Tj ETQq1 1 0.784314 rgBT /Overlock	1.4	21
7769	Bixbyite- and anatase-type phases in the system Scâ€“Taâ€“Oâ€“N. Journal of Solid State Chemistry, 2010, 183, 2051-2058.	1.4	14
7770	Effects of oxygen vacancy on the magnetic properties of Cr-doped SnO2: Density functional investigation. Journal of Solid State Chemistry, 2010, 183, 3073-3077.	1.4	22
7771	Magnetic structure and phonon spectra of iron-based superconductors: A first-principle study. Physica C: Superconductivity and Its Applications, 2010, 470, S430-S432.	0.6	1
7772	Pressure effects on iron-based superconductors: A first-principles study. Physica C: Superconductivity and Its Applications, 2010, 470, S387-S388.	0.6	1
7773	Structural, elastic, electronic properties and Fermi surface for superconducting Mo2GaC in comparison with V2GaC and Nb2GaC from first principles. Physica C: Superconductivity and Its Applications, 2010, 470, 533-537.	0.6	43
7774	First-principles calculations for anisotropy of iron-based superconductors. Physica C: Superconductivity and Its Applications, 2010, 470, 1066-1069.	0.6	2
7775	Stability of IIIâ€“V and IVâ€“VI nanowiresâ€”A theoretical study. Physica E: Low-Dimensional Systems and Nanostructures, 2010, 42, 795-798.	1.3	7
7776	An ab-initio study of photoabsorption spectrum of ultra small CdS clusters. Physica E: Low-Dimensional Systems and Nanostructures, 2010, 42, 1365-1371.	1.3	2

#	Article	IF	Citations
7777	A hierarchical research by large-scale and ab initio electronic structure theoriesâ€"Si and Ge cleavage and stepped surfaces. Physica E: Low-Dimensional Systems and Nanostructures, 2010, 42, 2784-2787.	1.3	1
7778	Neutral vacancy-defect-induced magnetism in SiC monolayer. Physica E: Low-Dimensional Systems and Nanostructures, 2010, 42, 2451-2454.	1.3	26
7779	The chemical modification of graphene antidot lattices. Physica E: Low-Dimensional Systems and Nanostructures, 2010, 43, 33-39.	1.3	3
7780	First-principles study of transition-metal atoms adsorption on GaN nanotube. Physica E: Low-Dimensional Systems and Nanostructures, 2010, 43, 22-27.	1.3	14
7781	Influences of Al doping on the electronic structure of Mg(0001) and dissociation properties of H2. Physics Letters, Section A: General, Atomic and Solid State Physics, 2010, 374, 975-980.	0.9	7
7782	Electronic structures of N- and C-doped NiO from first-principles calculations. Physics Letters, Section A: General, Atomic and Solid State Physics, 2010, 374, 1184-1187.	0.9	27
7783	Electronic structures and magnetic properties of Zn-doped colossal magnetoresistance materials. Physics Letters, Section A: General, Atomic and Solid State Physics, 2010, 374, 1555-1559.	0.9	1
7784	Ultra-incompressible superconducting phase of OsC predicted by phonon calculations. Physics Letters, Section A: General, Atomic and Solid State Physics, 2010, 374, 1880-1884.	0.9	18
7785	Hydrogen depassivation of the magnesium acceptor by beryllium in p-type GaN. Physics Letters, Section A: General, Atomic and Solid State Physics, 2010, 374, 2374-2378.	0.9	0
7786	Effect of orthorhombic distortion and electron correlation on the electronic structure of SrMnO3 from first principles. Physics Letters, Section A: General, Atomic and Solid State Physics, 2010, 374, 2388-2391.	0.9	5
7787	Investigation of tetragonal ReN2 and WN2 with high shear moduli from first-principles calculations. Physics Letters, Section A: General, Atomic and Solid State Physics, 2010, 374, 2569-2574.	0.9	39
7788	Strain-induced structural and direct-to-indirect band gap transition in ZnO nanotubes. Physics Letters, Section A: General, Atomic and Solid State Physics, 2010, 374, 2846-2849.	0.9	34
7789	Role of point defects on conductivity, magnetism and optical properties in In2O3. Physics Letters, Section A: General, Atomic and Solid State Physics, 2010, 374, 2879-2885.	0.9	12
7790	Stability and electronic properties of the O-terminated Cu2O(111) surfaces: First-principles investigation. Physics Letters, Section A: General, Atomic and Solid State Physics, 2010, 374, 2994-2998.	0.9	36
7791	First-principles study of the partitioning and site preference of Re or Ru in Co-based superalloys with interface. Physics Letters, Section A: General, Atomic and Solid State Physics, 2010, 374, 3238-3242.	0.9	21
7792	Preferential adsorption of gallium on GaAs(111)B surfaces during the initial growth of Au-assisted GaAs nanowires. Physics Letters, Section A: General, Atomic and Solid State Physics, 2010, 374, 3247-3253.	0.9	3
7793	A comparative first-principles study of the adsorption of a carbon atom on copper and nickel surfaces. Physics Letters, Section A: General, Atomic and Solid State Physics, 2010, 374, 4563-4567.	0.9	11
7794	Density functional theory studies on the adsorption, diffusion and dissociation of O2 on Pt(111). Physics Letters, Section A: General, Atomic and Solid State Physics, 2010, 374, 4713-4717.	0.9	31

#	Article	IF	Citations
7795	Magnetic properties of 3d transition metal chains on vicinal surface. Journal of Magnetism and Magnetic Materials, 2010, 322, 1296-1299.	1.0	9
7796	Ab initio investigation of local magnetic structures around substitutional 3d transition metal impurities at cation sites in IIIâ€“V and IIâ€“VI semiconductors. Journal of Magnetism and Magnetic Materials, 2010, 322, 290-297.	1.0	26
7797	Stability of Ferromagnetism in Fe, Co, and Ni Metals under High Pressure with GGA and GGA+U. Journal of Magnetism and Magnetic Materials, 2010, 322, 653-657.	1.0	42
7798	Concentration dependent magnetism induced by hydrogen adsorption on graphene and single walled carbon nanotubes. Journal of Magnetism and Magnetic Materials, 2010, 322, 838-843.	1.0	16
7799	Theoretical study of the electronic and magnetic properties of Co2Cr1â^'xVxAl. Journal of Magnetism and Magnetic Materials, 2010, 322, 2293-2297.	1.0	14
7800	Surface effects on the magnetic properties of Co2FeAl(001): An ab initio study. Journal of Magnetism and Magnetic Materials, 2010, 322, 3351-3354.	1.0	8
7801	Non-periodic finite-element formulation of Kohnâ€“Sham density functional theory. Journal of the Mechanics and Physics of Solids, 2010, 58, 256-280.	2.3	101
7802	Multiscale computations for carbon nanotubes based on a hybrid QM/QC (quantum mechanical and) Tj ETQq1 1 0.784314 rgBT /Ove	2.3	11
7803	First-principles study of ground-state properties and high pressure behavior of ThO2. Journal of Nuclear Materials, 2010, 399, 181-188.	1.3	68
7804	First principles study on elastic properties and phase transition of NpN. Journal of Nuclear Materials, 2010, 401, 113-117.	1.3	11
7805	First-principles study on dissolution and diffusion properties of hydrogen in molybdenum. Journal of Nuclear Materials, 2010, 404, 109-115.	1.3	49
7806	Ab initio-based diffusion theory and tracer diffusion in Niâ€“Cr and Niâ€“Fe alloys. Journal of Nuclear Materials, 2010, 405, 216-234.	1.3	126
7807	Ab initio simulation of yttrium oxide nanocluster formation on fcc Fe lattice. Journal of Nuclear Materials, 2010, 406, 345-350.	1.3	22
7808	Binary effect of He and H on the intra- and inter-granular embrittlement in Fe. Journal of Nuclear Materials, 2010, 407, 200-204.	1.3	22
7809	Study on the doping stability and electronic structure of wurtzite Zn1â^'xCdxO alloys by first-principle calculations. Journal of Physics and Chemistry of Solids, 2010, 71, 336-339.	1.9	20
7810	O-vacancy and surface on CeO2: A first-principles study. Journal of Physics and Chemistry of Solids, 2010, 71, 788-796.	1.9	29
7811	Dehydrogenation associated with Ti catalyst in sodium alanate. Journal of Physics and Chemistry of Solids, 2010, 71, 1073-1076.	1.9	8
7812	Chemical bonding and pseudogap formation in D022- and L12-structure (V, Ti)Al3. Journal of Physics and Chemistry of Solids, 2010, 71, 946-951.	1.9	14

#	Article	IF	Citations
7813	Transparent visible light activated Câ€“Nâ€“F-codoped TiO2 films for self-cleaning applications. Journal of Photochemistry and Photobiology A: Chemistry, 2010, 210, 181-187.	2.0	86
7814	The effect of Ti atom on hydrogenation of Al(111) surface: First-principles studies. International Journal of Hydrogen Energy, 2010, 35, 609-613.	3.8	18
7815	The adsorption and dissociation of H2O on TiO2(110) and M/TiO2(110) (MÂ=ÂPt, Au) surfacesâ€“A computational investigation. International Journal of Hydrogen Energy, 2010, 35, 1530-1536.	3.8	14
7816	An ab initio study of dissociative adsorption of H2 on FeTi surfaces. International Journal of Hydrogen Energy, 2010, 35, 1681-1692.	3.8	30
7817	Adsorption and desorption of hydrogen in Mg nanoclusters: Combined effects of size and Ti doping. International Journal of Hydrogen Energy, 2010, 35, 2344-2350.	3.8	12
7818	The role of Li and Ni metals in the adsorbate complex and their effect on the hydrogen storage capacity of single walled carbon nanotubes coated with metal hydrides, LiH and NiH2. International Journal of Hydrogen Energy, 2010, 35, 2368-2376.	3.8	38
7819	Effect of Mg, Ca, and Zn on stability of LiBH4 through computational thermodynamics. International Journal of Hydrogen Energy, 2010, 35, 6812-6821.	3.8	25
7820	First principles study to identify the reversible reaction step of a multinary hydrogen storage â€œLiâ€“Mgâ€“Bâ€“Nâ€“Hâ€•system. International Journal of Hydrogen Energy, 2010, 35, 9002-9011.	3.8	5
7821	First-principles studies of the structures and properties of Al- and Ag-substituted Mg2Ni alloys and their hydrides. International Journal of Hydrogen Energy, 2010, 35, 10349-10358.	3.8	23
7822	DFT-based FEM analysis of nonlinear effects on indentation process in diamond crystal. International Journal of Mechanical Sciences, 2010, 52, 303-308.	3.6	6
7823	Thermodynamics of carbon in iron nanoparticles at low temperature: Reduced solubility and size-induced nucleation of cementite. Physics Procedia, 2010, 6, 16-26.	1.2	5
7824	Structure, lattice dynamics and Fermi surface of the magnetic shape memory system Coâ€“Niâ€“Ga from first principles calculations. Physics Procedia, 2010, 10, 138-143.	1.2	0
7825	First-principles study electronic and optical properties of p-type Al-doped Î³-Si3N4. Physica B: Condensed Matter, 2010, 405, 828-833.	1.3	15
7826	First-principles study of extensive dopants in wurtzite ZnO. Physica B: Condensed Matter, 2010, 405, 158-160.	1.3	15
7827	Effect of uniaxial strain on the band gap of zigzag carbon nanotubes. Physica B: Condensed Matter, 2010, 405, 1329-1334.	1.3	12
7828	Surface structures of Heusler alloys: A first-principles study. Physica B: Condensed Matter, 2010, 405, 1580-1585.	1.3	3
7829	Adsorption of oxygen atom on the pristine and antisite defected SiC nanotubes. Physica B: Condensed Matter, 2010, 405, 2673-2679.	1.3	14
7830	First-principles study on the relaxed structures and electronic properties of Fe nanowires. Physica B: Condensed Matter, 2010, 405, 2726-2732.	1.3	1

#	Article	IF	Citations
7831	Hydrogen sensing properties of low-index surfaces of SnO2 from first-principles. Physica B: Condensed Matter, 2010, 405, 3458-3462.	1.3	22
7832	First-principles calculations on third-order elastic constants and internal relaxation for monolayer graphene. Physica B: Condensed Matter, 2010, 405, 3501-3506.	1.3	32
7833	Nucleation effect of Sia of 6Hâ€“SiC-(0 0 0 1)â€“(âˆš3Ã—âˆš3)R30Â° surface: First-principles study. Physica B: Condensed Matter, 2010, 405, 3576-3580.	1.3	5
7834	GGA and GGA+U calculations of the ground state of SrMnO3. Physica B: Condensed Matter, 2010, 405, 3638-3641.	1.3	5
7835	First-principles determination of the structure, elastic constant, phase diagram and thermodynamics of NiTi alloy. Physica B: Condensed Matter, 2010, 405, 3665-3672.	1.3	32
7836	The structural, electronic, elastic, vibrational, and thermodynamic properties of HoX (X=Sb, Bi). Physica B: Condensed Matter, 2010, 405, 3977-3985.	1.3	9
7837	Elastic and electronic properties of ScMn2 from first-principles calculations. Physica B: Condensed Matter, 2010, 405, 4812-4817.	1.3	10
7838	Magnetic properties in nitrogen-doped CeO2 from first-principles calculations. Physica B: Condensed Matter, 2010, 405, 4858-4862.	1.3	7
7839	Atomistic theoretical models for nanoporous hybrid materials. Microporous and Mesoporous Materials, 2010, 129, 304-318.	2.2	46
7840	Interaction of CO, CO2 and CH4 with mesoporous organosilica: Periodic DFT calculations with dispersion corrections. Microporous and Mesoporous Materials, 2010, 129, 62-67.	2.2	23
7841	Density functional study of the chemisorption of C1, C2 and C3 intermediates in propane dissociation on Pt(111). Journal of Molecular Catalysis A, 2010, 321, 42-49.	4.8	77
7842	Effects of the period vacancy on the structure, electronic and magnetic properties of the zigzag BN nanoribbon. Journal of Molecular Structure, 2010, 984, 344-349.	1.8	14
7843	Interface atomic structure of LaCuOSe:Mg epitaxial thin film and MgO substrate. Materials Science and Engineering B: Solid-State Materials for Advanced Technology, 2010, 173, 229-233.	1.7	3
7844	Impurities in FeAs-based superconductor, SrFe2As2, studied by first-principles calculations. Materials Science and Engineering B: Solid-State Materials for Advanced Technology, 2010, 173, 244-247.	1.7	4
7845	Electronic structures of MnP-based crystals: LaMnOP, BaMn2P2, and KMnP. Materials Science and Engineering B: Solid-State Materials for Advanced Technology, 2010, 173, 239-243.	1.7	8
7846	Realization of p-type ZnO by (nN, Mg) codoping from first-principles. Optical Materials, 2010, 32, 1216-1222.	1.7	24
7847	Engineering of the electronic structures of metal-porphyrin tapes and metal-hexaphyrin tapes: A first-principles study. Chemical Physics, 2010, 369, 66-70.	0.9	9
7848	Density-functional study for the NOx (x=1, 2) dissociation mechanism on the Cu(111) surface. Chemical Physics, 2010, 373, 300-306.	0.9	36

#	Article	IF	Citations
7849	Amorphous carbon and its surfaces. Chemical Physics, 2010, 374, 77-82.	0.9	6
7850	Thermal stabilities of delithiated olivine MPO4 (M=Fe, Mn) cathodes investigated using first principles calculations. Electrochemistry Communications, 2010, 12, 427-430.	2.3	224
7851	Fabrication and characterization of platinum nanoparticle arrays of controlled size, shape and orientation. Electrochimica Acta, 2010, 55, 7934-7938.	2.6	14
7852	First principle calculations of core-level binding energy and Auger kinetic energy shifts in metallic solids. Journal of Electron Spectroscopy and Related Phenomena, 2010, 178-179, 88-99.	0.8	25
7853	Water adsorption and dissociation on the Au(321) stepped surface. Computational and Theoretical Chemistry, 2010, 946, 51-56.	1.5	12
7854	Cluster and periodic DFT calculations of adsorption of hydroxyl on the Au(hkl) surfaces. Computational and Theoretical Chemistry, 2010, 946, 43-50.	1.5	28
7855	Electron and vibrational spectroscopies using DFT, plane waves and pseudopotentials: CASTEP implementation. Computational and Theoretical Chemistry, 2010, 954, 22-35.	1.5	205
7856	Magnetic and electronic properties of a single iron atomic chain encapsulated in carbon nanotubes: A first-principles study. Computational and Theoretical Chemistry, 2010, 962, 108-112.	1.5	8
7857	Electronic structure and optical properties in ZnO:M(Co, Cd). Thin Solid Films, 2010, 518, 4568-4571.	0.8	26
7858	Doping-induced modulation of electrical and optical properties of silicon nitride. Thin Solid Films, 2010, 518, 4918-4922.	0.8	5
7859	Electronic structure and crystallinity of the HfO2â€“TiO2 thin films. Thin Solid Films, 2010, 518, e107-e110.	0.8	4
7860	First-principles study on the formation of a vacancy in Ge under biaxial compressive strain. Thin Solid Films, 2010, 518, 6373-6377.	0.8	4
7861	Tunable properties of wide-band gap p-type BaCu(Ch1â^'xChxâ€²)F (Ch = S, Se, Te) thin-film solid solutions. Thin Solid Films, 2010, 518, 5494-5500.	0.8	21
7862	Ab initio study of the binding of collagen amino acids to graphene and A-doped (A=H, Ca) graphene. Thin Solid Films, 2010, 518, 6951-6961.	0.8	64
7863	Stability of strained thin films with interface misfit dislocations: A multiscale computational study. Thin Solid Films, 2010, 519, 809-817.	0.8	4
7864	Enhancement of optical absorption in Ga-chalcopyrite-based intermediate-band materials for high efficiency solar cells. Solar Energy Materials and Solar Cells, 2010, 94, 1903-1906.	3.0	48
7865	An ab initio study of Coâ€“Cr(V) disorder effects on the electronic structure and magnetic properties of. Solid State Communications, 2010, 150, 109-113.	0.9	3
7866	Elastic and electronic properties of a new MAX compound from first-principles calculations. Solid State Communications, 2010, 150, 49-53.	0.9	18

#	Article	IF	Citations
7867	First principles study of Jahnâ€“Teller effects in LixMnPO4. Solid State Communications, 2010, 150, 40-44.	0.9	95
7868	An ab initio study of 5d noble metal nitrides: OsN2, IrN2, PtN2 and AuN2. Solid State Communications, 2010, 150, 181-186.	0.9	37
7869	Ab initio investigation of oxygen adsorption on the stability of carbon nanotube field effect transistors (CNTFETs). Solid State Communications, 2010, 150, 258-261.	0.9	3
7870	Phase transition and thermodynamics of thorium from first-principles calculations. Solid State Communications, 2010, 150, 393-398.	0.9	13
7871	Structural stability and electronic properties of LiNiN. Solid State Communications, 2010, 150, 669-674.	0.9	8
7872	Defect-induced strong ferromagnetism in Cr-doped from first-principles theory. Solid State Communications, 2010, 150, 663-665.	0.9	6
7873	Crystal structure and physical properties of OsN: First-principle calculations. Solid State Communications, 2010, 150, 759-762.	0.9	18
7874	Ab initio prediction for the ionic conduction of lithium in <mml:math xmlns:mml="http://www.w3.org/1998/Math/MathML" altimg="si20.gif" display="inline" overflow="scroll"><mml:msub><mml:mrow><mml:mstyle mathvariant="normal"><mml:mi>LiInSiO</mml:mi></mml:mstyle></mml:mrow><mml:mrow><mml:mn>4</mml:mn></mml:mrow></mml and <mml:math xmlns:mml="http://www.w3.org/1998/Math/MathML" altimg="si21.gif" display="inline" overflow="scroll"><mml:msub><mml:mrow><mml:mstyle mathvariant="normal"><mml:mi>LiIn. Solid	0.9	11
7875	Bandgaps and band bowing in semiconductor alloys. Solid State Communications, 2010, 150, 888-892.	0.9	8
7876	Electronic structure and magnetic properties in Nitrogen-doped from density functional calculations. Solid State Communications, 2010, 150, 852-856.	0.9	11
7877	Formation energies of low-indexed surfaces of tin dioxide terminated by nonmetals. Solid State Communications, 2010, 150, 957-960.	0.9	7
7878	Ab initio studies of half-metallic ferromagnetism in carbon-doped. Solid State Communications, 2010, 150, 923-927.	0.9	13
7879	First-principles investigation of Cr doping effects on the structural, magnetic and electronic properties in. Solid State Communications, 2010, 150, 1069-1073.	0.9	8
7880	Defect-induced rigidity enhancement in layered semiconductors. Solid State Communications, 2010, 150, 1200-1203.	0.9	7
7881	A first-principles study on phase transition induced by charge ordering of <mml:math xmlns:mml="http://www.w3.org/1998/Math/MathML" altimg="si26.gif" display="inline" overflow="scroll"><mml:msup><mml:mrow><mml:mstyle mathvariant="normal"><mml:mi>Mn</mml:mi></mml:mstyle></mml:mrow><mml:mrow><mml:mn>3</mml:mn><mml:mo>+</mml:mo mathvariant="normal"><mml:mi>Mn</mml:mi></mml:mstyle></mml:mrow><mml:mrow><mml:mn>4</mml:mn><mml:mo>+</mml:mo Solid State Communications, 2010, 150, 1329-1333.	0.9	29
7882	Structural stability and hydrogen diffusion in alloys. Solid State Communications, 2010, 150, 1715-1718.	0.9	18
7883	The effect of magnetostructural coupling on mechanical behaviors in CrN. Solid State Communications, 2010, 150, 2045-2048.	0.9	19
7884	First principles investigation on the band gap of the ground state of. Solid State Communications, 2010, 150, 1983-1986.	0.9	18

#	Article	IF	Citations
7885	Vibrational signature of the Siâ€“N defect in Si-doped GaNxAs1âˆ’x. Solid State Communications, 2010, 150, 1967-1970.	0.9	5
7886	Electronic and magnetic properties of C-doped Mg3N2: A density functional theory study. Solid State Communications, 2010, 150, 2223-2226.	0.9	5
7887	A combined conductivity and DFT study of protons in PbZrO3 and alkaline earth zirconate perovskites. Solid State Ionics, 2010, 181, 130-137.	1.3	57
7888	Factors that affect activation energy for Li diffusion in LiFePO4: A first-principles investigation. Solid State Ionics, 2010, 181, 907-913.	1.3	24
7889	Structural, electronic and Li diffusion properties of LiFeSO4F. Solid State Ionics, 2010, 181, 1209-1213.	1.3	38
7890	Atomic modification of stepped metal surfaces using vertical single-atom manipulation with a trimer-apex tip: First-principles and semiempirical simulations. Surface and Coatings Technology, 2010, 204, 3254-3257.	2.2	1
7891	Instability, intermixing and electronic structure at the epitaxial <mml:math xmlns:mml="http://www.w3.org/1998/Math/MathML" altimg="si51.gif" display="inline" overflow="scroll"><mml:msub><mml:mrow><mml:mstyle mathvariant="normal"><mml:mi>LaAlO</mml:mi></mml:mstyle></mml:mrow><mml:mrow><mml:mn>3</mml:mn></mml:mrow></mm		

#	Article	IF	Citations
7903	Theoretical analysis of oxygen reduction reaction and H2O2 formation and the impact of CF3SO3H coverage on Pt (111). Surface Science, 2010, 604, 965-973.	0.8	14
7904	Cooperative phenomena in self-assembled nucleation of 3Ã—4-In/Si(100) surface magic clusters. Surface Science, 2010, 604, 1116-1120.	0.8	2
7905	Plasma nitridation of Ge(100) surface studied by scanning tunneling microscopy. Surface Science, 2010, 604, 1239-1246.	0.8	3
7906	Electric field induced oscillations in the catalytic water production on rhodium: A theoretical analysis. Surface Science, 2010, 604, 1353-1368.	0.8	22
7907	Structure determination of the p3Ã—3R30â˜ Biâ€“Ag(111) surface alloy using LEED Iâ€“V and DFT analyses. Surface Science, 2010, 604, 1395-1399.	0.8	14
7908	Role of sub-surface oxygen in Cu(100) oxidation. Surface Science, 2010, 604, 1425-1431.	0.8	25
7909	A reactive force-field (ReaxFF) Monte Carlo study of surface enrichment and step structure on yttria-stabilized zirconia. Surface Science, 2010, 604, 1438-1444.	0.8	24
7910	Thermodynamic driving forces governing assembly of disilicide nanowires. Surface Science, 2010, 604, 1481-1486.	0.8	8
7911	Adsorption of thin films of titanium on tungsten (111) surface. Surface Science, 2010, 604, 1524-1530.	0.8	4
7912	Theoretical study of the migration of the hydrogen atom adsorbed on aluminum nanowire. Surface Science, 2010, 604, 1718-1726.	0.8	7
7913	Structural and electronic properties of group III Rich In0.53Ga0.47As(001). Surface Science, 2010, 604, 1757-1766.	0.8	21
7914	Effects of bimetallic modification on the decomposition of CH3OH and H2O on Pt/W(110) bimetallic surfaces. Surface Science, 2010, 604, 1845-1853.	0.8	13
7915	Adsorption of atomic oxygen on cubic PbTiO3 and LaMnO3 (001) surfaces: A density functional theory study. Surface Science, 2010, 604, 1889-1893.	0.8	36
7916	Ab initio study of Yb on the Ge(111)â€“(3Ã—2) and Si(111)â€“(3Ã—2) surfaces. Surface Science, 2010, 604, 1899-1905.	0.8	2
7917	Adsorption of water monomer and clusters on platinum(111) terrace and related steps and kinks. Surface Science, 2010, 604, 1978-1986.	0.8	61
7918	Application of Neumannâ€“Kopp rule for the estimation of heat capacity of mixed oxides. Thermochimica Acta, 2010, 497, 7-13.	1.2	304
7919	Direct space structure solution from precession electron diffraction data: Resolving heavy and light scatterers in Pb13Mn9O25. Ultramicroscopy, 2010, 110, 881-890.	0.8	26
7920	Liquid structure as a guide for phase stability in the solid state: Discovery of a stable compound in the Auâ€“Si alloy system. Acta Materialia, 2010, 58, 449-456.	3.8	16

#	Article	IF	Citations
7921	First-principles study of soluteâ€“vacancy binding in magnesium. Acta Materialia, 2010, 58, 531-540.	3.8	113
7922	First-principles assessment of hydrogen absorption into FeAl and Fe3Si: Towards prevention of steel embrittlement. Acta Materialia, 2010, 58, 638-648.	3.8	46
7923	Ab initio calculations of the uraniumâ€“hydrogen system: Thermodynamics, hydrogen saturation of Î±-U and phase-transformation to UH3. Acta Materialia, 2010, 58, 1045-1055.	3.8	60
7924	Phase field modeling of defects and deformation. Acta Materialia, 2010, 58, 1212-1235.	3.8	365
7925	Plastic deformation of wadsleyite: IV Dislocation core modelling based on the Peierlsâ€“Nabarroâ€“Galerkin model. Acta Materialia, 2010, 58, 1467-1478.	3.8	22
7926	Prediction of structural, electronic and elastic properties of Y2Ti2O7 and Y2TiO5. Acta Materialia, 2010, 58, 1536-1543.	3.8	99
7927	Calculation of impurity diffusivities in Î±-Fe using first-principles methods. Acta Materialia, 2010, 58, 1982-1993.	3.8	117
7928	Effect of Re in Î³ phase, Î³â€²Î³â€² phase and Î³/Î³â€²Î³/Î³â€² interface of Ni-based single-crystal superalloys. Acta Materialia, 2010, 58, 2045-2055.	3.8	55
7929	The effect of platinum on Al diffusion kinetics in Î²-NiAl: Implications for thermal barrier coating lifetime. Acta Materialia, 2010, 58, 2726-2737.	3.8	41
7930	First-principles calculations of the elastic, phonon and thermodynamic properties of Al12Mg17. Acta Materialia, 2010, 58, 4012-4018.	3.8	103
7931	Ab initio study on plane defects in zirconiumâ€“hydrogen solid solution and zirconium hydride. Acta Materialia, 2010, 58, 3927-3938.	3.8	103
7932	Structural analysis of a new precipitate phase in high-temperature TiNiPt shape memory alloys. Acta Materialia, 2010, 58, 4660-4673.	3.8	77
7933	First-principles energetics of hydrogen traps in Î±-Fe: Point defects. Acta Materialia, 2010, 58, 4730-4741.	3.8	174
7934	Fundamental studies on stress-corrosion cracking in iron and underlying mechanisms. Acta Materialia, 2010, 58, 5142-5149.	3.8	19
7935	First-principles data for solid-solution strengthening of magnesium: From geometry and chemistry to properties. Acta Materialia, 2010, 58, 5704-5713.	3.8	325
7936	Effects of tantalum on the partitioning of tungsten between the Î³- and Î³â€²-phases in nickel-based superalloys: Linking experimental and computational approaches. Acta Materialia, 2010, 58, 5898-5911.	3.8	105
7937	Theoretical investigation of {110} generalized stacking faults and their relation to dislocation behavior in perovskite oxides. Acta Materialia, 2010, 58, 6072-6079.	3.8	40
7938	First-principles studies on alloying and simplified thermodynamic aqueous chemical stability of calcium-, zinc-, aluminum-, yttrium- and iron-doped magnesium alloysâ˜†. Acta Biomaterialia, 2010, 6, 1698-1704.	4.1	69

#	Article	IF	Citations
7939	Mechanism of incorporation of zinc into hydroxyapatite. Acta Biomaterialia, 2010, 6, 2289-2293.	4.1	122
7940	Ab initio study of thermodynamic, structural, and elastic properties of Mg-substituted crystalline calcite. Acta Biomaterialia, 2010, 6, 4506-4512.	4.1	44
7941	Inhibition of coking and CO poisoning of Pt catalysts by the formation of Au/Pt bimetallic surfaces. Applied Catalysis A: General, 2010, 375, 303-309.	2.2	61
7942	DFT study on the reaction of NO oxidation on a stepped gold surface. Applied Catalysis A: General, 2010, 379, 111-120.	2.2	28
7943	Density functional theory study of sulfur tolerance of CO adsorption and dissociation on Rhâ€“Ni binary metals. Applied Catalysis A: General, 2010, 389, 122-130.	2.2	17
7944	Impact of CO on the transformation of a model FCC gasoline over CoMoS/Al2O3 catalysts: A combined kinetic and DFT approach. Applied Catalysis B: Environmental, 2010, 97, 323-332.	10.8	11
7945	Generalized-stacking-fault energy and surface properties for HCP metals: A first-principles study. Applied Surface Science, 2010, 256, 3409-3412.	3.1	91
7946	Study of ammonia molecule adsorbing on diamond (100) surface. Applied Surface Science, 2010, 256, 4136-4141.	3.1	7
7947	Adsorption of 2-chlorophenol on Cu2O(111)â€“CuCUS: A first-principles density functional study. Applied Surface Science, 2010, 256, 4764-4770.	3.1	8
7948	Low-coverage alkali metal adsorption on the Ge(001)-p(12) surface. Applied Surface Science, 2010, 256, 4784-4788.	3.1	3
7949	Theoretical study of CO and Pb adsorption on the Ni(111) and Ni3Al(111) surfaces. Applied Surface Science, 2010, 256, 4806-4812.	3.1	19
7950	Fluorine, chlorine and iodine adsorption on the Ge(001) surface: Comparative study for the coverage of 0.75 and 1 monolayer. Applied Surface Science, 2010, 256, 4822-4828.	3.1	6
7951	Mechanics and energy analysis on molten pool spreading during laser solid forming. Applied Surface Science, 2010, 256, 4612-4620.	3.1	37
7952	Effects of the edge shape and the width on the structural and electronic properties of silicene nanoribbons. Applied Surface Science, 2010, 256, 6313-6317.	3.1	111
7953	Adsorption of oxygen molecular on pristine and defected SiC nanotubes. Applied Surface Science, 2010, 257, 282-289.	3.1	11
7954	Density functional theory simulation of titanium migration and reaction with oxygen in the early stages of oxidation of equiatomic NiTi alloy. Biomaterials, 2010, 31, 3439-3448.	5.7	55
7955	Density functional theory study on adsorption of thiophene on TiO2 anatase (001) surfaces. Catalysis Today, 2010, 149, 218-223.	2.2	48
7956	Catalyst size and morphological effects on the interaction of NO2 with BaO/Î³-Al2O3 materials. Catalysis Today, 2010, 151, 304-313.	2.2	8

#	Article	IF	Citations
7957	Non-equilibrium surface pattern formation during catalytic reactions with nanoscale resolution: Investigations of the electric field influence. Catalysis Today, 2010, 154, 75-84.	2.2	14
7958	Lattice anisotropy, electronic and chemical structures of uranyl carbonate, UO2CO3, from first principles. Chemical Physics, 2010, 372, 46-50.	0.9	6
7959	Density-functional studies of the adsorption and reaction of HCl and H2O molecules over the W(111) surface. Chemical Physics, 2010, 374, 22-29.	0.9	0
7960	Calculations of single-crystal elastic constants made simple. Computer Physics Communications, 2010, 181, 671-675.	3.0	182
7961	Finite-size modelling of electrodes for quantum transport calculations using k-space ab initio techniques. Computer Physics Communications, 2010, 181, 746-749.	3.0	3
7962	ATAT@WIEN2k: An interface for cluster expansion based on the linearized augmented planewave method. Computer Physics Communications, 2010, 181, 913-920.	3.0	10
7963	DFT and tight binding Monte Carlo calculations related to single-walled carbon nanotube nucleation and growth. Carbon, 2010, 48, 470-478.	5.4	44
7964	First-principles investigation into structural and magnetic properties of binary graphite 3d-transition metal intercalated compounds (XC6; X=Cr, Mn, Fe). Carbon, 2010, 48, 1341-1344.	5.4	7
7965	In situ observations of the nucleation and growth of atomically sharp graphene bilayer edges. Carbon, 2010, 48, 2354-2360.	5.4	33
7966	Graphane with defect or transition-metal impurity. Carbon, 2010, 48, 3901-3905.	5.4	39
7967	The effect of van der Waals interactions on the properties of intrinsic defects in graphite. Carbon, 2010, 48, 4145-4161.	5.4	37
7968	Edge reconstructions induce magnetic and metallic behavior in zigzag graphene nanoribbons. Carbon, 2010, 48, 4409-4413.	5.4	44
7969	Influence of Î±-alumina supports on oxygen binding to Pd, Ag, Pt, and Au. Chemical Physics Letters, 2010, 484, 231-236.	1.2	17
7970	Ab initio calculations on the structure and properties of hexagonal boron nitrides. Chemical Physics Letters, 2010, 490, 210-215.	1.2	12
7971	Role of hydroxyl groups for the O2 adsorption on CeO2 surface: A DFT+U study. Chemical Physics Letters, 2010, 493, 269-272.	1.2	18
7972	Ferromagnetic interaction between A-site Cu spins in A-site-ordered perovskites Aâ€²Cu3Sn4O12 with Aâ€²=Ca2+, Sr2+, Pb2+, and La3+. Chemical Physics Letters, 2010, 494, 213-217.	1.2	6
7973	Pressure induced structural changes in the potential hydrogen storage compound ammonia borane: A combined X-ray, neutron and theoretical investigation. Chemical Physics Letters, 2010, 495, 203-207.	1.2	28
7974	Spatial confinement of carriers and tunable band structures in InAs/InP-coreâ€“shell nanowires. Chemical Physics Letters, 2010, 495, 261-265.	1.2	22

#	Article	IF	Citations
7975	Potential existence of postperovskite nitrofluorides: In silico LaZrN2F. Chemical Physics Letters, 2010, 498, 77-80.	1.2	3
7976	Application of an empirical dispersion potential to van der Waals binding in nitromethane, pentaerythritol, and pentaerythritol tetranitrate. Chemical Physics Letters, 2010, 498, 97-100.	1.2	13
7977	Density functional calculations of the electronic structure and magnetism of the different phases of <mml:math xmlns:mml="http://www.w3.org/1998/Math/MathML" altimg="si45.gif" overflow="scroll"><mml:mrow><mml:msub><mml:mrow><mml:mtext>BaFe</mml:mtext></mml:mrow><mml:mrow><mml:mn>2</mm Chemical Physics Letters, 2010, 498, 281-286.	1.2	0
7978	Core-level shifts of the c(8Ã—2)-reconstructed InAs(100) and InSb(100) surfaces. Journal of Electron Spectroscopy and Related Phenomena, 2010, 177, 52-57.	0.8	13
7979	Local structure of Ca dopant in BaTiO3 by Ca K-edge X-ray absorption near-edge structure and first-principles calculations. Journal of Electron Spectroscopy and Related Phenomena, 2010, 180, 53-57.	0.8	17
7980	Structural polymorphism of pyrazinium hydrogen sulfate: extending chemistry of the pyrazinium salts with small anions. Acta Crystallographica Section B: Structural Science, 2010, 66, 451-457.	1.8	5
7981	Validation of experimental molecular crystal structures with dispersion-corrected density functional theory calculations. Acta Crystallographica Section B: Structural Science, 2010, 66, 544-558.	1.8	156
7982	Modulated Lanthanum Chains in the Crystal Structure of La3.65[Ru(C2)3]. Zeitschrift Fur Anorganische Und Allgemeine Chemie, 2010, 636, 41-49.	0.6	5
7983	Synthesis and Approximated Crystal and Electronic Structure of a Proposed New Tantalum Oxide Nitride Ta₃O₆NÂ. Zeitschrift Fur Anorganische Und Allgemeine Chemie, 2010, 636, 1006-1012.	0.6	9
7984	Electronic and transport properties of graphene nanoribbons. Physica Status Solidi (A) Applications and Materials Science, 2010, 207, 304-308.	0.8	31
7985	Structural models of aâ€Si:H with a low defect concentration: A firstâ€principles molecular dynamics study. Physica Status Solidi (A) Applications and Materials Science, 2010, 207, 605-608.	0.8	2
7986	Spectral properties of InN and its native oxide from first principles. Physica Status Solidi (A) Applications and Materials Science, 2010, 207, 1041-1053.	0.8	11
7987	Controlling the conductivity of InN. Physica Status Solidi (A) Applications and Materials Science, 2010, 207, 1024-1036.	0.8	72
7988	Origin of highâ€density hole doping and anisotropic hole transport in a wide gap layered semiconductor LaCuOSe studied by firstâ€principles calculations. Physica Status Solidi (A) Applications and Materials Science, 2010, 207, 1636-1641.	0.8	8
7989	Subgap states, doping and defect formation energies in amorphous oxide semiconductor aâ€InGaZnO₄ studied by density functional theory. Physica Status Solidi (A) Applications and Materials Science, 2010, 207, 1698-1703.	0.8	149
7990	Stability of diatomic hydrogen in oxygenâ€deficient ZnO. Physica Status Solidi (B): Basic Research, 2010, 247, 950-954.	0.7	6
7991	Do the atoms at second layer block the path of vacancies in the bulk? - The DFT study of vacancies below the Mg (0001) surface. Physica Status Solidi (B): Basic Research, 2010, 247, 259-264.	0.7	0
7992	Ab initio study of magnetoelectricity in composite multiferroics. Physica Status Solidi (B): Basic Research, 2010, 247, 1600-1607.	0.7	24

#	Article	IF	Citations
7993	Kinetic Monte Carlo study of selfâ€organization of lowâ€dimensional nanostructures on fcc (110) surfaces. Physica Status Solidi (B): Basic Research, 2010, 247, 1039-1047.	0.7	2
7994	Functionalization of graphene with transition metals. Physica Status Solidi (B): Basic Research, 2010, 247, 2920-2923.	0.7	12
7995	Structural evolution of double perovskite Sr2MgWO6 under high pressure. Physica Status Solidi (B): Basic Research, 2010, 247, 1773-1777.	0.7	13
7996	N-doped ZnO nanowires: Surface segregation, the effect of hydrogen passivation and applications in spintronics. Physica Status Solidi (B): Basic Research, 2010, 247, 2195-2201.	0.7	22
7997	Electronic structure and magnetism of monatomic oneâ€dimensional metal nanostructures on metal surfaces. Physica Status Solidi (B): Basic Research, 2010, 247, 2537-2549.	0.7	9
7998	First principles theoretical study of complex magnetic order in transitionâ€metal nanowires. Physica Status Solidi (B): Basic Research, 2010, 247, 2610-2620.	0.7	13
7999	Calculation of Oxygen and Sulfur Average Velocity on the Iron Surface: A Twoâ€dimensional Gas Model Study. Steel Research International, 2010, 81, 949-952.	1.0	5
8000	Firstâ€Principles Simulation on Piezoresistive Properties in Doped Silicon Nanosheets. IEEJ Transactions on Electrical and Electronic Engineering, 2010, 5, 157-163.	0.8	15
8001	On the performance of eleven DFT functionals in the description of the vibrational properties of aluminosilicates. International Journal of Quantum Chemistry, 2010, 110, 406-415.	1.0	121
8002	Nonhydrodynamic collective processes in molten salts: Theory and ab initio simulations. International Journal of Quantum Chemistry, 2010, 110, 38-45.	1.0	11
8003	Optical properties of amorphous and crystalline silicon surfaces functionalized with Ag_n adsorbates. International Journal of Quantum Chemistry, 2010, 110, 3005-3014.	1.0	18
8004	Firstâ€principle investigation of the relaxed structure and electronic properties of the Cu(110) vicinal surface. Surface and Interface Analysis, 2010, 42, 53-58.	0.8	0
8005	Theoretical Defect Energetics in Calcium Phosphate Bioceramics. Journal of the American Ceramic Society, 2010, 93, 1-14.	1.9	49
8006	Exploring Structures and Phase Relationships of Ceramics from First Principles. Journal of the American Ceramic Society, 2010, 93, 1201-1214.	1.9	16
8007	Ab Initio Study Of Double Oxides ZnX₂O₄(X=Al, Ga, In) Having Spinel Structure. Journal of the American Ceramic Society, 2010, 93, 3335-3341.	1.9	53
8008	Above-room-temperature ferroelectricity in a single-component molecular crystal. Nature, 2010, 463, 789-792.	13.7	659
8009	A strong ferroelectric ferromagnet created by means of spinâ€“lattice coupling. Nature, 2010, 466, 954-958.	13.7	668
8010	Surface modification of bioresorbable polymer scaffolds by laser treatment. Biophysics (Russian) Tj ETQq1 1 0.784314 rgBT /Overlock	0.2	5

#	Article	IF	Citations
8011	Composition of cementite in the dependence on the temperature. In situ neutron diffraction study and Ab initio calculations. JETP Letters, 2010, 91, 143-146.	0.4	25
8012	Ab initio calculation of the electronic structure, Fermi surface, and elastic properties of the new 7.5-K superconductor Nb2InC. JETP Letters, 2010, 91, 410-414.	0.4	13
8013	Reconstruction dependence of the etching and passivation of the GaAs(001) surface. JETP Letters, 2010, 91, 466-470.	0.4	5
8014	Metallic beta-phase silicon nanowires: Structure and electronic properties. JETP Letters, 2010, 92, 352-355.	0.4	3
8015	Using first principles to predict bimetallic catalysts for the ammonia decomposition reaction. Nature Chemistry, 2010, 2, 484-489.	6.6	381
8016	Synthesis of a metal oxide with a room-temperature photoreversible phase transition. Nature Chemistry, 2010, 2, 539-545.	6.6	221
8017	Structural evolution during the reduction of chemically derived graphene oxide. Nature Chemistry, 2010, 2, 581-587.	6.6	1,573
8018	State-selective dissociation of a single water molecule on an ultrathin MgO film. Nature Materials, 2010, 9, 442-447.	13.3	171
8019	Robust isothermal electric control of exchange bias at room temperature. Nature Materials, 2010, 9, 579-585.	13.3	528
8020	A multiferroic material to search for the permanent electric dipole moment of the electron. Nature Materials, 2010, 9, 649-654.	13.3	88
8021	Quantitative prediction of solute strengthening in aluminium alloys. Nature Materials, 2010, 9, 750-755.	13.3	256
8022	A joint effort with lasting impact. Nature Materials, 2010, 9, 690-692.	13.3	12
8023	Unusual infrared-absorption mechanism in thermally reduced graphene oxide. Nature Materials, 2010, 9, 840-845.	13.3	724
8024	An extended defect in graphene as a metallic wire. Nature Nanotechnology, 2010, 5, 326-329.	15.6	909
8025	A Theoretical Investigation of the Structural Properties of Chemically Modified Mo-S-I Nanowires. Chinese Journal of Catalysis, 2010, 31, 739-746.	6.9	1
8026	Diffusion on one-dimensional surfaces. , 0, , 183-260.		0
8027	Atomic pair interactions. , 0, , 696-734.		0
8028	Diffusion on two-dimensional surfaces. , 2010, , 261-422.		1

#	Article	IF	Citations
8029	Determination of adatom movements. , 2010, , 24-63.		0
8030	Diffusion in special environments. , 0, , 423-516.		0
8031	First-Principles Estimation of Hydrogen Occupancy around Lattice Defects in Al. Zairyo/Journal of the Society of Materials Science, Japan, 2010, 59, 596-603.	0.1	22
8032	Crystal and Electronic Structures, Photoluminescence Properties of Eu2+-Doped Novel Oxynitride Ba4Si6O16-3x/2Nx. Materials, 2010, 3, 1692-1708.	1.3	27
8033	Transformation Behavior of Ferrite at Steel/B1 Compounds Interface. Tetsu-To-Hagane/Journal of the Iron and Steel Institute of Japan, 2010, 96, 123-128.	0.1	14
8034	Properties of Carbon Nanotubes under External Factors. , 0, , .		0
8035	Multi-Physics Properties in Ferroelectric Nanowires and Related Structures from First-Principles. , 2010, , .		0
8036	Computational study of the dielectric properties of [La,Sc]2O3 solid solutions. Journal of Applied Physics, 2010, 107, 074104.	1.1	0
8037	Size-dependent structural and electronic properties of ZnS nanofilms: An ab initio study. Journal of Applied Physics, 2010, 108, 064317.	1.1	13
8038	First Principles Study of Oxygen Incorporation Reactions in Oxides. Transactions of the Materials Research Society of Japan, 2010, 35, 59-68.	0.2	2
8039	Deformation-Induced Electronic Structure Changes in Boron Nitride Nanotubes. Zairyo/Journal of the Society of Materials Science, Japan, 2010, 59, 604-609.	0.1	1
8040	Applications of the three-dimensional visualization system VESTA in mineralogical sciences. Ganseki Kobutsu Kagaku, 2010, 39, 136-145.	0.1	1
8041	First-Principles Investigation of the Electronic Structure and Magnetic Properties for Co-Doped Fe₃O₄. Materials Science Forum, 2010, 654-656, 1678-1681.	0.3	0
8042	Carbon nanotube-clamped metal atomic chain. Proceedings of the National Academy of Sciences of the United States of America, 2010, 107, 9055-9059.	3.3	36
8043	Anomalous molecular orbital variation upon adsorption on a wide band gap insulator. Journal of Chemical Physics, 2010, 132, 214706.	1.2	12
8044	Dynamical Simulations of Dry Oxidation and NO Annealing of SiO₂/4H-SiC Interface on C-Face at 1500K: From First Principles. Materials Science Forum, 0, 645-648, 483-486.	0.3	0
8045	Ab Initio Study of the Structural and Mechanical Properties of Hf-Si-N. Advanced Materials Research, 2010, 139-141, 22-25.	0.3	1
8046	First-Principles Study on Co-Doped ZnO with Oxygen Vacancy. Advanced Materials Research, 0, 154-155, 124-129.	0.3	0

#	Article	IF	Citations
8047	First principles study of vacancy and tungsten diffusion in fcc cobalt. Modelling and Simulation in Materials Science and Engineering, 2010, 18, 015008.	0.8	13
8048	The influence of exact exchange corrections in van der Waals layered narrow bandgap black phosphorus. Journal of Physics Condensed Matter, 2010, 22, 015502.	0.7	37
8049	Role of buffer layer in electronic structures of iron phthalocyanine molecules on Au(111). Chinese Physics B, 2010, 19, 097809.	0.7	4
8050	Rotation of hydrogen molecules during the dissociative adsorption on the Mg(0001) surface: a first-principles study. Chinese Physics B, 2010, 19, 058201.	0.7	3
8051	First-principles study of diffusion behaviour of point defects in the O-terminated (0001) surface in wurtzite ZnO. Chinese Physics B, 2010, 19, 013101-5.	0.7	5
8052	M atom (M = Cu, Ag and Au) interaction with Ag and Au substrates: a first-principles study using cluster and slab models. Journal of Physics Condensed Matter, 2010, 22, 435001.	0.7	12
8053	Density-functional investigation of hexagonal prism transition-metal-encapsulated cageM2Si18(M=) Tj ETQq0 0 0 rgBT /Overlock 10 Tf 5	0.8	4
8054	Benchmarking FeCr empirical potentials against density functional theory data. Modelling and Simulation in Materials Science and Engineering, 2010, 18, 075004.	0.8	12
8055	Mechanical and Magnetic Properties of Rh and RhH: First-Principles Calculations. Chinese Physics Letters, 2010, 27, 027101.	1.3	6
8056	Mechanism of Zn stabilization in hydroxyapatite and hydrated (0 0 1) surfaces of hydroxyapatite. Journal of Physics Condensed Matter, 2010, 22, 145502.	0.7	12
8057	First-principles investigation of site preference and bonding properties of alloying element in TiAl with O impurity. Modelling and Simulation in Materials Science and Engineering, 2010, 18, 015007.	0.8	11
8058	Electronic Structure and Characteristics of Chemical Bonds in CuInSe2, CuGaSe2, and CuAlSe2. Japanese Journal of Applied Physics, 2010, 49, 04DP07.	0.8	25
8059	Highly Strained Metastable Heterojunction between Wurtzite GaN(0001) and Cubic CrN(111). Journal of the Electrochemical Society, 2010, 157, D577.	1.3	4
8060	Proton Transfer in Perfluorosulfonic Acid Functionalized Carbon Nanotubes. Materials Research Society Symposia Proceedings, 2010, 1269, 60701.	0.1	1
8061	Tuning the electronic properties of armchair carbon nanoribbons by a selective boron doping. Journal of Physics Condensed Matter, 2010, 22, 505302.	0.7	11
8062	First-principles studies of liquid lithium under pressure. Journal of Physics Condensed Matter, 2010, 22, 095503.	0.7	9
8063	First-principles study of CuAlS2for p-type transparent conductive materials. Journal Physics D: Applied Physics, 2010, 43, 395405.	1.3	16
8064	New Lines and Issues Associated with Deep Defect Spectra in Electron, Proton and ⁴He Ion Irradiated 4H SiC. Materials Science Forum, 0, 645-648, 411-414.	0.3	4

#	Article	IF	Citations
8065	Ab-initio calculation of the vibrational influence on hole-trapping. , 2010, , .		1
8066	Dynamical stability of body center cubic iron at the Earthâ€™s core conditions. Proceedings of the National Academy of Sciences of the United States of America, 2010, 107, 9962-9964.	3.3	58
8067	Theoretical study of fcc-metal/MgO(110) interfacial potentials. Journal of Physics Condensed Matter, 2010, 22, 215001.	0.7	6
8068	First-principles Studies on Electronic Structures of Ga-doped ZnO and ZnS. Chinese Journal of Chemical Physics, 2010, 23, 527-532.	0.6	15
8069	Influence of Pb adatom on adsorption of oxygen molecules on Pb(111) surface: a first-principles study. Chinese Physics B, 2010, 19, 108201.	0.7	4
8070	Correcting the systematic error of the density functional theory calculation: the alternate combination approach of genetic algorithm and neural network. Chinese Physics B, 2010, 19, 076401.	0.7	2
8071	Structural, curvature and electronic properties of Rh adsorption on armchair single-walled carbon nanotube. Chinese Physics B, 2010, 19, 097104.	0.7	7
8072	Selenium: A Nonprecious Metal Cathode Catalyst for Oxygen Reduction. Journal of the Electrochemical Society, 2010, 157, B173.	1.3	10
8073	First-principles study of the structural and magnetic properties of graphene on a Fe/Ni(1â€‰1â€‰1) surface. Journal Physics D: Applied Physics, 2010, 43, 385002.	1.3	14
8074	Density functional study of the electronic structure and lattice dynamics of SrCl2. Journal of Physics Condensed Matter, 2010, 22, 445402.	0.7	7
8075	Atomistic nucleation and growth mechanism for single-wall carbon nanotubes on catalytic nanoparticle surfaces. Nanotechnology, 2010, 21, 115602.	1.3	6
8076	Active Materials Based on Implanted Si for Obtaining Intermediate Band Solar Cells. Advances in Science and Technology, 0, , .	0.2	5
8077	Impact of the Formation of Dimer Structures at the Surface on the Internal Atoms of Si Thin Film. Journal of the Electrochemical Society, 2010, 157, H323.	1.3	6
8078	First-Principles Calculations of Atomic and Electronic Properties of Tl and In on Si(111). Communications in Theoretical Physics, 2010, 54, 545-550.	1.1	0
8079	A first-principles study on the adhesion of Pt layers to NiO(100) and IrO₂(110) surfaces. Journal of Physics Condensed Matter, 2010, 22, 015003.	0.7	3
8080	Donor-donor binding in In2O3: Engineering shallow donor levels. Journal of Applied Physics, 2010, 107, 083704.	1.1	21
8081	Band Structures of Metal-Oxide Capped Graphene: A First Principles Study. Chinese Physics Letters, 2010, 27, 077201.	1.3	7
8082	Effects of H on Electronic Structure and Ideal Tensile Strength of W: A First-Principles Calculation. Chinese Physics Letters, 2010, 27, 127101.	1.3	13

#	Article	IF	Citations
8083	Atomic and Electronic Structure of Zinc and Copper Pyrovanadates with Negative Thermal Expansion. Advances in Science and Technology, 2010, 63, 358-363.	0.2	4
8084	First-principles modelling of magnesium titanium hydrides. Journal of Physics Condensed Matter, 2010, 22, 074208.	0.7	12
8085	First-principles investigation of Ge doping effects on the structural, electronic and magnetic properties in antiperovskite Mn₃CuN. Journal of Physics Condensed Matter, 2010, 22, 206003.	0.7	16
8086	Site preference of Ru in NiAl and valence band structure of NiAl containing Ru: First-principles study and photoelectron spectrum. Philosophical Magazine Letters, 2010, 90, 225-232.	0.5	5
8087	First-principles calculation of electronic and structural properties of<mml:math xmlns:mml="http://www.w3.org/1998/Math/MathML" display="inline"><mml:mrow><mml:msub><mml:mrow><mml:mtext>YBa</mml:mtext></mml:mrow><mml:mn>2</mml:mn></mml:ms Physical Review B, 2010, 82, .	1.1	17
8088	Characterizing electronic structure motifs in<mml:math xmlns:mml="http://www.w3.org/1998/Math/MathML" display="inline"><mml:mrow><mml:mi>Î²</mml:mi><mml:msub><mml:mrow><mml:mtext>-UH</mml:mtext></mml:mrow><mml:mr Physical Review B, 2010, 82, .	1.1	14
8089	Accurate ab initio predictions of IIIâ€“V direct-indirect band gap crossovers. Applied Physics Letters, 2010, 97, 091902.	1.5	43
8090	Inhibiting Adatom Diffusion through Surface Alloying. Physical Review Letters, 2010, 105, 015703.	2.9	11
8091	Quantum delocalization and correlation effects in one-dimensional chains of adsorbed hydrogen atoms. Physical Review B, 2010, 82, .	1.1	1
8092	Atomic-scale chemical fluctuation inLaSrVMoO6, a proposed half-metallic antiferromagnet. Physical Review B, 2010, 82, .	1.1	13
8093	Origin of high solubility of silicon in La2O3: A first-principles study. Applied Physics Letters, 2010, 97, .	1.5	12
8094	Direct Subangstrom Measurement of Surfaces of Oxide Particles. Physical Review Letters, 2010, 105, 226101.	2.9	60
8095	Phase stability and decomposition products of Tiâ€“Alâ€“Taâ€“N thin films. Applied Physics Letters, 2010, 97, .	1.5	57
8096	First-principles calculations on the energetics of nitrogen-doped hexagonal Ge2Sb2Te5. Journal of Applied Physics, 2010, 107, .	1.1	9
8097	Structures of neutral and anionic Au16 clusters revisited. Journal of Chemical Physics, 2010, 132, 194306.	1.2	33
8098	Optimizing photoelectrochemical properties of<mml:math xmlns:mml="http://www.w3.org/1998/Math/MathML" display="inline"><mml:mrow><mml:msub><mml:mrow><mml:mtext>TiO</mml:mtext></mml:mrow><mml:mn>2</mml:mn></mml:msub chemical codoping. Physical Review B, 2010, 82, .	1.1	62
8099	Theoretical study of the stabilization mechanisms of the different stable oxygen incorporated (101Â¯0) surface of III-nitrides. Journal of Applied Physics, 2010, 107, 043529.	1.1	4
8100	Molecular adsorption of small alkanes on a PdO(101) thin film: Evidence of Ïƒ-complex formation. Journal of Chemical Physics, 2010, 132, 024709.	1.2	71

#	Article	IF	Citations
8101	Effective band gap narrowing of anatase TiO2 by strain along a soft crystal direction. Applied Physics Letters, 2010, 96, .	1.5	185
8102	Theoretical calculations of hydrogen adsorption by SnO2 (110) surface: Effect of doping and calcination. Journal of Applied Physics, 2010, 107, 104504.	1.1	15
8103	Tunable magnetism on<mml:math xmlns:mml="http://www.w3.org/1998/Math/MathML" display="inline"><mml:mrow><mml:mtext>Si</mml:mtext><mml:mrow><mml:mo>(</mml:mo><mml:mrow><mml:mn>111</mml:mn></mml:mrow></mml:mrow></mml:mrow></mml:math> chemisorption of graphene nanoribbons. Physical Review B, 2010, 82, .	1.1	5
8104	Cr diffusion in<mml:math xmlns:mml="http://www.w3.org/1998/Math/MathML" display="inline"><mml:mrow><mml:mi>Î±</mml:mi><mml:msub><mml:mrow><mml:mtext>-Al</mml:mtext></mml:mrow><mml:mn>2</mml:mn></mml:msub></mml:mrow></mml:math> Secondary ion mass spectroscopy and first-principles study. Physical Review B, 2010, 82, .	1.1	10
8105	Atomic-Scale Compensation Phenomena at Polar Interfaces. Physical Review Letters, 2010, 105, 197602.	2.9	146
8106	Strong influence of complex band structure on tunneling electroresistance: A combined model andab initiostudy. Physical Review B, 2010, 82, .	1.1	22
8107	Role of oxygen vacancies in HfO2-based gate stack breakdown. Applied Physics Letters, 2010, 96, .	1.5	41
8108	Double-diamond NaAl via pressure: Understanding structure through Jones zone activation. Journal of Chemical Physics, 2010, 132, 114106.	1.2	8
8109	Pentagons and Heptagons in the First Water Layer on Pt(111). Physical Review Letters, 2010, 105, 026102.	2.9	211
8110	Controllable magnetic property of SiC by anion-cation codoping. Applied Physics Letters, 2010, 96, .	1.5	27
8111	Phase Stability and Electronic Structure of In-Free Photovoltaic Materials: Cu₂ZnSiSe₄, Cu₂ZnGeSe₄, and Cu₂ZnSnSe₄. Japanese Journal of Applied Physics, 2010, 49, 121203.	0.8	73
8112	Probing the existence of energetically degenerate cluster isomers by chemical tagging. Applied Physics Letters, 2010, 97, 223104.	1.5	1
8113	Mixed-Valency Signature in Vibrational Inelastic Electron Tunneling Spectroscopy. Physical Review Letters, 2010, 104, 136101.	2.9	39
8114	Similarity of optical properties of hydrides and semiconductors for antireflection coatings. Philosophical Magazine, 2010, 90, 2925-2937.	0.7	10
8115	Ab initiomulti-string Frenkelâ€“Kontorova model for a b =a/2[111] screw dislocation in bcc iron. Philosophical Magazine, 2010, 90, 1035-1061.	0.7	22
8116	Radioparagenesis: The formation of novel compounds and crystalline structures via radioactive decay. Philosophical Magazine Letters, 2010, 90, 435-446.	0.5	17
8117	First-principles study of substitutional metal impurities in graphene: structural, electronic and magnetic properties. New Journal of Physics, 2010, 12, 053012.	1.2	214
8118	Strain and coordination effects in the adsorption properties of early transition metals: A density-functional theory study. Physical Review B, 2010, 81, .	1.1	119

#	Article	IF	Citations
8119	Effect of trace moisture on friction. Applied Physics Letters, 2010, 96, .	1.5	18
8120	Ab initio simulations of molten Ni alloys. Journal of Applied Physics, 2010, 107, .	1.1	33
8121	Fluorine clustering and diffusion in silicon: Ab initio calculations and kinetic Monte Carlo model. Journal of Vacuum Science and Technology B:Nanotechnology and Microelectronics, 2010, 28, C1G1-C1G6.	0.6	3
8122	Effect of structural relaxation and oxidation conditions on interlayer exchange coupling in Fe|MgO|Fe tunnel junctions. Applied Physics Letters, 2010, 96, .	1.5	47
8123	Transport properties of corrugated graphene nanoribbons. Applied Physics Letters, 2010, 96, .	1.5	33
8124	Low-temperature adsorption of H2S on Ag(111). Journal of Chemical Physics, 2010, 133, 124705.	1.2	18
8125	Mapping antibonding electron states of a Pb adatom on Pb(111). Physical Review B, 2010, 81, .	1.1	12
8126	Exciton: a code for excitations in materials. Molecular Physics, 2010, 108, 3181-3188.	0.8	16
8127	First-principles study of atomic and electronic structures of amorphous HgTe. , 2010, , .		0
8128	First-principles determination of charge and orbital interactions in<mml:math xmlns:mml="http://www.w3.org/1998/Math/MathML" display="inline"><mml:mrow><mml:msub><mml:mrow><mml:mtext>Fe</mml:mtext></mml:mrow><mml:mn>3</mml:mn></mml:msub> Physical Review B, 2010, 81, .	1.1	21
8129	Understanding conductivity anomalies in CuI-based delafossite transparent conducting oxides: Theoretical insights. Journal of Chemical Physics, 2010, 132, 024707.	1.2	101
8130	Structural and dynamical heterogeneity in molten Si-rich oxides. Applied Physics Letters, 2010, 96, 043121.	1.5	6
8131	Fluorite transition metal hydride induced destabilization of the<mml:math xmlns:mml="http://www.w3.org/1998/Math/MathML" display="inline"><mml:mrow><mml:msub><mml:mrow><mml:mtext>MgH</mml:mtext></mml:mrow><mml:mn>2</mml:mn></mml:ms in<mml:math xmlns:mml="http://www.w3.org/1998/Math/MathML" display="inline"><mml:mrow><mml:msub><mml:mrow><mml:mtext>MgH</mml:mtext></mml:mrow><mml:mn>2</mml:mn></mml:ms Physical Review B, 2010, 82, .	1.1	37
8132	Armchair nanoribbons of silicon and germanium honeycomb structures. Physical Review B, 2010, 81, .	1.1	137
8133	Boron nitride formation on magnesium studied byab initiocalculations. Physical Review B, 2010, 81, .	1.1	5
8134	Oxygen and water-related impurities inC60crystals: A density-functional theory study. Physical Review B, 2010, 82, .	1.1	24
8135	Resistivity of thin Cu films coated with Ta, Ti, Ru, Al, and Pd barrier layers from first principles. Physical Review B, 2010, 81, .	1.1	62
8136	Magneto-optical properties and charge-spin coupling in the molecular(2,3-dmpyH)2CuBr4spin-ladder material. Physical Review B, 2010, 81, .	1.1	17

#	Article	IF	Citations
8137	Charge-induced spin polarization in nonmagnetic organic molecule<mml:math xmlns:mml="http://www.w3.org/1998/Math/MathML" display="inline"><mml:mrow><mml:msub><mml:mrow><mml:mtext>Alq</mml:mtext></mml:mrow><mml:mn>3</mml:mn></mml:msub></mml:mrow></mml:math>. Physical Review B, 2010, 82, .	1.1	32
8138	Diffusion of carbon in bcc Fe in the presence of Si. Physical Review B, 2010, 81, .	1.1	54
8139	Ab initiostudy of magnetism at iron surfaces under epitaxial in-plane strain. Physical Review B, 2010, 81, .	1.1	27
8140	Structure of chlorine on Ag(111): Evidence of the(3Ã—3)reconstruction. Physical Review B, 2010, 81, .	1.1	18
8141	Origin of bulklike optical response in noble-metal Ag and Au nanoparticles. Physical Review B, 2010, 82, .	1.1	14
8142	Effect of electron correlations on structural phase stability, magnetism, and spin-dependent transport in<mml:math xmlns:mml="http://www.w3.org/1998/Math/MathML" display="inline"><mml:mrow><mml:msub><mml:mrow><mml:mtext>CeMnNi</mml:mtext></mml:mrow><mml:mn>4</mml:mn></mml:msub></mml:mrow></mml:math>. Physical Review B, 2010, 81, .	1.1	6
8143	Anisotropic lattice dynamics of FePt<mml:math xmlns:mml="http://www.w3.org/1998/Math/MathML" display="inline"><mml:mrow><mml:mtext>L</mml:mtext><mml:msub><mml:mn>1</mml:mn><mml:mn>0</mml:mn></mml:msub></mml:mrow></mml:math>films. Physical Review B, 2010, 82, .	1.1	13
8144	Magnetism of small Cr clusters: Interplay between structure, magnetic order, and electron correlations. Physical Review B, 2010, 81, .	1.1	21
8145	Ab initiomodeling of diffusion in indium oxide. Physical Review B, 2010, 81, .	1.1	54
8146	Incipient plasticity of twin and stable/unstable grain boundaries during nanoindentation in copper. Physical Review B, 2010, 82, .	1.1	36
8147	High-pressure and high-temperature multianvil synthesis of metastable polymorphs of<mml:math xmlns:mml="http://www.w3.org/1998/Math/MathML" display="inline"><mml:mrow><mml:msub><mml:mrow><mml:mtext>Bi</mml:mtext></mml:mrow><mml:mn>2</mml:mn></mml:msub></mml:mrow></mml:math>Crystal structure and electronic properties. Physical Review B, 2010, 82, .	1.1	37
8148	Order, miscibility, and electronic structure of<mml:math xmlns:mml="http://www.w3.org/1998/Math/MathML" display="inline"><mml:mrow><mml:mtext>Ag</mml:mtext><mml:mrow><mml:mo>(</mml:mo><mml:mrow><mml:mtext>Bi</mml:mtext></mml:mrow></mml:mrow></mml:math>and (Ag,Bi,Sb)Te precipitates in rocksalt matrix: A first-principles study. Physical Review B, 2010, 81, .	1.1	17
8149	Electrical rectification by selective wave-function coupling in small Ag clusters on<mml:math xmlns:mml="http://www.w3.org/1998/Math/MathML" display="inline"><mml:mrow><mml:mtext>Si</mml:mtext><mml:mrow><mml:mo>(</mml:mo><mml:mrow><mml:mn>111</mml:mn></mml:mrow></mml:mrow></mml:math>Physical Review B, 2010, 81, .	1.1	11
8150	Electronic and structural properties of Laves-phase<mml:math xmlns:mml="http://www.w3.org/1998/Math/MathML" display="inline"><mml:mrow><mml:msub><mml:mrow><mml:mtext>MgZn</mml:mtext></mml:mrow><mml:mn>2</mml:mn></mml:msub></mml:mrow></mml:math>varying chemical disorder. Physical Review B, 2010, 82, .	1.1	11
8151	Atomic displacements in the charge ice pyrochlore<mml:math xmlns:mml="http://www.w3.org/1998/Math/MathML" display="inline"><mml:mrow><mml:msub><mml:mrow><mml:mtext>Bi</mml:mtext></mml:mrow><mml:mn>2</mml:mn></mml:msub></mml:mrow></mml:math>by neutron total scattering. Physical Review B, 2010, 81, .	1.1	52
8152	Mn-doped cubic BN as an atomiclike memory device: A density functional study. Physical Review B, 2010, 81, .	1.1	2
8153	Thermodynamic fluctuations between magnetic states from first-principles phonon calculations: The case of bcc Fe. Physical Review B, 2010, 82, .	1.1	42
8154	Adsorption-enhanced reactivity of the In/Si(001) system. Physical Review B, 2010, 81, .	1.1	14

#	Article	IF	Citations
8155	Reorientable dipolar<mml:math xmlns:mml="http://www.w3.org/1998/Math/MathML" display="inline"><mml:mrow><mml:msub><mml:mrow><mml:mtext>Cu</mml:mtext></mml:mrow><mml:mrow><mml:mtext>Ca</mml:mtext></mml:mrow></mml:msub></mml:mrow></mml:math> and anomalous screening in<mml:math xmlns:mml="http://www.w3.org/1998/Math/MathML" display="inline"><mml:mrow><mml:msub><mml:mrow><mml:mtext>CaCu</mml:mtext></mml:mrow><mml:mn>3</mml:mn></mml:msub></mml:mrow></mml:math> Physical Review B, 2010, 81, .	1.1	11
8156	Accurate defect levels obtained from the HSE06 range-separated hybrid functional. Physical Review B, 2010, 81, .	1.1	297
8157	Effects of bonding type and interface geometry on coherent transport through the single-molecule magnetMn12. Physical Review B, 2010, 81, .	1.1	19
8158	Homogeneous nanocables from double-walled boron-nitride nanotubes using first-principles calculations. Physical Review B, 2010, 82, .	1.1	10
8159	Role of structural disorder in optical absorption in silicon. Physical Review B, 2010, 82, .	1.1	6
8160	Building effective models from sparse but precise data: Application to an alloy cluster expansion model. Physical Review B, 2010, 81, .	1.1	33
8161	Positrons as interface-sensitive probes of polar semiconductor heterostructures. Physical Review B, 2010, 82, .	1.1	23
8162	Uniform spin-chain physics arising from Nâ€”Câ€”N bridges inCuNCN, the nitride analog of the copper oxides. Physical Review B, 2010, 81, .	1.1	16
8163	Band structures of delafossite transparent conductive oxides from a self-consistent<mml:math xmlns:mml="http://www.w3.org/1998/Math/MathML" display="inline"><mml:mrow><mml:mi>G</mml:mi><mml:mi>W</mml:mi></mml:mrow></mml:math>approach. Physical Review B, 2010, 82, .	1.1	63
8164	Rescaled Monte Carlo approach for magnetic systems:Ab initiothermodynamics of bcc iron. Physical Review B, 2010, 81, .	1.1	57
8165	Competing strain effects in reactivity of<mml:math xmlns:mml="http://www.w3.org/1998/Math/MathML" display="inline"><mml:mrow><mml:msub><mml:mrow><mml:mtext>LaCoO</mml:mtext></mml:mrow><mml:mn>3</mml:mn></mml:msub></mml:mrow></mml:math> oxygen. Physical Review B, 2010, 82, .	1.1	110
8166	Doping of hexagonal boron nitride via intercalation: A theoretical prediction. Physical Review B, 2010, 81, .	1.1	61
8167	Termination and Verwey transition of the (111) surface of magnetite studied by scanning tunneling microscopy and first-principles calculations. Physical Review B, 2010, 81, .	1.1	49
8168	Theoretical investigation of intermediate phases between<mml:math xmlns:mml="http://www.w3.org/1998/Math/MathML" display="inline"><mml:mrow><mml:msub><mml:mrow><mml:mtext>Li</mml:mtext></mml:mrow><mml:mn>2</mml:mn></mml:msub></mml:mrow></mml:math> and<mml:math xmlns:mml="http://www.w3.org/1998/Math/MathML" display="inline"><mml:mrow><mml:msub><mml:mrow><mml:mtext>LiNH</mml:mtext></mml:mrow><mml:mn>2</mml:mn></mml:msub></mml:mrow></mml:math>	1.1	5
8169	Strain-field effects on the formation and migration energies of self interstitials in<mml:math xmlns:mml="http://www.w3.org/1998/Math/MathML" display="inline"><mml:mrow><mml:mi>Î±</mml:mi><mml:mtext>-Fe</mml:mtext></mml:mrow></mml:math>from first principles. Physical Review B, 2010, 81, .	1.1	50
8170	Structure discovery for metallic glasses using stochastic quenching. Physical Review B, 2010, 82, .	1.1	24
8171	Experimental and theoretical investigation of the stability of the monoclinic<mml:math xmlns:mml="http://www.w3.org/1998/Math/MathML" display="inline"><mml:mrow><mml:msub><mml:mrow><mml:mtext>BaWO</mml:mtext></mml:mrow><mml:mn>4</mml:mn></mml:msub></mml:mrow></mml:math> phase at high pressure and high temperature. Physical Review B, 2010, 81, .	1.1	19
8172	Adsorption of a water molecule on Fe(100): Density-functional calculations. Physical Review B, 2010, 81, .	1.1	48

#	Article	IF	Citations
8173	Dynamical effects in x-ray absorption spectra of graphene and monolayered<mml:math xmlns:mml="http://www.w3.org/1998/Math/MathML" display="inline"><mml:mi>h</mml:mi></mml:math>-BN on Ni(111). Physical Review B, 2010, 81, .	1.1	27
8174	Reversible enhancement of the magnetism of ultrathin Co films by H adsorption. Physical Review B, 2010, 82, .	1.1	7
8175	Spin-lattice interactions through the quantum critical transition inCu(pyz)(NO3)2. Physical Review B, 2010, 81, .	1.1	10
8176	Strain effects on the stability and structure of vacancy clusters in Si: A first-principles study. Physical Review B, 2010, 81, .	1.1	4
8177	Nature of the negative thermal expansion in antiperovskite compound Mn3ZnN. Journal of Applied Physics, 2010, 108, .	1.1	33
8178	Low hole effective mass in thin InAs nanowires. Applied Physics Letters, 2010, 96, .	1.5	9
8179	Binding in alkali and alkaline-earth tetrahydroborates: Special position of magnesium tetrahydroborate. Physical Review B, 2010, 81, .	1.1	33
8180	Ferroelectric dead layer driven by a polar interface. Physical Review B, 2010, 82, .	1.1	51
8181	Structural investigation of the (110) surface of$\hat{1}^3$-Al4Cu9. Physical Review B, 2010, 82, .	1.1	25
8182	Antiferromagnetism with spin polarization of GaN-based diluted magnetic semiconductors. Physical Review B, 2010, 81, .	1.1	22
8183	Lattice instabilities in hexagonal NiSi: A NiAs prototype structure. Physical Review B, 2010, 81, .	1.1	4
8184	High-pressure structural phase transitions in<mml:math xmlns:mml="http://www.w3.org/1998/Math/MathML" display="inline"><mml:mrow><mml:msub><mml:mrow><mml:mtext>CuWO</mml:mtext></mml:mrow><mml:mn>4</mml:mn></mml:mrow> Physical Review B, 2010, 81, .	1.1	67
8185	Magnetic quantum oscillations for the surface states of topological insulator<mml:math xmlns:mml="http://www.w3.org/1998/Math/MathML" display="inline"><mml:mrow><mml:msub><mml:mrow><mml:mtext>Bi</mml:mtext></mml:mrow><mml:mn>2</mml:mn></mml:msub> Physical Review B, 2010, 82, .	1.1	31
8186	Polarity of ultrathin MgO(111) films deposited on a metal substrate. Physical Review B, 2010, 81, .	1.1	25
8187	Phase relations and hardness trends ofZrO2phases at high pressure. Physical Review B, 2010, 81, .	1.1	61
8188	Amorphous defect clusters of pure Si and type inversion in Si detectors. Physical Review B, 2010, 82, .	1.1	12
8189	Diffraction of swift atoms after grazing scattering from metal surfaces: N/Ag(111) system. Physical Review A, 2010, 82, .	1.0	9
8190	Substrate-induced cooperative effects in water adsorption from density functional calculations. Physical Review B, 2010, 82, .	1.1	6

#	Article	IF	Citations
8191	Near-surface microstructure ofNi-23â€‚at.â€‰%â€‚Pt: Grazing incidence diffraction and first-principles calculations. Physical Review B, 2010, 81, .	1.1	4
8192	Theory-guided growth of aluminum antimonide single crystals with optimal properties for radiation detection. Applied Physics Letters, 2010, 97, 142104.	1.5	10
8193	Mechanisms of atomic diffusion on the flat, stepped, and faceted surfaces of Al(110). Physical Review B, 2010, 81, .	1.1	22
8194	Polarization screening and induced carrier density at the interface of LaAlO3 overlayer on SrTiO3 (001). Journal of Applied Physics, 2010, 108, .	1.1	17
8195	Mechanical and electronic properties of ferromagnetic<mml:math xmlns:mml="http://www.w3.org/1998/Math/MathML" display="inline"><mml:mrow><mml:msub><mml:mrow><mml:mtext>Ga</mml:mtext></mml:mrow><mml:mrow><mml:mn>1</mml:mn> ultrafast coherent acoustic phonons. Physical Review B, 2010, 81, .	1.1	18
8196	Spin-polarized two-dimensional electron gas through electrostatic doping in<mml:math xmlns:mml="http://www.w3.org/1998/Math/MathML" display="inline"><mml:mrow><mml:msub><mml:mrow><mml:mtext>LaAlO</mml:mtext></mml:mrow><mml:mn>3</mml:mn></mml:mrow></mml:msub></mml:mrow></mml:math>. Physical Review B, 2010, 82, .	1.1	27
8197	Ab initio calculations and synthesis of the off-stoichiometric half-Heusler phase Ni1â^'xMn1+xSb. Journal of Applied Physics, 2010, 108, 093712.	1.1	10
8198	Ab initio study on copper ferrite. Journal of Applied Physics, 2010, 107, .	1.1	19
8199	Near-ultraviolet light emitting diodes using strained ultrathin InN/GaN quantum well grown by metal organic vapor phase epitaxy. Applied Physics Letters, 2010, 96, .	1.5	23
8200	Evidence for Strain-Induced Ferroelectric Order in Epitaxial Thin-Film<mml:math xmlns:mml="http://www.w3.org/1998/Math/MathML" display="inline"><mml:msub><mml:mi>KTaO</mml:mi><mml:mn>3</mml:mn></mml:msub></mml:math>. Physical Review Letters, 2010, 104, 227601.	2.9	72
8201	Electronic structure and thermoelectric properties of In32â^'xGexO48 (x=0, 1, 2, and 3) at low temperature. Applied Physics Letters, 2010, 97, 252106.	1.5	8
8202	The role of pentagonâ€“heptagon pair defect in carbon nanotube: The center of vacancy reconstruction. Applied Physics Letters, 2010, 97, 093106.	1.5	15
8203	Hypergolic fuel detection using individual single walled carbon nanotube networks. Journal of Applied Physics, 2010, 107, .	1.1	11
8204	High-pressure phase transformations in carbonates. Physical Review B, 2010, 82, .	1.1	31
8205	Valence-band splittings in cubic and hexagonal AlN, GaN, and InN. Applied Physics Letters, 2010, 97, .	1.5	28
8206	Density functional calculations of hole induced long ranged ferromagnetic ordering in Mn doped Cd28Se28 nanocluster. Applied Physics Letters, 2010, 96, .	1.5	11
8207	Investigation of possible half-metallic antiferromagnets on double perovskites LaABBâ€²O6 (A=Ca,Sr,Ba;) Tj ETQq0 0 0 rgBT /Overlock 1	1.1	20
8208	Ferroelectric polarization and domain walls in orthorhombic (K1â^'xNax)NbO3 lead-free ferroelectric ceramics. Applied Physics Letters, 2010, 96, .	1.5	11

#	Article	IF	Citations
8209	Electronic Mapping of Molecular Orbitals at the Molecule-Metal Interface. Physical Review Letters, 2010, 105, 066801.	2.9	23
8210	Effects of capping HfO2 with multivalent oxides toward reducing the number of charged defects. Applied Physics Letters, 2010, 96, 162906.	1.5	9
8211	Understanding of large auxetic properties of iron-gallium and iron-aluminum alloys. Journal of Applied Physics, 2010, 108, .	1.1	33
8212	Anomalous aggregation state of deuterium molecules in the nanoscale pores of a metal organic framework. Journal of Applied Physics, 2010, 108, 074310.	1.1	3
8213	Pressure-Induced Intermolecular Interactions in Crystalline Silane-Hydrogen. Physical Review Letters, 2010, 105, 215501.	2.9	18
8214	Electronic, structural, and magnetic effects of 3d transition metals in hematite. Journal of Applied Physics, 2010, 107, .	1.1	135
8215	Ab initiostudy of the low-temperature phases of lithium imide. Physical Review B, 2010, 82, .	1.1	18
8216	Enhanced electron-mediated ferromagnetism in Co-doped ZnO nanowires. Journal of Applied Physics, 2010, 108, .	1.1	11
8217	Density functional calculations of Ti nanoclusters in the metastable Mg-Ti system. Physical Review B, 2010, 82, .	1.1	12
8218	Hexagonal BaTi1â^'xCoxO3 phase stabilized by Co dopants. Applied Physics Letters, 2010, 96, .	1.5	22
8219	Simultaneous Segregation at Coherent and Semicoherent Heterophase Interfaces. Physical Review Letters, 2010, 105, 076102.	2.9	80
8220	Theory of a three-dimensional nanoporous silicon lattice with unsaturated bonding. Applied Physics Letters, 2010, 97, 121906.	1.5	3
8221	Elastic softening behavior of Tiâ€“Nb single crystal near martensitic transformation temperature. Journal of Applied Physics, 2010, 108, .	1.1	45
8222	Tuning magnetic properties of In ₂ O ₃ by control of intrinsic defects. Europhysics Letters, 2010, 89, 47005.	0.7	20
8223	Hole-Mediated Hydrogen Spillover Mechanism in Metal-Organic Frameworks. Physical Review Letters, 2010, 104, 236101.	2.9	34
8224	First-principle investigation of 3d transition metal elements in Î³â€²-Co3(Al,W). Journal of Applied Physics, 2010, 107, .	1.1	35
8225	Atomic structure and<mml:math xmlns:mml="http://www.w3.org/1998/Math/MathML" display="inline"><mml:mrow><mml:msub><mml:mrow><mml:mtext>SiH</mml:mtext></mml:mrow><mml:mn>4</mml:mn></mml:msu of<mml:math xmlns:mml="http://www.w3.org/1998/Math/MathML" display="inline"><mml:mrow><mml:msub><mml:mrow><mml:mtext>SiH</mml:mtext></mml:mrow><mml:mn>4</mml:mn></mml:msu Physical Review B, 2010, 82, .	1.1	13
8226	Robustness of Topologically Protected Surface States in Layering of<mml:math xmlns:mml="http://www.w3.org/1998/Math/MathML" display="inline"><mml:msub><mml:mi>Bi</mml:mi><mml:mn>2</mml:mn></mml:msub><mml:msub><mml:mi>Te</mml:mi><mml:mn Films. Physical Review Letters, 2010, 105, 186801.	2.9	136

#	Article	IF	Citations
8227	Significant elastic anisotropy in Ti1âˆ'xAlxN alloys. Applied Physics Letters, 2010, 97, .	1.5	107
8228	Charge Ordering Induced Ferromagnetic Insulator:<mml:math xmlns:mml="http://www.w3.org/1998/Math/MathML" display="inline"><mml:msub><mml:mi mathvariant="bold">K</mml:mi><mml:mn>2</mml:mn></mml:msub><mml:msub><mml:mi>Cr</mml:mi><mml:mn>8</mml:mn></mml:msub><mml:msub><mml:mi mathvariant="bold">O</mml:mi><mml:mn>16</mml:mn></mml:msub></mml:math>. Physical Review	2.98	39
8229	Electronic and optical properties of the<mml:math xmlns:mml="http://www.w3.org/1998/Math/MathML" display="inline"><mml:mrow><mml:msub><mml:mrow><mml:mtext>Mg</mml:mtext></mml:mrow><mml:mrow><mml:mn>2</mml:mn></mml:m From band insulator to Mott insulator. Physical Review B, 2010, 82, .	1.1	4
8230	Role of strain in polarization switching in semipolar InGaN/GaN quantum wells. Applied Physics Letters, 2010, 97, 181102.	1.5	34
8231	First-principles studies of interlayer exchange coupling in (Ga, Mn)As-based diluted magnetic semiconductor multilayers. Journal of Applied Physics, 2010, 108, 053703.	1.1	11
8232	Mechanical properties of defective single wall carbon nanotubes. Journal of Applied Physics, 2010, 107, 061803.	1.1	9
8233	Formation of core/shell-like ZnSe1âˆ'xTex nanocrystals due to equilibrium surface segregation. Applied Physics Letters, 2010, 96, .	1.5	7
8234	O-vacancy-mediated spin-spin interaction in Co-doped ZnO: First-principles total-energy calculations. Journal of Applied Physics, 2010, 107, 023909.	1.1	14
8235	Orientation-dependent work function of graphene on Pd(111). Applied Physics Letters, 2010, 97, .	1.5	122
8236	O-vacancy as the origin of negative bias illumination stress instability in amorphous Inâ€“Gaâ€“Znâ€“O thin film transistors. Applied Physics Letters, 2010, 97, .	1.5	380
8237	First-principles study of GaAs(001)-Î²2(2Ã—4) surface oxidation and passivation with H, Cl, S, F, and GaO. Journal of Applied Physics, 2010, 107, .	1.1	74
8238	Density functional calculations of the structural, electronic, and ferroelectric properties of high-k titanate Re2Ti2O7 (Re=La and Nd). Journal of Applied Physics, 2010, 108, .	1.1	41
8239	Vacancy clustering and diffusion in heavily P doped Si. Applied Physics Letters, 2010, 97, 251909.	1.5	6
8240	Highly anisotropic sliding at TiN/Fe interfaces: A first principles study. Journal of Applied Physics, 2010, 108, 113511.	1.1	9
8241	A density functional theory study of the CH2I2 reaction on Ag(111): Thermodynamics, kinetics, and electronic structures. Journal of Chemical Physics, 2010, 132, 024715.	1.2	6
8242	Phase stability of carbon clathrates at high pressure. Journal of Applied Physics, 2010, 107, .	1.1	31
8243	Molecular simulation on interfacial structure and gettering efficiency of direct silicon bonded (110)/(100) substrates. Journal of Applied Physics, 2010, 107, 113509.	1.1	4
8244	Ab initioand molecular dynamics studies of solid Î²-HMX: effects of hydrostatic pressure and high temperature. Molecular Simulation, 2010, 36, 670-681.	0.9	11

#	Article	IF	Citations
8245	Two-dimensional electron or hole gas at ZnO/6H-SiC interface. Applied Physics Letters, 2010, 96, 192109.	1.5	3
8246	Molecular chemisorption on open metal sites in Cu3(benzenetricarboxylate)2: A spatially periodic density functional theory study. Journal of Chemical Physics, 2010, 133, 094509.	1.2	87
8247	Thermophysical properties of liquid carbon dioxide under shock compressions: Quantum molecular dynamic simulations. Journal of Chemical Physics, 2010, 133, 134503.	1.2	14
8248	Magnetic properties in graphene-graphane superlattices. Applied Physics Letters, 2010, 97, 133102.	1.5	19
8249	Nonempirical prediction of impurity segregation in Î±-Fe from first principles. Journal of Applied Physics, 2010, 107, .	1.1	9
8250	Novel properties of boron nitride nanotubes encapsulated with Fe, Co, and Ni nanoclusters. Journal of Chemical Physics, 2010, 132, 164704.	1.2	21
8251	Hugoniot of shocked liquid deuterium up to 300 GPa: Quantum molecular dynamic simulations. Journal of Applied Physics, 2010, 108, .	1.1	9
8252	Energetic, mechanical, and vibrational stability of metastable OsC phase. Journal of Applied Physics, 2010, 108, .	1.1	7
8253	Silicon carbide oxidation in the presence of cesium: Modeling and analysis. Journal of Applied Physics, 2010, 108, 083512.	1.1	2
8254	A-site occupancy in the lead-free (Bi1/2Na1/2TiO3)0.94â€“(BaTiO3)0.06 piezoceramic: Combining first-principles study and TEM. Journal of Applied Physics, 2010, 107, .	1.1	16
8255	Stability of oxygen point defects in<mml:math xmlns:mml="http://www.w3.org/1998/Math/MathML" display="inline"><mml:mrow><mml:msub><mml:mrow><mml:mtext>UO</mml:mtext></mml:mrow><mml:mn>2</mml:mn></mml:msu first-principles<mml:math xmlns:mml="http://www.w3.org/1998/Math/MathML" display="inline"><mml:mrow><mml:mtext>DFT</mml:mtext><mml:mo>+</mml:mo><mml:mi>U</mml:mi></mml:mrow></mml:math>c Physical Review B, 2010, 82, .	1.1	185
8256	<mml:math xmlns:mml="http://www.w3.org/1998/Math/MathML" display="inline"><mml:mi>Y</mml:mi></mml:math>-cut, and<mml:math xmlns:mml="http://www.w3.org/1998/Math/MathML" display="inline"><mml:mrow><mml:msqrt><mml:mn>2</mml:mn></mml:msqrt><mml:mo>Ã—</mml:mo><mml:msqrt><mml:mn>2</mml:mn>	1.1	117
8257	and charge inhomogeneity at the surface of superconducting<mml:math xmlns:mml="http://www.w3.org/1998/Math/MathML" display="inline"><mml:mrow><mml:msub><mml:mrow><mml:mtext>BaFe</mml:mtext></mml:mrow><mml:mrow><mml:mn>2</mml:mn> Physical Review B, 2010, 81, .	1.1	34
8258	<mml:math xmlns:mml="http://www.w3.org/1998/Math/MathML" display="inline"><mml:msub><mml:mi>KO</mml:mi><mml:mn>2</mml:mn></mml:msub></mml:math>: Realization of Orbital Ordering in a<mml:math xmlns:mml="http://www.w3.org/1998/Math/MathML" display="inline"><mml:mi>p</mml:mi></mml:math>-Orbital System. Physical Review Letters, 2010, 105,	2.9	27
8259	Single-crystal elastic constants of ferromagnetic bcc Fe-based random alloys from first-principles theory. Physical Review B, 2010, 81, .	1.1	85
8260	Density functional analysis of key energetics in metal homoepitaxy: Quantum size effects in periodic slab calculations. Physical Review B, 2010, 81, .	1.1	31
8261	Temperature and pressure effects in CO titration of ensembles in PdAu(111) alloys using first principles. Physical Review B, 2010, 82, .	1.1	29
8262	Interplay of defect cluster and the stability of xenon in uranium dioxide from density functional calculations. Physical Review B, 2010, 82, .	1.1	79

#	Article	IF	Citations
8263	Coating geometries of metals on single-walled carbon nanotubes. Applied Physics Letters, 2010, 96, .	1.5	37
8264	Magnetism in two-dimensional<mml:math xmlns:mml="http://www.w3.org/1998/Math/MathML" display="inline"><mml:mrow><mml:msub><mml:mrow><mml:mtext>BN</mml:mtext></mml:mrow><mml:mrow><mml:mn>1</mml:mn> xmlns:mml="http://www.w3.org/1998/Math/MathML" display="inline"><mml:mrow><mml:msub><mml:mtext>B</mml:mtext><mml:mrow><mml:mn>1</mml:mn><mml:mo>â^'</mml:mo> Physical Review B, 2010, 81, .	1.1	7
8265	Electronic damping of anharmonic adsorbate vibrations at metallic surfaces. Physical Review B, 2010, 81, .	1.1	37
8266	Reversal of chloride-induced Cu(001) subsurface buckling in the electrochemical environment: Anin situsurface x-ray diffraction and density functional theory study. Physical Review B, 2010, 81, .	1.1	43
8267	Ferroelectricity in strained<mml:math xmlns:mml="http://www.w3.org/1998/Math/MathML" display="inline"><mml:mrow><mml:msub><mml:mrow><mml:mtext>Ca</mml:mtext></mml:mrow><mml:mrow><mml:mn>0.5</mml:m first principles. Physical Review B, 2010, 82, .	1.1	40
8268	Ab initiostudy of compressed<mml:math xmlns:mml="http://www.w3.org/1998/Math/MathML" display="inline"><mml:mrow><mml:mtext>Ar</mml:mtext><mml:msub><mml:mrow><mml:mrow><mml:mo>(</mml:mo><mml:mrow> Structural stability and anomalous melting. Physical Review B, 2010, 81, .	1.1	20
8269	Magnetic ordering in blocking layer and highly anisotropic electronic structure of high-<mml:math xmlns:mml="http://www.w3.org/1998/Math/MathML" display="inline"><mml:mrow><mml:msub><mml:mi>T</mml:mi><mml:mi>c</mml:mi></mml:msub></mml:mrow></mml:math>iron-bas superconductor<mml:math xmlns:mml="http://www.w3.org/1998/Math/MathML" display="inline"><mml:mrow><mml:msub><mml:mrow><mml:mtext>Sr</mml:mtext></mml:mrow><mml:mn>2</mml:mn></mml:msub Physical Review B, 2010, 82, .	1.1	24
8270	Doping of cobalt oxide with transition metal impurities:Ab initiostudy. Physical Review B, 2010, 81, .	1.1	19
8271	Valence band study of thermoelectric Zintl-phase<mml:math xmlns:mml="http://www.w3.org/1998/Math/MathML" display="inline"><mml:mrow><mml:msub><mml:mrow><mml:mtext>SrZn</mml:mtext></mml:mrow><mml:mn>2</mml:mn></mml:ms xmlns:mml="http://www.w3.org/1998/Math/MathML" display="inline"><mml:mrow><mml:msub><mml:mrow><mml:mtext>YbZn</mml:mtext></mml:mrow><mml:mn>2</mml:mn></mml:m Physical Review B, 2010, 81, .	1.1	32
8272	Diffraction of fast atoms during grazing scattering from the surface of an ultrathin silica film on Mo(112). Physical Review B, 2010, 82, .	1.1	59
8273	Theory of nitride oxide adsorption on transition metal (111) surfaces: a first-principles investigation. Physical Chemistry Chemical Physics, 2010, 12, 2459.	1.3	63
8274	Carrier wave effect in nonresonant inelastic scanning tunneling spectroscopy of molecules with delocalized frontier orbitals. Physical Review B, 2010, 81, .	1.1	2
8275	Electronic and magnetic properties of Co and Ni impurities in Cu wires: First-principles investigation of local moment formation in one dimension. Physical Review B, 2010, 82, .	1.1	3
8276	Si/Ge exchange mechanisms at the Ge(105) surface. Physical Review B, 2010, 81, .	1.1	6
8277	Point-defect-mediated dehydrogenation of AlH3. Applied Physics Letters, 2010, 97, .	1.5	8
8278	Excess carbon in silicon carbide. Journal of Applied Physics, 2010, 108, 123705.	1.1	26
8279	First-principles study of magnetic properties of<mml:math xmlns:mml="http://www.w3.org/1998/Math/MathML" display="inline"><mml:mrow><mml:mtext>L</mml:mtext><mml:msub><mml:mn>1</mml:mn><mml:mn>0</mml:mn></mml:msub></r MnPt and FePt alloys. Physical Review B, 2010, 81, .	1.1	73
8280	Chemical control of polar behavior in bicomponent short-period superlattices. Physical Review B, 2010, 81, .	1.1	14

#	Article	IF	Citations
8281	Diffusion of 1,4-butanedithiol onAu(100)â˜'(1Ã—1): A DFT-based master-equation approach. Physical Review B, 2010, 82, .	1.1	4
8282	Significance of Self-Trapping on Hydrogen Diffusion. Physical Review Letters, 2010, 105, 185901.	2.9	13
8283	Adatom-dependent diffusion mechanisms on aAg/Si(111)3Ã—3surface. Physical Review B, 2010, 81, .	1.1	10
8284	Adsorption structures of phenol on theSi(001)â˜'(2Ã—1)surface calculated using density functional theory. Physical Review B, 2010, 81, .	1.1	15
8285	Activated<mml:math xmlns:mml="http://www.w3.org/1998/Math/MathML" display="inline"><mml:mrow><mml:msub><mml:mtext>O</mml:mtext><mml:mn>2</mml:mn></mml:msub></mml:mrow></mml:math and formation of oxide islands on Be(0001): An atomistic model for metal oxidation. Physical Review B, 2010, 82, .	1.1	7
8286	Atomic transport in ordered compounds mediated by local disorder: Diffusion in<mml:math xmlns:mml="http://www.w3.org/1998/Math/MathML" display="inline"><mml:mrow><mml:mi>B</mml:mi><mml:mn>2</mml:mn><mml:msub><mml:mrow><mml:mtext>Ni</mml:mtext></ Physical Review B, 2010, 81, .	1.1	21
8287	Characterization of spin-state tuning in thermally annealed semiconductor quantum dots. Physical Review B, 2010, 82, .	1.1	12
8288	CO adsorption on Pt-induced Ge nanowires. Physical Review B, 2010, 81, .	1.1	8
8289	Ab initioand scanning tunneling microscopy study of an indium-terminated GaAs(100) surface: An indium-induced surface reconstruction change in the<mml:math xmlns:mml="http://www.w3.org/1998/Math/MathML" display="inline"><mml:mrow><mml:mi>c</mml:mi><mml:mrow><mml:mo>(</mml:mo><mml:mrow><mml:mn>8</mml:mn><mml:mo> Physical Review B, 2010, 81, .	1.1	18
8290	First-principles study of 1,4-butanedithiol molecules and radicals adsorbed on unreconstructed Au(111) and Au(100). Physical Review B, 2010, 81, .	1.1	9
8291	Structure and energetics of ferroelectric domain walls in<mml:math xmlns:mml="http://www.w3.org/1998/Math/MathML" display="inline"><mml:mrow><mml:msub><mml:mrow><mml:mtext>LiNbO</mml:mtext></mml:mrow><mml:mn>3</mml:mn></mml: atomic-level simulations. Physical Review B, 2010, 82, .	1.1	45
8292	<mml:math xmlns:mml="http://www.w3.org/1998/Math/MathML" display="inline"><mml:mrow><mml:mtext>BaCu</mml:mtext><mml:mi>C</mml:mi><mml:mi>h</mml:mi><mml:mtext>F</mml:mtext>	1.1	23
8293	Ab initiostudy of low-dimensional quantum spin systems<mml:math xmlns:mml="http://www.w3.org/1998/Math/MathML" display="inline"><mml:mrow><mml:msub><mml:mrow><mml:mtext>Sr</mml:mtext></mml:mrow><mml:mn>3</mml:mn></mml:msub> xmlns:mml="http://www.w3.org/1998/Math/MathML" display="inline"><mml:mrow><mml:msub><mml:mrow><mml:mtext>Sr</mml:mtext></mml:mrow><mml:mn>3</mml:mn></mml:msub> Physical Review B, 2010, 82, .	1.1	25
8294	Pathways for thermal phosphorus desorption from the silicon (001) surface. Physical Review B, 2010, 82, .	1.1	4
8295	Phase transformation in Si from semiconducting diamond to metallic<mml:math xmlns:mml="http://www.w3.org/1998/Math/MathML" display="inline"><mml:mrow><mml:mi>Î²</mml:mi><mml:mtext>-Sn</mml:mtext></mml:mrow></mml:math>phase in QMC and DFT under hydrostatic and anisotropic stress. Physical Review B, 2010, 82, .	1.1	65
8296	Structure of the (010) surface of the orthorhombic complex metallic alloy<mml:math xmlns:mml="http://www.w3.org/1998/Math/MathML" display="inline"><mml:mrow><mml:mi mathvariant="normal">T</mml:mi><mml:msub><mml:mrow><mml:mtext>-Al</mml:mtext></mml:mrow><mml:mn>3</mml:mn></ Physical Review B, 2010, 81, .	1.1	22
8297	Tailoring perpendicular magnetic anisotropy in ultrathin Co/Pt multilayers coupled to NiO. Physical Review B, 2010, 81, .	1.1	8
8298	Unusual compression behavior of<mml:math xmlns:mml="http://www.w3.org/1998/Math/MathML" display="inline"><mml:mrow><mml:msub><mml:mrow><mml:mtext>TiO</mml:mtext></mml:mrow><mml:mn>2</mml:mn> from first principles. Physical Review B, 2010, 82, .	1.1	28

#	Article	IF	Citations
8299	Ab initiomolecular dynamics simulations using a Chebyshev-filtered subspace iteration technique. Physical Review B, 2010, 82, .	1.1	14
8300	Hydrogen interaction with point defects in tungsten. Physical Review B, 2010, 82, .	1.1	216
8301	Extrinsic point defects in aluminum antimonide. Physical Review B, 2010, 81, .	1.1	21
8302	Ab initio study of shock compressed oxygen. Journal of Chemical Physics, 2010, 132, 154307.	1.2	10
8303	Structure and properties of surface and subsurface defects in graphite accounting for van der Waals and spin-polarization effects. Physical Review B, 2010, 82, .	1.1	17
8304	Ab initio study of oxygenreduction mechanism at Pt4cluster. Physical Chemistry Chemical Physics, 2010, 12, 614-620.	1.3	45
8305	Atomic structure of<mml:math xmlns:mml="http://www.w3.org/1998/Math/MathML" display="inline"><mml:mrow><mml:mtext>Yb</mml:mtext><mml:mo>/</mml:mo><mml:mtext>Si</mml:mtext><mml:mrow><mml:mo Interrelation between the silicon dimer arrangement and<mml:math xmlns:mml="http://www.. Physical Review B, 2010, 82, .	1.1	6
8306	Density functional study of<mml:math xmlns:mml="http://www.w3.org/1998/Math/MathML" display="inline"><mml:mrow><mml:msub><mml:mrow><mml:mtext>Li</mml:mtext></mml:mrow><mml:mn>4</mml:mn></mml:ms xmlns:mml="http://www.w3.org/1998/Math/MathML" display="inline"><mml:mrow><mml:msub><mml:mrow><mml:mtext>Li</mml:mtext></mml:mrow><mml:mrow><mml:mn>1.5</mml:mn> Physical Review B, 2010, 81, .	1.1	16
8307	Quantitative local environment characterization in amorphous oxides. Physical Review B, 2010, 81, .	1.1	16
8308	Point defect chemistry in amorphous<mml:math xmlns:mml="http://www.w3.org/1998/Math/MathML" display="inline"><mml:mrow><mml:msub><mml:mrow><mml:mtext>HfO</mml:mtext></mml:mrow><mml:mn>2</mml:mn></mml:ms Density functional theory calculations. Physical Review B, 2010, 81, .	1.1	36
8309	Working at the interface. Molecular Physics, 2010, 108, 3235-3248.	0.8	0
8310	Role of electronic friction during the scattering of vibrationally excited nitric oxide molecules from Au(111). Physical Review B, 2010, 82, .	1.1	67
8311	Recoverable degradation in InAs/AlSb high-electron mobility transistors: The role of hot carriers and metastable defects in AlSb. Journal of Applied Physics, 2010, 108, 114505.	1.1	5
8312	Rotational motion of<mml:math xmlns:mml="http://www.w3.org/1998/Math/MathML" display="inline"><mml:mrow><mml:msub><mml:mrow><mml:mtext>BH</mml:mtext></mml:mrow><mml:mn>4</mml:mn></mml:m in<mml:math xmlns:mml="http://www.w3.org/1998/Math/MathML" display="inline"><mml:mrow><mml:mi>M</mml:mi><mml:msub><mml:mrow><mml:mtext>BH</mml:mtext></mml:mrow><mml:mn> Reactive interface formation and Co-induced<mml:math xmlns:mml="http://www.w3.org/1998/Math/MathML" display="inline"><mml:mrow>. Physical Review B,	1.1	77
8313	xmlns:mml="http://www.w3.org/1998/Math/MathML" display="inline"><mml:mrow><mml:mrow><mml:mo>(</mml:mo><mml:mrow><mml:msqrt><mml:mn>7</mml:mn></mml:msqrt><mm on a GaN(0001) pseudo-<mml:math xmlns:mml="http://www.w3.org/1998/Math/MathML"		

#	Article	IF	Citations
8317	Effect of interfacial Cr on magnetoelectricity ofFe2/CrO2/BaTiO3(001). Physical Review B, 2010, 81, .	1.1	4
8318	Effects of Electronic and Lattice Polarization on the Band Structure of Delafossite Transparent Conductive Oxides. Physical Review Letters, 2010, 104, 136401.	2.9	88
8319	Anomalies in the response of V, Nb, and Ta to tensile and shear loading:Ab initiodensity functional theory calculations. Physical Review B, 2010, 81, .	1.1	59
8320	Density functional theory study of Pt-induced Ge(001) reconstructions. Physical Review B, 2010, 81, .	1.1	13
8321	First-principles studies of Au-induced nanowires on Ge(001). Physical Review B, 2010, 81, .	1.1	34
8322	Comment On â€œStructural Prediction and Phase Transformation Mechanisms in Calcium at High Pressureâ€• Physical Review Letters, 2010, 104, 209601; author reply 209602.	2.9	6
8323	Magnetostructural Effect in the Multiferroic<mml:math xmlns:mml="http://www.w3.org/1998/Math/MathML" display="inline"><mml:msub><mml:mi>BiFeO</mml:mi><mml:mn>3</mml:mn></mml:msub><mml:mtext mathvariant="normal">â^'</mml:mtext><mml:msub><mml:mi>BiMnO</mml:mi><mml:mn>3</mml:mn></mml:msub></mml:math>Che from First Principles. Physical Review Letters, 2010, 104, 037202.	2.9	25
8324	Oxidation and the origin of the two-dimensional electron gas in AlGaN/GaN heterostructures. Journal of Applied Physics, 2010, 107, .	1.1	94
8325	Single-monolayer<mml:math xmlns:mml="http://www.w3.org/1998/Math/MathML" display="inline"><mml:mrow><mml:msub><mml:mrow><mml:mtext>SiN</mml:mtext></mml:mrow><mml:mi>x</mml:mi></mml:msub> in TiN: A first-principles study. Physical Review B, 2010, 81, .	1.1	28
8326	Metastable polymeric nitrogen nanotube from a zigzag sheet phase and first-principles calculations. Physical Review B, 2010, 82, .	1.1	11
8327	Electronic effects of single H atoms on Ge(001) revisited. Journal of Chemical Physics, 2010, 133, 014703.	1.2	10
8328	Strong Quantum Size Effects in Pb(111) Thin Films Mediated by Anomalous Friedel Oscillations. Physical Review Letters, 2010, 105, 066101.	2.9	35
8329	First-principles investigation ofBaFe2As2(001). Physical Review B, 2010, 82, .	1.1	7
8330	Multivalent metal tetrahydroborides of Al, Sc, Y, Ti, and Zr. Physical Review B, 2010, 81, .	1.1	23
8331	First-principles study of quantum size effects in ultrathin Pb-Bi metal alloy films. Physical Review B, 2010, 81, .	1.1	10
8332	MgO/metal interfaces at low coverage: An order<mml:math xmlns:mml="http://www.w3.org/1998/Math/MathML" display="inline"><mml:mi>N</mml:mi></mml:math>, semiempirical Hartree-Fock simulation. Physical Review B, 2010, 81, .	1.1	12
8333	Ab initiostudy of the solubility and kinetics of hydrogen in austenitic high Mn steels. Physical Review B, 2010, 81, .	1.1	35
8334	Tuning surface metallicity and ferromagnetism by hydrogen adsorption at the polar ZnO(0001) surface. Physical Review B, 2010, 81, .	1.1	56

#	Article	IF	Citations
8335	Strong hydrogen trapping at helium in tungsten: Density functional theory calculations. Physical Review B, 2010, 81, .	1.1	83
8336	Multiferroic<mml:math xmlns:mml="http://www.w3.org/1998/Math/MathML" display="inline"><mml:mrow><mml:msub><mml:mrow><mml:mtext>BiFeO</mml:mtext></mml:mrow><mml:mn>3</mml:mn></mml:msub></mml:mrow></mml:math> checkerboard from first principles. Physical Review B, 2010, 82, .	1.1	16
8337	Cohesive and magnetic properties of grain boundaries in bcc Fe with Cr additions. Physical Review B, 2010, 81, .	1.1	79
8338	Characteristics of bamboo defects in peapod-grown double-walled carbon nanotubes. Physical Review B, 2010, 82, .	1.1	3
8339	The properties of small Ag clusters bound to DNA bases. Journal of Chemical Physics, 2010, 132, 195102.	1.2	108
8340	Ab initio study on noncompensated CrO codoping of GaN for enhanced solar energy conversion. Journal of Chemical Physics, 2010, 132, 104501.	1.2	38
8341	Thermal Conductivity of Periclase (MgO) from First Principles. Physical Review Letters, 2010, 104, 208501.	2.9	125
8342	Magic Monatomic Linear Chains for Mn Nanowire Self-Assembly on Si(001). Physical Review Letters, 2010, 105, 116102.	2.9	30
8343	Novel High Pressure Structures and Superconductivity of<mml:math xmlns:mml="http://www.w3.org/1998/Math/MathML" display="inline"><mml:mi>Ca</mml:mi><mml:msub><mml:mi>Li</mml:mi><mml:mn>2</mml:mn></mml:msub></mml:math>. Physical Review Letters, 2010, 104, 177005.	2.9	64
8344	Magnetic perturbation and associated energies of the antiphase boundaries in ordered Ni3Al. Journal of Applied Physics, 2010, 108, .	1.1	23
8345	Ideal tensile strength of cubic crystals under superimposed transverse biaxial stresses from first principles. Physical Review B, 2010, 82, .	1.1	51
8346	Structure and stability of phases within the NbNâ€“AlN system. Journal Physics D: Applied Physics, 2010, 43, 145403.	1.3	49
8347	Cohesive Properties and Asymptotics of the Dispersion Interaction in Graphite by the Random Phase Approximation. Physical Review Letters, 2010, 105, 196401.	2.9	330
8348	Ferromagnetically Coupled Shastry-Sutherland Quantum Spin Singlets in<mml:math xmlns:mml="http://www.w3.org/1998/Math/MathML" display="inline"><mml:mo stretchy="false">(</mml:mo><mml:mi>CuCl</mml:mi><mml:mo) Tj ETQq1 1 0.784314 rgBT /Overlock 10 Tf 50 222 Td (stretchy="false"> mathvariant="normal">O</mml:mi><mml:mn>7</mml:mn></mml:msub></mml:math>. Physical Review Letters, 2010, 105, 167205.	2.9	29
8349	First-principles calculation of H vibrational excitations at a dislocation core of Pd. Physical Review B, 2010, 82, .	1.1	13
8350	Structural phases of strained<mml:math xmlns:mml="http://www.w3.org/1998/Math/MathML" display="inline"><mml:mrow><mml:msub><mml:mrow><mml:mtext>LaAlO</mml:mtext></mml:mrow><mml:mn>3</mml:mn></mml:msub></mml:mrow></mml:math> by octahedral tilt instabilities. Physical Review B, 2010, 82, .	1.1	66
8351	Influence of exchange correlation on the symmetry and properties of siderite according to density-functional theory. Physical Review B, 2010, 82, .	1.1	16
8352	Thermodynamic stability of neutral Xe defects in diamond. Physical Review B, 2010, 82, .	1.1	12

#	Article	IF	Citations
8353	Facile abstraction of hydrogen atoms from graphane, diamond, and amorphous carbon surfaces: A first-principles study. Physical Review B, 2010, 82, .	1.1	5
8354	First-principles description of atomic gold chains on Ge(001). Physical Review B, 2010, 81, .	1.1	17
8355	Bismuth-stabilized<mml:math xmlns:mml="http://www.w3.org/1998/Math/MathML" display="inline"><mml:mrow><mml:mi>c</mml:mi><mml:mrow><mml:mo>(</mml:mo><mml:mrow><mml:mn>2</mml:mn><mml:mo> on a InSb(100) substrate: Violation of the electron counting model. Physical Review B, 2010, 81, .	1.1	19
8356	Magnetic states of<mml:math xmlns:mml="http://www.w3.org/1998/Math/MathML" display="inline"><mml:mrow><mml:mi>M</mml:mi><mml:mtext>-Fe</mml:mtext></mml:mrow></mml:math>wires<mml:math xmlns:mml="http://www.w3.org/1998/Math/MathML" display="inline"><mml:mrow><mml:mrow><mml:mo>(</mml:mo><mml:mrow><mml:mi>M</mml:mi><mml:mo>= vicinal Cu(111) from first principles. Physical Review B, 2010, 81, .	1.1	11
8357	Frozen thermal fluctuations in adsorbate-induced step restructuring. Physical Review B, 2010, 82, .	1.1	4
8358	Density functional theory andab initiomolecular dynamics study of NO adsorption on Pd(111) and Pt(111) surfaces. Physical Review B, 2010, 81, .	1.1	16
8359	Elastic constants of<mml:math xmlns:mml="http://www.w3.org/1998/Math/MathML" display="inline"><mml:mi>Î²</mml:mi></mml:math>-eucryptite studied by density functional theory. Physical Review B, 2010, 81, .	1.1	19
8360	Si atom adsorption and diffusion on Si(110)-(1Ã—1)and(2Ã—1). Physical Review B, 2010, 81, .	1.1	8
8361	Step structure of Si(110)-(16Ã—2)and adsorption ofH2O. Physical Review B, 2010, 82, .	1.1	13
8362	Effects of metal impurities on the optical properties of polyethylene in the warm dense-matter regime. Physical Review B, 2010, 81, .	1.1	15
8363	First-principles-based<mml:math xmlns:mml="http://www.w3.org/1998/Math/MathML" display="inline"><mml:mrow><mml:msup><mml:mi>s</mml:mi><mml:mo>Â±</mml:mo></mml:msup></mml:mrow></mml:math>-wav modeling for iron-based superconductors: Specific heat and nuclear magnetic relaxation rate. Physical Review B, 2010, 82, .	1.1	2
8364	Role of the self-interaction error in studying chemisorption on graphene from first-principles. Physical Review B, 2010, 81, .	1.1	23
8365	Molecular dynamics study of<mml:math xmlns:mml="http://www.w3.org/1998/Math/MathML" display="inline"><mml:mrow><mml:msub><mml:mtext>H</mml:mtext><mml:mn>2</mml:mn></mml:msub></mml:mrow></mml:math> on H-covered Pd(100). Physical Review B, 2010, 81, .	1.1	26
8366	Pt-induced nanowires on Ge(001): A density functional theory study. Physical Review B, 2010, 81, .	1.1	30
8367	Dispersive resonance bands within the space-charge layer of a metal-semiconductor junction. Physical Review B, 2010, 81, .	1.1	9
8368	Quantum conductance of a single magnetic atom: Anab initiostudy. Physical Review B, 2010, 82, .	1.1	19
8369	Theory of hot-carrier-induced phenomena in GaN high-electron-mobility transistors. Applied Physics Letters, 2010, 96, .	1.5	45
8370	Atomic-scale structure and electronic property of the LaAlO3/TiO2 interface. Journal of Applied Physics, 2010, 108, .	1.1	49

#	Article	IF	Citations
8371	Self-trapping in B-doped amorphous Si: Intrinsic origin of low acceptor efficiency. Physical Review B, 2010, 81, .	1.1	9
8372	Electronic structure of the<mml:math xmlns:mml="http://www.w3.org/1998/Math/MathML" display="inline"><mml:mrow><mml:mtext>Pb</mml:mtext><mml:mo>/</mml:mo><mml:mtext>Si</mml:mtext><mml:mrow><mml:mo rec. Physical Review B, 2010, 81, .	1.1	12
8373	Quasiperiodic Pb monolayer on the fivefold<mml:math xmlns:mml="http://www.w3.org/1998/Math/MathML" display="inline"><mml:mrow><mml:mi>i</mml:mi><mml:mtext>-Al-Pd-Mn</mml:mtext></mml:mrow></mml:math>surface: Structure and electronic properties. Physical Review B, 2010, 82, .	1.1	16
8374	Cluster expansion Monte Carlo study of phase stability of vanadium nitrides. Physical Review B, 2010, 81, .	1.1	23
8375	Structural and magnetic properties of<mml:math xmlns:mml="http://www.w3.org/1998/Math/MathML" display="inline"><mml:mrow><mml:msub><mml:mrow><mml:mtext>Tc</mml:mtext></mml:mrow><mml:mi>n</mml:mi></mml:msub metalofullerenes: First-principles predictions. Physical Review B, 2010, 81, .	1.1	19
8376	Tuning the magnetic and electronic properties of bilayer graphene nanoribbons on Si(001) by bias voltage. Physical Review B, 2010, 81, .	1.1	28
8377	Interfacial magnetoelectric coupling in tricomponent superlattices. Physical Review B, 2010, 81, .	1.1	69
8378	Dynamics of quantum tunneling: Effects on the rate and transition path of OH on Cu(110). Physical Review B, 2010, 81, .	1.1	14
8379	Theoretical study of the elasticity, mechanical behavior, electronic structure, interatomic bonding, and dielectric function of an intergranular glassy film model in prismaticÎ²-Si3N4. Physical Review B, 2010, 81, .	1.1	28
8380	Recovery of the half-metallicity of an<mml:math xmlns:mml="http://www.w3.org/1998/Math/MathML" display="inline"><mml:mrow><mml:msub><mml:mrow><mml:mtext>Fe</mml:mtext></mml:mrow><mml:mn>3</mml:mn> by atomic hydrogen adsorption. Physical Review B, 2010, 81, .	1.1	5
8381	Valence band structure of the icosahedral Ag-In-Yb quasicrystal. Physical Review B, 2010, 81, .	1.1	22
8382	Effect of phosphorus on cleavage fracture in<mml:math xmlns:mml="http://www.w3.org/1998/Math/MathML" display="inline"><mml:mi>Î²</mml:mi></mml:math>-carbide. Physical Review B, 2010, 81, .	1.1	11
8383	High-pressure structural and lattice dynamical study of<mml:math xmlns:mml="http://www.w3.org/1998/Math/MathML" display="inline"><mml:mrow><mml:msub><mml:mrow><mml:mtext>HgWO</mml:mtext></mml:mrow><mml:mn>4</mml:mn></mml: Physical Review B, 2010, 82, .	1.1	11
8384	Negative compressibility in platinum sulfide using density-functional theory. Physical Review B, 2010, 81, .	1.1	31
8385	Selenium adsorbed single wall carbon nanotubes as a potential candidate for nanoscale interconnects. Applied Physics Letters, 2010, 97, 163107.	1.5	7
8386	Multishell Intermetallic Onions by Symmetrical Configuration of Ordered Domains. Physical Review Letters, 2010, 105, 225501.	2.9	4
8387	High-pressure phase transitions and compressibility of wolframite-type tungstates. Journal of Applied Physics, 2010, 107, .	1.1	66
8388	A comparative DFT study of electronic properties of 2H-, 4H- and 6H-SiC(0001) and SiC(000 ar{1}) clean surfaces: significance of the surface Stark effect. New Journal of Physics, 2010, 12, 043024.	1.2	30

#	Article	IF	Citations
8389	A nitrogen-rich C₃N₁₂solid transformed from cyanuric triazide under high pressure and temperature. Journal of Physics Condensed Matter, 2010, 22, 505402.	0.7	12
8390	Comparisons of ZnO codoped by group IIIA elements (Al, Ga, In) and N: a first-principle study. Chinese Physics B, 2010, 19, 117102.	0.7	20
8391	Magnetism and clustering in Cr-doped InN. Applied Physics Letters, 2010, 97, .	1.5	20
8392	ADSORPTION PROPERTIES OF N2 ON Be(0001) SURFACE: A FIRST-PRINCIPLES CALCULATION. Modern Physics Letters B, 2010, 24, 859-865.	1.0	5
8393	Electron traps and their effect on the surface chemistry of TiO ₂ (110). Proceedings of the National Academy of Sciences of the United States of America, 2010, 107, 2391-2396.	3.3	264
8394	Crystal engineering using functionalized adamantane. Journal of Physics Condensed Matter, 2010, 22, 315303.	0.7	2
8395	Quantum States and Diffusion of Lithium Atom Motion on a Graphene. Journal of the Physical Society of Japan, 2010, 79, 014601.	0.7	20
8396	Ab initiomolecular dynamics study of liquid Se₃₀Te₇₀: structural, electronic and dynamical properties. Physica Scripta, 2010, 82, 035603.	1.2	12
8397	FIRST-PRINCIPLES STUDY OF MAGNETISM AND DEFECT STATE PROPERTIES OF ANTIPEROVSKITE GaC_{1-x}Mn₃. Modern Physics Letters B, 2010, 24, 953-962.	1.0	2
8398	Novel transport properties of gold-single wall carbon nanotubes composite contacts. Journal of Applied Physics, 2010, 108, 064318.	1.1	2
8399	Reactant-governing growth direction of indium nitride nanowires. Nanotechnology, 2010, 21, 245601.	1.3	13
8400	MAGNETIC COUPLING IN PSEUDOMORPHIC 2ML OVERLAYERS AND SANDWICH SUPERLATTICE STRUCTURES OF Cr, Mn, Fe, Co AND Ni ON FCC Cu(001). International Journal of Modern Physics B, 2010, 24, 405-412.	1.0	3
8401	Impact of strain on the surface properties of transition metal carbide films: First-principles study. Journal of Applied Physics, 2010, 107, 083521.	1.1	18
8402	DFT Study of Alkali Metal Atom Adsorption on Defect-Free MgO(001) Surface. Chinese Journal of Chemical Physics, 2010, 23, 538-542.	0.6	7
8403	A Beâ€“W interatomic potential. Journal of Physics Condensed Matter, 2010, 22, 352206.	0.7	26
8404	Electronic structures and stability of Ni/Bi₂Te₃and Co/Bi₂Te₃interfaces. Journal Physics D: Applied Physics, 2010, 43, 115303.	1.3	49
8405	FIRST-PRINCIPLES INVESTIGATION OF STRUCTURAL AND ELECTRONIC PROPERTIES OF THE RECONSTRUCTED ZnO$(000ar 1)$ and $(0001) (sqrt{3}imessqrt{3})-R30^circ$ SURFACES. Modern Physics Letters B, 2010, 24, 2803-2814.	1.0	1
8406	Magnetic properties of 3d transition metal wires on vicinal Cu(111) surfaces at finite temperature. Journal of Applied Physics, 2010, 107, .	1.1	11

#	Article	IF	Citations
8407	Effects of Single Vacancy on Electronic and Optical Properties for Î³-Si3N4. Chinese Journal of Chemical Physics, 2010, 23, 201-206.	0.6	2
8408	Magnetic ordering and magnetodielectric phenomena in CoSeO₄. Journal of Physics Condensed Matter, 2010, 22, 506003.	0.7	7
8409	Role of Iridium in Pt-based Alloy Catalysts for the ORR: Surface Adsorption and Stabilization Studies. Journal of the Electrochemical Society, 2010, 157, B959.	1.3	35
8410	Edge versus interior in the chemical bonding and magnetism of zigzag edged triangular graphene molecules. Journal of Chemical Physics, 2010, 133, 044708.	1.2	12
8411	A PROBABLE MECHANISM OF SPIN-STATE TRANSITION IN LaCoO₃. Modern Physics Letters B, 2010, 24, 1785-1790.	1.0	3
8412	Study on Chemical Reactivity Control of Sodium by Suspended Nanoparticles I. Journal of Nuclear Science and Technology, 2010, 47, 1165-1170.	0.7	12
8413	Kinetics versus thermodynamics in materials modeling: The case of the di-vacancy in iron. Philosophical Magazine, 2010, 90, 2585-2595.	0.7	24
8414	First-Principles Study of Ni Adatom Adsorption on Graphene for Ni-Catalyzed Carbonization of Wood as Electromagnetic Shielding (EMS) Materials. , 2010, , .		1
8415	The interaction of Cu with Bi nanolines on H-passivated Si(001): anab initioanalysis. Journal of Physics Condensed Matter, 2010, 22, 345001.	0.7	1
8416	Quantum Mechanical Study on Tunnelling and Ballistic Transport of Nanometer Si MOSFETs. Chinese Physics Letters, 2010, 27, 057101.	1.3	0
8417	A Simple Theoretical Method to Predict the Hardness of Pure Metal Crystals. Chinese Physics Letters, 2010, 27, 076201.	1.3	1
8418	First-principles analysis of C₂H₂molecule diffusion and its dissociation process on the ferromagnetic bcc-Fe(110) surface. Journal of Physics Condensed Matter, 2010, 22, 384214.	0.7	7
8419	Theoretical analysis of initial adsorption of high-Îº metal oxides on InxGa1â^'xAs(0â€,0â€,1)-(4Ã—2) surfaces. Journal of Chemical Physics, 2010, 133, 194702.	1.2	4
8420	First-principles study of the effect of water on the phase transitions in Mg₂SiO₄forsterite. High Pressure Research, 2010, 30, 318-324.	0.4	4
8421	First-principles sliding simulation of Al-terminated Î£13 pyramidal twin grain boundary inÎ±-Al₂O₃. Philosophical Magazine Letters, 2010, 90, 159-172.	0.5	6
8422	p H -dependence of conduction type in cuprous oxide synthesized from solution. Journal of Applied Physics, 2010, 107, .	1.1	61
8423	A first-principles study on magnetic coupling between carbon adatoms on graphene. New Journal of Physics, 2010, 12, 113021.	1.2	30
8424	Anchoring of a Single Molecular Rotor and Its Array on Metal Surfaces using Molecular Design and Self-Assembly. International Journal of Molecular Sciences, 2010, 11, 656-671.	1.8	9

#	Article	IF	Citations
8425	Methane dissociation and adsorption on Ni(111), Pt(111), Ni(100), Pt(100), and Pt(110)-(1Ã—2): Energetic study. Journal of Chemical Physics, 2010, 132, 054705.	1.2	156
8426	Investigation of osmium carbides with various stoichiometries: First-principles calculations. Journal of Applied Physics, 2010, 107, .	1.1	26
8427	Thermodynamic phase diagram for hydrogen on polar InP(111)B surfaces. Journal of Applied Physics, 2010, 107, 063516.	1.1	7
8428	First-principles studies for CO and O2 on gold nanocluster. Journal of Chemical Physics, 2010, 132, 244302.	1.2	27
8429	Ab initio statistical mechanics of surface adsorption and desorption. II. Nuclear quantum effects. Journal of Chemical Physics, 2010, 133, 044103.	1.2	10
8430	Alchemical derivatives of reaction energetics. Journal of Chemical Physics, 2010, 133, 084104.	1.2	57
8431	Identifying configuration and orientation of adsorbed molecules by inelastic electron tunneling spectra. Journal of Chemical Physics, 2010, 133, 064702.	1.2	6
8432	Shell-anchor-core structures for enhanced stability and catalytic oxygen reduction activity. Journal of Chemical Physics, 2010, 133, 134705.	1.2	18
8433	Atomic structure and formation mechanism of identically sized Au clusters grown on Si(111)-(7Ã—7) surface. Journal of Chemical Physics, 2010, 133, 124706.	1.2	20
8434	Multiple localized states and magnetic orderings in partially open zigzag carbon nanotube superlattices: An ab initio study. Journal of Chemical Physics, 2010, 133, 084702.	1.2	11
8435	Atomic imaging of the monolayer nucleation and unpinning of a compound semiconductor surface during atomic layer deposition. Journal of Chemical Physics, 2010, 133, 154704.	1.2	29
8436	Scanning tunneling microscopy/spectroscopy study of atomic and electronic structures of In2O on InAs and In0.53Ga0.47As(001)-(4Ã—2) surfaces. Journal of Chemical Physics, 2010, 133, 164704.	1.2	13
8437	Defects responsible for the Fermi level pinning in n+ poly-Si/HfO2 gate stacks. Applied Physics Letters, 2010, 97, .	1.5	7
8438	Passivation effects of fluorine and hydrogen at the SiCâ€“SiO2 interface. Applied Physics Letters, 2010, 97, .	1.5	13
8439	Predicting the melting temperatures of bulk materials. Europhysics Letters, 2010, 91, 46001.	0.7	2
8440	Nanostructural interpretation for elastic softening of amorphous carbon induced by the incorporation of silicon and hydrogen atoms. Journal of Applied Physics, 2010, 107, .	1.1	9
8441	Phonon Dispersion in Superionic Copper Selenide: Observation of Soft Phonon Modes in Superionic Phase Transition. Journal of the Physical Society of Japan, 2010, 79, 25-28.	0.7	11
8442	Electronic properties of WO3 quantum films. , 2010, , .		0

#	Article	IF	Citations
8443	Core-shell morphologies of FePt and CoPt nanoparticles: Anab initiocomparison. Journal of Physics: Conference Series, 2010, 200, 072039.	0.3	14
8444	Reassessment of the Mgâ€“Ge binary system using CALPHAD supported by first-principles calculation. International Journal of Materials Research, 2010, 101, 1489-1496.	0.1	8
8445	Recognition tunneling. Nanotechnology, 2010, 21, 262001.	1.3	70
8446	A First Principles Study on Dissociation and Adsorption Processes of H₂ on Pd₃Ag(111) Surface. Japanese Journal of Applied Physics, 2010, 49, 115702.	0.8	13
8447	Band structure and Fermi surface of atomically uniform lead films. New Journal of Physics, 2010, 12, 113034.	1.2	1
8448	Dimensionality-driven insulatorâ€“metal transition in A-site excess non-stoichiometric perovskites. Nature Communications, 2010, 1, 106.	5.8	70
8449	Pourbaix diagrams of alkaline earth metal elements by combination of first principles calculations and thermochemical data. Journal of Physics Condensed Matter, 2010, 22, 384206.	0.7	1
8450	First-principles determination of dislocation properties in magnesium based on the improved Peierlsâ€“Nabarro equation. Physica Scripta, 2010, 81, 065601.	1.2	20
8451	Structure of InSb(001) surface. Journal of Physics Condensed Matter, 2010, 22, 265001.	0.7	5
8452	Phase relationships and structures of inorganic crystals by a combination of the cluster expansion method and first principles calculations. Journal of Physics Condensed Matter, 2010, 22, 384207.	0.7	1
8453	Thioglycolic acid on the gold (111) surface and Raman vibrational spectra. Journal of Chemical Physics, 2010, 132, 064702.	1.2	6
8454	The equation of state and nonmetalâ€“metal transition of benzene under shock compression. Journal of Applied Physics, 2010, 107, 083502.	1.1	10
8455	Calculation of anharmonic OH phonon dispersion curves for the Mg(OH)2 crystal. Journal of Chemical Physics, 2010, 133, 034120.	1.2	3
8456	The effect of dopant at the Zr site on the proton conduction pathways of SrZrO3: An orthorhombic perovskite. Journal of Chemical Physics, 2010, 133, 064701.	1.2	15
8457	First-principles study of native defects in TlBr: Carrier trapping, compensation, and polarization phemomenon. Journal of Applied Physics, 2010, 108, .	1.1	36
8458	Structure of the B2 phase in the Tiâ€“25Alâ€“25Zr alloy: a density functional study. Journal of Physics Condensed Matter, 2010, 22, 345502.	0.7	3
8459	Vacancy-defectâ€“derived magnetism in titanium oxide nanosheet: A first-principles study. Europhysics Letters, 2010, 90, 66005.	0.7	4
8460	A density-functional study of the adsorption of methane-thiol on the (111) surfaces of the Ni-group metals: II. Vibrational spectroscopy. Journal of Physics Condensed Matter, 2010, 22, 265006.	0.7	68

#	Article	IF	Citations
8461	Efficacy of surface error corrections to density functional theory calculations of vacancy formation energy in transition metals. Journal of Physics Condensed Matter, 2010, 22, 345501.	0.7	17
8462	Entropy effects in hydrocarbon conversion reactions: free-energy integrations and transition-path sampling. Journal of Physics Condensed Matter, 2010, 22, 384201.	0.7	24
8463	DFT study of structure stability and elasticity of wadsleyite II. Journal of Physics Condensed Matter, 2010, 22, 145402.	0.7	6
8464	A density functional study of the adsorption of methane-thiol on the (111) surfaces of the Ni-group metals: I. Molecular and dissociative adsorption. Journal of Physics Condensed Matter, 2010, 22, 265005.	0.7	19
8465	The nature of the observed free-electron-like state in a PTCDA monolayer on Ag(111). New Journal of Physics, 2010, 12, 063014.	1.2	38
8466	Emergence of noncollinear magnetic ordering in bimetallic Co_{6â^'n}Mn_nclusters. Journal Physics D: Applied Physics, 2010, 43, 015006.	1.3	8
8467	First-principles study of the structural, elastic, and electronic properties of C₂₀, C₁₂B₈, and C₁₂N₈. Journal of Physics Condensed Matter, 2010, 22, 175505.	0.7	0
8468	Atomic structure and adhesion of the Nb(001)/Î±-Nb₅Si₃(001) interface: a first-principles study. Journal of Physics Condensed Matter, 2010, 22, 085004.	0.7	22
8469	First-Principles Simulation on Thickness Dependence of Piezoresistance Effect in Silicon Nanosheets. Japanese Journal of Applied Physics, 2010, 49, 06GH01.	0.8	10
8470	The ideal strength of gold under uniaxial stress: anab initiostudy. Journal of Physics Condensed Matter, 2010, 22, 295405.	0.7	25
8471	Tuning independently the Fermi energy and spin splitting in Rashba systems: ternary surface alloys on Ag(111). Journal of Physics Condensed Matter, 2010, 22, 385501.	0.7	10
8472	Conductivity engineering of graphene by defect formation. Journal Physics D: Applied Physics, 2010, 43, 045404.	1.3	89
8473	Design of type-II MgxZn1â^'xO:N/ZnO superlattices for UV photodetector applications. Semiconductor Science and Technology, 2010, 25, 045012.	1.0	1
8474	Predicting the segregation profile of the Pt₂₅Rh₇₅(100) surface from first-principles. Journal of Physics Condensed Matter, 2010, 22, 384203.	0.7	10
8475	Trapping of Holes and Excitons in Scintillators: CsI and ${m LaX}_{3}$ (${m X}={m Cl}$, Br). IEEE Transactions on Nuclear Science, 2010, 57, 2303-2308.	1.2	16
8476	Ab Initio Kinetics of Gas Phase Decomposition Reactions. Journal of Physical Chemistry A, 2010, 114, 12656-12661.	1.1	40
8477	Computational Investigation of FeS₂ Surfaces and Prediction of Effects of Sulfur Environment on Stabilities. Journal of Physical Chemistry C, 2010, 114, 8971-8980.	1.5	75
8478	Theoretical prediction of topological insulators in thallium-based III-V-VI ₂ ternary chalcogenides. Europhysics Letters, 2010, 90, 37002.	0.7	140

#	Article	IF	Citations
8479	Crystal-Field and Strain Effects on Minimum-Spin-Splitting Surfaces in Bulk Wurtzite Materials. Journal of the Physical Society of Japan, 2010, 79, 093705.	0.7	1
8480	First-principles<mml:math xmlns:mml="http://www.w3.org/1998/Math/MathML" display="inline"><mml:mrow><mml:mtext>LDA</mml:mtext><mml:mo>+</mml:mo><mml:mi>U</mml:mi></mml:mrow></mml:math><mml:math xmlns:mml="http://www.w3.org/1998/Math/MathML" display="inline"><mml:mrow><mml:mtext>GGA</mml:mtext><mml:mo>+</mml:mo><mml:mi>U</mml:mi></mml:mrow></mml:math> Electronic structure and excitonic absorption in<mml:math xmlns:mml="http://www.w3.org/1998/Math/MathML" display="inline"><mml:mrow><mml:mtext>BaCu</mml:mtext><mml:mi>C</mml:mi><mml:mi>h</mml:mi><mml:mtext>F</mml:mtext>	1.1	63
8481		1.1	21
8482	Defects Responsible for the Hole Gas in Ge/Si Coreâ˜Shell Nanowires. Nano Letters, 2010, 10, 116-121.	4.5	49
8483	The effect of acoustic phonon scattering on the carrier mobility in the semiconducting zigzag single wall carbon nanotubes. Applied Physics Letters, 2010, 96, 183108.	1.5	45
8484	Density Functional Theory Study of Catechol Adhesion on Silica Surfaces. Journal of Physical Chemistry C, 2010, 114, 20793-20800.	1.5	123
8485	Ultrathin epitaxial cobalt films on graphene for spintronic investigations and applications. New Journal of Physics, 2010, 12, 103040.	1.2	74
8486	Structure of Zeolite A (LTA) Surfaces and the Zeolite A/Water Interface. Journal of Physical Chemistry C, 2010, 114, 9739-9747.	1.5	43
8487	Structure Stability and Magnetic Properties of Ni₂XGa (X = Mn, Fe, Co) Ferromagnetic Shape Memory Alloys by DFT Approach. Solid State Phenomena, 0, 160, 69-74.	0.3	4
8488	Importance of London dispersion effects for the packing of molecular crystals: a case study for intramolecular stacking in a bis-thiophene derivative. Physical Chemistry Chemical Physics, 2010, 12, 8500.	1.3	115
8489	Density Functional Theory Studies of the Structure Sensitivity of Ethanol Oxidation on Palladium Surfaces. Journal of Physical Chemistry C, 2010, 114, 10489-10497.	1.5	92
8490	Computation of correlation-induced atomic displacements and structural transformations in paramagnetic<mml:math xmlns:mml="http://www.w3.org/1998/Math/MathML" display="inline"><mml:mrow><mml:msub><mml:mrow><mml:mtext>KCuF</mml:mtext></mml:mrow><mml:mn>3</mml:mn></mml:msub></mml:mrow></mml:math><mml:math xmlns:mml="http://www.w3.org/1998/Math/MathML" display="inline"><mml:mrow><mml:msub><mml:mrow><mml:mtext>LaMnO</mml:mtext></mml:mrow><mml:mn>3</mml:mn></mml:msub></mml:mrow></mml:math>. Physical Review B, 2010, 81, .	1.1	63
8491	Effect of doping and pressure on magnetism and lattice structure of iron-based superconductors. Physical Review B, 2010, 82, .	1.1	37
8492	Forcing Ferromagnetic Coupling Between Rare-Earth-Metal and<mml:math xmlns:mml="http://www.w3.org/1998/Math/MathML" display="inline"><mml:mn>3</mml:mn><mml:mi>d</mml:mi></mml:math>Ferromagnetic Films. Physical Review Letters, 2010, 104, 156402.	2.9	42
8493	Boron and nitrogen functionalized diamondoids: A first principles investigation. Diamond and Related Materials, 2010, 19, 837-840.	1.8	7
8494	The metallicity of B-doped diamond surface by first-principles study. Diamond and Related Materials, 2010, 19, 824-828.	1.8	6
8495	Atomic structure and mechanical properties of BC2N superlattice. Diamond and Related Materials, 2010, 19, 1341-1347.	1.8	5
8496	Antiferromagnetic order in (Ga,Mn)N nanocrystals: A density functional theory study. Physical Review B, 2010, 82, .	1.1	22

#	Article	IF	Citations
8497	Structure and magnetism of bulk Fe and Cr: from plane waves to LCAO methods. Journal of Physics Condensed Matter, 2010, 22, 295502.	0.7	43
8498	Origin of Colossal Ionic Conductivity in Oxide Multilayers: Interface Induced Sublattice Disorder. Physical Review Letters, 2010, 104, 115901.	2.9	124
8499	Density Functional Calculations on the Hydrogenation of Carbon Dioxide on Fe(111) and W(111) Surfaces. Journal of Physical Chemistry C, 2010, 114, 1194-1200.	1.5	27
8500	Hydrogen in oxides and nitrides: unexpected physics and impact on devices. IOP Conference Series: Materials Science and Engineering, 2010, 15, 012001.	0.3	3
8501	First Principles Studies of the Effect of Nickel Carbide Catalyst Composition on Carbon Nanotube Growth. Journal of Physical Chemistry C, 2010, 114, 18045-18050.	1.5	26
8502	Structure-Induced Ferromagnetic Stabilization in Free-Standing Hexagonal Fe1.3Ge Nanowires. Journal of the American Chemical Society, 2010, 132, 17447-17451.	6.6	23
8503	Bond-order potential for point and extended defect simulations in tungsten. Journal of Applied Physics, 2010, 107, .	1.1	76
8504	A DFT study of halogen atoms adsorbed on graphene layers. Nanotechnology, 2010, 21, 485701.	1.3	85
8505	First-principles study of defects and adatoms in silicon carbide honeycomb structures. Physical Review B, 2010, 81, .	1.1	344
8506	Epitaxial strain effects in the spinel ferrites<mml:math xmlns:mml="http://www.w3.org/1998/Math/MathML" display="inline"><mml:mrow><mml:msub><mml:mrow><mml:mtext>CoFe</mml:mtext></mml:mrow><mml:mn>2</mml:mn></mml	1.1	135
8507	Sequestration of Noble Gases in Giant Planet Interiors. Physical Review Letters, 2010, 104, 121101.	2.9	110
8508	Environmental Fate and Transport of Energetic Materials: The Aqueous Environment. , 2010, , .		0
8509	Magnetic cluster expansion model for bcc-fcc transitions in Fe and Fe-Cr alloys. Physical Review B, 2010, 81, .	1.1	111
8510	Oxygen vacancies and donor impurities in Î²-Ga2O3. Applied Physics Letters, 2010, 97, .	1.5	733
8511	Confinement effects on alloy reactivity. Physical Chemistry Chemical Physics, 2010, 12, 12466.	1.3	8
8512	Vibrational Properties of<mml:math xmlns:mml="http://www.w3.org/1998/Math/MathML" display="inline"><mml:mi>Î±</mml:mi></mml:math>- and<mml:math xmlns:mml="http://www.w3.org/1998/Math/MathML" display="inline"><mml:mi>Îƒ</mml:mi></mml:math>-Phase Fe-Cr Alloy. Physical Review Letters, 2010, 104,	2.9	29
8514	The effect of yttrium dopant on the proton conduction pathways of BaZrO3, a cubic perovskite. Journal of Chemical Physics, 2010, 132, 214709.	1.2	55
8515	DFT-Based Theoretical Calculations of Nb- and W-Doped Anatase TiO₂: Complex Formation between W Dopants and Oxygen Vacancies. Journal of Physical Chemistry C, 2010, 114, 12777-12783.	1.5	32

#	Article	IF	Citations
8516	Oxidative Decomposition of Methanol on Subnanometer Palladium Clusters: The Effect of Catalyst Size and Support Composition. Journal of Physical Chemistry C, 2010, 114, 10342-10348.	1.5	76
8517	Catalysis and Surface Organometallic Chemistry: A View from Theory and Simulations. Chemical Reviews, 2010, 110, 1788-1806.	23.0	121
8518	Structural stability and thermal properties of BeO from the quasiharmonic approximation. Journal of Physics Condensed Matter, 2010, 22, 045404.	0.7	29
8519	Magnetism in ZnO nanowire with Fe/Co codoping: First-principles density functional calculations. Physical Review B, 2010, 81, .	1.1	36
8520	Structural, electronic and magnetic properties of partially inverse spinel CoFe₂O₄: a first-principles study. Journal Physics D: Applied Physics, 2010, 43, 445003.	1.3	175
8521	Coverage-Dependent Adsorption Mode of Water on Fe₃O₄(001): Insights from First Principles Calculations. Journal of Physical Chemistry C, 2010, 114, 11148-11156.	1.5	66
8522	Density Functional Theory Modeling and Calculation of NMR Parameters: An ab Initio Study of the Polymorphs of Bulk Glycine. Crystal Growth and Design, 2010, 10, 3657-3667.	1.4	40
8523	Multifunctional Porous Graphene for Nanoelectronics and Hydrogen Storage: New Properties Revealed by First Principle Calculations. Journal of the American Chemical Society, 2010, 132, 2876-2877.	6.6	304
8524	Room temperature ferromagnetism in pristine MgO thin films. Applied Physics Letters, 2010, 96, .	1.5	105
8525	Size-Dependent Tuning of Mn²⁺ d Emission in Mn²⁺-Doped CdS Nanocrystals: Bulk vs Surface. Journal of Physical Chemistry C, 2010, 114, 18323-18329.	1.5	80
8526	Reconstruction and evaporation at graphene nanoribbon edges. Physical Review B, 2010, 81, .	1.1	55
8527	Modelling nano-clusters and nucleation. Physical Chemistry Chemical Physics, 2010, 12, 786-811.	1.3	174
8528	Adsorption of monovalent metal atoms on graphene: a theoretical approach. Nanotechnology, 2010, 21, 115701.	1.3	77
8529	Crystal structure prediction and isostructurality of three small organic halogen compounds. Physical Chemistry Chemical Physics, 2010, 12, 8571.	1.3	16
8530	Hydrogen vibrational modes on graphene and relaxation of the Câ€“H stretch excitation from first-principles calculations. Journal of Chemical Physics, 2010, 133, 054505.	1.2	40
8531	Morphology and texture evolution of nanostructured CaF₂films on amorphous substrates under oblique incidence flux. Nanotechnology, 2010, 21, 445701.	1.3	19
8532	Contrasting Behavior of Carbon Nucleation in the Initial Stages of Graphene Epitaxial Growth on Stepped Metal Surfaces. Physical Review Letters, 2010, 104, 186101.	2.9	194
8533	Determining the anisotropic exchange coupling of<mml:math xmlns:mml="http://www.w3.org/1998/Math/MathML" display="inline"><mml:mrow><mml:msub><mml:mrow><mml:mtext>CrO</mml:mtext></mml:mrow><mml:mn>2</mml:mn></mml:ms first-principles density functional theory calculations. Physical Review B, 2010, 81, .	1.1	28

#	Article	IF	Citations
8534	A Combined Experimentalâ^'Computational Investigation of Carbon Dioxide Capture in a Series of Isoreticular Zeolitic Imidazolate Frameworks. Journal of the American Chemical Society, 2010, 132, 11006-11008.	6.6	303
8535	Dopant-vacancy binding effects in Li-doped magnesium hydride. Physical Review B, 2010, 82, .	1.1	27
8536	High-pressure magnetic transition in hcp-Fe. American Mineralogist, 2010, 95, 880-883.	0.9	30
8537	Room-Temperature Synthesis of Agâ^'Ni and Pdâ^'Ni Alloy Nanoparticles. Journal of Physical Chemistry C, 2010, 114, 14309-14318.	1.5	82
8538	Variations of ferroelectric off-centering distortion and<mml:math xmlns:mml="http://www.w3.org/1998/Math/MathML" display="inline"><mml:mrow><mml:mn>3</mml:mn><mml:mi>d</mml:mi><mml:mtext>â^'</mml:mtext><mml:mn>4</mml:mn><mml:mi mixing in La-doped<mml:math xmlns:mml="http://www.w3.org/1998/Math/MathML" display="inline"><mml:mrow><mml:msub><mml:mrow><mml:mtext>BiFeO</mml:mtext></mml:mrow><mml:mn>3</mml:mn></mml:m	1.1	74
8539	Unconventional superconducting phase in the weakly correlated noncentrosymmetric<mml:math xmlns:mml="http://www.w3.org/1998/Math/MathML" display="inline"><mml:mrow><mml:msub><mml:mrow><mml:mtext>Mo</mml:mtext></mml:mrow><mml:mn>3</mml:mn></mml:m Physical Review B, 2010, 82, .	1.1	121
8540	Quantifying octahedral rotations in strained perovskite oxide films. Physical Review B, 2010, 82, .	1.1	293
8541	Understanding of Adsorption and Catalytic Properties of Bimetallic Ptâ^'Co Alloy Surfaces from First Principles: Insight from Disordered Alloy Surfaces. Journal of Physical Chemistry C, 2010, 114, 7141-7152.	1.5	16
8542	Electron Dynamics in Dye-Sensitized Solar Cells: Effects of Surface Terminations and Defects. Journal of Physical Chemistry B, 2010, 114, 17077-17083.	1.2	28
8543	Lattice dynamics and structural stability of ordered<mml:math xmlns:mml="http://www.w3.org/1998/Math/MathML" display="inline"><mml:mrow><mml:msub><mml:mrow><mml:mtext>Fe</mml:mtext></mml:mrow><mml:mn>3</mml:mn></mml:m xmlns:mml="http://www.w3.org/1998/Math/MathML" display="inline"><mml:mrow><mml:msub><mml:mrow><mml:mtext>Fe</mml:mtext></mml:mrow><mml:mn>3</mml:mn></mml:m	1.1	45
8544	Intrinsic point defects and complexes in the quaternary kesterite semiconductor<mml:math xmlns:mml="http://www.w3.org/1998/Math/MathML" display="inline"><mml:mrow><mml:msub><mml:mrow><mml:mtext>Cu</mml:mtext></mml:mrow><mml:mn>2</mml:mn></mml:msu Physical Review B, 2010, 81, .	1.1	624
8545	Numerical Methods for Electronic Structure Calculations of Materials. SIAM Review, 2010, 52, 3-54.	4.2	231
8546	Density functional theory plus U study of vacancy formations in bismuth ferrite. Applied Physics Letters, 2010, 96, .	1.5	69
8547	Theoretical study of interface structure and energetics in semicoherent<mml:math xmlns:mml="http://www.w3.org/1998/Math/MathML" display="inline"><mml:mrow><mml:mtext>Fe</mml:mtext><mml:mrow><mml:mo>(</mml:mo><mml:mrow><mml:mn>001</mml:m		

#	Article	IF	Citations
8552	Theoretical calculations of the thermodynamic stability of ionic substitutions in hydroxyapatite under an aqueous solution environment. Journal of Physics Condensed Matter, 2010, 22, 384210.	0.7	7
8553	Comparative Density Functional Study of Methanol Decomposition on Cu₄ and Co₄ Clusters. Journal of Physical Chemistry B, 2010, 114, 14458-14466.	1.2	35
8554	Interfacial properties of NM/CeO₂(111) (NM = noble metal atoms or clusters of Pd, Pt and) Tj ETQq0 0 0 rgBT /Overlock 10	0.7	34
8555	Theoretical Simulation of Temperature Programmed Desorption of Molecular Oxygen on Isolated Au Nanoparticles from Density Functional Calculations and Microkinetics Models. Journal of Physical Chemistry C, 2010, 114, 5101-5106.	1.5	13
8556	First-Principles Calculations of Electronic Structure and Solution Energies of Mn-Doped BaTiO3. Japanese Journal of Applied Physics, 2010, 49, 09MC01.	0.8	27
8557	First Principles Calculation Study of the Origin of the Tetragonal Structure of BiCoO3. Japanese Journal of Applied Physics, 2010, 49, 09ME08.	0.8	10
8558	Quantum anomalous Hall effect in graphene from Rashba and exchange effects. Physical Review B, 2010, 82, .	1.1	567
8559	Hydrostatic and uniaxial compression studies of 1,3,5-triamino- 2,4,6-trinitrobenzene using density functional theory with van der Waals correction. Journal of Applied Physics, 2010, 107, .	1.1	39
8560	Adsorption of small aromatic molecules on the (111) surfaces of noble metals: A density functional theory study with semiempirical corrections for dispersion effects. Journal of Chemical Physics, 2010, 132, 224701.	1.2	210
8561	Selectivity of Cobalt-Based Non-Platinum Oxygen Reduction Catalysts in the Presence of Methanol and Formic Acid. Journal of Physical Chemistry C, 2010, 114, 15190-15195.	1.5	19
8562	Size-dependent strain effects on electronic and optical properties of ZnO nanowires. Applied Physics Letters, 2010, 97, .	1.5	29
8563	Structure and energetics of imogolite: a quantum mechanical ab initio study with B3LYP hybrid functional. Journal of Materials Chemistry, 2010, 20, 10417.	6.7	41
8564	First-Principles Simulations of Lithium Melting: Stability of the bcc Phase Close to Melting. Physical Review Letters, 2010, 104, 185701.	2.9	67
8565	Structural and electronic trends in rare-earth technetate pyrochlores. Dalton Transactions, 2010, 39, 7207.	1.6	13
8566	Resolving the Structure of Active Sites on Platinum Catalytic Nanoparticles. Nano Letters, 2010, 10, 3073-3076.	4.5	101
8567	Stability, elastic and electronic properties of palladium nitride. Journal of Physics Condensed Matter, 2010, 22, 015404.	0.7	20
8568	Calculation of fast pipe diffusion along a dislocation stacking fault ribbon. Physical Review B, 2010, 82, .	1.1	19
8569	Magnetism of substitutional Co impurities in graphene: Realization of single<mml:math xmlns:mml="http://www.w3.org/1998/Math/MathML" display="inline"><mml:mi>Ï€</mml:mi></mml:math>vacancies. Physical Review B, 2010, 81, .	1.1	178

#	Article	IF	Citations
8570	First-principles study of H on the reconstructed W(100) surface. Physical Review B, 2010, 81, .	1.1	69
8571	First-principles investigations of Ti-substituted hydroxyapatite electronic structure. Physical Chemistry Chemical Physics, 2010, 12, 156-163.	1.3	22
8572	Visualization and analysis of atomistic simulation data with OVITOâ€“the Open Visualization Tool. Modelling and Simulation in Materials Science and Engineering, 2010, 18, 015012.	0.8	8,805
8573	Local atomic structure of Ca-Mg-Zn metallic glasses. Physical Review B, 2010, 82, .	1.1	44
8574	Density Functional Theory Study of Ag Adsorption on SrTiO3 (001) Surface. Journal of Physical Chemistry C, 2010, 114, 10917-10921.	1.5	32
8575	Stability and Reactivity of ÏµÂ˚Ï‡Â˚Î¸ Iron Carbide Catalyst Phases in FischerÂ˚Tropsch Synthesis: Controlling Î¼_C. Journal of the American Chemical Society, 2010, 132, 14928-14941.	6.6	426
8576	Magnetism in bcc and fcc Fe with carbon and manganese. Journal of Physics Condensed Matter, 2010, 22, 316002.	0.7	59
8577	Controlling Novel Red-Light Emissions by Doping In2O3 Nano/Microstructures with Interstitial Nitrogen. Journal of Physical Chemistry C, 2010, 114, 13234-13240.	1.5	21
8578	Magnetic properties of the half-metallic Heusler alloys<mml:math xmlns:mml="http://www.w3.org/1998/Math/MathML" display="inline"><mml:mrow><mml:msub><mml:mrow><mml:mtext>Co</mml:mtext></mml:mrow><mml:mn>2</mml:mn></mml:msu<mml:math xmlns:mml="http://www.w3.org/1998/Math/MathML" display="inline"><mml:mrow><mml:msub><mml:mrow><mml:mtext>Co</mml:mtext></mml:mrow><mml:mn>2</mml:mn></mml:msu<mml:mi>Î²</mml:mi></mml:math>phase in Ni-Ti shape-memory alloy. Physical Review B, 2010, 81, .	1.1	99
8579	Ab initio study of interacting lattice vibrations and stabilization of the<mml:math xmlns:mml="http://www.w3.org/1998/Math/MathML" display="inline"><mml:mi>Î²</mml:mi></mml:math>phase in Ni-Ti shape-memory alloy. Physical Review B, 2010, 81, .	1.1	33
8580	Electronic and magnetic properties of zigzag graphene nanoribbon with one edge saturated. Applied Physics Letters, 2010, 96, .	1.5	121
8581	Electronic structure of oxygen-terminated zigzag graphene nanoribbons: A hybrid density functional theory study. Physical Review B, 2010, 81, .	1.1	50
8582	Computational Study of BrÃ¸nsted Acidity of Mordenite. Effect of the Electric Field on the Infrared OH Stretching Frequencies. Journal of Physical Chemistry C, 2010, 114, 15424-15431.	1.5	21
8583	Electronic and magnetic properties of a BN sheet decorated with hydrogen and fluorine. Physical Review B, 2010, 81, .	1.1	278
8584	Functionalization of BN honeycomb structure by adsorption and substitution of foreign atoms. Physical Review B, 2010, 82, .	1.1	92
8585	Triangle defect states of hexagonal boron nitride atomic layer: Density functional theory calculations. Physical Review B, 2010, 81, .	1.1	60
8586	Method for locating low-energy solutions within<mml:math xmlns:mml="http://www.w3.org/1998/Math/MathML" display="inline"><mml:mrow><mml:mtext>DFT</mml:mtext><mml:mo>+</mml:mo><mml:mi>U</mml:mi></mml:mrow></mml:math>. Physical Review B, 2010, 82, .	1.1	215
8587	Deep versus Shallow Behavior of Intrinsic Defects in Rutile and Anatase TiO₂ Polymorphs. Journal of Physical Chemistry C, 2010, 114, 21694-21704.	1.5	138

#	Article	IF	Citations
8588	Spin-polarized energy-gap opening in asymmetric bilayer graphene nanoribbons. Applied Physics Letters, 2010, 97, .	1.5	12
8589	Molecular understanding of alkyne hydrogenation for the design of selective catalysts. Dalton Transactions, 2010, 39, 8412.	1.6	133
8590	Modeling and simulation of uniaxial strain effects in armchair graphene nanoribbon tunneling field effect transistors. Applied Physics Letters, 2010, 96, 252105.	1.5	33
8591	Evolutionary Crystal Structure Prediction as a Method for the Discovery of Minerals and Materials. Reviews in Mineralogy and Geochemistry, 2010, 71, 271-298.	2.2	182
8592	Ab initio molecular dynamics simulations of the initial stages of solidâ€“electrolyte interphase formation on lithium ion battery graphitic anodes. Physical Chemistry Chemical Physics, 2010, 12, 6583.	1.3	221
8593	Electronic and Defect Structures of CuSCN. Journal of Physical Chemistry C, 2010, 114, 9111-9117.	1.5	155
8594	On the Thermodynamic Stability of Î±,Ï‰-Alkanedithiols Self-Assembled Monolayers on Unreconstructed and Reconstructed Au(111). Langmuir, 2010, 26, 9589-9595.	1.6	12
8595	Electronic Structures and Magnetic Properties of GaN Sheets and Nanoribbons. Journal of Physical Chemistry C, 2010, 114, 11390-11394.	1.5	115
8596	Theoretical studies of acrolein hydrogenation on Au20 nanoparticle. Journal of Chemical Physics, 2010, 132, 184702.	1.2	15
8597	Density Functional Theory Study on Surface C_xH_y Formation from CO Activation on Fe₃C(100). Journal of Physical Chemistry C, 2010, 114, 21585-21592.	1.5	44
8598	Thermoelectric properties of Bi2Te3 atomic quintuple thin films. Applied Physics Letters, 2010, 97, .	1.5	96
8599	Role of molecular electronic structure in inelastic electron tunneling spectroscopy:<mml:math xmlns:mml="http://www.w3.org/1998/Math/MathML" display="inline"><mml:mrow><mml:msub><mml:mtext>O</mml:mtext><mml:mn>2</mml:mn></mml:msub></mml:mrow></mml:ma Ag(110). Physical Review B, 2010, 82, .	1.1	24
8600	Interphase energies of hcp precipitates in fcc metals: A density-functional theory study in Al-Ag. Physical Review B, 2010, 81, .	1.1	16
8601	Thiol with an Unusual Adsorptionâ^'Desorption Behavior: 6-Mercaptopurine on Au(111). Langmuir, 2010, 26, 17068-17074.	1.6	34
8602	Role of Hydrogen Species in Palladium-Catalyzed Alkyne Hydrogenation. Journal of Physical Chemistry C, 2010, 114, 2293-2299.	1.5	71
8603	First-principles study of structural and elastic properties of monoclinic and orthorhombic BiMnO₃. Journal of Physics Condensed Matter, 2010, 22, 295404.	0.7	8
8604	Lithium Insertion In Silicon Nanowires: An ab Initio Study. Nano Letters, 2010, 10, 3243-3249.	4.5	201
8605	Modeling the Electrochemical Hydrogen Oxidation and Evolution Reactions on the Basis of Density Functional Theory Calculations. Journal of Physical Chemistry C, 2010, 114, 18182-18197.	1.5	990

#	Article	IF	Citations
8606	Effects of Au nanoparticles on the magnetic and transport properties of<mml:math xmlns:mml="http://www.w3.org/1998/Math/MathML" display="inline"><mml:mrow><mml:msub><mml:mrow><mml:mtext>La</mml:mtext></mml:mrow><mml:mrow><mml:mn>0.67</mml: layers. Physical Review B, 2010, 81, .	1.1	39
8607	Revisiting Hydrogen Storage in Bulk BC₃. Journal of Physical Chemistry C, 2010, 114, 3260-3264.	1.5	23
8609	Theoretical Exploration of the Structural, Electronic, and Magnetic Properties of ZnO Nanotubes with Vacancies, Antisites, and Nitrogen Substitutional Defects. Journal of Physical Chemistry C, 2010, 114, 5760-5766.	1.5	39
8610	Intrinsic room temperature ferromagnetism in boron-doped ZnO. Applied Physics Letters, 2010, 97, .	1.5	66
8611	Electronic structure and magnetic properties of Mn-doped ZnO nanotubes: An ab initio study. Journal of Applied Physics, 2010, 108, 084308.	1.1	21
8612	Elastic and plastic deformation of graphene, silicene, and boron nitride honeycomb nanoribbons under uniaxial tension: A first-principles density-functional theory study. Physical Review B, 2010, 81, .	1.1	219
8613	First-principles study on ferroelectricity at PbTiO3surface steps. Journal of Physics Condensed Matter, 2010, 22, 355901.	0.7	21
8614	Ab initiostudy of ferroelectric closure domains in ultrathin<mml:math xmlns:mml="http://www.w3.org/1998/Math/MathML" display="inline"><mml:mrow><mml:msub><mml:mrow><mml:mtext>PbTiO</mml:mtext></mml:mrow><mml:mrow><mml:mn>3</mml:mn></mml:mrow><mml:mn></mml:mn> Physical Review B, 2010, 81, .	1.1	54
8615	Band structure engineering of semiconductors for enhanced photoelectrochemical water splitting: The case of<mml:math xmlns:mml="http://www.w3.org/1998/Math/MathML" display="inline"><mml:mrow><mml:msub><mml:mrow><mml:mtext>TiO</mml:mtext></mml:mrow><mml:mrow><mml:mn>2</mml:mn></mml:mrow></mml:msub> Physical Review B, 2010, 82, .	1.1	300
8616	First-Principles Study of Initial Growth of InP Nanowires: Self-Catalytic Effect and Nucleation Mechanism of In Adatoms. Journal of Physical Chemistry C, 2010, 114, 10195-10201.	1.5	5
8617	Effects on Electronic Properties of Molecule Adsorption on CuO Surfaces and Nanowires. Journal of Physical Chemistry C, 2010, 114, 17120-17126.	1.5	115
8618	Systematic Study of the Multiple-Element Filling in Caged Skutterudite CoSb₃. Chemistry of Materials, 2010, 22, 2384-2394.	3.2	40
8619	Hydrogenation: A Simple Approach To Realize Semiconductorâ^'Half-Metalâ^'Metal Transition in Boron Nitride Nanoribbons. Journal of the American Chemical Society, 2010, 132, 1699-1705.	6.6	277
8620	Strain-induced semiconducting-metallic transition for ZnO zigzag nanoribbons. Journal of Applied Physics, 2010, 107, .	1.1	18
8621	Fluorination induced half metallicity in two-dimensional few zinc oxide layers. Journal of Chemical Physics, 2010, 132, 204703.	1.2	32
8622	Surface-passivation-induced metallic and magnetic properties of ZnO graphitic sheet. Applied Physics Letters, 2010, 96, .	1.5	18
8623	Chemically Meaningful Atomic Charges That Reproduce the Electrostatic Potential in Periodic and Nonperiodic Materials. Journal of Chemical Theory and Computation, 2010, 6, 2455-2468.	2.3	365
8624	Reversible Bond Formation in a Gold-Atomâ€“Organic-Molecule Complex as a Molecular Switch. Physical Review Letters, 2010, 105, 266102.	2.9	142

#	Article	IF	Citations
8625	Superhard and superconducting structures of BC5. Journal of Applied Physics, 2010, 108, .	1.1	66
8626	First Principles Study on Hydrogen Desorption from a Metal (=Al, Ti, Mn, Ni) Doped MgH₂ (110) Surface. Journal of Physical Chemistry C, 2010, 114, 11328-11334.	1.5	69
8627	Tuning Hydrated Nanoceria Surfaces: Experimental/Theoretical Investigations of Ion Exchange and Implications in Organic and Inorganic Interactions. Langmuir, 2010, 26, 7188-7198.	1.6	35
8628	Energetics of Polar and Nonpolar Facets of PbSe Nanocrystals from Theory and Experiment. ACS Nano, 2010, 4, 211-218.	7.3	93
8629	Classification of spinel structures based on first-principles cluster expansion analysis. Physical Review B, 2010, 81, .	1.1	38
8630	Impurity clustering and impurity-induced bands in PbTe-, SnTe-, and GeTe-based bulk thermoelectrics. Physical Review B, 2010, 81, .	1.1	86
8631	Growth Kinetic Processes of AlN Molecules on the Al-Polar Surface of AlN. Journal of Physical Chemistry A, 2010, 114, 9028-9033.	1.1	10
8632	Origins of Hole Doping and Relevant Optoelectronic Properties of Wide Gap p-Type Semiconductor, LaCuOSe. Journal of the American Chemical Society, 2010, 132, 15060-15067.	6.6	43
8633	Performance Comparisons of Bilayer Graphene and Graphene Nanoribbon Field-Effect Transistors under Ballistic Transport. Japanese Journal of Applied Physics, 2010, 49, 110207.	0.8	13
8634	Li Ion Diffusion Mechanisms in Bulk Monoclinic Li₂CO₃ Crystals from Density Functional Studies. Journal of Physical Chemistry C, 2010, 114, 20903-20906.	1.5	70
8635	Electronic Structure of TiO₂ Surfaces and Effect of Molecular Adsorbates Using Different DFT Implementations. Journal of Physical Chemistry C, 2010, 114, 22659-22670.	1.5	134
8636	Electron-lattice instabilities suppress cuprate-like electronic structures in<mml:math xmlns:mml="http://www.w3.org/1998/Math/MathML" display="inline"><mml:mrow><mml:msub><mml:mrow><mml:mtext>SrFeO</mml:mtext></mml:mrow><mml:mn>3</mml:mn></mml:mr Physical Review B, 2010, 81, .	1.1	22
8637	Stability and Formation Mechanisms of Carbonyl- and Hydroxyl-Decorated Holes in Graphene Oxide. Journal of Physical Chemistry C, 2010, 114, 12053-12061.	1.5	129
8638	Electronic and phononic properties of cinnabar:Ab initiocalculations and some experimental results. Physical Review B, 2010, 82, .	1.1	24
8639	Giant Magnetoelastic Coupling in a Metallic Helical Metamagnet. Physical Review Letters, 2010, 104, 247202.	2.9	84
8640	The role of sp-hybridized atoms in carbon ferromagnetism: a spin-polarized density functional theory calculation. Journal of Physics Condensed Matter, 2010, 22, 046001.	0.7	5
8641	Quantum Conductance of Î¼-Borolyl Triple-Decker Sandwich Complexes. Journal of Physical Chemistry C, 2010, 114, 11266-11272.	1.5	6
8642	Dissolution and diffusion properties of carbon in tungsten. Journal of Physics Condensed Matter, 2010, 22, 445504.	0.7	29

#	Article	IF	Citations
8643	MoirÃ© Superstructures of Graphene on Faceted Nickel Islands. ACS Nano, 2010, 4, 6509-6514.	7.3	78
8644	Density functional theory investigation of<mml:math xmlns:mml="http://www.w3.org/1998/Math/MathML" display="inline"><mml:mrow><mml:mn>3</mml:mn><mml:mi>d</mml:mi></mml:mrow></mml:math>,<mml:math xmlns:mml="http://www.w3.org/1998/Math/MathML" display="inline"><mml:mrow><mml:mn>4</mml:mn><mml:mi>d</mml:mi></mml:mrow></mml:math>, and<mml:math xmlns:mml="http://www.w3.org/1998/Math/MathML" display="inline"><mml:mrow></mml:mrow></mml:math>	1.1	211
8645	Completeness of the exact muffin-tin orbitals: Application to hydrogenated alloys. Physical Review B, 2010, 81, .	1.1	7
8646	LiMSO4F (M = Fe, Co and Ni): promising new positive electrode materials through the DFT microscope. Physical Chemistry Chemical Physics, 2010, 12, 15512.	1.3	65
8647	EuAgxAl11â^'x with the BaHg11-Type Structure: Composition, Coloring, and Competition with the BaCd11-Type Structure. Chemistry of Materials, 2010, 22, 1798-1806.	3.2	13
8648	Theoretical study of the surface modification of indium tin oxide with trifluorophenyl phosphonic acid molecules: impact of coverage density and binding geometry. Journal of Materials Chemistry, 2010, 20, 2630.	6.7	76
8649	Ab initiodescription of heterostructural alloys: Thermodynamic and structural properties of<mml:math xmlns:mml="http://www.w3.org/1998/Math/MathML" display="inline"><mml:mrow><mml:msub><mml:mrow><mml:mtext>Mg</mml:mtext></mml:mrow><mml:mi>x</mml:mi></mml:msub> xmlns:mml="http://www.w3.org/1998/Math/MathM. Physical Review B, 2010, 81, .	1.1	49
8650	Structural, electronic, and magnetic properties of nanometer-sized iron-oxide atomic clusters: Comparison between GGA and<mml:math xmlns:mml="http://www.w3.org/1998/Math/MathML" display="inline"><mml:mrow><mml:mtext>GGA</mml:mtext><mml:mo>+</mml:mo><mml:mtext>U</mml:mtext></mml:mrow></mml:m Physical Review B, 2010, 81, .	1.1	24
8651	Simulation of hydrogenated graphene field-effect transistors through a multiscale approach. Physical Review B, 2010, 82, .	1.1	50
8652	Charge carrier scattering by defects in semiconductors. Physical Review B, 2010, 81, .	1.1	47
8653	Surface segregation and stability of coreâ€“shell alloy catalysts for oxygen reduction in acid medium. Physical Chemistry Chemical Physics, 2010, 12, 2209.	1.3	114
8654	Shock Compression of a Fifth Period Element: Liquid Xenon to 840ÂGPa. Physical Review Letters, 2010, 105, 085501.	2.9	84
8655	First-principles and classical molecular dynamics simulation of shocked polymers. Physical Review B, 2010, 81, .	1.1	261
8656	Diffusion and electrical conductivity in water at ultrahigh pressures. Physical Review B, 2010, 82, .	1.1	73
8657	AbÂInitioIndications for Giant Magnetoelectric Effects Driven by Structural Softness. Physical Review Letters, 2010, 105, 037208.	2.9	99
8658	Substrate coherency driven octahedral rotations in perovskite oxide films. Physical Review B, 2010, 82, .	1.1	95
8659	Phonon Mechanism of the Magnetostructural Phase Transition in MnAs. Physical Review Letters, 2010, 104, 147205.	2.9	25
8660	Curvature-induced excess surface energy of fullerenes: Density functional theory and Monte Carlo simulations. Physical Review B, 2010, 81, .	1.1	27

#	Article	IF	Citations
8661	First-principles study of structural and electronic properties of ultrathin silicon nanosheets. Physical Review B, 2010, 82, .	1.1	52
8662	Dramatic reduction of the oxygen vacancy formation energy in ceria particles: a possible key to their remarkable reactivity at the nanoscale. Journal of Materials Chemistry, 2010, 20, 10535.	6.7	192
8663	Impurity doping in<mml:math xmlns:mml="http://www.w3.org/1998/Math/MathML" display="inline"><mml:mrow><mml:msub><mml:mrow><mml:mtext>SiO</mml:mtext></mml:mrow><mml:mn>2</mml:mn> Formation energies and defect levels from first-principles calculations. Physical Review B, 2010, 82, .	1.1	39
8664	Structural, electronic and optical properties of ilmenite and perovskite CdSnO₃from DFT calculations. Journal of Physics Condensed Matter, 2010, 22, 435801.	0.7	20
8665	Theoretical prediction of multiferroicity in double perovskite<mml:math xmlns:mml="http://www.w3.org/1998/Math/MathML" display="inline"><mml:mrow><mml:msub><mml:mtext>Y</mml:mtext><mml:mn>2</mml:mn></mml:msub><mml:msub><mml:mrow> Physical Review B, 2010, 82, .	1.1	115
8666	Magnetic anisotropy in Li-phosphates and origin of magnetoelectricity in<mml:math xmlns:mml="http://www.w3.org/1998/Math/MathML" display="inline"><mml:mrow><mml:msub><mml:mrow><mml:mtext>LiNiPO</mml:mtext></mml:mrow><mml:mn>4</mml:mn></ Physical Review B, 2010, 81, .	1.1	24
8667	Magnetically induced ferroelectricity in<mml:math xmlns:mml="http://www.w3.org/1998/Math/MathML" display="inline"><mml:mrow><mml:msub><mml:mrow><mml:mtext>Cu</mml:mtext></mml:mrow><mml:mn>2</mml:mn></mml:msub> xmlns:mml="http://www.w3.org/1998/Math/MathML" display="inline"><mml:mrow><mml:msub><mml:mrow><mml:mtext>Cu</mml:mtext></mml:mrow><mml:mn>2</mml:mn></mml:msub> Physical Review B, 2010, 82, .	1.1	20
8668	Ab Initio Study of CO Hydrogenation to Oxygenates on Reduced Rh Terraces and Stepped Surfaces. Journal of Physical Chemistry C, 2010, 114, 10171-10182.	1.5	99
8669	High-pressure x-ray diffraction andab initiostudy of<mml:math xmlns:mml="http://www.w3.org/1998/Math/MathML" display="inline"><mml:mrow><mml:msub><mml:mrow><mml:mtext>Ni</mml:mtext></mml:mrow><mml:mn>2</mml:mn></mml:msub> xmlns:mml="http://www.w3.org/1998/Math/MathML" display="inline"><mml:mrow><mml:msub><mml:mrow><mml:mtext>Pd</mml:mtext></mml:mrow><mml:mn>2</mml:m. Physical Review B, 2010, 82, .	1.1	91
8670	Interplay between Charge Order, Ferroelectricity, and Ferroelasticity: Tungsten Bronze Structures as a Playground for Multiferroicity. Physical Review Letters, 2010, 105, 107202.	2.9	33
8671	NaMnFe₂(PO₄)₃ Alluaudite Phase: Synthesis, Structure, and Electrochemical Properties As Positive Electrode in Lithium and Sodium Batteries. Chemistry of Materials, 2010, 22, 5554-5562.	3.2	140
8672	Charge Transport in Self-Assembled Semiconducting Organic Layers: Role of Dynamic and Static Disorder. Journal of Physical Chemistry C, 2010, 114, 10592-10597.	1.5	44
8673	Thermodynamics and kinetics of the copper vacancy in CuInSe2, CuGaSe2, CuInS2, and CuGaS2 from screened-exchange hybrid density functional theory. Journal of Applied Physics, 2010, 108, .	1.1	79
8674	First-principles study of the mechanical and optical properties of amorphous hydrogenated silicon and silicon-rich silicon oxide. Physical Review B, 2010, 81, .	1.1	24
8675	First-Principles Study on the Origin of the Different Selectivities for Methanol Steam Reforming on Cu(111) and Pd(111). Journal of Physical Chemistry C, 2010, 114, 21539-21547.	1.5	137
8676	Transferable orthogonal tight-binding parameters for ZnS and CdS. Journal of Physics Condensed Matter, 2010, 22, 295304.	0.7	2
8677	AuS and SH Bond Formation/Breaking during the Formation of Alkanethiol SAMs on Au(111): A Theoretical Study. Journal of Physical Chemistry C, 2010, 114, 9444-9452.	1.5	89
8678	The Electronic Structure and Chemical Properties of a Ni/CeO₂Anode in a Solid Oxide Fuel Cell: A DFT +UStudy. Journal of Physical Chemistry C, 2010, 114, 21411-21416.	1.5	44

#	Article	IF	Citations
8679	Reversible high-pressure carbon nanotube vessel. Physical Review B, 2010, 81, .	1.1	7
8680	Electronic structure and lattice dynamics of the magnetic shape-memory alloy<mml:math xmlns:mml="http://www.w3.org/1998/Math/MathML" display="inline"><mml:mrow><mml:msub><mml:mrow><mml:mtext>Co</mml:mtext></mml:mrow><mml:mn>2</mml:mn></mml:msu Physical Review B, 2010, 82, .	1.1	36
8681	Intrinsic electrostatic effects in nanostructured ceramics. Physical Review B, 2010, 81, .	1.1	22
8682	Competing Mechanisms in Atomic Layer Deposition of Er₂O₃ versus La₂O₃ from Cyclopentadienyl Precursors. Chemistry of Materials, 2010, 22, 117-129.	3.2	29
8683	Embedded ribbons of graphene allotropes: an extended defect perspective. New Journal of Physics, 2010, 12, 125006.	1.2	68
8684	Theoretical Investigation of the Magnetic Structure and Ferroelectric Polarization of the Multiferroic Langasite Ba₃NbFe₃Si₂O₁₄. Chemistry of Materials, 2010, 22, 5290-5295.	3.2	26
8685	Elastic constants and thermophysical properties of Alâ€“Mgâ€“Si alloys from first-principles calculations. International Journal of Materials Research, 2010, 101, 1392-1397.	0.1	3
8686	Stability, geometry, and electronic structure of an alternative I-III-VI2 material, CuScS2: A hybrid density functional theory analysis. Applied Physics Letters, 2010, 97, 131904.	1.5	19
8687	Work-Function Modification beyond Pinning: When Do Molecular Dipoles Count?. Nano Letters, 2010, 10, 4369-4374.	4.5	70
8688	On the Nature and Behavior of Li Atoms in Si: A First Principles Study. Journal of Physical Chemistry C, 2010, 114, 17942-17946.	1.5	82
8689	Understanding Cooperativity in Hydrogen-Bond-Induced Supramolecular Polymerization: A Density Functional Theory Study. Journal of Physical Chemistry B, 2010, 114, 13667-13674.	1.2	119
8690	Electronic structures of fully fluorinated and semifluorinated zinc oxide sheets. Applied Physics Letters, 2010, 96, .	1.5	26
8691	Controlling Edge Morphology in Graphene Layers Using Electron Irradiation: From Sharp Atomic Edges to Coalesced Layers Forming Loops. Physical Review Letters, 2010, 105, 045501.	2.9	56
8692	Theoretical Simulation of n-Alkane Cracking on Zeolites. Journal of Physical Chemistry C, 2010, 114, 10229-10239.	1.5	73
8693	Positive Charge States and Possible Polymorphism of Gold Nanoclusters on Reduced Ceria. Journal of the American Chemical Society, 2010, 132, 2175-2182.	6.6	109
8694	Oxygen-Induced Transformations of an FeO(111) Film on Pt(111): A Combined DFT and STM Study. Journal of Physical Chemistry C, 2010, 114, 21504-21509.	1.5	90
8695	Core and Shell States of Silicon Nanowires under Strain. Journal of Physical Chemistry C, 2010, 114, 9702-9705.	1.5	15
8696	Defect Interactions of ${hbox{H}}_{2}$ in ${hbox{SiO}}_{2}$: Implications for ELDRS and Latent Interface Trap Buildup. IEEE Transactions on Nuclear Science, 2010, , .	1.2	18

#	Article	IF	Citations
8697	Ab-initio Study of Transition-Metal Dimers on MgO(001) Surfaces: Comparison of Atomic and Electronic Properties. Journal of the Physical Society of Japan, 2010, 79, 074718.	0.7	20
8698	Stability of graphene oxide phases from first-principles calculations. Physical Review B, 2010, 82, .	1.1	124
8699	Synthesis, Characterization, and Quantum-Chemical Studies of Ni(CN)₂MX (M = Rb, Cs; X =) Tj ETQq0 0 0 rgBT /Overlock 1	1.9	1
8700	Theoretical Study on Adsorption and Dissociation of NO₂Molecule on Fe(111) Surface. Langmuir, 2010, 26, 7157-7164.	1.6	27
8701	A HREELS and DFT Study of the Adsorption of Aromatic Hydrocarbons on Diamond (111). Langmuir, 2010, 26, 3286-3291.	1.6	4
8702	Role of Electronic Structure in the Martensitic Phase Transition of<mml:math xmlns:mml="http://www.w3.org/1998/Math/MathML" display="inline"><mml:msub><mml:mi>Ni</mml:mi><mml:mn>2</mml:mn></mml:msub><mml:msub><mml:mi>Mn</mml:mi><mml:mi mml: by Hard-X-Ray Photoelectron Spectroscopy andAbÂInitioCalc. Physical Review Letters, 2010, 104, 176401.	7.2	189
8703	First-Principles Characterization of Amorphous Phases of MB₁₂H₁₂, M = Mg, Ca. Journal of Physical Chemistry C, 2010, 114, 14601-14605.	1.5	29
8704	Electronic and Magnetic Structure of Transition-Metal Carbodiimides by Means of GGA+U Theory. Journal of Physical Chemistry A, 2010, 114, 12345-12352.	1.1	21
8705	<mml:math xmlns:mml="http://www.w3.org/1998/Math/MathML" display="inline"><mml:mi>J</mml:mi></mml:math>dependence in the<mml:math xmlns:mml="http://www.w3.org/1998/Math/MathML" display="inline"><mml:mrow><mml:mtext>LSDA</mml:mtext><mml:mo>+</mml:mo><mml:mi>U</mml:mi></mml:mrow></mml:math> of noncollinear magnets. Physical Review B, 2010, 82, .	1.1	57
8706	Density Functional Studies of the Adsorption and Dissociation of CO₂Molecule on Fe(111) Surface. Langmuir, 2010, 26, 775-781.	1.6	23
8707	Experimental and theoretical investigations on magnetic behavior of (Al,Co) co-doped ZnO nanoparticles. Nanoscale, 2010, 2, 1505.	2.8	16
8708	Ab initiostudy of the lattice dynamics of CsNiF₃. Journal of Physics Condensed Matter, 2010, 22, 435402.	0.7	4
8709	CO₂ Activation and Total Reduction on Titanium(0001) Surface. Journal of Physical Chemistry C, 2010, 114, 11456-11459.	1.5	34
8710	Diffusion of Atomic Oxygen on the Si(100) Surface. Journal of Physical Chemistry C, 2010, 114, 12649-12658.	1.5	18
8711	Thickness-Dependent Hydroxylation of MgO(001) Thin Films. Journal of Physical Chemistry C, 2010, 114, 18207-18214.	1.5	57
8712	Density Functional Theory Study of Surface Carbonate Formation on BaO(001). Journal of Physical Chemistry C, 2010, 114, 1867-1874.	1.5	10
8713	Relaxation of Photoexcited Electrons at a Nanostructured Si(111) Surface. Journal of Physical Chemistry Letters, 2010, 1, 1073-1077.	2.1	83
8714	Kinetic and Theoretical Study of the Hydrodechlorination of CH_{4â^'x}Cl_x (x = 1â^'4) Compounds on Palladium. Langmuir, 2010, 26, 16615-16624.	1.6	28

#	Article	IF	Citations
8715	Structural, Electronic, and Electrochemical Properties of Cathode Materials Li₂MSiO₄ (M = Mn, Fe, and Co): Density Functional Calculations. Journal of Physical Chemistry C, 2010, 114, 3693-3700.	1.5	92
8716	Hydration of Rutile TiO₂: Thermodynamics and Effects on n- and p-Type Electronic Conduction. Journal of Physical Chemistry C, 2010, 114, 9139-9145.	1.5	25
8717	Electrodeposited Aluminum-Doped Î±-Fe₂O₃ Photoelectrodes: Experiment and Theory. Chemistry of Materials, 2010, 22, 510-517.	3.2	240
8718	Behaviour of group IIIA impurities in PbTe: implications to improve thermoelectric efficiency. Journal Physics D: Applied Physics, 2010, 43, 405403.	1.3	32
8719	Density functional theory with nonlocal correlation: A key to the solution of the CO adsorption puzzle. Physical Review B, 2010, 81, .	1.1	83
8720	Control of Octahedral Tilts and Magnetic Properties of Perovskite Oxide Heterostructures by Substrate Symmetry. Physical Review Letters, 2010, 105, 227203.	2.9	211
8721	Strain-Enhanced Stabilization and Catalytic Activity of Metal Nanoclusters on Graphene. Journal of Physical Chemistry C, 2010, 114, 16541-16546.	1.5	108
8722	ZnO Nanostructures for Gas Sensing: Interaction of NO₂, NO, O, and N with the ZnO(101Ì…0) Surface. Journal of Physical Chemistry C, 2010, 114, 10881-10893.	1.5	101
8723	Structural Design and Two-Dimensional Conductivity of Sheet-Tube Frameworks. Journal of Physical Chemistry C, 2010, 114, 19673-19677.	1.5	11
8724	Modeling Localized Photoinduced Electrons in Rutile-TiO₂ Using Periodic DFT+U Methodology. Langmuir, 2010, 26, 16232-16238.	1.6	36
8725	Cooperative Cation Migrations upon CO Addition in CuI- and Alkali-Exchanged Faujasite: A DFT Study. Journal of Physical Chemistry C, 2010, 114, 17802-17811.	1.5	25
8726	Bonding and Microstructural Stability in Ni₅₅Ti₄₅ Studied by Experimental and Theoretical Methods. Journal of Physical Chemistry C, 2010, 114, 19704-19713.	1.5	11
8727	Defect Processes in a PbS Metal Organic Framework: A Quantum-Confined Hybrid Semiconductor. Journal of Physical Chemistry Letters, 2010, 1, 1284-1287.	2.1	38
8728	Ground-state properties and high-pressure behavior of plutonium dioxide: Density functional theory calculations. Physical Review B, 2010, 82, .	1.1	121
8729	The Theoretical Quest for Sulfate of Ag2+: Genuine Ag(II)SO4, Diamagnetic Ag(I)2S2O8, or Rather Mixed-Valence Ag(I)[Ag(III)(SO4)2]?. Inorganic Chemistry, 2010, 49, 2735-2742.	1.9	15
8730	Oxygen ion diffusivity in strained yttria stabilized zirconia: where is the fastest strain?. Journal of Materials Chemistry, 2010, 20, 4809.	6.7	296
8731	First Principles Studies of Nitrogen Doped Carbon Nanotubes for Dioxygen Reduction. Journal of Physical Chemistry C, 2010, 114, 3371-3375.	1.5	39
8732	Phase equilibria at<mml:math xmlns:mml="http://www.w3.org/1998/Math/MathML" display="inline"><mml:mrow><mml:msub><mml:mrow><mml:mtext>Si-HfO</mml:mtext></mml:mrow><mml:mn>2</mml:mn></mml: xmlns:mml="http://www.w3.org/1998/Math/MathML" display="inline"><mml:mrow><mml:msub><mml:mrow><mml:mtext>Pt-HfO</mml:mtext></mml:mrow><mml:mn>2</mml:mn></mml: from first principles thermodynamics. Physical Review B, 2010, 82, .	1.1	13

#	Article	IF	Citations
8733	Electronic Structure and Redox Properties of the Ti-Doped Zirconia (111) Surface. Journal of Physical Chemistry C, 2010, 114, 15403-15409.	1.5	20
8734	The Electronic Structure of Mixed Self-Assembled Monolayers. ACS Nano, 2010, 4, 6735-6746.	7.3	43
8735	Exploration of Half Metallicity in Edge-Modified Graphene Nanoribbons. Journal of Physical Chemistry C, 2010, 114, 3937-3944.	1.5	105
8736	Complex polarization ordering in<mml:math xmlns:mml="http://www.w3.org/1998/Math/MathML" display="inline"><mml:mrow><mml:msub><mml:mrow><mml:mtext>PbTiO</mml:mtext></mml:mrow><mml:mn>3</mml:mn></mml:msub></mml:mrow></mml:math> A first-principles computational study. Physical Review B, 2010, 82, .	3.1	37
8737	Formation, Characterization, and Reactivity of Adsorbed Oxygen on BaO/Pt(111). Journal of Physical Chemistry C, 2010, 114, 20195-20206.	1.5	6
8738	A Density Functional Theory Study of Adsorption and Decomposition of Nitroamine Molecules on the Al(111) Surface. Journal of Physical Chemistry C, 2010, 114, 9390-9397.	1.5	23
8739	SO₂Adsorption and Transformations on Î³-Al₂O₃Surfaces: A Density Functional Theory Study. Journal of Physical Chemistry C, 2010, 114, 10444-10454.	1.5	44
8740	First-Principles Calculations of Hydrogen Generation Due to Water Splitting on Polar GaN Surfaces. Journal of Physical Chemistry C, 2010, 114, 18228-18232.	1.5	41
8741	The CO Formation Reaction Pathway in Steam Methane Reforming by Rhodium. Langmuir, 2010, 26, 16339-16348.	1.6	29
8742	In-Situ Deposition of Alkali and Alkaline Earth Hydride Thin Films To Investigate the Formation of Reactive Hydride Composites. Journal of Physical Chemistry C, 2010, 114, 13895-13901.	1.5	11
8743	Structural Analysis and Electronic Properties of Negatively Charged TCNQ: 2D Networks of (TCNQ)2Mn Assembled on Cu(100). Journal of Physical Chemistry C, 2010, 114, 17197-17204.	1.5	28
8744	Possible Reaction Paths of Small Silicon Clusters with Oxygen Explored with Density Functional Theory. Journal of Physical Chemistry C, 2010, 114, 13196-13203.	1.5	3
8745	Coverage Dependence of the Structure of Acrolein Adsorbed on Ag(111). Journal of Physical Chemistry Letters, 2010, 1, 2546-2549.	2.1	17
8746	Oxygen vacancy induced structural variations of exfoliated monolayerMnO2sheets. Physical Review B, 2010, 81, .	1.1	24
8747	The Fermi Level Dependent Electronic Properties of the Smallest (2,2) Carbon Nanotube. Nano Letters, 2010, 10, 3290-3296.	4.5	9
8748	Curvature Effects on the Magnetism of Ultrashort Zigzag Carbon Nanotubes and Nanographenes. Journal of Physical Chemistry C, 2010, 114, 7553-7557.	1.5	7
8749	Density Functional Theory Study of the Interaction of Carbon Monoxide with Bimetallic Coâ^'Mn Clusters. Journal of Physical Chemistry A, 2010, 114, 10508-10514.	1.1	26
8750	Tunable Ionic and Electronic Conduction of Lithium Nitride via Phosphorus and Arsenic Substitution: A First-Principles Study. Journal of Physical Chemistry C, 2010, 114, 16706-16709.	1.5	9

#	Article	IF	Citations
8751	Uniaxial Strain in Molecular Nanowires: A Case Study of Î²-phase Polyfluorenes. Journal of Physical Chemistry Letters, 2010, 1, 1326-1331.	2.1	3
8752	Site Switching from Di-Ïƒ Ethylene to Ï€-Bonded Ethylene in the Presence of Coadsorbed Nitrogen on Pt(111). Journal of Physical Chemistry C, 2010, 114, 12230-12233.	1.5	5
8753	Protonated Forms of Monoclinic Zirconia: A Theoretical Study. Journal of Physical Chemistry C, 2010, 114, 8014-8025.	1.5	17
8754	Stabilizing Monomeric Iron Species in a Porous Silica/Mo(112) Film. ACS Nano, 2010, 4, 863-868.	7.3	11
8755	Pairing of (R,R)-2,3-Butanediol Molecules on a Si(001) Surface. Journal of Physical Chemistry C, 2010, 114, 17761-17767.	1.5	3
8756	Calibration of the Isomer Shift for Iodine Resonant Transitions by Ab Initio Calculations. Journal of Physical Chemistry A, 2010, 114, 7146-7152.	1.1	4
8757	First Principles Quasiharmonic Thermoelasticity of Mantle Minerals. Reviews in Mineralogy and Geochemistry, 2010, 71, 99-128.	2.2	45
8758	Optimization of Parameters Used in Algorithms of Ion-Mobility Calculation for Conformational Analyses. Journal of Physical Chemistry B, 2010, 114, 1204-1212.	1.2	51
8759	Ferromagnetic Properties of Y-Doped AlN Nanorods. Journal of Physical Chemistry C, 2010, 114, 15574-15577.	1.5	38
8760	First Principles Study of the Adsorption Structure of Ethylene on Ge(001) Surface. Journal of Physical Chemistry C, 2010, 114, 2200-2207.	1.5	14
8761	Structural and Magnetic Characteristics of Gd₅Ga_xSi_{4â^'x}. Inorganic Chemistry, 2010, 49, 4586-4593.	1.9	17
8762	Oxidative Dehydrogenation of Methanol to Formaldehyde by a Vanadium Oxide Cluster Supported on Rutile TiO₂(110): Which Oxygen is Involved?. Journal of Physical Chemistry C, 2010, 114, 13736-13738.	1.5	30
8763	Metallization of a Hypervalent Radical Dimer: Molecular and Band Perspectives. Journal of the American Chemical Society, 2010, 132, 4876-4886.	6.6	39
8764	Bifunctional Mechanism of CO₂ Methanation on Pd-MgO/SiO₂ Catalyst: Independent Roles of MgO and Pd on CO₂ Methanation. Journal of Physical Chemistry C, 2010, 114, 7128-7131.	1.5	156
8765	Phase Behavior of Pseudobinary Precious Metalâ^'Carbide Systems. Journal of Physical Chemistry C, 2010, 114, 21664-21671.	1.5	5
8766	Siâ^'Ge-based Oxynitrides: From Molecules to Solids. Chemistry of Materials, 2010, 22, 3884-3899.	3.2	9
8767	Single-Molecule Interfacial Electron Transfer in Donor-Bridge-Nanoparticle Acceptor Complexes. Journal of Physical Chemistry B, 2010, 114, 14309-14319.	1.2	26
8768	Structural motifs in oxidized graphene: A genetic algorithm study based on density functional theory. Physical Review B, 2010, 82, .	1.1	77

#	Article	IF	Citations
8769	First principles investigation on redox properties of<mml:math xmlns:mml="http://www.w3.org/1998/Math/MathML" display="inline"><mml:mi>M</mml:mi></mml:math>-doped<mml:math xmlns:mml="http://www.w3.org/1998/Math/MathML" display="inline"><mml:mrow><mml:msub><mml:mrow><mml:mtext>CeO</mml:mtext></mml:mrow><mml:mn>2</mml:mn></mml:ms	1.1	112
8770	xmlns:mml="http://www.w3.org/1998/Math/MathML" display="inline"><mml:mrow><mml:mrow><mml:m Improved Non-Pt Alloys for the Oxygen Reduction Reaction at Fuel Cell Cathodes Predicted from Quantum Mechanics. Journal of Physical Chemistry C, 2010, 114, 11527-11533.	1.5	43
8771	Theoretical Analysis of the Adsorption of Late Transition-Metal Atoms on the (001) Surface of Early Transition-Metal Carbides. Journal of Physical Chemistry C, 2010, 114, 1622-1626.	1.5	25
8772	Natural charge spatial separation and quantum confinement of ZnO/GaN-core/shell nanowires. Journal of Applied Physics, 2010, 108, 123707.	1.1	12
8773	Density Functional Theory Study of NH_x (x = 0â^'3) and N₂ Adsorption on IrO₂(110) Surfaces. Journal of Physical Chemistry C, 2010, 114, 18588-18593.	1.5	23
8774	Viscosity and mutual diffusion of deuterium-tritium mixtures in the warm-dense-matter regime. Physical Review E, 2010, 82, 036404.	0.8	55
8775	Nanoscale Alloying, Phase-Segregation, and Coreâ^'Shell Evolution of Goldâ^'Platinum Nanoparticles and Their Electrocatalytic Effect on Oxygen Reduction Reaction. Chemistry of Materials, 2010, 22, 4282-4294.	3.2	205
8776	Magnetic moment and local moment alignment in anionic and/or oxidized Fen clusters. Journal of Chemical Physics, 2010, 132, 194305.	1.2	41
8777	First Principles Investigation of Oxygen Vacancies in Columbite MNb₂O₆ (M =) Tj ETQq0 0 0 rgBT /Overlock 1	3.2	26
8778	Heterogeneous nucleation of solid Al from the melt by<mml:math xmlns:mml="http://www.w3.org/1998/Math/MathML" display="inline"><mml:mrow><mml:msub><mml:mrow><mml:mtext>TiB</mml:mtext></mml:mrow><mml:mn>2</mml:mn></mml:m xmlns:mml="http://www.w3.org/1998/Math/MathML" display="inline"><mml:mrow><mml:msub><mml:mrow><mml:mtext>Al</mml:mtext></mml:mrow><mml:mn>3</mml:mn></mml:ms Anab initiomolecular dynamics study. Physical Review B, 2010, 82, .	1.1	66
8779	Structural Modifications and Mechanical Properties of Molybdenum Borides from First Principles. Journal of Physical Chemistry C, 2010, 114, 6722-6725.	1.5	142
8780	MgO-Supported Gold Cages Identified by Their Vibrational Modes: First-Principles Simulations. Journal of Physical Chemistry C, 2010, 114, 13035-13038.	1.5	2
8781	Ab-initioStudy of Transition-Metal Dimers on Defective MgO(001) Surfaces: Atomic and Electronic Structures. Journal of the Physical Society of Japan, 2010, 79, 124703.	0.7	11
8782	Interconversion of Perovskite and Fluorite Structures in Ceâ^'Scâ^'O System. Inorganic Chemistry, 2010, 49, 1152-1157.	1.9	20
8783	Simultaneously Understanding the Geometric and Electronic Structure of Anthraceneselenolate on Au(111): A Combined Theoretical and Experimental Study. Journal of Physical Chemistry C, 2010, 114, 2677-2684.	1.5	34
8784	Surface Energies Control the Self-Organization of Oriented In₂O₃ Nanostructures on Cubic Zirconia. Nano Letters, 2010, 10, 3740-3746.	4.5	96
8785	First-Principles Study of Ethylene on Ge(001)â€"Electronic Structures and STM Images. Journal of Physical Chemistry C, 2010, 114, 14473-14481.	1.5	1
8786	Catalytically Active Structure of Bi Deposited on a Au(111) Electrode for the Hydrogen Peroxide Reduction Reaction. Langmuir, 2010, 26, 4590-4593.	1.6	20

#	Article	IF	Citations
8787	Calcium Borohydride for Hydrogen Storage: A Computational Study of Ca(BH₄)₂ Crystal Structures and the CaB₂H_x Intermediate. Journal of Physical Chemistry C, 2010, 114, 9503-9509.	1.5	26
8788	Proton transfer in adsorbed water dimers. Physical Chemistry Chemical Physics, 2010, 12, 3953.	1.3	28
8789	Structure of Dimeric Molybdenum(VI) Oxide Species on Î³-Alumina: A Periodic Density Functional Theory Study. Journal of Physical Chemistry C, 2010, 114, 19406-19414.	1.5	33
8790	Analysis of Bonding between Conjugated Organic Molecules and Noble Metal Surfaces Using Orbital Overlap Populations. Journal of Chemical Theory and Computation, 2010, 6, 3481-3489.	2.3	12
8791	Selective Small-Diameter Metallic Single-Walled Carbon Nanotube Removal by Mere Standing with Anthraquinone and Application to a Field-Effect Transistor. Journal of Physical Chemistry C, 2010, 114, 21035-21041.	1.5	13
8792	Interacting Quasi-Two-Dimensional Sheets of Interlinked Carbon Nanotubes: A High-Pressure Phase of Carbon. ACS Nano, 2010, 4, 3515-3521.	7.3	29
8793	Thermodynamics and structures of oxide crystals by a systematic set of first principles calculations. Journal of Materials Chemistry, 2010, 20, 10335.	6.7	7
8794	CO Electroxidation on Gold in Alkaline Media: A Combined Electrochemical, Spectroscopic, and DFT Study. Langmuir, 2010, 26, 12425-12432.	1.6	58
8795	Band Gap Narrowing versus Formation of Electronic States in the Gap in Nâˆ’TiO₂ Thin Films. Journal of Physical Chemistry C, 2010, 114, 22546-22557.	1.5	34
8796	On the Mechanism of Low-Temperature CO Oxidation on Ni(111) and NiO(111) Surfaces. Journal of Physical Chemistry C, 2010, 114, 21579-21584.	1.5	71
8797	Vanadia Aggregates on an Ultrathin Aluminum Oxide Film on NiAl(110). Journal of Physical Chemistry C, 2010, 114, 4983-4994.	1.5	20
8798	Adsorption of Thiophene-Conjugated Sensitizers on TiO₂ Anatase (101). Journal of Physical Chemistry C, 2010, 114, 20240-20248.	1.5	40
8799	Adsorption, Oxidation State, and Diffusion of Pt Atoms on the CeO₂(111) Surface. Journal of Physical Chemistry C, 2010, 114, 14202-14207.	1.5	71
8800	Origin of the Diverse Melting Behaviors of Intermediate-Size Nanoclusters: Theoretical Study of AlN(N= 51âˆ’58, 64). Journal of the American Chemical Society, 2010, 132, 18287-18291.	6.6	24
8801	Half-Metallic Antiferromagnet BaCrFeAs₂. Journal of Physical Chemistry C, 2010, 114, 11614-11617.	1.5	19
8802	Magnetism and perfect spin filtering effect in graphene nanoflakes. Nanotechnology, 2010, 21, 385201.	1.3	66
8803	First-Principles Calculation of Synergistic (N, P)-Codoping Effects on the Visible-Light Photocatalytic Activity of Anatase TiO₂. Journal of Physical Chemistry C, 2010, 114, 11984-11990.	1.5	55
8804	Density Functional Theory Study of Ethanol Decomposition on 3Ni/Î±-Al₂O₃(0001) Surface. Langmuir, 2010, 26, 15845-15851.	1.6	13

#	Article	IF	Citations
8805	Strong Kinetic Isotope Effect in the Dissociative Chemisorption of H₂ on a PdO(101) Thin Film. Journal of Physical Chemistry C, 2010, 114, 11485-11497.	1.5	47
8806	Sequential Observation of Ag_nS₄^{â˜’} (1 â‰¤ n â‰¤ 7) Gas Phase Clusters in MS/MS and Prediction of Their Structures. Journal of Physical Chemistry Letters, 2010, 1, 1423-1427.	2.1	35
8807	Nitric Oxide Adsorption Effects on Metal Phthalocyanines. Journal of Physical Chemistry B, 2010, 114, 10017-10021.	1.2	52
8808	Structural Transition and Thermal Stability of a Coronene Molecular Monolayer on Cu(110). Journal of Physical Chemistry C, 2010, 114, 11180-11184.	1.5	8
8809	Synergistic Effects on Band Gap-Narrowing in Titania by Codoping from First-Principles Calculations. Chemistry of Materials, 2010, 22, 1616-1623.	3.2	134
8810	Ab Initio Computational Studies of Mg Vacancy Diffusion in Doped MgB₂ Aimed at Hydriding Kinetics Enhancement of the LiBH₄ + MgH₂ System. Journal of Physical Chemistry C, 2010, 114, 21801-21807.	1.5	10
8811	Role of Step Sites and Surface Vacancies in the Adsorption and Activation of CO on Ï‡-Fe₅C₂ Surfaces. Journal of Physical Chemistry C, 2010, 114, 7863-7879.	1.5	43
8812	Insight from First-Principles Calculations into the Interactions between Hydroxybenzoic Acids and Alkali Chloride Surfaces. Journal of Physical Chemistry C, 2010, 114, 460-467.	1.5	14
8813	Density Functional Theory Study of Water Dissociative Chemisorption on the Fe₃O₄(111) Surface. Journal of Physical Chemistry C, 2010, 114, 21405-21410.	1.5	56
8814	Aerosol-Derived Bimetallic Alloy Powders: Bridging the Gap. Journal of Physical Chemistry C, 2010, 114, 17181-17190.	1.5	33
8815	Scaling Dopant States in a Semiconducting Nanostructure by Chemically Resolved Electron Energy-Loss Spectroscopy: A Case Study on Co-Doped ZnO. Journal of the American Chemical Society, 2010, 132, 6492-6497.	6.6	41
8816	A two-temperature model of radiation damage in Î±-quartz. Journal of Chemical Physics, 2010, 133, 144711.	1.2	26
8817	Temperature-dependent elastic stiffness constants of Î±- and Î¸-Al₂O₃from first-principles calculations. Journal of Physics Condensed Matter, 2010, 22, 375403.	0.7	70
8818	Structural Study of the Li0.5Na0.5MnFe2(PO4)3and Li0.75Na0.25MnFe2(PO4)3Alluaudite Phases and Their Electrochemical Properties As Positive Electrodes in Lithium Batteries. Inorganic Chemistry, 2010, 49, 10378-10389.	1.9	42
8819	Finite Magnetization Plateau from a Two-Dimensional Antiferromagnet: Density Functional Analysis of the Magnetic Structure of Cu₃(P₂O₆OH)₂. Inorganic Chemistry, 2010, 49, 9253-9256.	1.9	13
8820	Theoretical optoelectronic analysis of<mml:math xmlns:mml="http://www.w3.org/1998/Math/MathML" display="inline"><mml:mrow><mml:msub><mml:mrow><mml:mtext>MgIn</mml:mtext></mml:mrow><mml:mn>2</mml:mn></mml:m xmlns:mml="http://www.w3.org/1998/Math/MathML" display="inline"><mml:mrow><mml:msub><mml:mrow><mml:mtext>CdIn</mml:mtext></mml:mrow><mml:mn>2</mml:mn></mml:m Physical Review B, 2010, 81, .	1.1	45
8821	Diameter dependence of mechanical, electronic, and structural properties of InAs and InP nanowires: A first-principles study. Physical Review B, 2010, 81, .	1.1	64
8822	Catalytic activity of small MgO-supported Au clusters towards CO oxidation: A density functional study. Physical Review B, 2010, 81, .	1.1	40

#	Article	IF	Citations
8823	Magnetism in armchair BC2N nanoribbons. Applied Physics Letters, 2010, 96, 133103.	1.5	19
8824	Experimental and density-functional study of the electronic structure of<mml:math xmlns:mml="http://www.w3.org/1998/Math/MathML" display="inline"><mml:mrow><mml:msub><mml:mrow><mml:mtext>In</mml:mtext></mml:mrow><mml:mn>4</mml:mn></mml:ms Physical Review B, 2010, 81, .	1.1	13
8825	Field Emission Enhancement in Semiconductor Nanofilms by Engineering the Layer Thickness: First-Principles Calculations. Journal of Physical Chemistry C, 2010, 114, 11584-11587.	1.5	8
8826	Potential-Dependent Chemisorption of Carbon Monoxide at a Gold Coreâ"Platinum Shell Nanoparticle Electrode: A Combined Study by Electrochemical in Situ Surface-Enhanced Raman Spectroscopy and Density Functional Theory. Journal of Physical Chemistry C, 2010, 114, 403-411.	1.5	34
8827	Conductive Path Formation in the Ta₂O₅ Atomic Switch: First-Principles Analyses. ACS Nano, 2010, 4, 6477-6482.	7.3	50
8828	Electronic Structure and Origin of Visible-Light Activity of C-Doped Cubic In₂O₃ from First-Principles Calculations. Journal of Physical Chemistry C, 2010, 114, 13942-13946.	1.5	8
8829	Electronic and magnetic properties of zigzag graphene nanoribbons with periodic protruded edges. Physical Review B, 2010, 82, .	1.1	18
8830	Electron spectrum of epitaxial graphene monolayers. Physical Review B, 2010, 82, .	1.1	34
8831	How Surface Reactivity Depends on the Configuration of Coadsorbed Reactants: CO Oxidation on Rh(100). Journal of Physical Chemistry C, 2010, 114, 17127-17135.	1.5	15
8832	Strain-induced isosymmetric phase transition in<mml:math xmlns:mml="http://www.w3.org/1998/Math/MathML" display="inline"><mml:mrow><mml:msub><mml:mrow><mml:mtext>BiFeO</mml:mtext></mml:mrow><mml:mn>3</mml:mn></mml:m Physical Review B, 2010, 81, .	1.1	243
8833	Competing phases in<mml:math xmlns:mml="http://www.w3.org/1998/Math/MathML" display="inline"><mml:mrow><mml:msub><mml:mrow><mml:mtext>BiFeO</mml:mtext></mml:mrow><mml:mn>3</mml:mn></mml:m films under compressive epitaxial strain. Physical Review B, 2010, 81, .	1.1	93
8834	First-Principles Study of High-Pressure Behavior of Solid Î²-HMX. Journal of Physical Chemistry A, 2010, 114, 1082-1092.	1.1	53
8835	Pseudopotential and full-electron DFT calculations of thermodynamic properties of electrons in metals and semiempirical equations of state. Journal of Physics Condensed Matter, 2010, 22, 505501.	0.7	40
8836	Alumina as a Simultaneous Support and Co Catalyst: Cationic Hafnium Complex Evidenced by Experimental and DFT Analyses. Journal of Physical Chemistry C, 2010, 114, 18516-18528.	1.5	23
8837	The Formation of Gold Clusters Supported on Mesoporous Silica Material Surfaces: A Molecular Picture. Journal of Physical Chemistry C, 2010, 114, 9002-9007.	1.5	27
8838	A First Principles Study on Charge Dependent Diffusion of Point Defects in Rutile TiO2. Journal of Physical Chemistry C, 2010, 114, 19649-19652.	1.5	15
8839	Spin- and Energy-Dependent Tunneling through a Single Molecule with Intramolecular Spatial Resolution. Physical Review Letters, 2010, 105, 047204.	2.9	257
8840	Design of the Local Spin Polarization at the Organic-Ferromagnetic Interface. Physical Review Letters, 2010, 105, 066601.	2.9	284

#	Article	IF	Citations
8841	Density Functional Calculations and IR Reflection Absorption Spectroscopy on the Interaction of SO₂ with Oxide-Supported Pd Nanoparticles. Journal of Physical Chemistry C, 2010, 114, 13813-13824.	1.5	20
8842	DFT Studies of Solvation Effects on the Nanosize Bare, Thiolated, and Redox Active Ligated Au₅₅ Cluster. Journal of Physical Chemistry C, 2010, 114, 15941-15950.	1.5	12
8843	Control of Two-Dimensional Ordering of F16CuPc on Bi/Ag(111): Effect of Interfacial Interactions. Journal of Physical Chemistry C, 2010, 114, 11234-11241.	1.5	15
8844	Autocatalytic Reduction of a Cu₂O/Cu(111) Surface by CO: STM, XPS, and DFT Studies. Journal of Physical Chemistry C, 2010, 114, 17042-17050.	1.5	84
8845	Stability of Pt Monolayers on Irâ˜Co Cores with and without a Pd Interlayer. Journal of Physical Chemistry C, 2010, 114, 13055-13060.	1.5	19
8846	Surface Potential at the Airâ˜Water Interface Computed Using Density Functional Theory. Journal of Physical Chemistry Letters, 2010, 1, 496-499.	2.1	106
8847	Orientationally disordered<mml:math xmlns:mml="http://www.w3.org/1998/Math/MathML" display="inline"><mml:mrow><mml:msub><mml:mtext>H</mml:mtext><mml:mn>2</mml:mn></mml:msub></mml:mrow></mml:math> the high-pressure van der Waals compound<mml:math xmlns:mml="http://www.w3.org/1998/Math/MathML"		

#	Article	IF	Citations
8859	Electronic structures of boron nitride nanotubes subjected to tension, torsion, and flattening: A first-principles DFT study. Physical Review B, 2010, 82, .	1.1	22
8860	New Hydrides REScSiH and REScGeH (RE = La, Ce): Structure, Magnetism, and Chemical Bonding. Chemistry of Materials, 2010, 22, 5013-5021.	3.2	25
8861	Dopant-Induced Electronic Structure Modification of HOPG Surfaces: Implications for High Activity Fuel Cell Catalysts. Journal of Physical Chemistry C, 2010, 114, 506-515.	1.5	100
8862	Nature of Nâˆ’N Bonding within High-Pressure Noble-Metal Pernitrides and the Prediction of Lanthanum Pernitride. Journal of the American Chemical Society, 2010, 132, 2421-2429.	6.6	78
8863	The Effect of Environment on the Reaction of Water on the Ceria(111) Surface: A DFT+U Study. Journal of Physical Chemistry C, 2010, 114, 14891-14899.	1.5	105
8864	Deviations and polarity of [100] dislocations in bcc metals. Philosophical Magazine Letters, 2010, 90, 385-391.	0.5	3
8865	Origin of magnetism in undoped<mml:math xmlns:mml="http://www.w3.org/1998/Math/MathML" display="inline"><mml:mrow><mml:msub><mml:mrow><mml:mtext>MoO</mml:mtext></mml:mrow><mml:mn>2</mml:mn></mml:m by first-principles calculations. Physical Review B, 2010, 81, .	3.7	22
8866	Density-functional characterization of antiferromagnetism in oxygen-deficient anatase and rutile<mml:math xmlns:mml="http://www.w3.org/1998/Math/MathML" display="inline"><mml:mrow><mml:msub><mml:mrow><mml:mtext>TiO</mml:mtext></mml:mrow><mml:mn>2</mml:mn></mml:m Physical Review B, 2010, 81, .	1.1	135
8867	Density Functional Study of Boron-Doped Anatase TiO₂. Journal of Physical Chemistry C, 2010, 114, 19830-19834.	1.5	49
8868	A Direct Relation between Adsorbate Interactions, Configurations, and Reactivity: CO Oxidation on Rh(100) and Rh(111). Journal of Physical Chemistry C, 2010, 114, 21672-21680.	1.5	15
8869	Half-Solidity of Tetrahedral-like Al₅₅ Clusters. ACS Nano, 2010, 4, 1092-1098.	7.3	14
8870	Magnetic Properties of Cu_mO_n Clusters: A First Principles Study. Journal of Physical Chemistry A, 2010, 114, 8417-8422.	1.1	17
8871	Grafting of Lanthanide Complexes on Silica Surfaces: A Theoretical Investigation. Journal of Physical Chemistry A, 2010, 114, 6322-6330.	1.1	29
8872	Temperature-Dependent Synthetic Routes to and Thermochemical Ranking of Î±- and Î²-SrNCN. Inorganic Chemistry, 2010, 49, 2267-2272.	1.9	22
8873	First-Principles Study of Titania Nanoribbons: Formation, Energetics, and Electronic Properties. Journal of Physical Chemistry C, 2010, 114, 9234-9238.	1.5	17
8874	Diffusivity Control in Molecule-on-Metal Systems Using Electric Fields. Nano Letters, 2010, 10, 1184-1188.	4.5	64
8875	Titanium-decorated graphene for high-capacity hydrogen storage studied by density functional simulations. Journal of Physics Condensed Matter, 2010, 22, 445301.	0.7	91
8876	Superconductivity at â¼100ÂK in dense SiH ₄ (H ₂) ₂ predicted by first principles. Proceedings of the National Academy of Sciences of the United States of America, 2010, 107, 15708-15711.	3.3	132

#	Article	IF	Citations
8877	High-pressure crystal structures and superconductivity of Stannane (SnH ₄). Proceedings of the National Academy of Sciences of the United States of America, 2010, 107, 1317-1320.	3.3	168
8878	Superconducting high-pressure phases of disilane. Proceedings of the National Academy of Sciences of the United States of America, 2010, 107, 9969-9973.	3.3	102
8879	First-principles study of the magnetic, structural and electronic properties of LiFeAs. Journal of Physics Condensed Matter, 2010, 22, 046006.	0.7	9
8880	Pressure-induced elemental dissociation in zinc chalcogenides. New Journal of Physics, 2010, 12, 043058.	1.2	12
8881	First-principles study on mechanical and magnetic properties of the perovskite and post-perovskite polymorphs of pure end-member FeSiO₃at the coreâ€“mantle boundary. High Pressure Research, 2010, 30, 292-300.	0.4	2
8882	Does the MgO(100)-Support Facilitate the Reaction of Nitrogen and Hydrogen Molecules Catalyzed by Zr2Pd2 Clusters? A Computational Study. Inorganic Chemistry, 2010, 49, 2557-2567.	1.9	0
8883	On the Role of a Cobalt Promoter in a Water-Gas-Shift Reaction on Co-MoS₂. Journal of Physical Chemistry C, 2010, 114, 16669-16676.	1.5	42
8884	Adsorption of NO₂ on Oxygen Deficient ZnO(21Ì…1Ì…0) for Gas Sensing Applications: A DFT Study. Journal of Physical Chemistry C, 2010, 114, 16603-16610.	1.5	67
8885	Structural stability of TiO2at high pressure in density-functional theory based calculations. Journal of Physics Condensed Matter, 2010, 22, 295501.	0.7	30
8886	Cluster scattering effects on phonon conduction in graphene. Physical Review B, 2010, 81, .	1.1	93
8887	Pathways for Oxygen Incorporation in Mixed Conducting Perovskites: A DFT-Based Mechanistic Analysis for (La, Sr)MnO_{3â^'Î´}. Journal of Physical Chemistry C, 2010, 114, 3017-3027.	1.5	160
8888	Ab initio molecular dynamics simulations investigating proton transfer in perfluorosulfonic acid functionalized carbon nanotubes. Physical Chemistry Chemical Physics, 2010, 12, 8728.	1.3	55
8889	The effects of the hydrophobic environment on proton mobility in perfluorosulfonic acid systems: an ab initio molecular dynamics study. Journal of Materials Chemistry, 2010, 20, 6342.	6.7	53
8890	Theoretical and experimental study of the structural stability of<mml:math xmlns:mml="http://www.w3.org/1998/Math/MathML" display="inline"><mml:mrow><mml:msub><mml:mrow><mml:mtext>TbPO</mml:mtext></mml:mrow><mml:mn>4</mml:mn></mml:mrow></mml:math>high pressures. Physical Review B, 2010, 81, .	1.1	46
8891	Band bowing and band alignment in InGaN alloys. Applied Physics Letters, 2010, 96, .	1.5	319
8892	Recent atomistic modelling studies of energy materials: batteries included. Philosophical Transactions Series A, Mathematical, Physical, and Engineering Sciences, 2010, 368, 3255-3267.	1.6	35
8893	Adsorption of CO on Rutile TiO₂ (110)-1 Ã— 1 Surface with Preadsorbed O Adatoms. Journal of Physical Chemistry C, 2010, 114, 18222-18227.	1.5	38
8894	Theoretical investigation of the high pressure structure, lattice dynamics, phase transition, and thermal equation of state of titanium metal. Journal of Applied Physics, 2010, 107, .	1.1	70

#	Article	IF	Citations
8895	Synthesis and Optical Properties of Amorphous Si₃N_{4â˜'x}P_x Dielectrics and Complementary Insights from ab Initio Structural Simulations. Chemistry of Materials, 2010, 22, 5296-5305.	3.2	2
8896	First-Principles Study of Different Polymorphs of Crystalline Zirconium Hydride. Journal of Physical Chemistry C, 2010, 114, 22361-22368.	1.5	75
8897	Predicting impurity gases and phases during hydrogen evolution from complex metal hydrides using free energy minimization enabled by first-principles calculations. Physical Chemistry Chemical Physics, 2010, 12, 9918.	1.3	20
8898	Quantum computing with defects. Proceedings of the National Academy of Sciences of the United States of America, 2010, 107, 8513-8518.	3.3	588
8899	Oxygen vacancy migration in ceria and Pr-doped ceria: A DFT+U study. Journal of Chemical Physics, 2010, 132, 094104.	1.2	128
8900	Effects of silicon and germanium adsorbed on graphene. Applied Physics Letters, 2010, 96, .	1.5	63
8901	Systematic variations in structural and electronic properties of BiFeO3 by A-site substitution. Applied Physics Letters, 2010, 96, .	1.5	63
8902	Linear tuning of charge carriers in graphene by organic molecules and charge-transfer complexes. Physical Review B, 2010, 81, .	1.1	88
8903	Force-matched embedded-atom method potential for niobium. Physical Review B, 2010, 81, .	1.1	120
8904	Hybrid functional studies of the oxygen vacancy in<mml:math xmlns:mml="http://www.w3.org/1998/Math/MathML" display="inline"><mml:mrow><mml:msub><mml:mrow><mml:mtext>TiO</mml:mtext></mml:mrow><mml:mn>2</mml:mn></mml:msub></mml:mrow></mml:math> Physical Review B, 2010, 81, .	1.1	554
8905	Wave function extended Lagrangian Born-Oppenheimer molecular dynamics. Physical Review B, 2010, 82, .	1.1	59
8906	Evolutionary Crystal Structure Prediction and Novel High-Pressure Phases. NATO Science for Peace and Security Series B: Physics and Biophysics, 2010, , 293-323.	0.2	0
8907	Unveiling the atomic and electronic structure of the VN/MgO interface. Physical Review B, 2010, 82, .	1.1	3
8908	Efficient Band Gap Prediction for Solids. Physical Review Letters, 2010, 105, 196403.	2.9	398
8909	Graphene hydrate: theoretical prediction of a new insulating form of graphene. New Journal of Physics, 2010, 12, 125012.	1.2	46
8910	New Phases of Water Ice Predicted at Megabar Pressures. Physical Review Letters, 2010, 105, 195701.	2.9	84
8911	Prediction of Isothermal Equation of State of an Explosive Nitrate Ester by van der Waals Density Functional Theory. Journal of Physical Chemistry Letters, 2010, 1, 346-348.	2.1	5
8912	Optical second-harmonic and reflectance-anisotropy spectroscopy of clean and hydrogen-terminated vicinal Si(001) surfaces. Journal of the Optical Society of America B: Optical Physics, 2010, 27, 981.	0.9	8

#	Article	IF	Citations
8913	In situ observation of thermal expansion of tetragonal C11b phase in Zr2Cu(1â˜'x)Pdx alloys. Intermetallics, 2010, 18, 8-13.	1.8	6
8914	Ab initio study of formation energy and magnetism of sigma phase in Crâ€"Fe and Crâ€"Co systems. Intermetallics, 2010, 18, 212-220.	1.8	51
8915	The lattice dynamical and thermo-elastic properties of Rh3X (X=Ti, V) compounds. Intermetallics, 2010, 18, 286-291.	1.8	21
8916	Core properties of dislocations in YCu and YAg B2 intermetallic compounds. Intermetallics, 2010, 18, 312-318.	1.8	21
8917	Theoretical investigation of the Pt3Al ground state. Intermetallics, 2010, 18, 417-421.	1.8	36
8918	First-principles study of the structural, electronic and elastic properties of W5Si3. Intermetallics, 2010, 18, 688-693.	1.8	41
8919	Why is the slip direction in CuZn and FeAl different than in CoTi?. Intermetallics, 2010, 18, 1285-1287.	1.8	17
8920	Correlation between thermodynamics and glass forming ability in the Alâ€"Ceâ€"Ni system. Intermetallics, 2010, 18, 900-906.	1.8	24
8921	Entropy favored ordering: Phase stability of Ni3Pt revisited by first-principles. Intermetallics, 2010, 18, 961-964.	1.8	24
8922	The electronic, elastic, and structural properties of Tiâ€"Pd intermetallics and associated hydrides from first principles calculations. Intermetallics, 2010, 18, 998-1006.	1.8	40
8923	Monte-Carlo simulation of atom kinetics in intermetallics: Correcting the jump rates in Ni3Al. Intermetallics, 2010, 18, 1091-1098.	1.8	8
8924	Effects of alloying elements on elastic properties of Ni3Al by first-principles calculations. Intermetallics, 2010, 18, 1163-1171.	1.8	86
8925	Combined ab initio and experimental study of structural and elastic properties of Fe3Al-based ternaries. Intermetallics, 2010, 18, 1310-1315.	1.8	37
8926	The Feâ€"Ni system: Thermodynamic modelling assisted by atomistic calculations. Intermetallics, 2010, 18, 1148-1162.	1.8	149
8927	Ab initio study of the anomalous volume-composition dependence in Feâ€"Al alloys. Intermetallics, 2010, 18, 1316-1321.	1.8	37
8928	Prediction of the site occupations of the ThMn12-type intermetallics YFe12â˜'Mo by combining thermodynamic model with ab-initio calculations. Intermetallics, 2010, 18, 1465-1469.	1.8	8
8929	Ni and Al diffusion in Ni-rich NiAl and the effect of Pt additions. Intermetallics, 2010, 18, 1470-1479.	1.8	17
8930	On third-order elastic constants for ductile rare-earth intermetallic compounds: AÂfirst-principles study. Intermetallics, 2010, 18, 1653-1658.	1.8	11

#	Article	IF	Citations
8931	First-principles calculations and thermodynamic modeling of the Reâ€“Y system with extension to the Niâ€“Reâ€“Y system. Intermetallics, 2010, 18, 2412-2418.	1.8	10
8932	Ab initio calculations on the third-order elastic constants for selected B2â€“MgRE (REÂ=ÂY, Tb, Dy, Nd) intermetallics. Intermetallics, 2010, 18, 2472-2476.	1.8	20
8933	Local atomic and electronic structures of equiatomic liquid alloy KSb from 923 to 1773K. Journal of Non-Crystalline Solids, 2010, 356, 8-13.	1.5	4
8934	Changes of structure in potassium depleted binary silicate glass studied by MD. Journal of Non-Crystalline Solids, 2010, 356, 2473-2479.	1.5	5
8935	Molecular simulations of silicate melts doped with sulphur and nitrogen. Journal of Non-Crystalline Solids, 2010, 356, 2458-2464.	1.5	11
8936	Electronic structure and interfacial properties of Ge nanoclusters embedded in amorphous silica. Journal of Non-Crystalline Solids, 2010, 356, 2448-2453.	1.5	11
8937	From atomic and electronic structures of molten multicomponent alloys to their glass-forming ability: First-principles simulations. Journal of Non-Crystalline Solids, 2010, 356, 2807-2812.	1.5	6
8938	Thermodynamic assessments of Agâ€“Dy and Agâ€“Er binary systems. Journal of Alloys and Compounds, 2010, 489, 146-151.	2.8	6
8939	The role of trace element segregation in the eutectic modification of hypoeutectic Alâ€“Si alloys. Journal of Alloys and Compounds, 2010, 489, 415-420.	2.8	132
8940	The standard enthalpies of formation of binary intermetallic compounds of some late 4d and 5d transition metals by high temperature direct synthesis calorimetry. Journal of Alloys and Compounds, 2010, 492, 105-115.	2.8	36
8941	First-principles investigation of the structural and mechanical properties of Î²â€³ phase in Mgâ€“Gd alloy system. Journal of Alloys and Compounds, 2010, 492, 416-420.	2.8	25
8942	Molecular dynamics and first-principles studies on the deformation mechanisms of nanostructured cobalt. Journal of Alloys and Compounds, 2010, 504, S467-S471.	2.8	18
8943	Multi-scale modeling of shear banding in iron-based metallic glasses. Journal of Alloys and Compounds, 2010, 504, S56-S59.	2.8	2
8944	Temperature dependent elastic coefficients of Mg2X (X=Si, Ge, Sn, Pb) compounds from first-principles calculations. Journal of Alloys and Compounds, 2010, 498, 191-198.	2.8	53
8945	-Al13Co4, a new quasicrystal approximant. Journal of Alloys and Compounds, 2010, 500, 153-160.	2.8	34
8946	A series of BaAl2â^'xSixH2â^'x (0.4<x<1.6) hydrides with compositions and structures in between BaSi2 and BaAl2H2. Journal of Alloys and Compounds, 2010, 505, 1-5.	2.8	13
8947	Mechanochemically driven nonequilibrium processes in MNH2â€“CaH2 systems (M=Li or Na). Journal of Alloys and Compounds, 2010, 506, 224-230.	2.8	5
8948	First-principles study of elastic and electronic properties of MgZn2 and ScZn2 phases in Mgâ€“Scâ€“Zn alloy. Journal of Alloys and Compounds, 2010, 506, 412-417.	2.8	135

#	Article	IF	Citations
8949	Prediction of concomitant structures in binary metallic systems from RG map: With MgCu2 structure type as an example. Journal of Alloys and Compounds, 2010, 508, 55-61.	2.8	4
8950	Elastic properties of Ni2MnGa from first-principles calculations. Journal of Alloys and Compounds, 2010, 508, 177-183.	2.8	94
8951	Solvus boundaries of (meta)stable phases in the Alâ€“Mgâ€“Si system: First-principles phonon calculations and thermodynamic modeling. Calphad: Computer Coupling of Phase Diagrams and Thermochemistry, 2010, 34, 20-25.	0.7	34
8952	Thermodynamic assessment of the Vâ€“Zn system supported by key experiments and first-principles calculations. Calphad: Computer Coupling of Phase Diagrams and Thermochemistry, 2010, 34, 75-80.	0.7	13
8953	Thermodynamic properties of cementite (). Calphad: Computer Coupling of Phase Diagrams and Thermochemistry, 2010, 34, 129-133.	0.7	72
8954	First-principles calculations and thermodynamic modeling of Csâ€“In system. Calphad: Computer Coupling of Phase Diagrams and Thermochemistry, 2010, 34, 134-137.	0.7	3
8955	Thermodynamic remodeling of the Coâ€“Ga system. Calphad: Computer Coupling of Phase Diagrams and Thermochemistry, 2010, 34, 189-195.	0.7	14
8956	Thermodynamic modeling of Laves phases in the Crâ€“Hf and Crâ€“Ti systems: Reassessment using first-principles results. Calphad: Computer Coupling of Phase Diagrams and Thermochemistry, 2010, 34, 215-221.	0.7	37
8957	Assessment of the atomic mobility in fcc Alâ€“Cuâ€“Mg alloys. Calphad: Computer Coupling of Phase Diagrams and Thermochemistry, 2010, 34, 286-293.	0.7	19
8958	Thermodynamic modeling of the Pdâ€“S system supported by first-principles calculations. Calphad: Computer Coupling of Phase Diagrams and Thermochemistry, 2010, 34, 324-331.	0.7	8
8959	Ab initio ternary -phase diagram: The Crâ€“Moâ€“Re system. Calphad: Computer Coupling of Phase Diagrams and Thermochemistry, 2010, 34, 487-494.	0.7	21
8960	Ab initio and thermodynamic study of the Crâ€“Re system. Calphad: Computer Coupling of Phase Diagrams and Thermochemistry, 2010, 34, 495-503.	0.7	20
8961	Determination of the high-pressure properties of fayalite from first-principles calculations. Earth and Planetary Science Letters, 2010, 289, 449-456.	1.8	33
8962	Thermodynamics of mixing in MgSiO3â€“Al2O3 perovskite and ilmenite from ab initio calculations. Earth and Planetary Science Letters, 2010, 295, 477-486.	1.8	15
8963	Structural and electrochemical aspects of Mn substitution into Li2FeSiO4 from DFT calculations. Computational Materials Science, 2010, 47, 678-684.	1.4	36
8964	Bond analysis of phosphorus skutterudites: Elongated lanthanum electron buildup in LaFe4P12. Computational Materials Science, 2010, 47, 752-757.	1.4	8
8965	The structural, electronic, elastic, phonon, and thermodynamical properties of the SmX (X=P, Sb, Bi) compounds. Computational Materials Science, 2010, 47, 758-768.	1.4	5
8966	First-principles thermodynamics from phonon and Debye model: Application to Ni and Ni3Al. Computational Materials Science, 2010, 47, 1040-1048.	1.4	357

#	Article	IF	Citations
8967	Theoretical investigation of hydrogen storage ability of a carbon nanohorn. Computational Materials Science, 2010, 49, S378-S382.	1.4	14
8968	First principles modeling of stability mechanism of nonstoichiometric uranium dioxide. Computational Materials Science, 2010, 49, S364-S368.	1.4	3
8969	Composition-temperature phase diagram of BexZn1â^'xO from first principles. Computational Materials Science, 2010, 49, S29-S31.	1.4	25
8970	The effects of unit cell size on the bandgap range in the direct enumeration study of AlxGayIn1â^'xâ^'yP alloys. Computational Materials Science, 2010, 49, S114-S118.	1.4	1
8971	Dehydrogenation kinetics of magnesium hydride investigated by DFT and experiment. Computational Materials Science, 2010, 49, S144-S149.	1.4	26
8972	Structural and elastic properties of cubic and hexagonal TiN and AlN from first-principles calculations. Computational Materials Science, 2010, 48, 705-709.	1.4	126
8973	Auâ€“K co-deposition on MgO(2L)/Ag(001): A first principles study. Computational Materials Science, 2010, 48, 719-723.	1.4	0
8974	Dynamical properties of deeply undercooled and amorphous systems: Combined classical and ab initio molecular dynamics simulations approaches. Computational Materials Science, 2010, 49, S272-S275.	1.4	1
8975	First-principles calculations of pressure-induced phase transformation in AlN and GaN. Computational Materials Science, 2010, 48, 768-772.	1.4	39
8976	The natural valence band offset of dilute GaAs1â^'xNx and GaAs: The first-principles approach. Computational Materials Science, 2010, 49, S150-S152.	1.4	1
8977	First-principles calculations of pure elements: Equations of state and elastic stiffness constants. Computational Materials Science, 2010, 48, 813-826.	1.4	259
8978	Thermo-elastic and lattice dynamical properties of Rh3Hf compound. Computational Materials Science, 2010, 48, 859-865.	1.4	19
8979	First-principles study of the stability of NbC and NbN precipitates under coherency strains in Î±-iron. Computational Materials Science, 2010, 49, 60-63.	1.4	41
8980	DFT study on elastic and piezoelectric properties of tetragonal BaTiO3. Computational Materials Science, 2010, 49, S372-S377.	1.4	34
8981	Cluster expansion models for Feâ€“Cr alloys, the prototype materials for a fusion power plant. Computational Materials Science, 2010, 49, S199-S203.	1.4	22
8982	Properties of the bare, passivated and doped germanium nanowire: A density-functional theory study. Computational Materials Science, 2010, 49, 682-690.	1.4	7
8983	Ab initio studies of staggered Li adatoms on graphene. Computational Materials Science, 2010, 49, 787-791.	1.4	28
8984	First-principles investigation of CO adsorption on Pt/Ge(001)-(4Ã—2). Computational Materials Science, 2010, 49, 895-898.	1.4	3

#	Article	IF	Citations
8985	First-principles study of self-diffusion in hcp Mg and Zn. Computational Materials Science, 2010, 50, 301-307.	1.4	64
8986	Structural, elastic, and lattice dynamical properties of Germanium diiodide (GeI2). Computational Materials Science, 2010, 50, 349-355.	1.4	20
8987	Surface stability of potassium nitrate (KNO3) from density functional theory. Computational Materials Science, 2010, 50, 356-362.	1.4	6
8988	Theoretical investigation of moderate misfit and interface energetics in the Fe/VN system. Computational Materials Science, 2010, 50, 550-559.	1.4	23
8989	Ab initio lattice dynamics calculations on the combined effect of temperature and silicon on the stability of different iron phases in the Earth's inner core. Physics of the Earth and Planetary Interiors, 2010, 178, 2-7.	0.7	20
8990	A particularly strong organic acceptor for tuning the hole-injection barriers in modern organic devices. Synthetic Metals, 2010, 160, 1456-1462.	2.1	8
8991	A Theoretical Study of CO₂ Anions on Anatase (101) Surface. Journal of Physical Chemistry C, 2010, 114, 21474-21481.	1.5	159
8992	Density functional study of the Au-intercalated graphene/Ni(111) surface. Physical Review B, 2010, 82, .	1.1	61
8993	Tuning the Hydrogen Storage in Magnesium Alloys. Journal of Physical Chemistry Letters, 2010, 1, 1982-1986.	2.1	25
8994	Quasiparticle and optical properties of rutile and anatase<mml:math xmlns:mml="http://www.w3.org/1998/Math/MathML" display="inline"><mml:mrow><mml:msub><mml:mrow><mml:mtext>TiO</mml:mtext></mml:mrow><mml:mn>2</mml:mn></mml:msub></mml:mrow></mml:math> Physical Review B, 2010, 82, .	1.1	192
8995	Graphene-like silicon nanoribbons on Ag(110): A possible formation of silicene. Applied Physics Letters, 2010, 96, .	1.5	874
8996	First-Principles-Based Kinetic Monte Carlo Simulation of Nitric Oxide Reduction over Platinum Nanoparticles under Lean-Burn Conditions. Industrial & Engineering Chemistry Research, 2010, 49, 10364-10373.	1.8	36
8997	Quasi-single Crystal Semiconductors on Glass Substrates Through Biaxially Oriented Buffer Layers. Materials Research Society Symposia Proceedings, 2010, 1268, 1.	0.1	1
8998	Oxygen activation on gold nanoparticles: separating the influence of particle size, particle shape and support interaction. Dalton Transactions, 2010, 39, 8538.	1.6	134
8999	Intrinsic magnetism at silicon surfaces. Nature Communications, 2010, 1, 58.	5.8	144
9000	Step-by-step growth of epitaxially aligned polythiophene by surface-confined reaction. Proceedings of the National Academy of Sciences of the United States of America, 2010, 107, 11200-11204.	3.3	117
9001	Uniaxial Magnetic Anisotropy Energy of Fe Wires Embedded in Carbon Nanotubes. ACS Nano, 2010, 4, 2883-2891.	7.3	8
9002	Charge effect in S enhanced CO adsorption: A theoretical study of CO on Au, Ag, Cu, and Pd (111) surfaces coadsorbed with S, O, Cl, and Na. Journal of Chemical Physics, 2010, 133, 094703.	1.2	29

#	Article	IF	Citations
9003	Halide Ligated Iron Porphines: A DFT+U and UB3LYP Study. Journal of Physical Chemistry A, 2010, 114, 13381-13387.	1.1	31
9004	Dynamics simulation of N2 scattering onto W(100,110) surfaces: A stringent test for the recently developed flexible periodic Londonâ€“Eyringâ€“Polanyiâ€“Sato potential energy surface. Journal of Chemical Physics, 2010, 132, 204501.	1.2	27
9005	Templated Growth of Hexagonal Nickel Carbide Nanocrystals on Vertically Aligned Carbon Nanotubes. Journal of Physical Chemistry C, 2010, 114, 10424-10429.	1.5	24
9006	Effect of Particle Size on Hydrogen Release from Sodium Alanate Nanoparticles. ACS Nano, 2010, 4, 5647-5656.	7.3	85
9007	Firstâ€principles calculations of atomic and electronic properties of ZnO nanostructures. Physica Status Solidi (B): Basic Research, 2010, 247, 2581-2593.	0.7	7
9008	Atomistic modeling of interfaces and their impact on microstructure and properties. Acta Materialia, 2010, 58, 1117-1151.	3.8	430
9009	Hydrogen in tungsten: Absorption, diffusion, vacancy trapping, and decohesion. Journal of Materials Research, 2010, 25, 315-327.	1.2	230
9010	Surface and Quantum Confinement Effects in ZnO Nanocrystals. Journal of Physical Chemistry C, 2010, 114, 18293-18297.	1.5	53
9011	Hybrid functional study of proper and improper multiferroics. Physical Chemistry Chemical Physics, 2010, 12, 5405.	1.3	147
9012	CO Adsorption on Monometallic and Bimetallic Auâ^'Pd Nanoparticles Supported on Oxide Thin Films. Journal of Physical Chemistry C, 2010, 114, 17099-17104.	1.5	71
9013	Phase stability and nondilute Li diffusion in spinel<mml:math xmlns:mml="http://www.w3.org/1998/Math/MathML" display="inline"><mml:mrow><mml:msub><mml:mrow><mml:mtext>Li</mml:mtext></mml:mrow><mml:mrow><mml:mn>1</mml:mn> Physical Review B, 2010, 81, .	1.1	103
9014	The absorption of oxygenated silicon carbide nanoparticles. Journal of Chemical Physics, 2010, 133, 064705.	1.2	36
9015	<mml:math xmlns:mml="http://www.w3.org/1998/Math/MathML" display="inline"><mml:mrow><mml:mi>Î²</mml:mi><mml:msub><mml:mrow><mml:mtext>-Cu</mml:mtext></mml:mrow><mml:mn>2 A spin-<mml:math xmlns:mml="http://www.w3.org/1998/Math/MathML" display="inline"><mml:mrow><mml:mstyle scriptlevel="1"><mml:mfrac bevelled="false"><mml:mn>1</mml:mn><mml:mn>2. Physical Review B, 2010, 82, .	1.1	84
9016	First principles determination of the structure and elasticity of hydrous ringwoodite. Journal of Geophysical Research, 2010, 115, .	3.3	42
9017	EPR andab initiocalculation study on the EI4 center in<mml:math xmlns:mml="http://www.w3.org/1998/Math/MathML" display="inline"><mml:mrow><mml:mn>4</mml:mn><mml:mi>H</mml:mi></mml:mrow></mml:math>- and<mml:math xmlns:mml="http://www.w3.org/1998/Math/MathML" display="inline"><mml:mrow><mml:mn>6</mml:mn><mml:mi>H</mml:mi><mml:mtext>-SiC</mml:mtext></mml:mrow></mml:math>. Physical Review B, 2010, 82, .	1.1	12
9018	Geometric and electronic structures of graphitic-like and tubular silicon carbides:Ab-initiostudies. Physical Review B, 2010, 82, .	1.1	54
9019	Structural, electronic, optical and vibrational properties of nanoscale carbons and nanowires: a colloquial review. Journal of Physics Condensed Matter, 2010, 22, 334201.	0.7	10
9020	Electronic structure and magnetic properties of (Fe,Co)-codoped ZnO: Theory and experiment. Physical Review B, 2010, 81, .	1.1	33

#	Article	IF	Citations
9021	Impact of Interfacial Oxygen Content on Bonding, Stability, Band Offsets, and Interface States of GaAs:HfO₂ Interfaces. Journal of Physical Chemistry C, 2010, 114, 22610-22618.	1.5	82
9022	Electronic structure calculations with GPAW: a real-space implementation of the projector augmented-wave method. Journal of Physics Condensed Matter, 2010, 22, 253202.	0.7	1,451
9023	First-principles simulations of structural, electronic, and magnetic properties of vacancy-bearing Fe silicates. Physical Review B, 2010, 81, .	1.1	10
9024	Defect-controlled electronic transport in single, bilayer, and N-doped graphene: Theory. Physical Review B, 2010, 81, .	1.1	23
9025	First-principles investigation of bilayer graphene with intercalated C, N or O atoms. Journal of Physics Condensed Matter, 2010, 22, 245502.	0.7	21
9026	Adsorption and growth morphology of rare-earth metals on graphene studied byab initiocalculations and scanning tunneling microscopy. Physical Review B, 2010, 82, .	1.1	66
9027	Structurally driven metamagnetism in MnP and related<mml:math xmlns:mml="http://www.w3.org/1998/Math/MathML" display="inline"><mml:mrow><mml:mi>P</mml:mi><mml:mi>n</mml:mi><mml:mi>m</mml:mi><mml:mi>a</mml:mi></mml:mrow></m Physical Review B, 2010, 81, .	1.1	63
9028	First-principles prediction of partitioning of alloying elements between cementite and ferrite. Acta Materialia, 2010, 58, 6276-6281.	3.8	84
9029	JuNoLo â€“ JÃ¼lich nonlocal code for parallel post-processing evaluation of vdW-DF correlation energy. Computer Physics Communications, 2010, 181, 371-379.	3.0	40
9030	Magnetic transition of iron carbide at high pressures. Physics of the Earth and Planetary Interiors, 2010, 180, 1-6.	0.7	55
9031	Practical Materials Chemistry Approaches for Tuning Optical and Structural Properties of Group IV Semiconductors and Prototype Photonic Devices. IEEE Photonics Journal, 2010, 2, 924-941.	1.0	26
9032	Development of a Reactive Force Field for Ironâ“Oxyhydroxide Systems. Journal of Physical Chemistry A, 2010, 114, 6298-6307.	1.1	199
9033	Electronic structure of<mml:math xmlns:mml="http://www.w3.org/1998/Math/MathML" display="inline"><mml:mrow><mml:msub><mml:mrow><mml:mtext>LiCoO</mml:mtext></mml:mrow><mml:mn>2</mml:mn></mml:r films: A combined photoemission spectroscopy and density functional theory study. Physical Review B, 2010, 82, .	1.1	60
9034	A DFT study of PtAu bimetallic clusters adsorbed on MgO/Ag(100) ultrathin films. Physical Chemistry Chemical Physics, 2010, 12, 6352.	1.3	12
9035	Nearly Massless Electrons in the Silicon Interface with a Metal Film. Physical Review Letters, 2010, 104, 246803.	2.9	31
9036	Crystal Structures and Exotic Behavior of Magnesium under Pressure. Journal of Physical Chemistry C, 2010, 114, 21745-21749.	1.5	146
9037	Modeling surface segregation phenomena in the (111) surface of ordered Pt3Ti crystal. Journal of Chemical Physics, 2010, 133, 114701.	1.2	25
9038	Catalytic Reduction of NO₂with Hydrogen on Pt Field Emitter Tips: Kinetic Instabilities on the Nanoscale. Langmuir, 2010, 26, 16381-16391.	1.6	20

#	Article	IF	Citations
9039	Structural and Electronic Properties of Li-Ion Battery Cathode Material FeF₃. Journal of Physical Chemistry C, 2010, 114, 16813-16817.	1.5	59
9040	Ab initiocalculations of arsenic in silicon: Diffusion mechanism and strain dependence. Physical Review B, 2010, 81, .	1.1	4
9041	First-principles Calculation Assisted Thermodynamic Modeling of Ti-Co-Cu Ternary System. Journal of Materials Science and Technology, 2010, 26, 317-326.	5.6	4
9042	Oxygen-Induced Surface Reconstruction of SrRuO₃ and Its Effect on the BaTiO₃ Interface. ACS Nano, 2010, 4, 4190-4196.	7.3	44
9043	Controlled Interactions between Anhydrous Keggin-Type Heteropolyacids and Silica Support: Preparation and Characterization of Well-Defined Silica-Supported Polyoxometalate Species. Journal of Physical Chemistry C, 2010, 114, 19024-19034.	1.5	50
9044	Industry meets theory: computational R & D for innovative products. Journal of Physics Condensed Matter, 2010, 22, 384209.	0.7	9
9045	Origin of the Different Activity and Selectivity toward Hydrogenation of Single Metal Au and Pt on TiO₂ and Bimetallic Auâ"Pt/TiO₂ Catalysts. Langmuir, 2010, 26, 16607-16614.	1.6	77
9046	Strong Interplay between Structure and Electronic Properties in <mml:math xmlns:mml="http://www.w3.org/1998/Math/MathML" display="inline"><mml:mi>CuIn</mml:mi><mml:mo stretchy="false">(</mml:mo><mml:mi) Tj ETQq1 1 0.784314 rgBT /Overlock 10 Tf 50 462 Td (mathvariant="bold">S</mml:mi><mml:m	2.9	133
9048	Band gap tuning in GaN through equibiaxial in-plane strains. Applied Physics Letters, 2010, 96, .	1.5	76
9049	Density functional theory study ofZnX(X=O,â€,S,â€,Se,â€,Te)under uniaxial strain. Physical Review B, 2010, 81, .	1.1	66
9050	Effect of Electronic and Geometric Shell Closures on the Stability of Neutral and Anionic TiNa_n (n = 1â"13) Clusters. Journal of Physical Chemistry C, 2010, 114, 10739-10744.	1.5	26
9051	Electronic structure of <mml:math xmlns:mml="http://www.w3.org/1998/Math/MathML" display="inline"><mml:mrow><mml:msub><mml:mrow><mml:mtext>In</mml:mtext></mml:mrow><mml:mn>2</mml:mn></mml:ms Sn-doped <mml:math xmlns:mml="http://www.w3.org/1998/Math/MathML" display="inline"><mml:mrow><mml:msub><mml:mrow><mml:mtext>In</mml:mtext></mml:mrow><mml:mn>2</mml:mn></mml:ms	1.1	114
9052	Band offsets of semiconductor heterostructures: A hybrid density functional study. Applied Physics Letters, 2010, 97, 092119.	1.5	46
9053	Magnetic thermodynamics of fcc Ni from first-principles partition function approach. Journal of Applied Physics, 2010, 108, .	1.1	31
9054	Tungsten oxides. I. Effects of oxygen vacancies and doping on electronic and optical properties of different phases of WO3. Journal of Applied Physics, 2010, 108, .	1.1	119
9055	Thermodynamic limits of crystallization and the prediction of glass formation tendency. Physical Review B, 2010, 81, .	1.1	8
9056	Electronic and magnetic properties of graphane nanoribbons. Physical Review B, 2010, 81, .	1.1	136
9057	Tunable properties of PtxFe1â"x electrocatalysts and their catalytic activity towards the oxygen reduction reaction. Nanoscale, 2010, 2, 573.	2.8	40

#	Article	IF	Citations
9058	First-principles calculations of Znâ€“K XANES in Ca-deficient hydroxyapatite. Journal of Physics Condensed Matter, 2010, 22, 384213.	0.7	11
9059	Theoretical Confirmation of the Enhanced Facility to Increase Oxygen Vacancy Concentration in TiO₂by Iron Doping. Journal of Physical Chemistry C, 2010, 114, 6511-6517.	1.5	78
9060	Ab initiostudy of thermoelectric transport properties of pure and doped quaternary compounds. Physical Review B, 2010, 82, .	1.1	73
9061	Silicon nano-ribbons on Ag(110): a computational investigation. Journal of Physics Condensed Matter, 2010, 22, 045004.	0.7	65
9062	Coupling Epitaxy, Chemical Bonding, and Work Function at the Local Scale in Transition Metal-Supported Graphene. ACS Nano, 2010, 4, 5773-5782.	7.3	145
9063	Analysis of the Magnetic Structure and Ferroelectric Polarization of Monoclinic MnSb2S4by Density Functional Theory Calculations. Inorganic Chemistry, 2010, 49, 10956-10959.	1.9	16
9064	First-Principles Prediction on the High-Pressure Structures of Transition Metal Diborides (TMB₂, TM = Sc, Ti, Y, Zr). Inorganic Chemistry, 2010, 49, 6859-6864.	1.9	41
9065	Ferromagnetic and antiferromagnetic properties of the semihydrogenated SiC sheet. Applied Physics Letters, 2010, 96, .	1.5	56
9066	Magnetic anisotropy of Fe and Co ultrathin films deposited on Rh(111) and Pt(111) substrates: An experimental and first-principles investigation. Physical Review B, 2010, 82, .	1.1	106
9067	Cluster-Assembled Materials: Toward Nanomaterials with Precise Control over Properties. ACS Nano, 2010, 4, 235-240.	7.3	127
9068	Trends of Water Gas Shift Reaction on Close-Packed Transition Metal Surfaces. Journal of Physical Chemistry C, 2010, 114, 9826-9834.	1.5	98
9069	Noble and alkali adatoms on a mathrm {Si(111) sqrt {3} imes sqrt {3}} â€“Ag surface: a first-principles study. Journal of Physics Condensed Matter, 2010, 22, 085001.	0.7	9
9070	Atomic Structure of a CeO₂ Grain Boundary: The Role of Oxygen Vacancies. Nano Letters, 2010, 10, 4668-4672.	4.5	173
9071	Towards suppressing H blistering by investigating the physical origin of the Hâ€“He interaction in W. Nuclear Fusion, 2010, 50, 115010.	1.6	137
9072	An Improved Self-Consistent-Charge Density-Functional Tight-Binding (SCC-DFTB) Set of Parameters for Simulation of Bulk and Molecular Systems Involving Titanium. Journal of Chemical Theory and Computation, 2010, 6, 266-278.	2.3	177
9073	Hydrogen adsorption on polar ZnO(0001)-Zn: Extending equilibrium surface phase diagrams to kinetically stabilized structures. Physical Review B, 2010, 82, .	1.1	58
9074	First-principles determination of charge carrier mobility in disordered semiconducting polymers. Physical Review B, 2010, 82, .	1.1	26
9075	Synthesis and Characterization of the Crystal Structure and Magnetic Properties of the Ternary Manganese Vanadate NaMnVO₄. Inorganic Chemistry, 2010, 49, 8578-8582.	1.9	30

#	Article	IF	Citations
9076	Structure and diffusion of intrinsic defect complexes in LiNbO₃from density functional theory calculations. Journal of Physics Condensed Matter, 2010, 22, 135002.	0.7	39
9077	Interfacial oxygen and nitrogen induced dipole formation and vacancy passivation for increased effective work functions in TiN/HfO2 gate stacks. Applied Physics Letters, 2010, 96, .	1.5	29
9078	Selecting the tip electron orbital for scanning tunneling microscopy imaging with sub-Ã¥ngstrÃ¶m lateral resolution. Europhysics Letters, 2010, 92, 46003.	0.7	33
9079	Native defects in oxide semiconductors: a density functional approach. Journal of Physics Condensed Matter, 2010, 22, 384211.	0.7	47
9080	First-principle study of structure and stability of nickel carbides. Journal of Physics Condensed Matter, 2010, 22, 445503.	0.7	34
9081	Strain Effects on Electronic Properties of Boron Nitride Nanoribbons. Chinese Physics Letters, 2010, 27, 077101.	1.3	13
9082	Ab initiostudy of structural and magnetic properties of Si-doped<mml:math xmlns:mml="http://www.w3.org/1998/Math/MathML" display="inline"><mml:mrow><mml:msub><mml:mrow><mml:mtext>Fe</mml:mtext></mml:mrow><mml:mn>2</mml:mn></mml:msub> Physical Review B, 2010, 82, .	1.1	30
9083	Computational study of structural and elastic properties of random Al_xGa_yIn_{1 â^'xâ^'y}N alloys. Journal of Physics Condensed Matter, 2010, 22, 205801.	0.7	9
9084	Self-assembled monolayers of polar molecules on Au(111) surfaces: distributing the dipoles. Physical Chemistry Chemical Physics, 2010, 12, 4291.	1.3	28
9085	Efficient implementation of the nonequilibrium Green function method for electronic transport calculations. Physical Review B, 2010, 81, .	1.1	160
9086	Alkali-Stabilized Pt-OH _x Species Catalyze Low-Temperature Water-Gas Shift Reactions. Science, 2010, 329, 1633-1636.	6.0	639
9087	Defect formation and phase stability of<mml:math xmlns:mml="http://www.w3.org/1998/Math/MathML" display="inline"><mml:mrow><mml:msub><mml:mrow><mml:mtext>Cu</mml:mtext></mml:mrow><mml:mn>2</mml:mn></mml:msub> material. Physical Review B, 2010, 81, .	1.1	28
9088	Hydrogen Oxidation at the Ni/Yttria-Stabilized Zirconia Interface: A Study Based on Density Functional Theory. Journal of Physical Chemistry C, 2010, 114, 11209-11214.	1.5	52
9089	The physical and chemical properties of heteronanotubes. Reviews of Modern Physics, 2010, 82, 1843-1885.	16.4	239
9090	Group-V impurities in<mml:math xmlns:mml="http://www.w3.org/1998/Math/MathML" display="inline"><mml:mrow><mml:msub><mml:mrow><mml:mtext>SnO</mml:mtext></mml:mrow><mml:mn>2</mml:mn></mml:msub> first-principles calculations. Physical Review B, 2010, 81, .	1.1	52
9091	Density functional study of magnetic properties in Zn-doped SnO2. Journal of Applied Physics, 2010, 108, .	1.1	36
9092	Origin and passivation of fixed charge in atomic layer deposited aluminum oxide gate insulators on chemically treated InGaAs substrates. Applied Physics Letters, 2010, 96, .	1.5	148
9093	Prediction of a superhard material of ReN₄with a high shear modulus. Chinese Physics B, 2010, 19, 016201-4.	0.7	9

#	Article	IF	Citations
9094	Ab initiothermodynamics beyond the quasiharmonic approximation: W as a prototype. Physical Review B, 2010, 81, .	1.1	20
9095	Dissolution-Resistant Coreâ^'Shell Materials for Acid Medium Oxygen Reduction Electrocatalysts. Journal of Physical Chemistry Letters, 2010, 1, 724-728.	2.1	19
9096	Synthesis, Stability Range, and Fundamental Properties of Siâ^'Geâ^'Sn Semiconductors Grown Directly on Si(100) and Ge(100) Platforms. Chemistry of Materials, 2010, 22, 3779-3789.	3.2	61
9097	Methanol Synthesis from H₂and CO₂on a Mo₆S₈Cluster: A Density Functional Study. Journal of Physical Chemistry A, 2010, 114, 3888-3895.	1.1	83
9098	Oscillatory crossover from two-dimensional to three-dimensional topological insulators. Physical Review B, 2010, 81, .	1.1	459
9099	A Novel Excitation Control Equipment Design of Synchronous Motor. , 2010, , .		0
9100	Density functional theory studies of doping in titania. Molecular Simulation, 2010, 36, 618-632.	0.9	12
9101	First Principles Study of the Binding of 4d and 5d Transition Metals to Graphene. Journal of Physical Chemistry C, 2010, 114, 18548-18552.	1.5	49
9102	Understanding from First-Principles Why LiNH2BH3Â·NH3BH3 Shows Improved Dehydrogenation over LiNH2BH3 and NH3BH3. Journal of Physical Chemistry C, 2010, 114, 19089-19095.	1.5	27
9103	Functionalizing Single- and Multi-layer Graphene with Br and Br2. Journal of Physical Chemistry C, 2010, 114, 14939-14945.	1.5	43
9104	DFT Studies of Oxygen Vacancies on Undoped and Doped La₂O₃ Surfaces. Journal of Physical Chemistry C, 2010, 114, 12234-12244.	1.5	101
9105	Magnetic properties of small Pt-capped Fe, Co, and Ni clusters: A density functional theory study. Physical Review B, 2010, 82, .	1.1	68
9106	Zircon-monoclinic-scheelite transformation in nanocrystalline chromates. Physical Review B, 2010, 81, .	1.1	5
9107	Identifying Doping Strategies To Optimize the Oxide Ion Conductivity in Ceria-Based Materials. Journal of Physical Chemistry C, 2010, 114, 19062-19076.	1.5	28
9108	Defect physics of the kesterite thin-film solar cell absorber Cu2ZnSnS4. Applied Physics Letters, 2010, 96, .	1.5	454
9109	Effective method to identify the vacancies in crystalline GeTe. Applied Physics Letters, 2010, 97, .	1.5	30
9110	Stability and charge transfer levels of extrinsic defects in<mml:math xmlns:mml="http://www.w3.org/1998/Math/MathML" display="inline"><mml:mrow><mml:msub><mml:mrow><mml:mtext>LiNbO</mml:mtext></mml:mrow><mml:mn>3</mml:mn></mml:r Physical Review B, 2010, 82, .	1.1	41
9111	Hydrogen donors in<mml:math xmlns:mml="http://www.w3.org/1998/Math/MathML" display="inline"><mml:mrow><mml:msub><mml:mrow><mml:mtext>SnO</mml:mtext></mml:mrow><mml:mn>2</mml:mn></mml:msub></mml: by infrared spectroscopy and first-principles calculations. Physical Review B, 2010, 82, .	1.1	50

#	Article	IF	Citations
9112	Optical gaps of free and embedded Si nanoclusters: Density functional theory calculations. Physical Review B, 2010, 82, .	1.1	20
9113	Robust Dirac point in honeycomb-structure nanoribbons with zigzag edges. Physical Review B, 2010, 81, .	1.1	12
9114	Structure of the indium-rich InSb(001) surface. Physical Review B, 2010, 82, .	1.1	14
9115	First-principles study of structural, elastic, lattice dynamical and thermodynamical properties of GdX (X = Bi, Sb). Philosophical Magazine, 2010, 90, 1833-1852.	0.7	9
9116	A theoretical insight into the catalytic effect of a mixed-metal oxide at the nanometer level: The case of the highly active metal/CeOx/TiO2(110) catalysts. Journal of Chemical Physics, 2010, 132, 104703.	1.2	93
9117	Structural properties of warm dense matter. Journal of Physics: Conference Series, 2010, 220, 012001.	0.3	16
9118	Study of the interaction between short alkanethiols from ab initio calculations. Physical Chemistry Chemical Physics, 2010, 12, 7555.	1.3	17
9119	Anharmonicity-induced phonon broadening in aluminum at high temperatures. Physical Review B, 2010, 82, .	1.1	37
9120	Comparing efficiencies of genetic and minima hopping algorithms for crystal structure prediction. Physical Chemistry Chemical Physics, 2010, 12, 11617.	1.3	30
9121	First-principles study of the variation of electron transport in a single molecular junction with the length of the molecular wire. Physical Review B, 2010, 82, .	1.1	7
9122	Is there a Auâ€“S bond dipole in self-assembled monolayers on gold?. Physical Chemistry Chemical Physics, 2010, 12, 4287.	1.3	37
9123	Lattice dynamics of rhenium trioxide from the quasiharmonic approximation. Physical Review B, 2010, 82, .	1.1	29
9124	First-principles and Monte Carlo study of magnetostructural transition and magnetocaloric properties of<mml:math xmlns:mml="http://www.w3.org/1998/Math/MathML" display="inline"><mml:mrow><mml:msub><mml:mrow><mml:mtext>Ni</mml:mtext></mml:mrow><mml:mrow><mml:mn>2</mml:mn></mml:mrow> Physical Review B, 2010, 81, .	1.1	119
9125	Advances in computational studies of energy materials. Philosophical Transactions Series A, Mathematical, Physical, and Engineering Sciences, 2010, 368, 3379-3456.	1.6	119
9126	First-principles study of the thermodynamics of hydrogen-vacancy interaction in fcc iron. Physical Review B, 2010, 82, .	1.1	106
9127	Role of Auâ^'C Interactions on the Catalytic Activity of Au Nanoparticles Supported on TiC(001) toward Molecular Oxygen Dissociation. Journal of the American Chemical Society, 2010, 132, 3177-3186.	6.6	88
9128	Electronic structure and transport in thermoelectric compounds AZn2Sb2 (A = Sr, Ca, Yb, Eu). Dalton Transactions, 2010, 39, 1046-1054.	1.6	184
9129	Carbon impurities and the yellow luminescence in GaN. Applied Physics Letters, 2010, 97, .	1.5	531

#	Article	IF	Citations
9130	A multi-scale approach for performance assessment of hydrogenated graphene Field-Effect Transistors. , 2010, , .		0
9131	Periodicity, work function and reactivity of graphene on Ru(0001) from first principles. New Journal of Physics, 2010, 12, 043041.	1.2	104
9132	The electronic structure of Î²-Ga2O3. Applied Physics Letters, 2010, 97, .	1.5	146
9133	Improved Description of the Structure of Molecular and Layered Crystals: Ab Initio DFT Calculations with van der Waals Corrections. Journal of Physical Chemistry A, 2010, 114, 11814-11824.	1.1	895
9134	Ultrafast carrier dynamics in pristine and FeCl3-intercalated bilayer graphene. Applied Physics Letters, 2010, 97, 141910.	1.5	28
9135	Structural, Electronic, and Magnetic Properties of Defects in the BC₃ Sheet from First Principles. Journal of Physical Chemistry C, 2010, 114, 12416-12421.	1.5	37
9136	The Complex Thiolâ^'Palladium Interface: A Theoretical and Experimental Study. Langmuir, 2010, 26, 14655-14662.	1.6	33
9137	Spontaneous edge-defect formation and defect-induced conductance suppression in graphene nanoribbons. Physical Review B, 2010, 82, .	1.1	41
9138	Ferromagnetism in multiferroic<mml:math xmlns:mml="http://www.w3.org/1998/Math/MathML" display="inline"><mml:mrow><mml:msub><mml:mrow><mml:mtext>BiFeO</mml:mtext></mml:mrow><mml:mn>3</mml:mn></mml:m A first-principles-based study. Physical Review B, 2010, 81, .	3.1	116
9139	Planar Tetracoordinate Carbon Strips in Edge Decorated Graphene Nanoribbon. Journal of the American Chemical Society, 2010, 132, 5554-5555.	6.6	75
9140	Temperature-Dependent Magnetoelectric Effect from First Principles. Physical Review Letters, 2010, 105, 087202.	2.9	82
9141	Electron and phonon scattering in the high-temperature thermoelectric<mml:math xmlns:mml="http://www.w3.org/1998/Math/MathML" display="inline"><mml:mrow><mml:msub><mml:mrow><mml:mtext>La</mml:mtext></mml:mrow><mml:mn>3</mml:mn></mml:m xmlns:mml="http://www.w3.org/1998/Math/Math. Physical Review B, 2010, 81, .	1.1	44
9142	Origins of magnetism in transition metal doped CuI. Journal of Applied Physics, 2010, 108, 043713.	1.1	8
9143	Modeling the noble metal/TiO2 (110) interface with hybrid DFT functionals: A periodic electrostatic embedded cluster model study. Journal of Chemical Physics, 2010, 133, 164703.	1.2	59
9144	Hydrogen Adsorption on Monoclinic (1Ì...11) and (1Ì...01) ZrO₂ Surfaces: A Periodic ab Initio Study. Journal of Physical Chemistry C, 2010, 114, 11918-11923.	1.5	31
9145	Iron-Decorated, Functionalized Metal Organic Framework for High-Capacity Hydrogen Storage: First-Principles Calculations. Journal of Physical Chemistry C, 2010, 114, 14276-14280.	1.5	26
9146	Adsorption of an Mn atom on a ZnO sheet and nanotube: a density functional theory study. Journal of Physics Condensed Matter, 2010, 22, 175501.	0.7	26
9147	Quantum Chemical Modeling of Benzene Ethylation over H-ZSM-5 Approaching Chemical Accuracy: A Hybrid MP2:DFT Study. Journal of the American Chemical Society, 2010, 132, 11525-11538.	6.6	144

#	Article	IF	Citations
9148	Structures of [Ag₇(SR)₄]^{â^'}and [Ag₇(DMSA)₄]^{â^'}. Journal of the American Chemical Society, 2010, 132, 7355-7360.	6.6	60
9149	Direct and indirect electron transfer at a semiconductor surface with an adsorbate: Theory and application to Ag3Si(111):H. Journal of Chemical Physics, 2010, 132, 114702.	1.2	20
9150	Oxygen vacancy formation and migration in Ce1â^'xZrxO2 catalyst: A DFT+U calculation. Journal of Chemical Physics, 2010, 132, 214702.	1.2	57
9151	Theoretical and experimental studies of substitution of cadmium into hydroxyapatite. Physical Chemistry Chemical Physics, 2010, 12, 15490.	1.3	23
9152	Reconstruction of core and surface nanoparticles: The example of<mml:math xmlns:mml="http://www.w3.org/1998/Math/MathML" display="inline"><mml:mrow><mml:msub><mml:mrow><mml:mtext>Pt</mml:mtext></mml:mrow><mml:mrow><mml:mn>55</mml:m xmlns:mml="http://www.w3.org/1998/Math/MathML" display="inline"><mml:mrow><mml:msub><mml:mrow><mml:mtext>Au</mml:mtext></mml:mrow><mml:mrow><mml:mn>55</mml:n Physical Review B, 2010, 82, .	1.1	56
9153	Schottky barrier height and conduction mechanisms in ferroelectric bismuth titanate. Applied Physics Letters, 2010, 96, 052102.	1.5	10
9154	First-principles calculations of Born effective charges and spontaneous polarization of ferroelectric bismuth titanate. Journal of Physics Condensed Matter, 2010, 22, 165902.	0.7	27
9155	Trapping of oxygen vacancy at grain boundary and its correlation with local atomic configuration and resultant excess energy in barium titanate: A systematic computational analysis. Physical Review B, 2010, 82, .	1.1	52
9156	Lattice dynamics in<mml:math xmlns:mml="http://www.w3.org/1998/Math/MathML" display="inline"><mml:mrow><mml:msub><mml:mrow><mml:mtext>ZrB</mml:mtext></mml:mrow><mml:mrow><mml:mn>12</mml:m xmlns:mml="http://www.w3.org/1998/Math/MathML" display="inline"><mml:mrow><mml:msub><mml:mrow><mml:mtext>LuB</mml:mtext></mml:mrow><mml:mrow><mml:mn>12</mml: initiocalculations and inelastic neutron scattering. Physical Review B, 2010, 82, .	1.1	39
9157	Interpretation of high-resolution images of the best-bound wetting layers on Pt(111). Journal of Chemical Physics, 2010, 133, 154703.	1.2	42
9158	Cooperativity in Surface Bonding and Hydrogen Bonding of Water and Hydroxyl at Metal Surfaces. Journal of Physical Chemistry C, 2010, 114, 10240-10248.	1.5	51
9159	Conductometric chemical sensor based on individual CuO nanowires. Nanotechnology, 2010, 21, 485502.	1.3	139
9160	The response of mechanical and electronic properties of graphane to the elastic strain. Applied Physics Letters, 2010, 96, .	1.5	344
9161	Einstein modes in the phonon density of states of the single-filled skutterudite<mml:math xmlns:mml="http://www.w3.org/1998/Math/MathML" display="inline"><mml:mrow><mml:msub><mml:mrow><mml:mtext>Yb</mml:mtext></mml:mrow><mml:mrow><mml:mn>0.2</mml:mn Physical Review B, 2010, 82, .	1.1	77
9162	Structural Order-Disorder Transitions and Phonon Conductivity of Partially Filled Skutterudites. Physical Review Letters, 2010, 105, 265901.	2.9	56
9163	The ultimate diamond slab: GraphAne versus graphEne. Diamond and Related Materials, 2010, 19, 368-373.	1.8	71
9164	New Superconducting and Semiconducting Fe-B Compounds Predicted with anAbÂInitioEvolutionary Search. Physical Review Letters, 2010, 105, 217003.	2.9	182
9165	Effects of Hydration and Oxygen Vacancy on CO₂ Adsorption and Activation on Î²-Ga₂O₃(100). Langmuir, 2010, 26, 5551-5558.	1.6	118

#	Article	IF	Citations
9166	Communication: Coalescence of carbon atoms on Cu (111) surface: Emergence of a stable bridging-metal structure motif. Journal of Chemical Physics, 2010, 133, 071101.	1.2	72
9167	Lithium Coordination Sites in Li_xTiO₂(B): A Structural and Computational Study. Chemistry of Materials, 2010, 22, 6426-6432.	3.2	104
9168	Defect-induced defect-mediated magnetism in ZnO and carbon-based materials. Journal of Physics Condensed Matter, 2010, 22, 334210.	0.7	21
9169	Evaluation of Sn Nanowire Encapsulated Carbon Nanotube for a Li-Ion Battery Anode by DFT Calculations. Journal of Physical Chemistry C, 2010, 114, 8542-8545.	1.5	33
9170	Cobaltâ^'Porphyrin Catalyzed Electrochemical Reduction of Carbon Dioxide in Water. 2. Mechanism from First Principles. Journal of Physical Chemistry A, 2010, 114, 10174-10184.	1.1	130
9171	Cobaltâ^'Porphyrin Catalyzed Electrochemical Reduction of Carbon Dioxide in Water. 1. A Density Functional Study of Intermediates. Journal of Physical Chemistry A, 2010, 114, 10166-10173.	1.1	69
9172	Theoretical Analysis of the Spin Exchange and Magnetic Dipoleâ^'Dipole Interactions Leading to the Magnetic Structure of Ni₃TeO₆. Inorganic Chemistry, 2010, 49, 7545-7548.	1.9	38
9173	Bismuth doping of graphene. Applied Physics Letters, 2010, 96, .	1.5	30
9174	First-principles study of the dipole layer formation at metal-organic interfaces. Physical Review B, 2010, 81, .	1.1	48
9175	Structure and Stability of Tube and Cage Ge₆₀H₆₀. Journal of Physical Chemistry A, 2010, 114, 12755-12758.	1.1	4
9176	Limits for n-type doping in In2O3 and SnO2: A theoretical approach by first-principles calculations using hybrid-functional methodology. Journal of Applied Physics, 2010, 108, .	1.1	57
9177	Carbonâ^'Chlorine Bond Scission in Li-Doped Single-Walled Carbon Nanotubes: Reaction of CH₃Cl and Lithium. Journal of Physical Chemistry C, 2010, 114, 17148-17158.	1.5	9
9178	Unusual Physical and Chemical Properties of Ni in Ce_{1â^'x}Ni_xO_{2â^'y} Oxides: Structural Characterization and Catalytic Activity for the Water Gas Shift Reaction. Journal of Physical Chemistry C, 2010, 114, 12689-12697.	1.5	151
9179	Computer simulations of structures and properties of the biomaterial hydroxyapatite. Journal of Materials Chemistry, 2010, 20, 5376.	6.7	72
9180	First principles study of electronic transport through a Cu(111)â^£graphene junction. Applied Physics Letters, 2010, 97, 142105.	1.5	33
9181	On the transition-metal doping efficiency of zinc oxide nanocrystals. Applied Physics Letters, 2010, 97, .	1.5	17
9182	High-Pressure Phases of Calcium: Density-Functional Theory and Diffusion Quantum MonteÂCarlo Approach. Physical Review Letters, 2010, 105, 235503.	2.9	37
9183	Effects of surface reconstructions on oxygen adsorption at AlN polar surfaces. Europhysics Letters, 2010, 89, 56004.	0.7	8

#	Article	IF	Citations
9184	Magnetic behavior of SnO2 nanosheets at room temperature. Applied Physics Letters, 2010, 97, .	1.5	35
9185	Diffusion of hydrogen in bcc tungsten studied with first principle calculations. Journal of Applied Physics, 2010, 107, .	1.1	174
9186	Atomic Charges Derived from Electrostatic Potentials for Molecular and Periodic Systems. Journal of Physical Chemistry A, 2010, 114, 10225-10233.	1.1	70
9187	Near sulfur L-edge X-ray absorption spectra of methanethiol in isolation and adsorbed on a Au(111) surface: a theoretical study using the four-component static exchange approximation. Physical Chemistry Chemical Physics, 2010, 12, 5596.	1.3	16
9188	Carrier-Tunable Magnetic Ordering in Vanadiumâ^'Naphthalene Sandwich Nanowires. Journal of the American Chemical Society, 2010, 132, 10215-10217.	6.6	57
9189	Electronic structure of mixed-valence silver oxide AgO from hybrid density-functional theory. Physical Review B, 2010, 81, .	1.1	71
9190	Electronic structure and magnetism of transition metal doped Zn12O12 clusters: Role of defects. Journal of Applied Physics, 2010, 108, .	1.1	22
9191	First-principles study of the effect of vacancies on magnetic properties of Zn_{1 â^'x}Co_xO thin films. Journal of Physics Condensed Matter, 2010, 22, 076002.	0.7	4
9192	Adsorbate-Induced Changes in the Surface Composition of Bimetallic Clusters: Ptâ^'Au on TiO₂(110). Journal of Physical Chemistry C, 2010, 114, 21652-21663.	1.5	70
9193	Size dependence of the bulk modulus of semiconductor nanocrystals from first-principles calculations. Physical Review B, 2010, 82, .	1.1	34
9194	Absorption of Pt clusters and the induced magnetic properties of graphene. Journal of Physics Condensed Matter, 2010, 22, 316005.	0.7	22
9195	The intramolecular blue-shifting Câ€“Hâ‹¯Fâ€“C hydrogen bond: crystal structure of [4,4â€²-bis(HCF2CF2CF2CF2CH2OCH2)-2,2â€²-bpy]MCl2where M = Pt, Pd. CrystEngComm, 2010, 12, 538-542.	1.3	26
9196	Scintillation Properties of Eu^{2+}-Activated Barium Fluoroiodide. IEEE Transactions on Nuclear Science, 2010, 57, 1702-1705.	1.2	19
9197	First-Principles Simulations of Chemical Reactions in an HCl Molecule Embedded inside a C or BN Nanotube Induced by Ultrafast Laser Pulses. Physical Review Letters, 2010, 105, 248301.	2.9	16
9198	Electronic properties of strained Si/Ge core-shell nanowires. Applied Physics Letters, 2010, 96, .	1.5	83
9199	Investigating behaviours of hydrogen in a tungsten grain boundary by first principles: from dissolution and diffusion to a trapping mechanism. Nuclear Fusion, 2010, 50, 025016.	1.6	182
9200	CO 2 capture properties of alkaline earth metal oxides and hydroxides: A combined density functional theory and lattice phonon dynamics study. Journal of Chemical Physics, 2010, 133, 074508.	1.2	122
9201	Gate leakage current in double-gate MOSFETs with Si/SiO<inf>2</inf> interface model from first principle calculations. , 2010, , .		0

#	Article	IF	Citations
9202	First-principles study on variation of lattice parameters of mullite Al4+2xSi2-2xO10-x (x = 0.125, 0.250,) Tj ETQq0 0 0 rgBT /Overlock 10	0.9	8
9204	Electro-Oxidation of Borohydride on Rhodium, Iridium, and Rhodiumâ€“Iridium Bimetallic Nanoparticles with Implications to Direct Borohydride Fuel Cells. Journal of the Electrochemical Society, 2010, 157, B1201.	1.3	44
9205	Computational materials engineering: Capabilities of atomic-scale prediction of mechanical, thermal, and electrical properties of microelectronic materials. , 2010, , .		1
9206	Experimental and theoretical determination of adsorption heats of CO2 over alkali metal exchanged ferrierites with different Si/Al ratio. Physical Chemistry Chemical Physics, 2010, 12, 6413.	1.3	86
9207	High-pressure phase transitions of solid HF, HCl, and HBr: Anab initioevolutionary study. Physical Review B, 2010, 82, .	1.1	27
9208	Towards an understanding of the vibrational mode specificity for dissociative chemisorption of CH4 on Ni(111): a 15 dimensional study. Physical Chemistry Chemical Physics, 2010, 12, 7654.	1.3	36
9209	The interaction of NOx on Ni(111) surface investigated with quantum-chemical calculations. Physical Chemistry Chemical Physics, 2010, 12, 13707.	1.3	12
9210	Adsorption Properties of BF4-Anions on Graphene. Japanese Journal of Applied Physics, 2010, 49, 02BB04.	0.8	6
9211	Searching insight into the atomistic structure of SiCO ceramics. Journal of Materials Chemistry, 2010, 20, 10528.	6.7	52
9212	Understanding conductivity in SrCu₂O₂: stability, geometry and electronic structure of intrinsic defects from first principles. Journal of Materials Chemistry, 2010, 20, 1086-1096.	6.7	42
9213	STM fingerprint of moleculeâ€“adatom interactions in a self-assembled metalâ€“organic surface coordination network on Cu(111). Physical Chemistry Chemical Physics, 2010, 12, 8815.	1.3	62
9214	Databases of virtual inorganic crystal structures and their applications. Physical Chemistry Chemical Physics, 2010, 12, 8521.	1.3	6
9215	Pt promotion and spill-over processes during deposition and desorption of upd-Had and OHad on PtxRu1â^'x/Ru(0001) surface alloys. Physical Chemistry Chemical Physics, 2010, 12, 10388.	1.3	29
9216	First-principles investigation of electron-induced cross-linking of aromatic self-assembled monolayers on Au(111). Physical Chemistry Chemical Physics, 2010, 12, 1578.	1.3	10
9217	A solid-state NMR and DFT study of compositional modulations in AlxGa1â^'xAs. Physical Chemistry Chemical Physics, 2010, 12, 11517.	1.3	29
9218	Hydrogen saturation stabilizes vacancy-induced ferromagnetic ordering in graphene. Physical Chemistry Chemical Physics, 2010, 12, 13699.	1.3	31
9219	Adsorption of glycine on the anatase (101) surface: an ab initio study. Physical Chemistry Chemical Physics, 2010, 12, 11033.	1.3	38
9220	Using â€œradioparagenesisâ€•to design robust nuclear waste forms. Energy and Environmental Science, 2010, 3, 130-135.	15.6	20

#	Article	IF	Citations
9221	A highly ordered, aromatic bidentate self-assembled monolayer on Au(111): a combined experimental and theoretical study. Physical Chemistry Chemical Physics, 2010, 12, 6445.	1.3	23
9222	Rules for selectivity in oxidation processes on RuO2(110). Physical Chemistry Chemical Physics, 2010, 12, 12217.	1.3	20
9223	The relative strength and role in crystal packing of I^{â^'}â‹¯Ï€ and CHâ‹¯I^{â^'}interactions in iminium salts. CrystEngComm, 2010, 12, 186-191.	1.3	4
9224	Ab initio studies of hydrogen and acceptor defects in rutile TiO2. Physical Chemistry Chemical Physics, 2010, 12, 6817.	1.3	30
9225	The atomic level structure of the TiO2â€“NiTi interface. Physical Chemistry Chemical Physics, 2010, 12, 9742.	1.3	18
9226	Oxide and halide nanoclusters on ionic substrates: heterofilm formation and lattice mismatch. Journal of Materials Chemistry, 2010, 20, 10403.	6.7	6
9227	Styrene oligomerization as a molecular probe reaction for zeolite acidity: a UV-Vis spectroscopy and DFT study. Physical Chemistry Chemical Physics, 2010, 12, 7032.	1.3	42
9228	Geometric and electronic structure of Pd/4-aminothiophenol/Au(111) metalâ€“moleculeâ€“metal contacts: a periodic DFT study. Physical Chemistry Chemical Physics, 2010, 12, 4423.	1.3	11
9229	Monitoring the interaction of adsorbates on metal surfaces by surface site engineering: the case of ethoxy on Cu, Pd, Ag and Au regular and stepped surfaces. Physical Chemistry Chemical Physics, 2010, 12, 6492.	1.3	11
9230	Li+ ion conductivity and diffusion mechanism in Î±-Li3N and Î²-Li3N. Energy and Environmental Science, 2010, 3, 1524.	15.6	149
9231	Reconstruction and stability of Î²-cristobalite 001, 101, and 111 surfaces during dehydroxylation. Physical Chemistry Chemical Physics, 2010, 12, 14930.	1.3	60
9232	Evolutionary structure prediction and electronic properties of indium oxide nanoclusters. Physical Chemistry Chemical Physics, 2010, 12, 8446.	1.3	36
9233	Pourbaix-like phase diagram for lithium manganese spinels in acid. Journal of Materials Chemistry, 2010, 20, 369-374.	6.7	15
9234	The role of the extra-framework cations in the adsorption of CO2 on faujasite Y. Physical Chemistry Chemical Physics, 2010, 12, 13534.	1.3	117
9235	Zintl-phase compounds with<mml:math xmlns:mml="http://www.w3.org/1998/Math/MathML" display="inline"><mml:mrow><mml:msub><mml:mrow><mml:mtext>SnSb</mml:mtext></mml:mrow><mml:mn>4</mml:mn></mml:m anions: Electronic structure and thermoelectric properties. Physical Review B, 2010, 81, .	3.7	66
9236	Phase stability and mechanical properties of tungsten borides from first principles calculations. Physical Chemistry Chemical Physics, 2010, 12, 13158.	1.3	126
9237	Topography and work function measurements of thin MgO(001) films on Ag(001) by nc-AFM and KPFM. Physical Chemistry Chemical Physics, 2010, 12, 3203.	1.3	75
9238	Bidimensional versus tridimensional oxygen vacancy diffusion in SnO2â^'x under different gas environments. Physical Chemistry Chemical Physics, 2010, 12, 2401.	1.3	29

#	Article	IF	Citations
9239	Theoretical Study of H₂S Dissociation and Sulfur Oxidation on a W(111) Surface. Journal of Physical Chemistry C, 2010, 114, 19489-19495.	1.5	23
9240	Design of Superhard Ternary Compounds under High Pressure: SiC₂N₄and Si₂CN₄. Journal of Physical Chemistry C, 2010, 114, 8609-8613.	1.5	20
9241	Stabilization of a Complex Perovskite Superstructure under Ambient Conditions: Influence of Cation Composition and Ordering, and Evaluation as an SOFC Cathode. Chemistry of Materials, 2010, 22, 6598-6615.	3.2	19
9242	Modification of Au/TiO₂ Nanosystems by SiO₂ Monolayers: Toward the Control of the Catalyst Activity and Stability. Journal of Physical Chemistry C, 2010, 114, 2996-3002.	1.5	23
9243	Structural Stability and Electronic Properties of InAs Nanowires and Nanotubes: Effects of Surface and Size. Journal of Physical Chemistry C, 2010, 114, 17514-17518.	1.5	20
9244	Spin-Dependent Electronâ"Phonon Interaction in SmFeAsO by Low-Temperature Raman Spectroscopy. Journal of the American Chemical Society, 2010, 132, 15223-15227.	6.6	14
9245	Doping PbSe nanocrystals: Predictions based on a trapped-dopant model. Physical Review B, 2010, 81, .	1.1	14
9246	Electronic Conductivity and Stability of Doped Titania (Ti_{1â"X}M_XO₂, M = Nb, Ru, and Ta)â€"A Density Functional Theory-Based Comparison. Journal of Physical Chemistry C, 2010, 114, 13162-13167.	1.5	26
9247	Polarizable interatomic force field for<mml:math xmlns:mml="http://www.w3.org/1998/Math/MathML" display="inline"><mml:mrow><mml:msub><mml:mrow><mml:mtext>TiO</mml:mtext></mml:mrow><mml:mn>2</mml:mn></mml:msub></mml:mrow></mml:math>using density functional theory. Physical Review B, 2010, 81, .	1.1	27
9248	Trapping of multiple hydrogen atoms in a tungsten monovacancy from first principles. Physical Review B, 2010, 82, .	1.1	124
9249	Direct Measurement of the Attractive Interaction Forces on F⁰ Color Centers on MgO(001) by Dynamic Force Microscopy. ACS Nano, 2010, 4, 2510-2514.	7.3	29
9250	Density functional theory study of the high- and low-temperature phases of cubic iron sulfide. Physical Review B, 2010, 82, .	1.1	13
9251	Electron knock-on damage in hexagonal boron nitride monolayers. Physical Review B, 2010, 82, .	1.1	241
9252	Two bonding configurations for individually adsorbed<mml:math xmlns:mml="http://www.w3.org/1998/Math/MathML" display="inline"><mml:mrow><mml:msub><mml:mrow><mml:mtext>C</mml:mtext></mml:mrow><mml:mn>60</mml:mn></mml:msub></mml:mrow></mml:math>on Au(111). Physical Review B, 2010, 82, .	1.1	42
9253	Effects of substitutional impurity Au and Si atoms on antiphase boundary energies in Ti3Al: A first principles study. Philosophical Magazine, 2010, 90, 3919-3934.	0.7	3
9254	Two-dimensional carbon semiconductor: Density functional theory calculations. Physical Review B, 2010, 82, .	1.1	79
9255	High stability and electronic structures of noble-metal covered W(111) atom perfect pyramidal tips. Physical Review B, 2010, 81, .	1.1	5
9256	Understanding the role of structural disorder on spin polarization in<mml:math xmlns:mml="http://www.w3.org/1998/Math/MathML" display="inline"><mml:mrow><mml:msub><mml:mrow><mml:mtext>CeMnNi</mml:mtext></mml:mrow><mml:mn>4</mml:mn></mml:msub></mml:mrow></mml:math>XAFS. Physical Review B, 2010, 82, .	1.1	6

#	Article	IF	Citations
9257	Phonon-coupling enhanced absorption of alloyed amorphous silicon for solar photovoltaics. Physical Review B, 2010, 82, .	1.1	6
9258	Structural transformation and vibrational properties of<mml:math xmlns:mml="http://www.w3.org/1998/Math/MathML" display="inline"><mml:mrow><mml:msub><mml:mrow><mml:mtext>BaO</mml:mtext></mml:mrow><mml:mn>2</mml:mn></mml:msub></mml:mrow></mml:math> Electric and magnetic polarizabilities of hexagonal<mml:math xmlns:mml="http://www.w3.org/1998/Math/MathML"	1.1	18
9259			

#	Article	IF	Citations
9275	Gold cluster beyond hollow cage: A double shell structure of Au58. Journal of Chemical Physics, 2010, 132, 104301.	1.2	22
9276	Doping dependence of electronic and mechanical properties of<mml:math xmlns:mml="http://www.w3.org/1998/Math/MathML" display="inline"><mml:mrow><mml:msub><mml:mrow><mml:mtext>GaSe</mml:mtext></mml:mrow><mml:mrow><mml:mn>1</mml:mn></mml:mrow></mml:msub></mml:mrow></mml:math> xmlns:mml="http://www.w3.org/1998/Math/MathML" display="inline"><mml:mrow><mml:msub><mml:mrow><mml:mtext>. Physical Review B, 2010, 82, .	1.1	41
9277	Effects of spin-orbit coupling and strong correlation on the paramagnetic insulating state in plutonium dioxides. Physical Review B, 2010, 82, .	1.1	38
9278	Electronic transport properties of<mml:math xmlns:mml="http://www.w3.org/1998/Math/MathML" display="inline"><mml:mrow><mml:msub><mml:mrow><mml:mtext>SrTiO</mml:mtext></mml:mrow><mml:mrow><mml:mn>3</mml:mn></mml:mrow></mml:msub></mml:mrow></mml:math> its alloys:<mml:math xmlns:mml="http://www.w3.org/1998/Math/MathML" display="inline"><mml:mrow><mml:msub><mml:mrow><mml:mtext>Sr</mml:mtext></mml:mrow><mml:mrow><mml:mn>1</mml:mn></mml:mrow></mml:msub></mml:mrow></mml:math> Physical Review B, 2010, 82, .	1.1	45
9279	Spin-orbit effects in structural and electronic properties for the solid state of the group-14 elements from carbon to superheavy element 114. Physical Review B, 2010, 82, .	1.1	61
9280	Relativistic peculiarities at stepped surfaces: Energetics and diffusion patterns obtained fromab initiocalculations. Physical Review B, 2010, 82, .	1.1	3
9281	First-principles study of charge-density waves on Cu surfaces covered by In, Pb, and Bi atoms: Analysis of electronic structure and surface phonons. Physical Review B, 2010, 82, .	1.1	1
9282	Interaction of<mml:math xmlns:mml="http://www.w3.org/1998/Math/MathML" display="inline"><mml:mrow><mml:msub><mml:mrow><mml:mtext>O</mml:mtext></mml:mrow><mml:mrow><mml:mn>2</mml:mn></mml:mrow></mml:msub></mml:mrow></mml:math> xmlns:mml="http://www.w3.org/1998/Math/MathML" display="inline"><mml:mrow><mml:msub><mml:mrow><mml:mtext>H</mml:mtext></mml:mrow><mml:mrow><mml:mn>2</mml:mn></mml:mrow></mml:msub></mml:mrow></mml:math> xmlns:mml="http://www.w3.org/1998/Math/MathML" display="inline"><mml:mrow><mml:msub><mml:mrow><mml:mtext>N</mml:mtext></mml:mrow><mml:mrow><mml:mn>2</mml:mn></mml:mrow></mml:msub></mml:mrow></mml:math>. Physical Revi	1.1	24
9283	Nonconventional magnetism in pristine and alkali doped In2O3: Density functional study. Journal of Applied Physics, 2010, 108, .	1.1	29
9284	O 2 reduction by lithium on Au(111) and Pt(111). Journal of Chemical Physics, 2010, 133, 024703.	1.2	88
9285	Dissociation of methane under high pressure. Journal of Chemical Physics, 2010, 133, 144508.	1.2	101
9286	hcp metal nanoclusters with hexagonalAâ^'Abilayer stacking stabilized by enhanced covalent bonding. Physical Review B, 2010, 82, .	1.1	15
9287	Phase diagram up to 105 GPa and mechanical strength of<mml:math xmlns:mml="http://www.w3.org/1998/Math/MathML" display="inline"><mml:mrow><mml:msub><mml:mrow><mml:mtext>HfO</mml:mtext></mml:mrow><mml:mrow><mml:mn>2</mml:mn></mml:mrow></mml:msub></mml:mrow></mml:math> Physical Review B, 2010, 82, .	1.1	55
9288	Transmission electron microscopy and first-principles calculations of hydrogen ordering inÎ²-YH2+x. Physical Review B, 2010, 82, .	1.1	0
9289	First-principles thermodynamic modeling of atomic ordering in yttria-stabilized zirconia. Physical Review B, 2010, 82, .	1.1	28
9290	Gas adsorption and high-emission current induced degradation of field emission characteristics in solution-processed ZnO nanoneedles. Journal of Applied Physics, 2010, 108, 124318.	1.1	9
9292	Device characteristics of double-gate MOSFETs with Si-dielectric interface model from first principle calculations. , 2010, , .		0
9293	Structures of Pbn(n= 21â€“30) clusters from first-principles calculations. Journal of Physics Condensed Matter, 2010, 22, 465501.	0.7	5

#	Article	IF	Citations
9294	Segregation of Pt₂₈Rh₂₇bimetallic nanoparticles: a first-principles study. Journal of Physics Condensed Matter, 2010, 22, 245401.	0.7	21
9295	A first-principles study of H2O adsorption and dissociation on the SrTiO3(100) surface. Molecular Simulation, 2010, 36, 604-617.	0.9	21
9296	The crucial role of chemistry on mobile properties of dislocation. Philosophical Magazine, 2010, 90, 3757-3765.	0.7	0
9297	Electronic reconstruction and transport properties in SrTiO<inf>3</inf>/Sr<inf>1−x</inf>La<inf>x</inf>TiO<inf>3</inf> superlattice. , 2010, , .		0
9298	Investigation of structure and hydrogen bonding of superhydrous phase B (HT) under pressure using first-principles density functional calculations. High Pressure Research, 2010, 30, 198-206.	0.4	12
9299	First-Principles Study of the Adsorption of Water on Tri-s-triazine-based Graphitic Carbon Nitride. Japanese Journal of Applied Physics, 2010, 49, 115703.	0.8	59
9300	Tungsten oxides. II. The metallic nature of MagnÃ©li phases. Journal of Applied Physics, 2010, 108, .	1.1	101
9301	New insights into oxygen environments generated during phosphate glass alteration: a combined 17O MAS and MQMAS NMR and first principles calculations study. Physical Chemistry Chemical Physics, 2010, 12, 9053.	1.3	19
9302	Influence of dopants Ti and Ni on bonding interactions and dehydrogenation properties of lithium alanate. Physical Chemistry Chemical Physics, 2010, 12, 10942.	1.3	10
9303	Validation of dispersion-corrected density functional theory calculations for the crystal structure prediction of molecular salts: a crystal structure prediction study of pyridinium chloride. CrystEngComm, 2010, 12, 3827.	1.3	12
9304	First principles study of doped carbon supports for enhanced platinum catalysts. Physical Chemistry Chemical Physics, 2010, 12, 9461.	1.3	110
9305	Onset of diradical character in small nanosized graphene patches. Physical Chemistry Chemical Physics, 2010, 12, 9839.	1.3	30
9306	Enantiospecific adsorption of amino acids on hydroxylated quartz (10Ì„1)0). Physical Chemistry Chemical Physics, 2010, 12, 8024.	1.3	31
9307	Tuning magnetic properties of Mn4 cluster with gold coating. Physical Chemistry Chemical Physics, 2010, 12, 1493.	1.3	4
9308	Adsorption of DNA/RNA nucleobases on hexagonal boron nitride sheet: an ab initio study. Physical Chemistry Chemical Physics, 2011, 13, 12225.	1.3	96
9309	Molecular models for WH6 under pressure. New Journal of Chemistry, 2011, 35, 2349.	1.4	10
9310	Enhanced initial protein adsorption on engineered nanostructured cubic zirconia. Physical Chemistry Chemical Physics, 2011, 13, 6597.	1.3	30
9311	Ferroelectric phase transition in LiNbO<inf>3</inf>: Insights from molecular dynamics. , 2011, , .		0

#	Article	IF	Citations
9312	Titanium-decorated graphene oxide for carbon monoxide capture and separation. Physical Chemistry Chemical Physics, 2011, 13, 21126.	1.3	52
9313	The Zintl ion [As7]2â^': an example of an electron-deficient Asx radical anion. Chemical Communications, 2011, 47, 3126.	2.2	18
9314	Self-limited oxygen exchange kinetics at SnO2 surfaces. Physical Chemistry Chemical Physics, 2011, 13, 3223.	1.3	18
9315	H atom adsorption and diffusion on Si(110)-(1Ã—1) and (2Ã—1) surfaces. Physical Chemistry Chemical Physics, 2011, 13, 11367.	1.3	8
9316	First-principles study of electronic and magnetic properties of transition metal adsorbed h-BNC2 sheets. Physical Chemistry Chemical Physics, 2011, 13, 21593.	1.3	11
9317	Band gap engineering of double-cation-impurity-doped anatase-titania for visible-light photocatalysts: a hybrid density functional theory approach. Physical Chemistry Chemical Physics, 2011, 13, 13698.	1.3	39
9318	Modified Naples yellow in Renaissance majolica: study of Pbâ€“Sbâ€“Zn and Pbâ€“Sbâ€“Fe ternary pyroantimonates by X-ray absorption spectroscopy. Journal of Analytical Atomic Spectrometry, 2011, 26, 2500.	1.6	39
9319	The importance of ion size and electrode curvature on electrical double layers in ionic liquids. Physical Chemistry Chemical Physics, 2011, 13, 1152-1161.	1.3	173
9320	Epitaxial growth of diindenoperylene ultrathin films on Ag(111) investigated by LT-STM and LEED. Physical Chemistry Chemical Physics, 2011, 13, 20933.	1.3	17
9321	Computing the 7Li NMR chemical shielding of hydrated Li+ using cluster calculations and time-averaged configurations from ab initio molecular dynamics simulations. Physical Chemistry Chemical Physics, 2011, 13, 13629.	1.3	36
9322	Nitrogen/gold codoping of the TiO2(101) anatase surface. A theoretical study based on DFT calculations. Physical Chemistry Chemical Physics, 2011, 13, 11340.	1.3	38
9323	CdS:Co diluted magnetic semiconductor nanocrystals: synthesis and ferromagnetism study. CrystEngComm, 2011, 13, 5646.	1.3	40
9324	Silica hollow nanospheres as new nanoscaffold materials to enhance hydrogen releasing from ammonia borane. Physical Chemistry Chemical Physics, 2011, 13, 18592.	1.3	37
9325	Properties of self-assembled Bi nanolines on InAs(100) studied by core-level and valence-band photoemission, and first-principles calculations. Physical Review B, 2011, 83, .	1.1	9
9326	Raman evidence for the superconducting gap and spinâ€“phonon coupling in the superconductor Ca(Fe_{0.95}Co_{0.05})₂As₂. Journal of Physics Condensed Matter, 2011, 23, 255403.	0.7	9
9327	Molecular-Scale Structure of a Nitrobenzene Monolayer on Si(001). Journal of Physical Chemistry C, 2011, 115, 3011-3017.	1.5	6
9328	Behavior of Li Guest in KNb₅O₁₃ Host with One-Dimensional Tunnels and Multiple Interstitial Sites. Chemistry of Materials, 2011, 23, 3210-3216.	3.2	17
9329	Role of Long-Range Intermolecular Forces in the Formation of Inorganic Nanoparticle Clusters. Journal of Physical Chemistry A, 2011, 115, 12933-12940.	1.1	20

#	Article	IF	Citations
9330	Surface Structure and Environment-Dependent Hydroxylation of the Nonpolar Hematite (100) from Density Functional Theory Modeling. Journal of Physical Chemistry C, 2011, 115, 23023-23029.	1.5	21
9331	Mechanisms of Ion-Beam Modification of Terthiophene Oligomers from Atomistic Simulations. Journal of Physical Chemistry C, 2011, 115, 23936-23945.	1.5	6
9332	Nonspectral Methods for Solving the SchrÃ¶dinger Equation for Electronic and Vibrational Problems. Journal of Physical Chemistry Letters, 2011, 2, 2193-2199.	2.1	11
9333	Graphene Actuators: Quantum-Mechanical and Electrostatic Double-Layer Effects. Journal of the American Chemical Society, 2011, 133, 10858-10863.	6.6	101
9334	Pyridine Adsorption on Single-Layer Iron Phthalocyanine on Au(111). Journal of Physical Chemistry C, 2011, 115, 20201-20208.	1.5	34
9335	Adsorption and Diffusion of Fructose in Zeolite HZSM-5: Selection of Models and Methods for Computational Studies. Journal of Physical Chemistry C, 2011, 115, 21785-21790.	1.5	30
9336	Chemical Raman Enhancement of Organic Adsorbates on Metal Surfaces. Physical Review Letters, 2011, 106, 083003.	2.9	123
9337	On the Nature of the Spin Frustration in the CuO₂ Ribbon Chains of LiCuVO₄: Crystal Structure Determination at 1.6 K, Magnetic Susceptibility Analysis, and Density Functional Evaluation of the Spin Exchange Constants. Inorganic Chemistry, 2011, 50, 3582-3588.	1.9	29
9338	Perpendicular growth of carbon chains on graphene from first-principles. Physical Review B, 2011, 83, .	1.1	44
9339	Interaction between NO and Na, O, S, Cl on Au and Pd(111) surfaces. Physical Chemistry Chemical Physics, 2011, 13, 14466.	1.3	10
9340	Self assembled CdLa₂S₄hexagon flowers, nanoprisms and nanowires: novel photocatalysts for solar hydrogen production. Journal of Materials Chemistry, 2011, 21, 2624-2631.	6.7	40
9341	Intrinsic defects and dopants in LiNH2: a first-principles study. Physical Chemistry Chemical Physics, 2011, 13, 6043.	1.3	15
9342	Examining the robustness of first-principles calculations for metal hydride reaction thermodynamics by detection of metastable reaction pathways. Physical Chemistry Chemical Physics, 2011, 13, 21520.	1.3	14
9343	Exploring the structure and chemical activity of 2-D gold islands on graphene moirÃ©/Ru(0001). Faraday Discussions, 2011, 152, 267.	1.6	37
9344	Structural and electronic properties of graphene nanotubeâ€“nanoribbon hybrids. Physical Chemistry Chemical Physics, 2011, 13, 3925.	1.3	7
9345	Experimental verification of a subtle low-temperature phase transition suggested by DFT-D energy minimisation. CrystEngComm, 2011, 13, 1768.	1.3	12
9346	Morphology mapping of platinum catalysts over the entire nanoscale. Catalysis Science and Technology, 2011, 1, 1440.	2.1	26
9347	From Single to Multiple Ag-Layer Modification of Au Nanocavity Substrates: A Tunable Probe of the Chemical Surface-Enhanced Raman Scattering Mechanism. ACS Nano, 2011, 5, 5433-5443.	7.3	37

#	Article	IF	Citations
9348	Physical Properties of Thalliumâ€“Tellurium Based Thermoelectric Compounds Using First-Principles Simulations. Journal of Physical Chemistry A, 2011, 115, 8761-8766.	1.1	25
9349	Enhanced Deseleniumization of Selenophene Molecules Adsorbed on Si(100)-2 Ã— 1 Surface. Journal of Physical Chemistry C, 2011, 115, 17856-17860.	1.5	4
9350	Syntheses, Structures, and Magnetic and Thermoelectric Properties of Double-Tunnel Tellurides: A_xRE₂Cu_{6â€“x}Te₆ (A = Kâ€“Cs; RE = Laâ€“Nd). Chemistry of Materials, 2011, 23, 4910-4919.	3.2	38
9351	Replacing Platinum with Tungsten Carbide (WC) for Reforming Reactions: Similarities in Ethanol Decomposition on Ni/Pt and Ni/WC Surfaces. ACS Catalysis, 2011, 1, 390-398.	5.5	44
9352	Site- and Configuration-Selective Anchoring of Ironâ€“Phthalocyanine on the Step Edges of Au(111) Surface. Journal of Physical Chemistry C, 2011, 115, 10791-10796.	1.5	31
9353	Interplay between structure, stoichiometry and properties of technetium nitrides. Dalton Transactions, 2011, 40, 6738.	1.6	20
9354	The isomeric effect on the adjacent Si dimer didechlorination of trans and iso-dichloroethylene on Si(100)-2Ã—1. Physical Chemistry Chemical Physics, 2011, 13, 7121.	1.3	2
9355	Chemically reactive species remain alive inside carbon nanotubes: a density functional theory study. Physical Chemistry Chemical Physics, 2011, 13, 337-346.	1.3	17
9356	Tunable electrical and magnetic properties of half-metallic ZnxFe3â^'xO4 from first principles. Physical Chemistry Chemical Physics, 2011, 13, 21243.	1.3	21
9357	Interlayer interaction and relative vibrations of bilayer graphene. Physical Chemistry Chemical Physics, 2011, 13, 5687.	1.3	149
9358	Theoretical study of the vibrational properties of NaAlH4 with AlH3 vacancies. Faraday Discussions, 2011, 151, 243.	1.6	2
9359	Electronic<mml:math xmlns:mml="http://www.w3.org/1998/Math/MathML" display="inline"><mml:mrow><mml:mi>d</mml:mi></mml:mrow></mml:math>-band properties of gold nanoclusters grown on amorphous carbon. Physical Review B, 2011, 83, .	1.1	50
9360	Multi scale modeling of multi phonon hole capture in the context of NBTI. , 2011, , .		3
9361	Multilevel simulation for the investigation of fast diffusivity paths. , 2011, , .		0
9362	Dissipative dynamics within the electronic friction approach: the femtosecond laser desorption of H2/D2 from Ru(0001). Physical Chemistry Chemical Physics, 2011, 13, 8659.	1.3	63
9363	Modelling moleculeâ€“surface interactionsâ€”an automated quantum-classical approach using a genetic algorithm. Physical Chemistry Chemical Physics, 2011, 13, 10577.	1.3	14
9364	Low-temperature hydrogenation of the Cî€O bond of propanal over Niâ€“Pt bimetallic catalysts: from model surfaces to supported catalysts. Catalysis Science and Technology, 2011, 1, 638.	2.1	22
9365	The structural evolution and diffusion during the chemical transformation from cobalt to cobalt phosphide nanoparticles. Journal of Materials Chemistry, 2011, 21, 11498.	6.7	136

#	Article	IF	Citations
9366	Effects of deposited Pt particles on the reducibility of CeO2(111). Physical Chemistry Chemical Physics, 2011, 13, 11384.	1.3	89
9367	Dynamic factors in the reactions between the magic cluster Alâ˜'13 and HCl/HI. Physical Chemistry Chemical Physics, 2011, 13, 9871.	1.3	5
9368	Beryllium and boron decoration forms planar tetracoordinate carbon strips at the edge of graphene nanoribbons. Physical Chemistry Chemical Physics, 2011, 13, 2732-2737.	1.3	19
9369	Crystal-structure prediction of pyridine with four independent molecules. CrystEngComm, 2011, 13, 7135.	1.3	28
9370	Buried Pd slows self-diffusion on Cu(001). Physical Review B, 2011, 84, .	1.1	6
9371	Ab initio study of lithium transition metal fluorophosphate cathodes for rechargeable batteries. Journal of Materials Chemistry, 2011, 21, 12054.	6.7	18
9372	Vibrations of a single adsorbed organic molecule: anharmonicity matters!. Physical Chemistry Chemical Physics, 2011, 13, 612-618.	1.3	21
9373	The role of long-lived oxygen precursors on AuM alloys (M = Ni, Pd, Pt) in CO oxidation. Physical Chemistry Chemical Physics, 2011, 13, 5790.	1.3	23
9374	The effect of host relaxation and dynamics on guest molecule dynamics in H2/tetrahydrofuran-hydrate. Faraday Discussions, 2011, 151, 37.	1.6	5
9375	Trends in water monomer adsorption and dissociation on flat insulating surfaces. Physical Chemistry Chemical Physics, 2011, 13, 12447.	1.3	40
9376	Electronic structure of pyridine-based SAMs on flat Au(111) surfaces: extended charge rearrangements and Fermi level pinning. Physical Chemistry Chemical Physics, 2011, 13, 9747.	1.3	26
9377	Throwing jellium at galliumâ€"a systematic superatom analysis of metalloid gallium clusters. Physical Chemistry Chemical Physics, 2011, 13, 21109.	1.3	28
9378	Effect of transition metal (M = Co, Ni, Cu) substitution on electronic structure and vacancy formation of Li₃N. Journal of Materials Chemistry, 2011, 21, 165-170.	6.7	11
9379	Density functional theory investigation of the phonon instability, thermal equation of state and melting curve of Mo. Physical Chemistry Chemical Physics, 2011, 13, 1669-1675.	1.3	16
9380	The mechanism of the water-gas shift reaction on Cu/TiO2(110) elucidated from application of density-functional theory. Physical Chemistry Chemical Physics, 2011, 13, 20393.	1.3	20
9381	Dynamics of scattering and dissociative adsorption on a surface alloy: H2/W(100)-c(2 Ã— 2)Cu. Physical Chemistry Chemical Physics, 2011, 13, 4614.	1.3	7
9382	Interstitialcy diffusion of oxygen in tetragonal La₂CoO₄₊Î´. Physical Chemistry Chemical Physics, 2011, 13, 2242-2249.	1.3	104
9383	The role of low-coordinate oxygen on Co₃O₄(110) in catalyticCO oxidation. Physical Chemistry Chemical Physics, 2011, 13, 978-984.	1.3	121

#	Article	IF	Citations
9384	The active site structure of nitrided and oxynitrided graphite as a cathode catalyst in a fuel cell. Physical Chemistry Chemical Physics, 2011, 13, 2659-2662.	1.3	13
9385	Effective increasing of optical absorption and energy conversion efficiency of anatase TiO2 nanocrystals by hydrogenation. Physical Chemistry Chemical Physics, 2011, 13, 18063.	1.3	92
9386	Ab initiobased determination of thermodynamic properties of cementite including vibronic, magnetic, and electronic excitations. Physical Review B, 2011, 84, .	1.1	57
9387	Fast computation of DFT nuclear gradient with multiresolution*This article is dedicated to Dr. Russell J. Boyd for his distinguished career in chemical research.. Canadian Journal of Chemistry, 2011, 89, 657-662.	0.6	3
9388	The Adsorption Properties of Cu and Ni on the Ceria(111) Surface. Advanced Materials Research, 2011, 213, 166-171.	0.3	5
9389	B ₂ CO: A potential superhard material in the B-C-O system. Europhysics Letters, 2011, 95, 66006.	0.7	37
9390	A kinetic Monte Carlo study of Pt on Au(111) with applications to bimetallic catalysis. Journal of Physics Condensed Matter, 2011, 23, 015302.	0.7	3
9391	Theoretical Study on Electronic Structure and Conductivity of Y-Doped ZnO. , 2011, , .		2
9392	Computational Discovery of Hydrogen Storage Compounds. , 2011, , 481-502.		0
9393	Phase stability, point defects, and elastic properties of W-V and W-Ta alloys. Physical Review B, 2011, 84, .	1.1	139
9394	Phonon softening and metallization of a narrow-gap semiconductor by thermal disorder. Proceedings of the National Academy of Sciences of the United States of America, 2011, 108, 4725-4730.	3.3	96
9395	Design of ferromagnetism in Cu-doped ZnO nanowires: First-principles prediction. Europhysics Letters, 2011, 95, 47011.	0.7	17
9396	Application of graphene in tandem organic solar cells. , 2011, , .		0
9397	First-principles studies of Ce-doped RE2M2O7 (REâ€‰=â€‰Y, La; Mâ€‰=â€‰Ti, Zr, Hf): A class of nonscintillators. Journal of Applied Physics, 2011, 109, .	1.1	38
9398	GeSn technology: Extending the Ge electronics roadmap. , 2011, , .		84
9399	Induced Magnetoelectric Response in<mml:math xmlns:mml="http://www.w3.org/1998/Math/MathML" display="inline"><mml:mi>P</mml:mi><mml:mi>n</mml:mi><mml:mi>m</mml:mi><mml:mi>a</mml:mi></mml:math>-Perovskites. Physical Review Letters, 2011, 107, 197603.	7.6	58
9400	Intermolecular bridges and carrier traps in defective C<mml:math xmlns:mml="http://www.w3.org/1998/Math/MathML" display="inline"><mml:msub><mml:mrow /><mml:mn>60</mml:mn></mml:msub></mml:math>crystals. Physical Review B, 2011, 84, .	1.1	15
9401	Strain-tunable band gap of hydrogenated bilayer graphene. New Journal of Physics, 2011, 13, 063047.	1.2	19

#	Article	IF	Citations
9402	<mml:math xmlns:mml="http://www.w3.org/1998/Math/MathML" display="inline"><mml:mi>c</mml:mi><mml:mo stretchy="false">(</mml:mo><mml:mn>2</mml:mn><mml:mo>Ã—</mml:mo><mml:mn>2</mml:mn><mml:mo) TJETQq0 0 0 rgBT /Ov	2.5	0
9403	Intrinsic stoichiometry and oxygen-induced <mml:math xmlns:mml="http://www.w3.org/1998/Math/MathML" display="inline"><mml:mi>p</mml:mi></mml:math>-type conductivity of pyrite FeS<mml:math xmlns:mml="http://www.w3.org/1998/Math/MathML" display="inline"><mml:msub><mml:mrow /><mml:mn>2</mml:mn></mml:msub></mml:math>. Physical Review B, 2011, 84, .	1.1	65
9404	Including many-body screening into self-consistent calculations: Tight-binding model studies with the Gutzwiller approximation. Physical Review B, 2011, 83, .	1.1	20
9405	Twinning in bcc metals under shock loading: a challenge to empirical potentials. Philosophical Magazine Letters, 2011, 91, 731-740.	0.5	54
9406	Multiscale Modelling in Computational Heterogeneous Catalysis. Topics in Current Chemistry, 2011, 307, 69-107.	4.0	48
9407	Microstructure, optical property, and electronic band structure of cuprous oxide thin films. Journal of Applied Physics, 2011, 110, .	1.1	45
9408	Intrinsic defects and electronic conductivity of TaON: First-principles insights. Applied Physics Letters, 2011, 99, .	1.5	34
9409	Origin of charge separation in III-nitride nanowires under strain. Applied Physics Letters, 2011, 99, 262103.	1.5	6
9410	Oxygen Reduction by Lithium on Model Carbon and Oxidized Carbon Structures. Journal of the Electrochemical Society, 2011, 158, A1177.	1.3	66
9411	Promotion of water-mediated carbon removal by nanostructured barium oxide/nickel interfaces in solid oxide fuel cells. Nature Communications, 2011, 2, 357.	5.8	280
9412	Extended Lagrangian free energy molecular dynamics. Journal of Chemical Physics, 2011, 135, 164111.	1.2	19
9413	Electronic, optical, and mechanical properties of superhard cold-compressed phases of carbon. Applied Physics Letters, 2011, 99, .	1.5	68
9414	Electronic structure of oxygen-vacancy defects in amorphous In-Ga-Zn-O semiconductors. Physical Review B, 2011, 84, .	1.1	253
9415	The crystal structure of Â-Al(OH)3: Neutron diffraction measurements and ab initio calculations. American Mineralogist, 2011, 96, 854-859.	0.9	15
9416	A theoretical study of bipolar organic transport material: Disilanyl double-pillared bisanthracene (^{Si}DPBA). Canadian Journal of Chemistry, 2011, 89, 1257-1263.	0.6	0
9417	Theoretical Study of Electronâ€“Phonon Relaxation in PbSe and CdSe Quantum Dots: Evidence for Phonon Memory. Journal of Physical Chemistry C, 2011, 115, 21641-21651.	1.5	60
9418	Improved Stability and Catalytic Properties of Au16 Cluster Supported on Graphane. Journal of Physical Chemistry C, 2011, 115, 20168-20174.	1.5	38
9419	Ab Initio Study on the Size and Chirality Effects on the Encapsulation of Tetrafluorotetracyano-p-quinodimethane inside Carbon Nanotubes. Journal of Physical Chemistry C, 2011, 115, 5280-5285.	1.5	4

#	Article	IF	Citations
9420	First-Principles Study of H⁺ Intercalation in Layer-Structured LiCoO₂. Journal of Physical Chemistry C, 2011, 115, 12672-12676.	1.5	70
9421	Analysis of the Alloying System in Ni-Base Superalloys Based on <i>Ab Initio</i> Study of Impurity Segregation to Ni Grain Boundary. Advanced Materials Research, 0, 278, 192-197.	0.3	18
9422	Connecting the Chemical and Physical Viewpoints of What Determines Structure: From 1-D Chains to Î³-Brasses. Chemical Reviews, 2011, 111, 4522-4545.	23.0	50
9423	First-Principles Study of Isomorphic (â€˜Dual-Defectâ€™) Substitution in Kaolinite. Clays and Clay Minerals, 2011, 59, 501-506.	0.6	11
9424	Transition-metal 13-atom clusters assessed with solid and surface-biased functionals. Journal of Chemical Physics, 2011, 134, 134105.	1.2	27
9425	Comparison of the Carbonyl and Nitrosyl Complexes Formed by Adsorption of CO and NO on Monolayers of Iron Phthalocyanine on Au(111). Journal of Physical Chemistry C, 2011, 115, 24718-24727.	1.5	49
9426	Polarization and Electric Field Dependence of Electronic Properties in LaAlO₃/SrTiO₃ Heterostructures. ACS Applied Materials & Interfaces, 2011, 3, 3819-3823.	4.0	14
9427	Site Specific Optical and Photocatalytic Properties of Bi-Doped NaTaO₃. Journal of Physical Chemistry C, 2011, 115, 11846-11853.	1.5	71
9428	Toward Functional Inorganic/Organic Hybrids: Phenoxy-allyl-PTCDI Synthesis, Experimentally and Theoretically Determined Properties of the Isolated Molecule, Layer Characteristics, and the Interface Formation of Phenoxy-allyl-PTCDI on Si(111):H Determined by SXPS and DFT. Journal of Physical Chemistry C, 2011, 115, 21139-21150.	1.5	5
9429	Passivation of Metal Surface States: Microscopic Origin for Uniform Monolayer Graphene by Low Temperature Chemical Vapor Deposition. ACS Nano, 2011, 5, 1915-1920.	7.3	58
9430	Nature of Pt_n/TiO₂(110) Interface under Water-Gas Shift Reaction Conditions: A Constrained ab Initio Thermodynamics Study. Journal of Physical Chemistry C, 2011, 115, 19246-19259.	1.5	44
9431	Formation, Morphology, and Effect of Complex Defects in Boron Nitride Nanotubes: An ab initio Calculation. Journal of Physical Chemistry C, 2011, 115, 12782-12788.	1.5	7
9432	Evaluation of the Role of Au in Improving Catalytic Activity of Ni Nanoparticles for the Formation of One-Dimensional Carbon Nanostructures. Nano Letters, 2011, 11, 2464-2471.	4.5	52
9433	Direct Diffusion through Interpenetrating Networks: Oxygen in Titanium. Physical Review Letters, 2011, 107, 045504.	2.9	102
9434	Deposition of Nonstoichiometric Tritungsten Oxides on the TiO₂(110) Surface: A Possible Way to Stabilize the Unstable Clusters in the Gas Phase. Journal of Physical Chemistry C, 2011, 115, 15335-15344.	1.5	8
9435	Charge Localization and Transport in Lithiated Olivine Phosphate Materials. Journal of Physical Chemistry C, 2011, 115, 25001-25006.	1.5	23
9436	The First-Cycle Electrochemical Lithiation of Crystalline Ge: Dopant and Orientation Dependence and Comparison with Si. Journal of Physical Chemistry Letters, 2011, 2, 3092-3095.	2.1	48
9437	First-Principles Study of the Doping of InAs Nanowires: Role of Surface Dangling Bonds. Journal of Physical Chemistry C, 2011, 115, 14449-14454.	1.5	30

#	Article	IF	Citations
9438	Mechanics and Chemistry: Single Molecule Bond Rupture Forces Correlate with Molecular Backbone Structure. Nano Letters, 2011, 11, 1518-1523.	4.5	129
9439	Experimental and Computational Study of Functionality Impact on Sodaliteâ€“Zeolitic Imidazolate Frameworks for CO₂Separation. Journal of Physical Chemistry C, 2011, 115, 16425-16432.	1.5	128
9440	Large-Scale Patterning of Zwitterionic Molecules on a Si(111)-7â€‰Ã—â€‰7 Surface. ACS Nano, 2011, 5, 424-428.	8.3	12
9441	Confinement-Induced Polymerization of Ethylene. Journal of Physical Chemistry C, 2011, 115, 2134-2139.	1.5	8
9442	Interaction of BrPDI, BrGly, and BrAsp with the Rutile TiO2(110) Surface for Photovoltaic and Photocatalytic Applications: A First-Principles Study. Journal of Physical Chemistry C, 2011, 115, 9220-9226.	1.5	7
9443	Electronic structure and phonons in La<mml:math xmlns:mml="http://www.w3.org/1998/Math/MathML" display="inline"><mml:msub><mml:mrow /><mml:mn>2</mml:mn></mml:msub></mml:math>CoMnO<mml:math xmlns:mml="http://www.w3.org/1998/Math/MathML" display="inline"><mml:msub><mml:mrow /><mml:mn>6</mml:mn></mml:msub></mml:math>: A ferromagnetic insulator driven by Coulomb-assisted spin-orbit coupling. Physical Review B, 2011, 84, .	1.1	64
9444	CO Oxidation on Inverse CeO_x/Cu(111) Catalysts: High Catalytic Activity and Ceria-Promoted Dissociation of O₂. Journal of the American Chemical Society, 2011, 133, 3444-3451.	6.6	241
9445	The electronic and structural properties of novel organomodified Si nanosheets. Physical Chemistry Chemical Physics, 2011, 13, 15418.	1.3	35
9446	Structural and thermodynamic properties of liquid Na-Li and Ca-Li alloys at high pressure. Physical Review B, 2011, 83, .	1.1	18
9447	Resistive switching mechanisms in random access memory devices incorporating transition metal oxides: TiO₂, NiO and Pr_{0.7}Ca_{0.3}MnO₃. Nanotechnology, 2011, 22, 254029.	1.3	65
9448	Band Gap Opening by Two-Dimensional Manifestation of Peierls Instability in Graphene. ACS Nano, 2011, 5, 2964-2969.	7.3	70
9449	Ternary tetradymite compounds as topological insulators. Physical Review B, 2011, 83, .	1.1	81
9450	Density Functional Theory Study of O₂ and NO Adsorption on Heteroatom-Doped Graphenes Including the van der Waals Interaction. Journal of Physical Chemistry C, 2011, 115, 10971-10978.	1.5	34
9451	Antiferromagnetic superexchange via <mml:math xmlns:mml="http://www.w3.org/1998/Math/MathML" display="inline"><mml:mrow><mml:mn>3</mml:mn><mml:mi>d</mml:mi></mml:mrow></mml:math> states of titanium in EuTiO<mml:math xmlns:mml="http://www.w3.org/1998/Math/MathML" display="inline"><mml:mrow><mml:msub><mml:mrow /><mml:mrow><mml:mn>3</mml:mn></mml:mrow></mml:msub></mml:mrow></mml:math> as seen from hybrid Hartree-Fock density functional calculations. Physical Review B, 2011, 83, .	1.1	104
9452	Equilibrium and metastable phase transitions in silicon nitride at high pressure: A first-principles and experimental study. Physical Review B, 2011, 84, .	1.1	35
9453	Novel High-Pressure Phase of RhB: First-Principles Calculations. Journal of Physical Chemistry C, 2011, 115, 19910-19915.	1.5	16
9454	Quasi-one-dimensional antiferromagnetism and multiferroicity in CuCrO<mml:math xmlns:mml="http://www.w3.org/1998/Math/MathML" display="inline"><mml:msub><mml:mrow /><mml:mn>4</mml:mn></mml:msub></mml:math>. Physical Review B, 2011, 84, .	1.1	28
9455	First-Principles Study of the Structural, Electronic, and Optical Properties of Oxide-Sheathed Silicon Nanowires. ACS Nano, 2011, 5, 1713-1723.	7.3	20

#	Article	IF	Citations
9456	Phase stabilization in nitrogen-implanted nanocrystalline cubic zirconia. Physical Chemistry Chemical Physics, 2011, 13, 19517.	1.3	15
9457	Epitaxial Strain-Induced Chemical Ordering in La0.5Sr0.5CoO3â˜Î´Films on SrTiO3. Chemistry of Materials, 2011, 23, 984-988.	3.2	80
9458	DFT study of propane dehydrogenation on Pt catalyst: effects of step sites. Physical Chemistry Chemical Physics, 2011, 13, 3257.	1.3	173
9459	Ab initiostudy of IIâ€“(VI)₂dichalcogenides. Journal of Physics Condensed Matter, 2011, 23, 405801.	0.7	13
9460	Stability of the hydrogen-storage compound Li6Mg(NH)4from first principles. Physical Review B, 2011, 83, .	1.1	2
9461	Geometric and magnetic properties of Pt clusters supported on graphene: Relativistic density-functional calculations. Journal of Chemical Physics, 2011, 134, 154705.	1.2	60
9462	Hybrid DFT Functional-Based Static and Molecular Dynamics Studies of Excess Electron in Liquid Ethylene Carbonate. Journal of the Electrochemical Society, 2011, 158, A400.	1.3	71
9463	Electronic structure and transport properties of doped PbSe. Physical Review B, 2011, 84, .	1.1	53
9464	Ab initioInvestigations of Fe2+/Fe3+Bond Dimerization and Ferroelectricity Induced by Intermediate Site/Bond-Centered Charge Ordering in Magnetite. Journal of the Physical Society of Japan, 2011, 80, 014709.	0.7	10
9465	Properties of epitaxial (110) BaTiO<mml:math xmlns:mml="http://www.w3.org/1998/Math/MathML" display="inline"><mml:msub><mml:mrow /><mml:mn>3</mml:mn></mml:msub></mml:math>films from first principles. Physical Review B, 2011, 84, .	1.1	29
9466	Thermal Stability of Corrugated Epitaxial Graphene Grown on Re(0001). Physical Review Letters, 2011, 106, 216101.	2.9	106
9467	To Wet or Not to Wet? Dispersion Forces Tip the Balance for Water Ice on Metals. Physical Review Letters, 2011, 106, 026101.	2.9	159
9468	Density functional theory investigations of the structural and electronic properties of Ag<mml:math xmlns:mml="http://www.w3.org/1998/Math/MathML" display="inline"><mml:mrow><mml:msub><mml:mrow /><mml:mrow><mml:mn>2</mml:mn></mml:mrow></mml:msub></mml:mrow></mml:math>V<mml:math xmlns:mml="http://www.w3.org/1998/Math/MathML" display="inline"><mml:mrow><mml:msub><mml:mrow /><mml:mrow><mml:mn>4</mml:mn></mml:mrow></mml:msub></mml:mrow></mml:math>O	1.1	27
9469	Tailoring the Structure of Water at a Metal Surface: A Structural Analysis of the Water Bilayer Formed on an Alloy Template. Physical Review Letters, 2011, 106, 226101.	2.9	37
9470	Understanding Acetaldehyde Thermal Chemistry on the TiO₂ (110) Rutile Surface: From Adsorption to Reactivity. Journal of Physical Chemistry C, 2011, 115, 2819-2825.	1.5	22
9471	Unveiling the complex electronic structure of amorphous metal oxides. Proceedings of the National Academy of Sciences of the United States of America, 2011, 108, 6355-6360.	3.3	102
9472	An ab Initio Investigation of Hydrogen Adsorption in Li-Dopedcloso-Boranes. Journal of Physical Chemistry C, 2011, 115, 1450-1456.	1.5	40
9473	Stability of Î²-Mo₂C Facets from ab Initio Atomistic Thermodynamics. Journal of Physical Chemistry C, 2011, 115, 22360-22368.	1.5	108

#	Article	IF	Citations
9474	Electron and Electrostatic Properties of Three Crystal Forms of Piracetam. Crystal Growth and Design, 2011, 11, 2528-2539.	1.4	11
9475	Single-ion anisotropy, Dzyaloshinskii-Moriya interaction, and negative magnetoresistance of the spin-<mml:math xmlns:mml="http://www.w3.org/1998/Math/MathML" display="inline"><mml:mrow><mml:mfrac><mml:mrow><mml:mn>1</mml:mn></mml:mrow><mml:mrow><mml:mn>2</mml:mn></ xmlns:mml="http://www.w3.org/1998/Math/MathML" display="inline"><mml:mrow><mml:msub><mml:mi>R</mml:mi><mml:mrow><mml:mn>2</mml:mn></mml:mrow></mml:msub></m Physical Review B, 2011, 83, .	1.1	39
9476	Surface and Electronic Properties of Hydrogen Terminated Si [001] Nanowires. Journal of Physical Chemistry C, 2011, 115, 12586-12591.	1.5	6
9477	Advanced methods for the analysis of x-ray absorption spectroscopy data applied to semiconductors. Semiconductor Science and Technology, 2011, 26, 064004.	1.0	15
9478	Adsorption of Zn²⁺ on the (110) Surface of TiO₂ (Rutile): A Density Functional Molecular Dynamics Study. Journal of Physical Chemistry C, 2011, 115, 9608-9614.	1.5	12
9479	Effects of reduced dimensionality on the electronic structure and defect chemistry of semiconducting hybrid organicâ€“inorganic PbS solids. Proceedings of the Royal Society A: Mathematical, Physical and Engineering Sciences, 2011, 467, 1970-1985.	1.0	23
9480	DFT Study of 1,3-Dimethylimidazolium Tetrafluoroborate on Al and Cu(111) Surfaces. Journal of Physical Chemistry C, 2011, 115, 14718-14730.	1.5	19
9481	Local defects enhanced dehydrogenation kinetics of the NaBH4-added Liâ€“Mgâ€“Nâ€“H system. Physical Chemistry Chemical Physics, 2011, 13, 314-321.	1.3	34
9482	Density Functional Calculations to Study the Mechanism of the Fischerâ€“Tropsch Reaction on Fe(111) and W(111) Surfaces. Journal of Physical Chemistry C, 2011, 115, 11045-11055.	1.5	36
9483	Properties of Benzene Confined between Two Au(111) Surfaces Using a Combined Density Functional Theory and Classical Molecular Dynamics Approach. Journal of Physical Chemistry C, 2011, 115, 14707-14717.	1.5	33
9484	Graphyne- and graphdiyne-based nanoribbons: Density functional theory calculations of electronic structures. Applied Physics Letters, 2011, 98, .	1.5	277
9485	Versatile Electronic and Magnetic Properties of Corrugated V₂O₅ Two-Dimensional Crystal and Its Derived One-Dimensional Nanoribbons: A Computational Exploration. Journal of Physical Chemistry C, 2011, 115, 11983-11990.	1.5	33
9486	High-pressure Raman spectroscopy and lattice-dynamics calculations on scintillating MgWO<mml:math xmlns:mml="http://www.w3.org/1998/Math/MathML" display="inline"><mml:mrow><mml:msub><mml:mrow /><mml:mrow><mml:mn>4</mml:mn></mml:mrow></mml:msub></mml:mrow></mml:math>: Comparison with isomorphic compounds. Physical Review B, 2011, 83, .	1.1	78
9487	Theoretical study of structural, mechanical and spectroscopic properties of boehmite (Î³-AlOOH). Journal of Physics Condensed Matter, 2011, 23, 404201.	0.7	18
9488	Actinide Dioxides in Water: Interactions at the Interface. Journal of Physical Chemistry Letters, 2011, 2, 3130-3134.	2.1	38
9489	Hydrated Magnesium Cations Mg⁺(H₂O)_n, n â‰ˆ 20â€“60, Exhibit Chemistry of the Hydrated Electron in Reactions with O₂ and CO₂. Journal of Physical Chemistry A, 2011, 115, 10174-10180.	1.1	37
9490	Tuning Magnetism in Transition-Metal-Doped 3C Silicon Carbide Polytype. Journal of Physical Chemistry C, 2011, 115, 253-256.	1.5	28
9491	Interaction of Water with FeO(111)/Pt(111): Environmental Effects and Influence of Oxygen. Journal of Physical Chemistry C, 2011, 115, 19328-19335.	1.5	39

#	Article	IF	Citations
9492	Structure of Methyl Pyruvate and Î±-(1-Naphthyl)ethylamine on Pd(111). Journal of Physical Chemistry C, 2011, 115, 8790-8797.	1.5	24
9493	Stability of Group-V Endohedral Fullerenes. Journal of Physical Chemistry C, 2011, 115, 3528-3533.	1.5	7
9494	Structural Investigation of the (001) Surface of the Al₉Co₂ Complex Metallic Alloy. Journal of Physical Chemistry C, 2011, 115, 14922-14932.	1.5	20
9495	Are Azafullerene Encapsulated Single-Walled Carbon Nanotubes n-Type Semiconductors?. Journal of Physical Chemistry C, 2011, 115, 12760-12762.	1.5	12
9496	Sulfur-Induced Reconstruction of Ag(111) Surfaces Studied by DFT. Journal of Physical Chemistry C, 2011, 115, 9587-9592.	1.5	9
9497	Structural and Electronic Properties of Bismuth and Lead Nanowires Inside Carbon Nanotubes. Journal of Physical Chemistry C, 2011, 115, 10524-10530.	1.5	2
9498	Site Substitution of Ti in NaAlH₄ and Na₃AlH₆. Journal of Physical Chemistry C, 2011, 115, 21454-21464.	1.5	19
9499	Identifying Molecular Orbital Energies by Distance-Dependent Transition Voltage Spectroscopy. Journal of Physical Chemistry C, 2011, 115, 15025-15030.	1.5	22
9500	Geometric and Electronic Confinement Effects on Catalysis. Journal of Physical Chemistry C, 2011, 115, 21324-21333.	1.5	42
9501	Density Functional Theory Study of Acetaldehyde Hydrodeoxygenation on MoO₃. Journal of Physical Chemistry C, 2011, 115, 8155-8164.	1.5	64
9502	Impurity Concentration Dependence of Optical Absorption for Phosphorus-Doped Anatase TiO₂. Journal of Physical Chemistry C, 2011, 115, 8184-8188.	1.5	56
9503	Single Electron Tunneling through a Tailored Arylthio-coronene. Journal of Physical Chemistry C, 2011, 115, 9204-9209.	1.5	9
9504	Role of an Aluminum Atom on Graphene for Hydrogen Adsorption. Journal of the Physical Society of Japan, 2011, 80, 074705.	0.7	24
9505	Electronic structure of cation-codoped TiO2 for visible-light photocatalyst applications from hybrid density functional theory calculations. Applied Physics Letters, 2011, 98, 142103.	1.5	38
9506	<mml:math xmlns:mml="http://www.w3.org/1998/Math/MathML" display="inline"><mml:msub><mml:mi>BiFeO</mml:mi><mml:mn>3</mml:mn></mml:msub></mml:math>Films under Tensile Epitaxial Strain from First Principles. Physical Review Letters, 2011, 106, 237601.	2.9	56
9507	Effect of Hydrostatic Compression on Structure and Properties of 2-Diazo-4,6- Dinitrophenol Crystal: Density Functional Theory Studies. Journal of Physical Chemistry C, 2011, 115, 11738-11748.	1.5	23
9508	Chemical storage of hydrogen in few-layer graphene. Proceedings of the National Academy of Sciences of the United States of America, 2011, 108, 2674-2677.	3.3	229
9509	Orthogonal Interactions of CO Molecules on a One-Dimensional Substrate. ACS Nano, 2011, 5, 8877-8883.	7.3	24

#	Article	IF	Citations
9510	Mechanistic Switch between Oxidative (Andrussow) and Nonoxidative (Degussa) Formation of HCN on Pt(111) by Density Functional Theory. Journal of Physical Chemistry C, 2011, 115, 5667-5674.	1.5	24
9511	Vacancy and Oxygen Substitution for Nitrogen-Induced Structural Stability of Ta₂N₃. Journal of Physical Chemistry C, 2011, 115, 3129-3135.	1.5	12
9512	Reaction of NO on Niâ^'Pt Bimetallic Surfaces Investigated with Theoretical Calculations. Journal of Physical Chemistry C, 2011, 115, 7538-7544.	1.5	18
9513	Effect of Fluorination on Photocatalytic Degradation of Rhodamine B over In(OH)ySz: Promotion or Suppression?. Journal of Physical Chemistry C, 2011, 115, 460-467.	1.5	33
9514	Tuning the CO Dissociation Barriers by Low-Dimensional Surface Alloys. Journal of Physical Chemistry C, 2011, 115, 21320-21323.	1.5	9
9515	Electronic and structural properties of the oxygen vacancy in BaTiO3. Applied Physics Letters, 2011, 98, .	1.5	61
9516	Gold Cluster Diffusion Kinetics on Stoichiometric and Reduced Surfaces of Rutile TiO₂(110). Journal of Physical Chemistry C, 2011, 115, 11611-11617.	1.5	17
9517	Structures of the Ordered Water Monolayer on MgO(001). Journal of Physical Chemistry C, 2011, 115, 6764-6774.	1.5	88
9518	Mapping Complex Chiral Adlayers: A Truly Random 2-D Solid Solution of (RS)-3-Pyrroline-2-Carboxylic Acid on Cu(110). Journal of Physical Chemistry C, 2011, 115, 1180-1185.	1.5	12
9519	Irregular Modulation of Density-of-States of Nano-Peapods Encapsulating Gd@C₈₂Metallofullerenes. Journal of Physical Chemistry C, 2011, 115, 3968-3972.	1.5	4
9520	Dissociation of Methane on La₂O₃ Surfaces Doped with Cu, Mg, or Zn. Journal of Physical Chemistry C, 2011, 115, 18239-18246.	1.5	31
9521	Computational Studies of Experimentally Observed Structures of Sulfur on Metal Surfaces. Journal of Physical Chemistry C, 2011, 115, 17077-17091.	1.5	24
9522	Graphene Nucleation on Transition Metal Surface: Structure Transformation and Role of the Metal Step Edge. Journal of the American Chemical Society, 2011, 133, 5009-5015.	6.6	315
9523	Novel approaches to multiscale modelling in materials science. International Materials Reviews, 2011, 56, 207-225.	9.4	107
9524	Interaction of Water with the Fluorine-Covered Anatase TiO₂ (001) Surface. Journal of Physical Chemistry C, 2011, 115, 17092-17096.	1.5	21
9525	A Comparative First-Principles Study of the Structure, Energetics, and Properties of Liâ€“M (M = Si, Ge,) Tj ETQq1 1 0.784314 rgBT /O	1.5	125
9526	First-principles study of phonon linewidths in noble metals. Physical Review B, 2011, 84, .	1.1	51
9527	Control of the band-gap states of metal oxides by the application of epitaxial strain: The case of indium oxide. Physical Review B, 2011, 83, .	1.1	42

#	Article	IF	Citations
9528	Double-Hole-Mediated Coupling of Dopants and Its Impact on Band Gap Engineering in<mml:math xmlns:mml="http://www.w3.org/1998/Math/MathML" display="inline"><mml:msub><mml:mi>TiO</mml:mi><mml:mn>2</mml:mn></mml:msub></mml:math>. Physical Review Letters, 2011, 106, 066801.	2.9	134
9529	Nature of the Band Gap and Origin of the Conductivity of<mml:math xmlns:mml="http://www.w3.org/1998/Math/MathML" display="inline"><mml:msub><mml:mi>PbO</mml:mi><mml:mn>2</mml:mn></mml:msub></mml:math>Revealed by Theory and Experiment. Physical Review Letters, 2011, 107, 246402.	2.9	93
9530	Mechanistic Studies of Waterâ€“Gas-Shift Reaction on Transition Metals. Journal of Physical Chemistry C, 2011, 115, 18582-18588.	1.5	125
9531	Experimental and theoretical studies of ammonia decomposition activity on Fe-Pt, Co-Pt, and Cu-Pt bimetallic surfaces. Journal of Chemical Physics, 2011, 134, 184701.	1.2	34
9532	First-principles investigation of higher oxides of uranium and neptunium:<mml:math xmlns:mml="http://www.w3.org/1998/Math/MathML" display="inline"><mml:mrow><mml:msub><mml:mi mathvariant="normal">U</mml:mi><mml:mrow><mml:mn>3</mml:mn></mml:mrow></mml:msub></mml:mrow></mml:math>O<mml:math xmlns:mml="http://www.w3.org/1998/Math/MathML" display="inline"><mml:mrow><mml:msub><mml:mrow /><mml:mrow><mml:mn>8</mml:mn></mml:mrow></mml:msub></mml:mrow></mml:math>and Np<mml:	1.1	43
9533	Electrochemical Windows of Room-Temperature Ionic Liquids from Molecular Dynamics and Density Functional Theory Calculations. Chemistry of Materials, 2011, 23, 2979-2986.	3.2	337
9534	First-Principles Study of Silicon Nanowire Approaching the Bulk Limit. Nano Letters, 2011, 11, 4794-4799.	4.5	40
9535	Edge dislocation core structures in FCC metals determined fromab initiocalculations combined with the improved Peierlsâ€“Nabarro equation. Physica Scripta, 2011, 83, 045604.	1.2	23
9536	Crystal Chemistry and Electronic Structure of the Photovoltaic Buffer Layer, (In1-xAlx)2S3. Chemistry of Materials, 2011, 23, 5168-5176.	3.2	15
9537	Theoretical study of pressure-driven phase transitions in HgSe and HgTe. Physical Review B, 2011, 83, .	1.1	12
9538	Adsorption and Reaction of Furfural and Furfuryl Alcohol on Pd(111): Unique Reaction Pathways for Multifunctional Reagents. ACS Catalysis, 2011, 1, 1272-1283.	5.5	145
9539	Enhanced visible-light photocatalytic activity of anatase TiO2 through N and S codoping. Applied Physics Letters, 2011, 98, .	1.5	57
9540	Structural Stability of AB_y Phases in the (La,Mg)â€“Ni System Obtained by Density Functional Theory Calculations. Journal of Physical Chemistry C, 2011, 115, 25470-25478.	1.5	75
9541	Growth and Structural Properties of Mg_N (N = 10â€“56) Clusters: Density Functional Theory Study. Journal of Physical Chemistry A, 2011, 115, 12307-12314.	1.1	52
9542	Dissociation of O2 Molecules on Strained Pb(111) Surfaces. Journal of Physical Chemistry C, 2011, 115, 17378-17383.	1.5	2
9543	Transfer doping of a metallic carbon nanotube and graphene on metal surfaces. Physical Review B, 2011, 83, .	1.1	17
9544	The role of electron localization in the atomic structure of transition-metal 13-atom clusters: the example of Co13, Rh13, and Hf13. Physical Chemistry Chemical Physics, 2011, 13, 17242.	1.3	43
9545	A density functional theory study of Mn nanowires on the Si(001) surface. Journal of Physics Condensed Matter, 2011, 23, 305003.	0.7	7

#	Article	IF	Citations
9546	Lattice Stability of Si[100] Wires From First Principles. Journal of Physical Chemistry C, 2011, 115, 3286-3290.	1.5	1
9547	Density Functional Theory Study of Methyl Iodide Adsorption and Dissociation on Clean and K-Promoted Î²-Mo₂C Surfaces. Journal of Physical Chemistry C, 2011, 115, 2798-2804.	1.5	15
9548	Sensitivity of (5,5) SWSiCNTs and SWSiCNTs with Stoneâ€“Wales Defects toward Hazardous Molecules. Journal of Physical Chemistry C, 2011, 115, 11493-11499.	1.5	27
9549	Alkanethiol Adsorption on Platinum: Chain Length Effects on the Quality of Self-Assembled Monolayers. Journal of Physical Chemistry C, 2011, 115, 17788-17798.	1.5	34
9550	Intrinsic Spin-Orbit Coupling in Zigzag and Armchair Graphene Nanoribbons. Journal of Nanomaterials, 2011, 2011, 1-7.	1.5	0
9551	Molecular Dynamics Simulations of Surface Oxidation on Pt(111) and Pt/PtCo/Pt₃Co(111). Journal of Physical Chemistry C, 2011, 115, 4104-4113.	1.5	23
9552	Signature of Al₁₁Sm₃fragments in undercooled Al₉₀Sm₁₀liquid fromab initiomolecular dynamics simulations. Journal of Physics Condensed Matter, 2011, 23, 235104.	0.7	6
9553	Binding Structures of Pyrrole on Si(5 5 12)â€“2 Ã— 1 Surfaces. Journal of Physical Chemistry C, 2011, 115, 17111-17117.	1.5	3
9554	Nanocrystalline Graphite Growth on Sapphire by Carbon Molecular Beam Epitaxy. Journal of Physical Chemistry C, 2011, 115, 4491-4494.	1.5	113
9555	Role of Cu Doping in SnO₂ Sensing Properties Toward H₂S. Journal of Physical Chemistry C, 2011, 115, 18597-18602.	1.5	72
9556	Vacancy Diffusion in NaAlH₄ and Na₃AlH₆. Journal of Physical Chemistry C, 2011, 115, 21465-21472.	1.5	28
9557	Comparison of Cation Adsorption by Isostructural Rutile and Cassiterite. Langmuir, 2011, 27, 4585-4593.	1.6	29
9558	Structure of Lithium Peroxide. Journal of Physical Chemistry Letters, 2011, 2, 2483-2486.	2.1	53
9559	Chromium Porphyrin Arrays As Spintronic Devices. Journal of the American Chemical Society, 2011, 133, 9364-9369.	6.6	167
9560	The nature of electron lone pairs in BiVO4. Applied Physics Letters, 2011, 98, .	1.5	90
9561	Electronic and Magnetic Properties of Metalâ^'(4,4â€²-bipyridine) Sandwich Complexes and Their Nanowires. Journal of Physical Chemistry A, 2011, 115, 219-224.	1.1	4
9562	Experimental and First-Principles Thermodynamic Study of the Formation and Effects of Vacancies in Layered Lithium Nickel Cobalt Oxides. Chemistry of Materials, 2011, 23, 5388-5397.	3.2	89
9563	First-principles study of magnetic properties in Mo-doped graphene. Journal of Physics Condensed Matter, 2011, 23, 346001.	0.7	28

#	Article	IF	Citations
9564	Monolayer Graphene and h-BN on Metal Substrates as Versatile Templates for Metallic Nanoclusters. Journal of Physical Chemistry Letters, 2011, 2, 2341-2345.	2.1	63
9565	Structures and magnetic properties of Pd<mml:math xmlns:mml="http://www.w3.org/1998/Math/MathML" display="inline"><mml:msub><mml:mrow /><mml:mi>n</mml:mi></mml:msub></mml:math>clusters (<mml:math) Tj ETQq1 1 0.784314 rgBT /Overlock 10 Tf 50 702 Td (xmlns:m	1.0	28
9566	Energetics of Oxidation in MoS₂Nanoparticles by Density Functional Theory. Journal of Physical Chemistry C, 2011, 115, 10606-10616.	1.5	55
9567	Structure and Properties of Liâ^'Si Alloys: A First-Principles Study. Journal of Physical Chemistry C, 2011, 115, 2514-2521.	1.5	187
9568	In Situ Oxidation Study of Pt(110) and Its Interaction with CO. Journal of the American Chemical Society, 2011, 133, 20319-20325.	6.6	120
9569	Honeycomb-Patterned Quantum Dots beyond Graphene. Journal of Physical Chemistry C, 2011, 115, 17743-17749.	1.5	25
9570	Selective Nitrogen-Doping Structure of Nanosize Graphitic Layers. Journal of Physical Chemistry C, 2011, 115, 3737-3744.	1.5	52
9571	On the Formation and the Structure of the First Bimetallic Borohydride Borate, LiCa₃(BH₄)(BO₃)₂. Journal of Physical Chemistry C, 2011, 115, 10298-10304.	1.5	19
9572	Water Molecule-Induced Stiffening in ZnO Nanobelts. Nano Letters, 2011, 11, 2845-2848.	4.5	42
9573	Si₂H₆ Dissociative Chemisorption and Dissociation on Si(100)-(2Ã—1) and Ge(100)-(2Ã—1). Journal of Physical Chemistry C, 2011, 115, 24534-24548.	1.5	9
9574	Reactivity of Câ€“C Scission on Ni-Based Core/Shell Bimetallic Surfaces Investigated with Quantum-Chemical Calculations. Journal of Physical Chemistry C, 2011, 115, 19231-19238.	1.5	2
9575	Oxygen Reduction Reaction on Metal-Terminated MnCr₂O₄ Nano-octahedron Catalyzing MnS Dissolution in an Austenitic Stainless Steel. Journal of Physical Chemistry C, 2011, 115, 4127-4133.	1.5	4
9576	Transport Properties of Zigzag Graphene Nanoribbons Decorated by Carboxyl Group Chains. Journal of Physical Chemistry C, 2011, 115, 21893-21898.	1.5	8
9577	Native Defects and the Dehydrogenation of NaBH4. Journal of Physical Chemistry C, 2011, 115, 24429-24434.	1.5	13
9578	Emergent Multistability in Assembled Nanostructures. Nano Letters, 2011, 11, 2486-2489.	4.5	27
9579	Complete Titanium Substitution by Boron in a Tetragonal Prism: Exploring the Complex Boride Series Ti_{3âˆ'x}Ru_{5âˆ'y}Ir_yB_{2+x} (0 â‰¤) Tj ETQq1 1 0.784314	1.5	28
9580	sâ€“d Electronic Interaction Induced H₂ Dissociation on the Î³-U(100) Surface and Influences of Niobium Doping. Journal of Physical Chemistry C, 2011, 115, 23381-23386.	1.5	15
9581	Methane Dissociation on High and Low Indices Rh Surfaces. Journal of Physical Chemistry C, 2011, 115, 13027-13034.	1.5	35

#	Article	IF	Citations
9582	Heat-to-Connect: Surface Commensurability Directs Organometallic One-Dimensional Self-Assembly. ACS Nano, 2011, 5, 9093-9103.	7.3	64
9583	Comparison of Oâ^'H, Câ^'H, and Câ^'O Bond Scission Sequence of Methanol on Tungsten Carbide Surfaces Modified by Ni, Rh, and Au. Journal of Physical Chemistry C, 2011, 115, 6644-6650.	1.5	49
9584	Au/TiO₂(110) Interfacial Reconstruction Stability from ab Initio. Journal of Physical Chemistry C, 2011, 115, 17799-17805.	1.5	16
9585	The Influence of Antisite Defects on the Half-Metallic Properties in Disordered LaSrVMoO₆. Journal of Physical Chemistry C, 2011, 115, 13907-13910.	1.5	3
9586	Lithium Intercalation Induced Decoupling of Epitaxial Graphene on SiC(0001): Electronic Property and Dynamic Process. Journal of Physical Chemistry C, 2011, 115, 23992-23997.	1.5	32
9587	First-principles study of the oxygen evolution reaction of lithium peroxide in the lithium-air battery. Physical Review B, 2011, 84, .	1.1	191
9588	Rh-Decorated Cu Alloy Catalyst for Improved C₂Oxygenate Formation from Syngas. Journal of Physical Chemistry C, 2011, 115, 18247-18256.	1.5	62
9589	Vibrational Analysis of the Hydrogen-Bond Symmetrization in Ice. Journal of Physical Chemistry B, 2011, 115, 71-74.	1.2	12
9590	Electronic structure and magnetic properties of the graphene/Fe/Ni(111) intercalation-like system. Physical Chemistry Chemical Physics, 2011, 13, 7534.	1.3	110
9591	Indirect Magnetic Coupling of Manganese Porphyrin to a Ferromagnetic Cobalt Substrate. Journal of Physical Chemistry C, 2011, 115, 1295-1301.	1.5	44
9592	Physisorption Structure of Water on the GaN Polar Surface: Force Field Development and Molecular Dynamics Simulations. Journal of Physical Chemistry C, 2011, 115, 11684-11693.	1.5	13
9593	Electronic Structures of Porous Graphene, BN, and BC₂N Sheets with One- and Two-Hydrogen Passivations from First Principles. Journal of Physical Chemistry C, 2011, 115, 5334-5343.	1.5	48
9594	Hydrogen Bonds and van der Waals Forces in Ice at Ambient and High Pressures. Physical Review Letters, 2011, 107, 185701.	2.9	193
9595	Magnetism and bonding in graphene nanodots with H modified interior, edge, and apex. Journal of Chemical Physics, 2011, 135, 084707.	1.2	4
9596	Reactivity of Transition Metals (Pd, Pt, Cu, Ag, Au) toward Molecular Hydrogen Dissociation: Extended Surfaces versus Particles Supported on TiC(001) or Small Is Not Always Better and Large Is Not Always Bad. Journal of Physical Chemistry C, 2011, 115, 11666-11672.	1.5	82
9597	Pathways of Methanol Steam Reforming on PdZn and Comparison with Cu. Journal of Physical Chemistry C, 2011, 115, 20583-20589.	1.5	60
9598	Ab initioguided optimization of GaTe for radiation detection applications. Physical Review B, 2011, 84, .	1.1	25
9599	Structural, electronic, and magnetic properties of C-doped GaN nanoribbon. Journal of Applied Physics, 2011, 109, .	1.1	13

#	Article	IF	Citations
9600	X-ray Emission Spectroscopy of Nitrogen-Rich Compounds. Journal of Physical Chemistry A, 2011, 115, 3243-3250.	1.1	20
9601	Ab Initio Molecular Dynamics Study of Temperature Effects on the Structure and Stability of Energetic Solid Silver Azide. Journal of Physical Chemistry C, 2011, 115, 20782-20787.	1.5	24
9602	Structures of Pt clusters on graphene doped with nitrogen, boron, and silicon: a theoretical study. Chinese Physics B, 2011, 20, 056801.	0.7	13
9603	Understanding the Interaction of the Porphyrin Macrocycle to Reactive Metal Substrates: Structure, Bonding, and Adatom Capture. ACS Nano, 2011, 5, 1831-1838.	7.3	58
9604	Leapfrog Cracking and Nanoamorphization of ZnO Nanowires during In Situ Electrochemical Lithiation. Nano Letters, 2011, 11, 4535-4541.	4.5	169
9605	H₂S Adsorption on Î³-Al₂O₃ Surfaces: A Density Functional Theory Study. Journal of Physical Chemistry C, 2011, 115, 1899-1910.	1.5	23
9606	Thermodynamic Cartography and Structure/Property Mapping of Commercial Platinum Catalysts. ACS Catalysis, 2011, 1, 76-81.	5.5	26
9607	K₃B₆O₁₀Cl: A New Structure Analogous to Perovskite with a Large Second Harmonic Generation Response and Deep UV Absorption Edge. Journal of the American Chemical Society, 2011, 133, 7786-7790.	6.6	617
9608	Chemical bonding in copper-based transparent conducting oxides: CuMO₂(M = In, Ga, Sc). Journal of Physics Condensed Matter, 2011, 23, 334201.	0.7	25
9609	Thermopower of Amineâ^'Gold-Linked Aromatic Molecular Junctions from First Principles. ACS Nano, 2011, 5, 551-557.	7.3	87
9610	Sc-phthalocyanine sheet: Promising material for hydrogen storage. Applied Physics Letters, 2011, 99, .	1.5	32
9611	Reevaluation of the Structure and Fundamental Physical Properties of Dawsonites by DFT Studies. Inorganic Chemistry, 2011, 50, 2590-2598.	1.9	11
9612	[As₇M(CO)₃]^{3â€“} M = Cr, Mo, W: Bonding and Electronic Structure of Cluster Assemblies with Metal Carbonyls. Journal of Physical Chemistry C, 2011, 115, 23704-23710.	1.5	6
9613	Tip-Dependent Scanning Tunneling Microscopy Imaging of Ultrathin FeO Films on Pt(111). Journal of Physical Chemistry C, 2011, 115, 2089-2099.	1.5	55
9614	Role of Polytetrahedral Structures in the Elongation and Rupture of Gold Nanowires. ACS Nano, 2011, 5, 10065-10073.	7.3	18
9615	New Nickel Gallium Boride, B₁₄Ga₃Ni₂₇: Synthesis and Crystal Structure. Inorganic Chemistry, 2011, 50, 3907-3912.	1.9	9
9616	Structure phase transition and elastic properties of hafnium: First-principles study. Philosophical Magazine Letters, 2011, 91, 61-69.	0.5	20
9617	Theoretical Study of the Interaction of CO on TiC(001) and Au Nanoparticles Supported on TiC(001): Probing the Nature of the Au/TiC Interface. Journal of Physical Chemistry C, 2011, 115, 22495-22504.	1.5	17

#	Article	IF	Citations
9618	Hybrid density functional theory band structure engineering in hematite. Journal of Chemical Physics, 2011, 134, 224706.	1.2	152
9619	In-Phase Alignments of Asymmetric Building Units in Ln₄GaSbS₉(Ln = Pr, Nd,) Tj ETQq1 1 0.784314 rgBT /Ove Chemical Society, 2011, 133, 4617-4624.	6.6	191
9620	Atomistic Design of High Thermoelectricity on Si/Ge Superlattice Nanowires. Journal of Physical Chemistry C, 2011, 115, 20696-20702.	1.5	30
9621	Effect of Concentration on the Energetics and Dynamics of Li Ion Transport in Anatase and Amorphous TiO₂. Journal of Physical Chemistry C, 2011, 115, 15661-15673.	1.5	47
9622	Coupled Magnetic-Ferroelectric Metal-Insulator Transition in Epitaxially Strained<mml:math xmlns:mml="http://www.w3.org/1998/Math/MathML" display="inline"><mml:msub><mml:mi>SrCoO</mml:mi><mml:mn>3</mml:mn></mml:msub></mml:math>from First Principles. Physical Review Letters, 2011, 107, 067601.	2.9	73
9623	Dynamics of Hydration in Vanadiaâ€“Titania Catalysts at Low Loading: A Theoretical and Experimental Study. Journal of Physical Chemistry C, 2011, 115, 24133-24142.	1.5	29
9624	Elasticity and anisotropy of Fe3C at high pressures. American Mineralogist, 2011, 96, 1530-1536.	0.9	44
9625	First-Principles Study of Water Dissociation on PdZn near Surface Alloys. Journal of Physical Chemistry C, 2011, 115, 18752-18760.	1.5	21
9626	Adsorption and Reaction of Si2H5 on Clean and H-Covered Si(100)-(2 Ã— 1) Surfaces: A Computational Study. Journal of Physical Chemistry C, 2011, 115, 15369-15374.	1.5	5
9627	Glycolaldehyde as a Probe Molecule for Biomass Derivatives: Reaction of Câ€”OH and Câ•O Functional Groups on Monolayer Ni Surfaces. Journal of the American Chemical Society, 2011, 133, 20528-20535.	6.6	42
9628	Catalytic activity of Pd ensembles over Au(111) surface for CO oxidation: A first-principles study. Journal of Chemical Physics, 2011, 134, 054704.	1.2	25
9629	Ideal Strengths and Bonding Properties of PuO₂under Tension. Chinese Physics Letters, 2011, 28, 047101.	1.3	4
9630	Experimental and theoretical study of the metastable decay of negatively charged nucleosides in the gas phase. Physical Chemistry Chemical Physics, 2011, 13, 15283.	1.3	19
9631	Adsorption of NO Molecule on Spinel-Type CuFe₂O₄ Surface: A First-Principles Study. Journal of Physical Chemistry C, 2011, 115, 13035-13040.	1.5	54
9632	New Insights into the Strain Coupling to Surface Chemistry, Electronic Structure, and Reactivity of La_{0.7}Sr_{0.3}MnO₃. Journal of Physical Chemistry Letters, 2011, 2, 801-807.	2.1	145
9633	Periodic Density Functional Theory Study of VO_n Species Supported on the CeO₂(111) Surface. Journal of Physical Chemistry C, 2011, 115, 7399-7410.	1.5	61
9634	Stability and Quenching of Plasmon Resonance Absorption in Magnetic Gold Nanoparticles. Journal of Physical Chemistry Letters, 2011, 2, 2996-3001.	2.1	5
9635	Revisiting the Zintlâ€“Klemm Concept: Alkali Metal Trielides. Inorganic Chemistry, 2011, 50, 7625-7636.	1.9	38

#	Article	IF	Citations
9636	Catalytic properties of Al13Co4 studied by ab initio methods. Philosophical Magazine, 2011, 91, 2904-2912.	0.7	10
9637	Transport Properties of Double Quantum Dots Formed by Ferrocene Units. Journal of Physical Chemistry C, 2011, 115, 5257-5264.	1.5	7
9638	Origin of the Enhanced Visible-Light Absorption in N-Doped Bulk Anatase TiO₂ from First-Principles Calculations. Journal of Physical Chemistry C, 2011, 115, 19394-19404.	1.5	91
9639	Structure of the orthorhombic Al13Co4(100) surface using LEED, STM, andab initiostudies. Physical Review B, 2011, 84, .	1.1	41
9640	The Effects of Electronâ€“Hole Pair Coupling on the Infrared Laser-Controlled Vibrational Excitation of NO on Au(111). Journal of Physical Chemistry A, 2011, 115, 10698-10707.	1.1	11
9641	Gap Opening of Graphene by Dual FeCl₃-Acceptor and K-Donor Doping. Journal of Physical Chemistry Letters, 2011, 2, 2577-2581.	2.1	101
9642	CO-Induced Embedding of Pt Adatoms in a Partially Reduced FeOxFilm on Pt(111). Journal of the American Chemical Society, 2011, 133, 10692-10695.	6.6	27
9643	Atomic Layer Deposition of Pt on Tungsten Monocarbide (WC) for the Oxygen Reduction Reaction. Journal of Physical Chemistry C, 2011, 115, 3709-3715.	1.5	94
9644	Theoretical Study of the Adsorption of the Butanol Isomers in H-ZSM-5. Journal of Physical Chemistry C, 2011, 115, 8658-8669.	1.5	45
9645	On the High Magnetic-Ordering Temperature of the 5d Magnetic Oxide Ca₃LiOsO₆ Crystallizing in a Trigonal Crystal Structure: Density Functional Analysis. Inorganic Chemistry, 2011, 50, 4182-4186.	1.9	11
9646	Ferromagnetism in Two-Dimensional Carbon Chains Linked by 1,3,5-Benzenetriyl Units. Journal of Physical Chemistry C, 2011, 115, 19621-19625.	1.5	11
9647	Adsorption of Single Platinum Atom on the Graphene Oxide: The Role of the Carbon Lattice. Journal of Physical Chemistry C, 2011, 115, 12023-12032.	1.5	9
9648	Ferromagnetism in IV main group element (C) and transition metal (Mn) doped MgO: A density functional perspective. AIP Advances, 2011, 1, 032129.	0.6	19
9649	New Quaternary Hydride CeZnSnH1.5: Structure, Magnetism, and Chemical Bonding. Chemistry of Materials, 2011, 23, 1096-1104.	3.2	10
9650	Role of Deprotonation and Cu Adatom Migration in Determining the Reaction Pathways of Oxalic Acid Adsorption on Cu(111). Journal of Physical Chemistry C, 2011, 115, 21177-21182.	1.5	22
9651	Valence Excited States in Large Molecules via Local Multireference Singles and Doubles Configuration Interaction. Journal of Chemical Theory and Computation, 2011, 7, 103-111.	2.3	23
9652	Activities towardsp-type doping of ZnO. Journal of Physics: Conference Series, 2011, 265, 012002.	0.3	23
9653	Study of Native Defects and Transition-Metal (Mn, Fe, Co, and Ni) Doping in a Zinc-Blende CdS Photocatalyst by DFT and Hybrid DFT Calculations. Journal of Physical Chemistry C, 2011, 115, 5675-5682.	1.5	95

#	Article	IF	Citations
9654	Application of Density Functional Theory and Photoelectron Spectra to the Adsorption and Reaction of H2S on Si (100). Journal of Physical Chemistry C, 2011, 115, 19203-19209.	1.5	8
9655	Molecular Calipers Control Atomic Separation at a Metal Surface. Nano Letters, 2011, 11, 4113-4117.	4.5	18
9656	Density Functional Theory Study of Pyrophyllite and M-Montmorillonites (M = Li, Na, K, Mg, and Ca): Role of Dispersion Interactions. Journal of Physical Chemistry A, 2011, 115, 9695-9703.	1.1	75
9657	Structure of clean and hydrated Î±-Al2O3 (11Ì„02) surfaces: implication on surface charge. Physical Chemistry Chemical Physics, 2011, 13, 6531.	1.3	29
9658	Anisotropic Lithium Insertion Behavior in Silicon Nanowires: Binding Energy, Diffusion Barrier, and Strain Effect. Journal of Physical Chemistry C, 2011, 115, 9376-9381.	1.5	61
9659	Structural and Electronic Properties of the Adsorption of Oxygen on AlN (101Ì…0) and (112Ì…0) Surfaces: A First-Principles Study. Journal of Physical Chemistry C, 2011, 115, 1882-1886.	1.5	18
9660	Magnetic Cooperative Effects in Small Niâ€“Ru Clusters. Journal of Physical Chemistry A, 2011, 115, 13950-13955.	1.1	10
9661	Superhard phases of B2O: An isoelectronic compound of diamond. Diamond and Related Materials, 2011, 20, 501-504.	1.8	16
9662	Density functional theory study of La<mml:math xmlns:mml="http://www.w3.org/1998/Math/MathML" display="inline"><mml:msub><mml:mrow /><mml:mn>2</mml:mn></mml:msub></mml:math>Ce<mml:math xmlns:mml="http://www.w3.org/1998/Math/MathML" display="inline"><mml:msub><mml:mrow /><mml:mn>2</mml:mn></mml:msub></mml:math>O<mml:math xmlns:mml="http://www.w3.org/1998/Math/MathML" display="inline"><mml:msub><mml:mrow /><mml:mn>7</mml:mn></mml:msub></mml:math>	1.1	43
9663	Cu<mml:math xmlns:mml="http://www.w3.org/1998/Math/MathML" display="inline"><mml:msub><mml:mrow /><mml:mn>3</mml:mn></mml:msub></mml:math>VO<mml:math xmlns:mml="http://www.w3.org/1998/Math/MathML" display="inline"><mml:msub><mml:mrow /><mml:mn>4</mml:mn></mml:msub></mml:math> and Ag<mml:math xmlns:mml="http://www.w3.org/199	1.1	38
9664	Inverse Design and Synthesis of acac-Coumarin Anchors for Robust TiO₂ Sensitization. Journal of the American Chemical Society, 2011, 133, 9014-9022.	6.6	79
9665	Band structure of Si/Ge coreâ€“shell nanowires along the [110] direction modulated by external uniaxial strain. Journal of Physics Condensed Matter, 2011, 23, 115502.	0.7	34
9666	First-Principles Study of Nb Doping Effect on the Diffusion of Oxygen Atom in Î³-TiAl. Advanced Materials Research, 0, 304, 148-153.	0.3	6
9667	Synthesis and Stabilization of Subnanometric Gold Oxide Nanoparticles on Multiwalled Carbon Nanotubes and Their Catalytic Activity. Journal of the American Chemical Society, 2011, 133, 10251-10261.	6.6	87
9668	Stability of Donor-Pair Defects in Si_{1â€“x}Ge_x Alloy Nanowires. Journal of Physical Chemistry C, 2011, 115, 10345-10350.	1.5	7
9669	Doping properties of monoclinic BiVO<mml:math xmlns:mml="http://www.w3.org/1998/Math/MathML" display="inline"><mml:mrow><mml:msub><mml:mrow /><mml:mn>4</mml:mn></mml:msub></mml:mrow></mml:math>studied by first-principles density-functional theory. Physical Review B, 2011, 83, .	1.1	194
9670	First-Principles Study of Lattice Dynamics and Thermodynamics of TiO2Polymorphs. Inorganic Chemistry, 2011, 50, 6996-7003.	1.9	61
9671	Boron Nitride Nanoribbons Become Metallic. Nano Letters, 2011, 11, 3267-3273.	4.5	120

#	Article	IF	Citations
9672	Size Control of Charge-Orbital Order in Half-Doped Manganite<mml:math xmlns:mml="http://www.w3.org/1998/Math/MathML" display="inline"><mml:msub><mml:mi>La</mml:mi><mml:mn>0.5</mml:mn></mml:msub><mml:msub><mml:mi>Ca</mml:mi><mml:r Physical Review Letters, 2011, 107, 197202.	2.9	43
9673	Magneto-structural properties and magnetic anisotropy of small transition-metal clusters: a first-principles study. Journal of Physics Condensed Matter, 2011, 23, 136001.	0.7	32
9674	Density Functional Theory Study of Alkane-Alkoxide Hydride Transfer in Zeolites. ACS Catalysis, 2011, 1, 105-115.	5.5	42
9675	Acrolein hydrogenation on Pt(211) and Au(211) surfaces: a density functional theory study. Physical Chemistry Chemical Physics, 2011, 13, 21146.	1.3	48
9676	Chemisorption of CO and Mechanism of CO Oxidation on Supported Platinum Nanoclusters. Journal of the American Chemical Society, 2011, 133, 4498-4517.	6.6	448
9677	Effect of impurities on the mechanical and electronic properties of Au, Ag, and Cu monatomic chain nanowires. Physical Review B, 2011, 84, .	1.1	30
9678	Reactivity Descriptors for Borohydride Interaction with Metal Surfaces. Journal of Physical Chemistry C, 2011, 115, 19883-19889.	1.5	46
9679	Tunneling Magnetoresistance of Bilayer Hexagonal Boron Nitride and Its Linear Response to External Uniaxial Strain. Journal of Physical Chemistry C, 2011, 115, 8260-8264.	1.5	38
9680	Role of metal oxide support in redox reactions of iron oxide for chemical looping applications: experiments and density functional theory calculations. Energy and Environmental Science, 2011, 4, 3661.	15.6	138
9681	Doping effects of C, Si and Ge in wurtzite [0001] GaN, AlN, and InN nanowires. Journal of Applied Physics, 2011, 110, .	1.1	18
9682	The interplay between dopants and oxygen vacancies in the magnetism of V-doped TiO₂. Journal of Physics Condensed Matter, 2011, 23, 334216.	0.7	10
9683	Mechanism for amorphization of boron carbide B<mml:math xmlns:mml="http://www.w3.org/1998/Math/MathML" display="inline"><mml:msub><mml:mrow /><mml:mn>4</mml:mn></mml:msub></mml:math>C under uniaxial compression. Physical Review B, 2011, 84, .	1.1	74
9684	CO adsorption, CO dissociation, and C-C coupling on Cu monolayer-covered Fe(100). Journal of Fuel Chemistry and Technology, 2011, 39, 956-960.	0.9	20
9685	High-pressure behavior of iron carbide (Fe₇C₃) at inner core conditions. Journal of Geophysical Research, 2011, 116, .	3.3	75
9686	Elasticity and anisotropy of iron-nickel phosphides at high pressures. Geophysical Research Letters, 2011, 38, n/a-n/a.	1.5	6
9687	Parameter estimation by Density Functional Theory for a lattice-gas model of Br and Cl chemisorption on Ag (100). Journal of Electroanalytical Chemistry, 2011, 662, 130-136.	1.9	8
9688	Theoretical study on the effective methanol decomposition on Pd(111) surface facilitated in alkaline medium. Journal of Electroanalytical Chemistry, 2011, 662, 251-256.	1.9	15
9689	Role of Hydroxyl Groups on the Stability and Catalytic Activity of Au Clusters on a Rutile Surface. Journal of Physical Chemistry Letters, 2011, 2, 2918-2924.	2.1	35

#	Article	IF	Citations
9690	Pyrene: Hydrogenation, hydrogen evolution, and Ï€-band model. Journal of Chemical Physics, 2011, 134, 164703.	1.2	32
9691	Hybrid functional investigations of band gaps and band alignments for AlN, GaN, InN, and InGaN. Journal of Chemical Physics, 2011, 134, 084703.	1.2	256
9692	Electronic, Structural, and Electrochemical Properties of LiNi_xCu_yMn_{2â€“xâ€“y}O₄ (0) Tj ETQq0 0 0 rgBT /Overlo 23, 2832-2841.	3.2	122
9693	Interaction of hydrogen with zinc oxide nanorods: why the spacing is important. Nanotechnology, 2011, 22, 135704.	1.3	7
9694	Graphene on Ni(111): Coexistence of Different Surface Structures. Journal of Physical Chemistry Letters, 2011, 2, 759-764.	2.1	158
9695	First-principles investigation of the stability of MN and CrMN precipitates under coherency strains in Î±-Fe (Mâ€‰=â€‰V, Nb, Ta). Journal of Applied Physics, 2011, 109, .	1.1	17
9696	Li Ion Diffusion Mechanisms in LiFePO₄: An ab Initio Molecular Dynamics Study. Journal of Physical Chemistry A, 2011, 115, 13045-13049.	1.1	107
9697	Atomistic simulations of the implantation of low-energy boron and nitrogen ions into graphene. Physical Review B, 2011, 83, .	1.1	127
9698	Highly monodisperse coreâ€“shell particles created by solid-state reactions. Nature Materials, 2011, 10, 710-715.	13.3	98
9699	Strain-induced negative differential resistance in armchair-edge graphene nanoribbons. Applied Physics Letters, 2011, 98, .	1.5	43
9700	Development of a Transferable Variable Charge Potential for the Study of Energy Conversion Materials FeF₂ and FeF₃. Journal of Physical Chemistry C, 2011, 115, 24198-24205.	1.5	14
9701	Ideal shear strength under compression and tension in C, Si, Ge, and cubic SiC: anab initiodensity functional theory study. Journal of Physics Condensed Matter, 2011, 23, 385401.	0.7	17
9703	Graphene adhesion on MoS2 monolayer: An ab initio study. Nanoscale, 2011, 3, 3883.	2.8	346
9704	Small gold clusters on graphene, their mobility and clustering: a DFT study. Journal of Physics Condensed Matter, 2011, 23, 205301.	0.7	42
9705	Small Size Particles of Different Metal Alloys with Protective Shell for Hydrogen Storage. NATO Science for Peace and Security Series C: Environmental Security, 2011, , 167-175.	0.1	0
9706	Effect of Dopants on the Energy of Oxygen-Vacancy Formation at the Surface of Ceria: Local or Global?. Journal of Physical Chemistry C, 2011, 115, 17898-17909.	1.5	118
9707	Adsorption properties of chalcogen atoms on a golden buckyball Au₁₆^{â^'}from first principles. Journal of Physics Condensed Matter, 2011, 23, 505301.	0.7	5
9708	Diffusion and drift of graphene flake on graphite surface. Journal of Chemical Physics, 2011, 134, 104505.	1.2	43

#	Article	IF	Citations
9709	Prediction of a superconductive superhard material: Diamond-like BC7. Journal of Applied Physics, 2011, 110, 013501.	1.1	21
9710	Thermal Expansion of Supported and Freestanding Graphene: Lattice Constant versus Interatomic Distance. Physical Review Letters, 2011, 106, 135501.	2.9	148
9711	Stabilization of Electrocatalytic Metal Nanoparticles at Metalâ˜'Metal Oxideâ˜'Graphene Triple Junction Points. Journal of the American Chemical Society, 2011, 133, 2541-2547.	6.6	391
9712	Accurate electronic properties for (Hg,Cd)Te systems using hybrid density functional theory. Physical Review B, 2011, 84, .	1.1	75
9713	Hydrogenated cation vacancies in semiconducting oxides. Journal of Physics Condensed Matter, 2011, 23, 334212.	0.7	237
9714	Multi-component transparent conducting oxides: progress in materials modelling. Journal of Physics Condensed Matter, 2011, 23, 334210.	0.7	52
9715	Dynamical nature of the high-temperature Pb/Si(111)-1<mml:math xmlns:mml="http://www.w3.org/1998/Math/MathML" display="inline"><mml:mo>Ã—</mml:mo></mml:math>1 phase. Physical Review B, 2011, 84, .	1.1	5
9716	Impurity-related vibrational modes in a pentacene crystal. EPJ Applied Physics, 2011, 55, 23903.	0.3	1
9717	Comparative study of structural and electronic properties of Cu-based multinary semiconductors. Physical Review B, 2011, 84, .	1.1	95
9718	Magnetic ordering in tetragonal FeS: Evidence for strong itinerant spin fluctuations. Physical Review B, 2011, 83, .	1.1	57
9719	First-principles study of Cu₂ZnSnS₄and the related band offsets for photovoltaic applications. Journal of Physics Condensed Matter, 2011, 23, 404203.	0.7	90
9720	Controllable healing of defects and nitrogen doping of graphene by CO and NO molecules. Physical Review B, 2011, 83, .	1.1	67
9721	Structural Defects in W-Doped TiO₂ (101) Anatase Surface: Density Functional Study. Journal of Physical Chemistry C, 2011, 115, 16970-16976.	1.5	34
9722	Transition-Metal-Atom-Embedded Graphane and Its Spintronic Device Applications. Journal of Physical Chemistry C, 2011, 115, 22701-22706.	1.5	24
9724	CO Oxidation Facilitated by Robust Surface States on Au-Covered Topological Insulators. Physical Review Letters, 2011, 107, 056804.	2.9	128
9725	Pressure-induced structural transitions in europium to 92 GPa. Physical Review B, 2011, 83, .	1.1	33
9726	Hydrogen passivation and multiple hydrogenâ€“Hg vacancy complex impurities (nHâ€“VHg, nâ€‰=â€‰1,2,3,4) in Hg0.75Cd0.25Te. Journal of Applied Physics, 2011, 110, .	1.1	5
9727	Adsorption of carbon adatoms to graphene and its nanoribbons. Journal of Applied Physics, 2011, 109, 013704.	1.1	59

#	Article	IF	Citations
9728	Electronic Packing Frustration in Complex Intermetallic Structures: The Role of Chemical Pressure in Ca₂Ag₇. Journal of the American Chemical Society, 2011, 133, 10070-10073.	6.6	42
9729	First-principles approach to phase stability for a ternary<mml:math xmlns:mml="http://www.w3.org/1998/Math/MathML" display="inline"><mml:mrow><mml:mi>Ïƒ</mml:mi></mml:mrow></mml:math>phase: Application to Cr-Ni-Re. Physical Review B, 2011, 83, .	1.1	19
9730	Structural Relationship between Negative Thermal Expansion and Quartic Anharmonicity of Cubic<mml:math xmlns:mml="http://www.w3.org/1998/Math/MathML" display="inline"><mml:msub><mml:mi>ScF</mml:mi><mml:mn>3</mml:mn></mml:msub></mml:math>. Physical Review Letters, 2011, 107, 195504.	2.9	201
9731	Effects of H-, N-, and (H, N)-Doping on the Photocatalytic Activity of TiO₂. Journal of Physical Chemistry C, 2011, 115, 12224-12231.	1.5	144
9732	Gate-Voltage Control of Oxygen Diffusion on Graphene. Physical Review Letters, 2011, 106, 146802.	2.9	99
9733	Understanding CO₂ Capture Mechanisms in Aqueous Monoethanolamine via First Principles Simulations. Journal of Physical Chemistry Letters, 2011, 2, 522-526.	2.1	91
9734	Clean Coupling of Unfunctionalized Porphyrins at Surfaces To Give Highly Oriented Organometallic Oligomers. Journal of the American Chemical Society, 2011, 133, 12031-12039.	6.6	133
9735	Functionalization of Single-Layer MoS₂ Honeycomb Structures. Journal of Physical Chemistry C, 2011, 115, 13303-13311.	1.5	484
9736	Pressure-Induced Local Structure Distortions in Cu(pyz)F2(H2O)2. Inorganic Chemistry, 2011, 50, 6347-6352.	1.9	14
9737	Adsorption of gas molecules on transition metal embedded graphene: a search for high-performance graphene-based catalysts and gas sensors. Nanotechnology, 2011, 22, 385502.	1.3	280
9738	Adsorption of Cu, Ag, and Au atoms on graphene including van der Waals interactions. Journal of Physics Condensed Matter, 2011, 23, 395001.	0.7	117
9739	Single Terrace Growth of Graphene on a Metal Surface. Nano Letters, 2011, 11, 1895-1900.	4.5	68
9740	Pathways for methanol steam reforming involving adsorbed formaldehyde and hydroxyl intermediates on Cu(111): density functional theory studies. Physical Chemistry Chemical Physics, 2011, 13, 9622.	1.3	61
9741	Investigating the Quartz (101Ì…0)/Water Interface using Classical and Ab Initio Molecular Dynamics. Langmuir, 2011, 27, 8700-8709.	1.6	72
9742	Self-diffusion in MgOâ€”a density functional study. Journal of Physics Condensed Matter, 2011, 23, 345402.	0.7	13
9743	High pressure structural stability of BaLiF3. Journal of Applied Physics, 2011, 110, .	1.1	21
9744	Relating Trends in First-Principles Electronic Structure and Open-Circuit Voltage in Organic Photovoltaics. Journal of Physical Chemistry Letters, 2011, 2, 2531-2537.	2.1	45
9745	Electronic structure and thermoelectric properties of Sb-based semiconducting half-Heusler compounds. Physical Review B, 2011, 83, .	1.1	106

#	Article	IF	Citations
9746	Kinetic and Thermodynamic Evaluation of the Reversible N-Heterocyclic Carbeneâ^'Isothiocyanate Coupling Reaction: Applications in Latent Catalysis. Journal of Organic Chemistry, 2011, 76, 301-304.	1.7	41
9747	Interflake thermal conductance of edge-passivated graphene. Physical Review B, 2011, 84, .	1.1	8
9748	Three Dimensional Carbon-Nanotube Polymers. ACS Nano, 2011, 5, 7226-7234.	7.3	110
9749	Properties of nitrogen-vacancy centers in diamond: the group theoretic approach. New Journal of Physics, 2011, 13, 025025.	1.2	320
9750	First-Principles Study of the Graphene@MoSe₂ Heterobilayers. Journal of Physical Chemistry C, 2011, 115, 20237-20241.	1.5	121
9751	Phase Stability and Physical Properties of Manganese Borides: A First-Principles Study. Journal of Physical Chemistry C, 2011, 115, 21429-21435.	1.5	60
9752	Crystal Structure Refinement and Bonding Patterns of CrB₄: A Boron-Rich Boride with a Framework of Tetrahedrally Coordinated B Atoms. Inorganic Chemistry, 2011, 50, 10540-10542.	1.9	49
9753	The Mixing Mechanism during Lithiation of Si Negative Electrode in Li-Ion Batteries: An Ab Initio Molecular Dynamics Study. Nano Letters, 2011, 11, 5494-5500.	4.5	155
9754	Nitrogen-Doped Graphitic Layers Deposited on Silicon Nanowires for Efficient Lithium-Ion Battery Anodes. Journal of Physical Chemistry C, 2011, 115, 9451-9457.	1.5	131
9755	Choice of U for DFT+U Calculations for Titanium Oxides. Journal of Physical Chemistry C, 2011, 115, 5841-5845.	1.5	264
9756	Coexistence of rectilinear and vortex polarizations at twist boundaries in ferroelectric PbTiO<mml:math xmlns:mml="http://www.w3.org/1998/Math/MathML" display="inline"><mml:mrow><mml:msub><mml:mrow /><mml:mrow><mml:mn>3</mml:mn></mml:mrow></mml:msub></mml:mrow></mml:math>from first principles. Physical Review B, 2011, 83, .	1.1	24
9757	First-Principles Study of Lithium Borocarbide as a Cathode Material for Rechargeable Li ion Batteries. Journal of Physical Chemistry Letters, 2011, 2, 1129-1132.	2.1	36
9758	Strain-induced magnetic transitions in half-fluorinated single layers of BN, GaN and graphene. Nanoscale, 2011, 3, 2301.	2.8	124
9759	Electronic structures of silver oxides. Physical Review B, 2011, 84, .	1.1	62
9760	Identification of substitutional Li in<mml:math xmlns:mml="http://www.w3.org/1998/Math/MathML" display="inline"><mml:mrow><mml:mi>n</mml:mi></mml:mrow></mml:math>-type ZnO and its role as an acceptor. Physical Review B, 2011, 83, .	1.1	54
9761	Electronic Structure of Ligated CdSe Clusters: Dependence on DFT Methodology. Journal of Physical Chemistry C, 2011, 115, 15793-15800.	1.5	80
9762	Electronic and magnetic properties of pristine and chemically functionalized germanene nanoribbons. Nanoscale, 2011, 3, 4330.	2.8	93
9763	Crystal structure, electronic structure, and thermoelectric properties of Ca5Al2Sb6. Journal of Materials Chemistry, 2011, 21, 12497.	6.7	38

#	Article	IF	Citations
9764	Theoretical study of high photocatalytic performance of Ag<mml:math xmlns:mml="http://www.w3.org/1998/Math/MathML" display="inline"><mml:mrow><mml:msub><mml:mrow /><mml:mrow><mml:mn>3</mml:mn></mml:mrow></mml:msub></mml:mrow></mml:math>PO<mml:math xmlns:mml="http://www.w3.org/1998/Math/MathML" display="inline"><mml:mrow><mml:msub><mml:mrow /><mml:mrow><mml:mn>4</mml:mn></mml:mro	1.1	186
9765	Higher-Order Continuum Theory Applied to Fracture Simulation of Nanoscale Intergranular Glassy Film. Journal of Nanomechanics & Micromechanics, 2011, 1, 60-71.	1.4	91
9766	Understanding the p-type defect chemistry of CuCrO2. Journal of Materials Chemistry, 2011, 21, 3655.	6.7	176
9767	Molecular dynamics study of the adhesion of Cu/SiO<mml:math xmlns:mml="http://www.w3.org/1998/Math/MathML" display="inline"><mml:mrow><mml:msub><mml:mrow /><mml:mrow><mml:mn>2</mml:mn></mml:mrow></mml:msub></mml:mrow></mml:math>interfaces using a variable-charge interatomic potential. Physical Review B, 2011, 83, .	1.1	47
9768	Defects in SiC: Theory. Materials Science Forum, 2011, 679-680, 225-232.	0.3	4
9769	Structure, Properties, and Theoretical Electronic Structure of UCuOP and NpCuOP. Inorganic Chemistry, 2011, 50, 576-589.	1.9	8
9770	Pressure-induced structural transitions in BN fromab initiometadynamics. Physical Review B, 2011, 84, .	1.1	51
9771	Sources of Conductivity and Doping Limits in CdO from Hybrid Density Functional Theory. Journal of the American Chemical Society, 2011, 133, 15065-15072.	6.6	178
9772	(Barely) Solid Li(NH₃)₄: The Electronics of an Expanded Metal. Journal of the American Chemical Society, 2011, 133, 3535-3547.	6.6	35
9773	Mono- and Dicarbonyl-Bridged Tricyclic Heterocyclic Acceptors: Synthesis and Electronic Properties. Journal of Organic Chemistry, 2011, 76, 2660-2671.	1.7	33
9774	Half-metallicity in graphene nanoribbons with topological line defects. Physical Review B, 2011, 84, .	1.1	108
9775	Energetics and Mechanism for H₂S Adsorption by Ceria-Lanthanide Mixed Oxides: Implications for the Desulfurization of Biomass Gasifier Effluents. Journal of Physical Chemistry C, 2011, 115, 24178-24188.	1.5	24
9777	Effects of Lattice Constant and Sintering Atmosphere on Substitution of Sn^{2+} Ions at Ba Site in (Ba,Ca)TiO$_{3}$ Perovskites: Experimental and Theoretical Studies. Japanese Journal of Applied Physics, 2011, 50, 09NC11.	0.8	8
9778	Theoretical Study on Interactions between Oxygen Vacancy and Doped Rare-Earth Elements in Barium Titanate. Japanese Journal of Applied Physics, 2011, 50, 09NE01.	0.8	20
9779	Crystal Structure Engineering by Fine-Tuning the Surface Energy: The Case of CdE (E = S/Se) Nanocrystals. Journal of Physical Chemistry Letters, 2011, 2, 706-712.	2.1	51
9780	Ligand-Induced Structural Evolution of Pt₅₅ Nanoparticles: Amine versus Thiol. ACS Nano, 2011, 5, 8515-8522.	7.3	37
9781	Combined Experimental and Theoretical Investigations of Heterogeneous Dual Cation Sites in Cu,M-FER Zeolites. Journal of Physical Chemistry C, 2011, 115, 13312-13321.	1.5	20
9782	Quantum-mechanics-based design principles for solid oxide fuel cell cathode materials. Energy and Environmental Science, 2011, 4, 4933.	15.6	141

#	Article	IF	Citations
9783	Structural and Electronic Properties of (Al₂O₃)_n Clusters with n = 1â€“10 from First Principles Calculations. Journal of Physical Chemistry C, 2011, 115, 18111-18121.	1.5	60
9784	A Density Functional Theory Study of Spectroscopic and Thermodynamic Properties of Surfacic Hydrides on Ru (0001) Model Surface: The Influence of the Coordination Modes and the Coverage. Journal of Physical Chemistry C, 2011, 115, 2169-2178.	1.5	30
9785	Periodic Projector Augmented Wave Density Functional Calculations on the Hexachlorobenzene Crystal and Comparison with the Experimental Multipolar Charge Density Model. Journal of Physical Chemistry A, 2011, 115, 14484-14494.	1.1	43
9786	Thermoelectric nanocomposite from the metastable void filling in caged skutterudite. Journal of Materials Research, 2011, 26, 1848-1856.	1.2	13
9787	Tin dioxide from first principles: Quasiparticle electronic states and optical properties. Physical Review B, 2011, 83, .	1.1	145
9788	Predicting Two-Dimensional Boronâ€“Carbon Compounds by the Global Optimization Method. Journal of the American Chemical Society, 2011, 133, 16285-16290.	6.6	242
9789	Silver(ii) triflate with one-dimensional [Ag(ii)(SO3CF3)4/2]â^ž chains hosting antiferromagnetism. CrystEngComm, 2011, 13, 6871.	1.3	21
9790	Nature and Location of Cationic Lanthanum Species in High Alumina Containing Faujasite Type Zeolites. Journal of Physical Chemistry C, 2011, 115, 21763-21776.	1.5	105
9791	Formation of Superoxide Anions on Ceria Nanoparticles by Interaction of Molecular Oxygen with Ce³⁺ Sites. Journal of Physical Chemistry C, 2011, 115, 5817-5822.	1.5	107
9792	A dipole polarizable potential for reduced and doped CeO₂obtained from first principles. Journal of Physics Condensed Matter, 2011, 23, 255402.	0.7	31
9793	First-principles calculations of phase transition, elastic modulus, and superconductivity under pressure for zirconium. Journal of Applied Physics, 2011, 109, .	1.1	66
9794	Possibility of Gas Sensor Using Electronic Transport Properties of Ironâ^’Porphyrin Molecular Junction System. Journal of Physical Chemistry C, 2011, 115, 6886-6892.	1.5	20
9795	Tunable Electronic and Magnetic Properties in B_xN_yC_z Nanohybrids: Effect of Domain Segregation. Journal of Physical Chemistry C, 2011, 115, 10842-10850.	1.5	97
9796	Bi₂Ti₂O₇: It Is Not What You Have Read. Chemistry of Materials, 2011, 23, 4965-4974.	3.2	126
9797	Temperature-driven phase transitions from first principles including all relevant excitations: The fcc-to-bcc transition in Ca. Physical Review B, 2011, 84, .	1.1	52
9798	Electronic Structures of BC₂N Nanoribbons. Journal of Physical Chemistry C, 2011, 115, 3572-3577.	1.5	37
9799	Computational Investigation on Adsorption and Dissociation of the NH₃Molecule on the Fe(111) Surface. Journal of Physical Chemistry C, 2011, 115, 521-528.	1.5	32
9800	Strain Effects in Ge/Si and Si/Ge Core/Shell Nanowires. Journal of Physical Chemistry C, 2011, 115, 15739-15742.	1.5	17

#	Article	IF	Citations
9801	A density functional theory approach to mushroom-like platinum clusters on palladium-shell over Au core nanoparticles for high electrocatalytic activity. Physical Chemistry Chemical Physics, 2011, 13, 5441.	1.3	28
9802	Proton transfer in the hydrogen-bonded chains of lepidocrocite: a computational study. Physical Chemistry Chemical Physics, 2011, 13, 17864.	1.3	11
9803	CeO₂ â†" CuO_x Interactions and the Controlled Assembly of CeO₂(111) and CeO₂(100) Nanoparticles on an Oxidized Cu(111) Substrate. Journal of Physical Chemistry C, 2011, 115, 23062-23066.	1.5	44
9804	Selective Hydrogenolysis of Polyols and Cyclic Ethers over Bifunctional Surface Sites on Rhodiumâ€"Rhenium Catalysts. Journal of the American Chemical Society, 2011, 133, 12675-12689.	6.6	439
9805	Experimental (XAS, STEM, TPR, and XPS) and Theoretical (DFT) Characterization of Supported Rhenium Catalysts. Journal of Physical Chemistry C, 2011, 115, 5740-5755.	1.5	83
9806	Substitutional Alloy of Bi and Te at High Pressure. Physical Review Letters, 2011, 106, 145501.	2.9	363
9807	First-principles characterization of an AlSiVC center in cubic silicon carbide. Journal of Applied Physics, 2011, 110, 033711.	1.1	9
9808	First-Principles Study of Novel Conversion Reactions for High-Capacity Li-Ion Battery Anodes in the Liâ€"Mgâ€"Bâ€"Nâ€"H System. Journal of Physical Chemistry C, 2011, 115, 16681-16687.	1.5	21
9809	Coverage effects in the adsorption of H2 on Pd(100) studied by ab initio molecular dynamics simulations. Journal of Chemical Physics, 2011, 135, 174707.	1.2	35
9810	Asymmetric<mml:math xmlns:mml="http://www.w3.org/1998/Math/MathML" display="inline"><mml:mi>d</mml:mi></mml:math>-O 2<mml:math xmlns:mml="http://www.w3.org/1998/Math/MathML" display="inline"><mml:mi>p</mml:mi></mml:math>hybridization as the origin of hexagonal ferroelectricity in multiferroic HoMnO<mml:math xmlns:mml="http://www.w3.org/1998/Math/MathML" display="inline"><mml:msub><mml:mrow />	1.1	18
9811	Theoretical investigations into the enantiomeric and racemic forms of Î±-(trifluoromethyl)lactic acid. Physical Chemistry Chemical Physics, 2011, 13, 811-817.	1.3	17
9812	Band gap anomalies of the ZnM2IIIO4 (MIII = Co, Rh, Ir) spinels. Physical Chemistry Chemical Physics, 2011, 13, 9667.	1.3	65
9813	O K-energy loss near-edge structure change induced by tantalum impurity in monoclinic hafnium oxide. Journal of Applied Physics, 2011, 109, 053723.	1.1	3
9814	Energy density in density functional theory: Application to crystalline defects and surfaces. Physical Review B, 2011, 83, .	1.1	58
9815	The synergistic effects of the Cuâ€"CeO2(111) catalysts on the adsorption and dissociation of water molecules. Physical Chemistry Chemical Physics, 2011, 13, 9363.	1.3	31
9816	Uncovering the Complex Behavior of Hydrogen in<mml:math xmlns:mml="http://www.w3.org/1998/Math/MathML" display="inline"><mml:msub><mml:mi>Cu</mml:mi><mml:mn>2</mml:mn></mml:msub><mml:mi mathvariant="normal">O</mml:mi></mml:math>. Physical Review Letters, 2011, 106, 186403.	2.9	51
9817	Exceptionally strong magnetism in the 4<mml:math xmlns:mml="http://www.w3.org/1998/Math/MathML" display="inline"><mml:mrow><mml:mi>d</mml:mi></mml:mrow></mml:math>perovskites<mml:math xmlns:mml="http://www.w3.org/1998/Math/MathML" display="inline"><mml:mrow><mml:mi>R</mml:mi></mml:mrow></mml:math>TcO<mml:math xmlns:mml="http://www.w3.org/1998/Math/MathML" display="inline"><mml:mrow><mml:msub><mml:m	1.1	42
9818	Slow Release of NO by Microporous Titanosilicate ETS-4. Journal of the American Chemical Society, 2011, 133, 6396-6402.	6.6	44

#	Article	IF	Citations
9819	Influence of water on the properties of an Au/Mpy/Pd metal/molecule/metal junction. Beilstein Journal of Nanotechnology, 2011, 2, 384-393.	1.5	5
9820	Density functional theory study of NO ₂ -sensing mechanisms of pure and Ti-doped WO ₃ (002) surfaces. Chinese Physics B, 2011, 20, 102101.	0.7	18
9821	Electronic structures of Fe-terminated armchair boron nitride nanoribbons. Applied Physics Letters, 2011, 99, .	1.5	25
9822	Large ferroelectric polarization in the new double perovskite NaLaMnWO6 induced by non-polar instabilities. Physical Chemistry Chemical Physics, 2011, 13, 12186.	1.3	93
9823	Electronic structure of bismuth telluride quasi-two-dimensional crystal: A first principles study. Applied Physics Letters, 2011, 98, .	1.5	19
9824	Vibrational properties of the LiNbO3 z-surfaces. IEEE Transactions on Ultrasonics, Ferroelectrics, and Frequency Control, 2011, 58, 1751-1756.	1.7	9
9825	Ab Initio Study on a Novel Photocatalyst: Functionalized Graphitic Carbon Nitride Nanotube. ACS Catalysis, 2011, 1, 99-104.	5.5	118
9826	Structural basis for supercooled liquid fragility established by synchrotron-radiation method and computer simulation. Journal of Applied Physics, 2011, 110, 043519.	1.1	39
9827	Application to Ceramic Interfaces. , 2011, , 467-521.		0
9828	Dispersion of edge states and quantum confinement of electrons in graphene channels drawn on graphene fluoride. Physical Review B, 2011, 83, .	1.1	14
9829	First-principles study of competing mechanisms of nondilute Li diffusion in spinel Li<mml:math xmlns:mml="http://www.w3.org/1998/Math/MathML" display="inline"><mml:mrow><mml:msub><mml:mrow /><mml:mrow><mml:mi>x</mml:mi></mml:mrow></mml:msub></mml:mrow></mml:math>TiS<mml:math xmlns:mml="http://www.w3.org/1998/Math/MathML" display="inline"><mml:mrow><mml:msub><mml:mrow /><mml:mrow><mml:mn>2</mml:mn></mml:mro	1.1	67
9830	Density functional theory based study of graphene and dielectric oxide interfaces. Journal of Physics Condensed Matter, 2011, 23, 505503.	0.7	7
9832	Anisotropic interactions and strain-induced topological phase transition in Sb<mml:math xmlns:mml="http://www.w3.org/1998/Math/MathML" display="inline"><mml:msub><mml:mrow /><mml:mn>2</mml:mn></mml:msub></mml:math>Se<mml:math xmlns:mml="http://www.w3.org/1998/Math/MathML" display="inline"><mml:msub><mml:mrow /><mml:mn>3</mml:mn></mml:msub></mml:math>and Bi<mml:math xmlns:mml="http://www.w3.org/1998/Math/MathML" display="inline"><mml:msub><mml:mrow /><mml:mml:	1.1	101
9833	Graphitic GaNâ€“ZnO and corresponding nanotubes. Journal of Materials Chemistry, 2011, 21, 17071.	6.7	5
9834	Lattice dynamics of anharmonic solids from first principles. Physical Review B, 2011, 84, .	1.1	482
9835	Temperature-driven Î±-to-Î² phase transformation in Ti, Zr and Hf from first-principles theory combined with lattice dynamics. Europhysics Letters, 2011, 96, 66006.	0.7	27
9836	Density functional study of carbon doping in ZnO. Semiconductor Science and Technology, 2011, 26, 014038.	1.0	24
9837	Bonding Changes Along Solid-Solid Phase Transitions Using the Electron Localization Function Approach. , 2011, , 625-658.		3

#	Article	IF	Citations
9838	Structural and electronic properties of Sc<mml:math xmlns:mml="http://www.w3.org/1998/Math/MathML" display="inline"><mml:msub><mml:mrow /><mml:mi>n</mml:mi></mml:msub><mml:math>O<mml:math xmlns:mml="http://www.w3.org/1998/Math/MathML" display="inline"><mml:msub><mml:mrow		

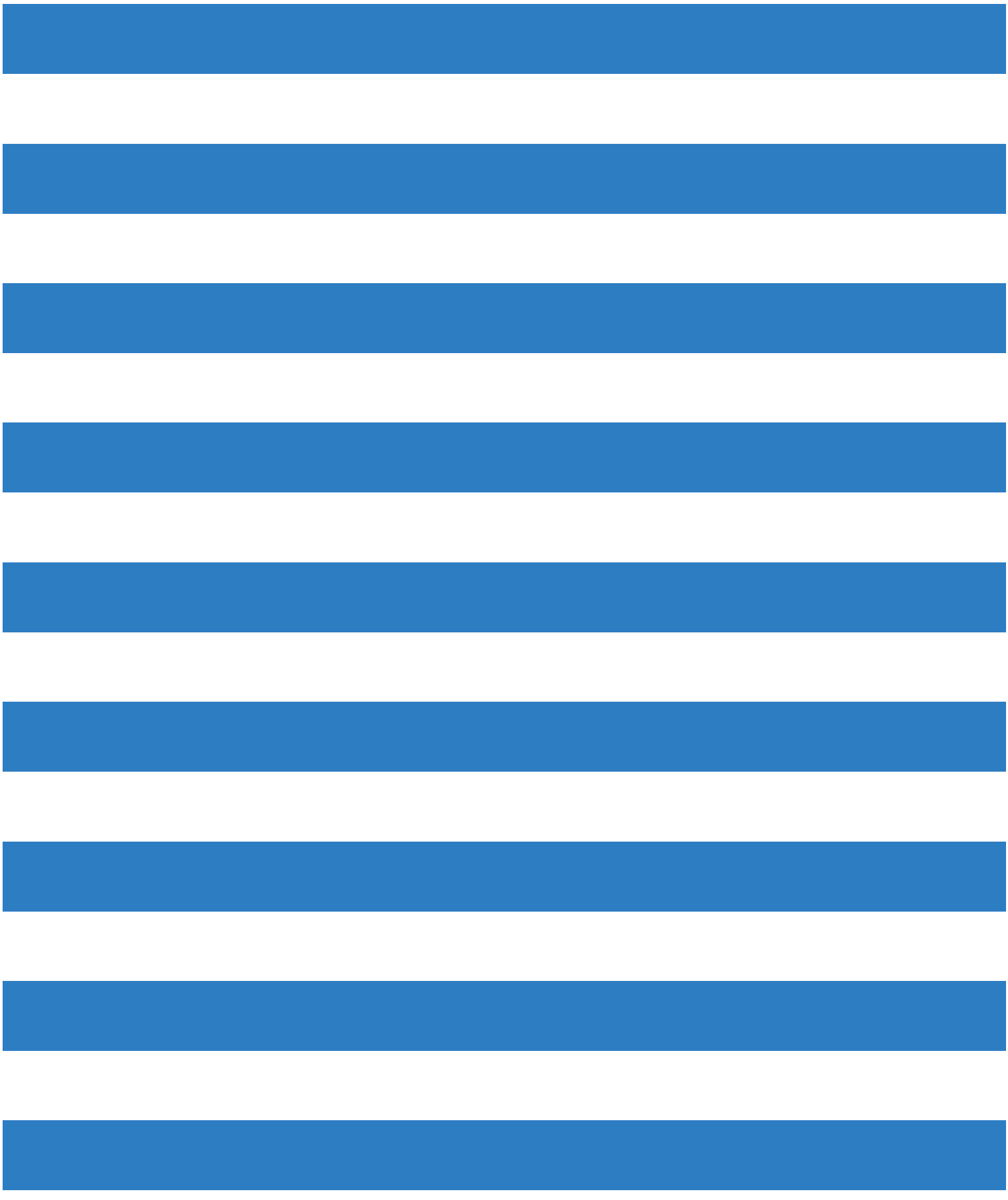

#	Article	IF	Citations
9856	Large Isosymmetric Reorientation of Oxygen Octahedra Rotation Axes in Epitaxially Strained Perovskites. Physical Review Letters, 2011, 106, 235502.	2.9	45
9857	Syntheses and Characterization of New Mid-Infrared Transparency Compounds: Centric Ba₂BiGaS₅ and Acentric Ba₂BiInS₅. Inorganic Chemistry, 2011, 50, 5679-5686.	1.9	90
9858	Electronic structures and bonding of graphyne sheet and its BN analog. Journal of Chemical Physics, 2011, 134, 174701.	1.2	182
9859	Multiscale Simulation of Nanostructured Materials and Systems. Japanese Journal of Applied Physics, 2011, 50, 05FE08.	0.8	0
9860	Thermodynamic properties of Pt nanoparticles: Size, shape, support, and adsorbate effects. Physical Review B, 2011, 84, .	1.1	50
9861	Density Functional Theory Analysis of the Interplay between Jahnâ^'Teller Instability, Uniaxial Magnetism, Spin Arrangement, Metalâ^'Metal Interaction, and Spinâ^'Orbit Coupling in Ca₃CoMO₆ (M = Co, Rh, Ir). Inorganic Chemistry, 2011, 50, 1758-1766.	1.9	25
9862	Switching and rectification of a single light-sensitive diarylethene molecule sandwiched between graphene nanoribbons. Journal of Chemical Physics, 2011, 135, 184703.	1.2	60
9863	Structural and magnetic properties of ternary Fe_{1â€“}_xMn_xPt nanoalloys from first principles. Beilstein Journal of Nanotechnology, 2011, 2, 162-172.	1.5	12
9864	Energetic Molecules Encapsulated Inside Carbon Nanotubes and between Graphene Layers: DFT Calculations. Journal of Physical Chemistry C, 2011, 115, 10985-10989.	1.5	60
9865	Ground states of group-IV nanostructures: Magic structures of diamond and silicon nanocrystals. Physical Review B, 2011, 83, .	1.1	13
9866	Computational studies of doped nanostructures. Reports on Progress in Physics, 2011, 74, 046501.	8.1	52
9867	Size effect of Pd clusters on hydrogen adsorption. Journal of Physics Condensed Matter, 2011, 23, 045503.	0.7	14
9868	Piezomagnetic behavior of Co-doped ZnO nanoribbons. Physical Review B, 2011, 84, .	1.1	7
9869	Mechanism for direct conversion of graphite to diamond. Physical Review B, 2011, 84, .	1.1	34
9870	Ab initiostudy of the magnetic ordering in Si/Mn digital alloys. Physical Review B, 2011, 84, .	1.1	12
9871	Point Defects on Graphene on Metals. Physical Review Letters, 2011, 107, 116803.	2.9	202
9872	Linear Alkane Polymerization on a Gold Surface. Science, 2011, 334, 213-216.	6.0	321
9873	Electrostatic Doping of Graphene through Ultrathin Hexagonal Boron Nitride Films. Nano Letters, 2011, 11, 4631-4635.	4.5	118

#	Article	IF	Citations
9874	Calculations of Li-Ion Diffusion in Olivine Phosphates. Chemistry of Materials, 2011, 23, 4032-4037.	3.2	249
9875	Identifying surface structural changes in layered Li-excess nickel manganese oxides in high voltage lithium ion batteries: A joint experimental and theoretical study. Energy and Environmental Science, 2011, 4, 2223.	15.6	728
9876	Hydrogen Adsorption on Ga₂O₃ Surface: A Combined Experimental and Computational Study. Journal of Physical Chemistry C, 2011, 115, 10140-10146.	1.5	61
9877	Chemical Transformation of Au-Tipped CdS Nanorods into AuS/Cd Core/Shell Particles by Electron Beam Irradiation. Nano Letters, 2011, 11, 4555-4561.	4.5	33
9878	Study on the Energy Band Structure of La Doped ZnO. Advanced Materials Research, 0, 233-235, 2119-2124.	0.3	1
9879	Tailoring Homochirality at Surfaces: Going Beyond Molecular Handedness. Journal of the American Chemical Society, 2011, 133, 15992-16000.	6.6	33
9880	Using Atomic Layer Deposition to Hinder Solvent Decomposition in Lithium Ion Batteries: First-Principles Modeling and Experimental Studies. Journal of the American Chemical Society, 2011, 133, 14741-14754.	6.6	174
9881	Zipping Up: Cooperativity Drives the Synthesis of Graphene Nanoribbons. Journal of the American Chemical Society, 2011, 133, 14884-14887.	6.6	110
9882	Density Functional Theory Study of the Oxidation of Ammonia on the IrO₂(110) Surface. Langmuir, 2011, 27, 14253-14259.	1.6	19
9883	Graphene Spintronics: The Role of Ferromagnetic Electrodes. Nano Letters, 2011, 11, 151-155.	4.5	137
9884	Methyl Formate Pathway in Methanol Steam Reforming on Copper: Density Functional Calculations. ACS Catalysis, 2011, 1, 1263-1271.	5.5	47
9885	Electronic structure and physical properties of the spinel-type phase of BeP2N4from all-electron density functional calculations. Physical Review B, 2011, 83, .	1.1	23
9886	Magnetic and electronic structure properties of Co-doped SnO2 nanoparticles synthesized by the sol-gel-hydrothermal technique. Journal of Applied Physics, 2011, 109, 083930.	1.1	32
9887	Enhanced one dimensional mobility of oxygen on strained LaCoO3(001) surface. Journal of Materials Chemistry, 2011, 21, 18983.	6.7	64
9888	Effect of Coverage and Defects on the Adsorption of Propanethiol on Au(111) Surface: A Theoretical Study. Langmuir, 2011, 27, 14514-14521.	1.6	29
9889	First-principles study of diffusion of interstitial and vacancy in Î± Uâ€“Zr. Journal of Physics Condensed Matter, 2011, 23, 205402.	0.7	26
9890	Effect of the external electric field on surface states: Anab initiostudy. Physical Review B, 2011, 84, .	1.1	17
9891	Electronic and Magnetic Properties and Structural Stability of BeO Sheet and Nanoribbons. ACS Applied Materials & Interfaces, 2011, 3, 4787-4795.	4.0	62

#	Article	IF	Citations
9892	Theoretical Study of Electrochemical Processes on Ptâ€“Ni Alloys. Journal of Physical Chemistry C, 2011, 115, 10640-10650.	1.5	79
9893	Structural and vibrational study of Bi<mml:math xmlns:mml="http://www.w3.org/1998/Math/MathML" display="inline"><mml:msub><mml:mrow /><mml:mn>2</mml:mn></mml:msub></mml:math>Se<mml:math xmlns:mml="http://www.w3.org/1998/Math/MathML" display="inline"><mml:msub><mml:mrow /><mml:mn>3</mml:mn></mml:msub></mml:math>under high pressure. Physical Review B, 2011, 84, .	1.1	138
9894	Revisiting Mn-doped Ge using the Heyd-Scuseria-Ernzerhof hybrid functional. Physical Review B, 2011, 83, .	1.1	59
9895	Electronic structures and work functions of BC3 nanotubes: A first-principle study. Journal of Applied Physics, 2011, 110, .	1.1	20
9896	Elementary Excitations at Magnetic Surfaces and Their Spin Dependence. Physical Review Letters, 2011, 106, 127201.	2.9	24
9897	Charge Transport in Strongly Coupled Molecular Junctions: â€œIn-Phaseâ€• and â€œOut-of-Phaseâ€• Contribution to Electron Tunneling. Journal of Physical Chemistry C, 2011, 115, 17564-17573.	1.5	8
9898	Stoichiometry of the<mml:math xmlns:mml="http://www.w3.org/1998/Math/MathML" display="inline"><mml:mrow><mml:msub><mml:mi mathvariant="normal">LaFeO</mml:mi><mml:mrow><mml:mn>3</mml:mn></mml:mrow></mml:msub></mml:mrow></mml:math>(01 surface determined from first-principles and thermodynamic calculations. Physical Review B, 2011, 83, .	1.1	33
9899	Doping of graphene by a Au(111) substrate: Calculation strategy within the local density approximation and a semiempirical van der Waals approach. Physical Review B, 2011, 83, .	1.1	90
9900	Lattice normal modes and electronic properties of the correlated metal LaNiO<mml:math xmlns:mml="http://www.w3.org/1998/Math/MathML" display="inline"><mml:msub><mml:mrow /><mml:mn>3</mml:mn></mml:msub></mml:math>. Physical Review B, 2011, 84, .	1.1	110
9901	Electronic and optical properties of potential solar absorber Cu3PSe4. Applied Physics Letters, 2011, 99, .	1.5	25
9902	CO2 adsorption on TiO2(110) rutile: Insight from dispersion-corrected density functional theory calculations and scanning tunneling microscopy experiments. Journal of Chemical Physics, 2011, 134, 104707.	1.2	91
9903	Native defects in Al2O3 and their impact on III-V/Al2O3 metal-oxide-semiconductor-based devices. Journal of Applied Physics, 2011, 109, .	1.1	149
9904	Feasibility of band gap engineering of pyrite FeS<mml:math xmlns:mml="http://www.w3.org/1998/Math/MathML" display="inline"><mml:msub><mml:mrow /><mml:mn>2</mml:mn></mml:msub></mml:math>. Physical Review B, 2011, 84, .	1.1	48
9905	U and Xe transport in UO<mml:math xmlns:mml="http://www.w3.org/1998/Math/MathML" display="inline"><mml:msub><mml:mrow /><mml:mrow><mml:mn>2</mml:mn><mml:mo>Â±</mml:mo><mml:mi>x</mml:mi></mml:mrow></mml:msub></mml:math>: Density functional theory calculations. Physical Review B, 2011, 84, .	1.1	110
9906	Imprinting self-assembled patterns of lines at a semiconductor surface, using heat, light, or electrons. Proceedings of the National Academy of Sciences of the United States of America, 2011, 108, 950-955.	3.3	26
9907	Hydrogen insertion in Pd core/Pt shell cubo-octahedral nanoparticles. Physical Review B, 2011, 83, .	1.1	12
9908	Syntheses, structures and properties of coordination polymers of cadmium(ii) with 4-methyl-1,2,4-triazole-3-thiol ligand. CrystEngComm, 2011, 13, 1697.	1.3	30
9909	Lattice dynamics of Sb<mml:math xmlns:mml="http://www.w3.org/1998/Math/MathML" display="inline"><mml:msub><mml:mrow /><mml:mn>2</mml:mn></mml:msub></mml:math>Te<mml:math xmlns:mml="http://www.w3.org/1998/Math/MathML" display="inline"><mml:msub><mml:mrow /><mml:mn>3</mml:mn></mml:msub></mml:math>at high pressures. Physical Review B, 2011, 84, .	1.1	108

#	Article	IF	Citations
9910	Charge-driven structural transformation and valence versatility of boron sheets in magnesium borides. Physical Review B, 2011, 83, .	1.1	18
9911	Theoretical study of the structure of self-assembled monolayers of short alkylthiolates on Au(111) and Ag(111): the role of induced substrate reconstruction and chainâ€“chain interactions. Physical Chemistry Chemical Physics, 2011, 13, 9353.	1.3	24
9912	Phase Transitions in Epitaxial (<mml:math xmlns:mml="http://www.w3.org/1998/Math/MathML") Tj ETQq0 0 0 rgBT /Overlock 10 Tf 50 6 xmlns:mml="http://www.w3.org/1998/Math/MathML" display="inline"><mml:msub><mml:mi>BiFeO</mml:mi><mml:mn>3</mml:mn></mml:msub></mml:math>Films from First Principles. Physical Review Letters, 2011, 107, 117602.	2.9	37
9913	Elastic properties of poly(vinyldene fluoride) (PVDF) crystals: A density functional theory study. Journal of Applied Physics, 2011, 109, .	1.1	35
9914	Enhanced photoelectrochemical activity for Cu and Ti doped hematite: The first principles calculations. Applied Physics Letters, 2011, 98, .	1.5	84
9915	Hybrid density functional theory description of N- and C-doping of NiO. Journal of Chemical Physics, 2011, 134, 224703.	1.2	34
9916	Ab initio calculations of the reaction pathways for methane decomposition over the Cu (111) surface. Journal of Chemical Physics, 2011, 135, 064707.	1.2	78
9918	Doping of graphene adsorbed on the a-SiO2 surface. Applied Physics Letters, 2011, 99, 163108.	1.5	46
9919	Bias in bonding behavior among boron, carbon, and nitrogen atoms in ion implanted a-BN, a-BC, and diamond like carbon films. Journal of Applied Physics, 2011, 110, .	1.1	20
9920	Ab initio studies of the Sn-doped ZnO transparent conductive oxide. Journal of Physics: Conference Series, 2011, 276, 012194.	0.3	4
9921	Carbon Monoxide-Tolerant Platinum Nanoparticle Catalysts on Defect-Engineered Graphene. ACS Nano, 2011, 5, 805-810.	7.3	127
9922	Experimental and computational study of crystalline formic acid composed of the higher-energy conformer. Journal of Chemical Physics, 2011, 134, 054506.	1.2	10
9923	Origin of the low thermal conductivity of the thermoelectric material Î²-Zn4Sb3: An ab initio theoretical study. Applied Physics Letters, 2011, 98, .	1.5	20
9924	Transport Properties of Hybrid Zigzag Graphene and Boron Nitride Nanoribbons. Journal of Physical Chemistry C, 2011, 115, 10836-10841.	1.5	45
9925	Ab initio Study of Half-Metallicity and Magnetism of Complex Organometallic Molecular Wires. Journal of Physical Chemistry C, 2011, 115, 7292-7297.	1.5	19
9926	Hydrolysis of Imidazole-2-ylidenes. Journal of the American Chemical Society, 2011, 133, 780-789.	6.6	135
9927	Formation of Self-Assembled Chains of Tetrathiafulvalene on a Cu(100) Surface. Journal of Physical Chemistry A, 2011, 115, 13080-13087.	1.1	6
9928	Density-based mixing parameter for hybrid functionals. Physical Review B, 2011, 83, .	1.1	338

#	Article	IF	Citations
9929	Magnetoelastic coupling in<mml:math xmlns:mml="http://www.w3.org/1998/Math/MathML" display="inline"><mml:mi>Î³</mml:mi></mml:math>-iron investigated within anab initiospin spiral approach. Physical Review B, 2011, 84, .	1.1	39
9930	Grain boundary atomic structures and light-element visualization in ceramics: combination of Cs-corrected scanning transmission electron microscopy and first-principles calculations. Microscopy (Oxford, England), 2011, 60, S173-S188.	0.7	20
9931	First-principles study on the interaction of H interstitials with grain boundaries in<mml:math xmlns:mml="http://www.w3.org/1998/Math/MathML" display="inline"><mml:mi>Î±</mml:mi></mml:math>- and<mml:math xmlns:mml="http://www.w3.org/1998/Math/MathML" display="inline"><mml:mi>Î³</mml:mi></mml:math>-Fe. Physical Review B, 2011, 84, .	1.1	211
9932	Optical properties of water at high temperature. Physics of Plasmas, 2011, 18, .	0.7	20
9933	First-principles investigation of Ca<mml:math xmlns:mml="http://www.w3.org/1998/Math/MathML" display="inline"><mml:mrow><mml:msub><mml:mrow /><mml:mrow><mml:mn>3</mml:mn></mml:mrow></mml:msub></mml:mrow></mml:math>(Ti, Zr, Hf,) Tj ETQq0 0 0 rgBT /Overlock 1	1.1	20
9934	<mml:math xmlns:mml="http://www.w3.org/1998/Math/MathML" display="inline"><mml:mrow><mml:msub><mml:mrow /><mml:mrow><mml:mn>2</mml:mn></mml:mrow></mml:msub></mml:mrow></mml:math>Fe<mml:math Role of iron in the incorporation of uranium in ferric garnet matrices. Physical Review B, 2011, 84, .	1.1	40
9935	Fe-Fe adatom interaction and growth morphology on graphene. Physical Review B, 2011, 84, .	1.1	23
9936	Periodically Modulated Electronic Properties of the Epitaxial Monolayer Graphene on Ru(0001). Journal of Physical Chemistry C, 2011, 115, 24858-24864.	1.5	36
9937	Ab initiostudy of ferromagnetic single-wall nickel nanotubes. Physical Review B, 2011, 84, .	1.1	17
9938	Ab initiostudy of palladium and silicon carbide. Philosophical Magazine, 2011, 91, 458-467.	0.7	4
9939	First-principles calculation and experimental study of oxygen diffusion in uranium dioxide. Physical Review B, 2011, 83, .	1.1	112
9940	Atomic-scale investigation on lithium storage mechanism in TiNb2O7,. Energy and Environmental Science, 2011, 4, 2638.	15.6	256
9941	Phase Stability and Elasticity of TiAlN. Materials, 2011, 4, 1599-1618.	1.3	80
9942	Crystal structure and dynamics of Mg(ND3)6Cl2. Physical Chemistry Chemical Physics, 2011, 13, 7644.	1.3	9
9943	Design of a low band gap oxide ferroelectric: Bi 6 Ti 4 O 17. Europhysics Letters, 2011, 94, 37006.	0.7	3
9944	Alloying effects on the elastic parameters of ferromagnetic and paramagnetic Fe from first-principles theory. Journal of Applied Physics, 2011, 110, .	1.1	22
9945	Vibrational Signatures in the Infrared Spectra of Single- and Double-Walled Carbon Nanotubes and Their Diameter Dependence. Journal of Physical Chemistry Letters, 2011, 2, 2079-2082.	2.1	15
9946	Interatomic potential for the Al-Cu system. Physical Review B, 2011, 83, .	1.1	123

#	Article	IF	Citations
9947	First-Principles Study of the Local Magnetic Moment on a N-Doped Cu ₂ O (111) Surface. Chinese Physics Letters, 2011, 28, 127102.	1.3	1
9948	A formation mechanism of oxygen vacancies in a MnO2 monolayer: a DFT + U study. Physical Chemistry Chemical Physics, 2011, 13, 11325.	1.3	37
9949	Bonding and charge transfer by metal adatom adsorption on graphene. Physical Review B, 2011, 83, .	1.1	167
9950	Tunable Band Gaps in Bilayer Grapheneâ^'BN Heterostructures. Nano Letters, 2011, 11, 1070-1075.	4.5	224
9951	Electronic and optical properties of Mg_xZn_{1â^'x}O and Cd_xZn_{1â^'x}O fromab initiocalculations. New Journal of Physics, 2011, 13, 085012.	1.2	60
9952	Structure-Dependent Ferromagnetism in Mn-Doped IIIâ€“V Nanowires. Nano Letters, 2011, 11, 3319-3323.	4.5	38
9953	Adsorption and (photo-) electrochemical splitting of water on rutile ruthenium dioxide. Europhysics Letters, 2011, 93, 68001.	0.7	11
9954	Ab Initio Simulations of the Effects of Nanoscale Confinement on Proton Transfer in Hydrophobic Environments. Journal of Physical Chemistry B, 2011, 115, 10826-10835.	1.2	18
9955	On the Magnetic Insulating States, Spin Frustration, and Dominant Spin Exchange of the Ordered Double-Perovskites Sr2CuOsO6and Sr2NiOsO6: Density Functional Analysis. Inorganic Chemistry, 2011, 50, 4142-4148.	1.9	27
9956	A First-Principles Model for Hydrogen Uptake Promoted by Sulfur on Ni(111). Journal of the Electrochemical Society, 2011, 158, F36.	1.3	17
9957	Interaction of Gold Clusters with a Hydroxylated Surface. Journal of Physical Chemistry Letters, 2011, 2, 1211-1215.	2.1	39
9958	Electronic structure and oxygen vacancies in PdO and ZnO: validation of DFT models. Physical Chemistry Chemical Physics, 2011, 13, 15947.	1.3	35
9959	Physical and chemical properties of a Ga-doped ZnO crystal. Physica Scripta, 2011, 83, 065604.	1.2	11
9960	Visible Light Photo-oxidation of Model Pollutants Using CaCu₃Ti₄O₁₂: An Experimental and Theoretical Study of Optical Properties, Electronic Structure, and Selectivity. Journal of the American Chemical Society, 2011, 133, 1016-1032.	6.6	130
9961	A comparative study of quantum transport properties of silver and copper nanowires using first principles calculations. Journal of Physics Condensed Matter, 2011, 23, 085501.	0.7	28
9962	Surface core-level shifts on Ge(111)<mml:math xmlns:mml="http://www.w3.org/1998/Math/MathML" display="inline"><mml:mrow><mml:mi>c</mml:mi><mml:mo stretchy="false">(</mml:mo><mml:mn>2</mml:mn><mml:mo>Ã—</mml:mo><mml:mn>8</mml:mn><mml:mo) TjETQq1 1 0.784314 rgBT /Overlock 10 Tf 50 22 Td (2011, 83, .		
9963	Synthesis and Electrochemical Properties of Monoclinic LiMnBO[sub 3] as a Li Intercalation Material. Journal of the Electrochemical Society, 2011, 158, A309.	1.3	94
9964	Prediction of solid oxide fuel cell cathode activity with first-principles descriptors. Energy and Environmental Science, 2011, 4, 3966.	15.6	464

#	Article	IF	Citations
9965	First-principles study of stability of the bcc and Ï‰ phases of a low Al concentration Nb_{1 â^’x}Al_xalloy. Journal of Physics Condensed Matter, 2011, 23, 295501.	0.7	3
9966	Classification of the critical resolved shear stress in the hexagonal-close-packed materials by atomic simulation: Application to Î±-zirconium and Î±-titanium. Journal of Applied Physics, 2011, 110, .	1.1	67
9967	A New Organicâ€“Inorganic Hybrid Oxyfluorotitanate [Hgua]₂Â·(Ti₅O₅F₁₂) as a Transparent UV Filter. Inorganic Chemistry, 2011, 50, 5671-5678.	1.9	13
9968	Tailoring Au-core Pd-shell Pt-cluster nanoparticles for enhanced electrocatalytic activity. Chemical Science, 2011, 2, 531-539.	3.7	172
9969	Emergence of Atypical Properties in Assembled Graphene Nanoribbons. Physical Review Letters, 2011, 107, 135501.	2.9	69
9970	Tunable band gaps in bilayer transition-metal dichalcogenides. Physical Review B, 2011, 84, .	1.1	538
9971	Density Functional Theory Study of H and CO Adsorption on Alkali-Promoted Mo₂C Surfaces. Journal of Physical Chemistry C, 2011, 115, 6870-6876.	1.5	59
9972	Raman spectroscopy of the internal strain of a graphene layer grown on copper tuned by chemical vapor deposition. Physical Review B, 2011, 84, .	1.1	49
9973	Wetting of Intact and Partially Dissociated Water Layer on Ru(0001): a Density Functional Study. Journal of Physical Chemistry C, 2011, 115, 5834-5840.	1.5	10
9974	First-principles calculations of lattice dynamics in CdTiO<mml:math xmlns:mml="http://www.w3.org/1998/Math/MathML" display="inline"><mml:msub><mml:mrow /><mml:mn>3</mml:mn></mml:msub></mml:math>and CaTiO<mml:math xmlns:mml="http://www.w3.org/1998/Math/MathML" display="inline"><mml:msub><mml:mrow /><mml:mn>3</mml:mn></mml:msub></mml:math>: Phase stability and ferroelectricity. Physical Review B, 2011, 84, .	1.1	58
9975	Thermal Dehydration and Vibrational Spectra of Hydrated Sodium Metaborates. Industrial & Engineering Chemistry Research, 2011, 50, 7746-7752.	1.8	30
9976	On the dissociation of molecular hydrogen by Au supported on transition metal carbides: choice of the most active support. Physical Chemistry Chemical Physics, 2011, 13, 6865.	1.3	31
9977	Temperature-induced martensitic phase transitions in gum-metal approximants: First-principles investigations for Ti<mml:math xmlns:mml="http://www.w3.org/1998/Math/MathML" display="inline"><mml:msub><mml:mrow /><mml:mn>3</mml:mn></mml:msub></mml:math>Nb. Physical Review B, 2011, 84, .	1.1	41
9978	First Principles Studies of the Effect of Ostwald Ripening on Carbon Nanotube Chirality Distributions. ACS Nano, 2011, 5, 771-779.	7.3	27
9979	Tuning the Electronic Transport Properties of Zigzag Graphene Nanoribbons via Hydrogenation Separators. Journal of Physical Chemistry C, 2011, 115, 24366-24372.	1.5	10
9980	First-principles studies of Te<mml:math xmlns:mml="http://www.w3.org/1998/Math/MathML" display="inline"><mml:mrow><mml:msub><mml:mrow /><mml:mrow><mml:mn>2</mml:mn></mml:mrow></mml:msub></mml:mrow></mml:math>O<mml:math xmlns:mml="http://www.w3.org/1998/Math/MathML" display="inline"><mml:mrow><mml:msub><mml:mrow /><mml:mrow><mml:mn>5</mml:mn></mml:mrow></mml:msub></mml:mrow></mml:math>polymorphs.	1.1	57
9981	Ultrafast Solid-State Transformation Pathway from New-Phased Goethite VOOH to Paramontroseite VO₂ to Rutile VO₂(R). Journal of Physical Chemistry C, 2011, 115, 791-799.	1.5	49
9982	Structural and electronic properties of silver/silicon interfaces and implications for solar cell performance. Physical Review B, 2011, 83, .	1.1	32

#	Article	IF	Citations
9983	First-principles study of the influence of (110)-oriented strain on the ferroelectric properties of rutile TiO2. Physical Review B, 2011, 84, .	1.1	20
9984	Tin Monoxide: Structural Prediction from First Principles Calculations with van der Waals Corrections. Journal of Physical Chemistry C, 2011, 115, 19916-19924.	1.5	95
9985	Comparison of the defective pyrochlore and ilmenite polymorphs of AgSb<mml:math xmlns:mml="http://www.w3.org/1998/Math/MathML" display="inline"><mml:mrow><mml:msub><mml:mi>O</mml:mi><mml:mrow><mml:mn>3</mml:mn></mml:mrow></mml:msub></mm GGA and hybrid DFT. Physical Review B, 2011, 83, .	1.1	23
9986	A guideline for atomistic design and understanding of ultrahard nanomagnets. Nature Communications, 2011, 2, 528.	5.8	67
9987	Vacancy-induced magnetism in BaTiO3(001) thin films based on density functional theory. Physical Chemistry Chemical Physics, 2011, 13, 4738.	1.3	29
9988	Effects of rhenium alloying on adhesion of Mo/HfC and Mo/ZrC interfaces: A first-principles study. Journal of Applied Physics, 2011, 110, .	1.1	14
9989	Defects in SiC for quantum computing. Journal of Applied Physics, 2011, 109, .	1.1	66
9990	Self-Assembly of Metal Phthalocyanines on Pb(111) and Au(111) Surfaces at Submonolayer Coverage. Journal of Physical Chemistry C, 2011, 115, 21750-21754.	1.5	41
9991	Adsorption and reaction of SO2 on clean and oxygen precovered Pd(100)â€"a combined HR-XPS and DF study. Physical Chemistry Chemical Physics, 2011, 13, 16227.	1.3	18
9992	A germanate transparent conductive oxide. Nature Communications, 2011, 2, 470.	5.8	88
9993	Hydrogen interaction with fullerenes: From C<mml:math xmlns:mml="http://www.w3.org/1998/Math/MathML" display="inline"><mml:msub><mml:mrow /><mml:mn>20</mml:mn></mml:msub></mml:math>to graphene. Physical Review B, 2011, 84, .	1.1	24
9994	Theory of structural trends within<mml:math xmlns:mml="http://www.w3.org/1998/Math/MathML" display="inline"><mml:mrow><mml:mn>4</mml:mn><mml:mi>d</mml:mi></mml:mrow></mml:math>and<mml:math xmlns:mml="http://www.w3.org/1998/Math/MathML" display="inline"><mml:mrow><mml:mn>5</mml:mn><mml:mi>d</mml:mi></mml:mrow></mml:math>transition metal topologically close-packed phases. Physical Review B, 2011, 83, .	1.1	58
9995	Optimization of the magnetic potential for Î±-Fe. Journal of Physics Condensed Matter, 2011, 23, 206001.	0.7	40
9996	Hydrogen in layered iron arsenides: Indirect electron doping to induce superconductivity. Physical Review B, 2011, 84, .	1.1	109
9997	Diffusion of Al, O, Pt, Hf, and Y atoms on Î±-Al₂O₃(0001): implications for the role of alloying elements in thermal barrier coatings. Journal of Materials Chemistry, 2011, 21, 1447-1456.	6.7	41
9998	From VO2 (B) to VO2 (A) nanobelts: first hydrothermal transformation, spectroscopic study and first principles calculation. Physical Chemistry Chemical Physics, 2011, 13, 15873.	1.3	99
9999	Direct hydrothermal synthesis of monoclinic VO2(M) single-domain nanorods on large scale displaying magnetocaloric effect. Journal of Materials Chemistry, 2011, 21, 4509.	6.7	106
10000	Magnetism of Phthalocyanine-Based Organometallic Single Porous Sheet. Journal of the American Chemical Society, 2011, 133, 15113-15119.	6.6	350

#	Article	IF	Citations
10001	Improved visible-light photocatalysis of nano-Bi2Sn2O7 with dispersed s-bands. Journal of Materials Chemistry, 2011, 21, 3872.	6.7	92
10002	Identification of <mml:math xmlns:mml="http://www.w3.org/1998/Math/MathML" display="inline"><mml:mi>p</mml:mi></mml:math>-type skutterudites<mml:math xmlns:mml="http://www.w3.org/1998/Math/MathML" display="inline"><mml:mi>R</mml:mi></mml:math>Fe<mml:math xmlns:mml="http://www.w3.org/1998/Math/MathML" display="inline"><mml:msub><mml:mrow /><mml:mn>4</mml:mn></mml:msub></mml:math>Sb<mml:math xmlns:mml="http://www.w3.org/1998/M	1.1	76
10003	Manganese Triazacyclononane Oxidation Catalysts Grafted under Reaction Conditions on Solid Cocatalytic Supports. Journal of the American Chemical Society, 2011, 133, 18684-18695.	6.6	44
10004	Novel Superhard Carbon: C-Centered Orthorhombic<mml:math xmlns:mml="http://www.w3.org/1998/Math/MathML" display="inline"><mml:msub><mml:mi mathvariant="normal">C</mml:mi><mml:mn>8</mml:mn></mml:msub></mml:math>. Physical Review Letters, 2011, 107, 215502.	2.9	225
10005	Denser than diamond:Ab initiosearch for superdense carbon allotropes. Physical Review B, 2011, 83, .	1.1	118
10006	High-Pressure Study of Lithium Azide from Density-Functional Calculations. Journal of Physical Chemistry A, 2011, 115, 4521-4529.	1.1	32
10007	DFT Studies on the Interaction of Defective Graphene-Supported Fe and Al Nanoparticles. Journal of Physical Chemistry C, 2011, 115, 8961-8970.	1.5	175
10008	Chemical Resolution at Ionic Crystal Surfaces Using Dynamic Atomic Force Microscopy with Metallic Tips. Physical Review Letters, 2011, 106, 216102.	2.9	56
10009	Facile Charge-Displacement at Silicon Gives Spaced-out Reaction. Journal of the American Chemical Society, 2011, 133, 16560-16565.	6.6	7
10010	Fluorinating Hexagonal Boron Nitride into Diamond-Like Nanofilms with Tunable Band Gap and Ferromagnetism. Journal of the American Chemical Society, 2011, 133, 14831-14838.	6.6	79
10011	Evaluation of Theoretical Approaches for Describing the Interaction of Water with Linear Acenes. Journal of Physical Chemistry A, 2011, 115, 5955-5964.	1.1	24
10012	Thermodynamic modelling of nanomorphologies of hematite and goethite. Journal of Materials Chemistry, 2011, 21, 11566.	6.7	114
10013	Structure and properties of the low-density phase Î¹-Al2O3from first principles. Physical Review B, 2011, 84, .	1.1	23
10014	Interface Control of Emergent Ferroic Order in Ruddlesden-Popper<mml:math xmlns:mml="http://www.w3.org/1998/Math/MathML" display="inline"><mml:msub><mml:mi>Sr</mml:mi><mml:mrow><mml:mi>n</mml:mi><mml:mo>+</mml:mo><mml:mn>1</mml:mn></mml:mrow></mml:msub></mml:math><mml:math xmlns:mml="http://www.w3.org/1998/Math/MathML" mathvariant="bold">O</mml:mi><mml:mrow><mml:mn>3</mml:mn><mml:mi>n</mml:mi><mml:mo>+</mml:mo><mml:mn>1</mml:mn></mml:mr	2.0	7
10015	Strain modulated band gap of edge passivated armchair graphene nanoribbons. Applied Physics Letters, 2011, 98, 023112.	1.5	69
10016	Energy gaps in nitrogen delta-doping graphene: A first-principles study. Applied Physics Letters, 2011, 99, 012107.	1.5	25
10017	Enhanced Hydrogen Storage on Li Functionalized BC₃ Nanotube. Journal of Physical Chemistry C, 2011, 115, 6136-6140.	1.5	38
10018	Controlling the Functionalizations of Hexagonal Boron Nitride Structures by Carrier Doping. Journal of Physical Chemistry Letters, 2011, 2, 2168-2173.	2.1	38

#	Article	IF	Citations
10019	Electronic Structure and Carrier Mobility in Graphdiyne Sheet and Nanoribbons: Theoretical Predictions. ACS Nano, 2011, 5, 2593-2600.	7.3	833
10020	The Energy of Hydroxyl Coadsorbed with Water on Pt(111). Journal of Physical Chemistry C, 2011, 115, 23008-23012.	1.5	45
10021	Structural and magnetic properties of CaFe<mml:math xmlns:mml="http://www.w3.org/1998/Math/MathML" display="inline"><mml:mrow><mml:msub><mml:mrow /><mml:mrow><mml:mn>2</mml:mn></mml:mrow></mml:msub></mml:mrow></mml:math>As<mml:math xmlns:mml="http://www.w3.org/1998/Math/MathML" display="inline"><mml:mrow><mml:msub><mml:mrow /><mml:mrow><mml:mn>2</mml:mn></mml:mrow></mml:msub></mml:mrow></mml:math>	1.1	44
10022	Electronic and Structural Properties of WO₃: A Systematic Hybrid DFT Study. Journal of Physical Chemistry C, 2011, 115, 8345-8353.	1.5	250
10023	Ab initiostudy of edge smoothing, atom attraction, and downward funneling in Ag/Ag(100). Physical Review B, 2011, 83, .	1.1	7
10024	Hybrid functional electronic structure of PbPdO₂, a small-gap semiconductor. Journal of Physics Condensed Matter, 2011, 23, 465501.	0.7	38
10025	Microstructure and Phase Behavior of a Quinquethiophene-Based Self-Assembled Monolayer as a Function of Temperature. Journal of Physical Chemistry C, 2011, 115, 22925-22930.	1.5	21
10026	On the physisorption of water on graphene: a CCSD(T) study. Physical Chemistry Chemical Physics, 2011, 13, 12041.	1.3	172
10027	Improvement of thermoelectric properties for half-Heusler TiNiSn by interstitial Ni defects. Journal of Applied Physics, 2011, 110, .	1.1	79
10028	Structural Stability and Catalytic Activity of Lanthanum-Based Perovskites. Journal of Physical Chemistry C, 2011, 115, 8709-8715.	1.5	20
10029	Universal Phase Transitions of B1-Structured Stoichiometric Transition Metal Carbides. Inorganic Chemistry, 2011, 50, 9266-9272.	1.9	11
10030	Predictability of the polymorphs of small organic compounds: Crystal structure predictions of four benchmark blind test molecules. Physical Chemistry Chemical Physics, 2011, 13, 20361.	1.3	16
10031	Polytypism of GaAs, InP, InAs, and InSb: Anab initiostudy. Physical Review B, 2011, 84, .	1.1	47
10032	Experimental and DFT studies of gold nanoparticles supported on MgO(111) nano-sheets and their catalytic activity. Physical Chemistry Chemical Physics, 2011, 13, 2582.	1.3	41
10033	Improving the Carbon Resistance of Ni-Based Steam Reforming Catalyst by Alloying with Rh: A Computational Study Coupled with Reforming Experiments and EXAFS Characterization. ACS Catalysis, 2011, 1, 574-582.	5.5	67
10034	Methods for Computing Accurate Atomic Spin Moments for Collinear and Noncollinear Magnetism in Periodic and Nonperiodic Materials. Journal of Chemical Theory and Computation, 2011, 7, 4146-4164.	2.3	77
10035	Natural Orbitals for Wave Function Based Correlated Calculations Using a Plane Wave Basis Set. Journal of Chemical Theory and Computation, 2011, 7, 2780-2785.	2.3	117
10036	Large-Area Graphene Films by Simple Solution Casting of Edge-Selectively Functionalized Graphite. ACS Nano, 2011, 5, 4974-4980.	7.3	98

#	Article	IF	Citations
10037	Kinetically Controlled Autocatalytic Chemical Process for Bulk Production of Bimetallic Coreâ€“Shell Structured Nanoparticles. ACS Nano, 2011, 5, 9370-9381.	7.3	67
10038	Coupling of magnetic edge states in Li-intercalated bilayer and multilayer zigzag graphene nanoribbons. Europhysics Letters, 2011, 94, 27007.	0.7	5
10039	Disorder-induced metallicity in amorphous graphene. Physical Review B, 2011, 84, .	1.1	56
10040	Kinetic modelling of the shape-dependent evolution of faceted gold nanoparticles. Journal of Materials Chemistry, 2011, 21, 12239.	6.7	25
10041	Ba4KFe3O9: A Novel Ferrite Containing Discrete 6-Membered Rings of Corner-Sharing FeO4Tetrahedra. Inorganic Chemistry, 2011, 50, 10310-10318.	1.9	10
10042	Chemical Pressure and Rare-Earth Orbital Contributions in Mixed Rare-Earth Silicides La_{5â€“x}Y_xSi₄ (0 â‰¤ x â‰¤ 5). Inorganic Chemistry, 2011, 50, 12714-12723.	1.9	14
10043	Density Functional Analysis of the Magnetic Structure of Li₃RuO₄: Importance of the Ruâ€“OÂ·Â·Â·Oâ€“Ru Spin-Exchange Interactions and Substitutional Ru Defects at the Li Sites. Inorganic Chemistry, 2011, 50, 9400-9405.	1.9	10
10044	Density Functional Analysis of the Spin Exchange Interactions and Charge Order Patterns in the Layered Magnetic Oxides YBaM2O5(M = Mn, Fe, Co). Inorganic Chemistry, 2011, 50, 10643-10647.	1.9	4
10045	Experimental and Theoretical Studies of the Vibrational and Electronic Spectra of a Lanthanide Ion at a Site of T_h Symmetry: Pr³⁺ in Cs₂NaPr(NO₂)₆. Inorganic Chemistry, 2011, 50, 9004-9013.	1.9	8
10046	Investigation of Counterion Influence on an Octahedral IrH6-Complex in the Solid State Hydrides AAeIrH6(A = Na, K and Ae = Ca, Sr, Ba, and Eu) with a New Structure Type. Inorganic Chemistry, 2011, 50, 11890-11895.	1.9	8
10047	Visualization of Hydrogen Bonding and Associated Chirality in Methanol Hexamers. Physical Review Letters, 2011, 107, 256101.	2.9	42
10048	Methyl Chloride Reactions on Lithiated Carbon Nanotubes: Lithium as Both Reactant and Catalyst. Journal of Physical Chemistry C, 2011, 115, 11694-11700.	1.5	8
10049	RbCN₃H₄: The First Structurally Characterized Salt of a New Class of Guanidinate Compounds. Inorganic Chemistry, 2011, 50, 3799-3803.	1.9	28
10050	Normal Mode Analysis in Zeolites: Toward an Efficient Calculation of Adsorption Entropies. Journal of Chemical Theory and Computation, 2011, 7, 1090-1101.	2.3	94
10051	Energy-Level Alignment in 4â€²-Substituted Stilbene-4-thiolate Self-Assembled Monolayers on Gold. Journal of Physical Chemistry C, 2011, 115, 7487-7495.	1.5	4
10052	Stability of edge states and edge magnetism in graphene nanoribbons. Physical Review B, 2011, 83, .	1.1	198
10053	Spin-crossover in cyanide-based bimetallic coordination polymersâ€”insight from first-principles calculations. Journal of Materials Chemistry, 2011, 21, 13832.	6.7	20
10054	Identification of the<mml:math xmlns:mml="http://www.w3.org/1998/Math/MathML" display="inline"><mml:msub><mml:mi>V</mml:mi><mml:mi>Al</mml:mi></mml:msub></mml:math>-O<mml:math xmlns:mml="http://www.w3.org/1998/Math/MathML" display="inline"><mml:msub><mml:mrow /><mml:mi mathvariant="normal">N</mml:mi></mml:msub></mml:math>defect complex in AlN single crystals. Physical Review B, 2011, 84, .	1.1	56

#	Article	IF	Citations
10055	Observation and electric current control of a local spin in a single-molecule magnet. Nature Communications, 2011, 2, 217.	5.8	373
10056	Magnetic behavior of Fe(Se,Te) systems: First-principles calculations. Journal of Applied Physics, 2011, 110, .	1.1	23
10057	Surface State Induced Ferromagnetism in Co- and Mn-Doped ZnO Surfaces. Journal of Physical Chemistry C, 2011, 115, 3368-3371.	1.5	13
10058	Enhanced Oxygen Reduction Activity of Platinum Monolayer on Gold Nanoparticles. Journal of Physical Chemistry Letters, 2011, 2, 67-72.	2.1	80
10059	Density Functional Modeling of the Interactions of Platinum Clusters with CeO₂ Nanoparticles of Different Size. Journal of Physical Chemistry C, 2011, 115, 16081-16086.	1.5	40
10060	Stacking sequence dependence of graphene layers on SiC (0001â^')â€"Experimental and theoretical investigation. Journal of Applied Physics, 2011, 109, .	1.1	78
10061	Enantioselective Hydrogenation of Î±-Ketoesters: An in Situ Surface-Enhanced Raman Spectroscopy (SERS) Study. Journal of Physical Chemistry C, 2011, 115, 21363-21372.	1.5	9
10062	Structural and Chemical Properties of Gold Rare Earth Disilicide Coreâ^'Shell Nanowires. ACS Nano, 2011, 5, 477-485.	7.3	4
10063	First-principles thermodynamics of La<mml:math xmlns:mml="http://www.w3.org/1998/Math/MathML" display="inline"><mml:msub><mml:mrow /><mml:mn>2</mml:mn></mml:msub></mml:math>O<mml:math xmlns:mml="http://www.w3.org/1998/Math/MathML" display="inline"><mml:msub><mml:mrow /><mml:mn>3</mml:mn></mml:msub></mml:math>-P<mml:math xmlns:mml="http://www.w3.org/1998/Math/MathML" display="inline"><mml:msub><mml:mrow /><mml:mml:	1.1	16
10064	Modeling W-V and W-Ta Alloys for Fusion Applications: Phase Stability, Short-Range Order and Point Defect Properties. Materials Research Society Symposia Proceedings, 2011, 1298, 49.	0.1	1
10065	Direct correlation of crystal structure and optical properties in wurtzite/zinc-blende GaAs nanowire heterostructures. Physical Review B, 2011, 83, .	1.1	193
10066	Dopant Modulated Li Insertion in Si for Battery Anodes: Theory and Experiment. Journal of Physical Chemistry C, 2011, 115, 18916-18921.	1.5	84
10067	Positive Vibrational Entropy of Chemical Ordering in FeV. Physical Review Letters, 2011, 107, 115501.	2.9	35
10068	Collectively Induced Quantum-Confined Stark Effect in Monolayers of Molecules Consisting of Polar Repeating Units. Journal of the American Chemical Society, 2011, 133, 18634-18645.	6.6	33
10069	Thermodynamic Analysis of the Cu-Sn-P Ternary System. High Temperature Materials and Processes, 2011, 30, .	0.6	1
10070	The Influence of Surface Oxide on the Growth of Metal/Semiconductor Nanowires. Nano Letters, 2011, 11, 2753-2758.	4.5	23
10071	Defect-induced magnetism in undoped wide band gap oxides: Zinc vacancies in ZnO as an example. AIP Advances, 2011, 1, .	0.6	179
10072	Strengthening mechanism of metallic nanoscale multilayer with negative enthalpy of mixing. Journal of Applied Physics, 2011, 110, .	1.1	13

#	Article	IF	Citations
10073	An all-inorganic type-II heterojunction array with nearly full solar spectral response based on ZnO/ZnSe core/shell nanowires. Journal of Materials Chemistry, 2011, 21, 6020.	6.7	120
10074	Facet-dependent lithium intercalation into Si crystals: Si(100) vs. Si(111). Physical Chemistry Chemical Physics, 2011, 13, 21282.	1.3	49
10075	Structural, electronic, and dynamical properties of methane under high pressure. Journal of Chemical Physics, 2011, 134, 064515.	1.2	12
10076	Electronic properties of bilayer AA-stacked zigzag nanographene ribbons. Diamond and Related Materials, 2011, 20, 505-508.	1.8	1
10077	Transition metal atoms encapsulated in adamantane molecules. Diamond and Related Materials, 2011, 20, 1222-1224.	1.8	14
10078	(Mo+N) codoped TiO2 for enhanced visible-light photoactivity. Applied Surface Science, 2011, 257, 9355-9361.	3.1	47
10079	Density functional study of TaSin (n=1â€“3, 12) clusters adsorbed to graphene surface. Applied Surface Science, 2011, 258, 705-710.	3.1	10
10080	Energy barriers for trimethylaluminum reaction with varying surface hydroxyl density. Applied Surface Science, 2011, 258, 225-229.	3.1	28
10081	Lithium and antimony adsorbed on graphene studied by first-principles calculations. Applied Surface Science, 2011, 258, 800-805.	3.1	9
10082	Diffusion of Li+ ion on graphene: A DFT study. Applied Surface Science, 2011, 258, 1651-1655.	3.1	111
10083	The location of atomic hydrogen in NiTi alloy: A first principles study. Computational Materials Science, 2011, 50, 820-823.	1.4	19
10084	High-pressure structural phase transitions and mechanical properties of calcite rock. Computational Materials Science, 2011, 50, 852-857.	1.4	28
10085	Ab initio investigation of Al/Mo2B interfacial adhesion. Computational Materials Science, 2011, 50, 880-885.	1.4	40
10086	Structural, elastic, and lattice dynamical properties of YB2 compound. Computational Materials Science, 2011, 50, 1057-1063.	1.4	11
10087	Structural and lattice dynamical properties of Zintl NaIn and NaTl compounds. Computational Materials Science, 2011, 50, 1070-1076.	1.4	25
10088	Solubility of carbon in Î±-iron under volumetric strain and close to the Î£5(3 1 0)[0 0 1] grain boundary: Comparison of DFT and empirical potential methods. Computational Materials Science, 2011, 50, 1088-1096.	1.4	47
10089	First-principles studies of typical long-period superstructures Al5Ti3, h-Al2Ti and r-Al2Ti in Al-rich TiAl alloys. Computational Materials Science, 2011, 50, 1467-1476.	1.4	28
10090	Theoretical investigation on the transition-metal borides with Ta3B4-type structure: A class of hard and refractory materials. Computational Materials Science, 2011, 50, 1559-1566.	1.4	169

#	Article	IF	Citations
10091	Magnetism in non-transition-metal doped CdS studied by density functional theory. Computational Materials Science, 2011, 50, 1661-1666.	1.4	41
10092	Reinvestigation of the tensile strength and fracture property of Ni(1 1 1)/Î±-Al2O3(0 0 0 1) interfaces by first-principle calculations. Computational Materials Science, 2011, 50, 1711-1716.	1.4	23
10093	Functionalization of low-dimensional honeycomb germanium with 3d transition-metal atoms. Computational Materials Science, 2011, 50, 1717-1724.	1.4	10
10094	Ab initio study of structural, elastic and vibrational properties of praseodymium chalcogenides. Computational Materials Science, 2011, 50, 1958-1964.	1.4	5
10095	Atomic diffusion in the Fe [001] â^=5 (310) and (210) symmetric tilt grain boundary. Computational Materials Science, 2011, 50, 2087-2095.	1.4	4
10096	Phonon and thermodynamic properties of Alâ€“Mn compounds: A first-principles study. Computational Materials Science, 2011, 50, 2096-2103.	1.4	23
10097	A high-throughput infrastructure for density functional theory calculations. Computational Materials Science, 2011, 50, 2295-2310.	1.4	787
10098	Adsorption and penetration of hydrogen in W: A first principles study. Computational Materials Science, 2011, 50, 2291-2294.	1.4	29
10099	The theoretical strength of fcc crystals under multiaxial loading. Computational Materials Science, 2011, 50, 2257-2261.	1.4	10
10100	Magnetic properties for the transition-metal aluminides XAl2 (X=V, Cr, Mn, and Co): A first-principles study. Computational Materials Science, 2011, 50, 2433-2438.	1.4	7
10101	The energetic and structural properties of bcc NiCu, FeCu alloys: A first-principles study. Computational Materials Science, 2011, 50, 2586-2591.	1.4	40
10102	Self-diffusion in Zn4Sb3 from first-principles molecular dynamics. Computational Materials Science, 2011, 50, 2663-2665.	1.4	11
10103	Mechanical properties and defective effects of bcc Vâ€“4Crâ€“4Ti and Vâ€“5Crâ€“5Ti alloys by first-principles simulations. Computational Materials Science, 2011, 50, 2727-2731.	1.4	22
10104	A simple tight-binding model for the study of 4d transition metals under pressure. Computational Materials Science, 2011, 50, 2732-2735.	1.4	3
10105	Interatomic potentials for Zirconium Diboride and Hafnium Diboride. Computational Materials Science, 2011, 50, 2828-2835.	1.4	15
10106	Influence of magnesium on hydrogenated ScAl1â^'xMgx alloys: A theoretical study. Computational Materials Science, 2011, 50, 2848-2853.	1.4	3
10107	Dehydrogenation properties of epitaxial (100) MgH2/TiH2 multilayers â€“ A DFT study. Computational Materials Science, 2011, 50, 2960-2966.	1.4	13
10108	First-principles investigation on metal tantalum under conditions of electronic excitation. Computational Materials Science, 2011, 50, 3110-3113.	1.4	6

#	Article	IF	Citations
10109	First-principles calculations on structural, magnetic and electronic properties of oxygen doped BiF3. Computational Materials Science, 2011, 50, 3131-3135.	1.4	17
10110	Stacking faults in B2-structured magnesium alloys from first principles calculations. Computational Materials Science, 2011, 50, 3198-3207.	1.4	11
10111	The structural and mechanical properties of CdN compound: A first principles study. Computational Materials Science, 2011, 50, 3208-3212.	1.4	31
10112	Interaction of C with vacancy in W: A first-principles study. Computational Materials Science, 2011, 50, 3213-3217.	1.4	39
10113	First-principles study of ground state properties of ZrH2. Computational Materials Science, 2011, 50, 3297-3302.	1.4	56
10114	Adsorption and dissociation of N2O molecule on Fe(1 1 1) surface: A DFT study. Computational Materials Science, 2011, 50, 3311-3314.	1.4	16
10115	Thermodynamics of zinc insertion in CuGaS2:Ti, used as a modulator agent in an intermediate-band photovoltaic material. Computational and Theoretical Chemistry, 2011, 975, 134-137.	1.1	10
10116	Coverage and charge dependent adsorption of butanethiol on the Au(111) surface: A density functional theory study. Computational and Theoretical Chemistry, 2011, 975, 116-121.	1.1	10
10117	Structural and electronic properties of a single C chain doped zigzag AlN nanoribbon. Computational and Theoretical Chemistry, 2011, 974, 151-158.	1.1	14
10118	A first principles study of gas adsorption on charged CuBTC. Computational and Theoretical Chemistry, 2011, 976, 153-160.	1.1	58
10119	First-principles study on substituted doping of BN nanotubes by transition metals V, Cr and Mn. Computational and Theoretical Chemistry, 2011, 976, 215-220.	1.1	52
10120	Structural and electronic properties of phosphorus-doped titanium clusters: A DFT study. Computational and Theoretical Chemistry, 2011, 977, 50-54.	1.1	9
10121	Magnetic and electronic properties of the nickel clusters Nin (nâ©½30). Computational and Theoretical Chemistry, 2011, 978, 41-46.	1.1	50
10122	Ab initio and thermodynamic modelling of alloying effects on activity of sacrificial aluminium anodes. Corrosion Science, 2011, 53, 1724-1731.	3.0	12
10123	Uranyl adsorption at (010) edge surfaces of kaolinite: A density functional study. Geochimica Et Cosmochimica Acta, 2011, 75, 706-718.	1.6	64
10124	Structure, thermodynamic and transport properties of liquid MgSiO3: Comparison of molecular models and laboratory results. Geochimica Et Cosmochimica Acta, 2011, 75, 1272-1296.	1.6	51
10125	First principles molecular dynamics simulations of diopside (CaMgSi2O6) liquid to high pressure. Geochimica Et Cosmochimica Acta, 2011, 75, 3792-3802.	1.6	60
10126	Aluminum coprecipitates with Fe (hydr)oxides: Does isomorphous substitution of Al3+ for Fe3+ in goethite occur?. Geochimica Et Cosmochimica Acta, 2011, 75, 4667-4683.	1.6	54

#	Article	IF	Citations
10127	First-principles calculations and thermodynamic modeling of the Alâ€“Pt binary system. Calphad: Computer Coupling of Phase Diagrams and Thermochemistry, 2011, 35, 20-29.	0.7	41
10128	Thermodynamic modeling of Laves phases in the Taâ€“V system: Reassessment using first-principles results. Calphad: Computer Coupling of Phase Diagrams and Thermochemistry, 2011, 35, 103-108.	0.7	15
10129	Structural and thermal properties of calcium using an MEAM potential. Calphad: Computer Coupling of Phase Diagrams and Thermochemistry, 2011, 35, 262-268.	0.7	6
10130	Structure, elastic and thermodynamic properties of the Niâ€“P system from first-principles calculations. Calphad: Computer Coupling of Phase Diagrams and Thermochemistry, 2011, 35, 284-291.	0.7	25
10131	Thermodynamic modeling of fcc order/disorder transformations in the Coâ€“Pt system. Calphad: Computer Coupling of Phase Diagrams and Thermochemistry, 2011, 35, 323-330.	0.7	25
10132	Experimental investigation and thermodynamic modeling of the Mnâ€“Niâ€“Si system. Calphad: Computer Coupling of Phase Diagrams and Thermochemistry, 2011, 35, 346-354.	0.7	20
10133	An overview on phase equilibria and thermodynamic modeling in multicomponent Al alloys: Focusing on the Alâ€“Cuâ€“Feâ€“Mgâ€“Mnâ€“Niâ€“Siâ€“Zn system. Calphad: Computer Coupling of Phase Diagrams and Thermochemistry, 2011, 35, 427-445.	0.7	90
10134	First principle energies of binary and ternary phases of the Feâ€“Nbâ€“Niâ€“Cr system. Calphad: Computer Coupling of Phase Diagrams and Thermochemistry, 2011, 35, 588-593.	0.7	41
10135	Thermodynamic description of the Alâ€“Cuâ€“Y ternary system. Calphad: Computer Coupling of Phase Diagrams and Thermochemistry, 2011, 35, 574-579.	0.7	28
10136	First-principles calculations of binary Al compounds: Enthalpies of formation and elastic properties. Calphad: Computer Coupling of Phase Diagrams and Thermochemistry, 2011, 35, 562-573.	0.7	81
10137	Configurational thermodynamics of Feâ€“Ni alloys at Earth's core conditions. Earth and Planetary Science Letters, 2011, 308, 90-96.	1.8	14
10138	Ab initio study of the diffusion barriers for iron and chromium impurities in silicon. Energy Procedia, 2011, 8, 23-27.	1.8	2
10139	T-Carbon: A Novel Carbon Allotrope. Physical Review Letters, 2011, 106, 155703.	2.9	421
10140	Trapping of metal atoms in the defects on graphene. Journal of Chemical Physics, 2011, 135, 224704.	1.2	116
10141	Formation of Carbon Clusters in the Initial Stage of Chemical Vapor Deposition Graphene Growth on Ni(111) Surface. Journal of Physical Chemistry C, 2011, 115, 17695-17703.	1.5	119
10142	Electric Field as a Switching Tool for Magnetic States in Atomic-Scale Nanostructures. Physical Review Letters, 2011, 106, 037202.	2.9	58
10143	Ab Initio Nonadiabatic Molecular Dynamics of the Ultrafast Electron Injection from a PbSe Quantum Dot into the TiO₂ Surface. Journal of the American Chemical Society, 2011, 133, 19240-19249.	6.6	120
10144	Tailoring the electronic structure of TiO<mml:math xmlns:mml="http://www.w3.org/1998/Math/MathML" display="inline"><mml:mrow><mml:msub><mml:mrow /><mml:mrow><mml:mn>2</mml:mn></mml:mrow></mml:msub></mml:mrow></mml:math>by cation codoping from hybrid density functional theory calculations. Physical Review B, 2011, 83, .	1.1	52

#	Article	IF	Citations
10145	Polaronic effects in TiO<mml:math xmlns:mml="http://www.w3.org/1998/Math/MathML" display="inline"><mml:mrow><mml:msub><mml:mrow /><mml:mrow><mml:mn>2</mml:mn></mml:mrow></mml:msub></mml:mrow></mml:math>calculated by the HSE06 hybrid functional: Dopant passivation by carrier self-trapping. Physical Review B, 2011, 83, .	1.1	176
10146	Calculation of carrier-concentration-dependent effective mass in Nb-doped anatase crystals of TiO2. Physical Review B, 2011, 83, .	1.1	45
10147	Interactions of same-row oxygen vacancies on rutile TiO2(110). Physical Review B, 2011, 84, .	1.1	2
10148	Anomalous energy pathway of vacancy migration and self-diffusion in hcp Ti. Physical Review B, 2011, 83, .	1.1	41
10149	<mml:math xmlns:mml="http://www.w3.org/1998/Math/MathML" display="inline"><mml:msub><mml:mi>VO</mml:mi><mml:mn>2</mml:mn></mml:msub></mml:math>: A Novel View from Band Theory. Physical Review Letters, 2011, 107, 016401.	2.9	201
10150	xmlns:mml="http://www.w3.org/1998/Math/MathML" display="inline"><mml:mrow><mml:msub><mml:mrow /><mml:mrow><mml:mi>x</mml:mi></mml:mrow></mml:msub></mml:mrow></mml:math>Ga<mml:math xmlns:mml="http://www.w3.org/1998/Math/MathML"	1.1	42
10151	First-principles electronic structure and relative stability of pyrite and marcasite: Implications for photovoltaic performance. Physical Review B, 2011, 83, .	1.1	122
10152	Electronic structure of tris(8-hydroxyquinolinato)aluminium(III) revisited using the Heyd-Scuseria-Ernzerhof hybrid functional: Theory and experiments. Physical Review B, 2011, 84, .	1.1	17
10153	Hybrid density functional study of oxygen vacancies in KTaO3and NaTaO3. Physical Review B, 2011, 83, .	1.1	26
10154	Quantum Confinement in CdTe Quantum Dots: Investigation through Cyclic Voltammetry Supported by Density Functional Theory (DFT). Journal of Physical Chemistry C, 2011, 115, 6243-6249.	1.5	134
10155	Hierarchically Porous Graphene as a Lithiumâ€“Air Battery Electrode. Nano Letters, 2011, 11, 5071-5078.	4.5	943
10156	Metallization in hydrogen-helium mixtures. Physical Review B, 2011, 84, .	1.1	78
10157	Modeling Thermal Decomposition Mechanisms in Gaseous and Crystalline Molecular Materials: Application to Î²-HMX. Journal of Physical Chemistry B, 2011, 115, 12677-12686.	1.2	66
10158	Hydrogen bonding and chemical shift assignments in carbazole functionalized isocyanides from solid-state NMR and first-principles calculations. Physical Chemistry Chemical Physics, 2011, 13, 13082.	1.3	28
10159	Hybrid Functionals Study of Band Bowing, Band Edges and Electronic Structures of Cd_{1â€“x}Zn_xS Solid Solution. Journal of Physical Chemistry C, 2011, 115, 19741-19748.	1.5	88
10160	xmlns:mml="http://www.w3.org/1998/Math/MathML" display="inline"><mml:msub><mml:mrow /><mml:mn>2</mml:mn></mml:msub></mml:math>Ti<mml:math xmlns:mml="http://www.w3.org/1998/Math/MathML" display="inline"><mml:msub><mml:mrow /><mml:mn>2</mml:mn></mml:msub></mml:math>O<mml:math	1.1	56
10161	Role of van der Waals interaction in crystalline ammonia borane. Applied Physics Letters, 2011, 99, 181904.	1.5	12
10162	The electronic structure of zircon-type orthovanadates: Effects of high-pressure and cation substitution. Journal of Applied Physics, 2011, 110, .	1.1	151

#	Article	IF	Citations
10163	Destabilization of Ag nanoislands on Ag(100) by adsorbed sulfur. Journal of Chemical Physics, 2011, 135, 154701.	1.2	16
10164	Structural, mechanical, and electronic properties of defect-patterned graphene nanomeshes from first principles. Physical Review B, 2011, 84, .	1.1	76
10165	Fingerprints of Dirac points in first-principles calculations of scanning tunneling spectra of graphene on a metal substrate. Physical Review B, 2011, 84, .	1.1	19
10166	First-principles study of diffusion and interactions of vacancies and hydrogen in hcp-titanium. Journal of Physics Condensed Matter, 2011, 23, 405401.	0.7	51
10167	DFT Studies of the Interactions of a Graphene Layer with Small Water Aggregates. Journal of Physical Chemistry A, 2011, 115, 12348-12356.	1.1	73
10168	Native defects in hexagonal <mml:math xmlns:mml="http://www.w3.org/1998/Math/MathML" display="inline"><mml:mrow><mml:mi>I2</mml:mi></mml:mrow></mml:math>-Si <mml:math xmlns:mml="http://www.w3.org/1998/Math/MathML" display="inline"><mml:mrow><mml:msub><mml:mi /><mml:mrow><mml:mn>3</mml:mn></mml:mrow></mml:msub></mml:mrow></mml:math> <mml:math xmlns:mml="http://www.w3.org/1998/Math/MathML" display="inline"><mml:mrow><mml:msub><mml:mi mathvariant="normal">N</mml:mi><mml:mrow><mml:mn>4</mml:mn></mml:mrow></mml:msub> Physics	1.1	35
10169	Evaluation of Tavorite-Structured Cathode Materials for Lithium-Ion Batteries Using High-Throughput Computing. Chemistry of Materials, 2011, 23, 3854-3862.	3.2	244
10170	Phase stability of intermetallic PtIn2 under pressure: An in-situ transport, structural and first principles investigations. Journal of Applied Physics, 2011, 109, 083531.	1.1	4
10171	Large-scale screening of metal hydrides for hydrogen storage from first-principles calculations based on equilibrium reaction thermodynamics. Physical Chemistry Chemical Physics, 2011, 13, 7218.	1.3	30
10172	Probing Lewis acidity of Y(BH4)3via its reactions with MBH4 (M = Li, Na, K, NMe4). Dalton Transactions, 2011, 40, 12808.	1.6	43
10173	Development of Interatomic ReaxFF Potentials for Auâ€“Sâ€“Câ€“H Systems. Journal of Physical Chemistry A, 2011, 115, 10315-10322.	1.1	77
10174	Formation of Graphene pâ€“n Superlattices on Pb Quantum Wedged Islands. ACS Nano, 2011, 5, 3707-3713.	7.3	9
10175	Designing shape-memory Heusler alloys from first-principles. Applied Physics Letters, 2011, 99, .	1.5	91
10176	Polymorph Prediction of Small Organic Molecules, Co-crystals and Salts. RSC Drug Discovery Series, 2011, , 44-88.	0.2	2
10177	Low-Temperature Growth of Graphene by Chemical Vapor Deposition Using Solid and Liquid Carbon Sources. ACS Nano, 2011, 5, 3385-3390.	7.3	353
10178	Engineering a Robust Quantum Spin Hall State in Graphene via Adatom Deposition. Physical Review X, 2011, 1, .	2.8	284
10179	Modulating Optical Properties of Graphene Oxide: Role of Prominent Functional Groups. ACS Nano, 2011, 5, 7640-7647.	7.3	216
10181	Stability and electronic structure of the Coâ€“P compounds from first-principle calculations. Journal of Alloys and Compounds, 2011, 509, 165-171.	2.8	82

#	Article	IF	Citations
10182	DFT studies of hydrogen storage properties of Mg0.75Ti0.25. Journal of Alloys and Compounds, 2011, 509, 210-216.	2.8	20
10183	Crystal structure of the mirror symmetry 10H-type long-period stacking order phase in Mgâ€“Yâ€“Zn alloy. Journal of Alloys and Compounds, 2011, 509, 669-674.	2.8	24
10184	Stability and mobility of native point defects in AlH3. Journal of Alloys and Compounds, 2011, 509, S658-S661.	2.8	7
10185	Mechanical and phonon properties of the superhard LuB2, LuB4, and LuB12 compounds. Journal of Alloys and Compounds, 2011, 509, 1711-1715.	2.8	47
10186	First-principles study of nickel-silicides ordered phases. Journal of Alloys and Compounds, 2011, 509, 2639-2644.	2.8	52
10187	Structural, elastic and electronic properties of Mg(Cu1â^'xZnx)2 alloys calculated by first-principles. Journal of Alloys and Compounds, 2011, 509, 2885-2890.	2.8	22
10188	Thermodynamic optimization of the Cuâ€“Nd system. Journal of Alloys and Compounds, 2011, 509, 2679-2683.	2.8	20
10189	Thermodynamic assessment of Auâ€“La and Auâ€“Er binary systems. Journal of Alloys and Compounds, 2011, 509, 4439-4444.	2.8	9
10190	The thermochemical behavior of some binary shape memory alloys by high temperature direct synthesis calorimetry. Journal of Alloys and Compounds, 2011, 509, 5256-5262.	2.8	12
10191	Electronic structures and Eu3+ photoluminescence behaviors in Y2Si2O7 and La2Si2O7. Journal of Alloys and Compounds, 2011, 509, 5023-5027.	2.8	13
10192	Ab initio electronic structure calculations and optical properties of ordered and disordered Ni3Al. Journal of Alloys and Compounds, 2011, 509, 5230-5237.	2.8	13
10193	Theoretical study on the electronic and optical properties of (N, Fe)-codoped anatase TiO2 photocatalyst. Journal of Alloys and Compounds, 2011, 509, 6067-6071.	2.8	83
10194	Investigating behaviors of H in a W single crystal by first-principles: From solubility to interaction with vacancy. Journal of Alloys and Compounds, 2011, 509, 8277-8282.	2.8	42
10195	Phase stability of magnesium-rare earth binary systems from first-principles calculations. Journal of Alloys and Compounds, 2011, 509, 6899-6907.	2.8	59
10196	Synthesis and visible-light photocatalytic activity of NdVO4 nanowires. Journal of Alloys and Compounds, 2011, 509, 7968-7972.	2.8	42
10197	Hydrogen solution in tetrahedral or octahedral interstitial sites in Al. Journal of Alloys and Compounds, 2011, 509, 9214-9217.	2.8	11
10198	First-principles phase stability calculations and estimation of finite temperature effects on pseudo-binary Mg6(PdxNi1â^'x) compounds. Intermetallics, 2011, 19, 502-510.	1.8	11
10199	First-principles calculations of phonon and thermodynamic properties of Fe-Si compounds. Intermetallics, 2011, 19, 1374-1384.	1.8	40

#	Article	IF	Citations
10200	Electronic structure and transport properties of SrAl2Si2: Effect of yttrium substitution. Intermetallics, 2011, 19, 1448-1454.	1.8	10
10201	Can twinning stabilize B19â€² structure in NiTi martensite?. Intermetallics, 2011, 19, 1567-1572.	1.8	21
10202	First-principles phonon calculations of thermodynamic properties for ductile rare-earth intermetallic compounds. Intermetallics, 2011, 19, 1599-1604.	1.8	17
10203	First-principles coexistence simulations of supercooled liquid silicon. Journal of Non-Crystalline Solids, 2011, 357, 442-445.	1.5	4
10204	First principles study of oxygen-deficient centers in pure and Ge-doped silica. Journal of Non-Crystalline Solids, 2011, 357, 1994-1999.	1.5	19
10205	Calculation and analysis of vibrational spectra of PbCl2â€“Sb2O3â€“TeO2 glass from first principles. Journal of Non-Crystalline Solids, 2011, 357, 2562-2570.	1.5	16
10206	The shoulder in the second peak of the pair correlation function of superheated liquid Fe80B20 alloy. Journal of Non-Crystalline Solids, 2011, 357, 3207-3211.	1.5	15
10207	Proximity of iron pnictide superconductors to a quantum tricritical point. Nature Communications, 2011, 2, 398.	5.8	72
10208	Native Defect Concentrations in NaAlH₄ and Na₃AlH₆. Journal of Physical Chemistry C, 2011, 115, 21443-21453.	1.5	27
10209	Density functional theory study of TiO<mml:math xmlns:mml="http://www.w3.org/1998/Math/MathML" display="inline"><mml:mrow><mml:msub><mml:mrow /><mml:mrow><mml:mn>2</mml:mn></mml:mrow></mml:msub></mml:mrow></mml:math>/Ag Formation enthalpies by mixing GGA and GGA<mml:math xmlns:mml="http://www.w3.org/1998/Math/MathML" display="inline"><mml:mrow><mml:mo>+</mml:mo></mml:mrow></mml:math><mml:math xmlns:mml="http://www.w3.org/1998/Math/MathML" display="inline"><mml:mrow><mml:mi>U</mml:mi></mml:mrow></mml:math>calculations. Physical Review B, 2011, 83, .	1.1	43
10210	Formation enthalpies by mixing GGA and GGA<mml:math xmlns:mml="http://www.w3.org/1998/Math/MathML" display="inline"><mml:mrow><mml:mo>+</mml:mo></mml:mrow></mml:math><mml:math xmlns:mml="http://www.w3.org/1998/Math/MathML" display="inline"><mml:mrow><mml:mi>U</mml:mi></mml:mrow></mml:math>calculations. Physical Review B, 2011, 84, .	1.1	853
10211	Interface engineering of quantum Hall effects in digital transition metal oxide heterostructures. Nature Communications, 2011, 2, 596.	5.8	395
10212	Ab Initio Study on Manganese Doped Cadmium Ferrite $(hbox{Cd}_{1-x}hbox{Mn}_{x}hbox{Fe}_{2}hbox{O}_{4})$. IEEE Transactions on Magnetics, 2011, 47, 324-332.	1.2	5
10213	Intralayer magnetic ordering in Ge/Mn digital alloys. Physical Review B, 2011, 83, .	1.1	7
10214	Density functional study of the phase diagram and thermodynamic properties of Zr. Computational Materials Science, 2011, 50, 835-840.	1.4	23
10215	Phonons of the anomalous element cerium. Proceedings of the National Academy of Sciences of the United States of America, 2011, 108, 9342-9345.	3.3	47
10216	Ammonia decomposition activity on monolayer Ni supported on Ru, Pt and WC substrates. Surface Science, 2011, 605, 2055-2060.	0.8	22
10217	The origin of interfacial electronic and magnetic degradation for a ferromagnet atop organic conjugated molecules. Synthetic Metals, 2011, 161, 575-580.	2.1	14

#	Article	IF	Citations
10218	Metallic and non-metallic properties of one-dimensional peanut-shaped fullerene polymers. Synthetic Metals, 2011, 161, 1546-1551.	2.1	6
10219	Structural and elastic properties of CaGeO3 perovskite at high pressures. Physics of the Earth and Planetary Interiors, 2011, 189, 151-156.	0.7	15
10220	Electronic properties of oxides: Chemical and theoretical approaches. Progress in Solid State Chemistry, 2011, 39, 70-95.	3.9	67
10221	First-principles calculation of structural and elastic properties of Pd3-xRhxV alloys. Transactions of Nonferrous Metals Society of China, 2011, 21, 388-394.	1.7	9
10222	Microstructure of 18R-type long period ordered structure phase in Mg97Y2Zn1 alloy. Transactions of Nonferrous Metals Society of China, 2011, 21, 801-806.	1.7	11
10223	Mechanical Properties and Defective Effects of 316LN Stainless Steel by First-Principles Simulations. Journal of Materials Science and Technology, 2011, 27, 1029-1033.	5.6	12
10224	Hybrid Graphene/Titania Nanocomposite: Interface Charge Transfer, Hole Doping, and Sensitization for Visible Light Response. Journal of Physical Chemistry Letters, 2011, 2, 894-899.	2.1	252
10225	First-principles investigation on optical properties of GaN and InGaN alloys. Journal Physics D: Applied Physics, 2011, 44, 495304.	1.3	17
10226	Metal oxide resistive memory switching mechanism based on conductive filament properties. Journal of Applied Physics, 2011, 110, .	1.1	416
10227	Highly Conductive Boron Nanotubes: Transport Properties, Work Functions, and Structural Stabilities. ACS Nano, 2011, 5, 4997-5005.	7.3	106
10228	Lattice dynamical analogies and differences between SrTiO<mml:math xmlns:mml="http://www.w3.org/1998/Math/MathML" display="inline"><mml:msub><mml:mrow /><mml:mn>3</mml:mn></mml:msub></mml:math>and EuTiO<mml:math xmlns:mml="http://www.w3.org/1998/Math/MathML" display="inline"><mml:msub><mml:mrow /><mml:mn>3</mml:mn></mml:msub></mml:math>revealed by phonon-dispersion relations and double-well potentials. Physical Review B, 2011, 84, .	1.1	45
10229	xmlns:mml="http://www.w3.org/1998/Math/MathML" display="inline"><mml:msub><mml:mrow /><mml:mn>2</mml:mn></mml:msub></mml:math>CoGe<mml:math xmlns:mml="http://www.w3.org/1998/Math/MathML" display="inline"><mml:msub><mml:mrow /><mml:mn>2</mml:mn></mml:msub></mml:math>O<mml:math	1.1	38
10230	Anisotropic splitting and spin polarization of metallic bands due to spin-orbit interaction at the Ge(111)(<mml:math xmlns:mml="http://www.w3.org/1998/Math/MathML") Tj ETQq0 0 0 rgBT /Overlock 10 Tf 50 272 Td (display="inlin xmlns:mml="http://www.w3.org/1998/Math/MathML" display="inline"><mml:mrow><mml:mi>R</mml:mi><mml:msup><mml:mn>30</mml:mn><mml:mo>â˜</mml:mo></mml:msup></mml: surface. Physical Review B, 2011, 84, .	1.1	17
10231	Anab initiomolecular dynamics study of iron phases at high pressure and temperature. Journal of Physics Condensed Matter, 2011, 23, 485402.	0.7	19
10232	Simulations of the Quartz(101Ì…1)/Water Interface: A Comparison of Classical Force Fields, Ab Initio Molecular Dynamics, and X-ray Reflectivity Experiments. Journal of Physical Chemistry C, 2011, 115, 2076-2088.	1.5	183
10233	Periodic Density Functional Theory Study of Water Adsorption on the Î±-Quartz (101) Surface. Journal of Physical Chemistry C, 2011, 115, 5756-5766.	1.5	73
10234	Self-doped SrTiO3â¯Î´ photocatalyst with enhanced activity for artificial photosynthesis under visible light. Energy and Environmental Science, 2011, 4, 4211.	15.6	244
10235	Atomic structure of Ag(111) saturated with chlorine: Formation of Ag3Cl7clusters. Physical Review B, 2011, 84, .	1.1	10

#	Article	IF	Citations
10236	Hexagonal TiO₂ for Photoelectrochemical Applications. Journal of Physical Chemistry C, 2011, 115, 18042-18045.	1.5	17
10237	Structural, Electronic, and Magnetic Properties of Quasi-1D Quantum Magnets [Ni(HF₂)(pyz)₂]X (pyz = pyrazine; X = PF₆^{â€“},) Tj ETQq1 1 0.784314 rgBT /Overlock Chemistry, 2011, 50, 5990-6009.	1.9	30
10238	Characterization of thermal transport in low-dimensional boron nitride nanostructures. Physical Review B, 2011, 84, .	1.1	264
10239	First principles study on interfacial electronic structures in exchange-spring magnets. Journal of Physics: Conference Series, 2011, 266, 012046.	0.3	19
10240	Band gap of InxGa1â^'xN: A first principles analysis. Applied Physics Letters, 2011, 98, .	1.5	50
10241	Using Chebyshev-Filtered Subspace Iteration and Windowing Methods to Solve the Kohn-Sham Problem. , 2011, , 167-189.		1
10242	Computational Approaches Towards Modeling Finite Molecular Assemblies: Role of Cation-Ï€, Ï€â€“Ï€ and Hydrogen Bonding Interactions. , 2011, , 517-555.		2
10243	Kirkendall Effect and Lattice Contraction in Nanocatalysts: A New Strategy to Enhance Sustainable Activity. Journal of the American Chemical Society, 2011, 133, 13551-13557.	6.6	255
10244	Designed metamagnetism in CoMnGe<mml:math xmlns:mml="http://www.w3.org/1998/Math/MathML" display="inline"><mml:mrow><mml:msub><mml:mrow /><mml:mrow><mml:mn>1</mml:mn><mml:mo>â^'</mml:mo><mml:mi>x</mml:mi></mml:mrow></mml:msub></mml:mrow></mml:m xmlns:mml="http://www.w3.org/1998/Math/MathML" display="inline"><mml:mrow><mml:msub><mml:mrow /><mml:mrow><mml:mi>x</mml:mi></mml:mrow></mml:msub></mml:mrow></mml:math>. Physical Revi	1.1	51
10245	Theoretical Study of the Interstitial Oxygen Atom in Anatase and Rutile TiO₂: Electron Trapping and Elongation of the r(Oâ^'O) Bond. Journal of Physical Chemistry C, 2011, 115, 8265-8273.	1.5	44
10246	Negative Differential Resistance of Oligo(Phenylene Ethynylene) Self-Assembled Monolayer Systems: The Electric-Field-Induced Conformational Change Mechanism. Journal of Physical Chemistry C, 2011, 115, 3722-3730.	1.5	23
10247	Competition between fcc and icosahedral short-range orders in pure and samarium-doped liquid aluminum from first principles. Physical Review B, 2011, 83, .	1.1	24
10248	Computational Investigation of CO Adsorption and Oxidation on Iron-Modified Cerium Oxide. Journal of Physical Chemistry C, 2011, 115, 14745-14753.	1.5	63
10249	Anderson Acceleration for Fixed-Point Iterations. SIAM Journal on Numerical Analysis, 2011, 49, 1715-1735.	1.1	358
10250	SiC₂ Silagraphene and Its One-Dimensional Derivatives: Where Planar Tetracoordinate Silicon Happens. Journal of the American Chemical Society, 2011, 133, 900-908.	6.6	171
10251	Chemistry of Doped Oxides: The Activation of Surface Oxygen and the Chemical Compensation Effect. Journal of Physical Chemistry C, 2011, 115, 3065-3074.	1.5	102
10252	Bulk structures of PtO and PtO2from density functional calculations. Physical Review B, 2011, 84, .	1.1	34
10253	Nature of adhesion of condensed organic films on platinum by first-principles simulations. Physical Chemistry Chemical Physics, 2011, 13, 11827.	1.3	8

#	Article	IF	Citations
10254	Phonon calculations in cubic and tetragonal phases of SrTiO<mml:math xmlns:mml="http://www.w3.org/1998/Math/MathML" display="inline"><mml:mrow><mml:msub><mml:mrow /><mml:mrow><mml:mn>3</mml:mn></mml:mrow></mml:msub></mml:mrow></mml:math>: A comparative LCAO and plane-wave study. Physical Review B, 2011, 83, .	1.1	81
10255	DFT calculations of crystal-field parameters for the lanthanide ions in the LaCl3crystal. Journal of Physics Condensed Matter, 2011, 23, 205502.	0.7	7
10256	DFT-Based Study on Oxygen Adsorption on Defective Graphene-Supported Pt Nanoparticles. Journal of Physical Chemistry C, 2011, 115, 22742-22747.	1.5	200
10257	High-pressure vibrational and optical study of Bi<mml:math xmlns:mml="http://www.w3.org/1998/Math/MathML" display="inline"><mml:msub><mml:mrow /><mml:mn>2</mml:mn></mml:msub></mml:math>Te<mml:math xmlns:mml="http://www.w3.org/1998/Math/MathML" display="inline"><mml:msub><mml:mrow /><mml:mn>3</mml:mn></mml:msub></mml:math>. Physical Review B, 2011, 84, .	1.1	100
10258	Hydride-Assisted Hydrogenation of Ti-Doped NaH/Al: A Density Functional Theory Study. Journal of Physical Chemistry C, 2011, 115, 2522-2528.	1.5	11
10259	A First Principles Study on the Dissociation and Rotation Processes of a Single O₂ Molecule on the Pt(111) Surface. Journal of Physical Chemistry C, 2011, 115, 6864-6869.	1.5	22
10260	Fluorinating Hexagonal Boron Nitride/Graphene Multilayers into Hybrid Diamondlike Nanofilms with Tunable Energy Gap. Journal of Physical Chemistry C, 2011, 115, 21678-21684.	1.5	25
10261	First-Principles Thermodynamics of Graphene Growth on Cu Surfaces. Journal of Physical Chemistry C, 2011, 115, 17782-17787.	1.5	317
10262	Impurity complexes and conductivity of Ga-doped ZnO. Physical Review B, 2011, 84, .	1.1	79
10263	Band Gap and Edge Engineering via Ferroic Distortion and Anisotropic Strain: The Case of<mml:math xmlns:mml="http://www.w3.org/1998/Math/MathML" display="inline"><mml:msub><mml:mi>SrTiO</mml:mi><mml:mn>3</mml:mn></mml:msub></mml:math>. Physical Review Letters, 2011, 107, 146804.	2.9	124
10264	First-principles study of the biomineral hydroxyapatite. Physical Review B, 2011, 84, .	1.1	91
10265	Quantum Spin Hall Effect in Silicene and Two-Dimensional Germanium. Physical Review Letters, 2011, 107, 076802.	2.9	1,972
10266	Elastic constants, phonon density of states, and thermal properties of UO<mml:math xmlns:mml="http://www.w3.org/1998/Math/MathML" display="inline"><mml:msub><mml:mrow /><mml:mn>2</mml:mn></mml:msub></mml:math>. Physical Review B, 2011, 84, .	1.1	82
10267	Orientational ordering of interstitial atoms and martensite formation in dilute Fe-based solid solutions. Physical Review B, 2011, 83, .	1.1	36
10268	Quantum confinement and spin-orbit interactions in PbSe and PbTe nanowires: First-principles calculation. Physical Review B, 2011, 84, .	1.1	10
10269	Tunable Dielectric Properties of Transition Metal Dichalcogenides. ACS Nano, 2011, 5, 5903-5908.	7.3	129
10270	Nonprecious Metal Catalysts for Low Temperature Solid Oxide Fuel Cells. Journal of Physical Chemistry C, 2011, 115, 11641-11648.	1.5	7
10271	Concise relation of substitution energy to macroscopic deformation in a deformed system. Physical Review B, 2011, 84, .	1.1	7

#	Article	IF	Citations
10272	A Comparative Study of Lattice Dynamics of Three- and Two-Dimensional MoS₂. Journal of Physical Chemistry C, 2011, 115, 16354-16361.	1.5	298
10273	Band structure engineering of multinary chalcogenide topological insulators. Physical Review B, 2011, 83, .	1.1	60
10274	Electronic transport coefficients fromab initiosimulations and application to dense liquid hydrogen. Physical Review B, 2011, 83, .	1.1	148
10275	Dynamical Screening and Ionic Conductivity in Water fromAbÂInitioSimulations. Physical Review Letters, 2011, 107, 185901.	2.9	41
10276	Properties of copper (fluoro-)phthalocyanine layers deposited on epitaxial graphene. Journal of Chemical Physics, 2011, 134, 194706.	1.2	77
10277	Density functional study of ternary topological insulator thin films. Physical Review B, 2011, 83, .	1.1	30
10278	Effect of Temperature on the Elastic Anisotropy of Pure Fe and<mml:math xmlns:mml="http://www.w3.org/1998/Math/MathML" display="inline"><mml:msub><mml:mi>Fe</mml:mi><mml:mn>0.9</mml:mn></mml:msub><mml:msub><mml:mi>Cr</mml:mi><mml:m Alloy. Physical Review Letters, 2011, 107, 205504	2.9	60
10279	<mml:math xmlns:mml="http://www.w3.org/1998/Math/MathML" display="inline"><mml:mrow><mml:msub><mml:mrow /><mml:mrow><mml:mn>2</mml:mn></mml:mrow></mml:msub></mml:mrow></mml:math>ZnSn(S,Se)<mml:math xmlns:mml="http://www.w3.org/1998/Math/MathML"	1.1	399
10280	High-temperature multiferroicity and strong magnetocrystalline anisotropy in<mml:math xmlns:mml="http://www.w3.org/1998/Math/MathML" display="inline"><mml:mrow><mml:mn>3</mml:mn><mml:mi>d</mml:mi></mml:mrow></mml:math>-<mml:math xmlns:mml="http://www.w3.org/1998/Math/MathML" display="inline"><mml:mrow><mml:mn>5</mml:mn><mml:mi>d</mml:mi></mml:mrow></mml:math>double perovskites. Physical Review B, 2011, 83, .	1.1	45
10281	The nature of chemical bonding in nitramide. Russian Chemical Bulletin, 2011, 60, 2161-2174.	0.4	8
10282	Topological and magnetic phase transitions in Bi<mml:math xmlns:mml="http://www.w3.org/1998/Math/MathML" display="inline"><mml:msub><mml:mrow /><mml:mn>2</mml:mn></mml:msub></mml:math>Se<mml:math xmlns:mml="http://www.w3.org/1998/Math/MathML" display="inline"><mml:msub><mml:mrow /><mml:mn>3</mml:mn></mml:msub></mml:math>thin films with magnetic impurities. Physical Review B, 2011, 84, .	1.1	29
10283	<mml:math xmlns:mml="http://www.w3.org/1998/Math/MathML" display="inline"><mml:mrow><mml:msub><mml:mrow /><mml:mrow><mml:mn>2</mml:mn></mml:mrow></mml:msub></mml:mrow></mml:math>O<mml:math xmlns:mml="http://www.w3.org/1998/Math/MathML"	1.1	18
10285	Density Functional Investigation of the Difference in the Magnetic Structures of the Layered Triangular Antiferromagnets CuFeO2and AgCrO2. Chemistry of Materials, 2011, 23, 4181-4185.	3.2	8
10286	Thermal conductivity of Siâ€“Ge quantum dot superlattices. Nanotechnology, 2011, 22, 155701.	1.3	22
10287	Chemical processes in the deep interior of Uranus. Nature Communications, 2011, 2, 203.	5.8	74
10288	Adsorption Behavior of 4-Methoxypyridine on Gold Nanoparticles. Langmuir, 2011, 27, 7258-7264.	1.6	18
10289	Theoretical Study of Adsorption of Ag Clusters on the Anatase TiO₂(100) Surface. Journal of Physical Chemistry C, 2011, 115, 17368-17377.	1.5	52
10290	<mml:math xmlns:mml="http://www.w3.org/1998/Math/MathML" display="inline"><mml:msub><mml:mrow /><mml:mn>3</mml:mn></mml:msub></mml:math>Ni<mml:math xmlns:mml="http://www.w3.org/1998/Math/MathML" display="inline"><mml:msub><mml:mrow /><mml:mn>2</mml:mn></mml:msub></mml:math>O<mml:math xmlns:mml="http://www.w3.org/1998/Math/MathML"	1.1	25

#	Article	IF	Citations
10291	Pressure-driven changes in electronic structure of BiCoO<mml:math xmlns:mml="http://www.w3.org/1998/Math/MathML" display="inline"><mml:mrow><mml:msub><mml:mrow /><mml:mrow><mml:mn>3</mml:mn></mml:mrow></mml:msub></mml:mrow></mml:math>. Physical Review B, 2011, 83, .	1.1	20
10292	Hydrogen Bonding and Molecular Rearrangement in 1,3,5-Triamino-2,4,6-trinitrobenzene under Compression. Journal of Physical Chemistry B, 2011, 115, 12085-12093.	1.2	31
10293	Achieving High Capacity by Vanadium Substitution into Li₂FeSiO₄. Journal of the Electrochemical Society, 2011, 159, A69-A74.	1.3	33
10294	Nanoporous carbon structures based on C<mml:math xmlns:mml="http://www.w3.org/1998/Math/MathML" display="inline"><mml:msub><mml:mrow /><mml:mn>20</mml:mn></mml:msub></mml:math>. Physical Review B, 2011, 84, .	1.1	7
10295	Ab initiostudy of structural stability of small 3<mml:math xmlns:mml="http://www.w3.org/1998/Math/MathML" display="inline"><mml:mi>d</mml:mi></mml:math>late transition metal clusters: Interplay of magnetization and hybridization. Physical Review B, 2011, 84, .	1.1	27
10296	Mechanism of ferroelectricity in<mml:math xmlns:mml="http://www.w3.org/1998/Math/MathML" display="inline"><mml:msup><mml:mi>d</mml:mi><mml:mn>3</mml:mn></mml:msup></mml:math>perovskites: A model study. Physical Review B, 2011, 84, .	1.1	18
10297	Engineering quantum anomalous/valley Hall states in graphene via metal-atom adsorption: Anab-initiostudy. Physical Review B, 2011, 84, .	1.1	217
10298	Calcium-Based Functionalization of Carbon Materials for CO₂Capture: A First-Principles Computational Study. Journal of Physical Chemistry C, 2011, 115, 10990-10995.	1.5	51
10299	From Point Defects in Graphene to Two-Dimensional Amorphous Carbon. Physical Review Letters, 2011, 106, 105505.	2.9	675
10300	First-principles study of polyacetylene derivatives bearing nitroxide radicals. Physical Review B, 2011, 84, .	1.1	7
10301	Accurate Static and Dynamic Properties of Liquid Electrolytes for Li-Ion Batteries from ab initio Molecular Dynamics. Journal of Physical Chemistry B, 2011, 115, 3085-3090.	1.2	115
10302	Bond-Order Potential for Erbium-Hydride System. Journal of Physical Chemistry C, 2011, 115, 25097-25104.	1.5	9
10303	Understanding Ti intermediate-band formation in partially inverse thiospinel MgIn<mml:math xmlns:mml="http://www.w3.org/1998/Math/MathML" display="inline"><mml:msub><mml:mrow /><mml:mn>2</mml:mn></mml:msub></mml:math>S<mml:math xmlns:mml="http://www.w3.org/1998/Math/MathML" display="inline"><mml:msub><mml:mrow /><mml:mn>4</mml:mn></mml:msub></mml:math>through many-body approaches. Physical Review B, 2011, 84, .	1.1	14
10304	Water induced electrical hysteresis in germanium nanowires: a theoretical study. Physical Chemistry Chemical Physics, 2011, 13, 11663.	1.3	12
10305	Computational Investigation of O₂ Reduction and Diffusion on 25% Sr-Doped LaMnO₃ Cathodes in Solid Oxide Fuel Cells. Langmuir, 2011, 27, 6787-6793.	1.6	36
10306	First-principles predictions of potential hydrogen storage materials: Nanosized Ti(core)/Mg(shell) hydrides. Physical Review B, 2011, 83, .	1.1	21
10307	Theoretical investigation of gold clusters supported on graphene sheets. New Journal of Chemistry, 2011, 35, 2153.	1.4	31
10308	Drastic Change of the Ferromagnetic Properties of the Ternary Germanide GdTiGe through Hydrogen Insertion. Inorganic Chemistry, 2011, 50, 11046-11054.	1.9	24

#	Article	IF	Citations
10309	Three-Dimensional Atomic Imaging of Colloidal Coreâ€“Shell Nanocrystals. Nano Letters, 2011, 11, 3420-3424.	4.5	134
10310	Phonon lifetimes from first-principles self-consistent lattice dynamics. Journal of Physics Condensed Matter, 2011, 23, 445401.	0.7	5
10311	SO₂ Adsorption on Pt(111) and Oxygen Precovered Pt(111): A Combined Infrared Reflection Absorption Spectroscopy and Density Functional Study. Journal of Physical Chemistry C, 2011, 115, 479-491.	1.5	61
10312	Organometallic Complexes of Graphene: Toward Atomic Spintronics Using a Graphene Web. ACS Nano, 2011, 5, 9939-9949.	7.3	70
10313	First-principles simulations of exciton diffusion in organic semiconductors. Physical Review B, 2011, 84, .	1.1	58
10314	Electronic structures of quasi-one-dimensional ferrimagnetic insulator Ca3Co2O6. Computer Physics Communications, 2011, 182, 93-95.	3.0	3
10315	Confinement-induced changes in magnetic behavior of a Ti monolayer on Pt. Chemical Physics Letters, 2011, 507, 117-121.	1.2	7
10316	Pt(111)-Alloy Surfaces for Non-Activated OOH Dissociation. E-Journal of Surface Science and Nanotechnology, 2011, 9, 352-356.	0.1	11
10317	Theory of Doping: Monovalent Adsorbates. , 0, , .		1
10318	The Effect of Particle Size on Hydrogen Release from Sodium Alanate. ECS Meeting Abstracts, 2011, , .	0.0	0
10320	Electronic and Magnetic Properties of the Graphene- Ferromagnet Interfaces: Theory vs. Experiment. , 2011, , .		4
10321	Experimental and theoretical investigations on effects of hydrostatic pressure on the electrical properties of rhombohedral Sb2Te3. AIP Advances, 2011, 1, .	0.6	5
10322	Metastable Solvent Epitaxy of SiC, the Other Diamond Synthetics. , 0, , .		0
10323	First Principles Study on the Adsorption and Dehydrogenation of Borohydride on Mn(111). E-Journal of Surface Science and Nanotechnology, 2011, 9, 257-264.	0.1	6
10324	Simulation of bonding effects in HRTEM images of light element materials. Beilstein Journal of Nanotechnology, 2011, 2, 394-404.	1.5	14
10325	Polarized Tips or Surfaces: Consequences in Kelvin Probe Force Microscopy. E-Journal of Surface Science and Nanotechnology, 2011, 9, 6-14.	0.1	20
10326	Atomistic Simulations of Flash Memory Materials Based on Chalcogenide Glasses. , 0, , .		0
10327	Structural and Electronic Properties of Hydrogenated Graphene. , 0, , .		0

#	Article	IF	Citations
10328	First-Principles Calculation on Initial Stage of Oxidation of Si (110)-(1 Ã— 1) Surface. Advances in Condensed Matter Physics, 2011, 2011, 1-5.	0.4	1
10329	The stability and work function of TaCxN1â^'x alloy surfaces. Journal of Applied Physics, 2011, 109, .	1.1	6
10330	Catalytic Reactions on Model Gold Surfaces: Effect of Surface Steps and of Surface Doping. Catalysts, 2011, 1, 40-51.	1.6	8
10331	Coinage metal (4, 4) nanotubes, simulated by first-principles calculations. Journal of Chemical Physics, 2011, 134, 244504.	1.2	7
10332	Layered transition-metal permanent-magnet structures. Journal of Applied Physics, 2011, 109, .	1.1	2
10333	Quantum Chemical Analysis of Electroless Deposition Processes. Hyomen Gijutsu/Journal of the Surface Finishing Society of Japan, 2011, 62, 657.	0.1	2
10334	Suppression of the formation of interstitial Li through (F, Li) codoping ZnO. Journal of Physics: Conference Series, 2011, 276, 012158.	0.3	2
10335	Ab initio study on the lithiation mechanism of Mg<inf>2</inf>Si electrode. , 2011, , .		1
10336	Ab initio structure determination of 3,4-diaminopyridin-1-ium dihydrogen phosphate. Powder Diffraction, 2011, 26, 321-325.	0.4	7
10337	Investigation of Cu precipitation in bcc-Fe â€“ Comparison of numerical analysis with experiment. International Journal of Materials Research, 2011, 102, 709-716.	0.1	8
10338	Zr segregation and associated Al vacancies in alumina grain boundaries. Journal of the Ceramic Society of Japan, 2011, 119, 840-844.	0.5	14
10340	The effects of Bi alloying in Cu delafossites: A density functional theory study. Journal of Applied Physics, 2011, 109, .	1.1	17
10341	The elastic properties of Mn3(Cu1â^'xGex)N compounds. AIP Advances, 2011, 1, 042125.	0.6	4
10342	Electronic origin of structure and mechanical properties in Y and Nb alloyed Tiâ€“Alâ€“N thin films. International Journal of Materials Research, 2011, 102, 735-742.	0.1	38
10343	NiSi crystal structure, site preference, and partitioning behavior of palladium in NiSi(Pd)/Si(100) thin films: Experiments and calculations. Applied Physics Letters, 2011, 99, .	1.5	23
10345	Anisotropy of zigzag chains of palladium. Journal of Applied Physics, 2011, 109, 07E322.	1.1	4
10346	Powder diffraction and solid state DFT study of thetrans-bis(5-methylsalicylato)-bis(N,N-diethylnicotinamide)-diaquacopper(II) complex structure. Zeitschrift FÃ¼r Kristallographie, 2011, 226, 756-761.	1.1	1
10347	Seeing oxygen disorder in YSZ/SrTiO₃colossal ionic conductor heterostructures using EELS. EPJ Applied Physics, 2011, 54, 33507.	0.3	52

#	Article	IF	Citations
10348	High electron mobility due to sodium ions in the gate oxide of SiC-metal-oxide-semiconductor field-effect transistors. Journal of Applied Physics, 2011, 109, .	1.1	27
10349	High-efficiency switching effect in porphyrin-ethyne-benzene conjugates. Journal of Chemical Physics, 2011, 135, 044706.	1.2	37
10350	Uncompensated antiferromagnetic moments in Mn-Ir/FM (FMâ€‰=â€‰Ni-Co, Co-Fe, Fe-Ni) bilayers: Compositional dependence and its origin. Journal of Applied Physics, 2011, 110, 123920.	1.1	20
10351	Scaling of flat band potential and dielectric constant as a function of Ta concentration in Ta-TiO2 epitaxial films. AIP Advances, 2011, 1, 022151.	0.6	17
10352	First Principles Calculations of the Electronic Structure of ZrN Allotropes. Journal of the Physical Society of Japan, 2011, 80, 114707.	0.7	3
10353	First principles study of the structural, electronic, and dielectric properties of amorphous HfO2. Journal of Applied Physics, 2011, 110, .	1.1	51
10354	Electronic and magnetic properties of early transition-metal substituted iron-cyclopentadienyl sandwich molecular wires: Parity-dependent half-metallicity. Journal of Chemical Physics, 2011, 135, 014702.	1.2	5
10355	Interaction of Bis-diethylaminosilane with a Hydroxylized Si (001) Surface for SiO2 Thin-Film Growth Using Density Functional Theory. IEICE Transactions on Electronics, 2011, E94-C, 771-774.	0.3	3
10357	Effective coordination concept applied for phase change (GeTe)m(Sb2Te3)n compounds. Journal of Applied Physics, 2011, 109, .	1.1	83
10358	Chemical speciation of adsorbed glycine on metal surfaces. Journal of Chemical Physics, 2011, 135, 034703.	1.2	20
10359	Gallium interstitial contributions to diffusion in gallium arsenide. AIP Advances, 2011, 1, .	0.6	8
10360	Manipulating absorption and diffusion of H atom on graphene by mechanical strain. AIP Advances, 2011, 1, 032109.	0.6	26
10361	A comparison of accelerators for direct energy minimization in electronic structure calculations. Journal of Chemical Physics, 2011, 134, 244104.	1.2	9
10362	Atomic and electronic properties of P/Si(1Â1Â1)-(2ÂÃ—Â1) surface. EPJ Applied Physics, 2011, 56, 31302.	0.3	1
10363	Work function engineering in silicides: Chlorine doping in NiSi. Journal of Applied Physics, 2011, 109, 083703.	1.1	7
10364	Computer simulation of coherent BaZrO3/MgO interfaces. Journal of the Ceramic Society of Japan, 2011, 119, 861-866.	0.5	1
10365	Microscopic Phase-Field Modeling of Edge and Screw Dislocation Core Structures and Peierls Stresses of BCC Iron. Nippon Kinzoku Gakkaishi/Journal of the Japan Institute of Metals, 2011, 75, 104-109.	0.2	7
10366	Stability and Electronic Structures of Pt-Rh Icosahedral Nanoparticles. Materials Transactions, 2011, 52, 1339-1343.	0.4	4

#	Article	IF	Citations
10367	Growth and structure of an ultrathin tin oxide film on Rh(111). Journal of Applied Physics, 2011, 109, .	1.1	7
10368	Transition Metal Solubilities in WC in Cemented Carbide Materials. Journal of the American Ceramic Society, 2011, 94, 605-610.	1.9	45
10369	Grain Boundaries in Uranium Dioxide: Scanning Electron Microscopy Experiments and Atomistic Simulations. Journal of the American Ceramic Society, 2011, 94, 1893-1900.	1.9	78
10370	Stabilization Mechanisms of LaFeO3 (010) Surfaces Determined with First Principles Calculations. Journal of the American Ceramic Society, 2011, 94, 1931-1939.	1.9	18
10371	Interfacial Stoichiometry and Adhesion at Metal/Î±â€Al₂O₃ Interfaces. Journal of the American Ceramic Society, 2011, 94, s154.	1.9	26
10372	Phase Stability, Electronic Structure, Compressibility, Elastic and Optical Properties of a Newly Discovered <scp>Ti₃SnC₂</scp>: A Firstâ€Principle Study. Journal of the American Ceramic Society, 2011, 94, 3907-3914.	1.9	27
10373	High Ion Conductivity in MgHf(WO4)3 Solids with Ordered Structure: 1-D Alignments of Mg2+ and Hf4+ Ions. Journal of the American Ceramic Society, 2011, 94, 2285-2288.	1.9	39
10374	Ab Initio Computations of Electronic, Mechanical, and Thermal Properties of <scp>ZrB₂</scp> and <scp>HfB₂</scp>. Journal of the American Ceramic Society, 2011, 94, 3494-3499.	1.9	64
10375	Europiumâ€Doped <scp>LaSi₃N₅</scp> Ternary Nitride: Synthesis, Spectroscopy, Computed Electronic Structure and Band Gaps. Journal of the American Ceramic Society, 2011, 94, 4345-4351.	1.9	13
10376	Directed long-range molecular migration energized by surface reaction. Nature Chemistry, 2011, 3, 400-408.	6.6	36
10377	Surface-mediated chain reaction through dissociative attachment. Nature Chemistry, 2011, 3, 85-89.	6.6	41
10378	Experimental analysis of charge redistribution dueÂto chemical bonding by high-resolution transmission electron microscopy. Nature Materials, 2011, 10, 209-215.	13.3	270
10379	Orbital reflectometry of oxide heterostructures. Nature Materials, 2011, 10, 189-193.	13.3	215
10380	The lithium intercalation process in the low-voltage lithium battery anode Li1+xV1â^'xO2. Nature Materials, 2011, 10, 223-229.	13.3	267
10381	Magnetization of zircon induced by 3d impurities: Ab initio calculations. Doklady Physical Chemistry, 2011, 438, 90-93.	0.2	2
10382	Atomic and electronic structure of mixed Au-Co nanowires: Ab initio molecular dynamics study. JETP Letters, 2011, 93, 129-132.	0.4	11
10383	Effect of hydrogen on the formation of the atomic structure of linear carbon chains: An ab initio approach. JETP Letters, 2011, 93, 652-656.	0.4	7
10384	Laser ablation of gold: Experiment and atomistic simulation. JETP Letters, 2011, 93, 642-647.	0.4	25

#	Article	IF	Citations
10385	Effect of stretching-contraction deformations on the magnetic ordering state of mixed Pd-Fe nanowires. JETP Letters, 2011, 94, 228-232.	0.4	13
10386	Modeling of the electronic structure, chemical bonding, and properties of ternary silicon carbide Ti3SiC2. Journal of Structural Chemistry, 2011, 52, 785-802.	0.3	57
10387	A theoretical study of lithium absorption in amorphous and crystalline silicon. Journal of Structural Chemistry, 2011, 52, 861-869.	0.3	12
10388	Generalized planner fault energies, twinning and ductility of L12 type Al3Sc and Al3Mg. Solid State Sciences, 2011, 13, 120-125.	1.5	24
10389	Ferromagnetism driven by vacancies and C/N substitution at SrO (100) surface. Solid State Sciences, 2011, 13, 126-130.	1.5	5
10390	A comparison of the electronic and optical properties of zinc-blende, rocksalt and wurtzite AlN: A DFT study. Solid State Sciences, 2011, 13, 331-336.	1.5	53
10391	Ab initio investigations of the perovskite and K2NiF4 phases in the Csâ€“Caâ€“H system. Solid State Sciences, 2011, 13, 569-573.	1.5	3
10392	Ab initio study of the hydrogenation effects on the electronic, chemical, and magnetic structures of CeIrSb. Solid State Sciences, 2011, 13, 948-952.	1.5	4
10393	The first principles study on the TmSb compound. Solid State Sciences, 2011, 13, 1291-1298.	1.5	5
10394	Ab initio investigations of the Ca2IrO4-type structure as a â€œpost-K2NiF4â€• Case study of Na2OsO4. Solid State Sciences, 2011, 13, 1396-1400.	1.5	8
10395	Density functional theory studies on elastic and electronic properties of tetragonal ZnP2. Solid State Sciences, 2011, 13, 1604-1607.	1.5	5
10396	First principles investigations of the hydrogenation effects on the electronic structure and the chemical bonding of CeIrAl. Solid State Sciences, 2011, 13, 1704-1708.	1.5	5
10397	Study on mechanical behavior and electronic structures of Alâ€“Cu intermetallic compounds based on first-principles calculations. Solid State Communications, 2011, 151, 1270-1274.	0.9	22
10398	First principles study on the structural, electronic, and elastic properties of Naâ€“As systems. Solid State Communications, 2011, 151, 1349-1354.	0.9	6
10399	First-principles study of phase transitions in antiferromagnetic Â(, Co and Ni). Solid State Communications, 2011, 151, 1475-1478.	0.9	9
10400	First-principles study of martensitic transformation of IrTi alloy. Solid State Communications, 2011, 151, 1433-1436.	0.9	6
10401	A theoretical investigation of the special properties of SrFe1â^'xCoxO3. Solid State Communications, 2011, 151, 1616-1621.	0.9	6
10402	Effects of copper and oxygen vacancies on the ferromagnetism of Mn- and Co-doped Cu2O. Solid State Communications, 2011, 151, 1583-1587.	0.9	7

#	Article	IF	Citations
10403	Mechanical properties and electronic structure of the incompressible rhenium carbides and nitrides: A first-principles study. Solid State Communications, 2011, 151, 1842-1845.	0.9	20
10404	Controlled modification of Schottky barrier height by partisan interlayer. Solid State Communications, 2011, 151, 1641-1644.	0.9	14
10405	From first principles: Phase transition mechanisms of hexagonal Sc and Y under pressure. Solid State Communications, 2011, 151, 1972-1975.	0.9	2
10406	Magnetism of Mg atomic chains on the NaCl(100) surface. Solid State Communications, 2011, 151, 1912-1915.	0.9	1
10407	Phase transition of cadmium fluoride under high pressure. Solid State Communications, 2011, 151, 1899-1902.	0.9	12
10408	Grain boundary-driven leakage path formation in HfO2 dielectrics. Solid-State Electronics, 2011, 65-66, 146-150.	0.8	110
10409	Understanding the catalytic effects of H2S on CVD-growth of Î±-alumina: Thermodynamic gas-phase simulations and density functional theory. Surface and Coatings Technology, 2011, 206, 1771-1779.	2.2	14
10410	Phase stability and alloy-related trends in Tiâ€“Alâ€“N, Zrâ€“Alâ€“N and Hfâ€“Alâ€“N systems from first principles. Surface and Coatings Technology, 2011, 206, 1698-1704.	2.2	112
10411	Intermediate band position modulated by Zn addition in Ti doped CuGaS2. Thin Solid Films, 2011, 519, 7517-7521.	0.8	20
10412	Optical properties of Cu(In,Ga)Se2 and Cu2ZnSn(S,Se)4. Thin Solid Films, 2011, 519, 7508-7512.	0.8	77
10413	First-principles calculations of vacancy formation in In-free photovoltaic semiconductor Cu2ZnSnSe4. Thin Solid Films, 2011, 519, 7513-7516.	0.8	38
10414	The structure of Tiâ€“Siâ€“N superhard nanocomposite coatings: ab initio study. Thin Solid Films, 2011, 520, 876-880.	0.8	13
10415	First-principles study of GaAs(001)-Î²2(2Ã—4) surface oxidation. Microelectronic Engineering, 2011, 88, 3419-3423.	1.1	11
10416	Interaction of gas molecules with crystalline polymer separation membranes: Atomic-scale modeling and first-principles calculations. Journal of Membrane Science, 2011, 384, 176-183.	4.1	5
10417	Nanocrystalline ZnSb2O6: Hydrothermal synthesis, electronic structure and photocatalytic activity. Journal of Molecular Catalysis A, 2011, 349, 80-85.	4.8	23
10418	Band structure and photocatalytic properties of N/Zr co-doped anatase TiO2 from first-principles study. Journal of Molecular Catalysis A, 2011, 351, 11-16.	4.8	45
10419	Alâ€“Pd interatomic potential and its application to nanoscale multilayer thin films. Materials Science & Engineering A: Structural Materials: Properties, Microstructure and Processing, 2011, 530, 73-86.	2.6	13
10420	Magnetic and electronic properties of Sn1â€“xCrxO2 diluted alloys. Materials Science and Engineering B: Solid-State Materials for Advanced Technology, 2011, 176, 1378-1381.	1.7	6

#	Article	IF	Citations
10421	Density functional study on helium and hydrogen interstitials in silicon carbide. Nuclear Instruments & Methods in Physics Research B, 2011, 269, 2067-2074.	0.6	15
10422	Simulating gamma-ray energy resolution in scintillators due to electronâ€“hole pair statistics. Nuclear Instruments & Methods in Physics Research B, 2011, 269, 2667-2675.	0.6	4
10423	Molecular dynamics simulation on ionic conduction process of oxygen in Ce1â^'xMxO2â^'x/2. Journal of the European Ceramic Society, 2011, 31, 3159-3169.	2.8	20
10424	First-principles study of the electronic and magnetic properties of a Nickelâ€“Zinc ferrite: ZnxNi1â^'xFe2O4. Journal of Magnetism and Magnetic Materials, 2011, 323, 3138-3142.	1.0	11
10425	First-principles investigation on the effect of carbon on hydrogen trapping in tungsten. Journal of Nuclear Materials, 2011, 415, S709-S712.	1.3	40
10426	Modeling of yttrium, oxygen atoms and vacancies in Î³-iron lattice. Journal of Nuclear Materials, 2011, 416, 40-44.	1.3	7
10427	Ab initio modeling of oxygen impurity atom incorporation into uranium mononitride surface and sub-surface vacancies. Journal of Nuclear Materials, 2011, 416, 200-204.	1.3	33
10428	Simulation of defect evolution in electron-irradiated dilute FeCr alloys. Journal of Nuclear Materials, 2011, 417, 1078-1081.	1.3	9
10429	Formation of vacancy clusters in tungsten crystals under hydrogen-rich condition. Journal of Nuclear Materials, 2011, 417, 1115-1118.	1.3	40
10430	Theoretical study on segregation of Cu, Mo and W impurities and stability of impurityâ€“vacancy pairs in bcc Fe. Journal of Nuclear Materials, 2011, 417, 1054-1057.	1.3	1
10431	Atomistic modelling of the Feâ€“Crâ€“C system. Journal of Nuclear Materials, 2011, 415, 316-319.	1.3	3
10432	First-principles study of the incorporation and diffusion of helium in cubic zirconia. Journal of Nuclear Materials, 2011, 418, 143-151.	1.3	16
10433	Ideal mechanical properties of vanadium by a first-principles computational tensile test. Journal of Nuclear Materials, 2011, 416, 345-349.	1.3	11
10434	First-principles study of H2 adsorption and dissociation on Zr(0001). Journal of Nuclear Materials, 2011, 418, 159-164.	1.3	16
10435	First principles study of hydrogen behaviors in hexagonal tungsten carbide. Journal of Nuclear Materials, 2011, 418, 233-238.	1.3	12
10436	Energetics of mixing in ThO2â€“CeO2 fluorite solid solutions. Journal of Nuclear Materials, 2011, 419, 72-75.	1.3	16
10437	Study of cerium solubility in Gd2Zr2O7 by DFT+U calculations. Journal of Nuclear Materials, 2011, 419, 105-111.	1.3	40
10438	Stability and dissolution of heliumâ€“vacancy complexes in vanadium solid. Journal of Nuclear Materials, 2011, 419, 1-8.	1.3	51

#	Article	IF	Citations
10439	Vacancyâ€“solute interactions in ferromagnetic and paramagnetic bcc iron: Ab initio calculations. Journal of Nuclear Materials, 2011, 419, 248-255.	1.3	63
10440	Photo-absorption spectra of small hydrogenated silicon clusters using the time-dependent density functional theory. Journal of Physics and Chemistry of Solids, 2011, 72, 1096-1100.	1.9	10
10441	First-principles based microkinetic modeling of borohydride oxidation on a Au(111) electrode. Journal of Power Sources, 2011, 196, 9228-9237.	4.0	95
10442	Effect of Cr and Mn ions on the structure and magnetic properties of GaFeO3: Role of the substitution site. Journal of Solid State Chemistry, 2011, 184, 2353-2359.	1.4	16
10443	Ab initio study on preferred growth of ZnO. Scripta Materialia, 2011, 64, 483-485.	2.6	29
10444	A universal scaling of planar fault energy barriers in face-centered cubic metals. Scripta Materialia, 2011, 64, 605-608.	2.6	118
10445	Basal-plane stacking-fault energies of Mg: A first-principles study of Li- and Al-alloying effects. Scripta Materialia, 2011, 64, 693-696.	2.6	130
10446	Structural relationship between one-dimensional crystals of Guinierâ€“Prestonâ€“Bagaryatsky zones in Alâ€“Cuâ€“Mg alloys. Scripta Materialia, 2011, 64, 999-1002.	2.6	33
10447	Ab initio calculations of the generalized stacking fault energy in aluminium alloys. Scripta Materialia, 2011, 64, 916-918.	2.6	110
10448	First-principles study of long-period stacking ordered-like multi-stacking fault structures in pure magnesium. Scripta Materialia, 2011, 64, 942-945.	2.6	47
10449	Structural, electronic and energetic properties of GaN[0 0 0 1]/Ga2O3[1 0 0] heterojunctions: A first-principles density functional theory study. Scripta Materialia, 2011, 65, 465-468.	2.6	5
10450	The effect of alloying elements on grain boundary and bulk cohesion in aluminum alloys: An ab initio study. Scripta Materialia, 2011, 65, 926-929.	2.6	56
10451	Metal (Pd, Pt)-decorated carbon nanotubes for CO and NO sensing. Sensors and Actuators B: Chemical, 2011, 159, 171-177.	4.0	87
10452	Strain-induced changes in electronic structures and work function for (001), (110) and (111) of AlCu3. Physica B: Condensed Matter, 2011, 406, 4046-4051.	1.3	9
10453	The stability and the nonlinear elasticity of 2D hexagonal structures of Si and Ge from first-principles calculations. Physica B: Condensed Matter, 2011, 406, 4080-4084.	1.3	50
10454	Ab initio molecular dynamics simulations on structural change of supercooled liquid Si at different temperatures from 1700 to 1100K. Physica B: Condensed Matter, 2011, 406, 3991-3996.	1.3	4
10455	Structural and electronic properties of U2Ti: A first principles study. Physica B: Condensed Matter, 2011, 406, 4317-4321.	1.3	12
10456	Origin of the intriguing physical properties in A-site-ordered LaCu3Fe4O12 double perovskite. Physica B: Condensed Matter, 2011, 406, 4432-4435.	1.3	4

#	Article	IF	Citations
10457	First-principles study of transition metal linear monoatomic chains adsorption on boron nitride nanotube. Physica B: Condensed Matter, 2011, 406, 4572-4577.	1.3	3
10458	First principle study on generalized-stacking-fault energy surfaces of B2-AlRE intermetallic compounds. Physica B: Condensed Matter, 2011, 406, 4529-4534.	1.3	8
10459	First-principles study of elastic and thermo-physical properties of kesterite-type Cu2ZnSnS4. Physica B: Condensed Matter, 2011, 406, 4604-4607.	1.3	34
10460	Distorted magnetic orders and electronic structures for FeSe under pressure. Physica C: Superconductivity and Its Applications, 2011, 471, 603-607.	0.6	2
10461	First-principles study of light-element doping effects on iron-based superconductors. Physica C: Superconductivity and Its Applications, 2011, 471, 662-665.	0.6	2
10462	Electronic bands, Fermi surface, and elastic properties of new 4.2K superconductor SrPtAs with a honeycomb structure from first principles calculations. Physica C: Superconductivity and Its Applications, 2011, 471, 594-596.	0.6	11
10463	First-principles study on structural, electronic and magnetic properties of ZnO nanotube filled with Fe, Co and Ni nanowires. Physica E: Low-Dimensional Systems and Nanostructures, 2011, 44, 405-410.	1.3	9
10464	Tuning electronic and magnetic properties of AlN nanosheets with hydrogen and fluorine: First-principles prediction. Physics Letters, Section A: General, Atomic and Solid State Physics, 2011, 375, 3583-3587.	0.9	31
10465	Theoretical study of the new compound VO2 (D). Physics Letters, Section A: General, Atomic and Solid State Physics, 2011, 375, 3474-3477.	0.9	22
10466	The active role played by nonmagnetic Sr in magnetostructural coupling in SrTcO3 from first principles. Physics Letters, Section A: General, Atomic and Solid State Physics, 2011, 375, 3615-3617.	0.9	11
10467	Electronic transport in large systems through a QUAMBOâ€“NEGF approach: Application to atomic carbon chains. Physics Letters, Section A: General, Atomic and Solid State Physics, 2011, 375, 3710-3715.	0.9	5
10468	The stable CaBe2Ge2 structures in antimonide compounds ATM2Sb2 (A = Ca, Sr, Ba; TM = Fe, Co, Ni, Cu): A first-principles study. Physics Letters, Section A: General, Atomic and Solid State Physics, 2011, 375, 4218-4224.	0.9	6
10469	Electronic and magnetic properties of perfect and defected germanium nanoribbons. Materials Chemistry and Physics, 2011, 130, 140-146.	2.0	12
10470	Effects of hydrogen on a tungsten grain boundary: A first-principles computational tensile test. Progress in Natural Science: Materials International, 2011, 21, 240-245.	1.8	35
10471	Influence of stacking fault energy on formation of long period stacking ordered structures in Mgâ€“Znâ€“Yâ€“Zr alloys. Progress in Natural Science: Materials International, 2011, 21, 485-490.	1.8	42
10472	Why is metallic Pt the best catalyst for methoxy decomposition?. Journal of Natural Gas Chemistry, 2011, 20, 90-98.	1.8	11
10473	Adsorption and dissociation of H2O on Cu2O(100): A computational study. Journal of Natural Gas Chemistry, 2011, 20, 155-161.	1.8	33
10474	Performance Limits of Monolayer Transition Metal Dichalcogenide Transistors. IEEE Transactions on Electron Devices, 2011, 58, 3042-3047.	1.6	428

#	Article	IF	Citations
10475	Magnetic Properties of Boron-Doped Co$_{2}$FeSi: A First-Principles Study. IEEE Transactions on Magnetics, 2011, 47, 2912-2915.	1.2	3
10476	Structure and Magnetic Properties of ${hbox {LiFePO}}_{4}$ Under Pressure. IEEE Transactions on Magnetics, 2011, 47, 3817-3820.	1.2	4
10477	First-Principles Study of Magnetic Exchange Interactions of $3{m -D}$ Transition Mental Adatoms on Graphene. IEEE Transactions on Magnetics, 2011, 47, 2425-2428.	1.2	1
10478	Phonon spectra and phonon-dependent properties of AgSO4, an unusual sulfate of divalent silver. Vibrational Spectroscopy, 2011, 57, 334-337.	1.2	7
10479	Determining factors of thermoelectric properties of semiconductor nanowires. Nanoscale Research Letters, 2011, 6, 502.	3.1	20
10480	Dehydrogenation of propane over ZnMOR. Static and dynamic reaction energy diagram. Journal of Catalysis, 2011, 277, 104-116.	3.1	43
10481	Methane oxidation on Pdâ€“Ceria: A DFT study of the mechanism over PdxCe1â^'xO2, Pd, and PdO. Journal of Catalysis, 2011, 278, 16-25.	3.1	145
10482	Mechanism of selective alcohol oxidation to aldehydes on gold catalysts: Influence of surface roughness on reactivity. Journal of Catalysis, 2011, 278, 50-58.	3.1	110
10483	Influence of particles alloying on the performances of Ptâ€“Ru/CNT catalysts for selective hydrogenation. Journal of Catalysis, 2011, 278, 59-70.	3.1	84
10484	Catalytic consequences of acid strength in the conversion of methanol to dimethyl ether. Journal of Catalysis, 2011, 278, 78-93.	3.1	178
10485	Complex intermetallic compounds as selective hydrogenation catalysts â€“ A case study for the (100) surface of Al13Co4. Journal of Catalysis, 2011, 278, 200-207.	3.1	54
10486	CO2 methanation on Ru-doped ceria. Journal of Catalysis, 2011, 278, 297-309.	3.1	328
10487	Monomolecular cracking of propane over acidic chabazite: An ab initio molecular dynamics and transition path sampling study. Journal of Catalysis, 2011, 279, 220-228.	3.1	98
10488	Hydrodeoxygenation pathways catalyzed by MoS2 and NiMoS active phases: A DFT study. Journal of Catalysis, 2011, 279, 276-286.	3.1	118
10489	Interaction of SO2 with Cu/TiC(001) and Au/TiC(001): Toward a new family of DeSOx catalysts. Journal of Catalysis, 2011, 279, 352-360.	3.1	28
10490	Conversion of furfural and 2-methylpentanal on Pd/SiO2 and Pdâ€“Cu/SiO2 catalysts. Journal of Catalysis, 2011, 280, 17-27.	3.1	323
10491	Superior catalytic properties in aerobic oxidation of olefins over Au nanoparticles on pyrrolidone-modified SBA-15. Journal of Catalysis, 2011, 281, 30-39.	3.1	65
10492	Insight into methanol synthesis from CO2 hydrogenation on Cu(111): Complex reaction network and the effects of H2O. Journal of Catalysis, 2011, 281, 199-211.	3.1	347

#	Article	IF	Citations
10493	Oxide clusters as source of the third oxygen atom for the formation of carbonates in alkaline earth dehydrated zeolites. Journal of Catalysis, 2011, 281, 212-221.	3.1	18
10494	Câ€“H bond activation of methane on clean and oxygen pre-covered metals: A systematic theoretical study. Journal of Catalysis, 2011, 282, 74-82.	3.1	101
10495	Selectivity of chemisorbed oxygen in Câ€“H bond activation and CO oxidation and kinetic consequences for CH4â€“O2 catalysis on Pt and Rh clusters. Journal of Catalysis, 2011, 283, 10-24.	3.1	81
10496	Oxygen reduction reaction mechanism on nitrogen-doped graphene: A density functional theory study. Journal of Catalysis, 2011, 282, 183-190.	3.1	545
10497	Mechanism for the waterâ€“gas shift reaction on monofunctional platinum and cause of catalyst deactivation. Journal of Catalysis, 2011, 282, 278-288.	3.1	58
10498	Stability and reactivity of active sites for direct benzene oxidation to phenol in Fe/ZSM-5: A comprehensive periodic DFT study. Journal of Catalysis, 2011, 284, 194-206.	3.1	69
10499	BrÃ¸nsted acidity of amorphous silicaâ€“alumina: The molecular rules of proton transfer. Journal of Catalysis, 2011, 284, 215-229.	3.1	96
10500	Selective conversion of furfural to methylfuran over silica-supported NiFe bimetallic catalysts. Journal of Catalysis, 2011, 284, 90-101.	3.1	463
10501	A Fortran program for calculating electron or hole mobility in disordered semiconductors from first-principles. Computer Physics Communications, 2011, 182, 2632-2637.	3.0	6
10502	Interaction of valine and valine radicals with single-walled carbon nanotube (5,0). Chemical Physics Letters, 2011, 511, 299-303.	1.2	11
10503	The geometric and electronic structure of Xe-adsorbed Fe(001) surface by first-principles calculations. Chemical Physics Letters, 2011, 512, 99-103.	1.2	1
10504	Pressure-induced structural phase transition in wide-gap molecular solid CF4. Chemical Physics Letters, 2011, 512, 223-226.	1.2	2
10505	First-principles study on absolute band edge positions for IIâ€“VI semiconductors at (110) surface. Chemical Physics Letters, 2011, 513, 72-76.	1.2	9
10506	Ab initio study of Kubas-type dihydrogen fixation onto d-orbital states of Ca adatoms. Chemical Physics Letters, 2011, 513, 256-260.	1.2	10
10507	First principles study on the structure and STM image of acetylene adsorption on Ge(001). Chemical Physics Letters, 2011, 514, 109-113.	1.2	1
10508	Analysis of band gap formation in graphene by Si impurities: Local bonding interaction rules. Chemical Physics Letters, 2011, 515, 85-90.	1.2	13
10509	Density functional calculations of Lithium-doped few-layer ABA-stacked graphene supported on Pt and Si-terminated SiC surfaces. Chemical Physics Letters, 2011, 515, 263-268.	1.2	5
10510	CO catalytic oxidation on iron-embedded hexagonal boron nitride sheet. Chemical Physics Letters, 2011, 515, 159-162.	1.2	87

#	Article	IF	Citations
10511	Work function modulation of AuCl4â˜ molecule adsorbed on graphene: A first-principles simulation. Chemical Physics Letters, 2011, 516, 88-91.	1.2	3
10512	Nickel induced iono-covalent character of hydrogen in RbMgH3 from first principles. Chemical Physics Letters, 2011, 516, 174-176.	1.2	3
10513	Oxidation of tin clusters: A first principles study. Chemical Physics Letters, 2011, 518, 70-75.	1.2	3
10514	The effect of humidity on the adsorption of the hydrazine on single-wall carbon nanotubes: First-principles electronic structure calculations. Chemical Physics Letters, 2011, 518, 93-98.	1.2	10
10515	A multiscale theoretical methodology for the calculation of electrochemical observables from ab initio data: Application to the oxygen reduction reaction in a Pt(111)-based polymer electrolyte membrane fuel cell. Electrochimica Acta, 2011, 56, 10842-10856.	2.6	68
10516	An implementation of core level spectroscopies in a real space Projector Augmented Wave density functional theory code. Journal of Electron Spectroscopy and Related Phenomena, 2011, 184, 427-439.	0.8	61
10517	Mechanistic analysis of direct N2O decomposition and reduction with H2 or NH3 over RuO2. Applied Catalysis B: Environmental, 2011, 110, 33-39.	10.8	8
10518	Interaction of H2 with fragments of MOF-5 and its implications for the design and development of new MOFs: A computational study. International Journal of Hydrogen Energy, 2011, 36, 10737-10747.	3.8	18
10519	Ab initio and periodic DFT investigation of hydrogen storage on light metal-decorated MOF-5. International Journal of Hydrogen Energy, 2011, 36, 10816-10827.	3.8	61
10520	First principle study of hydrogen diffusion in equilibrium rutile, rutile with deformation twins and fluorite polymorph of Mg hydride. International Journal of Hydrogen Energy, 2011, 36, 11802-11809.	3.8	29
10521	Intrinsic mechanisms on enhancement of hydrogen desorption from MgH2 by (001) surface doping. International Journal of Hydrogen Energy, 2011, 36, 12939-12949.	3.8	51
10522	First principles study on desorption of chemisorbed hydrogen atoms from single-walled carbon nanotubes under external electric field. International Journal of Hydrogen Energy, 2011, 36, 13645-13656.	3.8	11
10523	Ab initio and thermodynamic investigation on the Caâ€“H system. International Journal of Hydrogen Energy, 2011, 36, 13632-13639.	3.8	8
10524	Theoretical studies on hydrogen adsorption properties of lithium decorated diborene (B2H4Li2) and diboryne (B2H2Li2). International Journal of Hydrogen Energy, 2011, 36, 15681-15688.	3.8	17
10525	Dehydrogenation of pure and Ti-doped Na3AlH6 surfaces from first principles calculations. International Journal of Hydrogen Energy, 2011, 36, 15632-15641.	3.8	8
10526	Hybrid functional study on structural and electronic properties of oxides. Current Applied Physics, 2011, 11, S337-S340.	1.1	57
10527	Vacancy defects in indium oxide: An ab-initio study. Current Applied Physics, 2011, 11, S296-S300.	1.1	55
10528	Formation of oxygen active species in Ag-modified CeO2 catalyst for soot oxidation: A DFT study. Catalysis Today, 2011, 177, 31-38.	2.2	61

#	Article	IF	Citations
10529	Thin Film Growth on Quasicrystalline Surfaces. Israel Journal of Chemistry, 2011, 51, 1314-1325.	1.0	14
10530	Physical properties of the junction of scandium and carbon nanotubes. Journal of Zhejiang University: Science A, 2011, 12, 255-259.	1.3	1
10531	Calcium-Decorated Carbyne Networks as Hydrogen Storage Media. Nano Letters, 2011, 11, 2660-2665.	4.5	98
10532	Elastic, Electronic, and Optical Properties of Two-Dimensional Graphyne Sheet. Journal of Physical Chemistry C, 2011, 115, 20466-20470.	1.5	380
10533	High Capacity Hydrogen Storage in Ca Decorated Graphyne: A First-Principles Study. Journal of Physical Chemistry C, 2011, 115, 23221-23225.	1.5	210
10534	Size effects on silver nanoparticlesâ€™ properties. Nanotechnology, 2011, 22, 275708.	1.3	19
10535	First-principles study of noble gas impurities and defects in UO<mml:math xmlns:mml="http://www.w3.org/1998/Math/MathML" display="inline"><mml:msub><mml:mrow /><mml:mn>2</mml:mn></mml:msub></mml:math>. Physical Review B, 2011, 84, .	1.1	68
10536	Electronic Structure of Partially Reduced Rutile TiO₂(110) Surface: Where Are the Unpaired Electrons Located?. Journal of Physical Chemistry C, 2011, 115, 4696-4705.	1.5	153
10537	Electronic Structure of Pure and N-Doped TiO₂ Nanocrystals by Electrochemical Experiments and First Principles Calculations. Journal of Physical Chemistry C, 2011, 115, 6381-6391.	1.5	118
10538	Structural, elastic, vibrational and electronic properties of amorphous Al₂O₃fromab initiocalculations. Journal of Physics Condensed Matter, 2011, 23, 495401.	0.7	64
10539	Prediction of semiconductor band edge positions in aqueous environments from first principles. Physical Review B, 2011, 83, .	1.1	101
10540	Are glycine cyclic dimers stable in aqueous solution?. CrystEngComm, 2011, 13, 4391.	1.3	18
10541	Methanol conversion over TiO₂-anatase supported oxomolybdate catalysts: an integratedoperandoâ€“ DFT modeling approach. Phase Transitions, 2011, 84, 700-713.	0.6	8
10542	Using first-principles metadynamics simulation to predict new phases and probe the phase transition of NaAlH₄. Journal of Physics Condensed Matter, 2011, 23, 345401.	0.7	3
10543	Mn induced ferromagnetism and modulated topological surface states in Bi2Te3. Applied Physics Letters, 2011, 98, 252502.	1.5	68
10544	Accelerated Materials Design for Hydrogen Separation Membranes. ACS Symposium Series, 2011, , 27-38.	0.5	4
10545	Tuning the Metal Binding Energy and Hydrogen Storage in Alkali Metal Decorated MOF-5 Through Boron Doping: A Theoretical Investigation. Journal of Physical Chemistry C, 2011, 115, 16984-16991.	1.5	45
10546	Role of Water and Carbonates in Photocatalytic Transformation of CO₂ to CH₄ on Titania. Journal of the American Chemical Society, 2011, 133, 3964-3971.	6.6	416

#	Article	IF	Citations
10547	Reactivity of Chemisorbed Oxygen Atoms and Their Catalytic Consequences during CH₄â€“O₂ Catalysis on Supported Pt Clusters. Journal of the American Chemical Society, 2011, 133, 15958-15978.	6.6	184
10548	Structural and thermal properties of LaMnO3from neutron diffraction and first principles studies. Journal of Physics Condensed Matter, 2011, 23, 245402.	0.7	12
10549	Charge Transfer between Metal Clusters and Growing Carbon Structures in Chirality-Controlled Single-Walled Carbon Nanotube Growth. Journal of Physical Chemistry Letters, 2011, 2, 1009-1014.	2.1	21
10550	Reparameterization of the REBO-CHO potential for graphene oxide molecular dynamics simulations. Physical Review B, 2011, 84, .	1.1	35
10551	Freezing in Resonance Structures for Better Packing: XeF₂ Becomes (XeF⁺)(F^{â˜}) at Large Compression. Inorganic Chemistry, 2011, 50, 3832-3840.	1.9	55
10552	Crystal structures of thiazine-indigo pigments, determined from single-crystal and powder diffraction data. Zeitschrift FÃ¼r Kristallographie, 2011, 226, 822-831.	1.1	2
10553	First-principles investigation of C₆₀molecule adsorption on a diamond (1â€‰0â€‰0)-2 Ã— 1 surface. Modelling and Simulation in Materials Science and Engineering, 2011, 19, 045001.	0.8	1
10554	Atomic-Resolution Imaging of Spin-State Superlattices in Nanopockets within Cobaltite Thin Films. Nano Letters, 2011, 11, 973-976.	4.5	90
10555	Band Lineup and Charge Carrier Separation in Mixed Rutile-Anatase Systems. Journal of Physical Chemistry C, 2011, 115, 3443-3446.	1.5	162
10556	Structural, Mechanical Stability, and Physical Properties of Iridium Carbides with Various Stoichiometries: First-Principles Investigations. Journal of Physical Chemistry C, 2011, 115, 6948-6953.	1.5	9
10557	Surface properties of 3dtransition metals. Philosophical Magazine, 2011, 91, 3627-3640.	0.7	45
10558	Prediction of the chemical trends of oxygen vacancy levels in binary metal oxides. Applied Physics Letters, 2011, 99, .	1.5	42
10559	Ab Initio Molecular Dynamics Simulations of the Cooperative Adsorption of Hydrazine and Water on Copper Surfaces: Implications for Shape Control of Nanoparticles. Chemistry of Materials, 2011, 23, 2718-2728.	3.2	15
10560	Ab initiostudy of the thermodynamic properties of rare-earth-magnesium intermetallics MgRE (RE=Y, Dy, Pr, Tb). Physica Scripta, 2011, 83, 065707.	1.2	13
10561	Low-Temperature Phase Transformation from Graphite to<mml:math xmlns:mml="http://www.w3.org/1998/Math/MathML" display="inline"><mml:mi>s</mml:mi><mml:msup><mml:mi>p</mml:mi><mml:mn>3</mml:mn></mml:msup></mml:math>Orthorhombic Carbon. Physical Review Letters, 2011, 106, 075501.	2.9	259
10562	Breathing and Twisting: An Investigation of Framework Deformation and Guest Packing in Single Crystals of a Microporous Vanadium Benzenedicarboxylate. Inorganic Chemistry, 2011, 50, 2028-2036.	1.9	34
10563	Pressure induced high spin-low spin transition in FeSe superconductor studied by x-ray emission spectroscopy and ab initio calculations. Applied Physics Letters, 2011, 99, 061913.	1.5	13
10564	Coexistence of ferroelectric triclinic phases in highly strained BiFeO<mml:math xmlns:mml="http://www.w3.org/1998/Math/MathML" display="inline"><mml:msub><mml:mrow /><mml:mn>3</mml:mn></mml:msub></mml:math>films. Physical Review B, 2011, 84, .	1.1	99

#	Article	IF	Citations
10565	Strain effects on the electronic structure of SrTiO<mml:math xmlns:mml="http://www.w3.org/1998/Math/MathML" display="inline"><mml:msub><mml:mrow /><mml:mn>3</mml:mn></mml:msub></mml:math>: Toward high electron mobilities. Physical Review B, 2011, 84, .	1.1	79
10566	First-Principles Investigation of Morphotropic Transitions and Phase-Change Functional Responses in<mml:math xmlns:mml="http://www.w3.org/1998/Math/MathML" display="inline"><mml:msub><mml:mi>BiFeO</mml:mi><mml:mn>3</mml:mn></mml:msub><mml:mtext mathvariant="normal">â^'</mml:mtext><mml:msub><mml:mi>BiCoO</mml:mi><mml:mn>3</mml:mn></mml:msub></mml:math>	2.9	85
10567	First-principles predictions of low-energy phases of multiferroic BiFeO<mml:math xmlns:mml="http://www.w3.org/1998/Math/MathML" display="inline"><mml:mrow><mml:msub><mml:mi /><mml:mrow><mml:mn>3</mml:mn></mml:mrow></mml:msub></mml:mrow></mml:math>. Physical Review B, 2011, 83, .	1.1	216
10568	<mml:math xmlns:mml="http://www.w3.org/1998/Math/MathML" display="inline"><mml:mrow><mml:msub><mml:mrow /><mml:mn>2</mml:mn></mml:msub></mml:mrow></mml:math>O<mml:math xmlns:mml="http://www.w3.org/1998/Math/MathML"	1.1	73
10569	Discovery of the recoverable high-pressure iron oxide Fe₄O₅. Proceedings of the National Academy of Sciences of the United States of America, 2011, 108, 17281-17285.	3.3	120
10570	Density Functional Characterization of Pure and Alkaline Earth Metalâ€Doped Bi₁₂GeO₂₀, Bi₁₂SiO₂₀, and Bi₁₂TiO₂₀ Photocatalysts. ChemCatChem, 2011, 3, 378-385.	1.8	21
10571	CO+NO versus CO+O₂ Reaction on Monolayer FeO(111) Films on Pt(111). ChemCatChem, 2011, 3, 671-674.	1.8	29
10572	DFT Comparison of Nâ€Nitrosodimethylamine Decomposition Pathways Over Ni and Pd. ChemCatChem, 2011, 3, 898-903.	1.8	11
10573	Zircon to monazite phase transition in CeVO<mml:math xmlns:mml="http://www.w3.org/1998/Math/MathML" display="inline"><mml:mrow><mml:msub><mml:mrow /><mml:mn>4</mml:mn></mml:msub></mml:mrow></mml:math>: X-ray diffraction and Raman-scattering measurements. Physical Review B, 2011, 84, .	1.1	83
10574	Structure and electronic properties of cerium orthophosphate: Theory and experiment. Physical Review B, 2011, 83, .	1.1	36
10575	Stone-Wales-type transformations in carbon nanostructures driven by electron irradiation. Physical Review B, 2011, 83, .	1.1	226
10576	Polar distortions in hydrogen-bonded organic ferroelectrics. Physical Review B, 2011, 84, .	1.1	45
10577	Mechanical and Electronic Properties of MoS₂ Nanoribbons and Their Defects. Journal of Physical Chemistry C, 2011, 115, 3934-3941.	1.5	427
10578	Inducing and optimizing magnetism in graphene nanomeshes. Physical Review B, 2011, 84, .	1.1	69
10579	Structures of fluorinated graphene and their signatures. Physical Review B, 2011, 83, .	1.1	254
10580	Group IV Graphene- and Graphane-Like Nanosheets. Journal of Physical Chemistry C, 2011, 115, 13242-13246.	1.5	288
10581	High-pressure study of ScVO<mml:math xmlns:mml="http://www.w3.org/1998/Math/MathML" display="inline"><mml:mrow><mml:msub><mml:mrow /><mml:mn>4</mml:mn></mml:msub></mml:mrow></mml:math>by Raman scattering andab initiocalculations. Physical Review B, 2011, 83, .	1.1	54
10582	Developing high-capacity hydrogen storage materials via quantum simulations. MRS Bulletin, 2011, 36, 198-204.	1.7	15

#	Article	IF	Citations
10583	Cu and Co codoping effects on room-temperature ferromagnetism of (Co,Cu):ZnO dilute magnetic semiconductors. Journal of Applied Physics, 2011, 109, 103705.	1.1	28
10584	Electronic and magnetic properties of perfect, vacancy-doped, and nonmetal adsorbed MoSe2, MoTe2 and WS2 monolayers. Physical Chemistry Chemical Physics, 2011, 13, 15546.	1.3	428
10585	Metallic clusters on a model surface: Quantum versus geometric effects. Physical Review B, 2011, 84, .	1.1	2
10586	Selective Alignment of Carbon Nanotubes on Sapphire Surfaces: Bond Formation between Nanotubes and Substrates. Physical Review Letters, 2011, 107, 065501.	2.9	5
10587	Forces and Currents in Carbon Nanostructures: Are We Imaging Atoms?. Physical Review Letters, 2011, 106, 176101.	2.9	81
10588	Ab initioinvestigation of Ti<mml:math xmlns:mml="http://www.w3.org/1998/Math/MathML" display="inline"><mml:msub><mml:mrow /><mml:mn>2</mml:mn></mml:msub></mml:math>Al(C,N) solid solutions. Physical Review B, 2011, 84, .	1.1	19
10589	Local structure of Ba(Ti,Zr)O<mml:math xmlns:mml="http://www.w3.org/1998/Math/MathML" display="inline"><mml:mrow><mml:msub><mml:mrow /><mml:mrow><mml:mn>3</mml:mn></mml:mrow></mml:msub></mml:mrow></mml:math>perovskite-like solid solutions and its relation to the band-gap behavior. Physical Review B, 2011, 83, .	1.1	62
10590	Spin texture and magnetic anisotropy of Co impurities in Bi<mml:math xmlns:mml="http://www.w3.org/1998/Math/MathML" display="inline"><mml:msub><mml:mrow /><mml:mn>2</mml:mn></mml:msub></mml:math>Se<mml:math xmlns:mml="http://www.w3.org/1998/Math/MathML" display="inline"><mml:msub><mml:mrow	1.1	47
10591	Electronic and magnetic structure of the mixed-valence cobaltite CaBaCo<mml:math xmlns:mml="http://www.w3.org/1998/Math/MathML" display="inline"><mml:msub><mml:mrow /><mml:mn>4</mml:mn></mml:msub></mml:math>O<mml:math xmlns:mml="http://www.w3.org/1998/Math/MathML" display="inline"><mml:msub><mml:mrow /><mml:mn>7</mml:mn></mml:msub></mml:math>. Physical Review B, 2011, 84, .	1.1	10
10592	Energy gap of Kronig-Penney-type hydrogenated graphene superlattices. Physical Review B, 2011, 84, .	1.1	12
10593	Effects of Alkali Adatoms on CO and H₂S Adsorptions on the Fe(100) Surface: A Density Functional Theory Study. Journal of Physical Chemistry C, 2011, 115, 23893-23901.	1.5	19
10594	Peculiarities of the decoration of carbon nanotubes with transition metal atoms. Russian Journal of Physical Chemistry B, 2011, 5, 163-167.	0.2	5
10595	Activation of molecular hydrogen on platinum nanoparticles: Quantum-chemical modeling. Russian Journal of Inorganic Chemistry, 2011, 56, 1290-1300.	0.3	6
10596	Quantum-chemical modeling of the dissociative adsorption of molecular hydrogen onto the tin dioxide surface. Russian Journal of Inorganic Chemistry, 2011, 56, 1402-1409.	0.3	3
10597	Dissociative adsorption of molecular hydrogen onto Pt6 and Pt19 platinum clusters located on the tin dioxide surface: Quantum-chemical modeling. Russian Journal of Inorganic Chemistry, 2011, 56, 1579-1588.	0.3	8
10598	Quantum-chemical modeling of the hydrogen spillover effect in the H/Pt/SnO2 system. Russian Journal of Inorganic Chemistry, 2011, 56, 1765-1774.	0.3	3
10599	Theoretical study of the structure and properties of complexes formed by lithium and a boron Î± sheet. Russian Journal of Physical Chemistry A, 2011, 85, 1390-1393.	0.1	0
10600	Magnetic ordering in digital alloys of group-IV semiconductors with 3d-transition metals. Journal of Experimental and Theoretical Physics, 2011, 112, 625-636.	0.2	8

#	Article	IF	Citations
10601	Mobility of vacancies under deformation and their effect on the elastic properties of graphene. Journal of Experimental and Theoretical Physics, 2011, 112, 820-824.	0.2	17
10602	Role of magnetism in the formation of a short-range order in iron-silicon alloys. Journal of Experimental and Theoretical Physics, 2011, 112, 848-859.	0.2	23
10603	Hydrogenation of the nanopowders that form in a carbon-helium plasma stream during the introduction of Ni and Mg. Journal of Experimental and Theoretical Physics, 2011, 113, 1057-1062.	0.2	1
10604	Quantum-mechanical calculations and analysis of vibrational modes in lead magnoniobate. Physics of the Solid State, 2011, 53, 147-150.	0.2	3
10605	Effect of coverage by carbon on the possibility of forming an interstitial solid solution in Fe(001) and Fe(111) subsurface layers. Physics of the Solid State, 2011, 53, 599-605.	0.2	3
10606	Effect of alloying elements and impurities on interface properties in aluminum alloys. Physics of the Solid State, 2011, 53, 2189-2193.	0.2	12
10607	Modulation of the electronic and magnetic properties of the silicene nanoribbons by a singleÂC chain. European Physical Journal B, 2011, 79, 197-202.	0.6	19
10608	First-principles investigation of electronic structure and optical properties in N-F codoped ZnO with wurtzite structure. European Physical Journal B, 2011, 80, 25-30.	0.6	8
10609	Electronic structure of fluorides: general trends for ground and excited state properties. European Physical Journal B, 2011, 81, 115-120.	0.6	25
10610	Structural, electronic and magnetic properties of hcp Fe, Co and Ni nanowires encapsulated in zigzag carbon nanotubes. European Physical Journal B, 2011, 81, 459-465.	0.6	24
10611	Ferromagnetism in Rh-doped SnO2 from first-principles calculation. European Physical Journal B, 2011, 80, 337-341.	0.6	17
10612	Structural and electronic properties of Y2CrS4 from first-principles study. European Physical Journal B, 2011, 80, 307-310.	0.6	1
10613	Theoretical investigation of the hydrogenation induced atomic rearrangements in palladium rich intermetallic compounds MPd3 (M = Mg, In, Tl). European Physical Journal B, 2011, 82, 1-6.	0.6	11
10614	Spacer induced magnetism and its effect on interlayer exchange coupling in Fe/(Pd, Cu, Au, Ag) multilayered nanowires. European Physical Journal B, 2011, 80, 459-467.	0.6	4
10615	First-principle study of magnetism induced by vacancies in graphene. European Physical Journal B, 2011, 80, 343-349.	0.6	63
10616	Electronic and magnetic properties of SiC nanoribbons by F termination. European Physical Journal B, 2011, 84, 419-424.	0.6	3
10617	Sulphur overlayers on Ir(100) and its effect on the adsorption of CO: a DFT study. European Physical Journal B, 2011, 83, 437-443.	0.6	6
10618	Collisions between a single gold atom and 13 atom gold clusters: an abÂinitio approach. European Physical Journal D, 2011, 61, 87-93.	0.6	8

#	Article	IF	Citations
10619	Defect studies in small CdTe clusters. European Physical Journal D, 2011, 61, 609-619.	0.6	4
10620	Oxygen impact on quantum confinement effect for silicon clusters in different size regimes: ab initio investigations. European Physical Journal D, 2011, 64, 331-337.	0.6	1
10621	First-principles calculations of the structural, electronic and magnetic properties of BnN20â^'n (n =) Tj ETQq0 0 0 rgBT /Overlock 10 Tf 5	0.6	0
10622	The role of d-orbital polarization on rhodium cluster collisions. European Physical Journal D, 2011, 64, 45-51.	0.6	3
10623	Faster proton transfer dynamics of water on SnO2 compared to TiO2. Journal of Chemical Physics, 2011, 134, 044706.	1.2	34
10624	<mml:math xmlns:mml="http://www.w3.org/1998/Math/MathML" display="inline"><mml:mrow><mml:mi fontstyle="italic">Ab</mml:mi><mml:mi>a€,</mml:mi><mml:mi fontstyle="italic">initio</mml:mi></mml:mrow></mml:math>study of larger Pb<mml:math xmlns:mml="http://www.w3.org/1998/Math/MathML" display="inline"><mml:mrow><mml:msub><mml:mrow /><mml:mi>n</mml:mi></mml:msub></mml:mrow></mml:math>clusters	1.1	25
10625	Hydrogen-induced interactions in vanadium from first-principles calculations. Physical Review B, 2011, 83, .	1.1	45
10626	Formation of oxygen vacancies and charge carriers induced in the<mml:math xmlns:mml="http://www.w3.org/1998/Math/MathML" display="inline"><mml:mi>n</mml:mi></mml:math>-type interface of a LaAlO<mml:math xmlns:mml="http://www.w3.org/1998/Math/MathML" display="inline"><mml:msub><mml:mrow /><mml:mn>3</mml:mn></mml:msub></mml:math>overlayer on SrTiO<mml:math xmlns:mml="http://www.w3.org/1998/Math/MathML" display="inline"><mml:msub><mml:mrow />	1.1	99
10627	Defect states of complexes involving a vacancy on the boron site in boronitrene. Physical Review B, 2011, 84, .	1.1	36
10628	Ionization-Enhanced Decomposition of 2,4,6-Trinitrotoluene (TNT) Molecules. Journal of Physical Chemistry A, 2011, 115, 8142-8146.	1.1	12
10629	Evidence of Cobalt-Vacancy Complexes in<mml:math xmlns:mml="http://www.w3.org/1998/Math/MathML" display="inline"><mml:msub><mml:mi>Zn</mml:mi><mml:mrow><mml:mn>1</mml:mn><mml:mo>â^'</mml:mo><mml:mi>x</mml:mi></mml:mrow></mml:msub><mml:mi mathvariant="normal">O</mml:mi></mml:math>Dilute Magnetic Semiconductors. Physical Review Letters, 2011, 107, 127206.	2.9	86
10630	Asymmetric Split-Vacancy Defects in SiC Polytypes: A Combined Theoretical and Electron Spin Resonance Study. Physical Review Letters, 2011, 107, 195501.	2.9	22
10631	Reversible Transition between Thermodynamically Stable Phases with Low Density of Oxygen Vacancies on the<mml:math xmlns:mml="http://www.w3.org/1998/Math/MathML" display="inline"><mml:msub><mml:mi>SrTiO</mml:mi><mml:mn>3</mml:mn></mml:msub><mml:mo stretchy="false">(</mml:mo><mml:mn>110</mml:mn><mml:mo) Tj ETQq0 0 0 rgBT /Overlock 10 Tf 50 247 Td (stretchy="false">)</mml:mo	2.9	30
10632	High pressure partially ionic phase of water ice. Nature Communications, 2011, 2, 563.	5.8	208
10633	Predicted Novel High-Pressure Phases of Lithium. Physical Review Letters, 2011, 106, 015503.	2.9	499
10634	Phase Transitions of AlFeO₃ and GaFeO₃ from the Chiral Orthorhombic (Pna2₁) Structure to the Rhombohedral (R3̄...c) Structure. Inorganic Chemistry, 2011, 50, 9527-9532.	1.9	51
10635	Tailoring Native Defects in LiFePO₄: Insights from First-Principles Calculations. Chemistry of Materials, 2011, 23, 3003-3013.	3.2	155
10636	First-Principles Theory of Electrochemical Capacitance of Nanostructured Materials: Dipole-Assisted Subsurface Intercalation of Lithium in Pseudocapacitive TiO₂ Anatase Nanosheets. Journal of Physical Chemistry C, 2011, 115, 4909-4915.	1.5	56

#	Article	IF	Citations
10637	Electrical control of the chemical bonding of fluorine on graphene. Physical Review B, 2011, 83, .	1.1	76
10638	First-Principles Study of Photoinduced Water-Splitting on Fe₂O₃. Journal of Physical Chemistry C, 2011, 115, 12901-12907.	1.5	96
10639	Splitting Water on Metal Oxide Surfaces. Journal of Physical Chemistry C, 2011, 115, 19710-19715.	1.5	45
10640	Unusual ferromagnetic superexchange in CdVO<mml:math xmlns:mml="http://www.w3.org/1998/Math/MathML" display="inline"><mml:msub><mml:mrow /><mml:mn>3</mml:mn></mml:msub></mml:math>: The role of Cd. Physical Review B, 2011, 84, .	1.1	23
10641	Limits on Passivating Defects in Semiconductors: The Case of Si Edge Dislocations. Physical Review Letters, 2011, 107, 035503.	2.9	9
10642	Hydrogen effect on shearing and cleavage of Al: A first-principles study. Physical Review B, 2011, 84, .	1.1	15
10643	Hydrogen transport on graphene: Competition of mobility and desorption. Physical Review B, 2011, 84, .	1.1	36
10644	Voltage, stability and diffusion barrier differences between sodium-ion and lithium-ion intercalation materials. Energy and Environmental Science, 2011, 4, 3680.	15.6	1,236
10645	Bound and free self-interstitial defects in graphite and bilayer graphene: A computational study. Physical Review B, 2011, 84, .	1.1	32
10646	Radiation-induced damage and evolution of defects in Mo. Physical Review B, 2011, 84, .	1.1	53
10647	Effect of symmetry breaking on the optical absorption of semiconductor nanoparticles. Physical Review B, 2011, 84, .	1.1	8
10648	Thickness dependence of the strain, band gap and transport properties of epitaxial In₂O₃thin films grown on Y-stabilised ZrO₂(111). Journal of Physics Condensed Matter, 2011, 23, 334211.	0.7	45
10649	Nanovoids in thermoelectric Î²-Zn4Sb3: A possibility for nanoengineering via Zn diffusion. Acta Materialia, 2011, 59, 5266-5275.	3.8	35
10650	Prediction of thermal cross-slip stress in magnesium alloys from direct first-principles data. Acta Materialia, 2011, 59, 5652-5660.	3.8	99
10651	Binding of multiple H atoms to solute atoms in bcc Fe using first principles. Acta Materialia, 2011, 59, 5812-5820.	3.8	28
10652	Energetics of twinning in martensitic NiTi. Acta Materialia, 2011, 59, 5893-5904.	3.8	81
10653	Precipitates in Alâ€“Cu alloys revisited: Atom-probe tomographic experiments and first-principles calculations of compositional evolution and interfacial segregation. Acta Materialia, 2011, 59, 6187-6204.	3.8	206
10654	Local electronic structure of LiFePO4 nanoparticles in aged Li-ion batteries. Acta Materialia, 2011, 59, 6917-6926.	3.8	19

#	Article	IF	Citations
10655	First-principles-based mesoscale modeling of the solute-induced stabilization of ã€˜100ã€‰ tilt grain boundaries in an Alâ€“Pb alloy. Acta Materialia, 2011, 59, 7022-7028.	3.8	7
10656	Structure and energetics of the coherent interface between the Î¸â€² precipitate phase and aluminium in Alâ€“Cu. Acta Materialia, 2011, 59, 7043-7050.	3.8	176
10657	The structure and the properties of S-phase in AlCuMg alloys. Acta Materialia, 2011, 59, 7396-7405.	3.8	93
10658	Firstâ€principles study of CrB₄ as a high shear modulus compound. Physica Status Solidi - Rapid Research Letters, 2011, 5, 13-15.	1.2	25
10659	Dielectric properties of organosilicons from first principles. Journal of Materials Science, 2011, 46, 90-93.	1.7	14
10660	Phase equilibria and thermodynamic modeling in the Geâ€“Zr binary system. Journal of Materials Science, 2011, 46, 1405-1413.	1.7	3
10661	Structures of a Î£Â=Â9, [110]/{221} symmetrical tilt grain boundary in SrTiO3. Journal of Materials Science, 2011, 46, 4162-4168.	1.7	8
10662	Atomistic structure and energetics of interface between Mn-doped Î³-Ga2O3 and MgAl2O4. Journal of Materials Science, 2011, 46, 4169-4175.	1.7	12
10663	Indium adsorption and incorporation mechanisms in AlN. Journal of Materials Science, 2011, 46, 4377-4383.	1.7	4
10664	First-principles study of structure, vacancy formation, and strength of bcc Fe/V4C3 interface. Journal of Materials Science, 2011, 46, 4206-4215.	1.7	7
10665	Structure and thermodynamics of the key precipitated phases in the Alâ€“Mgâ€“Si alloys from first-principles calculations. Journal of Materials Science, 2011, 46, 7839-7849.	1.7	26
10666	Crystal Structure, Infrared Spectra and DFT Study of Benzyl 2,3-Anhydro-Î²-d-Ribopyranoside. Journal of Chemical Crystallography, 2011, 41, 167-174.	0.5	2
10667	Dihydrogen Phosphate and Hydrogen Sulphate of 1,4-Dimethyl-1,4-diazabicyclo[2.2.2]octane-1,4-diium: Crystal Structures, Hydrogen Bonding and Infrared Spectra. Journal of Chemical Crystallography, 2011, 41, 1539-1546.	0.5	3
10668	An analysis for the DIIS acceleration method used in quantum chemistry calculations. Journal of Mathematical Chemistry, 2011, 49, 1889-1914.	0.7	82
10669	Direct CO Oxidation by Lattice Oxygen on Zr-Doped Ceria Surfaces. Catalysis Letters, 2011, 141, 78-82.	1.4	39
10670	A DFT Study on the Adsorption of Formic Acid and Its Oxidized Intermediates on (100) Facets of Pt, Au, Monolayer and Decorated Pt@Au Surfaces. Catalysis Letters, 2011, 141, 1872-1882.	1.4	25
10671	Fabrication and modification of the supported Al nanoparticles on the Al(001) and (110) surfaces using the reversible vertical single-atom manipulation with the Cu and Pt trimer-apex tips: a first-principles study. Journal of Nanoparticle Research, 2011, 13, 1191-1196.	0.8	1
10672	Electronic structure effects on stability and quantum conductance in 2D gold nanowires. Journal of Nanoparticle Research, 2011, 13, 5225-5238.	0.8	6

#	Article	IF	Citations
10673	Gold Nanoparticles on Yttrium Modified Titania: Support Properties and Catalytic Activity. Topics in Catalysis, 2011, 54, 219-228.	1.3	25
10674	Creation of Low-Coordination Gold Sites on Au(111) Surface by 1,4-phenylene Diisocyanide Adsorption. Topics in Catalysis, 2011, 54, 20-25.	1.3	36
10675	Computational Investigation of the Thermochemistry and Kinetics of Steam Methane Reforming Over a Multi-Faceted Nickel Catalyst. Topics in Catalysis, 2011, 54, 828-844.	1.3	89
10676	Adsorption mechanism of single guanine and thymine on single-walled carbon nanotubes. Journal of Molecular Modeling, 2011, 17, 2773-2780.	0.8	12
10677	On possible existence of pseudobinary mixed valence fluorides of Ag(I) / Ag(II): a DFT study. Journal of Molecular Modeling, 2011, 17, 2237-2248.	0.8	7
10678	Crystal and electronic structures and high-pressure behavior of AgSO4, a unique narrow band gap antiferromagnetic semiconductor: LDA(+U) picture. Journal of Molecular Modeling, 2011, 17, 2259-2264.	0.8	9
10679	On the role of lattice dynamics on low-temperature oxygen mobility in solid oxides: a neutron diffraction and first-principles investigation of $$ {hbox{L}}{{hbox{a}}_2}{hbox{Cu}}{{hbox{O}}_{{4 + delta }}} $$. Journal of Solid State Electrochemistry, 2011, 15, 357-366.	1.2	29
10680	Hydrogenation mechanism in lanthanum-activated magnesium films. Applied Physics A: Materials Science and Processing, 2011, 102, 739-745.	1.1	3
10681	Antisite defects and Mg doping in LiFePO4: aÂfirst-principles investigation. Applied Physics A: Materials Science and Processing, 2011, 104, 529-537.	1.1	47
10682	Microscopic indium distribution and electron localization in zinc blende InGaN alloys and InGaN/GaN strained quantum wells. Applied Physics B: Lasers and Optics, 2011, 104, 105-111.	1.1	5
10683	Crossover of cation partitioning in olivines: a combination of ab initio and Monte Carlo study. Physics and Chemistry of Minerals, 2011, 38, 259-265.	0.3	9
10684	Solid solution behaviour of CaSiO3 and MgSiO3 perovskites. Physics and Chemistry of Minerals, 2011, 38, 311-319.	0.3	16
10685	The enigma of post-perovskite anisotropy: deformation versus transformation textures. Physics and Chemistry of Minerals, 2011, 38, 665-678.	0.3	33
10686	DFT study of Rb-TFA structure after high-pressure action. Physics and Chemistry of Minerals, 2011, 38, 819-824.	0.3	2
10687	Atomic carbon adsorption on Ni nanoclusters: a DFT study. Theoretical Chemistry Accounts, 2011, 128, 17-24.	0.5	32
10688	DFT and kinetics study of O/O2 mixtures reacting over a graphite (0001) basal surface. Theoretical Chemistry Accounts, 2011, 128, 683-694.	0.5	34
10689	Thermo-dynamical contours of electronic-vibrational spectra simulated using the statistical quantumâ€“mechanical methods. Theoretical Chemistry Accounts, 2011, 130, 609-632.	0.5	9
10690	Structural and electronic properties of tungsten trioxides: from cluster to solid surface. Theoretical Chemistry Accounts, 2011, 130, 103-114.	0.5	28

#	Article	IF	Citations
10691	Ag diffusion in cubic silicon carbide. Journal of Nuclear Materials, 2011, 408, 257-271.	1.3	91
10692	Electronic structures, mechanical and thermodynamic properties of ThN from first-principles calculations. Journal of Nuclear Materials, 2011, 408, 136-141.	1.3	37
10693	Assessment of radiation-induced segregation mechanisms in austenitic and ferriticâ€“martensitic alloys. Journal of Nuclear Materials, 2011, 411, 41-50.	1.3	119
10694	First principles calculation of the elastic constants and phonon modes of UO2 using GGA + U with orbital occupancy control. Journal of Nuclear Materials, 2011, 412, 301-307.	1.3	31
10695	Phase equilibrium of PuO2â^'xâ^'Pu2O3 based on first-principles calculations and configurational entropy change. Journal of Nuclear Materials, 2011, 412, 338-341.	1.3	3
10696	Elastic properties of cubic, tetragonal and monoclinic ZrO2 from first-principles calculations. Journal of Nuclear Materials, 2011, 415, 13-17.	1.3	82
10697	Ab initio study of ultra-incompressible ternary BeCN2 polymorph. Journal of Physics and Chemistry of Solids, 2011, 72, 667-672.	1.9	12
10698	Structure and magnetic properties of the Al1â^'xGaxFeO3 family of oxides: A combined experimental and theoretical study. Journal of Solid State Chemistry, 2011, 184, 494-501.	1.4	47
10699	Synthesis and magnetic property of FeMoO4 nanorods. Materials Science and Engineering B: Solid-State Materials for Advanced Technology, 2011, 176, 756-761.	1.7	42
10700	Gold might slow down the growth of helium bubble in iron. Nuclear Instruments & Methods in Physics Research B, 2011, 269, 1428-1430.	0.6	16
10701	Exploring the interaction between the boron nitride nanotube and biological molecules. Computer Physics Communications, 2011, 182, 39-42.	3.0	45
10702	CIF2Cell: Generating geometries for electronic structure programs. Computer Physics Communications, 2011, 182, 1183-1186.	3.0	128
10703	A theoretical study on the catalytic effect of nanoparticle confined in carbon nanotube. Chemical Physics Letters, 2011, 502, 96-100.	1.2	15
10704	Origin of doping effects on the oxygen storage capacity of Ce1â^'xMxO2 (M=Fe, Ru, Os, Sm, Pu). Chemical Physics Letters, 2011, 502, 169-172.	1.2	22
10705	The structure of FePc on Cu(100). Chemical Physics Letters, 2011, 503, 53-56.	1.2	7
10706	Cu-doped ceria: Oxygen vacancy formation made easy. Chemical Physics Letters, 2011, 510, 60-66.	1.2	53
10707	Structural and electronic properties of neutral and charged Ca8C12 metal carbides. Chemical Physics Letters, 2011, 507, 260-264.	1.2	4
10708	Theoretical study of the influence of Na on CO adsorption and dissociation on Pd(111): Long-range or short-range interactions between co-adsorbates?. Chemical Physics Letters, 2011, 511, 33-38.	1.2	11

#	Article	IF	Citations
10709	Two-color Thomson scattering at FLASH. High Energy Density Physics, 2011, 7, 145-149.	0.4	14
10710	Fast and metastable fragmentation of deprotonated d-fructose â€“ A combined experimental and computational study. International Journal of Mass Spectrometry, 2011, 305, 50-57.	0.7	11
10711	An efficient numerical method for the equations of steady and unsteady flows of homogeneous incompressible Newtonian fluid. Journal of Computational Physics, 2011, 230, 551-571.	1.9	4
10712	Stable structure and effects of oxygen on InN (101Â¯0) and (112Â¯0) surfaces. Journal of Crystal Growth, 2011, 327, 233-236.	0.7	2
10713	A computational study of thin cubic carbide films in WC/Co interfaces. Acta Materialia, 2011, 59, 171-181.	3.8	46
10714	Hole doping effect on ferromagnetism in Mn-doped ZnO nanowires. Current Applied Physics, 2011, 11, 236-240.	1.1	8
10715	Oxygen vacancy in LiTiPO5 and LiTi2(PO4)3: A first-principles study. Physics Letters, Section A: General, Atomic and Solid State Physics, 2011, 375, 934-938.	0.9	25
10716	Dissociation of hydrogen molecules on the clean and hydrogen-preadsorbed Be(0001) surface. Physics Letters, Section A: General, Atomic and Solid State Physics, 2011, 375, 2430-2436.	0.9	9
10717	Adsorption and diffusion of H2O molecule on the Be(0001) surface: A density-functional theory study. Physics Letters, Section A: General, Atomic and Solid State Physics, 2011, 375, 3208-3212.	0.9	8
10718	Atomic-level structure and structureâ€“property relationship in metallic glasses. Progress in Materials Science, 2011, 56, 379-473.	16.0	1,364
10719	Self-assembly and ordering of C60 on the WO2/W(110) surface. Nano Research, 2011, 4, 194-203.	5.8	19
10720	Patterning nanoroads and quantum dots on fluorinated graphene. Nano Research, 2011, 4, 143-152.	5.8	120
10721	Selective growth of ZnO nanorods on SiO2/Si substrates using a graphene buffer layer. Nano Research, 2011, 4, 440-447.	5.8	63
10722	Direct imaging of molecular orbitals of metal phthalocyanines on metal surfaces with an O2-functionalized tip of a scanning tunneling microscope. Nano Research, 2011, 4, 523-530.	5.8	27
10723	Fe nanoclusters on the Ge(001) surface studied by scanning tunneling microscopy, density functional theory calculations and X-ray magnetic circular dichroism. Nano Research, 2011, 4, 971-978.	5.8	4
10724	Ab initio molecular dynamic simulation on the elasticity of Mg3Al2Si3O12 pyrope. Journal of Earth Science (Wuhan, China), 2011, 22, 169-175.	1.1	13
10725	First principles study of Ag-doped, Nb-doped and Ag/Nb doped SrTiO3. Rare Metals, 2011, 30, 177-182.	3.6	2
10726	Effect of Fe ternary addition on ductility of NiAl intermetallic alloy. Rare Metals, 2011, 30, 316-319.	3.6	4

#	Article	IF	Citations
10727	First principles calculations of electronic properties and mechanical properties of bcc molybdenum and niobium. Rare Metals, 2011, 30, 354-358.	3.6	24
10728	First-principles study of carbon effects in a tungsten grain boundary: site preference, segregation and strengthening. Science China: Physics, Mechanics and Astronomy, 2011, 54, 2164-2169.	2.0	32
10729	Electronic origin of the anomalous solid solution hardening of Y and Gd in Mg: A first-principles study. Science Bulletin, 2011, 56, 1038-1042.	1.7	20
10730	First-principles calculations of the Î²â€²-Mg7Gd precipitate in Mg-Gd binary alloys. Science Bulletin, 2011, 56, 1142-1146.	1.7	25
10731	First-principle investigation of the electronic and magnetic properties of PbMn(SO4)2. Frontiers of Physics, 2011, 6, 96-99.	2.4	2
10732	Quantum simulation of molecular interaction and dynamics at surfaces. Frontiers of Physics, 2011, 6, 294-308.	2.4	10
10733	Metal-decorated defective BN nanosheets as hydrogen storage materials. Frontiers of Physics, 2011, 6, 224-230.	2.4	7
10734	First-Principles Study on the Grain Boundary Embrittlement of Metals by Solute Segregation: Part II. Metal (Fe, Al, Cu)-Hydrogen (H) Systems. Metallurgical and Materials Transactions A: Physical Metallurgy and Materials Science, 2011, 42, 330-339.	1.1	137
10735	First-Principles Study on the Grain Boundary Embrittlement of Metals by Solute Segregation: Part I. Iron (Fe)-Solute (B, C, P, and S) Systems. Metallurgical and Materials Transactions A: Physical Metallurgy and Materials Science, 2011, 42, 319-329.	1.1	139
10736	Effects of Additives and Impurity on the Adhesive Behavior of the NiAl(110)/Al2O3 (0001) Interface: An Ab Initio Study. Metallurgical and Materials Transactions A: Physical Metallurgy and Materials Science, 2011, 42, 4126-4136.	1.1	22
10737	Properties of Nitrogen Molecules in ZnO. Journal of Electronic Materials, 2011, 40, 440-445.	1.0	4
10738	Electronic Structures and Transport Properties of RFe4Sb12 (RÂ=ÂNa, Ca, Nd, Yb, Sn, In). Journal of Electronic Materials, 2011, 40, 974-979.	1.0	9
10739	Self-Diffusion Coefficient of fcc Mg: First-Principles Calculations and Semi-Empirical Predictions. Journal of Phase Equilibria and Diffusion, 2011, 32, 128-137.	0.5	13
10740	Valence band offsets of the strained and longitudinally relaxed diamond/c-BN superlattices. Journal of Shanghai University, 2011, 15, 218-222.	0.1	0
10741	Alkali metal atom adsorption on-top of the F s 0 defective center of MgO(001) surface. Journal of Shanghai University, 2011, 15, 223-228.	0.1	1
10742	First Isolated â€œHypoelectronicâ€•[In₆]^{6â€“} Cluster in Insulating Cs₂₂In₆(SiO₄)₄. Zeitschrift Fur Anorganische Und Allgemeine Chemie, 2011, 637, 834-839.	0.6	8
10743	Dimers of Ag²⁺ Ions â€“ Synthesis and Characterization of the Quaternary Silver Fluoride Ag₂ZnZr₂F₁₄ with [Ag₂F₇]^{3â€“} Units. Zeitschrift Fur Anorganische Und Allgemeine Chemie, 2011, 637, 1118-1121.	0.6	8
10744	In Search of Chemical Frustration in the Caâ€Cuâ€Cd System: Chemical Pressure Relief in the Crystal Structures of ÂCa₅Cu₂Cd and Ca₂Cu₂Cd₉. Zeitschrift Fur Anorganische Und Allgemeine Chemie, 2011, 637, 1961-1974.	0.6	19

#	Article	IF	Citations
10745	Crystal and electronic structure of PbTe/CdTe nanostructures. Nanoscale Research Letters, 2011, 6, 126.	3.1	13
10746	Electronic and magnetic properties of SnO2/CrO2 thin superlattices. Nanoscale Research Letters, 2011, 6, 146.	3.1	8
10747	Defect-related hysteresis in nanotube-based nano-electromechanical systems. Nanoscale Research Letters, 2011, 6, 245.	3.1	4
10748	Metal-functionalized single-walled graphitic carbon nitride nanotubes: a first-principles study on magnetic property. Nanoscale Research Letters, 2011, 6, 97.	3.1	18
10749	J-ICE: a newJmolinterface for handling and visualizing crystallographic and electronic properties. Journal of Applied Crystallography, 2011, 44, 225-229.	1.9	88
10750	VESTAâ€...3for three-dimensional visualization of crystal, volumetric and morphology data. Journal of Applied Crystallography, 2011, 44, 1272-1276.	1.9	16,580
10751	Bis(Î¼²-2-(dimethylamino)ethoxo-N,O,O)-di(phenolato-O)ditin(II): a high-resolution single-crystal X-ray diffraction and quantum chemical study. Acta Crystallographica Section B: Structural Science, 2011, 67, 315-323.	1.8	12
10752	Structural building principles of complex face-centered cubic intermetallics. Acta Crystallographica Section B: Structural Science, 2011, 67, 269-292.	1.8	50
10753	Towards crystal structure prediction of complex organic compounds â€“ a report on the fifth blind test. Acta Crystallographica Section B: Structural Science, 2011, 67, 535-551.	1.8	358
10754	First-principles investigation of the electronic structures of edge dislocations in GaN. Physica Status Solidi (A) Applications and Materials Science, 2011, 208, 1555-1557.	0.8	2
10755	Towards experimental identification of vacancy complexes in InN. Physica Status Solidi (A) Applications and Materials Science, 2011, 208, 1548-1550.	0.8	4
10756	Firstâ€principles study on structural, electronic and magnetic properties of iron nanowire encapsulated in carbon nanotube. Physica Status Solidi (A) Applications and Materials Science, 2011, 208, 97-103.	0.8	8
10757	Nanostructuring in Î²â€Zn₄Sb₃ with variable starting Zn compositions. Physica Status Solidi (A) Applications and Materials Science, 2011, 208, 1652-1657.	0.8	25
10758	Synthesis, characterization, and optical properties of Ag₂Mo₂O₇ nanowires. Physica Status Solidi (A) Applications and Materials Science, 2011, 208, 1937-1941.	0.8	16
10759	Firstâ€principles study on the structural, phonon, and thermodynamic properties of the ternary carbides in Tiâ€“Alâ€“C system. Physica Status Solidi (A) Applications and Materials Science, 2011, 208, 1879-1884.	0.8	23
10760	Melting curve of the cI16 sodium at high pressure from ab initio calculations. Physica Status Solidi (B): Basic Research, 2011, 248, 1143-1148.	0.7	2
10761	Adsorption of Sn on the Ge(111)â€(3â€‰Ã—â€‰3) surface studied by ab initio density functional theory. Physica Status Solidi (B): Basic Research, 2011, 248, 2142-2146.	0.7	1
10762	Accurate Kohnâ€“Sham DFT with the speed of tight binding: Current techniques and future directions in materials modelling. Physica Status Solidi (B): Basic Research, 2011, 248, 1309-1318.	0.7	57

#	Article	IF	Citations
10763	Elastic properties of superconducting MAX phases from firstâ€principles calculations. Physica Status Solidi (B): Basic Research, 2011, 248, 228-232.	0.7	68
10764	Timeâ€dependent density functional study on the excitation spectrum of point defects in semiconductors. Physica Status Solidi (B): Basic Research, 2011, 248, 1337-1346.	0.7	80
10765	Charge transport in organic crystals: Theory and modelling. Physica Status Solidi (B): Basic Research, 2011, 248, 511-525.	0.7	134
10766	Advances in electronic structure methods for defects and impurities in solids. Physica Status Solidi (B): Basic Research, 2011, 248, 19-27.	0.7	66
10767	Influence of hydrogen on electrical and optical properties of ZnO films. Physica Status Solidi (B): Basic Research, 2011, 248, 1702-1707.	0.7	23
10768	Structural and mechanical properties of dolomite rock under high pressure conditions: A firstâ€principles study. Physica Status Solidi (B): Basic Research, 2011, 248, 1894-1900.	0.7	18
10769	Single walled carbon nanotubes functionalized with hydrides as potential hydrogen storage media: A survey of intermolecular interactions. Physica Status Solidi (B): Basic Research, 2011, 248, 2147-2158.	0.7	12
10770	Effect of chirality and curvature of singleâ€walled carbon nanotubes on the adsorption of uracil. Physica Status Solidi (B): Basic Research, 2011, 248, 1431-1436.	0.7	13
10771	Substrate induced bandgap in multilayer epitaxial graphene on the 4Hâ€SiC ($000{ar {1}}$) surface. Physica Status Solidi (B): Basic Research, 2011, 248, 1690-1695.	0.7	6
10772	Elastic and electronic properties of hexagonal rhenium subâ€nitrides Re₃N and Re₂N in comparison withhcpâ€Re and wurtziteâ€like rhenium mononitride ReN. Physica Status Solidi (B): Basic Research, 2011, 248, 1369-1374.	0.7	41
10773	Elastic properties and electronic structures of Mgï£¿Ce intermetallic compounds from firstâ€principles calculations. Physica Status Solidi (B): Basic Research, 2011, 248, 2097-2102.	0.7	7
10774	Bandgap modulations of silicon carbon nanoribbons by transverse electric fields: A theoretical study. Physica Status Solidi (B): Basic Research, 2011, 248, 1676-1681.	0.7	26
10775	Elastic properties and interâ€atomic bonding in layered Feâ€“Cu arsenide oxide Sr₂Fe₂CuAs₂O₂. Physica Status Solidi (B): Basic Research, 2011, 248, 2165-2169.	0.7	0
10776	Magnetic coupling in dilute magnetic semiconductors: A new perspective. Physica Status Solidi (B): Basic Research, 2011, 248, 2032-2036.	0.7	2
10777	From electrons to materials. Physica Status Solidi (B): Basic Research, 2011, 248, 2213-2221.	0.7	4
10778	Energy landscape of silicon tetraâ€interstitials using an optimized classical potential. Physica Status Solidi (B): Basic Research, 2011, 248, 2050-2055.	0.7	14
10779	Pentagonal puckering in a sheet of amorphous graphene. Physica Status Solidi (B): Basic Research, 2011, 248, 2082-2086.	0.7	31
10780	Effects of Y and Zn atoms on the elastic properties of Mg solid solution from firstâ€principles calculations. Physica Status Solidi (B): Basic Research, 2011, 248, 2809-2815.	0.7	12

#	Article	IF	Citations
10781	Ultrathin monolayer of rubrene on Au(111) induced by charge transfer. Surface and Interface Analysis, 2011, 43, 1494-1497.	0.8	2
10782	Waterâ€Dependent Photonic Bandgap in Silica Artificial Opals. Small, 2011, 7, 1838-1845.	5.2	33
10783	Determining the Elasticity of Materials Employing Quantumâ€mechanical Approaches: From the Electronic Ground State to the Limits of Materials Stability. Steel Research International, 2011, 82, 86-100.	1.0	27
10784	Crystal and electronic structure of the room temperature organometallic ferrimagnet V(TCNE)₂. Analysis of numerical DoS and magnetic properties as related to orbital and spinâ€Hamiltonian models. International Journal of Quantum Chemistry, 2011, 111, 2490-2509.	1.0	1
10785	Dimorphism of the prodrug lâ€tyrosine ethyl ester: Pressureâ€“temperature state diagram and crystal structure of phase II. Journal of Pharmaceutical Sciences, 2011, 100, 4774-4782.	1.6	24
10786	Microstructure and Nanoscale Piezoelectric/Ferroelectric Properties in La₂Ti₂O₇ Thin Films Grown on (110)â€Oriented Doped Nb:SrTiO₃ Substrates. Advanced Engineering Materials, 2011, 13, 961-969.	1.6	22
10787	Surfaceâ€Modified Lowâ€Temperature Solid Oxide Fuel Cell. Advanced Functional Materials, 2011, 21, 4684-4690.	7.8	67
10788	Batteryless Chemical Detection with Semiconductor Nanowires. Advanced Materials, 2011, 23, 117-121.	11.1	22
10789	Evaluation of Charge Mobility in Organic Materials: From Localized to Delocalized Descriptions at a Firstâ€Principles Level. Advanced Materials, 2011, 23, 1145-1153.	11.1	127
10790	Mechanism of Visibleâ€Light Photocatalysis in Nitrogenâ€Doped TiO₂. Advanced Materials, 2011, 23, 2343-2347.	11.1	160
10791	Longâ€Range Visible Fluorescence Tunability Using Componentâ€Modulated Coupled Quantum Dots. Advanced Materials, 2011, 23, 1998-2003.	11.1	19
10792	Bandgap Engineering of Graphene by Physisorbed Adsorbates. Advanced Materials, 2011, 23, 2638-2643.	11.1	80
10793	Metal Nanostructure Formation on Graphene: Weak versus Strong Bonding. Advanced Materials, 2011, 23, 2082-2087.	11.1	69
10794	Mixed Magnetism for Refrigeration and Energy Conversion. Advanced Energy Materials, 2011, 1, 1215-1219.	10.2	227
10795	Lattice dynamics of ZnAl₂O₄ and ZnGa₂O₄ under high pressure. Annalen Der Physik, 2011, 523, 157-167.	0.9	47
10796	Silver(II) Fluorosulfate: A Thermally Fragile Ferromagnetic Derivative of Divalent Silver in an Oxaâ€Ligand Environment. European Journal of Inorganic Chemistry, 2011, 2011, 2499-2507.	1.0	20
10797	Ag3(SO3F)4: A Rare Example of a Mixed-Valent AgII/AgI Compound Showing 1D Antiferromagnetism. European Journal of Inorganic Chemistry, 2011, 2011, 2508-2516.	1.0	15
10798	Li2Sr4[Si2N5]N - A Layered Lithium Nitridosilicate Nitride. European Journal of Inorganic Chemistry, 2011, 2011, 2118-2123.	1.0	8

#	Article	IF	Citations
10799	Revisiting the Zintlâ€“Klemm Concept: A₂AuBi (A = Li or Na). European Journal of Inorganic Chemistry, 2011, 2011, 3989-3998.	1.0	14
10800	Mg11Cu6Al12, A New Link in the Structural Chemistry of MgCu2-Type Clusters. European Journal of Inorganic Chemistry, 2011, 2011, 3936-3949.	1.0	11
10801	Steric and Chain Length Effects in the (${sqrt {(3)} }$Ã—${sqrt {(3)} }$)R30Â° Structures of Alkanethiol Selfâ€Assembled Monolayers on Au(111). ChemPhysChem, 2011, 12, 999-1009.	1.0	35
10802	Variableâ€Temperature IR Spectroscopic and Theoretical Studies on CO₂ Adsorbed in Zeolite Kâ€FER. ChemPhysChem, 2011, 12, 1435-1443.	1.0	26
10803	Outer Helmholtz Plane of the Electrical Double Layer Formed at the Solid Electrodeâ€“Liquid Interface. ChemPhysChem, 2011, 12, 1430-1434.	1.0	85
10804	Adsorption of Supramolecular Building Blocks on Graphite: A Force Field and Density Functional Theory Study. ChemPhysChem, 2011, 12, 2242-2245.	1.0	12
10805	New Insights into the Bandâ€Gap Narrowing of (N, P)â€Codoped TiO₂ from Hybrid Density Functional Theory Calculations. ChemPhysChem, 2011, 12, 2604-2608.	1.0	29
10806	The Pseudopotential Approximation in Electronic Structure Theory. ChemPhysChem, 2011, 12, 3143-3155.	1.0	154
10807	A DFT Study of Carbon in the Subsurface Layer of Cobalt Surfaces. ChemPhysChem, 2011, 12, 2925-2928.	1.0	18
10808	Nitrogenâ€Doped Carbon Nanotubes: Growth, Mechanism and Structure. ChemPhysChem, 2011, 12, 2995-3001.	1.0	26
10809	Systemâ€Dependent Dispersion Coefficients for the DFTâ€D3 Treatment of Adsorption Processes on Ionic Surfaces. ChemPhysChem, 2011, 12, 3414-3420.	1.0	318
10810	Nanostructured Carbonâ€“Metal Oxide Hybrids as Amphiphilic Emulsion Catalysts. ChemSusChem, 2011, 4, 964-974.	3.6	49
10811	Computational study on the reactions of H₂O₂ on TiO₂ anatase (101) and rutile (110) surfaces. Journal of Computational Chemistry, 2011, 32, 1065-1081.	1.5	64
10812	Adsorption and dissociation of NH₃ on clean and hydroxylated TiO₂ rutile (110) surfaces: A computational study. Journal of Computational Chemistry, 2011, 32, 1101-1112.	1.5	13
10813	Giant magnetic moment of the coreâ€shell Co₁₃@Mn₂₀ clusters: Firstâ€principles calculations. Journal of Computational Chemistry, 2011, 32, 2474-2478.	1.5	13
10814	Firstâ€principles prediction on electronic and magnetic properties of hydrogenated AlN nanosheets. Journal of Computational Chemistry, 2011, 32, 3122-3128.	1.5	42
10815	Density functional theoryâ€based electrochemical models for the oxygen reduction reaction: Comparison of modeling approaches for electric field and solvent effects. Journal of Computational Chemistry, 2011, 32, 3399-3408.	1.5	61
10816	Theoretical insights on the electron doping and Curie temperature in Laâ€doped Sr₂CrWO₆. Journal of Computational Chemistry, 2011, 32, 3313-3318.	1.5	9

#	Article	IF	Citations
10827	Oxygenâ€Vacancy Ordering at Surfaces of Lithium Manganese(III,IV) Oxide Spinel Nanoparticles. Angewandte Chemie - International Edition, 2011, 50, 3053-3057.	7.2	127
10828	Activation of Oxygen on MgO: O₂^{.â”} Radical Ion Formation on Thin, Metalâ€Supported MgO(001) Films. Angewandte Chemie - International Edition, 2011, 50, 2635-2638.	7.2	101
10829	Templateâ€Assisted Formation of Fullerenes from Shortâ€Chain Hydrocarbons by Supported Platinum Nanoparticles. Angewandte Chemie - International Edition, 2011, 50, 4611-4614.	7.2	10
10830	[Cu(HF₂)₂(pyrazine)]_n: A Rectangular Antiferromagnetic Lattice with a Spin Exchange Path Made Up of Two Different FHF^{â”} Bridges. Angewandte Chemie - International Edition, 2011, 50, 1573-1576.	7.2	17
10831	The Mechanism of Potassium Promoter: Enhancing the Stability of Active Surfaces. Angewandte Chemie - International Edition, 2011, 50, 7403-7406.	7.2	141
10832	Carbon Chain Growth by Formyl Insertion on Rhodium and Cobalt Catalysts in Syngas Conversion. Angewandte Chemie - International Edition, 2011, 50, 5335-5338.	7.2	105
10833	The Particleâ€Size Dependence of the Activation Energy for Decomposition of Lithium Amide. Angewandte Chemie - International Edition, 2011, 50, 10170-10173.	7.2	19
10834	Electric Control of Magnetization and Interplay between Orbital Ordering and Ferroelectricity in a Multiferroic Metalâ€“Organic Framework. Angewandte Chemie - International Edition, 2011, 50, 5847-5850.	7.2	249
10835	Oxygen Defects and Novel Transport Mechanisms in Apatite Ionic Conductors: Combined ¹⁷Oâ€…NMR and Modeling Studies. Angewandte Chemie - International Edition, 2011, 50, 9328-9333.	7.2	57
10836	Tailoring the Shape of Metal Adâ€Particles by Doping the Oxide Support. Angewandte Chemie - International Edition, 2011, 50, 11525-11527.	7.2	99
10837	Construction of a highâ€performance computing cluster: A curriculum for engineering and science students. Computer Applications in Engineering Education, 2011, 19, 678-684.	2.2	5
10838	A New Phase in the Binary Iron Nitrogen System?â€”The Prediction of Iron Pernitride, FeN₂. Chemistry - A European Journal, 2011, 17, 2598-2603.	1.7	35
10839	Pyrazolateâ€Based Cobalt(II)â€Containing Metalâ€“Organic Frameworks in Heterogeneous Catalytic Oxidation Reactions: Elucidating the Role of Entatic States for Biomimetic Oxidation Processes. Chemistry - A European Journal, 2011, 17, 8671-8695.	1.7	138
10840	Hydrothermal Synthesis of Na_{0.5}La_{0.5}TiO₃â€“LaCrO₃ Solidâ€Solution Singleâ€Crystal Nanocubes for Visibleâ€Lightâ€Driven Photocatalytic H₂ Evolution. Chemistry - A European Journal, 2011, 17, 7858-7867.	1.7	43
10841	Progress in Crystal Structure Prediction. Chemistry - A European Journal, 2011, 17, 10736-10744.	1.7	79
10842	Facile Synthesis of Wideâ€Bandgap Fluorinated Graphene Semiconductors. Chemistry - A European Journal, 2011, 17, 8896-8903.	1.7	121
10843	Theoretical and Experimental Studies on the Carbonâ€Nanotube Surface Oxidation by Nitric Acid: Interplay between Functionalization and Vacancy Enlargement. Chemistry - A European Journal, 2011, 17, 11467-11477.	1.7	93
10844	Hierarchical TiO₂ Microspheres: Synergetic Effect of {001} and {101} Facets for Enhanced Photocatalytic Activity. Chemistry - A European Journal, 2011, 17, 15032-15038.	1.7	180

#	Article	IF	Citations
10845	Potassium Silanide (KSiH₃): A Reversible Hydrogen Storage Material. Chemistry - A European Journal, 2011, 17, 12302-12309.	1.7	46
10846	Is Electronegativity a Useful Descriptor for the Pseudoâ€Alkali Metal NH₄?. Chemistry - A European Journal, 2011, 17, 13197-13205.	1.7	16
10847	Novel Auâ€“TiC catalysts for CO oxidation and desulfurization processes. Catalysis Today, 2011, 166, 2-9.	2.2	37
10848	Low-temperature 1,3-butadiene hydrogenation over supported Pt/3d/Î³-Al2O3 bimetallic catalystsâ˜†. Catalysis Today, 2011, 160, 61-69.	2.2	33
10849	Precursor-mediated dissociation of n-butane on a PdO(101) thin film. Catalysis Today, 2011, 160, 213-227.	2.2	55
10850	A comparative density functional theory study of the direct synthesis of H2O2 on Pd, Pt and Au surfaces. Catalysis Today, 2011, 160, 242-248.	2.2	62
10851	Generation of defects on oxide supports by doping with metals and their role in oxygen activation. Catalysis Today, 2011, 169, 52-59.	2.2	20
10852	Challenges in the first-principles description of reactions in electrocatalysis. Catalysis Today, 2011, 165, 129-137.	2.2	135
10853	Does confinement effect always enhance catalytic activity? A theoretical study of H2 dissociation on CNT supported gold clusters. Catalysis Today, 2011, 165, 25-31.	2.2	12
10854	Understanding of ethanol decomposition on Rh(111) from density functional theory and kinetic Monte Carlo simulations. Catalysis Today, 2011, 165, 64-70.	2.2	82
10855	Adsorption and activation of CO2 over the Cuâ€“Co catalyst supported on partially hydroxylated Î³-Al2O3. Catalysis Today, 2011, 165, 10-18.	2.2	35
10856	Spontaneous reduction of O2 on PtVFe nanocatalysts. Catalysis Today, 2011, 165, 150-159.	2.2	31
10857	Density functional theory study of the effect of subsurface H, C, and Ag on C2H2 hydrogenation on Pd(111). Catalysis Today, 2011, 165, 106-111.	2.2	21
10858	Adsorption of selenium atoms at the Si(111)-7Ã—7 surface: A combination of scanning tunnelling microscopy and density functional theory studies. Chemical Physics, 2011, 382, 41-46.	0.9	9
10859	Influence of exchange-correlation functionals on dielectric properties of rutile TiO2. Current Applied Physics, 2011, 11, S293-S296.	1.1	27
10860	An experimental and theoretical examination of the effect of sulfur on the pyrolytically grown carbon nanotubes from sucrose-based solid state precursors. Carbon, 2011, 49, 508-517.	5.4	20
10861	Defect formation and hysteretic inter-tube displacement in multi-wall carbon nanotubes. Carbon, 2011, 49, 581-586.	5.4	7
10862	Structure, energy, and structural transformations of graphene grain boundaries from atomistic simulations. Carbon, 2011, 49, 2306-2317.	5.4	137

#	Article	IF	Citations
10863	First-principles based kinetic modeling of effect of hydrogen on growth of carbon nanotubes. Carbon, 2011, 49, 2508-2521.	5.4	28
10864	Analysis of the strong propensity for the delocalized diamagnetic ÏЄ electronic structure of hydrogenated graphenes. Carbon, 2011, 49, 2665-2670.	5.4	4
10865	Single Pd atoms in activated carbon fibers and their contribution to hydrogen storage. Carbon, 2011, 49, 4050-4058.	5.4	74
10866	Vacancy clusters as entry ports for cesium intercalation in graphite. Carbon, 2011, 49, 3937-3952.	5.4	28
10867	Oxygen migration on the graphene surface. 2. Thermochemistry of basal-plane diffusion (hopping). Carbon, 2011, 49, 4226-4238.	5.4	78
10868	Strain enhanced defect reactivity at grain boundaries in polycrystalline graphene. Carbon, 2011, 49, 3983-3988.	5.4	74
10869	Fermi level dependent optical transition energy in metallic single-walled carbon nanotubes. Carbon, 2011, 49, 4774-4780.	5.4	14
10870	Structural, electronic and magnetic properties of GaN nanotubes filled with nickel nanowires. Computational and Theoretical Chemistry, 2011, 963, 18-23.	1.1	9
10871	A theoretical study for the influence of coverage on Li, Na and K adsorption on Co(0001). Computational and Theoretical Chemistry, 2011, 963, 125-129.	1.1	7
10872	The effect of cluster thickness on the adsorption of CH4 on Pdn. Computational and Theoretical Chemistry, 2011, 963, 236-244.	1.1	14
10873	Comparison of electronic and magnetic properties of Fe, Co and Ni nanowires encapsulated in beryllium oxygen nanotubes. Computational and Theoretical Chemistry, 2011, 963, 273-278.	1.1	18
10874	DFT investigation of CO oxidation over Mg exchanged periodic zeolite models. Computational and Theoretical Chemistry, 2011, 964, 108-115.	1.1	16
10875	The effects of the dangling bond on the electronic and magnetic properties of AlN nanoribbon. Computational and Theoretical Chemistry, 2011, 967, 113-119.	1.1	18
10876	Electronic properties of rhombohedral graphite. Computer Physics Communications, 2011, 182, 77-80.	3.0	6
10877	XtalOpt: An open-source evolutionary algorithm for crystal structure prediction. Computer Physics Communications, 2011, 182, 372-387.	3.0	263
10878	The object-oriented DFT program library S/PHI/nX. Computer Physics Communications, 2011, 182, 543-554.	3.0	77
10879	Efficient self-consistency for magnetic tight binding. Computer Physics Communications, 2011, 182, 1350-1360.	3.0	14
10880	Speeding up plane-wave electronic-structure calculations using graphics-processing units. Computer Physics Communications, 2011, 182, 1421-1427.	3.0	48

#	Article	IF	Citations
10881	Phase stabilities and decomposition mechanism in the Zrâ€“Siâ€“N system studied by combined ab initio DFT and thermodynamic calculation. Acta Materialia, 2011, 59, 297-307.	3.8	37
10882	Phase equilibria, crystal chemistry, electronic structure and physical properties of Agâ€“Baâ€“Ge clathrates. Acta Materialia, 2011, 59, 2368-2384.	3.8	37
10883	Light emission from several-atom Inâ€“N clusters in wurtzite Ga-rich InGaN alloys and InGaN/GaN strained quantum wells. Acta Materialia, 2011, 59, 2773-2782.	3.8	14
10884	Hydrogen-enhanced local plasticity at dilute bulk H concentrations: The role of Hâ€“H interactions and the formation of local hydrides. Acta Materialia, 2011, 59, 2969-2980.	3.8	132
10885	First-principles study of the nucleation and stability of ordered precipitates in ternary Alâ€“Scâ€“Li alloys. Acta Materialia, 2011, 59, 3012-3023.	3.8	133
10886	First-principles calculations of impurity diffusion coefficients in dilute Mg alloys using the 8-frequency model. Acta Materialia, 2011, 59, 3214-3228.	3.8	124
10887	Study of spinodal decomposition and formation of nc-Al2O3/ZrO2 nanocomposites by combined ab initio density functional theory and thermodynamic modeling. Acta Materialia, 2011, 59, 3498-3509.	3.8	34
10888	First-principles phase stability, magnetic properties and solubility in aluminumâ€“rare-earth (Alâ€“RE) alloys and compounds. Acta Materialia, 2011, 59, 3659-3666.	3.8	68
10889	The equilibrium morphology of WC particles â€“ A combined ab initio and experimental study. Acta Materialia, 2011, 59, 3748-3757.	3.8	52
10890	Ab initio study of the modification of elastic properties of Î±-iron by hydrostatic strain and by hydrogen interstitials. Acta Materialia, 2011, 59, 4255-4263.	3.8	45
10891	Configuration and electronic properties of graphene nanoribbons on Si(211) surface. Applied Surface Science, 2011, 257, 2474-2480.	3.1	2
10892	Boron doped ZnO thin films fabricated by RF-magnetron sputtering. Applied Surface Science, 2011, 257, 2498-2502.	3.1	77
10893	Structures of CoAl(111) surface: A first principles study. Applied Surface Science, 2011, 257, 3341-3345.	3.1	1
10894	Study on the interface between the organic and inorganic semiconductors. Applied Surface Science, 2011, 257, 4994-4999.	3.1	4
10895	Interactions between tri-methylaluminum molecules and their effect on the reaction of tri-methylaluminum with an OH-terminated Si (0 0 1) surface. Applied Surface Science, 2011, 257, 6326-6331.	3.1	13
10896	Energy gap modulation of graphene nanoribbons by F termination. Applied Surface Science, 2011, 257, 6440-6444.	3.1	14
10897	Au adsorption and Au-mediated charge transfer on the SrO-termination of SrTiO3 (0 0 1) surface. Applied Surface Science, 2011, 257, 6607-6611.	3.1	18
10898	Density functional theory prediction for diffusion of lithium on boron-doped graphene surface. Applied Surface Science, 2011, 257, 7443-7446.	3.1	40

#	Article	IF	Citations
10899	Density functional theory study of selenium adsorption on Fe(110). Applied Surface Science, 2011, 257, 6878-6883.	3.1	5
10900	First principles study of Si etching by CHF3 plasma source. Applied Surface Science, 2011, 257, 8767-8771.	3.1	6
10901	Magnetic properties of the semifluorinated and semihydrogenated 2D sheets of group-IV and III-V binary compounds. Applied Surface Science, 2011, 257, 7845-7850.	3.1	75
10902	Density functional theory study on activity of Î±-Fe2O3 in chemical-looping combustion system. Applied Surface Science, 2011, 257, 8647-8652.	3.1	53
10903	The role of Ru atoms toward the dehydrogenation of ethanol on Ru/ZrO2(111) surface. Chemical Physics Letters, 2011, 501, 315-318.	1.2	2
10904	Periodic density functional study of Co3O4 surfaces. Chemical Physics Letters, 2011, 502, 63-68.	1.2	72
10905	First principles study of Ca2PtO4 in K2NiF4 and â€˜post-K2NiF4â€™ type structures. Chemical Physics Letters, 2011, 503, 49-52.	1.2	2
10906	Chemisorbed atomic oxygen inducing Pd segregation in PdAu(1 1 1) alloy: Energetic and electronic DFT analysis. Chemical Physics Letters, 2011, 503, 97-100.	1.2	35
10907	DFT study on the NO oxidation on a flat gold surface model. Chemical Physics Letters, 2011, 503, 129-133.	1.2	17
10908	Structure of the methylthiolate monolayer on Ag (111): The role of substrate vacancies. Chemical Physics Letters, 2011, 503, 71-74.	1.2	5
10909	DFT determination of ammonia adsorption configurations on the Pt{100}â€“(1Ã—1) surface at low coverage. Chemical Physics Letters, 2011, 505, 21-25.	1.2	5
10910	Bonding and vibrations of CHxO and CHx species (x=1â€“3) on a palladium nanoparticle representing model catalysts. Chemical Physics Letters, 2011, 506, 92-97.	1.2	15
10911	A theoretical study of ambipolar organic transport material: 1,4-Bis(pentafluorobenzyl)[60]-fullerene. Chemical Physics Letters, 2011, 506, 255-259.	1.2	7
10912	Theoretical study of weak chemical interactions in solid formamide. Chemical Physics Letters, 2011, 508, 54-58.	1.2	10
10913	Electronic structure and equation of state of PdO2 from ab initio. Chemical Physics Letters, 2011, 508, 215-218.	1.2	21
10914	Atomic Cu adsorption on defect-free SrTiO3(001) surface. Chemical Physics Letters, 2011, 510, 104-108.	1.2	12
10915	Observation of Significant enhancement in the efficiency of a DSSC by InN nanoparticles over TiO2-nanoparticle films. Chemical Physics Letters, 2011, 510, 126-130.	1.2	12
10916	Structures and energies of iron promoted Î³-Al2O3 surface: A computational study. Chemical Physics Letters, 2011, 510, 224-227.	1.2	23

#	Article	IF	Citations
10917	Acetate and phosphate anion adsorption linear sweep voltammograms simulated using density functional theory. Electrochimica Acta, 2011, 56, 3996-4006.	2.6	32
10918	XPS characterisation of in situ treated lanthanum oxide and hydroxide using tailored charge referencing and peak fitting procedures. Journal of Electron Spectroscopy and Related Phenomena, 2011, 184, 399-409.	0.8	449
10919	Vibrational and NMR properties of polyynes. Carbon, 2011, 49, 3340-3345.	5.4	11
10920	The extraordinary stability imparted to silver monolayers by chloride. Electrochimica Acta, 2011, 56, 1652-1661.	2.6	17
10921	Probing the conduction band edge of transition metal oxides by X-ray absorption spectroscopy. Journal of Electron Spectroscopy and Related Phenomena, 2011, 183, 107-113.	0.8	8
10922	First-principles study of the high pressure phase transition and lattice dynamics of cerium. Physica B: Condensed Matter, 2011, 406, 669-675.	1.3	11
10923	Tuning the electronic and magnetic properties of the Si nanoribbons through dangling bond. Physica B: Condensed Matter, 2011, 406, 699-704.	1.3	12
10924	Substitution mechanism of Zn ions in Î²-tricalcium phosphate. Physica B: Condensed Matter, 2011, 406, 890-894.	1.3	26
10925	Generalized-stacking-fault energy surfaces for B2-MgRE (RE=Y, Dy, Pr, Tb) intermetallic compounds: Ab initio calculations. Physica B: Condensed Matter, 2011, 406, 967-971.	1.3	10
10926	First-principles study on alloying stability, electronic structure, and mechanical properties of Al-based intermetallics. Physica B: Condensed Matter, 2011, 406, 1149-1153.	1.3	26
10927	Pâ€“n codoping induced enhancement of ferromagnetism in Mn-doped In2O3: A first-principles study. Physica B: Condensed Matter, 2011, 406, 1818-1821.	1.3	10
10928	Elastic properties of MBH4 (M=Na, K, Rb, Cs). Physica B: Condensed Matter, 2011, 406, 2196-2199.	1.3	24
10929	Structural and elastic properties of Ni2+xMn1âˆ’xGa alloys. Physica B: Condensed Matter, 2011, 406, 2240-2244.	1.3	14
10930	First principles study of structural, vibrational and electronic properties of graphene-like MX2 (M=Mo, Nb, W, Ta; X=S, Se, Te) monolayers. Physica B: Condensed Matter, 2011, 406, 2254-2260.	1.3	613
10931	Native defects and Pr impurities in orthorhombic CaTiO3 by first-principles calculations. Physica B: Condensed Matter, 2011, 406, 2697-2702.	1.3	11
10932	First-principles study of Friedel oscillations normal to the low index surfaces of Al. Physica B: Condensed Matter, 2011, 406, 2767-2771.	1.3	3
10933	Density functional study of oxygen adsorption on the Mg3Nd (001) surface. Physica B: Condensed Matter, 2011, 406, 2777-2782.	1.3	1
10934	Stability of half-metallic antiferromagnet La2VMnO6, first-principles calculation study. Physica B: Condensed Matter, 2011, 406, 2783-2787.	1.3	11

#	Article	IF	Citations
10935	Stability, structural, elastic, and electronic properties of polymorphs of the superconducting disilicide YIr2Si2. Physica B: Condensed Matter, 2011, 406, 3525-3530.	1.3	21
10936	Density functional calculations for Ni adsorption on Al(110). Physica B: Condensed Matter, 2011, 406, 2994-2998.	1.3	2
10937	First-principles study on structural and electronic properties of copper nanowire encapsulated into GaN nanotube. Physica B: Condensed Matter, 2011, 406, 3502-3507.	1.3	8
10938	The structural stability, elastic constants and electronic structure of Alâ€“Sr intermetallics by first-principles calculations. Physica B: Condensed Matter, 2011, 406, 3681-3686.	1.3	18
10939	Effect of doping V on the half-metallic and magnetic properties of Mn3Al intermetallic compound. Physica B: Condensed Matter, 2011, 406, 3726-3730.	1.3	6
10940	Density functional investigation of structural, electronic and optical properties of Ge-doped ZnO. Physica B: Condensed Matter, 2011, 406, 3926-3930.	1.3	6
10941	First-principles calculations on temperature-dependent elastic constants of rare-earth intermetallic compounds: YAg and YCu. Physica B: Condensed Matter, 2011, 406, 3951-3955.	1.3	13
10942	The phase diagram of water and the magnetic fields of Uranus and Neptune. Icarus, 2011, 211, 798-803.	1.1	195
10943	Stability of Frenkel pairs in Si(100) surface in the presence of germanium and oxygen atoms. Microelectronic Engineering, 2011, 88, 503-505.	1.1	0
10944	The role of oxygen-related defects and hydrogen impurities in HfO2 and ZrO2. Microelectronic Engineering, 2011, 88, 1452-1456.	1.1	88
10945	First-principles electronic-structure calculations on the stability and oxygen conductivity in Ba0.5Sr0.5Co0.8Fe0.2O3â^Î´. Journal of Membrane Science, 2011, 366, 92-96.	4.1	23
10946	Violating the general acidityâ€“activity correlation: Computational evidence in a CpNa-modified HMCM-22 zeolite for ethene protonation. Microporous and Mesoporous Materials, 2011, 144, 67-73.	2.2	2
10947	First-principles study of the structural and electronic properties of armchair silicene nanoribbons with vacancies. Journal of Molecular Structure, 2011, 990, 75-78.	1.8	42
10948	Electronic and structural properties of TiB2: Bulk, surface, and nanoscale effects. Materials Science and Engineering B: Solid-State Materials for Advanced Technology, 2011, 176, 484-489.	1.7	20
10949	From the interface energy to the solubility limit of aluminium in nickel from first-principles and Kinetic Monte Carlo calculations. Materials Science and Engineering B: Solid-State Materials for Advanced Technology, 2011, 176, 767-771.	1.7	5
10950	Grain boundary segregation in low Cr Feâ€“Cr alloys: The effect of radiation induced vacancies studied by metropolis Monte Carlo simulations. Nuclear Instruments & Methods in Physics Research B, 2011, 269, 1679-1683.	0.6	8
10951	First-principles study of hydrogen behavior in Vâ€“Crâ€“Ti alloys. Nuclear Instruments & Methods in Physics Research B, 2011, 269, 1735-1739.	0.6	22
10952	Stress effects on stability and diffusion of H in W: A first-principles study. Nuclear Instruments & Methods in Physics Research B, 2011, 269, 1731-1734.	0.6	35

#	Article	IF	Citations
10953	Classical and quantum mechanical rainbow-scattering of fast He atoms from a KCl(001) surface. Nuclear Instruments & Methods in Physics Research B, 2011, 269, 799-803.	0.6	12
10954	Electronic structure of MoO2. DFT periodic and cluster model studies. Applied Catalysis A: General, 2011, 391, 137-143.	2.2	30
10955	Adsorption and dissociation of ammonia on clean and metal-covered TiO2 rutile (1 1 0) surfaces: A comparative DFT study. Applied Catalysis B: Environmental, 2011, 106, 510-519.	10.8	29
10956	Structural and electronic properties of atomic oxygen adsorption on Pt(111): A density-functional theory study. Applied Surface Science, 2011, 257, 3047-3054.	3.1	23
10957	First-principle calculation on nearly half-metallic antiferromagnetic behavior of double perovskites La2VReO6. Journal of Magnetism and Magnetic Materials, 2011, 323, 175-178.	1.0	5
10958	Structures, stabilities and magnetic properties of FeConâ^'1 (nâ‰16) clusters. Journal of Magnetism and Magnetic Materials, 2011, 323, 842-848.	1.0	7
10959	Noble metals induced magnetic properties of graphene. Journal of Magnetism and Magnetic Materials, 2011, 323, 2441-2447.	1.0	44
10960	A comparative study of fracture in Al: Quantum mechanical vs. empirical atomistic description. Journal of the Mechanics and Physics of Solids, 2011, 59, 775-786.	2.3	11
10961	Thermodynamic study of the Npâ€“Zr system. Journal of Nuclear Materials, 2011, 409, 1-8.	1.3	8
10962	Ab-initio based modeling of diffusion in dilute bcc Feâ€“Ni and Feâ€“Cr alloys and implications for radiation induced segregation. Journal of Nuclear Materials, 2011, 411, 1-14.	1.3	101
10963	Structural, electronic, mechanical, and thermodynamic properties of UN2: Systematic density functional calculations. Journal of Nuclear Materials, 2011, 410, 46-51.	1.3	24
10964	Calphad thermodynamic description of some binary systems involving U. Journal of Nuclear Materials, 2011, 411, 131-143.	1.3	60
10965	Stability and migration property of helium and self defects in vanadium and Vâ€“4Crâ€“4Ti alloy by first-principles. Journal of Nuclear Materials, 2011, 413, 90-94.	1.3	38
10966	Effect of carbon on irradiation-induced grain-boundary phosphorus segregation in reactor pressure vessel steels using first-principles-based rate theory model. Journal of Nuclear Materials, 2011, 414, 328-335.	1.3	4
10967	Superconductivity and properties of FeTeO films. Journal of Physics and Chemistry of Solids, 2011, 72, 426-429.	1.9	10
10968	Ab initio study of 5d-shells Ir substitution for Fe-based SmOFe1â^'Ir As. Journal of Physics and Chemistry of Solids, 2011, 72, 329-332.	1.9	0
10969	Elastic, thermal and structural properties of platinum. Journal of Physics and Chemistry of Solids, 2011, 72, 169-175.	1.9	23
10970	Effect of the dangling bond on the electronic and magnetic properties of BN nanoribbon. Journal of Physics and Chemistry of Solids, 2011, 72, 256-262.	1.9	35

#	Article	IF	Citations
10971	Enhanced Li capacity at high lithiation potentials in graphene oxide. Journal of Power Sources, 2011, 196, 5697-5703.	4.0	58
10972	Structure, thermal stability and properties of Li3Sc(BO3)2. Journal of Solid State Chemistry, 2011, 184, 115-122.	1.4	9
10973	CO2 capture properties of Mâ€“Câ€“Oâ€“H (M=Li, Na, K) systems: A combined density functional theory and lattice phonon dynamics study. Journal of Solid State Chemistry, 2011, 184, 304-311.	1.4	74
10974	Neutron diffraction study of La4LiAuO8: Understanding Au3+ in an oxide environment. Journal of Solid State Chemistry, 2011, 184, 1439-1444.	1.4	7
10975	First-principle investigation of Jahnâ€“Teller distortion and topological analysis of chemical bonds in LiNiO2. Journal of Solid State Chemistry, 2011, 184, 1784-1790.	1.4	34
10976	Chemical order and local structure of the lead-free relaxor ferroelectric. Journal of Solid State Chemistry, 2011, 184, 2041-2046.	1.4	84
10977	Grain boundary mediated leakage current in polycrystalline HfO2 films. Microelectronic Engineering, 2011, 88, 1272-1275.	1.1	101
10978	Is interfacial chemistry correlated to gap states for high-k/IIIâ€“V interfaces?. Microelectronic Engineering, 2011, 88, 1061-1065.	1.1	62
10979	Strain-induced ferromagnetism in LaCoO3: Theory and growth on Si (100). Microelectronic Engineering, 2011, 88, 1444-1447.	1.1	15
10980	A DFT study on the adsorption and dissociation of methanol over MoS2 surface. Journal of Molecular Catalysis A, 2011, , .	4.8	9
10981	Role of CO2 in ethylbenzene dehydrogenation over Fe2O3(0 0 0 1) from first principles. Journal of Molecular Catalysis A, 2011, 344, 53-61.	4.8	16
10982	Vacancy formation and clustering behavior in Y2O3 by first principles. Nuclear Instruments & Methods in Physics Research B, 2011, 269, 1720-1723.	0.6	17
10983	Ab initio study of PrAg intermetallic compound. Physica B: Condensed Matter, 2011, 406, 388-392.	1.3	2
10984	Ab-initio study of fluorine-doped tin dioxide: A prospective catalyst support for water electrolysis. Physica B: Condensed Matter, 2011, 406, 471-477.	1.3	24
10985	Structural, elastic constants, hardness, and optical properties of pyrite-type dinitrides (CN2, SiN2,) Tj ETQq0 0 0 rgBT /Overlock 10 Tf 50	1.3	15
10986	Theoretical investigation of new type of ternary magnesium alloys AMgNi4 (A=Y, La, Ce, Pr and Nd). Physica B: Condensed Matter, 2011, 406, 1330-1335.	1.3	20
10987	Plane-wave pseudopotential study for the structural stability of Hf: The role of spinâ€“orbit interaction. Physica B: Condensed Matter, 2011, 406, 1744-1748.	1.3	16
10988	Direct or indirect semiconductor: The role of stacking fault in h-BN. Physica B: Condensed Matter, 2011, 406, 2293-2297.	1.3	12

#	Article	IF	Citations
10989	Aluminum and nitrogen impurities in Wurtzite ZnO: first-principles studies. Physica B: Condensed Matter, 2011, 406, 3125-3129.	1.3	38
10990	Atomic structure and diffusivity in liquid Al80Ni20 by ab initio molecular dynamics simulations. Physica B: Condensed Matter, 2011, 406, 3089-3097.	1.3	38
10991	The elastic and bonding properties of the sulvanite compounds: A first-principles study by local and semi-local functionals. Physica B: Condensed Matter, 2011, 406, 3788-3793.	1.3	20
10992	Fermi surface effect on intrinsic Lorenz number of Fermi liquids. Physica B: Condensed Matter, 2011, 406, 3674-3680.	1.3	0
10993	A mesh-free convex approximation scheme for Kohnâ€“Sham density functional theory. Journal of Computational Physics, 2011, 230, 5226-5238.	1.9	27
10994	Nonlinear elasticity of monolayer zinc oxide honeycomb structures: A first-principles study. Physica E: Low-Dimensional Systems and Nanostructures, 2011, 43, 914-918.	1.3	7
10995	Structural, electronic and magnetic properties of the 3d transition-metal-doped AlN nanotubes. Physica E: Low-Dimensional Systems and Nanostructures, 2011, 43, 1249-1254.	1.3	28
10996	Structural stability and electronic, magnetic properties of Ge adsorption on defected graphene: a first-principles study. Physica E: Low-Dimensional Systems and Nanostructures, 2011, 43, 1461-1464.	1.3	14
10997	First principles investigation on carbon nanostructures functionalized with borane: An analysis on their hydrogen storage capacity. Physica E: Low-Dimensional Systems and Nanostructures, 2011, 43, 1528-1534.	1.3	9
10998	Superhard and superconductive polymorphs of diamond-like BC3. Physics Letters, Section A: General, Atomic and Solid State Physics, 2011, 375, 771-774.	0.9	59
10999			

#	Article	IF	Citations
11007	REPRINT OF: Surface electronic structure of Ti-covered W(111) by photofield emission. Ultramicroscopy, 2011, 111, 386-391.	0.8	0
11008	First-principles study on the effects of point vacancies on the spectral properties of. Solid State Communications, 2011, 151, 29-32.	0.9	16
11009	Migration of adatom adsorption on graphene using DFT calculation. Solid State Communications, 2011, 151, 13-16.	0.9	268
11010	Structural, electronic and magnetic properties of the 3d transition metal-doped GaN nanotubes. Solid State Communications, 2011, 151, 139-143.	0.9	16
11011	Cobalt suppressed Jahnâ€“Teller effect in for lithium ion batteries. Solid State Communications, 2011, 151, 234-237.	0.9	23
11012	Crystal structures of under high pressure. Solid State Communications, 2011, 151, 388-391.	0.9	11
11013	Energetics and stability of vacancies in carbon nanotubes. Solid State Communications, 2011, 151, 482-486.	0.9	42
11014	Mechanical properties of superhard diamondlike BC5. Solid State Communications, 2011, 151, 478-481.	0.9	8
11015	The stable structures of iron pnictides AFeAs (AÂ= Âalkali and alkaline-earth metals): A first principles study. Solid State Communications, 2011, 151, 446-450.	0.9	8
11016	Bonding character of lithium atoms adsorbed on a graphene layer. Solid State Communications, 2011, 151, 529-531.	0.9	9
11017	Superhard polymorphs of diamond-like. Solid State Communications, 2011, 151, 716-719.	0.9	38
11018	Adsorption of Au and Pt dimers on Ge(001) and Si(001): A first-principles study. Solid State Communications, 2011, 151, 655-658.	0.9	3
11019	First-principles study on the structural and electronic properties of AlNCx nanosheet. Solid State Communications, 2011, 151, 834-837.	0.9	17
11020	The third-order elastic moduli and pressure derivatives for AlRE (RE=Y, Pr, Nd, Tb, Dy, Ce) intermetallics with B2-structure: A first-principles study. Solid State Communications, 2011, 151, 996-1000.	0.9	16
11021	Structural, elastic, electronic and magnetic properties of ThCr2Si2 from first-principles calculations. Solid State Communications, 2011, 151, 1165-1168.	0.9	10
11022	Manifestation of LOâ€“LA phonons in Raman scattering in graphene. Solid State Communications, 2011, 151, 1071-1074.	0.9	19
11023	Electronic and magnetic properties of silicon adsorption on graphene. Solid State Communications, 2011, 151, 1128-1130.	0.9	16
11024	Theoretical analysis of space charge layer formation at metal/ionic conductor interfaces. Solid State Ionics, 2011, 183, 20-25.	1.3	28

#	Article	IF	Citations
11025	Substitutional doping and oxygen vacancies in La2Zr2O7 pyrochlore oxide. Solid State Ionics, 2011, 189, 19-28.	1.3	33
11026	Electronic structures of Ga-induced incommensurate and commensurate overlayers on the Si(111) surface. Surface Science, 2011, 605, 146-152.	0.8	6
11027	The adsorption of a substituted benzene, the ethynyl-trifluoro-toluene on Si(100)-2Ã—1. Surface Science, 2011, 605, 166-173.	0.8	3
11028	Movement of a tungsten adatom on the W(112) surface. Surface Science, 2011, 605, 282-288.	0.8	9
11029	Density functional study of copper segregation in aluminum. Surface Science, 2011, 605, 341-350.	0.8	24
11030	The effect of Zr-doping on the interaction of water molecules with the ceria (111) surface. Surface Science, 2011, 605, 351-360.	0.8	8
11031	Adsorption and activation of CO coadsorbed with K on Fe(100) surface: A plane-wave DFT study. Surface Science, 2011, 605, 401-414.	0.8	44
11032	Formation of sulfite-like species on Cr2O3 after SO2 chemisorption. Surface Science, 2011, 605, 489-493.	0.8	13
11033	Adsorption of sulfur on Ag(100). Surface Science, 2011, 605, 520-527.	0.8	20
11034	Triple-domain effects on the electronic structure of Pb/Si(111)-(Ã—): Density-functional calculations. Surface Science, 2011, 605, 551-554.	0.8	12
11035	Electronic and structural properties of armchair SWCNT/TiO2(110)-(1Ã—2) system. Surface Science, 2011, 605, 593-596.	0.8	2
11036	Dispersion and induction interactions of graphene with nanostructures. Surface Science, 2011, 605, 1621-1632.	0.8	16
11037	Stability of gold nanostructures on rutile TiO2(110) surface. Surface Science, 2011, 605, 668-674.	0.8	7
11038	A theoretical study of CO adsorption on FeCo(100) and the effect of alloying. Surface Science, 2011, 605, 681-688.	0.8	34
11039	Ab initio determination of atomic structure and energy of surface states of bare and hydrogen covered GaN (0001) surface â€" Existence of the Surface States Stark Effect (SSSE). Surface Science, 2011, 605, 695-713.	0.8	36
11040	Disordered reconstructions of the reduced SnO2-(110) surface. Surface Science, 2011, 605, 714-722.	0.8	30
11041	Properties of rutile TiO2 surfaces from a Tight-Binding Variable-Charge model. Comparison with ab initio calculations. Surface Science, 2011, 605, 738-745.	0.8	20
11042	Initial steps in methanol steam reforming on PdZn and ZnO surfaces: Density functional theory studies. Surface Science, 2011, 605, 750-759.	0.8	58

#	Article	IF	Citations
11043	Decomposition of NH3 on Ir(110): A first-principle study. Surface Science, 2011, 605, 802-807.	0.8	20
11044	Surface reactions of AsH3, H2Se, and H2S on the Zn2TiO4(010) surface. Surface Science, 2011, 605, 818-823.	0.8	10
11045	Arrays of Ru nanoclusters with narrow size distribution templated by monolayer graphene on Ru. Surface Science, 2011, 605, 1676-1684.	0.8	70
11046	Tin-stabilized (1Ã—2) and (1Ã—4) reconstructions on GaAs(100) and InAs(100) studied by scanning tunneling microscopy, photoelectron spectroscopy, and ab initio calculations. Surface Science, 2011, 605, 883-888.	0.8	2
11047	The structure of Cu{100}-p(2Ã—6)-2mg-Sn studied by DFT and LEED. Surface Science, 2011, 605, 1000-1004.	0.8	1
11048	First-principles study of atomic hydrogen adsorption on Fe3O4(100). Surface Science, 2011, 605, 1067-1073.	0.8	32
11049	Adsorption and diffusion of an Au atom and dimer on a Î¸-Al2O3 (001) surface. Surface Science, 2011, 605, 1122-1128.	0.8	10
11050	Acetylene adsorption on silicon (100)-(4Ã—2) revisited. Surface Science, 2011, 605, 1341-1346.	0.8	14
11051	Adsorption of water molecule on (001) and (110) surfaces of MgH2. Surface Science, 2011, 605, 1224-1229.	0.8	3
11052	Theoretical study of hydrazine adsorption on Pt(111): Anti or cis?. Surface Science, 2011, 605, 1347-1353.	0.8	27
11053	Ag-mediated charge transfer from electron-doped SrTiO3 to CO and NO: A first-principles study. Surface Science, 2011, 605, 1331-1335.	0.8	7
11054	Cation mixing, band offsets and electric fields at LaAlO3/SrTiO3(001) heterojunctions with variable La:Al atom ratio. Surface Science, 2011, 605, 1381-1387.	0.8	74
11055	A first-principles study of oxygen adsorption and interaction with Al adatoms on Al(110). Surface Science, 2011, 605, 1391-1396.	0.8	6
11056	Structural dependence of intermediate species for the hydrogen evolution reaction on single crystal electrodes of Pt. Surface Science, 2011, 605, 1462-1465.	0.8	31
11057	Density functional theory calculation of platinum surface segregation energy in Pt3Ni (111) surface doped with a third transition metal. Surface Science, 2011, 605, 1577-1582.	0.8	35
11058	First principle simulations of the surface diffusion of Si and Me adatoms on the Si(111) Al, Ga, In, Pb. Surface Science, 2011, 605, 1866-1871.	0.8	6
11059	Thermodynamic description of the Alâ€“Cuâ€“Mgâ€“Mnâ€“Si quinary system and its application to solidification simulation. Thermochimica Acta, 2011, 512, 258-267.	1.2	35
11060	Vacuum-ultraviolet ellipsometry spectra and structural properties of Pb(Zr,Ti)O3 films. Thin Solid Films, 2011, 519, 2885-2888.	0.8	8

#	Article	IF	Citations
11061	Structural and electronic properties of Î²-In2X3 (X=O, S, Se, Te) using ab initio calculations. Thin Solid Films, 2011, 519, 5679-5683.	0.8	9
11062	Ab initio calculation of Co2MnSi/semiconductor (SC, =GaAs, Ge) heterostructures. Thin Solid Films, 2011, 519, 4400-4408.	0.8	14
11063	Influence of Zr on structure, mechanical and thermal properties of Tiâ€“Alâ€“N. Thin Solid Films, 2011, 519, 5503-5510.	0.8	102
11064	First-principles study on electronic structure, phase stability, and optical properties of In2X2O7 (Xâ•Ć,) Tj ETQq1 1 0.784314 rgBT /Ov	0.8	11
11065	Density Functional Theory Investigation on the Dissociation and Adsorption Processes of N₂ on Pd(111) and Pd₃Ag(111) Surfaces. Japanese Journal of Applied Physics, 2011, 50, 045701.	0.8	4
11066	Orientation dependent ionization potential of In₂O₃: a natural source for inhomogeneous barrier formation at electrode interfaces in organic electronics. Journal of Physics Condensed Matter, 2011, 23, 334203.	0.7	36
11067	Anab initiostudy of local vibration modes of the nitrogen-vacancy center in diamond. New Journal of Physics, 2011, 13, 025016.	1.2	42
11068	Ferromagnetism Induced by Vacancies in Bulk and the (1010) Surfaces of ZnO: Density Functional Theory Calculations. Japanese Journal of Applied Physics, 2011, 50, 01BE05.	0.8	3
11069	Textured growth of the high moment material Gd(0â€‰0â€‰0â€‰1)/Cr(0â€‰0â€‰0â€‰1)/Fe(0â€‰0â€‰0â€‰1). Journal Physics D: Applied Physics, 2011, 44, 265004.	1.3	10
11070	Spinâ€“orbit splitting in graphene on metallic substrates. Journal of Physics Condensed Matter, 2011, 23, 225502.	0.7	28
11071	The effect of carbon distribution on the manganese magnetic moment in bcc Feâ€“Mn alloy. Journal of Physics Condensed Matter, 2011, 23, 326003.	0.7	19
11072	Theoretical Calculations for Magnetic Property of FeRh Inter-Metallic Compound with Site-Exchange Defects. Japanese Journal of Applied Physics, 2011, 50, 105803.	0.8	5
11073	Ab initioStudy of Atomic Hydrogen on ZnO Surfaces. Applied Physics Express, 2011, 4, 125601.	1.1	9
11074	Energy Stabilities, Magnetic Properties, and Electronic Structures of Diluted Magnetic Semiconductor Zn1â^'xMnxS(001) Thin Films. Chinese Journal of Chemical Physics, 2011, 24, 47-54.	0.6	1
11075	Ab initiostudy of magnetoelectricity in Fe/BaTiO₃: the effects of n-doped perovskite interfaces. Journal of Physics Condensed Matter, 2011, 23, 455902.	0.7	3
11076	Study of the structural, elastic and electronic properties of ordered Ca(Mg1â^'xLix)2alloys from first-principles calculations. Physica Scripta, 2011, 84, 055603.	1.2	4
11077	Structural and electronic properties of hydrogen adsorptions on BC₃sheet and graphene: a comparative study. Nanotechnology, 2011, 22, 135703.	1.3	24
11078	Molecular and Electronic Tuning of Si/Carbon Nanotube Hybrid System. Japanese Journal of Applied Physics, 2011, 50, 045101.	0.8	1

#	Article	IF	Citations
11079	Electron Accumulation in LaAlO$_{3}$/SrTiO$_{3}$ Interfaces by the Broken Symmetry of Crystal Field. Japanese Journal of Applied Physics, 2011, 50, 10PF03.	0.8	0
11080	Mechanical properties and twin boundary drag in Feâ€“Pd ferromagnetic shape memory foilsâ€”experiments andab initiomodeling. New Journal of Physics, 2011, 13, 063034.	1.2	15
11081	Fine tuning of the electronic structure of Ï€-conjugated molecules for molecular electronics. Nanotechnology, 2011, 22, 145701.	1.3	10
11082	Stress tensor: A quantitative indicator of effective volume and stability of helium in metals. Europhysics Letters, 2011, 96, 66001.	0.7	26
11083	First-principle description of magnonic Pd_nFe_m multilayers. Journal of Applied Physics, 2011, 109, 07C110.	1.1	2
11084	Vacancies in CuInSe₂: new insights from hybrid-functional calculations. Journal of Physics Condensed Matter, 2011, 23, 422202.	0.7	25
11085	Towards the accurate electronic structure descriptions of typical high-constant dielectrics. Journal Physics D: Applied Physics, 2011, 44, 185402.	1.3	13
11086	First-principles study of NiSi2/HfO2interfaces: energetics and Schottky-barrier heights. Journal Physics D: Applied Physics, 2011, 44, 405302.	1.3	0
11087	Bonding characters of Al-containing bulk metallic glasses studied by²⁷Al NMR. Journal of Physics Condensed Matter, 2011, 23, 115501.	0.7	16
11088	Shear properties of potassium chloride films on iron obtained using density functional theory. Journal of Physics Condensed Matter, 2011, 23, 265003.	0.7	11
11089	LEEDIâ€“Vand DFT structure determination of the (surd 3imes surd 3)mathrm {R}30^{circ } Pbâ€“Ag(111) surface alloy. Journal of Physics Condensed Matter, 2011, 23, 265006.	0.7	2
11090	Surface magnetism in O₂dissociationâ€”from basics to application. Journal of Physics Condensed Matter, 2011, 23, 394207.	0.7	7
11091	Adsorbate and defect effects on electronic and transport properties of gold nanotubes. Nanotechnology, 2011, 22, 215702.	1.3	11
11092	Structure and energetics of 180Â° domain walls in PbTiO₃by density functional theory. Journal of Physics Condensed Matter, 2011, 23, 175902.	0.7	48
11093	Unexpected relationship between interlayer distances and surface/cleavage energies in Î³-TiAl: density functional study. Journal of Physics Condensed Matter, 2011, 23, 265009.	0.7	18
11094	Carbon release by selective alloying of transition metal carbides. Journal of Physics Condensed Matter, 2011, 23, 355401.	0.7	15
11095	Electronic structures and the spin polarization of Heusler alloy Co₂FeAl surface. Journal of Physics: Conference Series, 2011, 263, 012016.	0.3	3
11096	Quantum electronic stability of atomically uniform films. , 2011, , 22-51.		0

#	Article	IF	Citations
11097	Magnetostriction, elasticity, and D03 phase stability in Feâ€“Ga and Feâ€“Gaâ€“Ge alloys. Journal of Applied Physics, 2011, 109, 07A904.	1.1	8
11098	SOx on ceria from adsorbed SO2. Journal of Chemical Physics, 2011, 134, 184703.	1.2	32
11099	A unique vibrational signature of rotated water monolayers on Pt(111): Predicted and observed. Journal of Chemical Physics, 2011, 134, 204702.	1.2	31
11100	The initial growth behavior of perylene on Cu(100). Journal of Chemical Physics, 2011, 134, 194702.	1.2	6
11101	Interaction of He with Cu, V, and Ta in bcc Fe: A first-principles study. Journal of Applied Physics, 2011, 110, .	1.1	19
11102	Disorder effect on the electronic and magnetic properties of Sr2FeCoO6: A density-functional theoretical investigation. Journal of Applied Physics, 2011, 110, 083701.	1.1	8
11103	On the adsorption and formation of Pt dimers on the CeO2(111) surface. Journal of Chemical Physics, 2011, 135, 244708.	1.2	14
11104	Magnetic properties of Fe chains on Cu2N/Cu(100): A density functional theory study. Journal of Applied Physics, 2011, 110, 123915.	1.1	16
11105	Effects of O in a binary-phase TiAlâ€“Ti₃Al alloy: from site occupancy to interfacial energetics. Journal of Physics Condensed Matter, 2011, 23, 225504.	0.7	22
11106	Surfactant-enabled epitaxy through control of growth mode with chemical boundary conditions. Nature Communications, 2011, 2, 461.	5.8	23
11107	First principles study of adsorption of O2 on Al surface with hybrid functionals. Journal of Chemical Physics, 2011, 135, 214702.	1.2	42
11108	Robust acceleration of self consistent field calculations for density functional theory. Journal of Chemical Physics, 2011, 134, 134109.	1.2	10
11109	Li and Ca Co-decorated carbon nitride nanostructures as high-capacity hydrogen storage media. Journal of Applied Physics, 2011, 110, .	1.1	26
11110	Equilibrium compositional distribution in freestanding ternary semiconductor quantum dots: The case of InxGa1â”xAs. Journal of Chemical Physics, 2011, 135, 234701.	1.2	5
11111	Tilting, Bending, and Nonterminal Sites in<mml:math xmlns:mml="http://www.w3.org/1998/Math/MathML" display="inline"><mml:mi>CO</mml:mi><mml:mo>/</mml:mo><mml:mi>Cu</mml:mi><mml:mo stretchy="false">(</mml:mo><mml:mn>001</mml:mn><mml:mo) Tj ETQq0 0 0 rgBT /Overlock 10 Tf 50 167 Td (stretchy="false">)</mml:mo><mml:mi>Cu</mml:mi><mml:mo stretchy="false">(</mml:mo><mml:mn>001</mml:mn><mml:mo stretchy="false">)</mml:mo></mml:math> Surfaces. Physical Review Letters, 2011, 107, .	2.9	6
11112	Ab initio study of the intrinsic exchange bias at the SrRuO<mml:math xmlns:mml="http://www.w3.org/1998/Math/MathML" display="inline"><mml:mrow><mml:msub><mml:mrow /><mml:mn>3</mml:mn></mml:msub></mml:mrow></mml:math>/SrMnO<mml:math xmlns:mml="http://www.w3.org/1998/Math/MathML" display="inline"><mml:mrow><mml:msub><mml:mrow /><mml:mn>3</mml:mn></mml:msub></mml:mrow></mml:math> interface. Physical Review B, 2011, 84, .	1.1	38
11113	Pressure-induced electron topological transitions in Ba-doped Si clathrate. Physical Review B, 2011, 84, .	1.1	23
11114		1.1	17

#	Article	IF	Citations
11115	Quantum molecular dynamics simulations for the nonmetal-metal transition in shocked methane. Physical Review B, 2011, 84, .	1.1	15
11116	Towards predictive modeling of near-edge structures in electron energy-loss spectra of AlN-based ternary alloys. Physical Review B, 2011, 83, .	1.1	36
11117	Nanoscale hydride formation at dislocations in palladium:Ab initiotheory and inelastic neutron scattering measurements. Physical Review B, 2011, 83, .	1.1	8
11118	Scattered surface charge density: A tool for surface characterization. Physical Review B, 2011, 84, .	1.1	7
11119	Epitaxial Interfaces between Crystallographically Mismatched Materials. Physical Review Letters, 2011, 107, 026102.	2.9	15
11120	First-principles study of polar LaAlO (001) surface stabilization by point defects. Physical Review B, 2011, 84, .	1.1	34
11121	Disorder-induced reversal of spin polarization in the Heusler alloy Co<mml:math xmlns:mml="http://www.w3.org/1998/Math/MathML" display="inline"><mml:mrow><mml:msub><mml:mrow /><mml:mrow><mml:mn>2</mml:mn></mml:mrow></mml:msub></mml:mrow></mml:math>FeSi. Physical Review B, 2011, 83, .	1.1	38
11122	Metallic and superconducting gallane under high pressure. Physical Review B, 2011, 84, .	1.1	65
11123	Simulation of spin-polarized scanning tunneling microscopy on complex magnetic surfaces: Case of a Cr monolayer on Ag(111). Physical Review B, 2011, 84, .	1.1	16
11124	Trends in solubility between boron nitride and carbon. Physical Review B, 2011, 84, .	1.1	10
11125	Two-dimensional C/BN core/shell structures. Physical Review B, 2011, 83, .	1.1	27
11126	Intrinsic ferromagnetism in two-dimensional carbon structures: Triangular graphene nanoflakes linked by carbon chains. Physical Review B, 2011, 84, .	1.1	40
11127	Structural and magnetic ground-state properties of<mml:math xmlns:mml="http://www.w3.org/1998/Math/MathML" display="inline"><mml:mi>Î³</mml:mi></mml:math>-FeMn alloys fromab initiocalculations. Physical Review B, 2011, 84, .	1.1	56
11128	Predicting the spin-lattice order of frustrated systems from first principles. Physical Review B, 2011, 84, .	1.1	262
11129	Role of spin quantization in determining the thermodynamic properties of magnetic transition metals. Physical Review B, 2011, 83, .	1.1	45
11130	First-principles prediction of high-capacity, thermodynamically reversible hydrogen storage reactions based on (NH4)2B12H12. Physical Review B, 2011, 83, .	1.1	13
11131	Quantum molecular dynamics simulations of transport properties in liquid and dense-plasma plutonium. Physical Review E, 2011, 83, 026404.	0.8	38
11132	Thermal conductivity of compressed<mml:math xmlns:mml="http://www.w3.org/1998/Math/MathML" display="inline"><mml:mrow><mml:msub><mml:mi mathvariant="normal">H</mml:mi><mml:mrow><mml:mn>2</mml:mn></mml:mrow></mml:msub></mml:mrow></mml:math>O to 22 GPa: A test of the Leibfried-SchlÃ¶mann equation. Physical Review B, 2011, 83, .	1.1	68

#	Article	IF	Citations
11133	Effect of surface passivation on dopant distribution in Si quantum dots: The case of B and P doping. Applied Physics Letters, 2011, 98, .	1.5	26
11134	Electronic structures of graphene/boron nitride sheet superlattices. Physical Review B, 2011, 84, .	1.1	34
11135	Nanodopant-Induced Band Modulation in<mml:math xmlns:mml="http://www.w3.org/1998/Math/MathML" display="inline"><mml:msub><mml:mi>AgPb</mml:mi><mml:mi>m</mml:mi></mml:msub><mml:msub><mml:mi>SbTe</mml:mi><mml:mi><mm Thermoelectrics. Physical Review Letters, 2011, 106, 206601.	2.9	18
11136	xmlns:mml="http://www.w3.org/1998/Math/MathML" display="inline"><mml:msub><mml:mrow /><mml:mrow><mml:mn>1</mml:mn><mml:mo>â’</mml:mo><mml:mi>x</mml:mi></mml:mrow></mml:msub></mml:math>Ce<mml: xmlns:mml="http://www.w3.org/1998/Math/MathML" display="inline"><mml:msub><mml:mrow /><mml:mi>x</mml:mi></mml:msub></mml:math>O<mml:math	1.1	36
11137	Construction and performance of fully numerical optimum atomic basis sets. Physical Review B, 2011, 84, .	1.1	2
11138			

#	Article	IF	Citations
11151	Static charging of graphene and graphite slabs. Applied Physics Letters, 2011, 98, .	1.5	23
11152	Radiation-Induced Defect Evolution and Electrical Degradation of AlGaN/GaN High-Electron-Mobility Transistors. IEEE Transactions on Nuclear Science, 2011, 58, 2918-2924.	1.2	69
11153	Stabilizing and activating dopants in âŸ¨112âŸ© silicon nanowires by alkene adsorptions: A first-principles study. Applied Physics Letters, 2011, 98, 073115.	1.5	8
11154	Ab initiostudy of the adsorption, migration, clustering, and reaction of palladium on the surface of silicon carbide. Physical Review B, 2011, 83, .	1.1	16
11155	Properties of amorphous GaN from first-principles simulations. Physical Review B, 2011, 84, .	1.1	25
11156	Ab initiosimulation of solid electrolyte materials in liquid and glassy phases. Physical Review B, 2011, 83, .	1.1	17
11157	The half-metallic properties and geometrical structures of cubic BaMnO3 and BaTiO3/BaMnO3 superlattice. Journal of Applied Physics, 2011, 109, .	1.1	11
11158	Crystallographic, magnetic, and electronic structures of ferromagnetic shape memory alloys Ni2XGa (X=Mn,Fe,Co) from first-principles calculations. Journal of Applied Physics, 2011, 109, 014908.	1.1	54
11159	Compressive Surface Stress in Magnetic Transition Metals. Physical Review Letters, 2011, 106, 057202.	2.9	34
11160	Rotational transitions in a C<mml:math xmlns:mml="http://www.w3.org/1998/Math/MathML" display="inline"><mml:msub><mml:mrow /><mml:mn>60</mml:mn></mml:msub></mml:math>monolayer on the WO<mml:math xmlns:mml="http://www.w3.org/1998/Math/MathML" display="inline"><mml:mrow><mml:msub><mml:mrow /><mml:mn>2</mml:mn></mml:msub><mml:mo></mml:mo></mml:mrow></mml:math>W(110) surface.	1.1	16
11161	Anomalous vibrational dynamics in the Mg<mml:math xmlns:mml="http://www.w3.org/1998/Math/MathML" display="inline"><mml:mrow><mml:msub><mml:mrow /><mml:mrow><mml:mn>2</mml:mn></mml:mrow></mml:msub></mml:mrow></mml:math>Zn<mml:math xmlns:mml="http://www.w3.org/1998/Math/MathML" display="inline"><mml:mrow><mml:msub><mml:mrow /><mml:mrow><mml:mn>2</mml:mn></mml:mrow></mml:msub></mml:mrow></mml:math>	1.1	28
11162	Relativistic tight-binding model: Application to Pt surfaces. Physical Review B, 2011, 83, .	1.1	3
11163	Pressure- and temperature-induced structural phase transitions of CaFe<mml:math xmlns:mml="http://www.w3.org/1998/Math/MathML" display="inline"><mml:mrow><mml:msub><mml:mrow /><mml:mrow><mml:mn>2</mml:mn></mml:mrow></mml:msub></mml:mrow></mml:math>As<mml:math xmlns:mml="http://www.w3.org/1998/Math/MathML" display="inline"><mml:mrow><mml:msub><mml:mrow /><mml:mrow><mml:mn>2</mml:mn></mml:mrow></mml:msub></mml:mrow></mml:math>	1.1	18
11164	Electronic correlation effects in superconducting picene fromab initiocalculations. Physical Review B, 2011, 83, .	1.1	81
11165	<mml:math xmlns:mml="http://www.w3.org/1998/Math/MathML" display="inline"><mml:mrow><mml:mi>G</mml:mi><mml:mi>W</mml:mi></mml:mrow></mml:math>calculations including spin-orbit coupling: Application to Hg chalcogenides. Physical Review B, 2011, 84, .	1.1	87
11166	Tj ETQq1 1 0.784314 rgBT /Overlock 10 Tf 50 582 Td (<mml:math xmlns:mml="http://www.w3.org/1998/Math/MathML" display="inline"><mml:msub><mml:mrow /><mml:mn>3</mml:mn></mml:msub></mml:math>reconstruction of the Sm/Si(100)(<mml:math)	1.1	5
11167	surface studied by high-resolution photoelectron spectroscopy and density functional theory calcul Anionic and Hidden Hydrogen in ZnO. Physical Review Letters, 2011, 106, 115502.	2.9	84
11168	Role of copper interstitials in CuInSe<mml:math xmlns:mml="http://www.w3.org/1998/Math/MathML" display="inline"><mml:msub><mml:mrow /><mml:mn>2</mml:mn></mml:msub></mml:math>: First-principles calculations. Physical Review B, 2011, 84, .	1.1	25

#	Article	IF	Citations
11169	Pressure-induced half-metallic gap transformation in Co2MnSi observed by tunneling conductance spectroscopy. Physical Review B, 2011, 83, .	1.1	1
11170	Size effects on formation energies and electronic structures of oxygen and zinc vacancies in ZnO nanowires: A first-principles study. Journal of Applied Physics, 2011, 109, 044306-044306-5.	1.1	17
11171	Unusual structure and magnetism in manganese oxide nanoclusters. Physical Review B, 2011, 83, .	1.1	12
11172	Insulating state of ultrathin epitaxial LaNiO<mml:math xmlns:mml="http://www.w3.org/1998/Math/MathML" display="inline"><mml:msub><mml:mrow /><mml:mn>3</mml:mn></mml:msub></mml:math>thin films detected by hard x-ray photoemission. Physical Review B, 2011, 84, .	1.1	35
11173	Strain-induced formation of ultrathin mixed-oxide films. Physical Review B, 2011, 83, .	1.1	34
11174	Enhanced photoelectrochemical performance of rutile TiO2 by Sb-N donor-acceptor coincorporation from first principles calculations. Applied Physics Letters, 2011, 99, .	1.5	41
11175	Tunable two-dimensional or three-dimensional electron gases by submonolayer La doping of SrTiO<mml:math xmlns:mml="http://www.w3.org/1998/Math/MathML" display="inline"><mml:mrow><mml:msub><mml:mrow /><mml:mrow><mml:mn>3</mml:mn></mml:mrow></mml:msub></mml:mrow></mml:math>. Physical Review B, 2011, 83, .	1.1	23
11176	Ab initio based polarizable force field generation and application to liquid silica and magnesia. Journal of Chemical Physics, 2011, 135, 234512.	1.2	17
11177	Anomalous Lattice Dynamics near the Ferroelectric Instability in PbTe. Physical Review Letters, 2011, 107, 175503.	2.9	97
11178	Electronic structure, Born effective charges and spontaneous polarization in magnetoelectric gallium ferrite. Journal of Physics Condensed Matter, 2011, 23, 325902.	0.7	39
11179	Possible routes for synthesis of new boron-rich Feâ€“B and Fe1â^'xCrxB4 compounds. Applied Physics Letters, 2011, 98, .	1.5	46
11180	Atomic scale mechanism for the Ge-induced stabilization of the tetragonal, very high-Î², phase of ZrO2. Applied Physics Letters, 2011, 99, .	1.5	15
11181	Formation and diffusion of vacancy-polaron complex in olivine-type LiMnPO<mml:math xmlns:mml="http://www.w3.org/1998/Math/MathML" display="inline"><mml:msub><mml:mrow /><mml:mn>4</mml:mn></mml:msub></mml:math>and LiFePO<mml:math xmlns:mml="http://www.w3.org/1998/Math/MathML" display="inline"><mml:msub><mml:mrow /><mml:mn>4</mml:mn></mml:msub></mml:math>. Physical Review B, 2011, 84, .	1.1	40
11182	Transition-metal-molecular sandwich nanowires as magnetic on/off switch. Applied Physics Letters, 2011, 99, .	1.5	18
11183	Hydrogen impurity in paratellurite<mml:math xmlns:mml="http://www.w3.org/1998/Math/MathML" display="inline"><mml:mrow><mml:mi>Î±</mml:mi></mml:mrow></mml:math>-TeO<mml:math xmlns:mml="http://www.w3.org/1998/Math/MathML" display="inline"><mml:mrow><mml:msub><mml:mrow /><mml:mn>2</mml:mn></mml:msub></mml:mrow></mml:math>: Muon-spin rotation andab initiostudies. Physical Review B, 2011, 83, .	1.1	24
11184	Density functional calculations of electronic structure and magnetic properties of the hydrocarbon<mml:math xmlns:mml="http://www.w3.org/1998/Math/MathML" display="inline"><mml:mrow><mml:msub><mml:mi mathvariant="normal">K</mml:mi><mml:mrow><mml:mn>3</mml:mn></mml:mrow></mml:msub></mml:mrow></mml:math>picen superconductor near the metal-insulator transition. Physical Review B, 2011, 83, .	1.1	56
11185	First-principles calculations of Xe-adsorbed Pd(111) and Cu(111) surfaces with an empirical correction of van der Waals interactions. Journal of Applied Physics, 2011, 110, 103701.	1.1	8
11186	Catalytic Properties Dominated by Electronic Structures in PdZn, NiZn, and PtZn Intermetallic Compounds. Journal of the Physical Society of Japan, 2011, 80, 064801.	0.7	27

#	Article	IF	Citations
11187	Effects of nonhydrostatic pressure on the structural and magnetic properties of BaFe<mml:math xmlns:mml="http://www.w3.org/1998/Math/MathML" display="inline"><mml:mrow><mml:msub><mml:mrow /><mml:mrow><mml:mn>2</mml:mn></mml:mrow></mml:msub></mml:mrow></mml:math>As<mml:math xmlns:mml="http://www.w3.org/1998/Math/MathML" display="inline"><mml:mrow><mml:msub><mml:mrow /><mml:mrow><mml:mn>2</mml:mn></mml:mro	1.1	16
11188	Kinetic and relativistic effects on the surface alloy formation of submonolayer Au adsorbed on Si(111)-3Ã—3-Pb surface. Applied Physics Letters, 2011, 99, 211912.	1.5	0
11189	Effect of oxygen vacancy defect on the magnetic properties of Co-doped ZnO. Chinese Physics B, 2011, 20, 027103.	0.7	25
11190	Role of codeposited impurities during growth. I. Explaining distinctive experimental morphology on Cu(0 0 1). Physical Review B, 2011, 83, .	1.1	14
11191	Energetics of hydrogen in GeO2, Ge, and their interfaces. Applied Physics Letters, 2011, 99, 032902.	1.5	9
11192	Magnetoelectric effect and critical thickness for ferroelectricity in Co/BaTiO3/Co multiferroic tunnel junctions. Journal of Applied Physics, 2011, 109, .	1.1	53
11193	Band alignment at the SiO<mml:math xmlns:mml="http://www.w3.org/1998/Math/MathML" display="inline"><mml:msub><mml:mrow /><mml:mn>2</mml:mn></mml:msub></mml:math>/HfO<mml:math xmlns:mml="http://www.w3.org/1998/Math/MathML" display="inline"><mml:msub><mml:mrow /><mml:mn>2</mml:mn></mml:msub></mml:math>interface: Group IIIA versus group IIIB metal dopants. Physical Review B, 2011, 84, .	1.1	19
11194	<mml:math xmlns:mml="http://www.w3.org/1998/Math/MathML" display="inline"><mml:mrow><mml:msub><mml:mrow /><mml:mrow><mml:mn>4</mml:mn></mml:mrow></mml:msub></mml:mrow></mml:math>and YCrO<mml:math xmlns:mml="http://www.w3.org/1998/Math/MathML"	1.1	43
11195	First-principles calculations of electronic, vibrational, and structural properties of scheelite EuWO<mml:math xmlns:mml="http://www.w3.org/1998/Math/MathML" display="inline"><mml:msub><mml:mrow /><mml:mn>4</mml:mn></mml:msub></mml:math>under pressure. Physical Review B, 2011, 84, .	1.1	24
11196	Engineering the magnetic properties of hybrid organic-ferromagnetic interfaces by molecular chemical functionalization. Physical Review B, 2011, 84, .	1.1	52
11197	Multiple exchange interactions induced by Jahn-Teller distortions in dilute magnetic semiconductors. Physical Review B, 2011, 84, .	1.1	5
11198	Electron structure and dynamics at poly(3-hexylthiophene)/fullerene photovoltaic heterojunctions. Applied Physics Letters, 2011, 98, 083303.	1.5	12
11199	Signature of helium segregation in hydrogen-helium mixtures. Physical Review B, 2011, 84, .	1.1	13
11200	Monoatomic and dimer Mn adsorption on the Au(111) surface from first principles. Physical Review B, 2011, 83, .	1.1	8
11201	Polarity replication across m-plane GaN/ZnO interfaces. Applied Physics Letters, 2011, 99, 181910.	1.5	4
11202	Reciprocal-space cluster expansions for complex alloys with long-range interactions. Physical Review B, 2011, 83, .	1.1	11
11203	A comparison of the growth modes of (100)- and (110)-oriented CrO2 films through the calculation of surface and interface energies. Journal of Applied Physics, 2011, 110, 113910.	1.1	5
11204	Charge disproportionation and Jahn-Teller distortion in LiNiO<mml:math xmlns:mml="http://www.w3.org/1998/Math/MathML" display="inline"><mml:msub><mml:mrow /><mml:mn>2</mml:mn></mml:msub></mml:math>and NaNiO<mml:math xmlns:mml="http://www.w3.org/1998/Math/MathML" display="inline"><mml:msub><mml:mrow /><mml:mn>2</mml:mn></mml:msub></mml:math>: A density functional theory study. Physical Review B, 2011, 84, .	1.1	60

#	Article	IF	Citations
11205	Site specific metallic to semiconductor transition in selenium adsorbed armchair single wall carbon nanotubes. Journal of Applied Physics, 2011, 110, 104302.	1.1	1
11206	First-principles study of Ti intercalation between graphene and Au surface. Applied Physics Letters, 2011, 98, 261905.	1.5	3
11207	Understanding neutron scattering data in YMn<mml:math xmlns:mml="http://www.w3.org/1998/Math/MathML" display="inline"><mml:msub><mml:mrow /><mml:mn>2</mml:mn></mml:msub></mml:math>O<mml:math xmlns:mml="http://www.w3.org/1998/Math/MathML" display="inline"><mml:msub><mml:mrow /><mml:mn>5</mml:mn></mml:msub></mml:math>: An effective spin Hamiltonian. Physical Review B, 2011, 84, .	1.1	12
11208	Pressure induced crystallization in amorphous silicon. Journal of Applied Physics, 2011, 109, .	1.1	23
11209	Large spin-phonon coupling and magnetically induced phonon anisotropy in Sr<mml:math xmlns:mml="http://www.w3.org/1998/Math/MathML" display="inline"><mml:mi>M</mml:mi></mml:math>O<mml:math xmlns:mml="http://www.w3.org/1998/Math/MathML" display="inline"><mml:msub><mml:mrow		

#	Article	IF	Citations
11223	Electronic structure of a 4-Ã…diameter carbon nanotube placed on a patterned hydrogen-terminated Si(001):3Ã—1surface and the effect of electric field. Physical Review B, 2011, 83, .	1.1	1
11224	Ag-induced Si(100) reconstruction: Si(100)-(22Ã—22)R45â˜-Ag. Physical Review B, 2011, 84, .	1.1	3
11225	Possible interaction-driven topological phases in (111) bilayers of LaNiO<mml:math xmlns:mml="http://www.w3.org/1998/Math/MathML" display="inline"><mml:msub><mml:mrow /><mml:mn>3</mml:mn></mml:msub></mml:math>. Physical Review B, 2011, 84, .	1.1	139
11226	Epitaxial integration of ferromagnetic correlated oxide LaCoO3 with Si (100). Applied Physics Letters, 2011, 98, .	1.5	64
11227	Oxidized In-containing III-V(100) surfaces: Formation of crystalline oxide films and semiconductor-oxide interfaces. Physical Review B, 2011, 83, .	1.1	32
11228	Role of hydrogen on the ZnO(000<mml:math xmlns:mml="http://www.w3.org/1998/Math/MathML" 1 ET Q q 1 1 0.784314 rg BT /Over	1.1	13
11229	Density functional study of weak ferromagnetism in a thick BiCrO3 film. Journal of Applied Physics, 2011, 109, 103905.	1.1	6
11230	Impact of local lattice distortions on the structural stability of Fe-Pd magnetic shape-memory alloys. Physical Review B, 2011, 83, .	1.1	30
11231	Catalytic effect of near-surface alloying on hydrogen interaction on the aluminum surface. Physical Review B, 2011, 83, .	1.1	18
11232	Codoping in a single molecular junction from first principles. Physical Review B, 2011, 83, .	1.1	7
11233	Orbital-separation approach for consideration of finite electric bias within density-functional total-energy formalism. Physical Review B, 2011, 84, .	1.1	11
11234	Determinant influence of surfaces on the Co clustering trend at ZnO. Applied Physics Letters, 2011, 99,	1.5	3
11235	Short- and medium-range order in Zr<mml:math xmlns:mml="http://www.w3.org/1998/Math/MathML" display="inline"><mml:mrow><mml:msub><mml:mrow /><mml:mrow><mml:mn>80</mml:mn></mml:mrow></mml:msub></mml:mrow></mml:math>Pt<mml:math xmlns:mml="http://www.w3.org/1998/Math/MathML" display="inline"><mml:mrow><mml:msub><mml:mrow /><mml:mrow><mml:mn>20</mml:mn></mml:mrow></mml:msub></mml:mrow></mml:math>liquids. Phy	1.1	89
11237	Epitaxial strain and interfacial electronic topological transition in O-rich MgO/FeO/Fe(001) interfaces. Physical Review B, 2011, 83, .	1.1	24
11238	Dehydrogenation of defects and hot-electron degradation in GaN high-electron-mobility transistors. Journal of Applied Physics, 2011, 109, .	1.1	114
11239	The catalytic potential of high-Îº dielectrics for graphene formation. Applied Physics Letters, 2011, 98, .	1.5	63
11240	Room-temperature ferromagnetism in Mn-implanted amorphous Ge. Physical Review B, 2011, 83, .	1.1	25
11241	First-principles study of organic-inorganic hybrid framework compound Mn(C4H4O4). Physical Review B, 2011, 84, .	1.1	2

#	Article	IF	Citations
	Electronic structure of Si(110)-(<mml:math xmlns:mml="http://www.w3.org/1998/Math/MathML") Tj ETQq0 0 0 rgBT /Overlock 10 Tf 50		
11242	studied by scanning tunneling spectroscopy and density functional theory. Physical Review B, 2011, 84, .	1.1	22
11243	Carrier-induced antiferromagnet of graphene islands embedded in hexagonal boron nitride. Physical Review B, 2011, 84, .	1.1	73
11244	<mml:math xmlns:mml="http://www.w3.org/1998/Math/MathML" display="inline"><mml:msub><mml:mi>LaCo</mml:mi><mml:mn>2</mml:mn></mml:msub><mml:msub><mml:mi mathvariant="bold">B</mml:mi><mml:mn>2</mml:mn></mml:msub></mml:math>: A Co-Based Layered Superconductor with a<mml:math xmlns:mml="http://www.w3.org/1998/Math/MathML" display="inline"><mml:msub><mml:mi>ThCr</mml:mi><mml:mn>2</mml:mn></mml:msub><mml:msub><mml:mi>Si</mml:mi><mml:m Structure. Physical Review Letters, 2011, 106, 237001.	2.9	34
11245	Interplay of Conductance, Force, and Structural Change in Metallic Point Contacts. Physical Review Letters, 2011, 106, 016802.	2.9	124
11246	Substantial reduction of Stone-Wales activation barrier in fullerene. Physical Review B, 2011, 84, .	1.1	24
11247	Effect of onsite Coulomb repulsion on thermoelectric properties of full-Heusler compounds with pseudogaps. Physical Review B, 2011, 84, .	1.1	52
11248	First principles calculations in silicon: Structural and electronic properties of point defect. , 2011, , .		1
11249	Concentration effects on segregation behavior of Pt-Rh nanoparticles. Physical Review B, 2011, 84, .	1.1	27
11250	Assembly of iron phthalocyanine and pentacene molecules on a graphene monolayer grown on Ru(0001). Physical Review B, 2011, 84, .	1.1	102
11251	Atomic-scale study of the adsorption of calcium fluoride on Si(100) at low-coverage regime. Physical Review B, 2011, 84, .	1.1	10
11252	Strontium migration assisted by oxygen vacancies in SrTiO<mml:math xmlns:mml="http://www.w3.org/1998/Math/MathML" display="inline"><mml:mrow><mml:msub><mml:mrow /><mml:mrow><mml:mn>3</mml:mn></mml:mrow></mml:msub></mml:mrow></mml:math>from classical and quantum mechanical simulations. Physical Review B, 2011, 83, .	1.1	67
11253	A First Principles Study of O₂/Ag(111) â€“Adsorption and Magnetic Propertiesâ€“. Journal of the Physical Society of Japan, 2011, 80, 084605.	0.7	10
11254	Endotaxial Si nanolines in Si(001):H. Physical Review B, 2011, 84, .	1.1	11
11255	Engineering the magnetic properties of the Mn13cluster by doping. Physical Review B, 2011, 83, .	1.1	22
11256	Ab initiostudy of the electronic, mechanical, and vibrational properties of different Al2Si2Sr crystalline phases. Physical Review B, 2011, 83, .	1.1	4
11257	Binding block modeling technique: Application to ternary chalcogenide glasses g-Ge<mml:math xmlns:mml="http://www.w3.org/1998/Math/MathML" display="inline"><mml:mrow><mml:msub><mml:mrow /><mml:mrow><mml:mn>2</mml:mn></mml:mrow></mml:msub></mml:mrow></mml:math>As<mml:math xmlns:mml="http://www.w3.org/1998/Math/MathML"	1.1	7
11258	Thermodynamic stability, stoichiometry, and electronic structure of bcc-In<mml:math xmlns:mml="http://www.w3.org/1998/Math/MathML" display="inline"><mml:msub><mml:mrow /><mml:mn>2</mml:mn></mml:msub></mml:math>O<mml:math xmlns:mml="http://www.w3.org/1998/Math/MathML" display="inline"><mml:msub><mml:mrow /><mml:mn>3</mml:mn></mml:msub></mml:math>from first principles study.	1.1	77
11259	First principles study of the adsorption of Au atoms and Au<mml:math xmlns:mml="http://www.w3.org/1998/Math/MathML" display="inline"><mml:msub><mml:mrow /><mml:mn>2</mml:mn></mml:msub></mml:math>and Au<mml:math xmlns:mml="http://www.w3.org/1998/Math/MathML" display="inline"><mml:msub><mml:mrow /><mml:mn>4</mml:mn></mml:msub></mml:math>clusters on FeO/Pt(111). Physical Review B, 2011, 84, .	1.1	20

#	Author	Title	IF	Citations
11260	Nonlinear	structure-composition relationships in the Ge<mml:math xmlns:mml="http://www.w3.org/1998/Math/MathML" display="inline"><mml:msub><mml:mrow /><mml:mrow><mml:mn>1</mml:mn><mml:mo>â^'</mml:mo><mml:mi>y</mml:mi></mml:mrow></mml:msub></mml:math>Sn<mml:math xmlns:mml="http://www.w3.org/1998/Math/MathML" display="inline"><mml:msub><mml:mrow		

#	Article	IF	Citations
11278	Terminating Surface Electromigration at the Source. Physical Review Letters, 2011, 106, 156404.	2.9	15
11279	Stability of the Bulk Phase of Layered ZnO. Physical Review Letters, 2011, 107, 085508.	2.9	35
11280	Memetic figure selection for cluster expansion in binary alloy systems. , 2011, , .		0
11281	Rainbow scattering under axial surface channeling from a KCl(001) surface. Physical Review B, 2011, 84, .	1.1	16
11282	K<mml:math xmlns:mml="http://www.w3.org/1998/Math/MathML" display="inline"><mml:msub><mml:mrow /><mml:mn>2</mml:mn></mml:msub></mml:math>O<mml:math xmlns:mml="http://www.w3.org/1998/Math/MathML" display="inline"><mml:msub><mml:mrow /><mml:mn>2</mml:mn></mml:msub></mml:math>: The most stable oxide of K. Physical Review B, 2011, 84, .	1.1	9
11283	Unexpectedly Large Electronic Contribution to Linear Magnetoelectricity. Physical Review Letters, 2011, 106, 107202.	2.9	56
11284	Sodium chloride on Si(100) grown by molecular beam epitaxy. Physical Review B, 2011, 83, .	1.1	8
11285	The effects of alloying element Co on Niâ€“Mnâ€“Ga ferromagnetic shape memory alloys from first-principles calculations. Applied Physics Letters, 2011, 98, .	1.5	47
11286	Novel Cooperative Interactions and Structural Ordering in<mml:math xmlns:mml="http://www.w3.org/1998/Math/MathML" display="inline"><mml:msub><mml:mi mathvariant="normal">H</mml:mi><mml:mn>2</mml:mn></mml:msub><mml:mi mathvariant="normal">S</mml:mi><mml:mtext mathvariant="normal">â^'</mml:mtext><mml:msub><mml:mi mathvariant="normal">H</mml:mi><mml:mn>2</mml:mn></mml:msub></mml:math>. Physical Review Let	2.9	80
11287	Role of Electronic Excitation in the Amorphization of Ge-Sb-Te Alloys. Physical Review Letters, 2011, 107, 015501.	2.9	107
11288	Density functional theory study on the electronic structure of<mml:math xmlns:mml="http://www.w3.org/1998/Math/MathML" display="inline"><mml:mi>n</mml:mi></mml:math>-and<mml:math xmlns:mml="http://www.w3.org/1998/Math/MathML" display="inline"><mml:mi>p</mml:mi></mml:math>-type doped SrTiO<mml:math xmlns:mml="http://www.w3.org/1998/Math/MathML" display="inline"><mml:msub><mml:mrow /><mml:mn>3</mml:mn></mml:msub></mml:math>at anodic solid oxide fuel cell conditions. Physical	1.1	16
11289	Magnetically dead layers at<mml:math xmlns:mml="http://www.w3.org/1998/Math/MathML" display="inline"><mml:mrow><mml:mi>s</mml:mi><mml:mi>p</mml:mi></mml:mrow></mml:math>-impurity-decorated grain boundaries and surfaces in nickel. Physical Review B, 2011, 84, .	1.1	33
11290	Noncollinear magnetism in transition metal nanostructures: Exchange interaction and local environment effects in free and deposited clusters. Physical Review B, 2011, 84, .	1.1	7
11291	Phonon density of states of Fe<mml:math xmlns:mml="http://www.w3.org/1998/Math/MathML" display="inline"><mml:msub><mml:mrow /><mml:mn>2</mml:mn></mml:msub></mml:math>O<mml:math xmlns:mml="http://www.w3.org/1998/Math/MathML" display="inline"><mml:msub><mml:mrow /><mml:mn>3</mml:mn></mml:msub></mml:math>across high-pressure structural and electronic transitions. Physical Review B, 2011, 84, .	1.1	12
11292	Imaging and Control of Surface Magnetization Domains in a Magnetoelectric Antiferromagnet. Physical Review Letters, 2011, 106, 087202.	2.9	96
11293	A topological point defect regulates the evolution of extended defects in irradiated silicon. Applied Physics Letters, 2011, 98, 171915.	1.5	10
11294	Stable Cation Inversion at the<mml:math xmlns:mml="http://www.w3.org/1998/Math/MathML" display="inline"><mml:msub><mml:mi>MgAl</mml:mi><mml:mn>2</mml:mn></mml:msub><mml:msub><mml:mi mathvariant="normal">O</mml:mi><mml:mn>4</mml:mn></mml:msub><mml:mo stretchy="false">(</mml:mo><mml:mn>100</mml:mn><mml:mo) Tj ETQq0 0 0 rgBT /Overlock 10 Tf 50 87 Td (stretchy="false">)</mml	2.9	45
11295	First-principles study of phase stability of Gd-doped EuO and EuS. Physical Review B, 2011, 83, .	1.1	28

#	Article	IF	Citations
11296	Electronic origin of the phase transition in ternary alloy Mo(Si1â^'x,Alx)2. Applied Physics Letters, 2011, 98, 101903.	1.5	5
11297	Adhesion of TiC/Fe Cermet Interface with C Vacancy: A First-Principles Study. Advanced Materials Research, 0, 415-417, 368-371.	0.3	1
11298	Electronic structure and transport properties of single and double filled CoSb3 with atoms Ba, Yb and In. Journal of Applied Physics, 2011, 109, 113723.	1.1	18
11299	Noble gases on metal surfaces: Insights on adsorption site preference. Physical Review B, 2011, 84, .	1.1	33
11300	Neutron scattering andÎ¼SR investigations of quasi-one-dimensional magnetism in the spin=3/2compound Li3RuO4. Physical Review B, 2011, 84, .	1.1	9
11301	spingap opening accompanied by a strong magnetoelastic response in the<mml:math xmlns:mml="http://www.w3.org/1998/Math/MathML" display="inline"><mml:mrow><mml:mi>S</mml:mi><mml:mo>=</mml:mo><mml:mn>1</mml:mn></mml:mrow></mml:math>magnetic dimer system Ba<mml:math xmlns:mml="http://www.w3.org/1998/Math/MathML" display="inline"><mml:msub><mml:mrow /><mml:mn>3</mml:mn></mml:msub></mml:math>RuO<mml:math xmlns:mml="http://www.w3.org/1998/Math/MathML"	1.1	30
11302	Electronic versus Lattice Match for Metal-Semiconductor Epitaxial Growth: Pb on Ge(111). Physical Review Letters, 2011, 107, 066802.	2.9	20
11303	Computationally driven experimental discovery of the CeIr<mml:math xmlns:mml="http://www.w3.org/1998/Math/MathML" display="inline"><mml:mrow><mml:msub><mml:mrow /><mml:mrow><mml:mn>4</mml:mn></mml:mrow></mml:msub></mml:mrow></mml:math>In compound. Physical Review B, 2011, 83, .	1.1	12
11304	Commensurate-incommensurate phase transition in bilayer graphene. Physical Review B, 2011, 84, .	1.1	86
11305	van der Waals interactions in the ground state of Mg(BH<mml:math) Tj ETQq1 1 0.784314 rgBT /Overlock 10 Tf 50 407 Td (xmlns:mml="http://www.w3.org/1998/Math/MathML" display="inline"><mml:mrow><mml:msub><mml:mrow />	1.1	47
11306	Finite Volume Discretizations for Eigenvalue Problems with Applications to Electronic Structure Calculations. Multiscale Modeling and Simulation, 2011, 9, 208-240.	0.6	16
11307	First-principles prediction of the thermodynamic stability of xenon in monoclinic, tetragonal, and yttrium-stabilized cubic ZrO<mml:math xmlns:mml="http://www.w3.org/1998/Math/MathML" display="inline"><mml:mrow><mml:msub><mml:mrow /><mml:mrow><mml:mn>2</mml:mn></mml:mrow></mml:msub></mml:mrow></mml:math>. Physical Review B, 2011, 83, .	1.1	14
11308	The dynamical process of the phase transition from VO2(M) to VO2(R). Journal of Applied Physics, 2011, 110, .	1.1	20
11309	The effect of doping on the energetics and quantum conductance in graphene nanoribbons with a metallocene adsorbate. Journal of Chemical Physics, 2011, 135, 124708.	1.2	13
11310	Free energy of defect formation: Thermodynamics of anion Frenkel pairs in indium oxide. Physical Review B, 2011, 83, .	1.1	24
11311	First-principles study of dislocations in hcp metals through the investigation of the (<mml:math) Tj ETQq1 1 0.784314 rgBT /Overlock 10 twin boundary. Physical Review B, 2011, 84, .	1.1	49
11312	Mechanical properties of clusters in quasicrystal approximants: The example of the 1/1 Al-Cu-Fe approximant. Physical Review B, 2011, 84, .	1.1	1
11313	superconducting gap function in the organic superconductor (TMTSF)<mml:math xmlns:mml="http://www.w3.org/1998/Math/MathML" display="inline"><mml:mrow><mml:msub><mml:mrow /><mml:mrow><mml:mn>2</mml:mn></mml:mrow></mml:msub></mml:mrow></mml:math>ClO<mml:math xmlns:mml="http://www.w3.org/1998/Math/MathML" display="inline"><mml:mrow><mml:msub><mml:mrow /><mml:mrow><mml:mn>4</mml:mn></mml:mro	1.1	23

#	Article	IF	Citations
11314	Î±-iron facet with enhanced carbon mobility. Physical Review B, 2011, 83, .	1.1	4
11315	First-principles investigation of the very large perpendicular magnetic anisotropy at Fe<mml:math xmlns:mml="http://www.w3.org/1998/Math/MathML" display="inline"><mml:mrow><mml:mo>|</mml:mo></mml:mrow></mml:math>MgO and Co<mml:math xmlns:mml="http://www.w3.org/1998/Math/MathML" display="inline"><mml:mrow><mml:mo>|</mml:mo></mml:mrow></mml:math>MgO interfaces.	1.1	545
11316	Soft and isotropic phonons in PrFeAsO<mml:math xmlns:mml="http://www.w3.org/1998/Math/MathML" display="inline"><mml:msub><mml:mrow /><mml:mrow><mml:mn>1</mml:mn><mml:mo>â^'</mml:mo><mml:mi>y</mml:mi></mml:mrow></mml:msub></mml:math>. Physical Review B, 2011, 84, .	1.1	19
11317	First-Principles Calculations of the Urbach Tail in the Optical Absorption Spectra of Silica Glass. Physical Review Letters, 2011, 106, 027401.	2.9	53
11318	Origin of<mml:math xmlns:mml="http://www.w3.org/1998/Math/MathML" display="inline"><mml:mrow><mml:mi>p</mml:mi></mml:mrow></mml:math>-type conductivity in layered<mml:math xmlns:mml="http://www.w3.org/1998/Math/MathML" display="inline"><mml:mrow><mml:mi>n</mml:mi></mml:mrow></mml:math>GeTe<mml:math xmlns:mml="http://www.w3.org/1998/Math/MathML" display="inline"><mml:mrow><mml:mi>n</mml:mi></mml:mrow></mml:math>	1.1	41
11319	TiPO<mml:math xmlns:mml="http://www.w3.org/1998/Math/MathML" display="inline"><mml:mrow><mml:msub><mml:mrow /><mml:mrow><mml:mn>4</mml:mn></mml:mrow></mml:msub></mml:mrow></mml:math>featuring large intrachain coupling. Physical Review B, 2011, 83, .	1.1	32
11320	Ultrastiffness and metallicity of rhenium nitrides. Journal of Applied Physics, 2011, 109, .	1.1	15
11321	First-principles study of the solid solution of hydrogen in lanthanum. Physical Review B, 2011, 84, .	1.1	5
11322	First-principles study on oxidation effects in uranium oxides and high-pressure high-temperature behavior of point defects in uranium dioxide. Physical Review B, 2011, 84, .	1.1	32
11323	Magnetic Nanostructures by Adaptive Twinning in Strained Epitaxial Films. Physical Review Letters, 2011, 107, 206105.	2.9	27
11324	Crystalline diborane at high pressures. Physical Review B, 2011, 84, .	1.1	40
11325	Synthesis and properties of platinum hydride. Physical Review B, 2011, 83, .	1.1	75
11326	Relative Isomer Abundance of Fullerenes and Carbon Nanotubes Correlates with Kinetic Stability. Physical Review Letters, 2011, 107, 175506.	2.9	18
11327	Ab initiostudy of point defects in the strongly correlated system CoO. Physical Review B, 2011, 84, .	1.1	13
11328	Molecular ordering of glycine on Cu(100): Thep(2Ã—4) superstructure. Physical Review B, 2011, 84, .	1.1	3
11329	Hybrid density functional study of oligothiophene/ZnO interface for photovoltaics. Physical Review B, 2011, 83, .	1.1	28
11330	Dependence of magnetism on GdFeO<mml:math xmlns:mml="http://www.w3.org/1998/Math/MathML" display="inline"><mml:mrow><mml:msub><mml:mrow /><mml:mrow><mml:mn>3</mml:mn></mml:mrow></mml:msub></mml:mrow></mml:math>distortion in the<mml:math xmlns:mml="http://www.w3.org/1998/Math/MathML" display="inline"><mml:mrow><mml:msub><mml:mi>t</mml:mi><mml:mrow><mml:mn>2</mml:mn><mml:mi>g</mml:mi></mml:mrow> xmlns:mml="http://www.w3.org/1998/Math/MathML" display="inline"><mm. Physical Review B, 2011, 83, .	1.1	29
11331	Diamond membrane surface after ion-implantation-induced graphitization for graphite removal: Molecular dynamics simulation. Physical Review B, 2011, 83, .	1.1	16

#	Article	IF	Citations
11332	Local hydroxyl adsorption geometry on TiO<mml:math xmlns:mml="http://www.w3.org/1998/Math/MathML" display="inline"><mml:msub><mml:mrow /><mml:mn>2</mml:mn></mml:msub></mml:math>(110). Physical Review B, 2011, 84, .	1.1	9
11333	Fermi level pinning by integer charge transfer at electrode-organic semiconductor interfaces. Applied Physics Letters, 2011, 98, 113303.	1.5	42
11334	Compositional effects on the electronic structure of ZnSe1â^'xSx ternary quantum dots. Applied Physics Letters, 2011, 99, .	1.5	5
11335	Surface structures of complex intermetallic compounds: An<mml:math xmlns:mml="http://www.w3.org/1998/Math/MathML" display="inline"><mml:mrow><mml:mtext mathvariant="bold">a</mml:mtext><mml:mtext>b</mml:mtext><mml:mspace width="4.pt" /><mml:mtext>initio</mml:mtext></mml:mrow></mml:math>DFT study for the (100) surface of o-Al<mml:math xmlns:mml="http://www.w3.org/1998/Math/MathML" display="inline"><mml:msub><mml:mrow /><mml:mn>13</mml:mn></mml:msub></mml:math>Co<mml:ma	1.1	20
11336	Diffusion of Ag alongÎ£3 grain boundaries in 3C-SiC. Physical Review B, 2011, 84, .	1.1	44
11337	Ni(111)<mml:math xmlns:mml="http://www.w3.org/1998/Math/MathML" display="inline"><mml:mo>	</mml:mo></mml:math>graphene<mml:math xmlns:mml="http://www.w3.org/1998/Math/MathML" display="inline"><mml:mrow><mml:mo>	</mml:mo><mml:mi>h</mml:mi></mml:mrow></mml:math>-BN junctions as ideal spin injectors. Physical Review B, 2011, 84, .	1.1	69
11338	Simulation of the surface structure of lithium manganese oxide spinel. Physical Review B, 2011, 83, .	1.1	104
11339	Theoretical study of the role of the tip in enhancing the sensitivity of differential conductance tunneling spectroscopy on magnetic surfaces. Physical Review B, 2011, 83, .	1.1	17
11340	Theoretical analysis of the crystal structure, band-gap energy, polarization, and piezoelectric properties of ZnO-BeO solid solutions. Physical Review B, 2011, 84, .	1.1	22
11341	Charge-driven ordering and ferroelectric polarization in multiferroic TbMn<mml:math xmlns:mml="http://www.w3.org/1998/Math/MathML" display="inline"><mml:mrow><mml:msub><mml:mrow /><mml:mrow><mml:mn>2</mml:mn></mml:mrow></mml:msub></mml:mrow></mml:math>O<mml:math xmlns:mml="http://www.w3.org/1998/Math/MathML"	1.1	19
11342	Energetics and kinetics of the<mml:math xmlns:mml="http://www.w3.org/1998/Math/MathML" display="inline"><mml:mrow><mml:mi>c</mml:mi></mml:mrow></mml:math>(<mml:math) Tj ETQq0 0 0 rgBT /Overlock 10 Tf 50 352		

#	Article	IF	Citations
11350	Enhancing ionic conductivity of bulk single-crystal yttria-stabilized zirconia by tailoring dopant distribution. Physical Review B, 2011, 83, .	1.1	34
11351	Blueshifting the Onset of Optical UV Absorption for Water under Pressure. Physical Review Letters, 2011, 106, 187403.	2.9	30
11352	Room-temperature diffusive phenomena in semiconductors: The case of AlGaN. Physical Review B, 2011, 84, .	1.1	32
11353	Effects of hydrostatic pressure on the electrical properties of hexagonal Ge2Sb2Te5: Experimental and theoretical approaches. Applied Physics Letters, 2011, 98, .	1.5	10
11354	Emergence of surface states in nanoscale Cu<mml:math xmlns:mml="http://www.w3.org/1998/Math/MathML" display="inline"><mml:mrow><mml:msub><mml:mrow /><mml:mrow><mml:mn>2</mml:mn></mml:mrow></mml:msub></mml:mrow></mml:math>N islands. Physical Review B, 2011, 83, .	1.1	14
11355	Magnetism of covalently functionalized carbon nanotubes. Applied Physics Letters, 2011, 99, .	1.5	9
11356	Effects of composition and compositional distribution on the electronic structure of ZnSe1â^'xTex ternary quantum dots. Journal of Applied Physics, 2011, 110, 123509.	1.1	3
11357	Stability and electronic structure of bilayer graphone. Applied Physics Letters, 2011, 98, .	1.5	13
11358	Orientational Ordering of Nonplanar Phthalocyanines on Cu(111): Strength and Orientation of the Electric Dipole Moment. Physical Review Letters, 2011, 106, 156102.	2.9	48
11359	First-principles study of defect properties of zinc blende MgTe. Physical Review B, 2011, 83, .	1.1	24
11360	Superconducting high-pressure phase of platinum hydride from first principles. Physical Review B, 2011, 84, .	1.1	47
11361	Undulating Slip in Laves Phase and Implications for Deformation in Brittle Materials. Physical Review Letters, 2011, 106, 165505.	2.9	46
11362	Nature of the band gap of<mml:math xmlns:mml="http://www.w3.org/1998/Math/MathML" display="inline"><mml:mrow><mml:msub><mml:mrow><mml:mi mathvariant="normal">Tl</mml:mi></mml:mrow><mml:mrow><mml:mn>2</mml:mn></mml:mrow></mml:msub><mml:mi mathvariant="normal">O</mml:mi><mml:msub><mml:mrow /><mml:mrow><mml:mn>3</mml:mn></mml:mrow></mml:msub></mml:mrow></mml:math>. Physical	1.1	39
11363	<mml:math xmlns:mml="http://www.w3.org/1998/Math/MathML" display="inline"><mml:mrow><mml:msub><mml:mi>R</mml:mi><mml:mrow><mml:mn>1</mml:mn><mml:mo>â^'</mml:mo><mml:		

#	Article	IF	Citations
11368	Orthorhombic fluctuations in tetragonal<mml:math xmlns:mml="http://www.w3.org/1998/Math/MathML" display="inline"><mml:mi>A</mml:mi></mml:math>Fe<mml:math xmlns:mml="http://www.w3.org/1998/Math/MathML" display="inline"><mml:msub><mml:mrow /><mml:mn>2</mml:mn></mml:msub></mml:math>As<mml:math xmlns:mml="http://www.w3.org/1998/Math/MathML" display="inline"><mml:msub><mml:mrow /><mml:mi>	1.1	9
11369	Nonlinear variations in the electronic structure of IIâ€“VI and IIIâ€“V wurtzite semiconductors with biaxial strain. Applied Physics Letters, 2011, 98, .	1.5	24
11370	Defect-Induced Magnetism in Neutron Irradiated 6<mml:math xmlns:mml="http://www.w3.org/1998/Math/MathML" display="inline"><mml:mi>H</mml:mi></mml:math>-SiC Single Crystals. Physical Review Letters, 2011, 106, 087205.	2.9	143
11371	Native defects in LiNH<mml:math xmlns:mml="http://www.w3.org/1998/Math/MathML" display="inline"><mml:mrow><mml:msub><mml:mrow /><mml:mrow><mml:mn>2</mml:mn></mml:mrow></mml:msub></mml:mrow></mml:math>: A first-principles study. Physical Review B, 2011, 84, .	1.1	19
11372	Room-temperature ferromagnetism in CrSi2(core)/SiO2(shell) semiconducting nanocables. Applied Physics Letters, 2011, 98, 193104.	1.5	12
11373	Structural, electronic, and dielectric properties of amorphous hafnium silicates. Journal of Applied Physics, 2011, 110, .	1.1	16
11374	Noncontact atomic force microscopy imaging of atomic structure and cation defects of the polar MgAl<mml:math xmlns:mml="http://www.w3.org/1998/Math/MathML" display="inline"><mml:msub><mml:mrow /><mml:mn>2</mml:mn></mml:msub></mml:math>O<mml:math xmlns:mml="http://www.w3.org/1998/Math/MathML" display="inline"><mml:msub><mml:mrow /><mml:mn>4</mml:mn></mml:msub></mml:math>(100) surface: Experiments and first-principles simula	1.1	15
11375	First-principles studies on the dominant acceptor and the activation mechanism of phosphorus-doped ZnO. Applied Physics Letters, 2011, 99, 111902.	1.5	17
11376	Modeling the iron oxides and oxyhydroxides for the prediction of environmentally sensitive phase transformations. Physical Review B, 2011, 83, .	1.1	64
11377	Doping-Enhanced Lithium Diffusion in Lithium-Ion Batteries. Physical Review Letters, 2011, 107, 118302.	2.9	7
11378	The trapping of N2 molecules and the reduction in its bonding length in Ge(001) due to N2+ ion implantation. Journal of Applied Physics, 2011, 109, .	1.1	4
11379	Computational materials design for high-<mml:math xmlns:mml="http://www.w3.org/1998/Math/MathML" display="inline"><mml:mrow><mml:msub><mml:mi>T</mml:mi><mml:mrow><mml:mi>c</mml:mi></mml:mrow></mml:msub></mml:mr	1.1	24
11380	Ultrathin (1Ã—2)-Sn layer on GaAs(100) and InAs(100) substrates: A catalyst for removal of amorphous surface oxides. Applied Physics Letters, 2011, 98, .	1.5	3
11381	A route to multiferroics by non-d 0 cation B in magnetic perovskites. Europhysics Letters, 2011, 96, 67012.	0.7	6
11382	The theoretical search for half-metallic material: The non-stoichiometric peroskite oxide Sr2FeCoO6â^'Î´. Applied Physics Letters, 2011, 99, .	1.5	20
11383	Interface model for HfO2 gate stack from first principles calculations and its application to nanoscale device simulations. Applied Physics Letters, 2011, 98, .	1.5	9
11384	Tailoring band gap in GaN sheet by chemical modification and electric field: Ab initio calculations. Applied Physics Letters, 2011, 98, .	1.5	105
11385	Capturing dynamic cation hopping in cubic pyrochlores. Applied Physics Letters, 2011, 99, .	1.5	10

#	Article	IF	Citations
11386	Fragile magnetic ground state and metal-insulator transitions in CaCrO3: The first-principles calculations. Journal of Applied Physics, 2011, 110, .	1.1	10
11387	First principles phase diagram calculations for the wurtzite-structure quasibinary systems SiC-AlN, SiC-GaN and SiC-InN. Journal of Applied Physics, 2011, 110, .	1.1	24
11388	Electronic structural and electrochemical properties of lithium zirconates and their capabilities of CO2 capture: A first-principles density-functional theory and phonon dynamics approach. Journal of Renewable and Sustainable Energy, 2011, 3, .	0.8	51
11389	Piezoelectrics by design: A route through short-period Perovskite superlattices. Journal of Applied Physics, 2011, 109, .	1.1	5
11390	Unified cluster expansion method applied to the configurational thermodynamics of cubic Ti<mml:math xmlns:mml="http://www.w3.org/1998/Math/MathML" display="inline"><mml:mrow><mml:msub><mml:mrow /><mml:mrow><mml:mn>1</mml:mn><mml:mo>â^'</mml:mo><mml:mi>x</mml:mi></mml:mrow></mml:msub><mml:m xmlns:mml="http://www.w3.org/1998/Math/MathML" display="inline"><mml:mrow><mml:msub><mml:mrow /><mml:mrow><mml:mi>x</mml:mi></mml:mrow	1.1	38
11391	Electronic structure, vibrational spectrum, and thermal properties of yttrium nitride: A first-principles study. Journal of Applied Physics, 2011, 109, 073720.	1.1	49
11392	Accurate and efficient algorithm for Bader charge integration. Journal of Chemical Physics, 2011, 134, 064111.	1.2	1,393
11393	Theory of surface segregation in ternary semiconductor quantum dots. Applied Physics Letters, 2011, 98, .	1.5	13
11394	Anomalous structural transformation, spontaneous polarization, piezoelectric response, and band structure of semiconductor aluminum nitride under hydrostatic pressure. Journal of Applied Physics, 2011, 110, 103712.	1.1	14
11395	Theoretical study of C₆₀as catalyst for dehydrogenation in LiBH₄. Nanotechnology, 2011, 22, 335401.	1.3	24
11396	Combined electron beam imaging and ab initio modeling of T1 precipitates in Alâ€“Liâ€“Cu alloys. Applied Physics Letters, 2011, 98, .	1.5	104
11397	Tailoring electronic properties of InAs nanowires by surface functionalization. Journal of Applied Physics, 2011, 110, 103713.	1.1	13
11398	Improved calculation of vacancy properties in Ge using the Heyd-Scuseria-Ernzerhof range-separated hybrid functional. Journal of Applied Physics, 2011, 110, .	1.1	19
11399	Reaction mechanisms of thermal atomic oxygen interaction with organosilicate low k dielectric materials from ab initio molecular dynamics simulations. Journal of Vacuum Science and Technology A: Vacuum, Surfaces and Films, 2011, 29, .	0.9	10
11400	Notice of Violation of IEEE Publication Principles - The first principles study on the effects of alloying element on elastic properties of Ni. , 2011, , .		0
11401	CO2 adsorption on TiO2(101) anatase: A dispersion-corrected density functional theory study. Journal of Chemical Physics, 2011, 135, 124701.	1.2	119
11402	Multiphonon hole trapping from first principles. Journal of Vacuum Science and Technology B:Nanotechnology and Microelectronics, 2011, 29, 01A201.	0.6	29
11403	Novel hexagonal polytypes of silver: growth, characterization and first-principles calculations. Journal of Physics Condensed Matter, 2011, 23, 325401.	0.7	34

#	Article	IF	Citations
11404	Structure and X-ray powder reference patterns for hexagonal perovskite-related phases, (Sr_{0.8}Ca_{0.2})₅Co₄O₁₂ and Sr₆Co₅O₁₅. Powder Diffraction, 2011, 26, 22-30.	0.4	29
11405	A computational study of the molecular and crystal structure and selected physical properties of octahydridosilasequioxaneâ€"(Si₂O₃H₂)₄. I. Electronic and structural aspects. Proceedings of the Royal Society A: Mathematical, Physical and Engineering Sciences, 2011, 467, 928-953.	1.0	9
11406	The Configuration and Evolution of Ti-Si-N Island on TiN(<i>001</i>) Surface: <i>Ab Initio</i> Study. Advanced Materials Research, 0, 295-297, 301-306.	0.3	1
11407	Regarding the validity of the time-dependent Kohnâ€"Sham approach for electron-nuclear dynamics via trajectory surface hopping. Journal of Chemical Physics, 2011, 134, 024102.	1.2	178
11408	Magnetism Driven by Intrinsic Defect in GaN Nanowires. Advanced Materials Research, 2011, 236-238, 2160-2165.	0.3	0
11409	The Effect of Vacancy on the Phase Stability of TiNi Shape Memory Alloy from First-Principle Calculation. Materials Science Forum, 2011, 687, 528-532.	0.3	1
11410	First-Principle Calculations of the Electronic Structure and Elastic Constants of Arsenic Doped Î²-SiC. Materials Science Forum, 0, 704-705, 492-497.	0.3	0
11411	Theoretical Studies on P-Type Conduction in (S,Cu) Co-Doped ZnO. Advanced Materials Research, 2011, 306-307, 269-273.	0.3	1
11412	Thermodynamic and Elastic Properties of the Phases Appearing in the Lightweight La-Mg Alloys. Materials Science Forum, 2011, 690, 15-18.	0.3	1
11413	First-Principles Prediction of Optical Absorption Enhancement for Si Native Defect Clusters under Biaxial Strain. Electrochemical and Solid-State Letters, 2011, 14, P1.	2.2	0
11414	Electronic Structure of O-vacancy in High-k Dielectrics and Oxide Semiconductors. Materials Research Society Symposia Proceedings, 2011, 1370, 3.	0.1	0
11415	Mechanisms of Cr and H incorporation in stishovite determined by single-crystal EPR spectroscopy and DFT calculations. American Mineralogist, 2011, 96, 1331-1342.	0.9	8
11416	The Direct Oxidation of CO on the Highly Active Pt-Skin Pt₃Ni(111) Surface: a First Principles Study. Advanced Materials Research, 0, 213, 147-151.	0.3	0
11417	First-Principles Investigation of Structural, Elastic and Electronic Properties of Lanthanide Titanate Oxides Ln₂TiO₅. Materials Research Society Symposia Proceedings, 2011, 1298, 85.	0.1	4
11418	Synergistic effects on band gap-narrowing in titania by doping from first-principles calculations: density functional theory studies. Materials Research Society Symposia Proceedings, 2011, 1352, 9.	0.1	1
11419	First-Principles Modeling of Tungsten-Based Alloys for Fusion Power Plant Applications. Key Engineering Materials, 0, 465, 15-20.	0.4	16
11420	Influence of the Concentration of La High Doping on Conduction of ZnO. Advanced Materials Research, 0, 295-297, 1322-1325.	0.3	0
11421	Energetics and Properties of Vacancies, Anti-Sites, and Atomic Defects (B, C, and N) in Ductile B2-YM (M=Ag, Cu, Rh) Intermetallics. Materials Science Forum, 0, 689, 91-94.	0.3	2

#	Article	IF	Citations
11422	The dissociative chemisorption of methane on Ni(100): Reaction path description of mode-selective chemistry. Journal of Chemical Physics, 2011, 135, 114701.	1.2	113
11423	Elastic and Electronic Properties of Mg₂Ca and Mg₂Y Phases. Advanced Materials Research, 0, 233-235, 2231-2238.	0.3	3
11424	First Principles Analysis of Ultra-Thin Silicon Films with Dimer Structures. Materials Research Society Symposia Proceedings, 2011, 1370, 89.	0.1	0
11425	Thermodynamics of Oxygen Chemistry on PbTiO3 and LaMnO3 (001) Surfaces. Materials Research Society Symposia Proceedings, 2011, 1309, 151.	0.1	0
11426	First principles study of electronic structures of dopants in Mg2Si. Materials Research Society Symposia Proceedings, 2011, 1329, 1.	0.1	5
11427	Ab-initio modeling of Fe-Mn based alloys and nanoclusters. Materials Research Society Symposia Proceedings, 2011, 1296, 1.	0.1	0
11428	Effect of Sn and Nb on generalized stacking fault energy surfaces in zirconium and gamma hydride habit planes. Philosophical Magazine, 2011, 91, 1665-1678.	0.7	20
11429	Magnetic and structural properties of nanocrystalline PrCo₃. Journal of Physics: Conference Series, 2011, 303, 012028.	0.3	9
11430	First-principles Study of Defect Migration in RE-doped Ceria (RE = Pr, Gd). Materials Research Society Symposia Proceedings, 2011, 1311, 15801.	0.1	0
11431	Theoretical investigation of Er-O co-doping in hexagonal GaN. Materials Research Society Symposia Proceedings, 2011, 1342, 73.	0.1	1
11432	Theoretical Hardness of Zr ₃ N ₄ Films. Chinese Physics Letters, 2011, 28, 076102.	1.3	5
11433	First-principles study of electronic properties and stability of Nb₅SiB₂(001) surface. Chinese Physics B, 2011, 20, 037101.	0.7	6
11434	Structural and Electronic Properties of Sulfur-Passivated InAs(001) (2Ã—6) Surface. Chinese Physics Letters, 2011, 28, 086802.	1.3	3
11435	First-principles studies of Mn-doped LiCoPO ₄. Chinese Physics B, 2011, 20, 018201.	0.7	11
11436	A density functional theory study of structural, mechanical and electronic properties of crystalline phosphorus pentoxide. Journal of Chemical Physics, 2011, 135, 234513.	1.2	14
11437	Crystalline Inâ€“Gaâ€“Znâ€“O Density of States and Energy Band Structure Calculation Using Density Function Theory. Japanese Journal of Applied Physics, 2011, 50, 091102.	0.8	14
11438	Quantitative Advances in the Zintlâ€“Klemm Formalism. Structure and Bonding, 2011, , 1-55.	1.0	54
11439	Effects of Mg Addition on Thickness of Galvalume Coating: A First-Principles Study. Advanced Materials Research, 0, 291-294, 125-128.	0.3	1

#	Article	IF	Citations
11440	Surface alloy formation of noble adatoms adsorbed on Si(111)-sqrt {3}imes sqrt {3} â€“Pb surface: a first-principles study. Journal of Physics Condensed Matter, 2011, 23, 265001.	0.7	3
11441	Anisotropic Permittivity of Tetragonal BaTiO₃: A First-Principles Study. Japanese Journal of Applied Physics, 2011, 50, 09NE02.	0.8	17
11442	First Principles Study of Ideal Composites Reinforced by Coherent Nano-Fibres. Key Engineering Materials, 0, 465, 73-76.	0.4	3
11443	Synergy Effect of Ce/N Co-Doping on Anatase TiO₂ Photocatalysts from First Principles Calculation. Materials Science Forum, 2011, 675-677, 1045-1048.	0.3	0
11445	Theoretical Study of the Effect of Ca Doping on the Electronic Properties of LiCoO₂. Advanced Materials Research, 0, 415-417, 1643-1646.	0.3	2
11446	Ab initio Study of the Hydrogen Molecule on ZnO Surfaces. Materials Research Society Symposia Proceedings, 2011, 1327, 80401.	0.1	0
11447	Hydrogen Atom Adsorption on Î±-Al₂O₃(0001) Surface from First Principles. Advanced Materials Research, 2011, 399-401, 2261-2265.	0.3	2
11448	Theoretical Investigation on Microstructure of the Novel 24R-Type LPSO Phase in Mg₉₇Zn₁Y₂ Alloy. Advanced Materials Research, 0, 233-235, 2359-2366.	0.3	0
11449	Theoretical Study of the Effect of (F, Li) Codoping on P-Type Tendency in ZnO. Advanced Materials Research, 2011, 189-193, 1660-1663.	0.3	1
11450	Density Functional Theory Calculations of Properties of the Grain Boundaries in Aluminum. Materials Research Society Symposia Proceedings, 2011, 1297, 155.	0.1	3
11451	The Electronic and Magnetic Properties of Chemically Decorated Boron Nitride Sheet. Applied Mechanics and Materials, 2011, 130-134, 1439-1443.	0.2	0
11452	Computational Studies of the NiTi Alloy System: Bulk, Supercell, and Surface Calculations. Materials Research Society Symposia Proceedings, 2011, 1295, 15.	0.1	3
11453	Phase separation and surface segregation in ceriaâ€“zirconia solid solutions. Proceedings of the Royal Society A: Mathematical, Physical and Engineering Sciences, 2011, 467, 1925-1938.	1.0	45
11454	The Influence of Alloying Elements on Grain Boundary and Bulk Cohesion in Aluminum Alloys: Ab Initio Study. Advanced Materials Research, 2011, 409, 417-422.	0.3	1
11455	Ab Initio Studies of Nb Doping Effect on the Formation and Diffusion of Oxygen Vacancy and Ti Interstitial in Rutile TiO₂. Advanced Materials Research, 2011, 304, 142-147.	0.3	1
11456	A density functional theory study of the electronic structures and magnetic properties of Fe (1â^' x) Co x alloy nanowires encapsulated in (10,0) carbon nanotubes. Chinese Physics B, 2011, 20, 127302.	0.7	4
11457	Low temperature CVD growth of graphene nano-flakes directly on high K dielectrics. Materials Research Society Symposia Proceedings, 2011, 1284, 19.	0.1	2
11458	Alkaline-Earth and Rare-Earth Elements and Oxygen Vacancy in BaTiO₃: Analyses by First-Principles Calculations and EXAFS. Key Engineering Materials, 2011, 485, 23-26.	0.4	3

#	Article	IF	Citations
11459	Valence-band electronic structure of iron phthalocyanine: An experimental and theoretical photoelectron spectroscopy study. Journal of Chemical Physics, 2011, 134, 074312.	1.2	53
11460	First principles study of defects in solid electrolyte lithium thiophosphate Li7P3S11. Materials Research Society Symposia Proceedings, 2011, 1331, 50501.	0.1	0
11461	First principles study of segregation to the Î£5(310) grain boundary of cubic zirconia. Journal of Physics Condensed Matter, 2011, 23, 085005.	0.7	5
11462	High-pressure theoretical and experimental study of HgWO4. High Pressure Research, 2011, 31, 58-63.	0.4	1
11463	The use of dispersion-corrected DFT calculations to prevent an incorrect structure determination from powder data: the case of acetolone, C₁₁H₁₁N₃O₃. Zeitschrift FÃ¼r Kristallographie, 2011, 226, 476-482.	1.1	9
11464	Effect of biaxial strain on half-metallicity of transition metal alloyed zinc-blende ZnO and GaAs: a first-principles study. Journal Physics D: Applied Physics, 2011, 44, 205002.	1.3	5
11465	Contrast and Synergy between Electrocatalysis and Heterogeneous Catalysis. Advances in Physical Chemistry, 2011, 2011, 1-18.	2.0	23
11466	Study of Silicon-metal Interaction in Adsorption Process: An Ab-initio Approach. Materials Research Society Symposia Proceedings, 2011, 1305, 1.	0.1	0
11467	Structural, Electronic and Defect Properties of Cu2ZnSn(S,Se)4 Alloys. Materials Research Society Symposia Proceedings, 2011, 1370, 55.	0.1	5
11468	Combined inelastic neutron scattering and solid-state density functional theory study of dynamics of hydrogen atoms in muscovite 2M1. American Mineralogist, 2011, 96, 301-307.	0.9	5
11469	Tuning of the periodicity of stable self-organized metallic templates. Chinese Physics B, 2011, 20, 020513.	0.7	0
11470	First-principles study of CO oxidation on bismuth-promoted Pt(111) surfaces. Molecular Simulation, 2011, 37, 648-658.	0.9	8
11471	Control of carbon nanotube handedness using a supramolecular chiral surface. Journal of Chemical Physics, 2011, 135, 154703.	1.2	3
11472	Localised Phonon Modes at LiNbO₃(0001) Surfaces. Ferroelectrics, 2011, 419, 1-8.	0.3	11
11473	Effect of Lithium Absorption at Tetrahedral Site and Isomorphic Substitution on Montmorillonite Properties: A Density Functional Theory Study. Japanese Journal of Applied Physics, 2011, 50, 055701.	0.8	5
11474	Structural stability and electronic properties of the new superconductor (Ca₄Al₂O_{6 â^' x})(Fe₂As₂) from first-principles study. Superconductor Science and Technology, 2011, 24, 105014.	1.8	4
11475	Theoretical Studies of Structure and Doping of Hydrogenated Amorphous Silicon. Materials Research Society Symposia Proceedings, 2011, 1321, 297.	0.1	4
11476	Effect of impurities on structural, cohesive and magnetic properties of grain boundaries in Î±-Fe. Modelling and Simulation in Materials Science and Engineering, 2011, 19, 025001.	0.8	56

#	Article	IF	Citations
11477	Adsorption and Diffusion of Li and Ni on Graphene with Boron Substitution for Hydrogen Storage: Ab-initio Method. Japanese Journal of Applied Physics, 2011, 50, 06GJ02.	0.8	2
11478	Reactive Ability and Bong Strength Analysis on Al(OH)₃ Crystals with Three Different Crystalline. Advanced Materials Research, 0, 396-398, 614-619.	0.3	0
11479	Structural, electronic, and magnetic properties of CrN under high pressure. Chinese Physics B, 2011, 20, 077102.	0.7	10
11480	<i>Ab Initio</i> Calculations of Kinetic Properties in ZrC and TiC Carbides. Solid State Phenomena, 0, 172-174, 990-995.	0.3	12
11481	Vacancy and H Interactions in Nb. Chinese Physics Letters, 2011, 28, 127101.	1.3	4
11482	Self-standing nanoribbons of antimony selenide and antimony sulfide with well-defined size and band gap. Nanotechnology, 2011, 22, 175705.	1.3	39
11483	A simple molecular mechanics potential for Î¼m scale graphene simulations from the adaptive force matching method. Journal of Chemical Physics, 2011, 134, 184704.	1.2	51
11484	Ab initio studies on the mechanic and magnetic properties of PdH x. Chinese Physics B, 2011, 20, 026201.	0.7	7
11485	Excess of boron in TiB₂ superhard thin films: a combined experimental and ab initio study. Journal Physics D: Applied Physics, 2011, 44, 385402.	1.3	39
11486	Effect of Doping on the Thermoelectric Properties of Thallium Tellurides Using First Principles Calculations. Solid State Phenomena, 0, 172-174, 985-989.	0.3	2
11487	Occupation and Magnetic Property of Cr Additive in L1₀ FePt: First-Principle Study. Materials Science Forum, 2011, 689, 235-238.	0.3	0
11488	Electronic Excitation Induced Solid-State Amorphization in Ge-Sb-Te Alloy. Materials Research Society Symposia Proceedings, 2011, 1370, 77.	0.1	0
11489	Study on Electronic Structure and Optical Property of Silicon Doped with Transition Metal by First Principles. Advanced Materials Research, 0, 217-218, 930-935.	0.3	2
11490	A strong ferroelectric ferromagnet created by means of spinâ€“lattice coupling. Nature, 2011, 476, 114-114.	13.7	183
11491	Platinum metal silicides and germanides: superconductivity in non-centrosymmetric intermetallics. Journal of Physics: Conference Series, 2011, 273, 012078.	0.3	16
11492	Half metallicity and electronic structures in armchair BCN-hybrid nanoribbons. Journal of Chemical Physics, 2011, 134, 074708.	1.2	17
11493	Nanocatalyst structure as a template to define chirality of nascent single-walled carbon nanotubes. Journal of Chemical Physics, 2011, 134, 014705.	1.2	36
11494	Boron/nitrogen pairs Co-doping in metallic carbon nanotubes: a first-principle study. Chinese Physics B, 2011, 20, 027102.	0.7	7

#	Article	IF	Citations
11495	Electronic structures and thermodynamic stabilities of aluminum-based deuterides from first principles calculations. Chinese Physics B, 2011, 20, 017102.	0.7	2
11496	Atomic-scale insight and design principles for turbine engine thermal barrier coatings from theory. Proceedings of the National Academy of Sciences of the United States of America, 2011, 108, 5480-5487.	3.3	37
11497	On multiple adsorptions of hydrogen atoms on graphene. Physica Scripta, 2011, 84, 028108.	1.2	7
11498	Ammonia adsorption on iron phthalocyanine on Au(111): Influence on adsorbateâ€“substrate coupling and molecular spin. Journal of Chemical Physics, 2011, 134, 114710.	1.2	40
11499	Energy investigation of effects of O on mechanical properties of NiAl intermetallics. Journal of Physics Condensed Matter, 2011, 23, 025501.	0.7	9
11500	Ab-initiostudy of the electronic and elastic properties of beryllium chalcogenides BeX (X=S, Se and Te). Physica Scripta, 2011, 84, 035704.	1.2	25
11501	ELECTRON DOPING EFFECTS ON ELECTRONIC AND MAGNETIC PROPERTIES IN Sr2FeReO6. Modern Physics Letters B, 2011, 25, 2259-2267.	1.0	4
11502	Geometric and Electronic Structures at the Interface between Iron Phthalocyanine and Si (110). Chinese Physics Letters, 2011, 28, 116804.	1.3	3
11504	First principles theoretical study of the hole-assisted conversion of CO to CO2 on the anatase TiO2(101) surface. Journal of Chemical Physics, 2011, 134, 104701.	1.2	39
11505	First-principles study of Be doped CuAlS2 for p-type transparent conductive materials. Journal of Applied Physics, 2011, 109, .	1.1	10
11506	First-principles calculation of the elastic moduli of sheet silicates and their application to shale anisotropy. American Mineralogist, 2011, 96, 125-137.	0.9	92
11507	First Principles Calculations of Defect Formation in In-Free Photovoltaic Semiconductors Cu₂ZnSnS₄ and Cu₂ZnSnSe₄. Japanese Journal of Applied Physics, 2011, 50, 04DP07.	0.8	83
11508	Ferromagnetic interactions in hosted bipartite materialsâ€”generalized-double-exchange and generalized-superexchange interactions. Journal of Physics Condensed Matter, 2011, 23, 086004.	0.7	14
11509	A combined high-pressure experimental and theoretical study of the electronic band-structure of scheelite-type AWO4 (Aâ€‰=â€‰Ca, Sr, Ba, Pb) compounds. Journal of Applied Physics, 2011, 110, .	1.1	81
11510	Origins of dihydrogen binding to metal-inserted porphyrins: Electric polarization and Kubas interaction. Journal of Chemical Physics, 2011, 134, 234701.	1.2	6
11511	Conductivity and magnetic properties study on doped semiconductor material of 3C-SiC: A first-principle investigation. , 2011, , .		1
11512	Thermophysical properties for shock compressed polystyrene. Physics of Plasmas, 2011, 18, .	0.7	33
11513	Tailoring a two-dimensional electron gas at the LaAlO ₃ /SrTiO ₃ (001) interface by epitaxial strain. Proceedings of the National Academy of Sciences of the United States of America, 2011, 108, 4720-4724.	3.3	218

#	Article	IF	Citations
11514	ELASTIC AND THERMODYNAMIC PROPERTIES OF NiAl AND Ni3Al FROM FIRST-PRINCIPLES CALCULATIONS. International Journal of Modern Physics B, 2011, 25, 3623-3631.	1.0	14
11515	EFFECTS OF SULFUR SUBSTITUTIONAL IMPURITIES ON ZnO STRUCTURE USING DENSITY FUNCTIONAL THEORY. International Journal of Nanoscience, 2011, 10, 381-390.	0.4	1
11516	First-Principles Simulation on Piezoresistivity in Alpha and Beta Silicon Carbide Nanosheets. Japanese Journal of Applied Physics, 2011, 50, 06GE05.	0.8	30
11517	Size-dependent elastic properties of single-walled ZnO nanotubes: A first-principles study. Journal of Applied Physics, 2011, 109, .	1.1	11
11518	Interatomic potentials for mixed oxide and advanced nuclear fuels. Physical Review B, 2011, 83, .	1.1	25
11519	COMPUTATION OF INTERACTION POTENTIAL OF ADSORBATES ON ZIGZAG SWCNTs â€" APPLICATION TO FUNCTIONALIZATION AND HYDROGEN STORAGE. International Journal of Nanoscience, 2011, 10, 391-396.	0.4	10
11520	ELECTRONIC AND MAGNETIC STRUCTURE OF THE HIGH PRESSURE PHASE OF Li₂CuO₂. International Journal of Modern Physics B, 2011, 25, 3409-3414.	1.0	4
11521	Steric bulkiness of pyrrole substituents and the out-of-plane deformations of porphyrins: nickel(II) octaisopropylporphyrin and its meso-nitro derivative. Journal of Porphyrins and Phthalocyanines, 2011, 15, 727-741.	0.4	4
11522	Theoretical prediction of the growth and surface structure of Pt and Ni nanoparticles. Europhysics Letters, 2011, 96, 66005.	0.7	10
11523	Ab-initio aprroach to the electronic, structural, elastic, and finite-temperature thermodynamic properties of Ti2AX (Aâ€‰=â€‰Al or Ga and Xâ€‰=â€‰C or N). Journal of Applied Physics, 2011, 110, .	1.1	35
11524	The mechanical, electronic structure and thermodynamic properties of B2-based AgRE studied from first-principles. Physica Scripta, 2011, 83, 045301.	1.2	12
11525	SPIN-ORBIT COUPLING IN GRAPHENE UNDER UNIAXIAL STRAIN: TIGHT-BINDING APPROACH AND FIRST-PRINCIPLES CALCULATIONS. Modern Physics Letters B, 2011, 25, 823-830.	1.0	5
11526	On the p-type character of Cd-and Zn-doped InAs nanowires. Nanotechnology, 2011, 22, 265203.	1.3	11
11527	FIRST-PRINCIPLES CALCULATION OF THE ELECTRONIC STRUCTURE AND MAGNETISM AT THE GRAPHENE/Ni(111) INTERFACE. International Journal of Modern Physics B, 2011, 25, 2791-2800.	1.0	2
11528	Quantum molecular dynamic simulations of warm dense carbon monoxide. Journal of Chemical Physics, 2011, 135, 064501.	1.2	10
11529	Ab initiocharacterization of the electronic properties of PbTe quantum dots embedded in a CdTe matrix. Semiconductor Science and Technology, 2011, 26, 014005.	1.0	6
11530	Electronic structures of an epitaxial graphene monolayer on SiC(0001) after gold intercalation: a first-principles study. Nanotechnology, 2011, 22, 275704.	1.3	21
11531	Density functional investigations on structural and electronic properties of anionic and neutral sodium clusters Na_N(N= 40â€“147): comparison with the experimental photoelectron spectra. Journal of Physics Condensed Matter, 2011, 23, 405303.	0.7	5

#	Article	IF	Citations
11532	Band parameters and strain effects in ZnO and group-III nitrides. Semiconductor Science and Technology, 2011, 26, 014037.	1.0	56
11533	Theoretical studies on clean and adsorbed surfaces of Ag-In-Yb. Philosophical Magazine, 2011, 91, 2913-2919.	0.7	4
11534	First-Principles Studies for the Hydrogen Doping Effects on Iron-Based Superconductors. Journal of the Physical Society of Japan, 2011, 80, 073705.	0.7	8
11535	Calculations of the thermal conductivity of National Ignition Facility target materials at temperatures near 10 eV and densities near 10 g/cc using finite-temperature quantum molecular dynamics. Physics of Plasmas, 2011, 18, .	0.7	31
11536	First-principles study of low-index surfaces of the Al5Co2 complex metallic alloy. Philosophical Magazine, 2011, 91, 2894-2903.	0.7	6
11537	Effect of impurity atoms on Î±2/Î³ lamellar interfacial misfit in Tiâ€“Al alloy: a systematic first principles study. Philosophical Magazine, 2011, 91, 3685-3704.	0.7	7
11538	Lead adsorption on the Al₁₃Co₄(100) surface: heterogeneous nucleation and pseudomorphic growth. New Journal of Physics, 2011, 13, 103011.	1.2	17
11539	Ab initio investigations on the stability of seven-fold approximants. Philosophical Magazine, 2011, 91, 2567-2578.	0.7	10
11540	Platinum Monolayer Electrocatalysts for the Oxygen Reduction Reaction: Improvements Induced by Surface and Subsurface Modifications of Cores. Advances in Physical Chemistry, 2011, 2011, 1-16.	2.0	30
11541	Electronic Structure and Spin-Injection of Co-Based Heusler Alloy/ Semiconductor Junctions. Key Engineering Materials, 2011, 470, 54-59.	0.4	0
11542	Hydrogen Storage on Platinum-Decorated Carbon Nanotubes with Boron, Nitrogen Dopants or Sidewall Vacancies. Journal of Nano Research, 2011, 15, 29-40.	0.8	10
11543	Effect of alloying additions on the hydrogen-induced grain boundary embrittlement in iron. Journal of Physics Condensed Matter, 2011, 23, 015501.	0.7	24
11544	Site selectivity in the growth of copper islands on Au (111). New Journal of Physics, 2011, 13, 013044.	1.2	32
11545	Binding structures of propylene glycol stereoisomers on the Si(001)â˜2Ã—1 surface: A combined scanning tunneling microscopy and theoretical study. Journal of Chemical Physics, 2011, 134, 044704.	1.2	1
11546	First-principles study of void induced stresses at a diamond (100) grain boundary. Journal of Applied Physics, 2011, 109, 033518.	1.1	6
11547	Dimer pinning and the assignment of semiconductorâ€“adsorbate surface structures. Journal of Chemical Physics, 2011, 134, 064709.	1.2	4
11548	Structural and energetic origin of defects at the interface between germanium and a high-k dielectric from first principles. Applied Physics Letters, 2011, 98, 082904.	1.5	3
11549	First-principles investigation of the adsorption of the 2,5-pyridine di-carboxylic acid onto the Cu(011) surface. Journal of Chemical Physics, 2011, 134, 104708.	1.2	7

#	Article	IF	Citations
11550	Triplet states of zigzag edged hexagonal graphene molecules C6m**2H6m(m= 1, 2, 3, â€¦, 10) and carbon based magnetism. Journal of Chemical Physics, 2011, 134, 124706.	1.2	12
11551	Toward CH₄dissociation and C diffusion during Ni/Fe-catalyzed carbon nanofiber growth: A density functional theory study. Journal of Chemical Physics, 2011, 134, 134704.	1.2	30
11552	AX centers in II-VI semiconductors: Hybrid functional calculations. Applied Physics Letters, 2011, 98, .	1.5	18
11553	Fingerprints of the hydrogen bond in the photoemission spectra of croconic acid condensed phase: An x-ray photoelectron spectroscopy and ab-initio study. Journal of Chemical Physics, 2011, 134, 174505.	1.2	26
11554	Communication: Stable carbon nanoarches in the initial stages of epitaxial growth of graphene on Cu(111). Journal of Chemical Physics, 2011, 134, 171105.	1.2	80
11555	Rare earth chalcogenide Ce3Te4 as high efficiency high temperature thermoelectric material. Applied Physics Letters, 2011, 98, .	1.5	18
11556	The identification of a solvated electron pair in the gaseous clusters of Naâ^'(H2O)n and Liâ^'(H2O)n. Journal of Chemical Physics, 2011, 135, 064309.	1.2	5
11557	Isotopic effect on the vibrational lifetime of the carbon-deuterium stretch excitation on graphene. Journal of Chemical Physics, 2011, 135, 114506.	1.2	5
11558	Geometrical structure and spin order of Gd13 cluster. Journal of Chemical Physics, 2011, 135, 114512.	1.2	18
11559	C-N coupling on transition metal surfaces: A density functional theory study. Journal of Chemical Physics, 2011, 135, 124707.	1.2	4
11560	Density functional theory simulations of amorphous high-Îº oxides on a compound semiconductor alloy: a-Al2O3/InGaAs(100)-(4Ã—2), a-HfO2/InGaAs(100)-(4Ã—2), and a-ZrO2/InGaAs(100)-(4Ã—2). Journal of Chemical Physics, 2011, 135, 244705.	1.2	22
11561	First-principles study of structural stability, elastic, vibrational, and electronic properties of TaRu alloys. Europhysics Letters, 2011, 95, 18002.	0.7	0
11562	A hydronitrogen solid: high pressureab initioevolutionary structure searches. Journal of Physics Condensed Matter, 2011, 23, 022203.	0.7	21
11563	The effect of doping element Zr on anisotropy and microstructure of SmCo7â^'xZrx. Journal of Applied Physics, 2011, 109, 07A748.	1.1	12
11564	Electronic structures and optical properties of hexagonal boron nitride under hydrostatic pressures. Journal of Applied Physics, 2011, 109, 073708.	1.1	14
11565	Response of fcc metals andL1₂andD0₂₂type trialuminides to uniaxial loading along [100] and [001]:ab initioDFT calculations. Philosophical Magazine, 2011, 91, 491-516.	0.7	11
11566	First Principles Study on the Electronic Properties of Zn64Sb64â^'xTex Solid Solution (x = 0, 2, 3, 4). International Journal of Molecular Sciences, 2011, 12, 3162-3169.	1.8	7
11567	Design of Improved Metal-Organic Framework (MOF) H2 Adsorbents. Polymers, 2011, 3, 2133-2141.	2.0	8

#	Article	IF	Citations
11568	Memory and Spin Injection Devices Involving Half Metals. Journal of Nanomaterials, 2011, 2011, 1-6.	1.5	7
11569	Cell-constrained melt-quench simulation ofd-AlCoNi: Ni-rich versus Co-rich structures. Philosophical Magazine, 2011, 91, 2557-2566.	0.7	8
11570	Magnetism of two-dimensional triangular nanoflake-based kagome lattices. New Journal of Physics, 2012, 14, 033043.	1.2	18
11571	Assessment of correlation energies based on the random-phase approximation. New Journal of Physics, 2012, 14, 043002.	1.2	137
11572	The electronic and optical properties of warm dense nitrous oxide using quantum molecular dynamics simulations. Physics of Plasmas, 2012, 19, 112701.	0.7	3
11573	Al-Doped CuInSe₂: An <i>Ab Initio</i> Study of Structural and Electronic Properties of a Photovoltaic Material. Advanced Materials Research, 0, 512-515, 1543-1547.	0.3	1
11574	Magnetic behavior of Ba3Cu3Sc4O12. Journal of Physics Condensed Matter, 2012, 24, 236001.	0.7	15
11575	Formation Energy Calculations of Impurity Elements at Substitutional or Interstitial Sites in Silicon. Applied Mechanics and Materials, 0, 251, 431-435.	0.2	1
11576	Site Preference and Elastic Properties of 5d Transition Metals in Ductility YAg Alloys. Advanced Materials Research, 2012, 472-475, 1397-1401.	0.3	0
11577	Field Emission of Gallium-Doped Carbon Nanotubes. Advanced Materials Research, 2012, 535-537, 61-66.	0.3	0
11578	Structural, Electronic and Optical Properties of SiC Quantum Dots. Journal of Nano Research, 2012, 18-19, 77-87.	0.8	2
11579	A Possible New Parent Compound Sr4Al2O6Fe2As2 with High-TC Superconductivity. Journal of the Physical Society of Japan, 2012, 81, 024713.	0.7	4
11580	High Throughput Thin Film Pt-M Alloys for Fuel Electrooxidation: Low Concentrations of M (M = Sn,) Tj ETQq0 0 0 rgBT /Overlock 10 Tf 5 159, F880-F887.	1.3	16
11581	Nitric Oxide Adsorption and Dissociation on Nb(100) Surface. Journal of the Physical Society of Japan, 2012, 81, 044606.	0.7	2
11582	A first-principles density functional theory study of the electronic structural and thermodynamic properties of M2ZrO3 and M2CO3 (Mâ€‰=â€‰Na, K) and their capabilities for CO2 capture. Journal of Renewable and Sustainable Energy, 2012, 4, 013109.	0.8	25
11583	Ab Initio Study on the Structural and Magnetic Properties of Co-Pd and Co-Pt Linear and Zigzag Nanowires. Integrated Ferroelectrics, 2012, 136, 132-138.	0.3	1
11584	The effect of van der Waal's gap expansions on the surface electronic structure of layered topological insulators. New Journal of Physics, 2012, 14, 113030.	1.2	65
11585	Universal magnetic properties of sp³-type defects in covalently functionalized graphene. New Journal of Physics, 2012, 14, 043022.	1.2	87

#	Article	IF	Citations
11586	Spectroscopic evidence for spin-polarized edge states in graphitic Si nanowires. New Journal of Physics, 2012, 14, 103004.	1.2	21
11587	<i>Ab Initio</i> Calculation of Mechanical Properties of Stacking Fault in 3C-SiC: Effect of Stress and Doping. Materials Science Forum, 0, 717-720, 415-418.	0.3	2
11588	Different views on the electronic structure of nanoscale graphene: aromatic molecule versus quantum dot. New Journal of Physics, 2012, 14, 113008.	1.2	33
11589	Force and conductance during contact formation to a C₆₀molecule. New Journal of Physics, 2012, 14, 073032.	1.2	46
11590	Properties of Reaction Intermediates from Unzipping Nanotubes via the Diketone Formation: A Computational Study. Journal of Nanomaterials, 2012, 2012, 1-10.	1.5	2
11591	Multiscale Computational Model of Nitride Semiconductor Nanostructures. Advanced Materials Research, 2012, 560-561, 1133-1137.	0.3	0
11592	Twisted ZBâ€“CdTe/RSâ€“PbTe (111) heterojunction as a metastable interface structure. New Journal of Physics, 2012, 14, 113021.	1.2	13
11593	Ab initiostudy of Cu diffusion inÎ±-cristobalite. New Journal of Physics, 2012, 14, 113029.	1.2	16
11594	Advances in Electrocatalysis. Advances in Physical Chemistry, 2012, 2012, 1-4.	2.0	3
11595	Stability, interaction and influence of domain boundaries in Ge/Si(111)-5 Ã— 5. Journal of Physics Condensed Matter, 2012, 24, 445003.	0.7	3
11596	Surface structure and phase transition of K adsorption on Au(111): By ab initio atomistic thermodynamics. Journal of Chemical Physics, 2012, 136, 044510.	1.2	7
11597	Robust surface state of intrinsic topological insulator Bi₂Te₂Se thin films: a first-principles study. Journal of Physics Condensed Matter, 2012, 24, 035502.	0.7	17
11598	Magnetic Properties of Iron on Strained Graphene: Density Functional Theory Study. Japanese Journal of Applied Physics, 2012, 51, 06FD13.	0.8	0
11599	Effect of Electronegativity and Charge Balance on the Visible-Light-Responsive Photocatalytic Activity of Nonmetal Doped Anatase TiO₂. International Journal of Photoenergy, 2012, 2012, 1-8.	1.4	22
11600	C₆₀-mediated hydrogen desorption in Liâ€“Nâ€“H systems. Nanotechnology, 2012, 23, 485406.	1.3	5
11601	An unexpected softening from WB ₃ to WB ₄. Europhysics Letters, 2012, 98, 66004.	0.7	45
11602	Structure of the Al2Cu(001) and Al9Co2(001) surfaces: role of the covalent-like bonding network and off-stoichiometric effects. Materials Research Society Symposia Proceedings, 2012, 1517, 1.	0.1	1
11603	Density Functional Theory and <i>Ab Initio</i> Molecular Dynamics Study of the Effect of Ti and Zr Transition Metals in D0₃ Fe₃Al. Materials Science Forum, 0, 706-709, 1095-1099.	0.3	0

#	Article	IF	Citations
11604	Dissociation of water on Ti-decorated fullerene clusters. AIP Advances, 2012, 2, 012163.	0.6	3
11605	Influence of Synthesis Conditions on the Formation of a Kaolinitemethanol Complex and Simulation of its Vibrational Spectra. Clays and Clay Minerals, 2012, 60, 227-239.	0.6	46
11606	Crystal structures of (Mg _{1- x} ,Fe _x)SiO ₃ postperovskite at high pressures. Proceedings of the National Academy of Sciences of the United States of America, 2012, 109, 1035-1040.	3.3	15
11607	Application of Density Functional Theory to Point Defect Anelasticity of Carbon-Containing Austenitic Alloys. Solid State Phenomena, 2012, 184, 69-74.	0.3	0
11608	A reactive force field for lithiumâ€“aluminum silicates with applications to eucryptite phases. Modelling and Simulation in Materials Science and Engineering, 2012, 20, 015002.	0.8	51
11609	A computational study of the molecular and crystal structure and selected physical properties of octahydridosilasequioxane, (Si ₂ O ₃ H ₂) ₄ . II. Vibrational analysis. Proceedings of the Royal Society A: Mathematical, Physical and Engineering Sciences, 2012, 468, 851-870.	1.0	5
11610	Long-Range Interaction between H and (B or P) Dopant Atoms in Silicon Crystals Investigated by First Principles Calculation. Journal of the Electrochemical Society, 2012, 159, H450-H454.	1.3	1
11611	Anomalous Chemical Expansion Behavior of Pr_{0.2}Ce_{0.8}O_{2-Î´}Thin Films Grown by Pulsed Laser Deposition. Journal of the Electrochemical Society, 2012, 159, F799-F803.	1.3	19
11612	Identification of Niobium in 4H-SiC by EPR and <i>Ab Initio</i> Studies. Materials Science Forum, 0, 717-720, 217-220.	0.3	3
11613	Electronic effects on the melting of small gallium clusters. Journal of Chemical Physics, 2012, 137, 144307.	1.2	30
11614	Shallow donor levels enhanced ferromagnetism in the In 2 O 3 :Co nanocrystal. Europhysics Letters, 2012, 97, 57006.	0.7	9
11615	Effect of C doping on the structural and electronic properties of LiFePO ₄ : A first-principles investigation. Chinese Physics B, 2012, 21, 097401.	0.7	10
11616	A theoretical study of the reactivity of Cu2O(111) surfaces: the case of NO dissociation. Journal of Physics Condensed Matter, 2012, 24, 262001.	0.7	5
11617	Elastic properties of Nb-based alloys by using the density functional theory. Chinese Physics B, 2012, 21, 016202.	0.7	17
11618	Predicting active slip systems in Î²-Sn from ideal shear resistance. Modelling and Simulation in Materials Science and Engineering, 2012, 20, 035003.	0.8	32
11619	Theoretical predictions of a bucky-diamond SiC cluster. Nanotechnology, 2012, 23, 235705.	1.3	11
11620	Pulsed high harmonic generation of light due to pumped Bloch oscillations in noninteracting metals. Physica Scripta, 2012, T151, 014062.	1.2	5
11621	Theoretical Study of the Filling Fraction Limit of Fe-Substituted Ba-Filled Skutterudite <i>Ba_yFe_{4x}Co_{4-4x}Sb₁₂</i>. Key Engineering Materials, 0, 519, 169-173.		

#	Article	IF	Citations
11622	Ab initioinvestigation of the mechanical properties of copper. Chinese Physics B, 2012, 21, 096102.	0.7	11
11623	Strain effect on the diffusion of interstitial Mn in GaAs. Journal of Physics Condensed Matter, 2012, 24, 215801.	0.7	2
11624	Pt3 and Pt4 clusters on graphene monolayers supported on a Ni(111) substrate: Relativistic density-functional calculations. Journal of Chemical Physics, 2012, 137, 044710.	1.2	13
11625	Mechanical and electronic properties of novel tungsten nitride. Europhysics Letters, 2012, 100, 46001.	0.7	9
11626	Electronic structures and vibrational properties of coronene on Ru(0001): first-principles study. Chinese Physics B, 2012, 21, 036801.	0.7	4
11627	The Role of Na and Mg Doping on the Electronic Conductivity of LiFePO₄ : First-Principles Investigations. Advanced Materials Research, 0, 629, 64-69.	0.3	0
11628	Effect of Y and Zn Substitution on Tensile Properties of 6H-Type LPSO Phase in Mg₉₇Zn₁Y₂ Alloy. Advanced Materials Research, 0, 476-478, 2469-2475.	0.3	2
11629	Yellow-emitting Î³-Ca_2SiO_4:Ce^3+, Li^+ phosphor for solid-state lighting: luminescent properties, electronic structure, and white light-emitting diode application. Optics Express, 2012, 20, 2761.	1.7	76
11630	A first-principle investigation of antigorite up to 30 GPa: Structural behavior under compression. American Mineralogist, 2012, 97, 1177-1186.	0.9	14
11631	Models of Mixed Metal-Oxide Interfaces for Atomistic Materials Simulations. Materials Research Society Symposia Proceedings, 2012, 1444, 57.	0.1	0
11632	Graphene Electromechanical Actuation; Origins, Optimization and Applications. Materials Research Society Symposia Proceedings, 2012, 1407, 39.	0.1	0
11633	NO dissociation on Cu(111) and Cu₂O(111) surfaces: a density functional theory based study. Journal of Physics Condensed Matter, 2012, 24, 175005.	0.7	33
11634	Multi-Scale Modeling of Interstitial Dislocation Loop Growth in Irradiated Materials. Materials Research Society Symposia Proceedings, 2012, 1444, 37.	0.1	1
11635	Oscillation of the magnetic moment in modulated martensites in Ni2MnGa studied by ab initio calculations. Applied Physics Letters, 2012, 100, .	1.5	26
11636	Influence of the cluster dimensionality on the binding behavior of CO and O2 on Au13. Journal of Chemical Physics, 2012, 136, 024312.	1.2	19
11637	First Principles Investigation of Interaction of Oxygen with Low Index Surfaces of Î³-TiAl. Materials Science Forum, 0, 706-709, 1106-1114.	0.3	1
11638	JUPITER MODELS WITH IMPROVED AB INITIO HYDROGEN EQUATION OF STATE (H-REOS.2). Astrophysical Journal, 2012, 750, 52.	1.6	165
11639	First-Principles Investigation of Hexagonal WB2 Surfaces. Journal of the Physical Society of Japan, 2012, 81, 044712.	0.7	3

#	Article	IF	Citations
11640	Origin of magnetic anisotropy and spiral spin order in multiferroic BiFeO₃. Applied Physics Letters, 2012, 100, 242413.	1.5	29
11641	Understanding Cr segregation at the He bubble surface in Fe. Journal of Physics Condensed Matter, 2012, 24, 095009.	0.7	7
11642	First-principles investigations on the magnetic structure of Î±-NaMnO₂. Journal of Physics Condensed Matter, 2012, 24, 456002.	0.7	5
11643	First-principles calculation of structural, mechanical, magnetic and thermodynamic properties for Î³-M₂₃C₆(M = Fe, Cr) compounds. Journal of Physics Condensed Matter, 2012, 24, 505503.	0.7	34
11644	A First-Principles Study of the Ferroelectric Phase of AgNbO₃. Japanese Journal of Applied Physics, 2012, 51, 09LE02.	0.8	8
11645	Effect of high-pressure on the electronic and magnetic properties in double perovskite oxide Sr2FeMoO6. Journal of Applied Physics, 2012, 112, .	1.1	17
11646	Conductance of single-atom magnetic junctions: A first-principles study. Applied Physics Letters, 2012, 101, .	1.5	4
11647	Magnetic properties of Mn-doped Ge46and Ba8Ge46clathrates. Journal of Physics Condensed Matter, 2012, 24, 505501.	0.7	0
11648	Pt on graphene monolayers supported on a Ni(111) substrate: Relativistic density-functional calculations. Journal of Chemical Physics, 2012, 136, 074701.	1.2	17
11649	Electronic structure and elasticity of Z-phases in the Crâ€“Nbâ€“Vâ€“N system. Journal of Physics Condensed Matter, 2012, 24, 195502.	0.7	8
11650	Ab initiocalculation of strain effect on the magnetic properties of the thiogermanate [(CH₃)₄N]₂FeGe₄S₁₀. Journal of Physics Condensed Matter, 2012, 24, 245501.	0.7	4
11651	Band gap of Î²-PtO2 from first-principles. AIP Advances, 2012, 2, 022172.	0.6	22
11652	Transferable tight-binding potential for germanium. Journal of Physics Condensed Matter, 2012, 24, 305802.	0.7	8
11653	Self-Organized Nanostructures and High Blocking Temperatures in MgO-Based d^{0} Ferromagnets. Japanese Journal of Applied Physics, 2012, 51, 050201.	0.8	24
11654	Spin interactions in mineral libethenite series: evolution of low-dimensional magnetism. Journal of Physics Condensed Matter, 2012, 24, 436003.	0.7	1
11655	Ab-initio Study of Interactions of Gold Atoms with Hydroxylated MgO(001) Surfaces. Journal of the Physical Society of Japan, 2012, 81, 054601.	0.7	17
11656	First-principles study on the incipient oxidization of Nb(110). Journal of Physics Condensed Matter, 2012, 24, 225005.	0.7	5
11657	Helium, neon and argon diffraction from Ru(0001). Journal of Physics Condensed Matter, 2012, 24, 354002.	0.7	16

#	Article	IF	Citations
11658	First-principles study of nanometer-sharp domain walls in ferromagnetic Fe monolayers under in-plane strain. Journal of Physics Condensed Matter, 2012, 24, 095303.	0.7	3
11659	First-principles Study on Neutral Nitrogen Impurities in Zinc Oxide. Chinese Journal of Chemical Physics, 2012, 25, 48-52.	0.6	4
11660	Experimental and theoretical investigation of graphene layers on SiC(0001Â¯) in different stacking arrangements. Journal of Vacuum Science and Technology B:Nanotechnology and Microelectronics, 2012, 30, 03D117.	0.6	2
11661	First-principles study of the growth thermodynamics of Pt on SrTiO3 (001). Journal of Vacuum Science and Technology B:Nanotechnology and Microelectronics, 2012, 30, 04E108.	0.6	10
11662	Kinetics of the sulfur oxidation on palladium: A combined in situ x-ray photoelectron spectroscopy and density-functional study. Journal of Chemical Physics, 2012, 136, 094702.	1.2	19
11663	Theoretical model for artificial structure modulation of HfO2/SiOx/Si interface by deposition of a dopant material. Applied Physics Letters, 2012, 100, 092904.	1.5	3
11664	Rippled nanocarbons from periodic arrangements of reordered bivacancies in graphene or nanotubes. Journal of Chemical Physics, 2012, 136, 124705.	1.2	7
11665	Insight into the vertical detachment energy oscillation of NanC60â^' clusters. Journal of Chemical Physics, 2012, 136, 174314.	1.2	4
11666	Water dissociation on Cu (111): Effects of molecular orientation, rotation, and vibration on reactivity. Journal of Chemical Physics, 2012, 137, 094708.	1.2	29
11667	The origin of the conductivity maximum in molten salts. I. Bismuth chloride. Journal of Chemical Physics, 2012, 136, 124504.	1.2	16
11668	Helium mediated deposition: Modeling the Heâ^'TiO₂(110)-(1Ã—1) interaction potential and application to the collision of a helium droplet from density functional calculations. Journal of Chemical Physics, 2012, 136, 124703.	1.2	31
11669	Four-body interaction energy for compressed solid krypton from quantum theory. Journal of Chemical Physics, 2012, 137, 044108.	1.2	6
11670	Local atomic structure in equilibrium and supercooled liquid Zr75.5Pd24.5. Journal of Chemical Physics, 2012, 137, 044501.	1.2	26
11671	Density matrix treatment of non-adiabatic photoinduced electron transfer at a semiconductor surface. Journal of Chemical Physics, 2012, 137, 22A521.	1.2	15
11672	On the early stage of aluminum oxidation: An extraction mechanism via oxygen cooperation. Journal of Chemical Physics, 2012, 137, 094707.	1.2	42
11673	Validation of the reaction thermodynamics associated with NaSc(BH4)4 from first-principles calculations: Detecting metastable paths and identifying the minimum free energy path. Journal of Chemical Physics, 2012, 137, 084111.	1.2	4
11674	Effect of dispersion correction on the Au(1 1 1)-H2O interface: A first-principles study. Journal of Chemical Physics, 2012, 137, 114709.	1.2	49
11675	Uranyl ion interaction at the water/NiO(100) interface: A predictive investigation by first-principles molecular dynamic simulations. Journal of Chemical Physics, 2012, 137, 164701.	1.2	7

#	Article	IF	Citations
11676	Potential energy surface of H2O on Al{111} and Rh{111} from theoretical methods. Journal of Chemical Physics, 2012, 137, 204702.	1.2	11
11677	Electrically active Er doping in InAs, In0.53Ga0.47As, and GaAs. Applied Physics Letters, 2012, 101, .	1.5	2
11678	Structural, elastic, and vibrational properties of layered titanium dichalcogenides: A van der Waals density functional study. Journal of Chemical Physics, 2012, 137, 224509.	1.2	19
11679	Crystal field splitting and optical bandgap of hexagonal LuFeO3 films. Applied Physics Letters, 2012, 101, .	1.5	51
11680	A non-self-consistent range-separated time-dependent density functional approach for large-scale simulations. Journal of Physics Condensed Matter, 2012, 24, 205801.	0.7	20
11681	Diffusion and segregation of niobium in fcc-nickel. Journal of Physics Condensed Matter, 2012, 24, 095010.	0.7	15
11682	Ab-initio modeling of metastable precipitation processes in aluminum 7xxx alloys. International Journal of Materials Research, 2012, 103, 972-979.	0.1	6
11683	First principles study of the ternary complex model of EL2 defect in GaAs saturable absorber. Optics Express, 2012, 20, 6258.	1.7	25
11684	Templating of arrays of Ru nanoclusters by monolayer graphene/Ru MoirÃ©s with different periodicities. Journal of Physics Condensed Matter, 2012, 24, 314201.	0.7	11
11685	First principles study of Bismuth alloying effects in GaAs saturable absorber. Optics Express, 2012, 20, 11574.	1.7	20
11686	Predicting the acidity constant of a goethite hydroxyl group from first principles. Journal of Physics Condensed Matter, 2012, 24, 124105.	0.7	28
11687	Coexistence of spin glass and antiferromagnetic orders in Ba3Fe2.15W0.85O8.72. Journal of Physics Condensed Matter, 2012, 24, 206004.	0.7	3
11688	Epitaxial Fe films on ZnSe(001): effect of the substrate surface reconstruction on the magnetic anisotropy. Journal of Physics Condensed Matter, 2012, 24, 236006.	0.7	1
11689	Thermoelectric transport in strained Si and Si/Ge heterostructures. Journal of Physics Condensed Matter, 2012, 24, 275501.	0.7	27
11690	Acetylene on Cu(111): imaging a molecular surface arrangement with a constantly rearranging tip. Journal of Physics Condensed Matter, 2012, 24, 354005.	0.7	2
11691	Enhanced binding strength between metal nanoclusters and carbon nanotubes with an atomic nickel defect. Nanotechnology, 2012, 23, 205204.	1.3	11
11692	Non-contact atomic force microscopy study of hydroxyl groups on the spinel MgAl2O4(100) surface. Nanotechnology, 2012, 23, 325703.	1.3	19
11693	First-principles Study of Adsorption and Dissociation of Methanol on the Pt(100) Surface. Chinese Journal of Chemical Physics, 2012, 25, 199-203.	0.6	0

#	Article	IF	Citations
11694	Electronic structures of single-layer boron pnictides. Applied Physics Letters, 2012, 101, .	1.5	114
11695	Fermi level tuning using the Hf-Ni alloy system as a gate electrode in metal-oxide-semiconductor devices. Journal of Applied Physics, 2012, 112, .	1.1	12
11696	Hydrogen induced stabilization of meta-stable Mg-Ti. Applied Physics Letters, 2012, 100, 111902.	1.5	7
11697	Ferromagnetism and its stability in n-type Gd-doped GaN: First-principles calculation. Applied Physics Letters, 2012, 100, 232408.	1.5	20
11698	Correlation between local structure and electrical resistivity in gallium-antimony melts. Applied Physics Letters, 2012, 100, 171908.	1.5	1
11699	Kinetic behavior of nitrogen penetration into indium double layer improving the smoothness of InN film. Journal of Applied Physics, 2012, 111, .	1.1	7
11700	Mechanism of dangling bond elimination on As-rich InGaAs surface. , 2012, , .		3
11701	Spin-polarization of VGaON center in GaN and its application in spin qubit. Applied Physics Letters, 2012, 100, 192401.	1.5	25
11702	Quantum molecular dynamics simulations for the nonmetal-metal transition in fluid nitrogen oxide. Journal of Applied Physics, 2012, 112, 033501.	1.1	7
11703	Selection rule of preferred doping site for n-type oxides. Applied Physics Letters, 2012, 100, 262109.	1.5	10
11704	Self-assembly of C60 monolayer on epitaxially grown, nanostructured graphene on Ru(0001) surface. Applied Physics Letters, 2012, 100, .	1.5	42
11705	Strong current polarization and negative differential resistance in chiral graphene nanoribbons with reconstructed (2,1)-edges. Applied Physics Letters, 2012, 101, 073101.	1.5	15
11706	Migration mechanism for atomic hydrogen in porous carbon materials. Applied Physics Letters, 2012, 100, .	1.5	14
11707	Polymorphic phases of sp3-hybridized superhard CN. Journal of Chemical Physics, 2012, 137, 184506.	1.2	40
11708	Nanomodification of gold surface by picosecond soft x-ray laser pulse. Journal of Applied Physics, 2012, 112, .	1.1	44
11709	Pressure-induced phase transition and mechanical properties of molybdenum diboride: First principles calculations. Journal of Applied Physics, 2012, 112, .	1.1	11
11710	High pressure transport, structural, and first principles investigations on the fluorite structured intermetallic, PtAl2. Journal of Applied Physics, 2012, 111, .	1.1	2
11711	First principles study of the oxygen vacancy formation and the induced defect states in hafnium silicates. Journal of Applied Physics, 2012, 111, 074106.	1.1	14

#	Article	IF	Citations
11712	Low bias short channel impurity mobility in graphene from first principles. Applied Physics Letters, 2012, 101, 093102.	1.5	9
11713	Digital magnetic heterostructures based on GaN using GGA-1/2 approach. Applied Physics Letters, 2012, 101, .	1.5	18
11714	Conductive and ferromagnetic contributions of H in ZnCoO using H₂ hot isostatic pressure. Applied Physics Letters, 2012, 100, 112403.	1.5	18
11715	Electronic structure of buried Co-Cu interface studied with photoemission spectroscopy. Journal of Applied Physics, 2012, 112, 103702.	1.1	2
11716	Local-strain mapping on Ag(111) islands on Nb(110). Applied Physics Letters, 2012, 101, 063111.	1.5	10
11717	Structural properties and 4f â†' 5d absorptions in Ce-doped LuAlO₃: a first-principles study. Journal of Physics Condensed Matter, 2012, 24, 055502.	0.7	9
11718	ZnSnN2: A new earth-abundant element semiconductor for solar cells. , 2012, , .		13
11719	First-principles characterization of ferromagnetism in N-doped SrTiO3 and BaTiO3. Applied Physics Letters, 2012, 100, 062409.	1.5	44
11720	Reconstructions and electronic structure of (112Â¯2) and (112Â¯2Â¯) semipolar AlN surfaces. Journal of Applied Physics, 2012, 112, 033510.	1.1	7
11721	Disordered surface structure of an ultra-thin tin oxide film on Rh(100). Journal of Applied Physics, 2012, 111, 064907.	1.1	7
11722	Superconductivity in Defective Pyrite-Type Iridium Chalcogenides<mml:math xmlns:mml="http://www.w3.org/1998/Math/MathML" display="inline"><mml:msub><mml:mi>Ir</mml:mi><mml:mi>x</mml:mi></mml:msub><mml:msub><mml:mi>Ch</mml:mi><mml:mn>2	2.9	26
11723	2012, 109, 217002. Comment on â€œStability of the Bulk Phase of Layered ZnOâ€• Physical Review Letters, 2012, 108, 259601; discussion 259602.	2.9	11
11724	Observation of the hole state symmetry of MgB2 by inelastic scattering of fast electrons accompanied by boron K-shell excitation. Journal of Applied Physics, 2012, 112, 113920.	1.1	1
11725	Composition and crystallography dependence of the work function: Experiment and calculations of Pt-Al alloys. Physical Review B, 2012, 86, .	1.1	20
11726	Theoretical investigation of Fe substitution for Mn in complex hydride YMn2H6. Applied Physics Letters, 2012, 100, 021908.	1.5	10
11727	Electronic Correlations Stabilize the Antiferromagnetic Mott State in<mml:math xmlns:mml="http://www.w3.org/1998/Math/MathML" display="inline"><mml:msub><mml:mi>Cs</mml:mi><mml:mn>3</mml:mn></mml:msub><mml:msub><mml:mi mathvariant="bold">C</mml:mi><mml:mn>60</mml:mn></mml:msub></mml:math>. Physical Review Letters, 2012, 109, 166404.	2.9	8
11728	Influence of doping on the photoactive properties of magnetron-sputtered titania coatings: Experimental and theoretical study. Physical Review B, 2012, 86, .	1.1	23
11729	Observation of persistent centrosymmetricity in the hexagonal manganite family. Physical Review B, 2012, 85, .	1.1	57

#	Article	IF	Citations
11730	Ab initiostudy of spin-spiral noncollinear magnetism in a free-standing Fe(110) monolayer under in-plane strain. Physical Review B, 2012, 85, .	1.1	17
11731	Ab initiostudy revealing a layered structure in hydrogen-rich KH<mml:math xmlns:mml="http://www.w3.org/1998/Math/MathML" display="inline"><mml:msub><mml:mrow /><mml:mn>6</mml:mn></mml:msub></mml:math>under high pressure. Physical Review B, 2012, 86, .	1.1	79
11732	Adsorption of zwitterionic assemblies on Si(111)-7ÂÃ—Â7: A joint tunneling spectroscopy andab initiostudy. Physical Review B, 2012, 85, .	1.1	5
11733	First-principles modeling of temperature- and concentration-dependent solubility in the phase-separating alloy FexCu1â^'x. Physical Review B, 2012, 86, .	1.1	14
11734	Cu dimer formation mechanism on the ZnO(10<mml:math) Tj ETQq0 0 0 rgBT /Overlock 10 Tf 50 592 Td (xmlns:mml="http://www.w3.o Physical Review B, 2012, 86, .	1.1	13
11735	Role of Antisite Disorder on Preamorphization Swelling in Titanate Pyrochlores. Physical Review Letters, 2012, 108, 195504.	2.9	85
11736	Tuning the Growth Orientation of Epitaxial Films by Interface Chemistry. Physical Review Letters, 2012, 108, 066101.	2.9	27
11737	Magnetic impurities in graphane with dehydrogenated channels. Physical Review B, 2012, 85, .	1.1	15
11738	Ab initiocontinuum model for the influence of local stress on cross-slip of screw dislocations in fcc metals. Physical Review B, 2012, 86, .	1.1	19
11739	Atomic-resolution imaging of the polar (000<mml:math) Tj ETQq1 1 0.784314 rgBT /Overlock 10 Tf 50 402 Td (xmlns:mml="http://www surface of LiNbO<mml:math xmlns:mml="http://www.w3.org/1998/Math/MathML" display="inline"><mml:msub><mml:mrow /><mml:mn>3</mml:mn></mml:msub></mml:math>in aqueous solution by frequency modulation atomic force microscopy. Physical Review B, 2012, 86, .	1.1	33
11740	Simulation of spin-polarized scanning tunneling spectroscopy on complex magnetic surfaces: Case of a Cr monolayer on Ag(111). Physical Review B, 2012, 85, .	1.1	13
11741	Band alignment and electronic structure of the anatase TiO<mml:math xmlns:mml="http://www.w3.org/1998/Math/MathML" display="inline"><mml:msub><mml:mrow /><mml:mn>2</mml:mn></mml:msub></mml:math>/SrTiO<mml:math xmlns:mml="http://www.w3.org/1998/Math/MathML" display="inline"><mml:msub><mml:mrow /><mml:mn>3</mml:mn></mml:msub></mml:math>(001) heterostructure integrated on Si(001). Physical Review B, 2012, 86, .	1.1	40
11742	Influence of Al concentration on the optoelectronic properties of Al-doped MgO. Physical Review B, 2012, 86, .	1.1	5
11743	Incorporation and migration of hydrogen in yttria-stabilized cubic zirconia: Insights from semilocal and hybrid-functional calculations. Physical Review B, 2012, 86, .	1.1	23
11744	Mass transport and thermal stability of TiN/Al2O3/InGaAs nanofilms. Journal of Applied Physics, 2012, 112, .	1.1	21
11745	Room Temperature Ferromagnetism in Lithium-Doped ZnO. IEEE Transactions on Magnetics, 2012, 48, 3422-3425.	1.2	4
11746	Fluid like behavior of oxygen in cubic zirconia under extreme conditions. Applied Physics Letters, 2012, 101, .	1.5	8
11747	Tuning the electronic structure of ultrathin crystalline silica films on Ru(0001). Physical Review B, 2012, 85, .	1.1	85

#	Article	IF	Citations
11748	First-principles study of hexagonal tungsten trioxide: Nature of lattice distortions and effect of potassium doping. Physical Review B, 2012, 86, .	1.1	26
11749	Theoretical investigation of structural stability and electronic properties of hydrogenated silicon nanocrystals: Size, shape, and surface reconstruction. Physical Review B, 2012, 86, .	1.1	11
11750	Effect of charge-transfer complex on the energy level alignment between graphene and organic molecules. Applied Physics Letters, 2012, 100, 183102.	1.5	5
11751	Large bandwidths in synthetic one-dimensional stacks of biological molecules. Physical Review B, 2012, 86, .	1.1	7
11752	Atomically Abrupt Liquid-Oxide Interface Stabilized by Self-Regulated Interfacial Defects: The Case of<mml:math xmlns:mml="http://www.w3.org/1998/Math/MathML" display="inline"><mml:mi>Al</mml:mi><mml:mo>/</mml:mo><mml:msub><mml:mi>Al</mml:mi><mml:mn>2</mml:mn></mml:msub><mathvariant="bold">O</mml:mi><mml:mn>3</mml:mn></mml:msub></mml:math>Interfaces. Physical Review Letters, 2012, 108, 236105.	2.9	25
11753	<mml:mrow /><mml:mn>90</mml:mn></mml:msup></mml:math>SrF<mml:math xmlns:mml="http://www.w3.org/1998/Math/MathML" display="inline"><mml:msub><mml:mrow /><mml:mn>2</mml:mn></mml:msub></mml:math>: A density functional theory study of phase stability	1.1	3
11754	Hydrogen site occupancy and strength of forces in nanosized metal hydrides. Physical Review B, 2012, 85, .	1.1	28
11755	Impact of excess iron on the calculated electronic and magnetic properties of gallium ferrite. Physical Review B, 2012, 85, .	1.1	15
11756	Community Accessible Datastore of High-Throughput Calculations: Experiences from the Materials Project. , 2012, , .		8
11757	Potential enhancement in magnetoelectric effect at Mn-rich Co ₂ MnSi/BaTiO ₃ (001) interface. Europhysics Letters, 2012, 99, 57008.	0.7	16
11758	Adsorption of oxygen-containing functional groups on free and supported graphene using point contact. Physical Review B, 2012, 85, .	1.1	6
11759	Spin-dependent Smoluchowski effect. Physical Review B, 2012, 86, .	1.1	7
11760	Enhanced thermoelectric figure of merit in assembled graphene nanoribbons. Physical Review B, 2012, 86, .	1.1	81
11761	Computer simulations of crystallization kinetics in amorphous silicon under pressure. Journal of Applied Physics, 2012, 111, 063509.	1.1	7
11762	Microscopic Origin of Universal Quasilinear Band Structures of Transparent Conducting Oxides. Physical Review Letters, 2012, 108, 196404.	2.9	24
11763	Uniaxial versus hydrostatic pressure-induced phase transitions in CaFe<mml:math xmlns:mml="http://www.w3.org/1998/Math/MathML" display="inline"><mml:msub><mml:mrow /><mml:mn>2</mml:mn></mml:msub></mml:math>As<mml:math xmlns:mml="http://www.w3.org/1998/Math/MathML" display="inline"><mml:msub><mml:mrow /><mml:mn>2</mml:mn></mml:msub></mml:math>and BaFe<mml:math xmlns:mml="http://www.w3.org/1998/Math/MathML" display="inline"><mml:msub><mml:mrow />	1.1	49
11764	Interaction Effect of Protons on Their Migration in Bulk Undoped Barium Zirconate Using Density Functional Theory. Japanese Journal of Applied Physics, 2012, 51, 09MA01.	0.8	4
11765	Carbon tri-interstitial defect: A model for the D<mml:math xmlns:mml="http://www.w3.org/1998/Math/MathML" display="inline"><mml:msub><mml:mrow /><mml:mi>II</mml:mi></mml:msub></mml:math>center. Physical Review B, 2012, 86, .	1.1	33

#	Article	IF	Citations
11766	Nazca Lines by La ordering in La2/3â^'xLi3xTiO3 ion-conductive perovskite. Applied Physics Letters, 2012, 101, 073903.	1.5	8
11767	Adsorbed water-molecule hexagons with unexpected rotations in islands on Ru(0001) and Pd(111). Physical Review B, 2012, 85, .	1.1	27
11768	Defect and solute properties in dilute Fe-Cr-Ni austenitic alloys from first principles. Physical Review B, 2012, 85, .	1.1	61
11769	Circumstantial evidence for hydrogen-induced surface magnetism on Pd(110). Physical Review B, 2012, 85, .	1.1	4
11770	Adsorbate-induced reconstruction by C<mml:math xmlns:mml="http://www.w3.org/1998/Math/MathML" display="inline"><mml:msub><mml:mrow /><mml:mn>60</mml:mn></mml:msub></mml:math>on close-packed metal surfaces: Mechanism for different types of reconstruction. Physical Review B, 2012, 85, .	1.1	22
11771	Reflectivity of warm dense deuterium along the principal Hugoniot. Physical Review B, 2012, 85, .	1.1	13
11772	Structural analysis and superconductivity of CeFeAsO<mml:math xmlns:mml="http://www.w3.org/1998/Math/MathML" display="inline"><mml:msub><mml:mrow /><mml:mrow><mml:mn>1</mml:mn><mml:mo>â^'</mml:mo><mml:mi>x</mml:mi></mml:mrow></mml:msub></mml:math>H<mml:math xmlns:mml="http://www.w3.org/1998/Math/MathML" display="inline"><mml:msub><mml:mrow /><mml:mi>x</mml:mi></mml:msub></mml:math>. Physical Review B, 2012, 85, .	1.1	52
11773	Structure of Silicene Grown on Ag(111). Applied Physics Express, 2012, 5, 045802.	1.1	518
11774	Energy transport and scintillation of cerium-doped elpasolite Cs<mml:math xmlns:mml="http://www.w3.org/1998/Math/MathML" display="inline"><mml:msub><mml:mrow /><mml:mn>2</mml:mn></mml:msub></mml:math>LiYCl<mml:math xmlns:mml="http://www.w3.org/1998/Math/MathML" display="inline"><mml:msub><mml:mrow /><mml:mn>6</mml:mn></mml:msub></mml:math>: Hybrid density functional calculations. Physical Review B, 2012, 86, .	1.1	78
11775	Electronic structure, small polaron, and F center in LiCaAlF6. Journal of Applied Physics, 2012, 112, 123516.	1.1	11
11776	Design of strain-engineered quantum tunneling devices for topological surface states. Applied Physics Letters, 2012, 100, 131602.	1.5	26
11777	Ab initiodetermination of structure-property relationships in alloy nanoparticles. Physical Review B, 2012, 86, .	1.1	31
11778	Highâ€pressure phases of NaAlH4 from first principles. Applied Physics Letters, 2012, 100, 061905.	1.5	10
11779	Role of applied bias and tip electronic structure in the scanning tunneling microscopy imaging of highly oriented pyrolytic graphite. Physical Review B, 2012, 85, .	1.1	18
11780	Structural, electronic and optical properties of titania nanotubes. Advances in Applied Ceramics, 2012, 111, 72-93.	0.6	8
11781	Interplay of localized and itinerant character of Ru ions: Tl<mml:math xmlns:mml="http://www.w3.org/1998/Math/MathML" display="inline"><mml:msub><mml:mrow /><mml:mn>2</mml:mn></mml:msub></mml:math>Ru<mml:math xmlns:mml="http://www.w3.org/1998/Math/MathML" display="inline"><mml:msub><mml:mrow /><mml:mn>2</mml:mn></mml:msub></mml:math>O<mml:math xmlns:mml="http://www.w3.org/1998/Math/MathML" display="inline"><mml:msub><mml:mrow />	1.1	5
11782	First-principles analysis of structural and opto-electronic properties of indium tin oxide. Journal of Applied Physics, 2012, 111, .	1.1	16
11783	Hydrogen-induced disruption of the ZnO(0001) polar surface. Physical Review B, 2012, 86, .	1.1	12

#	Article	IF	Citations
11784	Periodic variations in the local surface potential of Si(111)-(5Ã—2)-Au. Physical Review B, 2012, 85, .	1.1	3
11785	Anharmonic phonons of NaZr<mml:math xmlns:mml="http://www.w3.org/1998/Math/MathML" display="inline"><mml:msub><mml:mrow /><mml:mn>2</mml:mn></mml:msub></mml:math>(PO<mml:math) Tj ETQq1 1 0.784314 rgBT /Overlock 10 Tf 50 707 Td (xmlns:mml	1.1	43
11786	Block antiferromagnetism and checkerboard charge ordering in the alkali-doped iron selenides<mml:math xmlns:mml="http://www.w3.org/1998/Math/MathML" display="inline"><mml:mi>R</mml:mi></mml:math><mml:math xmlns:mml="http://www.w3.org/1998/Math/MathML" display="inline"><mml:msub><mml:mrow /><mml:mn>1</mml:mn><mml:mo>â^’</mml:mo><mml:mi>x</mml:mi></mml:mrow></mml:msub></mml:math>Fe<mml:	1.1	34
11787	Microscopic origin of the structural phase transitions at<mml:math xmlns:mml="http://www.w3.org/1998/Math/MathML" display="inline"><mml:msub><mml:mrow /><mml:mn>2</mml:mn></mml:msub></mml:math><mml:math xmlns:mml="http://www.w3.org/1998/Math/MathML" display="inline"><mml:msub><mml:mrow /><mml:mn>3</mml:mn></mml:msub></mml:math>(0001) surface. Physical Review B, 2012, 86, .	1.1	13
11788	Directed assembly of Ru nanoclusters on Ru(0001)-supported graphene: STM studies and atomistic modeling. Physical Review B, 2012, 86, .	1.1	27
11789	Role of nonlocal exchange in the electronic structure of correlated oxides. Physical Review B, 2012, 85, .	1.1	65
11790	Scanning Tunneling Microscopy Contrast Mechanisms for<mml:math xmlns:mml="http://www.w3.org/1998/Math/MathML" display="inline"><mml:msub><mml:mi>TiO</mml:mi><mml:mn>2</mml:mn></mml:msub></mml:math>. Physical Review Letters, 2012, 109, 156105.	2.9	38
11791	Search for stable ferromagnets among<mml:math xmlns:mml="http://www.w3.org/1998/Math/MathML" display="inline"><mml:msup><mml:mi>A</mml:mi><mml:mi>IV</mml:mi></mml:msup></mml:math>/Fe digital alloys (<mml:math xmlns:mml="http://www.w3.org/1998/Math/MathML") Tj ETQq1 1 0.784314 rgBT /Overlock 10 Tf 50 457 Td (	1.1	50
11792	Quantum molecular dynamics simulations of thermophysical properties of fluid ethane. Physical Review E, 2012, 86, 061111.	0.8	5
11793	Modeling configurational energetics on multiple lattices through extended cluster expansion. Physical Review B, 2012, 85, .	1.1	12
11794	Ab initiostudy of the strain dependent thermodynamics of Bi doping in GaAs. Physical Review B, 2012, 86, .	1.1	50
11795	High Chalcocite<mml:math xmlns:mml="http://www.w3.org/1998/Math/MathML" display="inline"><mml:msub><mml:mi>Cu</mml:mi><mml:mn>2</mml:mn></mml:msub><mml:mi mathvariant="normal">S</mml:mi></mml:math>: A Solid-Liquid Hybrid Phase. Physical Review Letters, 2012, 108, 085703.	2.9	88
11796	Understanding controls on interfacial wetting at epitaxial graphene: Experiment and theory. Physical Review B, 2012, 85, .	1.1	95
11797	Excitation, relaxation, and quantum diffusion of CO on copper. Physical Review B, 2012, 86, .	1.1	23
11798	Cluster expansion with controlled accuracy for the MgO/ZnO pseudobinary system via first-principles calculations. Physical Review B, 2012, 86, .	1.1	9
11799	Hybrid molecular dynamics and first-principles study on the work function of a Pt(111) electrode immersed in aqueous solution at room temperature. Physical Review B, 2012, 86, .	1.1	18
11800	Effective on-site interaction for dynamical mean-field theory. Physical Review B, 2012, 86, .	1.1	60
11801	Formation and destabilization of Ga interstitials in GaAsN: Experiment and theory. Physical Review B, 2012, 86, .	1.1	12

#	Article	IF	Citations
11802	Clusters binding to the graphene moirÃ© on Ir(111): X-ray photoemission compared to density functional calculations. Physical Review B, 2012, 85, .	1.1	50
11803	Pseudodielectric function and critical-point energies of iron pyrite. Physical Review B, 2012, 86, .	1.1	34
11804	Drastically enhanced H2flux through asymmetric quantum Pd films. Physical Review B, 2012, 85, .	1.1	0
11805	Large organic molecule chemisorption on the SiC(0001) surface. Physical Review B, 2012, 85, .	1.1	18
11806	Electron paramagnetic resonance and theoretical studies of Nb in 4H- and 6H-SiC. Journal of Applied Physics, 2012, 112, .	1.1	11
11807	Charge Redistribution Mechanisms of Ceria Reduction. Physical Review Letters, 2012, 108, 135504.	2.9	24
11808	Semiempirical van der Waals interactions versusab initiononlocal correlation effects in the thiophene-Cu(111) system. Physical Review B, 2012, 86, .	1.1	22
11809	Theoretical study of the temperature dependence of the magnon dispersion relation in transition-metal wires and monolayers. Physical Review B, 2012, 86, .	1.1	7
11810	Anomalies in nonstoichiometric uranium dioxide induced by a pseudo phase transition of point defects. Physical Review B, 2012, 85, .	1.1	6
11811	Growth morphology and thermal stability of metal islands on graphene. Physical Review B, 2012, 86, .	1.1	38
11812	Spin-split silicon states at step edges of Si(553)-Au. Physical Review B, 2012, 85, .	1.1	21
11813	Phase stability of long-period stacking structures in Mg-Y-Zn: A first-principles study. Physical Review B, 2012, 86, .	1.1	44
11814	Energetics and approximate quasiparticle electronic structure of low-index surfaces of SnO<mml:math xmlns:mml="http://www.w3.org/1998/Math/MathML" display="inline"><mml:msub><mml:mrow /><mml:mn>2</mml:mn></mml:msub></mml:math>. Physical Review B, 2012, 86, .	1.1	31
11815	Doping domains in graphene on gold substrates: First-principles and scanning tunneling spectroscopy studies. Physical Review B, 2012, 85, .	1.1	19
11816	Electronic and transport properties of armchair and zigzag sp³-hybridized silicane nanoribbons. , 2012, , .		1
11817	The electronic and optical properties of Eu/Si-codoped anatase TiO₂ photocatalyst. Applied Physics Letters, 2012, 100, 102105.	1.5	16
11818	Relation between the work function and Young's modulus of RhSi and estimate of Schottky-barrier height at RhSi/Si interface: An ab-initio study. Journal of Applied Physics, 2012, 112, .	1.1	11
11819	Electronic structure of LaBr<mml:math xmlns:mml="http://www.w3.org/1998/Math/MathML" display="inline"><mml:msub><mml:mrow /><mml:mn>3</mml:mn></mml:msub></mml:math>from quasiparticle self-consistent<mml:math xmlns:mml="http://www.w3.org/1998/Math/MathML" display="inline"><mml:mrow><mml:mi>G</mml:mi><mml:mi>W</mml:mi></mml:mrow></mml:math>calculations. Physical Review B, 2012, 85, .	1.1	28

#	Article	IF	Citations
11820	First principles analysis on interaction between vacancy near surface and dimer structure of silicon crystal. Journal of Applied Physics, 2012, 111, 013521.	1.1	7
11821	Formation of monomer to tetramer Ag nanodots in a vanadium oxide nanomesh on Pd(111). Journal of Applied Physics, 2012, 112, 034902.	1.1	2
11822	Prediction of a metastable phase of silicon in theIbamstructure. Physical Review B, 2012, 85, .	1.1	41
11823	Intrinsic defect in BiNbO4: A density functional theory study. Journal of Applied Physics, 2012, 112, .	1.1	25
11824	Ab initio study of vacancy and self-interstitial properties near single crystal silicon surfaces. Journal of Applied Physics, 2012, 111, .	1.1	33
11825	LiB and its boron-deficient variants under pressure. Physical Review B, 2012, 86, .	1.1	23
11826	Density functional theory investigation of titanium-tungsten superlattices: Structure and mechanical properties. Physical Review B, 2012, 86, .	1.1	0
11827	Synchrotron x-ray spectroscopy studies of valence and magnetic state in europium metal to extreme pressures. Physical Review B, 2012, 85, .	1.1	20
11828	Intrinsic defects and conduction characteristics of Sc<mml:math xmlns:mml="http://www.w3.org/1998/Math/MathML" display="inline"><mml:msub><mml:mrow /><mml:mn>2</mml:mn></mml:msub></mml:math>O<mml:math xmlns:mml="http://www.w3.org/1998/Math/MathML" display="inline"><mml:msub><mml:mrow /><mml:mn>3</mml:mn></mml:msub></mml:math>in thermionic cathode systems. Physical Review B, 2012, 86, .	1.1	19
11829	Nature of the hole states in Li-doped NiO. Physical Review B, 2012, 85, .	1.1	45
11830	Phase stability of Ni<mml:math xmlns:mml="http://www.w3.org/1998/Math/MathML" display="inline"><mml:msub><mml:mrow		

#	Article	IF	Citations
11838	Quantum Monte Carlo study of small aluminum clusters Al<mml:math xmlns:mml="http://www.w3.org/1998/Math/MathML" display="inline"><mml:msub><mml:mrow /><mml:mi>n</mml:mi></mml:msub></mml:math>(<mml:math) Tj ETQq0 0 0 rgBT /Overlock 10 Tf 50 742 Td (xmlns:mml="http://www.	1.1	44
11839	Physical Review B, 2012, 85, . Nonlinear stress-strain relations for crystalline solids in initially deformed state. Journal of Applied Physics, 2012, 112, .	1.1	1
11840	Electronic properties of Si(111)-7Ã—7and related reconstructions: Density functional theory calculations. Physical Review B, 2012, 85, .	1.1	28
11841	Magnetic properties of O<mml:math xmlns:mml="http://www.w3.org/1998/Math/MathML" display="inline"><mml:msub><mml:mrow /><mml:mn>2</mml:mn></mml:msub></mml:math>adsorbed on Cu(100): A spin-polarized metastable He beam study. Physical Review B, 2012, 86, .	1.1	6
11842	Equation of state of paramagnetic CrN fromab initiomolecular dynamics. Physical Review B, 2012, 85, .	1.1	70
11843	Zero-bias anomaly in ferromagnetic Ni nanoconstrictions. Physical Review B, 2012, 86, .	1.1	18
11844	Low hole polaron migration barrier in lithium peroxide. Physical Review B, 2012, 85, .	1.1	158
11845	Role of structure of C-terminated<mml:math xmlns:mml="http://www.w3.org/1998/Math/MathML" display="inline"><mml:mrow><mml:mn>4</mml:mn><mml:mi>H</mml:mi></mml:mrow></mml:math>-SiC(<mml:math) Tj ETQq1 1 0.7	1.1	38
11846	surface in growth of graphene layers: Transmission electron microscopy and density functional theo Atomistic modeling of As diffusion in ZnO. Physical Review B, 2012, 85, .	1.1	23
11847	Competing allotropes of Bi deposited on the Al13Co4(100) alloy surface. Physical Review B, 2012, 86, .	1.1	10
11848	Magnetic and transport properties of Mn3âˆ’xGa/MgO/Mn3âˆ’xGa magnetic tunnel junctions: A first-principles study. Applied Physics Letters, 2012, 100, .	1.5	49
11849	Semimetal-antiferromagnetic insulator transition in graphene induced by biaxial strain. Physical Review B, 2012, 86, .	1.1	20
11850	Multi-oriented moirÃ© superstructures of graphene on Ir(111): experimental observations and theoretical models. Journal of Physics Condensed Matter, 2012, 24, 314214.	0.7	60
11851	Understanding image contrast formation in TiO<mml:math xmlns:mml="http://www.w3.org/1998/Math/MathML" display="inline"><mml:msub><mml:mrow /><mml:mn>2</mml:mn></mml:msub></mml:math>with force spectroscopy. Physical Review B, 2012, 85, .	1.1	52
11852	Unusual rigidity and ideal strength of CrB4 and MnB4. Applied Physics Letters, 2012, 100, .	1.5	54
11853	Role of functional groups in surface bonding of planar<mml:math xmlns:mml="http://www.w3.org/1998/Math/MathML" display="inline"><mml:mi>Ï€</mml:mi></mml:math>-conjugated molecules. Physical Review B, 2012, 86, .	1.1	66
11854	Orbital-dependent electron tunneling within the atom superposition approach: Theory and application to W(110). Physical Review B, 2012, 86, .	1.1	20
11855	structure and electronic properties of amorphous high-<mml:math xmlns:mml="http://www.w3.org/1998/Math/MathML" display="inline"><mml:mi>Î²</mml:mi></mml:math>oxides: HfO<mml:math xmlns:mml="http://www.w3.org/1998/Math/MathML" display="inline"><mml:msub><mml:mrow /><mml:mn>2</mml:mn></mml:msub></mml:math>, ZrO<mml:math xmlns:mml="http://www.w3.org/1998/Math/MathML" display="inline"><mml:msub><mml:mrow /><mml:mi>	1.1	55

#	Article	IF	Citations
11856	Equation of state of CH<mml:math xmlns:mml="http://www.w3.org/1998/Math/MathML" display="inline"><mml:msub><mml:mrow /><mml:mrow><mml:mn>1.36</mml:mn></mml:mrow></mml:msub></mml:math>: First-principles molecular dynamics simulations and shock-and-release wave speed measurements. Physical Review B, 2012, 86, .	1.1	57
11857	High-pressure behavior of dense hydrogen up to 3.5 TPa from density functional theory calculations. Journal of Applied Physics, 2012, 111, 063510.	1.1	34
11858	Flat bands near Fermi level of topological line defects on graphite. Applied Physics Letters, 2012, 101, .	1.5	30
11859	Photoisomerization for a molecular switch in contact with a surface. Physical Review B, 2012, 85, .	1.1	32
11860	Stable interstitial dopantâ€“vacancy complexes in ZnO. Physical Review B, 2012, 85, .	1.1	26
11861	Structural transformation and vibrational properties of BaC<mml:math xmlns:mml="http://www.w3.org/1998/Math/MathML" display="inline"><mml:msub><mml:mrow /><mml:mn>2</mml:mn></mml:msub></mml:math>at high pressure. Physical Review B, 2012, 85, .	1.1	25
11862	Magnetic ordering and multiferroicity in MnI<mml:math xmlns:mml="http://www.w3.org/1998/Math/MathML" display="inline"><mml:msub><mml:mrow /><mml:mn>2</mml:mn></mml:msub></mml:math>. Physical Review B, 2012, 86, .	1.1	24
11863	Effect of surface hydrogen on the anomalous surface segregation behavior of Cr in Fe-rich Fe-Cr alloys. Physical Review B, 2012, 86, .	1.1	3
11864	Structure and intermolecular bonding in NaBH<mml:math xmlns:mml="http://www.w3.org/1998/Math/MathML" display="inline"><mml:msub><mml:mrow /><mml:mn>4</mml:mn></mml:msub></mml:math><mml:math xmlns:mml="http://www.w3.org/1998/Math/MathML" display="inline"><mml:mo>Â·</mml:mo></mml:math>2H<mml:math xmlns:mml="http://www.w3.org/1998/Math/MathML" display="inline"><mml:msub><mml:mrow /><mml:	1.1	2
11865	Rocky Core Solubility in Jupiter and Giant Exoplanets. Physical Review Letters, 2012, 108, 111101.	2.9	119
11866	Electronic and vibrational properties of vanadium-carbide nanowires. Journal of Applied Physics, 2012, 112, .	1.1	3
11867	The role of 4f-electron on spin reorientation transition of NdFeO3: A first principle study. Journal of Applied Physics, 2012, 111, .	1.1	57
11868	Ab initiothermodynamics calculation of the relative concentration of NV<mml:math xmlns:mml="http://www.w3.org/1998/Math/MathML" display="inline"><mml:msup><mml:mrow /><mml:mo>â^’</mml:mo></mml:msup></mml:math>and NV<mml:math xmlns:mml="http://www.w3.org/1998/Math/MathML" display="inline"><mml:msup><mml:mrow /><mml:mn>0</mml:mn></mml:msup></mml:math>defects in diamond. Physical Review B, 2012, 85, .	1.1	16
11869	Lithiation of silica through partial reduction. Applied Physics Letters, 2012, 100, .	1.5	57
11870	Magnetic and electronic properties of D22-Mn3Ge (001) films. Applied Physics Letters, 2012, 101, .	1.5	88
11871	Nanoalloy composition-temperature phase diagram for catalyst design: Case study of Ag-Au. Physical Review B, 2012, 86, .	1.1	22
11872	Ab initiostudy of the factors affecting the ground state of rare-earth nickelates. Physical Review B, 2012, 85, .	1.1	18
11873	Adsorbate-induced segregation: First-principles study for C/Pt25Rh75(100). Physical Review B, 2012, 86, .	1.1	10

#	Article	IF	Citations
11874	Magnetic properties of ZnS doped with noble metals (Xâ€‰=â€‰Ru, Rh, Pd, and Ag). Journal of Applied Physics, 2012, 112, .	1.1	16
11875	Electronic and electrostatic properties of polar oxide nanostructures: MgO(111) islands on Au(111). Physical Review B, 2012, 86, .	1.1	20
11876	On the origin of the 265â€‰nm absorption band in AlN bulk crystals. Applied Physics Letters, 2012, 100, .	1.5	137
11877	Composition and local atomic arrangement of decagonal Al-Co-Cu quasicrystal surfaces. Physical Review B, 2012, 86, .	1.1	5
11878	First-principles study of point defects in solar cell semiconductor CuInS2. Journal of Applied Physics, 2012, 112, .	1.1	30
11879	An unusual variation of stability and hardness in molybdenum borides. Applied Physics Letters, 2012, 101, .	1.5	36
11880	Site preference of cation vacancies in Mn-doped Ga2O3 with defective spinel structure. Applied Physics Letters, 2012, 101, .	1.5	14
11881	Surface properties of the clean and Au/Pd covered Fe<mml:math xmlns:mml="http://www.w3.org/1998/Math/MathML" display="inline"><mml:msub><mml:mrow /><mml:mn>3</mml:mn></mml:msub></mml:math>O<mml:math xmlns:mml="http://www.w3.org/1998/Math/MathML" display="inline"><mml:msub><mml:mrow /><mml:mn>4</mml:mn></mml:msub></mml:math>(111): DFT andDFT+<mml:math xmlns:mml="http://www.w3.org/1998/Math/MathML" display="inline"><mml:mi>U</mml:mi></mml:math>	1.1	68
11882	Tailoring magnetoresistance at the atomic level: Anab initiostudy. Physical Review B, 2012, 85, .	1.1	2
11883	Graphene on cubic and hexagonal SiC: A comparative theoretical study. Physical Review B, 2012, 86, .	1.1	12
11884	Electronic and optical properties of free-standing and supported vanadium nanowires. Journal of Applied Physics, 2012, 111, 093506.	1.1	8
11885	High-temperature behavior of supported graphene: Electron-phonon coupling and substrate-induced doping. Physical Review B, 2012, 86, .	1.1	31
11886	Magnetic configuration, electronic structure, and stability of the low-index surfaces of<mml:math xmlns:mml="http://www.w3.org/1998/Math/MathML" display="inline"><mml:mi>Î·</mml:mi></mml:math>-Mn<mml:math xmlns:mml="http://www.w3.org/1998/Math/MathML" display="inline"><mml:msub><mml:mrow /><mml:mn>3</mml:mn></mml:msub></mml:math>N<mml:math xmlns:mml="http://www.w3.org/1998/Math/MathML" display="inline"><mml:msub><mml:mrow /><mml:mml:	1.1	5
11887	Engineering direct-indirect band gap transition in wurtzite GaAs nanowires through size and uniaxial strain. Applied Physics Letters, 2012, 100, 193108.	1.5	39
11888	Possible magnetic behavior in oxygen-deficient<mml:math xmlns:mml="http://www.w3.org/1998/Math/MathML" display="inline"><mml:mi>Î²</mml:mi></mml:math>-PtO<mml:math xmlns:mml="http://www.w3.org/1998/Math/MathML" display="inline"><mml:msub><mml:mrow /><mml:mn>2</mml:mn></mml:msub></mml:math>. Physical Review B, 2012, 85, .	1.1	9
11889	Magnetic exchange interactions and antiferromagnetism ofATcO3(A=Ca, Sr, Ba) studied from first principles. Physical Review B, 2012, 85, .	1.1	16
11890	Single well or double well: First-principles study of 8<mml:math xmlns:mml="http://www.w3.org/1998/Math/MathML" display="inline"><mml:mi>H</mml:mi></mml:math>and 3<mml:math xmlns:mml="http://www.w3.org/1998/Math/MathML" display="inline"><mml:mi>C</mml:mi></mml:math>inclusions in the 4<mml:math xmlns:mml="http://www.w3.org/1998/Math/MathML" display="inline"><mml:mi>H</mml:mi></mml:math>	1.1	6
11891	First-principles study on phase stability of MoSi<mml:math xmlns:mml="http://www.w3.org/1998/Math/MathML" display="inline"><mml:msub><mml:mrow /><mml:mn>2</mml:mn></mml:msub></mml:math>-NbSi<mml:math xmlns:mml="http://www.w3.org/1998/Math/MathML" display="inline"><mml:msub><mml:mrow /><mml:mn>2</mml:mn></mml:msub></mml:math>pseudobinary alloys. Physical Review B, 2012, 85, .	1.1	6

#	Article	IF	Citations
11892	Vibrations of Au₁₃and FeAu₁₂nanoparticles and the limits of the Debye temperature concept. Journal of Physics Condensed Matter, 2012, 24, 104026.	0.7	16
11893	Validity of the rigid band approximation in the study of the thermopower of narrow band gap semiconductors. Physical Review B, 2012, 85, .	1.1	93
11894	Enhancement of electron-nuclear hyperfine interaction at lattice defects in semiconducting single-walled carbon nanotubes studied byab initiodensity functional theory calculations. Physical Review B, 2012, 86, .	1.1	0
11895	Electrochemical cycling reversibility of LiMoS₂ using first-principles calculations. Applied Physics Letters, 2012, 100, 263901.	1.5	23
11896	Pressure-Driven Evolution of the Covalent Network inCaB6. Physical Review Letters, 2012, 109, 075501.	2.9	57
11897	Effect of Replacement of Fe²⁺ by Co²⁺ in W-Type Hexagonal Ferrite BaFe₁₈O₂₇ to its Electronic Properties from First Principles. Advanced Materials Research, 2012, 424-425, 137-140.	0.3	0
11898	Resolving quandaries surrounding NiTi. Applied Physics Letters, 2012, 101, 081907.	1.5	15
11899	A photoelectron spectroscopy study of the electronic structure evolution in CuInSe₂-related compounds at changing copper content. Applied Physics Letters, 2012, 101, 111607.	1.5	13
11900	Electronic and magnetic properties of substitutionally Fe-, Co-, and Ni-doped BC3 honeycomb structure. Journal of Applied Physics, 2012, 111, .	1.1	12
11901	Half metallic character of NiMoO₃ driven by the electron correlation and spin-orbit coupling. Applied Physics Letters, 2012, 101, 042414.	1.5	4
11902	Role of heteroepitaxial misfit strains on the band offsets of Zn1â^'xBexO/ZnO quantum wells: A first-principles analysis. Journal of Applied Physics, 2012, 111, 113714.	1.1	16
11903	Bandgap engineering of ZnSnP2 for high-efficiency solar cells. Applied Physics Letters, 2012, 100, .	1.5	116
11904	Poly â€“NÂ=ÂNâ€“ linked 1,5-dihydro-1,5-diazocine, the two-dimensional polymer withDirac insulatorproperties:ab initiostudy. Molecular Simulation, 2012, 38, 886-891.	0.9	3
11905	Stretch-induced softening of bending rigidity in graphene. Applied Physics Letters, 2012, 100, .	1.5	31
11906	Vacancy ordering and phonon spectrum of the iron-based superconductor K0.8Fe1.6Se2. Physical Review B, 2012, 85, .	1.1	30
11907	Band engineering in silicide alloys. Physical Review B, 2012, 85, .	1.1	10
11908	Electronic origin of the anomalous segregation behavior of Cr in Fe-rich Fe-Cr alloys. Physical Review B, 2012, 85, .	1.1	25
11909	Atomic ordering in Au-(42 to 50) at.<mml:math xmlns:mml="http://www.w3.org/1998/Math/MathML" display="inline"><mml:mo>%</mml:mo></mml:math>Pd: A diffuse scattering and first-principles investigation. Physical Review B, 2012, 85, .	1.1	6

#	ARTICLE	IF	CITATIONS
11910	First-principles study of impurities in TlBr. Journal of Applied Physics, 2012, 111, 073519.	1.1	5
11911	Epitaxial growth mechanisms of graphene and effects of substrates. Physical Review B, 2012, 85, .	1.1	39
11912	Spectroscopic characterization of a multiband complex oxide: Insulating and conducting cement 12CaOÂ·7Al2O3. Physical Review B, 2012, 85, .	1.1	21
11913	Atomistic method for analysis of electromigration. , 2012, , .		0
11914	<i>Ab initio</i>study on optoelectronic properties of interstitially versus substitutionally doped titania. Physical Review B, 2012, 86, .	1.1	6
11915	Atomic and electronic structures of SrTiO<mml:math xmlns:mml="http://www.w3.org/1998/Math/MathML" display="inline"><mml:msub><mml:mrow /><mml:mn>3</mml:mn></mml:msub></mml:math>/GaAs heterointerfaces: An 80-kV atomic-resolution electron energy-loss spectroscopy study. Physical Review B, 2012, 85, .	1.1	17
11916	First-Principles Study of the Influence of (110) Strain on the Ferroelectric Trends of TiO₂. Ferroelectrics, 2012, 429, 31-42.	0.3	8
11917	Analysis of the Heyd-Scuseria-Ernzerhof density functional parameter space. Journal of Chemical Physics, 2012, 136, 204117.	1.2	130
11918	Reversible mechanism for spin crossover in transition-metal cyanides. Physical Review B, 2012, 85, .	1.1	16
11919	Impact of Atomic Structure on the Magnon Dispersion Relation: A Comparison Between<mml:math xmlns:mml="http://www.w3.org/1998/Math/MathML" display="inline"><mml:mi>Fe</mml:mi><mml:mo stretchy="false">(</mml:mo><mml:mn>111</mml:mn><mml:mo) Tj ETQq1 1 0.784314 rgBT /Overlock 10 Tf 50 387 Td (stretchy="false mathvariant="bold">W</mml:mi><mml:mo stretchy="false">(</mml:mo><mml:mn>110</mml:mn><mml:mo) Tj ETQq1 1 0.784314 rgBT /Overlock 10 Tf 50 357 Td (stretchy="false	2.9	18
11920	Stability of Sb-Te layered structures: First-principles study. Physical Review B, 2012, 85, .	1.1	12
11921	Stability of Ge on Si (1 1 10) surfaces and the role of dimer tilting. Physical Review B, 2012, 85, .	1.1	25
11922	First-principles study of Zintl aluminide SrAl2. Physical Review B, 2012, 85, .	1.1	11
11923	First-principles calculation of x-ray absorption spectra and x-ray magnetic circular dichroism of ultrathin Fe films on BaTiO<mml:math xmlns:mml="http://www.w3.org/1998/Math/MathML" display="inline"><mml:msub><mml:mrow /><mml:mn>3</mml:mn></mml:msub></mml:math>(001). Physical Review B, 2012, 85, .	1.1	16
11924	AuCu intermetallic nanoparticles: surfactant-free synthesis and novel electrochemistry. Journal of Materials Chemistry, 2012, 22, 15769.	6.7	68
11925	Electronic structure of oxygen vacancies in<mml:math xmlns:mml="http://www.w3.org/1998/Math/MathML" display="inline"><mml:msub><mml:mrow><mml:mi mathvariant="normal">SrTiO</mml:mi></mml:mrow><mml:mn>3</mml:mn></mml:msub></mml:math>and<mml:math xmlns:mml="http://www.w3.org/1998/Math/MathML" display="inline"><mml:msub><mml:mrow><mml:mi mathvariant="normal">LaAlO</mml:mi></mml:mrow><mml:mn>3</mml:mn></mml:msub></mml:math>. Physical Review B, 2012, 86, .	1.1	146
11926	Catalytic growth of N-doped MgO on Mo(001). Physical Review B, 2012, 86, .	1.1	7
11927	Trapping of three-dimensional electrons and transition to two-dimensional transport in the three-dimensional topological insulator Bi<mml:math xmlns:mml="http://www.w3.org/1998/Math/MathML" display="inline"><mml:msub><mml:mrow /><mml:mn>2</mml:mn></mml:msub></mml:math>Se<mml:math xmlns:mml="http://www.w3.org/1998/Math/MathML" display="inline"><mml:msub><mml:mrow /><mml:mn>3</mml:mn></mml:msub></mml:math>under high pressure. Physical Review B, 2012, 85, .	1.1	29

#	Article	IF	Citations
11928	Ab initioatomistic thermodynamics study of the early stages of Cu(100) oxidation. Physical Review B, 2012, 86, .	1.1	42
11929	High-efficient tunable infrared laser from monatomic carbon chains. Europhysics Letters, 2012, 97, 27006.	0.7	12
11930	Structural, elastic, phonon and electronic properties of a MnPd alloy. Chinese Physics B, 2012, 21, 077102.	0.7	7
11931	CHARGE TRANSPORT AND LIGHT ABSORPTION IN CONJUGATED SYSTEMS FROM EXTENDED HÃœCKEL METHOD AND MARCUS THEORY. International Journal of Computational Materials Science and Engineering, 2012, 01, 1250020.	0.5	0
11932	UNIFORM BENDING EFFECT ON ELECTRONIC PROPERTIES OF BORON NITRIDE NANORIBBONS: A COMPUTATIONAL INVESTIGATION. Nano LIFE, 2012, 02, 1240005.	0.6	0
11933	SIZE-DEPENDENCE OF INFRARED SPECTRA IN NIOBIUM CARBIDE NANOCRYSTALS. International Journal of Modern Physics C, 2012, 23, 1240001.	0.8	4
11934	STRUCTURAL, MECHANICAL AND LATTICE DYNAMICAL STABILITY OF AgC AND AuC COMPOUNDS: A FIRST PRINCIPLES STUDY. Modern Physics Letters B, 2012, 26, 1250107.	1.0	3
11935	FIRST PRINCIPLES STUDY ON ELECTRONIC AND OPTICAL PROPERTIES OF Al-DOPED Î³-Ge₃N₄. International Journal of Modern Physics B, 2012, 26, 1250200.	1.0	5
11936	First-principles study of atomic and electronic structures of kaolinite in soft rock. Chinese Physics B, 2012, 21, 039101.	0.7	4
11937	Band gap engineering of (N, Si)-codoped TiO₂from hybrid density functional theory calculations. New Journal of Physics, 2012, 14, 053007.	1.2	26
11938	Structure and stability of weakly chemisorbed ethene adsorbed on low-index Cu surfaces: performance of density functionals with van der Waals interactions. Journal of Physics Condensed Matter, 2012, 24, 424217.	0.7	19
11939	HYDROGEN STORAGE ENHANCEMENT VIA TRANSITION METAL DECORATION ON METAL ORGANIC FRAMEWORKS: A FIRST-PRINCIPLES STUDY. Nano, 2012, 07, 1250044.	0.5	5
11940	Band engineering of type-II ZnO/ZnSe heterostructures for solar cell applications. Journal of Materials Research, 2012, 27, 730-733.	1.2	9
11941	Ab initio studying of topological insulator Bi2Se3under the stress. Journal of Physics: Conference Series, 2012, 394, 012022.	0.3	3
11942	Charge redistribution and local lattice structure of (F, Zn)-codoped LaFeAsO superconductor. New Journal of Physics, 2012, 14, 033005.	1.2	5
11943	Effect of site-disorder on magnetism and magneto-structural coupling in gallium ferrite: A first-principles study. Journal of Applied Physics, 2012, 111, .	1.1	16
11944	Melting and dissociation of ammonia at high pressure and high temperature. Journal of Chemical Physics, 2012, 137, 064507.	1.2	26
11945	Theoretical and experimental investigation of magnetotransport in iron chalcogenides. Science and Technology of Advanced Materials, 2012, 13, 054402.	2.8	18

#	Article	IF	Citations
11946	Interaction between impurity nitrogen and tungsten: a first-principles investigation. Chinese Physics B, 2012, 21, 016105.	0.7	18
11947	Static dielectric constants and molecular dipole distributions of liquid water and ice-Ih investigated by the PAW-PBE exchange-correlation functional. Journal of Chemical Physics, 2012, 137, 034510.	1.2	22
11948	Electrical transition of (3,3) carbon nanotube on patterned hydrogen terminated Si(001)-2â€‰Ã—â€‰1 driven by electric field. Journal of Applied Physics, 2012, 111, 123717.	1.1	1
11949	A first-principles study of the magnetic properties in boron-doped ZnO. Chinese Physics B, 2012, 21, 047504.	0.7	12
11950	First-principles molecular dynamics study for average structure and oxygen diffusivity at high temperature in cubic Bi₂O₃. Journal of Physics Condensed Matter, 2012, 24, 475402.	0.7	14
11951	Magnetic properties of Fe-pnictides superconductors as a function of pressure and doping. Materials Research Society Symposia Proceedings, 2012, 1434, 1.	0.1	0
11952	Strength and bonding nature of superhard Z-carbon from first-principle study. AIP Advances, 2012, 2, .	0.6	7
11953	Pairing symmetry in the iron-pnictide superconductor KFe ₂ As ₂. Europhysics Letters, 2012, 99, 57006.	0.7	12
11954	Chiral recognition of zinc phthalocyanine on Cu(100) surface. Applied Physics Letters, 2012, 100, 081602.	1.5	28
11955	d⁰ferromagnetic surface in HfO₂. Journal of Physics: Conference Series, 2012, 400, 032008.	0.3	0
11956	Theoretical Study on Hydrazine Chemisorption on Transition Metal Surfaces. Journal of the Physical Society of Japan, 2012, 81, 124705.	0.7	11
11957	Understanding the effect of the layer-to-layer distance on Li-intercalated graphite. Journal of Applied Physics, 2012, 111, .	1.1	27
11958	Surface concentration dependent structures of iodine on Pd(110). Journal of Chemical Physics, 2012, 137, 204703.	1.2	9
11959	Ab initiokinetic Monte Carlo model of ionic conduction in bulk yttria-stabilized zirconia. Modelling and Simulation in Materials Science and Engineering, 2012, 20, 065006.	0.8	12
11960	Predictions of Surface Electrochemistry of Saturated and Alkaline NH4Cl Solutions Interacting with Fe(110) from Ab Initio Calculations. Corrosion, 2012, 68, 591-599.	0.5	19
11961	Interface control of bulk ferroelectric polarization. Proceedings of the National Academy of Sciences of the United States of America, 2012, 109, 9710-9715.	3.3	212
11962	AB INITIO SIMULATIONS FOR MATERIAL PROPERTIES ALONG THE JUPITER ADIABAT. Astrophysical Journal, Supplement Series, 2012, 202, 5.	3.0	170
11963	Surface properties of clean and Au or Pd covered hematite (Î±-Fe₂O₃) (0001). Journal of Physics Condensed Matter, 2012, 24, 095003.	0.7	50

#	Article	IF	Citations
11964	Formation energies and the stability of the oxides of K. Molecular Simulation, 2012, 38, 1308-1314.	0.9	6
11965	First-principles investigation of diffusion behaviours of H isotopes: From W(110) surface into bulk and in bulk W. Chinese Physics B, 2012, 21, 126103.	0.7	5
11966	Dimensional reduction effect on momentum of carrier electrons in nanoscale silicon materials. , 2012, , .		2
11967	First-Principles Investigation of the Luminescence Mechanism of Eu²⁺in M₂SiO₄:Eu²⁺(M = Ba, Sr). ECS Journal of Solid State Science and Technology, 2012, 1, R87-R91.	0.9	17
11968	First-Principles Study on the Ideal Strengths of Typical Hcp Metals. Advanced Materials Research, 2012, 476-478, 2523-2529.	0.3	5
11969	A Formation Mechanism of X Level due to an Indium-Carbon Dimer in Silicon. Advanced Materials Research, 2012, 502, 154-158.	0.3	3
11970	Atomistic Simulation of Stress-Induced Grain Boundary Diffusion: For Tin-Whisker Problem. Materials Science Forum, 0, 706-709, 1545-1549.	0.3	2
11971	Site Preference and Elastic Properties of 3d Transition Metals Alloying Addition in Ductility YAg Alloys. Advanced Materials Research, 2012, 535-537, 1000-1004.	0.3	0
11972	Ab initioInvestigation of Hydrogen Atom Adsorption and Absorption on Pd(110) Surface. Journal of the Physical Society of Japan, 2012, 81, 114705.	0.7	19
11973	Superhard transition metal tetranitrides: XN₄(X = Re, Os, W). Journal of Materials Research, 2012, 27, 1705-1715.	1.2	20
11974	Ab initio description of quasiparticle band structures and optical near-edge absorption of transparent conducting oxides. Journal of Materials Research, 2012, 27, 2180-2189.	1.2	29
11975	The Effect of Pressure on Martensitic Phase Transformations. Advances in Science and Technology, 2012, 78, 13-18.	0.2	0
11976	Theory, Experiment and Computation of Half Metals for Spintronics: Recent Progress in Si-based Materials. The Nanoscale Systems: Mathematical Modelingory and Applications, 2012, 1, 1-22.	0.3	4
11977	Cerium-Doped Endohedral Fullerene: A Density-Functional Theory Study. , 2012, 2012, 1-8.		8
11978	The Synthetic Effects of Iron with Sulfur and Fluorine on Photoabsorption and Photocatalytic Performance in Codoped. International Journal of Photoenergy, 2012, 2012, 1-7.	1.4	2
11979	Carbon and other light element contents in the Earthâ€™s core based on first-principles molecular dynamics. Proceedings of the National Academy of Sciences of the United States of America, 2012, 109, 19579-19583.	3.3	77
11980	Catalytic Hydroxyl Radical Generation by CuO Confined in Multi-Walled Carbon Nanotubes. Advanced Materials Research, 0, 557-559, 448-455.	0.3	1
11981	Oxidation-Induced Epilayer Carbon Di-Interstitials as a Major Cause of Endemically Poor Mobilities in 4H-SiC/SiO₂ Structures. Materials Science Forum, 2012, 717-720, 445-448.	0.3	2

#	Article	IF	Citations
11982	Experimental and First Principles Study of the Ni-Ti-W System. Materials Science Forum, 0, 730-732, 775-780.	0.3	3
11983	Peculiar structure and tensile strength of WB4: nonstoichiometric origin. AIP Advances, 2012, 2, .	0.6	46
11984	Tuning electronic and magnetic properties of zigzag graphene nanoribbons by large-scale bending. Applied Physics Letters, 2012, 100, .	1.5	14
11985	Support effects on the dissociation of hydrogen over gold clusters on ZnO(101) surface: Theoretical insights. Journal of Chemical Physics, 2012, 137, 234704.	1.2	13
11986	Enhancing dissociative chemisorption of H ₂ O on Cu(111) via vibrational excitation. Proceedings of the National Academy of Sciences of the United States of America, 2012, 109, 10224-10227.	3.3	89
11987	Pulse-induced nonequilibrium dynamics of acetylene inside carbon nanotube studied by an ab initio approach. Proceedings of the National Academy of Sciences of the United States of America, 2012, 109, 8861-8865.	3.3	4
11988	First-principles study of the electronic and optical properties of the (Y, N)-codoped anatase TiO ₂ photocatalyst. Chinese Physics B, 2012, 21, 033103.	0.7	14
11989	Computational photonics from the bottom-up. , 2012, , .		0
11990	Defect properties of CuCrO₂: A density functional theory calculation. Chinese Physics B, 2012, 21, 087105.	0.7	13
11991	Visualizing frozen point defect tracks in Fe-containing olivines. Europhysics Letters, 2012, 98, 29001.	0.7	3
11992	Sensitizers in inelastic electron tunneling spectroscopy: a first-principles study of functional aromatics on Cu(111). Nanotechnology, 2012, 23, 315702.	1.3	6
11993	A New Insight into the Polaronâ€“Li Complex Diffusion in Cathode Material LiFe$_{1-y}$Mn$_{y}$PO$_{4}$ for Li Ion Batteries. Applied Physics Express, 2012, 5, 045801.	1.1	16
11994	Theory-Guided Materials Design of Multi-Phase Ti-Nb Alloys with Bone-Matching Elastic Properties. Materials, 2012, 5, 1853-1872.	1.3	70
11995	A density-functional theory investigation on desorption of O 2 on Sn(111) and its comparison with initial oxidation on the X (111) (X = Si, Ge, Sn, Pb) surfaces. Chinese Physics B, 2012, 21, 126803.	0.7	1
11996	Density functional theory study of the interaction of H ₂ with pure and Ti-doped WO ₃ (002) surfaces. Chinese Physics B, 2012, 21, 023101.	0.7	15
11997	Sulfur-induced embrittlement of nickel: a first-principles study. Modelling and Simulation in Materials Science and Engineering, 2012, 20, 065007.	0.8	28
11998	High-pressure structures of InBi predicted by particle swarm optimization algorithm. Chinese Physics B, 2012, 21, 026102.	0.7	4
11999	TAIPAN: First Results from the Thermal Triple-axis Spectrometer at OPAL Research Reactor. Journal of Physics: Conference Series, 2012, 340, 012003.	0.3	8

#	Article	IF	Citations
12000	Crystal Structure and Anomalous Sintering Behavior of (Sr0.7La0.3)1â^'xTiO3+Î´ Perovskites (0â€‰â‰€â€‰xâ€‰â‰€â€‰0.12) Synthesized by the Pechini Method. Journal of Fuel Cell Science and Technology, 2012, 9, .	0.8	16
12001	Ab-initioinvestigation of spin states of sodium cobaltate Na2/3CoO2. Journal of Physics: Conference Series, 2012, 394, 012019.	0.3	3
12002	Study on the effect of pressure on the properties of intrinsic point defects in monoclinic zirconia: Ab initio calculations. Journal of Applied Physics, 2012, 111, .	1.1	6
12003	Electronic and magnetic properties of oxygen patterned graphene superlattice. Journal of Applied Physics, 2012, 112, .	1.1	10
12004	Nitrogen induced ferromagnetism in Cobalt doped BaTiO3. AIP Advances, 2012, 2, 032148.	0.6	1
12005	A divide and conquer real-space approach for all-electron molecular electrostatic potentials and interaction energies. Journal of Chemical Physics, 2012, 136, 214104.	1.2	24
12006	A study on density functional theory of the effect of pressure on the formation and migration enthalpies of intrinsic point defects in growing single crystal Si. Journal of Applied Physics, 2012, 111, .	1.1	28
12007	Ferromagnetic nanostructures of oxygen on Ag(111). Journal of Physics: Conference Series, 2012, 379, 012013.	0.3	2
12008	Scanning Tunneling Microscopy and ab initio Studies of Precursor States of Ga-Induced Cluster on Si(001) Surface. Hyomen Kagaku, 2012, 33, 467-472.	0.0	0
12009	Ab-initio investigations of LuLiF4compound under pressure. Journal of Physics: Conference Series, 2012, 394, 012021.	0.3	0
12010	ENHANCEMENT OF GRAPHENE BINDING ENERGY BY Ti 1ML INTERCALATION BETWEEN GRAPHENE AND METAL SURFACES. International Journal of Modern Physics Conference Series, 2012, 11, 139-144.	0.7	1
12011	Ab-initio investigation of GdLiF4structure under pressure. Journal of Physics: Conference Series, 2012, 394, 012020.	0.3	1
12012	A Theoretical Study Showing K₂picene as a Parent Semiconductor for Organic Superconductivity. Journal of the Physical Society of Japan, 2012, 81, SB071.	0.7	3
12013	Transition-metal doping of small cadmium selenide clusters. Applied Physics Letters, 2012, 100, 053105.	1.5	5
12014	Diffusion of Transition Metals in 4H-SiC and Trials of Impurity Gettering. Applied Physics Express, 2012, 5, 031301.	1.1	16
12015	Monte Carlo simulation for the electron cascade due to gamma rays in semiconductor radiation detectors. Journal of Applied Physics, 2012, 111, 064910.	1.1	9
12016	Ab-initiostudy of metal-zirconia interfaces. IOP Conference Series: Materials Science and Engineering, 2012, 38, 012004.	0.3	4
12017	Electronic structures of graphane with vacancies and graphene adsorbed with fluorine atoms. AIP Advances, 2012, 2, 012173.	0.6	11

#	Article	IF	Citations
12018	A graphene composed of pentagons and octagons. AIP Advances, 2012, 2, .	0.6	14
12019	Effects of Co Addition on Crystal Structure, Thermal Stability and Magnetic Properties of Ni-Mn-Ga Ferromagnetic Shape Memory Alloys from First-Principles Calculations . Materials Science Forum, 0, 706-709, 1990-1995.	0.3	0
12020	Dispersion-corrected density functional theory calculations of the molecular binding of n-alkanes on Pd(111) and PdO(101). Journal of Chemical Physics, 2012, 136, 054702.	1.2	65
12021	Non-Idle-Spin Behavior and Field-Induced Magnetic Transitions of the Triple Chain Magnet Cu₃(OH)₄SO₄. Journal of the Physical Society of Japan, 2012, 81, 063704.	0.7	7
12022	Experimental Determination and Thermodynamic Assessment of Phase Equilibria in the Co–Mo System. Materials Transactions, 2012, 53, 1425-1435.	0.4	16
12023	New Growth Mechanism of Cubic Rh Clusters Composed of 8–12 Atoms Found by the Method of Euclidean Designs. Materials Transactions, 2012, 53, 459-462.	0.4	3
12024	Modulation effect of hydrogen and fluorine decoration on the surface work function of BN sheets. AIP Advances, 2012, 2, .	0.6	18
12025	Pulay forces from localized orbitals optimized in situ using a psinc basis set. Journal of Chemical Physics, 2012, 136, 234101.	1.2	41
12026	Oxidation of Germanium and Silicon surfaces (100): a comparative study through DFT methodology. IOP Conference Series: Materials Science and Engineering, 2012, 41, 012007.	0.3	9
12027	Electronic properties of rippled graphene. Journal of Physics: Conference Series, 2012, 402, 012004.	0.3	10
12028	Magnetic and structural properties of nanocrystalline PrCo3. IOP Conference Series: Materials Science and Engineering, 2012, 28, 012048.	0.3	5
12029	Excitation spectrum of point defects in semiconductors studied by time-dependent density functional theory. Journal of Materials Research, 2012, 27, 897-909.	1.2	31
12030	Shear strength and sliding behavior of Ni/Al₂O₃ interfaces: A first-principle study. Journal of Materials Research, 2012, 27, 1237-1244.	1.2	14
12031	A First-Principles Study of Pd-Pt Nanoclusters and their Hydrogen Adsorption Properties. Materials Research Society Symposia Proceedings, 2012, 1446, 49.	0.1	0
12032	Exit wave reconstruction from focal series of HRTEM images, single crystal XRD and total energy studies on Sb_xWO_{3+y}(xâ¼ 0.11). Zeitschrift Fur Kristallographie - Crystalline Materials, 2012, 227, 341-349.	0.4	8
12033	Hexamethoxytribenzocoronene, a Janus Double Concave Molecule to Selectively Assemble with Fullerene C60. Chemistry Letters, 2012, 41, 1588-1590.	0.7	4
12034	Hybrid Functional Study of the Structural and Electronic Properties of Co and Ni. Journal of the Physical Society of Japan, 2012, 81, 114715.	0.7	16
12035	First-Principles Calculations of Shocked Fluid Helium in Partially Ionized Region. Communications in Computational Physics, 2012, 12, 1121-1128.	0.7	3

#	Article	IF	Citations
12036	Electronâ€“Vibron Interaction Effects on Scanning Tunneling Microscopy Current through Melamine Adsorbed on Cu(100). Journal of the Physical Society of Japan, 2012, 81, 104711.	0.7	0
12037	Topological surface states scattering in antimony. Physical Review B, 2012, 86, .	1.1	21
12038	Mechanism and Kinetics for Ammonium Dinitramide (ADN) Sublimation: A First-Principles Study. Journal of Physical Chemistry A, 2012, 116, 10836-10841.	1.1	11
12039	Discriminative Separation of Gases by a â€œMolecular Trapdoorâ€•Mechanism in Chabazite Zeolites. Journal of the American Chemical Society, 2012, 134, 19246-19253.	6.6	321
12040	A canonical stabilityâ€“elasticity relationship verified for one million face-centred-cubic structures. Nature, 2012, 491, 740-743.	13.7	21
12041	Ferromagnetism and Orbital Order in a Topological Ferroelectric. Physical Review Letters, 2012, 109, 217202.	2.9	21
12042	Linear Magnetoelectric Effect by Orbital Magnetism. Physical Review Letters, 2012, 109, 197203.	2.9	52
12043	Evidence for Interlayer Coupling and MoirÃ© Periodic Potentials in Twisted Bilayer Graphene. Physical Review Letters, 2012, 109, 186807.	2.9	179
12044	Effects of Cu intercalation on the graphene/Ni(111) surface: Density-functional calculations. Journal of the Korean Physical Society, 2012, 61, 589-593.	0.3	5
12045	Co<mml:math xmlns:mml="http://www.w3.org/1998/Math/MathML" display="inline"><mml:mi>K</mml:mi></mml:math>-edge XANES of LiCoO<mml:math xmlns:mml="http://www.w3.org/1998/Math/MathML" display="inline"><mml:msub><mml:mrow /><mml:mn>2</mml:mn></mml:msub></mml:math>and CoO<mml:math xmlns:mml="http://www.w3.org/1998/Math/MathML" display="inline"><mml:msub><mml:mrow /><mml:mn>2</mml:mn></mml:msub></mml:math>with a variety of structures by supercell density fun	1.1	23
12046	Comparison of density functional approximations and the finite-temperature Hartree-Fock approximation in warm dense lithium. Physical Review E, 2012, 86, 056704.	0.8	26
12047	Natural torsion in chiral single-wall carbon nanotubes. Journal of Physics Condensed Matter, 2012, 24, 485302.	0.7	7
12048	Changes in a nanoparticleâ€™s spectroscopic signal mediated by the local environment. Nanotechnology, 2012, 23, 485202.	1.3	3
12049	Obtaining mixed ionic/electronic conductivity in perovskite oxides in a reducing environment: A computational prediction for doped SrTiO3. Solid State Ionics, 2012, 228, 37-45.	1.3	19
12050	STRUCTURAL, ELECTRONIC, AND MAGNETIC PROPERTIES OF BIMETALLIC TinMn13-n (n = 1â€“12) CLUSTERS FROM DENSITY FUNCTIONAL CALCULATIONS. Modern Physics Letters B, 2012, 26, 1250057.	1.0	2
12051	ATRâ€“FTIR and Density Functional Theory Study of the Structures, Energetics, and Vibrational Spectra of Phosphate Adsorbed onto Goethite. Langmuir, 2012, 28, 14573-14587.	1.6	142
12052	Binding of Pt Nanoclusters to Point Defects in Graphene: Adsorption, Morphology, and Electronic Structure. Journal of Physical Chemistry C, 2012, 116, 6543-6555.	1.5	224
12053	A Theoretical Study on the Structural and Energy Spectral Properties of Ce³⁺ Ions Doped in Various Fluoride Compounds. Journal of Physical Chemistry C, 2012, 116, 20513-20521.	1.5	39

#	Article	IF	Citations
12054	High pressure ices. Proceedings of the National Academy of Sciences of the United States of America, 2012, 109, 745-750.	3.3	92
12055	First-principles modeling of interfaces between solids with large lattice mismatch: The prototypical CoO(111)/Ni(111) interface. Physical Review B, 2012, 86, .	1.1	7
12056	Ab initio Calculations of Intrinsic Point Defects in ZnSb. Chemistry of Materials, 2012, 24, 2111-2116.	3.2	84
12057	Anisotropic Volume Expansion of Crystalline Silicon during Electrochemical Lithium Insertion: An Atomic Level Rationale. Nano Letters, 2012, 12, 5342-5347.	4.5	116
12058	Structural and Magnetic Properties of Small 4d Transition Metal Clusters: Role of Spinâ€“Orbit Coupling. Journal of Physical Chemistry A, 2012, 116, 11673-11684.	1.1	31
12059	Modifying the Atomic and Electronic Structures of Gold Nanocrystals via Changing the Chain Length of n-Alkanethiol Ligands. Journal of Physical Chemistry C, 2012, 116, 24999-25003.	1.5	16
12060	Making Câ€“C Bonds with Gold: Identification of Selective Gold Sites for Homo- and Cross-Coupling Reactions between Iodobenzene and Alkynes. Journal of Physical Chemistry C, 2012, 116, 24855-24867.	1.5	65
12061	Are MXenes Promising Anode Materials for Li Ion Batteries? Computational Studies on Electronic Properties and Li Storage Capability of Ti₃C₂ and Ti₃C₂X₂ (X = F, OH) Monolayer. Journal of the American Chemical Society, 2012, 134, 16909-16916.	6.6	1,768
12062	First-principles based thermodynamic model of phase equilibria in bcc Fe-Cr alloys. Physical Review B, 2012, 86, .	1.1	48
12063	Searching for active binary rutile oxide catalyst for water splitting from first principles. Physical Chemistry Chemical Physics, 2012, 14, 16612.	1.3	22
12064	Phonons in lanthanum manganite: Inelastic neutron scattering and density functional theory studies. Physical Review B, 2012, 86, .	1.1	2
12065	Effect of point defects on the electronic density of states of ScN studied by first-principles calculations and implications for thermoelectric properties. Physical Review B, 2012, 86, .	1.1	65
12066	Structure and diffusion in liquid complex hydrides viaab initiomolecular dynamics. Physical Review B, 2012, 86, .	1.1	8
12067	Domain formation on oxidized graphene. Physical Review B, 2012, 86, .	1.1	40
12068	Deciphering the Chemical Bonding in Anionic Thallium Clusters. Journal of the American Chemical Society, 2012, 134, 19884-19894.	6.6	15
12069	Solvent- and anion-controlled photochromism of viologen-based metalâ€“organic hybrid materials. Journal of Materials Chemistry, 2012, 22, 12212.	6.7	145
12070	The Electronic Structures, Born Effective Charges, and Interatomic Force Constants in <scp><scp>BaMO</scp></scp>₃ (MÂ=ÂTi, Zr, Hf, Sn): A Comparative Firstâ€Principles Study. Journal of the American Ceramic Society, 2012, 95, 3597-3604.	1.9	21
12071	<scp><scp>Y</scp></scp>₄<scp><scp>Si</scp></scp>₂<scp><scp>O</scp></scp>₇<scp><sc A New Oxynitride with Low Thermal Conductivity. Journal of the American Ceramic Society, 2012, 95, 3278-3284.	1.9	23

#	Article	IF	Citations
12072	Atomic Structure, Electronic Structure, and Optical Properties of <scp>YAG</scp> (110) Twin Grain Boundary. Journal of the American Ceramic Society, 2012, 95, 3894-3900.	1.9	3
12073	First-principles study of thermal properties and phase transition between Î²-Ti₃O₅and Î»-Ti₃O₅. Modelling and Simulation in Materials Science and Engineering, 2012, 20, 035020.	0.8	14
12074	Thermodynamic properties and structural stability of thorium dioxide. Journal of Physics Condensed Matter, 2012, 24, 225801.	0.7	68
12075	Synthesis, characterization and sorption properties of NH2-MIL-47. Physical Chemistry Chemical Physics, 2012, 14, 15562.	1.3	27
12076	Selectivity of Palladiumâ€“Cobalt Surface Alloy toward Oxygen Reduction Reaction. Journal of Physical Chemistry C, 2012, 116, 6200-6207.	1.5	24
12077	Bi on the Si(001) surface. Physical Review B, 2012, 86, .	1.1	4
12078	Charge Density Analysis and Topological Properties of Hal₃-Synthons and Their Comparison with Competing Hydrogen Bonds. Crystal Growth and Design, 2012, 12, 5373-5386.	1.4	78
12079	Two-dimensional organometallic porous sheets with possible high-temperature ferromagnetism. Nanoscale, 2012, 4, 5304.	2.8	23
12080	Uranyl adsorption on solvated edge surfaces of pyrophyllite: a DFT model study. Physical Chemistry Chemical Physics, 2012, 14, 5815.	1.3	46
12081	Polarization-Driven Topological Insulator Transition in a<mml:math xmlns:mml="http://www.w3.org/1998/Math/MathML" display="inline"><mml:mi>GaN</mml:mi><mml:mo>/</mml:mo><mml:mi>InN</mml:mi><mml:mo>/</mml:mo><mml:mi>GaN</mml:mi> Well. Physical Review Letters, 2012, 109, 186803.	2.9	158
12082	Half-metallic ferromagnetism in substitutionally doped boronitrene. Physical Review B, 2012, 86, .	1.1	10
12083	Tuning the band gap of bilayer graphene by ion implantation: Insight from computational studies. Physical Review B, 2012, 86, .	1.1	26
12084	Complete structural model for lanthanum tungstate: a chemically stable high temperature proton conductor by means of intrinsic defects. Journal of Materials Chemistry, 2012, 22, 1762-1764.	6.7	91
12085	Conductivity of an atomically defined metallic interface. Proceedings of the National Academy of Sciences of the United States of America, 2012, 109, 19097-19102.	3.3	25
12086	High-Pressure Phase Favored by a Symmetry-Recognized Nanoconfinement Effect. Journal of Physical Chemistry Letters, 2012, 3, 2154-2158.	2.1	2
12087	Method for defect stability diagram fromab initiocalculations: A case study of SrTiO<mml:math xmlns:mml="http://www.w3.org/1998/Math/MathML" display="inline"><mml:msub><mml:mrow /><mml:mn>3</mml:mn></mml:msub></mml:math>. Physical Review B, 2012, 86, .	1.1	28
12088	Phase Stability of the Earth-Abundant Tin Sulfides SnS, SnS₂, and Sn₂S₃. Journal of Physical Chemistry C, 2012, 116, 24262-24267.	1.5	201
12089	Charge-Selective Surface-Enhanced Raman Scattering Using Silver and Gold Nanoparticles Deposited on Siliconâ€“Carbon Coreâ€“Shell Nanowires. ACS Nano, 2012, 6, 2459-2470.	7.3	42

#	Article	IF	Citations
12090	Modeling charge transfer at organic donor-acceptor semiconductor interfaces. Applied Physics Letters, 2012, 100, 203302.	1.5	27
12091	Calculating Band Alignment between Materials with Different Structures: The Case of Anatase and Rutile Titanium Dioxide. Journal of Physical Chemistry C, 2012, 116, 20765-20768.	1.5	45
12092	Influence of polarizability on metal oxide properties studied by molecular dynamics simulations. Journal of Physics Condensed Matter, 2012, 24, 485401.	0.7	8
12093	Pressure-Induced Formation of Noble Metal Hydrides. Journal of Physical Chemistry C, 2012, 116, 1995-2000.	1.5	46
12094	Modulated structure and molecular dissociation of solid chlorine at high pressures. Journal of Chemical Physics, 2012, 137, 064502.	1.2	22
12095	First-principles models for phase stability and radiation defects in structural materials for future fusion power-plant applications. Journal of Materials Science, 2012, 47, 7385-7398.	1.7	26
12096	Identification of magnetic dopants on the surfaces of topological insulators: Experiment and theory for Fe on Bi<mml:math xmlns:mml="http://www.w3.org/1998/Math/MathML" display="inline"><mml:msub><mml:mrow /><mml:mn>2</mml:mn></mml:msub></mml:math>Te<mml:math xmlns:mml="http://www.w3.org/1998/Math/MathML" display="inline"><mml:msub><mml:mrow /><mml:mn>3</mml:mn></mml:msub></mml:math>(111). Physical Review B, 2012, 85, .	1.1	49
12097	Solidâ€“Electrolyte Interphase Formation and Electrolyte Reduction at Li-Ion Battery Graphite Anodes: Insights from First-Principles Molecular Dynamics. Journal of Physical Chemistry C, 2012, 116, 24476-24481.	1.5	111
12098	Physical properties of transparent perovskite oxides (Ba,La)SnO<mml:math xmlns:mml="http://www.w3.org/1998/Math/MathML" display="inline"><mml:msub><mml:mrow /><mml:mn>3</mml:mn></mml:msub></mml:math>with high electrical mobility at room temperature. Physical Review B, 2012, 86, .	1.1	264
12099	Attracting shallow donors: Hydrogen passivation in (Al,Ga,In)-doped ZnO. Physical Review B, 2012, 86, .	1.1	9
12100	First-principles calculations of electronic and magnetic properties in semi-fluorinated CdS sheet. Physics Letters, Section A: General, Atomic and Solid State Physics, 2012, 376, 3402-3406.	0.9	12
12101	Chlorine Adsorption on Graphene: Chlorographene. Journal of Physical Chemistry C, 2012, 116, 24075-24083.	1.5	135
12102	Large excitonic effects in monolayers of molybdenum and tungsten dichalcogenides. Physical Review B, 2012, 86, .	1.1	1,250
12103	Crystal and Electronic Structure and Magnetic Properties of Divalent Europium Perovskite Oxides EuMO₃ (M = Ti, Zr, and Hf): Experimental and First-Principles Approaches. Inorganic Chemistry, 2012, 51, 4560-4567.	1.9	54
12104	Theoretical Study of NO Conversion on Ag/TiO₂ Systems. I. Anatase (100) Surface. Journal of Physical Chemistry C, 2012, 116, 25262-25273.	1.5	11
12105	Dirac Fermions in Strongly Bound Graphene Systems. Physical Review Letters, 2012, 109, 206802.	2.9	53
12106	Theoretical Investigation of the Metal-Doped SrTiO₃ Photocatalysts for Water Splitting. Journal of Physical Chemistry C, 2012, 116, 7897-7903.	1.5	134
12107	First-principles study of the magnesiation of olivines: redox reaction mechanism, electrochemical and thermodynamic properties. Journal of Materials Chemistry, 2012, 22, 13517.	6.7	72

#	Article	IF	Citations
12108	Quantitative theory of the oxygen vacancy and carrier self-trapping in bulk TiO<mml:math xmlns:mml="http://www.w3.org/1998/Math/MathML" display="inline"><mml:msub><mml:mrow /><mml:mn>2</mml:mn></mml:msub></mml:math>. Physical Review B, 2012, 86, .	1.1	169
12109	Atomistic Description of Electron Beam Damage in Nitrogen-Doped Graphene and Single-Walled Carbon Nanotubes. ACS Nano, 2012, 6, 8837-8846.	7.3	119
12110	Morphological Dependence of Lithium Insertion in Nanocrystalline TiO₂(B) Nanoparticles and Nanosheets. Journal of Physical Chemistry Letters, 2012, 3, 2015-2019.	2.1	87
12111	Rietveld refinement and structure verification using `Morse' restraints. Journal of Applied Crystallography, 2012, 45, 1187-1197.	1.9	28
12112	Complex Surface Chemistry of 4-Mercaptopyridine Self-Assembled Monolayers on Au(111). Langmuir, 2012, 28, 6839-6847.	1.6	45
12113	Origin of the Structural Phase Transition in<mml:math xmlns:mml="http://www.w3.org/1998/Math/MathML" display="inline"><mml:msub><mml:mi>Li</mml:mi><mml:mn>7</mml:mn></mml:msub><mml:msub><mml:mi>La</mml:mi><mml:mn>3</mml:mn></mml:msub><mml:msub><mml:mi mathvariant="normal">O</mml:mi><mml:mn>12</mml:mn></mml:msub></mml:math>. Physical Review Letters, 2012, 109, 205702.	7.5	191
12114	Carbon Monoxide-Assisted Synthesis of Single-Crystalline Pd Tetrapod Nanocrystals through Hydride Formation. Journal of the American Chemical Society, 2012, 134, 7073-7080.	6.6	120
12115	Growth and electronic structure of nitrogen-doped graphene on Ni(111). Physical Review B, 2012, 86, .	1.1	77
12116	Ab initiosimulations of hot dense methane during shock experiments. Physical Review B, 2012, 86, .	1.1	31
12117	Visible-Light-Absorption in Graphitic C₃N₄ Bilayer: Enhanced by Interlayer Coupling. Journal of Physical Chemistry Letters, 2012, 3, 3330-3334.	2.1	138
12118	Magnetic Properties of Single Transition-Metal Atom Absorbed Graphdiyne and Graphyne Sheet from DFT+U Calculations. Journal of Physical Chemistry C, 2012, 116, 26313-26321.	1.5	264
12119	Tunable Hydrogen Separation in spâ€“sp² Hybridized Carbon Membranes: A First-Principles Prediction. Journal of Physical Chemistry C, 2012, 116, 16634-16638.	1.5	135
12120	Two-Dimensional Superlattice: Modulation of Band Gaps in Graphene-Based Monolayer Carbon Superlattices. Journal of Physical Chemistry Letters, 2012, 3, 3373-3378.	2.1	60
12121	Orientation of a Series of CO2 Reduction Catalysts on Single Crystal TiO2 Probed by Phase-Sensitive Vibrational Sum Frequency Generation Spectroscopy (PS-VSFG). Journal of Physical Chemistry C, 2012, 116, 24107-24114.	1.5	48
12122	DFT Study of CO₂ Adsorption and Hydrogenation on the In₂O₃ Surface. Journal of Physical Chemistry C, 2012, 116, 7817-7825.	1.5	265
12123	Pressure-induced group-subgroup phase transitions and post-cotunnite phases in actinide dioxides. Physical Review B, 2012, 85, .	1.1	17
12124	First-principles study of rare-earth-doped superconducting CaFe<mml:math xmlns:mml="http://www.w3.org/1998/Math/MathML" display="inline"><mml:msub><mml:mrow /><mml:mn>2</mml:mn></mml:msub></mml:math>As<mml:math xmlns:mml="http://www.w3.org/1998/Math/MathML" display="inline"><mml:msub><mml:mrow /><mml:mn>2</mml:mn></mml:msub></mml:math>. Physical Review B, 2012, 86, .	1.1	15
12125	MgFeGe as an isoelectronic and isostructural analog of the superconductor LiFeAs. Physical Review B, 2012, 85, .	1.1	14

#	Article	IF	Citations
12126	A comparison of destabilization mechanisms of the layered NaxMO2 and LixMO2 compounds upon alkali de-intercalation. Physical Chemistry Chemical Physics, 2012, 14, 15571.	1.3	158
12127	of CuInSe<mml:math xmlns:mml="http://www.w3.org/1998/Math/MathML" display="inline"><mml:msub><mml:mrow /><mml:mn>2</mml:mn></mml:msub></mml:math>and	1.1	70
12128	Electronic Structure of an Organic/Metal Interface: Pentacene/Cu(110). Journal of Physical Chemistry C, 2012, 116, 23465-23471.	1.5	49
12129	Interaction between graphene and the surface of SiO₂. Journal of Physics Condensed Matter, 2012, 24, 305004.	0.7	69
12130	DFT-based tight-binding modeling of iron-carbon. Physical Review B, 2012, 86, .	1.1	16
12131	Simulation of STM Images on a Flat Si (110)-(8Ã—2) Surface Using Density Functional Theory. Journal of the Electrochemical Society, 2012, 159, H201-H207.	1.3	4
12132	Giant Topological Insulator Gap in Graphene with<mml:math xmlns:mml="http://www.w3.org/1998/Math/MathML" display="inline"><mml:mn>5</mml:mn><mml:mi>d</mml:mi></mml:math>Adatoms. Physical Review Letters, 2012, 109, 266801.	2.9	186
12133	Modelling nanoscale cubic ZnS morphology and thermodynamic stability under sulphur-rich conditions. CrystEngComm, 2012, 14, 7749.	1.3	6
12134	Revealing non-covalent interactions in solids: NCI plots revisited. Physical Chemistry Chemical Physics, 2012, 14, 12165.	1.3	279
12135	Ab initio study of collective excitations in a disparate mass molten salt. Journal of Chemical Physics, 2012, 137, 224508.	1.2	11
12136	Catalytic Oxygen Activation on Helical Gold Nanowires. Journal of Physical Chemistry C, 2012, 116, 11189-11194.	1.5	13
12137	The adsorption of acrolein on a Pt (1 1 1): A study of chemical bonding and electronic structure. Applied Surface Science, 2012, 263, 79-85.	3.1	9
12138	Strain effects and band parameters in MgO, ZnO, and CdO. Applied Physics Letters, 2012, 101, .	1.5	67
12139	Type-I clathrate Ba8NixSi46â^'x: Phase relations, crystal chemistry and thermoelectric properties. Dalton Transactions, 2012, 41, 8839.	1.6	25
12140	First-Principles Predictions of Thermoelectric Figure of Merit for Organic Materials: Deformation Potential Approximation. Journal of Chemical Theory and Computation, 2012, 8, 3338-3347.	2.3	59
12141	A theoretical study of structural and electronic properties of pentacene/Al(1 0 0) interface. Journal of Molecular Graphics and Modelling, 2012, 38, 334-341.	1.3	10
12142	Homo-coupling of terminal alkynes on a noble metal surface. Nature Communications, 2012, 3, 1286.	5.8	350
12143	Scanning transmission electron microscopy: Albert Crewe's vision and beyond. Ultramicroscopy, 2012, 123, 90-98.	0.8	25

#	Article	IF	Citations
12144	First-principles prediction of oxygen octahedral rotations in perovskite-structure EuTiO<mml:math xmlns:mml="http://www.w3.org/1998/Math/MathML" display="inline"><mml:msub><mml:mrow /><mml:mn>3</mml:mn></mml:msub></mml:math>. Physical Review B, 2012, 85, .	1.1	55
12145	First-Principles Determination of the Structure of Magnesium Borohydride. Physical Review Letters, 2012, 109, 245503.	2.9	47
12146	Structural, electronic, and transport properties of silicane nanoribbons. Physical Review B, 2012, 86, .	1.1	28
12147	Transition Metal Decorated Porphyrin-like Porous Fullerene: Promising Materials for Molecular Hydrogen Adsorption. Journal of Physical Chemistry C, 2012, 116, 25184-25189.	1.5	68
12148	DFT investigation of molybdenum (oxo)carbide formation from MoO3. Structural Chemistry, 2012, 23, 1417-1424.	1.0	8
12149	Simulation of Spatially Resolved Electron Energy Loss Near-Edge Structure for Scanning Transmission Electron Microscopy. Physical Review Letters, 2012, 109, 246101.	2.9	21
12150	Amide Functionalization of Graphene and Carbon Nanotubes: Coverage- and Pattern-Dependent Electronic and Magnetic Properties. Journal of Physical Chemistry C, 2012, 116, 13722-13730.	1.5	20
12151	Octagraphene as a versatile carbon atomic sheet for novel nanotubes, unconventional fullerenes, and hydrogen storage. Journal of Applied Physics, 2012, 112, .	1.1	110
12152	Exotic Cubic Carbon Allotropes. Journal of Physical Chemistry C, 2012, 116, 24233-24238.	1.5	53
12153	Effects of Composition on Atomic Structure, Diffusivity, and Viscosity of Liquid Al-Zr Alloys. Metallurgical and Materials Transactions A: Physical Metallurgy and Materials Science, 2012, 43, [illegible]	1.1	21
12154	Helicoidal magnetic structure and ferroelectric polarization in Cu<mml:math xmlns:mml="http://www.w3.org/1998/Math/MathML" display="inline"><mml:msub><mml:mrow /><mml:mn>3</mml:mn></mml:msub></mml:math>Nb<mml:math xmlns:mml="http://www.w3.org/1998/Math/MathML" display="inline"><mml:msub><mml:mrow /><mml:mn>2</mml:mn></mml:msub></mml:math>O<mml:math xmlns:mml="http://www.w3.org/1998/Math/MathML" display="inline"><mml:msub><mml:mrow /><mml:mml:	1.1	8
12155	Hard magnetic ferrite with a gigantic coercivity and high frequency millimetre wave rotation. Nature Communications, 2012, 3, 1035.	5.8	184
12156	AbÂinitioCalculations of Deep-Level Carrier Nonradiative Recombination Rates in Bulk Semiconductors. Physical Review Letters, 2012, 109, 245501.	2.9	82
12157	CsHgInS₃: a New Quaternary Semiconductor for Î³-ray Detection. Chemistry of Materials, 2012, 24, 4434-4441.	3.2	56
12158	Strain-engineered artificial atom as a broad-spectrum solar energy funnel. Nature Photonics, 2012, 6, 866-872.	15.6	907
12159	Spin-orbit coupling effect by minority interface resonance states in single-crystal magnetic tunnel junctions. Physical Review B, 2012, 86, .	1.1	20
12160	Effects of strain on band structure and effective masses in MoS<mml:math xmlns:mml="http://www.w3.org/1998/Math/MathML" display="inline"><mml:msub><mml:mrow /><mml:mn>2</mml:mn></mml:msub></mml:math>. Physical Review B, 2012, 86, .	1.1	405
12161	A theoretical simulation on the catalytic oxidation of CO on Pt/graphene. Physical Chemistry Chemical Physics, 2012, 14, 16566.	1.3	297

#	Article	IF	Citations
12162	Hydrogen-induced reversible spin-reorientation transition and magnetic stripe domain phase in bilayer Co on Ru(0001). Physical Review B, 2012, 85, .	1.1	14
12163	Stepwise Photocatalytic Dissociation of Methanol and Water on TiO₂(110). Journal of the American Chemical Society, 2012, 134, 13366-13373.	6.6	244
12164	Energetic Driving Force of H Spillover between Rhodium and Titania Surfaces: A DFT View. Journal of Physical Chemistry C, 2012, 116, 25362-25367.	1.5	18
12165	Short-range order of Br and three-dimensional magnetism in (CuBr)LaNb<mml:math xmlns:mml="http://www.w3.org/1998/Math/MathML" display="inline"><mml:msub><mml:mrow /><mml:mn>2</mml:mn></mml:msub></mml:math>O<mml:math xmlns:mml="http://www.w3.org/1998/Math/MathML" display="inline"><mml:msub><mml:mrow /><mml:mn>7</mml:mn></mml:msub></mml:math>. Physical Review B, 2012, 85, .	1.1	7
12166	First-principles study of an interfacial phase diagram in the V-doped WC-Co system. Physical Review B, 2012, 86, .	1.1	35
12167	An effective structure prediction method for layered materials based on 2D particle swarm optimization algorithm. Journal of Chemical Physics, 2012, 137, 224108.	1.2	275
12168	Cyclometalated Ruthenium Oligomers with 2,3-Di(2-pyridyl)-5,6-diphenylpyrazine: A Combined Experimental, Computational, and Comparison Study with Noncyclometalated Analogous. Inorganic Chemistry, 2012, 51, 13312-13320.	1.9	15
12169	Low-energy structures of zinc borohydride Zn(BH<mml:math) 1j ETQq1 1 0.784314 rgBT /Overlock 10 Tf 50 477 Td (xmlns:mml="http://www.w3.org/1998/Math/MathML" display="inline"><mml:msub><mml:mrow /><mml:mn>2</mml:mn></mml:msub></mml:math>. Physical Review B, 2012, 86, .	1.1	27
12170	A new insight into the initial step in the Fischerâ€“Tropsch synthesis: CO dissociation on Ru surfaces. Physical Chemistry Chemical Physics, 2012, 14, 16686.	1.3	28
12171	Coherent and incoherent phase stabilities of thermoelectric rocksalt IV-VI semiconductor alloys. Physical Review B, 2012, 86, .	1.1	41
12172	Formation of twins in sapphire under shock wave loading: Atomistic simulations. Journal of Applied Physics, 2012, 111, .	1.1	16
12173	Polarization-dependent water adsorption on the LiNbO<mml:math xmlns:mml="http://www.w3.org/1998/Math/MathML" display="inline"><mml:msub><mml:mrow /><mml:mn>3</mml:mn></mml:msub></mml:math>(0001) surface. Physical Review B, 2012, 86, .	1.1	34
12174	Layered Hydride CaNiGeH with a ZrCuSiAs-type Structure: Crystal Structure, Chemical Bonding, and Magnetism Induced by Mn Doping. Journal of the American Chemical Society, 2012, 134, 11687-11694.	6.6	19
12175	Icosahedral Platinum Alloy Nanocrystals with Enhanced Electrocatalytic Activities. Journal of the American Chemical Society, 2012, 134, 11880-11883.	6.6	496
12176	High pressure structures of â€œ111â€•type iron-based superconductors predicted from first-principles. Physical Chemistry Chemical Physics, 2012, 14, 15029.	1.3	16
12177	Analysis of structural and electronic properties of Pr2NiO4through first-principles calculations. Journal of Physics Condensed Matter, 2012, 24, 405504.	0.7	13
12178	Spin Waves and Revised Crystal Structure of Honeycomb Iridate<mml:math xmlns:mml="http://www.w3.org/1998/Math/MathML" display="inline"><mml:msub><mml:mi>Na</mml:mi><mml:mn>2</mml:mn></mml:msub><mml:msub><mml:mi>IrO</mml:mi><mml:m Physical Review Letters, 2012, 108, 127204.	2.9	502
12179	Direct observation of a ferri-to-ferromagnetic transition in a fluoride-bridged 3dâ€“4f molecular cluster. Chemical Science, 2012, 3, 1024-1032.	3.7	78

#	Article	IF	Citations
12180	Effect of Subsurface Vacancies on Oxygen Reduction Reaction Activity of Pt-Based Alloys. Journal of Physical Chemistry C, 2012, 116, 14414-14422.	1.5	32
12181	Binding of an Oxide Layer to a Metal: The Case of Ti(101Ì…0)/TiO2(100). Journal of Physical Chemistry C, 2012, 116, 4224-4233.	1.5	8
12182	Atomic-Scale Modeling of the Dynamics of Titanium Oxidation. Journal of Physical Chemistry C, 2012, 116, 24201-24205.	1.5	15
12183	High Stability and Reactivity of Pt-Based Coreâ€“Shell Nanoparticles for Oxygen Reduction Reaction. Journal of Physical Chemistry C, 2012, 116, 13774-13780.	1.5	17
12184	Suppression of mixed-phase areas in highly elongated BiFeO<mml:math xmlns:mml="http://www.w3.org/1998/Math/MathML" display="inline"><mml:msub><mml:mrow /><mml:mn>3</mml:mn></mml:msub></mml:math>thin films on NdAlO<mml:math xmlns:mml="http://www.w3.org/1998/Math/MathML" display="inline"><mml:msub><mml:mrow /><mml:mn>3</mml:mn></mml:msub></mml:math>substrates. Physical Review B, 2012, 86, .	1.1	34
12185	Atomic and electronic structures of FeSe monolayer and bilayer thin films on SrTiO<mml:math xmlns:mml="http://www.w3.org/1998/Math/MathML" display="inline"><mml:msub><mml:mrow /><mml:mn>3</mml:mn></mml:msub></mml:math>(001): First-principles study. Physical Review B, 2012, 85, .	1.1	80
12186	Elucidation of Rh-Induced In-Gap States of Rh:SrTiO₃ Visible-Light-Driven Photocatalyst by Soft X-ray Spectroscopy and First-Principles Calculations. Journal of Physical Chemistry C, 2012, 116, 24445-24448.	1.5	89
12187	A multi scale modeling approach to non-radiative multi phonon transitions at oxide defects in MOS structures. Journal of Computational Electronics, 2012, 11, 218-224.	1.3	16
12188	High-pressure lattice dynamical study of bulk and nanocrystalline In2O3. Journal of Applied Physics, 2012, 112, .	1.1	55
12189	Ab initio calculations and thermodynamic modeling for the Feâ€“Mnâ€“Nb system. Calphad: Computer Coupling of Phase Diagrams and Thermochemistry, 2012, 38, 43-58.	0.7	46
12190	Understanding and Revisiting Properties of<mml:math xmlns:mml="http://www.w3.org/1998/Math/MathML" display="inline"><mml:msub><mml:mi>EuTiO</mml:mi><mml:mn>3</mml:mn></mml:msub></mml:math>Bulk Material and Films from First Principles. Physical Review Letters, 2012, 109, 267602.	2.9	46
12191	Contact-induced spin polarization in graphene/h-BN/Ni nanocomposites. Journal of Applied Physics, 2012, 112, .	1.1	20
12192	Rhombohedralâ€“orthorhombic morphotropic phase boundary in BiFeO3-based multiferroics: first-principles prediction. Journal of Materials Chemistry, 2012, 22, 1667-1672.	6.7	51
12193	Role of self-trapping in luminescence and<mml:math xmlns:mml="http://www.w3.org/1998/Math/MathML" display="inline"><mml:mi>p</mml:mi></mml:math>-type conductivity of wide-band-gap oxides. Physical Review B, 2012, 85, .	1.1	440
12194	A DFT study of methanol dehydrogenation on the PdIn(110) surface. Physical Chemistry Chemical Physics, 2012, 14, 16660.	1.3	27
12195	Electron correlation and spin-orbit coupling effects in US3 and USe3. Journal of Chemical Physics, 2012, 137, 214703.	1.2	1
12196	Electronic bands of III-V semiconductor polytypes and their alignment. Physical Review B, 2012, 86, .	1.1	134
12197	Generalization of Natural Bond Orbital Analysis to Periodic Systems: Applications to Solids and Surfaces via Plane-Wave Density Functional Theory. Journal of Chemical Theory and Computation, 2012, 8, 1902-1911.	2.3	177

#	Article	IF	Citations
12198	Effect of Rare Earth Elements and Alloy Composition on Hydrogenation Properties and Crystal Structures of Hydrides in Mg2â€“xRExNi4. Journal of Physical Chemistry C, 2012, 116, 19156-19163.	1.5	32
12199	Understanding of the Buckling Distortions in Silicene. Journal of Physical Chemistry C, 2012, 116, 24639-24648.	1.5	188
12200	Chemical and optical properties of carbon-doped TiO2: A density-functional study. Applied Physics Letters, 2012, 100, 102114.	1.5	54
12201	Low-frequency Raman modes and electronic excitations in atomically thin MoS<mml:math xmlns:mml="http://www.w3.org/1998/Math/MathML" display="inline"><mml:msub><mml:mrow /><mml:mn>2</mml:mn></mml:msub></mml:math>films. Physical Review B, 2012, 86, .	1.1	134
12202	Band gap control via tuning of inversion degree in CdIn2S4 spinel. Applied Physics Letters, 2012, 100, .	1.5	31
12203	Realization of tunable Dirac cone and insulating bulk states in topological insulators (Bi1â^'xSbx)2Te3. Scientific Reports, 2012, 2, 976.	1.6	24
12204	Atomic and electronic structure of superionic solid electrolyte Li₁₀GeP₂S₁₂. Materials Research Society Symposia Proceedings, 2012, 1440, 56.	0.1	2
12205	Ab initioprediction of pressure-induced structural phase transitions of CrVO<mml:math xmlns:mml="http://www.w3.org/1998/Math/MathML" display="inline"><mml:msub><mml:mrow /><mml:mn>4</mml:mn></mml:msub></mml:math>-type orthophosphates. Physical Review B, 2012, 86, .	1.1	39
12206	High-pressure transition to the post-barite phase in BaCrO<mml:math xmlns:mml="http://www.w3.org/1998/Math/MathML" display="inline"><mml:msub><mml:mrow /><mml:mn>4</mml:mn></mml:msub></mml:math>hashemite. Physical Review B, 2012, 86, .	1.1	27
12207	First principles study of foreign interstitial atom (carbon, nitrogen) interactions with intrinsic defects in tungsten. Journal of Nuclear Materials, 2012, 430, 270-278.	1.3	40
12208	Bonding Mechanisms of Graphene on Metal Surfaces. Journal of Physical Chemistry C, 2012, 116, 7360-7366.	1.5	133
12209	Achieving fast convergence of ab initio free energy perturbation calculations with the adaptive force-matching method. Theoretical Chemistry Accounts, 2012, 131, 1.	0.5	25
12210	Structural, magnetic and electronic properties of FeF2 by first-principle calculation. Transactions of Nonferrous Metals Society of China, 2012, 22, 386-390.	1.7	5
12211	Firstâ€"principles study of stacking fault energies in Ni3Al intermetallic alloys. Transactions of Nonferrous Metals Society of China, 2012, 22, 661-664.	1.7	35
12212	Band gap narrowing of TiO2 by compensated codoping for enhanced photocatalytic activity. Journal of Natural Gas Chemistry, 2012, 21, 302-307.	1.8	31
12213	First-Principles Calculations on Structure, Elastic and Thermodynamic Properties of Al2X (X=Sc, Y) under Pressure. Journal of Materials Science and Technology, 2012, 28, 155-163.	5.6	28
12214	First Principles Calculations for Structural, Electronic, and Magnetic Properties of Gadolinium-Doped Alumina Clusters. Journal of Physical Chemistry C, 2012, 116, 6115-6126.	1.5	11
12215	Site-Selective Cu Deposition on Pt Dendrimer-Encapsulated Nanoparticles: Correlation of Theory and Experiment. Journal of the American Chemical Society, 2012, 134, 4153-4162.	6.6	44

#	Article	IF	Citations
12216	Porous Carbon Nanotube Membranes for Separation of H₂/CH₄ and CO₂/CH₄ Mixtures. Journal of Physical Chemistry C, 2012, 116, 25904-25910.	1.5	59
12217	Empirical oscillating potentials for alloys fromab initiofits and the prediction of quasicrystal-related structures in the Al-Cu-Sc system. Physical Review B, 2012, 85, .	1.1	45
12218	Band structure of gold from many-body perturbation theory. Physical Review B, 2012, 86, .	1.1	91
12219	A novel phosphor for glareless white light-emitting diodes. Nature Communications, 2012, 3, 1132.	5.8	306
12220	Adsorption of Polyvinylpyrrolidone on Ag Surfaces: Insight into a Structure-Directing Agent. Nano Letters, 2012, 12, 997-1001.	4.5	173
12221	LaSrVMoO6: A case study forA-site covalency-driven local cationic order in double perovskites. Physical Review B, 2012, 86, .	1.1	5
12222	Nearly Equivalent Inter- and Intramolecular Hydrogen Bonding in 1,3,5-Triamino-2,4,6-trinitrobenzene at High Pressure. Journal of Physical Chemistry C, 2012, 116, 2116-2122.	1.5	46
12223	First-principles study of magnetoelastic effect in the diatomic compounds<mml:math xmlns:mml="http://www.w3.org/1998/Math/MathML" display="inline"><mml:mi>M</mml:mi></mml:math>F<mml:math xmlns:mml="http://www.w3.org/1998/Math/MathML" display="inline"><mml:msub><mml:mrow		

#	Article	IF	Citations
12236	Effects of contact oxidization on the transport properties of Au/ZGNR junctions. Physica Status Solidi - Rapid Research Letters, 2012, 6, 457-459.	1.2	4
12237	Combined inelastic neutron scattering and solid-state DFT study of dynamics of hydrogen atoms in trioctahedral 1M phlogopite. Physics and Chemistry of Minerals, 2012, 39, 779-787.	0.3	1
12238	Electronic structure and optical property of 3d transition metal doped (5,5) boron nitride nanotube. Applied Physics A: Materials Science and Processing, 2012, 109, 601-606.	1.1	5
12239	Elastic constants of La, LaH2, and LaH3. Monatshefte FÃ¼r Chemie, 2012, 143, 1325-1328.	0.9	4
12240	Electromechanical coupling effect on electronic properties of double-walled boron nitride nanotubes. Acta Mechanica Sinica/Lixue Xuebao, 2012, 28, 1532-1538.	1.5	5
12241	Tunable band structures of polycrystalline graphene by external and mismatch strains. Acta Mechanica Sinica/Lixue Xuebao, 2012, 28, 1539-1544.	1.5	10
12242	Vacancy-Driven Surface Segregation in Ni x Mg1âˆ'x O(100) Solid Solutions from First Principles Calculations. Catalysis Letters, 2012, 142, 1211-1217.	1.4	11
12243	Effects of pressure and vibration on the thermal decomposition of cubic Ti1-x Al x N, Ti1-x Zr x N, and Zr1-x Al x N coatings: a first-principles study. Journal of Materials Science, 2012, 47, 7621-7627.	1.7	26
12244	First principles investigation of the structure and stability of LiNiO2 doped with Co and Mn. Journal of Materials Science, 2012, 47, 7558-7563.	1.7	16
12245	Polarization, piezoelectric properties, and elastic coefficients of In x Ga1âˆ'x N solid solutions from first principles. Journal of Materials Science, 2012, 47, 7587-7593.	1.7	7
12246	A blend of first-principles and kinetic lattice Monte Carlo computation to optimize samarium-doped ceria. Journal of Materials Science, 2012, 47, 7530-7541.	1.7	30
12247	Dielectric permittivity of ultrathin PbTiO3 nanowires from first principles. Journal of Materials Science, 2012, 47, 7580-7586.	1.7	23
12248	GGA+U method from first principles: application to reductionâ€“oxidation properties in ceria-based oxides. Journal of Materials Science, 2012, 47, 7542-7548.	1.7	20
12249	Properties of amorphous and crystalline titanium dioxide from first principles. Journal of Materials Science, 2012, 47, 7515-7521.	1.7	173
12250	Hydrogen uptake by graphene and nucleation of graphane. Journal of Materials Science, 2012, 47, 7571-7579.	1.7	22
12251	Electron trapping at the lattice Ti atoms adjacent to the Nb dopant in Nb-doped rutile TiO2. Journal of Materials Science, 2012, 47, 7522-7529.	1.7	9
12252	First-principles study of CaCu3B4O12 (B=Co, Rh, Ir). Journal of Materials Science, 2012, 47, 7660-7664.	1.7	11
12253	Electronic structure of Li2O2 {0001} surfaces. Journal of Materials Science, 2012, 47, 7564-7570.	1.7	82

#	Article	IF	Citations
12254	Tracing magnetism and pairing in FeTe-based systems. Journal of Materials Science, 2012, 47, 7671-7677.	1.7	4
12255	First principles calculations of oxygen vacancy-ordering effects in resistance change memory materials incorporating binary transition metal oxides. Journal of Materials Science, 2012, 47, 7498-7514.	1.7	83
12256	Nanocluster Collisions as a Way to Understand the Role of d-Shell Polarization. Journal of Superconductivity and Novel Magnetism, 2012, 25, 2205-2212.	0.8	1
12257	Influences of Cd-Substitution and Intrinsic Vacancies on the Electronic Structures and Optical Properties of ZnO Nanotubes. Journal of Superconductivity and Novel Magnetism, 2012, 25, 2457-2463.	0.8	4
12258	Emergence of Magnetism in Doped Two-Dimensional Honeycomb Structures of IIIâ€“V Binary Compounds. Journal of Superconductivity and Novel Magnetism, 2012, 25, 2533-2537.	0.8	12
12259	Computer simulation in mechanical spectroscopy. Metal Science and Heat Treatment, 2012, 54, 217-220.	0.2	1
12260	Oxygen- and nitrogen-chemisorbed carbon nanostructures for Z-scheme photocatalysis applications. Journal of Nanoparticle Research, 2012, 14, 1.	0.8	8
12261	Magnetic properties of two dimensional silicon carbide triangular nanoflakes-based kagome lattices. Journal of Nanoparticle Research, 2012, 14, 1.	0.8	5
12262	Surface-induced structural modification in ZnO nanoparticles. Journal of Nanoparticle Research, 2012, 14, 1.	0.8	5
12263	First principles-based adsorption comparison of group IV elements (C, Si, Ge, and Sn) on Au(111)/Ag(111) surface. Journal of Nanoparticle Research, 2012, 14, 1.	0.8	1
12264	Double layers of H2 adsorption on an AlN sheet induced by electric field. Journal of Nanoparticle Research, 2012, 14, 1.	0.8	1
12265	Contribution to the Understanding of Tribological Properties of Graphite Intercalation Compounds with Metal Chloride. Tribology Letters, 2012, 47, 367-379.	1.2	4
12266	A combined HAADF STEM and density functional theory study of tantalum and niobium locations in the Moâ€“Vâ€“Teâ€“Ta(Nb)â€“O M1 phases. Catalysis Communications, 2012, 29, 68-72.	1.6	19
12267	Selective CO2 hydrogenation on the Î³-Al2O3 supported bimetallic Coâ€“Cu catalyst. Catalysis Today, 2012, 194, 30-37.	2.2	18
12268	Spin-polarized transport through heterobilayers of graphene nanoribbons and ruthenium-porphyrin tapes. Chemical Physics, 2012, 405, 148-154.	0.9	3
12269	Transformation and slip behavior of Ni2FeGa. International Journal of Plasticity, 2012, 39, 61-74.	4.1	38
12270	Investigation in the Ga-rich side of the Mnâ€“Ga system: Synthesis and crystal structure of MnGa4 and MnGa5â^'x (xÂâ^¼Â0.15). Intermetallics, 2012, 29, 147-154.	1.8	9
12271	Effects of transition metals in a binary-phase TiAlâ€“Ti3Al alloy: From site occupancy, interfacial energetics to mechanical properties. Intermetallics, 2012, 31, 105-113.	1.8	29

#	Article	IF	Citations
12272	Phase stability of ternary antifluorite type compounds in the quasi-binary systems Mg2Xâ€“Mg2Y (X, YÂ=ÂSi,) Tj ETQq0 0 0 rgBT /Overlo	1.8	44
12273	A DFT study of formation energies of Feâ€“Znâ€“Al intermetallics and solutes. Intermetallics, 2012, 31, 137-144.	1.8	15
12274	Phase relationship in the Tbâ€“Feâ€“Cr ternary system at 600Â°C. Journal of Alloys and Compounds, 2012, 541, 198-203.	2.8	1
12275	The atomic and electronic structure of amorphous BP4. Journal of Alloys and Compounds, 2012, 545, 144-147.	2.8	4
12276	Surface morphology of HÃgg iron carbide (Ï‡-Fe5C2) from ab initio atomistic thermodynamics. Journal of Catalysis, 2012, 294, 47-53.	3.1	90
12277	Adsorbate interactions on surface lead to a flattened Sabatier volcano plot in reduction of oxygen. Journal of Catalysis, 2012, 295, 59-69.	3.1	24
12278	The (210) surface of intermetallic B20 compound GaPd as a selective hydrogenation catalyst: A DFT study. Journal of Catalysis, 2012, 295, 70-80.	3.1	45
12279	First-principles studies on linear and nonlinear optical effects in Ln4GaSbS9 (Ln=Ceâ€“Nd, Sm, Gdâ€“Tm,) Tj ETQq1 1 0.784314 rgBT	1.4	8
12280	Atomic site preferences and its effect on magnetic structure in the intermetallic borides M2Fe(Ru0.8T0.2)5B2 (M=Sc, Ti, Zr; T=Ru, Rh, Ir). Journal of Solid State Chemistry, 2012, 196, 168-174.	1.4	8
12281	A photoactive titanate with a stereochemically active Sn lone pair: Electronic and crystal structure of Sn2TiO4 from computational chemistry. Journal of Solid State Chemistry, 2012, 196, 157-160.	1.4	24
12282	First-principles study of electronic structure and elasticity of UAlx (x=1,2,3) system. Physica B: Condensed Matter, 2012, 407, 748-755.	1.3	9
12283	Transition metal hydrido-complexes: Electronic structure and bonding properties. Progress in Solid State Chemistry, 2012, 40, 31-40.	3.9	8
12284	On the long-range magnetic order and the preferred spin orientation of the layered magnetic oxides Sr2MnSi2O7 and Ba2MnGe2O7. Solid State Communications, 2012, 152, 1116-1118.	0.9	5
12285	Compositional variation of magnetic moment, magnetic anisotropy energy and coercivity in Fe(1â^'x)M x (MÂ=ÂCo/Ni) nanowires: an ab initio study. Applied Nanoscience (Switzerland), 2012, 2, 409-415.	1.6	14
12286	The structural and electronic properties of silicon nanoribbons on Ag(110): A first principles study. Physica B: Condensed Matter, 2012, 407, 4695-4699.	1.3	34
12287	Struggle between inner atoms of ultra-thin silicon film and both its dimer surfaces. Results in Physics, 2012, 2, 185-189.	2.0	2
12288	Quantum mechanical calculations on FeOH nanoparticles. Geoderma, 2012, 189-190, 236-242.	2.3	10
12289	AN AB INITIO MOLECULAR DYNAMICS STUDY ON THE SOLVATION OF FORMATE ION AND FORMIC ACID IN WATER. Journal of Theoretical and Computational Chemistry, 2012, 11, 1019-1032.	1.8	9

#	Article	IF	Citations
12290	Density functional theory model study of size and structure effects on water dissociation by platinum nanoparticles. Journal of Chemical Physics, 2012, 137, 034701.	1.2	56
12291	antiferromagnetism of<mml:math xmlns:mml="http://www.w3.org/1998/Math/MathML" display="inline"><mml:mi>Î²</mml:mi></mml:math>-MnO<mml:math xmlns:mml="http://www.w3.org/1998/Math/MathML" display="inline"><mml:msub><mml:mrow /><mml:mn>2</mml:mn></mml:msub></mml:math>from DFT+<mml:math	1.1	72
12292	Prediction of Two-Dimensional Boron Sheets by Particle Swarm Optimization Algorithm. Journal of Physical Chemistry C, 2012, 116, 20075-20079.	1.5	148
12293	Prediction of CO₂ Adsorption Properties in Zeolites Using Force Fields Derived from Periodic Dispersion-Corrected DFT Calculations. Journal of Physical Chemistry C, 2012, 116, 10692-10701.	1.5	123
12294	Cauchy pressure and the generalized bonding model for nonmagnetic bcc transition metals. Physical Review B, 2012, 86, .	1.1	64
12295	Nonlinearâ€“Linear Transition of Magnetoelectric Effect in Magnetic Graphene Nanoflakes on Substrates. Journal of Physical Chemistry C, 2012, 116, 626-631.	1.5	13
12296	The stabilities, electronic structures and elastic properties of Rbâ€”As systems. Chinese Physics B, 2012, 21, 047101.	0.7	3
12297	Anisotropic ferromagnetism in carbon-doped zinc oxide from first-principles studies. Physical Review B, 2012, 86, .	1.1	31
12298	Extra-electron induced covalent strengthening and generalization of intrinsic ductile-to-brittle criterion. Scientific Reports, 2012, 2, 718.	1.6	165
12299	DFT Simulation and Vibrational Analysis of the IR and Raman Spectra of a CdSe Quantum Dot Capped by Methylamine and Trimethylphosphine Oxide Ligands. Journal of Physical Chemistry C, 2012, 116, 14674-14681.	1.5	52
12300	Density Functional Theory Study of Niâ€“N_x/C Electrocatalyst for Oxygen Reduction in Alkaline and Acidic Media. Journal of Physical Chemistry C, 2012, 116, 17378-17383.	1.5	120
12301	Density functional theory study of Al-doped hematite. Physica Scripta, 2012, 85, 015602.	1.2	28
12302	Underpinning energetics of lithium bonding and stability in the Liâ€“Ptâ€“Sn system. Solid State Sciences, 2012, 14, 1471-1475.	1.5	4
12303	Continuous transformation paths for the molecular crystals of the PCBM fullerene derivative. Synthetic Metals, 2012, 162, 2421-2427.	2.1	4
12304	Spin orbital effect in lanthanides doped silicon cage clusters. Chemical Physics Letters, 2012, 550, 134-137.	1.2	17
12305	First-principles Study on Structure and Hardness of the RuB2. Rare Metal Materials and Engineering, 2012, 41, 2086-2090.	0.8	16
12306	Study of NO oxidation reaction over the Pt cluster supported on Î³-Al2O3(111) surface. Current Applied Physics, 2012, 12, S110-S114.	1.1	4
12307	Electron localization morphology of the stacking faults in Mg: A first-principles study. Chemical Physics Letters, 2012, 551, 121-125.	1.2	37

#	Article	IF	Citations
12308	Phase transition effect on durability of WO3 hydrogen sensing films: An insight by experiment and first-principle method. Sensors and Actuators B: Chemical, 2012, 171-172, 1288-1291.	4.0	24
12309	Equation of state and elastic properties of ACrO3 (A=Pb, Ca, Sr and Ba) perovskites under high pressure. Physica B: Condensed Matter, 2012, 407, 4671-4675.	1.3	3
12310	First principles investigations of the electronic structure and chemical bonding of U3Si2C2 â€“ A uranium silicideâ€“carbide with the rare [SiC] unit. Chemical Physics Letters, 2012, 550, 88-93.	1.2	5
12311	Size effect of half-metallic properties of BN/C hybrid nanoribbons. Physica B: Condensed Matter, 2012, 407, 4770-4772.	1.3	11
12312	First-principles investigation of electronic structure and transport properties of CoSb3 under different pressures. Chemical Physics Letters, 2012, 549, 22-26.	1.2	17
12313	First principles study of orthoâ€“para H2 conversion on the O2(0.25ÂML)/Ag(111) system. Current Applied Physics, 2012, 12, S115-S118.	1.1	4
12314	Luminescence study of cerium-doped La2Hf2O7: Effects due to trivalent and tetravalent cerium and oxygen vacancies. Journal of Luminescence, 2012, 132, 2889-2896.	1.5	28
12315	Pressure-temperature phase diagram of Ti2O3and physical properties in the golden Th2S3-type phase. Physical Review B, 2012, 86, .	1.1	22
12316	Role of nitrogen vacancies in the luminescence of Mg-doped GaN. Applied Physics Letters, 2012, 100, .	1.5	136
12317	S doping effect on the properties of double perovskite La2FeMoO6. Applied Physics Letters, 2012, 100, .	1.5	14
12318	Influence of chemical pressure in Sn-substituted Ni2MnGa Heusler alloy: Experimental and theoretical studies. Journal of Applied Physics, 2012, 112, 073921.	1.1	12
12319	Crystal structure of CaRhO3 polymorph: High-pressure intermediate phase between perovskite and post-perovskite. American Mineralogist, 2012, 97, 159-163.	0.9	12
12320	Hybrid functional study rationalizes the simple cubic phase of calcium at high pressures. Journal of Chemical Physics, 2012, 137, 184502.	1.2	15
12321	Electronic Structure and Half-Metallic Properties of Cubic Perovskite BaRu_{1-X}Ti_xO₃ System. Key Engineering Materials, 0, 519, 174-178.	0.4	0
12322	Amorphization and amorphous stability of Bi2Te3 chalcogenide films. Applied Physics Letters, 2012, 100, .	1.5	10
12323	Phenolic polymerâ€“surface interactions from ab initio computations. Molecular Physics, 2012, 110, 2371-2380.	0.8	0
12324	Electronic and optical properties of CoX2O4 (Xâ€‰=â€‰Al, Ga, In) alloys. Applied Physics Letters, 2012, 100, .	1.5	15
12325	Hydrogen impurity in yttria:Ab initioand<mml:math xmlns:mml="http://www.w3.org/1998/Math/MathML" display="inline"><mml:mi>Î¼</mml:mi></mml:math>SR perspectives. Physical Review B, 2012, 85, .	1.1	32

#	Article	IF	Citations
12326	Origin of the anomalous magnetic behavior of the Fe<mml:math xmlns:mml="http://www.w3.org/1998/Math/MathML" display="inline"><mml:msub><mml:mrow /><mml:mn>13</mml:mn></mml:msub></mml:math><mml:math xmlns:mml="http://www.w3.org/1998/Math/MathML" display="inline"><mml:msup><mml:mrow /><mml:mo>+</mml:mo></mml:msup></mml:math>cluster. Physical Review B, 2012, 86, .	1.1	26
12327	Transition-metal dispersion on carbon-doped boron nitride nanostructures: Applications for high-capacity hydrogen storage. Physical Review B, 2012, 86, .	1.1	45
12328	Ferroelectricity and superparamagnetism in Sr/Ti nonstoichiometric SrTiO<mml:math xmlns:mml="http://www.w3.org/1998/Math/MathML" display="inline"><mml:msub><mml:mrow /><mml:mn>3</mml:mn></mml:msub></mml:math>. Physical Review B, 2012, 85, .	1.1	34
12329	The effect of group IIIA metal ion dopants on the photocatalytic activities of nanocrystalline Sr_{0.25}H_{1.5}Ta₂O₆·H₂O. Physical Chemistry Chemical Physics, 2012, 14, 1212-1222.	1.3	17
12330	Synthesis and structures of cyclic gold complexes containing diphosphine ligands and luminescent properties of the high nuclearity species. Dalton Transactions, 2012, 41, 4789.	1.6	30
12331	Charge-distribution-related regioisomerism of photoresponsive metalâ€“organic polymeric chains. Dalton Transactions, 2012, 41, 13441.	1.6	47
12332	High pressure driven structural and electrochemical modifications in layered lithium transition metal intercalation oxides. Energy and Environmental Science, 2012, 5, 6214.	15.6	31
12333	Electronic and magnetic properties of the two-dimensional C4H-type polymer with strain effects, intrinsic defects and foreign atom substitutions. Physical Chemistry Chemical Physics, 2012, 14, 3651.	1.3	21
12334	Hydrogenation properties of KSi and NaSi Zintl phases. Physical Chemistry Chemical Physics, 2012, 14, 13319.	1.3	19
12335	Nitrogen and hydrogen defect equilibria in Ca12Al14O33: a combined experimental and computational study. Journal of Materials Chemistry, 2012, 22, 15828.	6.7	14
12336	Crystal and electronic structure, lattice dynamics and thermal properties of Ag(i)(SO3)R (R = F, CF3) Lewis acids in the solid state. Dalton Transactions, 2012, 41, 2034-2047.	1.6	28
12337	Ab initio and empirical defect modeling of LaMnO_{3Â±Î´}for solid oxidefuel cell cathodes. Physical Chemistry Chemical Physics, 2012, 14, 290-302.	1.3	56
12338	A concerted migration mechanism of mixed oxide ion and electron conduction in reduced ceria studied by first-principles density functional theory. Physical Chemistry Chemical Physics, 2012, 14, 6079.	1.3	55
12339	Electronic properties and charge transfer phenomena in Pt nanoparticles on Î³-Al2O3: size, shape, support, and adsorbate effects. Physical Chemistry Chemical Physics, 2012, 14, 11766.	1.3	76
12340	Spin crossover transition of Fe(phen)2(NCS)2: periodic dispersion-corrected density-functional study. Physical Chemistry Chemical Physics, 2012, 14, 5389.	1.3	57
12341	Ab initio model of intrinsic defects in Sc<inf>2</inf>O<inf>3</inf> for thermionic cathode systems. , 2012, , .		1
12342	Oxidation mechanism of the intermetallic compound Ti3Al from ab initio thermodynamics. Physical Chemistry Chemical Physics, 2012, 14, 11160.	1.3	26
12343	Graphene substrate-mediated catalytic performance enhancement of Runanoparticles: a first-principles study. Dalton Transactions, 2012, 41, 1289-1296.	1.6	61

#	Article	IF	Citations
12344	Electrochemical properties of crystallized dilithium squarate: insight from dispersion-corrected density functional theory. Physical Chemistry Chemical Physics, 2012, 14, 11398.	1.3	23
12345	Reduced Pd density of states in Pd/SAM/Au junctions: the role of adsorbed hydrogen atoms. Physical Chemistry Chemical Physics, 2012, 14, 2353.	1.3	10
12346	Decomposition mechanism and the effects of metal additives on the kinetics of lithium alanate. Physical Chemistry Chemical Physics, 2012, 14, 2840.	1.3	19
12347	H₂dissociation on individual Pd atoms deposited on Cu(111). Physical Chemistry Chemical Physics, 2012, 14, 303-310.	1.3	39
12348	Stress induced half-metallicity in surface defected germanium nanowires. Physical Chemistry Chemical Physics, 2012, 14, 1166-1174.	1.3	2
12349	Unravelling the specific site preference in doping of calcium hydroxyapatite with strontium from ab initio investigations and Rietveld analyses. Physical Chemistry Chemical Physics, 2012, 14, 3435.	1.3	43
12350	Hydrogen-bonded assembly of methanol on Cu(111). Physical Chemistry Chemical Physics, 2012, 14, 11846.	1.3	28
12351	First-principles study of the triwing graphene nanoribbons: junction-dependent electronic structures and electric field modulations. Physical Chemistry Chemical Physics, 2012, 14, 2040.	1.3	3
12352	Study of the Initial Stage of Solid Electrolyte Interphase Formation upon Chemical Reaction of Lithium Metal and N-Methyl-N-Propyl-Pyrrolidinium-Bis(Fluorosulfonyl)Imide. Journal of Physical Chemistry C, 2012, 116, 19789-19797.	1.5	178
12353	Interatomic potential for uranium in a wide range of pressures and temperatures. Journal of Physics Condensed Matter, 2012, 24, 015702.	0.7	36
12354	Origin of synergistic effect over Ni-based bimetallic surfaces: A density functional theory study. Journal of Chemical Physics, 2012, 137, 014703.	1.2	64
12355	Much stronger binding of metal adatoms to silicene than to graphene: A first-principles study. Physical Review B, 2012, 86, .	1.1	208
12356	Spin Reorientation in the Square-Lattice Antiferromagnets RMnAsO (R = Ce, Nd): Density Functional Analysis of the Spin-Exchange Interactions between the Rare-Earth and Transition-Metal Ions. Inorganic Chemistry, 2012, 51, 6890-6897.	1.9	19
12357	Ultra-incompressible Orthorhombic Phase of Osmium Tetraboride (OsB₄) Predicted from First Principles. Journal of Physical Chemistry C, 2012, 116, 4293-4297.	1.5	41
12358	Performance of Cluster Expansions of Coverage-Dependent Adsorption of Atomic Oxygen on Pt(111). Journal of Chemical Theory and Computation, 2012, 8, 264-273.	2.3	87
12359	Computationally efficient determination of hydrogen isotope effects on the thermodynamic stability of metal hydrides. Physical Review B, 2012, 86, .	1.1	11
12360	Theoretical Model for CO Adsorption and Dissociation on Clean and K-Doped Î²-Mo₂C Surfaces. Journal of Physical Chemistry C, 2012, 116, 24573-24581.	1.5	26
12361	Predictions of Sulfur Resistance in Metal Membranes for H2 Purification Using First-Principles Calculations. Industrial & Engineering Chemistry Research, 2012, 51, 301-309.	1.8	6

#	Article	IF	Citations
12362	A density functional theory investigation of the molecular and dissociative adsorption of hydrazine on defective copper surfaces. Journal of Materials Chemistry, 2012, 22, 23210.	6.7	25
12363	Defect chemistry of a BaZrO3 Î£3 (111) grain boundary by first principles calculations and spaceâ€“charge theory. Physical Chemistry Chemical Physics, 2012, 14, 12339.	1.3	46
12364	First-principles studies of proton-Ba interactions in doped LaPO4. Journal of Materials Chemistry, 2012, 22, 3758.	6.7	5
12365	Thin silica films on Ru(0001): monolayer, bilayer and three-dimensional networks of [SiO4] tetrahedra. Physical Chemistry Chemical Physics, 2012, 14, 11344.	1.3	106
12366	Reconstruction of the (001) surface of TiO2 nanosheets induced by the fluorine-surfactant removal process under UV-irradiation for dye-sensitized solar cells. Physical Chemistry Chemical Physics, 2012, 14, 4763.	1.3	40
12367	Electronic structure of the indium-adsorbed Au/Si(111)-3Ã—3surface: A first-principles study. Physical Review B, 2012, 85, .	1.1	15
12368	Does Halogen Adsorption Activate the Oxygen Atom on an Oxide Surface? I. A Study of Br₂ and HBr Adsorption on La₂O₃ and La₂O₃ Doped with Mg or Zr. Journal of Physical Chemistry C, 2012, 116, 4137-4148.	1.5	20
12369	Theoretical Study of Properties of Goethite (Î±-FeOOH) at Ambient and High-Pressure Conditions. Journal of Physical Chemistry C, 2012, 116, 6703-6713.	1.5	46
12370	Non-local Effects on Oxygen-Induced Surface Core Level Shifts of Re(0001). Journal of Physical Chemistry C, 2012, 116, 23297-23307.	1.5	10
12371	Oxidation of Magnesia-Supported Pd₃₀ Nanoclusters and Catalyzed CO Combustion: Size-Selected Experiments and First-Principles Theory. Journal of Physical Chemistry C, 2012, 116, 9594-9607.	1.5	40
12372	First-Principle Study on Structural and Electronic Properties of Pristine and Adsorbed LiF Nanotubes. Journal of Physical Chemistry C, 2012, 116, 1650-1657.	1.5	9
12373	Ab Initio, Physically Motivated Force Fields for CO₂ Adsorption in Zeolitic Imidazolate Frameworks. Journal of Physical Chemistry C, 2012, 116, 1892-1903.	1.5	87
12374	Computational Study of the Vibrational Structure of the Ammonia Molecule Adsorbed on the fcc (111) Transition Metal Surfaces. Journal of Physical Chemistry C, 2012, 116, 14960-14969.	1.5	16
12375	Investigation of Adsorption Behavior of Mercury on Au(111) from First Principles. Environmental Science & Technology, 2012, 46, 7260-7266.	4.6	51
12376	Influence of Electric Field on SERS: Frequency Effects, Intensity Changes, and Susceptible Bonds. Journal of the American Chemical Society, 2012, 134, 4646-4653.	6.6	41
12377	Methyl Dynamics Flattens Barrier to Proton Transfer in Crystalline Tetraacetylethane. Journal of Physical Chemistry A, 2012, 116, 2283-2291.	1.1	6
12378	Importance of HalogenÂ·Â·Â·Halogen Contacts for the Structural and Magnetic Properties of CuX₂(pyrazine-N,Nâ€²-dioxide)(H₂O)₂ (X = Cl and Br). Inorganic Chemistry, 2012, 51, 2121-2129.	1.9	38
12379	Mechanisms for Substrate-Enhanced Growth during the Early Stages of Atomic Layer Deposition of Alumina onto Silicon Nitride Surfaces. Chemistry of Materials, 2012, 24, 1080-1090.	3.2	17

#	Article	IF	Citations
12380	Structures, stability and electronic properties of two- or four-segment BN/C nanotubes. , 2012, , .		0
12381	Suppression of Grain Boundaries in Graphene Growth on Superstructured Mn-Cu(111) Surface. Physical Review Letters, 2012, 109, 265507.	2.9	36
12382	Lithium niobate-tantalate mixed crystals electronic and optical properties calculated from first principles. , 2012, , .		2
12383	Interfacial Elastic Dipoles: A New EOT Shifting Mechanism in HKMG Devices. IEEE Electron Device Letters, 2012, 33, 884-886.	2.2	1
12384	Relating Dynamic Properties to Atomic Structure in Metallic Glasses. Jom, 2012, 64, 856-881.	0.9	110
12385	First-principles study of the structural and elastic properties of rhenium-based transition-metal alloys. Physical Review B, 2012, 86, .	1.1	26
12386	Perceiving molecular themes in the structures and bonding of intermetallic phases: the role of HÃ¼ckel theory in an ab initio era. Dalton Transactions, 2012, 41, 7801.	1.6	36
12387	First principles investigation of electronic structure change and energy transfer by redox in inverse spinel cathodes LiNiVO4 and LiCoVO4. Journal of Materials Chemistry, 2012, 22, 18968.	6.7	15
12388	Oxygen molecule dissociation on carbon nanostructures with different types of nitrogen doping. Nanoscale, 2012, 4, 1184-1189.	2.8	220
12389	Different catalytic behavior of amorphous and crystalline cobalt tungstate for electrochemical water oxidation. RSC Advances, 2012, 2, 10874.	1.7	77
12390	Structural stabilities and electronic properties of planar C4 carbon sheet and nanoribbons. Physical Chemistry Chemical Physics, 2012, 14, 11107.	1.3	52
12391	Hydrogen-assisted CO dissociation on the Co(211) stepped surface. Catalysis Science and Technology, 2012, 2, 491.	2.1	56
12392	Structure, bonding, vibration and ideal strength of primitive-centered tetragonal boron nitride. Physical Chemistry Chemical Physics, 2012, 14, 869-876.	1.3	55
12393	Reconstruction and electronic properties of silicon nanosheets as a function of thickness. Nanoscale, 2012, 4, 2906.	2.8	34
12394	The paradox of an insulating contact between a chemisorbed molecule and a wide band gap semiconductor surface. Physical Chemistry Chemical Physics, 2012, 14, 1700-1705.	1.3	18
12395	Octahedrality versus tetrahedrality in stoichiometric ceria nanoparticles. Chemical Communications, 2012, 48, 4199.	2.2	25
12396	Electronic structure and thermoelectric performance of Zintl compound Ca5Ga2As6. Journal of Materials Chemistry, 2012, 22, 20284.	6.7	24
12397	Nitrogen defects in wide band gap oxides: defect equilibria and electronic structure from first principles calculations. Physical Chemistry Chemical Physics, 2012, 14, 11808.	1.3	15

#	Article	IF	Citations
12398	Unique reactivity of Fe nanoparticlesâ€“defective graphene composites toward NHx (x = 0, 1, 2, 3) adsorption: a first-principles study. Physical Chemistry Chemical Physics, 2012, 14, 15036.	1.3	30
12399	Radical self-assembled monolayers on Au(111) formed by the adsorption of closed-shell molecules. Journal of Materials Chemistry, 2012, 22, 4269.	6.7	13
12400	Tuning Electronic Structure of Graphene: A First-Principles Study. IEEE Nanotechnology Magazine, 2012, 11, 534-541.	1.1	37
12401	A novel low compressible and superhard carbon nitride: Body-centered tetragonal CN2. Physical Chemistry Chemical Physics, 2012, 14, 13081.	1.3	108
12402	Pathways for Câ€“H bond cleavage of propane Ïƒ-complexes on PdO(101). Physical Chemistry Chemical Physics, 2012, 14, 12202.	1.3	34
12403	Curvature effects on electronic properties of armchair graphene nanoribbons without passivation. Physical Chemistry Chemical Physics, 2012, 14, 16409.	1.3	15
12404	First-principles density functional calculation of electrochemical stability of fast Li ion conducting garnet-type oxides. Physical Chemistry Chemical Physics, 2012, 14, 10008.	1.3	66
12405	Ferroelectric phase transition in LiNbO₃: Insights from molecular dynamics. IEEE Transactions on Ultrasonics, Ferroelectrics, and Frequency Control, 2012, 59, 1925-1928.	1.7	18
12406	How to get superhard MnB2: a first-principles study. Journal of Materials Chemistry, 2012, 22, 17630.	6.7	9
12407	Theoretical investigation on the structural and thermodynamic properties of FeSe at high pressure and high temperature. Dalton Transactions, 2012, 41, 9781.	1.6	6
12408	Effects of reactive elements on the structure and diffusivity of liquid chromia: Anab initiomolecular dynamics study. Physical Review B, 2012, 85, .	1.1	19
12409	Synthesis, structure and band gap energy of covalently linked cluster-assembled materials. Dalton Transactions, 2012, 41, 12365.	1.6	33
12410	DFT-study of the energetics of perovskite-type oxides LaMO3 (M = Scâ€“Cu). RSC Advances, 2012, 2, 10667.	1.7	10
12411	Hybrid density functional study of band alignment in ZnOâ€“GaN and ZnOâ€“(Ga1â^'xZnx)(N1â^'xOx)â€“GaN heterostructures. Physical Chemistry Chemical Physics, 2012, 14, 15693.	1.3	46
12412	Surface phase diagram of hematite pseudocubes in hydrous environments. Journal of Materials Chemistry, 2012, 22, 161-167.	6.7	12
12413	First-principles and experimental investigation of the morphology of layer-structured LiNiO2 and LiCoO2. Journal of Materials Chemistry, 2012, 22, 12874.	6.7	74
12414	RbFe²⁺Fe³⁺F₆: Synthesis, structure, and characterization of a new charge-ordered magnetically frustrated pyrochlore-related mixed-metal fluoride. Chemical Science, 2012, 3, 741-751.	3.7	20
12415	Reaction dynamics at a metal surface; halogenation of Cu(110). Faraday Discussions, 2012, 157, 337.	1.6	31

#	Article	IF	Citations
12416	Band gap tunable Sn-doped PbSe nanocrystals: solvothermal synthesis and first-principles calculations. CrystEngComm, 2012, 14, 7408.	1.3	16
12417	Role of complex defects in photocatalytic activities of nitrogen-doped anatase TiO2. Physical Chemistry Chemical Physics, 2012, 14, 5924.	1.3	51
12418	Ab initio method for electromigration analysis. , 2012, , .		0
12419	Effects of Cluster Size on Platinumâ€“Oxygen Bonds Formation in Small Platinum Clusters. Japanese Journal of Applied Physics, 2012, 51, 035002.	0.8	7
12420	ZnO nanostructures for sensing of H<inf>2</inf>S. , 2012, , .		0
12421	Ab initiostudy on the formation of chemically ordered Zr2Al phase by coupled replaciveâ€“displacive transformation. Philosophical Magazine, 2012, 92, 4040-4055.	0.7	6
12422	Vibrational fingerprints of LiNbO<inf>3</inf>-LiTaO<inf>3</inf> mixed crystals. , 2012, , .		0
12423	Electron Properties of F, and N Doped Hematite: The Application for Photocatalysis. Advanced Materials Research, 2012, 562-564, 298-301.	0.3	5
12424	Strain Effect on the Electrochemical Properties of Li₂MnO₃ Cathode Material: A First Principles Calculation. Key Engineering Materials, 2012, 519, 147-151.	0.4	1
12425	New Perspective on Formation Energies and Energy Levels of Point Defects in Nonmetals. Physical Review Letters, 2012, 108, 066404.	2.9	96
12426	Antisite Atom Segregation in Porous Boron Nitride Nanotubes: Formation Mechanism and Characterization. Journal of Physical Chemistry C, 2012, 116, 22051-22056.	1.5	2
12427	Anisotropic Chemical Pressure Effects in Single-Component Molecular Metals Based on Radical Dithiolene and Diselenolene Gold Complexes. Journal of the American Chemical Society, 2012, 134, 17138-17148.	6.6	73
12428	Ab initiocalculations of rare-earth diffusion in magnesium. Physical Review B, 2012, 85, .	1.1	48
12429	Nucleation, Growth, and Adsorbate-Induced Changes in Composition for Coâ€“Au Bimetallic Clusters on TiO₂. Journal of Physical Chemistry C, 2012, 116, 24616-24629.	1.5	31
12430	Atomistic modeling of an impurity element and a metalâ€“impurity system: pure P and Feâ€“P system. Journal of Physics Condensed Matter, 2012, 24, 225002.	0.7	15
12431	New Insights on Vibrational Dynamics of Corannulene. Journal of Physical Chemistry C, 2012, 116, 25089-25096.	1.5	14
12432	Non-innocent Dissociation of H₂O on GaP(110): Implications for Electrochemical Reduction of CO₂. Journal of the American Chemical Society, 2012, 134, 13600-13603.	6.6	48
12433	Boron Sheet Adsorbed on Metal Surfaces: Structures and Electronic Properties. Journal of Physical Chemistry C, 2012, 116, 18202-18206.	1.5	58

#	Article	IF	Citations
12434	Incipient ferroelectricity in 2.3<mml:math xmlns:mml="http://www.w3.org/1998/Math/MathML" display="inline"><mml:mo>%</mml:mo></mml:math>tensile-strained CaMnO<mml:math xmlns:mml="http://www.w3.org/1998/Math/MathML" display="inline"><mml:msub><mml:mrow /><mml:mn>3</mml:mn></mml:msub></mml:math>films. Physical Review B, 2012, 85, .	1.1	59
12435	Benzene, coronene, and circumcoronene adsorbed on gold, and a gold cluster adsorbed on graphene: Structural and electronic properties. Physical Review B, 2012, 85, .	1.1	57
12436	Intermetallic Compound AlPd As a Selective Hydrogenation Catalyst: A DFT Study. Journal of Physical Chemistry C, 2012, 116, 6307-6319.	1.5	47
12437	Information-Theoretic Approach for the Discovery of Design Rules for Crystal Chemistry. Journal of Chemical Information and Modeling, 2012, 52, 1812-1820.	2.5	40
12438	Frictional Figures of Merit for Single Layered Nanostructures. Physical Review Letters, 2012, 108, 126103.	2.9	110
12439	CO₂ Hydrogenation to Formic Acid on Ni(111). Journal of Physical Chemistry C, 2012, 116, 3001-3006.	1.5	141
12440	Thermodynamic and Electrochemical Properties of the Liâ€“Coâ€“O and Liâ€“Niâ€“O Systems. Chemistry of Materials, 2012, 24, 97-105.	3.2	42
12441	Environment-Controlled Tethering by Aggregation and Growth of Phosphonic Acid Monolayers on Silicon Oxide. Langmuir, 2012, 28, 8046-8051.	1.6	73
12442	Localized Reaction at a Smooth Metal Surface: p-Diiodobenzene at Cu(110). Journal of the American Chemical Society, 2012, 134, 9320-9326.	6.6	40
12443	Studies on the Encapsulation of F^{â€“} in Single Walled Nanotubes of Different Chiralities Using Density Functional Theory Calculations and Carâ€“Parrinello Molecular Dynamics Simulations. Journal of Physical Chemistry A, 2012, 116, 5519-5528.	1.1	13
12444	The Role of Atomic Vacancy on Water Dissociation over Titanium Dioxide Nanosheet: A Density Functional Theory Study. Journal of Physical Chemistry C, 2012, 116, 2477-2482.	1.5	35
12445	Surface Chemistry of 2-Iodoethanol on Pd(111): Orientation of Surface-Bound Alcohol Controls Selectivity. Journal of Physical Chemistry C, 2012, 116, 4201-4208.	1.5	13
12446	Interfacial Charge Transfer and Chemical Bonding in a Niâ€“LaNbO₄ Cermet for Proton-Conducting Solid-Oxide Fuel Cell Anodes. Chemistry of Materials, 2012, 24, 4152-4159.	3.2	16
12447	Role of Inter- and Intramolecular Bonding on Impact Sensitivity. Journal of Physical Chemistry A, 2012, 116, 11008-11014.	1.1	9
12448	Oxidation State of Uranium in A₆Cu₁₂U₂S₁₅ (A = K, Rb,) Tj ETQq0 0 0 rgBT /Overlo	1.9	28
12449	Investigation of the spin exchange interactions and the magnetic structure of the high-temperature multiferroic CuBr<mml:math xmlns:mml="http://www.w3.org/1998/Math/MathML" display="inline"><mml:msub><mml:mrow /><mml:mn>2</mml:mn></mml:msub></mml:math>. Physical Review B, 2012, 86, .	1.1	28
12450	Magnetic Excitations of Rare Earth Atoms and Clusters on Metallic Surfaces. Nano Letters, 2012, 12, 4805-4809.	4.5	37
12451	Influence of impurities on phase stability of martensites in titanium. Philosophical Magazine, 2012, 92, 2272-2285.	0.7	4

#	Article	IF	Citations
12452	SCC-DFTB Parametrization for Boron and Boranes. Journal of Chemical Theory and Computation, 2012, 8, 1153-1163.	2.3	26
12453	An Extended Charge Equilibration Method. Journal of Physical Chemistry Letters, 2012, 3, 2506-2511.	2.1	253
12454	Structures of uranyl peroxide hydrates: a first-principles study of studtite and metastudtite. Dalton Transactions, 2012, 41, 9748.	1.6	58
12455	Simulation of Aqueous Dissolution of Lithium Manganate Spinel from First Principles. Journal of Physical Chemistry C, 2012, 116, 4050-4059.	1.5	57
12456	Structural and vibrational properties of<mml:math xmlns:mml="http://www.w3.org/1998/Math/MathML" display="inline"><mml:mi>Î±</mml:mi></mml:math>-MoO<mml:math xmlns:mml="http://www.w3.org/1998/Math/MathML" display="inline"><mml:msub><mml:mrow /><mml:mn>3</mml:mn></mml:msub></mml:math>from van der Waals corrected density functional theory calculations. Physical Review B, 2012, 85, .	1.1	47
12457	Enhanced Charge-Transfer Kinetics by Anion Surface Modification of LiFePO₄. Chemistry of Materials, 2012, 24, 3212-3218.	3.2	62
12458	Role of Pr on the Semiconductor Properties of Nanotitania. An Experimental and First-Principles Investigation. Journal of Physical Chemistry C, 2012, 116, 23083-23093.	1.5	19
12459	Special Chemical Properties of RuO_x Nanowires in RuO_x/TiO₂(110): Dissociation of Water and Hydrogen Production. Journal of Physical Chemistry C, 2012, 116, 4767-4773.	1.5	25
12460	First-Principles Study on Cd Doping in Cu₂ZnSnS₄ and Cu₂ZnSnSe₄. Japanese Journal of Applied Physics, 2012, 51, 10NC11.	0.8	32
12461	Potassium Zinc Borohydrides Containing Triangular [Zn(BH₄)₃]^{â^'} and Tetrahedral [Zn(BH₄)_xCl_{4â€“x}]^{2â€“} Anions. Journal of Physical Chemistry C, 2012, 116, 1563-1571.	1.5	34
12462	Ab initiostudy of metastable layered perovskitesR2Ti2O7(R=Sm and Gd). Physical Review B, 2012, 86, .	1.1	11
12463	Ligand Field Effect at Oxideâ€“Metal Interface on the Chemical Reactivity of Ultrathin Oxide Film Surface. Journal of the American Chemical Society, 2012, 134, 10554-10561.	6.6	23
12464	Improved CO Adsorption Energies, Site Preferences, and Surface Formation Energies from a Meta-Generalized Gradient Approximation Exchangeâ€“Correlation Functional, M06-L. Journal of Physical Chemistry Letters, 2012, 3, 2975-2979.	2.1	63
12465	Adsorption of Pt and Bimetallic PtAu Clusters on the Partially Reduced Rutile (110) TiO₂ Surface: A First-Principles Study. Journal of Physical Chemistry C, 2012, 116, 5735-5746.	1.5	40
12466	SO₂ Poisoning Structures and the Effects on Pure and Mn Doped CeO₂: A First Principles Investigation. Journal of Physical Chemistry C, 2012, 116, 22930-22937.	1.5	58
12467	Stable p-Type Conduction from Sb-Decorated Head-to-Head Basal Plane Inversion Domain Boundaries in ZnO Nanowires. Nano Letters, 2012, 12, 1311-1316.	4.5	61
12468	First-Principles Study of EMIM-FAFSA Molecule Adsorption on a Li(100) Surface as a Model for Li-Ion Battery Electrodes. Journal of Physical Chemistry C, 2012, 116, 8493-8509.	1.5	32
12469	Ab initiothermodynamics of intrinsic oxygen vacancies in ceria. Physical Review B, 2012, 86, .	1.1	43

#	Article	IF	Citations
12470	Proton-Conducting Network in Lanthanum Orthophosphate. Journal of Physical Chemistry C, 2012, 116, 19117-19124.	1.5	42
12471	Hybrid density functional study of small Rh<mml:math xmlns:mml="http://www.w3.org/1998/Math/MathML" display="inline"><mml:msub><mml:mrow /><mml:mi>n</mml:mi></mml:msub></mml:math><mml:math xmlns:mml="http://www.w3.org/1998/Math/MathML" display="inline"><mml:mrow><mml:mo>(</mml:mo><mml:mi>n</mml:mi><mml:mo>=</mml:mo><mml:mn>2</mml:mn><mml:mo>a^' Physical Review B, 2012, 86, .	1.1	36
12472	Making Photo-selective TiO₂ Materials by Cationâ€“Anion Codoping: From Structure and Electronic Properties to Photoactivity. Journal of Physical Chemistry C, 2012, 116, 18759-18767.	1.5	29
12473	Effects of alloying element and temperature on the stacking fault energies of dilute Ni-base superalloys. Journal of Physics Condensed Matter, 2012, 24, 505403.	0.7	103
12474	Graphene-diamond interface: Gap opening and electronic spin injection. Physical Review B, 2012, 85, .	1.1	95
12475	Computational studies of graphene growth mechanisms. Physical Review B, 2012, 85, .	1.1	20
12476	Local Electronic Structure and Density of Edge and Facet Atoms at Rh Nanoclusters Self-Assembled on a Graphene Template. ACS Nano, 2012, 6, 3034-3043.	7.3	49
12477	Assessment of density functional theory for bonds formed between rare gases and open-shell atoms: a computational study of small molecules containing He, Ar, Kr and Xe. Physical Chemistry Chemical Physics, 2012, 14, 553-561.	1.3	10
12478	Crystal Structure, Energetics, And Electrochemistry of Li₂FeSiO₄ Polymorphs from First Principles Calculations. Chemistry of Materials, 2012, 24, 495-503.	3.2	102
12479	Two-Dimensional Superstructure Formation of Fluorinated Fullerene on Au(111): A Scanning Tunneling Microscopy Study. ACS Nano, 2012, 6, 2679-2685.	7.3	18
12480	First-Principle Studies on the Pressure-Induced Structural Changes in Energetic Ionic Salt 3-Azido-1,2,4-triazolium Nitrate Crystal. Journal of Physical Chemistry C, 2012, 116, 16144-16153.	1.5	28
12481	First-principles study of Î³-CuI for p-type transparent conducting materials. Journal Physics D: Applied Physics, 2012, 45, 145102.	1.3	40
12482	Effect of temperature and compositional changes on the phonon properties of Ni-Mn-Ga shape memory alloys. Physical Review B, 2012, 86, .	1.1	21
12483	Density functional theory studies on the electronic, structural, phonon dynamical and thermo-stability properties of bicarbonates MHCO₃, M = Li, Na, K. Journal of Physics Condensed Matter, 2012, 24, 325501.	0.7	11
12484	Efficient Approach for the Computational Study of Alcohol and Nitrile Adsorption in H-ZSM-5. Journal of Physical Chemistry C, 2012, 116, 5499-5508.	1.5	77
12485	Insight into the Adsorption of Water on the Clean CeO₂(111) Surface with van der Waals and Hybrid Density Functionals. Journal of Physical Chemistry C, 2012, 116, 13584-13593.	1.5	116
12486	Silicon-Containing Multidecker Organometallic Complexes and Nanowires: A Density Functional Theory Study. Journal of Physical Chemistry Letters, 2012, 3, 151-156.	2.1	8
12487	Successive hydrogenation starting from the edge(s): an effective approach to fine-tune the electronic and magnetic behaviors of SiC nanoribbons. Journal of Materials Chemistry, 2012, 22, 24166.	6.7	32

#	Article	IF	Citations
12488	Strain-driven spin-state transition and superexchange interaction in LaCoO<mml:math xmlns:mml="http://www.w3.org/1998/Math/MathML" display="inline"><mml:msub><mml:mrow /><mml:mn>3</mml:mn></mml:msub></mml:math>:<mml:math xmlns:mml="http://www.w3.org/1998/Math/MathML" display="inline"><mml:mrow><mml:mi>A</mml:mi><mml:mi>b</mml:mi></mml:mrow></mml:math>initiostudy. Physical Review B, 2012, 86, .	1.1	72
12489	Electronic and magnetic structure of Fe3O4/BiFeO3 multiferroic superlattices: First principles calculations. Journal of Applied Physics, 2012, 112, 063925.	1.1	22
12490	Single Gold Atom Adsorption on the Fe₃O₄(111) Surface. Journal of Physical Chemistry C, 2012, 116, 10632-10638.	1.5	57
12491	Anisotropic elasticity of DyScO₃substrates. Journal of Physics Condensed Matter, 2012, 24, 385404.	0.7	16
12492	Theoretical Analysis of Oxygen Vacancy Formation in Zr-Doped BaTiO$_{3}$. Japanese Journal of Applied Physics, 2012, 51, 09LE01.	0.8	6
12493	Effect of thermal disorder on high figure of merit in PbTe. Physical Review B, 2012, 86, .	1.1	39
12494	Nature of Pt_n/CeO₂ (111) Surface under Waterâ€“Gas Shift Reaction Conditions: A Constrained ab Initio Thermodynamics Study. Journal of Physical Chemistry C, 2012, 116, 9029-9042.	1.5	34
12495	Intrinsic defects in multiferroic BiFeO<mml:math xmlns:mml="http://www.w3.org/1998/Math/MathML" display="inline"><mml:msub><mml:mrow /><mml:mn>3</mml:mn></mml:msub></mml:math>and their effect on magnetism. Physical Review B, 2012, 85, .	1.1	153
12496	Electronic and structural properties of N-vacancy in AlN nanowires: A first-principles study. Chinese Physics B, 2012, 21, 087101.	0.7	8
12497	Hydrogen Storage in Yttrium-Decorated Single Walled Carbon Nanotube. Journal of Physical Chemistry C, 2012, 116, 22502-22508.	1.5	115
12498	The study of pressure induced structural phase transition in spin-frustrated Yb2Ti2O7 pyrochlore. Journal of Applied Physics, 2012, 111, .	1.1	12
12499	Surface orientation effects in crystallineâ€“amorphous silicon interfaces. Physical Chemistry Chemical Physics, 2012, 14, 15173.	1.3	18
12500	Cagelike Diamondoid Nitrogen at High Pressures. Physical Review Letters, 2012, 109, 175502.	2.9	176
12501	Superconductive sodalite-like clathrate calcium hydride at high pressures. Proceedings of the National Academy of Sciences of the United States of America, 2012, 109, 6463-6466.	3.3	630
12502	Spiral chain O ₄ form of dense oxygen. Proceedings of the National Academy of Sciences of the United States of America, 2012, 109, 751-753.	3.3	111
12503	Promoter Effect of Early Stage Grown Surface Oxides: A Near-Ambient-Pressure XPS Study of CO Oxidation on PtSn Bimetallics. Journal of Physical Chemistry Letters, 2012, 3, 3707-3714.	2.1	43
12504	Ligand-Assisted Enhancement of CO₂ Capture in Metalâ€“Organic Frameworks. Journal of the American Chemical Society, 2012, 134, 6714-6719.	6.6	95
12505	CO Oxidation at the Interface between Doped CeO₂ and Supported Au Nanoclusters. Journal of Physical Chemistry Letters, 2012, 3, 2194-2199.	2.1	102

#	Article	IF	Citations
12506	Kinetic-Dynamic Properties of Different Monomers and Two-Dimensional Homoepitaxy Growth on the Zn-Polar (0001) ZnO Surface. Crystal Growth and Design, 2012, 12, 2850-2855.	1.4	4
12507	Theoretical Study of the Role of a Metalâ€“Cation Ensemble at the Oxideâ€“Metal Boundary on CO Oxidation. Journal of Physical Chemistry C, 2012, 116, 7491-7498.	1.5	59
12508	Self-Improving Anode for Lithium-Ion Batteries Based on Amorphous to Cubic Phase Transition in TiO₂ Nanotubes. Journal of Physical Chemistry C, 2012, 116, 3181-3187.	1.5	110
12509	Impact of Fluorination on Initial Growth and Stability of Pentacene on Cu(111). Journal of Physical Chemistry C, 2012, 116, 7726-7734.	1.5	29
12510	Adsorption of CO₂ on a PdO(101) Thin Film. Journal of Physical Chemistry C, 2012, 116, 3007-3016.	1.5	20
12511	Adsorption, Dissociation, and Hydrogenation of CO₂ on WC(0001) and WC-Co Alloy Surfaces Investigated with Theoretical Calculations. Journal of Physical Chemistry C, 2012, 116, 13202-13209.	1.5	27
12512	Hydrogen Adsorption and Site-Selective Reduction of the Fe₃O₄(001) Surface: Insights From First Principles. Journal of Physical Chemistry C, 2012, 116, 16447-16453.	1.5	35
12513	An Assessment of the vdW-TS Method for Extended Systems. Journal of Chemical Theory and Computation, 2012, 8, 1503-1513.	2.3	112
12514	Are Deposited Bimetallic Clusters More Effective for SO₃ Decomposition? A Systematic Study Using First Principles Theory. Journal of Physical Chemistry C, 2012, 116, 25594-25601.	1.5	10
12515	Synthesis and Properties of Monocrystalline Al(As_{1â€“x}P_x)Si₃ Alloys on Si(100). Chemistry of Materials, 2012, 24, 2347-2355.	3.2	10
12516	As₂O₃ Polymorphs: Theoretical Insight into Their Stability and Ammonia Templated Claudetite II Crystallization. Crystal Growth and Design, 2012, 12, 5663-5670.	1.4	23
12517	Site-Selective Mott Transition in Rare-Earth-Element Nickelates. Physical Review Letters, 2012, 109, 156402.	2.9	254
12518	First-principles study of structural, magnetic, and electronic properties of small Fe-Rh alloy clusters. Physical Review B, 2012, 85, .	1.1	42
12519	Higher-order contributions to the Rashba-Bychkov effect with application to the Bi/Ag(111) surface alloy. Physical Review B, 2012, 85, .	1.1	108
12520	Formation of Active Sites on WO₃ Catalysts: A Density Functional Theory Study of Olefin Metathesis. ACS Catalysis, 2012, 2, 341-349.	5.5	27
12521	First-Principles Study of Electron Mobility in Cationic and Anionic Conjugated Polyelectrolytes. Journal of Physical Chemistry C, 2012, 116, 1205-1210.	1.5	8
12522	Threadlike Tin Clusters with High Thermal Stability Based on Fundamental Units. Journal of Physical Chemistry C, 2012, 116, 231-236.	1.5	8
12523	Hydrogen and deuterium in shock wave experiments, ab initio simulations and chemical picture modeling. European Physical Journal D, 2012, 66, 1.	0.6	16

#	Article	IF	Citations
12524	Adsorption of Dichlorobenzene on Au and Pt Stepped Surfaces Using van der Waals Density Functional Theory. Journal of Physical Chemistry C, 2012, 116, 20409-20416.	1.5	27
12525	First-Principles Study on the Initial Oxidization of a Nb(100) Surface. Journal of Physical Chemistry C, 2012, 116, 23371-23376.	1.5	4
12526	First-Principles Study of Biaxial Strain Effect on Hydrogen Adsorbed Mg (0001) Surface. Journal of Physical Chemistry C, 2012, 116, 14943-14949.	1.5	24
12527	Slab Thickness Effects for the Clean and Adsorbed Ge(001) Surface with Comparison to Si(001). Journal of Physical Chemistry C, 2012, 116, 6615-6622.	1.5	11
12528	A New Hypothesis for the Dissolution Mechanism of Silicates. Journal of Physical Chemistry C, 2012, 116, 17479-17491.	1.5	52
12529	Gd13Fe10C13: Indications of Feâ€“Fe Multiple Bonding Emerging from Chemical Frustration. Journal of the American Chemical Society, 2012, 134, 10361-10364.	6.6	13
12530	The Î¼₃ Model of Acids and Bases: Extending the Lewis Theory to Intermetallics. Inorganic Chemistry, 2012, 51, 4250-4264.	1.9	14
12531	Thermodynamic Properties of Ga27Si3 Cluster Using Density Functional Molecular Dynamics. Journal of Physical Chemistry A, 2012, 116, 11-17.	1.1	7
12532	Chemically Doped Radial Junction Characteristics in Silicon Nanowires. Nano Letters, 2012, 12, 6133-6138.	4.5	5
12533	Heteroatom-Transfer Coupled Photoreduction and Carbon Dioxide Fixation on Metal Oxides. Journal of Physical Chemistry C, 2012, 116, 9461-9471.	1.5	45
12534	Thermodynamics and elastic properties of Ta from first-principles calculations. Chinese Physics B, 2012, 21, 127102.	0.7	7
12535	Dynamics of the Oxygen Molecules Scattered from the Graphite (0001) Surface and Comparison with Experimental Data. Journal of Physical Chemistry C, 2012, 116, 21482-21488.	1.5	14
12536	A Pressure Induced Structural Dichotomy in Isostructural Bis-1,2,3-thiaselenazolyl Radical Dimers. Crystal Growth and Design, 2012, 12, 4676-4684.	1.4	15
12537	Li, Al, and Ni Substitutional Doping in MgO Ultrathin Films on Metals: Work Function Tuning via Charge Compensation. Journal of Physical Chemistry C, 2012, 116, 5781-5786.	1.5	30
12538	Formation of One-Dimensional Electronic States along the Step Edges of CeO₂(111). ACS Nano, 2012, 6, 1126-1133.	7.3	61
12539	Crystal and Electronic Structures of Neptunium Nitrides Synthesized Using a Fluoride Route. Journal of the American Chemical Society, 2012, 134, 3111-3119.	6.6	20
12540	On the Need for Spin Polarization in Heterogeneously Catalyzed Reactions on Nonmagnetic Metallic Surfaces. Journal of Chemical Theory and Computation, 2012, 8, 1737-1743.	2.3	21
12541	First-principles study of the effect of iron on the crystal structure, stability and chemical bonding in the Î²-based AlCu ordered Î·2-phase and the pretransition state of a solid solution. Philosophical Magazine, 2012, 92, 1649-1662.	0.7	5

#	Article	IF	Citations
12542	Tailoring Electronic Structure Through Alloying: The AgnCu34â€“n(n= 0â€“34) Nanoparticle Family. Journal of Physical Chemistry C, 2012, 116, 281-291.	1.5	31
12543	High Mobility in a Stable Transparent Perovskite Oxide. Applied Physics Express, 2012, 5, 061102.	1.1	338
12544	Structure of the Au/Pd(100) Alloy Surface. Journal of Physical Chemistry C, 2012, 116, 4692-4697.	1.5	8
12545	Water Adsorption on Na/Cu(111): State-Specific Coupling with Quantum Well States. Journal of Physical Chemistry C, 2012, 116, 17613-17618.	1.5	8
12546	Acetone-Assisted Oxygen Vacancy Diffusion on TiO₂(110). Journal of Physical Chemistry Letters, 2012, 3, 2970-2974.	2.1	18
12547	Halogen Adsorption on CeO₂: The Role of Lewis Acidâ€“Base Pairing. Journal of Physical Chemistry C, 2012, 116, 6664-6671.	1.5	48
12548	Stable Subnanometer Cobalt Oxide Clusters on Ultrananocrystalline Diamond and Alumina Supports: Oxidation State and the Origin of Sintering Resistance. Journal of Physical Chemistry C, 2012, 116, 24027-24034.	1.5	24
12549	Quantum-Chemical Calculations on the Mechanism of the Waterâ€“Gas Shift Reaction on Nanosized Gold Cluster. Journal of Physical Chemistry C, 2012, 116, 336-342.	1.5	30
12550	Porous Alumina Protective Coatings on Palladium Nanoparticles by Self-Poisoned Atomic Layer Deposition. Chemistry of Materials, 2012, 24, 2047-2055.	3.2	110
12551	Variable-Temperature Scanning Tunneling Microscopy and Computational Studies Examining Water and Potassium Adsorption on Au(100). Journal of Physical Chemistry C, 2012, 116, 555-562.	1.5	5
12552	Binding Modes of Fluorinated Benzylphosphonic Acids on the Polar ZnO Surface and Impact on Work Function. Journal of Physical Chemistry C, 2012, 116, 19125-19133.	1.5	56
12553	Scanning tunneling microscopy study of graphene on Au(111): Growth mechanisms and substrate interactions. Physical Review B, 2012, 85, .	1.1	89
12554	Band engineering of Ni1â^'xMgxO alloys for photocathodes of high efficiency dye-sensitized solar cells. Journal of Applied Physics, 2012, 112, .	1.1	27
12555	Cadmium-rare earth oxyborates Cd4ReO(BO3)3 (Re = Y, Gd, Lu): congruently melting compounds with large SHG responses. Journal of Materials Chemistry, 2012, 22, 19911.	6.7	61
12556	On the Mechanisms of Carbon Formation Reaction on Ni(111) Surface. Journal of Physical Chemistry C, 2012, 116, 16522-16531.	1.5	19
12557	From Nondissociative to Dissociative Adsorption of Benzene-thiol on Au(111): A Density Functional Theory Study. Journal of Physical Chemistry C, 2012, 116, 1002-1011.	1.5	14
12558	Analysis of Charge Transfer for in Situ Li Intercalated Carbon Nanotubes. Journal of Physical Chemistry C, 2012, 116, 11364-11369.	1.5	25
12559	Kinetics of Anatase Electrodes: The Role of Ordering, Anisotropy, and Shape Memory Effects. Chemistry of Materials, 2012, 24, 2894-2898.	3.2	90

#	Article	IF	Citations
12560	Validation of Interstitial Iron and Consequences of Nonstoichiometry in Mackinawite (Fe_{1+x}S). Journal of Physical Chemistry A, 2012, 116, 2234-2243.	1.1	18
12561	Ethanol and Water Adsorption on Close-Packed 3d, 4d, and 5d Transition-Metal Surfaces: A Density Functional Theory Investigation with van der Waals Correction. Journal of Physical Chemistry C, 2012, 116, 24695-24705.	1.5	103
12562	Methyl Radical Reactivity on the Basal Plane of Graphite. Journal of Physical Chemistry C, 2012, 116, 18347-18357.	1.5	16
12563	Drastic Au(111) Surface Reconstruction upon Insulin Growth Factor Tripeptide Adsorption. Journal of the American Chemical Society, 2012, 134, 6579-6583.	6.6	24
12564	Ordered Growth of Upright Melamine Species on Ni{111}: A Study with Scanning Tunnelling Microscopy and Reflection Absorption Infrared Spectroscopy. Journal of Physical Chemistry C, 2012, 116, 6685-6690.	1.5	18
12565	Electronic and lattice instability and its relaxation mechanism in Pt-Co interfaces. Physical Review B, 2012, 85, .	1.1	1
12566	Physisorption of nucleobases on graphene: a comparative van der Waals study. Journal of Physics Condensed Matter, 2012, 24, 424210.	0.7	83
12567	Comparison of the Site Occupancies Determined by Combined Rietveld Refinement and Density Functional Theory Calculations: Example of the Ternary Moâ€“Niâ€“Re Ïƒ Phase. Inorganic Chemistry, 2012, 51, 3071-3078.	1.9	30
12568	Unusual nonlinear strain dependence of valence-band splitting in ZnO. Physical Review B, 2012, 86, .	1.1	11
12569	Quasiclassical Trajectory Dynamics Study of Atomic Oxygen Collisions on an O-Preadsorbed Graphite (0001) Surface with a New Analytical Potential Energy Surface. Journal of Physical Chemistry C, 2012, 116, 13092-13103.	1.5	18
12570	Decomposition of Methanol on Clean and Oxygen-Predosed V(100): A First-Principles Study. Journal of Physical Chemistry C, 2012, 116, 25344-25353.	1.5	10
12571	Establishing the LaMnO₃ Surface Phase Diagram in an Oxygen Environment: An ab Initio Kinetic Monte Carlo Simulation Study. Journal of Physical Chemistry C, 2012, 116, 26349-26357.	1.5	21
12572	Kinetics and Mechanisms for the Adsorption, Dissociation, and Diffusion of Hydrogen in Ni and Ni/YSZ Slabs: A DFT Study. Langmuir, 2012, 28, 5596-5605.	1.6	34
12573	Câ€“H Bond Activation of Methane via Ïƒâ€“d Interaction on the IrO₂(110) Surface: Density Functional Theory Study. Journal of Physical Chemistry C, 2012, 116, 6367-6370.	1.5	95
12574	First-principles study of lithium ion migration in lithium transition metal oxides with spinel structure. Physical Chemistry Chemical Physics, 2012, 14, 13963.	1.3	64
12575	Influence of water on the electronic structure of metal-supported graphene: Insights from van der Waals density functional theory. Physical Review B, 2012, 85, .	1.1	70
12576	DFT Study of the Electronic Properties of LaOCl Surfaces. Journal of Physical Chemistry C, 2012, 116, 681-691.	1.5	13
12577	On the Reaction Mechanism of Acetaldehyde Decomposition on Mo(110). ACS Catalysis, 2012, 2, 468-478.	5.5	16

#	Article	IF	Citations
12578	Trends in the Electronic Structure of Extended Gold Compounds: Implications for Use of Gold in Heterogeneous Catalysis. Inorganic Chemistry, 2012, 51, 7569-7578.	1.9	7
12579	Importance of the correct Fermi energy on the calculation of defect formation energies in semiconductors. Applied Physics Letters, 2012, 101, 082105.	1.5	32
12580	Role of NH₃ in the Dehydrogenation of Calcium Amidoborane Ammoniate and Magnesium Amidoborane Ammoniate: A First-Principles Study. Inorganic Chemistry, 2012, 51, 76-87.	1.9	14
12581	Polymeric Fused-Ring Type Iron Phthalocyanine Nanosheet and Its Derivative Ribbons and Tubes. Journal of Physical Chemistry C, 2012, 116, 9235-9242.	1.5	18
12582	Linker Dependent Bond Rupture Force Measurements in Single-Molecule Junctions. Journal of the American Chemical Society, 2012, 134, 4003-4006.	6.6	121
12583	Sulfidization of Au(111) from Thioacetic Acid: An Experimental and Theoretical Study. Langmuir, 2012, 28, 15278-15285.	1.6	16
12584	An ab initio molecular dynamics study: liquid-Al/solid-TiB₂ interfacial structure during heterogeneous nucleation. Journal Physics D: Applied Physics, 2012, 45, 455307.	1.3	23
12585	Extending the Density Functional Tight Binding Method to Carbon Under Extreme Conditions. Journal of Physical Chemistry C, 2012, 116, 2198-2204.	1.5	29
12586	pâ€“n Junction at the Interface between Metallic Systems. Journal of Physical Chemistry Letters, 2012, 3, 818-825.	2.1	5
12587	Vacancy trapping mechanism for multiple hydrogen and helium in beryllium: a first-principles study. Journal of Physics Condensed Matter, 2012, 24, 095004.	0.7	19
12588	Harnessing Chemical Raman Enhancement for Understanding Organic Adsorbate Binding on Metal Surfaces. Journal of Physical Chemistry Letters, 2012, 3, 1357-1362.	2.1	26
12589	Giant Magnetoelastic Effect at the Opening of a Spin-Gap in Ba₃BiIr₂O₉. Journal of the American Chemical Society, 2012, 134, 3265-3270.	6.6	39
12590	Absolute Surface Step Energies: Accurate Theoretical Methods Applied to Ceria Nanoislands. Journal of Physical Chemistry Letters, 2012, 3, 1956-1961.	2.1	38
12591	Dynamic structure factor in warm dense beryllium. New Journal of Physics, 2012, 14, 055020.	1.2	52
12592	Electronic Spectra and Crystal-Field Analysis of Europium in Hexanitritolanthanate Systems. Inorganic Chemistry, 2012, 51, 2997-3006.	1.9	15
12593	Tuning Band Gap Energies in Pb3(C6X6) Extended Solid-State Structures. Journal of Physical Chemistry C, 2012, 116, 8370-8378.	1.5	9
12594	First-principles study of the electronic structure and optical properties of defect chalcopyrite CdGa ₂ Te ₄. Chinese Physics B, 2012, 21, 123101.	0.7	7
12595	Surface and Particle-Size Effects on Hydrogen Desorption from Catalyst-Doped MgH₂. Journal of Physical Chemistry C, 2012, 116, 20315-20320.	1.5	11

#	Article	IF	Citations
12596	N-Alkyldinaphthocarbazoles, Azaheptacenes, for Solution-Processed Organic Field-Effect Transistors. Journal of the American Chemical Society, 2012, 134, 18185-18188.	6.6	44
12597	Strain-Induced Spin Crossover in Phthalocyanine-Based Organometallic Sheets. Journal of Physical Chemistry Letters, 2012, 3, 3109-3114.	2.1	54
12598	First-Principle Study on High-Pressure Behavior of Crystalline Polyazido-1,3,5-triazine. Journal of Physical Chemistry C, 2012, 116, 6745-6753.	1.5	23
12599	Monolayer Formation of Molybdenum Carbonyl on Cu(111) Revealed by Scanning Tunneling Microscopy and Density Functional Theory. Journal of Physical Chemistry C, 2012, 116, 10617-10622.	1.5	12
12600	First-Principles Assessment of the Reactions of Boric Acid on NiO(001) and ZrO2(1Ì...11) Surfaces. Journal of Physical Chemistry C, 2012, 116, 10113-10119.	1.5	7
12601	The Role of Stable and Mobile Carbon Adspecies in Copper-Promoted Graphene Growth. Journal of Physical Chemistry C, 2012, 116, 5802-5809.	1.5	70
12602	Graphitic Carbon Growth on MgO(100) by Molecular Beam Epitaxy. Journal of Physical Chemistry C, 2012, 116, 7380-7385.	1.5	23
12603	Anisotropic Strain Enhanced Hydrogen Solubility in bcc Metals: The Independence on the Sign of Strain. Physical Review Letters, 2012, 109, 135502.	2.9	101
12604	Influence of Step Defects on the H2S Splitting on Copper Surfaces from First-Principles Microkinetic Modeling. Journal of Physical Chemistry C, 2012, 116, 20321-20331.	1.5	14
12605	1D Hydrogen Bond Chain on Pt(211) Stepped Surface Observed by O K-NEXAFS Spectroscopy. Journal of Physical Chemistry C, 2012, 116, 13980-13984.	1.5	19
12606	Surface Ferromagnetic p-Type ZnO Nanowires through Charge Transfer Doping. ACS Applied Materials & Interfaces, 2012, 4, 1365-1370.	4.0	5
12607	3-D Atomic-Scale Mapping of Manganese Dopants in Lead Sulfide Nanowires. Journal of Physical Chemistry C, 2012, 116, 6595-6600.	1.5	12
12608	Improved Atoms-in-Molecule Charge Partitioning Functional for Simultaneously Reproducing the Electrostatic Potential and Chemical States in Periodic and Nonperiodic Materials. Journal of Chemical Theory and Computation, 2012, 8, 2844-2867.	2.3	282
12609	A DFT+U study of acetylene selective hydrogenation on oxygen defective anatase (101) and rutile (110) TiO2 supported Pd4 cluster. Journal of Chemical Physics, 2012, 136, 104107.	1.2	54
12610	Mechanical properties of graphene and boronitrene. Physical Review B, 2012, 85, .	1.1	713
12611	Structure of Isolated Molybdenum(VI) and Molybdenum(IV) Oxide Species on Silica: Periodic and Cluster DFT Studies. Journal of Physical Chemistry C, 2012, 116, 5571-5584.	1.5	60
12612	Adsorption of small molecules on silver clusters. Journal of Chemical Physics, 2012, 136, 024314.	1.2	25
12613	Inelastic X-Ray Scattering from Shocked Liquid Deuterium. Physical Review Letters, 2012, 109, 265003.	2.9	43

#	Article	IF	Citations
12614	p-electron magnetism in CdS doped with main group elements. Journal of Physics Condensed Matter, 2012, 24, 476002.	0.7	9
12615	Ab Initio Prediction of Adsorption Isotherms for Small Molecules in Metalâ€“Organic Frameworks: The Effect of Lateral Interactions for Methane/CPO-27-Mg. Journal of the American Chemical Society, 2012, 134, 18354-18365.	6.6	90
12616	Syntheses and Characterization of Six Quaternary Uranium Chalcogenides A₂M₄U₆Q₁₇ (A = Rb or Cs; M = Pd or Pt; Q = S or Se). Inorganic Chemistry, 2012, 51, 8873-8881.	1.9	15
12617	Effect of Alkyl Chain-Length on Dissociative Attachment: 1-Bromoalkanes on Si(100)-c(4Ã—2). Journal of Physical Chemistry C, 2012, 116, 10129-10137.	1.5	12
12618	Palladium in the Gap: Cluster Assemblies with Band Edges Localized on Linkers. Journal of Physical Chemistry C, 2012, 116, 10207-10214.	1.5	9
12619	Photoabsorbance and Photovoltage of Crystalline and Amorphous Silicon Slabs with Silver Adsorbates. Journal of Physical Chemistry C, 2012, 116, 25525-25536.	1.5	28
12620	Structure of Glycine on Ge(100): Ab Initio Study of Its Scanning Tunneling Microscopy Images. Journal of Physical Chemistry C, 2012, 116, 13890-13895.	1.5	2
12621	Strain-Induced ZnO Spinterfaces. Journal of Physical Chemistry C, 2012, 116, 610-617.	1.5	14
12622	Effects of Intrinsic Surface Defects on Thiophenol Self-Assembly on Au(111): Surface Structures and Reaction Mechanisms. Journal of Physical Chemistry C, 2012, 116, 19909-19917.	1.5	4
12623	Tuning Semiconductor Band Edge Energies for Solar Photocatalysis via Surface Ligand Passivation. Nano Letters, 2012, 12, 383-388.	4.5	124
12624	Tuning Structural and Mechanical Properties of Two-Dimensional Molecular Crystals: The Roles of Carbon Side Chains. Nano Letters, 2012, 12, 1229-1234.	4.5	27
12625	A simple law governing coupled magnetic orders in perovskites. Journal of Physics Condensed Matter, 2012, 24, 312201.	0.7	54
12626	Hydrogen Interaction with the Al Surface Promoted by Subsurface Alloying with Transition Metals. Journal of Physical Chemistry C, 2012, 116, 18663-18668.	1.5	19
12627	Effect of Molecular Passivation on the Doping of InAs Nanowires. Journal of Physical Chemistry C, 2012, 116, 17928-17933.	1.5	16
12628	Modified Ion Pair Interaction for Water Dimers on Supported MgO Ultrathin Films. Journal of Physical Chemistry C, 2012, 116, 20349-20355.	1.5	19
12629	Maximally localized Wannier functions in LaMnO₃within PBE +U, hybrid functionals and partially self-consistent GW: an efficient route to constructab initiotight-binding parameters for e_gperovskites. Journal of Physics Condensed Matter, 2012, 24, 235602.	0.7	106
12630	Density Functional Theory Study of Oxygen Reduction Activity on Ultrathin Platinum Nanotubes. Journal of Physical Chemistry C, 2012, 116, 16499-16510.	1.5	18
12631	Magnetic properties of phthalocyanine-based organometallic nanowire. Applied Physics Letters, 2012, 101, 062405.	1.5	24

#	Article	IF	Citations
12632	New Implicit Solvation Scheme for Solid Surfaces. Journal of Physical Chemistry C, 2012, 116, 22458-22462.	1.5	47
12633	Subangstrom Profile Imaging of Relaxed ZnO(101Ì…0) Surfaces. Nano Letters, 2012, 12, 704-708.	4.5	25
12634	Formic Acid Dehydrogenation on Ni(111) and Comparison with Pd(111) and Pt(111). Journal of Physical Chemistry C, 2012, 116, 4149-4156.	1.5	115
12635	WORK FUNCTION OF BORON CARBIDE: A DFT CALCULATION. Surface Review and Letters, 2012, 19, 1250040.	0.5	7
12636	p-electron magnetism in doped BaTiO _{3â^'x} M _x (M=C, N, B). Europhysics Letters, 2012, 97, 67008.	0.7	7
12637	Catalytic Reactivity of CuNi Alloys toward H₂O and CO Dissociation for an Efficient Waterâ€“Gas Shift: A DFT Study. Journal of Physical Chemistry C, 2012, 116, 745-752.	1.5	71
12638	Redirecting focus in CuInSe<mml:math xmlns:mml="http://www.w3.org/1998/Math/MathML" display="inline"><mml:msub><mml:mrow /><mml:mn>2</mml:mn></mml:msub></mml:math>research towards selenium-related defects. Physical Review B, 2012, 86, .	1.1	26
12639	Microstructure evolution of diazonium functionalized graphene: A potential approach to change graphene electronic structure. Journal of Materials Chemistry, 2012, 22, 2063-2068.	6.7	38
12640	Comparative study of defect transition energy calculation methods: The case of oxygen vacancy in In<mml:math xmlns:mml="http://www.w3.org/1998/Math/MathML" display="inline"><mml:msub><mml:mrow /><mml:mn>2</mml:mn></mml:msub></mml:math>O<mml:math xmlns:mml="http://www.w3.org/1998/Math/MathML" display="inline"><mml:msub><mml:mrow /><mml:mn>3</mml:mn></mml:msub></mml:math>and ZnO. Physical Review B, 2012, 86, .	1.1	23
12641	Three Alkali-Metalâ€“Goldâ€“Gallium Systems. Ternary Tunnel Structures and Some Problems with Poorly Ordered Cations. Inorganic Chemistry, 2012, 51, 7711-7721.	1.9	40
12642	Formation of a Rhodium Surface Oxide Film in Rh_n/CeO₂(111) Relevant for Catalytic CO Oxidation: A Computational Study. Journal of Physical Chemistry C, 2012, 116, 22904-22915.	1.5	27
12643	Electronic Structure, Optical Properties, and Hydrogen Adsorption Characteristics of Supercubane-Based Three-Dimensional Porous Carbon. Journal of Physical Chemistry C, 2012, 116, 25015-25021.	1.5	20
12644	Controlled Synthesis of Rh Nanoparticles on TiO₂(110) via Rh(CO)₂(acac). Journal of Physical Chemistry C, 2012, 116, 11987-11993.	1.5	13
12645	Density Functional Theory Study on the Role of Ceria Addition in TixCe1â€“xO2 Adsorbents for Thiophene Adsorption. Journal of Physical Chemistry C, 2012, 116, 3457-3466.	1.5	25
12646	Monocrystalline Al(As_{1â€“x}N_x)Si₃ and Al(P_{1â€“x}N_x)_ySi_{5â€“2y} Alloys with Diamond-like Structures: New Chemical Approaches to Semiconductors Lattice Matched to Si. Chemistry of Materials, 2012, 24, 3219-3230.	3.2	10
12647	Half-Metallic Properties Induced by Fluorine in Aluminum Nitride Nanosheet. Journal of the Physical Society of Japan, 2012, 81, 044705.	0.7	2
12648	Oxidation of an Organic Adlayer: A Birdâ€™s Eye View. Journal of the American Chemical Society, 2012, 134, 8817-8822.	6.6	12
12649	Computational Differentiation of BrÃ¸nsted Acidity Induced by Alkaline Earth or Rare Earth Cations in Zeolites. Inorganic Chemistry, 2012, 51, 12165-12175.	1.9	9

#	Article	IF	Citations
12650	Dissociative Adsorption and Aggregation of Water on the Fe(100) Surface: A DFT Study. Journal of Physical Chemistry C, 2012, 116, 20306-20314.	1.5	49
12651	Interactions between Organics and Metal Surfaces in the Intermediate Regime between Physisorption and Chemisorption. Journal of Physical Chemistry C, 2012, 116, 23603-23607.	1.5	19
12652	Si/Ge Double-Layered Nanotube Array as a Lithium Ion Battery Anode. ACS Nano, 2012, 6, 303-309.	7.3	225
12653	Formaldehyde Decomposition and Coupling on V(100): A First-Principles Study. Journal of Physical Chemistry C, 2012, 116, 10639-10648.	1.5	7
12654	First principles calculation on thermal stability of metastable precipitates in Mgâ€“Gd binary alloys. Materials Science and Technology, 2012, 28, 794-798.	0.8	7
12655	(Nd_{1.5}Mg_{0.5})Ni₇-Based Compounds: Structural and Hydrogen Storage Properties. Inorganic Chemistry, 2012, 51, 2976-2983.	1.9	73
12656	Tuning of the Surface-Exposing and Photocatalytic Activity for AgX (X = Cl and Br): A Theoretical Study. Journal of Physical Chemistry C, 2012, 116, 19372-19378.	1.5	31
12657	Electronic Structure and Spin Polarization of Metal (Mn, Fe, Cu) Phthalocyanines on an Fe(100) Surface by First-Principles Calculations. Journal of Physical Chemistry C, 2012, 116, 18752-18758.	1.5	15
12658	Transition Metal Surface Passivation Induced Graphene Edge Reconstruction. Journal of the American Chemical Society, 2012, 134, 6204-6209.	6.6	127
12659	Structural, electronic, and polarization properties of Bi2ZnTiO6 supercell from first-principles. Journal of Applied Physics, 2012, 111, 114101.	1.1	9
12660	Bonding and Charge Transfer in Metalâ€“Organic Coordination Networks on Au(111) with Strong Acceptor Molecules. Journal of Physical Chemistry C, 2012, 116, 24558-24565.	1.5	112
12661	Size- and shape-dependent phase transformations in wurtzite ZnS nanostructures. Physical Chemistry Chemical Physics, 2012, 14, 9871.	1.3	27
12662	Spin Splitting in a Nickel Phthalocyanine Molecule on an Fe(100) Surface by First-principles Calculations. Journal of Physical Chemistry C, 2012, 116, 10976-10981.	1.5	7
12663	A Density Functional Theory and Experimental Study of CO₂ Interaction with Brookite TiO₂. Journal of Physical Chemistry C, 2012, 116, 19755-19764.	1.5	84
12664	Morphology Control of Nanostructures: Na-Doped PbTeâ€“PbS System. Nano Letters, 2012, 12, 5979-5984.	4.5	100
12665	Cation disorder in MgX2O4(X= Al, Ga, In) spinels from first principles. Physical Review B, 2012, 86, .	1.1	20
12666	Half-Metallicity in Organic Single Porous Sheets. Journal of the American Chemical Society, 2012, 134, 5718-5721.	6.6	101
12667	Growth of Pt Particles on the Anatase TiO₂ (101) Surface. Journal of Physical Chemistry C, 2012, 116, 12114-12123.	1.5	63

#	Article	IF	Citations
12668	Structures and Energetics of Pt Clusters on TiO₂: Interplay between Metalâ€“Metal Bonds and Metalâ€“Oxygen Bonds. Journal of Physical Chemistry C, 2012, 116, 21880-21885.	1.5	39
12669	Melanin films on Au(1 1 1): Adsorption and molecular conductance. Organic Electronics, 2012, 13, 1844-1852.	1.4	4
12670	Control of the Spatial Resolution in Ultimately High Resolution STM Experiments with [001]-Oriented Single Crystalline Tungsten Probes. Physics Procedia, 2012, 32, 785-788.	1.2	1
12671	First-principles studies of interlayer exchange coupling in (Ga, Co)N-based diluted magnetic semiconductor multilayers. Physica A: Statistical Mechanics and Its Applications, 2012, 391, 5090-5094.	1.2	1
12672	Comparison between various finite-size supercell correction schemes for charged defect calculations. Physica B: Condensed Matter, 2012, 407, 3063-3067.	1.3	23
12673	Phase diagrams of polar surface reconstructions of zinc oxide. Physica B: Condensed Matter, 2012, 407, 2871-2874.	1.3	3
12674	First-principles study of the segregation of boron dopants near the interface between crystalline Si and amorphous SiO2. Physica B: Condensed Matter, 2012, 407, 2989-2992.	1.3	7
12675	Effect of O-vacancy defects on the Schottky barrier heights in Ni/SiO2 and Ni/HfO2 interfaces. Physica B: Condensed Matter, 2012, 407, 2907-2910.	1.3	3
12676	Electronic structure and properties of NbS2 and TiS2 low dimensional structures. Physica B: Condensed Matter, 2012, 407, 3188-3191.	1.3	15
12677	Site preference and elastic properties of ternary alloying additions in B2 YAg alloys by first-principles calculations. Physica B: Condensed Matter, 2012, 407, 3749-3752.	1.3	1
12678	Structure, bonding and stability of semi-carbides M2C and sub-carbides M4C (M=V, Cr, Nb, Mo, Ta, W): A first principles investigation. Physica B: Condensed Matter, 2012, 407, 3833-3838.	1.3	28
12679	Controllable modification of the conduction properties of carbon nanotube devices through deposition of a metal overlayer onto the sidewalls. Physica E: Low-Dimensional Systems and Nanostructures, 2012, 44, 1539-1542.	1.3	3
12680	First-principles study of nitrogen-doped CuAlO2. Physics Letters, Section A: General, Atomic and Solid State Physics, 2012, 376, 2613-2616.	0.9	16
12681	The environmental dependence of redox energetics of PuO2 and Î±-Pu2O3: A quantitative solution from. Physics Letters, Section A: General, Atomic and Solid State Physics, 2012, 376, 2672-2676.	0.9	10
12682	Understanding the chiral selectivity of gold nanotubes. Physics Letters, Section A: General, Atomic and Solid State Physics, 2012, 376, 2707-2711.	0.9	6
12683	First principles prediction of the elastic, electronic, and optical properties of Sb2S3 and Sb2Se3 compounds. Solid State Sciences, 2012, 14, 1211-1220.	1.5	124
12684	Planar nano-block structures Tin+1Al0.5Cn and Tin+1Cn (n=1, and 2) from MAX phases: Structural, electronic properties and relative stability from first principles calculations. Superlattices and Microstructures, 2012, 52, 147-157.	1.4	59
12685	Imposing changes of band and spinâ€“orbit gaps in GaNBi. Solid State Communications, 2012, 152, 1700-1702.	0.9	15

#	Article	IF	Citations
12686	Density functional investigation of the magnetic superstructure of Cu2MnSnS4. Solid State Communications, 2012, 152, 1683-1685.	0.9	9
12687	New superhard carbon phases between graphite and diamond. Solid State Communications, 2012, 152, 1560-1563.	0.9	89
12688	Orbital-decomposed electronic structures of cubic zirconia. Solid State Communications, 2012, 152, 1673-1677.	0.9	8
12689	Interaction of zinc interstitial with oxygen vacancy in zinc oxide: An origin of n-type doping. Solid State Communications, 2012, 152, 1711-1714.	0.9	54
12690	First-principles studies on the structural and electronic properties of Li-ion battery cathode material CuF2. Solid State Communications, 2012, 152, 1703-1706.	0.9	20
12691	A density functional theory study on the origin of lithium-montmorillonite's conductivity at low water content: A first investigation. Solid State Communications, 2012, 152, 1862-1866.	0.9	7
12692	The important features of VHg-related defects in arsenic-doped HgCdTe. Solid State Communications, 2012, 152, 1725-1728.	0.9	1
12693	Functionalization of edge reconstructed graphene nanoribbons by H and Fe: A density functional study. Solid State Communications, 2012, 152, 1719-1724.	0.9	6
12694	Detailed insights into the structural properties and oxygen-pathways in orthorhombic Ba0.5Sr0.5Co0.8Fe0.2O3â€“Î´ by electronic-structure theory. Solid State Ionics, 2012, 222-223, 53-58.	1.3	20
12695	Surface structure of In2O3(111) (1Ã—1) determined by density functional theory calculations and low energy electron diffraction. Surface Science, 2012, 606, 1-6.	0.8	21
12696	Ionic and radical adsorption on the Au(hkl) surfaces: A DFT study. Surface Science, 2012, 606, 69-77.	0.8	32
12697	The mechanism of H2 dissociation and adsorption on Mn-modified Ni(111) surface: A density functional theory-based investigation. Surface Science, 2012, 606, 62-68.	0.8	9
12698	Fast atom diffraction during grazing scattering from a MgO(001) surface. Surface Science, 2012, 606, 161-173.	0.8	39
12699	Formation of a missing row reconstruction on a Cu(100) surface: An atom scale density functional theory based study. Surface Science, 2012, 606, 192-201.	0.8	11
12700	Adsorption of water monomer and clusters on platinum(111) terrace and related steps and kinks II. Surface diffusion. Surface Science, 2012, 606, 233-238.	0.8	15
12701	Stress-driven structural transformation of Sb-passivated Si(114). Surface Science, 2012, 606, 312-319.	0.8	5
12702	Coverage-dependent molecular tilt of carbon monoxide chemisorbed on Pt{110}: A combined LEED and DFT structural analysis. Surface Science, 2012, 606, 383-393.	0.8	10
12703	Atomic scale control of catalytic process in oxidation of Pb thin films. Surface Science, 2012, 606, 450-455.	0.8	0

#	Article	IF	Citations
12704	Passivation effect of allylamine molecule on the electronic structure of a Si(001)â˜'(2Ã—1) surface. Surface Science, 2012, 606, 470-474.	0.8	3
12705	Relative stability of armchair, zigzag and reczag graphene edges on the Ru(0001) surface. Surface Science, 2012, 606, 485-489.	0.8	10
12706	The adsorption and reconstruction of strong electron acceptor tetracyanoethylene (TCNE) on Si(001)-(2Ã—1): A density functional theory investigation. Surface Science, 2012, 606, 523-526.	0.8	1
12707	Structural and electronic properties of cobalt carbide Co2C and its surface stability: Density functional theory study. Surface Science, 2012, 606, 598-604.	0.8	79
12708	First-principles calculations of ammonia decomposition on Ni(110) surface. Surface Science, 2012, 606, 549-553.	0.8	57
12709	Effect of platinum promoters on the removal of O from the surface of cobalt catalysts: A DFT study. Surface Science, 2012, 606, 634-643.	0.8	27
12710	First-principles study of the water structure on flat and stepped gold surfaces. Surface Science, 2012, 606, 886-891.	0.8	74
12711	Energetics of Carbon deposition on Fe(100) and Fe(110) surfaces and subsurfaces. Surface Science, 2012, 606, 733-739.	0.8	30
12712	Study of the TiSi interface formed by Ti deposition on a clean Si (100) surface. Surface Science, 2012, 606, 754-761.	0.8	3
12713	First principles investigations of hydrazine adsorption conformations on Ni(111) surface. Surface Science, 2012, 606, 766-771.	0.8	45
12714	Density functional theory-based analysis on O2 molecular interaction with the tri-s-triazine-based graphitic carbon nitride. Surface Science, 2012, 606, 892-901.	0.8	56
12715	pH-dependent structure and energetics of H2O/MgO(100). Surface Science, 2012, 606, 902-907.	0.8	23
12716	Mechanism of oxygen adsorption on surfaces of Î³-TiAl. Surface Science, 2012, 606, 852-857.	0.8	39
12717	Fe3O4 surface electronic structures and stability from GGA+U. Surface Science, 2012, 606, 872-879.	0.8	115
12718	CO2 hydrogenation to formic acid on Ni(110). Surface Science, 2012, 606, 1050-1055.	0.8	76
12719	Structural, electronic, stability and reduction properties of perovskite surfaces: The case of rhombohedral BaCeO3. Surface Science, 2012, 606, 1078-1087.	0.8	23
12720	Surface interactions of Au(I) cyclo-trimer with Au(111) and Al(111) surfaces: A computational study. Surface Science, 2012, 606, 1100-1107.	0.8	7
12721	Theoretical study of hydrogen dissociation and diffusion on Nb and Ni co-doped Mg(0001): A synergistic effect. Surface Science, 2012, 606, L45-L49.	0.8	21

#	Article	IF	Citations
12722	Surface structure of bismuth terminated GaAs surfaces grown with molecular beam epitaxy. Surface Science, 2012, 606, 1203-1207.	0.8	27
12723	Stability of small chemical groups on hexagonal-SiC(0001) surfaces: A theoretical study. Surface Science, 2012, 606, 1195-1202.	0.8	2
12724	A density functional theory study of CF3CH2I adsorption and reaction on Ag(111). Surface Science, 2012, 606, 1227-1232.	0.8	15
12725	Effect of nitrogen incorporation and oxygen vacancy on electronic structure and the absence of a gap state in HfSiO films. Surface Science, 2012, 606, L64-L68.	0.8	4
12726	Controlling adsorption status of individual fullerene at room-temperature. Surface Science, 2012, 606, 1308-1312.	0.8	0
12727	Diffusion of a Ga adatom on the GaAs(001)â€¢(4Ã—4)â€heterodimer surface: A first principles study. Surface Science, 2012, 606, 1303-1307.	0.8	12
12728	Structure and properties of a model oxide-supported catalyst under redox conditions: WOx/Î±-Fe2O3 (0001). Surface Science, 2012, 606, 1367-1381.	0.8	6
12729	Pt-chain induced formation of Ge nanowires on the Ge(001) surface. Surface Science, 2012, 606, 1405-1411.	0.8	8
12730	Metallization of the Î²-SiC(100) 3Ã—2 surface: A DFT investigation. Surface Science, 2012, 606, 1471-1474.	0.8	3
12731	Interfacial structure of Co porphyrins on Au(111) electrode: Interaction of porphyrin molecules with substrate. Surface Science, 2012, 606, 1560-1564.	0.8	8
12732	Mechanistic understanding of hydrogenation of acetaldehyde on Au(111): A DFT investigation. Surface Science, 2012, 606, 1608-1617.	0.8	17
12733	Density functional theory study of water adsorption on FeOOH surfaces. Surface Science, 2012, 606, 1623-1632.	0.8	51
12734	Structure of ordered oxide on InAs(100) surface. Surface Science, 2012, 606, 1837-1841.	0.8	5
12735	Effect of oxygen on the stability of Ag islands on Si(111)-7Ã—7. Surface Science, 2012, 606, 1871-1878.	0.8	2
12736	First-principles study of Si(111)-In reconstruction. Surface Science, 2012, 606, 1914-1917.	0.8	7
12737	A theoretical study of the structure and stability of borohydride on 3d transition metals. Surface Science, 2012, 606, 1954-1959.	0.8	23
12738	3C-SiC(001)-3 Ã— 2 reconstructed surface analyzed by high-resolution medium energy ion scattering. Surface Science, 2012, 606, 1942-1947.	0.8	4
12739	Scandium-Decorated MOF-5 as Potential Candidates for Room-Temperature Hydrogen Storage: A Solution for the Clustering Problem in MOFs. Journal of Physical Chemistry C, 2012, 116, 17336-17342.	1.5	50

#	Article	IF	Citations
12740	First principles calculations of magnetism, dielectric properties and spinâ€“phonon coupling in double perovskite Bi2CoMnO6. Journal of Physics Condensed Matter, 2012, 24, 295901.	0.7	5
12741	Phase conversion from graphite toward a simple monoclinic sp3-carbon allotrope. Journal of Chemical Physics, 2012, 137, 024502.	1.2	38
12742	Graphene nanodots with intrinsically magnetic protrusions. Journal of Chemical Physics, 2012, 136, 064706.	1.2	5
12743	Strain dependence of polarization and piezoelectric response in epitaxial BiFeO₃thin films. Journal of Physics Condensed Matter, 2012, 24, 162202.	0.7	66
12744	Playing with Dimensions: Rational Design for Heteroepitaxial pâ€“n Junctions. Nano Letters, 2012, 12, 68-76.	4.5	29
12745	Ab initio carbon capture in open-site metalâ€“organic frameworks. Nature Chemistry, 2012, 4, 810-816.	6.6	310
12746	Van der Waals interactions at metal/organic interfaces at the single-molecule level. Nature Materials, 2012, 11, 872-876.	13.3	181
12747	First-Principles Study of Half-Metallic Materials in Double-Perovskite A₂FeMO₆ (M = Mo, Re, and W) with IVA Group Elements Set on the A-Site Position. Journal of Physical Chemistry C, 2012, 116, 18032-18037.	1.5	23
12748	First-principles investigation of the structural phases and enhanced response properties of the BiFeO<mml:math xmlns:mml="http://www.w3.org/1998/Math/MathML" display="inline"><mml:msub><mml:mrow /><mml:mn>3</mml:mn></mml:msub></mml:math>-LaFeO<mml:math xmlns:mml="http://www.w3.org/1998/Math/MathML" display="inline"><mml:msub><mml:mrow /><mml:mn>3</mml:mn></mml:msub></mml:math>multiferroic solid solution. Physical Review B, 2012,	1.1	58
12749	Symmetry-Driven Novel Kondo Effect in a Molecule. Physical Review Letters, 2012, 109, 086602.	2.9	138
12750	Ferroelectricity of Sn-doped SrTiO<mml:math xmlns:mml="http://www.w3.org/1998/Math/MathML" display="inline"><mml:msub><mml:mrow /><mml:mn>3</mml:mn></mml:msub></mml:math>perovskites with tin at both<mml:math xmlns:mml="http://www.w3.org/1998/Math/MathML" display="inline"><mml:mi>A</mml:mi></mml:math>and<mml:math xmlns:mml="http://www.w3.org/1998/Math/MathML"	1.1	33
12751	Stability of the high-pressure phases of CaTiO<mml:math xmlns:mml="http://www.w3.org/1998/Math/MathML" display="inline"><mml:msub><mml:mrow /><mml:mn>3</mml:mn></mml:msub></mml:math>perovskite at finite temperatures. Physical Review B, 2012, 86, .	1.1	15
12752	Structural and electronic properties of Pb<mml:math xmlns:mml="http://www.w3.org/1998/Math/MathML" display="inline"><mml:msub><mml:mrow /><mml:mrow><mml:mn>1</mml:mn><mml:mo>â^’</mml:mo><mml:mi>x</mml:mi></mml:mrow></mml:msub></mml:math>Cd<mml:math xmlns:mml="http://www.w3.org/1998/Math/MathML" display="inline"><mml:msub><mml:mrow /><mml:mi>x</mml:mi></mml:msub></mml:math>Te and Pb<mml:math xmlns:mml="http://www.w3.org/1998/Math/MathML" display="inline"><mml:msub><mml:mrow /><mml:mi>	1.1	20
12753	How Critical Are the van der Waals Interactions in Polymer Crystals?. Journal of Physical Chemistry A, 2012, 116, 9347-9352.	1.1	63
12754	Spin-filtering and switching effects of a single-molecule magnet Mn(dmit)2. Journal of Applied Physics, 2012, 111, 043713.	1.1	13
12755	Trace Flue Gas Contaminants Poison Coordinatively Unsaturated Metalâ€“Organic Frameworks: Implications for CO₂ Adsorption and Separation. Journal of Physical Chemistry C, 2012, 116, 20480-20488.	1.5	90
12756	Chiral graphene nanoribbon inside a carbon nanotube: ab initio study. Nanoscale, 2012, 4, 4522.	2.8	32
12757	Calcium-based functionalization of carbon nanostructures for peptide immobilization in aqueous media. Journal of Materials Chemistry, 2012, 22, 19684.	6.7	26

#	Article	IF	Citations
12758	Physical and Chemical Nature of the Scaling Relations between Adsorption Energies of Atoms on Metal Surfaces. Physical Review Letters, 2012, 108, 116103.	2.9	233
12759	How to fabricate a semihydrogenated graphene sheet? A promising strategy explored. Applied Physics Letters, 2012, 101, 073114.	1.5	34
12760	Experimental and theoretical investigations of the polymorphism of 5-chloroacetoxybenzoic acid (5-chloroaspirin). CrystEngComm, 2012, 14, 1672-1680.	1.3	15
12761	First Principles Simulations of the Electrochemical Lithiation and Delithiation of Faceted Crystalline Silicon. Journal of the American Chemical Society, 2012, 134, 14362-14374.	6.6	221
12762	Atomistic Insights into the Conversion Reaction in Iron Fluoride: A Dynamically Adaptive Force Field Approach. Journal of the American Chemical Society, 2012, 134, 8205-8211.	6.6	54
12763	First-principles calculations of uranium diffusion in uranium dioxide. Physical Review B, 2012, 86, .	1.1	83
12764	Two-Dimensional Boron Monolayer Sheets. ACS Nano, 2012, 6, 7443-7453.	7.3	690
12765	Guided Self-Assembly of Metal Atoms on Silicon Using Organic-Molecule Templating. Journal of the American Chemical Society, 2012, 134, 15312-15317.	6.6	17
12766	Asymmetric orientation of toluene molecules at oil-silica interfaces. Journal of Chemical Physics, 2012, 137, 064703.	1.2	15
12767	Molecular models of birnessite and related hydrated layered minerals. American Mineralogist, 2012, 97, 1505-1514.	0.9	36
12768	Native defects in second-generation topological insulators: Effect of spin-orbit interaction on Bi<mml:math xmlns:mml="http://www.w3.org/1998/Math/MathML" display="inline"><mml:msub><mml:mrow /><mml:mn>2</mml:mn></mml:msub></mml:math>Se<mml:math xmlns:mml="http://www.w3.org/1998/Math/MathML" display="inline"><mml:msub><mml:mrow /><mml:mn>3</mml:mn></mml:msub></mml:math>. Physical Review B, 2012, 86, .	1.1	117
12769	Effects of doping on the lattice parameter of SrTiO3. Applied Physics Letters, 2012, 100, .	1.5	114
12770	Effect of the electric field on magnetic properties of linear chains on a Pt(111) surface. Physical Review B, 2012, 85, .	1.1	25
12771	Understanding the Metal-Directed Growth of Single-Crystal M-TCNQF₄ Organic Nanowires with Time-Resolved, in Situ X-ray Diffraction and First-Principles Theoretical Studies. Journal of the American Chemical Society, 2012, 134, 14353-14361.	6.6	17
12772	Topological surface states and Dirac point tuning in ternary topological insulators. Physical Review B, 2012, 85, .	1.1	171
12773	Direct first-principles chemical potential calculations of liquids. Journal of Chemical Physics, 2012, 137, 094114.	1.2	14
12774	Microscopic Origin of Large Negative Magnetoelectric Coupling in<mml:math xmlns:mml="http://www.w3.org/1998/Math/MathML" display="inline"><mml:msub><mml:mi>Sr</mml:mi><mml:mrow><mml:mn>1</mml:mn><mml:mo>/</mml:mo><mml:mn>2</mml:mn> Physical Review Letters, 2012, 109, 107601.	2.9	42
12775	Unusual Stability and Activity of DI-Pd19 Clusters for O₂ Dissociation. Journal of Physical Chemistry C, 2012, 116, 19586-19589.	1.5	9

#	Article	IF	Citations
12776	Electronic and transport gaps of graphene opened by grain boundaries. Journal of Applied Physics, 2012, 112, .	1.1	34
12777	Semiconducting allotrope of graphene. Nanotechnology, 2012, 23, 385704.	1.3	36
12778	Oxygen density dependent band gap of reduced graphene oxide. Journal of Applied Physics, 2012, 111, .	1.1	160
12779	High-Pressure Raman and X-ray Diffraction Study of Î²- and Î³-Polymorphs of Aluminum Hydride. Journal of Physical Chemistry C, 2012, 116, 3808-3816.	1.5	14
12780	Ab initiostudy of the relation between electric polarization and electric field gradients in ferroelectrics. Physical Review B, 2012, 86, .	1.1	20
12781	Persistent Medium-Range Order and Anomalous Liquid Properties ofAl1âˆ’xCuxAlloys. Physical Review Letters, 2012, 108, 115901.	2.9	29
12782	Modified embedded atom method potential for Al, Si, Mg, Cu, and Fe alloys. Physical Review B, 2012, 85, .	1.1	267
12783	Large amplitude fluxional behaviour of elemental calcium under high pressure. Scientific Reports, 2012, 2, 372.	1.6	16
12784	Why the Heyd-Scuseria-Ernzerhof hybrid functional description of VO<mml:math xmlns:mml="http://www.w3.org/1998/Math/MathML" display="inline"><mml:msub><mml:mrow /><mml:mn>2</mml:mn></mml:msub></mml:math>phases is not correct. Physical Review B, 2012, 86, .	1.1	68
12785	Study of pressure-induced amorphization in sulfur usingab initiomolecular dynamics. Physical Review B, 2012, 85, .	1.1	12
12786	Li Absorption and Intercalation in Single Layer Graphene and Few Layer Graphene by First Principles. Nano Letters, 2012, 12, 4624-4628.	4.5	271
12787	Strong asymmetrical doping properties of spinel CoAl2O4. Journal of Applied Physics, 2012, 111, 093723.	1.1	6
12788	Prominently Improved Hydrogen Purification and Dispersive Metal Binding for Hydrogen Storage by Substitutional Doping in Porous Graphene. Journal of Physical Chemistry C, 2012, 116, 21291-21296.	1.5	76
12789	Simulation of crack propagation in alumina with ab initio based polarizable force field. Journal of Chemical Physics, 2012, 136, 084707.	1.2	18
12790	Feâ€“C and Feâ€“H systems at pressures of the Earth's inner core. Physics-Uspekhi, 2012, 55, 489-497.	0.8	71
12791	Strain-engineered magnetic order in (LaMnO<mml:math) Tj ETQq1 1 0.784314 rgBT /Overlock 10 Tf 50 167 Td (xmlns:mml="http://www.w3.org/1998/Math/MathML" display="inline"><mml:msub><mml:mrow		

#	Article	IF	Citations
12794	Modulating the bandgaps of graphdiyne nanoribbons by transverse electric fields. Journal of Physics Condensed Matter, 2012, 24, 165301.	0.7	37
12795	Influence of indium cluster on the high and constant background electron density in ternary In_xGa_{1â^'x}N alloys. Applied Physics Letters, 2012, 101, 062102.	1.5	8
12796	Computational study of the adsorption and dissociation of phenol on Pt and Rh surfaces. Physical Chemistry Chemical Physics, 2012, 14, 5849.	1.3	74
12797	Density functional theory study of phase stability, vibrational, and electronic properties of Mo3Al2C. Physical Review B, 2012, 86, .	1.1	10
12798	Zinc Oxide as a Model Transparent Conducting Oxide: A Theoretical and Experimental Study of the Impact of Hydroxylation, Vacancies, Interstitials, and Extrinsic Doping on the Electronic Properties of the Polar ZnO (0002) Surface. Chemistry of Materials, 2012, 24, 3044-3055.	3.2	110
12799	Stability and Segregation of B and P Dopants in Si/SiO₂ Coreâ€“Shell Nanowires. Nano Letters, 2012, 12, 5068-5073.	4.5	19
12800	Effect of Boron on Carbide Coarsening at 873ÂK (600ÂÂ°C) in 9Âto 12Âpct Chromium Steels. Metallurgical and Materials Transactions A: Physical Metallurgy and Materials Science, 2012, 43, 4053-4062.	1.1	60
12801	Adsorption and Separation of Xylene Isomers: CPO-27-Ni vs HKUST-1 vs NaY. Journal of Physical Chemistry C, 2012, 116, 21844-21855.	1.5	72
12802	Effects of shape and composition on the properties of CdS nanocrystals. Physical Review B, 2012, 86, .	1.1	16
12803	Synthesis and Characterization of the Crystal Structure and Magnetic Properties of the New Fluorophosphate LiNaCo[PO₄]F. Inorganic Chemistry, 2012, 51, 8729-8738.	1.9	15
12804	Catalysis by a Zinc-Porphyrin-Based Metalâ€“Organic Framework: From Theory to Computational Design. Journal of Physical Chemistry C, 2012, 116, 23494-23502.	1.5	33
12805	Effect of Mg-substitute and potassium doping on the<mml:math xmlns:mml="http://www.w3.org/1998/Math/MathML" display="inline"><mml:msub><mml:mi>A</mml:mi><mml:mrow><mml:mn>0.8</mml:mn></mml:mrow></mml:msub></mml:math>F<mml:math xmlns:mml="http://www.w3.org/1998/Math/MathML" display="inline"><mml:msub><mml:mrow /><mml:mrow><mml:mn>1.6</mml:mn></mml:mrow></mml:msub></mml:math>Se<mml:math xmlns:mml="http://www.w3.org/1998/Math/MathML" display="inline"><mml:msub><mml:mrow /><mml:mml:	1.1	14
12806	Deformation Potential Theory. Springer Briefs in Molecular Science, 2012, , 67-88.	0.1	11
12807	Detection of hidden structures for arbitrary scales in complex physical systems. Scientific Reports, 2012, 2, 329.	1.6	40
12809	Decay Kinetics of Cluster-Beam-Deposited Metal Particles. Journal of Physical Chemistry C, 2012, 116, 19327-19334.	1.5	10
12810	Pressure effects on the electronic and optical properties of<mml:math xmlns:mml="http://www.w3.org/1998/Math/MathML" display="inline"><mml:mi>A</mml:mi></mml:math>WO<mml:math xmlns:mml="http://www.w3.org/1998/Math/MathML" display="inline"><mml:msub><mml:mrow		

#	Article	IF	Citations
12813	First-principles study of bubble nucleation and growth behaviors in Î± Uâ€“Zr. Journal of Physics Condensed Matter, 2012, 24, 415404.	0.7	16
12814	Electronic Structure, Spin-States, and Spin-Crossover Reaction of Heme-Related Fe-Porphyrins: A Theoretical Perspective. Journal of Physical Chemistry B, 2012, 116, 5849-5859.	1.2	102
12815	Computational Methods for the Assignment of Vibrational Modes in Crystalline Materials. Springer Series in Optical Sciences, 2012, , 151-190.	0.5	3
12816	How low can you go? Minimum energy pathways for O2 dissociation on Pt(111). Physical Chemistry Chemical Physics, 2012, 14, 16677.	1.3	50
12817	Dehydrogenation of AlH₃ via the Vacancy Clustering Mechanism. Journal of Physical Chemistry C, 2012, 116, 12995-13002.	1.5	3
12818	Self-Assembled Monolayer Induced Au(111) and Ag(111) Reconstructions: Work Functions and Interface Dipole Formation. Journal of Physical Chemistry C, 2012, 116, 7826-7837.	1.5	64
12819	Quantum Tunneling Enabled Self-Assembly of Hydrogen Atoms on Cu(111). ACS Nano, 2012, 6, 10115-10121.	7.3	45
12820	Quasi-Molecular and Atomic Phases of Dense Solid Hydrogen. Journal of Physical Chemistry C, 2012, 116, 9221-9226.	1.5	78
12821	Strong single-ion anisotropy and anisotropic interactions of magnetic adatoms induced by topological surface states. Physical Review B, 2012, 85, .	1.1	22
12822	Maximally localized Wannier functions: Theory and applications. Reviews of Modern Physics, 2012, 84, 1419-1475.	16.4	2,159
12823	Raising the Thermoelectric Performance of p-Type PbS with Endotaxial Nanostructuring and Valence-Band Offset Engineering Using CdS and ZnS. Journal of the American Chemical Society, 2012, 134, 16327-16336.	6.6	308
12824	A multiscale physical model for the transient analysis of PEM water electrolyzer anodes. Physical Chemistry Chemical Physics, 2012, 14, 10215.	1.3	33
12825	Passivation of CuI Quantum Dots. Journal of Physical Chemistry C, 2012, 116, 21039-21045.	1.5	3
12826	Reversible tuning of the surface state in a pseudobinary Bi2(Te-Se)3topological insulator. Physical Review B, 2012, 86, .	1.1	12
12827	Defect Chemistry in Layered LiMO₂ (M = Co, Ni, Mn, and) Tj ETQq0 0 0 rgBT /Overlock 10 Tf 50 187 Td (Li<su 3886-3894.	3.2	128
12828	Assessment of ten DFT methods in predicting structures of sheet silicates: Importance of dispersion corrections. Journal of Chemical Physics, 2012, 137, 114105.	1.2	117
12829	Structural properties of amorphous metal carbides: Theory and experiment. Acta Materialia, 2012, 60, 4720-4728.	3.8	19
12830	Role of silicon in accelerating the nucleation of Al3(Sc,Zr) precipitates in dilute Alâ€“Scâ€“Zr alloys. Acta Materialia, 2012, 60, 4740-4752.	3.8	161

#	Article	IF	Citations
12831	Lattice dynamics, thermodynamics and elastic properties of monoclinic Li2CO3 from density functional theory. Acta Materialia, 2012, 60, 5204-5216.	3.8	64
12832	The effect of native point defect thermodynamics on off-stoichiometry in Î²-Mg17Al12. Acta Materialia, 2012, 60, 5135-5142.	3.8	18
12833	Soluteâ€“vacancy binding of the rare earths in magnesium from first principles. Acta Materialia, 2012, 60, 5151-5159.	3.8	50
12834	First-principles prediction of yield stress for basal slip in Mgâ€“Al alloys. Acta Materialia, 2012, 60, 5197-5203.	3.8	67
12835	Effect of H2O on catalytic performance of manganese oxides in NO reduction by NH3. Applied Catalysis A: General, 2012, 437-438, 139-148.	2.2	30
12836	Reaction mechanism for CO oxidation on Cu(311): A density functional theory study. Applied Surface Science, 2012, 258, 3980-3985.	3.1	7
12837	Nitric oxide adsorption on Nb(110) surface. Applied Surface Science, 2012, 258, 4428-4435.	3.1	10
12838	Tuning of CeO2 buffer layers for coated superconductors through doping. Applied Surface Science, 2012, 260, 32-35.	3.1	29
12839	Tuning electronic structure and photocatalytic properties by Ag incorporated on (001) surface of anatase TiO2. Applied Surface Science, 2012, 258, 4806-4812.	3.1	24
12840	First-principles study of the adsorption of lysine on hydroxyapatite (100) surface. Applied Surface Science, 2012, 258, 4911-4916.	3.1	38
12841	Effect of dangling bonds of ultra-thin silicon film surface on electronic states of internal atoms. Applied Surface Science, 2012, 258, 5265-5269.	3.1	7
12842	Adsorption and surface reaction of bis-diethylaminosilane as a Si precursor on an OH-terminated Si (0) Tj ETQq1 1 0.784314 rgBT /Ov	3.1	27
12843	First-principles study of CO and NO adsorption on transition metals doped (8,0) boron nitride nanotube. Applied Surface Science, 2012, 258, 6391-6397.	3.1	127
12844	Periodic DFT study of adsorption of nitroamine molecule on Î±-Al2O3(001) surface. Applied Surface Science, 2012, 258, 7334-7342.	3.1	13
12845	First-principles study of oxygen adsorption on Fe(110) surface. Applied Surface Science, 2012, 258, 8484-8491.	3.1	34
12846	Theoretical prediction of hydrogen storage on Li decorated planar boron sheets. Applied Surface Science, 2012, 258, 8874-8879.	3.1	29
12847	Influence of typical defects on thermal conductivity of graphene nanoribbons: An equilibrium molecular dynamics simulation. Applied Surface Science, 2012, 258, 9926-9931.	3.1	43
12848	The austenite/É› martensite interface: A first-principles investigation of the fcc Fe(1 1 1)/hcp Fe(0 0 0 1) system. Applied Surface Science, 2012, 258, 9977-9981.	3.1	69

#	Article	IF	Citations
12849	Synergetic effect of ZrO2 on the oxidationâ€“reduction reaction of Fe2O3 during chemical looping combustion. Applied Surface Science, 2012, 258, 10022-10027.	3.1	35
12850	The complex metal-rich boride Ti1+xRh2â^'x+yIr3â^'yB3 (x=0.68, y=1.06) with a new structure type containing B4 zigzag fragments: Synthesis, crystal chemistry and theoretical calculations. Journal of Solid State Chemistry, 2012, 192, 113-119.	1.4	23
12851	Defect and phase stability of solid solutions of Mg2X with an antifluorite structure: An ab initio study. Journal of Solid State Chemistry, 2012, 193, 133-136.	1.4	22
12852	Elastic and electronic properties of the Ti5X3 (X=Si, Ge, Sn, Pb) compounds from first-principles calculations. Journal of Solid State Chemistry, 2012, 194, 127-134.	1.4	8
12853	First-principles investigation of the thermo-physical properties of Ca3Si4. Journal of Solid State Chemistry, 2012, 194, 179-187.	1.4	13
12854	Crystal structure and magnetic properties of â€œÎ±â€²â€²-Fe16N2â€•containing residual Î±-Fe prepared by low-temperature ammonia nitridation. Journal of Solid State Chemistry, 2012, 194, 76-79.	1.4	42
12855	Carbonate â€œdoorâ€•in the NaKA zeolite as the reason of higher CO2 uptake relative to N2. Microporous and Mesoporous Materials, 2012, 162, 98-104.	2.2	20
12856	Synthesis and structure determination of tetrakis(4-iodoanilinum) Î²-octamolybdate dihydrate. Journal of Molecular Structure, 2012, 1021, 70-75.	1.8	4
12857	Direct octane fuel cells: A promising power for transportation. Nano Energy, 2012, 1, 448-455.	8.2	118
12858	GaN/ZnO superlattice nanowires as photocatalyst for hydrogen generation: A first-principles study on electronic and magnetic properties. Nano Energy, 2012, 1, 488-493.	8.2	60
12859	Experimental research on acetic acid steam reforming over Coâ€“Fe catalysts and subsequent density functional theory studies. International Journal of Hydrogen Energy, 2012, 37, 11122-11131.	3.8	67
12860	Energetics of Ti and Zr transition metals in D03-Fe3Al and its Î£5 (310) [001] grain boundary. Intermetallics, 2012, 22, 251-254.	1.8	7
12861	Ab initio study of competitive hydride formation in zirconium alloys. Intermetallics, 2012, 20, 24-32.	1.8	39
12862	Dimorphic LaPdSn and ErAgSn â€“ A first principles study. Intermetallics, 2012, 20, 33-38.	1.8	5
12863	Thermodynamic properties of Laves phases in the Mgâ€“Alâ€“Ca system at finite temperature from first-principles. Intermetallics, 2012, 22, 17-23.	1.8	28
12864	First-principles investigation of the Alâ€“Siâ€“Sr ternary system: Ground state determination and mechanical properties. Intermetallics, 2012, 21, 31-44.	1.8	19
12865	First-principles investigation on shear deformation of a TiAl/Ti3Al interface and effects of oxygen. Intermetallics, 2012, 22, 41-46.	1.8	21
12866	First-principles investigations of elastic, electronic and thermodynamic properties of Al12X (XÂ=ÂMo, W) Tj ETQq1 1 0.784314 rgBT /	1.8	17

#	Article	IF	Citations
12867	First-principles calculations on finite temperature elastic properties of B2-AlRE (REÂ=ÂY, Tb, Pr, Nd, Dy) intermetallics. Intermetallics, 2012, 26, 57-61.	1.8	5
12868	Structural, electronic, elastic properties and chemical bonding in LaNi2P2 and LaNi2Ge2 from first principles. Intermetallics, 2012, 26, 1-7.	1.8	12
12869	The nature of the atomic-level structure in the Cuâ€“Zr binary metallic glasses. Intermetallics, 2012, 26, 8-10.	1.8	17
12870	First principle study of the effect of Ti and Zr transition metals located in bulk D03Fe3Al and â^5 (310)[001] grain boundary. Intermetallics, 2012, 28, 1-10.	1.8	4
12871	First-principles studies of structural stabilities and enthalpies of formation of refractory intermetallics: TM and TM3 (TÂ=ÂTi, Zr, Hf; MÂ=ÂRu, Rh, Pd, Os, Ir, Pt). Intermetallics, 2012, 28, 16-24.	1.8	70
12872	Site occupation behavior of sulfur and phosphorus in NiAl, TiAl and FeAl. Intermetallics, 2012, 28, 156-163.	1.8	10
12873	A first-principles study of the effect of Ta on the superlattice intrinsic stacking fault energy of L12-Co3(Al,W). Intermetallics, 2012, 28, 138-143.	1.8	75
12874	Thermodynamic and mechanical properties of lanthanumâ€“magnesium phases from density functional theory. Journal of Alloys and Compounds, 2012, 512, 296-310.	2.8	64
12875	Structure, formation energies and elastic constants of uranium metal investigated by first principles calculations. Journal of Alloys and Compounds, 2012, 516, 139-143.	2.8	34
12876	Magnetism-induced ductility in NiAl intermetallic alloys with Fe additions: Theory and experiment. Journal of Alloys and Compounds, 2012, 519, 101-105.	2.8	8
12877	Elastic and thermo-physical properties of TiC, TiN, and their intermediate composition alloys using ab initio calculations. Journal of Alloys and Compounds, 2012, 528, 20-27.	2.8	80
12878	Structural, elastic, electronic properties and stability trends of 1111-like silicide arsenides and germanide arsenides MCuXAs (M=Ti, Zr, Hf; X=Si, Ge) from first principles. Journal of Alloys and Compounds, 2012, 533, 71-78.	2.8	13
12879	First principles investigation of temperature and pressure dependent elastic properties of ZrC and ZrN using Debyeâ€“Gruneisen theory. Journal of Alloys and Compounds, 2012, 540, 94-99.	2.8	33
12880	First principles study on the p-type transparent conducting properties of rutile Ti1â^'xInxO2. Journal of Alloys and Compounds, 2012, 539, 221-225.	2.8	7
12881	Aerobic epoxidation of propene over silver (111) and (100) facet catalysts. Journal of Catalysis, 2012, 292, 138-147.	3.1	56
12882	Periodic trends of oxygen vacancy formation and Câ€“H bond activation over transition metal-doped CeO2 (1 1 1) surfaces. Journal of Catalysis, 2012, 293, 103-115.	3.1	139
12883	Higher-order adaptive finite-element methods for orbital-free density functional theory. Journal of Computational Physics, 2012, 231, 6596-6621.	1.9	28
12884	The structure and electronic properties of AlN/SrTiO3 (111) interfaces. Journal of Crystal Growth, 2012, 353, 134-139.	0.7	7

#	Article	IF	Citations
12885	Chain structure of liquid Se at high temperature and pressure investigated by ab initio molecular dynamics simulations. Journal of Non-Crystalline Solids, 2012, 358, 873-879.	1.5	1
12886	Ab initio simulations of ironâ€“nickel alloys at Earth's core conditions. Earth and Planetary Science Letters, 2012, 345-348, 126-130.	1.8	16
12887	The elasticity of lawsonite at high pressure and the origin of low velocity layers in subduction zones. Earth and Planetary Science Letters, 2012, 349-350, 116-125.	1.8	35
12888	Reversal segregation driven by lattice vibration for alloy nanoparticles. Calphad: Computer Coupling of Phase Diagrams and Thermochemistry, 2012, 36, 151-154.	0.7	1
12889	Grid-increment cluster expansion for polymorphic structures in alloys. Calphad: Computer Coupling of Phase Diagrams and Thermochemistry, 2012, 36, 23-27.	0.7	3
12890	Thermodynamic modeling of the Geâ€“Sc system supported by key experiments and first-principles calculation. Calphad: Computer Coupling of Phase Diagrams and Thermochemistry, 2012, 37, 18-24.	0.7	11
12891	Thermodynamic description of the Geâ€“Na and Geâ€“K systems using the CALPHAD approach supported by first-principles calculations. Calphad: Computer Coupling of Phase Diagrams and Thermochemistry, 2012, 37, 72-76.	0.7	11
12892	Thermodynamic assessment of Auâ€“Ho and Auâ€“Tm binary systems. Calphad: Computer Coupling of Phase Diagrams and Thermochemistry, 2012, 37, 87-93.	0.7	9
12893	Elastic, phonon and thermodynamic properties of Mgâ€“Ga compounds from first-principles calculations. Calphad: Computer Coupling of Phase Diagrams and Thermochemistry, 2012, 37, 137-144.	0.7	11
12894	Thermodynamic description of the LiNiO2â€“NiO2 pseudo-binary system and extrapolation to the Li(Co,Ni)O2â€“(Co,Ni)O2 system. Calphad: Computer Coupling of Phase Diagrams and Thermochemistry, 2012, 37, 100-107.	0.7	32
12895	Structural, phonon and thermodynamic properties of fcc-based metal nitrides from first-principles calculations. Calphad: Computer Coupling of Phase Diagrams and Thermochemistry, 2012, 37, 126-131.	0.7	24
12896	First-principles thermal equation of state of tungsten carbide. Computational Materials Science, 2012, 59, 41-47.	1.4	16
12897	Ab initio study of the effect of Zr content on elastic and electronic properties of L12â€“Al3(Sc1â^'xZrx) alloys. Computational Materials Science, 2012, 59, 87-93.	1.4	22
12898	First principles study on the structural, magnetic and electronic properties of Te-doped BiF3. Computational Materials Science, 2012, 60, 212-216.	1.4	7
12899	Theoretical investigation on the magnetic and electronic properties of La2NiIrO6. Computational Materials Science, 2012, 60, 149-152.	1.4	6
12900	Metal decorated monolayer BC2N for hydrogen storage. Computational Materials Science, 2012, 60, 181-185.	1.4	22
12901	A pseudo-tetragonal phase of superhard B8C16(N6CO). Computational Materials Science, 2012, 62, 55-59.	1.4	4
12902	First-principles simulations of local structure contrast for liquid Ge1Sb2Te4, Ge2Sb2Te5, and Ge4Sb1Te5 alloys. Computational Materials Science, 2012, 61, 287-290.	1.4	10

#	Article	IF	Citations
12903	Point defect concentrations of impurity carbon in tungsten. Computational Materials Science, 2012, 62, 282-284.	1.4	16
12904	Adsorption and diffusion studies of an O adatom on anatase surfaces with first principles calculations. Computational Materials Science, 2012, 63, 58-65.	1.4	14
12905	First-principles study of the effect of BiGa heteroantisites in GaAs:Bi alloy. Computational Materials Science, 2012, 63, 178-181.	1.4	12
12906	First-principles calculations of the electronic structure, phase transition and properties of ZrSiO4 polymorphs. Computational and Theoretical Chemistry, 2012, 987, 62-70.	1.1	23
12907	First-principles study of the F-terminated Boron Nitride nanoribbons. Computational and Theoretical Chemistry, 2012, 979, 49-53.	1.1	12
12908	First principles study on the structural, magnetic and electronic properties of Co-doped FeF3. Computational and Theoretical Chemistry, 2012, 980, 44-48.	1.1	20
12909	A DFT+U study of structure and reducibility of CenO2nâ^'x (nâ©½4, 0â©½xâ©½n) nanoclusters. Computational and Theoretical Chemistry, 2012, 987, 25-31.	1.1	9
12910	Fullerene and graphene formation from carbon nanotube fragments. Computational and Theoretical Chemistry, 2012, 987, 115-121.	1.1	13
12911	Structural, electronic, and magnetic properties of Ni M clusters (M = Hf, Ta, W) with n= 1â€“12. Computational and Theoretical Chemistry, 2012, 984, 128-136.	1.1	12
12912	Classical dynamics study of atomic oxygen over graphite (0001) with new interpolated and analytical potential energy surfaces. Computational and Theoretical Chemistry, 2012, 990, 132-143.	1.1	17
12913	Energy dissipation channels in the adsorption of N on Ag(111). Computational and Theoretical Chemistry, 2012, 990, 126-131.	1.1	28
12914	The adsorption and reactions of SiClx (x=0â€“4) on hydroxylated TiO2 anatase (101) surface: A computational study on the functionalization of titania with Cl2Si(O)O adsorbate. Computational and Theoretical Chemistry, 2012, 993, 45-52.	1.1	9
12915	The effect of coadsorbed water on the stability, configuration and interconversion of formyl (HCO) and hydroxymethylidyne (COH) on platinum (111). Chemical Physics Letters, 2012, 541, 32-38.	1.2	25
12916	Impact energy dependence of defect formation in single-walled carbon nanotubes. Chemical Physics Letters, 2012, 541, 92-95.	1.2	5
12917	Core restructuring for magnetic Fe55 icosahedral nanoparticles. Chemical Physics Letters, 2012, 541, 101-104.	1.2	10
12918	Electronic structure and chemical bonding of Li4Pt3Si. Chemical Physics Letters, 2012, 542, 47-51.	1.2	3
12919	Importance of spinâ€“orbit coupling in M@Pb12 clusters (M=3d and 4d atoms). Chemical Physics Letters, 2012, 543, 106-110.	1.2	6
12920	Influence of Sn interaction on the structural evolution of Au clusters: A first principles study. Chemical Physics Letters, 2012, 543, 121-126.	1.2	9

#	Article	IF	Citations
12921	Comprehensive investigations on the feasibility of nitrogen as a p-type dopant in ZnO. Chemical Physics Letters, 2012, 543, 92-95.	1.2	8
12922	First-principles study of structural and mechanical properties of AgB2 and AuB2 compounds under pressure. Computational Materials Science, 2012, 51, 83-90.	1.4	43
12923	Prediction of elastic properties of precipitation-hardened aluminum cast alloys. Computational Materials Science, 2012, 51, 365-371.	1.4	5
12924	An improved molecular dynamics potential for the Alâ€“O system. Computational Materials Science, 2012, 53, 483-492.	1.4	16
12925	Improved Finnisâ€“Sinclair potential for bcc vanadium solid. Computational Materials Science, 2012, 53, 101-104.	1.4	8
12926	Structural, electronic and elastic properties of V5Si3 phases from first-principles calculations. Computational Materials Science, 2012, 53, 169-174.	1.4	20
12927	Spinâ€“orbit and modified Beckeâ€“Johnson potential effects on the electronic properties of bulk Ge: A density functional theory study. Computational Materials Science, 2012, 54, 37-42.	1.4	17
12928	Ab initio study of defect properties in YPO4. Computational Materials Science, 2012, 54, 170-175.	1.4	10
12929	The incorporation and solution of krypton in uranium dioxide: Density functional theory calculations. Computational Materials Science, 2012, 54, 188-194.	1.4	10
12930	Tailoring the band gap of GaN codoped by VO for enhanced solar energy conversion from first-principles calculations. Computational Materials Science, 2012, 54, 101-104.	1.4	2
12931	A theoretical investigation of the stability of crystalline silicon dicarbide. Computational Materials Science, 2012, 55, 186-191.	1.4	7
12932	A DFT-LDA study of electronic and optical properties of hexagonal boron nitride under uniaxial strain. Computational Materials Science, 2012, 54, 165-169.	1.4	14
12933	First-principles investigation on diffusion and permeation behaviors of hydrogen isotopes in molybdenum. Computational Materials Science, 2012, 54, 32-36.	1.4	13
12934	First-principles study of Fe-based superconductors: A comparison of screened hybrid functional with gradient corrected functional. Computational Materials Science, 2012, 55, 284-294.	1.4	4
12935	First-principles study of grain boundary embrittlement in Feâ€“Niâ€“S alloy. Computational Materials Science, 2012, 55, 17-22.	1.4	16
12936	Mechanical properties of the hexagonal boron nitride monolayer: Ab initio study. Computational Materials Science, 2012, 56, 11-17.	1.4	349
12937	First-principles investigation of adsorption of N2O on the anatase TiO2 (101) and the CO pre-adsorbed TiO2 surfaces. Computational Materials Science, 2012, 58, 24-30.	1.4	21
12938	Theoretical investigations of interstitial atoms in bcc metals: Local lattice distortion and diffusion barrier. Computational Materials Science, 2012, 58, 67-70.	1.4	6

#	Article	IF	Citations
12939	On the limitations of the DFT+U approach to energetics of actinides. Computational Materials Science, 2012, 59, 48-56.	1.4	6
12940	He diffusion and closure temperatures in apatite and zircon: A density functional theory investigation. Geochimica Et Cosmochimica Acta, 2012, 86, 228-238.	1.6	22
12941	Cation distribution and mixing thermodynamics in Fe/Ni thiospinels. Geochimica Et Cosmochimica Acta, 2012, 88, 275-282.	1.6	21
12942	Resonance Charges to Encode Selection Rules in Inelastic Electron Tunneling Spectroscopy. Journal of Physical Chemistry Letters, 2012, 3, 3007-3011.	2.1	6
12943	Periodic Trends in Adsorption and Activation Energies for Heterometallic Diffusion on (100) Transition Metal Surfaces. Journal of Physical Chemistry C, 2012, 116, 22469-22475.	1.5	8
12944	Coupling of a carbon nanotube and graphene nanoribbon by titanium and vanadium chains: a first-principles study. RSC Advances, 2012, 2, 9958.	1.7	3
12945	First-row transition metal atoms adsorption on rutile TiO2(110) surface. Structural Chemistry, 2012, 23, 1309-1321.	1.0	17
12946	Charged states and band-gap narrowing in codoped ZnO nanowires for enhanced photoelectrochemical responses: Density functional first-principles calculations. Physical Review B, 2012, 85, .	1.1	19
12947	Origin of enhanced water adsorption at âŸ¨11Â¯0âŸ© step edge on rutile TiO2(110) surface. Journal of Chemical Physics, 2012, 137, 114707.	1.2	8
12948	Orbital ordering under reduced symmetry in transition metal perovskites: Oxygen vacancy in SrTiO<mml:math xmlns:mml="http://www.w3.org/1998/Math/MathML" display="inline"><mml:msub><mml:mrow /><mml:mn>3</mml:mn></mml:msub></mml:math>. Physical Review B, 2012, 86, .	1.1	49
12949	In- and Out-Dependent Interactions of Iron with Carbon Nanotubes. Journal of Physical Chemistry C, 2012, 116, 16461-16466.	1.5	30
12950	Effects of temperature and ferromagnetism on the Î³-Ni/Î³â€²-Ni3Al interfacial free energy from first principles calculations. Journal of Materials Science, 2012, 47, 7653-7659.	1.7	30
12951	Geometric Arrangement of Components in Bimetallic PdZn/Pd(111) Surfaces Modified by CO Adsorption: A Combined Study by Density Functional Calculations, Polarization-Modulated Infrared Reflection Absorption Spectroscopy, and Temperature-Programmed Desorption. Journal of Physical Chemistry C, 2012, 116, 18768-18778.	1.5	40
12952	First-Principles Study on Relaxor-Type Ferroelectric Behavior without Chemical Inhomogeneity in BaTaO₂N and SrTaO₂N. Chemistry of Materials, 2012, 24, 4343-4349.	3.2	78
12953	Liâ€“Na ternary amidoborane for hydrogen storage: experimental and first-principles study. Dalton Transactions, 2012, 41, 4754.	1.6	18
12954	Capture Lithium in Î±MnO₂: Insights from First Principles. Chemistry of Materials, 2012, 24, 3943-3951.	3.2	114
12955	Predicted Lithiumâ€“Boron Compounds under High Pressure. Journal of the American Chemical Society, 2012, 134, 18599-18605.	6.6	113
12956	First-principles calculations and thermodynamic modeling of the Vâ€“Zr system. Calphad: Computer Coupling of Phase Diagrams and Thermochemistry, 2012, 36, 163-168.	0.7	22

#	Article	IF	Citations
12957	Cooperative effects at waterâ€“crystalline silica interfaces strengthen surface silanol hydrogen bonding. An ab initio molecular dynamics study. Physical Chemistry Chemical Physics, 2012, 14, 10507.	1.3	43
12958	Combined ab initio, experimental, and CALPHAD approach for an improved thermodynamic evaluation of the Mgâ€“Si system. Calphad: Computer Coupling of Phase Diagrams and Thermochemistry, 2012, 37, 77-86.	0.7	19
12961	Prominent Electronic and Geometric Modifications of Palladium Nanoparticles by Polymer Stabilizers for Hydrogen Production under Ambient Conditions. Angewandte Chemie - International Edition, 2012, 51, 11275-11278.	7.2	110
12962	On the Mechanism Behind the Instability of Isoreticular Metalâ€“Organic Frameworks (IRMOFs) in Humid Environments. Chemistry - A European Journal, 2012, 18, 12260-12266.	1.7	66
12963	Centralâ€Atom Size Effects on the Methyl Torsions of Groupâ€…XIV Tetratolyls. Chemistry - A European Journal, 2012, 18, 13018-13024.	1.7	8
12964	Initial Decomposition of Methanol and Water on In₂O₃(110): A Periodic DFT Study. Chinese Journal of Chemistry, 2012, 30, 2036-2040.	2.6	13
12965	Lowering Energy Barriers in Surface Reactions through Concerted Reaction Mechanisms. ChemPhysChem, 2012, 13, 3467-3471.	1.0	19
12966	9.4L: Lateâ€News Paper: Microscopic Mechanism of the Negative Bias and Illumination Stress Instability of Amorphous Oxide TFTs. Digest of Technical Papers SID International Symposium, 2012, 43, 95-97.	0.1	0
12967	Accelerating VASP electronic structure calculations using graphic processing units. Journal of Computational Chemistry, 2012, 33, 2581-2589.	1.5	143
12968	Gettering of transition metals by porous silicon in epitaxial silicon solar cells. Physica Status Solidi (A) Applications and Materials Science, 2012, 209, 1866-1871.	0.8	23
12969	Short range order and Ag diffusion threshold in Ag_x(Ge_{0.25}Se_{0.75})_{100â^'x} glasses. Physica Status Solidi (B): Basic Research, 2012, 249, 2028-2033.	0.7	12
12970	Alloy solid solution strengthening of Mg alloys: Valence effect. Physica Status Solidi (B): Basic Research, 2012, 249, 2089-2095.	0.7	15
12971	Lowering the symmetry group of carbon tetrachloride by high pressure. Physica Status Solidi (B): Basic Research, 2012, 249, 2113-2117.	0.7	6
12972	Structure, stability and electronic properties of tricycle type graphane. Physica Status Solidi - Rapid Research Letters, 2012, 6, 427-429.	1.2	43
12973	Sequential hydrogen dissociation from a charged Pt₁₃H₂₄ cluster modeled by ab initio molecular dynamics. International Journal of Quantum Chemistry, 2012, 112, 3896-3903.	1.0	29
12974	Roomâ€Temperature Intercalationâ€“Deintercalation Strategy Towards VO₂(B) Single Layers with Atomic Thickness. Small, 2012, 8, 3752-3756.	5.2	65
12975	Optical Properties of the Orchid Colored Silver(II) Fluoride Cs₂AgF₄. Zeitschrift Fur Anorganische Und Allgemeine Chemie, 2012, 638, 1792-1795.	0.6	7
12976	Interaction of oxygen with the platinum surface: A quantum-chemical modeling. Russian Journal of Inorganic Chemistry, 2012, 57, 1089-1099.	0.3	6

#	Article	IF	Citations
12977	Behavior of molecular hydrogen on the platinum crystal surface: Quantum-chemical modeling. Russian Journal of Inorganic Chemistry, 2012, 57, 1460-1469.	0.3	9
12978	An ab-initio study of silicon adsorption on metallic surfaces (Au/Ag): Novel perspective to explore chemical bonding. European Physical Journal B, 2012, 85, 1.	0.6	1
12979	Half-metallicity in Rh-doped TiO2 from ab initio calculations. European Physical Journal B, 2012, 85, 1.	0.6	5
12980	A density functional theory study of ordered oxygen overlayers on Ir(100). European Physical Journal B, 2012, 85, 1.	0.6	6
12981	Magnetic exchange at realistic CoO/Ni interfaces. European Physical Journal B, 2012, 85, 1.	0.6	4
12982	A first-principles study aided with Monte Carlo simulations of carbon doped iron-manganese alloys. European Physical Journal B, 2012, 85, 1.	0.6	6
12983	New hexagonal structure for silicon atoms. European Physical Journal B, 2012, 85, 1.	0.6	13
12984	Study of the oxygen vacancy influence on magnetic properties of Fe- and Co-doped SnO2 diluted alloys. Nanoscale Research Letters, 2012, 7, 540.	3.1	14
12985	g-B3N3C: a novel two-dimensional graphite-like material. Nanoscale Research Letters, 2012, 7, 624.	3.1	6
12986	H and Li Related Defects in ZnO and Their Effect on Electrical Properties. Journal of Physical Chemistry C, 2012, 116, 23764-23772.	1.5	33
12987	Low-energy silicon allotropes with strong absorption in the visible for photovoltaic applications. Physical Review B, 2012, 86, .	1.1	138
12988	Linear Band-Gap Modulation of Graphane Nanoribbons under Uniaxial Elastic Strain: A Density Functional Theory Study. Journal of Physical Chemistry C, 2012, 116, 9356-9359.	1.5	32
12989	Electronic properties of two-dimensional covalent organic frameworks. Journal of Chemical Physics, 2012, 137, 244703.	1.2	63
12990	Origin of the Room-Temperature Ferromagnetism in Sr₃YCo₄O_{10+Î´} (0.5 < Î´ < 1.0): Formation of Ferromagnetic Spin Bags in the Oxygen-Rich Perovskite Layers. Chemistry of Materials, 2012, 24, 3117-3119.	3.2	14
12991	Robust Room-Temperature Ferromagnetism with Giant Anisotropy in Nd-Doped ZnO Nanowire Arrays. Nano Letters, 2012, 12, 3994-4000.	4.5	157
12992	First-principles calculation of phase equilibrium of V-Nb, V-Ta, and Nb-Ta alloys. Physical Review B, 2012, 85, .	1.1	46
12993	d0Ferromagnetic Interface between Nonmagnetic Perovskites. Physical Review Letters, 2012, 109, 127207.	2.9	45
12994	Li⁺ionic conductivities and diffusion mechanisms in Li-based imides and lithium amide. Physical Chemistry Chemical Physics, 2012, 14, 1596-1606.	1.3	43

#	Article	IF	Citations
12995	Interface dipole between two metallic oxides caused by localized oxygen vacancies. Physical Review B, 2012, 86, .	1.1	56
12996	Effect of gadolinium doping on the electronic band structure of europium oxide. Physical Review B, 2012, 85, .	1.1	25
12997	Ground-state search in multicomponent magnetic systems. Physical Review B, 2012, 85, .	1.1	3
12998	First-principles calculations of the phase diagrams and band gaps in CuInSe2-CuGaSe2and CuInSe2-CuAlSe2pseudobinary systems. Physical Review B, 2012, 85, .	1.1	32
12999	First-principles study of pressure-induced phase transition and electronic property of PbCrO3. Journal of Applied Physics, 2012, 111, 013503.	1.1	16
13000	Substrate-mediated enhanced activity of Ru nanoparticles in catalytic hydrogenation of benzene. Nanoscale, 2012, 4, 2288.	2.8	47
13001	A fresh look at dense hydrogen under pressure. I. An introduction to the problem, and an index probing equalization of Hâ€“H distances. Journal of Chemical Physics, 2012, 136, 074501.	1.2	61
13002	A fresh look at dense hydrogen under pressure. III. Two competing effects and the resulting intra-molecular H-H separation in solid hydrogen under pressure. Journal of Chemical Physics, 2012, 136, 074503.	1.2	35
13003	A fresh look at dense hydrogen under pressure. IV. Two structural models on the road from paired to monatomic hydrogen, via a possible non-crystalline phase. Journal of Chemical Physics, 2012, 136, 074504.	1.2	29
13004	Spintronic Materials, Synthesis, Processing and Applications. , 2012, , 193-228.		2
13005	First-principles thermodynamic modeling of lanthanum chromate perovskites. Physical Review B, 2012, 85, .	1.1	10
13006	Topological electronic structure and Weyl semimetal in the TlBiSe<mml:math xmlns:mml="http://www.w3.org/1998/Math/MathML" display="inline"><mml:msub><mml:mrow /><mml:mn>2</mml:mn></mml:msub></mml:math>class of semiconductors. Physical Review B, 2012, 86, .	1.1	135
13007	Understanding and Controlling the Reactivity of the Calcium Silicate phases from First Principles. Chemistry of Materials, 2012, 24, 1262-1267.	3.2	113
13008	Self-Assembled Ti Quantum Wire on Zigzag Graphene Nanoribbons with One Edge Saturated. Journal of Physical Chemistry C, 2012, 116, 24824-24828.	1.5	2
13009	The halogen analogs of thiolated gold nanoclusters. Nanoscale, 2012, 4, 4234.	2.8	31
13010	Competition for Graphene: Graphynes with Direction-Dependent Dirac Cones. Physical Review Letters, 2012, 108, 086804.	2.9	995
13011	Prominent electrochromism through vacancy-order melting in a complex oxide. Nature Communications, 2012, 3, 799.	5.8	85
13012	Band gap opening of graphene by doping small boron nitride domains. Nanoscale, 2012, 4, 2157.	2.8	225

#	Article	IF	Citations
13013	Self-consistent measurement of the equation of state of liquid deuterium. High Energy Density Physics, 2012, 8, 76-80.	0.4	16
13014	Oxygen Bridges between NiO Nanosheets and Graphene for Improvement of Lithium Storage. ACS Nano, 2012, 6, 3214-3223.	7.3	977
13015	Development and Validation of a ReaxFF Reactive Force Field for Fe/Al/Ni Alloys: Molecular Dynamics Study of Elastic Constants, Diffusion, and Segregation. Journal of Physical Chemistry A, 2012, 116, 12163-12174.	1.1	61
13016	Intrinsic point-defect equilibria in tetragonal ZrO<mml:math xmlns:mml="http://www.w3.org/1998/Math/MathML" display="inline"><mml:msub><mml:mrow /><mml:mn>2</mml:mn></mml:msub></mml:math>: Density functional theory analysis with finite-temperature effects. Physical Review B, 2012, 86, .	1.1	74
13017	The difference between oxygen and sulfur adsorption on the InSb (110) surface. , 2012, , .		0
13018	First-principles study of defects distribution with different arsenic doping source in HgCdTe. , 2012, , .		0
13019	Structural, elastic, magnetic and electronic properties of 4d perovskite CaTcO3: a DFT+Uinvestigation. Journal of Physics Condensed Matter, 2012, 24, 185401.	0.7	3
13020	Compression of Silver Sulfide: X-ray Diffraction Measurements and Total-Energy Calculations. Inorganic Chemistry, 2012, 51, 5289-5298.	1.9	44
13021	A first-principles study of helium storage in oxides and at oxideâ€“iron interfaces. Journal of Applied Physics, 2012, 111, .	1.1	43
13022	Adsorption of NO on the Rh₁₃, Pd₁₃, Ir₁₃, and Pt₁₃ Clusters: A Density Functional Theory Investigation. Journal of Physical Chemistry C, 2012, 116, 20540-20549.	1.5	33
13023	The magnetoelectric effect in transition metal oxides: Insights and the rational design of new materials from first principles. Current Opinion in Solid State and Materials Science, 2012, 16, 227-242.	5.6	64
13024	From Wadeâ€“Mingos to Zintlâ€“Klemm at 100 GPa: Binary Compounds of Boron and Lithium. Journal of the American Chemical Society, 2012, 134, 18606-18618.	6.6	56
13025	Strain Induced Quantum Effect in Semiconductors. Journal of the Physical Society of Japan, 2012, 81, 074712.	0.7	4
13026	Graphyne: Hexagonal network of carbon with versatile Dirac cones. Physical Review B, 2012, 86, .	1.1	307
13027	Strain-induced phase transition in Î² -MnO ₂. Europhysics Letters, 2012, 99, 27005.	0.7	2
13028	Double Perovskite Structure: A Vibrational and Luminescence Investigation Providing a Perspective on Crystal Field Strength. Journal of Physical Chemistry A, 2012, 116, 7337-7344.	1.1	22
13029	A green-yellow emitting oxyfluoride solid solution phosphor Sr2Ba(AlO4F)1â^'x(SiO5)x:Ce3+ for thermally stable, high color rendition solid state white lighting. Journal of Materials Chemistry, 2012, 22, 18204.	6.7	105
13030	The origin of isotope-induced helical-sense bias in supramolecular polymers of benzene-1,3,5-tricarboxamides. Physical Chemistry Chemical Physics, 2012, 14, 13997.	1.3	3

#	Article	IF	Citations
13031	Four superhard carbon allotropes: a first-principles study. Physical Chemistry Chemical Physics, 2012, 14, 8410.	1.3	66
13032	Impact of point defects on electronic structure in Y2Ti2O7. RSC Advances, 2012, 2, 7235.	1.7	16
13034	Self-organization of extraframework cations in zeolites. Proceedings of the Royal Society A: Mathematical, Physical and Engineering Sciences, 2012, 468, 2070-2086.	1.0	73
13035	Confinement-dependent ferromagnetism in Mn-doped InAs quantum dots embedded in InP nanowires. Physical Review B, 2012, 86, .	1.1	3
13036	A Density Functional Theory Study on the Deformation Behaviors of Fe-Si-B Metallic Glasses. International Journal of Molecular Sciences, 2012, 13, 10401-10409.	1.8	9
13037	Design of SHG materials with mid-infrared transparency based on genetic engineering for Ba2BiInA5 (A) Tj ETQq1 1 0.784314 rgBT /O	6.7	20
13038	The role of titanium nitride supports for single-atom platinum-based catalysts in fuel cell technology. Physical Chemistry Chemical Physics, 2012, 14, 16552.	1.3	88
13039	Magnetic properties of Fe2GeMo3N; an experimental and computational study. Journal of Materials Chemistry, 2012, 22, 15606.	6.7	5
13040	Electronic properties and 4f â†' 5d transitions in Ce-doped Lu2SiO5: a theoretical investigation. Journal of Materials Chemistry, 2012, 22, 13723.	6.7	53
13041	Interaction of interstitial nitrogen atoms in Nb: Ab initio calculations. Bulletin of the Russian Academy of Sciences: Physics, 2012, 76, 1-6.	0.1	1
13042	Novel sp3 forms of carbon predicted by evolutionary metadynamics and analysis of their synthesizability using transition path sampling. Journal of Superhard Materials, 2012, 34, 350-359.	0.5	14
13043	Computational Modeling of Grain Boundaries in <scp><scp>ZrB</scp></scp>₂: Implications for Lattice Thermal Conductivity. Journal of the American Ceramic Society, 2012, 95, 3971-3978.	1.9	7
13044	First-principles study on the relaxed structures and electronic properties of Cu [110] nanowires. Journal of the Korean Physical Society, 2012, 61, 1015-1020.	0.3	2
13045	Chemical composition of the atomic chains formed on Pd(110) by Cu deposition: Density-functional calculations. Journal of the Korean Physical Society, 2012, 61, 1986-1989.	0.3	0
13046	Shallow n-type doping by transition-metal impurities (Hf, Zr, or Ti) in amorphous In2O3. Journal of the Korean Physical Society, 2012, 61, 933-937.	0.3	0
13047	Interplay between non-bridging oxygen, triclusters, and fivefold Al coordination in low silica content calcium aluminosilicate melts. Applied Physics Letters, 2012, 101, .	1.5	87
13048	Scaling Behavior and Beyond Equilibrium in the Hexagonal Manganites. Physical Review X, 2012, 2, .	2.8	119
13049	Modeling thermoelectric transport in organic materials. Physical Chemistry Chemical Physics, 2012, 14, 16505.	1.3	93

#	Article	IF	Citations
13050	Spin-phonon coupling effects in transition-metal perovskites: A DFTÂ+Â<mml:math xmlns:mml="http://www.w3.org/1998/Math/MathML" display="inline"><mml:mi>U</mml:mi></mml:math>and hybrid-functional study. Physical Review B, 2012, 85, .	1.1	145
13051	Simultaneous enhancement of electronic and Li+ ion conductivity in LiFePO4. Applied Physics Letters, 2012, 101, .	1.5	43
13052	Spin-wave method for the total energy of paramagnetic state. Physical Review B, 2012, 85, .	1.1	57
13053	Hydrogen sorption in titanium alloys with a symmetric Î£5(310) tilt grain boundary and a (310) surface. Journal of Experimental and Theoretical Physics, 2012, 115, 462-473.	0.2	7
13054	Structural, Electronic, and Magnetic Properties Of Co_nCu_m Nanoalloys (m + n = 12) from First Principles Calculations. Journal of Physical Chemistry A, 2012, 116, 9353-9360.	1.1	14
13055	Sulfides with Strong Nonlinear Optical Activity and Thermochromism: ACd₄Ga₅S₁₂ (A = K, Rb, Cs). Chemistry of Materials, 2012, 24, 3406-3414.	3.2	156
13056	Orbital degrees of freedom as origin of magnetoelectric coupling in magnetite. Physical Review B, 2012, 85, .	1.1	19
13057	First Principles Study of the Li₁₀GeP₂S₁₂ Lithium Super Ionic Conductor Material. Chemistry of Materials, 2012, 24, 15-17.	3.2	600
13058	Two-Dimensional Polaronic Behavior in the Binary Oxides<mml:math xmlns:mml="http://www.w3.org/1998/Math/MathML" display="inline"><mml:mi>m</mml:mi><mml:mtext mathvariant="normal">â^'</mml:mtext><mml:msub><mml:mi>HfO</mml:mi><mml:mn>2</mml:mn></mml:msub></mml:math>and<mml:math xmlns:mml="http://www.w3.org/1998/Math/MathML" display="inline"><mml:mi>m</mml:mi><mml:mtext mathvariant="normal">â^'</mml:mtext><mml:msub><mml:mi>ZrO</mml:mi><mml:mn>2</mml:mn></mml:msub></mml:math>. Physical Review Letters, 2012, 108, 116403.	2.9	56
13059	Initial geometries, interaction mechanism and high stability of silicene on Ag(111) surface. Scientific Reports, 2012, 2, 861.	1.6	183
13060	Bipolar magnetic semiconductors: a new class of spintronics materials. Nanoscale, 2012, 4, 5680.	2.8	241
13061	Prediction of orientational phase transition in boron carbide. Solid State Sciences, 2012, 14, 1648-1652.	1.5	31
13062	Electronic, magnetic and dielectric properties of multiferroic MnTiO3. Journal of Materials Research, 2012, 27, 1421-1429.	1.2	17
13063	Simulation of NMR Fermi Contact Shifts for Lithium Battery Materials: The Need for an Efficient Hybrid Functional Approach. Journal of Physical Chemistry C, 2012, 116, 17393-17402.	1.5	30
13064	The quantum hypernetted chain model of warm dense matter. High Energy Density Physics, 2012, 8, 150-153.	0.4	21
13065	<mml:math xmlns:mml="http://www.w3.org/1998/Math/MathML" display="inline"><mml:mi>p</mml:mi></mml:math>-Type Conductivity in N-Doped ZnO: The Role of the<mml:math xmlns:mml="http://www.w3.org/1998/Math/MathML" display="inline"><mml:msub><mml:mi mathvariant="normal">N</mml:mi><mml:mi>Zn</mml:mi></mml:msub><mml:mtext mathvariant="normal">â^'</mml:mtext><mml:msub><mml:mi>V</mml:mi><mml:mi mathvariant="normal">	2.9	143
13066	Electronic structure, lattice energies and Born exponents for alkali halides from first principles. AIP Advances, 2012, 2, .	0.6	42
13067	Design of a Polymerâ€“Carbon Nanohybrid Junction by Interface Modeling for Efficient Printed Transistors. ACS Nano, 2012, 6, 662-670.	7.3	29

#	Article	IF	Citations
13068	Configuring pnicogen rings in skutterudites for low phonon conductivity. Physical Review B, 2012, 86, .	1.1	30
13070	First principle study on generalized stacking fault energy and surface energy of B2-AgRE intermetallics. Physica B: Condensed Matter, 2012, 407, 4117-4122.	1.3	1
13071	Î³-Alumina: The Essential and Unexpected Role of Water for the Structure, Stability, and Reactivity of â€œDefectâ€•Sites. Journal of the American Chemical Society, 2012, 134, 14430-14449.	6.6	308
13072	Molecular adsorption on metal surfaces with van der Waals density functionals. Physical Review B, 2012, 85, .	1.1	89
13073	Hydration thermodynamics of pyrochlore structured oxides from TG and first principles calculations. Dalton Transactions, 2012, 41, 13343.	1.6	25
13074	Ab initioand semi-empirical van der Waals study of grapheneâ€“boron nitride interaction from a molecular point of view. Journal of Physics Condensed Matter, 2012, 24, 424214.	0.7	26
13075	Tuning of the Band Structures of Zigzag Graphene Nanoribbons by an Electric Field and Adsorption of Pyridine and BF3: A DFT Study. Journal of Physical Chemistry C, 2012, 116, 20054-20061.	1.5	10
13076	Interplay between Chemical and Magnetic Order in FeRh Clusters. Journal of Physical Chemistry C, 2012, 116, 17228-17238.	1.5	26
13077	A first-principles study for electronic and magnetic properties of LaFeO3/LaCrO3superlattices. Journal of Physics: Conference Series, 2012, 400, 032126.	0.3	2
13078	Enhanced optical absorption and photocatalytic activity of anatase TiO₂ through (Si,Ni) codoping. Applied Physics Letters, 2012, 101, 062106.	1.5	21
13079	All-Electron Path Integral Monte Carlo Simulations of Warm Dense Matter: Application to Water and Carbon Plasmas. Physical Review Letters, 2012, 108, 115502.	2.9	119
13080	Time-Dependent CO₂ Sorption Hysteresis in a One-Dimensional Microporous Octahedral Molecular Sieve. Journal of the American Chemical Society, 2012, 134, 7944-7951.	6.6	74
13081	Hydrogen Desorption from Ti-Doped MgH₂(110) Surfaces: Catalytic Effect on Reaction Pathways and Kinetic Barriers. Journal of Physical Chemistry C, 2012, 116, 7874-7878.	1.5	25
13082	Density functional theory study of CO2 capture with transition metal oxides and hydroxides. Journal of Chemical Physics, 2012, 136, 064516.	1.2	26
13083	Incorporation, valence state, and electronic structure of Mn and Cr in bulk single crystal Î²â€“Ga2O3. Journal of Applied Physics, 2012, 111, 123716.	1.1	40
13085	Controlling the Conductivity in Oxide Semiconductors. Springer Series in Materials Science, 2012, , 23-35.	0.4	8
13086	Revealing the coupled cation interactions behind the electrochemical profile of LixNi0.5Mn1.5O4. Energy and Environmental Science, 2012, 5, 6047.	15.6	67
13087	The solvation of two electrons in the gaseous clusters of Naâ¯(NH3)n and Liâ¯(NH3)n. Journal of Chemical Physics, 2012, 136, 124314.	1.2	5

#	Article	IF	Citations
13088	Induced ferromagnetism in one-side semihydrogenated silicene and germanene. Physical Chemistry Chemical Physics, 2012, 14, 3031.	1.3	166
13089	Edge Structural Stability and Kinetics of Graphene Chemical Vapor Deposition Growth. ACS Nano, 2012, 6, 3243-3250.	7.3	179
13090	Phonon spectrum and bonding properties of Bi2Se3: Role of strong spin-orbit interaction. Applied Physics Letters, 2012, 100, .	1.5	40
13091	A DFT-D study of structural and energetic properties of TiO₂modifications. Journal of Physics Condensed Matter, 2012, 24, 424206.	0.7	51
13092	Tetragonality of carbon-doped ferromagnetic iron alloys: A first-principles study. Physical Review B, 2012, 85, .	1.1	18
13093	Improved description of soft layered materials with van der Waals density functional theory. Journal of Physics Condensed Matter, 2012, 24, 424216.	0.7	150
13094	Effects of oxygen vacancy location on the electronic structure and spin density of Co-doped rutile TiO ₂ dilute magnetic semiconductors. Chinese Physics B, 2012, 21, 047503.	0.7	7
13095	Phononic filter effect of rattling phonons in the thermoelectric clathrate Ba<mml:math xmlns:mml="http://www.w3.org/1998/Math/MathML" display="inline"><mml:msub><mml:mrow /><mml:mn>8</mml:mn></mml:msub></mml:math>Ge<mml:math xmlns:mml="http://www.w3.org/1998/Math/MathML" display="inline"><mml:msub><mml:mrow /><mml:mrow><mml:mn>40</mml:mn><mml:mo>+</mml:mo><mml:mi>x</mml:mi></mml:mrow></mml:msub></mml:math>Ni<mml:	1.1	81
13096	Tailoring Magnetic Doping in the Topological Insulator<mml:math xmlns:mml="http://www.w3.org/1998/Math/MathML" display="inline"><mml:msub><mml:mi>Bi</mml:mi><mml:mn>2</mml:mn></mml:msub><mml:msub><mml:mi>Se</mml:mi><mml:mn Physical Review Letters, 2012, 109, 266405.	2.9	136
13097	First-Principles Study of LiBH4Nanoclusters and Their Hydrogen Storage Properties. Journal of Physical Chemistry C, 2012, 116, 18038-18047.	1.5	23
13098	Size-Dependent Catalytic Performance of CuO on Î³-Al₂O₃: NO Reduction versus NH₃ Oxidation. ACS Catalysis, 2012, 2, 1432-1440.	5.5	75
13099	The mechanical shear behavior of Al single crystals and grain boundaries. Journal of Applied Physics, 2012, 112, .	1.1	8
13100	A red anatase TiO2 photocatalyst for solar energy conversion. Energy and Environmental Science, 2012, 5, 9603.	15.6	379
13101	Nanocarbon-Based Photovoltaics. ACS Nano, 2012, 6, 8896-8903.	7.3	117
13102	Adsorption of silicon on Au(110): An ordered two dimensional surface alloy. Applied Physics Letters, 2012, 101, .	1.5	34
13103	The phase transition and elastic and optical properties of polymorphs of CuI. Journal of Physics Condensed Matter, 2012, 24, 475503.	0.7	11
13104	A theoretic insight into the catalytic activity promotion of CeO2 surfaces by Mn doping. Physical Chemistry Chemical Physics, 2012, 14, 5769.	1.3	122
13105	Magnetic cluster expansion simulation and experimental study of high temperature magnetic properties of Feâ€“Cr alloys. Journal of Physics Condensed Matter, 2012, 24, 326001.	0.7	17

#	Article	IF	Citations
13106	First principles molecular dynamics study of nitrogen vacancy complexes in boronitrene. Journal of Physics Condensed Matter, 2012, 24, 265002.	0.7	8
13107	Platinum-Based Nanoalloys Pt_nTM_{55â€“n} (TM = Co, Rh, Au): A Density Functional Theory Investigation. Journal of Physical Chemistry C, 2012, 116, 18432-18439.	1.5	65
13108	Edge-dependent structural, electronic and magnetic properties of MoS2 nanoribbons. Journal of Materials Chemistry, 2012, 22, 7280.	6.7	250
13109	Charge and Ion Transport in NiO and Aspects of Ni Oxidation from First Principles. Journal of Physical Chemistry C, 2012, 116, 1948-1954.	1.5	62
13110	Computational screening of dopants for photocatalytic two-electron reduction of CO2 on anatase (101) surfaces. Energy and Environmental Science, 2012, 5, 6196.	15.6	138
13111	Prediction of stable ferroelectricity in epitaxial BaTiO₃ on Si. Applied Physics Letters, 2012, 101, 102903.	1.5	3
13112	Highly stable Pt monolayer on PdAu nanoparticle electrocatalysts for the oxygen reduction reaction. Nature Communications, 2012, 3, 1115.	5.8	377
13113	Propene Epoxidation with H₂/H₂O/O₂ Mixtures Over Gold Atoms Supported on Defective Graphene: A Theoretical Study. Journal of Physical Chemistry C, 2012, 116, 19355-19362.	1.5	26
13114	Thermodynamic and stoichiometric stability of the Cd-terminated CdTe (111) surface. Physical Review B, 2012, 85, .	1.1	9
13116	Lattice Mismatch Induced Nonlinear Growth of Graphene. Journal of the American Chemical Society, 2012, 134, 6045-6051.	6.6	88
13117	H-atom relay reactions in real space. Nature Materials, 2012, 11, 167-172.	13.3	105
13118	Heteroepitaxial Growth of Single-Walled Carbon Nanotubes from Boron Nitride. Scientific Reports, 2012, 2, 971.	1.6	16
13119	Optimal Electron Density Mechanism for Hydrogen on the Surface and at a Vacancy in Tungsten. Chinese Physics Letters, 2012, 29, 077101.	1.3	7
13120	Tuning the Electronic Properties of Semiconducting Transition Metal Dichalcogenides by Applying Mechanical Strains. ACS Nano, 2012, 6, 5449-5456.	7.3	809
13121	Tetrahedral Palladium Nanocrystals: AÂNew Support for Platinum Monolayer Electrocatalysts with High Activity and Stability in the Oxygen Reduction Reaction. Zeitschrift Fur Physikalische Chemie, 2012, 226, 1025-1038.	1.4	15
13122	Adsorption of Small Palladium Clusters on the Î±-Al₂O₃(0001) Surface: A First Principles Study. Journal of Physical Chemistry C, 2012, 116, 2863-2871.	1.5	20
13123	Polymorphic Phases of sp³-Hybridized Carbon under Cold Compression. Journal of the American Chemical Society, 2012, 134, 7530-7538.	6.6	69
13124	Ethanol Reforming on Co(0001) Surfaces: A Density Functional Theory Study. Journal of Physical Chemistry A, 2012, 116, 1409-1416.	1.1	34

#	Article	IF	Citations
13125	Density functional theory calculations andab initiomolecular dynamics simulations for diffusion of Li⁺within liquid ethylene carbonate. Modelling and Simulation in Materials Science and Engineering, 2012, 20, 065004.	0.8	38
13126	Palladium Nanoparticles/Defective Graphene Composites as Oxygen Reduction Electrocatalysts: A First-Principles Study. Journal of Physical Chemistry C, 2012, 116, 2710-2719.	1.5	94
13127	Abundance of CuZnâ€‰+â€‰SnZn and 2CuZnâ€‰+â€‰SnZn defect clusters in kesterite solar cells. Applied Physics Letters, 2012, 101, .	1.5	178
13128	Magic Carbon Clusters in the Chemical Vapor Deposition Growth of Graphene. Journal of the American Chemical Society, 2012, 134, 2970-2975.	6.6	138
13129	Are 4-Mercaptobenzoic Acid Self Assembled Monolayers on Au(111) a Suitable System to Test Adatom Models?. Journal of Physical Chemistry C, 2012, 116, 25765-25771.	1.5	35
13130	First-Principles Study of Spontaneous Polarization in SbFeO₃. Journal of the Physical Society of Japan, 2012, 81, 074702.	0.7	5
13131	Hydrogen adsorption on and spillover from Au- and Cu-supported Pt3 and Pd3 clusters: a density functional study. Physical Chemistry Chemical Physics, 2012, 14, 16062.	1.3	28
13132	Self-assembly mechanisms of short atomic chains on single-layer graphene and boron nitride. Physical Review B, 2012, 86, .	1.1	24
13133	Strain-dependent electronic and magnetic properties of MoS2 monolayer, bilayer, nanoribbons and nanotubes. Physical Chemistry Chemical Physics, 2012, 14, 13035.	1.3	435
13134	Site occupancy of chromium in the Î³â€²-Ni₃Al phase of nickel-based superalloys: a combined 3D atom probe and first-principles study. Philosophical Magazine Letters, 2012, 92, 495-506.	0.5	24
13135	Global minimum structure search in LixCoO2 composition using a hybrid evolutionary algorithm. Physical Chemistry Chemical Physics, 2012, 14, 13095.	1.3	12
13136	Triethylamine on Si(001)-(2 Ã— 1) at 300 K: Molecular Adsorption and Site Configurations Leading to Dissociation. Journal of Physical Chemistry C, 2012, 116, 16473-16486.	1.5	26
13138	First-principles study of O-BN: A sp3-bonding boron nitride allotrope. Journal of Applied Physics, 2012, 112, .	1.1	53
13139	Ab Initio Thermodynamics Examination of Sulfur Species Present on Rh, Ni, and Binary Rhâ€“Ni Surfaces under Steam Reforming Reaction Conditions. Langmuir, 2012, 28, 5660-5668.	1.6	10
13140	An angular-dependent embedded atom method (A-EAM) interatomic potential to model thermodynamic and mechanical behavior of Al/Si composite materials. Modelling and Simulation in Materials Science and Engineering, 2012, 20, 035007.	0.8	21
13141	Rapid Materials Degradation Induced by Surfaces and Voids: Ab Initio Modeling of Î²-Octatetramethylene Tetranitramine. Journal of the American Chemical Society, 2012, 134, 11815-11820.	6.6	65
13142	Atomic structure of a Î£3 [110]/(111) grain boundary in CeO2. Applied Physics Letters, 2012, 100, .	1.5	22
13143	LiBeB: A predicted phase with structural and electronic peculiarities. Physical Review B, 2012, 86, .	1.1	14

#	Article	IF	Citations
13144	Chemical tip fingerprinting in scanning probe microscopy of an oxidized Cu(110) surface. Physical Review B, 2012, 86, .	1.1	21
13145	Electronic and Magnetic Properties of Fluorinated Graphene with Different Coverage of Fluorine. Journal of Physical Chemistry C, 2012, 116, 18193-18201.	1.5	142
13146	First principles calculations of alloying element diffusion coefficients in Ni using the five-frequency model. Chinese Physics B, 2012, 21, 109102.	0.7	48
13147	Rational Tuning of Water Vapor and CO₂ Adsorption in Highly Stable Zr-Based MOFs. Journal of Physical Chemistry C, 2012, 116, 23526-23532.	1.5	129
13148	Effects of Mg, Ca, and Fe(II) Doping on the Kaolinite (001) Surface with H₂O Adsorption. Clays and Clay Minerals, 2012, 60, 330-337.	0.6	16
13149	First-Principles Modeling of the Initial Stages of Organic Solvent Decomposition on Li_xMn₂O₄(100) Surfaces. Journal of Physical Chemistry C, 2012, 116, 9852-9861.	1.5	114
13150	Thermal conductivity of BN-C nanostructures. Physical Review B, 2012, 86, .	1.1	429
13151	A new first principles approach to calculate phonon spectra of disordered alloys. Journal of Physics Condensed Matter, 2012, 24, 015402.	0.7	15
13152	Stability and migration of large oxygen clusters in UO2+x: Density functional theory calculations. Journal of Chemical Physics, 2012, 136, 234702.	1.2	34
13153	Structural and electronic properties of CuSbS2 and CuBiS2: potential absorber materials for thin-film solar cells. Physical Chemistry Chemical Physics, 2012, 14, 7229.	1.3	144
13154	Dissociation of H<mml:math xmlns:mml="http://www.w3.org/1998/Math/MathML" display="inline"><mml:msub><mml:mrow /><mml:mn>2</mml:mn></mml:msub></mml:math>O at the vacancies of single-layer MoS<mml:math xmlns:mml="http://www.w3.org/1998/Math/MathML" display="inline"><mml:msub><mml:mrow /><mml:mn>2</mml:mn></mml:msub></mml:math>. Physical Review B, 2012, 85, .	1.1	132
13155	Mechanistic Insights into Selective Oxidation of Ethanol on Au(111): A DFT Study. Chinese Journal of Catalysis, 2012, 33, 407-415.	6.9	29
13156	Enhancing magnetocrystalline anisotropy of the Fe70Pd30 magnetic shape memory alloy by adding Cu. Acta Materialia, 2012, 60, 6920-6930.	3.8	13
13157	Emergence of ferromagnetism at a vacancy on a non-magnetic ferroelectric PbTiO3 surface: A first-principles study. Acta Materialia, 2012, 60, 6322-6330.	3.8	20
13158	Double-atomic-wall-based dynamic precipitates of the early-stage S-phase in AlCuMg alloys. Acta Materialia, 2012, 60, 6573-6580.	3.8	58
13159	Correlation of the atomic and electronic structures and the optical properties of the Î£5(210)/[001] symmetric tilt grain boundary in yttrium aluminum garnet. Acta Materialia, 2012, 60, 7041-7050.	3.8	2
13160	Hydrogen spillover storage on Ca-decorated graphene. International Journal of Hydrogen Energy, 2012, 37, 11835-11841.	3.8	53
13161	Computational analysis of atomic C and S adsorption on Ni, Cu, and Ni-Cu SOFC anode surfaces. International Journal of Hydrogen Energy, 2012, 37, 11941-11945.	3.8	29

#	Article	IF	Citations
13162	First-principles based modeling of hydrogen permeation through Pdâ€“Cu alloys. International Journal of Hydrogen Energy, 2012, 37, 12760-12764.	3.8	28
13163	Hydrogen adsorption on and diffusion through MoS2 monolayer: First-principles study. International Journal of Hydrogen Energy, 2012, 37, 14323-14328.	3.8	105
13164	Improving the hydrogen storage capacity of metal organic framework by chemical functionalization. International Journal of Hydrogen Energy, 2012, 37, 16070-16077.	3.8	30
13165	Hybrid functionals studies of structural and electronic properties of ZnxCd(1â^'x)S and (ZnxCd1â^'x)(SexS1â^'x) solid solution photocatalysts. International Journal of Hydrogen Energy, 2012, 37, 17870-17881.	3.8	27
13166	Hydrogen storage in lithium-decorated benzene complexes. International Journal of Hydrogen Energy, 2012, 37, 17153-17157.	3.8	8
13167	Environmentally dependent stability of low-index hematite surfaces. Journal of Colloid and Interface Science, 2012, 386, 315-324.	5.0	23
13168	Nanocrystalline CaSb2O5(OH)2 and Ca2Sb2O7: Controlled syntheses, electronic structures and photocatalytic activity. Applied Catalysis B: Environmental, 2012, 127, 205-211.	10.8	14
13169	First-principles study of hydrogen storage on Ti (Sc)-decorated boron-carbon-nitride sheet. Applied Surface Science, 2012, 263, 182-186.	3.1	23
13170	Thermodynamic modeling of the Srâ€“X (X=H, Li, Na, Sc) systems. Calphad: Computer Coupling of Phase Diagrams and Thermochemistry, 2012, 38, 17-22.	0.7	6
13171	Atomistic modeling of pure Co and Coâ€“Al system. Calphad: Computer Coupling of Phase Diagrams and Thermochemistry, 2012, 38, 7-16.	0.7	44
13172	First-principles calculations and thermodynamic re-modeling of the Hfâ€“W system. Calphad: Computer Coupling of Phase Diagrams and Thermochemistry, 2012, 38, 92-99.	0.7	17
13173	Phase stability and thermodynamic modeling of the Reâ€“Ti system supplemented by first-principles calculations. Calphad: Computer Coupling of Phase Diagrams and Thermochemistry, 2012, 38, 71-80.	0.7	11
13174	Pressure-induced solubility suppression for boronâ€“carbonâ€“nitride ternary alloys. Calphad: Computer Coupling of Phase Diagrams and Thermochemistry, 2012, 38, 81-84.	0.7	1
13175	Thermodynamic evaluations and optimizations of binary Mg-light Rare Earth (La, Ce, Pr, Nd, Sm) systems. Calphad: Computer Coupling of Phase Diagrams and Thermochemistry, 2012, 38, 100-116.	0.7	64
13176	Phase stability of Vâ€“Ta alloy using cluster expansion and Monte Carlo techniques. Calphad: Computer Coupling of Phase Diagrams and Thermochemistry, 2012, 39, 33-36.	0.7	5
13177	Thermodynamic modeling of the Hfâ€“Sn and Snâ€“Y systems. Calphad: Computer Coupling of Phase Diagrams and Thermochemistry, 2012, 39, 91-96.	0.7	10
13178	First principles phase diagram calculations for the octahedral-interstitial system Î±TiOX, 0â‰¤Xâ‰¤1/2. Calphad: Computer Coupling of Phase Diagrams and Thermochemistry, 2012, 39, 97-103.	0.7	20
13179	Ab initio study of the interaction of H with substitutional solute atoms in Î±-Fe: Trends across the transition-metal series. Computational Materials Science, 2012, 65, 235-238.	1.4	11

#	Article	IF	Citations
13180	Tunable band gap in half-fluorinated bilayer graphene under biaxial strains. Computational Materials Science, 2012, 65, 165-169.	1.4	7
13181	First-principles study of phonons and intrinsic dielectric response of Ba(Ni1/3Ta2/3)O3. Computational Materials Science, 2012, 65, 81-84.	1.4	4
13182	Graphene-like titanium carbides and nitrides Tin+1Cn, Tin+1Nn (n=1, 2, and 3) from de-intercalated MAX phases: First-principles probing of their structural, electronic properties and relative stability. Computational Materials Science, 2012, 65, 104-114.	1.4	286
13183	Modification of graphene as active hydrogen storage medium by strain engineering. Computational Materials Science, 2012, 65, 144-148.	1.4	21
13184	First-principles calculations of MnB4, TcB4, and ReB4 with the MnB4-type structure. Computational Materials Science, 2012, 65, 372-376.	1.4	18
13185	The electronic, mechanical and lattice dynamic properties of TiSiY from first-principles calculations. Computational Materials Science, 2012, 65, 485-489.	1.4	1
13186	Ionic interactions: Comparative topological approach. Computational and Theoretical Chemistry, 2012, 998, 193-201.	1.1	41
13187	Sequential adjacent Si dimer dechlorination mechanism of perchloroethylene adsorption on Si(100) with temperature evolution. Computational and Theoretical Chemistry, 2012, 999, 162-168.	1.1	0
13188	DFT study on stability and structure of bimetallic AumPdn (N=38, 55, 79, N=m+n, m/nâ‰ˆ2:1 and 5:1) clusters. Computational and Theoretical Chemistry, 2012, 999, 246-250.	1.1	13
13189	2,4-Diazido-5-iodo-pyrimidine crystal under high pressure: A comparison of DFT and DFT-D studies. Computational and Theoretical Chemistry, 2012, 1000, 60-69.	1.1	10
13190	Real-space density functional theory and time dependent density functional theory using finite/infinite element methods. Computer Physics Communications, 2012, 183, 2581-2588.	3.0	2
13191	Diffusion of transition metals in periclase by experiment and first-principles, with implications for coreâ€“mantle equilibration during metal percolation. Earth and Planetary Science Letters, 2012, 357-358, 42-53.	1.8	6
13192	First-principles studies on stabilities and electronic properties of AlN nanostructures. Superlattices and Microstructures, 2012, 52, 662-668.	1.4	9
13193	Protons in perovskite nitrides and oxide nitrides: A first principles study of ThTaN3 and SrTaO2N. Solid State Communications, 2012, 152, 1921-1923.	0.9	8
13194	Multiferroic and magnetoelectric nature of GaFeO3, AlFeO3 and related oxides. Solid State Communications, 2012, 152, 1964-1968.	0.9	55
13195	Influence of antiphase boundary period parameter Mâ€² on elastic and electronic properties of one dimensional long period structures of Al3Ti. Solid State Communications, 2012, 152, 1939-1944.	0.9	7
13196	First-principle study of the electronic structure and magnetic properties of CeRu2Al2B. Solid State Communications, 2012, 152, 2105-2108.	0.9	1
13197	Structural changes on cycling Li2FeSiO4 polymorphs from DFT calculations. Solid State Ionics, 2012, 228, 19-24.	1.3	20

#	Article	IF	Citations
13198	Intra-octahedral proton transfer in bulk orthorhombic perovskite barium cerate. Solid State Ionics, 2012, 226, 71-75.	1.3	8
13199	Increased thermal stability of Tiâ€“Alâ€“N thin films by Ta alloying. Surface and Coatings Technology, 2012, 211, 98-103.	2.2	104
13200	Transport properties of zigzag graphene nanoribbons with oxygen edge decoration. Organic Electronics, 2012, 13, 2494-2501.	1.4	15
13201	The low velocity layer in subduction zone: Structure and elasticity of glaucophane at high pressures. Physics of the Earth and Planetary Interiors, 2012, 208-209, 50-58.	0.7	26
13202	Structure of Defects, their Interactions and Positron Characteristics in Fe3 Alsystem. Physics Procedia, 2012, 35, 69-74.	1.2	4
13203	Electronic and magnetic properties for Co13 clusters deposited on graphene: A first-principles exploration. Physica E: Low-Dimensional Systems and Nanostructures, 2012, 46, 6-11.	1.3	27
13204	Room temperature ferromagnetic property of Ag2Mo2O7 nanowires. Physica E: Low-Dimensional Systems and Nanostructures, 2012, 46, 213-217.	1.3	7
13205	Enhanced magnetism of SiC with He defects. Physics Letters, Section A: General, Atomic and Solid State Physics, 2012, 376, 3363-3367.	0.9	4
13206	First-principles investigations of O2 dissociation on low-coordinated Pd ensembles over stepped Au surfaces. Physics Letters, Section A: General, Atomic and Solid State Physics, 2012, 376, 3432-3438.	0.9	11
13207	Predicting hard metallic osmiumâ€“carbon compounds under high pressure. Physics Letters, Section A: General, Atomic and Solid State Physics, 2012, 376, 3535-3539.	0.9	10
13208	Strain and chirality effects on the mechanical and electronic properties of silicene and silicane under uniaxial tension. Physics Letters, Section A: General, Atomic and Solid State Physics, 2012, 376, 3546-3550.	0.9	129
13209	First-principles calculation of structure and mechanical property of IrY. Procedia Engineering, 2012, 31, 665-670.	1.2	0
13210	Thermodynamic stability of Mgâ€“Yâ€“Zn long-period stacking ordered structures. Scripta Materialia, 2012, 67, 798-801.	2.6	53
13211	Surface energies of AlN allotropes from first principles. Scripta Materialia, 2012, 67, 760-762.	2.6	73
13212	Density functional analysis of the magnetic structures of Sr2MGe2O7 (M=Mn, Co). Journal of Magnetism and Magnetic Materials, 2012, 324, 3716-3718.	1.0	4
13213	Analysis of the magnetic structure of the manganese oxychalcogenides R2Mn2Se2O (R=LaO, BaF) by density functional calculations. Journal of Magnetism and Magnetic Materials, 2012, 324, 3859-3862.	1.0	5
13214	Interfacial electronic structure and magnetoelectric effect in M/BaTiO3 (M=Ni, Fe) superlattices. Journal of Magnetism and Magnetic Materials, 2012, 324, 3937-3943.	1.0	22
13215	First-principles calculations of adhesion, bonding and magnetism of the Fe/HfC interface. Journal of Magnetism and Magnetic Materials, 2012, 324, 4155-4160.	1.0	13

#	Article	IF	Citations
13216	Relationship between the short-range order and electrical resistivity in liquid indium-antimony. Journal of Non-Crystalline Solids, 2012, 358, 1892-1896.	1.5	2
13217	Electronic, mechanical and thermodynamic properties of Î±-UH3: A comparative study by using the LDA and LDA+U approaches. Journal of Nuclear Materials, 2012, 430, 137-141.	1.3	23
13218	Role of grain boundary and dislocation loop in H blistering in W: A density functional theory assessment. Journal of Nuclear Materials, 2012, 430, 132-136.	1.3	37
13219	Structural, electronic and magnetic properties of a symmetrical FeReO terminated (001)-oriented slab of double perovskite Sr2FeReO6. Materials Chemistry and Physics, 2012, 136, 570-576.	2.0	14
13220	Study of interatomic potential and thermal structural properties of Î²-Zn4Sb3. Materials Research Bulletin, 2012, 47, 3558-3567.	2.7	10
13221	An intermediate fcc Zr state observed in the Cuâ€“Zrâ€“Ni system upon ion beam mixing. Materials Letters, 2012, 89, 90-92.	1.3	2
13222	Interconnect reliability dependence on fast diffusivity paths. Microelectronics Reliability, 2012, 52, 1532-1538.	0.9	4
13223	The role of van der Waals interactions in the adsorption of noble gases on metal surfaces. Journal of Physics Condensed Matter, 2012, 24, 424211.	0.7	42
13224	First-Principles Modeling of the â€œClean-Upâ€•of Native Oxides during Atomic Layer Deposition onto IIIâ€“V Substrates. Journal of Physical Chemistry C, 2012, 116, 643-654.	1.5	50
13225	General Method for Determination of the Surface Composition in Bimetallic Nanoparticle Catalysts from the L Edge X-ray Absorption Near-Edge Spectra. ACS Catalysis, 2012, 2, 2433-2443.	5.5	16
13226	Oxidative Dehydrogenation of Cyclohexane on Cobalt Oxide (Co₃O₄) Nanoparticles: The Effect of Particle Size on Activity and Selectivity. ACS Catalysis, 2012, 2, 2409-2423.	5.5	113
13227	Electronic and Magnetic Properties of Graphene/Fluorographene Superlattices. Journal of Physical Chemistry C, 2012, 116, 18278-18283.	1.5	25
13228	Influence of Oxygen Evolution during Water Oxidation on the Surface of Perovskite Oxide Catalysts. Journal of Physical Chemistry Letters, 2012, 3, 3264-3270.	2.1	562
13229	Defect-Mediated Lattice Relaxation and Domain Stability in Ferroelectric Oxides. Physical Review Letters, 2012, 109, 117601.	2.9	34
13230	Electronic structure of assembled graphene nanoribbons: Substrate and many-body effects. Physical Review B, 2012, 86, .	1.1	43
13231	Synthesis of Ptâ€“Pd Coreâ€“Shell Nanostructures by Atomic Layer Deposition: Application in Propane Oxidative Dehydrogenation to Propylene. Chemistry of Materials, 2012, 24, 3525-3533.	3.2	104
13232	Hydration structures of U(III) and U(IV) ions from ab initio molecular dynamics simulations. Journal of Chemical Physics, 2012, 137, 074502.	1.2	15
13233	Z-BN: a novel superhard boron nitride phase. Physical Chemistry Chemical Physics, 2012, 14, 10967.	1.3	72

#	Article	IF	Citations
13234	Extreme Poisson's ratios and their electronic origin in B2 CsCl-type AB intermetallic compounds. Physical Review B, 2012, 85, .	1.1	42
13235	Analysis of Intrinsic Defects in CeO₂ Using a Koopmans-Like GGA+U Approach. Journal of Physical Chemistry C, 2012, 116, 2443-2452.	1.5	144
13236	Physics of bandgap formation in Cuâ€“Sbâ€“Se based novel thermoelectrics: the role of Sb valency and Cu d levels. Journal of Physics Condensed Matter, 2012, 24, 415502.	0.7	19
13237	Noncentrosymmetric Inorganic Open-Framework Chalcohalides with Strong Middle IR SHG and Red Emission: Ba₃AGa₅Se₁₀Cl₂ (A = Cs, Rb, K). Journal of the American Chemical Society, 2012, 134, 2227-2235.	6.6	220
13238	Superatomic orbitals in sixteen-coordinate M@Li16 bonded by metallic bonds. Nanoscale, 2012, 4, 2567.	2.8	12
13239	In Situ Formation of Pyridyl-Functionalized Poly(3-hexylthiophene)s via Quenching of the Grignard Metathesis Polymerization: Toward Ligands for Semiconductor Quantum Dots. Chemistry of Materials, 2012, 24, 4459-4467.	3.2	38
13240	The influence of charge ordering on the phase stability of spinel LiNi2O4. RSC Advances, 2012, 2, 12940.	1.7	14
13241	On the Structure of Î²-Molybdenum Dichloride. Inorganic Chemistry, 2012, 51, 4965-4971.	1.9	3
13242	The modification of central B/N atom chain on electron transport of graphene nanoribbons. Journal of Applied Physics, 2012, 112, 113713.	1.1	1
13244	CO₂ Reduction on Transition Metal (Fe, Co, Ni, and Cu) Surfaces: In Comparison with Homogeneous Catalysis. Journal of Physical Chemistry C, 2012, 116, 5681-5688.	1.5	247
13245	Electrically tunable band gap in silicene. Physical Review B, 2012, 85, .	1.1	997
13246	First-principles study of electronic, vibrational, elastic, and magnetic properties of FeF<mml:math xmlns:mml="http://www.w3.org/1998/Math/MathML" display="inline"><mml:msub><mml:mrow /><mml:mn>2</mml:mn></mml:msub></mml:math>as a function of pressure. Physical Review B, 2012, 85, .	1.1	50
13247	Particle-swarm structure prediction on clusters. Journal of Chemical Physics, 2012, 137, 084104.	1.2	453
13248	Sulfidation of Ceria Surfaces from Sulfur and Sulfur Diffusion. Journal of Physical Chemistry C, 2012, 116, 8417-8425.	1.5	19
13249	Transferable pair potentials for CdS and ZnS crystals. Journal of Chemical Physics, 2012, 136, 234111.	1.2	44
13250	Distribution of cations in wurtzitic In<mml:math xmlns:mml="http://www.w3.org/1998/Math/MathML" display="inline"><mml:msub><mml:mrow /><mml:mi>x</mml:mi></mml:msub></mml:math>Ga<mml:math xmlns:mml="http://www.w3.org/1998/Math/MathML" display="inline"><mml:msub><mml:mrow /><mml:mrow><mml:mn>1</mml:mn><mml:mo>â^’</mml:mo><mml:mi>x</mml:mi></mml:mrow></mml:msub></mml:math>N and In<mml:math xmlns:mml="http://www.w3.org/1998/Math/MathML" display="inline"><mml:msub><mml:mrow /><mml:mi>x</mml:mi></mml:msub></mml:math>Ga<mml:math xmlns:mml="http://www.w3.org/1998/Math/MathML" display="inline"><mml:msub><mml:mrow /><mml:mrow><mml:mn>1</mml:mn><mml:mo>â^’</mml:mo><mml:mi>x</mml:mi></mml:mrow></mml:msub></mml:math>N alloys. Physical Review	1.1	22
13251	Crystal facet-dependent photocatalytic oxidation and reduction reactivity of monoclinic WO3 for solar energy conversion. Journal of Materials Chemistry, 2012, 22, 6746.	6.7	356
13252	A Comprehensive Search for Stable Ptâ€“Pd Nanoalloy Configurations and Their Use as Tunable Catalysts. Nano Letters, 2012, 12, 4875-4880.	4.5	98

#	Article	IF	Citations
13253	Hydrogen Adsorption on PdGa(110): A DFT Study. Journal of Physical Chemistry C, 2012, 116, 17518-17524.	1.5	17
13254	First-principles study of the spin-gap system Sr<mml:math xmlns:mml="http://www.w3.org/1998/Math/MathML" display="inline"><mml:msub><mml:mrow /><mml:mn>2</mml:mn></mml:msub></mml:math>Cu(BO<mml:math) Tj ETQq1 1 0.784314 rgBT /Overlock 10 Tf 50 707 Td (xmlns:mml="http://www.w3.org/1998/Math/MathML" display="inline"><mml:msub><mml:mrow /></mml:msub>	1.1	7
13255	Ceâ€“Mn Oxides for High-Temperature Gasifier Effluent Desulfurization. Energy & Fuels, 2012, 26, 6765-6776.	2.5	30
13256	Single-Crystal Structures, Optical Absorptions, and Electronic Distributions of Thorium Oxychalcogenides ThOQ (Q = S, Se, Te). Inorganic Chemistry, 2012, 51, 8112-8118.	1.9	20
13257	Reaction of the Basal Plane of Graphite with the Methyl Radical. Journal of Physical Chemistry Letters, 2012, 3, 1680-1683.	2.1	21
13258	Selective Graphene Formation on Copper Twin Crystals. Journal of the American Chemical Society, 2012, 134, 12492-12498.	6.6	60
13259	High-Performance Graphene Oxide Electromechanical Actuators. Journal of the American Chemical Society, 2012, 134, 1250-1255.	6.6	44
13260	Thermodynamics of Lithium in TiO₂(B) from First Principles. Chemistry of Materials, 2012, 24, 1568-1574.	3.2	90
13261	Experimental and Computational Investigation of Au₂₅ Clusters and CO₂: A Unique Interaction and Enhanced Electrocatalytic Activity. Journal of the American Chemical Society, 2012, 134, 10237-10243.	6.6	361
13262	Electronic Fingerprints of DNA Bases on Graphene. Nano Letters, 2012, 12, 927-931.	4.5	65
13263	Feedback mechanism for the stability of the band gap of CuInSe<mml:math xmlns:mml="http://www.w3.org/1998/Math/MathML" display="inline"><mml:msub><mml:mrow /><mml:mn>2</mml:mn></mml:msub></mml:math>. Physical Review B, 2012, 86, .	1.1	29
13264	Interplay between quantum size effect and strain effect on growth of nanoscale metal thin films. Physical Review B, 2012, 86, .	1.1	22
13265	Direct Calculation of Li-Ion Transport in the Solid Electrolyte Interphase. Journal of the American Chemical Society, 2012, 134, 15476-15487.	6.6	524
13266	Chemical Origins of Frictional Aging. Physical Review Letters, 2012, 109, 186102.	2.9	82
13267	X-ray absorption from large molecules at metal surfaces: Theoretical and experimental results for Co-OEP on Ni(100). Journal of Chemical Physics, 2012, 137, 194703.	1.2	8
13268	Nonequilibrium electron-vibration coupling and conductance fluctuations in a C60junction. Physical Review B, 2012, 86, .	1.1	8
13269	First principles calculation on the adsorption of water on lithiumâ€“montmorillonite (Liâ€“MMT). Journal of Physics Condensed Matter, 2012, 24, 475506.	0.7	11
13270	Metal-Supported Metal Clusters: A Density Functional Study of Pt₃ and Pd₃. Journal of Physical Chemistry C, 2012, 116, 10057-10063.	1.5	12

#	Article	IF	Citations
13271	Linking 31P Magnetic Shielding Tensors to Crystal Structures: Experimental and Theoretical Studies on Metal(II) Aminotris(methylenephosphonates). Inorganic Chemistry, 2012, 51, 11466-11477.	1.9	19
13272	Hybrid Graphene and Graphitic Carbon Nitride Nanocomposite: Gap Opening, Electronâ€“Hole Puddle, Interfacial Charge Transfer, and Enhanced Visible Light Response. Journal of the American Chemical Society, 2012, 134, 4393-4397.	6.6	565
13273	The delocalized nature of holes in (Ga, N) cluster-doped ZnO. Journal of Physics Condensed Matter, 2012, 24, 415503.	0.7	4
13274	Mechanical properties of graphene oxides. Nanoscale, 2012, 4, 5910.	2.8	239
13275	Electronic structures of silicene fluoride and hydride. Applied Physics Letters, 2012, 100, .	1.5	165
13276	Novel Zn-doped SnO₂hierarchical architectures: synthesis, characterization, and gas sensing properties. CrystEngComm, 2012, 14, 1701-1708.	1.3	65
13277	First-principles study of a pressure-induced spin transition in multiferroic Bi<mml:math xmlns:mml="http://www.w3.org/1998/Math/MathML" display="inline"><mml:msub><mml:mrow /><mml:mn>2</mml:mn></mml:msub></mml:math>FeCrO<mml:math xmlns:mml="http://www.w3.org/1998/Math/MathML" display="inline"><mml:msub><mml:mrow /><mml:mn>6</mml:mn></mml:msub></mml:math>. Physical Review B, 2012, 86, .	1.1	20
13278	Elastic properties of hybrid graphene/boron nitride monolayer. Acta Mechanica, 2012, 223, 2591-2596.	1.1	77
13279	Structural and Electronic Properties of Neutral and Ionic (Ga₂O₃)_n Clusters with n = 1â€“10. Journal of Physical Chemistry C, 2012, 116, 2691-2701.	1.5	17
13280	Nonadiabatic dynamics at metal surfaces: Independent electron surface hopping with phonon and electron thermostats. Faraday Discussions, 2012, 157, 325.	1.6	18
13281	First-principles investigation of transition metal atom M (M = Cu, Ag, Au) adsorption on CeO2(110). Physical Chemistry Chemical Physics, 2012, 14, 1923.	1.3	52
13282	Photo-induced Charge Separation across the Grapheneâ€“TiO₂ Interface Is Faster than Energy Losses: A Time-Domain ab Initio Analysis. Journal of the American Chemical Society, 2012, 134, 14238-14248.	6.6	226
13283	A combined first principles and analytical treatment for determination of the surface elastic constants: application to Si(001) ideal and reconstructed surfaces. Philosophical Magazine Letters, 2012, 92, 7-19.	0.5	23
13284	Unravelling the Role of the Central Metal Ion in the Electronic Structure of Tris(8-hydroxyquinoline) Metal Chelates: Photoemission Spectroscopy and Hybrid Functional Calculations. Journal of Physical Chemistry A, 2012, 116, 11548-11552.	1.1	4
13285	Ab-Initio Modeling of the Resistance Switching Mechanism in RRAM Devices: Case Study of Hafnium Oxide (HfO2). Materials Research Society Symposia Proceedings, 2012, 1430, 72.	0.1	11
13286	Mechanisms of the Oxygen Reduction Reaction on Defective Graphene-Supported Pt Nanoparticles from First-Principles. Journal of Physical Chemistry C, 2012, 116, 3653-3660.	1.5	312
13287	Effect of alloying element on dislocation cross-slip in Î³â€²-Ni₃Al: a first-principles study. Philosophical Magazine, 2012, 92, 4028-4039.	0.7	20
13288	Systematic study of ferroelectric, interfacial, oxidative, and doping effects on conductance of Pt/BaTiO<mml:math xmlns:mml="http://www.w3.org/1998/Math/MathML" display="inline"><mml:msub><mml:mrow /><mml:mn>3</mml:mn></mml:msub></mml:math>/Pt ferroelectic tunnel junctions. Physical Review B, 2012, 85, .	1.1	23

#	Article	IF	Citations
13289	Improved oxygen surface exchange kinetics at grain boundaries in nanocrystalline yttria-stabilized zirconia. MRS Communications, 2012, 2, 107-111.	0.8	15
13290	Complex GdSc_{1â€“x}In_xO₃ Oxides: Synthesis and Structure Driven Tunable Electrical Properties. Chemistry of Materials, 2012, 24, 2186-2196.	3.2	49
13291	Realizing a SnO2-based ultraviolet light-emitting diode via breaking the dipole-forbidden rule. NPG Asia Materials, 2012, 4, e30-e30.	3.8	137
13292	Atomistic Simulations of Microelectronic Materials: Prediction of Mechanical, Thermal, and Electrical Properties. , 2012, , 3-24.		0
13293	Strain relief and disorder in commensurate water layers formed on Pd(111). Journal of Physics Condensed Matter, 2012, 24, 124102.	0.7	14
13294	Optical properties of Mg-doped VO2: Absorption measurements and hybrid functional calculations. Applied Physics Letters, 2012, 101, .	1.5	70
13295	CO₂ Activation and Methanol Synthesis on Novel Au/TiC and Cu/TiC Catalysts. Journal of Physical Chemistry Letters, 2012, 3, 2275-2280.	2.1	129
13296	The effects of Mo doping on 0.3Li[Li0.33Mn0.67]O2Â·0.7Li[Ni0.5Co0.2Mn0.3]O2 cathode material. Dalton Transactions, 2012, 41, 3053.	1.6	76
13297	Field-effect transistors fabricated from diluted magnetic semiconductor colloidal nanowires. Nanoscale, 2012, 4, 1263.	2.8	15
13298	Enhanced electronic conductivity by controlled self-doping in pyrochlores. Physical Chemistry Chemical Physics, 2012, 14, 6556.	1.3	10
13299	Possible nâ€“type carrier sources in In2O3(ZnO)k. Chemistry of Materials, 2012, 24, 106-114.	3.2	38
13300	A Density Functional Theory Study on Carbon Monoxide Adsorption on Platinumâ€“Osmium and Platinumâ€“Rutheniumâ€“Osmium Alloys. Journal of Physical Chemistry C, 2012, 116, 21447-21458.	1.5	13
13301	Role of Distant Al Atoms in Alkaline Earth Zeolites for Stabilization of Hydroxyl Groups. Journal of Physical Chemistry C, 2012, 116, 2399-2410.	1.5	10
13302	First-principles analysis of oxide-ion conduction mechanism in lanthanum silicate. Journal of Materials Chemistry, 2012, 22, 7265.	6.7	29
13303	Mechanism for enhanced oxygen reduction kinetics at the (La,Sr)CoO3â^Î´/(La,Sr)2CoO4+Î´ hetero-interface. Energy and Environmental Science, 2012, 5, 8598.	15.6	109
13304	Gaussian charge-transfer charge distributions for non-self-consistent electronic structure calculations. Physical Review B, 2012, 85, .	1.1	3
13305	On the origin of blue emission from ZnO quantum dots synthesized by a solâ€“gel route. Semiconductor Science and Technology, 2012, 27, 065020.	1.0	28
13306	First principle molecular dynamic simulation of the rapid solidification process of Ca50Mg20Cu30 alloy. Journal of Applied Physics, 2012, 112, 073517.	1.1	6

#	Article	IF	Citations
13307	Intrinsic Strength and Failure Behaviors of Graphene Grain Boundaries. ACS Nano, 2012, 6, 2704-2711.	7.3	197
13308	Tracking lithium transport and electrochemical reactions in nanoparticles. Nature Communications, 2012, 3, 1201.	5.8	254
13309	The Structural and Electronic Properties of Tin Oxide Nanowires: An Ab Initio Investigation. Journal of Physical Chemistry C, 2012, 116, 13382-13387.	1.5	8
13310	Combined Density Functional Theory and Monte Carlo Analysis of Monomolecular Cracking of Light Alkanes Over H-ZSM-5. Journal of Physical Chemistry C, 2012, 116, 23408-23417.	1.5	59
13311	Simulation of structural and electronic properties of amorphous tungsten oxycarbides. New Journal of Physics, 2012, 14, 113028.	1.2	5
13312	Advancing density functional theory to finite temperatures: methods and applications in steel design. Journal of Physics Condensed Matter, 2012, 24, 053202.	0.7	75
13313	Determinations of the high-pressure crystal structures of Sb₂Te₃. Journal of Physics Condensed Matter, 2012, 24, 475403.	0.7	42
13314	Composition-Controlled PtCo Alloy Nanocubes with Tuned Electrocatalytic Activity for Oxygen Reduction. ACS Applied Materials & Interfaces, 2012, 4, 6228-6234.	4.0	103
13315	New-phase VO2 micro/nanostructures: investigation of phase transformation and magnetic property. New Journal of Chemistry, 2012, 36, 619-625.	1.4	108
13316	Crystal Chemistry of CdIn₂S₄, MgIn₂S₄, and MnIn₂S₄ Thiospinels under High Pressure. Journal of Physical Chemistry C, 2012, 116, 14078-14087.	1.5	44
13317	Benzene adsorbed on metals: Concerted effect of covalency and van der Waals bonding. Physical Review B, 2012, 86, .	1.1	243
13318	Elastic constants, composition, and piezoelectric polarization in In<mml:math xmlns:mml="http://www.w3.org/1998/Math/MathML" display="inline"><mml:msub><mml:mrow /><mml:mi>x</mml:mi></mml:msub></mml:math>Al<mml:math xmlns:mml="http://www.w3.org/1998/Math/MathML" display="inline"><mml:msub><mml:mrow /><mml:mrow><mml:mn>1</mml:mn><mml:mo>â^’</mml:mo><mml:mi>x</mml:mi></mml:mrow></mml:msub></mml:math>N: From ab initio calculations to experimental implications for the applicability of Vegard's rule.	1.1	31
13319	Electronic and structural properties of InAs/InP core/shell nanowires: A first principles study. Journal of Applied Physics, 2012, 111, 054315.	1.1	14
13320	First principles study of the magnetism driven by cation defects in CeO₂: the important role of O2p states. Chinese Physics B, 2012, 21, 047505.	0.7	8
13321	Ni-Assisted Transformation of Graphene Flakes to Fullerenes. Journal of Physical Chemistry C, 2012, 116, 6572-6584.	1.5	38
13322	A density functional theory study of hydrogen dissociation and diffusion at the perimeter sites of Au/TiO2. Physical Chemistry Chemical Physics, 2012, 14, 3741.	1.3	52
13323	Transport Properties of Carbon Nanotubes: Effects of Vacancy Clusters and Disorder. Journal of Physical Chemistry C, 2012, 116, 1179-1184.	1.5	9
13324	Lattice dynamics, thermodynamics, and bonding strength of lithium-ion battery materials LiMPO₄(M = Mn, Fe, Co, and Ni): a comparative first-principles study. Journal of Materials Chemistry, 2012, 22, 1142-1149.	6.7	87

#	Article	IF	Citations
13325	Fragmentation of the Fluorite Type in Fe8Al17.4Si7.6: Structural Complexity in Intermetallics Dictated by the 18 Electron Rule. Inorganic Chemistry, 2012, 51, 10341-10349.	1.9	21
13326	Surface Reactions and Defect Formation in Irradiated Graphene Devices. IEEE Transactions on Nuclear Science, 2012, 59, 3039-3044.	1.2	12
13327	Epitaxially Constrained Hexagonal Ferroelectricity and Canted Triangular Spin Order in LuFeO₃ Thin Films. Chemistry of Materials, 2012, 24, 2426-2428.	3.2	77
13328	Band Alignment for Ambipolar-Doping of Sn _x Zn _{1â^' x} Te Alloys. Communications in Theoretical Physics, 2012, 57, 723-726.	1.1	3
13329	Oxygen Vacancy Induced Band-Gap Narrowing and Enhanced Visible Light Photocatalytic Activity of ZnO. ACS Applied Materials & Interfaces, 2012, 4, 4024-4030.	4.0	1,269
13330	Single-Layer [Cu₂Br(IN)₂]_n Coordination Polymer (CP): Electronic and Magnetic Properties, and Implication for Molecular Sensors. Journal of Physical Chemistry C, 2012, 116, 4119-4125.	1.5	27
13331	Edge-decorated graphene nanoribbons by scandium as hydrogen storage media. Nanoscale, 2012, 4, 915.	2.8	71
13332	Ab initiobased multiscale modeling of alloy surface segregation. Journal of Physics Condensed Matter, 2012, 24, 485006.	0.7	4
13333	Mild Bromination-Assisted Density-Gradient Ultracentrifugation to Sort Single-Walled Carbon Nanotubes by Metallicity. Journal of Physical Chemistry C, 2012, 116, 23027-23035.	1.5	5
13334	Many MÂ©Bn boron wheels are local, but not global minima. Physical Chemistry Chemical Physics, 2012, 14, 14898.	1.3	29
13335	Mechanical properties of graphyne monolayers: a first-principles study. Physical Chemistry Chemical Physics, 2012, 14, 13385.	1.3	222
13336	Mechanisms and Energies of Water Gas Shift Reaction on Fe-, Co-, and Ni-Promoted MoS₂ Catalysts. Journal of Physical Chemistry C, 2012, 116, 25368-25375.	1.5	53
13337	Atomic forces at finite magnetic temperatures: Phonons in paramagnetic iron. Physical Review B, 2012, 85, .	1.1	157
13338	Hole Trapping at Surfaces of m-ZrO₂ and m-HfO₂ Nanocrystals. Journal of Physical Chemistry C, 2012, 116, 25888-25897.	1.5	26
13339	CO Adsorption Behavior on Decorated Pt@Au Nanoelectrocatalysts: A Combined Experimental and DFT Theoretical Calculation Study. Journal of Physical Chemistry C, 2012, 116, 3851-3856.	1.5	20
13340	Density functional theory study of the structural and electronic properties of amorphous silicon nitrides: Si<mml:math xmlns:mml="http://www.w3.org/1998/Math/MathML" display="inline"><mml:msub><mml:mrow /><mml:mn>3</mml:mn></mml:msub></mml:math>N<mml:math xmlns:mml="http://www.w3.org/1998/Math/MathML" display="inline"><mml:msub><mml:mrow /><mml:mrow><mml:mn>4</mml:mn><mml:mo>â^'</mml:mo><mml:mi>x</mml:mi></mml:mrow></mml:msub></mml:math>:H. Physical Review B, 2012, 86, .	1.1	34
13341	Enhancement of Ag cluster mobility on Ag surfaces by chloridation. Journal of Chemical Physics, 2012, 137, 184705.	1.2	3
13342	Exchange coupling and helical spin order in the triangular lattice antiferromagnet CuCrO 2 using first principles. Chinese Physics B, 2012, 21, 077502.	0.7	14

#	Article	IF	Citations
13343	First-principles study of the adsorption of oxygen atoms on copper nanowires. Science China: Physics, Mechanics and Astronomy, 2012, 55, 413-418.	2.0	6
13344	The structural, electronic and magnetic properties of the 3d TM (V, Cr, Mn, Fe, Co, Ni and Cu) doped ZnO nanotubes: A first-principles study. Science China: Physics, Mechanics and Astronomy, 2012, 55, 428-435.	2.0	20
13345	Modulation of the electronic and magnetic properties of a GaN nanoribbon from dangling bonds. Science China: Physics, Mechanics and Astronomy, 2012, 55, 631-638.	2.0	6
13346	Stability and diffusion properties of self-interstitial atoms in tungsten: a first-principles investigation. Science China: Physics, Mechanics and Astronomy, 2012, 55, 614-618.	2.0	21
13347	AbÂInitio Studies of the Unreconstructed Polar CdTe (111) Surface. Journal of Electronic Materials, 2012, 41, 2745-2753.	1.0	13
13348	Elastic Coefficients of Zn1â^'x Be x O Solid Solutions: a First-Principles Study. Journal of Electronic Materials, 2012, 41, 3007-3012.	1.0	6
13349	First-principles investigation of cohesive energy and electronic structure in vanadium phosphides. Journal of Central South University, 2012, 19, 1796-1801.	1.2	10
13350	Structural transitions of tin clusters: Snn (n=34â€“44). Chemical Physics Letters, 2012, 552, 69-72.	1.2	5
13351	Magnesium amidoborane monoammoniate: Plane-wave DFT calculations. Chemical Physics Letters, 2012, 545, 26-28.	1.2	1
13352	Mobile effect of hydrogen on intergranular decohesion of iron: first-principles calculations. Philosophical Magazine, 2012, 92, 1349-1368.	0.7	67
13353	Ferromagnetism and manipulation of topological surface states in Bi2Se3 family by 2p light elements. Applied Physics Letters, 2012, 100, .	1.5	10
13354	Coadsorption properties of CO2 and H2O on TiO2 rutile (110): A dispersion-corrected DFT study. Journal of Chemical Physics, 2012, 137, 074704.	1.2	63
13355	Oxygen vacancy segregation and space-charge effects in grain boundaries of dry and hydrated BaZrO3. Applied Physics Letters, 2012, 100, .	1.5	52
13356	First-principles theoretical analysis of transition-metal doping of ZnSe quantum dots. Journal of Applied Physics, 2012, 112, 024301.	1.1	3
13357	Thermodynamic instability of ZnSe/ZnS core/shell quantum dots. Journal of Applied Physics, 2012, 111, 113526.	1.1	9
13358	Transport properties of hybrid graphene/graphane nanoribbons. Applied Physics Letters, 2012, 100, 103109.	1.5	10
13359	Magnetic moment of a single vacancy in graphene and semiconducting nanoribbons. Physical Review B, 2012, 86, .	1.1	45
13360	Average atom transport properties for pure and mixed species in the hot and warm dense matter regimes. Physics of Plasmas, 2012, 19, .	0.7	46

#	Article	IF	Citations
13361	Electronic Structure of the CuCl₂(100) Surface: A DFT First-Principle Study. Journal of Nanomaterials, 2012, 2012, 1-7.	1.5	5
13362	Early stages in the degradation of metalâ€“organic frameworks in liquid water from first-principles molecular dynamics. Physical Chemistry Chemical Physics, 2012, 14, 7240.	1.3	52
13363	Physical mechanisms for the unique optical properties of chalcogen-hyperdoped silicon. Europhysics Letters, 2012, 99, 46005.	0.7	37
13364	Simultaneous Control of Ionic and Electronic Conductivity in Materials: Thallium Bromide Case Study. Physical Review Letters, 2012, 108, 246604.	2.9	13
13365	Ab initio many-body study of the electronic and optical properties of MgAl2O4 spinel. Journal of Applied Physics, 2012, 111, .	1.1	27
13366	Reaction mechanisms of oxygen plasma interaction with organosilicate low-k materials containing organic crosslinking groups. Journal of Vacuum Science and Technology A: Vacuum, Surfaces and Films, 2012, 30, .	0.9	11
13367	Air-Protected Epitaxial Graphene/Ferromagnet Hybrids Prepared by Chemical Vapor Deposition and Intercalation. Journal of Physical Chemistry Letters, 2012, 3, 2059-2063.	2.1	54
13368	Strain-assisted bandgap modulation in Zn based II-VI semiconductors. Applied Physics Letters, 2012, 100, .	1.5	38
13369	Structural rotation of Al under uniaxial compression: A first-principles prediction. Journal of Applied Physics, 2012, 112, .	1.1	4
13370	Band gap engineering of silicene zigzag nanoribbons with perpendicular electric fields: a theoretical study. Journal of Physics Condensed Matter, 2012, 24, 455302.	0.7	33
13371	Magnetic structure and ferroelectric activity in orthorhombic YMnO3: Relative roles of magnetic symmetry breaking and atomic displacements. Physical Review B, 2012, 86, .	1.1	18
13372	Site preference and effect of alloying on elastic properties of ternary<mml:math xmlns:mml="http://www.w3.org/1998/Math/MathML" display="inline"><mml:mi>B</mml:mi></mml:math>2 NiAl-based alloys. Physical Review B, 2012, 85, .	1.1	53
13373	Quasiparticle and optical spectroscopy of the organic semiconductors pentacene and PTCDA from first principles. Physical Review B, 2012, 85, .	1.1	181
13374	Direct writing of electronic devices on graphene oxide by catalytic scanning probe lithography. Nature Communications, 2012, 3, 1194.	5.8	85
13375	First-principles calculations of the magnetic anisotropic constants of Coâ€“Pd multilayers: Effect of stacking faults. Europhysics Letters, 2012, 99, 17001.	0.7	6
13376	Multiferroics: theory, mechanisms, and materials. Science and Technology of Atomic, Molecular, Condensed Matter and Biological Systems, 2012, 2, 129-161.	0.6	2
13377	Hydration and proton conductivity in LaAsO₄. Journal of Materials Chemistry, 2012, 22, 1652-1661.	6.7	29
13379	n-type doping in Cu2O with F, Cl, and Br: A first-principles study. Journal of Applied Physics, 2012, 111, .	1.1	31

#	Article	IF	Citations
13380	Strength, hardness, and lattice vibrations of<mml:math xmlns:mml="http://www.w3.org/1998/Math/MathML" display="inline"><mml:mi>Z</mml:mi></mml:math>-carbon and<mml:math xmlns:mml="http://www.w3.org/1998/Math/MathML" display="inline"><mml:mi>W</mml:mi></mml:math>-carbon: First-principles calculations. Physical Review B, 2012, 85, .	1.1	51
13381	New Insight into the Atomic Structure of Electrochemically Delithiated O3-Li_(1â€“x)CoO₂ (0 â‰¤ x â‰¤ 0.5) Nanoparticles. Nano Letters, 2012, 12, 6192-6197.	12.5	128
13382	Ab initio and classical simulation of the defect formation in sapphire. Russian Metallurgy (Metally), 2012, 2012, 879-883.	0.1	1
13383	The electronic property of graphene adsorbed on the siloxane and silanol surface structures of SiO2: A theoretical prediction. Applied Physics Letters, 2012, 101, .	1.5	10
13384	Hydrogenated graphene: Structures and surface work function. , 2012, , .		2
13385	Why the Band Gap of Graphene Is Tunable on Hexagonal Boron Nitride. Journal of Physical Chemistry C, 2012, 116, 3142-3146.	1.5	103
13386	Multiferroic Materials Based on Organic Transition-Metal Molecular Nanowires. Journal of the American Chemical Society, 2012, 134, 14423-14429.	6.6	49
13387	Probing oxygen vacancy concentration and homogeneity in solid-oxide fuel-cell cathode materials on the subunit-cell level. Nature Materials, 2012, 11, 888-894.	13.3	282
13388	Ab initio investigations of the electronic structure and lithium stability in Li2UN2 and LiUN2. Monatshefte FÃ¼r Chemie, 2012, 143, 1341-1348.	0.9	2
13389	First-Principles Calculations on Stabilization of Iron Carbides (Fe3C, Fe5C2, and Î·-Fe2C) in Steels by Common Alloying Elements. Metallurgical and Materials Transactions A: Physical Metallurgy and Materials Science, 2012, 43, 4436-4444.	1.1	52
13390	Understanding the Interface Dipole of Copper Phthalocyanine (CuPc)/C₆₀: Theory and Experiment. Journal of Physical Chemistry Letters, 2012, 3, 2173-2177.	2.1	63
13391	Excellent Catalytic Effects of Graphene Nanofibers on Hydrogen Release of Sodium alanate. Journal of Physical Chemistry C, 2012, 116, 10861-10866.	1.5	33
13392	CO Oxidation Mechanism on CeO₂-Supported Au Nanoparticles. Journal of the American Chemical Society, 2012, 134, 1560-1570.	6.6	496
13393	Raman spectra of titanium dioxide (anatase, rutile) with identified oxygen isotopes (16, 17, 18). Physical Chemistry Chemical Physics, 2012, 14, 14567.	1.3	417
13394	Quantum chemical modeling of the structure formation and proton transfer in 2-hydroxybenzenesulfonic, 4-hydroxy-1,3-benzenedisulfonic, and 1,3-benzenedisulfonic acids. Russian Chemical Bulletin, 2012, 61, 1521-1530.	0.4	9
13395	Formation of native defects in the Î³-ray detector material Cs2Hg6S7. Applied Physics Letters, 2012, 101, .	1.5	11
13396	Wavefunction-based electron correlation methods for solids. Physical Chemistry Chemical Physics, 2012, 14, 7605.	1.3	79
13397	Comparative theoretical studies of high pressure effect on polymorph I of 2,2â€²,4,4â€²,6,6â€²-hexanitroazobenzene crystal. Structural Chemistry, 2012, 23, 1631-1642.	1.0	4

#	Article	IF	Citations
13398	Diffusion behaviors of hydrogen isotopes in niobium from first-principles. Science China: Physics, Mechanics and Astronomy, 2012, 55, 2378-2382.	2.0	5
13399	DFT Study of Furfural Conversion to Furan, Furfuryl Alcohol, and 2-Methylfuran on Pd(111). ACS Catalysis, 2012, 2, 2496-2504.	5.5	232
13400	High-pressure structures and metallization of sodium chloride. Europhysics Letters, 2012, 100, 26005.	0.7	16
13401	Crystal and electronic structures of CuxS solar cell absorbers. Applied Physics Letters, 2012, 100, .	1.5	105
13402	Interface enhancement of spin-polar phonon coupling in perovskite multiferroic superlattices. Europhysics Letters, 2012, 100, 17005.	0.7	7
13403	Route to high NÃ©el temperatures in 4<mml:math xmlns:mml="http://www.w3.org/1998/Math/MathML" display="inline"><mml:mi>d</mml:mi></mml:math>and 5<mml:math xmlns:mml="http://www.w3.org/1998/Math/MathML" display="inline"><mml:mi>d</mml:mi></mml:math>transition metal oxides. Physical Review B, 2012, 86, .	1.1	24
13404	Theoretical prediction of impurity effects on the internally oxidized metal/oxide interface: the case study of S on Cu/Al2O3. Physical Chemistry Chemical Physics, 2012, 14, 11178.	1.3	24
13405	Theoretical Study of Magnesium and Zinc Tantalates and Niobates as Prospective Catalyst Supports for Water Electrolysis. Journal of the Electrochemical Society, 2012, 159, F607-F616.	1.3	5
13406	Solubility and clustering of ruthenium fission products in uranium dioxide as determined by density functional theory. Physical Review B, 2012, 85, .	1.1	15
13407	Calculations of the thermodynamic and kinetic properties of Li<mml:math xmlns:mml="http://www.w3.org/1998/Math/MathML" display="inline"><mml:msub><mml:mrow /><mml:mrow><mml:mn>1</mml:mn><mml:mo>+</mml:mo><mml:mi>x</mml:mi></mml:mrow></mml:msub></mml:math>V<mml:math xmlns:mml="http://www.w3.org/1998/Math/MathML" display="inline"><mml:msub><mml:mrow /><mml:mn>3</mml:mn></mml:msub></mml:math>O<mml:math xmlns:mml="http://www.w3.org/1998/Math/MathML" display="inline"><mml:msub><mml:mrow /><mml:mn	1.1	16
13408	Computational design of low-band-gap double perovskites. Physical Review B, 2012, 86, .	1.1	70
13409	Mechanisms for the decomposition and dehydrogenation of Li amide/imide. Physical Review B, 2012, 85, .	1.1	27
13410	Ferrimagnetism, antiferromagnetism, and magnetic frustration in La<mml:math xmlns:mml="http://www.w3.org/1998/Math/MathML" display="inline"><mml:msub><mml:mrow /><mml:mrow><mml:mn>2</mml:mn><mml:mo>âˆ’</mml:mo><mml:mi>x</mml:mi></mml:mrow></mml:msub></mml:math>Sr<mml:math xmlns:mml="http://www.w3.org/1998/Math/MathML" display="inline"><mml:msub><mml:mrow /><mml:mi>x</mml:mi></mml:msub></mml:math>CuRuO<mml:math xmlns:mml="http://www.w3.org/1998/Math/MathML" display="inline"><mml:msub><mml:mrow /><mml:mn	1.1	20
13411	Electronic structure of Pb<mml:math xmlns:mml="http://www.w3.org/1998/Math/MathML" display="inline"><mml:msub><mml:mrow /><mml:mn>2</mml:mn></mml:msub></mml:math>Se<mml:math xmlns:mml="http://www.w3.org/1998/Math/MathML" display="inline"><mml:msub><mml:mrow /><mml:mn>3</mml:mn></mml:msub></mml:math>induced by the quantum size effects of Pb adlayers. Physical Review B, 2012, 86, .	1.1	19
13412	Electronic surface compensation of polarization in PbTiO3 films. Journal of Applied Physics, 2012, 112, .	1.1	16
13413	VO<mml:math xmlns:mml="http://www.w3.org/1998/Math/MathML" display="inline"><mml:msub><mml:mrow /><mml:mn>2</mml:mn></mml:msub></mml:math>: Orbital competition, magnetism, and phase stability. Physical Review B, 2012, 86, .	1.1	53
13414	Water Adsorption and Its Effect on the Stability of Low Index Stoichiometric and Reduced Surfaces of Ceria. Journal of Physical Chemistry C, 2012, 116, 7073-7082.	1.5	204
13415	Role of lone pair electrons in determining the optoelectronic properties of BiCuOSe. Physical Review B, 2012, 85, .	1.1	42

#	Article	IF	Citations
13416	First-Principles Assessment of H₂S and H₂O Reaction Mechanisms and the Subsequent Hydrogen Absorption on the CeO₂(111) Surface. Journal of Physical Chemistry C, 2012, 116, 2411-2424.	1.5	101
13417	Titanium and magnesium Co-alloyed hematite thin films for photoelectrochemical water splitting. Journal of Applied Physics, 2012, 111, 073502.	1.1	30
13419	First-Principles Optical Spectra for<mml:math xmlns:mml="http://www.w3.org/1998/Math/MathML" display="inline"><mml:mi>F</mml:mi></mml:math>Centers in MgO. Physical Review Letters, 2012, 108, 126404.	2.9	157
13420	Electronic and magnetic properties of La2NiMnO6 and La2CoMnO6 with cationic ordering. Applied Physics Letters, 2012, 100, .	1.5	61
13421	Quantum Tunneling of Magnetization in Ultrasmall Half-Metallic V3O4 Quantum Dots: Displaying Quantum Superparamagnetic State. Scientific Reports, 2012, 2, 755.	1.6	25
13422	First-Principles Calculations of Luminescence Spectrum Line Shapes for Defects in Semiconductors: The Example of GaN and ZnO. Physical Review Letters, 2012, 109, 267401.	2.9	187
13423	First-principles study of the SiN<mml:math xmlns:mml="http://www.w3.org/1998/Math/MathML" display="inline"><mml:msub><mml:mrow /><mml:mi>x</mml:mi></mml:msub></mml:math>/TiN(001) interface. Physical Review B, 2012, 85, .	1.1	17
13424	First-principles study of shear behavior of Al, TiN, and coherent Al/TiN interfaces. Journal of Applied Physics, 2012, 111, .	1.1	21
13425	Lithium Lanthanum Titanium Oxides: A Fast Ionic Conductive Coating for Lithium-Ion Battery Cathodes. Chemistry of Materials, 2012, 24, 2744-2751.	3.2	115
13426	First-principles study of the local structure and crystal field of Yb 2+ in sodium and potassium halides. Chinese Physics B, 2012, 21, 037102.	0.7	1
13427	Clustering of N impurities in ZnO. Applied Physics Letters, 2012, 100, 022107.	1.5	18
13428	Magnetic states and optical properties of single-layer carbon-doped hexagonal boron nitride. Applied Physics Letters, 2012, 100, .	1.5	74
13429	On the possibility of p-type SnO2. Journal of Materials Chemistry, 2012, 22, 25236.	6.7	154
13430	First-principles study of interstitial diffusion of oxygen in nickel chromium binary alloy. Applied Physics Letters, 2012, 100, 131904.	1.5	16
13431	Electronic structures of zigzag SiC nanoribbons with asymmetric hydrogen-terminations. Applied Physics Letters, 2012, 101, 013102.	1.5	42
13432	Electronic Properties of Graphene Altered by Substrate Surface Chemistry and Externally Applied Electric Field. Journal of Physical Chemistry C, 2012, 116, 6259-6267.	1.5	28
13433	Edge stresses of non-stoichiometric edges in two-dimensional crystals. Applied Physics Letters, 2012, 100, .	1.5	21
13434	Bimetallic IrNi core platinum monolayer shell electrocatalysts for the oxygen reduction reaction. Energy and Environmental Science, 2012, 5, 5297-5304.	15.6	156

#	Article	IF	Citations
13435	Multiple hydrogen trapping at monovacancies. Philosophical Magazine Letters, 2012, 92, 217-225.	0.5	22
13436	Ab initioparametrized model of strain-dependent solubility of H in Î±-iron. Modelling and Simulation in Materials Science and Engineering, 2012, 20, 035011.	0.8	5
13437	High precision electronic charge density determination for L1₀-ordered Î³-TiAl by quantitative convergent beam electron diffraction. Philosophical Magazine, 2012, 92, 4408-4424.	0.7	3
13438	Reversal of atomic contrast in scanning probe microscopy on (111) metal surfaces. Journal of Physics Condensed Matter, 2012, 24, 084003.	0.7	15
13439	Water Dissociation on Bimetallic Surfaces: General Trends. Journal of Physical Chemistry C, 2012, 116, 10120-10128.	1.5	32
13440	First-Principles Study of CO Adsorption and Oxidation on Ru-Doped CeO₂(111) Surface. Journal of Physical Chemistry C, 2012, 116, 6239-6246.	1.5	90
13441	Ordered Semiconducting Nitrogen-Graphene Alloys. Physical Review X, 2012, 2, .	2.8	50
13442	A Combined Experimental-Computational Study on the Effect of Topology on Carbon Dioxide Adsorption in Zeolitic Imidazolate Frameworks. Journal of Physical Chemistry C, 2012, 116, 24084-24090.	1.5	112
13443	Desorption of n-alkanes from graphene: a van der Waals density functional study. Journal of Physics Condensed Matter, 2012, 24, 424212.	0.7	27
13444	Covalency, double-counting, and the metal-insulator phase diagram in transition metal oxides. Physical Review B, 2012, 86, .	1.1	66
13445	Pressure and Temperature Control of Spin-Switchable Metal-Organic Coordination Polymers fromAbÂInitioCalculations. Physical Review Letters, 2012, 109, 077203.	2.9	38
13446	Selective nucleation induced by defect nanostructures: A way to control cobalt disilicide precipitation during ion implantation. Journal of Applied Physics, 2012, 112, 123504.	1.1	6
13447	Ab initiostudy of neutral (TiO₂)_nclusters and their interactions with water and transition metal atoms. Journal of Physics Condensed Matter, 2012, 24, 305301.	0.7	27
13448	Magnetism of Cr-doped ZnO with intrinsic defects. Journal of Applied Physics, 2012, 111, .	1.1	11
13449	Magnetism in transition-metal-doped ZnO: A first-principles study. Journal of Applied Physics, 2012, 112, .	1.1	31
13450	Surface Charge Transfer Induced Ferromagnetism in Nanostructured ZnO/Al. Journal of Physical Chemistry C, 2012, 116, 8541-8547.	1.5	15
13451	Kinetically Controlled Lithium-Staging in Delithiated LiFePO₄ Driven by the Fe Center Mediated Interlayer Liâ€“Li Interactions. Chemistry of Materials, 2012, 24, 4693-4703.	3.2	59
13452	Dissociative Hydrogen Adsorption on Close-Packed Cobalt Nanoparticle Surfaces. Journal of Physical Chemistry C, 2012, 116, 25868-25873.	1.5	35

#	Article	IF	Citations
13453	New Crystal Structures of IrB and IrB₂: First-Principles Calculations. Journal of Physical Chemistry C, 2012, 116, 21961-21966.	1.5	19
13454	Electronic shell structure in Ga12 icosahedra and the relation to the bulk forms of gallium. Physical Chemistry Chemical Physics, 2012, 14, 9912.	1.3	20
13455	ELECTRONIC, MAGNETIC, AND MECHANICAL PROPERTIES OF LINE-DEFECT EMBEDDED GRAPHENE NANORIBBONS: A FIRST-PRINCIPLES STUDY. Nano LIFE, 2012, 02, 1240003.	0.6	4
13456	Tunable ferromagnetism in assembled two dimensional triangular graphene nanoflakes. Physical Chemistry Chemical Physics, 2012, 14, 2065.	1.3	24
13457	Lithium Amide (LiNH₂) Under Pressure. Journal of Physical Chemistry A, 2012, 116, 10027-10036.	1.1	17
13458	Physical properties of thermoelectric zinc antimonide using first-principles calculations. Physical Review B, 2012, 85, .	1.1	59
13459	Surface Studies of Catalysis by Metals: Nanosize and Alloying Effects. Engineering Materials, 2012, , 369-404.	0.3	12
13460	Structural evolution of single-layer films during deposition of silicon on silver: a first-principles study. Journal of Physics Condensed Matter, 2012, 24, 442001.	0.7	38
13461	SOLUBILITY OF WATER ICE IN METALLIC HYDROGEN: CONSEQUENCES FOR CORE EROSION IN GAS GIANT PLANETS. Astrophysical Journal, 2012, 745, 54.	1.6	128
13462	Electronic Structure of Spatially Aligned Graphene Nanoribbons on Au(788). Physical Review Letters, 2012, 108, 216801.	2.9	212
13463	Donor Characteristics of Transition-Metal-Doped Oxides: Cr-Doped MgO versus Mo-Doped CaO. Journal of the American Chemical Society, 2012, 134, 11380-11383.	6.6	90
13464	Elastic and electronic properties of tI26-type Mg₁₂RE (RE = Ce, Pr and Nd) phases. Modelling and Simulation in Materials Science and Engineering, 2012, 20, 035018.	0.8	50
13465	Equation of State for Shock Compressed Xenon in the Ionization Regime: ab Initio Study. Communications in Theoretical Physics, 2012, 58, 160-164.	1.1	1
13466	Rationale for switching to nonlocal functionals in density functional theory. Journal of Physics Condensed Matter, 2012, 24, 424215.	0.7	18
13467	Nanotube-based scanning rotational microscope. Applied Physics Letters, 2012, 100, 173101.	1.5	8
13468	Highly Flexible Molecule â€œChameleonâ€• Reversible Thermochromism and Phase Transitions in Solid Copper(II) Diiminate Cu[CF3â€”C(NH)â€”CFâ•C(NH)â€”CF3]2. Inorganic Chemistry, 2012, 51, 10590-10602.	1.9	19
13469	Role of Si as carrier suppressor in amorphous Znâ€“Snâ€“O. Current Applied Physics, 2012, 12, S12-S16.	1.1	36
13470	Diverse Closed Cavities in Condensed Rare Earth Metalâ€“Chalcogenide Matrixes: Cs[Lu₇Q₁₁] and (ClCs₆)[RE₂₁Q₃₄] (RE =) Tj ETQq1 1 0.784314 rg	3.1	44

#	Article	IF	Citations
13471	Nucleation of Rh_n (n = 1â€“5) Clusters on Î³-Al₂O₃ Surfaces: A Density Functional Theory Study. Journal of Physical Chemistry C, 2012, 116, 10623-10631.	1.5	45
13472	Atomic structure and magnetic properties of Fe1â€“xCox alloys. Journal of Applied Physics, 2012, 111, 07E338.	1.1	19
13473	Optical Properties of Gallium Oxide Clusters from First-Principles Calculations. Journal of Physical Chemistry A, 2012, 116, 10559-10565.	1.1	11
13474	Making Sense of Boron-Rich Binary Beâ€“B Phases. Inorganic Chemistry, 2012, 51, 9066-9075.	1.9	20
13475	First-principles calculation of magnetoelastic coefficients and magnetostriction in the spinel ferrites CoFe<mml:math xmlns:mml="http://www.w3.org/1998/Math/MathML" display="inline"><mml:msub><mml:mrow /><mml:mn>2</mml:mn></mml:msub></mml:math>O<mml:math xmlns:mml="http://www.w3.org/1998/Math/MathML" display="inline"><mml:msub><mml:mrow /><mml:mn>4</mml:mn></mml:msub></mml:math>and NiFe<mml:math xmlns:mml="http://www.w3.org/1	1.1	103
13476	Structural characterization of amorphous YCrO 3 from first principles. Europhysics Letters, 2012, 99, 57010.	0.7	3
13477	Heteroatomic Effects on Charge-Transfer Mobility of Dianthra[2,3-b:2â€²,3â€²-f]thieno[3,2-b]thiophene (DATT) and Its Derivatives. Journal of Physical Chemistry C, 2012, 116, 19197-19202.	1.5	30
13478	Application of Pt Nanoparticle Dissolution and Oxidation Modeling to Understanding Degradation in PEM Fuel Cells. Journal of the Electrochemical Society, 2012, 159, B578-B591.	1.3	79
13479	Soft phonon mode coupled with antiferromagnetic order in incipient-ferroelectric Mott insulators Sr<mml:math xmlns:mml="http://www.w3.org/1998/Math/MathML" display="inline"><mml:msub><mml:mrow /><mml:mn>1</mml:mn><mml:mo>â^’</mml:mo><mml:mi>x</mml:mi></mml:mrow></mml:msub></mml:math>Ba<mml:math xmlns:mml="http://www.w3.org/1998/Math/MathML" display="inline"><mml:msub><mml:mrow />	1.1	35
13480	Spin-lattice coupling and phonon dispersion in orthorhombic <mml:math xmlns:mml="http://www.w3.org/1998/Math/MathML" display="inline"><mml:msub><mml:mrow /><mml:mn>2</mml:mn></mml:msub></mml:math>O<mml:math xmlns:mml="http://www.w3.org/1998/Math/MathML" display="inline"><mml:msub><mml:mrow /><mml:mn>4</mml:mn></mml:msub></mml:math> from first principles. Physical Review B, 2012, 86, .	1.1	25
13481	Hybrid functional study of the elastic and structural properties of wurtzite and zinc-blende group-III nitrides. Physical Review B, 2012, 86, .	1.1	39
13482	First-principles investigation of pressure-induced phase transition in LiNbO3. Journal of Applied Physics, 2012, 111, .	1.1	7
13483	Noncollinear magnetism and single-ion anisotropy in multiferroic perovskites. Physical Review B, 2012, 86, .	1.1	88
13484	First-Principles Study of the Effect of Organic Ligands on the Crystal Structure of CdS Nanoparticles. Journal of Physical Chemistry C, 2012, 116, 6507-6511.	1.5	22
13485	Spin-splitting calculation for zincblende semiconductors using an atomic bond-orbital model. Journal of Physics Condensed Matter, 2012, 24, 415802.	0.7	1
13486	Growth mechanisms of ZnO(0001) investigated using the first-principles calculation. Journal of Applied Physics, 2012, 112, 064301.	1.1	4
13487	Intriguing Behavior of Halogenated Two-Dimensional Tin. Journal of Physical Chemistry C, 2012, 116, 12977-12981.	1.5	54
13488	Isobutene Protonation in H-FAU, H-MOR, H-ZSM-5, and H-ZSM-22. Journal of Physical Chemistry C, 2012, 116, 18236-18249.	1.5	44

#	Article	IF	Citations
13489	Electronic structure mechanism of martensitic phase transformation in binary titanium alloys. Journal of Applied Physics, 2012, 112, 123718.	1.1	23
13490	Ideal tensile and shear strength of a gum metal approximant:Ab initiodensity functional calculations. Physical Review B, 2012, 85, .	1.1	19
13491	Pressure-induced phase transitions and structure of chemically ordered nanoregions in the lead-free relaxor ferroelectric Na<mml:math xmlns:mml="http://www.w3.org/1998/Math/MathML" display="inline"><mml:msub><mml:mrow /><mml:mrow><mml:mn>1</mml:mn><mml:mo>/</mml:mo><mml:mn>2</mml:mn></mml:mrow></mml:msub></mml:math>Bi<mml:math xmlns:mml="http://www.w3.org/1998/Math/MathML" display="inline"><mml:msub><mml:mrow /><mml:mrow><mml:mn>1</mml:mn><mml:mo>/</mml:mo><mml:mn>2</mml:mn></mml:mrow></mml:msub></mml:math>.	1.1	32
13492	Role of Defects in the Phase Transition of VO₂ Nanoparticles Probed by Plasmon Resonance Spectroscopy. Nano Letters, 2012, 12, 780-786.	4.5	196
13493	Formation of an intermediate band in isoreticular metalâ€“organic framework-993 (IRMOF-993) and metal-substituted analogues M-IRMOF-993. Journal of Materials Chemistry, 2012, 22, 16324.	6.7	37
13494	Ab Initio Thermodynamic Study of the CO2Capture Properties of Potassium Carbonate Sesquihydrate, K2CO3Â·1.5H2O. Journal of Physical Chemistry C, 2012, 116, 14461-14470.	1.5	36
13495	First-Principles Study of Lithium Adsorption and Diffusion on Graphene with Point Defects. Journal of Physical Chemistry C, 2012, 116, 21780-21787.	1.5	256
13496	First-principles calculations of interfacial and segregation energies in Î±-Cr₂O₃. Journal of Physics Condensed Matter, 2012, 24, 225001.	0.7	6
13497	Temperature-dependent ideal strength and stacking fault energy of fcc Ni: a first-principles study of shear deformation. Journal of Physics Condensed Matter, 2012, 24, 155402.	0.7	64
13498	Optical properties of Al-doped CuInSe2 from the first principle calculation. Physica B: Condensed Matter, 2012, 407, 4814-4818.	1.3	15
13499	Diffusion of hydrogen within idealized grains of bcc Fe: A kinetic Monte Carlo study. Physical Review B, 2012, 86, .	1.1	59
13500	What causes high resistivity in CdTe. New Journal of Physics, 2012, 14, 063020.	1.2	57
13501	A first-principles approach to transition states of diffusion. Journal of Physics Condensed Matter, 2012, 24, 305402.	0.7	9
13502	Trends in Selective Hydrogen Peroxide Production on Transition Metal Surfaces from First Principles. ACS Catalysis, 2012, 2, 2664-2672.	5.5	137
13503	The role of surface defects in large organic molecule adsorption: substrate configuration effects. Physical Chemistry Chemical Physics, 2012, 14, 10726.	1.3	19
13504	Local suppression of ferroelectricity at PbTiO₃surface steps: a density functional theory study. Journal of Physics Condensed Matter, 2012, 24, 045903.	0.7	9
13505	Theoretical prediction of mechanical stability of ferromagnetic fcc Fe-Cu alloys from first principles. Journal of Applied Physics, 2012, 111, 053517.	1.1	11
13506	Bifunctional Mixed-Lanthanide Cyano-Bridged Coordination Polymers Ln0.5Lnâ€²0.5(H2O)5[W(CN)8] (Ln/Lnâ€²) Tj ETQq1 1 0.7843	1.9	41

#	Article	IF	Citations
13507	Synthesis, Crystal Structure and Magnetic Properties of the New One-Dimensional Manganate Cs3Mn2O4. Journal of the American Chemical Society, 2012, 134, 11734-11739.	6.6	9
13508	Adsorption Equilibria of CO Coverage on Î²-Mo₂C Surfaces. Journal of Physical Chemistry C, 2012, 116, 6340-6348.	1.5	53
13509	Combined Scanning Tunneling Microscopy and High-Resolution Electron Energy Loss Spectroscopy Study on the Adsorption State of CO on Ag(001). Langmuir, 2012, 28, 13249-13252.	1.6	7
13510	Vacancy-driven ferromagnetism in ferroelectric PbTiO₃. Applied Physics Letters, 2012, 100, 162901.	1.5	61
13511	Highly Active Pt₃Pb and Coreâ€“Shell Pt₃Pbâ€“Pt Electrocatalysts for Formic Acid Oxidation. ACS Nano, 2012, 6, 2818-2825.	7.3	177
13512	Electrooxidation of Methanol at SnO_xâ€“Pt Interface: A Tunable Activity of Tin Oxide Nanoparticles. Journal of Physical Chemistry Letters, 2012, 3, 3286-3290.	2.1	44
13513	Ab Initio Study of Advanced Metallic Nuclear Fuels for Fast Breeder Reactors. Materials Research Society Symposia Proceedings, 2012, 1444, 67.	0.1	3
13514	Strain-induced changes to the electronic structure of germanium. Journal of Physics Condensed Matter, 2012, 24, 195802.	0.7	67
13515	Carbon allotropes with triple bond predicted by first-principle calculation: Triple bond modified diamond and<mml:math xmlns:mml="http://www.w3.org/1998/Math/MathML" display="inline"><mml:mrow><mml:mi>T</mml:mi></mml:mrow></mml:math>-carbon. Physical Review B, 2012, 86, .	1.1	72
13516	Lowest enthalpy polymorph of cold-compressed graphite phase. Physical Chemistry Chemical Physics, 2012, 14, 4347.	1.3	80
13517	Superhard F-carbon predicted byab initioparticle-swarm optimization methodology. Journal of Physics Condensed Matter, 2012, 24, 165504.	0.7	42
13518	Identifying a Structural Preference in Reduced Rare-Earth Metal Halides by Combining Experimental and Computational Techniques. Inorganic Chemistry, 2012, 51, 11356-11364.	1.9	29
13520	Near-infrared luminescent cubic silicon carbide nanocrystals for in vivo biomarker applications: an ab initio study. Nanoscale, 2012, 4, 7720.	2.8	39
13521	Structural investigation of aluminium doped ZnO nanoparticles by solid-state NMR spectroscopy. Physical Chemistry Chemical Physics, 2012, 14, 11610.	1.3	60
13522	Giant piezoelectric resistance effect of nanoscale zinc oxide tunnel junctions: first principles simulations. Physical Chemistry Chemical Physics, 2012, 14, 7051.	1.3	14
13523	Electronic Spectra and Crystal Field Analysis of Tb3+in Cs2NaTb(NO2)6: Tb3+Situated at a Site ofThSymmetry. Journal of Physical Chemistry C, 2012, 116, 12764-12771.	1.5	3
13524	Tetragonal Allotrope of Group 14 Elements. Journal of the American Chemical Society, 2012, 134, 12362-12365.	6.6	170
13525	Revealing the Surface Reactivity of Zirconia by Periodic DFT Calculations. Journal of Physical Chemistry C, 2012, 116, 6636-6644.	1.5	58

#	Article	IF	Citations
13526	Effect of Indium Doping of Î³-Alumina on the Stabilization of PtSn Alloyed Clusters Prepared by Surface Organostannic Chemistry. Journal of Physical Chemistry C, 2012, 116, 10073-10083.	1.5	25
13527	Mechanical properties of graphdiyne sheet. Physica B: Condensed Matter, 2012, 407, 4436-4439.	1.3	112
13528	Effects of alloying elements and temperature on the elastic properties of dilute Ni-base superalloys from first-principles calculations. Journal of Applied Physics, 2012, 112, .	1.1	77
13529	Electrical and thermal conductivity of Al liquid at high pressures and temperatures fromab initiocomputations. Physical Review B, 2012, 85, .	1.1	37
13530	Stability of Graphene Edges under Electron Beam: Equilibrium Energetics versus Dynamic Effects. ACS Nano, 2012, 6, 671-676.	7.3	120
13531	Activation of Surface Hydroxyl Groups by Modification of H-Terminated Si(111) Surfaces. Journal of the American Chemical Society, 2012, 134, 8869-8874.	6.6	68
13532	On the stability of single-walled carbon nanotubes and their binding strengths. Theoretical Chemistry Accounts, 2012, 131, 1.	0.5	7
13533	High-pressure studies on azido-tetrazole chainâ€“ring conversion in crystalline 2-azido-4,6-dichloro-1,3,5-triazine. Theoretical Chemistry Accounts, 2012, 131, 1.	0.5	2
13534	Ab initio investigation of the structural stability and optical properties of low-density amorphous carbon doped with N, B, and Fe. Theoretical Chemistry Accounts, 2012, 131, 1.	0.5	1
13535	Electrical transport properties of Co-based skutterudites filled with Ag and Au. Physical Review B, 2012, 86, .	1.1	15
13536	Thermodynamic properties of neptunium nitride: a first principles study. Journal of Nuclear Science and Technology, 2012, 49, 328-333.	0.7	6
13537	Ab initiotheory of phase stability and structural selectivity in Fe-Pd alloys. Physical Review B, 2012, 85, .	1.1	36
13538	Silicene structures on silver surfaces. Journal of Physics Condensed Matter, 2012, 24, 314211.	0.7	141
13539	Exotic Topological Insulator States and Topological Phase Transitions in Sb2Se3â€“Bi2Se3 Heterostructures. ACS Nano, 2012, 6, 2345-2352.	7.3	56
13540	A systematic study of polarons due to oxygen vacancy formation at the rutile TiO₂(110) surface by GGA +Uand HSE06 methods. Journal of Physics Condensed Matter, 2012, 24, 435504.	0.7	63
13541	Electronic structures of an epitaxial graphene monolayer on SiC(0001) after metal intercalation (metalâ€‰=â€‰Al, Ag, Au, Pt, and Pd): A first-principles study. Applied Physics Letters, 2012, 100, 063115.	1.5	28
13542	Dislocations and Grain Boundaries in Two-Dimensional Boron Nitride. ACS Nano, 2012, 6, 7053-7058.	7.3	216
13543	Chemical bonding, conductive network, and thermoelectric performance of the ternary semiconductors Cu<mml:math xmlns:mml="http://www.w3.org/1998/Math/MathML" display="inline"><mml:msub><mml:mrow /><mml:mn>2</mml:mn></mml:msub></mml:math>Sn<mml:math xmlns:mml="http://www.w3.org/1998/Math/MathML"		

#	Article	IF	Citations
13544	Formation of Perpendicular Graphene Nanosheets on LiFePO₄: A First-Principles Characterization. Journal of Physical Chemistry C, 2012, 116, 17650-17656.	1.5	28
13545	Lateral in-plane coupling between graphene nanoribbons: A density functional study. Journal of Applied Physics, 2012, 111, 043714.	1.1	2
13546	Polyoxometalates adsorbed on metallic surfaces: immediate reduction of [SiW12O40]4â^' on Ag(100). Chemical Science, 2012, 3, 2020.	3.7	32
13547	First-Principles Study on Structural Properties and 4f â†' 5d Transitions of Locally Charge-Compensated Ce³⁺ in CaF₂. Journal of Physical Chemistry C, 2012, 116, 18419-18426.	1.5	22
13548	Structure, bonding, and possible superhardness of CrB<mml:math xmlns:mml="http://www.w3.org/1998/Math/MathML" display="inline"><mml:msub><mml:mrow /><mml:mn>4</mml:mn></mml:msub></mml:math>. Physical Review B, 2012, 85, .	1.1	154
13549	Lithium Peroxide Surfaces Are Metallic, While Lithium Oxide Surfaces Are Not. Journal of the American Chemical Society, 2012, 134, 1093-1103.	6.6	331
13550	Density Functional Theory Analysis on Behavior of Metal Impurities in Ge (100) / Si (100). Materials Science Forum, 0, 725, 243-246.	0.3	0
13551	Evidence for Dirac Fermions in a Honeycomb Lattice Based on Silicon. Physical Review Letters, 2012, 109, 056804.	2.9	634
13552	Improved gas sensing activity in structurally defected bilayer graphene. Nanotechnology, 2012, 23, 505501.	1.3	61
13553	Enhanced Oxidation Reactivity of WO3(001) Surface through the Formation of Oxygen Radical Centers. Journal of Physical Chemistry C, 2012, 116, 5067-5075.	1.5	27
13554	Effect of carbon on hydrogen behaviour in tungsten: first-principle calculations. Nuclear Fusion, 2012, 52, 123003.	1.6	16
13555	First principles study of phosphorus and boron substitutional defects in Si-XII. Journal of Physics Condensed Matter, 2012, 24, 055505.	0.7	2
13556	LiCe(BH₄)₃Cl, a New Lithium-Ion Conductor and Hydrogen Storage Material with Isolated Tetranuclear Anionic Clusters. Chemistry of Materials, 2012, 24, 1654-1663.	3.2	128
13557	Water-hydroxyl phases on an open metal surface: breaking the ice rules. Chemical Science, 2012, 3, 93-102.	3.7	45
13558	Surface defects on ZnO nanowires: implications for design of sensors. Journal of Physics Condensed Matter, 2012, 24, 305001.	0.7	23
13559	Elastic phase transitions in metals at high pressures. Journal of Physics Condensed Matter, 2012, 24, 195402.	0.7	11
13560	Evidence of the Existence of Magnetism in Pristine VX₂ Monolayers (X = S, Se) and Their Strain-Induced Tunable Magnetic Properties. ACS Nano, 2012, 6, 1695-1701.	7.3	733
13561	Mechanistic Insights on the Hydrogenation of Î±,Î²-Unsaturated Ketones and Aldehydes to Unsaturated Alcohols over Metal Catalysts. ACS Catalysis, 2012, 2, 671-683.	5.5	206

#	Article	IF	Citations
13562	Fe-Anchored Graphene Oxide: A Low-Cost and Easily Accessible Catalyst for Low-Temperature CO Oxidation. Journal of Physical Chemistry C, 2012, 116, 2507-2514.	1.5	189
13563	Gold-embedded zigzag graphene nanoribbons as spin gapless semiconductors. Physical Review B, 2012, 86, .	1.1	48
13564	Folded graphene nanoribbons with single and double closed edges. Physical Review B, 2012, 85, .	1.1	15
13565	Density functional study of water-gas shift reaction on M3O3x/Cu(111). Physical Chemistry Chemical Physics, 2012, 14, 16626.	1.3	23
13566	Dominant Factors Governing the Rate Capability of a TiO₂ Nanotube Anode for High Power Lithium Ion Batteries. ACS Nano, 2012, 6, 8308-8315.	7.3	184
13567	Development of EAM Potential for Fe with Pseudo-Hydrogen Effects and Molecular Dynamics Simulation of Hydrogen Embrittlement. Zairyo/Journal of the Society of Materials Science, Japan, 2012, 61, 175-182.	0.1	10
13568	First Principles Calculations of 1-methoxymethyl-1-methylpyrrolidinium and 1-ethyl-3-methylimidazolium Adsorption on Graphene. Journal of the Vacuum Society of Japan, 2012, 55, 198-203.	0.3	2
13569	Atomistic Modeling of Corrosion Events at the Interface between a Metal and Its Environment. International Journal of Corrosion, 2012, 2012, 1-13.	0.6	33
13570	Origin of the Giant Negative Thermal Expansion in<mml:math xmlns:mml="http://www.w3.org/1998/Math/MathML" id="M1"><mml:mrow><mml:msub><mml:mrow><mml:mtext>Mn</mml:mtext></mml:mrow><mml:mtext>3</mml:mtext></mml:msub		

#	Article	IF	Citations
13581	Catalytic Hydrogen Production from Bioethanol. , 2012, , .		3
13582	Structural and electronic properties of oligo- and polythiophenes modified by substituents. Beilstein Journal of Nanotechnology, 2012, 3, 909-919.	1.5	39
13583	Application of Molecular Dynamics Simulation to Small Systems. , 0, , .		0
13584	Towards atomic resolution in sodium titanate nanotubes using near-edge X-ray-absorption fine-structure spectromicroscopy combined with multichannel multiple-scattering calculations. Beilstein Journal of Nanotechnology, 2012, 3, 789-797.	1.5	22
13585	CaCuO₂ antiferromagnetism using shallow well added solely to atomic potential for generating O^{2â^'} basis set of periodic molecular orbitals with consideration of coulomb potential in solid in an LDA. International Journal of Quantum Chemistry, 2012, 112, 44-52.	1.0	7
13586	Double icosahedronâ€based motif of Ni_n (n = 20â^'30). International Journal of Quantum Chemistry, 2012, 112, 1717-1724.	1.0	17
13587	Electronic structure and optical absorbance of doped amorphous silicon slabs. International Journal of Quantum Chemistry, 2012, 112, 300-313.	1.0	9
13588	Bonding and electronic properties of ice at high pressure. International Journal of Quantum Chemistry, 2012, 112, 314-320.	1.0	1
13589	Competition between ordering, twinning, and segregation in binary magnetic 3dâ€5d nanoparticles: A supercomputing perspective. International Journal of Quantum Chemistry, 2012, 112, 277-288.	1.0	18
13590	Interfacial interaction between ZnO thin film and polyimide substrate investigated by XPS and DFT calculation. Surface and Interface Analysis, 2012, 44, 308-317.	0.8	4
13591	Stable structure and effects of sulfur in CdTe/CdS heterojunctions. Surface and Interface Analysis, 2012, 44, 434-438.	0.8	10
13592	Combined XPS and first principle study of metastable Mgâ€“Ti thin films. Surface and Interface Analysis, 2012, 44, 986-988.	0.8	6
13593	Hybrid functional calculations of native point defects in InN. Physica Status Solidi (A) Applications and Materials Science, 2012, 209, 65-70.	0.8	31
13594	Ferromagnetic coupling in Mgâ€doped passivated AlN nanowires: A firstâ€principles study. Physica Status Solidi (B): Basic Research, 2012, 249, 185-189.	0.7	10
13595	CO adsorption on metalâ€oxide surfaces doped with transitionâ€metal adatoms. Physica Status Solidi (B): Basic Research, 2012, 249, 1046-1057.	0.7	11
13596	Structural and electronic properties of conducting Cu nanowire encapsulated in semiconducting zigzag carbon nanotubes: A firstâ€principles study. Physica Status Solidi (B): Basic Research, 2012, 249, 1033-1038.	0.7	8
13597	Ab initio density functional theory calculation of stacking fault energy and stress in 3Câ€SiC. Physica Status Solidi (B): Basic Research, 2012, 249, 1229-1234.	0.7	23
13598	Instability of amorphous oxide semiconductors via carrierâ€mediated structural transition between disorder and peroxide state. Physica Status Solidi (B): Basic Research, 2012, 249, 1277-1281.	0.7	107

#	Article	IF	Citations
13599	Understanding Dissipative Tipâ€“Molecule Interactions with Submolecular Resolution on an Organic Adsorbate. Small, 2012, 8, 602-611.	5.2	12
13600	Local structures and roles of Fe³⁺ and Cr³⁺ in pâ€type semiconductor CuAlO₂. Physica Status Solidi (B): Basic Research, 2012, 249, 1559-1565.	0.7	6
13601	Mechanical properties of L1₂ type Al₃X (Xâ€‰=â€‰Mg, Sc, Zr) from firstâ€principles study. Physica Status Solidi (B): Basic Research, 2012, 249, 1510-1516.	0.7	23
13602	Migration of nitrogen in hexagonal Ge₂Sb₂Te₅: An abâ€initio study. Physica Status Solidi - Rapid Research Letters, 2012, 6, 108-110.	1.2	2
13603	Density functional study of Î±â€“Î² phase transition of polyvinylidene difluoride. Physica Status Solidi - Rapid Research Letters, 2012, 6, 217-219.	1.2	4
13604	Computational modeling of wet TiO₂ (001) anatase surfaces functionalized by transition metal doping. International Journal of Quantum Chemistry, 2012, 112, 3867-3873.	1.0	24
13605	Computational simulation of the pâ€n doped silicon quantum dot. International Journal of Quantum Chemistry, 2012, 112, 3879-3888.	1.0	32
13606	Realâ€Time Microscopy of Graphene Growth on Epitaxial Metal Films: Role of Template Thickness and Strain. Small, 2012, 8, 2250-2257.	5.2	21
13607	Tuning the Doping Type and Level of Graphene with Different Gold Configurations. Small, 2012, 8, 3129-3136.	5.2	70
13608	The structural, elastic and thermodynamic properties of intermetallic compound CeGa2. Open Physics, 2012, 10, .	0.8	0
13609	Switching Magnetization by 180Â° with an Electric Field. Physical Review Letters, 2012, 108, 197206.	2.9	81
13610	Octahedral Rotationâ€Induced Ferroelectricity in Cation Ordered Perovskites. Advanced Materials, 2012, 24, 1961-1968.	11.1	288
13611	High-pressure melting curve of platinum fromab initioZ method. Physical Review B, 2012, 85, .	1.1	50
13612	Hydrogen Adsorption on Co Surfaces: A Density Functional Theory and Temperature Programmed Desorption Study. ACS Catalysis, 2012, 2, 1097-1107.	5.5	107
13613	Origin of the Increase of Activity and Selectivity of Nickel Doped by Au, Ag, and Cu for Acetylene Hydrogenation. ACS Catalysis, 2012, 2, 1027-1032.	5.5	162
13614	Dipole-Assisted Charge Separation in Organicâ€“Inorganic Hybrid Photovoltaic Heterojunctions: Insight from First-Principles Simulations. Journal of Physical Chemistry C, 2012, 116, 9845-9851.	1.5	25
13615	Properties of short polystyrene chains confined between two gold surfaces through a combined density functional theory and classical molecular dynamics approach. Soft Matter, 2012, 8, 6320.	1.2	33
13616	A search model for topological insulators with high-throughput robustness descriptors. Nature Materials, 2012, 11, 614-619.	13.3	244

#	Article	IF	Citations
13617	Multivariate Method-Assisted Ab Initio Study of Olivine-Type LiMXO₄ (Main Group) Tj ETQq0 0 0 rgBT /Overlock 10 T Solid Electrolytes. Chemistry of Materials, 2012, 24, 1357-1364.	3.2	57
13618	Structural phase transition in LiFeSi2O6fromab initiocalculations. Journal of Physics Condensed Matter, 2012, 24, 195401.	0.7	4
13619	Ab InitioPhonon Structure ofh-YMnO₃in Low-Symmetry Ferroelectric Phase. Ferroelectrics, 2012, 426, 90-96.	0.3	4
13620	Classical interatomic potential for orthorhombic uranium. Journal of Physics Condensed Matter, 2012, 24, 235403.	0.7	23
13621	Extended X-ray Absorption Fine Structure and X-ray Diffraction Examination of Sputtered Nickel Carbon Binary Thin Films for Fuel Cell Applications. Journal of Physical Chemistry C, 2012, 116, 6159-6165.	1.5	10
13622	Predicting Nanocrystal Shape through Consideration of Surface-Ligand Interactions. ACS Nano, 2012, 6, 2118-2127.	7.3	236
13623	Oxygen-Storage Materials BaYMn2O5+Î´ from the Quantum-Chemical Point of View. Chemistry of Materials, 2012, 24, 1910-1916.	3.2	27
13624	Pd-Modified Tungsten Carbide for Methanol Electro-oxidation: From Surface Science Studies to Electrochemical Evaluation. ACS Catalysis, 2012, 2, 751-758.	5.5	84
13625	Surface-Enhanced Decomposition Kinetics of Molecular Materials Illustrated with Cyclotetramethylene-tetranitramine. Journal of Physical Chemistry C, 2012, 116, 11077-11081.	1.5	52
13626	Domain Structure in the Tetragonal Phase of BaTiO₃â€“ from Bulk to Nanoparticles. Ferroelectrics, 2012, 426, 21-30.	0.3	14
13627	Orthorhombic carbon allotrope of compressed graphite:Ab initiocalculations. Physical Review B, 2012, 85, .	1.1	80
13628	Water-Mediated Proton Hopping on an Iron Oxide Surface. Science, 2012, 336, 889-893.	6.0	242
13629	mathcal{O}(N) methods in electronic structure calculations. Reports on Progress in Physics, 2012, 75, 036503.	8.1	432
13630	First-Principles Prediction of Metal-Free Magnetism and Intrinsic Half-Metallicity in Graphitic Carbon Nitride. Physical Review Letters, 2012, 108, 197207.	2.9	272
13631	Symmetrical Negative Differential Resistance Behavior of a Resistive Switching Device. ACS Nano, 2012, 6, 2517-2523.	7.3	103
13632	xmlns:mml="http://www.w3.org/1998/Math/MathML" display="inline"><mml:msub><mml:mi>BaTiO</mml:mi><mml:mn>3</mml:mn></mml:msub><mml:mo mathvariant="bold" stretchy="false">(</mml:mo><mml:mn>001</mml:mn><mml:mo mathvariant="bold") Tj ETQq1 1 0.784314 rgBT / mathvariant="bold" stretchy="false">(</mml:mo><mml:mn>2</mml:mn><mml:mo) Tj ETQq1 1 0.784314 rgBT /Overlock 10 Tf 50 127	2.9	16
13633	Harvesting Energy from Water Flow over Graphene?. Nano Letters, 2012, 12, 1736-1741.	4.5	132
13634	Trends in the elastic response of binary early transition metal nitrides. Physical Review B, 2012, 85, .	1.1	136

#	Article	IF	Citations
13635	Room temperature ferromagnetism in Teflon due to carbon dangling bonds. Nature Communications, 2012, 3, 727.	5.8	56
13636	Acceptor doping of single-walled carbon nanotubes by encapsulation of zinc halogenides. European Physical Journal B, 2012, 85, 1.	0.6	49
13637	Metastable decay of DNA components and their compositions â€“ a perspective on the role of reactive electron scattering in radiation damage. European Physical Journal D, 2012, 66, 1.	0.6	15
13638	Origin of Ferroelectricity in High-<mml:math xmlns:mml="http://www.w3.org/1998/Math/MathML" display="inline"><mml:msub><mml:mi>T</mml:mi><mml:mi>c</mml:mi></mml:msub></mml:math>Magnetic Ferroelectric Oxide Bismuth Ferrite. Journal of the American Chemical Society, 2012, 134, 19285-19292.	2.9	43
13639	Ab initio modeling of the structural, electronic, and optical properties of A<mml:math xmlns:mml="http://www.w3.org/1998/Math/MathML" display="inline"><mml:msup><mml:mrow /><mml:mi>II</mml:mi></mml:msup></mml:math>B<mml:math xmlns:mml="http://www.w3.org/1998/Math/MathML" display="inline"><mml:msup><mml:mrow /><mml:mi>IV</mml:mi></mml:msup></mml:math>C<mml:math xmlns:mml="http://www.w3.org/1998/Math/MathML" display="inline"><mml:msubsup><mml:mrow /><m	1.1	121
13640	Vacancy formation energies in fcc metals: Influence of exchange-correlation functionals and correction schemes. Physical Review B, 2012, 85, .	1.1	85
13641	Stability of hydrogenation states of graphene and conditions for hydrogen spillover. Physical Review B, 2012, 85, .	1.1	39
13642	Thermoelectric properties of Ba-Cu-Si clathrates. Physical Review B, 2012, 85, .	1.1	35
13643	Silicene: Compelling Experimental Evidence for Graphenelike Two-Dimensional Silicon. Physical Review Letters, 2012, 108, 155501.	2.9	3,275
13644	Structural Origins of the Excellent Glass Forming Ability of<mml:math xmlns:mml="http://www.w3.org/1998/Math/MathML" display="inline"><mml:msub><mml:mi>Pd</mml:mi><mml:mn>40</mml:mn></mml:msub><mml:msub><mml:mi>Ni</mml:mi><mml:mn>40</mml:mn></mml:msub><mml:msub><mml:mi mathvariant="normal">P</mml:mi><mml:mn>20</mml:mn></mml:msub></mml:math>. Physical Review	2.9	115
13645	Coupled phonons, magnetic excitations, and ferroelectricity in AlFeO<mml:math xmlns:mml="http://www.w3.org/1998/Math/MathML" display="inline"><mml:msub><mml:mrow /><mml:mn>3</mml:mn></mml:msub></mml:math>: Raman and first-principles studies. Physical Review B, 2012, 85, .	1.1	31
13646	Arylthio-substituted coronenes as tailored building blocks for molecular electronics. Physical Chemistry Chemical Physics, 2012, 14, 1635-1641.	1.3	2
13647	Shallow versus Deep Nature of Mg Acceptors in Nitride Semiconductors. Physical Review Letters, 2012, 108, 156403.	2.9	230
13648	Ultrathin SnO₂ Nanosheets: Oriented Attachment Mechanism, Nonstoichiometric Defects, and Enhanced Lithium-Ion Battery Performances. Journal of Physical Chemistry C, 2012, 116, 4000-4011.	1.5	325
13649	Perspective on density functional theory. Journal of Chemical Physics, 2012, 136, 150901.	1.2	1,236
13650	Embedded atom method potentials for Al-Pd-Mn phases. Physical Review B, 2012, 85, .	1.1	27
13651	Phonon spectrum, thermal expansion and heat capacity of UO2 from first-principles. Journal of Nuclear Materials, 2012, 426, 109-114.	1.3	75
13652	Configuration and binding energy of multiple hydrogen atoms trapped in monovacancy in bcc transition metals. Physical Review B, 2012, 85, .	1.1	100

#	Article	IF	Citations
13653	A red metallic oxide photocatalyst. Nature Materials, 2012, 11, 595-598.	13.3	430
13654	Structure and Energetics of Shuttlecock-Shaped Tin-Phthalocyanine on Ag(111): A Density Functional Study Employing Dispersion Correction. Journal of Physical Chemistry C, 2012, 116, 9487-9497.	1.5	25
13655	A Universal Method to Produce Lowâ€“Work Function Electrodes for Organic Electronics. Science, 2012, 336, 327-332.	6.0	1,878
13656	Time-dependent density-functional theory in massively parallel computer architectures: the octopus project. Journal of Physics Condensed Matter, 2012, 24, 233202.	0.7	181
13657	Band-gap engineering in chemically conjugated bilayer graphene:Ab initiocalculations. Physical Review B, 2012, 85, .	1.1	29
13658	Nature of Ag Islands and Nanoparticles on the CeO₂(111) Surface. Journal of Physical Chemistry C, 2012, 116, 1122-1132.	1.5	92
13659	Covalently bonded three-dimensional carbon nanotube solids via boron induced nanojunctions. Scientific Reports, 2012, 2, 363.	1.6	329
13660	xmlns:mml="http://www.w3.org/1998/Math/MathML" display="inline"><mml:msub><mml:mrow /><mml:mn>2</mml:mn></mml:msub></mml:math>/(LaAlO<mml:math) Tj ETQq1 1 0.784314 rgBT /Overlock 10 Tf 5 0 457 Td (xmlns	1.5	
13661	Effects of pressure on the structure and lattice dynamics of TmPO<mml:math xmlns:mml="http://www.w3.org/1998/Math/MathML" display="inline"><mml:msub><mml:mrow /><mml:mn>4</mml:mn></mml:msub></mml:math>: Experiments and calculations. Physical Review B, 2012, 85, .	1.1	32
13662	Novel Structural Motifs in Low Energy Phases of<mml:math xmlns:mml="http://www.w3.org/1998/Math/MathML" display="inline"><mml:msub><mml:mi>LiAlH</mml:mi><mml:mn>4</mml:mn></mml:msub></mml:math>. Physical Review Letters, 2012, 108, 205505.	2.9	43
13663	Magnetic properties of Co2C and Co3C nanoparticles and their assemblies. Applied Physics Letters, 2012, 101, .	1.5	64
13664	Graphing and grafting graphene: Classifying finite topological defects. Physical Review B, 2012, 85, .	1.1	24
13665	Comparison of Nb- and Ta-doping of anatase TiO2 for transparent conductor applications. Journal of Applied Physics, 2012, 112, .	1.1	36
13666	Study on the electronic structure and hydrogen adsorption by transition metal decorated single wall carbon nanotubes. Journal of Physics Condensed Matter, 2012, 24, 185505.	0.7	53
13667	Stable, Single-Layer MX₂ Transition-Metal Oxides and Dichalcogenides in a Honeycomb-Like Structure. Journal of Physical Chemistry C, 2012, 116, 8983-8999.	1.5	1,196
13668	Atomic Layer Deposition of Dielectrics on Graphene Using Reversibly Physisorbed Ozone. ACS Nano, 2012, 6, 2722-2730.	7.3	115
13669	Ab initioinvestigation of FeAs/GaAs heterostructures for potential spintronic and superconducting applications. Physical Review B, 2012, 85, .	1.1	6
13670	Graphene coatings: An efficient protection from oxidation. Physical Review B, 2012, 85, .	1.1	178

#	Article	IF	Citations
13671	Effect of Surface Motion on the Rotational Quadrupole Alignment Parameter of<mml:math xmlns:mml="http://www.w3.org/1998/Math/MathML" display="inline"><mml:msub><mml:mi mathvariant="bold">D</mml:mi><mml:mn>2</mml:mn></mml:msub></mml:math>Reacting on Cu(111). Physical Review Letters, 2012, 108, 236104.	2.9	95
13672	Dispersion-Corrected Density Functional Theory and Classical Force Field Calculations of Water Loading on a Pyrophyllite(001) Surface. Journal of Physical Chemistry C, 2012, 116, 17134-17141.	1.5	40
13673	Transport properties of HfO<mml:math xmlns:mml="http://www.w3.org/1998/Math/MathML" display="inline"><mml:msub><mml:mrow /><mml:mrow><mml:mn>2</mml:mn><mml:mo>â^'</mml:mo><mml:mi>x</mml:mi></mml:mrow></mml:msub></mml:math>based resistive-switching memories. Physical Review B, 2012, 85, .	1.1	51
13674	First-principles study of lithium intercalated bilayer graphene. Science China: Physics, Mechanics and Astronomy, 2012, 55, 1376-1382.	2.0	28
13675	Nitrogen-doped graphene nanosheets as anode materials for lithium ion batteries: a first-principles study. Journal of Materials Chemistry, 2012, 22, 8911.	6.7	517
13676	Emergence of non-centrosymmetric topological insulating phase in BiTeI under pressure. Nature Communications, 2012, 3, 679.	5.8	220
13677	Surface Ligands Increase Photoexcitation Relaxation Rates in CdSe Quantum Dots. ACS Nano, 2012, 6, 6515-6524.	7.3	128
13678	Encapsulation of small magnetic clusters in fullerene cages: A density functional theory investigation within van der Waals corrections. Physical Review B, 2012, 85, .	1.1	36
13679	Charge transfer between carbon nanotubes and sulfuric acid as determined by Raman spectroscopy. Physical Review B, 2012, 85, .	1.1	24
13680	Molecular doping of graphene with ammonium groups. Physical Review B, 2012, 85, .	1.1	34
13681	Quantum size effects in the atomistic structure of armchair nanoribbons. Physical Review B, 2012, 85, .	1.1	17
13682	Energy gaps in graphene nanomeshes. Physical Review B, 2012, 85, .	1.1	72
13683	Effects of static charging and exfoliation of layered crystals. Physical Review B, 2012, 85, .	1.1	35
13684	Evolution of Structure and of Grafting Properties of Î³-Alumina with Pretreatment Temperature. Journal of Physical Chemistry C, 2012, 116, 834-843.	1.5	37
13685	P-type doping of lithium peroxide with carbon sheets. Applied Physics Letters, 2012, 101, .	1.5	19
13686	The roles of Ï€ electrons in the electronic structures and optical properties of graphyne. Science Bulletin, 2012, 57, 3080-3085.	1.7	15
13687	Highly entangled K0.5V2O5 superlong nanobelt membranes for flexible nonvolatile memory devices. Journal of Materials Chemistry, 2012, 22, 18214.	6.7	22
13688	Calculating the energy of vacancies and adatoms in a hexagonal SiC monolayer. Russian Journal of Physical Chemistry A, 2012, 86, 1091-1095.	0.1	3

#	Article	IF	Citations
13689	Catalyzed activation of CO2 by a Lewis-base site in Wâ€“Cuâ€“BTC hybrid metal organic frameworks. Chemical Science, 2012, 3, 2708.	3.7	32
13690	First-principles study of hydrogen ordering in lanthanum hydride and its effect on the metal-insulator transition. Physical Review B, 2012, 86, .	1.1	5
13691	Finite-size supercell correction schemes for charged defect calculations. Physical Review B, 2012, 86, .	1.1	371
13692	Lithium intercalation into TiO<mml:math xmlns:mml="http://www.w3.org/1998/Math/MathML" display="inline"><mml:msub><mml:mrow /><mml:mn>2</mml:mn></mml:msub></mml:math>(B): A comparison of LDA, GGA, and GGA+<mml:math xmlns:mml="http://www.w3.org/1998/Math/MathML" display="inline"><mml:mi>U</mml:mi></mml:math>density functional calculations. Physical Review B, 2012, 86, .	1.1	52
13693	Convergence of many-body wave-function expansions using a plane-wave basis: From homogeneous electron gas to solid state systems. Physical Review B, 2012, 86, .	1.1	101
13694	Artificial Construction of the Layered Ruddlesdenâ€“Popper Manganite La₂Sr₂Mn₃O₁₀ by Reflection High Energy Electron Diffraction Monitored Pulsed Laser Deposition. Journal of the American Chemical Society, 2012, 134, 7700-7714.	6.6	29
13695	A Comparative Density Functional Theory Study of Water Gas Shift Over PdZn(111) and NiZn(111). Topics in Catalysis, 2012, 55, 313-321.	1.3	12
13696	Controlled Catalytic Properties of Platinum Clusters on Strained Graphene. Journal of Physical Chemistry Letters, 2012, 3, 1989-1996.	2.1	46
13697	Geometry, Electronic Structure, and Bonding in CuMCh₂(M = Sb, Bi; Ch = S, Se): Alternative Solar Cell Absorber Materials?. Journal of Physical Chemistry C, 2012, 116, 7334-7340.	1.5	97
13698	Topological crystalline insulators in the SnTe material class. Nature Communications, 2012, 3, 982.	5.8	1,146
13699	Empirical van der Waals corrections to solidâ€state density functional theory: Iodine and phosphorous containing molecular crystals. Journal of Computational Chemistry, 2012, 33, 1615-1622.	1.5	6
13700	Adsorption of metadiiodobenzene on Cu(110): A theoretical study. Journal of Computational Chemistry, 2012, 33, 1623-1631.	1.5	5
13701	Density functional theory study of highâ€pressure effect on crystalline 4,4â€²,6,6â€²â€tetra(azido)hydrazoâ€1,3,5â€triazine. Journal of Computational Chemistry, 2012, 33, 1820-1830.	1.5	10
13702	Implementation of empirical dispersion corrections to density functional theory for periodic systems. Journal of Computational Chemistry, 2012, 33, 2023-2031.	1.5	130
13703	Self-consistent GW calculation of the electronic structure of co-doped ZnO. Journal of the Korean Physical Society, 2012, 60, 292-296.	0.3	1
13704	Initial oxidation structure of chlorinated Si(001). Journal of the Korean Physical Society, 2012, 60, 398-402.	0.3	0
13705	Van der Waals interaction between P4 molecules: Density functional theory calculations with dispersion correction. Journal of the Korean Physical Society, 2012, 60, 410-414.	0.3	2
13706	Electronic structures and spin magnetic properties of CoFe: Lattice strain effects. Journal of the Korean Physical Society, 2012, 60, 445-449.	0.3	1

#	Article	IF	Citations
13707	Origin of the diverse behavior of oxygen vacancies inABO3perovskites: A symmetry based analysis. Physical Review B, 2012, 85, .	1.1	28
13708	Influence of surface segregation on the elastic property of Ptâ€“Ni alloy nanowires. Computational Materials Science, 2012, 55, 81-84.	1.4	5
13709	High-capacity electrode material BC<mml:math xmlns:mml="http://www.w3.org/1998/Math/MathML" display="inline"><mml:msub><mml:mrow /><mml:mn>3</mml:mn></mml:msub></mml:math>for lithium batteries proposed byab initiosimulations. Physical Review B, 2012, 85, .	1.1	42
13710	Systematic search for low-enthalpy<mml:math xmlns:mml="http://www.w3.org/1998/Math/MathML" display="inline"><mml:mrow><mml:mi>s</mml:mi><mml:msup><mml:mi>p</mml:mi><mml:mn>3</mml:mn></mml:msup></mml:mrow allotropes using evolutionary metadynamics. Physical Review B, 2012, 85, .	1.1	82
13711	Investigation of band offsets of interface BiOCl:Bi2WO6: a first-principles study. Physical Chemistry Chemical Physics, 2012, 14, 2450.	1.3	34
13712	Prediction on the existence and chemical stability of cuprous fluoride. Chemical Science, 2012, 3, 2565.	3.7	22
13713	Trends in methanol decomposition on transition metal alloy clusters from scaling and BrÃ¸nstedâ€“Evansâ€“Polanyi relationships. Physical Chemistry Chemical Physics, 2012, 14, 8644.	1.3	30
13714	CALYPSO: A method for crystal structure prediction. Computer Physics Communications, 2012, 183, 2063-2070.	3.0	2,085
13715	Graphyne and Graphdiyne: Promising Materials for Nanoelectronics and Energy Storage Applications. Journal of Physical Chemistry C, 2012, 116, 5951-5956.	1.5	430
13716	Lattice instabilities in metallic elements. Reviews of Modern Physics, 2012, 84, 945-986.	16.4	448
13717	New cubic carbon phase via graphitic sheet rumpling. Physical Review B, 2012, 85, .	1.1	30
13718	Comparison of Reaction Pathways of Ethylene Glycol, Acetaldehyde, and Acetic Acid on Tungsten Carbide and Ni-Modified Tungsten Carbide Surfaces. Journal of Physical Chemistry C, 2012, 116, 5720-5729.	1.5	29
13719	Structural properties and quasiparticle band structures of Cu-based quaternary semiconductors for photovoltaic applications. Journal of Applied Physics, 2012, 111, .	1.1	67
13720	Symmetry and Stability of the Rutile-Based TiO₂ Nanowires: Models and Comparative LCAO-Plane Wave DFT Calculations. Journal of Physical Chemistry C, 2012, 116, 13395-13402.	1.5	21
13721	The effect of concentration on Li diffusivity and conductivity in rutile TiO2. Physical Chemistry Chemical Physics, 2012, 14, 4565.	1.3	32
13722	Enhancement of magnetoelectric effect by combining different interfacial coupling mechanisms. Journal of Applied Physics, 2012, 111, .	1.1	24
13723	Band Gap Engineering of MnO via ZnO Alloying: A Potential New Visible-Light Photocatalyst. Journal of Physical Chemistry C, 2012, 116, 9876-9887.	1.5	118
13724	Tunable Magnetism in a Nonmetal-Substituted ZnO Monolayer: A First-Principles Study. Journal of Physical Chemistry C, 2012, 116, 11336-11342.	1.5	180

#	Article	IF	Citations
13725	Tuning the Electronic and Magnetic Properties of MoS₂ Nanoribbons by Strain Engineering. Journal of Physical Chemistry C, 2012, 116, 11752-11757.	1.5	212
13726	High-pressureâ€“high-temperature equation of state of KCl and KBr. Physical Review B, 2012, 85, .	1.1	122
13727	First-principles study of point defects under varied chemical potentials in Li4BN3H10. Physical Review B, 2012, 85, .	1.1	9
13728	Anharmonic vibrations of the dicarbon antisite defect in 4H-SiC. Applied Physics Letters, 2012, 100, .	1.5	5
13729	Halogenated two-dimensional germanium: candidate materials for being of Quantum Spin Hall state. Journal of Materials Chemistry, 2012, 22, 12587.	6.7	79
13730	Intrinsic Metallic and Semiconducting Cubic Boron Nitride Nanofilms. Nano Letters, 2012, 12, 3650-3655.	4.5	42
13731	High-temperature phonon stabilization of<mml:math xmlns:mml="http://www.w3.org/1998/Math/MathML" display="inline"><mml:mi>Î³</mml:mi></mml:math>-uranium from relativistic first-principles theory. Physical Review B, 2012, 85, .	1.1	59
13732	Properties of IRMOF-14 and its analogues M-IRMOF-14 (M = Cd, alkaline earth metals): electronic structure, structural stability, chemical bonding, and optical properties. Physical Chemistry Chemical Physics, 2012, 14, 4713.	1.3	45
13733	About the Nitrogen Location in Nanocrystalline N-Doped TiO₂: Combined DFT and EXAFS Approach. Journal of Physical Chemistry C, 2012, 116, 1764-1771.	1.5	74
13734	Metals on graphene: correlation between adatom adsorption behavior and growth morphology. Physical Chemistry Chemical Physics, 2012, 14, 9157.	1.3	145
13735	Light-Controlled Plasmon Switching Using Hybrid Metal-Semiconductor Nanostructures. Nano Letters, 2012, 12, 2690-2696.	4.5	17
13736	Catalytic Role of Gold Nanoparticle in GaAs Nanowire Growth: A Density Functional Theory Study. Nano Letters, 2012, 12, 943-948.	4.5	30
13737	A hybrid density functional study on the electron and hole trap states in anatase titanium dioxide. Physical Chemistry Chemical Physics, 2012, 14, 589-598.	1.3	67
13738	Effect of atomic impurities on the helical surface states of the topological insulator Bi₂Te₃. Journal of Physics Condensed Matter, 2012, 24, 175001.	0.7	17
13739	Two-dimensional materials with Dirac cones: Graphynes containing heteroatoms. Physical Review B, 2012, 86, .	1.1	99
13740	First-principles calculations of phonon and thermodynamic properties of AlRE (RE = Y, Gd, Pr, Yb) intermetallic compounds. Physica Scripta, 2012, 85, 035705.	1.2	10
13741	Comparing van der Waals Density Functionals for CO₂ Adsorption in Metal Organic Frameworks. Journal of Physical Chemistry C, 2012, 116, 16957-16968.	1.5	72
13742	Influence of Surface Segregation on the Mechanical Property of Metallic Alloy Nanowires. Materials Research Society Symposia Proceedings, 2012, 1424, 127.	0.1	0

#	Article	IF	Citations
13743	On the Origin of Photoluminescence in Silicon Nanocrystals: Pressure-Dependent Structural and Optical Studies. Nano Letters, 2012, 12, 4200-4205.	4.5	133
13744	Theoretical Design of a Shallow Donor in Diamond by Lithium-Nitrogen Codoping. Physical Review Letters, 2012, 108, 226404.	2.9	20
13745	Preferential sites for adsorption of methanol and methoxy on Pt and Pt-alloy surfaces. Physica Scripta, 2012, 85, 015605.	1.2	5
13746	X-ray absorption Debye-Waller factors fromab initiomolecular dynamics. Physical Review B, 2012, 85, .	1.1	31
13747	Direct observation of a positive spin polarization at the (111) surface of magnetite. Physical Review B, 2012, 85, .	1.1	25
13748	Biaxial strain effect of spin dependent tunneling in MgO magnetic tunnel junctions. Applied Physics Letters, 2012, 101, 042407.	1.5	18
13749	Emergence of giant magnetic anisotropy in freestanding Au/Co nanowires. Applied Physics Letters, 2012, 101, 043108.	1.5	21
13750	Understanding the Magnetic Shape Memory System Feâ€“Pdâ€“X by Thin Film Experiments and First Principle Calculations. Advanced Engineering Materials, 2012, 14, 724-749.	1.6	16
13751	The Role of Adaptive Martensite in Magnetic Shape Memory Alloys. Advanced Engineering Materials, 2012, 14, 562-581.	1.6	99
13752	A Firstâ€Principles Investigation of the Compositional Dependent Properties of Magnetic Shape Memory Heusler Alloys. Advanced Engineering Materials, 2012, 14, 530-546.	1.6	54
13753	Ab Initioâ€Based Prediction of Phase Diagrams: Application to Magnetic Shape Memory Alloys. Advanced Engineering Materials, 2012, 14, 547-561.	1.6	37
13754	Understanding Chemical Expansion in Nonâ€Stoichiometric Oxides: Ceria and Zirconia Case Studies. Advanced Functional Materials, 2012, 22, 1958-1965.	7.8	305
13755	Oriented Growth of Al₂O₃:ZnO Nanolaminates for Use as Electronâ€Selective Electrodes in Inverted Polymer Solar Cells. Advanced Functional Materials, 2012, 22, 1531-1538.	7.8	47
13756	Nanoscale Ferroelectricity in Crystalline Î³â€Glycine. Advanced Functional Materials, 2012, 22, 2996-3003.	7.8	119
13757	Controlling Bulk Conductivity in Topological Insulators: Key Role of Antiâ€Site Defects. Advanced Materials, 2012, 24, 2154-2158.	11.1	258
13758	Metal Oxide Thin Film Phototransistor for Remote Touch Interactive Displays. Advanced Materials, 2012, 24, 2631-2636.	11.1	143
13759	Twoâ€Dimensional Nanostructured Growth of Nanoclusters and Molecules on Insulating Surfaces. Advanced Materials, 2012, 24, 3228-3232.	11.1	22
13760	Sulfurâ€Bridged Annuleneâ€TCNQ Coâ€Crystal: A Selfâ€Assembled â€˜â€˜Molecular Level Heterojunctionâ€™â€™ with Air Stable Ambipolar Charge Transport Behavior. Advanced Materials, 2012, 24, 2603-2607.	11.1	207

#	Article	IF	Citations
13761	Polarity Switching of Charge Transport and Thermoelectricity in Selfâ€Assembled Monolayer Devices. Advanced Materials, 2012, 24, 4403-4407.	11.1	22
13762	Optically Tunable Aminoâ€Functionalized Graphene Quantum Dots. Advanced Materials, 2012, 24, 5333-5338.	11.1	756
13763	Functionalized Graphene Sheets as Molecular Templates for Controlled Nucleation and Selfâ€Assembly of Metal Oxideâ€Graphene Nanocomposites. Advanced Materials, 2012, 24, 5136-5141.	11.1	92
13764	A Novel Codoping Approach for Enhancing the Performance of LiFePO₄ Cathodes. Advanced Energy Materials, 2012, 2, 1028-1032.	10.2	72
13765	Ionic transfer mechanism of COS reaction with CaO: Inert marker experiment and density functional theory (DFT) calculation. AICHE Journal, 2012, 58, 2617-2620.	1.8	7
13766	Spin excitations in Co₂NiGa under pressure from a theoretical approach. Annalen Der Physik, 2012, 524, 212-226.	0.9	4
13767	Chemical Bonding and Atomic Structure in Y₂O₃:ZrO₂â€SrTiO₃ Layered Heterostructures. Angewandte Chemie, 2012, 124, 3474-3478.	1.6	2
13771	Chemical Bonding and Atomic Structure in Y₂O₃:ZrO₂â€SrTiO₃ Layered Heterostructures. Angewandte Chemie - International Edition, 2012, 51, 3418-3422.	7.2	9
13772	The Surface Science Approach for Understanding Reactions on Oxide Powders: The Importance of IR Spectroscopy. Angewandte Chemie - International Edition, 2012, 51, 4731-4734.	7.2	68
13773	Modeling Zeolites with Metalâ€Supported Twoâ€Dimensional Aluminosilicate Films. Angewandte Chemie - International Edition, 2012, 51, 6005-6008.	7.2	96
13774	Reversible Wurtziteâ€“Tetragonal Reconstruction in ZnO(10$ar 1$0) Surfaces. Angewandte Chemie - International Edition, 2012, 51, 7744-7747.	7.2	41
13775	Adsorbate Alignment in Surface Halogenation: Standing Up is Better than Lying Down. Angewandte Chemie - International Edition, 2012, 51, 9061-9065.	7.2	6
13776	Molecular Understanding of Enyne Hydrogenation over Palladium and Copper Catalysts. ChemCatChem, 2012, 4, 1420-1427.	1.8	18
13777	DFT Study of Steam Reforming of Formaldehyde on Cu, PdZn, and Ir. ChemCatChem, 2012, 4, 1311-1320.	1.8	14
13778	Theoretical Study of the Reduction of Uranium(VI) Aquo Complexes on Titania Particles and by Alcohols. Chemistry - A European Journal, 2012, 18, 7117-7127.	1.7	29
13779	Sizeâ€Dependent Surface Activity of Rutile and Anatase TiO₂ Nanocrystals: Facile Surface Modification and Enhanced Photocatalytic Performance. Chemistry - A European Journal, 2012, 18, 4759-4765.	1.7	30
13780	Highâ€Potential Reversible Li Deintercalation in a Substituted Tetrahydroxyâ€pâ€benzoquinone Dilithium Salt: An Experimental and Theoretical Study. Chemistry - A European Journal, 2012, 18, 8800-8812.	1.7	68
13781	Photocatalytic Generation of Syngas Using Combustionâ€Synthesized Silver Bismuth Tungstate. ChemPhysChem, 2012, 13, 2945-2955.	1.0	30

#	Article	IF	Citations
13782	The Role of Effective Mass of Carrier in the Photocatalytic Behavior of Silver Halideâ€Based Ag@AgX (X=Cl, Br, I): A Theoretical Study. ChemPhysChem, 2012, 13, 2304-2309.	1.0	99
13783	A Firstâ€Principle Calculation of Sulfur Oxidation on Metallic Ni(111) and Pt(111), and Bimetallic Ni@Pt(111) and Pt@Ni(111) Surfaces. ChemPhysChem, 2012, 13, 3194-3203.	1.0	16
13784	Sizeâ€Dependent Lattice Expansion in Nanoparticles: Reality or Anomaly?. ChemPhysChem, 2012, 13, 2443-2454.	1.0	186
13785	Quantifying Large Effects of Framework Flexibility on Diffusion in MOFs: CH₄ and CO₂ in ZIFâ€8. ChemPhysChem, 2012, 13, 3449-3452.	1.0	185
13786	Modification of nâ€Type Organic Semiconductor Performance of Perylene Diimides by Substitution in Different Positions: Twoâ€Dimensional Ï€â€Stacking and Hydrogen Bonding. ChemSusChem, 2012, 5, 879-887.	3.6	102
13787	Mechanistic Investigation on the Formation and Dehydrogenation of Calcium Amidoborane Ammoniate. ChemSusChem, 2012, 5, 927-931.	3.6	10
13788	CO Oxidation at the Perimeters of an FeO/Pt(111) Interface and how Water Promotes the Activity: A Firstâ€Principles Study. ChemSusChem, 2012, 5, 871-878.	3.6	37
13789	Design of a Highly Nanodispersed Pdâ€“MgO/SiO₂ Composite Catalyst with Multifunctional Activity for CH₄ Reforming. ChemSusChem, 2012, 5, 1474-1481.	3.6	35
13790	Ab Initio Simulation of Complex Dielectric Function for Dense Aluminum Plasma. Contributions To Plasma Physics, 2012, 52, 145-148.	0.5	19
13791	Solar hydrogen production with semiconductor metal oxides: new directions in experiment and theory. Physical Chemistry Chemical Physics, 2012, 14, 49-70.	1.3	198
13792	Density Functional Theory Study of the Interaction of Hydrogen with Li₆C₆₀. Journal of Physical Chemistry Letters, 2012, 3, 1084-1088.	2.1	48
13793	Lithium Adsorption on Graphene: From Isolated Adatoms to Metallic Sheets. Journal of Chemical Theory and Computation, 2012, 8, 1064-1071.	2.3	79
13794	Modeling oxidation of Pt-based alloy surfaces for fuel cell cathode electrocatalysts. Catalysis, 0, , 323-357.	0.6	0
13795	Efficient Defect Healing in Catalytic Carbon Nanotube Growth. Physical Review Letters, 2012, 108, 245505.	2.9	100
13796	Vibrational Davydov Splittings and Collective Mode Polarizations in Oriented Organic Semiconductor Crystals. Journal of Physical Chemistry C, 2012, 116, 14491-14503.	1.5	25
13797	Near room-temperature synthesis of transfer-free graphene films. Nature Communications, 2012, 3, 645.	5.8	205
13798	Magnetic properties of PbFe<mml:math xmlns:mml="http://www.w3.org/1998/Math/MathML" display="inline"><mml:msub><mml:mrow /><mml:mrow><mml:mn>1</mml:mn><mml:mo>/</mml:mo><mml:mn>2</mml:mn></mml:mrow></mml:msub></mml:math>Nb<mml: xmlns:mml="http://www.w3.org/1998/Math/MathML" display="inline"><mml:msub><mml:mrow /><mml:mrow><mml:mn>1</mml:mn><mml:mo>/</mml:mo><mml:mn>2</mml:mn></mml:mrow></mml:msub></mml:math>O<mml:r xmlns:mml="http://www.w3.org/1998/Math/MathML" display="inline"><mml:msub><mml:mrow />	1.1	69
13799	Physic Compensating Edge Polarity: A Means To Alter the Growth Orientation of MgO Nanostructures on Au(111). Journal of Physical Chemistry C, 2012, 116, 11126-11132.	1.5	15

#	Article	IF	Citations
13800	Structural, Electronic, and Thermoelectric Properties of InSe Nanotubes: First-Principles Calculations. Journal of Physical Chemistry C, 2012, 116, 3956-3961.	1.5	14
13801	Theoretical Calculations on the Oxidation of CO on Au₅₅, Ag₁₃Au₄₂, Au₁₃Ag₄₂, and Ag₅₅ Clusters of Nanometer Size. Journal of Physical Chemistry C, 2012, 116, 13196-13201.	1.5	25
13802	Energetic and thermodynamic aspects of structural transitions in Fe-Pd ferromagnetic shape memory thin films: Anab initiostudy. Physical Review B, 2012, 85, .	1.1	13
13803	Molecular Dynamics Simulation: From â€œAb Initioâ€•to â€œCoarse Grainedâ€•, 2012, , 195-238.		11
13804	Fundamental Structural, Electronic, and Chemical Properties of Carbon Nanostructures: Graphene, Fullerenes, Carbon Nanotubes, and Their Derivatives. , 2012, , 793-867.		17
13805	Density functional theory analysis of dopants in cupric oxide. Journal of Applied Physics, 2012, 111, .	1.1	57
13806	Adsorption and Diffusion of Li on Pristine and Defective Graphene. ACS Applied Materials & Interfaces, 2012, 4, 2432-2438.	4.0	363
13807	Thermal transport in graphyne nanoribbons. Physical Review B, 2012, 85, .	1.1	103
13808	Evolutionary metadynamics: a novel method to predict crystal structures. CrystEngComm, 2012, 14, 3596.	1.3	62
13809	Mapping the shape and phase of palladium nanocatalysts. Catalysis Science and Technology, 2012, 2, 1485.	2.1	18
13810	Electronic Structure Changes across the Metamagnetic Transition in FeRh via Hard X-Ray Photoemission. Physical Review Letters, 2012, 108, 257208.	2.9	68
13811	Symmetry Breaking: Polymorphic Form Selection by Enantiomers of the Melatonin Agonist and Its Missing Polymorph. Crystal Growth and Design, 2012, 12, 3964-3976.	1.4	16
13812	Unveiling Structureâ€“Property Relationships in Sr₂Fe_{1.5}Mo_{0.5}O_{6â^Î´}, an Electrode Material for Symmetric Solid Oxide Fuel Cells. Journal of the American Chemical Society, 2012, 134, 6826-6833.	6.6	172
13813	WH_nunder pressure. Journal of Physics Condensed Matter, 2012, 24, 155701.	0.7	29
13814	Atom-by-Atom Observation of Grain Boundary Migration in Graphene. Nano Letters, 2012, 12, 3168-3173.	4.5	178
13815	Constraints on the phase diagram of molybdenum from first-principles free-energy calculations. Physical Review B, 2012, 85, .	1.1	55
13816	Ab initiobased empirical potential used to study the mechanical properties of molybdenum. Physical Review B, 2012, 85, .	1.1	71
13817	Structure and stability of<mml:math xmlns:mml="http://www.w3.org/1998/Math/MathML" display="inline"><mml:msub><mml:mrow /><mml:mn>2</mml:mn></mml:msub></mml:math>Fe and Al<mml:math xmlns:mml="http://www.w3.org/1998/Math/MathML" display="inline"><mml:msub><mml:mrow /><mml:mn>5</mml:mn></mml:msub></mml:math>Fe<mml:math xmlns:mml="http://www.w3.org/1998/Math/MathML" display="inline"><mml:msub><mml:mrow /><mml:	1.1	42

#	Article	IF	Citations
13818	Terraces at ohmic contact in SiC electronics: Structure and electronic states. Journal of Applied Physics, 2012, 111, 113717.	1.1	10
13819	Local fields in conductor surface electromigration: A first-principles study in the low-bias ballistic limit. Physical Review B, 2012, 85, .	1.1	10
13820	Remarkable Hydrogen Storage Capacity In Li-Decorated Graphyne: Theoretical Predication. Journal of Physical Chemistry C, 2012, 116, 13837-13841.	1.5	136
13821	Effect of Surface Deposited Pt on the Photoactivity of TiO₂. Journal of Physical Chemistry C, 2012, 116, 10138-10149.	1.5	92
13822	Effect of Li-doping on the magnetic properties of ZnO with Zn vacancies. Journal of Applied Physics, 2012, 111, 093902.	1.1	19
13823	Mechanical properties of bcc Fe-Cr alloys by first-principles simulations. Frontiers of Physics, 2012, 7, 360-365.	2.4	20
13824	Multiferroic behavior of Aurivillius Bi4Mn3O12from first principles. Physical Review B, 2012, 85, .	1.1	6
13825	Clustering and magnetic anisotropy of Fe adatoms on graphene. Physical Review B, 2012, 85, .	1.1	29
13826	Magnetic structure of hydrogen-induced defects on graphene. Physical Review B, 2012, 85, .	1.1	46
13827	Engineering the work function of armchair graphene nanoribbons using strain and functional species: a first principles study. Journal of Physics Condensed Matter, 2012, 24, 075501.	0.7	61
13828	Hole polaron formation and migration in olivine phosphate materials. Physical Review B, 2012, 85, .	1.1	77
13829	First-principles theoretical investigation of monoatomic and dimer Mn adsorption on noble metal (111) surfaces. Physical Review B, 2012, 85, .	1.1	13
13830	Advances in ab-initio theory of multiferroics. European Physical Journal B, 2012, 85, 1.	0.6	35
13831	First-principles prediction of charge mobility in carbon and organic nanomaterials. Nanoscale, 2012, 4, 4348.	2.8	551
13832	Effects of Cu and Al on the crystal structure and composition of Î· (MgZn2) phase in over-aged Alâ€“Znâ€“Mgâ€“Cu alloys. Journal of Materials Science, 2012, 47, 5419-5427.	1.7	64
13833	Ab initio prediction of new 3D-like phases ThCuSiAs, ThCuGeAs and their structural, mechanical, and electronic properties. Journal of Materials Science, 2012, 47, 6741-6747.	1.7	4
13834	Magnetic Moments in SmCo5 and SmCo5â^'x Cu x Films. Journal of Superconductivity and Novel Magnetism, 2012, 25, 1947-1950.	0.8	14
13835	Study of the Cuâ€“Liâ€“Mgâ€“H system by thermal analysis. Journal of Thermal Analysis and Calorimetry, 2012, 108, 733-739.	2.0	3

#	Article	IF	Citations
13836	Preventing the CO poisoning on Pt nanocatalyst using appropriate substrate: a first-principles study. Journal of Nanoparticle Research, 2012, 14, 1.	0.8	34
13837	Electric field-induced metallic transition of (3,3) carbon nanotube supported on patterned hydrogen-terminated Si(001):1ÂÃ—Â1 surface. Journal of Nanoparticle Research, 2012, 14, 1.	0.8	0
13838	Physical and chemical properties of Co nâ^'m Cu m nanoclusters with nÂ=Â2â€“6 atoms via ab-initio calculations. Journal of Nanoparticle Research, 2012, 14, 1.	0.8	10
13839	First-principles study of the structure, mechanical properties, and phase stability of crystalline zirconia under high pressure. Structural Chemistry, 2012, 23, 601-611.	1.0	13
13840	Adsorption of 2,4,6-trinitrotoluene on Al(111) ultrathin film: periodic DFT calculations. Structural Chemistry, 2012, 23, 921-930.	1.0	7
13841	Comprehensive study of the structure of aluminum trihalides from electron diffraction and computation. Structural Chemistry, 2012, 23, 879-893.	1.0	12
13842	Reactions of Propylene Oxide on Supported Silver Catalysts: Insights into Pathways Limiting Epoxidation Selectivity. Topics in Catalysis, 2012, 55, 3-12.	1.3	21
13843	Influence of Sulfur Poisoning on CO Adsorption on Pd(100). Topics in Catalysis, 2012, 55, 267-279.	1.3	10
13844	Enantiospecific Chemisorption of Amino Acids on Step Decorated Chiral Cu Surfaces. Topics in Catalysis, 2012, 55, 243-259.	1.3	20
13845	Aqueous N2O Reduction with H2 Over Pd-Based Catalyst: Mechanistic Insights From Experiment and Simulation. Topics in Catalysis, 2012, 55, 300-312.	1.3	11
13846	Platinum Nanoclusters Exhibit Enhanced Catalytic Activity for Methane Dehydrogenation. Topics in Catalysis, 2012, 55, 345-352.	1.3	16
13847	Density Functional Theory Study of Selectivity Considerations for Câ€“C Versus Câ€“O Bond Scission in Glycerol Decomposition on Pt(111). Topics in Catalysis, 2012, 55, 280-289.	1.3	41
13848	Selectivity of Adsorption of Thiophene and its Derivatives on Titania Anatase Surfaces: A Density Functional Theory Study. Topics in Catalysis, 2012, 55, 229-242.	1.3	9
13849	Investigation of Ti Addition Effects on the Thickness of 55Âpct Al-Zn-1.6Âpct Si Coating by First-Principles Calculation. Metallurgical and Materials Transactions A: Physical Metallurgy and Materials Science, 2012, 43, 2012-2017.	1.1	11
13850	Electronic structures of the F-terminated AlN nanoribbons. Pramana - Journal of Physics, 2012, 78, 469-474.	0.9	10
13851	An exchange intercalation mechanism for the formation of a two-dimensional Si structure underneath graphene. Nano Research, 2012, 5, 352-360.	5.8	71
13852	Ab-initio study of silicon and tin as a negative electrode materials for lithium-ion batteries. International Journal of Precision Engineering and Manufacturing, 2012, 13, 1191-1197.	1.1	31
13853	Electronic structures of Heusler alloy Co2FeAl1â^'x Si x surface. Rare Metals, 2012, 31, 107-111.	3.6	17

#	Article	IF	Citations
13854	Electronic structures of new tunnel barrier spinel MgAl2O4: first-principles calculations. Rare Metals, 2012, 31, 112-116.	3.6	10
13855	Role of step sites on water dissociation on stoichiometric ceria surfaces. Theoretical Chemistry Accounts, 2012, 131, 1.	0.5	30
13856	Ab initio parametrized polarizable force field for rutile-type SnO2. Theoretical Chemistry Accounts, 2012, 131, 1.	0.5	9
13857	Effects of Ti doping at the reduced SnO2(110) surface with different oxygen vacancies: a first principles study. Theoretical Chemistry Accounts, 2012, 131, 1.	0.5	6
13858	First-principles molecular dynamics simulations of the H2O / Cu(111) interface. Journal of Molecular Modeling, 2012, 18, 2433-2442.	0.8	17
13859	Structural, electronic, and elastic properties of K-As compounds: a first principles study. Journal of Molecular Modeling, 2012, 18, 3101-3112.	0.8	11
13860	Acetylene hydrogenation on anatase TiO2(101) supported Pd4 cluster: oxygen deficiency effect. Journal of Molecular Modeling, 2012, 18, 3329-3339.	0.8	15
13861	No miscibility gap in Ptâ€“Rh binary alloys: A first-principles study. Acta Materialia, 2012, 60, 1093-1098.	3.8	18
13862	Kinetic pathways for phase separation: An atomic-scale study in Niâ€“Alâ€“Cr alloys. Acta Materialia, 2012, 60, 1871-1888.	3.8	53
13863	Why is the slip direction different in different B2 alloys?. Acta Materialia, 2012, 60, 881-888.	3.8	30
13864	An ab initio study of Tiâ€“Yâ€“O nanocluster energetics in nanostructured ferritic alloys. Acta Materialia, 2012, 60, 935-947.	3.8	46
13865	Core structure of a screw dislocation in Ti from density functional theory and classical potentials. Acta Materialia, 2012, 60, 1287-1292.	3.8	81
13866	First-principles study of the thermodynamic and elastic properties of eutectic Feâ€“Ti alloys. Acta Materialia, 2012, 60, 1594-1602.	3.8	36
13867	Effects of alloying elements on thermal expansions of Î³-Ni and Î³â€²-Ni3Al by first-principles calculations. Acta Materialia, 2012, 60, 1846-1856.	3.8	42
13868	The ternary system Auâ€“Baâ€“Si: Clathrate solution, electronic structure, physical properties, phase equilibria and crystal structures. Acta Materialia, 2012, 60, 2324-2336.	3.8	24
13869	Prediction of thermal cross-slip stress in magnesium alloys from a geometric interaction model. Acta Materialia, 2012, 60, 2350-2358.	3.8	103
13870	On the possibility of rhenium clustering in nickel-based superalloys. Acta Materialia, 2012, 60, 2866-2872.	3.8	78
13871	The relation between ductility and stacking fault energies in Mg and Mgâ€“Y alloys. Acta Materialia, 2012, 60, 3011-3021.	3.8	481

#	Article	IF	Citations
13872	The effect of electronic and magnetic valences on the martensitic transformation of CoNiGa shape memory alloys. Acta Materialia, 2012, 60, 3545-3558.	3.8	28
13873	Solute strengthening from first principles and application to aluminum alloys. Acta Materialia, 2012, 60, 3873-3884.	3.8	185
13874	Ab initio analysis of Guinierâ€“Prestonâ€“Bagaryatsky zone nucleation in Alâ€“Cuâ€“Mg alloys. Acta Materialia, 2012, 60, 3861-3872.	3.8	40
13875	Mechanical properties and chemical bonding of the Osâ€“B system: A first-principles study. Acta Materialia, 2012, 60, 4208-4217.	3.8	42
13876	Effects of defects and non-coordinating molecular overlayers on the work function of graphene and energy-level alignment with organic molecules. Carbon, 2012, 50, 851-856.	5.4	20
13877	Two-beam-laser interference mediated reduction, patterning and nanostructuring of graphene oxide for the production of a flexible humidity sensing device. Carbon, 2012, 50, 1667-1673.	5.4	290
13878	On the interaction of polycyclic aromatic compounds with graphene. Carbon, 2012, 50, 2482-2492.	5.4	66
13879	In situ transmission electron microscopy of electrochemical lithiation, delithiation and deformation of individual graphene nanoribbons. Carbon, 2012, 50, 3836-3844.	5.4	98
13880	Hydrogen-mediated support effects on acrolein hydrogenation over ZnO supported gold clusters. Catalysis Communications, 2012, 17, 164-167.	1.6	11
13881	The adsorption of CO on potassium doped molybdenum carbide surface: An ab-initio study. Catalysis Today, 2012, 181, 102-107.	2.2	13
13882	Effect of Ag on the control of Ni-catalyzed carbon formation: A density functional theory study. Catalysis Today, 2012, 186, 54-62.	2.2	52
13883	Integrated operando X-ray absorption and DFT characterization of Cuâ€“SSZ-13 exchange sites during the selective catalytic reduction of NO with NH3. Catalysis Today, 2012, 184, 129-144.	2.2	212
13884	Theoretical and experimental analysis for site preference of rare earth elements in BaTiO3. Ceramics International, 2012, 38, S25-S28.	2.3	21
13885	Lithium ion migration pathways in Li3xLa2/3â˜’xâ–¡1/3â˜’2xTiO3. Ceramics International, 2012, 38, S467-S470.	2.3	20
13886	On the electric dipole moments of small sodium clusters from different theoretical approaches. Chemical Physics, 2012, 399, 252-257.	0.9	9
13887	Ab initio calculation of chromium oxide containing Ti dopant. Chemical Physics, 2012, 393, 148-152.	0.9	30
13888	Hydrogen storage on Ti decorated SiC nanostructures: A first principles study. International Journal of Hydrogen Energy, 2012, 37, 3733-3740.	3.8	39
13889	Theoretical calculation of hydrogen desorption energies of calcium hydride clusters. International Journal of Hydrogen Energy, 2012, 37, 3767-3771.	3.8	3

#	Article	IF	Citations
13890	A first principle study of SO3 decomposition on silver nano-clusters: Implications toward hydrogen production. International Journal of Hydrogen Energy, 2012, 37, 3645-3651.	3.8	6
13891	Stability of transition metals on Mg(0001) surfaces and their effects on hydrogen adsorption. International Journal of Hydrogen Energy, 2012, 37, 309-317.	3.8	48
13892	Atomic-scale mechanisms of oxygen electrode delamination in solid oxide electrolyzer cells. International Journal of Hydrogen Energy, 2012, 37, 1280-1291.	3.8	59
13893	Hydrogen energetics and charge transfer in the Ni/LaNbO4 interface from DFT calculations. International Journal of Hydrogen Energy, 2012, 37, 8033-8042.	3.8	6
13894	Novel (Ir,Sn,Nb)O2 anode electrocatalysts with reduced noble metal content for PEM based water electrolysis. International Journal of Hydrogen Energy, 2012, 37, 3001-3013.	3.8	64
13895	Local structural arrangements around oxygen and hydrogen-related defects in proton conducting LaP3O9 investigated by first principles calculations. International Journal of Hydrogen Energy, 2012, 37, 7995-8003.	3.8	10
13896	First-principles study on hydrogen storage by graphitic carbon nitride nanotubes. International Journal of Hydrogen Energy, 2012, 37, 4170-4178.	3.8	96
13897	The role of B-site cations on proton conductivity in double perovskite oxides La2MgTiO6 and La2MgZrO6. International Journal of Hydrogen Energy, 2012, 37, 7983-7994.	3.8	5
13898	Stability of erbium hydrides studied by DFT calculations. International Journal of Hydrogen Energy, 2012, 37, 4246-4253.	3.8	12
13899	Defects at the (1 1 0) surface of rutile TiO2 from ab initio calculations. International Journal of Hydrogen Energy, 2012, 37, 8110-8117.	3.8	13
13900	Mechanism for the decomposition of lithium borohydride. International Journal of Hydrogen Energy, 2012, 37, 5825-5832.	3.8	32
13901	First-principles study of the hydrogen absorption at Î£5 symmetrical tilt grain boundary in B2-TiFe alloy. International Journal of Hydrogen Energy, 2012, 37, 6666-6673.	3.8	18
13902	Atomistic study of LaNbO4; surface properties and hydrogen adsorption. International Journal of Hydrogen Energy, 2012, 37, 6674-6685.	3.8	13
13903	Hydrogenation of CO on molybdenum and cobalt molybdenum carbides. Applied Catalysis A: General, 2012, 423-424, 192-204.	2.2	43
13904	Red phosphorus: An elemental photocatalyst for hydrogen formation from water. Applied Catalysis B: Environmental, 2012, 111-112, 409-414.	10.8	265
13905	VASP on a GPU: Application to exact-exchange calculations of the stability of elemental boron. Computer Physics Communications, 2012, 183, 1422-1426.	3.0	115
13906	Linear scaling algorithm of real-space density functional theory of electrons with correlated overlapping domains. Computer Physics Communications, 2012, 183, 1664-1673.	3.0	25
13907	Introducing k-point parallelism into VASP. Computer Physics Communications, 2012, 183, 1696-1701.	3.0	33

#	Article	IF	Citations
13908	A distributed approach to verification and validation of electronic structure simulation data using ESTEST. Computer Physics Communications, 2012, 183, 1744-1748.	3.0	2
13909	Detailed check of the LDA+U and GGA+U corrected method for defect calculations in wurtzite ZnO. Computer Physics Communications, 2012, 183, 1749-1752.	3.0	61
13910	Quantum mechanical modeling of electronic excitations in metal oxides: Magnesia as a prototype. Chemical Physics Letters, 2012, 519-520, 18-24.	1.2	29
13911	DFT study of the M segregation on MAu alloys (M=Ni, Pd, Pt) in presence of adsorbed oxygen O and O2. Chemical Physics Letters, 2012, 521, 98-103.	1.2	47
13912	Effect of the environment on the hydroxyl density of Î±-quartz (111). Chemical Physics Letters, 2012, 522, 46-50.	1.2	6
13913	First-principles study of substitutional carbon pair and Stoneâ€“Wales defect complexes in boron nitride nanotubes. Chemical Physics Letters, 2012, 522, 79-82.	1.2	20
13914	Formation dynamics of FeN thin films on Cu(100). Chemical Physics Letters, 2012, 523, 78-82.	1.2	2
13915	Native point defects in ZnS: First-principles studies based on LDA, LDA+U and an extrapolation scheme. Chemical Physics Letters, 2012, 531, 75-79.	1.2	25
13916	Improved convergence of rutile-TiO2(110) slab properties with thickness by one-side saturation. Chemical Physics Letters, 2012, 531, 90-93.	1.2	5
13917	Structural, electronic and magnetic properties of single transition-metal adsorbed BN sheet: A density functional study. Chemical Physics Letters, 2012, 532, 40-46.	1.2	42
13918	Far-infrared spectroscopy investigation of sulfurâ€“oxygen interactions in Ï€-conjugated oligomers. Chemical Physics Letters, 2012, 535, 116-119.	1.2	2
13919	Barriers to motion and rotation of graphene layers based on measurements of shear mode frequencies. Chemical Physics Letters, 2012, 536, 82-86.	1.2	43
13920	Structural and electronic properties of Agâ€“Pd bimetallic clusters on Al2O3 substrates: A first principles study. Chemical Physics Letters, 2012, 537, 69-74.	1.2	6
13921	Ab initio investigation of the electronic structure of CeRh2Sb2. Chemical Physics Letters, 2012, 537, 48-52.	1.2	0
13922	The electronic properties at the iron-phthalocyanine/Ag(110) interface. Chemical Physics Letters, 2012, 537, 53-57.	1.2	7
13923	Doping and temperature dependence of thermoelectric properties of AgGaTe2: First principles investigations. Chemical Physics Letters, 2012, 537, 62-64.	1.2	25
13924	Novel D-Ï€-A system based on zinc porphyrin dyes for dye-sensitized solar cells: Synthesis, electrochemical, and photovoltaic properties. Dyes and Pigments, 2012, 94, 143-149.	2.0	76
13925	A mixed-cation mixed-anion borohydride NaY(BH4)2Cl2. International Journal of Hydrogen Energy, 2012, 37, 8428-8438.	3.8	33

#	Article	IF	Citations
13926	Structural, electronic and thermodynamic properties of Al- and Si-doped Î±-, Î³-, and Î²-MgH2: Density functional andÂhybrid density functional calculations. International Journal of Hydrogen Energy, 2012, 37, 9112-9122.	3.8	27
13927	Density functional studies on the hydrogen storage capacity of boranes and alanes based cages. International Journal of Hydrogen Energy, 2012, 37, 9730-9741.	3.8	17
13928	Unprecedented selectivity to the direct desulfurization (DDS) pathway in a highly active FeNi bimetallic phosphide catalyst. Journal of Catalysis, 2012, 285, 1-5.	3.1	73
13929	An integrated approach to Deacon chemistry on RuO2-based catalysts. Journal of Catalysis, 2012, 285, 273-284.	3.1	111
13930	Deoxygenation mechanisms on Ni-promoted MoS2 bulk catalysts: A combined experimental and theoretical study. Journal of Catalysis, 2012, 286, 153-164.	3.1	107
13931	Unraveling the mechanism of the NO reduction by CO on gold based catalysts. Journal of Catalysis, 2012, 289, 11-20.	3.1	36
13932	Ab initio molecular dynamics simulation of lithiation-induced phase-transition of crystalline silicon. Electrochimica Acta, 2012, 62, 73-76.	2.6	28
13933	Competitive anion/anion interactions on copper surfaces relevant for Damascene electroplating. Electrochimica Acta, 2012, 70, 286-295.	2.6	56
13934	Study of the electrochemical deposition of Mg in the atomic level: Why it prefers the non-dendritic morphology. Electrochimica Acta, 2012, 76, 270-274.	2.6	262
13935	Modification of the adsorption properties of O and OH on Ptâ€“Ni bimetallic surfaces by subsurface alloying. Electrochimica Acta, 2012, 76, 440-445.	2.6	25
13936	Mechanical Properties and Electronic Structure of Mullite Phases Using Firstâ€Principles Modeling. Journal of the American Ceramic Society, 2012, 95, 2075-2088.	1.9	46
13937	Abnormal Partial Dispersion in Pyrochlore Lanthanum Zirconate Transparent Ceramics. Journal of the American Ceramic Society, 2012, 95, 2899-2905.	1.9	17
13938	<scp><scp>N</scp></scp>Â+Â<scp><scp>Ni</scp></scp> Codoped Anatase <scp><scp>TiO</scp></scp>₂ Nanocrystals with Exposed {001} Facets Through Twoâ€Step Hydrothermal Route. Journal of the American Ceramic Society, 2012, 95, 2951-2956.	1.9	35
13939	Effect of Y and Zn substitution on elastic properties of 6H-type ABCBCB LPSO structure in Mg97Zn1Y2 alloy. Materials Chemistry and Physics, 2012, 131, 634-641.	2.0	7
13940	A new approach to establish both stable and metastable phase equilibria for fcc ordered/disordered phase transition: application to the Alâ€“Ni and Niâ€“Si systems. Materials Chemistry and Physics, 2012, 135, 94-105.	2.0	23
13941	Grain boundary stoichiometry and interactions with defects in SrTiO3. Scripta Materialia, 2012, 66, 105-108.	2.6	25
13942	Generalized stacking fault energy in magnesium alloys: Density functional theory calculations. Scripta Materialia, 2012, 66, 219-222.	2.6	157
13943	Effects of transition metals on the grain boundary cohesion in tungsten. Scripta Materialia, 2012, 66, 558-561.	2.6	117

#	Article	IF	Citations
13944	Structural stability and generalized stacking fault energies in Î² Tiâ€“Nb alloys: Relation to dislocation properties. Scripta Materialia, 2012, 66, 682-685.	2.6	35
13945	Copper precipitation in cobalt-alloyed precipitation-hardened stainless steel. Scripta Materialia, 2012, 66, 943-946.	2.6	33
13946	First-principles calculations of the stability and incorporation of helium, xenon and krypton in uranium. Journal of Nuclear Materials, 2012, 425, 2-7.	1.3	23
13947	Threshold concentration for H blistering in defect free W. Journal of Nuclear Materials, 2012, 421, 176-180.	1.3	10
13948	First-principles calculations of phase transition, elasticity, and thermodynamic properties for TiZr alloy. Journal of Nuclear Materials, 2012, 420, 501-507.	1.3	31
13949	Cs diffusion in cubic silicon carbide. Journal of Nuclear Materials, 2012, 421, 89-96.	1.3	17
13950	Ab initio modelling of volatile fission products in uranium mononitride. Journal of Nuclear Materials, 2012, 422, 137-142.	1.3	33
13951	Retention and diffusion of H, He, O, C impurities in Be. Journal of Nuclear Materials, 2012, 423, 164-169.	1.3	34
13952	Adsorption and dissociation of H2O on Zr(0001) with density-functional theory studies. Journal of Nuclear Materials, 2012, 424, 51-56.	1.3	8
13953	A DFT+U study of cerium solubility in La2Zr2O7. Journal of Nuclear Materials, 2012, 424, 69-74.	1.3	18
13954	First-principles study of surface properties of PuO2: Effects of thickness and O-vacancy on surface stability and chemical activity. Journal of Nuclear Materials, 2012, 426, 139-147.	1.3	40
13955	First-principles study of the stability of fission products in uranium monocarbide. Journal of Nuclear Materials, 2012, 426, 189-197.	1.3	22
13956	Role of water on the stability of oxygen vacancies in ZrO2: An ab initio based study. Journal of Nuclear Materials, 2012, 429, 173-176.	1.3	5
13957	Stability of self-interstitial atoms in hcp-Zr. Journal of Nuclear Materials, 2012, 429, 233-236.	1.3	43
13958	Trapping of multiple hydrogen atoms in a vanadium monovacancy: A first-principles study. Journal of Nuclear Materials, 2012, 429, 216-220.	1.3	34
13959	Ab initio studies of Nb doping effect on the formation of oxygen vacancy in rutile TiO2. Journal of Physics and Chemistry of Solids, 2012, 73, 84-93.	1.9	15
13960	Transition metal impurity effect on charge and spin density in iron: Ab initio calculations and comparison with MÃ¶ssbauer data. Journal of Physics and Chemistry of Solids, 2012, 73, 317-323.	1.9	10
13961	First-principles study of high-capacity hydrogen storage on graphene with Li atoms. Journal of Physics and Chemistry of Solids, 2012, 73, 245-251.	1.9	88

#	Article	IF	Citations
13962	Ab initio based investigation of interstitial interactions and Snoek relaxation in Nbâ€“O. Journal of Physics and Chemistry of Solids, 2012, 73, 182-187.	1.9	5
13963	Structural, electronic and magnetic properties of Fe(1â^'x)Cox alloy nanowires encapsulated inside (10,0) boron nitride nanotube. Journal of Physics and Chemistry of Solids, 2012, 73, 530-534.	1.9	12
13964	Crystal structures, elastic, and lattice dynamical properties of BeB2, NaB2, and CaB2 from the first principles. Journal of Physics and Chemistry of Solids, 2012, 73, 593-598.	1.9	7
13965	Ab initio calculations on the structural and lattice dynamical properties of TmX (X=As, P) compounds. Journal of Physics and Chemistry of Solids, 2012, 73, 917-924.	1.9	3
13966	Half-metallic ferromagnetic nature of the double perovskite Pb2FeMoO6 from first-principle calculations. Journal of Physics and Chemistry of Solids, 2012, 73, 1116-1121.	1.9	34
13967	Electronic states of metal (Cu, Ag, Au) atom on CeO2(111) surface: The role of local structural distortion. Journal of Power Sources, 2012, 197, 28-37.	4.0	46
13968	Exploring calcium tantalates and niobates as prospective catalyst supports for water electrolysis. Journal of Power Sources, 2012, 202, 190-199.	4.0	8
13969	Effect of Mg-doping on the degradation of LiNiO2-based cathode materials by combined spectroscopic methods. Journal of Power Sources, 2012, 205, 449-455.	4.0	104
13970	First-principles studies of the effects of impurities on the ionic and electronic conduction in LiFePO4. Journal of Power Sources, 2012, 206, 274-281.	4.0	56
13971	Elastic behavior of crystalline Liâ€“Sn phases with increasing Li concentration. Journal of Power Sources, 2012, 208, 165-169.	4.0	57
13972	A combined first-principles computational/experimental study on LiNi0.66Co0.17Mn0.17O2 as a potential layered cathode material. Journal of Power Sources, 2012, 211, 12-18.	4.0	25
13973	Stability and hydrogen storage properties of various metal-decorated benzene complexes. Journal of Power Sources, 2012, 211, 27-32.	4.0	11
13974	Electronic structure and anisotropic chemical bonding in TiNF from ab initio study. Journal of Solid State Chemistry, 2012, 185, 25-30.	1.4	6
13975	Structural, energetic and thermodynamic analyses of Ca(BH4)2Â·2NH3 from first principles calculations. Journal of Solid State Chemistry, 2012, 185, 206-212.	1.4	10
13976	Electronic structure and chemical bonding of Î±- and Î²-CeIr2Si2 intermediate valence compounds. Journal of Solid State Chemistry, 2012, 186, 81-86.	1.4	5
13977	Atomic Pt and molecular H2O adsorptions on SrTiO3 with and without Nb-doping: Electron trapping center and mediating roles of Pt in charge transfer from semiconductor to water. Journal of Solid State Chemistry, 2012, 187, 64-69.	1.4	4
13978	Effects of oxygen vacancy and N-doping on the electronic and photocatalytic properties of Bi2MO6 (M=Mo, W). Journal of Solid State Chemistry, 2012, 187, 103-108.	1.4	78
13979	The T2 phase in the Nbâ€“Siâ€“B system studied by ab initio calculations and synchrotron X-ray diffraction. Journal of Solid State Chemistry, 2012, 190, 111-117.	1.4	11

#	Article	IF	Citations
13980	First-principles study of hydrogen storage on Ti-decorated B2C sheet. Journal of Solid State Chemistry, 2012, 190, 126-129.	1.4	8
13981	Ab initio investigations of the electronic structure and chemical bonding of Li2ZrN2. Journal of Solid State Chemistry, 2012, 190, 191-195.	1.4	6
13982	Decohesion of Ti3SiC2 induced by He impurities. Materials Letters, 2012, 83, 23-26.	1.3	22
13983	Ab initio study of boron segregation and deactivation at Si/SiO2 interface. Microelectronic Engineering, 2012, 89, 120-123.	1.1	16
13984	Revisiting lithium K and iron M2,3 edge superimposition: The case of lithium battery material LiFePO4. Micron, 2012, 43, 16-21.	1.1	20
13985	First-principles study of the methyl formate pathway of methanol steam reforming on PdZn(111) with comparison to Cu(111). Journal of Molecular Catalysis A, 2012, 356, 165-170.	4.8	30
13986	Ammonia decomposition on Fe(1 1 0), Co(1 1 1) and Ni(1 1 1) surfaces: A density functional theory study. Journal of Molecular Catalysis A, 2012, 357, 81-86.	4.8	114
13987	Ideal strength and deformation-induced phase transformation of hcp metals Re, Ru, and Os: A first-principles study. Materials Science & Engineering A: Structural Materials: Properties, Microstructure and Processing, 2012, 534, 353-364.	2.6	12
13988	The effects of alloying elements on generalized stacking fault energies, strength and ductility of Î³â€²-Ni3Al. Materials Science & Engineering A: Structural Materials: Properties, Microstructure and Processing, 2012, 539, 38-41.	2.6	61
13989	Mechanical properties and work function of L21 structure AlCu2X (X=Ti, Mn, Zr, or Hf) intermetallics. Materials Science & Engineering A: Structural Materials: Properties, Microstructure and Processing, 2012, 545, 13-19.	2.6	11
13990	Impeding effect of Ce on He bubble growth in bcc Fe. Nuclear Instruments & Methods in Physics Research B, 2012, 280, 22-25.	0.6	19
13991	Electronic structure and chemical bonding of LiYSi. Solid State Sciences, 2012, 14, 375-380.	1.5	7
13992	7Li and 29Si solid state NMR and chemical bonding of La2Li2Si3. Solid State Sciences, 2012, 14, 367-374.	1.5	10
13993	Structural, electronic, elastic, thermodynamic and vibration properties of TbN compound from first principles calculations. Solid State Sciences, 2012, 14, 401-408.	1.5	22
13994	Elastic properties and electronic structures of typical Alâ€“Ce structures from first-principles calculations. Solid State Sciences, 2012, 14, 555-561.	1.5	41
13995	Electronic structure and bonding of the hydrides Mg3TH7 (TÂ=ÂMn, Re) from first principles. Solid State Sciences, 2012, 14, 639-643.	1.5	2
13996	Zigzag graphene nanoribbons: Flexible and robust transparent conductors. Solid State Sciences, 2012, 14, 711-714.	1.5	6
13997	Evaluation of vanadium substituted In2S3 as a material for intermediate band solar cells. Solar Energy Materials and Solar Cells, 2012, 98, 88-93.	3.0	10

#	Article	IF	Citations
13998	First principles studies of Fe/Co superlattices and multilayers with bcc (001) and (110) orientations. Superlattices and Microstructures, 2012, 51, 92-102.	1.4	8
13999	Electronic and magnetic properties of single-wall GeC nanotubes filled with iron nanowires. Superlattices and Microstructures, 2012, 51, 754-764.	1.4	16
14000	Electrical properties and Raman scattering investigation of Ag doped ZnO thin films. Solid State Communications, 2012, 152, 147-150.	0.9	49
14001	Effects of uniaxial strain on magnetic interactions in Co-doped ZnO nanowires: First-principles calculations. Solid State Communications, 2012, 152, 19-23.	0.9	13
14002	Magnetic and electronic properties of Cr, Mn, and Fe adatoms on Si(001): A first-principles study. Solid State Communications, 2012, 152, 127-131.	0.9	8
14003	Crystal and electronic structures of superhard B2CN : An ab initio study. Solid State Communications, 2012, 152, 71-75.	0.9	16
14004	Theoretical search for half-metallic material: Y MnS3. Solid State Communications, 2012, 152, 288-291.	0.9	3
14005	Superconducting compounds with metallic square net. Solid State Communications, 2012, 152, 666-670.	0.9	7
14006	The predominance of the rutile phase of SnO2 : First principles study. Solid State Communications, 2012, 152, 349-353.	0.9	6
14007	Ab initio study of V doping effects on electronic structure and magnetic properties in Co2Fe1â^'xV xAl. Solid State Communications, 2012, 152, 450-454.	0.9	3
14008	Quasiparticle band structures of IIâ€“VI semiconductors containing semicore states in the approach. Solid State Communications, 2012, 152, 588-592.	0.9	5
14009	Investigation of possible half-metal material on double perovskites Sr2BBO6 (B, B=3d transition metal) using first-principle calculations. Solid State Communications, 2012, 152, 968-973.	0.9	21
14010	First principles calculations on the effect of pressure on SiH4(H2)2. Solid State Communications, 2012, 152, 873-877.	0.9	4
14011	First-principles calculations reveal the n-type doping difficulties of group IIIA elements in zinc blende ZnS. Solid State Communications, 2012, 152, 864-867.	0.9	1
14012	A first principles study of constitutional and thermal defects in D8m-Si3Nb5. Solid State Communications, 2012, 152, 989-993.	0.9	3
14013	First-principles investigation on high-pressure structural evolution of MnTiO3. Solid State Communications, 2012, 152, 984-988.	0.9	6
14014	First-principles study on the origin of ferromagnetism in n-type Cu-doped ZnO. Solid State Communications, 2012, 152, 1057-1060.	0.9	11
14015	Evidence of a medium-range ordered phase and mechanical instabilities in strontium under high pressure. Solid State Communications, 2012, 152, 1172-1175.	0.9	2

#	Article	IF	Citations
14016	InN doped with Zn: Bulk and surface investigation from first principles. Solid State Communications, 2012, 152, 1168-1171.	0.9	5
14017	Theoretical investigation on electronic structure and mechanical properties of cubic crystallographic structures with point defects in Al-based alloys. Solid State Communications, 2012, 152, 1263-1269.	0.9	11
14018	Temperature-induced magnetization reversal and ultra-fast magnetic switch at low field in SmFeO3. Solid State Communications, 2012, 152, 1112-1115.	0.9	92
14019	Ferromagnetic half-metallic characteristic in bulk Ni0.5M0.5O (M=Cu, Zn and Cd): A GGA+U study. Solid State Communications, 2012, 152, 1108-1111.	0.9	10
14020	Strong excitonic effect in organicâ€“inorganic hybrid crystals. Solid State Communications, 2012, 152, 1259-1262.	0.9	1
14021	First-principle study of energy band structure of armchair graphene nanoribbons. Solid State Communications, 2012, 152, 1089-1093.	0.9	35
14022	Energy barriers for proton migration in yttrium-doped barium zirconate super cell with Î£5 (310)/[001] tilt grain boundary. Solid State Ionics, 2012, 213, 18-21.	1.3	23
14023	Proton transport mechanism and pathways in the superprotonic phase of CsHSO4 from experiment and theory. Solid State Ionics, 2012, 213, 72-75.	1.3	9
14024	Periodic long range proton conduction pathways in pseudo-cubic and orthorhombic perovskites. Solid State Ionics, 2012, 213, 8-13.	1.3	10
14025	Thermodynamic assessment of the Snâ€“Sr system supported by first-principles calculations. Thermochimica Acta, 2012, 529, 74-79.	1.2	6
14026	Characterization and analysis of epitaxial silicon phosphorus alloys for use in n-channel transistors. Thin Solid Films, 2012, 520, 3158-3162.	0.8	31
14027	Under-surface observation of thin-film alumina on NiAl(100) with scanning tunneling microscopy. Thin Solid Films, 2012, 520, 3952-3959.	0.8	6
14028	The adsorption of O on (001) and (111) CdTe surfaces: A first-principles study. Thin Solid Films, 2012, 520, 3960-3964.	0.8	6
14029	First-principles study of the (001) and (110) surfaces of superhard ReB2. Thin Solid Films, 2012, 520, 4951-4955.	0.8	4
14030	Epitaxial growth of NiTiO3 with a distorted ilmenite structure. Thin Solid Films, 2012, 520, 5534-5541.	0.8	24
14031	The structural, electronic and magnetic properties of a symmetrical FeMoO terminated (001)-oriented slab of double perovskite Sr2FeMoO6. Thin Solid Films, 2012, 520, 5695-5701.	0.8	2
14032	Theoretical characterization of the TTF/Au (111) interface: STM imaging, band alignment and charging energy. Organic Electronics, 2012, 13, 399-408.	1.4	16
14033	Theoretical study on charge transport properties of cyanovinyl-substituted oligothiophenes. Organic Electronics, 2012, 13, 1213-1222.	1.4	48

#	Article	IF	Citations
14034	First principles study of native defects in BeO. Physics Procedia, 2012, 28, 79-83.	1.2	13
14035	The temperature-dependent elastic properties of B2-MgRE intermetallic compounds from first principles. Physica B: Condensed Matter, 2012, 407, 96-102.	1.3	13
14036	Comparison of the structural and magnetic properties of ground-state SrTcO3 and CaTcO3 from first principles. Physica B: Condensed Matter, 2012, 407, 218-221.	1.3	5
14037	A first-principle study of the structural, elastic, lattice dynamical and thermodynamic properties of PrX (X=P, As). Physica B: Condensed Matter, 2012, 407, 316-323.	1.3	8
14038	Structural, electronic, magnetic and elastic properties of tetragonal layered diselenide KCo2Se2 from first principles calculations. Physica B: Condensed Matter, 2012, 407, 271-275.	1.3	22
14039	First-principles study of martensitic phase transformation of TiRh alloy. Physica B: Condensed Matter, 2012, 407, 347-351.	1.3	7
14040	Electronic structures of zigzag AlN, GaN nanoribbons and AlxGa1â^'xN nanoribbon heterojunctions: First-principles study. Physica B: Condensed Matter, 2012, 407, 515-518.	1.3	16
14041	First-principles study of ferromagnetism in Ti-doped ZnO with oxygen vacancy. Physica B: Condensed Matter, 2012, 407, 743-747.	1.3	9
14042	Structural and electronic properties of copper nanowire encapsulated into BeO nanotube: First-principles study. Physica B: Condensed Matter, 2012, 407, 784-789.	1.3	3
14043	Effects of Zn impurities on the electronic properties of Pr doped CaTiO3. Physica B: Condensed Matter, 2012, 407, 849-854.	1.3	13
14044	Effect of impurity ions configurations on the magnetic properties of Mn-doped ZnO. Physica B: Condensed Matter, 2012, 407, 883-887.	1.3	6
14045	Orbital-decomposed electronic and magnetic properties of the double perovskite Sr2FeReO6. Physica B: Condensed Matter, 2012, 407, 912-917.	1.3	16
14046	A first-principles study of the electronic structure of the sulvanite compounds. Physica B: Condensed Matter, 2012, 407, 985-991.	1.3	17
14047	Electronic properties of anatase TiO2 doped by lanthanides: A DFT+U study. Physica B: Condensed Matter, 2012, 407, 1038-1043.	1.3	61
14048	Ab initio calculations of band structure and thermophysical properties for SnS2 and SnSe2. Physica B: Condensed Matter, 2012, 407, 1146-1152.	1.3	41
14049	A comparison of electronic structure and optical properties between N-doped Î²-Ga2O3 and Nâ€“Zn co-doped Î²-Ga2O3. Physica B: Condensed Matter, 2012, 407, 1227-1231.	1.3	33
14050	Structure, electronic and magnetic properties of Ca-doped chromium oxide studied by the DFT method. Physica B: Condensed Matter, 2012, 407, 1262-1267.	1.3	24
14051	First-principles investigation of Fe-doped MgSiO3-ilmenite. Physica B: Condensed Matter, 2012, 407, 2037-2043.	1.3	5

#	Article	IF	Citations
14052	Structural relative stabilities and pressure-induced phase transitions for lanthanide trihydrides REH3 (RE=Sm, Gd, Tb, Dy, Ho, Er, Tm, and Lu). Physica B: Condensed Matter, 2012, 407, 2050-2057.	1.3	16
14053	Magnetic properties and electronic structures of hcp Fe, Co and Ni nanowires encapsulated in a zigzag (12,0) BN nanotube. Physica B: Condensed Matter, 2012, 407, 2136-2140.	1.3	6
14054	Chemical analysis using coincidence Doppler broadening and supporting first-principles theory: Applications to vacancy defects in compound semiconductors. Physica B: Condensed Matter, 2012, 407, 2684-2688.	1.3	3
14055	First-principles study on structural and electronic properties of AlNSix heterosheet. Physica B: Condensed Matter, 2012, 407, 2301-2305.	1.3	9
14056	Origins of ferromagnetism in transition metal doped diamond. Physica B: Condensed Matter, 2012, 407, 2347-2350.	1.3	4
14057	Structural, electronic and magnetic properties of the double perovskite Pb2FeReO6. Physica B: Condensed Matter, 2012, 407, 2617-2621.	1.3	14
14058	Electronic band structure, stability, structural, and elastic properties of IrTi alloys. Physica B: Condensed Matter, 2012, 407, 2744-2748.	1.3	3
14059	Magnetic properties of (Ga,Mn)N ternaries and structural, electronic, and magnetic properties of cation-mixed (Ga,Mn)(As,N) and (In,Mn)(As,N) quaternaries. Physica B: Condensed Matter, 2012, 407, 2650-2658.	1.3	3
14060	An ab-initio study of (Mn,Al) doped ZnO including strong correlation effects. Physica E: Low-Dimensional Systems and Nanostructures, 2012, 44, 1095-1097.	1.3	4
14061	Modeling of graphene-based NEMS. Physica E: Low-Dimensional Systems and Nanostructures, 2012, 44, 949-954.	1.3	41
14062	First-principles study of the structural, magnetic, and electronic properties of LiMBO3 (M=Mn, Fe, Co). Physics Letters, Section A: General, Atomic and Solid State Physics, 2012, 376, 179-184.	0.9	18
14063	Li and Na Co-decorated carbon nitride nanotubes as promising new hydrogen storage media. Physics Letters, Section A: General, Atomic and Solid State Physics, 2012, 376, 631-636.	0.9	21
14064	Mechanical and electronic properties of monolayer MoS2 under elastic strain. Physics Letters, Section A: General, Atomic and Solid State Physics, 2012, 376, 1166-1170.	0.9	313
14065	First-principles studies of the hydrogenation effects in silicene sheets. Physics Letters, Section A: General, Atomic and Solid State Physics, 2012, 376, 1230-1233.	0.9	119
14066	Influence of spinâ€“orbit coupling on electronic structures of TM@Au12 (<mml:math) Tj ETQq0 0 0 rgBT /Overlock 10 Tf 50 197 Td (xm 1300-1305.	0.9	14
14067	High inertness of W@Si12 cluster toward O2 molecule. Physics Letters, Section A: General, Atomic and Solid State Physics, 2012, 376, 1454-1459.	0.9	6
14068	Effects of oxygen-containing defect complex on the electronic structures and transport properties of single-walled carbon nanotubes. Physics Letters, Section A: General, Atomic and Solid State Physics, 2012, 376, 1686-1691.	0.9	12
14069	Gas sensing applications of 1D-nanostructured zinc oxide: Insights from density functional theory calculations. Progress in Materials Science, 2012, 57, 437-486.	16.0	195

#	Article	IF	Citations
14070	Approximation of the electron density of Aluminium clusters in tensor-product format. Journal of Computational Physics, 2012, 231, 2551-2564.	1.9	9
14071	First-principles calculations of oxygen vacancies and cerium substitution in lutetium pyrosilicate. Journal of Luminescence, 2012, 132, 164-170.	1.5	5
14072	Anisotropy of the electrical conductivity in W-type hexagonal ferrites BaFe18O27 and BaCo2Fe16O27 from first principles. Journal of Magnetism and Magnetic Materials, 2012, 324, 1498-1502.	1.0	20
14073	Co doping effects on structural, electronic and magnetic properties in Mn2VGa. Journal of Magnetism and Magnetic Materials, 2012, 324, 1463-1467.	1.0	13
14074	First-principles study of ferromagnetism in Zn- and Cd-doped SnO2. Journal of Magnetism and Magnetic Materials, 2012, 324, 1764-1769.	1.0	14
14075	Effect of Au proximity on the LSMO surface: An ab initio study. Journal of Magnetism and Magnetic Materials, 2012, 324, 2659-2663.	1.0	5
14076	On the cause for the no spin-gap behavior of the triangular spin tube system CsCrF4. Journal of Magnetism and Magnetic Materials, 2012, 324, 2806-2808.	1.0	11
14077	High-pressure phase transitions and equations of state in NiSi. I.Ab initiosimulations. Journal of Applied Crystallography, 2012, 45, 186-196.	1.9	13
14078	Parameters for temperature dependence of mean-square displacements for B-, Bi- and Tl-containing binary IIIâ€“V compounds. Acta Crystallographica Section A: Foundations and Advances, 2012, 68, 319-323.	0.3	3
14079	Ab-initio crystal structure analysis and refinement approaches of oligo p-benzamides based on electron diffraction data. Acta Crystallographica Section B: Structural Science, 2012, 68, 171-181.	1.8	49
14080	Constrained evolutionary algorithm for structure prediction of molecular crystals: methodology and applications. Acta Crystallographica Section B: Structural Science, 2012, 68, 215-226.	1.8	146
14081	Comparisons of Performance Potentials of Si and InAs Nanowire MOSFETs Under Ballistic Transport. IEEE Transactions on Electron Devices, 2012, 59, 206-211.	1.6	20
14082	Computer simulation and experimental investigation of the crystal structure and electronic properties of InN/Si and GaN/Si thin films. Bulletin of the Russian Academy of Sciences: Physics, 2012, 76, 696-698.	0.1	0
14083	Features of the structure and properties of Î²-FeSi2 nanofilms and a Î²-FeSi2/Si interface. JETP Letters, 2012, 95, 20-24.	0.4	3
14084	Theoretical study of the diffusion of lithium in crystalline and amorphous silicon. JETP Letters, 2012, 95, 143-147.	0.4	16
14085	Ab initio study of 2DEG at the surface of topological insulator Bi2Te3. JETP Letters, 2012, 95, 213-218.	0.4	22
14086	Ab initio study of the structure of oriented films of linearly chain carbon. JETP Letters, 2012, 95, 462-466.	0.4	6
14087	New interatomic potential for computation of mechanical and thermodynamic properties of uranium in a wide range of pressures and temperatures. Physics of Metals and Metallography, 2012, 113, 107-116.	0.3	12

#	Article	IF	Citations
14088	A first-principles investigation of the effect of relaxation on the alloy formation in the aluminum-3d-transition-metal system. Physics of Metals and Metallography, 2012, 113, 427-437.	0.3	1
14089	Interaction of scandium and titanium atoms with a carbon surface containing five- and seven-membered rings. Journal of Experimental and Theoretical Physics, 2012, 114, 80-84.	0.2	0
14090	Adhesion at the interfaces between BCC metals and Î±-Al2O3. Journal of Experimental and Theoretical Physics, 2012, 114, 305-313.	0.2	12
14091	Theoretical investigation of the atomic and electronic structure of Li x BC3 intercalated compounds. Journal of Experimental and Theoretical Physics, 2012, 114, 1018-1021.	0.2	3
14092	Atomistic simulation of laser ablation of gold: Effect of pressure relaxation. Journal of Experimental and Theoretical Physics, 2012, 114, 792-800.	0.2	66
14093	Magnetism and unusual Cu valency in quadruple perovskites. European Physical Journal B, 2012, 85, 1.	0.6	10
14094	The role of size in spin properties of zigzag graphene nanoribbon. European Physical Journal B, 2012, 85, 1.	0.6	1
14095	The Mechanism of Lowâ€Temperature CO Oxidation on IB Group Metals and Metal Oxides. ChemCatChem, 2012, 4, 100-111.	1.8	25
14096	Adsorption of Uranyl Species onto the Rutile (110) Surface: A Periodic DFT Study. Chemistry - A European Journal, 2012, 18, 1458-1466.	1.7	37
14097	Selective Response of Mesoporous Silicon to Adsorbants with Nitro Groups. Chemistry - A European Journal, 2012, 18, 2912-2922.	1.7	6
14098	The effect of structure and phase transformation on the mechanical properties of Re₂N and the stability of Mn₂N. Journal of Computational Chemistry, 2012, 33, 18-24.	1.5	11
14099	Firstâ€principle investigation of magnetic coupling mechanism in hypothesized Aâ€siteâ€ordered perovskite YMn₃Sc₄O₁₂. Journal of Computational Chemistry, 2012, 33, 82-87.	1.5	4
14100	Electronic structure and low temperature thermoelectric properties of In₂₄ M₈ O₄₈ (M = Ge⁴⁺, Sn⁴⁺, Ti⁴⁺, and) Tj ETQq0 0 1 rgBT /Overlock 10	1.5	8
14101	Dispersive interactions in water bilayers at metallic surfaces: A comparison of the PBE and RPBE functional including semiempirical dispersion corrections. Journal of Computational Chemistry, 2012, 33, 695-701.	1.5	136
14102	Structure and Electronic Properties and Phase Stabilities of the Cd_{1â^'x}Zn_xS Solid Solution in the Range of 0â‰¤xâ‰¤1. ChemPhysChem, 2012, 13, 147-154.	1.0	21
14103	Isentropic Compression of Deuterium by Quantum Molecular Dynamics. Contributions To Plasma Physics, 2012, 52, 33-36.	0.5	17
14104	Multiscale prediction of mechanical behavior of ferriteâ€“pearlite steel with numerical material testing. International Journal for Numerical Methods in Engineering, 2012, 89, 829-845.	1.5	44
14105	Metalâ€“Organic Hybrid Interface States of A Ferromagnet/Organic Semiconductor Hybrid Junction as Basis For Engineering Spin Injection in Organic Spintronics. Advanced Functional Materials, 2012, 22, 989-997.	7.8	122

#	Article	IF	Citations
14106	Halfâ€Metallic Antiferromagnet as a Prospective Material for Spintronics. Advanced Materials, 2012, 24, 294-298.	11.1	117
14107	Surface Modification of Indiumâ€Tinâ€Oxide Via Selfâ€Assembly of a Donorâ€Acceptor Complex: A Density Functional Theory Study. Advanced Materials, 2012, 24, 687-693.	11.1	10
14108	Valence Stateâ€Dependent Ferromagnetism in Mnâ€Doped NiO Thin Films. Advanced Materials, 2012, 24, 353-357.	11.1	40
14109	Polarizationâ€Induced Charge Distribution at Homogeneous Zincblende/Wurtzite Heterostructural Junctions in ZnSe Nanobelts. Advanced Materials, 2012, 24, 1328-1332.	11.1	30
14111	The Atomic Structure of a Metalâ€Supported Vitreous Thin Silica Film. Angewandte Chemie - International Edition, 2012, 51, 404-407.	7.2	207
14112	A first-principles study of site occupancy and interfacial energetics of an H-doped TiAl-Ti3Al alloy. Science China: Physics, Mechanics and Astronomy, 2012, 55, 228-234.	2.0	12
14113	Effects of 3d Transition Metal Elements in the B2-FeAl Structure. Metallurgical and Materials Transactions A: Physical Metallurgy and Materials Science, 2012, 43, 757-762.	1.1	4
14114	Microstructure and Thickness of 55 pct Al-Zn-1.6 pct Si-0.2 pct RE Hot-Dip Coatings: Experiment, Thermodynamic, and First-Principles Study. Metallurgical and Materials Transactions B: Process Metallurgy and Materials Processing Science, 2012, 43, 198-205.	1.0	16
14115	Thermodynamic Optimization of the Sc-X (XÂ=ÂLa, Li, Ca, Cr) Systems. Journal of Phase Equilibria and Diffusion, 2012, 33, 40-45.	0.5	3
14116	Shear-induced low-dimension electron transport in (LaMnO3)2/(SrMnO3)2 superlattice. Applied Physics A: Materials Science and Processing, 2012, 106, 119-124.	1.1	2
14117	Conduction modulation of Ï€-stacked ethylbenzene wires on Si(100) with substituent groups. Theoretical Chemistry Accounts, 2012, 131, 1.	0.5	9
14118	Thermodynamic Properties of MgSc and AlSc from First-Principles Phonon Calculations. International Journal of Thermophysics, 2012, 33, 300-310.	1.0	16
14119	Elastic properties of random L12â€“Al3(Sc0.5TM0.5) alloys from first-principle SQSs calculations. Journal of Materials Science, 2012, 47, 3793-3800.	1.7	7
14120	Structural, elastic, electronic, and optical properties of defect-chalcopyrite structure CdGa2 X 4 (XÂ=ÂS, Se) compounds. Journal of Materials Science, 2012, 47, 3849-3854.	1.7	34
14121	Spin/Charge Redistributions and Oxygen Atom Displacements Induced by Spin Flip and Hole Doping in the CuO2 Layer of High-Temperature Superconductors. Journal of Superconductivity and Novel Magnetism, 2012, 25, 55-59.	0.8	2
14122	Theoretical study of the surface properties of poly(dimethylsiloxane) and poly(tetrafluoroethylene). Journal of Molecular Modeling, 2012, 18, 239-250.	0.8	3
14123	Noncovalent and covalent functionalization of a (5, 0) single-walled carbon nanotube with alanine and alanine radicals. Journal of Molecular Modeling, 2012, 18, 771-781.	0.8	19
14124	Assessing structural bonding aspects of multiband superconductors through impurityâ€induced local lattice distortions: A case study on MgB₂. International Journal of Quantum Chemistry, 2013, 113, 643-650.	1.0	0

#	Article	IF	Citations
14125	Lead adsorption on the pseudoâ€10â€fold surface of the Al₁₃Co₄ complex metallic alloy: A first principle study. International Journal of Quantum Chemistry, 2013, 113, 840-846.	1.0	5
14126	Firstâ€principles investigation of magnetic property and defect formation energy in Niâ€Mnâ€Ga ferromagnetic shape memory alloy. International Journal of Quantum Chemistry, 2013, 113, 847-851.	1.0	10
14127	Crystal structures and thermodynamic investigations of NaSc(BH₄)₄ from firstâ€principles calculations. International Journal of Quantum Chemistry, 2013, 113, 119-124.	1.0	6
14128	Scanning tunneling microscopy and density functional theory combined studies of rutile TiO₂(1 1 0) surface chemistry: Watch surface processes at the atomic scale. International Journal of Quantum Chemistry, 2013, 113, 89-95.	1.0	7
14129	Geometric and magnetic properties of Co adatom decorated nitrogen-doped graphene. Journal of Applied Physics, 2013, 113, .	1.1	11
14130	Low-Potential Sodium Insertion in a NASICON-Type Structure through the Ti(III)/Ti(II) Redox Couple. Journal of the American Chemical Society, 2013, 135, 3897-3903.	6.6	213
14131	Exocyclobutadieneite. Journal of Mathematical Chemistry, 2013, 51, 868-880.	0.7	1
14132	Adsorption of Single Li and the Formation of Small Li Clusters on Graphene for the Anode of Lithium-Ion Batteries. ACS Applied Materials & Interfaces, 2013, 5, 7793-7797.	4.0	190
14133	Numerical Solution of the Kohn-Sham Equation by Finite Element Methods with an Adaptive Mesh Redistribution Technique. Journal of Scientific Computing, 2013, 55, 372-391.	1.1	19
14134	A density functional theory analysis of trends in glycerol decomposition on close-packed transition metal surfaces. Physical Chemistry Chemical Physics, 2013, 15, 6475.	1.3	72
14135	Nickel Dimers Adsorbed on Graphene: First-Principles Study. Journal of Superconductivity and Novel Magnetism, 2013, 26, 3515-3522.	0.8	4
14136	Structural and Magnetic Properties of MnTe Phases from Ab Initio Calculations. Journal of Superconductivity and Novel Magnetism, 2013, 26, 1963-1972.	0.8	26
14137	Magnetism in Double Perovskites. Journal of Superconductivity and Novel Magnetism, 2013, 26, 1991-1995.	0.8	36
14138	Magnetism of Nano-Graphene with Defects: A Monte Carlo Study. Journal of Superconductivity and Novel Magnetism, 2013, 26, 679-685.	0.8	70
14139	Investigation on electronic, mechanical and thermal properties of Hfâ€“H system. Journal of Nuclear Materials, 2013, 443, 99-106.	1.3	7
14140	Ferric garnet matrices for immobilization of actinides. Journal of Nuclear Materials, 2013, 436, 1-7.	1.3	17
14141	Kinetic theory molecular dynamics; numerical considerations. High Energy Density Physics, 2013, 9, 696-701.	0.4	6
14142	Inversion domain boundaries on tin (Sn)-doped ZnO nanobelts: Aberration-corrected scanning transmission electron microscopy study. Applied Physics Letters, 2013, 102, 033103.	1.5	7

#	Article	IF	Citations
14143	Analysis of the origin of lateral interactions in the adsorption of small organic molecules on oxide surfaces. Theoretical Chemistry Accounts, 2013, 132, 1.	0.5	5
14144	An insight into evolution of electronic, magnetic, optical, and vibrational properties of ultrathin Pd nanowires. Journal of Nanoparticle Research, 2013, 15, 1.	0.8	4
14145	Manipulation of half-metallicity and ferromagnetism in N-doped CdS nanowire. Journal of Nanoparticle Research, 2013, 15, 1.	0.8	6
14146	Finite size effects on the magnetocrystalline anisotropy energy in Fe magnetic nanowires from first principles. Journal of Nanoparticle Research, 2013, 15, 1.	0.8	11
14148	Cs₂M^{II}M^{IV}₃Q₈ (Q = S, Se, Te): An Extensive Family of Layered Semiconductors with Diverse Band Gaps. Chemistry of Materials, 2013, 25, 3344-3356.	3.2	75
14149	Thermodynamic modeling of the Uâ€“Zr system â€“ A revisit. Journal of Nuclear Materials, 2013, 443, 331-341.	1.3	60
14150	First-Principles Study of Microporous Magnets M-MOF-74 (M = Ni, Co, Fe, Mn): the Role of Metal Centers. Inorganic Chemistry, 2013, 52, 9356-9362.	1.9	94
14151	Vacancies and defect levels in IIIâ€“V semiconductors. Journal of Applied Physics, 2013, 114, .	1.1	53
14152	Python Materials Genomics (pymatgen): A robust, open-source python library for materials analysis. Computational Materials Science, 2013, 68, 314-319.	1.4	2,392
14153	Electronic Structures of Antimony Oxides. Journal of Physical Chemistry C, 2013, 117, 14759-14769.	1.5	80
14154	Density Functional Theory Models for Radiation Damage. Annual Review of Materials Research, 2013, 43, 35-61.	4.3	101
14155	First-principles study of carbon atoms adsorbed on MgO(100) related to graphene growth. Current Applied Physics, 2013, 13, 327-330.	1.1	27
14156	Octahedral tilting-induced ferroelectricity in<mml:math xmlns:mml="http://www.w3.org/1998/Math/MathML" display="inline"><mml:mi>A</mml:mi></mml:math>SnO<mml:math xmlns:mml="http://www.w3.org/1998/Math/MathML" display="inline"><mml:msub><mml:mrow /><mml:mn>3</mml:mn></mml:msub></mml:math>/<mml:math xmlns:mml="http://www.w3.org/1998/Math/MathML" display="inline"><mml:msup><mml:mi>A</mml:mi>	1.1	30
14157	Stable cycling of lithium sulfide cathodes through strong affinity with a bifunctional binder. Chemical Science, 2013, 4, 3673.	3.7	412
14158	Defect Chemistry of Rutile TiO₂ from First Principles Calculations. Journal of Physical Chemistry C, 2013, 117, 5919-5930.	1.5	45
14159	SAM-like arrangement of thiolated graphene nanoribbons: decoupling the edge state from the metal substrate. Physical Chemistry Chemical Physics, 2013, 15, 3233.	1.3	2
14160	DFT Study of the Adsorption of <scp>d</scp>-(<scp>l</scp>-)Cysteine on Flat and Chiral Stepped Gold Surfaces. Langmuir, 2013, 29, 8856-8864.	1.6	50
14161	Noncrystalline-to-Crystalline Transformations in Pt Nanoparticles. Journal of the American Chemical Society, 2013, 135, 13062-13072.	6.6	71

#	Article	IF	Citations
14162	DFT study on crystalline 1,1-diamino-2,2-dintroethylene under high pressures. Journal of Molecular Modeling, 2013, 19, 4039-4047.	0.8	25
14163	Hole-lattice coupling and photoinduced insulator-metal transition in VO<mml:math xmlns:mml="http://www.w3.org/1998/Math/MathML" display="inline"><mml:msub><mml:mrow /><mml:mn>2</mml:mn></mml:msub></mml:math>. Physical Review B, 2013, 88, .	1.1	62
14164	Reversible anionic redox chemistry in high-capacity layered-oxide electrodes. Nature Materials, 2013, 12, 827-835.	13.3	1,192
14165	Higher-order adaptive finite-element methods for Kohnâ€“Sham density functional theory. Journal of Computational Physics, 2013, 253, 308-343.	1.9	98
14166	Competing atomic and molecular mechanisms of thermal oxidationâ€”SiC versus Si. Journal of Applied Physics, 2013, 114, .	1.1	14
14167	Copper(II) Complexes with Aromatico-Phosphorylated Phenols - Synthesis, Crystal Structures, and X-ray Photoelectron Spectroscopy. European Journal of Inorganic Chemistry, 2013, 2013, 4823-4831.	1.0	10
14168	On the Stereochemical Inertness of the Auride Lone Pair: Ab Initio Studies of AAu (A = K, Rb, Cs). Inorganic Chemistry, 2013, 52, 8183-8189.	1.9	26
14169	Ab initio calculation of transport and optical properties of aluminum: Influence of simulation parameters. Computational Materials Science, 2013, 79, 817-829.	1.4	44
14170	Dielectric and magnetic properties of BiFe1-4x/3TixO3 ceramics with iron vacancies: Experimental and first-principles studies. Journal of Applied Physics, 2013, 114, .	1.1	19
14171	DFT+U Study of Arsenate Adsorption on FeOOH Surfaces: Evidence for Competing Binding Mechanisms. Journal of Physical Chemistry C, 2013, 117, 15571-15582.	1.5	43
14172	Two-dimensional carbon allotropes from graphene to graphyne. Journal of Materials Chemistry C, 2013, 1, 3677.	2.7	116
14173	Prediction of a new two-dimensional metallic carbon allotrope. Physical Chemistry Chemical Physics, 2013, 15, 2024-2030.	1.3	124
14174	Magnetic and electronic properties of Fe/Cu multilayered nanowires: A first-principles investigation. Physica E: Low-Dimensional Systems and Nanostructures, 2013, 50, 1-5.	1.3	24
14175	Role of Phenolic Groups in the Stabilization of Palladium Nanoparticles. Industrial & Engineering Chemistry Research, 2013, 52, 9783-9789.	1.8	28
14176	First principle and ReaxFF molecular dynamics investigations of formaldehyde dissociation on Fe(100) surface. Journal of Computational Chemistry, 2013, 34, 1982-1996.	1.5	11
14177	First-principles investigation of Li ion diffusion in Li2FeSiO4. Solid State Ionics, 2013, 247-248, 8-14.	1.3	25
14178	First-principles study of structure and stability in Siâ€“Câ€“O-based materials. Theoretical Chemistry Accounts, 2013, 132, 1.	0.5	8
14179	The Unusual and the Expected in the Si/C Phase Diagram. Journal of the American Chemical Society, 2013, 135, 11651-11656.	6.6	42

#	Article	IF	Citations
14180	Buckled Silicene Formation on Ir(111). Nano Letters, 2013, 13, 685-690.	4.5	1,074
14181	A sum rule for inelastic electron tunneling spectroscopy: an ab initio study of a donor (TTF) and acceptors (TCNE, TCNQ and DCNQI) parallelly oriented on Cu(100). Physical Chemistry Chemical Physics, 2013, 15, 16111.	1.3	6
14182	Structural stability of higher-energy phases in Cu and Cuâ€“Fe alloy revealed by ab initio calculations. Computational Materials Science, 2013, 79, 463-467.	1.4	8
14183	Determination of the Insulation Gap of Uranium Oxides by Spectroscopic Ellipsometry and Density Functional Theory. Journal of Physical Chemistry C, 2013, 117, 16540-16551.	1.5	57
14184	The Feâ€“Mn enthalpy phase diagram from first principles. Journal of Alloys and Compounds, 2013, 577, 370-375.	2.8	15
14185	Commentary: The Materials Project: A materials genome approach to accelerating materials innovation. APL Materials, 2013, 1, .	2.2	6,913
14186	Absence and presence of Dirac electrons in silicene on substrates. Physical Review B, 2013, 87, .	1.1	195
14187	Formation of CO₂ and Ethane from Propionyl over Platinum: A Density Functional Theory Study. ACS Catalysis, 2013, 3, 1730-1738.	5.5	5
14188	A first-principles study on magnetocrystalline anisotropy at interfaces of Fe with non-magnetic metals. Journal of Applied Physics, 2013, 113, 233908.	1.1	29
14189	Stacking and electric field effects in atomically thin layers of GaN. Journal of Physics Condensed Matter, 2013, 25, 345302.	0.7	68
14190	Electronic structures of silicene/GaS heterosheets. Applied Physics Letters, 2013, 103, .	1.5	105
14191	Strain induced variations in band offsets and built-in electric fields in InGaN/GaN multiple quantum wells. Journal of Applied Physics, 2013, 114, .	1.1	24
14192	Theoretical study of selective hydrogenation in a mixture of acetylene and ethylene over Fe@W(111) bimetallic surfaces. Applied Catalysis A: General, 2013, 462-463, 296-301.	2.2	5
14193	First principles investigations of structural, electronic, elastic, and dielectric properties of KMgF3. Journal of Materials Science, 2013, 48, 7635-7641.	1.7	19
14194	Density Functional Theory-Computed Mechanisms of Ethylene and Diethyl Ether Formation from Ethanol on Î³-Al₂O₃(100). ACS Catalysis, 2013, 3, 1965-1975.	5.5	130
14195	Tunable Bandgap in Bilayer Armchair Graphene Nanoribbons: Concurrent Influence of Electric Field and Uniaxial Strain. IEEE Transactions on Electron Devices, 2013, 60, 2464-2470.	1.6	19
14196	Two-step spin-switchable tetranuclear Fe(II) molecular solid:Ab initiotheory and predictions. Physical Review B, 2013, 88, .	1.1	12
14197	The first transition metal iodato peroxido complex: the synthesis, vibrational spectra and crystal structure from powder diffraction data of K3[V2O2(O2)4(IO3)]Â·H2O. Open Chemistry, 2013, 11, 1352-1359.	1.0	0

#	Article	IF	Citations
14198	Lattice Dynamics Study of HgGa₂Se₄ at High Pressures. Journal of Physical Chemistry C, 2013, 117, 15773-15781.	1.5	21
14199	Environment-driven reactivity of H2 on PdRu surface alloys. Physical Chemistry Chemical Physics, 2013, 15, 14936.	1.3	15
14200	Magnetic hollow cages with colossal moments. Journal of Chemical Physics, 2013, 139, 044301.	1.2	6
14201	Structural and electronic properties of grapheneâ€“ZnO interfaces: dispersion-corrected density functional theory investigations. Nanotechnology, 2013, 24, 305401.	1.3	67
14202	First-principles calculations of ferroelectric properties in AAâ€²BBâ€²O6 double perovskites with different types of cation ordering. Physica Status Solidi (B): Basic Research, 2013, 250, 1888-1897.	0.7	8
14203	Mechanical and Electronic Properties of Graphyne and Its Family under Elastic Strain: Theoretical Predictions. Journal of Physical Chemistry C, 2013, 117, 14804-14811.	1.5	151
14204	Joined edges in MoS₂: metallic and half-metallic wires. Journal of Physics Condensed Matter, 2013, 25, 312201.	0.7	21
14205	Interface effects at a ferromagnetic and ferroelectric junction. Thin Solid Films, 2013, 540, 92-95.	0.8	5
14206	Atomic structure and electronic properties of folded graphene nanoribbons: A first-principles study. Journal of Applied Physics, 2013, 113, .	1.1	17
14207	Thermodynamic reassessment of the Alâ€“Crâ€“Si system with the refined description of the Alâ€“Cr system. Thermochimica Acta, 2013, 561, 77-90.	1.2	28
14208	Site preference, magnetism and lattice vibrations of intermetallics M7â^'xTxB3 (MÂ=ÂRh, Ru; TÂ=ÂFe, Co). Intermetallics, 2013, 42, 112-119.	1.8	8
14209	Structural, elastic and electronic properties of new layered superconductor HfCuGe2 in comparison with isostructural HfCuSi2, ZrCuGe2, and ZrCuSi2 from first-principles calculations. Intermetallics, 2013, 42, 130-136.	1.8	6
14210	Heating of Zeolites under Microwave Irradiation: A Density Functional Theory Approach to the Ion Movements Responsible of the Dielectric Loss in Na, K, and Ca A-Zeolites. Journal of Physical Chemistry C, 2013, 117, 15659-15666.	1.5	16
14211	Adsorption of formaldehyde and formyl intermediates on Pt, PtRu-, and PtRuMo-alloy surfaces: A density functional study. Applied Surface Science, 2013, 266, 405-409.	3.1	10
14212	Ab initio study of CO adsorption on PdGa(110). Computational Materials Science, 2013, 71, 192-196.	1.4	9
14213	Many-body quasiparticle spectrum of Co-doped ZnO: A<mml:math xmlns:mml="http://www.w3.org/1998/Math/MathML" display="inline"><mml:mrow><mml:mi>G</mml:mi><mml:mi>W</mml:mi></mml:mrow></mml:math>perspective. Physical Review B, 2013, 87, .	1.1	22
14214	Electronic and thermoelectric properties of assembled graphene nanoribbons with elastic strain and structural dislocation. Applied Physics Letters, 2013, 102, .	1.5	31
14215	Theoretical Studies on Ethylene Selectivity in the Oxidative Dehydrogenation Reaction on Undoped and Doped Nanostructured Carbon Catalysts. Chemistry - an Asian Journal, 2013, 8, 2605-2608.	1.7	18

#	Article	IF	Citations
14216	Interaction of dioxygen with the platinum Pt19/SnO2/H2 cluster: DFT calculation. Russian Journal of Inorganic Chemistry, 2013, 58, 311-319.	0.3	1
14217	Properties of Disorder-Engineered Black Titanium Dioxide Nanoparticles through Hydrogenation. Scientific Reports, 2013, 3, 1510.	1.6	317
14218	Carbon-supported bimetallic Pdâ€“Fe catalysts for vapor-phase hydrodeoxygenation of guaiacol. Journal of Catalysis, 2013, 306, 47-57.	3.1	384
14219	Ab initio molecular dynamics study of the structure of undercooled Ni melt. Journal of Non-Crystalline Solids, 2013, 376, 216-220.	1.5	12
14220	Improving microstructure of silicon/carbon nanofiber composites as a Li battery anode. Journal of Power Sources, 2013, 221, 455-461.	4.0	50
14221	Nanoscale Dielectric Capacitors Composed of Graphene and Boron Nitride Layers: A First-Principles Study of High Capacitance at Nanoscale. Journal of Physical Chemistry C, 2013, 117, 15327-15334.	1.5	45
14222	Two-Dimensional Materials from Data Filtering andAb InitioCalculations. Physical Review X, 2013, 3, .	2.8	180
14223	Effect of Moleculeâ€“Surface Reaction Mechanism on the Electronic Characteristics and Photovoltaic Performance of Molecularly Modified Si. Journal of Physical Chemistry C, 2013, 117, 22351-22361.	1.5	25
14224	Exceptional Tunability of Band Energy in a Compressively Strained Trilayer MoS₂ Sheet. ACS Nano, 2013, 7, 7126-7131.	7.3	550
14225	Highly sensitive spin-crossover transition in a metal-organic molecular crystal. Physical Review B, 2013, 88, .	1.1	1
14226	C4 Carbon allotropes with triple-bonds predicted by first-principles calculations. Solid State Communications, 2013, 169, 50-56.	0.9	9
14227	Dirac Cones in Two-Dimensional Lattices: Janugraphene and Chlorographene. Journal of Physical Chemistry Letters, 2013, 4, 2471-2476.	2.1	25
14228	An ab initio study on the transition paths from graphite to diamond under pressure. Journal of Physics Condensed Matter, 2013, 25, 145402.	0.7	22
14229	First-principles study of L12â€“Al3(Sc1â^'xTMx) alloys using special quasirandom structures. Computational Materials Science, 2013, 79, 136-142.	1.4	10
14230	The Physics of Copper Oxide (Cu2O). Semiconductors and Semimetals, 2013, , 201-226.	0.4	34
14231	Structural stabilities and uniaxial strain modulated electronic properties of AlN/SiC-coreâ€“shell nanowires: A first-principles study. Superlattices and Microstructures, 2013, 57, 19-26.	1.4	5
14232	Scalable properties of metal clusters: A comparative DFT study of ionic-core treatments. Chemical Physics Letters, 2013, 578, 92-96.	1.2	8
14233	Magnetic and electronic properties of Cu1â^'xFexO from first principles calculations. RSC Advances, 2013, 3, 4447.	1.7	3

#	Article	IF	Citations
14234	Topological Signatures in the Electronic Structure of Graphene Spirals. Scientific Reports, 2013, 3, 1632.	1.6	36
14235	Unidirectional Molecular Stacking of Tribenzotriquinacenes in the Solid State: A Combined Xâ€ray and Theoretical Study. Chemistry - A European Journal, 2013, 19, 9930-9938.	1.7	46
14236	First-principles calculations of finite-temperature elastic properties of Ti2AlX (X=C or N). Computational Materials Science, 2013, 79, 296-302.	1.4	24
14237	Elastic properties of VO2 from first-principles calculation. Solid State Communications, 2013, 167, 1-4.	0.9	17
14238	Graphane- and Fluorographene-Based Quantum Dots. Journal of Physical Chemistry C, 2013, 117, 16242-16247.	1.5	14
14239	Unusual Magnetic Properties of Functionalized Graphene Nanoribbons. Journal of Physical Chemistry Letters, 2013, 4, 2482-2488.	2.1	22
14240	Theoretical Understanding of Enhanced Photoelectrochemical Catalytic Activity of Sn-Doped Hematite: Anisotropic Catalysis and Effects of Morin Transition and Sn Doping. Journal of Physical Chemistry C, 2013, 117, 3779-3784.	1.5	51
14241	Syntheses, Structures, and Nonlinear Optical Properties of Quaternary Chalcogenides: Pb₄Ga₄GeQ₁₂ (Q = S, Se). Inorganic Chemistry, 2013, 52, 8334-8341.	1.9	50
14242	Stabilization mechanism for the polar ZnO(000<mml:math) Tj ETQq0 0 0 rgBT /Overlock 10 Tf 50 432 Td (xmlns:mml="http://www.w3.c Physical Review B, 2013, 87, .	1.1	77
14243	Understanding the Influence of Nickel Doping in a Tungsten Grain Boundary on Mechanical Strength. , 2013, , .		0
14244	How relevant is the choice of classical potentials in finding minimal energy cluster conformations?. Computational and Theoretical Chemistry, 2013, 1021, 155-163.	1.1	8
14245	Properties of Fe8â^'NCoN nanoribbons and nanowires: A DFT approach. Journal of Magnetism and Magnetic Materials, 2013, 339, 75-80.	1.0	2
14246	Preparation-method-dependent morphological, band structural, microstructural, and photocatalytic properties of noble metalâ€“GaNbO4 nanocomposites. RSC Advances, 2013, 3, 16817.	1.7	10
14247	Defective Graphene Supported MPd₁₂ (M = Fe, Co, Ni, Cu, Zn, Pd) Nanoparticles as Potential Oxygen Reduction Electrocatalysts: A First-Principles Study. Journal of Physical Chemistry C, 2013, 117, 1350-1357.	1.5	88
14248	Single-Layer Group-III Monochalcogenide Photocatalysts for Water Splitting. Chemistry of Materials, 2013, 25, 3232-3238.	3.2	675
14249	Effect of Rb and Ta Doping on the Ionic Conductivity and Stability of the Garnet Li_{7+2xâ€“y}(La_{3â€“x}Rb_x)(Zr_{2â€“y}Ta_y (0 â‰¤ x â‰¤ 0.375, 0 â‰¤ y â‰¤ 1) Superionic Conductor: A First Principles Investigation. Chemistry of Materials, 2013, 25, 3048-3055.	3.2	185
14250	Squaroglitter: A 3,4-Connected Carbon Net. Journal of Chemical Theory and Computation, 2013, 9, 3855-3859.	2.3	8
14251	Electronic states of disordered grain boundaries in graphene prepared by chemical vapor deposition. Carbon, 2013, 64, 178-186.	5.4	36

#	Article	IF	Citations
14252	Mapping the 3D surface potential in Bi2Se3. Nature Communications, 2013, 4, 2277.	5.8	46
14253	Magnetic Properties of bcc-Fe(001)/C₆₀ Interfaces for Organic Spintronics. ACS Applied Materials & Interfaces, 2013, 5, 837-841.	4.0	39
14254	Origin of the unique activity of Pt/TiO2 catalysts for the waterâ€“gas shift reaction. Journal of Catalysis, 2013, 306, 78-90.	3.1	76
14255	Electronic Properties of Silver Doped TiO2 Anatase (100) Surface. ACS Symposium Series, 2013, , 187-218.	0.5	11
14256	Magnetic Properties of the RbMnPO4Zeolite-ABW-Type Material: A Frustrated Zigzag Spin Chain. Inorganic Chemistry, 2013, 52, 9627-9635.	1.9	15
14257	Graphene-Oxide-Stabilized Atomic Ti for H₂O₂ Activation and Propylene Epoxidation: A First-Principle Study. Journal of Physical Chemistry C, 2013, 117, 16005-16011.	1.5	15
14258	Thermodynamic stability of various phases of zinc tin oxides from ab initio calculations. Journal of Materials Chemistry C, 2013, 1, 6364.	2.7	28
14259	Anions vs. Cations of Pt13H24 Cluster Models: Ab Initio Molecular Dynamics Investigation of Electronic Properties and Photocatalytic Activity. ACS Symposium Series, 2013, , 173-185.	0.5	2
14260	Effects of pressure on the electronic structures of LaOFeP. Physics Letters, Section A: General, Atomic and Solid State Physics, 2013, 377, 1479-1485.	0.9	0
14261	Unified model of ferroelectricity induced by spin order. Physical Review B, 2013, 88, .	1.1	41
14262	Paramagnetic Silicon Nanoparticles Without Magnetic Ion Doping: An Ab-Initio Study Prediction. Silicon, 2013, 5, 255-262.	1.8	4
14263	High pressure iso-structural phase transition in BiMn₂O₅. Journal of Physics Condensed Matter, 2013, 25, 325401.	0.7	8
14264	Coherent electron transport through freestanding graphene junctions with metal contacts: a materials approach. Journal of Computational Electronics, 2013, 12, 145-164.	1.3	8
14265	Effect of zinc oxide as a sintering aid on proton migration across Î£5 (310)/[001] tilt grain boundary of barium zirconate. Journal of Electroceramics, 2013, 30, 19-23.	0.8	1
14266	Atomic structure of hardening precipitates in an Alâ€“Mgâ€“Znâ€“Cu alloy determined by HAADF-STEM and first-principles calculations: relation to Î·-MgZn2. Journal of Materials Science, 2013, 48, 3638-3651.	1.7	85
14267	First-principles study of native point defects in Bi2Se3. AIP Advances, 2013, 3, .	0.6	73
14268	Rationale of Drug Encapsulation and Release from Biocompatible Porous Metalâ€“Organic Frameworks. Chemistry of Materials, 2013, 25, 2767-2776.	3.2	412
14269	Charge transport in lithium peroxide: relevance for rechargeable metalâ€“air batteries. Energy and Environmental Science, 2013, 6, 2370.	15.6	293

#	Article	IF	Citations
14271	Crystal Structure Prediction of a Flexible Molecule of Pharmaceutical Interest with Unusual Polymorphic Behavior. Crystal Growth and Design, 2013, 13, 581-589.	1.4	53
14272	Structures, mobilities, electronic and magnetic properties of point defects in silicene. Nanoscale, 2013, 5, 9785.	2.8	230
14273	Hydrogen trapping in Î´-Pu: insights from electronic structure calculations. Journal of Physics Condensed Matter, 2013, 25, 265001.	0.7	12
14274	Antiferromagnetic-like coupling in the cationic iron cluster of thirteen atoms. Physical Chemistry Chemical Physics, 2013, 15, 14458.	1.3	15
14275	Crystallinity-dependent substitutional nitrogen doping in ZnO and its improved visible light photocatalytic activity. Journal of Colloid and Interface Science, 2013, 400, 18-23.	5.0	61
14276	Recent advances in computational predictions of NMR parameters for the structure elucidation of carbohydrates: methods and limitations. Chemical Society Reviews, 2013, 42, 8376.	18.7	113
14277	Electronic structure and magnetism of Ti 2 FeSi: A first-principles study. Journal of Magnetism and Magnetic Materials, 2013, 345, 171-175.	1.0	18
14278	First principles LDA +Uand GGA +Ustudy of protactinium and protactinium oxides: dependence on the effectiveUparameter. Journal of Physics Condensed Matter, 2013, 25, 145603.	0.7	20
14279	Magnetic properties of transition-metal nanoalloys. , 2013, , 247-281.		1
14280	Temperature-driven phase transformation in Y3Co: Neutron scattering and first-principles studies. Physical Review B, 2013, 88, .	1.1	6
14281	Silicene on hydrogenâ€passivated Si(111) and Ge(111) substrates. Physica Status Solidi - Rapid Research Letters, 2013, 7, 538-541.	1.2	29
14282	Carbon Coating of LiFePO₄ Can Be Strengthened by Sc and Ti. Journal of Physical Chemistry C, 2013, 117, 276-279.	1.5	15
14283	First-Principles Investigations of Metal (Cu, Ag, Au, Pt, Rh, Pd, Fe, Co, and Ir) Doped Hexagonal Boron Nitride Nanosheets: Stability and Catalysis of CO Oxidation. Journal of Physical Chemistry C, 2013, 117, 17319-17326.	1.5	300
14284	Effect of Anchoring Groups on Single Molecule Charge Transport through Porphyrins. Journal of Physical Chemistry C, 2013, 117, 14890-14898.	1.5	88
14285	Structures and Mechanisms of Water Adsorption on ZnO(0001) and GaN(0001) Surface. Journal of Physical Chemistry C, 2013, 117, 15976-15983.	1.5	52
14286	Bandgap Opening by Patterning Graphene. Scientific Reports, 2013, 3, 2289.	1.6	176
14287	Bandgap engineering of graphene by corrugation on lattice-mismatched MgO (111). Journal of Materials Chemistry C, 2013, 1, 1595.	2.7	25
14288	Self-Ordered Titanium Dioxide Nanotube Arrays: Anodic Synthesis and Their Photo/Electro-Catalytic Applications. Materials, 2013, 6, 2892-2957.	1.3	92

#	Article	IF	Citations
14289	The effect of out-of-plane strain on the electronic properties of zigzag graphene nanoribbons. , 2013, , .		1
14290	Unraveling Convoluted Structural Transitions in SnTe at High Pressure. Journal of Physical Chemistry C, 2013, 117, 5352-5357.	1.5	36
14291	Vibrational properties and the stability of the KCuF3phases. Journal of Physics Condensed Matter, 2013, 25, 115404.	0.7	3
14292	Quasiparticle band gaps of graphene nanowiggles and their magnetism on Au(111). Physical Review B, 2013, 88, .	1.1	15
14293	Molecular flexibility and structural instabilities in crystalline l-methionine. Biophysical Chemistry, 2013, 180-181, 76-85.	1.5	13
14294	Vacancy-cluster mechanism of metal-atom diffusion in substoichiometric carbides. Physical Review B, 2013, 87, .	1.1	31
14295	The role of an oxometallic complex in OH dissociation during water oxidation: a microscopic insight from DFT study. Journal of Materials Chemistry A, 2013, 1, 10422.	5.2	4
14296	Origins of CH₄/CO₂ Adsorption Selectivity in Zeolitic Imidazolate Frameworks: A van der Waals Density Functional Study. Journal of Physical Chemistry C, 2013, 117, 14642-14651.	1.5	16
14297	Electronic and spin transport properties of graphene nanoribbon mediated by metal adatoms: a study by the QUAMBOâ€“NEGF approach. Journal of Physics Condensed Matter, 2013, 25, 105302.	0.7	7
14298	A computational DFT study of CO oxidation on a Au nanorod supported on CeO2(110): on the role of the support termination. Catalysis Science and Technology, 2013, 3, 3020.	2.1	60
14299	Metallicity retained by covalent functionalization of graphene with phenyl groups. Nanoscale, 2013, 5, 7537.	2.8	9
14300	Electronic structure of oxygen-functionalized armchair graphene nanoribbons. Physical Review B, 2013, 88, .	1.1	30
14301	Formation and switching of defect dipoles in acceptor-doped lead titanate: A kinetic model based on first-principles calculations. Physical Review B, 2013, 88, .	1.1	75
14302	First-principles investigation of B- and N-doped fluorographene. Physical Review B, 2013, 88, .	1.1	11
14303	First-principles study on doping and temperature dependence of thermoelectric property of Bi2S3 thermoelectric material. Materials Research Bulletin, 2013, 48, 1984-1988.	2.7	44
14304	Finite temperature and pressure molecular dynamics for BaFe<mml:math xmlns:mml="http://www.w3.org/1998/Math/MathML" display="inline"><mml:msub><mml:mrow /><mml:mn>2</mml:mn></mml:msub></mml:math>As<mml:math xmlns:mml="http://www.w3.org/1998/Math/MathML" display="inline"><mml:msub><mml:mrow	1.1	8
14305	Energetics and kinetics of native point defects in Ga<mml:math xmlns:mml="http://www.w3.org/1998/Math/MathML" display="inline"><mml:msub><mml:mrow /><mml:mn>2</mml:mn></mml:msub></mml:math>Se<mml:math xmlns:mml="http://www.w3.org/1998/Math/MathML" display="inline"><mml:msub><mml:mrow /><mml:mn>3</mml:mn></mml:msub></mml:math>from first principles. Physical Review B, 2013, 88, .	1.1	4
14306	Solution softening in magnesium alloys: the effect of solid solutions on the dislocation core structure and nonbasal slip. Journal of Physics Condensed Matter, 2013, 25, 022202.	0.7	54

#	Article	IF	Citations
14307	Two phases of Ga2S3: promising infrared second-order nonlinear optical materials with very high laser induced damage thresholds. Journal of Materials Chemistry C, 2013, 1, 4754.	2.7	243
14308	Ab initio molecular dynamics simulation of the liquid and amorphous structure of Mg65Cu25Gd10 alloy. Physica B: Condensed Matter, 2013, 426, 65-70.	1.3	3
14309	Insights into electrochemical performance of Li2FeSiO4 from first-principles calculations. Electrochimica Acta, 2013, 111, 172-178.	2.6	30
14310	Structural phase diagrams of supported oxide nanowires from extended Frenkel-Kontorova models of diatomic chains. Journal of Chemical Physics, 2013, 139, 084703.	1.2	5
14311	Prediction of a multiferroic state with large electric polarization in tensile-strained TbMnO<mml:math xmlns:mml="http://www.w3.org/1998/Math/MathML" display="inline"><mml:msub><mml:mrow /><mml:mn>3</mml:mn></mml:msub></mml:math>. Physical Review B, 2013, 88, .	1.1	14
14312	Artificial neural network prediction indicators of density functional theory metal hydride models. International Journal of Hydrogen Energy, 2013, 38, 11920-11929.	3.8	8
14313	Phase Separation Induced by Au Catalysts in Ternary InGaAs Nanowires. Nano Letters, 2013, 13, 643-650.	4.5	79
14314	Surface effects on the structure and lithium behavior in lithiated silicon: A first principles study. Surface Science, 2013, 612, 16-23.	0.8	30
14315	A theoretical study of CH4 dissociation on NiPd(111) surface. Surface Science, 2013, 612, 63-68.	0.8	29
14316	Melting curve of face-centered-cubic nickel from first-principles calculations. Physical Review B, 2013, 88, .	1.1	40
14317	The influence of hydrogen impurities on the atomic and electronic structures of carbyne crystals. Moscow University Physics Bulletin (English Translation of Vestnik Moskovskogo Universiteta,) Tj ETQq0 0 0 rgBT /Overlock 10 Tf 50 33	0.1	10
14318	Investigation of the mechanical and electronic properties of Ag-Au and Co-Au nanocontacts by the method of first-principle molecular dynamics. Moscow University Physics Bulletin (English) Tj ETQq1 1 0.784314 rgBT /Overlock 10 Tf 5	0.1	3
14319	Structural, electronic and magnetic properties of transition metal binary alloy clusters with isoelectronic components: case study with Mn_mTc_n, Ti_mZr_nand Mn_mRe_n. Journal of Physics Condensed Matter, 2013, 25, 225302.	0.7	11
14320	Ab initioprediction of the critical thickness of a precipitate. Journal of Physics Condensed Matter, 2013, 25, 355005.	0.7	7
14321	CO Hydrogenation on Pd(111): Competition between Fischerâ€“Tropsch and Oxygenate Synthesis Pathways. Journal of Physical Chemistry C, 2013, 117, 14667-14676.	1.5	30
14322	Room Temperature Nanoscale Ferroelectricity in MagnetoelectricGaFeO3Epitaxial Thin Films. Physical Review Letters, 2013, 111, 087601.	2.9	99
14323	Toward the Microscopic Identification of Anions and Cations at the Ionic Liquid|Ag(111) Interface: A Combined Experimental and Theoretical Investigation. ACS Nano, 2013, 7, 7773-7784.	7.3	100
14324	Structural phase transition and mechanical properties of TiO₂ under high pressure. Physica Status Solidi (B): Basic Research, 2013, 250, 2206-2214.	0.7	33

#	Article	IF	Citations
14325	First-Principles Calculation of Nb2AlC/Nb Interfaces. Jom, 2013, 65, 326-330.	0.9	2
14326	Electronic structure and band gap engineering of ZnO-based semiconductor alloy films. Molecular Simulation, 2013, 39, 1007-1012.	0.9	3
14327	Electronic and optical properties of agglomerated hydrogen terminated silicon nanoparticles. European Physical Journal D, 2013, 67, 1.	0.6	6
14328	Experimental and theoretical investigations on the polymorphism and metastability of BiPO4. Dalton Transactions, 2013, 42, 14999.	1.6	70
14329	Adsorption and decomposition of NH3 on Ir(111): A density functional theory study. Surface Science, 2013, 616, 29-35.	0.8	11
14330	Theoretical and experimental study of the interaction of CO on TiC surfaces: Regular versus low coordinated sites. Surface Science, 2013, 613, 63-73.	0.8	5
14331	Comparison of wurtzite and zinc-blende GaAs surfaces as possible nanowire side walls: DFT stability calculations. Surface Science, 2013, 613, 74-79.	0.8	14
14332	Graphene moirÃ© structure grown on a pseudomorphic metal overlayer supported on Ru(0001). Surface Science, 2013, 611, 67-73.	0.8	17
14333	Monolayer Doping via Phosphonic Acid Grafting on Silicon: Microscopic Insight from Infrared Spectroscopy and Density Functional Theory Calculations. Advanced Functional Materials, 2013, 23, 3471-3477.	7.8	64
14334	Density Functional Theory Study of the Silicene-like SiX and XSi₃ (X = B, C, N, Al, P) Honeycomb Lattices: The Various Buckled Structures and Versatile Electronic Properties. Journal of Physical Chemistry C, 2013, 117, 18266-18278.	1.5	271
14335	Dyeâ€Sensitized Solar Cells based on Organic Dualâ€Channel Anchorable Dyes with Wellâ€Defined Core Bridge Structures. ChemSusChem, 2013, 6, 2069-2073.	3.6	27
14336	Atomistic study of soft-mode dynamics in PbTiO<mml:math xmlns:mml="http://www.w3.org/1998/Math/MathML" display="inline"><mml:msub><mml:mrow /><mml:mn>3</mml:mn></mml:msub></mml:math>. Physical Review B, 2013, 88, .	1.1	34
14337	Role of van der Waals corrections for the Pt<mml:math xmlns:mml="http://www.w3.org/1998/Math/MathML" display="inline"><mml:msub><mml:mi>X</mml:mi><mml:mn>2</mml:mn></mml:msub></mml:math>(<mml:math) Tj ETQq0 0 0 rgBT /	1.1	26
14338	Electrical and dielectric characteristics of Al/Dy2O3/p-Si heterostructure. Physica B: Condensed Matter, 2013, 429, 79-84.	1.3	13
14339	Topological classification of crystalline insulators with space group symmetry. Physical Review B, 2013, 88, .	1.1	128
14340	First-principles study of the structure and band structure of Ga₂Se₃. Journal of Physics Condensed Matter, 2013, 25, 225503.	0.7	17
14341	CO2 hydrogenation on Au/TiC, Cu/TiC, and Ni/TiC catalysts: Production of CO, methanol, and methane. Journal of Catalysis, 2013, 307, 162-169.	3.1	214
14342	Proxies from Ab Initio Calculations for Screening Efficient Ce³⁺ Phosphor Hosts. Journal of Physical Chemistry C, 2013, 117, 17955-17959.	1.5	176

#	Article	IF	Citations
14343	Theoretical study of structural stabilities and magnetic properties of doped transition metals in MnTe vs ZnTe and CdTe: Reduced clustering trend and enhanced magnetic coupling. Journal of Applied Physics, 2013, 114, .	1.1	2
14344	Chiral, Racemic, and Meso-Lithium Tartrate Framework Polymorphs: A Detailed Structural Analysis. Crystal Growth and Design, 2013, 13, 3705-3715.	1.4	23
14345	Influence of lone pair doping on the multiferroic property of orthorhombic HoMnO3:ab initioprediction. Journal of Physics Condensed Matter, 2013, 25, 385901.	0.7	0
14346	Effect of alloying elements on in-plane ordering and disordering of solute clusters in Mg-based long-period stacking ordered structures: A first-principles analysis. Scripta Materialia, 2013, 69, 594-597.	2.6	54
14347	Dramatic increase in the Raman signal of functional groups on carbon nanotube surfaces. Carbon, 2013, 56, 235-242.	5.4	9
14348	K+-hydration in a low-energy two-dimensional wetting layer on the basal surface of muscovite. Journal of Chemical Physics, 2013, 139, 074705.	1.2	7
14349	Thermodynamic modeling of Auâ€“Ceâ€“Sn ternary system. Calphad: Computer Coupling of Phase Diagrams and Thermochemistry, 2013, 42, 38-50.	0.7	20
14350	Dynamical response and instability in ceria under lattice expansion. Physical Review B, 2013, 87, .	1.1	48
14351	A density functional theory study of oxygen reduction reaction on Meâ€“N4 (Me = Fe, Co, or Ni) clusters between graphitic pores. Journal of Materials Chemistry A, 2013, 1, 10790.	5.2	253
14352	Effect of boron, nitrogen, and oxygen impurities on the electronic structure and deformation behavior of Ti3SiC2. Physics of the Solid State, 2013, 55, 551-555.	0.2	1
14353	<mml:math xmlns:mml="http://www.w3.org/1998/Math/MathML" display="inline"><mml:mi>d</mml:mi><mml:mo>+</mml:mo><mml:mi>i</mml:mi><mml:msup><mml:mi>d</mml:mi><mml:mn>â€²</mml:mn> Superconductivity in Bilayer Silicene. Physical Review Letters, 2013, 111, 066804.	2.9	156
14354	Effect of fluorine, nitrogen, and carbon impurities on the electronic and magnetic properties of WO3. Semiconductors, 2013, 47, 740-744.	0.2	3
14355	Shallow Impurity Level Calculations in Semiconductors UsingAbÂInitioMethods. Physical Review Letters, 2013, 110, 166404.	2.9	26
14356	Dynamical Crossover at the Liquid-Liquid Transformation of a Compressed Molten Alkali Metal. Physical Review Letters, 2013, 111, 077801.	2.9	28
14357	Band structure design of semiconductors for enhanced photocatalytic activity: The case of TiO2. Progress in Natural Science: Materials International, 2013, 23, 402-407.	1.8	220
14358	Dependence of the Minority-Carrier Lifetime on the Stoichiometry of CdTe Using Time-Resolved Photoluminescence and First-Principles Calculations. Physical Review Letters, 2013, 111, 067402.	2.9	124
14359	A physical organogel electrolyte: characterized by in situ thermo-irreversible gelation and single-ion-predominent conduction. Scientific Reports, 2013, 3, 1917.	1.6	45
14360	First-Principles Studies of the Activation of Oxygen Molecule and Its Role in Partial Oxidation of Methane on Boron-Doped Single-Walled Carbon Nanotubes. Journal of Physical Chemistry C, 2013, 117, 17485-17492.	1.5	17

#	Article	IF	Citations
14361	Density Functional Investigation of the Adsorption of Ethanolâ€“Water Mixture on the Pt(111) Surface. Journal of Physical Chemistry C, 2013, 117, 16942-16952.	1.5	25
14362	Catalytically favorable surface patterns in Ptâ€“Au nanoclusters. RSC Advances, 2013, 3, 15350.	1.7	8
14363	X-ray photoelectron spectroscopy investigation of magnetron sputtered Mgâ€“Tiâ€“H thin films. International Journal of Hydrogen Energy, 2013, 38, 10704-10715.	3.8	21
14364	Toward an Ideal Polymer Binder Design for High-Capacity Battery Anodes. Journal of the American Chemical Society, 2013, 135, 12048-12056.	6.6	332
14365	Onset of Chiral Adenine Surface Growth. ChemPhysChem, 2013, 14, 3294-3302.	1.0	2
14366	How Do Li Atoms Pass through the Al₂O₃ Coating Layer during Lithiation in Li-ion Batteries?. Journal of Physical Chemistry Letters, 2013, 4, 2681-2685.	2.1	166
14367	Atomistic origin of rapid crystallization of Ag-doped Ge-Sb-Te alloys: A joint experimental and theoretical study. Physica Status Solidi (B): Basic Research, 2013, 250, 1785-1790.	0.7	12
14368	TEM study of structural and microstructural characteristics of a precipitate phase in Ni-rich Niâ€“Tiâ€“Hf and Niâ€“Tiâ€“Zr shape memory alloys. Acta Materialia, 2013, 61, 6191-6206.	3.8	169
14369	Structure Sensitivity Study of Waterborne Contaminant Hydrogenation Using Shape- and Size-Controlled Pd Nanoparticles. ACS Catalysis, 2013, 3, 453-463.	5.5	74
14370	Origin of the vanishing critical thickness for ferroelectricity in free-standing PbTiO3 ultrathin films from first principles. Journal of Applied Physics, 2013, 114, .	1.1	11
14371	First-Principles Study of p-n-Doped Silicon Quantum Dots: Charge Transfer, Energy Dissipation, and Time-Resolved Emission. Journal of Physical Chemistry Letters, 2013, 4, 2906-2913.	2.1	53
14372	Structure of kaolinite and influence of stacking faults: Reconciling theory and experiment using inelastic neutron scattering analysis. Journal of Chemical Physics, 2013, 138, 194501.	1.2	12
14373	Simulation of Titanium Metal/Titanium Dioxide Etching with Chlorine and Hydrogen Chloride Gases Using the ReaxFF Reactive Force Field. Journal of Physical Chemistry A, 2013, 117, 5655-5663.	1.1	32
14374	Structure and mechanical properties of tungsten mononitride under high pressure from first-principles calculations. Computational Materials Science, 2013, 79, 456-462.	1.4	23
14375	Variable cell nudged elastic band method for studying solidâ€“solid structural phase transitions. Computer Physics Communications, 2013, 184, 2111-2118.	3.0	71
14376	Strain driven enhancement of ferroelectricity and magnetoelectric effect in multiferroic tunnel junction. Physical Chemistry Chemical Physics, 2013, 15, 14770.	1.3	10
14377	Firstâ€Principles Investigations of the Structural, Vibrational and Thermochemical Properties of Barium Cerate â€“ Another Test Case for Densityâ€Functional Theory. Zeitschrift Fur Anorganische Und Allgemeine Chemie, 2013, 639, 1227-1231.	0.6	20
14378	CO Oxidation at the Auâ€“Cu Interface of Bimetallic Nanoclusters Supported on CeO₂(111). Journal of Physical Chemistry Letters, 2013, 4, 2943-2947.	2.1	80

#	Article	IF	Citations
14379	NH3/Ir(100): Electronic structure and dehydrogenation. International Journal of Hydrogen Energy, 2013, 38, 2965-2972.	3.8	16
14381	Orthorhombic C32: a novel superhard sp3 carbon allotrope. Physical Chemistry Chemical Physics, 2013, 15, 14120.	1.3	62
14382	Energy barriers for point-defect reactions in<mml:math xmlns:mml="http://www.w3.org/1998/Math/MathML" display="inline"><mml:mrow><mml:mn>3</mml:mn><mml:mi>C</mml:mi></mml:mrow></mml:math>-SiC. Physical Review B, 2013, 88, .	1.1	50
14383	A Molecular Mechanism for the Waterâ€“Hydroxyl Balance during Wetting of TiO₂. Journal of Physical Chemistry C, 2013, 117, 17078-17083.	1.5	22
14384	Interplay of Electronic Structure and Atomic Mobility in Nanoalloys of Au and Pt. Journal of Physical Chemistry C, 2013, 117, 17268-17273.	1.5	30
14385	Oxygen behavior on the platinum surface: A quantum-chemical modeling. Russian Journal of Inorganic Chemistry, 2013, 58, 803-807.	0.3	5
14386	Effect of pentagonâ€“heptagon defect on thermal transport properties in graphene nanoribbons. Carbon, 2013, 65, 181-186.	5.4	53
14387	Possibility of a 2D SiC monolayer formation on Mg(0001) and MgO(111) substrates. Russian Journal of Physical Chemistry A, 2013, 87, 1332-1335.	0.1	7
14388	Tuning the band gap of hematite Î±-Fe2O3 by sulfur doping. Physics Letters, Section A: General, Atomic and Solid State Physics, 2013, 377, 1943-1947.	0.9	98
14389	Deformation potentials in AlGaN and InGaN alloys and their impact on optical polarization properties of nitride quantum wells. Physical Review B, 2013, 88, .	1.1	19
14390	Comparative optical study of colloidal anatase titania nanorods and atomically thin wires. Nanoscale, 2013, 5, 1465.	2.8	15
14391	Syntheses of three members of A(II)M(IV)(PO4)2: luminescence properties of PbGe(PO4)2 and its Eu3+-doped powders. CrystEngComm, 2013, 15, 7089.	1.3	23
14393	Effects of charging and perpendicular electric field on the properties of silicene and germanene. Journal of Physics Condensed Matter, 2013, 25, 305007.	0.7	45
14394	An ab initio study of the peak tensile strength of tungsten with an account of helium point defects. International Journal of Plasticity, 2013, 48, 54-71.	4.1	19
14395	Strain-controlled oxygen vacancy formation and ordering in CaMnO<mml:math xmlns:mml="http://www.w3.org/1998/Math/MathML" display="inline"><mml:msub><mml:mrow /><mml:mn>3</mml:mn></mml:msub></mml:math>. Physical Review B, 2013, 88, .	1.1	315
14396	Electric control of the magnetization in BiFeO<mml:math xmlns:mml="http://www.w3.org/1998/Math/MathML" display="inline"><mml:msub><mml:mrow /><mml:mn>3</mml:mn></mml:msub></mml:math>/LaFeO<mml:math xmlns:mml="http://www.w3.org/1998/Math/MathML" display="inline"><mml:msub><mml:mrow /><mml:mn>3</mml:mn></mml:msub></mml:math> superlattices. Physical Review B, 2013, 88, .	1.1	63
14397	Twinning stress in shape memory alloys: Theory and experiments. Acta Materialia, 2013, 61, 6790-6801.	3.8	67
14398	Calculation of arrangement of oxygen ions and vacancies in double perovskite GdBaCo2O5+Î´ by first-principles DFT with Monte Carlo simulations. Physical Chemistry Chemical Physics, 2013, 15, 10494.	1.3	18

#	Article	IF	Citations
14399	F-doped VO2 nanoparticles for thermochromic energy-saving foils with modified color and enhanced solar-heat shielding ability. Physical Chemistry Chemical Physics, 2013, 15, 11723.	1.3	160
14400	Thermodynamic properties and phase stability of wadsleyite II. Physics and Chemistry of Minerals, 2013, 40, 251-257.	0.3	2
14401	Ligand-Directed Formation of Gold Tetrapod Nanostructures. Journal of Physical Chemistry C, 2013, 117, 17143-17150.	1.5	30
14402	Mechanical properties of g-GaN: a first principles study. Applied Physics A: Materials Science and Processing, 2013, 113, 483-490.	1.1	80
14403	Mechanistic Insights in the Catalytic Synthesis of Vinyl Acetate on Palladium and Gold/Palladium Alloy Surfaces. Topics in Catalysis, 2013, 56, 1314-1332.	1.3	29
14404	Vapor Phase Ketonization of Acetic Acid on Ceria Based Metal Oxides. Topics in Catalysis, 2013, 56, 1782-1789.	1.3	33
14405	Deactivation of Cu2O(100) by CO Poisoning. Topics in Catalysis, 2013, 56, 1082-1087.	1.3	4
14406	Near Surface Phase Transition of Solute Derived Pt Monolayers. Topics in Catalysis, 2013, 56, 1065-1073.	1.3	8
14407	Spectroscopic Evidences of Charge Transfer Phenomena and Stabilization of Unusual Phases at Iron Oxide Monolayers Grown on Pt(111). Topics in Catalysis, 2013, 56, 1074-1081.	1.3	11
14408	Local structures and structural phase change in Ni-Zr-Nb glassy alloys composed of Ni5Zr5Nb3 icosahedral clusters. Journal of Applied Physics, 2013, 114, 063501.	1.1	9
14409	Geometrical and magnetic properties of vanadium clusters supported on graphene. Journal of the Korean Physical Society, 2013, 63, 225-228.	0.3	4
14410	Design of self-organized nanostructures to achieve high blocking temperatures in MgO-based d 0 ferromagnets. Journal of the Korean Physical Society, 2013, 62, 1807-1811.	0.3	5
14411	Ab initio calculations on the effect of Mn substitution in the Î²-carbide Fe3AlC. Journal of the Korean Physical Society, 2013, 62, 481-485.	0.3	14
14412	Electronic structures of a Zn vacancy on the ZnO(10 $ar 1$ 0) surface: Density functional theory calculations. Journal of the Korean Physical Society, 2013, 62, 508-512.	0.3	7
14413	Completing a family: LiCN3H4, the lightest alkali metal guanidinate. Dalton Transactions, 2013, 42, 15080.	1.6	17
14414	Effects of hydrogen in a vanadium grain boundary: From site occupancy to mechanical properties. Science China: Physics, Mechanics and Astronomy, 2013, 56, 1389-1395.	2.0	4
14415	Elastic and thermo-physical properties of stannite-type Cu2ZnSnS4 and Cu2ZnSnSe4 from first-principles calculations. Acta Metallurgica Sinica (English Letters), 2013, 26, 285-292.	1.5	14
14416	Critical electronic structures controlling phase transitions induced by lithium ion intercalation in molybdenum disulphide. Science Bulletin, 2013, 58, 1632-1641.	1.7	44

#	Article	IF	Citations
14417	Application of the density-functional theory to calculation of the reflectivity from shocked xenon. Doklady Physics, 2013, 58, 277-281.	0.2	4
14418	Efficient step-mediated intercalation of silver atoms deposited on the Bi2Se3 surface. JETP Letters, 2013, 96, 714-718.	0.4	16
14419	Nanocolumnar Germanium Thin Films as a High-Rate Sodium-Ion Battery Anode Material. Journal of Physical Chemistry C, 2013, 117, 18885-18890.	1.5	175
14420	Atomistic Simulation of Orientation Dependence in Shock-Induced Initiation of Pentaerythritol Tetranitrate. Journal of Physical Chemistry B, 2013, 117, 928-936.	1.2	55
14421	Precipitates in a near-equiatomic (Ni+Pt)-rich TiNiPt alloy. Scripta Materialia, 2013, 69, 713-715.	2.6	7
14422	Syntheses, Structures, and Electronic Properties of a New Series of Tellurides of the Type [Sequestered Cation]₂(Te_x) (x = 1â€“4). Zeitschrift Fur Anorganische Und Allgemeine Chemie, 2013, 639, 2809-2815.	0.6	11
14423	Equation of state and elasticity of B2-type FeSi: Implications for silicon in the inner core. Physics of the Earth and Planetary Interiors, 2013, 224, 32-37.	0.7	11
14424	Twin-induced one-dimensional homojunctions yield high quantum efficiency for solar hydrogen generation. Nature Communications, 2013, 4, 2278.	5.8	325
14425	Conductance of ferro- and antiferro-magnetic single-atom contacts: A first-principles study. Journal of Applied Physics, 2013, 114, 063711.	1.1	4
14426	Magnetic properties of 3d transition metals and nitrogen functionalized armchair graphene nanoribbon. RSC Advances, 2013, 3, 21110.	1.7	10
14427	Ti- and Zr-based metal-air batteries. Journal of Power Sources, 2013, 242, 400-404.	4.0	12
14428	Solution Properties of the System ZrSiO₄â€“HfSiO₄: A Computational and Experimental Study. Journal of Physical Chemistry C, 2013, 117, 10013-10019.	1.5	14
14429	An empirical model for silver tantalate. Modelling and Simulation in Materials Science and Engineering, 2013, 21, 055002.	0.8	12
14430	Magnetic Hardening Induced by Nonmagnetic Organic Molecules. Physical Review Letters, 2013, 111, 106805.	2.9	89
14431	Atomistic study of stress-induced switching of 90Â° ferroelectric domain walls in PbTiO3: size, temperature and structural effect. Modelling and Simulation in Materials Science and Engineering, 2013, 21, 065019.	0.8	4
14432	Atomistic processes of grain boundary motion and annihilation in graphene. Journal of Physics Condensed Matter, 2013, 25, 155301.	0.7	6
14433	Elastic properties of an Mgâ€“Znâ€“Y alloy single crystal with a long-period stacking-ordered structure. Acta Materialia, 2013, 61, 6338-6351.	3.8	125
14434	Growth and Structure of Cu and Au on the Nonpolar ZnO(101Ì…0) Surface: STM, XPS, and DFT Studies. Journal of Physical Chemistry C, 2013, 117, 18386-18397.	1.5	27

#	Article	IF	Citations
14435	First-Principles Studies of Photoinduced Charge Transfer in Noncovalently Functionalized Carbon Nanotubes. Journal of Physical Chemistry C, 2013, 117, 17909-17918.	1.5	13
14436	First-principles investigation of thiophene adsorption on Ni13 and Zn@Ni12 nanoclusters. Computational and Theoretical Chemistry, 2013, 1020, 136-142.	1.1	13
14437	Effect of magnetism on the solubility of 3d elements in BCC iron: Results of first-principle investigations. Physics of Metals and Metallography, 2013, 114, 642-653.	0.3	25
14438	Computing Gibbs free energy differences by interface pinning. Physical Review B, 2013, 88, .	1.1	64
14439	Electrochemical formation and surface characterisation of Cu2â^'xTe thin films with adjustable content of Cu. RSC Advances, 2013, 3, 21648.	1.7	8
14440	Tunable electronic and magnetic properties of WS2 nanoribbons. Journal of Applied Physics, 2013, 114, .	1.1	48
14441	Solid-liquid coexistence in small systems: A statistical method to calculate melting temperatures. Journal of Chemical Physics, 2013, 139, 094114.	1.2	48
14442	Effect of defects and dopants in graphene on hydrogen interaction in graphene-supported NaAlH4. International Journal of Hydrogen Energy, 2013, 38, 3670-3680.	3.8	22
14443	The rational design of polyurea & polyurethane dielectric materials. Polymer, 2013, 54, 3529-3533.	1.8	82
14444	First principles computational study on the electrochemical stability of Ptâ€“Co nanocatalysts. Nanoscale, 2013, 5, 8625.	2.8	71
14445	Why (1 0 0) Terraces Break and Make Bonds: Oxidation of Dimethyl Ether on Platinum Single-Crystal Electrodes. Journal of the American Chemical Society, 2013, 135, 14329-14338.	6.6	46
14446	Fermi level influence on the adsorption at semiconductor surfacesâ€”ab initio simulations. Journal of Applied Physics, 2013, 114, .	1.1	35
14447	On the mobility of vacancy clusters in reduced activation steels: an atomistic study in the Feâ€“Crâ€“W model alloy. Journal of Physics Condensed Matter, 2013, 25, 315401.	0.7	25
14448	Melilite-type blue chromophores based on Mn3+ in a trigonal-bipyramidal coordination induced by interstitial oxygen. Journal of Materials Chemistry C, 2013, 1, 5843.	2.7	24
14449	Quantum Degeneracy in Atomic Point Contacts Revealed by Chemical Force and Conductance. Physical Review Letters, 2013, 111, 106803.	2.9	23
14450	Theoretical study of sorption and diffusion of lithium atoms on the surface of crystalline silicon and inside it. JETP Letters, 2013, 97, 634-638.	0.4	3
14451	Linear infinite cadmium chains in CaAu4Cd2 and other intermetallics with YbMo2Al4-type structure. Monatshefte FÃ¼r Chemie, 2013, 144, 751-760.	0.9	19
14452	Multi-physics analysis of nano-structured ferroelectrics by first-principles simulations. Acta Mechanica, 2013, 224, 1261-1270.	1.1	2

#	Article	IF	Citations
14453	A synergistic strategy established by the combination of two H-enriched Bâ€“N based hydrides towards superior dehydrogenation. Journal of Materials Chemistry A, 2013, 1, 10155.	5.2	26
14454	Oxygen subsurface adsorption on the Cu(110)-c(6Ã—2) surface. Surface Science, 2013, 615, 57-64.	0.8	15
14455	Photoemission and density functional theory study of Ge(100): Clean surface and Yb-induced (2Ã—4) reconstruction. Surface Science, 2013, 615, 88-96.	0.8	6
14456	First-principles study of Bi and Sb intercalated graphene on SiC(0001) substrate. Surface Science, 2013, 616, 149-154.	0.8	26
14457	Vibrational spectra of an RDX film over an aluminum substrate from molecular dynamics simulations and density functional theory. Journal of Molecular Modeling, 2013, 19, 2773-2778.	0.8	5
14458	The melting point of lithium: an orbital-free first-principles molecular dynamics study. Molecular Physics, 2013, 111, 3448-3456.	0.8	41
14459	Adsorption and decomposition mechanism of hexogen (RDX) on Al(111) surface by periodic DFT calculations. Journal of Molecular Modeling, 2013, 19, 2451-2458.	0.8	37
14460	Interaction Between AsHg and V Hg in Arsenic-Doped Hg1â^'x Cd x Te. Journal of Electronic Materials, 2013, 42, 3054-3058.	1.0	1
14461	Elastic properties of MgSiO3-perovskite under lower mantle conditions and the composition of the deep Earth. Earth and Planetary Science Letters, 2013, 379, 1-12.	1.8	55
14462	Near Infrared Emission Band and Origin in Ni(II)-Doped CdS Nanoribbons by CVD Technique. Journal of Physical Chemistry C, 2013, 117, 17777-17785.	1.5	52
14463	Structural, electronic and thermodynamic properties of R3ZnH5 (R=K, Rb, Cs): A first-principle calculation. Journal of Solid State Chemistry, 2013, 198, 433-439.	1.4	6
14464	ELECTRONIC PROPERTIES OF HgTe WITHIN DIFFERENT STRUCTURES. International Journal of Modern Physics B, 2013, 27, 1350086.	1.0	0
14465	Size and Shape Effects of Pd@Pt Coreâ€“Shell Nanoparticles: Unique Role of Surface Contraction and Local Structural Flexibility. Journal of Physical Chemistry C, 2013, 117, 16144-16149.	1.5	62
14466	The origin of perpendicular magneto-crystalline anisotropy in L1₀â€“FeNi under tetragonal distortion. Journal of Physics Condensed Matter, 2013, 25, 106005.	0.7	92
14467	Effect of sodium incorporation into CuInSe2 from first principles. Journal of Applied Physics, 2013, 114, .	1.1	67
14468	Improved electron field emission from metal grafted graphene composites. Carbon, 2013, 62, 337-345.	5.4	39
14469	Exotic High Activity Surface Patterns in PtAu Nanoclusters. Journal of Physical Chemistry C, 2013, 117, 9275-9280.	1.5	10
14470	Site preference and interaction energies of Co and Cr in gamma prime Ni₃Al: a first-principles study. Modelling and Simulation in Materials Science and Engineering, 2013, 21, 055006.	0.8	17

#	Article	IF	Citations
14471	Orbital-Ordering-Induced Ferroelectricity in<mml:math xmlns:mml="http://www.w3.org/1998/Math/MathML" display="inline"><mml:msub><mml:mi>SrCrO</mml:mi><mml:mn>3</mml:mn></mml:msub></mml:math>. Physical Review Letters, 2013, 111, 077601.	2.9	24
14472	Computational testing of trivalent dopants in CeO₂for improved high-Îº dielectric behaviour. Journal of Materials Chemistry C, 2013, 1, 1093-1098.	2.7	35
14473	First-principles study of small palladium clusters on NiAl(110) alloy surface. Physica E: Low-Dimensional Systems and Nanostructures, 2013, 53, 7-13.	1.3	9
14474	Graphene oxide and lithium amidoborane: a new way to bridge chemical and physical approaches for hydrogen storage. Journal of Materials Chemistry A, 2013, 1, 8016.	5.2	27
14475	Trends in spin and orbital magnetism of free and encapsulated FePt nanoparticles. Physica Status Solidi (A) Applications and Materials Science, 2013, 210, 1282-1297.	0.8	6
14476	Interaction of O2 with reduced rutile TiO2(110) surface. Surface Science, 2013, 610, 33-41.	0.8	18
14477	Spinâ€“orbit splitting in the Si(335)â€“Au surface. Surface Science, 2013, 609, 44-47.	0.8	8
14478	A DFT study of adsorption and decomposition of hexahydro-1,3,5-trinitro-1,3,5-triazine on Mg(0001) surface. Journal of Molecular Modeling, 2013, 19, 4459-4465.	0.8	1
14479	Identification of [1,3]dithiolo[4,5- d]dithiazolyl radicals by in situ EPR spectroscopy and cyclic voltammetry. Tetrahedron, 2013, 69, 8790-8797.	1.0	6
14480	A Facile Mechanism for Recharging Li₂O₂ in Liâ€“O₂ Batteries. Chemistry of Materials, 2013, 25, 3328-3336.	3.2	179
14481	Understanding Chemical Changes across the Î±-Cristobalite to Stishovite Transition Path in Silica. Journal of Physical Chemistry C, 2013, 117, 8950-8958.	1.5	15
14482	Examination of Oxygen Vacancy Formation in Mn-Doped CeO₂ (111) Using DFT+U and the Hybrid Functional HSE06. Langmuir, 2013, 29, 10120-10131.	1.6	53
14483	Evolution of Topological Surface States in Antimony Ultra-Thin Films. Scientific Reports, 2013, 3, 2010.	1.6	38
14484	The low/room-temperature forms of the lithiated salt of 3,6-dihydroxy-2,5-dimethoxy-p-benzoquinone: a combined experimental and dispersion-corrected density functional study. CrystEngComm, 2013, 15, 2809.	1.3	8
14485	Atomic and electronic structure of molybdenum carbide phases: bulk and low Miller-index surfaces. Physical Chemistry Chemical Physics, 2013, 15, 12617.	1.3	189
14486	Study on UV-shielding mechanism of layered double hydroxide materials. Physical Chemistry Chemical Physics, 2013, 15, 18217.	1.3	52
14487	Electromechanical properties of zigzag-shaped carbon nanotubes. Physical Chemistry Chemical Physics, 2013, 15, 17134.	1.3	12
14488	The vibration properties of the (n,0) boron nitride nanotubes from ab initio quantum chemical simulations. Journal of Chemical Physics, 2013, 138, 054906.	1.2	44

#	Article	IF	Citations
14489	Decoherence reduces thermal energy loss in graphene quantum dots. Applied Physics Letters, 2013, 103, .	1.5	10
14490	Pathway and energetics of xenon migration in uranium dioxide. Physical Review B, 2013, 87, .	1.1	30
14491	Ab initio study of the formation of structural kinks in carbon chains. Journal of Surface Investigation, 2013, 7, 479-484.	0.1	0
14492	Investigation into the adsorption of atomic nitrogen on an Al2O3 (0001) surface. Journal of Surface Investigation, 2013, 7, 76-80.	0.1	0
14493	First-principles investigation into the effect of Cr on the segregation of multi-H at the Fe Î£3 (111) grain boundary. Journal of Nuclear Materials, 2013, 441, 301-305.	1.3	27
14494	First principles methods for elpasolite halide crystal structure prediction at finite temperatures. Journal of Alloys and Compounds, 2013, 577, 463-468.	2.8	9
14495	First-principle study of electronic, structural properties and stability of Sn0.5M0.5O2, M=Ti, Mn, Sb, Pb. Physica B: Condensed Matter, 2013, 421, 132-137.	1.3	7
14496	First principles study of Î±2-Ti3Al(0001) surface and Î³-TiAl(111)/Î±2-Ti3Al(0001) interfaces. Applied Surface Science, 2013, 276, 198-202.	3.1	27
14497	Effects of hydroxyl group on H2 dissociation on graphene: A density functional theory study. Journal of Energy Chemistry, 2013, 22, 493-497.	7.1	8
14498	Water co-adsorption and electric field effects on borohydride structures on Os(111) by first-principles calculations. Journal of Alloys and Compounds, 2013, 580, S6-S9.	2.8	1
14499	The standard enthalpies of formation of some binary intermetallic compounds of lanthanideâ€“iron systems by high temperature direct synthesis calorimetry. Journal of Alloys and Compounds, 2013, 554, 232-239.	2.8	30
14500	Phase transition and possible metallization in CeVO4 under pressure. Journal of Solid State Chemistry, 2013, 203, 273-280.	1.4	37
14501	Structure sensitivity of ammonia decomposition over Ni catalysts: A computational and experimental study. Fuel Processing Technology, 2013, 108, 112-117.	3.7	56
14502	Oxygen induced transformations of the Î´-Pu(111) surface. Surface Science, 2013, 618, 101-108.	0.8	9
14503	First principles simulation on the K0.8Fe2Se2 high-temperature structural superconductor. Physica C: Superconductivity and Its Applications, 2013, 493, 55-57.	0.6	1
14504	Sound velocities and elastic properties of PbTiO3 and PbZrO3 under pressure: First principles study. Ceramics International, 2013, 39, S277-S281.	2.3	5
14505	First principle study of Ce doping and related complexes in GaN. Computational Materials Science, 2013, 72, 32-37.	1.4	8
14506	First-principles calculations for the surface termination of Li2TiO3(001) surfaces. Journal of Nuclear Materials, 2013, 442, S705-S709.	1.3	3

#	Article	IF	Citations
14507	Scaffolds of magnetically active 3d metals in the valence electron controlled borides Ti9â˜xM2+xRu18B8 (M=Crâ€“Ni; x=0.5â€“1): Structutral, electronic and magnetic properties. Journal of Solid State Chemistry, 2013, 204, 283-290.	1.4	5
14508	First principles study of the spontaneous electric polarization in. Thin Solid Films, 2013, 533, 93-96.	0.8	10
14509	On the dual deuterium/deuteron nature of D charge distribution in the Ti host matrix: A DFT analysis. International Journal of Hydrogen Energy, 2013, 38, 16477-16484.	3.8	0
14510	Nature of SnO6 octahedron in bulk and nanoparticles of Y2Sn2O7 probed by experimental and theoretical methods. Chemical Physics Letters, 2013, 590, 77-82.	1.2	3
14511	Structure of La2Ni7 hydride from first-principles calculations. Journal of Alloys and Compounds, 2013, 580, S76-S80.	2.8	1
14512	Composition-dependent ground state of martensite in Niâ€“Mnâ€“Ga alloys. Acta Materialia, 2013, 61, 3858-3865.	3.8	45
14513	Dehydrogenation mechanisms of Ca(NH2BH3)2: TheÂless the charge transfer, the lower the barrier. International Journal of Hydrogen Energy, 2013, 38, 11313-11320.	3.8	8
14514	Theoretical study of oxidationâ€“reduction reaction of Fe2O3 supported on MgO during chemical looping combustion. Applied Surface Science, 2013, 266, 350-354.	3.1	35
14515	Structural and reaction pathway analyses of Mg(BH4)2Â·2NH3 for hydrogen storage : A first-principles study. International Journal of Hydrogen Energy, 2013, 38, 2836-2845.	3.8	7
14516	The crystallographic and morphological evolution of the strengthening precipitates in Cuâ€“Niâ€“Si alloys. Acta Materialia, 2013, 61, 1210-1219.	3.8	115
14517	First principles screening of B2 stabilizers in CuPd-based hydrogen separation membranes: (1) Substitution for Pd. Journal of Alloys and Compounds, 2013, 574, 368-376.	2.8	16
14518	Electronic structure and magnetism of various surfaces of the catalytic material Pt3Ni: Density-functional study. Journal of Magnetism and Magnetic Materials, 2013, 339, 89-93.	1.0	2
14519	Behaviors of alloying element titanium in vanadium: From energetics to tensile/shear deformation. Computational Materials Science, 2013, 77, 348-354.	1.4	9
14520	Electronic and mechanical properties of ordered (Pu, U) O2 compounds: A density functional theory +U study. Journal of Nuclear Materials, 2013, 433, 345-350.	1.3	40
14521	Stabilization of metastable ferroelectric Ba1â˜xCaxTi2O5 by breaking Ca-site selectivity via crystallization from glass. Scientific Reports, 2013, 3, 3010.	1.6	7
14522	Emission energy barriers of scandate surfaces with adsorbed Ba and Ba-O using density functional theory. , 2013, , .		0
14523	Thermal conductivity and phonon linewidths of monolayer MoS2 from first principles. Applied Physics Letters, 2013, 103, .	1.5	273
14524	CuSbS2 and CuBiS2 as potential absorber materials for thin-film solar cells. Journal of Renewable and Sustainable Energy, 2013, 5, .	0.8	63

#	Article	IF	Citations
14525	Electron-phonon superconductivity near charge-density-wave instability in LaO0.5F0.5BiS2: Density-functional calculations. Physical Review B, 2013, 87, .	1.1	139
14526	Thermoelectric effects in silicene nanoribbons. Physical Review B, 2013, 88, .	1.1	120
14527	Insights into the phase diagram of bismuth ferrite from quasiharmonic free-energy calculations. Physical Review B, 2013, 88, .	1.1	50
14528	First-principles investigation of graphene on the ferroelectric LiNbO ₃ (001) surface. Europhysics Letters, 2013, 104, 17009.	0.7	20
14529	Ab initiocharacterization of a Ni-related defect in diamond: The W8 center. Physical Review B, 2013, 87, .	1.1	15
14530	Ab initiostudy of the split silicon-vacancy defect in diamond: Electronic structure and related properties. Physical Review B, 2013, 88, .	1.1	143
14531	Monolayer semiconducting transition metal dichalcogenide alloys: Stability and band bowing. Journal of Applied Physics, 2013, 113, .	1.1	214
14532	Electronic structure of a single-layer InN quantum well in a GaN matrix. Applied Physics Letters, 2013, 102, .	1.5	27
14533	Interface defects and impurities at the growth zone of Auâ€catalyzed GaAs nanowire from first principles. Physica Status Solidi - Rapid Research Letters, 2013, 7, 882-885.	1.2	1
14534	Vibrational, elastic properties and sound velocities of zinc aluminate spinel. Computational Materials Science, 2013, 69, 505-509.	1.4	22
14535	Hydrogen storage in polylithiated BC3 monolayer sheet. Solid State Communications, 2013, 170, 39-43.	0.9	29
14536	Stability maps to predict anomalous ductility in B2 materials. Physical Review B, 2013, 87, .	1.1	17
14537	Molecular dynamics simulations of an electrified water/Pt(111) interface using point charge dissociative water. Electrochimica Acta, 2013, 101, 308-325.	2.6	21
14538	Ordering determination of Li2CoSiO4 polymorphs by first-principles calculations. Chemical Physics Letters, 2013, 580, 115-119.	1.2	11
14539	Band offsets for mismatched interfaces: The special case of ZnO on CdTe (001). Journal of Vacuum Science and Technology A: Vacuum, Surfaces and Films, 2013, 31, 061102.	0.9	4
14540	Substantial enhancement in intrinsic coercivity on M-type strontium hexaferrite through the increase in magneto-crystalline anisotropy by co-doping of group-V and alkali elements. Applied Physics Letters, 2013, 103, 242417.	1.5	11
14541	Mechanics and Mechanically Tunable Band Gap in Single-Layer Hexagonal Boron-Nitride. Materials Research Letters, 2013, 1, 200-206.	4.1	141
14542	A first-principles study of magnetism of lithium fluorosulphate LiFeSO4F. Journal of Applied Physics, 2013, 113, .	1.1	11

#	Article	IF	Citations
14543	Anionâ€Doped Mixed Metal Oxide Nanostructures Derived from Layered Double Hydroxide as Visible Light Photocatalysts. Advanced Functional Materials, 2013, 23, 2348-2356.	7.8	86
14544	Device Performance of Heterojunction Tunneling Field-Effect Transistors Based on Transition Metal Dichalcogenide Monolayer. IEEE Electron Device Letters, 2013, 34, 1331-1333.	2.2	62
14545	Tunable band gap in few-layer graphene by surface adsorption. Scientific Reports, 2013, 3, .	1.6	55
14546	Nanometer size 3dâ€“4d and 3dâ€“5d substitutional clusters: Promising candidates for magnetic storageapplications. Journal of Magnetism and Magnetic Materials, 2013, 334, 31-35.	1.0	9
14547	Structure, elastic and dynamical properties of KN3 and RbN3: A van der Waals density functional study. Solid State Sciences, 2013, 23, 17-25.	1.5	9
14548	First-principles study of mechanical properties of one-dimensional carbon nanotube intramolecular junctions. Computational Materials Science, 2013, 70, 1-7.	1.4	27
14549	Spin-Orbit Splitting in Single-Layer<mml:math xmlns:mml="http://www.w3.org/1998/Math/MathML" display="inline"><mml:msub><mml:mi>MoS</mml:mi><mml:mn>2</mml:mn></mml:msub></mml:math>Revealed by Triply Resonant Raman Scattering. Physical Review Letters, 2013, 111, 126801.	2.9	137
14550	First-principle insights into the catalytic role of indium oxide in methanol steam reforming. Chinese Journal of Catalysis, 2013, 34, 1855-1860.	6.9	11
14551	Density functional theory calculations for the oxygen dissociation on nitrogen and transition metal doped graphenes. Chemical Physics Letters, 2013, 586, 104-107.	1.2	15
14552	First-principles study of the electronic and optical properties of the (Eu,N)-codoped anatase TiO2 photocatalyst. Computational Materials Science, 2013, 68, 234-237.	1.4	10
14553	Near-edge band structures and band gaps of Cu-based semiconductors predicted by the modified Becke-Johnson potential plus an on-site Coulomb U. Journal of Chemical Physics, 2013, 139, 184706.	1.2	43
14554	A comprehensive study of thermoelectric and transport properties of Î²-silicon carbide nanowires. Journal of Applied Physics, 2013, 114, .	1.1	36
14555	Electronic and optical performances of Si and Fe-codoped TiO2 nanoparticles: A photocatalyst for the degradation of methylene blue. Applied Catalysis B: Environmental, 2013, 142-143, 38-44.	10.8	24
14557	Growth, disorder, and physical properties of ZnSnN2. Applied Physics Letters, 2013, 103, .	1.5	111
14558	Methane dissociation on Pt(111), Ir(111) and PtIr(111) surface: A density functional theory study. Applied Surface Science, 2013, 284, 784-791.	3.1	60
14559	Nonlinear elastic response of cubic crystals to biaxial strain. Computational Materials Science, 2013, 79, 284-288.	1.4	3
14560	Universal infrared absorbance of two-dimensional honeycomb group-IV crystals. Physical Review B, 2013, 87, .	1.1	157
14561	Structure and stability of acrolein and allyl alcohol networks on Ag(111) from density functional theory based calculations with dispersion corrections. Surface Science, 2013, 617, 175-182.	0.8	6

#	Article	IF	Citations
14562	Spin polarization study of graphene on the Ni(111) surface by density functional theory calculations with a semiempirical long-range dispersion correction. Journal of Applied Physics, 2013, 114, 143713.	1.1	13
14563	Effective ionâ€“ion potentials in warm dense matter. High Energy Density Physics, 2013, 9, 178-186.	0.4	16
14564	Antiphase inversion domains in lithium cobaltite thin films deposited on single-crystal sapphire substrates. Acta Materialia, 2013, 61, 7671-7678.	3.8	29
14565	Structural, electronic and elastic properties of the C14 NbCr2 Laves phase under hydrostatic pressure. Solid State Communications, 2013, 174, 46-49.	0.9	8
14566	Experimental and theoretical investigations for mitigating NaAlH4 reactivity risks during postulated accident scenarios involving exposure to air or water. Chemical Engineering Research and Design, 2013, 91, 463-475.	2.7	12
14567	Light elements-induced iono-covalent character in MgH2: An ab-initio approach. Computational Materials Science, 2013, 69, 424-427.	1.4	15
14568	Tuning the Ferroelectric Polarization in a Multiferroic Metalâ€“Organic Framework. Journal of the American Chemical Society, 2013, 135, 18126-18130.	6.6	252
14569	High-throughput screening of small-molecule adsorption in MOF. Journal of Materials Chemistry A, 2013, 1, 13597.	5.2	92
14570	The pressure dependence of the solid state structure of biphenyl from DFT calculations. Physical Chemistry Chemical Physics, 2013, 15, 20288.	1.3	3
14571	Structural Behaviors of Cytosine into the Hydrated Interlayer of Na⁺-Montmorillonite Clay. An ab Initio Molecular Dynamics Study. Journal of Physical Chemistry C, 2013, 117, 26179-26189.	1.5	17
14572	Theoretical and Experimental Investigations of N2-selective Membranes. Energy Procedia, 2013, 37, 1093-1103.	1.8	1
14573	Origin of the temperature dependence of the band gap of PbS and PbSe quantum dots. Solid State Communications, 2013, 165, 49-54.	0.9	81
14574	Artificially imposed hexagonal ferroelectricity in canted antiferromagnetic YFeO3 epitaxial thin films. Materials Chemistry and Physics, 2013, 138, 929-936.	2.0	29
14575	Electronic structure and static dielectric response of Ba(Mn1/3Nb2/3)O3 from first principles. Solid State Communications, 2013, 154, 1-5.	0.9	8
14576	First principles calculations of oxygen vacancy formation in barium-strontium-cobalt-ferrite. RSC Advances, 2013, 3, 12267.	1.7	33
14577	Band gap engineering of graphene/h-BN hybrid superlattices nanoribbons. Journal of Applied Physics, 2013, 113, 033703.	1.1	21
14578	Gap renormalization of molecular crystals from density-functional theory. Physical Review B, 2013, 88, .	1.1	239
14579	Electronic structure and quasiparticle bandgap of silicene structures. Applied Physics Letters, 2013, 102, .	1.5	79

#	Article	IF	Citations
14580	A Possible Reaction Pathway to Fabricate a Halfâ€Metallic Wire on a Silicon Surface. Advanced Functional Materials, 2013, 23, 2233-2238.	7.8	12
14581	Pressure induced semiconductor to half metal transition in Sr2NiReO6. Journal of Applied Physics, 2013, 114, 163705.	1.1	4
14582	Electrical conductivity in oxygen-deficient phases of tantalum pentoxide from first-principles calculations. Journal of Applied Physics, 2013, 114, .	1.1	36
14583	Direct and diffuse reflection of electron waves at armchair edges of epitaxial graphene. RSC Advances, 2013, 3, 25735.	1.7	6
14584	Epitaxial cobalt oxide films on Ir(100)â€"the importance of crystallographic analyses. Journal of Physics Condensed Matter, 2013, 25, 173001.	0.7	65
14585	A thermodynamic criterion for designing superhard transition-metal borides with ultimate boron content. Computational Materials Science, 2013, 68, 222-228.	1.4	47
14586	Role of ReOx in Re-modified Rh/ZrO2 and Ir/ZrO2 catalysts in glycerol hydrogenolysis: Insights from first-principles study. Chinese Journal of Catalysis, 2013, 34, 1656-1666.	6.9	18
14587	Nitrogen-induced local spin polarization in graphene on cobalt. Journal of Magnetism and Magnetic Materials, 2013, 342, 144-148.	1.0	2
14588	Grain misorientation and grain-boundary rotation dependent mechanical properties in polycrystalline graphene. Journal of the Mechanics and Physics of Solids, 2013, 61, 1421-1432.	2.3	109
14589	Crystal structure and properties of high-pressure-synthesized BiRhO3, LuRhO3, and NdRhO3. Journal of Solid State Chemistry, 2013, 200, 271-278.	1.4	16
14590	Electronic and structural influence of Ni by Pd substitution on the hydrogenation properties of TiNi. Journal of Solid State Chemistry, 2013, 198, 475-484.	1.4	14
14591	Theory of magnetic enhancement in strontium hexaferrite through Znâ€“Sn pair substitution. Journal of Magnetism and Magnetic Materials, 2013, 348, 75-81.	1.0	33
14592	An atomic study of hydrogen effect on the early stage oxidation of transition metal surfaces. International Journal of Hydrogen Energy, 2013, 38, 1644-1656.	3.8	29
14593	A first-principles study of the diffusion of atomic oxygen in nickel. Corrosion Science, 2013, 75, 248-255.	3.0	21
14594	Hexagonal MIn₂S₄ (M = Mn, Fe, Co): Formation and Phase Transition. Journal of Physical Chemistry C, 2013, 117, 20054-20059.	1.5	11
14595	Tunable band gap and hydrogen adsorption property of a two-dimensional porous polymer by nitrogen substitution. Physical Chemistry Chemical Physics, 2013, 15, 666-670.	1.3	20
14596	DFT study of the adsorption of the corrosion inhibitor 2-mercaptoimidazole onto Fe(100) surface. Electrochimica Acta, 2013, 112, 577-586.	2.6	78
14597	Synthesis of nitrogen-doped single-walled carbon nanotubes and monitoring of doping by Raman spectroscopy. Chinese Physics B, 2013, 22, 086101.	0.7	7

#	Article	IF	Citations
14598	Graphene on amorphous HfO2surface: Anab initioinvestigation. Physical Review B, 2013, 87, .	1.1	12
14599	First principles study of transport properties of LaAlO3/SrTiO3 heterostructure with water adsorbates. Solid State Communications, 2013, 169, 46-49.	0.9	3
14600	First principles investigation on the stability, magnetic and electronic properties of the fully and partially hydrogenated BN nanoribbons in different conformers. Journal of Materials Chemistry C, 2013, 1, 6890.	2.7	17
14601	Hybrid nanotubeâ€“graphene junctions: spin degeneracy breaking and tunable electronic structure. Physical Chemistry Chemical Physics, 2013, 15, 20281.	1.3	5
14602	Photo-active and optical properties of bismuth ferrite (BiFeO3): An experimental and theoretical study. Chemical Physics Letters, 2013, 572, 78-84.	1.2	67
14603	First-principle prediction of half-metallic ferrimagnetism in Mn-based full-Heusler alloys with highly ordered structure. Journal of Magnetism and Magnetic Materials, 2013, 333, 162-168.	1.0	54
14604	Evolving Structural Diversity and Metallicity in Compressed Lithium Azide. Journal of Physical Chemistry C, 2013, 117, 20838-20846.	1.5	51
14605	Synthesis and Characterization of MnCrO4, a New Mixed-Valence Antiferromagnet. Inorganic Chemistry, 2013, 52, 11850-11858.	1.9	8
14606	Fluorine-Doped IrO₂: A Potential Electrocatalyst for Water Electrolysis. Journal of Physical Chemistry C, 2013, 117, 20542-20547.	1.5	35
14607	The origin of the high work function of chlorinated indium tin oxide. NPG Asia Materials, 2013, 5, e57-e57.	3.8	41
14608	Shock-induced plasticity in tantalum single crystals: Interatomic potentials and large-scale molecular-dynamics simulations. Physical Review B, 2013, 88, .	1.1	216
14609	Substrate Mediated Short- and Long-Range Adsorption Patterns of CO on Ag(110). Physical Review Letters, 2013, 110, 196101.	2.9	5
14610	How a single aluminum atom makes a difference to gallium: First-principles simulations of bimetallic cluster melting. Journal of Chemical Physics, 2013, 139, 094309.	1.2	9
14611	Ferromagnetism in Nd-doped ZnO nanowires and the influence of oxygen vacancies: ab initio calculations. Physical Chemistry Chemical Physics, 2013, 15, 17793.	1.3	18
14612	Water adsorption and dissociation on Ni surface: Effects of steps, dopants, coverage and self-aggregation. Physical Chemistry Chemical Physics, 2013, 15, 17804.	1.3	28
14613	Predicting a new photocatalyst and its electronic properties by density functional theory. Journal of Applied Physics, 2013, 114, .	1.1	24
14614	Tuning the physical properties of antiferromagnetic perovskite oxide NiCrO3 by high-pressure from density-functional calculations. Solid State Communications, 2013, 170, 24-29.	0.9	5
14615	Effect of Metal Impurities on the Tensile Strength of Carbon Nanotubes: A Theoretical Study. Journal of Physical Chemistry C, 2013, 117, 5470-5474.	1.5	12

#	Article	IF	Citations
14616	Ab initiostudy of the electronic and magnetic structure of the TiO<mml:math xmlns:mml="http://www.w3.org/1998/Math/MathML" display="inline"><mml:msub><mml:mrow /><mml:mn>2</mml:mn></mml:msub></mml:math>rutile (110)/Fe interface. Physical Review B, 2013, 88, .	1.1	5
14617	Interaction Mechanisms of Ammonia and Tin Oxide: A Combined Analysis Using Single Nanowire Devices and DFT Calculations. Journal of Physical Chemistry C, 2013, 117, 3520-3526.	1.5	52
14618	Electronic transport through ordered and disordered graphene grain boundaries. Carbon, 2013, 64, 101-110.	5.4	35
14619	Carbyne from First Principles: Chain of C Atoms, a Nanorod or a Nanorope. ACS Nano, 2013, 7, 10075-10082.	7.3	375
14620	Thermodynamic assessment of the Gaâ€“X (X=B, Ca, Sr, Ba) systems supported by first-principles calculations. Calphad: Computer Coupling of Phase Diagrams and Thermochemistry, 2013, 43, 52-60.	0.7	8
14621	Fe-substituted indium thiospinels: New intermediate band semiconductors with better absorption of solar energy. Journal of Applied Physics, 2013, 113, 213509.	1.1	27
14622	Stable ferromagnetism and half-metallicity in two-dimensional polyporphyrin frameworks. RSC Advances, 2013, 3, 7016.	1.7	43
14623	Î²-Technetium Dichloride: Solid-State Modulated Structure, Electronic Structure, and Physical Properties. Journal of the American Chemical Society, 2013, 135, 15955-15962.	6.6	10
14624	Crystal Structure, Optical Properties, and Electronic Structure of Calcium Strontium Tungsten Oxynitrides Ca_xSr_{1â€“x}WO₂N. Journal of Physical Chemistry C, 2013, 117, 18529-18539.	1.5	12
14625	Growth and properties of GaSbBi alloys. Applied Physics Letters, 2013, 103, 142106.	1.5	84
14626	High-Pressure Synthesis and Characterization of Li₂Ca₃[N₂]₃â€”An Uncommon Metallic Diazenide with [N₂]^{2â€“} Ions. Journal of the American Chemical Society, 2013, 135, 16668-16679.	6.6	19
14627	Ab initio design of GaN-based photocatalyst: ZnO-codoped GaN nanotubes. Journal of Power Sources, 2013, 232, 323-331.	4.0	22
14628	Antisites and anisotropic diffusion in GaAs and GaSb. Applied Physics Letters, 2013, 103, 142107.	1.5	11
14629	Large-Gap Quantum Spin Hall Insulators in Tin Films. Physical Review Letters, 2013, 111, 136804.	2.9	1,140
14630	Tailoring magnetic properties of metallic thin films with quantum well states and external electric fields. Physical Review B, 2013, 88, .	1.1	23
14631	Graphene-mediated exchange coupling between a molecular spin and magnetic substrates. Physical Review B, 2013, 88, .	1.1	17
14632	Mixing and non-stoichiometry in Feâ€“Niâ€“Crâ€“Znâ€“O spinel compounds: density functional theory calculations. Physical Chemistry Chemical Physics, 2013, 15, 15550.	1.3	44
14633	Hidden surface states at non-polar GaN (101Â¯) facets: Intrinsic pinning of nanowires. Applied Physics Letters, 2013, 103, .	1.5	45

#	Article	IF	Citations
14634	A dispersion-corrected density functional theory case study on ethyl acetate conformers, dimer, and molecular crystal. Theoretical Chemistry Accounts, 2013, 132, 1.	0.5	18
14635	Zinc Blende 0D Quantum Dots to Wurtzite 1D Quantum Wires: The Oriented Attachment and Phase Change in ZnSe Nanostructures. Journal of Physical Chemistry Letters, 2013, 4, 3292-3297.	2.1	41
14636	Ligand-Field Theory-Based Analysis of the Adsorption Properties of Ruthenium Nanoparticles. ACS Nano, 2013, 7, 9823-9835.	7.3	22
14637	Promoted Ceria: A Structural, Catalytic, and Computational Study. ACS Catalysis, 2013, 3, 2256-2268.	5.5	92
14638	Isolated catalyst sites on amorphous supports: A systematic algorithm for understanding heterogeneities in structure and reactivity. Journal of Chemical Physics, 2013, 138, 204105.	1.2	41
14639	Effect of strain on thermoelectric properties of SrTiO3: First-principles calculations. Chemical Physics Letters, 2013, 586, 159-163.	1.2	31
14640	Methods for First-Principles Alloy Thermodynamics. Jom, 2013, 65, 1523-1532.	0.9	64
14641	Structure sensitivity of CO methanation on Co (0001), and surfaces: Density functional theory calculations. Catalysis Today, 2013, 215, 36-42.	2.2	72
14642	Hydrogen Deposition on Pt(111) during Electrochemical Hydrogen Evolution from a First-Principles Multiadsorption-Site Study. Journal of Physical Chemistry C, 2013, 117, 22696-22704.	1.5	45
14643	Full control of magnetism in a manganite bilayer by ferroelectric polarization. Physical Review B, 2013, 88, .	1.1	46
14644	Mechanism of the CaIrO<mml:math xmlns:mml="http://www.w3.org/1998/Math/MathML" display="inline"><mml:msub><mml:mrow /><mml:mn>3</mml:mn></mml:msub></mml:math>post-perovskite phase transition under pressure. Physical Review B, 2013, 88, .	1.1	16
14645	Fermi surface nesting and magnetic quantum phase transition in graphenelike BC<mml:math xmlns:mml="http://www.w3.org/1998/Math/MathML" display="inline"><mml:msub><mml:mrow /><mml:mn>3</mml:mn></mml:msub></mml:math>: A first-principles study. Physical Review B, 2013, 88, .	1.1	15
14646	Direct observation of a highly spin-polarized organic spinterface at room temperature. Scientific Reports, 2013, 3, 1272.	1.6	118
14647	Real-Space Density Functional Theory on Graphical Processing Units: Computational Approach and Comparison to Gaussian Basis Set Methods. Journal of Chemical Theory and Computation, 2013, 9, 4360-4373.	2.3	53
14648	Condensed Astatine: Monatomic and Metallic. Physical Review Letters, 2013, 111, 116404.	2.9	38
14649	Enhancing the Thermoelectric Properties of Layered Transition-Metal Dichalcogenides 2H-MQ₂ (M = Mo, W; Q = S, Se, Te) by Layer Mixing: Density Functional Investigation. Chemistry of Materials, 2013, 25, 3745-3752.	3.2	81
14650	Interface-Induced Topological Insulator Transition in<mml:math xmlns:mml="http://www.w3.org/1998/Math/MathML" display="inline"><mml:mi>GaAs</mml:mi><mml:mo>/</mml:mo><mml:mi>Ge</mml:mi><mml:mo>/</mml:mo><mml:mi>GaAs</mml:m Wells. Physical Review Letters, 2013, 111, 156402.	2.9	123
14651	display="inline"><mml:msub><mml:mrow /><mml:mn>2</mml:mn></mml:msub></mml:math>Se<mml:math xmlns:mml="http://www.w3.org/1998/Math/MathML" display="inline"><mml:msub><mml:mrow /><mml:mn>3</mml:mn></mml:msub></mml:math>(111) surface doped with transition metals: Anab initioinvestigation. Physical Review B, 2013, 88, .	1.1	52

#	Article	IF	Citations
14652	Understanding the Role of Different Conductive Polymers in Improving the Nanostructured Sulfur Cathode Performance. Nano Letters, 2013, 13, 5534-5540.	4.5	601
14653	Lithium Chalcogenidotetrelates: LiChTâ€"Synthesis and Characterization of New Li⁺ Ion Conducting Li/Sn/Se Compounds. Chemistry of Materials, 2013, 25, 2961-2969.	3.2	32
14654	Understanding Scanning Tunneling Microscopy Contrast Mechanisms on Metal Oxides: A Case Study. ACS Nano, 2013, 7, 10233-10244.	7.3	53
14655	Vision for Designing High-Energy, Hybrid Li Ion/Liâ€"O₂ Cells. Journal of Physical Chemistry Letters, 2013, 4, 3607-3611.	2.1	26
14656	Prediction of Novel SiCN Compounds: First-Principles Calculations. Journal of Physical Chemistry C, 2013, 117, 21943-21948.	1.5	20
14657	Silicon spin chains at finite temperature: Dynamics of Si(553)-Au. Physical Review B, 2013, 87, .	1.1	18
14658	New Layered Structures of Cuprous Chalcogenides as Thin Film Solar Cell Materials:<mml:math xmlns:mml="http://www.w3.org/1998/Math/MathML" display="inline"><mml:msub><mml:mi>Cu</mml:mi><mml:mn>2</mml:mn></mml:msub><mml:mi>Te</mml:mi></mml:math>and<mm xmlns:mml="http://www.w3.org/1998/Math/MathML" display="inline"><mml:msub><mml:mi>Cu</mml:mi><mml:mn>2</mml:mn></mml:msub><mml:mi>Se</mml:mi></mml:math>.	2.9	103
14659	Lattice Instability and Competing Spin Structures in the Double Perovskite Insulator<mml:math xmlns:mml="http://www.w3.org/1998/Math/MathML" display="inline"><mml:msub><mml:mi>Sr</mml:mi><mml:mn>2</mml:mn></mml:msub><mml:msub><mml:mi>FeOsO</mml:mi><mml:mi><m Physical Review Letters, 2013, 111, 167205.	2.9	100
14660	Solid-State Chemistry of Cuprous Delafossites: Synthesis and Stability Aspects. Chemistry of Materials, 2013, 25, 4423-4435.	3.2	114
14661	Room-Temperature Reactions for Self-Cleaning Molecular Nanosensors. Nano Letters, 2013, 13, 798-802.	4.5	18
14662	Deliquescence of NaBH4 from Density Functional Theory and Experiments. Industrial & Engineering Chemistry Research, 2013, 52, 13849-13861.	1.8	4
14663	Observation and magnetism of Cr<mml:math xmlns:mml="http://www.w3.org/1998/Math/MathML" display="inline"><mml:msub><mml:mrow /><mml:mn>2</mml:mn></mml:msub></mml:math>[BP<mml:math xmlns:mml="http://www.w3.org/1998/Math/MathML" display="inline"><mml:msub><mml:mrow /><mml:mn>3</mml:mn></mml:msub></mml:math>O<mml:math xmlns:mml="http://www.w3.org/1998/Math/MathML" display="inline"><mml:msub><mml:mrow />	1.1	15
14664	Hopping transport through defect-induced localized states in molybdenum disulphide. Nature Communications, 2013, 4, 2642.	5.8	935
14665	CH4 dissociation on NiM(111) (M=Co, Rh, Ir) surface: A first-principles study. Surface Science, 2013, 617, 149-155.	0.8	32
14666	First-principles and experimental studies of the IR emissivity of Sn-doped ZnO. Materials Science in Semiconductor Processing, 2013, 16, 1447-1453.	1.9	18
14667	Limitations of the hybrid functional approach to electronic structure of transition metal oxides. Physical Review B, 2013, 88, .	1.1	24
14668	On-Surface Azideâ€"Alkyne Cycloaddition on Au(111). ACS Nano, 2013, 7, 8509-8515.	7.3	115
14669	Visualizing spin-dependent bulk scattering and breakdown of the linear dispersion relation in Bi<mml:math xmlns:mml="http://www.w3.org/1998/Math/MathML" display="inline"><mml:msub><mml:mrow /><mml:mn>2</mml:mn></mml:msub></mml:math>Te<mml:math xmlns:mml="http://www.w3.org/1998/Math/MathML" display="inline"><mml:msub><mml:mrow /><mml:mn>3</mml:mn></mml:msub></mml:math>. Physical Review B, 2013, 88, .	1.1	34

#	Article	IF	Citations
14670	Trapping of Hydrochloric and Hydrofluoric Acid at Vacancies on and underneath the Ice I_h Basal-Plane Surface. Journal of Physical Chemistry A, 2013, 117, 11066-11071.	1.1	5
14671	Incorporation of Lithium by MgH₂: An Ab Initio Study. Journal of Physical Chemistry C, 2013, 117, 22467-22477.	1.5	23
14672	Relative Photooxidation and Photoreduction Activities of the {100}, {101}, and {001} Surfaces of Anatase TiO₂. Langmuir, 2013, 29, 13647-13654.	1.6	86
14673	Accurate determination of thermodynamic properties for liquid alloys based on ab initio molecular dynamics simulation. Fluid Phase Equilibria, 2013, 360, 44-53.	1.4	10
14674	CO Adsorption on Defective Graphene-Supported Pt₁₃ Nanoclusters. Journal of Physical Chemistry C, 2013, 117, 19927-19933.	1.5	62
14675	Bond Length and Charge Density Variations within Extended Arm Chair Defects in Graphene. ACS Nano, 2013, 7, 9860-9866.	7.3	38
14676	Tetragonal Phase Germanium Nanocrystals in Lithium Ion Batteries. ACS Nano, 2013, 7, 9075-9084.	7.3	120
14677	Role of Chemical Potential in Tuning Equilibrium Crystal Shape and Electronic Properties of Wurtzite GaAs Nanowires. Journal of Physical Chemistry C, 2013, 117, 23349-23356.	1.5	15
14678	Adsorption of CO₂ at ZnO: A Surface Structure Effect from DFT+U Calculations. Journal of Physical Chemistry C, 2013, 117, 22954-22966.	1.5	107
14679	High-throughput screening of monometallic catalysts for aqueous-phase hydrogenation of biomass-derived oxygenates. Applied Catalysis B: Environmental, 2013, 140-141, 98-107.	10.8	78
14680	Structural Stability of La₂Ce₂O₇ as a Proton Conductor: A First-Principles Study. Journal of Physical Chemistry C, 2013, 117, 20379-20386.	1.5	26
14681	Adsorption of gas molecules on monolayer MoS2 and effect of applied electric field. Nanoscale Research Letters, 2013, 8, 425.	3.1	581
14682	Nanosized CoO Films on the Î±-Al₂O₃ (0001) Surface: A Density Functional Study. Journal of Physical Chemistry C, 2013, 117, 22714-22722.	1.5	6
14683	Phase stability, thermodynamic and mechanical properties of AlZr2, FeZr2 and Al2FeZr6 from first-principles calculations. Journal of Nuclear Materials, 2013, 440, 6-10.	1.3	13
14684	Point defects in Cd(Zn)Te and TlBr: Theory. Journal of Crystal Growth, 2013, 379, 84-92.	0.7	32
14685	Theoretical Insights into Adsorption of Cobalt Phthalocyanine on Ag(111): A Combination of Chemical and van der Waals Bonding. Journal of Physical Chemistry C, 2013, 117, 23887-23898.	1.5	23
14686	Unusual Metallic Microporous Boron Nitride Networks. Journal of Physical Chemistry Letters, 2013, 4, 3484-3488.	2.1	80
14687	First-Principles Study of Alkali and Alkaline Earth Ion Intercalation in Iron Hexacyanoferrate: The Important Role of Ionic Radius. Journal of Physical Chemistry C, 2013, 117, 21158-21165.	1.5	177

#	Source	IF	Citations
14688	Superconductivity in Ba<mml:math xmlns:mml="http://www.w3.org/1998/Math/MathML" display="inline"><mml:msub><mml:mrow /><mml:mrow><mml:mi>n</mml:mi><mml:mo>+</mml:mo><mml:mn>2</mml:mn></mml:mrow></mml:msub></mml:math>Ir<mml:ma xmlns:mml="http://www.w3.org/1998/Math/MathML" display="inline"><mml:msub><mml:mrow /><mml:mrow><mml:mn>4</mml:mn><mml:mi>n</mml:mi></mml:mrow></mml:msub></mml:math>Ge<mml:math xmlns:mml="http://www.w3.org/1998/Math/MathML" display="inline"><mml:msub><mml:mrow /><mml:mml:	1.1	12
14689	Atomic-scale investigation of Îµ and Î¸ precipitates in bainite in 100Cr6 bearing steel by atom probe tomography and ab initio calculations. Acta Materialia, 2013, 61, 7582-7590.	3.8	62
14690	Interaction of Phase Transformation and Magnetic Properties of Heusler Alloys: A Density Functional Theory Study. Jom, 2013, 65, 1540-1549.	0.9	21
14691	Phase stability, mechanical properties and thermal stability of Y alloyed Tiâ€“Alâ€“N coatings. Surface and Coatings Technology, 2013, 235, 174-180.	2.2	47
14692	Polarization discontinuity induced two-dimensional electron gas at ZnO/Zn(Mg)O interfaces: A first-principles study. Physical Review B, 2013, 88, .	1.1	31
14693	Co_xCu_{1â€“x}Cr₂S₄ Nanocrystals: Synthesis, Magnetism, and Band Structure Calculations. Chemistry of Materials, 2013, 25, 4003-4009.	3.2	19
14694	Density functional theory simulation of liquid helium-4 in aerogel. JETP Letters, 2013, 98, 209-213.	0.4	1
14695	Theory of Carriers Transport in III-Nitride Materials: State of the Art and Future Outlook. IEEE Transactions on Electron Devices, 2013, 60, 3204-3215.	1.6	33
14696	Charge, Spin, and Heat Transport in the Proximity of Metal/Ferromagnet Interface. Solid State Physics, 2013, 64, 53-82.	1.3	3
14697	Magnetic properties of strained La_{2/3}Sr_{1/3}MnO₃perovskites from first principles. Journal of Physics Condensed Matter, 2013, 25, 136005.	0.7	9
14698	Real-Space Identification of Intermolecular Bonding with Atomic Force Microscopy. Science, 2013, 342, 611-614.	6.0	365
14699	High-temperature ferro-electricity in two-dimensional atomic crystal. Applied Physics Letters, 2013, 103, .	1.5	30
14700	The structural, electronic and magnetic properties of bi-layered MoS2 with transition-metals doped in the interlayer. RSC Advances, 2013, 3, 12939.	1.7	33
14701	Structural control of magnetic anisotropy in a strain-driven multiferroic EuTiO<mml:math xmlns:mml="http://www.w3.org/1998/Math/MathML" display="inline"><mml:msub><mml:mrow /><mml:mn>3</mml:mn></mml:msub></mml:math>thin film. Physical Review B, 2013, 88, .	1.1	20
14702	Effect of sulphur vacancy on geometric and electronic structure of MoS2 induced by molecular hydrogen treatment at room temperature. RSC Advances, 2013, 3, 18424.	1.7	47
14703	Quantification of curvature effects in boron and carbon nanotubes: Band structures and ballistic current. Physical Review B, 2013, 87, .	1.1	9
14704	Problem Solving with Pentagons: Tsai-Type Quasicrystal as a Structural Response to Chemical Pressure. Inorganic Chemistry, 2013, 52, 12875-12877.	1.9	21
14705	New Roles for Icosahedral Clusters in Intermetallic Phases: Micelle-like Segregation of Caâ€“Cd and Cuâ€“Cd Interactions in Ca₁₀Cd₂₇Cu₂. Journal of the American Chemical Society, 2013, 135, 17369-17378.	6.6	22

#	Article	IF	Citations
14706	Continuous transformations of C₆₀crystals: polymorphs, polymers, and the ideal strength of fullerites. Journal of Physics Condensed Matter, 2013, 25, 435303.	0.7	6
14707	Stable three-dimensional metallic carbon with interlocking hexagons. Proceedings of the National Academy of Sciences of the United States of America, 2013, 110, 18809-18813.	3.3	134
14708	Molecular adsorption study of nicotine and caffeine on single-walled carbon nanotubes from first principles. Chemical Physics Letters, 2013, 580, 57-61.	1.2	23
14709	Insights into the Surface Chemistry of Tin Oxide Atomic Layer Deposition from Quantum Chemical Calculations. Journal of Physical Chemistry C, 2013, 117, 19056-19062.	1.5	20
14710	Strain-controlled interface engineering of binding and charge doping at metal-graphene contacts. Applied Physics Letters, 2013, 103, 143107.	1.5	4
14711	Nanocrystalline tungsten hydrides at high pressures. Physical Review B, 2013, 87, .	1.1	32
14712	Intrinsic Magnetism of Grain Boundaries in Two-Dimensional Metal Dichalcogenides. ACS Nano, 2013, 7, 10475-10481.	7.3	232
14713	Unraveling the Role of Metalâ€“Support Interactions in Heterogeneous Catalysis: Oxygenate Selectivity in Fischerâ€“Tropsch Synthesis. ACS Catalysis, 2013, 3, 2881-2890.	5.5	54
14714	Band-Gap States of TiO₂(110): Major Contribution from Surface Defects. Journal of Physical Chemistry Letters, 2013, 4, 3839-3844.	2.1	76
14715	Self-healing of vacancy defects in single-layer graphene and silicene. Physical Review B, 2013, 88, .	1.1	119
14716	Hyperfine coupling of point defects in semiconductors by hybrid density functional calculations: The role of core spin polarization. Physical Review B, 2013, 88, .	1.1	79
14717	Electronic and magnetic properties of an organic multiferroic: (C2H5NH3)2CuCl4. Journal of Magnetism and Magnetic Materials, 2013, 346, 91-95.	1.0	14
14718	Two novel derivatives of ammonia borane for hydrogen storage: synthesis, structure, and hydrogen desorption investigation. Journal of Materials Chemistry A, 2013, 1, 12263.	5.2	18
14719	The Role of Surface Oxygen in the Growth of Large Single-Crystal Graphene on Copper. Science, 2013, 342, 720-723.	6.0	977
14720	Stabilizing the magnetic moment of single holmium atoms by symmetry. Nature, 2013, 503, 242-246.	13.7	129
14721	Adsorption and diffusion of Pb(II) on the kaolinite(001) surface: A density-functional theory study. Applied Clay Science, 2013, 85, 74-79.	2.6	25
14722	Stress-induced anisotropic diffusion in alloys: Complex Si solute flow near a dislocation core in Ni. Physical Review B, 2013, 88, .	1.1	47
14723	Structure and electronic properties of Au intercalated hexagonal-boron-nitride/graphene bilayer. Physica E: Low-Dimensional Systems and Nanostructures, 2013, 49, 111-116.	1.3	9

#	Article	IF	Citations
14724	The visible transmittance and solar modulation ability of VO2 flexible foils simultaneously improved by Ti doping: an optimization and first principle study. Physical Chemistry Chemical Physics, 2013, 15, 17537.	1.3	101
14725	External electric field effects on electronic and magnetic properties at molecule-metal interfaces: Cu-phthalocyanine adsorbed on Fe(001) surface. Journal of Applied Physics, 2013, 114, .	1.1	5
14726	Stability of graphitic-like zinc oxide layers under carriers doping: a first-principles study. Nanoscale, 2013, 5, 12111.	2.8	10
14727	Graphene-Based Topological Insulator with an Intrinsic Bulk Band Gap above Room Temperature. Nano Letters, 2013, 13, 6251-6255.	4.5	116
14728	Vibrational Fingerprints of LiNbO₃-LiTaO₃Mixed Crystals. Ferroelectrics, 2013, 447, 63-68.	0.3	7
14729	LiNb_{1-x}Ta_xO₃Electronic Structure and Optical Response fromFirst-PrinciplesCalculations. Ferroelectrics, 2013, 447, 78-85.	0.3	6
14730	Insights into the Role of Surface Distortion in Promoting the Separation and Transfer of Photogenerated Carriers in Anatase TiO₂. Journal of Physical Chemistry C, 2013, 117, 24496-24502.	1.5	32
14731	Effect of A-site cation disorder on oxygen diffusion in perovskite-type Ba0.5Sr0.5Co1â^'xFexO2.5. Journal of Materials Chemistry A, 2013, 1, 10345.	5.2	22
14732	Atomistic modeling of He embrittlement at grain boundaries ofÎ±-Fe: a common feature over different grain boundaries. Modelling and Simulation in Materials Science and Engineering, 2013, 21, 085013.	0.8	10
14733	Standard enthalpies of formation of some Lanthanideâ€“Cobalt binary alloys by high temperature direct synthesis calorimetry. Journal of Alloys and Compounds, 2013, 578, 465-470.	2.8	15
14734	Zigzag Inversion Domain Boundaries in Indium Zinc Oxide-Based Nanowires: Structure and Formation. ACS Nano, 2013, 7, 10747-10751.	7.3	19
14735	Phase Evolution of Tin Nanocrystals in Lithium Ion Batteries. ACS Nano, 2013, 7, 11103-11111.	7.3	105
14736	Optical Absorption and Band Gap Reduction in (Fe1â€“xCrx)2O3 Solid Solutions: A First-Principles Study. Journal of Physical Chemistry C, 2013, 117, 25504-25512.	1.5	43
14737	Effect of ZnO Nanostructure Morphology on the Sensing of H2S Gas. Journal of Physical Chemistry C, 2013, 117, 26106-26118.	1.5	39
14738	Quantum Monte Carlo applied to solids. Physical Review B, 2013, 88, .	1.1	81
14739	First-principles free energy calculations of the structural phase transition in LiBH<mml:math xmlns:mml="http://www.w3.org/1998/Math/MathML"><mml:msub><mml:mrow /><mml:mn>4</mml:mn></mml:msub></mml:math>with I, Cl, Na, and K substitution. Physical Review B, 2013, 88, .	1.1	6
14740	Stability, electronic, and magnetic properties of the magnetically doped topological insulators<mml:math xmlns:mml="http://www.w3.org/1998/Math/MathML"><mml:msub><mml:mtext>Bi</mml:mtext><mml:mn>2</mml:mn></mml:msub><mml:msub><mml:mtext>Te</mml:mtext><mml:mn>3</mml:mn></mml:msub></mml:math>, <mml:math xmlns:mml="http://www.w3.org/1998/Math/MathML"><mml:msub><mml:mrow /><mml:mn>3</mml:mn></mml:msub></mml:math>, Bi<mml:math xmlns:mml="http://www.w3.org/1998/Math/MathML"><mml:msub><mml:mrow /><mml:mn>2</mml:mn></mml:msub></mml:math>Se<mml:math xmlns:mml="http://www.w3.org/1998/Math/MathML"><mml:msub><mml:mrow /><mml:mn>3</mml:mn></mml:msub></mml:math>, and Bi<mml:math xmlns:mml="http://www.w3.org/1998/Math/MathML"><mml:msub><mml:mrow /><mml:mn>2</mml:mn></mml:msub></mml:math>Te<mml:math xmlns:mml="http://www.w3.org/1998/Math/MathML"><mml:msub><mml:mrow /><mml:mn>3</mml:mn></mml:msub></mml:math>. Physical Review B, 2013, 88, .	1.1	126
14741	Isotopic differentiation and sublattice melting in dense dynamic ice. Physical Review B, 2013, 88, .	1.1	14

#	Article	IF	Citations
14742	Energy Band Alignment between Anatase and Rutile TiO₂. Journal of Physical Chemistry Letters, 2013, 4, 4182-4187.	2.1	210
14743	Superlubricity through graphene multilayers between Ni(111) surfaces. Physical Review B, 2013, 87, .	1.1	63
14744	Magnetic properties in zinc-blende CdS induced by Cd vacancies. Physics Letters, Section A: General, Atomic and Solid State Physics, 2013, 377, 572-576.	0.9	23
14745	First principles study of hydroxyapatite surface. Journal of Chemical Physics, 2013, 139, 044714.	1.2	40
14746	The impact of crystal symmetry on the electronic structure and functional properties of complex lanthanum chromium oxides. Journal of Materials Chemistry C, 2013, 1, 4527.	2.7	42
14747	Insight in the activity and diastereoselectivity of various Lewis acid catalysts for the citronellal cyclization. Journal of Catalysis, 2013, 305, 118-129.	3.1	51
14748	A computational investigation of CO oxidation on ruthenium-embedded hexagonal boron nitride nanosheet. Computational and Theoretical Chemistry, 2013, 1011, 5-10.	1.1	107
14749	Magnetic field strength influence on the reactive magnetron sputter deposition of Ta₂O₅. Journal Physics D: Applied Physics, 2013, 46, 335203.	1.3	15
14750	Amorphization Driven by Defect-Induced Mechanical Instability. Physical Review Letters, 2013, 111, 155501.	2.9	35
14751	Electrical and Photoresponse Properties of Printed Thin-Film Transistors Based on Poly(9,9-dioctylfluorene-co-bithiophene) Sorted Large-Diameter Semiconducting Carbon Nanotubes. Journal of Physical Chemistry C, 2013, 117, 18243-18250.	1.5	76
14752	Structure, energetics, and electronic states of IIIâ€“V compound polytypes. Journal of Physics Condensed Matter, 2013, 25, 273201.	0.7	101
14753	Thermodynamics of the Zr-O system from first-principles calculations. Physical Review B, 2013, 88, .	1.1	190
14754	Critical thickness for ferroelectricity and magnetoelectric effect in multiferroic tunnel junction with symmetrical and asymmetrical electrodes. European Physical Journal B, 2013, 86, 1.	0.6	38
14755	Strain-Induced NÃ©el Temperature Enhancement in Corundum-Type Cr₂O₃and Fe₂O₃. Applied Physics Express, 2013, 6, 113007.	1.1	29
14756	Importance of dispersion in density functional calculations of cesium chloride and its related halides. Physical Review B, 2013, 88, .	1.1	29
14757	Investigation of the diffusion of atomic fission products in UC by density functional calculations. Journal of Nuclear Materials, 2013, 434, 240-247.	1.3	18
14758	Adsorption and Stability of Ï€-Bonded Ethylene on GaP(110). Journal of Physical Chemistry C, 2013, 117, 26091-26096.	1.5	5
14759	Effects of strain on the valence band structure and exciton-polariton energies in ZnO. Physical Review B, 2013, 88, .	1.1	42

#	Article	IF	Citations
14760	Investigation of new superhard carbon allotropes with promising electronic properties. Journal of Applied Physics, 2013, 114, 183708.	1.1	10
14761	Magnetoelastic effects in doped Fe<mml:math xmlns:mml="http://www.w3.org/1998/Math/MathML" display="inline"><mml:msub><mml:mrow /><mml:mn>2</mml:mn></mml:msub></mml:math>P. Physical Review B, 2013, 88, .	1.1	40
14762	Extremely Long CuÂ·Â·Â·O Contact as a Possible Pathway for Magnetic Interactions in Na₂Cu(CO₃)₂. Inorganic Chemistry, 2013, 52, 14355-14363.	1.9	15
14763	First-principles study of thermoelectric and lattice vibrational properties of chalcopyrite CuGaTe2. Journal of Alloys and Compounds, 2013, 570, 150-155.	2.8	53
14764	Study of B1 (NaCl-type) to B2 (CsCl-type) pressure-induced structural phase transition in BaS, BaSe and BaTe usingab initiocomputations. Journal of Physics Condensed Matter, 2013, 25, 075401.	0.7	8
14765	Theoretical QTAIM, ELI-D, and Hirshfeld Surface Analysis of the Cuâ€“(H)B Interaction in [Cu₂(bipy)₂B₁₀H₁₀]. Journal of Physical Chemistry A, 2013, 117, 13138-13150.	1.1	43
14766	Proton-Induced Dehydrogenation of Defects in AlGaN/GaN HEMTs. IEEE Transactions on Nuclear Science, 2013, 60, 4080-4086.	1.2	136
14767	First-principles study of the ideal strength of Fe3C cementite. Materials Science & Engineering A: Structural Materials: Properties, Microstructure and Processing, 2013, 572, 25-29.	2.6	14
14768	First-principles DFT+U modeling of defect behaviors in anti-ferromagnetic uranium mononitride. Journal of Applied Physics, 2013, 114, .	1.1	21
14769	First-principles identifications of superstructures of germanene on Ag(111) surface and h-BN substrate. Physical Chemistry Chemical Physics, 2013, 15, 16853.	1.3	56
14770	Reducing self-compensating Mn interstitials in (Ga, Mn)As via nanostructure engineering. Journal Physics D: Applied Physics, 2013, 46, 175005.	1.3	8
14771	Thallium Mercury Chalcobromides, TlHg6Q4Br5 (Q = S, Se). Inorganic Chemistry, 2013, 52, 11875-11880.	1.9	14
14772	Transition Metal Decorated Graphyne: An Efficient Catalyst for Oxygen Reduction Reaction. Journal of Physical Chemistry C, 2013, 117, 26021-26028.	1.5	82
14773	Theoretical study on the interaction of pristine, defective and strained graphene with Fen and Nin (n=13, 38, 55) clusters. Chemical Physics Letters, 2013, 588, 203-207.	1.2	32
14774	Crystal structure prediction for supersaturated AZO: the case of Zn3Al2O6. CrystEngComm, 2013, 15, 10440.	1.3	3
14775	Realistic multisite lattice-gas modeling and KMC simulation of catalytic surface reactions: Kinetics and multiscale spatial behavior for CO-oxidation on metal (100) surfaces. Progress in Surface Science, 2013, 88, 393-521.	3.8	61
14776	Thermodynamic assessment of the Feâ€“Nbâ€“V system. Calphad: Computer Coupling of Phase Diagrams and Thermochemistry, 2013, 43, 143-148.	0.7	8
14777	The Role of Passivants on the Stoichiometry of CdSe and GaAs Nanocrystals. Journal of Physical Chemistry C, 2013, 117, 21981-21987.	1.5	4

#	Article	IF	Citations
14778	Toward First Principles Prediction of Voltage Dependences of Electrolyte/Electrolyte Interfacial Processes in Lithium Ion Batteries. Journal of Physical Chemistry C, 2013, 117, 24224-24235.	1.5	68
14779	Pseudopotential-based studies of electron transport in graphene and graphene nanoribbons. Journal of Physics Condensed Matter, 2013, 25, 473202.	0.7	58
14780	Catalytic Properties of Near-Surface Alloy of Transition Metal in Aluminum: A Density Functional Theory Study of Structural and Electronic Properties. Journal of Physical Chemistry C, 2013, 117, 25077-25089.	1.5	15
14781	First-principles study of the nano-scaling effect on the electrochemical behavior in LiNi_{0.5}Mn_{1.5}O₄. Nanotechnology, 2013, 24, 424007.	1.3	27
14782	Adsorption and pathways of single atomistic processes on TiN (111) surfaces: A first principle study. Computational Materials Science, 2013, 77, 102-107.	1.4	19
14783	Complex magnetic ordering as a driving mechanism of multifunctional properties of Heusler alloys from first principles. European Physical Journal B, 2013, 86, 1.	0.6	88
14784	Self-Organization of Gold Chloride Molecules on Au(111) Surface. Journal of Physical Chemistry C, 2013, 117, 24948-24954.	1.5	16
14785	Beyond standard local density approximation in the study of magnetoelectric effects in Fe/BaTiO₃and Co/BaTiO₃interfaces. Journal of Physics Condensed Matter, 2013, 25, 485500.	0.7	14
14786	Ab initiostudy of magnetic coupling in CaCu<mml:math xmlns:mml="http://www.w3.org/1998/Math/MathML" display="inline"><mml:msub><mml:mrow /><mml:mn>3</mml:mn></mml:msub></mml:math><mml:math xmlns:mml="http://www.w3.org/1998/Math/MathML" display="inline"><mml:msub><mml:mi>B</mml:mi><mml:mn>4</mml:mn></mml:msub></mml:math>O<mml:math xmlns:mml="http://www.w3.org/1998/Math/MathML" display="inline"><mml:msub><mml:mrow /><mml:mml:	1.1	31
14787	Dynamical Orientation of Large Molecules on Oxide Surfaces and its Implications for Dye-Sensitized Solar Cells. Chemistry of Materials, 2013, 25, 4354-4363.	3.2	15
14788	Critical Importance of van der Waals Stabilization in Strongly Chemically Bonded Surfaces: Cu(110):O. Journal of Chemical Theory and Computation, 2013, 9, 5578-5584.	2.3	10
14789	Defect identification in semiconductors with positron annihilation: Experiment and theory. Reviews of Modern Physics, 2013, 85, 1583-1631.	16.4	600
14790	Controllable Disorder Engineering in Oxygen-Incorporated MoS₂ Ultrathin Nanosheets for Efficient Hydrogen Evolution. Journal of the American Chemical Society, 2013, 135, 17881-17888.	6.6	2,107
14791	Average and Local Structural Origins of the Optical Properties of the Nitride Phosphor La_{3â€“x}Ce_xSi₆N₁₁ (0 < x â‰ 3). Inorganic Chemistry, 2013, 52, 13730-13741.	1.9	103
14792	Metalâ€“organic frameworks constructed from flexible ditopic ligands: conformational diversity of an aliphatic ligand. New Journal of Chemistry, 2013, 37, 4130.	1.4	22
14793	Ann-body potential for a Zrâ€“Nb system based on the embedded-atom method. Journal of Physics Condensed Matter, 2013, 25, 105404.	0.7	23
14794	Neutron powder diffraction and molecular dynamics study of superionic SrBr₂. Journal of Physics Condensed Matter, 2013, 25, 454205.	0.7	4
14795	Atomistic linear response voltage drop calculations for quantum transport in materials: The high conductance regime. Journal of Applied Physics, 2013, 114, .	1.1	2

#	Article	IF	Citations
14796	Ba₄Ta₂O₉ Oxide Prepared from an Oxalate-Based Molecular Precursorâ€"Characterization and Properties. Inorganic Chemistry, 2013, 52, 14299-14308.	1.9	25
14797	CO Dissociation Mechanism on Cu-Doped Fe(100) Surfaces. Journal of Physical Chemistry C, 2013, 117, 24920-24931.	1.5	38
14798	Mechanism of magnetization enhancement at CoO/permalloy interfaces. Applied Physics Letters, 2013, 103, 071603.	1.5	2
14799	Energetics and kinetics of direct phase conversion from graphite to diamond. Science China: Physics, Mechanics and Astronomy, 2013, 56, 2266-2271.	2.0	2
14800	Small Photocarrier Effective Masses Featuring Ambipolar Transport in Methylammonium Lead Iodide Perovskite: A Density Functional Analysis. Journal of Physical Chemistry Letters, 2013, 4, 4213-4216.	2.1	675
14801	Defects Are Needed for Fast Photo-Induced Electron Transfer from a Nanocrystal to a Molecule: Time-Domain Ab Initio Analysis. Journal of the American Chemical Society, 2013, 135, 18892-18900.	6.6	61
14802	A new hard phase of ReB4 predicted from first principles. Journal of Alloys and Compounds, 2013, 573, 20-26.	2.8	34
14803	Physical properties of the thermoelectric cubic lanthanum chalcogenides La<mml:math xmlns:mml="http://www.w3.org/1998/Math/MathML" display="inline"><mml:mrow><mml:msub><mml:mrow /><mml:mrow><mml:mn>3</mml:mn><mml:mo>â^'</mml:mo><mml:mi>y</mml:mi></mml:mrow></mml:msub><mml:msub><mml:mrow /><mml:mrow><mml:mn>2</mml:mn></mml:mrow></mml:msub><mml:mi>	1.1	22
14804	Interaction of Pyridine Derivatives with a Gold (111) Surface as a Model for Adsorption to Large Nanoparticles. Journal of Physical Chemistry C, 2013, 117, 4470-4479.	1.5	45
14805	Mechanical Properties and Stacking Fault Energies of NiFeCrCoMn High-Entropy Alloy. Jom, 2013, 65, 1780-1789.	0.9	596
14806	Effects of alloying and transmutation impurities on stability and mobility of helium in tungsten under a fusion environment. Nuclear Fusion, 2013, 53, 073049.	1.6	43
14807	Cuâ€"Cr, Cuâ€"Mn, and Cuâ€"Fe Spinel-Oxide-Type Catalysts for Reforming of Oxygenated Hydrocarbons. Journal of Physical Chemistry C, 2013, 117, 23757-23765.	1.5	35
14808	Adsorbate-Induced Oxygen Vacancy Mobility in Ultrathin Oxide Films. Journal of Physical Chemistry C, 2013, 117, 23806-23811.	1.5	7
14809	Curvature Effects on the Interfacial Capacitance of Carbon Nanotubes in an Ionic Liquid. Journal of Physical Chemistry C, 2013, 117, 23539-23546.	1.5	53
14810	Comparison of ReaxFF, DFTB, and DFT for Phenolic Pyrolysis. 1. Molecular Dynamics Simulations. Journal of Physical Chemistry A, 2013, 117, 11115-11125.	1.1	88
14811	Unidirectional suppression of hydrogen oxidation on oxidized platinum clusters. Nature Communications, 2013, 4, 2500.	5.8	197
14812	Mechanism of Preferential Adsorption of SO₂ into Two Microporous Paddle Wheel Frameworks M(bdc)(ted)_{0.5}. Chemistry of Materials, 2013, 25, 4653-4662.	3.2	127
14813	Theory of local electric polarization and its relation to internal strain: Impact on polarization potential and electronic properties of group-III nitrides. Physical Review B, 2013, 88, .	1.1	101

#	Article	IF	Citations
14814	Modeling the Impact of Alkanethiol SAMs on the Morphology of Gold Nanocrystals. Crystal Growth and Design, 2013, 13, 5433-5441.	1.4	13
14815	Correlation and relativistic effects in U metal and U-Zr alloy: Validation ofab initioapproaches. Physical Review B, 2013, 88, .	1.1	74
14816	Electrical properties of point defects in CdS and ZnS. Applied Physics Letters, 2013, 103, .	1.5	62
14817	Structural and mechanical stability of rare-earth diborides. Chinese Physics B, 2013, 22, 046202.	0.7	63
14818	Adsorption and diffusion of the Rh and Au adatom on graphene moirÃ©/Ru(0001). Journal of Chemical Physics, 2013, 138, 184710.	1.2	22
14819	Synthetic Route to Metal Nitrides: High-Pressure Solid-State Metathesis Reaction. Inorganic Chemistry, 2013, 52, 13356-13362.	1.9	44
14820	Investigation on the thermoelectric properties of nanostructured. Journal of Solid State Chemistry, 2013, 199, 90-95.	1.4	30
14821	Hydrogen generation from formic acid decomposition on Ni(211), Pd(211) and Pt(211). Journal of Molecular Catalysis A, 2013, 379, 169-177.	4.8	38
14822	Contributions of point defects, chemical disorder, and thermal vibrations to electronic properties of Cd<mml:math xmlns:mml="http://www.w3.org/1998/Math/MathML" display="inline"><mml:msub><mml:mrow /><mml:mrow><mml:mn>1</mml:mn><mml:mo>â^’</mml:mo><mml:mi>x</mml:mi></mml:mrow></mml:msub></mml:math>Zn<mml:math xmlns:mml="http://www.w3.org/1998/Math/MathML" display="inline"><mml:msub><mml:mrow /><mml:mi>x</mml:mi></mml:msub></mml:math>Te alloys. Physical Review B, 2013, 88, .	1.1	11
14823	Enhanced photosensitized activity of a BiOClâ€“Bi2WO6 heterojunction by effective interfacial charge transfer. Physical Chemistry Chemical Physics, 2013, 15, 19387.	1.3	108
14824	Structural and electronic properties of hybrid perovskites for high-efficiency thin-film photovoltaics from first-principles. APL Materials, 2013, 1, .	2.2	517
14825	The transition behavior of FePc on Ag(110). Chemical Physics Letters, 2013, 582, 90-94.	1.2	5
14826	First-principles study of the behavior of O, N and C impurities in vanadium solids. Journal of Nuclear Materials, 2013, 435, 71-76.	1.3	33
14827	Magnetic properties of Co2â^’xTMxC and Co3â^’xTMxC nanoparticles. Journal of Applied Physics, 2013, 114, 243909.	1.1	7
14828	Investigation of NaY Zeolite with adsorbed CO2 by neutron powder diffraction. Microporous and Mesoporous Materials, 2013, 172, 95-104.	2.2	59
14829	Structural Evolution of Carbon Dioxide under High Pressure. Journal of the American Chemical Society, 2013, 135, 14167-14171.	6.6	111
14830	Adiabatic release measurements in<mml:math xmlns:mml="http://www.w3.org/1998/Math/MathML" display="inline"><mml:mi>Î±</mml:mi></mml:math>-quartz between 300 and 1200 GPa: Characterization of<mml:math xmlns:mml="http://www.w3.org/1998/Math/MathML" display="inline"><mml:mi>Î±</mml:mi></mml:math>-quartz as a shock standard in the multimegabar regime. Physical Review B, 2013, 88, .	1.1	105
14831	A procedure for bypassing metastable states in local basis set DFT+U calculations and its application to uranium dioxide surfaces. Computational Materials Science, 2013, 71, 157-164.	1.4	26

#	Article	IF	Citations
14832	Interstitial zinc clusters in zinc oxide. Physical Review B, 2013, 88, .	1.1	68
14833	Highly efficient and robust cathode materials for low-temperature solid oxide fuel cells: PrBa0.5Sr0.5Co2â^'xFexO5+Î´. Scientific Reports, 2013, 3, 2426.	1.6	285
14834	High-Pressure Phase Transitions and Structures of Topological Insulator BiTeI. Journal of Physical Chemistry C, 2013, 117, 25677-25683.	1.5	50
14835	Vanadium sulfide nanoribbons: Electronic and magnetic properties. Physics Letters, Section A: General, Atomic and Solid State Physics, 2013, 377, 3154-3157.	0.9	13
14836	Role of the Siâ€“Si bond stability in the first stages of Ti diffusion on a Si(111) 2Ã—1 surface. A periodic DFT study. Applied Surface Science, 2013, 273, 496-501.	3.1	2
14837	Topological phase transition and two-dimensional topological insulators in Ge-based thin films. Physical Review B, 2013, 88, .	1.1	19
14838	Density functional study of structural defects in h-BNC2sheets. Journal of Physics Condensed Matter, 2013, 25, 025304.	0.7	4
14839	Case study of Rb+(aq), quasi-chemical theory of ion hydration, and the no split occupancies rule. Annual Reports on the Progress of Chemistry Section C, 2013, 109, 266.	4.4	31
14840	Temperature-dependent effective third-order interatomic force constants from first principles. Physical Review B, 2013, 88, .	1.1	266
14841	Microstructural study of high-temperature Crâ€“Niâ€“Alâ€“Ti alloys supported by first-principles calculations. Intermetallics, 2013, 35, 33-40.	1.8	9
14842	Experimental and theoretical study of NiMoW, NiMo, and NiW sulfide catalysts supported on an AlTiMg mixed oxide during the hydrodesulfurization of dibenzothiophene. Fuel, 2013, 113, 733-743.	3.4	44
14843	Hole Transport in Diketopyrrolopyrrole (DPP) Small Molecules: A Joint Theoretical and Experimental Study. Journal of Physical Chemistry C, 2013, 117, 6730-6740.	1.5	21
14844	Native defects in tetradymite Bi<mml:math xmlns:mml="http://www.w3.org/1998/Math/MathML" display="inline"><mml:msub><mml:mrow		

#	Article	IF	Citations
14850	Electron tunneling characteristics of a cubic quantum dot, (PbS)32. Journal of Chemical Physics, 2013, 139, 244307.	1.2	13
14851	Structural properties and high-temperature spin and electronic transitions in GdCoO3: Experiment and theory. Physical Review B, 2013, 88, .	1.1	33
14852	Structures, Energetics, and Electronic Properties of Layered Materials and Nanotubes of Cadmium Chalcogenides. Journal of Physical Chemistry C, 2013, 117, 25817-25825.	1.5	26
14853	Effects of NaOH in Solid NaH: Solution/Segregation Phase Transition and Diffusion Acceleration. Journal of Physical Chemistry C, 2013, 117, 23575-23581.	1.5	6
14854	New Functionalized Metalâ€“Organic Frameworks MIL-47-X (X = â^'Cl, â^'Br, â^'CH₃,) Tj ETQq0 0 0 rgBT /Overlock 10 Tf 50 Adsorption Properties. Journal of Physical Chemistry C, 2013, 117, 22784-22796.	1.5	79
14855	Tailoring the Adsorption of Benzene on PdFe Surfaces: A Density Functional Theory Study. Journal of Physical Chemistry C, 2013, 117, 24317-24328.	1.5	45
14856	Graphyne and Graphdiyne: Versatile Catalysts for Dehydrogenation of Light Metal Complex Hydrides. Journal of Physical Chemistry C, 2013, 117, 21643-21650.	1.5	40
14857	Role of magnetism in Cu precipitation in<mml:math xmlns:mml="http://www.w3.org/1998/Math/MathML" display="inline"><mml:mi>Î±</mml:mi></mml:math>-Fe. Physical Review B, 2013, 88, .	1.1	31
14858	Temperature-dependent lithium storage behavior in tetragonal boron (B50) thin film anode for Li-ion batteries. Electrochimica Acta, 2013, 87, 230-235.	2.6	8
14859	Stability and electronic properties of two-dimensional silicene and germanene on graphene. Physical Review B, 2013, 88, .	1.1	173
14860	Shock-induced phase transformations in gallium single crystals by atomistic methods. Physical Review B, 2013, 88, .	1.1	15
14861	Trimetallic Borohydride Li₃MZn₅(BH₄)₁₅ (M = Mg,) Tj ETQq1 1 0.784314 rgBT /O	1.9	51
14862	Band Structure Engineering in Topological Insulator Based Heterostructures. Nano Letters, 2013, 13, 6064-6069.	4.5	57
14863	Magnetic properties of Mn₂NiSn shape memory alloy. Journal of Physics Condensed Matter, 2013, 25, 236005.	0.7	9
14864	Thermal effects on electronic properties of CO/Pt(111) in water. Physical Chemistry Chemical Physics, 2013, 15, 13619.	1.3	2
14865	Energy stabilization of the<mml:math xmlns:mml="http://www.w3.org/1998/Math/MathML" display="inline"><mml:mi>s</mml:mi></mml:math>-symmetry superatom molecular orbital by endohedral doping of C<mml:math xmlns:mml="http://www.w3.org/1998/Math/MathML" display="inline"><mml:msub><mml:mrow /><mml:mn>82</mml:mn></mml:msub></mml:math>fullerene with a lanthanum atom. Physical Review B, 2013, 88, .	1.1	13
14866	Theoretical investigation of FeTe magnetic ordering under hydrostatic pressure. Physical Review B, 2013, 87, .	1.1	17
14867	Support effect on H adsorption on a metal atom. Chemical Physics Letters, 2013, 565, 45-51.	1.2	6

#	Article	IF	Citations
14868	Study of multivacancies in alpha Fe. Journal of Nuclear Materials, 2013, 441, 168-177.	1.3	20
14869	Optimization of a hybrid exchangeâ€“correlation functional for silicon carbides. Chemical Physics Letters, 2013, 579, 58-63.	1.2	9
14870	The effect of uniaxial pressure on the magnetic anisotropy of the Mn ₁₂ -Ac single-molecule magnet. Europhysics Letters, 2013, 102, 47008.	0.7	3
14871	Structural, electronic, mechanical, and magnetic properties and relative stability of polymorphic modifications of ReN2 from Ab initio calculation data. Physics of the Solid State, 2013, 55, 1821-1825.	0.2	4
14872	Carrier Separation at Dislocation Pairs in CdTe. Physical Review Letters, 2013, 111, 096403.	2.9	51
14873	Understanding the defect chemistry of tin monoxide. Journal of Materials Chemistry C, 2013, 1, 8194.	2.7	75
14874	Thermally and Vibrationally Induced Tautomerization of Single Porphycene Molecules on a Cu(110) Surface. Physical Review Letters, 2013, 111, 246101.	2.9	93
14875	Anisotropy of the elastic properties of crystalline cellulose Iβ from first principles density functional theory with Van der Waals interactions. Cellulose, 2013, 20, 2703-2718.	2.4	150
14876	Phase transformations in the nitrocarburizing surface of carbon steels revisited by microstructure and property characterizations. Acta Materialia, 2013, 61, 3963-3972.	3.8	41
14877	Ab initiostudy of thermodynamic, electronic, magnetic, structural, and elastic properties of Ni<mml:math xmlns:mml="http://www.w3.org/1998/Math/MathML" display="inline"><mml:msub><mml:mrow /><mml:mn>4</mml:mn></mml:msub></mml:math>N allotropes. Physical Review B, 2013, 88, .	1.1	19
14878	The electronic structure of organicâ€“inorganic hybrid compounds: (NH₄)₂CuCl₄, (CH₃NH₃)₂CuCl₄and (C₂H₅NH₃)₂CuCl₄. Journal of Physics Condensed Matter, 2013, 25, 295502.	0.7	39
14879	Synthesis, Characterization, and Electronic Structure of Single-Crystal SnS, Sn₂S₃, and SnS₂. Chemistry of Materials, 2013, 25, 4908-4916.	3.2	388
14880	On the role of halides and thiols in additive-assisted copper electroplating. Electrochimica Acta, 2013, 89, 537-548.	2.6	54
14881	Ultrafast band-gap oscillations in iron pyrite. Physical Review B, 2013, 88, .	1.1	18
14882	First-principles investigation of dual substitutional impurity-induced electronic structural modulation of PbTe on cationic and anionic sites. Acta Materialia, 2013, 61, 6428-6442.	3.8	6
14883	The Influence of Functionals on Density Functional Theory Calculations of the Properties of Reducible Transition Metal Oxide Catalysts. Journal of Physical Chemistry C, 2013, 117, 25562-25578.	1.5	47
14884	Functionalization of monolayer MoS2 by substitutional doping: A first-principles study. Physics Letters, Section A: General, Atomic and Solid State Physics, 2013, 377, 1362-1367.	0.9	285
14885	Catalyzed Surface-Aligned Reaction, H(ad)Â+ÂH2(ad)Â=ÂH2(g)Â+ÂH(ad) on Coinage Metals. Zeitschrift Fur Physikalische Chemie, 2013, , 130722000303001.	1.4	2

#	Article	IF	Citations
14886	Multiscale Modeling of Chemistry in Water: Are We There Yet?. Journal of Chemical Theory and Computation, 2013, 9, 5567-5577.	2.3	59
14887	Vacancy dependent structural, electronic, and magnetic properties of zigzag silicene nanoribbons:Co. Journal of Applied Physics, 2013, 114, .	1.1	17
14888	First-principles investigation of quantum transport through an endohedral N@C₆₀in the Coulomb blockade regime. Journal of Physics Condensed Matter, 2013, 25, 495302.	0.7	1
14889	Methane adsorption on graphite(0001) films: A first-principles study. Chinese Physics B, 2013, 22, 016802.	0.7	6
14890	Facile one-pot synthesis and band gap calculations of ZnxCd1â^'xS nanorods. Materials Letters, 2013, 102-103, 94-97.	1.3	20
14891	Interface formation of scandium nitride on the GaN(0001) surface: A first-principles study. Computational Materials Science, 2013, 70, 77-81.	1.4	6
14892	Thermodynamic assessment of Snâ€“Cuâ€“Ce system. Calphad: Computer Coupling of Phase Diagrams and Thermochemistry, 2013, 43, 124-132.	0.7	8
14893	HCl Oxidation on IrO₂-Based Catalysts: From Fundamentals to Scale-Up. ACS Catalysis, 2013, 3, 2813-2822.	5.5	52
14894	First principles modeling of zirconium solution in bulk UO2. Journal of Applied Physics, 2013, 113, .	1.1	22
14895	Bonding Schemes for Polar Intermetallics through Molecular Orbital Models: Ca-Supported Ptâ€“Pt Bonds in Ca10Pt7Si3. Crystals, 2013, 3, 504-516.	1.0	11
14896	Negative-<mml:math xmlns:mml="http://www.w3.org/1998/Math/MathML"><mml:mi>U</mml:mi></mml:math>carbon vacancy in 4<mml:math xmlns:mml="http://www.w3.org/1998/Math/MathML"><mml:mi>H</mml:mi></mml:math>-SiC: Assessment of charge correction schemes and identification of the negative carbon vacancy at the quasicubic site. Physical Review B, 2013, 88, .	1.1	45
14897	Electronic structure study of N, O related defects in GaP for photoelectrochemical applications. Journal of Materials Chemistry A, 2013, 1, 8425.	5.2	4
14898	Design of semiconductor ternary quantum dots with optimal optoelectronic function. AICHE Journal, 2013, 59, 3223-3236.	1.8	9
14899	Formation of the OOH radical at steps of the boehmite surface and its inhibition by gallic acid: A theoretical study including DFT-based dynamics. Journal of Inorganic Biochemistry, 2013, 128, 164-173.	1.5	19
14900	The first principles studies of the MgB7 compound: Hard material. Intermetallics, 2013, 39, 84-88.	1.8	29
14901	Magnetic, transport and electronic properties of SmNi4Si compound. Journal of Alloys and Compounds, 2013, 577, 19-24.	2.8	8
14902	Binary nature of monolayer boron sheets from ab initio global searches. Journal of Chemical Physics, 2013, 138, 024701.	1.2	44
14903	An Atomistic Study of Perfluoropolyether Lubricant Thermal Stability in Heat Assisted Magnetic Recording. IEEE Transactions on Magnetics, 2013, 49, 3748-3751.	1.2	3

#	Article	IF	Citations
14904	Manageable N-doped Graphene for High Performance Oxygen Reduction Reaction. Scientific Reports, 2013, 3, 2771.	1.6	182
14905	Ab initio calculation of the thermodynamic properties and phase diagram of gallium nitride. Physica B: Condensed Matter, 2013, 431, 115-119.	1.3	4
14906	Ab initio calculations on elastic properties in L12 structure Al3X and X3Al-type (X=transition or main) Tj ETQq0 0 0 rgBT /Overlock 10 Tf	0.9	59
14907	Hydrogen-enhanced vacancy embrittlement of grain boundaries in iron. Physical Review B, 2013, 88, .	1.1	51
14908	Proton or Deuteron Transfer in Phase IV of Solid Hydrogen and Deuterium. Physical Review Letters, 2013, 110, 025903.	2.9	59
14909	Stability and migration of charged oxygen interstitials in ThO2 and CeO2. Acta Materialia, 2013, 61, 7639-7645.	3.8	30
14910	Strong anisotropic influence of local-field effects on the dielectric response of<mml:math xmlns:mml="http://www.w3.org/1998/Math/MathML" display="inline"><mml:mi>Î±</mml:mi></mml:math>-MoO<mml:math xmlns:mml="http://www.w3.org/1998/Math/MathML" display="inline"><mml:msub><mml:mrow /><mml:mn>3</mml:mn></mml:msub></mml:math>. Physical Review B, 2013, 88, .	1.1	88
14911	The structural, electronic, elastic, vibration and thermodynamic properties of GdMg. Solid State Sciences, 2013, 16, 168-174.	1.5	12
14912	Possible doping strategies for MoS<mml:math xmlns:mml="http://www.w3.org/1998/Math/MathML" display="inline"><mml:msub><mml:mrow /><mml:mn>2</mml:mn></mml:msub></mml:math>monolayers: Anab initiostudy. Physical Review B, 2013, 88, .	1.1	489
14913	Structural and electronic properties of<mml:math xmlns:mml="http://www.w3.org/1998/Math/MathML" display="inline"><mml:mi>Î±</mml:mi></mml:math>-tin nanocrystals from first principles. Physical Review B, 2013, 87, .	1.1	29
14914	Magnetic Order in NbS$_2$ Nanoribbons. IEEE Transactions on Magnetics, 2013, 49, 4538-4541.	1.2	1
14915	Bio-oil catalytic reforming without steam addition: Application to hydrogen production and studies on its mechanism. International Journal of Hydrogen Energy, 2013, 38, 16038-16047.	3.8	94
14916	Mixing of equations of state for xenon-deuterium using density functional theory. Physics of Plasmas, 2013, 20, .	0.7	10
14917	Electronic structure of silicene on Ag(111): Strong hybridization effects. Physical Review B, 2013, 88, .	1.1	186
14918	Theoretical and experimental studies on the electronic structure of crystalline and amorphous ZnSnO3 thin films. Applied Physics Letters, 2013, 102, .	1.5	25
14919	Structural, electronic, and optical properties of Cu3-V-VI4 compound semiconductors. Applied Physics Letters, 2013, 103, .	1.5	36
14920	Orbital ordering in La<mml:math xmlns:mml="http://www.w3.org/1998/Math/MathML" display="inline"><mml:msub><mml:mrow /><mml:mrow><mml:mn>0.5</mml:mn></mml:mrow></mml:msub></mml:math>Sr<mml:math xmlns:mml="http://www.w3.org/1998/Math/MathML" display="inline"><mml:msub><mml:mrow /><mml:mrow><mml:mn>1.5</mml:mn></mml:mrow></mml:msub></mml:math>MnO<mml:math xmlns:mml="http://www.w3.org/1998/Math/MathML" display="inline"><mml:msub><mml:mrow /><mml:mn	1.1	0
14921	Influence of c-axis orientation and scandium concentration on infrared active modes of magnetron sputtered ScxAl1â^'xN thin films. Applied Physics Letters, 2013, 103, .	1.5	9

#	Article	IF	Citations
14922	CO2 in the mantle: Melting and solidâ€“solid phase boundaries. Earth and Planetary Science Letters, 2013, 373, 228-232.	1.8	24
14923	A first-principles study of the mechanical properties of g-GeC. Mechanics of Materials, 2013, 64, 135-141.	1.7	81
14924	Biaxial strain effects on adatom surface diffusion on tungsten from first principles. Physical Review B, 2013, 88, .	1.1	12
14925	Multiclass classification of distributed memory parallel computations. Pattern Recognition Letters, 2013, 34, 322-329.	2.6	8
14926	The spin and orbital moment of Fen (n = 2â€“20) clusters. Journal of Chemical Physics, 2013, 139, 034314.	1.2	42
14927	Pressure-induced phase-transition sequence in CoF<mml:math xmlns:mml="http://www.w3.org/1998/Math/MathML" display="inline"><mml:msub><mml:mrow /><mml:mn>2</mml:mn></mml:msub></mml:math>: An experimental and first-principles study on the crystal, vibrational, and electronic properties. Physical Review B, 2013, 88, .	1.1	29
14928	Ionic current and polarization effect in TlBr. Physical Review B, 2013, 87, .	1.1	27
14929	Realization of free-standing silicene using bilayer graphene. Applied Physics Letters, 2013, 103, .	1.5	80
14930	First-principles study of the structural, mechanical, magnetic, and electronic properties of Cr4AlN3 under pressure. Intermetallics, 2013, 43, 71-78.	1.8	9
14931	Dimethylammonium copper formate [(CH3)2NH2]Cu(HCOO)3: A metal-organic framework with quasi-one-dimensional antiferromagnetism and magnetostriction. Physical Review B, 2013, 87, .	1.1	62
14932	Abundant topological states in silicene with transition metal adatoms. Physical Review B, 2013, 88, .	1.1	57
14933	Strong coupling of Jahn-Teller distortion to oxygen-octahedron rotation and functional properties in epitaxially strained orthorhombic LaMnO<mml:math xmlns:mml="http://www.w3.org/1998/Math/MathML" display="inline"><mml:msub><mml:mrow /><mml:mn>3</mml:mn></mml:msub></mml:math>. Physical Review B, 2013, 88, .	1.1	82
14934	Magnetism and stability of noncompensated anion-cation codoped ZnO. Journal of Applied Physics, 2013, 113, .	1.1	11
14935	First-principles study of hydrogen vacancies in lithium amide doped with titanium and niobium. International Journal of Hydrogen Energy, 2013, 38, 11303-11312.	3.8	9
14936	Electronic-structure modification of graphene on Ni(111) surface by the intercalation of a noble metal. Physical Review B, 2013, 87, .	1.1	23
14937	Ab initiostudy of the stabilities of and mechanism of superionic transport in lithium-rich antiperovskites. Physical Review B, 2013, 87, .	1.1	135
14938	Bandgap engineering of Cu2CdxZn1â^'xSnS4 alloy for photovoltaic applications: A complementary experimental and first-principles study. Journal of Applied Physics, 2013, 114, .	1.1	88
14939	Dual-channel anchorable organic dye with triphenylamine-based core bridge unit for dye-sensitized solar cells. Dyes and Pigments, 2013, 99, 599-606.	2.0	23

#	Article	IF	Citations
14940	Contribution of core-loss fine structures to the characterization of ion irradiation damages in the nanolaminated ceramic Ti3AlC2. Acta Materialia, 2013, 61, 7348-7363.	3.8	45
14941	Theoretical study on tetragonal transition metal dinitrides from first principles calculations. Journal of Alloys and Compounds, 2013, 581, 508-514.	2.8	26
14942	Adhesion of the TiN/Fe interface with point defects from first principles. Journal of Applied Physics, 2013, 113, 014905.	1.1	11
14943	First-principles phonon calculations on the lattice dynamics and thermodynamics of rare-earth intermetallics TbCu and TbZn. Intermetallics, 2013, 43, 65-70.	1.8	7
14944	Effects of Potassium Ion Substitution on Lattice Parameters and Proton Migration in Barium Phosphate. Japanese Journal of Applied Physics, 2013, 52, 117101.	0.8	4
14945	Three-band tight-binding model for monolayers of group-VIB transition metal dichalcogenides. Physical Review B, 2013, 88, .	1.1	715
14946	Band alignment in SnS thin-film solar cells: Possible origin of the low conversion efficiency. Applied Physics Letters, 2013, 102, .	1.5	130
14947	Stabilities and Reconstructions of PbTe Crystal Surfaces from Density-Functional Theory. Journal of Physical Chemistry C, 2013, 117, 24455-24461.	1.5	20
14948	Catalytic properties of extraframework iron-containing species in ZSM-5 for N2O decomposition. Journal of Catalysis, 2013, 308, 386-397.	3.1	43
14949	First-principles study of negative thermal expansion in zinc oxide. Journal of Applied Physics, 2013, 114, .	1.1	38
14950	Optical isotropization of anisotropic wurtzite Al-rich AlGaN via asymmetric modulation with ultrathin (GaN) _m /(AlN) _n superlattices. Laser and Photonics Reviews, 2013, 7, 572-579.	4.4	17
14951	Thermoelectric performance of p-type skutterudites YbxFe4â^'yPtySb12 (0.8â€‰â‰€â€‰xâ€‰â‰€â€‰1, yâ€‰=â€‰1 and 0.5). Journal of Applied Physics, 2013, 113, .	1.1	13
14952	Band-Filling Correction Method for Accurate Adsorption Energy Calculations: A Cu/ZnO Case Study. Journal of Chemical Theory and Computation, 2013, 9, 4673-4678.	2.3	9
14953	Recent progress in R&D on tungsten alloys for divertor structural and plasma facing materials. Journal of Nuclear Materials, 2013, 442, S181-S189.	1.3	272
14954	Quantum energy density: Improved efficiency for quantum Monte Carlo calculations. Physical Review B, 2013, 88, .	1.1	7
14955	Atomistic Modeling of the Sorption Free Energy of Dioxins at Clayâ€“Water Interfaces. Journal of Physical Chemistry C, 2013, 117, 24975-24984.	1.5	22
14956	<mml:math xmlns:mml="http://www.w3.org/1998/Math/MathML" display="inline"><mml:msub><mml:mi>MnSb</mml:mi><mml:mn>2</mml:mn></mml:msub><mml:msub><mml:mi mathvariant="bold">O</mml:mi><mml:mn>6</mml:mn></mml:msub></mml:math>: A Polar Magnet with a Chiral Crystal Structure. Physical Review Letters, 2013, 111, 017202.	2.9	32
14957	Effect of hydrogen incorporation on the negative bias illumination stress instability in amorphous In-Ga-Zn-O thin-film-transistors. Journal of Applied Physics, 2013, 113, .	1.1	62

#	Article	IF	Citations
14958	First-principles study on the magnetic properties in Mg doped BiFeO3 with and without oxygen vacancies. Journal of Applied Physics, 2013, 114, 233912.	1.1	25
14959	Strain Effects To Optimize Thermoelectric Properties of Doped Bi₂O₂Se via Tranâ€“Blaha Modified Beckeâ€“Johnson Density Functional Theory. Journal of Physical Chemistry C, 2013, 117, 21597-21602.	1.5	111
14960	Three-Dimensional Metallic Boron Nitride. Journal of the American Chemical Society, 2013, 135, 18216-18221.	6.6	145
14961	Mechanical and electronic properties of A1â^'xBxHy (A and B=Ti, Zr, Hf) hydride alloys: A first-principles study. Journal of Alloys and Compounds, 2013, 581, 404-412.	2.8	5
14962	Thermal Stability of Li₂O₂and Li₂O for Li-Air Batteries: In Situ XRD and XPS Studies. Journal of the Electrochemical Society, 2013, 160, A824-A831.	1.3	278
14963	Density functional theory study of the structure and vibrational modes of acrylonitrile adsorbed on Cu(100). Physical Chemistry Chemical Physics, 2013, 15, 1288-1295.	1.3	11
14964	Cation disorder as the major electron scattering source in crystalline InGaZnO. Applied Physics Letters, 2013, 102, 152104.	1.5	29
14965	Structures and stabilities of alkaline earth metal peroxides XO2 (X = Ca, Be, Mg) studied by a genetic algorithm. RSC Advances, 2013, 3, 22135.	1.7	20
14966	Extended X-ray absorption fine structure study of Gd doped ZrO2 systems. Journal of Applied Physics, 2013, 113, .	1.1	15
14967	First-principles study on competing phases of silicene: Effect of substrate and strain. Physical Review B, 2013, 88, .	1.1	45
14968	Topological insulators in transition-metal intercalated graphene: The role of<mml:math xmlns:mml="http://www.w3.org/1998/Math/MathML" display="inline"><mml:mi>d</mml:mi></mml:math>electrons in significantly increasing the spin-orbit gap. Physical Review B, 2013, 87, .	1.1	43
14969	Low-energy electron reflectivity of graphene on copper and other substrates. Physical Review B, 2013, 87, .	1.1	43
14970	First-principles study of bismuth films on the Ni(111) surface. Physical Review B, 2013, 88, .	1.1	7
14971	Edge-adsorption of potassium adatoms on graphene nanoribbon: A first principle study. Applied Surface Science, 2013, 280, 698-704.	3.1	19
14972	Polar oxide substrates for graphene growth: A first-principles investigation of graphene on MgO(111). Current Applied Physics, 2013, 13, 803-807.	1.1	13
14973	Pressure-induced topological phase transitions in rocksalt chalcogenides. Physical Review B, 2013, 88, .	1.1	70
14974	Adsorption configurations of carbon monoxide on gold monolayer supported by graphene or monolayer hexagonal boron nitride: a first-principles study. European Physical Journal B, 2013, 86, 1.	0.6	6
14975	First-principles study of hydrogen storage on Li-decorated silicene. Journal of Nanoparticle Research, 2013, 15, 1.	0.8	23

#	Article	IF	Citations
14976	Oxidation of Cr2AlC (0001): Insights from Ab Initio Calculations. Jom, 2013, 65, 1487-1491.	0.9	13
14977	Oxygen Atom Adsorption on and Diffusion into Nb(110) and Nb(100) from First Principles. Jom, 2013, 65, 1473-1481.	0.9	8
14978	Materials Design and Discovery with High-Throughput Density Functional Theory: The Open Quantum Materials Database (OQMD). Jom, 2013, 65, 1501-1509.	0.9	1,461
14979	Elastic Properties of New Pt-based Superconductors CaPt3P and SrPt3P as Evaluated from First-Principles Calculations. Journal of Superconductivity and Novel Magnetism, 2013, 26, 3167-3170.	0.8	3
14980	Effect of van der Waals interactions on H2 dissociation on clean and defected Ru(0001) surface. European Physical Journal B, 2013, 86, 1.	0.6	6
14981	Theoretical study of the adsorption of 3d- and 4d-metals on a WC(0001) surface. Journal of Experimental and Theoretical Physics, 2013, 117, 309-319.	0.2	1
14982	Liquid metal material genome: Initiation of a new research track towards discovery of advanced energy materials. Frontiers in Energy, 2013, 7, 317-332.	1.2	31
14983	Structures and properties of AunScm (n + m = 6) clusters. European Physical Journal D, 2013, 67, 1.	0.6	6
14984	Multiferroicity in vanadium-doped La2Ti2O7: insights from first principles. European Physical Journal B, 2013, 86, 1.	0.6	12
14985	Low-energy nanoscale clusters of (TiC) n nÂ=Â6, 12: a structural and energetic comparison with MgO. Theoretical Chemistry Accounts, 2013, 132, 1.	0.5	7
14986	Platinum nanoparticles on the antimony-doped tin dioxide surface: Quantum-chemical modeling. Russian Journal of Inorganic Chemistry, 2013, 58, 1489-1495.	0.3	3
14987	A novel layer-structured PtN2: First-principles calculations. Journal of Superhard Materials, 2013, 35, 339-349.	0.5	2
14988	Activation energy of hydrogen migration by relay in the O2/Pt19/SnO2/H2 + n H2O system. Russian Chemical Bulletin, 2013, 62, 363-373.	0.4	5
14989	Magnetic interactions between native defects in ZnO: A first-principles study. Journal of the Korean Physical Society, 2013, 63, 2170-2174.	0.3	1
14990	Writing with atoms: Oxygen adatoms on the MoO2/Mo(110) surface. Nano Research, 2013, 6, 929-937.	5.8	13
14991	Energy investigations on the mechanical properties of magnesium alloyed by X = C, B, N, O and vacancy. Frontiers of Materials Science, 2013, 7, 405-412.	1.1	3
14992	Study of the polarizations of (Al,Ga,AlGa)N nitride compounds and the charge density of various interfaces based on them. Semiconductors, 2013, 47, 1621-1625.	0.2	9
14993	Negative differential resistance in graphene-nanoribbonâ€“carbon-nanotube crossbars: a first-principles multiterminal quantum transport study. Journal of Computational Electronics, 2013, 12, 542-552.	1.3	17

#	Article	IF	Citations
14994	Band-gap modulations of armchair silicene nanoribbons by transverse electric fields. European Physical Journal B, 2013, 86, 1.	0.6	21
14995	Prediction of A2 to B2 Phase Transition in the High-Entropy Alloy Mo-Nb-Ta-W. Jom, 2013, 65, 1772-1779.	0.9	87
14996	Prediction of Semimetallic Tetragonal<mml:math xmlns:mml="http://www.w3.org/1998/Math/MathML" display="inline"><mml:msub><mml:mi>Hf</mml:mi><mml:mn>2</mml:mn></mml:msub><mml:msub><mml:mi mathvariant="bold">O</mml:mi><mml:mn>3</mml:mn></mml:msub></mml:math>and<mml:math xmlns:mml="http://www.w3.org/1998/Math/MathML" display="inline"><mml:msub><mml:mi>Zr</mml:mi><mml:mn>2</mml:mn></mml:msub><mml:msub><mml:mi mathvariant="bold">O</mml:mi><mml:mn>3</mml:mn></mml:msub></mml:math>from First Principles.	2.9	77
14997	Molecular Heterogeneity of Polystyrene-Modified Fullerene Core Stars. Macromolecules, 2013, 46, 7451-7457.	2.2	3
14998	The effect of hydrogen atoms on the screw dislocation mobility in bcc iron: A first-principles study. Acta Materialia, 2013, 61, 6857-6867.	3.8	140
14999	Theoretical and Experimental Investigations on the Growth of SnS van der Waals Epitaxies on Graphene Buffer Layer. Crystal Growth and Design, 2013, 13, 4755-4759.	1.4	18
15000	Theoretical prediction of microstructure evolution during the internal oxidation fabrication of metal-oxide composites: the case of Cuâ€“Al2O3. RSC Advances, 2013, 3, 16136.	1.7	4
15001	Graphene on Ru(0001) MoirÃ© Corrugation Studied by Scanning Tunneling Microscopy on Au/Graphene/Ru(0001) Heterostructures. Journal of Physical Chemistry C, 2013, 117, 20675-20680.	1.5	11
15002	La-doped BaSnO3â€”Degenerate perovskite transparent conducting oxide: Evidence from synchrotron x-ray spectroscopy. Applied Physics Letters, 2013, 103, .	1.5	81
15003	Tuning the electronic and magnetic properties of triangular boron nitride quantum dots via carbon doping. Physica E: Low-Dimensional Systems and Nanostructures, 2013, 49, 52-60.	1.3	17
15004	Magnetic properties of a SnO2 quantum dot. Physica E: Low-Dimensional Systems and Nanostructures, 2013, 53, 72-77.	1.3	9
15005	Predicted giant magnetic anisotropy energy of highly stable Ir dimer on single-vacancy graphene. Physical Review B, 2013, 87, .	1.1	28
15006	Trends in Adsorption Characteristics of Benzene on Transition Metal Surfaces: Role of Surface Chemistry and van der Waals Interactions. Journal of Physical Chemistry C, 2013, 117, 20572-20583.	1.5	147
15007	Ab initiostudy of symmetrical tilt grain boundaries in bcc Fe: structural units, magnetic moments, interfacial bonding, local energy and local stress. Journal of Physics Condensed Matter, 2013, 25, 135004.	0.7	52
15008	Ambipolar doping in SnO. Applied Physics Letters, 2013, 103, .	1.5	94
15009	A DFT study on CO oxidation on Pd4 and Rh4 clusters and adsorbed Pd and Rh atoms on CeO2 and Ce0.75Zr0.25O2 supports for TWC applications. Applied Surface Science, 2013, 285, 927-936.	3.1	19
15010	Two-Dimensional Transition Metal Honeycomb Realized: Hf on Ir(111). Nano Letters, 2013, 13, 4671-4674.	4.5	102
15011	Design Principles of Heteroepitaxial Bimetallic Catalysts. ACS Catalysis, 2013, 3, 2248-2255.	5.5	31

#	Article	IF	Citations
15012	Theoretical identification of carbonate geometry in zeolites from IR spectra. Microporous and Mesoporous Materials, 2013, 173, 15-21.	2.2	12
15013	xmlns:mml="http://www.w3.org/1998/Math/MathML" display="inline"><mml:msub><mml:mrow		

#	Article	IF	Citations
15031	Light metals decorated covalent triazine-based frameworks as a high capacity hydrogen storage medium. Journal of Materials Chemistry A, 2013, 1, 11705.	5.2	47
15032	Coupling of Cobaltâ€“Tetraphenylporphyrin Molecules to a Copper Nitride Layer. Journal of Physical Chemistry C, 2013, 117, 15984-15990.	1.5	15
15033	From Antiferromagnetic to Ferromagnetic Interaction in Cyanido-Bridged Fe(III)â€“Ru(II)â€“Fe(III) Complexes by Change of the Central Diamagnetic Cyanido-Metal Geometry. Inorganic Chemistry, 2013, 52, 11343-11350.	1.9	32
15034	Symmetrization driven spin transition in Îµ-FeOOH at high pressure. Earth and Planetary Science Letters, 2013, 379, 49-55.	1.8	54
15035	Lithiation Behavior of Silicon-Rich Oxide (SiO_{1/3}): A First-Principles Study. Chemistry of Materials, 2013, 25, 3435-3440.	3.2	80
15036	Rippling Graphene at the Nanoscale through Dislocation Addition. Nano Letters, 2013, 13, 4937-4944.	4.5	59
15037	Amorphous silicon nanomaterials: Quantum dots versus nanowires. Journal of Renewable and Sustainable Energy, 2013, 5, .	0.8	12
15038	Structure and dynamics studies of the short strong hydrogen bond in the 3,5-dinitrobenzoic acidâ€“nicotinic acid molecular complex. CrystEngComm, 2013, 15, 7576.	1.3	11
15039	Obtaining Detailed Structural Information about Supramolecular Systems on Surfaces by Combining High-Resolution Force Microscopy with ab Initio Calculations. ACS Nano, 2013, 7, 9098-9105.	7.3	56
15040	GGA+U studies of the early actinide mononitrides and dinitrides. Journal of Nuclear Materials, 2013, 442, 235-244.	1.3	33
15041	Investigation of boron antimonide as hot carrier absorber material. Solar Energy Materials and Solar Cells, 2013, 111, 123-126.	3.0	27
15042	Recent advances in metal hydrides for clean energy applications. MRS Bulletin, 2013, 38, 452-458.	1.7	48
15043	Field-Effect Birefringent Spin Lens in Ultrathin Film of Magnetically Doped Topological Insulators. Physical Review Letters, 2013, 111, 116601.	2.9	15
15044	Synthesis, Characterization, and Atomistic Modeling of Stabilized Highly Pyrophoric Al(BH₄)₃ via the Formation of the Hypersalt K[Al(BH₄)₄]. Journal of Physical Chemistry C, 2013, 117, 19905-19915.	1.5	50
15045	Enhanced lithium adsorption and diffusion on silicene nanoribbons. RSC Advances, 2013, 3, 20338.	1.7	26
15046	Tuning the Catalytic Selectivity of Copper Using TiO₂: Waterâ€Gas Shift versus CO Oxidation. ChemCatChem, 2013, 5, 3673-3679.	1.8	14
15047	Direct Observation of Molecular Orbitals in an Individual Single-Molecule Magnet Mn₁₂ on Bi(111). ACS Nano, 2013, 7, 6825-6830.	7.3	19
15048	Origin of the Bipolar Doping Behavior of SnO from X-ray Spectroscopy and Density Functional Theory. Chemistry of Materials, 2013, 25, 3114-3123.	3.2	135

#	Article	IF	Citations
15049	Stability and electronic structure of Cu<mml:math xmlns:mml="http://www.w3.org/1998/Math/MathML" display="inline"><mml:msub><mml:mrow /><mml:mn>2</mml:mn></mml:msub></mml:math>ZnSnS<mml:math xmlns:mml="http://www.w3.org/1998/Math/MathML" display="inline"><mml:msub><mml:mrow /><mml:mn>4</mml:mn></mml:msub></mml:math>surfaces: First-principles study. Physical Review B, 2013, 88, .	1.1	55
15050	sp3-Bonded silicon allotropes based on the Kelvin problem. Physical Chemistry Chemical Physics, 2013, 15, 17619.	1.3	15
15051	Ab-initio molecular dynamics simulation of Î´-Bi3YO6. Solid State Ionics, 2013, 245-246, 43-48.	1.3	7
15052	Formation and development of dislocation in graphene. Applied Physics Letters, 2013, 102, .	1.5	31
15053	Ordered bilayer rutheniumâ€“platinum core-shell nanoparticles as carbon monoxide-tolerant fuel cell catalysts. Nature Communications, 2013, 4, 2466.	5.8	200
15054	Piezoelectric properties of ScAlN thin films for piezo-MEMS devices. , 2013, , .		52
15055	Density functional theory study of Fe adatoms adsorbed monolayer and bilayer MoS2 sheets. Journal of Applied Physics, 2013, 114, .	1.1	35
15056	High pressure high-temperature behavior and magnetic properties of Fe₄N: experiment and theory. High Pressure Research, 2013, 33, 684-696.	0.4	27
15057	Improved Density Dependent Correction for the Description of London Dispersion Forces. Journal of Chemical Theory and Computation, 2013, 9, 4293-4299.	2.3	183
15058	Efficient Atomic-Scale Kinetics through a Complex Heterophase Interface. Physical Review Letters, 2013, 111, 046102.	2.9	42
15059	Decafluorocyclohex-1-ene at 4.2â€¦K â€“ crystal structure and theoretical analysis of weak interactions. Acta Crystallographica Section B: Structural Science, Crystal Engineering and Materials, 2013, 69, 395-404.	0.5	4
15060	First-principles study of cubane-type ZnO: Another ZnO polymorph. Chemical Physics Letters, 2013, 557, 102-105.	1.2	12
15061	Ab initiocalculation of traction separation laws for a grain boundary in molybdenum with segregated C impurites. Modelling and Simulation in Materials Science and Engineering, 2013, 21, 075005.	0.8	55
15062	On the thermal stability of late blooming phases in reactor pressure vessel steels: An atomistic study. Journal of Nuclear Materials, 2013, 442, 282-291.	1.3	83
15063	Caesium in high oxidation states and as a p-block element. Nature Chemistry, 2013, 5, 846-852.	6.6	177
15064	Chemical bonding in 1-(chlorodimethylstannylmethyl)-2-piperidone and its Si and Ge analogues. General trends and Oâ†'M (M=Si, Ge, Sn) coordination bond energy. Journal of Molecular Structure, 2013, 1051, 49-55.	1.8	14
15065	How ligands improve the hydrothermal stability and affect the adsorption in the IRMOF family. Physical Chemistry Chemical Physics, 2013, 15, 17696.	1.3	29
15066	A combined first principles and analytical determination of the modulus of cohesion, surface energy, and the additional constants in the second strain gradient elasticity. International Journal of Solids and Structures, 2013, 50, 3967-3974.	1.3	33

#	Article	IF	Citations
15067	Anomalous surface segregation behaviour of some 3d elements in ferromagnetic iron. Journal of Physics Condensed Matter, 2013, 25, 415502.	0.7	6
15068	Electronic, magnetic, optical and elastic properties of Fe2YAl (Y=Ti, V and Cr) using first principles methods. Journal of Magnetism and Magnetic Materials, 2013, 339, 142-150.	1.0	36
15069	Accessing 4f-states in single-molecule spintronics. Nature Communications, 2013, 4, 2425.	5.8	71
15070	Room-temperature spin-spiral multiferroicity in high-pressure cupric oxide. Nature Communications, 2013, 4, 2511.	5.8	76
15071	Î²-Mn-Type Co_{8+<i>x</i>}Zn_{12â€"<i>x</i>} as a Defect Cubic Laves Phase: Site Preferences, Magnetism, and Electronic Structure. Inorganic Chemistry, 2013, 52, 9399-9408.	1.9	34
15072	Spin state of iron in Fe<mml:math xmlns:mml="http://www.w3.org/1998/Math/MathML" display="inline"><mml:msub><mml:mrow /><mml:mn>3</mml:mn></mml:msub></mml:math>O<mml:math xmlns:mml="http://www.w3.org/1998/Math/MathML" display="inline"><mml:msub><mml:mrow /><mml:mn>4</mml:mn></mml:msub></mml:math>magnetite and<mml:math xmlns:mml="http://www.w3.org/1998/Math/MathML" display="inline"><mml:mi>h</mml:mi></mml:math>-	1.1	34
15073	Zhang-Rice physics and anomalous copper states in A-site ordered perovskites. Scientific Reports, 2013, 3, 1834.	1.6	44
15074	Fast Mass Transport Kinetics in B₂₀H₁₆: A High-Capacity Hydrogen Storage Material. Journal of Physical Chemistry C, 2013, 117, 19295-19301.	1.5	12
15075	Interstitial oxygens and cation deficiency in Mo-doped ceria, an anode material for SOFCs. Journal of Materials Chemistry A, 2013, 1, 8344.	5.2	5
15076	Controllable modulation of the electronic properties of graphene and silicene by interface engineering and pressure. Journal of Materials Chemistry C, 2013, 1, 4869.	2.7	28
15077	Electronic and magnetic properties of silicene nanoflakes by first-principles calculations. Physics Letters, Section A: General, Atomic and Solid State Physics, 2013, 377, 2792-2795.	0.9	12
15078	Tunable band gap of AlN, GaN nanoribbons and AlN/GaN nanoribbon heterojunctions: A first-principle study. Solid State Communications, 2013, 172, 24-28.	0.9	26
15079	Understanding Photoelectrochemical Properties of Bâ€"N Codoped Anatase TiO₂ for Solar Energy Conversion. Journal of Physical Chemistry C, 2013, 117, 15911-15917.	1.5	33
15080	Defects at Ge/oxide and IIIâ€"V/oxide interfaces. Microelectronic Engineering, 2013, 109, 211-215.	1.1	32
15081	LiH as a Li+ and Hâˆ' ion provider. Solid State Ionics, 2013, 253, 53-56.	1.3	7
15082	Structural and electronic properties of SiC nanotubes filled with Cu nanowires: A first-principles study. Physica E: Low-Dimensional Systems and Nanostructures, 2013, 54, 319-325.	1.3	6
15083	The Intrinsic Ferromagnetism in a MnO₂ Monolayer. Journal of Physical Chemistry Letters, 2013, 4, 3382-3386.	2.1	171
15084	Vacancy and doping driven ferromagnetism in BaTiO3 perovskite. Physica B: Condensed Matter, 2013, 424, 79-83.	1.3	26

#	Article	IF	Citations
15085	Comparison of Cluster, Slab, and Analytic Potential Models for the Dimethyl Methylphosphonate (DMMP)/TiO₂(110) Intermolecular Interaction. Journal of Physical Chemistry C, 2013, 117, 17613-17622.	1.5	18
15086	Systematic First-Principles Investigation of Mixed Transition Metal Olivine Phosphates LiM_{1-y}Mâ€²_yPO₄ (M/Mâ€² = Mn, Fe, and Co) as Cathode Materials. Journal of Physical Chemistry C, 2013, 117, 17919-17926.	1.5	30
15087	Segregation of Impurities in GaAs and InAs Nanowires. Journal of Physical Chemistry C, 2013, 117, 20361-20370.	1.5	12
15088	Characterization of Electronic States inside Metallic Nanopores. Journal of Physical Chemistry C, 2013, 117, 18406-18413.	1.5	3
15089	Metal desorption from Fe(110) and its alloyed surfaces. Chemical Physics Letters, 2013, 585, 162-166.	1.2	8
15090	Changes in valence, coordination and reactivity that occur upon oxidation of fresh metal surfaces. Philosophical Magazine, 2013, 93, 4286-4310.	0.7	14
15091	Universal Rule on Chiralityâ€Dependent Bandgaps in Graphene Antidot Lattices. Small, 2013, 9, 1405-1410.	5.2	34
15092	Nature of the band gap and origin of the electro-/photo-activity of Co3O4. Journal of Materials Chemistry C, 2013, 1, 4628.	2.7	176
15093	Ab Initio Study of the Vibrational Signatures for the Covalent Functionalization of Graphene. Journal of Physical Chemistry C, 0, , 130917155202007.	1.5	5
15094	Density functional theory study into H2O dissociative adsorption on the Fe5C2(010) surface. Applied Catalysis A: General, 2013, 468, 370-383.	2.2	25
15095	Electronic Structure and Thermoelectric Properties of ZnO Single-Walled Nanotubes and Nanowires. Journal of Physical Chemistry C, 2013, 117, 21037-21042.	1.5	19
15096	Thermochemical modeling of the U1âˆ’yGdyO2Â±x phase. Journal of Nuclear Materials, 2013, 443, 588-595.	1.3	13
15097	Fast and Accurate Electrostatics in Metal Organic Frameworks with a Robust Charge Equilibration Parameterization for High-Throughput Virtual Screening of Gas Adsorption. Journal of Physical Chemistry Letters, 2013, 4, 3056-3061.	2.1	90
15098	First-principles investigations of electronic structure and magnetic properties of superlattice between BaMnO3 and cubic perovskite compound. Superlattices and Microstructures, 2013, 61, 42-49.	1.4	4
15099	Electronic and magnetic properties of pristine and transition metal doped ZnTe nanowires. Journal of Physics Condensed Matter, 2013, 25, 266003.	0.7	5
15100	Electronic properties of graphene on the C-decorated Si(111) surface: An ab initio study. Current Applied Physics, 2013, 13, 1512-1519.	1.1	2
15101	Band structure engineering of TiO2 nanowires by nâ€“p codoping for enhanced visible-light photoelectrochemical water-splitting. Physical Chemistry Chemical Physics, 2013, 15, 18523.	1.3	38
15102	Evidence To Challenge the Universality of the Horiutiâ€“Polanyi Mechanism for Hydrogenation in Heterogeneous Catalysis: Origin and Trend of the Preference of a Non-Horiutiâ€“Polanyi Mechanism. Journal of the American Chemical Society, 2013, 135, 15244-15250.	6.6	101

#	Article	IF	Citations
15103	Structure of Pd/Au Alloy Nanoparticles from a Density Functional Theory-Based Embedded-Atom Potential. Journal of Physical Chemistry C, 2013, 117, 21810-21822.	1.5	22
15104	Ab initio study of the highâ€temperature phase transition in crystalline GeO₂. Journal of Computational Chemistry, 2013, 34, 2320-2326.	1.5	16
15105	Energy benchmarks for water clusters and ice structures from an embedded many-body expansion. Journal of Chemical Physics, 2013, 139, 114101.	1.2	60
15106	Na₂AgF₄: 1D antiferromagnet with unusually short Ag²⁺â‹¯Ag²⁺separation. Dalton Transactions, 2013, 42, 2167-2173.	1.6	12
15107	Decomposition mechanism of Al1â^'xSixNy solid solution and possible mechanism of the formation of covalent nanocrystalline AlN/Si3N4 nanocomposites. Acta Materialia, 2013, 61, 4226-4236.	3.8	21
15108	Organometallic Hexahapto-Functionalized Graphene: Band Gap Engineering with Minute Distortion to the Planar Structure. Journal of Physical Chemistry C, 2013, 117, 22156-22161.	1.5	31
15109	Theoretical study on copper's energetics and magnetism in TiO2 polymorphs. Journal of Applied Physics, 2013, 113, .	1.1	48
15110	All-scale hierarchical thermoelectrics: MgTe in PbTe facilitates valence band convergence and suppresses bipolar thermal transport for high performance. Energy and Environmental Science, 2013, 6, 3346.	15.6	646
15111	Designing Fe Nanostructures at Graphene/h-BN Interfaces. Journal of Physical Chemistry C, 2013, 117, 21763-21771.	1.5	7
15112	First-principles study of valence band offsets at ZnSnP2/CdS, ZnSnP2/ZnS, and related chalcopyrite/zincblende heterointerfaces. Journal of Applied Physics, 2013, 114, .	1.1	24
15113	Mechanistic Study of the Oxidative Steam Reforming of EtOH on Rh(111): The Importance of the Oxygen Effect. ChemCatChem, 2013, 5, 3164-3174.	1.8	11
15114	Thermal Decomposition Mechanisms of Nitroesters: Ab Initio Modeling of Pentaerythritol Tetranitrate. Journal of Physical Chemistry C, 2013, 117, 18144-18153.	1.5	41
15115	Different solvates of the dinuclear cyclometallated gold(i) complex [Au2(Î¼-2-C6H4AsMe2)2]: a computational study insight into solvent-effected optical properties. Dalton Transactions, 2013, 42, 12883.	1.6	8
15116	A variational method for density functional theory calculations on metallic systems with thousands of atoms. Journal of Chemical Physics, 2013, 139, 054107.	1.2	51
15117	First-principles study of helium, carbon, and nitrogen in austenite, dilute austenitic iron alloys, and nickel. Physical Review B, 2013, 88, .	1.1	71
15118	Defect formation energy and magnetic properties of off-stoichiometric Ni-Mn-In alloys by first-principles calculations. Journal of Applied Physics, 2013, 113, .	1.1	12
15119	Enhancement of p-type mobility in tin monoxide by native defects. Applied Physics Letters, 2013, 102, .	1.5	51
15120	Computational Search for Single-Layer Transition-Metal Dichalcogenide Photocatalysts. Journal of Physical Chemistry C, 2013, 117, 20440-20445.	1.5	468

#	Article	IF	Citations
15121	Electronic Structural MoirÃ© Pattern Effects on MoS₂/MoSe₂ 2D Heterostructures. Nano Letters, 2013, 13, 5485-5490.	4.5	296
15122	Evolution of Structure and Activity of Alloy Electrocatalysts during Electrochemical Cycles: Combined Activity, Stability, and Modeling Analysis of PtIrCo(7:1:7) and Comparison with PtCo(1:1). Journal of Physical Chemistry C, 2013, 117, 23224-23234.	1.5	6
15123	Origin of giant spin-lattice coupling and the suppression of ferroelectricity in EuTiO<mml:math xmlns:mml="http://www.w3.org/1998/Math/MathML" display="inline"><mml:msub><mml:mrow /><mml:mn>3</mml:mn></mml:msub></mml:math>from first principles. Physical Review B, 2013, 88, .	1.1	45
15124	Simulations of the elastic properties of nanomaterials using multiscale modelling methods. Mechanics of Materials, 2013, 67, 74-78.	1.7	4
15125	First principles studies of structural, electrical and magnetic properties of semiconductor nanowires. Physica Status Solidi - Rapid Research Letters, 2013, 7, 739-753.	1.2	2
15126	Competing Effects of Fluorination on the Orientation of Aromatic and Aliphatic Phosphonic Acid Monolayers on Indium Tin Oxide. Journal of Physical Chemistry C, 2013, 117, 15139-15147.	1.5	40
15127	Origin of the phase transition in IrTe<mml:math xmlns:mml="http://www.w3.org/1998/Math/MathML" display="inline"><mml:msub><mml:mrow /><mml:mn>2</mml:mn></mml:msub></mml:math>: Structural modulation and local bonding instability. Physical Review B, 2013, 88, .	1.1	62
15128	On the forming-free operation of HfOx based RRAM devices: Experiments and ab initio calculations. , 2013, , .		5
15129	First-Principles Study of Point Defect Formation in AgNbO₃. Japanese Journal of Applied Physics, 2013, 52, 09KF08.	0.8	22
15130	Modeling of processes in fuel cells based on sulfonic acid membranes and platinum clusters. Russian Journal of Electrochemistry, 2013, 49, 788-793.	0.3	10
15131	Ab initio calculations of thermal conductivity of metals with hot electrons. Doklady Physics, 2013, 58, 334-338.	0.2	6
15132	Enhance ferromagnetism by stabilizing the cation vacancies in GaN. European Physical Journal B, 2013, 86, 1.	0.6	7
15133	In situ Raman spectroscopy of LiFePO₄: size and morphology dependence during charge and self-discharge. Nanotechnology, 2013, 24, 424009.	1.3	69
15134	Lithium Adsorption on Hexagonal Boron Nitride Nanosheet Using Dispersion-Corrected Density Functional Theory Calculations. Japanese Journal of Applied Physics, 2013, 52, 06GG08.	0.8	20
15135	First-principle calculations on the structural stability and electronic properties of superhard B_xC_ycompounds. Journal of Physics Condensed Matter, 2013, 25, 425502.	0.7	8
15136	Defect Control in Zinc Oxynitride Semiconductor for High-Performance and High-Stability Thin-Film Transistors. Solid State Phenomena, 0, 205-206, 446-450.	0.3	7
15137	Design of Shallow Acceptors in GaN through Zincâ€“Magnium Codoping: First-Principles Calculation. Applied Physics Express, 2013, 6, 042104.	1.1	5
15138	Cuâ€“Biâ€“Se-based pavonite homologue: a promising thermoelectric material with low lattice thermal conductivity. Journal of Materials Chemistry A, 2013, 1, 9768.	5.2	13

#	Article	IF	Citations
15139	Giant reduction of the phase transition temperature for beryllium doped VO2. Physical Chemistry Chemical Physics, 2013, 15, 4687.	1.3	29
15140	Semiconducting layered technetium dichalcogenides: insights from first-principles. Dalton Transactions, 2013, 42, 15288.	1.6	23
15141	Alternating chirality in the monolayer H2TPP on Cu(110)â€“(2 Ã— 1)O. Physical Chemistry Chemical Physics, 2013, 15, 4691.	1.3	7
15142	Si:WO3heterostructure for Z-scheme water splitting: an ab initio study. Journal of Materials Chemistry A, 2013, 1, 1078-1085.	5.2	32
15143	Spin-polarization and ferromagnetism of graphitic carbon nitride materials. Journal of Materials Chemistry C, 2013, 1, 6265.	2.7	82
15144	Bond-energy decoupling: principle and application to heterogeneous catalysis. Chemical Science, 2013, 4, 606-611.	3.7	12
15145	Strain effects on hydrogen storage in Ti decorated pyridinic N-doped graphene. Physical Chemistry Chemical Physics, 2013, 15, 12757.	1.3	14
15146	LixFeF6 (x = 2, 3, 4) battery materials: structural, electronic and lithium diffusion properties. Physical Chemistry Chemical Physics, 2013, 15, 20473.	1.3	17
15147	Relative contributions of quantum and double layer capacitance to the supercapacitor performance of carbon nanotubes in an ionic liquid. Physical Chemistry Chemical Physics, 2013, 15, 19741-19747.	1.3	68
15148	Dimension-dependent phase transition and magnetic properties of VS2. Journal of Materials Chemistry A, 2013, 1, 10821.	5.2	183
15149	First-principles structural design of superhard material of ZrB4. Physical Chemistry Chemical Physics, 2013, 15, 20894.	1.3	52
15150	First principles studies on the redox ability of (Ga1â^'xZnx)N1â^'xOx solid solutions and thermal reactions for H2 and O2 production on their surfaces. Physical Chemistry Chemical Physics, 2013, 15, 19807.	1.3	12
15151	Strain-induced Dirac cone-like electronic structures and semiconductorâ€“semimetal transition in graphdiyne. Physical Chemistry Chemical Physics, 2013, 15, 8179.	1.3	81
15152	[CoI(CN)2(CO)3]â^', a new discovery from an 80-year-old reaction. Chemical Communications, 2013, 49, 7382.	2.2	4
15153	First-principles melting of gallium clusters down to nine atoms: structural and electronic contributions to melting. Physical Chemistry Chemical Physics, 2013, 15, 15325.	1.3	37
15154	Intrinsic thermodynamic and kinetic properties of Sb electrodes for Li-ion and Na-ion batteries: experiment and theory. Journal of Materials Chemistry A, 2013, 1, 7985.	5.2	226
15155	Computational characterization of the internal bonding and solvation structure for [Nb10O28]aq6â^'. Physical Chemistry Chemical Physics, 2013, 15, 20929.	1.3	1
15156	Stability of Si epoxide defects in Si nanowires: a mixed reactive force field/DFT study. Physical Chemistry Chemical Physics, 2013, 15, 15091.	1.3	3

#	Article	IF	Citations
15157	Mitigation of CO poisoning on functionalized Ptâ€“TiN surfaces. Physical Chemistry Chemical Physics, 2013, 15, 19450.	1.3	27
15158	Control of spin in a La(Mn,Zn)AsO alloy by carrier doping. Journal of Materials Chemistry C, 2013, 1, 7197.	2.7	17
15159	Bilayer silicene with an electrically-tunable wide band gap. RSC Advances, 2013, 3, 21943.	1.7	32
15160	A detailed evaluation of model defects as candidates for the bias temperature instability. , 2013, , .		4
15161	First Principles Simulations of Nanoscale Silicon Devices With Uniaxial Strain. IEEE Transactions on Electron Devices, 2013, 60, 3527-3533.	1.6	12
15162	Simulation Studies of the Phase Stability of the Ruddlesdenâ€“Popper Phases. Journal of the American Ceramic Society, 2013, 96, 2316-2321.	1.9	14
15163	Atomic layer deposition of photoactive CoO/SrTiO3 and CoO/TiO2 on Si(001) for visible light driven photoelectrochemical water oxidation. Journal of Applied Physics, 2013, 114, .	1.1	29
15164	A Nanoporous PdCo Alloy as a Highly Active Electrocatalyst for the Oxygenâ€Reduction Reaction and Formic Acid Electrooxidation. Chemistry - an Asian Journal, 2013, 8, 2721-2728.	1.7	31
15165	Atomically resolved spectroscopic study of Sr2IrO4: Experiment and theory. Scientific Reports, 2013, 3, 3073.	1.6	55
15166	Theoretical perspective of photocatalytic properties of single-layer SnS<mml:math xmlns:mml="http://www.w3.org/1998/Math/MathML" display="inline"><mml:msub><mml:mrow /><mml:mn>2</mml:mn></mml:msub></mml:math>. Physical Review B, 2013, 88, .	1.1	215
15167	Electronic structure of defects and doping in ZnO: Oxygen vacancy and nitrogen doping. Physica Status Solidi (B): Basic Research, 2013, 250, 2091-2101.	0.7	21
15168	Structures, stability, mechanical and electronic properties of Î±-boron andÎ±*-boron. AIP Advances, 2013, 3, .	0.6	18
15169	Substrate-mediated band-dispersion of adsorbate molecular states. Nature Communications, 2013, 4, 1514.	5.8	63
15170	The effect of vibrational entropy on the solubility and stability of ordered Al3Li phases in Al-Li alloys. APL Materials, 2013, 1, .	2.2	11
15171	Enantioselectivity of (321) chiral noble metal surfaces: A density functional theory study of lactate adsorption. Journal of Chemical Physics, 2013, 139, 224709.	1.2	5
15172	MODELLING OF NEUTRAL VACANCIES IN FORSTERITE MINERAL. International Journal of Modern Physics B, 2013, 27, 1350141.	1.0	2
15173	Electronic and Magnetic Properties of Li_{1.5}Mn_{0.5}As Alloys in the Cu₂Sb Structure. Advanced Materials Research, 0, 702, 231-235.	0.3	1
15174	First principle study of elastic and thermodynamic properties of FeB4 under high pressure. Journal of Applied Physics, 2013, 114, .	1.1	42

#	Article	IF	Citations
15175	First-principles calculation of intrinsic carrier mobility of silicene. Journal of Applied Physics, 2013, 114, .	1.1	211
15176	Stability and superconductivity of Ca-B phases at ambient and high pressure. Physical Review B, 2013, 88, .	1.1	32
15177	Tuning the conductance of monatomic carbon chain. Journal of Applied Physics, 2013, 114, 154309.	1.1	5
15178	Computational identification of single-layer CdO for electronic and optical applications. Applied Physics Letters, 2013, 103, .	1.5	52
15179	Pressure effects on structural, electronic, absorption, and thermodynamic properties of crystalline 2,4,6-triamino-3,5-dinitropyridine-1-oxide: A DFT study. Journal of Physical Organic Chemistry, 2013, 26, 589-595.	0.9	6
15180	H₂S splitting on Cu(110): Insight from combined periodic density functional theory calculations and microkinetic simulation. International Journal of Quantum Chemistry, 2013, 113, 1992-2001.	1.0	26
15181	Computational investigation of the adsorption and reactions of SiH_x (x =) Tj ETQq0 0 0 rgBT /Overlock 10 Tf Chemistry, 2013, 113, 1696-1708.	1.0	4
15182	First-principles Thermodynamic Models in Heterogeneous Catalysis. RSC Catalysis Series, 2013, , 59-115.	0.1	9
15183	Density Functional Theory Methods for Electrocatalysis. RSC Catalysis Series, 2013, , 116-156.	0.1	5
15184	Computing Accurate Net Atomic Charges, Atomic Spin Moments, and Effective Bond Orders in Complex Materials. RSC Catalysis Series, 2013, , 192-222.	0.1	2
15185	Accuracy of density functional theory in the prediction of carbon dioxide adsorbent materials. Dalton Transactions, 2013, 42, 4670.	1.6	15
15186	Hydrogen adsorption and desorption at the Pt(110)-(1Ã—2) surface: experimental and theoretical study. Physical Chemistry Chemical Physics, 2013, 15, 6323.	1.3	67
15187	Spectroscopic properties of crystalline elemental boron and the implications on B11Câ€“CBC. RSC Advances, 2013, 3, 25374.	1.7	10
15188	Dynamic behaviour of carbocations on zeolites: mobility and rearrangement of the C4H7+ system. Chemical Communications, 2013, 49, 4480.	2.2	8
15189	Stability and migration barriers of small vanadium oxide clusters on the CeO2(111) surface studied by density functional theory. Faraday Discussions, 2013, 162, 233.	1.6	25
15190	The CO oxidation mechanism and reactivity on PdZn alloys. Physical Chemistry Chemical Physics, 2013, 15, 7768.	1.3	55
15191	Experimental and theoretical studies of tetramethoxy-p-benzoquinone: infrared spectra, structural and lithium insertion properties. RSC Advances, 2013, 3, 19081.	1.7	21
15192	Half-metallicity of a kagome spin lattice: the case of a manganese bis-dithiolene monolayer. Nanoscale, 2013, 5, 10404.	2.8	84

#	Article	IF	Citations
15193	Thermodynamic and electronic properties of tunable IIâ€“VI and IVâ€“VI semiconductor based metalâ€“organic frameworks from computational chemistry. Journal of Materials Chemistry C, 2013, 1, 95-100.	2.7	23
15194	Mn ion dissolution from MnS: a density functional theory study. Physical Chemistry Chemical Physics, 2013, 15, 17112.	1.3	11
15195	Entropies of defect formation in ceria from first principles. Physical Chemistry Chemical Physics, 2013, 15, 15935.	1.3	48
15196	Ribbon aromaticity in double-chain planar BnH22â^' and Li2BnH2 nanoribbon clusters up to n = 22: lithiated boron dihydride analogues of polyenes. Physical Chemistry Chemical Physics, 2013, 15, 18872.	1.3	31
15197	Zigzag graphene nanoribbons with curved edges. RSC Advances, 2013, 3, 10014.	1.7	6
15198	Tunable topological surface and realization of insulating massive Dirac fermion state in Bi2Te2Se with co-substitution. Journal of Materials Chemistry C, 2013, 1, 114-120.	2.7	4
15199	Thermodynamics of native point defects in Î±-Fe2O3: an ab initio study. Physical Chemistry Chemical Physics, 2013, 15, 18906.	1.3	91
15200	Effects of Al-doping on the properties of Liâ€“Mnâ€“Niâ€“O cathode materials for Li-ion batteries: an ab initio study. Journal of Materials Chemistry A, 2013, 1, 9273.	5.2	84
15201	Local surface structure effect on reactivity of molecules confined between metallic surfaces. Physical Chemistry Chemical Physics, 2013, 15, 1647-1654.	1.3	9
15202	A biocompatible calcium bisphosphonate coordination polymer: towards a metal-linker synergistic therapeutic effect?. CrystEngComm, 2013, 15, 9899.	1.3	49
15203	Dual passivation of GaAs (110) surfaces using O2/H2O and trimethylaluminum. Journal of Chemical Physics, 2013, 139, 244706.	1.2	7
15204	Hydrogenolysis of ethylene glycol to methanol over modified RANEYÂ® catalysts. Physical Chemistry Chemical Physics, 2013, 15, 9043.	1.3	22
15205	A grand canonical genetic algorithm for the prediction of multi-component phase diagrams and testing of empirical potentials. Journal of Physics Condensed Matter, 2013, 25, 495401.	0.7	52
15206	Protons crossing triple phase boundaries based on a metal catalyst, Pd or Ni, and barium zirconate. Physical Chemistry Chemical Physics, 2013, 15, 12525.	1.3	16
15207	Prediction of stable hafnium carbides: Stoichiometries, mechanical properties, and electronic structure. Physical Review B, 2013, 88, .	1.1	51
15208	The donor/acceptor edge-modification: an effective strategy to modulate the electronic and magnetic behaviors of zigzag silicon carbon nanoribbons. Physical Chemistry Chemical Physics, 2013, 15, 18039.	1.3	23
15209	From Boron Cluster to Two-Dimensional Boron Sheet on Cu(111) Surface: Growth Mechanism and Hole Formation. Scientific Reports, 2013, 3, 3238.	1.6	206
15210	Nature of proton transport in a water-filled carbon nanotube and in liquid water. Physical Chemistry Chemical Physics, 2013, 15, 6344.	1.3	51

#	Article	IF	Citations
15211	Suppression of Sr surface segregation in La_{1â^'x}Sr_xCo_{1â^'y}Fe_yO_{3â^'Î´}: a first principles study. Physical Chemistry Chemical Physics, 2013, 15, 489-496.	1.3	182
15212	Selective adsorption of olefinâ€“paraffin on diamond-like frameworks: diamondyne and PAF-302. Journal of Materials Chemistry A, 2013, 1, 9433.	5.2	41
15213	Control of one-dimensional magnetism in graphene via spontaneous hydrogenation of the grain boundary. Physical Chemistry Chemical Physics, 2013, 15, 8271.	1.3	5
15214	First-principles study of the formation and migration of native defects in LiNH₂BH₃. Physical Chemistry Chemical Physics, 2013, 15, 893-900.	1.3	7
15215	Structural and electronic properties of Li8ZrO6 and its CO2 capture capabilities: an ab initio thermodynamic approach. Physical Chemistry Chemical Physics, 2013, 15, 9752.	1.3	36
15216	Integrated X-ray photoelectron spectroscopy and DFT characterization of benzene adsorption on Pt(111), Pt(355) and Pt(322) surfaces. Physical Chemistry Chemical Physics, 2013, 15, 20662.	1.3	25
15217	Structure and local reactivity of PdAg/Pd(111) surface alloys. Physical Chemistry Chemical Physics, 2013, 15, 1497-1508.	1.3	45
15218	Active sites on hydrogen evolution photocatalyst. Journal of Materials Chemistry A, 2013, 1, 15258.	5.2	96
15219	Computational investigation of defect segregation at the (001) surface of BaCeO3 and BaZrO3: the role of metalâ€“oxygen bond strength in controlling vacancy segregation. Journal of Materials Chemistry A, 2013, 1, 2840.	5.2	18
15220	Oxide ion transport in Sr2Fe1.5Mo0.5O6â^'Î´, a mixed ion-electron conductor: new insights from first principles modeling. Physical Chemistry Chemical Physics, 2013, 15, 6250.	1.3	59
15221	Crystal growth and efficient second-harmonic-generation of the monoclinic LaCa4O(BO3)3 crystal. CrystEngComm, 2013, 15, 6035.	1.3	19
15222	Mode selectivity in methane dissociative chemisorption on Ni(111). Chemical Science, 2013, 4, 3249.	3.7	115
15223	Modulating the electronic properties of germanium nanowires via applied strain and surface passivation. Physical Chemistry Chemical Physics, 2013, 15, 5927.	1.3	12
15224	Electronic and magnetic properties of one dimensional sandwich polymers: [(Ge5)TM]â^ž (TM = Ti, V, Cr,) Tj ETQq1 1 0.784314 rgBT /	2.7	9
15225	Ln3GaS6 (Ln = Dy, Y): new infrared nonlinear optical materials with high laser induced damage thresholds. Dalton Transactions, 2013, 42, 14223.	1.6	63
15226	Synthesis and photocatalytic hydrogen production of a novel photocatalyst LaCO3OH. Journal of Materials Chemistry A, 2013, 1, 6629.	5.2	61
15227	High-Pressure Synthesis, Crystal Structure, and Properties of In₂NiMnO₆ with Antiferromagnetic Order and Field-Induced Phase Transition. Inorganic Chemistry, 2013, 52, 14108-14115.	1.9	25
15228	Polarity effects in unsupported polar nanoribbons. Physical Review B, 2013, 87, .	1.1	16

#	Article	IF	Citations
15229	Oxygen adsorption and dissociation during the oxidation of monolayer Ti2C. Journal of Materials Chemistry A, 2013, 1, 13672.	5.2	77
15230	Atomic-scale structure and electronic property of the La₂FeCrO₆/SrTiO₃ interface. Journal of Applied Physics, 2013, 114, 113705.	1.1	6
15231	Charge-Induced Spin Polarization in Î±-Sexithienyl Studied by First-Principles Calculations. Journal of Physical Chemistry C, 2013, 117, 16238-16241.	1.5	8
15232	On the Relationship between Mo K-Edge Energies and DFT Computed Partial Charges. Journal of Physical Chemistry C, 2013, 117, 2769-2773.	1.5	18
15233	Spin-Peierls distortions in TiPO<mml:math xmlns:mml="http://www.w3.org/1998/Math/MathML" display="inline"><mml:msub><mml:mrow /><mml:mn>4</mml:mn></mml:msub></mml:math>. Physical Review B, 2013, 88, .	1.1	17
15234	Surface passivation and orientation dependence in the electronic properties of silicon nanowires. Journal of Physics Condensed Matter, 2013, 25, 145501.	0.7	15
15235	Oxygen reduction and transport on the La1â^'xSrxCo1â^'yFeyO3â^'Î´ cathode in solid oxide fuel cells: a first-principles study. Journal of Materials Chemistry A, 2013, 1, 12932.	5.2	55
15236	Cobalt-doped ZnO nanocrystals: quantum confinement and surface effects from ab initio methods. Physical Chemistry Chemical Physics, 2013, 15, 15863.	1.3	12
15237	Lithium intercalation behaviors in Ge and Sn crystalline surfaces. Physical Chemistry Chemical Physics, 2013, 15, 13586.	1.3	13
15238	First-principles thermodynamic calculations and experimental investigation of Srâ€“Siâ€“Nâ€“O systemâ€”synthesis of Sr₂Si₅N₈:Eu phosphor. Journal of Materials Chemistry C, 2013, 1, 69-78.	2.7	34
15239	Thermodynamic screening of metal-substituted MOFs for carbon capture. Physical Chemistry Chemical Physics, 2013, 15, 4573.	1.3	62
15240	Quantum state-resolved CH4 dissociation on Pt(111): coverage dependent barrier heights from experiment and density functional theory. Physical Chemistry Chemical Physics, 2013, 15, 20526.	1.3	47
15241	Lithium and oxygen adsorption at the Î²-MnO2 (110) surface. Journal of Materials Chemistry A, 2013, 1, 14879.	5.2	58
15242	Cu3MCh3 (M = Sb, Bi; Ch = S, Se) as candidate solar cell absorbers: insights from theory. Physical Chemistry Chemical Physics, 2013, 15, 15477.	1.3	71
15243	Methane storage capabilities of diamond analogues. Physical Chemistry Chemical Physics, 2013, 15, 20937.	1.3	10
15244	High performance robust F-doped tin oxide based oxygen evolution electro-catalysts for PEM based water electrolysis. Journal of Materials Chemistry A, 2013, 1, 4026.	5.2	66
15245	Insights into the nature of Cu doping in amorphous mesoporous alumina. Journal of Materials Chemistry A, 2013, 1, 14592.	5.2	49
15246	Polymerization of nitrogen in lithium azide. Journal of Chemical Physics, 2013, 139, 164710.	1.2	69

#	Article	IF	Citations
15247	Anisotropic two-dimensional electron gas at the LaAlO3/SrTiO3 (110) interface. Nature Communications, 2013, 4, 1838.	5.8	96
15248	Thermodynamic properties of magnesium alloys. , 2013, , 85-124.		0
15249	Tuning the chemical activity through PtAu nanoalloying: a first principles study. Journal of Materials Chemistry A, 2013, 1, 9885.	5.2	19
15250	Adsorption, dissociation, penetration, and diffusion of N2 on and in bcc Fe: first-principles calculations. Physical Chemistry Chemical Physics, 2013, 15, 5186.	1.3	34
15251	Introduction of nitrogen with controllable configuration into graphene via vacancies and edges. Journal of Materials Chemistry A, 2013, 1, 14927.	5.2	39
15252	Anticorrelation between the Evolution of Molecular Dipole Moments and Induced Work Function Modifications. Journal of Physical Chemistry Letters, 2013, 4, 3521-3526.	2.1	25
15253	Tuning the electronic and magnetic properties of zigzag silicene nanoribbons by edge hydrogenation and doping. RSC Advances, 2013, 3, 24075.	1.7	63
15254	Trapping of interstitial defects: filling the gap between the experimental measurements and DFT calculations. Journal of Physics Condensed Matter, 2013, 25, 435402.	0.7	3
15255	Six-dimensional quantum dynamics study for the dissociative adsorption of HCl on Au(111) surface. Journal of Chemical Physics, 2013, 139, 184705.	1.2	56
15256	Theoretical study of amino derivatives and anticancer platinum drug grafted on various carbon nanostructures. Journal of Chemical Physics, 2013, 139, 174704.	1.2	12
15257	Simple pair-wise interactions for hybrid Monte Carloâ€“molecular dynamics simulations of titania/yttria-doped iron. Journal of Physics Condensed Matter, 2013, 25, 055402.	0.7	9
15258	First-principles study of CaFe<mml:math xmlns:mml="http://www.w3.org/1998/Math/MathML" display="inline"><mml:msub><mml:mrow /><mml:mn>2</mml:mn></mml:msub></mml:math>As<mml:math xmlns:mml="http://www.w3.org/1998/Math/MathML" display="inline"><mml:msub><mml:mrow /><mml:mn>2</mml:mn></mml:msub></mml:math>under pressure. Physical Review B, 2013, 88, .	1.1	15
15259	Development of the ReaxFF reactive force field for aluminumâ€“molybdenum alloy. Journal of Materials Research, 2013, 28, 1155-1164.	1.2	10
15260	Interface effects on tunneling magnetoresistance in organic spintronics with flexible amineâ€“Au links. Nanotechnology, 2013, 24, 415201.	1.3	13
15261	Mechanism of Ferroelectricity in Half-Doped Manganites with Pseudocubic and Bilayer Structure. Journal of the Physical Society of Japan, 2013, 82, 113703.	0.7	11
15262	Topological phase transitions in (Bi<mml:math xmlns:mml="http://www.w3.org/1998/Math/MathML") Tj ETQq1 1 0.784314 rgBT /Overlo	1.1	45
15263	Ferroelectric Domains in Multiferroic<mml:math xmlns:mml="http://www.w3.org/1998/Math/MathML" display="inline"><mml:msub><mml:mi>BiFeO</mml:mi><mml:mn>3</mml:mn></mml:msub></mml:math>Films under Epitaxial Strains. Physical Review Letters, 2013, 110, 187601.	2.9	54
15264	Uniaxial strain-induced ferroelectric phase with a giant axial ratio in a (110) BiFeO<mml:math xmlns:mml="http://www.w3.org/1998/Math/MathML" display="inline"><mml:msub><mml:mrow /><mml:mn>3</mml:mn></mml:msub></mml:math>thin film. Physical Review B, 2013, 87, .	1.1	27

#	Article	IF	Citations
15265	Distribution of Al and adsorption of NH₃ and pyridine in ZSM-12: a computational study. Canadian Journal of Chemistry, 2013, 91, 925-934.	0.6	19
15266	Surface Coverage and SEI Induced Electrochemical Surface Stress Changes during Li Deposition in a Model System for Li-Ion Battery Anodes. Journal of the Electrochemical Society, 2013, 160, A888-A896.	1.3	55
15267	Study of band-structure, optical properties and native defects inA^IB^{III}O₂(A^I= Cu or) Tj ETQq0 0 0 rgBT /Overlock 10 Tf 50 66 065003.	1.0	49
15268	Dependence of intrinsic performance of transition metal dichalcogenide transistors on materials and number of layers at the 5 nm channel-length limit. , 2013, , .		20
15269	High Temperature Interconnect and Die Attach Technology: Auâ€“Sn SLID Bonding. IEEE Transactions on Components, Packaging and Manufacturing Technology, 2013, 3, 904-914.	1.4	46
15270	Partition behavior of alloying elements and phase transformation temperatures inÂCoâ€“Alâ€“W-base quaternary systems. Intermetallics, 2013, 32, 274-283.	1.8	193
15271	Thermodynamic, structural and elastic properties of Co3X (XÂ=ÂTi, Ta, W, V, Al) compounds from first-principles calculations. Intermetallics, 2013, 32, 303-311.	1.8	55
15272	Crystal structure and phase stability of the Î¦ phase in the Alâ€“Mgâ€“Zn system. Intermetallics, 2013, 32, 259-273.	1.8	14
15273	Magnetic CrX and MnX (X=Si, Ge, and As) nanowires: Stability enhancement and linearization. Journal of Alloys and Compounds, 2013, 547, 138-146.	2.8	2
15274	Structure, electronic characteristic and thermodynamic properties of K2ZnH4 hydride crystal: A first-principles study. Journal of Alloys and Compounds, 2013, 549, 30-37.	2.8	6
15275	UV-irradiation-enhanced ferromagnetism of barium vanadate (Ba3V2O8) nanoflowers. Journal of Alloys and Compounds, 2013, 550, 389-394.	2.8	17
15276	Theoretical investigation on structural and thermodynamic properties of the intermetallic compound in Mgâ€“Znâ€“Ag alloy under high pressure and high temperature. Journal of Alloys and Compounds, 2013, 550, 406-411.	2.8	18
15277	Microkinetics of steam methane reforming on platinum and rhodium metal surfaces. Journal of Catalysis, 2013, 297, 227-235.	3.1	43
15278	A simplified approach to the band gap correction of defect formation energies: Al, Ga, and In-doped ZnO. Journal of Physics and Chemistry of Solids, 2013, 74, 45-50.	1.9	38
15279	Sources of carrier compensation in arsenic-doped HgCdTe. Journal of Physics and Chemistry of Solids, 2013, 74, 57-64.	1.9	3
15280	Structural and electronic properties of coaxial nanocables of AlN nanowire core and SiC nanotube sheath: A first-principles study. Journal of Physics and Chemistry of Solids, 2013, 74, 366-369.	1.9	3
15281	Growth and structure of Si and Ge in vanadium oxide nanomesh on Pd(111) studied by STM and DFT. Applied Surface Science, 2013, 265, 291-295.	3.1	1
15282	First-principles based phenomenological study of Ni nanocubes: The effects of nanostructuring on carbon poisoning of Ni(0 0 1) nanofacets. Applied Surface Science, 2013, 265, 339-345.	3.1	8

#	Article	IF	Citations
15283	Reaction mechanism for methanol oxidation on Au(111): A density functional theory study. Applied Surface Science, 2013, 265, 443-451.	3.1	29
15284	Insights into the preference of CHx(x=1â€“3) formation from CO hydrogenation on Cu(111) surface. Applied Surface Science, 2013, 265, 720-730.	3.1	51
15285	The adsorption of bisulfate and sulfate anions over a Pt(111) electrode: A first principle study of adsorption configurations, vibrational frequencies and linear sweep voltammogram simulations. Catalysis Today, 2013, 202, 20-35.	2.2	60
15286	Structure of water layers on hydrogen-covered Pt electrodes. Catalysis Today, 2013, 202, 183-190.	2.2	90
15287	Atomic ensemble effects on formic acid oxidation on PdAu electrode studied by first-principles calculations. Journal of Power Sources, 2013, 224, 241-249.	4.0	58
15288	Elastic softening of alloy negative electrodes for Na-ion batteries. Journal of Power Sources, 2013, 225, 207-214.	4.0	87
15289	Synthesis and crystal structure of Mg0.5NbO2: An ion-exchange reaction with Mg2+ between trigonal [NbO2]â^' layers. Journal of Solid State Chemistry, 2013, 197, 471-474.	1.4	4
15290	DFT+U study of the oxide-ion conductor pentalanthanum hexamolybdenum henicosaoxide. Journal of Solid State Chemistry, 2013, 197, 304-311.	1.4	16
15291	Hybrid functional calculation of electronic and phonon structure of BaSnO. Journal of Solid State Chemistry, 2013, 197, 134-138.	1.4	42
15292	Calcium-decorated graphyne nanotubes as promising hydrogen storage media: A first-principles study. Journal of Solid State Chemistry, 2013, 197, 323-328.	1.4	57
15293	Theoretical calculation on electronic excitation and compression effect in tungsten. Physica B: Condensed Matter, 2013, 413, 69-72.	1.3	2
15294	Two types of meta-crystals for IV group elements: Density functional theory calculations. Physica B: Condensed Matter, 2013, 410, 17-21.	1.3	0
15295	Structural, elastic, and electronic properties of new 211 MAX phase Nb2GeC from first-principles calculations. Physica B: Condensed Matter, 2013, 410, 42-48.	1.3	28
15296	Tellurium-evaporation-annealing for p-type bismuthâ€“antimonyâ€“telluride thermoelectric materials. Journal of Alloys and Compounds, 2013, 548, 126-132.	2.8	14
15297	Effects of iron concentration and cationic site disorder on the optical properties of magnetoelectric gallium ferrite thin films. RSC Advances, 2013, 3, 3124.	1.7	11
15298	High pressure effect on structure, electronic structure, and thermoelectric properties of MoS2. Journal of Applied Physics, 2013, 113, .	1.1	101
15299	Orientation of Phenylphosphonic Acid Self-Assembled Monolayers on a Transparent Conductive Oxide: A Combined NEXAFS, PM-IRRAS, and DFT Study. Langmuir, 2013, 29, 2166-2174.	1.6	61
15300	Predicting Dislocations and Grain Boundaries in Two-Dimensional Metal-Disulfides from the First Principles. Nano Letters, 2013, 13, 253-258.	4.5	310

#	Article	IF	Citations
15301	First principles study on the adsorption of CO2 and H2O on the K2CO3 (001) surface. Surface Science, 2013, 609, 140-146.	0.8	33
15302	Bending Rigidity and Gaussian Bending Stiffness of Single-Layered Graphene. Nano Letters, 2013, 13, 26-30.	4.5	299
15303	First principles calculation of mixing enthalpy of Î²-Ti with transition elements. Journal of Alloys and Compounds, 2013, 550, 501-508.	2.8	14
15304	First-Principles Study of the Interfaces between Fe and Transition Metal Carbides. Journal of Physical Chemistry C, 2013, 117, 187-193.	1.5	27
15305	First-principles calculations of vibrational and thermodynamical properties of rare-earth diborides. Computational Materials Science, 2013, 68, 307-313.	1.4	4
15306	A rational interpretation of improved catalytic performances of additive-impregnated dried CoMo hydrotreating catalysts: a combined theoretical and experimental study. Catalysis Science and Technology, 2013, 3, 140-151.	2.1	37
15307	Exfoliated graphene-supported Pt and Pt-based alloys as electrocatalysts for direct methanol fuel cells. Carbon, 2013, 52, 595-604.	5.4	117
15308	Tuning the Catalytic Activity of Ru@Pt Coreâ€“Shell Nanoparticles for the Oxygen Reduction Reaction by Varying the Shell Thickness. Journal of Physical Chemistry C, 2013, 117, 1748-1753.	1.5	140
15309	van der Waals Epitaxial Growth of Graphene on Sapphire by Chemical Vapor Deposition without a Metal Catalyst. ACS Nano, 2013, 7, 385-395.	7.3	211
15310	Theoretical design and experimental implementation of Ag/Au electrodes for the electrochemical reduction of nitrate. Physical Chemistry Chemical Physics, 2013, 15, 3196.	1.3	98
15311	Predicted crystal structures of molybdenum under high pressure. Journal of Alloys and Compounds, 2013, 556, 116-120.	2.8	15
15312	Bonding, structures, and band gap closure of hydrogen at high pressures. Physical Review B, 2013, 87, .	1.1	54
15313	Evolutionary search for BiInS3 crystal structure and predicting its second-order nonlinear optical property. Journal of Solid State Chemistry, 2013, 199, 78-83.	1.4	6
15314	First-principles study of Caâ€“Feâ€“Ptâ€“As-type iron-based superconductors. Physica C: Superconductivity and Its Applications, 2013, 484, 39-42.	0.6	10
15315	Effects of strain on ferroelectric polarization and magnetism in orthorhombic HoMnO<mml:math xmlns:mml="http://www.w3.org/1998/Math/MathML" display="inline"><mml:msub><mml:mrow /><mml:mn>3</mml:mn></mml:msub></mml:math>. Physical Review B, 2013, 87, .	1.1	17
15316	Effect of the Al Siting on the Structure of Co(II) and Cu(II) Cationic Sites in Ferrierite. A Periodic DFT Molecular Dynamics and FTIR Study. Journal of Physical Chemistry C, 2013, 117, 3958-3968.	1.5	42
15317	Domain walls in a perovskite oxide with two primary structural order parameters: First-principles study of BiFeO<mml:math xmlns:mml="http://www.w3.org/1998/Math/MathML" display="inline"><mml:msub><mml:mrow /><mml:mn>3</mml:mn></mml:msub></mml:math>. Physical Review B, 2013, 87, .	1.1	69
15318	Band offsets and heterostructures of two-dimensional semiconductors. Applied Physics Letters, 2013, 102, .	1.5	1,361

#	Article	IF	Citations
15319	Reversible control of magnetic interactions by electric field in a single-phase material. Nature Communications, 2013, 4, 1334.	5.8	67
15320	Relation between spontaneous polarization and crystal field from first principles. Physical Review B, 2013, 87, .	1.1	35
15321	Ab initio study of edge effect on relative motion of walls in carbon nanotubes. Journal of Chemical Physics, 2013, 138, 024703.	1.2	22
15322	The role of van der Waals forces in water adsorption on metals. Journal of Chemical Physics, 2013, 138, 024708.	1.2	173
15323	Impact of hydrogen and oxygen defects on the lattice parameter of chemical vapor deposited zinc sulfide. Journal of Applied Physics, 2013, 113, .	1.1	19
15324	Theoretical Study of Sensitizer Candidates for Dye-Sensitized Solar Cells: Peripheral Substituted Dizinc Pyrazinoporphyrazineâ€“Phthalocyanine Complexes. Journal of Physical Chemistry A, 2013, 117, 430-438.	1.1	50
15325	Orbital chirality and Rashba interaction in magnetic bands. Physical Review B, 2013, 87, .	1.1	78
15326	Tuning the Electronic and Chemical Properties of Monolayer MoS₂ Adsorbed on Transition Metal Substrates. Nano Letters, 2013, 13, 509-514.	4.5	262
15327	Motion of in-channel dimers on W(112): A DFT study. Surface Science, 2013, 608, 115-121.	0.8	4
15328	Structural and mechanical stability of dilute yttrium doped chromium. Applied Physics Letters, 2013, 102, 021901.	1.5	4
15329	Ab initio investigation of a possible liquidâ€“liquid phase transition in MgSiO3 at megabar pressures. High Energy Density Physics, 2013, 9, 152-157.	0.4	18
15330	Two viable three-dimensional carbon semiconductors with an entirely sp²configuration. Physical Chemistry Chemical Physics, 2013, 15, 680-684.	1.3	48
15331	New V^{IV}-Based Metalâ€“Organic Framework Having Framework Flexibility and High CO₂ Adsorption Capacity. Inorganic Chemistry, 2013, 52, 113-120.	1.9	68
15332	A first principles investigation of the mechanical properties of g-ZnO: The graphene-like hexagonal zinc oxide monolayer. Computational Materials Science, 2013, 68, 320-324.	1.4	63
15333	Undoped visible-light-sensitive titania photocatalyst. Journal of Materials Science, 2013, 48, 108-114.	1.7	30
15334	A comprehensive study of the heat capacity of CsF from T= 5 K to T= 1400 K. Journal of Chemical Thermodynamics, 2013, 57, 92-100.	1.0	15
15335	Trivalent Actinide and Lanthanide Complexation of 5,6-Dialkyl-2,6-bis(1,2,4-triazin-3-yl)pyridine (RBTP; R =) Tj ETQq0 0 0 rgBT /Overlock 52, 761-776.	1.9	18
15336	Charge distribution and oxygen diffusion in hyperstoichiometric uranium dioxide UO2+x (xâ©½0.25). Journal of Nuclear Materials, 2013, 434, 422-433.	1.3	11

#	Article	IF	Citations
15337	N- and Mo-doping Bi2WO6 in photocatalytic water splitting. Computational Materials Science, 2013, 67, 88-92.	1.4	39
15338	Structural and electronic properties of the Co-induced Si(111) <mml:math xmlns:mml="http://www.w3.org/1998/Math/MathML" altimg="si7.gif" overflow="scroll"><mml:mrow><mml:msqrt><mml:mn>13</mml:mn></mml:msqrt><mml:mo>Ã—</mml:mo><mml:msqrt><mml:mn surface reconstruction. Surface Science, 2013, 607, 111-117.	0.8	8
15339	Graphene with line defect as a membrane for gas separation: Design via a first-principles modeling. Surface Science, 2013, 607, 153-158.	0.8	55
15340	The first principles investigation of lattice dynamical and thermodynamical properties of Al2Ca and Al2Mg compounds in the cubic Laves structure. Computational Materials Science, 2013, 68, 27-31.	1.4	32
15341	Inelastic neutron scattering, Raman and DFT investigations of the adsorption of phenanthrenequinone on onion-like carbon. Carbon, 2013, 52, 150-157.	5.4	14
15342	Theoretical Approaches to Excited-State-Related Phenomena in Oxide Surfaces. Chemical Reviews, 2013, 113, 4456-4495.	23.0	80
15343	Band gap change induced by defect complexes in Cu2ZnSnS4. Thin Solid Films, 2013, 535, 265-269.	0.8	91
15344	Stability of xenon oxides at high pressures. Nature Chemistry, 2013, 5, 61-65.	6.6	118
15345	Ab initio study of ZnCoO diluted magnetic semiconductor and its magnetic properties. Journal of Alloys and Compounds, 2013, 551, 306-311.	2.8	19
15346	Redetermination of crystal structure of Ag(<scp>ii</scp>)SO₄and its high-pressure behavior up to 30 GPa. CrystEngComm, 2013, 15, 192-198.	1.3	17
15347	Optimization of smart Heusler alloys from first principles. Journal of Alloys and Compounds, 2013, 577, S107-S112.	2.8	46
15348	Periodic density functional theory study of the high-pressure behavior of energetic crystalline 1,4-dinitrofurazano[3, 4-b]piperazine. Journal of Molecular Modeling, 2013, 19, 305-314.	0.8	7
15349	Adsorption of CH3S and CF3S on Pt(111) surface: a density functional theory study. Journal of Materials Science, 2013, 48, 2277-2283.	1.7	7
15350	P-type reduced graphene oxide membranes induced by iodine doping. Journal of Materials Science, 2013, 48, 2284-2289.	1.7	28
15351	Cathode properties of Na3M2(PO4)2F3 [MÂ=ÂTi, Fe, V] for sodium-ion batteries. Journal of Power Sources, 2013, 227, 80-85.	4.0	181
15352	Mechanism of Alcoholâ€“Water Separation in Metalâ€“Organic Frameworks. Journal of Physical Chemistry C, 2013, 117, 4124-4130.	1.5	33
15353	Binding of Polyvinylpyrrolidone to Ag Surfaces: Insight into a Structure-Directing Agent from Dispersion-Corrected Density Functional Theory. Journal of Physical Chemistry C, 2013, 117, 1163-1171.	1.5	93
15354	Selective Hydrogenation of Î±,Î²â€Unsaturated Aldehydes and Ketones using Novel Manganese Oxide and Platinum Supported on Manganese Oxide Octahedral Molecular Sieves as Catalysts. ChemCatChem, 2013, 5, 506-512.	1.8	62

#	Article	IF	Citations
15355	Effects of suboxide layers on the electronic properties of Si(100)/SiO2 interfaces: Atomistic multi-scale approach. Journal of Applied Physics, 2013, 113, .	1.1	13
15356	First principles investigation of the effects of Bi vacancy on the magnetic, conductive and electrochemical properties of BiF3. Computational Materials Science, 2013, 68, 117-120.	1.4	4
15358	Charge Delocalization Induces Reaction in Molecular Chains at a Surface. Angewandte Chemie - International Edition, 2013, 52, 320-324.	7.2	23
15359	A Theoretical Study on the Mechanism of Photocatalytic Oxygen Evolution on BiVO₄ in Aqueous Solution. Chemistry - A European Journal, 2013, 19, 1320-1326.	1.7	161
15360	Relating the Composition of Pt_xRu_{100â^'x}/C Nanoparticles to Their Structural Aspects and Electrocatalytic Activities in the Methanol Oxidation Reaction. Chemistry - A European Journal, 2013, 19, 905-915.	1.7	8
15361	A Highly Efficient, Cleanâ€Surface, Porous Platinum Electrocatalyst and the Inhibition Effect of Surfactants on Catalytic Activity. Chemistry - A European Journal, 2013, 19, 240-248.	1.7	71
15362	Structure Sensitivity of CO Oxidation on Co₃O₄: A DFT Study. ChemPhysChem, 2013, 14, 204-212.	1.0	64
15363	Ketonic Decarboxylation Reaction Mechanism: A Combined Experimental and DFT Study. ChemSusChem, 2013, 6, 141-151.	3.6	121
15364	Structural and Photoelectrochemical Evaluation of Nanotextured Snâ€Doped AgInS₂ Films Prepared by Spray Pyrolysis. ChemSusChem, 2013, 6, 102-109.	3.6	11
15365	Nanoporous PdTi Alloys as Nonâ€Platinum Oxygenâ€Reduction Reaction Electrocatalysts with Enhanced Activity and Durability. ChemSusChem, 2013, 6, 78-84.	3.6	52
15366	Effect of Spinâ€Crossoverâ€Induced Pore Contraction on CO₂â€“Host Interactions in the Porous Coordination Polymers [Fe(pyrazine)M(CN)₄] (M = Ni, Pt). European Journal of Inorganic Chemistry, 2013, 2013, 511-519.	1.0	15
15367	Iron Particle Nanodrilling of Few Layer Graphene at Low Electron Beam Accelerating Voltages. Particle and Particle Systems Characterization, 2013, 30, 76-82.	1.2	9
15368	Spinâ€Polarized Semiconductors: Tuning the Electronic Structure of Graphene by Introducing a Regular Pattern of sp³ Carbons on the Graphene Plane. Small, 2013, 9, 306-311.	5.2	9
15369	Diisopropylammonium Bromide Is a High-Temperature Molecular Ferroelectric Crystal. Science, 2013, 339, 425-428.	6.0	703
15370	Electronic structure, chemical bonding and magnetism of the metal-rich borides MRh6B3 (MÂ=ÂCr, Mn,) Tj ETQq0 0 0 rgBT /Overlock 10 14-20.	1.5	13
15371	Substrate-Induced Symmetry Breaking in Silicene. Physical Review Letters, 2013, 110, 076801.	2.9	358
15372	First-principles study of stacking fault energies in Mg-based binary alloys. Computational Materials Science, 2013, 79, 564-569.	1.4	107
15373	Adsorbed CO induced change of the adsorption site and charge of Au adatoms on FeO(111)/Ru(0001). Chinese Journal of Catalysis, 2013, 34, 1820-1825.	6.9	3

#	Article	IF	Citations
15374	Spin polarization of single-layer graphene epitaxially grown on Ni(111) thin film. Carbon, 2013, 61, 134-139.	5.4	16
15375	Thermodynamic analysis using first-principles calculations of phases andÂstructures of LixNi0.5Mn1.5O4 (0Ââ‰ÂxÂâ‰Â1). Journal of Power Sources, 2013, 241, 1-5.	4.0	9
15376	The detailed orbital-decomposed electronic structures of tetragonal ZrO2. Physica B: Condensed Matter, 2013, 411, 126-130.	1.3	8
15377	Energetics and diffusion of hydrogen in Î±-Al2O3 and Er2O3. Fusion Engineering and Design, 2013, 88, 2646-2649.	1.0	14
15378	Vacancy trapping mechanism for multiple helium in monovacancy and small void of vanadium solid. Journal of Nuclear Materials, 2013, 440, 557-561.	1.3	32
15379	Zinc oxide flower-like synthesized under hydrothermal conditions. Thin Solid Films, 2013, 537, 97-101.	0.8	12
15380	Introduction of vacancy drag effect to first-principles-based rate theory model for irradiation-induced grain-boundary phosphorus segregation. Journal of Nuclear Materials, 2013, 440, 627-632.	1.3	10
15381	Synthesis and magnetic property of Fe doped LaPO4 nanorods. Applied Surface Science, 2013, 268, 458-463.	3.1	9
15382	Ferroelectricity at a junction structure of a 180Â° domain wall and a (001) surface in PbTiO3: A density functional theory study. Physica B: Condensed Matter, 2013, 410, 22-27.	1.3	5
15383	Technetium and ruthenium incorporation into rutile TiO2. Journal of Nuclear Materials, 2013, 441, 380-389.	1.3	16
15384	Tight-binding studies of bulk properties and hydrogen vacancies in KBH4. Computational Materials Science, 2013, 79, 888-895.	1.4	3
15385	First-principles characterization of formate and carboxyl adsorption on stoichiometric CeO2(111) and CeO2(110) surfaces. Journal of Energy Chemistry, 2013, 22, 524-532.	7.1	12
15386	Generalized planar fault energies and mechanical twinning in gamma TiAl alloys. Scripta Materialia, 2013, 68, 759-762.	2.6	32
15387	Behaviors of helium in vanadium: Stability, diffusion, vacancy trapping and ideal tensile strength. Progress in Natural Science: Materials International, 2013, 23, 459-463.	1.8	14
15388	Ab initio study of structurally bound water at cation vacancy sites in Fe- and Al-oxyhydroxide materials. Geochimica Et Cosmochimica Acta, 2013, 114, 94-111.	1.6	29
15389	On the delithiation mechanism of Li2FeSiO4â^'ySy compounds: A first-principles investigation. Electrochimica Acta, 2013, 112, 670-677.	2.6	14
15390	Thermodynamic assessment of the Cdâ€“X (X= Sr, Ti, B, V) systems. Calphad: Computer Coupling of Phase Diagrams and Thermochemistry, 2013, 42, 6-12.	0.7	2
15391	The feasibility of tunable p-type Mg doping in a GaN monolayer nanosheet. Acta Materialia, 2013, 61, 7720-7725.	3.8	81

#	Article	IF	Citations
15392	Realization of high thermoelectric performance in p-type unfilled ternary skutterudites FeSb2+xTe1â^'x via band structure modification and significant point defect scattering. Acta Materialia, 2013, 61, 7693-7704.	3.8	44
15393	Revelation of the crucial interactions in spin-hybrid systems by means of X-ray absorption spectroscopy. Journal of Electron Spectroscopy and Related Phenomena, 2013, 189, 171-177.	0.8	2
15394	Efficient iterative method for solving the Diracâ€"Kohnâ€"Sham density functional theory. Journal of Computational Physics, 2013, 245, 205-217.	1.9	6
15395	Energetic and structural analysis of N2H4BH3 inorganic solid and its modified material for hydrogen storage. International Journal of Hydrogen Energy, 2013, 38, 6718-6725.	3.8	7
15396	Electronic structures and Li intercalation of AuCN and CuCN crystals and nanowires. Computational and Theoretical Chemistry, 2013, 1020, 157-162.	1.1	2
15397	The catalytic adsorption and dissociation of carbon dioxide on a double icosahedral Ru19 nanocluster â€" A theoretical study. Chemical Physics Letters, 2013, 585, 149-152.	1.2	11
15398	Hexavalent hydrogen complex in hypothetical Y2CrH6. Journal of Alloys and Compounds, 2013, 580, S274-S277.	2.8	7
15399	Universal ground state hexagonal phases and mechanical properties of stoichiometric transition metal tetraborides: TMB4 (TM=W, Tc, and Re). Computational Materials Science, 2013, 68, 371-378.	1.4	26
15400	Electronic and magnetic properties of triangular graphene nanoflakes embedded in fluorographene. Chemical Physics Letters, 2013, 572, 48-52.	1.2	5
15401	Protons in Al doped BaZrO3 escape dopant traps to access long range proton conduction highways. Solid State Ionics, 2013, 252, 40-47.	1.3	18
15402	Optical response characteristics arising from delocalized electrons in phase change materials. Acta Materialia, 2013, 61, 1757-1763.	3.8	11
15403	Thermodynamic stability of Coâ€"Alâ€"W L12 Î³â€². Acta Materialia, 2013, 61, 2330-2338.	3.8	76
15404	Formation of pre-silicide layers below Ni1â^'xPtxSi/Si interfaces. Acta Materialia, 2013, 61, 2481-2488.	3.8	4
15405	Reactivity of adducts relevant to the deposition of hexagonal BN from first-principles calculations. Chemical Physics Letters, 2013, 583, 119-124.	1.2	40
15406	Structural stability and electronic structure study of YCu2â€"YZn2 Laves phases by first-principles calculations. Computational Materials Science, 2013, 77, 366-371.	1.4	9
15407	Adsorption behaviors of Cs and I atoms on the graphite surface by the first-principles. Journal of Nuclear Materials, 2013, 441, 113-118.	1.3	11
15408	Hydrogenâ€"Te antisite complex impurity (Hâ€"TeHg) in Hg0.75Cd0.25Te: First-principles study. Journal of Physics and Chemistry of Solids, 2013, 74, 1086-1092.	1.9	4
15409	Catalytic behavior and surface species investigation over Î³-Al2O3 in dimethyl ether hydrolysis. Applied Catalysis A: General, 2013, 460-461, 99-105.	2.2	13

#	Article	IF	Citations
15410	Stability and migration of vacancy in Vâ€“4Crâ€“4Ti alloy: Effects of Al, Si, Y trace elements. Journal of Nuclear Materials, 2013, 442, 370-376.	1.3	21
15411	On spectral quadrature for linear-scaling Density Functional Theory. Chemical Physics Letters, 2013, 584, 182-187.	1.2	32
15412	First-principles aided thermodynamic modeling of the Nbâ€“Re system. Calphad: Computer Coupling of Phase Diagrams and Thermochemistry, 2013, 41, 119-127.	0.7	16
15413	First-principles study of water activation on Cu-ZnO catalysts. Chinese Journal of Catalysis, 2013, 34, 1705-1711.	6.9	11
15414	Nucleation behavior of supported Rh nanoparticles fabricated from Rh(CO)2(acac) on Al2O3/Ni3Al(111). Chemical Physics Letters, 2013, 555, 7-11.	1.2	7
15415	Atomistic study of plastic deformation in Mgâ€“Al alloys. Materials Science & Engineering A: Structural Materials: Properties, Microstructure and Processing, 2013, 586, 245-252.	2.6	30
15416	First-principles investigation on vacancy trapping behaviors of hydrogen in vanadium. Journal of Nuclear Materials, 2013, 442, S688-S693.	1.3	27
15417	Microscopic nature of mobile fluoride anions on sp2 carbon surfaces. Chemical Physics Letters, 2013, 570, 85-89.	1.2	4
15418	Water adsorption on MnO:ZnO(001) â€” From single molecules to bilayer coverage. Surface Science, 2013, 617, 218-224.	0.8	9
15419	Valence band electronic structure of Nd1â^'xYxMnO3 using X-ray absorption, photoemission and GGA+U calculations. Journal of Electron Spectroscopy and Related Phenomena, 2013, 189, 51-55.	0.8	2
15420	A first-principles study of the structure, electronic properties, and oxygen binding of FeO/Pt(111) and FeO2/Pt(111). Chinese Journal of Catalysis, 2013, 34, 973-978.	6.9	12
15421	Effect of polar distortion on electronic structures of (001) LaGaO3/SrTiO3 interface. Physics Letters, Section A: General, Atomic and Solid State Physics, 2013, 377, 577-581.	0.9	9
15422	Density functional studies of selected metal dioxides. Journal of Physics and Chemistry of Solids, 2013, 74, 1632-1639.	1.9	15
15423	Thermodynamic modeling of the (U,La)O2Â±x solid solution phase. Journal of Nuclear Materials, 2013, 433, 227-232.	1.3	21
15424	Dielectric response of Fe2O3 crystals and thin films. Chemical Physics Letters, 2013, 586, 67-69.	1.2	53
15425	Diffusivities and atomic mobilities in fcc_A1 Niâ€“X (X=Ge, Ti and V) alloys. Calphad: Computer Coupling of Phase Diagrams and Thermochemistry, 2013, 41, 108-118.	0.7	20
15426	An atomistic thermodynamics study of the structural evolution of the Pt3Ni(111) surface in an oxygen environment. Chinese Journal of Catalysis, 2013, 34, 1434-1442.	6.9	10
15427	The carbon-tolerance mechanism of Ni-based alloy with coinage metals. Physics Letters, Section A: General, Atomic and Solid State Physics, 2013, 377, 2189-2194.	0.9	16

#	Article	IF	Citations
15428	B24 cluster as promising material for lithium storage and hydrogen storage applications. Computational Materials Science, 2013, 77, 31-34.	1.4	8
15429	Adsorption of H atoms on cubic Er2O3 (001) surface: A DFT study. Journal of Nuclear Materials, 2013, 443, 555-561.	1.3	4
15430	Ab initio study of He point defects in fcc Auâ€“Ag alloys. Journal of Alloys and Compounds, 2013, 557, 5-10.	2.8	6
15432	Stability and electronic properties of polar and non-polar surfaces of CuI. Applied Surface Science, 2013, 268, 87-91.	3.1	11
15433	Unexpectedly hard and highly stable WB3 with a noncompact structure. Chemical Physics Letters, 2013, 580, 48-52.	1.2	42
15434	Ab initio study of the structural, mechanical, and dynamical properties of the rare-earth dihydrides XH2 (X=Sc, Y, and La). Physica B: Condensed Matter, 2013, 429, 119-126.	1.3	22
15435	Role of nano in catalysis: Palladium catalyzed hydrogen desorption from nanosized magnesium hydride. Nano Energy, 2013, 2, 742-748.	8.2	25
15436	First-principles investigation of electronic, mechanical and thermodynamic properties of L12 ordered Co3(M, W) (M = Al, Ge, Ga) phases. Acta Materialia, 2013, 61, 5437-5448.	3.8	72
15437	First principles study of the electronic and magnetic structures and bonding properties of UCoC2 ternary, characteristic of Câ€“C units. Solid State Sciences, 2013, 17, 128-133.	1.5	1
15438	Compositional trends and magnetic excitations in binary and ternary Feâ€“Pdâ€“X magnetic shape memory alloys. Journal of Alloys and Compounds, 2013, 577, S333-S337.	2.8	10
15439	Study of interaction between radioactive nuclides and graphite surface by the first-principles and statistic physics. Applied Surface Science, 2013, 285, 278-286.	3.1	16
15440	Alkali metal induced effects on coadsorbed carbon monoxide on Co(0001): A density functional theory study. Computational and Theoretical Chemistry, 2013, 1009, 55-59.	1.1	6
15441	Study of the half-metallic materials double perovskites Sr2ZnBO6 (B=Tc, Re, Ru, Os, Co, Pd, and Au) via first-principle calculations. Journal of Magnetism and Magnetic Materials, 2013, 341, 25-29.	1.0	25
15442	Predicted ferromagnetism in hole doped armchair nanoribbons: A first principles study. Chemical Physics Letters, 2013, 555, 173-177.	1.2	4
15443	Binary cluster collision dynamics and minimum energy conformations. Physica B: Condensed Matter, 2013, 427, 76-84.	1.3	6
15444	Molecular oxygen adsorption on ferromagnetic platinum. Chemical Physics Letters, 2013, 555, 125-130.	1.2	9
15445	Energetics of interstitial oxygen in Î²-TiX (X=transition elements) alloys using first principles methods. Journal of Alloys and Compounds, 2013, 571, 107-113.	2.8	8
15446	Dynamical properties of physically adsorbed water molecules at the TiO2 rutile-(110) surface. Chemical Physics Letters, 2013, 583, 125-130.	1.2	18

#	Article	IF	Citations
15447	Structural, electronic properties and stability of Ag-doped GaAs nanowires: First-principles study. Physica E: Low-Dimensional Systems and Nanostructures, 2013, 54, 301-307.	1.3	5
15448	Phonon-mediated thermal transport: Confronting theory and microscopic simulation with experiment. Current Opinion in Solid State and Materials Science, 2013, 17, 1-9.	5.6	25
15449	Computational Mechanistic Study of Borohydride Electrochemical Oxidation on Au₃Ni(111). Journal of Physical Chemistry C, 2013, 117, 3818-3825.	1.5	19
15450	Monovalent Cation-Exchanged Natrolites and Their Behavior under Pressure. A Computational Study. Journal of Physical Chemistry C, 2013, 117, 19020-19030.	1.5	18
15451	Metal-decorated graphene oxide for ammonia adsorption. Europhysics Letters, 2013, 103, 28007.	0.7	17
15452	VSb(SeO₃)₄, First Selenite Containing V³⁺ Cation: Synthesis, Structure, Characterization, Magnetic Properties, and Calculations. Inorganic Chemistry, 2013, 52, 14224-14230.	1.9	10
15453	Catalytic activity of Coâ€“N_x/C electrocatalysts for oxygen reduction reaction: a density functional theory study. Physical Chemistry Chemical Physics, 2013, 15, 148-153.	1.3	303
15454	Theoretical Investigation of the Adsorption and Câ€“C Bond Scission of CCH₃ on the (111) and (100) Surfaces of Pd: Comparison with Pt. Journal of Physical Chemistry C, 2013, 117, 18131-18138.	1.5	8
15455	Magnetism of an adatom on bilayer graphene and its control: A first-principles perspective. Physical Review B, 2013, 88, .	1.1	19
15456	Magnetism in Lithiumâ€“Oxygen Discharge Product. ChemSusChem, 2013, 6, 1196-1202.	3.6	23
15457	Atomic-scale inversion of spin polarization at an organic-antiferromagnetic interface. Physical Review B, 2013, 88, .	1.1	30
15458	Conducting Boron Sheets Formed by the Reconstruction of the<mml:math xmlns:mml="http://www.w3.org/1998/Math/MathML" display="inline"><mml:mi>Î±</mml:mi></mml:math>-Boron (111) Surface. Physical Review Letters, 2013, 111, 136101.	2.9	40
15459	Insights into the atomic and electronic structure triggered by ordered nitrogen vacancies in CrN. Physical Review B, 2013, 87, .	1.1	22
15460	Free energies of (Co, Fe, Ni, Zn)Fe₂O₄spinels and oxides in water at high temperatures and pressure from density functional theory: results for stoichiometric NiO and NiFe₂O₄surfaces. Journal of Physics Condensed Matter, 2013, 25, 445008.	0.7	47
15461	Ion Dependence of Gate Dielectric Behavior of Alkali Metal Ion-Incorporated Aluminas in Oxide Field-Effect Transistors. Chemistry of Materials, 2013, 25, 3788-3796.	3.2	58
15462	Origination of the direct-indirect band gap transition in strained wurtzite and zinc-blende GaAs nanowires: A first principles study. Physical Review B, 2013, 87, .	1.1	48
15463	Hybrid density functional study of structural and electronic properties of functionalized Ti<mml:math xmlns:mml="http://www.w3.org/1998/Math/MathML" display="inline"><mml:mrow><mml:msub><mml:mrow		

#	Article	IF	Citations
15465	Influence of orbital contributions to the valence band alignment of Bi<mml:math xmlns:mml="http://www.w3.org/1998/Math/MathML" display="inline"><mml:msub><mml:mrow /><mml:mn>2</mml:mn></mml:msub></mml:math>O<mml:math xmlns:mml="http://www.w3.org/1998/Math/MathML" display="inline"><mml:msub><mml:mrow /><mml:mn>3</mml:mn></mml:msub></mml:math>, Fe<mml:math xmlns:mml="http://www.w3.org/1998/Math/MathML" display="inline"><mml:msub><mml:mrow /><mml:mn>2</mml:mn></mml:msub></mml:math>O<mml:math xmlns:mml="http://www.w3.org/1998/Math/MathML" display="inline"><mml:msub><mml:mrow /><mml:mn>3</mml:mn></mml:msub></mml:math>, and LaFeO<mml:math xmlns:mml="http://www.w3.org/1998/Math/MathML" display="inline"><mml:msub><mml:mrow /><mml:mn>3</mml:mn></mml:msub></mml:math> polymorphs: Role of oxide/oxide interfaces and dipole renormalization. Physical Review B, 2013, 88, .	1.1	53
15466	Determination of the Electronic Structure and UVâ€“Vis Absorption Properties of (Na2â€“xCux)Ta4O11 from First-Principle Calculations. Journal of Physical Chemistry C, 2013, 117, 17477-17484.	1.1	20
15467	CaLi2superconductor under the pressure of 100 GPa: the thermodynamic critical field and the specific heat. Physica Scripta, 2013, 88, 025704.	1.5	32
15468	Arbitrary tip orientation in STM simulations: 3D WKB theory and application to W(110). Journal of Physics Condensed Matter, 2013, 25, 445009.	1.2	5
15469	PbCu₃TeO₇: an $S=rac{1}{2}$ staircase kagome lattice with significant intra-plane and inter-plane couplings. Journal of Physics Condensed Matter, 2013, 25, 336003.	0.7	11
15470	Dependence of equilibrium stacking fault width in fcc metals on theÎ³-surface. Modelling and Simulation in Materials Science and Engineering, 2013, 21, 025015.	0.7	18
15471	Promotional Effect of Carbon on Fe Catalysts for Ammonia Decomposition: A Density Functional Theory Study. Industrial & Engineering Chemistry Research, 2013, 52, 17151-17155.	0.8	45
15472	Coreâ€“Shell Nanocatalyst Design by Combining Highâ€Throughput Experiments and Firstâ€Principles Simulations. ChemCatChem, 2013, 5, 3712-3718.	1.8	11
15473	Mechanistic Insight into the Au-3d Metal Alloy-Catalyzed Borohydride Electro-Oxidation: From Electronic Properties to Thermodynamics. ACS Catalysis, 2013, 3, 3031-3040.	1.8	8
15474	Quantum Anomalous Hall Effect and Tunable Topological States in 3d Transition Metals Doped Silicene. Scientific Reports, 2013, 3, 2908.	5.5	25
15475	Spin gap in the adjacent Cu-O chains of <mml:math xmlns:mml="http://www.w3.org/1998/Math/MathML" display="inline"><mml:msub><mml:mrow /><mml:mn>2</mml:mn></mml:msub></mml:math>(OH)<mml:math xmlns:mml="http://www.w3.org/1998/Math/MathML" display="inline"><mml:msub><mml:mrow /><mml:mn>2</mml:mn></mml:msub></mml:math>CO<mml:math xmlns:mml="http://www.w3.org/1998/Math/MathML" display="inline"><mml:msub><mml:mrow /><mml:mn>	1.6	163
15476	Two-dimensional carbon topological insulators superior to graphene. Scientific Reports, 2013, 3, 3532.	1.1	42
15477	Controllable Magnetic Doping of the Surface State of a Topological Insulator. Physical Review Letters, 2013, 110, 126804.	1.6	140
15478	Structural, electronic, and magnetic properties of the period vacancy in zigzag Ga<scp>N</scp> nanoribbons. Physica Status Solidi (B): Basic Research, 2013, 250, 1510-1518.	2.9	98
15479	The structure and properties of (aluminum, oxygen) defect complexes in silicon. Journal of Applied Physics, 2013, 114, 063520.	0.7	13
15480	Reaction Barriers and Cooperative Effects for the Adsorption of Pyridine on Si(100). Journal of Physical Chemistry C, 2013, 117, 26644-26651.	1.1	10
15481	Antiâ€ferrodistortiveâ€Like Oxygenâ€Octahedron Rotation Induced by the Oxygen Vacancy in Cubic SrTiO₃. Advanced Materials, 2013, 25, 86-90.	1.5	9
15482		11.1	94

#	Article	IF	Citations
15483	Phase Stability and Transport Mechanisms in Antiperovskite Li₃OCl and Li₃OBr Superionic Conductors. Chemistry of Materials, 2013, 25, 4663-4670.	3.2	204
15484	Spin/orbital coupling and charge ordering in LaMnO3/SrMnO3 superlattice. Journal of Magnetism and Magnetic Materials, 2013, 333, 8-12.	1.0	6
15485	Changes in electronic, magnetic and bonding properties from Zr2FeH5 to Zr3FeH7 addressed from ab initio. Solid State Sciences, 2013, 25, 55-62.	1.5	2
15486	First-principles study of alkali metal-graphite intercalation compounds. Journal of Power Sources, 2013, 243, 585-587.	4.0	336
15487	High-pressure polymorphs of TbVO4: A Raman and ab initio study. Journal of Alloys and Compounds, 2013, 577, 327-335.	2.8	45
15488	Lithium transport investigation in LixFeSiO4: A promising cathode material. Solid State Communications, 2013, 173, 9-13.	0.9	12
15489	Atomistic simulations of solid solution strengthening in Ni-based superalloy. Computational Materials Science, 2013, 68, 132-137.	1.4	20
15490	Electronic, mechanical, and thermodynamic properties of americium dioxide. Journal of Nuclear Materials, 2013, 441, 411-420.	1.3	33
15491	The optical absorption and hydrogen production by water splitting of (Si,Fe)-codoped anatase TiO2 photocatalyst. International Journal of Hydrogen Energy, 2013, 38, 5209-5214.	3.8	58
15492	Structural and electronic properties of CuI doped with Zn, Ga and Al. Journal of Physics and Chemistry of Solids, 2013, 74, 1122-1126.	1.9	19
15493	Vibrational modes and electrical transport in Sr2GdTaO6. Materials Chemistry and Physics, 2013, 143, 26-33.	2.0	10
15494	The synergetic effect of metal oxide support on Fe2O3 for chemical looping combustion: A theoretical study. Applied Surface Science, 2013, 282, 718-723.	3.1	44
15495	Electronic and magnetic properties of 3d transition metal-doped strontium clusters: Prospective magnetic superatoms. Chemical Physics, 2013, 417, 37-44.	0.9	15
15496	Effect of vacancy on the dissolution and diffusion properties of hydrogen and helium in molybdenum. Journal of Nuclear Materials, 2013, 433, 167-173.	1.3	31
15497	An examination of nickel doping effect on the mechanical strength of a tungsten grain boundary. Computational Materials Science, 2013, 77, 131-138.	1.4	14
15498	C-REDOR curves of extended spin systems. Solid State Nuclear Magnetic Resonance, 2013, 49-50, 12-22.	1.5	9
15499	The mechanism of sulfur poisoning on the nickel/yttrium-stabilized zirconia anode of solid oxide fuel cells: The role of the oxygen vacancy. Journal of Power Sources, 2013, 237, 128-131.	4.0	26
15500	Raman spectroscopy and dielectric properties of nanoceramic NdFeO3. Materials Research Bulletin, 2013, 48, 1688-1693.	2.7	56

#	Article	IF	Citations
15501	Mn adsorption on C substituted BN sheet: First-principle study. Superlattices and Microstructures, 2013, 62, 175-181.	1.4	8
15502	Enhanced photoelectrochemical performance of anatase TiO2 by metal-assisted Sâ€“O coupling for water splitting. International Journal of Hydrogen Energy, 2013, 38, 1251-1257.	3.8	27
15503	Dissolution and diffusion behaviors of hydrogen in copper: A first-principles investigation. Computational Materials Science, 2013, 79, 923-928.	1.4	21
15504	Theoretical investigations of metal-free dyes for solar cells: Effects of electron donor and acceptor groups on sensitizers. Journal of Power Sources, 2013, 242, 464-471.	4.0	20
15505	Band-offset effect on localization of carriers and p-type doping of InAs/GaAs coreâ€“shell nanowires. Physics Letters, Section A: General, Atomic and Solid State Physics, 2013, 377, 1464-1468.	0.9	6
15506	Formation of aluminides on Ni-based superalloy 690 substrate, their characterization and first-principle Ni(111)/NiAl(110) interface simulations. Surface and Coatings Technology, 2013, 235, 741-747.	2.2	17
15507	Effect of hydrogen on the surface energy of ferrite and austenite. Corrosion Science, 2013, 77, 379-384.	3.0	46
15508	Study of thermodynamic properties of SiH4(H2)2 superconductor under high pressure. Physica C: Superconductivity and Its Applications, 2013, 485, 145-148.	0.6	9
15509	First-principles thermodynamic calculations of diffusion characteristics of impurities in Î³-iron. Journal of Nuclear Materials, 2013, 442, S684-S687.	1.3	7
15510	Enhanced nucleation of Al islands on H-dosed Si(100)-2 Ã— 1 surface: A combined density functional theory and kinetic Monte Carlo study. Surface Science, 2013, 617, 73-80.	0.8	8
15511	Quantum size effects in Î±-plutonium (020) surface layers. Solid State Communications, 2013, 172, 29-32.	0.9	2
15512	Oxygen adsorption on Î³-TiAl surfaces and the related surface phase diagrams: A density-functional theory study. Acta Materialia, 2013, 61, 1726-1738.	3.8	32
15513	A theoretical investigation of the slip systems of Ta2C. Acta Materialia, 2013, 61, 3914-3922.	3.8	26
15514	Significant effects of graphite fragments on hydrogen storage performances of LiBH4: A first-principles approach. International Journal of Hydrogen Energy, 2013, 38, 13717-13727.	3.8	13
15515	Neutron-induced dpa, transmutations, gas production, and helium embrittlement of fusion materials. Journal of Nuclear Materials, 2013, 442, S755-S760.	1.3	122
15516	Hydrogen storage properties of the pseudo binary laves phase (Sc1â^'xZrx)(Co1â^'yNiy)2 system. International Journal of Hydrogen Energy, 2013, 38, 9772-9778.	3.8	5
15517	Static dielectric response and polar phonons of Ba(Mn1/3Nb2/3)O3 and Ba(Ni1/3Nb2/3)O3 complex perovskites. Computational Materials Science, 2013, 79, 918-922.	1.4	3
15518	Structural and electronic properties of sodium azide at high pressure: A first principles study. Solid State Communications, 2013, 161, 13-18.	0.9	47

#	Article	IF	Citations
15519	Thermodynamic optimization of Coâ€“Ge binary system. Thermochimica Acta, 2013, 572, 94-100.	1.2	6
15520	Mechanisms of dopants influence on hydrogen uptake in COF-108: A first principles study. International Journal of Hydrogen Energy, 2013, 38, 14668-14674.	3.8	9
15521	Effects of Zn atoms on the basal dislocation in magnesium solution from Peierlsâ€“Nabarro model. Materials Science & Engineering A: Structural Materials: Properties, Microstructure and Processing, 2013, 582, 299-304.	2.6	8
15522	Enhanced chemical reactions of oxygen at grain boundaries in polycrystalline graphene. Polyhedron, 2013, 64, 158-162.	1.0	27
15523	Synergetic effect of H and He with vacancy in vanadium solid from first-principles simulations. Nuclear Instruments & Methods in Physics Research B, 2013, 303, 75-80.	0.6	15
15524	Electronic and optical properties of S/I-codoped anatase TiO2 from ab initio calculations. Solid State Communications, 2013, 171, 17-21.	0.9	4
15525	Ordered surface-alloys formation in the Hf/W(100) adsorption system. Journal of Alloys and Compounds, 2013, 554, 246-253.	2.8	1
15526	Chair like NiAu6: Clusters assemblies and CO oxidation study by ab initio methods. Chemical Physics Letters, 2013, 584, 108-112.	1.2	13
15527	The ternary germanides UMnGe and U2Mn3Ge. Solid State Sciences, 2013, 21, 73-80.	1.5	5
15528	First-principles studies of carbon dioxide adsorption in cryptomelane/hollandite-type manganese dioxide. Chemical Physics Letters, 2013, 580, 120-125.	1.2	11
15529	Ab initio theoretical and photoemission studies on formation of 4H-SiC(0001)/SiO2 interface. Applied Surface Science, 2013, 280, 500-503.	3.1	2
15530	Effects of van der Waals interaction for first-principles calculations on iron-based superconductors. Physica C: Superconductivity and Its Applications, 2013, 494, 9-12.	0.6	3
15531	Electronic and magnetism properties of half-bare zigzag silicon carbon nanoribbons from hybrid density functional calculations. Solid State Communications, 2013, 158, 25-28.	0.9	7
15532	Surface step enhanced H2 splitting on Ti-doped Al(111) surface. Chemical Physics Letters, 2013, 565, 86-91.	1.2	2
15533	Density functional theory investigations of bismuth vanadate: Effect of hybrid functionals. Computational Materials Science, 2013, 74, 33-39.	1.4	28
15534	Influence of alloying elements on phase stability and elastic properties of aluminum and magnesium studied by first principles. Computational Materials Science, 2013, 74, 86-91.	1.4	8
15535	Theoretical study on the dissociative adsorption of CH4 on Pd-doped Ni surfaces. Chinese Journal of Catalysis, 2013, 34, 911-922.	6.9	32
15536	First principles investigation of the electronic, elastic and vibrational properties of tungsten disilicide. Journal of Alloys and Compounds, 2013, 553, 93-98.	2.8	10

#	Article	IF	Citations
15537	Drastic changes of electronic, magnetic, mechanical and bonding properties in Zr2Co by hydrogenation. Intermetallics, 2013, 36, 25-30.	1.8	9
15538	Low-energy electron reflectivity from graphene: First-principles computations and approximate models. Ultramicroscopy, 2013, 130, 101-108.	0.8	24
15539	Electronic, mechanical and optical properties of Y2O3 with hybrid density functional (HSE06). Computational Materials Science, 2013, 71, 19-24.	1.4	32
15540	Ab initio molecular dynamics study of temperature dependent structure properties of liquid leadâ€“bismuth eutectic alloy. Physica B: Condensed Matter, 2013, 429, 6-11.	1.3	12
15541	Insight of volume-compression-induced changes in SrRuO3 from first-principles calculations. Physica B: Condensed Matter, 2013, 415, 10-13.	1.3	1
15542	First-principles study of point defects in solar cell semiconductor CuI. Physica B: Condensed Matter, 2013, 413, 116-119.	1.3	29
15543	Ferromagnetism and antiferromagnetism in hydrogenated g-C3N4: A first-principles study. Physica B: Condensed Matter, 2013, 421, 46-49.	1.3	14
15544	A theoretical study of thorium titanium-based alloys. Journal of Nuclear Materials, 2013, 440, 229-235.	1.3	14
15545	Ab initio investigation of the crystal and electronic structures ofÂtheÂnitride fluoride ThNF. Solid State Sciences, 2013, 18, 123-126.	1.5	4
15546	Large anisotropy of electrical conductivity induced high thermoelectric performance of p-type CrSi2. Journal of Alloys and Compounds, 2013, 581, 413-417.	2.8	10
15547	Elastic, vibrational and thermodynamic properties of based group IV semiconductors and GeC under pressure. Journal of Physics and Chemistry of Solids, 2013, 74, 1615-1625.	1.9	16
15548	Nitrogen-tuned bonding mechanism of Li and Ti adatom embedded graphene. Journal of Solid State Chemistry, 2013, 205, 160-164.	1.4	7
15549	Synergistic effects of codopants on photocatalytic O2 evolution in BiVO4. Solid State Sciences, 2013, 24, 79-84.	1.5	20
15550	Prediction of the site ordering behaviours of elements in C15 NbCr2-based intermetallics by combining thermodynamic model with ab-initio calculation. Intermetallics, 2013, 35, 104-109.	1.8	13
15551	Methanol adsorption and decomposition on <mml:math xmlns:mml="http://www.w3.org/1998/Math/MathML" altimg="si11.gif" overflow="scroll"><mml:mrow><mml:mtext>ZnO</mml:mtext><mml:mo stretchy="false">(</mml:mo><mml:mn>10</mml:mn><mml:mover) Tj ETQq0 0 0 rgBT /Overlock 10 Tf 50 177 Td (accent="true"><mml	1.2	11
15552	First-principles study on stability of Li, Na and Ca in Lu2SiO5. Journal of Luminescence, 2013, 139, 1-5.	1.5	11
15553	Vacancy trapping behaviors of oxygen in tungsten: A first-principles study. Journal of Nuclear Materials, 2013, 437, 6-10.	1.3	17
15554	Segregation of alloying atoms on the Fe(100) surface and their effects on oxygen adsorption. Physica B: Condensed Matter, 2013, 425, 42-47.	1.3	12

#	Article	IF	Citations
15555	Lithium storage in amorphous TiNi hydride: Electrode for rechargeable lithium-ion batteries. Materials Chemistry and Physics, 2013, 141, 348-354.	2.0	15
15556	Half metal to insulator transition driven by electron doping in Ba2FeReO6. Journal of Magnetism and Magnetic Materials, 2013, 339, 163-167.	1.0	7
15557	Na adsorption on SrTiO3 (0 0 1) surface and its interaction with water: A DFT calculation. Applied Surface Science, 2013, 270, 359-363.	3.1	6
15558	Density functional theory study of lactic acid adsorption and dehydration reaction on monoclinic 0 1 1,<mml:math xmlns:mml="http://www.w3.org/1998/Math/MathML" altimg="si1.gif" overflow="scroll"><mml:mrow><mml:mover accent="true"><mml:mrow><mml:mn>1</mml:mn></mml:mrow><mml:mrow><mml:mo>Â¯</mml:mo></mml:mrow></mml:mover><mml:mspace width="0.12em" /><mml:mn>0</mml:mn><mml:mspace width="0.12em" /><mml:mn>1</mml:mn></mml:mrow></mml:math>, and<mml:math xmlns:mml="http://www.w3.org/1998	3.1	18
15559	The spin-filter role of the ill-defined layer in FM/Alq3/FM organic spin valve: A first-principle study. Synthetic Metals, 2013, 177, 82-88.	2.1	1
15560	Adsorption and dissociation of methanol on defective rutile TiO2 (110) surface with bridging oxygen-vacancy pairs. Chemical Physics Letters, 2013, 584, 98-102.	1.2	5
15561	Phase stability and thermal expansion behavior of Cu6Sn5 intermetallics doped with Zn, Au and In. Intermetallics, 2013, 43, 85-98.	1.8	41
15562	Investigating permeation and transport of H isotopes in tungsten by first-principles. Fusion Engineering and Design, 2013, 88, 368-373.	1.0	16
15563	Atomic modeling of structural and optical properties of amorphous silicon. Chemical Physics Letters, 2013, 570, 95-99.	1.2	6
15564	Hybrid preconditioning for iterative diagonalization of ill-conditioned generalized eigenvalue problems in electronic structure calculations. Journal of Computational Physics, 2013, 255, 16-30.	1.9	11
15565	NbF5 and TaF5: Assignment of 19F NMR resonances and chemical bond analysis from GIPAW calculations. Journal of Solid State Chemistry, 2013, 207, 208-217.	1.4	22
15566	Significant charge transfer between a single-molecule magnet Mn12 and a Bi substrate. Polyhedron, 2013, 66, 157-161.	1.0	4
15567	Structural transformation of sputtered o-LiMnO2 thin-film cathodes induced by electrochemical cycling. Thin Solid Films, 2013, 549, 263-267.	0.8	8
15568	Diluted ferromagnetic graphene by compensated nâ€“p codoping. Carbon, 2013, 61, 609-615.	5.4	28
15569	Band gap tuning in HgTe through uniaxial strains. Solid State Communications, 2013, 166, 1-5.	0.9	3
15570	A popular metastable omega phase in body-centered cubic steels. Materials Chemistry and Physics, 2013, 139, 830-835.	2.0	50
15571	Local structure analysis on (La,Ba)(Ga,Mg)O3â˜Î´ by the pair distribution function method using a neutron source and density functional theory calculations. Solid State Communications, 2013, 163, 46-49.	0.9	5
15572	The phase stability and elastic properties of MgZn2 and Mg4Zn7 in Mgâ€“Zn alloys. Scripta Materialia, 2013, 68, 495-498.	2.6	69

#	Article	IF	Citations
15573	The detailed geometrical and electronic structures of monoclinic zirconia. Journal of Physics and Chemistry of Solids, 2013, 74, 518-523.	1.9	24
15574	Theoretical study of the Fluorine doped anatase surfaces. Surface Science, 2013, 618, 154-158.	0.8	25
15575	High resolution STM imaging with oriented single crystalline tips. Applied Surface Science, 2013, 267, 219-223.	3.1	16
15576	High activation energy for proton migration at <mml:math xmlns:mml="http://www.w3.org/1998/Math/MathML" altimg="si6.gif" overflow="scroll"><mml:mstyle displaystyle="true"><mml:mo>â^'</mml:mo><mml:mrow><mml:mn>3</mml:mn><mml:mfenced open="(") Tj ETQq1 1 0.784314 rgB open="[" close="]"><mml:mrow><mml:mn>1</mml:mn><mml:mover	1.3	14
15577	Hydrogen retention to impurities in tungsten: A multi-scale study. Journal of Nuclear Materials, 2013, 438, S1001-S1004.	1.3	15
15578	Elastic and electronic properties of Ce2O3 from first principles. Journal of Alloys and Compounds, 2013, 551, 672-676.	2.8	13
15579	Ab initio calculations of optical properties of Li and K at high pressures. Journal of Physics and Chemistry of Solids, 2013, 74, 1221-1226.	1.9	2
15580	First-principle study of amorphous SiZnSnO thin-film transistor with excellent stability. Thin Solid Films, 2013, 534, 609-613.	0.8	29
15581	Effects of Li and Na intercalation on electronic, bonding and thermoelectric transport properties of MX2 (M=Ta; X=S or Se) dichalcogenides â€“ Ab initio investigation. Journal of Alloys and Compounds, 2013, 581, 731-740.	2.8	19
15582	Ab initio study of ã€^111ã€‰ {110} superdislocation properties in B2-MgRE (RE=Laâ€“Er) intermetallics. Computational Materials Science, 2013, 69, 168-172.	1.4	5
15583	Magnetic ordering and electron correlation of iron-based superconductor (Ca3Al2O5â^'x)(Fe2As2) from first-principles study. Solid State Communications, 2013, 172, 41-48.	0.9	0
15584	Effect of carbon on helium trapping in tungsten: A first-principles investigation. Journal of Nuclear Materials, 2013, 440, 338-343.	1.3	16
15585	Surface dynamics of Cu and Ag atoms on hydroxylated MgO(001) surfaces. Journal of the Korean Physical Society, 2013, 62, 79-85.	0.3	10
15586	Correlation between charge-transfer and rotation of C60 on WO2/W(110). Nanoscale, 2013, 5, 3380.	2.8	10
15587	Nitrogen-Doped Fullerene as a Potential Catalyst for Hydrogen Fuel Cells. Journal of the American Chemical Society, 2013, 135, 3315-3318.	6.6	167
15588	Can hematite nanoparticles be an environmental indicator?. Energy and Environmental Science, 2013, 6, 561-569.	15.6	28
15589	Zipping and Unzipping of a Paddlewheel Metalâ€“Organic Framework to Enable Twoâ€Step Synthetic and Structural Transformation. Chemistry - A European Journal, 2013, 19, 3552-3557.	1.7	28
15590	Dicalcium nitride as a two-dimensional electride with an anionic electron layer. Nature, 2013, 494, 336-340.	13.7	386

#	Article	IF	Citations
15591	Exotic spin-orbital Mott insulating states in BaIrO3. Physical Review B, 2013, 87, .	1.1	16
15592	Alkali metal organocyclotrisiloxanolates [RSi(O)OM]3 with vinyl and alkyl substituents at the silicon center. Journal of Organometallic Chemistry, 2013, 729, 86-94.	0.8	7
15593	A Mechanistic Study of Graphene Fluorination. Journal of Physical Chemistry C, 2013, 117, 5407-5415.	1.5	18
15594	Topological states ruled by stacking faults in Bi2Se3 and Bi2Te3. Journal of Applied Physics, 2013, 113, 023705.	1.1	21
15595	Phase stability, electrochemical stability and ionic conductivity of the Li_{10Â±1}MP₂X₁₂(M = Ge, Si, Sn, Al or P, and X = O, S or Se) family of superionic conductors. Energy and Environmental Science, 2013, 6, 148-156.	15.6	545
15596	Methane dehydrogenation on Au/Ni surface alloys â€“ a first-principles study. Catalysis Science and Technology, 2013, 3, 1343.	2.1	36
15597	Decomposition and Oxidation of Methanol on Ir(111): A First-Principles Study. Journal of Physical Chemistry C, 2013, 117, 4574-4584.	1.5	23
15598	Mineralâ€“Water Interface Reactions of Actinides. Chemical Reviews, 2013, 113, 1016-1062.	23.0	271
15599	Interaction of platinum nanoparticles with different types of tin dioxide surface: Quantum-chemical modeling. Russian Journal of Inorganic Chemistry, 2013, 58, 56-61.	0.3	10
15600	Spin-polarized electronic current induced by sublattice engineering of graphene sheets with boron/nitrogen. Physical Review B, 2013, 87, .	1.1	24
15601	Electrochemical water splitting by gold: evidence for an oxide decomposition mechanism. Chemical Science, 2013, 4, 2334.	3.7	229
15602	Binary Compounds of Boron and Beryllium: A Rich Structural Arena with Space for Predictions. Chemistry - A European Journal, 2013, 19, 4184-4197.	1.7	26
15603	Noncovalent Interactions of DNA Bases with Naphthalene and Graphene. Journal of Chemical Theory and Computation, 2013, 9, 2090-2096.	2.3	73
15604	Chiral â€œPinwheelâ€•Heterojunctions Self-Assembled from C₆₀ and Pentacene. ACS Nano, 2013, 7, 3086-3094.	7.3	16
15605	Thermoelectric performance of MX2 (Mâ€‰=â€‰Mo,W; Xâ€‰=â€‰S,Se) monolayers. Journal of Applied Physics, 2013, 113, .	1.1	202
15606	Low-Energy Electronic Properties of Graphene and Armchair Ribbon Superlattices. Journal of Physical Chemistry C, 2013, 117, 7326-7333.	1.5	3
15607	Chern Insulators from Heavy Atoms on Magnetic Substrates. Physical Review Letters, 2013, 110, 116802.	2.9	99
15608	Band structure and phase stability of the copper oxides Cu<mml:math xmlns:mml="http://www.w3.org/1998/Math/MathML" display="inline"><mml:msub><mml:mrow /><mml:mn>2</mml:mn></mml:msub></mml:math>O, CuO, and Cu<mml:math xmlns:mml="http://www.w3.org/1998/Math/MathML" display="inline"><mml:msub><mml:mrow /><mml:mn>4</mml:mn></mml:msub></mml:math>O<mml:math xmlns:mml="http://www.w3.org/1998/Math/MathML" display="inline"><mml:msub><mml:mrow /><mml:	1.1	309

#	Article	IF	Citations
15609	Stable p- and n-type doping of few-layer graphene/graphite. Carbon, 2013, 57, 507-514.	5.4	42
15610	Tunable electronic and dielectric behavior of GaS and GaSe monolayers. Physical Chemistry Chemical Physics, 2013, 15, 7098.	1.3	182
15611	Coke-Tolerant Ni/BaCe_{1â€“x}Y_xO_{3â^'Î´} Anodes for Solid Oxide Fuel Cells: DFT+U Study. Journal of Physical Chemistry C, 2013, 117, 7086-7096.	1.5	26
15612	First-principles calculations of H, O and OH adsorption on metallic layered supported thin films. Journal of Physics Condensed Matter, 2013, 25, 175002.	0.7	6
15613	Effective Mass-Driven Structural Transition in a Mn-Doped ZnS Nanoplatelet. Journal of Physical Chemistry Letters, 2013, 4, 1023-1027.	2.1	6
15614	DFT+U Study of Polaronic Conduction in Li₂O₂ and Li₂CO₃: Implications for Liâ€“Air Batteries. Journal of Physical Chemistry C, 2013, 117, 5568-5577.	1.5	142
15615	Effect of film thickness and biaxial strain on the curie temperature of EuO. Applied Physics Letters, 2013, 102, .	1.5	23
15616	Prediction of Water Adsorption in Copper-Based Metalâ€“Organic Frameworks Using Force Fields Derived from Dispersion-Corrected DFT Calculations. Journal of Physical Chemistry C, 2013, 117, 7519-7525.	1.5	56
15617	Theoretical Studies of the Adsorption of CO and C on Ni(111) and Ni/CeO₂(111): Evidence of a Strong Metalâ€“Support Interaction. Journal of Physical Chemistry C, 2013, 117, 8241-8250.	1.5	100
15618	Understanding the Nucleation and Growth of Metals on TiO₂: Co Compared to Au, Ni, and Pt. Journal of Physical Chemistry C, 2013, 117, 7191-7201.	1.5	84
15619	Construction and application of multi-element EAM potential (Niâ€“Alâ€“Re) inÎ³/Î³â€² Ni-based single crystal superalloys. Modelling and Simulation in Materials Science and Engineering, 2013, 21, 015007.	0.8	49
15620	Dimethyl Disulfide on Cu(111): From Nondissociative to Dissociative Adsorption. Journal of Physical Chemistry C, 2013, 117, 6587-6593.	1.5	5
15621	Functionalized Graphitic Carbon Nitride for Efficient Energy Storage. Journal of Physical Chemistry C, 2013, 117, 6055-6059.	1.5	171
15622	Atomistic Modeling of Warm Dense Matter in the Twoâ€Temperature State. Contributions To Plasma Physics, 2013, 53, 129-139.	0.5	52
15623	Surface-enhanced Raman scattering (SERS) from Au:Ag bimetallic nanoparticles: the effect of the molecular probe. Chemical Science, 2013, 4, 509-515.	3.7	183
15624	PbO₂: from semi-metal to transparent conducting oxide by defect chemistry control. Chemical Communications, 2013, 49, 448-450.	2.2	27
15625	DFT+U Investigation of Propene Oxidation over Bismuth Molybdate: Active Sites, Reaction Intermediates, and the Role of Bismuth. Journal of Physical Chemistry C, 2013, 117, 7123-7137.	1.5	70
15626	On the Origin of the Enhanced Supercapacitor Performance of Nitrogen-Doped Graphene. Journal of Physical Chemistry C, 2013, 117, 5610-5616.	1.5	230

#	Article	IF	Citations
15627	Ab initiostudy of collective dynamics in the liquid phase of the equimolar alloy CsAu: Evidence for a nonmetallic state. Physical Review B, 2013, 87, .	1.1	5
15628	Structurally and Electronically Designed TiO₂N_x Nanofibers for Lithium Rechargeable Batteries. ACS Applied Materials & Interfaces, 2013, 5, 691-696.	4.0	63
15629	Adsorption and absorption of boron, nitrogen, aluminum, and phosphorus on silicene: Stability and electronic and phonon properties. Physical Review B, 2013, 87, .	1.1	186
15630	Identifying Molecular Species on Surfaces by Scanning Tunneling Microscopy: Methyl Pyruvate on Pd(111). Journal of Physical Chemistry C, 2013, 117, 4505-4514.	1.5	15
15631	Two-Dimensional Carbon Compounds Derived from Graphyne with Chemical Properties Superior to Those of Graphene. Scientific Reports, 2013, 3, 1271.	1.6	36
15632	Experimental and theoretical studies of donorâ€“acceptor scintillation from PbI2. Journal of Luminescence, 2013, 134, 28-34.	1.5	37
15633	Proximity-induced giant spin-orbit interaction in epitaxial graphene on a topological insulator. Physical Review B, 2013, 87, .	1.1	94
15634	Magnetic orders and electronic structure in LaMnO3/SrTiO3 superlattices. Journal of Applied Physics, 2013, 113, .	1.1	10
15635	An Effective Approach to Achieve a Spin Gapless Semiconductorâ€“Halfâ€Metalâ€“Metal Transition in Zigzag Graphene Nanoribbons: Attaching A Floating Induced Dipole Field via Ï€â€“Ï€ Interactions. Advanced Functional Materials, 2013, 23, 1507-1518.	7.8	37
15636	Surface-Accelerated Decomposition of Î´-HMX. Journal of Physical Chemistry Letters, 2013, 4, 730-734.	2.1	49
15637	A ternary EAM interatomic potential for Uâ€“Mo alloys with xenon. Modelling and Simulation in Materials Science and Engineering, 2013, 21, 035011.	0.8	71
15638	Activation of Photocatalytic Water Oxidation on N-Doped ZnO Bundle-like Nanoparticles under Visible Light. Journal of Physical Chemistry C, 2013, 117, 4937-4942.	1.5	143
15639	Temperature-Mediated Magnetism in Fe-Doped ZnO Semiconductors. Journal of Physical Chemistry C, 2013, 117, 5338-5342.	1.5	17
15640	The role of impurity oxygen in hydrogen bubble nucleation in tungsten. Journal of Nuclear Materials, 2013, 433, 357-363.	1.3	45
15641	Prediction of stable insulating intermetallic compounds. Physical Review B, 2013, 87, .	1.1	6
15642	Postsynthetic Exchanges of the Pillaring Ligand in Three-Dimensional Metalâ€“Organic Frameworks. Chemistry of Materials, 2013, 25, 1047-1054.	3.2	56
15643	Atomic scale morphology, growth behaviour and electronic properties of semipolar ${ 1 0ar {1}3} $ GaN surfaces. Journal of Physics Condensed Matter, 2013, 25, 045008.	0.7	3
15644	The surface states of lithium tetraborate. Journal of Physics Condensed Matter, 2013, 25, 045014.	0.7	2

#	Article	IF	Citations
15645	Sulfur- and Oxygen-Induced Alterations of the Iron (001) Surface Magnetism and Work Function: A Theoretical Study. Journal of Physical Chemistry C, 2013, 117, 6161-6171.	1.5	17
15646	Nonlinear elastic behavior of two-dimensional molybdenum disulfide. Physical Review B, 2013, 87, .	1.1	400
15647	Phonon frequencies of tetragonally strained PbTiO₃from first principles. Phase Transitions, 2013, 86, 200-205.	0.6	4
15648	Formation and properties of graphane superstructures. Journal of Physics Condensed Matter, 2013, 25, 085301.	0.7	6
15649	The Impact of Functionalization on the Stability, Work Function, and Photoluminescence of Reduced Graphene Oxide. ACS Nano, 2013, 7, 1638-1645.	7.3	247
15650	Concerted Migration Mechanism in the Li Ion Dynamics of Garnet-Type Li₇La₃Zr₂O₁₂. Chemistry of Materials, 2013, 25, 425-430.	3.2	206
15651	Surface-Confined Reaction of Aliphatic Diamines with Aromatic Diisocyanates on Au{111} Leads to Ordered Oligomer Assemblies. Journal of Physical Chemistry C, 2013, 117, 4515-4520.	1.5	10
15652	Composition- and Band-Gap-Tunable Synthesis of Wurtzite-Derived Cu₂ZnSn(S_{1â€“x}Se_x)₄ Nanocrystals: Theoretical and Experimental Insights. ACS Nano, 2013, 7, 1454-1463.	7.3	89
15653	Improving the optical absorption of BiFeO3 for photovoltaic applications via uniaxial compression or biaxial tension. Applied Physics Letters, 2013, 102, .	1.5	54
15654	Control of the Magnetism and Magnetic Anisotropy of a Single-Molecule Magnet with an Electric Field. Physical Review Letters, 2013, 110, 097202.	2.9	135
15655	Hybrid Improper Ferroelectricity in a Multiferroic and Magnetoelectric Metalâ€Organic Framework. Advanced Materials, 2013, 25, 2284-2290.	11.1	280
15656	Theoretical prediction of new carbon allotropes. Journal of Chemical Physics, 2013, 138, 024502.	1.2	30
15657	Cu3BiS3 as a potential photovoltaic absorber with high optical efficiency. Applied Physics Letters, 2013, 102, .	1.5	59
15658	Magnetic properties and origins of ferroelectric polarization in multiferroic CaMn<mml:math xmlns:mml="http://www.w3.org/1998/Math/MathML" display="inline"><mml:msub><mml:mrow /><mml:mn>7</mml:mn></mml:msub></mml:math>O<mml:math xmlns:mml="http://www.w3.org/1998/Math/MathML" display="inline"><mml:msub><mml:mrow /><mml:mn>12</mml:mn></mml:msub></mml:math>. Physical Review B, 2013, 87, .	1.1	29
15659	Effects of Charging and Electric Field on Graphene Oxide. Journal of Physical Chemistry C, 2013, 117, 5943-5952.	1.5	47
15660	Enhanced Optical Absorption Due to Symmetry Breaking in TiO_{2(1â€“x)}S_{2x} Alloys. Journal of Physical Chemistry C, 2013, 117, 4189-4193.	1.5	13
15661	Electronic structure of Î±-SrB₄O₇: experiment and theory. Journal of Physics Condensed Matter, 2013, 25, 085503.	0.7	24
15662	Transition-metal acceptor complexes in zinc oxide. Physical Review B, 2013, 87, .	1.1	12

#	Article	IF	Citations
15663	Electronic and optical properties of cadmium fluoride: The role of many-body effects. Physical Review B, 2013, 87, .	1.1	20
15664	Approaching chemical accuracy with density functional calculations: Diatomic energy corrections. Physical Review B, 2013, 87, .	1.1	75
15665	Strain-induced topological insulator phase transition in HgSe. Physical Review B, 2013, 87, .	1.1	33
15666	Massive Dirac surface states in topological insulator/magnetic insulator heterostructures. Physical Review B, 2013, 87, .	1.1	132
15667	Structural domain walls in polar hexagonal manganites. Nature Communications, 2013, 4, 1540.	5.8	103
15668	Alloying route to tailor giant magnetic anisotropy in transition-metal nanowires. Physical Review B, 2013, 87, .	1.1	12
15669	Insight into the initial oxidation of 4<mml:math xmlns:mml="http://www.w3.org/1998/Math/MathML" display="inline"><mml:mi>H</mml:mi></mml:math>-SiC from first-principles thermodynamics. Physical Review B, 2013, 87, .	1.1	15
15670	Effect of substitutional doping on the Néel temperature of <mml:math xmlns:mml="http://www.w3.org/1998/Math/MathML" display="inline"><mml:mrow><mml:msub><mml:mi mathvariant="bold">Cr</mml:mi><mml:mn mathvariant="bold">2</mml:mn></mml:msub><mml:msub><mml:mi	1.1	51
15671	Field effect doping of graphene in metal<mml:math xmlns:mml="http://www.w3.org/1998/Math/MathML" display="inline"><mml:mo>|</mml:mo></mml:math>dielectric<mml:math xmlns:mml="http://www.w3.org/1998/Math/MathML" display="inline"><mml:mo>|</mml:mo></mml:math>graphene heterostructures: A model based upon first-principles calculations. Physical Review B, 2013, 87, .	1.1	33
15672	Systematic modulation and enhancement of CO2â€‰:â€‰N2 selectivity and water stability in an isoreticular series of bio-MOF-11 analogues. Chemical Science, 2013, 4, 1746.	3.7	182
15673	Two-dimensional carbon allotrope with strong electronic anisotropy. Physical Review B, 2013, 87, .	1.1	108
15674	H<mml:math xmlns:mml="http://www.w3.org/1998/Math/MathML" display="inline"><mml:msub><mml:mrow /><mml:mn mathvariant="bold">4</mml:mn></mml:msub></mml:math>O and other hydrogen-oxygen compounds at giant-planet core pressures. Physical Review B, 2013, 87, .	1.1	18
15675	First-principles investigation of incipient ferroelectric trends of rutile TiO2in bulk and at the (110) surface. Physical Review B, 2013, 87, .	1.1	16
15676	Multiscale Modeling of CdTe Thin Film Deposition Process. Materials Research Society Symposia Proceedings, 2013, 1524, 1.	0.1	0
15677	Solid state adaptive natural density partitioning: a tool for deciphering multi-center bonding in periodic systems. Physical Chemistry Chemical Physics, 2013, 15, 5022.	1.3	143
15678	Cross-sectional aspect ratio modulated electronic properties in Si/Ge core/shell nanowires. Journal Physics D: Applied Physics, 2013, 46, 135302.	1.3	5
15679	High-pressure phase transitions and equations of state in NiSi. III. A new high-pressure phase of NiSi. Journal of Applied Crystallography, 2013, 46, 14-24.	1.9	12
15680	Peierls potential of screw dislocations in bcc transition metals: Predictions from density functional theory. Physical Review B, 2013, 87, .	1.1	89

#	Article	IF	Citations
15681	Strain-induced self-doping in silicene and germanene from first-principles. Solid State Communications, 2013, 155, 6-11.	0.9	131
15682	The Modulated Structure of Co₃Al₄Si₂: Incommensurability and Coâ€“Co Interactions in Search of Filled Octadecets. Inorganic Chemistry, 2013, 52, 3178-3189.	1.9	25
15683	DFT study on stability and H2 adsorption activity of bimetallic Au79â^'Pd (n= 1â€“55) clusters. Chemical Physics, 2013, 415, 179-185.	0.9	20
15684	High Surface Reactivity and Water Adsorption on NiFe₂O₄ (111) Surfaces. Journal of Physical Chemistry C, 2013, 117, 5678-5683.	1.5	52
15685	Formation of an oxygen vacancy-dinitrogen complex in nitrogen-doped hafnium oxide. Journal of Analytical Atomic Spectrometry, 2013, 28, 482.	1.6	8
15686	Chemical Expansion and Change in Lattice Constant of Yâ€Doped <scp><scp>BaZrO</scp></scp>₃ by Hydration/Dehydration Reaction and Final Heatâ€Treating Temperature. Journal of the American Ceramic Society, 2013, 96, 879-884.	1.9	65
15687	Ab initio study on magnetic anisotropy change of SrCoxTixFe12â^'2xO19. Journal of Applied Physics, 2013, 113, 17D909.	1.1	15
15691	n-Diamond: Dynamical stability of proposed structures. Diamond and Related Materials, 2013, 34, 60-64.	1.8	12
15692	Phonon softening and direct to indirect band gap crossover in strained single-layer MoSe<mml:math xmlns:mml="http://www.w3.org/1998/Math/MathML" display="inline"><mml:msub><mml:mrow /><mml:mn>2</mml:mn></mml:msub></mml:math>. Physical Review B, 2013, 87, .	1.1	200
15693	Intrinsic nanofilamentation in resistive switching. Journal of Applied Physics, 2013, 113, 114503.	1.1	69
15694	Oxygen reduction reaction on active sites of heteroatom-doped graphene. RSC Advances, 2013, 3, 5498.	1.7	59
15695	New insight into the structure of saturated chlorine layer on Ag(111): LT-STM and DFT study. Applied Surface Science, 2013, 267, 21-25.	3.1	10
15696	Li2O clusters for high-capacity hydrogen storage: A first principles study. Chemical Physics, 2013, 415, 26-30.	0.9	8
15697	Global Structural Optimization of Tungsten Borides. Physical Review Letters, 2013, 110, 136403.	2.9	253
15698	Liquid-phase thermodynamics and structures in the Cuâ€“Nb binary system. Modelling and Simulation in Materials Science and Engineering, 2013, 21, 025005.	0.8	32
15699	Cage-Forming Compounds in the Baâ€“Rhâ€“Ge System: From Thermoelectrics to Superconductivity. Inorganic Chemistry, 2013, 52, 931-943.	1.9	20
15700	Norm-conserving pseudopotentials with chemical accuracy compared to all-electron calculations. Journal of Chemical Physics, 2013, 138, 104109.	1.2	95
15701	Role of Magnetism in Catalysis: RuO₂ (110) Surface. Journal of Physical Chemistry C, 2013, 117, 6353-6357.	1.5	98

#	Article	IF	Citations
15702	Ab initiostudy of boron in<mml:math xmlns:mml="http://www.w3.org/1998/Math/MathML" display="inline"><mml:mi>Î±</mml:mi></mml:math>-iron: Migration barriers and interaction with point defects. Physical Review B, 2013, 87, .	1.1	29
15703	Role of Sodium Doping in Lead Chalcogenide Thermoelectrics. Journal of the American Chemical Society, 2013, 135, 4624-4627.	6.6	128
15704	Stabilization criteria for cubic AlN in TiN/AlN and CrN/AlN bi-layer systems. Journal Physics D: Applied Physics, 2013, 46, 045305.	1.3	34
15705	Cu₂(OH)PO₄, a Nearâ€Infraredâ€Activated Photocatalyst. Angewandte Chemie - International Edition, 2013, 52, 4810-4813.	7.2	220
15706	Incorporation of nitrogen in Co:ZnO studied by x-ray absorption spectroscopy and x-ray linear dichroism. Physical Review B, 2013, 87, .	1.1	9
15707	A computational study of the influence of the ceria surface termination on the mechanism of CO oxidation of isolated Rh atoms. Faraday Discussions, 2013, 162, 281.	1.6	37
15708	Is there a Difference in Van Der Waals Interactions between Rare Gas Atoms Adsorbed on Metallic and Semiconducting Single-Walled Carbon Nanotubes?. Physical Review Letters, 2013, 110, 135503.	2.9	19
15709	Solid-State Structure and Calculated Electronic Structure, Formation Energy, Chemical Bonding, and Optical Properties of Zn₄O(FMA)₃ and Its Heavier Congener Cd₄O(FMA)₃. Inorganic Chemistry, 2013, 52, 4217-4228.	1.9	24
15710	In-Plane Coassembly Route to Atomically Thick Inorganicâ€“Organic Hybrid Nanosheets. ACS Nano, 2013, 7, 1682-1688.	7.3	45
15711	Cu<mml:math xmlns:mml="http://www.w3.org/1998/Math/MathML" display="inline"><mml:msub><mml:mrow /><mml:mn>2</mml:mn></mml:msub></mml:math>Zn(Sn,Ge)Se<mml:math xmlns:mml="http://www.w3.org/1998/Math/MathML" display="inline"><mml:msub><mml:mrow /><mml:mn>4</mml:mn></mml:msub></mml:math>and Cu<mml:math xmlns:mml="http://www.w3.org/1998/Math/MathML" display="inline"><mml:msub><mml:mrow /></mml:msub></mml:math>	1.1	90
15712	Axial ratio dependence of the stability of self-interstitials in HCP structures. Journal of Nuclear Materials, 2013, 437, 293-296.	1.3	10
15713	Towards ab initio screening of co-crystal formation through lattice energy calculations and crystal structure prediction of nicotinamide, isonicotinamide, picolinamide and paracetamol multi-component crystals. CrystEngComm, 2013, 15, 3799.	1.3	100
15714	Cation vacancies in the alloy compounds of Cu2ZnSn(S1â^'Se)4 and CuIn(S1â^'Se)2. Thin Solid Films, 2013, 535, 318-321.	0.8	15
15715	Structural stability of Cr-related defect complex in diamond for single photon sources: A first-principles study. Journal of Applied Physics, 2013, 113, .	1.1	6
15716	A Detailed Model Grid for Solid Planets from 0.1 through 100 Earth Masses. Publications of the Astronomical Society of the Pacific, 2013, 125, 227-239.	1.0	185
15717	Metal-induced charge transfer, structural distortion, and orbital order in SrTiO<mml:math xmlns:mml="http://www.w3.org/1998/Math/MathML" display="inline"><mml:msub><mml:mrow /><mml:mn>3</mml:mn></mml:msub></mml:math>thin films. Physical Review B, 2013, 87, .	1.1	12
15718	Fischerâ€“Tropsch Synthesis over Supported Ptâ€“Mo Catalyst: Toward Bimetallic Catalyst Optimization. Journal of Physical Chemistry C, 2013, 117, 4450-4458.	1.5	3
15719	Platinum-Modulated Cobalt Nanocatalysts for Low-Temperature Aqueous-Phase Fischerâ€“Tropsch Synthesis. Journal of the American Chemical Society, 2013, 135, 4149-4158.	6.6	116

#	Article	IF	Citations
15720	Chemical trend of the formation energies of the group-III and group-V dopants in Si quantum dots. Physical Review B, 2013, 87, .	1.1	5
15721	Topological surface states revealed by Sb thin films adsorbed with impurity atoms. Physical Review B, 2013, 87, .	1.1	7
15722	Comment on â€œTopological Insulators in Ternary Compounds with a Honeycomb Latticeâ€• Physical Review Letters, 2013, 110, 129701.	2.9	4
15723	Effect of nitrogen induced defects in Li dispersed graphene onÂhydrogen storage. International Journal of Hydrogen Energy, 2013, 38, 4611-4617.	3.8	59
15724	Density Functional Theory Calculations of UO₂ Oxidation: Evolution of UO_{2+x}, U₄O_{9â€“y}, U₃O₇, and U₃O₈. Inorganic Chemistry, 2013, 52, 2769-2778.	1.9	96
15725	Thermodynamic functions of the heated electron subsystem in the field of cold nuclei. High Energy Density Physics, 2013, 9, 309-314.	0.4	43
15726	Chiralityâ€Đependent Reactivity of Individual Singleâ€Walled Carbon Nanotubes. Small, 2013, 9, 1379-1386.	5.2	41
15727	A Quantum Alloy: The Ligand-Protected Au_{25â€“x}Ag_x(SR)₁₈ Cluster. Journal of Physical Chemistry C, 2013, 117, 7914-7923.	1.5	124
15728	Spontaneous Symmetry Breaking and Dynamic Phase Transition in Monolayer Silicene. Physical Review Letters, 2013, 110, 085504.	2.9	205
15729	Combined theoretical and experimental analysis of processes determining cathode performance in solid oxide fuel cells. Physical Chemistry Chemical Physics, 2013, 15, 5443.	1.3	240
15730	Quasiparticle band structures and optical properties of strained monolayer MoS<mml:math xmlns:mml="http://www.w3.org/1998/Math/MathML" display="inline"><mml:msub><mml:mrow /><mml:mn>2</mml:mn></mml:msub></mml:math>and WS<mml:math xmlns:mml="http://www.w3.org/1998/Math/MathML" display="inline"><mml:msub><mml:mrow /><mml:mn>2</mml:mn></mml:msub></mml:math>. Physical Review B, 2013, 87, .	1.1	764
15731	The behaviour of oxygen at metal electrodes in HfO2 based resistive switching devices. Microelectronic Engineering, 2013, 109, 346-350.	1.1	29
15732	Tin clusters formed by fundamental units: a potential way to assemble tin nanowires. Physical Chemistry Chemical Physics, 2013, 15, 1831-1836.	1.3	14
15733	Chiral-Selective CoSO₄/SiO₂ Catalyst for (9,8) Single-Walled Carbon Nanotube Growth. ACS Nano, 2013, 7, 614-626.	7.3	101
15734	Effects of strain on the electron effective mass in GaN and AlN. Applied Physics Letters, 2013, 102, .	1.5	66
15735	CO and O overlayers on Pd nanocrystals supported on TiO2(110). Faraday Discussions, 2013, 162, 191.	1.6	6
15736	Structural and electronic properties of BaCrO4 at high-pressures. Solid State Communications, 2013, 155, 45-48.	0.9	3
15737	Influence of scandium concentration on power generation figure of merit of scandium aluminum nitride thin films. Applied Physics Letters, 2013, 102, .	1.5	159

#	Article	IF	Citations
15738	Structure of Monomeric Chromium(VI) Oxide Species Supported on Silica: Periodic and Cluster DFT Studies. Journal of Physical Chemistry C, 2013, 117, 8138-8149.	1.5	63
15739	Electronic states of intrinsic surface and bulk vacancies in FeS₂. Journal of Physics Condensed Matter, 2013, 25, 045004.	0.7	35
15740	Electronic, Thermal, and Structural Properties of Graphene Oxide Frameworks. Journal of Physical Chemistry C, 2013, 117, 8276-8281.	1.5	26
15741	Realization of insulating massive Dirac fermion state in Bi2Te3 by co-substitution of magnetic and non-magnetic elements. Applied Physics Letters, 2013, 102, .	1.5	4
15742	First-principles study of structure and properties of Ï‰-Ti2Zr. Computational Materials Science, 2013, 74, 129-137.	1.4	8
15743	A Beaded-String Silicon Anode. ACS Nano, 2013, 7, 2717-2724.	7.3	68
15744	Single-Electron Induces Double-Reaction by Charge Delocalization. Journal of the American Chemical Society, 2013, 135, 6220-6225.	6.6	41
15745	Ab initioanalysis of the defect structure of ceria. Physical Review B, 2013, 87, .	1.1	125
15746	Spin crossover in a single Fe(phen<mml:math xmlns:mml="http://www.w3.org/1998/Math/MathML") Tj ETQq0 0 0 rgBT /Overlock 10 Tf 5 adsorbed onto metallic substrates: Anab initiocalculation. Physical Review B, 2013, 87, .	1.1	49
15747	Use of ab initio methods for the interpretation of the experimental IR reflectance spectra of crystalline compounds. Journal of Computational Chemistry, 2013, 34, 1476-1485.	1.5	12
15748	Mechanisms of Halogen-Based Covalent Self-Assembly on Metal Surfaces. Journal of the American Chemical Society, 2013, 135, 5768-5775.	6.6	216
15749	Engineering of Facets, Band Structure, and Gasâ€Sensing Properties of Hierarchical Sn²⁺â€Doped SnO₂ Nanostructures. Advanced Functional Materials, 2013, 23, 4847-4853.	7.8	108
15750	Theoretical study of adhesion at the metal-zirconium dioxide interfaces. Technical Physics, 2013, 58, 325-334.	0.2	4
15751	d0 magnetism in semiconductors through confining delocalized atomic orbitals. Applied Physics Letters, 2013, 102, 022422.	1.5	10
15752	Tunable topological electronic structures in Sb(111) bilayers: A first-principles study. Applied Physics Letters, 2013, 102, .	1.5	107
15753	Theoretical Study of the Interaction of Electron Donor and Acceptor Molecules with Graphene. Journal of Physical Chemistry C, 2013, 117, 2411-2420.	1.5	79
15754	Nitrogen-doped layered oxide Sr5Ta4O15â^'xNx for water reduction and oxidation under visible light irradiation. Journal of Materials Chemistry A, 2013, 1, 5651.	5.2	89
15755	Band offsets in complex-oxide thin films and heterostructures of SrTiO3/LaNiO3 and SrTiO3/GdTiO3 by soft and hard X-ray photoelectron spectroscopy. Journal of Applied Physics, 2013, 113, .	1.1	29

#	Article	IF	Citations
15756	Atom-specific forces and defect identification on surface-oxidized Cu(100) with combined 3D-AFM and STM measurements. Physical Review B, 2013, 87, .	1.1	36
15757	Adsorption capacity of H2O, NH3, CO, and NO2 on the pristine graphene. Journal of Applied Physics, 2013, 113, .	1.1	80
15758	Computationally Assisted Identification of Functional Inorganic Materials. Science, 2013, 340, 847-852.	6.0	62
15759	Density-functional study of perovskite-type hydride LiNiH<mml:math xmlns:mml="http://www.w3.org/1998/Math/MathML" display="inline"><mml:msub><mml:mrow /><mml:mn>3</mml:mn></mml:msub></mml:math>and its synthesis: Mechanism for formation of metallic perovskite. Physical Review B, 2013, 87, .	1.1	18
15760	Theoretical study of the influence of vacancies in the magnetic stability of V-, Cr-, and Mn-doped SnO2. Applied Surface Science, 2013, 267, 115-118.	3.1	7
15761	Covalent magnetism and magnetic impurities. Journal of Physics Condensed Matter, 2013, 25, 186002.	0.7	2
15762	Multi-component perovskite-type oxides CaCu3V4â˜xMnxO12: Synthesis and electronic properties. Solid State Communications, 2013, 162, 57-60.	0.9	6
15763	Enhanced hydrogen storage properties under external electric fields of N-doped graphene with Li decoration. Physical Chemistry Chemical Physics, 2013, 15, 3243.	1.3	29
15764	Optical anisotropy and blue-shift phenomenon in tetragonal BiFeO₃. Journal Physics D: Applied Physics, 2013, 46, 135102.	1.3	16
15765	Band Gap Engineering of BN Sheets by Interlayer Dihydrogen Bonding and Electric Field Control. ChemPhysChem, 2013, 14, 1787-1792.	1.0	36
15766	AB INITIOMOLECULAR DYNAMICS SIMULATIONS ON LOCAL STRUCTURE AND ELECTRONIC PROPERTIES IN LIQUIDSbFROM 913 K TO 1193 K. International Journal of Modern Physics B, 2013, 27, 1350012.	1.0	6
15767	Adsorption and Diffusion of Oxygen Atoms on a Pt(211) Stepped Surface. Journal of Physical Chemistry C, 2013, 117, 9772-9778.	1.5	24
15768	Ab initio study of single-crystalline and polycrystalline elastic properties of Mg-substituted calcite crystals. Journal of the Mechanical Behavior of Biomedical Materials, 2013, 20, 296-304.	1.5	32
15769	Insights into the adsorption and energy transfer of Ag clusters on the AgCl(100) surface. Physical Chemistry Chemical Physics, 2013, 15, 8722.	1.3	48
15770	Optically Controlled Switching of the Charge State of a Single Nitrogen-Vacancy Center in Diamond at Cryogenic Temperatures. Physical Review Letters, 2013, 110, 167402.	2.9	179
15771	New form of polymeric nitrogen from dynamic shock simulation. Journal of Chemical Physics, 2013, 138, 054503.	1.2	9
15772	Prediction of ferroelectric stability and magnetoelectric effect of asymmetric multiferroic tunnel junctions. Applied Physics Letters, 2013, 102, 152906.	1.5	8
15773	Tunable Band Gap Photoluminescence from Atomically Thin Transition-Metal Dichalcogenide Alloys. ACS Nano, 2013, 7, 4610-4616.	7.3	543

#	Article	IF	Citations
15774	High-performance giant-magnetoresistance junctions based on the all-Heusler architecture with matched energy bands and Fermi surfaces. Applied Physics Letters, 2013, 102, 152403.	1.5	15
15775	Structural and electronic properties of ultrathin copper nanowires: A density-functional theory study. Physica B: Condensed Matter, 2013, 410, 105-111.	1.3	11
15776	First-principles study on the structural stability and electronic properties of AlN/GaN heterostructure nanoribbons. Superlattices and Microstructures, 2013, 57, 37-43.	1.4	2
15777	Graphene layers on Cu and Ni (111) surfaces in layer controlled graphene growth. RSC Advances, 2013, 3, 3046.	1.7	36
15778	Electronic structure and vibrational entropies of fcc Au-Fe alloys. Physical Review B, 2013, 87, .	1.1	16
15779	Site Preference and Ordering Induced by Au Substitution in the Î³-Brass Related Complex Auâ€“Crâ€“Zn Phases. Inorganic Chemistry, 2013, 52, 4812-4818.	1.9	8
15780	First-principles simulations of iron with nitrogen: from surface adsorption to bulk diffusion. Modelling and Simulation in Materials Science and Engineering, 2013, 21, 045004.	0.8	14
15781	Codetermination of crystal structures at high pressure: Combined application of theory and experiment to the intermetallic compound AuGa<mml:math xmlns:mml="http://www.w3.org/1998/Math/MathML" display="inline"><mml:msub><mml:mrow /><mml:mn>2</mml:mn></mml:msub></mml:math>. Physical Review B, 2013, 87, .	1.1	6
15782	Role of Interface in the Lithiation of Silicon-Graphene Composites: A First Principles Study. Journal of Physical Chemistry C, 2013, 117, 9598-9604.	1.5	36
15783	Dynamic Effect of Solvation on the Optical Properties of a CdTe Nanocrystal. Advanced Optical Materials, 2013, 1, 239-243.	3.6	2
15784	Stability and strength of covalent crystals under uniaxial and triaxial loading from first principles. Journal of Physics Condensed Matter, 2013, 25, 035401.	0.7	11
15785	Density Functional Study of the First Wetting Layer on the GaN (0001) Surface. Journal of Physical Chemistry C, 2013, 117, 8774-8783.	1.5	28
15786	Atomic steps on the MgO(100) surface. Physical Review B, 2013, 87, .	1.1	12
15787	Comment on â€œTwo-Dimensional Boron Monolayer Sheetsâ€• ACS Nano, 2013, 7, 879-879.	7.3	6
15788	Full band calculations of the intrinsic lower limit of contact resistivity. Applied Physics Letters, 2013, 102, .	1.5	31
15789	Computational Studies on Nonâ€covalent Interactions of Carbon and Boron Fullerenes with Graphene. ChemPhysChem, 2013, 14, 1844-1852.	1.0	25
15790	DFT study on the reaction of O2 dissociation catalyzed by gold surfaces doped with transition metal atoms. Applied Catalysis A: General, 2013, 458, 90-102.	2.2	23
15791	Structural Stability and Electronic and Magnetic Properties of Fluorinated Bilayer Graphene. Journal of Physical Chemistry C, 2013, 117, 3572-3579.	1.5	38

#	Article	IF	Citations
15792	Novel half-metal and spin gapless semiconductor properties in N-doped silicene nanoribbons. Journal of Applied Physics, 2013, 113, .	1.1	37
15793	Silicene beyond mono-layersâ€"different stacking configurations and their properties. Journal of Physics Condensed Matter, 2013, 25, 085508.	0.7	74
15794	He, Kr and Xe diffusion in ZrN â€“ An atomic scale study. Journal of Nuclear Materials, 2013, 438, 7-14.	1.3	12
15795	Nitrogen: unraveling the secret to stable carbon-supported Pt-alloy electrocatalysts. Energy and Environmental Science, 2013, 6, 2957.	15.6	99
15796	Characterization of sodium ion electrochemical reaction with tin anodes: Experiment and theory. Journal of Power Sources, 2013, 234, 48-59.	4.0	186
15797	Interaction and electronic structures of oxygen divacancy in HfO₂. Physica Status Solidi (B): Basic Research, 2013, 250, 352-355.	0.7	16
15798	Dual behavior of excess electrons in rutile TiO₂. Physica Status Solidi - Rapid Research Letters, 2013, 7, 199-203.	1.2	140
15799	Carrier Mobility in Graphyne Should Be Even Larger than That in Graphene: A Theoretical Prediction. Journal of Physical Chemistry Letters, 2013, 4, 1443-1448.	2.1	328
15800	Direct visualization of reversible dynamics in a Si6 cluster embedded in a graphene pore. Nature Communications, 2013, 4, 1650.	5.8	104
15801	Degenerate n-Doping of Few-Layer Transition Metal Dichalcogenides by Potassium. Nano Letters, 2013, 13, 1991-1995.	4.5	651
15802	Understanding the Electronic Structures of Graphene Quantum Dot Physisorption and Chemisorption onto the TiO₂ (110) Surface: A Firstâ€Principles Calculation. ChemPhysChem, 2013, 14, 579-582.	1.0	36
15803	Scalable and Effective Enrichment of Semiconducting Single-Walled Carbon Nanotubes by a Dual Selective Naphthalene-Based Azo Dispersant. Journal of the American Chemical Society, 2013, 135, 5569-5581.	6.6	36
15804	Quantitative experimental determination of site-specific magnetic structures by transmitted electrons. Nature Communications, 2013, 4, 1395.	5.8	66
15805	Carbon clusters near the step of Rh surface: implication for the initial stage of graphene nucleation. European Physical Journal D, 2013, 67, 1.	0.6	6
15806	Electronic properties of the MoS<mml:math xmlns:mml="http://www.w3.org/1998/Math/MathML" display="inline"><mml:msub><mml:mrow /><mml:mn>2</mml:mn></mml:msub></mml:math>-WS<mml:math xmlns:mml="http://www.w3.org/1998/Math/MathML" display="inline"><mml:msub><mml:mrow /><mml:mn>2</mml:mn></mml:msub></mml:math>heterojunction. Physical Review B, 2013, 87, .	1.1	424
15807	Phonon Lifetime Investigation of Anharmonicity and Thermal Conductivity of<mml:math xmlns:mml="http://www.w3.org/1998/Math/MathML" display="inline"><mml:msub><mml:mi>UO</mml:mi><mml:mn>2</mml:mn></mml:msub></mml:math>by Neutron Scattering and Theory. Physical Review Letters, 2013, 110, 157401.	2.9	132
15808	Band Gap Bowing at Nanoscale: Investigation of CdS_xSe_{1â€“x} Alloy Quantum Dots through Cyclic Voltammetry and Density Functional Theory. Journal of Physical Chemistry C, 2013, 117, 7376-7383.	1.5	52
15809	Assessment of density functionals for van der Waals complexes of sodium and benzene. Molecular Physics, 2013, 111, 1211-1218.	0.8	5

#	Article	IF	Citations
15810	A Systematic Investigation of p-Nitrophenol Reduction by Bimetallic Dendrimer Encapsulated Nanoparticles. Journal of Physical Chemistry C, 2013, 117, 7598-7604.	1.5	349
15811	Charging of Gold Atoms on Doped MgO and CaO: Identifying the Key Parameters by DFT Calculations. Journal of Physical Chemistry C, 2013, 117, 9943-9951.	1.5	45
15812	Initial-stage behaviors of tin and lead adsorption on vanadium surface oxide nanomesh on Pd(111). Surface Science, 2013, 613, 35-39.	0.8	0
15813	Pressure-Induced Stabilization and Insulator-Superconductor Transition of BH. Physical Review Letters, 2013, 110, 165504.	2.9	76
15814	Superionic to Superionic Phase Change in Water: Consequences for the Interiors of Uranus and Neptune. Physical Review Letters, 2013, 110, 151102.	2.9	80
15815	Quantum chemical elucidation of the mechanism for hydrogenation of TiO2 anatase crystals. Journal of Chemical Physics, 2013, 138, 154705.	1.2	35
15816	Stability and physical properties of a tri-ring based porous g-C4N3 sheet. Physical Chemistry Chemical Physics, 2013, 15, 7142.	1.3	64
15817	Active Sites of Pd-Doped Flat and Stepped Cu(111) Surfaces for H₂ Dissociation in Heterogeneous Catalytic Hydrogenation. ACS Catalysis, 2013, 3, 1245-1252.	5.5	79
15818	Computational discovery of single-layer III-V materials. Physical Review B, 2013, 87, .	1.1	318
15819	Ion Impacts on Graphene/Ir(111): Interface Channeling, Vacancy Funnels, and a Nanomesh. Nano Letters, 2013, 13, 1948-1955.	4.5	81
15820	CO adsorption on the Ni2Pb/Ni(111) surface alloy: A DFT study. Applied Surface Science, 2013, 267, 4-7.	3.1	7
15821	Tkatchenko-Scheffler van der Waals correction method with and without self-consistent screening applied to solids. Physical Review B, 2013, 87, .	1.1	293
15822	Structure, Stability, and Property Modulations of Stoichiometric Graphene Oxide. Journal of Physical Chemistry C, 2013, 117, 1064-1070.	1.5	22
15823	Novel mercury selenidoantimonates with structures ranging from one-dimensional ribbon to three-dimensional open-framework. Dalton Transactions, 2013, 42, 5454.	1.6	17
15824	Hydrogen behaviors in molybdenum and tungsten and a generic vacancy trapping mechanism for H bubble formation. Journal of Nuclear Materials, 2013, 434, 395-401.	1.3	74
15825	Atomistic Theory of Ostwald Ripening and Disintegration of Supported Metal Particles under Reaction Conditions. Journal of the American Chemical Society, 2013, 135, 1760-1771.	6.6	352
15826	Graphene surface induced specific self-assembly of poly(3-hexylthiophene) for nanohybrid optoelectronics: from first-principles calculation to experimental characterizations. Soft Matter, 2013, 9, 5355.	1.2	50
15827	Equations of state and transport properties of warm dense beryllium: A quantum molecular dynamics study. Physical Review E, 2013, 87, 043105.	0.8	18

#	Article	IF	Citations
15828	Topâ€“down fabrication of sub-nanometre semiconducting nanoribbons derived from molybdenum disulfide sheets. Nature Communications, 2013, 4, 1776.	5.8	220
15829	Visible-light-responsive copper(<scp>ii</scp>) borate photocatalysts with intrinsic midgap states for water splitting. Journal of Materials Chemistry A, 2013, 1, 1553-1556.	5.2	38
15830	Defect engineering of BaSnO<mml:math xmlns:mml="http://www.w3.org/1998/Math/MathML" display="inline"><mml:msub><mml:mrow /><mml:mn>3</mml:mn></mml:msub></mml:math>for high-performance transparent conducting oxide applications. Physical Review B, 2013, 87, .	1.1	183
15831	Grain-boundary structural transformation induced by geometry and chemistry. Physical Review B, 2013, 87, .	1.1	14
15832	Ab initio Probing of Magnetic and Electronic Properties of Monoclinic Îµ-WO3 Doped with 3d Transition Metals Within GGA and GGA+U. Journal of Superconductivity and Novel Magnetism, 2013, 26, 2343-2346.	0.8	1
15833	Giant magnetic moments of B and C doped cuboctahedral Mn13 clusters. Nanoscale, 2013, 5, 2114.	2.8	5
15834	Magnetism of Cu<mml:math xmlns:mml="http://www.w3.org/1998/Math/MathML" display="inline"><mml:msub><mml:mi>X</mml:mi><mml:mn>2</mml:mn></mml:msub></mml:math>frustrated chains (<mml:math xmlns:mml="http://www.w3.org/1998/Math/MathML") Tj ETQq0 0 0 rgBT /Overlock 10 Tf 50 497 Td (display="inline" 2013, 87, .	1.1	14
15835	Comparative Investigation of Benzene Steam Reforming over Spinel Supported Rh and Ir Catalysts. ACS Catalysis, 2013, 3, 1133-1143.	5.5	39
15836	Effect of van der Waals Interactions on the Adsorption of Olympicene Radical on Cu(111): Characteristics of Weak Physisorption versus Strong Chemisorption. Journal of Physical Chemistry C, 2013, 117, 2893-2902.	1.5	52
15837	Silicene on Substrates: A Way To Preserve or Tune Its Electronic Properties. Journal of Physical Chemistry C, 2013, 117, 10353-10359.	1.5	237
15838	Novel stable compounds in the Mgâ€“O system under high pressure. Physical Chemistry Chemical Physics, 2013, 15, 7696.	1.3	102
15839	An advanced cathode for Na-ion batteries with high rate and excellent structural stability. Physical Chemistry Chemical Physics, 2013, 15, 3304.	1.3	501
15840	Thermodynamics of Tiâ€“Ni shape memory alloys. Calphad: Computer Coupling of Phase Diagrams and Thermochemistry, 2013, 41, 128-139.	0.7	40
15841	Electronic Structure of Semiconducting and Metallic Tubes in TiO₂/Carbon Nanotube Heterojunctions: Density Functional Theory Calculations. Journal of Physical Chemistry Letters, 2013, 4, 1340-1346.	2.1	55
15842	Selective Semihydrogenation of Alkynes on Shapeâ€Controlled Palladium Nanocrystals. Chemistry - an Asian Journal, 2013, 8, 919-925.	1.7	39
15843	Density functional theory study on the adsorption and decomposition of the formic acid catalyzed by highly active mushroom-like Au@Pd@Pt tri-metallic nanoparticles. Physical Chemistry Chemical Physics, 2013, 15, 4625.	1.3	22
15844	Coupled polaron-phonon effects on Seebeck coefficient and lattice conductivity of B<mml:math xmlns:mml="http://www.w3.org/1998/Math/MathML" display="inline"><mml:msub><mml:mrow /><mml:mn>13</mml:mn></mml:msub></mml:math>C<mml:math xmlns:mml="http://www.w3.org/1998/Math/MathML" display="inline"><mml:msub><mml:mrow /><mml:mn>2</mml:mn></mml:msub></mml:math>from first principles. Physical Review B, 2013, 87, .	1.1	8
15845	Comprehensive examination of dopants and defects in BaTiO<mml:math xmlns:mml="http://www.w3.org/1998/Math/MathML" display="inline"><mml:msub><mml:mrow /><mml:mn>3</mml:mn></mml:msub></mml:math>from first principles. Physical Review B, 2013, 87, .	1.1	43

#	Article	IF	Citations
15846	Designing band gap of graphene by B and N dopant atoms. RSC Advances, 2013, 3, 802-812.	1.7	396
15847	DFT+U Study of Molecular and Dissociative Water Adsorptions on the Fe₃O₄(110) Surface. Journal of Physical Chemistry C, 2013, 117, 7648-7655.	1.5	46
15848	Graphene-analogous low-dimensional materials. Progress in Materials Science, 2013, 58, 1244-1315.	16.0	684
15849	Effect of local metal microstructure on adsorption on bimetallic surfaces: Atomic nitrogen on Ni/Pt(111). Journal of Chemical Physics, 2013, 138, 174702.	1.2	21
15850	Effect of Packing on Formation of Deep Carrier Traps in Amorphous Conjugated Polymers. Journal of Physical Chemistry Letters, 2013, 4, 1453-1459.	2.1	16
15851	Parameterization of Reactive Force Field: Dynamics of the [Nb6O19Hx](8â€“x)â€“ Lindqvist Polyoxoanion in Bulk Water. Journal of Physical Chemistry A, 2013, 117, 6967-6974.	1.1	11
15852	Quantum Zeno Effect Rationalizes the Phonon Bottleneck in Semiconductor Quantum Dots. Physical Review Letters, 2013, 110, 180404.	2.9	230
15853	Isomers of C12N12 as potential hydrogen storage materials and the effect of the electric field therein. RSC Advances, 2013, 3, 6991.	1.7	12
15854	Î²-MnO2 as a cathode material for lithium ion batteries from first principles calculations. Physical Chemistry Chemical Physics, 2013, 15, 9075.	1.3	74
15855	Theoretical study on the reactivity of the surface of pure oxides: The Influence of the support and oxygen vacancies. Applied Surface Science, 2013, 274, 1-6.	3.1	11
15856	Effective increasing of optical absorption of TiO2 by introducing trivalent titanium. Applied Physics Letters, 2013, 102, .	1.5	14
15857	Silicon clathrates as anode materials for lithium ion batteries?. Journal of Materials Chemistry A, 2013, 1, 7782.	5.2	42
15858	Defect Thermodynamics and Diffusion Mechanisms in Li₂CO₃ and Implications for the Solid Electrolyte Interphase in Li-Ion Batteries. Journal of Physical Chemistry C, 2013, 117, 8579-8593.	1.5	228
15859	Nanostructured Electrocatalysts for Oxygen Reduction Reaction: First-Principles Computational Insights. Lecture Notes in Energy, 2013, , 613-635.	0.2	0
15860	Scalable Patterning of One-Dimensional Dangling Bond Rows on Hydrogenated Si(001). ACS Nano, 2013, 7, 4422-4428.	7.3	13
15861	Mechanism of Framework Oxygen Exchange in Feâ€Zeolites: A Combined DFT and Mass Spectrometry Study. ChemPhysChem, 2013, 14, 520-531.	1.0	10
15862	The most stable crystal structure and the formation processes of an order-disorder (OD) intermetallic phase in the Mgâ€“Alâ€“Gd ternary system. Philosophical Magazine, 2013, 93, 2826-2846.	0.7	45
15863	STM imaging, spectroscopy and manipulation of a self-assembled PTCDI monolayer on epitaxial graphene. Physical Chemistry Chemical Physics, 2013, 15, 4939.	1.3	23

#	Article	IF	Citations
15864	Xâ€ray Crystallographic and Firstâ€Principles Theoretical Studies of K₂[TcOCl₅] and UV/Vis Investigation of the [TcOCl₅]^{2â€“} and [TcOCl₄]^{â€“} Ions. European Journal of Inorganic Chemistry, 2013, 2013, 1097-1104.	1.0	3
15865	The dissociative chemisorption of methane on Ni(111): The effects of molecular vibration and lattice motion. Journal of Chemical Physics, 2013, 138, 174705.	1.2	95
15866	Role of screening in the density functional applied to transition-metal defects in semiconductors. Physical Review B, 2013, 87, .	1.1	35
15867	First-principles calculations of the vacancy defects in BiOF as cathode materials for Li-ion batteries. Computational Materials Science, 2013, 74, 50-54.	1.4	10
15868	High temperature defect chemistry in layered lithium transition-metal oxides based on first-principles calculations. Journal of Power Sources, 2013, 244, 592-596.	4.0	16
15869	Surfaces of intermetallic compounds: Anab initioDFT study for B20-type AlPd. Physical Review B, 2013, 87, .	1.1	18
15870	Band structure and optical transitions in atomic layers of hexagonal gallium chalcogenides. Physical Review B, 2013, 87, .	1.1	181
15871	Theoretical Prediction of Multiferroicity in SmBaMn₂O₆. Journal of the Physical Society of Japan, 2013, 82, 043702.	0.7	15
15872	Ab initio study of the stable phases of 1:1 tantalum nitride. Acta Materialia, 2013, 61, 3799-3807.	3.8	28
15873	Square-lattice magnetism of diabolette Pb<mml:math xmlns:mml="http://www.w3.org/1998/Math/MathML" display="inline"><mml:msub><mml:mrow /><mml:mn>2</mml:mn></mml:msub></mml:math>Cu(OH)<mml:math xmlns:mml="http://www.w3.org/1998/Math/MathML" display="inline"><mml:msub><mml:mrow /><mml:mn>4</mml:mn></mml:msub></mml:math>Cl<mml:math xmlns:mml="http://www.w3.org/1998/Math/MathML" display="inline"><mml:msub><mml:mrow /></mml:msub></mml:math>	1.1	23
15874	Exploration of Structures of Two-Dimensional Boronâ€“Silicon Compounds with sp² Silicon. Journal of Physical Chemistry Letters, 2013, 4, 561-567.	2.1	75
15875	First-principles study of temperature-dependent diffusion coefficients: Hydrogen, deuterium, and tritium in Î±-Ti. Journal of Applied Physics, 2013, 113, .	1.1	26
15876	The equation of state for hydrogen at high densities. High Energy Density Physics, 2013, 9, 448-456.	0.4	15
15877	Simultaneous Measurement of Force and Conductance Across Single Molecule Junctions. Conference Proceedings of the Society for Experimental Mechanics, 2013, , 75-84.	0.3	0
15878	Toward Single-Layer Uniform Hexagonal Boron Nitrideâ€“Graphene Patchworks with Zigzag Linking Edges. Nano Letters, 2013, 13, 3439-3443.	4.5	242
15879	Atomic-Scale Observation of Lithiation Reaction Front in Nanoscale SnO₂ Materials. ACS Nano, 2013, 7, 6203-6211.	7.3	134
15880	Development of a ReaxFF Reactive Force Field for Titanium Dioxide/Water Systems. Langmuir, 2013, 29, 7838-7846.	1.6	96
15881	Acrolein Hydrogenation on Ni(111). Journal of Physical Chemistry C, 2013, 117, 12715-12724.	1.5	14

#	Article	IF	Citations
15882	An experimental and first-principles study of the effect of B/N doping in TiO2 thin films for visible light photo-catalysis. Journal of Photochemistry and Photobiology A: Chemistry, 2013, 254, 25-34.	2.0	27
15883	Template-directed assembly of pentacene molecules on epitaxial graphene on Ru(0001). Nano Research, 2013, 6, 131-137.	5.8	31
15884	Ab initioinvestigations of the strontium gallium nitride ternaries Sr₃GaN₃and Sr₆GaN₅: promising materials for optoelectronic. Semiconductor Science and Technology, 2013, 28, 085005.	1.0	6
15885	Enhancement of the Thermoelectric Performance of Bi0.4Sb1.6Te3 Alloys by In and Ga Doping. Journal of Electronic Materials, 2013, 42, 1617-1621.	1.0	24
15886	First-principles study of structural, elastic, electronic, vibrational and thermodynamic properties of UN. Journal of Nuclear Materials, 2013, 440, 63-69.	1.3	37
15887	First-principles analysis of MoS<mml:math xmlns:mml="http://www.w3.org/1998/Math/MathML" display="inline"><mml:msub><mml:mrow /><mml:mn>2</mml:mn></mml:msub></mml:math>/Ti<mml:math xmlns:mml="http://www.w3.org/1998/Math/MathML" display="inline"><mml:msub><mml:mrow /><mml:mn>2</mml:mn></mml:msub></mml:math>C and MoS<mml:math xmlns:mml="http://www.w3.org/1998/Math/MathML" display="inline"><mml:msub><mml:mrow />	1.1	166
15888	Electronically Induced Ferromagnetic Transitions inSm5Ge4-Type Magnetoresponsive Phases. Physical Review Letters, 2013, 110, 077204.	2.9	12
15889	Solute effect on oxygen diffusion in Î±-titanium. Journal of Applied Physics, 2013, 113, .	1.1	15
15890	Electronic structure of III-V zinc-blende semiconductors from first principles. Physical Review B, 2013, 87, .	1.1	47
15891	Interactions of platinum clusters with a graphite substrate. Physical Chemistry Chemical Physics, 2013, 15, 11950.	1.3	66
15892	Energy Level Alignment and Charge Carrier Mobility in Noncovalently Functionalized Graphene. Journal of Physical Chemistry Letters, 2013, 4, 2158-2165.	2.1	83
15893	Observation of He bubbles in ion irradiated fusion materials by conductive atomic force microscopy. Journal of Nuclear Materials, 2013, 441, 54-58.	1.3	11
15894	First-principles study of single-layer C-terminated BN quantum dots. Physica E: Low-Dimensional Systems and Nanostructures, 2013, 53, 115-119.	1.3	2
15895	â€œIn-Silico Seedingâ€• Isostructurality and Pseudoisostructurality in a Family of Aspirin Derivatives. Crystal Growth and Design, 2013, 13, 2906-2915.	1.4	7
15896	Orientation-dependent binding energy of graphene on palladium. Applied Physics Letters, 2013, 102, 051606.	1.5	10
15897	Self-interstitial defects in hexagonal close packed metals revisited: Evidence for low-symmetry configurations in Ti, Zr, and Hf. Physical Review B, 2013, 87, .	1.1	66
15898	Interfacial bonding and electronic structure of HfO2/GaSb interfaces: A first principles study. Applied Physics Letters, 2013, 102, 022901.	1.5	18
15899	Selective Hydrodeoxygenation of Biomassâ€Derived Oxygenates to Unsaturated Hydrocarbons using Molybdenum Carbide Catalysts. ChemSusChem, 2013, 6, 798-801.	3.6	173

#	Article	IF	Citations
15900	Antibacterial and photocatalytic activity of TiO2 and ZnO nanomaterials in phosphate buffer and saline solution. Applied Microbiology and Biotechnology, 2013, 97, 5565-5573.	1.7	38
15901	Surface work function of chemically derived graphene: A first-principles study. Physics Letters, Section A: General, Atomic and Solid State Physics, 2013, 377, 1760-1765.	0.9	7
15902	Origin of Novel Diffusions of Cu and Ag in Semiconductors: The Case of CdTe. Physical Review Letters, 2013, 110, 235901.	2.9	49
15903	CsCdInQ₃ (Q = Se, Te): New Photoconductive Compounds As Potential Materials for Hard Radiation Detection. Chemistry of Materials, 2013, 25, 2089-2099.	3.2	50
15904	Structures, phase stabilities, and electrical potentials of Li-Si battery anode materials. Physical Review B, 2013, 87, .	1.1	41
15905	Screened Coulomb Hybrid DFT Study on Electronic Structure and Optical Properties of Anionic and Cationic Te-Doped Anatase TiO₂. Journal of Physical Chemistry C, 2013, 117, 12942-12948.	1.5	28
15906	First principles calculations of the structure and elastic constants of Î±, Î² and Î³ uranium. Journal of Nuclear Materials, 2013, 433, 143-151.	1.3	91
15907	Periodic Density-Functional Calculations on Work-Function Change Induced by Adsorption of Halogens on Cu(111). Physical Review Letters, 2013, 110, 156804.	2.9	81
15908	Comparison of the Binding of Polyvinylpyrrolidone and Polyethylene Oxide to Ag Surfaces: Elements of a Successful Structure-Directing Agent. Journal of Physical Chemistry C, 2013, 117, 11444-11448.	1.5	35
15909	The mechanical and thermo-physical properties and electronic structures of SnS and SnSe in orthorhombic structure. Journal of Alloys and Compounds, 2013, 556, 86-93.	2.8	45
15910	First-principles study of the structural stability of cubic, tetragonal and hexagonal phases in Mn₃Z (Z=Ga, Sn and Ge) Heusler compounds. Journal of Physics Condensed Matter, 2013, 25, 206006.	0.7	67
15911	Half-Metallic and Magnetic Silicon Nanowires Functionalized by Transition-Metal Atoms. Springer Series in Materials Science, 2013, , 149-169.	0.4	1
15912	Cation Size Mismatch and Charge Interactions Drive Dopant Segregation at the Surfaces of Manganite Perovskites. Journal of the American Chemical Society, 2013, 135, 7909-7925.	6.6	468
15913	Structural, electronic and optical properties of silver delafossite oxides: A first-principles study with hybrid functional. Physica B: Condensed Matter, 2013, 422, 20-27.	1.3	12
15914	Electroreduction of Carbon Dioxide to Methane on Copper, Copperâ€“Silver, and Copperâ€“Gold Catalysts: A DFT Study. Journal of Physical Chemistry C, 2013, 117, 8262-8268.	1.5	87
15915	Deposition of (WO3)3 nanoclusters on the MgO(001) surface: A possible way to identify the charge states of the defect centers. Journal of Chemical Physics, 2013, 138, 034711.	1.2	9
15916	Atomistic Modelling and Simulation of Warm Dense Matter. Conductivity and Reflectivity. Contributions To Plasma Physics, 2013, 53, 300-310.	0.5	25
15917	Two-Dimensional Hexagonal Beryllium Sulfide Crystal. Journal of Physical Chemistry Letters, 2013, 4, 1856-1860.	2.1	38

#	Article	IF	Citations
15918	Study of the magnetic and electronic properties of nanocrystalline PrCo3by neutron powder diffraction and density functional theory. Journal of Physics Condensed Matter, 2013, 25, 116001.	0.7	13
15919	Experimental and Theoretical Comparison of Gas Desorption Energies on Metallic and Semiconducting Single-Walled Carbon Nanotubes. Journal of the American Chemical Society, 2013, 135, 7768-7776.	6.6	20
15920	Mn-doped monolayer MoS<mml:math xmlns:mml="http://www.w3.org/1998/Math/MathML" display="inline"><mml:msub><mml:mrow /><mml:mn>2</mml:mn></mml:msub></mml:math>: An atomically thin dilute magnetic semiconductor. Physical Review B, 2013, 87, .	1.1	413
15921	Structure, Energetic and Tribological Properties, and Possible Applications in Nanoelectromechanical Systems of Argon-Separated Double-Layer Graphene. Journal of Physical Chemistry C, 2013, 117, 11428-11435.	1.5	7
15922	First-principles study of possible shallow donors in ZnAl<mml:math xmlns:mml="http://www.w3.org/1998/Math/MathML" display="inline"><mml:msub><mml:mrow /><mml:mn>2</mml:mn></mml:msub></mml:math>O<mml:math xmlns:mml="http://www.w3.org/1998/Math/MathML" display="inline"><mml:msub><mml:mrow /><mml:mn>2</mml:mn></mml:msub></mml:math>. Physica B: Condensed Matter, 2013, 417, 67.	1.1	55
15923	Structure, Energetic and Tribological Properties, and Possible Applications in Nanoelectromechanical Systems of Argon-Separated Double-Layer Graphene. Journal of Physical Chemistry C, 2013, 117, 11428-11435.	1.1	26
15924	Novel Soft-Chemistry Route of Ag₂Mo₃O₁₀Â·2H₂O Nanowires and in Situ Photogeneration of a Ag@Ag₂Mo₃O₁₀Â·2H₂O Plasmonic Heterostructure. Inorganic Chemistry, 2013, 52, 6440-6449.	1.9	29
15925	Reversible Intercalation of Hexagonal Boron Nitride with BrÃ¸nsted Acids. Journal of the American Chemical Society, 2013, 135, 8372-8381.	6.6	88
15926	Local Structure of Proton-Conducting Lanthanum Tungstate La_{28â€“x}W_{4+x}O_{54+Î´}: a Combined Density Functional Theory and Pair Distribution Function Study. Chemistry of Materials, 2013, 25, 2378-2384.	3.2	25
15927	Ethanol Photoreaction on RuO_x/Ru-Modified TiO₂(110). Journal of Physical Chemistry C, 2013, 117, 11149-11158.	1.5	34
15928	Elastic properties of tetragonal BiFeO3 from first-principles calculations. Applied Physics Letters, 2013, 102, .	1.5	55
15929	First-Principles Investigation of Selective Oxidation of Propane on Clean and Sulfided V₂O₅ (010) Surfaces. Journal of Physical Chemistry C, 2013, 117, 11258-11274.	1.5	10
15930	Theoretical prediction of hydrogen storage on Li-decorated boron nitride atomic chains. Journal of Applied Physics, 2013, 113, .	1.1	17
15931	KAg11(VO4)4 as a candidate p-type transparent conducting oxide. Journal of Chemical Physics, 2013, 138, 194703.	1.2	6
15932	First principles assessment of perovskite dopants for proton conductors with chemical stability and high conductivity. RSC Advances, 2013, 3, 3333.	1.7	28
15933	Stability, electronic structures and transport properties of armchair (10, 10) BN/C nanotubes. Journal of Solid State Chemistry, 2013, 200, 294-298.	1.4	10
15934	Electrocatalytic Reduction of Nitrate on a Pt Electrode Modified by pâ€Block Metal Adatoms in Acid Solution. ChemCatChem, 2013, 5, 1773-1783.	1.8	45
15935	Electronic and optical properties of nanocrystalline WO₃thin films studied by optical spectroscopy and density functional calculations. Journal of Physics Condensed Matter, 2013, 25, 205502.	0.7	43

#	Article	IF	Citations
15936	Magnetic Coupling of Porphyrin Molecules Through Graphene. Advanced Materials, 2013, 25, 3473-3477.	11.1	72
15937	Cation and magnetic orders in MnFe2O4 from density functional calculations. Journal of Applied Physics, 2013, 113, .	1.1	46
15938	Reconstruction of Clean and Oxygen-Covered Pt(110) Surfaces. Journal of Physical Chemistry C, 2013, 117, 11251-11257.	1.5	24
15939	Electronic structure and quantum dynamics of photoinitiated dissociation of O2 on rutile TiO2 nanocluster. Journal of Chemical Physics, 2013, 138, 194705.	1.2	5
15940	Effect of surface reconstruction on the electronic structure of ZnO(0001). Physical Review B, 2013, 87, .	1.1	21
15941	Direct atomic-scale confirmation of three-phase storage mechanism in Li4Ti5O12 anodes for room-temperature sodium-ion batteries. Nature Communications, 2013, 4, 1870.	5.8	628
15942	CO-Induced Smoluchowski Ripening of Pt Cluster Arrays on the Graphene/Ir(111) MoirÃ©. ACS Nano, 2013, 7, 2020-2031.	7.3	62
15943	Theoretical Study on the Structure and Energetics of Cd Insertion and Cu Depletion of CuIn5Se8. Journal of Physical Chemistry C, 2013, 117, 10892-10900.	1.5	24
15944	Synthesis, Crystal Structure, and Physical Properties of Sr₂FeOsO₆. Inorganic Chemistry, 2013, 52, 6713-6719.	1.9	68
15945	On the properties of binary rutile MO2 compounds, M = Ir, Ru, Sn, and Ti: A DFT study. Journal of Chemical Physics, 2013, 138, 194706.	1.2	50
15946	Mechanisms of Atomic Motion Through Crystalline GeTe. Chemistry of Materials, 2013, 25, 2220-2226.	3.2	38
15947	Nanostructuring of Î²-MnO₂: The Important Role of Surface to Bulk Ion Migration. Chemistry of Materials, 2013, 25, 536-541.	3.2	99
15948	Impurity-related degradation in a prototype organic photovoltaic material: A first-principles study. Organic Electronics, 2013, 14, 1242-1248.	1.4	10
15949	Growth of Single- and Bilayer ZnO on Au(111) and Interaction with Copper. Journal of Physical Chemistry C, 2013, 117, 11211-11218.	1.5	108
15950	Active Oxygen Vacancy Site for Methanol Synthesis from CO₂ Hydrogenation on In₂O₃(110): A DFT Study. ACS Catalysis, 2013, 3, 1296-1306.	5.5	530
15951	Giant Molecular Magnetocapacitance. Physical Review Letters, 2013, 110, 217205.	2.9	15
15952	Absence of Metallicity in K-doped Picene: Importance of Electronic Correlations. Physical Review Letters, 2013, 110, 216403.	2.9	53
15953	Growth Intermediates for CVD Graphene on Cu(111): Carbon Clusters and Defective Graphene. Journal of the American Chemical Society, 2013, 135, 8409-8414.	6.6	132

#	Article	IF	Citations
15954	Element-specific quantitative determination of the local atomic order in CoPt alloy nanoparticles: Experiment and theory. Physical Review B, 2013, 87, .	1.1	33
15955	Computational modelling of inorganic solids. Annual Reports on the Progress of Chemistry Section A, 2013, 109, 421.	0.8	3
15956	Electronic and elastic properties of yttrium gallium garnet under pressure fromab initiostudies. Journal of Applied Physics, 2013, 113, 183505.	1.1	19
15957	Temperature and pressure dependent geometry optimization and elastic constant calculations for arbitrary symmetry crystals: Applications to MgSiO3 perovskites. Journal of Applied Physics, 2013, 113, .	1.1	23
15958	Defect segregation at grain boundary and its impact on photovoltaic performance of CuInSe2. Applied Physics Letters, 2013, 102, .	1.5	50
15959	Mg-doped VO2 nanoparticles: hydrothermal synthesis, enhanced visible transmittance and decreased metalâ€“insulator transition temperature. Physical Chemistry Chemical Physics, 2013, 15, 7505.	1.3	178
15960	Role of high-order electromechanical coupling terms in thermodynamics of ferroelectric thin films. Physical Review B, 2013, 87, .	1.1	27
15961	Phase Behavior of Ag₂CrO₄ under Compression: Structural, Vibrational, and Optical Properties. Journal of Physical Chemistry C, 2013, 117, 12239-12248.	1.5	23
15962	CO Chemisorption and Dissociation at High Coverages during CO Hydrogenation on Ru Catalysts. Journal of the American Chemical Society, 2013, 135, 6107-6121.	6.6	204
15963	Caffeine Confinement into a Series of Functionalized Porous Zirconium MOFs: A Joint Experimental/Modeling Exploration. Journal of Physical Chemistry C, 2013, 117, 11694-11704.	1.5	70
15964	Insight into the Preference Mechanism of CH_x (x = 1â€“3) and Câ€“C Chain Formation Involved in C₂ Oxygenate Formation from Syngas on the Cu(110) Surface. Journal of Physical Chemistry C, 2013, 117, 6594-6606.	1.5	59
15965	Endohedral Metallofullerenes Containing Lanthanides: A Robust Yet Simple Computational Approach. Journal of Physical Chemistry C, 2013, 117, 12916-12921.	1.5	15
15966	Sum-Frequency-Generation Vibration Spectroscopy and Density Functional Theory Calculations with Dispersion Corrections (DFT-D2) for Cellulose Iα and Iβ. Journal of Physical Chemistry B, 2013, 117, 6681-6692.	1.2	90
15967	Carbon dioxide activation and dissociation on ceria (110): A density functional theory study. Journal of Chemical Physics, 2013, 138, 014702.	1.2	141
15968	Scanning Tunneling Microscopy and Density Functional Theory Studies of Adatom-Involved Adsorption of Methylnitrene on Copper(110) Surface. Journal of Physical Chemistry C, 2013, 117, 12111-12116.	1.5	5
15969	Formation and Healing of Vacancies in Graphene Chemical Vapor Deposition (CVD) Growth. Journal of the American Chemical Society, 2013, 135, 4476-4482.	6.6	91
15970	Oxygen vacancy-mediated room-temperature ferromagnetism in insulating cobalt-substituted SrTiO<mml:math xmlns:mml="http://www.w3.org/1998/Math/MathML" display="inline"><mml:msub><mml:mrow /><mml:mn>3</mml:mn></mml:msub></mml:math>epitaxially integrated with silicon. Physical Review B, 2013, 87, .	1.1	26
15971	Wetting at the BaTiO3/Pt interface. Journal of Applied Physics, 2013, 113, 184102.	1.1	10

#	Article	IF	Citations
15972	In Situ Growth of Cellular Two-Dimensional Silicon Oxide on Metal Substrates. ACS Nano, 2013, 7, 5175-5180.	7.3	31
15973	In Situ Raman Study of Phase Stability of Î±-Li₃V₂(PO₄)₃ upon Thermal and Laser Heating. Journal of Physical Chemistry C, 2013, 117, 11994-12002.	1.5	39
15974	Orbital-selective charge transfer at oxygen-deficient LaAlO<mml:math xmlns:mml="http://www.w3.org/1998/Math/MathML" display="inline"><mml:msub><mml:mrow /><mml:mn>3</mml:mn></mml:msub></mml:math>/SrTiO<mml:math xmlns:mml="http://www.w3.org/1998/Math/MathML" display="inline"><mml:msub><mml:mrow /><mml:mn>3</mml:mn></mml:msub></mml:math>(001) interfaces. Physical Review B, 2013, 87, .	1.1	8
15975	Size Dependence in the Stabilities and Electronic Properties of Î±-Graphyne and Its Boron Nitride Analogue. Journal of Physical Chemistry C, 2013, 117, 2175-2182.	1.5	117
15976	Ab initiocalculation of optical properties with excitonic effects in wurtzite InxGa1â^'xN and InxAl1â^'xN alloys. Physical Review B, 2013, 87, .	1.1	14
15977	Crystal Structure and Local Structure of Mg2â€“xPrxNi4(x= 0.6 and 1.0) Deuteride Using in Situ Neutron Total Scattering. Inorganic Chemistry, 2013, 52, 7010-7019.	1.9	28
15978	Pressure-Induced Superconductivity in SnTe: A First-Principles Study. Journal of Physical Chemistry C, 2013, 117, 12266-12271.	1.5	31
15979	Operando Effects on the Structure and Dynamics of Pt_nSn_m/Î³-Al₂O₃ from Ab Initio Molecular Dynamics and X-ray Absorption Spectra. Journal of Physical Chemistry C, 2013, 117, 12446-12457.	1.5	33
15980	Anomalous Melting Behavior of Solid Hydrogen at High Pressures. Journal of Physical Chemistry C, 2013, 117, 11873-11877.	1.5	13
15981	Effect of Support Structure and Composition on the Catalytic Activity of Pt Nanoclusters for Methane Dehydrogenation. Industrial & Engineering Chemistry Research, 2013, 52, 15447-15454.	1.8	26
15982	Charge transfer and formation of Ce3+ upon adsorption of metal atom M (MÂ=ÂCu, Ag, Au) on CeO2 (100) surface. Journal of Power Sources, 2013, 234, 69-81.	4.0	32
15983	Comparison of stress and total energy methods for calculation of elastic properties of semiconductors. Journal of Physics Condensed Matter, 2013, 25, 025803.	0.7	30
15984	Optimized geometry and electronic structure of graphyne-like silicyne nanoribbons. Chinese Physics B, 2013, 22, 057303.	0.7	7
15985	On-Surface Formation of One-Dimensional Polyphenylene through Bergman Cyclization. Journal of the American Chemical Society, 2013, 135, 8448-8451.	6.6	154
15986	First-Principles Elucidation of Atomic Size Effects Using DFT-Chemical Pressure Analysis: Origins of Ca₃₆Sn₂₃â€™s Long-Period Superstructure. Journal of Chemical Theory and Computation, 2013, 9, 3170-3180.	2.3	32
15987	Rationale for the Higher Reactivity of Interfacial Sites in Methanol Decomposition on Au₁₃/TiO₂(110). Journal of the American Chemical Society, 2013, 135, 7629-7635.	6.6	56
15988	The catalytic synergetic effect of carbon nanotubes on CuO during advanced oxidation processes: A theoretical account. Chemical Physics Letters, 2013, 572, 53-57.	1.2	2
15989	NaBa2Cu3S5: A Doped p-Type Degenerate Semiconductor. Inorganic Chemistry, 2013, 52, 7210-7217.	1.9	16

#	Article	IF	Citations
15990	Adsorption Site Determination of a Molecular Monolayer via Inelastic Tunneling. Nano Letters, 2013, 13, 2346-2350.	4.5	17
15991	Pressure-Induced Half-Metallic Ferrimagnetism in La₂VMnO₆. Journal of Physical Chemistry C, 2013, 117, 7231-7235.	1.5	15
15992	Evolutionary method for predicting surface reconstructions with variable stoichiometry. Physical Review B, 2013, 87, .	1.1	99
15993	Work function and Young's modulus of platinum nanotubes: Density functional study. Physica Status Solidi (B): Basic Research, 2013, 250, 1519-1525.	0.7	2
15994	Periodic Trends in 3d Metal Mediated CO2 Activation. ACS Symposium Series, 2013, , 67-88.	0.5	3
15995	Visualization of Compression and Spillover in a Coadsorbed System: Syngas on Cobalt Nanoparticles. ACS Nano, 2013, 7, 4384-4392.	7.3	24
15996	Sodium Storage and Transport Properties in Layered Na₂Ti₃O₇ for Roomâ€Temperature Sodiumâ€Ion Batteries. Advanced Energy Materials, 2013, 3, 1186-1194.	10.2	456
15997	Intrinsic Mechanical Properties of 20 MAXâ€Phase Compounds. Journal of the American Ceramic Society, 2013, 96, 2292-2297.	1.9	95
15998	Cationic vacancies and anomalous spectral-weight transfer in Ti<mml:math xmlns:mml="http://www.w3.org/1998/Math/MathML" display="inline"><mml:msub><mml:mrow /><mml:mrow><mml:mn>1</mml:mn><mml:mo>â”</mml:mo><mml:mi>x</mml:mi></mml:mrow></mml:msub></mml:math>Ta<mml:math xmlns:mml="http://www.w3.org/1998/Math/MathML" display="inline"><mml:msub><mml:mrow /><mml:mi>x</mml:mi></mml:msub></mml:math>O<mml:math xmlns:mml="http://www.w3.org/1998/Math/MathML" display="inline"><mml:msub><mml:mrow /><mml:	1.1	20
15999	Bulk modulus prediction of austenitic stainless steel using a hybrid GAâ€“ANN as a data mining tools. Computational Materials Science, 2013, 77, 330-334.	1.4	16
16000	Atomic and electronic structure of La2CoMnO6 on SrTiO3 and LaAlO3 substrates from first principles. Journal of Applied Physics, 2013, 113, .	1.1	6
16001	Electronic structure and thermoelectric properties of half-Heusler Zr0.5Hf0.5NiSn by first-principles calculations. Journal of Applied Physics, 2013, 113, .	1.1	60
16002	The canonical work function-strain relationship of the platinum metal: A first-principles approach to metal-gate transistor optimization. Applied Physics Letters, 2013, 102, .	1.5	20
16003	Nonpolar GaN films on high-index silicon: Lattice matching by design. Physical Review B, 2013, 87, .	1.1	7
16004	Density Functional Theory Study of Water-Gas-Shift Reaction on 3Cu/Î±-Al2O3(0001) Surface. Journal of Physical Chemistry C, 2013, 117, 12045-12053.	1.5	10
16005	Four-States Multiferroic Memory Embodied Using Mn-Doped BaTiO₃ Nanorods. ACS Nano, 2013, 7, 5522-5529.	7.3	71
16006	Self-modulated band gap in boron nitride nanoribbons and hydrogenated sheets. Nanoscale, 2013, 5, 6381.	2.8	53
16007	Efficient hydrogenation over single-site bimetallic RuSn clusters. Physical Chemistry Chemical Physics, 2013, 15, 9694.	1.3	15

#	Article	IF	Citations
16008	Ni6Cr5MoO18: A compensated half metal predicted from first-principles. Journal of Applied Physics, 2013, 113, 043718.	1.1	2
16009	Dissociative Chemisorption of Methane on Pt(110)-(1Ã—2): Effects of Lattice Motion on Reactions at Step Edges. Journal of Physical Chemistry A, 2013, 117, 8651-8659.	1.1	36
16010	Obtaining an intermediate band photovoltaic material through the Bi insertion in CdTe. Solar Energy Materials and Solar Cells, 2013, 114, 99-103.	3.0	18
16011	Frustrated Octahedral Tilting Distortion in the Incommensurately Modulated Li3xNd2/3â€“xTiO3Perovskites. Chemistry of Materials, 2013, 25, 2670-2683.	3.2	41
16012	Mechanistic study of the electrochemical extraction of K+ from KFeSO4F. Journal of Materials Chemistry A, 2013, 1, 8000.	5.2	15
16013	Phase Stability and Elastic Properties of Chromium Borides with Various Stoichiometries. ChemPhysChem, 2013, 14, 1245-1255.	1.0	23
16014	A comparative study of the reversible hydrogen storage behavior in several metal decorated graphyne. International Journal of Hydrogen Energy, 2013, 38, 3987-3993.	3.8	96
16015	Relative stability of normal vs. inverse spinel for 3d transition metal oxides as lithium intercalation cathodes. Physical Chemistry Chemical Physics, 2013, 15, 6486.	1.3	42
16016	Dangling bonds and vacancies in germanium. Physical Review B, 2013, 87, .	1.1	52
16017	Thermodynamics of Al-substitution in Fe-oxyhydroxides. Geochimica Et Cosmochimica Acta, 2013, 120, 514-530.	1.6	33
16018	Correlating the hydrogen evolution reaction activity in alkaline electrolytes with the hydrogen binding energy on monometallic surfaces. Energy and Environmental Science, 2013, 6, 1509.	15.6	869
16019	Atomistic modeling of the directed-assembly of bimetallic Pt-Ru nanoclusters on Ru(0001)-supported monolayer graphene. Journal of Chemical Physics, 2013, 138, 134703.	1.2	10
16020	Nanostructured materials for rechargeable batteries: synthesis, fundamental understanding and limitations. Current Opinion in Chemical Engineering, 2013, 2, 151-159.	3.8	7
16021	Electronic structure engineering of elpasolites: Case of Cs2AgYCl6. Journal of Luminescence, 2013, 143, 710-714.	1.5	22
16022	Adsorption of alkali, alkaline-earth, and 3<mml:math xmlns:mml="http://www.w3.org/1998/Math/MathML" display="inline"><mml:mi>d</mml:mi></mml:math>transition metal atoms on silicene. Physical Review B, 2013, 87, .	1.1	282
16023	The helical surface states of the S-covered topological insulator Sb₂Te₃(0001). Journal of Physics Condensed Matter, 2013, 25, 265005.	0.7	2
16024	Theoretical study of strained porous graphene structures and their gas separation properties. Carbon, 2013, 54, 359-364.	5.4	54
16025	Quaternary Diamondâ€Like Chalcogenidometalate Networks as Efficient Anode Material in Lithiumâ€Ion Batteries. Advanced Functional Materials, 2013, 23, 5693-5699.	7.8	26

#	Article	IF	Citations
16026	Energy-Level Matching of Fe(III) Ions Grafted at Surface and Doped in Bulk for Efficient Visible-Light Photocatalysts. Journal of the American Chemical Society, 2013, 135, 10064-10072.	6.6	263
16027	Mechanics and morphology of single-walled carbon nanotubes: from graphene to the elastica. Philosophical Magazine, 2013, 93, 2057-2088.	0.7	20
16028	Topology-Driven Magnetic Quantum Phase Transition in Topological Insulators. Science, 2013, 339, 1582-1586.	6.0	206
16029	Towards Direct-Gap Silicon Phases by the Inverse Band Structure Design Approach. Physical Review Letters, 2013, 110, 118702.	2.9	136
16030	Discussion on the structural anisotropy of wÃ¼rtzite-type compounds. Solid State Sciences, 2013, 21, 81-84.	1.5	3
16031	Temperature dependence of stacking-fault and anti-phase boundary energies in Al Sc fromab initiocalculations. Philosophical Magazine, 2013, 93, 3423-3441.	0.7	5
16032	Solvent-Exfoliated and Functionalized Graphene with Assistance of Supercritical Carbon Dioxide. ACS Sustainable Chemistry and Engineering, 2013, 1, 144-151.	3.2	80
16033	The structural and electronic properties of tubular gold clusters with a spinal support. Physical Chemistry Chemical Physics, 2013, 15, 12340.	1.3	11
16034	First-principles study on the mechanism of coking inhibition by the Ni(111) surface doped with IB-group metals at the anode of solid oxide fuel cells. Journal of Power Sources, 2013, 242, 762-767.	4.0	10
16035	Electronic Control of the Tip-Induced Hopping of an Hexaphenyl-Benzene Molecule Physisorbed on a Bare Si(100) Surface at 9 K. Journal of Physical Chemistry C, 2013, 117, 13663-13675.	1.5	13
16036	High capacity reversible hydrogen storage by metallo-carbohedrenes: An ab initio molecular dynamics simulation study. Applied Physics Letters, 2013, 102, .	1.5	8
16037	Ab initio study of iron nanowires encapsulated inside silicon nitride nanotubes. Physica E: Low-Dimensional Systems and Nanostructures, 2013, 49, 97-104.	1.3	5
16038	Ab initio study of the fracture energy of LiFePO 4 /FePO 4 interfaces. Journal of Power Sources, 2013, 243, 706-714.	4.0	21
16039	Dissociative Adsorption of Hydrogen on PdO(101) Studied by HRCLS and DFT. Journal of Physical Chemistry C, 2013, 117, 13510-13519.	1.5	25
16040	Ab initiocalculations on the defect structure of<mml:math xmlns:mml="http://www.w3.org/1998/Math/MathML" display="inline"><mml:mi>Î²</mml:mi></mml:math>-Ga<mml:math xmlns:mml="http://www.w3.org/1998/Math/MathML" display="inline"><mml:msub><mml:mrow /><mml:mn>2</mml:mn></mml:msub></mml:math>O<mml:math xmlns:mml="http://www.w3.org/1998/Math/MathML" display="inline"><mml:msub><mml:mrow />	1.1	123
16041	The Impacts of Cation Stoichiometry and Substrate Surface Quality on Nucleation, Structure, Defect Formation, and Intermixing in Complex Oxide Heteroepitaxyâ€“LaCrO₃ on SrTiO₃(001). Advanced Functional Materials, 2013, 23, 2953-2963.	7.8	48
16042	Initial reaction of silicon precursors with a varying number of dimethylamino ligands on a hydroxyl-terminated silicon (001) surface. Applied Surface Science, 2013, 280, 207-211.	3.1	23
16043	Two-dimensional electron gas at the metastable twisted interfaces of CdTe/PbTe (111) single heterojunctions. Physical Review B, 2013, 87, .	1.1	27

#	Article	IF	Citations
16044	Surface antiferromagnetism and incipient metal-insulator transition in strained manganite films. Physical Review B, 2013, 87, .	1.1	11
16045	First-principles thermodynamic study of the electrochemical stability ofÂPtÂnanoparticles in fuel cell applications. Journal of Power Sources, 2013, 238, 137-143.	4.0	40
16046	Effect of Pt and Ru promoters on deactivation of Co catalysts by C deposition during Fischerâ€“Tropsch synthesis: A DFT study. Applied Catalysis A: General, 2013, 462-463, 107-115.	2.2	20
16047	STM and STS Studies on the Density of States Modulation of Pr@C₈₂ and Sc₃C₂@C₈₀ Binary-Metallofullerene Peapods. Journal of Physical Chemistry C, 2013, 117, 6966-6971.	1.5	3
16048	Electronic and Magnetic Properties of Infinite 1D Chains of Paddlewheel Carboxylates M₂(COOR)₄ (M = Mo, W, Ru, Rh, Ir, Cu). Journal of Physical Chemistry C, 2013, 117, 5462-5469.	1.5	10
16049	Role of oxygen vacancies in TiO2-based resistive switches. Journal of Applied Physics, 2013, 113, .	1.1	26
16050	Surface Temperature Effects on Dissociative Chemisorption of H₂ on Cu(100). Journal of Physical Chemistry C, 2013, 117, 8851-8863.	1.5	33
16051	Structure analysis of a precipitate phase in an Ni-rich high-temperature NiTiHf shape memory alloy. Acta Materialia, 2013, 61, 3335-3346.	3.8	138
16052	Electronic structure and transport properties of N₂^{AA}-doped armchair and zigzag graphene nanoribbons. Nanotechnology, 2013, 24, 235701.	1.3	9
16053	Fullerene Interfaced with a TiO₂(110) Surface May Not Form an Efficient Photovoltaic Heterojunction: First-Principles Investigation of Electronic Structures. Journal of Physical Chemistry Letters, 2013, 4, 2223-2229.	2.1	36
16054	First-principles study of atomic hydrogen adsorption and initial hydrogenation of Zr(0001) surface. Journal of Applied Physics, 2013, 113, .	1.1	9
16055	Role of electronic correlation in high-low temperature phase transition of hexagonal nickel sulfide: A comparative density functional theory study with and without correction for on-site Coulomb interaction. Journal of Chemical Physics, 2013, 138, 244703.	1.2	13
16056	Ab-initio study of free standing TiO2 clusters: Stability and magnetism. Journal of Applied Physics, 2013, 113, 17B526.	1.1	23
16057	Oxygen Vacancies and Ordering of dâ€levels Control Voltage Suppression in Oxide Cathodes: the Case of Spinel LiNi_{0.5}Mn_{1.5}O_{4â€î}. Advanced Functional Materials, 2013, 23, 5530-5535.	7.8	69
16058	Molecular adsorption induces the transformation of rhombohedral- to Bernal-stacking order in trilayer graphene. Nature Communications, 2013, 4, 2074.	5.8	34
16059	Anatase Nanoparticle Surface Reactivity in NaCl Media: A CDâ€“MUSIC Model Interpretation of Combined Experimental and Density Functional Theory Studies. Langmuir, 2013, 29, 8572-8583.	1.6	11
16060	First-principles investigations of oxygen adsorption at TiNi surface and the TiO2/TiOâ€“TiNi interface. Physica B: Condensed Matter, 2013, 426, 118-126.	1.3	17
16061	Magnetic properties of small cobaltâ€“copper clusters. Journal of Physics Condensed Matter, 2013, 25, 216003.	0.7	7

#	Article	IF	Citations
16062	Stabilization of 9/10-Fold Structure in Bismuth Selenide at High Pressures. Journal of Physical Chemistry C, 2013, 117, 10045-10050.	1.5	43
16063	Concentration-Dependent Ordering of Lithiated Amorphous TiO2. Journal of Physical Chemistry C, 2013, 117, 3834-3845.	1.5	18
16064	Core-shell magnetic exchange model for Co3O4 nanowires. Applied Physics Letters, 2013, 102, 203102.	1.5	5
16065	Rhombohedrally Distorted Î³-Au5â€“xZn8+y Phases in the Auâ€“Zn System. Inorganic Chemistry, 2013, 52, 1328-1337.	1.9	12
16066	High-entropy Alloys with High Saturation Magnetization, Electrical Resistivity and Malleability. Scientific Reports, 2013, 3, 1455.	1.6	436
16067	Defect-Induced and UV-Irradiation-Enhanced Ferromagnetism in Cubic Barium Niobate. Journal of Physical Chemistry C, 2013, 117, 14281-14288.	1.5	12
16068	Ferroelectric distortions in doped ferroelectrics: BaTiO<mml:math xmlns:mml="http://www.w3.org/1998/Math/MathML" display="inline"><mml:msub><mml:mrow /><mml:mn>3</mml:mn></mml:msub></mml:math>:<mml:math xmlns:mml="http://www.w3.org/1998/Math/MathML"		

#	Article	IF	Citations
16080	Structural and Electronic Properties of Superlattice Composed of Graphene and Monolayer MoS₂. Journal of Physical Chemistry C, 2013, 117, 15347-15353.	1.5	99
16081	Electronic Structure of Epitaxial Sn-Doped Anatase Grown on SrTiO₃(001) by Dip Coating. Journal of Physical Chemistry C, 2013, 117, 15221-15228.	1.5	10
16082	First-Principles Study on Electronic Properties and Optical Spectra of Ce-Doped La₂CaB₁₀O₁₉ Crystal. Journal of Physical Chemistry C, 2013, 117, 15241-15246.	1.5	20
16083	Anionic or Cationic S-Doping in Bulk Anatase TiO₂: Insights on Optical Absorption from First Principles Calculations. Journal of Physical Chemistry C, 2013, 117, 8892-8902.	1.5	78
16084	Surface Reduction Mechanism of Ceriumâ€“Gallium Mixed Oxides with Enhanced Redox Properties. Journal of Physical Chemistry C, 2013, 117, 8822-8831.	1.5	33
16085	On the role of lanthanum substitution defects in reducing lattice thermal conductivity of the AgSbTe2 (P4/mmm) thermoelectric compound for energy conversion applications. Computational Materials Science, 2013, 78, 98-103.	1.4	26
16086	Benzene adsorption on PtCo(111): A DFT study. Applied Surface Science, 2013, 282, 17-24.	3.1	7
16087	van der Waals bonding and the quasiparticle band structure of SnO from first principles. Physical Review B, 2013, 87, .	1.1	55
16088	Mechanistic Studies of Water Electrolysis and Hydrogen Electro-Oxidation on High Temperature Ceria-Based Solid Oxide Electrochemical Cells. Journal of the American Chemical Society, 2013, 135, 11572-11579.	6.6	90
16089	Thermodynamics of glycerol hydrogenolysis to propanediols over supported copper clusters: Insights from first-principles study. Science China Chemistry, 2013, 56, 763-772.	4.2	11
16090	Can H2S poison the surface of yttria-stabilized zirconia?. International Journal of Hydrogen Energy, 2013, 38, 8974-8979.	3.8	16
16091	Influence of Crystal Packing on an Organometallic Ruthenium(IV) Complex Structure: The Right Distance for the Right Reason. Organometallics, 2013, 32, 3784-3787.	1.1	27
16092	Magnetization and spin dynamics of the spin<mml:math xmlns:mml="http://www.w3.org/1998/Math/MathML" display="inline"><mml:mrow><mml:mi>S</mml:mi><mml:mo>=</mml:mo><mml:mfrac><mml:mn>1</mml:mn><mml:mn>2</mml:mn> nanomagnet Cu<mml:math xmlns:mml="http://www.w3.org/1998/Math/MathML" display="inline"><mml:msub><mml:mrow /><mml:mn>5</mml:mn></mml:msub></mml:math>(OH)<mml:math xmlns:mml="http://www.w3.org/1998/	1.1	20
16093	Nucleation of Graphene Precursors on Transition Metal Surfaces: Insights from Theoretical Simulations. Journal of Physical Chemistry C, 2013, 117, 14858-14864.	1.5	39
16094	Ultranarrow and Widely TunableMn2+-Induced Photoluminescence from Single Mn-Doped Nanocrystals of ZnS-CdS Alloys. Physical Review Letters, 2013, 110, 267401.	2.9	84
16095	Structure and local reactivity of the Au(111) surface reconstruction. Physical Review B, 2013, 87, .	1.1	125
16096	Assigning EXAFS results for uranyl adsorption on minerals via formal charges of bonding oxygen centers. Surface Science, 2013, 615, 21-25.	0.8	9
16097	First-principles study of sulfur multi-absorption in nickel and its segregation to the Ni(100) and Ni(111) surfaces. Surface Science, 2013, 617, 15-21.	0.8	19

#	Article	IF	Citations
16098	Atomic-Scale Study of Calcite Nucleation in Calcium Oxide. Journal of Physical Chemistry C, 2013, 117, 8813-8821.	1.5	30
16099	Effects of strain on the electrical properties of silicon carbide. Journal of Applied Physics, 2013, 114, .	1.1	12
16100	Accelerated Materials Design of Lithium Superionic Conductors Based on Firstâ€Principles Calculations and Machine Learning Algorithms. Advanced Energy Materials, 2013, 3, 980-985.	10.2	178
16101	Benzene adsorption on binary Pt3M alloys and surface alloys: a DFT study. Physical Chemistry Chemical Physics, 2013, 15, 12197.	1.3	28
16102	van der Waals interaction in iron-chalcogenide superconductors. Physical Review B, 2013, 87, .	1.1	23
16103	Influence of surface structures, subsurface carbon and hydrogen, and surface alloying on the activity and selectivity of acetylene hydrogenation on Pd surfaces: A density functional theory study. Journal of Catalysis, 2013, 305, 264-276.	3.1	214
16104	Enhanced catalytic activity in strained chemically exfoliated WS2 nanosheets for hydrogen evolution. Nature Materials, 2013, 12, 850-855.	13.3	2,326
16105	Density Functional Calculations of the Structural and Electronic Properties of (Y2O3)n0,Â±1 Clusters with n = 1â€“10. Journal of Physical Chemistry A, 2013, 117, 5542-5550.	1.1	22
16106	Tuning electronic and magnetic properties of MoO3 sheets by cutting, hydrogenation, and external strain: a computational investigation. Nanoscale, 2013, 5, 5321.	2.8	65
16107	Structureâ€“property relationship of polyimides based on pyromellitic dianhydride and shortâ€chain aliphatic diamines for dielectric material applications. Journal of Applied Polymer Science, 2013, 130, 1276-1280.	1.3	34
16108	Insight into oxygen stability and vacancy formation on Co3O4 model slabs. Computational Materials Science, 2013, 72, 15-25.	1.4	29
16109	Ab initio calculations of characteristic lengths of crystalline materials in first strain gradient elasticity. Mechanics of Materials, 2013, 61, 73-78.	1.7	52
16110	Tuning the vertical location of helical surface states in topological insulator heterostructures via dual-proximity effects. Scientific Reports, 2013, 3, 1233.	1.6	38
16111	Pressure induced phase transitions in multiferroic BiFeO3. Solid State Communications, 2013, 154, 72-76.	0.9	15
16112	First-principle study on structural and electronic properties of CeO<mml:math xmlns:mml="http://www.w3.org/1998/Math/MathML" display="inline"><mml:msub><mml:mrow /><mml:mn>2</mml:mn></mml:msub></mml:math>and ThO<mml:math xmlns:mml="http://www.w3.org/1998/Math/MathML" display="inline"><mml:msub><mml:mrow /><mml:mn>2</mml:mn></mml:msub></mml:math>. Physical Review B, 2013, 87, .	1.1	22
16113	<mml:math xmlns:mml="http://www.w3.org/1998/Math/MathML" display="inline"><mml:msub><mml:mrow /><mml:mn>3</mml:mn></mml:msub></mml:math>B<mml:math xmlns:mml="http://www.w3.org/1998/Math/MathML" display="inline"><mml:msub><mml:mrow /><mml:mn>2</mml:mn></mml:msub></mml:math>O<mml:math	1.1	37
16114	Structure change, layer sliding, and metallization in high-pressure MoS<mml:math xmlns:mml="http://www.w3.org/1998/Math/MathML" display="inline"><mml:msub><mml:mrow /><mml:mn>2</mml:mn></mml:msub></mml:math>. Physical Review B, 2013, 87, .	1.1	116
16115	Structureâ€“activity relationship of Au/ZrO2 catalyst on formation of hydroxyl groups and its influence on CO oxidation. Journal of Materials Chemistry A, 2013, 1, 6051.	5.2	36

#	Article	IF	Citations
16116	Half-metallic hole-doped Mn/Si trilayers. Journal Physics D: Applied Physics, 2013, 46, 165502.	1.3	3
16117	Density functional theory study of the electronic structure of fluorite Cu2Se. Journal of Physics Condensed Matter, 2013, 25, 125503.	0.7	41
16118	A generic tight-binding model for monolayer, bilayer and bulk MoS2. AIP Advances, 2013, 3, .	0.6	174
16119	Stability and electronic properties of ultrathin films of silicon and germanium. Physical Chemistry Chemical Physics, 2013, 15, 9710.	1.3	65
16120	Selective CO2 Adsorption on Metal-Organic Frameworks Based on Trinuclear Cu3-Pyrazolato Complexes: An Experimental and Computational Study. Crystal Growth and Design, 2013, 13, 2628-2635.	1.4	18
16121	The Effect of N and B Doping on Graphene and the Adsorption and Migration Behavior of Pt Atoms. Journal of Physical Chemistry C, 2013, 117, 10523-10535.	1.5	71
16122	Novel electronic and magnetic properties in N or B doped silicene nanoribbons. Journal of Materials Chemistry C, 2013, 1, 2735.	2.7	73
16123	One-Dimensional Ni-Based Nanostructures and Their Application as Solid Oxide Fuel Cell Anodes: A DFT Investigation. Journal of Physical Chemistry C, 2013, 117, 1315-1322.	1.5	8
16124	Magnetic Silicon Nanotube: Role of Encapsulated Europium Atoms. Journal of Physical Chemistry C, 2013, 117, 10764-10769.	1.5	10
16125	Low energy three-dimensional hydrocarbon crystal from cold compression of benzene. Journal of Physics Condensed Matter, 2013, 25, 205403.	0.7	10
16126	Electrostatic tuning of Kondo effect in a rare-earth-doped wide-band-gap oxide. Physical Review B, 2013, 87, .	1.1	49
16127	Pressure induced phase transitions in TiH2. Journal of Applied Physics, 2013, 113, 103512.	1.1	17
16128	Competition of shape and interaction patchiness for self-assembling nanoplates. Nature Chemistry, 2013, 5, 466-473.	6.6	278
16129	Topological Dangling Bonds with Large Spin Splitting and Enhanced Spin Polarization on the Surfaces of Bi₂Se₃. Nano Letters, 2013, 13, 1915-1919.	4.5	36
16130	Unusual Temperature Dependence of Band Dispersion in<mml:math xmlns:mml="http://www.w3.org/1998/Math/MathML" display="inline"><mml:mi>Ba</mml:mi><mml:mo stretchy="false">(</mml:mo><mml:msub><mml:mi>Fe</mml:mi><mml:mrow><mml:mn>1</mml:mn><mml:mo>−</mml:mo><mml:m its Conseque. Physical Review Letters, 2013, 110, 067002.	7.9	42
16131	Magnetic Ordering in Tetragonal 3d Metal Arsenides M2As (M = Cr, Mn, Fe): An Ab Initio Investigation. Inorganic Chemistry, 2013, 52, 3013-3021.	1.9	8
16132	Activation Volume Tensor for Oxygen-Vacancy Migration in Strained<mml:math xmlns:mml="http://www.w3.org/1998/Math/MathML" display="inline"><mml:msub><mml:mi>CeO</mml:mi><mml:mn>2</mml:mn></mml:msub></mml:math>Electrolytes. Physical Review Letters, 2013, 110, 205901.	7.9	55
16133	Theoretical modeling of defect segregation and space-charge formation in the BaZrO3 (210)[001] tilt grain boundary. Solid State Ionics, 2013, 252, 121-125.	1.3	26

#	Article	IF	Citations
16134	Bonding Characteristics of TiC and TiN. Modeling and Numerical Simulation of Material Science, 2013, 03, 7-11.	0.5	22
16135	Energetics of Câ€“N coupling reactions on Pt(111) and Ni(111) surfaces from application of density-functional theory. Physical Chemistry Chemical Physics, 2013, 15, 10395.	1.3	3
16136	How Cr changes the dislocation core structure of Î±-Fe: the role of magnetism. Journal of Physics Condensed Matter, 2013, 25, 085403.	0.7	1
16137	Boron diffusion induced symmetry reduction and scattering in CoFeB/MgO/CoFeB magnetic tunnel junctions. Physical Review B, 2013, 87, .	1.1	33
16138	Pressure and Temperature Effects on the Formation of a Pd/C Surface Carbide: Insights into the Role of Pd/C as a Selective Catalytic State for the Partial Hydrogenation of Acetylene. Journal of Physical Chemistry C, 2013, 117, 11059-11065.	1.5	14
16139	Photoinduced Charge Transfer from Titania to Surface Doping Site. Journal of Physical Chemistry C, 2013, 117, 9673-9692.	1.5	59
16140	Fibrous Hybrid of Graphene and Sulfur Nanocrystals for High-Performance Lithiumâ€“Sulfur Batteries. ACS Nano, 2013, 7, 5367-5375.	7.3	722
16141	Lowâ€Density Equation of State for Water from a Chemical Model. Contributions To Plasma Physics, 2013, 53, 336-346.	0.5	9
16142	Pressure-induced structural phase transition and equation of state of LiTaO₃. Journal of Physics Condensed Matter, 2013, 25, 215401.	0.7	4
16143	First-principles model for phase stability, radiation defects and elastic properties Of Wâ€“Ta and Wâ€“V alloys. Journal of Nuclear Materials, 2013, 442, S680-S683.	1.3	28
16144	Trapping and diffusion behaviors of helium at vacancy in iron from first principles. Science China: Physics, Mechanics and Astronomy, 2013, 56, 1100-1106.	2.0	7
16145	Atomic positions and diffusion paths of h and he in the Î±-Ti lattice. Physics of the Solid State, 2013, 55, 367-372.	0.2	26
16146	Single-layer MoS2 as an efficient photocatalyst. Catalysis Science and Technology, 2013, 3, 2214.	2.1	271
16147	Investigation of magnetic properties induced by group-V element in doped ZnO. Physical Chemistry Chemical Physics, 2013, 15, 5208.	1.3	38
16148	Novel Two-Dimensional Tetragonal Monolayer: Metalâ€“TCNQ Networks. Journal of Physical Chemistry A, 2013, 117, 5171-5177.	1.1	32
16149	Probing Nitrosyl Ligation of Surface-Confined Metalloporphyrins by Inelastic Electron Tunneling Spectroscopy. ACS Nano, 2013, 7, 5273-5281.	7.3	26
16150	Electrochemistry of Hollandite Î±-MnO₂: Li-Ion and Na-Ion Insertion and Li₂O Incorporation. Chemistry of Materials, 2013, 25, 2515-2526.	3.2	172
16151	Review on cerium intermetallic compounds: A bird's eye outlook through DFT. Progress in Solid State Chemistry, 2013, 41, 55-85.	3.9	28

#	Article	IF	Citations
16152	Tailoring the electronic and optical properties of rutile TiO2 by (Nb + Sb, C) codoping from DFT + U calculations. Chemical Physics Letters, 2013, 567, 34-38.	1.2	27
16153	The Oxidation of Cobalt Nanoparticles into Kirkendall-Hollowed CoO and Co₃O₄: The Diffusion Mechanisms and Atomic Structural Transformations. Journal of Physical Chemistry C, 2013, 117, 14303-14312.	1.5	128
16154	Adsorption of NO₂ on YSZ(111) and Oxygen-Enriched YSZ(111) Surfaces. Journal of Physical Chemistry C, 2013, 117, 12472-12482.	1.5	9
16155	Hybrid Hartree-Fock density functional study of charged point defects in ferroelectric PbTiO<mml:math xmlns:mml="http://www.w3.org/1998/Math/MathML" display="inline"><mml:msub><mml:mrow /><mml:mn>3</mml:mn></mml:msub></mml:math>. Physical Review B, 2013, 87, .	1.1	63
16156	Interstitialâ€“interstitial interactions in bcc VB group metals: Ab initiocalculations. Journal of Physics and Chemistry of Solids, 2013, 74, 716-722.	1.9	3
16157	Catalyst studies on the ring opening of tetrahydrofuranâ€“dimethanol to 1,2,6-hexanetriol. Catalysis Today, 2013, 210, 106-116.	2.2	67
16158	Theoretical Considerations on the Electroreduction of CO to C₂ Species on Cu(100) Electrodes. Angewandte Chemie - International Edition, 2013, 52, 7282-7285.	7.2	677
16159	Geometric and Electronic Structures as well as Thermodynamic Stability of Hexyl-Modified Silicon Nanosheet. Journal of Physical Chemistry C, 2013, 117, 13283-13288.	1.5	16
16160	Ab initio investigations of the electronic structures and chemical bonding in LiCo6P4 and Li2Co12P7. Journal of Solid State Chemistry, 2013, 202, 227-233.	1.4	4
16161	Structure determination of ultra dense magnesium borohydride: A first-principles study. Journal of Chemical Physics, 2013, 138, 214503.	1.2	3
16162	Structural and electronic properties of a single C chain doped zigzag silicene nanoribbon. Physica E: Low-Dimensional Systems and Nanostructures, 2013, 53, 173-177.	1.3	14
16163	Structural and electronic properties of substitutionally doped armchair silicene nanoribbons. Physica B: Condensed Matter, 2013, 425, 66-71.	1.3	43
16164	A DFT study of the NO dissociation on gold surfaces doped with transition metals. Journal of Chemical Physics, 2013, 138, 074701.	1.2	9
16165	Origin of site preference of CO and NO adsorption on Pd(111) at different coverages: A density functional theory study. Computational and Theoretical Chemistry, 2013, 1004, 22-30.	1.1	12
16166	Extraordinary Sunlight Absorption and One Nanometer Thick Photovoltaics Using Two-Dimensional Monolayer Materials. Nano Letters, 2013, 13, 3664-3670.	4.5	1,681
16167	First-Principles Study of the Electronic Properties of B/N Atom Doped Silicene Nanoribbons. Journal of Physical Chemistry C, 2013, 117, 13620-13626.	1.5	49
16168	C/B codoping effect on band gap narrowing and optical performance of TiO2 photocatalyst: a spin-polarized DFT study. Journal of Materials Chemistry A, 2013, 1, 4516.	5.2	42
16169	Equation of state calculations of hydrogen-helium mixtures in solar and extrasolar giant planets. Physical Review B, 2013, 87, .	1.1	82

#	Article	IF	Citations
16170	Formalism to model stacking fault effects on surface phase stability in alloys. Physical Review B, 2013, 87, .	1.1	5
16171	Dielectric properties of carbon-, silicon-, and germanium-based polymers: A first-principles study. Physical Review B, 2013, 87, .	1.1	31
16172	Mechanical and electronic properties of stoichiometric silicene and germanene oxides from firstâ€principles. Physica Status Solidi - Rapid Research Letters, 2013, 7, 410-413.	1.2	38
16173	Phase transition and elastic and optical properties of Lu2SiO5. Optical Materials, 2013, 35, 1659-1663.	1.7	5
16174	Spectroscopy of Donorâ˜Ï€â€“Acceptor Porphyrins for Dye-Sensitized Solar Cells. Journal of Physical Chemistry C, 2013, 117, 13357-13364.	1.5	36
16175	Effects of Dy on the adherence of Al2O3/NiAl interface: A combined first-principles and experimental studies. Corrosion Science, 2013, 66, 59-66.	3.0	39
16176	Cyclic oxidation of Î²-NiAl with various reactive element dopants at 1200Â°C. Corrosion Science, 2013, 66, 125-135.	3.0	164
16177	The first-principles study of martensitic transformations in MnMe (MeÂ=ÂRh, Pd) alloys at low temperatures. Intermetallics, 2013, 34, 83-88.	1.8	3
16178	A simulation study of the shape of Î²â€² precipitates in Mgâ€“Y and Mgâ€“Gd alloys. Acta Materialia, 2013, 61, 453-466.	3.8	150
16179	The graphene-supported palladium and palladiumâ€“yttrium nanoparticles for the oxygen reduction and ethanol oxidation reactions: Experimental measurement and computational validation. Applied Catalysis B: Environmental, 2013, 129, 163-171.	10.8	86
16180	Substitutional adsorption mechanism and controllable magnetic properties of Mn on PbTe(111) surface. Applied Surface Science, 2013, 265, 120-123.	3.1	2
16181	First-principles investigation of structural phase transitions and electronic properties of CuGaSe2 up to 100 GPa. Computational Materials Science, 2013, 67, 21-26.	1.4	19
16182	Elastic constants of austenitic stainless steel: Investigation by the first-principles calculations and the artificial neural network approach. Computational Materials Science, 2013, 67, 353-358.	1.4	37
16183	First-principles investigation of the mechanical, electronic and thermophysical properties of Q-phase in Alâ€“Mgâ€“Siâ€“Cu alloys. Computational Materials Science, 2013, 67, 334-340.	1.4	8
16184	Enhanced magnetization and conductive phase in NiFe2O4. Journal of Magnetism and Magnetic Materials, 2013, 325, 144-146.	1.0	18
16185	Origin of ferromagnetism in Zn-doped SnO2 from first-principles study. Journal of Magnetism and Magnetic Materials, 2013, 325, 7-12.	1.0	23
16186	Possible ferromagnetism in Li, Na and K-doped AlN: A first-principle study. Journal of Magnetism and Magnetic Materials, 2013, 326, 45-49.	1.0	19
16187	Carbon doped ZnO: Synthesis, characterization and interpretation. Journal of Magnetism and Magnetic Materials, 2013, 329, 146-152.	1.0	132

#	Article	IF	Citations
16188	First-principles study on the half-metallic Tc-doped Sr2FeReO6. Journal of Magnetism and Magnetic Materials, 2013, 329, 30-33.	1.0	4
16189	Coarse-graining Kohnâ€“Sham Density Functional Theory. Journal of the Mechanics and Physics of Solids, 2013, 61, 38-60.	2.3	46
16190	First-principles prediction of an intrinsic half-metallic graphitic hydrogenated carbon nitride. Physics Letters, Section A: General, Atomic and Solid State Physics, 2013, 377, 347-350.	0.9	30
16191	Accommodation at the interface of highly dissimilar GaN(0001)/Sc2O3(111) heteroepitaxial systems. Scripta Materialia, 2013, 68, 211-214.	2.6	2
16192	Structural mechanism for ultrahigh-strength Co-based metallic glasses. Scripta Materialia, 2013, 68, 257-260.	2.6	12
16193	Manipulation of surface energy anisotropy in iron using surface segregation of phosphorus: An atomistic simulation. Scripta Materialia, 2013, 68, 329-332.	2.6	13
16194	Oxygen-induced Y surface segregation in a CuPdY ternary alloy. Surface Science, 2013, 608, 61-66.	0.8	5
16195	Comparative study of friction properties for hydrogen- and fluorine-modified diamond surfaces: A first-principles investigation. Surface Science, 2013, 608, 74-79.	0.8	30
16196	Hydroxylation-induced surface stability of AnO2 (An=U, Np, Pu) from first-principles. Surface Science, 2013, 608, 180-187.	0.8	59
16197	In-situ transmission electron microscopy and first-principles study of Au (100) surface dislocation dynamics. Surface Science, 2013, 608, 154-164.	0.8	5
16198	Structural transformations of Cu(110) surface induced by adsorption of molecular chlorine. Surface Science, 2013, 608, 135-145.	0.8	23
16199	Ab initio molecular dynamics study of H2 adsorption on sulfur- and chlorine-covered Pd(100). Surface Science, 2013, 608, 249-254.	0.8	19
16200	Thermodynamic assessment of the Laâ€“Sb and the Hoâ€“Sb systems using the associate model. Thermochimica Acta, 2013, 551, 104-109.	1.2	0
16201	The Mechanism for the Thermally Driven Self-Assembly of Pyrazine into Ordered Lines on Si(100). Journal of Physical Chemistry C, 2013, 117, 15749-15753.	1.5	8
16202	Structure and thermoelectric properties of EuTi(O,N)3â€‰Â±â€‰Î´. Journal of Applied Physics, 2013, 114,	1.1	24
16203	Influence of Step Defects on Methanol Decomposition: Periodic Density Functional Studies on Pd(211) and Kinetic Monte Carlo Simulations. Journal of Physical Chemistry C, 2013, 117, 451-459.	1.5	28
16204	Structural Acidâ€“Base Chemistry in the Metallic State: How Î¼₃-Neutralization Drives Interfaces and Helices in Ti₂₁Mn₂₅. Inorganic Chemistry, 2013, 52, 8349-8359.	1.9	9
16205	Effect of Transition Metal Dopants on Initial Mass Transport in the Dehydrogenation of NaAlH₄: Density Functional Theory Study. Journal of Physical Chemistry C, 2013, 117, 3-14.	1.5	19

#	Article	IF	Citations
16206	Linear Compressibility and Thermal Expansion of KMn[Ag(CN)₂]₃ Studied by Raman Spectroscopy and First-Principles Calculations. Journal of Physical Chemistry C, 2013, 117, 25704-25713.	1.5	18
16207	Dirac cone in Î±-graphdiyne: a first-principles study. Nanoscale Research Letters, 2013, 8, 469.	3.1	36
16208	Do silicene nanoribbons have high carrier mobilities?. Europhysics Letters, 2013, 101, 27005.	0.7	18
16209	Determination of a Density Functional Tight Binding Model with an Extended Basis Set and Three-Body Repulsion for Carbon Under Extreme Pressures and Temperatures. Journal of Physical Chemistry C, 2013, 117, 7885-7894.	1.5	28
16210	First Principles Study on Ta₃N₅:Ti₃O₃N₂ Solid Solution As a Water-Splitting Photocatalyst. Journal of Physical Chemistry C, 2013, 117, 24710-24715.	1.5	16
16211	Transition metal atoms pathways on rutile TiO2 (110) surface: Distribution of Ti3+ states and evidence of enhanced peripheral charge accumulation. Journal of Chemical Physics, 2013, 138, 154711.	1.2	47
16212	Multiscale quantum/atomistic coupling using constrained density functional theory. Physical Review B, 2013, 87, .	1.1	32
16213	DFT+U Calculations and XAS Study: Further Confirmation of the Presence of CoO5 Square-Based Pyramids with IS-Co3+ in Li-Overstoichiometric LiCoO2. Journal of Physical Chemistry C, 2013, 117, 26493-26500.	1.5	17
16214	Structures and Electronic Properties of the SiAu_n (n = 17â€“20) Clusters. Journal of Physical Chemistry A, 2013, 117, 2672-2677.	1.1	16
16215	Structural Transformations and Absorption Properties of Crystalline 7-Amino-6-nitrobenzodifuroxan under High Pressures. Journal of Physical Chemistry C, 2013, 117, 16830-16839.	1.5	36
16216	Structural, Electronic, and Magnetic Properties of the Semifluorinated Boron Nitride Bilayer: A First-Principles Study. Journal of Physical Chemistry C, 2013, 117, 3114-3121.	1.5	12
16217	Consequences of Metalâ€“Oxide Interconversion for Câ€“H Bond Activation during CH₄ Reactions on Pd Catalysts. Journal of the American Chemical Society, 2013, 135, 15425-15442.	6.6	256
16218	Oligomeric Vanadium Oxide Species Supported on the CeO₂(111) Surface: Structure and Reactivity Studied by Density Functional Theory. Journal of Physical Chemistry C, 2013, 117, 5274-5285.	1.5	60
16219	Theoretical Study on the Diffusion Mechanism of Cd in the Cu-Poor Phase of CuInSe₂ Solar Cell Material. Journal of Physical Chemistry C, 2013, 117, 25933-25938.	1.5	21
16220	Revisiting the Dependence of the Optical and Mobility Gaps of Hydrogenated Amorphous Silicon on Hydrogen Concentration. Journal of Physical Chemistry C, 2013, 117, 23956-23963.	1.5	23
16221	An SCC-DFTB Repulsive Potential for Various ZnO Polymorphs and the ZnOâ€“Water System. Journal of Physical Chemistry C, 2013, 117, 17004-17015.	1.5	42
16222	Properties of Weakly Bound Molecular Oxygen on the Rutile TiO₂(110) Surface from Density Functional Theory. Journal of Physical Chemistry C, 2013, 117, 17151-17158.	1.5	2
16223	Methane Dissociation on Li-, Na-, K-, and Cu-Doped Flat and Stepped CaO(001). Journal of Physical Chemistry C, 2013, 117, 7114-7122.	1.5	24

#	Article	IF	Citations
16224	Temperature dependence of TiN elastic constants fromab initiomolecular dynamics simulations. Physical Review B, 2013, 87, .	1.1	78
16225	Interaction of Titanium Oxide Nanostructures with Graphene and Functionalized Graphene Nanoribbons: A DFT Study. Journal of Physical Chemistry C, 2013, 117, 25424-25432.	1.5	32
16226	Magnetic structure of bixbyite<mml:math xmlns:mml="http://www.w3.org/1998/Math/MathML" display="inline"><mml:mi>Î±</mml:mi></mml:math>-Mn<mml:math xmlns:mml="http://www.w3.org/1998/Math/MathML" display="inline"><mml:msub><mml:mrow /><mml:mn>2</mml:mn></mml:msub></mml:math>O<mml:math xmlns:mml="http://www.w3.org/1998/Math/MathML" display="inline"><mml:msub><mml:mrow /><mml:mn>3</mml:mn></mml:msub></mml:math>: A combined DFT<mml:math xmlns:mml="http://www.	1.1	61
16227	First-principles study of group III impurity doped PbSe: Bulk and nanowire. Physical Review B, 2013, 87, .	1.1	8
16228	Au-Decorated Silicene: Design of a High-Activity Catalyst toward CO Oxidation. Journal of Physical Chemistry C, 2013, 117, 483-488.	1.5	63
16229	The Effects of the Formation of Stoneâ€“Wales Defects on the Electronic and Magnetic Properties of Silicon Carbide Nanoribbons: A Firstâ€Principles Investigation. ChemPhysChem, 2013, 14, 2841-2852.	1.0	37
16230	d0 magnetism and large magnetoelectric effect in BC4N nanoribbons. Journal of Applied Physics, 2013, 113, 133705.	1.1	3
16231	Rational Design of Monocrystalline (InP)_yGe_{5â€“2y}/Ge/Si(100) Semiconductors: Synthesis and Optical Properties. Journal of the American Chemical Society, 2013, 135, 12388-12399.	6.6	4
16232	DFT Simulations of Titanium Oxide Films on Titanium Metal. Journal of Physical Chemistry C, 2013, 117, 358-367.	1.5	20
16233	Combined LDA and LDA-1/2 method to obtain defect formation energies in large silicon supercells. Physical Review B, 2013, 88, .	1.1	22
16234	Carbon-Based Electrodes for Lithium Air Batteries: Scientific and Technological Challenges from a Modeling Perspective. ECS Journal of Solid State Science and Technology, 2013, 2, M3084-M3100.	0.9	66
16235	Formation of Stable Nitrene Surface Species by the Reaction of Adsorbed Phenyl Isocyanate at the Ge(100)-2 Ã— 1 Surface. Langmuir, 2013, 29, 15842-15850.	1.6	8
16236	First-Principles Study of Structural Prototypes for NaAlH4: Elevated Pressure Polymorph in Symmetry Fmm2 Leads to a Single-Step Decomposition Pathway. Journal of Physical Chemistry C, 2013, 117, 8864-8870.	1.5	3
16237	Single-Site and Monolayer Surface Hydration Energy of Anatase and Rutile Nanoparticles Using Density Functional Theory. Journal of Physical Chemistry C, 2013, 117, 26084-26090.	1.5	18
16238	Facet Recognition and Molecular Ordering of Ionic Liquids on Metal Surfaces. Journal of Physical Chemistry C, 2013, 117, 25969-25981.	1.5	80
16239	First-Principle Electronic Properties of Dilute-As GaNAs Alloy for Visible Light Emitters. Journal of Display Technology, 2013, 9, 272-279.	1.3	102
16240	Suppression of hydride precipitates in niobium superconducting radio-frequency cavities. Superconductor Science and Technology, 2013, 26, 105003.	1.8	13
16241	Liquidâ€“Liquid Miscibility Gaps in Drugâ€“Water Binary Systems: Crystal Structure and Thermodynamic Properties of Prilocaine and the Temperatureâ€“Composition Phase Diagram of the Prilocaineâ€“Water System. Molecular Pharmaceutics, 2013, 10, 1332-1339.	2.3	13

#	Article	IF	Citations
16242	Experimental Investigation and Thermodynamic Modeling for the Mg-Nd-Sr System. Metallurgical and Materials Transactions A: Physical Metallurgy and Materials Science, 2013, 44, 5634-5641.	1.1	6
16243	Theoretical Study on Structural Stability of Fully Filled p-Type Skutterudites RETM4Sb12 (REÂ=ÂRare) Tj ETQq1 1 0.784314 rgBT /Ove	1.0	20
16244	Sulfur dioxide adsorbed on graphene and heteroatom-doped graphene: a first-principles study. European Physical Journal B, 2013, 86, 1.	0.6	79
16245	Ab initio study of I2 and T2 stacking faults in C14 Laves phase MgZn2. European Physical Journal B, 2013, 86, 1.	0.6	16
16246	First principles study on magnetic properties in ZnS doped with palladium. European Physical Journal B, 2013, 86, 1.	0.6	18
16247	The mystery of abnormally large volume of PbCrO3 with a structurally consistent Hubbard U from first-principles. European Physical Journal B, 2013, 86, 1.	0.6	4
16248	Multiscale modeling of submonolayer growth for Fe/Mo (110). European Physical Journal B, 2013, 86, 1.	0.6	2
16249	Structural and electronic properties of BeO nanotubes filled with Cu nanowires. European Physical Journal B, 2013, 86, 1.	0.6	3
16250	Elucidating hydrogen assisting vacancy formation in metals: Mo and Nb as examples. European Physical Journal B, 2013, 86, 1.	0.6	15
16251	Structural, electronic, vibrational, and elastic properties of SWCNTs doped with B and N: an ab initio study. European Physical Journal D, 2013, 67, 1.	0.6	10
16252	Unveiling Stable Group IV Alloy Nanowires via a Comprehensive Search and Their Electronic Band Characteristics. Nano Letters, 2013, 13, 4951-4956.	4.5	21
16253	First-principles studies of phase stability and crystal structures in Li-Zn mixed-metal borohydrides. Physical Review B, 2013, 88, .	1.1	11
16254	Scattering of Nitrogen Atoms off Ag(111) Surfaces: A Theoretical Study. Journal of Physical Chemistry C, 2013, 117, 9779-9790.	1.5	20
16255	Excess manganese as the origin of the low-temperature anomaly in NiMnSb. Physical Review B, 2013, 88, .	1.1	9
16256	Manipulation of band structures in wurtzite and zinc-blende GaAs/InAs-core-shell nanowires. Journal of Applied Physics, 2013, 114, .	1.1	4
16257	Ab Initio Molecular Dynamics Simulations of Ti₂ on C₂₀ Collisions and C₂₀Ti₂ Configurations. Journal of Physical Chemistry C, 2013, 117, 4287-4291.	1.5	1
16258	Theoretical study of the ground-state structures and properties of niobium hydrides under pressure. Physical Review B, 2013, 88, .	1.1	63
16259	First-principles prediction and experimental verification of glass-forming ability in Zr-Cu binary metallic glasses. Scientific Reports, 2013, 3, 2124.	1.6	34

#	Article	IF	Citations
16260	Selecting the suitable dopants: electronic structures of transition metal and rare earth doped thermoelectric sodium cobaltate. RSC Advances, 2013, 3, 1442-1449.	1.7	13
16261	Preferential Adsorption of Zigzag Single-Walled Carbon Nanotubes on the ST-Cut Surface of Quartz. Journal of Physical Chemistry C, 2013, 117, 4639-4646.	1.5	3
16262	Stabilizing intrinsic defects in SnO<mml:math xmlns:mml="http://www.w3.org/1998/Math/MathML" display="inline"><mml:msub><mml:mrow /><mml:mn>2</mml:mn></mml:msub></mml:math>. Physical Review B, 2013, 87, .	1.1	40
16263	3dâ€“4f Magnetic Interaction with Density Functional Theory Plus U Approach: Local Coulomb Correlation and Exchange Pathways. Journal of Physical Chemistry A, 2013, 117, 13194-13204.	1.1	10
16264	First-principles study of the structural transformation, electronic structure, and optical properties of crystalline 2,6-diamino-3,5-dinitropyrazine-1-oxide under high pressure. Journal of Molecular Modeling, 2013, 19, 5159-5170.	0.8	26
16265	Quantum mechanical modeling of the structures, energetics and spectral properties of Îł and Îł2 cellulose. Cellulose, 2013, 20, 9-23.	2.4	39
16266	Valence band offsets at zinc-blende heterointerfaces with misfit dislocations: A first-principles study. Physical Review B, 2013, 88, .	1.1	15
16267	Self-Assembly of Upright, Partially Dehydrogenated Melamine on Pd(111). Journal of Physical Chemistry C, 2013, 117, 22874-22879.	1.5	17
16268	Tuning from Half-Metallic to Semiconducting Behavior in SiC Nanoribbons. Journal of Physical Chemistry C, 2013, 117, 15447-15455.	1.5	26
16269	Functionalization Based on the Substitutional Flexibility: Strong Middle IR Nonlinear Optical Selenides AX^{II}₄X^{III}₅Se₁₂. Journal of the American Chemical Society, 2013, 135, 12914-12921.	6.6	183
16270	Effect of Heat Treatment on the Lithium Ion Conduction of the LiBH₄â€“LiI Solid Solution. Journal of Physical Chemistry C, 2013, 117, 3249-3257.	1.5	65
16271	Structure and stability of borohydride on Au(111) and Au₃M(111) (M = Cr, Mn, Fe, Co, Ni) surfaces. Dalton Transactions, 2013, 42, 770-775.	1.6	34
16272	Variation of Kondo Peak Observed in the Assembly of Heteroleptic 2,3-Naphthalocyaninato Phthalocyaninato Tb(III) Double-Decker Complex on Au(111). ACS Nano, 2013, 7, 1092-1099.	7.3	47
16273	First-Principles Study on a Potential Hydrogen Storage Medium of Mg/TiAl Sandwiched Films. Journal of Physical Chemistry C, 2013, 117, 25374-25380.	1.5	11
16274	Can cation vacancy defects induce room temperature ferromagnetism in GaN?. Applied Physics Letters, 2013, 102, 062411.	1.5	28
16275	Formation, Stabilities, and Electronic and Catalytic Performance of Platinum Catalyst Supported on Non-Metal-Doped Graphene. Journal of Physical Chemistry C, 2013, 117, 5258-5268.	1.5	78
16276	New Insights into the Origin of Visible-Light Photocatalytic Activity in Se-Modified Anatase TiO₂ from Screened Coulomb Hybrid DFT Calculations. Journal of Physical Chemistry C, 2013, 117, 25229-25235.	1.5	28
16277	Magnetic and electronic properties of Fe3O4/graphene heterostructures: First principles perspective. Journal of Applied Physics, 2013, 113, .	1.1	6

#	Article	IF	Citations
16278	Investigations on the gate oxide dependence of AC RTN characteristics in nanoscaled MOSFETs: SiON vs. HfO<inf>2</inf>. , 2013, , .		0
16279	Enhancement of gettering in epitaxial thin-film silicon solar cells by tuning the properties of porous silicon. , 2013, , .		1
16280	Formation and migration energies of the vacancy in Si calculated using the HSE06 range-separated hybrid functional. Physical Review B, 2013, 88, .	1.1	35
16281	Ferroelectric control of magnetic anisotropy of FePt/BaTiO3 magnetoelectric heterojunction: A density functional theory study. Journal of Applied Physics, 2013, 113, .	1.1	17
16282	Enhancement of the hole-induced d⁰-ferromagnetism in ZnO through compensated donorâ€“acceptor complexes: a first-principles study. Semiconductor Science and Technology, 2013, 28, 035017.	1.0	8
16283	Insights into the Mechanism of Fe(II) Adsorption and Oxidation at Feâ€“Clay Mineral Surfaces from First-Principles Calculations. Journal of Physical Chemistry C, 2013, 117, 22880-22886.	1.5	53
16284	Metal-insulator transition at the LaAlO<mml:math xmlns:mml="http://www.w3.org/1998/Math/MathML" display="inline"><mml:msub><mml:mrow /><mml:mn>3</mml:mn></mml:msub></mml:math>/SrTiO<mml:math xmlns:mml="http://www.w3.org/1998/Math/MathML" display="inline"><mml:msub><mml:mrow /><mml:mn>3</mml:mn></mml:msub></mml:math>interface revisited: A hybrid functional study. Physical Review B, 2013, 88, .	1.1	20
16285	Effect of Metal Surfaces in On-Surface Glaser Coupling. Journal of Physical Chemistry C, 2013, 117, 18595-18602.	1.5	95
16286	Modeling Water Adsorption on Rutile (110) Using van der Waals Density Functional and DFT+U Methods. Journal of Physical Chemistry C, 2013, 117, 23638-23644.	1.5	33
16287	Examining the Effects of Different Ring Configurations and Equatorial Fluorine Atom Positions on CO₂ Sorption in [Cu(bpy)₂SiF₆]. Crystal Growth and Design, 2013, 13, 4542-4548.	1.4	17
16288	Mixed Termination of Hematite (Î±-Fe₂O₃)(0001) Surface. Journal of Physical Chemistry C, 2013, 117, 24339-24344.	1.5	48
16289	First-Principles Investigation on Elastic Constants of TiN under High Pressure. Advanced Materials Research, 0, 802, 109-113.	0.3	1
16290	Thermally Induced Desulfurization: Structural Transformation of Thiophene on the Si(100) Surface. Journal of Physical Chemistry C, 2013, 117, 11731-11737.	1.5	9
16291	Role of Te in the low-dimensional multiferroic material FeTe<mml:math xmlns:mml="http://www.w3.org/1998/Math/MathML" display="inline"><mml:msub><mml:mrow /><mml:mn>2</mml:mn></mml:msub></mml:math>O<mml:math xmlns:mml="http://www.w3.org/1998/Math/MathML" display="inline"><mml:msub><mml:mrow /><mml:mn>5</mml:mn></mml:msub></mml:math>: Physical Review B, 2013, 88, .	1.1	10
16292	Thermal properties of UO₂with a non-local exchange-correlation pressure correction: a systematic first principles DFT + U study. Modelling and Simulation in Materials Science and Engineering, 2013, 21, 065014.	0.8	18
16293	Magnetic Order Through Super-Superexchanges in the Polar Magnetoelectric Organicâ€“Inorganic Hybrid Cr[(D3N-(CH2)2-PO3)(Cl)(D2O)]. Inorganic Chemistry, 2013, 52, 753-760.	1.9	8
16294	Spontaneous Reduction and Assembly of Graphene oxide into Three-Dimensional Graphene Network on Arbitrary Conductive Substrates. Scientific Reports, 2013, 3, 2065.	1.6	157
16295	Electronic structures and thermoelectric properties of layered BiCuOCh oxychalcogenides (Ch = S,) Tj ETQq1 1 0.784314 rgBT /Overlock	5.2	128

#	Article	IF	Citations
16296	Atomic Imaging of the Irreversible Sensing Mechanism of NO₂ Adsorption on Copper Phthalocyanine. Journal of the American Chemical Society, 2013, 135, 14600-14609.	6.6	53
16297	New Carbon Allotropes with Helical Chains of Complementary Chirality Connected by Ethene-type Ï€-Conjugation. Scientific Reports, 2013, 3, 3077.	1.6	52
16298	On the CO₂ Capture in Water-Free Monoethanolamine Solution: An ab Initio Molecular Dynamics Study. Journal of Physical Chemistry B, 2013, 117, 5971-5977.	1.2	30
16299	Elementary Reaction Processes Involving Atomic and Molecular Oxygen on ZrB2(0001) Surface. Journal of Physical Chemistry C, 2013, 117, 5831-5839.	1.5	5
16300	High CO2 Selectivity of ZnO Powder Catalysts for Methanol Steam Reforming. Journal of Physical Chemistry C, 2013, 117, 6493-6503.	1.5	27
16301	A reduced moment-based model for oxygen precipitation in silicon. Journal of Applied Physics, 2013, 114, 243508.	1.1	11
16302	Contacting a Conjugated Molecule with a Surface Dangling Bond Dimer on a Hydrogenated Ge(001) Surface Allows Imaging of the Hidden Ground Electronic State. ACS Nano, 2013, 7, 10105-10111.	7.3	28
16303	X-Ray Imaging and Multiferroic Coupling of Cycloidal Magnetic Domains in Ferroelectric Monodomain<mml:math xmlns:mml="http://www.w3.org/1998/Math/MathML" display="inline"><mml:msub><mml:mi>BiFeO</mml:mi><mml:mn>3</mml:mn></mml:msub></mml:math>. Physical Review Letters, 2013, 110, 217206.	2.9	67
16304	Catalytic Activity of Single Transition-Metal Atom Doped in Cu(111) Surface for Heterogeneous Hydrogenation. Journal of Physical Chemistry C, 2013, 117, 14618-14624.	1.5	77
16305	Selectively strong molecular adsorption on boron nitride monolayer induced by transition metal substrate. Current Applied Physics, 2013, 13, 2059-2063.	1.1	12
16306	Cr segregation at C11b/C40 interface in MoSi2-based alloys: A first-principles study. Intermetallics, 2013, 42, 165-169.	1.8	14
16307	Structural differences existing in bulk and nanoparticles of Y2Sn2O7: Investigated by experimental and theoretical methods. Journal of Solid State Chemistry, 2013, 200, 202-208.	1.4	17
16308	Solvated protons in density functional theoryâ€"A few examples. Electrochimica Acta, 2013, 105, 248-253.	2.6	27
16309	Hydrogen absorption and hydrogen-induced reverse segregation in palladiumâ€“silver surface. International Journal of Hydrogen Energy, 2013, 38, 14715-14724.	3.8	31
16310	Ab initio studies of Mo-based alloys: Mechanical, elastic, and vibrational properties. Intermetallics, 2013, 38, 116-125.	1.8	36
16311	MoirÃ© superstructures of silicene on hexagonal boron nitride: A first-principles study. Physics Letters, Section A: General, Atomic and Solid State Physics, 2013, 377, 2628-2632.	0.9	51
16312	Ab initio study the effects of Si and Mg dopants on point defects and Y diffusion in YAG. Computational Materials Science, 2013, 69, 261-266.	1.4	47
16313	Chemical ordering rather than random alloying in SbAs. Physical Review B, 2013, 87, .	1.1	14

#	Article	IF	Citations
16314	Modified embedded-atom method interatomic potentials for pure Y and the Vâ€“Pdâ€“Y ternary system. Modelling and Simulation in Materials Science and Engineering, 2013, 21, 085008.	0.8	15
16315	Drastic changes in electronic, magnetic, mechanical and bonding properties from Zr2CoH5 to Mg2CoH5. Journal of Solid State Chemistry, 2013, 200, 209-214.	1.4	5
16316	Origin of the Visible Light Absorption of Boron/Nitrogen Co-doped Anatase TiO₂. Journal of Physical Chemistry C, 2013, 117, 26454-26459.	1.5	25
16317	Atomic Structure of an Ultrathin Fe-Silicate Film Grown on a Metal: AÂMonolayer of Clay?. Journal of the American Chemical Society, 2013, 135, 19222-19228.	6.6	35
16318	Anatomy of perpendicular magnetic anisotropy in Fe/MgO magnetic tunnel junctions: First-principles insight. Physical Review B, 2013, 88, .	1.1	117
16319	Semihydrogenated BN Sheet: A Promising Visible-light Driven Photocatalyst for Water Splitting. Scientific Reports, 2013, 3, 1858.	1.6	127
16320	Hydrogenation and Disorder in Engineered Black<mml:math xmlns:mml="http://www.w3.org/1998/Math/MathML" display="inline"><mml:msub><mml:mi>TiO</mml:mi><mml:mn>2</mml:mn></mml:msub></mml:math>. Physical Review Letters, 2013, 111, 065505.	2.9	199
16321	Tailoring of defect levels by deformations: Te-antisite in CdTe. Journal of Physics Condensed Matter, 2013, 25, 415801.	0.7	10
16322	Hydroxyl-decorated graphene systems as candidates for organic metal-free ferroelectrics, multiferroics, and high-performance proton battery cathode materials. Physical Review B, 2013, 87, .	1.1	100
16323	Defect mediated manipulation of nanoclusters on an insulator. Scientific Reports, 2013, 3, 1270.	1.6	14
16324	Pressure-induced polymerization of nitrogen in potassium azides. Europhysics Letters, 2013, 104, 16005.	0.7	39
16325	Effect of MgO(100) support on structure and properties of Pd and Pt nanoparticles with 49-155 atoms. Journal of Chemical Physics, 2013, 139, 084701.	1.2	41
16326	Strain-induced modification in the magnetic properties of Mn5Ge3 thin films. Journal of Applied Physics, 2013, 114, .	1.1	17
16327	Pressure-induced half-metallicity in Co2MnGe0.75Ga0.25. Journal of Magnetism and Magnetic Materials, 2013, 346, 192-195.	1.0	1
16328	Orbital-selective single molecule rectifier on graphene-covered Ru(0001) surface. Applied Physics Letters, 2013, 102, 163506.	1.5	10
16329	A new family of star-like icosahedral structures for small cobalt clusters. Chemical Physics, 2013, 415, 106-111.	0.9	12
16330	Density functional theory (DFT) study of Zn, O2 and O adsorption on polar ZnO(0001) and ZnO (0001) surfaces. Journal of Crystal Growth, 2013, 374, 53-59.	0.7	10
16331	Optimized purification for density matrix calculation. Chemical Physics Letters, 2013, 555, 291-295.	1.2	20

#	Article	IF	Citations
16332	Characterization of Te-antisite-related defects in HgCdTe. Physics Letters, Section A: General, Atomic and Solid State Physics, 2013, 377, 2663-2667.	0.9	0
16333	display="inline"><mml:msub><mml:mrow /><mml:mrow><mml:mn>3</mml:mn><mml:mo>â^'</mml:mo><mml:mi>x</mml:mi></mml:mrow></mml:msub></mml:math>Fe<mml:math xmlns:mml="http://www.w3.org/1998/Math/MathML" display="inline"><mml:msub><mml:mrow /><mml:mi>x</mml:mi></mml:msub></mml:math>Sn<mml:math	1.1	7
16334	On the role of strong electron correlations in the surface properties and chemistry of uranium dioxide. Dalton Transactions, 2013, 42, 4570.	1.6	32
16335	Synthesis and Characterization of Patronite Form of Vanadium Sulfide on Graphitic Layer. Journal of the American Chemical Society, 2013, 135, 8720-8725.	6.6	300
16336	High-precision X-ray diffraction data, experimental and theoretical study of 2H-MoS2. Russian Chemical Bulletin, 2013, 62, 1852-1857.	0.4	9
16337	Ab initio study of the distribution of point defects at grain boundaries in crystalline silicon. JETP Letters, 2013, 98, 76-79.	0.4	2
16338	Electronic structures and half-metallicity in perovskite BaRu1â^'xFexO3: first-principles studies. European Physical Journal B, 2013, 86, 1.	0.6	4
16339	Influence of spin-phonon coupling on antiferromagnetic spin fluctuations in FeSe under pressure: First-principles calculations with van der Waals corrections. Physical Review B, 2013, 88, .	1.1	23
16340	First Observation of a Kondo Resonance for a Stable Neutral Pure Organic Radical, 1,3,5-Triphenyl-6-oxoverdazyl, Adsorbed on the Au(111) Surface. Journal of the American Chemical Society, 2013, 135, 651-658.	6.6	56
16341	Insights into graphene functionalization by single atom doping. Nanotechnology, 2013, 24, 505715.	1.3	10
16342	Carrier-mediated magnetism in transition metal doped Bi2Se3 topological insulator. Journal of Physics Condensed Matter, 2013, 25, 445003.	0.7	5
16343	Structure Sensitivity in CO Oxidation by a Single Au Atom Supported on Ceria. Journal of Physical Chemistry C, 2013, 117, 7721-7726.	1.5	45
16344	Ï‡ and Ïƒ Phases in Binary Rheniumâ€“Transition Metal Systems: a Systematic First-Principles Investigation. Inorganic Chemistry, 2013, 52, 3674-3686.	1.9	31
16345	Establishing the Accuracy of Broadly Used Density Functionals in Describing Bulk Properties of Transition Metals. Journal of Chemical Theory and Computation, 2013, 9, 1631-1640.	2.3	184
16346	4,4â€²-Dithiodipyridine on Au(111): A Combined STM, STS, and DFT Study. Journal of Physical Chemistry C, 2013, 117, 20060-20067.	1.5	9
16347	Low-energy electron reflectivity from graphene. Physical Review B, 2013, 87, .	1.1	83
16348	Steering On-Surface Self-Assembly of High-Quality Hydrocarbon Networks with Terminal Alkynes. Journal of Physical Chemistry C, 2013, 117, 3987-3995.	1.5	40
16349	Blue luminescence and Zn acceptor in GaN. Physical Review B, 2013, 88, .	1.1	53

#	Article	IF	Citations
16350	Tuning the Structure of Ultrathin<mml:math xmlns:mml="http://www.w3.org/1998/Math/MathML" display="inline"><mml:msub><mml:mi>BaTiO</mml:mi><mml:mn>3</mml:mn></mml:msub></mml:math>Films on Me(001) (<mml:math xmlns:mml="http://www.w3.org/1998/Math/MathML") Tj ETQq0 0 0 rgBT /Overlock 10 Tf 50 737 Td [(display=" Surfaces. Physical Review Letters, 2013, 111, 105501.	7.9	14
16351	The electrostatic interaction of an external charged system with a metal surface: a simplified density functional theory approach. Journal of Physics Condensed Matter, 2013, 25, 355006.	0.7	9
16352	Pressure-Driven Enhancement of Topological Insulating State in Tin Telluride. Journal of Physical Chemistry C, 2013, 117, 8437-8442.	1.5	16
16353	Interface engineering through atomic dopants in HfO2-based gate stacks. Journal of Applied Physics, 2013, 114, .	1.1	14
16354	Structural Phase Transitions on AgCuS Stromeyerite Mineral under Compression. Inorganic Chemistry, 2013, 52, 355-361.	1.9	26
16355	Noncovalent Functionalization with Alkali Metal to Separate Semiconducting from Metallic Carbon Nanotubes: A Theoretical Study. Journal of Physical Chemistry C, 2013, 117, 4309-4313.	1.5	13
16356	Role of the Anchored Groups in the Bonding and Self-Organization of Macrocycles: Carboxylic versus Pyrrole Groups. Journal of Physical Chemistry C, 2013, 117, 7661-7668.	1.5	8
16357	CO Oxidation at the Interface of Au Nanoclusters and the Stepped-CeO₂(111) Surface by the Marsâ€“van Krevelen Mechanism. Journal of Physical Chemistry Letters, 2013, 4, 216-221.	2.1	148
16358	Local Reconstructions of Silicene Induced by Adatoms. Journal of Physical Chemistry C, 2013, 117, 26305-26315.	1.5	91
16359	Optical Transition and Photocatalytic Performance of d¹ Metallic Perovskites. Journal of Physical Chemistry C, 2013, 117, 5593-5598.	1.5	31
16360	Computational Investigation of CO Adsorption and Oxidation on Mn/CeO₂(111) Surface. Journal of Physical Chemistry C, 2013, 117, 433-441.	1.5	75
16361	Li Segregation Induces Structure and Strength Changes at the Amorphous Si/Cu Interface. Nano Letters, 2013, 13, 4759-4768.	4.5	75
16362	Photoelectron and Absorption Spectroscopy Studies of Metal-Free Phthalocyanine on Au(111): Experiment and Theory. Journal of Physical Chemistry C, 2013, 117, 7018-7025.	1.5	17
16363	First-principles approaches to simulate lithiation in silicon electrodes. Modelling and Simulation in Materials Science and Engineering, 2013, 21, 074001.	0.8	32
16364	Hydrogen Bond Dynamics in Proton-Conducting Lanthanum Arsenate. Journal of Physical Chemistry C, 2013, 117, 18006-18012.	1.5	11
16365	Effects of Sn²⁺ Ion Size on Sn Doped SrTiO₃. Japanese Journal of Applied Physics, 2013, 52, 09KC04.	0.8	5
16366	Heterogeneous Mercury Oxidation on Au(111) from First Principles. Environmental Science & Technology, 2013, 47, 8515-8522.	4.6	103
16367	Possibility of a Field Effect Transistor Based on Dirac Particles in Semiconducting Anatase-TiO₂ Nanowires. Nano Letters, 2013, 13, 1073-1079.	4.5	10

#	Article	IF	Citations
16368	Stability of Extraframework Iron-Containing Complexes in ZSM-5 Zeolite. Journal of Physical Chemistry C, 2013, 117, 413-426.	1.5	75
16369	Driving Magnetostructural Transitions in Layered Intermetallic Compounds. Physical Review Letters, 2013, 110, 217211.	2.9	48
16370	Defect Suppression in AlN Epilayer Using Hierarchical Growth Units. Journal of Physical Chemistry C, 2013, 117, 14158-14164.	1.5	11
16371	Microkinetic Simulation of Temperature-Programmed Desorption. Journal of Physical Chemistry C, 2013, 117, 6136-6142.	1.5	14
16372	Pits confined in ultrathin cerium(IV) oxide for studying catalytic centers in carbon monoxide oxidation. Nature Communications, 2013, 4, 2899.	5.8	326
16373	Thermal Lattice Expansion Effect on Reactive Scattering of H₂ from Cu(111) at T_s = 925 K. Journal of Physical Chemistry A, 2013, 117, 8770-8781.	1.1	50
16374	Pressure depended elastic, vibration and optical properties of NbIrSn from first principles calculations. Materials Science and Technology, 2013, 29, 925-930.	0.8	8
16375	Noncollinear Spin States for Density Functional Calculations of Open-Shell and Multi-Configurational Systems: Dissociation of MnO and NiO and Barrier Heights of O₃, BeH₂, and H₄. Journal of Chemical Theory and Computation, 2013, 9, 5349-5355.	2.3	14
16376	NiO-MgO and CoO-MgO Thin-Film Solid Oxide Solutions on a Mo(100) Support: Formation, Reduction, and Influence of the Support. Journal of Physical Chemistry C, 2013, 117, 280-287.	1.5	9
16377	A Pathway to Type-I Band Alignment in Ge/Si Coreâ€“Shell Nanowires. Journal of Physical Chemistry Letters, 2013, 4, 121-126.	2.1	14
16378	Viscosity of Ultrathin Water Films Confined between Aluminol Surfaces of Kaolinite: Ab Initio Simulations. Journal of Physical Chemistry C, 2013, 117, 6088-6095.	1.5	26
16379	Electronic structures of zigzag silicene nanoribbons with asymmetric sp2â^'sp3 edges. Applied Physics Letters, 2013, 102, .	1.5	74
16380	Origin of anomalous strain effects on the molecular adsorption on boron-doped graphene. Journal of Chemical Physics, 2013, 139, 044709.	1.2	6
16381	Giant electroresistance and tunable magnetoelectricity in a multiferroic junction. Physical Review B, 2013, 88, .	1.1	3
16382	Grain Boundary Induced Conductivity in Li₂O₂. Journal of Physical Chemistry C, 2013, 117, 25222-25228.	1.5	45
16383	Firstâ€Principles Study of Hydrolysis Reaction Barriers in a Sodium Borosilicate Glass. International Journal of Applied Glass Science, 2013, 4, 395-407.	1.0	66
16384	Connecting bulk symmetry and orbital polarization in strained RNiO<mml:math xmlns:mml="http://www.w3.org/1998/Math/MathML" display="inline"><mml:msub><mml:mrow /><mml:mn>3</mml:mn></mml:msub></mml:math>ultrathin films. Physical Review B, 2013, 88, .	1.1	40
16385	First principles study of the interface between silicone and undoped/doped BaTiO3. Journal of Applied Physics, 2013, 113, .	1.1	5

#	Article	IF	Citations
16386	Nontrivial topological electronic structures in a single Bi(111) bilayer on different substrates: A first-principles study. Physical Review B, 2013, 88, .	1.1	83
16387	Dipole Orientation Dependent Symmetry Reduction of Chloroaluminum Phthalocyanine on Cu(111). Journal of Physical Chemistry C, 2013, 117, 1013-1019.	1.5	38
16388	Crystal structure and magnetic properties of a new layered sodium nickel hydroxide phosphate, Na2Ni3(OH)2(PO4)2. Dalton Transactions, 2013, 42, 14718.	1.6	15
16389	Insight into Organometallic Intermediate and Its Evolution to Covalent Bonding in Surface-Confined Ullmann Polymerization. ACS Nano, 2013, 7, 8190-8198.	7.3	190
16390	Elucidating Band-Selective Sensitization in Iron(II) Polypyridine-TiO₂ Assemblies. Inorganic Chemistry, 2013, 52, 8621-8628.	1.9	48
16391	Long Range Chiral Imprinting of Cu(110) by Tartaric Acid. Journal of Physical Chemistry C, 2013, 117, 22290-22297.	1.5	53
16392	Multi-Scale Characterization Studies of Aged Li-Ion Large Format Cells for Improved Performance: An Overview. Journal of the Electrochemical Society, 2013, 160, A2111-A2154.	1.3	50
16393	Tetrahydrofuran in TiCl₄/THF/MgCl₂: a Non-Innocent Ligand for Supported Zieglerâ€“Natta Polymerization Catalysts. ACS Catalysis, 2013, 3, 52-56.	5.5	58
16394	Magnetic Structure and Electromagnetic Properties of LnCrAsO with a ZrCuSiAs-type Structure (Ln =) Tj ETQq0 0 0 rgBT /Overlock 10 Tf	1.9	34
16395	Hydration Dynamics for Vanadia/Titania Catalysts at High Loading: A Combined Theoretical and Experimental Study. Journal of Physical Chemistry C, 2013, 117, 25535-25544.	1.5	17
16396	Understanding Structure and Bonding of Multilayered Metalâ€“Organic Nanostructures. Journal of Physical Chemistry C, 2013, 117, 3055-3061.	1.5	36
16397	Hydrogen Dynamics in Nanoconfined Lithiumborohydride. Journal of Physical Chemistry C, 2013, 117, 3789-3798.	1.5	51
16398	DFT Studies of Pristine Hexagonal Ge₁Sb₂Te₄(0001), Ge₂Sb₂Te₅(0001), and Ge₁Sb₄Te₇(0001) Surfaces. Journal of Physical Chemistry C, 2013, 117, 15075-15089.	1.5	29
16399	Patterning Graphitic Câ€“N Sheets into a Kagome Lattice for Magnetic Materials. Journal of Physical Chemistry Letters, 2013, 4, 259-263.	2.1	55
16400	Identification of the Scaling Relations for Binary Noble-Metal Nanoparticles. Journal of Physical Chemistry C, 2013, 117, 2849-2854.	1.5	17
16401	Electrospun sillenite Bi12MO20 (M = Ti, Ge, Si) nanofibers: general synthesis, band structure, and photocatalytic activity. Physical Chemistry Chemical Physics, 2013, 15, 20698.	1.3	106
16402	Yellow Luminescence of Gallium Nitride Generated by Carbon Defect Complexes. Physical Review Letters, 2013, 110, 087404.	2.9	208
16403	The Influence of Water and Hydroxyl on a Bimetallic (âˆš3 Ã— âˆš3)R30Â° Sn/Pt Surface Alloy. Journal of Physical Chemistry C, 2013, 117, 4032-4039.	1.5	11

#	Article	IF	Citations
16404	Reduction Mechanisms of Ethylene Carbonate on Si Anodes of Lithium-Ion Batteries: Effects of Degree of Lithiation and Nature of Exposed Surface. ACS Applied Materials & Interfaces, 2013, 5, 13457-13465.	4.0	68
16405	Dispersive Electronic States of the Ï€-Orbitals Stacking in Single Molecular Lines on the Si(001)-(2Ã—1)-H Surface. Journal of Physical Chemistry Letters, 2013, 4, 1199-1204.	2.1	2
16406	Tunable Anderson Localization in Hydrogenated Graphene Based on the Electric Field Effect. Physical Review Letters, 2013, 111, 216801.	2.9	4
16407	Surface Interactions of C₂ and C₃ Polyols with Î³-Al₂O₃ and the Role of Coadsorbed Water. Langmuir, 2013, 29, 581-593.	1.6	66
16408	Photoswitchable Molecular Rings for Solar-Thermal Energy Storage. Journal of Physical Chemistry Letters, 2013, 4, 854-860.	2.1	74
16409	First-Principles Investigations on the Na₂MnPO₄F as a Cathode Material for Na-Ion Batteries. Journal of the Electrochemical Society, 2013, 160, A927-A932.	1.3	34
16410	Origin of the Voltage Hysteresis in the CoP Conversion Material for Li-Ion Batteries. Journal of Physical Chemistry C, 2013, 117, 837-849.	1.5	87
16411	Oxidative Dehydrogenation of Methane by Isolated Vanadium Oxide Clusters Supported on Au (111) and Ag (111) Surfaces. Journal of Physical Chemistry C, 2013, 117, 18475-18483.	1.5	8
16412	Modeling the Interaction of Nanoparticles with Mineral Surfaces: Adsorbed C₆₀ on Pyrophyllite. Journal of Physical Chemistry A, 2013, 117, 6602-6611.	1.1	15
16413	Unit cell structure of the wurtzite phase of GaP nanowires: X-ray diffraction studies and density functional theory calculations. Physical Review B, 2013, 88, .	1.1	28
16414	Effects of interface bonding and defects on boron diffusion at Si/SiO2 interface. Journal of Applied Physics, 2013, 114, .	1.1	12
16415	Ferroelectric ground state and polarization-switching path of orthorhombic YMnO3with coexistingE-type and cycloidal spin phases. Physical Review B, 2013, 88, .	1.1	6
16416	Selective Excitation of Atomic-Scale Dynamics by Coherent Exciton Motion in the Non-Bornâ€“Oppenheimer Regime. Journal of Physical Chemistry Letters, 2013, 4, 4260-4266.	2.1	8
16417	Possible Bose-condensate behavior in a quantum phase originating in a collective excitation in the chemically and optically doped Mott-Hubbard system UO<mml:math xmlns:mml="http://www.w3.org/1998/Math/MathML" display="inline"><mml:msub><mml:mrow /><mml:mrow><mml:mn>2</mml:mn><mml:mo>+</mml:mo><mml:mi>x</mml:mi></mml:mrow></mml:msub></mml:math>. Physical Review B, 2013, 88, .	1.1	39
16418	Structure of Stoichiometric and Oxygen-Rich Ultrathin FeO(111) Films Grown on Pd(111). Journal of Physical Chemistry C, 2013, 117, 15155-15163.	1.5	52
16419	Response of silicane and germanane to uni-axial compression: Superstructures, polymorph nano-ribbons, and extreme bending. Journal of Chemical Physics, 2013, 139, 124709.	1.2	26
16420	The origin of magnetism in transition metal-doped ZrO₂thin films: experiment and theory. Journal of Physics Condensed Matter, 2013, 25, 436003.	0.7	20
16421	Intrinsic Spin Seebeck Effect in<mml:math xmlns:mml="http://www.w3.org/1998/Math/MathML" display="inline"><mml:mi>Au</mml:mi><mml:mo>/</mml:mo><mml:mi>YIG</mml:mi></mml:math>. Physical Review Letters, 2013, 110, 067206.	2.9	246

#	Article	IF	Citations
16422	Electronic structure and the groundâ€state properties of cobalt antimonide skutterudites: Revisited with different theoretical methods. Physica Status Solidi (A) Applications and Materials Science, 2013, 210, 131-139.	0.8	22
16423	ScPdZn and ScPtZn with YAlGe Type Structure â€“ Groupâ€Subgroup Relation and ⁴⁵Sc Solid State NMR Spectroscopy. Zeitschrift Fur Anorganische Und Allgemeine Chemie, 2013, 639, 246-253.	0.6	6
16424	Novel Nanoscale Twinned Phases in Perovskite Oxides. Advanced Functional Materials, 2013, 23, 234-240.	7.8	101
16425	Steering the Growth of Metal Adâ€particles via Interface Interactions Between a MgO Thin Film and a Mo Support. Advanced Functional Materials, 2013, 23, 75-80.	7.8	24
16426	Novel Nanorod Precipitate Formation in Neodymium and Titanium Codoped Bismuth Ferrite. Advanced Functional Materials, 2013, 23, 683-689.	7.8	29
16427	Synthesis, Characterization, and Structural Modeling of Highâ€Capacity, Dual Functioning MnO₂ Electrode/Electrocatalysts for Liâ€O₂ Cells. Advanced Energy Materials, 2013, 3, 75-84.	10.2	111
16428	Inverse Design of High Absorption Thinâ€Film Photovoltaic Materials. Advanced Energy Materials, 2013, 3, 43-48.	10.2	316
16429	Highâ€Throughput Computational Screening of New Liâ€ion Battery Anode Materials. Advanced Energy Materials, 2013, 3, 252-262.	10.2	150
16430	Realization of the Switching Mechanism in Resistance Random Access Memoryâ„¢ Devices: Structural and Electronic Properties Affecting Electron Conductivity in a Hafnium Oxideâ€“Electrode System Through First-Principles Calculations. Journal of Electronic Materials, 2013, 42, 143-150.	1.0	10
16431	Scrutinizing negative thermal expansion in MOF-5 by scattering techniques and ab initio calculations. Dalton Transactions, 2013, 42, 1996-2007.	1.6	59
16432	First principle study of cobalt impurity in bcc Fe with Cu precipitates. Journal of Materials Science, 2013, 48, 1377-1386.	1.7	17
16433	Hydrogen-induced nanotunnel opening within semiconductor subsurface. Nature Communications, 2013, 4, .	5.8	10
16434	Stress Formulation in the All-Electron Full-Potential Linearized Augmented Plane Wave Method: II. Accuracy Check in the Generalized Gradient Approximation. Journal of the Physical Society of Japan, 2013, 82, 044701.	0.7	1
16435	Electronic and Oxygen Migration Properties of Monoclinic La₂GeO_{5-Î´}. Journal of the Physical Society of Japan, 2013, 82, 084702.	0.7	0
16436	Alloying-related trends from first principles: An application to the Tiâ€“Alâ€“Xâ€“N system. Journal of Applied Physics, 2013, 113, .	1.1	55
16437	Ab initio Investigations of Carbon Atoms Adsorbed on Î±-Al2O3 Surfaces in Relation to Graphene Growth. Journal of the Physical Society of Japan, 2013, 82, 114709.	0.7	2
16438	Bilipid membrane phase characterization by reflectance anisotropy spectroscopy (RAS). Proceedings of SPIE, 2013, , .	0.8	0
16439	Sign-inverted response of aluminum work function to tangential strain. Journal of Physics Condensed Matter, 2013, 25, 445012.	0.7	3

#	Article	IF	Citations
16440	Zn_xCd_{1â^'x}Se nanomultipods with tunable band gaps: synthesis and first-principles calculations. Nanotechnology, 2013, 24, 235706.	1.3	12
16441	Structure of the clean Gd5Ge4(010) surface. Journal of Physics Condensed Matter, 2013, 25, 485002.	0.7	0
16442	Extended Czjzek model applied to NMR parameter distributions in sodium metaphosphate glass. Journal of Physics Condensed Matter, 2013, 25, 255402.	0.7	15
16443	Pathways and kinetics of methane and ethane Câ€“H bond cleavage on PdO(101). Journal of Chemical Physics, 2013, 139, 104702.	1.2	49
16444	Adhesion of the ironâ€“chromium oxide interface from first-principles theory. Journal of Physics Condensed Matter, 2013, 25, 495501.	0.7	10
16445	Site preference of Mg acceptors and improvement of p-type doping efficiency in nitride alloys. Journal of Physics Condensed Matter, 2013, 25, 245801.	0.7	1
16446	Oxygen adsorption on the Al₉Co₂(001) surface: first-principles and STM study. Journal of Physics Condensed Matter, 2013, 25, 355003.	0.7	7
16447	Prediction of a Superhard Material: B₄C₄. Journal of the Physical Society of Japan, 2013, 82, 073702.	0.7	11
16448	A density-functional theory study of tip electronic structures in scanning tunneling microscopy. Nanotechnology, 2013, 24, 105201.	1.3	7
16449	Enhanced ferromagnetism by adding electrons in triple-decker Gdâ€“phthalocyanine. Physica Scripta, 2013, 87, 045701.	1.2	1
16450	Observation of a pressure-induced Asâ€“As hybridization associated with a change in the electronic state of Fe in the tetragonal phase of EuFe₂As₂. Journal of Physics Condensed Matter, 2013, 25, 022201.	0.7	8
16451	Molecular dynamics evidence for alkali-metal rattling in the Î²-pyrochlores, AOs₂O₆(A = K, Rb, Cs). Journal of Physics Condensed Matter, 2013, 25, 475404.	0.7	3
16452	Energy ordering of grain boundaries in Cr2O3: insights from theory. Journal of Physics Condensed Matter, 2013, 25, 485005.	0.7	5
16453	Electronic structure and thermodynamic stability of uranium-doped yttrium iron garnet. Journal of Physics Condensed Matter, 2013, 25, 495502.	0.7	13
16454	Phase stability and elastic properties of Crâ€“V alloys. Journal of Physics Condensed Matter, 2013, 25, 075402.	0.7	31
16455	Size-dependent permittivity and intrinsic optical anisotropy of nanometric gold thin films: a density functional theory study. Optics Express, 2013, 21, 11827.	1.7	52
16456	Fine band gap modulation effects of aGNRs by an organic functional group: a first-principles study. Journal Physics D: Applied Physics, 2013, 46, 235101.	1.3	5
16457	Hybridization between Cuâ€“O chain and Cu(110) surface states in the O(2Ã—1)/Cu(110) surface from first principles. Journal of Physics Condensed Matter, 2013, 25, 135003.	0.7	6

#	Article	IF	Citations
16458	Epitaxial strain induced magnetic transitions and phonon instabilities in tetragonal SrRuO3. Journal of Physics Condensed Matter, 2013, 25, 165504.	0.7	1
16459	Substrate dependence of Pt4 electronic properties. Journal of Physics Condensed Matter, 2013, 25, 222001.	0.7	3
16460	Structure and phase transitions at the interface between Î±-Al₂O₃and Pt. Journal of Physics Condensed Matter, 2013, 25, 232202.	0.7	8
16461	Magnetic anisotropy of FeO and CoO: the influence of gradient corrections on exchange and correlation. Journal of Physics Condensed Matter, 2013, 25, 486002.	0.7	6
16462	Chemical evolution via beta decay: a case study in strontium-90. Journal of Physics Condensed Matter, 2013, 25, 065504.	0.7	17
16463	Optical absorption and emission of Î±-Sn nanocrystals from first principles. Nanotechnology, 2013, 24, 405702.	1.3	13
16464	The atomic and electronic structures of NiO(001)/Au(001) interfaces. Journal of Chemical Physics, 2013, 139, 144705.	1.2	7
16465	STM imagery and density functional calculations of C60fullerene adsorption on the 6H-SiC(0001)-3Ã—3 surface. Physical Review B, 2013, 87, .	1.1	10
16466	Roles of core-shell and Î´-ray kinetics in layered BN Î±-voltaic efficiency. Journal of Applied Physics, 2013, 113, 063703.	1.1	2
16467	Non-polar p-type Zn0.94Mn0.05Na0.01O texture: Growth mechanism and codoping effect. Journal of Applied Physics, 2013, 113, 083513.	1.1	8
16468	Structure and chemical reactivity of the polar three-fold surfaces of GaPd: A density-functional study. Journal of Chemical Physics, 2013, 138, 124703.	1.2	19
16469	Single domain Bi2Se3 films grown on InP(111)A by molecular-beam epitaxy. Applied Physics Letters, 2013, 102, .	1.5	45
16470	Origin of the unusual reflectance and density contrasts in the phase-change material Cu₂GeTe₃. Applied Physics Letters, 2013, 102, 224105.	1.5	37
16471	Exploration on pressure-induced phase transition of cerium mononitride from first-principles calculations. Applied Physics Letters, 2013, 102, .	1.5	16
16472	Thermal conductivity of argon at high pressure from first principles calculations. Journal of Applied Physics, 2013, 114, 064902.	1.1	14
16473	Local order of Ge atoms in amorphous GeTe nanoscale ultrathin films. Applied Physics Letters, 2013, 103, .	1.5	21
16474	Unusual sevenfold coordination of Ru in complex hydride Na3RuH7: Prospect for formation of [FeH7]3â€“ anion. Applied Physics Letters, 2013, 103, 113903.	1.5	10
16475	AA stacking, tribological and electronic properties of double-layer graphene with krypton spacer. Journal of Chemical Physics, 2013, 139, 154705.	1.2	23

#	Article	IF	Citations
16476	The dissociative chemisorption of methane on Ni(100) and Ni(111): Classical and quantum studies based on the reaction path Hamiltonian. Journal of Chemical Physics, 2013, 139, 194701.	1.2	44
16477	Electronic structural and magnetic properties of Mn5Ge3 clusters. Journal of Chemical Physics, 2013, 139, 204307.	1.2	3
16478	Tuning the Magnetism by CO Adsorption in Graphene-Like ZnO with Defect. Journal of the Physical Society of Japan, 2013, 82, 064702.	0.7	2
16479	Appearance of Flat Bands and Edge States in Boronâ€“Carbonâ€“Nitride Nanoribbons. Journal of the Physical Society of Japan, 2013, 82, 083710.	0.7	6
16480	Correlation between the variation in observed melting temperatures and structural motifs of the global minima of gallium clusters: An ab initio study. Journal of Chemical Physics, 2013, 138, 014303.	1.2	14
16481	Oxidation of the two-phase Nb/Nb5Si3 composite: The role of energetics, thermodynamics, segregation, and interfaces. Journal of Chemical Physics, 2013, 138, 014708.	1.2	17
16482	Full DFT-D description of a nanoporous supramolecular network on a silicon surface. Journal of Chemical Physics, 2013, 138, 084704.	1.2	11
16483	Strain-engineered A-type antiferromagnetic order in YTiO3: A first-principles calculation. Journal of Applied Physics, 2013, 113, .	1.1	18
16484	First-principles analyses of unusual ferromagnetism observed in CrSi2(core)/SiO2(shell) nanocables. Journal of Applied Physics, 2013, 113, 17E140.	1.1	3
16485	First-principles investigations on the magnetic property in tripotassium doped picene. Journal of Applied Physics, 2013, 113, 17E131.	1.1	14
16486	Effects of intrinsic defects on methanthiol monolayers on Cu(111): A density functional theory study. Journal of Chemical Physics, 2013, 138, 134708.	1.2	0
16487	Density functional study of methanol decomposition on clean and O or OH adsorbed PdZn(111). Journal of Chemical Physics, 2013, 138, 184701.	1.2	13
16488	Absorption induced modulation of magnetism in two-dimensional metal-phthalocyanine porous sheets. Journal of Chemical Physics, 2013, 138, 204706.	1.2	17
16489	Bottom-up modeling of Al/Ni multilayer combustion: Effect of intermixing and role of vacancy defects on the ignition process. Journal of Applied Physics, 2013, 113, 204301.	1.1	8
16490	Grain boundary composition and conduction in HfO2: An ab initio study. Applied Physics Letters, 2013, 102, .	1.5	54
16491	Comparison of density functionals for nitrogen impurities in ZnO. Journal of Chemical Physics, 2013, 138, 234702.	1.2	13
16492	The structure of SrTiO3(001)-2â€‰Ã—â€‰1 surface analyzed by high-resolution medium energy ion scattering coupled with ab initio calculations. Journal of Chemical Physics, 2013, 138, 244705.	1.2	4
16493	Determination of effective work function of Pr0.7Ca0.3MnO3 and Pt films on ZrOx using terraced-oxide method. Applied Physics Letters, 2013, 103, 033516.	1.5	2

#	Article	IF	Citations
16494	First-principles study of energetic and electronic properties of Î´-Re6MO12 (Reâ€‰=â€‰Ho, Gd, Y; Mâ€‰=â€‰U, W). Journal of Applied Physics, 2013, 114, .	1.1	5
16495	A first-principles study of ZnO polar surface growth: Adsorption of ZnxOy clusters. Journal of Chemical Physics, 2013, 139, 124704.	1.2	7
16496	Adsorption and dissociation of oxygen molecules on Si(111)-(7Ã—7) surface. Journal of Chemical Physics, 2013, 139, 194709.	1.2	12
16497	Oxidation of step edges on vicinal 4H-SiC(0001) surfaces. Applied Physics Letters, 2013, 103, 211603.	1.5	7
16498	Strain-induced orbital polarization and multiple phase transitions in Ba2MnWO6 from first principles. Journal of Chemical Physics, 2013, 139, 204707.	1.2	3
16499	Effects of temperature and pressure on phonons in FeSi<mml:math xmlns:mml="http://www.w3.org/1998/Math/MathML" display="inline"><mml:msub><mml:mrow /><mml:mrow><mml:mn>1</mml:mn><mml:mo>â^’</mml:mo><mml:mi>x</mml:mi></mml:mrow></mml:msub><mml:mi>Al</mml:mi><mml:msub><mml:mrow /><mml:mrow><mml:mi>x</mml:mi></mml:mrow></mml:msub></mml:math>. Physical Review B, 2013, 87, .	1.1	21
16500	Investigation of Mn adatoms adsorption on graphene using first-principles calculation. Journal of Physics: Conference Series, 2013, 417, 012003.	0.3	0
16501	Role of Nanolaminated Crystal Structure on the Radiation Damage Tolerance of Ti₃SiC₂: Theoretical Investigation of Native Point Defects. Journal of Nanomaterials, 2013, 2013, 1-5.	1.5	13
16502	Systematic theoretical search for alloys with increased thermal stability for advanced hard coatings applications. New Journal of Physics, 2013, 15, 095010.	1.2	15
16503	Defect-Driven Restructuring of TiO2 Surface and Modified Reactivity Toward Deposited Gold Atoms. Catalysts, 2013, 3, 276-287.	1.6	5
16504	Investigation of single-walled carbon nanotubes with a low-energy electron point projection microscope. New Journal of Physics, 2013, 15, 043015.	1.2	13
16505	Magnetic-field-enhanced carbon solution in proeutectoid ferrite. Journal Physics D: Applied Physics, 2013, 46, 385002.	1.3	2
16506	Dynamic nano-pulling effect of the boron-functionalized graphene monovacancy for molecule dissociation. Journal Physics D: Applied Physics, 2013, 46, 385302.	1.3	10
16507	A theoretical study of the dynamical switching of a single spin by exchange forces. New Journal of Physics, 2013, 15, 013011.	1.2	15
16508	The ageing effect in topological insulators: evolution of the surface electronic structure of Bi₂Se₃upon K adsorption. New Journal of Physics, 2013, 15, 113031.	1.2	43
16509	DFT study of structural, electronic, and absorption properties of crystalline Î²-RDX under pressures. Canadian Journal of Chemistry, 2013, 91, 968-973.	0.6	5
16510	Size-selective self-assembly of magnetic Mn nanoclusters on Si(111). Journal of Chemical Physics, 2013, 138, 164705.	1.2	7
16511	Atypical charge redistribution over a charge-transfer monolayer on a metal. New Journal of Physics, 2013, 15, 083048.	1.2	16

#	Article	IF	Citations
16512	Unusual Bi-Containing Surface Layers of IIIâ€“V Compound Semiconductors. Springer Series in Materials Science, 2013, , 225-261.	0.4	0
16513	Structure and Optical Properties of Superlattices ZnO Doped with Mg. Advanced Materials Research, 0, 659, 30-35.	0.3	0
16514	First-Principles Study on Cl Adsorption on Î³-TiAl(100) Surface. Advanced Materials Research, 2013, 803, 370-374.	0.3	3
16515	First-Principles Study on Structural and Electronic Properties of the Armchair GaN Nanoribbons. Advanced Materials Research, 0, 703, 67-70.	0.3	0
16516	First-principles density functional theory study of strained wurtzite InP and InAs. Journal Physics D: Applied Physics, 2013, 46, 505106.	1.3	14
16517	Multiscale analysis of adsorption-induced surface stress of alkanethiol on microcantilever. Journal Physics D: Applied Physics, 2013, 46, 035301.	1.3	5
16518	Chemical and hydrostatic pressure effect on charge density waves of SmNiC₂. New Journal of Physics, 2013, 15, 123018.	1.2	14
16519	Enhanced upper critical fields in a new quasi-one-dimensional superconductor Nb₂Pd_xSe₅. New Journal of Physics, 2013, 15, 123031.	1.2	35
16520	Ab initioand atomistic study of generalized stacking fault energies in Mg and Mgâ€“Y alloys. New Journal of Physics, 2013, 15, 043020.	1.2	97
16521	Elastic Properties, Mechanical Stability, and State Densities of Aluminnides. Acta Physica Polonica A, 2013, 123, 668-672.	0.2	5
16522	Electronic Structure of the Cubic Perovskites BiMO_3 (M = Al, Ga, In, Sc). Acta Physica Polonica A, 2013, 124, 852-854.	0.2	13
16523	The evolution of structural and electronic properties during the glass transition process of Alâ€“Niâ€“Nd alloy. Journal Physics D: Applied Physics, 2013, 46, 105303.	1.3	4
16524	Interactions between stacked layers of phenyl-modified silicene. New Journal of Physics, 2013, 15, 125018.	1.2	13
16525	Activity of Fe₂O₃ and its Effect on Co Oxidation in the Chemical Looping Combustion: An Theoretical Account. Advanced Materials Research, 0, 726-731, 2040-2044.	0.3	3
16526	First-Principle Study of Electronic Structure and Enhanced Visible-Light Photocatalytic Activity of Anatase TiO₂ through C and F Codoping. Advanced Materials Research, 0, 746, 400-405.	0.3	3
16527	First-Principles Study of Thin-Film Properties of Transition-Metal Oxide SrTcO₃. Advanced Materials Research, 2013, 763, 17-22.	0.3	0
16528	The Effect of Carbon Monoxide Co-Adsorption on Ni-Catalysed Water Dissociation. International Journal of Molecular Sciences, 2013, 14, 23301-23314.	1.8	10
16529	First-Principles Study on Electronic Structure and Magnetic Properties of Freestanding Ni Nanobelts. Advanced Materials Research, 0, 661, 57-61.	0.3	1

#	Article	IF	Citations
16530	The Structural and Electronic Properties of the Zigzag GaN Nanoribbons: A First-Principles Study. Advanced Materials Research, 2013, 700, 79-82.	0.3	0
16531	Improvement in the hydrogen desorption from MgH2 upon transition metals doping: A hybrid density functional calculations. AIP Advances, 2013, 3, .	0.6	11
16532	Multi-Scale Simulation of Transport via a Mo/n+-GaAs Schottky Contact. Materials Research Society Symposia Proceedings, 2013, 1553, 1.	0.1	1
16533	Study of Nickel Segregation at the TiNi-Titanium Oxide Interface. Materials Science Forum, 0, 738-739, 269-273.	0.3	4
16534	Theoretical Study on Reactivity of Cu-Based Oxygen Carrier for CO Chemical Looping Combustion. Advanced Materials Research, 2013, 805-806, 1336-1339.	0.3	0
16535	The Role of Defects in Li3ClO Solid Electrolyte: Calculations and Experiments. Materials Research Society Symposia Proceedings, 2013, 1526, 1.	0.1	10
16536	Comparative study of metallic silicideâ€“germanide orthorhombic MnP systems. Journal of Physics Condensed Matter, 2013, 25, 355403.	0.7	3
16537	Hydrogenated K4 carbon: A new stable cubic gauche structure of carbon hydride. Journal of Chemical Physics, 2013, 138, 024702.	1.2	18
16538	Valence-Band Offset ofm-Plane GaN(11Ì„00) Films Grown on LiAlO₂(100) Substrates. Applied Physics Express, 2013, 6, 071001.	1.1	0
16539	Polar and Magneto-Electric Properties of Anti-Ferrodistortive Ordered Jahn-Teller Distortions in a multiferroic metal-organic framework. Journal of Physics: Conference Series, 2013, 428, 012029.	0.3	15
16540	Ab initioscreening methodology applied to the search for new permanent magnetic materials. New Journal of Physics, 2013, 15, 125023.	1.2	50
16541	First-Principles Calculation of the Electronic Properties of Single-Walled Carbon Nanotubes under Torsions. Materials Research Society Symposia Proceedings, 2013, 1505, 1.	0.1	0
16542	Defect controlled magnetism in FeP/graphene/Ni(111). Scientific Reports, 2013, 3, 3405.	1.6	31
16543	Ab initio evaluation of oxygen diffusivity in LaFeO3: the role of lanthanum vacancies. MRS Communications, 2013, 3, 161-166.	0.8	26
16544	Ternary Cu3BiY3 (Y = S, Se, and Te) for Thin-Film Solar Cells. Materials Research Society Symposia Proceedings, 2013, 1538, 235-240.	0.1	3
16545	First principles calculations and experiments for Cu-Mg/Li hydrides negative electrodes. Materials Research Society Symposia Proceedings, 2013, 1496, 1.	0.1	0
16546	Electronic Properties of Zno Doped by Rare-Earth Elements from First-Principles. Advanced Materials Research, 2013, 690-693, 623-626.	0.3	0
16547	Thermodynamic modeling of chromium: strong and weak magnetic coupling. Journal of Physics Condensed Matter, 2013, 25, 425401.	0.7	18

#	Article	IF	Citations
16548	Introducing Color Centers to Silicon Carbide Nanocrystals for In Vivo Biomarker Applications: A First Principles Study. Materials Science Forum, 2013, 740-742, 641-644.	0.3	1
16549	Iron pairs in beryl: New insights from electron paramagnetic resonance, synchrotron X-ray absorption spectroscopy, and ab initio calculations. American Mineralogist, 2013, 98, 1745-1753.	0.9	15
16550	Stability of Pristine and Defective SnTe Surfaces from First Principles. ChemPhysChem, 2013, 14, 3108-3111.	1.0	26
16551	Modulation of Dirac points and band-gaps in graphene via periodic fullerene adsorption. AIP Advances, 2013, 3, .	0.6	18
16552	Energetics of Protonic Species in Yttrium-doped Barium Zirconate: A Density Functional Theory Study. Materials Research Society Symposia Proceedings, 2013, 1495, 1.	0.1	0
16553	First Principles Prediction on the Formation and Properties of Polyanion Deficient Iron Phosphate. ECS Electrochemistry Letters, 2013, 2, A111-A113.	1.9	2
16554	Accelerating atomic orbital-based electronic structure calculation via pole expansion and selected inversion. Journal of Physics Condensed Matter, 2013, 25, 295501.	0.7	50
16555	Formation Energy Calculations of Impurity Elements at Substitutional or Interstitial Sites in Silicon. Advanced Materials Research, 0, 681, 48-52.	0.3	1
16556	Quantum-Mechanical Study of Single-Crystalline and Polycrystalline Elastic Properties of Mg-Substituted Calcite Crystals. Key Engineering Materials, 0, 592-593, 335-341.	0.4	2
16557	First-principles study of one-dimensional sandwich wires [(P)5TM]âˆž (TM = Ti, V, Cr, Mn, Fe, Co). Journal of Physics Condensed Matter, 2013, 25, 395503.	0.7	1
16558	SURFACE ENERGY ENGINEERING OF Cu SURFACE BY STRAIN: FIRST-PRINCIPLES CALCULATIONS. Surface Review and Letters, 2013, 20, 1350054.	0.5	6
16559	Band offsets at zincblende-wurtzite GaAs nanowire sidewall surfaces. Applied Physics Letters, 2013, 103, .	1.5	28
16560	Structural and Electronic Properties of Armchair GaN Nanoribbons with AlN Edges: First-Principles Study. Advanced Materials Research, 2013, 771, 101-104.	0.3	0
16561	A first-principles study of the structural and elastic properties of orthorhombic and tetragonal Ca₃Mn₂O₇. Chinese Physics B, 2013, 22, 066201.	0.7	6
16562	Extra metal adatom surface diffusion simulation on 1/3 ML Si(111) $sqrt {3}imes sqrt {3}$ metal-induced surfaces. Physica Scripta, 2013, 88, 035604.	1.2	2
16563	Ground-state structure determination and mechanical properties of palladium seminitride. Chinese Physics B, 2013, 22, 116104.	0.7	4
16564	Science than art of Si many-body potentials: Reproducibility and transferability. Europhysics Letters, 2013, 102, 33002.	0.7	1
16565	Novel high-pressure phase with pseudo-benzene â€œN ₆ â€•molecule of LiN ₃. Europhysics Letters, 2013, 101, 26004.	0.7	55

#	Article	IF	Citations
16566	Quasi-Three-Dimensional Diffusion of Li ions in Li3FePO4CO3: First-Principles Calculations for Cathode Materials of Li-Ion Batteries. Applied Physics Express, 2013, 6, 115801.	1.1	12
16567	First-Principles Study of Ag-Doped GaAs Nanowires. Chinese Physics Letters, 2013, 30, 066101.	1.3	1
16568	The Predicted fcc Superconducting Phase for Compressed Se and Te. Chinese Physics Letters, 2013, 30, 027401.	1.3	5
16569	Differences in the adsorption of FePc on coinage metal surfaces. Chinese Physics B, 2013, 22, 063101.	0.7	3
16570	Density functional theory calculations of phenol-modified monolayer silicon nanosheets. , 2013, , .		2
16571	First-principles study on the elastic properties of Bâ€² and Q phase in Alâ€“Mgâ€“Si (â€“Cu) alloys. Physica Scripta, 2013, 87, 015601.	1.2	22
16572	Hybrid Functional Studies on Impurity-Concentration-Controlled Band Engineering of Chalcogen-Hyperdoped Silicon. Applied Physics Express, 2013, 6, 085801.	1.1	18
16573	A First-Principles Investigation of the Carrier Doping Effect on the Magnetic Properties of Defective Graphene. Chinese Physics Letters, 2013, 30, 077502.	1.3	4
16574	Foundations of ab initio simulations of electric charges and fields at semiconductor surfaces within slab models. Journal of Applied Physics, 2013, 114, .	1.1	32
16575	Effects of chromium on structure and mechanical properties of vanadium: A first-principles study. Chinese Physics B, 2013, 22, 106109.	0.7	2
16576	Dispersion corrections in graphenic systems: a simple and effective model of binding. Journal of Physics Condensed Matter, 2013, 25, 445010.	0.7	31
16577	An accidental visualization of the Brillouin zone in an Niâ€“W alloyviadiffuse scattering. Journal of Applied Crystallography, 2013, 46, 1211-1215.	1.9	10
16578	The new phase of HgF ₂ at high pressure. Europhysics Letters, 2013, 102, 36002.	0.7	8
16579	First-Principles Calculations of Elastic Properties of HoBi and ErBi. Advanced Materials Research, 2013, 664, 672-676.	0.3	0
16580	Magnetic Properties and Stability of Quasi-One-Dimensional Cr Chains Embedded in (Zn,Cr)Te. Applied Physics Express, 2013, 6, 073006.	1.1	2
16581	First-Principles Studies on Cd Doping in CuInSe₂ and Related Compounds during Chemical Bath Deposition of CdS Buffer Layer. Japanese Journal of Applied Physics, 2013, 52, 061201.	0.8	11
16582	Analysis of dissociation of âŒ©câŒª and âŒ©c+aâŒª dislocations to nucleate $(1,0,ar{1},2)$ twins in Mg. Modelling and Simulation in Materials Science and Engineering, 2013, 21, 055007.	0.8	45
16583	First-Principles Investigations on Magnetic Properties in Off-Stoichiometric Ni₂MnIn Magnetic Shape Memory Alloys. Advanced Materials Research, 2013, 750-752, 730-733.	0.3	0

#	Article	IF	Citations
16584	Role of Inter-Dopant Interactions on the Diffusion of Li and Na Atoms in Bulk Si Anodes. Materials Research Society Symposia Proceedings, 2013, 1541, 75601.	0.1	2
16585	Theoretical prediction of ion conductivity in solid state HfO₂. Chinese Physics B, 2013, 22, 016601.	0.7	8
16586	Polar P6 ₃ cm phase as a marginally stable ground-state structure of InMnO ₃ : First-principles study. Europhysics Letters, 2013, 104, 57001.	0.7	1
16587	Bayesian inference as a tool for analysis of first-principles calculations of complex materials: an application to the melting point of Ti2GaN. Modelling and Simulation in Materials Science and Engineering, 2013, 21, 075001.	0.8	7
16588	From Used Oxide Nuclear Fuel to Rechargeable Battery: A First-Principles Study. Materials Research Society Symposia Proceedings, 2013, 1541, 73201.	0.1	0
16589	Ab initiostudy of the alloying effect of transition metals on structure, stability and ductility of CrN. Journal Physics D: Applied Physics, 2013, 46, 365301.	1.3	38
16590	Protons Crossing Triple Phase Boundaries based on Pd and Barium Zirconate: A Density Functional Theory Study. Materials Research Society Symposia Proceedings, 2013, 1542, 1.	0.1	0
16591	The bonding, charge distribution, spin ordering, optical, and elastic properties of four MAX phases Cr2AX (Aâ€‰=â€‰Al or Ge, Xâ€‰=â€‰C or N): From density functional theory study. Journal of Applied Physics, 2013, 114, .	2.2	13
16592	First-principles study on ferromagnetism in W-doped graphene. RSC Advances, 2013, 3, 26261.	1.7	20
16593	Photocatalytic and Antipathogenic Effects of TiO₂/Cu_xO (1<x<2). Journal of the Korean Chemical Society, 2013, 57, 483-488.	0.2	0
16594	Searching for Next Single-Phase High-Entropy Alloy Compositions. Entropy, 2013, 15, 4504-4519.	1.1	256
16595	Nanostructured ZnOâ€“X Alloys with Tailored Optoelectronic Properties for Solar-energy Technologies. Materials Research Society Symposia Proceedings, 2013, 1558, 1.	0.1	0
16596	Formation of the â€“N(NO)N(NO)â€“ polymer at high pressure and stabilization at ambient conditions. Proceedings of the National Academy of Sciences of the United States of America, 2013, 110, 5321-5325.	3.3	10
16597	Theoretical Study on Reactivity of Fe-Based Oxygen Carrier with CH₄ during Chemical Looping Combustion. Applied Mechanics and Materials, 0, 345, 298-301.	0.2	3
16598	Using First Principles Thermodynamics to Predict the Shape Surface Structure and Reactivity of Solvated Nanoparticles at High Temperatures and Pressures.. Materials Research Society Symposia Proceedings, 2013, 1546, 1.	0.1	0
16599	Design of Ptâ€Based Bimetallic Alloys for the Oxidation of H₂O₂: A Combined Computational and Experimental Approach. ChemCatChem, 2013, 5, 1709-1712.	1.8	2
16600	Atomicâ€Scale Probing the Priority of Oxidation Sites of an Organic Molecule Adsorbed at the Cuï£¿O/Cu(1â€‰1â€‰0) Interface. ChemCatChem, 2013, 5, 2662-2666.	1.8	0
16601	Airâ€Promoted Adsorptive Desulfurization over Ti_{0.9}Ce_{0.1}O₂ Mixed Oxides from Diesel Fuel under Ambient Conditions. ChemCatChem, 2013, 5, 3582-3586.	1.8	17

#	Article	IF	Citations
16602	Elastic Properties of CaSiO3 Perovskite from ab initio Molecular Dynamics. Entropy, 2013, 15, 4300-4309.	1.1	3
16603	Computational Chemistry Approach for White LED (Oxy)Nitride Phosphors. ECS Journal of Solid State Science and Technology, 2013, 2, R3048-R3058.	0.9	32
16604	Influence of normal and shear strain on magnetic anisotropy energy of hcp cobalt: An ab initio study. Journal of Materials Research, 2013, 28, 1559-1566.	1.2	3
16605	Correlation effects and spin-orbit interactions in two-dimensional hexagonal 5d transition metal carbides, Ta _{n+1} C _n (n = 1,2,3). Europhysics Letters, 2013, 101, 57004.	0.7	54
16606	The core structure and pseudo-magnetic field of the dislocation in graphene. Europhysics Letters, 2013, 104, 26002.	0.7	7
16607	Density Functional Study of the Structure, Stability and Oxygen Reduction Activity of Ultrathin Platinum Nanowires. Journal of the Electrochemical Society, 2013, 160, F548-F553.	1.3	7
16608	Density functional theory periodic slab calculations of adsorption and dissociation of H₂O on the Cu₂O(110):CuO surface. Canadian Journal of Physics, 2013, 91, 1101-1106.	0.4	10
16609	Influence of H, C, N and O impurities on the stability of Mg and Al from first-principles calculations. Modelling and Simulation in Materials Science and Engineering, 2013, 21, 055014.	0.8	4
16610	Sodiumâ€“gold binaries: novel structures for ionic compounds from anab initiostructural search. New Journal of Physics, 2013, 15, 115007.	1.2	58
16611	Bis(4-methylanilinium) and bis(4-iodoanilinium) pentamolybdates from laboratory X-ray powder data and total energy minimization. Acta Crystallographica Section C: Crystal Structure Communications, 2013, 69, 1367-1372.	0.4	5
16612	Combined in-situ photoemission spectroscopy and density functional theory of the Sr Zintl template for oxide heteroepitaxy on Si(001). Journal of Vacuum Science and Technology B:Nanotechnology and Microelectronics, 2013, 31, 04D107.	0.6	7
16613	Atomic structure, energetics, and chemical bonding of Y doped Î£13 grain boundaries in Î±-Al₂O₃. Philosophical Magazine, 2013, 93, 1158-1171.	0.7	10
16614	NMR study of small molecule adsorption in MOF-74-Mg. Journal of Chemical Physics, 2013, 138, 154704.	1.2	31
16615	Structure, Electrical and Optical Properties of the Polar ZnO(0001) Surfaces. Advanced Materials Research, 2013, 659, 25-29.	0.3	1
16616	First-Principle Calculation for a Novel Hydrogen Storage Material Mg₂Ni and its Substitutes. Advanced Materials Research, 0, 781-784, 19-23.	0.3	1
16617	First-Principles Study on the Thermodynamic Properties of Nb, Cr₂Nb and Nb₅Si₃ Alloys. Materials Science Forum, 0, 749, 466-472.	0.3	4
16618	Piezoelectricity in PbZrxTi1-xO3Studied by Density-Functional Perturbation Theory Supercell Calculations. Japanese Journal of Applied Physics, 2013, 52, 091101.	0.8	4
16619	Mechanics of metal-catecholate complexes: The roles of coordination state and metal types. Scientific Reports, 2013, 3, 2914.	1.6	173

#	Article	IF	Citations
16620	Study of intrinsic defects in 3C-SiC using first-principles calculation with a hybrid functional. Journal of Chemical Physics, 2013, 139, 124707.	1.2	27
16621	Towards a specific reaction parameter density functional for reactive scattering of H2 from Pd(111). Journal of Chemical Physics, 2013, 139, 244707.	1.2	14
16622	Vacancy-suppressed lattice conductivity of high-<mml:math xmlns:mml="http://www.w3.org/1998/Math/MathML" display="inline"><mml:mrow><mml:mi mathvariant="italic">ZT</mml:mi></mml:mrow></mml:math>In<mml:math xmlns:mml="http://www.w3.org/1998/Math/MathML" display="inline"><mml:msub><mml:mrow /><mml:mn>4</mml:mn></mml:msub></mml:math>Se<mml:math xmlns:mml="http://www.w3.org/1998/Math/MathML" display="inline"><mml:msub><mml:mrow /><mml:	1.1	33
16623	Isentropic compression of hydrogen: Probing conditions deep in planetary interiors. Physical Review B, 2013, 88, .	1.1	27
16624	Arrays of carbon nanoscrolls as deep subwavelength magnetic metamaterials. Physical Review B, 2013, 88, .	1.1	1
16625	Nonvolatile Resistive Switching in<mml:math xmlns:mml="http://www.w3.org/1998/Math/MathML" display="inline"><mml:mi>Pt</mml:mi><mml:mo>/</mml:mo><mml:msub><mml:mi>LaAlO</mml:mi><mml:mn>3</mml:mn></mml:msub></mml:math>/Nb:SrTiO3Interfaces. Physical Review X, 2013, 3, .	2.8	49
16626	Critical thickness for the two-dimensional electron gas in LaTiO3/SrTiO3superlattices. Physical Review B, 2013, 88, .	1.1	22
16627	Strainâ€Engineered Modulation on the Electronic Properties of Phosphorousâ€Doped ZnO. ChemPhysChem, 2013, 14, 3916-3924.	1.0	13
16628	First-principles investigation of phase stability and electronic structure of tetragonal (P4/m) Ga_{3â^'}_xAl_xTi₂(xâ€‰=â€‰0â€“3) compounds. Philosophical Magazine Letters, 2013, 93, 273-282.	1.0	1
16629	DNA sequencing with titanium nitride electrodes. International Journal of Quantum Chemistry, 2013, 113, 2295-2305.	1.0	6
16630	Effect of transition-metal additives on hydrogen desorption kinetics of MgH2. Applied Physics Letters, 2013, 102, .	1.5	38
16631	Influence of oxygen and hydrogen adsorption on the magnetic structure of an ultrathin iron film on an Ir(001) surface. Physical Review B, 2013, 88, .	1.1	11
16632	Probing the generalized magicity of Ag nanoclusters constructed on Si(111) by atomic manipulation. Physical Review B, 2013, 88, .	1.1	7
16633	Hybrid functional versus quasiparticle calculations for the Schottky barrier and effective work function at TiN/HfO<mml:math xmlns:mml="http://www.w3.org/1998/Math/MathML" display="inline"><mml:msub><mml:mrow /><mml:mn>2</mml:mn></mml:msub></mml:math>interface. Physical Review B, 2013, 87, .	1.1	15
16634	Strain engineering of topological properties in leadâ€salt semiconductors. Physica Status Solidi - Rapid Research Letters, 2013, 7, 1102-1106.	1.2	26
16635	Positive exchange bias in thin film multilayers produced with nano-oxide layer. Applied Physics Letters, 2013, 102, 252406.	1.5	2
16636	First Principle Molecular Dynamic Simulation of the Ge_xAs_xS_{100-2x} Glasses. Advanced Materials Research, 2013, 798-799, 101-106.	0.3	0
16637	Dependence of silicon oxidation channel on distribution of surface electrons at initial stage of oxide growth on Si(001). Applied Physics Letters, 2013, 103, 163113.	1.5	4

#	Article	IF	Citations
16638	Schottky barrier at the AlN/metal junction. Journal of Applied Physics, 2013, 113, .	1.1	6
16639	Thermophysical properties of hydrogen-helium mixtures: Re-examination of the mixing rules via quantum molecular dynamics simulations. Physical Review E, 2013, 88, 033106.	0.8	8
16640	Plasmonic excitations in quantum-sized sodium nanoparticles studied by time-dependent density functional calculations. Physical Review B, 2013, 88, .	1.1	35
16641	Considerations for surface reconstruction stability prediction on GaAs(001). Physical Review B, 2013, 87, .	1.1	8
16642	Phonon spectrum, thermodynamic properties, and pressure-temperature phase diagram of uranium dioxide. Physical Review B, 2013, 88, .	1.1	75
16643	Detection of surface carbon and hydrocarbons in hot spot regions of niobium superconducting rf cavities by Raman spectroscopy. Physical Review Special Topics: Accelerators and Beams, 2013, 16, .	1.8	26
16644	Large resistivity change and phase transition in the antiferromagnetic semiconductors LiMnAs and LaOMnAs. Physical Review B, 2013, 88, .	1.1	34
16645	Lattice distortion effects on topological phases in (LaNiO<mml:math) Tj ETQq1 1 0.784314 rgBT /Overlock 10 Tf 50 487 Td (xmlns:mml="http://www.w3.org/1998/Math/MathML" display="inline"><mml:msub><mml:mrow		

#	Article	IF	Citations
16656	Superconductivity in a single-layer alkali-doped FeSe: A weakly coupled two-leg ladder system. Physical Review B, 2013, 88, .	1.1	11
16657	Synthesis, characterization, electronic structure, and phonon properties of the noncentrosymmetric superconductor LaPtSi. Physical Review B, 2013, 88, .	1.1	39
16658	Large spin splitting in the conduction band of transition metal dichalcogenide monolayers. Physical Review B, 2013, 88, .	1.1	341
16659	Mechanism of Strong Affinity of Clay Minerals to Radioactive Cesium: First-Principles Calculation Study for Adsorption of Cesium at Frayed Edge Sites in Muscovite. Journal of the Physical Society of Japan, 2013, 82, 033802.	0.7	71
16660	The electronic properties of point defects in earth-abundant photovoltaic material Zn3P2: A hybrid functional method study. Journal of Applied Physics, 2013, 113, .	1.1	26
16661	Caged clusters in Al<mml:math xmlns:mml="http://www.w3.org/1998/Math/MathML" display="inline"><mml:msub><mml:mrow /><mml:mn>11</mml:mn></mml:msub></mml:math>Ir<mml:math xmlns:mml="http://www.w3.org/1998/Math/MathML" display="inline"><mml:msub><mml:mrow /><mml:mn>4</mml:mn></mml:msub></mml:math>: Structural transition and insulating phase. Physical Review B, 2013, 87, .	1.1	16
16662	Defects and defect healing in amorphous Si<mml:math xmlns:mml="http://www.w3.org/1998/Math/MathML" display="inline"><mml:msub><mml:mrow /><mml:mn>3</mml:mn></mml:msub></mml:math>N<mml:math xmlns:mml="http://www.w3.org/1998/Math/MathML" display="inline"><mml:msub><mml:mrow /><mml:mrow><mml:mn>4</mml:mn><mml:mo>â^’</mml:mo><mml:mi>x</mml:mi></mml:mrow></mml:msub></mml:math>H<mml:math xmlns:mml="http://www.w3.org/1998/Math/MathML" display="inline"><mml:msub><mml:mrow /><mml:mi>	1.1	19
16663	Experimental and first-principles study of ferromagnetism in Mn-doped zinc stannate nanowires. Journal of Applied Physics, 2013, 114, .	1.1	7
16664	Environment-dependent noncollinear magnetic orders and spin-wave spectra of Fe chains and stripes. Physical Review B, 2013, 87, .	1.1	9
16665	Spin coupling around a carbon atom vacancy in graphene. Physical Review B, 2013, 88, .	1.1	34
16666	Electronic thermal conductivity as derived by density functional theory. Physical Review B, 2013, 88, .	1.1	14
16667	Electron doping limit in Al-doped ZnO by donor-acceptor interactions. Journal of Applied Physics, 2013, 113, 153703.	1.1	38
16668	Strain tuning of optical emission energy and polarization in monolayer and bilayer MoS<mml:math xmlns:mml="http://www.w3.org/1998/Math/MathML" display="inline"><mml:msub><mml:mrow /><mml:mn>2</mml:mn></mml:msub></mml:math>. Physical Review B, 2013, 88, .	1.1	365
16669	Surface reconstruction stability and configurational disorder on Bi-terminated GaAs(001). Physical Review B, 2013, 87, .	1.1	22
16670	Thermal conductivity of bulk and nanowire InAs, AlN, and BeO polymorphs from first principles. Journal of Applied Physics, 2013, 114, .	1.1	48
16671	Low energy structures of lithium-ion battery materials Li(MnxNixCo1â^’2x)O2 revealed by first-principles calculations. Applied Physics Letters, 2013, 103, .	1.5	9
16672	Toughness enhancement in hard ceramic thin films by alloy design. APL Materials, 2013, 1, .	2.2	109
16673	Properties of threading screw dislocation core in wurtzite GaN studied by Heyd-Scuseria-Ernzerhof hybrid functional. Applied Physics Letters, 2013, 103, .	1.5	13

#	Article	IF	Citations
16674	Carbon monoxide-induced reduction and healing of graphene oxide. Journal of Vacuum Science and Technology A: Vacuum, Surfaces and Films, 2013, 31, .	0.9	17
16675	Spin-dependent resonant tunneling of multiferroic tunnel junction via head-to-head 180Â° domain wall. Journal of Applied Physics, 2013, 114, 163703.	1.1	6
16676	Simulation and modeling of the electronic structure of GaAs damage clusters. Journal of Applied Physics, 2013, 113, 093706.	1.1	1
16677	First-principles study of graphene adsorbed on WS2 monolayer. Journal of Applied Physics, 2013, 114, 183709.	1.1	22
16678	Structure Prediction of Binary Pernitride MN₂ Compounds (M=Ca, Sr, Ba, La, and Ti). Chemistry - an Asian Journal, 2013, 8, 743-754.	1.7	22
16679	Gold-titania interface toughening and thermal conductance enhancement using an organophosphonate nanolayer. Applied Physics Letters, 2013, 102, 201605.	1.5	15
16680	Phase stabilities at a glance: Stability diagrams of nickel dipnictides. Journal of Chemical Physics, 2013, 139, 214705.	1.2	13
16681	Guest host interaction and low energy host structure dynamics in tin clathrates. Journal of Applied Physics, 2013, 113, 084902.	1.1	10
16682	Theory of near-interface trap quenching by impurities in SiC-based metal-oxide-semiconductor devices. Applied Physics Letters, 2013, 102, .	1.5	7
16683	Defect states and disorder in charge transport in semiconductor nanowires. Journal of Applied Physics, 2013, 114, .	1.1	9
16684	Potential barrier and band structure of closed edge graphene. Journal of Applied Physics, 2013, 114, 074305.	1.1	3
16685	Elastic moduli and hardness of highly incompressible platinum perpnictide PtAs2. Applied Physics Letters, 2013, 103, 101901.	1.5	7
16686	Surface-induced charge at a Ge (100) dimer surface and its interaction with vacancies and self-interstitials. Journal of Applied Physics, 2013, 113, .	1.1	8
16687	Dissolving, trapping and detrapping mechanisms of hydrogen in bcc and fcc transition metals. AIP Advances, 2013, 3, .	0.6	82
16688	Diffusion and desorption of oxygen atoms on graphene. Journal of Physics Condensed Matter, 2013, 25, 405301.	0.7	24
16689	A computational study of the thermoelectric performance of ultrathin Bi2Te3 films. Applied Physics Letters, 2013, 102, .	1.5	78
16690	Three-chain B6n+14 cages as possible precursors for the syntheses of boron fullerenes. Journal of Chemical Physics, 2013, 139, 224307.	1.2	16
16691	Mass transport in CuInSe2 from first principles. Journal of Applied Physics, 2013, 113, .	1.1	22

#	Article	IF	Citations
16692	Amorphous thermal stability of Al-doped Sb2Te3 films for phase-change memory application. Applied Physics Letters, 2013, 103, .	1.5	35
16693	Density functional theory study on the impact of heavy doping on Si intrinsic point defect properties and implications for single crystal growth from a melt. Journal of Applied Physics, 2013, 114, .	1.1	50
16694	Large negative magnetoresistance in reactive sputtered polycrystalline GdNx films. Applied Physics Letters, 2013, 102, .	1.5	4
16695	Coupled theoretical and experimental studies for the radiation hardening of silica-based optical fibers. , 2013, , .		1
16696	Structural, electronic, and linear optical properties of organic photovoltaic PBTTT-C14 crystal. Journal of Chemical Physics, 2013, 138, 164503.	1.2	12
16697	Can nitrogen-based cobalt pnictides exist?. Journal of Applied Physics, 2013, 114, 093701.	1.1	0
16698	Chemistry at molecular junctions: Rotation and dissociation of O2 on the Ag(110) surface induced by a scanning tunneling microscope. Journal of Chemical Physics, 2013, 139, 074702.	1.2	21
16699	Ab initio study on the structural characteristics of amorphous Zn2SnO4. Applied Physics Letters, 2013, 103, 252102.	1.5	10
16700	Charge transfer in Sr Zintl template on Si(001). Applied Physics Letters, 2013, 102, 031604.	1.5	19
16701	Surface electronic structure for various surface preparations of Nb-doped SrTiO₃ (001). Journal of Applied Physics, 2013, 114, 103710.	1.1	33
16702	Metal to semiconductor transition in metallic transition metal dichalcogenides. Journal of Applied Physics, 2013, 114, 174307.	1.1	31
16703	Ordering-enhanced dislocation glide in III-V alloys. Journal of Applied Physics, 2013, 114, .	1.1	20
16704	High-temperature neutron diffraction and first-principles study of temperature-dependent crystal structures and atomic vibrations in Ti3AlC2, Ti2AlC, and Ti5Al2C3. Journal of Applied Physics, 2013, 113, .	1.1	44
16705	On the fly first principles study of the classical scattering of an Ar atom from the LiF(100) surface. Journal of Chemical Physics, 2013, 139, 044707.	1.2	6
16706	Thin film bulk acoustic wave resonators tuning from first principles. Journal of Applied Physics, 2013, 113, .	1.1	5
16707	Dihydride structures of deuterium on germanium (001) surfaces. Journal of Applied Physics, 2013, 113, 023703.	1.1	1
16708	Spatially non-uniform field response in arrays of silicon quantum dots: DFT computation. , 2013, , .		0
16709	Electronic structure of magnetic semiconductor CdCr2Te4: A possible spin-dependent symmetry filter. Applied Physics Letters, 2013, 103, 192402.	1.5	9

#	Article	IF	Citations
16710	Theoretical studies of the passivantsâ€™ effect on the SixGe1-x nanowires: Composition profiles, diameter, shape, and electronic properties. Journal of Chemical Physics, 2013, 139, 154713.	1.2	0
16711	Effects of alloying and local order in AuNi contacts for Ohmic radio frequency micro electro mechanical systems switches via multi-scale simulation. Journal of Applied Physics, 2013, 113, 203510.	1.1	2
16712	Lead incorporation mechanism in LiF crystals. Applied Physics Letters, 2013, 102, 081107.	1.5	5
16713	First-principles study of electronic structures and photocatalytic activity of low-Miller-index surfaces of ZnO. Journal of Applied Physics, 2013, 113, 034903.	1.1	16
16714	Role of gold nanoclusters supported on TiO2(110) model catalyst in CO oxidation reaction. Journal of Vacuum Science and Technology A: Vacuum, Surfaces and Films, 2013, 31, 061404.	0.9	10
16715	Site-preference and valency for rare-earth sites in (R-Ce)2Fe14B magnets. Applied Physics Letters, 2013, 102, .	1.5	112
16716	Modulation of Fermi velocities of Dirac electrons in single layer graphene by moirÃ© superlattice. Applied Physics Letters, 2013, 103, .	1.5	5
16717	Atomistic modeling of the Au dropletâ€“GaAs interface for size-selective nanowire growth. Physical Review B, 2013, 88, .	1.1	21
16718	Effects of a finite Dirac cone on the dispersion properties of graphite. Physical Review B, 2013, 87, .	1.1	15
16719	Common effect of chemical and external pressures on the magnetic properties of <mml:math xmlns:mml="http://www.w3.org/1998/Math/MathML"		

#	Article	IF	Citations
16728	Monopole-based formalism for the diagonal magnetoelectric response. Physical Review B, 2013, 88, .	1.1	93
16729	Half-filled orbital and unconventional geometry of a common dopant in Si(001). Physical Review B, 2013, 88, .	1.1	2
16730	First-principles insights into the structure of the incipient magnesium oxide and its instability to decomposition: Oxygen chemisorption to Mg(0001) and thermodynamic stability. Physical Review B, 2013, 87, .	1.1	39
16731	A Photoelectrochemical Investigation on the Synergetic Effect between CdS and Reduced Graphene Oxide for Solarâ€Energy Conversion. Chemistry - an Asian Journal, 2013, 8, 2395-2400.	1.7	45
16732	Indications of strong neutral impurity scattering in Ba(Sn,Sb)O<mml:math xmlns:mml="http://www.w3.org/1998/Math/MathML" display="inline"><mml:msub><mml:mrow /><mml:mn>3</mml:mn></mml:msub></mml:math>single crystals. Physical Review B, 2013, 88, .	1.1	48
16733	First-principles study of temperature-dependent diffusion coefficients for helium in Î±-Ti. Journal of Applied Physics, 2013, 114, 153507.	1.1	11
16734	Interstitial-boron solution strengthened WB3+x. Applied Physics Letters, 2013, 103, .	1.5	72
16735	Simulated doping of Si from first principles using pseudoatoms. Physical Review B, 2013, 87, .	1.1	16
16736	Relative entropy as model selection tool in cluster expansions. Physical Review B, 2013, 87, .	1.1	10
16737	Influence of Cr doping on the magnetic structure of the FeAs-strips compound CaFe4As3: A single-crystal neutron diffraction study. Physical Review B, 2013, 88, .	1.1	1
16738	Epilayer thickness and strain dependence of Ge(113) surface energies. Physical Review B, 2013, 87, .	1.1	10
16739	Two-dimensional electron gas generated by La-doping at SrTiO3(001) surface: A first-principles study. AIP Advances, 2013, 3, 062116.	0.6	2
16740	Origin of the Bismuth-Induced Decohesion of Nickel and Copper Grain Boundaries. Physical Review Letters, 2013, 111, 055502.	2.9	30
16741	Monolayer graphene oxide as a building block for artificial muscles. Applied Physics Letters, 2013, 102, 021903.	1.5	26
16742	Vacancy compensation and related donor-acceptor pair recombination in bulk AlN. Applied Physics Letters, 2013, 103, .	1.5	80
16743	Influence of monolayer contamination on electric-field-noise heating in ion traps. Physical Review A, 2013, 87, .	1.0	27
16744	Ferroelectric functionality in SrTiO3/Si heterojunctions. Journal of Applied Physics, 2013, 114, .	1.1	17
16745	Characterization of Co distribution in ZnO by x-ray magnetic circular dichroism. Journal of Applied Physics, 2013, 113, 203913.	1.1	10

#	Article	IF	Citations
16746	Accuracy of exchange-correlation functionals and effect of solvation on the surface energy of copper. Physical Review B, 2013, 87, .	1.1	211
16747	Stability of MnB2 with AlB2-type structure revealed by first-principles calculations and experiments. Applied Physics Letters, 2013, 102, .	1.5	14
16748	Synthesis and formation process of Al2CuHx: A new class of interstitial aluminum-based alloy hydride. APL Materials, 2013, 1, .	2.2	20
16749	Rationalizing strain engineering effects in rare-earth nickelates. Physical Review B, 2013, 88, .	1.1	58
16750	Theoretical Characterization of Chiral Carbon Nanotube Encapsulating Ellipsoidal C70. Chinese Journal of Chemical Physics, 2013, 26, 780-783.	0.6	0
16751	First-principles study of band gap engineering of ZnO by alloying with LiGaO2 for ultraviolet applications. Journal of Applied Physics, 2013, 114, .	1.1	9
16752	First principles study on InP (001)-(2 Ã— 4) surface oxidation. Journal of Applied Physics, 2013, 113, 103705.	1.1	18
16753	Ab initio study on the size effect of symmetric and asymmetric ferroelectric tunnel junctions: A comprehensive picture with regard to the details of electrode/ferroelectric interfaces. Journal of Applied Physics, 2013, 114, 064105.	1.1	23
16754	Magnetic exchange forces andd-state filling: Antiferromagnetic MnO(001) and NiO(001) surfaces. Physical Review B, 2013, 88, .	1.1	4
16755	Structural variants and the modified Slater-Pauling curve for transition-metal-based half-Heusler alloys. Journal of Applied Physics, 2013, 113, .	1.1	20
16756	Cr incorporation in Cu<scp>G</scp>a<scp>S</scp>₂ chalcopyrite: A new intermediateâ€band photovoltaic material with wideâ€spectrum solar absorption. Physica Status Solidi (A) Applications and Materials Science, 2013, 210, 1098-1102.	0.8	65
16757	Ab initio determination of basic dielectric properties. , 2013, , .		0
16758	The Close Relationships between the Crystal Structures of MO and MSO4(M = Group 10, 11, or 12) Tj ETQq0 0 0 rgBT /Overlock 10 Tf 5 2013, 2013, 5094-5102.	1.0	5
16759	Investigation of the role of electrodes on the retention performance of HfO<inf>x</inf> based RRAM cells by experiments, atomistic simulations and device physical modeling. , 2013, , .		7
16760	Electronic and structural properties of carbon nanotubes modulated by external strain. Journal of Applied Physics, 2013, 113, .	1.1	6
16761	Formation of nickel-platinum silicides on a silicon substrate: Structure, phase stability, and diffusion from ab initio computations. Journal of Applied Physics, 2013, 114, .	1.1	13
16762	Electronic, dielectric, and optical properties of the B phase of niobium pentoxide and tantalum pentoxide by firstâ€principles calculations. Physica Status Solidi (B): Basic Research, 2013, 250, 1644-1650.	0.7	24
16763	Ab initiostudy of magnetic anisotropy in cobalt doped zinc oxide with electron-filling. Journal of Applied Physics, 2013, 113, 17C728.	1.1	1

#	Article	IF	Citations
16764	High-throughput ab initio screening of binary solid solutions in olivine phosphates for Li-ion battery cathodes. Modelling and Simulation in Materials Science and Engineering, 2013, 21, 074004.	0.8	5
16765	Arsenic decapping and pre-atomic layer deposition trimethylaluminum passivation of Al2O3/InGaAs(100) interfaces. Applied Physics Letters, 2013, 103, .	1.5	40
16766	Atomistic simulations of stainless steels: a many-body potential for the Feâ€“Crâ€“C system. Journal of Physics Condensed Matter, 2013, 25, 445401.	0.7	51
16767	Kinetic Origin of Divergent Decompression Pathways in Silicon and Germanium. Physical Review Letters, 2013, 110, 165503.	2.9	44
16768	Effects of irradiation on the mechanical behavior of twined SiC nanowires. Journal of Applied Physics, 2013, 113, 104309.	1.1	7
16769	Refractive Index of BAs_{1-x}P_x Semiconductors. Solid State Phenomena, 0, 209, 225-228.	0.3	0
16770	Methane dissociative chemisorption and detailed balance on Pt(111): Dynamical constraints and the modest influence of tunneling. Journal of Chemical Physics, 2013, 139, 214707.	1.2	13
16771	Abnormal Photocurrent Response and Enhanced Photocatalytic Activity Induced by Charge Transfer between WS₂ Nanosheets and WO₃ Nanoparticles. ChemPhysChem, 2013, 14, 4069-4073.	1.0	37
16772	Proximity Effects Induced in Graphene by Magnetic Insulators: First-Principles Calculations on Spin Filtering and Exchange-Splitting Gaps. Physical Review Letters, 2013, 110, 046603.	2.9	287
16773	Ice phases under ambient and high pressure: Insights from density functional theory. Physical Review B, 2013, 87, .	1.1	28
16774	Equilibrium shape of graphene domains on Ni(111). Physical Review B, 2013, 88, .	1.1	14
16775	Possible origin of the discrepancy in Peierls stresses of fcc metals: First-principles simulations of dislocation mobility in aluminum. Physical Review B, 2013, 88, .	1.1	53
16776	First-principles study of fcc-Ag/bcc-Fe interfaces. Physical Review B, 2013, 87, .	1.1	64
16777	Mode conversion and long-lived vibrational modes in lead monolayers on silicon (111) after femtosecond laser excitation: A molecular dynamics simulation. Physical Review B, 2013, 88, .	1.1	15
16778	Elliptic Preconditioner for Accelerating the Self-Consistent Field Iteration in Kohn–Sham Density Functional Theory. SIAM Journal of Scientific Computing, 2013, 35, S277-S298.	1.3	51
16779	Electronic reconstruction and surface two-dimensional electron gas in a polarized heterostructure with a hole-doped single copper-oxygen plane. Physical Review B, 2013, 87, .	1.1	3
16780	As vacancies, Ga antisites, and Au impurities in zinc blende and wurtzite GaAs nanowire segments from first principles. Physical Review B, 2013, 87, .	1.1	27
16781	Electronic, elastic, vibrational, and thermodynamic properties of type-VIII clathrates Ba8Ga16Sn30 and Ba8Al16Sn30 by first principles. Journal of Applied Physics, 2013, 114, 163509.	1.1	12

#	Article	IF	Citations
16782	Computational studies of catalyst-free single walled carbon nanotube growth. Journal of Chemical Physics, 2013, 139, 054308.	1.2	1
16783	First-principles studies of interlayer exchange coupling in (Ga, Cr)N-based diluted magnetic semiconductor multilayers. Journal of Applied Physics, 2013, 113, 054302.	1.1	3
16784	Distortion of electronic structure in HfO2 induced by the out-diffused As from GaAs substrate. Journal of Applied Physics, 2013, 113, 186101.	1.1	0
16785	Band offsets of CuInSe<mml:math xmlns:mml="http://www.w3.org/1998/Math/MathML" display="inline"><mml:msub><mml:mrow /><mml:mn>2</mml:mn></mml:msub></mml:math>/CdS and CuInSe<mml:math xmlns:mml="http://www.w3.org/1998/Math/MathML" display="inline"><mml:msub><mml:mrow /><mml:mn>2</mml:mn></mml:msub></mml:math>/ZnS (110) interfaces: A hybrid density functional theory study. Physical Review B, 2013, 88, .	1.1	50
16786	Carrier-tunable magnetism of graphene with single-atom vacancy. Journal of Applied Physics, 2013, 113, 213709.	1.1	7
16787	Ab initio studies of effect of copper substitution on the electronic and magnetic properties of Ni<mml:math xmlns:mml="http://www.w3.org/1998/Math/MathML" display="inline"><mml:msub><mml:mrow /><mml:mn>2</mml:mn></mml:msub></mml:math>MnGa and Mn<mml:math xmlns:mml="http://www.w3.org/1998/Math/MathML" display="inline"><mml:msub><mml:mrow /><mml:mn>2</mml:mn></mml:msub></mml:math>NiGa. Physical Review B, 2013, 88, .	1.1	60
16788	La doped SrTiO3 thin films on SrLaAlO4 (001) as transparent conductor. Journal of Applied Physics, 2013, 113, 183711.	1.1	10
16789	Cation composition effects on electronic structures of In-Sn-Zn-O amorphous semiconductors. Journal of Applied Physics, 2013, 113, .	1.1	67
16790	Ferroelectric Transition in the Inorganic Supramolecular Complex (Hg₆P₄)(CuCl₃)₂. Chemistry - an Asian Journal, 2013, 8, 2925-2931.	1.7	9
16791	High pressure and high temperature stabilization of cubic AlN in Ti0.60Al0.40N. Journal of Applied Physics, 2013, 113, .	1.1	34
16792	Gate-tunable exchange coupling between cobalt clusters on graphene. Physical Review B, 2013, 87, .	1.1	29
16793	Dissimilar-electrodes-induced asymmetric characteristic and diode effect of current transport in zinc oxide tunnel junctions. Journal of Applied Physics, 2013, 114, 044111.	1.1	10
16794	Coexistence of weak ferromagnetism and polar lattice distortion in epitaxial NiTiO3 thin films of the LiNbO3-type structure. Journal of Vacuum Science and Technology B:Nanotechnology and Microelectronics, 2013, 31, 030603.	0.6	17
16795	Environment-dependent interfacial strength using first principles thermodynamics: The example of the Pt-HfO2 interface. Journal of Applied Physics, 2013, 114, 163503.	1.1	6
16796	Potential thermoelectric performance of hole-doped Cu₂O. New Journal of Physics, 2013, 15, 043029.	1.2	47
16797	Polarity compensation in low-dimensional oxide nanostructures: The case of metal-supported MgO nanoribbons. Physical Review B, 2013, 87, .	1.1	16
16798	Dielectric permittivity enhancement in hydroxyl functionalized polyolefins via cooperative interactions with water. Applied Physics Letters, 2013, 102, 152901.	1.5	11
16799	Role of lone-pair electrons in Sb-doped amorphous InGaZnO4: Suppression of the hole-induced lattice instability. Applied Physics Letters, 2013, 102, 152101.	1.5	7

#	Article	IF	Citations
16800	Formation and annealing behaviors of qubit centers in 4H-SiC from first principles. Journal of Applied Physics, 2013, 114, .	1.1	18
16801	Efficient Separation of Photogenerated Electronâ€Hole Pairs by the Combination of a Heterolayered Structure and Internal Polar Field in Pyroelectric BiOIO₃ Nanoplates. Chemistry - A European Journal, 2013, 19, 14777-14780.	1.7	158
16802	Theory and synthesis of bilayer graphene intercalated with ICl and IBr for low power device applications. Journal of Applied Physics, 2013, 114, .	1.1	7
16803	Molecular switches from benzene derivatives adsorbed on metal surfaces. Nature Communications, 2013, 4, 2569.	5.8	82
16804	Manipulation of spin state of iron porphyrin by chemisorption on magnetic substrates. Physical Review B, 2013, 88, .	1.1	50
16805	Chemical bonds and vibrational properties of ordered (U, Np, Pu) mixed oxides. Journal of Applied Physics, 2013, 113, 013501.	1.1	12
16806	Local and chemical environment dependence of the magnetic properties of CoRh core-shell nanoparticles. Physical Review B, 2013, 88, .	1.1	17
16807	Electronic structure of the spin gapless material Co-doped PbPdO₂. Journal of Applied Physics, 2013, 114, 103709.	1.1	11
16808	Thermodynamic and mechanical stabilities of Î±- and Î²-Ta4AlC3 via first-principles investigations. Journal of Applied Physics, 2013, 114, 213517.	1.1	4
16809	Theory of kâ†'â‹…Ï€â†'+U formalism for diluted magnetic semiconductors: Application to p-type Sn1â^'xGdxTe. Journal of Applied Physics, 2013, 113, 103902.	1.1	6
16810	k<mml:math xmlns:mml="http://www.w3.org/1998/Math/MathML" display="inline"><mml:mo>Â·</mml:mo></mml:math>p subband structure of the LaAlO<mml:math xmlns:mml="http://www.w3.org/1998/Math/MathML" display="inline"><mml:msub><mml:mrow /><mml:mn>3</mml:mn></mml:msub></mml:math>/SrTiO<mml:math xmlns:mml="http://www.w3.org/1998/Math/MathML" display="inline"><mml:msub><mml:mrow /><mml:mn>3</mml:mn></mml:msub></mml:math> heterostructures: The formation	1.1	25
16811	Identification of a N-related shallow acceptor and electron paramagnetic resonance center in ZnO: N<mml:math xmlns:mml="http://www.w3.org/1998/Math/MathML" display="inline"><mml:mrow><mml:msub><mml:mrow /><mml:mn>2</mml:mn></mml:msub><mml:msup><mml:mrow /><mml:mo>+</mml:mo></mml:msup></mml:mrow></mml:math> on the Zn site. Physical Review B, 2013, 87, .	1.1	33
16812	A-Site Diffusion in La_{1 â^' x}Sr_xMnO₃: Ab Initio and Kinetic Monte Carlo Calculations. Journal of the Electrochemical Society, 2013, 160, F877-F882.	1.3	12
16813	Nanoscale assembly of silicon-like [Al(As<mml:math) Tj ETQq0 0 0 rgBT /Overlock 10 Tf 50 207 Td (xmlns:mml="http://www.w3.org/199	1.1	5
16814	xmlns:mml="http://www.w3.org/1998/Math/MathML" display="inline"><mml:msub><mml:mrow /><mml:	1.1	30
16815	Phase stability of ScN-based solid solutions for thermoelectric applications from first-principles calculations. Journal of Applied Physics, 2013, 114, 073512.	1.1	5
16816	Favorable magnetoelectric phenomenon in Co2MnSi/PbTiO3 (001) ultrathin bilayer: A density functional theory study. Journal of Applied Physics, 2013, 114, 144101.	1.2	6
16817	One-dimensional embedded cluster approach to modeling CdS nanowires. Journal of Chemical Physics, 2013, 139, 124101.		

#	Article	IF	Citations
16818	Controlling the charge state of single Mo dopants in a CaO film. Physical Review B, 2013, 88, .	1.1	24
16819	Indirect to direct bandgap transition under uniaxial strain in layered ZnO. Applied Physics Letters, 2013, 102, .	1.5	17
16820	Asymmetric electron transport and highest occupied molecular orbital assisted tunneling through Zn-porphyrin molecular junctions. Applied Physics Letters, 2013, 103, .	1.5	8
16821	Effects of Li doping on H-diffusion in MgH2: A first-principles study. Journal of Applied Physics, 2013, 114, .	1.1	12
16822	ELECTRONIC STRUCTURES AND MAGNETISM IN Cu-DOPED ZnO MONOLAYER. Modern Physics Letters B, 2013, 27, 1350204.	1.0	4
16823	Parallel kinetic Monte Carlo simulation framework incorporating accurate models of adsorbate lateral interactions. Journal of Chemical Physics, 2013, 139, 224706.	1.2	122
16824	Prediction of the bias voltage dependent magnetic contrast in spin-polarized scanning tunneling microscopy. Physical Review B, 2013, 87, .	1.1	10
16825	First principles investigation of Ti adsorption and migration on Si(100) surfaces. Journal of Applied Physics, 2013, 114, 243505.	1.1	3
16826	Development of a ReaxFF potential for Pd/O and application to palladium oxide formation. Journal of Chemical Physics, 2013, 139, 044109.	1.2	83
16827	Direct ab-initio molecular dynamic study of ultrafast phase change in Ag-alloyed Ge2Sb2Te5. Applied Physics Letters, 2013, 102, .	1.5	24
16828	Large magnetoresistance of paracyclophane-based molecular tunnel junctions: A first-principles study. Journal of Applied Physics, 2013, 114, 213906.	1.1	12
16829	Effect of Feâ€“O distance on magnetocrystalline anisotropy energy at the Fe/MgO(001) interface. Journal of Applied Physics, 2013, 113, .	1.1	21
16830	Strain-Induced Defect Superstructure on the<mml:math xmlns:mml="http://www.w3.org/1998/Math/MathML" display="inline"><mml:msub><mml:mi>SrTiO</mml:mi><mml:mn>3</mml:mn></mml:msub><mml:mo stretchy="false">(</mml:mo><mml:mn>110</mml:mn><mml:mo) Tj ETQq0 0 0 rgBT /Overlock 10 Tf 50 247 Td (stretchy="false">)</mm	2.9	32
16831	Magnetic and electronic structure of the film-stabilized Mott insulator BaCrO<mml:math xmlns:mml="http://www.w3.org/1998/Math/MathML" display="inline"><mml:msub><mml:mrow /><mml:mn>3</mml:mn></mml:msub></mml:math>. Physical Review B, 2013, 87, .	1.1	11
16832	Comment on â€œStructural and Electronic Properties ofTGraphene: A Two-Dimensional Carbon Allotrope with Tetraringsâ€• Physical Review Letters, 2013, 110, 029601.	2.9	22
16833	Low-energy planar magnetic defects in BaFe<mml:math xmlns:mml="http://www.w3.org/1998/Math/MathML" display="inline"><mml:msub><mml:mrow /><mml:mn>2</mml:mn></mml:msub></mml:math>As<mml:math xmlns:mml="http://www.w3.org/1998/Math/MathML" display="inline"><mml:msub><mml:mrow /><mml:mn>2</mml:mn></mml:msub></mml:math>: Nanotwins, twins, antiphase, and domain walls	1.1	2
16834	General model for explicitly hole-doped superconductor parent compounds: Electronic structure of Ca<mml:math xmlns:mml="http://www.w3.org/1998/Math/MathML" display="inline"><mml:msub><mml:mrow /><mml:mn>2</mml:mn><mml:mo>â^’</mml:mo><mml:mi>x</mml:mi></mml:mrow></mml:msub></mml:math>Na<mml:math xmlns:mml="http://www.w3.org/1998/Math/MathML" display="inline"><mml:msub><mml:mrow /><mml:mi>x</mml:mi></mml:msub></mml:math>CuO<mml:math xmlns:mml="http://www.w3.org/1998/M	1.1	5
16835	Two types of surface states in topological crystalline insulators. Physical Review B, 2013, 88, .	1.1	181

#	Article	IF	Citations
16836	Biaxial strain effect on the electronic and magnetic phase transitions in double perovskite La2FeMnO6: A first-principles study. Journal of Applied Physics, 2013, 114, .	1.1	23
16837	Decay behavior of localized states at reconstructed armchair graphene edges. Physical Review B, 2013, 88, .	1.1	15
16838	Temperature Effects in the Vibrational Spectra of Self-Assembled Monolayers. Physical Review Letters, 2013, 111, 086102.	2.9	9
16839	Detecting p-type conduction in Ba-doped InN. Applied Physics Letters, 2013, 102, 042109.	1.5	6
16840	Theoretical Photovoltaic Conversion Efficiencies of ZnSnP₂, CdSnP₂, and Zn_{1-x}Cd_xSnP₂Alloys. Applied Physics Express, 2013, 6, 061201.	1.1	39
16841	Optical conductivity of highly mismatched GaP alloys. Applied Physics Letters, 2013, 102, 023901.	1.5	3
16842	Thermodynamic stability of alkali-metalâ€“zinc double-cation borohydrides at low temperatures. Physical Review B, 2013, 88, .	1.1	29
16843	First-principles study of quantum confinement and surface effects on the electronic properties of InAs nanowires. Journal of Applied Physics, 2013, 114, .	1.1	31
16844	High-pressure study of the structural and elastic properties of defect-chalcopyrite HgGa2Se4. Journal of Applied Physics, 2013, 113, .	1.1	28
16845	Controlling on-surface molecular diffusion behaviors by functionalizing the organic molecules with tert-butyl groups. Applied Physics Letters, 2013, 103, 013103.	1.5	8
16846	Correlation-assisted phonon softening and the orbital-selective Peierls transition in VO<mml:math xmlns:mml="http://www.w3.org/1998/Math/MathML" display="inline"><mml:msub><mml:mrow /><mml:mn>2</mml:mn></mml:msub></mml:math>. Physical Review B, 2013, 87, .	1.1	76
16847	Electron-limiting defect complex in hyperdoped GaAs: TheDDXcenter. Physical Review B, 2013, 87, .	1.1	3
16848	Epitaxial Zintl aluminide SrAl4grown on a LaAlO3substrate. Physical Review B, 2013, 88, .	1.1	3
16849	First-principles study of elastic properties of cubic Cr1â^’xAlxN alloys. Journal of Applied Physics, 2013, 113, .	1.1	55
16850	Tunneling electron induced rotation of a copper phthalocyanine molecule on Cu(111). Physical Review B, 2013, 88, .	1.1	15
16851	Adsorption of phosphorus molecules evaporated from an InP solid source on the Si(100) surface. Physical Review B, 2013, 87, .	1.1	5
16852	Geometrically induced melting variation in gallium clusters from first principles. Physical Review B, 2013, 88, .	1.1	17
16853	In4d and Ga3d levels in In_xX_{1â^’}_xN (Xâ€‰=â€‰Ga, Al) alloys. Applied Physics Letters, 2013, 102, 172105.	1.5	2

#	Article	IF	Citations
16854	Origin of Space Charge in Grain Boundaries of Protonâ€Conducting BaZrO₃. Fuel Cells, 2013, 13, 19-28.	1.5	51
16855	Band offset of GaAs/AlxGa1â^'xAs heterojunctions from atomistic first principles. Applied Physics Letters, 2013, 102, .	1.5	37
16856	ELECTRONIC AND MAGNETIC PROPERTIES OF SILICENE AND SILICANE NANORIBBONS. International Journal of Computational Materials Science and Engineering, 2013, 02, 1350011.	0.5	3
16857	First principles study of aluminum-oxygen complexes in silicon. , 2013, , .		0
16858	Superior Field Emission Properties of Layered WS2-RGO Nanocomposites. Scientific Reports, 2013, 3, 3282.	1.6	218
16859	Adsorption of methylamine on mackinawite (FES) surfaces: A density functional theory study. Journal of Chemical Physics, 2013, 139, 124708.	1.2	45
16860	The effects of Zn vacancies on ferromagnetism in Cu-doped ZnO films controlled by oxygen pressure and Li doping. Chinese Physics B, 2013, 22, 067503.	0.7	7
16861	Impact of Group-II Acceptors on the Electrical and Optical Properties of GaN. Japanese Journal of Applied Physics, 2013, 52, 08JJ04.	0.8	44
16862	Structural, elastic, thermodynamic and lattice dynamic properties of PrX (Xâ€‰=â€‰Sb, Bi). International Journal of Materials Research, 2013, 104, 99-108.	0.1	3
16863	Multiscale simulations in face-centered cubic metals: A method coupling quantum mechanics and molecular mechanics. Chinese Physics B, 2013, 22, 027101.	0.7	1
16864	Adsorption and Electronic Structure of Sr and Ag Atoms on Graphite Surfaces: a First-Principles Study. Chinese Physics Letters, 2013, 30, 066801.	1.3	4
16865	Towards understanding the carbon trapping mechanism in copper by investigating the carbonâ€"vacancy interaction. Chinese Physics B, 2013, 22, 076104.	0.7	9
16866	Hidden Structural Order in Orthorhombic<mml:math xmlns:mml="http://www.w3.org/1998/Math/MathML" display="inline"><mml:msub><mml:mi>Ta</mml:mi><mml:mn>2</mml:mn></mml:msub><mml:msub><mml:mi mathvariant="bold">O</mml:mi><mml:mn>5</mml:mn></mml:msub></mml:math>. Physical Review Letters, 2013, 110, 235502.	2.9	79
16867	Quantum molecular dynamics simulations of the thermophysical properties of shocked liquid ammonia for pressures up to 1.3 TPa. Journal of Chemical Physics, 2013, 139, 134505.	1.2	11
16868	THE FIRST-PRINCIPLES STABILITY STUDY OF PdC AND CdC COMPOUNDS. International Journal of Modern Physics B, 2013, 27, 1350016.	1.0	1
16869	Anisotropic thermal anharmonicity of CdSiP2 and ZnGeP2: Ab initio calculations. Journal of Applied Physics, 2013, 114, .	1.1	12
16870	ELECTRONIC AND OPTICAL PROPERTIES OF PERFECT MgO AND MgO WITH F CENTER UNDER HIGH PRESSURE. International Journal of Modern Physics C, 2013, 24, 1350052.	0.8	5
16871	Electrically tunable topological state in [111] perovskite materials with an antiferromagnetic exchange field. New Journal of Physics, 2013, 15, 063031.	1.2	63

#	Article	IF	Citations
16872	Synergistic Modification of Electronic and Photocatalytic Properties of TiO 2 Nanotubes by Implantation of Au and N Atoms. ChemPhysChem, 2013, 14, 2800-2807.	1.0	7
16873	Adsorption of lactic acid on chiral Pt surfacesâ€"A density functional theory study. Journal of Chemical Physics, 2013, 138, 084705.	1.2	13
16874	Ab-initio studies of some rare-earth borides: CeB₂, PrB₂, NdB₂, and PmB₂. International Journal of Materials Research, 2013, 104, 858-864.	0.1	0
16875	Theoretical study on the tungsten-induced reduction of transition temperature and the degradation of optical properties for VO2. Journal of Chemical Physics, 2013, 138, 114705.	1.2	76
16876	Effects of Na Substitution on Li Ion Migration in Li₂CoSiO₄Cathode Material. Journal of the Electrochemical Society, 2013, 160, A658-A661.	1.3	15
16877	Initial reduction of the NiO(100) surface in hydrogen. Journal of Chemical Physics, 2013, 139, 024704.	1.2	9
16878	Rational syntheses of core-shell Fex@Pt nanoparticles for the study of electrocatalytic oxygen reduction reaction. Scientific Reports, 2013, 3, 2872.	1.6	75
16879	THERMAL PROPERTIES OF THE XB₂(X = Ag, Au) COMPOUNDS: A FIRST-PRINCIPLES STUDY. International Journal of Modern Physics B, 2013, 27, 1350046.	1.0	0
16880	Engineering a topological phase transition in Î²-InSe via strain. New Journal of Physics, 2013, 15, 073008.	1.2	29
16881	CARBON-DOPEDTiO₂NANOTUBES: EXPERIMENTAL AND COMPUTATIONAL STUDIES. Journal of Theoretical and Computational Chemistry, 2013, 12, 1350007.	1.8	8
16882	AB INITIO MOLECULAR DYNAMICS SIMULATIONS ON LOCAL STRUCTURE AND ELECTRONIC PROPERTIES IN LIQUID Mg_xBi_{1-x} ALLOYS. International Journal of Modern Physics B, 2013, 27, 1350011.	1.0	2
16883	INTRINSIC ROOM TEMPERATURE FERROMAGNETISM OF SILICON-DOPED ZnO THIN FILMS. Modern Physics Letters B, 2013, 27, 1350092.	1.0	1
16884	ELECTRONIC STRUCTURE OF K_{0.8}Fe₂Se₂ FROM DENSITY FUNCTIONAL THEORY GW METHOD SIMULATION. International Journal of Modern Physics B, 2013, 27, 1362017.	1.0	0
16885	THE STRUCTURE, MAGNETISM AND CONDUCTIVITY OF Li3V2(PO4)3: A THEORETICAL AND EXPERIMENTAL STUDY. Modern Physics Letters B, 2013, 27, 1350199.	1.0	5
16886	Pressure dependent stability and structure of carbon dioxideâ€"A density functional study including long-range corrections. Journal of Chemical Physics, 2013, 139, 174501.	1.2	18
16887	A first-principles study on defect association and oxygen ion migration of Sm³⁺and Gd³⁺co-doped ceria. Journal of Physics Condensed Matter, 2013, 25, 225401.	0.7	20
16888	FIRST PRINCIPLES DENSITY FUNCTIONAL INVESTIGATION OF SUPPORTED TUNGSTEN CLUSTER (W_n; n = 1 TO 6) ON ANCHORED GRAPHITE (0001) SURFACE. International Journal of Computational Materials Science and Engineering, 2013, 02, 1350015.	0.5	0
16889	Effect of electronic structures on catalytic properties of CuNi alloy and Pd in MeOH-related reactions. Journal of Chemical Physics, 2013, 138, 144701.	1.2	7

#	Article	IF	Citations
16890	Analysis of dissociated dislocations in a deformed bicrystal close to the rhombohedral twin orientation in Î±-alumina. Philosophical Magazine, 2013, 93, 1182-1196.	0.7	2
16891	Structural and dynamical change of liquid carbon with pressure:ab initiomolecular dynamics simulations. Physica Scripta, 2013, 88, 045601.	1.2	2
16892	Lattice stability and formation energies of intrinsic defects in Mg2Si and Mg2Ge via first principles simulations. Journal of Physics Condensed Matter, 2013, 25, 035403.	0.7	36
16893	Structural and Optoelectronic Characterization of RF Sputtered ZnSnN₂. Advanced Materials, 2013, 25, 2562-2566.	11.1	161
16895	Topologically close-packed phases in binary transition-metal compounds: matching high-throughputab initiocalculations to an empirical structure map. New Journal of Physics, 2013, 15, 115016.	1.2	40
16896	Templated three-dimensional growth of quasicrystalline lead. Nature Communications, 2013, 4, 2715.	5.8	36
16897	First-Principles Studies of the Electronic and Dielectric Properties of Si/SiO₂/HfO₂ Interfaces. Japanese Journal of Applied Physics, 2013, 52, 041803.	0.8	7
16898	Pure and Li-doped NiTiH: Potential anode materials for Li-ion rechargeable batteries. Applied Physics Letters, 2013, 103, 033902.	1.5	11
16899	The electronic structure of gas phase croconic acid compared to the condensed phase: More insight into the hydrogen bond interaction. Journal of Chemical Physics, 2013, 138, 014308.	1.2	24
16900	Superconductivity at 44 K in K intercalated FeSe system with excess Fe. Scientific Reports, 2013, 3, 1216.	1.6	58
16901	Coupling the valley degree of freedom to antiferromagnetic order. Proceedings of the National Academy of Sciences of the United States of America, 2013, 110, 3738-3742.	3.3	263
16902	Electronic structures and properties of lanthanide hexaboride nanowires. Journal of Applied Physics, 2013, 114, 143709.	1.1	5
16903	Theoretical study of Zn and Cd interstitials and substitutional interstitials in CuInSe2 via hybrid functional calculations. , 2013, , .		1
16904	Water dissociation on Ni(100) and Ni(111): Effect of surface temperature on reactivity. Journal of Chemical Physics, 2013, 139, 174707.	1.2	40
16905	Firstâ€Principles Calculations of Lithiumâ€Ion Migration at a Coherent Grain Boundary in a Cathode Material, LiCoO₂. Advanced Materials, 2013, 25, 618-622.	11.1	149
16906	Vacancy breathing by grain boundariesâ€"a mechanism of memristive switching in polycrystalline oxides. MRS Communications, 2013, 3, 167-170.	0.8	9
16907	Ab initio study of the effect of oxygen vacancy on magnetism in Co doped ZnO. Materials Research Society Symposia Proceedings, 2013, 1494, 31-36.	0.1	1
16908	Cu Grain Boundary Embrittlement by Liquid Hg: A Comparison between Experiment and ab-initio Modeling. Materials Research Society Symposia Proceedings, 2013, 1515, 1.	0.1	0

#	Article	IF	Citations
16909	Surface and substrate induced effects on thin films of the topological insulators Bi<mml:math xmlns:mml="http://www.w3.org/1998/Math/MathML" display="inline"><mml:msub><mml:mrow /><mml:mn>2</mml:mn></mml:msub></mml:math>Se<mml:math xmlns:mml="http://www.w3.org/1998/Math/MathML" display="inline"><mml:msub><mml:mrow /><mml:mn>3</mml:mn></mml:msub></mml:math>and Bi<mml:math xmlns:mml="http://www.w3.org/1998/Math/MathML" display="inline"><mml:msub><mml:mrow /><mml:mml:	1.1	49
16910	Ferroelectricity Driven by Twisting of Silicate Tetrahedral Chains. Angewandte Chemie - International Edition, 2013, 52, 8088-8092.	7.2	62
16911	Formation Energy of Intrinsic Point Defects in Si and Ge and Implications for Ge Crystal Growth. ECS Journal of Solid State Science and Technology, 2013, 2, P104-P109.	0.9	19
16912	Mixed-mode mechanical responses of Ni(111)/Î±-Al2O3(0001) interface by first-principle calculations. Journal of Materials Research, 2013, 28, 3018-3028.	1.2	11
16913	The crystal structure of p-type transparent conductive oxide CuBO2. MRS Communications, 2013, 3, 157-160.	0.8	12
16914	Local environment of silicon in cubic boron nitride. Journal of Applied Physics, 2013, 114, 233502.	1.1	10
16915	Quantifying stoichiometry-induced variations in structure and energy of a SrTiO₃symmetric Î£13 {510}/<100â€‰>â€‰grain boundary. Philosophical Magazine, 2013, 93, 1219-1229.	0.7	13
16916	On the accuracy of van der Waals inclusive density-functional theory exchange-correlation functionals for ice at ambient and high pressures. Journal of Chemical Physics, 2013, 139, 154702.	1.2	119
16917	Molecular distortion and charge transfer effects in ZnPc/Cu(111). Scientific Reports, 2013, 3, .	1.6	19
16919	First-principles calculations of niobium hydride formation in superconducting radio-frequency cavities. Superconductor Science and Technology, 2013, 26, 095002.	1.8	17
16920	Predicting Atomic Arrangement of Solute Clusters in Dilute Mg Alloys. Materials Research Letters, 2013, 1, 213-219.	4.1	44
16921	Physical Guiding Principles for High Quality Resistive Random Access Memory Stack with Al₂O₃ Insertion Layer. Japanese Journal of Applied Physics, 2013, 52, 04CD11.	0.8	12
16922	Morphology and surface structure of cubic BaTiO₃ using first-principles density functional theory. Journal of the Ceramic Society of Japan, 2013, 121, 611-613.	0.5	9
16923	Investigation of PbTiO₃ thin films with reduced and re-oxidized treatment using Raman spectroscopy. Journal of the Ceramic Society of Japan, 2013, 121, 859-862.	0.5	5
16924	Density Function Theoretical Investigation on the Ni3PP Structure and the Hydrogen Adsorption Property of the Ni2P(0001) Surface. Chemistry Letters, 2013, 42, 1481-1483.	0.7	25
16925	Temperature Effect on the Synthesis of Gibbsite and Boehmite. Chemistry Letters, 2013, 42, 1463-1465.	0.7	3
16926	Accelerating materials property predictions using machine learning. Scientific Reports, 2013, 3, 2810.	1.6	574
16928	Graphene Synthesis. , 2013, , 45-72.		0

#	Article	IF	Citations
16929	Effects of Hindered Rotation on H₂Nuclear Spin Conversion on Ag(111). Journal of the Physical Society of Japan, 2013, 82, 023601.	0.7	9
16930	Chemical State Analysis of Li1^|^minus;xNi0.5Mn1.5O4 by Soft X-ray Absorption Spectroscopy. Hyomen Kagaku, 2013, 34, 415-420.	0.0	1
16931	Introduction to carbon-based nanostructures. , 0, , 1-10.		0
16932	Electronic properties of carbon-based nanostructures. , 0, , 11-90.		0
16933	The effect of Si impurity at the Al Î£5 grain boundary: a first principle computational tensile test study. Acta Metallurgica Sinica (English Letters), 2013, 26, 675-680.	1.5	8
16934	Hybrid functional study on diffusion of silicate cathode material Li₂NiSiO₄. Journal of Physics: Conference Series, 2013, 454, 012061.	0.3	13
16935	Systematic chemical functionalization of hybrid moleculeâ€“surface interfaces. Physica Status Solidi (B): Basic Research, 2013, 250, 2267-2276.	0.7	1
16936	Changes in the Structural Dimensionality of Selenidostannates in Ionic Liquids: Formation, Structures, Stability, and Photoconductivity. Chemistry - A European Journal, 2013, 19, 8806-8813.	1.7	49
16937	Self-consistent Scale-bridging Approach to Compute the Elasticity of Multi-phase Polycrystalline Materials. Materials Research Society Symposia Proceedings, 2013, 1524, 301.	0.1	28
16938	Ferroic phase transition in LaEr(MoO₄)₃. Powder Diffraction, 2013, 28, S86-S93.	0.4	2
16939	The effect of Si and S on the stability of bcc iron with respect to tetragonal strain at the Earth's inner core conditions. Geophysical Research Letters, 2013, 40, 2958-2962.	1.5	8
16940	Magnetic ordering and structural stability of La_{2/3}Sr_{1/3}MnO₃/SrTiO₃ (001) interfaces: A densityâ€functional theory study. Physica Status Solidi (B): Basic Research, 2013, 250, 402-410.	0.7	0
16941	Magnesium and Cadmium in Covalentlyâ€Bonded Lonsdaleite Networks: Synthesis, Structure, and Bonding of AETMg₂ and SrTCd₂ (AE = Ca, Sr; T = Pd,) Tj ETQq0 0 0 rgBT /Overlock	0.0	15
16942	Path aggregation techniques for EXAFS visualization and analysis. Journal of Physics: Conference Series, 2013, 430, 012006.	0.3	1
16943	Low intensity conduction states in FeS₂: implications for absorption, open-circuit voltage and surface recombination. Journal of Physics Condensed Matter, 2013, 25, 465801.	0.7	38
16944	Nature of the Interfaces Between Stoichiometric and Underâ€Stoichiometric MoO₃ and 4,4â€²â€²â€²N,Nâ€²â€²dicarbazoleâ€biphenyl: A Combined Theoretical and Experimental Study. Advanced Functional Materials, 2013, 23, 6091-6099.	7.8	26
16945	ã€ˆ110ã€‰{111} dislocation core properties in L1₂ Al₃ Sc and Al₃ Mg based on the Peierls-Nabarro model. Physica Status Solidi (B): Basic Research, 2013, 250, 1825-1831.	0.7	1
16946	Extracting the hybrid functional mixing parameter from a GW quasiparticle approach. Physica Status Solidi (B): Basic Research, 2013, 250, 1449-1452.	0.7	2

#	Article	IF	Citations
16947	On the Control Parameters of the Quasiâ€One Dimensional Superconductivity in Sc₃CoC₄. Zeitschrift Fur Anorganische Und Allgemeine Chemie, 2013, 639, 1985-1995.	0.6	19
16948	The application of molecular dynamics to fitting EXAFS data. Journal of Physics: Conference Series, 2013, 430, 012009.	0.3	1
16950	Multiferroicity in V-doped PbTiO₃. Journal of Physics: Conference Series, 2013, 470, 012013.	0.3	6
16951	Ab initio-aided CALPHAD thermodynamic modeling of the Sn-Pb binary system under current stressing. Scientific Reports, 2013, 3, 2731.	1.6	17
16952	First-principles study of structural and electronic properties of Laves phases structures YM2(M = Cu) Tj ETQq0 0 0 rgBT /Overlock 10 Tf 5	0.1	5
16953	Rational design of Nb-based alloys for hydrogen separation: A first principles study. AIP Advances, 2013, 3, .	0.6	2
16954	Antiferromagnetic FeSe monolayer on SrTiO3: The charge doping and electric field effects. Scientific Reports, 2013, 3, 2213.	1.6	64
16955	Thermodynamic Analysis of Phase Equilibria in the Mg–Al–Ho Ternary System. Materials Transactions, 2013, 54, 647-655.	0.4	6
16956	Direction and Size of Ir Magnetic Moment Induced in MnIr/Co1-xFexExchange Bias Bilayers from Resonant X-ray Magnetic Scattering Experiments at the Ir L3Absorption Edge. Journal of the Physical Society of Japan, 2013, 82, 034711.	0.7	1
16957	Electronic structures of oxygen-deficient Ta2O5. AIP Advances, 2013, 3, .	0.6	26
16959	The interaction of hydrogen with the {010} surfaces of Mg and Fe olivine as models for interstellar dust grains: a density functional theory study. Philosophical Transactions Series A, Mathematical, Physical, and Engineering Sciences, 2013, 371, 20110592.	1.6	17
16960	Turning Indium Oxide into a Superior Electrocatalyst: Deterministic Heteroatoms. Scientific Reports, 2013, 3, 3109.	1.6	28
16961	Promising ferrimagnetic double perovskite oxides towards high spin polarization at high temperature. AIP Advances, 2013, 3, .	0.6	14
16962	Adsorption of hydrogen atoms on graphene with TiO2 decoration. Journal of Applied Physics, 2013, 113, 153708.	1.1	9
16963	Ab-initio study of Mg-doped InN(0001) surface. AIP Advances, 2013, 3, .	0.6	3
16964	Mechanical properties of bilayer graphene with twist and grain boundaries. Journal of Applied Physics, 2013, 113, .	1.1	34
16965	Aluminum doping induced columnar growth of homoepitaxial ZnO films by metalorganic chemical vapor deposition. Applied Physics Letters, 2013, 103, 141907.	1.5	5
16966	Rotational Effects on the Dissociative Adsorption and Abstraction Dynamics of O₂/Al(111). Journal of the Physical Society of Japan, 2013, 82, 113602.	0.7	4

#	Article	IF	Citations
16967	First-Principles Prediction of Possible Synthesis of Li-Fe Based Complex Hydride Li4FeH6. Nippon Kinzoku Gakkaishi/Journal of the Japan Institute of Metals, 2013, 77, 604-608.	0.2	10
16968	First Principles Calculations of Solute Ordering in Mg–Zn–Y Alloys. Materials Transactions, 2013, 54, 656-660.	0.4	3
16969	Thermodynamic Analysis of the Mg–RE–Zn (RE = Y, La) Ternary hcp Phase Using the Cluster Variation Method. Materials Transactions, 2013, 54, 636-640.	0.4	22
16970	First-Principles Investigation on the Lithium Ion Insertion/Extraction in Trirutile LixFeF3. Electrochemistry, 2013, 81, 12-15.	0.6	8
16971	Oxide-Ion Conduction, Average and Local Structures of LaSrGa1^|^minus;xMgxO4^|^minus;^|^delta; with Layered Perovskite Structure. Electrochemistry, 2013, 81, 448-453.	0.6	14
16972	Adsorption and Surface Diffusion of Pt Atoms on Hydroxylated MgO(001) Surfaces. Journal of the Physical Society of Japan, 2013, 82, 034603.	0.7	16
16973	Electronic Structure and Functions of Point Defects in Oxide and Nitride Semiconductors: Renewed Understanding from First-Principles Calculations. Materia Japan, 2013, 52, 350-356.	0.1	0
16974	First-Principles-Based Modeling of Energetic Stability for Alloy Nanoparticles with Multiple Shapes. Nippon Kinzoku Gakkaishi/Journal of the Japan Institute of Metals, 2013, 77, 276-280.	0.2	0
16975	Energetic Stability and Thermoelectric Property of Alkali-Metal-Encapsulated Type-I Silicon-Clathrate from First-Principles Calculation. Materials Transactions, 2013, 54, 276-285.	0.4	16
16976	Energetic Analysis of Deformation Twins and Twinning Dislocations in Magnesium. Materials Transactions, 2013, 54, 1524-1527.	0.4	12
16977	Phonon Scattering and Electron Transport in Single Wall Carbon Nanotube. , 2013, , .		43
16978	Ab-initio Investigation of Hydrogen Trap State by Cementite in bcc-Fe. ISIJ International, 2013, 53, 709-713.	0.6	32
16979	Cs Adsorption in Clay Minerals and Zeolites: First Principle Calculation Studies toward Understanding Their Microscopic Mechanism. Hyomen Kagaku, 2013, 34, 135-142.	0.0	5
16980	Picosecond amorphization of chalcogenides material: From scattering to ionization. Applied Physics Letters, 2013, 102, .	1.5	4
16981	Elements Science and Technology Project: Design of Precious Metal Free Catalyst for NO Dissociation. Journal of the Japan Petroleum Institute, 2013, 56, 357-365.	0.4	4
16982	First-Principles Calculation of Hydrogen Effects on the Formation and Diffusion of Vacancies in Alpha Iron: Discussion of the Hydrogen-Enhanced Strain-Induced Vacancy Mechanism. Zairyo/Journal of the Society of Materials Science, Japan, 2014, 63, 182-187.	0.1	27
16983	Theoretical study of the adsorption of benzene on coinage metals. Beilstein Journal of Organic Chemistry, 2014, 10, 1775-1784.	1.3	53
16984	Performance Analysis of Electronic Structure Codes on HPC Systems: A Case Study of SIESTA. PLoS ONE, 2014, 9, e95390.	1.1	13

#	Article	IF	Citations
16985	Preparation of Zirconium Oxide Powder Using Zirconium Carboxylate Precursors. Advances in Physical Chemistry, 2014, 2014, 1-8.	2.0	8
16986	Revisiting the Zinc-Blende/Wurtzite Heterocrystalline Structure in CdS. Advances in Condensed Matter Physics, 2014, 2014, 1-7.	0.4	5
16987	Heterospin Junctions in Zigzag-Edged Graphene Nanoribbons. Applied Sciences (Switzerland), 2014, 4, 351-365.	1.3	1
16988	From Stable ZnO and GaN Clusters to Novel Double Bubbles and Frameworks. Inorganics, 2014, 2, 248-263.	1.2	10
16989	Quasi-1D physics in metal-organic frameworks: MIL-47(V) from first principles. Beilstein Journal of Nanotechnology, 2014, 5, 1738-1748.	1.5	23
16990	First-Principles Calculation of the Effects of Carbon on Tetragonality and Magnetic Moment of BCC-Fe. Tetsu-To-Hagane/Journal of the Iron and Steel Institute of Japan, 2014, 100, 1329-1338.	0.1	10
16991	First-Principles Study of Ferroelectric-Ferromagnetic Coupling in Multiferroic BiFeO3. Zairyo/Journal of the Society of Materials Science, Japan, 2014, 63, 168-173.	0.1	1
16992	Density Functional Theory Calculations of Charge-Induced Spin Polarization in Pentacene. Chinese Journal of Chemical Physics, 2014, 27, 519-522.	0.6	1
16993	Analysis of the Changes in Electronic Structures and Work Function Variation in Alkali Metal^|^mdash;Metal Surface Systems. Journal of the Vacuum Society of Japan, 2014, 57, 27-31.	0.3	7
16994	Hybrid Density Functional Study on Plutonium Dioxide. , 2014, , .		2
16995	Degenerate Phases of Iodine on Pt(110) at Half-Monolayer Coverage. Journal of Physical Chemistry C, 2014, 118, 29919-29927.	1.5	5
16996	Fe₃S₄and Fe₃O₄magnetic nanocrystals: magneto-optical and MÃ¶ssbauer spectroscopy study. Materials Research Express, 2014, 1, 025033.	0.8	13
16997	Structural stability and electronic properties of carbon star lattice monolayer. Chinese Physics B, 2014, 23, 096104.	0.7	0
16998	Solute effect on basal and prismatic slip systems of Mg. Journal of Physics Condensed Matter, 2014, 26, 445004.	0.7	21
16999	The generalized planar fault energy, ductility, and twinnability of Al and Alâ€”RE(RE= Sc, Y,) Tj ETQq0 0 0 rgBT /Overlock 1	0.7	6
17000	Electronic and Optical Properties at Organic/Organic Interfaces in Organic Solar Cells. Topics in Current Chemistry, 2014, 352, 103-150.	4.0	6
17001	Hydrogen on graphene investigated by inelastic neutron scattering. Journal of Physics: Conference Series, 2014, 554, 012009.	0.3	20
17002	Stability and mobility of rhenium and osmium in tungsten: first principles study. Modelling and Simulation in Materials Science and Engineering, 2014, 22, 075006.	0.8	81

#	Article	IF	Citations
17003	Effect of temperature on elastic constants, generalized stacking fault energy and dislocation cores in MgO and CaO. Computational Condensed Matter, 2014, 1, 38-44.	0.9	13
17004	Ultrahigh thermoelectricity of atomically thick Bi2Se3 single layers: A computational study. Applied Surface Science, 2014, 321, 525-530.	3.1	11
17005	First Principles Study on the Electrochemical, Thermal and Mechanical Properties of LiCoO2 for Thin Film Rechargeable Battery. Materials Today: Proceedings, 2014, 1, 82-93.	0.9	28
17006	Vibrational Excitation Induces Double Reaction. ACS Nano, 2014, 8, 12468-12475.	7.3	14
17007	Promoting alkali and alkaline-earth metals on MgO for enhancing CO₂capture by first-principles calculations. Physical Chemistry Chemical Physics, 2014, 16, 24818-24823.	1.3	37
17008	Electrical Stress and Total Ionizing Dose Effects on <formula formulatype="inline"><tex Notation="TeX">${hbox {MoS}}_{2}$</tex> </formula> Transistors. IEEE Transactions on Nuclear Science, 2014, 61, 2862-2867.	1.2	20
17009	DFT study on the interaction between atomic aluminum and graphene. Journal of Theoretical and Computational Chemistry, 2014, 13, 1450055.	1.8	7
17010	Ab initio study of topological surface states of strained HgTe. Europhysics Letters, 2014, 107, 57006.	0.7	21
17011	Propane Ammoxidation over Moâ€“Vâ€“Teâ€“Nbâ€“O M1 Phase Investigated by DFT: Elementary Steps of Ammonia Adsorption, Activation and NH Insertion into Ï€-Allyl Intermediate. Topics in Catalysis, 2014, 57, 1145-1151.	1.3	11
17012	Effects of C impurities on the elastic properties of NiAl intermetallics. Progress in Natural Science: Materials International, 2014, 24, 637-641.	1.8	9
17013	Optical properties of organometallic perovskite: An ab initio study using relativistic GW correction and Bethe-Salpeter equation. Europhysics Letters, 2014, 108, 67015.	0.7	47
17014	Stacking stability of MoS ₂ bilayer: An ab initio study. Chinese Physics B, 2014, 23, 106801.	0.7	38
17015	DFT-supported phase-field study on the effect of mechanically driven fluxes in Ni₄Ti₃precipitation. Modelling and Simulation in Materials Science and Engineering, 2014, 22, 034003.	0.8	14
17016	Absence of significant structural changes near the magnetic ordering temperature in small-ion rare earth perovskiteRMnO3. Journal of Physics Condensed Matter, 2014, 26, 495402.	0.7	4
17017	Band alignment in visible-light photo-active CoO/SrTiO3 (001) heterostructures. Journal of Applied Physics, 2014, 116, .	1.1	10
17018	Unusual coordination structure in undercooled eutectic Ga-In alloy melt. Europhysics Letters, 2014, 107, 36004.	0.7	8
17019	Ceria Nanocrystals Exposing Wide (100) Facets: Structure and Polarity Compensation. Advanced Materials Interfaces, 2014, 1, 1400404.	1.9	49
17020	GEOMETRY OF DOPAMINE ADSORPTION ON RUTILE (110) SURFACE. International Journal of Modern Physics B, 2014, 28, 1450071.	1.0	4

#	Article	IF	Citations
17021	Influences ofB-site Cations on Intrinsic Dielectric Properties of Ba(Bâ€²1/3Bâ€²â€²2/3)O3Materials. Ferroelectrics, 2014, 467, 22-32.	0.3	1
17022	Duality of Topological Defects in Hexagonal Manganites. Physical Review Letters, 2014, 113, 267602.	2.9	40
17023	DENSITY FUNCTIONAL THEORY STUDIES ON THE ADSORPTION OF 4-METHYLBENZENETHIOL AND 4-ETHYLBENZENETHIOL MOLECULES ONAu(111) SURFACE. Surface Review and Letters, 2014, 21, 1450087.	0.5	1
17024	Stability and electronic properties of isomers of B/N co-doped graphene. Applied Nanoscience (Switzerland), 2014, 4, 989-996.	1.6	47
17025	First-principles study of the stability of silicane and germanane under strain. Modern Physics Letters B, 2014, 28, 1450138.	1.0	4
17026	Selective Hostâ€“Guest Interaction between Metal Ions and Metalâ€“Organic Frameworks Using Dynamic Nuclear Polarization Enhanced Solidâ€State NMR Spectroscopy. Chemistry - A European Journal, 2014, 20, 16308-16313.	1.7	35
17027	Combining Kohn-Sham and orbital-free density-functional theory for Hugoniot calculations to extreme pressures. Physical Review E, 2014, 90, 063314.	0.8	28
17028	Interplay of Photoabsorption, Electronic Structure, and Recombination Rate of Charge Carriers on Visible Light Driven Photocatalytic Activity of Cu- and N-Doped Ba3V2O8. European Journal of Inorganic Chemistry, 2014, 2014, 5585-5595.	1.0	8
17029	Ab initio design of nanostructures for solar energy conversion: a case study on silicon nitride nanowire. Nanoscale Research Letters, 2014, 9, 531.	3.1	2
17031	High pressure effect on the electronic structure and thermoelectric properties of BiCuSeO: first-principles calculations. RSC Advances, 2014, 4, 54819-54825.	1.7	33
17032	Spin and Orbital Magnetism in Free Nanoparticles. Frontiers of Nanoscience, 2014, 6, 33-84.	0.3	1
17033	Criticality of surface topology for charge-carrier transport characteristics in two-dimensional borocarbonitrides: design principles for an efficient electronic material. Nanoscale, 2014, 6, 13430-13434.	2.8	15
17034	Thermodynamic modeling of the Inâ€“Ptâ€“Sb system. International Journal of Materials Research, 2014, 105, 525-536.	0.1	5
17035	Structural evolution and stabilities of negatively charged lead telluride clusters. Journal of Theoretical and Computational Chemistry, 2014, 13, 1450043.	1.8	1
17036	Defect properties of Sb- and Bi-doped CuInSe2: The effect of the deep lone-pair s states. Applied Physics Letters, 2014, 105, .	1.5	21
17037	Chemical scissors cut phosphorene nanostructures. Materials Research Express, 2014, 1, 045041.	0.8	20
17038	Activation of n â†' Ï€* Transitions in Two-Dimensional Conjugated Polymers for Visible Light Photocatalysis. Journal of Physical Chemistry C, 2014, 118, 29981-29989.	1.5	326
17039	Structure and energetics of<mml:math xmlns:mml="http://www.w3.org/1998/Math/MathML"><mml:msub><mml:mi>LaAlO</mml:mi><mml:mn>3</mml:mn></mml:msub><m surfaces. Physical Review B, 2014, 90, .	1.1	26

#	Article	IF	Citations
17040	Electrochemical and Photoelectrochemical Properties of the Copper Hydroxyphosphate Mineral Libethenite. ChemElectroChem, 2014, 1, 663-672.	1.7	15
17041	Thermal expansion, diffusion and melting of Li₂O using a compact forcefield derived fromab initiomolecular dynamics. Modelling and Simulation in Materials Science and Engineering, 2014, 22, 075009.	0.8	9
17042	Dimerization-Induced Fermi-Surface Reconstruction in<mml:math xmlns:mml="http://www.w3.org/1998/Math/MathML" display="inline"><mml:mrow><mml:msub><mml:mrow><mml:mi>IrTe</mml:mi></mml:mrow><mml:mrow><mml:mn>2</mml:mn></m Physical Review Letters, 2014, 113, 266406.	2.9	26
17043	Effect of hydrostatic pressure on the thermoelectric properties of<mml:math xmlns:mml="http://www.w3.org/1998/Math/MathML"><mml:mrow><mml:msub><mml:mi mathvariant="bold">Bi</mml:mi><mml:mn>2</mml:mn></mml:msub><mml:msub><mml:mi mathvariant="bold">Te</mml:mi><mml:mn>3</mml:mn></mml:msub></mml:mrow></mml:math>. Physical Review B, 2014, 90, .	1.1	29
17044	Electronic excitations and self-trapping of electrons and holes in CaSO4. Physica Scripta, 2014, 89, 044013.	1.2	8
17045	Direct experimental determination of onset of electronâ€“electron interactions in gap opening of zigzag graphene nanoribbons. Nature Communications, 2014, 5, 4311.	5.8	83
17046	Quantum magnetoresistance in the Ca-intercalated graphite superconductorCaC6. Physical Review B, 2014, 90, .	1.1	0
17047	Covalency-driven structural instability and spin-phonon coupling in barium cobalt oxychloride. Physical Review B, 2014, 90, .	1.1	4
17048	Anharmonicity and atomic distribution of SnTe and PbTe thermoelectrics. Physical Review B, 2014, 90, .	1.1	64
17049	Temperature-driven band inversion in<mml:math xmlns:mml="http://www.w3.org/1998/Math/MathML"><mml:mrow><mml:msub><mml:mi>Pb</mml:mi><mml:mrow><mml:mn>0.77 Optical and Hall effect studies. Physical Review B, 2014, 90, .	1.1	9
17050	Electronic, phononic, and thermoelectric properties of graphyne sheets. Applied Physics Letters, 2014, 105, 223108.	1.5	64
17051	Study of Shallow Backside Junctions for Backside Illumination of CMOS Image Sensors. Journal of Electronic Materials, 2014, 43, 3933-3941.	1.0	0
17052	Adsorption and diffusion of oxygen atom on UN2(100) surface and subsurface: a density functional theory study (DFT and DFTÂ+ÂU). Journal of Nanostructure in Chemistry, 2014, 4, 143-151.	5.3	4
17053	Using structural disorder to enhance the magnetism and spin-polarization in FexSi1 â^'xthin films for spintronics. Materials Research Express, 2014, 1, 026102.	0.8	11
17054	Ab-initio study of the interfacial properties in ultrathin MgO films on O-rich FeO/Fe(001) surfaces. Journal of the Korean Physical Society, 2014, 65, 702-708.	0.3	4
17055	Influence of Ni on Cu precipitation in Feâ€“Cuâ€“Ni ternary alloy by an atomic study. Chinese Physics B, 2014, 23, 063601.	0.7	14
17056	Anisotropy and temperature dependence of structural, thermodynamic, and elastic properties of crystalline cellulose I_{Î²}: a first-principles investigation. Modelling and Simulation in Materials Science and Engineering, 2014, 22, 085012.	0.8	25
17057	Stability and electronic structure studies of LaAlO 3 /SrTiO 3 (110) heterostructures. Chinese Physics B, 2014, 23, 087302.	0.7	6

#	Article	IF	Citations
17058	Hybrid density functional studies of cadmium vacancy in CdTe. Chinese Physics B, 2014, 23, 077103.	0.7	7
17059	Electronic and transport properties of V-shaped defect zigzag MoS 2 nanoribbons. Chinese Physics B, 2014, 23, 047307.	0.7	11
17060	DFT study of nitrogenâ€“vacancy complexions in (fcc) Fe. Modelling and Simulation in Materials Science and Engineering, 2014, 22, 055004.	0.8	5
17061	Physical properties of FePt nanocomposite doped with Ag atoms: First-principles study. Chinese Physics B, 2014, 23, 076105.	0.7	7
17062	High-pressure-activated carbon tetrachloride decomposition. Chinese Physics B, 2014, 23, 023302.	0.7	0
17063	Conditions for electronic reconstruction at stoichiometric polar/polar interfaces. Journal of Physics Condensed Matter, 2014, 26, 485010.	0.7	6
17064	Anab initio-based Erâ€“He interatomic potential in hcp Er. Modelling and Simulation in Materials Science and Engineering, 2014, 22, 065009.	0.8	3
17065	Effects of electron-beam irradiation on Inâ€“Gaâ€“Znâ€“O thin films. Japanese Journal of Applied Physics, 2014, 53, 115502.	0.8	2
17066	Ab initiostudy on stacking sequences, free energy, dynamical stability and potential energy surfaces of graphite structures. Modelling and Simulation in Materials Science and Engineering, 2014, 22, 035016.	0.8	13
17067	Effects of the 3d transition metal doping on the structural, electronic, and magnetic properties of BeO nanotubes. Chinese Physics B, 2014, 23, 017103.	0.7	1
17068	Modulating magnetism of nitrogen-doped zigzag graphene nanoribbons. Chinese Physics B, 2014, 23, 067305.	0.7	7
17069	Twisted ultrathin silicon nanowires: A possible torsion electromechanical nanodevice. Europhysics Letters, 2014, 108, 36006.	0.7	5
17070	First-principles investigation of chemical modification on two-dimensional ironâ”phthalocyanine sheet. Chinese Physics B, 2014, 23, 018103.	0.7	3
17071	Energetics, structure and composition of nanoclusters in oxide dispersion strengthened Feâ€“Cr alloys. Modelling and Simulation in Materials Science and Engineering, 2014, 22, 085003.	0.8	11
17072	Structural stability and electrical properties of AlB₂-type MnB₂under high pressure. Chinese Physics B, 2014, 23, 016102.	0.7	8
17073	Corrosion related properties of iron (100) surface in liquid lead and bismuth environments: A first-principles study. Chinese Physics B, 2014, 23, 056801.	0.7	7
17074	Symmetry-resolved surface-derived electronic structure of MoS₂(0â€‰0â€‰0â€‰1). Journal of Physics Condensed Matter, 2014, 26, 455501.	0.7	9
17075	Role of helium in the sliding and mechanical properties of a vanadium grain boundary: A first-principles study. Chinese Physics B, 2014, 23, 056104.	0.7	5

#	Article	IF	Citations
17076	Structure Sensitivity in the Decomposition of Ethylene Carbonate on Si Anodes. ChemPhysChem, 2014, 15, 3950-3954.	1.0	11
17077	Ferromagnetism in Gd doped ZnO nanowires: A first principles study. Journal of Applied Physics, 2014, 116, .	1.1	48
17078	A DFT study on surface dependence of Î²-Ga2O3 for CO2 hydrogenation to CH3OH. Journal of Molecular Modeling, 2014, 20, 2543.	0.8	11
17079	Computational Study of In-Plane Phonon Transport in Si Thin Films. Scientific Reports, 2014, 4, 6399.	1.6	73
17080	DEFECT PHYSICS AND INTRINSIC p-TYPE CONDUCTIVITY IN TOPOLOGICAL INSULATOR AuTlS2. Modern Physics Letters B, 2014, 28, 1450008.	1.0	1
17081	Theoretical and experimental investigation of the excellent pâ€“n control in yttrium aluminoborides. Science and Technology of Advanced Materials, 2014, 15, 035012.	2.8	14
17082	One-dimensional CuO nanowire: synthesis, electrical, and optoelectronic devices application. Nanoscale Research Letters, 2014, 9, 637.	3.1	71
17083	RRS-PBC: a molecular approach for periodic systems. Science China Chemistry, 2014, 57, 1399-1404.	4.2	8
17084	Prediction of Irradiation Spectrum Effects in Pyrochlores. Jom, 2014, 66, 2578-2582.	0.9	6
17085	Ab initio calculation of the thermal conductivity of indium antimonide. Semiconductor Science and Technology, 2014, 29, 124002.	1.0	6
17086	A first principles scanning tunneling potentiometry study of an opaque graphene grain boundary in the ballistic transport regime. Nanotechnology, 2014, 25, 415701.	1.3	10
17087	The Electronic Structure and Formation Energies of Ni-doped CuAlO ₂ by Density Functional Theory Calculation. Chinese Physics Letters, 2014, 31, 037101.	1.3	4
17088	Elastic and Dynamical Properties of YB ₄ : First-Principles Study. Chinese Physics Letters, 2014, 31, 116201.	1.3	16
17089	First-principles study of band alignments in the p-type hosts BaM₂X₂(M= Cu, Ag;X= S, Se). Journal of Physics Condensed Matter, 2014, 26, 155802.	0.7	10
17090	DFT Studies on a Series of Nitramines Containing Pyridine Ring. Polycyclic Aromatic Compounds, 2014, 34, 588-605.	1.4	3
17091	Experimental and theoretical identification of a high-pressure polymorph of Ga2S3 with Î±-Bi2Te3-type structure. Journal of Applied Physics, 2014, 116, 193507.	1.1	6
17092	Boron-tuning transition temperature of vanadium dioxide from rutile to monoclinic phase. Journal of Chemical Physics, 2014, 141, 194707.	1.2	18
17093	Origin of the band dispersion in a metal phthalocyanine crystal. Physical Review B, 2014, 90, .	1.1	15

#	Article	IF	Citations
17094	Vibrational lifetimes of hydrogen on lead films: An ab initio molecular dynamics with electronic friction (AIMDEF) study. Journal of Chemical Physics, 2014, 141, 234702.	1.2	40
17095	Simple bond-order-type interatomic potential for an intermixed Fe-Cr-C system of metallic and covalent bondings in heat-resistant ferritic steels. Journal of Applied Physics, 2014, 116, 244311.	1.1	2
17096	DFT study of pressure effects in molecular crystal 4,10-dinitro-2,6,8,12-tetraoxa-4,10-diazatetracyclo-[5.5.0.05,903,11]-dodecane. Canadian Journal of Chemistry, 2014, 92, 616-624.	0.6	9
17097	Multiple adsorption of CO on Na-exchanged Y faujasite: a DFT investigation. Molecular Simulation, 2014, 40, 33-44.	0.9	15
17098	High-pressure synthesis and Sn valence state analysis of BaTiO3â€“SnO solid solution. Journal of Materials Research, 2014, 29, 2928-2933.	1.2	1
17099	First-principles simulation on orientation dependence of piezoresistivity in graphene nanoribbon. , 2014, , .		1
17100	Comparative modelling of chemical ordering in palladium-iridium nanoalloys. Journal of Chemical Physics, 2014, 141, 224307.	1.2	23
17101	Formation of 2D transition metal dichalcogenides on TiC_{1â^’x}A_x surfaces (A = S, Se, Te): A theoretical study. Journal of Materials Research, 2014, 29, 207-214.	1.2	2
17102	Spin-coupling in dimers of 2,3-dicyano-5,6-dichlorosemiquinone radical anions in the crystalline state. Acta Crystallographica Section B: Structural Science, Crystal Engineering and Materials, 2014, 70, 181-190.	0.5	16
17103	Understanding the Behavior of Native Point Defects in <scp><scp>ZrC</scp></scp> by Firstâ€Principles Calculations. Journal of the American Ceramic Society, 2014, 97, 4024-4030.	1.9	18
17104	Fluorinated graphene and hexagonal boron nitride as ALD seed layers for graphene-based van der Waals heterostructures. Nanotechnology, 2014, 25, 355202.	1.3	5
17105	Stokes-anti-Stokes contribution to double resonance Raman processes in graphene. Physica Status Solidi (B): Basic Research, 2014, 251, 2525-2529.	0.7	2
17106	Ab-initio Prediction of Magnetoelectricity in Infinite-Layer CaFeO₂and MgFeO₂. Journal of the Physical Society of Japan, 2014, 83, 094712.	0.7	8
17107	Enhanced visible light photocatalytic activity of anatase TiO₂ through C, N, and F codoping. Canadian Journal of Physics, 2014, 92, 71-75.	0.4	7
17108	High temperature phase decomposition in TixZryAlzN. AIP Advances, 2014, 4, .	0.6	13
17109	Elastic properties and lattice dynamics of ruthenium at high pressures. Journal of Physics: Conference Series, 2014, 490, 012059.	0.3	4
17110	Manipulating topological phase transition by strain. Acta Crystallographica Section C, Structural Chemistry, 2014, 70, 118-122.	0.2	32
17112	Inâ€Gap States in Electronic Structure of Nonpolar Surfaces of Insulating Metal Oxides. Advanced Materials Interfaces, 2014, 1, 1300131.	1.9	11

#	Article	IF	Citations
17113	Uniform B-C-N Ternary Monolayer from Non-Metal Filled g-C3N4 Sheet. Chinese Journal of Chemical Physics, 2014, 27, 394-398.	0.6	4
17114	Analytical Green's function of the multidimensional frequency-dependent phonon Boltzmann equation. Physical Review B, 2014, 90, .	1.1	35
17115	Electronic properties of two-dimensional ZnO atomically sheet on Cu substrate: a first-principles study. Modern Physics Letters B, 2014, 28, 1450204.	1.0	3
17116	Atomic structure and bonding of the interfacial bilayer between Au nanoparticles and epitaxially regrown MgAl2O4 substrates. Applied Physics Letters, 2014, 105, .	1.5	16
17117	Electronic and thermoelectric properties of InN studied using ab initio density functional theory and Boltzmann transport calculations. Journal of Applied Physics, 2014, 116, 223706.	1.1	8
17118	Band structure engineering through orbital interaction for enhanced thermoelectric power factor. Applied Physics Letters, 2014, 104, .	1.5	64
17119	Ab initio study of point defects in PbSe and PbTe: Bulk and nanowire. Journal of Applied Physics, 2014, 116, .	1.1	10
17120	Experimental and theoretical investigation on the compression mechanism of FeF₃up to 62.0â€...GPa. Acta Crystallographica Section B: Structural Science, Crystal Engineering and Materials, 2014, 70, 801-808.	0.5	7
17121	Complex borides based on AlLiB₁₄ as high-temperature thermoelectric compounds. Physical Chemistry Chemical Physics, 2014, 16, 25337-25341.	1.3	14
17122	Band engineering of GaN/AlN quantum wells by Si dopants. Journal of Applied Physics, 2014, 115, 124305.	1.1	6
17123	Structure, electronic and electrochemical properties of Li-rich metal phosphate by first-principles study. Journal Physics D: Applied Physics, 2014, 47, 025301.	1.3	2
17124	Lattice structures and electronic properties of CIGS/CdS interface: First-principles calculations. Chinese Physics B, 2014, 23, 077301.	0.7	11
17125	Adsorption and Surface Diffusion of Au Monomers and Dimers on Strongly Correlated NiO(001) Surfaces. Journal of the Physical Society of Japan, 2014, 83, 113602.	0.7	6
17126	Segregation of alloying atoms at a tilt symmetric grain boundary in tungsten and their strengthening and embrittling effects. Chinese Physics B, 2014, 23, 106107.	0.7	17
17127	Analysis of SnS₂hyperdoped with V proposed as efficient absorber material. Journal of Physics Condensed Matter, 2014, 26, 395501.	0.7	5
17128	Spin-orbital entangled molecular jeff states in lacunar spinel compounds. Nature Communications, 2014, 5, 3988.	5.8	52
17129	First Principles Study of Structural Stability and Magnetic Property of Non-equilibrium Coâ€“Mo Alloys. Acta Metallurgica Sinica (English Letters), 2014, 27, 1057-1062.	1.5	2
17130	Electron dynamics in charged wet TiO2anatase (001) surface functionalised by ruthenium ions. Molecular Physics, 2014, 112, 441-452.	0.8	20

#	Article	IF	Citations
17131	Electronic properties of tantalum pentoxide polymorphs from first-principles calculations. Applied Physics Letters, 2014, 105, 202108.	1.5	30
17132	Identification of Active Sites in a Realistic Model of Strong Metalâ€“Support Interaction Catalysts: The Case of Platinumâ€‰(1â€‰1â€‰1)â€Supported Iron Oxide Film. ChemCatChem, 2014, 6, 185-190.	1.8	19
17133	Strong enhancement of phonon scattering through nanoscale grains in lead sulfide thermoelectrics. NPG Asia Materials, 2014, 6, e108-e108.	3.8	140
17134	Dirac fermions in blue-phosphorus. 2D Materials, 2014, 1, 031002.	2.0	34
17135	Architectured van der Waals epitaxy of ZnO nanostructures on hexagonal BN. NPG Asia Materials, 2014, 6, e145-e145.	3.8	43
17136	Mechanistic Study of CO Titration on Cu_xO/Cu(1â€‰1â€‰1) (xâ‰2) Surfaces. ChemCatChem, 2014, 6, 2364-2372.	1.8	31
17137	Nitrogen Vacancies and Oxygen Substitution of Ta₃N₅: First-Principles Investigation. Journal of the Physical Society of Japan, 2014, 83, 114707.	0.7	17
17138	Origin of ferromagnetism in aluminum-doped TiO2 thin films: Theory and experiments. Applied Physics Letters, 2014, 105, .	1.5	44
17139	Effect of vacancy defects on generalized stacking fault energy of fcc metals. Journal of Physics Condensed Matter, 2014, 26, 115404.	0.7	21
17140	Interfacial charge transfer and enhanced photocatalytic performance for the heterojunction WO₃/BiOCl: first-principles study. Journal of Materials Chemistry A, 2014, 2, 20770-20775.	5.2	52
17141	Quantum size effect on dielectric function of ultrathin metal film: a first-principles study of Al(1â€‰1â€‰1). Journal of Physics Condensed Matter, 2014, 26, 505302.	0.7	16
17142	Charge transition levels of Mn-doped Si calculated with the GGA-1/2 method. Physical Review B, 2014, 90, .	1.1	10
17143	Unexpected Roomâ€Temperature Ferromagnetism in Nanostructured Bi₂Te₃. Angewandte Chemie - International Edition, 2014, 53, 729-733.	7.2	33
17144	Magnetic anisotropy in Ta/CoFeB/MgO investigated by x-ray magnetic circular dichroism and first-principles calculation. Applied Physics Letters, 2014, 105, .	1.5	47
17145	Structure and magnetic properties of the perovskite YCo0.5Fe0.5O3. AIP Advances, 2014, 4, .	0.6	22
17146	Atomic-scale structure and properties of highly stable antiphase boundary defects in Fe3O4. Nature Communications, 2014, 5, 5740.	5.8	112
17147	Computing total energies in complex materials using charge self-consistent DFTâ€‰+â€‰DMFT. Physical Review B, 2014, 90, .	1.1	73
17148	Towards numerically accurate many-body perturbation theory: Short-range correlation effects. Journal of Chemical Physics, 2014, 141, 164127.	1.2	24

#	Article	IF	Citations
17149	Multistage reaction pathways in detonating high explosives. Applied Physics Letters, 2014, 105, .	1.5	25
17150	Tunable topological electronic structure of silicene on a semiconducting Bi/Si(111)-3Ã—3substrate. Physical Review B, 2014, 90, .	1.1	11
17151	The Electronic and Structural Properties of 3C-SiC: A First-Principles Study. Advanced Materials Research, 0, 971-973, 208-212.	0.3	2
17152	Density Functional Study of Bulk and Surface Properties of Rhodium Hydride. Acta Physica Polonica A, 2014, 125, 29-35.	0.2	6
17153	Structure and Properties of the GeAsS Glasses from <i>Ab initio</i> Calculations. Advanced Materials Research, 0, 1035, 502-507.	0.3	0
17154	DFT Simulation of the Extra Me Adatom Diffusion on the Ge(111) â^š3Ã—â^š3 1/3 ML Me Induced Surfaces. Solid State Phenomena, 0, 213, 12-18.	0.3	1
17155	Grain Refinement Mechanism of Al-5Ti-1B Master Alloy by <i>Ab Initio</i> Calculations. Materials Science Forum, 0, 794-796, 746-751.	0.3	0
17156	Thermomechanical Processed Steels. , 2014, , 191-216.		15
17157	The structure and phase transitions of crystalline polydimethylsilane [Me2Si] n revisited. Russian Chemical Bulletin, 2014, 63, 2515-2526.	0.4	1
17158	The hydroxylated and reduced rutile TiO2(011)-2Ã—1 surfaces: A first-principles study. Surface Science, 2014, 628, 126-131.	0.8	6
17159	Atomic imaging and modeling of passivation, functionalization, and atomic layer deposition nucleation of the SiGe(001) surface via H2O2(g) and trimethylaluminum dosing. Surface Science, 2014, 630, 273-279.	0.8	16
17160	Interface structure of a topological insulator/superconductor heterostructure. New Journal of Physics, 2014, 16, 123043.	1.2	25
17161	Reversible switching of magnetic states by electric fields in nitrogenized-divacancies graphene decorated by tungsten atoms. Scientific Reports, 2014, 4, 7575.	1.6	10
17162	A First Principle Comparative Study on Chemisorption of H2on C60, C80, and Sc3N@C80in Gas Phase and Chemisorption of H2on Solid Phase C60. Journal of Nanomaterials, 2014, 2014, 1-7.	1.5	1
17163	Magnetocrystalline anisotropy and its electric-field-assisted switching of Heusler-compound-based perpendicular magnetic tunnel junctions. New Journal of Physics, 2014, 16, 103033.	1.2	43
17164	Pressure-induced drastic collapse of a high oxygen coordination shell in quartz-likeÎ±-GeO₂. New Journal of Physics, 2014, 16, 023022.	1.2	11
17165	The two aluminum sites in the 27Al MAS NMR spectrum of kaolinite: Accurate determination of isotropic chemical shifts and quadrupolar interaction parameters. American Mineralogist, 2014, 99, 393-400.	0.9	11
17166	Tunable Band Gap and Conductivity Type of ZnSe/Si Core-Shell Nanowire Heterostructures. Materials, 2014, 7, 7276-7288.	1.3	1

#	Article	IF	Citations
17167	Silicene on metal and metallized surfaces:ab initiostudies. New Journal of Physics, 2014, 16, 075004.	1.2	24
17168	Hydrogen-induced anomalous Hall effect in Co-doped ZnO. New Journal of Physics, 2014, 16, 073030.	1.2	7
17169	Optical Properties of BN and BBi Compounds. Acta Physica Polonica A, 2014, 125, 574-576.	0.2	3
17170	Vacancy-induced toughening in hard single-crystal V 0.5 Mo 0.5 N x /MgO(0 0 1) thin films. Acta Materialia, 2014, 77, 394-400.	3.8	75
17171	A comparative DFT study of the structural and electronic properties of nonpolar GaN surfaces. Applied Surface Science, 2014, 314, 794-799.	3.1	12
17172	Site preference and magnetic orderings in the intermetallic boride series M 1.5 Rh 5.5 B 3 (M = Cr, Mn,) Tj ETQq1 1 0.784314 rgBT /O	1.4	4
17173	The formation energy and bonding characteristics of small heliumâ€“vacancy clusters on the low-index surface of Î±-Fe by first principles calculations. Computational Materials Science, 2014, 92, 387-394.	1.4	6
17174	Short range orders in molten Al: An ab initio molecular dynamics study. Computational Materials Science, 2014, 93, 97-103.	1.4	5
17175	Ab initio prediction of the Li5Ge2 Zintl compound. Computational Materials Science, 2014, 93, 133-136.	1.4	8
17176	First-principle investigations of the magnetic properties and possible martensitic transformation in Ni2MnX (X=Al, Ga, In, Si, Ge and Sn). Journal of Magnetism and Magnetic Materials, 2014, 371, 135-138.	1.0	13
17177	First-principles study of water adsorption and dissociation on the UO2 (1 1 1), (1 1 0) and (1 0 0) surfaces. Journal of Nuclear Materials, 2014, 454, 446-454.	1.3	36
17178	Phonon softening and failure of graphene under tensile strain. Solid State Communications, 2014, 200, 51-55.	0.9	7
17179	Atomistic Simulations as Part of an Integrated Computational Environment for Structural Design. , 2014, , .		0
17180	Electronic and magnetic states of Mn2and Mn2H on Ag(111). New Journal of Physics, 2014, 16, 063021.	1.2	7
17181	Novel Hybrid Polymer Dielectrics Based on Group 14 Chemical Motifs. International Journal of High Speed Electronics and Systems, 2014, 23, 1420002.	0.3	2
17182	Mechanical Properties of Tetragonal and Orthorhombic Phases of Quasi-One-Dimensional Antiferromagnet KCuF_{3}. Acta Physica Polonica A, 2014, 126, 14-15.	0.2	2
17183	Exchange Interactions in a Low-Dimensional Magnetic System Cu(H_{2}O)_{2}(en)SO_{4}. Acta Physica Polonica A, 2014, 126, 50-51.	0.2	2
17184	First-Principles Surface Stress Calculations and Multiscale Deformation Analysis of a Self-Assembled Monolayer Adsorbed on a Micro-Cantilever. Sensors, 2014, 14, 7435-7450.	2.1	6

#	Article	IF	Citations
17185	Superspin glass phase and hierarchy of interactions in multiferroic PbFe_{1/2}Sb_{1/2}O₃: an analog of ferroelectric relaxors?. New Journal of Physics, 2014, 16, 113041.	1.2	45
17186	Curie Temperature and Density of States at the Fermi Level for Al-Cu-Fe Phases: Î²-Solid State Solution-Approximants-Icosahedral Quasicrystals. Acta Physica Polonica A, 2014, 126, 572-576.	0.2	3
17187	Elemental vacancy diffusion database from high-throughput first-principles calculations for fcc and hcp structures. New Journal of Physics, 2014, 16, 015018.	1.2	67
17188	Protective Transition Metal Nitride Coatings. , 2014, , 355-388.		32
17189	Engineering electronic properties of metalâ€“MoSe₂ interfaces using self-assembled monolayers. Journal of Materials Chemistry C, 2014, 2, 9842-9849.	2.7	25
17190	Depleted Uranium as Hydrogen Storage Material. Advances in Science and Technology, 2014, 94, 32-37.	0.2	0
17191	Energetics of Slip Deformation in Beta-Sn: A First-Principles Study. Key Engineering Materials, 0, 626, 46-49.	0.4	3
17192	Influence of Nd-Doping on Electronic Structure and Optical Properties of ZnO. Advanced Materials Research, 0, 941-944, 658-661.	0.3	0
17193	Molar Volume of Fcc Phase in the Ni-Cr-Mo System. Advanced Materials Research, 2014, 936, 1209-1215.	0.3	2
17194	Sensitization of Perovskite Strontium Stannate SrSnO₃towards Visible-Light Absorption by Doping. International Journal of Photoenergy, 2014, 2014, 1-3.	1.4	15
17195	Theory of Superhard Materials. , 2014, , 59-79.		3
17196	Half metal in two-dimensional hexagonal organometallic framework. Nanoscale Research Letters, 2014, 9, 2414.	3.1	30
17197	Adsorption and reconstruction of metal-phthalocyanine molecules on Pt(001) investigated by density functional theory. Surface Science, 2014, 630, 202-207.	0.8	5
17198	Deblocking effect of carbonates and hydrogen carbonates in the alkali form zeolites with narrow pores. Microporous and Mesoporous Materials, 2014, 200, 35-45.	2.2	8
17199	Theoretical Study of the Chemical Pressure Effect on Tc in the Cuprate Superconductors. Physics Procedia, 2014, 58, 34-37.	1.2	0
17200	Electrically engineered polymer-carbon hybrid heterojunction for high-performance printed transistors. , 2014, , .		0
17201	Structural and electronic distortions in hydrogenated single-walled zigzag carbon nanotubes. , 2014, , .		0
17202	Prediction of subgap states in Zn- and Sn-based oxides using various exchange-correlation functionals. Physical Review B, 2014, 90, .	1.1	12

#	Article	IF	Citations
17203	Magnetic pyroxenes<mml:math xmlns:mml="http://www.w3.org/1998/Math/MathML"><mml:msub><mml:mrow><mml:mi mathvariant="normal">LiCrGe</mml:mi></mml:mrow><mml:mn>2</mml:mn></mml:msub><mml:msub><mml:mrow><mml:mi mathvariant="normal">O</mml:mi></mml:mrow><mml:mn>6</mml:mn></mml:msub></mml:math>and<mml:math xmlns:mml="http://www.w3.org/1998/Math/MathML"><mml:msub><mml:mrow><mml:mi mathvariant="normal">LiCrSi</mml:mi></mml:mrow><mml:mn>2</mml:mn></mml:msub><mml:msub><mml:mrow><mml:mi	1.1	17
17204	Transforming a surface state of a topological insulator by a Bi capping layer. Physical Review B, 2014, 90, .	1.1	9
17205	Stable structure of high In coverage onSi(111)â˜Î±â˜3Ã—3-Au. Physical Review B, 2014, 90, .	1.1	5
17206	Charge transfer across transition-metal oxide interfaces: Emergent conductance and electronic structure. Physical Review B, 2014, 90, .	1.1	22
17207	Ordering phenomena and formation of nanostructures in<mml:math xmlns:mml="http://www.w3.org/1998/Math/MathML"><mml:msub><mml:mrow><mml:mi mathvariant="normal">In</mml:mi></mml:mrow><mml:mrow><mml:mi>x</mml:mi></mml:mrow></mml:msub><mml:msub><mml:mrow><mml:mi mathvariant="normal">Ga</mml:mi></mml:mrow><mml:mrow><mml:mn>1</mml:mn><mml:mo>â˜</mml:mo><mml:mi>x</mml:mi><mml:mi mathvariant="normal">N</mml:mi></mml:mrow></mml:math>layers coherently grown on GaN(0001). Physical Review B, 2014, 90, .	1.1	20
17208	Silicene phases on Ag(111). , 2014, , .		2
17209	Communication: Ab initio simulations of hydrogen-bonded ferroelectrics: Collective tunneling and the origin of geometrical isotope effects. Journal of Chemical Physics, 2014, 140, 041103.	1.2	19
17210	Origin of major donor states in Inâ€“Gaâ€“Zn oxide. Journal of Applied Physics, 2014, 116, .	1.1	43
17211	Ba2phenanthrene is the main component in the Ba-doped phenanthrene superconductor. Journal of Chemical Physics, 2014, 141, 224501.	1.2	6
17212	Six-dimensional quantum dynamics for dissociative chemisorption of H₂and D₂on Ag(111) on a permutation invariant potential energy surface. Physical Chemistry Chemical Physics, 2014, 16, 24704-24715.	1.3	59
17213	Ab initio calculations on magnetism induced by composite defects in magnesium oxide. Journal of Applied Physics, 2014, 115, 17A926.	1.1	5
17214	Ab initio study of electron-ion structure factors in binary liquids with different types of chemical bonding. Journal of Chemical Physics, 2014, 141, 214504.	1.2	4
17215	Monoxides of small terbium clusters: A density functional theory investigation. Journal of Chemical Physics, 2014, 141, 244304.	1.2	2
17216	Topological states of Sb thin films contacted by a single sheet of heterogeneous atoms. New Journal of Physics, 2014, 16, 093006.	1.2	2
17217	Silicane and germanane: tight-binding and first-principles studies. 2D Materials, 2014, 1, 011005.	2.0	59
17218	Implications of coverage-dependent O adsorption for catalytic NO oxidation on the late transition metals. Catalysis Science and Technology, 2014, 4, 4356-4365.	2.1	59
17219	Why do the [PhSiO_{1.5}]_{8,10,12} cages self-brominate primarily in the ortho position? Modeling reveals a strong cage influence on the mechanism. Physical Chemistry Chemical Physics, 2014, 16, 25760-25764.	1.3	18
17220	Prediction of solute diffusivity in Al assisted by first-principles molecular dynamics. Journal of Physics Condensed Matter, 2014, 26, 025403.	0.7	5

#	Article	IF	Citations
17221	Thermodynamic description of the Taâ€“Wâ€“Zr system. International Journal of Materials Research, 2014, 105, 1048-1056.	0.1	6
17222	Clusters, molecular layers, and 3D crystals of water on Ni(111). Journal of Chemical Physics, 2014, 141, 18C520.	1.2	36
17223	Ab initio Study on Spectral Properties of Charge-Compensated Ce3+ in NaF. Chinese Journal of Chemical Physics, 2014, 27, 512-518.	0.6	3
17224	Electronic and optical properties of quaternary alloy GaAsBiN lattice-matched to GaAs. Optics Express, 2014, 22, 30633.	1.7	15
17225	Crystal structure search and electronic properties of alkali-doped phenanthrene and picene. Physical Review B, 2014, 90, .	1.1	20
17226	Electronic and optical excitations of the PTB7 crystal: First-principles GW-BSE calculations. Physical Review B, 2014, 90, .	1.1	18
17227	Magnetic structure map for face-centered tetragonal iron: Appearance of a collinear spin structure. Physical Review B, 2014, 90, .	1.1	4
17228	Validation of molecular crystal structures from powder diffraction data with dispersion-corrected density functional theory (DFT-D). Acta Crystallographica Section B: Structural Science, Crystal Engineering and Materials, 2014, 70, 1020-1032.	0.5	222
17229	Chemical-Potential-Dependent Gap Opening at the Dirac Surface States of<mml:math xmlns:mml="http://www.w3.org/1998/Math/MathML" display="inline"><mml:mrow><mml:msub><mml:mrow><mml:mi>Bi</mml:mi></mml:mrow><mml:mrow><mml:mn>2</mml:mn></mml:mrow></mml:msub></mml:mrow></mml:math> by Aggregated Substitutional Cr Atoms. Physical Review Letters, 2014, 112, 056801.	2.9	102
17230	Theory of vibrationally assisted tunneling for hydroxyl monomer flipping on Cu(110). Physical Review B, 2014, 90, .	1.1	4
17231	Magneto-optical Kerr effect in L1 FePdPt ternary alloys: Experiments and first-principles calculations. Journal of Applied Physics, 2014, 115, .	1.1	5
17232	Magnetoelectric properties of the<mml:math xmlns:mml="http://www.w3.org/1998/Math/MathML"><mml:mtext>Co</mml:mtext><mml:mo>/</mml:mo><mml:msub><mml:mtext xmlns:mml="http://www.w3.org/1998/Math/MathML"><mml:msub><mml:mtext>Ti</mml:mtext><mml:mrow><mml:mn>1</mml:mn> xmlns:mml="http://www.w3.org/1998/Math/MathML"><mml:msub><mml:mtext>O</mml:mtext><mml:mn>3</mml:mn></mml:msub></mml:mrow></mml:msub></mml:mtext></mml:msub></mml:math> Physical Review B, 2014, 89, .	1.1	20
17233	Deterministic switching of ferromagnetism at room temperature using an electric field. Nature, 2014, 516, 370-373.	13.7	570
17234	The impact of argon admixture on the c-axis oriented growth of direct current magnetron sputtered ScxAl1â^'xN thin films. Journal of Applied Physics, 2014, 115, .	1.1	29
17235	Temperature effects on the energy bandgap and conductivity effective masses of charge carriers in lead telluride from first-principles calculations. Journal of Applied Physics, 2014, 116, .	1.1	7
17236	Double-hole-induced oxygen dimerization in transition metal oxides. Physical Review B, 2014, 89, .	1.1	26
17237	Indirect-direct band gap transition through electric tuning in bilayer MoS2. Journal of Chemical Physics, 2014, 140, 174707.	1.2	40
17238	Point defects at cleaved<mml:math xmlns:mml="http://www.w3.org/1998/Math/MathML"><mml:mrow><mml:msub><mml:mi>Sr</mml:mi><mml:mrow><mml:mi>n</mml:mi> mathvariant="normal">O</mml:mi><mml:mrow><mml:mn>3</mml:mn><mml:mi>n</mml:mi><mml:mo>+</mml:mo><mml:mn>1</mml:mn> surfaces. Physical Review B, 2014, 90, .	1.1	12

#	Article	IF	Citations
17239	Prediction of Near-Room-Temperature Quantum Anomalous Hall Effect on Honeycomb Materials. Physical Review Letters, 2014, 113, 256401.	2.9	263
17240	Atomic-resolution characterization of the effects of CdCl₂treatment on poly-crystalline CdTe thin films. Applied Physics Letters, 2014, 105, 071910.	1.5	23
17241	Intermediate Phases during Decomposition of Metal Borohydrides, M(BH₄)_n (M = Na, Mg, Y). Journal of Physical Chemistry C, 2014, 118, 28456-28461.	1.5	16
17242	Mixed valency and site-preference chemistry for cerium and its compounds: A predictive density-functional theory study. Physical Review B, 2014, 89, .	1.1	60
17243	Structural stability and thermodynamics of CrN magnetic phases fromab initiocalculations and experiment. Physical Review B, 2014, 90, .	1.1	95
17244	Microscopic first-principles model of strain-induced interaction in concentrated size-mismatched alloys. Physical Review B, 2014, 90, .	1.1	6
17245	The role of the isolated 6s states in BiVO4 on the electronic and atomic structures. Applied Physics Letters, 2014, 105, .	1.5	15
17246	High-pressure structural and elastic properties of Tl2O3. Journal of Applied Physics, 2014, 116, .	1.1	20
17247	First-principles study of the effect of phosphorus on nickel grain boundary. Journal of Applied Physics, 2014, 115, .	1.1	26
17248	Microscopic origin of pressure-induced isosymmetric transitions in fluoromanganate cryolites. Physical Review B, 2014, 90, .	1.1	4
17249	Ab initio modeling of resistive switching mechanism in binary metal oxides. , 2014, , .		2
17250	Theoretical study on electronic properties of MoS2 antidot lattices. Journal of Applied Physics, 2014, 116, .	1.1	12
17251	Dynamic structural disorder in supported nanoscale catalysts. Journal of Chemical Physics, 2014, 140, 134701.	1.2	9
17252	Effect of tensile strain on the electronic structure of Ge: A first-principles calculation. Journal of Applied Physics, 2014, 116, 113105.	1.1	17
17253	First-principles calculation of elastic moduli of early-late transition metal alloys. Physical Review B, 2014, 89, .	1.1	8
17254	Alignment of the diamond nitrogen vacancy center by strain engineering. Applied Physics Letters, 2014, 105, .	1.5	22
17255	Comment on â€œIdeal strength and phonon instability in single-layer<mml:math xmlns:mml="http://www.w3.org/1998/Math/MathML"><mml:msub><mml:mi mathvariant="bold">MoS</mml:mi><mml:mn>2</mml:mn></mml:msub></mml:math>â€• Physical Review B, 2014, 90, .	1.1	7
17256	Plasticity of hexagonal systems: Split slip modes and inverse Peierls relation in<mml:math xmlns:mml="http://www.w3.org/1998/Math/MathML"><mml:mi>Î±</mml:mi></mml:math>-Ti. Physical Review B, 2014, 89, .	1.1	35

#	Article	IF	Citations
17257	An experimental and first-principles study on band alignments at interfaces of Cu₂ZnSnS₄/CdS/ZnO heterojunctions. Journal Physics D: Applied Physics, 2014, 47, 075304.	1.3	44
17258	Tuning of noble metal work function with organophosphonate nanolayers. Applied Physics Letters, 2014, 105, .	1.5	10
17259	Ab initiofriction forces on the nanoscale: A density functional theory study of fcc Cu(111). Physical Review B, 2014, 90, .	1.1	25
17260	Valence-band density of states and surface electron accumulation in epitaxial<mml:math xmlns:mml="http://www.w3.org/1998/Math/MathML"><mml:msub><mml:mi>SnO</mml:mi><mml:mn>2</mml:mn></mml:msub></mml:math> Physical Review B, 2014, 90, .	1.1	62
17261	Hindered magnetic order from mixed dimensionalities in<mml:math xmlns:mml="http://www.w3.org/1998/Math/MathML"><mml:msub><mml:mrow><mml:mtext>CuP</mml:mtext></mml:mrow><mml:mn>2</mml:mn></mml:msub></mml:math> Physical Review B, 2014, 89, .	1.1	28
17262	Influence of alloying elements Nb, Zr, Sn, and oxygen on structural stability and elastic properties of the Ti2448 alloy. Physical Review B, 2014, 89, .	1.1	11
17263	Energy band modulation of graphane by hydrogen-vacancy chains: A first-principles study. AIP Advances, 2014, 4, .	0.6	5
17264	Self-Doping of Ultrathin Insulating Films by Transition Metal Atoms. Physical Review Letters, 2014, 112, 026102.	2.9	23
17265	Electronic and optical properties of NbO2. Journal of Applied Physics, 2014, 116, .	1.1	67
17266	Octahedral tilting and ferroelectricity in Rb<mml:math xmlns:mml="http://www.w3.org/1998/Math/MathML"><mml:mi>A</mml:mi></mml:math><mml:math xmlns:mml="http://www.w3.org/1998/Math/MathML"><mml:msub><mml:mrow /><mml:mn>2</mml:mn></mml:msub></mml:math>O<mml:math xmlns:mml="http://www.w3.org/1998/Math/MathML"><mml:msub><mml:mrow		

#	Article	IF	Citations
17275	Atomic and electronic structure of the ferroelectric BaTiO3/Ge(001) interface. Applied Physics Letters, 2014, 104, .	1.5	45
17276	Hydrogen Peroxide Synthesis via Enhanced Two-Electron Oxygen Reduction Pathway on Carbon-Coated Pt Surface. Journal of Physical Chemistry C, 2014, 118, 30063-30070.	1.5	248
17277	How to Chemically Tailor Metal-Porphyrin-Like Active Sites on Carbon Nanotubes and Graphene for Minimal Overpotential in the Electrochemical Oxygen Evolution and Oxygen Reduction Reactions. Journal of Physical Chemistry C, 2014, 118, 29482-29491.	1.5	36
17278	Discovery of the Last Remaining Binary Platinumâ€Group Pernitride RuN₂. Chemistry - A European Journal, 2014, 20, 13885-13888.	1.7	57
17279	Dirac Cones in two-dimensional conjugated polymer networks. Nature Communications, 2014, 5, 5842.	5.8	69
17280	Structure and gap of low-x(Ga_{1-x}In_x)₂O₃alloys. Journal of Physics: Conference Series, 2014, 566, 012016.	0.3	9
17281	Spin state ofMn2+and magnetism in vanadate-carbonate compound,K2Mn3(VO4)2CO3. Physical Review B, 2014, 90, .	1.1	4
17282	Pairwise chemical interactions of charged transition-metal impurities in insulators. Physical Review B, 2014, 90, .	1.1	2
17283	Initial and secondary oxidation products on the Si(111)-(7â€‰Ã—â€‰7) surface identified by atomic force microscopy and first principles calculations. Applied Physics Letters, 2014, 104, 133107.	1.5	9
17284	Competition between heavy fermion and Kondo interaction in isoelectronic A-site-ordered perovskites. Nature Communications, 2014, 5, 5818.	5.8	15
17285	Helium bubble nucleation and growth in Î±-Fe: insights from firstâ€“principles simulations. Journal of Physics Condensed Matter, 2014, 26, 255401.	0.7	14
17286	Antisites in III-V semiconductors: Density functional theory calculations. Journal of Applied Physics, 2014, 116, .	1.1	12
17287	Superconductivity in noncentrosymmetric<mml:math xmlns:mml="http://www.w3.org/1998/Math/MathML"><mml:mrow><mml:mi>Ba</mml:mi><mml:msub><mml:mi>Al</mml:mi></mml:msub><mml:m structures. Physical Review B, 2014, 90, .	1.1	32
17288	Magnetic orders of LaTiO3 under epitaxial strain: A first-principles study. Journal of Applied Physics, 2014, 115, 17E108.	1.1	14
17289	Origin of the unusually strong luminescence of<mml:math xmlns:mml="http://www.w3.org/1998/Math/MathML"><mml:mi>a</mml:mi></mml:math>-type screw dislocations in GaN. Physical Review B, 2014, 90, .	1.1	19
17290	Schottky Barrier Formation and Strain at the (011)<mml:math xmlns:mml="http://www.w3.org/1998/Math/MathML" display="inline"><mml:mrow><mml:mi>GdN</mml:mi><mml:mo>/</mml:mo><mml:mi>GaN</mml:mi></mml:mrow></mml:math>Int from First Principles. Physical Review Applied, 2014, 2, .	1.5	8
17291	Electrical Activity of Boron and Phosphorus in Hydrogenated Amorphous Silicon. Physical Review Applied, 2014, 2, .	1.5	8
17292	Density-functional investigation of molecular graphene: CO on Cu(111). Physical Review B, 2014, 90, .	1.1	10

#	Article	IF	Citations
17293	Formation and stability of dense arrays of Au nanoclusters on hexagonal boron nitride/Rh(111). Physical Review B, 2014, 89, .	1.1	29
17294	Magnetic analytic bond-order potential for modeling the different phases of Mn at zero Kelvin. Physical Review B, 2014, 89, .	1.1	11
17295	Ni-La Electrocatalysts for Direct Hydrazine Alkaline Anion-Exchange Membrane Fuel Cells. Journal of the Electrochemical Society, 2014, 161, H3106-H3112.	1.3	12
17296	Finding Unprecedentedly Low-Thermal-Conductivity Half-Heusler Semiconductors via High-Throughput Materials Modeling. Physical Review X, 2014, 4, .	2.8	210
17297	Electronic structure and phonon instabilities in the vicinity of the quantum phase transition and superconductivity of<mml:math xmlns:mml="http://www.w3.org/1998/Math/MathML"><mml:msub><mml:mrow><mml:mo>(</mml:mo><mml:mtext>x</mml:mtext><mml:mtext>Sr</mml:mtext><mml:mtext><mml:msub><mml:mtext>Ir</mml:mtext><mml:mn>4</mml:mn></mml:msub><mml:mo>)</mml:mo></mml:mrow><mml:mn>1</mml:mn><mml:mo>−</mml:mo><mml:mtext>x</mml:mtext></mml:msub></mml:math> xmlns:mml="http://www.w3.org/1998/Math/MathML"><mml:msub><mml:mtext>Ir</mml:mtext><mml:mn>4</mml:mn></mml:msub><mml:mo><</mml:mo> xmlns:mml="http://ww. Physical Review B, 2014, 89, .	4	
17298	Modulation of the electron transport properties in graphene nanoribbons doped with BN chains. AIP Advances, 2014, 4, 067123.	0.6	5
17299	Comment on â€œFirst-principles-based embedded atom method for PdAu nanoparticlesâ€• Physical Review B, 2014, 89, .	1.1	3
17300	On-surface synthesis of a two-dimensional porous coordination network: Unraveling adsorbate interactions. Physical Review B, 2014, 90, .	1.1	61
17301	Reply to â€œComment on â€˜Ideal strength and phonon instability in single-layer<mml:math xmlns:mml="http://www.w3.org/1998/Math/MathML"><mml:msub><mml:mi mathvariant="bold">MoS</mml:mi><mml:mn>2</mml:mn></mml:msub></mml:math>â€™ â€• Physical Review B, 2014, 90, .	1.1	12
17302	Interfacial Carbon Nanoplatelet Formation by Ion Irradiation of Graphene on Iridium(111). ACS Nano, 2014, 8, 12208-12218.	7.3	29
17303	Effect of cation arrangement on the electronic structures of the perovskite solid solutions <span class="aps-inline-formula"><math		

#	Article	IF	Citations
17311	Correlation between the ionic potential and thermal stability of metal borohydrides: First-principles investigations. Physical Review B, 2014, 90, .	1.1	12
17312	Origin of the Increased Photocatalytic Performance of TiO2Nanocrystal Composed of Pure Core and Heavily Nitrogen-Doped Shell: A Theoretical Study. ACS Applied Materials & Interfaces, 2014, 6, 22815-22822.	4.0	25
17313	Defect interactions with stepped CeO2/SrTiO3 interfaces: Implications for radiation damage evolution and fast ion conduction. Journal of Chemical Physics, 2014, 140, 194701.	1.2	21
17314	Tuning the electronic structure of SrTiO3/SrFeO3â^'x superlattices via composition and vacancy control. APL Materials, 2014, 2, .	2.2	7
17315	Intrinsic spin dependent and ferromagnetic stability on edge saturated zigzag graphene-like carbon-nitride nanoribbons. Applied Physics Letters, 2014, 104, 172111.	1.5	8
17316	Ab initiosimulations of MgO under extreme conditions. Physical Review B, 2014, 89, .	1.1	39
17317	Phase stability analysis of the InAs/GaAs (001) wetting layer from first principles. Physical Review B, 2014, 89, .	1.1	1
17318	Properties of Pt-supported iron oxide ultra-thin films: Similarity of Hubbard-corrected and hybrid density functional theory description. Journal of Chemical Physics, 2014, 141, 144702.	1.2	19
17319	Stacking-dependent energetics and electronic structure of ultrathin polymorphic<mml:math xmlns:mml="http://www.w3.org/1998/Math/MathML"><mml:msub><mml:mi mathvariant="normal">V</mml:mi><mml:mn>2</mml:mn></mml:msub><mml:mi mathvariant="normal">VI</mml:mi><mml:mn>3</mml:mn></mml:msub></mml:math>topological insulator nanofilms. Physical Review B, 2014, 90, .	1.1	8
17320	Magnetic spiral induced by strong correlations in<mml:math xmlns:mml="http://www.w3.org/1998/Math/MathML"><mml:msub><mml:mi>MnAu</mml:mi><mml:mn>2</mml:mn></mml:msub><m Physical Review B, 2014, 90, .	1.1	11
17321	Nearly compensated exchange in the dimer compound callaghaniteCu2Mg2(CO3)(oH)6Â·2H2O. Physical Review B, 2014, 89, .	1.1	15
17322	Do Agn (up to n = 8) clusters retain their identity on graphite? Insights from first-principles calculations including dispersion interactions. Journal of Chemical Physics, 2014, 140, 164705.	1.2	13
17323	Piezo-antiferromagnetic effect of sawtooth-like graphene nanoribbons. Applied Physics Letters, 2014, 104, .	1.5	3
17324	Xenon Suboxides Stable under Pressure. Journal of Physical Chemistry Letters, 2014, 5, 4336-4342.	2.1	49
17325	The role of the carbon-silicon complex in eliminating deep ultraviolet absorption in AlN. Applied Physics Letters, 2014, 104, .	1.5	59
17326	Conduction paths in Cu/amorphous-Ta2O5/Pt atomic switch: First-principles studies. Journal of Applied Physics, 2014, 115, .	1.1	30
17327	First-principles study of the structure of Mg/Nb multilayers. Applied Physics Letters, 2014, 105, 071602.	1.5	26
17328	Effects of non-local exchange on core level shifts for gas-phase and adsorbed molecules. Journal of Chemical Physics, 2014, 141, 034706.	1.2	29

#	Article	IF	Citations
17329	Optical anisotropy in bismuth titanate: An experimental and theoretical study. Journal of Applied Physics, 2014, 115, 133509.	1.1	3
17330	Band structure and pressure-induced metallic transition in iodine â€“ GW calculation. High Pressure Research, 2014, 34, 215-221.	0.4	4
17331	Multi-scale simulations of metal-semiconductor contacts for nano-MOSFETs. , 2014, , .		0
17332	Band gap and electronic structure of MgSiN2. Applied Physics Letters, 2014, 105, 112108.	1.5	20
17333	Intrinsic nature of visible-light absorption in amorphous semiconducting oxides. APL Materials, 2014, 2, .	2.2	23
17334	Shockley-Read-Hall lifetimes in CdTe. Journal of Applied Physics, 2014, 116, .	1.1	11
17335	High-pressure phase transition of MH3 (M: Er, Ho). Journal of Chemical Physics, 2014, 141, 054703.	1.2	6
17336	Anti-site disorder and improved functionality of Mn2NiX (X = Al, Ga, In, Sn) inverse Heusler alloys. Journal of Applied Physics, 2014, 116, .	1.1	16
17337	Energetics of Adsorbed CH₂ and CH on Pt(111) by Calorimetry: The Dissociative Adsorption of Diiodomethane. Journal of Physical Chemistry C, 2014, 118, 29310-29321.	1.5	13
17338	Local structure and structural rigidity of the green phosphor Î²-SiAlON:Eu²⁺. Applied Physics Letters, 2014, 105, 181904.	1.5	39
17339	Electrical, thermal, and species transport properties of liquid eutectic Ga-In and Ga-In-Sn from first principles. Journal of Chemical Physics, 2014, 140, 064303.	1.2	109
17340	An efficient approach to ab initio Monte Carlo simulation. Journal of Chemical Physics, 2014, 140, 034106.	1.2	9
17341	Origins of optical absorption and emission lines in AlN. Applied Physics Letters, 2014, 105, .	1.5	127
17342	Effect of lattice deformation on exchange coupling constants in Cr2O3. Journal of Applied Physics, 2014, 115, 17D719.	1.1	13
17343	First-principles study of vacancy-assisted impurity diffusion in ZnO. APL Materials, 2014, 2, 096101.	2.2	35
17344	Anomalous magneto-structural behavior of MnBi explained: A path towards an improved permanent magnet. APL Materials, 2014, 2, .	2.2	35
17345	In situ measurement of CuPt alloy ordering using strain anisotropy. Journal of Applied Physics, 2014, 115, 053502.	1.1	16
17346	Metamorphic Ga0.76In0.24As/GaAs0.75Sb0.25 tunnel junctions grown on GaAs substrates. Journal of Applied Physics, 2014, 116, .	1.1	23

#	Article	IF	Citations
17347	Ellipsometric characterization and density-functional theory analysis of anisotropic optical properties of single-crystal Î±-SnS. Journal of Applied Physics, 2014, 116, .	1.1	59
17348	Freestanding atomically-thin cuprous oxide sheets for improved visible-light photoelectrochemical water splitting. Nano Energy, 2014, 8, 205-213.	8.2	54
17349	All-electron GW quasiparticle band structures of group 14 nitride compounds. Journal of Chemical Physics, 2014, 141, 044709.	1.2	17
17350	A Model to Determine the Chemical Expansion in Non-Stoichiometric Oxides Based on the Elastic Force Dipole. Journal of the Electrochemical Society, 2014, 161, F3060-F3064.	1.3	9
17351	First-principles electronic structure and formation energies of group V and VII impurities in the Î±-Fe2O3 alloys. Journal of Applied Physics, 2014, 116, .	1.1	4
17352	Diverse and tunable electronic structures of single-layer metal phosphorus trichalcogenides for photocatalytic water splitting. Journal of Chemical Physics, 2014, 140, 054707.	1.2	99
17353	Tunable ferroelectric polarization and its interplay with spinâ€“orbit coupling in tin iodide perovskites. Nature Communications, 2014, 5, 5900.	5.8	247
17354	Identification of critical stacking faults in thin-film CdTe solar cells. Applied Physics Letters, 2014, 105, .	1.5	48
17355	Monolayers of MoS2 as an oxidation protective nanocoating material. Journal of Applied Physics, 2014, 116, .	1.1	55
17356	Magnetism of theFe2+andCe3+sublattices inCe2O2FeSe2: A combined neutron powder diffraction, inelastic neutron scattering, and density functional study. Physical Review B, 2014, 90, .	1.1	12
17357	Coherence penalty functional: A simple method for adding decoherence in Ehrenfest dynamics. Journal of Chemical Physics, 2014, 140, 194107.	1.2	86
17358	Magnetoelectric effect in Fe linear chains on Pt(001). Journal of Applied Physics, 2014, 115, 17C733.	1.1	2
17359	Band gap of epitaxial in-plane-dimerized single-phase NbO₂films. Applied Physics Letters, 2014, 104, 092901.	1.5	40
17360	Anharmonicity, mechanical instability, and thermodynamic properties of the Cr-Re Ïƒ-phase. Journal of Chemical Physics, 2014, 140, 144502.	1.2	6
17361	A new crystal: layer-structured rhombohedral In3Se4. CrystEngComm, 2014, 16, 393-398.	1.3	31
17362	Structure of screw dislocation core in Ta at high pressure. Journal of Applied Physics, 2014, 115, 093505.	1.1	4
17363	Structural, electronic, and optical properties of GaInO3: A hybrid density functional study. Journal of Applied Physics, 2014, 115, .	1.1	33
17364	Discovering low-permittivity materials: Evolutionary search for MgAl2O4 polymorphs. Applied Physics Letters, 2014, 105, .	1.5	4

#	Article	IF	Citations
17365	Oxygen and nitrogen diffusion in Î±-hafnium from first principles. Applied Physics Letters, 2014, 104, .	1.5	9
17366	Structures and electronic properties of oxidized graphene from first-principles study. Europhysics Letters, 2014, 105, 37005.	0.7	8
17367	The Electronic Properties of Graphene Adsorbed on the (111) HfO2 Surface â€“ A First Principles Study. Procedia Engineering, 2014, 79, 583-589.	1.2	4
17368	Boron deactivation in heavily boron-doped Czochralski silicon during rapid thermal anneal: Atomic level understanding. Applied Physics Letters, 2014, 104, 032102.	1.5	2
17369	Evolution of optical properties of tin film from solid to liquid studied by spectroscopic ellipsometry and ab initio calculation. Applied Physics Letters, 2014, 104, 121907.	1.5	14
17370	Hydrogen activation, diffusion, and clustering on CeO2(111): A DFT+U study. Journal of Chemical Physics, 2014, 141, 014703.	1.2	109
17371	Enhanced tunability of thermodynamic stability of complex hydrides by the incorporation of Hâ€“ anions. Applied Physics Letters, 2014, 104, .	1.5	24
17372	GeTe sequences in superlattice phase change memories and their electrical characteristics. Applied Physics Letters, 2014, 104, .	1.5	57
17373	Superhard sp 3 carbon allotrope: Ab initio calculations. Europhysics Letters, 2014, 108, 46006.	0.7	7
17374	Modeling intrinsic defects in LiNbO₃ within the Slater-Janak transition state model. Journal of Chemical Physics, 2014, 140, 234113.	1.2	33
17375	Structure and phonon behavior of crystalline GeTe ultrathin film. Applied Physics Letters, 2014, 105, .	1.5	12
17376	Effect of surface structure on workfunction and Schottky-barrier height in SrRuO3/SrTiO3 (001) heterojunctions. Journal of Applied Physics, 2014, 115, 173705.	1.1	21
17377	Effects of the Cu off-stoichiometry on transport properties of wide gap p-type semiconductor, layered oxysulfide LaCuSO. Applied Physics Letters, 2014, 105, .	1.5	24
17378	Source and major species of CH_x (x = 1â€“3) in acetic acid synthesis from methaneâ€“syngas on Rh catalyst: a theoretical study. RSC Advances, 2014, 4, 58631-58642.	1.7	5
17379	Assessing hafnium on hafnia as an oxygen getter. Journal of Applied Physics, 2014, 115, .	1.1	37
17380	Adsorption structure of water molecules on the Be(0001) surface. Journal of Applied Physics, 2014, 115, 213511.	1.1	9
17381	Detailed formation processes of stable dislocations in graphene. Nanoscale, 2014, 6, 14836-14844.	2.8	29
17382	First-Principles Study on the Surface Energies of Rutile TiO₂(110) vs (011)-2Ã—1 Surfaces. Advanced Materials Research, 0, 937, 113-117.	0.3	0

#	Article	IF	Citations
17383	An ab initio study on the electronic and magnetic properties of MgO with intrinsic defects. RSC Advances, 2014, 4, 51366-51373.	1.7	24
17384	Enhancement of Initial Growth of ZnO Films on Layer-Structured Bi₂Te₃ by Atomic Layer Deposition. Chemistry of Materials, 2014, 26, 6448-6453.	3.2	14
17385	Electrostatics-based finite-size corrections for first-principles point defect calculations. Physical Review B, 2014, 89, .	1.1	320
17386	Quantum spin Hall and<mml:math xmlns:mml="http://www.w3.org/1998/Math/MathML"><mml:msub><mml:mi>Z</mml:mi><mml:mn>2</mml:mn></mml:msub></mml:math> states in an organic material. Physical Review B, 2014, 90, .	1.1	11
17387	Unraveling Crystalline Structure of High-Pressure Phase of Silicon Carbonate. Physical Review X, 2014, 4, .	2.8	7
17388	Tailoring Li adsorption on graphene. Physical Review B, 2014, 90, .	1.1	42
17389	First-principles study of octahedral tilting and ferroelectric-like transition in metallic<mml:math xmlns:mml="http://www.w3.org/1998/Math/MathML"><mml:msub><mml:mi mathvariant="normal">LiOsO</mml:mi><mml:mn>3</mml:mn></mml:msub></mml:math>. Physical Review B, 2014, 89, .	1.1	44
17390	Metal-dichalcogenide hetero-TFETs: Are they a viable option for low power electronics?. , 2014, , .		18
17391	Electronic and Structural Differences between Wurtzite and Zinc Blende InAs Nanowire Surfaces: Experiment and Theory. ACS Nano, 2014, 8, 12346-12355.	7.3	78
17392	Interfacial Structures and Bonding in Metal-Coated Gold Nanorods. Structure and Bonding, 2014, , 67-90.	1.0	7
17393	Enhanced half-metallicity in the zigzag graphene nanoribbons by adsorption of the zigzag hydrogen fluoride molecular chains. AIP Advances, 2014, 4, 067132.	0.6	0
17394	Structural and Vibrational Study of Pseudocubic CdIn₂Se₄ under Compression. Journal of Physical Chemistry C, 2014, 118, 26987-26999.	1.5	7
17395	Ytterbium-driven strong enhancement of electron-phonon coupling in graphene. Physical Review B, 2014, 90, .	1.1	19
17396	Ab inito and <scp>FTIR</scp> Studies of <scp>HfSiCNO</scp> Processed from the Polymer Route. Journal of the American Ceramic Society, 2014, 97, 742-749.	1.9	14
17397	Graphene on Crystalline Metal Surfaces. , 0, , 691-736.		0
17398	Optimal packing size of non-ligated CdSe nanoclusters for microstructure synthesis. Journal of Applied Physics, 2014, 116, .	1.1	2
17399	Spontaneous Formation of O₈ Clusters and Chains within Nanostructures. Journal of Physical Chemistry C, 2014, 118, 24741-24745.	1.5	2
17400	First principles study of the magnetic properties of LaOMnAs. Journal of Applied Physics, 2014, 115, 17D723.	1.1	10

#	Article	IF	Citations
17401	Prediction of Mode Specificity, Bond Selectivity, Normal Scaling, and Surface Lattice Effects in Water Dissociative Chemisorption on Several Metal Surfaces Using the Sudden Vector Projection Model. Journal of Physical Chemistry C, 2014, 118, 26851-26858.	1.5	29
17402	First-principle investigations of K2NiF4-type double perovskite oxides La4Bâ€²Bâ€³O8 (Bâ€²Bâ€³â€‰=â€‰Fe, Co, Ni). Journal of Applied Physics, 2014, 115, 213910.	1.1	2
17403	Ring-Opening and Oxidation Pathways of Furanic Oxygenates on Oxygen-Precovered Pd(111). Journal of Physical Chemistry C, 2014, 118, 27933-27943.	1.5	20
17404	Acidâ€“Base Interaction and Its Role in Alkane Dissociative Chemisorption on Oxide Surfaces. Journal of Physical Chemistry C, 2014, 118, 27336-27342.	1.5	54
17405	Two-dimensional quasi-freestanding molecular crystals for high-performance organic field-effect transistors. Nature Communications, 2014, 5, 5162.	5.8	315
17406	Combined Computational and Experimental Study of Li Exchange Reaction at the Surface of Spinel LiMn₂O₄ as a Rechargeable Li-Ion Battery Cathode. Journal of Physical Chemistry C, 2014, 118, 27245-27251.	1.5	31
17407	Manipulation of electronic and magnetic properties of M2C (M = Hf, Nb, Sc, Ta, Ti, V, Zr) monolayer by applying mechanical strains. Applied Physics Letters, 2014, 104, .	1.5	139
17408	A DFT+UStudy of Strain-Dependent Ionic Migration in Sm-Doped Ceria. Journal of the Physical Society of Japan, 2014, 83, 094707.	0.7	15
17409	Toward Modeling Clay Mineral Nanoparticles: The Edge Surfaces of Pyrophyllite and Their Interaction with Water. Journal of Physical Chemistry C, 2014, 118, 27308-27317.	1.5	48
17410	Preferential Location of Germanium in the UTL and IPC-2a Zeolites. Journal of Physical Chemistry C, 2014, 118, 26939-26946.	1.5	17
17411	Superconducting properties of<mml:math xmlns:mml="http://www.w3.org/1998/Math/MathML"><mml:msub><mml:mi mathvariant="normal">K</mml:mi><mml:mrow><mml:mn>1</mml:mn><mml:mtext>â^’</mml:mtext><mml:mi>x</mml:mi></mml:mrow><mml:mi mathvariant="normal">Na</mml:mi><mml:mi>x</mml:mi></mml:msub><mml:msub><mml:mi mathvariant="normal">Fe</mml:mi><mml:mn>2</mml:mn></mml:msub><mml:msub><mml:mi mathvariant="normal">As</mml:mi><mml:mn>2</mml:mn></mml:msub></mml:math>under pressure. Ph	1.1	13
17412	The Role of Ru and RuO₂ in the Catalytic Transfer Hydrogenation of 5â€Hydroxymethylfurfural for the Production of 2,5â€Dimethylfuran. ChemCatChem, 2014, 6, 848-856.	1.8	136
17413	Electronic Properties of Transitionâ€Metalâ€Decorated Silicene. ChemPhysChem, 2014, 15, 4095-4099.	1.0	15
17414	Electronic and bonding analysis of hardness in pyrite-type transition-metal pernitrides. Physical Review B, 2014, 90, .	1.1	108
17415	Band alignment at bandâ€insulator/Mottâ€insulator interfaces. Physica Status Solidi - Rapid Research Letters, 2014, 8, 577-582.	1.2	5
17416	Ethanol Synthesis from Syngas on the Stepped Rh(211) Surface: Effect of Surface Structure and Composition. Journal of Physical Chemistry C, 2014, 118, 22691-22701.	1.5	46
17417	Ab initioinvestigation of tensile strengths of metal(1Â1Â1)/Î±-Al₂O₃(0Â0Â0Â1) interfaces. Philosophical Magazine, 2014, 94, 265-284.	0.7	13
17418	An ab initio investigation of flexoelectric effect in ultrathin BaTiO3 nanotubes. Journal of Applied Physics, 2014, 115, .	1.1	9

#	Article	IF	Citations
17419	First-principles calculations of a robust two-dimensional boron honeycomb sandwiching a triangular molybdenum layer. Physical Review B, 2014, 90, .	1.1	70
17420	Experimental and Numerical Study of Submonolayer Sputter Deposition of Polystyrene Fragments on Silver for the Storing Matter Technique. Analytical Chemistry, 2014, 86, 11217-11225.	3.2	4
17421	The electronic properties and lattice dynamics of (Na0.5Bi0.5)TiO3: From cubic to tetragonal and rhombohedral phases. Journal of Applied Physics, 2014, 115, 124107.	1.1	24
17422	Simultaneous Presence of Two Different Magnetic Structures in a Single-Crystalline Solid? Hydrogen-Distribution-Dependent Magnetism. Inorganic Chemistry, 2014, 53, 10800-10802.	1.9	0
17423	Adsorption of a Pt₁₃ Cluster on Graphene Oxides at Varied Ratios of Oxygen to Carbon and Its Catalytic Reactions for CO Removal Investigated with Quantum-Chemical Calculations. Journal of Physical Chemistry C, 2014, 118, 26764-26771.	1.5	17
17424	Electronic structures and optical properties of two-dimensional ScN and YN nanosheets. Journal of Applied Physics, 2014, 115, .	1.1	30
17425	Effect of Cu alloying on S poisoning of Ni surface viaab initiothermodynamics calculations. Physica Status Solidi (A) Applications and Materials Science, 2014, 211, 1882-1888.	0.8	4
17426	Adsorption of Water Dimer on Platinum(111): Identification of the â^'OHÂ·Â·Â·Pt Hydrogen Bond. ACS Nano, 2014, 8, 11583-11590.	7.3	34
17427	Clustering of H and He, and their effects on vacancy evolution in tungsten in a fusion environment. Nuclear Fusion, 2014, 54, 103007.	1.6	69
17428	Total Ionizing Dose Effects on hBN Encapsulated Graphene Devices. IEEE Transactions on Nuclear Science, 2014, 61, 2868-2873.	1.2	27
17429	Coexistence of two diffusion mechanisms: W on W(100). Physical Review B, 2014, 89, .	1.1	7
17430	Cyanoâ€Functionalized Triarylamines on Au(111): Competing Intermolecular versus Molecule/Substrate Interactions. Advanced Materials Interfaces, 2014, 1, 1300025.	1.9	52
17431	Theory of melting at high pressures: Amending density functional theory with quantum Monte Carlo. Physical Review B, 2014, 90, .	1.1	16
17432	Surface Supported Goldâ€“Organic Hybrids: Onâ€Surface Synthesis and Surface Directed Orientation. Small, 2014, 10, 1361-1368.	5.2	62
17433	Study of charged defects for substitutionally doped chromium in hexagonal barium titanate from firstâ€principles theory. Physica Status Solidi - Rapid Research Letters, 2014, 8, 527-531.	1.2	15
17434	Electronic and structural properties at the interface between iron-phthalocyanine and Cu(110). Journal of Chemical Physics, 2014, 140, 094704.	1.2	12
17435	New stable Reâ€“B phases for ultra-hard materials. Journal of Physics Condensed Matter, 2014, 26, 455401.	0.7	6
17436	Phonon thermal transport in<mml:math xmlns:mml="http://www.w3.org/1998/Math/MathML"><mml:msub><mml:mi mathvariant="normal">Bi</mml:mi><mml:mn>2</mml:mn></mml:msub><mml:msub><mml:mi mathvariant="normal">Te</mml:mi><mml:mn>3</mml:mn></mml:msub></mml:math>from first principles. Physical Review B, 2014, 90, .	1.1	150

#	Article	IF	Citations
17437	The role of stoichiometric vacancy periodicity in pressure-induced amorphization of the Ga2SeTe2 semiconductor alloy. Applied Physics Letters, 2014, 105, 051908.	1.5	6
17438	Magnetic phase diagram and multiferroicity of<mml:math xmlns:mml="http://www.w3.org/1998/Math/MathML"><mml:msub><mml:mi mathvariant="normal">Ba</mml:mi><mml:mn>3</mml:mn></mml:msub><mml:msub><mml:mi mathvariant="normal">MnNb</mml:mi><mml:mn>2</mml:mn></mml:msub><mml:msub><mml:mi mathvariant="normal">O</mml:mi><mml:mn>9</mml:mn></mml:msub></mml:math>: A spin-<mml:math xmlns:mml="http://www.w3.org/1998/Math/MathML"><mml:mfrac><mml:mn>5</mml:mn><mml:mn>2</mml:mn></mml:mfrac></mml	1.1	60
17439	Understanding the interactions between oxygen vacancies atSrTiO3(001) surfaces. Physical Review B, 2014, 90, .	1.1	26
17440	Crystal Surface and State of Charge Dependencies of Electrolyte Decomposition on LiMn₂O₄Cathode. Journal of the Electrochemical Society, 2014, 161, E3059-E3065.	1.3	63
17441	Electronic properties of InP (001)/HfO2 (001) interface: Band offsets and oxygen dependence. Journal of Applied Physics, 2014, 115, .	1.1	15
17442	The electronic structure changes and the origin of the enhanced optical properties in N-doped anatase TiO2â€"A theoretical revisit. Journal of Applied Physics, 2014, 116, 093709.	1.1	6
17443	First-Principles Investigation of Câ€“H Bond Scission and Formation Reactions in Ethane, Ethene, and Ethyne Adsorbed on Ru(0001). Journal of Physical Chemistry C, 2014, 118, 26683-26694.	1.5	24
17444	Electronic surface states and dielectric self-energy profiles in colloidal nanoscale platelets of CdSe. Physical Chemistry Chemical Physics, 2014, 16, 25182-25190.	1.3	30
17445	First-Principles Characterization of the Critical Thickness for Forming Metallic States in Strained LaAlO₃/SrTiO₃(001) Heterostructure. ACS Applied Materials & Interfaces, 2014, 6, 22351-22358.	4.0	37
17446	A comparative study on magnetism in Zn-doped AlN and GaN from first-principles. Journal of Applied Physics, 2014, 116, .	1.1	9
17447	Ambiguity of Experimental Spin Information from States with Mixed Orbital Symmetries. Physical Review Letters, 2014, 113, 116402.	2.9	36
17448	Phase diagram of electron-doped dichalcogenides. Physical Review B, 2014, 90, .	1.1	59
17449	Mechanism of charge transfer/disproportionation inLnCu3Fe4O12(LnÂ=Âlanthanides). Physical Review B, 2014, 89, .	1.1	9
17450	AB INITIO EQUATIONS OF STATE FOR HYDROGEN (H-REOS.3) AND HELIUM (He-REOS.3) AND THEIR IMPLICATIONS FOR THE INTERIOR OF BROWN DWARFS. Astrophysical Journal, Supplement Series, 2014, 215, 21.	3.0	121
17451	Approximate Hessian for acceleratingab initiostructure relaxation by force fitting. Physical Review B, 2014, 89, .	1.1	5
17452	The formation and electronic properties of hydrogenated bilayer silicene from first-principles. Journal of Applied Physics, 2014, 116, 024303.	1.1	20
17453	Hydrogenated vacancies and hidden hydrogen in SrTiO3. Physical Review B, 2014, 89, .	1.1	36
17454	Field-induced magnetic transitions in<mml:math		

#	Article	IF	Citations
17455	Shallow halogen vacancies in halide optoelectronic materials. Physical Review B, 2014, 90, .	1.1	119
17456	Structure, hydrogen bonding and thermal expansion of ammonium carbonate monohydrate. Acta Crystallographica Section B: Structural Science, Crystal Engineering and Materials, 2014, 70, 948-962.	0.5	14
17457	First-Principles Approach to Calculating Energy Level Alignment at Aqueous Semiconductor Interfaces. Physical Review Letters, 2014, 113, 176802.	2.9	72
17458	Proximity effects on H absorption in ultrathin V layers. Physical Review B, 2014, 90, .	1.1	5
17459	Exploration of stable compounds, crystal structures, and superconductivity in the Be-H system. AIP Advances, 2014, 4, .	0.6	25
17460	Preparation of gallium nitride surfaces for atomic layer deposition of aluminum oxide. Journal of Chemical Physics, 2014, 141, 104702.	1.2	22
17461	Dissociative Chemisorption of<mml:math xmlns:mml="http://www.w3.org/1998/Math/MathML" display="inline"><mml:mrow><mml:msub><mml:mrow><mml:mi mathvariant="normal">O</mml:mi></mml:mrow><mml:mrow><mml:mn>2</mml:mn></mml:mrow></mml:msub></mml:mrow></mml: Stress Corrosion Cracking in Silicon Crystals. Physical Review Letters, 2014, 112, 115501.	2.9	33
17462	Nuclear forward scattering and first-principles studies of the iron oxide phase<mml:math xmlns:mml="http://www.w3.org/1998/Math/MathML"><mml:msub><mml:mrow><mml:mi mathvariant="normal">Fe</mml:mi></mml:mrow><mml:mn>4</mml:mn></mml:msub><mml:msub><mml:mrow><mml:mi mathvariant="normal">O</mml:mi></mml:mrow><mml:mn>5</mml:mn></mml:msub></mml:math>. Physical Review B, 2014, 90, .	1.1	8
17463	Chern insulator at a magnetic rocksalt interface. Physical Review B, 2014, 90, .	1.1	47
17464	Temperature measurements of shocked silica aerogel foam. Physical Review E, 2014, 90, 033107.	0.8	23
17465	Fermi level pinning and the charge transfer contribution to the energy of adsorption at semiconducting surfaces. Journal of Applied Physics, 2014, 115, 043529.	1.1	21
17466	Unoccupied electronic states of icosahedral Al-Pd-Mn quasicrystals: Evidence of image potential resonance and pseudogap. Physical Review B, 2014, 90, .	1.1	10
17467	<mml:math xmlns:mml="http://www.w3.org/1998/Math/MathML" display="inline"><mml:mi>s</mml:mi><mml:msup><mml:mi>d</mml:mi><mml:mn>2</mml:mn></mml:msup></mml:math>-Graphene: Kagome Band in a Hexagonal Lattice. Physical Review Letters, 2014, 113, 236802.	2.9	68
17468	Local versus global electronic properties of chalcopyrite alloys: X-ray absorption spectroscopy and ab initio calculations. Journal of Applied Physics, 2014, 116, 093703.	1.1	12
17469	Effects of Concentration, Crystal Structure, Magnetism, and Electronic Structure Method on First-Principles Oxygen Vacancy Formation Energy Trends in Perovskites. Journal of Physical Chemistry C, 2014, 118, 28776-28790.	1.5	105
17470	Cooperativity in spin-crossover transition in metalorganic complexes: Interplay of magnetic and elastic interactions. Physical Review B, 2014, 90, .	1.1	16
17471	The Virtue of Defects: Stable Bromine Production by Catalytic Oxidation of Hydrogen Bromide on Titanium Oxide. Angewandte Chemie - International Edition, 2014, 53, 8628-8633.	7.2	38
17472	Successes and failures of Hubbard-corrected density functional theory: The case of Mg doped LiCoO2. Journal of Chemical Physics, 2014, 141, 164706.	1.2	22

#	Article	IF	Citations
17473	Lone-pair interactions and photodissociation of compressed nitrogen trifluoride. Journal of Chemical Physics, 2014, 141, 064706.	1.2	8
17474	Structural defects in epitaxial graphene layers synthesized on C-terminated 4H-SiC (0001Â¯) surfaceâ€"Transmission electron microscopy and density functional theory studies. Journal of Applied Physics, 2014, 115, 054310.	1.1	7
17475	Water adsorption and dissociation on Ni(110): How is it different from its close packed counterparts?. Journal of Chemical Physics, 2014, 140, 174704.	1.2	21
17476	Insight into the description of van der Waals forces for benzene adsorption on transition metal (111) surfaces. Journal of Chemical Physics, 2014, 140, 084704.	1.2	158
17477	Grain Boundary Controlled Electron Mobility in Polycrystalline Titanium Dioxide. Advanced Materials Interfaces, 2014, 1, 1400078.	1.9	52
17478	Ab-initio modeling of electromechanical coupling at Si surfaces. Journal of Applied Physics, 2014, 116, 073507.	1.1	4
17479	Anisotropic In distribution in InGaN core-shell nanowires. Journal of Applied Physics, 2014, 116, .	1.1	8
17480	ORGANIC SPINTRONICS: PAST, PRESENT AND FUTURE. Spin, 2014, 04, 1440013.	0.6	10
17481	<mml:math xmlns:mml="http://www.w3.org/1998/Math/MathML"><mml:mrow><mml:msub><mml:mi>J</mml:mi><mml:mi>eff</mml:mi></mml:ms spin-orbit insulating state close to the cubic limit in<mml:math xmlns:mml="http://www.w3.org/1998/Math/MathML"><mml:msub><mml:mtext>Ca</mml:mtext><mml:mn>4</mml:mn></mml:msub> xmlns:mml="http://www.w3.org/1998/Math/MathML"><mml:msub><mml:mtext>IrO</mml:mtext><m. Physical Review B, 2014, 89, .	1.1	27
17482	xmlns:mml="http://www.w3.org/1998/Math/MathML"><mml:msub><mml:mi>Ti</mml:mi><mml:mi>n</mml:mi></mml:msub><mml:ms mathvariant="normal">O</mml:mi><mml:mrow><mml:mn>2</mml:mn><mml:mi>n</mml:mi><mml:mo>â^'</mml:mo><mml:mn>1< phases studied using density functional theory. Physical Review B, 2014, 90, .	1.1	33
17483	Imprint Control of Nonvolatile Shape Memory with Asymmetric Ferroelectric Multilayers. Chemistry of Materials, 2014, 26, 6911-6914.	3.2	17
17484	Molecularâ€Scale Imaging of Water Near Charged Surfaces. ChemElectroChem, 2014, 1, 431-435.	1.7	13
17485	Structure and magnetism of Tm atoms and monolayers on W(110). Physical Review B, 2014, 90, .	1.1	11
17486	Importance of tetrahedral coordination for high-valent transition-metal oxides:<mml:math xmlns:mml="http://www.w3.org/1998/Math/MathML"><mml:msub><mml:mrow><mml:mi mathvariant="normal">YCrO</mml:mi></mml:mrow><mml:mn>4</mml:mn></mml:msub></mml:math>as a model system. Physical Review B, 2014, 90, .	1.1	9
17487	Nonlinear lattice dynamics as a basis for enhanced superconductivity in YBa2Cu3O6.5. Nature, 2014, 516, 71-73.	13.7	391
17488	Ab initio study of electronic, magnetic, and spectroscopic properties in <mml:math xmlns:mml="http://www.w3.org/1998/Math/MathML"><mml:mi>A</mml:mi></mml:math>- and<mml:math xmlns:mml="http://www.w3.org/1998/Math/MathML"><mml:mi>B</mml:mi></mml:math>-site-ordered perovskite<mml:math xmlns:mml="http://www.w3.org/1998/Math/MathML"><mml:mi>Ca</mml:mi><mml:msub><mml:mi>Cu</mml:mi><mml:mn>3</mml:mn> Physical Review B, 2014, 90, .	1.1	10
17489	Pressure variation of Rashba spin splitting toward topological transition in the polar semiconductor BiTeI. Physical Review B, 2014, 90, .	1.1	31
17490	Structures and magnetic properties of Fe clusters on graphene. Physical Review B, 2014, 90, .	1.1	28

#	Article	IF	Citations
17491	First-principles study of the minimal model of magnetic interactions in Fe-based superconductors. Physical Review B, 2014, 89, .	1.1	29
17492	Stable two-dimensional dumbbell stanene: A quantum spin Hall insulator. Physical Review B, 2014, 90, .	1.1	154
17493	Atomic structure of the<mml:math xmlns:mml="http://www.w3.org/1998/Math/MathML"><mml:mrow><mml:msqrt><mml:mn>3</mml:mn></mml:msqrt><mml:mspace width="0.16em" /><mml:mo>Ã—</mml:mo><mml:mspace width="0.16em" /><mml:msqrt><mml:mn>3</mml:mn></mml:msqrt></mml:mrow></mml:math>phase of silicene on Ag(111). Physical Review B, 2014, 90, .	1.1	107
17494	Electronic structure of<mml:math xmlns:mml="http://www.w3.org/1998/Math/MathML"><mml:msub><mml:mi>Ba</mml:mi><mml:mn>3</mml:mn></mml:msub><mml:msub><mml:mi mathvariant="normal">O</mml:mi><mml:mn>9</mml:mn></mml:msub></mml:math>: A candidate quantum spin liquid compound. Physical Review B, 2014, 89, .	1.1	16
17495	Li intercalation in graphite: A van der Waals density-functional study. Physical Review B, 2014, 90, .	1.1	63
17496	High Resolution Scanning Tunneling Microscopy of a 1D Coordination Polymer with Imidazoleâ€Based N,N,O Ligands on HOPG. Chemistry - A European Journal, 2014, 20, 11863-11869.	1.7	5
17497	Nature and evolution of the band-edge states in<mml:math xmlns:mml="http://www.w3.org/1998/Math/MathML"><mml:msub><mml:mi>MoS</mml:mi><mml:mn>2</mml:mn></mml:msub></mml:math>From monolayer to bulk. Physical Review B, 2014, 90, .	1.1	138
17498	Thermal stability and structural evolution of quaternary Tiâ€“Taâ€“Bâ€“N coatings. Surface and Coatings Technology, 2014, 259, 698-706.	2.2	9
17499	Two-dimensional square ternary Cu<mml:math xmlns:mml="http://www.w3.org/1998/Math/MathML"><mml:msub><mml:mrow /><mml:mn>2</mml:mn></mml:msub></mml:math>MX<mml:math xmlns:mml="http://www.w3.org/1998/Math/MathML"><mml:msub><mml:mrow		

#	Article	IF	Citations
17509	Orbital polarization in strained<mml:math xmlns:mml="http://www.w3.org/1998/Math/MathML"><mml:msub><mml:mi mathvariant="normal">LaNiO</mml:mi><mml:mn>3</mml:mn></mml:msub></mml:math>: Structural distortions and correlation effects. Physical Review B, 2014, 90, .	1.1	41
17510	Synthesis of Colloidal 2D/3D MoS₂ Nanostructures by Pulsed Laser Ablation in an Organic Liquid Environment. Journal of Physical Chemistry C, 2014, 118, 30120-30126.	1.5	34
17511	Doubleâ€Cubeâ€Shaped Mixed Chalcogen/Pentele Clusters from GaCl₃ Melts. European Journal of Inorganic Chemistry, 2014, 2014, 3043-3052.	1.0	20
17512	Three-dimensional polymeric structures of single-wall carbon nanotubes. Journal of Chemical Physics, 2014, 140, 204709.	1.2	8
17513	SiN-SiC nanofilm: A nano-functional ceramic with bipolar magnetic semiconducting character. Applied Physics Letters, 2014, 104, .	1.5	26
17514	Indirect-to-direct gap transition in strained and unstrained<mml:math xmlns:mml="http://www.w3.org/1998/Math/MathML"><mml:msub><mml:mi>Sn</mml:mi><mml:mi>x</mml:mi></mml:msub></mml:math> Physical Review B, 2014, 89, .	1.1	107
17515	Selectively localized Wannier functions. Physical Review B, 2014, 90, .	1.1	24
17516	Elastic anisotropy and shear-induced atomistic deformation of tetragonal silicon carbon nitride. Journal of Applied Physics, 2014, 116, .	1.1	2
17517	Self-consistent determination of Hubbard<mml:math xmlns:mml="http://www.w3.org/1998/Math/MathML"><mml:mi>U</mml:mi></mml:math>for explaining the anomalous magnetism of the Gd<mml:math xmlns:mml="http://www.w3.org/1998/Math/MathML"><mml:msub><mml:mrow /><mml:mn>13</mml:mn></mml:msub></mml:math>cluster. Physical Review B, 2014, 89, .	1.1	26
17518	First-Principles and Kinetic Monte Carlo Simulation Studies of the Reactivity of Tc(0001), MoTc(111) and MoTc(110) Surfaces. Journal of the Electrochemical Society, 2014, 161, C83-C88.	1.3	11
17519	Tuning the hydrogen desorption of<mml:math xmlns:mml="http://www.w3.org/1998/Math/MathML"><mml:mrow><mml:msub><mml:mrow><mml:mi>Mg</mml:mi><mml:mo>(</mml:mo> Zn alloying. Physical Review B, 2014, 90, .	1.1	4
17520	Turning<mml:math xmlns:mml="http://www.w3.org/1998/Math/MathML"><mml:msub><mml:mi>SrTiO</mml:mi><mml:mn>3</mml:mn></mml:msub></mml:math> a Mott insulator. Physical Review B, 2014, 90, .	1.1	25
17521	Boron diffusion in MgO and emergence of magnetic ground states: A first-principles study. Physical Review B, 2014, 89, .	1.1	6
17522	First-principles evidence of Mn moment canting in hole-doped<mml:math xmlns:mml="http://www.w3.org/1998/Math/MathML"><mml:mi>Ba</mml:mi><mml:msub><mml:mrow /><mml:mrow><mml:mn>1</mml:mn><mml:mo>â^’</mml:mo><mml:mn>2</mml:mn><mml:mi>x</mml:mi></mml:mrow></mml:msub></mml:math><mml:math xmlns:mml="http://www.w3.org/1998/Math/MathML"><mml:mi>K</mml:mi><mml:msub><mml:mrow /><mml:mrow><mml:mn>2</mml:mn><mml:mi>x</mml:mi></mml:mrow></mml:msub></mml:math>	1.1	13
17523	Efficacy of the DFTÂ+Â <mml:math xmlns:mml="http://www.w3.org/1998/Math/MathML"><mml:mi>U</mml:mi></mml:math> formalism for modeling hole polarons in perovskite oxides. Physical Review B, 2014, 90, .	1.1	86
17524	Structural evolution in high-pressure amorphous<mml:math xmlns:mml="http://www.w3.org/1998/Math/MathML"><mml:msub><mml:mi mathvariant="normal">CO</mml:mi><mml:mn>2</mml:mn></mml:msub></mml:math>fromab initiomolecular dynamics. Physical Review B, 2014, 89, .	1.1	9
17525	Origin of High-Resolution IETS-STM Images of Organic Molecules with Functionalized Tips. Physical Review Letters, 2014, 113, 226101.	2.9	165
17526	Effect of As-chain layers in<mml:math xmlns:mml="http://www.w3.org/1998/Math/MathML"><mml:msub><mml:mtext>CaFeAs</mml:mtext><mml:mn>2</mml:mn></mml:msub></mml:math> Physical Review B, 2014, 89, .	1.1	41

#	Article	IF	Citations
17527	Shape-dependent photocatalytic activity of Bi₅O₇I caused by facets synergetic and internal electric field effects. RSC Advances, 2014, 4, 65056-65064.	1.7	36
17528	Thermoelectric transport properties of molybdenum from<mml:math xmlns:mml="http://www.w3.org/1998/Math/MathML"><mml:mi mathvariant="italic">ab</mml:mi><mml:mspace width="0.28em" /><mml:mi mathvariant="italic">initio</mml:mi></mml:math>simulations. Physical Review B, 2014, 90, .	1.1	27
17529	Electrical switching effect of a single-unit-cell CrO2 layer on rutile TiO2 surface. Applied Physics Letters, 2014, 104, 122408.	1.5	4
17530	Unraveling the<mml:math xmlns:mml="http://www.w3.org/1998/Math/MathML"><mml:msub><mml:mrow><mml:mtext>LiNbO</mml:mtext></mml:mrow><mml: surface by atomic force microscopy and density functional theory. Physical Review B, 2014, 89, .	1.1	10
17531	A Highâ€Temperature Neutron Diffraction and Firstâ€Principles Study of <scp><scp>Ti</scp></scp>₃<scp><scp>AlC</scp></scp>₂ and <scp><scp>Ti</scp></scp>₃(<scp><scp>Al</scp></scp>_{0.8}<scp><scp>Sn</scp></scp>_{0.2})<sc Journal of the American Ceramic Society, 2014, 97, 570-576.	1.9	14
17532	Topological transition and edge states in HgTe quantum wells from first principles. Physical Review B, 2014, 89, .	1.1	17
17533	Scalable Oxygenâ€Ion Transport Kinetics in Metalâ€Oxide Films: Impact of Thermally Induced Lattice Compaction in Acceptor Doped Ceria Films. Advanced Functional Materials, 2014, 24, 1562-1574.	7.8	65
17534	Density Functional Theory Study on Spin States of LaCoO3 at Room Temperature. Chinese Journal of Chemical Physics, 2014, 27, 274-278.	0.6	5
17535	The effects of chemical bonding on the topological property of half- Heusler compounds: First principle calculation. Computational Condensed Matter, 2014, 1, 8-13.	0.9	2
17536	Topological crystalline insulator PbxSn1-xTe thin films on SrTiO3 (001) with tunable Fermi levels. APL Materials, 2014, 2, .	2.2	15
17537	Inâ€situ Raman spectroscopy of currentâ€carrying graphene microbridge. Journal of Raman Spectroscopy, 2014, 45, 168-172.	1.2	11
17538	On the room-temperature phase diagram of high pressure hydrogen: An ab initio molecular dynamics perspective and a diffusion Monte Carlo study. Journal of Chemical Physics, 2014, 141, 024501.	1.2	19
17539	Origin of High Photoconductive Gain in Fully Transparent Heterojunction Nanocrystalline Oxide Image Sensors and Interconnects. Advanced Materials, 2014, 26, 7102-7109.	11.1	65
17540	First-principles calculations of the electronic, vibrational, and elastic properties of the magnetic laminate Mn2GaC. Journal of Applied Physics, 2014, 116, .	1.1	23
17541	Increasing the Visible Light Absorption of Graphitic Carbon Nitride (Melon) Photocatalysts by Homogeneous Selfâ€Modification with Nitrogen Vacancies. Advanced Materials, 2014, 26, 8046-8052.	11.1	658
17542	Configuration dependence of the properties of Cd_{1â€“x}<scp>Z</scp>n_x<scp>S</scp> solid solutions by firstâ€principles calculations. Physica Status Solidi (B): Basic Research, 2014, 251, 655-660.	0.7	5
17543	Hydrogen dynamics and metallic phase stabilization in VO2. Applied Physics Letters, 2014, 104, .	1.5	34
17544	Atomic imaging and modeling of H2O2(g) surface passivation, functionalization, and atomic layer deposition nucleation on the Ge(100) surface. Journal of Chemical Physics, 2014, 140, 204708.	1.2	14

#	Article	IF	Citations
17545	Edge effects on the electronic properties of phosphorene nanoribbons. Journal of Applied Physics, 2014, 116, .	1.1	157
17546	Hardness of FeB4: Density functional theory investigation. Journal of Chemical Physics, 2014, 140, 174505.	1.2	80
17547	Failure of DFT-based computations for a stepped-substrate-supported correlated Co wire. Physical Review B, 2014, 89, .	1.1	10
17548	Lattice dynamics and lattice thermal conductivity of thorium dicarbide. Journal of Nuclear Materials, 2014, 454, 142-148.	1.3	10
17549	A six-dimensional potential energy surface for Ru(0001)(2Ã—2):CO. Journal of Chemical Physics, 2014, 141, 094704.	1.2	12
17550	Communication: Origin of the difference between carbon nanotube armchair and zigzag ends. Journal of Chemical Physics, 2014, 140, 091102.	1.2	13
17551	Electronic structure and stability of low symmetry Ta₂O₅polymorphs. Physica Status Solidi - Rapid Research Letters, 2014, 8, 560-565.	1.2	26
17552	Catalytically active Au-O(OH) _x - species stabilized by alkali ions on zeolites and mesoporous oxides. Science, 2014, 346, 1498-1501.	6.0	544
17553	Benchmarking the performance of density functional theory and point charge force fields in their description of sI methane hydrate against diffusion Monte Carlo. Journal of Chemical Physics, 2014, 140, 174703.	1.2	41
17554	Ag and Au atoms intercalated in bilayer heterostructures of transition metal dichalcogenides and graphene. APL Materials, 2014, 2, 092801.	2.2	11
17555	Density functional theory study of the mechanism of Li diffusion in rutile RuO2. AIP Advances, 2014, 4, .	0.6	24
17556	Ternary chalcogenides<mml:math xmlns:mml="http://www.w3.org/1998/Math/MathML"><mml:mrow><mml:mi mathvariant="normal">C</mml:mi><mml:msub><mml:mi mathvariant="normal">s</mml:mi><mml:mn>2</mml:mn></mml:msub><mml:mi mathvariant="normal">Z</mml:mi><mml:msub><mml:mi mathvariant="normal">n</mml:mi><mml:mn>3</mml:mn></mml:msub><mml:mi mathvariant="normal">	1.1	9
17557	Diversity of hydrogen configuration and its roles in SrTiO3â˜Î˙. APL Materials, 2014, 2, 012103.	2.2	26
17558	Characterization of the nitrogen split interstitial defect in wurtzite aluminum nitride using density functional theory. Journal of Applied Physics, 2014, 116, .	1.1	9
17559	Oxygen vacancies at the surface of SrTiO₃ thin films. Journal of Applied Physics, 2014, 115, 033710.	1.1	14
17560	Manipulation of graphene work function using a self-assembled monolayer. Journal of Applied Physics, 2014, 116, 084312.	1.1	20
17561	First-Principles Prediction of Oxygen Reduction Activity on Pdâ€“Cuâ€“Si Metallic Glasses. Journal of Physical Chemistry C, 2014, 118, 28609-28615.	1.5	11
17562	Ab initio characterization of layered MoS2 as anode for sodium-ion batteries. Journal of Power Sources, 2014, 268, 279-286.	4.0	377

#	Article	IF	Citations
17563	Theoretical investigation of charge accumulation layer on the Bi-induced InAs(111)-(2â€‰Ã—â€‰2) surface. Journal of Applied Physics, 2014, 115, 163702.	1.1	0
17564	First-Principles Screening of Complex Transition Metal Hydrides for High Temperature Applications. Inorganic Chemistry, 2014, 53, 11833-11848.	1.9	20
17565	Polymerization of nitrogen in cesium azide under modest pressure. Journal of Chemical Physics, 2014, 141, 044717.	1.2	50
17566	Investigating atomic contrast in atomic force microscopy and Kelvin probe force microscopy on ionic systems using functionalized tips. Physical Review B, 2014, 90, .	1.1	59
17567	High Stability of Faceted Nanotubes and Fullerenes of Multiphase Layered Phosphorus: A Computational Study. Physical Review Letters, 2014, 113, 226801.	2.9	91
17568	A Stable Binary BeB2 phase. Scientific Reports, 2014, 4, 6993.	1.6	25
17569	Lithium Concentration Dependent Elastic Properties of Battery Electrode Materials from First Principles Calculations. Journal of the Electrochemical Society, 2014, 161, F3010-F3018.	1.3	231
17570	Determination of Polarizationâ€Fields Across Polytype Interfaces in InAs Nanopillars. Advanced Materials, 2014, 26, 1052-1057.	11.1	27
17571	Ab Initio Thermodynamics of Oxygen Vacancies and Zinc Interstitials in ZnO. Journal of Physical Chemistry Letters, 2014, 5, 4238-4242.	2.1	14
17572	Controlling orbital-selective Kondo effects in a single molecule through coordination chemistry. Journal of Chemical Physics, 2014, 141, 054702.	1.2	27
17573	The Extended Stability Range of Phosphorus Allotropes. Angewandte Chemie - International Edition, 2014, 53, 11629-11633.	7.2	138
17574	Negatively Charged Ions on Mg(0001) Surfaces: Appearance and Origin of Attractive Adsorbate-Adsorbate Interactions. Physical Review Letters, 2014, 113, 136102.	2.9	21
17575	(Sr,Ba)(Si,Ge)2 for thin-film solar-cell applications: First-principles study. Journal of Applied Physics, 2014, 115, .	1.1	61
17576	Bonding Nature of Local Structural Motifs in Amorphous GeTe. Angewandte Chemie - International Edition, 2014, 53, 10817-10820.	7.2	125
17577	First principles studies of proton conduction in KTaO3. Journal of Chemical Physics, 2014, 141, 024707.	1.2	9
17578	Modeling and stabilities of Mg/MgH2 interfaces: A first-principles investigation. AIP Advances, 2014, 4, .	0.6	13
17579	Phthalocyanineâ€Based Organometallic Nanocages: Properties and Gas Storage. ChemPhysChem, 2014, 15, 126-131.	1.0	9
17580	Inclusion flotation-driven channel segregation in solidifying steels. Nature Communications, 2014, 5, 5572.	5.8	79

#	Article	IF	Citations
17581	First-principles predicted low-energy structures of NaSc(BH4)4. Journal of Chemical Physics, 2014, 140, 124708.	1.2	25
17582	Direct Observation of Atomic Dynamics and Silicon Doping at a Topological Defect in Graphene. Angewandte Chemie - International Edition, 2014, 53, 8908-8912.	7.2	37
17583	Origin of deep subgap states in amorphous indium gallium zinc oxide: Chemically disordered coordination of oxygen. Applied Physics Letters, 2014, 104, .	1.5	67
17584	Lattice thermal conductivity of UO2usingab-initioand classical molecular dynamics. Journal of Applied Physics, 2014, 115, 123510.	1.1	35
17585	Extended Klein Edges in Graphene. ACS Nano, 2014, 8, 12272-12279.	7.3	41
17586	Affinity of the Interface between Hydroxyapatite (0001) and Titanium (0001) Surfaces: A First-Principles Investigation. ACS Applied Materials & Interfaces, 2014, 6, 20738-20751.	4.0	15
17587	Configurational Thermodynamics of Alloyed Nanoparticles with Adsorbates. Nano Letters, 2014, 14, 7077-7084.	4.5	37
17588	Mechanical Properties, Electronic Structures, and Potential Applications in Lithium Ion Batteries: A First-Principles Study toward SnSe₂ Nanotubes. Journal of Physical Chemistry C, 2014, 118, 28291-28298.	1.5	37
17589	The work functions of Au/Mg decorated Au(100), Mg(001), and AuMg alloy surfaces: A theoretical study. Journal of Chemical Physics, 2014, 141, 094705.	1.2	6
17590	DFT characterization of nanostructured germanium surfaces induced by cobalt atoms. Surface and Interface Analysis, 2014, 46, 92-97.	0.8	0
17591	Theoretical Study on the Mechanism of Anisotropic Thermal Properties of <scp><scp>Ti</scp></scp>₂<scp><scp>AlC</scp></scp> and <scp><scp>Cr</scp></scp>₂<scp><scp>AlC</scp></scp>. Journal of the American Ceramic Society, 2014, 97, 1202-1208.	1.9	31
17592	Semiconductor to metal transition by tuning the location of N2AA in armchair graphene nanoribbons. Journal of Applied Physics, 2014, 115, 053707.	1.1	12
17593	First principles investigation of the initial stage of H-induced missing-row reconstruction of Pd(110) surface. Journal of Chemical Physics, 2014, 140, 244707.	1.2	11
17594	Spin dependent transport properties of Mn-Ga/MgO/Mn-Ga magnetic tunnel junctions with metal(Mg,) Tj ETQq1 1 0.784314 rgBT /Ov	1.1	8
17595	Camel-back band-induced power factor enhancement of thermoelectric lead-tellurium from Boltzmann transport calculations. Applied Physics Letters, 2014, 104, .	1.5	14
17596	Adsorption of Large Hydrocarbons on Coinage Metals: A van der Waals Density Functional Study. ChemPhysChem, 2014, 15, 2851-2858.	1.0	45
17597	Structure-property relations in amorphous carbon for photovoltaics. Applied Physics Letters, 2014, 105, 043903.	1.5	14
17598	In-Depth Atomic Structure of the Pentacene/Cu(110) Interface in the Monolayer Coverage Regime: Theory and X-ray Diffraction Results. Journal of Physical Chemistry C, 2014, 118, 27815-27822.	1.5	4

#	Article	IF	Citations
17599	Enhancing interfacial conductivity and spatial charge confinement of LaAlO3/SrTiO3 heterostructures via strain engineering. Applied Physics Letters, 2014, 105, .	1.5	47
17600	Exceptionally Stiff Two-Dimensional Molecular Crystal by Substrate-Confinement. ACS Nano, 2014, 8, 11425-11431.	7.3	6
17601	The structural and electronic properties of Au_nclusters on the Î±-Al₂O₃(0001) surface: a first principles study. Physical Chemistry Chemical Physics, 2014, 16, 26561-26569.	1.3	14
17602	Ultrathin Silica Films: The Atomic Structure of Twoâ€Dimensional Crystals and Glasses. Chemistry - A European Journal, 2014, 20, 9176-9183.	1.7	51
17603	A first principles analysis of the effect of hydrogen concentration in hydrogenated amorphous silicon on the formation of strained Si-Si bonds and the optical and mobility gaps. Journal of Applied Physics, 2014, 115, .	1.1	16
17604	Fast and Anisotropic Proton Conduction in a Crystalline Polyphosphate. Journal of Physical Chemistry C, 2014, 118, 29629-29635.	1.5	21
17605	Identification of the Au Coverage and Structure of the<mml:math xmlns:mml="http://www.w3.org/1998/Math/MathML" display="inline"><mml:mrow><mml:mi>Au</mml:mi><mml:mo>/</mml:mo><mml:mi>Si</mml:mi><mml:mo stretchy="false">(</mml:mo><mml:mn>111</mml:mn><mml:mo) Tj ETQq0 0 0 rgBT /Overlock 10 Tf 50 492 Td (stretchy="false">)</mm		

#	Article	IF	Citations
17617	Tuning the Fermi level beyond the equilibrium doping limit through quenching: The case of CdTe. Physical Review B, 2014, 90, .	1.1	66
17618	<mml:math xmlns:mml="http://www.w3.org/1998/Math/MathML"><mml:mrow><mml:mo>(</mml:mo><mml:mn>111</mml:mn><mml:mo>)</m states of SnTe. Physical Review B, 2014, 90, .	1.1	27
17619	Inter- and Intralayer Compression of Germanane. Journal of Physical Chemistry C, 2014, 118, 28196-28201.	1.5	7
17620	Ab Initio Transport Calculations for Single-Atom Copper Junctions in the Presence of Hydrogen Chloride. Journal of Physical Chemistry C, 2014, 118, 28252-28257.	1.5	4
17621	First-principles study of bismuth films at transition-metal grain boundaries. Physical Review B, 2014, 90, .	1.1	16
17622	Image formation and contrast inversion in noncontact atomic force microscopy imaging of oxidized Cu(110) surfaces. Physical Review B, 2014, 90, .	1.1	8
17623	Lifshitz and other transitions in alkaline-earth 122 pnictides under pressure. Physical Review B, 2014, 90, .	1.1	8
17624	Formation and stability of point defects in monolayer rhenium disulfide. Physical Review B, 2014, 89, .	1.1	151
17625	Ab initio molecular dynamics calculations on scattering of hyperthermal H atoms from Cu(111) and Au(111). Journal of Chemical Physics, 2014, 141, 054705.	1.2	41
17626	First-principles study of NO reduction by CO on transition metal atoms-doped CeO2(111). Chinese Journal of Catalysis, 2014, 35, 1937-1943.	6.9	9
17627	Advances in interaction mechanism of water (gas) on clay minerals in China. International Journal of Mining Science and Technology, 2014, 24, 727-735.	4.6	11
17628	Elastic properties and stress-temperature phase diagrams of high-temperature phases with low-temperature lattice instabilities. Physical Review B, 2014, 90, .	1.1	23
17629	Two-Dimensional Ordering of Solute Nanoclusters at a Close-Packed Stacking Fault: Modeling and Experimental Analysis. Scientific Reports, 2014, 4, 7318.	1.6	37
17630	Synthesis of Cu@Pd core-shell nanowires with enhanced activity and stability for formic acid oxidation. Electrochimica Acta, 2014, 143, 44-48.	2.6	52
17631	Morphology and surface properties of LiVOPO₄: a first principles study. Physical Chemistry Chemical Physics, 2014, 16, 24604-24609.	1.3	18
17632	A Complexed Sol-Gel (CSG) Approach to High Surface Area (HSA) Durable Ultra Active Platinum-Ruthenium Electro-Catalysts for Direct Methanol Fuel Cells. Journal of the Electrochemical Society, 2014, 161, F1053-F1060.	1.3	2
17633	Contact-induced spin polarization in BNNT(CNT)/TM (TM=Co, Ni) nanocomposites. Journal of Applied Physics, 2014, 116, 084309.	1.1	9
17634	Multigap absorption inCaCu3Ti4O12and the prediction capability ofab initiomethods. Physical Review B, 2014, 90, .	1.1	2

#	Article	IF	Citations
17635	Achieving a direct band gap in oxygen functionalized-monolayer scandium carbide by applying an electric field. Physical Chemistry Chemical Physics, 2014, 16, 26273-26278.	1.3	82
17636	Roomâ€Temperature Ferroelectricity in Hexagonal TbMnO₃ Thin Films. Advanced Materials, 2014, 26, 7660-7665.	11.1	32
17637	Dispersion corrected RPBE studies of liquid water. Journal of Chemical Physics, 2014, 141, 064501.	1.2	102
17638	First-principle investigations of the peculiar magnetic behavior of Sr₂ FeOsO₆. Physica Status Solidi - Rapid Research Letters, 2014, 08, 776-780.	1.2	10
17639	Enhancing the three-dimensional electronic structure in 1111-type iron arsenide superconductors by H substitution. Physical Review B, 2014, 89, .	1.1	16
17640	Intrinsic Noise from Neighboring Bases in the DNA Transverse Tunneling Current. Physical Review Applied, 2014, 1, .	1.5	8
17641	A DFT investigation of the interactions of Pd, Ag, Sn, and Cs with silicon carbide. International Journal of Quantum Chemistry, 2014, 114, 1534-1545.	1.0	8
17642	Uniaxial strain-induced magnetic order transition from E-type to A-type in orthorhombic YMnO3 from first-principles. Journal of Applied Physics, 2014, 116, .	1.1	6
17643	Pressure-induced phase transition and superconductivity in<mml:math xmlns:mml="http://www.w3.org/1998/Math/MathML"><mml:msub><mml:mrow><mml:mi mathvariant="normal">YBa</mml:mi></mml:mrow><mml:mn>2</mml:mn></mml:msub><mml:msub><mml:mrow><mml:mi mathvariant="normal">Cu</mml:mi></mml:mrow><mml:mn>4</mml:mn></mml:msub><mml:msub><mml:mrow><mml:mi mathvariant="normal">O</mml:mi></mml:mrow><mml:mn>8</mml:mn></mml:msub></mml:math>. Physical Review B, 2014, 90, .	1.1	13
17644	Revisiting the adsorption of copper-phthalocyanine on Au(111) including van der Waals corrections. Journal of Chemical Physics, 2014, 140, 124711.	1.2	11
17645	Mechanical properties, electronic properties and phase stability of Mg under pressure: A first-principles study. International Journal of Modern Physics B, 2014, 28, 1450200.	1.0	5
17646	Most spin-1/2 transition-metal ions do have single ion anisotropy. Journal of Chemical Physics, 2014, 141, 124113.	1.2	27
17647	Density Functional Theory Beyond the Generalized Gradient Approximation for Surface Chemistry. Topics in Current Chemistry, 2014, , 25-51.	4.0	9
17648	Phase Stability and Defect Physics of a Ternary ZnSnN₂ Semiconductor: First Principles Insights. Advanced Materials, 2014, 26, 311-315.	11.1	81
17649	Interaction of Mo(CO)₆ and its derivative fragments with the Cu(001) surface: Influence on the decomposition process. International Journal of Quantum Chemistry, 2014, 114, 1630-1635.	1.0	5
17650	Effects of dilute substitutional solutes on interstitial carbon in<mml:math xmlns:mml="http://www.w3.org/1998/Math/MathML"><mml:mi>Î±</mml:mi></mml:math>-Fe: Interactions and associated carbon diffusion from first-principles calculations. Physical Review B, 2014, 90, .	1.1	38
17651	Correlation of interfacial bonding mechanism and equilibrium conductance of molecular junctions. Frontiers of Physics, 2014, 9, 780-788.	2.4	13
17652	Dual nature of the ferroelectric and metallic state in<mml:math xmlns:mml="http://www.w3.org/1998/Math/MathML"><mml:msub><mml:mi mathvariant="normal">LiOsO</mml:mi><mml:mn>3</mml:mn></mml:msub></mml:math>. Physical Review B, 2014, 90, .	1.1	57

#	Article	IF	Citations
17653	Vibrational free energy and phase stability of paramagnetic and antiferromagnetic CrN fromab initiomolecular dynamics. Physical Review B, 2014, 89, .	1.1	46
17654	Electronic structure and polaronic charge distributions of Fe vacancy clusters inFe1â^'xO. Physical Review B, 2014, 90, .	1.1	6
17655	Wurtzite structure in ultrathin ZnO films on Fe(110): Surface x-ray diffraction andab initiocalculations. Physical Review B, 2014, 90, .	1.1	6
17656	Rationalizing the role of structural motif and underlying electronic structure in the finite temperature behavior of atomic clusters. Journal of Chemical Physics, 2014, 140, 154307.	1.2	3
17657	Influence of shape anisotropy of self-interstitials on dislocation sink efficiencies in Zr: Multiscale modeling. Physical Review B, 2014, 90, .	1.1	16
17658	Topological phase transition and quantum spin Hall state in TlBiS2. Journal of Applied Physics, 2014, 116, 033704.	1.1	12
17659	Understanding surface core-level shifts using the Auger parameter: A study of Pd atoms adsorbed on ultrathin SiO<mml:math xmlns:mml="http://www.w3.org/1998/Math/MathML"><mml:msub><mml:mrow /><mml:mn>2</mml:mn></mml:msub></mml:math>films. Physical Review B, 2014, 89, .	1.1	38
17660	Hydrogen intercalation of single and multiple layer graphene synthesized on Si-terminated SiC(0001) surface. Journal of Applied Physics, 2014, 116, .	1.1	14
17661	Structure and properties of complex hydride perovskite materials. Nature Communications, 2014, 5, 5706.	5.8	168
17662	Ab initiostudy of H-vacancy interactions in fcc metals: Implications for the formation of superabundant vacancies. Physical Review B, 2014, 89, .	1.1	104
17663	Correlation between the electronic structures and diffusion paths of interstitial defects in semiconductors: The case of CdTe. Physical Review B, 2014, 90, .	1.1	24
17664	Dynamics of tungsten hexacarbonyl, dicobalt octacarbonyl, and their fragments adsorbed on silica surfaces. Journal of Chemical Physics, 2014, 140, 184706.	1.2	6
17665	Local structures around<mml:math xmlns:mml="http://www.w3.org/1998/Math/MathML"><mml:mn>3</mml:mn><mml:mi>d</mml:mi></mml:math>metal dopants in topological insulator<mml:math xmlns:mml="http://www.w3.org/1998/Math/MathML"><mml:msub><mml:mrow><mml:mi mathvariant="normal">Bi</mml:mi></mml:mrow><mml:mn>2</mml:mn></mml:msub><mml:msub><mml:mrow><mml:mi mathvariant="normal">Se</mml:mi></mml:mrow><mml:mn>3</mml:mn></mml:msub></mml:math>studied	1.1	18
17666	Waltzing of a helium pair in tungsten: Migration barrier and trajectory revealed from first-principles. AIP Advances, 2014, 4, .	0.6	8
17667	The effects of dangling bond on the electronic and magnetic properties of armchair AlN/SiC heterostructure nanoribbons. Computational Materials Science, 2014, 92, 372-376.	1.4	3
17668	Defect formation energy and magnetic properties of aluminum-substituted M-type barium hexaferrite. Computational Condensed Matter, 2014, 1, 45-50.	0.9	26
17669	Theory of action spectroscopy for single-molecule reactions induced by vibrational excitations with STM. Physical Review B, 2014, 89, .	1.1	29
17670	Effect of the VAsVGa complex defect doping on properties of the semi-insulating GaAs. Journal of Applied Physics, 2014, 115, .	1.1	10

#	Article	IF	Citations
17671	Superconductivity in noncentrosymmetric ternary equiatomic pnictides LaMP(<mml:math) Tj ETQq0 0 0 rgBT /Overlock 10 Tf 50	1.1	40
17672	Electronic and magnetic properties of the<mml:math xmlns:mml="http://www.w3.org/1998/Math/MathML"><mml:msub><mml:mi mathvariant="normal">Ti</mml:mi><mml:mn>5</mml:mn></mml:msub><mml:msub><mml:mi mathvariant="normal">O</mml:mi><mml:mn>9</mml:mn></mml:msub></mml:math>MagnÃ©li phase. Physical Review B, 2014, 90, .	1.1	10
17674	Quantum confinement and band offsets in amorphous silicon quantum wells. Physical Review B, 2014, 90, .	1.1	6
17675	Multiple Ï€-bands and Bernal stacking of multilayer graphene on C-face SiC, revealed by nano-Angle Resolved Photoemission. Scientific Reports, 2014, 4, 4157.	1.6	33
17676	Theoretical investigation of the adsorption and diffusion of hydrogen on the surface and in the bulk of the intermetallic compound Mg2Ni. Physics of the Solid State, 2014, 56, 2035-2042.	0.2	1
17677	A RESTful API for exchanging materials data in the AFLOWLIB.org consortium. Computational Materials Science, 2014, 93, 178-192.	1.4	148
17678	Enhanced efficiency of p-type doping by band-offset effect in wurtzite and zinc-blende GaAs/InAs-core-shell nanowires. Journal of Applied Physics, 2014, 116, 093704.	1.1	2
17679	Impurity-vacancy complexes and ferromagnetism in doped sesquioxides. Physical Review B, 2014, 89, .	1.1	9
17680	The role of native defects in the transport of charge and mass and the decomposition of Li₄BN₃H₁₀. Physical Chemistry Chemical Physics, 2014, 16, 25314-25320.	1.3	6
17681	Combined experimental and theoretical study of fast atom diffraction on the<mml:math xmlns:mml="http://www.w3.org/1998/Math/MathML"><mml:msub><mml:mi>Î²</mml:mi><mml:mn>2</mml:mn></mml:msub><mml:m GaAs(001) surface. Physical Review B, 2014, 90, .	1.1	11
17682	Intrinsic Rashba-like splitting in asymmetric Bi2Te3/Sb2Te3 heterogeneous topological insulator films. Applied Physics Letters, 2014, 105, 082401.	1.5	3
17683	A first-principles study of lithium-decorated hybrid boron nitride and graphene domains for hydrogen storage. Journal of Chemical Physics, 2014, 141, 084711.	1.2	29
17684	Magnetic properties and heat capacity of the three-dimensional frustrated<mml:math xmlns:mml="http://www.w3.org/1998/Math/MathML"><mml:mrow><mml:mi>S</mml:mi><mml:mo>=</mml:mo><mml:mfrac><mml:m xmlns:mml="http://www.w3.org/1998/Math/MathML"><mml:msub><mml:mrow><mml:mi mathvariant="normal">PbCuTe</mml:mi></mml:mrow><mml:mn>2</mml:mn></mml:msub><mml:msub><mml:mrow><mml:mi Lattice-tuned magnetism of<mml:math xmlns:mml="http://www.w3.org/1998/Math/MathML"><mml:mrow><mml:mn>6. Physical Review B, 2014, 90, .	1.1	52
17685	xmlns:mml="http://www.w3.org/1998/Math/MathML"><mml:mrow><mml:msup><mml:mrow><mml:mi>Ru</mml:mi></mml:mrow><mml:mi in single crystals of the layered honeycomb ruthenates<mml:math xmlns:mml="http://www.w3.org/1998/Math/MathML"><mml:mrow><mml:msub><mml:mi>Li</mml:mi><mml:mn>2</mml:mn></mml:mm. Physical Review B, 2014, 90, .	1.1	54
17686	Microalloying Boron Carbide with Silicon to Achieve Dramatically Improved Ductility. Journal of Physical Chemistry Letters, 2014, 5, 4169-4174.	2.1	46
17687	Role of atomic radius and<mml:math xmlns:mml="http://www.w3.org/1998/Math/MathML"><mml:mi>d</mml:mi></mml:math>-states hybridization in the stability of the crystal structure of<mml:math xmlns:mml="http://www.w3.org/1998/Math/MathML"><mml:msub><mml:mi>M</mml:mi><mml:mn>2</mml:mn></mml:msub><mml:m mathvariant="normal">O</mml:mi></mml:mrow><mml:mn>3</mml:mn></mml:msub></mml:math><mml:math		

#	Article	IF	Citations
17690	Electronic structure and mechanical properties of ternary ZrTaN alloys studied byab initiocalculations and thin-film growth experiments. Physical Review B, 2014, 90, .	1.1	45
17691	NaOsO3: A high Neel temperature 5doxide. Physical Review B, 2014, 89, .	1.1	21
17692	The Key Role of van der Waals Interactions in MPc/Au(111) (M = Co, Fe, H₂) Systems Based on First-Principles Calculations. Journal of Physical Chemistry C, 2014, 118, 27843-27849.	1.5	14
17693	Electronic Structure Modulation of Metalâ€“Organic Frameworks for Hybrid Devices. ACS Applied Materials & Interfaces, 2014, 6, 22044-22050.	4.0	75
17694	Bandgap Tunability in Zn(Sn,Ge)N₂ Semiconductor Alloys. Advanced Materials, 2014, 26, 1235-1241.	11.1	75
17695	Comment on â€œCorrelation and relativistic effects in U metal and U-Zr alloy: Validation ofab initioapproachesâ€• Physical Review B, 2014, 90, .	1.1	37
17696	Ferroelectricity in wurtzite structure simple chalcogenide. Applied Physics Letters, 2014, 104, .	1.5	52
17697	Theory of Mn-doped II-II-V semiconductors. Physical Review B, 2014, 90, .	1.1	54
17698	Electromigration of bivalent functional groups on graphene. Physical Review B, 2014, 89, .	1.1	13
17699	Characterization of few-layer 1T-MoSe2 and its superior performance in the visible-light induced hydrogen evolution reaction. APL Materials, 2014, 2, .	2.2	222
17700	Crystal facet effect on structural stability and electronic properties of wurtzite InP nanowires. Journal of Applied Physics, 2014, 115, .	1.1	6
17701	Complex trend of magnetic order in Fe clusters on4dtransition-metal surfaces. II. First-principles calculations. Physical Review B, 2014, 89, .	1.1	6
17702	Computational prediction and characterization of single-layer CrS₂. Applied Physics Letters, 2014, 104, 022116.	1.5	108
17703	Termination-dependent electronic and magnetic properties of ultrathin<mml:math xmlns:mml="http://www.w3.org/1998/Math/MathML"><mml:msub><mml:mi mathvariant="normal">SrRuO</mml:mi><mml:mn>3</mml:mn></mml:msub></mml:math>(111) films on<mml:math xmlns:mml="http://www.w3.org/1998/Math/MathML"><mml:msub><mml:mi mathvariant="normal">SrTiO</mml:mi><mml:mn>3</mml:mn></mml:msub></mml:math>. Physical Review B, 2014, 89, .	1.1	15
17704	Revealing an unusual transparent phase of superhard iron tetraboride under high pressure. Proceedings of the National Academy of Sciences of the United States of America, 2014, 111, 17050-17053.	3.3	23
17705	First-principles investigation of the electronic and Li-ion diffusion properties of LiFePO4 by sulfur surface modification. Journal of Applied Physics, 2014, 116, .	1.1	29
17706	Novel K rattling: A new route to thermoelectric materials?. Journal of Applied Physics, 2014, 115, 033703.	1.1	5
17707	Weak competing interactions control assembly of strongly bonded TCNQ ionic acceptor molecules on silver surfaces. Physical Review B, 2014, 90, .	1.1	11

#	Article	IF	Citations
17708	Electrochemical Cycling of Sodiumâ€Filled Silicon Clathrate. ChemElectroChem, 2014, 1, 347-353.	1.7	29
17709	Dissociative adsorption of CH3X (X = Br and Cl) on a silicon(100) surface revisited by density functional theory. Journal of Chemical Physics, 2014, 141, 174701.	1.2	11
17710	Scaling up the shape: A novel growth pattern of gallium clusters. Journal of Chemical Physics, 2014, 141, 054308.	1.2	10
17711	Magnetic moment enhancement and spin polarization switch of the manganese phthalocyanine molecule on an IrMn(100) surface. Journal of Chemical Physics, 2014, 141, 034703.	1.2	9
17712	Shape-Memory Transformations of NiTi: Minimum-Energy Pathways between Austenite, Martensites, and Kinetically Limited Intermediate States. Physical Review Letters, 2014, 113, 265701.	2.9	34
17713	Formation energies of carbon related defects in Cu<inf>2</inf>ZnSnS<inf>4</inf>. , 2014, , .		0
17714	Impurity-induced enhancement of perpendicular magnetic anisotropy in Fe/MgO tunnel junctions. Physical Review B, 2014, 90, .	1.1	24
17715	Magnetoresistance in multilayer fullerene spin valves: A first-principles study. Physical Review B, 2014, 90, .	1.1	20
17716	Pressure and temperature dependence of the zero-field splitting in the ground state of NV centers in diamond: A first-principles study. Physical Review B, 2014, 90, .	1.1	97
17717	Perovskite to Postperovskite Transition in NaFeF₃. Inorganic Chemistry, 2014, 53, 12205-12214.	1.9	19
17718	Influences of Surface Substitutional Ti Atom on Hydrogen Adsorption, Dissociation, and Diffusion Behaviors on the Î±-U(001) Surface. Journal of Physical Chemistry C, 2014, 118, 26634-26640.	1.5	12
17719	Theoretical Study of Optical Properties of Native Point Defects in Î±-Al₂O₃. Integrated Ferroelectrics, 2014, 156, 79-85.	0.3	14
17720	Chainâ€like structures of gold supported by silicon substrate. Physica Status Solidi (B): Basic Research, 2014, 251, 924-932.	0.7	0
17721	Indirect-Direct Band Gap Transition by Van Der Waals Interaction Engineering in MoS₂/WS₂ Bilayer Heterojunction. Applied Mechanics and Materials, 0, 614, 70-74.	0.2	4
17722	Exploring High-Pressure Structures of N₂CO. Journal of Physical Chemistry C, 2014, 118, 27252-27257.	1.5	16
17723	Thermodynamic Aspects of Cathode Coatings for Lithiumâ€Ion Batteries. Advanced Energy Materials, 2014, 4, 1400690.	10.2	99
17724	Band structure engineering of anatase TiO2 by metal-assisted P-O coupling. Journal of Chemical Physics, 2014, 140, 174705.	1.2	29
17725	Stress stabilization of a new ferroelectric phase incorporated into SrTaO2N thin films. Journal of Applied Physics, 2014, 116, 053505.	1.1	9

#	Article	IF	Citations
17726	Origin of resolution enhancement by co-doping of scintillators: Insight from electronic structure calculations. Applied Physics Letters, 2014, 104, .	1.5	34
17727	Surface reconstruction stability of Bi/GaSb surfaces. Journal of Applied Physics, 2014, 116, .	1.1	5
17728	Photo-induced change of dielectric response in BaCoSiO4 stuffed tridymite. Journal of Applied Physics, 2014, 115, .	1.1	19
17729	Massive Surface Reshaping Mediated by Metalâ€“Organic Complexes. Journal of Physical Chemistry C, 2014, 118, 29704-29712.	1.5	28
17730	Tuning nucleation density of metal island with charge doping of graphene substrate. Applied Physics Letters, 2014, 105, 071609.	1.5	8
17731	Interrelation between Structure â€“ Magnetic Properties in La_{0.5}Sr_{0.5}CoO₃. Advanced Materials Interfaces, 2014, 1, 1400203.	1.9	20
17732	Crystal Structure and Elastic Properties of Hypothesized <scp>MAX</scp> Phaseâ€Like Compound (<scp><scp>Cr</scp></scp>₂<scp><scp>Hf</scp></scp>)₂<scp><scp>Al</scp></scp>₃<scp><scp>C</scp></scp>₂. Journal of the American Ceramic Society, 2014, 97, 2646-2653.	1.9	8
17733	Theoretical study of the ammonia nitridation rate on an Fe (100) surface: A combined density functional theory and kinetic Monte Carlo study. Journal of Chemical Physics, 2014, 141, 134108.	1.2	3
17735	Impact of Functionalized Polystyrenes as the Electron Injection Layer on Gold and Aluminum Surfaces: A Combined Theoretical and Experimental Study. Israel Journal of Chemistry, 2014, 54, 779-788.	1.0	2
17736	Pressure induced phase transition in MH2 (M = V, Nb). Journal of Chemical Physics, 2014, 140, 114703.	1.2	18
17737	A Firstâ€Principles Investigation on Microscopic Atom Distribution and Configurationâ€Averaged Properties in Cd_{1â^'x}Zn_xS Solid Solutions. ChemPhysChem, 2014, 15, 3125-3132.	1.0	6
17738	New Reconstructions of the (110) Surface of Rutile<mml:math xmlns:mml="http://www.w3.org/1998/Math/MathML" display="inline"><mml:mrow><mml:msub><mml:mrow><mml:mi>TiO</mml:mi></mml:mrow><mml:mrow><mml:mn>2</mml:mn></mml:mrow> by an Evolutionary Method. Physical Review Letters, 2014, 113, 266101.	7.9	61
17739	Study of the Mechanical and Thermodynamic Properties on NiAl and Ni₃Al. Applied Mechanics and Materials, 0, 584-586, 1256-1263.	0.2	6
17740	Vegard's law-like behavior for Mn_mTc_nalloy clusters: a first-principles prediction. Journal of Physics Condensed Matter, 2014, 26, 185004.	0.7	6
17741	Electronic structure and magnetic properties of iridate superlattice SrIrO₃/SrTiO₃. Journal of Physics Condensed Matter, 2014, 26, 185501.	0.7	20
17742	Ab Initio Research on a New Type of Half-Metallic Double Perovskites, A2CrMO6 (A = IVA Group) Tj ETQq1 1 0.784314 rgBT /Overlock	1.0	11
17743	²²⁹Thorium-doped calcium fluoride for nuclear laser spectroscopy. Journal of Physics Condensed Matter, 2014, 26, 105402.	0.7	44
17744	Giant Birefringence in Layered Compound LaOBiS 2. Chinese Physics Letters, 2014, 31, 047802.	1.3	8

#	Article	IF	Citations
17745	The design ofd-character Dirac cones based on graphene. Journal of Physics Condensed Matter, 2014, 26, 385501.	0.7	4
17746	New materials graphyne, graphdiyne, graphone, and graphane: review of properties, synthesis, and application in nanotechnology. Nanotechnology, Science and Applications, 2014, 7, 1.	4.6	241
17747	The crystal structure of IrB₂: a first-principle calculation. RSC Advances, 2014, 4, 63442-63446.	1.7	10
17748	Properties of the silver cyclic amide Ag2(C4H4NO2)2(H2O) crystal from the periodic DFT computations. Journal of Structural Chemistry, 2014, 55, 621-628.	0.3	0
17749	Surface-Specific Catalytic Activity of Carbon Nanotube Encapsulated with Metal-Oxide Clusters. Applied Mechanics and Materials, 0, 490-491, 113-117.	0.2	0
17750	Ab initio study of H, He, Li and Be impurity effect in tungsten Î£3{1â€‰1â€‰2} and Î£27{5â€‰5â€‰2} grain boundaries. Journal of Physics Condensed Matter, 2014, 26, 135004.	0.7	23
17751	The interaction of oxygen with theÎ±-U(001) surface: anab initiostudy. Physica Scripta, 2014, 89, 075701.	1.2	5
17752	Trapping Behavior of He in Ti Revisited by ab initio Calculations. Chinese Physics Letters, 2014, 31, 017102.	1.3	0
17753	First-principles evaluation of penetration energy of metal atom into Si substrate. Japanese Journal of Applied Physics, 2014, 53, 058006.	0.8	8
17754	Stacking sequence dependence of electronic properties in double-layer graphene heterostructures. Japanese Journal of Applied Physics, 2014, 53, 06JD03.	0.8	4
17755	Point defect-assisted doping mechanism and related thermoelectric transport properties in Pb-doped BiCuOTe. Journal of Materials Chemistry A, 2014, 2, 19759-19764.	5.2	40
17756	Effect of amino ligand size of Si precursors on initial reaction with an â€“OH-terminated Si(001) surface for atomic layer deposition. Japanese Journal of Applied Physics, 2014, 53, 08NE04.	0.8	8
17757	Data-driven discovery of energy materials: efficient BaM₂Si₃O₁₀â€‰:â€‰Eu²⁺(M = Sc, Lu) phosphors for application in solid state white lighting. Faraday Discussions, 2014, 176, 333-347.	1.6	20
17758	High-pressure structural behaviour of HoVO₄: combined XRD experiments andab initiocalculations. Journal of Physics Condensed Matter, 2014, 26, 265402.	0.7	58
17759	The common effects of surface and internal bonds on the electronic structure of Bi₂Te₃ nano-films by first-principles calculation. Materials Research Express, 2014, 1, 025043.	0.8	1
17760	Ab-initio simulations of MoS<inf>2</inf> transistors: From mobility calculation to device performance evaluation. , 2014, , .		6
17761	First-principles theory of the luminescence lineshape for the triplet transition in diamond NV centres. New Journal of Physics, 2014, 16, 073026.	1.2	183
17762	Preparation, Characterization and Origin of Highly Active and Thermally Stable Pdâ€“Ce_{0.8}Zr_{0.2}O₂ Catalysts via Sol-Evaporation Induced Self-Assembly Method. Environmental Science & Technology, 2014, 48, 12403-12410.	4.6	31

#	Article	IF	Citations
17763	Theoretical Study of the Lithium Diffusion in the Crystalline and Amorphous Silicon as well as on its Surface. Solid State Phenomena, 0, 213, 29-34.	0.3	2
17764	Computational analysis of the contributions to the piezoelectric coefficient $$e_{33}$$ e 33 in ZnO nanowires: first-principles calculations. Journal of Computational Electronics, 2014, 13, 983-988.	1.3	1
17765	First-Principles Study on Structural, Electronic, and Magnetic Properties of 3d Transition-Metal Nanowires Encapsulated Inside GaN Nanotubes. Journal of Superconductivity and Novel Magnetism, 2014, 27, 2539-2545.	0.8	2
17766	DFT-D studies on structural variation and absorption properties of crystalline benzotrifuroxan under high pressure. Canadian Journal of Chemistry, 2014, 92, 1131-1137.	0.6	5
17767	Boron-Phosphorus Pairs in Compensated Crystalline Silicon. ECS Solid State Letters, 2014, 3, N23-N25.	1.4	0
17769	Electronic and magnetic properties of boron nitride nanoribbons with squareâ€“octagon (4â€‰|â€‰8) line defects. Nanotechnology, 2014, 25, 115702.	1.3	14
17770	The effect of helium nano-bubbles on the structures stability and electronic properties of palladium tritides: a density functional theory study. Proceedings of the Royal Society A: Mathematical, Physical and Engineering Sciences, 2014, 470, 20140357.	1.0	4
17771	BaSi₂as a promising low-cost, earth-abundant material with large optical activity for thin-film solar cells: A hybrid density functional study. Applied Physics Express, 2014, 7, 071203.	1.1	103
17772	Hybrid Bi-Cells for Water Independent Direct Methanol Fuel Cells. Journal of the Electrochemical Society, 2014, 161, F1037-F1052.	1.3	2
17773	Adsorption and diffusion of lithium on 1T-MoS2 monolayer. Computational Materials Science, 2014, 93, 86-90.	1.4	62
17774	Chain Length Effect on Surface Stress of Alkanethiolates Adsorbed onto AU(111) Surface: a van der Waals Density Functional Study. Journal of Mechanics, 2014, 30, 241-246.	0.7	8
17775	Effects of surface charge doping on magnetic anisotropy in capping 3dâ€“5d(4d) multilayers deposited on highly polarizable substrates. Journal Physics D: Applied Physics, 2014, 47, 105006.	1.3	10
17776	Activity and Durability of PEFCs Alloy Core-Shell Catalysts: Role of Surface Oxidation. Advances in Science and Technology, 2014, 93, 31-40.	0.2	1
17777	Transport Properties of the Layered Transition Metal Oxypnictide Sr₂ScMPO₃withMP layers (M=Mn, Ni and) Tj ETQq1 1 0.784314 rgBT/Overlock 10 Tf 50	3.3	8
17778	Switchable S = 1/2 and J = 1/2 Rashba bands in ferroelectric halide perovskites. Proceedings of the National Academy of Sciences of the United States of America, 2014, 111, 6900-6904.	3.3	252
17779	Dynamics of charge transfer at Au/Si metal-semiconductor nano-interface. Molecular Physics, 2014, 112, 474-484.	0.8	23
17780	First principle predictions of anomalous yield strength in L1₂materials. Materials Research Innovations, 2014, 18, S4-1021-S4-1025.	1.0	5
17781	Structures and Electronic Properties of Graphene with Vacancy Defects. Materials Research Society Symposia Proceedings, 2014, 1658, 70.	0.1	0

#	Article	IF	Citations
17782	Noble Metals Can Have Different Effects on Photocatalysis Over Metalâ€“Organic Frameworks (MOFs): A Case Study on M/NH₂â€MILâ€125(Ti) (M=Pt and Au). Chemistry - A European Journal, 2014, 20, 4780-4788.	1.7	247
17783	Theoretical study of intermolecular interactions in nanoporous networks on boron doped silicon surface. Chemical Physics Letters, 2014, 615, 117-123.	1.2	0
17784	First-Principles Prediction on Long-Range Ferromagnetism Induced by Vacancies in SnO₂ Nanosheet. Journal of the Physical Society of Japan, 2014, 83, 104601.	0.7	1
17785	Phases Stability of Ni-Mn-Ga Alloys Studied by <i>Ab Initio</i> Calculations. Materials Science Forum, 0, 783-786, 1646-1651.	0.3	1
17786	Contact Resistance of Screen Printed Ag-Contacts to Si Emitters: Mathematical Modeling and Microstructural Characterization. Journal of the Electrochemical Society, 2014, 161, E3180-E3187.	1.3	2
17787	Quantum chemical modeling of the structure and proton conductivity of mesitylenesulfonic acid dihydrate 2,4,6-Me3C6H2SO3 â¯Â·H5O2 +. Russian Chemical Bulletin, 2014, 63, 1765-1773.	0.4	2
17788	Helium Interaction with Y2Ti2O7: A First Principles Study. Materials Research Society Symposia Proceedings, 2014, 1645, 1.	0.1	0
17789	Spectroscopic and atomic force studies of the functionalisation of carbon surfaces: new insights into the role of the surface topography and specific chemical states. Faraday Discussions, 2014, 173, 257-272.	1.6	18
17790	Enhancement of Spin Correlation in Cr₂O₃ Film Above NÃ©el Temperature Induced by Forming a Junction With Fe₂O₃ Layer: First-Principles and Monte-Carlo Study. IEEE Transactions on Magnetics, 2014, 50, 1-4.	1.2	11
17791	A neural network based approach to predict high voltage li-ion battery cathode materials. , 2014, , .		5
17792	Theoretical investigations of the electronic properties of functionalized zinc-oxide nanowires. Proceedings of SPIE, 2014, , .	0.8	0
17793	Occupied and unoccupied electronic structure of Na doped MoS2(0001). Applied Physics Letters, 2014, 105, .	1.5	30
17794	Circular Patterned Test Structures for Precise Determination of Piezoelectric Thin Film Constants: Application to ScxAl1-xN. Procedia Engineering, 2014, 87, 112-115.	1.2	1
17795	Multi-scale simulations of a Mo/n⁺â€“GaAs Schottky contact for nano-scale IIIâ€“V MOSFETs. Semiconductor Science and Technology, 2014, 29, 054003.	1.0	8
17796	Direct dâ€“d interactions among transition metal impurities in IIIâ€“V semiconductors. Applied Physics Express, 2014, 7, 023004.	1.1	3
17797	Arsenic Adsorption onto Minerals: Connecting Experimental Observations with Density Functional Theory Calculations. Minerals (Basel, Switzerland), 2014, 4, 208-240.	0.8	58
17798	Theoretical Investigations on Graphite Oxide Immersed in Water or Methanol. Chinese Journal of Chemical Physics, 2014, 27, 9-14.	0.6	4
17799	Large potential steps at weakly interacting metal-insulator interfaces. Physical Review B, 2014, 90, .	1.1	24

#	Article	IF	Citations
17800	Study on Electronic Structure of GaN under Pressure. Advanced Materials Research, 2014, 900, 217-221.	0.3	0
17801	Quantum valley Hall states and topological transitions in Pt(Ni, Pd)-decorated silicene: A first-principles study. Journal of Chemical Physics, 2014, 141, 244701.	1.2	3
17802	Protons in acceptor doped langasite, La3Ga5SiO14. Solid State Ionics, 2014, 264, 76-84.	1.3	10
17803	Ab Initio Study on MoS2 and Its Family: Chemical Trend, Band Alignment, Alloying, and Gap Modulation. Lecture Notes in Nanoscale Science and Technology, 2014, , 77-101.	0.4	1
17804	Crystal structure prediction and hydrogen-bond symmetrization of solid hydrazine under high pressure: a first-principles study. Acta Crystallographica Section C, Structural Chemistry, 2014, 70, 112-117.	0.2	2
17805	Electrocatalysis - Basic Concepts, Theoretical Treatments in Electrocatalysis via DFT-Based Simulations. , 2014, , 397-402.		0
17806	Giant electronic polarization induced by a helical spin order in SrMn ₇ O ₁₂ : First-principles calculations. Europhysics Letters, 2014, 108, 67012.	0.7	5
17807	Thermodynamic description of Ge-Mn-Si. Materials Research Society Symposia Proceedings, 2014, 1642, 1.	0.1	0
17808	Spin Polarization Properties of Na Doped Meridianal Tris(8-Hydroxyquinoline) Aluminum Studied by First Principles Calculations. Chinese Physics Letters, 2014, 31, 048502.	1.3	4
17809	First principles calculations of solution energies of dopants around stacking faults in Si crystal. Japanese Journal of Applied Physics, 2014, 53, 061302.	0.8	11
17810	Strain driven sequential magnetic transitions in strained GdTiO₃on compressive substrates: a first-principles study. Journal of Physics Condensed Matter, 2014, 26, 476001.	0.7	5
17811	Structural, magnetic and conduction properties of 3d-metal monoatomic wires. Materials Research Express, 2014, 1, 026302.	0.8	0
17812	Adsorption Mechanism of Carbon Monoxide on PtRu and PtRuMo Surfaces in the Density Functional Theory Perspective. Advanced Materials Research, 0, 896, 537-540.	0.3	4
17813	Optimal stoichiometry for nucleation and growth of conductive filaments in HfO_x. Modelling and Simulation in Materials Science and Engineering, 2014, 22, 025001.	0.8	31
17814	Quantum Chemical Study of Point Defects in Tin Dioxide. Lecture Notes in Electrical Engineering, 2014, , 13-24.	0.3	6
17815	Superconducting state above the boiling point of liquid nitrogen in the GaH3compound. Superconductor Science and Technology, 2014, 27, 015003.	1.8	32
17817	Progress on New Approaches to Old Ideas: Orbital-Free Density Functionals. Letters in Mathematical Physics, 2014, , 113-134.	0.4	30
17818	Hydrogenated ultra-thin tin films predicted as two-dimensional topological insulators. New Journal of Physics, 2014, 16, 115008.	1.2	56

#	Article	IF	Citations
17819	Theoretical Modeling of Oxide-Photocatalysts for PEC Water Splitting. Nanostructure Science and Technology, 2014, , 113-134.	0.1	0
17820	Diffusion in CdS of Cd and S vacancies and Cu, Cd, Cl, S and Te interstitials studied with first-principles computations. Materials Research Express, 2014, 1, 025904.	0.8	10
17821	Transmission electron microscopy/electron energy loss spectroscopy measurements andab initiocalculation of local magnetic moments at nickel grain boundaries. Science and Technology of Advanced Materials, 2014, 15, 015005.	2.8	7
17822	Electronic Properties of Hydrogenated Graphene-Like Materials Under Strains. Materials Research Society Symposia Proceedings, 2014, 1658, 76.	0.1	0
17823	Solute-Vacancy Interactions in Nickel. Materials Research Society Symposia Proceedings, 2014, 1645, 1.	0.1	4
17824	A DFT Study of B, N and BN Doped Graphene. Materials Research Society Symposia Proceedings, 2014, 1701, 7.	0.1	4
17825	Ti and Zr Transition Metals Effect in the D03 Fe3Al by <i>Ab Initio</i> Study Approach. Materials Science Forum, 0, 783-786, 1640-1645.	0.3	0
17826	Defects and Sintering-Induced Diffusion Processes in Yttria-Stabilised Zirconia Nanomaterials Studied by Positron Annihilation Spectroscopy. , 0, 1, 155-172.		2
17827	Electronic structures and optical properties of cuprous oxide and hydroxide. Materials Research Society Symposia Proceedings, 2014, 1675, 185-190.	0.1	1
17828	Can slow-diffusing solute atoms reduce vacancy diffusion in advanced high-temperature alloys?. Materials Science & Engineering A: Structural Materials: Properties, Microstructure and Processing, 2014, 617, 194-199.	2.6	11
17829	Spin-correlations and magnetic structure in an Fe monolayer on 5dtransition metal surfaces. Journal of Physics Condensed Matter, 2014, 26, 186001.	0.7	17
17830	A Density Functional Theory Study of the Adsorption of Benzene on Hematite (Î±-Fe2O3) Surfaces. Minerals (Basel, Switzerland), 2014, 4, 89-115.	0.8	105
17831	Quantum-Mechanical Methods for Quantifying Incorporation of Contaminants in Proximal Minerals. Minerals (Basel, Switzerland), 2014, 4, 690-715.	0.8	28
17832	Low-energy nanoscale clusters of (TiC)n n = 6, 12: a structural and energetic comparison with MgO. Highlights in Theoretical Chemistry, 2014, , 213-218.	0.0	2
17833	Electronic and Optical Properties of Sn-Doped Zno with and without O Vacancy. Applied Mechanics and Materials, 0, 576, 9-13.	0.2	0
17834	Direct observation of adsorption geometry for the van der Waals adsorption of a single Ï€-conjugated hydrocarbon molecule on Au(111). Journal of Chemical Physics, 2014, 140, 074709.	1.2	13
17835	Structure and dynamics in liquid bismuth and Bin clusters: A density functional study. Journal of Chemical Physics, 2014, 141, 194503.	1.2	21
17836	DX-like centers in NaI:Tl upon aliovalent codoping. Journal of Applied Physics, 2014, 116, .	1.1	18

#	Article	IF	Citations
17837	Origin of the Bloch-type polarization components at the 180Â° domain walls in ferroelectric PbTiO3. Journal of Applied Physics, 2014, 116, .	1.1	20
17838	Spin polarization of Co(0001)/graphene junctions from first principles. Journal of Physics Condensed Matter, 2014, 26, 104204.	0.7	15
17839	Cluster expansion of multicomponent ionic systems with controlled accuracy: importance of long-range interactions in heterovalent ionic systems. Journal of Physics Condensed Matter, 2014, 26, 115403.	0.7	17
17840	A comparative first-principles study of martensitic phase transformations in TiPd₂ and TiPd intermetallics. Journal of Physics Condensed Matter, 2014, 26, 135401.	0.7	1
17841	First-principles study of hydrogen configurations at the core of a high-angle grain boundary in cubic yttria-stabilized zirconia. Journal of Physics Condensed Matter, 2014, 26, 025502.	0.7	7
17842	Magnetic effect on the interfacial energy of the Ni(1â€‰1â€‰1)/Cr(1â€‰1â€‰0) interface. Journal of Physics Condensed Matter, 2014, 26, 355001.	0.7	11
17843	Tunneling anisotropic magnetoresistance effect of single adatoms on a noncollinear magnetic surface. Journal of Physics Condensed Matter, 2014, 26, 394010.	0.7	7
17844	Electric tuning of the surface and quantum well states in Bi2Se3 films: a first-principles study. Journal of Physics Condensed Matter, 2014, 26, 395005.	0.7	0
17845	Modelling [1â€‰0â€‰0] and [0â€‰1â€‰0] screw dislocations in MgSiO₃perovskite based on the Peierlsâ€“Nabarroâ€“Galerkin model. Modelling and Simulation in Materials Science and Engineering, 2014, 22, 025020.	0.8	16
17846	Van der Waals interaction in a boron nitride bilayer. New Journal of Physics, 2014, 16, 113015.	1.2	37
17847	First-principles study of electronic structures and stability of body-centered cubic Tiâ€“Mo alloys by special quasirandom structures. Science and Technology of Advanced Materials, 2014, 15, 035014.	2.8	23
17848	Single Cation Contributions to the Polarization in GaFeO₃ (Mars 2014). IEEE Transactions on Magnetics, 2014, 50, 1-4.	1.2	1
17849	Optical and other material properties of SiO2 fromab initiostudies. Optical Engineering, 2014, 53, 071808.	0.5	4
17850	Structural, electronic, and magnetic properties of double perovskite Pb2CrMO6 (M=Mo, W and Re) from first-principles investigation. Journal of Magnetism and Magnetic Materials, 2014, 349, 74-79.	1.0	18
17851	Elastic properties, lattice dynamics and structural transitions in molybdenum at high pressures. Computational Materials Science, 2014, 81, 313-318.	1.4	23
17852	First-principles-based phase diagrams and thermodynamic properties of TCP phases in Reâ€“X systems (X=Ta, V, W). Computational Materials Science, 2014, 81, 433-445.	1.4	32
17853	First-principles investigation of the electronic and magnetic properties of ZnO nanosheet with intrinsic defects. Computational Materials Science, 2014, 81, 259-263.	1.4	27
17854	First-principle prediction of robust half-metallic Te-based half-Heusler alloys. Journal of Magnetism and Magnetic Materials, 2014, 350, 119-123.	1.0	24

#	Article	IF	Citations
17855	Dislocation slip stress prediction in shape memory alloys. International Journal of Plasticity, 2014, 54, 247-266.	4.1	50
17856	Controlling Câ€“O, Câ€“C and Câ€“H bond scission for deoxygenation, reforming, and dehydrogenation of ethanol using metal-modified molybdenum carbide surfaces. Green Chemistry, 2014, 16, 777-784.	4.6	51
17857	Semi-metallic to semiconducting transition in graphene nanosheet with site specific co-doping of boron and nitrogen. Physica E: Low-Dimensional Systems and Nanostructures, 2014, 56, 64-68.	1.3	50
17858	The mixed intermetallic silicide Nb5â^'xTaxSi3 (0â©½xâ©½5). Crystal and electronic structure. Journal of Alloys and Compounds, 2014, 584, 385-392.	2.8	9
17859	Influence of adsorbates on the segregation properties of Auâ€“Pd bimetallic clusters. Computational Materials Science, 2014, 81, 253-258.	1.4	5
17860	Effect of size and aspect ratio on structural parameters and evidence of shape transition in zinc oxide nanostructures. Journal of Physics and Chemistry of Solids, 2014, 75, 543-549.	1.9	53
17861	Electron transfer through solid-electrolyte-interphase layers formed on Si anodes of Li-ion batteries. Electrochimica Acta, 2014, 140, 250-257.	2.6	59
17862	The effect of chemical potential on the thermodynamic stability of carbonate ions in hydroxyapatite. Acta Biomaterialia, 2014, 10, 3716-3722.	4.1	27
17863	Tuning the band gap of PbCrO4 through high-pressure: Evidence of wide-to-narrow semiconductor transitions. Journal of Alloys and Compounds, 2014, 587, 14-20.	2.8	60
17864	Structural and dynamical properties of MgSiO3 melt over the pressure range 200â€“500GPa: Ab initio molecular dynamics. Journal of Non-Crystalline Solids, 2014, 385, 169-174.	1.5	8
17865	Detailed atomistic insight into the Î²â€³ phase in Alâ€“Mgâ€“Si alloys. Acta Materialia, 2014, 69, 126-134.	3.8	156
17866	Electrochemical properties of NaNi1/3Co1/3Fe1/3O2 as a cathode material for Na-ion batteries. Electrochemistry Communications, 2014, 38, 79-81.	2.3	135
17867	Thermophysical properties of LiFePO4 cathodes with carbonized pitch coatings and organic binders: Experiments and first-principles modeling. Journal of Power Sources, 2014, 251, 8-13.	4.0	30
17868	First-principles study of electronic structure and optical properties of (Zrâ€“Al)-codoped ZnO. Computational Materials Science, 2014, 82, 70-75.	1.4	34
17869	The effect of intermolecular interactions on the charge transport properties of thiazole/thiophene-based oligomers with trifluoromethylphenyl. Journal of Molecular Graphics and Modelling, 2014, 51, 79-85.	1.3	5
17870	Effect of alloying on elastic properties of ZrN based transition metal nitride alloys. Surface and Coatings Technology, 2014, 255, 140-145.	2.2	34
17871	Theoretical studies of elastic properties of orthorhombic LiBH4. Computational Materials Science, 2014, 81, 378-385.	1.4	38
17872	Proton migration in bulk orthorhombic barium cerate using density functional theory. Solid State Ionics, 2014, 259, 1-8.	1.3	17

#	Article	IF	Citations
17873	Large magnetoelectric coupling in ferromagnetic/ferroelectric superlattices with asymetric interfaces. Journal of Magnetism and Magnetic Materials, 2014, 354, 299-302.	1.0	3
17874	Prediction of two-dimensional materials with half-metallic Dirac cones: Ni2C18H12 and Co2C18H12. Carbon, 2014, 73, 382-388.	5.4	48
17875	Identifying the nature of interaction between LiBH4 and two-dimensional substrates: DFT study with van der Waals correction. Journal of Alloys and Compounds, 2014, 587, 428-436.	2.8	4
17876	The effect of biaxial mechanical strain on the physical properties of double perovskite Sr2FeMoO6: A theoretical study. Solid State Communications, 2014, 191, 70-75.	0.9	21
17877	Vibrational and dielectric properties of Î±-Si3N4 from density functional theory. Materials Chemistry and Physics, 2014, 147, 42-49.	2.0	16
17878	Structural and electronic properties of linear and angular polycyclic aromatic hydrocarbons. Physics Letters, Section A: General, Atomic and Solid State Physics, 2014, 378, 1379-1382.	0.9	13
17879	Chlorine molecule adsorbed on graphene and doped graphene: A first-principle study. Physica B: Condensed Matter, 2014, 436, 54-58.	1.3	20
17880	Facet dependent binding and etching: Ultra-sensitive colorimetric visualization of blood uric acid by unmodified silver nanoprisms. Biosensors and Bioelectronics, 2014, 59, 227-232.	5.3	55
17881	The influence of Ti- and Si-doping on the structure, morphology and photo-response properties of Î±-Fe2O3 for efficient water-splitting: Insights from experiment and first-principles calculations. Chemical Physics Letters, 2014, 592, 242-246.	1.2	18
17882	First-principles calculations of structural, elastic and electronic properties of Li2B12H12. Journal of Alloys and Compounds, 2014, 593, 169-175.	2.8	12
17883	Premixed TiCâ€“Ni composite powder prepared by mechanical milling of Tiâ€“Ni alloy/graphite mixture and subsequent heat treatment. Powder Technology, 2014, 253, 681-685.	2.1	6
17884	Realization of controlling the band alignment via atomic substitution. Carbon, 2014, 69, 495-501.	5.4	3
17885	First-principle study on the X (X=N, P, As, Sb) doped (9.0) single-walled SiC nanotubes. Physica B: Condensed Matter, 2014, 447, 56-61.	1.3	14
17886	Effects of F and Cl on the stability of MgH2. International Journal of Hydrogen Energy, 2014, 39, 877-883.	3.8	36
17887	Ab initio study of effects of Al and Y co-doping on destabilizing of MgH2. International Journal of Hydrogen Energy, 2014, 39, 9254-9261.	3.8	20
17888			

#	Article	IF	Citations
17891	Drastic changes in the electronic and magnetic structures of hydrogenated U2Ti intermetallic from first principles. Journal of Magnetism and Magnetic Materials, 2014, 358-359, 70-75.	1.0	5
17892	Hybrid functional calculations of potential hydrogen storage material: Complex dimagnesium iron hydride. International Journal of Hydrogen Energy, 2014, 39, 9709-9717.	3.8	39
17893	Structural and mechanical properties of Laves phases YCu2 and YZn2: First principles calculation analyzed with data mining approach. Computational Materials Science, 2014, 89, 176-181.	1.4	27
17894	Coverage dependence of the level alignment for methanol on TiO2(110). Computational and Theoretical Chemistry, 2014, 1040-1041, 259-265.	1.1	13
17895	First-principles study of electronic properties of F-terminated silicon nanoribbons. Physica E: Low-Dimensional Systems and Nanostructures, 2014, 57, 21-27.	1.3	14
17896	Screening study of light-metal and transition-metal-doped NiTiH hydrides as Li-ion battery anode materials. Solid State Ionics, 2014, 258, 88-91.	1.3	9
17897	Realizing high visible-light-induced carriers mobility in TiO2-based photoanodes. Journal of Power Sources, 2014, 251, 195-201.	4.0	3
17898	Influence of titanium and nickel dopants on the dehydrogenation properties of Mg(AlH4)2: Electronic structure mechanisms. International Journal of Hydrogen Energy, 2014, 39, 9276-9287.	3.8	8
17899	Vacancy trapping behaviors of hydrogen in Ti3SiC2: A first-principles study. Materials Letters, 2014, 116, 322-327.	1.3	18
17900	The adsorption of Cs and residual gases on Ga0.5Al0.5As (001) Î²2 (2Ã—4) surface: A first principles research. Applied Surface Science, 2014, 290, 142-147.	3.1	15
17901	Formaldehyde molecule adsorbed on doped graphene: A first-principles study. Applied Surface Science, 2014, 293, 216-219.	3.1	49
17902	Heterojunction nanowires having high activity and stability for the reduction of oxygen: Formation by self-assembly of iron phthalocyanine with single walled carbon nanotubes (FePc/SWNTs). Journal of Colloid and Interface Science, 2014, 419, 61-67.	5.0	24
17903	Effect of oxygen vacancy concentration on the absorption spectra of Dy2Ti2O7 crystal. Journal of Alloys and Compounds, 2014, 599, 170-174.	2.8	9
17904	Core structure and dissociation energetics of basal edge dislocation in Î±-Al2O3: A combined atomistic simulation and transmission electron microscopy analysis. Acta Materialia, 2014, 65, 76-84.	3.8	14
17905	First-principles calculations on sulfur interacting with ternary Pdâ€“Ag-transition metal alloy membrane alloys. Journal of Membrane Science, 2014, 453, 525-531.	4.1	16
17906	Hydrogenation induced deformation mode and thermal conductivity variations in graphene sheets. Carbon, 2014, 72, 185-191.	5.4	9
17907	Oxygen vacancy formation and the induced defect states in HfO2 and Hf-silicates â€“ A first principles hybrid functional study. Microelectronics Reliability, 2014, 54, 1119-1124.	0.9	7
17908	Electronic structure and electrical properties of Ba2LaTaO6. Journal of Alloys and Compounds, 2014, 593, 275-282.	2.8	9

#	Article	IF	Citations
17909	First-principles study of the dislocation core structures on basal plane in magnesium. European Journal of Mechanics, A/Solids, 2014, 45, 1-7.	2.1	3
17910	A first-principles study of methyl lactate adsorption on the chiral Cu (643) surface. Surface Science, 2014, 629, 28-34.	0.8	4
17911	Phonon scattering and thermal conductance properties in two coupled graphene nanoribbons modulated with bridge atoms. Physics Letters, Section A: General, Atomic and Solid State Physics, 2014, 378, 1952-1955.	0.9	8
17912	Temperature effects on the generalized planar fault energies and twinnabilities of Al, Ni and Cu: First principles calculations. Computational Materials Science, 2014, 88, 124-130.	1.4	31
17913	Strongly reduced band gap in NiMn2O4 due to cation exchange. Journal of Magnetism and Magnetic Materials, 2014, 358-359, 149-152.	1.0	5
17914	Crystal structure and formation mechanism of (Cr2/3Ti1/3)3AlC2 MAX phase. Acta Materialia, 2014, 73, 186-193.	3.8	146
17915	Structural and crystal chemical properties of rare-earth titanate pyrochlores. Journal of Alloys and Compounds, 2014, 605, 63-70.	2.8	90
17916	Ni-doping effect of Mg(0001) surface to use it as a hydrogen storage material. Journal of Alloys and Compounds, 2014, 609, 93-99.	2.8	10
17917	Maximum energy product at elevated temperatures for hexagonal strontium ferrite (SrFe12O19) magnet. Journal of Magnetism and Magnetic Materials, 2014, 355, 1-6.	1.0	50
17918	A systematic, first-principles study of the structural preference and magnetic properties of mononitrides of the d-block metals. Journal of Alloys and Compounds, 2014, 603, 172-179.	2.8	22
17919	First-principles investigation of the intrinsic defects in Ti3SiC2. Journal of Physics and Chemistry of Solids, 2014, 75, 384-390.	1.9	17
17920	Lithium-doped triazine-based graphitic C3N4 sheet for hydrogen storage at ambient temperature. Computational Materials Science, 2014, 81, 275-279.	1.4	75
17921	DFT study of the adsorption and dissociation of water on Ni(111), Ni(110) and Ni(100) surfaces. Surface Science, 2014, 627, 1-10.	0.8	109
17922	Ab initio study of metastability of Eu3+ defect complexes in GaN. Physica B: Condensed Matter, 2014, 439, 141-143.	1.3	6
17923	Interface structure of nanodiamond composite films: First-principles studies. Journal of Alloys and Compounds, 2014, 599, 183-187.	2.8	9
17924	Structural stability in Aurivillius phases based on ab initio thermodynamics. Journal of Physics and Chemistry of Solids, 2014, 75, 1088-1093.	1.9	3
17925	DFT calculations for SO4/graphene with and without a Pd atom. Computational Materials Science, 2014, 83, 418-425.	1.4	3
17926	Oxygen assisted H2O dissociation on the Pt{110}(1Ã—2) surface from first principles. Surface Science, 2014, 627, 42-48.	0.8	13

#	Article	IF	Citations
17927	First principles study about Fe adsorption on planar SiC nanostructures: Monolayer and nanoribbon. Microelectronic Engineering, 2014, 126, 37-41.	1.1	5
17928	Thermoelectric properties of Au-containing type-I clathrates Ba8AuxGa16â^'3xGe30+2x. Journal of Alloys and Compounds, 2014, 587, 747-754.	2.8	8
17929	Motion of small cross-channel clusters on W(211) surface: A density functional theory study. Applied Surface Science, 2014, 299, 146-155.	3.1	2
17930	First principles study of the electronic structure and magnetism of oxygen-deficient anatase TiO2 (001) surface. Applied Surface Science, 2014, 292, 475-479.	3.1	23
17931	Contributions of dispersion forces to R-3-methylcyclohexanone physisorption on low and high Miller index Cu surfaces. Surface Science, 2014, 629, 35-40.	0.8	7
17932	Influence of Î±-Al2O3 (0001) surface reconstruction on wettability of Al/Al2O3 interface: A first-principle study. Computational Materials Science, 2014, 85, 193-199.	1.4	43
17933	Site occupation of Nb atoms in ternary Niâ€“Tiâ€“Nb shape memory alloys. Acta Materialia, 2014, 74, 85-95.	3.8	36
17934	Nitrogen and Boron substitutional doped zigzag silicene nanoribbons: Ab initio investigation. Physica E: Low-Dimensional Systems and Nanostructures, 2014, 60, 112-117.	1.3	21
17935	Electronic structure and bonding of small Pd clusters on stoichiometric and reduced SnO2(110) surfaces. Vacuum, 2014, 106, 86-93.	1.6	13
17936	Novel high-pressure crystal structures of boron trifluoride. Journal of Physics and Chemistry of Solids, 2014, 75, 1094-1098.	1.9	2
17937	Functionalization of hydrogenated graphene by polylithiated species for efficient hydrogen storage. International Journal of Hydrogen Energy, 2014, 39, 2560-2566.	3.8	40
17938	Electronic and optical properties of C and Nb co-doped anatase TiO2. Computational Materials Science, 2014, 85, 164-171.	1.4	19
17939	First-principles calculations of Ag addition on the diffusion mechanisms of Cuâ€“Fe alloys. Solid State Communications, 2014, 183, 60-63.	0.9	17
17940	He-induced vacancy formation in bcc Fe solid from first-principles simulation. Journal of Nuclear Materials, 2014, 444, 147-152.	1.3	48
17941	Structural and electronic effects of helium interstitials in Y2Ti2O7: A first-principles study. Journal of Nuclear Materials, 2014, 452, 189-196.	1.3	20
17942	Structural evolution and stabilities of (PbTe)n(n=1â€“20) clusters. Computational and Theoretical Chemistry, 2014, 1039, 40-49.	1.1	8
17943	Application of attractive potential by DFT+U to predict the electronic properties of materials without highly localized bands. Computational Materials Science, 2014, 81, 290-295.	1.4	5
17944	Hydrogen atom absorption in hydrogen-covered Pd(110) (1ÂÃ—Â2) missing-row surface. International Journal of Hydrogen Energy, 2014, 39, 6598-6603.	3.8	16

#	Article	IF	Citations
17945	Electronic structure and ionic diffusion of green battery cathode material: Mg2Mo6S8. Solid State Ionics, 2014, 261, 17-20.	1.3	23
17946	Structural and electronic properties of copper nanowires inside zigzag carbon nanotubes. Physica B: Condensed Matter, 2014, 447, 77-82.	1.3	2
17947	Magnetic properties of graphene/BN/Co(111) and potential spintronics. Journal of Magnetism and Magnetic Materials, 2014, 355, 7-11.	1.0	15
17948	Interactions of solute (3 p , 4 p , 5 p and 6 p) with solute, vacancy and divacancy in bcc Fe. Journal of Nuclear Materials, 2014, 455, 68-72.	1.3	13
17949	Synthesis and phase separation of (Ti,Zr)C. Acta Materialia, 2014, 66, 209-218.	3.8	47
17950	Structure and elasticity of phlogopite under compression: Geophysical implications. Physics of the Earth and Planetary Interiors, 2014, 233, 1-12.	0.7	36
17951	Nitrogen atom diffusion into TiO2 anatase bulk via surfaces. Computational Materials Science, 2014, 82, 107-113.	1.4	12
17952	Benefits of oxygen in CuInSe2 and CuGaSe2 containing Se-rich grain boundaries. Physics Letters, Section A: General, Atomic and Solid State Physics, 2014, 378, 1956-1960.	0.9	5
17953	Stability domains of Nb(CN) during the carburization/nitridation of metallic niobium. Ceramics International, 2014, 40, 8911-8914.	2.3	10
17954	The disproportionation reaction phase transition, mechanical, and lattice dynamical properties of the lanthanum dihydrides under highÂpressure: A first principles study. Solid State Sciences, 2014, 32, 76-82.	1.5	9
17955	Modeling of pseudoelasticity via reversible slip in Fe3Ga. Computational Materials Science, 2014, 87, 34-42.	1.4	2
17956	Ferromagnetism in stacked bilayers of Pd/C60. Journal of Magnetism and Magnetic Materials, 2014, 349, 128-134.	1.0	9
17957	Chlorine ion mobility in Cl-mayenite (Ca12Al14O32Cl2): An investigation combining high-temperature neutron powder diffraction, impedance spectroscopy and quantum-chemical calculations. Solid State Ionics, 2014, 254, 48-58.	1.3	33
17958	Density functional study of GaN(0001)/AlN(0001) high electron mobility transistor structures. Journal of Crystal Growth, 2014, 401, 30-32.	0.7	3
17959	A DFT study of adsorption and decomposition of nitroamine molecule on Mg(001) surface. Structural Chemistry, 2014, 25, 409-417.	1.0	8
17960	Elastic and Electronic Properties of Superconducting CaPd 2 As 2 and SrPd 2 As 2 vs. Non-superconducting BaPd 2 As 2. Journal of Superconductivity and Novel Magnetism, 2014, 27, 155-161.	0.8	10
17961	Precipitation in Î± $alpha$ -Fe based Fe-Cu-Ni-Mn-alloys: behaviour of Ni and Mn modelled by ab initio and kinetic Monte Carlo simulations. Applied Physics A: Materials Science and Processing, 2014, 115, 679-687.	1.1	11
17962	Rational design of mixed ionic and electronic conducting perovskite oxides for solid oxide fuel cell anode materials: A case study for doped SrTiO3. Journal of Power Sources, 2014, 245, 875-885.	4.0	19

#	Article	IF	Citations
17963	Solution enthalpy of Po and Te in solid leadâ€“bismuth eutectic. Journal of Nuclear Materials, 2014, 450, 287-291.	1.3	9
17964	Engineering Grain Boundaries in Cu₂ZnSnSe₄ for Better Cell Performance: A Firstâ€Principle Study. Advanced Energy Materials, 2014, 4, 1300712.	10.2	135
17965	Firstâ€principles study of structural, elastic, and electronic properties of M₂₃<scp>C</scp>₆ and <scp>MC</scp> carbides (<scp>M</scp>â€‰=â€‰<scp>R</scp>u, Rh, Pd, Os, Ir, and Pt). Physica Status Solidi (B): Basic Research, 2014, 251, 148-154.	0.7	3
17966	Structural and elastic properties of defect chalcopyrite HgGa2S4 under high pressure. Journal of Alloys and Compounds, 2014, 583, 70-78.	2.8	32
17967	Quantum mechanical calculations on celluloseâ€“water interactions: structures, energetics, vibrational frequencies and NMR chemical shifts for surfaces of Iİ± and Iİ² cellulose. Cellulose, 2014, 21, 909-926.	2.4	27
17968	Structural and electronic properties of armchair graphene nanoribbons under uniaxial strain. Physica E: Low-Dimensional Systems and Nanostructures, 2014, 56, 55-58.	1.3	9
17969	Hierarchical SnO₂ Nanostructures: Recent Advances in Design, Synthesis, and Applications. Chemistry of Materials, 2014, 26, 123-133.	3.2	532
17970	Highly Selective SAMâ€“Nanowire Hybrid NO₂ Sensor: Insight into Charge Transfer Dynamics and Alignment of Frontier Molecular Orbitals. Advanced Functional Materials, 2014, 24, 595-602.	7.8	71
17971	Three-dimensional Wentzel-Kramers-Brillouin approach for the simulation of scanning tunneling microscopy and spectroscopy. Frontiers of Physics, 2014, 9, 711-747.	2.4	14
17972	Stability, composition and properties of Li2FeSiO4 surfaces studied by DFT. Journal of Solid State Electrochemistry, 2014, 18, 1401-1413.	1.2	25
17973	Magnetism in Cu-Doped Rutile SnO2 Semiconductor Induced by the RKKY Interaction. Journal of Superconductivity and Novel Magnetism, 2014, 27, 581-586.	0.8	11
17974	Experimental and theoretical investigations on high-pressure phase transition of Sr2Fe2O5. Physics and Chemistry of Minerals, 2014, 41, 449-459.	0.3	6
17975	Periodic DFT study of structural, electronic, absorption, and thermodynamic properties of crystalline Î±-RDX under hydrostatic compression. Structural Chemistry, 2014, 25, 451-461.	1.0	7
17976	DFT studies on 7-nitrotetrazolo [1,5]furazano[4,5-b]pyridine 1-oxide: crystal structure, detonation properties, sensitivity and effect of hydrostatic compression. Structural Chemistry, 2014, 25, 239-249.	1.0	4
17977	DFT analysis: Fe4 cluster and Fe(110) surface interaction studies with pyrrole, furan, thiophene, and selenophene molecules. Structural Chemistry, 2014, 25, 115-126.	1.0	20
17978	Interplay of the doped Ge atoms and the N vacancies with the negative thermal expansion of M3(Cu1â^'x) Tj ETQq1 1 0.784314 rgBT	1.1	2
17979	Toward high capacity and stable manganese-spinel electrode materials: A case study of Ti-substituted system. Journal of Power Sources, 2014, 245, 570-578.	4.0	59
17980	Stability of spinel Li4Ti5O12 in air. Journal of Power Sources, 2014, 245, 684-690.	4.0	40

#	Article	IF	Citations
17981	Impact of Dynamic Interlayer Interactions on Thermal Conductivity of Ca3Co4O9. Journal of Electronic Materials, 2014, 43, 1905-1915.	1.0	8
17982	Experimental investigation and thermodynamic assessment of the Hfâ€“Ge system. Journal of Materials Science, 2014, 49, 1306-1316.	1.7	0
17983	Properties of interfaces between iron-group metals (Fe, Co, Ni) and HfC via first-principles modeling. Journal of Materials Science, 2014, 49, 407-414.	1.7	8
17984	Thermodynamic Properties of Elements and Compounds in Al-Sc Binary System from Ab Initio Calculations Based on Density Functional Theory. Metallurgical and Materials Transactions A: Physical Metallurgy and Materials Science, 2014, 45, 1720-1735.	1.1	10
17985	Quantum-Chemical Modeling of Energetic Materials. Advances in Quantum Chemistry, 2014, , 71-145.	0.4	24
17986	Surface reconstruction and chemical evolution of stoichiometric layered cathode materials for lithium-ion batteries. Nature Communications, 2014, 5, 3529.	5.8	1,118
17987	Broadband Fewâ€Layer MoS₂ Saturable Absorbers. Advanced Materials, 2014, 26, 3538-3544.	11.1	645
17988	Magnetic properties and origin of the half-metallicity of Ti2MnZ (Z=Al, Ga, In, Si, Ge, Sn) Heusler alloys with the Hg2CuTi-type structure. Journal of Magnetism and Magnetic Materials, 2014, 349, 104-108.	1.0	46
17989	A DFT study of oxygen dissociation on platinum based nanoparticles. Nanoscale, 2014, 6, 1153-1165.	2.8	74
17990	A first-principles study on the role of hydrogen in early stage of graphene growth during the CH4 dissociation on Cu(111) and Ni(111) surfaces. Carbon, 2014, 74, 255-265.	5.4	54
17991	IntrinsicLiNbO3point defects from hybrid density functional calculations. Physical Review B, 2014, 89, .	1.1	36
17992	A possible superhard orthorhombic carbon. Diamond and Related Materials, 2014, 43, 49-54.	1.8	27
17993	Structural stability and topological surface states of the SnTe (111) surface. Physical Review B, 2014, 89, .	1.1	31
17994	First-principles investigation of the structural, mechanical and electronic properties of the NbO-structured 3d, 4d and 5d transition metal nitrides. Computational Materials Science, 2014, 84, 365-373.	1.4	78
17995	Insights into structural and thermodynamic properties of the intermetallic compound in ternary Mgâ€“Znâ€“Cu alloy under high pressure and high temperature. Journal of Alloys and Compounds, 2014, 597, 119-123.	2.8	22
17996	Phase stability and physical properties of technetium borides: A first-principles study. Computational Materials Science, 2014, 82, 86-91.	1.4	14
17997	Selective Trans-Membrane Transport of Alkali and Alkaline Earth Cations through Graphene Oxide Membranes Based on Cationâ^'Ï€ Interactions. ACS Nano, 2014, 8, 850-859.	7.3	333
17998	First-principles study on the elastic properties of Srâ€“Tiâ€“O ceramics. Solid State Communications, 2014, 182, 43-46.	0.9	16

#	Article	IF	Citations
17999	High pressure phase transitions in SnO2 polymorphs by first-principles calculations. Journal of Alloys and Compounds, 2014, 587, 638-645.	2.8	29
18000	Theoretical investigation and design of high-efficiency dithiafulvenyl-based sensitizers for dye-sensitized solar cells: the impacts of elongating Ï€-spacers and rigidifying dithiophene. Physical Chemistry Chemical Physics, 2014, 16, 9458.	1.3	40
18001	The crystallization process of liquid vanadium studied byab initiomolecular dynamics. Journal of Physics Condensed Matter, 2014, 26, 155101.	0.7	12
18002	Mechanical properties and atomistic deformation mechanism of spinel-type BeP2N4. Computational Materials Science, 2014, 83, 457-462.	1.4	10
18003	Vibrational, elastic properties and sound velocities of ZnGa2O4 spinel. Computational Materials Science, 2014, 85, 259-263.	1.4	8
18004	Ab initio study of the structural, elastic, thermodynamic, electronic and vibration properties of TbMg intermetallic compound. Superlattices and Microstructures, 2014, 71, 46-61.	1.4	6
18005	First-principle calculations of structural, elastic and thermodynamic properties of Feâ€“B compounds. Intermetallics, 2014, 46, 211-221.	1.8	72
18006	Coâ€crystallization with Nicotinamide in Two Conformations Lowers Energy but Expands Volume. Journal of Pharmaceutical Sciences, 2014, 103, 2896-2903.	1.6	9
18007	Comparative study of A-site order in the lead-free bismuth titanates M1/2Bi1/2TiO3 (M=Li, Na, K, Rb, Cs,) Tj ETQq0 0 0 rgBT /Overlock 10	1.4	18
18008	Black phosphorus field-effect transistors. Nature Nanotechnology, 2014, 9, 372-377.	15.6	7,071
18009	Incorporating Isolated Molybdenum (Mo) Atoms into Bilayer Epitaxial Graphene on 4H-SiC(0001). ACS Nano, 2014, 8, 970-976.	7.3	23
18010	Theoretical investigation on compressibility, electronic and thermodynamic properties of single crystal PtAs2 under high pressure. Computational Materials Science, 2014, 86, 124-129.	1.4	13
18011	Generating electricity by moving a droplet of ionic liquid along graphene. Nature Nanotechnology, 2014, 9, 378-383.	15.6	488
18012	Experimental Charge Density Study of a Silylone. Angewandte Chemie - International Edition, 2014, 53, 2766-2770.	7.2	115
18013	Impact of the metal substrate on the electronic structure of armchair graphene nanoribbons. Chemical Physics Letters, 2014, 597, 148-152.	1.2	4
18014	Influence of the dislocation core on the glide of the Â½ã€ˆ111ã€‰{110} edge dislocation in bcc-iron: An embedded atom method study. Computational Materials Science, 2014, 87, 274-282.	1.4	16
18015	Breakdown of the Arrhenius Law in Describing Vacancy Formation Energies: The Importance of Local Anharmonicity Revealed byAb initioThermodynamics. Physical Review X, 2014, 4, .	2.8	92
18016	Electronic structure and thermodynamic properties of millerite NiS from first principles: Complex fermi surface and large thermal expansion coefficient. Computational Materials Science, 2014, 83, 412-417.	1.4	12

#	Article	IF	Citations
18017	Vacancy mechanism of oxygen diffusivity in bcc Fe: A first-principles study. Corrosion Science, 2014, 83, 94-102.	3.0	56
18018	Anisotropic Etching of Graphite Flakes with Water Vapor to Produce Armchairâ€Edged Graphene. Small, 2014, 10, 2809-2814.	5.2	23
18019	Influence of alkali cations on the inter-conversion of extra-framework aluminium species in dealuminated zeolites. Microporous and Mesoporous Materials, 2014, 189, 173-180.	2.2	7
18020	Molecular dynamics simulation of liquidâ€“vapor phase diagrams of metals modeled using modified empirical pair potentials. Fluid Phase Equilibria, 2014, 361, 181-187.	1.4	5
18021	Density functional theory in the solid state. Philosophical Transactions Series A, Mathematical, Physical, and Engineering Sciences, 2014, 372, 20130270.	1.6	242
18022	Ab initio study of the anion vacancy on anatase TiO2 (101) surface. Modern Physics Letters B, 2014, 28, 1450076.	1.0	5
18023	Will a graphitic-like ZnO single-layer be an ideal substrate for graphene?. RSC Advances, 2014, 4, 17478.	1.7	16
18024	Vanadium doping of LiMnPO4: Vibrational spectroscopy and first-principle studies. Chemical Physics Letters, 2014, 591, 21-24.	1.2	14
18025	Constructing molecular structures on periodic superstructure of graphene/Ru(0001). Philosophical Transactions Series A, Mathematical, Physical, and Engineering Sciences, 2014, 372, 20130015.	1.6	10
18026	Temperature-dependent mechanical properties of alpha-/beta-Nb5Si3 phases from first-principles calculations. Intermetallics, 2014, 46, 72-79.	1.8	30
18027	Inorganic Doubleâ€Helix Nanotoroid of Simple Lithiumï£¿Phosphorus Species. Chemistry - A European Journal, 2014, 20, 2431-2435.	1.7	15
18028	Efficient hydrogen storage in boron doped graphene decorated by transition metals â€“ A first-principles study. Carbon, 2014, 73, 132-140.	5.4	123
18029	High-capacity hydrogen storage in Li-decorated (AlN)n (nÂ=Â12, 24, 36) nanocages. International Journal of Hydrogen Energy, 2014, 39, 3780-3789.	3.8	39
18030	Dangling bond modulating the electronic and magnetic properties of zigzag SiGe nanoribbon. Physica E: Low-Dimensional Systems and Nanostructures, 2014, 58, 1-5.	1.3	4
18031	Structural, electronic and magnetic properties of C atom doped AlN nanoribbons. Superlattices and Microstructures, 2014, 69, 10-16.	1.4	9
18032	Oxygen vacancy induced carbon deposition at the triple phase boundary of the nickel/yttrium-stabilized zirconia (YSZ) interface. Journal of Power Sources, 2014, 261, 136-140.	4.0	18
18033	Ab initio based study of finite-temperature structural, elastic and thermodynamic properties of FeTi. Intermetallics, 2014, 45, 11-17.	1.8	16
18034	Dynamical magnetic charges and linear magnetoelectricity. Physical Review B, 2014, 89, .	1.1	13

#	Article	IF	Citations
18035	First-principles study of influence of Ti vacancy and Nb dopant on the bonding of TiAl/TiO2 interface. Intermetallics, 2014, 49, 1-6.	1.8	39
18036	Activity and coke formation of nickel and nickel carbide in dry reforming: A deactivation scheme from density functional theory. Journal of Catalysis, 2014, 311, 469-480.	3.1	231
18037	Quantum molecular dynamics study of warm dense iron. Physical Review E, 2014, 89, 023101.	0.8	13
18038	Adsorption of hydrazine on the perfect and defective copper (111) surface: A dispersion-corrected DFT study. Surface Science, 2014, 622, 1-8.	0.8	76
18039	DFT computational study of the RGD peptide interaction with the rutile TiO2 (110) surface. Surface Science, 2014, 624, 8-14.	0.8	30
18040	Kondo effect of a cobalt adatom on a zigzag graphene nanoribbon. Physical Review B, 2014, 89, .	1.1	19
18041	Chromium coordination compounds with bis(3,5-dimethylpyrazol-1-yl)acetic acid or its anion. Polyhedron, 2014, 70, 119-124.	1.0	2
18042	Reaction Mechanism for Direct Propylene Epoxidation by Alumina-Supported Silver Aggregates: The Role of the Particle/Support Interface. ACS Catalysis, 2014, 4, 32-39.	5.5	82
18043	Shedding light on the self-assembly of stable SiC based cage nanostructures: A comprehensive molecular dynamics study. Computational Materials Science, 2014, 84, 49-62.	1.4	5
18044	Design of ferromagnetism in Co-doped SnO2 nanosheets: a first-principles study. RSC Advances, 2014, 4, 9602.	1.7	17
18045	Electronic Chemical Potentials of Porous Metalâ€“Organic Frameworks. Journal of the American Chemical Society, 2014, 136, 2703-2706.	6.6	262
18046	Bonds, bands, and band gaps in tetrahedrally bonded ternary compounds: The role of group V lone pairs. Journal of Physics and Chemistry of Solids, 2014, 75, 477-485.	1.9	27
18047	Density functional theory investigation of the electronic structure and thermoelectric properties of layered MoS2, MoSe2 and their mixed-layer compound. Journal of Solid State Chemistry, 2014, 211, 113-119.	1.4	40
18048	First principles calculations in Vâ€“Si system. Defects in A15-V3Si phase. Computational Materials Science, 2014, 85, 94-101.	1.4	9
18049	Interplay between Subnanometer Ag and Pt Clusters and Anatase TiO2 (101) Surface: Implications for Catalysis and Photocatalysis. Journal of Physical Chemistry C, 2014, 118, 4702-4714.	1.5	38
18050	Spin-dependent optical response of multiferroic EuO: First-principles DFT calculations. Physical Review B, 2014, 89, .	1.1	21
18051	Defective Graphene as a High-Capacity Anode Material for Na- and Ca-Ion Batteries. ACS Applied Materials & Interfaces, 2014, 6, 1788-1795.	4.0	365
18052	Methane Storage in Metal-Substituted Metalâ€“Organic Frameworks: Thermodynamics, Usable Capacity, and the Impact of Enhanced Binding Sites. Journal of Physical Chemistry C, 2014, 118, 2929-2942.	1.5	43

#	Article	IF	Citations
18053	Understanding the reactivity of metallic nanoparticles: beyond the extended surface model for catalysis. Chemical Society Reviews, 2014, 43, 4922-4939.	18.7	156
18054	Effect of Grain Boundary Stresses on Sink Strength. Materials Research Letters, 2014, 2, 100-106.	4.1	51
18055	Band structure engineering of CdSe nanosheet by strain: A first-principles study. Chemical Physics Letters, 2014, 595-596, 91-96.	1.2	5
18056	Atomistic simulation of stacking faults in (001), (010), and (100) planes of cementite. Physics of Metals and Metallography, 2014, 115, 85-97.	0.3	13
18057	First-principles study of the phonon dispersion and dielectric properties of wurtzite InP: Role of In<mml:math xmlns:mml="http://www.w3.org/1998/Math/MathML"><mml:mi>4</mml:mi><mml:mi>d</mml:mi></mml:math>electrons. Physical Review B, 2014, 89, .	1.1	13
18058	Protected Surface States and a Superconducting Phase in<mml:math xmlns:mml="http://www.w3.org/1998/Math/MathML" display="inline"><mml:mrow><mml:mo stretchy="false">[</mml:mo><mml:msub><mml:mrow><mml:mi>Tl</mml:mi></mml:mrow><mml:mrow><mml:mn>4</mml:mn></mml:m stretchy="false">]</mml:mo><mml:mo		

#	Article	IF	Citations
18071	Structural and electronic properties of chiral single-wall copper nanotubes. Science China: Physics, Mechanics and Astronomy, 2014, 57, 644-651.	2.0	6
18072	Spinâ€“orbit effects on the structural, homotop, and magnetic configurations of small pure and Fe-doped Pt clusters. Journal of Nanoparticle Research, 2014, 16, 1.	0.8	8
18073	The search for the good Pd-based catalyst for oxygen reduction reaction: coreâ€“shell M4@Pd20 nanowires. Journal of Nanoparticle Research, 2014, 16, 1.	0.8	5
18074	Soft picosecond X-ray laser nanomodification of gold and aluminum surfaces. Applied Physics B: Lasers and Optics, 2014, 116, 1005-1016.	1.1	26
18075	Theoretical investigation of the structure and properties of the VN(111) monolayer on the MgO(111) surface. Physics of the Solid State, 2014, 56, 229-234.	0.2	6
18076	Density Functional Study of the Î²â€³ Phase in Al-Mg-Si Alloys. Metallurgical and Materials Transactions A: Physical Metallurgy and Materials Science, 2014, 45, 2916-2924.	1.1	20
18077	Nitrogen-doped graphene as an excellent candidate for selective gas sensing. Science China Chemistry, 2014, 57, 911-917.	4.2	55
18078	Crystal structure and magnetic properties of CuSb2O4. Journal of Materials Science, 2014, 49, 3497-3510.	1.7	11
18079	Ab initio perspective of the âŒ©110âŒª symmetrical tilt grain boundaries in bcc Fe: application of local energy and local stress. Journal of Materials Science, 2014, 49, 3980-3995.	1.7	41
18080	Ferromagnetism Induced by As Doping in ZnO: First-Principles Calculations. Journal of Superconductivity and Novel Magnetism, 2014, 27, 835-838.	0.8	1
18081	High Mg effective incorporation in Al-rich Al x Ga1 - xN by periodic repetition of ultimate V/III ratio conditions. Nanoscale Research Letters, 2014, 9, 40.	3.1	23
18082	Electronic band structure, Fermi surface, structural and elastic properties of two polymorphs of MgFeSeO as possible new superconducting systems. JETP Letters, 2014, 98, 609-613.	0.4	0
18083	A theoretical study of possible point defects incorporated into Î±-alumina deposited by chemical vapor deposition. Theoretical Chemistry Accounts, 2014, 133, 1.	0.5	4
18084	Theoretical study on the adsorption mechanism of iodine molecule on platinum surface in dye-sensitized solar cells. Theoretical Chemistry Accounts, 2014, 133, 1.	0.5	13
18085	A DFT study of vibrational frequencies and 13C NMR chemical shifts of model cellulosic fragments as a function of size. Cellulose, 2014, 21, 53-70.	2.4	21
18086	An approximate eigensolver for self-consistent field calculations. Numerical Algorithms, 2014, 66, 609-641.	1.1	1
18087	Novel metalâ€“organic framework linkers for light harvesting applications. Chemical Science, 2014, 5, 2081-2090.	3.7	152
18088	Linking Interfacial Step Structure and Chemistry with Locally Enhanced Radiationâ€Induced Amorphization at Oxide Heterointerfaces. Advanced Materials Interfaces, 2014, 1, 1300142.	1.9	25

#	Structure of the Co/Si(111) <mml:math altimg="si10.gif" overflow="scroll" xmlns:xocs="http://www.elsevier.com/xml/xocs/dtd" xmlns:xs="http://www.w3.org/2001/XMLSchema" xmlns:xsi="http://www.w3.org/2001/XMLSchema-instance" xmlns="http://www.elsevier.com/xml/ja/dtd" xmlns:ja="http://www.elsevier.com/xml/ja/dtd" xmlns:mml="http://www.w3.org/1998/Math/MathML" xmlns:tb="http://www.elsevier.com/xml/common/table/dtd" xmlns:sb="http://www.elsevier.com/xml/common/struct-bib/dtd" xmlns:ce="http://www.elsevier.com/x	IF	Citations
18089		0.8	4
18090	Intrinsic insulating ferromagnetism in manganese oxide thin films. Physical Review B, 2014, 89, .	1.1	47
18091	Vibrational zero point energy for H-doped silicon. Chemical Physics Letters, 2014, 601, 49-53.	1.2	4
18092	Strain-induced magnetism in MoS2 monolayer with defects. Journal of Applied Physics, 2014, 115, .	1.1	112
18093	Metallization and superconductivity of BeH2 under high pressure. Journal of Chemical Physics, 2014, 140, 124707.	1.2	50
18094	The segregation behavior of manganese and silicon at the coherent interfaces of copper precipitates in ferritic steels. Journal of Nuclear Materials, 2014, 445, 43-49.	1.3	12
18095	Adsorption and energetics of H2O molecules and O atoms on the Ï‡-Fe5C2 (111), (â^’411) and (001) surfaces from DFT. Applied Catalysis A: General, 2014, 475, 186-194.	2.2	14
18096	Tuning the electronic and optical properties of monatomic carbon chains. Carbon, 2014, 68, 487-492.	5.4	14
18097	Critic2: A program for real-space analysis of quantum chemical interactions in solids. Computer Physics Communications, 2014, 185, 1007-1018.	3.0	497
18098	Mechanism of excitonic dephasing in layered InSe crystals. Physical Review B, 2014, 89, .	1.1	23
18099	Experimental and DFT study on the catalytic asymmetric hydrogenation performance of (1S,2S)-DPEN-Ru(TPP)2 encapsulated in zeolite. Journal of Molecular Catalysis A, 2014, 385, 85-90.	4.8	5
18100	K6 carbon: A metallic carbon allotrope in sp3 bonding networks. Journal of Chemical Physics, 2014, 140, 054514.	1.2	52
18101	First-principles study of high-pressure crystal structures and superconductivity of Li3Be alloy. Computational Materials Science, 2014, 88, 45-49.	1.4	0
18102	Enhanced magnetic anisotropy in cobalt-carbide nanoparticles. Applied Physics Letters, 2014, 104, 023111.	1.5	44
18103	Formation of two-dimensional uranium silicide film and its electronic structure study. Physica B: Condensed Matter, 2014, 436, 215-219.	1.3	4
18104	Selective semi-hydrogenation of acetylene: Atomistic scenario for reactions on the polar threefold surfaces of GaPd. Journal of Catalysis, 2014, 312, 232-248.	3.1	41
18105	Generalized BrÃ¸nstedâ€“Evansâ€“Polanyi relationships and descriptors for Oâ€“H bond cleavage of organic molecules on transition metal surfaces. Journal of Catalysis, 2014, 313, 24-33.	3.1	42
18106	Lattice dynamics of cubic AuZn from first principles. Physical Review B, 2014, 89, .	1.1	4

#	Article	IF	Citations
18107	Chemical routes to modify, uplift, and detach a silicene layer from a metal substrate. Physical Chemistry Chemical Physics, 2014, 16, 5183.	1.3	21
18108	Amorphous LiLaTiO₃as Solid Electrolyte Material. Journal of the Electrochemical Society, 2014, 161, A473-A479.	1.3	41
18109	Mechanical properties and electronic structure of anti-ReO3 structured cubic nitrides, M3N, of d block transition metals M: An ab initio study. Journal of Alloys and Compounds, 2014, 595, 80-86.	2.8	55
18110	Quantum Anomalous Hall Effect in Graphene Proximity Coupled to an Antiferromagnetic Insulator. Physical Review Letters, 2014, 112, 116404.	2.9	361
18111	Kinetics of Catalytic Dehydrogenation of Propane over Pt-Based Catalysts. Advances in Chemical Engineering, 2014, 44, 61-125.	0.5	17
18112	Density functional study of the mechanical and phonon properties of Al12X (XÂ=ÂMo, Tc, Ru, W, Re, and) Tj ETQq1 1 0.784314 rgBT	1.8	13
18113	Hydrogen storage on calcium-decorated BC7 sheet: A first-principles study. International Journal of Hydrogen Energy, 2014, 39, 2142-2148.	3.8	25
18114	High pressure studies of terbium trihydride. X-ray, Raman and DFT investigations. Journal of Alloys and Compounds, 2014, 597, 58-62.	2.8	4
18115	Geometric ferroelectricity in fluoroperovskites. Physical Review B, 2014, 89, .	1.1	61
18116	Mechanisms of the paraelectric to ferroelectric phase transition in RbH<mml:math xmlns:mml="http://www.w3.org/1998/Math/MathML"><mml:msub><mml:mrow /><mml:mn>2</mml:mn></mml:msub></mml:math>PO<mml:math xmlns:mml="http://www.w3.org/1998/Math/MathML"><mml:msub><mml:mrow /><mml:mn>4</mml:mn></mml:msub></mml:math>probed by purely resonant x-ray diffraction. Physical Review B, 2014, 89, .	1.1	12
18117	Photocatalytic hydrogen production with visible light over Mo and Cr-doped BiNb(Ta)O4. International Journal of Hydrogen Energy, 2014, 39, 1220-1227.	3.8	24
18118	Thermodynamic modeling and first-principles calculations of the Moâ€“O system. Calphad: Computer Coupling of Phase Diagrams and Thermochemistry, 2014, 45, 178-187.	0.7	30
18119	Theoretical prediction and experimental verification of low loading of platinum on titanium carbide as low-cost and stable electrocatalysts. Journal of Catalysis, 2014, 312, 216-220.	3.1	56
18120	Investigating the Gas Sorption Mechanism in an rht-Metalâ€“Organic Framework through Computational Studies. Journal of Physical Chemistry C, 2014, 118, 439-456.	1.5	40
18121	Mechanistic investigation of the cis/trans isomerization of 2-butene on Pt(111): DFT study of the influence of the hydrogen coverage. Journal of Catalysis, 2014, 311, 190-198.	3.1	23
18122	Epitaxial growth of gold on Si(001). Surface Science, 2014, 624, 15-20.	0.8	8
18123	Gd doped Au nanoclusters: Molecular magnets with novel properties. Chemical Physics Letters, 2014, 592, 217-221.	1.2	4
18124	Phase transition and thermodynamic properties of beryllium from first-principles calculations. Computational Materials Science, 2014, 84, 139-144.	1.4	15

#	Article	IF	Citations
18125	Ab-initio calculation of electronic and optical properties of nitrogen and boron doped graphene nanosheet. Carbon, 2014, 73, 275-282.	5.4	165
18126	New insights into the properties and interactions of carbon chains as revealed by HRTEM and DFT analysis. Carbon, 2014, 66, 436-441.	5.4	58
18127	Identification of the active Cu site in standard selective catalytic reduction with ammonia on Cu-SSZ-13. Journal of Catalysis, 2014, 312, 87-97.	3.1	286
18128	The nitrogen vacancy and oxygen substitution of OsN2: First-principles investigation. Journal of Alloys and Compounds, 2014, 590, 27-32.	2.8	1
18129	Ferromagnetic (Mn, N)-codoped ZnO nanopillars array: Experimental and computational insights. Applied Physics Letters, 2014, 104, 022412.	1.5	59
18130	Investigation of the adsorption of amino acids on Pd(111): A density functional theory study. Applied Surface Science, 2014, 301, 199-207.	3.1	13
18131	Thermoelectric properties of atomically thin silicene and germanene nanostructures. Physical Review B, 2014, 89, .	1.1	164
18132	Hydrogen defects in tetragonal ZrO₂studied using density functional theory. Physical Chemistry Chemical Physics, 2014, 16, 1354-1365.	1.3	36
18133	Post-annealing effects on structural and magnetic properties of Mnâ€“N codoped ZnO thin films. Materials Science in Semiconductor Processing, 2014, 21, 52-57.	1.9	7
18134	Unusual defect physics in CH3NH3PbI3 perovskite solar cell absorber. Applied Physics Letters, 2014, 104, .	1.5	2,142
18135	van der Waals trilayers and superlattices: modification of electronic structures of MoS₂ by intercalation. Nanoscale, 2014, 6, 4566-4571.	2.8	111
18136	Electronic structures and mechanical properties of iron borides from first principles. Solid State Communications, 2014, 187, 28-32.	0.9	18
18137	On equation of state, elastic, and lattice dynamic stability of bcc bismuth under high pressure: Ab-initio calculations. Journal of Applied Physics, 2014, 115, .	1.1	11
18138	Controlling the CO oxidation rate over Pt/TiO2 catalysts by defect engineering of the TiO2 support. Journal of Catalysis, 2014, 311, 306-313.	3.1	71
18139	Gap opening and tuning of the electronic instability in Au intercalated bilayer graphene. Carbon, 2014, 71, 76-86.	5.4	9
18140	Influence of Electronic Type Purity on the Lithiation of Single-Walled Carbon Nanotubes. ACS Nano, 2014, 8, 2399-2409.	7.3	16
18141	Resonant Raman scattering of graphite intercalation compounds KC₈, KC₂₄, and KC₃₆. Journal of Raman Spectroscopy, 2014, 45, 219-223.	1.2	15
18142	Electrocatalysis of oxygen reduction with platinum supported on molybdenum carbideâ€“carbon composite. Journal of Electroanalytical Chemistry, 2014, 720-721, 34-40.	1.9	42

#	Article	IF	Citations
18143	The role of cerium in the improved SO2 tolerance for NO reduction with NH3 over Mn-Ce/TiO2 catalyst at low temperature. Applied Catalysis B: Environmental, 2014, 148-149, 582-588.	10.8	332
18144	Theoretical and kinetic assessment of the mechanism of ethane hydrogenolysis on metal surfaces saturated with chemisorbed hydrogen. Journal of Catalysis, 2014, 311, 350-356.	3.1	55
18145	Unveiling the Atomic Structure of Singleâ€Wall Boron Nanotubes. Advanced Functional Materials, 2014, 24, 4127-4134.	7.8	29
18146	NO oxidation: A probe reaction on Cu-SSZ-13. Journal of Catalysis, 2014, 312, 179-190.	3.1	155
18147	Experimental investigation and thermodynamic analysis of the Scâ€“Ni system supplemented with first-principles calculations. Thermochimica Acta, 2014, 586, 30-39.	1.2	13
18148	Single molecule tunneling spectroscopy investigation of reversibly switched dipolar vanadyl phthalocyanine on graphite. Applied Physics Letters, 2014, 104, .	1.5	13
18149	Probing Weak Intermolecular Interactions by Using the Invariom Approach: A Comparative Study of sâ€Tetrazine. Chemistry - A European Journal, 2014, 20, 6978-6984.	1.7	20
18150	CO adsorption on Pt clusters supported on graphite. Journal of Electroanalytical Chemistry, 2014, 716, 23-30.	1.9	18
18151	Electric field as a novel switch for magnetization of Fe/graphene system. Journal of Magnetism and Magnetic Materials, 2014, 362, 93-96.	1.0	11
18152	Structural, elastic, and thermal properties of cementite (<mml:math) Tj ETQq1 1 0.784314 rgBT /Overlock 10 Tf 50 387 Td (xmlns:mml= calculated using a modified embedded atom method. Physical Review B, 2014, 89, .	1.1	81
18153	Density functional investigation of why Ba 2 BiFeS 5 and Ba 2 SbFeS 5 differ in their magnetic properties. Journal of Magnetism and Magnetic Materials, 2014, 360, 152-156.	1.0	0
18154	Quantum modelling of hydrogen chemisorption on graphene and graphite. Journal of Chemical Physics, 2014, 140, 124702.	1.2	18
18155	Degenerate Perturbation in Band-Gap Opening of Graphene Superlattice. Journal of Physical Chemistry C, 2014, 118, 8174-8180.	1.5	15
18156	Hybrid density functional investigations of Li2MSiO4 (M=Mn, Fe and Co) cathode materials. Computational Materials Science, 2014, 83, 45-50.	1.4	14
18157	Alkali metal adsorption on Ge(001)-c(2Ã—4) surface: 0.25 monolayer of Na, K, Rb and Cs. Applied Surface Science, 2014, 301, 112-118.	3.1	0
18158	Field-regulated switching of the magnetization of Co-porphyrin on graphene. Physical Review B, 2014, 89, .	1.1	17
18159	Stable surface terminations of orthorhombic Mo2C catalysts and their CO activation mechanisms. Applied Catalysis A: General, 2014, 478, 146-156.	2.2	37
18160	Homologous series of layered structures in binary and ternary Bi-Sb-Te-Se systems:Ab initiostudy. Physical Review B, 2014, 89, .	1.1	5

#	Article	IF	Citations
18161	Tuning electronic and magnetic properties of armchair|zigzag hybrid graphene nanoribbons by the choice of supercell model of grain boundaries. Journal of Applied Physics, 2014, 115, 104303.	1.1	10
18162	Strain engineering of selective chemical adsorption on monolayer MoS₂. Nanoscale, 2014, 6, 5156-5161.	2.8	177
18163	Crystal electron binding energy and surface work function control of tin dioxide. Physical Review B, 2014, 89, .	1.1	48
18164	Atomistic modeling of intrinsic and radiation-enhanced fission gas (Xe) diffusion in <mml:math xmlns:mml="http://www.w3.org/1998/Math/MathML" altimg="si236.gif" overflow="scroll"><mml:mrow><mml:msub><mml:mrow><mml:mi mathvariant="normal">UO</mml:mi></mml:mrow><mml:mrow><mml:mn>2</mml:mn><mml:mo>Â±</mml:mo><mml:mi>x</mml:mi></mml:mrow></mml:msub></mml:mrow></mml:math> Implications for nuclear fuel performance modeling. Journal of Nuclear Materials, 2014, 451, 225-242.	1.3	83
18165	Pressureâ€“composition phase diagram of Tiâ€“<scp>C</scp> from first principles. Physica Status Solidi (B): Basic Research, 2014, 251, 533-536.	0.7	11
18166	On the origin of the significant difference in lithiation behavior between silicon and germanium. Journal of Power Sources, 2014, 263, 252-258.	4.0	44
18168	Highâ€Performance Pseudocubic Thermoelectric Materials from Nonâ€cubic Chalcopyrite Compounds. Advanced Materials, 2014, 26, 3848-3853.	11.1	269
18169	Topological domain walls and quantum valley Hall effects in silicene. Physical Review B, 2014, 89, .	1.1	59
18170	Using the electron localization function to correct for confinement physics in semi-local density functional theory. Journal of Chemical Physics, 2014, 140, 18A536.	1.2	18
18171	DFT study of optical properties of pure and doped graphene. Physica E: Low-Dimensional Systems and Nanostructures, 2014, 62, 28-35.	1.3	159
18172	Sn1â^'xTixS2 ternary alloys: A new visible optical material. Acta Materialia, 2014, 72, 223-228.	3.8	29
18173	Theoretical study of <mml:math xmlns:mml="http://www.w3.org/1998/Math/MathML" altimg="si30.gif" overflow="scroll"><mml:mrow><mml:msub><mml:mrow><mml:mi mathvariant="italic">Ga</mml:mi></mml:mrow><mml:mrow><mml:mn>2</mml:mn></mml:mrow></mml:msub><mml:msub><mml:mi mathvariant="italic">Se</mml:mi></mml:mrow><mml:mrow><mml:mn>3</mml:mn></mml:mrow></mml:msub><mml:mtext>,</mml:mtext><mml:msub><mml:mi mathvariant="italic">Ga</mml:mi></mml:mrow><mml:mrow><mml:mn>2</mml:mn></mml:mrow></mml:msub><m. Acta Materialia, 2014, 71, 349-369.	3.8	16
18174	Calculations of complex surface structures based on the example of (4Ã—2) InAs (001). Surface Science, 2014, 623, 41-46.	0.8	1
18175	A DFT study of the stoichiometric and reduced anatase (001) surfaces. Applied Surface Science, 2014, 294, 42-48.	3.1	23
18176	First-principles study on armchair AlN nanoribbons with different edge terminations. Superlattices and Microstructures, 2014, 67, 40-46.	1.4	23
18177	First-principles thermal conductivity of warm-dense deuterium plasmas for inertial confinement fusion applications. Physical Review E, 2014, 89, 043105.	0.8	69
18178	Silicene-derived phases on Ag(111) substrate versus coverage:Ab initiostudies. Physical Review B, 2014, 89, .	1.1	60
18179	First-principles study of 4d solute diffusion in nickel. Journal of Materials Science, 2014, 49, 4038-4044.	1.7	17

#	Article	IF	Citations
18180	Structural, vibrational, and quasiparticle band structure of 1,1-diamino-2,2-dinitroethelene from ab initio calculations. Journal of Chemical Physics, 2014, 140, 014105.	1.2	39
18181	From Ag2Sb2O6 to Cd2Sb2O7: Investigations on an anion-deficient to ideal pyrochlore solid solution. Journal of Solid State Chemistry, 2014, 210, 65-73.	1.4	8
18182	First-principles reaction site model for coverage-sensitive surface reactions: Pt(111)â€“O temperature programmed desorption. Surface Science, 2014, 622, L1-L6.	0.8	24
18183	N-doped graphene as catalysts for oxygen reduction and oxygen evolution reactions: Theoretical considerations. Journal of Catalysis, 2014, 314, 66-72.	3.1	537
18184	Elastic and mechanical properties of intrinsic and doped PbSe and PbTe studied by first-principles. Materials Chemistry and Physics, 2014, 146, 472-477.	2.0	19
18185	Transport properties of graphene/metal planar junction. Physics Letters, Section A: General, Atomic and Solid State Physics, 2014, 378, 1321-1325.	0.9	14
18186	First-principles study on surface structure, thickness and composition dependence of the stability of Pt-skin/Pt3Co oxygen-reduction-reaction catalysts. Journal of Power Sources, 2014, 247, 562-571.	4.0	22
18187	Structural tristability and deep Dirac states in bilayer silicene on Ag(111) surfaces. Physical Review B, 2014, 89, .	1.1	58
18188	Carbon Support Effects on the Hydrogen Storage Properties of LiBH₄ Nanoparticles: A First-Principles Study. Journal of Physical Chemistry C, 2014, 118, 5102-5109.	1.5	12
18189	Effects of hole localization on limiting p-type conductivity in oxide and nitride semiconductors. Journal of Applied Physics, 2014, 115, 012014.	1.1	55
18190	Confinement of Dirac electrons in graphene quantum dots. Physical Review B, 2014, 89, .	1.1	36
18191	Energetics and diffusion of gold in bismuth telluride-based thermoelectric compounds. Journal of Applied Physics, 2014, 115, 063705.	1.1	16
18192	Hydrogen Adsorption Structures and Energetics on Iron Surfaces at High Coverage. Journal of Physical Chemistry C, 2014, 118, 4181-4188.	1.5	84
18193	Oxygen vacancy formation and the ion migration mechanism in layered perovskite (Sr,La)₃Fe₂O_{7â^Î´}. Physical Chemistry Chemical Physics, 2014, 16, 10875-10882.	1.3	43
18194	Electrical and optical properties of fluid iron from compressed to expanded regime. Physics of Plasmas, 2014, 21, 032711.	0.7	5
18195	The adsorption of NO on YSZ(111) and oxygen-enriched YSZ(111) surfaces. Chemical Physics Letters, 2014, 593, 61-68.	1.2	3
18196	Atomistic spin model simulations of magnetic nanomaterials. Journal of Physics Condensed Matter, 2014, 26, 103202.	0.7	542
18197	Sulfur dioxide molecule sensors based on zigzag graphene nanoribbons with and without Cr dopant. Physics Letters, Section A: General, Atomic and Solid State Physics, 2014, 378, 667-671.	0.9	38

#	Article	IF	Citations
18198	Photocatalytic Water Splitting under Visible Light by Mixed-Valence Sn₃O₄. ACS Applied Materials & Interfaces, 2014, 6, 3790-3793.	4.0	148
18199	Atomistic Origins of High-Performance in Hybrid Halide Perovskite Solar Cells. Nano Letters, 2014, 14, 2584-2590.	4.5	2,068
18200	Impact of local strain on Ti-L_{2,3}electron energy-loss near-edge structures of BaTiO₃: a first-principles multiplet study. Microscopy (Oxford, England), 2014, 63, 249-254.	0.7	10
18201	The stability, magnetism and electronic structure of Fe15TMN2 and Fe14TM2N2 (TM=Cr, Mn, Co, and Ni). Journal of Magnetism and Magnetic Materials, 2014, 364, 1-4.	1.0	13
18202	Computational study of hydrogen induced lattice rearrangement and its influence on hydrogen permeance in Pdâ€“Au alloys. Journal of Alloys and Compounds, 2014, 609, 244-252.	2.8	12
18203	Designing a robustly metallic noncenstrosymmetric ruthenate oxide with large thermopower anisotropy. Nature Communications, 2014, 5, 3432.	5.8	134
18204	Ab initio atomistic thermodynamics study on the sulfur tolerance mechanism of the oxygen-enriched yttria-stabilized zirconia surface. Surface Science, 2014, 622, 16-23.	0.8	1
18205	Energetics and configurations of Heâ€“He pair in vacancy of transition metals. Nuclear Instruments & Methods in Physics Research B, 2014, 322, 34-40.	0.6	9
18206	Interaction of carbonâ€“vacancy complex with minor alloying elements of ferritic steels. Journal of Nuclear Materials, 2014, 451, 82-87.	1.3	29
18207	Interlayer coupling enhancement in graphene/hexagonal boron nitride heterostructures by intercalated defects or vacancies. Journal of Chemical Physics, 2014, 140, 134706.	1.2	52
18208	Semimetallic Two-Dimensional Boron Allotrope with Massless Dirac Fermions. Physical Review Letters, 2014, 112, .	2.9	497
18209	Reducing Lattice Thermal Conductivity of the Thermoelectric Compound AgSbTe2 (P4/mmm) by Lanthanum Substitution: Computational and Experimental Approaches. Journal of Electronic Materials, 2014, 43, 3772-3779.	1.0	19
18210	Effect of WN content on toughness enhancement in V1â^'xWxN/MgO(001) thin films. Journal of Vacuum Science and Technology A: Vacuum, Surfaces and Films, 2014, 32, .	0.9	45
18211	Electronic structure engineering in chemically modified ultrathin ZnO nanofilms via a built-in heterointerface. RSC Advances, 2014, 4, 18718-18723.	1.7	7
18212	Waving potential in graphene. Nature Communications, 2014, 5, 3582.	5.8	246
18213	Self-assembled ultrathin nanotubes on diamond (100) surface. Nature Communications, 2014, 5, 3666.	5.8	164
18214	Hydrogen storage in TiO2 functionalized (10, 10) single walled carbon nanotube (SWCNT) â€“ First principles study. International Journal of Hydrogen Energy, 2014, 39, 4973-4980.	3.8	26
18215	Vapor Phase Growth and Imaging Stacking Order of Bilayer Molybdenum Disulfide. Journal of Physical Chemistry C, 2014, 118, 9203-9208.	1.5	47

#	Article	IF	Citations
18216	Dye Self-Association Identified by Intermolecular Couplings between Vibrational Modes As Revealed by Infrared Spectroscopy, and Implications for Electron Injection. Journal of Physical Chemistry C, 2014, 118, 5854-5861.	1.5	33
18217	Polymorphism of Paracetamol: A New Understanding of Molecular Flexibility through Local Methyl Dynamics. Molecular Pharmaceutics, 2014, 11, 1032-1041.	2.3	26
18218	Vibrationally Promoted Dissociation of Water on Ni(111). Science, 2014, 344, 504-507.	6.0	175
18219	Comment on â€œLiH as a Li+ and Hâ¯ ion provider by Khang Hoang, Chris G. Van de Walle, Solid State Ionics 253 (2013) 53â€•. Solid State Ionics, 2014, 261, 26-27.	1.3	20
18220	From the Lindlar Catalyst to Supported Ligandâ€Modified Palladium Nanoparticles: Selectivity Patterns and Accessibility Constraints in the Continuousâ€Flow Threeâ€Phase Hydrogenation of Acetylenic Compounds. Chemistry - A European Journal, 2014, 20, 5926-5937.	1.7	141
18221	LSDA+U calculations of the electronic and optical properties of rutile TiO2(110) vs (011)-2Ã—1 surfaces. Computational Materials Science, 2014, 90, 1-6.	1.4	4
18222	First-principles study of a single Fe-chain doped zigzag AlN nanoribbons. Superlattices and Microstructures, 2014, 69, 136-143.	1.4	2
18223	Partially oxidized gold nanoparticles: A catalytic base-free system for the aerobic homocoupling of alkynes. Journal of Catalysis, 2014, 315, 6-14.	3.1	30
18224	Designing pâ€Type Semiconductorâ€“Metal Hybrid Structures for Improved Photocatalysis. Angewandte Chemie - International Edition, 2014, 53, 5107-5111.	7.2	176
18225	Adsorption of perfluoropentacene on aluminum (100) surface: Structural and electronic properties from first principle study. Computational Materials Science, 2014, 89, 216-223.	1.4	2
18226	DFT Simulations of Water Adsorption and Activation on Lowâ€Index Î±â€Ga₂O₃ Surfaces. Chemistry - A European Journal, 2014, 20, 6915-6926.	1.7	32
18227	Novel electronic structures of superlattice composed of graphene and silicene. Materials Research Bulletin, 2014, 50, 268-272.	2.7	12
18228	Band-gap engineering in fluorographene nanoribbons under uniaxial strain. Journal of Applied Physics, 2014, 115, 044305.	1.1	5
18229	First principles study of electronic structure, structural and optical properties of Mg3Si2O5(OH)4. Applied Clay Science, 2014, 93-94, 8-11.	2.6	6
18230	Atomic-scale analysis of liquid-gallium embrittlement of aluminum grain boundaries. Acta Materialia, 2014, 73, 312-325.	3.8	105
18231	Integrating computational modeling and first-principles calculations to predict stacking fault energy of dilute multicomponent Ni-base alloys. Computational Materials Science, 2014, 91, 50-55.	1.4	17
18232	Armchair graphene nanoribbons under shear strain. Physica E: Low-Dimensional Systems and Nanostructures, 2014, 60, 156-159.	1.3	7
18233	Propane ammoxidation over Moâ€“Vâ€“Teâ€“Nbâ€“O M1 phase: Density functional theory study of propane oxidative dehydrogenation steps. Catalysis Today, 2014, 238, 28-34.	2.2	21

#	Article	IF	Citations
18234	The wurtziteâ€“rocksalt phase transition for a BexMgyZn1â^'xâ^'yO alloy: Be content vs Mg content. Journal of Alloys and Compounds, 2014, 608, 197-201.	2.8	6
18235	Growth Mechanism of Metal Clusters on a Graphene/Ru(0001) Template. Advanced Materials Interfaces, 2014, 1, 1300104.	1.9	24
18236	Study on structural, electronic and magnetic properties of Sn atom adsorbed on defective graphene by first-principle calculations. Applied Surface Science, 2014, 307, 158-164.	3.1	29
18237	Structures and catalytic properties of Pdm(Au)n (m+n=4) clusters supported on MgO(100) surface. altimg="si1.gif" overflow="scroll"><mml:msub><mml:mrow><mml:mi mathvariant="normal">Pd</mml:mi></mml:mrow><mml:mrow><mml:mi>m</mml:mi></mml:mrow></mml:msub><mml:msub><mml:m mathvariant="normal">Au</mml:mi></mml:mrow><mml:mrow><mml:mi>n</mml:mi></mml:mrow></mml:msub></mml:math>		

#	Article	IF	Citations
18252	Perfect spin filtering and large spin thermoelectric effects in organic transition-metal molecular junctions. Physical Chemistry Chemical Physics, 2014, 16, 11349.	1.3	32
18253	NO Adsorption on Copper Phthalocyanine Functionalized Graphite. Journal of Physical Chemistry C, 2014, 118, 10076-10082.	1.5	23
18254	Electronic and magnetic properties of F atoms adsorbed on TiO₂:Mn(001) diluted magnetic semiconductor surfaces: First-principles calculations. International Journal of Modern Physics B, 2014, 28, 1450096.	1.0	1
18255	First-principles investigation of the bulk and low-index surfaces of<mml:math xmlns:mml="http://www.w3.org/1998/Math/MathML"><mml:mi>Mo</mml:mi><mml:msub><mml:mi>Se</mml:mi><mml:mn>2</mml:mn> Physical Review B, 2014, 89, .	1.1	12
18256	C<scp>RYSTAL14</scp>: A program for the ab initio investigation of crystalline solids. International Journal of Quantum Chemistry, 2014, 114, 1287-1317.	1.0	1,151
18257	A stable three-dimensional topological Dirac semimetal Cd3As2. Nature Materials, 2014, 13, 677-681.	13.3	1,242
18258	Unexpected symmetry and AA stacking of bilayer silicene on<mml:math xmlns:mml="http://www.w3.org/1998/Math/MathML"><mml:mi>Ag</mml:mi><mml:mrow><mml:mn>(111)</mml:mn></mml:mrow></ Physical Review B, 2014, 89, .	1.1	32
18259	Observation of a three-dimensional topological Dirac semimetal phase in high-mobility Cd3As2. Nature Communications, 2014, 5, 3786.	5.8	1,166
18260	Six-dimensional potential energy surface of the dissociative chemisorption of HCl on Au(111) using neural networks. Science China Chemistry, 2014, 57, 147-155.	4.2	50
18261	Carrier induced magnetic coupling transitions in phthalocyanine-based organometallic sheet. Nanoscale, 2014, 6, 328-333.	2.8	44
18262	Ionic Conduction in Cubic Na₃TiP₃O₉N, a Secondary Na-Ion Battery Cathode with Extremely Low Volume Change. Chemistry of Materials, 2014, 26, 3295-3305.	3.2	68
18263	New Mn₂â€based Heusler Compounds. Zeitschrift Fur Anorganische Und Allgemeine Chemie, 2014, 640, 738-752.	0.6	68
18264	Effect of Si doping on the electronic properties of BN monolayer. Nanoscale, 2014, 6, 5526-5531.	2.8	42
18265	BN-decorated graphene nanoflakes with tunable opto-electronic and charge transport properties. Journal of Materials Chemistry C, 2014, 2, 2918-2928.	2.7	35
18266	Atomistic simulation of transport phenomena in nanoelectronic devices. Chemical Society Reviews, 2014, 43, 4357-4367.	18.7	27
18267	Elemental tellurium as a chiral<mml:math xmlns:mml="http://www.w3.org/1998/Math/MathML"><mml:mi>p</mml:mi></mml:math>-type thermoelectric material. Physical Review B, 2014, 89, .	1.1	165
18268	Chemical trends of Mn⁴⁺emission in solids. Journal of Materials Chemistry C, 2014, 2, 2475-2481.	2.7	214
18269	Multiple Twinning As a Structure Directing Mechanism in Layered Rock-Salt-Type Oxides: NaMnO₂ Polymorphism, Redox Potentials, and Magnetism. Chemistry of Materials, 2014, 26, 3306-3315.	3.2	56

#	Article	IF	Citations
18270	Band-Edge Noise Spectroscopy of a Magnetic Tunnel Junction. Physical Review Letters, 2014, 112, .	2.9	8
18271	Substitutional doping of graphene: The role of carbon divacancies. Physical Review B, 2014, 89, .	1.1	52
18272	Gate Bias Dependence of Defect-Mediated Hot-Carrier Degradation in GaN HEMTs. IEEE Transactions on Electron Devices, 2014, 61, 1316-1320.	1.6	40
18273	A Combined <italic>Ab Initio</italic> and Experimental Study on the Nature of Conductive Filaments in <inline-formula> <tex-math notation="TeX">${m Pt}/{m Hf}{m O}_{2}/{m Pt}$ </tex-math></inline-formula> Resistive Random Access Memory. IEEE Transactions on Electron Devices, 2014, 61, 1394-1402.	1.6	55
18274	Tuning Interlayer Coupling in Large-Area Heterostructures with CVD-Grown MoS₂ and WS₂ Monolayers. Nano Letters, 2014, 14, 3185-3190.	4.5	683
18275	Controllable Synthesis of Ceria Nanoparticles with Uniform Reactive {100} Exposure Planes. Journal of Physical Chemistry C, 2014, 118, 4437-4443.	1.5	29
18276	DFT Study on Ce-Doped Anatase TiO₂: Nature of Ce³⁺ and Ti³⁺ Centers Triggered by Oxygen Vacancy Formation. Journal of Physical Chemistry C, 2014, 118, 9677-9689.	1.5	51
18277	Robust Diffusive Proton Motions in Phase IV of Solid Hydrogen. Journal of Physical Chemistry C, 2014, 118, 11902-11905.	1.5	7
18278	Red Photoluminescence from Bi³⁺ and the Influence of the Oxygen-Vacancy Perturbation in ScVO₄: A Combined Experimental and Theoretical Study. Journal of Physical Chemistry C, 2014, 118, 7515-7522.	1.5	164
18279	Hybrid functional calculations of<mml:math xmlns:mml="http://www.w3.org/1998/Math/MathML"><mml:mrow><mml:mi>D</mml:mi><mml:mi>X</mml:mi></mml:mrow></mml in AlN and GaN. Physical Review B, 2014, 89, .	1.1	119
18280	Dielectric Relaxation Processes, Electronic Structure, and Band Gap Engineering of MFUâ€4â€type Metalâ€Organic Frameworks: Towards a Rational Design of Semiconducting Microporous Materials. Advanced Functional Materials, 2014, 24, 3885-3896.	7.8	95
18281	InN growth on BaTiO3 (111) substrates: A first-principles study. Journal of Crystal Growth, 2014, 395, 98-103.	0.7	0
18282	Theoretical aspects of WS₂ nanotube chemical unzipping. Nanoscale, 2014, 6, 8400-8404.	2.8	5
18283	Oxygen adsorption characteristics on hybrid carbon and boronâ€nitride nanotubes. Journal of Computational Chemistry, 2014, 35, 1058-1063.	1.5	13
18284	Gas adsorption on MoS2 monolayer from first-principles calculations. Chemical Physics Letters, 2014, 595-596, 35-42.	1.2	328
18285	Theoretical study on strain induced variations in electronic properties of 2H-MoS2 bilayer sheets. Applied Physics Letters, 2014, 104, .	1.5	36
18286	Large-scale SCC-DFTB calculations of reconstructed polar ZnO surfaces. Surface Science, 2014, 628, 50-61.	0.8	10
18287	Electronic and magnetic structures and bonding properties of Ce2T2X (TÂ=ÂInd element; XÂ=ÂMg, Cd, Pb or) Tj ETQq1 1 0.784314 rg	1.8	9

#	Article	IF	Citations
18288	Stacking-dependent electronic structure of bilayer silicene. Applied Physics Letters, 2014, 104, .	1.5	70
18289	Interaction of tetraethoxysilane with OH-terminated SiO2 (001) surface: A first principles study. Applied Surface Science, 2014, 305, 247-251.	3.1	10
18290	Identifying Active Functionalities on Fewâ€Layered Graphene Catalysts for Oxidative Dehydrogenation of Isobutane. ChemSusChem, 2014, 7, 483-491.	3.6	56
18291	Electronic structure of spinel-type LiNi1/2Ge3/2O4 and LiNi1/2Mn3/2O4 as positive electrodes for rechargeable Li-ion batteries studied by first-principles density functional theory. Solid State Ionics, 2014, 262, 74-76.	1.3	5
18292	Electronic structure and thermoelectric properties of In4Se3â^'x (x=0, 0.25, 0.5, 0.75): First-principles calculations. Journal of Alloys and Compounds, 2014, 589, 125-131.	2.8	6
18293	First-principles study of thermodynamic properties and solubility of aluminum-rare-earth intermetallics. Computational Materials Science, 2014, 90, 56-60.	1.4	22
18294	A first-principles study on the electronic and magnetic properties of armchair SiC/AlN nanoribbons. Journal of Alloys and Compounds, 2014, 586, 176-179.	2.8	5
18295	Thermodynamic assessment of the Alâ€“Dy, Dyâ€“Zr and Alâ€“Dyâ€“Zr systems. Science Bulletin, 2014, 59, 1738-1746.	1.7	6
18296	Catalytic Activity of Pt Nano-Particles for H2 Formation. Topics in Catalysis, 2014, 57, 273-281.	1.3	26
18297	Molecular dynamics simulations of CO2 reduction on Cu(111) and Cu/ZnO(10 <mml:math) Tj ETQq1 1 0.784314 rgBT /Overlock 10 T	1.6	24
18298	Rechargeable magnesium battery: Current status and key challenges for the future. Progress in Materials Science, 2014, 66, 1-86.	16.0	538
18299	Ab initio investigation on hybrid graphite-like structure made up of silicene and boron nitride. Physics Letters, Section A: General, Atomic and Solid State Physics, 2014, 378, 1162-1169.	0.9	12
18300	Solid-state dimer method for calculating solid-solid phase transitions. Journal of Chemical Physics, 2014, 140, 174104.	1.2	112
18301	Behavior of Li defects in solid electrolyte lithium thiophosphate Li7P3S11: A first principles study. Computational Materials Science, 2014, 90, 44-49.	1.4	18
18302	Tailoring Exciton Dynamics by Elastic Strainâ€Gradient in Semiconductors. Advanced Materials, 2014, 26, 2572-2579.	11.1	76
18303	Qualitative link between work of adhesion and thermal conductance of metal/diamond interfaces. Journal of Applied Physics, 2014, 115, .	1.1	46
18304	Double-decker phthalocyanine complex: Scanning tunneling microscopy study of film formation and spin properties. Progress in Surface Science, 2014, 89, 127-160.	3.8	40
18305	Chiral Co(II) Metalâ€“Organic Framework in the Heterogeneous Catalytic Oxidation of Alkenes under Aerobic and Anaerobic Conditions. ACS Catalysis, 2014, 4, 1032-1039.	5.5	53

#	Article	IF	Citations
18306	Simultaneous reduction in leakage current and enhancement in magnetic moment in BiFeO₃ nanofibers via optimized Sn doping. Physica Status Solidi - Rapid Research Letters, 2014, 8, 653-657.	1.2	13
18307	p-Type conductivity and stability of Agâ€“N codoped ZnO thin films. Journal of Alloys and Compounds, 2014, 609, 173-177.	2.8	60
18308	Using Room Temperature Current Noise To Characterize Single Molecular Spectra. ACS Nano, 2014, 8, 2111-2117.	7.3	5
18309	Theoretical and electron paramagnetic resonance studies of hyperfine interaction in nitrogen doped 4H and 6H SiC. Journal of Applied Physics, 2014, 115, .	1.1	17
18310	Phase stability and hot corrosion behavior of ZrO2â€“Ta2O5 compound in Na2SO4â€“V2O5 mixtures at elevated temperatures. Ceramics International, 2014, 40, 4077-4083.	2.3	40
18311	Unique Properties of Halide Perovskites as Possible Origins of the Superior Solar Cell Performance. Advanced Materials, 2014, 26, 4653-4658.	11.1	1,735
18312	Structural, electronic and optical properties of a large random network model of amorphous SiO2 glass. Journal of Non-Crystalline Solids, 2014, 383, 28-32.	1.5	56
18313	The stability and electronic structure of Fe atoms embedded in zigzag graphene nanoribbons. Physica B: Condensed Matter, 2014, 441, 28-32.	1.3	15
18314	Oxidation and hydrogen uptake in zirconium, Zircaloy-2 and Zircaloy-4: Computational thermodynamics and ab initio calculations. Journal of Nuclear Materials, 2014, 444, 65-75.	1.3	38
18315	The stability and diffusion properties of foreign impurity atoms on the surface and in the bulk of vanadium: A first-principles study. Computational Materials Science, 2014, 81, 191-198.	1.4	21
18316	Twin-boundary segregation energies and solute-diffusion activation enthalpies in Mg-based binary systems: A first-principles study. Scripta Materialia, 2014, 80, 17-20.	2.6	85
18317	First-principles calculations of transition metalâ€“solute interactions with point defects in tungsten. Acta Materialia, 2014, 66, 172-183.	3.8	132
18318	Half-metallicity in carbon-substituted CdS monolayer. Physica E: Low-Dimensional Systems and Nanostructures, 2014, 59, 230-234.	1.3	8
18319	Structural and Electronic Properties of TM_n[(BN)₃H₆]_m Complexes with TM = Co (n, m = 1â€“3) and with TM = Fe, Ni, Ru, Rh, Pd (n = m = 1â€“3). Journal of Physical Chemistry A, 2014, 118, 2976-2983.	1.1	7
18320	Inversion Symmetry Breaking by Oxygen Octahedral Rotations in the Ruddlesden-Popper<mml:math xmlns:mml="http://www.w3.org/1998/Math/MathML" display="inline"><mml:mrow><mml:mi>Na</mml:mi><mml:mi>R</mml:mi><mml:msub><mml:mrow><mml:mi>TiO</mml:mi></mml:mr	2.9	60
18321	First-principles microscopic model of exchange-driven magnetoelectric response with application to<mml:math xmlns:mml="http://www.w3.org/1998/Math/MathML"><mml:msub><mml:mrow><mml:mtext>Cr</mml:mtext></mml:mrow><mml:mn>2</mml:mn></mml:msub><mml:msub><mml:mrow><mml:mtext>O</mml:mtext></mml:mrow><mml:mn>3</mml:mn></mml:msub></mml:math>. Physical Review B, 2014, 89, .	3.7	11
18322	Competition and cooperation between antiferrodistortive and ferroelectric instabilities in the model perovskite SrTiO₃. Journal of Physics Condensed Matter, 2014, 26, 122203.	0.7	92
18323	Ballistic Transport Performance of Silicane and Germanane Transistors. IEEE Transactions on Electron Devices, 2014, 61, 1590-1598.	1.6	51

#	Article	IF	Citations
18324	Redox Targeting of Anatase TiO₂ for Redox Flow Lithiumâ€ion Batteries. Advanced Energy Materials, 2014, 4, 1400567.	10.2	82
18325	Sublattice Localized Electronic States in Atomically Resolved Graphene-Pt(111) Edge-Boundaries. ACS Nano, 2014, 8, 3590-3596.	7.3	19
18326	Following Molecules through Reactive Networks: Surface Catalyzed Decomposition of Methanol on Pd(111), Pt(111), and Ni(111). Journal of Physical Chemistry C, 2014, 118, 12364-12383.	1.5	35
18327	Prediction of Large-Gap Two-Dimensional Topological Insulators Consisting of Bilayers of Group III Elements with Bi. Nano Letters, 2014, 14, 2505-2508.	4.5	173
18328	Surface Structure Evolution of LiMn₂O₄ Cathode Material upon Charge/Discharge. Chemistry of Materials, 2014, 26, 3535-3543.	3.2	223
18329	Formation of Chiral Self-Assembled Structures of Amino Acids on Transition-Metal Surfaces: Alanine on Pd(111). Journal of Physical Chemistry C, 2014, 118, 6856-6865.	1.5	26
18330	Electronic ferroelectricity induced by charge and orbital orderings. Journal of Physics Condensed Matter, 2014, 26, 103201.	0.7	42
18331	Magnetoelectric effects at the interfaces between nonmagnetic perovskites: Ab initio prediction. Europhysics Letters, 2014, 105, 27002.	0.7	3
18332	Hydroxylation of the surface of PbS nanocrystals passivated with oleic acid. Science, 2014, 344, 1380-1384.	6.0	404
18333	N incorporation and associated localized vibrational modes in GaSb. Physical Review B, 2014, 89, .	1.1	14
18334	Ab initiostudy of point defects in NiTi-based alloys. Physical Review B, 2014, 89, .	1.1	28
18335	First-principles study of point defects in an fcc Fe-10Ni-20Cr model alloy. Physical Review B, 2014, 89, .	1.1	61
18336	An unconventional bilayer ice structure on a NaCl(001) film. Nature Communications, 2014, 5, 4056.	5.8	64
18337	Stabilized silicene within bilayer graphene: A proposal based on molecular dynamics and density-functional tight-binding calculations. Physical Review B, 2014, 89, .	1.1	51
18338	Efficient carrier transport in halide perovskites: theoretical perspectives. Journal of Materials Chemistry A, 2014, 2, 9091-9098.	5.2	414
18339	Elucidation of the Na_{2/3}FePO₄ and Li_{2/3}FePO₄ Intermediate Superstructure Revealing a Pseudouniform Ordering in 2D. Journal of the American Chemical Society, 2014, 136, 9144-9157.	6.6	67
18340	Thermal Expansion, Heat Capacity, and Thermal Conductivity of Nickel Ferrite (NiFe₂O₄). Journal of the American Ceramic Society, 2014, 97, 1559-1565.	1.9	51
18341	Anisotropic Mo₂â€“Phthalocyanine Sheet: A New Member of the Organometallic Family. Journal of Physical Chemistry A, 2014, 118, 304-307.	1.1	13

#	Article	IF	Citations
18342	The promoting role of minor amount of water in solvent-free hydrogenation of halogenated nitrobenzenes. Chinese Chemical Letters, 2014, 25, 205-208.	4.8	6
18343	Adaptive cluster expansions and redox-dependent atomic ordering. Computational Materials Science, 2014, 83, 207-211.	1.4	2
18344	Diffusion of Co, Ru and Re in Ni-based superalloys: A first-principles study. Journal of Alloys and Compounds, 2014, 588, 163-169.	2.8	40
18345	Density functional theory study of propane steam reforming on Rhâ€“Ni bimetallic surface: Sulfur tolerance and scaling/BrÃ¸nstedâ€“Evansâ€“Polanyi relations. Journal of Catalysis, 2014, 309, 248-259.	3.1	28
18346	Broadband, site selective and time resolved photoluminescence spectroscopic studies of finely size-modulated Y2O3:Eu3+ phosphors synthesized by a complex based precursor solution method. Current Applied Physics, 2014, 14, 72-81.	1.1	24
18347	Design of a Metalâ€“Organic Framework with Enhanced Back Bonding for Separation of N₂ and CH₄. Journal of the American Chemical Society, 2014, 136, 698-704.	6.6	157
18348	Molecular dynamics simulations of influence of Re on lattice trapping and fracture stress of cracks in Ni. Computational Materials Science, 2014, 83, 196-206.	1.4	24
18349	Surface-assisted cisâ€“trans isomerization of an alkene molecule on Cu(110). Chemical Communications, 2014, 50, 1728-1730.	2.2	13
18350	Electronic properties on GaN(0001) surface â€“ ab initio investigation. Vacuum, 2014, 99, 166-174.	1.6	12
18351	DFT study of benzene and CO co-adsorption on PtCo(111). Applied Surface Science, 2014, 289, 502-510.	3.1	8
18352	Electronic properties of 2D and 3D hybrid organic/inorganic perovskites for optoelectronic and photovoltaic applications. Optical and Quantum Electronics, 2014, 46, 1225-1232.	1.5	60
18353	Self-assembled monolayers of methylselenolate on the Au(111) surface: A combined STM and DFT study. Surface Science, 2014, 619, 67-70.	0.8	4
18354	Laves phases in the Vâ€“Zr system below room temperature: Stability analysis using ab initio results and phase diagram. Calphad: Computer Coupling of Phase Diagrams and Thermochemistry, 2014, 44, 62-69.	0.7	8
18355	Thermodynamic assessment of the Srâ€“In and Srâ€“Bi systems supported by first-principles calculations. Calphad: Computer Coupling of Phase Diagrams and Thermochemistry, 2014, 45, 49-54.	0.7	7
18356	Microscopic Origin for Electrically Benign Small-angle Grain Boundaries in Low-cost Semiconductors. Materials Research Letters, 2014, 2, 51-56.	4.1	3
18357	Suppression effect of oxygen on the Î² to Ï‰ transformation in a Î²-type Ti alloy: insights from first-principles. Modelling and Simulation in Materials Science and Engineering, 2014, 22, 015007.	0.8	22
18358	Scalable enhancement of graphene oxide properties by thermally driven phase transformation. Nature Chemistry, 2014, 6, 151-158.	6.6	326
18359	Carbon-14 decay as a source of non-canonical bases in DNA. Biochimica Et Biophysica Acta - General Subjects, 2014, 1840, 526-534.	1.1	3

#	Article	IF	Citations
18360	Modelling of P3HT:PCBM interface using coarse-grained forcefield derived from accurate atomistic forcefield. Physical Chemistry Chemical Physics, 2014, 16, 4653.	1.3	42
18361	CO Adsorption on Clean and Oxidized Pd(111). Journal of Physical Chemistry C, 2014, 118, 1118-1128.	1.5	69
18362	M585, a low energy superhard monoclinic carbon phase. Solid State Communications, 2014, 181, 24-27.	0.9	25
18363	Temperature-dependent elastic stiffness constants of fcc-based metal nitrides from first-principles calculations. Journal of Materials Science, 2014, 49, 424-432.	1.7	9
18364	Initial stages of Cu3Au(111) oxidation: oxygen induced Cu segregation and the protective Au layer profile. Physical Chemistry Chemical Physics, 2014, 16, 3815.	1.3	16
18365	The microstructure, stability, and elastic properties of 14H long-period stacking-ordered phase in Mgâ€“Znâ€“Y alloys: a first-principles study. Journal of Materials Science, 2014, 49, 737-748.	1.7	24
18366	Combined XPS and first principles study of double-perovskite Ca2GdTaO6. Journal of Materials Science, 2014, 49, 819-826.	1.7	16
18367	Large positive spin polarization and giant inverse tunneling magnetoresistance in Fe/PbTiO3/Fe multiferroic tunnel junction. Journal of Magnetism and Magnetic Materials, 2014, 351, 29-36.	1.0	4
18368	Recent NMR developments applied to organicâ€“inorganic materials. Progress in Nuclear Magnetic Resonance Spectroscopy, 2014, 77, 1-48.	3.9	78
18369	Ab-initio calculations of Juddâ€“Ofelt intensity parameters for transitions between crystal-field levels. Journal of Luminescence, 2014, 152, 54-57.	1.5	14
18370	Tunable Electronic Properties of Two-Dimensional Transition Metal Dichalcogenide Alloys: A First-Principles Prediction. Journal of Physical Chemistry Letters, 2014, 5, 285-291.	2.1	98
18371	Atomically resolved STM imaging with a diamond tip: simulation and experiment. Nanotechnology, 2014, 25, 025706.	1.3	14
18372	Hydrogen adsorption in lithium decorated conjugated microporous polymers: a DFT investigation. RSC Advances, 2014, 4, 4170-4176.	1.7	19
18373	Electron correlation and relativity of the 5f electrons in the Uâ€“Zr alloy system. Journal of Nuclear Materials, 2014, 444, 356-358.	1.3	38
18374	Point defects and diffusion in ordered alloys: An ab initio study of the effect of vibrations. Intermetallics, 2014, 45, 38-45.	1.8	6
18375	First principles study of structural and electronic properties of cubic phase of ZrO2 and HfO2. Physica B: Condensed Matter, 2014, 434, 7-13.	1.3	43
18376	Effect of alloying elements on the properties of Zr and the Zrâ€“H system. Journal of Nuclear Materials, 2014, 445, 241-250.	1.3	51
18377	Effect of surface strain on oxygen adsorption on Zr (0001) surface. Journal of Nuclear Materials, 2014, 445, 1-6.	1.3	19

#	Article	IF	Citations
18378	Magnetism, structure and chemical order in small CoPd clusters: A first-principles study. Journal of Magnetism and Magnetic Materials, 2014, 349, 109-115.	1.0	13
18379	Oxygen vacancy formation energies in Sr-doped complex perovskites: ab initio thermodynamic study. Solid State Ionics, 2014, 254, 11-16.	1.3	26
18380	Bandgap engineering through nanoporosity. Nanoscale, 2014, 6, 1181-1187.	2.8	26
18381	Silicene on metal substrates: A first-principles study on the emergence of a hierarchy of honeycomb structures. Applied Surface Science, 2014, 291, 93-97.	3.1	24
18382	Elastic, electronic properties and intra-atomic bonding in orthorhombic and tetragonal polymorphs of BaZn2As2 from first-principles calculations. Journal of Alloys and Compounds, 2014, 583, 100-105.	2.8	16
18383	High performance fluorine doped (Sn,Ru)O2 oxygen evolution reactionÂelectro-catalysts for proton exchange membrane based water electrolysis. Journal of Power Sources, 2014, 245, 362-370.	4.0	42
18384	Interaction of minor alloying elements of high-Cr ferritic steels with lattice defects: An ab initio study. Journal of Nuclear Materials, 2014, 444, 237-246.	1.3	38
18385	First-principles study of Mn, Al and C distribution and their effect on stacking fault energies in fcc Fe. Journal of Alloys and Compounds, 2014, 582, 475-482.	2.8	113
18386	Pseudopotentials for high-throughput DFT calculations. Computational Materials Science, 2014, 81, 446-452.	1.4	1,114
18387	Ag (100)/MgO (100) interface: A van der Waals density functional study. Applied Surface Science, 2014, 288, 115-121.	3.1	7
18388	Multiple exciton generation in silicon quantum dot arrays: density functional perturbation theory computation. Molecular Physics, 2014, 112, 430-440.	0.8	21
18389	Inorganic chemistry solutions to semiconductor nanocrystal problems. Coordination Chemistry Reviews, 2014, 263-264, 182-196.	9.5	35
18390	Synergistic effect of rhenium and ruthenium in nickel-based single-crystal superalloys. Journal of Alloys and Compounds, 2014, 582, 299-304.	2.8	44
18391	Hybrid Monte Carlo/Molecular Dynamics Simulation of a Refractory Metal High Entropy Alloy. Metallurgical and Materials Transactions A: Physical Metallurgy and Materials Science, 2014, 45, 196-200.	1.1	157
18392	Structures and stabilities of small carbon interstitial clusters in cubic silicon carbide. Acta Materialia, 2014, 62, 162-172.	3.8	22
18393	Elasticity behavior, phonon spectra, and the pressureâ€“temperature phase diagram of HfTi alloy: A density-functional theory study. Computational Materials Science, 2014, 82, 5-11.	1.4	15
18394	Metal atom adsorption on a defective TiO2â€“x support. Chemical Physics Letters, 2014, 594, 23-29.	1.2	5
18395	NiTiSn a material of technological interest: Ab initio calculations ofÂphase stability and defects. Intermetallics, 2014, 46, 103-110.	1.8	44

#	Article	IF	Citations
18396	Deep-Ultraviolet Nonlinear Optical Crystals: Ba₃P₃O₁₀X (X = Cl,) Tj ETQq0 0 0 rgBT /Overlock 10	6.6	386
18397	Does the fcc phase exist in the Fe bccâ€“hcp transition? A conclusion from first-principles studies. Modelling and Simulation in Materials Science and Engineering, 2014, 22, 025007.	0.8	26
18398	Effect of Na adsorption on the structural and electronic properties of Si(111)$ sqrt {ext {sffamily 3}}imes sqrt {ext {sffamily 3}}$ -Au surface. Journal of Physics Condensed Matter, 2014, 26, 055009.	0.7	9
18399	GGA+U Study on the Mechanism of Photodecomposition of Water Adsorbed on Rutile TiO₂(110) Surface: Free vs Trapped Hole. Journal of Physical Chemistry C, 2014, 118, 1027-1034.	1.5	41
18400	Understanding the surface chemistry of carbon nanotubes: Toward a rational design of Ru nanocatalysts. Journal of Catalysis, 2014, 309, 185-198.	3.1	71
18401	Effects of different nitrogen-to-titanium atomic ratios on the evolution of Tiâ€“Siâ€“N islands on TiN(001) surfaces: First-principle studies. Journal of Alloys and Compounds, 2014, 586, 431-435.	2.8	3
18402	DFT study of chromium-doped SnO2 materials. Journal of Materials Science, 2014, 49, 2904-2911.	1.7	33
18403	Size-Dependent Halogenated Nitrobenzene Hydrogenation Selectivity of Pd Nanoparticles. Journal of Physical Chemistry C, 2014, 118, 2594-2601.	1.5	98
18404	Predicting self-diffusion in metal oxides from first principles: The case of oxygen in tetragonal ZrO<mml:math xmlns:mml="http://www.w3.org/1998/Math/MathML"><mml:msub><mml:mrow /><mml:mn>2</mml:mn></mml:msub></mml:math>. Physical Review B, 2014, 89, .	1.1	26
18405	First-Principles Study on the Electronic and Magnetic Properties of Zigzag AlN-SiC Nanoribbons. Journal of Superconductivity and Novel Magnetism, 2014, 27, 1079-1082.	0.8	4
18406	Theoretical Study of Li Migration in Lithiumâ€“Graphite Intercalation Compounds with Dispersion-Corrected DFT Methods. Journal of Physical Chemistry C, 2014, 118, 2273-2280.	1.5	141
18407	Quantum wells formed in transition-metal dichalcogenide nanosheet-superlattices: stability and electronic structures from first principles. Physical Chemistry Chemical Physics, 2014, 16, 1393-1398.	1.3	25
18408	Modulating the atomic and electronic structures through alloying and heterostructure of single-layer MoS₂. Journal of Materials Chemistry A, 2014, 2, 2101-2109.	5.2	92
18409	First-principles molecular dynamics modeling of the LiClâ€“KCl molten salt system. Computational Materials Science, 2014, 83, 362-370.	1.4	89
18410	Molecular phenomena in colloidal nanostructure synthesis. Molecular Simulation, 2014, 40, 134-140.	0.9	14
18411	Tuning photocatalytic performance of the near-infrared-driven photocatalyst Cu2(OH)PO4 based on effective mass and dipole moment. Physical Chemistry Chemical Physics, 2014, 16, 3267.	1.3	69
18412	The effect of water on the structural, electronic and photocatalytic properties of graphitic carbon nitride. Physical Chemistry Chemical Physics, 2014, 16, 3299.	1.3	97
18413	Direct chemical conversion of graphene to boron- and nitrogen- and carbon-containing atomic layers. Nature Communications, 2014, 5, 3193.	5.8	198

#	Article	IF	Citations
18414	Atomic structure evolution during solidification of liquid niobium fromab initiomolecular dynamics simulations. Journal of Physics Condensed Matter, 2014, 26, 055004.	0.7	16
18415	Ferromagnetism in MnX2 (X = S, Se) monolayers. Physical Chemistry Chemical Physics, 2014, 16, 4990.	1.3	199
18416	Strain Induced Metastable Phase and Phase Revolution in PbTiO 3 -CoFe 2 O 4 Nanocomposite Film. Chinese Physics Letters, 2014, 31, 017701.	1.3	4
18417	Cr adsorption induced magnetism in Bi2Se3 film by proximity effects. Physica E: Low-Dimensional Systems and Nanostructures, 2014, 55, 9-12.	1.3	8
18418	Anionogenic Mixed Valency in KxBa1â€“xO2â^Î´. Inorganic Chemistry, 2014, 53, 496-502.	1.9	4
18419	Hydroxyl Identification on ZnO by Infrared Spectroscopies: Theory and Experiments. Journal of Physical Chemistry C, 2014, 118, 1492-1505.	1.5	40
18420	Mechanistic Study of 1,3-Butadiene Formation in Acetylene Hydrogenation over the Pd-Based Catalysts Using Density Functional Calculations. Journal of Physical Chemistry C, 2014, 118, 1560-1567.	1.5	68
18421	Emergence of spin-filter states in Ptâ€“Fe nanowires. Physical Chemistry Chemical Physics, 2014, 16, 8360-8366.	1.3	15
18422	The origin of p-type conductivity in ZnM2O4 (M = Co, Rh, Ir) spinels. Physical Chemistry Chemical Physics, 2014, 16, 2588.	1.3	57
18423	Two-dimensional bismuthâ€“silver structures on Si(111). Surface Science, 2014, 623, 17-24.	0.8	15
18424	A Bâ€“Câ€“N hybrid porous sheet: an efficient metal-free visible-light absorption material. Physical Chemistry Chemical Physics, 2014, 16, 4299.	1.3	13
18425	Dissociative adsorption of 2,3,7,8-TCDD on the surfaces of typical metal oxides: a first-principles density functional theory study. Physical Chemistry Chemical Physics, 2014, 16, 5553.	1.3	10
18426	Room-temperature ferromagnetism in hydrogenated ZnO nanoparticles. Journal of Applied Physics, 2014, 115, .	1.1	38
18427	On the mechanism of sulfur fast diffusion in 3-D transition metals. Acta Materialia, 2014, 67, 95-101.	3.8	16
18428	Structural and Electronic Properties of Micellar Au Nanoparticles: Size and Ligand Effects. ACS Nano, 2014, 8, 6671-6681.	7.3	36
18429	Theoretical Prediction and Experimental Confirmation of Unusual Ternary Ordered Semiconductor Compounds in Srâ€“Pbâ€“S System. Journal of the American Chemical Society, 2014, 136, 1628-1635.	6.6	33
18430	Strongly correlated one-dimensional magnetic behavior of<mml:math xmlns:mml="http://www.w3.org/1998/Math/MathML"><mml:msub><mml:mi>NiTa</mml:mi><mml:mn>2</mml:mn></mml:msub></mml xmlns:mml="http://www.w3.org/1998/Math/MathML"><mml:msub><mml:mi mathvariant="normal">O</mml:mi><mml:mn>6</mml:mn></mml:msub></mml:math>. Physical Review B, 2014, 89, .	1.1	26
18431	The Changing Colors of a Quantum-Confined Topological Insulator. ACS Nano, 2014, 8, 1222-1230.	7.3	39

#	Article	IF	Citations
18432	Polymorphism of dislocation core structures at the atomic scale. Nature Communications, 2014, 5, 3239.	5.8	85
18433	Densification of a continuous random network model of amorphous SiO₂glass. Physical Chemistry Chemical Physics, 2014, 16, 1500-1514.	1.3	56
18434	Characterization of Fe Substitution into La-Hexaaluminate Systems and the Effect on N₂O Catalytic Decomposition. Journal of Physical Chemistry C, 2014, 118, 1999-2010.	1.5	21
18435	Thermodynamic modeling of Feâ€“Tiâ€“Bi system assisted with key experiments. Calphad: Computer Coupling of Phase Diagrams and Thermochemistry, 2014, 46, 34-41.	0.7	5
18436	MoS₂/MX₂ heterobilayers: bandgap engineering via tensile strain or external electrical field. Nanoscale, 2014, 6, 2879-2886.	2.8	326
18437	Ab initiostudy of the effects of interfacial structure on the ferroelectric, magnetic, and magnetoelectric coupling properties ofFe/BaTiO3multiferroic tunnel junctions. Physical Review B, 2014, 89, .	1.1	11
18438	Lattice vibrational modes and phonon thermal conductivity of monolayer MoS<mml:math xmlns:mml="http://www.w3.org/1998/Math/MathML"><mml:msub><mml:mrow /><mml:mn>2</mml:mn></mml:msub></mml:math>. Physical Review B, 2014, 89, .	1.1	387
18439	Graphene,<mml:math xmlns:mml="http://www.w3.org/1998/Math/MathML"><mml:mi>h</mml:mi></mml:math>-BN,<mml:math xmlns:mml="http://www.w3.org/1998/Math/MathML"><mml:mi>h</mml:mi></mml:math>-MoS<mml:math xmlns:mml="http://www.w3.org/1998/Math/MathML"><mml:msub><mml:mrow /><mml:mn>2</mml:mn></mml:msub></mml:math>, and<mml:math xmlns:mml="http://www.w3.org/1998/	1.1	133
18440	Exploring CO dissociation on Fe nanoparticles by density functional theory-based methods: Fe13 as a case study. Theoretical Chemistry Accounts, 2014, 133, 1.	0.5	7
18441	First-principles study of the high-pressure behavior of solid 1,7-diamino-1,7-dinitrimino-2,4,6-trinitro-2,4,6-triazaheptane. Computational and Theoretical Chemistry, 2014, 1030, 38-43.	1.1	4
18442	High Coverage CO Adsorption and Dissociation on the Orthorhombic Mo₂C(100) Surface. Journal of Physical Chemistry C, 2014, 118, 3162-3171.	1.5	52
18443	First-principles study of anhydrite, polyhalite and carnallite. Chemical Physics Letters, 2014, 594, 1-5.	1.2	17
18444	A Force Field for Describing the Polyvinylpyrrolidone-Mediated Solution-Phase Synthesis of Shape-Selective Ag Nanoparticles. Journal of Physical Chemistry C, 2014, 118, 3366-3374.	1.5	52
18445	A combined DFT + U and Monte Carlo study on rare earth doped ceria. Physical Chemistry Chemical Physics, 2014, 16, 9974.	1.3	111
18446	Nature of the ferromagnetic ground state in the Mn<mml:math xmlns:mml="http://www.w3.org/1998/Math/MathML"><mml:msub><mml:mrow /><mml:mn>4</mml:mn></mml:msub></mml:math>molecular magnet. Physical Review B, 2014, 89, .	1.1	7
18447	Experimental investigation and thermodynamic modeling of the Gaâ€“Zr system. Journal of Alloys and Compounds, 2014, 587, 497-505.	2.8	6
18448	Anisotropic growth of gold nanoparticles using cationic gemini surfactants: effects of structure variations in head and tail groups. Journal of Materials Chemistry C, 2014, 2, 994-1003.	2.7	39
18449	A metallic carbon allotrope with superhardness: a first-principles prediction. Journal of Materials Chemistry C, 2014, 2, 2751-2757.	2.7	40

#	Article	IF	Citations
18450	The orbital minimization method for electronic structure calculations with finite-range atomic basis sets. Computer Physics Communications, 2014, 185, 873-883.	3.0	20
18451	Thermochemical Ranking and Dynamic Stability of TeO₂ Polymorphs from Ab Initio Theory. Crystal Growth and Design, 2014, 14, 871-878.	1.4	32
18452	Direct observation of the transition from indirect to direct bandgap in atomically thin epitaxial MoSe2. Nature Nanotechnology, 2014, 9, 111-115.	15.6	1,129
18453	van der Waals corrected DFT study of high coverage benzene adsorptions on Si(100) surface and STM simulations. Surface Science, 2014, 621, 152-161.	0.8	11
18454	Multichannel scanning probe microscopy and spectroscopy of graphene moirÃ© structures. Physical Chemistry Chemical Physics, 2014, 16, 3894.	1.3	24
18455	First principles studies on hydrogen storage in single-walled carbon nanotube functionalized with TiO2. Solid State Communications, 2014, 183, 1-7.	0.9	19
18456	Graphene/g-C3N4 bilayer: considerable band gap opening and effective band structure engineering. Physical Chemistry Chemical Physics, 2014, 16, 4230.	1.3	138
18457	First-principles calculation on p-type conduction of (Sb, N) codoping in ZnO. Journal of Physics and Chemistry of Solids, 2014, 75, 42-47.	1.9	16
18458	Lonsdaleite Films with Nanometer Thickness. Journal of Physical Chemistry Letters, 2014, 5, 541-548.	2.1	56
18459	Monolayer behaviour in bulk ReS2 due to electronic and vibrational decoupling. Nature Communications, 2014, 5, 3252.	5.8	906
18460	Solvent-Induced Proton Hopping at a Waterâ€“Oxide Interface. Journal of Physical Chemistry Letters, 2014, 5, 474-480.	2.1	82
18461	The structural stability and magnetic properties of the ferromagnetic Heusler alloy Niâ€“Mnâ€“Sn: A first principle investigation. Journal of Magnetism and Magnetic Materials, 2014, 355, 173-179.	1.0	18
18462	Cerium Substitution in Yttrium Iron Garnet: Valence State, Structure, and Energetics. Chemistry of Materials, 2014, 26, 1133-1143.	3.2	53
18463	Computational Design of Core/Shell Nanoparticles for Oxygen Reduction Reactions. Journal of Physical Chemistry Letters, 2014, 5, 292-297.	2.1	71
18464	Enhanced mechanical property of Feâ€“Al alloy due to Mn insertion: ab initio study. Journal of Alloys and Compounds, 2014, 583, 295-299.	2.8	19
18465	Theoretical Investigation of the Mechanism of the Waterâ€“Gas Shift Reaction on Cobalt@Gold Coreâ€“Shell Nanocluster. Journal of Physical Chemistry C, 2014, 118, 298-309.	1.5	13
18466	Computational thermodynamics of the CoNiGa high temperature shape memory alloy system. Calphad: Computer Coupling of Phase Diagrams and Thermochemistry, 2014, 45, 167-177.	0.7	4
18467	Adsorption of Pd, Pt, Cu, Ag, and Au Monomers on NiAl(110) Surface: A Comparative Study from DFT Calculations. Journal of Physical Chemistry A, 2014, 118, 5748-5755.	1.1	11

#	Article	IF	Citations
18468	H2 dissociation on Î³-Al2O3 supported Cu/Pd atoms: A DFT investigation. Applied Surface Science, 2014, 290, 154-160.	3.1	24
18469	Tunable Electrical Conductivity in Metal-Organic Framework Thin-Film Devices. Science, 2014, 343, 66-69.	6.0	1,061
18470	Mechanism of Hydrogen Spillover on WO₃(001) and Formation of H_xWO₃ (x = 0.125, 0.25, 0.375, and 0.5). Journal of Physical Chemistry C, 2014, 118, 494-501.	1.5	89
18471	Two-dimensional semiconductor alloys: Monolayer Mo1â^'xWxSe2. Applied Physics Letters, 2014, 104, .	1.5	154
18472	Toward an Accurate Description of Methane Physisorption on Carbon Nanotubes. Journal of Physical Chemistry C, 2014, 118, 544-550.	1.5	22
18473	Photocatalyst AgInS2 for active overall water-splitting: A first-principles study. Chemical Physics Letters, 2014, 591, 189-192.	1.2	43
18474	High Coverage CO Activation Mechanisms on Fe(100) from Computations. Journal of Physical Chemistry C, 2014, 118, 1095-1101.	1.5	54
18475	Bulk magnetoelectricity in the hexagonal manganites and ferrites. Nature Communications, 2014, 5, 2998.	5.8	181
18476	Interatomic potential for accurate phonons and defects in UO2. Journal of Nuclear Materials, 2014, 446, 155-162.	1.3	10
18477	Strong band hybridization between silicene and Ag(111) substrate. Physica E: Low-Dimensional Systems and Nanostructures, 2014, 58, 38-42.	1.3	43
18478	Theoretical Description of the Role of Halides, Silver, and Surfactants on the Structure of Gold Nanorods. Nano Letters, 2014, 14, 871-875.	4.5	146
18479	Unexpected magnetic properties in carbon-doped SnO2 from first-principles calculation. Computational Materials Science, 2014, 83, 5-11.	1.4	26
18480	Structures and Phase Transition of a MoS₂ Monolayer. Journal of Physical Chemistry C, 2014, 118, 1515-1522.	1.5	432
18481	Spin-chain magnetism and uniform Dzyaloshinsky-Moriya anisotropy in BaV<mml:math xmlns:mml="http://www.w3.org/1998/Math/MathML"><mml:msub><mml:mrow /><mml:mn>3</mml:mn></mml:msub></mml:math>O<mml:math xmlns:mml="http://www.w3.org/1998/Math/MathML"><mml:msub><mml:mrow /><mml:mn>8</mml:mn></mml:msub></mml:math>. Physical Review B, 2014, 89, .	1.1	19
18482	Adsorption and diffusion of atoms on the Si(335)â€“Au surface. Surface Science, 2014, 622, 9-15.	0.8	5
18483	Ground-state and spin-wave dynamics in Brownmillerite SrCoO_{2.5}â€”a combined hybrid functional and LSDA + U study. Journal of Physics Condensed Matter, 2014, 26, 036004.	0.7	13
18484	A metal-free organicâ€“inorganic aqueous flow battery. Nature, 2014, 505, 195-198.	13.7	1,333
18485	New type of ferromagnetic insulator: Double perovskite La2NiMO6 (M=Mn, Tc, Re, Ti, Zr, and Hf). Journal of Magnetism and Magnetic Materials, 2014, 357, 7-12.	1.0	25

#	Article	IF	Citations
18486	First-principles study of the mechanical properties and phase stability of TiO2. Computational Materials Science, 2014, 83, 114-119.	1.4	32
18487	Negatively curved carbon as the anode for lithium ion batteries. Carbon, 2014, 66, 39-47.	5.4	72
18488	High-pressure formation and stabilization of binary iridium hydrides. Physical Chemistry Chemical Physics, 2014, 16, 3220.	1.3	15
18489	Self-Accelerating CO Sorption in a Soft Nanoporous Crystal. Science, 2014, 343, 167-170.	6.0	434
18490	An adaptive genetic algorithm for crystal structure prediction. Journal of Physics Condensed Matter, 2014, 26, 035402.	0.7	120
18491	Pressure-induced topological quantum phase transition in Sb<mml:math xmlns:mml="http://www.w3.org/1998/Math/MathML"><mml:msub><mml:mrow /><mml:mn>2</mml:mn></mml:msub></mml:math>Se<mml:math xmlns:mml="http://www.w3.org/1998/Math/MathML"><mml:msub><mml:mrow /><mml:mn>3</mml:mn></mml:msub></mml:math>. Physical Review B, 2014, 89, .	1.1	47
18492	Amorphous Fe2O3 as a high-capacity, high-rate and long-life anode material for lithium ion batteries. Nano Energy, 2014, 4, 23-30.	8.2	307
18493	Phase stability, electronic structure and optical properties of BiInO3under strain. Journal Physics D: Applied Physics, 2014, 47, 055302.	1.3	4
18494	Proposed Photosynthesis Method for Producing Hydrogen from Dissociated Water Molecules Using Incident Near-Infrared Light. Physical Review Letters, 2014, 112, 018301.	2.9	237
18495	Interfacial effects on the spin density wave in FeSe/SrTiO<mml:math xmlns:mml="http://www.w3.org/1998/Math/MathML"><mml:msub><mml:mrow /><mml:mn>3</mml:mn></mml:msub></mml:math>thin films. Physical Review B, 2014, 89, .	1.1	52
18496	Effects of rare-earth dopants on the thermally grown Al2O3/Ni(Al) interface: the first-principles prediction. Journal of Materials Science, 2014, 49, 2640-2646.	1.7	17
18497	Theoretical studies on the hole transport property of tetrathienoarene derivatives: The influence of the position of sulfur atom, substituent and Ï€-conjugated core. Organic Electronics, 2014, 15, 602-613.	1.4	42
18498	Hydrogen-free graphene edges. Nature Communications, 2014, 5, 3040.	5.8	74
18499	Unlocking the Potential of Cation-Disordered Oxides for Rechargeable Lithium Batteries. Science, 2014, 343, 519-522.	6.0	943
18500	Transparent Conducting Oxides of Relevance to Organic Electronics: Electronic Structures of Their Interfaces with Organic Layers. Chemistry of Materials, 2014, 26, 631-646.	3.2	48
18501	Predictive Morphology Control of Hydrogen-Terminated Silicon Nanoparticles. Journal of Physical Chemistry C, 2014, 118, 2580-2586.	1.5	12
18502	Real-space imaging of interfacial water with submolecular resolution. Nature Materials, 2014, 13, 184-189.	13.3	173
18503	Energy Level Realignment in Weakly Interacting Donorâ€“Acceptor Binary Molecular Networks. ACS Nano, 2014, 8, 1699-1707.	7.3	35

#	Article	IF	Citations
18504	Discovery of a Three-Dimensional Topological Dirac Semimetal, Na ₃ Bi. Science, 2014, 343, 864-867.	6.0	1,889
18505	Modeling Water and Ammonia Adsorption in Hydrophobic Metalâ€“Organic Frameworks: Single Components and Mixtures. Journal of Physical Chemistry C, 2014, 118, 1102-1110.	1.5	57
18506	Indirect-to-direct band gap transition of the ZrS2 monolayer by strain: first-principles calculations. RSC Advances, 2014, 4, 7396.	1.7	91
18507	Hydrogen- and oxygen-related effects in phthalocyanine crystals: formation of carrier traps and a change in the magnetic state. Physical Chemistry Chemical Physics, 2014, 16, 3317.	1.3	9
18508	Pressure-induced phase transitions in UN: A density functional theory study. Journal of Alloys and Compounds, 2014, 588, 648-653.	2.8	9
18509	Structural and electronic properties of CdTe:Cl from first-principles. Materials Chemistry and Physics, 2014, 143, 637-641.	2.0	15
18510	Influence of carbonâ€“vacancy interaction on carbon and vacancy diffusivity in tungsten. Computational Materials Science, 2014, 83, 1-4.	1.4	21
18511	Atomic-level structures and physical properties of magnetic CoSiB metallic glasses. Journal of Magnetism and Magnetic Materials, 2014, 352, 49-55.	1.0	8
18512	First principles study of pyrophosphate defects and dopantâ€“defect interactions in stronium-doped lanthanum orthophosphate. Journal of Materials Chemistry A, 2014, 2, 1047-1053.	5.2	6
18513	Gold catalyzed hydrogenations of small imines and nitriles: enhanced reactivity of Au surface toward H₂via collaboration with a Lewis base. Chemical Science, 2014, 5, 1082-1090.	3.7	91
18514	Ceria in an oxygen environment: Surface phase equilibria and its descriptors. Surface Science, 2014, 619, 49-58.	0.8	27
18515	Constructing metallic nanoroads on a MoS₂monolayer via hydrogenation. Nanoscale, 2014, 6, 1691-1697.	2.8	48
18516	Cu cluster deposition on ZnO<mml:math xmlns:mml="http://www.w3.org/1998/Math/MathML" altimg="si10.gif" overflow="scroll"><mml:mfenced open="(") Tj ETQq0 0 0 rgBT /Overlock 10 Tf 50 272 Td (close=")"><mml:mrow><mml:mover accent="true"><mml:mn>1</mml:mn><mml:mo stretchy="true">Â¯</mml:mo></mml:mover><mml:mn>0</mml:mn></mml:mrow></mml:mfenced></mml:math>: Morphology and growth mode predicted from molecular dynamics simulations. Surface Science, 2014,	0.8	16
18517	Structural, electronic and magnetic properties of binary transition metal aluminum clusters: absence of electronic shell structure. Journal of Physics Condensed Matter, 2014, 26, 015006.	0.7	7
18518	Two-dimensional silicene nucleation on a Ag(111) surface: structural evolution and the role of surface diffusion. Physical Chemistry Chemical Physics, 2014, 16, 304-310.	1.3	30
18519	High-pressure close-packed structure of boron. RSC Advances, 2014, 4, 203-207.	1.7	18
18520	Tailoring the performance of graphene-based supercapacitors using topological defects: A theoretical assessment. Carbon, 2014, 68, 734-741.	5.4	78
18521	Tuning the near-gap electronic structure of tin-halide and lead-halide perovskites via changes in atomic layering. Physical Review B, 2014, 90, .	1.1	39

#	Article	IF	Citations
18522	Cooperative Interplay of van der Waals Forces and Quantum Nuclear Effects on Adsorption: H at Graphene and at Coronene. ACS Nano, 2014, 8, 9905-9913.	7.3	42
18523	Dopant-Induced Surface Magnetism in Î²-SiC Controlled by Dopant Depth. Journal of Physical Chemistry C, 2014, 118, 25429-25433.	1.5	7
18524	The different roles of Pu-oxide overlayers in the hydrogenation of Pu-metal: An ab initio molecular dynamics study based on van der Waals density functional (vdW-DF)+U. Journal of Chemical Physics, 2014, 140, 164709.	1.2	22
18525	Nanostructuration of CoSi by mechanical milling and mechanical alloying. Solid State Sciences, 2014, 38, 129-137.	1.5	12
18526	Theoretical prediction of hydrogen storage on Li-decorated monolayer black phosphorus. Journal Physics D: Applied Physics, 2014, 47, 465302.	1.3	47
18527	Boron phosphide under pressure: In situ study by Raman scattering and X-ray diffraction. Journal of Applied Physics, 2014, 116, .	1.1	33
18528	Kondo Effect Mediated Topological Protection: Co on Sb(111). ACS Nano, 2014, 8, 11576-11582.	7.3	5
18529	Graphene Oxide as a Promising Hole Injection Layer for MoS₂-Based Electronic Devices. ACS Nano, 2014, 8, 11432-11439.	7.3	68
18530	Structurally unstable<mml:math xmlns:mml="http://www.w3.org/1998/Math/MathML"><mml:msup><mml:mi>A</mml:mi><mml:mi>III</mml:mi></mml:msup><mml:ms mathvariant="normal">BiO</mml:mi><mml:mn>3</mml:mn></mml:msub></mml:math>perovskites are predicted to be topological insulators but their stable structural forms are trivial band insulators. Physical Review B, 2014, 90, .	1.1	21
18531	Crystal structures and stabilities of cristobalite-helium phases at high pressures. American Mineralogist, 2014, 99, 184-189.	0.9	11
18532	Quantum study of boron nitride nanotubes functionalized with anticancer molecules. Physical Chemistry Chemical Physics, 2014, 16, 18425-18432.	1.3	54
18533	Long-range magnetic coupling between nanoscale organicâ€“metal hybrids mediated by a nanoskyrmion lattice. Nature Nanotechnology, 2014, 9, 1018-1023.	15.6	44
18534	Assessing the Performances of Dispersion-Corrected Density Functional Methods for Predicting the Crystallographic Properties of High Nitrogen Energetic Salts. Journal of Chemical Theory and Computation, 2014, 10, 4982-4994.	2.3	22
18535	Magnetism in undoped ZnS studied from density functional theory. Journal of Applied Physics, 2014, 115, .	1.1	34
18536	Fluorine Adsorption on Single and Bilayer Graphene: Role of Sublattice and Layer Decoupling. Journal of Physical Chemistry C, 2014, 118, 27074-27080.	1.5	20
18537	Study of electronic properties, stabilities and magnetic quenching of molybdenum-doped germanium clusters: a density functional investigation. RSC Advances, 2014, 4, 64825-64834.	1.7	59
18538	The structures and thermodynamic stability of copper(<scp>ii</scp>) chloride surfaces. Physical Chemistry Chemical Physics, 2014, 16, 24209-24215.	1.3	13
18539	Synthesis of Oneâ€Dimensional Copper Sulfide Nanorods as Highâ€Performance Anode in Lithium Ion Batteries. ChemSusChem, 2014, 7, 3328-3333.	3.6	80

#	Article	IF	Citations
18540	First-principles investigations of defect and phase stabilities in thermoelectric (GeTe)x(AgSbTe2)1â^'x. Japanese Journal of Applied Physics, 2014, 53, 111201.	0.8	6
18541	Bonding and Charge Transfer in Nitrogen-Donor Uranyl Complexes: Insights from NEXAFS Spectra. Inorganic Chemistry, 2014, 53, 11415-11425.	1.9	15
18542	Synthesis and Crystal Structure of Î´-TaON, a Metastable Polymorph of Tantalum Oxide Nitride. Inorganic Chemistry, 2014, 53, 11691-11698.	1.9	27
18543	Nitrite Reduction Mechanism on a Pd Surface. Environmental Science & Technology, 2014, 48, 12768-12774.	4.6	188
18544	The quantum nature of skyrmions and half-skyrmions in Cu2OSeO3. Nature Communications, 2014, 5, 5376.	5.8	108
18545	Continuous Tuning of Band Gap for Ï€-Conjugated Ni Bis(dithiolene) Complex Bilayer. Journal of Physical Chemistry C, 2014, 118, 25626-25632.	1.5	15
18546	Modeling the Partial Atomic Charges in Inorganometallic Molecules and Solids and Charge Redistribution in Lithium-Ion Cathodes. Journal of Chemical Theory and Computation, 2014, 10, 5640-5650.	2.3	73
18547	Third-order elastic constants of ZnO and size effect in ZnO nanowires. Journal of Applied Physics, 2014, 115, 213516.	1.1	17
18548	P-type zinc oxide spinels: application to transparent conductors and spintronics. New Journal of Physics, 2014, 16, 055011.	1.2	28
18549	Selenium adsorption at different coverages on Fe(1 0 0) and Fe(1 1 1): A DFT study. Applied Surface Science, 2014, 315, 252-260.	3.1	11
18550	Weak topological insulators induced by the interlayer coupling: A first-principles study of stacked Bi<mml:math xmlns:mml="http://www.w3.org/1998/Math/MathML"><mml:msub><mml:mrow /><mml:mn>2</mml:mn></mml:msub></mml:math>TeI. Physical Review B, 2014, 89, .	1.1	46
18551	Ab initiostudy of the magnetoelectric effect and critical thickness for ferroelectricity in Co₂FeSi/BaTiO₃multiferroic tunnel junctions. Modelling and Simulation in Materials Science and Engineering, 2014, 22, 015008.	0.8	13
18552	Elementary Surface Chemistry during CuO/Al Nanolaminate-Thermite Synthesis: Copper and Oxygen Deposition on Aluminum (111) Surfaces. ACS Applied Materials & Interfaces, 2014, 6, 15086-15097.	4.0	47
18553	An atomistic picture of the diffusion of two vacancies forming a diâ€vacancy in Si. Physica Status Solidi (B): Basic Research, 2014, 251, 2185-2188.	0.7	4
18554	Ice Carbons. Journal of Physical Chemistry C, 2014, 118, 27502-27508.	1.5	4
18555	Hinge-like structure induced unusual properties of black phosphorus and new strategies to improve the thermoelectric performance. Scientific Reports, 2014, 4, 6946.	1.6	202
18556	Liâ€“Si phase diagram: Enthalpy of mixing, thermodynamic stability, and coherent assessment. Journal of Alloys and Compounds, 2014, 616, 581-593.	2.8	36
18557	On factors controlling activity of submonolayer bimetallic catalysts: Nitrogen desorption. Journal of Chemical Physics, 2014, 140, 014703.	1.2	6

#	Article	IF	Citations
18558	Lithiation of SiO₂ in Li-Ion Batteries: In Situ Transmission Electron Microscopy Experiments and Theoretical Studies. Nano Letters, 2014, 14, 7161-7170.	4.5	115
18559	Part-crystalline part-liquid state and rattling-like thermal damping in materials with chemical-bond hierarchy. Proceedings of the National Academy of Sciences of the United States of America, 2014, 111, 15031-15035.	3.3	225
18560	Spontaneous Graphitization of Ultrathin Cubic Structures: A Computational Study. Nano Letters, 2014, 14, 7126-7130.	4.5	31
18561	Tuning electronic and magnetic properties of SnSe₂ armchair nanoribbons via edge hydrogenation. Journal of Materials Chemistry C, 2014, 2, 10175-10183.	2.7	17
18562	DFT comparison of intrinsic WGS kinetics over Pd and Pt. Journal of Catalysis, 2014, 320, 106-117.	3.1	106
18563	Effect of nitrogen and vacancy defects on the thermal conductivity of diamond: Anab initioGreen's function approach. Physical Review B, 2014, 90, .	1.1	87
18564	Adsorption of the Herbicide 4-Chloro-2-methylphenoxyacetic Acid (MCPA) by Goethite. Environmental Science & Technology, 2014, 48, 11803-11810.	4.6	38
18565	Ab initio investigations of the phase stability in tantalum carbides. Acta Materialia, 2014, 80, 341-349.	3.8	72
18566	First-Principles Prediction of New Complex Transition Metal Hydrides for High Temperature Applications. Inorganic Chemistry, 2014, 53, 11849-11860.	1.9	12
18568	Metallization of vanadium dioxide driven by large phonon entropy. Nature, 2014, 515, 535-539.	13.7	252
18569	Structures and thermoelectric properties of double-filled (CaxCe1â^'x)Fe4Sb12 skutterudites. Journal of Solid State Chemistry, 2014, 218, 221-229.	1.4	18
18570	A Highly Selective and Selfâ€Powered Gas Sensor Via Organic Surface Functionalization of pâ€Si/nâ€ZnO Diodes. Advanced Materials, 2014, 26, 8017-8022.	11.1	103
18571	Interplay of hydrogen treatment and nitrogen doping in ZnO nanoparticles: a first-principles study. Nanotechnology, 2014, 25, 145204.	1.3	7
18572	Interactions between silver nanoparticles and polyvinyl alcohol nanofibers. AIP Advances, 2014, 4, .	0.6	28
18573	Perovskite oxides: New candidate materials for low work function electron emitters. , 2014, , .		0
18574	Selective Hydrogenation of Cinnamaldehyde to Cinnamal Alcohol over Platinum/Graphene Catalysts. ChemCatChem, 2014, 6, 3246-3253.	1.8	80
18575	Graphitic Phase of NaCl. Bulk Properties and Nanoscale Stability. Journal of Physical Chemistry Letters, 2014, 5, 4014-4019.	2.1	16
18576	Identifying the Structure of the Intermediate, Li_{2/3}CoPO₄, Formed during Electrochemical Cycling of LiCoPO₄. Chemistry of Materials, 2014, 26, 6193-6205.	3.2	54

#	Article	IF	Citations
18577	Photocatalytic activity of Î±-PbO₂-type TiO₂. Physica Status Solidi - Rapid Research Letters, 2014, 8, 822-826.	1.2	13
18578	Computational and Experimental Investigation of Ti Substitution in Li₁(Ni_xMn_xCo_{1â€“2xâ€“y}Ti_y)O₂ for Lithium Ion Batteries. Journal of Physical Chemistry Letters, 2014, 5, 3649-3655.	6.1	38
18579	Magnetism of zigzag edge phosphorene nanoribbons. Applied Physics Letters, 2014, 105, .	1.5	97
18580	Intrinsic carrier mobility of germanene is larger than graphene's: first-principle calculations. RSC Advances, 2014, 4, 21216-21220.	1.7	144
18581	Manyâ€body and spinâ€orbit effects on directâ€indirect band gap transition of strained monolayer MoS₂ and WS₂. Annalen Der Physik, 2014, 526, L7.	0.9	87
18582	A local topological view of pressure-induced polymorphs in SiO2. Theoretical Chemistry Accounts, 2014, 133, 1.	0.5	6
18583	Unexpected Reconstruction of theÎ±-Boron (111) Surface. Physical Review Letters, 2014, 113, 176101.	2.9	29
18584	Impurity-related effects in poly(3-hexylthiophene) crystals. Physical Chemistry Chemical Physics, 2014, 16, 25557-25563.	1.3	13
18585	Quantum spin Hall effect in two-dimensional transition metal dichalcogenides. Science, 2014, 346, 1344-1347.	6.0	1,558
18586	The extraordinary magnetoelectric response in silicene doped with Fe and Cr atoms. Applied Physics Letters, 2014, 105, .	1.5	18
18587	On the role of long range interactions for the adsorption of sexithiophene on Ag(110) surface. Journal of Chemical Physics, 2014, 140, 144703.	1.2	16
18588	Exchange integrals in magnetoelectric hexagonal ferrite (SrCo2Ti2Fe8O19): A density functional study. Journal of Applied Physics, 2014, 115, 17D908.	1.1	10
18589	The modulation of metalâ€“insulator transition temperature of vanadium dioxide: a density functional theory study. Journal of Materials Chemistry C, 2014, 2, 9283-9293.	2.7	58
18590	Phase transitions and antiferroelectricity in<mml:math xmlns:mml="http://www.w3.org/1998/Math/MathML"><mml:mrow><mml:mi>BiFe</mml:mi><mml:msub><mml:mi mathvariant="normal">O</mml:mi><mml:mn>3</mml:mn></mml:msub></mml:mrow></mml:math>from atomic-level simulations. Physical Review B, 2014, 90, .	1.1	18
18591	Synthesis, transport properties, and electronic structure of Cu2CdSnTe4. Applied Physics Letters, 2014, 104, .	1.5	25
18592	Dynamics of H2 Eley-Rideal abstraction from W(110): Sensitivity to the representation of the molecule-surface potential. Journal of Chemical Physics, 2014, 141, 024701.	1.2	15
18593	Initial stages of ITO/Si interface formation: In situ x-ray photoelectron spectroscopy measurements upon magnetron sputtering and atomistic modelling using density functional theory. Journal of Applied Physics, 2014, 115, 083705.	1.1	16
18594	Permutation invariant polynomial neural network approach to fitting potential energy surfaces. III. Molecule-surface interactions. Journal of Chemical Physics, 2014, 141, 034109.	1.2	120

#	Article	IF	Citations
18595	Dynamical properties and their strain-dependence of ZnSe(ZnSe:N): Zinc-blende and wurtzite. AIP Advances, 2014, 4, .	0.6	7
18596	Quasi-Free-Standing Graphene Monolayer on a Ni Crystal through Spontaneous Na Intercalation. Physical Review X, 2014, 4, .	2.8	11
18597	Tetravalent Doping of <scp><scp>CeO</scp></scp>₂: The Impact of Valence Electron Character on Group IV Dopant Influence. Journal of the American Ceramic Society, 2014, 97, 258-266.	1.9	36
18598	Vanadium Oxide Compounds: Structure, Properties, and Growth from the Gas Phase. Chemical Vapor Deposition, 2014, 20, 299-311.	1.4	135
18599	Predicting polymeric crystal structures by evolutionary algorithms. Journal of Chemical Physics, 2014, 141, 154102.	1.2	41
18600	Adsorption and dissociation of O₂ on MoSe₂ and MoTe₂ monolayers: ab initio study. International Journal of Modern Physics B, 2014, 28, 1450195.	1.0	10
18601	Accelerating the Design of Solar Thermal Fuel Materials through High Throughput Simulations. Nano Letters, 2014, 14, 7046-7050.	4.5	27
18602	<mml:math xmlns:mml="http://www.w3.org/1998/Math/MathML"><mml:mrow><mml:mi>G</mml:mi><mml:mi>W</mml:mi></mml:mrow></mml:m on post-transition-metal oxides. Physical Review B, 2014, 89, .	1.1	24
18603	Band alignment of semiconductors from density-functional theory and many-body perturbation theory. Physical Review B, 2014, 90, .	1.1	271
18604	Structural, electronic, vibrational and dielectric properties of selected high-shape K semiconductor oxides. Journal Physics D: Applied Physics, 2014, 47, 413001.	1.3	5
18605	Topological<mml:math xmlns:mml="http://www.w3.org/1998/Math/MathML"><mml:mi>Î±</mml:mi></mml:math>-Sn surface states versus film thickness and strain. Physical Review B, 2014, 90, .	1.1	26
18606	Thermal equation of state of solid naphthalene to 13 GPa and 773 K: In situ X-ray diffraction study and first principles calculations. Journal of Chemical Physics, 2014, 140, 164508.	1.2	26
18607	Theoretical Study of Electronic Properties of X-Doped (X = F, Cl, Br, I) VO₂ Nanoparticles for Thermochromic Energy-Saving Foils. Journal of Physical Chemistry A, 2014, 118, 11114-11118.	1.1	24
18608	Metallic filament formation by aligned oxygen vacancies in ZnO-based resistive switches. Journal of Applied Physics, 2014, 115, .	1.1	10
18609	Quinoneâ€Modified Surfaces for Enhanced Enzymeâ€“Electrode Interactions in Pyrroloquinolineâ€Quinoneâ€Dependent Glucose Dehydrogenase Anodes. ChemElectroChem, 2014, 1, 2017-2028.	1.7	14
18610	Binding and Diffusion of Lithium in Graphite: Quantum Monte Carlo Benchmarks and Validation of van der Waals Density Functional Methods. Journal of Chemical Theory and Computation, 2014, 10, 5318-5323.	2.3	117
18611	Surface structures of In-Pd intermetallic compounds. II. A theoretical study. Journal of Chemical Physics, 2014, 141, 084703.	1.2	11
18612	Lattice dynamics and thermal conductivity of skutterudites<mml:math xmlns:mml="http://www.w3.org/1998/Math/MathML"><mml:msub><mml:mi mathvariant="normal">CoSb</mml:mi><mml:mn>3</mml:mn></mml:msub></mml:math>and<mml:math xmlns:mml="http://www.w3.org/1998/Math/MathML"><mml:msub><mml:mi mathvariant="normal">IrSb</mml:mi><mml:mn>3</mml:mn></mml:msub></mml:math>from first principles: Why<mml:math xmlns:mml="http://www.w3.org/1998/Math/MathML"><mml:msub><mml:mi m	1.1	51

#	Article	IF	Citations
18613	Electronic structures and magnetic stabilities of 2D Mn-doped GaAs nanosheets: The role of long-range exchange interactions and doping strategies. Journal of Applied Physics, 2014, 116, .	1.1	16
18614	Undercoordinated indium as an intrinsic electron-trap center in amorphous InGaZnO4. NPG Asia Materials, 2014, 6, e143-e143.	3.8	36
18615	Dopant-site-dependent scattering by dislocations in epitaxial films of perovskite semiconductor BaSnO3. APL Materials, 2014, 2, .	2.2	61
18616	The effects of surface bond relaxation on electronic structure of Sb2Te3nano-films by first-principles calculation. AIP Advances, 2014, 4, 107115.	0.6	3
18617	A theoretical investigation on phase transition and dissociation of ammonium bromide under high pressure. Science Bulletin, 2014, 59, 5272-5277.	1.7	2
18618	Elinvar effect in Co-doped TiNi strain glass alloys. Applied Physics Letters, 2014, 105, .	1.5	31
18619	Firstâ€principles study of the electronic and magnetic properties of 4â€8 lineâ€defectâ€embedded BN sheets decorated with transition metals. Annalen Der Physik, 2014, 526, 415-422.	0.9	18
18621	Propene epoxidation with O₂or H₂â€“O₂mixtures over silver catalysts: theoretical insights into the role of the particle size. Physical Chemistry Chemical Physics, 2014, 16, 26600-26612.	1.3	18
18622	Fe adsorption on hematite (Î±-Fe2O3) (0001) and magnetite (Fe3O4) (111) surfaces. Journal of Chemical Physics, 2014, 141, 134707.	1.2	14
18623	Electronic structure and crystal phase stability of palladium hydrides. Journal of Applied Physics, 2014, 116, .	1.1	37
18624	Organic molecule-functionalized Zn3P2 nanowires for photochemical H2 production: DFT and experimental analyses. International Journal of Hydrogen Energy, 2014, 39, 19887-19898.	3.8	5
18625	Correlated Optical and Magnetic Properties in Photoreduced Graphene Oxide. Journal of Physical Chemistry C, 2014, 118, 28258-28265.	1.5	21
18626	Alloy Negative Electrodes for Li-Ion Batteries. Chemical Reviews, 2014, 114, 11444-11502.	23.0	1,675
18627	Laser surface alloying of molybdenum on aluminum for enhanced wear resistance. Surface and Coatings Technology, 2014, 258, 337-342.	2.2	35
18628	Incorporation effects of Si in TiC x thin films. Surface and Coatings Technology, 2014, 258, 392-397.	2.2	17
18629	Kinetics and Thermodynamics of H₂O Dissociation on Reduced CeO₂(111). Journal of Physical Chemistry C, 2014, 118, 27402-27414.	1.5	91
18630	Integral equation model for warm and hot dense mixtures. Physical Review E, 2014, 90, 033110.	0.8	28
18631	Artificial chemical and magnetic structure at the domain walls of an epitaxial oxide. Nature, 2014, 515, 379-383.	13.7	146

#	Article	IF	Citations
18632	Unusual role of epilayerâ€“substrate interactions in determining orientational relations in van der Waals epitaxy. Proceedings of the National Academy of Sciences of the United States of America, 2014, 111, 16670-16675.	3.3	64
18633	Ion Intercalation into Two-Dimensional Transition-Metal Carbides: Global Screening for New High-Capacity Battery Materials. Journal of the American Chemical Society, 2014, 136, 16270-16276.	6.6	528
18634	First-Principles Analysis of Defect-Mediated Li Adsorption on Graphene. ACS Applied Materials & Interfaces, 2014, 6, 21141-21150.	4.0	120
18635	First-Principles Predictions and in Situ Experimental Validation of Alumina Atomic Layer Deposition on Metal Surfaces. Chemistry of Materials, 2014, 26, 6752-6761.	3.2	68
18636	Localization of metallicity and magnetic properties of graphene and of graphene nanoribbons doped with boron clusters. Philosophical Magazine, 2014, 94, 1841-1858.	0.7	8
18637	Experimental verification of the high pressure crystal structures in NH3BH3. Journal of Chemical Physics, 2014, 140, 244507.	1.2	11
18638	Characterization of oxygen impurity in silicon nitride storage layer: A first-principles investigation. Physica Status Solidi (B): Basic Research, 2014, 251, 1212-1218.	0.7	7
18639	Modelling of monovacancy diffusion in W over wide temperature range. Journal of Applied Physics, 2014, 115, 123504.	1.1	16
18640	Adsorption of formic acid on rutile TiO2 (110) revisited: An infrared reflection-absorption spectroscopy and density functional theory study. Journal of Chemical Physics, 2014, 140, 034705.	1.2	49
18641	Modification of the Galliumâ€Doped Zinc Oxide Surface with Selfâ€Assembled Monolayers of Phosphonic Acids: A Joint Theoretical and Experimental Study. Advanced Functional Materials, 2014, 24, 3593-3603.	7.8	31
18642	Inelastic Neutron Scattering and Density Functional Theoryâ€“Molecular Dynamics Study of Si Dynamics in <scp><scp>Ti</scp></scp>₃<scp><scp>SiC</scp></scp>₂. Journal of the American Ceramic Society, 2014, 97, 916-922.	1.9	2
18643	Structural and electrical properties of armchair CdS nanotubes. Journal of Applied Physics, 2014, 115, 214307.	1.1	8
18644	Sulfur dimers adsorbed on Au(111) as building blocks for sulfur octomers formation: A density functional study. Journal of Chemical Physics, 2014, 141, 044713.	1.2	7
18645	Ferromagnetic-nonmagnetic and metal-insulator phase transitions at the interfaces of KTaO3 and PbTiO3. Journal of Applied Physics, 2014, 116, .	1.1	10
18646	Switchable Dielectric, Piezoelectric, and Secondâ€Harmonic Generation Bistability in a New Improper Ferroelectric above Room Temperature. Advanced Materials, 2014, 26, 4515-4520.	11.1	146
18647	Photoelectrochemical Hydrogen Production on Î±â€Fe₂O₃ (0001): Insights from Theory and Experiments. ChemSusChem, 2014, 7, 162-171.	3.6	27
18648	Water on BN doped benzene: A hard test for exchange-correlation functionals and the impact of exact exchange on weak binding. Journal of Chemical Physics, 2014, 141, 18C530.	1.2	25
18649	Direct tunneling through high-Îºamorphous HfO2: Effects of chemical modification. Journal of Applied Physics, 2014, 116, 023703.	1.1	15

#	Article	IF	Citations
18650	Phonons and electronâ€phonon coupling in grapheneâ€hâ€BN heterostructures. Annalen Der Physik, 2014, 526, 381-386.	0.9	40
18651	Signatures of a Twoâ€Dimensional Ferromagnetic Electron Gas at the La_{0.7}Sr_{0.3}MnO₃/SrTiO₃ Interface Arising From Orbital Reconstruction. Advanced Materials, 2014, 26, 7516-7520.	11.1	23
18652	First-principles study for stability and binding mechanism of graphene/Ni(111) interface: Role of vdW interaction. Journal of Chemical Physics, 2014, 141, 044708.	1.2	56
18653	Computational synthesis of single-layer GaN on refractory materials. Applied Physics Letters, 2014, 105, .	1.5	46
18654	Selective Dissociation of Dihydrogen over Dioxygen on a Hindered Platinum Surface for the Direct Synthesis of Hydrogen Peroxide. ChemCatChem, 2014, 6, 2836-2842.	1.8	23
18655	A first principle study of adsorption of two proximate nitrogen atoms on graphene. International Journal of Quantum Chemistry, 2014, 114, 1619-1629.	1.0	8
18656	A Tailored Catalyst for the Sustainable Conversion of Glycerol to Acrolein: Mechanistic Aspect of Sequential Dehydration. ChemSusChem, 2014, 7, 2193-2201.	3.6	25
18657	Water Reaction Mechanism in Metal Organic Frameworks with Coordinatively Unsaturated Metal Ions: MOF-74. Chemistry of Materials, 2014, 26, 6886-6895.	3.2	149
18658	Edge and interfacial states in a two-dimensional topological insulator: Bi(111) bilayer on<mml:math xmlns:mml="http://www.w3.org/1998/Math/MathML"><mml:msub><mml:mi>Bi</mml:mi><mml:mn>2</mml:mn></mml:msub><mml:m Physical Review B, 2014, 89, .	1.1	78
18659	Electronic structure and thermoelectric properties of orthorhombic SrLiAs. Journal of Applied Physics, 2014, 116, 033705.	1.1	6
18661	Dissociative chemisorption of methane on metal surfaces: Tests of dynamical assumptions using quantum models and ab initio molecular dynamics. Journal of Chemical Physics, 2014, 141, 054102.	1.2	80
18662	Multi-scale computational study of the molten salt based recycling of spent nuclear fuels. International Journal of Energy Research, 2014, 38, 1987-1993.	2.2	10
18663	Low thermal conductivity and triaxial phononic anisotropy of SnSe. Applied Physics Letters, 2014, 105, .	1.5	226
18664	Li4FeH6: Iron-containing complex hydride with high gravimetric hydrogen density. APL Materials, 2014, 2, .	2.2	31
18665	Ab initio study of molecular and atomic oxygen on GeTe(111) surfaces. Journal of Applied Physics, 2014, 116, .	1.1	10
18666	Modelling near-surface bound electron states in a 3D topological insulator: analytical and numerical approaches. Journal of Physics Condensed Matter, 2014, 26, 485003.	0.7	12
18667	Electronic structures and optical properties of SnSe2(1â^'x)O2x alloys. Computational Materials Science, 2014, 95, 712-717.	1.4	9
18669	Nonfrustrated Interlayer Order and Its Relevance to the Bose-Einstein Condensation of Magnons in<mml:math xmlns:mml="http://www.w3.org/1998/Math/MathML" display="inline"><mml:mrow><mml:msub><mml:mrow><mml:mi>BaCuSi</mml:mi></mml:mrow><mml:mrow><mml:mn>2</mml:mn></mml:mrow></mml:msub><mml:mi>O</mml:mi><mml:mrow><mml:mn>6</mml:mn></mml:mrow></mml:msub></mml:mrow></mml:mi> mathvariant="normal"> Physical Review Letters, 2014, 112, 187202.	2.0	94

#	Article	IF	Citations
18670	First-principle calculations of high-pressure phase transformations in RuC. Europhysics Letters, 2014, 105, 46004.	0.7	5
18671	Density functional theory study of adsorption of H2O, H, O, and OH on stepped platinum surfaces. Journal of Chemical Physics, 2014, 140, 134708.	1.2	83
18672	Exploration for Two-Dimensional Electrides via Database Screening andAbÂInitioCalculation. Physical Review X, 2014, 4, .	2.8	84
18673	Validating density-functional theory simulations at high energy-density conditions with liquid krypton shock experiments to 850 GPa on Sandia's Z machine. Physical Review B, 2014, 90, .	1.1	29
18674	Interlaced crystals having a perfect Bravais lattice and complex chemical order revealed by real-space crystallography. Nature Communications, 2014, 5, 5431.	5.8	29
18675	Density functional theory calculations of stability and diffusion mechanisms of impurity atoms in Ge crystals. Journal of Applied Physics, 2014, 116, .	1.1	12
18676	Costless Derivation of Dispersion Coefficients for Metal Surfaces. Journal of Chemical Theory and Computation, 2014, 10, 5002-5009.	2.3	49
18677	Ab Initio Study of Thin Oxideâ€“Metal Overlayers as an Inverse Catalytic System for Dioxygen Reduction and Enhanced CO Tolerance. ACS Catalysis, 2014, 4, 4074-4080.	5.5	42
18678	High Coverage Water Aggregation and Dissociation on Fe(100): A Computational Analysis. Journal of Physical Chemistry C, 2014, 118, 26139-26154.	1.5	47
18679	New phases of binary compounds: CsCl-type RuGe and RuSn. Europhysics Letters, 2014, 107, 56003.	0.7	6
18680	Probing the Coverage Dependence of Site and Adsorbate Configurational Correlations on (111) Surfaces of Late Transition Metals. Journal of Physical Chemistry C, 2014, 118, 25597-25602.	1.5	29
18681	Molecular Dynamics of the Electron-Induced Reaction of Diiodomethane on Cu(110). Journal of Physical Chemistry C, 2014, 118, 25525-25533.	1.5	12
18682	Structural, optical, and electrical properties of strained La-doped SrTiO3 films. Journal of Applied Physics, 2014, 116, .	1.1	53
18683	Density functional theory simulation of hydrogen-bonding structure and vibrational densities of states at the quartz (1â€‰0â€‰1)-water interface and its relation to dissolution as a function of solution pH and ionic strength. Journal of Physics Condensed Matter, 2014, 26, 244101.	0.7	20
18684	Density Functional Theory (DFT) simulations of porous tantalum pentoxide. Journal of Physics: Conference Series, 2014, 500, 032005.	0.3	0
18685	Oxygen Transport in Perovskite-Type Solid Oxide Fuel Cell Materials: Insights from Quantum Mechanics. Accounts of Chemical Research, 2014, 47, 3340-3348.	7.6	121
18686	Visualization of electron orbitals in scanning tunneling microscopy. JETP Letters, 2014, 99, 731-741.	0.4	5
18687	Platinum nanoparticles on different types of titanium dioxide surface: A quantum-chemical modeling. Russian Journal of Inorganic Chemistry, 2014, 59, 816-823.	0.3	9

#	Article	IF	Citations
18688	Theoretical study of the thermodynamic stability and electronic structure of thin films of 3C, 2H, and 2D silicon carbides. Physics of the Solid State, 2014, 56, 1654-1658.	0.2	1
18689	Quantum molecular dynamics simulation of hydrogen diffusion in zirconium hydride. Physics of the Solid State, 2014, 56, 1879-1885.	0.2	11
18690	Ideal stoichiometric technetium nitrides under pressure: A first-principles study. Journal of Superhard Materials, 2014, 36, 288-295.	0.5	7
18691	Phonon Self-Energy and Origin of Anomalous Neutron Scattering Spectra in SnTe and PbTe Thermoelectrics. Physical Review Letters, 2014, 112, 175501.	2.9	125
18692	Two-Dimensional Transition-Metal Electride Y₂C. Chemistry of Materials, 2014, 26, 6638-6643.	3.2	151
18693	First-principles<mml:math xmlns:mml="http://www.w3.org/1998/Math/MathML"><mml:mrow><mml:mi>DFT</mml:mi><mml:mo>+</mml:mo><mml:mi>G</mml:mi> of oxygen vacancies in rutile<mml:math xmlns:mml="http://www.w3.org/1998/Math/MathML"><mml:msub><mml:mtext>TiO</mml:mtext><mml:mn>2</mml:mn></mml:msub> Physical Review B, 2014, 89, .	1.1	80
18694	Dissociative Adsorption of Molecules on Graphene and Silicene. Journal of Physical Chemistry C, 2014, 118, 27574-27582.	1.5	43
18695	Defectâ€Driven Interfacial Electronic Structures at an Organic/Metalâ€Oxide Semiconductor Heterojunction. Advanced Materials, 2014, 26, 4711-4716.	11.1	46
18696	Intrinsic and interfacial effect of electrode metals on the resistive switching behaviors of zinc oxide films. Nanotechnology, 2014, 25, 425204.	1.3	49
18697	Fitting of interatomic potentials without forces: A parallel particle swarm optimization algorithm. Computer Physics Communications, 2014, 185, 3090-3093.	3.0	7
18698	Point charges and atomic multipole moments of Si and O in amorphous SiO2 for the estimation of the electrostatic field and potential. Journal of Structural Chemistry, 2014, 55, 398-408.	0.3	1
18699	Oxide interfaces for novel electronic applications. New Journal of Physics, 2014, 16, 025005.	1.2	157
18700	Full Determination of Individual Reconstructed Atomic Columns in Intermixed Heterojunctions. Nano Letters, 2014, 14, 6584-6589.	4.5	1
18701	A charge optimized many-body potential for titanium nitride (TiN). Journal of Physics Condensed Matter, 2014, 26, 265004.	0.7	10
18702	Band gap opening in bilayer silicene by alkali metal intercalation. Journal of Physics Condensed Matter, 2014, 26, 475303.	0.7	30
18703	Design of the Alkali-Metal-Doped WO₃ as a Near-Infrared Shielding Material for Smart Window. Industrial & Engineering Chemistry Research, 2014, 53, 17981-17988.	1.8	68
18704	Superconductivity of Ca2InN with a layered structure embedding an anionic indium chain array. Superconductor Science and Technology, 2014, 27, 055005.	1.8	3
18705	Efficient determination of alloy ground-state structures. Physical Review B, 2014, 90, .	1.1	11

#	Article	IF	Citations
18706	Ab Initio Structure Search and in Situ ⁷Li NMR Studies of Discharge Products in the Liâ€“S Battery System. Journal of the American Chemical Society, 2014, 136, 16368-16377.	6.6	132
18707	Computational Study on Removal of Epoxide from Narrow Zigzag Graphene Nanoribbons. Journal of Physical Chemistry C, 2014, 118, 27123-27130.	1.5	2
18708	Vacancy formation on C60/Pt (111): unraveling the complex atomistic mechanism. Nanotechnology, 2014, 25, 385602.	1.3	25
18709	Impact of exact exchange in the description of the electronic structure of organic charge-transfer molecular crystals. Physical Review B, 2014, 90, .	1.1	24
18710	Optoelectronic excitations and photovoltaic effect in strongly correlated materials. Physical Review B, 2014, 90, .	1.1	26
18711	Performance Limits Projection of Black Phosphorous Field-Effect Transistors. IEEE Electron Device Letters, 2014, 35, 963-965.	2.2	84
18712	First principles study of point defects in SnS. Physical Chemistry Chemical Physics, 2014, 16, 26176-26183.	1.3	75
18713	Kinetic, Spectroscopic, and Theoretical Assessment of Associative and Dissociative Methanol Dehydration Routes in Zeolites. Angewandte Chemie - International Edition, 2014, 53, 12177-12181.	7.2	122
18714	What Makes Hydroxamate a Promising Anchoring Group in Dye-Sensitized Solar Cells? Insights from Theoretical Investigation. Journal of Physical Chemistry Letters, 2014, 5, 3992-3999.	2.1	61
18715	Computational studies of electrochemical CO₂ reduction on subnanometer transition metal clusters. Physical Chemistry Chemical Physics, 2014, 16, 26584-26599.	1.3	62
18716	Room-temperature magnetic order on zigzag edges of narrow graphene nanoribbons. Nature, 2014, 514, 608-611.	13.7	662
18717	Density-Functional Prediction of a Surface Magnetic Phase in<mml:math xmlns:mml="http://www.w3.org/1998/Math/MathML" display="inline"><mml:mrow><mml:msub><mml:mrow><mml:mi>SrTiO</mml:mi></mml:mrow><mml:mrow><mml:mn>3</mml:mn></mml:mrow>	2.9	26
18718	<mml:math xmlns:mml="http://www.w3.org/1998/Math/MathML" display="inline"><mml:mrow><mml:msub><mml:mrow><mml:mi>BaFe</mml:mi></mml:mrow><mml:mrow><mml:mn>2</mml:mn></mml:mrow></ mathvariant="normal">S</mml:mi><mml:msub><mml:mrow><mml:mi mathvariant="normal">e</mml:mi></mml:mrow><mml:mrow><mml:mn>3</mml:mn></mml:mrow></mml:msub></mml:mrow></mml: A High<mml:math xmlns:mml="http://www.w3.org/1998/Math/MathML" display="inline"><mml:mrow><mml:msub><mml:mrow><mml:mi>T</mml:mi></mml:mrow><mml: Physic	2.9	67
18719	Band convergence in the non-cubic chalcopyrite compounds Cu₂MGeSe₄. Journal of Materials Chemistry C, 2014, 2, 10189-10194.	2.7	57
18720	The stability, electronic properties, and hardness of SiN2 under high pressure. RSC Advances, 2014, 4, 55023-55027.	1.7	9
18721	Structures and energies of Cu clusters on Fe and Fe₃C surfaces from density functional theory computation. Physical Chemistry Chemical Physics, 2014, 16, 26997-27011.	1.3	11
18722	Luminescence and electronic properties of Ba₂MgSi₂O₇:Eu²⁺: a combined experimental and hybrid density functional theory study. Journal of Materials Chemistry C, 2014, 2, 8328-8332.	2.7	35
18723	The first principles studies on the reaction pathway of the oxidative dehydrogenation of ethane on the undoped and doped carbon catalyst. Journal of Materials Chemistry A, 2014, 2, 5287.	5.2	45

#	Article	IF	Citations
18724	Theory of mass transport in sodium alanate. Journal of Materials Chemistry A, 2014, 2, 4438-4448.	5.2	10
18725	Magnesium ion dynamics in Mg(BH₄)_{2(1â^'x)}X_{2x}(X = Cl or) Tj ETQq1 1 0.784314 rgBT /Overlock 1366-1370.	1.7	28
18726	Hydrogen storage on metal oxide model clusters using density-functional methods and reliable van der Waals corrections. Physical Chemistry Chemical Physics, 2014, 16, 5382.	1.3	21
18727	Ab initio study of graphene-like monolayer molybdenum disulfide as a promising anode material for rechargeable sodium ion batteries. RSC Advances, 2014, 4, 43183-43188.	1.7	88
18728	A study on adatom transport through (â^š3 Ã— â^š3)â€“R30Â°â€“CH₃S self-assembled monolayers on Au(111) using first principles calculations. Physical Chemistry Chemical Physics, 2014, 16, 23067-23073.	1.3	3
18729	Mode coupling between nonpolar and polar phonons as the origin of improper ferroelectricity in hexagonal LuMnO₃. Journal of Materials Chemistry C, 2014, 2, 4126-4132.	2.7	13
18730	Insulatorâ€“half metal transition driven by hole doping: a density functional study of Sr-doped La2VMnO6. Dalton Transactions, 2014, 43, 8698.	1.6	5
18731	Pressure-induced isostructural phase transition in CaB₄. RSC Advances, 2014, 4, 42523-42529.	1.7	6
18732	Understanding the defect chemistry of alkali metal strontium silicate solid solutions: insights from experiment and theory. Journal of Materials Chemistry A, 2014, 2, 17919-17924.	5.2	34
18733	Poisoning effect of adsorbed CO during CO₂ electroreduction on late transition metals. Physical Chemistry Chemical Physics, 2014, 16, 20429-20435.	1.3	63
18734	The effect of the supramolecular network of (Z)-3-(4-(diphenylamino)phenyl)-2-(pyridin-2-yl)-acrylonitrile on the fluorescence behavior of a single crystal: experimental and theoretical studies. CrystEngComm, 2014, 16, 8591-8604.	1.3	10
18735	Low effective mass leading to an improved ZT value by 32% for n-type BiCuSeO: a first-principles study. Journal of Materials Chemistry A, 2014, 2, 13923.	5.2	42
18736	Ab initio DFT+U analysis of oxygen transport in LaCoO₃: the effect of Co³⁺ magnetic states. Journal of Materials Chemistry A, 2014, 2, 8060-8074.	5.2	76
18737	Engineering the Effective p-Type Dopant in GaAs/InAs Coreâ€“Shell Nanowires with Surface Dangling Bonds. Journal of Physical Chemistry C, 2014, 118, 25209-25214.	1.5	1
18738	Formation and catalytic activity of Pt supported on oxidized graphene for the CO oxidation reaction. Physical Chemistry Chemical Physics, 2014, 16, 7887-7895.	1.3	75
18739	The magnetism of Fe₄N/oxides (MgO, BaTiO₃, BiFeO₃) interfaces from first-principles calculations. RSC Advances, 2014, 4, 48848-48859.	1.7	12
18740	Theoretical insight into chlorine adsorption on the Fe(100) surface. Physical Chemistry Chemical Physics, 2014, 16, 8575-8581.	1.3	20
18741	The adsorption behaviour of CH4 on microporous carbons: effects of surface heterogeneity. Physical Chemistry Chemical Physics, 2014, 16, 11037.	1.3	55

#	Article	IF	Citations
18742	Role of the nano amorphous interface in the crystallization of Sb2Te3 towards non-volatile phase change memory: insights from first principles. Physical Chemistry Chemical Physics, 2014, 16, 10810.	1.3	24
18743	Orientation effects in morphology and electronic properties of anatase TiO2 one-dimensional nanostructures. II. Nanotubes. Physical Chemistry Chemical Physics, 2014, 16, 9490.	1.3	15
18744	Vacancy patterning and patterning vacancies: controlled self-assembly of fullerenes on metal surfaces. Nanoscale, 2014, 6, 10850-10858.	2.8	6
18745	Large polarization but small electron transfer for water around Al3+ in a highly hydrated crystal. Physical Chemistry Chemical Physics, 2014, 16, 9351.	1.3	4
18746	Effect of oxygen vacancy on the structural and electronic characteristics of crystalline Zn₂SnO₄. Journal of Materials Chemistry C, 2014, 2, 8381-8387.	2.7	19
18747	First-principles calculations of finite-temperature thermodynamic properties of binary solid solutions in the Alâ€“Cuâ€“Mg system. Calphad: Computer Coupling of Phase Diagrams and Thermochemistry, 2014, 47, 196-210.	0.7	7
18748	Ga-vacancy induced room temperature ferromagnetism observed in N-irradiated GaN films. Chemical Physics Letters, 2014, 616-617, 161-164.	1.2	18
18749	Surfaces of Rutile MnO₂ Are Electronically Conducting, Whereas the Bulk Material Is Insulating. Journal of Physical Chemistry C, 2014, 118, 25009-25015.	1.5	25
18750	Pressure dependence of structural and dynamical properties in melt sulfur: Evidence for two successive chain breakages. Chemical Physics Letters, 2014, 616-617, 131-136.	1.2	7
18751	Transport and optical properties of warm dense aluminum in the two-temperature regime: Ab initio calculation and semiempirical approximation. Physics of Plasmas, 2014, 21, .	0.7	50
18752	Computational study of the energetics and defect clustering tendencies for Y- and La-doped UO2. Acta Materialia, 2014, 78, 282-289.	3.8	19
18753	Electronic and Magnetic Properties of BiFeO₃: Gd³⁺. Ferroelectrics, 2014, 461, 85-91.	0.3	6
18754	Structural characterization of slightly boron-deficient LiB, LiB_{0.9} and LiB_{0.8}, under pressure. Journal of Physics Condensed Matter, 2014, 26, 475402.	0.7	1
18755	First-principles investigation on dimerization of metal-encapsulated gold nanoclusters. RSC Advances, 2014, 4, 192-198.	1.7	7
18756	Site-specific catalytic activity in exfoliated MoS₂single-layer polytypes for hydrogen evolution: basal plane and edges. Journal of Materials Chemistry A, 2014, 2, 20545-20551.	5.2	150
18757	Ab initio ORTEP drawings: a case study of N-based molecular crystals with different chemical nature. CrystEngComm, 2014, 16, 10907-10915.	1.3	32
18758	Nitranilic acid hexahydrate, a novel benchmark system of the Zundel cation in an intrinsically asymmetric environment: spectroscopic features and hydrogen bond dynamics characterised by experimental and theoretical methods. Physical Chemistry Chemical Physics, 2014, 16, 998-1007.	1.3	14
18759	Modeling Catalytic Steps on Extra-Framework Metal Centers in Zeolites. A Case Study on Ethylene Dimerization. Journal of Physical Chemistry C, 2014, 118, 25077-25088.	1.5	16

#	Article	IF	Citations
18760	The adsorption and dissociation of methane on cobalt surfaces: thermochemistry and reaction barriers. RSC Advances, 2014, 4, 43004-43011.	1.7	25
18761	Photophysical, bandstructural, and textural properties of o-FeNbO₄ in relation to its cocatalyst-assisted photoactivity for water oxidation. RSC Advances, 2014, 4, 33435-33445.	1.7	26
18762	Oxygen vacancies in self-assemblies of ceria nanoparticles. Journal of Materials Chemistry A, 2014, 2, 18329-18338.	5.2	33
18763	First-principles study of borohydride adsorption properties on osmium nanoparticles and surfaces: understanding the effects of facets, size and local sites. Catalysis Science and Technology, 2014, 4, 1301-1312.	2.1	5
18764	New manifold two-dimensional single-layer structures of zinc-blende compounds. Journal of Materials Chemistry A, 2014, 2, 17971-17978.	5.2	107
18765	Density functional study of the Ge(111)c(2 Ã— 8) surface using the modified Becke-Johnson exchange potential with LDA correlation and spinâ€“orbit interactions. RSC Advances, 2014, 4, 48245-48253.	1.7	2
18766	Origin and effect of Inâ€“Sn ordering in InSnCo₃S₂: a neutron diffraction and DFT study. RSC Advances, 2014, 4, 42183-42189.	1.7	21
18767	Mechanical and electronic properties of pristine and Ni-doped Si, Ge, and Sn sheets. Physical Chemistry Chemical Physics, 2014, 16, 1667-1671.	1.3	46
18768	Formation of a G-Quartet-Fe Complex and Modulation of Electronic and Magnetic Properties of the Fe Center. ACS Nano, 2014, 8, 11799-11805.	7.3	35
18769	Thermodynamics of thorium substitution in yttrium iron garnet: comparison of experimental and theoretical results. Journal of Materials Chemistry A, 2014, 2, 16945-16954.	5.2	22
18770	Study of structural, electronic and optical properties of tungsten doped bismuth oxychloride by DFT calculations. Physical Chemistry Chemical Physics, 2014, 16, 21349-21355.	1.3	37
18771	High throughput first-principles calculations of bixbyite oxides for TCO applications. Physical Chemistry Chemical Physics, 2014, 16, 17724-17733.	1.3	25
18772	A semiconductive superhard FeB₄phase from first-principles calculations. Physical Chemistry Chemical Physics, 2014, 16, 22008-22013.	1.3	15
18773	A comparative computational study on the synthesis prescriptions, structures and acid properties of B-, Al- and G-incorporated MTW-type zeolites. RSC Advances, 2014, 4, 47906-47920.	1.7	17
18774	Band structure engineering of monolayer MoS₂by surface ligand functionalization for enhanced photoelectrochemical hydrogen production activity. Nanoscale, 2014, 6, 13565-13571.	2.8	62
18775	Tuning electronic and optical properties of a new class of covalent organic frameworks. Journal of Materials Chemistry C, 2014, 2, 2404.	2.7	32
18776	Interaction of acetone with the Ge(001) surface. RSC Advances, 2014, 4, 12672.	1.7	4
18777	What are grain boundary structures in graphene?. Nanoscale, 2014, 6, 4309-4315.	2.8	34

#	Article	IF	Citations
18778	A DFT study of furan hydrogenation and ring opening on Pd(111). Green Chemistry, 2014, 16, 736-747.	4.6	80
18779	Activation of H2 oxidation at sulphur-exposed Ni surfaces under low temperature SOFC conditions. Physical Chemistry Chemical Physics, 2014, 16, 9383.	1.3	10
18780	Reported and predicted structures of Ba(Co,Nb)1â^'Î´O3 hexagonal perovskite phases. Physical Chemistry Chemical Physics, 2014, 16, 21073-21081.	1.3	3
18781	Density-functional description of electrides. Physical Chemistry Chemical Physics, 2014, 16, 14584-14593.	1.3	76
18782	Computational design of inorganic nonlinear optical crystals based on a genetic algorithm. CrystEngComm, 2014, 16, 10569-10580.	1.3	67
18783	Geometrically induced transitions between semimetal and semiconductor in graphene. Physical Review B, 2014, 90, .	1.1	15
18784	Robust 2D Topological Insulators in van der Waals Heterostructures. ACS Nano, 2014, 8, 10448-10454.	7.3	88
18785	Predictions for p-Type CH₃NH₃PbI₃ Perovskites. Journal of Physical Chemistry C, 2014, 118, 25350-25354.	1.5	71
18786	Assignment of Raman-active vibrational modes of tetragonal mackinawite: Raman investigations and ab initio calculations. RSC Advances, 2014, 4, 25827-25834.	1.7	17
18787	Low energy effective Hamiltonian for giant-gap quantum spin Hall insulators in honeycomb<mml:math xmlns:mml="http://www.w3.org/1998/Math/MathML"><mml:mi>X</mml:mi></mml:math>-hydride/halide<mml:math xmlns:mml="http://www.w3.org/1998/Math/MathML"><mml:mo>(</mml:mo><mml:mi>X</mml:mi><mml:mo>=</mml:mo><mml:mi) Tj 2014, 90, .	1.1	119
18788	Silicane as an Inert Substrate of Silicene: A Promising Candidate for FET. Journal of Physical Chemistry C, 2014, 118, 25278-25283.	1.5	64
18789	Structure, fragmentation patterns, and magnetic properties of small cobalt oxide clusters. Physical Chemistry Chemical Physics, 2014, 16, 21732-21741.	1.3	25
18790	Halide adsorption on close-packed metal electrodes. Physical Chemistry Chemical Physics, 2014, 16, 13630-13634.	1.3	54
18791	A DFT based prediction of gold fullerene Au92Si12 with the aid of silicon. RSC Advances, 2014, 4, 13927.	1.7	18
18792	Sb- and Bi-doped Mg₂Si: location of the dopants, micro- and nanostructures, electronic structures and thermoelectric properties. Dalton Transactions, 2014, 43, 14983-14991.	1.6	55
18793	Mechanical and metallic properties of tantalum nitrides from first-principles calculations. RSC Advances, 2014, 4, 10133.	1.7	55
18794	(Pb,Cd)â€“O covalency in PbTiO3â€“CdTiO3 with enhanced negative thermal expansion. Physical Chemistry Chemical Physics, 2014, 16, 5237.	1.3	11
18795	Investigations on V₂C and V₂CX₂ (X = F, OH) Monolayer as a Promising Anode Material for Li Ion Batteries from First-Principles Calculations. Journal of Physical Chemistry C, 2014, 118, 24274-24281.	1.5	301

#	Article	IF	Citations
18796	Computational investigation of structural and electronic properties of aqueous interfaces of GaN, ZnO, and a GaN/ZnO alloy. Physical Chemistry Chemical Physics, 2014, 16, 12057-12066.	1.3	39
18797	Shape Effect of Pd-Promoted Ga₂O₃ Nanocatalysts for Methanol Synthesis by CO₂ Hydrogenation. Journal of Physical Chemistry C, 2014, 118, 24452-24466.	1.5	73
18798	H-Bond Interaction-Enhanced Dissociation of H₂O on Si(100)-2Ã—1. Journal of Physical Chemistry C, 2014, 118, 24603-24610.	1.5	4
18799	Oxygen Vacancy Formation and Reduction Properties of Î²-MnO₂ Grain Boundaries and the Potential for High Electrochemical Performance. ACS Applied Materials & Interfaces, 2014, 6, 17776-17784.	4.0	39
18800	Anomalous Interfacial Lithium Storage in Graphene/TiO₂ for Lithium Ion Batteries. ACS Applied Materials & Interfaces, 2014, 6, 18147-18151.	4.0	65
18801	A new assisted molecular cycloaddition on boron doped silicon surfaces: a predictive DFT-D study. Physical Chemistry Chemical Physics, 2014, 16, 12164.	1.3	6
18802	Cation Disorder Regulation by Microstate Configurational Entropy in Photovoltaic Absorber Materials Cu2ZnSn(S,Se)4. Journal of Physical Chemistry C, 2014, 118, 24884-24889.	1.5	18
18803	Electron energy level engineering in Zn_{1â^'x}Cd_xSe nanocrystals. Journal of Materials Chemistry C, 2014, 2, 8077-8082.	2.7	8
18804	Thermodynamic study of benzene and hydrogen coadsorption on Pd(111). Physical Chemistry Chemical Physics, 2014, 16, 23754-23768.	1.3	25
18805	C60 molecules grown on a Si-supported nanoporous supramolecular network: a DFT study. Physical Chemistry Chemical Physics, 2014, 16, 14722-14729.	1.3	1
18806	Screened coulomb hybrid DFT investigation of band gap and optical absorption predictions of CuVO₃, CuNbO₃ and Cu₅Ta₁₁O₃₀ materials. Physical Chemistry Chemical Physics, 2014, 16, 18198-18204.	1.3	40
18807	The Family of LiCo₆P₄ Type Compounds â€“ Trends in Electronic Structure and Chemical Bonding. Zeitschrift Fur Anorganische Und Allgemeine Chemie, 2014, 640, 1641-1647.	0.6	5
18808	Two-dimensional layered transition metal disulphides for effective encapsulation of high-capacity lithium sulphide cathodes. Nature Communications, 2014, 5, 5017.	5.8	530
18809	Li₂FePO₄F and its metal-doping for Li-ion batteries: an ab initio study. RSC Advances, 2014, 4, 50195-50201.	1.7	6
18810	High pressure phases of different tetraboranes. High Pressure Research, 2014, 34, 59-69.	0.4	3
18811	Chemical Modification and Energetically Favorable Atomic Disorder of a Layered Thermoelectric Material TmCuTe₂ Leading to High Performance. Chemistry - A European Journal, 2014, 20, 15401-15408.	1.7	35
18812	On-surface synthesis of organometallic complex via metalâ€“alkene interactions. Chemical Communications, 2014, 50, 15924-15927.	2.2	10
18813	First-principles GGA+Ustudy of the different conducting properties in pentavalent-ion-doped anatase and rutile TiO₂. Journal Physics D: Applied Physics, 2014, 47, 275101.	1.3	36

#	Article	IF	Citations
18814	The effect of simultaneous substitution on the electronic band structure and thermoelectric properties of Se-doped Co3SnInS2 with the Kagome lattice. Solid State Communications, 2014, 199, 56-60.	0.9	16
18815	Honeycomb network of indium trimers and monomers on Si(111)-(2Ã—2). Physical Review B, 2014, 89, .	1.1	13
18816	Water clustering on nanostructured iron oxide films. Nature Communications, 2014, 5, 4193.	5.8	65
18817	Non-collinear spin DFT for lanthanide ions in doped hexagonal NaYF₄. Molecular Physics, 2014, 112, 546-556.	0.8	19
18818	Large and robust electrical spin injection into GaAs at zero magnetic field using an ultrathin CoFeB/MgO injector. Physical Review B, 2014, 90, .	1.1	56
18819	Theoretical investigation of the<mml:math xmlns:mml="http://www.w3.org/1998/Math/MathML"><mml:mi>Ï‰</mml:mi></mml:math>-related phases in<mml:math xmlns:mml="http://www.w3.org/1998/Math/MathML"><mml:mi mathvariant="normal">TiAl</mml:mi><mml:mo>â^'</mml:mo><mml:mi mathvariant="normal">Nb</mml:mi></mml:math> Mo alloys. Physical Review B, 2014, 90, .	1.1	32
18820	Nature of Tunable Optical Reflectivity of Rocksalt Hafnium Nitride Films. Journal of Physical Chemistry C, 2014, 118, 20511-20520.	1.5	23
18821	The healing of N-vacancy in boron nitride nanotube by using NO and NO2 molecules: a density functional theoretical study. RSC Advances, 2014, 4, 22688.	1.7	18
18822	Structural and Electronic Properties of Silicene on MgX₂ (X = Cl, Br, and I). ACS Applied Materials & Interfaces, 2014, 6, 11675-11681.	4.0	55
18823	Giant spin-driven ferroelectric polarization in TbMnO3 under high pressure. Nature Communications, 2014, 5, 4927.	5.8	131
18824	Orbital Origins of Helices and Magic Electron Counts in the Nowotny Chimney Ladders: the 18 â€“ n Rule and a Path to Incommensurability. Inorganic Chemistry, 2014, 53, 10627-10631.	1.9	51
18825	Could Li/Ni Disorder be Utilized Positively? Combined Experimental and Computational Investigation on Pillar Effect of Ni at Li Sites on LiCoO 2 at High Voltages. Electrochimica Acta, 2014, 146, 784-791.	2.6	47
18826	Effects of Mg and Al doping on the electronic structure and dehydrogenation of LiBH4Â·NH3. International Journal of Hydrogen Energy, 2014, 39, 17144-17152.	3.8	8
18827	First-Principles Study of Water Reaction and H₂ Formation on UO₂ (111) and (110) Single Crystal Surfaces. Journal of Physical Chemistry C, 2014, 118, 21935-21944.	1.5	35
18828	Adsorption Energy of tert-Butyl on Pt(111) by Dissociation of tert-Butyl Iodide: Calorimetry and DFT. Journal of Physical Chemistry C, 2014, 118, 427-438.	1.5	22
18829	Structure, magnetism and spin polarization in (Ni 1â^'x Co x) 2 MnGa alloys: Unusual composition dependences. Europhysics Letters, 2014, 105, 47010.	0.7	0
18830	High Catalytic Activity of Au Clusters Supported on ZnO Nanosheets. Journal of Physical Chemistry C, 2014, 118, 21038-21041.	1.5	19
18831	Waterâ€“Gas Shift Catalysis at Corner Atoms of Pt Clusters in Contact with a TiO₂ (110) Support Surface. ACS Catalysis, 2014, 4, 3654-3662.	5.5	56

#	Article	IF	Citations
18832	Theoretical study of heavy metal Cd, Cu, Hg, and Ni(II) adsorption on the kaolinite(001) surface. Applied Surface Science, 2014, 317, 718-723.	3.1	69
18833	Stress/strain aging mechanisms in Al alloys from first principles. Transactions of Nonferrous Metals Society of China, 2014, 24, 2130-2137.	1.7	8
18834	Tuning the properties of visible-light-responsive tantalum (oxy)nitride photocatalysts by non-stoichiometric compositions: a first-principles viewpoint. Physical Chemistry Chemical Physics, 2014, 16, 20548-20560.	1.3	86
18835	Theoretical investigation of La monopnictides: Electronic properties and pressure-induced phase transition. Journal of Applied Physics, 2014, 116, .	1.1	12
18836	Spin-Orbit Coupling, Quantum Dots, and Qubits in Monolayer Transition Metal Dichalcogenides. Physical Review X, 2014, 4, .	2.8	222
18837	Metal-Free Ketjenblack Incorporated Nitrogen-Doped Carbon Sheets Derived from Gelatin as Oxygen Reduction Catalysts. Nano Letters, 2014, 14, 1870-1876.	4.5	155
18838	Structural Stability and Elastic and Electronic Properties of W₂X (X = B, C, N): First-Principles Investigations. Journal of the Physical Society of Japan, 2014, 83, 014708.	0.7	2
18839	Intermixing at the absorber-buffer layer interface in thin-film solar cells: The electronic effects of point defects in Cu(In,Ga)(Se,S)2 and Cu2ZnSn(Se,S)4 devices. Journal of Applied Physics, 2014, 116, .	1.1	25
18840	Prediction of Two-Dimensional Topological Crystalline Insulator in PbSe Monolayer. Nano Letters, 2014, 14, 5717-5720.	4.5	93
18841	A first principle study on Fe incorporated MTW-type zeolite. Microporous and Mesoporous Materials, 2014, 199, 83-92.	2.2	13
18842	First-principles study of fast Na diffusion in Na3P. Chemical Physics Letters, 2014, 612, 129-133.	1.2	26
18843	Local environment dependent<mml:math xmlns:mml="http://www.w3.org/1998/Math/MathML"><mml:mtext>GGA</mml:mtext><mml:mo>+</mml:mo><mml:mi>U</mml:mi> for accurate thermochemistry of transition metal compounds. Physical Review B, 2014, 90, .	1.1	82
18844	Identification of Grain Boundary Segregation Mechanisms during Silicon Bi-Crystal Solidification. Materials Science Forum, 2014, 790-791, 329-334.	0.3	1
18845	Layered uranium(<scp>vi</scp>) hydroxides: structural and thermodynamic properties of dehydrated schoepite Î±-UO₂(OH)₂. Dalton Transactions, 2014, 43, 17191-17199.	1.6	35
18846	Photo-active and dynamical properties of hematite (Fe2O3)â€“water interfaces: an experimental and theoretical study. Physical Chemistry Chemical Physics, 2014, 16, 14445.	1.3	26
18847	Core polarity of screw dislocations in Feâ€“Co alloys. Philosophical Magazine Letters, 2014, 94, 334-341.	0.5	17
18848	Electronic structure at nanocontacts of surface passivated CdSe nanorods with gold clusters. Physical Chemistry Chemical Physics, 2014, 16, 10823-10829.	1.3	5
18849	Twin-driven thermoelectric figure-of-merit enhancement of Bi₂Te₃ nanowires. Nanoscale, 2014, 6, 6158-6165.	2.8	60

#	Article	IF	Citations
18850	Pressure-induced hydrogen transfer and polymerization in crystalline furoxan. RSC Advances, 2014, 4, 15995-16004.	1.7	12
18851	Surface oxygen vacancies in gold based catalysts for CO oxidation. RSC Advances, 2014, 4, 13145-13152.	1.7	24
18852	The chemical origin and catalytic activity of coinage metals: from oxidation to dehydrogenation. Physical Chemistry Chemical Physics, 2014, 16, 7481-7490.	1.3	14
18853	Enhanced photocatalytic mechanism for the hybrid g-C₃N₄/MoS₂ nanocomposite. Journal of Materials Chemistry A, 2014, 2, 7960-7966.	5.2	347
18854	Effects of hydrogen and water on the activity and selectivity of acetic acid hydrogenation on ruthenium. Green Chemistry, 2014, 16, 911-924.	4.6	49
18855	Lithium and sodium battery cathode materials: computational insights into voltage, diffusion and nanostructural properties. Chemical Society Reviews, 2014, 43, 185-204.	18.7	899
18856	Does Bi form clusters in GaAs1 â^'xBixalloys?. Semiconductor Science and Technology, 2014, 29, 115007.	1.0	11
18857	Detecting gas molecules via atomic magnetization. Dalton Transactions, 2014, 43, 13070-13075.	1.6	5
18858	Remarkable chemical adsorption of manganese-doped titanate for direct carbon dioxide electrolysis. Journal of Materials Chemistry A, 2014, 2, 6904-6915.	5.2	137
18859	The decomposition of Î±-LiN₂H₃BH₃: an unexpected hydrogen release from a homopolar protonâ€“proton pathway. Journal of Materials Chemistry A, 2014, 2, 15627.	5.2	7
18860	Narrow Bandgap in Î²-BaZn₂As₂ and Its Chemical Origins. Journal of the American Chemical Society, 2014, 136, 14959-14965.	6.6	33
18861	An experimental and computational investigation of the oxygen storage properties of BaLnFe2O5+Î´ and BaLnCo2O5+Î´ (Ln = La, Y) perovskites. Journal of Materials Chemistry A, 2014, 2, 2397.	5.2	22
18862	Hydrothermal synthesis, structure refinement, and electrochemical characterization of Li₂CoGeO₄ as an oxygen evolution catalyst. Journal of Materials Chemistry A, 2014, 2, 18428-18434.	5.2	6
18863	Size- effect induced high thermoelectric figure of merit in PbSe and PbTe nanowires. Physical Chemistry Chemical Physics, 2014, 16, 8114-8118.	1.3	15
18864	CO₂ Adsorption on Anatase TiO₂ (101) Surfaces in the Presence of Subnanometer Ag/Pt Clusters: Implications for CO₂ Photoreduction. Journal of Physical Chemistry C, 2014, 118, 26236-26248.	1.5	57
18865	Enhancement of the p-channel performance of sulfur-bridged annulene through a donorâ€“acceptor co-crystal approach. Journal of Materials Chemistry C, 2014, 2, 8886-8891.	2.7	28
18866	Structural stability and compressive behavior of ZrH₂under hydrostatic pressure and nonhydrostatic pressure. RSC Advances, 2014, 4, 46780-46786.	1.7	13
18867	Strontium influence on the oxygen electrocatalysis of La_{2â^'x}Sr_xNiO_{4Â±Î´} (0.0 â‰¤ x_{Sr} â‰¤ 1.0) thin films. Journal of Materials Chemistry A, 2014, 2, 6480-6487.	5.2	37

#	Article	IF	Citations
18868	Interactions of adsorbed CO2 on water ice at low temperatures. Physical Chemistry Chemical Physics, 2014, 16, 15630.	1.3	25
18869	Variable-composition structural optimization and experimental verification of MnB₃and MnB₄. Physical Chemistry Chemical Physics, 2014, 16, 15866-15873.	1.3	49
18870	Oxygen vacancy effects on an amorphous-TaO_x-based resistance switch: a first principles study. Nanoscale, 2014, 6, 10169-10178.	2.8	45
18871	Highly efficient Pd-based coreâ€“shell nanowire catalysts for O₂ dissociation. Physical Chemistry Chemical Physics, 2014, 16, 20532-20536.	1.3	5
18872	Tin-decorated ruthenium nanoparticles: a way to tune selectivity in hydrogenation reaction. Nanoscale, 2014, 6, 9806-9816.	2.8	24
18873	CrXTe₃(X = Si, Ge) nanosheets: two dimensional intrinsic ferromagnetic semiconductors. Journal of Materials Chemistry C, 2014, 2, 7071.	2.7	332
18874	Doping indium in Î²-Bi₂O₃to tune the electronic structure and improve the photocatalytic activities: first-principles calculations and experimental investigation. Physical Chemistry Chemical Physics, 2014, 16, 23476-23482.	1.3	40
18875	Emergence of electric polarity in BiTeX (X = Br and I) monolayers and the giant Rashba spin splitting. Physical Chemistry Chemical Physics, 2014, 16, 17603.	1.3	73
18876	Effects of cationic substitution on structural defects in layered cathode materials LiNiO2. Journal of Materials Chemistry A, 2014, 2, 7988.	5.2	132
18877	Tailoring on-surface supramolecular architectures based on adenine directed self-assembly. Chemical Communications, 2014, 50, 356-358.	2.2	5
18878	O vacancies on steps on the CeO2(111) surface. Physical Chemistry Chemical Physics, 2014, 16, 7823.	1.3	33
18879	Double bubbles: a new structural motif for enhanced electronâ€“hole separation in solids. Physical Chemistry Chemical Physics, 2014, 16, 21098-21105.	1.3	11
18880	Eu(<scp>ii</scp>) luminescence in the perovskite host lattices KMgH₃, NaMgH₃ and mixed crystals LiBa_xSr_{1â^'x}H₃. Journal of Materials Chemistry C, 2014, 2, 4799-4804.	2.7	24
18881	Self-assembled monolayers of CH3S from the adsorption of CH3SSCH3 on Au(111). Physical Chemistry Chemical Physics, 2014, 16, 2533.	1.3	2
18882	Prediction of a Dirac state in monolayer<mml:math xmlns:mml="http://www.w3.org/1998/Math/MathML"><mml:msub><mml:mi mathvariant="normal">TiB</mml:mi><mml:mn>2</mml:mn></mml:msub></mml:math>. Physical Review B, 2014, 90, .	1.1	134
18883	The facet-dependent enhanced catalytic activity of Pd nanocrystals. Chemical Communications, 2014, 50, 9454.	2.2	43
18884	Novel Li₃ClO based glasses with superionic properties for lithium batteries. Journal of Materials Chemistry A, 2014, 2, 5470-5480.	5.2	158
18885	Novel Si Networks in the Ca/Si Phase Diagram under Pressure. Journal of Physical Chemistry C, 2014, 118, 25167-25175.	1.5	15

#	Article	IF	Citations
18886	Size-dependent magnetic order and giant magnetoresistance in organic titaniumâ€“benzene multidecker cluster. Physical Chemistry Chemical Physics, 2014, 16, 1902-1908.	1.3	8
18887	Dihalogen edge-modification: an effective approach to realize the half-metallicity and metallicity in zigzag silicon carbon nanoribbons. Journal of Materials Chemistry C, 2014, 2, 7836-7850.	2.7	28
18888	Spin-induced band modifications of graphene through intercalation of magnetic iron atoms. Nanoscale, 2014, 6, 3824-3829.	2.8	51
18889	Theoretical investigation of layered zeolites with MWW topology: MCM-22P vs. MCM-56. Dalton Transactions, 2014, 43, 10443-10450.	1.6	33
18890	Softest elastic mode governs materials hardness. Science Bulletin, 2014, 59, 1747-1754.	1.7	14
18891	Tuning of the electronic and optical properties of single-layer black phosphorus by strain. Physical Review B, 2014, 90, .	1.1	279
18892	Strain and structure heterogeneity in MoS2 atomic layers grown by chemical vapour deposition. Nature Communications, 2014, 5, 5246.	5.8	453
18893	Positional disorder in ammonia borane at ambient conditions. Physical Review B, 2014, 89, .	1.1	5
18894	Oxygen diffusion pathways in brownmillerite SrCoO2.5: Influence of structure and chemical potential. Journal of Chemical Physics, 2014, 141, 084710.	1.2	64
18895	WS₂ As an Excellent High-Temperature Thermoelectric Material. Chemistry of Materials, 2014, 26, 6628-6637.	3.2	92
18896	Toward Stronger Alâ€“BN Nanotube Composite Materials: Insights into Bonding at the Al/BN Interface from First-Principles Calculations. Journal of Physical Chemistry C, 2014, 118, 26894-26901.	1.5	24
18897	Using light-switching molecules to modulate charge mobility in a quantum dot array. Physical Review B, 2014, 89, .	1.1	8
18898	Ab Initio Calculations of Band Gaps and Absolute Band Positions of Polymorphs of RbPbI₃ and CsPbI₃: Implications for Main-Group Halide Perovskite Photovoltaics. Journal of Physical Chemistry C, 2014, 118, 27721-27727.	1.5	117
18899	Effect of hydrogen gas impurities on the hydrogen dissociation on iron surface. International Journal of Quantum Chemistry, 2014, 114, 626-635.	1.0	49
18900	First-Principles Studies of Lithium Adsorption and Diffusion on Graphene with Grain Boundaries. Journal of Physical Chemistry C, 2014, 118, 28055-28062.	1.5	70
18901	Atomic corrugation and electron localization due to MoirÃ© patterns in twisted bilayer graphenes. Physical Review B, 2014, 90, .	1.1	208
18902	Intrinsic Barrier to Electrochemically Decompose Li₂CO₃ and LiOH. Journal of Physical Chemistry C, 2014, 118, 26591-26598.	1.5	162
18903	Significant variation of surface spin polarization through group IV atom (C, Si, Ge, Sn) adsorption on Fe₃O₄(100). Physical Chemistry Chemical Physics, 2014, 16, 95-102.	1.3	10

#	Article	IF	Citations
18904	High pressure superconducting phase of BI3: an ab initio study. RSC Advances, 2014, 4, 32068-32074.	1.7	4
18905	Properties of two-dimensional insulators: a DFT study of Co adsorption on NaCl and MgO ultrathin films. Physical Chemistry Chemical Physics, 2014, 16, 21838-21845.	1.3	20
18906	Electro-reduction of nitrogen on molybdenum nitride: structure, energetics, and vibrational spectra from DFT. Physical Chemistry Chemical Physics, 2014, 16, 3014.	1.3	55
18907	Understanding the electronic and ionic conduction and lithium over-stoichiometry in LiMn₂O₄ spinel. Journal of Materials Chemistry A, 2014, 2, 18271-18280.	5.2	68
18908	Dipolar polarization and piezoelectricity of a hexagonal boron nitride sheet decorated with hydrogen and fluorine. Physical Chemistry Chemical Physics, 2014, 16, 6575.	1.3	92
18909	An atomistic insight into the corrosion of the oxide film in liquid leadâ€“bismuth eutectic. Physical Chemistry Chemical Physics, 2014, 16, 7417.	1.3	10
18910	Chemical trends of electronic and optical properties of ns² ions in halides. Journal of Materials Chemistry C, 2014, 2, 4784-4791.	2.7	26
18911	Ideal two-dimensional systems with a gain Rashba-type spin splitting: SrFBiS₂and BiOBiS₂nanosheets. Journal of Materials Chemistry C, 2014, 2, 8539-8545.	2.7	13
18912	Studies on phase stability, mechanical, optical and electronic properties of a new Gd2CaZnO5 phosphor system for LEDs. CrystEngComm, 2014, 16, 1652.	1.3	10
18913	Mechanisms of enhanced sulfur tolerance on samarium (Sm)-doped cerium oxide (CeO₂) from first principles. Physical Chemistry Chemical Physics, 2014, 16, 10727-10733.	1.3	16
18914	Electronic and magnetic properties of transition-metal-doped sodium superatom clusters: TM@Na8 (TM=3d, 4d and 5d transition metal). Computational Materials Science, 2014, 95, 440-445.	1.4	7
18915	The synthesis and performance of Zr-doped and Wâ€“Zr-codoped VO₂ nanoparticles and derived flexible foils. Journal of Materials Chemistry A, 2014, 2, 15087-15093.	5.2	131
18916	Stable phase domains of the TiO₂â€“Ti₃O₅â€“Ti₂O₃â€“TiOâ€“Ti(C_xO_y)â system examined experimentally and via first principles calculations. Journal of Materials Chemistry A, 2014, 2, 2641-2647.	5.2	44
18917	Vacancy inter-layer migration in multi-layered graphene. Nanoscale, 2014, 6, 5729-5734.	2.8	20
18918	Pauling's third rule beyond the bulk: chemical bonding at quartz-type GeO2surfaces. Chemical Science, 2014, 5, 894-903.	3.7	17
18919	The impact of orbital hybridization on the electronic structure of crystalline InGaZnO: a new perspective on the compositional dependence. Journal of Materials Chemistry C, 2014, 2, 9196-9204.	2.7	24
18920	Ab initio calculation of magnetic properties of p-block element doped ZnO. RSC Advances, 2014, 4, 45598-45602.	1.7	22
18921	Ligand field density functional theory for the prediction of future domestic lighting. Physical Chemistry Chemical Physics, 2014, 16, 14625-14634.	1.3	24

#	Article	IF	Citations
18922	A facile and versatile method for preparation of colored TiO₂ with enhanced solar-driven photocatalytic activity. Nanoscale, 2014, 6, 10216-10223.	2.8	382
18923	First-principles study of ground-state properties of U₂Mo. Physical Chemistry Chemical Physics, 2014, 16, 26974-26982.	1.3	26
18924	Defect chemistry in layered transition-metal oxides from screened hybrid density functional calculations. Journal of Materials Chemistry A, 2014, 2, 5224-5235.	5.2	96
18925	Morphological evolution and electronic alteration of ZnO nanomaterials induced by Ni/Fe co-doping. Nanoscale, 2014, 6, 7312-7318.	2.8	10
18926	Free-floating ultrathin tin monoxide sheets for solar-driven photoelectrochemical water splitting. Journal of Materials Chemistry A, 2014, 2, 10647.	5.2	54
18927	Oxygen Vacancy Effect on Photoluminescence Properties of Self-Activated Yttrium Tungstate. Journal of Physical Chemistry C, 2014, 118, 25633-25642.	1.5	45
18928	Ab initio molecular dynamics simulations of aqueous triflic acid confined in carbon nanotubes. Physical Chemistry Chemical Physics, 2014, 16, 16465-16479.	1.3	20
18929	The catalytic reactions in the Cuâ€“Liâ€“Mgâ€“H high capacity hydrogen storage system. Physical Chemistry Chemical Physics, 2014, 16, 23012-23025.	1.3	10
18930	The role of water co-adsorption on the modification of ZnO nanowires using acetic acid. Physical Chemistry Chemical Physics, 2014, 16, 8509-8514.	1.3	8
18931	Tensile strain induced switching of magnetic states in NbSe₂and NbS₂single layers. Nanoscale, 2014, 6, 12929-12933.	2.8	59
18932	Adsorption-geometry induced transformation of self-assembled nanostructures of an aldehyde molecule on Cu(110). Nanoscale, 2014, 6, 11062-11065.	2.8	3
18933	Atomically resolved orientational ordering of C60molecules on epitaxial graphene on Cu(111). Nanoscale, 2014, 6, 11835-11840.	2.8	36
18934	Defect-induced semiconductor to metal transition in graphene monoxide. Physical Chemistry Chemical Physics, 2014, 16, 13477-13482.	1.3	12
18935	Adsorption of a dihydro-TTF derivative on Au(111) via a thiolate complex bonding to gold adatoms. Chemical Communications, 2014, 50, 10140-10143.	2.2	8
18936	CO oxidation on single and multilayer Pd oxides on Pd(111): mechanistic insights from RAIRS. Catalysis Science and Technology, 2014, 4, 3826-3834.	2.1	29
18937	The bending machine: CO₂ activation and hydrogenation on Î´-MoC(001) and Î²-Mo₂C(001) surfaces. Physical Chemistry Chemical Physics, 2014, 16, 14912-14921.	1.3	175
18938	Understanding doping anomalies in degenerate p-type semiconductor LaCuOSe. Journal of Materials Chemistry C, 2014, 2, 3429-3438.	2.7	55
18939	Porous Graphitic Carbon Nitride: A Possible Metal-free Photocatalyst for Water Splitting. Journal of Physical Chemistry C, 2014, 118, 26479-26484.	1.5	172

#	Article	IF	Citations
18940	Ferroelectric-like structural transition in metallic LiOsO3. RSC Advances, 2014, 4, 26843.	1.7	7
18941	Correlation of intercalation potential with d-electron configurations for cathode compounds of lithium-ion batteries. Physical Chemistry Chemical Physics, 2014, 16, 13255-13261.	1.3	5
18942	Mapping of single-site magnetic anisotropy tensors in weakly coupled spin clusters by torque magnetometry. Physical Chemistry Chemical Physics, 2014, 16, 17220.	1.3	24
18943	The characteristics of n- and p-type dopants in SnS2monolayer nanosheets. Physical Chemistry Chemical Physics, 2014, 16, 19674.	1.3	98
18944	Reduction mechanisms of additives on Si anodes of Li-ion batteries. Physical Chemistry Chemical Physics, 2014, 16, 17091-17098.	1.3	80
18945	Origin of blue emission in ThO₂ nanorods: exploring it as a host for photoluminescence of Eu³⁺, Tb³⁺ and Dy³⁺. RSC Advances, 2014, 4, 51244-51255.	1.7	45
18946	A first-principles investigation of oxygen reduction reaction catalysis capabilities of As decorated defect graphene. Dalton Transactions, 2014, 43, 15038-15047.	1.6	5
18947	Several different charge transfer and Ce³⁺localization scenarios for Rhâ€“CeO₂(111). Journal of Materials Chemistry A, 2014, 2, 2333-2345.	5.2	26
18948	Investigation of the local environment of iodate in hydroxyapatite by combination of X-ray absorption spectroscopy and DFT modeling. RSC Advances, 2014, 4, 14700-14707.	1.7	25
18949	Tuning electronic and magnetic properties of silicene with magnetic superhalogens. Physical Chemistry Chemical Physics, 2014, 16, 22979-22986.	1.3	35
18950	Engineering electronic properties of layered transition-metal dichalcogenide compounds through alloying. Nanoscale, 2014, 6, 5820-5825.	2.8	122
18951	The role of the CO adsorption on Pt monolayers supported on flat and stepped Au surfaces: a density functional investigation. RSC Advances, 2014, 4, 9247-9254.	1.7	18
18952	Electron transport enhanced by electrode surface reconstruction: a case study of C60-based molecular junctions. RSC Advances, 2014, 4, 44718-44725.	1.7	1
18953	Effect of Bi bilayers on the topological states of<mml:math xmlns:mml="http://www.w3.org/1998/Math/MathML"><mml:mrow><mml:msub><mml:mi>Bi</mml:mi><mml:mn>21</mml:mn></mml:msub></mml:mrow></mml:math>: A first-principles study. Physical Review B, 2014, 90, .	3.1	31
18954	The surface chemistry of NO_x on mackinawite (FeS) surfaces: a DFT-D2 study. Physical Chemistry Chemical Physics, 2014, 16, 15444-15456.	1.3	40
18955	Theoretical prediction of carbon dioxide reduction to methane at coordinatively unsaturated ferric site in the presence of Cu impurities. Physical Chemistry Chemical Physics, 2014, 16, 3515.	1.3	4
18956	A density functional theory-based study on the dissociation of NO on a CuO(110) surface. CrystEngComm, 2014, 16, 2260.	1.3	18
18957	First-principles study of nitrogen adsorption and dissociation on Î±-uranium (001) surface. RSC Advances, 2014, 4, 57308-57321.	1.7	15

#	Article	IF	Citations
18958	Charge inhomogeneity of graphene on SiO₂: dispersion-corrected density functional theory study on the effect of reactive surface sites. RSC Advances, 2014, 4, 37236-37243.	1.7	18
18959	Atomistic Structure and Ab Initio Electrochemical Properties of Li₄Ti₅O₁₂Defect Spinel for Li Ion Batteries. Journal of the Electrochemical Society, 2014, 161, A439-A444.	1.3	67
18960	Aliovalent doping of CeO₂: DFT study of oxidation state and vacancy effects. Journal of Materials Chemistry A, 2014, 2, 13723-13737.	5.2	93
18961	Tunable band gap and doping type in silicene by surface adsorption: towards tunneling transistors. Nanoscale, 2014, 6, 7609-7618.	2.8	151
18962	Electron transport via phenylâ€“perfluorophenyl interaction in crystals of fluorine-substituted dibenzalacetones. RSC Advances, 2014, 4, 50188-50194.	1.7	5
18963	Doping of rhenium disulfide monolayers: a systematic first principles study. Physical Chemistry Chemical Physics, 2014, 16, 16771-16779.	1.3	62
18964	Spin polarization gives rise to Cu precipitation in Fe-matrix. Physical Chemistry Chemical Physics, 2014, 16, 7222.	1.3	11
18965	A study on the influence of local doping in atomic layer deposited Al:ZnO thin film transistors. Journal of Materials Chemistry C, 2014, 2, 9274-9282.	2.7	21
18966	Facile synthesis of intense green light emitting LiGdF₄:Yb,Er-based upconversion bipyramidal nanocrystals and their polymer composites. Nanoscale, 2014, 6, 7461-7468.	2.8	53
18967	Theoretical investigation of the adsorption, IR, and electron injection of hydroxamate anchor at the TiO₂ anatase (1 0 1) surface. RSC Advances, 2014, 4, 19690-19693.	1.7	26
18968	Optical Absorption Energies of Molecular Defects in Pentaerythritol Tetranitrate Crystals: Quantum Chemical Modeling. Journal of Physical Chemistry C, 2014, 118, 26530-26542.	1.5	13
18969	Stacking interactions of nickel bis(dithiolene) with graphene and beyond. RSC Advances, 2014, 4, 13361.	1.7	9
18970	Two-dimensional g-C₃N₄: an ideal platform for examining facet selectivity of metal co-catalysts in photocatalysis. Chemical Communications, 2014, 50, 6094-6097.	2.2	225
18971	Electronic structure and band alignment of zinc nitride, Zn₃N₂. RSC Advances, 2014, 4, 3306-3311.	1.7	38
18972	Theoretical predictions of the structural, mechanical and lattice dynamical properties of XW2(Xâ€‰=â€‰Zr,) Tj ETQq0 0 0 rgBT /Overl	0.7	21
18973	Influence of vacancy defects on the thermal stability of silicene: a reactive molecular dynamics study. RSC Advances, 2014, 4, 1133-1137.	1.7	66
18974	Metallic three-coordinated carbon networks with eight-membered rings showing high density of states at the Fermi level. Physical Chemistry Chemical Physics, 2014, 16, 7102.	1.3	9
18975	Significant enhancement in the thermoelectric performance of strained nanoporous Si. Physical Chemistry Chemical Physics, 2014, 16, 2425-2429.	1.3	11

#	Article	IF	Citations
18976	A DFT + U computational study on stoichiometric and oxygen deficient Mâ€“CeO2 systems (M = Pd1, Rh1,) Tj ETQq0 0 0 rgBT /Overlock	1.3	19
18977	Modulated T carbon-like carbon allotropes: an ab initio study. RSC Advances, 2014, 4, 17364.	1.7	29
18978	First principles study of dopant solubility and defect chemistry in LiCoO₂. Journal of Materials Chemistry A, 2014, 2, 11235-11245.	5.2	52
18979	Transition metal-doped BiFeO₃nanofibers: forecasting the conductivity limit. Physical Chemistry Chemical Physics, 2014, 16, 23089-23095.	1.3	15
18980	Polycrystalline boron nitride constructed from hexagonal boron nitride. RSC Advances, 2014, 4, 38589-38593.	1.7	7
18981	Van der Waals density functional study of the energetics of alkali metal intercalation in graphite. RSC Advances, 2014, 4, 3973-3983.	1.7	145
18982	Electronic properties of silicene superlattices: roles of degenerate perturbation and inversion symmetry breaking. Journal of Materials Chemistry C, 2014, 2, 8773-8779.	2.7	13
18983	Electronic decoupling by h-BN layer between silicene and Cu(111): A DFT-based analysis. New Journal of Physics, 2014, 16, 105019.	1.2	20
18984	Air Stable p-Doping of WSe₂ by Covalent Functionalization. ACS Nano, 2014, 8, 10808-10814.	7.3	208
18985	Tin Disulfideâ€”An Emerging Layered Metal Dichalcogenide Semiconductor: Materials Properties and Device Characteristics. ACS Nano, 2014, 8, 10743-10755.	7.3	449
18986	Interfacial Interactions of Semiconductor with Graphene and Reduced Graphene Oxide: CeO₂ as a Case Study. ACS Applied Materials & Interfaces, 2014, 6, 20350-20357.	4.0	71
18987	First principles study of photo-oxidation degradation mechanisms in P3HT for organic solar cells. Physical Chemistry Chemical Physics, 2014, 16, 8092-8099.	1.3	70
18988	Photophysical properties of open-framework germanates templated by nickel complexes. Physical Chemistry Chemical Physics, 2014, 16, 10891.	1.3	2
18989	Magnetically stabilized Fe₈(Î¼₄-S)₆S₈ clusters in Ba₆Fe₂₅S₂₇. Dalton Transactions, 2014, 43, 14612-14624.	1.6	9
18990	Phonon-Assisted Crossover from a Nonmagnetic Peierls Insulator to a Magnetic Stoner Metal. Physical Review Letters, 2014, 113, 176401.	2.9	22
18991	A DFT study of the structures, stabilities and redox behaviour of the major surfaces of magnetite Fe₃O₄. Physical Chemistry Chemical Physics, 2014, 16, 21082-21097.	1.3	178
18992	Formation of nickelâ€“carbon heterofullerenes under electron irradiation. Dalton Transactions, 2014, 43, 7499-7513.	1.6	12
18993	Adsorption properties of nitrogen dioxide on hybrid carbon and boron-nitride nanotubes. Physical Chemistry Chemical Physics, 2014, 16, 22853-22860.	1.3	31

#	Article	IF	Citations
18994	Tuning the Band Gap in Silicene by Oxidation. ACS Nano, 2014, 8, 10019-10025.	7.3	175
18995	Thermodynamics of native defects in In₂O₃ crystals using a first-principles method. RSC Advances, 2014, 4, 36983-36989.	1.7	11
18996	High throughput exploration of ZrxSi1â^'xO2 dielectrics by evolutionary first-principles approaches. Physics Letters, Section A: General, Atomic and Solid State Physics, 2014, 378, 3549-3553.	0.9	7
18997	Crystal structures and properties of the CH4H2compound under high pressure. RSC Advances, 2014, 4, 37569.	1.7	7
18998	Ultrahard boron-rich tantalum boride: Monoclinic TaB 4. Journal of Alloys and Compounds, 2014, 617, 660-664.	2.8	28
18999	Hydrogen generation by water splitting on hematite (0001) surfaces: first-principles calculations. Physical Chemistry Chemical Physics, 2014, 16, 25442-25448.	1.3	32
19001	Ionic and Covalent Stabilization of Intermediates and Transition States in Catalysis by Solid Acids. Journal of the American Chemical Society, 2014, 136, 15229-15247.	6.6	43
19002	Re-visiting the O/Cu(111) system â€“ when metastable surface oxides could become an issue!. Physical Chemistry Chemical Physics, 2014, 16, 26735-26740.	1.3	18
19003	Magnetic and Ferroelectric Properties of BiCrO ₃ from First-Principles Calculations. Chinese Physics Letters, 2014, 31, 107501.	1.3	3
19004	Molecular chemisorption on passivated and defective boron doped silicon surfaces: a â€œforcedâ€•dative bond. Physical Chemistry Chemical Physics, 2014, 16, 24866-24873.	1.3	0
19005	Novel heterostructures by stacking layered molybdenum disulfides and nitrides for solar energy conversion. Journal of Materials Chemistry A, 2014, 2, 15389-15395.	5.2	87
19006	Multiple phases in the Îµ-VPO₄Oâ€“LiVPO₄Oâ€“Li₂VPO₄O system: a combined solid state electrochemistry and diffraction structural study. Journal of Materials Chemistry A, 2014, 2, 10182-10192.	5.2	79
19007	Role of MoO₃ on a Rhodium Catalyst in the Selective Hydrogenolysis of Biomass-Derived Tetrahydrofurfuryl Alcohol into 1,5-Pentanediol. Journal of Physical Chemistry C, 2014, 118, 25555-25566.	1.5	63
19008	Prediction of magnetic anisotropy of 5d transition metal-doped g-C₃N₄. Journal of Materials Chemistry C, 2014, 2, 8817-8821.	2.7	57
19010	Computational design of p-type transparent conductors for photovoltaic applications. , 2014, , .		2
19011	Interplay between the ionic and electronic transport and its effects on the reaction pattern during the electrochemical conversion in an FeF₂ nanoparticle. Physical Chemistry Chemical Physics, 2014, 16, 11690-11697.	1.3	12
19012	Electron spin-polarization and spin lattices in the boron- and nitrogen-doped organic framework COF-5. Physical Chemistry Chemical Physics, 2014, 16, 23286-23291.	1.3	17
19013	Charge Separation and Exciton Dynamics at Polymer/ZnO Interface from First-Principles Simulations. Journal of Physical Chemistry Letters, 2014, 5, 2649-2656.	2.1	48

#	Article	IF	Citations
19014	Experimental and Theoretical Analysis of Fast Lithium Ionic Conduction in a LiBH₄â€“C₆₀ Nanocomposite. Journal of Physical Chemistry C, 2014, 118, 21755-21761.	1.5	21
19015	Colorâ€Tunable Luminescence of Y₄Si₂N₂O₇:Ce³⁺, Tb³⁺, Dy³⁺ Phosphors Prepared by the Softâ€Chemical Ammonolysis Method. European Journal of Inorganic Chemistry, 2014, 2014, 1955-1964.	1.0	12
19016	Opening a band gap without breaking lattice symmetry: a new route toward robust graphene-based nanoelectronics. Nanoscale, 2014, 6, 7474.	2.8	16
19017	Impact of intrinsic atomic defects on the electronic structure of MoS₂monolayers. Nanotechnology, 2014, 25, 375703.	1.3	244
19018	Diffusion of Si impurities in Ni under stress: A first-principles study. Physical Review B, 2014, 90, .	1.1	26
19019	Electronic Structure at the Interface between Rubrene and Perylenediimide Single Crystals: Impact of Interfacial Charge Transfer and its Modulation. Advanced Materials Interfaces, 2014, 1, 1400362.	1.9	7
19020	Atom-Level Understanding of the Sodiation Process in Silicon Anode Material. Journal of Physical Chemistry Letters, 2014, 5, 1283-1288.	2.1	127
19021	Dynamic stability of the single-layer transition metal dichalcogenides. Computational Materials Science, 2014, 92, 206-212.	1.4	19
19022	Depolarized and Fully Active Cathode Based on Li(Ni_{0.5}Co_{0.2}Mn_{0.3})O₂ Embedded in Carbon Nanotube Network for Advanced Batteries. Nano Letters, 2014, 14, 4700-4706.	4.5	95
19023	Structural modeling of liquid and amorphous Al91Tb9 by Monte Carlo simulations. Journal of Non-Crystalline Solids, 2014, 405, 27-32.	1.5	7
19024	High ZT in p-Type (PbTe)_{1â€“2x}(PbSe)_x(PbS)_x Thermoelectric Materials. Journal of the American Chemical Society, 2014, 136, 3225-3237.	6.6	228
19025	Atomistic modeling of the orderâ€“disorder phase transformation in the Ni2Cr model alloy. Acta Materialia, 2014, 81, 258-271.	3.8	33
19026	A Comparative Theoretical Study of Proton-Coupled Hole Transfer for H2O and Small Organic Molecules (CH3OH, HCOOH, H2CO) on the Anatase TiO2(101) Surface. Journal of Physical Chemistry C, 2014, 118, 21457-21462.	1.5	32
19027	Hidden Thermodynamic Ground State of Calcium Diazenide. Journal of Physical Chemistry C, 2014, 118, 650-656.	1.5	8
19028	Synthesis of Extended Graphdiyne Wires by Vicinal Surface Templating. Nano Letters, 2014, 14, 1891-1897.	4.5	165
19029	Accelerated discovery of cathode materials with prolonged cycle life for lithium-ion battery. Nature Communications, 2014, 5, 4553.	5.8	108
19030	Meta-Positioning of Carbonitrile Functional Groups Induces Interfacial Edge-On Phase of Oligophenyl Derivatives. Journal of Physical Chemistry C, 2014, 118, 2622-2633.	1.5	6
19031	Magnetic Moment Enhancement for Mn₇ Cluster on Graphene. Journal of Physical Chemistry C, 2014, 118, 19123-19128.	1.5	12

#	Article	IF	Citations
19032	Single-layer Group-IVB nitride halides as promising photocatalysts. Journal of Materials Chemistry A, 2014, 2, 6755.	5.2	90
19033	Modeling LiNbO₃ Surfaces at Ambient Conditions. Journal of Physical Chemistry C, 2014, 118, 10213-10220.	1.5	16
19034	One- and two-particle effects in the electronic and optical spectra of barium fluoride. Journal of Physics Condensed Matter, 2014, 26, 125501.	0.7	6
19035	Dimensionality of Nanoscale TiO₂ Determines the Mechanism of Photoinduced Electron Injection from a CdSe Nanoparticle. Nano Letters, 2014, 14, 1790-1796.	4.5	38
19036	Silicon Monomer Formation and Surface Patterning of Si(001)-2 Ã— 1 Following Tetraethoxysilane Dissociative Adsorption at Room Temperature. Journal of Physical Chemistry C, 2014, 118, 1887-1893.	1.5	4
19037	Full Color Emission in ZnGa₂O₄: Simultaneous Control of the Spherical Morphology, Luminescent, and Electric Properties via Hydrothermal Approach. Advanced Functional Materials, 2014, 24, 6581-6593.	7.8	82
19038	Nanostructureâ€“Property Control in AlPSi₃/Si(100) Semiconductors Using Direct Molecular Assembly: Theory Meets Experiment at the Atomic Level. Chemistry of Materials, 2014, 26, 4092-4101.	3.2	6
19039	DFT +Uinvestigation of charged point defects and clusters in UO₂. Journal of Physics Condensed Matter, 2014, 26, 325501.	0.7	43
19040	Study of the interaction of solutes with Î£5 (013) tilt grain boundaries in iron using density-functional theory. Journal of Applied Physics, 2014, 115, .	1.1	71
19041	Real space pseudopotential calculations for size trends in Ga- and Al-doped zinc oxide nanocrystals with wurtzite and zincblende structures. Journal of Chemical Physics, 2014, 141, 094309.	1.2	7
19042	An effective method of tuning conducting properties: First-principles studies on electronic structures of graphene nanomeshes. Carbon, 2014, 79, 646-653.	5.4	18
19043	Dimerization of Propene Catalyzed by BrÃ¸nsted Acid Sites Inside the Main Channel of Zeolite SAPO-5: A Computational Study. Journal of Physical Chemistry C, 2014, 118, 18496-18504.	1.5	38
19044	Novel Delta-Ta₂O₅ Structure Obtained from DFT Calculations. Journal of Physical Chemistry C, 2014, 118, 13652-13658.	1.5	10
19045	Silicite: The layered allotrope of silicon. Physical Review B, 2014, 90, .	1.1	59
19046	Tunable Indirect to Direct Band Gap Transition of Monolayer Sc₂CO₂ by the Strain Effect. ACS Applied Materials & Interfaces, 2014, 6, 14724-14728.	4.0	175
19047	Electron-Deficient Telluride Cs₃Cu₂₀Te₁₃ with Sodalite-Type Network: Syntheses, Structures, and Physical Properties. Inorganic Chemistry, 2014, 53, 5575-5580.	1.9	20
19048	First Principles Calculations on Crystal and Electronic Structure of Co2P4O12. Integrated Ferroelectrics, 2014, 156, 115-121.	0.3	3
19049	CO₂ Adsorption Thermodynamics over N-Substituted/Grafted Graphanes: A DFT Study. Langmuir, 2014, 30, 1837-1844.	1.6	30

#	Article	IF	Citations
19050	Possible charge-density wave, superconductivity, and<mml:math xmlns:mml="http://www.w3.org/1998/Math/MathML"><mml:mi>f</mml:mi></mml:math>-electron valence instability in<mml:math xmlns:mml="http://www.w3.org/1998/Math/MathML"><mml:msub><mml:mi mathvariant="normal">EuBiS</mml:mi><mml:mn>2</mml:mn></mml:msub><mml:mtext>F</mml:mtext></mml:math>. Physical Review B, 2014, 90, .	1.1	112
19051	Theoretical Predictions of Freestanding Honeycomb Sheets of Cadmium Chalcogenides. Journal of Physical Chemistry C, 2014, 118, 16236-16245.	1.5	48
19052	Lithium and oxygen vacancies and their role in Li₂O₂charge transport in Liâ€“O₂batteries. Energy and Environmental Science, 2014, 7, 720-727.	15.6	84
19053	Tuning magnetism of monolayer MoS2 by doping vacancy and applying strain. Applied Physics Letters, 2014, 104, .	1.5	198
19054	Spatial variation in the electronic structures of carpetlike graphene nanoribbons and sheets. Current Applied Physics, 2014, 14, 1687-1691.	1.1	1
19055	Mechanistic Investigation of the Catalytic Decomposition of Ammonia (NH₃) on an Fe(100) Surface: A DFT Study. Journal of Physical Chemistry C, 2014, 118, 5309-5316.	1.5	51
19056	Role of Charge Transfer in Dehydrogenation of M(NH₂BH₃)₂ (M =) Tj ETQq0 0 0 rgBT /Overlock	1.5	4
19057	Dramatic changes in the electronic structure upon transition to the collapsed tetragonal phase in CaFe<mml:math xmlns:mml="http://www.w3.org/1998/Math/MathML"><mml:msub><mml:mrow /><mml:mn>2</mml:mn></mml:msub></mml:math>As<mml:math xmlns:mml="http://www.w3.org/1998/Math/MathML"><mml:msub><mml:mrow /><mml:mn>2</mml:mn></mml:msub></mml:math>. Physical Review B, 2014, 89, .	1.1	48
19058	Atomistic simulations of the interaction of alloying elements with grain boundaries in Mg. Acta Materialia, 2014, 80, 194-204.	3.8	45
19059	Atomic-Scale Investigation on the Facilitation and Inhibition of Guanine Tautomerization at Au(111) Surface. ACS Nano, 2014, 8, 1804-1808.	7.3	38
19060	DFT study of anatase-derived TiO2nanosheets/graphene hybrid materials. Physica Status Solidi (B): Basic Research, 2014, 251, 1471-1479.	0.7	29
19061	Low-temperature structural and transport anomalies in<mml:math xmlns:mml="http://www.w3.org/1998/Math/MathML"><mml:msub><mml:mi mathvariant="normal">Cu</mml:mi><mml:mn>2</mml:mn></mml:msub><mml:mi mathvariant="normal">Se</mml:mi></mml:math>. Physical Review B, 2014, 89, .	1.1	54
19062	Pseudopotentials periodic table: From H to Pu. Computational Materials Science, 2014, 95, 337-350.	1.4	1,196
19063	Role of oxygen vacancies in room-temperature ferromagnetism in cobalt-substituted<mml:math xmlns:mml="http://www.w3.org/1998/Math/MathML"><mml:msub><mml:mi>SrTiO</mml:mi><mml:mn>3</mml:mn></mml:msub></mml:math>. Physical Review B, 2014, 90, .	1.1	14
19064	Efficient Method for Fast Simulation of Scanning Tunneling Microscopy with a Tip Effect. Journal of Physical Chemistry A, 2014, 118, 8953-8959.	1.1	7
19065	Microkinetic Simulation of Ammonia Oxidation on the RuO₂(110) Surface. ACS Catalysis, 2014, 4, 639-648.	5.5	21
19066	Magnetism and electronic structure in Zn and Ti doped CoO: A first-principles study. Computational Materials Science, 2014, 93, 193-200.	1.4	9
19067	Characteristics of p-type Mg-doped GaS and GaSe nanosheets. Physical Chemistry Chemical Physics, 2014, 16, 18799.	1.3	44

#	Article	IF	Citations
19068	Electronic Properties of Edge-Hydrogenated Phosphorene Nanoribbons: A First-Principles Study. Journal of Physical Chemistry C, 2014, 118, 22368-22372.	1.5	117
19069	High-Throughput Calculations of Molecular Properties in the MedeA Environment: Accuracy of PM7 in Predicting Vibrational Frequencies, Ideal Gas Entropies, Heat Capacities, and Gibbs Free Energies of Organic Molecules. Journal of Chemical & Engineering Data, 2014, 59, 3136-3143.	1.0	26
19070	Role of van der Waals Forces in Thermodynamics and Kinetics of Layered Transition Metal Oxide Electrodes: Alkali and Alkaline-Earth Ion Insertion into V₂O₅. Journal of Physical Chemistry C, 2014, 118, 19599-19607.	1.5	79
19071	Hydrogen diffusion behavior and its effect on magnetic properties in (Mn, N)-codoped ZnO. Physica B: Condensed Matter, 2014, 454, 115-119.	1.3	2
19072	Stabilization of graphene nanopore. Proceedings of the National Academy of Sciences of the United States of America, 2014, 111, 7522-7526.	3.3	76
19073	Non-Radiative Electronâ€“Hole Recombination in Silicon Clusters: Ab Initio Non-Adiabatic Molecular Dynamics. Journal of Physical Chemistry C, 2014, 118, 20702-20709.	1.5	41
19074	Efficient Determination of Accurate Force Fields for Porous Materials Using ab Initio Total Energy Calculations. Journal of Physical Chemistry C, 2014, 118, 2693-2701.	1.5	23
19075	Major Difference in Visible-Light Photocatalytic Features between Perfect and Self-Defective Ta₃N₅ Materials: A Screened Coulomb Hybrid DFT Investigation. Journal of Physical Chemistry C, 2014, 118, 20784-20790.	1.5	39
19076	Ab initioself-consistent total-energy calculations within the EXX/RPA formalism. Physical Review B, 2014, 90, .	1.1	35
19077	Ferromagnetism in Nanostructured TiO₂/Al System Due to Surface Charge Transfer. Journal of Physical Chemistry C, 2014, 118, 3789-3794.	1.5	5
19078	The Role of the Bridging Atom in Stabilizing Odd Numbered Graphene Vacancies. Nano Letters, 2014, 14, 3972-3980.	4.5	44
19079	Pressure-stabilized lithium caesides with caesium anions beyond the â^'1 state. Nature Communications, 2014, 5, 4861.	5.8	45
19080	Spontaneous High Piezoelectricity in Poly(vinylidene fluoride) Nanoribbons Produced by Iterative Thermal Size Reduction Technique. ACS Nano, 2014, 8, 9311-9323.	7.3	110
19081	Charge Transfer between PbSe and NbSe2 in [(PbSe)1.14]m(NbSe2)1 Ferecrystalline Compounds. Chemistry of Materials, 2014, 26, 1859-1866.	3.2	37
19082	Unravelling the role of Li2S2 in lithiumâ€“sulfur batteries: A first principles study of its energetic and electronic properties. Journal of Power Sources, 2014, 272, 518-521.	4.0	72
19083	Global Flux Surface Hopping Approach for Mixed Quantum-Classical Dynamics. Journal of Chemical Theory and Computation, 2014, 10, 3598-3605.	2.3	125
19084	Potassium-Exchanged Natrolite Under Pressure. Computational Study vs Experiment. Journal of Physical Chemistry C, 2014, 118, 22030-22039.	1.5	5
19085	Initial Assessment of an Empirical Potential as a Portable Tool for Rapid Investigation of Li⁺ Diffusion in Li⁺-Battery Cathode Materials. Journal of Physical Chemistry C, 2014, 118, 11203-11214.	1.5	12

#	Article	IF	Citations
19086	CO dissociation on magnetic Fe_n clusters. Physical Chemistry Chemical Physics, 2014, 16, 20703-20713.	1.3	16
19087	First-principles studies of hydrogen behavior interacting with oxygen-enriched nanostructured particles in the ODS steels. International Journal of Hydrogen Energy, 2014, 39, 18506-18519.	3.8	7
19088	Oxygen-induced lattice distortion in Î²-Ti3Nb and its suppression effect on Î² to Îµâ€³ transformation. Acta Materialia, 2014, 81, 194-203.	3.8	19
19089	Variation of Kondo Temperature Induced by Moleculeâ€“Substrate Decoupling in Film Formation of Bis(phthalocyaninato)terbium(III) Molecules on Au(111). ACS Nano, 2014, 8, 4866-4875.	7.3	43
19090	Catalytic Performance of Vanadium MILâ€47 and Linkerâ€Substituted Variants in the Oxidation of Cyclohexene: A Combined Theoretical and Experimental Approach. ChemPlusChem, 2014, 79, 1183-1197.	1.3	20
19091	Graphene spintronics: Spin injection and proximity effects from first principles. Physical Review B, 2014, 90, .	1.1	43
19092	The electronic structure of silver orthophosphate: experiment and theory. Journal of Materials Chemistry A, 2014, 2, 6092-6099.	5.2	21
19093	First-principles calculation on oxygen ion migration in alkaline-earth doped La₂GeO₅. Journal of Physics Condensed Matter, 2014, 26, 255503.	0.7	1
19094	First-Principles Prediction of Ternary Interstitial Hydride Phase Stability in the Thâ€“Zrâ€“H System. Journal of Chemical & Engineering Data, 2014, 59, 3232-3241.	1.0	3
19095	Thermodynamic evaluation of the Npâ€“Zr system using CALPHAD and ab initio methods. Journal of Nuclear Materials, 2014, 452, 569-577.	1.3	9
19096	Cobalt incorporation in calcite: Thermochemistry of (Ca,Co)CO 3 solid solutions from density functional theory simulations. Geochimica Et Cosmochimica Acta, 2014, 142, 205-216.	1.6	18
19097	Single-walled carbon nanotubes as high pressure nanocontainer. International Journal of Modern Physics B, 2014, 28, 1450074.	1.0	1
19098	Dissociative Chemisorption of Methane on Ni and Pt Surfaces: Mode-Specific Chemistry and the Effects of Lattice Motion. Journal of Physical Chemistry A, 2014, 118, 9615-9631.	1.1	106
19099	Adsorption Properties of Two-Dimensional NaCl: A Density Functional Theory Study of the Interaction of Co, Ag, and Au Atoms with NaCl/Au(111) Ultrathin Films. Journal of Physical Chemistry C, 2014, 118, 12353-12363.	1.5	7
19100	First principles investigation of the conversion of N2O and CO to N2 and CO2 on a modified N + Fe/TiO2 (101) surface. RSC Advances, 2014, 4, 17896.	1.7	2
19101	Electronic Structure and Photoelectrochemical Properties of an Ir-Doped SrTiO₃ Photocatalyst. Journal of Physical Chemistry C, 2014, 118, 20222-20228.	1.5	63
19102	Spin-Polarized Surface State in EuO(100). Physical Review Letters, 2014, 112, 016803.	2.9	14
19103	Semiconductor to Metal to Half-Metal Transition in Pt-Embedded Zigzag Graphene Nanoribbons. Journal of Physical Chemistry C, 2014, 118, 16133-16139.	1.5	22

#	Article	IF	Citations
19104	Study of Phase Stability and Hydride Diffusion Mechanism of BaTiO₃ Oxyhydride from First-Principles. Journal of Physical Chemistry C, 2014, 118, 17254-17259.	1.5	31
19105	Influence of the Ba²⁺/Sr²⁺content and oxygen vacancies on the stability of cubic Ba_xSr_{1â^'x}Co_{0.75}Fe_{0.25}O_{3â^'Î´}. Physical Chemistry Chemical Physics, 2014, 16, 1333-1338.	1.3	7
19106	Role of the Nitrogen Source in Determining Structure and Morphology of N-Doped Nanocrystalline TiO2. Journal of Physical Chemistry C, 2014, 118, 4797-4807.	1.5	33
19107	Elasticity and dislocations in ice X under pressure. Physics of the Earth and Planetary Interiors, 2014, 236, 10-15.	0.7	18
19108	Composition-dependent stability of the medium-range order responsible for metallic glass formation. Acta Materialia, 2014, 81, 337-344.	3.8	24
19109	First-principles study of vibrational and noncollinear magnetic properties of the perovskite to postperovskite pressure transition of<mml:math xmlns:mml="http://www.w3.org/1998/Math/MathML"><mml:msub><mml:mi>NaMnF</mml:mi><mml:mn>3</mml:mn></mml:msub><[illegible] Physical Review B, 2014, 90, .	1.1	17
19110	Strain-engineered direct-indirect band gap transition and its mechanism in two-dimensional phosphorene. Physical Review B, 2014, 90, .	1.1	797
19111	Structures and Bonding Properties of Goldâ€“Arg-Cys Complexes: DFT Study of Simple Peptide-Coated Metal. Journal of Physical Chemistry C, 2014, 118, 20840-20847.	1.5	11
19112	Conformational Electroresistance and Hysteresis in Nanoclusters. Nano Letters, 2014, 14, 4476-4479.	4.5	6
19113	Ketonization of Carboxylic Acids in Biomass Conversion over TiO₂ and ZrO₂ Surfaces: A DFT Perspective. ACS Catalysis, 2014, 4, 2874-2888.	5.5	132
19114	Modeling the Effect of Dissolved Hydrogen Sulfide on Mg²⁺â€“Water Complex on Dolomite {104} Surfaces. Journal of Physical Chemistry C, 2014, 118, 15716-15722.	1.5	27
19115	Resistance to sulfur poisoning of the gold doped nickel/yttria-stabilized zirconia with interface oxygen vacancy. Journal of Power Sources, 2014, 271, 516-521.	4.0	13
19116	Room-Temperature Half-Metallicity in La(Mn,Zn)AsO Alloy via Element Substitutions. Journal of the American Chemical Society, 2014, 136, 5664-5669.	6.6	88
19117	Structure, magnetic, and transport properties of epitaxial ZnFe2O4 films: An experimental and first-principles study. Journal of Applied Physics, 2014, 115, .	1.1	35
19118	Temperature dependent transition of intragranular plastic to intergranular brittle failure in electrodeposited Cu micro-tensile samples. Materials Science & Engineering A: Structural Materials: Properties, Microstructure and Processing, 2014, 618, 398-405.	2.6	37
19119	Thermodynamic Control of Halogen-Terminated Silicon Nanoparticle Morphology. Crystal Growth and Design, 2014, 14, 4468-4474.	1.4	7
19120	Parametrization of the Stillinger-Weber potential for Si/N/H system and its application to simulations of silicon nitride film deposition with SiH4/NH3. Journal of Applied Physics, 2014, 115, .	1.1	3
19121	Role of oxygen in Cu(1 1 0) surface restructuring in the vicinity of step edges. Chemical Physics Letters, 2014, 613, 64-69.	1.2	15

#	Article	IF	Citations
19122	Liquid-metal electrode to enable ultra-low temperature sodiumâ€“beta alumina batteries for renewable energy storage. Nature Communications, 2014, 5, 4578.	5.8	158
19123	Migration mechanisms of helium in copper and tungsten. Journal of Materials Science, 2014, 49, 8127-8139.	1.7	34
19124	Electronic and thermodynamic properties of Î± -Pu 2 O 3. Physics Letters, Section A: General, Atomic and Solid State Physics, 2014, 378, 3060-3065.	0.9	16
19125	Stretching of BDT-gold molecular junctions: thiol or thiolate termination?. Nanoscale, 2014, 6, 14495-14507.	2.8	40
19126	Removal of Phosphorus in Metallurgical Silicon by Rare Earth Elements. Metallurgical and Materials Transactions E, 2014, 1, 257-262.	0.5	1
19127	Impact of Collective Electrostatic Effects on Charge Transport through Molecular Monolayers. Journal of Physical Chemistry C, 2014, 118, 22395-22401.	1.5	22
19128	Atomic-Scale Understanding of the Interaction of Poly(3-hexylthiophene) with the NiO (100) Surface: A First-Principles Study. Journal of Physical Chemistry C, 2014, 118, 20298-20305.	1.5	13
19129	Surfaceâ€Confined Singleâ€Layer Covalent Organic Framework on Singleâ€Layer Graphene Grown on Copper Foil. Angewandte Chemie - International Edition, 2014, 53, 9564-9568.	7.2	139
19130	Uniformly Wetting Deposition of Co Atoms on MoS₂ Monolayer: A Promising Two-Dimensional Robust Half-Metallic Ferromagnet. ACS Applied Materials & Interfaces, 2014, 6, 16835-16840.	4.0	57
19131	Proximity-induced topological state in graphene. Physical Review B, 2014, 90, .	1.1	19
19132	A mechanism of gas-phase alcohol oxidation at the interface of Au nanoparticles and a MgCuCr₂O₄spinel support. Catalysis Science and Technology, 2014, 4, 2997-3003.	2.1	23
19133	First-Principles Study on Electronic Structure of 15R-SiC Polytypes. Advanced Materials Research, 2014, 971-973, 77-80.	0.3	2
19134	H₂ Desorption from MgH₂ Surfaces with Steps and Catalyst-Dopants. Journal of Physical Chemistry C, 2014, 118, 6641-6649.	1.5	10
19135	On the origin of anisotropic lithiation in crystalline silicon over germanium: A first principles study. Applied Surface Science, 2014, 323, 78-81.	3.1	14
19136	Catalytic propane reforming mechanism over Zr-doped CeO₂(111). Catalysis Science and Technology, 2014, 4, 3278.	2.1	12
19137	Electronic and magnetic structures of coronene-based graphitic nanoribbons. Physical Chemistry Chemical Physics, 2014, 16, 3603.	1.3	10
19138	Ionic Liquid Chiral Resolution: Methyl 2-Ammonium Chloride Propanoate on Al(854)^S Surface. Journal of Physical Chemistry C, 2014, 118, 1568-1575.	1.5	3
19139	Ultrafast Bulk Diffusion of AlH_x in High-Entropy Dehydrogenation Intermediates of NaAlH₄. Journal of Physical Chemistry C, 2014, 118, 18356-18361.	1.5	3

#	Article	IF	Citations
19140	High-resolution scanning tunneling microscopy imaging of Si(1â€‰1â€‰1)-7â€‰Ã—â€‰7 structure and intrinsic molecular states. Journal of Physics Condensed Matter, 2014, 26, 394001.	0.7	6
19141	Theoretical Insights on the C2Hy Formation Mechanism During CH4 Dissociation on Cu(100) Surface. Journal of Physical Chemistry C, 2014, 118, 17662-17669.	1.5	3
19142	Oxygen vacancy diffusion in bare ZnO nanowires. Nanoscale, 2014, 6, 11882-11886.	2.8	29
19143	Tailoring Electronâ€Transfer Barriers for Zinc Oxide/C₆₀ Fullerene Interfaces. Advanced Functional Materials, 2014, 24, 7381-7389.	7.8	54
19144	Electronic structure of CdTe using GGA+USIC. Physica B: Condensed Matter, 2014, 452, 119-123.	1.3	21
19145	High-Pressure Raman Scattering of CaWO₄ Up to 46.3 GPa: Evidence of a New High-Pressure Phase. Inorganic Chemistry, 2014, 53, 9729-9738.	1.9	29
19146	A Density Functional Tight Binding Model with an Extended Basis Set and Three-Body Repulsion for Hydrogen under Extreme Thermodynamic Conditions. Journal of Physical Chemistry A, 2014, 118, 5520-5528.	1.1	18
19147	Phase transition, lattice dynamical and thermodynamic properties of yttrium antimonide with the rock salt structure under high pressure: first-principles investigations. High Pressure Research, 2014, 34, 78-88.	0.4	1
19148	Charge and magnetic states of Mn-, Fe-, and Co-doped monolayer MoS2. Journal of Applied Physics, 2014, 116, .	1.1	92
19149	Understanding the Mechanisms of CaO Carbonation: Role of Point Defects in CaCO₃ by Atomic-Scale Simulations. Journal of Physical Chemistry C, 2014, 118, 22583-22591.	1.5	11
19150	Improved Interaction of Hydrogen on Transition-Metal-Doped Al(100) Stepped Surface. Journal of Physical Chemistry C, 2014, 118, 7442-7450.	1.5	7
19151	Discrimination of the mechanism of CH₄ formation in Fischerâ€“Tropsch synthesis on Co catalysts: a combined approach of DFT, kinetic isotope effects and kinetic analysis. Catalysis Science and Technology, 2014, 4, 3534-3543.	2.1	46
19152	Unraveling the Cooperative Mechanism of Visible-Light Absorption in Bulk N,Nb Codoped TiO₂ Powders of Nanomaterials. Journal of Physical Chemistry C, 2014, 118, 24152-24164.	1.5	47
19153	Strain-induced metal-insulator transition in ultrathin films of<mml:math xmlns:mml="http://www.w3.org/1998/Math/MathML"><mml:msub><mml:mtext>SrRuO</mml:mtext><mml:mn>3</mml:mn></mml:msub></mml:math> Physical Review B, 2014, 90, .	3.7	26
19154	Density Functional Theory Calculations and Analysis of Reaction Pathways for Reduction of Nitric Oxide by Hydrogen on Pt(111). ACS Catalysis, 2014, 4, 3307-3319.	5.5	93
19155	Thermal Stability of Colloidal InP Nanocrystals: Small Inorganic Ligands Boost High-Temperature Photoluminescence. ACS Nano, 2014, 8, 977-985.	7.3	57
19156	Structural and electronic properties of the adsorbed and defected Cu nanowires: A density-functional theory study. Physica B: Condensed Matter, 2014, 454, 110-114.	1.3	4
19157	Theoretical Investigation of H₂ Oxidation on the Sr₂Fe_{1.5}Mo_{0.5}O₆ (001) Perovskite Surface under Anodic Solid Oxide Fuel Cell Conditions. Journal of the American Chemical Society, 2014, 136, 8374-8386.	6.6	68

#	Article	IF	Citations
19158	Effect of N- and P-Type Doping on the Oxygen-Binding Energy and Oxygen Spillover of Supported Palladium Clusters. Journal of Physical Chemistry C, 2014, 118, 20306-20313.	1.5	16
19159	First-Principles Analysis of Potential-Dependent Proton Coupled Electron Transfer between Polypyridylâ€“Ruthenium Complexes and Oxygen-Modified Graphene Electrodes. Journal of Physical Chemistry C, 2014, 118, 12097-12105.	1.5	0
19160	Significance of Î²-dehydrogenation in ethanol electro-oxidation on platinum doped with Ru, Rh, Pd, Os and Ir. Physical Chemistry Chemical Physics, 2014, 16, 13248-13254.	1.3	44
19161	Pressure evolution of two polymorphs of Tb2(MoO4)3. High Pressure Research, 2014, 34, 184-190.	0.4	3
19162	Transition from half metal to semiconductor in Li doped g-C4N3. Journal of Applied Physics, 2014, 115, .	1.1	10
19163	Thermodynamically constrained correction to ab initio equations of state. Journal of Applied Physics, 2014, 116, .	1.1	12
19164	Temperature and composition dependence of short-range order and entropy, and statistics of bond length: the semiconductor alloy (GaN)_{1â^'x}(ZnO)_x. Journal of Physics Condensed Matter, 2014, 26, 274204.	0.7	3
19165	Atom manipulation on an insulating surface at room temperature. Nature Communications, 2014, 5, 4403.	5.8	49
19166	First-principles study of full a-dislocations in pure magnesium. Journal of Applied Mechanics and Technical Physics, 2014, 55, 672-681.	0.1	3
19167	Stability of the hcp Ruthenium at high pressures from first principles. Journal of Applied Physics, 2014, 116, .	1.1	15
19168	Large spin Seebeck effects in zigzag-edge silicene nanoribbons. AIP Advances, 2014, 4, .	0.6	15
19169	CN-mayenite Ca12Al14O32(CN)2: Replacing mobile oxygen ions by cyanide ions. Solid State Sciences, 2014, 38, 69-78.	1.5	20
19170	Tuning the Work Function of Graphene-on-Quartz with a High Weight Molecular Acceptor. Journal of Physical Chemistry C, 2014, 118, 4784-4790.	1.5	50
19171	Unique Reaction Path in Heterogeneous Catalysis: The Concerted Semi-Hydrogenation of Propyne to Propene on CeO₂. ACS Catalysis, 2014, 4, 4015-4020.	5.5	55
19172	Efficient Spin Injection into Graphene through a Tunnel Barrier: Overcoming the Spin-Conductance Mismatch. Physical Review Applied, 2014, 2, .	1.5	39
19173	Investigation of the bulk and surface properties of CdSe: insights from theory. Physical Chemistry Chemical Physics, 2014, 16, 23251-23259.	1.3	17
19174	Determination of interfacial atomic structure, misfits and energetics of Î© phase in Alâ€“Cuâ€“Mgâ€“Ag alloy. Acta Materialia, 2014, 81, 501-511.	3.8	92
19175	High-mobility transport anisotropy and linear dichroism in few-layer black phosphorus. Nature Communications, 2014, 5, 4475.	5.8	3,568

#	Article	IF	Citations
19176	Density Functional Theory Study of the Adsorption of Hydrazine on the Perfect and Defective Copper (100), (110), and (111) Surfaces. Journal of Physical Chemistry C, 2014, 118, 26103-26114.	1.5	58
19177	First principles investigations on the electronic structure of anchor groups on ZnO nanowires and surfaces. Journal of Applied Physics, 2014, 115, .	1.1	16
19178	Adsorption Structures and Energies of Cun Clusters on the Fe(110) and Fe3C(001) Surfaces. Journal of Physical Chemistry C, 2014, 118, 21963-21974.	1.5	14
19179	CO Oxidation on the Pd(111) Surface. ACS Catalysis, 2014, 4, 3435-3443.	5.5	62
19180	Adsorption of CO Molecules on Si(001) at Room Temperature. Journal of Physical Chemistry C, 2014, 118, 21463-21468.	1.5	5
19181	On the nature of point defect and its effect on electronic structure of rocksalt hafnium nitride films. Acta Materialia, 2014, 81, 315-325.	3.8	31
19182	Optical characteristics of an epitaxial Fe3Si/Si(111) iron silicide film. JETP Letters, 2014, 99, 565-569.	0.4	9
19183	Polaronic Relaxation by Three-Electron Bond Formation in Graphitic Carbon Nitrides. Journal of Physical Chemistry C, 2014, 118, 4023-4032.	1.5	25
19184	Tuning the Magnetic Exchange via a Control of Orbital Hybridization in<mml:math xmlns:mml="http://www.w3.org/1998/Math/MathML" display="inline"><mml:mrow><mml:msub><mml:mrow><mml:mi>Cr</mml:mi></mml:mrow><mml:mrow><mml:mn>2</mml:mn></mml:mrow><mml:mm		

#	Article	IF	Citations
19194	Ab initiostudy of multiferroic<mml:math xmlns:mml="http://www.w3.org/1998/Math/MathML"><mml:mi>Bi</mml:mi><mml:mi>Fe</mml:mi><mml:msub><mml:mi mathvariant="normal">O</mml:mi><mml:mn>3</mml:mn></mml:msub></mml:math>(110) surfaces. Physical Review B, 2014, 89, .	1.1	16
19195	Direct Observation of a Long-Lived Single-Atom Catalyst Chiseling Atomic Structures in Graphene. Nano Letters, 2014, 14, 450-455.	4.5	81
19196	Fermi-level pinning, charge transfer, and relaxation of spin-momentum locking at metal contacts to topological insulators. Physical Review B, 2014, 90, .	1.1	45
19197	Density functional theory study of carbon dioxide electrochemical reduction on the Fe(100) surface. Physical Chemistry Chemical Physics, 2014, 16, 13708-13717.	1.3	25
19198	Hydrogen adsorption and diffusion around Si(0â€‰0â€‰1)/Si(1â€‰1â€‰0) corners in nanostructures. Journal of Physics Condensed Matter, 2014, 26, 295301.	0.7	2
19199	Embedding Covalency into Metal Catalysts for Efficient Electrochemical Conversion of CO₂. Journal of the American Chemical Society, 2014, 136, 11355-11361.	6.6	192
19200	Polar Surface Energies of Ionoâ€Covalent Materials: Implications of a Chargeâ€Transfer Model Tested on Li₂FeSiO₄ Surfaces. ChemPhysChem, 2014, 15, 2058-2069.	1.0	11
19201	Alloying InAs and InP nanowires for optoelectronic applications: A first principles study. Physics Letters, Section A: General, Atomic and Solid State Physics, 2014, 378, 2872-2875.	0.9	3
19202	Fluorite TiO₂(111) Surface Phase for Enhanced Visible-Light Solar Energy Conversion. Journal of Physical Chemistry C, 2014, 118, 20107-20111.	1.5	15
19203	Phosphorus vacancy cluster model for phosphorus diffusion gettering of metals in Si. Journal of Applied Physics, 2014, 115, 054906.	1.1	24
19204	Modelling of the influence of alloy composition on flow stress in high-strength nickel-based superalloys. Acta Materialia, 2014, 75, 356-370.	3.8	127
19205	Uncovering the True Atomic Structure of Disordered Materials: The Structure of a Hydrated Amorphous Magnesium Carbonate (MgCO₃Â·3D₂O). Chemistry of Materials, 2014, 26, 2693-2702.	3.2	26
19206	Visibility of Al Surface Sites of Î³-Alumina: A Combined Computational and Experimental Point of View. Journal of Physical Chemistry C, 2014, 118, 15292-15299.	1.5	97
19207	Controlling the Dimensionality of On-Surface Coordination Polymers via Endo- or Exoligation. Journal of the American Chemical Society, 2014, 136, 9355-9363.	6.6	65
19208	High-Pressure Studies of Bi₂S₃. Journal of Physical Chemistry A, 2014, 118, 1713-1720.	1.1	81
19209	Prediction of superconductivity of Ta₂AlC: in situ Raman spectrometry and density functional investigations. Journal of Raman Spectroscopy, 2014, 45, 202-207.	1.2	2
19210	A Novel Superhard Tetragonal Carbon Mononitride. Journal of Physical Chemistry C, 2014, 118, 3202-3208.	1.5	32
19211	Immobilizing Metal Nanoparticles on Single Wall Nanotubes. Effect of Surface Curvature. Journal of Physical Chemistry C, 2014, 118, 8907-8916.	1.5	32

#	Article	IF	Citations
19212	Glycerol Adsorption on Platinum Surfaces: A Density Functional Theory Investigation with van der Waals Corrections. Journal of Physical Chemistry C, 2014, 118, 15251-15259.	1.5	36
19213	Tuning selectivity and stability in propane dehydrogenation by shaping Pt particles: A combined experimental and DFT study. Journal of Molecular Catalysis A, 2014, 395, 329-336.	4.8	48
19214	Electronic and Magnetic Properties of Vanadium Dichalcogenides Monolayers Tuned by Hydrogenation. Journal of Physical Chemistry C, 2014, 118, 13248-13253.	1.5	109
19215	Anomalous Alloy Properties in Mixed Halide Perovskites. Journal of Physical Chemistry Letters, 2014, 5, 3625-3631.	2.1	231
19216	Nanoporous PdFe alloy as highly active and durable electrocatalyst for oxygen reduction reaction. International Journal of Hydrogen Energy, 2014, 39, 18247-18255.	3.8	52
19217	Phosphorene as a Superior Gas Sensor: Selective Adsorption and Distinct Iâ€“V Response. Journal of Physical Chemistry Letters, 2014, 5, 2675-2681.	2.1	877
19218	Theoretical Investigation of Small Transition-Metal Clusters Supported on the CeO₂(111) Surface. Journal of Physical Chemistry C, 2014, 118, 21438-21446.	1.5	35
19219	Tuning the phase transition in transition-metal-based magnetocaloric compounds. Physical Review B, 2014, 89, .	1.1	58
19220	Defect Evolution in Graphene upon Electrochemical Lithiation. ACS Applied Materials & Interfaces, 2014, 6, 17626-17636.	4.0	30
19221	The Role of Hydrogen on the Adsorption Behavior of Carboxylic Acid on TiO₂ Surfaces. Journal of Physical Chemistry C, 2014, 118, 10771-10779.	1.5	28
19222	Point defects and p-type conductivity in Zn1â€“xMnxGeAs2. Journal of Applied Physics, 2014, 116, 023501.	1.1	1
19223	Structure of Î´-Alumina: Toward the Atomic Level Understanding of Transition Alumina Phases. Journal of Physical Chemistry C, 2014, 118, 18051-18058.	1.5	72
19224	Visualizing the roles of graphene for excellent lithium storage. Journal of Materials Chemistry A, 2014, 2, 17808-17814.	5.2	48
19225	The effects of alloying and segregation for the reactivity and diffusion of oxygen on Cu₃Au(111). Physical Chemistry Chemical Physics, 2014, 16, 19702.	1.3	14
19226	First-principles studies on vacancy-modified interstitial diffusion mechanism of oxygen in nickel, associated with large-scale atomic simulation techniques. Journal of Applied Physics, 2014, 115, .	1.1	33
19227	Atomic-Level Understanding of Interfaces in the Synthesis of Crystalline Oxides on Semiconductors: Sr- and Ba/Si(100)(2 Ã— 3) Reconstructions. Journal of Physical Chemistry C, 2014, 118, 1894-1902.	1.5	12
19228	Surface properties of Î±-MnO₂: relevance to catalytic and supercapacitor behaviour. Journal of Materials Chemistry A, 2014, 2, 15509-15518.	5.2	121
19229	First-Principles Study of the Reaction Mechanism in Sodiumâ€“Oxygen Batteries. Chemistry of Materials, 2014, 26, 1048-1055.	3.2	91

#	Article	IF	Citations
19230	Valence State Driven Site Preference in the Quaternary Compound Ca5MgAgGe5: An Electron-Deficient Phase with Optimized Bonding. Inorganic Chemistry, 2014, 53, 4724-4732.	1.9	10
19231	Computational Study for Reactions of H Atoms with Adsorbed SiH₃ and Si₂H₅ on H-Covered Si(100)-(2 Ã— 1) Surface. Journal of Physical Chemistry C, 2014, 118, 20314-20322.	1.5	2
19232	Light-dependent controlled synthesis and photocatalytic properties of stable Ag 3 nanocrystals. Materials Research Bulletin, 2014, 60, 783-793.	2.7	7
19233	Oxygen-vacancy-induced local ferromagnetism as a driving mechanism in enhancing the magnetic response of ferrites. Physical Review B, 2014, 89, .	1.1	80
19234	Dissociative Hydrogen Adsorption on the Hexagonal Mo₂C Phase at High Coverage. Journal of Physical Chemistry C, 2014, 118, 8079-8089.	1.5	60
19235	Molecular Strategies for Configurational Sulfur Doping of Group IV Semiconductors Grown on Si(100) Using S(MH3)2(M = Si,Ge) Delivery Sources: An Experimental and Theoretical Inquiry. Chemistry of Materials, 2014, 26, 4447-4458.	3.2	5
19236	Tunable band gaps in graphene/GaN van der Waals heterostructures. Journal of Physics Condensed Matter, 2014, 26, 295304.	0.7	17
19237	High-throughput screening of high-capacity electrodes for hybrid Li-ionâ€“Liâ€“O₂cells. Physical Chemistry Chemical Physics, 2014, 16, 22073-22082.	1.3	30
19238	Effect of Pt on adherence of Î³â€²-Ni₃Al/Al₂O₃ interface of thermal barrier coatings investigated by first-principle molecular dynamics. Materials Research Innovations, 2014, 18, S2-1001-S2-1007.	1.0	2
19239	Assessing the Performance of Dispersionless and Dispersion-Accounting Methods: Helium Interaction with Cluster Models of the TiO₂(110) Surface. Journal of Physical Chemistry A, 2014, 118, 6367-6384.	1.1	30
19240	Energetic, Optical, and Electronic Properties of Intrinsic Electron-Trapping Defects in YAlO₃: A Hybrid DFT Study. Journal of Physical Chemistry C, 2014, 118, 19940-19947.	1.5	34
19241	Bandâ€Structure Engineering of ZnO by Anionâ€“Cation Coâ€Doping for Enhanced Photoâ€Electrochemical Activity. ChemPhysChem, 2014, 15, 1611-1618.	1.0	29
19242	Materials properties of magnesium and calcium hydroxides from first-principles calculations. Computational Materials Science, 2014, 95, 693-705.	1.4	35
19243	Ultrafast Carrier Thermalization and Cooling Dynamics in Few-Layer MoS₂. ACS Nano, 2014, 8, 10931-10940.	7.3	236
19244	Unraveling Mechanism on Reducing Thermal Hysteresis Width of VO₂ by Ti Doping: A Joint Experimental and Theoretical Study. Journal of Physical Chemistry C, 2014, 118, 18938-18944.	1.5	64
19245	Strong and weak adsorption of CO 2 on PuO 2 (1 1 0) surfaces from first principles calculations. Applied Surface Science, 2014, 316, 625-631.	3.1	24
19246	Obtaining Two-Dimensional Electron Gas in Free Space without Resorting to Electron Doping: An Electride Based Design. Journal of the American Chemical Society, 2014, 136, 13313-13318.	6.6	280
19247	Shear Instability in Nanoporous Si. Nano Letters, 2014, 14, 5081-5084.	4.5	2

#	Article	IF	Citations
19248	First-order liquidâ€“liquid phase transition in AsS melt caused by change of intermediate-range order. Journal of Non-Crystalline Solids, 2014, 404, 135-139.	1.5	3
19249	Thermal conductivity of fully filled skutterudites: Role of the filler. Physical Review B, 2014, 89, .	1.1	137
19250	Surface Modification of ITO Nanoparticles by Trimesic Acid: A Combined Experimental and DFT Study. Journal of Physical Chemistry C, 2014, 118, 21244-21249.	1.5	8
19251	Bending Poisson Effect in Two-Dimensional Crystals. Physical Review Letters, 2014, 112, .	2.9	30
19252	Graphitic Carbon Nitride Nanotubes As Li-Ion Battery Materials: A First-Principles Study. Journal of Physical Chemistry C, 2014, 118, 9318-9323.	1.5	62
19253	Polymersâ€™ surface interactions with molten iron: A theoretical study. Chemical Physics, 2014, 443, 107-111.	0.9	11
19254	Topological crystalline insulators and Dirac octets in antiperovskites. Physical Review B, 2014, 90, .	1.1	143
19256	Ti atoms in Ru0.3Ti0.7O2 mixed oxides form active and selective sites for electrochemical chlorine evolution. Electrochimica Acta, 2014, 146, 733-740.	2.6	44
19257	BaC: a thermodynamically stable layered superconductor. Physical Chemistry Chemical Physics, 2014, 16, 20780-20784.	1.3	8
19258	The ELPA library: scalable parallel eigenvalue solutions for electronic structure theory and computational science. Journal of Physics Condensed Matter, 2014, 26, 213201.	0.7	173
19259	Electronic Structure of Zn₃V₂O₈and Mg₃V₂O₈. Ferroelectrics, 2014, 461, 92-98.	0.3	5
19260	First-principles study of Cu/TiN and Al/TiN interfaces: weak versus strong interfaces. Modelling and Simulation in Materials Science and Engineering, 2014, 22, 035020.	0.8	28
19261	Revealing the Substrate Origin of the Linear Dispersion of Silicene/Ag(111). Nano Letters, 2014, 14, 5189-5193.	4.5	72
19262	Doped h-BN monolayer as efficient noble metal-free catalysts for CO oxidation: the role of dopant and water in activity and catalytic de-poisoning. Journal of Materials Chemistry A, 2014, 2, 12812-12820.	5.2	76
19263	First principles study of fluorine substitution on two-dimensional germanane. Journal of Physics Condensed Matter, 2014, 26, 335302.	0.7	14
19264	Structural paradox in submonolayer chlorine coverage on Au(111). Physical Review B, 2014, 89, .	1.1	15
19265	Silicon Monoxide at 1 atm and Elevated Pressures: Crystalline or Amorphous?. Journal of the American Chemical Society, 2014, 136, 3410-3423.	6.6	26
19266	Initial stages of oxygen adsorption onIn/Si(111)-4Ã—1. Physical Review B, 2014, 90, .	1.1	10

#	Article	IF	Citations
19267	Real Time Determination of the Electronic Structure of Unstable Reaction Intermediates during Au₂O₃ Reduction. Journal of Physical Chemistry Letters, 2014, 5, 80-84.	2.1	30
19268	Ab initiocalculation of the solution enthalpies of substitutional and interstitial impurities in paramagnetic fcc Fe. Physical Review B, 2014, 90, .	1.1	38
19269	Structural instability and the Mott-Peierls transition in a half-metallic hollandite :<mml:math xmlns:mml="http://www.w3.org/1998/Math/MathML"><mml:msub><mml:mi mathvariant="normal">K</mml:mi><mml:mn>2</mml:mn></mml:msub><mml:msub><mml:mi>Cr</mml:mi><mml:mn>8</mml:mn></mml:msub><mml:msub><mml:mi mathvariant="normal">O</mml:mi><mml:mn>16</mml:mn></mml:msub></mml:math>. Physical Review B, 2014, 90, .	1.1	12
19270	Energies of Electronic Transitions of Pentaerythritol Tetranitrate Molecules and Crystals. Journal of Physical Chemistry C, 2014, 118, 9324-9335.	1.5	20
19271	Novel rattling of K atoms in aluminium-doped defect pyrochlore tungstate. Journal of Physics Condensed Matter, 2014, 26, 305401.	0.7	2
19272	Metal-Free Magnetism and Half-Metallicity of Carbon Nitride Nanotubes: A First-Principles Study. Journal of Physical Chemistry C, 2014, 118, 22491-22498.	1.5	22
19273	Selective metal deposition at graphene line defects by atomic layer deposition. Nature Communications, 2014, 5, 4781.	5.8	243
19274	Bilayer Phosphorene: Effect of Stacking Order on Bandgap and Its Potential Applications in Thin-Film Solar Cells. Journal of Physical Chemistry Letters, 2014, 5, 1289-1293.	2.1	762
19275	Versatile Electronic and Magnetic Properties of SnSe₂ Nanostructures Induced by the Strain. Journal of Physical Chemistry C, 2014, 118, 9251-9260.	1.5	68
19276	Electronic structure of Zrâ€“Niâ€“Sn systems: role of clustering and nanostructures in half-Heusler and Heusler limits. Journal of Physics Condensed Matter, 2014, 26, 275501.	0.7	36
19277	An ab Initio Investigation of Proton Stability at BaZrO₃ Interfaces. Chemistry of Materials, 2014, 26, 4915-4924.	3.2	12
19278	Atomic Structure of <scp><scp>ZnO</scp></scp> Î£13 [0001]/{130} Symmetric Tilt Grain Boundary. Journal of the American Ceramic Society, 2014, 97, 617-621.	1.9	6
19279	Equilibrium Adsorption of <scp>d</scp>- and <scp>l</scp>-Alanine Mixtures on Naturally Chiral Cu{3,1,17}^{R&S} Surfaces. Journal of Physical Chemistry C, 2014, 118, 14957-14966.	1.5	28
19280	Three-dimensional metallic and two-dimensional insulating behavior in octahedral tantalum dichalcogenides. Physical Review B, 2014, 90, .	1.1	124
19281	Molecular Dynamics Simulations of Proposed Intermediates in the CO₂ + Aqueous Amine Reaction. Journal of Physical Chemistry Letters, 2014, 5, 1151-1156.	2.1	27
19282	Vibrational and thermodynamic properties ofÎ±-,Î²-,Î³-, and 6, 6, 12-graphyne structures. Nanotechnology, 2014, 25, 185701.	1.3	64
19283	Nanoalloy catalysts for electrochemical energy conversion and storage reactions. RSC Advances, 2014, 4, 42654-42669.	1.7	31
19284	First-Principles Hybrid Functional Study of the Organicâ€“Inorganic Perovskites CH₃NH₃SnBr₃ and CH₃NH₃SnI₃. Journal of Physical Chemistry C, 2014, 118, 24383-24388.	1.5	125

#	Article	IF	Citations
19285	First-principles-based optimization of electronic structures for bimetallic nanoparticles. Calphad: Computer Coupling of Phase Diagrams and Thermochemistry, 2014, 47, 144-147.	0.7	4
19286	Stability of Carbon on Cobalt Surfaces in Fischerâ€“Tropsch Reaction Conditions: A DFT Study. Journal of Physical Chemistry C, 2014, 118, 22479-22490.	1.5	30
19287	Modeling Load-displacement Curve and Pop-in Effect in Nanoindentation Tests. , 2014, 3, 1111-1116.		2
19288	An ab-initio investigation of the effect of graphene on the strength-electron density correlation in SiC grain boundaries. Computational Materials Science, 2014, 92, 422-430.	1.4	3
19289	Effect of Al substitution on Ti, Al, and N adatom dynamics on TiN(001), (011), and (111) surfaces. Surface Science, 2014, 630, 28-40.	0.8	37
19290	Hydrogen-related phenomena due to decreases in lattice defect energiesâ€”Molecular dynamics simulations using the embedded atom method potential with pseudo-hydrogen effects. Computational Materials Science, 2014, 92, 362-371.	1.4	24
19291	Adsorption of alkali metal atoms on germanene: A first-principles study. Applied Surface Science, 2014, 314, 15-20.	3.1	57
19292	Polaron states and migration in F-doped Li2MnO3. Physics Letters, Section A: General, Atomic and Solid State Physics, 2014, 378, 2449-2452.	0.9	20
19293	Ti2FeZ (Z=Al, Ga, Ge) alloys: Structural, electronic, and magnetic properties. Journal of Magnetism and Magnetic Materials, 2014, 369, 205-210.	1.0	16
19294	Trapping of oxide ions in Î´-Bi3YO6. Solid State Ionics, 2014, 264, 49-53.	1.3	9
19295	Constituents of magnetic anisotropy and a screening of spinâ€“orbit coupling in solids. Solid State Communications, 2014, 194, 35-38.	0.9	82
19296	Chebyshev-filtered subspace iteration method free of sparse diagonalization for solving the Kohnâ€“Sham equation. Journal of Computational Physics, 2014, 274, 770-782.	1.9	57
19297	Crystal structure and free energy of Ti 2 Ni 3 precipitates in Tiâ€“Ni alloys from first principles. Computational Materials Science, 2014, 93, 46-49.	1.4	11
19298	Composition dependent phase stability of Niâ€“Mnâ€“Ga alloys studied by ab initio calculations. Journal of Alloys and Compounds, 2014, 614, 126-130.	2.8	13
19299	Electronic structure and lattice dynamics of orthorhombic BiGaO3. Journal of Alloys and Compounds, 2014, 613, 175-180.	2.8	10
19300	Effect of vacancies (O, Ti) on the interfacial bonding strength and magnetoelectricity in Fe/BaTiO 3 : A first-principles study. Computational Materials Science, 2014, 93, 6-10.	1.4	0
19301	First-principles calculations of structural stability and mechanical properties of tungsten carbide under high pressure. Journal of Physics and Chemistry of Solids, 2014, 75, 1234-1239.	1.9	19
19302	Interaction of aluminium with hydrogen in twinning-induced plasticity steel. Scripta Materialia, 2014, 87, 9-12.	2.6	33

#	Article	IF	Citations
19303	Effects of strain on PdZn(100) for methoxide decomposition: A DFT study. Journal of Molecular Catalysis A, 2014, 393, 296-301.	4.8	2
19304	The structural, elastic, electronic and thermodynamic properties of hexagonal Î·-Cu6âˆ'xNixSn5 (xÂ=Â0, 0.5,) Tj ETQq1 1 0.784314 rgBT	1.8	14
19305	Interface properties in lamellar TiAl microstructures from density functional theory. Intermetallics, 2014, 54, 154-163.	1.8	39
19306	Distribution of Al and adsorption of NH3 in mordenite: A computational study. Journal of Fuel Chemistry and Technology, 2014, 42, 582-590.	0.9	8
19307	Parametrization of a classical force field for iron oxyhydroxide/water interfaces based on Density Functional Theory calculations. Computational Materials Science, 2014, 92, 343-352.	1.4	15
19308	Influence of Mn doping content on magnetic properties of a (Mn, N) co-doped ZnO system. Journal of Magnetism and Magnetic Materials, 2014, 369, 219-222.	1.0	6
19309	First principles modeling of the temperature dependent ternary phase diagram for the Cuâ€"Pdâ€"S system. Computational Materials Science, 2014, 92, 377-386.	1.4	1
19310	Adsorption of Ni, Pd, Pt, Cu, Ag and Au on the Fe3O4(111) surface. Surface Science, 2014, 628, 141-147.	0.8	42
19311	Synthesis, characterization, and electronic structure of few-layer MoSe₂ granular films. Physica Status Solidi (A) Applications and Materials Science, 2014, 211, 2671-2676.	0.8	13
19312	Slave mode expansion for obtainingab initiointeratomic potentials. Physical Review B, 2014, 90, .	1.1	15
19313	Self-consistent relativistic band structure of the<mml:math xmlns:mml="http://www.w3.org/1998/Math/MathML"><mml:mi mathvariant="normal">CH</mml:mi><mml:msub><mml:mrow /><mml:mn>3</mml:mn></mml:msub><mml:mi mathvariant="normal">NH</mml:mi><mml:msub><mml:mrow /><mml:mn>3</mml:mn></mml:msub><mml:mi mathvariant="normal">PbI</mml:mi><mml:msub><mml:mr	1.1	245
19314	A molecular dynamics simulation of hydrogen atoms collisions on an H-preadsorbed silica surface. Plasma Sources Science and Technology, 2014, 23, 045016.	1.3	19
19315	Equilibration dynamics and conductivity of warm dense hydrogen. Physical Review E, 2014, 90, 013104.	0.8	22
19316	Surface Structural Reconstruction for Optical Response in Iodine-Modified TiO₂ Photocatalyst System. Journal of Physical Chemistry C, 2014, 118, 13726-13732.	1.5	19
19317	Band gaps in incommensurable graphene on hexagonal boron nitride. Physical Review B, 2014, 89, .	1.1	97
19318	Fluorinated Boron Nitride Nanotube Quantum Dots: A Spin Filter. Journal of the American Chemical Society, 2014, 136, 11494-11498.	6.6	26
19319	Phase stability and its impact on the electrochemical performance of VOPO₄and LiVOPO₄. Journal of Materials Chemistry A, 2014, 2, 12330.	5.2	50
19320	First-principles study of native point defects in LiNi1/3Co1/3Mn1/3O2and Li2MnO3. Physical Chemistry Chemical Physics, 2014, 16, 16798.	1.3	20

#	Article	IF	Citations
19321	Diffusion on Demand to Control Precipitation Aging: Application to Al-Mg-Si Alloys. Physical Review Letters, 2014, 112, 225701.	2.9	132
19322	Spin-correlated electronic state on the surface of a spin-orbit Mott system. Physical Review B, 2014, 90, .	1.1	11
19323	Critical Role of the Semiconductorâ€“Electrolyte Interface in Photocatalytic Performance for Water-Splitting Reactions Using Ta₃N₅ Particles. Chemistry of Materials, 2014, 26, 4812-4825.	3.2	98
19324	Reliability evaluation of thermophysical properties from first-principles calculations. Journal of Physics Condensed Matter, 2014, 26, 335401.	0.7	9
19325	Generalized stacking fault energies, cleavage energies, ionicity and brittleness of Cu(Al/Ga/In)Se₂and CuGa(S/Se/Te)₂. Modelling and Simulation in Materials Science and Engineering, 2014, 22, 035002.	0.8	2
19326	Theoretical unification of hybrid-DFT and<mml:math xmlns:mml="http://www.w3.org/1998/Math/MathML"><mml:mtext>DFT</mml:mtext><mml:mo>â€‰</mml:mo><mml:mi>m</mml:mi></mml:math> for the treatment of localized orbitals. Physical Review B, 2014, 90, .	1.1	46
19327	Distinct Electronic Structure of the Electrolyte Gate-Induced Conducting Phase in Vanadium Dioxide Revealed by High-Energy Photoelectron Spectroscopy. ACS Nano, 2014, 8, 5784-5789.	7.3	27
19328	Symbiotic CeH 2.73 /CeO 2 catalyst: A novel hydrogen pump. Nano Energy, 2014, 9, 80-87.	8.2	159
19329	Thermodynamic re-assessment of the Alâ€“Gd and Gdâ€“Zr systems. Thermochimica Acta, 2014, 591, 51-56.	1.2	11
19330	A route to form initial hydrocarbon pool species in methanol conversion to olefins over zeolites. Journal of Catalysis, 2014, 317, 277-283.	3.1	151
19331	The Î³-Fe[N] and Î³â€²-Fe4N1â^'x phase boundaries in high-nitrogen steels: The cube cluster approximation and the effect of vibrational energy contributions. Computational Materials Science, 2014, 95, 8-12.	1.4	2
19332	The effect of hydrogen on the mechanical properties of FeTi for hydrogen storage applications. International Journal of Hydrogen Energy, 2014, 39, 12667-12675.	3.8	24
19333	Atomistic interaction between silicon and manganese in pearlitic steel: Combined atom probe tomography and first-principle calculations. Materials Letters, 2014, 134, 84-86.	1.3	18
19334	Comparison between cluster and slab model for Pt-group atom adsorption on gold and silver substrate. Surface Science, 2014, 630, 78-84.	0.8	4
19335	Atomic and electronic structure of tetrahedral amorphous carbon surfaces from density functional theory: Properties and simulation strategies. Carbon, 2014, 77, 1168-1182.	5.4	41
19336	Giant spinâ€“orbit splitting in ultrathin Ir(111) film. Physics Letters, Section A: General, Atomic and Solid State Physics, 2014, 378, 2640-2643.	0.9	2
19337	Impact of short-range ordering on yield strength of high manganese austenitic steels. Materials Science & Engineering A: Structural Materials: Properties, Microstructure and Processing, 2014, 614, 122-128.	2.6	48
19338	Nanoporous PtFe alloys as highly active and durable electrocatalysts for oxygen reduction reaction. Journal of Power Sources, 2014, 269, 589-596.	4.0	36

#	Article	IF	Citations
19339	Design of sustainable V-based hydrogen separation membranes based on grain boundary segregation. International Journal of Hydrogen Energy, 2014, 39, 12031-12044.	3.8	19
19340	Shape-dependent catalytic activity of oxygen reduction reaction (ORR) on silver nanodecahedra and nanocubes. Journal of Power Sources, 2014, 269, 152-157.	4.0	89
19341	Configuration-dependent geometric and electronic properties of bilayer graphene nanoribbons. Carbon, 2014, 77, 1031-1039.	5.4	18
19342	Structural, electronic and thermoelectric behaviour of CaMnO₃ and CaMnO_(3â^'Î'). Journal of Materials Chemistry A, 2014, 2, 14109-14117.	5.2	98
19343	Catalysis by Dynamically Formed Defects in a Metalâ€“Organic Framework Structure: Knoevenagel Reaction Catalyzed by Copper Benzeneâ€1,3,5â€tricarboxylate. ChemCatChem, 2014, 6, 2821-2824.	1.8	54
19344	Homolytic Cleavage of Molecular Oxygen by Manganese Porphyrins Supported on Ag(111). ACS Nano, 2014, 8, 5190-5198.	7.3	52
19345	Coronene Encapsulation in Singleâ€Walled Carbon Nanotubes: Stacked Columns, Peapods, and Nanoribbons. ChemPhysChem, 2014, 15, 1660-1665.	1.0	28
19346	Magnetic Exciton Relaxation and Spinâ€“Spin Interaction by the Time-Delayed Photoluminescence Spectra of ZnO:Mn Nanowires. ACS Applied Materials & Interfaces, 2014, 6, 10353-10366.	4.0	24
19347	Electronic structure, lattice dynamics and thermodynamic stability of paramelaconite Cu4O3. Materials Chemistry and Physics, 2014, 148, 293-298.	2.0	23
19348	Metastable host-guest structure of carbon. Journal of Superhard Materials, 2014, 36, 246-256.	0.5	2
19349	Quasiparticle electronic structure and optical absorption of diamond nanoparticles from ab initio many-body perturbation theory. Journal of Chemical Physics, 2014, 140, 214315.	1.2	6
19350	Density-Functional Tight-Binding Simulations of Curvature-Controlled Layer Decoupling and Band-Gap Tuning in Bilayer<mml:math xmlns:mml="http://www.w3.org/1998/Math/MathML" display="inline"><mml:mrow><mml:msub><mml:mrow><mml:mi>MoS</mml:mi></mml:mrow><mml:mrow><mml:mn>2</mml:mn></mml:mrow> Physical Review Letters, 2014, 112, 186802.	2.9	36
19351	Computational Investigation of NO₂ Adsorption and Reduction on Ceria and M-Doped CeO₂ (111) (M = Mn, Fe) Surfaces. Journal of Physical Chemistry C, 2014, 118, 10043-10052.	1.5	20
19352	Bilayer Graphene Growth via a Penetration Mechanism. Journal of Physical Chemistry C, 2014, 118, 6201-6206.	1.5	44
19353	Periodic DFT Study of Benzene Adsorption on Pd(100) and Pd(110) at Medium and Saturation Coverage. Journal of Physical Chemistry C, 2014, 118, 21483-21499.	1.5	16
19354	Solute strengthening of twinning dislocations in Mg alloys. Acta Materialia, 2014, 80, 278-287.	3.8	112
19355	Large-Gap Quantum Spin Hall Insulator in Single Layer Bismuth Monobromide Bi₄Br₄. Nano Letters, 2014, 14, 4767-4771.	4.5	156
19356	Collective Descriptors for the Adsorption of Sugar Alcohols on Pt and Pd(111). Journal of Physical Chemistry C, 2014, 118, 17531-17537.	1.5	23

#	Article	IF	Citations
19357	Applicability of density functional theory in reproducing accurate vibrational spectra of surface bound species. Journal of Computational Chemistry, 2014, 35, 1921-1929.	1.5	2
19358	High-Pressure Structural Stability and Optical Properties of Scheelite-type ZrGeO4 and HfGeO4 X-ray Phosphor Hosts. Journal of Physical Chemistry C, 2014, 118, 4325-4333.	1.5	11
19359	Site-Dependent Lewis Acidity of Î³-Al₂O₃ and Its Impact on Ethanol Dehydration and Etherification. Journal of Physical Chemistry C, 2014, 118, 12899-12907.	1.5	80
19360	Removal of Water Adsorbates on GaN Surfaces via Hopping Processes and with the Aid of a Pt₄ Cluster: An Ab Initio Study. Journal of Physical Chemistry C, 2014, 118, 20383-20392.	1.5	5
19361	Surface Polarization Matters: Enhancing the Hydrogenâ€Evolution Reaction by Shrinking Pt Shells in Ptâ€“Pdâ€“Graphene Stack Structures. Angewandte Chemie - International Edition, 2014, 53, 12120-12124.	7.2	436
19362	Magnetism in Dopant-Free Hexagonal CdS Nanorods: Experiments and First-Principles Analysis. Journal of Physical Chemistry C, 2014, 118, 11426-11431.	1.5	11
19363	Understanding the Interface of Liquids with an Organic Crystal Surface from Atomistic Simulations and AFM Experiments. Journal of Physical Chemistry C, 2014, 118, 2058-2066.	1.5	23
19364	Crystal Growth and Characterization of the Narrow-Band-Gap Semiconductors OsPn₂ (Pn) Tj ETQq1 1 0.784314 rgBT /O	1.9	18
19365	Understanding Adsorption-Induced Effects on Platinum Nanoparticles: An Energy-Decomposition Analysis. Journal of Physical Chemistry Letters, 2014, 5, 3120-3124.	2.1	37
19366	Effect of Polar Surfaces on Decomposition of Molecular Materials. Journal of the American Chemical Society, 2014, 136, 13289-13302.	6.6	44
19367	Toward New Fuel Cell Support Materials: A Theoretical and Experimental Study of Nitrogenâ€Doped Graphene. ChemSusChem, 2014, 7, 2609-2620.	3.6	45
19368	Half-Metallicity in MnPSe₃ Exfoliated Nanosheet with Carrier Doping. Journal of the American Chemical Society, 2014, 136, 11065-11069.	6.6	353
19369	Effect of Niobium on the Defect Chemistry and Oxidation Kinetics of Tetragonal ZrO₂. Journal of Physical Chemistry C, 2014, 118, 20122-20131.	1.5	26
19370	Enhanced Polymeric Dielectrics through Incorporation of Hydroxyl Groups. Macromolecules, 2014, 47, 1122-1129.	2.2	43
19371	Unraveling the Mechanism of the Covalent Coupling Between Terminal Alkynes on a Noble Metal. Journal of Physical Chemistry C, 2014, 118, 3181-3187.	1.5	73
19372	Enhanced Fe₂O₃ Reducibility via Surface Modification with Pd: Characterizing the Synergy within Pd/Fe Catalysts for Hydrodeoxygenation Reactions. ACS Catalysis, 2014, 4, 3381-3392.	5.5	114
19373	Effect of Pressure on Elastic Constants, Generalized Stacking Fault Energy, and Dislocation Properties in Antiperovskite-Type Ni-Rich Nitrides ZnNNi3 and CdNNi3. Journal of Superconductivity and Novel Magnetism, 2014, 27, 2607-2615.	0.8	1
19374	Quantum coherence of bulk electrons on metals revealed by scanning tunneling spectroscopy. Physical Review B, 2014, 89, .	1.1	1

#	Article	IF	Citations
19375	Ab initio simulations of optical materials. , 2014, , .		0
19376	Three New Silver Uranyl Diphosphonates: Structures and Properties. Inorganic Chemistry, 2014, 53, 2787-2796.	1.9	23
19377	Formation of an Organic/Metal Interface State from a Shockley Resonance. Journal of Physical Chemistry Letters, 2014, 5, 50-55.	2.1	41
19378	Stimulation of Electro-oxidation Catalysis by Bulk-Structural Transformation in Intermetallic ZrPt₃ Nanoparticles. ACS Applied Materials & Interfaces, 2014, 6, 16124-16130.	4.0	35
19379	The study of the P doped silicene nanoribbons with first-principles. Computational Materials Science, 2014, 95, 429-434.	1.4	25
19380	Electronic Structures of Carbon-Based KagomÃ© Lattices. Chinese Physics Letters, 2014, 31, 028102.	1.3	4
19381	Initial Stages of Oxygen Chemisorption on the Ge(001) Surface. Journal of Physical Chemistry C, 2014, 118, 15795-15803.	1.5	10
19382	Silica-Based Materials as Drug Adsorbents: First Principle Investigation on the Role of Water Microsolvation on Ibuprofen Adsorption. Journal of Physical Chemistry A, 2014, 118, 5801-5807.	1.1	47
19383	Decomposition of Metal Alkylamides, Alkyls, and Halides at Reducible Oxide Surfaces: Mechanism of â€˜Clean-upâ€™ During Atomic Layer Deposition of Dielectrics onto IIIâ€“V Substrates. Chemistry of Materials, 2014, 26, 2427-2437.	3.2	16
19384	Fast Energy Relaxation by Trap States Decreases Electron Mobility in TiO2 Nanotubes: Time-Domain Ab Initio Analysis. Journal of Physical Chemistry Letters, 2014, 5, 1642-1647.	2.1	31
19385	Superior mechanical flexibility of phosphorene and few-layer black phosphorus. Applied Physics Letters, 2014, 104, .	1.5	881
19386	Theoretical and experimental search for ZnSb-based thermoelectric materials. Journal of Physics Condensed Matter, 2014, 26, 365401.	0.7	17
19387	Surface design of alloy protection against CO-poisoning from first principles. Journal of Physics Condensed Matter, 2014, 26, 355006.	0.7	2
19389	A combined study of the equation of state of monazite-type lanthanum orthovanadate usingin situhigh-pressure diffraction andab initiocalculations. Acta Crystallographica Section B: Structural Science, Crystal Engineering and Materials, 2014, 70, 533-538.	0.5	16
19390	Small Cu Clusters Adsorbed on ZnO(101Ì…0) Show Evenâ€“Odd Alternations in Stability and Charge Transfer. Journal of Physical Chemistry C, 2014, 118, 6480-6490.	1.5	15
19391	Steering On-Surface Supramolecular Nanostructures by tert-Butyl Group. Journal of Physical Chemistry C, 2014, 118, 3088-3092.	1.5	11
19392	Theoretical Study on Equation of State of Porous Mo and Sn. Chinese Physics Letters, 2014, 31, 016402.	1.3	1
19393	A Hybrid Density Functional Theory/Molecular Mechanics Approach for Linear Response Properties in Heterogeneous Environments. Journal of Chemical Theory and Computation, 2014, 10, 989-1003.	2.3	39

#	Article	IF	Citations
19394	SO_x Oxidation Kinetics on Pt(111) and Pd(111): First-Principles Computations Meet Microkinetic Modeling. Journal of Physical Chemistry C, 2014, 118, 6934-6940.	1.5	18
19395	Nb-doped CaO: an efficient electron donor system. Journal of Physics Condensed Matter, 2014, 26, 315004.	0.7	5
19396	Substrate engineering in stabilizing epitaxial MgO(1â€‰1â€‰1) polar ultrathin films: first-principles calculations. Journal of Physics Condensed Matter, 2014, 26, 315014.	0.7	0
19397	Trends in Electrochemical Stability of Transition Metal Carbides and Their Potential Use As Supports for Low-Cost Electrocatalysts. ACS Catalysis, 2014, 4, 1558-1562.	5.5	142
19398	Ab initiostudies of thermodynamic and electronic properties of phosphorene nanoribbons. Physical Review B, 2014, 90, .	1.1	126
19399	Quaternary Sulfide Ba₆Zn₆ZrS₁₄: Synthesis, Crystal Structure, Band Structure, and Multiband Physical Properties. Chemistry - A European Journal, 2014, 20, 5977-5982.	1.7	19
19400	Characterization of the spin-<mml:math xmlns:mml="http://www.w3.org/1998/Math/MathML"><mml:mfrac><mml:mn>1</mml:mn><mml:mn>2</mml:mn></mml:mfrac></mml ferromagnet CuAs<mml:math xmlns:mml="http://www.w3.org/1998/Math/MathML"><mml:msub><mml:mrow /><mml:mn>2</mml:mn></mml:msub></mml:math>O<mml:math xmlns:mml="http://www.w3.org/1998/Math/MathML"><mml:msub><mml:mrow /><mml:mn>4</mml:mn><<	1.1	19
19401	Theoretical and Experimental Studies of Câ€“C versus Câ€“O Bond Scission of Ethylene Glycol Reaction Pathways via Metal-Modified Molybdenum Carbides. ACS Catalysis, 2014, 4, 1409-1418.	5.5	45
19402	Defect Engineering of BiI₃ Single Crystals: Enhanced Electrical and Radiation Performance for Room Temperature Gamma-Ray Detection. Journal of Physical Chemistry C, 2014, 118, 3244-3250.	1.5	72
19403	Interactions between hydrogen and tungsten carbide: a first principles study. RSC Advances, 2014, 4, 39912.	1.7	17
19404	Theoretical investigation of the effects of doping on the electronic structure and thermoelectric properties of ZnO nanowires. Physical Chemistry Chemical Physics, 2014, 16, 3771.	1.3	27
19405	Mechanism for Limiting Thickness of Thin Oxide Films on Aluminum. Physical Review Letters, 2014, 112, 146103.	2.9	74
19406	Emergence of Antiferromagnetic Ordering in Tb_n (n = 2â€“33) Clusters. Journal of Physical Chemistry A, 2014, 118, 1936-1947.	1.1	4
19407	Digermane Deposition on Si(100) and Ge(100): from Adsorption Mechanism to Epitaxial Growth. Journal of Physical Chemistry C, 2014, 118, 482-493.	1.5	6
19408	Enthalpyâ€“Entropy Compensation Effect in Hydrogen Storage Materials: Striking Example of Alkali Silanides MSiH3(M = K, Rb, Cs). Journal of Physical Chemistry C, 2014, 118, 3409-3419.	1.5	29
19409	Tuning the reactivity of Ru nanoparticles by defect engineering of the reduced graphene oxide support. RSC Advances, 2014, 4, 22230-22240.	1.7	20
19410	Trends in Atomic Adsorption on Pt₃M(111) Transition Metal Bimetallic Surface Overlayers. Journal of Physical Chemistry C, 2014, 118, 8342-8349.	1.5	16
19411	SnO2: A comprehensive review on structures and gas sensors. Progress in Materials Science, 2014, 66, 112-255.	16.0	933

#	Article	IF	Citations
19412	New Basic Insights into the Low Hot Electron Injection Efficiency of Gold-Nanoparticle-Photosensitized Titanium Dioxide. ACS Applied Materials & Interfaces, 2014, 6, 12388-12394.	4.0	36
19413	Pbca-Type In₂O₃: The High-Pressure Post-Corundum phase at Room Temperature.. Journal of Physical Chemistry C, 2014, 118, 20545-20552.	1.5	27
19414	First-Principles Calculations and Electron Density Topological Analysis of Covellite (CuS). Journal of Physical Chemistry A, 2014, 118, 5823-5831.	1.1	111
19415	Tunable Exciton Funnel Using MoirÃ© Superlattice in Twisted van der Waals Bilayer. Nano Letters, 2014, 14, 5350-5357.	4.5	55
19416	Effects of Ni vacancy, Ni antisite, Cr and Pt on the third-order elastic constants and mechanical properties of NiAl. Intermetallics, 2014, 55, 108-117.	1.8	23
19417	Metal adatoms-decorated silicene as hydrogen storage media. International Journal of Hydrogen Energy, 2014, 39, 14027-14032.	3.8	72
19418	Atomic structure and physical properties of fused porphyrin nanoclusters. Journal of Porphyrins and Phthalocyanines, 2014, 18, 552-568.	0.4	2
19419	Adsorption of tetrathiafulvalene (TTF) on Cu(1 0 0): can Ï€-stacked 1-D aggregates be formed at low temperature?. Chemical Physics Letters, 2014, 612, 45-50.	1.2	0
19420	An efficient method to generate amorphous structures based on local geometry. Computational Materials Science, 2014, 95, 256-262.	1.4	18
19421	Theoretical study of the structural phase transition and elastic properties of HfN under high pressures. Journal of Physics and Chemistry of Solids, 2014, 75, 1295-1300.	1.9	4
19422	Ab initio study of MgH 2 : Destabilizing effects of selective substitutions by transition metals. Solid State Sciences, 2014, 36, 47-51.	1.5	5
19423	Nitrogen and vanadium Co-doped TiO 2 mesosponge layers for enhancement in visible photocatalytic activity. Applied Surface Science, 2014, 315, 131-137.	3.1	27
19424	High Band Degeneracy Contributes to High Thermoelectric Performance in pâ€Type Halfâ€Heusler Compounds. Advanced Energy Materials, 2014, 4, 1400600.	10.2	261
19425	18-Electron rule inspired Zintl-like ions composed of all transition metals. Physical Chemistry Chemical Physics, 2014, 16, 20241-20247.	1.3	7
19426	Structural and electronic origin of the magnetic structures in hexagonal<mml:math xmlns:mml="http://www.w3.org/1998/Math/MathML"><mml:msub><mml:mrow><mml:mi mathvariant="normal">LuFeO</mml:mi></mml:mrow><mml:mn>3</mml:mn></mml:msub></mml:math>. Physical Review B, 2014, 90, .	1.1	38
19427	Induced Magnetization in<mml:math xmlns:mml="http://www.w3.org/1998/Math/MathML" display="inline"><mml:mrow><mml:msub><mml:mrow><mml:mi>La</mml:mi></mml:mrow><mml:mrow><mml:mn>0.7</mml:mn> Physical Review Letters, 2014, 113, 047204.	2.9	59
19428	Computational studies on magnetism and the optical properties of transition metal embedded graphitic carbon nitride sheets. Journal of Materials Chemistry C, 2014, 2, 7943-7951.	2.7	128
19429	AEMnSb₂(AE=Sr, Ba): a new class of Dirac materials. Journal of Physics Condensed Matter, 2014, 26, 042201.	0.7	57

#	Article	IF	Citations
19430	<mml:math xmlns:mml="http://www.w3.org/1998/Math/MathML"><mml:msub><mml:mrow><mml:mi mathvariant="normal">CaBaCo</mml:mi></mml:mrow><mml:mn>4</mml:mn></mml:msub></mml:math><mml:math xmlns:mml="http://www.w3.org/1998/Math/MathML"><mml:msub><mml:mrow><mml:mi mathvariant="normal">O</mml:mi></mml:mrow><mml:mn>7</mml:mn></mml:msub></mml:math>: A ferrimagnetic pyroelectric. Physical Review B, 2014, 90, .	1.1	42
19431	Electronic Structure of Half-Metal Antiferromagnetism in Double-Perovskite BiPbVRuO₆and BiPbVOsO₆. Journal of the Physical Society of Japan, 2014, 83, 054715.	0.7	4
19432	Modeling graphite under stress: Equations of state, vibrational modes, and interlayer friction. Physical Review B, 2014, 90, .	1.1	7
19433	Ceâ€“O Covalence in Silicate Oxyapatites and Its Influence on Luminescence Dynamics. Journal of Physical Chemistry C, 2014, 118, 16051-16059.	1.5	28
19434	Mechanism of insulator-to-metal transition in heavily Nb doped anatase TiO₂. Materials Research Express, 2014, 1, 015911.	0.8	9
19435	Crystal structure and physical properties of Mo2B: First-principle calculations. Journal of Applied Physics, 2014, 115, .	1.1	21
19436	Tunneling magnetoresistance of FePt/NaCl/FePt(001). Europhysics Letters, 2014, 105, 58003.	0.7	13
19437	Quantum molecular dynamics simulation of shock-wave experiments in aluminum. Journal of Applied Physics, 2014, 115, .	1.1	68
19438	Wavelength-Tuned Light Emission via Modifying the Band Edge Symmetry: Doped SnO₂ as an Example. Journal of Physical Chemistry C, 2014, 118, 6365-6371.	1.5	28
19439	Dopamine Adsorption on TiO₂ Anatase Surfaces. Journal of Physical Chemistry C, 2014, 118, 20688-20693.	1.5	47
19440	Degradation Mechanism against Hydrogenation Cycles in Mg_{2â€“x}Pr_xNi₄ (x = 0.6 and 1.0). Journal of Physical Chemistry C, 2014, 118, 6697-6705.	1.5	23
19441	Modeling of pseudotwinning in Fe₃Ga. Modelling and Simulation in Materials Science and Engineering, 2014, 22, 055008.	0.8	10
19442	Hybrid Quantum Mechanics/Molecular Mechanics Solvation Scheme for Computing Free Energies of Reactions at Metalâ€“Water Interfaces. Journal of Chemical Theory and Computation, 2014, 10, 3354-3368.	2.3	42
19443	Sulfidation and Sulfur Recovery from SO₂ over Ceria. Journal of Physical Chemistry C, 2014, 118, 17499-17504.	1.5	11
19444	[ZnBi₄]^{3â€“} Pentagon in K₆ZnBi₅: Aromatic All-Metal Heterocycle. Inorganic Chemistry, 2014, 53, 1266-1268.	1.9	6
19445	Precise Determination of the Threshold Diameter for a Single-Walled Carbon Nanotube To Collapse. ACS Nano, 2014, 8, 9657-9663.	7.3	43
19446	First-principles study of<mml:math xmlns:mml="http://www.w3.org/1998/Math/MathML"><mml:msup><mml:mrow><mml:mn>180</mml:mn></mml:mrow><mml:mo>â˜ walls in<mml:math xmlns:mml="http://www.w3.org/1998/Math/MathML"><mml:msub><mml:mrow><mml:mi mathvariant="normal">BaTiO</mml:mi></mml:mrow><mml:mn>3</mml:mn></mml:msub></mml:math>: Mixed Bloch-NÃ©el-Ising character. Physical Review B, 2014, 90, .	1.1	42
19447	Adsorption of Rh, Pd, Ir, and Pt on the Au(111) and Cu(111) Surfaces: A Density Functional Theory Investigation. Journal of Physical Chemistry C, 2014, 118, 19051-19061.	1.5	38

#	Article	IF	Citations
19448	Na_{2+x}Ti₆O₁₃ as Potential Negative Electrode Material for Na-Ion Batteries. Inorganic Chemistry, 2014, 53, 8250-8256.	1.9	57
19449	Molecular Motion Induced by Multivibronic Excitation on Semiconductor Surface. Journal of Physical Chemistry C, 2014, 118, 1554-1559.	1.5	5
19450	Pdâ€“Ir alloy as an anode material for borohydride oxidation. Journal of Power Sources, 2014, 269, 498-508.	4.0	45
19451	Theoretical and experimental studies of the adsorption geometry and reaction pathways of furfural over FeNi bimetallic model surfaces and supported catalysts. Journal of Catalysis, 2014, 317, 253-262.	3.1	88
19452	Hydrogen diffusion along grain boundaries in erbium oxide coatings. Journal of Nuclear Materials, 2014, 455, 360-365.	1.3	13
19453	Structure and reactivity of zero-, two- and three-dimensional Pd supported on SrTiO3(001). Surface Science, 2014, 630, 46-63.	0.8	6
19454	Exceptionally long-ranged lattice relaxation in oxygen-deficient Ta2O5. Solid State Communications, 2014, 195, 16-20.	0.9	10
19455	Tuning<mml:math xmlns:mml="http://www.w3.org/1998/Math/MathML" altimg="si1.gif" overflow="scroll"><mml:mi>p</mml:mi><mml:mo stretchy="false">/</mml:mo><mml:mi>n</mml:mi></mml:math>conductivity in wurtzite transition metal monoxide: Role of native defects in CoO and MnO. Physics Letters, Section A: General, Atomic and Solid State Physics, 2014, 378, 2685-2689.	0.9	8
19456	Solute/impurity diffusivities in bcc Fe: A first-principles study. Journal of Nuclear Materials, 2014, 455, 354-359.	1.3	14
19457	Cooperatively enhanced catalytic properties of Ti@Al(100) near-surface alloy for aluminum hydrogenation. International Journal of Hydrogen Energy, 2014, 39, 11963-11975.	3.8	1
19458	Structures, Energetics, and Electronic Properties of Multifarious Stacking Patterns for High-Buckled and Low-Buckled Silicene on the MoS₂ Substrate. Journal of Physical Chemistry C, 2014, 118, 19129-19138.	1.5	76
19459	Ti₃C₂ MXene as a High Capacity Electrode Material for Metal (Li, Na, K, Ca) Ion Batteries. ACS Applied Materials & Interfaces, 2014, 6, 11173-11179.	4.0	1,165
19460	Density Functional Theory (DFT) Computation of the Oxygen Reduction Reaction (ORR) on Titanium Nitride (TiN) Surface. Electrochimica Acta, 2014, 141, 25-32.	2.6	42
19461	The structural and electronic properties of amorphous HgCdTe from first-principles calculations. Journal Physics D: Applied Physics, 2014, 47, 025304.	1.3	2
19462	Selective oxidation of vinyl chloride on Ag2O(100), Cu2O(100), and Au2O(100) surfaces: A density functional theory study. Surface Science, 2014, 630, 116-124.	0.8	4
19463	Electronic structure and phase stability of plutonium hydrides: Role of Coulomb repulsion and spin-orbital coupling. International Journal of Hydrogen Energy, 2014, 39, 13255-13265.	3.8	23
19464	Hydrogen storage in Li dispersed graphene with Stoneâ€“Wales defects: A first-principles study. International Journal of Hydrogen Energy, 2014, 39, 13189-13194.	3.8	50
19465	Two-dimensional topological insulators with binary honeycomb lattices:<mml:math xmlns:mml="http://www.w3.org/1998/Math/MathML"><mml:mi>Si</mml:mi><mml:msub><mml:mi mathvariant="normal">C</mml:mi><mml:mn>3</mml:mn></mml:msub></mml:math>siligraphene and its analogs. Physical Review B, 2014, 89, .	1.1	83

#	Article	IF	Citations
19466	Charge Transfer, Luminescence, and Phonon Bottleneck in TiO₂ Nanowires Computed by Eigenvectors of Liouville Superoperator. Journal of Chemical Theory and Computation, 2014, 10, 3996-4005.	2.3	26
19467	Strong interaction between graphene edge and metal revealed by scanning tunneling microscopy. Carbon, 2014, 78, 190-195.	5.4	15
19468	Electronic structures and optical properties of rutile TiO2 with different point defects from DFT+U calculations. Physics Letters, Section A: General, Atomic and Solid State Physics, 2014, 378, 2719-2724.	0.9	49
19469	Ab initio study on the adsorption mechanism of oxygen on Cr2AlC (0 0 0 1) surface. Applied Surface Science, 2014, 315, 45-54.	3.1	16
19470	Growth morphology of thin films on metallic and oxide surfaces. Journal of Physics Condensed Matter, 2014, 26, 053001.	0.7	5
19471	Role of Dispersive Interactions in Determining Structural Properties of Organicâ€“Inorganic Halide Perovskites: Insights from First-Principles Calculations. Journal of Physical Chemistry Letters, 2014, 5, 2728-2733.	2.1	199
19472	Antiferromagnetism in Nanofilms of Mn-Doped GaN. Journal of Physical Chemistry C, 2014, 118, 18064-18068.	1.5	7
19473	First-Principles Study of Methanol Oxidation into Methyl Formate on Rutile TiO₂(110). Journal of Physical Chemistry C, 2014, 118, 19859-19868.	1.5	33
19474	Lithium hydroxide, LiOH, at elevated densities. Journal of Chemical Physics, 2014, 141, 024505.	1.2	20
19475	Dynamic layer rearrangement during growth of layered oxide films by molecular beam epitaxy. Nature Materials, 2014, 13, 879-883.	13.3	133
19476	Formation, migration, and clustering of point defects in CuInSe₂from first principles. Journal of Physics Condensed Matter, 2014, 26, 345501.	0.7	31
19477	First-Principles Study on Site Preference and 4f â† 5d Transitions of Ce³⁺ in Sr₃AlO₄F. Journal of Physical Chemistry A, 2014, 118, 986-992.	1.1	25
19478	Dense Network of One-Dimensional Midgap Metallic Modes in Monolayer<mml:math xmlns:mml="http://www.w3.org/1998/Math/MathML" display="inline"><mml:mrow><mml:msub><mml:mrow><mml:mi>MoSe</mml:mi></mml:mrow><mml:mrow><mml:mn>2</mml:mn></ Their Spatial Undulations. Physical Review Letters, 2014, 113, 066105.	2.9	172
19479	Interfacial adhesion between graphene and silicon dioxide by density functional theory with van der Waals corrections. Journal Physics D: Applied Physics, 2014, 47, 255301.	1.3	109
19480	A novel three dimensional semimetallic MoS2. Journal of Applied Physics, 2014, 115, .	1.1	6
19481	Phase diagram of the CuInSe2-CuGaSe2 pseudobinary system studied by combined ab initio density functional theory and thermodynamic calculation. Journal of Applied Physics, 2014, 116, .	1.1	16
19482	Computational exploration of newly synthesized zirconium metalâ€“organic frameworks UiO-66, -67, -68 and analogues. Journal of Materials Chemistry C, 2014, 2, 7111-7125.	2.7	89
19483	Pt@Au Nanorods Uniformly Decorated on Pyridyne Cycloaddition Graphene as a Highly Effective Electrocatalyst for Oxygen Reduction. ACS Applied Materials & Interfaces, 2014, 6, 13448-13454.	4.0	38

#	Article	IF	Citations
19484	A density functional theory investigation of the electronic structure and spin moments of magnetite. Science and Technology of Advanced Materials, 2014, 15, 044202.	2.8	81
19485	Polychiral Semiconducting Carbon Nanotubeâ€“Fullerene Solar Cells. Nano Letters, 2014, 14, 5308-5314.	4.5	109
19486	A strong linear correlation between the surface charge density on Ag nanoparticles and the amount of propylene adsorbed. Journal of Materials Chemistry A, 2014, 2, 6987.	5.2	6
19487	The role of Bi vacancies in the electrical conduction of BiFeO₃: a first-principles approach. Dalton Transactions, 2014, 43, 10787-10793.	1.6	47
19488	Adsorption of small mono- and poly-alcohols on rutile TiO2: a density functional theory study. Physical Chemistry Chemical Physics, 2014, 16, 14750.	1.3	13
19489	Computational materials design of negative effectiveUsystem in hole-doped chalcopyrite CuFeS₂. Journal of Physics Condensed Matter, 2014, 26, 355502.	0.7	8
19490	Deformation Induced Solidâ€“Solid Phase Transitions in Gamma Boron. Chemistry of Materials, 2014, 26, 4289-4298.	3.2	9
19491	Interesting Evidence for Templateâ€Induced Ferroelectric Behavior in Ultraâ€Thin Titanium Dioxide Films Grown on (110) Neodymium Gallium Oxide Substrates. Advanced Functional Materials, 2014, 24, 2844-2851.	7.8	16
19492	Green luminescence in Mg-doped GaN. Physical Review B, 2014, 90, .	1.1	120
19493	Intercalated graphitic carbon nitride: a fascinating two-dimensional nanomaterial for an ultra-sensitive humidity nanosensor. Nanoscale, 2014, 6, 9250.	2.8	108
19494	The search for the most stable structures of siliconâ€“carbon monolayer compounds. Nanoscale, 2014, 6, 11685-11691.	2.8	68
19495	Role of Au in Graphene Growth on a Ni Surface. ACS Catalysis, 2014, 4, 892-902.	5.5	8
19496	Phase transformations of nano-sized cubic boron nitride to white graphene and white graphite. Applied Physics Letters, 2014, 104, 093104.	1.5	21
19497	Formation of NV centers in diamond: A theoretical study based on calculated transitions and migration of nitrogen and vacancy related defects. Physical Review B, 2014, 89, .	1.1	149
19498	Nanoscale Stabilization of Sodium Oxides: Implications for Naâ€“O₂ Batteries. Nano Letters, 2014, 14, 1016-1020.	4.5	162
19499	Impact of Surface on the <inline-formula> <tex-math notation="TeX">d^{0} </tex-math></inline-formula> Ferromagnetism of Lithium-Doped Zinc Oxide Nanowires. IEEE Transactions on Magnetics, 2014, 50, 1-7.	1.2	3
19500	Optical band gap of SrTcO3 from first-principles calculations. Modern Physics Letters B, 2014, 28, 1450049.	1.0	5
19501	Tunable electronic properties induced by a defect-substrate in graphene/BC₃heterobilayers. Physical Chemistry Chemical Physics, 2014, 16, 22861-22866.	1.3	30

#	Article	IF	Citations
19502	Dislocation motion and grain boundary migration in two-dimensional tungsten disulphide. Nature Communications, 2014, 5, 4867.	5.8	192
19503	Origin of polar distortion in<mml:math xmlns:mml="http://www.w3.org/1998/Math/MathML"><mml:msub><mml:mi>LiNbO</mml:mi><mml:mn>3</mml:mn></mml:msub></mml:math> â€œferroelectricâ€•metals: Role of<mml:math xmlns:mml="http://www.w3.org/1998/Math/MathML"><mml:mi>A</mml:mi></mml:math>-site instability and short-range interactions. Physical Review B, 2014, 90, .	1.1	75
19504	The edge termination controlled kinetics in graphene chemical vapor deposition growth. Chemical Science, 2014, 5, 4639-4645.	3.7	41
19505	Stability, transparency, and conductivity of MgxZn1â^'xO and CdxZn1â^'xO: Designing optimum transparency conductive oxides. Journal of Applied Physics, 2014, 115, .	1.1	10
19506	Prediction and Characterization of MXene Nanosheet Anodes for Non-Lithium-Ion Batteries. ACS Nano, 2014, 8, 9606-9615.	7.3	814
19507	Insights into Diffusion Mechanisms in P2 Layered Oxide Materials by First-Principles Calculations. Chemistry of Materials, 2014, 26, 5208-5214.	3.2	149
19508	Enhanced lithiation in defective graphene. Carbon, 2014, 80, 305-310.	5.4	186
19509	Atomically-thin molybdenum nitride nanosheets with exposed active surface sites for efficient hydrogen evolution. Chemical Science, 2014, 5, 4615-4620.	3.7	455
19510	Impact of Graphene Edges on Enhancing the Performance of Electrochemical Double Layer Capacitors. Journal of Physical Chemistry C, 2014, 118, 21770-21777.	1.5	54
19511	Siliconâ€“Carbon Bond Inversions Driven by 60-keV Electrons in Graphene. Physical Review Letters, 2014, 113, 115501.	2.9	123
19512	Computational prediction of two-dimensional group-IV mono-chalcogenides. Applied Physics Letters, 2014, 105, .	1.5	245
19513	Testing the Jacob's ladder of density functionals for electronic structure and magnetism of rutile<mml:math xmlns:mml="http://www.w3.org/1998/Math/MathML"><mml:msub><mml:mi mathvariant="normal">VO</mml:mi><mml:mn>2</mml:mn></mml:msub></mml:math>. Physical Review B, 2014, 90, .	1.1	20
19514	Effects of substrate defects on the carbon cluster formation in graphene growth on Ni(111) surface. Physics Letters, Section A: General, Atomic and Solid State Physics, 2014, 378, 3055-3059.	0.9	4
19515	Development of interatomic potential for Ndâ€“Feâ€“B permanent magnet and evaluation of magnetic anisotropy near the interface and grain boundary. Modelling and Simulation in Materials Science and Engineering, 2014, 22, 065014.	0.8	12
19516	Nanoscale Spin-State Ordering in LaCoO₃ Epitaxial Thin Films. Chemistry of Materials, 2014, 26, 2496-2501.	3.2	74
19517	Atomic Structure of a Spinel-Like Transition<mml:math xmlns:mml="http://www.w3.org/1998/Math/MathML" display="inline"><mml:mrow><mml:msub><mml:mrow><mml:mi>Al</mml:mi></mml:mrow><mml:mrow><mml:mn>2</mml:mn></mml:mrow></mml:msub><mml:msub><mml:mrow><mml:mi mathvariant="normal">O</mml:mi></mml:mrow><mml:mrow><mml:mn>3</mml:mn></mml:mrow></mml:msub><mml:mo stretchy="false">(</mml:mo><mml:mn>100</mml:mn><mml:mo) Tj ETQq1 1 0.784314 rgBT /Overlock 10 Tf 50 127 Td (stretchy="false	2.9	13
19518	High Chemical Activity of a Perovskite Surface: Reaction of CO with<mml:math xmlns:mml="http://www.w3.org/1998/Math/MathML" display="inline"><mml:mrow><mml:msub><mml:mrow><mml:mi>Sr</mml:mi></mml:mrow><mml:mrow><mml:mn>3</mml:mn></mml:mrow></mml:msub><mml:msub><mml:mrow><mml:mi mathvariant="normal">O</mml:mi></mml:mrow><mml:mrow><mml:mn>7</mml:mn></mml:mrow></mml:msub></mml:mrow></mml: Physical Review Letters, 2014, 113, 116101.	2.9	18
19519	Monolayer Nanoislands of Pt on Au and Cu: A First-Principles Computational Study. Journal of Physical Chemistry C, 2014, 118, 22102-22110.	1.5	8

#	Article	IF	Citations
19520	Half-metallicity in graphitic C3 N4 nanoribbons: An ab initio study. Physica Status Solidi (B): Basic Research, 2014, 251, 1386-1392.	0.7	12
19521	Phosphorene nanoribbon as a promising candidate for thermoelectric applications. Scientific Reports, 2014, 4, 6452.	1.6	308
19522	First-Principles Study of Lead Iodide Perovskite Tetragonal and Orthorhombic Phases for Photovoltaics. Journal of Physical Chemistry C, 2014, 118, 19565-19571.	1.5	220
19523	Role of the Li⁺node in the Li-BH₄substructure of double-cation tetrahydroborates. Acta Crystallographica Section B: Structural Science, Crystal Engineering and Materials, 2014, 70, 871-878.	0.5	10
19524	Potential rare earth free permanent magnet: interstitial boron doped FeCo. Journal Physics D: Applied Physics, 2014, 47, 415002.	1.3	17
19525	Ab Initio Predicted Impact of Pt on Phase Stabilities in Ni-Mn-Ga Heusler Alloys. Journal of Phase Equilibria and Diffusion, 2014, 35, 695-700.	0.5	11
19526	Edge engineering of a topological Bi(111) bilayer. Physical Review B, 2014, 90, .	1.1	32
19527	Reorganization of a topological surface state: Theory for<mml:math xmlns:mml="http://www.w3.org/1998/Math/MathML"><mml:mrow><mml:msub><mml:mi>Bi</mml:mi><mml:mn>21</mml:mn></mml:m covered by noble metals. Physical Review B, 2014, 90, .	1.1	2
19528	Facet development during platinum nanocube growth. Science, 2014, 345, 916-919.	6.0	429
19529	First principles molecular dynamics studies of elastic constants, ideal tensile strength, chemistry of crack initiation, and surface and cohesive energies in amorphous silicon. Philosophical Magazine, 2014, 94, 2913-2936.	0.7	8
19530	Band Structure Tuning of TiO₂ for Enhanced Photoelectrochemical Water Splitting. Journal of Physical Chemistry C, 2014, 118, 7451-7457.	1.5	95
19531	Gapless<mml:math xmlns:mml="http://www.w3.org/1998/Math/MathML"><mml:msub><mml:mtext>MoS</mml:mtext><mml:mn>2</mml:mn><mml:ms possessing both massless Dirac and heavy fermions. Physical Review B, 2014, 89, .	1.1	109
19532	Utilizing the Gate-Opening Mechanism in ZIF-7 for Adsorption Discrimination between N₂O and CO₂. Journal of Physical Chemistry C, 2014, 118, 17831-17837.	1.5	51
19533	Tunable electronic and magnetic properties in germanene by alkali, alkaline-earth, group III and 3d transition metal atom adsorption. Physical Chemistry Chemical Physics, 2014, 16, 15968.	1.3	61
19534	Crystal Structure and Magnetic Properties of FeSeO₃Fâ€"Alternating Antiferromagnetic S = 5/2 chains. Inorganic Chemistry, 2014, 53, 4250-4256.	1.9	37
19535	Electronic Structure of Cesium Butyratouranylate(VI) as Derived from DFT-assisted Powder X-ray Diffraction Data. Journal of Physical Chemistry A, 2014, 118, 9745-9752.	1.1	17
19536	Analyzing the errors of DFT approximations for compressed water systems. Journal of Chemical Physics, 2014, 141, 014104.	1.2	16
19537	Defining the Proton Topology of the Zr₆-Based Metalâ€"Organic Framework NU-1000. Journal of Physical Chemistry Letters, 2014, 5, 3716-3723.	2.1	228

#	Article	IF	Citations
19538	First-principles study of O₂ reduction on BaZr_{1â^'x}Co_xO₃ cathodes in protonic-solid oxide fuel cells. Journal of Materials Chemistry A, 2014, 2, 16707-16714.	5.2	29
19539	Aligned Fe2TiO5-containing nanotube arrays with low onset potential for visible-light water oxidation. Nature Communications, 2014, 5, 5122.	5.8	161
19540	Influence of Defects and Synthesis Conditions on the Photovoltaic Performance of Perovskite Semiconductor CsSnI₃. Chemistry of Materials, 2014, 26, 6068-6072.	3.2	256
19541	Adsorption of phenol on Fe (110) and Pd (111) from first principles. Surface Science, 2014, 630, 244-253.	0.8	52
19542	Interdependency of Subsurface Carbon Distribution and Grapheneâ€"Catalyst Interaction. Journal of the American Chemical Society, 2014, 136, 13698-13708.	6.6	95
19543	Epitaxial growth of large-gap quantum spin Hall insulator on semiconductor surface. Proceedings of the National Academy of Sciences of the United States of America, 2014, 111, 14378-14381.	3.3	205
19544	An atlas of two-dimensional materials. Chemical Society Reviews, 2014, 43, 6537-6554.	18.7	1,159
19545	The metallization and superconductivity of dense hydrogen sulfide. Journal of Chemical Physics, 2014, 140, 174712.	1.2	612
19546	Theoretical studies of geometry asymmetry in tellurium nanostructures: intrinsic dipole, charge separation, and semiconductorâ€"metal transition. RSC Advances, 2014, 4, 44004-44010.	1.7	2
19547	An Acentric Calcium Borate Ca₂[B₅O₉]Â·(OH)Â·H₂O: Synthesis, Structure, and Nonliner Optical Property. Inorganic Chemistry, 2014, 53, 11757-11763.	1.9	84
19548	The Structure and Properties of Amorphous Indium Oxide. Chemistry of Materials, 2014, 26, 5401-5411.	3.2	179
19549	Electronic properties and hydrogen storage application of designed porous nanotubes from a polyphenylene network. International Journal of Hydrogen Energy, 2014, 39, 18966-18975.	3.8	33
19550	Structural Properties of Nickel Dimethylglyoxime at High Pressure: Single-Crystal X-ray Diffraction and DFT Studies. Journal of Physical Chemistry C, 2014, 118, 24705-24713.	1.5	22
19551	Nonlinear Valley and Spin Currents from Fermi Pocket Anisotropy in 2D Crystals. Physical Review Letters, 2014, 113, 156603.	2.9	80
19552	Ab initiosynthesis of single-layer III-V materials. Physical Review B, 2014, 89, .	1.1	112
19553	Al₂C monolayer: the planar tetracoordinate carbon global minimum. Nanoscale, 2014, 6, 10784.	2.8	82
19554	Electroconductive properties in doped spinel oxides. Optical Materials, 2014, 37, 656-665.	1.7	13
19555	First-principles high-pressure unreacted equation of state and heat of formation of crystal 2,6-diamino-3, 5-dinitropyrazine-1-oxide (LLM-105). Journal of Chemical Physics, 2014, 141, 064702.	1.2	36

#	Article	IF	Citations
19556	First-principles study on CuAlTe 2 and AgAlTe 2 for water splitting. Materials Chemistry and Physics, 2014, 148, 882-886.	2.0	13
19557	Development of a ReaxFF Reactive Force Field for Tetrabutylphosphonium Glycinate/CO₂ Mixtures. Journal of Physical Chemistry B, 2014, 118, 12008-12016.	1.2	46
19558	Support Effect in Oxide Catalysis: Methanol Oxidation on Vanadia/Ceria. Journal of the American Chemical Society, 2014, 136, 14616-14625.	6.6	101
19559	Understanding the role of silicon oxide shell in oxide-assisted SiNWs growth. Materials Chemistry and Physics, 2014, 148, 1145-1148.	2.0	2
19560	Reactions of Methanol with Pristine and Defective Ceria (111) Surfaces: A Comparison of Density Functionals. Journal of Physical Chemistry C, 2014, 118, 23690-23700.	1.5	33
19561	In Silico Design of Three-Dimensional Porous Covalent Organic Frameworks via Known Synthesis Routes and Commercially Available Species. Journal of Physical Chemistry C, 2014, 118, 23790-23802.	1.5	40
19562	Energy and diffusion of hydrogen atoms in titanium substituted vanadium hydrides from ab initio calculations. Materials Chemistry and Physics, 2014, 148, 533-539.	2.0	5
19563	Stability and properties of 2D porous nanosheets based on tetraoxa[8]circulene analogues. Nanoscale, 2014, 6, 14962-14970.	2.8	27
19564	Insights into the effect of coverage on CO adsorption and dissociation over Rh(1 0 0) surface: A theoretical study. Applied Surface Science, 2014, 320, 681-688.	3.1	11
19565	Charge Distribution View: Large Difference in Friction Performance Between Graphene and Hydrogenated Graphene Systems. Tribology Letters, 2014, 55, 405-412.	1.2	31
19566	Ab Initio Investigation of Bi-Rich Bi1â€“x Sb x Alloys. Journal of Electronic Materials, 2014, 43, 3110-3116.	1.0	2
19567	Using a scale-bridging technique to determine the effect of elastic properties on stress distribution around the femoral stem of an artificial hip joint with a simplified geometry. Metals and Materials International, 2014, 20, 593-600.	1.8	1
19568	Structures, Thermodynamics, and Li⁺Mobility of Li₁₀GeP₂S₁₂: A First-Principles Analysis. Journal of Physical Chemistry C, 2014, 118, 10590-10595.	1.5	51
19569	Role of Water and Adsorbed Hydroxyls on Ethanol Electrochemistry on Pd: New Mechanism, Active Centers, and Energetics for Direct Ethanol Fuel Cell Running in Alkaline Medium. Journal of Physical Chemistry C, 2014, 118, 5762-5772.	1.5	73
19570	Chemical Basis of the Tribological Properties of AgTaO₃ Crystal Surfaces. Journal of Physical Chemistry C, 2014, 118, 17577-17584.	1.5	18
19571	Mechanism of n-Butane Hydrogenolysis Promoted by Ta-Hydrides Supported on Silica. ACS Catalysis, 2014, 4, 1868-1874.	5.5	25
19572	Theoretical Study of a â€œSurface Explosionâ€• Decomposition of Acetic Acid on Rh Surfaces. ACS Catalysis, 2014, 4, 944-953.	5.5	7
19573	Photoinduced Câ€“C Reactions on Insulators toward Photolithography of Graphene Nanoarchitectures. Journal of the American Chemical Society, 2014, 136, 4651-4658.	6.6	45

#	Article	IF	Citations
19574	Quantum spin Hall effect on germanene nanorod embedded in completely hydrogenated germanene. Physical Review B, 2014, 89, .	1.1	57
19575	First-principles versus semi-empirical modeling of global and local electronic transport properties of graphene nanopore-based sensors for DNA sequencing. Journal of Computational Electronics, 2014, 13, 847-856.	1.3	27
19576	Li decorated 6,6,12-graphyne: A new star for hydrogen storage material. International Journal of Hydrogen Energy, 2014, 39, 17112-17117.	3.8	45
19577	Modulation of the Electronic Properties of Ultrathin Black Phosphorus by Strain and Electrical Field. Journal of Physical Chemistry C, 2014, 118, 23970-23976.	1.5	252
19578	Mechanism of Sulfur Poisoning of Sr₂Fe_{1.5}Mo_{0.5}O_{6-Î´} Perovskite Anode under Solid Oxide Fuel Cell Conditions. Journal of Physical Chemistry C, 2014, 118, 23545-23552.	1.5	23
19579	Density functional plus dynamical mean-field theory of the metal-insulator transition in early transition-metal oxides. Physical Review B, 2014, 90, .	1.1	37
19580	Key Structureâ€“Property Relationships in CO₂ Capture by Supported Alkanolamines. Journal of Physical Chemistry C, 2014, 118, 19252-19258.	1.5	8
19581	Feasible Catalytic Strategy for Writing Conductive Nanoribbons on a Single-Layer Graphene Fluoride. Journal of Physical Chemistry C, 2014, 118, 22643-22648.	1.5	0
19582	Giant charge fluctuations with Se height and Fe-vacancy formation inMxFe2â^'ySe2. Physical Review B, 2014, 89, .	1.1	1
19583	Spins of adsorbed molecules investigated by the detection of Kondo resonance. Surface Science, 2014, 630, 343-355.	0.8	18
19584	Testing epitaxial Co1.5Fe1.5Ge(001) electrodes in MgO-based magnetic tunnel junctions. Applied Physics Letters, 2014, 104, 252412.	1.5	11
19585	The Characterization, Stability, and Reactivity of Synthetic Calcium Silicate Surfaces from First Principles. Journal of Physical Chemistry C, 2014, 118, 15214-15219.	1.5	58
19586	Observation of Majorana fermions in ferromagnetic atomic chains on a superconductor. Science, 2014, 346, 602-607.	6.0	1,581
19587	Molecular simulations of physical and chemical adsorption under gas and liquid environments using force field- and quantum mechanics-based methods. Molecular Simulation, 2014, 40, 678-689.	0.9	9
19588	Spin-polarized quantum confinement in nanostructures: Scanning tunneling microscopy. Reviews of Modern Physics, 2014, 86, 1127-1168.	16.4	65
19589	Resolving Ultrafast Heating of Dense Cryogenic Hydrogen. Physical Review Letters, 2014, 112, 105002.	2.9	95
19590	Phase diagram of<mml:math xmlns:mml="http://www.w3.org/1998/Math/MathML"><mml:msub><mml:mi mathvariant="normal">BiFeO</mml:mi><mml:mn>3</mml:mn></mml:msub><mml:mo>/</mml:mo><mml:msub><mml:mi mathvariant="normal">LaFeO</mml:mi><mml:mn>3</mml:mn></mml:msub></mml:math>superlattices studied by x-ray diffraction experiments and first-principles calculations. Physical Review B, 2014, 90, .	1.1	9
19591	Unexpected magnetic anisotropy induced by oxygen vacancy in anatase TiO2: A first-principles study. Journal of Applied Physics, 2014, 115, 17A915.	1.1	10

#	Article	IF	Citations
19592	Covalency of hydrogen bonds in solids revisited. Chemical Communications, 2014, 50, 11547-11549.	2.2	50
19593	Structure of liquid Al and Al₆₇Mg₃₃alloy: comparison between experiment and simulation. Philosophical Magazine, 2014, 94, 1876-1892.	0.7	12
19594	Exchange processes in the contact formation of Pb electrodes. Electrochimica Acta, 2014, 140, 505-510.	2.6	23
19595	A Mechanism for TiO₂ Formation on Stepped TiN(001) from First-Principles Calculations. Journal of Physical Chemistry C, 2014, 118, 384-388.	1.5	8
19596	Strong Enhancement of Raman Scattering from a Bulk-Inactive Vibrational Mode in Few-Layer MoTe₂. ACS Nano, 2014, 8, 3895-3903.	7.3	275
19597	Group Additivity for Estimating Thermochemical Properties of Furanic Compounds on Pd(111). Industrial & Engineering Chemistry Research, 2014, 53, 11929-11938.	1.8	27
19598	Unraveling the Factors That Control Soft Landing of Small Silyl Ions on Fluorinated Self-Assembled Monolayers. Journal of Physical Chemistry C, 2014, 118, 10159-10169.	1.5	5
19599	Signature of the Dirac cone in the properties of linear oligoacenes. Nature Communications, 2014, 5, 5000.	5.8	33
19600	Rational design of all organic polymer dielectrics. Nature Communications, 2014, 5, 4845.	5.8	259
19601	Electronic structure and peculiar bonding properties of NdNiMg5 from first principles. Solid State Sciences, 2014, 38, 1-6.	1.5	5
19602	Low-temperature carbon monoxide oxidation catalysed by regenerable atomically dispersed palladium on alumina. Nature Communications, 2014, 5, 4885.	5.8	498
19603	Indirectâ€“direct bandgap transition and gap width tuning in bilayer MoS 2 superlattices. Chemical Physics Letters, 2014, 613, 74-79.	1.2	22
19604	Magnetism and Sound Velocities of Iron Carbide (Fe3C) under Pressure. Chinese Journal of Chemical Physics, 2014, 27, 297-301.	0.6	2
19605	Topological insulator states in a honeycomb lattice of s-triazines. Nanoscale, 2014, 6, 11157-11162.	2.8	79
19606	Transition metal doping of Mg₂FeH₆â€“ a DFT insight into synthesis and electronic structure. Physical Chemistry Chemical Physics, 2014, 16, 12356-12361.	1.3	20
19607	Structural and Electronic Properties of Monolayer 1T-MoS₂ Phase, and Its Interaction with Water Adsorbed on Perfect, Single S-Vacated and MoS₂-Unit-Vacated Surface: Density Functional Theory Calculations. Integrated Ferroelectrics, 2014, 156, 93-101.	0.3	15
19608	Nitrogen Adsorption, Dissociation, and Subsurface Diffusion on the Vanadium (110) Surface: A DFT Study for the Nitrogen-Selective Catalytic Membrane Application. Journal of Physical Chemistry C, 2014, 118, 4238-4249.	1.5	39
19609	CO₂ Adsorption As a Flat-Lying, Tridentate Carbonate on CeO₂(100). Journal of Physical Chemistry C, 2014, 118, 9042-9050.	1.5	73

#	Article	IF	Citations
19610	Reversible nano-structuring of SrCrO3-Î´ through oxidation and reduction at low temperature. Nature Communications, 2014, 5, 4669.	5.8	60
19611	Ferroelectricity from strain in<mml:math xmlns:mml="http://www.w3.org/1998/Math/MathML"><mml:msub><mml:mi mathvariant="normal">RbHgF</mml:mi><mml:mn>3</mml:mn></mml:msub></mml:math>perovskite and hybrid improper ferroelectricity in<mml:math xmlns:mml="http://www.w3.org/1998/Math/MathML"><mml:mo>(</mml:mo><mml:mtext>Na</mml:mtext><mml:mo>,</mml:mo><mml:mi mathvariant="normal">Hg</mml:mi><mml:mn>2</mml:mn></mml:msub><mml:msub><mml:mi mathvaria	1.1	14
19612	Structure, Magnetism, and Valence States of Cobalt and Platinum in Quasi-One-Dimensional Oxides A₃CoPtO₆ with A = Ca, Sr. Journal of Physical Chemistry C, 2014, 118, 5463-5469.	1.5	9
19613	Reversible Achiral-to-Chiral Switching of Single Mnâ€“Phthalocyanine Molecules by Thermal Hydrogenation and Inelastic Electron Tunneling Dehydrogenation. ACS Nano, 2014, 8, 2246-2251.	7.3	32
19614	Functionalization of Nanographenes: Metallic and Insulating Hexabenzocoronene Derivatives. Journal of Physical Chemistry C, 2014, 118, 1347-1352.	1.5	9
19615	Modeling the thermal conductivities of the zinc antimonides ZnSb and Zn<mml:math xmlns:mml="http://www.w3.org/1998/Math/MathML"><mml:msub><mml:mrow /><mml:mn>4</mml:mn></mml:msub></mml:math>Sb<mml:math xmlns:mml="http://www.w3.org/1998/Math/MathML"><mml:msub><mml:mrow /><mml:mn>3</mml:mn></mml:msub></mml:math>. Physical Review B, 2014, 89, .	1.1	102
19616	NO Chemisorption on Cu/SSZ-13: A Comparative Study from Infrared Spectroscopy and DFT Calculations. ACS Catalysis, 2014, 4, 4093-4105.	5.5	139
19617	Atomistic Explanation of Shear-Induced Amorphous Band Formation in Boron Carbide. Physical Review Letters, 2014, 113, 095501.	2.9	138
19618	High-Pressure Synthesis, Crystal Structure, and Phase Stability Relations of a LiNbO₃-Type Polar Titanate ZnTiO₃ and Its Reinforced Polarity by the Second-Order Jahnâ€“Teller Effect. Journal of the American Chemical Society, 2014, 136, 2748-2756.	6.6	122
19619	Ab initio study of Tl on Si(111)-(3Ã—1) surface. Physica Status Solidi (B): Basic Research, 2014, 251, 1570-1573.	0.7	4
19620	Modeling Electrochemical Decomposition of Fluoroethylene Carbonate on Silicon Anode Surfaces in Lithium Ion Batteries. Journal of the Electrochemical Society, 2014, 161, A213-A221.	1.3	132
19621	Bottom-Up Graphene-Nanoribbon Fabrication Reveals Chiral Edges and Enantioselectivity. ACS Nano, 2014, 8, 9181-9187.	7.3	187
19622	High-pressure phase transition of cesium chloride and cesium bromide. Physical Chemistry Chemical Physics, 2014, 16, 17924-17929.	1.3	15
19623	Point defect balance in epitaxial GaSb. Applied Physics Letters, 2014, 105, .	1.5	10
19624	Mechanical anisotropy and origin of shear plastic deformation of tetragonal B ₄ C ₄. Europhysics Letters, 2014, 108, 16001.	0.7	4
19625	Tunable atomic termination in nano-necklace BiFeO3. Applied Physics Letters, 2014, 104, 051606.	1.5	15
19626	Polyoxometalateâ€coupled Graphene via Polymeric Ionic Liquid Linker for Supercapacitors. Advanced Functional Materials, 2014, 24, 7301-7309.	7.8	107
19627	BrÃ¸nstedâ€“Evansâ€“Polanyi and Transition State Scaling Relations of Furan Derivatives on Pd(111) and Their Relation to Those of Small Molecules. ACS Catalysis, 2014, 4, 604-612.	5.5	68

#	Article	IF	Citations
19628	Manipulation of edge magnetism in hexagonal graphene nanoflakes. Physical Review B, 2014, 90, .	1.1	42
19629	Cl Species Transformation on CeO₂(111) Surface and Its Effects on CVOCs Catalytic Abatement: A First-Principles Investigation. Journal of Physical Chemistry C, 2014, 118, 6758-6766.	1.5	35
19630	Versatile Bottom-Up Construction of Diverse Macromolecules on a Surface Observed by Scanning Tunneling Microscopy. ACS Nano, 2014, 8, 8856-8870.	7.3	65
19631	Phosphonic Acid Adsorbates Tune the Surface Potential of TiO₂ in Gas and Liquid Environments. Journal of Physical Chemistry Letters, 2014, 5, 2450-2454.	2.1	15
19632	First principles prediction of structural stability, elastic, lattice dynamical and thermal properties of osmium carbides. Materials Science and Technology, 2014, 30, 842-849.	0.8	8
19633	Comparative density functional theory based study of the reactivity of Cu, Ag, and Au nanoparticles and of (111) surfaces toward CO oxidation and NO2 reduction. Journal of Molecular Modeling, 2014, 20, 2448.	0.8	12
19634	Modeling of molar volume of the sigma phase involving transition elements. Computational Materials Science, 2014, 95, 540-550.	1.4	10
19635	Role of oxygen impurity on the mechanical stability and atomic cohesion of Ta₃N₅ semiconductor photocatalyst. Physical Chemistry Chemical Physics, 2014, 16, 15375-15380.	1.3	37
19636	First-principles studies of the TE properties of [110]-Ge/Si core/shell nanowires with different surface structures. Journal of Materials Chemistry A, 2014, 2, 2538.	5.2	7
19637	Oxygen Reduction at a Cu-Modified Pt(111) Model Electrocatalyst in Contact with Nafion Polymer. ACS Catalysis, 2014, 4, 3772-3778.	5.5	47
19638	Quasiparticle Level Alignment for Photocatalytic Interfaces. Journal of Chemical Theory and Computation, 2014, 10, 2103-2113.	2.3	60
19639	Excitation-Assisted Disordering of GeTe and Related Solids with Resonant Bonding. Journal of Physical Chemistry C, 2014, 118, 10248-10253.	1.5	27
19640	Photoelectrochemical Properties of CuCrO2: Characterization of Light Absorption and Photocatalytic H2 Production Performance. Catalysis Letters, 2014, 144, 1487-1493.	1.4	32
19641	Role of Lewis and BrÃ¸nsted Acid Sites in the Dehydration of Glycerol over Niobia. ACS Catalysis, 2014, 4, 3180-3192.	5.5	163
19642	Li-decorated graphyne as high-capacity hydrogen storage media: First-principles plane wave calculations. International Journal of Hydrogen Energy, 2014, 39, 17104-17111.	3.8	67
19643	Suppression of boron segregation by interface Ge atoms at SiGe/SiO2 interface. Current Applied Physics, 2014, 14, 1557-1563.	1.1	1
19644	Characterization of interface and border traps in ALD Al2O3/GaN MOS capacitors with two-step surface pretreatments on Ga-polar GaN. Applied Surface Science, 2014, 317, 1022-1027.	3.1	23
19645	High-Sensitivity Photodetectors Based on Multilayer GaTe Flakes. ACS Nano, 2014, 8, 752-760.	7.3	319

#	Article	IF	Citations
19646	Detectable spinâ€“orbit splitting in Ni doped graphene. Physics Letters, Section A: General, Atomic and Solid State Physics, 2014, 378, 3196-3199.	0.9	1
19647	First-principles study of point defects in chalcopyrite<mml:math xmlns:mml="http://www.w3.org/1998/Math/MathML"><mml:msub><mml:mi>ZnSnP</mml:mi><mml:mn>2</mml:mn></mml:msub></m Physical Review B, 2014, 90, .	1.1	49
19648	Electronic structure, stacking energy, partial charge, and hydrogen bonding in four periodic B-DNA models. Physical Review E, 2014, 90, 022705.	0.8	21
19649	Computational Metallurgy. , 2014, , 2807-2835.		4
19650	Titanium in silicon: Lattice positions and electronic properties. Applied Physics Letters, 2014, 104, 152105.	1.5	20
19651	Formation of magnetic skyrmions with tunable properties in PdFe bilayer deposited on Ir(111). Physical Review B, 2014, 90, .	1.1	76
19652	Electronic and magnetic properties at the edges of nanostructures in an electric field:ab initiostudy. Journal of Physics Condensed Matter, 2014, 26, 445005.	0.7	0
19653	Edge-Specific Au/Ag Functionalization-Induced Conductive Paths in Armchair MoS₂ Nanoribbons. Chemistry of Materials, 2014, 26, 5625-5631.	3.2	26
19654	Tuning the band structure and superconductivity in single-layer FeSe by interface engineering. Nature Communications, 2014, 5, 5044.	5.8	202
19655	Single nickel-related defects in molecular-sized nanodiamonds for multicolor bioimaging: an ab initio study. Nanoscale, 2014, 6, 12018-12025.	2.8	18
19656	Theoretical insight into highly durable iron phthalocyanine derived non-precious catalysts for oxygen reduction reactions. Journal of Materials Chemistry A, 2014, 2, 19707-19716.	5.2	52
19657	Kinetic Barriers of the Phase Transition in the Oxygen Chemisorbed Cu(110)-(2 Ã— 1)-O as a Function of Oxygen Coverage. Journal of Physical Chemistry C, 2014, 118, 20858-20866.	1.5	24
19658	Density Functional Investigation of the Adsorption of Isooctane, Ethanol, and Acetic Acid on a Water-Covered Fe(100) Surface. Journal of Physical Chemistry C, 2014, 118, 21428-21437.	1.5	17
19659	B-Doped Graphene as Catalyst To Improve Charge Rate of Lithiumâ€“Air Battery. Journal of Physical Chemistry C, 2014, 118, 22412-22418.	1.5	81
19660	Elucidation of Aqueous Solvent-Mediated Hydrogen-Transfer Reactions by ab Initio Molecular Dynamics and Nudged Elastic-Band Studies of $NaBH_4$ Hydrolysis. Journal of Physical Chemistry C, 2014, 118, 21385-21399.	1.5	37
19661	Impact of the Selenolate Ligand on the Bonding Behavior of Au_{25} Nanoclusters. Journal of Physical Chemistry C, 2014, 118, 21730-21737.	1.5	14
19662	Intrinsic Ligand Effect Governing the Catalytic Activity of Pd Oxide Thin Films. ACS Catalysis, 2014, 4, 3330-3334.	5.5	79
19663	Coâ€“Co_2C and Coâ€“Co_2C/AC Catalysts for Hydroformylation of 1-Hexene under Low Pressure: Experimental and Theoretical Studies. Journal of Physical Chemistry C, 2014, 118, 19114-19122.	1.5	41

#	Article	IF	Citations
19664	Microwave and Conventional Hydro(solvo)thermal Syntheses of Three Co(II) Coordination Polymers: Supramolecular Isomerism and Structural Transformations Accompanied by Tunable Magnetic Properties. Crystal Growth and Design, 2014, 14, 4430-4438.	1.4	26
19665	Structure and IR Vibrational Spectra of Na₈[AlSiO₄]₆(BH₄)₂: Comparison of Theory and Experiment. Journal of Physical Chemistry A, 2014, 118, 7066-7073.	1.1	11
19666	How Adsorbate Alignment Leads to Selective Reaction. ACS Nano, 2014, 8, 8669-8675.	7.3	10
19667	Oxygen Adsorption on Irreducible Oxides Doped with Higher Valence Ions: O₂ Binding to the Dopant. Journal of Physical Chemistry C, 2014, 118, 23070-23082.	1.5	5
19668	Identifying Potential BO₂ Oxide Polymorphs for Epitaxial Growth Candidates. ACS Applied Materials & Interfaces, 2014, 6, 3630-3639.	4.0	26
19669	CO Activation Pathways of Fischerâ€“Tropsch Synthesis on Ï‡-Fe5C2 (510): Direct versus Hydrogen-Assisted CO Dissociation. Journal of Physical Chemistry C, 2014, 118, 10170-10176.	1.5	104
19670	Atomistic insights into milling mechanisms in an Feâ€“Y2O3 model alloy. Applied Physics A: Materials Science and Processing, 2014, 115, 851-858.	1.1	19
19671	First principles calculations of electronic and optical properties of Mo and C co-doped anatase TiO2. Applied Physics A: Materials Science and Processing, 2014, 117, 831-839.	1.1	12
19672	Effect of vacancies on magnetic behaviors of Cu-doped 6H-SiC. Applied Physics A: Materials Science and Processing, 2014, 117, 841-845.	1.1	2
19673	ReaxFF molecular dynamics simulations of CO collisions on an O-preadsorbed silica surface. Journal of Molecular Modeling, 2014, 20, 2160.	0.8	5
19674	Mechanical, electronic, and optical properties of Bi2S3 and Bi2Se3 compounds: first principle investigations. Journal of Molecular Modeling, 2014, 20, 2180.	0.8	68
19675	CO, CO2 and H2 adsorption on ZnO, CeO2, and ZnO/CeO2 surfaces: DFT simulations. Journal of Molecular Modeling, 2014, 20, 2270.	0.8	40
19676	Understanding the structural and electronic properties of the cathode material NaFeF3 in a Na-ion battery. Journal of Solid State Electrochemistry, 2014, 18, 2071-2075.	1.2	14
19677	Replacing Platinum with Tungsten Carbide for Decalin Dehydrogenation. Catalysis Letters, 2014, 144, 1443-1449.	1.4	13
19678	Toward a mechanism of rattler coupling in the Î²-pyrochlores AOs2O6 (AÂ=ÂK, Rb, Cs). Journal of Materials Science, 2014, 49, 5468-5480.	1.7	0
19679	First-principles study of A-site substitution in ferroelectric bismuth titanate. Journal of Materials Science, 2014, 49, 6363-6372.	1.7	4
19680	Theoretical study on strain-induced variations in electronic properties of monolayer MoS2. Journal of Materials Science, 2014, 49, 6762-6771.	1.7	65
19681	Nonlinear Elastic Properties of Superconducting Antiperovskites MNNi3 (M =Zn, Cd, Mg, Al, Ga, and In) from First Principles. Journal of Superconductivity and Novel Magnetism, 2014, 27, 1851-1859.	0.8	7

#	Article	IF	Citations
19682	A structural investigation of tris(ethyl acetoacetate)aluminium (III). Journal of Sol-Gel Science and Technology, 2014, 71, 217-223.	1.1	4
19683	DFT studies of oxygen dissociation on the 116-atom platinum truncated octahedron particle. Physical Chemistry Chemical Physics, 2014, 16, 26539-26545.	1.3	23
19684	Mechanisms for CO oxidation on Fe(<scp>iii</scp>)â€“OHâ€“Pt interface: a DFT study. Faraday Discussions, 2014, 176, 381-392.	1.6	7
19685	Assessing Carbon-Based Anodes for Lithium-Ion Batteries: A Universal Description of Charge-Transfer Binding. Physical Review Letters, 2014, 113, 028304.	2.9	93
19686	Semiconducting Layered Blue Phosphorus: A Computational Study. Physical Review Letters, 2014, 112, 176802.	2.9	996
19687	The effect of electron localization on the electronic structure and migration barrier of oxygen vacancies in rutile. Journal of Physics Condensed Matter, 2014, 26, 055602.	0.7	11
19688	Charge-density correlations in pressurized liquid lithium calculated usingab initiomolecular dynamics. Physical Review B, 2014, 90, .	1.1	9
19689	Search for Organic Thermoelectric Materials with High Mobility: The Case of 2,7-Dialkyl[1]benzothieno[3,2-b][1]benzothiophene Derivatives. Chemistry of Materials, 2014, 26, 2669-2677.	3.2	79
19690	Physical Adsorption and Charge Transfer of Molecular Br₂ on Graphene. ACS Nano, 2014, 8, 2943-2950.	7.3	58
19691	Transition Metal Embedded Two-Dimensional C₃N₄â€“Graphene Nanocomposite: A Multifunctional Material. Journal of Physical Chemistry C, 2014, 118, 15487-15494.	1.5	93
19692	First-principles study of luminescence in Eu<mml:math xmlns:mml="http://www.w3.org/1998/Math/MathML"><mml:msup><mml:mrow /><mml:mrow><mml:mn>2</mml:mn><mml:mo>+</mml:mo></mml:mrow></mml:msup></mml:math>-doped inorganic scintillators. Physical Review B, 2014, 89, .	1.1	77
19693	Ideal strength and phonon instability of strained monolayer materials. Physical Review B, 2014, 89, .	1.1	26
19694	Mechanisms of the Adsorption and Self-Assembly of Molecules with Polarized Functional Groups on Insulating Surfaces. Journal of Physical Chemistry C, 2014, 118, 14569-14578.	1.5	28
19695	Unexpected strong magnetism of Cu doped single-layer MoS₂ and its origin. Physical Chemistry Chemical Physics, 2014, 16, 8990-8996.	1.3	107
19696	Al_xC Monolayer Sheets: Two-Dimensional Networks with Planar Tetracoordinate Carbon and Potential Applications as Donor Materials in Solar Cell. Journal of Physical Chemistry Letters, 2014, 5, 2058-2065.	2.1	95
19697	On the Importance of the Associative Carboxyl Mechanism for the Water-Gas Shift Reaction at Pt/CeO₂ Interface Sites. Journal of Physical Chemistry C, 2014, 118, 6314-6323.	1.5	47
19698	Spin Exchange and Magnetic Dipoleâ€“Dipole Interactions Leading to the Magnetic Superstructures of MAs₂O₆ (M = Mn, Co, Ni). Inorganic Chemistry, 2014, 53, 3812-3817.	1.9	13
19699	Using surface plasmonics to turn on fullerene's dark excitons. Physical Review B, 2014, 89, .	1.1	12

#	Article	IF	Citations
19700	Ferromagnetism and topological surface states of manganese doped Bi2Te3: Insights from density-functional calculations. Journal of Chemical Physics, 2014, 140, 124704.	1.2	19
19701	Electron quantum conductance of bimetallic Pt-Fe nanowires. Bulletin of the Russian Academy of Sciences: Physics, 2014, 78, 149-151.	0.1	1
19702	First-principles study of bilayer graphene on BN/Co(111): van der Waals density functional approach. Journal of the Korean Physical Society, 2014, 64, 1370-1374.	0.3	2
19703	Effect of van der Waals interaction on the structural and cohesive properties of black phosphorus. Journal of the Korean Physical Society, 2014, 64, 547-553.	0.3	21
19704	Atomistic processes of Ni and Pd atoms on MgO(001) surfaces with surface-functional hydroxyl groups: Ab-initio calculations. Journal of the Korean Physical Society, 2014, 64, 554-560.	0.3	10
19705	First-principles calculations of the thermodynamic properties of transuranium elements in a molten salt medium. Journal of the Korean Physical Society, 2014, 64, 806-812.	0.3	5
19706	The relation of mechanical properties and local structures in bulk Mg 54 (Cu 1â˜' x Ag x) 35 Y 11 metallic glasses: Ab initio molecular dynamics simulations. Computational Materials Science, 2014, 92, 313-317.	1.4	6
19707	Phase stabilities at a glance II: Ternary ordering variants of pyrite and marcasite type structures. Computational Materials Science, 2014, 89, 114-121.	1.4	12
19708	Oxidation of Technetium Metal as Simulated by First Principles. Journal of Physical Chemistry C, 2014, 118, 10017-10023.	1.5	12
19709	From kesterite to stannite photovoltaics: Stability and band gaps of the Cu2(Zn,Fe)SnS4 alloy. Applied Physics Letters, 2014, 104, .	1.5	76
19710	Effect of enzymatic orientation through the use of syringaldazine molecules on multiple multi-copper oxidase enzymes. Physical Chemistry Chemical Physics, 2014, 16, 13367-13375.	1.3	39
19711	Analytic bond-order potentials for the bcc refractory metals Nb, Ta, Mo and W. Journal of Physics Condensed Matter, 2014, 26, 195501.	0.7	14
19712	Ab InitioSimulations for the Ion-Ion Structure Factor of Warm Dense Aluminum. Physical Review Letters, 2014, 112, 145007.	2.9	63
19713	Spin-orbit-coupled quantum wires and Majorana fermions on zigzag edges of monolayer transition-metal dichalcogenides. Physical Review B, 2014, 89, .	1.1	60
19714	Dislocation slip and twinning in Ni-based L12 type alloys. Intermetallics, 2014, 52, 20-31.	1.8	38
19715	Graphene nucleation on a surface-molten copper catalyst: quantum chemical molecular dynamics simulations. Chemical Science, 2014, 5, 3493-3500.	3.7	40
19716	Structural and electronic properties of single-side fluorinated graphene C4F under equibiaxial strains. Physica E: Low-Dimensional Systems and Nanostructures, 2014, 58, 59-62.	1.3	6
19717	Ab initio study of low-temperature magnetic properties of double perovskite <mml:math xmlns:mml="http://www.w3.org/1998/Math/MathML"><mml:msub><mml:mi mathvariant="normal">Sr</mml:mi><mml:mn>2</mml:mn></mml:msub></mml:math><mml:math xmlns:mml="http://www.w3.org/1998/Math/MathML"><mml:msub><mml:mi mathvariant="normal">FeOsO</mml:mi><mml:mn>6</mml:mn></mml:msub></mml:math>. Physical Review B, 2014, 89, .	1.1	52

#	Article	IF	Citations
19718	First-Principles Study on the Mechanism of Photoselective Catalytic Reduction of NO by NH₃ on Anatase TiO₂(101) Surface. Journal of Physical Chemistry C, 2014, 118, 6359-6364.	1.5	24
19719	Multiscale thermodynamic analysis on fracture toughness loss induced by solute segregation in steel. Philosophical Magazine, 2014, 94, 2131-2149.	0.7	21
19720	Vibrational and thermodynamic properties of GeSe in the quasiharmonic approximation. Physical Review B, 2014, 89, .	1.1	59
19721	Epitaxial growth and electronic structure of a layered zinc pnictide semiconductor, Î²-BaZn2As2. Thin Solid Films, 2014, 559, 100-104.	0.8	13
19722	Phonon density of states and anharmonicity of<mml:math xmlns:mml="http://www.w3.org/1998/Math/MathML"><mml:msub><mml:mi>UO</mml:mi><mml:mn>2</mml:mn></mml:msub></mml Physical Review B, 2014, 89, .	1.1	48
19723	Hydrogen Ordering and New Polymorph of Layered Perovskite Oxyhydrides: Sr₂VO_{4â€“x}H_x. Journal of the American Chemical Society, 2014, 136, 7221-7224.	6.6	63
19724	First-principles study on electronic and magnetic properties of twisted graphene nanoribbon and MÃ¶bius strips. Carbon, 2014, 71, 150-158.	5.4	23
19725	Asymmetry in the Electron and Hole Transfer at a Polymerâ€“Carbon Nanotube Heterojunction. Nano Letters, 2014, 14, 3335-3341.	4.5	67
19726	Thermodynamic modeling of the Crâ€“Niâ€“Ti system using a four-sublattice model for ordered/disordered bcc phases. Thermochimica Acta, 2014, 578, 35-42.	1.2	20
19727	Edge-, width- and strain-dependent semiconductorâ€“metal transition in SnSe nanoribbons. RSC Advances, 2014, 4, 6933.	1.7	23
19728	Density functional theory study of ethylene adsorption on clean anatase TiO2 (001) surface. Surface Science, 2014, 619, 59-66.	0.8	18
19729	Rationally Designed Polyimides for High-Energy Density Capacitor Applications. ACS Applied Materials & Interfaces, 2014, 6, 10445-10451.	4.0	98
19730	An ab initio study of the structureâ€“strength correlation in impact damaged SiC grain boundaries. Computational Materials Science, 2014, 82, 331-336.	1.4	5
19731	Structural, mechanical and electronic properties of 3d transition metal nitrides in cubic zincblende, rocksalt and cesium chloride structures: a first-principles investigation. Journal of Physics Condensed Matter, 2014, 26, 025404.	0.7	86
19732	Insights into an intriguing gas sorption mechanism in a polar metalâ€“organic framework with open-metal sites and narrow channels. Chemical Communications, 2014, 50, 7283-7286.	2.2	16
19733	Hole bipolaron formation at (100) MgO/CaO epitaxial interface. Physical Review B, 2014, 89, .	1.1	8
19734	Ferromagnetism in Cr-based<mml:math xmlns:mml="http://www.w3.org/1998/Math/MathML"><mml:mn>3</mml:mn><mml:mi>d</mml:mi></mml:math>-<mml:math xmlns:mml="http://www.w3.org/1998/Math/MathML"><mml:mn>5</mml:mn><mml:mi>d</mml:mi></mml:math>double perovskites: Effective model analysis and simulations. Physical Review B, 2014, 89, .	1.1	14
19735	First-principles calculation of the instability leading to giant inverse magnetocaloric effects. Physical Review B, 2014, 89, .	1.1	73

#	Article	IF	Citations
19736	Peierlsâ€Distorted Monoclinic MnB₄ with a Mnï£¿Mn Bond. Angewandte Chemie - International Edition, 2014, 53, 1684-1688.	7.2	52
19737	Effects of van der Waals density functional corrections on trends in furfural adsorption and hydrogenation on close-packed transition metal surfaces. Surface Science, 2014, 622, 51-59.	0.8	101
19738	Adsorption and dissociation of H2S on Mo(100) surface by first-principles study. Applied Surface Science, 2014, 292, 328-335.	3.1	36
19739	Reaction mechanisms of CO2 electrochemical reduction on Cu(111) determined with density functional theory. Journal of Catalysis, 2014, 312, 108-122.	3.1	382
19740	Instantaneous Generation of Charge-Separated State on TiO₂ Surface Sensitized with Plasmonic Nanoparticles. Journal of the American Chemical Society, 2014, 136, 4343-4354.	6.6	221
19741	Long-Range Periodicity of S/Au(111) Structures at Low and Intermediate Coverages. Journal of Physical Chemistry C, 2014, 118, 290-297.	1.5	18
19742	The ternary Niâ€”Alâ€”Co embedded-atom-method potential for Î³/Î³â€² Ni-based single-crystal superalloys: Construction and application. Chinese Physics B, 2014, 23, 033401.	0.7	11
19743	Magnetic properties and half-metallic in bulk and (001) surface of Ti2MnAl Heusler alloy with Hg2CuTi-type structure. Thin Solid Films, 2014, 558, 241-246.	0.8	16
19744	The structure determination of Al20Cu2Mn3 by near atomic resolution chemical mapping. Journal of Alloys and Compounds, 2014, 601, 25-30.	2.8	67
19745	Prediction of diffusivities in fcc phase of the Alâ€“Cuâ€“Mg system: First-principles calculations coupled with CALPHAD technique. Computational Materials Science, 2014, 90, 32-43.	1.4	6
19746	Can picolinamide be a promising cocrystal former?. CrystEngComm, 2014, 16, 4365-4368.	1.3	23
19747	Mechanisms of charge transfer and redistribution in LaAlO3/SrTiO3 revealed by high-energy optical conductivity. Nature Communications, 2014, 5, 3663.	5.8	70
19748	Ab initiocalculation of anisotropic interfacial excess free energies. Physical Review B, 2014, 89, .	1.1	12
19749	Interface Structure Prediction from First-Principles. Journal of Physical Chemistry C, 2014, 118, 9524-9530.	1.5	39
19750	Electronic structure and magnetic properties of diluted magnetic semiconductor K and Mn co-doped BaCd2As2 from first-principles calculations. Modern Physics Letters B, 2014, 28, 1450111.	1.0	1
19751	Tuning the crystal structure and electronic states of<mml:math xmlns:mml="http://www.w3.org/1998/Math/MathML"><mml:msub><mml:mtext>Ag</mml:mtext><mml:mn>2</mml:mn></mml:msu Structural transitions and metallization under pressure. Physical Review B, 2014, 89, .	1.1	24
19752	An energetic evaluation of dissolution corrosion capabilities of liquid metals on iron surface. Physical Chemistry Chemical Physics, 2014, 16, 16837.	1.3	29
19753	First-principles calculations and thermodynamic modeling of the Snâ€“Sr and Mgâ€“Snâ€“Sr systems. Calphad: Computer Coupling of Phase Diagrams and Thermochemistry, 2014, 46, 237-248.	0.7	19

#	Article	IF	Citations
19754	Ab initio calculations of mechanical stability of bcc Cu under pressure. Solid State Communications, 2014, 184, 25-28.	0.9	4
19755	CO₂ Adsorption in Fe₂(dobdc): A Classical Force Field Parameterized from Quantum Mechanical Calculations. Journal of Physical Chemistry C, 2014, 118, 12230-12240.	1.5	45
19756	Ion-exchange between Na2Ti3O7 and H2Ti3O7 nanosheets at different pH levels: An experimental and first-principles study. Physica E: Low-Dimensional Systems and Nanostructures, 2014, 60, 210-213.	1.3	10
19757	Molybdenum carbide catalysed hydrogen production from formic acid â€“ A density functional theory study. Journal of Power Sources, 2014, 246, 548-555.	4.0	45
19758	Effects of Alloying Elements on Stacking Fault Energies and Electronic Structures of Binary Mg Alloys: A First-Principles Study. Materials Research Letters, 2014, 2, 29-36.	4.1	95
19759	Electronics, Vacancies, Optical Properties, and Band Engineering of Red Photocatalyst SrNbO₃: A Computational Investigation. Journal of Physical Chemistry C, 2014, 118, 11267-11270.	1.5	9
19760	Electric field control and effect of Pd capping on magnetocrystalline anisotropy in FePd thin films: A first-principles study. Physical Review B, 2014, 89, .	1.1	41
19761	Alkali metal doped nickel oxide clusters: A density functional study. Computational and Theoretical Chemistry, 2014, 1035, 19-27.	1.1	3
19762	Reassigning the most stable surface of hydroxyapatite to the water resistant hydroxyl terminated (010) surface. Surface Science, 2014, 623, 55-63.	0.8	21
19763	Modulating magnetic characteristics of Pt embedded graphene by gas adsorption (N2, O2, NO2, SO2). Applied Surface Science, 2014, 289, 445-449.	3.1	103
19764	ComprehensiveAb InitioStudy of Doping in Bulk ZnO with Group-V Elements. Physical Review Applied, 2014, 1, .	1.5	32
19765	Making Câ€“C Bonds with Gold Catalysts: A Theoretical Study of the Influence of Gold Particle Size on the Dissociation of the Câ€“X Bond in Aryl Halides. Journal of Physical Chemistry C, 2014, 118, 9018-9029.	1.5	11
19766	First-principles study of intergranular embrittlement induced by Te in the Ni Î£ 5 grain boundary. Computational Materials Science, 2014, 88, 22-27.	1.4	40
19767	Pressure stabilization of long-missing bare C6 hexagonal rings in binary sesquicarbides. Chemical Science, 2014, 5, 3936-3940.	3.7	21
19768	The electronic structure of the antimony chalcogenide series: Prospects for optoelectronic applications. Journal of Solid State Chemistry, 2014, 213, 116-125.	1.4	86
19769	Computational materials discovery: the case of the Wâ€“B system. Acta Crystallographica Section C, Structural Chemistry, 2014, 70, 85-103.	0.2	87
19770	Understanding the influence of grain boundary thickness variation on the mechanical strength of a nickel-doped tungsten grain boundary. International Journal of Plasticity, 2014, 53, 135-147.	4.1	14
19771	Catalytic Dissociation of Water on the (001), (011), and (111) Surfaces of Violarite, FeNi₂S₄: A DFT-D2 Study. Journal of Physical Chemistry C, 2014, 118, 1958-1967.	1.5	41

#	Article	IF	Citations
19772	Physical factors controlling the observed high-strength precipitate morphology in Mgâ€“rare earth alloys. Acta Materialia, 2014, 65, 240-250.	3.8	69
19773	Effective potentials for simulations of the thermal conductivity of type-I semiconductor clathrate systems. Physical Review B, 2014, 89, .	1.1	17
19774	CCl Radicals As a Carbon Source for Diamond Thin Film Deposition. Journal of Physical Chemistry Letters, 2014, 5, 481-484.	2.1	5
19775	Reaction Pathway for Oxygen Reduction on FeN₄ Embedded Graphene. Journal of Physical Chemistry Letters, 2014, 5, 452-456.	2.1	307
19776	Giant Faraday effect due to Pauli exclusion principle in 3D topological insulators. Journal of Physics Condensed Matter, 2014, 26, 082201.	0.7	4
19777	Atomic structure and energetics of large vacancies in graphene. Physical Review B, 2014, 89, .	1.1	30
19778	Ab initio calculation of the electronic, mechanical, and thermodynamic properties of yttrium nitride with the rocksalt structure. Physica Status Solidi (B): Basic Research, 2014, 251, 792-802.	0.7	7
19779	Structures and magnetic properties of Mn-doped NiO thin films. Journal Physics D: Applied Physics, 2014, 47, 295001.	1.3	11
19780	Density functional theory study of the influence of Ti and V partitioning to cementite in ferritic steels. Physica Status Solidi (B): Basic Research, 2014, 251, 950-957.	0.7	9
19781	Strain-Induced Indirect to Direct Bandgap Transition in Multilayer WSe₂. Nano Letters, 2014, 14, 4592-4597.	4.5	572
19782	Germanium multiphase equation of state. Journal of Physics: Conference Series, 2014, 500, 032006.	0.3	7
19783	Metal-dioxidoterephthalate MOFs of the MOF-74 type: Microporous basic catalysts with well-defined active sites. Journal of Catalysis, 2014, 317, 1-10.	3.1	138
19784	Methanol synthesis from CO2 hydrogenation over a Pd4/In2O3 model catalyst: A combined DFT and kinetic study. Journal of Catalysis, 2014, 317, 44-53.	3.1	196
19785	Ab initio study on mechanical-bending-induced ferroelectric phase transition in ultrathin perovskite nanobelts. Acta Materialia, 2014, 76, 472-481.	3.8	11
19786	Rapid Microwave Preparation and ab Initio Studies of the Stability of the Complex Noble Metal Oxides La₂BaPdO₅ and La₂BaPtO₅. Inorganic Chemistry, 2014, 53, 2628-2634.	1.9	10
19787	Theoretical Study of Hydrogen Permeation through Mixed NiOâ€“MgO Films Supported on Mo(100): Role of the Oxideâ€“Metal Interface. Journal of Physical Chemistry A, 2014, 118, 5756-5761.	1.1	3
19788	Water Structures at Metal Electrodes Studied by Ab Initio Molecular Dynamics Simulations. Journal of the Electrochemical Society, 2014, 161, E3015-E3020.	1.3	81
19789	Cooperative H₂ Activation at Ag Cluster/Î¸-Al₂O₃(110) Dual Perimeter Sites: A Density Functional Theory Study. Journal of Physical Chemistry C, 2014, 118, 7996-8006.	1.5	31

#	Article	IF	Citations
19790	Crystal Structure, Physical Properties, and Electronic and Magnetic Structure of the Spin S = ⁵/₂ Zigzag Chain Compound Bi₂Fe(SeO₃)₂OCl₃. Inorganic Chemistry, 2014, 53, 5830-5838.	1.9	23
19791	xmlns:mml="http://www.w3.org/1998/Math/MathML"><mml:mi mathvariant="normal">RbFe</mml:mi><mml:mo>(</mml:mo><mml:mi) Tj ETQq1 1 0.784314 rgBT /Overlock 10 Tf 50 702 Td (mathvari	1.1	10
19792	Intrinsic ductility of Mg-based binary alloys: A first-principles study. Scripta Materialia, 2014, 89, 13-16.	2.6	39
19793	Thermodynamics, structure, and charge state of hydrogen-vacancy complexes in Î´-plutonium. Physical Review B, 2014, 89, .	1.1	9
19794	Tuning Electronic and Magnetic Properties of Early Transition-Metal Dichalcogenides via Tensile Strain. Journal of Physical Chemistry C, 2014, 118, 7242-7249.	1.5	216
19795	From Ab Initio Calculations to Multiscale Design of Si/C Coreâ€“Shell Particles for Li-Ion Anodes. Nano Letters, 2014, 14, 2140-2149.	4.5	29
19796	Tuning Ideal Tensile Strengths and Intrinsic Ductility of bcc Refractory Alloys. Physical Review Letters, 2014, 112, 115503.	2.9	139
19797	Understanding the Mechanism of Photocatalysis Enhancements in the Graphene-like Semiconductor Sheet/TiO2 Composites. Journal of Physical Chemistry C, 2014, 118, 5954-5960.	1.5	65
19798	Structural and Mechanical Properties of Platinum Carbide. Inorganic Chemistry, 2014, 53, 5797-5802.	1.9	19
19799	Catalytic activity of Pd-doped Cu nanoparticles for hydrogenation as a single-atom-alloy catalyst. Physical Chemistry Chemical Physics, 2014, 16, 8367-8375.	1.3	57
19800	Lattice-dynamical model for the filled skutterudite<mml:math xmlns:mml="http://www.w3.org/1998/Math/MathML"><mml:msub><mml:mi mathvariant="normal">LaFe</mml:mi><mml:mn>4</mml:mn></mml:msub><mml:msub><mml:mi mathvariant="normal">Sb</mml:mi><mml:mn>12</mml:mn></mml:msub></mml:math>: Harmonic and anharmonic couplings. Physical Review B, 2014, 89, .	1.1	12
19801	Soft-phonon mediated structural phase transition in GeTe. Physical Review B, 2014, 89, .	1.1	56
19802	Density functional theory based calculation of small-polaron mobility in hematite. Physical Review B, 2014, 89, .	1.1	53
19803	Use of elastic constants based onab initiocomputation in materials optimisation of austenitic stainless steels. Canadian Metallurgical Quarterly, 2014, 53, 282-291.	0.4	5
19804	Grapheneâ€“BODIPY as a photocatalyst in the photocatalyticâ€“biocatalytic coupled system for solar fuel production from CO2. Journal of Materials Chemistry A, 2014, 2, 5068.	5.2	99
19805	Structural Conditions for Cesium Migration to Si(100) Surface Employing Electronic Structure Calculations. Journal of Physical Chemistry C, 2014, 118, 3443-3450.	1.5	6
19806	Undoped ZnO abundant with metal vacancies. Nano Energy, 2014, 9, 71-79.	8.2	151
19807	Structures of Late Transition Metal Monoxides from Jahn-Teller Instabilities in the Rock Salt Lattice. Physical Review Letters, 2014, 113, 025505.	2.9	22

#	Article	IF	Citations
19808	Spin-Crossover and Massive Anisotropy Switching of 5d Transition Metal Atoms on Graphene Nanoflakes. Nano Letters, 2014, 14, 3364-3368.	4.5	28
19809	A Density Functional Theory Study of the Reconstruction of Gold (111) Surfaces. Journal of Physical Chemistry C, 2014, 118, 15624-15629.	1.5	15
19810	Origin of Ferroelectricity in a Family of Polar Oxides: The Dionâ€"Jacobson Phases. Inorganic Chemistry, 2014, 53, 3769-3777.	1.9	80
19811	Temperature dependence of alkali-metal rattling dynamics in theÎ²-pyrochlores, AOs2O6(A = K, Rb, Cs), from MD simulation. Journal of Physics Condensed Matter, 2014, 26, 235401.	0.7	0
19812	Physical properties of quasi-one-dimensional MgO and<mml:math xmlns:mml="http://www.w3.org/1998/Math/MathML"><mml:msub><mml:mi>Fe</mml:mi><mml:mn>3</mml:mn></mml:msub><mml:mathvariant="normal">O</mml:mi><mml:mn>4</mml:mn></mml:msub></mml:math>-based nanostructures. Physical Review B, 2014, 90, .	1.1	9
19813	Properties of warm dense polystyrene plasmas along the principal Hugoniot. Physical Review E, 2014, 89, 063104.	0.8	37
19814	Nucleation driven by orientational order in supercooled niobium as seen viaab initiomolecular dynamics. Physical Review B, 2014, 89, .	1.1	23
19815	Role of oxygen in materials properties of yttrium trihydride. Solid State Communications, 2014, 194, 39-42.	0.9	22
19816	New Phases of Germanene. Journal of Physical Chemistry Letters, 2014, 5, 2694-2699.	2.1	56
19817	Introducing the Triangular Defect to Effectively Engineer the Wide Band Gap of Boron Nitride Nanoribbons with Zigzag and Even Armchair Edges. Journal of Physical Chemistry C, 2014, 118, 12880-12889.	1.5	20
19818	Electronic and magnetic properties of honeycomb transition metal monolayers: first-principles insights. Physical Chemistry Chemical Physics, 2014, 16, 13383-13389.	1.3	33
19819	Exploiting Differential Electrochemical Stripping Behaviors of Fe₃O₄Nanocrystals toward Heavy Metal Ions by Crystal Cutting. ACS Applied Materials & Interfaces, 2014, 6, 12203-12213.	4.0	71
19820	Reversible Switching of a Single-Dipole Molecule Imbedded in Two-Dimensional Hydrogen-Bonded Binary Molecular Networks. Journal of Physical Chemistry C, 2014, 118, 1712-1718.	1.5	33
19821	Liquidlike correlations in single-crystalline Y<mml:math xmlns:mml="http://www.w3.org/1998/Math/MathML"><mml:msub><mml:mrow/><mml:mn>2</mml:mn></mml:msub></mml:math>Mo<mml:math xmlns:mml="http://www.w3.org/1998/Math/MathML"><mml:msub><mml:mrow/><mml:mn>2</mml:mn></mml:msub><mml:math>O<mml:math xmlns:mml="http://www.w3.org/1998/Math/MathML"><mml:msub><mml:mrow/><mml:mn>7</mml:mn></mml:msub></mml:math>	1.1	62
19822	Conjoined structures of carbon nanotubes and graphene nanoribbons. Physica Scripta, 2014, 89, 044008.	1.2	8
19823	Lead-iodide nanowire perovskite with methylviologen showing interfacial charge-transfer absorption: a DFT analysis. Physical Chemistry Chemical Physics, 2014, 16, 17955-17959.	1.3	23
19824	First-principles study of the electronic structure of CdS/ZnSe coupled quantum dots. Physical Review B, 2014, 89, .	1.1	10
19825	Giant pressure-induced volume collapse in the pyrite mineral MnS ₂. Proceedings of the National Academy of Sciences of the United States of America, 2014, 111, 5106-5110.	3.3	37

#	Article	IF	Citations
19826	Orientation effects in morphology and electronic properties of anatase TiO2 one-dimensional nanostructures. I. Nanowires. Physical Chemistry Chemical Physics, 2014, 16, 9479.	1.3	18
19827	Correlation of intrinsic point defects and the Raman modes of cuprous oxide. Physical Review B, 2014, 90, .	1.1	88
19828	Tetrahedral node diamondyne frameworks for CO2 adsorption and separation. Journal of Materials Chemistry A, 2014, 2, 4899.	5.2	16
19829	One Hydrogen Bondâ€"Two Ways To Build a Structure. The Role of Nâ€“HÂ·Â·Â·O Hydrogen Bonds in Crystal Structures of N,N-Dimethylglycine. Crystal Growth and Design, 2014, 14, 1851-1864.	1.4	17
19830	First-Principles Analysis of Phase Stability in Layeredâ€“Layered Composite Cathodes for Lithium-Ion Batteries. Chemistry of Materials, 2014, 26, 2407-2413.	3.2	32
19831	Na⁺ and K⁺ ion selectivity by size-controlled biomimetic graphene nanopores. Nanoscale, 2014, 6, 10666-10672.	2.8	89
19832	Ferromagnetic Exchange Coupling between Fe Phthalocyanine and Ni(111) Surface Mediated by the Extended States of Graphene. Journal of Physical Chemistry C, 2014, 118, 17670-17676.	1.5	36
19833	Ab initio molecular dynamics simulations of water and an excess proton in water confined in carbon nanotubes. Physical Chemistry Chemical Physics, 2014, 16, 17756.	1.3	32
19834	A Stable, Magnetic, and Metallic Li3O4Compound as a Discharge Product in a Liâ€“Air Battery. Journal of Physical Chemistry Letters, 2014, 5, 2516-2521.	2.1	52
19835	Pressure-induced structure and properties of crystalline Î²-FOX-7 by LDA and GGA calculations. Structural Chemistry, 2014, 25, 1625-1633.	1.0	5
19836	Expanding and Reducing Complexity in Materials Science Models with Relevance in Catalysis and Energy. Topics in Catalysis, 2014, 57, 14-24.	1.3	9
19837	Adsorption and Diffusion of 4d and 5d Transition Metal Adatoms on Graphene/Ru(0001) and the Implications for Cluster Nucleation. Topics in Catalysis, 2014, 57, 69-79.	1.3	28
19838	Ethanol Synthesis from Syngas on Transition Metal-Doped Rh(111) Surfaces: A Density Functional Kinetic Monte Carlo Study. Topics in Catalysis, 2014, 57, 125-134.	1.3	30
19839	Comparison of the effect of hydrogen incorporation and oxygen vacancies on the properties of anatase TiO2: electronics, optical absorption, and interaction with water. Science Bulletin, 2014, 59, 2175-2180.	1.7	9
19840	Electronic and magnetic structures of chain structured iron selenide compounds. Frontiers of Physics, 2014, 9, 465-471.	2.4	12
19841	Structural and Energetic Analysis of GroupÂV Impurities in p-Type HgCdTe: The Case of As and Sb. Journal of Electronic Materials, 2014, 43, 2849-2853.	1.0	1
19842	The Systems Tantalum (Niobium)-Cobalt-Boron. Journal of Phase Equilibria and Diffusion, 2014, 35, 43-85.	0.5	6
19843	Enthalpies of Formation and Electronic Densities of States of Vanadium Borides. Journal of Phase Equilibria and Diffusion, 2014, 35, 396-405.	0.5	7

#	Article	IF	Citations
19844	Multiscale Modeling of Phase Transformations in Steels. Jom, 2014, 66, 740-746.	0.9	12
19845	Spin-resolved self-doping tunes the intrinsic half-metallicity of AlN nanoribbons. Nano Research, 2014, 7, 63-70.	5.8	13
19846	TiO2 nanotube branched tree on a carbon nanofiber nanostructure as an anode for high energy and power lithium ion batteries. Nano Research, 2014, 7, 491-501.	5.8	42
19847	Strain-tunable electronic and transport properties of MoS2 nanotubes. Nano Research, 2014, 7, 518-527.	5.8	89
19848	The electronic structure of Nb3Al/Nb3Sn, a new test case for flat/steep band model of superconductivity. Journal of Modern Transportation, 2014, 22, 183-186.	2.5	8
19849	Ab initio investigation of phonon spectra in GdLiF4 compound under hydrostatic pressure. Optics and Spectroscopy (English Translation of Optika I Spektroskopiya), 2014, 116, 868-871.	0.2	0
19850	Methods for calculating the resonant part of the atomic factor in crystals with partial filling of the crystallographic position. Journal of Surface Investigation, 2014, 8, 384-390.	0.1	0
19851	The key role of carbon in hydrogen solubility in copper. European Physical Journal B, 2014, 87, 1.	0.6	2
19852	Structure and elastic anisotropy of uranium under pressure up to 100 GPa. European Physical Journal B, 2014, 87, 1.	0.6	5
19853	Investigation of aniline by high pressure Raman scattering spectroscopy and quantum chemical calculation. European Physical Journal D, 2014, 68, 1.	0.6	4
19854	Site-selective substitutional doping with atomic precision on stepped Al (111) surface by single-atom manipulation. Nanoscale Research Letters, 2014, 9, 235.	3.1	2
19855	Ferromagnetism in homogeneous (Al,Co)-codoped 4H-silicon carbides. Journal of Magnetism and Magnetic Materials, 2014, 363, 34-42.	1.0	16
19856	Mechanical and Electronic Properties of Ï€-Conjugated Metal Bis(dithiolene) Complex Sheets. Chemistry of Materials, 2014, 26, 2967-2974.	3.2	30
19857	Stability and electronic structures of native defects in single-layer<mml:math xmlns:mml="http://www.w3.org/1998/Math/MathML"><mml:msub><mml:mi mathvariant="normal">MoS</mml:mi><mml:mn>2</mml:mn></mml:msub></mml:math>. Physical Review B, 2014, 89, .	1.1	262
19858	First-principles determination of the enthalpy of formation of Mnâ€“Si phases. Solid State Communications, 2014, 188, 49-52.	0.9	11
19859	van der Waals density functional made accurate. Physical Review B, 2014, 89, .	1.1	524
19860	High-pressure behavior of Fe3P and the role of phosphorus in planetary cores. Earth and Planetary Science Letters, 2014, 390, 296-303.	1.8	34
19861	Room Temperature Ferromagnetism in Shuttle-like BaMoO₄ Microcrystals. Journal of Physical Chemistry C, 2014, 118, 13826-13832.	1.5	9

#	Article	IF	Citations
19862	Theoretical investigation of triphenylamine-based sensitizers with different Ï€-spacers for DSSC. Spectrochimica Acta - Part A: Molecular and Biomolecular Spectroscopy, 2014, 118, 1144-1151.	2.0	46
19863	High voltage sulphate cathodes Li₂M(SO₄)₂ (M = Fe, Mn, Co): atomic-scale studies of lithium diffusion, surfaces and voltage trends. Journal of Materials Chemistry A, 2014, 2, 7446-7453.	5.2	57
19864	Influence of substitutional impurities on hydrogen diffusion in B2-TiFe alloy. International Journal of Hydrogen Energy, 2014, 39, 12213-12220.	3.8	19
19865	Conductivity of Si(111)-(<mml:math xmlns:mml="http://www.w3.org/1998/Math/MathML") Tj ETQq1 1 0.784314 rgBT /Overlock 10 T The Role of a Single Atomic Step. Physical Review Letters, 2014, 112, 246802.	2.9	30
19866	A charge optimized many-body (comb) potential for titanium and titania. Journal of Physics Condensed Matter, 2014, 26, 315007.	0.7	21
19867	Quantum dots with single-atom precision. Nature Nanotechnology, 2014, 9, 505-508.	15.6	77
19868	Stabilizing forces acting on ZnO polar surfaces: STM, LEED, and DFT. Physical Review B, 2014, 89, .	1.1	54
19869	Adsorption of Li, Na, K, and Mg Atoms on Amorphous and Crystalline Silica Bilayers on Ru(0001): A DFT Study. Journal of Physical Chemistry C, 2014, 118, 15884-15891.	1.5	13
19870	Importance of oxygen spillover for fuel oxidation on Ni/YSZ anodes in solid oxide fuel cells. Physical Chemistry Chemical Physics, 2014, 16, 8536.	1.3	16
19871	Structural phase transitions in two-dimensional Mo- and W-dichalcogenide monolayers. Nature Communications, 2014, 5, 4214.	5.8	832
19872	Ground-state phase in the three-dimensional topological Dirac semimetal<mml:math xmlns:mml="http://www.w3.org/1998/Math/MathML"><mml:msub><mml:mi>Na</mml:mi><mml:mn>3</mml:mn></mml:msub><mml: Physical Review B, 2014, 89, .	1.1	36
19873	Protonic defects in yttria stabilized zirconia: incorporation, trapping and migration. Physical Chemistry Chemical Physics, 2014, 16, 4814.	1.3	15
19874	Ab Initio Atomistic Thermodynamics of Water Reacting with Uranium Dioxide Surfaces. Journal of Physical Chemistry C, 2014, 118, 8491-8500.	1.5	26
19875	Occupation matrix control of d- and f-electron localisations using DFT + U. Physical Chemistry Chemical Physics, 2014, 16, 21016-21031.	1.3	160
19876	Stability of the D8m-Ti5Sn2Ga compound. Experimental determinations and first principle calculations. Journal of Chemical Thermodynamics, 2014, 78, 269-277.	1.0	2
19877	Insights into Changes of Lattice and Electronic Structure Associated with Electrochemistry of Li₂CoSiO₄ Polymorphs. Journal of Physical Chemistry C, 2014, 118, 7351-7356.	1.5	14
19878	Alkali cation specific adsorption onto fcc(111) transition metal electrodes. Physical Chemistry Chemical Physics, 2014, 16, 13699-13707.	1.3	93
19879	Electronic structures and magnetism of transition metal doped BiAlO3: An ab initio study. Physica B: Condensed Matter, 2014, 451, 76-79.	1.3	3

#	Article	IF	Citations
19880	Direct Band Gap Silicon Allotropes. Journal of the American Chemical Society, 2014, 136, 9826-9829.	6.6	151
19881	Adsorbed and Subsurface Absorbed Hydrogen Atoms on Bare and MgO(100)-Supported Pd and Pt Nanoparticles. Journal of Physical Chemistry C, 2014, 118, 15242-15250.	1.5	33
19882	Role of Surface Structure on Li-Ion Energy Storage Capacity of Two-Dimensional Transition-Metal Carbides. Journal of the American Chemical Society, 2014, 136, 6385-6394.	6.6	1,164
19883	Tunable Spin-Dependent Properties of Zigzag Silicene Nanoribbons. Physical Review Applied, 2014, 1, .	1.5	26
19884	Optical and Magnetic Excitations of Metal-Encapsulating Si Cages: A Systematic Study by Time-Dependent Density Functional Theory. Journal of Physical Chemistry C, 2014, 118, 11377-11384.	1.5	25
19885	Molecular and Electronic Structure of Cyclic Trinuclear Gold(I) Carbeniate Complexes: Insights for Structure/Luminescence/Conductivity Relationships. Inorganic Chemistry, 2014, 53, 7485-7499.	1.9	32
19886	From spin-polarized interfaces to giant magnetoresistance in organic spin valves. Physical Review B, 2014, 89, .	1.1	15
19887	Large Capacitance Enhancement Induced by Metal-Doping in Graphene-Based Supercapacitors: A First-Principles-Based Assessment. ACS Applied Materials & Interfaces, 2014, 6, 12168-12176.	4.0	40
19888	Prediction of Quaternary Spinel Oxides as Li-Battery Cathodes: Cation Site Preference, Metal Mixing, Voltage and Phase Stability. Journal of the Electrochemical Society, 2014, 161, A1440-A1446.	1.3	14
19889	Hydrogen embrittlement of a carbon segregated <mml:math xmlns:mml="http://www.w3.org/1998/Math/MathML" altimg="si0032.gif" overflow="scroll"><mml:mi>Î£</mml:mi><mml:mn>5</mml:mn><mml:mo>(</mml:mo><mml:mn>310</mml:mn><mml:mo>)</mml:mo></mml:math> symmetrical tilt grain boundary in Î±-Fe. Materials Science & Engineering A: Structural Materials: Properties, Microstructure and Processing, 2014, 612, 462-467.	2.6	39
19890	Development of a ReaxFF Reactive Force Field for Ammonium Nitrate and Application to Shock Compression and Thermal Decomposition. Journal of Physical Chemistry A, 2014, 118, 1469-1478.	1.1	29
19891	Mechanically Induced Metalâ€“Insulator Transition in Carbyne. Nano Letters, 2014, 14, 4224-4229.	4.5	130
19892	Experimental and theoretical study of the electronic properties of Cu-doped anatase TiO2. Physical Chemistry Chemical Physics, 2014, 16, 3835.	1.3	111
19893	Dynamic Effects on the Charge Transport in an Organic Near-Infrared Absorber Material. Journal of Physical Chemistry C, 2014, 118, 6537-6547.	1.5	15
19894	Morphology dependence of catalytic properties of Ni nanoparticles at the tips of carbon nanofibers for ammonia decomposition to generate hydrogen. International Journal of Hydrogen Energy, 2014, 39, 20722-20730.	3.8	16
19895	Development of an Atomic Level Model for BiFeO3from First-Principles. Ferroelectrics, 2014, 461, 61-67.	0.3	2
19896	Response of MoS 2 nanosheet field effect transistor under different gas environments and its long wavelength photoresponse characteristics. Journal of Alloys and Compounds, 2014, 615, 989-993.	2.8	24
19897	CO Adsorption on Pd(100) Revisited by Sum Frequency Generation: Evidence for Two Adsorption Sites in the Compression Stage. Journal of Physical Chemistry C, 2014, 118, 19688-19700.	1.5	14

#	Article	IF	Citations
19898	First-principles study of high-field-related electronic behavior of group-III nitrides. Physical Review B, 2014, 90, .	1.1	20
19899	Band gap engineering of FeS₂ under biaxial strain: a first principles study. Physical Chemistry Chemical Physics, 2014, 16, 24466-24472.	1.3	38
19900	First-principles study of van der Waals interactions in MoS₂and MoO₃. Journal of Physics Condensed Matter, 2014, 26, 305502.	0.7	45
19901	Catalytic enhancement in dissociation of nitric oxide over rhodium and nickel small-size clusters: a DFT study. Physical Chemistry Chemical Physics, 2014, 16, 5393.	1.3	10
19902	Interdistance Effects on Flat and Buckled Silicene Like-bilayers. Journal of Physics: Conference Series, 2014, 491, 012006.	0.3	6
19903	An experimental and computational study to understand the lithium storage mechanism in molybdenum disulfide. Nanoscale, 2014, 6, 10243-10254.	2.8	103
19904	Analysis of the Difference between the Pyroxenes LiFeSi₂O₆ and LiFeGe₂O₆ in Their Spin Order, Spin Orientation, and Ferrotoroidal Order. Chemistry of Materials, 2014, 26, 1745-1750.	3.2	15
19905	First Principles <I>Ab Initio</I> Study of Co₂ Adsorption On The Kaolinite (001) Surface. Clays and Clay Minerals, 2014, 62, 153-160.	0.6	12
19906	Electrical contacts to monolayer black phosphorus: A first-principles investigation. Physical Review B, 2014, 90, .	1.1	122
19907	Calculated Stability and Structure of Nickel Ferrite Crystal Surfaces in Hydrothermal Environments. Journal of Physical Chemistry C, 2014, 118, 5414-5423.	1.5	35
19908	Understanding the local environment of Sm³⁺ in doped SrZrO₃ and energy transfer mechanism using time-resolved luminescence: a combined theoretical and experimental approach. RSC Advances, 2014, 4, 29202-29215.	1.7	83
19909	Preparation, Crystal Structure, and Magnetotransport Properties of the New CdCu₃Mn₄O₁₂ Perovskite: A Comparison with Density Functional Theory Calculations. Journal of Physical Chemistry C, 2014, 118, 9652-9658.	1.5	9
19910	Impact of cation-based localized electronic states on the conduction and valence band structure of Al1â^'xInxN alloys. Applied Physics Letters, 2014, 104, .	1.5	21
19911	Second generation Carâ€“Parrinello molecular dynamics. Wiley Interdisciplinary Reviews: Computational Molecular Science, 2014, 4, 391-406.	6.2	130
19912	First-principle study of the physics properties of DO3â€“Mg3Nd compound under high pressure. Superlattices and Microstructures, 2014, 73, 359-369.	1.4	6
19913	Minimizing Electronâ€“Hole Recombination on TiO₂ Sensitized with PbSe Quantum Dots: Time-Domain Ab Initio Analysis. Journal of Physical Chemistry Letters, 2014, 5, 2941-2946.	2.1	63
19914	A metallic carbon consisting of helical carbon triangle chains. Journal of Physics Condensed Matter, 2014, 26, 235402.	0.7	10
19915	Structure of Feâ€“N_xâ€“C Defects in Oxygen Reduction Reaction Catalysts from First-Principles Modeling. Journal of Physical Chemistry C, 2014, 118, 14388-14393.	1.5	167

#	Article	IF	Citations
19916	On the variation of dissolution rates at the orthoclase (0 0 1) surface with pH and temperature. Geochimica Et Cosmochimica Acta, 2014, 141, 598-611.	1.6	16
19917	Hole localization, migration, and the formation of peroxide anion in perovskite<mml:math xmlns:mml="http://www.w3.org/1998/Math/MathML"><mml:msub><mml:mrow><mml:mi>Sr</mml:mi><mml:mi>Ti</mml:mi></mml:mrow><mml:mn>3</mml:mn></mml:msub></mml:math>. Physical Review B, 2014, 90, .	1.1	29
19918	Phase Coexistence and Metal-Insulator Transition in Few-Layer Phosphorene: A Computational Study. Physical Review Letters, 2014, 113, 046804.	2.9	556
19919	First-principles theory of nonradiative carrier capture via multiphonon emission. Physical Review B, 2014, 90, .	1.1	263
19920	Linear optical and electronic properties of the polar metallic ruthenate (Sr,Ca)Ru2O6. Journal of Physics Condensed Matter, 2014, 26, 265501.	0.7	2
19921	Acidâ€“Base Chemistry in the Formation of Mackay-Type Icosahedral Clusters: Î¼₃-Acidity Analysis of Sc-Rich Phases of the Scâ€“Ir System. Inorganic Chemistry, 2014, 53, 5280-5293.	1.9	10
19922	Implications of Transition State Confinement within Small Voids for Acid Catalysis. Journal of Physical Chemistry C, 2014, 118, 17787-17800.	1.5	115
19923	Er60Ni132: A new structure from the Ni occupied the 4b sites in cubic laves superstructure synthesized under high pressure and high temperature. Intermetallics, 2014, 55, 195-198.	1.8	0
19924	Ground-state properties of rare-earth metals: an evaluation of density-functional theory. Journal of Physics Condensed Matter, 2014, 26, 416001.	0.7	43
19925	Tailoring the Electronic Structure of Mesoporous Spinel Î³-Al₂O₃ at Atomic Level: Cu-Doped Case. Journal of Physical Chemistry C, 2014, 118, 14299-14315.	1.5	24
19926	Engineering Preferential Adsorption of Single-Walled Carbon Nanotubes on Functionalized ST-cut Surfaces of Quartz. ACS Applied Materials & Interfaces, 2014, 6, 12665-12673.	4.0	1
19927	Atomic-Scale Perspective of Ultrafast Charge Transfer at a Dyeâ€“Semiconductor Interface. Journal of Physical Chemistry Letters, 2014, 5, 2753-2759.	2.1	79
19928	Formation of Large Polysulfide Complexes during the Lithium-Sulfur Battery Discharge. Physical Review Applied, 2014, 2, .	1.5	105
19929	First-principles study of crystalline CoWO4 as oxygen evolution reaction catalyst. RSC Advances, 2014, 4, 24692.	1.7	68
19930	Ultrathin rhodium nanosheets. Nature Communications, 2014, 5, 3093.	5.8	428
19931	Ab-initiostudy of long-period superstructures and anti-phase boundaries in Al-richÎ³-TiAl (L1₀)-based alloys. Philosophical Magazine, 2014, 94, 1202-1218.	0.7	7
19932	Roles of Plasmonic Excitation and Protonation on Photoreactions of p-Aminobenzenethiol on Ag Nanoparticles. Journal of Physical Chemistry C, 2014, 118, 6893-6902.	1.5	33
19933	Room-Temperature Ferrimagnet with Frustrated Antiferroelectricity: Promising Candidate Toward Multiple-State Memory. Physical Review X, 2014, 4, .	2.8	29

#	Article	IF	Citations
19934	Multiphase equation of state for carbon addressing high pressures and temperatures. Physical Review B, 2014, 89, .	1.1	127
19935	A Density Functional Study of Oxygen Adatoms on a Step-Doubled Platinum Surface. Journal of Physical Chemistry C, 2014, 118, 23675-23681.	1.5	3
19936	Computational design ofin vivobiomarkers. Journal of Physics Condensed Matter, 2014, 26, 143202.	0.7	13
19937	Helium bubble clustering in copper from first principles. Modelling and Simulation in Materials Science and Engineering, 2014, 22, 035019.	0.8	19
19938	First-principles study of a novel superhardsp3carbon allotrope. Physics Letters, Section A: General, Atomic and Solid State Physics, 2014, 378, 3326-3330.	0.9	27
19939	Extraordinary Photoluminescence and Strong Temperature/Angle-Dependent Raman Responses in Few-Layer Phosphorene. ACS Nano, 2014, 8, 9590-9596.	7.3	604
19940	Tailoring the Electronic Structure in Bilayer Molybdenum Disulfide via Interlayer Twist. Nano Letters, 2014, 14, 3869-3875.	4.5	278
19941	Achieving High-Quality Single-Atom Nitrogen Doping of Graphene/SiC(0001) by Ion Implantation and Subsequent Thermal Stabilization. ACS Nano, 2014, 8, 7318-7324.	7.3	81
19942	Structure and stability of two dimensional phosphorene with î€O or î€NH functionalization. RSC Advances, 2014, 4, 48017-48021.	1.7	68
19943	Striking Effect of Intra- versus Intermolecular Hydrogen Bonding on Zwitterions: Physical and Electronic Properties. Journal of the American Chemical Society, 2014, 136, 11614-11617.	6.6	12
19944	Angle-Resolved Thermal Dissociative Sticking of Light Alkanes on Pt(111): Transitioning from Dynamical to Statistical Behavior. Journal of Physical Chemistry C, 2014, 118, 22003-22011.	1.5	2
19945	Raman scattering investigation of the electron-phonon coupling in superconducting Nd(O,F)<mml:math xmlns:mml="http://www.w3.org/1998/Math/MathML"><mml:msub><mml:mi mathvariant="normal">BiS</mml:mi><mml:mn>2</mml:mn></mml:msub></mml:math>. Physical Review B, 2014, 90, .	1.1	36
19946	Silver and Cesium Diffusion Dynamics at the Î²-SiC Î£5 Grain Boundary Investigated with Density Functional Theory Molecular Dynamics and Metadynamics. Journal of Physical Chemistry A, 2014, 118, 915-926.	1.1	20
19947	Photo-induced current transient spectroscopy of single crystal Tl₆I₄Se. Semiconductor Science and Technology, 2014, 29, 115002.	1.0	6
19948	Palladium nanoparticles supported on graphitic carbon nitride-modified reduced graphene oxide as highly efficient catalysts for formic acid and methanol electrooxidation. Journal of Materials Chemistry A, 2014, 2, 19084-19094.	5.2	146
19949	Ln(IO3)3 (Ln = Ce, Nd, Eu, Gd, Er, Yb) Polycrystals As Novel Photocatalysts for Efficient Decontamination under Ultraviolet Light Irradiation. Inorganic Chemistry, 2014, 53, 4989-4993.	1.9	15
19950	Band-Gap Energy as a Descriptor of Catalytic Activity for Propene Oxidation over Mixed Metal Oxide Catalysts. Journal of the American Chemical Society, 2014, 136, 13684-13697.	6.6	120
19951	Chemical control of electrical contact to sp2 carbon atoms. Nature Communications, 2014, 5, 3659.	5.8	22

#	Article	IF	Citations
19952	Diffusion of Te vacancy and interstitials of Te, Cl, O, S, P and Sb in CdTe: A density functional theory study. Solar Energy Materials and Solar Cells, 2014, 128, 343-350.	3.0	9
19953	A Minimal Cluster Model of Valence Electrons in Adatom-Assisted Adsorbed Molecules: NCH₃/Cu(110) and OCH₃/Cu(110). Journal of Physical Chemistry C, 2014, 118, 9443-9449.	1.5	0
19954	Effect of temperature-induced solute distribution on stacking fault energy in Mgâ€“X(Xâ€‰=â€‰Li, Cu, Zn, Al, Y) Tj ETQq0 0 0 rgBT /C	0.7	31
19955	Catalytic NO activation and NOâ€“H 2 reaction pathways. Journal of Catalysis, 2014, 319, 95-109.	3.1	31
19956	Selective Hydrogenation of Acetylene over Pdâ€“Boron Catalysts: A Density Functional Theory Study. Journal of Physical Chemistry C, 2014, 118, 3664-3671.	1.5	51
19957	Piezoelectric properties of graphene oxide: A first-principles computational study. Applied Physics Letters, 2014, 105, .	1.5	58
19958	Anomalous properties of antiferroelectric<mml:math xmlns:mml="http://www.w3.org/1998/Math/MathML"><mml:msub><mml:mtext>PbZrO</mml:mtext><mml:mn>3</mml:mn></mml:msub></mml:ms hydrostatic pressure. Physical Review B, 2014, 89, .	1.1	11
19959	Computational Investigation of Electron Small Polarons in Î±-MoO₃. Journal of Physical Chemistry C, 2014, 118, 15565-15572.	1.5	44
19960	First principles calculations predict stable 50 nm nickel ferrite particles in PWR coolant. Journal of Nuclear Materials, 2014, 454, 77-80.	1.3	6
19961	Magnetism by Interfacial Hybridization and p-type Doping of MoS₂ in Fe₄N/MoS₂ Superlattices: A First-Principles Study. ACS Applied Materials & Interfaces, 2014, 6, 4587-4594.	4.0	54
19962	Constructing a Metallic/Semiconducting TaB₂/Ta₂O₅ Core/Shell Heterostructure for Photocatalytic Hydrogen Evolution. Advanced Energy Materials, 2014, 4, 1400057.	10.2	44
19963	Equation of state of lead from high-pressure neutron diffraction up to 8.9 GPa and its implication for the NaCl pressure scale. Physical Review B, 2014, 90, .	1.1	48
19964	Hierarchical Carbonâ€“Nitrogen Architectures with Both Mesopores and Macrochannels as Excellent Cathodes for Rechargeable Liâ€“O₂ Batteries. Advanced Functional Materials, 2014, 24, 6826-6833.	7.8	161
19965	Injection of spin polarization into Si from the heterostructure LaMnO3/Si interface. Applied Physics Express, 2014, 7, 093003.	1.1	1
19966	Magnetic and thermodynamic properties of face-centered cubic Feâ€“Ni alloys. Physical Chemistry Chemical Physics, 2014, 16, 16049.	1.3	54
19967	The Role of Surface States in the Oxygen Evolution Reaction on Hematite. Angewandte Chemie - International Edition, 2014, 53, 13404-13408.	7.2	128
19968	First-principles study of siloxene and germoxene: stable conformations, electronic properties, and defects. Journal of Physics Condensed Matter, 2014, 26, 285301.	0.7	11
19969	DFT study of reaction processes of methane combustion on PdO(100). Chemical Physics, 2014, 443, 53-60.	0.9	25

#	Article	IF	Citations
19970	Self-Catalyzed Carbon Dioxide Adsorption by Metalâ€“Organic Chains on Gold Surfaces. ACS Nano, 2014, 8, 8644-8652.	7.3	35
19971	Exploring the Structural Complexity of Intermetallic Compounds by an Adaptive Genetic Algorithm. Physical Review Letters, 2014, 112, 045502.	2.9	97
19972	Preparation of MoS₂â€“MoO₃ Hybrid Nanomaterials for Lightâ€Emitting Diodes. Angewandte Chemie - International Edition, 2014, 53, 12560-12565.	7.2	133
19973	Reactivity of the Defective Rutile TiO₂ (110) Surfaces with Two Bridging-Oxygen Vacancies: Water Molecule as a Probe. Journal of Physical Chemistry C, 2014, 118, 20257-20263.	1.5	20
19974	Influence of Surface Chemistry of Activated Carbon on the Activity of Gold/Activated Carbon Catalyst in Acetylene Hydrochlorination. Industrial & Engineering Chemistry Research, 2014, 53, 14272-14281.	1.8	56
19975	Correlation effects in (111) bilayers of perovskite transition-metal oxides. Physical Review B, 2014, 89, .	1.1	63
19976	Microscopic Theory of Cation Exchange in CdSe Nanocrystals. Physical Review Letters, 2014, 113, 156803.	2.9	64
19977	Absolute surface energies of polar and nonpolar planes of GaN. Physical Review B, 2014, 89, .	1.1	89
19978	An improved interatomic potential for xenon in UO₂: a combined density functional theory/genetic algorithm approach. Journal of Physics Condensed Matter, 2014, 26, 105501.	0.7	8
19979	Point defects engineering in graphene/h-BN bilayer: A first principle study. Applied Surface Science, 2014, 320, 502-508.	3.1	11
19980	Semimetallic molybdenum disulfide ultrathin nanosheets as an efficient electrocatalyst for hydrogen evolution. Nanoscale, 2014, 6, 8359-8367.	2.8	248
19981	Thermodynamic optimizations on the binary Liâ€“Sn system and ternary Mgâ€“Snâ€“Li system. Calphad: Computer Coupling of Phase Diagrams and Thermochemistry, 2014, 47, 100-113.	0.7	23
19982	Stabilization of the tetragonal distortion of Fe<mml:math xmlns:mml="http://www.w3.org/1998/Math/MathML"><mml:msub><mml:mrow /><mml:mi>x</mml:mi></mml:msub></mml:math>Co<mml:math xmlns:mml="http://www.w3.org/1998/Math/MathML"><mml:msub><mml:mrow /><mml:mrow><mml:mn>1</mml:mn><mml:mo>â^’</mml:mo><mml:mi>x</mml:mi></mml:mrow></mml:msub></mml:math>alloys by C impurities: A potential new permanent magnet. Physical Review B, 2014, 89, .	1.1	60
19983	Tunable electronic structures of p-type Mg doping in AlN nanosheet. Journal of Applied Physics, 2014, 116, .	1.1	33
19984	Prediction of giant magnetoelectric effect in LaMnO3/BaTiO3/SrMnO3 superlattice: The role of n-type SrMnO3/LaMnO3 interface. Journal of Applied Physics, 2014, 116, 074102.	1.1	11
19985	Surface energy and work function of fcc and bcc crystals: Density functional study. Surface Science, 2014, 630, 216-224.	0.8	173
19986	Mechanical and thermal properties of h-MX₂ (Mâ€‰=â€‰Cr, Mo, W; Xâ€‰=â€‰O, S, Se, Te) monolayers: A comparative study. Applied Physics Letters, 2014, 104, 203110.	1.5	157
19987	Electronic and magnetic properties of BiFeO 3 with intrinsic defects: First-principles prediction. Chinese Physics B, 2014, 23, 067102.	0.7	5

#	Article	IF	Citations
19988	Bulk Properties of Transition Metals: A Challenge for the Design of Universal Density Functionals. Journal of Chemical Theory and Computation, 2014, 10, 3832-3839.	2.3	245
19989	Adsorption of methanethiol on Au(1 1 1): Role of hydrogen bonds. Chemical Physics Letters, 2014, 610-611, 381-387.	1.2	2
19990	Control of Metalâ€“Organic Framework Crystal Topology by Ligand Functionalization: Functionalized HKUST-1 Derivatives. Crystal Growth and Design, 2014, 14, 6122-6128.	1.4	48
19991	Tuning the Adsorption of Aromatic Molecules on Platinum via Halogenation. Journal of Physical Chemistry C, 2014, 118, 6235-6241.	1.5	21
19992	Compressibility Systematics of Calcite-Type Borates: An Experimental and Theoretical Structural Study on ABO₃ (A = Al, Sc, Fe, and In). Journal of Physical Chemistry C, 2014, 118, 4354-4361.	1.5	22
19993	Structure and Charge Transfer in Binary Ordered Monolayers of Two Sulfur-Containing Donor Molecules and TNAP on the Au(111) Surface. Journal of Physical Chemistry C, 2014, 118, 3035-3048.	1.5	9
19994	Novel band structures in silicene on monolayer zinc sulfide substrate. Journal of Physics Condensed Matter, 2014, 26, 395003.	0.7	13
19995	First-principles study of AlN nanosheets with chlorination. RSC Advances, 2014, 4, 7500.	1.7	17
19996	Effects of surface-bulk hybridization in three-dimensional topological metals. Physical Review B, 2014, 89, .	1.1	13
19997	Hydrogen Bond Disruption in DNA Base Pairs from ¹⁴C Transmutation. Journal of Physical Chemistry B, 2014, 118, 10430-10435.	1.2	5
19998	Density functional theory study of pâ€chloroaniline adsorption on Pd surfaces and clusters. International Journal of Quantum Chemistry, 2014, 114, 895-899.	1.0	6
19999	Copper Promotion in CO Adsorption and Dissociation on the Fe(100) Surface. Journal of Physical Chemistry C, 2014, 118, 20472-20480.	1.5	30
20000	Versatile Electronic Properties of VSe₂ Bulk, Few-Layers, Monolayer, Nanoribbons, and Nanotubes: A Computational Exploration. Journal of Physical Chemistry C, 2014, 118, 21264-21274.	1.5	114
20001	Oxygen and Hydroxyl Species Induce Multiple Reaction Pathways for the Partial Oxidation of Allyl Alcohol on Gold. Journal of the American Chemical Society, 2014, 136, 6489-6498.	6.6	37
20002	Exploring Hardness and the Distorted sp² Hybridization of Bâ€“B Bonds in WB₃. Chemistry of Materials, 2014, 26, 5297-5302.	3.2	80
20003	Nanocatalyst Superior to Pt for Oxygen Reduction Reactions: The Case of Core/Shell Ag(Au)/CuPd Nanoparticles. Journal of the American Chemical Society, 2014, 136, 15026-15033.	6.6	172
20004	Thermo-selective Tm_xTi_{1â^'x}O_{2â^'x/2}nanoparticles: from Tm-doped anatase TiO₂to a rutile/pyrochlore Tm₂Ti₂O₇mixture. An experimental and theoretical study with a photocatalytic application. Nanoscale, 2014, 6, 12740-12757.	2.8	32
20005	Overcoming the polarization catastrophe in the rocksalt oxides MgO and CaO. Physical Review B, 2014, 90, .	1.1	13

#	Article	IF	Citations
20006	Quantitative Bond Energetics in Atomic-Scale Junctions. ACS Nano, 2014, 8, 7522-7530.	7.3	17
20007	Tunneling magnetoresistance in Fe3Si/MgO/Fe3Si(001) magnetic tunnel junctions. Applied Physics Letters, 2014, 104, .	1.5	23
20008	Direct evidence of active and inactive phases of Fe catalyst nanoparticles for carbon nanotube formation. Journal of Catalysis, 2014, 319, 54-60.	3.1	57
20009	Adsorption of Au and Pd on Ruthenium-Supported Bilayer Silica. Journal of Physical Chemistry C, 2014, 118, 20959-20969.	1.5	46
20010	Bipolaron Formation Induced by Oxygen Vacancy at Rutile TiO₂(110) Surfaces. Journal of Physical Chemistry C, 2014, 118, 9429-9435.	1.5	31
20011	Analysis of Charged State Stability for Monoclinic LiMnBO₃ Cathode. Chemistry of Materials, 2014, 26, 4200-4206.	3.2	24
20012	Study of the Electronic and Optical Properties of Hybrid Triangular (BN)xCy Foams. Journal of Physical Chemistry C, 2014, 118, 22181-22187.	1.5	2
20013	The mechanisms for the high resistance to sulfur poisoning of the Ni/yttria-stabilized zirconia system treated with Sn vapor. Physical Chemistry Chemical Physics, 2014, 16, 1033-1040.	1.3	14
20014	Toward Equatorial Planarity about Uranyl: Synthesis and Structure of Tridentate Nitrogen-Donor {UO₂}²⁺ Complexes. Inorganic Chemistry, 2014, 53, 2506-2515.	1.9	17
20015	Electron Emission Energy Barriers and Stability of Sc₂O₃ with Adsorbed Ba and Baâ€“O. Journal of Physical Chemistry C, 2014, 118, 19742-19758.	1.5	24
20016	Bayesian uncertainty quantification in the evaluation of alloy properties with the cluster expansion method. Computer Physics Communications, 2014, 185, 2885-2892.	3.0	19
20017	Oxygen evolution in Co-doped RuO2 and IrO2: Experimental and theoretical insights to diminish electrolysis overpotential. Journal of Power Sources, 2014, 268, 69-76.	4.0	98
20018	Effects of van der Waals Interactions in the Adsorption of Isooctane and Ethanol on Fe(100) Surfaces. Journal of Physical Chemistry C, 2014, 118, 17608-17615.	1.5	61
20019	Activity of ZnO polar surfaces: an insight from surface energies. Physical Chemistry Chemical Physics, 2014, 16, 22139-22144.	1.3	87
20020	Revisiting the Crystal Structure of Rhombohedral Lead Metaniobate. Inorganic Chemistry, 2014, 53, 9715-9721.	1.9	10
20021	SurfKin: An ab initio kinetic code for modeling surface reactions. Journal of Computational Chemistry, 2014, 35, 1890-1899.	1.5	20
20022	Magic numbers in small iron clusters: A first-principles study. Chemical Physics Letters, 2014, 613, 59-63.	1.2	36
20023	Fullerene growth from encapsulated graphene flakes. Nanoscale, 2014, 6, 11213-11218.	2.8	7

#	Article	IF	Citations
20024	Magnetic ordering in TbMn0.5Cr0.5O3 studied by neutron diffraction and first-principles calculations. Journal of Applied Physics, 2014, 116, 033919.	1.1	15
20025	Convergence of an analytic bond-order potential for collinear magnetism in Fe. Modelling and Simulation in Materials Science and Engineering, 2014, 22, 034005.	0.8	16
20026	Periodic Trends of Pnictogen Substitution into a Graphene Monovacancy: A First-Principles Investigation. Chemistry of Materials, 2014, 26, 5735-5744.	3.2	12
20027	Lithium Migration Pathways and van der Waals Effects in the LiFeSO₄OH Battery Material. Chemistry of Materials, 2014, 26, 3672-3678.	3.2	26
20028	Chemical Transformation of Carboxyl Groups on the Surface of Silicon Carbide Quantum Dots. Journal of Physical Chemistry C, 2014, 118, 19995-20001.	1.5	16
20029	Single-molecule magnet<mml:math xmlns:mml="http://www.w3.org/1998/Math/MathML"><mml:msub><mml:mi mathvariant="normal">Mn</mml:mi><mml:mn>12</mml:mn></mml:msub></mml:math>on graphene. Physical Review B, 2014, 90, .	1.1	12
20030	Predicting the Chiral Enrichment of Metallic SWCNTs on Niâ€“Cu Bimetallic Surfaces. Chemistry of Materials, 2014, 26, 4943-4950.	3.2	7
20031	Effects of strain on the band structure of group-III nitrides. Physical Review B, 2014, 90, .	1.1	100
20032	Nonstoichiometric Perovskite CaMnO_{3â^Î´} for Oxygen Electrocatalysis with High Activity. Inorganic Chemistry, 2014, 53, 9106-9114.	1.9	202
20033	Density functional theory study on the interaction of CO with the Fe3O4(001) surface. Applied Surface Science, 2014, 317, 752-759.	3.1	28
20034	Highly effective catalysis of the double-icosahedral Ru19 cluster for dinitrogen dissociation â€“ a first-principles investigation. Physical Chemistry Chemical Physics, 2014, 16, 7394.	1.3	4
20035	Role of Surface Hydroxyl Groups on Zinc Adsorption Characteristics on Î±-Al₂O₃(0001) Surfaces: First-Principles Study. Journal of Physical Chemistry C, 2014, 118, 13578-13589.	1.5	33
20036	Band alignments and polarization properties of BN polymorphs. Applied Physics Express, 2014, 7, 031001.	1.1	46
20037	Multi-intermediate-band character of Ti-substitutedCuGaS2: Implications for photovoltaic applications. Physical Review B, 2014, 90, .	1.1	24
20038	Chirality effect of mechanical and electronic properties of monolayer MoS2 with vacancies. Physics Letters, Section A: General, Atomic and Solid State Physics, 2014, 378, 2910-2914.	0.9	38
20039	Complex antipolar<mml:math xmlns:mml="http://www.w3.org/1998/Math/MathML"><mml:mrow><mml:msqrt><mml:mn>2</mml:mn></mml:msqrt><mml:mo>Ã— with<mml:math xmlns:mml="http://www.w3.org/1998/Math/MathML"><mml:mrow><mml:mi>P</mml:mi><mml:mi>n</mml:mi><mml:mi>m</mml:mi> in<mml:math xmlns:mml="http://www.w3.org/1998/Math/MathML"><mml:msub. Physical Review B, 2014, 90, .	1.1	18
20040	Sodium Ion Diffusion in Al₂O₃: A Distinct Perspective Compared with Lithium Ion Diffusion. Nano Letters, 2014, 14, 6559-6563.	4.5	91
20041	Bottom-up approach for the low-cost synthesis of graphene-alumina nanosheet interfaces using bimetallic alloys. Nature Communications, 2014, 5, 5062.	5.8	37

#	Article	IF	Citations
20042	Atomically-thin non-layered cobalt oxide porous sheets for highly efficient oxygen-evolving electrocatalysts. Chemical Science, 2014, 5, 3976.	3.7	332
20043	Coupled Theoretical and Experimental Studies for the Radiation Hardening of Silica-Based Optical Fibers. IEEE Transactions on Nuclear Science, 2014, 61, 1819-1825.	1.2	23
20044	Isolobal Analogies in Intermetallics: The Reversed Approximation MO Approach and Applications to CrGa4- and Ir3Ge7-Type Phases. Inorganic Chemistry, 2014, 53, 2730-2741.	1.9	51
20046	Adsorption and diffusion of Rh and Au dimers and trimers on graphene/Ru(0001). Surface Science, 2014, 626, 6-13.	0.8	8
20047	Stability and electronic properties of carbon in Î±-Al2O3. Journal of Physics and Chemistry of Solids, 2014, 75, 379-383.	1.9	27
20048	Density functional theory study of the adsorption and reaction of C2H4 on Fe3C(100). Chinese Journal of Catalysis, 2014, 35, 28-37.	6.9	7
20049	First-principles study of hydrogen adsorption and permeation in reconstructed cubic erbium oxide surfaces. Fusion Engineering and Design, 2014, 89, 1294-1298.	1.0	2
20050	The inter-adsorbate interaction mediated by Shockley-type surface state electrons and dipole moment: Cs and Ba atoms absorbed on Ag (111) films. Applied Surface Science, 2014, 289, 81-88.	3.1	2
20051	Termination, stability and electronic structures of Î±-Al2O3 (<mml:math) Tj ETQq0 0 0 rgBT /Overlock 10 Tf 50 437 Td (xmlns:mml="http surface: An ab initio study. Applied Surface Science, 2014, 303, 210-216.	3.1	7
20052	Electronic properties of experimentally observed Pb/Ru(0001) adsorbate structures: A DFT study. Applied Surface Science, 2014, 304, 115-121.	3.1	10
20053	First-principles study of thermophysical properties of uranium dioxide. Journal of Alloys and Compounds, 2014, 603, 282-286.	2.8	20
20054	Density functional theory calculations for Pd adsorption on SO4 adsorbed on h-BN. Computational Materials Science, 2014, 82, 231-236.	1.4	16
20055	Orthorhombic BN: A novel superhard boron nitride allotrope. Physics Letters, Section A: General, Atomic and Solid State Physics, 2014, 378, 741-744.	0.9	33
20056	Pressure induced metallization of fordite SnNb2O6 from first principles. Computational Materials Science, 2014, 84, 355-359.	1.4	3
20057	Engineering by Mn embedment and adsorption in defective boron nitrogen sheet. Physica E: Low-Dimensional Systems and Nanostructures, 2014, 56, 24-31.	1.3	3
20058	Negatively curved cubic carbon crystals with octahedral symmetry. Carbon, 2014, 76, 266-274.	5.4	48
20059	Density functional study of NO adsorption on undefected and oxygen defective Auâ€“BaO(100) surfaces. Applied Surface Science, 2014, 307, 165-171.	3.1	3
20060	Hydrogen storage on nitrogen induced defects in palladium-decorated graphene: A first-principles study. Applied Surface Science, 2014, 292, 921-927.	3.1	53

#	Article	IF	Citations
20061	Cooperativity of Halogen, Chalcogen, and Pnictogen Bonds in Infinite Molecular Chains by Electronic Structure Theory. Journal of Physical Chemistry A, 2014, 118, 3193-3200.	1.1	90
20062	Jahn-Teller distortion and charge, orbital, and magnetic order in <mml:math xmlns:mml="http://www.w3.org/1998/Math/MathML"><mml:msub><mml:mi mathvariant="normal">NaMn</mml:mi><mml:mn>7</mml:mn></mml:msub></mml:math><mml:math xmlns:mml="http://www.w3.org/1998/Math/MathML"><mml:msub><mml:mi mathvariant="normal">O</mml:mi><mml:mn>12</mml:mn></mml:msub></mml:math>. Physical Review B, 2014, 89, .	1.1	29
20063	Semihydrogenation of Acetylene on the (010) Surface of GaPd₂: Ga Enrichment Improves Selectivity. Journal of Physical Chemistry C, 2014, 118, 12285-12301.	1.5	30
20064	Electronâ€“Hole Pair Generation of the Visible-Light Plasmonic Photocatalyst Ag@AgCl: Enhanced Optical Transitions Involving Midgap Defect States of AgCl. Journal of Physical Chemistry C, 2014, 118, 12133-12140.	1.5	48
20065	Borohydrides: from sheet to framework topologies. Dalton Transactions, 2014, 43, 7726.	1.6	20
20066	Impact of co-adsorbed oxygen on crotonaldehyde adsorption over gold nanoclusters: a computational study. Physical Chemistry Chemical Physics, 2014, 16, 11202-11210.	1.3	3
20067	Chain-Length and Temperature Dependence of Self-Assembled Monolayers of Alkylthiolates on Au(111) and Ag(111) Surfaces. Journal of Physical Chemistry A, 2014, 118, 4138-4146.	1.1	23
20068	Flexoelectricity and ferroelectric domain wall structures: Phase-field modeling and DFT calculations. Physical Review B, 2014, 89, .	1.1	101
20069	What Limits Turnover Number in NH3Synthesis on a PNP Pincer Molecule?. Comments on Inorganic Chemistry, 2014, 34, 3-16.	3.0	1
20070	Homolytic Products from Heterolytic Paths in H₂ Dissociation on Metal Oxides: The Example of CeO₂. Journal of Physical Chemistry C, 2014, 118, 10921-10926.	1.5	174
20071	A ReaxFF Investigation of Hydride Formation in Palladium Nanoclusters via Monte Carlo and Molecular Dynamics Simulations. Journal of Physical Chemistry C, 2014, 118, 4967-4981.	1.5	53
20072	Exciton diffusion in disordered small molecules for organic photovoltaics: insights from first-principles simulations. Journal of Physics Condensed Matter, 2014, 26, 185006.	0.7	8
20073	Electronic properties of MoS ₂ sandwiched between graphene monolayers. Europhysics Letters, 2014, 106, 47003.	0.7	12
20074	Atomic-Scale Theory and Simulations for Colloidal Metal Nanocrystal Growth. Journal of Chemical & Engineering Data, 2014, 59, 3113-3119.	1.0	18
20075	Catalytic Transparency of Hexagonal Boron Nitride on Copper for Chemical Vapor Deposition Growth of Large-Area and High-Quality Graphene. ACS Nano, 2014, 8, 5478-5483.	7.3	48
20076	Investigation on AgGaSe 2 for water splitting from first-principles calculations. Europhysics Letters, 2014, 105, 37007.	0.7	8
20077	Rutile (Î²-)MnO₂ Surfaces and Vacancy Formation for High Electrochemical and Catalytic Performance. Journal of the American Chemical Society, 2014, 136, 1418-1426.	6.6	186
20078	Effects of a Carbon Surface Environment on the Decomposition Properties of Nanoparticle LiBH₄: A First-Principles Study. Journal of Physical Chemistry C, 2014, 118, 8852-8858.	1.5	17

#	Article	IF	Citations
20079	Silicene on Ag(111): A honeycomb lattice without Dirac bands. Physical Review B, 2014, 89, .	1.1	102
20080	Experimental and Firstâ€Principles Studies of the Ternary Borides Ta₃Ru₅B₂ and M_{3â€“x}Ru_{5+x}B₂ (M = Zr, Hf). European Journal of Inorganic Chemistry, 2014, 2014, 3085-3094.	1.0	10
20081	A systematic first-principles study of surface energies, surface relaxation and Friedel oscillation of magnesium surfaces. Journal Physics D: Applied Physics, 2014, 47, 115305.	1.3	39
20082	Optical Properties and Quasiparticle Band Gaps of Transition-Metal Atoms Encapsulated by Silicon Cages. Journal of Physical Chemistry C, 2014, 118, 5501-5509.	1.5	42
20083	Structural and electronic properties of germanene/MoS2 monolayer and silicene/MoS2 monolayer superlattices. Nanoscale Research Letters, 2014, 9, 110.	3.1	69
20084	Dielectric Properties of Selected Metalâ€“Organic Frameworks. Journal of Physical Chemistry C, 2014, 118, 11799-11805.	1.5	40
20085	Electronic and Structural Properties of Highly Aluminum Ion Doped TiO₂ Nanoparticles: A Combined Experimental and Theoretical Study. ChemPhysChem, 2014, 15, 2267-2280.	1.0	29
20086	Density functional theory simulations of complex catalytic materials in reactive environments: beyond the ideal surface at low coverage. Catalysis Science and Technology, 2014, 4, 2797-2813.	2.1	57
20087	Synthesis and Systematic Trends in Structure and Electrical Properties of [(SnSe)1.15]m(VSe2)1, m = 1, 2, 3, and 4. Chemistry of Materials, 2014, 26, 2862-2872.	3.2	33
20088	Effect of alloying of magnetic and non-magnetic low reactivity atoms into atomic chain. Physica Status Solidi (B): Basic Research, 2014, 251, 871-876.	0.7	9
20089	Effect of dispersion on surface interactions of cobalt(<scp>ii</scp>) octaethylporphyrin monolayer on Au(111) and HOPG(0001) substrates: a comparative first principles study. Physical Chemistry Chemical Physics, 2014, 16, 14096-14107.	1.3	58
20090	Cation Role in Structural and Electronic Properties of 3D Organicâ€“Inorganic Halide Perovskites: A DFT Analysis. Journal of Physical Chemistry C, 2014, 118, 12176-12183.	1.5	174
20091	Anisotropic thermal expansion in molecular solids: Theory and experiment on<mml:math xmlns:mml="http://www.w3.org/1998/Math/MathML"><mml:msub><mml:mi>LiBH</mml:mi><mml:mn>4</mml:mn></mml:msub></mml:math>. Physical Review B, 2014, 89, .	1.1	9
20092	Crystallographic and Magnetic Structure of the Perovskite-Type Compound BaFeO_{2.5}: Unrivaled Complexity in Oxygen Vacancy Ordering. Inorganic Chemistry, 2014, 53, 5911-5921.	1.9	44
20093	The molecular spin filter constructed from 1D organic chain. Physics Letters, Section A: General, Atomic and Solid State Physics, 2014, 378, 2020-2023.	0.9	5
20094	Ductility improvement of Mg alloys by solid solution: Ab initio modeling, synthesis and mechanical properties. Acta Materialia, 2014, 70, 92-104.	3.8	250
20095	LDA+U evaluation of the stability of low-index facets of LaCoO3 perovskite. Surface Science, 2014, 619, 71-76.	0.8	23
20096	Photoelectrochemical water oxidation of LaTaON2 under visible-light irradiation. International Journal of Hydrogen Energy, 2014, 39, 7697-7704.	3.8	53

#	Article	IF	Citations
20097	Electronic structures of long periodic stacking order structures in Mg: A first-principles study. Journal of Alloys and Compounds, 2014, 586, 656-662.	2.8	42
20098	Effect of oxygen and zinc vacancies in ferromagnetic C-doped ZnO: Density-functional calculations. Journal of Magnetism and Magnetic Materials, 2014, 354, 257-261.	1.0	15
20099	Superhard and high-strength yne-diamond semimetals. Diamond and Related Materials, 2014, 46, 15-20.	1.8	18
20100	First-principles study of hydrogen dissociation and diffusion on transition metal-doped Mg(0001) surfaces. Applied Surface Science, 2014, 305, 40-45.	3.1	31
20101	Adsorption and oxidation of sulfur dioxide on the yttria-stabilized zirconia surface: ab initio atomistic thermodynamics study. Physics Letters, Section A: General, Atomic and Solid State Physics, 2014, 378, 659-666.	0.9	5
20102	Fluorine doped (Ir,Sn,Nb)O2 anode electro-catalyst for oxygen evolution via PEM based water electrolysis. International Journal of Hydrogen Energy, 2014, 39, 664-674.	3.8	47
20103	A comparative computational study of the diffusion of Na and Li atoms in Sn(111) nanosheets. Solid State Ionics, 2014, 268, 273-276.	1.3	7
20104	Half-metallicity of C/BN hybrid nanoribbons containing a topological defective interface. Physica E: Low-Dimensional Systems and Nanostructures, 2014, 60, 224-228.	1.3	1
20105	Nitrogen-containing carbon nanostructures: A promising carrier for catalysis of ammonia borane dehydrogenation. Carbon, 2014, 68, 462-472.	5.4	27
20106	Generalized stacking fault energy, ideal strength and twinnability of dilute Mg-based alloys: A first-principles study of shear deformation. Acta Materialia, 2014, 67, 168-180.	3.8	193
20107	Atomic scale insights into ethanol oxidation on Pt, Pd and Au metallic nanofilms: A DFT with van der Waals interactions. Applied Surface Science, 2014, 288, 564-571.	3.1	39
20108	Diffusion of Cd vacancy and interstitials of Cd, Cu, Ag, Au and Mo in CdTe: A first principles investigation. Solar Energy, 2014, 101, 245-253.	2.9	21
20109	On the effect of deformation twins on stability of B19â€² structure in NiTi martensite. Computational Materials Science, 2014, 87, 107-111.	1.4	11
20110	The influence of pre-adsorbed Pt on hydrogen adsorption on B2 FeTi(111). International Journal of Hydrogen Energy, 2014, 39, 8621-8630.	3.8	6
20111	Ultra-high temperature steam corrosion of complex silicates for nuclear applications: A computational study. Journal of Nuclear Materials, 2014, 444, 56-64.	1.3	8
20112	The highly effective catalytic behavior of a metal nanocluster Ru79 on the dissociation of a N2 moleculeâ€"A quantum-chemical calculation. Catalysis Communications, 2014, 52, 5-9.	1.6	3
20113	Graphene: An impermeable or selectively permeable membrane for atomic species?. Carbon, 2014, 67, 58-63.	5.4	162
20114	Bismuth-containing c(4Ã—4) surface structure of the GaAs(100) studied by synchrotron-radiation photoelectron spectroscopy and ab initio calculations. Journal of Electron Spectroscopy and Related Phenomena, 2014, 193, 34-38.	0.8	3

#	Article	IF	Citations
20115	Influences of alloying elements and oxygen on the stability and elastic properties of Mg17Al12. Journal of Alloys and Compounds, 2014, 595, 142-147.	2.8	14
20116	Strain-dependent diffusion behavior of H within tungsten. Physica B: Condensed Matter, 2014, 443, 76-79.	1.3	10
20117	Electronic effects of isolated halogen atoms on the Ge(001) surface. Surface Science, 2014, 627, 49-56.	0.8	5
20118	First-principles thermodynamic description of hydrogen electroadsorption on the Pt(111) surface. Surface Science, 2014, 625, 104-111.	0.8	41
20119	Low formation energy and kinetic barrier of Stoneâ€“Wales defect in infinite and finite silicene. Chemical Physics Letters, 2014, 592, 52-55.	1.2	22
20120	Strengthening by the percolating intergranular eutectic in an HPDC Mgâ€“Ce alloy. Materials Science & Engineering A: Structural Materials: Properties, Microstructure and Processing, 2014, 599, 204-211.	2.6	23
20121	First principles study of oxygen reduction reaction mechanisms on N-doped graphene with a transition metal support. Electrochimica Acta, 2014, 140, 225-231.	2.6	50
20122	The photo-catalytic activities of MP (M=Ba, Ca, Cu, Sr, Ag; P=PO43â^', HPO42â^') microparticles. Applied Surface Science, 2014, 292, 570-575.	3.1	9
20123	Investigation into the formation of 13-6 helical multi-shell gold nanowires. Computational Materials Science, 2014, 82, 226-230.	1.4	1
20124	First-principles analysis on proton diffusivity in La3NbO7. Solid State Ionics, 2014, 262, 472-475.	1.3	9
20125	First-principles equation of state and phase stability of niobium pentoxide. Computational Materials Science, 2014, 81, 133-140.	1.4	59
20126	Asymmetry of radiation damage properties in Alâ€“Ti nanolayers. Journal of Nuclear Materials, 2014, 445, 261-271.	1.3	8
20127	Theoretical prediction of half-metallic materials in double perovskites Sr2Cr(Co)Bâ€²O6 (Bâ€²=Y, La, Zr, and) Tj ETQq0 0 0 rgBT /Overlo	2.8	24
20128	Influence of a parallel electric field on the dispersion relation of graphene â€“ A new route to Dirac logics. Journal of Crystal Growth, 2014, 401, 869-873.	0.7	2
20129	CO adsorption on PdCa(1 0 0), (1 1 1) and<mml:math xmlns:mml="http://www.w3.org/1998/Math/MathML" altimg="si3.gif" overflow="scroll"><mml:mrow><mml:mo stretchy="false">(</mml:mo><mml:mover) Tj ETQq0 0 0 rgBT /Overlock 10 Tf	3.1	12
20130	467 First-principles study of lattice stability of ReO3-type hypothetical TaO3. Computational Materials Science, 2014, 90, 177-181.	1.4	7
20131	Thermodynamic and kinetic properties of intrinsic defects and Mg transmutants in 3Câ€“SiC determined by density functional theory. Journal of Nuclear Materials, 2014, 448, 121-128.	1.3	11
20132	Ferromagnetism in Cu-doped polar and nonpolar GaN surfaces. Computational Materials Science, 2014, 83, 217-221.	1.4	7

#	Article	IF	Citations
20133	First-principles investigation of structural stability, mechanical properties and electronic structure of Ru1â^'xRexB2 and Re1â^'xRuxB2 borides. Computational Materials Science, 2014, 89, 19-23.	1.4	11
20134	First-principles molecular dynamics modeling of the molten fluoride salt with Cr solute. Journal of Nuclear Materials, 2014, 449, 148-157.	1.3	72
20135	Atomic and electronic structures of the (<mml:math) Tj ETQq0 0 0 rgBT /Overlock 10 Tf 50 672 Td (xmlns:mml="http://www.w3.org/199 of silicene sheet on Ag(1 1 1). Applied Surface Science, 2014, 303, 61-66.	3.1	49
20136	Magneto-elastic effects and thermodynamic properties of ferromagnetic hcp Co. Physica B: Condensed Matter, 2014, 441, 72-79.	1.3	6
20137	The competition for graphene formation on Re(0001): A complex interplay between carbon segregation, dissolution and carburisation. Carbon, 2014, 73, 389-402.	5.4	23
20138	Glass formability of W-based alloys through thermodynamic modeling: Wâ€"Feâ€"Hfâ€"Pdâ€"Ta and Wâ€"Feâ€"Siâ€"C. Intermetallics, 2014, 48, 79-85.	1.8	6
20139	First-principles study of Si atoms adsorbed on ZnO (0001) surface and the effect on electronic and optical properties. Surface Science, 2014, 625, 30-36.	0.8	21
20140	A key factor improving the thermoelectric properties of Zintl compounds A5M2Pn6 (A=Ca, Sr, Ba;) Tj ETQq1 1 0.784314 rgBT /Overlo	1.4	8
20141	First principles calculations of the stability of the T2 and D88 phases in the Vâ€"Siâ€"B system. Intermetallics, 2014, 50, 108-116.	1.8	9
20142	First-principles study of O2 adsorption on the Î±-U(001) surface. Journal of Physics and Chemistry of Solids, 2014, 75, 130-135.	1.9	14
20143	First-principles investigations on the electronic properties and stabilities of low-index surfaces of L12â€"Al3Sc intermetallic. Applied Surface Science, 2014, 288, 609-618.	3.1	45
20144	First-principles study of structural, electronic, and optical properties of the rutile TiO2(011)-2Ã—1 surface. Surface Science, 2014, 621, 88-93.	0.8	12
20145	Lithium ion conduction in tavorite-type LiMXO4F (Mâ€"X: Al P, Mg S) candidate solid electrolyte materials. Solid State Ionics, 2014, 262, 589-592.	1.3	15
20146	A DF-vdW study of the CH4 adsorption on different Ni surfaces. Surface Science, 2014, 625, 64-68.	0.8	27
20147	Orbital-free density functional theory study of crystalline Liâ€"Si alloys. Journal of Power Sources, 2014, 254, 62-72.	4.0	18
20148	Discovery of a meta-stable Alâ€"Sm phase with unknown stoichiometry using a genetic algorithm. Scripta Materialia, 2014, 81, 32-35.	2.6	13
20149	Magnetic properties and possible martensitic transformation in Mn2NiSi and Ni2MnSi Heusler alloys. Journal of Magnetism and Magnetic Materials, 2014, 362, 42-46.	1.0	16
20150	Effect of carbon vacancies on thermodynamic properties of TiCâ€"ZrC mixed carbides. Calphad: Computer Coupling of Phase Diagrams and Thermochemistry, 2014, 46, 87-91.	0.7	28

#	Article	IF	Citations
20151	Magnetism of hydrogen-irradiated silicon carbide. Physics Letters, Section A: General, Atomic and Solid State Physics, 2014, 378, 1897-1902.	0.9	3
20152	Theoretical study on the Si-doped graphene as an efficient metal-free catalyst for CO oxidation. Applied Surface Science, 2014, 308, 402-407.	3.1	115
20153	DFT+U study on the oxygen adsorption and dissociation on CeO2-supported platinum cluster. Applied Surface Science, 2014, 288, 244-250.	3.1	26
20154	Dynamics of point defect formation, clustering and pit initiation on the pyrite surface. Electrochimica Acta, 2014, 127, 416-426.	2.6	52
20155	A DFT study of methanol oxidation on Co3O4. Catalysis Communications, 2014, 45, 83-90.	1.6	30
20156	Band engineering of dichalcogenide MX2 nanosheets (M = Mo, W and X = S, Se) by out-of-plane pressure. Physics Letters, Section A: General, Atomic and Solid State Physics, 2014, 378, 745-749.	0.9	19
20157	Synthesis and photoluminescence of heavily La-doped Î±-Si3N4 nanowires via nitriding cyromilled nanocrystalline La-doped silicon powder. Journal of Luminescence, 2014, 151, 66-70.	1.5	9
20158	Cerium-doped LaSi3N5: Computed electronic structure and band gaps. Journal of the European Ceramic Society, 2014, 34, 2705-2712.	2.8	11
20159	Theoretical study on SmxSr1â^'xMnO3 as a potential solid oxide fuel cell cathode. Journal of Power Sources, 2014, 253, 138-142.	4.0	17
20160	Ab initio study on magnetism at TiO2/SrTiO3 interface. Computational Materials Science, 2014, 86, 43-48.	1.4	1
20161	Design of half-metallic ferromagnetism in germanene/silicene hybrid sheet. Solid State Communications, 2014, 191, 49-53.	0.9	18
20162	Theoretical study of mixing energetics in homovalent fluorite-structured oxide solid solutions. Journal of Nuclear Materials, 2014, 444, 292-297.	1.3	8
20163	Phase stability in the ternary Reâ€“Wâ€“Zr system. Acta Materialia, 2014, 70, 56-65.	3.8	8
20164	Surface phases of Cu2O(111) under CO2 electrochemical reduction conditions. Catalysis Communications, 2014, 52, 88-91.	1.6	49
20165	First principles investigation of the structure and electronic properties of Cu2Te. Computational Materials Science, 2014, 81, 163-169.	1.4	32
20166	Thermodynamic stability of oxide phases of Feâ€“Cr based ODS steels via quantum mechanical calculations. Calphad: Computer Coupling of Phase Diagrams and Thermochemistry, 2014, 45, 188-193.	0.7	32
20167	Magnetism in Ni-doped AlN with N vacancy: A first-principles study. Computational Materials Science, 2014, 91, 1-5.	1.4	6
20168	Influence of Cr/Zr doping on the electronic structure and hydrogen storage properties of the Mg2Ni (010) surface: A first principles study. Journal of Alloys and Compounds, 2014, 601, 280-288.	2.8	7

#	Article	IF	Citations
20169	A thermodynamic adsorption/entrapment model for selenium(IV) coprecipitation with calcite. Geochimica Et Cosmochimica Acta, 2014, 134, 16-38.	1.6	46
20170	Phase equilibrium of a CuInSe2â€“CuInS2 pseudobinary system studied by combined first-principles calculations and cluster expansion Monte Carlo simulations. Materials Science in Semiconductor Processing, 2014, 25, 251-257.	1.9	20
20171	Pressure and disorder effects on the half-metallic character and magnetic properties of the full-Heusler alloy Co2FeSi. Journal of Physics and Chemistry of Solids, 2014, 75, 391-396.	1.9	14
20172	Displacement threshold energy and recovery in an Alâ€“Ti nanolayered system with intrinsic point defect partitioning. Computational Materials Science, 2014, 85, 269-279.	1.4	3
20173	ShengBTE: A solver of the Boltzmann transport equation for phonons. Computer Physics Communications, 2014, 185, 1747-1758.	3.0	1,931
20174	Structural, half-metallic and elastic properties of the half-Heusler compounds NiMnM (MÂ=ÂSb, As and) Tj ETQq1 1 0.784314 rgBT /O	1.8	46
20175	Effects of interfacial electron transfer on the magnetic structure of SrMnO3 in LaAlO3/SrMnO3 heterostructures. Computational Materials Science, 2014, 81, 483-487.	1.4	6
20176	Synergetic effects of Mn and Si in the interaction with point defects in bcc Fe. Journal of Nuclear Materials, 2014, 455, 5-9.	1.3	16
20177	Electronic, magnetic and ferroelectric properties of multiferroic TlNiO3: A first principles study. Computational Materials Science, 2014, 82, 191-196.	1.4	1
20178	Charge separation across P3HT/carbon nanotube interface: First-principles calculations of electronic structures. Chemical Physics Letters, 2014, 597, 45-50.	1.2	3
20179	Tuning the catalytic property of non-noble metallic impurities in graphene. Carbon, 2014, 71, 139-149.	5.4	85
20180	Contribution of stacking fault in lowering the theoretical density of nickel. Computational Materials Science, 2014, 81, 249-252.	1.4	2
20181	Relating the electronic structure and reactivity of the 3d transition metal monoxide surfaces. Catalysis Communications, 2014, 52, 60-64.	1.6	19
20182	A first-principles prediction on the magnetism in CoO with Co and O Vacancies. Journal of Alloys and Compounds, 2014, 610, 422-427.	2.8	18
20183	Ab initio study on the effects of dopantâ€“defect cluster on the electronic properties of TiO2-based photocatalysts. International Journal of Hydrogen Energy, 2014, 39, 2049-2055.	3.8	17
20184	Oxygen chemisorption-induced surface phase transitions on Cu(110). Surface Science, 2014, 627, 75-84.	0.8	40
20185	When reconstruction comes around: Ni, Cu, and Au adatoms on Î´-MoC(001). Surface Science, 2014, 624, 32-36.	0.8	5
20186	Stability of 41 metalâ€“boron systems at 0GPa and 30GPa from first principles. Calphad: Computer Coupling of Phase Diagrams and Thermochemistry, 2014, 46, 184-204.	0.7	89

#	Article	IF	Citations
20187	Electronic structure and point defect concentrations of C11b MoSi2 by first-principles calculations. Journal of Alloys and Compounds, 2014, 605, 45-50.	2.8	21
20188	Room-temperature ferromagnetism properties of monoclinic VO2 (M1) nanobelts. Materials Research Bulletin, 2014, 53, 102-106.	2.7	11
20189	Quantitative computational screening of Pd-based intermetallic membranes for hydrogen separation. Journal of Membrane Science, 2014, 453, 516-524.	4.1	15
20190	Thermodynamic stability of Mg-based ternary long-period stacking ordered structures. Acta Materialia, 2014, 68, 325-338.	3.8	134
20191	Synthesis of hierarchical Sn3O4 microflowers self-assembled by nanosheets. Materials Letters, 2014, 120, 140-142.	1.3	24
20192	First-principles core structures of edge and screw dislocations in Mg. Scripta Materialia, 2014, 75, 42-45.	2.6	73
20193	STM contrast inversion of the Fe(110) surface. Applied Surface Science, 2014, 304, 65-72.	3.1	13
20194	Functional electrospun polymeric nanofibers incorporating geraniolâ€“cyclodextrin inclusion complexes: High thermal stability and enhanced durability of geraniol. Food Research International, 2014, 62, 424-431.	2.9	131
20195	Highly selective electrochemical reduction of CO2 to HCOOH on a gallium oxide cathode. Electrochemistry Communications, 2014, 43, 95-97.	2.3	46
20196	Predicted a novel high-pressure superhard boron nitride phase. Journal of Alloys and Compounds, 2014, 598, 54-56.	2.8	26
20197	Comparative study of metal atom adsorption on free-standing h-BN and h-BN/Ni (111) surfaces. Applied Surface Science, 2014, 299, 29-34.	3.1	36
20198	and <mml:math xmlns:mml="http://www.w3.org/1998/Math/MathML" altimg="si19.gif" overflow="scroll"><mml:mfenced open="(") Tj ETQq1 1 0.784314 rgBT /Overlock 10 Tf 50 287 Td (close=")"><mml:mrow><mml:mn>	0.8	8
20199	Vacancy migration energy dependence on local chemical environment in Feâ€“Cr alloys: A Density Functional Theory study. Journal of Nuclear Materials, 2014, 452, 425-433.	1.3	19
20200	O H versus C H bond scission sequence in ethanol decomposition on Pd(111). Surface Science, 2014, 619, 114-118.	0.8	22
20201	Electronic, magnetic and optical properties of Î²-Ti3O5 and Î»-Ti3O5: A density functional study. Computational Materials Science, 2014, 81, 158-162.	1.4	35
20202	Selective conversion of m-cresol to toluene over bimetallic Niâ€“Fe catalysts. Journal of Molecular Catalysis A, 2014, 388-389, 47-55.	4.8	243
20203	Alpha to omega martensitic phase transformation pathways in pure Zr. Journal of Alloys and Compounds, 2014, 586, 693-698.	2.8	24
20204	Stable sites and diffusion pathways of interstitial oxide ions in lanthanum germanate. Solid State Ionics, 2014, 262, 512-516.	1.3	17

#	Article	IF	Citations
20205	Physical and electrical characteristics of metal/Dy2O3/p-GaAs structure. Physica B: Condensed Matter, 2014, 444, 58-64.	1.3	18
20206	Local structure, magnetic and electronic properties of N-doped Î±-Cr2O3 from the first-principles. Computational Materials Science, 2014, 81, 353-357.	1.4	12
20207	Electronic and atomic structures of KFe2Se2 grain boundaries. Physica C: Superconductivity and Its Applications, 2014, 497, 110-118.	0.6	1
20208	The effect of oxygen vacancy on the half-metallic nature of double perovskite Sr2FeMoO6: A theoretical study. Solid State Communications, 2014, 177, 57-60.	0.9	22
20209	Ordered phases of ethylene adsorbed on charged fullerenes and their aggregates. Carbon, 2014, 69, 206-220.	5.4	14
20210	Ab initio study of stacking faults and deformation mechanism in C15 Laves phases Cr2X (XÂ=ÂNb, Zr, Hf). Materials Chemistry and Physics, 2014, 143, 702-706.	2.0	20
20211	Interactions of extrinsic interstitial atoms (H, He, O, C) with vacancies in beryllium from first-principles. Computational Materials Science, 2014, 90, 116-122.	1.4	3
20212	Temperature dependent LiNbO3(0001): Surface reconstruction and surface charge. Applied Surface Science, 2014, 301, 70-78.	3.1	28
20213	Insights into structural stability and Li superionic conductivity of Li10GeP2S12 from first-principles calculations. Chemical Physics Letters, 2014, 591, 16-20.	1.2	36
20214	First-principles study of oxygen and aluminum defects in Î²-Si3N4: Compensation and charge trapping. Computational Materials Science, 2014, 81, 178-183.	1.4	14
20215	A first-principles study on hydrogen behavior in helium-implanted tungsten and molybdenum. Journal of Nuclear Materials, 2014, 450, 64-68.	1.3	11
20216	First-principles study of the hydrogen adsorption and diffusion on ordered Ni3Fe(111) surface and in the bulk. Intermetallics, 2014, 44, 64-72.	1.8	5
20217	First principles thermodynamic studies for recycling spent nuclear fuels using electrorefining with a molten salt electrolyte. Energy, 2014, 68, 751-755.	4.5	14
20218	First-principles study of antisite defects effect on electronic and magnetic properties of Mn2+xCo1â^'xGa. Journal of Magnetism and Magnetic Materials, 2014, 349, 144-148.	1.0	7
20219	Ferroelectric Transitions at Ferroelectric Domain Walls Found from First Principles. Physical Review Letters, 2014, 112, 247603.	2.9	88
20220	Atomic Structure and Dynamics of Metal Dopant Pairs in Graphene. Nano Letters, 2014, 14, 3766-3772.	4.5	219
20221	Electric Field Tuning of the Rashba Effect in the Polar Perovskite Structures. Physical Review Letters, 2014, 112, .	2.9	77
20222	Equations of state for mixtures: results from density-functional (DFT) simulations compared to high accuracy validation experiments on Z. Journal of Physics: Conference Series, 2014, 500, 162004.	0.3	10

#	Article	IF	Citations
20223	First-Principles Studies of Paramagnetic Vivianite Fe₃(PO₄)₂Â·8H₂O Surfaces. Journal of Physical Chemistry C, 2014, 118, 6110-6121.	1.5	8
20224	Total energy calculations using DFT+DMFT: Computing the pressure phase diagram of the rare earth nickelates. Physical Review B, 2014, 89, .	1.1	77
20225	Giant Thermoelectric Effect in Graphene-Based Topological Insulators with Heavy Adatoms and Nanopores. Nano Letters, 2014, 14, 3779-3784.	4.5	89
20226	Geometric and Electronic Structures of Two-Dimensional SiC₃ Compound. Journal of Physical Chemistry C, 2014, 118, 4509-4515.	1.5	74
20227	Stable Single-Layer Honeycomblike Structure of Silica. Physical Review Letters, 2014, 112, 246803.	2.9	83
20228	Elastic Constants and Pressure-Induced Effects in MoS₂. Journal of Physical Chemistry C, 2014, 118, 12073-12076.	1.5	60
20229	Porous Boron Nitride with Tunable Pore Size. Journal of Physical Chemistry Letters, 2014, 5, 393-398.	2.1	81
20230	Tuning the electronic properties of half- and full-hydrogenated germanene by chlorination and hydroxylation: A first-principles study. Computational Materials Science, 2014, 92, 244-252.	1.4	23
20231	First-principles study of transition-metal atoms adsorption on MoS2 monolayer. Physica E: Low-Dimensional Systems and Nanostructures, 2014, 63, 276-282.	1.3	88
20232	Spectroscopic Distinctions between Two Types of Ce³⁺ Ions in X2-Y₂SiO₅: A Theoretical Investigation. Journal of Physical Chemistry A, 2014, 118, 4988-4994.	1.1	37
20233	<mml:math xmlns:mml="http://www.w3.org/1998/Math/MathML"><mml:msub><mml:mrow><mml:mi mathvariant="normal">LaSrVO</mml:mi></mml:mrow><mml:mn>4</mml:mn></mml:msub></mml:math>: A candidate for the spin-orbital liquid state. Physical Review B, 2014, 89, .	1.1	9
20234	Pt Skin on AuCu Intermetallic Substrate: A Strategy to Maximize Pt Utilization for Fuel Cells. Journal of the American Chemical Society, 2014, 136, 9643-9649.	6.6	220
20235	Phosphorene: An Unexplored 2D Semiconductor with a High Hole Mobility. ACS Nano, 2014, 8, 4033-4041.	7.3	5,474
20236	Phosphorene Nanoribbons, Phosphorus Nanotubes, and van der Waals Multilayers. Journal of Physical Chemistry C, 2014, 118, 14051-14059.	1.5	544
20237	Density Functional Theory Study of the Water Dissociation on Platinum Surfaces: General Trends. Journal of Physical Chemistry A, 2014, 118, 5832-5840.	1.1	106
20238	Dependence of the electronic and transport properties of<mml:math xmlns:mml="http://www.w3.org/1998/Math/MathML"><mml:msub><mml:mtext>metal-MoSe</mml:mtext><mml:mn>2</mml:mn></mml:msub></mml:math> on contact structures. Physical Review B, 2014, 89, .	1.1	48
20239	Hyperfine local probe study of alkaline-earth manganites SrMnO₃ and BaMnO₃. Journal of Physics Condensed Matter, 2014, 26, 215401.	0.7	8
20240	Magnetic properties of A^{II}â€“B^{IV}â€“C₂^V chalcopyrite semiconductors doped with 3dâ€elements. Physica Status Solidi (B): Basic Research, 2014, 251, 1007-1019.	0.7	5

#	Article	IF	Citations
20241	Role of the main adsorption modes in the interaction of the dye [COOHâ€“TPP-Zn(ii)] on a periodic TiO2 slab exposing a rutile (110) surface in a dye-sentized solar cell. RSC Advances, 2014, 4, 9639.	1.7	12
20242	Quantum Monte Carlo Benchmark of Exchange-Correlation Functionals for Bulk Water. Journal of Chemical Theory and Computation, 2014, 10, 2355-2362.	2.3	39
20243	Orbital mixture effect on the Fermi-surfaceâ€“<mml:math xmlns:mml="http://www.w3.org/1998/Math/MathML"><mml:msub><mml:mi>T</mml:mi><mml:mi>c</mml:mi></mml:msub></mml:ma in the cuprate superconductors: Bilayer vs. single layer. Physical Review B, 2014, 89, .	1.1	33
20244	Functionalization of Graphene Grown on Metal Substrate with Atomic Oxygen: Enolate vs Epoxide. Journal of the American Chemical Society, 2014, 136, 8528-8531.	6.6	20
20245	Probing the Orbital Origin of Conductance Oscillations in Atomic Chains. Nano Letters, 2014, 14, 2988-2993.	4.5	22
20246	Fast Prediction of Adsorption Properties for Platinum Nanocatalysts with Generalized Coordination Numbers. Angewandte Chemie - International Edition, 2014, 53, 8316-8319.	7.2	366
20247	A Unique Semiconductorâ€“Metalâ€“Graphene Stack Design to Harness Charge Flow for Photocatalysis. Advanced Materials, 2014, 26, 5689-5695.	11.1	134
20248	Buckled Germanene Formation on Pt(111). Advanced Materials, 2014, 26, 4820-4824.	11.1	770
20249	Vertical Heterostructures of Layered Metal Chalcogenides by van der Waals Epitaxy. Nano Letters, 2014, 14, 3047-3054.	4.5	135
20250	First-principles prediction of a promising p-type transparent conductive material CsGeCl₃. Applied Physics Express, 2014, 7, 041201.	1.1	14
20251	Single Pd Atom Embedded in CeO₂(111) for NO Reduction with CO: A First-Principles Study. Journal of Physical Chemistry C, 2014, 118, 12216-12223.	1.5	98
20252	Charge and magnetic states of rutile TiO2doped with Cr ions. Journal of Physics Condensed Matter, 2014, 26, 146003.	0.7	10
20253	Effects of Sulfur-Deficient Defect and Water on Rearrangements of Formamide on Pyrite (100) Surface. Journal of Physical Chemistry A, 2014, 118, 4079-4086.	1.1	18
20254	Mechanism of Oxygen Exchange between CO₂ and TiO₂(101) Anatase. Journal of Physical Chemistry C, 2014, 118, 1628-1639.	1.5	31
20255	Room temperature ferromagnetic ordering in 4 MeV Ar⁵⁺irradiated TiO₂. Journal Physics D: Applied Physics, 2014, 47, 025001.	1.3	27
20256	Monolithic graphene oxide sheets with controllable composition. Nature Communications, 2014, 5, 3383.	5.8	31
20257	Relative Stability of F-Covered TiO₂ Anatase (101) and (001) Surfaces from Periodic DFT Calculations and ab Initio Atomistic Thermodynamics. Journal of Physical Chemistry C, 2014, 118, 13667-13673.	1.5	29
20258	Effect of K doping on the quasifreestanding graphene formed on Au/Ni(111): Density-functional calculations. Physical Review B, 2014, 89, .	1.1	0

#	Article	IF	Citations
20260	Perspectives on point defect thermodynamics. Physica Status Solidi (B): Basic Research, 2014, 251, 97-129.	0.7	58
20261	Zinc inclusion to heterogeneous nickel catalysts reduces oligomerization during the semi-hydrogenation of acetylene. Journal of Catalysis, 2014, 316, 164-173.	3.1	82
20262	Spin Switch of the Transition-Metal-Doped Boron Nitride Sheet through H/F Chemical Decoration. Journal of Physical Chemistry C, 2014, 118, 8899-8906.	1.5	27
20263	Metallic magnetism at finite temperatures studied by relativistic disordered moment description: Theory and applications. Physical Review B, 2014, 89, .	1.1	41
20264	Magnetoelastic coupling and the formation of adaptive martensite in magnetic shape memory alloys. Physica Status Solidi (B): Basic Research, 2014, 251, 2067-2079.	0.7	26
20265	Interacting magnetic clusterâ€spin glasses and strain glasses in Niâ€“Mn based Heusler structured intermetallics. Physica Status Solidi (B): Basic Research, 2014, 251, 2135-2148.	0.7	37
20266	Surface Dipoles and Electron Transfer at the Metal Oxideâ€“Metal Interface: A 2PPE Study of Size-Selected Metal Oxide Clusters Supported on Cu(111). Journal of Physical Chemistry C, 2014, 118, 13697-13706.	1.5	30
20267	Weak topological insulators in PbTe/SnTe superlattices. Physical Review B, 2014, 89, .	1.1	46
20268	First-Principles Study of Barium and Zirconium Stability in Uranium Mononitride Nuclear Fuels. Journal of Physical Chemistry C, 2014, 118, 14579-14585.	1.5	11
20269	Electronic and optical properties of silicon based porous sheets. Physical Chemistry Chemical Physics, 2014, 16, 16832.	1.3	16
20270	In Silico Veritas. ACS Nano, 2014, 8, 6520-6525.	7.3	11
20271	Influence of Hydroxyls on Pd Atom Mobility and Clustering on Rutile TiO₂(011)-2 Ã— 1. ACS Nano, 2014, 8, 6321-6333.	7.3	49
20272	Quasiparticle band structure and tight-binding model for single- and bilayer black phosphorus. Physical Review B, 2014, 89, .	1.1	577
20273	Electrons and phonons in single layers of hexagonal indium chalcogenides fromab initiocalculations. Physical Review B, 2014, 89, .	1.1	281
20274	The dependence of SO3 dissociation on the diameter of single-wall carbon nanotubes based on first-principles calculations. Chemical Physics Letters, 2014, 608, 1-5.	1.2	4
20275	First-Principles Study of Lanthanum Strontium Manganite: Insights into Electronic Structure and Oxygen Vacancy Formation. Journal of Physical Chemistry C, 2014, 118, 13346-13356.	1.5	82
20276	Bandâ€Gap Manipulations of Monolayer Graphene by Phenyl Radical Adsorptions: A Density Functional Theory Study. ChemPhysChem, 2014, 15, 2610-2617.	1.0	0
20277	Slide Fastener Reduction of Grapheneâ€Oxide Edges by Calcium: Insight from Ab Initio Molecular Dynamics. ChemPhysChem, 2014, 15, 2707-2711.	1.0	3

#	Article	IF	Citations
20278	Giant Magnetic Anisotropy of Transition-Metal Dimers on Defected Graphene. Nano Letters, 2014, 14, 1853-1858.	4.5	128
20279	Anomalous Capacitive Behaviors of Graphene Oxide Based Solid-State Supercapacitors. Nano Letters, 2014, 14, 1938-1943.	4.5	78
20280	Molecular-Level Understanding of CeO₂ as a Catalyst for Partial Alkyne Hydrogenation. Journal of Physical Chemistry C, 2014, 118, 5352-5360.	1.5	112
20281	Predicting Î²â€² precipitate morphology and evolution in Mgâ€“RE alloys using a combination of first-principles calculations and phase-field modeling. Acta Materialia, 2014, 76, 259-271.	3.8	93
20282	Catalytic Reactions on the Open-Edge Sites of Nitrogen-Doped Carbon Nanotubes as Cathode Catalyst for Hydrogen Fuel Cells. ACS Catalysis, 2014, 4, 1267-1273.	5.5	33
20283	Theoretical investigation on RuO2 nanoclusters adsorbed on TiO2 rutile (110) and anatase (101) surfaces. Theoretical Chemistry Accounts, 2014, 133, 1.	0.5	15
20284	Determination of ground-state and low-energy structures of perovskite superlattices from first principles. Physical Review B, 2014, 89, .	1.1	9
20285	First-principles study of atomic structures and electronic properties of ultrathin Bi films on Ge(111). Surface Science, 2014, 626, 68-75.	0.8	9
20286	Adsorption of hydrogen and hydrocarbon molecules on SiC(001). Surface Science Reports, 2014, 69, 55-104.	3.8	13
20287	First principles study of helium trapping by solute elements in tungsten. Journal of Nuclear Materials, 2014, 455, 151-156.	1.3	24
20288	Enhanced Charge Transport in Amorphous Li₂O₂. Chemistry of Materials, 2014, 26, 2952-2959.	3.2	202
20289	Size, Shape, Stability, and Color of Plasmonic Silver Nanoparticles. Journal of Physical Chemistry C, 2014, 118, 9128-9136.	1.5	156
20290	Mechanistic Aspects of the Waterâ€“Gas Shift Reaction on Isolated and Clustered Au Atoms on CeO₂(110): A Density Functional Theory Study. ACS Catalysis, 2014, 4, 1885-1892.	5.5	120
20291	Coverage-Dependent CO Adsorption and Dissociation Mechanisms on Iron Surfaces from DFT Computations. ACS Catalysis, 2014, 4, 1991-2005.	5.5	95
20292	DFT-D3 Study of Some Molecular Crystals. Journal of Physical Chemistry C, 2014, 118, 7615-7621.	1.5	457
20293	Effects of carbon on the electrical and optical properties of InN, GaN, and AlN. Physical Review B, 2014, 89, .	1.1	357
20294	Effects of extrinsic and intrinsic perturbations on the electronic structure of graphene: Retaining an effective primitive cell band structure by band unfolding. Physical Review B, 2014, 89, .	1.1	424
20295	Quasiparticle spectra, absorption spectra, and excitonic properties of NaI and<mml:math xmlns:mml="http://www.w3.org/1998/Math/MathML"><mml:msub><mml:mrow><mml:mi>SrI</mml:mi></mml:mrow><mml:mn>2</mml:mn> many-body perturbation theory. Physical Review B, 2014, 89, .	1.1	32

#	Article	IF	Citations
20296	Density functional theory study of the oxygen reduction reaction mechanism in a BN co-doped graphene electrocatalyst. Journal of Materials Chemistry A, 2014, 2, 10273.	5.2	88
20297	A density functional theory study of oxygen reduction reaction on non-PGM Feâ€“Nxâ€“C electrocatalysts. Physical Chemistry Chemical Physics, 2014, 16, 13800.	1.3	170
20298	Mechanical properties of Mgâ€“RE (RE = Sc, Y, Gdâ€“Tm) solid solutions: first-principles determination. Modelling and Simulation in Materials Science and Engineering, 2014, 22, 055017.	0.8	11
20299	Generalized stacking fault energies of alloys. Journal of Physics Condensed Matter, 2014, 26, 265005.	0.7	66
20300	Fragment Hamiltonian model potential for nickel: metallic character and defects in crystalline lattices. Modelling and Simulation in Materials Science and Engineering, 2014, 22, 045013.	0.8	4
20301	Consequences of Optimal Bond Valence on Structural Rigidity and Improved Luminescence Properties in Sr_xBa_{2â€“x}SiO₄:Eu²⁺ Orthosilicate Phosphors. Chemistry of Materials, 2014, 26, 2275-2282.	3.2	323
20302	Doping Nature of Native Defects in<mml:math xmlns:mml="http://www.w3.org/1998/Math/MathML" display="inline"><mml:mrow><mml:mn>1</mml:mn><mml:mi>T</mml:mi><mml:mtext>â^’</mml:mtext><mml:msub><mml:mrow><m Physical Review Letters, 2014, 112, 197001.	7.1	
20303	A new method for development of bond-order potentials for transition bcc metals. Modelling and Simulation in Materials Science and Engineering, 2014, 22, 034002.	0.8	17
20304	Atomic and electronic structures of ZnO Divacancy in hexagonal ZnO. Journal of the Korean Physical Society, 2014, 64, 543-546.	0.3	4
20305	A comparative first-principles study of the electronic, mechanical, defect and acoustic properties of Ti₂AlC and Ti₃AlC. Journal Physics D: Applied Physics, 2014, 47, 215301.	1.3	27
20306	Theoretical study of thermoelectric properties of few-layer MoS2 and WSe2. Physical Chemistry Chemical Physics, 2014, 16, 10866.	1.3	174
20307	Interfacial Effects in Iron-Nickel Hydroxideâ€“Platinum Nanoparticles Enhance Catalytic Oxidation. Science, 2014, 344, 495-499.	6.0	591
20308	A simplified density functional theory method for investigating charged adsorbates on an ultrathin, insulating film supported by a metal substrate. Journal of Physics Condensed Matter, 2014, 26, 135003.	0.7	7
20309	Microscopic model for the strain-driven direct to indirect band-gap transition in monolayer<mml:math xmlns:mml="http://www.w3.org/1998/Math/MathML"><mml:msub><mml:mi>MoS</mml:mi><mml:mn>2</mml:mn></mml:msub></ ZnO. Physical Review B, 2014, 89, .	1.1	26
20310	Effect of spin orbit coupling and Hubbard<mml:math xmlns:mml="http://www.w3.org/1998/Math/MathML"><mml:mi>U</mml:mi></mml:math>on the electronic structure of IrO<mml:math xmlns:mml="http://www.w3.org/1998/Math/MathML"><mml:msub><mml:mrow /><mml:mn>2</mml:mn></mml:msub></mml:math>. Physical Review B, 2014, 89, .	1.1	35
20311	Electronic structure and excitations in oxygen deficient<mml:math xmlns:mml="http://www.w3.org/1998/Math/MathML"><mml:msub><mml:mrow><mml:mtext>CeO</mml:mtext></mml:mrow><mml: DFT calculations. Physical Review B, 2014, 89, .	1.1	18
20312	AB INITIO FREE ENERGY CALCULATIONS OF THE SOLUBILITY OF SILICA IN METALLIC HYDROGEN AND APPLICATION TO GIANT PLANET CORES. Astrophysical Journal, 2014, 787, 79.	1.6	59
20313	Effect of pressure on<mml:math xmlns:mml="http://www.w3.org/1998/Math/MathML"><mml:msub><mml:mtext>La</mml:mtext><mml:mn>2</mml:mn></mml:msub> xmlns:mml="http://www.w3.org/1998/Math/MathML"><mml:mi>(</mml:mi><mml:msub><mml:mtext>WO</mml:mtext><mml:mn>4 xmlns:mml="http://www.w3.org/1998/Math/MathML"><mml:msub><mml:mrow /><mml:mn>3</mml:mn></mml:msub></mml:math>with a modulated scheelite-type structure. Physical Review B, 2014, 89, .	1.1	9

#	Article	IF	Citations
20314	Crystal Structure Prediction and Its Application in Earth and Materials Sciences. Topics in Current Chemistry, 2014, 345, 223-256.	4.0	12
20315	Solute effect on the <mml:math xmlns:mml="http://www.w3.org/1998/Math/MathML" altimg="si26.gif" overflow="scroll"><mml:mrow><mml:mo stretchy="false">â€˜</mml:mo><mml:mi>a</mml:mi><mml:mo>+</mml:mo><mml:mi>c</mml:mi><mml:mo stretchy="false">â€‰</mml:mo></mml:mrow></mml:math> dislocation nucleation mechanism in magnesium. Acta Materialia, 2014, 75, 106-112.	3.8	56
20316	Optical properties of PuO2 and Î±-Pu2O3 by GGA+U+QA studies. Journal of Nuclear Materials, 2014, 452, 414-418.	1.3	19
20317	Non-collinear magnetic order and spinâ€“orbit coupling effect in 4d transition metal monatomic chains. Journal of Magnetism and Magnetic Materials, 2014, 368, 262-266.	1.0	2
20318	Expansion research on half-metallic materials in double perovskites of Sr 2 BB â€²O 6 (B = Co, Cu, and Ni;) Tj ETQq0 0 0 rgBT /Overlock	1.4	25
20319	Dimethylamine formation from N-nitrosodimethylamine adsorbed on the Ni{111} surface from first principles. Journal of Molecular Catalysis A, 2014, 392, 157-163.	4.8	6
20320	Uniaxial loading response of one dimensional long period structures of Al3Ti. Computational Materials Science, 2014, 91, 153-158.	1.4	15
20321	Beryllium decorated armchair boron nitride nanoribbon: A new planar tetracoordinate nitride containing system with enhanced conductivity. Chemical Physics Letters, 2014, 608, 277-283.	1.2	4
20322	Mechanisms of Zr surface corrosion determined via molecular dynamics simulations with charge-optimized many-body (COMB) potentials. Journal of Nuclear Materials, 2014, 452, 285-295.	1.3	29
20323	Microstructural characteristics of the microphase Y-Ti2SC in nickel-based superalloys. Journal of Alloys and Compounds, 2014, 611, 104-110.	2.8	8
20324	Designing Heusler nanoprecipitates by elastic misfit stabilization in Feâ€“Mn maraging steels. Acta Materialia, 2014, 76, 94-105.	3.8	65
20325	Synthesis of PtCu nanowires in nonaqueous solvent with enhanced activity and stability for oxygen reduction reaction. Journal of Power Sources, 2014, 267, 380-387.	4.0	56
20326	Atomistic structure and energetics of GdN clusters in Gd-doped GaN. Acta Materialia, 2014, 76, 87-93.	3.8	4
20327	In silico CrNF, a half-metallic ferromagnetic nitrideâ€“fluoride mimicking CrO2. Journal of Magnetism and Magnetic Materials, 2014, 368, 105-110.	1.0	7
20328	First principles study on the adsorption of Ptn (n=1â€“4) on Î³-Al2O3(110) surface. Applied Surface Science, 2014, 313, 424-431.	3.1	33
20329	Highly active and stable MgAl2O4-supported Rh and Ir catalysts for methane steam reforming: A combined experimental and theoretical study. Journal of Catalysis, 2014, 316, 11-23.	3.1	104
20330	Bulk properties of InN films determined by experiments and theory. Journal of Crystal Growth, 2014, 403, 124-127.	0.7	5
20331	Effect of 3d transition elements substitution for Ni in Ni2Mn1+xSn1-x on the phase stability and magnetic properties: A first principle investigation. Journal of Magnetism and Magnetic Materials, 2014, 368, 286-294.	1.0	12

#	Article	IF	Citations
20332	CO oxidation on Ag(111): The catalytic role of H2O. Surface Science, 2014, 628, 104-110.	0.8	10
20333	Theoretical investigation on carrier mobilities of armchair graphene nanoribbons with substituted edges. Chemical Physics, 2014, 439, 57-62.	0.9	3
20334	Point defects in garnet-type solid electrolyte (c-Li7La3Zr2O12) for Li-ion batteries. Solid State Ionics, 2014, 261, 100-105.	1.3	34
20335	Phase behavior and mechanical properties of Niâ€“W studied by first-principles calculations and ab initio based thermodynamics. Acta Materialia, 2014, 75, 307-315.	3.8	15
20336	Adsorption of water on UO2 (111) surface: Density functional theory calculations. Computational Materials Science, 2014, 91, 364-371.	1.4	28
20337	Adsorption of sulfamethoxazole molecule on silver colloids: A joint SERS and DFT study. Journal of Molecular Structure, 2014, 1073, 71-76.	1.8	19
20338	Spin polarization, orbital occupation and band gap opening in vanadium dioxide: The effect of screened Hartreeâ€“Fock exchange. Chemical Physics Letters, 2014, 608, 126-129.	1.2	16
20339	Stable configurations and electronic structures of hydrogenated graphyne. Computational Materials Science, 2014, 91, 274-278.	1.4	7
20340	Energy investigations on the adhesive properties of Al/TiC interfaces: First-principles study. Physica B: Condensed Matter, 2014, 449, 269-273.	1.3	30
20341	Investigating energetics of Au8 on graphene/Ru(0001) using a genetic algorithm and density functional theory. Surface Science, 2014, 628, 98-103.	0.8	2
20342	Integrated experimental and theoretical approach for corrosion and wear evaluation of laser surface nitrided, Tiâ€“6Alâ€“4V biomaterial in physiological solution. Journal of the Mechanical Behavior of Biomedical Materials, 2014, 37, 153-164.	1.5	22
20343	Possible origin of ferromagnetism in undoped monoclinic HfO 2 film. Computational Materials Science, 2014, 92, 120-126.	1.4	8
20344	First-principles calculation of self-diffusion coefficients in Ni3Al. Journal of Alloys and Compounds, 2014, 612, 361-364.	2.8	20
20345	Control of optical absorption edge of TiO2 through co-doped acceptors: The chemical trend. Physics Letters, Section A: General, Atomic and Solid State Physics, 2014, 378, 2275-2279.	0.9	3
20346	Segregation of hydrogen to defects in nickel using first-principles calculations: The case of self-interstitials and cavities. Journal of Alloys and Compounds, 2014, 614, 211-220.	2.8	46
20347	Interplay between Water and<mml:math xmlns:mml="http://www.w3.org/1998/Math/MathML" display="inline"><mml:mrow><mml:msub><mml:mrow><mml:mi>TiO</mml:mi></mml:mrow><mml:mrow><mml:mn>2</mml:mn></mml:mrow></mml:msub></mml:mrow></mml:math> (101) Surface with Subsurface Oxygen Vacancy. Physical Review Letters, 2014, 112, .	8.1	84
20348	High Thermoelectric Performance of p-Type SnTe via a Synergistic Band Engineering and Nanostructuring Approach. Journal of the American Chemical Society, 2014, 136, 7006-7017.	6.6	553
20349	Computational Evaluation of Optoelectronic Properties for Organic/Carbon Materials. Accounts of Chemical Research, 2014, 47, 3301-3309.	7.6	71

#	Article	IF	Citations
20350	Microscopic magnetic modeling for the<mml:math xmlns:mml="http://www.w3.org/1998/Math/MathML"><mml:mrow><mml:mi>S</mml:mi><mml:mspace width="0.16em" /><mml:mo>=</mml:mo><mml:mspace width="0.16em" /><mml:mfrac><mml:mn>1</mml:mn><mml:mn>2</mml:mn></mml:mfrac></mml:mrow></mml:math>alternating-chain compounds<mml:math xmlns:mml="http://www.w3.org/1998/Math/MathML"><mml:msub><mml:mi>Na</mml:mi><mml:mn>3</mml:mn></mml:msub><mml:m	1.1	30
20351	Interplay between Electronic Properties and Interatomic Spacing in Artificial Gold Chains on NiAl(110). Journal of Physical Chemistry C, 2014, 118, 29001-29006.	1.5	4
20352	Ab Initio Calculation of Proton Transport in DyPO₄. Journal of Physical Chemistry C, 2014, 118, 5073-5080.	1.5	3
20353	Polarization Dependence of Aragonite Calcium L-Edge XANES Spectrum Indicates c and bAxes Orientation. Journal of Physical Chemistry B, 2014, 118, 6758-6766.	1.2	17
20354	Design of Ferroelectric Organic Molecular Crystals with Ultrahigh Polarization. Journal of the American Chemical Society, 2014, 136, 6428-6436.	6.6	44
20355	Ab Initio Calculations of the Energy Dependence of Siâ€“Oâ€“Si Angles in Silica and Geâ€“Oâ€“Ge Angles in Germania Crystalline Systems. Chemistry of Materials, 2014, 26, 1523-1527.	3.2	20
20356	Nonmetallic substrates for growth of silicene: anab initioprediction. Journal of Physics Condensed Matter, 2014, 26, 185002.	0.7	45
20357	Anomalous Interface and Surface Strontium Segregation in (La_{1â€“y}Sr_y)₂CoO_{4Â±Î´}/La_{1â€“x}Sr<sub>x Heterostructured Thin Films. Journal of Physical Chemistry Letters, 2014, 5, 1027-1034.	7.3	73
20358	Gas Membrane Selectivity Enabled by Zeolitic Imidazolate Framework Electrostatics. Chemistry of Materials, 2014, 26, 3976-3985.	3.2	25
20359	Stability of NNO and NPO Nanotube Crystals. Journal of Physical Chemistry Letters, 2014, 5, 485-489.	2.1	6
20360	Many-body central force potentials for tungsten. Modelling and Simulation in Materials Science and Engineering, 2014, 22, 053001.	0.8	72
20361	A DFT + U study of acetylene selective hydrogenation over anatase supported PdaAgb(a + b = 4) cluster. Physical Chemistry Chemical Physics, 2014, 16, 17541.	1.3	35
20362	Theory of nonlinear phononics for coherent light control of solids. Physical Review B, 2014, 89, .	1.1	178
20363	CO- and NO-Induced Disintegration and Redispersion of Three-Way Catalysts Rhodium, Palladium, and Platinum: An ab Initio Thermodynamics Study. Journal of Physical Chemistry C, 2014, 118, 9588-9597.	1.5	56
20364	Proton Channels along Oxygen Octahedral Chains in La₃NbO₇. Journal of Physical Chemistry C, 2014, 118, 9377-9384.	1.5	12
20365	Significant Quantum Effects in Hydrogen Activation. ACS Nano, 2014, 8, 4827-4835.	7.3	44
20366	Improving SO2 gas sensing properties of graphene by introducing dopant and defect: A first-principles study. Applied Surface Science, 2014, 313, 405-410.	3.1	102
20367	Structure and stability of hydrogenated carbon atom vacancies in graphene. Carbon, 2014, 77, 165-174.	5.4	30

#	Article	IF	Citations
20368	First-Principles Investigation of Dehydrogenation on Cu-Doped MgH₂ (001) and (110) Surfaces. Journal of Physical Chemistry C, 2014, 118, 13607-13616.	1.5	23
20369	Unified mechanism for hydrogen trapping at metal vacancies. International Journal of Hydrogen Energy, 2014, 39, 11321-11327.	3.8	30
20370	Interaction of oxygen interstitials with lattice faults in Ti. Acta Materialia, 2014, 76, 82-86.	3.8	45
20371	Optimization and assessment of the Agâ€“Ca phase diagram. Journal of Alloys and Compounds, 2014, 612, 280-286.	2.8	3
20372	Ab initio studies of Th3N4, Th2N3 and Th2N2(NH). Solid State Communications, 2014, 193, 41-44.	0.9	10
20373	Graphene and graphite, low-temperature catalysts producing weakly-excited hydrogen molecules. Chemical Physics, 2014, 439, 117-120.	0.9	3
20374	The nature of oxygen states on the surfaces of CeO2 and La-doped CeO2. Chemical Physics Letters, 2014, 608, 239-243.	1.2	31
20375	Martensite modulus dilemma in monoclinic NiTi-theory and experiments. International Journal of Plasticity, 2014, 61, 17-31.	4.1	62
20376	First-principles prediction of the glass-forming ability in Zrâ€“Ni binary metallic glasses. Intermetallics, 2014, 53, 177-182.	1.8	8
20377	Ordered surface-alloys formation in the Zr/W(100) adsorption system. Journal of Alloys and Compounds, 2014, 612, 195-203.	2.8	1
20378	Effect of In and N dopants on the structural and magnetic properties of ZnO:Mn thin films. Superlattices and Microstructures, 2014, 73, 152-159.	1.4	2
20379	Grain boundaries in hybrid two-dimensional materials. Journal of the Mechanics and Physics of Solids, 2014, 70, 62-70.	2.3	11
20380	Three-dimensional three-connected tetragonal BN: Ab initio calculations. Physics Letters, Section A: General, Atomic and Solid State Physics, 2014, 378, 2303-2307.	0.9	33
20381	Ab initio molecular dynamics simulation of interstitial diffusion in Niâ€“Cr alloys and implications for radiation induced segregation. Journal of Nuclear Materials, 2014, 449, 225-233.	1.3	31
20382	Electronic, magnetic and multiferroic properties of magnetoelectric NiTiO3. Journal of Alloys and Compounds, 2014, 613, 401-406.	2.8	30
20383	Chemical and physical adsorption of a H2O molecule on a metal doped Zr (0001) surface. Journal of Nuclear Materials, 2014, 452, 493-499.	1.3	6
20384	Compositional evolution of Q-phase precipitates in an aluminum alloy. Acta Materialia, 2014, 75, 322-336.	3.8	83
20385	First-principles study of single atom adsorption on capped single-walled carbon nanotubes. International Journal of Hydrogen Energy, 2014, 39, 10161-10168.	3.8	10

#	Article	IF	Citations
20386	Combined atom probe tomography and first-principles calculations for studying atomistic interactions between tungsten and tantalum in nickel-based alloys. Acta Materialia, 2014, 74, 296-308.	3.8	38
20387	The relationship between intermolecular interactions and charge transport properties of trifluoromethylated polycyclic aromatic hydrocarbons. Organic Electronics, 2014, 15, 1896-1905.	1.4	24
20388	Molecular dynamics simulation of framework flexibility effects on noble gas diffusion in HKUST-1 and ZIF-8. Microporous and Mesoporous Materials, 2014, 194, 190-199.	2.2	75
20389	Structural properties of ultrathin Pb layers on Ru(0001) revealed by LEED, AES and DFT. Applied Surface Science, 2014, 311, 426-434.	3.1	8
20390	Density functional theory study of tin and titanium dioxides: Structural and mechanical properties in the tetragonal rutile phase. Materials Science in Semiconductor Processing, 2014, 28, 59-65.	1.9	4
20391	Clathrate formation in the systems Srâ€“Cuâ€“Ge and {Ba,Sr}â€“Cuâ€“Ge. Journal of Solid State Chemistry, 2014, 217, 169-179.	1.4	4
20392	Spin-polarized bandgap of graphene induced by alternative chemisorption with MgO (1 1 1) substrate. Carbon, 2014, 77, 208-214.	5.4	9
20393	Structure and energetics of Ni from ab initio molecular dynamics calculations. Computational Materials Science, 2014, 89, 242-246.	1.4	16
20394	Structural, magnetic and electronic properties of FenPt13â^'n clusters with n=0â€“13: A first-principle study. Journal of Magnetism and Magnetic Materials, 2014, 369, 27-33.	1.0	11
20395	Origin of piezoelectricity in monolayer halogenated graphane piezoelectrics. Chemical Physics Letters, 2014, 603, 62-66.	1.2	30
20396	Crystal structure, disorder and composition of the 2/1 approximant in the Alâ€“Mgâ€“Zn system revisited. Intermetallics, 2014, 53, 67-84.	1.8	10
20397	Oxygen-doped boron nitride nanosheets with excellent performance in hydrogen storage. Nano Energy, 2014, 6, 219-224.	8.2	210
20398	Critical evaluation and thermodynamic optimization of Mgâ€“Ga system and effect of low pressure on phase equilibria. Calphad: Computer Coupling of Phase Diagrams and Thermochemistry, 2014, 46, 168-175.	0.7	10
20399	Polarization enhancement in perovskite superlattices by oxygen octahedral tilts. Computational Materials Science, 2014, 91, 310-314.	1.4	24
20400	Excitons in Mg(OH)2 and Ca(OH)2 from ab initio calculations. Solid State Communications, 2014, 193, 11-15.	0.9	11
20401	Effect of the tetragonal distortion on the electronic structure, phonons and superconductivity in the Mo3Sb7 superconductor. Intermetallics, 2014, 53, 150-156.	1.8	8
20402	An ab initio computational study of pure Zn3N2 and its native point defects and dopants Cu, Ag and Au. Thin Solid Films, 2014, 564, 331-338.	0.8	29
20403	Hydrogen concentration estimation in metals at finite temperature using first-principles calculations and vibrational analysis. Computational Materials Science, 2014, 91, 211-222.	1.4	22

#	Article	IF	Citations
20404	Temperature dependent phase stability of nanolaminated ternaries from first-principles calculations. Computational Materials Science, 2014, 91, 251-257.	1.4	32
20405	First-principles investigation of boron defects in nickel ferrite spinel. Journal of Nuclear Materials, 2014, 452, 446-452.	1.3	14
20406	First-principles studies of oxygen chemisorption on Co(0001). Surface Science, 2014, 619, 90-97.	0.8	22
20407	First-principles study of soluteâ€“vacancy binding in Cu. Journal of Alloys and Compounds, 2014, 608, 334-337.	2.8	28
20408	Structural and electromagnetic properties of double C chains decorated zigzag silicene nanoribbon. Physica E: Low-Dimensional Systems and Nanostructures, 2014, 56, 205-210.	1.3	4
20409	Dynamical stability of NiTi under high pressure and high temperature. Journal of Alloys and Compounds, 2014, 608, 258-260.	2.8	4
20410	The U4Re7Si6 type â€“ Trends in electronic structure and chemical bonding. Solid State Sciences, 2014, 27, 5-10.	1.5	5
20411	First-principles study of helium trapping in cementite Fe3C. Journal of Nuclear Materials, 2014, 444, 368-372.	1.3	7
20412	On the importance of metalâ€“oxide interface sites for the waterâ€“gas shift reaction over Pt/CeO2 catalysts. Journal of Catalysis, 2014, 309, 314-324.	3.1	142
20413	Drastic changes of electronic structure, bonding properties and crystal symmetry in Zr2Cu by hydrogenation, from ab initio. Intermetallics, 2014, 45, 5-10.	1.8	3
20414	Density functional theory study of the adsorption of methanthiol on Au(111): Role of gold adatoms. Physica E: Low-Dimensional Systems and Nanostructures, 2014, 59, 248-253.	1.3	9
20415	The effect of defects on the magnetic properties and spin polarization of Ti2FeAl Heusler alloy. Journal of Magnetism and Magnetic Materials, 2014, 351, 25-28.	1.0	18
20416	Kinetic Monte Carlo modeling of reaction-induced phase separation in Au/Ni(111) surface alloy. Surface and Coatings Technology, 2014, 255, 15-21.	2.2	4
20417	Thermodynamic reassessment of Uâ€“Gdâ€“O system. Journal of Nuclear Materials, 2014, 452, 397-406.	1.3	24
20418	Structural Stability, Electronic and Magnetic Properties of Cu Adsorption on Defected Graphene: A First Principles Study. Journal of Superconductivity and Novel Magnetism, 2014, 27, 115-120.	0.8	10
20419	Raman and Infrared Spectroscopic Studies on Li₄RuH₆ Combined with First-Principles Calculations. Materials Transactions, 2014, 55, 1117-1121.	0.4	18
20420	New Thermoelectric Materials Possessing Pseudo-gap or Narrow-gap Near the Fermi Level. Materia Japan, 2014, 53, 260-264.	0.1	0
20421	Electronic and Local Crystal Structures of the ZrNiSn Half-Heusler Thermoelectric Material. Materials Transactions, 2014, 55, 1209-1214.	0.4	25

#	Article	IF	Citations
20422	Relations between Parameters in Different Sublattice Configurations for CALPHAD-Type Thermodynamic Assessments. Materials Transactions, 2014, 55, 1683-1688.	0.4	0
20423	Modelling ternary effects on antiphase boundary energy of Ni3Al. MATEC Web of Conferences, 2014, 14, 11005.	0.1	17
20424	Thermodynamic Analysis of Phase Equilibria in the Mn-Bi-Sb Ternary System. Nippon Kinzoku Gakkaishi/Journal of the Japan Institute of Metals, 2014, 78, 327-336.	0.2	4
20425	Alkali Ion Transport in Tavorite-Type ABTO4X (A: Li, Na; B-T: Al-P, Mg-S; X: F). Electrochemistry, 2014, 82, 851-854.	0.6	3
20426	Multi layer ceramic capacitors materials research using first-principles calculations. Journal of the Ceramic Society of Japan, 2014, 122, 367-372.	0.5	0
20427	Preparation and photocatalytic properties of new calcium and lead bismuthates. Journal of the Ceramic Society of Japan, 2014, 122, 509-512.	0.5	18
20428	Tuning of calcium silicate ceramics for environment-friendly material applications. Journal of the Ceramic Society of Japan, 2014, 122, 858-862.	0.5	4
20429	Magnetic properties and electronic structures of (YTiO3)2/(BaTiO3)n superlattices. Journal of Applied Physics, 2014, 115, 17D710.	1.1	8
20430	Computational design of model Re/Ru bearing Ni-base superalloys. MATEC Web of Conferences, 2014, 14, 17007.	0.1	3
20431	Control of defect binding and magnetic interaction energies in dilute magnetic semiconductors by charge state manipulation. Journal of Applied Physics, 2014, 115, 012008.	1.1	9
20432	Understanding the Adsorption of CuPc and ZnPc on Noble Metal Surfaces by Combining Quantum-Mechanical Modelling and Photoelectron Spectroscopy. Molecules, 2014, 19, 2969-2992.	1.7	69
20433	The adsorption of h-BN monolayer on the Ni(111) surface studied by density functional theory calculations with a semiempirical long-range dispersion correction. Journal of Applied Physics, 2014, 115, 17C117.	1.1	11
20434	The effect of the exchange-correlation functional on H2 dissociation on Ru(0001). Journal of Chemical Physics, 2014, 140, 084702.	1.2	57
20435	On the sensitivity of positron annihilation signals to alloy homogeneity in In_xGa_{1-x}N. Journal of Physics: Conference Series, 2014, 505, 012042.	0.3	4
20436	The nature of hydrogen in Î³-alumina. Journal of Applied Physics, 2014, 115, .	1.1	15
20437	First principles study of structural stability and site preference in Co₃(W,X). MATEC Web of Conferences, 2014, 14, 18001.	0.1	7
20438	Unusually large shear wave anisotropy for chlorite in subduction zone settings. Geophysical Research Letters, 2014, 41, 1506-1513.	1.5	58
20439	Interfacial Nb-substitution induced anomalous enhancement of polarization and conductivity in BaTiO3 ferroelectric tunnel junctions. AIP Advances, 2014, 4, 127148.	0.6	3

#	Article	IF	Citations
20440	Interface electronic structures of reversible double-docking self-assembled monolayers on an Au(111) surface. Philosophical Transactions Series A, Mathematical, Physical, and Engineering Sciences, 2014, 372, 20130018.	1.6	8
20441	Magnetic interactions in a quasi-one-dimensional antiferromagnet Cu(H2O)2(en)SO4. Journal of Applied Physics, 2014, 115, .	1.1	7
20442	Comparative Study of Sodium and Lithium Intercalation and Diffusion Mechanism in Black Phosphorus from First-principles Simulation. Chemistry Letters, 2014, 43, 1940-1942.	0.7	40
20443	First-principle Calculation Evaluations for MTW-type Zeolite Synthesis Prescriptions. Chemistry Letters, 2014, 43, 1026-1028.	0.7	5
20444	Lambda transitions in materials science: Recent advances in CALPHAD and firstâ€principles modelling. Physica Status Solidi (B): Basic Research, 2014, 251, 53-80.	0.7	75
20445	Ferroelectric Material Research Using First-principles Calculations â€“ Ferroelectricity in AgNbO3 â€“. Funtai Oyobi Fummatsu Yakin/Journal of the Japan Society of Powder and Powder Metallurgy, 2014, 61, 387-391.	0.1	0
20446	Effect of Hydrogen in a Vanadium Grain Boundary by First Principles. Fusion Science and Technology, 2014, 66, 106-111.	0.6	3
20447	Predictions of an alternative pathway for grain-boundary driven twinning. Applied Physics Letters, 2014, 104, .	1.5	10
20448	Nuclear quantum effects in a 1-D model of hydrogen bonded ferroelectrics. Journal of Physics: Conference Series, 2014, 571, 012012.	0.3	7
20449	Pressureâ€Induced Intersite Bï£¿M (M=Ru,â€…Ir) Valence Transitions in Hexagonal Perovskites. Angewandte Chemie - International Edition, 2014, 53, 3414-3417.	7.2	14
20450	Investigating individual arsenic dopant atoms in silicon using low-temperature scanning tunnelling microscopy. Journal of Physics Condensed Matter, 2014, 26, 012001.	0.7	28
20451	An investigation of muon sites in YBa₂Cu₃O₆by using Density Functional Theory. Journal of Physics: Conference Series, 2014, 551, 012052.	0.3	9
20452	Search for potential minimum positions in metal-organic hybrids, (C₂H₅NH₃)₂CuCl₄ and (C₆H₅CH₂CH₂NH₃)₂CuCl₄, by using density functional theory. Journal of Physics: Conference Series, 2014, 551, 012054.	0.3	10
20455	An Effect of the Supercell Calculation on Muon Positions and Local Deformations of Crystal Structure in La₂CuO₄. Journal of Physics: Conference Series, 2014, 551, 012051.	0.3	11
20456	Muon sites in Ce(Ru,Rh)₂Al₁₀ investigated by using Density Functional Theory from the view point of electronic potential. Journal of Physics: Conference Series, 2014, 551, 012053.	0.3	10
20459	First principles analysis of proton conduction behavior in electrolytes of protonic ceramic fuel cells. , 2014, , .		0
20460	Computational materials designÂ®: Realization of the switching mechanism in RRAM. , 2014, , .		0
20461	Theoretical Analysis on the Band Structure Variance of the Electron Doped 1111 Iron-based Superconductors. Physics Procedia, 2014, 58, 38-41.	1.2	0

#	Article	IF	Citations
20462	Intrinsic defects, nonstoichiometry, and aliovalent doping of ABO perovskite scintillators. Physica Status Solidi (B): Basic Research, 2014, 251, 2279-2286.	0.7	15
20463	Diffusion of cesium in silicon during SIMS experiments investigated by numerical simulations. Surface and Interface Analysis, 2014, 46, 7-10.	0.8	5
20464	Structural and Chemical Evolution of the Layered Liâ€Excess Li_xMnO₃ as a Function of Li Content from Firstâ€Principles Calculations. Advanced Energy Materials, 2014, 4, 1400498.	10.2	173
20465	Impact of <scp>M</scp>n on the solution enthalpy of hydrogen in austenitic <scp>F</scp>eâ€<scp>M</scp>n alloys: A firstâ€principles study. Journal of Computational Chemistry, 2014, 35, 2239-2244.	1.5	8
20466	Effect of Incorporating Aromatic and Chiral Groups on the Dielectric Properties of Poly(dimethyltin) Tj ETQq0 0 0 rgBT /Overlock 10 Tf 50	2.0	29
20468	Fluorine in Shark Teeth: Its Direct Atomicâ€Resolution Imaging and Strengthening Function. Angewandte Chemie - International Edition, 2014, 53, 1543-1547.	7.2	26
20469	Review on simulation of filamentary switching in binary metal oxide based RRAM devices. , 2014, , .		2
20470	Thermodynamic Stability of Oxide Phases of Fe-Cr Based ODS Steels via Quantum Mechanical Calculations. Procedia Engineering, 2014, 86, 788-798.	1.2	12
20471	Simulation of Probe Position-Dependent Electron Energy-Loss Fine Structure. Microscopy and Microanalysis, 2014, 20, 784-797.	0.2	12
20472	Influence of Static Atomic Displacements on Composition Quantification of AlGaN/GaN Heterostructures from HAADF-STEM Images. Microscopy and Microanalysis, 2014, 20, 1463-1470.	0.2	11
20473	Silver Nanoparticles for Catalysis of Hydrogen Peroxide Decomposition: Atomistic Modeling. Materials Research Society Symposia Proceedings, 2015, 1787, 21-25.	0.1	5
20474	Accurate Nanoscale Crystallography in Real-Space Using Scanning Transmission Electron Microscopy. Microscopy and Microanalysis, 2015, 21, 946-952.	0.2	35
20475	Direct evaluation of free energy for large system through structure integration approach. Journal of Physics Condensed Matter, 2015, 27, 385201.	0.7	5
20476	A study of the oxygen effect on the properties of magnetic anisotropy of Co nanowires on the Cu(210) surface: An ab initio approach. Physics of the Solid State, 2015, 57, 1366-1371.	0.2	3
20477	Examination of the impact of electronâ€“phonon coupling on fission enhanced diffusion in uranium dioxide using classical molecular dynamics. Journal of Materials Research, 2015, 30, 1485-1494.	1.2	12
20478	Irradiation-induced ordering in Pt-Cu alloy focusing on Pt7Cu. Materials Research Society Symposia Proceedings, 2015, 1760, 114.	0.1	0
20479	Effect of Al substitution on Thermoelectric Performance of CuInTe2 compounds. Materials Research Society Symposia Proceedings, 2015, 1735, 136.	0.1	4
20480	Electronic properties of monolayer molybdenum dichalcogenides under strains. Materials Research Society Symposia Proceedings, 2015, 1726, 31.	0.1	0

#	Article	IF	Citations
20481	Ab Initio Analysis of Charge Carrier Dynamics in Organic-Inorganic Lead Halide Perovskite Solar Cells. Materials Research Society Symposia Proceedings, 2015, 1776, 19-29.	0.1	4
20482	On the rotational alignment of graphene domains grown on Ge(110) andGe(111). MRS Communications, 2015, 5, 539-546.	0.8	19
20483	Thermodynamics of Pdâ€“Mn phases and extension to the Feâ€“Mnâ€“Pd system. Calphad: Computer Coupling of Phase Diagrams and Thermochemistry, 2015, 51, 314-333.	0.7	5
20484	Dynamic Stabilization of Cubic AuZn. Materials Today: Proceedings, 2015, 2, S569-S572.	0.9	0
20485	Prediction of the Xeâ€“He binary phase diagram at high pressures. Chemical Physics Letters, 2015, 640, 115-118.	1.2	11
20486	Data in support of crystal structures of highly-ordered long-period stacking-ordered phases with 18R, 14H and 10H-type stacking sequences in the Mgâ€“Znâ€“Y system. Data in Brief, 2015, 5, 314-320.	0.5	11
20487	The AFLOW standard for high-throughput materials science calculations. Computational Materials Science, 2015, 108, 233-238.	1.4	244
20488	DFT study of electron affinity of alkali metal termination on clean and oxygenated Î²-Si3N4. Diamond and Related Materials, 2015, 58, 214-220.	1.8	7
20489	Band and scattering tuning for high performance thermoelectric Sn1âˆ’xMnxTe alloys. Journal of Materiomics, 2015, 1, 307-315.	2.8	193
20490	The study of electronic structure and absorption coefficient of ZnTe:O alloys: A GGA+U method. Computational Materials Science, 2015, 109, 225-230.	1.4	5
20491	Composition and temperature dependences of site occupation for Al, Cr, W, and Nb in MoSi ₂. Chinese Physics B, 2015, 24, 120502.	0.7	8
20492	First-Principles Study of Oxygen Transfer and Hydrogen Oxidation Processes at the Ni-YSZ-Gas Triple Phase Boundaries in a Solid Oxide Fuel Cell Anode. Journal of Physical Chemistry C, 2015, 119, 27603-27608.	1.5	17
20493	A model for the direct-to-indirect band-gap transition in monolayer MoSe2 under strain. Pramana - Journal of Physics, 2015, 84, 1033-1040.	0.9	3
20494	Data set for diffusion coefficients of alloying elements in dilute Mg alloys from first-principles. Data in Brief, 2015, 5, 900-912.	0.5	18
20495	First-principles studies of lattice dynamics and thermal properties of Mg₂Si_{1âˆ’x}Sn_x. Journal of Materials Research, 2015, 30, 2578-2584.	1.2	10
20496	A high degree of enhancement of strength of sputter deposited Al/Al2O3 multilayers upon post annealing. Acta Materialia, 2015, 95, 378-385.	3.8	22
20497	Identifying defect-tolerant semiconductors with high minority-carrier lifetimes: beyond hybrid lead halide perovskites. MRS Communications, 2015, 5, 265-275.	0.8	662
20498	Photophysical electronic structure of double-perovskites A2GdTaO6 (AÂ=ÂBa and Sr). Journal of Alloys and Compounds, 2015, 648, 111-115.	2.8	6

#	Article	IF	Citations
20499	Structures and vibrational frequencies of CO adsorbed on transition metals from calculations using the vdW-DF2 functional. Computational and Theoretical Chemistry, 2015, 1069, 147-154.	1.1	16
20500	Ferromagnetic origin of Mn-doped Sr3La2O5Zn2As2: Ab initio study. JETP Letters, 2015, 101, 798-801.	0.4	0
20501	<i>Ab Initio</i> Study of MgSe Self-Interstitial (Mg<i>_i) Tj ETQq0 0 0 rgBT /Overlock 10 Tf 50 662	0.3	8
20502	Optical Properties of the Narrow-Band Ferroelectrics: First Principle Calculations. Ferroelectrics, 2015, 483, 43-52.	0.3	5
20503	Phonon-limited performance of single-layer, single-gate black phosphorus n- and p-type field-effect transistors. , 2015, , .		19
20504	Toward First-Principles Description of Carrier Relaxation in Nanoparticles. ACS Symposium Series, 2015, , 201-213.	0.5	0
20505	Pressure-induced novel compounds in the Hf-O system from first-principles calculations. Physical Review B, 2015, 92, .	1.1	44
20506	ab initio electronic transport model for photovoltaics. , 2015, , .		0
20507	Strontium vanadate: An ultra-low work function electron emission material. , 2015, , .		0
20508	Elastic properties of solids at high pressure. Physics-Uspekhi, 2015, 58, 1106-1114.	0.8	8
20509	Retention of Bond Direction in Surface Reaction: A Comparative Study of Variously Aligned p-Dihalobenzenes on Cu(110). Journal of Physical Chemistry C, 2015, 119, 26038-26045.	1.5	10
20510	Effect of Subsurface Oxygen on Selective Catalytic Reduction of NO by H₂ on Pt(100): A First-Principles Study. Journal of Physical Chemistry C, 2015, 119, 24819-24826.	1.5	14
20511	Electron dynamics of solvated titanium hydroxide. Molecular Physics, 2015, 113, 397-407.	0.8	7
20512	Alloying ZnS to create transparent conducting materials. , 2015, , .		0
20513	Anionâ€“Anion Bonding and Topology in Ternary Iridium Selenoâ€“Stannides. Inorganic Chemistry, 2015, 54, 11993-12001.	1.9	5
20514	Band Gap Dependence on Cation Disorder in ZnSnN₂ Solar Absorber. Advanced Energy Materials, 2015, 5, 1501462.	10.2	96
20515	Theory of Hydrogen Migration in Organicâ€“Inorganic Halide Perovskites. Angewandte Chemie, 2015, 127, 12614-12618.	1.6	8
20516	Red-light emission induced by Mn-doped magnesium fluorogermanate. Journal Physics D: Applied Physics, 2015, 48, 475101.	1.3	1

#	Article	IF	Citations
20517	Simulation Evidence of Hexagonalâ€toâ€Tetragonal ZnSe Structure Transition: A Monolayer Material with a Wideâ€Range Tunable Direct Bandgap. Advanced Science, 2015, 2, 1500290.	5.6	44
20518	Electronic Structures, Bonding Configurations, and Bandâ€Gapâ€Opening Properties of Graphene Binding with Lowâ€Concentration Fluorine. ChemistryOpen, 2015, 4, 642-650.	0.9	22
20519	Firstâ€principles theory of acceptors in nitride semiconductors. Physica Status Solidi (B): Basic Research, 2015, 252, 900-908.	0.7	115
20520	Cu adatom charging on Mo supported ScN, MgO and NaF. RSC Advances, 2015, 5, 94436-94445.	1.7	3
20521	Hybrid functional study on the ferroelectricity of domain walls with O-vacancies in PbTiO₃. Mechanical Engineering Journal, 2015, 2, 15-00037-15-00037.	0.2	3
20522	Preparation and phase transformation of Ag or Bi ion-exchanged layered niobate perovskite and their photocatalytic properties. Journal of the Ceramic Society of Japan, 2015, 123, 690-694.	0.5	7
20523	A First Principles study on Boron-doped Graphene decorated by Ni-Ti-Mg atoms for Enhanced Hydrogen Storage Performance. Scientific Reports, 2015, 5, 16797.	1.6	49
20524	Stable magnesium peroxide at high pressure. Scientific Reports, 2015, 5, 13582.	1.6	30
20525	Atomic-configuration modeling of ion-conducting crystalline oxide by diffraction technique and theoretical calculation. Journal of the Ceramic Society of Japan, 2015, 123, 637-642.	0.5	9
20526	Phase Diagram and High-Temperature Superconductivity of Compressed Selenium Hydrides. Scientific Reports, 2015, 5, 15433.	1.6	71
20527	Structure Prediction at High Pressures. , 2015, , 105-130.		1
20528	Calix[4]arene-p-sulfonic acid hydrates [CH2(OH)C6H2SO3H]4â€¢nH2O (n = 6, 8, 9, 10, 12): a quantum chemical study. Russian Chemical Bulletin, 2015, 64, 2632-2641.	0.4	1
20530	<mml:math xmlns:mml="http://www.w3.org/1998/Math/MathML" display="inline"><mml:mrow><mml:mi>DFT</mml:mi><mml:mo>+</mml:mo><mml:mi>U</mml:mi></mml:mrow></mml:math>Simulat of the<mml:math xmlns:mml="http://www.w3.org/1998/Math/MathML" display="inline"><mml:mrow><mml:msub><mml:mrow><mml:mi>Ti</mml:mi></mml:mrow><mml:mrow><mml:mn>4</mml:mn></mml:mrow></mml:msub><mml:mrow><mml:mi mathvariant="normal">O</mml:mi></mml:mrow><mml:mrow><mml:mn>7</mml:mn></mml:mrow></mml:msub><mml:mtext>â^'</mml:mtext><mml:mn	1.5	15
20531	Physical Review Applied, 2015, 3, . Defect Physics, Delithiation Mechanism, and Electronic and Ionic Conduction in Layered Lithium Manganese Oxide Cathode Materials. Physical Review Applied, 2015, 3, .	1.5	56
20532	Entropy-Driven Clustering in Tetrahedrally Bonded Multinary Materials. Physical Review Applied, 2015, 3, .	1.5	61
20533	Electronic Structure of Oxygen Interstitial Defects in Amorphous In-Ga-Zn-O Semiconductors and Implications for Device Behavior. Physical Review Applied, 2015, 3, .	1.5	58
20534	Discrete Electronic Bands in Semiconductors and Insulators: Potential High-Light-Yield Scintillators. Physical Review Applied, 2015, 3, .	1.5	51
20535	Formation of a Positive Fixed Charge at<mml:math xmlns:mml="http://www.w3.org/1998/Math/MathML" display="inline"><mml:mrow><mml:mi>c</mml:mi><mml:mtext>â^'</mml:mtext><mml:mi>Si</mml:mi><mml:mo stretchy="false">(</mml:mo><mml:mn>111</mml:mn><mml:mo) Tj ETQq1 1 0.784314 rgBT /Overlock 10 Tf 50 57 Td (stretchy="false" mathvariant="normal">N</mml:mi></mml:mrow><mml:mo. Physical Review Applied, 2015, 3, .	1.5	

#	Article	IF	Citations
20536	Molecular Oxygen as Charge-Compensating and Magnetic Centers in Anatase<mml:math xmlns:mml="http://www.w3.org/1998/Math/MathML" display="inline"><mml:mrow><mml:mi>Ti</mml:mi><mml:msub><mml:mrow><mml:mi mathvariant="normal">O</mml:mi></mml:mrow><mml:mrow><mml:mn>2</mml:mn></mml:mrow></mml:msub></mml:mrow></mml: Physical Review Applied, 2015, 3, .	1.5	7
20537	Anisotropic Nature of Anatase <mml:math xmlns:mml="http://www.w3.org/1998/Math/MathML" display="inline"><mml:mrow><mml:msub><mml:mrow><mml:mi>TiO</mml:mi></mml:mrow><mml:mrow><mml:mn>2</mml:mn></mml:mrow></mml:msub></mml:mrow></mml:math> and Its Intrinsic (001) Surface Electronic States. Physical Review Applied, 2015, 4, .	1.5	14
20538	Electronic Structure and Optical Properties of<mml:math xmlns:mml="http://www.w3.org/1998/Math/MathML" display="inline"><mml:mrow><mml:msub><mml:mrow><mml:mi>Cu</mml:mi></mml:mrow><mml:mrow><mml:mn>2</mml:mn></mml:mrow></mml:msub></mml:mrow></mml:math> First-Principles Calculations and Vacuum-Ultraviolet Spectroscopic Ellipsometric Studies. Physical Review Applied, 2015, 4, .	1.5	19
20539	Vacancy Ordering in <mml:math xmlns:mml="http://www.w3.org/1998/Math/MathML" display="inline"><mml:mi>O</mml:mi><mml:mn>3</mml:mn></mml:math> -Type Layered Metal Oxide Behavior of <mml:math xmlns:mml="http://www.w3.org/1998/Math/MathML" display="inline"><mml:mi mathvariant="normal">Ïƒ</mml:mi><mml:mn>3</mml:mn></mml:math>Grain Boundaries in	1.5	82
20540	<mml:math xmlns:mml="http://www.w3.org/1998/Math/MathML" display="inline"><mml:mrow><mml:msub><mml:mrow><mml:mi>CuInSe</mml:mi></mml:mrow><mml:mrow><mml:mn>2</mml:mn></mml:mrow></mml:msub></mml:mrow></mml:math>	1.5	7
20541	<mml:math xmlns:mml="http://www.w3.org/1998/Math/MathML" display="inline"><mml:msub><mml:mi>CuGaSe</mml:mi><mml:mn>2</mml:mn></mml:msub></mml:math>. Physical Review Applie Construction of a thermodynamic potential for the water ices VII and X. Physical Review B, 2015, 91, .	1.1	36
20542	Charge oscillations and interaction between potassium adatoms on graphene studied by first-principles calculations. Physical Review B, 2015, 91, .	1.1	9
20543	Finding the right substrate support for magnetic superatom assembly from density functional calculations. Physical Review B, 2015, 91, .	1.1	4
20544	Highly unconventional surface reconstruction of<mml:math xmlns:mml="http://www.w3.org/1998/Math/MathML"><mml:mrow><mml:msub><mml:mi>Na</mml:mi><mml:mn>2</mml:mn></mml:msub></mml:mrow></mml: persistent energy gap. Physical Review B, 2015, 91, .	1.1	12
20545	<mml:math xmlns:mml="http://www.w3.org/1998/Math/MathML"><mml:mi		

#	Article	IF	Citations
20554	Volume-dependent electron localization in ceria. Physical Review B, 2015, 91, .	1.1	16
20555	Weak electronic correlations and absence of heavy-fermion state in<mml:math xmlns:mml="http://www.w3.org/1998/Math/MathML"><mml:mi mathvariant="normal">KNi</mml:mi><mml:msub><mml:mrow /><mml:mn>2</mml:mn></mml:msub><mml:mi mathvariant="normal">Se</mml:mi><mml:msub><mml:mrow /><mml:mn>2</mml:mn></mml:msub></mml:math>. Physical Review B, 2015, 91, .	1.1	6
20556	Fully self-consistent solution of the Dyson equation using a plane-wave basis set. Physical Review B, 2015, 91, .	1.1	13
20557	Interaction-induced quantum anomalous Hall phase in (111) bilayer of<mml:math xmlns:mml="http://www.w3.org/1998/Math/MathML"><mml:msub><mml:mi>LaCoO</mml:mi><mml:mn>3</mml:mn></mml:msub></mml:math>/<mml:math xmlns:mml="http://www.w3.org/1998/Math/MathML"><mml:msub><mml:mi>LaCoO</mml:mi><mml:mn>3</mml:mn></mml:msub></mml:math>. Physical Review B, 2015, 91, .	1.1	47
20558	Large electropositive cations as surfactants for the growth of polar epitaxial films. Physical Review B, 2015, 91, .	1.1	1
20559	Noncentrosymmetric structural transitions in ultrashort ferroelectricAGaO3/Aâ€²GaO3superlattices. Physical Review B, 2015, 91, .	1.1	6
20560	<mml:math xmlns:mml="http://www.w3.org/1998/Math/MathML"><mml:mi>A</mml:mi></mml:math>-site-driven ferroelectricity in strained ferromagnetic<mml:math xmlns:mml="http://www.w3.org/1998/Math/MathML"><mml:msub><mml:mi mathvariant="normal">La</mml:mi><mml:mn>2</mml:mn></mml:msub><mml:msub><mml:mi mathvariant="normal">NiMnO</mml:mi><mml:mn>6</mml:mn></mml:msub></mml:math>thin films. Phy	1.1	42
20561	Ethane-xenon mixtures under shock conditions. Physical Review B, 2015, 91, .	1.1	11
20562	First-principles study of a sodium borosilicate glass-former. I. The liquid state. Physical Review B, 2015, 91, .	1.1	27
20563	Time-reversal-invariant topological superconductivity inn-doped BiH. Physical Review B, 2015, 91, .	1.1	18
20564	Synchrotron-radiation-based MÃ¶ssbauer spectroscopy of<mml:math xmlns:mml="http://www.w3.org/1998/Math/MathML"><mml:mrow><mml:mmultiscripts><mml:mi mathvariant="normal">K</mml:mi><mml:mprescripts /><mml:none /><mml:mrow><mml:mn>40</mml:mn></mml:mrow></mml:mmultiscripts></mml:mrow></mml:math>in antiferromagnetic potassium nanoclusters in sodalite. Physical Review B, 2015, 91, .	1.1	11
20565	Density functional theory calculations of the turbostratically disordered compound[(SnSe)1+y]m(VSe2)n. Physical Review B, 2015, 91, .	1.1	7
20566	Phonon anharmonicity of monoclinic zirconia and yttrium-stabilized zirconia. Physical Review B, 2015, 91, .	1.1	13
20567	Ultralow lattice thermal conductivity of the fully filled skutterudite<mml:math xmlns:mml="http://www.w3.org/1998/Math/MathML"><mml:mrow><mml:msub><mml:mtext>YbFe</mml:mtext><mml:mn>4</mml:mn></mml:msub></mml:math>Sb<mml:math xmlns:mml="http://www.w3.org/1998/Math/MathML"><mml:msub><mml:mn>12</mml:mn></mml:msub></mml:math>due to the flat avoided-crossing filler modes. Physical Review B, 2015, 91, .	1.1	46
20568	Raman study of magnetic excitations and magnetoelastic coupling in<mml:math xmlns:mml="http://www.w3.org/1998/Math/MathML"><mml:mrow><mml:mi>Î±</mml:mi><mml:msub><mml:mtext>-SrCr</mml:mtext><mml:mn>8</mml:mn></mml:msub></mml:mrow></mml:math>O<mml:math xmlns:mml="http://www.w3.org/1998/Math/MathML"><mml:msub><mml:mn>19</mml:mn></mml:msub></mml:math>. Physical Review B, 2015, 91, .	1.1	9
20569	Chromium point defects in hexagonal<mml:math xmlns:mml="http://www.w3.org/1998/Math/MathML"><mml:msub><mml:mi>BaTiO</mml:mi><mml:mn>3</mml:mn></mml:msub></mml:math>: A comparative study of first-principles calculations and experiments. Physical Review B, 2015, 91, .	1.1	17
20570	Hole-induced insulator-to-metal transition in<mml:math xmlns:mml="http://www.w3.org/1998/Math/MathML"><mml:mrow><mml:mi mathvariant="normal">L</mml:mi><mml:msub><mml:mi mathvariant="normal">a</mml:mi><mml:mrow><mml:mn>1</mml:mn><mml:mo>â^’</mml:mo><mml:mi>x</mml:mi></mml:mrow></mml:msub><mml:mi mathvariant="normal">S</mml:mi><mml:msub><mml:mi mathvariant="normal">r</mml:mi><mml:mi>x</mml:mi></mml:msub><mml:msub><mml:mi mathvariant="normal">Cr</mml:mi><mml:msub><mml:mi mathvariant="normal">O	1.1	74
20571	Atomically thin dilute magnetism in Co-doped phosphorene. Physical Review B, 2015, 91, .	1.1	130

#	Article	IF	Citations
20572	Two distinct topological phases in the mixed-valence compound<mml:math xmlns:mml="http://www.w3.org/1998/Math/MathML"><mml:msub><mml:mtext>YbB</mml:mtext><mml:mn>6</mml:mn></mml:msub> its differences from<mml:math xmlns:mml="http://www.w3.org/1998/Math/MathML"><mml:msub><mml:mtext>SmB</mml:mtext><mml:mn>6</mml:mn></mml:msub> Physical Review B, 2015, 91, .	1.1	19
20573	<mml:math xmlns:mml="http://www.w3.org/1998/Math/MathML"><mml:msub><mml:mi mathvariant="normal">C</mml:mi><mml:mn>60</mml:mn></mml:msub></mml:math>superstructure and carbide formation on the Al-terminated<mml:math xmlns:mml="http://www.w3.org/1998/Math/MathML"><mml:mrow><mml:msub><mml:mi>Al</mml:mi><mml:mn>9</mml:mn></mml:msub>	1.1	7
20574	Stoichiometry engineering of ternary oxide ultrathin films:<mml:math xmlns:mml="http://www.w3.org/1998/Math/MathML"><mml:msub><mml:mi mathvariant="normal">Ba</mml:mi><mml:mi>x</mml:mi></mml:msub><mml:msub><mml:mi mathvariant="normal">Ti</mml:mi><mml:mn>2</mml:mn></mml:msub><mml:msub><mml:mi mathvariant="normal">O</mml:mi><mml:mn>3</mml:mn></mml:msub></mml:math>on Au(111). Physical Review B, 2015, 91, .	1.1	27
20575	Thermodynamic stability of transition metals on the Mg-terminated<mml:math xmlns:mml="http://www.w3.org/1998/Math/MathML"><mml:msub><mml:mi>MgB</mml:mi><mml:mn>2</mml:mn></mml:msub> surface and their effects on hydrogen dissociation and diffusion. Physical Review B, 2015, 91, .	1.1	8
20576	Controlling the Schottky barrier at<mml:math xmlns:mml="http://www.w3.org/1998/Math/MathML"><mml:msub><mml:mrow><mml:mi mathvariant="normal">MoS</mml:mi></mml:mrow><mml:mn>2</mml:mn></mml:msub></mml:math>/metal contacts by inserting a BN monolayer. Physical Review B, 2015, 91, .	1.1	172
20577	Electronic structure of<mml:math xmlns:mml="http://www.w3.org/1998/Math/MathML"><mml:mrow><mml:msub><mml:mi>Ce</mml:mi><mml:mn>2</mml:mn></mml:msub> A two-dimensional heavy-fermion system studied by angle-resolved photoemission spectroscopy. Physical Review B, 2015, 91, .	1.1	9
20578	Biquadratic and ring exchange interactions in orthorhombic perovskite manganites. Physical Review B, 2015, 91, .	1.1	55
20579	Phonon softenings and the charge density wave instability in<mml:math xmlns:mml="http://www.w3.org/1998/Math/MathML"><mml:mrow><mml:msub><mml:mi>R</mml:mi><mml:mn>2</mml:mn></mml:msub>		

#	Article	IF	Citations
20590	Spectroscopic evidence in the visible-ultraviolet energy range of surface functionalization sites in the multilayer<mml:math xmlns:mml="http://www.w3.org/1998/Math/MathML"><mml:mrow><mml:msub><mml:mi>Ti</mml:mi><mml:mn>3</mml:mn></mml:msub><mml:msub><mml:mi mathvariant="normal">C</mml:mi><mml:mn>2</mml:mn></mml:msub></mml:mrow></mml:math>MXene. Physical Review B, 2015, 91, .	1.1	75
20591	Phase transition, and high-pressure semiconductor-metal transition in Si and<mml:math xmlns:mml="http://www.w3.org/1998/Math/MathML"><mml:msub><mml:mi mathvariant="normal">Si</mml:mi><mml:mrow><mml:mn>0.991</mml:mn></mml:mrow></mml:msub><mml:msub><mml:mi mathvariant="normal">Ge</mml:mi><mml:mrow><mml:mn>0.009</mml:mn></mml:mrow></mml:msub></mml:math>. Physical Review B, 2015, 91, .	1.1	28
20592	Atomic and electronic structure of bismuth-bilayer-terminated<mml:math xmlns:mml="http://www.w3.org/1998/Math/MathML"><mml:mrow><mml:msub><mml:mtext>Bi</mml:mtext><mml:mn>2</mml:mn></mml:msub></mml:mrow></mml:math> prepared by atomic hydrogen etching. Physical Review B, 2015, 91, .	1.1	25
20593	Structure classification and melting temperature prediction in octet AB solids via machine learning. Physical Review B, 2015, 91, .	1.1	65
20594	Anharmonicity and phase stability of antiperovskite<mml:math xmlns:mml="http://www.w3.org/1998/Math/MathML"><mml:msub><mml:mrow><mml:mi mathvariant="normal">Li</mml:mi></mml:mrow><mml:mn>3</mml:mn></mml:msub><mml:mi mathvariant="normal">OCl</mml:mi></mml:math>. Physical Review B, 2015, 91, .	1.1	47
20595	Improved method of calculatingab initiohigh-temperature thermodynamic properties with application to ZrC. Physical Review B, 2015, 91, .	1.1	86
20596	Achieving large magnetocaloric effects in Co- and Cr-substituted Heusler alloys: Predictions from first-principles and Monte Carlo studies. Physical Review B, 2015, 91, .	1.1	36
20597	Effect of disorder on the dilute equilibrium vacancy concentrations of multicomponent crystalline solids. Physical Review B, 2015, 91, .	1.1	17
20598	Influence of interstitial Mn on magnetism in the room-temperature ferromagnet<mml:math xmlns:mml="http://www.w3.org/1998/Math/MathML"><mml:mrow><mml:msub><mml:mi>Mn</mml:mi><mml:mrow><mml:mn>1</mml:mn></mml:mrow></mml:msub></mml:mrow></mml:math>. Physical Review B, 2015, 91, .	1.1	19
20599	Bulk electronic structure of Zn-Mg-Y and Zn-Mg-Dy icosahedral quasicrystals. Physical Review B, 2015, 91, .	1.1	13
20600	Ab initioelectronic transport model with explicit solution to the linearized Boltzmann transport equation. Physical Review B, 2015, 91, .	1.1	57
20601	Electronic structure, spin-orbit coupling, and interlayer interaction in bulk<mml:math xmlns:mml="http://www.w3.org/1998/Math/MathML"><mml:msub><mml:mrow><mml:mi mathvariant="normal">MoS</mml:mi></mml:mrow><mml:mn>2</mml:mn></mml:msub></mml:math>and<mml:math xmlns:mml="http://www.w3.org/1998/Math/MathML"><mml:msub><mml:mrow><mml:mi mathvariant="normal">WS</mml:mi></mml:mrow><mml:mn>2</mml:mn></mml:msub></mml:math>. Physical Review B, 2015, 91, .	1.1	116
20602	Two-dimensional inversion-asymmetric topological insulators in functionalized III-Bi bilayers. Physical Review B, 2015, 91, .	1.1	60
20603	Initial growth of Ba on<mml:math xmlns:mml="http://www.w3.org/1998/Math/MathML"><mml:mrow><mml:mi>Ge</mml:mi><mml:mo>(</mml:mo><mml:mn>001</mml:mn></mml:mrow></mml:math>: An STM and DFT study. Physical Review B, 2015, 91, .	1.1	7
20604	Magnetic ground state of semiconducting transition-metal trichalcogenide monolayers. Physical Review B, 2015, 91, .	1.1	352
20605	Single-layer crystalline phases of antimony: Antimonenes. Physical Review B, 2015, 91, .	1.1	261
20606	Kitaev magnetism in honeycomb<mml:math xmlns:mml="http://www.w3.org/1998/Math/MathML"><mml:msub><mml:mtext>RuCl</mml:mtext><mml:mn>3</mml:mn></mml:msub></mml:math> intermediate spin-orbit coupling. Physical Review B, 2015, 91, .	1.1	252
20607	Density functional plus dynamical mean-field theory of the spin-crossover molecule<mml:math xmlns:mml="http://www.w3.org/1998/Math/MathML"><mml:msub><mml:mrow><mml:mtext>Fe(phen)</mml:mtext></mml:mrow></mml:msub></mml:math>. Physical Review B, 2015, 91, .	1.1	40

#	Article	IF	Citations
20608	Surface versus bulk Dirac state tuning in a three-dimensional topological Dirac semimetal. Physical Review B, 2015, 91, .	1.1	16
20609	Electronic and geometric structure of graphene/SiC(0001) decoupled by lithium intercalation. Physical Review B, 2015, 91, .	1.1	56
20610	Portlandite crystal: Bulk, bilayer, and monolayer structures. Physical Review B, 2015, 91, .	1.1	34
20611	Transition metal solute interactions with point defects in fcc iron from first principles. Physical Review B, 2015, 92, .	1.1	28
20612	Jahn-Teller distortions as a novel source of multiferroicity. Physical Review B, 2015, 92, .	1.1	25
20613	Configurational order-disorder induced metal-nonmetal transition in<mml:math xmlns:mml="http://www.w3.org/1998/Math/MathML"><mml:mrow><mml:msub><mml:mtext>B</mml:mtext><mml:mn>13</mml:mn></mml:msub></mml:mrow></mml:math>with first-principles superatom-special quasirandom structure method. Physical Review B, 2015, 92, .	1.1	22
20614	Anisotropic lattice dynamics and intermediate-phase magnetism in delafossite<mml:math xmlns:mml="http://www.w3.org/1998/Math/MathML"><mml:msub><mml:mi>CuFeO</mml:mi><mml:mn>2</mml:mn></mml:msub></mml:math>. Physical Review B, 2015, 92, .	1.1	16
20615	Structure and dynamics of the fullerene polymer<mml:math xmlns:mml="http://www.w3.org/1998/Math/MathML"><mml:mrow><mml:msub><mml:mi>Li</mml:mi><mml:mn>4</mml:mn></mml:msub><mml:mi mathvariant="normal">C</mml:mi><mml:mn>60</mml:mn></mml:mrow></mml:math>studied by ab initio molecular dynamics. Physical Review B, 2015, 92, .	1.1	9
20616	Superexchange interaction in the <mml:math xmlns:mml="http://www.w3.org/1998/Math/MathML"><mml:mi>A</mml:mi></mml:math> -site ordered perovskite <mml:math xmlns:mml="http://www.w3.org/1998/Math/MathML"><mml:mrow><mml:msub><mml:mi>YMn</mml:mi><mml:mn>3</mml:mn></mml:msub><mml:mi mathvariant="normal">O</mml:mi><mml:mn>12</mml:mn></mml:mrow></mml:math>. Physical Review B, 2015, 92, .	1.1	12
20617	Intrinsic low thermal conductivity in weakly ionic rocksalt structures. Physical Review B, 2015, 92, .	1.1	9
20618	Superconductivity and spin fluctuations in the actinoidâ€“platinum metal borides{Th,U}Pt3B. Physical Review B, 2015, 92, .	1.1	2
20619	Origin of tunnel electroresistance effect in<mml:math xmlns:mml="http://www.w3.org/1998/Math/MathML"><mml:mrow><mml:mi>PbTi</mml:mi><mml:msub><mml:mi mathvariant="normal">O</mml:mi><mml:mn>3</mml:mn></mml:msub></mml:mrow></mml:math>-based multiferroic tunnel junctions. Physical Review B, 2015, 92, .	1.1	29
20620	Doping<mml:math xmlns:mml="http://www.w3.org/1998/Math/MathML"><mml:msub><mml:mtext>SrTiO</mml:mtext><mml:mn>3</mml:mn></mml:msub></mml:math>FeSe by excess atoms and oxygen vacancies. Physical Review B, 2015, 92, .	1.1	23
20621	Towards improved exact exchange functionals relying onGWquasiparticle methods for parametrization. Physical Review B, 2015, 92, .	1.1	7
20622	Three-center tight-binding potential model for C and Si. Physical Review B, 2015, 92, .	1.1	17
20623	First-principles studies on molecular beam epitaxy growth of <mml:math xmlns:mml="http://www.w3.org/1998/Math/MathML"><mml:mrow><mml:mi>GaA</mml:mi><mml:msub><mml:mi mathvariant="normal">s</mml:mi><mml:mrow><mml:mn>1</mml:mn><mml:mo>â”</mml:mo><mml:mi>x</mml:mi></mml:mrow></mml:msub><mml:msub><mml:mi mathvariant="normal">B</mml:mi><mml:msub><mml:mi mathvariant="normal">i</mml:mi><mml:mi>x</mml:mi></mml:msub></mml:msub></mml:mrow></mml:math>.	1.1	11
20624	Ab initiosimulation of single- and few-layer<mml:math xmlns:mml="http://www.w3.org/1998/Math/MathML"><mml:msub><mml:mi mathvariant="normal">MoS</mml:mi><mml:mn>2</mml:mn></mml:msub></mml:math>transistors: Effect of electron-phonon scattering. Physical Review B, 2015, 92, .	1.1	85
20625	Controlling the electronic structure of graphene using surface-adsorbate interactions. Physical Review B, 2015, 92, .	1.1	8

#	Article	IF	Citations
20626	Oxygen deficiency in<mml:math xmlns:mml="http://www.w3.org/1998/Math/MathML"><mml:mrow><mml:mi>Ti</mml:mi><mml:msub><mml:mi mathvariant="normal">O</mml:mi><mml:mn>2</mml:mn></mml:msub></mml:mrow></mml:math>: Similarities and differences between the Ti self-interstitial and the O vacancy in bulk rutile and anatase. Physical Review B, 2015, 92, .	1.1	57
20627	Defects as qubits in<mml:math xmlns:mml="http://www.w3.org/1998/Math/MathML"><mml:mn>3</mml:mn><mml:mi>C</mml:mi><mml:mtext>â€'</mml:mtext><mml:mn>4</mml:mn><mml:mi>H</mml:mi><mml:mtext>â€'</mml:mtext> Physical Review B, 2015, 92, .	1.1	88
20628	Beyond the Tamm-Dancoff approximation for extended systems using exact diagonalization. Physical Review B, 2015, 92, .	1.1	101
20629	Pressure-induced structural phase transition in CeNi: X-ray and neutron scattering studies and first-principles calculations. Physical Review B, 2015, 92, .	1.1	3
20630	Effect of epitaxial strain on cation and anion vacancy formation in MnO. Physical Review B, 2015, 92, .	1.1	26
20631	Stability analysis of the martensitic phase transformation in<mml:math xmlns:mml="http://www.w3.org/1998/Math/MathML"><mml:mrow><mml:msub><mml:mi>Co</mml:mi><mml:mn>2</mml:mn> alloy. Physical Review B, 2015, 92, .	1.1	11
20632	Raman vibrational spectra of bulk to monolayer<mml:math xmlns:mml="http://www.w3.org/1998/Math/MathML"><mml:mrow><mml:mi>Re</mml:mi><mml:msub><mml:mi mathvariant="normal">S</mml:mi><mml:mn>2</mml:mn></mml:msub></mml:mrow></mml:math>with lower symmetry. Physical Review B, 2015, 92, .	1.1	140
20633	Ferroelectricity ind0double perovskite fluoroscandates. Physical Review B, 2015, 92, .	1.1	1
20634	First-principles interatomic potentials for ten elemental metals via compressed sensing. Physical Review B, 2015, 92, .	1.1	71
20635	Effect of magnetism and atomic order on static atomic displacements in the Invar alloy Fe-27 at.% Pt. Physical Review B, 2015, 92, .	1.1	3
20636	Self-consistent phonon calculations of lattice dynamical properties in cubic<mml:math xmlns:mml="http://www.w3.org/1998/Math/MathML"><mml:msub><mml:mi>SrTiO</mml:mi><mml:mn>3</mml:mn> first-principles anharmonic force constants. Physical Review B, 2015, 92, .	1.1	324
20637	Anisotropic magnetic couplings and structure-driven canted to collinear transitions in<mml:math xmlns:mml="http://www.w3.org/1998/Math/MathML"><mml:mrow><mml:msub><mml:mi>Sr</mml:mi><mml:mn>2</mml:mn> magnetically constrained noncollinear DFT. Physical Review B, 2015, 92, .	1.1	70
20638	Pressure-induced transition in the multiferroic<mml:math xmlns:mml="http://www.w3.org/1998/Math/MathML"><mml:mrow><mml:mi>CoC</mml:mi><mml:msub><mml:mi mathvariant="normal">r</mml:mi><mml:mn>2</mml:mn></mml:msub><mml:msub><mml:mi mathvariant="normal">O</mml:mi><mml:mn>4</mml:mn></mml:msub></mml:mrow></mml:math>spinel. Physical Review B, 2015, 92, .	1.1	35
20639	Structural transformations of<mml:math xmlns:mml="http://www.w3.org/1998/Math/MathML"><mml:mrow><mml:msub><mml:mi>Li</mml:mi><mml:mn>2</mml:mn><mml:msub><mml:mi mathvariant="normal">C</mml:mi><mml:mn>2</mml:mn></mml:msub></mml:mrow></mml:math>at high pressure. Physical Review B, 2015, 92, .	1.1	8
20640	Anharmonic properties in<mml:math xmlns:mml="http://www.w3.org/1998/Math/MathML"><mml:mrow><mml:mi mathvariant="normal">M</mml:mi><mml:msub><mml:mi mathvariant="normal">g</mml:mi><mml:mn>2</mml:mn></mml:msub><mml:mi>X</mml:mi></mml:mrow></mml:math><mml:math		

#	Article	IF	Citations
20644	High-temperature superconductivity in heavily N- or B-doped graphene. Physical Review B, 2015, 92, .	1.1	45
20645	DFT+<mml:math xmlns:mml="http://www.w3.org/1998/Math/MathML"><mml:mi>U</mml:mi></mml:math>study of electrical levels and migration barriers of early<mml:math xmlns:mml="http://www.w3.org/1998/Math/MathML"><mml:mrow><mml:mn>3</mml:mn><mml:mi>d</mml:mi></mml:mrow></mml:math>-<mml:math xmlns:mml="http://www.w3.org/1998/Math/MathML"><mml:mrow><mml:mn>4</mml:mn><mml:mi>d</mml:mi></mml:mrow></mml:math>	1.1	16
20646	Spin-dependent transport in a multiferroic tunnel junction: Theory for<mml:math xmlns:mml="http://www.w3.org/1998/Math/MathML"><mml:mi>Co</mml:mi><mml:mo>/</mml:mo><mml:msub><mml:mi mathvariant="normal">PbTiO</mml:mi><mml:mn>3</mml:mn></mml:msub><mml:mo>/</mml:mo><mml:mi>Co</mml:mi></mml:math> Physical Review B, 2015, 92, .	1.1	31
20647	Spatially extended underscreened Kondo state from collective molecular spin. Physical Review B, 2015, 92, .	1.1	22
20648	Variational polaron self-interaction-corrected total-energy functional for charge excitations in insulators. Physical Review B, 2015, 92, .	1.1	35
20649	<mml:math xmlns:mml="http://www.w3.org/1998/Math/MathML"><mml:msub><mml:mi>TiS</mml:mi><mml:mn>3</mml:mn></mml:msub></mml:math> Width-independent band gap and strain-tunable electronic properties. Physical Review B, 2015, 92, .	1.1	58
20650	Nature of the bias-dependent symmetry reduction of iron phthalocyanine on Cu(111). Physical Review B, 2015, 92, .	1.1	22
20651	Large-gap two-dimensional topological insulator in oxygen functionalized MXene. Physical Review B, 2015, 92, .	1.1	229
20652	Scanning tunneling microscopy of the charge density wave in<mml:math xmlns:mml="http://www.w3.org/1998/Math/MathML"><mml:mrow><mml:mn>1</mml:mn><mml:mi>T</mml:mi></mml:mrow></mml:math>-<mml:math xmlns:mml="http://www.w3.org/1998/Math/MathML"><mml:msub><mml:mi mathvariant="normal">TaS</mml:mi><mml:mn>2</mml:mn></mml:msub></mml:math> the presence of single atom defects. Physical Review B, 2015, 92, .	1.1	36
20653	Large-gap quantum spin Hall states in decorated stanene grown on a substrate. Physical Review B, 2015, 92, .	1.1	108
20654	Thermal properties of black and blue phosphorenes from a first-principles quasiharmonic approach. Physical Review B, 2015, 92, .	1.1	140
20655	Testing predictions from density functional theory at finite temperatures:<mml:math xmlns:mml="http://www.w3.org/1998/Math/MathML"><mml:msub><mml:mi>Î²</mml:mi><mml:mn>2</mml:mn></mml:msub></mml:math> ground states in Co-Pt. Physical Review B, 2015, 92, .	1.1	6
20656	Structural and electronic properties of<mml:math xmlns:mml="http://www.w3.org/1998/Math/MathML"><mml:msub><mml:mi>SrZrO</mml:mi><mml:mn>3</mml:mn></mml:msub></mml:math> Sr(Ti,Zr)<mml:math xmlns:mml="http://www.w3.org/1998/Math/MathML"><mml:msub><mml:mi mathvariant="normal">O</mml:mi><mml:mn>3</mml:mn></mml:msub></mml:math>alloys. Physical Review B, 2015, 92, .	1.1	27
20657	Multidimensional quasiballistic thermal transport in transient grating spectroscopy. Physical Review B, 2015, 92, .	1.1	22
20658	Role of biaxial strain and microscopic ordering for structural and electronic properties of<mml:math xmlns:mml="http://www.w3.org/1998/Math/MathML"><mml:mrow><mml:msub><mml:mi mathvariant="normal">In</mml:mi><mml:mi>x</mml:mi></mml:msub><mml:msub><mml:mi>Ga</mml:mi><mml:mrow><mml:mn>1</mml:mn></mml:mrow></mml:msub><mml:mi mathvariant="normal">N</mml:mi></mml:mrow></mml:math>. Physical Review B, 2015, 92, .	1.1	6
20659	<mml:math xmlns:mml="http://www.w3.org/1998/Math/MathML"><mml:mrow><mml:msub><mml:mrow><mml:mo>(</mml:mo></mml:mrow></mml:msub></mml:mrow></mml:math> for transparent electronics. Physical Review B, 2015, 92, .	1.1	100
20660	Spin-polarized surface electronic structure of Ta(110): Similarities and differences to W(110). Physical Review B, 2015, 92, .	1.1	10
20661	Phosphorene analogues: Isoelectronic two-dimensional group-IV monochalcogenides with orthorhombic structure. Physical Review B, 2015, 92, .	1.1	391

#	Article	IF	Citations
20662	Toward a realistic description of multilayer black phosphorus: From<mml:math xmlns:mml="http://www.w3.org/1998/Math/MathML"><mml:mrow><mml:mi>G</mml:mi><mml:mi>W</mml:mi></mml:mrow></mml:m to large-scale tight-binding simulations. Physical Review B, 2015, 92, .	1.1	187
20663	Structural and phononic characteristics of nitrogenated holey graphene. Physical Review B, 2015, 92, .	1.1	80
20664	Quantum spin Hall effect and topological phase transition in two-dimensional square transition-metal dichalcogenides. Physical Review B, 2015, 92, .	1.1	117
20665	Xe irradiation of graphene on Ir(111): From trapping to blistering. Physical Review B, 2015, 92, .	1.1	32
20666	Stable xenon nitride at high pressures. Physical Review B, 2015, 92, .	1.1	50
20667	Graphite under uniaxial compression along the<mml:math xmlns:mml="http://www.w3.org/1998/Math/MathML"><mml:mi>c</mml:mi></mml:math>axis: A parameter to relate out-of-plane strain to in-plane phonon frequency. Physical Review B, 2015, 92, .	1.1	9
20668	Learning scheme to predict atomic forces and accelerate materials simulations. Physical Review B, 2015, 92, .	1.1	162
20669	All-thermal switching of amorphous Gd-Fe alloys: Analysis of structural properties and magnetization dynamics. Physical Review B, 2015, 92, .	1.1	41
20670	Ferromagnetic superexchange in insulating<mml:math xmlns:mml="http://www.w3.org/1998/Math/MathML"><mml:mrow><mml:mi mathvariant="normal">C</mml:mi><mml:msub><mml:mi mathvariant="normal">r</mml:mi><mml:mn>2</mml:mn></mml:msub><mml:mi>Mo</mml:mi><mml:msub><mml:mi mathvariant="normal">O</mml:mi><mml:mn>6</mml:mn></mml:msub></mml:mrow></mml:math>by controlling orbital hybridization. Physical Review B, 2015, 92, .	1.1	14
20671	Local atomic and electronic structures in ferromagnetic topological insulator Cr-doped<mml:math xmlns:mml="http://www.w3.org/1998/Math/MathML"><mml:mrow><mml:msub><mml:mrow><mml:mo>(</mml:mo> by. Physical Review B, 2015, 92, .	1.1	6
20672	Lattice stability and high-pressure melting mechanism of dense hydrogen up to 1.5 TPa. Physical Review B, 2015, 92, .	1.1	20
20673	Electronic structure and magnetism of K-intercalated iron chalcogenides. Physical Review B, 2015, 92, .	1.1	3
20674	Magnetism and metal-insulator transition in oxygen-deficient<mml:math xmlns:mml="http://www.w3.org/1998/Math/MathML"><mml:msub><mml:mi>SrTiO</mml:mi><mml:mn>3</mml:mn></mml:msub></m Physical Review B, 2015, 92, .	1.1	42
20675	First-principles calculation of charged capacitors under open-circuit conditions using the orbital-separation approach. Physical Review B, 2015, 92, .	1.1	2
20676	Tunable site- and orbital-selective Mott transition and quantum confinement effects in<mml:math xmlns:mml="http://www.w3.org/1998/Math/MathML"><mml:mrow><mml:msub><mml:mtext>La</mml:mtext><mml:mrow><mml:mn> Physical Review B, 2015, 92, .	1.1	16
20677	First-principles study of anisotropic thermoelectric transport properties of IV-VI semiconductor compounds SnSe and SnS. Physical Review B, 2015, 92, .	1.1	383
20678	Rashba effect in single-layer antimony telluroiodide SbTeI. Physical Review B, 2015, 92, .	1.1	60
20679	Reconstruction of electrostatic field at the interface leads to formation of two-dimensional electron gas at multivalent<mml:math xmlns:mml="http://www.w3.org/1998/Math/MathML"><mml:mrow><mml:mrow><mml:mo>(</mml:mo><mml:mn>110</mml:mn> width="0.28em" /><mml:mi>LaAl</mml:mi><mml:msub><mml:mi mathvariant="normal">O</mml:mi><mml:mn>3</mml:mn></mml:msub><mml:mtext></mml:mtext><mml:mi>SrTi</mml:mi> mathvariant="normal">O</mml:mi><mml:mn>3</mml:mn></mml:ms. Physical Review B, 2015, 92, .	1.1	11

#	Article	IF	Citations
20680	Monolayer II-VI semiconductors: A first-principles prediction. Physical Review B, 2015, 92, .	1.1	226
20681	Dynamical behavior of a dangling bond dimer on a hydrogenated semiconductor: Ge(001):H. Physical Review B, 2015, 92, .	1.1	11
20682	Topological surface states and Fermi arcs of the noncentrosymmetric Weyl semimetals TaAs, TaP, NbAs, and NbP. Physical Review B, 2015, 92, .	1.1	163
20683	Deep-to-shallow level transition of Re and Nb dopants in monolayer<mml:math xmlns:mml="http://www.w3.org/1998/Math/MathML"><mml:msub><mml:mi mathvariant="normal">MoS</mml:mi><mml:mn>2</mml:mn></mml:msub></mml:math>with dielectric environments. Physical Review B, 2015, 92, .	1.1	54
20684	Tunable spin helical Dirac quasiparticles on the surface of three-dimensional HgTe. Physical Review B, 2015, 92, .	1.1	19
20685	Energy splitting of image states induced by the surface potential corrugation of <mml:math xmlns:mml="http://www.w3.org/1998/Math/MathML"><mml:mtext>InAs</mml:mtext><mml:mo>(</mml:mo><mml:mn>111</mml:mn> Physical Review B, 2015, 92, .	1.1	19
20686	Breakdown of<mml:math xmlns:mml="http://www.w3.org/1998/Math/MathML"><mml:mrow><mml:mi>J</mml:mi><mml:mo>=</mml:mo><mml:mn>0</mml:mn> state in<mml:math xmlns:mml="http://www.w3.org/1998/Math/MathML"><mml:msup><mml:mi>d</mml:mi><mml:mn>4</mml:mn></mml:msup> double perovskites: A first-principles study. Physical Review B, 2015, 92, .	1.1	59
20687	Giant and tunable valley degeneracy splitting in<mml:math xmlns:mml="http://www.w3.org/1998/Math/MathML"><mml:msub><mml:mi>MoTe</mml:mi><mml:mn>2</mml:mn> Physical Review B, 2015, 92, .	1.1	284
20688	Origin of the metal-insulator transition in ultrathin films of<mml:math xmlns:mml="http://www.w3.org/1998/Math/MathML"><mml:mrow><mml:mi mathvariant="normal">L</mml:mi><mml:msub><mml:mi mathvariant="normal">a</mml:mi><mml:mrow><mml:mn>2</mml:mn><mml:mo>/</mml:mo><mml:mn>3</mml:mn></mml:mrow></mml:msub><mml:mi mathvariant="normal">S</mml:mi><mml:msub><mml:mi mathvariant="normal">r</mml:mi><mml:mrow><mml:mn>2</mml:mn><mml:mo>/</mml:mo><mml:mn>3</mml:mn></mml:mrow></m	1.1	80
20689	Topological phase transitions in group IV-VI semiconductors by phonons. Physical Review B, 2015, 92, .	1.1	18
20690	Hexagonal rare-earth manganites as promising photovoltaics and light polarizers. Physical Review B, 2015, 92, .	1.1	100
20691	Prediction of a two-dimensional crystalline structure of nitrogen atoms. Physical Review B, 2015, 92, .	1.1	109
20692	Atomic structure, alloying behavior, and magnetism in small Fe-Pt clusters. Physical Review B, 2015, 92, .	1.1	13
20693	Pressure-induced cation-cation bonding in<mml:math xmlns:mml="http://www.w3.org/1998/Math/MathML"><mml:mrow><mml:msub><mml:mi mathvariant="normal">V</mml:mi><mml:mn>2</mml:mn></mml:msub><mml:msub><mml:mi mathvariant="normal">O</mml:mi><mml:mn>3</mml:mn></mml:msub></mml:mrow></mml:math>. Physical Review B, 2015, 92, .	1.1	17
20694	Development and application of a Ni-Ti interatomic potential with high predictive accuracy of the martensitic phase transition. Physical Review B, 2015, 92, .	1.1	187
20695	Unoccupied electronic structure and momentum-dependent scattering dynamics in Pb/Si(557) nanowire arrays. Physical Review B, 2015, 92, .	1.1	4
20696	Localized itinerant electrons and unique magnetic properties of<mml:math xmlns:mml="http://www.w3.org/1998/Math/MathML"><mml:mrow><mml:msub><mml:mi>SrRu</mml:mi><mml:mn>2</mml:mn></mml:msub><mml:msub><mml:mi mathvariant="normal">O</mml:mi><mml:mn>6</mml:mn></mml:msub></mml:mrow></mml:math>. Physical Review B, 2015, 92, .	1.1	35
20697	Origins and implications of the ordering of oxygen vacancies and localized electrons on partially reduced<mml:math xmlns:mml="http://www.w3.org/1998/Math/MathML"><mml:msub><mml:mi>CeO</mml:mi><mml:mn>2</mml:mn></mml:msub> Physical Review B, 2015, 92, .	1.1	37

#	Article	IF	Citations
20698	Tracking the continuous spin-flop transition in<mml:math xmlns:mml="http://www.w3.org/1998/Math/MathML"><mml:mrow><mml:msub><mml:mi>Ni</mml:mi><mml:mn>3</mml:mn></mml:msub></mml:mrow></mml:math> infrared spectroscopy. Physical Review B, 2015, 92, .	1.1	26
20699	Common effect of chemical and external pressures on the magnetic properties ofRCoPOÂ(R=La,Pr,Nd,Sm). II.. Physical Review B, 2015, 92, .	1.1	5
20700	Geometric, electronic, and magnetic structure of<mml:math xmlns:mml="http://www.w3.org/1998/Math/MathML"><mml:mrow><mml:msub><mml:mtext>Fe</mml:mtext><mml:mi>x</mml:mi></mml:msub></mml:mrow></mml:math> Physical Review B, 2015, 92, .	1.1	19
20701	Optical spectroscopy and the nature of the insulating state of rare-earth nickelates. Physical Review B, 2015, 92, .	1.1	38
20702	First-principles study of the adsorption of MgO molecules on a clean Fe(001) surface. Physical Review B, 2015, 92, .	1.1	11
20703	van der Waals bilayer energetics: Generalized stacking-fault energy of graphene, boron nitride, and graphene/boron nitride bilayers. Physical Review B, 2015, 92, .	1.1	105
20704	Controlled confinement of half-metallic two-dimensional electron gas inBaTiO3/Ba2FeReO6/BaTiO3heterostructures: A first-principles study. Physical Review B, 2015, 92, .	1.1	11
20705	Prediction of Weyl semimetal in orthorhombic<mml:math xmlns:mml="http://www.w3.org/1998/Math/MathML"><mml:msub><mml:mi>MoTe</mml:mi><mml:mn>2</mml:mn></mml:msub></mml:math> Physical Review B, 2015, 92, .	1.1	511
20706	Spin-orbit influence ondz2-type surface state at Ta(110). Physical Review B, 2015, 92, .	1.1	7
20707	First-principles study of the organometallic<mml:math xmlns:mml="http://www.w3.org/1998/Math/MathML"><mml:mi>S</mml:mi><mml:mo>=</mml:mo><mml:mfrac><mml:mn>1</mml:mn></mml:math> compound Cu(1,3-bdc). Physical Review B, 2015, 92, .	1.1	7
20708	Spin-dependent properties and images of MnO, FeO, CoO, and NiO(001) surfaces. Physical Review B, 2015, 92, .	1.1	16
20709	Polaron mobility in oxygen-deficient and lithium-doped tungsten trioxide. Physical Review B, 2015, 92, .	1.1	52
20710	Breaking time-reversal symmetry at the topological insulator surface by metal-organic coordination networks. Physical Review B, 2015, 92, .	1.1	18
20711	Significant effect of stacking on the electronic and optical properties of few-layer black phosphorus. Physical Review B, 2015, 92, .	1.1	152
20712	Robust quantum anomalous Hall effect in graphene-based van der Waals heterostructures. Physical Review B, 2015, 92, .	1.1	93
20713	Phase separation of full-Heusler nanostructures in half-Heusler thermoelectrics and vibrational properties from first-principles calculations. Physical Review B, 2015, 92, .	1.1	65
20714	Role of vibrational and configurational excitations in stabilizing the<mml:math xmlns:mml="http://www.w3.org/1998/Math/MathML"><mml:mrow><mml:mi>L</mml:mi><mml:msub><mml:mn>1</mml:mn></mml:math> in Co-rich Co-Al-W alloys. Physical Review B, 2015, 92, .	1.1	19
20715	Large piezoelectric response of quarternary wurtzite nitride alloys and its physical origin from first principles. Physical Review B, 2015, 92, .	1.1	41

#	Article	IF	Citations
20716	Multiferroic heterostructures for spin filter applications: Anab initiostudy. Physical Review B, 2015, 92, .	1.1	3
20717	Topological<mml:math xmlns:mml="http://www.w3.org/1998/Math/MathML"><mml:mrow><mml:mi>p</mml:mi><mml:mo>+</mml:mo><mml:mi>i</mml:mi> in doped graphene-like single-sheet materials<mml:math xmlns:mml="http://www.w3.org/1998/Math/MathML"><mml:msub><mml:mi>BC</mml:mi><mml:mn>3</mml:mn></mml:msub></mml Physical Review B, 2015, 92, .	1.1	24
20718	Edge states and local electronic structure around an adsorbed impurity in a topological superconductor. Physical Review B, 2015, 92, .	1.1	5
20719	Electronic structure and spin-orbit driven magnetism in<mml:math xmlns:mml="http://www.w3.org/1998/Math/MathML"><mml:msup><mml:mi>d</mml:mi><mml:mrow><mml:mn>4.5</mml:mn></mml xmlns:mml="http://www.w3.org/1998/Math/MathML"><mml:mrow><mml:msub><mml:mtext>Ba</mml:mtext><mml:mn>3</mml:mn> Physical Review B, 2015, 92, .	1.1	18
20720	Spin-orbit driven magnetic insulating state with<mml:math xmlns:mml="http://www.w3.org/1998/Math/MathML"><mml:mrow><mml:msub><mml:mi>J</mml:mi><mml:mi>eff</mml:mi></mml:ms in a<mml:math xmlns:mml="http://www.w3.org/1998/Math/MathML"><mml:mrow><mml:mn>4</mml:mn><mml:mi>d</mml:mi></mml:mrow></mml:n Physical Review B, 2015, 92, .	1.1	10
20721	Ab initiostudy of the anharmonic lattice dynamics of iron at theÎ³âˆ'Îµphase transition. Physical Review B, 2015, 92, .	1.1	10
20722	Linear magnetoelectricity at room temperature in perovskite superlattices by design. Physical Review B, 2015, 92, .	1.1	20
20723	Magnetic moment formation in metal-organic monolayers. Physical Review B, 2015, 92, .	1.1	11
20724	Topological magnetic phase in<mml:math xmlns:mml="http://www.w3.org/1998/Math/MathML"><mml:msub><mml:mtext>LaMnO</mml:mtext><mml:mn>3</mml:mn> bilayer. Physical Review B, 2015, 92, .	1.1	33
20725	Reaction thermochemistry of metal sulfides with GGA and<mml:math xmlns:mml="http://www.w3.org/1998/Math/MathML"><mml:mrow><mml:mi mathvariant="normal">GGA</mml:mi><mml:mo>+</mml:mo><mml:mi>U</mml:mi></mml:mrow></mml:math>calculations. Physical Review B, 2015, 92, .	1.1	22
20726	Deep recombination centers in<mml:math xmlns:mml="http://www.w3.org/1998/Math/MathML"><mml:mrow><mml:mi mathvariant="normal">C</mml:mi><mml:msub><mml:mi mathvariant="normal">u</mml:mi><mml:mn>2</mml:mn></mml:msub><mml:mi>ZnSnS</mml:mi><mml:msub><mml:mi mathvariant="normal"></mml:mi><mml:mn>4</mml:mn></mml:msub></mml:mrow></mml:math>revealed by admittance spectroscopy. Physical Review B, 2015, 92, .	1.1	34
20727	xmlns:mml="http://www.w3.org/1998/Math/MathML"><mml:mrow><mml:mn>4</mml:mn><mml:mi>f</mml:mi></mml:mrow></mml:mn><mml:mi>p</mml:mi></mml:mrow></mml:m Au<mml:math xmlns:mml="http://www.w3.org/1998/Math/MathML"><mml:mrow><mml:mn>4</mml:mn><mml:mi>f</mml:mi></mml:mrow></mml:m core-level shifts on Au/Si(111)-(<mml:math) Tj ETQq1 1 0.784314 rgBT /Overlock 10 Tf 50 282 Td (xmlns:mml="http://www.w3.org/199	1.1	7
20728	Near valence-band electronic properties of semiconducting<mml:math xmlns:mml="http://www.w3.org/1998/Math/MathML"><mml:mrow><mml:mi>Î²</mml:mi><mml:msub><mml:mrow><mml:mo>â^'</mml:mo> mathvariant="normal">O</mml:mi><mml:mn>3</mml:mn></mml:msub></mml:mrow></mml:math>(100) single crystals. Physical Review B, 2015, 92, .	1.1	47
20729	Molecular induced skyhook effect for magnetic interlayer softening. Physical Review B, 2015, 92, .	1.1	19
20730	Anomalous charge and negative-charge-transfer insulating state in cuprate chain compound<mml:math xmlns:mml="http://www.w3.org/1998/Math/MathML"><mml:msub><mml:mi>KCuO</mml:mi><mml:mn>2</mml:mn></mml:msub></m Physical Review B, 2015, 92, .	1.1	20
20731	Nonequilibrium spin texture within a thin layer below the surface of current-carrying topological insulator<mml:math xmlns:mml="http://www.w3.org/1998/Math/MathML"><mml:mrow><mml:msub><mml:mi>Bi</mml:mi><mml:mn>2</mml:mn></mml:mn></mml A first-principles quantum transport study. Physical Review B, 2015, 92, .	1.1	41
20732	Physical properties and electronic structure of<mml:math xmlns:mml="http://www.w3.org/1998/Math/MathML"><mml:mrow><mml:msub><mml:mi>Sr</mml:mi><mml:mn>2</mml:mn></mml:mn></mml:r mathvariant="normal">O</mml:mi><mml:mn>2</mml:mn></mml:msub></mml:mrow></mml:math>containing<mml:math xmlns:mml="http://www.w3.org/1998/Math/MathML"><mml:msub><mml:mi>CrO</mml:mi><mml:mn>2</mml:mn></mml:msu. Physical Review B, 2015, 92, .	1.1	27
20733	Ab initio tight-binding Hamiltonian for transition metal dichalcogenides. Physical Review B, 2015, 92, .	1.1	158

#	Article	IF	Citations
20734	Converting normal insulators into topological insulators via tuning orbital levels. Physical Review B, 2015, 92, .	1.1	21
20735	Electronic and magnetic properties of the cation vacancy defect in<mml:math xmlns:mml="http://www.w3.org/1998/Math/MathML"><mml:mrow><mml:mi>m</mml:mi><mml:mtext>â^'</mml:mtext><mml:msub Physical Review B, 2015, 92, .	1.1	21
20736	Screened moments and absence of ferromagnetism in FeAl. Physical Review B, 2015, 92, .	1.1	29
20737	Strain-induced band alignment in wurtzite/zinc-blende InAs heterostructured nanowires. Physical Review B, 2015, 92, .	1.1	12
20738	Two-dimensional oxide topological insulator with iron-pnictide superconductor LiFeAs structure. Physical Review B, 2015, 92, .	1.1	150
20739	Ferromagnetism and perfect spin filtering in transition-metal-doped graphyne nanoribbons. Physical Review B, 2015, 92, .	1.1	39
20740	Tunable magnetic interaction in hydrogenated epitaxial graphene modulated by the SiC substrate. Physical Review B, 2015, 92, .	1.1	3
20741	Enhanced piezoelectricity and modified dielectric screening of two-dimensional group-IV monochalcogenides. Physical Review B, 2015, 92, .	1.1	179
20742	How the aggregation of oxygen vacancies in rutile-based<mml:math xmlns:mml="http://www.w3.org/1998/Math/MathML"><mml:msub><mml:mi>TiO</mml:mi><mml:mrow><mml:mn>2 causes memristive behavior. Physical Review B, 2015, 92, .	1.1	18
20743	Proton configurations in the hydrogen bonds ofKH2PO4as seen by resonant x-ray diffraction. Physical Review B, 2015, 92, .	1.1	15
20744	Proposal for ultrafast switching of ferroelectrics using midinfrared pulses. Physical Review B, 2015, 92, .	1.1	56
20745	Multiband electronic characterization of the complex intermetallic cage system<mml:math xmlns:mml="http://www.w3.org/1998/Math/MathML"><mml:mrow><mml:msub><mml:mi mathvariant="normal">Y</mml:mi><mml:mrow><mml:mn>1</mml:mn><mml:mo>â^'</mml:mo><mml:mi>x</mml:mi></mml:mrow> Physical Review B, 2015, 92, .	1.1	10
20746	Selectively doping barlowite for quantum spin liquid: A first-principles study. Physical Review B, 2015, 92, .	1.1	31
20747	Paramagnetism in the kagome compounds<mml:math xmlns:mml="http://www.w3.org/1998/Math/MathML"><mml:mrow><mml:mrow><mml:mo>(</mml:mo><mml:mi>Zn Physical Review B, 2015, 92, .	1.1	73
20748	Influence of epitaxial strain on clustering of iron in<mml:math xmlns:mml="http://www.w3.org/1998/Math/MathML"><mml:mi mathvariant="normal">Pb</mml:mi><mml:mo>(</mml:mo><mml:mrow><mml:msub><mml:mi>Fe</mml:mi><mml:mrow><mml:mn>1 mathvariant="normal">O</mml:mi><mml:mn>3</mml:mn></mml:m. Physical Review B, 2015, 92, .	1.1	19
20749	Systematic defect donor levels in III-V and II-VI semiconductors revealed by hybrid functional density-functional theory. Physical Review B, 2015, 92, .	1.1	7
20750	Electronic structure, magnetism, and antisite disorder in CoFeCrGe and CoMnCrAl quaternary Heusler alloys. Physical Review B, 2015, 92, .	1.1	73
20751	Brillouin zone spin filtering mechanism of enhanced tunneling magnetoresistance and correlation effects in a<mml:math xmlns:mml="http://www.w3.org/1998/Math/MathML"><mml:mtext>Co</mml:mtext><mml:mo>(</mml:mo><mml:mn>0001 tunnel junction. Physical Review B, 2015, 92, .	1.1	21

#	Article	IF	Citations
20752	New class of planar ferroelectric Mott insulators via first-principles design. Physical Review B, 2015, 92, .	1.1	4
20753	Incomplete Peierls-like chain dimerization as a mechanism for intrinsic conductivity and optical transparency: A La-Cu-O-S phase with mixed-anion layers as a case study. Physical Review B, 2015, 92, .	1.1	4
20754	Competing mechanism driving diverse pressure dependence of thermal conductivity of<mml:math xmlns:mml="http://www.w3.org/1998/Math/MathML"><mml:mi>X</mml:mi><mml:mtext>Te</mml:mtext></mml:math><mml:math		

#	Article	IF	Citations
20770	Candidate Source of Flux Noise in SQUIDs: Adsorbed Oxygen Molecules. Physical Review Letters, 2015, 115, 077002.	2.9	43
20771	Design of a Mott Multiferroic from a Nonmagnetic Polar Metal. Physical Review Letters, 2015, 115, 087202.	2.9	64
20772	Observation of Magnetoelectric Multiferroicity in a Cubic Perovskite System:<mml:math xmlns:mml="http://www.w3.org/1998/Math/MathML" display="inline"><mml:mrow><mml:msub><mml:mrow><mml:mi>LaMn</mml:mi></mml:mrow><mml:mrow><mml:mn>3</mml:mn></mml:mrow></mml:msub><mml:mrow><mml:mi mathvariant="normal">O</mml:mi></mml:mrow><mml:mrow><mml:mn>12</mml:mn></mml:mrow></mml:msub></mml:mrow></mml:math>. Physical Review Letters, 2015, 115, 087601.	2.9	105
20773	Charge Redistribution and Transport in Molecular Contacts. Physical Review Letters, 2015, 115, 136101.	2.9	22
20774	Band Engineering of Dirac Surface States in Topological-Insulator-Based van der Waals Heterostructures. Physical Review Letters, 2015, 115, 136801.	2.9	34
20775	Comment on â€œInterplay between Water andTiO2Anatase (101) Surface with Subsurface Oxygen Vacancyâ€• Physical Review Letters, 2015, 115, 149601.	2.9	10
20776	First-Principles Study of the Magnetic Structure ofNa2IrO3. Physical Review Letters, 2015, 115, 167204.	2.9	20
20777	Atomic-Level Understanding of â€œAsymmetric Twinsâ€•in Boron Carbide. Physical Review Letters, 2015, 115, 175501.	2.9	56
20778	Development of Path Integral MonteÂCarlo Simulations with Localized Nodal Surfaces for Second-Row Elements. Physical Review Letters, 2015, 115, 176403.	2.9	71
20779	Anomalous Stress Response of Ultrahard<mml:math xmlns:mml="http://www.w3.org/1998/Math/MathML" display="inline"><mml:mrow><mml:msub><mml:mrow><mml:mi>WB</mml:mi></mml:mrow><mml:mrow><mml:mi>n</mml:mi></mml:mrow></mml:msub></mml:mrow></mml:math>. Physical Review Letters, 2015, 115, 185502.	2.9	107
20780	Intrinsic Quantum Anomalous Hall Effect in the Kagome Lattice<mml:math xmlns:mml="http://www.w3.org/1998/Math/MathML" display="inline"><mml:mrow><mml:msub><mml:mrow><mml:mi>Cs</mml:mi></mml:mrow><mml:mrow><mml:mn>2</mml:mn></mml:mrow></mml:msub><mml:mrow><mml:mi mathvariant="normal">F</mml:mi></mml:mrow><mml:mrow><mml:mn>12</mml:mn></mml:mrow></mml:m. Physical Review Letters, 2015, 115, 186802.	2.9	134
20781	Field Effect and Strongly Localized Carriers in the Metal-Insulator Transition MaterialVO2. Physical Review Letters, 2015, 115, 196401.	2.9	31
20782	Shock Response and Phase Transitions of MgO at Planetary Impact Conditions. Physical Review Letters, 2015, 115, 198501.	2.9	74
20783	Prediction of Low-Thermal-Conductivity Compounds with First-Principles Anharmonic Lattice-Dynamics Calculations and Bayesian Optimization. Physical Review Letters, 2015, 115, 205901.	2.9	343
20784	Quantum Critical Origin of the Superconducting Dome in<mml:math xmlns:mml="http://www.w3.org/1998/Math/MathML" display="inline"><mml:mrow><mml:msub><mml:mrow><mml:mi>SrTiO</mml:mi></mml:mrow><mml:mrow><mml:mn>3</mml:mn></mml:mrow></mml:msub></mml:mrow></mml:math>. Physical Review Letters, 2015, 115, 247002.	2.9	148
20785	Structure of Self-Assembled Mn Atom Chains on Si(001). Physical Review Letters, 2015, 115, 256104.	2.9	9
20786	Anatomy of Dzyaloshinskii-Moriya Interaction at<mml:math xmlns:mml="http://www.w3.org/1998/Math/MathML" display="inline"><mml:mrow><mml:mi>Co</mml:mi><mml:mo>/</mml:mo><mml:mi>Pt</mml:mi></mml:mrow></mml:math>Interface. Physical Review Letters, 2015, 115, 267210.	2.9	507
20787	First-principles calculation of defect free energies: General aspects illustrated in the case of bcc Fe. Physical Review B, 2015, 92, .	1.1	29

#	Article	IF	Citations
20788	Coupled Nonpolar-Polar Metal-Insulator Transition in1âˆ¶1SrCrO3/SrTiO3Superlattices: A First-Principles Study. Physical Review Letters, 2015, 115, 106401.	2.9	12
20789	Incorporation of Li dopant into Cu2ZnSnSe4 photovoltaic absorber: hybrid-functional calculations. Journal Physics D: Applied Physics, 2015, 48, 482001.	1.3	5
20790	Optical properties of F- and H-terminated armchair silicon nanoribbons. Chinese Physics B, 2015, 24, 127802.	0.7	3
20791	Strain-compensated GaAs_{1â^'y}P_y/GaAs_{1â^'z}Bi_z/GaAs_{1â^'y} wells for laser applications. Semiconductor Science and Technology, 2015, 30, 094011.	1.8	8
20792	Three-Phase Model for the Reversible Lithiation-Delithiation of SnO Anodes in Li-Ion Batteries. Physical Review Applied, 2015, 4, .	1.5	6
20793	Electron-Injection-Assisted Generation of Oxygen Vacancies in Monoclinic<mml:math xmlns:mml="http://www.w3.org/1998/Math/MathML" display="inline"><mml:mrow><mml:msub><mml:mrow><mml:mi>HfO</mml:mi></mml:mrow><mml:mrow><mml:mn>2</mml:mn> Physical Review Applied, 2015, 4, .	1.5	67
20794	Covalency-driven low-temperature structural distortion and its effect on electronic structure of<mml:math xmlns:mml="http://www.w3.org/1998/Math/MathML"><mml:msub><mml:mi mathvariant="normal">Hg</mml:mi><mml:mn>2</mml:mn></mml:msub><mml:msub><mml:mi mathvariant="normal">Ru</mml:mi><mml:mn>2</mml:mn></mml:msub><mml:msub><mml:mi mathvariant="normal">O</mml:mi><mml:mn>7</mml:mn></mml:msub></mml:math>. Physical Review B, 2015, 91, .	1.1	3
20795	Nature of the metal-insulator transition in<mml:math xmlns:mml="http://www.w3.org/1998/Math/MathML"><mml:mrow><mml:mi>Nb</mml:mi><mml:msub><mml:mi mathvariant="normal">O</mml:mi><mml:mn>2</mml:mn></mml:msub></mml:mrow></mml:math>. Physical Review B, 2015, 91, .	1.1	47
20796	Phase stability and transformations in the halide perovskite<mml:math xmlns:mml="http://www.w3.org/1998/Math/MathML"><mml:msub><mml:mi>CsSnI</mml:mi><mml:mn>3</mml:mn></mml:msub></mml:math>. Physical Review B, 2015, 91, .	1.1	133
20797	High-pressure structure, decomposition, and superconductivity of<mml:math xmlns:mml="http://www.w3.org/1998/Math/MathML"><mml:msub><mml:mi mathvariant="normal">MoS</mml:mi><mml:mn>2</mml:mn></mml:msub></mml:math>. Physical Review B, 2015, 91, .	1.1	18
20798	Influence of wave-function updates inGWcalculations on titanates. Physical Review B, 2015, 91, .	1.1	15
20799	Controlling adsorption and spin configurations of Co atoms on<mml:math xmlns:mml="http://www.w3.org/1998/Math/MathML"><mml:mrow><mml:mi>Si</mml:mi><mml:mo>(</mml:mo><mml:mn>111</mml:mn> Physical Review B, 2015, 91, .	1.1	6
20800	Stoichiometry dependence of potential screening at<mml:math xmlns:mml="http://www.w3.org/1998/Math/MathML"><mml:mi mathvariant="normal">La</mml:mi><mml:msub><mml:mrow /><mml:mrow><mml:mo>(</mml:mo><mml:mn>1</mml:mn><mml:mo>â^'</mml:mo><mml:mi>Î´</mml:mi><mml:mo>)</mml:mo></mml:mrow></mml:msub><mml:mi mathvariant="normal">Al</mml:mi><mml:msub><mml:mrow /><mml:mrow><mml:mo>(</mml:mo><mml:mn>1</mml:mn><mml:mo>+</mml:mo><mml:mi>Î´</mml:mi><mml:mo>)</mml:mo></mml:mrow></mml:msub><mml:mi mathvariant="normal">O</mml:mi><mml:mn>3</mml:mn></mml:math>/<mml:math xmlns:mml="http://www.w3.org/1998/Math/MathML"><mml:msub><mml:mi mathvariant="normal">SrTiO</mml:mi><mml:mn>3</mml:mn></mml:msub></mml:math>	1.1	14
20801	First-principles study of codoping in lanthanum bromide. Physical Review B, 2015, 91, .	1.1	27
20802	Chen's derivative rule revisited: Role of tip-orbital interference in STM. Physical Review B, 2015, 91, .	1.1	31
20803	Spectral signatures of thermal spin disorder and excess Mn in half-metallic NiMnSb. Physical Review B, 2015, 91, .	1.1	8
20804	Strain control of electronic phase in rare-earth nickelates. Physical Review B, 2015, 91, .	1.1	20
20805	Charge transfer and hybrid ferroelectricity in<mml:math xmlns:mml="http://www.w3.org/1998/Math/MathML"><mml:mo>(</mml:mo><mml:msub><mml:mi>YFeO</mml:mi><mml:mn>3</mml:mn> /><mml:mi>n</mml:mi></mml:msub><mml:mo>/</mml:mo><mml:mo>(</mml:mo><mml:msub><mml:mi>YTiO</mml:mi><mml:mn>3</mml:mn> /><mml:mi>n</mml:mi></mml:msub></mml:math>magnetic superlattices. Physical Review B, 2015, 91, .	1.1	35

#	Article	IF	Citations
20806	Computational prediction of body-centered cubic carbon in an all-<mml:math xmlns:mml="http://www.w3.org/1998/Math/MathML"><mml:mrow><mml:mi>s</mml:mi><mml:msup><mml:mi>p</mml:mi><mml:mn>3</mml:mn></mml:msup></mml:mrow></mml:math> ring configuration. Physical Review B, 2015, 91, .	1.1	49
20807	Exchange correlation induced ferroelectric polarization in copper-based multiferroic material<mml:math xmlns:mml="http://www.w3.org/1998/Math/MathML"><mml:mi>Î±</mml:mi><mml:mo>â^'</mml:mo><mml:msub><mml:mi mathvariant="normal">Cu</mml:mi><mml:mn>2</mml:mn></mml:msub><mml:msub><mml:mi mathvariant="normal">V</mml:mi><mml:mn>2</mml:mn></mml:msub><mml:msub><mml:mi mathvariant="normal">O</mml:mi><mml:mn>7</mml:mn></mml:msub></mml:math>. Physical Review B,	1.1	41
20808	High-pressure layered structure of carbon disulfide. Physical Review B, 2015, 91, .	1.1	10
20809	Surface states of perovskite iridatesAlrO3: Signatures of a topological crystalline metal with nontrivialZ2index. Physical Review B, 2015, 91, .	1.1	41
20810	Effective tight-binding model forMX2under electric and magnetic fields. Physical Review B, 2015, 91, .	1.1	32
20811	Hybrid density functional calculations of the surface electronic structure of GdN. Physical Review B, 2015, 91, .	1.1	1
20812	Multivalley effective mass theory simulation of donors in silicon. Physical Review B, 2015, 91, .	1.1	49
20813	Double-charge model for classical force-field simulations. Physical Review B, 2015, 91, .	1.1	7
20814	Implications of the band gap problem on oxidation and hydration in acceptor-doped barium zirconate. Physical Review B, 2015, 91, .	1.1	36
20815	Improved predictions of the physical properties of Zn- and Cd-based wide band-gap semiconductors: A validation of the ACBN0 functional. Physical Review B, 2015, 91, .	1.1	56
20816	Crystal and electronic structure of BiTeI, AuTeI, and PdTeI compounds: A dispersion-corrected density-functional study. Physical Review B, 2015, 91, .	1.1	13
20817	Antiferromagnetic spin structure and negative thermal expansion ofLi2Ni(WO4)2. Physical Review B, 2015, 92, .	1.1	11
20818	Band-filling effect on magnetic anisotropy using a Green's function method. Physical Review B, 2015, 92, .	1.1	42
20819	Topological orbital magnetization and emergent Hall effect of an atomic-scale spin lattice at a surface. Physical Review B, 2015, 92, .	1.1	41
20820	Giant voltage modulation of magnetic anisotropy in strained heavy metal/magnet/insulator heterostructures. Physical Review B, 2015, 92, .	1.1	79
20821	Density functional versus spin-density functional and the choice of correlated subspace in multivariable effective action theories of electronic structure. Physical Review B, 2015, 92, .	1.1	34
20822	Hexagonal indium double layer on<mml:math xmlns:mml="http://www.w3.org/1998/Math/MathML"><mml:mrow><mml:mi>Si</mml:mi><mml:mrow><mml:mo>(</mml:mo></mml:mrow></mml:math> Physical Review B, 2015, 92, .	1.1	13
20823	First-principles structure determination of interface materials: The<mml:math xmlns:mml="http://www.w3.org/1998/Math/MathML"><mml:mrow><mml:msub><mml:mtext>Ni</mml:mtext><mml:mi>x</mml:mi></mml:msub></mml:mrow></mml:math> Physical Review B, 2015, 92, .	1.1	12

#	Article	IF	Citations
20824	Phonon quarticity induced by changes in phonon-tracked hybridization during lattice expansion and its stabilization of rutile<mml:math xmlns:mml="http://www.w3.org/1998/Math/MathML"><mml:msub><mml:mi>TiO</mml:mi><mml:mn>2</mml:mn></mml:msub></mml Physical Review B, 2015, 92, .	1.1	16
20825	Observation of a Raman-active phonon with Fano line shape in the quasi-one-dimensional superconductor<mml:math xmlns:mml="http://www.w3.org/1998/Math/MathML"><mml:mrow><mml:msub><mml:mi mathvariant="normal">K</mml:mi><mml:mn>2</mml:mn></mml:msub><mml:msub><mml:mi>Cr</mml:mi><mml:mn>3</mml:mn></ Physical Review B, 2015, 92, .	1.1	20
20826	Optical properties and Zeeman spectroscopy of niobium in silicon carbide. Physical Review B, 2015, 92, .	1.1	6
20827	Charge neutrality in epitaxial graphene on<mml:math xmlns:mml="http://www.w3.org/1998/Math/MathML"><mml:mrow><mml:mn>6</mml:mn><mml:mi>H</mml:mi></mml:mrow></mml via nitrogen intercalation. Physical Review B, 2015, 92, .	1.1	29
20828	Importance of anisotropic Coulomb interaction in<mml:math xmlns:mml="http://www.w3.org/1998/Math/MathML"><mml:msub><mml:mi>LaMnO</mml:mi><mml:mn>3</mml:mn></mml:msub></ Physical Review B, 2015, 92, .	1.1	47
20829	Effects of ferroelectric polarization on surface phase diagram: Evolutionary algorithm study of the<mml:math xmlns:mml="http://www.w3.org/1998/Math/MathML"><mml:msub><mml:mi mathvariant="normal">BaTiO</mml:mi><mml:mn>3</mml:mn></mml:msub></mml:math>(001) surface. Physical Review B, 2015, 92, .	1.1	18
20830	Tuning the magnetic anisotropy in single-layer crystal structures. Physical Review B, 2015, 92, .	1.1	37
20831	Electronic and magnetic properties of<mml:math xmlns:mml="http://www.w3.org/1998/Math/MathML"><mml:msub><mml:mi>GaFeO</mml:mi><mml:mn>3</mml:mn></mml:msub> initiocalculations for varying Fe/Ga ratio, inner cationic site disorder, and epitaxial strain. Physical Review B, 2015, 92, .	1.1	37
20832	Antiferromagnetism atT>500Kin the layered hexagonal ruthenateSrRu2O6. Physical Review B, 2015, 92, .	1.1	43
20833	Effects of strain and oxygen vacancies on the ferroelectric and antiferrodistortive distortions in<mml:math xmlns:mml="http://www.w3.org/1998/Math/MathML"><mml:mrow><mml:msub><mml:mi>PbTiO</mml:mi><mml:mn>3</mml:mn></ Physical Review B, 2015, 92, .	1.1	36
20834	Low-loss electron energy loss spectroscopy: An atomic-resolution complement to optical spectroscopies and application to graphene. Physical Review B, 2015, 92, .	1.1	29
20835	Proposal of a general scheme to obtain room-temperature spin polarization in asymmetric antiferromagnetic semiconductors. Physical Review B, 2015, 92, .	1.1	23
20836	Interpreting core-level spectra of oxidizing phosphorene: Theory and experiment. Physical Review B, 2015, 92, .	1.1	35
20837	Soft modes and anharmonicity in<mml:math xmlns:mml="http://www.w3.org/1998/Math/MathML"><mml:mrow><mml:msub><mml:mi mathvariant="normal">H</mml:mi><mml:mn>3</mml:mn></mml:msub><mml:mrow><mml:mo>[</mml:mo><mml:mrow><mml:mi> Raman spectroscopy and first-principles calculations. Physical Review B, 2015, 92, .	1.1	17
20838	Ab initiostudy of the structure and dynamics of bulk liquid Fe. Physical Review B, 2015, 92, .	1.1	31
20839	Synthesis of a predicted layered LiB via cold compression. Physical Review B, 2015, 92, .	1.1	21
20840	Large magneto-optical Kerr effect in noncollinear antiferromagnets<mml:math xmlns:mml="http://www.w3.org/1998/Math/MathML"><mml:mrow><mml:msub><mml:mi mathvariant="normal">Mn</mml:mi><mml:mn>3</mml:mn></mml:msub><mml:mi>X</mml:mi></mml:mrow><mml:mspace width="0.28em"		

#	Article	IF	Citations
20842	Complexes of silicon, vacancy, and hydrogen in diamond: A density functional study. Physical Review B, 2015, 92, .	1.1	30
20843	Layer- and strain-dependent optoelectronic properties of hexagonal AlN. Physical Review B, 2015, 92, .	1.1	53
20844	Hidden scale invariance of metals. Physical Review B, 2015, 92, .	1.1	36
20845	Vibrational contributions to the phase stability of PbS-PbTe alloys. Physical Review B, 2015, 92, .	1.1	18
20846	Pressure-induced spin reorientation and spin state transition inSrCoO3. Physical Review B, 2015, 92, .	1.1	18
20847	Heterostructures of graphene and nitrogenated holey graphene: MoirÃ© pattern and Dirac ring. Physical Review B, 2015, 92, .	1.1	34
20848	Ferromagnetic instability of interlayer floating electrons in the quasi-two-dimensional electrideY2C. Physical Review B, 2015, 92, .	1.1	40
20849	Theory of the Dirac half metal and quantum anomalous Hall effect in Mn-intercalated epitaxial graphene. Physical Review B, 2015, 92, .	1.1	50
20850	Intrinsic large gap quantum anomalous Hall insulators in<mml:math xmlns:mml="http://www.w3.org/1998/Math/MathML"><mml:mrow><mml:mi>La</mml:mi><mml:mi>X</mml:mi><mml:mo>(</mml:mo> Physical Review B, 2015, 92, .	1.1	19
20851	Origin of and tuning the optical and fundamental band gaps in transparent conducting oxides: The case of<mml:math xmlns:mml="http://www.w3.org/1998/Math/MathML"><mml:mrow><mml:msub><mml:mi>M</mml:mi><mml:mn>2</mml:mn></mml:msub><mml:mi mathvariant="normal">O</mml:mi><mml:mn>3</mml:mn></mml:msub><mml:mrow><mml:mo>(</mml:mo><mml:mi>M</mml:mi> Physical Review B, 2015, 92, .	1.1	17
20852	Structural diversity in lithium carbides. Physical Review B, 2015, 92, .	1.1	26
20853	Small polarons and point defects in barium cerate. Physical Review B, 2015, 92, .	1.1	33
20854	Electron-phonon coupling and thermal transport in the thermoelectric compound<mml:math xmlns:mml="http://www.w3.org/1998/Math/MathML"><mml:mrow><mml:msub><mml:mi>Mo</mml:mi><mml:mn>3</mml:mn></mml:msub> Physical Review B, 2015, 92, .	1.1	19
20855	First-principles modeling of three-body interactions in highly compressed solid helium. Physical Review B, 2015, 92, .	1.1	11
20856	Molecular orbital polarization in<mml:math xmlns:mml="http://www.w3.org/1998/Math/MathML"><mml:mrow><mml:msub><mml:mtext>Na</mml:mtext><mml:mn>2</mml:mn> Microscopic route to metal-metal transition without spontaneous symmetry breaking. Physical Review B, 2015, 92, .	1.1	4
20857	Impact of strain-induced electronic topological transition on the thermoelectric properties of<mml:math xmlns:mml="http://www.w3.org/1998/Math/MathML"><mml:msub><mml:mi>PtCoO</mml:mi><mml:mn>2</mml:mn></mml:msub> <mml:math xmlns:mml="http://www.w3.org/1998/Math/MathML"><mml:msub><mml:mi>PdCoO</mml:mi><mml:mn>2</mml:mn></mml:msub> Physical Review B, 2015, 92, .	1.1	21
20858	H-stabilized shallow acceptors in N-doped ZnO. Physical Review B, 2015, 92, .	1.1	23
20859	Excitonic emissions and above-band-gap luminescence in the single-crystal perovskite semiconductors<mml:math xmlns:mml="http://www.w3.org/1998/Math/MathML"><mml:mrow><mml:mi>CsPbB</mml:mi><mml:msub><mml:mi mathvariant="normal">r</mml:mi><mml:mn>3</mml:mn></mml:msub></mml:mrow></mml:math>and<mml:math xmlns:mml="http://www.w3.org/1998/Math/MathML"><mml:mrow><mml:mi>CsPbC</mml:mi><mml:msub><mml:mi mathvariant="normal">I</mml:mi><mml:mn>3</mml:mn></mml:msub></mml:mrow></mml:math>. Physi	1.1	250

#	Article	IF	Citations
20860	Systematic study of structural, electronic, and optical properties of atomic-scale defects in the two-dimensional transition metal dichalcogenides<mml:math		

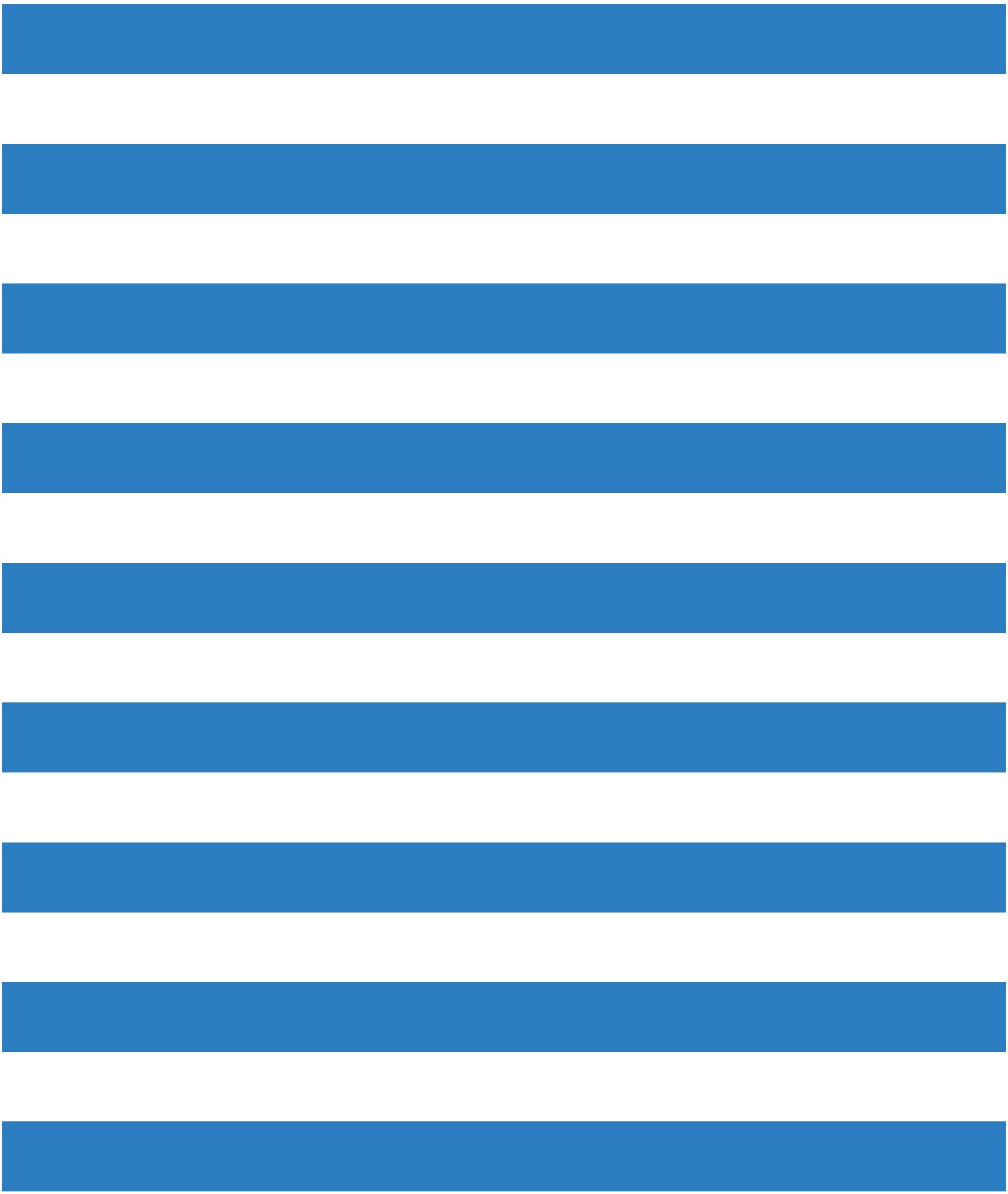

#	Article	IF	Citations
20878	The Open Quantum Materials Database (OQMD): assessing the accuracy of DFT formation energies. Npj Computational Materials, 2015, 1, .	3.5	1,200
20879	Topological nature and the multiple Dirac cones hidden in Bismuth high-Tc superconductors. Scientific Reports, 2015, 5, 10435.	1.6	30
20880	Nanostructured fuzz growth on tungsten under low-energy and high-flux He irradiation. Scientific Reports, 2015, 5, 10959.	1.6	64
20881	Electronic Topological Transition in Ag2Te at High-pressure. Scientific Reports, 2015, 5, 14681.	1.6	20
20882	Single Layer Bismuth Iodide: Computational Exploration of Structural, Electrical, Mechanical and Optical Properties. Scientific Reports, 2015, 5, 17558.	1.6	67
20883	Origin of interfacial perpendicular magnetic anisotropy in MgO/CoFe/metallic capping layer structures. Scientific Reports, 2015, 5, 18173.	1.6	120
20884	Stacked bilayer phosphorene: strain-induced quantum spin Hall state and optical measurement. Scientific Reports, 2015, 5, 13927.	1.6	64
20885	Perfect spin filtering effect and negative differential behavior in phosphorus-doped zigzag graphene nanoribbons. Scientific Reports, 2015, 5, 15966.	1.6	28
20886	Anisotropic electronic conduction in stacked two-dimensional titanium carbide. Scientific Reports, 2015, 5, 16329.	1.6	107
20887	Practical concept of an all-optical hot carrier solar cell. Japanese Journal of Applied Physics, 2015, 54, 08KA03.	0.8	5
20888	Predicted Growth of Two-Dimensional Topological Insulator Thin Films of III-V Compounds on Si(111) Substrate. Scientific Reports, 2015, 5, 15463.	1.6	46
20889	Novel lithium-nitrogen compounds at ambient and high pressures. Scientific Reports, 2015, 5, 14204.	1.6	66
20890	Strain-driven band inversion and topological aspects in Antimonene. Scientific Reports, 2015, 5, 16108.	1.6	203
20891	van der Waals Heteroepitaxy of Semiconductor Nanowires. Semiconductors and Semimetals, 2015, , 125-172.	0.4	7
20892	Ab initio investigation of CaO-ZnO alloys under high pressure. Scientific Reports, 2015, 5, 11003.	1.6	13
20893	Lattice Strain Mapping of Platinum Nanoparticles on Carbon and SnO2 Supports. Scientific Reports, 2015, 5, 13126.	1.6	65
20894	Controlling single-molecule junction conductance by molecular interactions. Scientific Reports, 2015, 5, 11796.	1.6	19
20895	A New Silicon Phase with Direct Band Gap and Novel Optoelectronic Properties. Scientific Reports, 2015, 5, 14342.	1.6	74

#	Article	IF	Citations
20896	Band Structure Engineering and Thermoelectric Properties of Charge-Compensated Filled Skutterudites. Scientific Reports, 2015, 5, 14641.	1.6	41
20897	Defective Ti2Nb10O27.1: an advanced anode material for lithium-ion batteries. Scientific Reports, 2015, 5, 17836.	1.6	81
20898	Structural stability and mechanical property of Ni(111)â€“grapheneâ€“Ni(111) layered composite: A first-principles study. Japanese Journal of Applied Physics, 2015, 54, 125503.	0.8	3
20899	Ab Initio Description of Thermoelectric Properties Based on the Boltzmann Theory. , 2015, , 187-221.		0
20900	The electrical conductivity of Al2O3 under shock-compression. Scientific Reports, 2015, 5, 12823.	1.6	8
20901	Observation of Fermi Arcs in Non-Centrosymmetric Weyl Semi-Metal Candidate NbP. Chinese Physics Letters, 2015, 32, 107101.	1.3	59
20902	Strain induced piezoelectric effect in black phosphorus and MoS2 van der Waals heterostructure. Scientific Reports, 2015, 5, 16448.	1.6	88
20903	Structural, electronic and vibrational properties of few-layer 2H- and 1T-TaSe2. Scientific Reports, 2015, 5, 16646.	1.6	44
20904	Charting the complete elastic properties of inorganic crystalline compounds. Scientific Data, 2015, 2, 150009.	2.4	642
20905	Quantum Spin Hall States in Stanene/Ge(111). Scientific Reports, 2015, 5, 14196.	1.6	38
20906	Layered polymeric nitrogen in RbN3 at high pressures. Scientific Reports, 2015, 5, 16677.	1.6	33
20907	Graphdiyne as a promising material for detecting amino acids. Scientific Reports, 2015, 5, 16720.	1.6	59
20908	Nitrogen oxides under pressure: stability, ionization, polymerization and superconductivity. Scientific Reports, 2015, 5, 16311.	1.6	9
20909	Alternative, Lead-free, Hybrid Organicâ€“Inorganic Perovskites for Solar Applications: A DFT Analysis. Chemistry Letters, 2015, 44, 826-828.	0.7	65
20910	First-Principles Study of Antimony Doping Effects on the Iron-Based Superconductor CaFe(Sb_xAs_{1â^’}_x)₂. Journal of the Physical Society of Japan, 2015, 84, 093702.	0.7	5
20911	Structural properties of Bi2â^’xMnxSe3 thin films grown via molecular beam epitaxy. Journal of Applied Physics, 2015, 118, .	1.1	6
20912	Magnetostructural, mechanical and electronic properties of manganese tetraboride. AIP Advances, 2015, 5, 117208.	0.6	4
20913	Highly tunable magnetism in silicene doped with Cr and Fe atoms under isotropic and uniaxial tensile strain. Applied Physics Letters, 2015, 107, .	1.5	14

#	Article	IF	Citations
20914	An accurate full-dimensional potential energy surface for Hâ€“Au(111): Importance of nonadiabatic electronic excitation in energy transfer and adsorption. Journal of Chemical Physics, 2015, 143, 124708.	1.2	62
20915	Size and structure effects of PtN (N = 12 â^' 13) clusters for the oxygen reduction reaction: First-principles calculations. Journal of Chemical Physics, 2015, 143, 184312.	1.2	36
20916	Electrical Levels and Diffusion Barriers of Early 3d and 4d Transition Metals in Silicon. Solid State Phenomena, 0, 242, 264-270.	0.3	1
20917	Ab initio structure determination of n-diamond. Scientific Reports, 2015, 5, 13447.	1.6	13
20918	Graphene-enhanced intermolecular interaction at interface between copper- and cobalt-phthalocyanines. Journal of Chemical Physics, 2015, 143, 134706.	1.2	4
20919	Methane dissociation on Ni(111): A fifteen-dimensional potential energy surface using neural network method. Journal of Chemical Physics, 2015, 143, 144701.	1.2	68
20920	Accuracy of Lagrange-sinc functions as a basis set for electronic structure calculations of atoms and molecules. Journal of Chemical Physics, 2015, 142, 094116.	1.2	18
20921	Direct assignment of molecular vibrations via normal mode analysis of the neutron dynamic pair distribution function technique. Journal of Chemical Physics, 2015, 143, 124201.	1.2	9
20922	Pressure-driven formation and stabilization of superconductive chromium hydrides. Scientific Reports, 2015, 5, 17764.	1.6	37
20923	Prediction of a Superhard Carbon-Rich Câ€“N Compound Comparable to Diamond. Journal of Physical Chemistry C, 2015, 119, 28614-28619.	1.5	26
20924	Ab initio calculations of the optical properties of crystalline and liquid InSb. AIP Advances, 2015, 5, 117110.	0.6	5
20925	Reliable and cost effective design of intermetallic Ni2Si nanowires and direct characterization of its mechanical properties. Scientific Reports, 2015, 5, 15050.	1.6	19
20926	The Landauâ€“Lifshitz equation in atomistic models. Low Temperature Physics, 2015, 41, 705-712.	0.2	44
20927	Identifying site-dependent effects of an extra Co atom on electronic states of single Co-phthalocyanine molecule. Journal of Chemical Physics, 2015, 143, 034701.	1.2	6
20928	Pressure-induced phase transition and electrical properties of thermoelectric Al-doped Mg2Si. Journal of Applied Physics, 2015, 118, .	1.1	12
20929	Diameter Dependence of Lattice Thermal Conductivity of Single-Walled Carbon Nanotubes: Study from Ab Initio. Scientific Reports, 2015, 5, 15440.	1.6	35
20930	Bandgap engineering of MagnÃ©li phase TinO2nâ^'1: Electron-hole self-compensation. Journal of Chemical Physics, 2015, 143, 054701.	1.2	10
20931	Site preference and magnetic properties of Ga/In-substituted strontium hexaferrite: An ab initio study. Journal of Applied Physics, 2015, 118, .	1.1	19

#	Article	IF	Citations
20932	A first-principles study of cementite (Fe3C) and its alloyed counterparts: Elastic constants, elastic anisotropies, and isotropic elastic moduli. AIP Advances, 2015, 5, .	0.6	46
20933	Effects of biaxial stress and layer thickness on octahedral tilts in LaNiO3. Applied Physics Letters, 2015, 107, 261901.	1.5	3
20934	Tensile-strain effect of inducing the indirect-to-direct band-gap transition and reducing the band-gap energy of Ge. Journal of Applied Physics, 2015, 118, 105704.	1.1	13
20935	Rational design of inorganic dielectric materials with expected permittivity. Scientific Reports, 2015, 5, 16769.	1.6	14
20936	Ab initio molecular dynamics study of the properties of cerium in liquid sodium at 1000â€‰K temperature. Journal of Applied Physics, 2015, 118, .	1.1	7
20937	Ab initiostudy of anisotropic mechanical properties of LiCoO2 during lithium intercalation and deintercalation process. Journal of Applied Physics, 2015, 118, .	1.1	56
20938	Structural, electronic and optical properties of well-known primary explosive: Mercury fulminate. Journal of Chemical Physics, 2015, 143, 204704.	1.2	6
20939	Pressure-induced localisation of the hydrogen-bond network in KOH-VI. Journal of Chemical Physics, 2015, 143, 244706.	1.2	7
20940	The roles of Eu during the growth of eutectic Si in Al-Si alloys. Scientific Reports, 2015, 5, 13802.	1.6	35
20941	Electronic Band Structure and Sub-band-gap Absorption of Nitrogen Hyperdoped Silicon. Scientific Reports, 2015, 5, 10513.	1.6	31
20942	Effects of cation concentration on photocatalytic performance over magnesium vanadates. APL Materials, 2015, 3, 104405.	2.2	11
20943	Theoretical discovery of stable structures of group III-V monolayers: The materials for semiconductor devices. Applied Physics Letters, 2015, 107, .	1.5	31
20944	Hydrogen reverses the clustering tendency of carbon in amorphous silicon oxycarbide. Scientific Reports, 2015, 5, 13051.	1.6	14
20945	Density functional theory meta-GGA + U study of water incorporation in the metal-organic framework material Cu-BTC. Journal of Chemical Physics, 2015, 143, 024701.	1.2	14
20946	A tunable amorphous p-type ternary oxide system: The highly mismatched alloy of copper tin oxide. Journal of Applied Physics, 2015, 118, 105702.	1.1	5
20947	Robustness of Rashba and Dirac Fermions against Strong Disorder. Scientific Reports, 2015, 5, 11285.	1.6	11
20948	Electronic and magnetic properties of Si substituted Fe3Ge. Journal of Applied Physics, 2015, 118, .	1.1	15
20949	Anisotropic lattice thermal conductivity in chiral tellurium from first principles. Applied Physics Letters, 2015, 107, .	1.5	38

#	Article	IF	Citations
20950	Study of lattice vibration and thermal conductivity of BiCuSeO from first-principles calculations. Materials Research Society Symposia Proceedings, 2015, 1735, 110.	0.1	0
20951	Implementation of density functional embedding theory within the projector-augmented-wave method and applications to semiconductor defect states. Journal of Chemical Physics, 2015, 143, 102806.	1.2	46
20952	Quantitative analysis on electric dipole energy in Rashba band splitting. Scientific Reports, 2015, 5, 13488.	1.6	12
20953	DGDFT: A massively parallel method for large scale density functional theory calculations. Journal of Chemical Physics, 2015, 143, 124110.	1.2	55
20954	Magnetic Transition to Antiferromagnetic Phase in Gadolinium Substituted Topological Insulator Bi2Te3. Scientific Reports, 2015, 5, 10309.	1.6	37
20955	Phase engineering of monolayer transition-metal dichalcogenide through coupled electron doping and lattice deformation. Applied Physics Letters, 2015, 107, .	1.5	33
20956	The Schottky barrier modulation at PtSi/Si interface by strain and structural deformation. AIP Advances, 2015, 5, 087109.	0.6	6
20957	Dibenzothiophene adsorption at boron doped carbon nanoribbons studied within density functional theory. Journal of Applied Physics, 2015, 117, .	1.1	5
20958	Classification of octet AB-type binary compounds using dynamical charges: A materials informatics perspective. Scientific Reports, 2015, 5, 17504.	1.6	14
20959	Electronic, Dielectric and Plasmonic Properties of Two-Dimensional Electride Materials X2N (X=Ca,) Tj ETQq1 1 0.784314 rgBT /Overlock	1.6	73
20960	Hypervalent Iodine with Linear Chain at High Pressure. Scientific Reports, 2015, 5, 14393.	1.6	13
20961	Presence of a Doubly-Splitting Site and Its Effect on Thermoelectric Properties of Cu₄SnS₄. Materials Transactions, 2015, 56, 858-863.	0.4	12
20962	First Principles Calculation of Thermal Expansion of Carbon and Boron Nitrides Based on Quasi-Harmonic Approximation. Materials Transactions, 2015, 56, 1452-1456.	0.4	12
20963	First-Principles Based Phonon Calculation and Raman Spectroscopy Measurement of RuGa₂ and RuAl₂ with High Thermoelectric Power Factor. Nippon Kinzoku Gakkaishi/Journal of the Japan Institute of Metals, 2015, 79, 591-596.	0.2	0
20964	The electronic properties of impurities (N, C, F, Cl and S) in Ag3PO4: A hybrid functional method study. Scientific Reports, 2015, 5, 12750.	1.6	6
20965	Effects of Hydrogen Atoms on Vacancy Formation at fcc Fe(111) Surfaces. Nippon Kinzoku Gakkaishi/Journal of the Japan Institute of Metals, 2015, 79, 447-451.	0.2	2
20966	Stability of 12CaO·7Al₂O₃ Crystal under High-Pressure: Experimental and First-Principles Approaches. Materials Transactions, 2015, 56, 1350-1353.	0.4	6
20967	Yet Another Marked Difference among Impurities as Modifier Elements for Refinement of Eutectic Si in Al-Si Alloys. Materials Transactions, 2015, 56, 1475-1483.	0.4	5

#	Article	IF	Citations
20968	Local Environment Analysis of Na Ions in β-Tricalcium Phosphate by X-ray Absorption Near-Edge Structure Measurements and First-Principles Calculations. Materials Transactions, 2015, 56, 1457-1460.	0.4	2
20969	Adsorption Structure and Electronic Structure of Ethylene on Pt₃Ti(001) and PtTi₃(001) Surfaces: a DFT Study. Materials Transactions, 2015, 56, 479-484.	0.4	1
20970	Electronic, vibrational and thermodynamic properties of Ca10(AsO4)6(OH)2: first principles study. EPJ Applied Physics, 2015, 72, 31201.	0.3	3
20971	Study of Σ3 BaZrO₃ (210)[001] tilt grain boundaries using density functional theory and a space charge layer model. Journal of the Ceramic Society of Japan, 2015, 123, 245-249.	0.5	9
20972	Characterization of Baddeleyite-structure NbON Films Deposited by RF Reactive Sputtering for Solar Hydrogen Production Devices. Electrochemistry, 2015, 83, 711-714.	0.6	12
20973	Bonding Nature of LiCoO₂ by Topological Analysis of Electron Density from X-ray Diffraction. Electrochemistry, 2015, 83, 840-842.	0.6	9
20974	Average and Local Crystal Structure and Electronic Structure of 0.4Li₂MnO₃-0.6LiMn_{1/3}Ni_{1/3}Co<sub&g Using First-principles Calculations and Neutron Beam and Synchrotron X-Ray Sources. Electrochemistry, 2015, 83, 879-884.	0.6	10
20975	Oxygen Vacancy Induced Flat Phonon Mode at FeSe /SrTiO3 interface. Scientific Reports, 2015, 5, 10011.	1.6	39
20976	Electronic Structures of Clusters of Hydrogen Vacancies on Graphene. Scientific Reports, 2015, 5, 15310.	1.6	5
20977	Alloy composition of half-Heusler compounds for high thermoelectric performance. Transactions of the JSME (in Japanese), 2015, 81, 14-00652-14-00652.	0.1	0
20978	Influences of carbon concentration on crystal structures and ideal strengths of B2CxO compounds in the B-C-O system. Scientific Reports, 2015, 5, 15481.	1.6	23
20979	Al4SiC4 wurtzite crystal: Structural, optoelectronic, elastic, and piezoelectric properties. APL Materials, 2015, 3, .	2.2	14
20980	Partial Geometric Frustration in Inorganic Supramolecular Spin Systems with One-Dimensional Trigonally Aligned Magnetic Chains â^ž1(MCl4)2â^' (Mâ€‰=â€‰Fe2+, Co2+). Scientific Reports, 2015, 5, 17344.	1.6	2
20981	Effects of residual hydrogen in sputtering atmosphere on structures and properties of amorphous In-Ga-Zn-O thin films. Journal of Applied Physics, 2015, 118, .	1.1	34
20982	Ferroelectricity driven magnetism at domain walls in LaAlO3/PbTiO3 superlattices. Scientific Reports, 2015, 5, 13052.	1.6	16
20983	A coupled cluster and MÃ̊ller-Plesset perturbation theory study of the pressure induced phase transition in the LiH crystal. Journal of Chemical Physics, 2015, 143, 102817.	1.2	32
20984	Unraveling the luminescence signatures of chemical defects in polyethylene. Journal of Chemical Physics, 2015, 143, 124907.	1.2	21
20985	First-principles analysis of anharmonic nuclear motion and thermal transport in thermoelectric materials. AIP Conference Proceedings, 2015, , .	0.3	2

#	Article	IF	Citations
20986	Theoretical study on low dielectric loss perovskites Ba(Zn1/3Ta2/3)O3by first-principles calculations. Japanese Journal of Applied Physics, 2015, 54, 10NE01.	0.8	1
20987	Magnetism in Na-filled Fe-based skutterudites. Scientific Reports, 2015, 5, 10782.	1.6	12
20988	Heteroepitaxial growth of SnSe films by pulsed laser deposition using Se-rich targets. Journal of Applied Physics, 2015, 118, .	1.1	38
20989	Research Update: Plentiful magnetic moments in oxygen deficient SrTiO3. APL Materials, 2015, 3, .	2.2	21
20990	Surface stability and the selection rules of substrate orientation for optimal growth of epitaxial II-VI semiconductors. Applied Physics Letters, 2015, 107, 141607.	1.5	5
20991	Subspace formulation of time-dependent density functional theory for large-scale calculations. Journal of Chemical Physics, 2015, 143, 064110.	1.2	24
20992	Synergistic effect of alloying elements doping and external pressure on the elastic property of Ni3Al: A first-principles study. AIP Advances, 2015, 5, 077136.	0.6	5
20993	Spin-polarization inversion at small organic molecule/Fe4N interfaces: A first-principles study. Journal of Applied Physics, 2015, 118, 115301.	1.1	9
20994	Experimental and ab initio studies on sub-lattice ordering and magnetism in Co2Fe(Ge1â^'xSix) alloys. Journal of Applied Physics, 2015, 118, 133906.	1.1	3
20995	Universal roles of hydrogen in electrochemical performance of graphene: high rate capacity and atomistic origins. Scientific Reports, 2015, 5, 16190.	1.6	15
20996	Pressure-induced superconductivity in H2-containing hydride PbH4(H2)2. Scientific Reports, 2015, 5, 16475.	1.6	35
20997	The strain induced band gap modulation from narrow gap semiconductor to half-metal on Ti2CrGe: A first principles study. AIP Advances, 2015, 5, 117225.	0.6	4
20998	Band energy control of molybdenum oxide by surface hydration. Applied Physics Letters, 2015, 107, .	1.5	26
20999	Yttrium aluminium garnet under pressure: Structural, elastic, and vibrational properties from ab initio studies. Journal of Applied Physics, 2015, 118, .	1.1	11
21000	Remarkably stable amorphous metal oxide grown on Zr-Cu-Be metallic glass. Scientific Reports, 2015, 5, 18196.	1.6	16
21001	Many-body ab initio diffusion quantum Monte Carlo applied to the strongly correlated oxide NiO. Journal of Chemical Physics, 2015, 143, 164710.	1.2	39
21002	Effects of strain on electronic and optic properties of holey two-dimensional C2N crystals. Applied Physics Letters, 2015, 107, .	1.5	144
21003	Determination of the hyperfine magnetic field in magnetic carbon-based materials: DFT calculations and NMR experiments. Scientific Reports, 2015, 5, 14761.	1.6	20

#	Article	IF	Citations
21004	Optical signatures of bulk and solutions of KC8 and KC24. Journal of Applied Physics, 2015, 118, 044304.	1.1	8
21005	Temperature-dependent elastic properties of Ti1â^'xAlxN alloys. Applied Physics Letters, 2015, 107, .	1.5	46
21006	On the Stability and Abundance of Single Walled Carbon Nanotubes. Scientific Reports, 2015, 5, 16850.	1.6	31
21007	Two-dimensional topological insulators with tunable band gaps: Single-layer HgTe and HgSe. Scientific Reports, 2015, 5, 14115.	1.6	50
21008	Defect induced d ferromagnetism in a ZnO grain boundary. Journal of Chemical Physics, 2015, 143, 224703.	1.2	48
21009	A Giant Reconstruction of Î±-quartz (0001) Interpreted as Three Domains of Nano Dauphine Twins. Scientific Reports, 2015, 5, 14545.	1.6	11
21010	Atomically precise semiconductorâ€"graphene and hBN interfaces by Ge intercalation. Scientific Reports, 2015, 5, 17700.	1.6	24
21011	Bonding and structure in dense multi-component molecular mixtures. Journal of Chemical Physics, 2015, 143, 164513.	1.2	16
21012	First-principles study of nitric oxide oxidation on Pt(111) versus Pt overlayer on 3d transition metals. Journal of Vacuum Science and Technology A: Vacuum, Surfaces and Films, 2015, 33, 021402.	0.9	3
21013	Enhanced surface modification engineering (H, F, Cl, Br, and NO2) of CdS nanowires with and without surface dangling bonds. Journal of Applied Physics, 2015, 118, .	1.1	3
21014	Self-regulation of charged defect compensation and formation energy pinning in semiconductors. Scientific Reports, 2015, 5, 16977.	1.6	56
21015	Insights in the electronic structure and redox reaction energy in LiFePO4 battery material from an accurate Tran-Blaha modified Becke Johnson potential. Journal of Applied Physics, 2015, 118, 125107.	1.1	1
21016	First-principles equation of state and electronic properties of warm dense oxygen. Journal of Chemical Physics, 2015, 143, 164507.	1.2	38
21017	Exploration of tetrahedral structures in silicate cathodes using a motif-network scheme. Scientific Reports, 2015, 5, 15555.	1.6	27
21018	Role of force-constant difference in phonon scattering by nano-precipitates in PbTe. Journal of Applied Physics, 2015, 118, .	1.1	12
21019	Cu diffusion in single-crystal and polycrystalline TiN barrier layers: A high-resolution experimental study supported by first-principles calculations. Journal of Applied Physics, 2015, 118, .	1.1	36
21020	Computational phase diagrams of noble gas hydrates under pressure. Journal of Chemical Physics, 2015, 143, 154507.	1.2	30
21021	Detection of Cu2Zn5SnSe8 and Cu2Zn6SnSe9 phases in co-evaporated Cu2ZnSnSe4 thin-films. Applied Physics Letters, 2015, 107, .	1.5	6

#	Article	IF	Citations
21022	Controlling the Electronic Structures and Properties of in-Plane Transition-Metal Dichalcogenides Quantum Wells. Scientific Reports, 2015, 5, 17578.	1.6	28
21023	Rise and fall of ferromagnetism in O-irradiated Al2O3 single crystals. Journal of Applied Physics, 2015, 117, 233904.	1.1	7
21024	Electronic and magnetic properties of N-N split substitution in GaAs: A hybrid density functional study. AIP Advances, 2015, 5, 077187.	0.6	3
21025	DFT study of phonon dispersion in pure graphene. AIP Conference Proceedings, 2015, , .	0.3	6
21026	A projection-free method for representing plane-wave DFT results in an atom-centered basis. Journal of Chemical Physics, 2015, 143, 104109.	1.2	4
21027	Type I band alignment in GaAs81Sb19/GaAs core-shell nanowires. Applied Physics Letters, 2015, 107, .	1.5	14
21028	Relevance of non-equilibrium defect generation processes to resistive switching in TiO2. Journal of Applied Physics, 2015, 118, .	1.1	11
21029	The dissociative chemisorption of water on Ni(111): Mode- and bond-selective chemistry on metal surfaces. Journal of Chemical Physics, 2015, 142, 234705.	1.2	50
21030	The electronic structure and thermoelectric properties of BiTl9Te6 and SbTl9Te6: First-principles calculations. Journal of Applied Physics, 2015, 118, 235703.	1.1	1
21031	Unconventional interplay between heterovalent dopant elements: Switch-and-modulator band-gap engineering in (Y, Co)-Codoped CeO2 nanocrystals. Scientific Reports, 2015, 5, 15415.	1.6	12
21032	Greatly Enhancing Catalytic Activity of Graphene by Doping the Underlying Metal Substrate. Scientific Reports, 2015, 5, 12058.	1.6	23
21033	The mechanism of charge density wave in Pt-based layered superconductors: SrPt2As2 and LaPt2Si2. Scientific Reports, 2015, 5, 15052.	1.6	24
21034	Small hole polaron in CdTe: Cd-vacancy revisited. Scientific Reports, 2015, 5, 14509.	1.6	29
21035	Site occupancy and magnetic properties of Al-substituted M-type strontium hexaferrite. Journal of Applied Physics, 2015, 117, .	1.1	48
21036	Surface properties of atomically flat poly-crystalline SrTiO3. Scientific Reports, 2015, 5, 8822.	1.6	57
21037	Structural phase transitions in Bi2Se3 under high pressure. Scientific Reports, 2015, 5, 15939.	1.6	56
21038	Exotic stable cesium polynitrides at high pressure. Scientific Reports, 2015, 5, 16902.	1.6	58
21039	Spin splitting in 2D monochalcogenide semiconductors. Scientific Reports, 2015, 5, 17044.	1.6	55

#	Article	IF	Citations
21040	Stanene cyanide: a novel candidate of Quantum Spin Hall insulator at high temperature. Scientific Reports, 2015, 5, 18604.	1.6	14
21041	Electrical/thermal transport and electronic structure of the binary cobalt pnictides CoPn2 (Pn = As) Tj ETQq1 1 0.784314 rgBT /Overlo	0.6	10
21042	Site-specific dissociation dynamics of H2/D2 on Ag(111) and Co(0001) and the validity of the site-averaging model. Journal of Chemical Physics, 2015, 143, 114706.	1.2	34
21043	Electronic structure and photovoltaic application of BiI3. Applied Physics Letters, 2015, 107, .	1.5	125
21044	Giant piezoelectricity of monolayer group IV monochalcogenides: SnSe, SnS, GeSe, and GeS. Applied Physics Letters, 2015, 107, .	1.5	569
21045	Diverse lattice dynamics in ternary Cu-Sb-Se compounds. Scientific Reports, 2015, 5, 13643.	1.6	51
21046	Half-Metallic Behavior in Doped Sr2CrOsO6 Double Perovskite with High Transition Temperature. Scientific Reports, 2015, 5, 15010.	1.6	43
21047	Dielectric tensor of monoclinic Ga₂O₃ single crystals in the spectral range 0.5â€“8.5 eV. APL Materials, 2015, 3, 106106.	2.2	81
21048	Interlayer coupling effects on Schottky barrier in the arsenene-graphene van der Waals heterostructures. Applied Physics Letters, 2015, 107, .	1.5	128
21049	The role of acoustic phonon anharmonicity in determining thermal conductivity of CdSiP2 and AgGaS2: First principles calculations. AIP Advances, 2015, 5, .	0.6	16
21050	Orientation and strain modulated electronic structures in puckered arsenene nanoribbons. AIP Advances, 2015, 5, .	0.6	19
21051	An ab initio method for the prediction of the lattice thermal transport properties of oxide systems: Case study of Li2O and K2O. Journal of Applied Physics, 2015, 118, .	1.1	19
21052	Thermoelectric properties of rocksalt ZnO from first-principles calculations. Journal of Applied Physics, 2015, 118, .	1.1	16
21053	Electronic transport in VO2â€”Experimentally calibrated Boltzmann transport modeling. Applied Physics Letters, 2015, 107, .	1.5	7
21054	A room-temperature sodium rechargeable battery using an SO2-based nonflammable inorganic liquid catholyte. Scientific Reports, 2015, 5, 12827.	1.6	27
21055	Adsorption and diffusion of Ru adatoms on Ru(0001)-supported graphene: Large-scale first-principles calculations. Journal of Chemical Physics, 2015, 143, 164706.	1.2	8
21056	Design of exceptionally strong and conductive Cu alloys beyond the conventional speculation via the interfacial energy-controlled dispersion of Î³-Al2O3 nanoparticles. Scientific Reports, 2015, 5, 17364.	1.6	31
21057	Application of Grid Increment Cluster Expansion to Modeling Potential Energy Surface of Cu-Based Alloys. Materials Transactions, 2015, 56, 1077-1080.	0.4	1

#	Article	IF	Citations
21058	First Principles Calculations of Solute Sweeping and Stacking Faults in Mg-Zn-Y Alloy. Materials Transactions, 2015, 56, 933-936.	0.4	4
21059	Substitution-induced spin-splitted surface states in topological insulator (Bi1â˜'xSbx)2Te3. Scientific Reports, 2015, 5, 8830.	1.6	19
21060	Structure, stability, and superconductivity of new Xeâ€“H compounds under high pressure. Journal of Chemical Physics, 2015, 143, 124310.	1.2	13
21061	Nitrogen Backbone Oligomers. Scientific Reports, 2015, 5, 13239.	1.6	28
21062	Computational discovery of lanthanide doped and Co-doped Y3Al5O12 for optoelectronic applications. Applied Physics Letters, 2015, 107, 112109.	1.5	10
21063	Stabilization of weak ferromagnetism by strong magnetic response to epitaxial strain in multiferroic BiFeO3. Scientific Reports, 2015, 5, 12969.	1.6	17
21064	Antiperovskite Chalco-Halides Ba3(FeS4)Cl, Ba3(FeS4)Br and Ba3(FeSe4)Br with Spin Super-Super Exchange. Scientific Reports, 2015, 5, 15910.	1.6	15
21065	Experimental and theoretical investigations of the electronic band structure of metal-organic frameworks of HKUST-1 type. Applied Physics Letters, 2015, 107, .	1.5	57
21066	Thermal surface free energy and stress of iron. Scientific Reports, 2015, 5, 14860.	1.6	66
21067	A novel Gaussian-Sinc mixed basis set for electronic structure calculations. Journal of Chemical Physics, 2015, 143, 064108.	1.2	11
21068	N2 dissociation on W(110): An ab initio molecular dynamics study on the effect of phonons. Journal of Chemical Physics, 2015, 142, 104702.	1.2	22
21069	Improving p-type doping efficiency in Al0.83Ga0.17N alloy substituted by nanoscale (AlN)5/(GaN)1 superlattice with MgGa-ONâ€ˆÎ´-codoping: Role of O-atom in GaN monolayer. AIP Advances, 2015, 5, .	0.6	6
21070	Structures and magnetic properties of Co-Zr-B magnets studied by first-principles calculations. Journal of Applied Physics, 2015, 117, .	1.1	15
21071	Dopant-mediated structural and magnetic properties of TbMnO3. Applied Physics Letters, 2015, 107, .	1.5	18
21072	Adhesion at TiNi interfaces with Ta, Mo and Si. MATEC Web of Conferences, 2015, 33, 03006.	0.1	1
21073	Ab initiostudy of Ni2MnGa under shear deformation. MATEC Web of Conferences, 2015, 33, 05006.	0.1	3
21074	Controlling electronic structure through epitaxial strain in ZnSe/ZnTe nano-heterostructures. Journal of Applied Physics, 2015, 118, 015701.	1.1	7
21075	Surface confined quantum well state in MoS2(0001) thin film. Applied Physics Letters, 2015, 107, .	1.5	4

#	Article	IF	Citations
21076	Change of Electronic Structures by Dopant-Induced Local Strain. Scientific Reports, 2015, 5, 11227.	1.6	8
21077	Structure of a zinc oxide ultra-thin film on Rh(100). Journal of Chemical Physics, 2015, 143, 174701.	1.2	8
21078	Mechanisms for pressure-induced crystal-crystal transition, amorphization, and devitrification of SnI4. Journal of Chemical Physics, 2015, 143, 164508.	1.2	13
21079	Electronic Properties of Fluoride and Halfâ€“fluoride Superlattices KZnF3/KAgF3 and SrTiO3/KAgF3. Scientific Reports, 2015, 5, 15849.	1.6	14
21080	On the reactions of cyclohexyl phenyl sulfide with water by means of density functional theory. AIP Conference Proceedings, 2015, , .	0.3	0
21081	Sculpting the band gap: a computational approach. Scientific Reports, 2015, 5, 15522.	1.6	14
21082	Accurate thermoelastic tensor and acoustic velocities of NaCl. AIP Advances, 2015, 5, 127222.	0.6	5
21083	Enhanced electrical activation in In-implanted Ge by C co-doping. Applied Physics Letters, 2015, 107, .	1.5	3
21084	Ab-initio Study of Cation-rich InP(001) and GaP(001) Surface Reconstructions and Iodine Adsorption. IOP Conference Series: Materials Science and Engineering, 2015, 77, 012004.	0.3	1
21085	Singles correlation energy contributions in solids. Journal of Chemical Physics, 2015, 143, 102816.	1.2	39
21086	Quantum dynamical simulation of the scattering of Ar from a frozen LiF(100) surface based on a first principles interaction potential. Journal of Chemical Physics, 2015, 143, 014705.	1.2	2
21087	Transferability and accuracy by combining dispersionless density functional and incremental post-Hartree-Fock theories: Noble gases adsorption on coronene/graphene/graphite surfaces. Journal of Chemical Physics, 2015, 143, 194701.	1.2	34
21088	Non-uniform Solute Segregation at Semi-Coherent Metal/Oxide Interfaces. Scientific Reports, 2015, 5, 13086.	1.6	21
21089	High-temperature quantum anomalous Hall effect in honeycomb bilayer consisting of Au atoms and single-vacancy graphene. Scientific Reports, 2015, 5, 16843.	1.6	10
21090	On cooperative effects and aggregation of GNNQQNY and NNQQNY peptides. Journal of Chemical Physics, 2015, 143, 135103.	1.2	10
21091	Nature of the first-order liquid-liquid phase transition in supercooled silicon. Journal of Chemical Physics, 2015, 143, 054508.	1.2	14
21092	Tuning molecule-substrate coupling via deposition of metal adatoms. Journal of Chemical Physics, 2015, 143, 184704.	1.2	1
21093	Dry (Mg,Fe)SiO₃ perovskite in the Earth's lower mantle. Journal of Geophysical Research: Solid Earth, 2015, 120, 894-908.	1.4	47

#	Article	IF	Citations
21094	Structural and electrical properties of In-implanted Ge. Journal of Applied Physics, 2015, 118, .	1.1	7
21095	Robust half-metallicity and topological aspects in two-dimensional Cu-TPyB. Scientific Reports, 2015, 5, 14098.	1.6	29
21096	On the accuracy of commonly used density functional approximations in determining the elastic constants of insulators and semiconductors. Journal of Chemical Physics, 2015, 143, 144104.	1.2	52
21097	Adsorption of Fe atoms on strongly-correlated NiO(001) surfaces with surface oxygen vacancies: Oxide support effects. Journal of the Korean Physical Society, 2015, 67, 1798-1803.	0.3	0
21098	Cuprate-like Electronic Properties in Superlattices with AgIIF2 Square Sheet. Scientific Reports, 2014, 4, 5420.	1.6	18
21099	First principles study of electronic structure for cubane-like and ring-shaped structures of M4O4, M4S4 clusters (M = Mn, Fe, Co, Ni, Cu). AIP Advances, 2015, 5, 117231.	0.6	12
21100	Type-I clathrates of K_{7.69(2)}Cu_{2.94(6)}Ge_{43.06(6)}and Rb₈Ag_{2.79(4)}Ge_{43.21(4)}. RSC Advances, 2015, 5, 53829-53834.	1.7	5
21102	Effect of uniaxial strain on the site occupancy of hydrogen in vanadium from density-functional calculations. Scientific Reports, 2015, 5, 10301.	1.6	16
21103	A computational study of diffusion in a glass-forming metallic liquid. Scientific Reports, 2015, 5, 10956.	1.6	11
21104	A route to possible civil engineering materials: the case of high-pressure phases of lime. Scientific Reports, 2015, 5, 12330.	1.6	1
21105	Nanoclusters first: a hierarchical phase transformation in a novel Mg alloy. Scientific Reports, 2015, 5, 14186.	1.6	40
21106	Quantum Oscillation Signatures of Pressure-induced Topological Phase Transition in BiTeI. Scientific Reports, 2015, 5, 15973.	1.6	25
21107	First-Principles Study of Lithium and Sodium Atoms Intercalation in Fluorinated Graphite. Engineering, 2015, 1, 243-246.	3.2	16
21108	A multi-level cell for STT-MRAM realized by capping layer adjustment. , 2015, , .		0
21109	The nonchalant magnetic ordering of vacancies in graphene. Carbon, 2015, 91, 358-369.	5.4	10
21110	Effect of Zn Additions on the Mechanical Properties of Cu6Sn5-Based IMCs: Theoretical and Experimental Investigations. Journal of Electronic Materials, 2015, 44, 3920-3926.	1.0	21
21111	Site preference of Hf dopant in Ni3Al alloys: A perturbed angular correlation study. Journal of Alloys and Compounds, 2015, 622, 541-547.	2.8	3
21112	High-temperature stability of Î´â€²-ZrO. Calphad: Computer Coupling of Phase Diagrams and Thermochemistry, 2015, 51, 292-298.	0.7	21

#	Article	IF	Citations
21113	Insulatorâ€“metal transition in 1Tâ€²-MoS2 under uniaxial strain. Physics Letters, Section A: General, Atomic and Solid State Physics, 2015, 379, 2883-2889.	0.9	7
21114	Synergistic interplay between H and He in molybdenum: A first-principles study. Journal of Nuclear Materials, 2015, 466, 194-200.	1.3	11
21115	Plasticity of the dense hydrous magnesium silicate phase A at subduction zones conditions. Physics of the Earth and Planetary Interiors, 2015, 248, 1-11.	0.7	1
21116	Hybrid functional calculations on the Na and K impurities in substitutional and interstitial positions in Cu2ZnSnSe4. , 2015, , .		1
21117	Effect of Doping on Hydrogen Evolution Reaction of Vanadium Disulfide Monolayer. Nanoscale Research Letters, 2015, 10, 480.	3.1	31
21118	Thermodynamics of the pseudobinary GaAs1-xBix (0Âa‰ÂxÂa‰Â1) alloys studied by different exchange-correlation functionals, special quasi-random structures and Monte Carlo simulations. Computational Condensed Matter, 2015, 5, 7-13.	0.9	5
21119	Effect of Alloying Elements and Impurity (N) on Bulk and Grain Boundary Cohesion in Cr-Base Alloys. Advanced Materials Research, 0, 1119, 569-574.	0.3	1
21120	Origin of high data retention for Ge1Cu2Te3 phase-change memory. , 2015, , .		0
21121	Classical interaction potentials for diverse materials fromab initiodata: a review ofpotfit. Modelling and Simulation in Materials Science and Engineering, 2015, 23, 074002.	0.8	76
21122	Mechanochemically Reduced SiO₂ by Ti Incorporation as Lithium Storage Materials. ChemSusChem, 2015, 8, 3111-3117.	3.6	17
21123	Van der Waals Effects on semiconductor clusters. Journal of Computational Chemistry, 2015, 36, 1919-1927.	1.5	5
21124	Electricâ€fieldâ€induced magnetism of firstâ€row d⁰ semiconductor nanowires and nanotubes. Physica Status Solidi (B): Basic Research, 2015, 252, 484-489.	0.7	2
21125	Effect of chlorination on the TlBr band edges for improved room temperature radiation detectors. Physica Status Solidi (B): Basic Research, 2015, 252, 1266-1271.	0.7	4
21126	Coulombâ€correlation effects on the optical properties of Î²â€Mn₂V₂O₇. Physica Status Solidi (B): Basic Research, 2015, 252, 2853-2857.	0.7	9
21127	On the van der Waals interactions and the stability of polypeptide chains in helical conformations. International Journal of Quantum Chemistry, 2015, 115, 1613-1620.	1.0	12
21128	Metallic High-Angle Grain Boundaries in Monolayer Polycrystalline WS₂. Small, 2015, 11, 4503-4507.	5.2	43
21129	On the Structure and Stability of BaAl₄â€Type Ordered Derivatives in the Srâ€“Auâ€“Sn System for the 600 Â°C Section. Zeitschrift Fur Anorganische Und Allgemeine Chemie, 2015, 641, 375-382.	0.6	3
21130	Formation and Movement of Cationic Defects During Forming and Resistive Switching in SrTiO₃ Thin Film Devices. Advanced Functional Materials, 2015, 25, 6360-6368.	7.8	56

#	Article	IF	Citations
21131	Synthetic Crystals of Silver with Carbon: 3D Epitaxy of Carbon Nanostructures in the Silver Lattice. Advanced Functional Materials, 2015, 25, 4768-4777.	7.8	27
21132	A New Cubic Phase for a NaYF₄ Host Matrix Offering High Upconversion Luminescence Efficiency. Advanced Materials, 2015, 27, 5528-5533.	11.1	94
21133	Mechanistic insights into the structureâ€dependent selectivity of catalytic furfural conversion on platinum catalysts. AIChE Journal, 2015, 61, 3812-3824.	1.8	53
21136	Synthesis, Structure, and Properties of SrC(NH)₃, a Nitrogenâ€Based Carbonate Analogue with the Trinacria Motif. Angewandte Chemie - International Edition, 2015, 54, 12171-12175.	7.2	12
21137	Supercubooctahedron (Cs₆Cl)₂Cs₅[Ga₁₅Ge₉Se₄₈] Exhibiting Both Cation and Anion Exchange. Chemistry - A European Journal, 2015, 21, 9809-9815.	1.7	13
21138	Organic Dyes with Wellâ€Defined Structures for Highly Efficient Dyeâ€Sensitised Solar Cells Based on a Cobalt Electrolyte. Chemistry - A European Journal, 2015, 21, 14804-14811.	1.7	36
21139	Polymorphism of M₃AlX Phases (MÂ=ÂTi, Zr, Hf; XÂ=ÂC, N) and Thermomechanical Properties of Ti₃AlN Polymorphs. Journal of the American Ceramic Society, 2015, 98, 2570-2578.	1.9	14
21140	Na2TeS3, Na2TeSe3-mP24, and Na2TeSe3-mC48: Crystal Structures and Optical and Electrical Properties of Sodium Chalcogenidotellurates(IV). Inorganic Chemistry, 2015, 54, 11457-11464.	1.9	3
21141	Hydrogen-Substituted Superconductors SmFeAsO_{1â€“x}H_x Misidentified As Oxygen-Deficient SmFeAsO_{1â€“x}. Inorganic Chemistry, 2015, 54, 11567-11573.	1.9	13
21142	Photofragmentation of the Gas-Phase Lanthanum Isopropylcyclopentadienyl Complex: Computational Modeling vs Experiment. Journal of Physical Chemistry A, 2015, 119, 10838-10848.	1.1	26
21143	Structural Changes in Self-Catalyzed Adsorption of Carbon Monoxide on 1,4-Phenylene Diisocyanide Modified Au(111). Journal of Physical Chemistry C, 2015, 119, 18317-18325.	1.5	9
21144	Revising morphology of â©111âª-oriented silicon and germanium nanowires. Nano Convergence, 2015, 2, .	6.3	8
21145	Quantum mechanical ab initio calculations of the structural, electronic and optical properties of bulk gold nitrides. European Physical Journal B, 2015, 88, 1.	0.6	3
21146	Stable Metallic 1Tâ€WS₂ Nanoribbons Intercalated with Ammonia Ions: The Correlation between Structure and Electrical/Optical Properties. Advanced Materials, 2015, 27, 4837-4844.	11.1	207
21147	Hybrid Organicâ€“Inorganic Perovskites (HOIPs): Opportunities and Challenges. Advanced Materials, 2015, 27, 5102-5112.	11.1	372
21148	Understanding Defectâ€Stabilized Noncovalent Functionalization of Graphene. Advanced Materials Interfaces, 2015, 2, 1500277.	1.9	19
21149	Sulfur Atoms Bridging Fewâ€Layered MoS₂ with Sâ€Doped Graphene Enable Highly Robust Anode for Lithiumâ€Ion Batteries. Advanced Energy Materials, 2015, 5, 1501106.	10.2	165
21150	Elucidation of Pathways for NO Electroreduction on Pt(111) from First Principles. Angewandte Chemie, 2015, 127, 8373-8376.	1.6	22

#	Article	IF	Citations
21151	Twoâ€Dimensional Boron Monolayers Mediated by Metal Substrates. Angewandte Chemie - International Edition, 2015, 54, 13022-13026.	7.2	288
21152	Synergistic Effect of Nitrogen in Cobalt Nitride and Nitrogenâ€Doped Hollow Carbon Spheres for the Oxygen Reduction Reaction. ChemCatChem, 2015, 7, 1826-1832.	1.8	62
21153	Oxygenâ€Assisted Synthesis of Mesoporous Palladium Nanoparticles as Highly Active Electrocatalysts. Chemistry - A European Journal, 2015, 21, 18671-18676.	1.7	6
21154	Topochemical Transformations of CaX₂ (X=C, Si, Ge) to Form Freeâ€Standing Twoâ€Dimensional Materials. Chemistry - A European Journal, 2015, 21, 18454-18460.	1.7	31
21155	Bournonite PbCuSbS₃: Stereochemically Active Loneâ€Pair Electrons that Induce Low Thermal Conductivity. ChemPhysChem, 2015, 16, 3264-3270.	1.0	56
21156	Sensing Characteristics of a Grapheneâ€like Boron Carbide Monolayer towards Selected Toxic Gases. ChemPhysChem, 2015, 16, 3511-3517.	1.0	25
21157	Timeâ€and Energyâ€Efficient Solution Combustion Synthesis of Binary Metal Tungstate Nanoparticles with Enhanced Photocatalytic Activity. ChemSusChem, 2015, 8, 1652-1663.	3.6	44
21158	Synergy of atom-probe structural data and quantum-mechanical calculations in a theory-guided design of extreme-stiffness superlattices containing metastable phases. New Journal of Physics, 2015, 17, 093004.	1.2	15
21159	The Effects of Embedded Dipoles in Aromatic Selfâ€Assembled Monolayers. Advanced Functional Materials, 2015, 25, 3943-3957.	7.8	90
21160	Synthesis of Layerâ€Tunable Graphene: A Combined Kinetic Implantation and Thermal Ejection Approach. Advanced Functional Materials, 2015, 25, 3666-3675.	7.8	43
21161	Direct Detection of the Superoxide Anion as a Stable Intermediate in the Electroreduction of Oxygen in a Nonâ€Aqueous Electrolyte Containing Phenol as a Proton Source. Angewandte Chemie, 2015, 127, 8283-8286.	1.6	19
21164	Theory of Hydrogen Migration in Organicâ€“Inorganic Halide Perovskites. Angewandte Chemie - International Edition, 2015, 54, 12437-12441.	7.2	134
21165	Selective Stereochemical Catalysis Controlled by Specific Atomic Arrangement of Ordered Alloys. ChemCatChem, 2015, 7, 3472-3479.	1.8	28
21166	A Composite of Complex and Chemical Hydrides Yields the First Alâ€Based Amidoborane with Improved Hydrogen Storage Properties. Chemistry - A European Journal, 2015, 21, 14562-14570.	1.7	31
21167	Combined Experimental and Computational Studies of a Na₂Ni_{1â^'x}Cu_xFe(CN)₆ Cathode with Tunable Potential for Aqueous Rechargeable Sodiumâ€ion Batteries. Chemistry - A European Journal, 2015, 21, 15686-15691.	1.7	19
21168	Theoretical Study of Cubic and Orthorhombic Nd_{1â€“}_xSr_xMnO₃ as a Potential Solid Oxide Fuel Cell Cathode. Fuel Cells, 2015, 15, 839-844.	1.5	6
21169	Spontaneous polarization and piezoelectric properties of AlN nanowires: Maximally localized Wannier functions analysis. Europhysics Letters, 2015, 111, 67003.	0.7	9
21170	Prediction and theoretical investigation of new 2D and 3D periodical structures, having graphene-like bandstructures. Physica Status Solidi (B): Basic Research, 2015, 252, 2407-2411.	0.7	2

#	Article	IF	Citations
21171	A systematic first-principles study of the tungsten trioxide polymorphs. Physica Status Solidi (B): Basic Research, 2015, 252, 2290-2295.	0.7	2
21172	Surfaceâ€Supported Robust 2D Lanthanideâ€Carboxylate Coordination Networks. Small, 2015, 11, 6358-6364.	5.2	43
21173	MD modeling of screw dislocation influence upon initiation and mechanism of BCC-HCP polymorphous transition in iron. EPJ Web of Conferences, 2015, 94, 04023.	0.1	6
21174	Density Functional Theory Study on Defect Feature of AsGaGaAsin Gallium Arsenide. Journal of Nanomaterials, 2015, 2015, 1-5.	1.5	0
21175	The photorefractive characteristics of bismuth-oxide doped lithium niobate crystals. AIP Advances, 2015, 5, 017132.	0.6	13
21177	Engineering Solar Cell Absorbers by Exploring the Band Alignment and Defect Disparity: The Case of Cuâ€• and Agâ€Based Kesterite Compounds. Advanced Functional Materials, 2015, 25, 6733-6743.	7.8	284
21178	Tuning the Electronic Structure of Graphene through Collective Electrostatic Effects. Advanced Materials Interfaces, 2015, 2, 1500323.	1.9	8
21179	Adsorption of nitrogenâ€•and sulfurâ€•containing compounds on NiMoS for hydrotreating reactions: A DFT and vdWâ€•corrected study. AIChE Journal, 2015, 61, 4036-4050.	1.8	39
21180	Improvement in Hydrogen Desorption from Î²â€•and Î³â€•MgH₂ upon Transitionâ€•Metal Doping. ChemPhysChem, 2015, 16, 2557-2561.	1.0	22
21181	Enhancing the Efficiency of Water Oxidation by Boronâ€Doped BiVO₄ under Visible Light: Hole Trapping by BO₄ Tetrahedra. ChemPlusChem, 2015, 80, 1113-1118.	1.3	15
21182	Modeling and simulations of interface properties with firstâ€•principles electronic structure computations. Mathematical Methods in the Applied Sciences, 2015, 38, 4495-4501.	1.2	1
21183	Electronic structure and magnetic properties of an ironâ€•and tantalumâ€based double perovskite. Physica Status Solidi (B): Basic Research, 2015, 252, 2723-2726.	0.7	0
21184	Sulfur doping of AlN and AlGaN for improved n-type conductivity. Physica Status Solidi - Rapid Research Letters, 2015, 9, 462-465.	1.2	12
21185	V₁₆N_{1.5}: Metastable or Missing in the Binary Phase Diagram?. Zeitschrift Fur Anorganische Und Allgemeine Chemie, 2015, 641, 2610-2616.	0.6	3
21186	Phonons of Fe-based superconductor Ca₁₀Pt₄As₈(Fe_{1â^'x}Pt_xAs)₁₀. Journal of Physics Condensed Matter, 2015, 27, 465701.	0.7	1
21187	Building chessboard-like supramolecular structures on Au(111) surfaces. Nanotechnology, 2015, 26, 385601.	1.3	7
21188	Bending-induced phase transition in monolayer black phosphorus. Chinese Physics B, 2015, 24, 086401.	0.7	7
21189	Multi-scale Simulations of Metal-Semiconductor Nanoscale Contacts. Journal of Physics: Conference Series, 2015, 647, 012030.	0.3	2

#	Article	IF	Citations
21190	Brewster angle of shock-compressed xenon plasmas. Journal of Physics: Conference Series, 2015, 653, 012111.	0.3	7
21191	First-principles study of oxygen adsorption and diffusion on the UN(001) surface. Physica Scripta, 2015, 90, 125801.	1.2	3
21192	Treatment of delocalized electron transfer in periodic and embedded cluster <scp>DFT</scp> calculations: The case of <scp>C</scp>u on <scp>Z</scp>n<scp>O</scp> (100). Journal of Computational Chemistry, 2015, 36, 2394-2405.	1.5	2
21193	High hydrogen storage capacity in calciumâ€decorated silicene nanostructures. Physica Status Solidi (B): Basic Research, 2015, 252, 2072-2078.	0.7	12
21194	Properties of armchair and zigzag CdS nanoribbons: A density functional study. Physica Status Solidi (B): Basic Research, 2015, 252, 2280-2289.	0.7	3
21195	Tellurium vacancy in cadmium telluride revisited: Size effects in the electronic properties. Physica Status Solidi (B): Basic Research, 2015, 252, 2649-2656.	0.7	11
21196	Complex magnetic states in Ni/Fe bi-segmented nanorods. Physica Status Solidi - Rapid Research Letters, 2015, 9, 740-744.	1.2	4
21197	Carbonates in zeolites: Formation, properties, reactivity. International Journal of Quantum Chemistry, 2015, 115, 1709-1717.	1.0	10
21198	Innovation and discovery of grapheneâ€like materials via densityâ€functional theory computations. Wiley Interdisciplinary Reviews: Computational Molecular Science, 2015, 5, 360-379.	6.2	205
21199	Structural transitions in Pb(In1âˆ•2Nb1âˆ•2)O₃ under pressure. Journal of Advanced Dielectrics, 2015, 05, 1550033.	1.5	2
21200	The 2015 H. H. Uhlig Summer Research Fellowship -- Summary Report: Optimizing the Interfacial Capacitance of Graphene Oxide-Based Supercapacitors through Basal Hydroxyl Group Coverage. Electrochemical Society Interface, 2015, 24, 76-77.	0.3	0
21201	Study of electronic and magnetic properties and related x-ray absorption spectroscopy of ultrathin Co films on BaTiO₃. Journal of Physics Condensed Matter, 2015, 27, 426003.	0.7	2
21202	Crystal structure and photoluminescence of (Gd,Ce)₄(SiS₄)₃and (Y,Ce)₄(SiS₄)₃. Materials Research Express, 2015, 2, 036203.	0.8	5
21203	Functionalized Graphene Superlattice as a Singleâ€Sheet Solar Cell. Advanced Functional Materials, 2015, 25, 5199-5205.	7.8	7
21204	Buckling Patterns of Grapheneâ€“Boron Nitride Alloy on Ru(0001). Advanced Materials Interfaces, 2015, 2, 1500322.	1.9	9
21205	Manganese Tetraboride, MnB₄: Highâ€Temperature Crystal Structure, pâ€“n Transition, ⁵⁵Mn NMR Spectroscopy, Solid Solutions, and Mechanical Properties. Chemistry - A European Journal, 2015, 21, 8177-8181.	1.7	26
21206	Cooperative interplay between impurities and charge density wave in the phase transition of atomic wires. New Journal of Physics, 2015, 17, 093026.	1.2	10
21207	Mechanical, electronic, and thermodynamic properties of zirconium carbide from first-principles calculations. Chinese Physics B, 2015, 24, 116301.	0.7	17

#	Article	IF	Citations
21208	Flux Crystal Growth of the Ternary Polygermanide LaPtGe₂, a pâ€Type Metal. European Journal of Inorganic Chemistry, 2015, 2015, 2164-2172.	1.0	10
21209	Interplay of strain and interdiffusion in Heusler alloy bilayers. Physica Status Solidi - Rapid Research Letters, 2015, 9, 321-325.	1.2	5
21210	Hybrid density functional study of optically active Er³⁺ centers in GaN. Physica Status Solidi - Rapid Research Letters, 2015, 9, 722-725.	1.2	14
21211	Hard Radiation Detection from the Selenophosphate Pb₂P₂Se₆. Advanced Functional Materials, 2015, 25, 4874-4881.	7.8	33
21212	Effect of Nitrogen and Fluorine Coâ€substitution on the Structure and Magnetic Properties of Cr₂O₃. ChemPhysChem, 2015, 16, 1502-1508.	1.0	15
21213	Phase stability of transition metal dichalcogenide by competing ligand field stabilization and charge density wave. 2D Materials, 2015, 2, 035019.	2.0	29
21214	Gram-Scale Aqueous Synthesis of Stable Few-Layered 1T-MoS₂: Applications for Visible-Light-Driven Photocatalytic Hydrogen Evolution. Small, 2015, 11, 5556-5564.	5.2	508
21215	Type II Bi_{1â€…â^'â€…x}W_xO_{1.5â€…+â€…1.5x}: a (3â€…+â€…3)-dimensional commensurate modulation that stabilizes the fast-ion conducting delta phase of bismuth oxide. Acta Crystallographica Section B: Structural Science, Crystal Engineering and Materials, 2015, 71, 679-687.	0.5	6
21216	On Intensifying Carrier Impurity Scattering to Enhance Thermoelectric Performance in Crâ€Doped Ce_yCo₄Sb₁₂. Advanced Functional Materials, 2015, 25, 6660-6670.	7.8	77
21217	In Situ Fabrication of PtCo Alloy Embedded in Nitrogenâ€Doped Graphene Nanopores as Synergistic Catalyst for Oxygen Reduction Reaction. Advanced Materials Interfaces, 2015, 2, 1500365.	1.9	21
21218	Atomic Scale Structure and Reduction of Cerium Oxide at the Interface with Platinum. Advanced Materials Interfaces, 2015, 2, 1500375.	1.9	25
21219	CuSbSe₂ as a Potential Photovoltaic Absorber Material: Studies from Theory to Experiment. Advanced Energy Materials, 2015, 5, 1501203.	10.2	99
21221	Deciphering a Nanocarbonâ€Based Artificial Peroxidase: Chemical Identification of the Catalytically Active and Substrateâ€Binding Sites on Graphene Quantum Dots. Angewandte Chemie, 2015, 127, 7282-7286.	1.6	39
21223	Hybridization Gap and Dresselhaus Spin Splitting in EuIr₄In₂Ge₄. Angewandte Chemie - International Edition, 2015, 54, 9186-9191.	7.2	7
21224	Boosting Photocatalytic Water Splitting: Interfacial Charge Polarization in Atomically Controlled Coreâ€“Shell Cocatalysts. Angewandte Chemie - International Edition, 2015, 54, 14810-14814.	7.2	131
21225	Enhanced CO Oxidation on the Oxide/Metal Interface: From Ultraâ€High Vacuum to Nearâ€Atmospheric Pressures. ChemCatChem, 2015, 7, 2620-2627.	1.8	47
21226	DFT Investigation on the Competition of the Waterâ€“Gas Shift Reaction Versus Methanation on Clean and Potassiumâ€Modified Nickel(1â€‰1â€‰1) Surfaces. ChemCatChem, 2015, 7, 3928-3935.	1.8	54
21227	Cyclotrimerizationâ€Induced Chiral Supramolecular Structures of 4â€Ethynyltriphenylamine on Au(111) Surface. Chemistry - A European Journal, 2015, 21, 12978-12983.	1.7	17

#	Article	IF	Citations
21228	The Solid Solution Sr_{1â^'x}Ba_xGa₂: Substitutional Disorder and Chemical Bonding Visited by NMR Spectroscopy and Quantum Mechanical Calculations. Chemistry - A European Journal, 2015, 21, 13971-13982.	1.7	8
21229	Electronic Structure and Partial Charge Distribution of Doxorubicin in Different Molecular Environments. ChemPhysChem, 2015, 16, 1451-1460.	1.0	26
21230	Linear Alkane Cï£¿C Bond Chemistry Mediated by Metal Surfaces. ChemPhysChem, 2015, 16, 1356-1360.	1.0	12
21231	Ammine Calcium and Strontium Borohydrides: Syntheses, Structures, and Properties. ChemSusChem, 2015, 8, 3472-3482.	3.6	24
21232	The Effects of Alkaline-Earth Counterions on the Architectures, Band-Gap Energies, and Proton Transfer of Triazole-Based Coordination Polymers. European Journal of Inorganic Chemistry, 2015, 2015, 2085-2091.	1.0	8
21233	Density functional theory study of the effect of helium clusters on tritium-containing palladium lattices. Journal of Physics Condensed Matter, 2015, 27, 475002.	0.7	4
21234	Significance of Surface Trivalent Manganese in the Electrocatalytic Activity of Water Oxidation in Undoped and Doped MnO₂ Nanowires. ChemCatChem, 2015, 7, 1848-1856.	1.8	44
21235	Potassiumâ€Induced Effect on the Structure and Chemical Activity of the Cu_xO/Cu(1â€‰1â€‰1) (x â‰ˆ 2) Surface: A Combined Scanning Tunneling Microscopy and Density Functional Theory Study. ChemCatChem, 2015, 7, 3865-3872.	1.8	38
21236	Highly Luminescent, Waterâ€Soluble Lanthanide Fluorobenzoates: Syntheses, Structures and Photophysics, Part I: Lanthanide Pentafluorobenzoates. Chemistry - A European Journal, 2015, 21, 17921-17932.	1.7	58
21237	A Study of Overheating of Thermostatically Controlled TiO₂ Thin Films by Using Raman Spectroscopy. ChemPhysChem, 2015, 16, 3949-3958.	1.0	0
21238	The Active Molybdenum Oxide Phase in the Methanol Oxidation to Formaldehyde (Formox Process): A DFT Study. ChemSusChem, 2015, 8, 2231-2239.	3.6	29
21239	Molecular Dynamics Simulations of Warm Dense Carbon. Contributions To Plasma Physics, 2015, 55, 390-398.	0.5	11
21240	An analytical bondâ€order potential for carbon. Journal of Computational Chemistry, 2015, 36, 1719-1735.	1.5	36
21241	SCCâ€DFTB parameters for simulating hybrid goldâ€thiolates compounds. Journal of Computational Chemistry, 2015, 36, 2075-2087.	1.5	82
21242	Effect of ferromagnetic ordering on phonons in KCo2Se2. Journal of Physics Condensed Matter, 2015, 27, 415403.	0.7	3
21243	Rapid theory-guided prototyping of ductile Mg alloys: from binary to multi-component materials. New Journal of Physics, 2015, 17, 093009.	1.2	35
21244	Structural and elastic properties of ternary silicides ScTSi (Tâ•Co, Ni, Cu, Ru, Rh, Pd, Ir, Pt) and of the equiatomic intermetallic compounds YTX (Tâ•Ni, Ir and Xâ•Si, Ge, Sn, Pb). Physica Status Solidi (B): Basic Research, 2015, 252, 2769-2777.	0.7	5
21245	Towards a metallic quasiâ€d⁹ system without copper: AgO at high pressure. Physica Status Solidi - Rapid Research Letters, 2015, 9, 401-404.	1.2	6

#	Article	IF	Citations
21246	Shallow donor in natural MoS2. Physica Status Solidi - Rapid Research Letters, 2015, 9, 707-710.	1.2	5
21247	Unoccupied titanium 3dstates due to subcluster formation in stoichiometric TiO₂nanoparticles. International Journal of Quantum Chemistry, 2015, 115, 1175-1180.	1.0	4
21248	Aligned Growth of Hexagonal Boron Nitride Monolayer on Germanium. Small, 2015, 11, 5375-5380.	5.2	56
21249	Î²â€Phase Formation in Feâ€“Mnâ€“Alâ€“C Austenitic Steels. Steel Research International, 2015, 86, 1161-1169.	1.0	61
21250	K₅Mn₃O₆ and Rb₈Mn₅O₁₀, New Charge Ordered Quasi Oneâ€Dimensional Oxomanganates (II, III). Zeitschrift Fur Anorganische Und Allgemeine Chemie, 2015, 641, 316-321.	0.6	9
21251	Influence of Valence Electron Concentration on Laves Phases: Structures and Phase Stability of Pseudoâ€Binary MgZn_{2â€“x}Pd_x. Zeitschrift Fur Anorganische Und Allgemeine Chemie, 2015, 641, 1486-1494.	0.6	9
21252	A Nonâ€rareâ€Earth Ions Selfâ€Activated White Emitting Phosphor under Single Excitation. Advanced Functional Materials, 2015, 25, 6833-6838.	7.8	48
21253	Nitrogen Terminated Diamond. Advanced Materials Interfaces, 2015, 2, 1500079.	1.9	61
21254	Lead Replacement in CH₃NH₃PbI₃ Perovskites. Advanced Electronic Materials, 2015, 1, 1500089.	2.6	67
21255	Cation Size Effects on the Electronic and Structural Properties of Solutionâ€Processed Inâ€“Xâ€“O Thin Films. Advanced Electronic Materials, 2015, 1, 1500146.	2.6	36
21257	Direct Detection of the Superoxide Anion as a Stable Intermediate in the Electroreduction of Oxygen in a Nonâ€Aqueous Electrolyte Containing Phenol as a Proton Source. Angewandte Chemie - International Edition, 2015, 54, 8165-8168.	7.2	78
21258	Elucidation of Pathways for NO Electroreduction on Pt(111) from First Principles. Angewandte Chemie - International Edition, 2015, 54, 8255-8258.	7.2	111
21259	Titanium Trisulfide Monolayer: Theoretical Prediction of a New Directâ€Gap Semiconductor with High and Anisotropic Carrier Mobility. Angewandte Chemie - International Edition, 2015, 54, 7572-7576.	7.2	239
21260	Ammoniaâ€“(Dinitramido)boranes: Highâ€Energyâ€Density Materials. Angewandte Chemie - International Edition, 2015, 54, 11730-11734.	7.2	45
21261	Theoretical calculations on the structural, electronic, and optical properties of bulk silver nitrides. Physica Status Solidi (B): Basic Research, 2015, 252, 2840-2852.	0.7	10
21262	In situ TEM study of reversible and irreversible electroforming in Pt/Ti:NiO/Pt heterostructures. Physica Status Solidi - Rapid Research Letters, 2015, 9, 301-306.	1.2	10
21263	First principles study of isostructural phase transition in Sb₂Te₃ under high pressure. Physica Status Solidi - Rapid Research Letters, 2015, 9, 379-383.	1.2	13
21264	On the Faceted and Inclined Twin Boundary of Titanium Carbide Derived from Nanolaminated Ti₃AlC₂. Journal of the American Ceramic Society, 2015, 98, 1664-1667.	1.9	4

#	Article	IF	Citations
21265	Optimization of active nanomaterials and transparent electrodes using printing and vacuum processes. , 2015, , 253-284.		0
21266	First-Principles Study of La Doping Effects on the Electronic Structures and Photocatalytic Properties of Anatase TiO2. Chinese Journal of Chemical Physics, 2015, 28, 681-687.	0.6	6
21268	Search for Effective Sites of Proximity Gettering Induced by Ion Implantation in Si Wafers with First Principles Calculation. Solid State Phenomena, 2015, 242, 271-276.	0.3	0
21269	Ultrafast defect dynamics: A new approach to all optical broadband switching employing amorphous selenium thin films. AIP Advances, 2015, 5, 077164.	0.6	6
21270	The graph-theoretic minimum energy path problem for ionic conduction. AIP Advances, 2015, 5, 107107.	0.6	3
21271	Controlled switching of single-molecule junctions by mechanical motion of a phenyl ring. Beilstein Journal of Nanotechnology, 2015, 6, 2088-2095.	1.5	9
21272	Electronic Structure and Magnetism of Mn-Doped ZnO Nanowires. Nanomaterials, 2015, 5, 885-894.	1.9	18
21273	Piezoelectric, Mechanical and Acoustic Properties of KNaNbOF5 from First-Principles Calculations. Materials, 2015, 8, 8578-8589.	1.3	5
21274	Calculations of helium separation via uniform pores of stanene-based membranes. Beilstein Journal of Nanotechnology, 2015, 6, 2470-2476.	1.5	9
21275	High-mobility material research for thin-film transistor with amorphous thalliumâ€“zincâ€“tin oxide semiconductor. Japanese Journal of Applied Physics, 2015, 54, 104101.	0.8	2
21276	Irregular Homogeneity Domains in Ternary Intermetallic Systems. Applied Sciences (Switzerland), 2015, 5, 1570-1589.	1.3	9
21277	Pt Monolayer Electrocatalyst for Oxygen Reduction Reaction on Pd-Cu Alloy: First-Principles Investigation. Catalysts, 2015, 5, 1193-1201.	1.6	12
21278	Optical Properties of Silicon-Rich Silicon Nitride (SixNyHz) from First Principles. Computation, 2015, 3, 657-669.	1.0	10
21279	Enthalpies of Formation of Transition Metal Diborides: A First Principles Study. Crystals, 2015, 5, 562-582.	1.0	11
21280	A Density Functional Tight Binding Study of Acetic Acid Adsorption on Crystalline and Amorphous Surfaces of Titania. Molecules, 2015, 20, 3371-3388.	1.7	40
21281	A simple method for understanding the triangular growth patterns of transition metal dichalcogenide sheets. AIP Advances, 2015, 5, .	0.6	19
21282	Itinerant Magnetism in Metallic CuFe2Ge2. PLoS ONE, 2015, 10, e0121186.	1.1	5
21283	First-Principles Calculations, Experimental Study, and Thermodynamic Modeling of the Al-Co-Cr System. PLoS ONE, 2015, 10, e0121386.	1.1	14

#	Article	IF	Citations
21284	Shock compression response of poly(4-methyl-1-pentene) plastic to 985â€‰GPa. Journal of Applied Physics, 2015, 118, .	1.1	19
21285	Opening the way to molecular cycloaddition of large molecules on supported silicene. Journal of Chemical Physics, 2015, 143, 154706.	1.2	6
21286	Temperature dependent spectroscopic ellipsometry and Raman scattering of PbTiO_3-based relaxor ferroelectric single crystals around MPB region. Optical Materials Express, 2015, 5, 2478.	1.6	3
21287	Structural and Electronic Properties of GaN (0001)/Î±-Al₂O₃(0001) Interface. Advances in Condensed Matter Physics, 2015, 2015, 1-6.	0.4	5
21288	Effect of Dopant Compensation on the Behavior of Dissolved Iron and Iron-Boron Related Complexes in Silicon. International Journal of Photoenergy, 2015, 2015, 1-6.	1.4	1
21289	Synthesis of the ZnGa₂S₄Nanocrystals and Their Visible-Light Photocatalytic Degradation Property. Journal of Nanomaterials, 2015, 2015, 1-7.	1.5	3
21290	Prediction of a New Phase of CuxS near Stoichiometric Composition. International Journal of Photoenergy, 2015, 2015, 1-7.	1.4	8
21291	Near Surface Stoichiometry in UO₂: A Density Functional Theory Study. Journal of Chemistry, 2015, 2015, 1-8.	0.9	2
21292	First Principles Study of Electronic and Magnetic Properties of Co-Doped Armchair Graphene Nanoribbons. Journal of Nanomaterials, 2015, 2015, 1-9.	1.5	3
21293	First-Principle and Experimental Study of a Gadolinium-Praseodymium-Cobalt Pseudobinary Intermetallic Compound. Journal of Materials, 2015, 2015, 1-9.	0.1	5
21294	First-Principles Study on Electronic and Optical Properties of Graphene-Like Boron Phosphide Sheets. Chinese Journal of Chemical Physics, 2015, 28, 588-594.	0.6	66
21295	First-Principles Study of Field Emission from Zigzag Graphene Nanoribbons Terminated with Ether Groups. Chinese Journal of Chemical Physics, 2015, 28, 573-578.	0.6	1
21296	Automatic and Systematic Atomistic Simulations in the MedeA^{Â®}Software Environment: Application to EU-REACH. Oil and Gas Science and Technology, 2015, 70, 405-417.	1.4	8
21297	Improvement of Anti-aging Property at Low Temperature by Cr Addition in Bake Hardenable Ultra Low Nitrogen Steels. ISIJ International, 2015, 55, 2648-2656.	0.6	2
21298	Ab initio Studies of O2 Adsorption on (110) Nickel-Rich Pentlandite (Fe4Ni5S8) Mineral Surface. Minerals (Basel, Switzerland), 2015, 5, 665-678.	0.8	23
21299	What superconducts in sulfur hydrides under pressure and why. Physical Review B, 2015, 91, .	1.1	220
21300	Pt atoms adsorbed on<mml:math xmlns:mml="http://www.w3.org/1998/Math/MathML"><mml:mrow><mml:msub><mml:mi>TiO</mml:mi><mml:mn>2</mml:mn></mml	1.1	11
	with noncontact atomic force microscopy and first-principles simulations. Physical Review B, 2015, 91, .		
21301	Structural and thermoelectric properties ofFeSb3skutterudite thin films. Physical Review B, 2015, 91, .	1.1	11

#	Article	IF	Citations
21302	Hexagonal AlN: Dimensional-crossover-driven band-gap transition. Physical Review B, 2015, 91, .	1.1	121
21303	Role of N defects in paramagnetic CrN at finite temperatures from first principles. Physical Review B, 2015, 91, .	1.1	30
21304	Hydrogen influence on diffusion in nickel from first-principles calculations. Physical Review B, 2015, 91, .	1.1	19
21305	Superconducting dome in<mml:math xmlns:mml="http://www.w3.org/1998/Math/MathML"><mml:msub><mml:mi>MoS</mml:mi><mml:mn>2</mml:mn></mml:msub></mm xmlns:mml="http://www.w3.org/1998/Math/MathML"><mml:msub><mml:mi>TiSe</mml:mi><mml:mn>2</mml:mn></mml:msub></m by quasiparticle-phonon coupling. Physical Review B, 2015, 91, .	1.1	44
21306	Modulation of electronic and mechanical properties of phosphorene through strain. Physical Review B, 2015, 91, .	1.1	172
21307	Effects of Lifshitz Transition on Charge Transport in Magnetic Phases of Fe-Based Superconductors. Physical Review Letters, 2015, 114, 097003.	2.9	22
21308	Novel stable hard transparent conductors in TiO2-TiC system: Design materials from scratch. Scientific Reports, 2015, 4, 7503.	1.6	8
21309	Pressure-induced zigzag phosphorus chain and superconductivity in boron monophosphide. Scientific Reports, 2015, 5, 8761.	1.6	16
21310	Effect of solute atoms on dislocation motion in Mg: An electronic structure perspective. Scientific Reports, 2015, 5, 8793.	1.6	69
21311	High-temperature Superconductivity in compressed Solid Silane. Scientific Reports, 2015, 5, 8845.	1.6	25
21312	Bottom-up formation of robust gold carbide. Scientific Reports, 2015, 5, 8891.	1.6	11
21313	Coexistence of metallic and insulating-like states in graphene. Scientific Reports, 2015, 5, 8974.	1.6	3
21314	Structural band-gap tuning in g-C₃N₄. Physical Chemistry Chemical Physics, 2015, 17, 957-962.	1.3	107
21315	Confinement of massless Dirac fermions in the graphene matrix induced by the B/N heteroatoms. Physical Chemistry Chemical Physics, 2015, 17, 5586-5593.	1.3	4
21316	On the mechanism of catalytic hydrogenation of thiophene on hydrogen tungsten bronze. Physical Chemistry Chemical Physics, 2015, 17, 9698-9705.	1.3	11
21317	Understanding chemical expansion in perovskite-structured oxides. Physical Chemistry Chemical Physics, 2015, 17, 10028-10039.	1.3	89
21318	4d transition-metal doped hematite for enhancing photoelectrochemical activity: theoretical prediction and experimental confirmation. RSC Advances, 2015, 5, 19353-19361.	1.7	26
21319	Coverage dependent water dissociative adsorption on Fe(110) from DFT computation. Physical Chemistry Chemical Physics, 2015, 17, 8811-8821.	1.3	60

#	Article	IF	Citations
21320	Dumbbell stanane: a large-gap quantum spin hall insulator. Physical Chemistry Chemical Physics, 2015, 17, 16624-16629.	1.3	25
21321	Type VIII Si based clathrates: prospects for a giant thermoelectric power factor. Physical Chemistry Chemical Physics, 2015, 17, 8850-8859.	1.3	23
21322	Structure and dynamics of metallic and carburized catalytic Ni nanoparticles: effects on growth of single-walled carbon nanotubes. Physical Chemistry Chemical Physics, 2015, 17, 15056-15064.	1.3	5
21323	Facet-dependent photocatalytic and antibacterial properties of Î±-Ag₂WO₄crystals: combining experimental data and theoretical insights. Catalysis Science and Technology, 2015, 5, 4091-4107.	2.1	123
21324	Band engineering via biaxial strain for enhanced thermoelectric performance in stannite-type Cu₂ZnSnSe₄. RSC Advances, 2015, 5, 24908-24914.	1.7	13
21325	The effect of the aliphatic carboxylate linkers on the electronic structures, chemical bonding and optical properties of the uranium-based metalâ€“organic frameworks. RSC Advances, 2015, 5, 26735-26748.	1.7	9
21326	Effects of magnetic ordering and electron correlations on the stability of FeN. RSC Advances, 2015, 5, 31270-31274.	1.7	13
21327	Theoretical insight into the roles of cocatalysts in the Niâ€“NiO/Î²-Ga₂O₃ photocatalyst for overall water splitting. Journal of Materials Chemistry A, 2015, 3, 10309-10319.	5.2	26
21328	Electronic properties of tin dichalcogenide monolayers and effects of hydrogenation and tension. Journal of Materials Chemistry C, 2015, 3, 3714-3721.	2.7	34
21329	Two-dimensional metalloporphyrin monolayers with intriguing electronic and spintronic properties. Journal of Materials Chemistry C, 2015, 3, 6901-6907.	2.7	22
21330	Origin of the smaller conductances of Rh, Pb, and Co atomic junctions in hydrogen environment. Journal of Applied Physics, 2015, 117, 064310.	1.1	1
21331	Direct observation of charge mediated lattice distortions in complex oxide solid solutions. Applied Physics Letters, 2015, 106, .	1.5	33
21332	Atomic-scale observation of dynamical fluctuation and three-dimensional structure of gold clusters. Journal of Applied Physics, 2015, 117, .	1.1	22
21333	Theoretical investigations on the layer-anion interaction in Mgâ€“Al layered double hydroxides: Influence of the anion nature and layer composition. Journal of Chemical Physics, 2015, 142, 094704.	1.2	7
21334	Benchmarking DFT and semiempirical methods on structures and lattice energies for ten ice polymorphs. Journal of Chemical Physics, 2015, 142, 124104.	1.2	84
21335	Mechanistic Study of the Persistent Luminescence of CaAl₂O₄:Eu,Nd. Chemistry of Materials, 2015, 27, 2195-2202.	3.2	186
21336	Effective Way to Control the Performance of a Ceria-Based DeNO_x Catalyst with Improved Alkali Resistance: Acidâ€“Base Adjusting. Journal of Physical Chemistry C, 2015, 119, 15077-15084.	1.5	24
21337	Structure Sensitivity of NO Adsorptionâ€“Dissociation on Pd_n (n = 8, 13, 19, 25) Clusters. Journal of Physical Chemistry C, 2015, 119, 12941-12948.	1.5	23

#	Article	IF	Citations
21338	Hydrogen Adsorption and Associated Electronic and Magnetic Properties of Rh-Decorated (8,0) Carbon Nanotubes Using Density Functional Theory. Journal of Physical Chemistry C, 2015, 119, 13238-13247.	1.5	32
21339	Molecular Design to Enhance the Thermal Stability of a Photo Switchable Molecular Junction Based on Dimethyldihydropyrene and Cyclophanediene Isomerization. Journal of Physical Chemistry C, 2015, 119, 11468-11474.	1.5	14
21340	Electronic Properties of Phosphorene/Graphene and Phosphorene/Hexagonal Boron Nitride Heterostructures. Journal of Physical Chemistry C, 2015, 119, 13929-13936.	1.5	295
21341	Entropic Separation of Styrene/Ethylbenzene Mixtures by Exploitation of Subtle Differences in Molecular Configurations in Ordered Crystalline Nanoporous Adsorbents. Langmuir, 2015, 31, 3771-3778.	1.6	46
21342	Electronic Properties of Electrical Vortices in Ferroelectric Nanocomposites from Large-Scale Ab Initio Computations. Nano Letters, 2015, 15, 3224-3229.	4.5	16
21343	Monolayer Ti₂CO₂: A Promising Candidate for NH₃ Sensor or Capturer with High Sensitivity and Selectivity. ACS Applied Materials & Interfaces, 2015, 7, 13707-13713.	4.0	524
21344	Photoinduced Water Oxidation at the Aqueous GaN (101Ì…0) Interface: Deprotonation Kinetics of the First Proton-Coupled Electron-Transfer Step. ACS Catalysis, 2015, 5, 2317-2323.	5.5	33
21345	Exploring Furfural Catalytic Conversion on Cu(111) from Computation. ACS Catalysis, 2015, 5, 4020-4032.	5.5	109
21346	Dependence on Size of Supported Rh Nanoclusters in the Decomposition of Methanol. ACS Catalysis, 2015, 5, 4276-4287.	5.5	25
21347	Mechanistic Insights into Metal Lewis Acid-Mediated Catalytic Transfer Hydrogenation of Furfural to 2-Methylfuran. ACS Catalysis, 2015, 5, 3988-3994.	5.5	244
21348	Substrate Facet Effect on the Growth of Monolayer MoS₂ on Au Foils. ACS Nano, 2015, 9, 4017-4025.	7.3	97
21349	Lateral Manipulation of Atomic Vacancies in Ultrathin Insulating Films. ACS Nano, 2015, 9, 5318-5325.	7.3	17
21350	Direct Visualization of Catalytically Active Sites at the FeOâ€“Pt(111) Interface. ACS Nano, 2015, 9, 7804-7814.	7.3	67
21351	Polymorph Selectivity of Superconducting CuSe₂ Through Kinetic Control of Solid-State Metathesis. Journal of the American Chemical Society, 2015, 137, 3827-3833.	6.6	38
21352	Theoretical Investigation on Incorporation and Diffusion Properties of Xe in Uranium Mononitride. Journal of Physical Chemistry C, 2015, 119, 5783-5789.	1.5	14
21353	DFT Study of the Conversion of Furfuryl Alcohol to 2-Methylfuran on RuO₂ (110). Journal of Physical Chemistry C, 2015, 119, 5938-5945.	1.5	37
21354	Size and Temperature Dependence of Electron Transfer between CdSe Quantum Dots and a TiO₂ Nanobelt. Journal of Physical Chemistry C, 2015, 119, 5639-5647.	1.5	19
21355	Shear-Induced Mechanochemistry: Pushing Molecules Around. Journal of Physical Chemistry C, 2015, 119, 7115-7123.	1.5	65

#	Article	IF	Citations
21356	Elucidating the Optical Properties of Novel Heterolayered Materials Based on MoTe₂â€“InN for Photovoltaic Applications. Journal of Physical Chemistry C, 2015, 119, 11886-11895.	1.5	56
21357	Ni Deposition on Yttria-Stabilized ZrO₂(111) Surfaces: A Density Functional Theory Study. Journal of Physical Chemistry C, 2015, 119, 6581-6591.	1.5	22
21358	The Nature and Role of the Goldâ€“Krypton Interactions in Small Neutral Gold Clusters. Journal of Physical Chemistry A, 2015, 119, 3075-3088.	1.1	11
21359	Growth of Close-Packed Semiconducting Single-Walled Carbon Nanotube Arrays Using Oxygen-Deficient TiO₂ Nanoparticles as Catalysts. Nano Letters, 2015, 15, 403-409.	4.5	59
21360	Extended Halogen Bonding between Fully Fluorinated Aromatic Molecules. ACS Nano, 2015, 9, 2574-2583.	7.3	119
21361	Edge dislocation slows down oxide ion diffusion in doped CeO2 by segregation of charged defects. Nature Communications, 2015, 6, 6294.	5.8	138
21362	Large enhancement of magnetic moment inL1₀ordered FePt thin films by Nd substitutional doping. Journal Physics D: Applied Physics, 2015, 48, 255001.	1.3	9
21363	X-ray absorption spectroscopy on magnetic nanoscale systems for modern applications. Reports on Progress in Physics, 2015, 78, 062501.	8.1	15
21364	Structural stability of single-layer MoS₂ under large strain. Journal of Physics Condensed Matter, 2015, 27, 105401.	0.7	29
21365	Searching for new TiO2crystal phases with better photoactivity. Journal of Physics Condensed Matter, 2015, 27, 134203.	0.7	22
21366	Transformation of electronic properties and structural phase transition from HfN to Hf₃N₄. Journal of Physics Condensed Matter, 2015, 27, 225501.	0.7	7
21367	Capacity retention behavior and morphology evolution of Si_xGe_{1â^'x}nanoparticles as lithium-ion battery anode. Nanotechnology, 2015, 26, 255702.	1.3	13
21368	Special quasirandom structure modeling of fluorite-structured oxide solid solutions with aliovalent cation substitutions. Modelling and Simulation in Materials Science and Engineering, 2015, 23, 055001.	0.8	4
21369	Mechanical stability of Ni and Ir under hydrostatic and uniaxial loading. Modelling and Simulation in Materials Science and Engineering, 2015, 23, 055010.	0.8	14
21370	Theoretical study on the removal of adsorbed sulfur on Pt anchored graphene surfaces. International Journal of Hydrogen Energy, 2015, 40, 6942-6949.	3.8	14
21371	Nitrogen and fluorine co-doped graphite nanofibers as high durable oxygen reduction catalyst in acidic media for polymer electrolyte fuel cells. Carbon, 2015, 93, 130-142.	5.4	130
21372	Thermal conductivity of skutterudite CoSb3 from first principles: Substitution and nanoengineering effects. Scientific Reports, 2015, 5, 7806.	1.6	70
21373	Conductivity-limiting bipolar thermal conductivity in semiconductors. Scientific Reports, 2015, 5, 10136.	1.6	107

#	Article	IF	Citations
21374	First-Principles Study of Ca3Sc2Si3O12:Ce3+ Phosphors. Chinese Journal of Chemical Physics, 2015, 28, 150-154.	0.6	5
21375	The best nanoparticle size distribution for minimum thermal conductivity. Scientific Reports, 2015, 5, 8995.	1.6	45
21376	Prediction of novel crystal structures and superconductivity of compressed HBr. RSC Advances, 2015, 5, 45812-45816.	1.7	6
21377	Charge Mediated Semiconducting-to-Metallic Phase Transition in Molybdenum Disulfide Monolayer and Hydrogen Evolution Reaction in New 1Tâ€² Phase. Journal of Physical Chemistry C, 2015, 119, 13124-13128.	1.5	295
21378	A computational study of interfaces in WCâ€“Co cemented carbides. Modelling and Simulation in Materials Science and Engineering, 2015, 23, 045001.	0.8	26
21379	Triggering the electrocatalytic hydrogen evolution activity of the inert two-dimensional MoS₂ surface via single-atom metal doping. Energy and Environmental Science, 2015, 8, 1594-1601.	15.6	1,109
21380	First-principles study of the inversion thermodynamics and electronic structure of<mml:math xmlns:mml="http://www.w3.org/1998/Math/MathML"><mml:mrow><mml:mi>Fe</mml:mi><mml:msub><mml:mi>M</mml:mi><mml:mi><mml:m		

#	Article	IF	Citations
21392	Electronic, structural, and substrate effect properties of single-layer covalent organic frameworks. Journal of Chemical Physics, 2015, 142, 184708.	1.2	19
21393	Density Functional Characterization of the Electronic Structures and Band Bending of Rutile RuO₂/TiO₂(110) Heterostructures. Journal of Physical Chemistry C, 2015, 119, 12394-12399.	1.5	13
21394	Stable half-metallic monolayers of FeCl2. Applied Physics Letters, 2015, 106, .	1.5	108
21395	Transformation pathways in high-pressure solid nitrogen: From molecular N2 to polymeric cg-N. Journal of Chemical Physics, 2015, 142, 094505.	1.2	27
21396	Interaction of rhyolite melts with monazite, xenotime, and zircon surfaces. Contributions To Mineralogy and Petrology, 2015, 169, 1.	1.2	3
21397	Dominance of Interface Chemistry over the Bulk Properties in Determining the Electronic Structure of Epitaxial Metal/Perovskite Oxide Heterojunctions. Chemistry of Materials, 2015, 27, 4093-4098.	3.2	4
21398	Epitaxial Growth of a Single-Crystal Hybridized Boron Nitride and Graphene Layer on a Wide-Band Gap Semiconductor. Journal of the American Chemical Society, 2015, 137, 6897-6905.	6.6	55
21399	Nanostructured robust cobalt metal alloy based anode electro-catalysts exhibiting remarkably high performance and durability for proton exchange membrane fuel cells. Journal of Materials Chemistry A, 2015, 3, 14015-14032.	5.2	27
21400	First-Principles Study on the Thermal Stability of LiNiO₂ Materials Coated by Amorphous Al₂O₃ with Atomic Layer Thickness. ACS Applied Materials & Interfaces, 2015, 7, 11599-11603.	4.0	47
21401	Unexpected buckled structures and tunable electronic properties in arsenic nanosheets: insights from first-principles calculations. Journal of Physics Condensed Matter, 2015, 27, 225304.	0.7	33
21402	Energy and dose dependence of proton-irradiation damage in graphene. RSC Advances, 2015, 5, 31861-31865.	1.7	21
21403	XRD analysis of TRAM composed from [Sb2Te3/GeTe] superlattice film and its switching characteristics. Materials Research Society Symposia Proceedings, 2015, 1729, 41-45.	0.1	0
21404	Improving the photocatalytic activity of TiO2 through reduction. RSC Advances, 2015, 5, 35661-35666.	1.7	19
21405	Two-dimensional metallic behavior at polar MgO/BaTiO ₃ (110) interfaces. Chinese Physics B, 2015, 24, 037301.	0.7	4
21406	Light-Driven and Phonon-Assisted Dynamics in Organic and Semiconductor Nanostructures. Chemical Reviews, 2015, 115, 5929-5978.	23.0	160
21407	First principles study of defect formation in thermoelectric zinc antimonide, Î²-Zn4Sb3. Journal of Physics Condensed Matter, 2015, 27, 125502.	0.7	12
21408	Kondo effect in binuclear metal-organic complexes with weakly interacting spins. Physical Review B, 2015, 91, .	1.1	14
21409	In situ investigation of two-step nucleation and growth of CdS nanoparticles from solution. Nanoscale, 2015, 7, 11328-11333.	2.8	30

#	Article	IF	Citations
21410	Two-dimensional arsenic monolayer sheet predicted from first-principles. Chinese Physics B, 2015, 24, 036301.	0.7	8
21411	Modeling accumulation capacitance-voltage characteristic of MoS2 thin flake transistors. Semiconductor Science and Technology, 2015, 30, 055013.	1.0	1
21412	A theoretical investigation of mixing thermodynamics, age-hardening potential and electronic structure of ternary M11â€“xM2xB2 alloys with AlB2 type structure. Scientific Reports, 2015, 5, 9888.	1.6	44
21413	Temperature dependent electron paramagnetic resonance (EPR) of SrZrO. Journal of Magnetism and Magnetic Materials, 2015, 391, 101-107.	1.0	14
21414	Spectroscopy of transmission resonances through a C₆₀junction. Journal of Physics Condensed Matter, 2015, 27, 015001.	0.7	7
21415	Ab initiodefect energetics of perovskite (001) surfaces for solid oxide fuel cells: A comparative study of<mml:math xmlns:mml="http://www.w3.org/1998/Math/MathML"><mml:mrow><mml:mi>LaMn</mml:mi><mml:msub><mml:mi mathvariant="normal">O</mml:mi><mml:mn>3</mml:mn></mml:msub></mml:mrow></mml:math>versus<mml:math xmlns:mml="http://www.w3.org/1998/Math/MathML"><mml:mrow><mml:mi>SrTi</mml:mi><mml:msub><mml:mi mathvariant="normal">O</mml:mi><mml:mn>3</mml:mn></mml:msub></mml:mrow></mml:math>and<mml:math	1.1	39
21416	First-principles investigations on vibrational, thermodynamic, mechanical properties and thermal conductivity of L1₂Al₃X (X = Sc, Er, Tm, Yb) intermetallics. Physica Scripta, 2015, 90, 065701.	1.2	18
21417	Reactivity of Hydrated Monovalent First Row Transition Metal Ions [M(H2O)n]+, M = Cr, Mn, Fe, Co, Ni, Cu, and Zn, n < 50, Toward Acetonitrile. Journal of Physical Chemistry A, 2015, 119, 5566-5578.	1.1	13
21418	Spin rotation driven ferroelectric polarization with a 180Â° flop in double-perovskite Lu2CoMnO6. RSC Advances, 2015, 5, 43432-43439.	1.7	8
21419	Development of a new dipole model: interatomic potential for yttria-stabilized zirconia for bulk and surface. Journal of Physics Condensed Matter, 2015, 27, 015005.	0.7	3
21420	Anisotropy in the Raman scattering of a CaFeO_{2.5} single crystal and its link with oxygen ordering in Brownmillerite frameworks. Journal of Physics Condensed Matter, 2015, 27, 225403.	0.7	19
21421	Structures of the metallic and superconducting high pressure phases of solid CS2. Scientific Reports, 2015, 5, 10458.	1.6	18
21422	Informatics-Aided Density Functional Theory Study on the Li Ion Transport of Tavorite-Type LiMTO₄F (M³⁺â€“T⁵⁺, M²⁺â€“T⁶⁺). Journal of Chemical Information and Modeling, 2015, 55, 1158-1168.	2.5	42
21423	Understanding Anharmonicity in fcc Materials: From its Origin toabÂinitioStrategies beyond the Quasiharmonic Approximation. Physical Review Letters, 2015, 114, 195901.	2.9	115
21424	Half-metallicity induced by boron adsorption on an Fe₃O₄(100) surface. Physical Chemistry Chemical Physics, 2015, 17, 15386-15391.	1.3	7
21425	Complex magnetism of Mn-based Pnma ternary alloys: Three exchange interactions induced by the position of Mn atoms. Physics Letters, Section A: General, Atomic and Solid State Physics, 2015, 379, 2370-2373.	0.9	1
21426	Thin-film Sb2Se3 photovoltaics with oriented one-dimensional ribbons and benign grain boundaries. Nature Photonics, 2015, 9, 409-415.	15.6	781
21427	Chemical modifications and stability of phosphorene with impurities: a first principles study. Physical Chemistry Chemical Physics, 2015, 17, 15209-15217.	1.3	78

#	Article	IF	Citations
21428	Methanol Oxidation to Formaldehyde on VSiBEA Zeolite: A Combined DFT/vdW/Transition Path Sampling and Experimental Study. Journal of Physical Chemistry C, 2015, 119, 13619-13631.	1.5	14
21429	First-Principles Energetics of Some Nonmetallic Impurity Atoms in Plutonium Dioxide. Journal of Physical Chemistry C, 2015, 119, 14879-14889.	1.5	24
21430	Predicting Methane Storage in Open-Metal-Site Metalâ€“Organic Frameworks. Journal of Physical Chemistry C, 2015, 119, 13451-13458.	1.5	62
21431	Electronic and Vibrational States of Single Tinâ€“Phthalocyanine Molecules in Double Layers on Ag(111). Journal of Physical Chemistry C, 2015, 119, 15716-15722.	1.5	16
21432	Insight Into the Effect of CuNi(111) and FeNi(111) Surface Structure and Second Metal Composition on Surface Carbon Elimination by O or OH: A Comparison Study with Ni(111) Surface. Journal of Physical Chemistry C, 2015, 119, 14135-14144.	1.5	25
21433	Crystalline LiN₅ Predicted from First-Principles as a Possible High-Energy Material. Journal of Physical Chemistry Letters, 2015, 6, 2363-2366.	2.1	145
21434	Flicker Noise as a Probe of Electronic Interaction at Metalâ€“Single Molecule Interfaces. Nano Letters, 2015, 15, 4143-4149.	4.5	109
21435	The phase diagram and hardness of carbon nitrides. Scientific Reports, 2015, 5, 9870.	1.6	78
21436	Unraveling the mechanism of 720 nm sub-band-gap optical absorption of a Ta₃N₅ semiconductor photocatalyst: a hybrid-DFT calculation. Physical Chemistry Chemical Physics, 2015, 17, 8166-8171.	1.3	34
21437	Dissociative dynamics of O₂ on Ag(110). Physical Chemistry Chemical Physics, 2015, 17, 9436-9445.	1.3	22
21438	Oxidation of SO2 and NO by epoxy groups on graphene oxides: the role of the hydroxyl group. RSC Advances, 2015, 5, 22802-22810.	1.7	44
21439	Giant magnetocrystalline anisotropy of 5d transition metal-based phthalocyanine sheet. Physical Chemistry Chemical Physics, 2015, 17, 17182-17189.	1.3	19
21440	Pyrimidine and s-triazine as structural motifs for ordered adsorption on Si(100): a first principles study. Physical Chemistry Chemical Physics, 2015, 17, 16876-16885.	1.3	6
21441	Electronic structures of anatase (TiO₂)_{1â^'x}(TaON)_x solid solutions: a first-principles study. Physical Chemistry Chemical Physics, 2015, 17, 17980-17988.	1.3	5
21442	Ab initio atomistic thermodynamics study on the oxidation mechanism of binary and ternary alloy surfaces. Journal of Chemical Physics, 2015, 142, 064705.	1.2	18
21443	Plasmas, 2015, 22, 056319.	0.7	11
21444	Induce magnetism into silicene by embedding transition-metal atoms. Applied Physics Letters, 2015, 106, .	1.5	28
21445	Electronic and magnetic properties of epitaxial perovskite SrCrO₃(0â€‰0â€‰1). Journal of Physics Condensed Matter, 2015, 27, 245605.	0.7	11

#	Article	IF	Citations
21446	Topological phase transitions of (BixSb1â^'x)2Se3 alloys by density functional theory. Journal of Physics Condensed Matter, 2015, 27, 255501.	0.7	10
21447	A new phase of phosphorus: the missed tricycle type red phosphorene. Journal of Physics Condensed Matter, 2015, 27, 265301.	0.7	47
21448	A metallic metal oxide (Ti₅O₉)-metal oxide (TiO₂) nanocomposite as the heterojunction to enhance visible-light photocatalytic activity. Nanotechnology, 2015, 26, 255705.	1.3	16
21449	Application of a VanÂDerÂWaals Density Functional to Small Molecular Complexes and Solids. , 2015, , .		1
21450	Band Symmetries of Mixed-Valence Topological Insulator: SmB₆. Journal of the Physical Society of Japan, 2015, 84, 024722.	0.7	34
21451	First-Principles Calculation of Phonon and Schottky Heat Capacities of Plutonium Dioxide. Journal of the Physical Society of Japan, 2015, 84, 053602.	0.7	4
21452	Tuning magnetism by biaxial strain in native ZnO. Physical Chemistry Chemical Physics, 2015, 17, 16536-16544.	1.3	19
21453	Stability, electronic and magnetic properties of Co-anchored on graphene sheets towards S, SH and H₂S molecules. EPJ Applied Physics, 2015, 70, 31301.	0.3	3
21454	First-principles study on the effect of alloying elements on the elastic deformation response in Î²-titanium alloys. Journal of Applied Physics, 2015, 117, .	1.1	14
21455	Bonding Effects on the Slip Differences in the<mml:math xmlns:mml="http://www.w3.org/1998/Math/MathML" display="inline"><mml:mi>B</mml:mi><mml:mn>1</mml:mn></mml:math>Monocarbides. Physical Review Letters, 2015, 114, 165502.	2.9	59
21456	Phase stability, chemical bonding and mechanical properties of titanium nitrides: a first-principles study. Physical Chemistry Chemical Physics, 2015, 17, 11763-11769.	1.3	126
21457	Mechanistic Insights into the Electrochemical Reduction of CO₂ to CO on Nanostructured Ag Surfaces. ACS Catalysis, 2015, 5, 4293-4299.	5.5	476
21458	Tuning the acidâ€“metal balance in Pd/ and Pt/zeolite catalysts for the hydroalkylation of m-cresol. Journal of Catalysis, 2015, 328, 173-185.	3.1	42
21459	Catechol and HCl Adsorption on TiO₂(110) in Vacuum and at the Waterâ€“TiO₂ Interface. Journal of Physical Chemistry Letters, 2015, 6, 2277-2281.	2.1	32
21460	Dual Passivation of Intrinsic Defects at the Compound Semiconductor/Oxide Interface Using an Oxidant and a Reductant. ACS Nano, 2015, 9, 4843-4849.	7.3	2
21461	Defect Engineering and Phase Junction Architecture of Wide-Bandgap ZnS for Conflicting Visible Light Activity in Photocatalytic H₂ Evolution. ACS Applied Materials & Interfaces, 2015, 7, 13915-13924.	4.0	193
21462	Remote p-type Doping in GaSb/InAs Core-shell Nanowires. Scientific Reports, 2015, 5, 10813.	1.6	11
21463	Synthesis of black ultrathin BiOCl nanosheets for efficient photocatalytic H2 production under visible light irradiation. Journal of Power Sources, 2015, 293, 409-415.	4.0	125

#	Article	IF	Citations
21464	Mechanism of CO methanation on the Ni4/Î³-Al2O3 and Ni3Fe/Î³-Al2O3 catalysts: A density functional theory study. International Journal of Hydrogen Energy, 2015, 40, 8864-8876.	3.8	34
21465	Intrinsic half-metallicity in fractal carbon nitride honeycomb lattices. Physical Chemistry Chemical Physics, 2015, 17, 21837-21844.	1.3	14
21466	A computational study on water adsorption on Cu2O(111) surfaces: The effects of coverage and oxygen defect. Applied Surface Science, 2015, 343, 33-40.	3.1	59
21467	DFT study of CO adsorption on Pd-SnO2(1 1 0) surfaces. Applied Surface Science, 2015, 347, 291-298.	3.1	39
21468	In situ hybridization of carbon nanotubes with bacterial cellulose for three-dimensional hybrid bioscaffolds. Biomaterials, 2015, 58, 93-102.	5.7	82
21469	Improvement in dehydrogenation performance ofÂMg(BH4)2Â·2NH3 doped with transition metal: First-principles investigation. International Journal of Hydrogen Energy, 2015, 40, 8721-8731.	3.8	15
21470	Electronic and structural characterization of InN heterostructures grown on Î²-LiGaO2 (001) substrates. Vacuum, 2015, 119, 106-111.	1.6	9
21471	Prediction of ordered omega phase formation by coupled replaciveâ€“displacive processes in Zr3Al2Nb and Zr4AlNb alloy: a first-principles study. Philosophical Magazine, 2015, 95, 1201-1220.	0.7	5
21472	Improvement of the Half-Metallic Stability of Co₂FeAl Heusler Alloys by GeTe-Doping. IEEE Transactions on Magnetics, 2015, 51, 1-4.	1.2	2
21473	Topological Metal of NaBi with Ultralow Lattice Thermal Conductivity and Electron-phonon Superconductivity. Scientific Reports, 2015, 5, 8446.	1.6	7
21474	A combined theoretical and experimental investigation of uranium dioxide under high static pressure. Journal of Physics Condensed Matter, 2015, 27, 265401.	0.7	9
21475	Bipolar doping of double-layer graphene vertical heterostructures with hydrogenated boron nitride. Physical Chemistry Chemical Physics, 2015, 17, 11692-11699.	1.3	9
21476	Multiple Redox Modes in the Reversible Lithiation of High-Capacity, Peierls-Distorted Vanadium Sulfide. Journal of the American Chemical Society, 2015, 137, 8499-8508.	6.6	127
21477	Metalâ€“Organic Framework Nodes as Nearly Ideal Supports for Molecular Catalysts: NU-1000- and UiO-66-Supported Iridium Complexes. Journal of the American Chemical Society, 2015, 137, 7391-7396.	6.6	228
21478	Atomic origin of high-temperature electron trapping in metal-oxide-semiconductor devices. Applied Physics Letters, 2015, 106, .	1.5	20
21479	Interactions of point defects with stacking faults in oxygen-free phosphorus-containing copper. Journal of Nuclear Materials, 2015, 462, 160-164.	1.3	9
21480	Examining the thermal conductivity of the half-Heusler alloy TiNiSn by first-principles calculations. Journal Physics D: Applied Physics, 2015, 48, 235302.	1.3	31
21481	Ligand-Hole in [SnI6] Unit and Origin of Band Gap in Photovoltaic Perovskite Variant Cs2SnI6. Bulletin of the Chemical Society of Japan, 2015, 88, 1250-1255.	2.0	130

#	Article	IF	Citations
21482	Strain-induced coupling of electrical polarization and structural defects in SrMnO3 films. Nature Nanotechnology, 2015, 10, 661-665.	15.6	153
21483	Effect of isovalent non-magnetic Fe-site doping on the electronic structure and spontaneous polarization of BiFeO3. Journal of Applied Physics, 2015, 117, 184104.	1.1	11
21484	Electrospun nylon 6,6 nanofibers functionalized with cyclodextrins for removal of toluene vapor. Journal of Applied Polymer Science, 2015, 132, .	1.3	24
21485	Electronic structure and microscopic chargeâ€transport properties of a newâ€type diketopyrrolopyrroleâ€based material. Journal of Computational Chemistry, 2015, 36, 695-706.	1.5	14
21486	Novel compounds in the Zrâ€“O system, their crystal structures and mechanical properties. Physical Chemistry Chemical Physics, 2015, 17, 17301-17310.	1.3	29
21487	The local structure of molten Ni 1â^'x Al x : An ab initio molecular dynamics study. Journal of Non-Crystalline Solids, 2015, 425, 11-19.	1.5	11
21488	Establishing a Link between Well-Ordered Pt(100) Surfaces and Real Systems: How Do Random Superficial Defects Influence the Electro-oxidation of Glycerol?. ACS Catalysis, 2015, 5, 4227-4236.	5.5	48
21489	Trade-Off between Accuracy and Universality in Linear Energy Relations for Alcohol Dehydrogenation on Transition Metals. Journal of Physical Chemistry C, 2015, 119, 12988-12998.	1.5	46
21490	Interplay between Switching Driven by the Tunneling Current and Atomic Force of a Bistable Four-Atom Si Quantum Dot. Nano Letters, 2015, 15, 4356-4363.	4.5	17
21491	Enhancement of photocatalytic activity of a two-dimensional GeH/graphene heterobilayer under visible light. RSC Advances, 2015, 5, 52264-52268.	1.7	18
21492	Formation of As-As Interlayer Bonding in the collapsed tetragonal phase of NaFe2As2 under pressure. Scientific Reports, 2015, 5, 9868.	1.6	16
21493	H-treatment impact on conductive-filament formation and stability in Ta2O5-based resistive-switching memory cells. Journal of Applied Physics, 2015, 117, .	1.1	20
21494	Modulation of Electronic Properties in Laterally and Commensurately Repeating Graphene and Boron Nitride Composite Nanostructures. Journal of Physical Chemistry C, 2015, 119, 13248-13256.	1.5	21
21495	Effect of van der Waals interactions in the DFT description of self-assembled monolayers of thiols on gold. Theoretical Chemistry Accounts, 2015, 134, 1.	0.5	17
21496	First-Principles Study of Ferromagnetic Nanowires Encapsulated Inside Silicon Carbide Nanotubes. Journal of Superconductivity and Novel Magnetism, 2015, 28, 2605-2611.	0.8	4
21497	Analysis on Dissociation of Pyramidal I Dislocation in Magnesium by Generalized-Stacking-Fault Energy. Acta Metallurgica Sinica (English Letters), 2015, 28, 876-882.	1.5	13
21498	Metallic nanoparticles for catalysis applications. , 2015, , 253-288.		2
21499	Characterization of bismuthâ€“cerium-molybdate selective propylene ammoxidation catalysts. Applied Catalysis A: General, 2015, 495, 115-123.	2.2	25

#	Article	IF	Citations
21500	Electronic structure modification of platinum on titanium nitride resulting in enhanced catalytic activity and durability for oxygen reduction and formic acid oxidation. Applied Catalysis B: Environmental, 2015, 174-175, 35-42.	10.8	63
21501	Formation of Ag nanowires on graphite stepped surfaces. A DFT study. Applied Surface Science, 2015, 324, 710-717.	3.1	9
21502	Periodic DFT study of Ti deposition on defective Si(100) surfaces. Applied Surface Science, 2015, 335, 160-166.	3.1	1
21503	Selectivity of Ni-based surface alloys toward hydrazine adsorption: A DFT study with van der Waals interactions. Applied Surface Science, 2015, 339, 36-45.	3.1	20
21504	Adsorption properties of transition metal atoms on strongly correlated NiO(001) surfaces with surface oxygen vacancies. Current Applied Physics, 2015, 15, 679-682.	1.1	12
21505	Unravelling the roles of surface chemical composition and geometry for the grapheneâ€“metal interaction through C1s core-level spectroscopy. Carbon, 2015, 93, 187-198.	5.4	18
21506	Investigation of thermophysical, electronic and lattice dynamic properties for CaX2Si2 (X=Ni,Zn,Cu,Ag,Au) via first-principles calculations. Computational Materials Science, 2015, 102, 167-173.	1.4	7
21507	Structural, electronic, and magnetic properties of AgnCo (n=1â€“9) clusters: A first-principles study. Computational and Theoretical Chemistry, 2015, 1066, 55-61.	1.1	18
21508	Phonon Transport Simulator (PhonTS). Computer Physics Communications, 2015, 192, 196-204.	3.0	64
21509	MEAMfit: A reference-free modified embedded atom method (RF-MEAM) energy and force-fitting code. Computer Physics Communications, 2015, 196, 439-445.	3.0	29
21510	Intercalated aromatic molecule effect on super-hard C20 fullerene materials. Diamond and Related Materials, 2015, 55, 139-143.	1.8	3
21511	Electrochemical specific adsorption of halides on Cu 111 , 100 , and 211 : A Density Functional Theory study. Electrochimica Acta, 2015, 173, 302-309.	2.6	82
21512	Local structure and thermoelectric properties of Mg2Si0.977â^'Ge Bi0.023 (0.1 â©½xâ©½ 0.4). Journal of Alloys and Compounds, 2015, 644, 249-255.	2.8	19
21513	Oxygen trapped by rare earth tetrahedral clusters in Nd4FeOS6: Crystal structure, electronic structure, and magnetic properties. Journal of Solid State Chemistry, 2015, 229, 41-48.	1.4	6
21514	Lithiation of ZnO nanowires studied by in-situ transmission electron microscopy and theoretical analysis. Mechanics of Materials, 2015, 91, 313-322.	1.7	32
21515	Interaction between vacancies and the Î±-Fe/Y 2 O 3 interface: A first-principles study. Nuclear Instruments & Methods in Physics Research B, 2015, 352, 67-71.	0.6	9
21516	Size and shape of oxygen vacancies and protons in acceptor-doped barium zirconate. Solid State Ionics, 2015, 275, 2-8.	1.3	60
21517	Water interaction with perfect and fluorine-doped Co3O4 (100) surface. Solid State Ionics, 2015, 277, 77-82.	1.3	24

#	Article	IF	Citations
21518	Electronic State and Piezoresistivity Analysis of Zinc Oxide Nanowires for Force Sensing Devices. Key Engineering Materials, 0, 644, 16-21.	0.4	3
21519	Enhancement Mechanism of the Conversion Effficiency of Dye-Sensitized Solar Cells Based on Nitrogen-, Fluorine-, and Iodine-Doped TiO₂ Photoanodes. Journal of Physical Chemistry C, 2015, 119, 13425-13432.	1.5	21
21520	Structure of magnesium selenate enneahydrate, MgSeO4Â·9H2O, from 5 to 250â€…K using neutron time-of-flight Laue diffraction. Acta Crystallographica Section B: Structural Science, Crystal Engineering and Materials, 2015, 71, 313-327.	0.5	4
21521	Anomalous doping effect in black phosphorene using first-principles calculations. Physical Chemistry Chemical Physics, 2015, 17, 16351-16358.	1.3	109
21522	Spin-state transition in unstrained & strained ultra-thin BiCoO₃ films. Dalton Transactions, 2015, 44, 10882-10887.	1.6	6
21523	First-principles design of silicene/Sc2CF2 heterojunction as a promising candidate for field effect transistor. Journal of Applied Physics, 2015, 117, .	1.1	27
21524	Thermodynamics of H₂O Splitting and H₂ Formation at the Cu(110)â€“Water Interface. Journal of Physical Chemistry C, 2015, 119, 14102-14113.	1.5	31
21525	Electronic Properties and Chemical Reactivity of TiS₂ Nanoflakes. Journal of Physical Chemistry C, 2015, 119, 15707-15715.	1.5	47
21526	Strategies to suppress cation vacancies in metal oxide alloys: consequences for solar energy conversion. Journal of Materials Science, 2015, 50, 5715-5722.	1.7	8
21527	Theoretical study of Î³â€²-Fe4N and É›-Fe x N iron nitrides at pressures up to 500 GPa. JETP Letters, 2015, 101, 371-375.	0.4	11
21528	Intrinsic defects in gallium sulfide monolayer: a first-principles study. RSC Advances, 2015, 5, 50883-50889.	1.7	27
21529	Stability of Ni Clusters and the Adsorption of CH₄: First-Principles Calculations. Journal of Physical Chemistry C, 2015, 119, 12378-12384.	1.5	38
21530	First-principles study of point defects in cerium dioxide and comparison to uranium dioxide. Materials Research Society Symposia Proceedings, 2015, 1743, 14.	0.1	0
21531	Atomistic modeling of the self-diffusion in Î³-U and Î³-U-Mo. Physics of Metals and Metallography, 2015, 116, 445-455.	0.3	31
21532	A density functional (PBE, PBEsol, HSE06) study of the structural, electronic and optical properties of the ternary compounds AgAlX2 (X = S, Se, Te). European Physical Journal B, 2015, 88, 1.	0.6	35
21533	Engineering Complex, Layered Metal Oxides: High-Performance Nickelate Oxide Nanostructures for Oxygen Exchange and Reduction. ACS Catalysis, 2015, 5, 4013-4019.	5.5	30
21534	Gap tuning and effective electron correlation energy in amorphous silicon: A first principles density functional theory-based molecular dynamics study. Computational Materials Science, 2015, 102, 110-118.	1.4	3
21535	Magnetic and optical anisotropy in the infinite-chains iron oxide Sr ₂ FeO ₃ : A first-principle investigation. Europhysics Letters, 2015, 110, 37006.	0.7	0

#	Article	IF	Citations
21536	Theory of Electromagnons in CuO. Physical Review Letters, 2015, 114, 197201.	2.9	18
21537	Defect complexes in congruent<mml:math xmlns:mml="http://www.w3.org/1998/Math/MathML"><mml:msub><mml:mi mathvariant="normal">LiNbO</mml:mi><mml:mn>3</mml:mn></mml:msub></mml:math>and their optical signatures. Physical Review B, 2015, 91, .	1.1	45
21538	Comparative study ofab initiononradiative recombination rate calculations under different formalisms. Physical Review B, 2015, 91, .	1.1	68
21539	Electronic Structure of Sodium Superoxide Bulk, (100) Surface, and Clusters using Hybrid Density Functional: Relevance for Naâ€“O₂ Batteries. Journal of Physical Chemistry Letters, 2015, 6, 2027-2031.	2.1	37
21540	Elucidating the real-time Ag nanoparticle growth on Î±-Ag₂WO₄during electron beam irradiation: experimental evidence and theoretical insights. Physical Chemistry Chemical Physics, 2015, 17, 5352-5359.	1.3	54
21541	Tuning oxygen vacancy photoluminescence in monoclinic Y2WO6 by selectively occupying yttrium sites using lanthanum. Scientific Reports, 2015, 5, 9443.	1.6	46
21542	Synthesis, Crystal Structure, and Photoelectric Properties of a New Layered Bismuth Oxysulfide. Inorganic Chemistry, 2015, 54, 5768-5773.	1.9	49
21543	Geometric and electronic structure and magnetic properties of Feâ€“Au nanoalloys: insights from ab initio calculations. Physical Chemistry Chemical Physics, 2015, 17, 28177-28185.	1.3	12
21544	Structural and magnetic properties of PrCo3â^'xFex by neutron powder diffraction and electronic structure investigations. Journal of Solid State Chemistry, 2015, 230, 19-25.	1.4	5
21545	Lattice structures and electronic properties of WZ-CuInS2/MoS2 interface from first-principles calculations. Applied Surface Science, 2015, 351, 382-391.	3.1	10
21546	Misfit accommodation mechanism at the heterointerface between diamond and cubic boron nitride. Nature Communications, 2015, 6, 6327.	5.8	66
21547	Structures, electronic properties and stability phase diagrams for copper(<scp>i</scp>/<scp>ii</scp>) bromide surfaces. Physical Chemistry Chemical Physics, 2015, 17, 9341-9351.	1.3	14
21548	Vacancy-dependent stability of cubic and wurtzite Ti1â^'xAlxN. Surface and Coatings Technology, 2015, 275, 214-218.	2.2	40
21549	Density Functional Theory-Assisted Microkinetic Analysis of Methane Dry Reforming on Ni Catalyst. Industrial & Engineering Chemistry Research, 2015, 54, 5901-5913.	1.8	158
21550	Insight into the mechanism and possibility of ethanol formation from syngas on Cu(100) surface. Journal of Molecular Catalysis A, 2015, 404-405, 115-130.	4.8	46
21551	Nanophotonics. , 2015, , 351-370.		0
21552	First-principles investigation of wet-chemical routes for the hydrogenation of graphene. Carbon, 2015, 93, 421-430.	5.4	3
21553	Lattice-Directed Formation of Covalent and Organometallic Molecular Wires by Terminal Alkynes on Ag Surfaces. ACS Nano, 2015, 9, 6305-6314.	7.3	114

#	Article	IF	Citations
21554	Intrinsic Conductivity in Sodiumâ€“Air Battery Discharge Phases: Sodium Superoxide vs Sodium Peroxide. Chemistry of Materials, 2015, 27, 3852-3860.	3.2	73
21555	Structure and segregation of dopantâ€“defect complexes at grain boundaries in nanocrystalline doped ceria. Physical Chemistry Chemical Physics, 2015, 17, 15375-15385.	1.3	33
21556	First principles study of magnetoelectric coupling in Co2FeAl/BaTiO3 tunnel junctions. Physical Chemistry Chemical Physics, 2015, 17, 14986-14993.	1.3	16
21557	High temperature oxidation resistance in titaniumâ€“niobium alloys. Journal of Alloys and Compounds, 2015, 643, 100-105.	2.8	26
21558	Physics of grain boundaries in polycrystalline photovoltaic semiconductors. Journal of Applied Physics, 2015, 117, .	1.1	52
21559	Crystal Phase and Facet Effects on the Structural Stability and Electronic Properties of GaP Nanowires. Journal of Physical Chemistry C, 2015, 119, 12030-12036.	1.5	8
21560	Theoretical Study of Graphene Doping Mechanism by Iodine Molecules. Journal of Physical Chemistry C, 2015, 119, 12071-12078.	1.5	35
21561	Effects of Interlayer Distance and van der Waals Energy on Electrochemical Activation of Partially Reduced Graphite Oxide. Electrochimica Acta, 2015, 173, 827-833.	2.6	12
21562	A first-principles study on the magnetic properties of nonmetal atom doped phosphorene monolayers. Physical Chemistry Chemical Physics, 2015, 17, 16341-16350.	1.3	91
21563	Ferroelectric Polarization of CH₃NH₃PbI₃: A Detailed Study Based on Density Functional Theory and Symmetry Mode Analysis. Journal of Physical Chemistry Letters, 2015, 6, 2223-2231.	2.1	179
21564	Phase stability and Raman vibration of the molybdenum ditelluride (MoTe₂) monolayer. Physical Chemistry Chemical Physics, 2015, 17, 14866-14871.	1.3	104
21565	Photoelectron Spectroscopy Characterization and Computational Modeling of Gadolinium Nitride Thin Films Synthesized by Chemical Vapor Deposition. Materials Research Society Symposia Proceedings, 2015, 1729, 131-136.	0.1	1
21566	Optimizing the Volmer Step by Single-Layer Nickel Hydroxide Nanosheets in Hydrogen Evolution Reaction of Platinum. ACS Catalysis, 2015, 5, 3801-3806.	5.5	142
21567	Hydrogen generation by the reaction of H₂O with Al₂O₃-based materials: a computational analysis. Physical Chemistry Chemical Physics, 2015, 17, 6834-6843.	1.3	28
21568	Monolayer PtSe₂, a New Semiconducting Transition-Metal-Dichalcogenide, Epitaxially Grown by Direct Selenization of Pt. Nano Letters, 2015, 15, 4013-4018.	4.5	560
21569	Theoretical prediction of a highly conducting solid electrolyte for sodium batteries: Na₁₀GeP₂S₁₂. Journal of Materials Chemistry A, 2015, 3, 12992-12999.	5.2	74
21570	Carbon Dimers as the Dominant Feeding Species in Epitaxial Growth and Morphological Phase Transition of Graphene on Different Cu Substrates. Physical Review Letters, 2015, 114, 216102.	2.9	73
21571	High-performance transition metalâ€“doped Pt ₃ Ni octahedra for oxygen reduction reaction. Science, 2015, 348, 1230-1234.	6.0	1,623

#	Article	IF	Citations
21572	Spin gapless semiconducting behavior in equiatomic quaternary CoFeMnSi Heusler alloy. Physical Review B, 2015, 91, .	1.1	212
21573	Insights into the effects of steam on propane dehydrogenation over a Pt/Al₂O₃ catalyst. Catalysis Science and Technology, 2015, 5, 3991-4000.	2.1	21
21574	Steric Effect on the Nucleophilic Reactivity of Nickel(III) Peroxo Complexes. Inorganic Chemistry, 2015, 54, 6176-6183.	1.9	39
21575	Structural defects in pristine and Mn-doped monolayer WS2: A first-principles study. Superlattices and Microstructures, 2015, 85, 339-347.	1.4	32
21576	The sulfur poisoning of the nickel/oxygen-enriched yttria-stabilized zirconia. Journal of Power Sources, 2015, 293, 635-641.	4.0	11
21577	Dâ€“Ï€â€“A organic dyes with various bulky amine-typed donor moieties for dye-sensitized solar cells employing the cobalt electrolyte. Organic Electronics, 2015, 25, 1-5.	1.4	16
21578	Theoretical gas to liquid shift of ¹⁵N isotropic nuclear magnetic shielding in nitromethane using ab initio molecular dynamics and GIAO/GIPAW calculations. Physical Chemistry Chemical Physics, 2015, 17, 12222-12227.	1.3	9
21579	Understanding corrosion inhibition with van der Waals DFT methods: the case of benzotriazole. Faraday Discussions, 2015, 180, 439-458.	1.6	60
21580	Cobalt-doped TiO2: a computational analysis of dopant placement and charge transfer direction on thin film anatase. Molecular Physics, 2015, , 1-15.	0.8	3
21581	The element features and criterion of formation of LPSO in magnesium alloys. Materials Research Innovations, 2015, 19, S133-S137.	1.0	8
21582	Promoting Ï‡-Fe₅C₂(100)_{0.25} with copper â€“ a DFT study. Journal of Lithic Studies, 2015, 1, 11-18.	0.1	6
21583	Fundamental properties of GaN(0001) films grown directly on Gd<inf>2</inf>O<inf>3</inf>(0001) platforms: Ab initio structural simulations. , 2015, , .		0
21584	Exceptional Friction Mitigation via Subsurface Plastic Shear in Defective Nanocrystalline Ceramics. Materials Research Letters, 2015, 3, 23-29.	4.1	7
21585	X-ray photoemission analysis of clean and carbon monoxide-chemisorbed platinum(111) stepped surfaces using a curved crystal. Nature Communications, 2015, 6, 8903.	5.8	48
21586	Intercalation and Pushâ€Out Process with Spinelâ€toâ€Rocksalt Transition on Mg Insertion into Spinel Oxides in Magnesium Batteries. Advanced Science, 2015, 2, 1500072.	5.6	153
21587	On Structural Features Necessary for Nearâ€IRâ€Light Photocatalysts. Chemistry - A European Journal, 2015, 21, 13583-13587.	1.7	13
21588	Scalable and Fault-Tolerant Cloud Computations: Modelling and Implementation. , 2015, , .		7
21589	A first-principles study of CO dissociative adsorption on iron nanoparticles supported on doped graphene. Solid State Communications, 2015, 223, 50-53.	0.9	6

#	Article	IF	Citations
21590	Electronic structures and elastic properties of monolayer and bilayer transition metal dichalcogenides MX ₂ (M = Mo, W; X = O, S, Se, Te): A comparative first-principles study. Chinese Physics B, 2015, 24, 097103.	0.7	98
21591	Atomic carbon adsorption on Ni38/Co38 clusters and three low-index Ni/Co surfaces: a density functional theory study. Materials Research Innovations, 2015, 19, S5-94-S5-100.	1.0	0
21592	Modeling of inter-ribbon tunneling in graphene. , 2015, , .		2
21593	Room-temperature tracking of chiral recognition process at the single-molecule level. Nano Research, 2015, 8, 3505-3511.	5.8	5
21594	Redox condition in molten salts and solute behavior: A first-principles molecular dynamics study. Journal of Nuclear Materials, 2015, 465, 224-235.	1.3	42
21595	Point Defects and Defect-Induced Optical Response in Ternary LiInSe₂ Crystals: First-Principles Insight. Journal of Physical Chemistry C, 2015, 119, 29123-29131.	1.5	12
21596	Effect of Sb Segregation on Conductance and Catalytic Activity at Pt/Sb-Doped SnO₂ Interface: A Synergetic Computational and Experimental Study. ACS Applied Materials & Interfaces, 2015, 7, 27782-27795.	4.0	19
21597	Spin-orbit engineering in transition metal dichalcogenide alloy monolayers. Nature Communications, 2015, 6, 10110.	5.8	176
21598	Topological states on the gold surface. Nature Communications, 2015, 6, 10167.	5.8	148
21599	Quantum chemical modeling of hydrogen migration on the Pt29/SnO2 composite catalyst. Russian Chemical Bulletin, 2015, 64, 752-758.	0.4	1
21600	Insight into the relationship between structure and magnetic properties in icosahedral Fe n Pt 55â^'n () Tj ETQq0 0 0 rgBT /Overlock 10 T	1.3	5
21601	Zn₁₇ Superatom Cage Doped with 3d Transition-Metal (TM) Impurities (TM = Sc, Ti, V, Cr, Mn,) Tj ETQq1 1 0.784314 rgB	1.5	7
21602	Band structure and characterization of dilute Ge:C alloys. , 2015, , .		0
21603	High-temperature in situ crystallographic observation of reversible gas sorption in impermeable organic cages. Proceedings of the National Academy of Sciences of the United States of America, 2015, 112, 14156-14161.	3.3	27
21604	The influence of the composition of eight-atom Ptâ€“Ir clusters on the magnetic properties. Molecular Physics, 2015, 113, 3628-3636.	0.8	5
21605	Tuning magnetic anistropy by charge injection and strain in Fe/MoS₂bilayer heterostructures. Journal Physics D: Applied Physics, 2015, 48, 485001.	1.3	13
21606	Ab initiophonon properties of half-Heusler NiTiSn, NiZrSn and NiHfSn. Journal of Physics Condensed Matter, 2015, 27, 425401.	0.7	23
21607	Thermodynamics of confined gallium clusters. Journal of Physics Condensed Matter, 2015, 27, 445502.	0.7	5

#	Article	IF	Citations
21608	Experimental and theoretical study ofÎ±â€“Eu₂(MoO₄)₃under compression. Journal of Physics Condensed Matter, 2015, 27, 465401.	0.7	5
21609	Zero-dipole molecular organic cations in mixed organicâ€“inorganic halide perovskites: possible chemical solution for the reported anomalous hysteresis in the currentâ€“voltage curve measurements. Nanotechnology, 2015, 26, 442001.	1.3	38
21610	Evolutionary algorithm based structure search for hard ruthenium carbides. Modelling and Simulation in Materials Science and Engineering, 2015, 23, 085006.	0.8	8
21611	Nature of the band gap of halide perovskites ABX ₃ (A = CH ₃ NH) Tj ETQq1 1 0.784314 rgBT /(2015, 24, 116302.	0.7	121
21612	Electronic properties of the SnSeâ€“metal contacts: First-principles study. Chinese Physics B, 2015, 24, 117308.	0.7	7
21613	First-principles study of FeSe epitaxial films on SrTiO 3. Chinese Physics B, 2015, 24, 117402.	0.7	8
21614	Silicene on MoS ₂ : role of the van der Waals interaction. 2D Materials, 2015, 2, 045004.	2.0	22
21615	Reliable structural data from Rietveld refinementsviarestraint consistency. Journal of Applied Crystallography, 2015, 48, 1777-1784.	1.9	19
21616	Theoretical Evidence for Low Charging Overpotentials of Superoxide Discharge Products in Metalâ€“Oxygen Batteries. Chemistry of Materials, 2015, 27, 8406-8413.	3.2	59
21617	Period-doubling reconstructions of semiconductor partial dislocations. NPG Asia Materials, 2015, 7, e216-e216.	3.8	12
21618	Band-Gap and Band-Edge Engineering of Multicomponent Garnet Scintillators from First Principles. Physical Review Applied, 2015, 4, .	1.5	62
21619	Reactions of CO, H₂O, CO₂, and H₂ on the Clean and Precovered Fe(110) Surfaces â€“ A DFT Investigation. Journal of Physical Chemistry C, 2015, 119, 28377-28388.	1.5	40
21620	Origin of High Photocatalytic Efficiency in Monolayer g-C₃N₄/CdS Heterostructure: A Hybrid DFT Study. Journal of Physical Chemistry C, 2015, 119, 28417-28423.	1.5	345
21621	Kinetic Role of Carbon in Solid-State Synthesis of Zirconium Diboride using Nanolaminates: Nanocalorimetry Experiments and First-Principles Calculations. Nano Letters, 2015, 15, 8266-8270.	4.5	13
21622	Role of edge dehydrogenation in magnetization and spin transport of zigzag graphene nanoribbons with line defects. Organic Electronics, 2015, 27, 212-220.	1.4	5
21623	Covalency-Dependent Vibrational Dynamics in Two-Dimensional Titanium Carbides. Journal of Physical Chemistry A, 2015, 119, 12977-12984.	1.1	34
21624	An Adsorption Study of CH₄ on ZSM-5, MOR, and ZSM-12 Zeolites. Journal of Physical Chemistry C, 2015, 119, 28970-28978.	1.5	32
21625	Effects of Interatomic Coupling on Magnetic Anisotropy and Order of Spins on Metallic Surfaces. Journal of Physical Chemistry C, 2015, 119, 26237-26241.	1.5	10

#	Article	IF	Citations
21626	Computational Studies of the Interaction of Carbon Dioxide with Graphene-Supported Titanium Dioxide. Journal of Physical Chemistry C, 2015, 119, 29044-29051.	1.5	15
21627	Nanocatalyst shape and composition during nucleation of single-walled carbon nanotubes. RSC Advances, 2015, 5, 106377-106386.	1.7	15
21628	Pressure-induced changes in the structural and absorption properties of crystalline 5-nitramino-3,4-dinitropyrazole. Journal of Chemical Sciences, 2015, 127, 1777-1784.	0.7	4
21629	Site Dependency of the High Conductivity of Ga₂In₆Sn₂O₁₆: The Role of the 7-Coordinate Site. Chemistry of Materials, 2015, 27, 8084-8093.	3.2	4
21630	Tip-Induced Molecule Anchoring in Niâ€“Phthalocyanine on Au(111) Substrate. Journal of Physical Chemistry C, 2015, 119, 27721-27726.	1.5	8
21631	Development of a ReaxFF Reactive Force Field for Fe/Cr/O/S and Application to Oxidation of Butane over a Pyrite-Covered Cr₂O₃ Catalyst. ACS Catalysis, 2015, 5, 7226-7236.	5.5	98
21632	Interfacial Effects in Îµ-Li_xVOPO₄ and Evolution of the Electronic Structure. Chemistry of Materials, 2015, 27, 8211-8219.	3.2	37
21633	A rational computational study of surface defect-mediated stabilization of low-dimensional Pt nanostructures on TiN(100). Physical Chemistry Chemical Physics, 2015, 17, 9680-9686.	1.3	6
21634	Structural and electronic properties of alkali metal peroxides at high pressures. RSC Advances, 2015, 5, 104337-104342.	1.7	12
21635	The Mechanism of Industrial Ammonia Synthesis Revisited: Calculations of the Role of the Associative Mechanism. Journal of Physical Chemistry C, 2015, 119, 26554-26559.	1.5	60
21636	Effect of carbon content and electronic strong correlation on the mechanical and thermodynamic properties of ytterbium carbides. RSC Advances, 2015, 5, 103082-103090.	1.7	5
21637	First-principles study of structurally modulated multiferroic<mml:math xmlns:mml="http://www.w3.org/1998/Math/MathML"><mml:mrow><mml:msub><mml:mtext>CaMn</mml:mtext><mml:mn>7</mml:mn> Physical Review B, 2015, 91, .	1.7	17
21638	Electronic Origin of Doping-Induced Enhancements of Reactivity: Case Study of Tricalcium Silicate. Journal of Physical Chemistry C, 2015, 119, 25991-25999.	1.5	32
21639	First principles study of Ca in BaTiO₃and Bi_{0.5}Na_{0.5}TiO₃. Philosophical Magazine, 2015, 95, 3785-3797.	0.7	4
21640	Piezoelectricity in two-dimensional group-III monochalcogenides. Nano Research, 2015, 8, 3796-3802.	5.8	219
21641	Real-Space Imaging of the Atomic Structure of Organicâ€“Inorganic Perovskite. Journal of the American Chemical Society, 2015, 137, 16049-16054.	6.6	155
21642	Mechanisms of Oxidase and Superoxide Dismutation-like Activities of Gold, Silver, Platinum, and Palladium, and Their Alloys: A General Way to the Activation of Molecular Oxygen. Journal of the American Chemical Society, 2015, 137, 15882-15891.	6.6	407
21643	Combined experimentalâ€“theoretical study of the optoelectronic properties of non-stoichiometric pyrochlore bismuth titanate. Journal of Materials Chemistry C, 2015, 3, 12032-12039.	2.7	29

#	Article	IF	Citations
21644	Identifying and rationalizing the morphological, structural, and optical properties of Î²-Ag₂MoO₄ microcrystals, and the formation process of Ag nanoparticles on their surfaces: combining experimental data and first-principles calculations. Science and Technology of Advanced Materials, 2015, 16, 065002.	2.8	61
21645	Melting curves of metals with excited electrons in the quasiharmonic approximation. Physical Review B, 2015, 92, .	1.1	58
21646	Crystal behavior of potassium bromate under compression. Acta Crystallographica Section B: Structural Science, Crystal Engineering and Materials, 2015, 71, 798-804.	0.5	3
21647	Li2Se:Te as a neutron scintillator. Journal of Alloys and Compounds, 2015, 647, 906-910.	2.8	7
21648	Vibrational and optical properties of MoS2: From monolayer to bulk. Surface Science Reports, 2015, 70, 554-586.	3.8	178
21649	â€œGuanigmaâ€• The Revised Structure of Biogenic Anhydrous Guanine. Chemistry of Materials, 2015, 27, 8289-8297.	3.2	74
21650	Two-Dimensional MnO₂ as a Better Cathode Material for Lithium Ion Batteries. Journal of Physical Chemistry C, 2015, 119, 28783-28788.	1.5	98
21651	First principles investigation of the diffusion of interstitial Cu, Ag and Au in ZnTe. International Journal of Modern Physics B, 2015, 29, 1550130.	1.0	0
21652	Study on the intrinsic defects in ZnO by combing first-principle and thermodynamic calculations. Modern Physics Letters B, 2015, 29, 1550194.	1.0	2
21653	First-principles study of oxygen and hydrogen adsorption on Pt(111) and PtML/Pd(111) surfaces. Modern Physics Letters B, 2015, 29, 1550199.	1.0	2
21654	ADSORPTION AND DISSOCIATION OF O2 ON Ti3Al (0001) STUDIED BY FIRST-PRINCIPLES. Surface Review and Letters, 2015, 22, 1550053.	0.5	9
21655	Synthesis of borophenes: Anisotropic, two-dimensional boron polymorphs. Science, 2015, 350, 1513-1516.	6.0	2,047
21656	Pushing back the limit of ab-initio quantum transport simulations on hybrid supercomputers. , 2015, , .		16
21657	Mechanistic Study on Water Gas Shift Reaction on the Fe₃O₄ (111) Reconstructed Surface. Journal of Physical Chemistry C, 2015, 119, 28934-28945.	1.5	44
21658	First-Principles Treatment of Photoluminescence in Semiconductors. Journal of Physical Chemistry C, 2015, 119, 27954-27964.	1.5	52
21659	Upward Shift in Conduction Band of Ta2O5 Due to Surface Dipoles Induced by N-Doping. Journal of Physical Chemistry C, 2015, 119, 26925-26936.	1.5	27
21660	Nanoscale Characterization and Unexpected Photovoltaic Behavior of Low Band Gap Sulfur-Overrich-Thiophene/Benzothiadiazole Decamers and Polymers. Journal of Physical Chemistry C, 2015, 119, 27200-27211.	1.5	19
21661	Isostructural Phase Transition in Bismuth Oxide Chloride Induced by Redistribution of Charge under High Pressure. Journal of Physical Chemistry C, 2015, 119, 27657-27665.	1.5	24

#	Article	IF	Citations
21662	Fundamental Insights into High-Temperature Water Electrolysis Using Ni-Based Electrocatalysts. Journal of Physical Chemistry C, 2015, 119, 26980-26988.	1.5	26
21663	Anisotropic Lattice Thermal Conductivity and Suppressed Acoustic Phonons in MOF-74 from First Principles. Journal of Physical Chemistry C, 2015, 119, 26000-26008.	1.5	39
21664	Frustrated Etching during H/Si(111) Methoxylation Produces Fissured Fluorinated Surfaces, Whereas Direct Fluorination Preserves the Atomically Flat Morphology. Journal of Physical Chemistry C, 2015, 119, 26029-26037.	1.5	6
21665	Quasi-Free-Standing Features of Stanene/Stanane on InSe and GaTe Nanosheets: A Computational Study. Journal of Physical Chemistry C, 2015, 119, 27848-27854.	1.5	24
21666	Computational Study on the Intramolecular Charge Separation of D-A-Ï€-A Organic Sensitizers with Different Linker Groups. Journal of Physical Chemistry C, 2015, 119, 26355-26361.	1.5	12
21667	A DFT Study of CO Oxidation at the Pdâ€“CeO₂(110) Interface. Journal of Physical Chemistry C, 2015, 119, 27505-27511.	1.5	57
21668	Computational Study of Cation Diffusion in Ceria. Journal of Physical Chemistry C, 2015, 119, 27307-27315.	1.5	45
21669	Migration of Single Iridium Atoms and Tri-iridium Clusters on MgO Surfaces: Aberration-Corrected STEM Imaging and Ab Initio Calculations. Journal of Physical Chemistry Letters, 2015, 6, 4675-4679.	2.1	12
21670	Tolerance of Intrinsic Defects in PbS Quantum Dots. Journal of Physical Chemistry Letters, 2015, 6, 4711-4716.	2.1	44
21671	Electrically Tunable Bandgaps in Bilayer MoS₂. Nano Letters, 2015, 15, 8000-8007.	4.5	161
21672	Synergistic Strain Engineering Effect of Hybrid Plasmonic, Catalytic, and Magnetic Coreâ€“Shell Nanocrystals. Nano Letters, 2015, 15, 8347-8353.	4.5	21
21673	How to Optimize the Interface between Photosensitizers and TiO₂ Nanocrystals with Molecular Engineering to Enhance Performances of Dye-Sensitized Solar Cells?. ACS Applied Materials & Interfaces, 2015, 7, 25341-25351.	4.0	28
21674	Nature and Catalytic Role of Extraframework Aluminum in Faujasite Zeolite: A Theoretical Perspective. ACS Catalysis, 2015, 5, 7024-7033.	5.5	92
21675	Experimental Observation of Redox-Induced Feâ€“N Switching Behavior as a Determinant Role for Oxygen Reduction Activity. ACS Nano, 2015, 9, 12496-12505.	7.3	499
21676	A hybrid density functional study on the visible light photocatalytic activity of (Mo,Cr)â€“N codoped KNbO₃. Physical Chemistry Chemical Physics, 2015, 17, 28743-28753.	1.3	67
21677	Enhancement of Tc in the atomic phase of iodine-doped hydrogen at high pressures. Physical Chemistry Chemical Physics, 2015, 17, 32335-32340.	1.3	15
21678	Initial reduction of CO₂ on perfect and O-defective CeO₂ (111) surfaces: towards CO or COOH?. RSC Advances, 2015, 5, 97528-97535.	1.7	36
21679	A comparative study of SrCo_{0.8}Nb_{0.2}O_{3â^Î´}and SrCo_{0.8}Ta_{0.2}O_{3â^Î´}as low-temperature solid oxide fuel cell cathodes: effect of non-geometry factors on the oxygen reduction reaction. Journal of Materials Chemistry A, 2015, 3, 24064-24070.	5.2	52

#	Article	IF	Citations
21680	Zn vacancy induced ferromagnetism in K doped ZnO. Journal of Materials Chemistry C, 2015, 3, 11953-11958.	2.7	43
21681	YB₆: A â€˜Ductileâ€™ and Soft Ceramic with Strong Heterogeneous Chemical Bonding for Ultrahigh-Temperature Applications. Materials Research Letters, 2015, 3, 210-215.	4.1	22
21682	Electronic and magnetic properties of 1 T-TiSe ₂ nanoribbons. 2D Materials, 2015, 2, 044002.	2.0	21
21683	Equation of State, Nonlinear Elastic Response, and Anharmonic Properties of Diamond-Cubic Silicon and Germanium: First-Principles Investigation. Zeitschrift Fur Naturforschung - Section A Journal of Physical Sciences, 2015, 70, 403-412.	0.7	4
21684	From soft to hard magnetic Feâ€“Coâ€“B by spontaneous strain: a combined first principles and thin film study. Journal of Physics Condensed Matter, 2015, 27, 476002.	0.7	29
21685	Defect-impurity complex induced long-range ferromagnetism in GaN nanowires. Materials Research Express, 2015, 2, 126104.	0.8	9
21686	Point Defects in TiNi-based Alloys from Ab-initio Calculations. Materials Today: Proceedings, 2015, 2, S615-S618.	0.9	5
21687	Comparison of electronic structure between monolayer silicenes on Ag (111). Chinese Physics B, 2015, 24, 087307.	0.7	8
21688	Effect of Ru on interdiffusion dynamics of Î²-NiAl/DD6 system: A combined experimental and first-principles studies. Materials and Design, 2015, 88, 667-674.	3.3	34
21689	First-Principle Calculations of the MgYA4 (AÂ=ÂCo and Ni) Phase with AuBe5-Type Structure. Acta Metallurgica Sinica (English Letters), 2015, 28, 1326-1331.	1.5	4
21690	Hindered rotational physisorption states of H2 on Ag(111) surfaces. Physical Chemistry Chemical Physics, 2015, 17, 19625-19630.	1.3	3
21691	On the energetics of cation ordering in tungsten-bronze-type oxides. Physical Chemistry Chemical Physics, 2015, 17, 30343-30351.	1.3	15
21692	Determining dilute-limit solvus boundaries in multi-component systems using defect energetics: Na in PbTe and PbS. Journal of Materials Chemistry C, 2015, 3, 10630-10649.	2.7	27
21693	Chemisorptive enantioselectivity of chiral epoxides on tartaric-acid modified Pd(111): three-point bonding. Physical Chemistry Chemical Physics, 2015, 17, 5450-5458.	1.3	10
21694	Energy and temperature dependence of rigid unit modes in AlPO₄-5. Physical Chemistry Chemical Physics, 2015, 17, 21547-21554.	1.3	4
21695	First principles study of oxygen diffusion in aÎ±-alumina twin grain boundary. Philosophical Magazine, 2015, 95, 3985-3999.	0.7	5
21696	Co-Graphene heterostructures with giant perpendicular magnetocrystalline anisotropy. , 2015, , .		0
21697	Enhanced Ab Initio Molecular Dynamics Simulation of the Temperature-Dependent Thermodynamics for the Diffusion of Carbon Monoxide on Ru(0001) Surface. Journal of Physical Chemistry C, 2015, 119, 26422-26428.	1.5	9

#	Article	IF	Citations
21698	First principles study of the electronic properties of a Ni₃(2,3,6,7,10,11-hexaaminotriphenylene)₂ monolayer under biaxial strain. RSC Advances, 2015, 5, 55186-55190.	1.7	16
21699	Quantifying electronic correlation strength in a complex oxide: A combined DMFT and ARPES study of<mml:math xmlns:mml="http://www.w3.org/1998/Math/MathML"><mml:msub><mml:mtext>LaNiO</mml:mtext><mml:mn>3</mml:mn></mml:msub></mml:math>. Physical Review B, 2015, 92, .	1.1	32
21700	Accelerated materials property predictions and design using motif-based fingerprints. Physical Review B, 2015, 92, .	1.1	136
21701	Lattice dynamics of binary and ternary phases in Tiâ€“Siâ€“C system: A combined Raman spectroscopy and density functional theory study. Materials Chemistry and Physics, 2015, 168, 58-65.	2.0	17
21702	Electronic structure and photocatalytic activities of (Bi2âˆ’Y)Sn2O7 solid solution. Applied Surface Science, 2015, 357, 2364-2371.	3.1	9
21703	Adsorption patterns of caffeic acid on titania: affinity, charge transfer and sunscreen applications. Molecular Physics, 0, , 1-11.	0.8	6
21704	Ab Initio Investigation on Cu/Cr Codoped Amorphous Carbon Nanocomposite Films with Giant Residual Stress Reduction. ACS Applied Materials & Interfaces, 2015, 7, 27878-27884.	4.0	38
21705	Hydrogenated boron arsenide nanosheet: A promising candidate for bipolar magnetic semiconductor. Applied Physics Express, 2015, 8, 113001.	1.1	18
21706	Tetragonal bismuth bilayer: a stable and robust quantum spin hall insulator. 2D Materials, 2015, 2, 045010.	2.0	34
21707	Predicted Formation of H₃⁺ in Solid Halogen Polyhydrides at High Pressures. Journal of Physical Chemistry A, 2015, 119, 11059-11065.	1.1	19
21708	(Ti/Zr,N) codoped hematite for enhancing the photoelectrochemical activity of water splitting. Physical Chemistry Chemical Physics, 2015, 17, 22179-22186.	1.3	41
21709	Computational prediction of the electronic structure and optical properties of graphene-like Î²-CuN₃. Physical Chemistry Chemical Physics, 2015, 17, 31872-31876.	1.3	7
21710	Mechanisms of Pyrrole Hydrogenation on Ru(0001) and Hydrogen Molybdenum Bronze Surfaces. Journal of Physical Chemistry C, 2015, 119, 22477-22485.	1.5	7
21711	Influential Electronic and Magnetic Properties of the Gallium Sulfide Monolayer by Substitutional Doping. Journal of Physical Chemistry C, 2015, 119, 29148-29156.	1.5	40
21712	A novel stable hydrogen-rich SnH8 under high pressure. RSC Advances, 2015, 5, 107637-107641.	1.7	9
21713	Interface engineering of electronic properties of graphene/boron nitride lateral heterostructures. 2D Materials, 2015, 2, 041001.	2.0	40
21714	Electronic structure and optical properties of CaTiO₃: An ab initio study. Proceedings of SPIE, 2015, , .	0.8	1
21715	First-principles study of the structural and electronic properties of ultrathin silver nanowires. European Physical Journal B, 2015, 88, 1.	0.6	4

#	Article	IF	Citations
21716	Fermi arcs and pseudogap emerging from dimensional crossover at the Fermi surface in La 2â^'x Sr x CuO 4. Europhysics Letters, 2015, 112, 37011.	0.7	5
21717	Ground state of bilayer hÎ±-silica: mechanical and electronic properties. Nanotechnology, 2015, 26, 505702.	1.3	7
21718	First-principles study of migration mechanisms and diffusion of carbon in GaN. Journal of Physics: Conference Series, 2015, 633, 012143.	0.3	3
21719	The mechanical exfoliation mechanism of black phosphorus to phosphorene: A first-principles study. Europhysics Letters, 2015, 112, 37003.	0.7	28
21720	High-T_c Layered Ferrielectric Crystals by Coherent Spinodal Decomposition. ACS Nano, 2015, 9, 12365-12373.	7.3	67
21721	Carrier-mediated ferromagnetism in the magnetic topological insulator Cr-doped (Sb,Bi)2Te3. Nature Communications, 2015, 6, 8913.	5.8	53
21722	Robust intrinsic ferromagnetism and half semiconductivity in stable two-dimensional single-layer chromium trihalides. Journal of Materials Chemistry C, 2015, 3, 12457-12468.	2.7	569
21723	Mechanism of effect of intrinsic defects on electrical and optical properties of Cu₂CdSnS₄: an experimental and first-principles study. Journal Physics D: Applied Physics, 2015, 48, 445105.	1.3	16
21724	Charge Transfer Stabilization of Late Transition Metal Oxide Nanoparticles on a Layered Niobate Support. Journal of the American Chemical Society, 2015, 137, 16216-16224.	6.6	60
21725	K₁₁Cd₂Sb₅built of an unprecedented planar CdSb₃triangle. Dalton Transactions, 2015, 44, 18316-18319.	1.6	4
21726	Crystal Growth, Structures, and Properties of the Complex Borides, LaOs₂Al₂B and La₂Os₂AlB₂. Inorganic Chemistry, 2015, 54, 8049-8057.	1.9	7
21727	Understanding Oxygen-Vacancy Migration in the Fluorite Oxide CeO2: An Ab Initio Study of Impurity-Anion Migration. Journal of Physical Chemistry C, 2015, 119, 28269-28275.	1.5	27
21728	New metastable phases in a trititanium pentoxide compound. Materials Research Express, 2015, 2, 126101.	0.8	4
21729	Enhanced photocatalytic activity of Î±-Bi2O3 with high electron-hole mobility by codoping approach: A first-principles study. Applied Surface Science, 2015, 358, 449-456.	3.1	25
21730	Gadolinium-Vacancy Clusters in the (111) Surface of Gadolinium-Doped Ceria: A Density Functional Theory Study. Chemistry of Materials, 2015, 27, 7910-7917.	3.2	26
21731	Defect stability in thorium monocarbide: An ab initio study. Chinese Physics B, 2015, 24, 097101.	0.7	4
21732	Bandgap engineering in van der Waals heterostructures of blue phosphorene and MoS2: A first principles calculation. Journal of Solid State Chemistry, 2015, 231, 64-69.	1.4	55
21733	Ab initio study of thermoelectric properties of doped SnO2 superlattices. Journal of Solid State Chemistry, 2015, 231, 123-131.	1.4	5

#	Article	IF	Citations
21734	Investigating the Energetic Ordering of Stable and Metastable TiO₂ Polymorphs Using DFT+U and Hybrid Functionals. Journal of Physical Chemistry C, 2015, 119, 21060-21071.	1.5	81
21735	Electronic structure of Î²-Ga2O3 single crystals investigated by hard X-ray photoelectron spectroscopy. Applied Physics Letters, 2015, 107, .	1.5	15
21736	Facet-controlled phase separation in supersaturated Au-Ni nanoparticles upon shape equilibration. Applied Physics Letters, 2015, 107, .	1.5	22
21737	Antiferromagnetic and topological states in silicene: A mean field study. Chinese Physics B, 2015, 24, 087503.	0.7	1
21738	Nickel Sulfide Nanoparticles Synthesized by Microwave-assisted Method as Promising Supercapacitor Electrodes: An Experimental and Computational Study. Electrochimica Acta, 2015, 182, 361-367.	2.6	99
21739	Role of Na⁺ Interstitials and Dopants in Enhancing the Na⁺ Conductivity of the Cubic Na₃PS₄ Superionic Conductor. Chemistry of Materials, 2015, 27, 8318-8325.	3.2	202
21740	Magnetic Exchange in Mn^{II}[TCNE] (TCNE = Tetracyanoethylene) Molecule-Based Magnets with Two- and Three-Dimensional Magnetic Networks. Journal of Physical Chemistry C, 2015, 119, 25036-25046.	1.5	8
21741	Interplay between Hydrogen Bonding, Epitaxy, and Charge Transfer in the Self-Assembly of Croconic Acid on Au(111) and Ag(111). Journal of Physical Chemistry C, 2015, 119, 26429-26437.	1.5	9
21742	Kinetically Trapped Two-Component Self-Assembled Adlayer. Journal of Physical Chemistry C, 2015, 119, 25364-25376.	1.5	27
21743	Facile one-pot fabrication and high photocatalytic performance of vanadium doped TiO2-based nanosheets for visible-light-driven degradation of RhB or Cr(VI). Applied Surface Science, 2015, 359, 435-448.	3.1	46
21744	Investigating Interfacial Electron Transfer in Highly Efficient Porphyrin-Sensitized Solar Cells. ACS Symposium Series, 2015, , 169-188.	0.5	0
21745	Understanding Hematite Doping with Group IV Elements: A DFT+U Study. Journal of Physical Chemistry C, 2015, 119, 26303-26310.	1.5	66
21746	Electronic Structure Evolution across the Peierls Metal-Insulator Transition in a Correlated Ferromagnet. Physical Review X, 2015, 5, .	2.8	10
21747	Adsorption of Water on Yttria-Stabilized Zirconia. Journal of Physical Chemistry C, 2015, 119, 22526-22533.	1.5	24
21748	Enhanced spin-phonon-electronic coupling in a 5d oxide. Nature Communications, 2015, 6, 8916.	5.8	45
21749	Random phase approximation up to the melting point: Impact of anharmonicity and nonlocal many-body effects on the thermodynamics of Au. Physical Review B, 2015, 91, .	1.1	18
21750	Direct surface charging and alkali-metal doping for tuning the interlayer magnetic order in planar nanostructures. Physical Review B, 2015, 92, .	1.1	3
21751	Extended antisite defects in tetrahedrally bonded semiconductors. Physical Review B, 2015, 92, .	1.1	17

#	Article	IF	Citations
21752	Effect of electron correlations on the<mml:math xmlns:mml="http://www.w3.org/1998/Math/MathML"><mml:msub><mml:mi mathvariant="normal">Fe</mml:mi><mml:mn>3</mml:mn></mml:msub><mml:mtext>Si</mml:mtext></mml:math>and<mml:math xmlns:mml="http://www.w3.org/1998/Math/MathML"><mml:mi>Î±</mml:mi><mml:mtext>â^'</mml:mtext><mml:msub><mml:mi mathvariant="normal">FeSi</mml:mi><mml:mn>2</mml:mn></mml:msub></mml:math>band structure and optical properties. Physical Review B, 2015, 92, .	1.1	21
21753	Strain-induced phenomena in layered materials. , 2015, , .		0
21754	First-Principles Investigation on Structural and Electronic Properties of Ferromagnetic Fe2P4O12. Ferroelectrics, 2015, 482, 113-120.	0.3	2
21755	Defect-induced faceted blue phosphorene nanotubes. Physical Review B, 2015, 92, .	1.1	26
21756	Probing magnetostructural correlations in multiferroicHoAl3(BO3)4. Physical Review B, 2015, 92, .	1.1	2
21757	Modeling of the magnetic free energy of self-diffusion in bcc Fe. Physical Review B, 2015, 92, .	1.1	22
21758	Growth and electronic structure of epitaxial single-layer<mml:math xmlns:mml="http://www.w3.org/1998/Math/MathML"><mml:msub><mml:mtext>WS</mml:mtext><mml:mn>2</mml:mn></mml:msub></mml:math>on Au(111). Physical Review B, 2015, 92, .	1.1	70
21759	<i>Ab Initio</i> Study of the Oxygen Effect on Magnetic Interactions within 3d Metal Nanowires on Vicinal Rh (553) Surface. Solid State Phenomena, 0, 233-234, 546-549.	0.3	0
21760	Strain-induced asymmetric modulation of band gap in narrow armchair-edge graphene nanoribbon. Modern Physics Letters B, 2015, 29, 1550224.	1.0	2
21761	Magnetic and electronic properties of frustrated spin dimer compound K2Fe2B2O7: A first-principles calculation. Solid State Communications, 2015, 220, 77-80.	0.9	0
21762	Current limitations of molecular dynamic simulations as probes of thermo-physical behavior of silicate melts. American Mineralogist, 2015, 100, 1866-1882.	0.9	14
21763	Hybrid carbon nanomaterials for electrochemical detection of biomolecules. Physica Scripta, 2015, 90, 094006.	1.2	3
21764	Determining surface structure and stability of Îµ-Fe2C, Ï‡-Fe5C2, Î¸-Fe3C and Fe4C phases under carburization environment from combined DFT and atomistic thermodynamic studies. Journal of Lithic Studies, 2015, 1, 44-60.	0.1	50
21765	Theoretical model of dynamic spin polarization of nuclei coupled to paramagnetic point defects in diamond and silicon carbide. Physical Review B, 2015, 92, .	1.1	59
21766	Physical modeling - A new paradigm in device simulation. , 2015, , .		15
21767	Theoretical investigation on the solution behaviors of Ba and Zr in uranium dinitride. Science China Chemistry, 2015, 58, 1891-1897.	4.2	3
21768	Ab InitioSimulations and Electronic Structure of Lithium-Doped Ionic Liquids: Structure, Transport, and Electrochemical Stability. Journal of Physical Chemistry B, 2015, 119, 14705-14719.	1.2	49
21769	Calculation of proton conductivity at the Î£3111/11Â¯0 tilt grain boundary of barium zirconate using density functional theory. Solid State Ionics, 2015, 279, 60-65.	1.3	15

#	Article	IF	Citations
21770	Peeling Silicene From Model Silver Substrates in Molecular Dynamics Simulations. Journal of Applied Mechanics, Transactions ASME, 2015, 82, .	1.1	8
21771	Molecular Orbital-Based Verification of Conductivity of Tetramethylammonium Pentaiodide and Pentaiodide-Based Electrolytes in Dye-Sensitized Solar Cells. Journal of the Electrochemical Society, 2015, 162, E263-E270.	1.3	8
21772	Order and disorder in quaternary atomic laminates from first-principles calculations. Physical Chemistry Chemical Physics, 2015, 17, 31810-31821.	1.3	71
21773	Accurate calculations of the high-pressure elastic constants based on the first-principles. Chinese Physics B, 2015, 24, 086201.	0.7	1
21774	First-principles study of the relaxor ferroelectricity of Ba(Zr, Ti)O ₃. Chinese Physics B, 2015, 24, 127702.	0.7	5
21775	Polymorph engineering of CuMO₂ (M = Al, Ga, Sc, Y) semiconductors for solar energy applications: from delafossite to wurtzite. Acta Crystallographica Section B: Structural Science, Crystal Engineering and Materials, 2015, 71, 702-706.	0.5	10
21776	ZenGen, a tool to generate ordered configurations for systematic first-principles calculations: The Crâ€“Moâ€“Niâ€“Re system as a case study. Calphad: Computer Coupling of Phase Diagrams and Thermochemistry, 2015, 51, 233-240.	0.7	39
21777	Observation ofSâ€‰â€‰= 1/2 quasi-1D magnetic and magneto-dielectric behavior in a cubic SrCuTe₂O₆. Journal of Physics Condensed Matter, 2015, 27, 426001.	0.7	15
21778	Elastic properties and electronic structures of lanthanide hexaborides. Chinese Physics B, 2015, 24, 096201.	0.7	18
21779	Dynamics of ultrathin gold layers on vitreous silica probed by density functional theory. Physical Chemistry Chemical Physics, 2015, 17, 27488-27495.	1.3	7
21780	Adiabatic release measurements in aluminum between 400 and 1200 GPa: Characterization of aluminum as a shock standard in the multimegabar regime. Physical Review B, 2015, 91, .	1.1	26
21781	antimonates<mml:math xmlns:mml="http://www.w3.org/1998/Math/MathML"><mml:mrow><mml:msub><mml:mi>A</mml:mi><mml:mn>3</mml:mn></mml:msub><mml:mi mathvariant="normal">N</mml:mi><mml:msub><mml:mi mathvariant="normal">i</mml:mi><mml:mn>2</mml:mn></mml:msub><mml:mi>Sb</mml:mi><mml:msub><mml:mi mathvariant="normal">O</mml:mi><mml:mn>6</mml:mn></mml:msub><mml:mspace width="0.28em" />	1.1	63
21782	Effects of Applied Bias and High Field Stress on the Radiation Response of GaN/AlGaN HEMTs. IEEE Transactions on Nuclear Science, 2015, 62, 2423-2430.	1.2	84
21783	The Electronic Structure of Structurally Strained Mn₃O₄Postspinel and the Relationship with Mn₃O₄Spinel. Journal of the Physical Society of Japan, 2015, 84, 114702.	0.7	15
21784	Methylene Blue Adsorption on the Basal Surfaces of Kaolinite: Structure and Thermodynamics from Quantum and Classical Molecular Simulation. Clays and Clay Minerals, 2015, 63, 185-198.	0.6	45
21785	E-beam-induced in situ structural transformation in one-dimensional nanomaterials. Science Bulletin, 2015, 60, 71-75.	4.3	8
21786	How Dopants Can Enhance Charge Transport in Li₂O₂. Chemistry of Materials, 2015, 27, 839-847.	3.2	79
21787	Anisotropic Impact Sensitivity and Shock Induced Plasticity of TKX-50 (Dihydroxylammonium) Tj ETQq1 1 0.784314 rgBT /Overlock 10 Journal of Physical Chemistry C, 2015, 119, 2196-2207.	1.5	67

#	Article	IF	Citations
21788	The structural, elastic and electronic properties of A₂C₂ (A = Li, Na, K, Rb and) Tj ETQq0 0 0 rgBT /Overlock 10 Tf 50 742 1550003.	0.8	4
21789	Phase transition of iron doped MgO under high pressure by first-principles study. International Journal of Modern Physics C, 2015, 26, 1550020.	0.8	1
21790	Temperature Dependent EXAFS Study of Chromium-Doped GaFeO₃ at Gallium and Iron Edges. Journal of Physical Chemistry C, 2015, 119, 2029-2037.	1.5	12
21791	Structural evolution and electronic mechanism for KBH4 phase transition from first-principles calculations. Chemical Physics Letters, 2015, 620, 88-91.	1.2	0
21792	The effects of the presence of metal Fe in the CO oxidation over Ir/FeOx catalyst. Catalysis Communications, 2015, 61, 83-87.	1.6	10
21793	Plasmon Resonances of Highly Doped Two-Dimensional MoS₂. Nano Letters, 2015, 15, 883-890.	4.5	167
21794	Synthesis and photocatalytic activity of TiO2 nanotubes co-doped by erbium ions. Applied Surface Science, 2015, 328, 115-119.	3.1	21
21795	Local structure evolution of Li2Fe0.5Mn0.5SiO4 during delithiation/lithiation processes: A first-principles investigation. Computational Materials Science, 2015, 99, 96-104.	1.4	4
21796	Correlating coreâ€level shifts and structure of zincâ€oxide surfaces. Physica Status Solidi (B): Basic Research, 2015, 252, 755-764.	0.7	6
21797	Room-Temperature Ordered Spin Structures in Cluster-Assembled Single V@Si₁₂ Sheets. Journal of Physical Chemistry C, 2015, 119, 1517-1523.	1.5	50
21798	Size effect on the structural and electronic properties of lead telluride clusters. International Journal of Quantum Chemistry, 2015, 115, 197-207.	1.0	4
21799	Sub-10â€‰nm rutile titanium dioxide nanoparticles for efficient visible-light-driven photocatalytic hydrogen production. Nature Communications, 2015, 6, 5881.	5.8	653
21800	The Nature of Photocatalytic â€œWater Splittingâ€•on Silicon Nanowires. Angewandte Chemie - International Edition, 2015, 54, 2980-2985.	7.2	97
21801	Ultrafast palladium diffusion in germanium. Journal of Materials Chemistry A, 2015, 3, 3832-3838.	5.2	14
21802	Charge Disproportionation in Tetragonal La₂MoO₅, a Small Band Gap Semiconductor Influenced by Direct Moâ€“Mo Bonding. Journal of the American Chemical Society, 2015, 137, 1245-1257.	6.6	8
21803	Thermodynamics of hydrogen-induced superabundant vacancy in tungsten. Journal of Nuclear Materials, 2015, 458, 187-197.	1.3	30
21804	Experimental Study of Strontium Adsorption on Anatase Nanoparticles as a Function of Size with a Density Functional Theory and CD Model Interpretation. Langmuir, 2015, 31, 703-713.	1.6	12
21805	Large resistivity modulation in mixed-phase metallic systems. Nature Communications, 2015, 6, 5959.	5.8	154

#	Article	IF	Citations
21806	Pressure-induced phase transition of BiOF: novel two-dimensional layered structures. Physical Chemistry Chemical Physics, 2015, 17, 4434-4440.	1.3	15
21807	Hydrogen Adsorption on Small Zeolite-Supported Rhodium Clusters. A Density Functional Study. Journal of Physical Chemistry C, 2015, 119, 1121-1129.	1.5	13
21808	Solid-State Materials and Molecular Cavities and Containers for the Supramolecular Recognition and Storage of NOX-Species: A Review. Comments on Inorganic Chemistry, 2015, 35, 128-178.	3.0	8
21809	DFT investigations on the structure and properties of MBP dimers and crystal with strong hydrogen-bonding interactions. Structural Chemistry, 2015, 26, 845-858.	1.0	4
21810	Anisotropic intrinsic lattice thermal conductivity of phosphorene from first principles. Physical Chemistry Chemical Physics, 2015, 17, 4854-4858.	1.3	379
21811	A new magnetic superatom: Cr@Zn₁₇. Physical Chemistry Chemical Physics, 2015, 17, 28033-28043.	1.3	17
21812	Highâ€Pressure Investigation in the System SiO₂â€“GeO₂: Mutual Solubility of Si and Ge in Quartz, Coesite and Rutile Phases. Journal of the American Ceramic Society, 2015, 98, 982-989.	1.9	8
21813	Ultralow thermal conductivity of <mml:math xmlns:mml="http://www.w3.org/1998/Math/MathML" altimg="si1.gif" overflow="scroll"><mml:mrow><mml:mi>Î²</mml:mi></mml:mrow></mml:math>-Cu2Se by atomic fluidity and structure distortion. Acta Materialia, 2015, 86, 247-253.	3.8	82
21814	Magnetic and electrode properties, structure and phase relations of the layered triangular-lattice tellurate Li4NiTeO6. Journal of Solid State Chemistry, 2015, 225, 89-96.	1.4	24
21815	The effect of in-plane strain on the electronic properties of LaAlO3/SrTiO3 interface. Computational Materials Science, 2015, 99, 57-61.	1.4	16
21816	Cs₂Hg₃S₄: A Low-Dimensional Direct Bandgap Semiconductor. Chemistry of Materials, 2015, 27, 370-378.	3.2	26
21817	Semiempirical and DFT computations of the influence of Tb(III) dopant on unit cell dimensions of cerium(III) fluoride. Journal of Computational Chemistry, 2015, 36, 193-199.	1.5	7
21818	Charge order at magnetite Fe₃O₄(0â€‰0â€‰1): surface and Verwey phase transitions. Journal of Physics Condensed Matter, 2015, 27, 012001.	0.7	10
21819	Domain boundaries and their influence on Li migration in solid-state electrolyte (La,Li)TiO3. Journal of Power Sources, 2015, 276, 203-207.	4.0	75
21820	A Theoretical Study on the Adsorption of CO2 on CuO(110) Surface. Journal of the Physical Society of Japan, 2015, 84, 015003.	0.7	5
21821	Î²â€CuN₃: The Overlooked Groundâ€State Polymorph of Copper Azide with Heterographeneâ€Like Layers. Angewandte Chemie - International Edition, 2015, 54, 1954-1959.	7.2	30
21822	Strain effects in monolayer iron-chalcogenide superconductors. 2D Materials, 2015, 2, 015001.	2.0	15
21823	Influence of the Exchangeâ€“Correlation Functional on the Electronic Properties of ZnSb as a Promising Thermoelectric Material. Journal of Electronic Materials, 2015, 44, 1540-1546.	1.0	14

#	Article	IF	Citations
21824	Dehydrogenation of Propane to Propylene by a Pd/Cu Single-Atom Catalyst: Insight from First-Principles Calculations. Journal of Physical Chemistry C, 2015, 119, 1016-1023.	1.5	64
21825	Design Principles for Metal Oxide Redox Materials for Solarâ€Driven Isothermal Fuel Production. Advanced Energy Materials, 2015, 5, 1401082.	10.2	52
21826	Carrier-dependent magnetic anisotropy of cobalt doped titanium dioxide. Scientific Reports, 2014, 4, 7496.	1.6	8
21827	Structural, vibrational and thermodynamic properties of <mml:math xmlns:mml="http://www.w3.org/1998/Math/MathML" altimg="si566.gif" overflow="scroll"><mml:mrow><mml:msub><mml:mrow><mml:mtext>Mg</mml:mtext></mml:mrow><mml:mrow><mml:mn>2</mml:mn> and <mml:math xmlns:mml="http://www.w3.org/1998/Math/MathML" altimg="si567.gif" overflow="scroll"><mml:mrow><mml:msu. Physics of the Earth and Planetary Interiors, 2015, 240, 1-24.	0.7	30
21828	New Insight into Structural Evolution in Layered NaCrO₂ during Electrochemical Sodium Extraction. Journal of Physical Chemistry C, 2015, 119, 166-175.	1.5	152
21829	Adsorption of Group IV Elements on Graphene, Silicene, Germanene, and Stanene: Dumbbell Formation. Journal of Physical Chemistry C, 2015, 119, 845-853.	1.5	45
21830	Impact of W on structural evolution and diffusivity of Niâ€“W melts: an ab initio molecular dynamics study. Journal of Materials Science, 2015, 50, 1071-1081.	1.7	11
21831	Coverage-Induced Conformational Effects on Activity and Selectivity: Hydrogenation and Decarbonylation of Furfural on Pd(111). ACS Catalysis, 2015, 5, 104-112.	5.5	172
21832	Charge optimized many-body potential for aluminum. Journal of Physics Condensed Matter, 2015, 27, 015003.	0.7	7
21833	Atomic insight into electrochemical inactivity of lithium chromate (LiCrO2): Irreversible migration of chromium into lithium layers in surface regions. Journal of Power Sources, 2015, 273, 1218-1225.	4.0	45
21834	First-principles study of negative thermal expansion mechanism in A-site-ordered perovskite SrCu₃Fe₄O₁₂. RSC Advances, 2015, 5, 1801-1807.	1.7	10
21835	Large magnetocrystalline anisotropy of Fe _{3â^'x} Cr _x Se ₄ single crystals due to Cr substitution. Europhysics Letters, 2015, 109, 37004.	0.7	12
21836	Structural stability of ternary D8mâ€“Ti5Sb2X (X=Al, Ga, In, Si, Ge, Sn) compounds. Calphad: Computer Coupling of Phase Diagrams and Thermochemistry, 2015, 49, 8-18.	0.7	2
21837	Thermodynamic study of the Geâ€“Mnâ€“Si system. Journal of Alloys and Compounds, 2015, 632, 10-16.	2.8	5
21838	Effect of interfaces of grain boundary Al2CuLi plates on fracture behavior of Alâ€“3Cuâ€“2Li. Acta Materialia, 2015, 87, 399-410.	3.8	28
21839	Alkali metal â€“ yttrium borohydrides: The link between coordination of small and large rare-earth. Journal of Solid State Chemistry, 2015, 225, 231-239.	1.4	27
21840	Understanding the mechanism of H atom absorption in the Pd(1 1 0) surface. Journal of Alloys and Compounds, 2015, 645, S123-S127.	2.8	10
21841	On the influence of polarization effects in predicting the interfacial structure and capacitance of graphene-like electrodes in ionic liquids. Journal of Chemical Physics, 2015, 142, 024701.	1.2	44

#	Article	IF	Citations
21842	Non-empirical phase equilibria in the Crâ€“Mo system: A combination of first-principles calculations, cluster expansion and Monte Carlo simulations. Solid State Sciences, 2015, 41, 19-24.	1.5	11
21843	A DFT study of CO2 electrochemical reduction on Pb(211) and Sn(112). Science China Chemistry, 2015, 58, 607-613.	4.2	30
21844	First-principles calculations of structural stability and elastic properties of REB12 strengthening phases in boriding Mgâ€“RE alloys. Journal of Alloys and Compounds, 2015, 632, 68-72.	2.8	9
21845	Unusual structural and electronic properties of porous silicene and germanene: insights from first-principles calculations. Nanoscale Research Letters, 2015, 10, 13.	3.1	29
21846	Feature-rich electronic properties in graphene ripples. Carbon, 2015, 86, 207-216.	5.4	37
21847	Unusual ferromagnetism in CoSi nanowires from internal and interfacial defects. Nanotechnology, 2015, 26, 065707.	1.3	6
21848	The vapour phase detection of explosive markers and derivatives using two fluorescent metalâ€“organic frameworks. Journal of Materials Chemistry A, 2015, 3, 6351-6359.	5.2	69
21849	Surface effects on the Frenkel pair defects stability in the vicinity of the Si(001) surface. Materials Science in Semiconductor Processing, 2015, 32, 179-187.	1.9	1
21850	Atomistic simulation of hydrogen dynamics near dislocations in vanadium hydrides. Journal of Alloys and Compounds, 2015, 645, S205-S208.	2.8	1
21851	Relationship between monolayer stacking faults and twins in nanocrystals. Acta Materialia, 2015, 88, 207-217.	3.8	26
21852	First-principles study of H2S adsorption and dissociation on Mo(1 1 0). Computational Materials Science, 2015, 101, 47-55.	1.4	13
21853	Pressure-induced planar N6 rings in potassium azide. Scientific Reports, 2014, 4, 4358.	1.6	53
21854	Carbon nitride with simultaneous porous network and O-doping for efficient solar-energy-driven hydrogen evolution. Nano Energy, 2015, 12, 646-656.	8.2	537
21855	Engineering the magnetic anisotropy of atomic-scale nanostructure under electric field. Journal of Physics Condensed Matter, 2015, 27, 076003.	0.7	4
21856	Simulation studies on the structural stability and properties of beta uranium. Journal of the Korean Physical Society, 2015, 66, 234-239.	0.3	3
21857	Structure, Activity, and Deactivation Mechanisms in Double Metal Cyanide Catalysts for the Production of Polyols. ChemCatChem, 2015, 7, 928-935.	1.8	34
21858	Novel Hydrogen Hydrate Structures under Pressure. Scientific Reports, 2014, 4, 5606.	1.6	41
21859	An amorphous SiO2/4H-SiC(0001) interface: Band offsets and accurate charge transition levels of typical defects. Solid State Communications, 2015, 205, 28-32.	0.9	22

#	Article	IF	Citations
21860	Isothermal reverse water gas shift chemical looping on La0.75Sr0.25Co(1â^')Fe O3 perovskite-type oxides. Catalysis Today, 2015, 258, 691-698.	2.2	72
21861	Reaction Pathways of GaN (0001) Growth from Trimethylgallium and Ammonia versus Triethylgallium and Hydrazine Using First Principle Calculations. Journal of Physical Chemistry C, 2015, 119, 4095-4103.	1.5	24
21862	Organicâ€“Inorganic Hybrid Lead Iodide Perovskite Featuring Zero Dipole Moment Guanidinium Cations: A Theoretical Analysis. Journal of Physical Chemistry C, 2015, 119, 4694-4701.	1.5	132
21863	N-substituted defective graphene sheets: promising electrode materials for Na-ion batteries. RSC Advances, 2015, 5, 17042-17048.	1.7	27
21864	Superior Photovoltaic Properties of Lead Halide Perovskites: Insights from First-Principles Theory. Journal of Physical Chemistry C, 2015, 119, 5253-5264.	1.5	246
21865	Effective Hamiltonians for phosphorene and silicene. New Journal of Physics, 2015, 17, 025004.	1.2	51
21866	Electronic excitation induced amorphization in titanate pyrochlores: an ab initio molecular dynamics study. Scientific Reports, 2015, 5, 8265.	1.6	20
21867	DFT study of electron affinity of hydrogen terminated Î²-Si3N4. Diamond and Related Materials, 2015, 53, 52-57.	1.8	16
21868	The Interaction of Formic Acid with Zinc Oxide: A Combined Experimental and Theoretical Study on Single Crystal and Powder Samples. Topics in Catalysis, 2015, 58, 174-183.	1.3	32
21869	Prediction of structural and metal-to-semiconductor phase transitions in nanoscale<mml:math xmlns:mml="http://www.w3.org/1998/Math/MathML"><mml:msub><mml:mi>MoS</mml:mi><mml:mn>2</mml:mn></mml:msub></mml:math xmlns:mml="http://www.w3.org/1998/Math/MathML"><mml:msub><mml:mi>WS</mml:mi><mml:mn>2</mml:mn></mml:msub></mml:math and other transition metal dichalcogenide zigzag ribbons. Physical Review B, 2015, 91, .	1.1	38
21870	Experimental and theoretical investigations of monolayer and few-layer talc. 2D Materials, 2015, 2, 015004.	2.0	37
21871	Evaluating Pristine and Modified SnS₂ as a Lithium-Ion Battery Anode: A First-Principles Study. ACS Applied Materials & Interfaces, 2015, 7, 4000-4009.	4.0	75
21872	Density Functional Theory of the Water Splitting Reaction on Fe(0): Comparison of Local and Nonlocal Correlation Functionals. ACS Catalysis, 2015, 5, 2070-2080.	5.5	28
21873	A Series of Noncentrosymmetric Antimony Sulfides Ln₈Sb₂S₁₅ (Ln) Tj ETQq1 1 0.784314 rgB Inorganic Chemistry, 2015, 2015, 964-968.	1.0	17
21874	Quantum Mechanical Rippling of a<mml:math xmlns:mml="http://www.w3.org/1998/Math/MathML" display="inline"><mml:mrow><mml:msub><mml:mrow><mml:mi>MoS</mml:mi></mml:mrow><mml:mrow><mml:mn>2</mml:mn></mml:mrow Controlled by Interlayer Bilayer Coupling. Physical Review Letters, 2015, 114, 065501.	2.9	20
21875	Local strain effect on the band gap engineering of graphene by a first-principles study. Applied Physics Letters, 2015, 106, .	1.5	30
21876	Understanding on the carbon deposition on the Nickel/Yttriumâ€“Stabilized Zirconia anode caused by the CO containing fuels. Journal of Power Sources, 2015, 279, 759-765.	4.0	14
21877	Effect of Cu doping on the catalytic activity of Fe3O4 in water-gas shift reactions. International Journal of Hydrogen Energy, 2015, 40, 2193-2198.	3.8	28

#	Article	IF	Citations
21878	The origin of the low efficiency of carbon removal from the Nickel/Yttriumâ€“Stabilized Zirconia triple-phase boundary by adsorbed water. Journal of Power Sources, 2015, 279, 224-230.	4.0	4
21879	A density-functional study on the electronic and vibrational properties of layered antimony telluride. Journal of Physics Condensed Matter, 2015, 27, 085402.	0.7	18
21880	Oxidative methane activation over yttrium stabilised zirconia. Chemical Communications, 2015, 51, 5856-5859.	2.2	6
21881	Interfacial-Strain-Induced Structural and Polarization Evolutions in Epitaxial Multiferroic BiFeO₃ (001) Thin Films. ACS Applied Materials & Interfaces, 2015, 7, 2944-2951.	4.0	32
21882	Energetic Stability of Absorbed H in Pd and Pt Nanoparticles in a More Realistic Environment. Journal of Physical Chemistry C, 2015, 119, 5180-5186.	1.5	25
21883	Formation of Bioinorganic Complexes by the Corrosive Adsorption of (S)-Proline on Ni/Au(111). Langmuir, 2015, 31, 262-271.	1.6	13
21884	Facet-Dependent Electrocatalytic Performance of Co₃O₄ for Rechargeable Liâ€“O₂ Battery. Journal of Physical Chemistry C, 2015, 119, 4516-4523.	1.5	99
21885	Point defect stability in a semicoherent metallic interface. Physical Review B, 2015, 91, .	1.1	23
21886	Ultrafast and Directional Diffusion of Lithium in Phosphorene for High-Performance Lithium-Ion Battery. Nano Letters, 2015, 15, 1691-1697.	4.5	628
21887	First principles study of the elastic properties of Li₂MnSiO_{4â^'y}S_y. Journal of Materials Chemistry A, 2015, 3, 5449-5456.	5.2	24
21888	First-principles nickel database: Energetics of impurities and defects. Computational Materials Science, 2015, 101, 77-87.	1.4	40
21889	An ab initio investigation of the effect of alloying elements on the elastic properties and magnetic behavior of Ni3Al. Computational Materials Science, 2015, 101, 39-46.	1.4	31
21890	Superdiffusive heat conduction in semiconductor alloys. I. Theoretical foundations. Physical Review B, 2015, 91, .	1.1	75
21891	Top cited articles in thermodynamic research. Journal of Engineering Thermophysics, 2015, 24, 68-85.	0.6	59
21892	Ab initio description of segregation and cohesion of grain boundaries in Wâ€“25 at.% Re alloys. Acta Materialia, 2015, 88, 180-189.	3.8	87
21893	Synthesis, Structure, and Thermal Instability of the Cu₂Ta₄O₁₁ Phase. Crystal Growth and Design, 2015, 15, 552-558.	1.4	11
21894	Enhanced ferromagnetic properties of Cu doped two-dimensional GaN monolayer. International Journal of Modern Physics C, 2015, 26, 1550009.	0.8	10
21895	Atomic-scale origin of piezoelectricity in wurtzite ZnO. Physical Chemistry Chemical Physics, 2015, 17, 7857-7863.	1.3	20

#	Article	IF	Citations
21896	Improving the adsorption behavior and reaction activity of Co-anchored graphene surface toward CO and O2 molecules. Sensors and Actuators B: Chemical, 2015, 211, 227-234.	4.0	63
21897	Optimised three-dimensional Fourier interpolation: An analysis of techniques and application to a linear-scaling density functional theory code. Computer Physics Communications, 2015, 187, 8-19.	3.0	7
21898	Oxidation of CO on a carbon-based material composed of nickel hydroxide and hydroxyl graphene oxide, (Ni4(OH)3â€“hGO) â€“ a first-principles calculation. Physical Chemistry Chemical Physics, 2015, 17, 7555-7563.	1.3	2
21899	A DFT study on the correlation between topology and Bader charges: Part I, effects of compression and expansion of As2O5. Solid State Sciences, 2015, 41, 1-7.	1.5	10
21900	Martensitic transformation in Ni-rich Ni55Mn25In20 Heusler alloy: Experiment and first-principles calculations. Journal of Alloys and Compounds, 2015, 633, 18-21.	2.8	10
21901	van der Waals Heterostructure of Phosphorene and Graphene: Tuning the Schottky Barrier and Doping by Electrostatic Gating. Physical Review Letters, 2015, 114, 066803.	2.9	445
21902	Ab initio study on the stability of N-doped ZnO under high pressure. RSC Advances, 2015, 5, 16774-16779.	1.7	3
21903	Room-Temperature Polar Order in [NH₄][Cd(HCOO)₃] - A Hybrid Inorganicâ€“Organic Compound with a Unique Perovskite Architecture. Inorganic Chemistry, 2015, 54, 2109-2116.	1.9	78
21904	Vacancy formation energies in metals: A comparison of MetaGGA with LDA and GGA exchangeâ€“correlation functionals. Computational Materials Science, 2015, 101, 96-107.	1.4	69
21905	Unveiling the charge migration mechanism in Na₂O₂: implications for sodiumâ€“air batteries. Physical Chemistry Chemical Physics, 2015, 17, 8203-8209.	1.3	30
21906	Promoted ceria catalysts for alkyne semi-hydrogenation. Journal of Catalysis, 2015, 324, 69-78.	3.1	65
21907	Molecular bonding-based descriptors for surface adsorption and reactivity. Journal of Catalysis, 2015, 324, 50-58.	3.1	17
21908	Simulation of IRRAS Spectra for Molecules on Oxide Surfaces: CO on TiO₂(110). Journal of Physical Chemistry C, 2015, 119, 5403-5411.	1.5	16
21909	Quantum Anomalous Hall Effect in Magnetic Insulator Heterostructure. Nano Letters, 2015, 15, 2019-2023.	4.5	50
21910	Prediction of new high pressure phase of TaB3: First-principles. Journal of Alloys and Compounds, 2015, 632, 37-43.	2.8	14
21911	PdIIâ€“PdII bonding interaction in dinuclear PdII complex with non-macrocyclic (O&N) chelates: Characterization, kinetics and DFT study. Polyhedron, 2015, 89, 101-109.	1.0	16
21912	Electrical control of carriers' spin orientation in the FeVTiSi Heusler alloy. Journal of Materials Chemistry C, 2015, 3, 2563-2567.	2.7	30
21913	Robust Two-Dimensional Topological Insulators in Methyl-Functionalized Bismuth, Antimony, and Lead Bilayer Films. Nano Letters, 2015, 15, 1083-1089.	4.5	166

#	Article	IF	Citations
21914	Magnetically Frustrated Double Perovskites: Synthesis, Structural Properties, and Magnetic Order of Sr₂BOsO₆ (B = Y, In, Sc). Zeitschrift Fur Anorganische Und Allgemeine Chemie, 2015, 641, 197-205.	0.6	47
21915	Incommensurate magnetic structure, Fe/Cu chemical disorder, and magnetic interactions in the high-temperature multiferroic<mml:math xmlns:mml="http://www.w3.org/1998/Math/MathML"><mml:mi mathvariant="normal">YBaCuFeO</mml:mi><mml:msub><mml:mrow /><mml:mn>5</mml:mn></mml:msub></mml:math>. Physical Review B, 2015, 91, .	1.1	39
21916	Titanium-Defected Undoped Anatase TiO₂ with p-Type Conductivity, Room-Temperature Ferromagnetism, and Remarkable Photocatalytic Performance. Journal of the American Chemical Society, 2015, 137, 2975-2983.	6.6	549
21917	Role of Chemical Potential in Flake Shape and Edge Properties of Monolayer MoS₂. Journal of Physical Chemistry C, 2015, 119, 4294-4301.	1.5	178
21918	Dynamic and structural stability of cubic vanadium nitride. Physical Review B, 2015, 91, .	1.1	71
21919	A Hybrid Quantum Mechanical Approach: Intimate Details of Electron Transfer between Type-I CdSe/ZnS Quantum Dots and an Anthraquinone Molecule. Journal of Physical Chemistry B, 2015, 119, 7651-7658.	1.2	23
21920	Exploring the activity of a novel Au/TiC(001) model catalyst towards CO and CO2 hydrogenation. Surface Science, 2015, 640, 141-149.	0.8	17
21921	Thermoelectric Response of Bulk and Monolayer MoSe₂ and WSe₂. Chemistry of Materials, 2015, 27, 1278-1284.	3.2	308
21923	Binding of SO3 to fly ash components: CaO, MgO, Na2O and K2O. Fuel, 2015, 145, 79-83.	3.4	35
21924	Surface-induced size-dependent ultimate tensile strength of thin films. Physics Letters, Section A: General, Atomic and Solid State Physics, 2015, 379, 471-481.	0.9	7
21925	A first-principles study of structure, elasticity and thermal decomposition of Ti1â^'xTMxN alloys (TM=Y,) Tj ETQq0 0 0 rgBT /Overlock 10	2.2	36
21926	The role of potassium promoter in surface carbon hydrogenation on HÃgg carbide surfaces. Applied Catalysis A: General, 2015, 493, 68-76.	2.2	22
21927	Airâ€promoted adsorptive desulfurization of diesel fuel over <scp>T</scp>iâ€<scp>C</scp>e mixed metal oxides. AICHE Journal, 2015, 61, 631-639.	1.8	53
21928	Increasing the band gap of FeS2 by alloying with Zn and applying biaxial strain: A first-principles study. Journal of Alloys and Compounds, 2015, 629, 43-48.	2.8	25
21929	Thermodynamic assessment of the Uâ€“Yâ€“O system. Journal of Nuclear Materials, 2015, 460, 5-12.	1.3	8
21930	Alloying effects of Ta on the mechanical properties of Î³â€™ Co3(Al, W): A first-principles study. Scripta Materialia, 2015, 100, 5-8.	2.6	27
21931	First-principles study of the phonon, dielectric, and piezoelectric response in Bi2ZnTiO6 supercell. Computational Materials Science, 2015, 101, 227-232.	1.4	7
21932	A first principles study of the energetics and core level shifts of anion-doped TiO2 photocatalysts. Chinese Journal of Catalysis, 2015, 36, 181-187.	6.9	3

#	Article	IF	Citations
21933	Effect of boron in Fe/MgO interface on structural stability and state coupling. Computational Materials Science, 2015, 101, 138-142.	1.4	3
21934	Crystal structure determination of incommensurate modulated martensite in Niâ€“Mnâ€“In Heusler alloys. Acta Materialia, 2015, 88, 375-388.	3.8	83
21935	Spectral neighbor analysis method for automated generation of quantum-accurate interatomic potentials. Journal of Computational Physics, 2015, 285, 316-330.	1.9	608
21936	Atomic study on the ordered structure in Al melts induced by liquid/substrate interface with Ti solute. Applied Physics Letters, 2015, 106, .	1.5	16
21937	Towards graphyne molecular electronics. Nature Communications, 2015, 6, 6321.	5.8	135
21938	Optical properties of transition metal atom adsorbed graphene: A density functional theoretical calculation. Physica E: Low-Dimensional Systems and Nanostructures, 2015, 69, 306-315.	1.3	19
21939	Enhancing phase stability and kinetics of lithium-rich layered oxide for an ultra-high performing cathode in Li-ion batteries. Journal of Power Sources, 2015, 281, 77-84.	4.0	39
21940	First principles lattice dynamics study of SnO2 polymorphs. Journal of Alloys and Compounds, 2015, 633, 272-279.	2.8	7
21941	Unraveling the Structure of Iron(III) Oxalate Tetrahydrate and Its Reversible Li Insertion Capability. Chemistry of Materials, 2015, 27, 1631-1639.	3.2	30
21942	Effect of substitution on elastic stability, electronic structure and magnetic property of Niâ€“Mn based Heusler alloys: An ab initio comparison. Journal of Alloys and Compounds, 2015, 632, 822-829.	2.8	38
21943	Stability, magnetic, and electronic properties of <mml:math xmlns:mml="http://www.w3.org/1998/Math/MathML" altimg="si33.gif" overflow="scroll"><mml:mrow><mml:mi>L</mml:mi><mml:msub><mml:mrow><mml:mn>2</mml:mn></mml:mrow><mml:mrow><mm and <mml:math xmlns:mml="http://www.w3.org/1998/Math/MathML" altimg="si34.gif" overflow="scroll"><mml:mrow><mml:mi>B</mml:mi><mml:mn>2</mml:mn></mml:mrow></mml:math> phases in Co2MnAl Heusler alloy. Journal of Alloys and Compounds, 2015, 632, 528-532.	2.8	20
21944	Bandgap tunability at single-layer molybdenum disulphide grain boundaries. Nature Communications, 2015, 6, 6298.	5.8	358
21945	Enhanced magnetism of Cun clusters capped with N and endohedrally doped with Cr. Journal of Chemical Physics, 2015, 142, 024309.	1.2	5
21946	Giant Phononic Anisotropy and Unusual Anharmonicity of Phosphorene: Interlayer Coupling and Strain Engineering. Advanced Functional Materials, 2015, 25, 2230-2236.	7.8	198
21947	First-Principles Investigation of Transition Metal Dichalcogenide Nanotubes for Li and Mg Ion Battery Applications. Journal of Physical Chemistry C, 2015, 119, 4302-4311.	1.5	47
21948	Optical function spectra and bandgap energy of Cu2SnSe3. Applied Physics Letters, 2015, 106, .	1.5	27
21949	Cation ordering induced polarization enhancement for<mml:math xmlns:mml="http://www.w3.org/1998/Math/MathML"><mml:msub><mml:mi>PbTiO</mml:mi><mml:mn>3</mml:mn></mml:msub><mml:mi></mml:mi></mml:msub><m superlattices. Physical Review B, 2015, 91, .	1.1	6
21950	Synthesis, Structure Determination and Electronic Structure of Magnesium Nitride Chloride, Mg₂NCl. Zeitschrift Fur Anorganische Und Allgemeine Chemie, 2015, 641, 266-269.	0.6	7

#	Article	IF	Citations
21951	Fluorinated Graphene in Interface Engineering of Geâ€Based Nanoelectronics. Advanced Functional Materials, 2015, 25, 1805-1813.	7.8	40
21952	Electrical Characteristics of Fieldâ€Effect Transistors based on Chemically Synthesized Graphene Nanoribbons. Advanced Electronic Materials, 2015, 1, 1400010.	2.6	32
21953	Computational Identification and Experimental Realization of Lithium Vacancy Introduction into the Olivine LiMgPO₄. Chemistry of Materials, 2015, 27, 2074-2091.	3.2	33
21954	Porphyrin-based porous sheet: Optoelectronic properties and hydrogen storage. International Journal of Hydrogen Energy, 2015, 40, 3689-3696.	3.8	22
21955	Atomically Precise Graphene Nanoribbon Heterojunctions for Excitonic Solar Cells. Journal of Physical Chemistry C, 2015, 119, 775-783.	1.5	34
21956	Dispersion Corrected DFT Study of Pentacene Thin Films on Flat and Vicinal Au(111) Surfaces. Journal of Physical Chemistry C, 2015, 119, 3596-3604.	1.5	6
21957	Auger-Mediated Electron Relaxation Is Robust to Deep Hole Traps: Time-Domain Ab Initio Study of CdSe Quantum Dots. Nano Letters, 2015, 15, 2086-2091.	4.5	57
21958	Free Energy Assessment of Water Structures and Their Dissociation on Ru(0001). Journal of Physical Chemistry C, 2015, 119, 5478-5483.	1.5	4
21959	Oxygen Atom Exchange between Gaseous CO₂ and TiO₂ Nanoclusters. Journal of Physical Chemistry C, 2015, 119, 3605-3612.	1.5	18
21960	Theoretical Study of Phase Separation of Scandium Hydrides under High Pressure. Journal of Physical Chemistry C, 2015, 119, 5614-5625.	1.5	37
21961	CO₂ Hydrate Nucleation Kinetics Enhanced by an Organo-Mineral Complex Formed at the Montmorilloniteâ€“Water Interface. Environmental Science & Technology, 2015, 49, 1197-1205.	4.6	47
21962	Quasiparticle Interfacial Level Alignment of Highly Hybridized Frontier Levels: H₂O on TiO₂(110). Journal of Chemical Theory and Computation, 2015, 11, 239-251.	2.3	28
21963	Strongest Second Harmonic Generation in the Polar R₃MTQ₇ Family: Atomic Distribution Induced Nonlinear Optical Cooperation. Chemistry of Materials, 2015, 27, 1876-1884.	3.2	70
21964	Ab Initio Studies of Segregation, Ordering, and Magnetic Behavior in (Feâ€“Pt)n, n = 55 and 147: Design of Fe75Pt72 Nanoparticle. Journal of Physical Chemistry C, 2015, 119, 11062-11071.	1.5	4
21965	Investigation of the Optical Absorbance, Electronic, and Photocatalytic Properties of (Cu1â€“xCox)2(OH)PO4 Solid Solutions. Journal of Physical Chemistry C, 2015, 119, 4684-4693.	1.5	7
21966	Theoretical Study on the Composition Location of the Best Glass Formers in Cuâ€“Zr Amorphous Alloys. Journal of Physical Chemistry A, 2015, 119, 806-814.	1.1	16
21967	Ultrathin Gold Nanowires: Soft-Templating versus Liquid Phase Synthesis, a Quantitative Study. Journal of Physical Chemistry C, 2015, 119, 4422-4430.	1.5	40
21968	Linear Metal Chains in Ca₂M₂X (M = Pd, Pt; X = Al, Ge): Origin of the Pairwise Distortion and Its Role in the Structure Stability. Chemistry of Materials, 2015, 27, 304-315.	3.2	27

#	Article	IF	Citations
21969	Adsorption of Benzene on Cu(100) and on Cu(100) Covered with an Ultrathin NaCl Film: Moleculeâ€“Substrate Interaction and Decoupling. Journal of Physical Chemistry C, 2015, 119, 4062-4071.	1.5	20
21970	Halogen Phases on Pd(110): Compression Structures, Domain Walls, and Corrosion. Journal of Physical Chemistry C, 2015, 119, 3613-3623.	1.5	4
21971	Interlayer Electronic Coupling in Arbitrarily Stacked MoS₂ Bilayers Controlled by Interlayer Sâ€“S Interaction. Journal of Physical Chemistry C, 2015, 119, 1247-1252.	1.5	25
21972	Adsorption and Dehydrogenation Behaviors of the NH₃ Molecule on the W(111) Surface: A First-Principles Study. Journal of Physical Chemistry C, 2015, 119, 4188-4198.	1.5	7
21973	Carbonation of Wollastonite(001) Competing Hydration: Microscopic Insights from Ion Spectroscopy and Density Functional Theory. ACS Applied Materials & Interfaces, 2015, 7, 4706-4712.	4.0	41
21974	Electronic Structures and Transport Properties of n-Type-Doped Indium Oxides. Journal of Physical Chemistry C, 2015, 119, 4789-4795.	1.5	20
21975	Theoretical Study of the Stoichiometric and Reduced Ce-Doped TiO2Anatase (001) Surfaces. Journal of Physical Chemistry C, 2015, 119, 4805-4816.	1.5	24
21976	Competitive Coadsorption of CO₂ with H₂O, NH₃, SO₂, NO, NO₂, N₂, O₂, and CH₄ in M-MOF-74 (M = Mg, Co, Ni): The Role of Hydrogen Bonding. Chemistry of Materials, 2015, 27, 2203-2217.	3.2	158
21977	Nitrogen(II) Oxide Charge Transfer Complexes on TiO₂: A New Source for Visible-Light Activity. Journal of Physical Chemistry C, 2015, 119, 4488-4501.	1.5	33
21978	Integer Charge Transfer and Hybridization at an Organic Semiconductor/Conductive Oxide Interface. Journal of Physical Chemistry C, 2015, 119, 4865-4873.	1.5	59
21979	Rb⁺ Adsorption at the Quartz(101)â€“Aqueous Interface: Comparison of Resonant Anomalous X-ray Reflectivity with ab Initio Calculations. Journal of Physical Chemistry C, 2015, 119, 4778-4788.	1.5	34
21980	Modulated Two-Dimensional Charge-Carrier Density in LaTiO₃â€“Layer-Doped LaAlO₃/SrTiO₃ Heterostructure. ACS Applied Materials & Interfaces, 2015, 7, 5305-5311.	4.0	26
21981	Reaction of Trimethylaluminum with Water on Pt(111) and Pd(111) from 10^{â€“5} to 10^{â€“1} Millibar. Journal of Physical Chemistry C, 2015, 119, 2399-2411.	1.5	21
21982	Pathways for Ethanol Dehydrogenation and Dehydration Catalyzed by Ceria (111) and (100) Surfaces. Journal of Physical Chemistry C, 2015, 119, 2447-2455.	1.5	46
21983	A Potential Regularity for Enhancing the Hydrogenation Properties of Ni₂P. Journal of Physical Chemistry C, 2015, 119, 2557-2565.	1.5	20
21984	Composition-Dependent Structural and Electronic Properties of Mg95â€“xZnxCa5Metallic Glasses: An Ab Initio Molecular Dynamics Study. Journal of Physical Chemistry B, 2015, 119, 3608-3618.	1.2	9
21985	First-Principles Investigation of Optoelectronic and Redox Properties of (Ta_{1â€“x}Nb_x)ON Compounds for Photocatalysis. Journal of Physical Chemistry C, 2015, 119, 4565-4572.	1.5	26
21986	Formation of Induced-Fit Chiral Templates by Amino Acid-Functionalized Pd(111) Surfaces. Journal of Physical Chemistry C, 2015, 119, 3556-3563.	1.5	12

#	Article	IF	Citations
21987	Lithium Ion Solvation and Diffusion in Bulk Organic Electrolytes from First-Principles and Classical Reactive Molecular Dynamics. Journal of Physical Chemistry B, 2015, 119, 1535-1545.	1.2	154
21988	GaN as an Interfacial Passivation Layer: Tuning Band Offset and Removing Fermi Level Pinning for IIIâ€“V MOS Devices. ACS Applied Materials & Interfaces, 2015, 7, 5141-5149.	4.0	41
21989	Energetics and Atomic Structures of Cu₂Te Overlayers on CdTe(111). Journal of Physical Chemistry C, 2015, 119, 4843-4847.	1.5	1
21990	CO Oxidation at Rutile TiO₂(110): Role of Oxygen Vacancies and Titanium Interstitials. ACS Catalysis, 2015, 5, 2042-2050.	5.5	65
21991	Convergence of Atomic Charges with the Size of the Enzymatic Environment. Journal of Chemical Information and Modeling, 2015, 55, 564-571.	2.5	17
21992	Study of Metal/Epoxy Interfaces between Epoxy Precursors and Metal Surfaces Using a Newly Developed Reactive Force Field for Aluminaâ€“Amine Adhesion. Journal of Physical Chemistry C, 2015, 119, 4796-4804.	1.5	13
21993	Theoretical Insight into the Reaction Mechanism of Ethanol Steam Reforming on Co(0001). Journal of Physical Chemistry C, 2015, 119, 2680-2691.	1.5	22
21994	NiAl(110) Surface as a Template for Growing Transition Metal Linear Atomic Chains: A DFT Investigation. Journal of Physical Chemistry C, 2015, 119, 2456-2461.	1.5	5
21995	Tailoring Native Defects and Zinc Impurities in Li₄Ti₅O₁₂: Insights from First-Principles Study. Journal of Physical Chemistry C, 2015, 119, 5238-5245.	1.5	23
21996	Optical properties of transition metal oxide quantum wells. Journal of Applied Physics, 2015, 117, .	1.1	12
21997	Cu impurity in insulators and in metal-insulator-metal structures: Implications for resistance-switching random access memories. Journal of Applied Physics, 2015, 117, 054504.	1.1	14
21998	Structural and electrochemical properties of Gd-doped Li4Ti5O12 as anode material with improved rate capability for lithium-ion batteries. Journal of Power Sources, 2015, 280, 355-362.	4.0	120
21999	Endowing single-electron-trapped oxygen vacancy self-modified titanium dioxide with visible-light photocatalytic activity by grafting Fe(III) nanocluster. Applied Catalysis B: Environmental, 2015, 172-173, 37-45.	10.8	30
22000	Ultimately short ballistic vertical graphene Josephson junctions. Nature Communications, 2015, 6, 6181.	5.8	94
22001	Strain-induced semiconductor to metal transition in few-layer black phosphorus from first principles. Chemical Physics Letters, 2015, 622, 109-114.	1.2	34
22002	Surface Electronic States of 18 Valence Electron Halfâ€Heusler Semiconductors. Advanced Materials Interfaces, 2015, 2, 1400340.	1.9	5
22003	Low In solubility and band offsets in the small-xÎ²-Ga₂O₃/(Ga_{1â^'}_xIn_x)₂O<su Applied Physics Express, 2015, 8, 021102.	1.5	19
22004	Silicene: A Promising Surface to Achieve Morphological Transformation in Gold Clusters. Journal of Physical Chemistry C, 2015, 119, 3192-3198.	1.5	9

#	Article	IF	Citations
22005	A density functional theory study of ethylene hydrogenation on MgO- and Î³-Al₂O₃-supported carbon-containing Ir₄ clusters. Physical Chemistry Chemical Physics, 2015, 17, 4899-4908.	1.3	19
22006	Catalytic reaction on FeN4/C site of nitrogen functionalized carbon nanotubes as cathode catalyst for hydrogen fuel cells. Catalysis Communications, 2015, 62, 79-82.	1.6	13
22007	Adsorption and ring-opening of lactide on the chiral metal surface Pt(321)S studied by density functional theory. Journal of Chemical Physics, 2015, 142, 044703.	1.2	2
22008	Ti-decorated zigzag graphene nanoribbons for hydrogen storage. A van der Waals-corrected density-functional study. International Journal of Hydrogen Energy, 2015, 40, 4960-4968.	3.8	65
22009	Density Functional Theory Study of Nucleation and Growth of Pt Nanoparticles on MoS₂(001) Surface. Crystal Growth and Design, 2015, 15, 642-652.	1.4	32
22010	Decoupling the electronic, geometric and interfacial contributions to support effects in heterogeneous catalysis. Molecular Simulation, 2015, 41, 123-133.	0.9	16
22011	Phonon anharmonicity in silicon from 100 to 1500 K. Physical Review B, 2015, 91, .	1.1	47
22012	Choosing a density functional for modeling adsorptive hydrogen storage: reference quantum mechanical calculations and a comparison of dispersion-corrected density functionals. Physical Chemistry Chemical Physics, 2015, 17, 6423-6432.	1.3	33
22013	Betheâ€“Salpeter calculation of optical-absorption spectra of In₂O₃and Ga₂O₃. Semiconductor Science and Technology, 2015, 30, 024010.	1.0	38
22014	Nitride-based high-electron-mobility transistor with single-layer InN for mobility-enhanced channel. Applied Physics Express, 2015, 8, 024302.	1.1	8
22015	First-principle and molecular dynamics calculations for physical properties of Niâ€“Sn alloy system. Computational Materials Science, 2015, 99, 274-284.	1.4	21
22016	First-Principles Phase Diagram of Magic-Sized Carbon Clusters on Ru(0001) and Rh(111) Surfaces. Journal of Physical Chemistry C, 2015, 119, 11086-11093.	1.5	14
22017	Metal and F dual-doping to synchronously improve electron transport rate and lifetime for TiO₂ photoanode to enhance dye-sensitized solar cells performances. Journal of Materials Chemistry A, 2015, 3, 5692-5700.	5.2	29
22018	Theoretical limits on the stability of single-phase kesterite-Cu2ZnSnS4. Journal of Applied Physics, 2015, 117, .	1.1	22
22019	Energetics, Charge Transfer, and Magnetism of Small Molecules Physisorbed on Phosphorene. Journal of Physical Chemistry C, 2015, 119, 3102-3110.	1.5	347
22020	Topological states in<mml:math xmlns:mml="http://www.w3.org/1998/Math/MathML"><mml:mi>Î±</mml:mi><mml:mo>â^'</mml:mo><mml:mi>Sn</mml:mi><mml:mi>1</mml:mi></mml:mo></mml:ma HgTe quantum wells: A comparison ofab initioresults. Physical Review B, 2015, 91, .	1.1	20
22021	Optical, electronic, and photoelectrochemical properties of the p-type Cu_{3â^'x}VO₄ semiconductor. Journal of Materials Chemistry A, 2015, 3, 4501-4509.	5.2	75
22022	Metalâ€“organic Kagome lattices M₃(2,3,6,7,10,11-hexaiminotriphenylene)₂ (M =) Tj ETQq1 1 0.784314 rg Physics, 2015, 17, 5954-5958.	1.3	108

#	Article	IF	Citations
22023	DFT-driven multi-site microkinetic modeling of ethanol conversion to ethylene and diethyl ether on Î³-Al2O3(1 1 1). Journal of Catalysis, 2015, 323, 121-131.	3.1	54
22024	New Phase of MnSb₂O₆ Prepared by Ion Exchange: Structural, Magnetic, and Thermodynamic Properties. Inorganic Chemistry, 2015, 54, 1705-1711.	1.9	21
22025	Native point defects in few-layer phosphorene. Physical Review B, 2015, 91, .	1.1	104
22026	Effect of helium and vacancies in a vanadium grain boundary by first-principles. Nuclear Instruments & Methods in Physics Research B, 2015, 352, 121-124.	0.6	8
22027	Structure dependent active sites of Ni_xS_y as electrocatalysts for hydrogen evolution reaction. Nanoscale, 2015, 7, 5157-5163.	2.8	121
22028	From carbon atom to graphene on Cu(111): an ab-initio study. European Physical Journal B, 2015, 88, 1.	0.6	17
22029	Katoite under pressure: an ab initio investigation of its structural, elastic and vibrational properties sheds light on the phase transition. Physical Chemistry Chemical Physics, 2015, 17, 2660-2669.	1.3	16
22030	CO Oxidation at the Au/TiO₂ Boundary: The Role of the Au/Ti_{5c} Site. ACS Catalysis, 2015, 5, 1589-1595.	5.5	99
22031	Competition between Direct and Indirect Exchange Couplings in MnFeAs: A First-Principles Investigation. Journal of Physical Chemistry C, 2015, 119, 580-589.	1.5	7
22032	Local Measurement of the Eliashberg Function of Pb Islands: Enhancement of Electron-Phonon Coupling by Quantum Well States. Physical Review Letters, 2015, 114, 047002.	2.9	37
22033	Quantum Size Effects in the Sizeâ€“Temperature Phase Diagram of Gallium: Structural Characterization of Shapeâ€Shifting Clusters. Chemistry - A European Journal, 2015, 21, 2862-2869.	1.7	16
22034	Effects of solute size on solid-solution hardening in vanadium alloys: A first-principles calculation. Scripta Materialia, 2015, 100, 106-109.	2.6	17
22035	Crystalline structures of polymeric hydrocarbon with 3,4-fold helical chains. Scientific Reports, 2015, 5, 7723.	1.6	9
22036	The Effect of Antisite Disorder and Particle Size on Li Intercalation Kinetics in Monoclinic LiMnBO₃. Advanced Energy Materials, 2015, 5, 1401916.	10.2	30
22037	B₈₄: a quasi-planar boron cluster stabilized with hexagonal holes. Nanoscale, 2015, 7, 4055-4062.	2.8	44
22038	Dirac point movement and topological phase transition in patterned graphene. Nanoscale, 2015, 7, 3645-3650.	2.8	18
22039	The role of the V_{Zn}â€“N_Oâ€“H complex in the p-type conductivity in ZnO. Physical Chemistry Chemical Physics, 2015, 17, 5485-5489.	1.3	21
22040	Tensile strain induced half-metallicity in graphene-like carbon nitride. Physical Chemistry Chemical Physics, 2015, 17, 6028-6035.	1.3	45

#	Article	IF	Citations
22041	Formation of Stoichiometric CsFn Compounds. Scientific Reports, 2015, 5, 7875.	1.6	20
22042	Elucidating the mechanism and active site of the cyclohexanol dehydrogenation on copper-based catalysts: A density functional theory study. Surface Science, 2015, 640, 181-189.	0.8	38
22043	Enhanced Ferromagnetism in a Mn₃C₁₂N₁₂H₁₂ Sheet. ChemPhysChem, 2015, 16, 614-620.	1.0	39
22044	Antiferromagnetic ground state with pair-checkerboard order in FeSe. Physical Review B, 2015, 91, .	1.1	59
22045	Two-Dimensional Mineral [Pb2BiS3][AuTe2]: High-Mobility Charge Carriers in Single-Atom-Thick Layers. Journal of the American Chemical Society, 2015, 137, 2311-2317.	6.6	14
22046	Giant Topological Nontrivial Band Gaps in Chloridized Gallium Bismuthide. Nano Letters, 2015, 15, 1296-1301.	4.5	92
22047	Semiconductor to metal transition in bilayer phosphorene under normal compressive strain. Nanotechnology, 2015, 26, 075701.	1.3	83
22048	Chemical insight from density functional modeling of molecular adsorption: Tracking the bonding and diffusion of anthracene derivatives on Cu(111) with molecular orbitals. Journal of Chemical Physics, 2015, 142, 101907.	1.2	7
22049	Atomistic insight into the oxidation of monolayer transition metal dichalcogenides: from structures to electronic properties. RSC Advances, 2015, 5, 17572-17581.	1.7	183
22050	Polymorphs of CaSeO₄ under Pressure: A First-Principles Study of Structural, Electronic, and Vibrational Properties. Inorganic Chemistry, 2015, 54, 1765-1777.	1.9	31
22051	A first-principles study on uniaxial strain effects of nonplanar oxygen-functionalized armchair graphene nanoribbons. Journal of Alloys and Compounds, 2015, 631, 219-224.	2.8	7
22052	Identification of a potential superhard compound ReCN. Journal of Alloys and Compounds, 2015, 631, 321-327.	2.8	9
22053	Evolution of Raman Scattering and Electronic Structure of Ultrathin Molybdenum Disulfide by Oxygen Chemisorption. Advanced Electronic Materials, 2015, 1, 1400037.	2.6	13
22054	Structural instabilities and mechanical properties of U2Mo from first principles calculations. Physical Chemistry Chemical Physics, 2015, 17, 4089-4095.	1.3	8
22055	Electronic structure and transport properties of Cu-deficient kuramite Cu_{3â^'}_xSnS₄. Japanese Journal of Applied Physics, 2015, 54, 021801.	0.8	10
22056	New insights into the electrochemical performance of Li₂MnSiO₄: effect of cationic substitutions. Journal of Materials Chemistry A, 2015, 3, 6004-6011.	5.2	27
22057	Organic molecules deposited on graphene: A computational investigation of self-assembly and electronic structure. Journal of Chemical Physics, 2015, 142, 044301.	1.2	23
22058	Effects of nitrogen on hydrogen retention in tungsten: First-principles calculations. Journal of Nuclear Materials, 2015, 459, 143-149.	1.3	18

#	Article	IF	Citations
22059	Mechanical Origin of the Structural Phase Transition in Methylammonium Lead Iodide CH₃NH₃PbI₃. Journal of Physical Chemistry Letters, 2015, 6, 681-685.	2.1	63
22060	Synthesis and Characterization of Melt-Spun Metastable Al6Ge5. Journal of Electronic Materials, 2015, 44, 948-952.	1.0	4
22061	Boron- and Nitrogen-Substituted Graphene Nanoribbons as Efficient Catalysts for Oxygen Reduction Reaction. Chemistry of Materials, 2015, 27, 1181-1186.	3.2	219
22062	Effects of Oxygen Adsorption on the Surface State of Epitaxial Silicene on Ag(111). Scientific Reports, 2014, 4, 7543.	1.6	70
22063	Atomic-Scale Mechanisms of Sliding along an Interdiffused Liâ€“Siâ€“Cu Interface. Nano Letters, 2015, 15, 1716-1721.	4.5	15
22064	Electronic structure, stability, and oxidation of boron-magnesium clusters and cluster solids. Journal of Chemical Physics, 2015, 142, 054304.	1.2	17
22065	Phase stabilities of pyrite-related MTCh compounds (M=Ni, Pd, Pt; T=Si, Ge, Sn, Pb; Ch=S, Se, Te): A systematic DFT study. Journal of Solid State Chemistry, 2015, 226, 29-35.	1.4	18
22066	Fragment-Based Design of NbRuB as a New Metal-Rich Boride Superconductor. Chemistry of Materials, 2015, 27, 1149-1152.	3.2	27
22067	Characterization of deep level defects in Tl6I4S single crystals by photo-induced current transient spectroscopy. Journal Physics D: Applied Physics, 2015, 48, 075303.	1.3	2
22068	Is hexagonal boron nitride always good as a substrate for carbon nanotube-based devices?. Physical Chemistry Chemical Physics, 2015, 17, 5072-5077.	1.3	6
22069	A first-principles study on three-dimensional covalently-bonded hexagonal boron nitride nanoribbons. Journal of Physics Condensed Matter, 2015, 27, 075301.	0.7	1
22070	Graphene versus MoS2: A short review. Frontiers of Physics, 2015, 10, 287-302.	2.4	176
22071	First principles simulations of elastic properties of radiopaque NiTiPt. Journal of Alloys and Compounds, 2015, 630, 54-59.	2.8	13
22072	Atomic Structure of Luminescent Centers in High-Efficiency Ce-doped w-AlN Single Crystal. Scientific Reports, 2014, 4, 3778.	1.6	43
22073	On-the-fly machine-learning for high-throughput experiments: search for rare-earth-free permanent magnets. Scientific Reports, 2014, 4, 6367.	1.6	212
22074	Structural phases driven by oxygen vacancies at the La0.7Sr0.3MnO3/SrTiO3 hetero-interface. Applied Physics Letters, 2015, 106, .	1.5	42
22075	Toward Optimizing the Performance of Self-Regenerating Pt-Based Perovskite Catalysts. ACS Catalysis, 2015, 5, 1112-1118.	5.5	20
22076	Monoclinic structure and electrical properties of metastable Sb₂Te₃and Bi_{0.4}Sb_{1.6}Te₃phases. Physica Status Solidi (B): Basic Research, 2015, 252, 267-273.	0.7	12

#	Article	IF	Citations
22077	Energy band alignment and electronic states of amorphous carbon surfaces in vacuo and in aqueous environment. Journal of Applied Physics, 2015, 117, 034502.	1.1	9
22078	Hierarchical nanoporous PtTi alloy as highly active and durable electrocatalyst toward oxygen reduction reaction. Journal of Power Sources, 2015, 280, 483-490.	4.0	65
22079	Searching for Low-Sensitivity Cast-Melt High-Energy-Density Materials: Synthesis, Characterization, and Decomposition Kinetics of 3,4-Bis(4-nitro-1,2,5-oxadiazol-3-yl)-1,2,5-oxadiazole-2-oxide. Journal of Physical Chemistry C, 2015, 119, 3509-3521.	1.5	64
22080	Magnetic and Electronic Evolutions of Hydrogenated VTe2 Monolayer under Tension. Scientific Reports, 2014, 4, 7524.	1.6	58
22081	Origin of dramatic oxygen solute strengthening effect in titanium. Science, 2015, 347, 635-639.	6.0	255
22082	Converting Chemically Functionalized Few-Layer Graphene to Diamond Films: A Computational Study. Journal of Physical Chemistry C, 2015, 119, 2828-2836.	1.5	50
22083	Al₂₀⁺does melt, albeit above the bulk melting temperature of aluminium. Physical Chemistry Chemical Physics, 2015, 17, 3741-3748.	1.3	10
22084	Stable structures of He and<mml:math xmlns:mml="http://www.w3.org/1998/Math/MathML"><mml:mrow><mml:msub><mml:mi mathvariant="normal">H</mml:mi><mml:mn>2</mml:mn></mml:msub><mml:mi mathvariant="normal">O</mml:mi></mml:mrow></mml:math>at high pressure. Physical Review B, 2015, 91, .	1.1	58
22085	Hydrogen bonds in Al2O3 as dissipative two-level systems in superconducting qubits. Scientific Reports, 2014, 4, 7590.	1.6	43
22086	First-principles simulations and shock Hugoniot calculations of warm dense neon. Physical Review B, 2015, 91, .	1.1	40
22087	N₂H: a novel polymeric hydronitrogen as a high energy density material. Journal of Materials Chemistry A, 2015, 3, 4188-4194.	5.2	49
22088	Phase stability of ternary fcc and bcc Fe-Cr-Ni alloys. Physical Review B, 2015, 91, .	1.1	114
22089	Brillouin zone and band structure of Î²â€Ca₂O₃. Physica Status Solidi (B): Basic Research, 2015, 252, 828-832.	0.7	242
22090	Shape-controlled octahedral cobalt disulfide nanoparticles supported on nitrogen and sulfur-doped graphene/carbon nanotube composites for oxygen reduction in acidic electrolyte. Journal of Materials Chemistry A, 2015, 3, 6340-6350.	5.2	100
22091	Study of the thermodynamic properties of CeO2 from ab initio calculations: The effect of phonon-phonon interaction. Journal of Chemical Physics, 2015, 142, 014503.	1.2	9
22092	Ferromagnetism in Fe-doped Bi2Se3 topological insulators with Se vacancies. Physics Letters, Section A: General, Atomic and Solid State Physics, 2015, 379, 417-420.	0.9	15
22093	Superconductivity at 52â€…K in hydrogen-substituted LaFeAsO1-xHx under high pressure. Scientific Reports, 2015, 5, 7829.	1.6	34
22094	Stabilizing CuPc Coordination Networks on Ag(100) by Ag Atoms. Journal of Physical Chemistry C, 2015, 119, 1442-1450.	1.5	23

#	Article	IF	Citations
22095	Pressure in electronically excited warm dense metals. Contributions To Plasma Physics, 2015, 55, 164-171.	0.5	14
22096	High Performance 3D Si/Ge Nanorods Array Anode Buffered by TiN/Ti Interlayer for Sodiumâ€•Ion Batteries. Advanced Functional Materials, 2015, 25, 1386-1392.	7.8	79
22097	The Nature of Photocatalytic â€œWater Splittingâ€•on Silicon Nanowires. Angewandte Chemie, 2015, 127, 3023-3028.	1.6	7
22098	Few-quintuple Bi2Te3 nanofilms as potential thermoelectric materials. Scientific Reports, 2015, 5, 8099.	1.6	56
22099	On the prismatic precipitate plates in Mgâ€“Caâ€“In alloys. Scripta Materialia, 2015, 101, 16-19.	2.6	12
22100	Quaternary rare-earth selenides with closed cavities: Cs[RE₉Mn₄Se₁₈] (RE = Hoâ€“Lu). Inorganic Chemistry Frontiers, 2015, 2, 298-305.	3.0	22
22101	Surface ReO_x Sites on Al₂O₃ and Their Molecular Structureâ€“Reactivity Relationships for Olefin Metathesis. ACS Catalysis, 2015, 5, 1432-1444.	5.5	64
22102	Relating voltage and thermal safety in Li-ion battery cathodes: a high-throughput computational study. Physical Chemistry Chemical Physics, 2015, 17, 5942-5953.	1.3	44
22103	C-vacancy concentration in cementite, Fe3C1âˆ', in equilibrium with Î±-Fe[C] and Î³-Fe[C]. Acta Materialia, 2015, 86, 374-384.	3.8	20
22104	Penta-graphene: A new carbon allotrope. Proceedings of the National Academy of Sciences of the United States of America, 2015, 112, 2372-2377.	3.3	1,114
22105	Conversion of CO₂ and C₂H₆ to Propanoic Acid on an Iridium-Modified Graphene Oxide Surface: Quantum-Chemical Investigation. Industrial & Engineering Chemistry Research, 2015, 54, 1539-1546.	1.8	5
22106	Pressure, relaxation volume, and elastic interactions in charged simulation cells. Physical Review B, 2015, 91, .	1.1	38
22107	Controlled Surface Segregation Leads to Efficient Cokeâ€Resistant Nickel/Platinum Bimetallic Catalysts for the Dry Reforming of Methane. ChemCatChem, 2015, 7, 819-829.	1.8	78
22108	Reformulation of<mml:math xmlns:mml="http://www.w3.org/1998/Math/MathML" display="inline"><mml:mrow><mml:mi>DFT</mml:mi><mml:mo>+</mml:mo><mml:mi>U</mml:mi></mml:mrow></mml:math>as a Pseudohybrid Hubbard Density Functional for Accelerated Materials Discovery. Physical Review X, 2015, 5, .	2.8	127
22109	The nature of interfaces and charge trapping sites in photocatalytic mixed-phase TiO2 from first principles modeling. Journal of Chemical Physics, 2015, 142, 024708.	1.2	40
22110	A Novel and Functional Single-Layer Sheet of ZnSe. ACS Applied Materials & Interfaces, 2015, 7, 1458-1464.	4.0	38
22111	Structural Phase Transition between Î³-Ti₃O₅ and Î´-Ti₃O₅ by Breaking of a One-Dimensionally Conducting Pathway. Crystal Growth and Design, 2015, 15, 653-657.	1.4	44
22112	First-Principles Analysis of Structure Sensitivity in NO Oxidation on Pt. ACS Catalysis, 2015, 5, 1087-1099.	5.5	35

#	Article	IF	Citations
22113	Contracted interlayer distance in graphene/sapphire heterostructure. Nano Research, 2015, 8, 1535-1545.	5.8	26
22114	Nudged-elastic band method with two climbing images: Finding transition states in complex energy landscapes. Journal of Chemical Physics, 2015, 142, 024106.	1.2	78
22115	First-principles study of magnetic frustration in FeSe epitaxial films on<mml:math xmlns:mml="http://www.w3.org/1998/Math/MathML"><mml:msub><mml:mi>SrTiO</mml:mi><mml:mn>3</mml:mn></mml:msub></m Physical Review B, 2015, 91, .	1.1	21
22116	Half-filled energy bands induced negative differential resistance in nitrogen-doped graphene. Nanoscale, 2015, 7, 4156-4162.	2.8	32
22117	The functionalisation of graphite surfaces with nitric acid: Identification of functional groups and their effects on gold deposition. Journal of Catalysis, 2015, 323, 10-18.	3.1	59
22118	Atomistic approach to predict the glass-forming ability in Zrâ€“Cuâ€“Al ternary metallic glasses. Journal of Alloys and Compounds, 2015, 627, 48-53.	2.8	27
22119	Structural and electronic properties of submonolayer-thick Sn films on Ru(0001). Applied Surface Science, 2015, 329, 376-383.	3.1	6
22120	Thermal conductivity of UO2 and PuO2 from first-principles. Journal of Alloys and Compounds, 2015, 628, 267-271.	2.8	27
22121	Diffusivity of heavy elements in Jupiter and Saturn. Icarus, 2015, 250, 400-404.	1.1	3
22122	Strain effects on the electronic structure of ZnSnP2 via modified Beckeâ€“Johnson exchange potential. Physics Letters, Section A: General, Atomic and Solid State Physics, 2015, 379, 427-430.	0.9	9
22123	Structural stability of Fe-based topologically close-packed phases. Intermetallics, 2015, 59, 59-67.	1.8	28
22124	Diffusion of fluorine on and between graphene layers. Physical Review B, 2015, 91, .	1.1	17
22125	Electronic structure and lattice dynamics in the<mml:math xmlns:mml="http://www.w3.org/1998/Math/MathML"><mml:msub><mml:mi>FeSb</mml:mi><mml:mn>3</mml:mn></mml:msub></mr from density functional theory. Physical Review B, 2015, 91, .	1.1	10
22126	Modulated spin structure responsible for the magnetic-field-induced polarization switching in multiferroicTbMn2O5. Physical Review B, 2015, 91, .	1.1	5
22127	The Effect of Uranium Cations on the Redox Properties of CeO2 Within the Context of Hydrogen Production from Water. Topics in Catalysis, 2015, 58, 143-148.	1.3	21
22128	Density functional theory calculations of atomic, electronic and thermodynamic properties of cubic LaCoO3and La1â^'xSrxCoO3surfaces. RSC Advances, 2015, 5, 760-769.	1.7	43
22129	Cluster Models for Studying CO2 Reduction on Semiconductor Photoelectrodes. Topics in Catalysis, 2015, 58, 46-56.	1.3	30
22130	Anisotropic optical properties of graphene/graphane superlattices. Solid State Sciences, 2015, 40, 71-76.	1.5	6

#	Article	IF	Citations
22131	First principle simulations of piezotronic transistors. Nano Energy, 2015, 14, 355-363.	8.2	45
22132	Stability and electronic structures of triazine-based carbon nitride nanotubes. RSC Advances, 2015, 5, 10892-10898.	1.7	11
22133	First principles studies of GeTe based dilute magnetic semiconductors. Journal of Physics Condensed Matter, 2015, 27, 015501.	0.7	17
22134	Improved ground-state electronic structure and optical dielectric constants with a semilocal exchange functional. Physical Review B, 2015, 91, .	1.1	19
22135	CO oxidation mechanism on AlAun. Journal of Molecular Structure, 2015, 1085, 1-12.	1.8	0
22136	Estimating Bulk-Composition-Dependent H₂ Adsorption Energies on Cu_xPd_{1â€“x} Alloy (111) Surfaces. ACS Catalysis, 2015, 5, 1020-1026.	5.5	24
22137	Pressure control of magnetic clusters in strongly inhomogeneous ferromagnetic chalcopyrites. Scientific Reports, 2015, 5, 7720.	1.6	11
22138	Initial Decomposition Reactions of Bicyclo-HMX [BCHMX or cis-1,3,4,6-Tetranitrooctahydroimidazo-[4,5-d]imidazole] from Quantum Molecular Dynamics Simulations. Journal of Physical Chemistry C, 2015, 119, 2290-2296.	1.5	17
22139	Oxygen surface exchange kinetics and stability of (La,Sr)₂CoO_{4Â±Î´}/La_{1â^'x}Sr_xMO_{3â^'Î´} (M = Co) Tj ETQq0 0 0 rgBT /Ove 2144-2157.	5.2	65
22140	Stability of surface and subsurface hydrogen on and in Au/Ni near-surface alloys. Surface Science, 2015, 640, 190-197.	0.8	4
22141	Photoluminescence Quenching and Charge Transfer in Artificial Heterostacks of Monolayer Transition Metal Dichalcogenides and Few-Layer Black Phosphorus. ACS Nano, 2015, 9, 555-563.	7.3	183
22142	Nature of ferroelectric-paraelectric phase transition and origin of negative thermal expansion in<mml:math xmlns:mml="http://www.w3.org/1998/Math/MathML"><mml:mrow><mml:mi>PbTi</mml:mi><mml:msub><mml:mi mathvariant="normal">O</mml:mi><mml:mn>3</mml:mn></mml:msub></mml:mrow></mml:math>.	1.1	37
22143	First-principles studies of lone-pair-induced distortions in epitaxial phases of perovskite<mml:math xmlns:mml="http://www.w3.org/1998/Math/MathML"><mml:msub><mml:mi>SnTiO</mml:mi><mml:mn>3</mml:mn></mml:msub></m xmlns:mml="http://www.w3.org/1998/Math/MathML"><mml:msub><mml:mi>PbTiO</mml:mi><mml:mn>3</mml:mn></mml:msub></m Physical Review B, 2015, 91, .	1.1	29
22144	Silicene, a promising new 2D material. Progress in Surface Science, 2015, 90, 46-83.	3.8	221
22145	Band alignments at interface of Cu2ZnSnS4/ZnO heterojunction: An X-ray photoelectron spectroscopy and first-principles study. Journal of Alloys and Compounds, 2015, 628, 293-297.	2.8	26
22146	Interplay of Spin-Orbit Interactions, Dimensionality, and Octahedral Rotations in Semimetallic<mml:math xmlns:mml="http://www.w3.org/1998/Math/MathML" display="inline"><mml:msub><mml:mtext mathvariant="bold">SrIrO</mml:mtext><mml:mn>3</mml:mn></mml:msub></mml:math>. Physical	2.9	189
22147	Superhard<mml:math xmlns:mml="http://www.w3.org/1998/Math/MathML" display="inline"><mml:msub><mml:mi>BC</mml:mi><mml:mn>3</mml:mn></mml:msub></mml:math>in Cubic Diamond Structure. Physical Review Letters, 2015, 114, 015502.	2.9	180
22148	Polytypism in superhard transition-metal triborides. Scientific Reports, 2014, 4, 5063.	1.6	17

#	Article	IF	Citations
22149	Chemical stability and Ce doping of LiMgAlF6 neutron scintillator. Journal of Alloys and Compounds, 2015, 622, 925-928.	2.8	2
22150	Carrier density modulation in a germanium heterostructure by ferroelectric switching. Nature Communications, 2015, 6, 6067.	5.8	75
22151	Density Functional Theory Comparison of Methanol Decomposition and Reverse Reactions on Metal Surfaces. ACS Catalysis, 2015, 5, 1027-1036.	5.5	83
22152	Novel Magnetic Monolayers of Transition Metal Silicide. Journal of Superconductivity and Novel Magnetism, 2015, 28, 1755-1758.	0.8	17
22153	Effective mineralization of organic dye under visible-light irradiation over electronic-structure-modulated Sn(Nb 1â˜'x Ta x) 2 O 6 solid solutions. Applied Catalysis B: Environmental, 2015, 168-169, 243-249.	10.8	23
22154	Electronic and magnetic properties of C60â€"Fenâ€"graphene intercalating nanostructures (n=1â€"6) predicted from first-principles calculations. Chemical Physics Letters, 2015, 618, 127-131.	1.2	1
22155	Scrutinizing individual CoTPP molecule adsorbed on coinage metal surfaces from the interplay of STM experiment and theory. Surface Science, 2015, 635, 108-114.	0.8	12
22156	A first-principles study on hydrogen in ZnS: Structure, stability and diffusion. Physics Letters, Section A: General, Atomic and Solid State Physics, 2015, 379, 487-490.	0.9	4
22157	Electronic and structural properties at the interface between CuPc and graphene. Journal of Applied Physics, 2015, 117, 013701.	1.1	7
22158	Crystallization-induced red emission of a facilely synthesized biodegradable indigo derivative. Chemical Communications, 2015, 51, 3375-3378.	2.2	47
22159	Frustration and Dzyaloshinsky-Moriya anisotropy in the kagome francisites<mml:math xmlns:mml="http://www.w3.org/1998/Math/MathML"><mml:msub><mml:mi mathvariant="normal">Cu</mml:mi><mml:mn>3</mml:mn></mml:msub><mml:mi mathvariant="normal">Bi</mml:mi><mml:mo>(</mml:mo><mml:mrow><mml:msub><mml:mi) Tj ETQq0 0 0 rgBT /Overlock 10 Tf 50 33	1.1	46
22160	mathvariant="normal">O</mml:mi><mml:mn. Physical Review B, 2015, 91, . Gas-phase dehydration of vicinal diols to epoxides: Dehydrative epoxidation over a Cs/SiO2 catalyst. Journal of Catalysis, 2015, 323, 85-99.	3.1	31
22161	Effect of alumina hydroxylation on glycerol hydrogenolysis to 1,2-propanediol over Cu/Al₂O₃: combined experiment and DFT investigation. RSC Advances, 2015, 5, 11188-11197.	1.7	42
22162	Highâ€Gain and Lowâ€Drivingâ€Voltage Photodetectors Based on Organolead Triiodide Perovskites. Advanced Materials, 2015, 27, 1912-1918.	11.1	560
22163	On the DFT Ground State of Crystalline Bromine and Iodine. ChemPhysChem, 2015, 16, 728-732.	1.0	20
22164	Deviation from high-entropy configurations in the atomic distributions of a multi-principal-element alloy. Nature Communications, 2015, 6, 5964.	5.8	530
22165	Numerical modeling of the core structure of [100] dislocations in Fe 3 C cementite. Scripta Materialia, 2015, 99, 61-64.	2.6	2
22166	High pressure structures and superconductivity of AlH₃(H₂) predicted by first principles. RSC Advances, 2015, 5, 5096-5101.	1.7	33

#	Article	IF	Citations
22167	Ab initio simulation of alloying effect on stacking fault energy in fcc Fe. Computational Materials Science, 2015, 99, 253-255.	1.4	44
22168	Tilt engineering of spontaneous polarization and magnetization above 300 K in a bulk layered perovskite. Science, 2015, 347, 420-424.	6.0	181
22169	Increasing the Thermoelectric Figure of Merit of Tetrahedrites by Co-Doping with Nickel and Zinc. Chemistry of Materials, 2015, 27, 408-413.	3.2	193
22170	Diffusion of Zr, Ru, Ce, Y, La, Sr and Ba fission products in UO2. Journal of Nuclear Materials, 2015, 459, 90-96.	1.3	15
22171	Facet-Dependent Electron Trapping in TiO₂ Nanocrystals. Journal of Physical Chemistry C, 2015, 119, 1913-1920.	1.5	55
22172	Coupling of Crystal Structure and Magnetism in the Layered, Ferromagnetic Insulator CrI₃. Chemistry of Materials, 2015, 27, 612-620.	3.2	729
22173	First-principles study of electronic structure of CuSbS2 and CuSbSe2 photovoltaic semiconductors. Thin Solid Films, 2015, 582, 401-407.	0.8	44
22174	Hydroxylation of the Rutile TiO₂(110) Surface Enhancing Its Reducing Power for Photocatalysis. Journal of Physical Chemistry C, 2015, 119, 1451-1456.	1.5	48
22175	Sulfur and Silicon Doping in Ag₃PO₄. Journal of Physical Chemistry C, 2015, 119, 2284-2289.	1.5	18
22176	Ab initio study on the adsorption of oxygen on Co(111) and its subsurface incorporation. European Physical Journal B, 2015, 88, 1.	0.6	4
22177	Significant contribution of As<mml:math xmlns:mml="http://www.w3.org/1998/Math/MathML"><mml:mrow><mml:mn>4</mml:mn><mml:mi>p</mml:mi></mml:mrow></mml:m to the low-lying electronic structure of the 112-type iron-based superconductor<mml:math xmlns:mml="http://www.w3.org/1998/Math/MathML"><mml:mi mathvariant="normal">Ca</mml:mi><mml:msub><mml:mrow /><mml:mrow><mml:mn>0.9</mml:mn></mml:mrow></mml:msub><mml:mi mathvariant="normal">La</	1.1	31
22178	A new high-pressure polymeric nitrogen phase in potassium azide. RSC Advances, 2015, 5, 11825-11830.	1.7	23
22179	Systematic study on the anisotropic elastic properties of tetragonal XYSb (XÂ=ÂTi, Zr, Hf; YÂ=ÂSi, Ge) compounds. Solid State Sciences, 2015, 40, 92-100.	1.5	50
22180	O2 Dissociation on M@Pt Coreâ€“Shell Particles for 3d, 4d, and 5d Transition Metals. Journal of Physical Chemistry C, 2015, 119, 11031-11041.	1.5	37
22181	A first-principles investigation on the effect of the divacancy defect on the band structures of boron nitride (BN) nanoribbons. Physica E: Low-Dimensional Systems and Nanostructures, 2015, 69, 65-74.	1.3	12
22182	Magnetoelectric coupling at the epitaxial Ni/PbTiO3 heterointerface from first principles. Physica B: Condensed Matter, 2015, 456, 383-387.	1.3	5
22183	First-principles calculations of the mechanic and vibration properties of AgRE (RE = Ho, Er, Tm) intermetallic compounds under pressure. Physica Scripta, 2015, 90, 025701.	1.2	4
22184	Electric field improved hydrogen storage of Ca-decorated monolayer MoS2. Physics Letters, Section A: General, Atomic and Solid State Physics, 2015, 379, 815-819.	0.9	25

#	Article	IF	Citations
22185	HfO ₂ on UVâ€“O ₃ exposed transition metal dichalcogenides: interfacial reactions study. 2D Materials, 2015, 2, 014004.	2.0	98
22186	Selective Propylene Oxidation to Acrolein by Gold Dispersed on MgCuCr₂O₄ Spinel. ACS Catalysis, 2015, 5, 1100-1111.	5.5	40
22187	Tailoring the electronic structure of Î²-Ga₂O₃ by non-metal doping from hybrid density functional theory calculations. Physical Chemistry Chemical Physics, 2015, 17, 5817-5825.	1.3	34
22188	Improving Performance in Colloidal Quantum Dot Solar Cells by Tuning Band Alignment through Surface Dipole Moments. Journal of Physical Chemistry C, 2015, 119, 2996-3005.	1.5	58
22189	Interface Structure in Cu/Ta₂O₅/Pt Resistance Switch: A First-Principles Study. ACS Applied Materials & Interfaces, 2015, 7, 519-525.	4.0	15
22190	Strain-induced metal-semimetal transition of BeB₂ monolayer. RSC Advances, 2015, 5, 11392-11396.	1.7	19
22191	A density functional theory study on 3d metal/graphene for the removal of CO from H2feed gas in hydrogen fuel cells. RSC Advances, 2015, 5, 16394-16399.	1.7	9
22192	Structures of FePt clusters and their interactions with the O 2 molecule. Chemical Physics Letters, 2015, 622, 34-41.	1.2	15
22193	The effect of dopant incorporation on the elastic properties of Ti metal. Modelling and Simulation in Materials Science and Engineering, 2015, 23, 015005.	0.8	5
22194	Adaptive machine learning framework to accelerate ab initio molecular dynamics. International Journal of Quantum Chemistry, 2015, 115, 1074-1083.	1.0	313
22195	Achieving High Specific Capacity through a Two-Electron Reaction in Hypothetical Li₂VFSiO₄: A First-Principles Investigation. Journal of the Electrochemical Society, 2015, 162, A787-A792.	1.3	6
22196	Two-dimensional square-pyramidal VO₂ with tunable electronic properties. Journal of Materials Chemistry C, 2015, 3, 3189-3197.	2.7	20
22197	Phase stability and transition of<mml:math xmlns:mml="http://www.w3.org/1998/Math/MathML"><mml:msub><mml:mtext>BaSi</mml:mtext><mml:mn>2</mml:mn></mml:msub> disilicides and digermanides. Physical Review B, 2015, 91, .	1.1	10
22198	A spectral scheme for Kohnâ€“Sham density functional theory of clusters. Journal of Computational Physics, 2015, 287, 226-253.	1.9	24
22199	Topological multiferroics. Phase Transitions, 2015, 88, 953-961.	0.6	4
22200	New insights into organicâ€“inorganic hybrid perovskite CH₃NH₃PbI₃nanoparticles. An experimental and theoretical study of doping in Pb²⁺sites with Sn²⁺, Sr²⁺, Cd²⁺and Ca²⁺. Nanoscale, 2015, 7, 6216-6229.	2.8	216
22201	Topological phase driven by confinement effects in Bi bilayers. Physical Review B, 2015, 91, .	1.1	16
22202	Cationic surface segregation in doped LaMnO3. Journal of Materials Science, 2015, 50, 3051-3056.	1.7	23

#	Article	IF	Citations
22203	The electronic origin of strengthening and ductilizing magnesium by solid solutes. Acta Materialia, 2015, 89, 225-233.	3.8	62
22204	Hydroxyapatite: Vibrational spectra and monoclinic to hexagonal phase transition. Journal of Applied Physics, 2015, 117, 074701.	1.1	15
22205	Structureâ€“property correlations in Eu-doped tetra calcium phosphate phosphor: A key to solid-state lighting application. Journal of Luminescence, 2015, 162, 25-30.	1.5	8
22206	Proximity enhanced quantum spin Hall state in graphene. Carbon, 2015, 87, 418-423.	5.4	29
22207	Energetic, structural and electronic properties of metal vacancies in strained AlN/GaN interfaces. Journal of Physics Condensed Matter, 2015, 27, 125006.	0.7	5
22208	Low-energy description of the metal-insulator transition in the rare-earth nickelates. Physical Review B, 2015, 91, .	1.1	106
22209	An ab initio study of TiS₃: a promising electrode material for rechargeable Li and Na ion batteries. RSC Advances, 2015, 5, 21455-21463.	1.7	58
22210	Material design for magnesium alloys with high deformability. Philosophical Magazine, 2015, 95, 869-885.	0.7	29
22211	Hydrogen diffusion behavior and vacancy interaction behavior in OsO2 and RuO2 by ab initio calculations. Computational Materials Science, 2015, 102, 14-20.	1.4	2
22212	Phase transition and thermodynamic properties of YAg alloy from first-principles calculations. Computational Materials Science, 2015, 102, 21-26.	1.4	5
22213	Nanoalloy electrocatalysis: simulating cyclic voltammetry from configurational thermodynamics with adsorbates. Physical Chemistry Chemical Physics, 2015, 17, 28103-28111.	1.3	6
22214	DFT-based Metadynamics simulation of proton diffusion in tetragonal zirconia at 1500 K. Journal of Nuclear Materials, 2015, 459, 30-36.	1.3	18
22215	Evidence of a graphene-like Sn-sheet on a Au(111) substrate: electronic structure and transport properties from first principles calculations. Physical Chemistry Chemical Physics, 2015, 17, 6705-6712.	1.3	33
22216	Defect kinetics and resistance to amorphization in zirconium carbide. Journal of Nuclear Materials, 2015, 457, 343-351.	1.3	22
22217	Hydrogen isotope in erbium oxide: Adsorption, penetration, diffusion, and vacancy trapping. Fusion Engineering and Design, 2015, 92, 35-40.	1.0	9
22218	Mechanism of Phosphorus and Chlorine Passivating a Nickel Catalyst: A Density Functional Theory Study. Electrochimica Acta, 2015, 167, 147-150.	2.6	12
22219	Graphdiyneâ€“metal contacts and graphdiyne transistors. Nanoscale, 2015, 7, 2116-2127.	2.8	94
22220	Oxygen-assisted water partial dissociation on copper: a model study. Physical Chemistry Chemical Physics, 2015, 17, 8231-8238.	1.3	29

#	Article	IF	Citations
22221	Thermoelastic properties of<mml:math xmlns:mml="http://www.w3.org/1998/Math/MathML"><mml:mi>Î±</mml:mi></mml:math>-iron from first-principles. Physical Review B, 2015, 91, .	1.1	40
22222	Electrical control of memristance and magnetoresistance in oxide magnetic tunnel junctions. Nanoscale, 2015, 7, 6334-6339.	2.8	21
22223	Multiscale simulations of the early stages of the growth of graphene on copper. Surface Science, 2015, 637-638, 11-18.	0.8	18
22224	Staging and In-Plane Superstructures Formed in Layered NaMO₂{M = Sc, Ti, V, Cr, Mn} during Na De-Intercalation: A Computational Study. Journal of the Electrochemical Society, 2015, 162, A511-A519.	1.3	13
22225	Interstitial H+-Mediated Ferromagnetism in Co-Doped ZnS. Journal of Superconductivity and Novel Magnetism, 2015, 28, 1389-1393.	0.8	7
22226	The Effects of Dangling Bonds on AlN Nanoribbons: A First-Principles Study. Journal of Superconductivity and Novel Magnetism, 2015, 28, 271-275.	0.8	1
22227	High temperature and pressure effects on the elastic properties of B2 intermetallics AgRE. Open Physics, 2015, 13, .	0.8	1
22228	Half-Metallic Ferromagnetism in Cu-Doped ZnO Nanostructures from First-Principle Prediction. Journal of Superconductivity and Novel Magnetism, 2015, 28, 2033-2038.	0.8	9
22229	High pressure equation of state for molten CaCO3 from first principles simulations. Diqiu Huaxue, 2015, 34, 13-20.	0.5	16
22230	Spin-orbit coupling, strong correlation, and insulator-metal transitions: The<mml:math xmlns:mml="http://www.w3.org/1998/Math/MathML"><mml:mrow><mml:msub><mml:mi mathvariant="normal">J</mml:mi><mml:mi>eff</mml:mi></mml:msub><mml:mo>=</mml:mo><mml:mfrac><mml:mn>3</mml:mn><mml:mn> Dirac-Mott insulator<mml:math xmlns:mml="http://www.w3.org/1998/Math/MathML"><mml:mrow><mml:msub><mml:mi>Ba</mml:mi><mml:mn>2</mml:mn></mml:msub> Physical Review B, 2015, 91, .	1.1	35
22231	Vibrational and magnetic properties of crystalline CuTe2O5. JETP Letters, 2015, 100, 652-656.	0.4	10
22232	Structural relaxation effects on the lowest $$4f{-}5d$$ 4 f - 5 d transition of $$hbox {Ce}^{3+}$$ Ce 3 + in garnets. Theoretical Chemistry Accounts, 2015, 134, 1.	0.5	12
22233	Two-temperature equation of state for aluminum and gold with electrons excited by an ultrashort laser pulse. Applied Physics B: Lasers and Optics, 2015, 119, 401-411.	1.1	34
22234	The Study on the Medium-Sized Carbon Islands on Ru(0001) Surface. Journal of Cluster Science, 2015, 26, 347-360.	1.7	10
22235	Observation of Single-Spin Dirac Fermions at the Graphene/Ferromagnet Interface. Nano Letters, 2015, 15, 2396-2401.	4.5	82
22236	Grain Boundary Plane Effect on Pr Segregation Site in ZnO Î£13 [0001] Symmetric Tilt Grain Boundaries. Journal of the American Ceramic Society, 2015, 98, 1932-1936.	1.9	10
22237	Atomistic mechanisms for bilayer growth of graphene on metal substrates. Physical Review B, 2015, 91, .	1.1	33
22238	Dynamics and stability of icosahedral Feâ€“Pt nanoparticles. Physical Chemistry Chemical Physics, 2015, 17, 28096-28102.	1.3	6

#	Article	IF	Citations
22239	First principles study of magnetic properties of Co_{1ML}/Ni_{2ML}/Cu(111) multilayer structure. Japanese Journal of Applied Physics, 2015, 54, 043001.	0.8	0
22240	Ultrathin undoped tetrahedral amorphous carbon films: thickness dependence of the electronic structure and implications for their electrochemical behaviour. Physical Chemistry Chemical Physics, 2015, 17, 9020-9031.	1.3	18
22241	Local order origin of thermal stability enhancement in amorphous Ag doping GeTe. Applied Physics Letters, 2015, 106, .	1.5	21
22242	Electronic structure calculations of oxygen-doped diamond using DFT technique. Microelectronic Engineering, 2015, 146, 26-31.	1.1	14
22243	Adsorption of insoluble polysulfides Li2Sx (x = 1, 2) on Li2S surfaces. Physical Chemistry Chemical Physics, 2015, 17, 9032-9039.	1.3	53
22244	First-principles study on the lattice dynamics and thermodynamic properties of Cu ₂ GeSe ₃. Europhysics Letters, 2015, 109, 47004.	0.7	20
22245	Interstitial impurity-induced magnetism inÎ±-PbO surface. Journal of Physics Condensed Matter, 2015, 27, 016002.	0.7	1
22246	A critical evaluation of GGA +Umodeling for atomic, electronic and magnetic structure of Cr₂AlC, Cr₂GaC and Cr₂GeC. Journal of Physics Condensed Matter, 2015, 27, 095601.	0.7	23
22247	Sources ofn-type conductivity in GaInO₃. Journal Physics D: Applied Physics, 2015, 48, 015101.	1.3	13
22248	Coadsorption of gold with chlorine on CeO ₂ (111) surfaces: A first principles study. Chinese Physics B, 2015, 24, 026801.	0.7	3
22249	Atomic structure and polarity compensation of BaTiO3(1â€‰1â€‰1) surface. Journal of Physics Condensed Matter, 2015, 27, 095901.	0.7	2
22250	Tuning metalâ€“graphene interaction by non-metal intercalation: a case study of the graphene/oxygen/Ni (1â€‰1â€‰1) system. Journal Physics D: Applied Physics, 2015, 48, 015308.	1.3	8
22251	Structural, Electrical, and Lithium Ion Dynamics of Li ₂ MnO ₃ from Density Functional Theory. Chinese Physics Letters, 2015, 32, 017102.	1.3	11
22252	Unfolding spinor wave functions and expectation values of general operators: Introducing the unfolding-density operator. Physical Review B, 2015, 91, .	1.1	274
22253	On the interplay between geometrical structure and magnetic anisotropy: a relativistic density-functional study of mixed Ptâ€“Co and Ptâ€“Fe trimers and tetramers in the gas-phase and supported on graphene. Journal of Physics Condensed Matter, 2015, 27, 046002.	0.7	5
22254	Strain effects on the electronic properties in Î´-doped oxide superlattices. Journal Physics D: Applied Physics, 2015, 48, 085303.	1.3	3
22255	Spin excitations in the two-dimensional strongly coupled dimer system malachite. Physical Review B, 2015, 91, .	1.1	4
22256	Gradient-dependent upper bound for the exchange-correlation energy and application to density functional theory. Physical Review B, 2015, 91, .	1.1	31

#	Article	IF	Citations
22257	Strategies for increasing the NÃ©el temperature of magnetoelectric Fe2TeO6. Journal of Physics Condensed Matter, 2015, 27, 022203.	0.7	9
22258	Energetic stability of soluteâ€“carbonâ€“vacancy complexes in bcc iron. Nuclear Instruments & Methods in Physics Research B, 2015, 352, 47-50.	0.6	7
22259	Manipulating magnetism of MnO nano-clusters by tuning the stoichiometry and charge state. Journal of Physics Condensed Matter, 2015, 27, 056002.	0.7	6
22260	The mechanical and electronic properties of Al/TiC interfaces alloyed by Mg, Zn, Cu, Fe and Ti: First-principles study. Physica Scripta, 2015, 90, 035701.	1.2	13
22261	H inÎ±-Zr and in zirconium hydrides: solubility, effect on dimensional changes, and the role of defects. Journal of Physics Condensed Matter, 2015, 27, 025402.	0.7	47
22262	Reduced tight-binding models for elemental Si and N, and ordered binary Si-N systems. Physical Review B, 2015, 91, .	1.1	11
22263	Exploring atomic defects in molybdenum disulphide monolayers. Nature Communications, 2015, 6, 6293.	5.8	1,124
22264	Ordering-induced direct-to-indirect band gap transition in multication semiconductor compounds. Physical Review B, 2015, 91, .	1.1	20
22265	Lithium decoration of three dimensional boron-doped graphene frameworks for high-capacity hydrogen storage. Applied Physics Letters, 2015, 106, .	1.5	21
22266	Effects of the vacancy and doping on the half-metallicity in La0.5Sr0.5MnO3. Journal of Magnetism and Magnetic Materials, 2015, 384, 229-234.	1.0	7
22267	Ab initiocalculation of shocked xenon reflectivity. Physical Review E, 2015, 91, 023105.	0.8	20
22268	Visualization and thermodynamic encoding of single-molecule partition function projections. Nature Communications, 2015, 6, 6210.	5.8	23
22269	A DFT perspective of potassium promotion of Ï‡-Fe5C2(100). Applied Catalysis A: General, 2015, 496, 64-72.	2.2	30
22270	Metallic ferroelectricity induced by anisotropic unscreened Coulomb interaction in<mml:math xmlns:mml="http://www.w3.org/1998/Math/MathML"><mml:msub><mml:mi>LiOsO</mml:mi><mml:mn>3</mml:mn></mml:msub><mml:mn>1</mml:mn></mml:msub><mml:msub><mml:mi>n</mml:mi> Physical Review B, 2015, 91, .	1.1	30
22271	First principles prediction on the interfaces of Fe/MoS2, Co/MoS2 and Fe3O4/MoS2. Computational Materials Science, 2015, 99, 326-335.	1.4	22
22272	Hydrogen in palladium: Anharmonicity of lattice dynamics from first principles. Physics of the Solid State, 2015, 57, 260-265.	0.2	7
22273	Novel monolayer pyrite FeS2 with atomic-thickness for magnetic devices. Computational Materials Science, 2015, 101, 255-259.	1.4	27
22274	First-principles study of point defects at a semicoherent interface. Scientific Reports, 2014, 4, 7567.	1.6	11

#	Article	IF	Citations
22275	Complex transition metal hydrides incorporating ionic hydrogen: Synthesis and characterization of Na2Mg2FeH8 and Na2Mg2RuH8. Journal of Alloys and Compounds, 2015, 645, S347-S352.	2.8	19
22276	A density functional theory study of hydrocarbon combustion and synthesis on Ni surfaces. Journal of Molecular Modeling, 2015, 21, 46.	0.8	7
22277	Formation of titanium monoxide (001) single-crystalline thin film induced by ion bombardment of titanium dioxide (110). Nature Communications, 2015, 6, 6147.	5.8	44
22278	First-principles-based kinetic Monte Carlo studies of diffusion of hydrogen in Niâ€“Al and Niâ€“Fe binary alloys. Journal of Materials Science, 2015, 50, 3361-3370.	1.7	7
22279	Establishing the most favorable metalâ€“carbon bond strength for carbon nanotube catalysts. Journal of Materials Chemistry C, 2015, 3, 3422-3427.	2.7	36
22280	Superiority of the bi-phasic mixture of a tin-based alloy nanocomposite as the anode for lithium ion batteries. Journal of Materials Chemistry A, 2015, 3, 3794-3800.	5.2	43
22281	Experimental and first-principles DFT studies of electronic, optical and magnetic properties of ceriumâ€“manganese codoped zinc oxide nanostructures. Materials Science in Semiconductor Processing, 2015, 34, 27-38.	1.9	36
22282	Lattice swelling and modulus change in a helium-implanted tungsten alloy: X-ray micro-diffraction, surface acoustic wave measurements, and multiscale modelling. Acta Materialia, 2015, 89, 352-363.	3.8	123
22283	Tunable topological quantum states in three- and two-dimensional materials. Frontiers of Physics, 2015, 10, 161-176.	2.4	15
22284	Low-Energy Structures of Binary Ptâ€“Sn Clusters from Global Search Using Genetic Algorithm and Density Functional Theory. Journal of Cluster Science, 2015, 26, 389-409.	1.7	34
22285	Electronic structure and optical properties of Î±-(Fe1-xVx)2O3 solid-solution thin films. Applied Physics Letters, 2015, 106, .	1.5	13
22286	Constrained density functional for noncollinear magnetism. Physical Review B, 2015, 91, .	1.1	68
22287	Interaction of aluminum dimer with defective graphene. Computational and Theoretical Chemistry, 2015, 1059, 27-34.	1.1	11
22288	Stiffness and toughness prediction of Coâ€“Feâ€“Taâ€“B metallic glasses, alloyed with Y, Zr, Nb, Mo, Hf, W, C, N and O byab initiomolecular dynamics. Journal of Physics Condensed Matter, 2015, 27, 105502.	0.7	5
22289	High-Pressure Electrides: The Chemical Nature of Interstitial Quasiatoms. Journal of the American Chemical Society, 2015, 137, 3631-3637.	6.6	134
22290	Effects of stress on lithium transport in amorphous silicon electrodes for lithium-ion batteries. Nano Energy, 2015, 13, 192-199.	8.2	58
22291	Core level shifts in Cuâ€“Pd alloys as a function of bulk composition and structure. Surface Science, 2015, 640, 127-132.	0.8	11
22292	Selective etherification of Î²-citronellene catalyzed by zeolite beta. Green Chemistry, 2015, 17, 2840-2845.	4.6	3

#	Article	IF	Citations
22293	Surface Morphology of Cu Adsorption on Different Terminations of the HÃgg Iron Carbide (Ï‡-Fe₅C₂) Phase. Journal of Physical Chemistry C, 2015, 119, 7371-7385.	1.5	14
22294	Carbon-monoxide adsorption and dissociation on Nb(110) surface. Applied Surface Science, 2015, 328, 641-648.	3.1	6
22295	Insight into CÂ+ O(OH) reaction for carbon elimination on different types of CoNi(111) surfaces: a DFT study. RSC Advances, 2015, 5, 19970-19982.	1.7	22
22296	Carbonâ€“Carbon Bond Formation by Activation of CH₃F on Alumina. Journal of Physical Chemistry C, 2015, 119, 7156-7163.	1.5	28
22297	Ring Activation of Furanic Compounds on Ruthenium-Based Catalysts. Journal of Physical Chemistry C, 2015, 119, 6075-6085.	1.5	29
22298	Estimation of the temperature dependent interaction between uncharged point defects in Si. AIP Advances, 2015, 5, .	0.6	5
22299	Anomalous temperature-induced volume contraction in GeTe. Physical Review B, 2015, 91, .	1.1	49
22300	Influence of Ti⁴⁺ on the Electrochemical Performance of Li-Rich Layered Oxides - High Power and Long Cycle Life of Li₂Ru_{1â€“x}Ti_xO₃ Cathodes. ACS Applied Materials & Interfaces, 2015, 7, 7118-7128.	4.0	34
22301	Robust Gapless Surface State and Rashba-Splitting Bands upon Surface Deposition of Magnetic Cr on Bi₂Se₃. Nano Letters, 2015, 15, 2031-2036.	4.5	33
22302	Probing the Stress Reduction Mechanism of Diamond-Like Carbon Films by Incorporating Ti, Cr, or W Carbide-Forming Metals: Ab Initio Molecular Dynamics Simulation. Journal of Physical Chemistry C, 2015, 119, 6086-6093.	1.5	33
22303	Intriguing electronic properties of two-dimensional MoS₂/TM₂CO₂ (TM = Ti, Zr, or Hf) hetero-bilayers: type-II semiconductors with tunable band gaps. Nanotechnology, 2015, 26, 135703.	1.3	57
22304	The roles of the temperature on the structural and electronic properties of deep-level VAsVGa defects in gallium arsenide. Journal of Alloys and Compounds, 2015, 637, 16-19.	2.8	3
22305	High resolution energy dispersive spectroscopy mapping of planar defects in L12-containing Co-base superalloys. Acta Materialia, 2015, 89, 423-437.	3.8	127
22306	Metallic Nickel Nitride Nanosheets Realizing Enhanced Electrochemical Water Oxidation. Journal of the American Chemical Society, 2015, 137, 4119-4125.	6.6	1,004
22307	Defect states at organicâ€“inorganic interfaces: Insight from first principles calculations for pentaerythritol tetranitrate on MgO surface. Surface Science, 2015, 637-638, 19-28.	0.8	17
22308	First-principles investigation on the structural, electronic properties and diffusion barriers of Mg/Al doped NaCoO₂as the cathode material of rechargeable sodium batteries. RSC Advances, 2015, 5, 27229-27234.	1.7	33
22309	Arcâ€Melting to Narrow the Bandgap of Oxide Semiconductors. Advanced Materials, 2015, 27, 2589-2594.	11.1	52
22310	Atomic Scale Microstructure and Properties of Se-Deficient Two-Dimensional MoSe₂. ACS Nano, 2015, 9, 3274-3283.	7.3	213

#	Article	IF	Citations
22311	Stable kagome lattices from group IV elements. Physical Review B, 2015, 91, .	1.1	13
22312	A first principles investigation of zinc induced embrittlement at grain boundaries in bcc iron. Acta Materialia, 2015, 90, 69-76.	3.8	73
22313	Identification and thermodynamic mechanism of the phase transition in hafnium nitride films. Acta Materialia, 2015, 90, 59-68.	3.8	31
22314	Strain tunable electronic and magnetic properties of pristine and semihydrogenated hexagonal boron phosphide. Applied Physics Letters, 2015, 106, .	1.5	35
22315	The performance and stability of the oxygen reduction reaction on Ptâ€“M (M = Pd, Ag and Au) nanorods: an experimental and computational study. Chemical Communications, 2015, 51, 6605-6608.	2.2	44
22316	Interaction of carbon, nitrogen and oxygen with vacancies and solutes in tungsten. RSC Advances, 2015, 5, 23261-23270.	1.7	21
22317	Breaking of Symmetry in Graphene Growth on Metal Substrates. Physical Review Letters, 2015, 114, 115502.	2.9	68
22318	Enhanced photocatalytic activities of Bi₂WO₆ by introducing Zn to replace Bi lattice sites: a first-principles study. RSC Advances, 2015, 5, 29058-29065.	1.7	38
22319	Manipulation of magnetic state in phosphorene layer by non-magnetic impurity doping. New Journal of Physics, 2015, 17, 023056.	1.2	81
22320	Novel Evolution Process of Zn-Induced Nanoclusters on Si(111)-(7Ã—7) Surface. Nano-Micro Letters, 2015, 7, 194-202.	14.4	2
22321	First-principles multiple-barrier diffusion theory: The case study of interstitial diffusion in CdTe. Physical Review B, 2015, 91, .	1.1	33
22322	Active Sites on Tiâ€“Ce Mixed Metal Oxides for Reactive Adsorption of Thiophene and Its Derivatives: A DFT Study. Journal of Physical Chemistry C, 2015, 119, 5903-5913.	1.5	15
22323	Highly luminescent flexible amino-functionalized graphene quantum dots@cellulose nanofiberâ€“clay hybrids for white-light emitting diodes. Journal of Materials Chemistry C, 2015, 3, 3536-3541.	2.7	83
22324	Synthesis and Characterization of a Cu₁₄ Hydride Cluster Supported by Neutral Donor Ligands. Chemistry - A European Journal, 2015, 21, 5341-5344.	1.7	60
22325	First-principles prediction on silicene-based heterobilayers as a promising candidate for FET. Materials Chemistry and Physics, 2015, 156, 89-94.	2.0	9
22326	Geometry Dependence of Electronic and Energetic Properties of One-Dimensional Peanut-Shaped Fullerene Polymers. Journal of Physical Chemistry A, 2015, 119, 3048-3055.	1.1	12
22327	Nucleation of metastable aragonite CaCO ₃ in seawater. Proceedings of the National Academy of Sciences of the United States of America, 2015, 112, 3199-3204.	3.3	187
22328	Theoretical investigation of effect of alloying elements on phase stability in body-centered cubic Ti-X alloys (X=V, Cr, Fe, Co, Nb, and Mo). Journal of Alloys and Compounds, 2015, 634, 193-199.	2.8	22

#	Article	IF	Citations
22329	Formation and Evolution of the High-Surface-Energy Facets of Anatase TiO₂. Journal of Physical Chemistry C, 2015, 119, 6094-6100.	1.5	37
22330	Deformation of singleâ€walled carbon nanotubes by interaction with graphene: A firstâ€principles study. Journal of Computational Chemistry, 2015, 36, 717-722.	1.5	8
22331	Lattice-Mismatch-Induced Twinning for Seeded Growth of Anisotropic Nanostructures. ACS Nano, 2015, 9, 3307-3313.	7.3	86
22332	Effect of Surface Structure on the Photoreactivity of TiO₂. Journal of Physical Chemistry C, 2015, 119, 6121-6127.	1.5	43
22333	Cooperative insertion of CO2 in diamine-appended metal-organic frameworks. Nature, 2015, 519, 303-308.	13.7	1,026
22334	Artificial layered perovskite oxides A(B0.5Bâ€²0.5)O3 as potential solar energy conversion materials. Journal of Applied Physics, 2015, 117, 055106.	1.1	4
22335	Effects of Pb Doping on Hole Transport Properties and Thin-Film Transistor Characteristics of SnO Thin Films. ECS Journal of Solid State Science and Technology, 2015, 4, Q26-Q30.	0.9	19
22336	Extraordinary deformation capacity of smallest carbohelicene springs. Physical Chemistry Chemical Physics, 2015, 17, 18684-18690.	1.3	13
22337	Ideal Strengths and Bonding Properties of UO ₂ under Tension. Chinese Physics Letters, 2015, 32, 037102.	1.3	3
22338	Unexpected band structure and half-metal in non-metal-doped arsenene sheet. Applied Physics Express, 2015, 8, 065202.	1.1	33
22339	Two-dimensional boronâ€“nitrogenâ€“carbon monolayers with tunable direct band gaps. Nanoscale, 2015, 7, 12023-12029.	2.8	74
22340	Identification of Novel Cu, Ag, and Au Ternary Oxides from Global Structural Prediction. Chemistry of Materials, 2015, 27, 4562-4573.	3.2	56
22341	Optical Polarization of Nuclear Spins in Silicon Carbide. Physical Review Letters, 2015, 114, 247603.	2.9	109
22342	Rare-earth free p-type filled skutterudites: Mechanisms for low thermal conductivity and effects of Fe/Co ratio on the band structure and charge transport. Acta Materialia, 2015, 92, 152-162.	3.8	34
22343	Argon Interaction with Gold Surfaces: Ab Initio-Assisted Determination of Pair Arâ€“Au Potentials for Molecular Dynamics Simulations. Journal of Physical Chemistry A, 2015, 119, 6897-6908.	1.1	18
22344	Study on the Effect of Pt Intercalation into Layered Niobate Perovskite for Photocatalytic Behavior. Langmuir, 2015, 31, 7660-7665.	1.6	11
22345	Crucial Role of Site Disorder and Frustration in Unusual Magnetic Properties of Quasi-2D Triangular Lattice Antimonate Na4FeSbO6. Applied Magnetic Resonance, 2015, 46, 1121-1145.	0.6	11
22346	Interface Coupling in Twisted Multilayer Graphene by Resonant Raman Spectroscopy of Layer Breathing Modes. ACS Nano, 2015, 9, 7440-7449.	7.3	127

#	Article	IF	Citations
22347	Unraveling the Atomistic Sodiation Mechanism of Black Phosphorus for Sodium Ion Batteries by First-Principles Calculations. Journal of Physical Chemistry C, 2015, 119, 15041-15046.	1.5	135
22348	Schottky barrier formation and band bending revealed by first- principles calculations. Scientific Reports, 2015, 5, 11374.	1.6	75
22349	Magnetic domain wall induced ferroelectricity in double perovskites. Applied Physics Letters, 2015, 106, 152901.	1.5	18
22350	Electric-Field Tunable Band Offsets in Black Phosphorus and MoS₂ van der Waals p-n Heterostructure. Journal of Physical Chemistry Letters, 2015, 6, 2483-2488.	2.1	193
22351	Activity of N-coordinated multi-metal-atom active site structures for Pt-free oxygen reduction reaction catalysis: Role of *OH ligands. Scientific Reports, 2015, 5, 9286.	1.6	109
22352	Coexistence pressure for a martensitic transformation from theory and experiment: Revisiting the bcc-hcp transition of iron under pressure. Physical Review B, 2015, 91, .	1.1	30
22353	Magnetic and superconducting phase diagram of the half-Heusler topological semimetal HoPdBi. Journal of Physics Condensed Matter, 2015, 27, 275701.	0.7	26
22354	Structure, Electronic, and Magnetic Properties of Binary Pt_nTM_{55â€“n} (TM = Fe, Co, Ni, Cu, Zn) Nanoclusters: A Density Functional Theory Investigation. Journal of Physical Chemistry C, 2015, 119, 15669-15679.	1.5	66
22355	1,4-Dithiineâ€”Puckered in the Gas Phase but Planar in Crystals: Role of Cooperativity. Journal of Physical Chemistry C, 2015, 119, 15770-15776.	1.5	22
22356	Trends of Oxygen Reduction Reaction on Platinum Alloys: A Computational and Experimental Study. Journal of Physical Chemistry C, 2015, 119, 15224-15231.	1.5	52
22357	A two-dimensional Ï€â€“d conjugated coordination polymer with extremely high electrical conductivity and ambipolar transport behaviour. Nature Communications, 2015, 6, 7408.	5.8	609
22358	Quantum Anomalous Hall Effect in Graphene-based Heterostructure. Scientific Reports, 2015, 5, 10629.	1.6	49
22359	Prediction of Diffusion Coefficients in Liquid and Solids. Defect and Diffusion Forum, 0, 364, 182-191.	0.4	10
22360	Defusing Complexity in Intermetallics: How Covalently Shared Electron Pairs Stabilize the FCC Variant Mo₂Cu_xGa_{6â€“x} (x â‰ˆ 0.9). Inorganic Chemistry, 2015, 54, 8103-8110.	1.9	13
22361	Pressure-driven dome-shaped superconductivity and electronic structural evolution in tungsten ditelluride. Nature Communications, 2015, 6, 7805.	5.8	324
22362	Hydrogen-doping induced reduction in the phase transition temperature of VO₂: a first-principles study. Physical Chemistry Chemical Physics, 2015, 17, 20998-21004.	1.3	47
22363	First-principles calculations of properties of orthorhombic iron carbide<mml:math xmlns:mml="http://www.w3.org/1998/Math/MathML"><mml:mrow><mml:msub><mml:mi>Fe</mml:mi><mml:mn>7</mml:mn></mml:r mathvariant="normal">C</mml:mi><mml:mn>3</mml:mn></mml:msub></mml:mrow></mml:math>at the Earth's core conditions. Physical Review B, 2015, 91, .	1.1	20
22364	Hydrogenation properties of Li Sr1â^'AlSi studied by quantum-chemical methods (0â‰¤xâ‰¤1) and in-situ neutron powder diffraction (x=1). Journal of Solid State Chemistry, 2015, 221, 318-324.	1.4	4

#	Article	IF	Citations
22365	Combined Experimental and ab Initio Study of Site Preference of Ce³⁺ in SrAl₂O₄. Journal of Physical Chemistry C, 2015, 119, 19326-19332.	1.5	31
22366	Direct Imaging Single Methanol Molecule Photocatalysis on Titania. Journal of Physical Chemistry C, 2015, 119, 17748-17754.	1.5	37
22367	Computational Identification of Descriptors for Selectivity in Syngas Reactions on a Mo₂C Catalyst. ACS Catalysis, 2015, 5, 5174-5185.	5.5	24
22368	Dynamic DMF Binding in MOF-5 Enables the Formation of Metastable Cobalt-Substituted MOF-5 Analogues. ACS Central Science, 2015, 1, 252-260.	5.3	123
22369	Unusual Mn coordination and redox chemistry in the high capacity borate cathode Li₇Mn(BO₃)₃. Physical Chemistry Chemical Physics, 2015, 17, 22259-22265.	1.3	17
22370	Trends in non-metal doping of the SrTiO₃ surface: a hybrid density functional study. Physical Chemistry Chemical Physics, 2015, 17, 21611-21621.	1.3	31
22371	Size effects and strain localization in atomic-scale cleavage modeling. Journal of Physics Condensed Matter, 2015, 27, 345002.	0.7	7
22372	Enhanced stability of the strengthening phase Ni2(Cr,Mo) in Niâ€“Crâ€“Mo alloys by adjacent instability. Computational Materials Science, 2015, 109, 111-114.	1.4	3
22373	Study of Poly (3,4-ethylenedioxythiophene)/MnO2 as Composite Cathode Materials for Aluminum-Air Battery. Electrochimica Acta, 2015, 176, 1324-1331.	2.6	23
22374	Electronic Structure of the Peryleneâ€“Zinc Oxide Interface: Computational Study of Photoinduced Electron Transfer and Impact of Surface Defects. Journal of Physical Chemistry C, 2015, 119, 18843-18858.	1.5	10
22375	Understanding Polyol Decomposition on Bimetallic Ptâ€“Mo Catalystsâ€”A DFT Study of Glycerol. ACS Catalysis, 2015, 5, 4942-4950.	5.5	25
22376	Designing Isoelectronic Counterparts to Layered Group V Semiconductors. ACS Nano, 2015, 9, 8284-8290.	7.3	128
22377	Quantifying the origin of inter-adsorbate interactions on reactive surfaces for catalyst screening and design. Physical Chemistry Chemical Physics, 2015, 17, 22227-22234.	1.3	2
22378	Half-metallic and magnetic properties in nonmagnetic element embedded graphitic carbon nitride sheets. Physical Chemistry Chemical Physics, 2015, 17, 22136-22143.	1.3	25
22379	Insight into the limited electrochemical activity of NaVP₂O₇. RSC Advances, 2015, 5, 64991-64996.	1.7	48
22380	Adsorption of nucleobases on 2D transition-metal dichalcogenides and graphene sheet: a first principles density functional theory study. RSC Advances, 2015, 5, 67427-67434.	1.7	112
22381	Thermodynamic investigation of Ti doping in MgAl₂O₄ based on the first-principles method. Journal of Materials Chemistry C, 2015, 3, 8970-8978.	2.7	12
22382	Electronic analog of chiral metamaterial: Helicity-resolved filtering and focusing of Dirac fermions in thin films of topological materials. Physical Review B, 2015, 92, .	1.1	9

#	Article	IF	Citations
22383	Atomic and electronic structure of CdS-based quantum dots. Journal of Structural Chemistry, 2015, 56, 517-522.	0.3	8
22384	Half-metallic ferromagnetism in Fe-chain-embedded zigzag boron-nitride nanoribbons with line defect. Physica E: Low-Dimensional Systems and Nanostructures, 2015, 74, 431-437.	1.3	2
22385	Predicted two-dimensional electrides: Lithiumâ€“carbon monolayer sheet. Physics Letters, Section A: General, Atomic and Solid State Physics, 2015, 379, 2511-2514.	0.9	11
22386	Ab initio study of magnetism in nonmagnetic metal substituted monolayer MoS2. Solid State Communications, 2015, 220, 67-71.	0.9	21
22387	Energetics of Rutile TiO₂ Vicinal Surfaces with âŸ¨001âŸ© Steps from the Energy Density Method. Journal of Physical Chemistry C, 2015, 119, 18203-18209.	1.5	8
22388	Trends in the Reactivity of Molecular O₂ with Copper Clusters: Influence of Size and Shape. Journal of Physical Chemistry C, 2015, 119, 19832-19846.	1.5	63
22389	Grain Boundary Structures and Electronic Properties of Hexagonal Boron Nitride on Cu(111). Nano Letters, 2015, 15, 5804-5810.	4.5	117
22390	A high performance cathode for proton conducting solid oxide fuel cells. Journal of Materials Chemistry A, 2015, 3, 8405-8412.	5.2	113
22391	First principles study of the structural, mechanical, phonon, optical, and thermodynamic properties of half-Heusler (HH) compound NbFeSb. Physica Scripta, 2015, 90, 095701.	1.2	17
22392	Composition-dependent structural and transport properties of amorphous transparent conducting oxides. Physical Review B, 2015, 91, .	1.1	37
22393	Phase patterning for ohmic homojunction contact in MoTe ₂. Science, 2015, 349, 625-628.	6.0	918
22394	Stabilization of wurtzite Sc0.4Al0.6N in pseudomorphic epitaxial Sc Al1â^'N/In Al1â^'N superlattices. Acta Materialia, 2015, 94, 101-110.	3.8	19
22395	Synthesis and properties of crystalline thin film of antimony trioxide on the Si(1 0 0) substrate. Applied Surface Science, 2015, 349, 259-263.	3.1	13
22396	High coverage hydrogen adsorption on the Fe3O4(110) surface. Applied Surface Science, 2015, 353, 973-978.	3.1	16
22397	Assessments of molar volume of the binary C14 Laves phase. Calphad: Computer Coupling of Phase Diagrams and Thermochemistry, 2015, 50, 82-91.	0.7	6
22398	The role of density functional theory methods in the prediction of nanostructured gas-adsorbent materials. Coordination Chemistry Reviews, 2015, 300, 142-163.	9.5	36
22399	Electronic structures and magnetic properties in nonmetallic element substituted MoS2 monolayer. Computational Materials Science, 2015, 107, 72-78.	1.4	55
22400	Multiscale ab initio simulation of Ni-based alloys: Real-space distribution of atoms in Î³ + Î³ â€² phase. Computational Materials Science, 2015, 108, 192-204.	1.4	13

#	Article	IF	Citations
22401	A theoretical prediction on huge hole and electron mobilities of 6,6,18-graphdiyne nanoribbons. Chemical Physics Letters, 2015, 633, 30-34.	1.2	7
22402	Restarted Pulay mixing for efficient and robust acceleration of fixed-point iterations. Chemical Physics Letters, 2015, 635, 69-74.	1.2	41
22403	The structure of waterâ€“methanol mixtures under an electric field: Ab initio molecular dynamics simulations. Chemical Physics Letters, 2015, 635, 99-106.	1.2	5
22404	Solubility and ordering of Ti, Ta, Mo and W on the Al sublattice in L12-Co3Al. Intermetallics, 2015, 64, 44-50.	1.8	27
22405	Effects of the defects on the structural, electronic and magnetic properties of Sr2FeMoO6. Journal of Alloys and Compounds, 2015, 648, 374-381.	2.8	10
22406	Electronic properties and relative stabilities of heterogeneous edge-decorated zigzag boron nitride nanoribbons. Journal of Alloys and Compounds, 2015, 649, 1130-1135.	2.8	7
22407	High spin polarization and spin splitting in equiatomic quaternary CoFeCrAl Heusler alloy. Journal of Magnetism and Magnetic Materials, 2015, 394, 82-86.	1.0	79
22408	Experimental investigation of phase equilibria in the Zrâ€“Nbâ€“Cr system at 1573ÂK and 1373ÂK. Journal of Nuclear Materials, 2015, 465, 626-632.	1.3	2
22409	Synthesis and crystal structure of Ba26B12Si5N27 containing [Si2] dumbbells. Journal of Solid State Chemistry, 2015, 230, 390-396.	1.4	7
22410	Electronic and atomic structure of complex defects in Al- and Ga-highly doped ZnO films. Materials Chemistry and Physics, 2015, 160, 420-428.	2.0	8
22411	Mapping Structural Changes in Electrode Materials: Application of the Hybrid Eigenvector-Following Density Functional Theory (DFT) Method to Layered Li_{0.5}MnO₂. Chemistry of Materials, 2015, 27, 5550-5561.	3.2	23
22412	Water Oxidation Mechanism on Alkaline-Earth-Cation Containing Birnessite-Like Manganese Oxides. Journal of Physical Chemistry C, 2015, 119, 18487-18494.	1.5	19
22413	Effects of stacking order, layer number and external electric field on electronic structures of few-layer C₂N-h2D. Nanoscale, 2015, 7, 14062-14070.	2.8	177
22414	Polymorphism of dioctyl-terthiophene within thin films: The role of the first monolayer. Chemical Physics Letters, 2015, 630, 12-17.	1.2	23
22415	Structure of the Hydroxyl Groups and Adsorbed D₂O Sites in the DX Zeolite: DFT and Experimental NMR Data. Journal of Physical Chemistry C, 2015, 119, 19548-19557.	1.5	9
22416	Understanding complete oxidation of methane on spinel oxides at a molecular level. Nature Communications, 2015, 6, 7798.	5.8	237
22417	Ideal Spintronics in Molecule-Based Novel Organometallic Nanowires. Scientific Reports, 2015, 5, 12772.	1.6	11
22418	Mechanism of Li intercalation/deintercalation into/from the surface of LiCoO₂. Physical Chemistry Chemical Physics, 2015, 17, 22917-22922.	1.3	23

#	Article	IF	Citations
22419	The ferroelectric polarization of Y2CoMnO6aligns along the b-axis: the first-principles calculations. Physical Chemistry Chemical Physics, 2015, 17, 20961-20970.	1.3	20
22420	Understanding the origin of phase segregation of nano-crystalline in a BexZn1â^'xO random alloy: a novel phase of Be1/3Zn2/3O. Nanoscale, 2015, 7, 9852-9858.	2.8	7
22421	Prediction of Ir0.5M0.5O2 (MÂ=ÂCr, Ru or Pb) Mixed Oxides as Active Catalysts for Oxygen Evolution Reaction from First-Principles Calculations. Topics in Catalysis, 2015, 58, 675-681.	1.3	15
22422	CO Dissociation at Vacancy Sites on HÃgg Iron Carbide: Direct Versus Hydrogen-Assisted Routes Investigated with DFT. Topics in Catalysis, 2015, 58, 665-674.	1.3	25
22423	Estimation of the activation energy for surface diffusion during metastable phase formation. Acta Materialia, 2015, 98, 135-140.	3.8	41
22424	Ab initio study of Fe adsorption on the (001) surface of transition metal carbides and nitrides. Computational Materials Science, 2015, 106, 149-154.	1.4	26
22425	First principles study on the phase stability and mechanical properties of MoSi2 alloyed with Al, Mg and Ge. Intermetallics, 2015, 67, 26-34.	1.8	24
22426	Effective p-type N-doped WS2 monolayer. Journal of Alloys and Compounds, 2015, 649, 357-361.	2.8	33
22427	Lattice properties of supersaturated Niâ€“Sn solid solutions. Materials Letters, 2015, 160, 72-74.	1.3	5
22428	Novel 2D RuPt core-edge nanocluster catalyst for CO electro-oxidation. Surface Science, 2015, 640, 50-58.	0.8	15
22429	Magnetite Fe₃O₄ (111) Surfaces: Impact of Defects on Structure, Stability, and Electronic Properties. Chemistry of Materials, 2015, 27, 5856-5867.	3.2	93
22430	Anomalous Stagewise Lithiation of Gold-Coated Silicon Nanowires: A Combined In Situ Characterization and First-Principles Study. ACS Applied Materials & Interfaces, 2015, 7, 16976-16983.	4.0	9
22431	A van der Waals Density Functional Investigation on the Improved Adsorption Properties of NO on the Rhn/MgO (100) Interface. ACS Applied Materials & Interfaces, 2015, 7, 17499-17509.	4.0	4
22432	Ordered Fe(II)Ti(IV)O₃ Mixed Monolayer Oxide on Rutile TiO₂(011). ACS Nano, 2015, 9, 8627-8636.	7.3	14
22433	Beating the Stoner criterion using molecular interfaces. Nature, 2015, 524, 69-73.	13.7	151
22434	DFT studies of the bonding mechanism of 8-hydroxyquinoline and derivatives on the (111) aluminum surface. Physical Chemistry Chemical Physics, 2015, 17, 22243-22258.	1.3	36
22435	The effect of impurities in ultra-thin hydrogenated silicene and germanene: a first principles study. Physical Chemistry Chemical Physics, 2015, 17, 22210-22216.	1.3	30
22436	A first-principles examination of conducting monolayer 1Tâ€²-MX₂(M = Mo, W; X = S, Se, Te): promising catalysts for hydrogen evolution reaction and its enhancement by strain. Physical Chemistry Chemical Physics, 2015, 17, 21702-21708.	1.3	117

#	Article	IF	Citations
22437	Tuning the charge state of Ag and Au atoms and clusters deposited on oxide surfaces by doping: a DFT study of the adsorption properties of nitrogen- and niobium-doped TiO₂ and ZrO₂. Physical Chemistry Chemical Physics, 2015, 17, 22342-22360.	1.3	42
22438	Geometric stability, electronic structure, and intercalation mechanism of Co adatom anchors on graphene sheets. Journal of Physics Condensed Matter, 2015, 27, 255009.	0.7	7
22439	Stability and electronic structure of two-dimensional allotropes of group-IV materials. Physical Review B, 2015, 92, .	1.1	124
22440	Origin of Excess Irreversible Capacity in Lithium-Ion Batteries Based on Carbon Nanostructures. Journal of the Electrochemical Society, 2015, 162, A2106-A2115.	1.3	29
22441	Guided design of copper oxysulfide superconductors. Europhysics Letters, 2015, 111, 17002.	0.7	8
22442	First-principles calculation of sulfurâ€“selenium segregation in ZnSe1â^'xSx: The role of lattice vibration. Materials Science in Semiconductor Processing, 2015, 39, 96-102.	1.9	6
22443	Vibrational spectra of Ruthenium Carbide structures yielded by the structure search employing evolutionary algorithm. Materials Science in Semiconductor Processing, 2015, 40, 484-490.	1.9	8
22444	Scattering of H(D) from LiF(100) under fast grazing incidence conditions: To what extent is classical dynamics a useful tool?. Nuclear Instruments & Methods in Physics Research B, 2015, 354, 9-15.	0.6	9
22445	Electronic structures and magnetic properties in Cu-doped two-dimensional dichalcogenides. Physica E: Low-Dimensional Systems and Nanostructures, 2015, 73, 69-75.	1.3	33
22446	Mechanical properties and spinodal decomposition of Ti Al1â^'â^'Zr N coatings. Physics Letters, Section A: General, Atomic and Solid State Physics, 2015, 379, 2037-2040.	0.9	4
22447	Computational study of <mml:math xmlns:mml="http://www.w3.org/1998/Math/MathML" altimg="si1.gif" overflow="scroll"><mml:mrow><mml:mo><</mml:mo><mml:mn>1</mml:mn><mml:mspace width="0.12em" /><mml:mover accent="true"><mml:mrow><mml:mn>1</mml:mn></mml:mrow><mml:mrow><mml:mo>Â¯</mml:mo></mml:mrow></mml:mover><m width="0.12em" /><mml:mn>0</mml:mn><mml:mspace width="0.12em" /><mml:mn>0</mml:mn><mml:mo>	2.6	22
22448	Pressure-induced structural phase transition, elastic and thermodynamic properties of ReC under high pressure. Solid State Sciences, 2015, 48, 49-55.	1.5	5
22449	A DFT study on the correlation between topology and Bader charges: Part III, the development of charge, â€œsizeâ€•and coordination in alkali and alkaline earth titanates(IV). Solid State Sciences, 2015, 48, 61-71.	1.5	3
22450	Decomposition pathways of C2 oxygenates on Rh-modified tungsten carbide surfaces. Surface Science, 2015, 640, 89-95.	0.8	5
22451	Cutting a chemical bond with demon's scissors: Mode- and bond-selective reactivity of methane on metal surfaces. Surface Science, 2015, 640, 25-35.	0.8	41
22452	A systematic DFT study of substrate reconstruction effects due to thiolate and selenolate adsorption. Surface Science, 2015, 640, 18-24.	0.8	15
22453	Reactions of methyl groups on a non-reducible metal oxide: The reaction of iodomethane on stoichiometric Î±-Cr2O3(0001). Surface Science, 2015, 641, 148-153.	0.8	3
22454	Screened Hybrid Exact Exchange Correction Scheme for Adsorption Energies on Perovskite Oxides. Journal of Physical Chemistry C, 2015, 119, 17662-17666.	1.5	7

#	Article	IF	Citations
22455	Observation of Surface-Bound Negatively Charged Hydride and Hydroxide on GaP(110) in H₂O Environments. Journal of Physical Chemistry C, 2015, 119, 17762-17772.	1.5	39
22456	Electric Field and Strain Effect on Graphene-MoS₂ Hybrid Structure: Ab Initio Calculations. Journal of Physical Chemistry Letters, 2015, 6, 3269-3275.	2.1	110
22457	Solubility of Boron, Carbon, and Nitrogen in Transition Metals: Getting Insight into Trends from First-Principles Calculations. Journal of Physical Chemistry Letters, 2015, 6, 3263-3268.	2.1	50
22458	Uncovering the Veil of the Degradation in Perovskite CH₃NH₃PbI₃ upon Humidity Exposure: A First-Principles Study. Journal of Physical Chemistry Letters, 2015, 6, 3289-3295.	2.1	171
22459	Exploring the metallic phase of N2O under high pressure. RSC Advances, 2015, 5, 65745-65749.	1.7	5
22460	Electronic Origins of Anomalous Twin Boundary Energies in Hexagonal Close Packed Transition Metals. Physical Review Letters, 2015, 115, 065501.	2.9	23
22461	Effect of Er doping on microstructure and optical properties of ZnO thin films prepared by solâ€“gel method. Journal of Materials Science: Materials in Electronics, 2015, 26, 8732-8739.	1.1	18
22462	First-principles calculations of the twin boundary energies and adhesion energies of interfaces for cubic face-centered transition-metal nitrides and carbides. Applied Surface Science, 2015, 355, 1132-1135.	3.1	27
22463	An alternative approach to investigate the origin of p-type conductivity in arsenic doped ZnO. Current Applied Physics, 2015, 15, 1256-1261.	1.1	13
22464	Theoretical study of the interaction between metallic fission products and defective graphite. Computational Materials Science, 2015, 106, 129-134.	1.4	9
22465	The phase stability, magnetic and vibrational properties of A2Ni21B6 Â(A=Th,ÂU) and Ce3Pd20Si6. Computer Physics Communications, 2015, 193, 72-77.	3.0	3
22466	High pressure stability of the monosilicides of cobalt and the platinum group elements. Journal of Alloys and Compounds, 2015, 626, 375-380.	2.8	16
22467	New Ag(F 1â^'x Cl x) phases for energy storage applications. Journal of Fluorine Chemistry, 2015, 174, 22-29.	0.9	10
22468	The electronic and magnetic properties of the F-doped CrO2 from first-principles study. Journal of Magnetism and Magnetic Materials, 2015, 379, 196-201.	1.0	2
22469	First-principles calculations of the lattice thermal conductivity of the lower mantle. Earth and Planetary Science Letters, 2015, 427, 11-17.	1.8	44
22470	Rotating Anisotropic Crystalline Silicon Nanoclusters in Graphene. ACS Nano, 2015, 9, 9497-9506.	7.3	15
22471	Two-Dimensional, Ordered, Double Transition Metals Carbides (MXenes). ACS Nano, 2015, 9, 9507-9516.	7.3	1,395
22472	Edge reconstruction in armchair phosphorene nanoribbons revealed by discontinuous Galerkin density functional theory. Physical Chemistry Chemical Physics, 2015, 17, 31397-31404.	1.3	37

#	Article	IF	Citations
22473	Computational screening for effective Ge_{1â^'x}Si_x nanowire photocatalyst. Physical Chemistry Chemical Physics, 2015, 17, 20391-20397.	1.3	14
22474	Ti-substituted Li[Li_{0.26}Mn_{0.6â^'x}Ti_xNi_{0.07}Co_{0.07}]O₂ layered cathode material with improved structural stability and suppressed voltage fading. Journal of Materials Chemistry A, 2015, 3, 17376-17384.	5.2	40
22475	Charge states of point defects in plutonium oxide: A first-principles study. Journal of Alloys and Compounds, 2015, 649, 544-552.	2.8	30
22476	Preparation and Instability of Nanocrystalline Cuprous Nitride. Inorganic Chemistry, 2015, 54, 6356-6362.	1.9	22
22477	Highly Anisotropic Dirac Fermions in Square Graphynes. Journal of Physical Chemistry Letters, 2015, 6, 2959-2962.	2.1	75
22478	Raman scattering efficiency in<mml:math xmlns:mml="http://www.w3.org/1998/Math/MathML"><mml:msub><mml:mi>LiTaO</mml:mi><mml:mn>3</mml:mn></mml:msub><mml:m xmlns:mml="http://www.w3.org/1998/Math/MathML"><mml:msub><mml:mi>LiNbO</mml:mi><mml:mn>3</mml:mn></mml:msub><mml:m Physical Review B, 2015, 91, .	1.1	94
22479	First-principles investigation of hydrogen trapping and diffusion at grain boundaries in nickel. Acta Materialia, 2015, 98, 306-312.	3.8	132
22480	Effect of surface composition on electronic properties of methylammonium lead iodide perovskite. Journal of Materiomics, 2015, 1, 213-220.	2.8	49
22481	Interrelationships among Grain Size, Surface Composition, Air Stability, and Interfacial Resistance of Al-Substituted Li₇La₃Zr₂O₁₂ Solid Electrolytes. ACS Applied Materials & Interfaces, 2015, 7, 17649-17655.	4.0	220
22482	Two-dimensional van der Waals C60 molecular crystal. Scientific Reports, 2015, 5, 12221.	1.6	24
22483	Semiconductorâ€“metal transition induced by nanoscale stabilization. Physical Chemistry Chemical Physics, 2015, 17, 5569-5573.	1.3	17
22484	Selective gas adsorption in microporous metalâ€“organic frameworks incorporating urotropine basic sites: an experimental and theoretical study. Chemical Communications, 2015, 51, 13918-13921.	2.2	29
22485	Relative stability and reducibility of CeO2 and Rh/CeO2 species on the surface and in the cavities of Î³-Al2O3: a periodic DFT study. Physical Chemistry Chemical Physics, 2015, 17, 22389-22401.	1.3	6
22486	The Birmingham parallel genetic algorithm and its application to the direct DFT global optimisation of Ir_N (N = 10â€“20) clusters. Nanoscale, 2015, 7, 14032-14038.	2.8	74
22487	Electronic structure and thermoelectric properties of Zintl compounds A₃AlSb₃ (A = Ca and Sr): first-principles study. RSC Advances, 2015, 5, 65133-65138.	1.7	14
22488	Electronic structure, optical and dielectric properties of BaTiO₃/CaTiO₃/SrTiO₃ ferroelectric superlattices from first-principles calculations. Journal of Materials Chemistry C, 2015, 3, 8625-8633.	2.7	96
22489	Au and Ti induced charge redistributions on monolayer WS ₂. Chinese Physics B, 2015, 24, 077301.	0.7	1
22490	Nitrogen atom shift and the structural change in chromium nitride. Acta Materialia, 2015, 98, 119-127.	3.8	6

#	Article	IF	Citations
22491	Interaction of metallic clusters with biologically active curcumin molecules. Chemical Physics Letters, 2015, 636, 163-166.	1.2	0
22492	Elastic properties of ferropericlase at lower mantle conditions and its relevance to ULVZs. Earth and Planetary Science Letters, 2015, 417, 40-48.	1.8	28
22493	Experimental (FTIR and FT-Raman) and theoretical investigation of some pyridine-dicarboxylic acids. Journal of Molecular Structure, 2015, 1100, 43-58.	1.8	16
22494	Density functional theory study of the structural, electronic and optical properties of C-doped anatase TiO2 (101) surface. Physics Letters, Section A: General, Atomic and Solid State Physics, 2015, 379, 1666-1670.	0.9	29
22495	Investigating new polyphorms of Znâ€“O from variable composition. Solid State Communications, 2015, 220, 36-38.	0.9	7
22496	Rational Composition Optimization of the Lithium-Rich Li₃OCl_{1â€“x}Br_x Anti-Perovskite Superionic Conductors. Chemistry of Materials, 2015, 27, 3749-3755.	3.2	130
22497	Influence of Structural Fluctuations, Proton Transfer, and Electric Field on Polarization Switching of Supported Two-Dimensional Hydrogen-Bonded Oxocarbon Monolayers. Chemistry of Materials, 2015, 27, 4839-4847.	3.2	13
22498	First-Principles Study of Carbon and Vacancy Structures in Niobium. Journal of Physical Chemistry C, 2015, 119, 14728-14736.	1.5	15
22499	Water-Induced, Spin-Dependent Defects on the Silicon (001) Surface. Journal of Physical Chemistry C, 2015, 119, 11612-11618.	1.5	4
22500	Early Stage Hydration of Wollastonite: Kinetic Aspects of the Metal-Proton Exchange Reaction. Journal of Physical Chemistry C, 2015, 119, 10493-10499.	1.5	23
22501	Reconstruction of Low-Index Î±-V₂O₅ Surfaces. Journal of Physical Chemistry C, 2015, 119, 10500-10506.	1.5	12
22502	First-Principles Calculation of Terahertz Absorption with Dispersion Correction of 2,2â€²-Bithiophene as Model Compound. Journal of Physical Chemistry C, 2015, 119, 12598-12607.	1.5	15
22503	Tuning the Surface Chemistry of Chiral Cu(531)^S for Enhanced Enantiospecific Adsorption of Amino Acids. Journal of Physical Chemistry C, 2015, 119, 15195-15203.	1.5	16
22504	First-Principles Calculations of Lithiation of a Hydroxylated Surface of Amorphous Silicon Dioxide. Journal of Physical Chemistry C, 2015, 119, 16424-16431.	1.5	43
22505	Prediction of Adsorption Properties of Cyclic Hydrocarbons in MOFs Using DFT-Derived Force Fields. Journal of Physical Chemistry C, 2015, 119, 16920-16926.	1.5	18
22506	Nanopatterning on H-Terminated Si(111) Explained as Dynamic Equilibrium of the Chemical Reaction with Methanol. Journal of Physical Chemistry C, 2015, 119, 16947-16953.	1.5	10
22507	Correlating Local Structure with Electrochemical Activity in Li₂MnO₃. Journal of Physical Chemistry C, 2015, 119, 18022-18029.	1.5	26
22508	Ïƒâ€“Ï€-Band Inversion in a Novel Two-Dimensional Material. Journal of Physical Chemistry C, 2015, 119, 19469-19474.	1.5	96

#	Article	IF	Citations
22509	Water on the MgO(001) Surface: Surface Reconstruction and Ion Solvation. Journal of Physical Chemistry Letters, 2015, 6, 2310-2314.	2.1	34
22510	Stabilization of 1T-MoS2 Sheets by Imidazolium Molecules in Self-Assembling Hetero-layered Nanocrystals. Langmuir, 2015, 31, 8953-8960.	1.6	34
22511	Solvent Control of Surface Plasmon-Mediated Chemical Deposition of Au Nanoparticles from Alkylgold Phosphine Complexes. ACS Applied Materials & Interfaces, 2015, 7, 13384-13394.	4.0	8
22512	(Ag,Cu)â€“Taâ€“O Ternaries As High-Temperature Solid-Lubricant Coatings. ACS Applied Materials & Interfaces, 2015, 7, 15422-15429.	4.0	32
22513	Quantum Chemical Design of Doped Ca₂MnAlO_{5+Î´} as Oxygen Storage Media. ACS Applied Materials & Interfaces, 2015, 7, 14518-14527.	4.0	15
22514	Chemical structure imaging of a single molecule by atomic force microscopy at room temperature. Nature Communications, 2015, 6, 7766.	5.8	81
22515	Sodium and Lithium Storage Properties of Spray-Dried Molybdenum Disulfide-Graphene Hierarchical Microspheres. Scientific Reports, 2015, 5, 11989.	1.6	58
22516	Density functional theory calculations of the hydrazine decomposition mechanism on the planar and stepped Cu(111) surfaces. Physical Chemistry Chemical Physics, 2015, 17, 21533-21546.	1.3	39
22517	Surface-dependence of interfacial binding strength between zinc oxide and graphene. RSC Advances, 2015, 5, 65719-65724.	1.7	15
22518	Electrocatalytic properties of iron chalcogenides as low-cost counter electrode materials for dye-sensitized solar cells. RSC Advances, 2015, 5, 72553-72561.	1.7	20
22519	Na_{2.44}Mn_{1.79}(SO₄)₃: a new member of the alluaudite family of insertion compounds for sodium ion batteries. Journal of Materials Chemistry A, 2015, 3, 18564-18571.	5.2	99
22520	Carbon dioxide sorption in a nanoporous octahedral molecular sieve. Journal Physics D: Applied Physics, 2015, 48, 335304.	1.3	7
22521	Free energy dependence of pure phase iron doped bismuth titanate from first principles calculations. Journal of Physics Condensed Matter, 2015, 27, 315502.	0.7	5
22522	How General is the Conversion Reaction in Mg Battery Cathode: A Case Study of the Magnesiation of Î±-MnO₂. Chemistry of Materials, 2015, 27, 5799-5807.	3.2	125
22523	Alkane reforming on partially sulfided CeO2 (1 1 1) surfaces. Journal of Catalysis, 2015, 330, 167-176.	3.1	17
22524	Mechanistic Insight into the Facet-Dependent Adsorption of Methanol on a Pt₃Ni Nanocatalyst. Journal of Physical Chemistry C, 2015, 119, 18352-18363.	1.5	19
22525	Phase diagram, mechanical properties, and electronic structure of Nbâ€“N compounds under pressure. Physical Chemistry Chemical Physics, 2015, 17, 22837-22845.	1.3	27
22526	Photovoltaic performance and the energy landscape of CH₃NH₃PbI₃. Physical Chemistry Chemical Physics, 2015, 17, 22604-22615.	1.3	35

#	Article	IF	Citations
22527	An atomistic investigation into the nature of fracture of Ni/Al2O3 interface with yttrium dopant under tension. Engineering Fracture Mechanics, 2015, 150, 239-247.	2.0	12
22528	Trapping of He clusters by inert-gas impurities in tungsten: First-principles predictions and experimental validation. Nuclear Instruments & Methods in Physics Research B, 2015, 352, 86-91.	0.6	45
22529	Trends in adsorbate induced core level shifts. Surface Science, 2015, 640, 59-64.	0.8	21
22530	Structural, electronic and magnetic properties of 5d transition metal mediated benzene adsorption on graphene: A first-principles study. Synthetic Metals, 2015, 209, 225-231.	2.1	11
22531	Strain-dependence of the structure and ferroic properties of epitaxial Ni1â˜'xTi1â˜'yO3 thin films grown on sapphire substrates. Thin Solid Films, 2015, 578, 113-123.	0.8	7
22532	Long-range structural correlations in amorphous ternary In-based oxides. Vacuum, 2015, 114, 142-149.	1.6	9
22533	First-Principles Design and Analysis of an Efficient, Pb-Free Ferroelectric Photovoltaic Absorber Derived from ZnSnO₃. Chemistry of Materials, 2015, 27, 5899-5906.	3.2	24
22534	van der Waals Interactions in Layered Lithium Cobalt Oxides. Journal of Physical Chemistry C, 2015, 119, 19053-19058.	1.5	103
22535	Electronic Structure and Carrier Mobility of Two-Dimensional Î± Arsenic Phosphide. Journal of Physical Chemistry C, 2015, 119, 20210-20216.	1.5	65
22536	Room Temperature Multiferroicity of Charge Transfer Crystals. ACS Nano, 2015, 9, 9373-9379.	7.3	38
22537	Electronic and Chemical Properties of Donor, Acceptor Centers in Graphene. ACS Nano, 2015, 9, 9180-9187.	7.3	36
22538	Polarity compensation in ultra-thin films of complex oxides: The case of a perovskite nickelate. Scientific Reports, 2014, 4, 6819.	1.6	54
22539	Origin of hydrogen evolution activity on MS₂ (M = Mo or Nb) monolayers. Journal of Materials Chemistry A, 2015, 3, 18898-18905.	5.2	30
22540	Mechanical Properties of Metal Nitrides for Radiation Resistant Coating Applications: A DFT Study. Physics Procedia, 2015, 66, 576-585.	1.2	8
22541	Spin and photophysics of carbon-antisite vacancy defect in<mml:math xmlns:mml="http://www.w3.org/1998/Math/MathML"><mml:mrow><mml:mn>4</mml:mn><mml:mi>H</mml:mi></mml:mrow></mml:m carbide: A potential quantum bit. Physical Review B, 2015, 91, .	1.1	50
22542	Analysis of optical and magnetooptical spectra of Fe5Si3 and Fe3Si magnetic silicides using spectral magnetoellipsometry. Journal of Experimental and Theoretical Physics, 2015, 120, 886-893.	0.2	12
22543	Fast rechargeable all-solid-state lithium ion batteries with high capacity based on nano-sized Li2FeSiO4 cathode by tuning temperature. Nano Energy, 2015, 16, 112-121.	8.2	37
22544	First-principles study of group V and VII impurities in SnS2. Superlattices and Microstructures, 2015, 85, 664-671.	1.4	20

#	Article	IF	Citations
22545	Computational Analysis of Stable Hard Structures in the Tiâ€“B System. ACS Applied Materials & Interfaces, 2015, 7, 15607-15617.	4.0	48
22546	Atomic species identification at the (101) anatase surface by simultaneous scanning tunnelling and atomic force microscopy. Nature Communications, 2015, 6, 7265.	5.8	49
22547	Nanoscale control of phonon excitations in graphene. Nature Communications, 2015, 6, 7528.	5.8	48
22548	Single layer of MX₃ (M = Ti, Zr; X = S, Se, Te): a new platform for nano-electronics and optics. Physical Chemistry Chemical Physics, 2015, 17, 18665-18669.	1.3	128
22549	Structural stability and defect energetics of ZnO from diffusion quantum Monte Carlo. Journal of Chemical Physics, 2015, 142, 164705.	1.2	55
22550	Stability and electronic structure of the low-Î£grain boundaries in CdTe: a density functional study. New Journal of Physics, 2015, 17, 013027.	1.2	31
22551	A Multilevel Cell for STT-MRAM Realized by Capping Layer Adjustment. IEEE Transactions on Magnetics, 2015, 51, 1-4.	1.2	14
22552	Electronic properties of semiconducting Ca₂Si silicide: From bulk to nanostructures by means of first principles calculations. Japanese Journal of Applied Physics, 2015, 54, 07JA03.	0.8	13
22553	Cation exchange mediated elimination of the Fe-antisites in the hydrothermal synthesis of LiFePO4. Nano Energy, 2015, 16, 256-267.	8.2	54
22554	Oxygen adsorption on Fe(110) surface revisited. Surface Science, 2015, 637-638, 35-41.	0.8	39
22555	The electronic structure of quasi-free-standing germanene on monolayer MX (M = Ga, In; X = S, Se, Te). Physical Chemistry Chemical Physics, 2015, 17, 19039-19044.	1.3	26
22556	Nature of Acid Sites in Silica-Supported Zirconium Oxide: A Combined Experimental and Periodic DFT Study. Journal of Physical Chemistry C, 2015, 119, 15150-15159.	1.5	22
22557	Probing the Dynamics of the Metallic-to-Semiconducting Structural Phase Transformation in MoS₂ Crystals. Nano Letters, 2015, 15, 5081-5088.	4.5	174
22558	Modulation of the molecular spintronic properties of adsorbed copper corroles. Nature Communications, 2015, 6, 7547.	5.8	40
22559	Probing local site environments and distribution of manganese in SrZrO3:Mn; PL and EPR spectroscopy complimented by DFT calculations. RSC Advances, 2015, 5, 17501-17513.	1.7	51
22560	Magnetic charges and magnetoelectricity in hexagonal rare-earth manganites and ferrites. Physical Review B, 2015, 92, .	1.1	22
22561	Dislocation core reconstruction induced by carbon segregation in bcc iron. Physical Review B, 2015, 91, .	1.1	81
22562	Pseudoelasticity in Fe3Ga with boron-A combined atomisticâ€“micromechanical treatment. International Journal of Plasticity, 2015, 72, 185-199.	4.1	5

#	Article	IF	Citations
22563	Carbon induced magnetism of SnO2 surfaces. Journal of Magnetism and Magnetic Materials, 2015, 394, 280-286.	1.0	2
22564	In Situ-Generated Co⁰-Co₃O₄/N-Doped Carbon Nanotubes Hybrids as Efficient and Chemoselective Catalysts for Hydrogenation of Nitroarenes. ACS Catalysis, 2015, 5, 4783-4789.	5.5	363
22565	Atomic-Scale Interfacial Magnetism in Fe/Graphene Heterojunction. Scientific Reports, 2015, 5, 11911.	1.6	30
22566	High coverage adsorption and co-adsorption of CO and H₂ on Ru(0001) from DFT and thermodynamics. Physical Chemistry Chemical Physics, 2015, 17, 19446-19456.	1.3	50
22567	Enhanced thermoelectric performance of layered SnS crystals: the synergetic effect of temperature and carrier concentration. RSC Advances, 2015, 5, 56382-56390.	1.7	37
22568	Vibrational properties and bonding nature of Sb₂Se₃and their implications for chalcogenide materials. Chemical Science, 2015, 6, 5255-5262.	3.7	89
22569	Magnetism in graphene oxide induced by epoxy groups. Applied Physics Letters, 2015, 106, .	1.5	41
22570	Magnetic evolution and anomalous Wilson transition in diagonal phosphorene nanoribbons driven by strain. Nanotechnology, 2015, 26, 295402.	1.3	5
22571	First-principles investigation of the structural characteristics of LiMO2 cathode materials for lithium secondary batteries. Journal of Molecular Structure, 2015, 1099, 317-322.	1.8	12
22572	Origin of the Formation of Nanoislands on Cobalt Catalysts during Fischerâ€“Tropsch Synthesis. ACS Catalysis, 2015, 5, 4756-4760.	5.5	30
22573	Accelerated materials design of Na_{0.5}Bi_{0.5}TiO₃ oxygen ionic conductors based on first principles calculations. Physical Chemistry Chemical Physics, 2015, 17, 18035-18044.	1.3	104
22574	Compressed sodalite-like MgH₆ as a potential high-temperature superconductor. RSC Advances, 2015, 5, 59292-59296.	1.7	147
22575	Lithium transport through lithium-ion battery cathode coatings. Journal of Materials Chemistry A, 2015, 3, 17248-17272.	5.2	109
22576	Calculation of the energetics of water incorporation in majorite garnet. American Mineralogist, 2015, 100, 1065-1075.	0.9	10
22577	Electronic properties of energy harvesting Cu-chalcogenides: pâ€“d hybridization and d-electron localization. Computational Materials Science, 2015, 108, 239-249.	1.4	49
22578	Synergistic effect of co-alloying elements on site preferences and elastic properties of Ni3Al: A first-principles study. Intermetallics, 2015, 65, 75-80.	1.8	29
22579	Ab-initio study of phase stability, elastic and thermodynamic properties of AlY alloy under pressure. Journal of Alloys and Compounds, 2015, 648, 67-74.	2.8	7
22580	Electro-oxidation of water on hematite: Effects of surface termination and oxygen vacancies investigated by first-principles. Surface Science, 2015, 640, 45-49.	0.8	43

#	Article	IF	Citations
22581	Reconciling the electronic and geometric corrugations of the hexagonal boron nitride and graphene nanomeshes. Surface Science, 2015, 642, L16-L19.	0.8	9
22582	An atomic scale study of ultralow friction between phosphorus-doped nanocrystalline diamond films. Tribology International, 2015, 86, 85-90.	3.0	9
22583	Complexities in the Molecular Spin Crossover Transition. Journal of Physical Chemistry C, 2015, 119, 16293-16302.	1.5	41
22584	Molecular Orientation and Structural Transformations in Phthalic Anhydride Thin Films on MgO(100)/Ag(100). Langmuir, 2015, 31, 7806-7814.	1.6	16
22585	Two-Dimensional Pnictogen Honeycomb Lattice: Structure, On-Site Spin-Orbit Coupling and Spin Polarization. Scientific Reports, 2015, 5, 11512.	1.6	93
22586	Embedded atom model for the liquid Uâ€“10Zr alloy based on density functional theory calculations. RSC Advances, 2015, 5, 61495-61501.	1.7	6
22587	Nature of defects in blue light emitting CaZrO₃: spectroscopic and theoretical study. RSC Advances, 2015, 5, 56526-56533.	1.7	58
22588	Possibility of designing catalysts beyond the traditional volcano curve: a theoretical framework for multi-phase surfaces. Chemical Science, 2015, 6, 5703-5711.	3.7	40
22589	Understanding the stable boron clusters: A bond model and first-principles calculations based on high-throughput screening. Journal of Chemical Physics, 2015, 142, 214307.	1.2	27
22590	First Principles Studies of the Phonon, Polarization, Dielectric and Piezoelectric Responses of Pyrochlore Cd₂Nb₂O₇. Ferroelectrics, 2015, 478, 106-117.	0.3	4
22591	Geometric Stability, Electronic Structure and Reactivity of Pt₄Cluster Supported on Defective Graphene. Integrated Ferroelectrics, 2015, 159, 57-65.	0.3	6
22592	Electronic phase transitions in ultrathin magnetite films. Journal of Physics Condensed Matter, 2015, 27, 293202.	0.7	8
22593	Charge optimized many-body (COMB) potential for Al₂O₃materials, interfaces, and nanostructures. Journal of Physics Condensed Matter, 2015, 27, 305004.	0.7	17
22594	Oxygen Effect on Magnetic Anisotropy Energy of Co Nanowires on Cu(210) Surface - An <i>Ab Initio</i> Study. Solid State Phenomena, 0, 233-234, 530-533.	0.3	0
22595	First-principles investigation on structural and electrochemical properties of NaCoO2 for rechargeable Na-ion batteries. Journal of Central South University, 2015, 22, 2036-2042.	1.2	6
22596	Anomalous structural dynamics in liquid Al80Cu20: An ab initio molecular dynamics study. Acta Materialia, 2015, 97, 75-85.	3.8	62
22597	Predictions on the compositions, structures, and mechanical properties of intermediate phases in binary Mgâ€“X (X = Sn, Y, Sc, Ag) alloys. Computational Materials Science, 2015, 106, 180-187.	1.4	15
22598	Effects of the defects on the half-metallic characters and magnetic properties in double perovskite Pb2FeMoO6. Materials Chemistry and Physics, 2015, 162, 711-723.	2.0	3

#	Article	IF	Citations
22599	Au₁₃: CO Adsorbs, Nanoparticle Responds. Journal of Physical Chemistry C, 2015, 119, 18196-18202.	1.5	15
22600	Rational Design of Pt₃Ni Surface Structures for the Oxygen Reduction Reaction. Journal of Physical Chemistry C, 2015, 119, 17735-17747.	1.5	44
22601	Assessing the Use of BiCuOS for Photovoltaic Application: From DFT to Macroscopic Simulation. Journal of Physical Chemistry C, 2015, 119, 17585-17595.	1.5	31
22602	Electronic Properties of Halogen-Adsorbed Graphene. Journal of Physical Chemistry C, 2015, 119, 17271-17277.	1.5	42
22603	Electron Injection from Copper Diimine Sensitizers into TiO₂: Structural Effects and Their Implications for Solar Energy Conversion Devices. Journal of the American Chemical Society, 2015, 137, 9670-9684.	6.6	60
22604	n-type conversion of SnS by isovalent ion substitution: Geometrical doping as a new doping route. Scientific Reports, 2015, 5, 10428.	1.6	59
22605	Structural, mechanical and electronic properties of Rh2B and RhB2: first-principles calculations. Scientific Reports, 2015, 5, 10500.	1.6	14
22606	Development and applications of the LFDFT: the non-empirical account of ligand field and the simulation of the fâ€“d transitions by density functional theory. Physical Chemistry Chemical Physics, 2015, 17, 18547-18557.	1.3	23
22607	Electronic and magnetic properties of silicon supported organometallic molecular wires: a density functional theory (DFT) study. Nanoscale, 2015, 7, 13734-13746.	2.8	8
22608	Tunable catalytic reactivity of small palladium clusters supported on graphene: a first-principles study. RSC Advances, 2015, 5, 61861-61867.	1.7	9
22609	Hydrogen-bonding-mediated structural stability and electrochemical performance of iron fluoride cathode materials. Journal of Materials Chemistry A, 2015, 3, 16222-16228.	5.2	34
22610	Computational discovery of ferromagnetic semiconducting single-layer<mml:math xmlns:mml="http://www.w3.org/1998/Math/MathML"><mml:msub><mml:mi>CrSnTe</mml:mi><mml:mn>3</mml:mn></mml:msub><i Physical Review B, 2015, 92, .	3.6	212
22611	Comparative DFT-D studies on structural and absorption properties of crystalline 3,3â€²-dinitroamino-4,4â€²-azoxyfurazan, 3,3â€²-dinitro-4,4â€²-azoxyfurazan, and 3,4-bis(3-nitrofurazan-4-yl)furoxan under high pressures. Canadian Journal of Chemistry, 2015, 93, 1191-1198.	0.6	0
22612	Using graphene to control magnetic anisotropy and interaction between supported clusters. New Journal of Physics, 2015, 17, 053052.	1.2	4
22613	Interface Energetics and Charge Carrier Density Amplification by Sn-Doping in LaAlO₃/SrTiO₃ Heterostructure. ACS Applied Materials & Interfaces, 2015, 7, 14294-14302.	4.0	24
22614	Ionic transport in hybrid lead iodide perovskite solar cells. Nature Communications, 2015, 6, 7497.	5.8	2,154
22615	The nontrivial electronic structure of Bi/Sb honeycombs on SiC(0001). New Journal of Physics, 2015, 17, 025005.	1.2	100
22616	First-principles study of structural, elastic, and thermodynamic properties of ZrHf alloy. Chinese Physics B, 2015, 24, 043102.	0.7	6

#	Article	IF	Citations
22617	Electronic Structure of BiFeO₃in Different Crystal Phases. Acta Physica Polonica A, 2015, 127, 266-268.	0.2	8
22618	The first example of a mixed valence ternary compound of silver with random distribution of Ag(<scp>i</scp>) and Ag(<scp>ii</scp>) cations. Dalton Transactions, 2015, 44, 10957-10968.	1.6	20
22619	Calculation of the stability of nonperiodic solids using classical force fields and the method of increments: N₂o as an example. Journal of Computational Chemistry, 2015, 36, 1420-1427.	1.5	5
22620	First-principles study of structural, electronic, and ferroelectric properties of rare-earth-doped BiFeO3. Journal of Materials Science, 2015, 50, 6227-6235.	1.7	35
22621	First-principles calculations of divalent substitution of Ca2+ in tricalcium phosphates. Acta Biomaterialia, 2015, 23, 329-337.	4.1	58
22622	Adsorption mechanisms of lithium oxides (LixO2) on a graphene-based electrode: A density functional theory approach. Applied Surface Science, 2015, 351, 193-202.	3.1	30
22623	Structure, elastic and piezoelectric properties of A 3 BO 7 (A = Ga, Al; B = P, As) compounds: A DFT study. Computational Materials Science, 2015, 106, 1-4.	1.4	8
22624	Hydrogen sorption in the LaNi5-xAlx-H system (0Ââ‰ÂxÂâ‰Â1). Intermetallics, 2015, 62, 7-16.	1.8	25
22625	High pressure phase transitions in scheelite structured fluoride: ErLiF4. Journal of Solid State Chemistry, 2015, 229, 164-172.	1.4	6
22626	Structural distortion and charge redistribution in SrTiO 3 (111) polar surfaces. Vacuum, 2015, 120, 83-88.	1.6	12
22627	In Situ Electrical Conductivity of Li_xMnO₂ Nanowires as a Function of x and Size. Chemistry of Materials, 2015, 27, 3494-3504.	3.2	13
22628	Exploring the Adsorption and the Potential Energy Surface of Acrylonitrile on Cu(100) and Cu(100) Coated with NaCl Layers. Journal of Physical Chemistry C, 2015, 119, 15125-15136.	1.5	6
22629	Dependence of the Structure and Electronic Properties of Dâ€“Aâ€“D Based Molecules on the D/A Ratio and the Strength of the Acceptor Moiety. Journal of Physical Chemistry C, 2015, 119, 14890-14899.	1.5	12
22630	Do â€œHotâ€•Charge-Transfer Excitons Promote Free Carrier Generation in Organic Photovoltaics?. Journal of Physical Chemistry C, 2015, 119, 15028-15035.	1.5	27
22631	Role of the dispersion force in modeling the interfacial properties of molecule-metal interfaces: adsorption of thiophene on copper surfaces. Scientific Reports, 2014, 4, 5036.	1.6	62
22632	Realization of Large-Area Wrinkle-Free Monolayer Graphene Films Transferred to Functional Substrates. Scientific Reports, 2015, 5, 9610.	1.6	22
22633	Covalent nitrophenyl diazonium functionalized silicene for spintronics: a first-principles study. Physical Chemistry Chemical Physics, 2015, 17, 17957-17961.	1.3	13
22634	Shape and composition control of Bi₁₉S₂₇(Br_{3â^'x},I_x) alloyed nanowires: the role of metal ions. Chemical Science, 2015, 6, 4615-4622.	3.7	24

#	Article	IF	Citations
22635	Deep red emission in Eu²⁺-activated Sr₄(PO₄)₂O phosphors for blue-pumped white LEDs. Journal of Materials Chemistry C, 2015, 3, 7356-7362.	2.7	21
22636	Stabilized quasi-Newton optimization of noisy potential energy surfaces. Journal of Chemical Physics, 2015, 142, 034112.	1.2	23
22637	Large perpendicular magnetic anisotropy of single Co atom on MgO monolayer: A first-principles study. Journal of Applied Physics, 2015, 117, 17B316.	1.1	3
22638	Experimental evidence for the formation of CoFe2C phase with colossal magnetocrystalline-anisotropy. Applied Physics Letters, 2015, 106, .	1.5	35
22639	Density functional theory study of the electrochemical interface between a Pt electrode and an aqueous electrolyte using an implicit solvent method. Journal of Chemical Physics, 2015, 142, 234107.	1.2	103
22640	Temperature dependent energy levels of methylammonium lead iodide perovskite. Applied Physics Letters, 2015, 106, .	1.5	159
22641	Stacking dependent electronic properties of the nanofilms composing of super-aligned single-walled carbon nanotubes. Journal Physics D: Applied Physics, 2015, 48, 215307.	1.3	0
22642	Theoretical study of the interaction of electron donor and acceptor molecules with monolayer WS₂. Journal Physics D: Applied Physics, 2015, 48, 285303.	1.3	25
22643	Optical properties of GaAsBi/GaAs quantum wells: Photoreflectance, photoluminescence and time-resolved photoluminescence study. Semiconductor Science and Technology, 2015, 30, 094005.	1.0	30
22644	Ionic compound mediated rearrangement of 3, 4, 9, 10-perylene tetracarboxylic dianhydride molecules on Ag(100) surface. Nanotechnology, 2015, 26, 275603.	1.3	7
22645	Quantum spin Hall effect in two-dimensional transition-metal dichalcogenide haeckelites. Physical Review B, 2015, 91, .	1.1	80
22646	Magnetic coupling in transition-metalâ€“doped LaSiFe _{11.5} TM _{0.5} (TM=Cr, Mn,) Tj ETQq1 1 0.784314 rgB	0.7	9
22647	Interatomic spacing distribution in multicomponent alloys. Acta Materialia, 2015, 97, 156-169.	3.8	92
22648	Van der Waals density functional theory study for bulk solids with BCC, FCC, and diamond structures. Current Applied Physics, 2015, 15, 885-891.	1.1	43
22649	Mechanical properties of ettringite and thaumasiteâ€”DFT and experimental study. Cement and Concrete Research, 2015, 77, 9-15.	4.6	29
22650	Crystallographic information of intermediate phases in binary Mgâ€“ X (X =Sn, Y, Sc, Ag) alloys. Data in Brief, 2015, 4, 190-192.	0.5	3
22651	Equation of state and electronic properties of EuVO4: A high-pressure experimental and computational study. Journal of Alloys and Compounds, 2015, 648, 1005-1016.	2.8	17
22652	The solubility of cerium in La2Ti2O7 by DFTÂ+ÂU calculations. Journal of Alloys and Compounds, 2015, 648, 609-614.	2.8	6

#	Article	IF	Citations
22653	First-principles study of native point defects and diffusion behaviors of helium in zirconium carbide. Journal of Nuclear Materials, 2015, 465, 161-166.	1.3	26
22654	Unique adsorption behaviors of carboxylic acids at rutile TiO2(110). Surface Science, 2015, 641, 82-90.	0.8	17
22655	Thin-Film Preparation and Characterization of Cs₃Sb₂I₉: A Lead-Free Layered Perovskite Semiconductor. Chemistry of Materials, 2015, 27, 5622-5632.	3.2	653
22656	Influence of Clusterâ€“Support Interactions on Reactivity of Size-Selected Nb_xO_y Clusters. Journal of Physical Chemistry C, 2015, 119, 14756-14768.	1.5	29
22657	Exploring the Self-Assembly Behaviors of an Organic Molecule Functionalized by Terminal Alkyne and Aldehyde Groups on Au(111). Journal of Physical Chemistry C, 2015, 119, 12935-12940.	1.5	6
22658	Thermodynamic and Kinetic Origins of Lithiation-Induced Amorphous-to-Crystalline Phase Transition of Phosphorus. Journal of Physical Chemistry C, 2015, 119, 12130-12137.	1.5	25
22659	Molecular-Level Details about Liquid H₂O Interactions with CO and Sugar Alcohol Adsorbates on Pt(111) Calculated Using Density Functional Theory and Molecular Dynamics. Journal of Physical Chemistry C, 2015, 119, 13642-13651.	1.5	44
22660	Hydrogen Activation on the Promoted and Unpromoted ReS2 (001) Surfaces under the Sulfidation Conditions: A First-Principles Study. Journal of Physical Chemistry C, 2015, 119, 17092-17101.	1.5	12
22661	The surface structure of silver-coated gold nanocrystals and its influence on shape control. Nature Communications, 2015, 6, 7664.	5.8	53
22662	The dipole moment of the spin density as a local indicator for phase transitions. Scientific Reports, 2014, 4, 5760.	1.6	20
22663	Length-dependent rectification and negative differential resistance in heterometallic n-alkanedithiol junctions. RSC Advances, 2015, 5, 13917-13922.	1.7	4
22664	Engineering the electronic bandgaps and band edge positions in carbon-substituted 2D boron nitride: a first-principles investigation. Physical Chemistry Chemical Physics, 2015, 17, 13547-13552.	1.3	35
22665	Molecular charge transfer via Ï€â€“Ï€ interaction: an effective approach to realize the half-metallicity and spin-gapless-semiconductor in zigzag graphene nanoribbon. RSC Advances, 2015, 5, 53003-53011.	1.7	11
22666	First principles study of ruthenium(<scp>ii</scp>) sensitizer adsorption on anatase TiO₂ (001) surface. RSC Advances, 2015, 5, 60230-60236.	1.7	7
22667	Structure imaging and vanadium substitution in cubic TiCr₂Laves phase. Philosophical Magazine, 2015, 95, 2403-2426.	0.7	9
22668	A first-principles study of oxygen vacancy induced changes in structural, electronic and magnetic properties of La2/3Sr1/3MnO3. Journal of Alloys and Compounds, 2015, 649, 973-980.	2.8	13
22669	Photocatalytic H2 production from spinels ZnGa2â^'Cr O4 (0â‰¤xâ‰¤2) solid solutions. Journal of Solid State Chemistry, 2015, 230, 95-101.	1.4	38
22670	First-principles investigation of intrinsic dielectric response in Ba(Bâ€²1/3Bâ€³2/3)O3 with Bâ€² as transition metal cations. Materials Chemistry and Physics, 2015, 159, 6-9.	2.0	3

#	Article	IF	Citations
22671	Reducing Systematic Errors in Oxide Species with Density Functional Theory Calculations. Journal of Physical Chemistry C, 2015, 119, 17596-17601.	1.5	29
22672	Interfacial Adsorption and Redox Coupling of Li₄Ti₅O₁₂ with Nanographene for High-Rate Lithium Storage. ACS Applied Materials & Interfaces, 2015, 7, 16565-16572.	4.0	32
22673	Zr5Sb3â^'xRux, a new superconductor in the W5Si3 structure type. Journal of Materials Chemistry C, 2015, 3, 8235-8240.	2.7	13
22674	Stacking fault energy, yield stress anomaly, and twinnability of Ni ₃ Al: A first principles study. Chinese Physics B, 2015, 24, 077102.	0.7	12
22675	Negative thermal expansion in isostructural cubic ReO 3 and ScF 3 : A comparative study. Computational Materials Science, 2015, 107, 157-162.	1.4	33
22676	Shedding Light on Aging of N-Doped Titania Photocatalysts. Journal of Physical Chemistry C, 2015, 119, 18663-18670.	1.5	19
22677	Ultrathin Ti-Silicate Film on a Ru(0001) Surface. Journal of Physical Chemistry C, 2015, 119, 15443-15448.	1.5	17
22678	How does the multiple constituent affect the carrier generation and charge transport in multicomponent TCOs of Inâ€“Znâ€“Sn oxide. Journal of Materials Chemistry C, 2015, 3, 7727-7737.	2.7	15
22679	The possibilities to lower the stacking fault energies of aluminum materials investigated by first-principles energy calculations. Computational Materials Science, 2015, 108, 136-146.	1.4	36
22680	Al3Pd2, a novel intermetallic compound: A first-principles study. Journal of Alloys and Compounds, 2015, 649, 54-61.	2.8	6
22681	Ab initio study of hydrogen on beryllium surfaces. Surface Science, 2015, 641, 198-203.	0.8	8
22682	Carbyne Fiber Synthesis within Evaporating Metallic Liquid Carbon. Journal of Physical Chemistry C, 2015, 119, 21605-21611.	1.5	32
22683	Reactivity of Perovskites with Water: Role of Hydroxylation in Wetting and Implications for Oxygen Electrocatalysis. Journal of Physical Chemistry C, 2015, 119, 18504-18512.	1.5	88
22684	Toggling the Local Electric Field with an Embedded Adatom Switch. Nano Letters, 2015, 15, 5564-5568.	4.5	5
22685	Nano-sized Superlattice Clusters Created by Oxygen Ordering in Mechanically Alloyed Fe Alloys. Scientific Reports, 2015, 5, 11772.	1.6	11
22686	Insights into the growth of bismuth nanoparticles on 2D structured BiOCl photocatalysts: an in situ TEM investigation. Dalton Transactions, 2015, 44, 15888-15896.	1.6	27
22687	Density functional theory calculations of magnetocrystalline anisotropy energies for () Tj ETQq0 0 0 rgBT /Overlock 10 Tf 50 107 Td (Fe< 2015, 27, 266002.	0.7	11
22688	A first-principles investigation of various gas (CO, H₂O, NO, and O₂) absorptions on a WS₂monolayer: stability and electronic properties. Journal of Physics Condensed Matter, 2015, 27, 305005.	0.7	80

#	Article	IF	Citations
22689	Ab-Initio Study of the Role of Mg₂Si and Al₂CuMg Phases in Electrochemical Corrosion of Al Alloys. Journal of the Electrochemical Society, 2015, 162, C503-C508.	1.3	24
22690	Geometrical structures, and electronic and transport properties of a novel two-dimensional Î²-GaS transparent conductor. Nano Research, 2015, 8, 3177-3185.	5.8	3
22691	Influence of one CO molecule on structural and electronic properties of monatomic Cu chain. Physica E: Low-Dimensional Systems and Nanostructures, 2015, 73, 89-95.	1.3	1
22692	First principles modeling of Ag adsorption on the LaMnO3 (001) surfaces. Solid State Ionics, 2015, 273, 46-50.	1.3	1
22693	Trends in Syntheses, Structures, and Properties for Three Series of Ammine Rare-Earth Metal Borohydrides, M(BH₄)₃Â·nNH₃ (M = Y, Gd, and Dy). Inorganic Chemistry, 2015, 54, 7402-7414.	1.9	41
22694	Theoretical and Experimental Studies of the Dechlorination Mechanism of Carbon Tetrachloride on a Vivianite Ferrous Phosphate Surface. Journal of Physical Chemistry A, 2015, 119, 5714-5722.	1.1	14
22695	Ab initio GGA+U study of oxygen evolution and oxygen reduction electrocatalysis on the (001) surfaces of lanthanum transition metal perovskites LaBO₃(B = Cr, Mn, Fe, Co and Ni). Physical Chemistry Chemical Physics, 2015, 17, 21643-21663.	1.3	98
22696	Magnetic properties of 2D nickel nanostrips: structure dependent magnetism and Stoner criterion. Journal of Physics Condensed Matter, 2015, 27, 316002.	0.7	1
22697	Complementary ab initio and X-ray nanodiffraction studies of Ta2O5. Acta Materialia, 2015, 83, 276-284.	3.8	24
22698	Thermodynamic modelling of the general NiAs-type structure: A study of first principle energies of formation for binary Ni-containing B8 compounds. Calphad: Computer Coupling of Phase Diagrams and Thermochemistry, 2015, 50, 174-181.	0.7	7
22699	New bismuth borophosphate Bi4BPO10: Synthesis, crystal structure, optical and band structure analysis. Materials Chemistry and Physics, 2015, 163, 286-292.	2.0	3
22700	Stable ScS2 nanostructures with tunable electronic and magnetic properties. Solid State Communications, 2015, 220, 12-16.	0.9	12
22701	The Electronic Structure and Bonding of Acetylene on PdGa(110). Journal of Physical Chemistry C, 2015, 119, 18229-18238.	1.5	15
22702	DFT+U Study of the Adsorption and Oxidation of an Iron Oxide Cluster on CeO₂ Support. Journal of Physical Chemistry C, 2015, 119, 17202-17208.	1.5	13
22703	Tailoring low-dimensional structures of bismuth on monolayer epitaxial graphene. Scientific Reports, 2015, 5, 11623.	1.6	18
22704	Thermal conductivity in PbTe from first principles. Physical Review B, 2015, 91, .	1.1	98
22705	CO Oxidation on Gold-Supported Iron Oxides: New Insights into Strong Oxideâ€“Metal Interactions. Journal of Physical Chemistry C, 2015, 119, 16614-16622.	1.5	62
22706	Elastic constants of random solid solutions by SQS and CPA approaches: the case of fcc Ti-Al. Journal of Physics Condensed Matter, 2015, 27, 315702.	0.7	33

#	Article	IF	Citations
22707	Platinum-based nanocages with subnanometer-thick walls and well-defined, controllable facets. Science, 2015, 349, 412-416.	6.0	854
22708	Three dimensional graphdiyne polymers with tunable band gaps. Carbon, 2015, 91, 518-526.	5.4	35
22709	Ab initio and empirical modeling of lithium atoms penetration into silicon. Computational Materials Science, 2015, 109, 76-83.	1.4	3
22710	Ab initio study of La 10â^'x Sr x (Si,Ge) 6 O 27â^'0.5x apatite for SOFC electrolyte. Computational Materials Science, 2015, 109, 25-33.	1.4	4
22711	Hybrid functional studies on the electronic properties of ultrathin black phosphorus under normal strain. Computational Materials Science, 2015, 109, 20-24.	1.4	22
22712	Electronic and transmission properties of magnetotunnel junctions of cobalt/iron intercalated bilayer two dimensional sheets. Physics Letters, Section A: General, Atomic and Solid State Physics, 2015, 379, 2661-2666.	0.9	1
22713	Probing the Protonation State and the Redox-Active Sites of Pendant Base Iron(II) and Zinc(II) Pyridinediimine Complexes. Inorganic Chemistry, 2015, 54, 7239-7248.	1.9	17
22714	Mechanistic Study of Carbon Monoxide Methanation over Pure and Rhodium- or Ruthenium-Doped Nickel Catalysts. Journal of Physical Chemistry C, 2015, 119, 16537-16551.	1.5	44
22715	Hydrogen Abstraction Energies and Ammonia Binding to BEA, ZSM-5, and Î±-Quartz Doped with Al, Sc, B, or Ga. Journal of Physical Chemistry C, 2015, 119, 16106-16114.	1.5	11
22716	Atomic-Scale View of VO_Xâ€“WO_X Coreduction on the Î±-Al₂O₃ (0001) Surface. Journal of Physical Chemistry C, 2015, 119, 16179-16187.	1.5	9
22717	Atomic Level Distributed Strain within Graphene Divacancies from Bond Rotations. ACS Nano, 2015, 9, 8599-8608.	7.3	21
22718	Origin of spin gapless semiconductor behavior in CoFeCrGa: Theory and Experiment. Physical Review B, 2015, 92, .	1.1	130
22719	Ab initiocalculation of the ion feature in x-ray Thomson scattering. Physical Review E, 2015, 92, 013103.	0.8	30
22720	The effect of cluster size on the optical band gap energy of Zn-based metalâ€“organic frameworks. Dalton Transactions, 2015, 44, 13464-13468.	1.6	6
22721	Structural and electronic properties of cubic KNbO3 (001) surfaces: A first-principles study. Applied Surface Science, 2015, 351, 558-564.	3.1	14
22722	The role of the defect on the adsorption and dissociation of water on graphitic carbon nitride. Applied Surface Science, 2015, 358, 363-369.	3.1	28
22723	Thermodynamically self-consistent method to predict thermophysical properties of ionic oxides. Computational Materials Science, 2015, 108, 17-26.	1.4	20
22724	Electronic structures and thermoelectric properties of La or Ce-doped Bi2Te3 alloys from first principles calculations. Journal of Physics and Chemistry of Solids, 2015, 85, 239-244.	1.9	11

#	Article	IF	Citations
22725	Important Role of Functional Groups for Sodium Ion Intercalation in Expanded Graphite. Chemistry of Materials, 2015, 27, 5402-5406.	3.2	79
22726	Theoretical and Experimental Study of the Crystal Structures, Lattice Vibrations, and Band Structures of Monazite-Type PbCrO₄, PbSeO₄, SrCrO₄, and SrSeO₄. Inorganic Chemistry, 2015, 54, 7524-7535.	1.9	90
22727	Adsorption and Reaction of C₂H₄ and O₂ on a Nanosized Gold Cluster: A Computational Study. Journal of Physical Chemistry A, 2015, 119, 8547-8555.	1.1	15
22728	Synthesis and Characterization of Nanobuilding Blocks [o-RStyrPhSiO_{1.5}]_{10,12} (R = Me, MeO, NBoc, and CN). Unexpected Photophysical Properties Arising from Apparent Asymmetric Cage Functionalization as Supported by Modeling Studies. Journal of Physical Chemistry C, 2015, 119, 15846-15858.	1.5	10
22729	Highly Sensitive and Selective Gas Detection Based on Silicene. Journal of Physical Chemistry C, 2015, 119, 16934-16940.	1.5	174
22730	Cooperative Reformable Channel System with Unique Recognition of Gas Molecules in a Zeolitic Imidazolate Framework with Multilevel Flexible Ligands. Journal of Physical Chemistry C, 2015, 119, 16762-16768.	1.5	9
22731	Passivation of InGaAs(001)-(2 Ã— 4) by Self-Limiting Chemical Vapor Deposition of a Silicon Hydride Control Layer. Journal of the American Chemical Society, 2015, 137, 8526-8533.	6.6	8
22732	Probing ketoâ€“enol tautomerism using photoelectron spectroscopy. Physical Chemistry Chemical Physics, 2015, 17, 19991-19996.	1.3	5
22733	Effect of annealing in oxygen on alloy structures of Pdâ€“Au bimetallic model catalysts. Physical Chemistry Chemical Physics, 2015, 17, 20588-20596.	1.3	23
22734	Super-saturated hydrogen effects on radiation damages in tungsten under the high-flux divertor plasma irradiation. Nuclear Fusion, 2015, 55, 083019.	1.6	35
22735	Catalytic effect of Ti and Ni on dehydrogenation of AlH3: A first principles investigation. Applied Surface Science, 2015, 347, 139-146.	3.1	7
22736	Theoretical investigation on electronic properties and carrier mobilities of armchair graphyne nanoribbons. Chemical Physics, 2015, 457, 114-121.	0.9	11
22737	Understanding the selectivity of methanol steam reforming on the (1 1 1) surfaces of NiZn, PdZn and PtZn: Insights from DFT. Journal of Catalysis, 2015, 330, 6-18.	3.1	35
22738	Reaction path analysis for 1-butanol dehydration in H-ZSM-5 zeolite: Ab initio and microkinetic modeling. Journal of Catalysis, 2015, 330, 28-45.	3.1	65
22739	Magnetism and electronic structure in La-doped CoO: A first-principles study. Physica E: Low-Dimensional Systems and Nanostructures, 2015, 74, 226-232.	1.3	2
22740	Lightweight superhard carbon allotropes obtained by transversely compressing the smallest CNTs under high pressure. Physics Letters, Section A: General, Atomic and Solid State Physics, 2015, 379, 2116-2119.	0.9	13
22741	Quantum Spin-Quantum Anomalous Hall Insulators and Topological Transitions in Functionalized Sb(111) Monolayers. Nano Letters, 2015, 15, 5149-5155.	4.5	52
22742	First principles study on stability and hydrogen adsorption properties of Mg/Ti interface. Physical Chemistry Chemical Physics, 2015, 17, 16594-16600.	1.3	13

#	Article	IF	Citations
22743	Merging open metal sites and Lewis basic sites in a NbO-type metalâ€“organic framework for improved C₂H₂/CH₄ and CO₂/CH₄ separation. Dalton Transactions, 2015, 44, 14823-14829.	1.6	39
22744	Generalized evolutionary metadynamics for sampling the energy landscapes and its applications. Physical Review B, 2015, 92, .	1.1	33
22745	Low-energy tetrahedral polymorphs of carbon, silicon, and germanium. Physical Review B, 2015, 91, .	1.1	90
22746	Density Functional Theory and Conductivity Studies of Boron-Based Anion Receptors. Journal of the Electrochemical Society, 2015, 162, A1927-A1934.	1.3	8
22747	Insight into structural, mechanical, electronic and thermodynamic properties of intermetallic phases in Zrâ€“Sn system from first-principles calculations. Journal of Physics and Chemistry of Solids, 2015, 86, 177-185.	1.9	21
22748	Photocatalytic Hydrogen Production over Chromium Doped Layered Perovskite Sr₂TiO₄. Inorganic Chemistry, 2015, 54, 7445-7453.	1.9	84
22749	Novel Superconducting Phases of HCl and HBr under High Pressure: An Ab Initio Study. Journal of Physical Chemistry C, 2015, 119, 17039-17043.	1.5	18
22750	Reaction of Phthalocyanines with Graphene on Ir(111). Journal of the American Chemical Society, 2015, 137, 9452-9458.	6.6	40
22751	Relationship between crystal structure and thermo-mechanical properties of kaolinite clay: beyond standard density functional theory. Dalton Transactions, 2015, 44, 12550-12560.	1.6	40
22752	Cation ordering induced semiconductor to half metal transition in La₂NiCrO₆. RSC Advances, 2015, 5, 50913-50918.	1.7	9
22753	Stability, elastic properties, and electronic structure of germanane nanoribbons. Journal of Physics Condensed Matter, 2015, 27, 245303.	0.7	4
22754	Development of a tight-binding model for Cu and its application to a Cu-heat-sink under irradiation. Journal of Materials Science, 2015, 50, 5684-5693.	1.7	17
22755	Optimal thermoelectric figure of merit of Si/Ge core-shell nanowires. Nano Research, 2015, 8, 2611-2619.	5.8	19
22756	Coverage Dependent Water Dissociative Adsorption on the Clean and O-Precovered Fe(111) Surfaces. Journal of Physical Chemistry C, 2015, 119, 11714-11724.	1.5	27
22757	Epitaxial phases of<mml:math xmlns:mml="http://www.w3.org/1998/Math/MathML"><mml:msub><mml:mtext>BiMnO</mml:mtext><mml:mn>3</mml:mn></mml:msub></mml:math> first principles. Physical Review B, 2015, 91, .	k	27
22758	Air Stable Doping and Intrinsic Mobility Enhancement in Monolayer Molybdenum Disulfide by Amorphous Titanium Suboxide Encapsulation. Nano Letters, 2015, 15, 4329-4336.	4.5	167
22759	Structural and electronic investigations of PbTa4O11 and BiTa7O19 constructed from Î±-U3O8 types of layers. Journal of Solid State Chemistry, 2015, 229, 310-321.	1.4	8
22760	EQeq+C: An Empirical Bond-Order-Corrected Extended Charge Equilibration Method. Journal of Chemical Theory and Computation, 2015, 11, 3364-3374.	2.3	15

#	Article	IF	Citations
22761	Nature of Nitrogen-Doped Anatase TiO₂ and the Origin of Its Visible-Light Activity. Journal of Physical Chemistry C, 2015, 119, 15890-15895.	1.5	32
22762	Combining density functional and incremental post-Hartree-Fock approaches for van der Waals dominated adsorbate-surface interactions: Ag2/graphene. Journal of Chemical Physics, 2015, 143, 102804.	1.2	34
22763	Electronic and Optical Properties of Oxides Nanostructures by First-Principles Approaches. , 2015, , 1-15.		0
22764	Surface states of FeF2 (110) and its uncompensated magnetization. Journal of Magnetism and Magnetic Materials, 2015, 393, 226-232.	1.0	4
22765	Extremely large magnetoresistance and ultrahigh mobility in the topological Weyl semimetal candidate NbP. Nature Physics, 2015, 11, 645-649.	6.5	893
22766	Study of temperature and ligand flexibility effects on coordination polymer formation from cyclobutanetetracarboxylic acid. CrystEngComm, 2015, 17, 5921-5931.	1.3	11
22767	Mechanical and dynamical stability of TiAsTe compound from ab initio calculations. Philosophical Magazine, 2015, 95, 2294-2305.	0.7	17
22768	Effects of stacking sequence and short-range ordering of solute atoms on elastic properties of Mgâ€“Znâ€“Y alloys with long-period stacking ordered structures. Acta Materialia, 2015, 96, 170-188.	3.8	42
22769	Structural and electronic properties of SimCn graphyne-like monolayers. Computational Materials Science, 2015, 107, 8-14.	1.4	12
22770	Pressure-induced structural phase transition in iron phosphide. Computational Materials Science, 2015, 107, 204-209.	1.4	7
22771	Computational study of the adsorption of benzene and hydrogen onÂpalladiumâ€“iridium nanoalloys. Journal of Organometallic Chemistry, 2015, 792, 190-193.	0.8	10
22772	Epitaxial ZrSe2/MoSe2 semiconductor v.d. Waals heterostructures on wide band gap AlN substrates. Microelectronic Engineering, 2015, 147, 269-272.	1.1	42
22773	Magnetic properties of two nearest Cu-doped monolayer WS 2 : A first-principles study. Solid State Communications, 2015, 217, 66-69.	0.9	29
22774	Reaction pathways of model compounds of biomass-derived oxygenates on Fe/Ni bimetallic surfaces. Surface Science, 2015, 640, 159-164.	0.8	10
22775	Trends in the Adsorption and Growth Morphology of Metals on the MoS₂(001) Surface. Crystal Growth and Design, 2015, 15, 3190-3200.	1.4	46
22776	Classical and Quantum Modeling of Li and Na Diffusion in FePO₄. Journal of Physical Chemistry C, 2015, 119, 15801-15809.	1.5	29
22777	A Comparative First-Principles Study on Sodiation of Silicon, Germanium, and Tin for Sodium-Ion Batteries. Journal of Physical Chemistry C, 2015, 119, 14843-14850.	1.5	95
22778	Single-Atom Alloy Pdâ€“Ag Catalyst for Selective Hydrogenation of Acrolein. Journal of Physical Chemistry C, 2015, 119, 18140-18148.	1.5	150

#	Article	IF	Citations
22779	Preferential Adsorption of TiO₂ Nanostructures on Functionalized Single-Walled Carbon Nanotubes: A DFT Study. Journal of Physical Chemistry C, 2015, 119, 15085-15093.	1.5	18
22780	Gold and Silver Clusters on TiO₂ and ZrO₂ (101) Surfaces: Role of Dispersion Forces. Journal of Physical Chemistry C, 2015, 119, 15381-15389.	1.5	70
22781	Energy Barrier Reduction for the Double Proton-Transfer Reaction in Guanineâ€“Cytosine DNA Base Pair on a Gold Surface. Journal of Physical Chemistry C, 2015, 119, 15735-15741.	1.5	14
22782	CO Oxidation over Strained Pt(100) Surface: A DFT Study. Journal of Physical Chemistry C, 2015, 119, 15500-15505.	1.5	48
22783	Structure and Reactivity of Alucone-Coated Films on Si and Li_xSi_y Surfaces. ACS Applied Materials & Interfaces, 2015, 7, 11948-11955.	4.0	39
22784	Design of Highly Active Perovskite Oxides for Oxygen Evolution Reaction by Combining Experimental and ab Initio Studies. ACS Catalysis, 2015, 5, 4337-4344.	5.5	107
22785	Mechanistic Investigation of Isopropanol Conversion on Alumina Catalysts: Location of Active Sites for Alkene/Ether Production. ACS Catalysis, 2015, 5, 4423-4437.	5.5	92
22786	Atomic picture of elastic deformation in a metallic glass. Scientific Reports, 2015, 5, 9184.	1.6	22
22787	Spin Polarization Inversion at Benzene-Absorbed Fe4N Surface. Scientific Reports, 2015, 5, 10602.	1.6	21
22788	Adsorption of uranyl on hydroxylated Î±-SiO₂(001): a first-principle study. Dalton Transactions, 2015, 44, 1646-1654.	1.6	23
22789	Stability and ionic mobility in argyrodite-related lithium-ion solid electrolytes. Physical Chemistry Chemical Physics, 2015, 17, 16494-16506.	1.3	109
22790	The synergistic effect between effective mass and built-in electric field for the transfer of carriers in nonlinear optical materials. Physical Chemistry Chemical Physics, 2015, 17, 17710-17717.	1.3	17
22791	Thermodynamics of technetium: reconciling theory and experiment using density functional perturbation analysis. Dalton Transactions, 2015, 44, 12735-12742.	1.6	11
22792	Structure and magnetic properties of open-ended silicon carbide nanotubes. RSC Advances, 2015, 5, 52754-52758.	1.7	2
22793	Ten-fold coordinated polymorph and metallization of TiO₂under high pressure. RSC Advances, 2015, 5, 54253-54257.	1.7	16
22794	CO₂ induced phase transitions in diamine-appended metalâ€“organic frameworks. Chemical Science, 2015, 6, 5177-5185.	3.7	45
22795	Characterization of adsorbed water in MIL-53(Al) by FTIR spectroscopy and ab-initio calculations. Journal of Chemical Physics, 2015, 142, 124702.	1.2	47
22796	MoS2 on an amorphous HfO2 surface: An ab initio investigation. Journal of Applied Physics, 2015, 117, 194303.	1.1	11

#	Article	IF	Citations
22797	Localized states induced by an oxygen vacancy in rutile TiO2. Journal of Applied Physics, 2015, 117, .	1.1	34
22798	Hydrogen and fluorine co-decorated silicene: A first principles study of piezoelectric properties. Journal of Applied Physics, 2015, 117, .	1.1	29
22799	Influence of support morphology on the bonding of molecules to nanoparticles. Proceedings of the National Academy of Sciences of the United States of America, 2015, 112, 7903-7908.	3.3	15
22800	On Theoretical Study of Magnetic Behavior of Diamond Doped with Transition Metals. Acta Physica Polonica A, 2015, 127, 823-826.	0.2	0
22801	Crossover between silicene and ultra-thin Si atomic layers on Ag(111) surfaces. New Journal of Physics, 2015, 17, 045028.	1.2	14
22802	Detection of concealed targets using spintronic microwave sensor. , 2015, , .		0
22803	Experimental and Theoretical Investigations on Structural and Vibrational Properties of Melilite-Type Sr₂ZnGe₂O₇ at High Pressure and Delineation of a High-Pressure Monoclinic Phase. Inorganic Chemistry, 2015, 54, 6594-6605.	1.9	23
22804	Superconductivity in Hf₅Sb_{3â€“x}Ru_x: Are Ru and Sb a Critical Charge-Transfer Pair for Superconductivity?. Chemistry of Materials, 2015, 27, 4511-4514.	3.2	17
22805	Inapplicability of Martin transformation to elastic constants of zinc-blende and wurtzite group-III nitride alloys. Journal of Applied Physics, 2015, 117, 105703.	1.1	16
22806	K2Hg2Se3: Large-Scale Synthesis of a Photoconductor Material Prototype with a Columnar Polyanionic Substructure. Chemistry of Materials, 2015, 27, 4114-4118.	3.2	18
22807	Predicting a Ferrimagnetic Phase of<mml:math xmlns:mml="http://www.w3.org/1998/Math/MathML" display="inline"><mml:mrow><mml:msub><mml:mrow><mml:mi>Zn</mml:mi></mml:mrow><mml:mrow><mml:mn>2</mml:mn></mml:mrow></mml:msub><mml:mn></mml:mn></mml:mrow></mml:math> Strong Magnetoelectric Coupling. Physical Review Letters, 2015, 114, 147204.	2.9	73
22808	Strong Asymmetric Charge Carrier Dependence in Inelastic Electron Tunneling Spectroscopy of Graphene Phonons. Physical Review Letters, 2015, 114, 245502.	2.9	41
22809	Materials Design On-the-Fly. Journal of Chemical Theory and Computation, 2015, 11, 3955-3960.	2.3	25
22810	Versatile Single-Layer Sodium Phosphidostannate(II): Strain-Tunable Electronic Structure, Excellent Mechanical Flexibility, and an Ideal Gap for Photovoltaics. Journal of Physical Chemistry Letters, 2015, 6, 2682-2687.	2.1	60
22811	Thermodynamic modeling of Crâ€“Nb and Zrâ€“Cr with extension to the ternary Zrâ€“Nbâ€“Cr system. Calphad: Computer Coupling of Phase Diagrams and Thermochemistry, 2015, 50, 134-143.	0.7	33
22812	Targeted Single-Site MOF Node Modification: Trivalent Metal Loading via Atomic Layer Deposition. Chemistry of Materials, 2015, 27, 4772-4778.	3.2	116
22813	Computational Study of Structure and Reactivity of Oligomeric Vanadia Clusters Supported on Anatase and Rutile TiO₂ Surfaces. Journal of Physical Chemistry C, 2015, 119, 15160-15167.	1.5	20
22814	Comparing Quasiparticle H₂O Level Alignment on Anatase and Rutile TiO₂. ACS Catalysis, 2015, 5, 4242-4254.	5.5	50

#	Article	IF	Citations
22815	Palladiumâ€“platinum core-shell icosahedra with substantially enhanced activity and durability towards oxygen reduction. Nature Communications, 2015, 6, 7594.	5.8	440
22816	Vertical twinning of the Dirac cone at the interface between topological insulators and semiconductors. Nature Communications, 2015, 6, 7630.	5.8	26
22817	Pressure and electric field-induced metallization in the phase-engineered ZrX₂(X = S, Se,) Tj ETQq0 0 0 rgBT /Overlock 10 T	1.5	36
22818	A porous nitrogen and phosphorous dual doped graphene blocking layer for high performance Liâ€“S batteries. Journal of Materials Chemistry A, 2015, 3, 16670-16678.	5.2	241
22819	Raman scattering investigation of large positive magnetoresistance material WTe2. Applied Physics Letters, 2015, 106, 081906.	1.5	66
22820	Adsorption of glycine on diamond (001): Role of bond angle of carbon atoms. Chinese Physics B, 2015, 24, 056803.	0.7	1
22821	Device Performance of the Mott Insulator<mml:math xmlns:mml="http://www.w3.org/1998/Math/MathML" display="inline"><mml:mrow><mml:msub><mml:mrow><mml:mi>LaVO</mml:mi></mml:mrow><mml:mrow><mml:mn>3</mml:mn></ a Photovoltaic Material. Physical Review Applied, 2015, 3, .	1.5	73
22822	Compositional dependence of structures of NiTi martensite from first principles. Acta Materialia, 2015, 95, 184-191.	3.8	10
22823	Heterogeneous nucleation at inoculant particles in a glass forming alloy: An ab initio molecular dynamics investigation of interfacial properties and local chemical bonding. Computational Materials Science, 2015, 108, 94-102.	1.4	10
22824	First principles investigation of the crystal and electronic structures of CeNCl and â€œCeNFâ€. Solid State Sciences, 2015, 48, 1-6.	1.5	2
22825	Selective Crystal Growth and Structural, Optical, and Electronic Studies of Mn3Ta2O8. Inorganic Chemistry, 2015, 54, 6513-6519.	1.9	6
22826	First-Principles Study on Structural, Electronic, and Spectroscopic Properties of Î³-Ca₂SiO₄:Ce³⁺ Phosphors. Journal of Physical Chemistry A, 2015, 119, 8031-8039.	1.1	23
22827	Thiolate-Bonded Self-Assembled Monolayers on Ni(111): Bonding Strength, Structure, and Stability. Journal of Physical Chemistry C, 2015, 119, 15455-15468.	1.5	21
22828	Sodium Ion Diffusion and Voltage Trends in Phosphates Na₄M₃(PO₄)₂P₂O₇ (M = Fe,) Tj ETQq1 1 0.784314 rg	1.5	126
22829	Interlayer orientation-dependent light absorption and emission in monolayer semiconductor stacks. Nature Communications, 2015, 6, 7372.	5.8	154
22830	Electronic and magnetism properties of two-dimensional stacked nickel hydroxides and nitrides. Scientific Reports, 2015, 5, 11656.	1.6	10
22831	Theoretical investigation of H₂S removal on Î³-Al₂O₃ surfaces of different hydroxyl coverage. RSC Advances, 2015, 5, 55372-55382.	1.7	11
22832	Intense red emitting monoclinic LaPO₄:Eu³⁺ nanoparticles: hostâ€“dopant energy transfer dynamics and photoluminescence properties. RSC Advances, 2015, 5, 58832-58842.	1.7	81

#	Article	IF	Citations
22833	Ab initio calculation of thermodynamic, transport, and optical properties of CH2 plastics. Physics of Plasmas, 2015, 22, 053303.	0.7	14
22834	Mechanism of charge transfer and its impacts on Fermi-level pinning for gas molecules adsorbed on monolayer WS2. Journal of Chemical Physics, 2015, 142, 214704.	1.2	124
22835	Modeling the surface photovoltage of silicon slabs with varying thickness. Journal of Physics Condensed Matter, 2015, 27, 134204.	0.7	9
22836	p-type conduction in Zn-ion implanted InN films. Journal Physics D: Applied Physics, 2015, 48, 215102.	1.3	2
22837	Revealing the Atomic Site-Dependent<mml:math xmlns:mml="http://www.w3.org/1998/Math/MathML" display="inline"><mml:mrow><mml:mi>g</mml:mi></mml:mrow></mml:math>Factor within a Single Magnetic Molecule via the Extended Kondo Effect. Physical Review Letters, 2015, 114, 126601.	2.9	26
22838	Bulk moduli of the silicon and germanium fullerenes Si60 and Ge60. Physics of the Solid State, 2015, 57, 1073-1078.	0.2	1
22839	Approximations to the Ground State. Springer Theses, 2015, , 19-46.	0.0	0
22840	Electronic and magnetic structures of ternary iron telluride KFe2Te2. Frontiers of Physics, 2015, 10, 1-6.	2.4	5
22841	The Ab Initio Treatment of High-Pressure and High-Temperature Mineral Properties and Behavior. , 2015, , 369-392.		2
22842	A new class of high strength high temperature Cobalt based Î³â€“Î³â€² Coâ€“Moâ€“Al alloys stabilized with Ta addition. Acta Materialia, 2015, 97, 29-40.	3.8	151
22843	Pressure-induced phase transition of zinc nitride chlorine. Computational Materials Science, 2015, 106, 175-179.	1.4	0
22844	Theoretical investigation of adsorption and dissociation of H2 on cluster Al6Si. International Journal of Hydrogen Energy, 2015, 40, 8911-8916.	3.8	23
22845	The structural, electronic and magnetic properties of Ga8â^'Mn As8 clusters. Journal of Magnetism and Magnetic Materials, 2015, 384, 155-159.	1.0	2
22846	Integrated study of first principles calculations and experimental measurements for Li-ionic conductivity in Al-doped solid-state LiGe2(PO4)3 electrolyte. Journal of Power Sources, 2015, 293, 11-16.	4.0	73
22847	Framework and Channel Modifications in Mayenite (12CaOÂ·7Al2O3) Nanocages By Cationic Doping. Chemistry of Materials, 2015, 27, 4731-4741.	3.2	43
22848	Synthesis of {111}-Faceted Au Nanocrystals Mediated by Polyvinylpyrrolidone: Insights from Density-Functional Theory and Molecular Dynamics. Journal of Physical Chemistry C, 2015, 119, 11982-11990.	1.5	32
22849	Electronic Structure of Nitrogen-Doped Graphene in the Ground and Core-Excited States from First-Principles Simulations. Journal of Physical Chemistry C, 2015, 119, 16660-16666.	1.5	31
22850	Vertical and Bidirectional Heterostructures from Graphyne and MSe₂ (M = Mo, W). Journal of Physical Chemistry Letters, 2015, 6, 2694-2701.	2.1	35

#	Article	IF	Citations
22851	Multiscale Experimental and Theoretical Investigations of Spin Crossover FeII Complexes: Examples of [Fe(phen)2(NCS)2] and [Fe(PM-BiA)2(NCS)2]. International Journal of Molecular Sciences, 2015, 16, 4007-4027.	1.8	16
22852	Rotational Spectromicroscopy: Imaging the Orbital Interaction between Molecular Hydrogen and an Adsorbed Molecule. Physical Review Letters, 2015, 114, 206101.	2.9	27
22853	Low-temperature phase transformation from nanotube to sp ³ superhard carbon phase. Chinese Physics B, 2015, 24, 066102.	0.7	0
22854	Bonding Analysis of BiFeO₃Substituted by Gd³⁺. Acta Physica Polonica A, 2015, 127, 362-364.	0.2	3
22855	Dynamics of Water Dissociative Chemisorption on Ni(111): Effects of Impact Sites and Incident Angles. Physical Review Letters, 2015, 114, 166101.	2.9	90
22856	Formation of As-As bond and its effect on absence of superconductivity in the collapsed tetragonal phase of<mml:math xmlns:mml="http://www.w3.org/1998/Math/MathML"><mml:mrow><mml:msub><mml:mi>Ca</mml:mi><mml:mrow><mml:mn>0.86</mml:mn></mml:mrow></mml:msub></mml:mrow></mml:math>An optical spectroscopy study. Physical Review B, 2015, 91, .	1.1	9
22857	Element-Resolved Thermodynamics of Magnetocaloric<mml:math xmlns:mml="http://www.w3.org/1998/Math/MathML" display="inline"><mml:msub><mml:mi>LaFe</mml:mi><mml:mrow><mml:mn>13</mml:mn><mml:mo>â^'</mml:mo><mml:mi>x</mml:mi></mml:mrow></mml:msub></mml:math>Physical Review Letters, 2015, 114, 057202.	2.9	78
22858	Impact of Rattlers on Thermal Conductivity of a Thermoelectric Clathrate: A First-Principles Study. Physical Review Letters, 2015, 114, 095501.	2.9	174
22859	Spin Crossover in Ferropericlase from First-Principles Molecular Dynamics. Physical Review Letters, 2015, 114, 117202.	2.9	56
22860	Surface Structure ofV2O3(0001)Revisited. Physical Review Letters, 2015, 114, 216101.	2.9	30
22861	Direct observation of an abrupt insulator-to-metal transition in dense liquid deuterium. Science, 2015, 348, 1455-1460.	6.0	241
22862	Optical properties and electronic transitions of DNA oligonucleotides as a function of composition and stacking sequence. Physical Chemistry Chemical Physics, 2015, 17, 4589-4599.	1.3	17
22863	An auxilliary grid method for the calculation of electrostatic terms in density functional theory on a real-space grid. Physical Chemistry Chemical Physics, 2015, 17, 31550-31557.	1.3	12
22864	Intrinsic defects in a photovoltaic perovskite variant Cs₂SnI₆. Physical Chemistry Chemical Physics, 2015, 17, 18900-18903.	1.3	191
22865	Interfacial bonding and electronic structure of GaN/GaAs interface: A first-principles study. Journal of Applied Physics, 2015, 117, .	1.1	14
22866	The evolution of polarization inside ultrathin PbTiO₃films: a theoretical study. Philosophical Magazine, 2015, 95, 2067-2077.	0.7	2
22867	Topological edge states in single- and multi-layer Bi₄Br₄. New Journal of Physics, 2015, 17, 015004.	1.2	32
22868	Thickness dependent of phase shift between surface energy and work function in Pb ultrathin films. New Journal of Physics, 2015, 17, 053006.	1.2	4

#	Article	IF	Citations
22869	The effects of electric field and gate bias pulse on the migration and stability of ionized oxygen vacancies in amorphous Inâ€“Gaâ€“Znâ€“O thin film transistors. Science and Technology of Advanced Materials, 2015, 16, 034902.	2.8	18
22870	Linear optical properties of defective KDP with oxygen vacancy: First-principles calculations. Chinese Physics B, 2015, 24, 077802.	0.7	12
22871	Electronic Structure and Carrier Mobilities of Arsenene and Antimonene Nanoribbons: A First-Principle Study. Nanoscale Research Letters, 2015, 10, 955.	3.1	137
22872	Optical Properties of a Monoclinic Insulator Cu(H2O)2(en)SO4. Acta Physica Polonica A, 2015, 127, 469-471.	0.2	1
22873	Physical properties of tetragonal transition-metal borides Nb 2 MB 2 (MÂ=ÂMo, W, Re or Os) with a new superstructure. Current Applied Physics, 2015, 15, 970-976.	1.1	3
22874	Study of sulfur adlayers on Au(1 1 1) from basic hydrolysis of piperazine bis(dithiocarbamate) sodium salt. Applied Surface Science, 2015, 345, 394-399.	3.1	7
22875	Dense or Porous Packing? Twoâ€Dimensional Selfâ€Assembly of Starâ€Shaped Monoâ€, Biâ€, and Terpyridine Derivatives. ChemPhysChem, 2015, 16, 949-953.	1.0	13
22876	Electro-mechanical anisotropy of phosphorene. Nanoscale, 2015, 7, 9746-9751.	2.8	223
22877	Study of Wetting on Chemically Soften Interfaces by Using Combined Solution Thermodynamics and DFT Calculations: Forecasting Effective Softening Elements. ACS Applied Materials & Interfaces, 2015, 7, 7576-7583.	4.0	8
22878	First-Principles Investigation of the Molecular Adsorption and Dissociation of Hydrazine on Niâ€“Fe Alloy Surfaces. Journal of Physical Chemistry C, 2015, 119, 8763-8774.	1.5	19
22879	Liquid Crystal (8CB) Molecular Adsorption on Lithium Niobate Z-Cut Surfaces. Journal of Physical Chemistry C, 2015, 119, 9342-9346.	1.5	11
22880	Density Functional Theory of MHâ€“MOH Solid Solubility (M = Alkali) and Experiments in NaHâ€“NaOH. Journal of Physical Chemistry C, 2015, 119, 8062-8069.	1.5	1
22881	Reductions of Oxygen, Carbon Dioxide, and Acetonitrile by the Magnesium(II)/Magnesium(I) Couple in Aqueous Media: Theoretical Insights from a Nano-Sized Water Droplet. Journal of Physical Chemistry A, 2015, 119, 2780-2792.	1.1	8
22882	Molten LiCl Layer Supported on MgO: Its Possible Role in Enhancing the Oxidative Dehydrogenation of Ethane. Journal of Physical Chemistry C, 2015, 119, 8681-8691.	1.5	18
22883	First-Principles Analysis of Proton Conduction Mechanism in Pyrochlore-Structured Lanthanum Zirconate. Journal of Physical Chemistry C, 2015, 119, 8480-8487.	1.5	26
22884	DFT Study of Oxidation States on Pyrite Surface Sites. Journal of Physical Chemistry C, 2015, 119, 7704-7710.	1.5	32
22885	Powder X-ray Diffraction Electron Density of Cubic Boron Nitride. Journal of Physical Chemistry C, 2015, 119, 6164-6173.	1.5	18
22886	One-Dimensional Oxygen Diffusion Mechanism in Sr₂ScGaO₅ Electrolyte Explored by Neutron and Synchrotron Diffraction, ¹⁷O NMR, and Density Functional Theory Calculations. Journal of Physical Chemistry C, 2015, 119, 11447-11458.	1.5	12

#	Article	IF	Citations
22887	On-Surface Construction of Network Structures by the tert-Butyl-Substituted Organic Molecules. Journal of Physical Chemistry C, 2015, 119, 8155-8159.	1.5	3
22888	Reliable Energy Level Alignment at Physisorbed Moleculeâ€“Metal Interfaces from Density Functional Theory. Nano Letters, 2015, 15, 2448-2455.	4.5	112
22889	Electronic Properties of Biphenylthiolates on Au(111): The Impact of Coverage Revisited. Journal of Physical Chemistry C, 2015, 119, 7817-7825.	1.5	20
22890	Self-Assembled Patterns and Youngâ€™s Modulus of Single-Layer Naphthalocyanine Molecules on Ag(111). Journal of Physical Chemistry C, 2015, 119, 8208-8212.	1.5	18
22891	Structural, Electronic, and Magnetic Properties of Adatom Adsorptions on Black and Blue Phosphorene: A First-Principles Study. Journal of Physical Chemistry C, 2015, 119, 10610-10622.	1.5	196
22892	Crystal Structure of Sinhalite MgAlBO4 under High Pressure. Journal of Physical Chemistry C, 2015, 119, 6777-6784.	1.5	5
22893	Unipolar self-doping behavior in perovskite CH3NH3PbBr3. Applied Physics Letters, 2015, 106, .	1.5	181
22894	Greatly improved electrochemical performance of lithiumâ€“oxygen batteries with a bimetallic platinumâ€“copper alloy catalyst. Journal of Power Sources, 2015, 288, 296-301.	4.0	49
22895	Impacts of electrode potentials and solvents on the electroreduction of CO₂: a comparison of theoretical approaches. Physical Chemistry Chemical Physics, 2015, 17, 13949-13963.	1.3	90
22896	Improved All-Carbon Spintronic Device Design. Scientific Reports, 2015, 5, 7634.	1.6	52
22897	AFFCK: Adaptive Force-Field-Assisted ab Initio Coalescence Kick Method for Global Minimum Search. Journal of Chemical Theory and Computation, 2015, 11, 2385-2393.	2.3	41
22898	Elastic anisotropy of iron carbides with trigonal-prismatic coordination of C by Fe. Journal of Alloys and Compounds, 2015, 633, 390-394.	2.8	8
22899	Insight into structural, elastic, phonon, and thermodynamic properties of Î±-sulfur and energy-related sulfides: a comprehensive first-principles study. Journal of Materials Chemistry A, 2015, 3, 8002-8014.	5.2	33
22900	Phase transitions of boron carbide: Pair interaction model of high carbon limit. Solid State Sciences, 2015, 47, 21-26.	1.5	22
22901	Spin-driven ordering of Cr in the equiatomic high entropy alloy NiFeCrCo. Applied Physics Letters, 2015, 106, .	1.5	158
22902	Single-Molecule Imaging of Activated Nitrogen Adsorption on Individual Manganese Phthalocyanine. Nano Letters, 2015, 15, 3181-3188.	4.5	22
22903	Origin of high thermal stability of amorphous Ge1Cu2Te3 alloy: A significant Cu-bonding reconfiguration modulated by Te lone-pair electrons for crystallization. Acta Materialia, 2015, 90, 88-93.	3.8	42
22904	Challenges of modelling real nanoparticles: Ni@Pt electrocatalysts for the oxygen reduction reaction. Physical Chemistry Chemical Physics, 2015, 17, 28286-28297.	1.3	30

#	Article	IF	Citations
22905	Toward Enhanced Photocatalytic Oxygen Evolution: Synergetic Utilization of Plasmonic Effect and Schottky Junction via Interfacing Facet Selection. Advanced Materials, 2015, 27, 3444-3452.	11.1	371
22906	Martensitic transformation between competing phases in Tiâ€“Ta alloys: a solid-state nudged elastic band study. Journal of Physics Condensed Matter, 2015, 27, 115401.	0.7	14
22907	Formation and binding energies of vacancies in the Al(111) surface: Density functional theory calculations confirm simple bond model. Surface Science, 2015, 637-638, 85-89.	0.8	5
22908	Magnetic anisotropy of C and N doped bulk FeCo alloy: A first principles study. Journal of Magnetism and Magnetic Materials, 2015, 388, 101-105.	1.0	12
22909	First-principles study of a sodium borosilicate glass-former. II. The glass state. Physical Review B, 2015, 91, .	1.1	33
22910	Ab-initio calculations and CALPHAD description of Crâ€“Geâ€“Mn and Crâ€“Geâ€“Si. Calphad: Computer Coupling of Phase Diagrams and Thermochemistry, 2015, 49, 50-57.	0.7	10
22911	Thermoelectric properties of IVâ€“VI-based heterostructures and superlattices. Journal of Solid State Chemistry, 2015, 227, 123-131.	1.4	8
22912	Reference diffraction patterns, microstructure, and pore-size distribution for the copper (II) benzene-1,3,5-tricarboxylate metal organic framework (Cu-BTC) compounds. Powder Diffraction, 2015, 30, 2-13.	0.4	23
22913	Fluorinated Carbide-Derived Carbon: More Hydrophilic, Yet Apparently More Hydrophobic. Journal of the American Chemical Society, 2015, 137, 5969-5979.	6.6	18
22914	Modulation of band gap by an applied electric field in silicene-based hetero-bilayers. Physical Chemistry Chemical Physics, 2015, 17, 11324-11328.	1.3	58
22915	Synthesis and characterization of ZnS with controlled amount of S vacancies for photocatalytic H2 production under visible light. Scientific Reports, 2015, 5, 8544.	1.6	171
22916	Realization of a pâ€“n junction in a single layer boron-phosphide. Physical Chemistry Chemical Physics, 2015, 17, 13013-13020.	1.3	112
22917	Transition Metal Doped Phosphorene: First-Principles Study. Journal of Physical Chemistry C, 2015, 119, 9198-9204.	1.5	227
22918	First-principles study of magnetic properties of stoichiometric and O deficient low-index surfaces of rutile SnO2 and TiO2. Journal of Magnetism and Magnetic Materials, 2015, 374, 197-204.	1.0	14
22919	Octahedral tilt transitions in the relaxor ferroelectric Na1/2Bi1/2TiO3. Journal of Solid State Chemistry, 2015, 227, 117-122.	1.4	20
22920	Prediction of novel hard phases of Si3N4: First-principles calculations. Journal of Solid State Chemistry, 2015, 228, 20-26.	1.4	20
22921	Self-organizing nanostructured lamellar (Ti,Zr)C â€" A superhard mixed carbide. International Journal of Refractory Metals and Hard Materials, 2015, 51, 25-28.	1.7	28
22922	First-principles studies of interlayer exchange coupling in (Ga, Mn)N-based diluted magnetic semiconductor multilayers. Optik, 2015, 126, 903-906.	1.4	2

#	Article	IF	Citations
22923	Half metallicity in Sr2CrOsO6 via Na doping. Journal of Alloys and Compounds, 2015, 636, 257-260.	2.8	11
22924	First-Principles Studies on Cation Dopants and Electrolyte | Cathode Interphases for Lithium Garnets. Chemistry of Materials, 2015, 27, 4040-4047.	3.2	279
22925	First principles study of structural, magnetic and electronic properties of C-doped monoclinic ZrO2. Journal of Magnetism and Magnetic Materials, 2015, 389, 90-94.	1.0	14
22926	Distortions of the calcite and aragonite atomic structures from interstitial water. Materials Chemistry and Physics, 2015, 157, 56-62.	2.0	5
22927	Stability and formation of long period stacking order structure in Mg-based ternary alloys. Computational Materials Science, 2015, 103, 90-96.	1.4	21
22928	A DFT study on the correlation between topology and Bader charges: Part II, effects of compression and dilatation of V2O5. Solid State Sciences, 2015, 43, 1-8.	1.5	6
22929	Structural, electronic and elastic properties of several metal organic frameworks as a new kind of energetic materials. Chemical Physics Letters, 2015, 628, 76-80.	1.2	13
22930	Designing thin film materials â€" Ternary borides from first principles. Thin Solid Films, 2015, 583, 46-49.	0.8	36
22931	Non-ferromagnetic behavior in Agâ€"N codoped ZnO: First-principle calculations. Materials Science in Semiconductor Processing, 2015, 35, 139-143.	1.9	3
22932	A new diluted magnetic semiconductor based on the expanded phase of ZnS: surmounting the random distribution of magnetic impurities. Physical Chemistry Chemical Physics, 2015, 17, 13117-13122.	1.3	7
22933	Catalytic effects of magnesium grain boundaries on H 2 dissociation. International Journal of Hydrogen Energy, 2015, 40, 5683-5688.	3.8	1
22934	Ab initio study of the electronic structure and band gaps of Eu-doped LaSi3N5 phosphors: A role of oxygen atom. Journal of the European Ceramic Society, 2015, 35, 3249-3253.	2.8	2
22935	Irradiation-induced formation of a spinel phase at the FeCr/MgO interface. Acta Materialia, 2015, 93, 87-94.	3.8	8
22936	First-principles study of soluteâ€"solute binding in magnesium alloys. Computational Materials Science, 2015, 103, 97-104.	1.4	23
22937	Electronic structure and energy level schemes of RE3+:LaSi3N5 and RE2+:LaSi3N5â^'xOx phosphors (RE=Ce, Pr, ND, Pm, Sm, Eu) from first principles. Journal of Luminescence, 2015, 164, 131-137.	1.5	21
22938	Chlorine adsorption on Cu(111) revisited: LT-STM and DFT study. Surface Science, 2015, 639, 7-12.	0.8	13
22939	First-principles investigation of novel polymorphs of Mg₂C. Physical Chemistry Chemical Physics, 2015, 17, 12970-12977.	1.3	8
22940	Luminescence properties and first principles calculations of Dy³⁺ activated Sr₃B₂O₆ phosphors. Functional Materials Letters, 2015, 08, 1550022.	0.7	7

#	Article	IF	Citations
22941	Formation and interaction of point defects in group IVb transition metal carbides and nitrides. Computational Materials Science, 2015, 104, 147-154.	1.4	36
22942	Materials discovery via CALYPSO methodology. Journal of Physics Condensed Matter, 2015, 27, 203203.	0.7	93
22943	Fatigue Crack Growth Fundamentals in Shape Memory Alloys. Shape Memory and Superelasticity, 2015, 1, 18-40.	1.1	36
22944	Na+ intercalation pseudocapacitance in graphene-coupled titanium oxide enabling ultra-fast sodium storage and long-term cycling. Nature Communications, 2015, 6, 6929.	5.8	969
22945	Mechanism of Oxidation of Ethane to Ethanol at Iron(IV)â€“Oxo Sites in Magnesium-Diluted Fe₂(dobdc). Journal of the American Chemical Society, 2015, 137, 5770-5781.	6.6	156
22946	Reaction mechanism from quantum molecular dynamics for the initial thermal decomposition of 2,4,6-triamino-1,3,5-triazine-1,3,5-trioxide (MTO) and 2,4,6-trinitro-1,3,5-triazine-1,3,5-trioxide (MTO3N), promising green energetic materials. Journal of Materials Chemistry A, 2015, 3, 12044-12050.	5.2	18
22947	Graphdiyne: A two-dimensional thermoelectric material with high figure of merit. Carbon, 2015, 90, 255-259.	5.4	124
22948	First-Principles Study about the Effect of Coverage on H₂ Adsorption and Dissociation over a Rh(100) Surface. Journal of Physical Chemistry C, 2015, 119, 10355-10364.	1.5	17
22949	Achieving Highly Efficient, Selective, and Stable CO₂ Reduction on Nitrogen-Doped Carbon Nanotubes. ACS Nano, 2015, 9, 5364-5371.	7.3	546
22950	Carbon Doping in Boron Suboxide: Structure, Energetics, and Elastic Properties. Journal of the American Ceramic Society, 2015, 98, 2223-2233.	1.9	5
22951	Spinâ€“orbit coupling in the band structure of monolayer WSe₂. Journal of Physics Condensed Matter, 2015, 27, 182201.	0.7	67
22952	Evolution behavior of C and Si atoms on diamond (001) surface: A first principle study. Applied Surface Science, 2015, 346, 464-469.	3.1	9
22953	Molecular dynamics simulations of mechanical properties of monolayer MoS₂. Nanotechnology, 2015, 26, 185705.	1.3	96
22954	Functional approach to electrodynamics of media. Photonics and Nanostructures - Fundamentals and Applications, 2015, 14, 1-34.	1.0	14
22955	Picosecond electric field pulse induced coherent magnetic switching in MgO/FePt/Pt(001)-based tunnel junctions: a multiscale study. Scientific Reports, 2014, 4, 4117.	1.6	38
22956	Thin Film Thermoelectric Metalâ€“Organic Framework with High Seebeck Coefficient and Low Thermal Conductivity. Advanced Materials, 2015, 27, 3453-3459.	11.1	227
22957	Rational Design of Organotin Polyesters. Macromolecules, 2015, 48, 2422-2428.	2.2	54
22958	Mg Intercalation in Layered and Spinel Host Crystal Structures for Mg Batteries. Inorganic Chemistry, 2015, 54, 4394-4402.	1.9	110

#	Article	IF	Citations
22959	When the Solvent Locks the Cage: Theoretical Insight into the Transmetalation of MOF-5 Lattices and Its Kinetic Limitations. Chemistry of Materials, 2015, 27, 3422-3429.	3.2	23
22960	A first principles study of the mechanical properties of Liâ€“Sn alloys. RSC Advances, 2015, 5, 36022-36029.	1.7	41
22961	Nano-scale displacement sensing based on van der Waals interactions. Nanoscale, 2015, 7, 8962-8967.	2.8	18
22962	Functional materials integrated on IIIâ€“V semiconductors. Microelectronic Engineering, 2015, 147, 117-121.	1.1	11
22963	Effect of dynamic disorder on charge carrier dynamics in Ph4DP and Ph4DTP molecules. RSC Advances, 2015, 5, 38722-38732.	1.7	10
22964	Finite-temperature properties of antiferroelectric<mml:math xmlns:mml="http://www.w3.org/1998/Math/MathML"><mml:msub><mml:mi>PbZrO</mml:mi><mml:mn>3</mml:mn></mml:msub> atomistic simulations. Physical Review B, 2015, 91, .	1.1	13
22965	Origin of different thermoelectric properties between Zintl compounds Ba3Al3P5 and Ba3Ga3P5: A first-principles study. Journal of Alloys and Compounds, 2015, 636, 387-394.	2.8	16
22966	Adsorption of RGD tripeptide on anatase (001) surface â€“ A first principle study. Computational Materials Science, 2015, 104, 124-129.	1.4	16
22967	Elastic properties of ferrous bearing MgSiO3 and their relevance to ULVZs. Geophysical Journal International, 2015, 201, 496-504.	1.0	12
22968	Structural and magnetic effects on thermal emittance of La1â^'xSrxMnO3 from the first principles calculation. Journal of Magnetism and Magnetic Materials, 2015, 390, 31-35.	1.0	2
22969	Mg intercalation into Ti2C building block. Chemical Physics Letters, 2015, 629, 36-39.	1.2	16
22970	Group Additivity and Modified Linear Scaling Relations for Estimating Surface Thermochemistry on Transition Metal Surfaces: Application to Furanics. Journal of Physical Chemistry C, 2015, 119, 10417-10426.	1.5	28
22971	The magnetic and half-metal properties of iron clusters adsorbed on armchair graphene nanoribbon. Computational and Theoretical Chemistry, 2015, 1062, 84-89.	1.1	13
22972	Loss of Linear Band Dispersion and Trigonal Structure in Silicene on Ir(111). Journal of Physical Chemistry Letters, 2015, 6, 1065-1070.	2.1	20
22973	Strengthening and ductilization potentials of nonmetallic solutes in magnesium: First-principles calculation of generalized stacking fault energies. Materials Letters, 2015, 150, 111-113.	1.3	16
22974	Effects of rare-earth on the cohesion of Ni Î£5 (0 1 2) grain boundary from first-principles calculations. Computational Materials Science, 2015, 96, 374-378.	1.4	23
22975	Experimental study and thermodynamic assessment of the Zrâ€“Alâ€“Gd system. Thermochimica Acta, 2015, 609, 36-48.	1.2	1
22976	Role of the third element in accelerating Fe diffusivities in Cu from first principles. Journal of Alloys and Compounds, 2015, 639, 642-647.	2.8	18

#	Article	IF	Citations
22977	Caesium incorporation and retention in illite interlayers. Applied Clay Science, 2015, 108, 128-134.	2.6	155
22978	A first-principles study on gas sensing properties of graphene and Pd-doped graphene. Applied Surface Science, 2015, 343, 121-127.	3.1	217
22979	First-principles investigation of site preference and diffusion behaviors of carbon in copper. Nuclear Instruments & Methods in Physics Research B, 2015, 352, 72-76.	0.6	4
22980	Low-index surfaces of CoSb3 skutterudites from first principles. Surface Science, 2015, 637-638, 124-131.	0.8	12
22981	Ab-initio study on the electronic, optical and ferroelectric properties of LiOsO3. Computational Materials Science, 2015, 105, 11-17.	1.4	12
22982	Dopants and dopantâ€“vacancy complexes in tetragonal lead titanate: A systematic first principles study. Computational Materials Science, 2015, 103, 224-230.	1.4	11
22983	Syntheses, Characterization, and Optical Properties of Centrosymmetric Ba₃(BS₃)_{1.5}(MS₃)_{0.5} and Noncentrosymmetric Ba₃(BQ₃)(SbQ₃). Inorganic Chemistry, 2015, 54, 4761-4767.	1.9	33
22984	A periodic density functional theory calculation: The structure of isolated copper(I) oxide species on Î³-Al2O3 (110) surface and its adsorption ability toward thiophene and benzene. Applied Surface Science, 2015, 346, 165-171.	3.1	5
22985	Electronic Band Structures and Native Point Defects of Ultrafine ZnO Nanocrystals. ACS Applied Materials & Interfaces, 2015, 7, 10617-10622.	4.0	14
22986	Ab initio simulation of elastic and mechanical properties of Zn- and Mg-doped hydroxyapatite (HAP). Journal of the Mechanical Behavior of Biomedical Materials, 2015, 47, 135-146.	1.5	49
22987	Origin of the structural diversity of M2O3 (M = Al, Ga, In). Computational Materials Science, 2015, 104, 35-39.	1.4	2
22988	Enhancement of the oxygen reduction on nitride stabilized pt-M (M=Fe, Co, and Ni) coreâ€“shell nanoparticle electrocatalysts. Nano Energy, 2015, 13, 442-449.	8.2	104
22989	First principles prediction of interfacial magnetoelectric coupling in tetragonal La2/3Sr1/3MnO3/BiFeO3 multiferroic superlattices. Physical Chemistry Chemical Physics, 2015, 17, 13647-13653.	1.3	5
22990	First principles study of structural, magnetic and electronic properties of N-doped monoclinic ZrO 2. Journal of Magnetism and Magnetic Materials, 2015, 387, 58-61.	1.0	5
22991	On Why the Two Polymorphs of NaFePO4Exhibit Widely Different Magnetic Structures: Density Functional Analysis. Inorganic Chemistry, 2015, 54, 4966-4971.	1.9	11
22992	First hydrothermal synthesis of Bi5O7Br and its photocatalytic properties for molecular oxygen activation and RhB degradation. Applied Surface Science, 2015, 346, 311-316.	3.1	74
22993	O₂ sensing dynamics of BiFeO₃ nanofibers: effect of minor carrier compensation. Nanotechnology, 2015, 26, 175501.	1.3	19
22994	Quantum-Chemical Characterization of the Properties and Reactivities of Metalâ€“Organic Frameworks. Chemical Reviews, 2015, 115, 6051-6111.	23.0	241

#	Article	IF	Citations
22995	Structure and energy level alignment at the dyeâ€“electrode interface in p-type DSSCs: new hints on the role of anchoring modes from ab initio calculations. Physical Chemistry Chemical Physics, 2015, 17, 12238-12246.	1.3	38
22996	Average and Local Structure, Debye Temperature, and Structural Rigidity in Some Oxide Compounds Related to Phosphor Hosts. ACS Applied Materials & Interfaces, 2015, 7, 7264-7272.	4.0	159
22997	Bandgap Widening of Phase Quilted, 2D MoS₂ by Oxidative Intercalation. Advanced Materials, 2015, 27, 3152-3158.	11.1	76
22998	Pristine and defect-containing phosphorene as promising anode materials for rechargeable Li batteries. Journal of Materials Chemistry A, 2015, 3, 11246-11252.	5.2	136
22999	Exploring d 0 magnetism in doped SnO 2 â€“a first principles DFT study. Journal of Magnetism and Magnetic Materials, 2015, 385, 207-216.	1.0	20
23000	Magnetism in SrTiO3 before and after UV irradiation. Applied Surface Science, 2015, 335, 115-120.	3.1	34
23001	Electron holography ofÂnanowires â€“ Part 1. , 2015, , 221-251.		1
23002	Metal-atom-induced charge redistributions and their effects on the electrical contacts to WS₂ monolayers. Physica Status Solidi (B): Basic Research, 2015, 252, 1783-1791.	0.7	2
23003	Looking for Auger signatures in III-nitride light emitters: A full-band Monte Carlo perspective. Applied Physics Letters, 2015, 106, .	1.5	30
23004	Role of Fe impurity complexes in the degradation of GaN/AlGaN high-electron-mobility transistors. Applied Physics Letters, 2015, 106, .	1.5	45
23005	Twisting phonons in complex crystals with quasi-one-dimensional substructures. Nature Communications, 2015, 6, 6723.	5.8	75
23006	Criteria for Predicting the Formation of Single-Phase High-Entropy Alloys. Physical Review X, 2015, 5, .	2.8	123
23007	The electronic properties tuned by the phase transition between the semiconducting and metallic phase of monolayer MoS₂/WS₂. Phase Transitions, 2015, 88, 726-734.	0.6	2
23008	Strong Long-Range Relaxations of Structural Defects in Graphene Simulated Using a New Semiempirical Potential. Journal of Physical Chemistry C, 2015, 119, 9646-9655.	1.5	20
23009	The oxygen reduction reaction on Pt(111) and Pt(100) surfaces substituted by subsurface Cu: a theoretical perspective. Journal of Materials Chemistry A, 2015, 3, 11444-11452.	5.2	102
23010	Ab initio calculations of mechanical properties: Methods and applications. Progress in Materials Science, 2015, 73, 127-158.	16.0	114
23011	Lateral heterojunctions within monolayer h-BN/graphene: a first-principles study. RSC Advances, 2015, 5, 33037-33043.	1.7	37
23012	Revealing chemical ordering in Ptâ€“Co nanoparticles using electronic structure calculations and X-ray photoelectron spectroscopy. Physical Chemistry Chemical Physics, 2015, 17, 28298-28310.	1.3	24

#	Article	IF	Citations
23013	A hierarchical microstructure due to chemical ordering in the bcc lattice: Early stages of formation in a ferritic Feâ€“Alâ€“Crâ€“Niâ€“Ti alloy. Acta Materialia, 2015, 92, 220-232.	3.8	58
23014	Interaction of cesium adatoms with free-standing graphene and graphene-veiled SiO₂ surfaces. RSC Advances, 2015, 5, 38623-38629.	1.7	2
23015	Origin of High Electronic Quality in Structurally Disordered CH₃NH₃PbI₃ and the Passivation Effect of Cl and O at Grain Boundaries. Advanced Electronic Materials, 2015, 1, 1500044.	2.6	175
23016	Theoretical Study of WS-9-Based Organic Sensitizers for Unusual Vis/NIR Absorption and Highly Efficient Dye-Sensitized Solar Cells. Journal of Physical Chemistry C, 2015, 119, 9782-9790.	1.5	121
23017	High-Pressure Hydrogen Sulfide from First Principles: A Strongly Anharmonic Phonon-Mediated Superconductor. Physical Review Letters, 2015, 114, 157004.	2.9	377
23018	Reactivity of transition metal atoms supported or not on TiO2(110) toward CO and H adsorption. Theoretical Chemistry Accounts, 2015, 134, 1.	0.5	4
23019	Montmorillonite interlayer surface chemistry: effect of magnesium ion substitution on cation adsorption. Theoretical Chemistry Accounts, 2015, 134, 1.	0.5	16
23020	Compressibilities of MnFe2O4 polymorphs. Physics and Chemistry of Minerals, 2015, 42, 569-577.	0.3	11
23021	Room-temperature ferromagnetism in carbon- and nitrogen-doped rutile TiO2. Applied Physics A: Materials Science and Processing, 2015, 118, 725-731.	1.1	12
23022	Reaction mechanisms for CO catalytic oxidation on monodisperse Mo atom-embedded graphene. Applied Physics A: Materials Science and Processing, 2015, 119, 475-485.	1.1	35
23023	Quantum Chemical Study of Mechanisms of the Reaction of Cyclohexyl Phenyl Sulfide with Water. Chemistry and Technology of Fuels and Oils, 2015, 51, 113-116.	0.2	3
23024	Reduction of the repulsive interaction as origin of helium trapping inside a monovacancy in BCC metals. Journal of Materials Science, 2015, 50, 3727-3739.	1.7	17
23025	Effects of Sr and Zn Doping on the Metallicity and Superconductivity of LSCO and YBCO. Journal of Superconductivity and Novel Magnetism, 2015, 28, 1299-1303.	0.8	5
23026	Tin content effect on the structural and energetic properties of lead telluride clusters. Structural Chemistry, 2015, 26, 573-585.	1.0	1
23027	The adsorption and dissociation of multilayer CH3OH on TiO2 (110). Science China Chemistry, 2015, 58, 614-619.	4.2	7
23028	Structural phase transition and electronic structure evolution in Ir 1â€“x Pt x Te 2 studied by scanning tunneling microscopy. Science Bulletin, 2015, 60, 798-805.	4.3	10
23029	HRTEM investigation of phase stability in aluminaâ€“zirconia multilayer thin films. Bulletin of Materials Science, 2015, 38, 401-407.	0.8	2
23030	Mechanical properties of U-0.95Âmass fraction of Ti alloy quenching and aging treatment: a first principles study. Advances in Manufacturing, 2015, 3, 244-251.	3.2	1

#	Article	IF	Citations
23031	First-principles molecular dynamics study of water dissociation on theÎ³-U(1â€‰0â€‰0) surface. Journal of Physics Condensed Matter, 2015, 27, 175005.	0.7	8
23032	Selection of Surface Coatings for High H₂ Permeability Group 5 Metal Membranes Using First-Principles Calculations. Journal of Physical Chemistry C, 2015, 119, 7848-7855.	1.5	9
23033	Effects of non-metal dopants and defects on electronic properties of barium titanate as photocatalyst. International Journal of Hydrogen Energy, 2015, 40, 4766-4776.	3.8	16
23034	RuPd Alloy Nanoparticles Supported on N-Doped Carbon as an Efficient and Stable Catalyst for Benzoic Acid Hydrogenation. ACS Catalysis, 2015, 5, 3100-3107.	5.5	136
23035	Mo₂C/Graphene Nanocomposite As a Hydrodeoxygenation Catalyst for the Production of Diesel Range Hydrocarbons. ACS Catalysis, 2015, 5, 3292-3303.	5.5	71
23036	Synthesis, characterization, in silico approach and in vitro antiproliferative activity of RPF151, a benzodioxole sulfonamide analogue designed from capsaicin scaffold. Journal of Molecular Structure, 2015, 1088, 138-146.	1.8	13
23037	Competing magnetic states, disorder, and the magnetic character of<mml:math xmlns:mml="http://www.w3.org/1998/Math/MathML"><mml:mrow><mml:msub><mml:mi>Fe</mml:mi><mml:mn>1</mml:mn> Physical Review B, 2015, 91, .	1.1	17
23038	Thermodynamic modeling of the Coâ€“Hf system supported by key experiments and first-principles calculations. Thermochimica Acta, 2015, 608, 49-58.	1.2	10
23039	Intrinsic defects and Na doping in Cu2ZnSnS4: A density-functional theory study. Solar Energy, 2015, 116, 125-132.	2.9	49
23040	First-principles calculation of metal-doped CaAlSiN₃: material design for new phosphors. RSC Advances, 2015, 5, 39319-39323.	1.7	16
23041	Phase stability in nanoscale material systems: extension from bulk phase diagrams. Nanoscale, 2015, 7, 9868-9877.	2.8	66
23042	Insight into the role of Li₂S₂ in Liâ€“S batteries: a first-principles study. Journal of Materials Chemistry A, 2015, 3, 8865-8869.	5.2	68
23043	The effects of thermal and electric fields on the electronic structures of silicene. Physical Chemistry Chemical Physics, 2015, 17, 13366-13373.	1.3	13
23044	Al15Ge4Ni3: A new intergrowth structure with Cu3Au- and CaF2-type building blocks. Journal of Solid State Chemistry, 2015, 225, 240-248.	1.4	5
23045	Ni cluster nucleation and growth on the anatase TiO₂(101) surface: a density functional theory study. RSC Advances, 2015, 5, 16582-16591.	1.7	17
23046	Aluminum Migration and Intrinsic Defect Interaction in Single-Crystal Zinc Oxide. Physical Review Applied, 2015, 3, .	1.5	38
23047	Environment-Controlled Dislocation Migration and Superplasticity in Monolayer MoS₂. Nano Letters, 2015, 15, 3495-3500.	4.5	30
23048	Ab Initio Approach for Prediction of Oxide Surface Structure, Stoichiometry, and Electrocatalytic Activity in Aqueous Solution. Journal of Physical Chemistry Letters, 2015, 6, 1785-1789.	2.1	64

#	Article	IF	Citations
23049	Coverage dependent adsorption and co-adsorption of CO and H₂ on the CdI₂-antitype metallic Mo₂C(001) surface. Physical Chemistry Chemical Physics, 2015, 17, 1907-1917.	1.3	17
23050	Ab initio study of intrinsic point defects in PbTe: an insight into phase stability. Acta Materialia, 2015, 92, 72-80.	3.8	46
23051	Understanding the Initial Stages of Reversible Mg Deposition and Stripping in Inorganic Nonaqueous Electrolytes. Chemistry of Materials, 2015, 27, 3317-3325.	3.2	105
23052	Effect of the components' interface on the synthesis of methanol over Cu/ZnO from CO₂/H₂: a microkinetic analysis based on DFT + U calculations. Physical Chemistry Chemical Physics, 2015, 17, 7317-7333.	1.3	28
23053	Discussion on the Structure Stability and the Luminescence Switch under Irradiation of a Ceâ€Doped Elpasolite Compound. Chemistry - A European Journal, 2015, 21, 5242-5251.	1.7	6
23054	Grain boundary in phosphorene and its unique roles on C and O doping. Europhysics Letters, 2015, 109, 47003.	0.7	12
23055	A robust carbon tolerant anode for solid oxide fuel cells. Science China Materials, 2015, 58, 204-212.	3.5	19
23056	Theoretical study of oxygen sorption and diffusion in the volume and on the surface of a Î³-TiAl alloy. Journal of Experimental and Theoretical Physics, 2015, 120, 257-267.	0.2	19
23057	Characterization of tetragonal phases of SrRuO3 under epitaxial strain by density functional theory. European Physical Journal B, 2015, 88, 1.	0.6	16
23058	Catalytic activities of noble metal atoms on WO3 (001): nitric oxide adsorption. Nanoscale Research Letters, 2015, 10, 60.	3.1	8
23059	Incorporation of Mg2+ in surface Ca2+ sites of aragonite: an ab initio study. Progress in Earth and Planetary Science, 2015, 2, .	1.1	14
23060	First-principles calculations of the lattice instability and the symmetry-lowering modulation of PtSi. Journal of the Korean Physical Society, 2015, 66, 612-616.	0.3	8
23061	Density-functional-theory study of monatomic and diatomic vacancies on the non-polar ZnO $$(10ar) Tj ETQq0 0 0 rgBT /Overlock 10 Tf	0.3	3
23062	Strain-induced metal-semiconductor transition in monolayers and bilayers of gray arsenic: A computational study. Physical Review B, 2015, 91, .	1.1	178
23063	Nanoflower-like weak crystallization manganese oxide for efficient removal of low-concentration NO at room temperature. Journal of Materials Chemistry A, 2015, 3, 7631-7638.	5.2	37
23064	Ab initio study of germanium-hydride compounds under high pressure. RSC Advances, 2015, 5, 19432-19438.	1.7	13
23065	B-doped 3C-SiC nanowires with a finned microstructure for efficient visible light-driven photocatalytic hydrogen production. Nanoscale, 2015, 7, 8955-8961.	2.8	80
23066	High energy density titanium doped-vanadium oxide-vertically aligned CNT composite electrodes for supercapacitor applications. Journal of Materials Chemistry A, 2015, 3, 8413-8432.	5.2	64

#	Article	IF	Citations
23067	Luminescence signature of free exciton dissociation and liberated electron transfer across the junction of graphene/GaN hybrid structure. Scientific Reports, 2015, 5, 7687.	1.6	18
23068	Realization of a reversible switching in TaO2 polymorphs via Peierls distortion for resistance random access memory. Applied Physics Letters, 2015, 106, 091903.	1.5	19
23069	Graphyne on metallic surfaces: A density functional theory study. Physical Review B, 2015, 91, .	1.1	17
23070	Route to n-type doping in SnS. Applied Physics Letters, 2015, 106, .	1.5	49
23071	Efficient Visible Light Nitrogen Fixation with BiOBr Nanosheets of Oxygen Vacancies on the Exposed {001} Facets. Journal of the American Chemical Society, 2015, 137, 6393-6399.	6.6	1,468
23072	Hydrogen diffusion in MgH₂ doped with Ti, Mn andÂFe. RSC Advances, 2015, 5, 34894-34899.	1.7	25
23073	Three-dimensional sp²-hybridized carbons consisting of orthogonal nanoribbons of graphene and net C. Physical Chemistry Chemical Physics, 2015, 17, 13028-13033.	1.3	22
23074	A Novel Phase of Li₁₅Si₄ Synthesized under Pressure. Advanced Energy Materials, 2015, 5, 1500214.	10.2	14
23075	Migration Barriers and Evolution of Mechanical Properties of Oxide Nanoclusters Containing Helium. Materials Research Society Symposia Proceedings, 2015, 1743, 20.	0.1	0
23076	The role of charge transfer in the oxidation state change of Ce atoms in the TM₁₃â€“CeO₂(111) systems (TM = Pd, Ag, Pt, Au): a DFT + U investigation. Physical Chemistry Chemical Physics, 2015, 17, 13520-13530.	1.3	41
23077	Doping effect in graphene on oxide substrates: MgO(111) and SiO2(0001). Current Applied Physics, 2015, 15, S103-S107.	1.1	6
23078	The structural and electronic properties of spinel MnCo2O4 bulk and low-index surfaces: From first principles studies. Applied Surface Science, 2015, 349, 510-515.	3.1	32
23079	Electronic and magnetic properties of diluted ferromagnetic semiconductor (La1â^'xBax)(Zn1â^'yMny)AsO from first-principles calculations. European Physical Journal B, 2015, 88, 1.	0.6	2
23080	Determination of Formation and Ionization Energies of Charged Defects in Two-Dimensional Materials. Physical Review Letters, 2015, 114, 196801.	2.9	89
23081	Novel ultra-incompressible phases of Ru2C. Journal of Physics Condensed Matter, 2015, 27, 175505.	0.7	1
23082	Interplay of Metal-Atom Ordering, Fermi Level Tuning, and Thermoelectric Properties in Cobalt Shandites Co₃M₂S₂ (M = Sn, In). Chemistry of Materials, 2015, 27, 3946-3956.	3.2	47
23083	Relationships between the surface electronic and chemical properties of doped 4d and 5d late transition metal dioxides. Journal of Chemical Physics, 2015, 142, 104703.	1.2	28
23084	Physics of Plasmas, 2015, 22, 056307.	0.7	14

#	Article	IF	Citations
23085	Band engineering of AgSb1â^'xBixO3 for photocatalytic water oxidation under visible light. Journal of Materials Chemistry A, 2015, 3, 8466-8474.	5.2	18
23086	Electronic structure and magnetism in g-C4N3 controlled by strain engineering. Applied Physics Letters, 2015, 106, .	1.5	23
23087	Obtaining strong ferromagnetism in diluted Gd-doped ZnO thin films through controlled Gd-defect complexes. Journal of Applied Physics, 2015, 117, .	1.1	52
23088	Theoretical capacity achieved in a LiMn_{0.5}Fe_{0.4}Mg_{0.1}BO₃ cathode by using topological disorder. Energy and Environmental Science, 2015, 8, 1790-1798.	15.6	27
23089	Band gap modulation of Janus graphene nanosheets by interlayer hydrogen bonding and the external electric field: a computational study. Journal of Materials Chemistry C, 2015, 3, 3416-3421.	2.7	50
23090	Synthesis of the Layered Quaternary Uranium-Containing Oxide Cs2Mn3U6O22and Characterization of its Magnetic Properties. Inorganic Chemistry, 2015, 54, 5495-5503.	1.9	5
23091	Functionalization of germanene by metal atoms adsorption: A first-principles study. Canadian Journal of Physics, 2015, 93, 1310-1318.	0.4	19
23092	An impurity intermediate band due to Pb doping induced promising thermoelectric performance of Ca₅In₂Sb₆. Physical Chemistry Chemical Physics, 2015, 17, 15156-15164.	1.3	10
23093	Magnetism in Quasi-One-Dimensional A ₂ Cr ₃ As ₃ (A=K,Rb) Superconductors. Chinese Physics Letters, 2015, 32, 057401.	1.3	55
23094	Theoretical investigation of thermodynamic stability and mobility of the intrinsic point defects in Ti₃AC₂ (A = Si, Al). Physical Chemistry Chemical Physics, 2015, 17, 8927-8934.	1.3	41
23095	Prediction of half-semiconductor antiferromagnets with vanishing net magnetization. RSC Advances, 2015, 5, 46640-46647.	1.7	21
23096	First principle study of the electrochemical properties of Li2FeSiS4. Computational Materials Science, 2015, 106, 135-139.	1.4	9
23097	Hole-doping of mechanically exfoliated graphene by confined hydration layers. Nano Research, 2015, 8, 3020-3026.	5.8	19
23098	Coherent view of crystal chemistry and ab initio analyses of Pb(II) and Bi(III) lone pair in square planar coordination. Progress in Solid State Chemistry, 2015, 43, 82-97.	3.9	21
23099	Adsorption of Aun (n = 1â€“4) clusters on Fe3O4(001) B-termination. RSC Advances, 2015, 5, 45446-45453.	1.7	16
23100	Superconductivity in bulk polycrystalline metastable phases of Sb2Te3 and Bi2Te3 quenched after high-pressureâ€“high-temperature treatment. Chemical Physics Letters, 2015, 631-632, 97-102.	1.2	20
23101	Stabilizing and increasing the magnetic moment of half-metals: The role of Li in half-Heusler<mml:math xmlns:mml="http://www.w3.org/1998/Math/MathML"><mml:mi mathvariant="normal">LiMn</mml:mi><mml:mi>Z</mml:mi></mml:math><mml:math xmlns:mml="http://www.w3.org/1998/Math/MathML"><mml:mo>(</mml:mo><mml:mi>Z</mml:mi><mml:mo>=</mml:mo><mml:mtext Physical Review B, 2015, 91, .	1.1	35
23102	Superconductivity in room-temperature stable electride and high-pressure phases of alkali metals. Philosophical Transactions Series A, Mathematical, Physical, and Engineering Sciences, 2015, 373, 20140450.	1.6	39

#	Article	IF	Citations
23103	Thermodynamic modeling of KF-CrF3 binary system. Chemical Research in Chinese Universities, 2015, 31, 461-465.	1.3	8
23104	Prediction of large-gap quantum spin hall insulator and Rashba-Dresselhaus effect in two-dimensional g-TlA (A = N, P, As, and Sb) monolayer films. Nano Research, 2015, 8, 2954-2962.	5.8	46
23105	Unusual stability of multiply charged organo-metallic complexes. RSC Advances, 2015, 5, 44003-44008.	1.7	16
23106	Why Sn doping significantly enhances the dielectric properties of Ba(Ti1-xSnx)O3. Scientific Reports, 2015, 5, 8606.	1.6	84
23107	Bismuth-induced surface structure and morphology in III-V semiconductors. , 2015, , .		0
23108	Advances in theory and their application within the field of zeolite chemistry. Chemical Society Reviews, 2015, 44, 7044-7111.	18.7	405
23109	A low-surface energy carbon allotrope: the case for bcc-C₆. Physical Chemistry Chemical Physics, 2015, 17, 14083-14087.	1.3	13
23110	Catalytic propane reforming mechanism over Mn-Doped CeO2 (111). Surface Science, 2015, 640, 119-126.	0.8	14
23111	Understanding the Anchoring Effect of Two-Dimensional Layered Materials for Lithiumâ€“Sulfur Batteries. Nano Letters, 2015, 15, 3780-3786.	4.5	779
23112	Two-dimensional graphene-like C₂N: an experimentally available porous membrane for hydrogen purification. Physical Chemistry Chemical Physics, 2015, 17, 15115-15118.	1.3	111
23113	Room-temperature ferromagnetism in Fe-doped wide band gap ferroelectric Bi0.5K0.5TiO3 nanocrystals. Materials Letters, 2015, 156, 129-133.	1.3	48
23114	Enhancing methane dissociation with nickel nanoclusters. Computational and Theoretical Chemistry, 2015, 1064, 7-14.	1.1	8
23115	H₂O Adsorption/Desorption in MOF-74: Ab Initio Molecular Dynamics and Experiments. Journal of Physical Chemistry C, 2015, 119, 13021-13031.	1.5	43
23116	Adsorption of Hydrogen at the GaN(0001Ì…) Surface: An Ab Initio Study. Journal of Physical Chemistry C, 2015, 119, 11563-11569.	1.5	15
23117	Dispersion Corrected Structural Properties and Quasiparticle Band Gaps of Several Organic Energetic Solids. Journal of Physical Chemistry A, 2015, 119, 6574-6581.	1.1	23
23118	Biexciton formation and exciton coherent coupling in layered GaSe. Journal of Chemical Physics, 2015, 142, 212422.	1.2	31
23119	Structure and energy of point defects in TiC: Anab initiostudy. Physical Review B, 2015, 91, .	1.1	23
23120	Hybrid functional band gap calculation of SnO6 containing perovskites and their derived structures. Journal of Solid State Chemistry, 2015, 228, 214-220.	1.4	8

#	Article	IF	Citations
23121	Stability and morphology-dependence of Sc3+ ions incorporation and substitution kinetics within ZnO host lattice. Materials Science in Semiconductor Processing, 2015, 39, 103-111.	1.9	15
23122	Two-dimensional electron gas and its electric control at the interface between ferroelectric and antiferromagnetic insulator studied from first principles. Physical Chemistry Chemical Physics, 2015, 17, 12812-12825.	1.3	10
23123	Elastic properties of perovskite ATiO3 (Aâ€‰=â€‰Be, Mg, Ca, Sr, and Ba) and PbBO3 (Bâ€‰=â€‰Ti, Zr, and Hf): First principles calculations. Journal of Applied Physics, 2015, 117, .	1.1	30
23124	In situ unravelling structural modulation across the charge-density-wave transition in vanadium disulfide. Physical Chemistry Chemical Physics, 2015, 17, 13333-13339.	1.3	24
23125	k Â· p theory for two-dimensional transition metal dichalcogenide semiconductors. 2D Materials, 2015, 2, 022001.	2.0	676
23126	The role of spatial constraints and entropy in the adsorption and transformation of hydrocarbons catalyzed by zeolites. Journal of Catalysis, 2015, 329, 32-48.	3.1	61
23127	Linker dependence of interfacial electron transfer rates in Fe(II)-polypyridine sensitized solar cells. Journal of Physics Condensed Matter, 2015, 27, 134205.	0.7	19
23128	Unraveling the structure sensitivity in methanol conversion on CeO2: A DFT+U study. Journal of Catalysis, 2015, 327, 58-64.	3.1	91
23129	Structure and Reactivity of Supported Hybrid Platinum Nanoparticles for the Flow Hydrogenation of Functionalized Nitroaromatics. ACS Catalysis, 2015, 5, 3767-3778.	5.5	81
23130	Diffusion of Cd and Te adatoms on CdTe(111) surfaces: A computational study using density functional theory. AIP Advances, 2015, 5, .	0.6	5
23131	Pristine-state structure of lithium-ion-battery cathode material Li_{1.2}Mn_{0.4}Co_{0.4}O₂ derived from NMR bond pathway analysis. Journal of Materials Chemistry A, 2015, 3, 11471-11477.	5.2	17
23132	Effects of in-plane stiffness and charge transfer on thermal expansion of monolayer transition metal dichalcogenide*. Chinese Physics B, 2015, 24, 026501.	0.7	29
23133	Polymorph Engineering of TiO₂: Demonstrating How Absolute Reference Potentials Are Determined by Local Coordination. Chemistry of Materials, 2015, 27, 3844-3851.	3.2	113
23134	Atomistic mechanisms of nonstoichiometry-induced twin boundary structural transformation in titanium dioxide. Nature Communications, 2015, 6, 7120.	5.8	90
23135	Combined first-principles and thermodynamic approach to<mml:math xmlns:mml="http://www.w3.org/1998/Math/MathML"><mml:mi>M</mml:mi></mml:math>-nitronyl nitroxide<mml:math xmlns:mml="http://www.w3.org/1998/Math/MathML"><mml:mo>(</mml:mo><mml:mi>M</mml:mi></mml:math>=) Tj ETQq0 0 0 rgBT	1.1	15
23136	First-principles investigation on the mechanical, vibrational and thermodynamics properties of AuCu3-type X3Sc (X=Al, Ga, In) intermetallic compounds. Computational Materials Science, 2015, 106, 38-44.	1.4	14
23137	Role of Cooperative Interactions in the Intercalation of Heteroatoms between Graphene and a Metal Substrate. Journal of the American Chemical Society, 2015, 137, 7099-7103.	6.6	50
23138	Impact of Surface Passivation on the Electronic Structure and Optical Properties oftheSi _{1â’ x} Ge _x Nanowires. Chinese Physics Letters, 2015, 32, 027301.	1.3	2

#	Article	IF	Citations
23139	Efficient photocatalytic dechlorination of chlorophenols over a nonlinear optical material Na₃VO₂B₆O₁₁ under UV-visible light irradiation. Journal of Materials Chemistry A, 2015, 3, 12179-12187.	5.2	54
23140	The use of ultrasonic cavitation for near-surface structuring of robust and low-cost AlNi catalysts for hydrogen production. Green Chemistry, 2015, 17, 2745-2749.	4.6	37
23141	Phase-Field Simulation of Orowan Strengthening by Coherent Precipitate Plates in an Aluminum Alloy. Metallurgical and Materials Transactions A: Physical Metallurgy and Materials Science, 2015, 46, 3287-3301.	1.1	41
23142	The electronic and magnetic properties of transition-metal element doped three-dimensional topological Dirac semimetal in Cd₃As₂. Journal of Materials Chemistry C, 2015, 3, 3547-3551.	2.7	19
23143	Interfacial Effects of CeO₂-Supported Pd Nanorod in Catalytic CO Oxidation: A Theoretical Study. Journal of Physical Chemistry C, 2015, 119, 12923-12934.	1.5	82
23144	Continuously tunable electronic structure of transition metal dichalcogenides superlattices. Scientific Reports, 2015, 5, 8356.	1.6	16
23145	Integrated digital inverters based on two-dimensional anisotropic ReS2 field-effect transistors. Nature Communications, 2015, 6, 6991.	5.8	505
23146	Ab-Initio Simulation of van der Waals MoTe₂â€“SnS₂ Heterotunneling FETs for Low-Power Electronics. IEEE Electron Device Letters, 2015, 36, 514-516.	2.2	74
23147	Carbon-Coated Coreâ€“Shell Feâ€“Cu Nanoparticles as Highly Active and Durable Electrocatalysts for a Znâ€“Air Battery. ACS Nano, 2015, 9, 6493-6501.	7.3	167
23148	Tunable zinc interstitial related defects in ZnMgO and ZnCdO films. Journal of Applied Physics, 2015, 117, .	1.1	46
23149	Synthesis of Surface Covalent Organic Frameworks via Dimerization and Cyclotrimerization of Acetyls. Journal of the American Chemical Society, 2015, 137, 4904-4907.	6.6	98
23150	Electronic and magnetic properties of MoS2 nanoribbons with sulfur line vacancy defects. Applied Surface Science, 2015, 346, 470-476.	3.1	25
23151	First-principles phase stability and elastic properties of Alâ€“La binary system intermetallic compounds. Intermetallics, 2015, 60, 92-97.	1.8	13
23152	Origin of Extraordinary Stability of Squareâ€Planar Carbon Atoms in Surface Carbides of Cobalt and Nickel. Angewandte Chemie - International Edition, 2015, 54, 5312-5316.	7.2	67
23153	Vibrational models for a crystal with 36 water molecules in the unit cell: IR spectra from experiment and calculation. Physical Chemistry Chemical Physics, 2015, 17, 10520-10531.	1.3	20
23154	The stability and surface termination of hexagonal LuFeO₃. Journal of Physics Condensed Matter, 2015, 27, 175004.	0.7	8
23155	Magnetism, electronic structure and half-metallic property of transition metal (V, Cr, Mn, Fe, Co) substituted Zn3P2 dilute magnetic semiconductors: An ab-initio study. Computational Materials Science, 2015, 102, 85-94.	1.4	16
23156	Electronic structure and optical properties of orthorhombic and rhombohedral RAlO3 (RÂ=ÂSm, Nd). Solid State Sciences, 2015, 42, 37-44.	1.5	10

#	Article	IF	Citations
23157	Versatile electronic properties and exotic edge states of single-layer tetragonal silicon carbides. Physical Chemistry Chemical Physics, 2015, 17, 11211-11216.	1.3	13
23158	Site- and bond-centered ordering driven ferroelectricity in DyNiO3. Journal of Alloys and Compounds, 2015, 639, 45-50.	2.8	1
23159	Heterovalent Substitution to Enrich Electrical Conductivity in Cu2CdSn1-xGaxSe4 Series for High Thermoelectric Performances. Scientific Reports, 2015, 5, 9365.	1.6	7
23160	Lithium boride sheet and nanotubes: structure and hydrogen storage. Physical Chemistry Chemical Physics, 2015, 17, 13821-13828.	1.3	18
23161	Insights into HÃgg Iron-Carbide-Catalyzed Fischerâ€“Tropsch Synthesis: Suppression of CH₄ Formation and Enhancement of Câ€“C Coupling on Ï‡-Fe₅C₂ (510). ACS Catalysis, 2015, 5, 2203-2208.	5.5	122
23162	First-principles calculations of the equations of state and relative stability of iron carbides at the Earthâ€™s core pressures. Russian Geology and Geophysics, 2015, 56, 164-171.	0.3	12
23164	An oxygen reduction catalytic process through superoxo adsorption states on n-type doped h-BN: A first-principles study. Current Applied Physics, 2015, 15, 727-732.	1.1	15
23165	A DFT study of oxygen reduction reaction mechanism over O-doped graphene-supported Pt4, Pt3Fe and Pt3V alloy catalysts. International Journal of Hydrogen Energy, 2015, 40, 5126-5134.	3.8	36
23166	Hydration entropy of BaZrO₃ from first principles phonon calculations. Journal of Materials Chemistry A, 2015, 3, 7639-7648.	5.2	68
23167	High capacity group-15 alloy anodes for Na-ion batteries: Electrochemical and mechanical insights. Journal of Power Sources, 2015, 285, 29-36.	4.0	75
23168	Line and rotational defects in boron-nitrene: Structure, energetics, and dependence on mechanical strain from first-principles calculations. Physica Status Solidi (B): Basic Research, 2015, 252, 1725-1730.	0.7	7
23169	Origin of the Zn-induced Al intergranular corrosion of the outermost surface layer of the aluminium grain boundary: An ab initio study. Computational Materials Science, 2015, 102, 78-84.	1.4	1
23170	Site occupancy of Ce3+ in Î²-Ca2SiO4: A combined experimental and ab initio study. Optical Materials, 2015, 44, 67-72.	1.7	19
23171	Origin of nonlinear piezoelectricity in III-V semiconductors: Internal strain and bond ionicity from hybrid-functional density functional theory. Physical Review B, 2015, 91, .	1.1	40
23172	Origin of Degradation Phenomenon under Drain Bias Stress for Oxide Thin Film Transistors using IGZO and IGO Channel Layers. Scientific Reports, 2015, 5, 7884.	1.6	30
23173	First-principles calculations of the dissolution and coalescence properties of Pt nanoparticle ORR catalysts: The effect of nanoparticle shape. Nano Research, 2015, 8, 1689-1697.	5.8	37
23174	Coverage-dependent thermodynamic analysis of the formation of water and hydrogen peroxide on a platinum model catalyst. Physical Chemistry Chemical Physics, 2015, 17, 11392-11400.	1.3	20
23175	Achieving Type I, II, and III Heterojunctions Using Functionalized MXene. ACS Applied Materials & Interfaces, 2015, 7, 7163-7169.	4.0	120

#	Article	IF	Citations
23176	Ultrabright X-ray laser scattering for dynamic warm dense matter physics. Nature Photonics, 2015, 9, 274-279.	15.6	208
23177	2D Nanovaristors at Grain Boundaries Account for Memristive Switching in Polycrystalline BiFeO₃. Advanced Electronic Materials, 2015, 1, 1500019.	2.6	11
23178	Strong IR NLO Material Ba₄MGa₄Se₁₀Cl₂: Highly Improved Laser Damage Threshold via Dual Ion Substitution Synergy. Advanced Optical Materials, 2015, 3, 957-966.	3.6	75
23179	Structural and Electronic Properties of Pb- Intercalated Graphene on Ru(0001). Journal of Physical Chemistry C, 2015, 119, 9839-9844.	1.5	30
23180	Real-space grids and the Octopus code as tools for the development of new simulation approaches for electronic systems. Physical Chemistry Chemical Physics, 2015, 17, 31371-31396.	1.3	376
23181	Rigid/Flexible Organic Structure Directing Agents for Directing the Synthesis of Multipore Zeolites: A Computational Approach. Journal of Physical Chemistry C, 2015, 119, 7711-7720.	1.5	13
23182	Electronic properties of nickel-doped TiO2 anatase. Journal of Physics Condensed Matter, 2015, 27, 134207.	0.7	15
23183	Enhancement of Ionic Transport in Complex Oxides through Soft Lattice Modes and Epitaxial Strain. Chemistry of Materials, 2015, 27, 2647-2652.	3.2	61
23184	Comment on â€œDynamic transition of supercritical hydrogen: Defining the boundary between interior and atmosphere in gas giantsâ€. Physical Review E, 2015, 91, 036101.	0.8	3
23185	Adsorption behavior of Co anchored on graphene sheets toward NO, SO2, NH3, CO and HCN molecules. Applied Surface Science, 2015, 342, 191-199.	3.1	132
23186	Anomalous breakdown of Bloch's rule in the Mott-Hubbard insulator<mml:math xmlns:mml="http://www.w3.org/1998/Math/MathML"><mml:msub><mml:mi>MnTe</mml:mi><mml:mn>2</mml:mn></mml:msub></m Physical Review B, 2015, 91, .	1.1	4
23187	Unexpected Magnetic Semiconductor Behavior in Zigzag Phosphorene Nanoribbons Driven by Half-Filled One Dimensional Band. Scientific Reports, 2015, 5, 8921.	1.6	88
23188	Rich stoichiometries of stable Ca-Bi system: Structure prediction and superconductivity. Scientific Reports, 2015, 5, 9326.	1.6	12
23189	An atomic-level strategy for the design of a low overpotential catalyst for Liâ^'O2 batteries. Nano Energy, 2015, 13, 679-686.	8.2	68
23190	A density functional study of oxygen vacancy formation on Î±-Fe2O3(0001) surface and the effect of supported Au nanoparticles. Research on Chemical Intermediates, 2015, 41, 9587-9601.	1.3	20
23191	Intramolecularly resolved Kondo resonance of high-spin<mml:math xmlns:mml="http://www.w3.org/1998/Math/MathML"><mml:mrow><mml:mi>Fe</mml:mi><mml:mo>(</mml:mo><mml:mi>II</mml:mi> adsorbed on<mml:math xmlns:mml="http://www.w3.org/1998/Math/MathML"><mml:mrow><mml:mrow><mml:mi>Au</mml:mi><mml:mo>(</mml:mo></mml: Physical Review B, 2015, 91, .	1.1	45
23192	Electronic Structure Calculations for Antiferromagnetism of Cuprates Using SIWB Method for Anions in DV and a Density Functional Theory Confirming from Finite Element Method. Advances in Quantum Chemistry, 2015, 70, 1-29.	0.4	1
23193	Aqueous proton transfer across single-layer graphene. Nature Communications, 2015, 6, 6539.	5.8	214

#	Article	IF	Citations
23194	Electronic Properties of Ce³⁺-Doped Sr₃Al₂O₅Cl₂: A Combined Spectroscopic and Theoretical Study. Journal of Physical Chemistry C, 2015, 119, 6785-6792.	1.5	41
23195	Ab Initio Study of the Dielectric and Electronic Properties of Multilayer GaS Films. Journal of Physical Chemistry Letters, 2015, 6, 1059-1064.	2.1	34
23196	Tailoring Electronic and Magnetic Properties of MoS₂ Nanotubes. Journal of Physical Chemistry C, 2015, 119, 6405-6413.	1.5	40
23197	Continuous Germanene Layer on Al(111). Nano Letters, 2015, 15, 2510-2516.	4.5	559
23198	Improved hydrogen storage in Ca-decorated boron heterofullerenes: a theoretical study. Journal of Materials Chemistry A, 2015, 3, 7710-7714.	5.2	28
23199	Strain engineering the magnetic states of vacancy-doped monolayer MoSe 2. Journal of Alloys and Compounds, 2015, 635, 307-313.	2.8	35
23200	Facile preparation of semimetallic MoP₂ as a novel visible light driven photocatalyst with high photocatalytic activity. Journal of Materials Chemistry A, 2015, 3, 10360-10367.	5.2	42
23201	Theoretical Prediction of Phosphorene and Nanoribbons As Fast-Charging Li Ion Battery Anode Materials. Journal of Physical Chemistry C, 2015, 119, 6923-6928.	1.5	96
23202	High intrinsic carrier mobility and photon absorption in the perovskite CH₃NH₃PbI₃. Physical Chemistry Chemical Physics, 2015, 17, 11516-11520.	1.3	182
23203	Enhanced O₂ Selectivity versus N₂ by Partial Metal Substitution in Cu-BTC. Chemistry of Materials, 2015, 27, 2018-2025.	3.2	72
23204	Effect of the Electrolyte Composition on SEI Reactions at Si Anodes of Li-Ion Batteries. Journal of Physical Chemistry C, 2015, 119, 7060-7068.	1.5	68
23205	Organicâ€“Clay Interfacial Chemical Bonds Probed by ab Initio Calculations. Journal of Physical Chemistry C, 2015, 119, 6511-6517.	1.5	9
23206	First-Principles Study of Structure Sensitivity of Ethylene Glycol Conversion on Platinum. ACS Catalysis, 2015, 5, 2623-2631.	5.5	60
23207	Noncollinear magnetism in postâ€perovskites from first principles: Comparison between CaRhO₃ and NaNiF₃. Physica Status Solidi (B): Basic Research, 2015, 252, 689-694.	0.7	5
23208	Deciphering a Nanocarbonâ€Based Artificial Peroxidase: Chemical Identification of the Catalytically Active and Substrateâ€Binding Sites on Graphene Quantum Dots. Angewandte Chemie - International Edition, 2015, 54, 7176-7180.	7.2	380
23209	Nanostructure formation mechanism and ion diffusion in ironâ€“titanium composite materials with chemical looping redox reactions. Journal of Materials Chemistry A, 2015, 3, 11302-11312.	5.2	68
23210	Synergy between Pd and Au in a Pdâ€“Au(100) bimetallic surface for the water gas shift reaction: a DFT study. RSC Advances, 2015, 5, 47066-47073.	1.7	14
23211	Transient dynamics of magnetic Coâ€“graphene systems. Nanoscale, 2015, 7, 10030-10038.	2.8	12

#	Article	IF	Citations
23212	The doping effect on the catalytic activity of graphene for oxygen evolution reaction in a lithiumâ€“air battery: a first-principles study. Physical Chemistry Chemical Physics, 2015, 17, 14605-14612.	1.3	77
23213	Length Dependent Thermal Conductivity Measurements Yield Phonon Mean Free Path Spectra in Nanostructures. Scientific Reports, 2015, 5, 9121.	1.6	55
23214	Thermodynamics of the hydrogen dominant potassium hydride superconductor at high pressure. Solid State Communications, 2015, 212, 1-4.	0.9	5
23215	Control of selectivity in allylic alcohol oxidation on gold surfaces: the role of oxygen adatoms and hydroxyl species. Physical Chemistry Chemical Physics, 2015, 17, 4730-4738.	1.3	22
23216	Bio-inspired design of electrocatalysts for oxalate oxidation: a combined experimental and computational study of Mnâ€“Nâ€“C catalysts. Physical Chemistry Chemical Physics, 2015, 17, 13235-13244.	1.3	26
23217	FeCoCp₃ Molecular Magnets as Spin Filters. Journal of Physical Chemistry C, 2015, 119, 12119-12129.	1.5	33
23218	Insights into How Fluorine-Adsorption and n-Type Doping Affect the Relative Stability of the (001) and (101) Surfaces of TiO₂: Enhancing the Exposure of More Active but Thermodynamically Less Stable (001). Journal of Physical Chemistry Letters, 2015, 6, 1876-1882.	2.1	36
23219	Tailoring Band Structure of TiO₂ To Enhance Photoelectrochemical Activity by Codoping S and Mg. Journal of Physical Chemistry C, 2015, 119, 11557-11562.	1.5	34
23220	P2-Na0.6[Cr0.6Ti0.4]O2 cation-disordered electrode for high-rate symmetric rechargeable sodium-ion batteries. Nature Communications, 2015, 6, 6954.	5.8	426
23221	Electronic structures and current conductivities of B, C, N and F defects in amorphous titanium dioxide. Physical Chemistry Chemical Physics, 2015, 17, 11908-11913.	1.3	19
23222	The band gap modulation of monolayer Ti₂CO₂ by strain. RSC Advances, 2015, 5, 30438-30444.	1.7	82
23223	Bandgap opening in few-layered monoclinic MoTe2. Nature Physics, 2015, 11, 482-486.	6.5	800
23224	Configuration-Induced Rich Electronic Properties of Bilayer Graphene. Journal of Physical Chemistry C, 2015, 119, 10623-10630.	1.5	16
23225	Structure and Stoichiometry in Supervalent Doped Li₇La₃Zr₂O₁₂. Chemistry of Materials, 2015, 27, 3658-3665.	3.2	99
23226	First-principles study of SO2 molecule adsorption on the pristine and Mn-doped boron nitride nanotubes. Applied Surface Science, 2015, 347, 485-490.	3.1	44
23227	Superior Properties of Energetically Stable La_{2/3}Sr_{1/3}MnO₃/Tetragonal BiFeO₃ Multiferroic Superlattices. ACS Applied Materials & Interfaces, 2015, 7, 10612-10616.	4.0	38
23228	Electronic Structure, Phonon Dynamical Properties, andCO2Capture Capability ofNa2âˆ’xMxZrO3(M=Li,K): Density-Functional Calculations and Experimental Validations. Physical Review Applied, 2015, 3, .	1.5	20
23229	A first-principles study of a single C-chain doped AlN nanoribbons. Superlattices and Microstructures, 2015, 84, 36-44.	1.4	14

#	Article	IF	Citations
23230	Stabilization and Band-Gap Tuning of the 1T-MoS₂ Monolayer by Covalent Functionalization. Chemistry of Materials, 2015, 27, 3743-3748.	3.2	297
23231	Strong increase in superconducting Tc for Nb2InC under compressive strain. Journal of Applied Physics, 2015, 117, 093908.	1.1	3
23232	Native defects in Tl6SI4: Density functional calculations. Journal of Applied Physics, 2015, 117, .	1.1	7
23233	Atomic-scale dynamics of triangular hole growth in monolayer hexagonal boron nitride under electron irradiation. Nanoscale, 2015, 7, 10600-10605.	2.8	63
23234	Ion diffusion mechanism in Pn Na_xLi_{2â^'x}MnSiO₄. CrystEngComm, 2015, 17, 2123-2128.	1.3	21
23235	The Electronic Properties of Single-Layer and Multilayer MoS₂ under High Pressure. Journal of Physical Chemistry C, 2015, 119, 10189-10196.	1.5	89
23236	A facile synthesis of high quality nanostructured CeO₂ and Gd₂O₃-doped CeO₂ solid electrolytes for improved electrochemical performance. Physical Chemistry Chemical Physics, 2015, 17, 14193-14200.	1.3	22
23237	Insight into the effect of CaMnO 3 support on the catalytic performance of platinum catalysts. Chemical Engineering Science, 2015, 135, 179-186.	1.9	6
23238	Vacancy Formation and Oxidation Characteristics of Single Layer TiS₃. Journal of Physical Chemistry C, 2015, 119, 10709-10715.	1.5	51
23239	Study of electronic structure of Co2MnSn Heusler alloy by resonant photoemission spectroscopy and ab initio calculations. Journal of Alloys and Compounds, 2015, 645, 112-117.	2.8	18
23240	Kinetics of Energy Selective Cs Encapsulation in Single-Walled Carbon Nanotubes for Damage-Free and Position-Selective Doping. Journal of Physical Chemistry C, 2015, 119, 11903-11908.	1.5	5
23241	Stabilization of fullerene-like boron cages by transition metal encapsulation. Nanoscale, 2015, 7, 10482-10489.	2.8	72
23242	Face-sharing octahedra in Cs3Al2F9 and Cs2AlF5. Powder Diffraction, 2015, 30, 130-138.	0.4	1
23243	Oxygen Activation and Reaction on Pdâ€“Au Bimetallic Surfaces. Journal of Physical Chemistry C, 2015, 119, 11754-11762.	1.5	57
23244	DMSOâ€“Li₂O₂ Interface in the Rechargeable Liâ€“O₂ Battery Cathode: Theoretical and Experimental Perspectives on Stability. ACS Applied Materials & Interfaces, 2015, 7, 11402-11411.	4.0	66
23245	The Intercalation Phase Diagram of Mg in V₂O₅ from First-Principles. Chemistry of Materials, 2015, 27, 3733-3742.	3.2	130
23246	Insights into the Anomalous Vibrational Frequency Shifts of CO₂ Adsorbed to Metal Sites in Microporous Frameworks. Journal of Physical Chemistry C, 2015, 119, 5293-5300.	1.5	17
23247	Adsorption of C and CH_x Radicals on Anatase (001) and the Influence of Oxygen Vacancies. Journal of Physical Chemistry C, 2015, 119, 4908-4921.	1.5	19

#	Article	IF	Citations
23248	Single Layer Molybdenum Disulfide under Direct Out-of-Plane Compression: Low-Stress Band-Gap Engineering. Nano Letters, 2015, 15, 3139-3146.	4.5	75
23249	Unusual Deprotonated Alkynyl Hydrogen Bonding in Metal-Supported Hydrocarbon Assembly. Journal of Physical Chemistry C, 2015, 119, 9669-9679.	1.5	39
23250	Dehydrogenation of Ammonia on Ru(0001) by Electronic Excitations. Journal of Physical Chemistry C, 2015, 119, 10520-10525.	1.5	3
23251	Mode- and Bond-Selective Chemistry on Metal Surfaces: The Dissociative Chemisorption of CHD₃ on Ni(111). Journal of Physical Chemistry C, 2015, 119, 14769-14779.	1.5	32
23252	General method to predict voltage-dependent ionic conduction in a solid electrolyte coating on electrodes. Physical Review B, 2015, 91, .	1.1	141
23253	The role of uniaxial strain in tailoring the interfacial properties of LaAlO₃/SrTiO₃heterostructure. RSC Advances, 2015, 5, 15682-15689.	1.7	30
23254	Hydriding and dehydriding energies of PuHx from ab initio calculations. Physics Letters, Section A: General, Atomic and Solid State Physics, 2015, 379, 1649-1653.	0.9	19
23255	Pseudo Jahnâ€“Teller Origin of Buckling Distortions in Two-Dimensional Triazine-Based Graphitic Carbon Nitride (g-C₃N₄) Sheets. Journal of Physical Chemistry C, 2015, 119, 12008-12015.	1.5	40
23256	Plasmonics in strained monolayer black phosphorus. Journal of Applied Physics, 2015, 117, .	1.1	33
23257	Theoretical insight into the strain effect on the intercalation potential of Liâ€“FePO₄ materials. RSC Advances, 2015, 5, 35667-35674.	1.7	9
23258	A New Core/Shell NiAu/Au Nanoparticle Catalyst with Pt-like Activity for Hydrogen Evolution Reaction. Journal of the American Chemical Society, 2015, 137, 5859-5862.	6.6	274
23259	Greatly Enhanced Electronic Conduction and Lithium Storage of Faceted TiO₂ Crystals Supported on Metallic Substrates by Tuning Crystallographic Orientation of TiO₂. Advanced Materials, 2015, 27, 3507-3512.	11.1	79
23260	Challenges in the synthetic routes to Mn(BH₄)₂: insight into intermediate compounds. Dalton Transactions, 2015, 44, 6571-6580.	1.6	19
23261	The Reaction Mechanism with Free Energy Barriers for Electrochemical Dihydrogen Evolution on MoS₂. Journal of the American Chemical Society, 2015, 137, 6692-6698.	6.6	173
23262	Novel diffusions of interstitial atoms in IIâ€“VI compounds zinc selenide. Modern Physics Letters B, 2015, 29, 1550044.	1.0	0
23263	Enhancement of multiferroic in BiFeO3 by Co doping. Journal of Alloys and Compounds, 2015, 645, 78-84.	2.8	29
23264	Topological crystalline insulator and quantum anomalous Hall states in IV-VI-based monolayers and their quantum wells. Physical Review B, 2015, 91, .	1.1	37
23265	Proton conduction at BaO-terminated (001) BaZrO3 surface using density functional theory. Solid State Ionics, 2015, 275, 19-22.	1.3	25

#	Article	IF	Citations
23266	Hydrazine network on Cu(111) surface: A Density Functional Theory approach. Surface Science, 2015, 637-638, 140-148.	0.8	21
23267	Electronic structures, magnetic properties and half-metallicity in Heusler alloys Zr2CoZ (Z=Al, Ga, In,) Tj ETQq1 1 0.784314 rgBT /Overlo	1.0	43
23268	Strain-induced directâ€“indirect bandgap transition and phonon modulation in monolayer WS2. Nano Research, 2015, 8, 2562-2572.	5.8	323
23269	Structural transformation between long and short-chain form of liquid sulfur from ab initio molecular dynamics. Journal of Chemical Physics, 2015, 142, 154502.	1.2	18
23270	Thermostructural behaviour of Niâ€“Cr materials: modelling of bulk and nanoparticle systems. Physical Chemistry Chemical Physics, 2015, 17, 15912-15920.	1.3	13
23271	Molecular Mechanisms for the Lithiation of Ruthenium Oxide Nanoplates as Lithium-Ion Battery Anode Materials: An Experimentally Motivated Computational Study. Journal of Physical Chemistry C, 2015, 119, 9705-9713.	1.5	24
23272	Ambient Pressure Structural Quantum Critical Point in the Phase Diagram of<mml:math xmlns:mml="http://www.w3.org/1998/Math/MathML" display="inline"><mml:mrow><mml:msub><mml:mrow><mml:mo stretchy="false">(</mml:mo><mml:msub><mml:mrow><mml:mi>Ca</mml:mi></mml:mrow><mml:mrow><mml:mi>x</mml:mi></mml:mrow>	2.9	81
23273	097002. Geometric stability and reaction activity of Pt clusters adsorbed graphene substrates for catalytic CO oxidation. Physical Chemistry Chemical Physics, 2015, 17, 11598-11608.	1.3	20
23274	Prediction of quantum anomalous Hall effect on graphene nanomesh. RSC Advances, 2015, 5, 9875-9880.	1.7	26
23275	Superhard-driven search of the covalent network in the B₃NO system. RSC Advances, 2015, 5, 35882-35887.	1.7	18
23276	Symmetry-Based Computational Tools for Magnetic Crystallography. Annual Review of Materials Research, 2015, 45, 217-248.	4.3	244
23277	Achieving optimum carrier concentrations in p-doped SnS thermoelectrics. Physical Chemistry Chemical Physics, 2015, 17, 9161-9166.	1.3	23
23278	Bandgap engineering of oxygen-rich TiO2+x for photocatalyst with enhanced visible-light photocatalytic ability. Journal of Materials Science, 2015, 50, 4324-4329.	1.7	20
23279	Theoretical search for half-Heusler topological insulators. Physical Review B, 2015, 91, .	1.1	54
23280	Sulfisoxazole/cyclodextrin inclusion complex incorporated in electrospun hydroxypropyl cellulose nanofibers as drug delivery system. Colloids and Surfaces B: Biointerfaces, 2015, 128, 331-338.	2.5	98
23281	Impact of homogeneous strain on uranium vacancy diffusion in uranium dioxide. Physical Review B, 2015, 91, .	1.1	27
23282	Giant Rashba-type splitting in molybdenum-driven bands of<mml:math xmlns:mml="http://www.w3.org/1998/Math/MathML"><mml:msub><mml:mi>MoS</mml:mi><mml:mn>2</mml:mn></mml:msub><mml:mathvariant="normal">Bi</mml:mi><mml:mo>(</mml:mo><mml:mn>111</mml:mn><mml:mo>)</mml:mo></mml:math>heterostructu Physical Review B, 2015, 91, .	1.1	46
23283	First-principles study of oxygen coverage effect on hydrogen oxidation on Ni(111) surface. Applied Surface Science, 2015, 333, 86-91.	3.1	20

#	Article	IF	Citations
23284	First-principles calculations study of Na adsorbed on silicene. Applied Surface Science, 2015, 341, 69-74.	3.1	31
23285	Crystal Field Effect Induced Topological Crystalline Insulators In Monolayer IVâ€“VI Semiconductors. Nano Letters, 2015, 15, 2657-2661.	4.5	104
23286	Effect of the crystal plane figure on the catalytic performance of MnO₂for the total oxidation of propane. CrystEngComm, 2015, 17, 3005-3014.	1.3	183
23287	Vacancy-induced initial decomposition of condensed phase NTO via bimolecular hydrogen transfer mechanisms at high pressure: a DFT-D study. Physical Chemistry Chemical Physics, 2015, 17, 10568-10578.	1.3	21
23288	Multiphysics modelling, quantum chemistry and risk analysis for corrosion inhibitor design and lifetime prediction. Faraday Discussions, 2015, 180, 459-477.	1.6	22
23289	Cu-deficiency induced structural transition of Cu_{2â^'x}Te. CrystEngComm, 2015, 17, 2878-2885.	1.3	41
23290	Magnetic properties of double-side partially fluorinated graphene from first principles calculations. Carbon, 2015, 89, 300-307.	5.4	30
23291	Origin of First-Order-Type Electronic and Structural Transitions in<mml:math xmlns:mml="http://www.w3.org/1998/Math/MathML" display="inline"><mml:msub><mml:mi>IrTe</mml:mi><mml:mn>2</mml:mn></mml:msub></mml:math>. Physical Review Letters, 2015, 114, 136401.	2.9	39
23292	Nanoscale Magnetization Reversal Caused by Electric Field-Induced Ion Migration and Redistribution in Cobalt Ferrite Thin Films. ACS Nano, 2015, 9, 4210-4218.	7.3	60
23293	SnS₂ nanotubes: a promising candidate for the anode material for lithium ion batteries. RSC Advances, 2015, 5, 32505-32510.	1.7	24
23295	Lateral interaction and spectroscopic constants of CO adsorbed on ZnO. Theoretical Chemistry Accounts, 2015, 134, 1.	0.5	6
23296	Hybrid functional studies on the optical and electronic properties of graphane and silicane. Solid State Communications, 2015, 209-210, 59-65.	0.9	6
23297	Driving a GaAs film to a large-gap topological insulator by tensile strain. Scientific Reports, 2015, 5, 8441.	1.6	55
23298	Defect Formation Energy in Spinel LiNi_{0.5}Mn_{1.5}O_{4-Î´} Using Ab Initio DFT Calculations. Journal of Physical Chemistry C, 2015, 119, 9117-9124.	1.5	37
23299	Compounds based on Group 14 elements: building blocks for advanced insulator dielectrics design. Journal of Materials Science, 2015, 50, 801-807.	1.7	13
23300	A Strategy to Stabilize Kesterite CZTS for High-Performance Solar Cells. Chemistry of Materials, 2015, 27, 2920-2927.	3.2	63
23301	First-Principles Study of Metal Adatom Adsorption on Black Phosphorene. Journal of Physical Chemistry C, 2015, 119, 8199-8207.	1.5	207
23302	A uniformly porous 2D CN (1â€‰:â€‰1) network predicted by first-principles calculations. RSC Advances, 2015, 5, 11791-11796.	1.7	6

#	Article	IF	Citations
23303	Ab initioapproach to model x-ray diffraction in warm dense matter. Physical Review E, 2015, 91, 033112.	0.8	15
23304	Prediction of new thermodynamically stable aluminum oxides. Scientific Reports, 2015, 5, 9518.	1.6	18
23305	Structural and electronic properties of Li-ion battery cathode material MoF3 from first-principles. Journal of Solid State Chemistry, 2015, 227, 25-29.	1.4	4
23306	Evaluation of the Electrochemical Stability of Model Cu-Pt(111) Near-Surface Alloy Catalysts. Electrochimica Acta, 2015, 179, 469-474.	2.6	12
23307	Layer-Dependent Dopant Stability and Magnetic Exchange Coupling of Iron-Doped MoS₂ Nanosheets. ACS Applied Materials & Interfaces, 2015, 7, 7534-7541.	4.0	90
23308	Does the Dirac Cone Exist in Silicene on Metal Substrates?. Scientific Reports, 2014, 4, 5476.	1.6	92
23309	Two-dimensional hexagonal V₂O nanosheet and nanoribbons. Applied Physics Express, 2015, 8, 035201.	1.1	2
23310	Energies and Forces. Springer Series in Solid-state Sciences, 2015, , 129-161.	0.3	0
23311	Conductance and spin-filter effects of oxygen-incorporated Au, Cu, and Fe single-atom chains. Journal of Applied Physics, 2015, 117, 043902.	1.1	11
23312	Ordered and Reversible Hydrogenation of Silicene. Physical Review Letters, 2015, 114, 126101.	2.9	127
23313	Electronic structure of ferromagnetic semiconductor material on the monoclinic and rhombohedral ordered double perovskites La2FeCoO6. Journal of Applied Physics, 2015, 117, .	1.1	16
23314	Modeling thermal properties of plutonium mononitride. Journal of Nuclear Materials, 2015, 461, 51-55.	1.3	0
23315	Strong spin-lattice coupling in CrSiTe3. APL Materials, 2015, 3, .	2.2	192
23316	Density Functional Calculations of Native Defects in CH₃NH₃PbI₃: Effects of Spinâ€“Orbit Coupling and Self-Interaction Error. Journal of Physical Chemistry Letters, 2015, 6, 1461-1466.	2.1	301
23317	Probing carbonate in bone forming minerals on the nanometre scale. Acta Biomaterialia, 2015, 20, 129-139.	4.1	28
23318	Morphology effects in photoactive ZnO nanostructures: photooxidative activity of polar surfaces. Journal of Materials Chemistry A, 2015, 3, 8782-8792.	5.2	39
23319	The low coordination number of nitrogen in hard tungsten nitrides: a first-principles study. Physical Chemistry Chemical Physics, 2015, 17, 13397-13402.	1.3	23
23320	Tunable electronic properties in the van der Waals heterostructure of germanene/germanane. Physical Chemistry Chemical Physics, 2015, 17, 12194-12198.	1.3	20

#	Article	IF	Citations
23321	Cycloaddition of Metal Porphines on Metal-Supported Graphene: A Computational Study. Journal of Physical Chemistry C, 2015, 119, 9234-9241.	1.5	8
23322	Effect of Metal in M₃(btc)₂ and M₂(dobdc) MOFs for O₂/N₂ Separations: A Combined Density Functional Theory and Experimental Study. Journal of Physical Chemistry C, 2015, 119, 6556-6567.	1.5	65
23323	Platinum Nanoparticle During Electrochemical Hydrogen Evolution: Adsorbate Distribution, Active Reaction Species, and Size Effect. ACS Catalysis, 2015, 5, 2376-2383.	5.5	102
23324	Bandstructure modulation of two-dimensional WSe2 by electric field. Journal of Applied Physics, 2015, 117, .	1.1	29
23325	Strain induced modulation to the magnetism of antisite defects doped monolayer MoS2. Journal of Magnetism and Magnetic Materials, 2015, 386, 155-160.	1.0	16
23326	Structural and Electronic Properties of Layered Arsenic and Antimony Arsenide. Journal of Physical Chemistry C, 2015, 119, 6918-6922.	1.5	210
23327	Role of hydrogen-bonding and its interplay with octahedral tilting in CH₃NH₃PbI₃. Chemical Communications, 2015, 51, 6434-6437.	2.2	173
23328	Molecular functionalization of silicene/Ag(111) by covalent bonds: a DFT study. Physical Chemistry Chemical Physics, 2015, 17, 14495-14501.	1.3	20
23329	General microscopic model of magnetoelastic coupling from first principles. Physical Review B, 2015, 91, .	1.1	22
23330	Tuning the Electronic and Magnetic Properties of Phosphorene by Vacancies and Adatoms. Journal of Physical Chemistry C, 2015, 119, 6530-6538.	1.5	125
23331	A facile solvothermal growth of single crystal mixed halide perovskite CH₃NH₃Pb(Br_{1â^'x}Cl_x)₃. Chemical Communications, 2015, 51, 7820-7823.	2.2	135
23332	Thermodynamic and kinetic modeling of oxide precipitation in nanostructured ferritic alloys. Acta Materialia, 2015, 91, 340-354.	3.8	40
23333	Raman spectroscopy of NdFeO₃at pressures up to 11â€…GPa. High Pressure Research, 2015, 35, 170-175.	0.4	4
23334	Hydrogen storage mechanism and lithium dynamics in Li12C60 investigated by Î¼SR. Carbon, 2015, 90, 130-137.	5.4	16
23335	Effect of Sn-Substitution on Thermoelectric Properties of Copper-Based Sulfide, Famatinite Cu₃SbS₄. Journal of the Physical Society of Japan, 2015, 84, 044706.	0.7	47
23336	High-Efficiency Thermoelectrics with Functionalized Graphene. Nano Letters, 2015, 15, 2830-2835.	4.5	67
23337	First principle study on the temperature dependent elastic constants, anisotropy, generalized stacking fault energy and dislocation core of NiAl and FeAl. Computational Materials Science, 2015, 103, 116-125.	1.4	40
23338	Nine New Phosphorene Polymorphs with Non-Honeycomb Structures: A Much Extended Family. Nano Letters, 2015, 15, 3557-3562.	4.5	275

#	Article	IF	Citations
23339	First-principles prediction of graphene/SnO2 heterostructure as a promising candidate for FET. RSC Advances, 2015, 5, 35377-35383.	1.7	5
23340	How Voltage Drops Are Manifested by Lithium Ion Configurations at Interfaces and in Thin Films on Battery Electrodes. Journal of Physical Chemistry C, 2015, 119, 10234-10246.	1.5	51
23341	Band gap narrowing in nitrogen-doped La₂Ti₂O₇ predicted by density-functional theory calculations. Physical Chemistry Chemical Physics, 2015, 17, 8994-9000.	1.3	37
23342	Effect of irradiation defects on the corrosion behaviors of steels exposed to lead bismuth eutectic in ADS: a first-principles study. Physical Chemistry Chemical Physics, 2015, 17, 12292-12298.	1.3	20
23343	Electronic structure and magnetism on FeSiAl alloy: A DFT study. Journal of Magnetism and Magnetic Materials, 2015, 389, 73-76.	1.0	11
23344	Magnetostriction and ferroelectric state in AgCrS₂. Journal of Physics Condensed Matter, 2015, 27, 165601.	0.7	11
23345	First principles calculations of (La,Mg)2Ni7 hydrides. Journal of Alloys and Compounds, 2015, 645, S5-S8.	2.8	13
23346	The influence of oxygen vacancies and La doping on the surface structure of NaTaO 3. Computational Materials Science, 2015, 103, 1-7.	1.4	21
23347	High-quality single crystal growth and spin flop of multiferroic Co4Nb2O9. Journal of Crystal Growth, 2015, 420, 90-93.	0.7	25
23348	High Pressure Effects on the Properties of âŒ©110âŒª {001} Dislocation in Superconducting ZnCNi3 and MgCNi3 Determined from First Principles Calculations Combined with an Improved Peierls-Nabarro Equation. Journal of Superconductivity and Novel Magnetism, 2015, 28, 2281-2291.	0.8	0
23349	Li adsorption, hydrogen storage and dissociation using monolayer MoS₂: an ab initio random structure searching approach. Physical Chemistry Chemical Physics, 2015, 17, 11367-11374.	1.3	65
23350	Computational Prediction of Metal Organic Frameworks Suitable for Molecular Infiltration as a Route to Development of Conductive Materials. Journal of Physical Chemistry Letters, 2015, 6, 1586-1591.	2.1	39
23351	Enhanced photocatalytic oxidation of propylene over V-doped TiO2 photocatalyst: Reaction mechanism between V5+ and single-electron-trapped oxygen vacancy. Applied Catalysis B: Environmental, 2015, 176-177, 160-172.	10.8	78
23352	Coupled ferroelectric polarization and magnetization in spinel FeCr2S4. Scientific Reports, 2014, 4, 6530.	1.6	38
23353	Ab initio molecular dynamics study of the local atomic structures in monatomic metallic liquid and glass. Materials & Design, 2015, 77, 1-5.	5.1	54
23354	Functionalization of a GaSe monolayer by vacancy and chemical element doping. Physical Chemistry Chemical Physics, 2015, 17, 10737-10748.	1.3	40
23355	Theoretic Insight into the Desulfurization Mechanism: Removal of H₂S by Ceria (110). Journal of Physical Chemistry C, 2015, 119, 7678-7688.	1.5	11
23356	Band-gap modulation of two-dimensional saturable absorbers for solid-state lasers. Photonics Research, 2015, 3, A10.	3.4	23

#	Article	IF	Citations
23357	Insights into the roles of two constituents CL-20 and HMX in the CL-20:HMX cocrystal at high pressure: a DFT-D study. RSC Advances, 2015, 5, 34216-34225.	1.7	24
23358	Ferromagnetism induced by entangled charge and orbital orderings in ferroelectric titanate perovskites. Nature Communications, 2015, 6, 6677.	5.8	85
23359	Ab-initio calculation of optical properties of AA-stacked bilayer graphene with tunable layer separation. Current Applied Physics, 2015, 15, 691-697.	1.1	24
23360	Toward â€œrocking-chair typeâ€•Mgâ€“Li dual-salt batteries. Journal of Materials Chemistry A, 2015, 3, 10188-10194.	5.2	72
23361	CO₂ Electrochemical Reduction to Methane and Methanol on Copper-Based Alloys: Theoretical Insight. Journal of Physical Chemistry C, 2015, 119, 8238-8249.	1.5	157
23362	Tuning the Electrical Transport Properties of Multilayered Molybdenum Disulfide Nanosheets by Intercalating Phosphorus. Journal of Physical Chemistry C, 2015, 119, 9560-9567.	1.5	40
23363	Introducing structural sensitivity into adsorptionâ€“energy scaling relations by means of coordination numbers. Nature Chemistry, 2015, 7, 403-410.	6.6	600
23364	Influence of Support Effects on CO Oxidation Kinetics on CO-Saturated Graphene-Supported Pt₁₃ Nanoclusters. Journal of Physical Chemistry C, 2015, 119, 8703-8710.	1.5	46
23365	Electrical conductivity enhancement by boron-doping in diamond using first principle calculations. Applied Surface Science, 2015, 334, 40-44.	3.1	32
23366	An ab-initio analysis of the influence of knock-on atom induced damage on the peak tensile strength of 3C-SiC grain boundaries. International Journal of Damage Mechanics, 2015, 24, 446-467.	2.4	2
23367	Theoretical Prediction of Anode Materials in Li-Ion Batteries on Layered Black and Blue Phosphorus. Journal of Physical Chemistry C, 2015, 119, 8662-8670.	1.5	169
23368	Compositional Engineering of Perovskite Oxides for Highly Efficient Oxygen Reduction Reactions. ACS Applied Materials & Interfaces, 2015, 7, 8562-8571.	4.0	66
23369	Composition-dependent structural and magnetic properties of Niâ€“Mnâ€“Ga alloys studied by ab initio calculations. Journal of Materials Science, 2015, 50, 3825-3834.	1.7	16
23370	Structural, electronic and magnetic properties of 3d transition metal atom adsorbed germanene: A first-principles study. Materials Chemistry and Physics, 2015, 160, 96-104.	2.0	50
23371	Codoping in SnTe: Enhancement of Thermoelectric Performance through Synergy of Resonance Levels and Band Convergence. Journal of the American Chemical Society, 2015, 137, 5100-5112.	6.6	394
23372	Optical properties of a conjugated-polymer-sensitised solar cell: the effect of interfacial structure. Physical Chemistry Chemical Physics, 2015, 17, 14489-14494.	1.3	0
23373	Modeling atomic force microscopy at LiNbO 3 surfaces from first-principles. Computational Materials Science, 2015, 103, 145-150.	1.4	11
23374	Vibrational spectra and lattice thermal conductivity of kesterite-structured Cu2ZnSnS4 and Cu2ZnSnSe4. APL Materials, 2015, 3, .	2.2	69

#	Article	IF	Citations
23375	Possible martensitic transformation and ferrimagnetic properties in Heusler alloy Mn2NiSn. Journal of Magnetism and Magnetic Materials, 2015, 386, 102-106.	1.0	12
23376	Tuning Carrier Confinement in the MoS₂/WS₂ Lateral Heterostructure. Journal of Physical Chemistry C, 2015, 119, 9580-9586.	1.5	74
23377	Structural Transitions in Monolayer MoS₂by Lithium Adsorption. Journal of Physical Chemistry C, 2015, 119, 10602-10609.	1.5	109
23378	Firstâ€principles calculation of Cu₂SnS₃ and related compounds. Physica Status Solidi (B): Basic Research, 2015, 252, 1230-1234.	0.7	36
23379	The role of low-lying optical phonons in lattice thermal conductance of rare-earth pyrochlores: A first-principle study. Acta Materialia, 2015, 91, 304-317.	3.8	58
23380	Diffusion of alkali metals in the first stage graphite intercalation compounds by vdW-DFT calculations. RSC Advances, 2015, 5, 15985-15992.	1.7	64
23381	Ab initio study of sodium intercalation into disordered carbon. Journal of Materials Chemistry A, 2015, 3, 9763-9768.	5.2	193
23382	Nb-doped LiBH 4 (010) surface for hydrogen desorption: First-principles calculations. International Journal of Hydrogen Energy, 2015, 40, 6365-6372.	3.8	8
23383	A new phase of ThC at high pressure predicted from a first-principles study. Physics Letters, Section A: General, Atomic and Solid State Physics, 2015, 379, 1607-1611.	0.9	17
23384	Na₄IrO₄: Squareâ€Planar Coordination of a Transition Metal in d⁵ Configuration due to Weak Onâ€Site Coulomb Interactions. Angewandte Chemie - International Edition, 2015, 54, 5417-5420.	7.2	13
23385	n and p type character of single molecule diodes. Scientific Reports, 2015, 5, 8350.	1.6	12
23386	Facile synthesis of Ag nanowireâ€“rGO composites and their promising field emission performance. RSC Advances, 2015, 5, 41887-41893.	1.7	34
23387	LaMgX and CeMgX (XÂ=ÂGa, In, Tl, Pd, Ag, Pt, Au) with ZrNiAl type structure â€“ A systematic view on electronic structure and chemical bonding. Solid State Sciences, 2015, 43, 28-34.	1.5	3
23388	Structure and thermodynamic properties of hafniaâ€“silica glasses with low hafnia content. Journal of Non-Crystalline Solids, 2015, 416, 14-20.	1.5	1
23389	Cubic C₉₆: a novel carbon allotrope with a porous nanocube network. Journal of Materials Chemistry A, 2015, 3, 10448-10452.	5.2	47
23390	In situ high-energy synchrotron X-ray diffraction studies and first principles modeling of Î±-MnO₂ electrodes in Liâ€“O₂ and Li-ion coin cells. Journal of Materials Chemistry A, 2015, 3, 7389-7398.	5.2	43
23391	Electronâ€transfer transparency of graphene: Fast reduction of metal ions on grapheneâ€covered donor surfaces. Physica Status Solidi - Rapid Research Letters, 2015, 9, 180-186.	1.2	14
23392	Large-Area Epitaxial Monolayer MoS₂. ACS Nano, 2015, 9, 4611-4620.	7.3	712

#	Article	IF	Citations
23393	Correlation of Electronic Structure with Catalytic Activity: H₂â€“D₂ Exchange across Cu_xPd_{1â€“x} Composition Space. ACS Catalysis, 2015, 5, 3137-3147.	5.5	18
23394	Atomistic modeling of the behavior of materials in rechargeable lithium-ion and lithiumâ€“air batteries. , 2015, , 233-259.		0
23395	Ru_{0.01}Ti_{0.99}Nb₂O₇ as an intercalation-type anode material with a large capacity and high rate performance for lithium-ion batteries. Journal of Materials Chemistry A, 2015, 3, 8627-8635.	5.2	131
23396	Porous BN for hydrogen generation and storage. Journal of Materials Chemistry A, 2015, 3, 9632-9637.	5.2	83
23397	Effects of single- and co-substitution of Ti on dehydrogenation of Mg 2 NiH 4 : A first-principles study. Computational Materials Science, 2015, 103, 45-51.	1.4	12
23398	Boron Suboxide and Boron Subphosphide Crystals: Hard Ceramics That Shear without Brittle Failure. Chemistry of Materials, 2015, 27, 2855-2860.	3.2	42
23399	Ammonia borane modified zirconium borohydride octaammoniate with enhanced dehydrogenation properties. Journal of Materials Chemistry A, 2015, 3, 5299-5304.	5.2	22
23400	Surface-Mediated Solvent Decomposition in Liâ€“Air Batteries: Impact of Peroxide and Superoxide Surface Terminations. Journal of Physical Chemistry C, 2015, 119, 9050-9060.	1.5	36
23401	A density functional study of silver clusters on a stepped graphite surface: formation of self-assembled nano-wires. Physical Chemistry Chemical Physics, 2015, 17, 12708-12716.	1.3	5
23402	Achieving a high magnetization in sub-nanostructured magnetite films by spin-flipping of tetrahedral Fe3+ cations. Nano Research, 2015, 8, 2935-2945.	5.8	21
23403	Towards full-spectrum photocatalysis: Achieving a Z-scheme between Ag2S and TiO2 by engineering energy band alignment with interfacial Ag. Nano Research, 2015, 8, 3621-3629.	5.8	65
23404	Superionic Phases of the 1:1 Waterâ€“Ammonia Mixture. Journal of Physical Chemistry A, 2015, 119, 10582-10588.	1.1	36
23405	Molecular Precursor Induced Surface Reconstruction at Graphene/Pt(111) Interfaces. Journal of Physical Chemistry C, 2015, 119, 22534-22541.	1.5	15
23406	What Is the Role of Pyridinium in Pyridine-Catalyzed CO₂ Reduction on p-GaP Photocathodes?. Journal of the American Chemical Society, 2015, 137, 13248-13251.	6.6	63
23407	Fluorographane: a promising material for bipolar doping of MoS2. Physical Chemistry Chemical Physics, 2015, 17, 27636-27641.	1.3	7
23408	Mechanical properties of monolayer sulphides: a comparative study between MoS₂, HfS₂ and TiS₃. Physical Chemistry Chemical Physics, 2015, 17, 27742-27749.	1.3	99
23409	Structure and properties of type-II clathrate Cs₈Na_{16â^'x}Tl_xGe₁₃₆. Dalton Transactions, 2015, 44, 16937-16945.	1.6	6
23410	Density functional studies of zirconia with different crystal phases for oxygen reduction reaction. RSC Advances, 2015, 5, 85122-85127.	1.7	11

#	Article	IF	Citations
23411	Reaction kinetics of the electrochemical oxidation of CO and syngas fuels on a Sr₂Fe_{1.5}Mo_{0.5}O_{6â^'Î´} perovskite anode. Journal of Materials Chemistry A, 2015, 3, 21618-21629.	5.2	13
23412	Low-energy electron diffraction and density functional theory study of potassium adsorbed on Pb(1â€‰0â€‰0). Journal of Physics Condensed Matter, 2015, 27, 345001.	0.7	1
23413	Strong correlation in 1D oxygen-ion conduction of apatite-type lanthanum silicate. Journal of Physics Condensed Matter, 2015, 27, 365601.	0.7	12
23414	Comparative study of van der Waals corrections to the bulk properties of graphite. Journal of Physics Condensed Matter, 2015, 27, 415502.	0.7	43
23415	Scanning tunneling spectroscopy reveals a silicon dangling bond charge state transition. New Journal of Physics, 2015, 17, 073023.	1.2	44
23416	Adsorption behavior of Fe atoms on a naphthalocyanine monolayer on Ag(111) surface. Chinese Physics B, 2015, 24, 076802.	0.7	6
23417	Realization of Dirac Cones in Few Bilayer Sb(111) Films by Surface Modification. Nanoscale Research Letters, 2015, 10, 1043.	3.1	9
23418	A Cu₂₅ Nanocluster with Partial Cu(0) Character. Journal of the American Chemical Society, 2015, 137, 13319-13324.	6.6	234
23419	Graphene-covered perovskites: an effective strategy to enhance light absorption and resist moisture degradation. RSC Advances, 2015, 5, 82346-82350.	1.7	43
23420	Thermal stability and mechanical properties of boron enhanced Moâ€“Si coatings. Surface and Coatings Technology, 2015, 280, 282-290.	2.2	19
23421	Topological Insulating Phases in Two-Dimensional Bismuth-Containing Single Layers Preserved by Hydrogenation. Journal of Physical Chemistry C, 2015, 119, 23599-23606.	1.5	95
23422	Oxygen Intercalation of Graphene on Transition Metal Substrate: An Edge-Limited Mechanism. Journal of Physical Chemistry Letters, 2015, 6, 4099-4105.	2.1	35
23423	Descriptor Analysis in Methanol Conversion on Doped CeO2(111): Guidelines for Selectivity Tuning. ACS Catalysis, 2015, 5, 6473-6480.	5.5	30
23424	Phase stability and lattice dynamics of ammonium azide under hydrostatic compression. Physical Chemistry Chemical Physics, 2015, 17, 29210-29225.	1.3	20
23425	Enhanced thermoelectric performance of n-type Cu_{0.008}Bi₂Te_{2.7}Se_{0.3} by band engineering. Journal of Materials Chemistry C, 2015, 3, 10604-10609.	2.7	34
23426	Prediction of a metalâ€“insulator transition and a two-dimensional electron gas in orthoferrite LaTiO₃/tetragonal BiFeO₃ heterostructures. Journal of Materials Chemistry C, 2015, 3, 11066-11075.	2.7	13
23427	The structural behavior of SrTiO3 under 400ÂkeV Ne2+ ion irradiation. Applied Physics A: Materials Science and Processing, 2015, 121, 1211-1217.	1.1	0
23428	Robust Large Gap Two-Dimensional Topological Insulators in Hydrogenated IIIâ€“V Buckled Honeycombs. Nano Letters, 2015, 15, 6568-6574.	4.5	105

#	Article	IF	Citations
23429	Rationalization of Au Concentration and Distribution in AuNi@Pt Coreâ€“Shell Nanoparticles for Oxygen Reduction Reaction. ACS Catalysis, 2015, 5, 6328-6336.	5.5	49
23430	Strong interface-induced spinâ€“orbit interaction in graphene on WS2. Nature Communications, 2015, 6, 8339.	5.8	314
23431	Facts and fictions about polymorphism. Chemical Society Reviews, 2015, 44, 8619-8635.	18.7	499
23432	First-principles computational study of highly stable and active ternary PtCuNi nanocatalyst for oxygen reduction reaction. Nano Research, 2015, 8, 3394-3403.	5.8	46
23433	Repulsion-Induced Surface-Migration by Ballistics and Bounce. Journal of Physical Chemistry Letters, 2015, 6, 4093-4098.	2.1	8
23434	Unravelling Doping Effects on PEDOT at the Molecular Level: From Geometry to Thermoelectric Transport Properties. Journal of the American Chemical Society, 2015, 137, 12929-12938.	6.6	176
23435	Melting of Pb Charge Glass and Simultaneous Pbâ€“Cr Charge Transfer in PbCrO₃ as the Origin of Volume Collapse. Journal of the American Chemical Society, 2015, 137, 12719-12728.	6.6	45
23436	Hydride ion formation in stoichiometric UO₂. Chemical Communications, 2015, 51, 16209-16212.	2.2	17
23437	NO adsorption and diffusion on hydroxylated rutile TiO₂(110). Physical Chemistry Chemical Physics, 2015, 17, 26594-26598.	1.3	16
23438	Transition metal selenides as efficient counter-electrode materials for dye-sensitized solar cells. Physical Chemistry Chemical Physics, 2015, 17, 28985-28992.	1.3	59
23439	Study of the electronic structure, stability and magnetic quenching of CrGe_n (nÂ= 1â€“17) clusters: a density functional investigation. RSC Advances, 2015, 5, 83004-83012.	1.7	36
23440	Ab initiostudy of the photocurrent at the Au/Si metalâ€“semiconductor nanointerface. Molecular Physics, 2015, 113, 327-335.	0.8	25
23441	Equation of state of solid, liquid and gaseous tantalum from first principles. Calphad: Computer Coupling of Phase Diagrams and Thermochemistry, 2015, 51, 133-143.	0.7	21
23442	Combined quantum-mechanical and Calphad approach to description of heat capacity of pure elements below room temperature. Calphad: Computer Coupling of Phase Diagrams and Thermochemistry, 2015, 51, 161-171.	0.7	9
23443	Numerical study on sequential period-doubling bifurcations of graphene wrinkles on a soft substrate. Solid State Communications, 2015, 222, 14-17.	0.9	10
23444	Complex Catalytic Behaviors of CuTiO_x Mixed-Oxide during CO Oxidation. Journal of Physical Chemistry C, 2015, 119, 22985-22991.	1.5	17
23445	Size-Dependent Reaction Mechanism and Kinetics for Propane Dehydrogenation over Pt Catalysts. ACS Catalysis, 2015, 5, 6310-6319.	5.5	189
23446	Photocatalytic splitting of water on s-triazine based graphitic carbon nitride: an ab initio investigation. Journal of Materials Chemistry A, 2015, 3, 23011-23016.	5.2	53

#	Article	IF	Citations
23447	Ab initio studies on the adsorption and implantation of Al and Fe to nitride materials. Journal of Applied Physics, 2015, 118, 125306.	1.1	4
23448	First-principles study of trimethylamine adsorption on anatase TiO2 nanorod surfaces. Theoretical Chemistry Accounts, 2015, 134, 1.	0.5	7
23449	The electrocatalytic properties of doped TiO2. Electrochimica Acta, 2015, 180, 514-527.	2.6	34
23450	Impact of apatite chemical composition on (U-Th)/He thermochronometry: An atomistic point of view. Geochimica Et Cosmochimica Acta, 2015, 167, 162-176.	1.6	74
23451	Combined experimental and theoretical assessments of the lattice dynamics and optoelectronics of TaON and Ta3N5. Journal of Solid State Chemistry, 2015, 229, 219-227.	1.4	88
23452	Substrate Vibrations as Promoters of Chemical Reactivity on Metal Surfaces. Journal of Physical Chemistry A, 2015, 119, 12434-12441.	1.1	25
23453	Bond-Selective and Mode-Specific Dissociation of CH₃D and CH₂D₂ on Pt(111). Journal of Physical Chemistry A, 2015, 119, 12442-12448.	1.1	29
23454	Multifunctional pure and Eu³⁺ doped Î²-Ag₂MoO₄: photoluminescence, energy transfer dynamics and defect induced properties. Dalton Transactions, 2015, 44, 19097-19110.	1.6	62
23455	Energy transfer dynamics and luminescence properties of Eu³⁺ in CaMoO₄ and SrMoO₄. Dalton Transactions, 2015, 44, 18957-18969.	1.6	137
23456	Energetics of proton transfer in alkali carbonates: a first principles calculation. RSC Advances, 2015, 5, 56205-56209.	1.7	10
23457	Low-activated Li-ion mobility and metal to semiconductor transition in CdP₂@Li phases. Journal of Materials Chemistry A, 2015, 3, 6484-6491.	5.2	8
23458	Interface effect on structural and electronic properties of graphdiyne adsorbed on SiO ₂ and h-BN substrates: A first-principles study. Chinese Physics B, 2015, 24, 096806.	0.7	0
23459	Muon Site Estimations by DFT Calculations in Metal and Insulating Systems. Materials Science Forum, 0, 827, 347-354.	0.3	5
23460	Theoretical study of H2 adsorption on metal-doped graphene sheets with nitrogen-substituted defects. International Journal of Hydrogen Energy, 2015, 40, 14154-14162.	3.8	37
23461	Full elastic constants of Cu 6 Sn 5 intermetallic by Resonant Ultrasound Spectroscopy (RUS) and ab initio calculations. Scripta Materialia, 2015, 107, 26-29.	2.6	10
23462	Self-Assembled Oligomeric Structures from 1,4-Benzenedithiol on Au(111) and the Formation of Conductive Linkers between Gold Nanoparticles. Journal of Physical Chemistry C, 2015, 119, 23042-23051.	1.5	20
23463	Electronic storage capacity of ceria: role of peroxide in Au_x supported on CeO₂(111) facet and CO adsorption. Physical Chemistry Chemical Physics, 2015, 17, 27758-27768.	1.3	14
23464	A study on AB2O6 compounds, Part V: a DFT study on charge balance as driving force for structural organisation. Zeitschrift Fur Kristallographie - Crystalline Materials, 2015, 230, 449-458.	0.4	2

#	Article	IF	Citations
23465	Tailoring Metal-Porphyrin-Like Active Sites on Graphene to Improve the Efficiency and Selectivity of Electrochemical CO₂ Reduction. Journal of Physical Chemistry C, 2015, 119, 21345-21352.	1.5	79
23466	Antiferromagnetic Order at The First Fe₄N Atomic Layer in Benzene Adsorbed Fe₄N Structures. Journal of Physical Chemistry C, 2015, 119, 23619-23626.	1.5	10
23467	Experimental and Theoretical Insights into the Hydrogen-Efficient Direct Hydrodeoxygenation Mechanism of Phenol over Ru/TiO₂. ACS Catalysis, 2015, 5, 6509-6523.	5.5	219
23468	The electronic structures of group-Vâ€“group-IV hetero-bilayer structures: a first-principles study. Physical Chemistry Chemical Physics, 2015, 17, 27769-27776.	1.3	54
23469	Hâ€“Si bonding-induced unusual electronic properties of silicene: a method to identify hydrogen concentration. Physical Chemistry Chemical Physics, 2015, 17, 26443-26450.	1.3	28
23470	Highly selective and efficient adsorption dyes self-assembled by 3D hierarchical architecture of molybdenum oxide. RSC Advances, 2015, 5, 85248-85255.	1.7	29
23471	Electron spin-polarization and band gap engineering in carbon-modified graphitic carbon nitrides. Journal of Materials Chemistry C, 2015, 3, 10886-10891.	2.7	13
23472	Pressure-induced emergence of unusually high-frequency transverse excitations in a liquid alkali metal: Evidence of two types of collective excitations contributing to the transverse dynamics at high pressures. Journal of Chemical Physics, 2015, 143, 104502.	1.2	32
23473	Assessing photocatalytic power of g-C3N4 for solar fuel production: A first-principles study involving quasi-particle theory and dispersive forces. Journal of Chemical Physics, 2015, 143, 094705.	1.2	11
23474	Ab initio calculations of polarization, piezoelectric constants, and elastic constants of InAs and InP in the wurtzite phase. Journal of Experimental and Theoretical Physics, 2015, 121, 246-249.	0.2	11
23475	The role of alloying element on the behaviors of helium in vanadium: Ti as an example. Computational Condensed Matter, 2015, 3, 1-8.	0.9	7
23476	Discharge and Charge Reaction Paths in Sodiumâ€“Oxygen Batteries: Does NaO₂ Form by Direct Electrochemical Growth or by Precipitation from Solution?. Journal of Physical Chemistry C, 2015, 119, 22778-22786.	1.5	91
23477	Crystal Structures and Chemical Bonding of Magnesium Carbide at High Pressure. Journal of Physical Chemistry C, 2015, 119, 23168-23174.	1.5	18
23478	Role of Site Stability in Methane Activation on Pd_xCe_{1â€“x}O_{Î´} Surfaces. ACS Catalysis, 2015, 5, 6187-6199.	5.5	69
23479	Câ€“O cleavage of aromatic oxygenates over ruthenium catalysts. A computational study of reactions at step sites. Physical Chemistry Chemical Physics, 2015, 17, 15324-15330.	1.3	26
23480	A novel crystalline SiCO compound. Physical Chemistry Chemical Physics, 2015, 17, 25055-25060.	1.3	7
23481	MoS2 decoration by Mo-atoms and the MoS2â€“Moâ€“graphene heterostructure: a theoretical study. Physical Chemistry Chemical Physics, 2015, 17, 28770-28773.	1.3	12
23482	Catalytic potential of highly defective (211) surfaces of zinc blende ZnO. Physical Chemistry Chemical Physics, 2015, 17, 27683-27689.	1.3	7

#	Article	IF	Citations
23483	Identifying systematic DFT errors in catalytic reactions. Catalysis Science and Technology, 2015, 5, 4946-4949.	2.1	144
23484	Impact of alkoxy chain length on carbazole-based, visible light-driven, dye sensitized photocatalytic hydrogen production. Journal of Materials Chemistry A, 2015, 3, 21713-21721.	5.2	33
23485	On sulfur core level binding energies in thiol self-assembly and alternative adsorption sites: An experimental and theoretical study. Journal of Chemical Physics, 2015, 143, 104702.	1.2	34
23486	First-principles calculations of half-metallic ferromagnetism in zigzag boron-nitride nanoribbons jointed with a single Fe-chain. Journal of Semiconductors, 2015, 36, 082003.	2.0	2
23487	Functionalized single-walled carbon nanotube (5, 0) as a carrier for isoniazid â€" A tuberculosis drug. International Journal of Computational Materials Science and Engineering, 2015, 04, 1550014.	0.5	3
23488	Unraveling the Origin of Structural Disorder in High Temperature Transition Al₂O₃: Structure of Î¸-Al₂O₃. Chemistry of Materials, 2015, 27, 7042-7049.	3.2	51
23489	Anionic Ordering and Thermal Properties of FeF₃·3H₂O. Inorganic Chemistry, 2015, 54, 9619-9625.	1.9	24
23490	Solvation Mechanism of Task-Specific Ionic Liquids in Water: A Combined Investigation Using Classical Molecular Dynamics and Density Functional Theory. Journal of Physical Chemistry B, 2015, 119, 12894-12904.	1.2	16
23491	First-Principles Theoretical Studies and Nanocalorimetry Experiments on Solid-State Alloying of Zrâ€"B. Nano Letters, 2015, 15, 6553-6558.	4.5	26
23492	High-Temperature Ferroelectricity and Photoluminescence in a Hybrid Organicâ€"Inorganic Compound: (3-Pyrrolinium)MnCl₃. Journal of the American Chemical Society, 2015, 137, 13148-13154.	6.6	246
23493	Combined experimental and computational NMR study of crystalline and amorphous zeolitic imidazolate frameworks. Physical Chemistry Chemical Physics, 2015, 17, 25191-25196.	1.3	28
23494	Magnetism tuned by the charge states of defects in bulk C-doped SnO₂materials. Physical Chemistry Chemical Physics, 2015, 17, 26429-26434.	1.3	8
23495	Study of morphology effects on magnetic interactions and band gap variations for 3d late transition metal bi-doped ZnO nanostructures by hybrid DFT calculations. Journal of Chemical Physics, 2015, 143, 084309.	1.2	4
23496	Density functional studies on edge-contacted single-layer MoS2 piezotronic transistors. Applied Physics Letters, 2015, 107, .	1.5	20
23497	Density functional theory for dielectric properties of warm dense matter. Molecular Physics, 2015, , 1-7.	0.8	3
23498	Electronic structure and optical properties of boron-sulfur symmetric codoping in 4 Ã— 4 graphene systems. European Physical Journal B, 2015, 88, 1.	0.6	11
23499	Solid solution hardening of vacancy stabilized Ti W1â^'B2. Acta Materialia, 2015, 101, 55-61.	3.8	45
23500	The roles of Yb-substitution on thermoelectric properties of In4â^'Yb Se3. Acta Materialia, 2015, 101, 16-21.	3.8	12

#	Article	IF	Citations
23501	Stability of Two-Dimensional Iron Carbides Suspended across Graphene Pores: First-Principles Particle Swarm Optimization. Journal of Physical Chemistry C, 2015, 119, 22954-22960.	1.5	30
23502	Predicting Two-Dimensional Silicon Carbide Monolayers. ACS Nano, 2015, 9, 9802-9809.	7.3	177
23503	A novel surface modification scheme for ITO nanocrystals by acetylene: a combined experimental and DFT study. Physical Chemistry Chemical Physics, 2015, 17, 26740-26744.	1.3	1
23504	Structural and electrical behaviour in Bi14YO22.5. RSC Advances, 2015, 5, 83471-83479.	1.7	2
23505	An efficient blue-emitting Sr₅(PO₄)₃Cl:Eu²⁺ phosphor for application in near-UV white light-emitting diodes. Journal of Materials Chemistry C, 2015, 3, 11219-11227.	2.7	141
23506	Hydrogen-induced stabilization and tunable electronic structures of penta-silicene: a computational study. Journal of Materials Chemistry C, 2015, 3, 11341-11348.	2.7	85
23507	Structure and electronic properties of Cu nanoclusters supported on Mo2C(001) and MoC(001) surfaces. Journal of Chemical Physics, 2015, 143, 114704.	1.2	25
23508	New insight into the helium-induced damage in MAX phase Ti3AlC2 by first-principles studies. Journal of Chemical Physics, 2015, 143, 114707.	1.2	26
23509	Estimation of Macroscopic Physical Property in Disordered States: Special Microscopic States Approach. Journal of the Physical Society of Japan, 2015, 84, 084801.	0.7	23
23510	A new C=C embedded porphyrin sheet with superior oxygen reduction performance. Nano Research, 2015, 8, 2901-2912.	5.8	35
23511	Influences of Al, Ti and Nb doping on the structure and hydrogen storage property of Mg(BH 4) 2 (001) surface â€“ A theoretical study. International Journal of Hydrogen Energy, 2015, 40, 10516-10526.	3.8	12
23512	Study of the thermodynamic stability of iron at inner core from first-principles theory combined with lattice dynamics. Physics of the Earth and Planetary Interiors, 2015, 248, 12-19.	0.7	7
23513	Phonon softening induced cubic-to-tetragonal phase transition in ReO 3. Physics Letters, Section A: General, Atomic and Solid State Physics, 2015, 379, 2756-2760.	0.9	3
23514	Electronic Structure of Pd Multilayers on Re(0001): The Role of Charge Transfer. Journal of Physical Chemistry C, 2015, 119, 23436-23444.	1.5	37
23515	Anisotropic Spin Transport and Strong Visible-Light Absorbance in Few-Layer SnSe and GeSe. Nano Letters, 2015, 15, 6926-6931.	4.5	290
23516	In Situ Probing of the Active Site Geometry of Ultrathin Nanowires for the Oxygen Reduction Reaction. Journal of the American Chemical Society, 2015, 137, 12597-12609.	6.6	46
23517	Combined crystal structure prediction and high-pressure crystallization in rational pharmaceutical polymorph screening. Nature Communications, 2015, 6, 7793.	5.8	193
23518	A modelling approach for MOF-encapsulated metal catalysts and application to n-butane oxidation. Physical Chemistry Chemical Physics, 2015, 17, 27596-27608.	1.3	19

#	Article	IF	Citations
23519	A first-principles study of orthorhombic CN as a potential superhard material. Physical Chemistry Chemical Physics, 2015, 17, 27821-27825.	1.3	27
23520	Invariom approach as a new tool in electron density studies of ionic liquids: a model case of 1-butyl-2,3-dimethylimidazolium chloride BDMIM[Cl]. RSC Advances, 2015, 5, 75360-75373.	1.7	13
23521	Atomic structure of the La/Pt(111) and Ce/Pt(111) surfaces revealed by DFT+U calculations. RSC Advances, 2015, 5, 521-528.	1.7	11
23522	Adsorption of alkali, alkaline-earth, simple and 3d transition metal, and nonmetal atoms on monolayer MoS2. AIP Advances, 2015, 5, .	0.6	43
23523	Structures and stability of metal-doped GenM (n = 9, 10) clusters. AIP Advances, 2015, 5, .	0.6	14
23524	Electrical and optical properties of warm dense beryllium along the principal Hugoniot. Physics of Plasmas, 2015, 22, 092705.	0.7	4
23525	Modulation of the electronic property of phosphorene by wrinkle and vertical electric field. Applied Physics Letters, 2015, 107, .	1.5	12
23526	Analysis of the Trajectory Surface Hopping Method from the Markov State Model Perspective. Journal of the Physical Society of Japan, 2015, 84, 094002.	0.7	17
23527	A DFT+U study of Pu immobilization in Gd2Zr2O7. Journal of Nuclear Materials, 2015, 467, 937-948.	1.3	17
23528	Highly Conducting, n-Type Bi₁₂O₁₅Cl₆ Nanosheets with Superlattice-like Structure. Chemistry of Materials, 2015, 27, 7710-7718.	3.2	55
23529	Lithium Intercalation in Graphene/MoS₂ Composites: First-Principles Insights. Journal of Physical Chemistry C, 2015, 119, 25860-25867.	1.5	78
23530	First-Principles Investigation of Mercury Adsorption on the Î±-Fe₂O₃(11Ì…02) Surface. Journal of Physical Chemistry C, 2015, 119, 26512-26518.	1.5	60
23531	A comparative first principles study on trivalent ion incorporated SSZ-13 zeolites. Physical Chemistry Chemical Physics, 2015, 17, 29586-29596.	1.3	18
23532	Stability of two-dimensional PN monolayer sheets and their electronic properties. Physical Chemistry Chemical Physics, 2015, 17, 32009-32015.	1.3	47
23533	Unexpected Photoreactivity in a NO₂-Functionalized Aluminum-MOF. Journal of Physical Chemistry C, 2015, 119, 26401-26408.	1.5	9
23534	Atomic Structure of Graphene Subnanometer Pores. ACS Nano, 2015, 9, 11599-11607.	7.3	75
23535	Theoretical study of polyiodide formation and stability on monolayer and bilayer graphene. Physical Chemistry Chemical Physics, 2015, 17, 30045-30051.	1.3	25
23536	Au_{13â^'n}Ag_n clusters: a remarkably simple trend. Physical Chemistry Chemical Physics, 2015, 17, 30492-30498.	1.3	22

#	Article	IF	Citations
23537	Computational investigation of NH₃ adsorption and dehydrogenation on a W-modified Fe(111) surface. Physical Chemistry Chemical Physics, 2015, 17, 30598-30605.	1.3	6
23538	Crystal structure and thermoelectric properties of Srâ€“Mo substituted CaMnO₃: a combined experimental and computational study. Journal of Materials Chemistry C, 2015, 3, 12245-12259.	2.7	37
23539	From generalized stacking fault energies to dislocation properties: Five-energy-point approach and solid solution effects in magnesium. Physical Review B, 2015, 92, .	1.1	26
23540	Orientation-dependent ferroelectricity of strained PbTiO3 films. Frontiers of Physics, 2015, 10, 1.	2.4	6
23541	A combined calorimetric and computational study of the energetics of rare earth substituted UO2 systems. Acta Materialia, 2015, 97, 191-198.	3.8	11
23542	Failure of single phenolic chains and cross-links: Energetics, mechanisms, and alternative linker design. Polymer, 2015, 80, 265-274.	1.8	5
23543	Metastable Ni₇B₃: A New Paramagnetic Boride from Solution Chemistry, Its Crystal Structure and Magnetic Properties. Inorganic Chemistry, 2015, 54, 10873-10877.	1.9	25
23544	Strain Tuning of Ferroelectric Polarization in Hybrid Organic Inorganic Perovskite Compounds. Journal of Physical Chemistry Letters, 2015, 6, 4553-4559.	2.1	67
23545	The Nature of the Interlayer Interaction in Bulk and Few-Layer Phosphorus. Nano Letters, 2015, 15, 8170-8175.	4.5	252
23546	A theoretical study of O₂ activation by the Au₇-cluster on Mg(OH)₂: roles of surface hydroxyls and hydroxyl defects. Physical Chemistry Chemical Physics, 2015, 17, 30736-30743.	1.3	10
23547	Engineering the optical transitions of self-assembled quantum dots. , 2015, , .		0
23548	Stability of dioctahedral 2:1 phyllosilicate edge structures based on pyrophyllite models. Theoretical Chemistry Accounts, 2015, 134, 1.	0.5	19
23549	Novel BN polymorphs transformed from the smallest BNNTs under high pressure. Computational Materials Science, 2015, 110, 241-246.	1.4	22
23550	Hole traps in sodium silicate: First-principles calculations of the mobility edge. Journal of Non-Crystalline Solids, 2015, 430, 9-15.	1.5	7
23551	Electronic and Optical Properties of Low-Dimensional TiO2: From Minority Surfaces to Nanocomposites. ACS Symposium Series, 2015, , 47-80.	0.5	1
23552	Elucidating the structure of the magnesium aluminum chloride complex electrolyte for magnesium-ion batteries. Energy and Environmental Science, 2015, 8, 3718-3730.	15.6	131
23553	Beryllium decorated armchair BC2N nanoribbons: coexistence of planar tetracoordinate carbon and nitrogen moieties. RSC Advances, 2015, 5, 73945-73950.	1.7	8
23554	Effects of Ga doping and hollow structure on the band-structures and photovoltaic properties of SnO₂ photoanode dye-sensitized solar cells. RSC Advances, 2015, 5, 93765-93772.	1.7	10

#	Article	IF	Citations
23555	Toward Rational Design of Catalysts Supported on a Topological Insulator Substrate. ACS Catalysis, 2015, 5, 7063-7067.	5.5	73
23556	Exploring PtSO4 and PdSO4 phases: an evolutionary algorithm based investigation. Physical Chemistry Chemical Physics, 2015, 17, 18146-18151.	1.3	13
23557	Structures and electronic properties of GaSe and GaS nanoribbons. RSC Advances, 2015, 5, 94679-94684.	1.7	15
23558	Synthesis of surfactant-free SnS nanoplates in an aqueous solution. RSC Advances, 2015, 5, 94796-94801.	1.7	18
23559	Ab initio study of the adsorption, diffusion, and intercalation of alkali metal atoms on the (0001) surface of the topological insulator Bi2Se3. Journal of Experimental and Theoretical Physics, 2015, 121, 465-476.	0.2	11
23560	Long-range interactions of bismuth growth on monolayer epitaxial graphene at room temperature. Carbon, 2015, 93, 180-186.	5.4	22
23561	Cation-Mutation Design of Quaternary Nitride Semiconductors Lattice-Matched to GaN. Chemistry of Materials, 2015, 27, 7757-7764.	3.2	23
23562	New Family of Quantum Spin Hall Insulators in Two-dimensional Transition-Metal Halide with Large Nontrivial Band Gaps. Nano Letters, 2015, 15, 7867-7872.	4.5	104
23563	Carbocation Stability in H-ZSM5 at High Temperature. Journal of Physical Chemistry A, 2015, 119, 11397-11405.	1.1	14
23564	Defect-strain engineering for multiferroic and magnetoelectric properties in epitaxial (110) ferroelectric lead titanate. Physical Review B, 2015, 92, .	1.1	17
23565	Magnetic Properties of Shandite-Phase Co_{3â^'}_xFe_xSn₂S₂ (x =) Tj ET Q q 0 0 0 rg BT /Overlo	0.7	13
23566	Small Organic Molecules for Efficient Singlet Fission: Role of Silicon Substitution. Journal of Physical Chemistry C, 2015, 119, 25696-25702.	1.5	36
23567	Crystal Structures and Electronic Properties of Cesium Xenides at High Pressures. Journal of Physical Chemistry C, 2015, 119, 24996-25002.	1.5	15
23568	Stable Si-based pentagonal monolayers: high carrier mobilities and applications in photocatalytic water splitting. Journal of Materials Chemistry A, 2015, 3, 24055-24063.	5.2	132
23569	Assessment of the TCA functional in computational chemistry and solid-state physics. Theoretical Chemistry Accounts, 2015, 134, 1.	0.5	10
23570	Investigations on average and local structures of Li(Li1/6Mn1/2Ni1/6Co1/6)O2 by the pair distribution function and the density functional theory. Journal of Power Sources, 2015, 299, 280-285.	4.0	2
23571	Highly Stable Bimetallic AuIr/TiO₂ Catalyst: Physical Origins of the Intrinsic High Stability against Sintering. Nano Letters, 2015, 15, 8141-8147.	4.5	40
23572	Electronic structure and luminescence properties of Tb3+-activated NaBaBO3 green-emitting phosphor. Journal of Rare Earths, 2015, 33, 933-938.	2.5	14

#	Article	IF	Citations
23573	Nitrogen Activation in a Marsâ€“van Krevelen Mechanism for Ammonia Synthesis on Co₃Mo₃N. Journal of Physical Chemistry C, 2015, 119, 28368-28376.	1.5	135
23574	Catalytic Upgrading of Biomass-Derived Compounds via Câ€“C Coupling Reactions: Computational and Experimental Studies of Acetaldehyde and Furan Reactions in HZSM-5. Journal of Physical Chemistry C, 2015, 119, 24025-24035.	1.5	19
23575	Polymorphic, Porous, and Hostâ€“Guest Nanostructures Directed by Monolayerâ€“Substrate Interactions: Epitaxial Self-Assembly Study of Cyclic Trinuclear Au(I) Complexes on HOPG at the Solutionâ€“Solid Interface. Journal of Physical Chemistry C, 2015, 119, 24844-24858.	1.5	15
23576	Individual Titanate Nanoribbons Studied by 3D-Resolved Polarization Dependent X-ray Absorption Spectra Measured with Scanning Transmission X-ray Microscopy. Journal of Physical Chemistry C, 2015, 119, 24192-24200.	1.5	10
23577	Anionic Chemistry of Noble Gases: Formation of Mgâ€“NG (NG = Xe, Kr, Ar) Compounds under Pressure. Journal of the American Chemical Society, 2015, 137, 14122-14128.	6.6	91
23578	A polar/Ï€ model of interactions explains face-to-face stacked quinoid rings: a case study of the crystal of potassium hydrogen chloranilate dihydrate. CrystEngComm, 2015, 17, 8645-8656.	1.3	9
23579	Porous P-doped graphitic carbon nitride nanosheets for synergistically enhanced visible-light photocatalytic H₂ production. Energy and Environmental Science, 2015, 8, 3708-3717.	15.6	1,146
23580	Oxidation and Dissociation of Formyl on Ni(111), Ni(110) and Ni(100) Surfaces: A Comparative Density Functional Theory Study. Topics in Catalysis, 2015, 58, 1136-1149.	1.3	2
23581	Study of the anisotropic segregation behavior of Sn on the surfaces of zirconium alloys by XPS. Applied Surface Science, 2015, 356, 769-775.	3.1	8
23582	On the role of hydrogen filled vacancies on the embrittlement of zirconium: An ab initio investigation. Journal of Nuclear Materials, 2015, 467, 311-319.	1.3	26
23583	Selective Oxidation of 1,2-Propanediol in Alkaline Anion-Exchange Membrane Electrocatalytic Flow Reactors: Experimental and DFT Investigations. ACS Catalysis, 2015, 5, 6926-6936.	5.5	29
23584	Methanol electro-oxidation on platinum modified tungsten carbides in direct methanol fuel cells: a DFT study. Physical Chemistry Chemical Physics, 2015, 17, 25235-25243.	1.3	46
23585	Two-dimensional silicon-carbon hybrids with a honeycomb lattice: New family for two-dimensional photovoltaic materials. Science China: Physics, Mechanics and Astronomy, 2015, 58, 1.	2.0	13
23586	From Silicene to Half-Silicane by Hydrogenation. ACS Nano, 2015, 9, 11192-11199.	7.3	97
23587	Mechanical properties of zirconium alloys and zirconium hydrides predicted from density functional perturbation theory. Dalton Transactions, 2015, 44, 18769-18779.	1.6	60
23588	Predicting the solar thermochemical water splitting ability and reaction mechanism of metal oxides: a case study of the hercynite family of water splitting cycles. Energy and Environmental Science, 2015, 8, 3687-3699.	15.6	68
23589	Strain control of the electronic structures, magnetic states, and magnetic anisotropy of Fe doped single-layer MoS2. Computational Materials Science, 2015, 110, 102-108.	1.4	51
23590	Atomistic modeling of high temperature uraniumâ€“zirconium alloy structure and thermodynamics. Journal of Nuclear Materials, 2015, 467, 802-819.	1.3	42

#	Article	IF	Citations
23591	Electronic properties of two-dimensional van der Waals GaS/GaSe heterostructures. Journal of Materials Chemistry C, 2015, 3, 11548-11554.	2.7	66
23592	Factors Contributing to Path Hysteresis of Displacement and Conversion Reactions in Li Ion Batteries. Chemistry of Materials, 2015, 27, 7593-7600.	3.2	27
23593	(CH₃NH₃)₂Pb(SCN)₂I₂: A More Stable Structural Motif for Hybrid Halide Photovoltaics?. Journal of Physical Chemistry Letters, 2015, 6, 4594-4598.	2.1	117
23594	Reversible Tuning of Interfacial and Intramolecular Charge Transfer in Individual MnPc Molecules. Nano Letters, 2015, 15, 8091-8098.	4.5	12
23595	First-principles calculation of the reflectance of shock-compressed xenon. Journal of Experimental and Theoretical Physics, 2015, 120, 894-904.	0.2	4
23596	Density functional theory study on the reaction between hematite and methane during chemical looping process. Applied Energy, 2015, 159, 132-144.	5.1	77
23597	Reconstructions and stabilities of PbTe(1 1 1) crystal surface from experiments and density-functional theory. Applied Surface Science, 2015, 356, 742-746.	3.1	6
23598	Magnetism in olivine-type LiCo_{1â^'x}Fe_xPO₄cathode materials: bridging theory and experiment. Physical Chemistry Chemical Physics, 2015, 17, 31202-31215.	1.3	16
23599	Prediction of spinâ€“orbital coupling effects on the electronic structure of two dimensional van der Waals heterostructures. Physical Chemistry Chemical Physics, 2015, 17, 31253-31259.	1.3	17
23600	Pressure evolution of the potential barriers for transformations of layered BN to dense structures. RSC Advances, 2015, 5, 87550-87555.	1.7	3
23601	Density Functional Theory and Electrochemical Studies: Structureâ€“Efficiency Relationship on Corrosion Inhibition. Journal of Chemical Information and Modeling, 2015, 55, 2391-2402.	2.5	53
23602	Benzoic Acid and Phthalic Acid on Atomically Well-Defined MgO(100) Thin Films: Adsorption, Interface Reaction, and Thin Film Growth. Journal of Physical Chemistry C, 2015, 119, 26968-26979.	1.5	22
23603	Carbon nanodot decorated graphitic carbon nitride: new insights into the enhanced photocatalytic water splitting from ab initio studies. Physical Chemistry Chemical Physics, 2015, 17, 31140-31144.	1.3	105
23604	Atomistic bond relaxation, energy entrapment, and electron polarization of the RbN and CsN clusters (N â‰¤ 58). Physical Chemistry Chemical Physics, 2015, 17, 30389-30397.	1.3	2
23605	Atomic scale modeling of shock response of fused silica and Î±-quartz. Journal of Materials Science, 2015, 50, 8128-8141.	1.7	37
23606	Tuning carrier confinement in the MoS2/WS2 heterostructure. Superlattices and Microstructures, 2015, 88, 12-17.	1.4	3
23607	Hybrid-Functional Calculations on the Incorporation of Na and K Impurities into the CuInSe₂ and CuIn₅Se₈ Solar-Cell Materials. Journal of Physical Chemistry C, 2015, 119, 25197-25203.	1.5	45
23608	Opposite correlations between cation disordering and amorphization resistance in spinels versus pyrochlores. Nature Communications, 2015, 6, 8750.	5.8	62

#	Article	IF	Citations
23609	Remarkably low-energy one-dimensional fault line defects in single-layered phosphorene. Nanoscale, 2015, 7, 19073-19079.	2.8	19
23610	Homogeneous vertical ZnO nanorod arrays with high conductivity on an in situ Gd nanolayer. RSC Advances, 2015, 5, 94670-94678.	1.7	52
23611	Urtra-Hard Bonds in P -Carbon Stronger than Diamond. Chinese Physics Letters, 2015, 32, 096201.	1.3	4
23612	Determination of crystal structures and tautomeric states of 2-ammoniobenzenesulfonates by laboratory X-ray powder diffraction. Zeitschrift Fur Kristallographie - Crystalline Materials, 2015, 230, 611-620.	0.4	7
23613	A Comparative DFT and DFT+U Study on Magnetism in Nickel-Doped Wurtzite AlN. Journal of Superconductivity and Novel Magnetism, 2015, 28, 3185-3192.	0.8	3
23614	Atomic and electronic structure of the TiN/MgO interface from first principles. Computational Materials Science, 2015, 105, 83-89.	1.4	18
23615	Efficient ab initio free energy calculations by classically assisted trajectory sampling. Computer Physics Communications, 2015, 197, 1-6.	3.0	1
23616	Simulation of He embrittlement at grain boundaries in bcc transition metals. Journal of Nuclear Materials, 2015, 465, 695-701.	1.3	14
23617	A comparative study for Hydrogen storage in metal decorated graphyne nanotubes and graphyne monolayers. Journal of Solid State Chemistry, 2015, 231, 53-57.	1.4	30
23618	Effect of structural defects on electronic and magnetic properties of pristine and Mn-doped MoS2 monolayer. Solid State Communications, 2015, 220, 31-35.	0.9	41
23619	Direct Observation of Sublimation Behaviors in One-Dimensional In2Se3/In2O3 Nanoheterostructures. Analytical Chemistry, 2015, 87, 5584-5588.	3.2	10
23620	Microscopic Origin of Thermal Conductivity Reduction in Disordered van der Waals Solids. Chemistry of Materials, 2015, 27, 5511-5518.	3.2	33
23621	Decoherence Allows Model Reduction in Nonadiabatic Dynamics Simulations. Journal of Physical Chemistry A, 2015, 119, 8846-8853.	1.1	11
23622	First-Principles Analysis of Defect Thermodynamics and Ion Transport in Inorganic SEI Compounds: LiF and NaF. ACS Applied Materials & Interfaces, 2015, 7, 18985-18996.	4.0	191
23623	Guidelines for the Rational Design of Ni-Based Double Hydroxide Electrocatalysts for the Oxygen Evolution Reaction. ACS Catalysis, 2015, 5, 5380-5387.	5.5	472
23624	Atomic-Scale Dynamics of Surface-Catalyzed Hydrogenation/Dehydrogenation: NH on Pt(111). ACS Nano, 2015, 9, 8303-8311.	7.3	6
23625	Six-dimensional quantum dynamics of dissociative chemisorption of H2 on Co(0001) on an accurate global potential energy surface. Physical Chemistry Chemical Physics, 2015, 17, 23346-23355.	1.3	23
23626	Adsorption properties of trifluoroacetic acid on anatase (101) and (001) surfaces: a density functional theory study. Physical Chemistry Chemical Physics, 2015, 17, 23627-23633.	1.3	6

#	Article	IF	Citations
23627	Sub-surface alloying largely influences graphene nucleation and growth over transition metal substrates. Physical Chemistry Chemical Physics, 2015, 17, 30270-30278.	1.3	4
23628	The gold/ampicillin interface at the atomic scale. Nanoscale, 2015, 7, 14515-14524.	2.8	20
23629	Photocatalytic H₂ generation over In₂TiO₅, Ni substituted In₂TiO₅ and NiTiO₃ â€“ a combined theoretical and experimental study. RSC Advances, 2015, 5, 61218-61229.	1.7	23
23630	Gold-rich R₃Au₇Sn₃: establishing the interdependence between electronic features and physical properties. Journal of Materials Chemistry C, 2015, 3, 8311-8321.	2.7	20
23631	Designing electronic anisotropy of three-dimensional carbon allotropes for the all-carbon device. Applied Physics Letters, 2015, 107, 021905.	1.5	2
23632	Solid-Solution Hardening in Mg-Gd-TM (TMÂ=ÂAg, Zn, and Zr) Alloys: An Integrated Density Functional Theory and Electron Work Function Study. Jom, 2015, 67, 2433-2441.	0.9	17
23633	First-Principles Study of Molybdenum Chalcogenide Halide Nanowires for Mg-Ion Battery Cathode Application. Chemistry of Materials, 2015, 27, 5878-5885.	3.2	8
23634	Ba and Sr Binary Phosphides: Synthesis, Crystal Structures, and Bonding Analysis. Inorganic Chemistry, 2015, 54, 8608-8616.	1.9	31
23635	Photophysical properties of quinoxaline-fused [7]carbohelicene derivatives. RSC Advances, 2015, 5, 72907-72915.	1.7	14
23636	Lowering the hydrogen desorption temperature of NH3BH3 through B-group substitutions. Journal of Materials Chemistry A, 2015, 3, 18528-18534.	5.2	6
23637	Influence of interstitial impurities on the Griffith work in Ti-based alloys. Physica Scripta, 2015, 90, 094010.	1.2	7
23638	Sensing polarization effects through the analysis of the effective C6 dispersion coefficients in NaCl solutions. Journal of Chemical Physics, 2015, 142, 014504.	1.2	1
23639	Steady-state heat transport: Ballistic-to-diffusive with Fourier's law. Journal of Applied Physics, 2015, 117, .	1.1	63
23640	Effect of gold subsurface layer on the surface activity and segregation in Pt/Au/Pt3M (where M =) Tj ETQq1 1 0.784314 rgBT /Overloc 034707.	1.2	25
23641	Computing the crystal growth rate by the interface pinning method. Journal of Chemical Physics, 2015, 142, 044104.	1.2	15
23642	Orientation-dependent magnetism and orbital structure of strained YTiO3 films on LaAlO3 substrates. Journal of Applied Physics, 2015, 117, 17C703.	1.1	4
23643	Chiral selectivity of amino acid adsorption on chiral surfacesâ€”The case of alanine on Pt. Journal of Chemical Physics, 2015, 142, 054708.	1.2	3
23644	Communication: Surface-to-bulk diffusion of isolated versus interacting C atoms in Ni(111) and Cu(111) substrates: A first principle investigation. Journal of Chemical Physics, 2015, 142, 061101.	1.2	13

#	Article	IF	Citations
23645	Thickness effect on magnetocrystalline anisotropy of Co/Pd(111) films: A density functional study. Journal of Applied Physics, 2015, 117, 17E105.	1.1	5
23646	The onset of sub-surface oxidation induced by defects in a chemisorbed oxygen layer. Journal of Chemical Physics, 2015, 142, 084701.	1.2	10
23647	Symmetry-dependent interfacial reconstruction to compensate polar discontinuity at perovskite oxide interfaces (LaAlO3/SrTiO3 and LaAlO3/CaTiO3). Applied Physics Letters, 2015, 106, .	1.5	7
23648	Phase selection during solidification of liquid magnesium viaab initiomolecular dynamics simulations. Journal of Applied Physics, 2015, 117, 114905.	1.1	12
23649	Structural properties of Ge on SrTiO3 (001) surface and Ge/SrTiO3 interface. Journal of Applied Physics, 2015, 117, .	1.1	3
23650	Cation ordering and effect of biaxial strain in double perovskite CsRbCaZnCl6. Journal of Applied Physics, 2015, 117, .	1.1	8
23651	Towards enhancing two-dimensional electron gas quantum confinement effects in perovskite oxide heterostructures. Journal of Applied Physics, 2015, 117, .	1.1	17
23652	Structural stability and electronic properties of InSb nanowires: A first-principles study. Journal of Applied Physics, 2015, 117, .	1.1	6
23653	Dirac cones in transition metal doped boron nitride. Journal of Applied Physics, 2015, 117, .	1.1	5
23654	Elastic anisotropy, vibrational, and thermodynamic properties of U2Ti intermetallic compound with AlB2-type structure under high pressure up to 100â€‰GPa. Journal of Applied Physics, 2015, 117, .	1.1	5
23655	Effect of adatom deposition on surface magnetism and exchange coupling parameter in (0001) SmCo5 slabs. Journal of Applied Physics, 2015, 117, 133902.	1.1	1
23656	Optimal electron irradiation as a tool for functionalization of MoS2: Theoretical and experimental investigation. Journal of Applied Physics, 2015, 117, .	1.1	22
23657	Observing and tuning the density distribution of localized states of monolayer graphene oxide by using external electric field. Applied Physics Letters, 2015, 106, .	1.5	6
23658	Half-metallic antiferromagnetism in double perovskite BiPbCrCuO6. Journal of Applied Physics, 2015, 117, 17D716.	1.1	5
23659	Magnetic and ferroelectric orders in strained Gd1/2Na1/2TiO3: First-principles calculations. Journal of Applied Physics, 2015, 117, 17C742.	1.1	1
23660	Atomic and molecular oxygen adsorbed on (111) transition metal surfaces: Cu and Ni. Journal of Chemical Physics, 2015, 142, 154702.	1.2	52
23661	Centrality measures highlight proton traps and access points to proton highways in kinetic Monte Carlo trajectories. Journal of Chemical Physics, 2015, 142, 154110.	1.2	14
23662	Effect of surface adsorption and non-stoichiometry on the workfunction of ZnO surfaces: A first principles study. Journal of Applied Physics, 2015, 117, 165304.	1.1	9

#	Article	IF	Citations
23663	Electronic structures and formation energies of pentavalent-ion-doped SnO2: First-principles hybrid functional calculations. Journal of Applied Physics, 2015, 117, .	1.1	46
23664	First-principles study on stability of transition metal solutes in aluminum by analyzing the underlying forces. Journal of Applied Physics, 2015, 117, 175901.	1.1	2
23665	Stability and migration of small copper clusters in amorphous dielectrics. Journal of Applied Physics, 2015, 117, .	1.1	24
23666	Communication: Water on hexagonal boron nitride from diffusion Monte Carlo. Journal of Chemical Physics, 2015, 142, 181101.	1.2	56
23667	Coverage dependent work function of graphene on a Cu(111) substrate with intercalated alkali metals. Applied Physics Letters, 2015, 106, .	1.5	17
23668	Mesoscale elucidation of laser-assisted chemical deposition of Sn nanostructured electrodes. Journal of Applied Physics, 2015, 117, 214301.	1.1	2
23669	Spontaneous formation of suboxidic coordination around Co in ferromagnetic rutile Ti0.95Co0.05O2 film. Applied Physics Letters, 2015, 106, .	1.5	43
23670	Brittle fracture toughnesses of GaN and AlN from first-principles surface-energy calculations. Applied Physics Letters, 2015, 106, .	1.5	21
23671	Optimization of L1 FePt/Fe45Co55 thin films for rare earth free permanent magnet applications. Journal of Applied Physics, 2015, 117, .	1.1	17
23672	First-principles modeling of quantum nuclear effects and atomic interactions in solid<mml:math xmlns:mml="http://www.w3.org/1998/Math/MathML"><mml:mmultiscripts><mml:mi mathvariant="normal">He</mml:mi><mml:mprescripts /><mml:none /><mml:mrow><mml:mn>4</mml:mn></mml:mrow></mml:mmultiscripts></mml:math>at high pressure. Physical Review B, 2015, 91, .	1.1	18
23673	Special quasirandom structure in heterovalent ionic systems. Physical Review B, 2015, 91, .	1.1	6
23674	Lattice dynamics of the heavy-fermion compound<mml:math xmlns:mml="http://www.w3.org/1998/Math/MathML"><mml:mrow><mml:msub><mml:mi>URu</mml:mi><mml:mn>2</mml:mn></mml:msub></mml:mrow></mml:math>: Physical Review B, 2015, 91, .	1.1	18
23675	Ab initiostudies of Cs on GaAs (100) and (110) surfaces. Physical Review B, 2015, 91, .	1.1	14
23676	Lattice-mismatched heteroepitaxy of IV-VI thin films on PbTe(001): Anab initiostudy. Physical Review B, 2015, 91, .	1.1	7
23677	Polaronic deformation at the<mml:math xmlns:mml="http://www.w3.org/1998/Math/MathML"><mml:msup><mml:mtext>Fe</mml:mtext><mml:mrow><mml:mn>2</mml:mn></mml:mrow></mml:msup></mml:math> site in<mml:math xmlns:mml="http://www.w3.org/1998/Math/MathML"><mml:msub><mml:mtext>Fe:LiNbO</mml:mtext><mml:mn>3</mml:mn></mml:msub></mml:math>: Physical Review B, 2015, 91, .	1.1	33
23678	Pressure-induced phase transitions and metallization in<mml:math xmlns:mml="http://www.w3.org/1998/Math/MathML"><mml:msub><mml:mi>VO</mml:mi><mml:mn>2</mml:mn></mml:msub></mml:math>: Physical Review B, 2015, 91, .	1.1	82
23679	Switchable conductivity at the ferroelectric interface: Nonpolar oxides. Physical Review B, 2015, 91, .	1.1	78
23680	Stability Domains of NbC and Nb(CN) During Carbothermal Reduction of Niobium Oxide. Journal of the American Ceramic Society, 2015, 98, 315-319.	1.9	21

#	Article	IF	Citations
23681	A Highâ€Temperature Neutron Diffraction Study of Nb₂AlC and TiNbAlC. Journal of the American Ceramic Society, 2015, 98, 940-947.	1.9	13
23682	Explaining Performance-Limiting Mechanisms in Fluorophosphate Na-Ion Battery Cathodes through Inactive Transition-Metal Mixing and First-Principles Mobility Calculations. Chemistry of Materials, 2015, 27, 6008-6015.	3.2	74
23683	Pressure-Modulated Conductivity, Carrier Density, and Mobility of Multilayered Tungsten Disulfide. ACS Nano, 2015, 9, 9117-9123.	7.3	120
23684	Y-doped Li₈ZrO₆: A Li-Ion Battery Cathode Material with High Capacity. Journal of the American Chemical Society, 2015, 137, 10992-11003.	6.6	54
23685	Stress reduction of Cu-doped diamond-like carbon films from ab initio calculations. AIP Advances, 2015, 5, .	0.6	9
23686	Effect of Pt Doping on B2-Phase Ordering Temperature of Co-Based Heusler Alloy: An <italic>Ab Initio</italic> Study. IEEE Transactions on Magnetics, 2015, 51, 1-4.	1.2	0
23687	Sensitivity of CoSi2 precipitation in silicon to extra-low dopant concentrations. II. First-principles calculations. Journal of Applied Physics, 2015, 117, 045704.	1.1	2
23688	Electronic and magnetic properties of zigzag silicene nanoribbons with Stoneâ€“Wales defects. Journal of Applied Physics, 2015, 117, .	1.1	16
23689	Effects of partitioned enthalpy of mixing on glass-forming ability. Journal of Chemical Physics, 2015, 142, 144504.	1.2	6
23690	Strain control magnetocrystalline anisotropy of Ta/FeCo/MgO heterostructures. Journal of Applied Physics, 2015, 117, .	1.1	18
23691	Dirac points and van Hove singularities of silicene under uniaxial strain. Journal of Applied Physics, 2015, 117, 164305.	1.1	14
23692	The temperature-dependent diffusion coefficient of helium in zirconium carbide studied with first-principles calculations. Journal of Applied Physics, 2015, 117, .	1.1	13
23693	Ba2TeO as an optoelectronic material: First-principles study. Journal of Applied Physics, 2015, 117, 195705.	1.1	3
23694	Effectiveness of organic molecules for spin filtering in an organic spin valve: Reaction-induced spin polarization for Co atop<mml:math xmlns:mml="http://www.w3.org/1998/Math/MathML"><mml:mi mathvariant="normal">Alq</mml:mi><mml:msub><mml:mrow /><mml:mn>3</mml:mn></mml:msub></mml:math>. Physical Review B, 2015, 91, .	1.1	14
23695	Linear Scaling of the Exciton Binding Energy versus the Band Gap of Two-Dimensional Materials. Physical Review Letters, 2015, 115, 066403.	2.9	175
23696	Theoretical investigation of dielectric properties of rare earth stillwellite compounds. International Journal of Modern Physics B, 2015, 29, 1550154.	1.0	0
23697	First principles study of normal and fast diffusing metallic impurities in hcp titanium. Computational Materials Science, 2015, 109, 380-387.	1.4	9
23698	Generation of Cuâ€“In alloy surfaces from CuInO₂as selective catalytic sites for CO₂electroreduction. Journal of Materials Chemistry A, 2015, 3, 19085-19092.	5.2	99

#	Article	IF	Citations
23699	Strain-induced dimensionality crossover of precursor modulations in Ni2MnGa. Applied Physics Letters, 2015, 106, 021910.	1.5	3
23700	Construction of single-crystalline supramolecular networks of perchlorinated hexa-peri-hexabenzocoronene on Au(111). Journal of Chemical Physics, 2015, 142, 101911.	1.2	13
23701	1D self-assembly of chemisorbed thymine on Cu(110) driven by dispersion forces. Journal of Chemical Physics, 2015, 142, 101916.	1.2	11
23702	Oxidation state and interfacial effects on oxygen vacancies in tantalum pentoxide. Journal of Applied Physics, 2015, 117, .	1.1	9
23703	Magnetic property and possible half-metal behavior in Co-doped graphene. Journal of Applied Physics, 2015, 117, 084311.	1.1	12
23704	Magnetism and electronic structure of (001)- and (111)-oriented LaTiO3 bilayers sandwiched in LaScO3 barriers. Journal of Applied Physics, 2015, 117, .	1.1	7
23705	Pressure effect on structural, elastic, and thermodynamic properties of tetragonal B4C4. AIP Advances, 2015, 5, .	0.6	8
23706	Amphoteric doping of praseodymium Pr3+ in SrTiO3 grain boundaries. Applied Physics Letters, 2015, 106, .	1.5	9
23707	Magnetocrystalline anisotropy of 4d/5d transition metals on a Co(0001) surface: A first-principles study. Journal of Applied Physics, 2015, 117, 17A327.	1.1	4
23708	Jump rates for surface diffusion of large molecules from first principles. Journal of Chemical Physics, 2015, 142, 154105.	1.2	1
23709	Towards a predictive route for selection of doping elements for the thermoelectric compound PbTe from first-principles. Journal of Applied Physics, 2015, 117, 175102.	1.1	16
23710	Lattice dynamics and chemical bonding in Sb2Te3 from first-principles calculations. Journal of Chemical Physics, 2015, 142, 174702.	1.2	22
23711	A periodic energy decomposition analysis method for the investigation of chemical bonding in extended systems. Journal of Chemical Physics, 2015, 142, 194105.	1.2	82
23712	Hybridab-initio/experimental high temperature equations of state: Application to the NaCl pressure scale. Journal of Applied Physics, 2015, 117, 215902.	1.1	8
23713	Insight on the ferroelectric properties in a (BiFeO3)2(SrTiO3)4 superlattice from experiment and ab initio calculations. Applied Physics Letters, 2015, 107, 042904.	1.5	11
23714	Al2O3 as a suitable substrate and a dielectric layer for n-layer MoS2. Applied Physics Letters, 2015, 107, 053106.	1.5	30
23715	Effects of Carbide Formation in Graphene Growth. Chinese Journal of Chemical Physics, 2015, 28, 65-69.	0.6	3
23716	Quantum anomalous Hall effect and related topological electronic states. Advances in Physics, 2015, 64, 227-282.	35.9	374

#	Article	IF	Citations
23717	Piezoelectric coefficients and spontaneous polarization of ScAlN. Journal of Physics Condensed Matter, 2015, 27, 245901.	0.7	209
23718	Database optimization for empirical interatomic potential models. Modelling and Simulation in Materials Science and Engineering, 2015, 23, 065011.	0.8	5
23719	Effects of single O vacancy on the magnetism and electronic structure of Ti doped CoO: A first principle study. Journal of Magnetism and Magnetic Materials, 2015, 396, 91-96.	1.0	1
23720	From the Ternary Eu(Au/In)₂ and EuAu₄(Au/In)₂ with Remarkable Au/In Distributions to a New Structure Type: The Gold-Rich Eu₅Au₁₆(Au/In)₆ Structure. Inorganic Chemistry, 2015, 54, 8187-8196.	1.9	23
23721	Systematic Enumeration of sp³ Nanothreads. Nano Letters, 2015, 15, 5124-5130.	4.5	80
23722	Competing Forces during Contact Formation between a Tip and a Single Molecule. Nano Letters, 2015, 15, 5156-5160.	4.5	9
23723	Site preference of NH₃-adsorption on Co, Pt and CoPt surfaces: the role of charge transfer, magnetism and strain. Physical Chemistry Chemical Physics, 2015, 17, 9335-9340.	1.3	9
23724	A DFT+U study of A-site and B-site substitution in BaFeO_{3â^Î´}. Physical Chemistry Chemical Physics, 2015, 17, 23511-23520.	1.3	46
23725	Unraveling the effect of La A-site substitution on oxygen ion diffusion and oxygen catalysis in perovskite BaFeO₃by data-mining molecular dynamics and density functional theory. Physical Chemistry Chemical Physics, 2015, 17, 24011-24019.	1.3	42
23726	Multilayered silicene: the bottom-up approach for a weakly relaxed Si(111) with Dirac surface states. Nanoscale, 2015, 7, 15880-15885.	2.8	28
23727	Hydroxide-ion incorporation and conduction mechanisms in tin pyrophosphate â€“ a first-principles study. Journal of Materials Chemistry A, 2015, 3, 11905-11911.	5.2	6
23728	The accessibility of nitrogen sites makes a difference in selective CO2 adsorption of a family of isostructural metalâ€“organic frameworks. Journal of Materials Chemistry A, 2015, 3, 19417-19426.	5.2	80
23729	Elucidating the origins of phase transformation hysteresis during electrochemical cycling of Liâ€“Sb electrodes. Journal of Materials Chemistry A, 2015, 3, 18928-18943.	5.2	48
23730	Benzene derivatives adsorbed to the Ag(111) surface: Binding sites and electronic structure. Journal of Chemical Physics, 2015, 142, 101924.	1.2	22
23731	Electronic structure and magnetic properties of zigzag blue phosphorene nanoribbons. Journal of Applied Physics, 2015, 118, 054301.	1.1	19
23732	Energy benchmarks for methane-water systems from quantum Monte Carlo and second-order MÃ¸ller-Plesset calculations. Journal of Chemical Physics, 2015, 143, 102812.	1.2	14
23733	First-principles study of the atomic structure and edge state of zigzag carbon nanoscrolls. Modern Physics Letters B, 2015, 29, 1550110.	1.0	0
23734	On the possibility of contact-induced spin polarization in interfaces of armchair nanotubes with transition metal substrates. Journal of Magnetism and Magnetic Materials, 2015, 396, 102-105.	1.0	2

#	Article	IF	Citations
23735	The effect of Se doping on the growth of Te nanorods. CrystEngComm, 2015, 17, 5734-5743.	1.3	8
23736	Computational and experimental investigation of TmAgTe₂and XYZ₂compounds, a new group of thermoelectric materials identified by first-principles high-throughput screening. Journal of Materials Chemistry C, 2015, 3, 10554-10565.	2.7	99
23737	Optical and transport properties of dense liquid silica. Physics of Plasmas, 2015, 22, 062706.	0.7	22
23738	Density functional theory calculation of ideal strength of SiC and GaN: Effect of multi-axial stress. Computational Materials Science, 2015, 109, 105-110.	1.4	25
23739	Mechanisms of LiCoO₂ Cathode Degradation by Reaction with HF and Protection by Thin Oxide Coatings. ACS Applied Materials & Interfaces, 2015, 7, 24265-24278.	4.0	98
23740	SnS44â€“, SbS43â€“, and AsS33â€“ Metal Chalcogenide Surface Ligands: Couplings to Quantum Dots, Electron Transfers, and All-Inorganic Multilayered Quantum Dot Sensitized Solar Cells. Journal of the American Chemical Society, 2015, 137, 13827-13835.	6.6	32
23741	Orbitally driven giant phonon anharmonicity inÂSnSe. Nature Physics, 2015, 11, 1063-1069.	6.5	539
23742	The interactions between TiO₂ and graphene with surface inhomogeneity determined using density functional theory. Physical Chemistry Chemical Physics, 2015, 17, 29734-29746.	1.3	38
23743	Graphyne as a promising substrate for high density magnetic storage bits. RSC Advances, 2015, 5, 87841-87846.	1.7	19
23744	The effect of Co doping on the conductive properties of ferromagnetic Zn_xCo_{1â^'x}O films. Journal of Materials Chemistry C, 2015, 3, 10188-10194.	2.7	17
23745	Uranyl adsorption at solvated edge surfaces of 2â€‰:â€‰1 smectites. A density functional study. Physical Chemistry Chemical Physics, 2015, 17, 13757-13768.	1.3	33
23746	Cation-Poor Complex Metallic Alloys in Ba(Eu)â€“Auâ€“Al(Ga) Systems: Identifying the Keys that Control Structural Arrangements and Atom Distributions at the Atomic Level. Inorganic Chemistry, 2015, 54, 10296-10308.	1.9	30
23747	In-Plane Intermolecular Interaction Assisted Assembly and Modified Electronic States of Metallofullerene Gd@C₈₂. Langmuir, 2015, 31, 11438-11442.	1.6	3
23748	Modelling of oxygen vacancy aggregates in monoclinic HfO₂: can they contribute to conductive filament formation?. Journal of Physics Condensed Matter, 2015, 27, 415401.	0.7	43
23749	Charge carrier transport and separation in pristine and nitrogen-doped graphene nanowiggle heterostructures. Carbon, 2015, 95, 833-842.	5.4	16
23750	Structure and thermoelectric properties of the n-type clathrate Ba8Cu5.1Ge40.2Sn0.7. Journal of Materials Chemistry A, 2015, 3, 19100-19106.	5.2	17
23751	Molecular Beam Epitaxyâ€Grown SnSe in the Rockâ€Salt Structure: An Artificial Topological Crystalline Insulator Material. Advanced Materials, 2015, 27, 4150-4154.	11.1	83
23752	A density functional theory study of CO oxidation on CuO1-x(111). Journal of Molecular Modeling, 2015, 21, 195.	0.8	17

#	Article	IF	Citations
23753	Hydrogen-induced nanotunnel structure on the C-terminated Î²-SiC(0 0 1)-c(2 Ã— 2) surface investigated by ab-initio calculations. Applied Surface Science, 2015, 357, 1753-1757.	3.1	5
23754	A thermodynamic re-assessment of Alâ€“V toward an assessment of the ternary Alâ€“Tiâ€“V system. Calphad: Computer Coupling of Phase Diagrams and Thermochemistry, 2015, 51, 75-88.	0.7	36
23755	Patched bimetallic surfaces are active catalysts for ammonia decomposition. Nature Communications, 2015, 6, 8619.	5.8	70
23756	Anisotropic thermoelectric properties of layered compounds in SnX₂ (X = S, Se): a promising thermoelectric material. Physical Chemistry Chemical Physics, 2015, 17, 29844-29853.	1.3	116
23757	DFT-based force field development for noble gas adsorption in metal organic frameworks. Journal of Materials Chemistry A, 2015, 3, 23539-23548.	5.2	33
23758	Structural modifications and electron beam damage in aluminium alloy precipitate Î¸'â€“AL₂. Philosophical Magazine, 2015, 95, 3524-3534.	0.7	14
23759	First Principles Study of Electronic Structure, Magnetic, and Mechanical Properties of Transition Metal Monoxides TMO(TM=Co and Ni). Zeitschrift Fur Naturforschung - Section A Journal of Physical Sciences, 2015, 70, 797-804.	0.7	11
23760	A first-principle prediction on the magnetism and electronic structure of Ti-doped CoO with two O vacancies. Current Applied Physics, 2015, 15, 1549-1555.	1.1	2
23761	Polymorphism in Thermoelectric As₂Te₃. Inorganic Chemistry, 2015, 54, 9936-9947.	1.9	25
23762	Significant Contribution of Intrinsic Carbon Defects to Oxygen Reduction Activity. ACS Catalysis, 2015, 5, 6707-6712.	5.5	519
23763	Metal cluster-deposited graphene as an adsorptive material for m-xylene. New Journal of Chemistry, 2015, 39, 9650-9658.	1.4	19
23764	First principle study on electronic properties of two-dimensional atomic crystals. , 2015, , .		0
23765	Hydrogen permeance studies in ordered ternary Cuâ€“Pd alloys. International Journal of Hydrogen Energy, 2015, 40, 14885-14899.	3.8	11
23766	Correlation between theoretical descriptor and catalytic oxygen reduction activity of graphene supported palladium and palladium alloy electrocatalysts. Journal of Power Sources, 2015, 300, 1-9.	4.0	38
23767	Characterizing the Greater-Than-Bulk Melting Behavior of Gaâ€“Al Nanoalloys. Journal of Physical Chemistry C, 2015, 119, 24095-24103.	1.5	3
23768	Tetrahedral Silsesquioxane Framework: A Feasible Candidate for Hydrogen Storage. Journal of Physical Chemistry C, 2015, 119, 23820-23829.	1.5	10
23769	Semiconductor Behavior of a Three-Dimensional Strontium-Based Metalâ€“Organic Framework. ACS Applied Materials & Interfaces, 2015, 7, 22767-22774.	4.0	71
23770	Understanding Selective Hydrogenation of Î±,Î²-Unsaturated Ketones to Unsaturated Alcohols on the Au₂₅(SR)₁₈ Cluster. ACS Catalysis, 2015, 5, 6624-6629.	5.5	66

#	Article	IF	Citations
23771	Understanding catalysis in a multiphasic two-dimensional transition metal dichalcogenide. Nature Communications, 2015, 6, 8311.	5.8	260
23772	Controllable synthesis of uniform BiOF nanosheets and their improved photocatalytic activity by an exposed high-energy (002) facet and internal electric field. RSC Advances, 2015, 5, 88936-88942.	1.7	28
23773	Amorphous Na₂Si₂O₅ as a fast Na⁺ conductor: an ab initio molecular dynamics simulation. Journal of Materials Chemistry A, 2015, 3, 19920-19927.	5.2	44
23774	Activation Energies for Oxide- and Interface-Trap Charge Generation Due to Negative-Bias Temperature Stress of Si-Capped SiGe-pMOSFETs. IEEE Transactions on Device and Materials Reliability, 2015, 15, 352-358.	1.5	9
23775	The origin of two-dimensional electron gas formed in LaGaO 3 /SrTiO 3. Applied Surface Science, 2015, 355, 1316-1320.	3.1	9
23776	(Sub)surface-Promoted Disproportionation and Absolute Band Alignment in High-Power LiMn₂O₄ Cathodes. Journal of Physical Chemistry C, 2015, 119, 21358-21368.	1.5	29
23777	Competitive Deposition of C and O Species on Cobalt Surface in Fischerâ€“Tropsch Synthesis Conditions: A Plausible Origin of Deactivation. Journal of Physical Chemistry C, 2015, 119, 23515-23526.	1.5	7
23778	Anisotropic Effective Mass, Optical Property, and Enhanced Band Gap in BN/Phosphorene/BN Heterostructures. ACS Applied Materials & Interfaces, 2015, 7, 23489-23495.	4.0	58
23779	Large-area synthesis of high-quality and uniform monolayer WS2 on reusable Au foils. Nature Communications, 2015, 6, 8569.	5.8	336
23780	Investigation of stable germane structures under high-pressure. Physical Chemistry Chemical Physics, 2015, 17, 27630-27635.	1.3	16
23781	Electronic structures of in-plane two-dimensional transition-metal dichalcogenide heterostructures. Physical Chemistry Chemical Physics, 2015, 17, 29380-29386.	1.3	34
23782	Solid-state chemistry of glassy antimony oxides. Journal of Materials Chemistry C, 2015, 3, 11349-11356.	2.7	12
23783	CO₂ Electroreduction Performance of Transition Metal Dimers Supported on Graphene: A Theoretical Study. ACS Catalysis, 2015, 5, 6658-6664.	5.5	227
23784	Elucidating Hydrogen Oxidation/Evolution Kinetics in Base and Acid by Enhanced Activities at the Optimized Pt Shell Thickness on the Ru Core. ACS Catalysis, 2015, 5, 6764-6772.	5.5	197
23785	Atomistic description of wave function localization effects in In_xGa_{1-x}N alloys and quantum wells. Proceedings of SPIE, 2015, , .	0.8	8
23786	Role of Alumina Coatings for Selective and Controlled Bonding of DNA on Technologically Relevant Oxide Surfaces. Journal of Physical Chemistry C, 2015, 119, 23527-23543.	1.5	17
23787	Structural and Electronic Features of Î²-Ni(OH)₂ and Î²-NiOOH from First Principles. Journal of Physical Chemistry C, 2015, 119, 24315-24322.	1.5	145
23788	New Phosphorene Allotropes Containing Ridges with 2- and 4-Coordination. Journal of Physical Chemistry C, 2015, 119, 24674-24680.	1.5	37

#	Article	IF	Citations
23789	First-principles study on the doping effects of Al in Î±-MnO2. Current Applied Physics, 2015, 15, 1556-1561.	1.1	12
23790	Imaging and spectrum of monolayer graphene oxide in external electric field. Carbon, 2015, 93, 843-850.	5.4	16
23791	Energetics and electronic structure of UAl4 with point defects. Journal of Nuclear Materials, 2015, 466, 539-550.	1.3	4
23792	Heâ€“He and Heâ€“metal interactions in transition metals from first-principles. Journal of Nuclear Materials, 2015, 467, 465-471.	1.3	25
23793	DFT-based ab initio MD simulation of the ionic conduction in doped ZrO₂systems under epitaxial strain. Physical Chemistry Chemical Physics, 2015, 17, 29057-29063.	1.3	21
23794	Metastable cubic and tetragonal phases of transition metals predicted by density-functional theory. RSC Advances, 2015, 5, 69680-69689.	1.7	14
23795	Electronic structure of porphyrin-based metalâ€“organic frameworks and their suitability for solar fuel production photocatalysis. Journal of Materials Chemistry A, 2015, 3, 23458-23465.	5.2	59
23796	Germanene: the germanium analogue of graphene. Journal of Physics Condensed Matter, 2015, 27, 443002.	0.7	304
23797	Giant Switchable Rashba Effect in Oxide Heterostructures. Advanced Materials Interfaces, 2015, 2, 1400445.	1.9	29
23798	Enhanced magnetic response and metallicity in AB stacked bilayer graphene via Cr-doping. Journal of Alloys and Compounds, 2015, 649, 1300-1305.	2.8	15
23799	Bâ€“N@Graphene: Highly Sensitive and Selective Gas Sensor. Journal of Physical Chemistry C, 2015, 119, 24827-24836.	1.5	112
23800	P-V-Tequation of state and high-pressure behavior of CaCO₃aragonite. American Mineralogist, 2015, 100, 2323-2329.	0.9	27
23801	Equation of state and elasticity of the 3.65 Ã... phase: Implications for the X-discontinuity. American Mineralogist, 2015, 100, 2199-2208.	0.9	17
23802	Effect of uniaxial strain on the structural, electronic and elastic properties of orthorhombic BiMnO3. Journal of Semiconductors, 2015, 36, 032002.	2.0	0
23803	Enhanced electron field emission from NiCo₂O₄nanosheet arrays. Materials Research Express, 2015, 2, 095011.	0.8	26
23804	Two-dimensional Pbâ€“Sn alloy monolayer films on Ag(111). Applied Surface Science, 2015, 351, 83-88.	3.1	6
23805	A first principle study on the magnetic properties of Cu2O surfaces. Current Applied Physics, 2015, 15, 1303-1311.	1.1	23
23806	Density functional theories study on the properties of Ga1â^'xCrxAs. Materials and Design, 2015, 87, 877-882.	3.3	4

#	Article	IF	Citations
23807	Impregnation versus Bulk Synthesis: How the Synthetic Route Affects the Photocatalytic Efficiency of Nb/Ta:N Codoped TiO₂ Nanomaterials. Journal of Physical Chemistry C, 2015, 119, 24104-24115.	1.5	36
23808	Core/Shell Face-Centered Tetragonal FePd/Pd Nanoparticles as an Efficient Non-Pt Catalyst for the Oxygen Reduction Reaction. ACS Nano, 2015, 9, 11014-11022.	7.3	165
23809	Tuning magnetic properties of antiferromagnetic chains by exchange interactions: ab initio studies. Physical Chemistry Chemical Physics, 2015, 17, 26302-26306.	1.3	12
23810	Crystal structure, electronic structure, temperature-dependent optical and scintillation properties of CsCe₂Br₇. Journal of Materials Chemistry C, 2015, 3, 11366-11376.	2.7	14
23811	Chiral solitons in a coupled double Peierls chain. Science, 2015, 350, 182-185.	6.0	96
23812	Finding optimal surface sites on heterogeneous catalysts by counting nearest neighbors. Science, 2015, 350, 185-189.	6.0	725
23813	Catalytic activities of platinum nanotubes: a density functional study. European Physical Journal B, 2015, 88, 1.	0.6	2
23814	Impact of Ferroelectric Distortion on Thermopower in BaTiO₃. Journal of the Physical Society of Japan, 2015, 84, 054701.	0.7	4
23815	Local structure study of Fe dopants in Niâ€“deficit Ni3Al alloys. Journal of Alloys and Compounds, 2015, 651, 705-711.	2.8	6
23816	Activating and tuning basal planes of MoO₂, MoS₂, and MoSe₂ for hydrogen evolution reaction. Physical Chemistry Chemical Physics, 2015, 17, 29305-29310.	1.3	60
23817	Benchmarking density functional theory predictions of framework structures and properties in a chemically diverse test set of metalâ€“organic frameworks. Journal of Materials Chemistry A, 2015, 3, 22432-22440.	5.2	64
23818	An ab initio study of oxide ion dynamics in type-II Bi3NbO7. Journal of Materials Chemistry A, 2015, 3, 21882-21890.	5.2	4
23819	Colorimetric Signal Amplification Assay for Mercury Ions Based on the Catalysis of Gold Amalgam. Analytical Chemistry, 2015, 87, 10963-10968.	3.2	57
23820	Thermodynamic Modeling of the Niâ€“H System. Journal of Physical Chemistry C, 2015, 119, 24546-24557.	1.5	6
23821	Activity versus Selectivity of the Methanol Oxidation at Ceria Surfaces: A Comparative First-Principles Study. Journal of Physical Chemistry C, 2015, 119, 23021-23031.	1.5	31
23822	Investigation of Bismuth Triiodide (BiI₃) for Photovoltaic Applications. Journal of Physical Chemistry Letters, 2015, 6, 4297-4302.	2.1	176
23823	Investigation of the Role of Polysaccharide in the Dolomite Growth at Low Temperature by Using Atomistic Simulations. Langmuir, 2015, 31, 10435-10442.	1.6	29
23824	Realization of a Strained Atomic Wire Superlattice. ACS Nano, 2015, 9, 10621-10627.	7.3	13

#	Article	IF	Citations
23825	Dopants Control Electronâ€“Hole Recombination at Perovskiteâ€“TiO₂ Interfaces: Ab Initio Time-Domain Study. ACS Nano, 2015, 9, 11143-11155.	7.3	108
23826	Electrically tunable multiple Dirac cones in thin films of the (LaO)2(SbSe2)2 family of materials. Nature Communications, 2015, 6, 8517.	5.8	25
23827	Quantum engineering of spin and anisotropy in magnetic molecular junctions. Nature Communications, 2015, 6, 8536.	5.8	68
23828	Electric-dipole effect of defects on the energy band alignment of rutile and anatase TiO₂. Physical Chemistry Chemical Physics, 2015, 17, 29079-29084.	1.3	24
23829	On the origin of preferred bicarbonate production from carbon dioxide (CO₂) capture in aqueous 2-amino-2-methyl-1-propanol (AMP). Physical Chemistry Chemical Physics, 2015, 17, 29184-29192.	1.3	38
23830	Quantum spin hall insulators in strain-modified arsenene. Nanoscale, 2015, 7, 19152-19159.	2.8	151
23831	Strain-induced semimetal-to-semiconductor transition and indirect-to-direct band gap transition in monolayer 1T-TiS₂. RSC Advances, 2015, 5, 83876-83879.	1.7	34
23832	Substitution of silicon within the rhombohedral boron carbide (B₄C) crystal lattice through high-energy ball-milling. Journal of Materials Chemistry C, 2015, 3, 11705-11716.	2.7	40
23833	Complex centers of hydrogen in tin dioxide. Theoretical Chemistry Accounts, 2015, 134, 1.	0.5	5
23834	Hydrogen embrittlement in nickel, visited by first principles modeling, cohesive zone simulation and nanomechanical testing. International Journal of Hydrogen Energy, 2015, 40, 16892-16900.	3.8	93
23835	Structure, electronic properties, luminescence and chromaticity investigations of rare earth doped KMgBO3 phosphors. Materials Chemistry and Physics, 2015, 165, 168-176.	2.0	18
23836	Crystal and Electronic Structures of Complex Bismuth Iodides A₃Bi₂I₉ (A = K, Rb, Cs) Related to Perovskite: Aiding the Rational Design of Photovoltaics. Chemistry of Materials, 2015, 27, 7137-7148.	3.2	413
23837	Structural Evolution in Methylammonium Lead Iodide CH₃NH₃PbI₃. Journal of Physical Chemistry A, 2015, 119, 11033-11038.	1.1	66
23838	Improved Ductility of Boron Carbide by Microalloying with Boron Suboxide. Journal of Physical Chemistry C, 2015, 119, 24649-24656.	1.5	27
23839	Electronic Structure and Optical Properties of Î±-CH₃NH₃PbBr₃ Perovskite Single Crystal. Journal of Physical Chemistry Letters, 2015, 6, 4304-4308.	2.1	136
23840	2D Electrides as Promising Anode Materials for Na-Ion Batteries from First-Principles Study. ACS Applied Materials & Interfaces, 2015, 7, 24016-24022.	4.0	181
23841	First-principles study of the alkali earth metal atoms adsorption on graphene. Applied Surface Science, 2015, 356, 668-673.	3.1	90
23842	Insights into the Lithium-Ion Conduction Mechanism of Garnet-Type Cubic Li₅La₃Ta₂O₁₂ by ab-Initio Calculations. Journal of Physical Chemistry C, 2015, 119, 20783-20791.	1.5	25

#	Article	IF	Citations
23843	Hydrogen Dissociative Adsorption on Lanthana: Polaron Formation and the Role of Acidâ€“Base Interactions. Journal of Physical Chemistry C, 2015, 119, 19876-19882.	1.5	22
23844	Flexible structural and electronic properties of a pentagonal B₂C monolayer via external strain: a computational investigation. Physical Chemistry Chemical Physics, 2015, 17, 24151-24156.	1.3	127
23845	Thermoelectric properties of single-layered SnSe sheet. Nanoscale, 2015, 7, 15962-15970.	2.8	256
23846	A global view of the phase transitions of SnO₂ in rechargeable batteries based on results of high throughput calculations. Journal of Materials Chemistry A, 2015, 3, 19483-19489.	5.2	21
23847	WO₃ based solid solution oxide â€“ promising proton exchange membrane fuel cell anode electro-catalyst. Journal of Materials Chemistry A, 2015, 3, 18296-18309.	5.2	28
23848	First-principles study on lattice thermal conductivity of thermoelectrics HgTe in different phases. Journal of Applied Physics, 2015, 117, .	1.1	16
23849	Cl-doping of Te-rich CdTe: Complex formation, self-compensation and self-purification from first principles. AIP Advances, 2015, 5, 087101.	0.6	18
23850	Calculations of Al dopant inÎ±-quartz using a variational implementation of the Perdewâ€“Zunger self-interaction correction. New Journal of Physics, 2015, 17, 083006.	1.2	26
23851	Theoretical insights on the influence of doped Ni in the early stage of graphene growth during the CH4 dissociation on Niâ€“Cu(111) surface. Applied Catalysis A: General, 2015, 506, 1-7.	2.2	14
23852	Transition metal adatoms on graphene: A systematic density functional study. Carbon, 2015, 95, 525-534.	5.4	144
23853	Strain effect on the NÃ©el temperature of SrTcO3 from first-principles calculations. Solid State Communications, 2015, 219, 25-27.	0.9	7
23854	Intrinsic Charge Storage Capability of Transition Metal Dichalcogenides as Pseudocapacitor Electrodes. Journal of Physical Chemistry C, 2015, 119, 20864-20870.	1.5	43
23855	Effects of proton irradiation on Si-nanocrystal/SiO2 multilayers: study of photoluminescence and first-principles calculations. Journal of Materials Chemistry C, 2015, 3, 8574-8581.	2.7	9
23856	Electronic structure and soft magnetic properties of Se/FeSiAl (110) films. Applied Surface Science, 2015, 354, 401-407.	3.1	8
23857	Encapsulated Silicene: A Robust Large-Gap Topological Insulator. ACS Applied Materials & Interfaces, 2015, 7, 19226-19233.	4.0	31
23858	On-Surface Synthesis of BN-Substituted Heteroaromatic Networks. ACS Nano, 2015, 9, 9228-9235.	7.3	78
23859	First-principles study on phase transition and ferroelectricity in lithium niobate and tantalate. Journal of Applied Physics, 2015, 118, .	1.1	36
23860	Theoretical Study of Epoxy Group Adsorption and Diffusion on Pristine, Defected Graphene Sheets. Integrated Ferroelectrics, 2015, 164, 112-121.	0.3	1

#	Article	IF	Citations
23861	Dislocation modelling in Ti₂AlN MAX phase based on the Peierlsâ€“Nabarro model. Philosophical Magazine, 2015, 95, 2539-2552.	0.7	27
23862	Shape memory behavior in Fe₃Al-modeling and experiments. Philosophical Magazine, 2015, 95, 2553-2570.	0.7	7
23863	Energy levels of the Ce activator relative to the YAP(Ce) scintillator host. Journal of Physics Condensed Matter, 2015, 27, 185501.	0.7	3
23864	An ab-initio study of CuInSe2 based ordered defect compounds. Materials Chemistry and Physics, 2015, 162, 372-379.	2.0	0
23865	Novel electronic properties in silicene on MoSe2 monolayer: An excellent prediction for FET. Materials Chemistry and Physics, 2015, 164, 150-156.	2.0	23
23866	Interplay of Octahedral Rotations and Lone Pair Ferroelectricity in CsPbF₃. Inorganic Chemistry, 2015, 54, 8536-8543.	1.9	54
23867	Theory and X-ray Absorption Spectroscopy for Aluminum Coordination Complexes â€“ Al K-Edge Studies of Charge and Bonding in (BDI)Al, (BDI)AlR₂, and (BDI)AlX₂ Complexes. Journal of the American Chemical Society, 2015, 137, 10304-10316.	6.6	21
23868	Hydrogenation-induced large-gap quantum-spin-Hall insulator states in a germaniumâ€“tin dumbbell structure. RSC Advances, 2015, 5, 72462-72468.	1.7	12
23869	Impact of biaxial compressive strain on the heterostructures of paraelectrics KTaO3 and SrTiO3. AIP Advances, 2015, 5, 057147.	0.6	3
23870	Enhanced p-type dopability of P and As in CdTe using non-equilibrium thermal processing. Journal of Applied Physics, 2015, 118, .	1.1	60
23871	Structural transformations among austenite, ferrite and cementite in Feâ€“C alloys: A unified theory based on ab initio simulations. Acta Materialia, 2015, 99, 281-289.	3.8	59
23872	A first-principles study of light non-metallic atom substituted blue phosphorene. Applied Surface Science, 2015, 356, 110-114.	3.1	95
23873	Chemisorption of benzene on Pt (1 1 1) surface: A DFT study with van der Waals interaction. Chemical Physics Letters, 2015, 637, 182-188.	1.2	15
23874	Applicability of special quasi-random structure models in thermodynamic calculations using semi-empirical Debyeâ€“GrÃ¼neisen theory. Journal of Alloys and Compounds, 2015, 650, 564-571.	2.8	16
23875	CO adsorption on cobalt: Prediction of stable surface phases. Surface Science, 2015, 642, L6-L10.	0.8	44
23876	Performance of a Non-Local van der Waals Density Functional on the Dissociation of H₂ on Metal Surfaces. Journal of Physical Chemistry A, 2015, 119, 12146-12158.	1.1	44
23877	Atomically controlled substitutional boron-doping of graphene nanoribbons. Nature Communications, 2015, 6, 8098.	5.8	400
23878	Laser irradiation-induced modification of the amorphous phase in GeTe films: the role of intermediate Geâ€“Te bonding in the crystallization mechanism. Journal of Materials Chemistry C, 2015, 3, 9393-9402.	2.7	12

#	Article	IF	Citations
23879	A first-principles study of Pt thin films on SrTiO3(100): Support effects on CO adsorption. Journal of Chemical Physics, 2015, 142, 124704.	1.2	13
23880	First-principles study of the structures and electronic band properties of Bi2Te3{11Ì„5} nanoribbons. AIP Advances, 2015, 5, .	0.6	7
23881	First-Principles Calculations of the Quantum Size Effects on the Stability and Reactivity of Ultrathin Ru(0001) Films. Chinese Physics Letters, 2015, 32, 067302.	1.3	1
23882	Structure and chemical bonding in MgNi2H3 from combined high resolution synchrotron and neutron diffraction studies and ab initio electronic structure calculations. Acta Materialia, 2015, 98, 416-422.	3.8	13
23883	Experimental investigation and thermodynamic description of the Liâ€“Siâ€“Ni ternary system. Calphad: Computer Coupling of Phase Diagrams and Thermochemistry, 2015, 51, 13-23.	0.7	3
23884	Revisit of polystyrene-modified fullerene core stars: A computational study. Journal of Molecular Graphics and Modelling, 2015, 61, 102-106.	1.3	1
23885	Novel <mml:math altimg="si1.gif" overflow="scroll" xmlns:xocs="http://www.elsevier.com/xml/xocs/dtd" xmlns:xs="http://www.w3.org/2001/XMLSchema" xmlns:xsi="http://www.w3.org/2001/XMLSchema-instance" xmlns="http://www.elsevier.com/xml/ja/dtd" xmlns:ja="http://www.elsevier.com/xml/ja/dtd" xmlns:mml="http://www.w3.org/1998/Math/MathML" xmlns:tb="http://www.elsevier.com/xml/common/table/dtd" xmlns:sb="http://www.elsevier.com/xml/common/struct-bib/dtd" xmlns:ce="http://www.elsevier.com/x	0.9	2
23886	Discovery of Î³-MnP₄ and the Polymorphism of Manganese Tetraphosphide. Inorganic Chemistry, 2015, 54, 8761-8768.	1.9	8
23887	Characterization of AlPO₄(110) Surface in Adsorption of Rh Dimer and Its Comparison with Î³-Al₂O₃(100) Surface: A Theoretical Study. Journal of Physical Chemistry C, 2015, 119, 19752-19762.	1.5	17
23888	Understanding Deviations in Hydrogen Solubility Predictions in Transition Metals through First-Principles Calculations. Journal of Physical Chemistry C, 2015, 119, 19642-19653.	1.5	31
23889	Controlling Electronic Structure and Transport Properties of Zigzag Graphene Nanoribbons by Edge Functionalization with Fluorine. Journal of Physical Chemistry C, 2015, 119, 21227-21233.	1.5	17
23890	Trapping and Characterization of a Single Hydrogen Molecule in a Continuously Tunable Nanocavity. Journal of Physical Chemistry Letters, 2015, 6, 3453-3457.	2.1	21
23891	Antagonism between Spinâ€“Orbit Coupling and Steric Effects Causes Anomalous Band Gap Evolution in the Perovskite Photovoltaic Materials CH₃NH₃Sn_{1â€“x}Pb_xI₃. Journal of Physical Chemistry Letters, 2015, 6, 3503-3509.	2.1	202
23892	Phagraphene: A Low-Energy Graphene Allotrope Composed of 5â€“6â€“7 Carbon Rings with Distorted Dirac Cones. Nano Letters, 2015, 15, 6182-6186.	4.5	482
23893	Adatom bond-induced geometric and electronic properties of passivated armchair graphene nanoribbons. Physical Chemistry Chemical Physics, 2015, 17, 16545-16552.	1.3	8
23894	Chirality control of nonplanar lead phthalocyanine (PbPc) and its potential application in high-density storage: a theoretical investigation. Physical Chemistry Chemical Physics, 2015, 17, 23651-23656.	1.3	9
23895	A novel phase of beryllium fluoride at high pressure. Physical Chemistry Chemical Physics, 2015, 17, 26283-26288.	1.3	11
23896	The nature of photogenerated charge separation among different crystal facets of BiVO₄studied by density functional theory. Physical Chemistry Chemical Physics, 2015, 17, 23503-23510.	1.3	112

#	Article	IF	Citations
23897	Global minimization of gold clusters by combining neural network potentials and the basin-hopping method. Nanoscale, 2015, 7, 14817-14821.	2.8	90
23898	Band gap control and transformation of monolayer-MoS₂-based hetero-bilayers. Journal of Materials Chemistry C, 2015, 3, 9403-9411.	2.7	30
23899	Lattice vibration modes of the layered material BiCuSeO and first principles study of its thermoelectric properties. New Journal of Physics, 2015, 17, 083012.	1.2	51
23900	Domain boundaries in silicene: Density functional theory calculations on electronic properties. Chinese Physics B, 2015, 24, 086806.	0.7	3
23901	Impurity migration and effects on vacancy formation enthalpy in polycrystalline depleted uranium. Journal of Nuclear Materials, 2015, 466, 343-350.	1.3	10
23902	Insights into the Nature of Formate Species in the Decomposition and Reaction of Methanol over Cerium Oxide Surfaces: A Combined Infrared Spectroscopy and Density Functional Theory Study. Journal of Physical Chemistry C, 2015, 119, 21452-21464.	1.5	47
23903	Role of the surface effect on the structural, electronic and mechanical properties of the carbide MXenes. Europhysics Letters, 2015, 111, 26007.	0.7	262
23904	Atomic configurations of various kinds of structural intergrowth in the polytypic M2B-type boride precipitated in the Ni-based superalloy. Acta Materialia, 2015, 100, 64-72.	3.8	18
23905	A first-principles study of cementite (Fe3C) and its alloyed counterparts: Structural properties, stability, and electronic structure. Computational Materials Science, 2015, 110, 169-181.	1.4	34
23906	Atomistic modeling study of surface effect on oxide ion diffusion in yttria-stabilized zirconia. Solid State Ionics, 2015, 279, 46-52.	1.3	4
23907	Chemisorbed oxygen atom on the activation of Câ€“H bond in methane: a Rh model study. RSC Advances, 2015, 5, 66221-66230.	1.7	10
23908	Electronic structures and optical properties of Î±-Fe2O3-xSex alloys for solar absorber. Modern Physics Letters B, 2015, 29, 1550050.	1.0	1
23909	Tunable electronic structures in the two-dimension SnX 2 (X = S and Se) nanosheets by stacking effects. Applied Surface Science, 2015, 356, 1200-1206.	3.1	17
23910	Behavior of fission gases in nuclear fuel: XAS characterization of Kr in UO2. Journal of Nuclear Materials, 2015, 466, 379-392.	1.3	22
23911	Structural Phase Stability Control of Monolayer MoTe₂ with Adsorbed Atoms and Molecules. Journal of Physical Chemistry C, 2015, 119, 21674-21680.	1.5	74
23912	Dynamic Structural Response and Deformations of Monolayer MoS₂ Visualized by Femtosecond Electron Diffraction. Nano Letters, 2015, 15, 6889-6895.	4.5	93
23913	AgPO₂F₂and Ag₉(PO₂F₂)₁₄: the first Ag(<scp>i</scp>) and Ag(<scp>i</scp>)/Ag(<scp>ii</scp>) difluorophosphates with complex crystal structures. Dalton Transactions, 2015, 44, 19478-19486.	1.6	8
23914	Theoretical study of hydration in Y2Mo3O12: Effects on structure and negative thermal expansion. AIP Advances, 2015, 5, .	0.6	17

#	Article	IF	Citations
23915	The effect of oxygen vacancy on holes-induced d0 magnetism in CaTiO3 and CaZrO3. Modern Physics Letters B, 2015, 29, 1550137.	1.0	3
23916	Experimental investigation and thermodynamic modeling of the Alâ€“Dyâ€“Zr system. Journal of Materials Science, 2015, 50, 6427-6436.	1.7	1
23917	Tuning the catalytic activity of Agâ€“Pd alloy cluster for hydrogen dissociation by controlling the Pd ratio. Computational and Theoretical Chemistry, 2015, 1071, 39-45.	1.1	9
23918	Atomic-Scale Insight into Tautomeric Recognition, Separation, and Interconversion of Guanine Molecular Networks on Au(111). Journal of the American Chemical Society, 2015, 137, 11795-11800.	6.6	41
23919	Magnetoelectric coupling and spin-dependent tunneling in Fe/PbTiO3/Fe multiferroic heterostructure with a Ni monolayer inserted at one interface. Journal of Applied Physics, 2015, 118, .	1.1	9
23920	Electronic and magnetic properties of nonmetal atoms adsorbed ReS2 monolayers. Journal of Applied Physics, 2015, 118, 064306.	1.1	26
23921	Atomic-scale luminescence measurement and theoretical analysis unveiling electron energy dissipation at ap-type GaAs(110) surface. Nanotechnology, 2015, 26, 365402.	1.3	12
23922	Hydrogen Isotopic Effects of Uranium Hydrides: First-Principles Calculations. Materials Science Forum, 2015, 817, 675-684.	0.3	1
23923	An Updated Thermodynamic Modeling of the Al-Zr System. Journal of Phase Equilibria and Diffusion, 2015, 36, 404-413.	0.5	34
23924	Efficient helium separation of graphitic carbon nitride membrane. Carbon, 2015, 95, 51-57.	5.4	115
23925	Investigation of interfaces in Mg/Nb multilayer thin films. Computational Materials Science, 2015, 108, 212-225.	1.4	10
23926	Band gap engineering of graphenylene by hydrogenation and halogenation: a density functional theory study. RSC Advances, 2015, 5, 70766-70771.	1.7	26
23927	The role of point defects in PbS, PbSe and PbTe: afirst principlesstudy. Journal of Physics Condensed Matter, 2015, 27, 355801.	0.7	23
23928	Prediction of Stable Nitride Perovskites. Chemistry of Materials, 2015, 27, 5957-5963.	3.2	102
23929	Band Gap on/off Switching of Silicene Superlattice. Journal of Physical Chemistry C, 2015, 119, 20747-20754.	1.5	21
23930	Tuning the Electronic Structure of Graphene by Molecular Dopants: Impact of the Substrate. ACS Applied Materials & Interfaces, 2015, 7, 19134-19144.	4.0	34
23931	A first-principles study on the hydrogen evolution reaction of VS₂ nanoribbons. Physical Chemistry Chemical Physics, 2015, 17, 24820-24825.	1.3	88
23932	Towards high throughput screening of electrochemical stability of battery electrolytes. Nanotechnology, 2015, 26, 354003.	1.3	160

#	Article	IF	Citations
23933	Pressure-tuning the nonlinear-optical properties of AgGaS_2 crystal: a first-principle study. Optical Materials Express, 2015, 5, 1738.	1.6	10
23934	Prospecting Lighting Applications with Ligand Field Tools and Density Functional Theory: A First-Principles Account of the 4f⁷â€“4f⁶5d¹ Luminescence of CsMgBr₃:Eu²⁺. Inorganic Chemistry, 2015, 54, 8319-8326.	1.9	39
23935	Critical Factors Driving the High Volumetric Uptake of Methane in Cu₃(btc)₂. Journal of the American Chemical Society, 2015, 137, 10816-10825.	6.6	73
23936	Chemical bonding in equiatomic cerium intermetallics â€“ The case of CeMgSn, CePdSn, and CeMgPb. Solid State Sciences, 2015, 48, 205-211.	1.5	2
23937	Ultrafast Electron and Hole Relaxation Pathways in Few-Layer MoS₂. Journal of Physical Chemistry C, 2015, 119, 20698-20708.	1.5	47
23938	Design principles for solid-state lithium superionic conductors. Nature Materials, 2015, 14, 1026-1031.	13.3	1,079
23939	Weyl semimetal phase in the non-centrosymmetric compound TaAs. Nature Physics, 2015, 11, 728-732.	6.5	796
23940	Revealing the role of Pb²⁺ in the stability of organicâ€“inorganic hybrid perovskite CH₃NH₃Pb_{1â^'x}Cd_xI₃: an experimental and theoretical study. Physical Chemistry Chemical Physics, 2015, 17, 23886-23896.	1.3	38
23941	Tuning the electronic properties of transition-metal trichalcogenides via tensile strain. Nanoscale, 2015, 7, 15385-15391.	2.8	79
23942	Magnetism in a nonmetal-substituted blue phosphorene: A first-principles study. , 2015, , .		0
23943	Crystal structures of highly-ordered long-period stacking-ordered phases with 18R, 14H and 10H-type stacking sequences in the Mgâ€“Znâ€“Y system. Acta Materialia, 2015, 99, 228-239.	3.8	145
23944	Single-Spin Dirac Fermion and Chern Insulator Based on Simple Oxides. Nano Letters, 2015, 15, 6434-6439.	4.5	87
23945	Janus Solidâ€“Liquid Interface Enabling Ultrahigh Charging and Discharging Rate for Advanced Lithium-Ion Batteries. Nano Letters, 2015, 15, 6102-6109.	4.5	90
23946	Predicting suitable optoelectronic properties of monoclinic VON semiconductor crystals for photovoltaics using accurate first-principles computations. Physical Chemistry Chemical Physics, 2015, 17, 25244-25249.	1.3	10
23947	Single layer lead iodide: computational exploration of structural, electronic and optical properties, strain induced band modulation and the role of spinâ€“orbital-coupling. Nanoscale, 2015, 7, 15168-15174.	2.8	80
23948	Ba₄AgGa₅Pn₈ (Pn = P, As): new pnictide-based compounds with nonlinear optical potential. Journal of Materials Chemistry C, 2015, 3, 9695-9700.	2.7	16
23949	Atomic-scale properties of Ni-based FCC ternary, and quaternary alloys. Acta Materialia, 2015, 99, 307-312.	3.8	159
23950	DFT-based modeling of benzene hydrogenation on Pt at industrially relevant coverage. Journal of Catalysis, 2015, 330, 406-422.	3.1	34

#	Article	IF	Citations
23951	Chemical Functionalization of GaN Monolayer by Adatom Adsorption. Journal of Physical Chemistry C, 2015, 119, 20911-20916.	1.5	65
23952	Impact of Anchoring Groups on Ballistic Transport: Single Molecule vs Monolayer Junctions. Journal of Physical Chemistry C, 2015, 119, 21198-21208.	1.5	40
23953	Ab Initio Prediction of Piezoelectricity in Two-Dimensional Materials. ACS Nano, 2015, 9, 9885-9891.	7.3	445
23954	Valence Band Modification and High Thermoelectric Performance in SnTe Heavily Alloyed with MnTe. Journal of the American Chemical Society, 2015, 137, 11507-11516.	6.6	371
23955	Zn-dopant dependent defect evolution in GaN nanowires. Nanoscale, 2015, 7, 16237-16245.	2.8	27
23956	Atomistic study on the cross-slip process of a screwâ€‰â€‰<a>â€‰â€‰dislocation in magnesium. Modelling and Simulation in Materials Science and Engineering, 2015, 23, 065002.	0.8	15
23957	Numerical Microscale Modeling of Solidification. , 2015, , 379-434.		0
23958	Tuning an Atomic Switch on a Surface with Electric and Magnetic Fields. Journal of Physical Chemistry Letters, 2015, 6, 3698-3701.	2.1	7
23959	Tunable band gap and magnetism of the two-dimensional nickel hydroxide. RSC Advances, 2015, 5, 77154-77158.	1.7	24
23960	Defects responsible for abnormal n-type conductivity in Ag-excess doped PbTe thermoelectrics. Journal of Applied Physics, 2015, 118, .	1.1	17
23961	Activation and dissociation of CO2 on the (001), (011), and (111) surfaces of mackinawite (FeS): A dispersion-corrected DFT study. Journal of Chemical Physics, 2015, 143, 094703.	1.2	46
23962	Theoretical understanding of magnetic and electronic structures of Ti3C2 monolayer and its derivatives. Solid State Communications, 2015, 222, 9-13.	0.9	41
23963	Kinetic and Mechanistic Assessment of Alkanol/Alkanal Decarbonylation and Deoxygenation Pathways on Metal Catalysts. Journal of the American Chemical Society, 2015, 137, 11984-11995.	6.6	55
23964	Adsorbing a PVDF polymer via noncovalent interactions to effectively tune the electronic and magnetic properties of zigzag SiC nanoribbons. Physical Chemistry Chemical Physics, 2015, 17, 24038-24047.	1.3	11
23965	DFT+U studies of Cu doping and p-type compensation in crystalline and amorphous ZnS. Physical Chemistry Chemical Physics, 2015, 17, 26270-26276.	1.3	27
23966	Modulation of Electronic Structure of Armchair MoS₂ Nanoribbon. Journal of Physical Chemistry C, 2015, 119, 22164-22171.	1.5	39
23967	Atomic-Scale Magnetism of Cr-Doped Bi₂Se₃ Thin Film Topological Insulators. ACS Nano, 2015, 9, 10237-10243.	7.3	54
23968	Anisotropic displacement parameters from dispersion-corrected DFT methods and their experimental validation by temperature-dependent X-ray diffraction. CrystEngComm, 2015, 17, 7414-7422.	1.3	27

#	Article	IF	Citations
23969	The effect of the morphology of supported subnanometer Pt clusters on the first and key step of CO₂ photoreduction. Physical Chemistry Chemical Physics, 2015, 17, 25379-25392.	1.3	25
23970	Synergistically optimized electrical and thermal transport properties of SnTe via alloying high-solubility MnTe. Energy and Environmental Science, 2015, 8, 3298-3312.	15.6	268
23971	Organicâ€“inorganic hybrid perovskites ABI₃(A = CH₃NH₃,) Tj ETQq0 0 0 rgBT /Overlock 10 Tf 5 functional evaluation. RSC Advances, 2015, 5, 78701-78707.	1.7	69
23972	A chemical link between Geâ€“Sbâ€“Te and Inâ€“Sbâ€“Te phase-change materials. Journal of Materials Chemistry C, 2015, 3, 9519-9523.	2.7	44
23973	Many-body dispersion effects in the binding of adsorbates on metal surfaces. Journal of Chemical Physics, 2015, 143, 102808.	1.2	69
23974	Manifestation of axion electrodynamics through magnetic ordering on edges of a topological insulator. Proceedings of the National Academy of Sciences of the United States of America, 2015, 112, 11514-11518.	3.3	11
23975	Migration of rhenium and osmium interstitials in tungsten. Journal of Nuclear Materials, 2015, 467, 418-423.	1.3	46
23976	First-principles calculations of the interaction between hydrogen and 3d alloying atom in nickel. Journal of Nuclear Materials, 2015, 465, 254-259.	1.3	8
23977	Bond Network Topology and Antiferroelectric Order in Cuprice CuOH. Inorganic Chemistry, 2015, 54, 8969-8977.	1.9	21
23978	A Combinatorial Genetic Algorithm for Computational Doping based Material Design. , 2015, , .		2
23979	Thermo-Elastic and Lattice Dynamical Properties of Pd3X (Xâ€‰=â€‰Ti, Zr, Hf) Alloys: An Ab Initio Study. Brazilian Journal of Physics, 2015, 45, 604-614.	0.7	3
23980	First principles investigation of hydrogen physical adsorption on graphynes' layers. Carbon, 2015, 95, 1076-1081.	5.4	64
23981	Energetics of gaseous and volatile fission products in molten Uâ€“10Zr alloy: A density functional theory study. Journal of Nuclear Materials, 2015, 466, 583-587.	1.3	1
23982	First-principles study of structural, electronic and Li-ion diffusion properties of N-doped LiFePO4 (010) surface. Solid State Ionics, 2015, 281, 1-5.	1.3	30
23983	Computational Exploration of the Binary A₁B₁ Chemical Space for Thermoelectric Performance. Chemistry of Materials, 2015, 27, 6213-6221.	3.2	38
23984	Brittle Failure Mechanism in Thermoelectric Skutterudite CoSb₃. Chemistry of Materials, 2015, 27, 6329-6336.	3.2	60
23985	Resolving the Controversy about the Band Alignment between Rutile and Anatase: The Role of OH^{â€“}/H⁺ Adsorption. Journal of Physical Chemistry C, 2015, 119, 21952-21958.	1.5	43
23986	In Situ Ambient Pressure X-ray Photoelectron Spectroscopy Studies of Methanol Oxidation on Pt(111) and Ptâ€“Re Alloys. Journal of Physical Chemistry C, 2015, 119, 23082-23093.	1.5	20

#	Article	IF	Citations
23987	Calculation Evidence of Staged Mott and Peierls Transitions in VO₂ Revealed by Mapping Reduced-Dimension Potential Energy Surface. Journal of Physical Chemistry Letters, 2015, 6, 3650-3656.	2.1	23
23988	Accurate Ab Initio Quantum Mechanics Simulations of Bi₂Se₃ and Bi₂Te₃ Topological Insulator Surfaces. Journal of Physical Chemistry Letters, 2015, 6, 3792-3796.	2.1	40
23989	Observation of an Excitonic Quantum Coherence in CdSe Nanocrystals. Nano Letters, 2015, 15, 6875-6882.	4.5	28
23990	Rashba and Dresselhaus Effects in Hybrid Organicâ€“Inorganic Perovskites: From Basics to Devices. ACS Nano, 2015, 9, 11557-11567.	7.3	304
23991	Monolayered Bi2WO6 nanosheets mimicking heterojunction interface with open surfaces for photocatalysis. Nature Communications, 2015, 6, 8340.	5.8	578
23992	Efficient hydrogen evolution catalysis using ternary pyrite-type cobalt phosphosulphide. Nature Materials, 2015, 14, 1245-1251.	13.3	1,162
23993	Dissociation of CO₂ on rhodium nanoclusters (Rh₁₃) in various structures supported on unzipped graphene oxide â€“ a DFT study. Physical Chemistry Chemical Physics, 2015, 17, 11028-11035.	1.3	10
23994	Pt-nanoparticle functionalized carbon nano-onions for ultra-high energy supercapacitors and enhanced field emission behaviour. RSC Advances, 2015, 5, 80990-80997.	1.7	52
23995	Pressure modulates the phase stability and physical properties of zinc nitride iodine. RSC Advances, 2015, 5, 78754-78759.	1.7	1
23996	On the mechanical stability of uranyl peroxide hydrates: implications for nuclear fuel degradation. RSC Advances, 2015, 5, 79090-79097.	1.7	46
23997	The accurate calculation of the band gap of liquid water by means of GW corrections applied to plane-wave density functional theory molecular dynamics simulations. Physical Chemistry Chemical Physics, 2015, 17, 365-375.	1.3	54
23998	Crystal feature and electronic structure of novel mixed alanate LiCa(AlH4)3: a density functional theory investigation. RSC Advances, 2015, 5, 16439-16445.	1.7	6
23999	Hydrocarbon chain growth and hydrogenation on V(100): a density functional theory study. RSC Advances, 2015, 5, 4909-4917.	1.7	0
24000	The system Ceâ€“Znâ€“Si for <33.3 at.% Ce: phase relations, crystal structures and physical properties. RSC Advances, 2015, 5, 36480-36497.	1.7	3
24001	Bonding between graphene and MoS2 monolayers without and with Li intercalation. Applied Physics Letters, 2015, 107, 043903.	1.5	20
24002	Precise control of defects in graphene using oxygen plasma. Journal of Vacuum Science and Technology A: Vacuum, Surfaces and Films, 2015, 33, .	0.9	32
24003	A lattice theory of the Stone-Wales defect as dipole of dislocation and anti-dislocation. European Physical Journal B, 2015, 88, 1.	0.6	11
24004	Assessing the reliability of van der Waals DFT functionals to study the physisorption of molecular hydrogen on aromatic systems. Theoretical Chemistry Accounts, 2015, 134, 1.	0.5	6

#	Article	IF	Citations
24005	Aromatic-based hydrocarbon pool mechanism for methanol-to-olefins conversion in H-SAPO-18: A van der Waals density functional study. Chinese Journal of Catalysis, 2015, 36, 1573-1579.	6.9	24
24006	CellMatch: Combining two unit cells into a common supercell with minimal strain. Computer Physics Communications, 2015, 197, 324-334.	3.0	60
24007	Li-Filled, B-Substituted Carbon Clathrates. Journal of the American Chemical Society, 2015, 137, 12639-12652.	6.6	42
24008	Bismuth and chromium co-doped strontium titanates and their photocatalytic properties under visible light irradiation. Physical Chemistry Chemical Physics, 2015, 17, 26320-26329.	1.3	57
24009	A visualized probe method for localization of surface oxygen vacancy on TiO₂: Au in situ reduction. Nanoscale, 2015, 7, 17488-17495.	2.8	14
24010	A promising way to open an energy gap in bilayer graphene. Nanoscale, 2015, 7, 17096-17101.	2.8	13
24011	Computational and experimental studies on the effect of hydrogenation of Ni-doped TiO₂ anatase nanoparticles for the application of water splitting. RSC Advances, 2015, 5, 81371-81377.	1.7	12
24012	Electronic properties and lithium storage capacities of two-dimensional transition-metal nitride monolayers. Journal of Materials Chemistry A, 2015, 3, 21486-21493.	5.2	79
24013	Hydrogen adsorption induced antiferrodistortive distortion and metallization at the (001) surface of SrTiO3. Journal of Applied Physics, 2015, 118, .	1.1	5
24014	Mechanical and thermal properties of Î³-Mg2SiO4 under high temperature and high pressure conditions such as in mantle: A first principles study. Journal of Chemical Physics, 2015, 143, 104503.	1.2	14
24015	Vacancy induced Jahnâ€“Teller distortion in silicon and its influence to the electronic structure. Modern Physics Letters B, 2015, 29, 1550136.	1.0	0
24016	Group 14 element-based non-centrosymmetric quantum spin Hall insulators with large bulk gap. Nano Research, 2015, 8, 3412-3420.	5.8	30
24017	Insights into dynamic processes of cations in pyrochlores and other complex oxides. Physical Chemistry Chemical Physics, 2015, 17, 24215-24223.	1.3	18
24018	Hydrogen binding energies and electronic structure of Niâ€“Pd particles: a clue to their special catalytic properties. Physical Chemistry Chemical Physics, 2015, 17, 26140-26148.	1.3	15
24019	First-principles study on alkali-metal effect of Li, Na, and K in CuInSe₂and CuGaSe₂. Japanese Journal of Applied Physics, 2015, 54, 08KC20.	0.8	38
24020	Microstructure and piezoelectric response of Y Al1â^'N thin films. Acta Materialia, 2015, 100, 81-89.	3.8	60
24021	Electron affinity and ionization potential of two-dimensional honeycomb sheets: A first principle study. Chemical Physics Letters, 2015, 637, 26-31.	1.2	20
24022	Al3AuIr: A New Compound in the Alâ€“Auâ€“Ir System. Inorganic Chemistry, 2015, 54, 7898-7905.	1.9	6

#	Article	IF	Citations
24023	Modulation of Electronic Structure of Armchair MoS2Nanoribbon. Journal of Physical Chemistry A, 2015, , 150902124434000.	1.1	1
24024	Role of Surface Termination in Atomic Layer Deposition of Silicon Nitride. Journal of Physical Chemistry Letters, 2015, 6, 3610-3614.	2.1	54
24025	Effect of Ca²⁺ codoping on the Eu²⁺ luminescence properties in the Sr₂Si₅N₈ host lattice: a theoretical approach. Physical Chemistry Chemical Physics, 2015, 17, 24925-24930.	1.3	17
24026	Anisotropy in elasticity and thermodynamic properties of zirconium tetraboride under high pressure. RSC Advances, 2015, 5, 77399-77406.	1.7	10
24027	Rhenium-phthalocyanine molecular nanojunction with high magnetic anisotropy and high spin filtering efficiency. Applied Physics Letters, 2015, 107, .	1.5	17
24028	Large Tunability of Physical Properties of Manganite Thin Films by Epitaxial Strain. Chinese Physics Letters, 2015, 32, 087504.	1.3	7
24029	Momentum microscopy of the layered semiconductor TiS₂and Ni intercalated Ni_{1/3}TiS₂. New Journal of Physics, 2015, 17, 083010.	1.2	23
24030	Optimized geometry and electronic structure of three-dimensionalÎ²-graphyne. Journal of Semiconductors, 2015, 36, 072002.	2.0	0
24031	A first-principles investigation of interstitial defects in dilute tungsten alloys. Journal of Nuclear Materials, 2015, 467, 448-456.	1.3	39
24032	Density functional theory screening of gas-treatment strategies for stabilization of high energy-density lithium metal anodes. Journal of Power Sources, 2015, 296, 150-161.	4.0	57
24033	Real-Time Study of CVD Growth of Silicon Oxide on Rutile TiO₂(110) Using Tetraethyl Orthosilicate. Journal of Physical Chemistry C, 2015, 119, 19149-19161.	1.5	10
24034	Fine-tuning the theoretically predicted structure of MIL-47(V) with the aid of powder X-ray diffraction. CrystEngComm, 2015, 17, 8612-8622.	1.3	7
24035	Coro-graphene and circumcoro-graphyne: novel two-dimensional materials with exciting electronic properties. RSC Advances, 2015, 5, 78910-78916.	1.7	26
24036	First-principles studies of p-type nitrogen-doped Î±-Fe2O3-xSx alloys. Journal of Applied Physics, 2015, 117, .	1.1	0
24037	Effect of interstitial impurities on grain boundary cohesive strength in vanadium. Computational Materials Science, 2015, 110, 163-168.	1.4	10
24038	Mechanistic studies of aldol condensations in UiO-66 and UiO-66-NH 2 metal organic frameworks. Journal of Catalysis, 2015, 331, 1-12.	3.1	88
24039	Observation of intervalley quantum interference in epitaxial monolayer tungsten diselenide. Nature Communications, 2015, 6, 8180.	5.8	55
24040	Hybrid cathode architectures for lithium batteries based on TiS₂ and sulfur. Journal of Materials Chemistry A, 2015, 3, 19857-19866.	5.2	119

#	Article	IF	Citations
24041	A novel two-dimensional material B₂S₃and its structural implication to new carbon and boron nitride allotropes. Journal of Materials Chemistry C, 2015, 3, 9921-9927.	2.7	13
24042	Structural, elastic, electronic, phonon and thermal properties of Ir₃Ta and Rh₃Ta alloys. Philosophical Magazine Letters, 2015, 95, 392-400.	0.5	7
24043	Selective Oxidation of Hydrogen in the Presence of Propylene over Pt-Based Coreâ€“Shell Nanocatalysts. Journal of Physical Chemistry C, 2015, 119, 21386-21394.	1.5	15
24044	Ligand-Conformation Energy Landscape of Thiolate-Protected Gold Nanoclusters. Journal of Physical Chemistry C, 2015, 119, 21555-21560.	1.5	21
24045	Methane Oxidation over PdO(101) Revealed by First-Principles Kinetic Modeling. Journal of the American Chemical Society, 2015, 137, 12035-12044.	6.6	104
24046	First-charge instabilities of layered-layered lithium-ion-battery materials. Physical Chemistry Chemical Physics, 2015, 17, 24382-24391.	1.3	63
24047	Exponential size-dependent tunability of strain on the transport behavior in ZnO tunnel junctions: an ab initio study. Physical Chemistry Chemical Physics, 2015, 17, 25583-25592.	1.3	6
24048	Li-ion conductivity in Li₉S₃N. Journal of Materials Chemistry A, 2015, 3, 20338-20344.	5.2	28
24049	Structural, elastic and electronic properties of Cu-X compounds from first-principles calculations. Journal of Central South University, 2015, 22, 1585-1594.	1.2	3
24050	Catalytic Role of the Substrate Defines Specificity of Therapeutic l-Asparaginase. Journal of Molecular Biology, 2015, 427, 2867-2885.	2.0	25
24051	First-principles investigation of titanium doping into Î²-SiAlON crystal in TiNâ€“SiAlON composites for EDM applications. Materials Chemistry and Physics, 2015, 162, 781-786.	2.0	7
24052	Origin of a Wide and Asymmetric Blue Luminescence Band in AlN Nanowires: VN, VAl, ON, and 3ONâ€“VAl Surface Defects. Journal of Physical Chemistry C, 2015, 119, 21688-21693.	1.5	4
24053	Pdâ€“Ir Coreâ€“Shell Nanocubes: A Type of Highly Efficient and Versatile Peroxidase Mimic. ACS Nano, 2015, 9, 9994-10004.	7.3	254
24054	Edge effects on band gap energy in bilayer 2H-MoS2 under uniaxial strain. Journal of Applied Physics, 2015, 117, .	1.1	20
24055	Supercritical phenomenon of hydrogen beyond the liquidâ€“liquid phase transition. New Journal of Physics, 2015, 17, 063023.	1.2	12
24056	Segregation and Î· phase formation along stacking faults during creep at intermediate temperatures in a Ni-based superalloy. Acta Materialia, 2015, 100, 19-31.	3.8	128
24057	Thermal and mechanical stability, electronic structure and energetic properties of Pu-containing pyrochlores: La2-Pu Zr2O7 and La2Zr2-Pu O7 (0Ââ‰ÂyÂâ‰Â2). Journal of Nuclear Materials, 2015, 466, 162-171.	1.3	18
24058	The Effect of Dispersion Correction on the Adsorption of CO on Metallic Nanoparticles. Journal of Physical Chemistry A, 2015, 119, 9703-9709.	1.1	60

#	Article	IF	Citations
24059	Heavy-Metal Adsorption Behavior of Two-Dimensional Alkalization-Intercalated MXene by First-Principles Calculations. Journal of Physical Chemistry C, 2015, 119, 20923-20930.	1.5	193
24060	The Strength of BrÃ¸nsted Acid Sites in Microporous Aluminosilicates. ACS Catalysis, 2015, 5, 5741-5755.	5.5	209
24061	High and anisotropic carrier mobility in experimentally possible Ti₂CO₂(MXene) monolayers and nanoribbons. Nanoscale, 2015, 7, 16020-16025.	2.8	225
24062	Elastic properties of magnesium with virtual long-period stacking-ordered structure: First-principles study. Computational Materials Science, 2015, 110, 191-197.	1.4	9
24063	Effects of polar and nonpolar on band structures in ultrathin ZnO/GaN type-II superlattices. Solid State Communications, 2015, 221, 14-17.	0.9	4
24064	Indirect-direct band gap transition of two-dimensional arsenic layered semiconductorsâ€”cousins of black phosphorus. Science China: Physics, Mechanics and Astronomy, 2015, 58, 1.	2.0	26
24065	Interfacial chemical bonding between carbon nanotube and aluminum substrate modulated by alloying elements. Diamond and Related Materials, 2015, 59, 1-6.	1.8	5
24066	Methanol on ZnO (101Ì…0): From Adsorption over Initial Dehydrogenation to Monolayer Formation. Journal of Physical Chemistry C, 2015, 119, 21574-21584.	1.5	6
24067	Observation of the Long Afterglow in AlN Helices. Nano Letters, 2015, 15, 6575-6581.	4.5	33
24068	Electrochemical Formation of Reactive Oxygen Species at Pt (111)â€”A Density Functional Theory Study. ACS Catalysis, 2015, 5, 6090-6098.	5.5	29
24069	Red-to-Ultraviolet Emission Tuning of Two-Dimensional Gallium Sulfide/Selenide. ACS Nano, 2015, 9, 9585-9593.	7.3	163
24070	Compositional bowing of band energies and their deformation potentials in strained InGaAs ternary alloys: A first-principles study. Applied Physics Letters, 2015, 107, .	1.5	13
24071	The preferred orientation of Mn3 spins in magnetic multiferroic CaMn7O12. Journal of Magnetism and Magnetic Materials, 2015, 396, 135-139.	1.0	5
24072	Synthesis, crystal and electronic structure, and optical property of the pentanary chalcohalide Ba3KSb4S9Cl. Journal of Solid State Chemistry, 2015, 232, 37-41.	1.4	14
24073	Reduction mechanism of hydroxyl group from graphene oxide with and without â€“NH2 agent. Physica B: Condensed Matter, 2015, 477, 70-74.	1.3	16
24074	Using Force-Matched Potentials To Improve the Accuracy of Density Functional Tight Binding for Reactive Conditions. Journal of Chemical Theory and Computation, 2015, 11, 4530-4535.	2.3	28
24075	Strain Tuning of Tinâ€“Halide and Leadâ€“Halide Perovskites: A First-Principles Atomic and Electronic Structure Study. Journal of Physical Chemistry C, 2015, 119, 22832-22837.	1.5	129
24076	Adsorption of aromatics on the (111) surface of PtM and PtM₃ (M = Fe, Ni) alloys. RSC Advances, 2015, 5, 85705-85719.	1.7	14

#	Article	IF	Citations
24077	Theoretical studies of heteroatom-doping in TiO₂ to enhance the electron injection in dye-sensitized solar cells. RSC Advances, 2015, 5, 79868-79873.	1.7	16
24078	Structural and electronic properties of the transition layer at the SiO2/4H-SiC interface. AIP Advances, 2015, 5, .	0.6	14
24079	Pentagonal monolayer crystals of carbon, boron nitride, and silver azide. Journal of Applied Physics, 2015, 118, .	1.1	91
24080	Solvation and Reaction of Ammonia in Molecularly Thin Water Films. Journal of Physical Chemistry C, 2015, 119, 23052-23058.	1.5	28
24081	Different Product Distributions and Mechanistic Aspects of the Hydrodeoxygenation of m-Cresol over Platinum and Ruthenium Catalysts. ACS Catalysis, 2015, 5, 6271-6283.	5.5	137
24082	Density-functional calculations of the conversion of methane to methanol on platinum-decorated sheets of graphene oxide. Physical Chemistry Chemical Physics, 2015, 17, 26191-26197.	1.3	27
24083	Edge State-Induced Novel Electronic Structures and Magnetic Properties of Zigzag AlN/SiC Nanoribbons. Journal of Superconductivity and Novel Magnetism, 2015, 28, 3053-3057.	0.8	0
24084	Prediction on elastic properties of off-stoichiometric L12-Al3Li intermetallic due to point defects. Computational Materials Science, 2015, 107, 184-189.	1.4	10
24085	Electronic and magnetic properties of C-doped Î±-Al2O3 by DFT calculations. Computational Materials Science, 2015, 110, 368-374.	1.4	16
24086	Prediction on anisotropic elasticity, sound velocity, and thermodynamic properties of MoSi2 under pressure. Journal of Alloys and Compounds, 2015, 652, 106-115.	2.8	32
24087	Monitoring the stability of organometallic perovskite thin films. Journal of Materials Chemistry A, 2015, 3, 21940-21945.	5.2	13
24088	Multifaceted Thermodynamics of Pbn (n = 16â€“24) Clusters: A Case Study. Journal of Physical Chemistry C, 2015, 119, 23698-23707.	1.5	1
24089	The pivotal role of the dopant choice on the thermodynamics of hydration and associations in proton conducting BaCe_{0.9}X_{0.1}O_{3â^'Î´} (X = Sc, Ga, Y, In, Gd and Er). Journal of Materials Chemistry A, 2015, 3, 23289-23298.	5.2	45
24090	Geometry, electronic structures and optical properties of phosphorus nanotubes. Nanotechnology, 2015, 26, 415702.	1.3	41
24091	Tuning and understanding the supercapacitance of heteroatom-doped graphene. Energy Storage Materials, 2015, 1, 103-111.	9.5	50
24092	Large-Scale Computational Screening of Binary Intermetallics for Membrane-Based Hydrogen Separation. Journal of Physical Chemistry C, 2015, 119, 26319-26326.	1.5	9
24093	Enhanced wetting of Cu on ZnO by migration of subsurface oxygen vacancies. Nature Communications, 2015, 6, 8845.	5.8	57
24094	Electronic and Magnetic Structure under Lattice Distortion in SrIrO₃/SrTiO₃Superlattice: A First-Principles Study. Journal of Physics: Conference Series, 2015, 592, 012139.	0.3	13

#	Article	IF	Citations
24095	Optical properties of g-C4N3/BN bilayer film: A first-principles study. Journal of the Korean Physical Society, 2015, 67, 1624-1629.	0.3	4
24096	Density functional study of lithium vacancy in Li4SiO4: Trapping of tritium and helium. Journal of Nuclear Materials, 2015, 467, 519-526.	1.3	20
24097	First-Principles Study of Lithiation of Type I Ba-Doped Silicon Clathrates. Journal of Physical Chemistry C, 2015, 119, 28247-28257.	1.5	22
24098	Pressure-induced structural changes and elemental dissociation of cadmium and mercury chalcogenides. RSC Advances, 2015, 5, 104426-104432.	1.7	5
24099	Another Way of Looking at Reactivity Enhancement in Large-Area Graphene: The Role of Exchange Splitting from First-Principles Methods. Journal of Physical Chemistry C, 2015, 119, 26636-26642.	1.5	1
24100	Electron Confinement in Channel Spaces for One-Dimensional Electride. Journal of Physical Chemistry Letters, 2015, 6, 4966-4971.	2.1	74
24101	Surface Structure Dependence of SO₂ Interaction with Ceria Nanocrystals with Well-Defined Surface Facets. Journal of Physical Chemistry C, 2015, 119, 28895-28905.	1.5	26
24102	First-Principles Study of Phosphorene and Graphene Heterostructure as Anode Materials for Rechargeable Li Batteries. Journal of Physical Chemistry Letters, 2015, 6, 5002-5008.	2.1	274
24103	Assessment of Hybrid Organicâ€“Inorganic Antimony Sulfides for Earth-Abundant Photovoltaic Applications. Journal of Physical Chemistry Letters, 2015, 6, 5009-5014.	2.1	47
24104	How to determine accurate chemical ordering in several nanometer large bimetallic crystallites from electronic structure calculations. Chemical Science, 2015, 6, 3868-3880.	3.7	70
24105	Strain-induced band structure and mobility modulation in graphitic blue phosphorus. Applied Surface Science, 2015, 356, 626-630.	3.1	33
24106	Pressure induced structural instability of FeV intermetallic compound with B2 ordering. Journal of Alloys and Compounds, 2015, 650, 537-541.	2.8	3
24107	Effect of alloying elements on hydrogen absorption properties of palladium-based solid solution alloys. Journal of Alloys and Compounds, 2015, 653, 444-452.	2.8	14
24108	Convergence of valence bands for high thermoelectric performance for p-type InN. Physica B: Condensed Matter, 2015, 479, 1-5.	1.3	6
24109	Computational materials design of attractive Fermion system with large negative effective Ueff in the hole-doped Delafossite of CuAlO2, AgAlO2 and AuAlO2: Charge-excitation induced Ueff < 0. Physica C: Superconductivity and Its Applications, 2015, 519, 168-183.	0.6	4
24110	Impurity distribution and ferromagnetism in Mn-doped GaAs nanowires: A first-principle study. Physics Letters, Section A: General, Atomic and Solid State Physics, 2015, 379, 2745-2749.	0.9	23
24111	Vacancy-induced insulator â€“ direct spin gapless semiconductor â€“ half-metal transition in double perovskite La2CrFeO6: A first-principles study. Physics Letters, Section A: General, Atomic and Solid State Physics, 2015, 379, 2897-2901.	0.9	8
24112	Investigation on the magnetic properties and spin polarization of Gd-substituted Fe3O4 films prepared by reactive sputtering. Thin Solid Films, 2015, 594, 162-167.	0.8	1

#	Article	IF	Citations
24113	Oxygen Activation and Dissociation on Transition Metal Free Perovskite Surfaces. Chemistry of Materials, 2015, 27, 8273-8281.	3.2	87
24114	Formation and Growth Mechanisms of Solid-Electrolyte Interphase Layers in Rechargeable Batteries. Chemistry of Materials, 2015, 27, 7990-8000.	3.2	225
24115	Thermodynamics of Hydrogen Adsorption and Incorporation at the ZnO(101Ì…0) Surface. Journal of Physical Chemistry C, 2015, 119, 26560-26565.	1.5	13
24116	DFT Study of CO₂ Activation on Doped and Ultrathin MgO Films.. Journal of Physical Chemistry C, 2015, 119, 27594-27602.	1.5	36
24117	Density-Functional Theory Molecular Dynamics Simulations and Experimental Characterization of a-Al₂O₃/SiGe Interfaces. ACS Applied Materials & Interfaces, 2015, 7, 26275-26283.	4.0	8
24118	Warm dense gold: effective ionâ€“ion interaction and ionisation. Molecular Physics, 0, , 1-10.	0.8	7
24119	Surface properties and work function changes induced by atomic oxygen adsorbed on HfC(1 1 1) surface. Applied Surface Science, 2015, 357, 1046-1052.	3.1	15
24120	Quantum states of hydrogen atom on Pd(1 1 0) surface. Applied Surface Science, 2015, 359, 687-691.	3.1	4
24121	Structural, electronic, and optical properties of bulk Cu2Se. Current Applied Physics, 2015, 15, 1417-1420.	1.1	13
24122	Patterning germanene into superlattices: An efficient method for tuning conducting properties. Chemical Physics Letters, 2015, 638, 187-190.	1.2	10
24123	A theoretical study on the selective oxygen K-edge soft X-ray emission spectroscopy of liquid acetic acid. Chemical Physics Letters, 2015, 640, 55-60.	1.2	3
24124	Atomic Mechanism of Electrocatalytically Active Coâ€“N Complexes in Graphene Basal Plane for Oxygen Reduction Reaction. ACS Applied Materials & Interfaces, 2015, 7, 27405-27413.	4.0	139
24125	Bipolar Conductance Switching of Single Anthradithiophene Molecules. ACS Nano, 2015, 9, 12506-12512.	7.3	37
24126	Covalent Functionalization of Boron Nitride Nanotubes via Reduction Chemistry. ACS Nano, 2015, 9, 12573-12582.	7.3	105
24127	Ion implantation of low energy Si into graphene: insight from computational studies. RSC Advances, 2015, 5, 99920-99926.	1.7	12
24128	Significant band engineering effect of YbTe for high performance thermoelectric PbTe. Journal of Materials Chemistry C, 2015, 3, 12410-12417.	2.7	61
24129	Combining 2d-Periodic Quantum Chemistry with Molecular Force Fields: A Novel QM/MM Procedure for the Treatment of Solid-State Surfaces and Interfaces. Journal of Chemical Theory and Computation, 2015, 11, 5873-5887.	2.3	19
24130	Strongly Interacting C₆₀/Ir(111) Interface: Transformation of C₆₀ into Graphene and Influence of Graphene Interlayer. Journal of Physical Chemistry C, 2015, 119, 27550-27555.	1.5	13

#	Article	IF	Citations
24131	Complex Surface Diffusion Mechanisms of Cobalt Phthalocyanine Molecules on Ag(100). Journal of the American Chemical Society, 2015, 137, 14920-14929.	6.6	33
24132	Defect chemistry and lithium transport in Li₃OCl anti-perovskite superionic conductors. Physical Chemistry Chemical Physics, 2015, 17, 32547-32555.	1.3	105
24133	Spin-orbit-induced gap modification in buckled honeycomb XBi and XBi₃(Xâ€‰â€‰=â€‰â€‰B, Al, Ga) Tj ETQq0	0.7	36
24134	Band parameters of phosphorene. Journal of Physics: Conference Series, 2015, 633, 012042.	0.3	8
24135	High performance bipolar spin filtering and switching functions of poly-(terphenylene-butadiynylene) between zigzag graphene nanoribbon electrodes. RSC Advances, 2015, 5, 96455-96463.	1.7	22
24136	Near-unity photoluminescence quantum yield in MoS ₂. Science, 2015, 350, 1065-1068.	6.0	993
24137	Useful Database of Effective Gettering Sites for Metal Impurities in Si Wafers with First Principles Calculation. ECS Journal of Solid State Science and Technology, 2015, 4, P351-P355.	0.9	16
24138	Optical, Electrical, and Catalytic Properties of Metal Nanoclusters Investigated by ab initio Molecular Dynamics Simulation: A Mini Review. ACS Symposium Series, 2015, , 215-234.	0.5	0
24139	Theoretical and experimental investigation of vacancy-based doping of monolayer MoS ₂ on oxide. 2D Materials, 2015, 2, 045009.	2.0	47
24140	Crystal structure, thermal behaviour and parageneses of koninckite, FePO₄Â·2.75H₂O. Mineralogical Magazine, 2015, 79, 1159-1173.	0.6	2
24141	Lattice distortion induced anomalous ferromagnetism and electronic structure in FCC Fe and Fe-TM (TMÂ=ÂCr, Ni, Ta and Zr) alloys. Materials Chemistry and Physics, 2015, 162, 748-756.	2.0	17
24142	Ab initio investigation of native point defects in Mg 24 Y 5. Materials Chemistry and Physics, 2015, 167, 70-76.	2.0	6
24143	Generality of the 18-n Rule: Intermetallic Structural Chemistry Explained through Isolobal Analogies to Transition Metal Complexes. Inorganic Chemistry, 2015, 54, 11385-11398.	1.9	86
24144	Competitive Paths for Methanol Decomposition on Ruthenium: A DFT Study. Journal of Physical Chemistry C, 2015, 119, 27382-27391.	1.5	25
24145	Density Functional Theory Computational Study of Alkali Cation-Exchanged Sodalite-like Zeolitelike Metalâ€“Organic Framework for CO2, N2, and CH4 Adsorption. Journal of Physical Chemistry C, 2015, 119, 27449-27456.	1.5	7
24146	Molecular Electronic Effects on the Thermal Grafting of Aryl Iodides to TiO₂ Surfaces. Journal of Physical Chemistry C, 2015, 119, 27972-27981.	1.5	0
24147	Role of Interlayer Coupling on the Evolution of Band Edges in Few-Layer Phosphorene. Journal of Physical Chemistry Letters, 2015, 6, 4876-4883.	2.1	38
24148	Thickness-Dependent Dielectric Constant of Few-Layer In₂Se₃ Nanoflakes. Nano Letters, 2015, 15, 8136-8140.	4.5	99

#	Article	IF	Citations
24149	Self-Assembly Strategy for Fabricating Connected Graphene Nanoribbons. ACS Nano, 2015, 9, 12035-12044.	7.3	81
24150	Tuning oxide activity through modification of the crystal and electronic structure: from strain to potential polymorphs. Physical Chemistry Chemical Physics, 2015, 17, 28943-28949.	1.3	31
24151	Sn(ii,iv) steric and electronic structure effects enable self-selective doping on Fe/Si-sites of Li2FeSiO4 nanocrystals for high performance lithium ion batteries. Journal of Materials Chemistry A, 2015, 3, 24437-24445.	5.2	15
24152	Fermi level engineering of topological insulator films by tuning the substrates. Journal of Physics Condensed Matter, 2015, 27, 435003.	0.7	2
24153	Two-dimensional Ni(OH) ₂ -XS ₂ (X = Mo and W) heterostructures. 2D Materials, 2015, 2, 034014.	2.0	11
24154	Effect of oxygen on the magnetic property of Bis(8-hydroxyquinoline)copper (CuQ2): An experimental and theoretical study. International Journal of Modern Physics B, 2015, 29, 1542027.	1.0	1
24155	Mixed-halide Cs2SnI3Br3 perovskite as low resistance hole-transporting material in dye-sensitized solar cells. Electrochimica Acta, 2015, 184, 466-474.	2.6	49
24156	Atomically Thin Transition-Metal Dinitrides: High-Temperature Ferromagnetism and Half-Metallicity. Nano Letters, 2015, 15, 8277-8281.	4.5	168
24157	Aqueous-Phase Preparation of Model HDS Catalysts on Planar Alumina Substrates: Support Effect on Mo Adsorption and Sulfidation. Journal of the American Chemical Society, 2015, 137, 15915-15928.	6.6	52
24158	Selective Catalytic Hydrogenolysis of Carbonâ€“Carbon Ïƒ Bonds in Primary Aliphatic Alcohols over Supported Metals. ACS Catalysis, 2015, 5, 7199-7207.	5.5	19
24159	A New Superhard Phase of C₃N₂ Polymorphs. Zeitschrift Fur Naturforschung - Section A Journal of Physical Sciences, 2015, 70, 1001-1005.	0.7	5
24160	Electric-Field-Driven Dual Vacancies Evolution in Ultrathin Nanosheets Realizing Reversible Semiconductor to Half-Metal Transition. Journal of the American Chemical Society, 2015, 137, 15043-15048.	6.6	43
24161	Pseudocapacitive slurry electrodes using redox-active quinone for high-performance flow capacitors: an atomic-level understanding of pore texture and capacitance enhancement. Journal of Materials Chemistry A, 2015, 3, 23323-23332.	5.2	58
24162	Exploration of High-Performance Single-Atom Catalysts on Support M₁/FeO_x for CO Oxidation via Computational Study. ACS Catalysis, 2015, 5, 544-552.	5.5	217
24163	Photon cascade emission in Pr3+ doped fluorides with CaF2 structure: Application of a model for its prediction. Chemical Physics Letters, 2015, 620, 29-34.	1.2	11
24164	In Situ TEM Characterization of Shear-Stress-Induced Interlayer Sliding in the Cross Section View of Molybdenum Disulfide. ACS Nano, 2015, 9, 1543-1551.	7.3	93
24165	Investigation of point defects diffusion in bcc uranium and Uâ€“Mo alloys. Journal of Nuclear Materials, 2015, 458, 304-311.	1.3	51
24166	On-surface formation of two-dimensional polymer via direct Câ€“H activation of metal phthalocyanine. Chemical Communications, 2015, 51, 2836-2839.	2.2	46

#	Article	IF	Citations
24167	Oxygen adsorption properties on a palladium promoted La_{1â^'x}Sr_xMnO₃solid oxide fuel cell cathode. RSC Advances, 2015, 5, 7761-7765.	1.7	16
24168	Stability of iron crystal structures at 0.3â€“1.5 TPa. Earth and Planetary Science Letters, 2015, 409, 299-306.	1.8	23
24169	Cyclometalated Fe(II) Complexes as Sensitizers in Dye-Sensitized Solar Cells. Inorganic Chemistry, 2015, 54, 560-569.	1.9	78
24170	Covalent coupling via dehalogenation on Ni(111) supported boron nitride and graphene. Chemical Communications, 2015, 51, 2440-2443.	2.2	52
24171	Low Resistance Metal Contacts to MoS₂ Devices with Nickel-Etched-Graphene Electrodes. ACS Nano, 2015, 9, 869-877.	7.3	184
24172	Mechanistic Details and Reactivity Descriptors in Oxidation and Acid Catalysis of Methanol. ACS Catalysis, 2015, 5, 666-682.	5.5	49
24173	Phenol Deoxygenation Mechanisms on Fe(110) and Pd(111). ACS Catalysis, 2015, 5, 523-536.	5.5	116
24174	Carbon-Induced Surface Transformations of Cobalt. ACS Catalysis, 2015, 5, 596-601.	5.5	44
24175	Effects of vertical strain on zigzag graphene nanoribbon with a topological line defect. Physica E: Low-Dimensional Systems and Nanostructures, 2015, 67, 116-120.	1.3	5
24176	Monodisperse Srâ€“La₂O₃hybrid nanofibers for oxidative coupling of methane to synthesize C₂hydrocarbons. Nanoscale, 2015, 7, 2260-2264.	2.8	111
24177	Structure evolution of nanoparticulate Fe₂O₃. Nanoscale, 2015, 7, 2960-2969.	2.8	47
24178	Impact of Process Conditions on the Sintering Behavior of an Alumina-Supported Cobalt Fischerâ€“Tropsch Catalyst Studied with an in Situ Magnetometer. ACS Catalysis, 2015, 5, 841-852.	5.5	83
24179	Ab initio calculations of the ideal tensile and shear strengths of uranium metal. Journal of Nuclear Materials, 2015, 458, 122-128.	1.3	7
24180	Insights into the PhCâ‰¡C/Au Interface. Journal of Physical Chemistry C, 2015, 119, 10804-10810.	1.5	50
24181	Adsorption and dissociation of ammonia on small iron clusters. International Journal of Hydrogen Energy, 2015, 40, 346-352.	3.8	23
24182	Predicting crystal structures and properties of matter under extreme conditions via quantum mechanics: the pressure is on. Physical Chemistry Chemical Physics, 2015, 17, 2917-2934.	1.3	99
24183	Dissolution energetics and its strain dependence of transition metal alloying elements in tungsten. Journal of Nuclear Materials, 2015, 456, 260-265.	1.3	18
24184	Spontaneous spin polarization in rubrene studied by density functional theory calculations. Physica E: Low-Dimensional Systems and Nanostructures, 2015, 66, 299-302.	1.3	3

#	Article	IF	Citations
24185	Quantum molecular dynamics study of expanded beryllium: Evolution from warm dense matter to atomic fluid. Scientific Reports, 2014, 4, 5898.	1.6	19
24186	Special quasirandom structures of alon. Computational Materials Science, 2015, 96, 312-318.	1.4	22
24187	Li₂O₂ Wetting on the (110) Surface of RuO₂, TiO₂, and SnO₂: An Initiating Force for Polycrystalline Growth. Journal of Physical Chemistry C, 2015, 119, 1024-1031.	1.5	24
24188	Hybrid Inorganicâ€"Organic Materials with an Optoelectronically Active Aromatic Cation: (C₇H₇)₂SnI₆ and C₇H₇PbI₃. Inorganic Chemistry, 2015, 54, 370-378.	1.9	86
24189	Self-assembly of metal atoms (Na, K, Ca) on graphene. Nanoscale, 2015, 7, 2352-2359.	2.8	10
24190	Spatially Dependent Lattice Deformations for Dislocations at the Edges of Graphene. ACS Nano, 2015, 9, 656-662.	7.3	12
24191	Complex doping of group 13 elements In and Ga in caged skutterudite CoSb3. Acta Materialia, 2015, 85, 112-121.	3.8	29
24192	Comparing hydrostatic-pressure- and epitaxial-strain-induced phase transitions in multiferroic PbNiO3 from first principles. Solid State Communications, 2015, 203, 75-80.	0.9	11
24193	Plasmaâ€Plasma and Liquidâ€Liquid Firstâ€Order Phase Transitions. Contributions To Plasma Physics, 2015, 55, 215-221.	0.5	25
24194	Magnesium interatomic potential for simulating plasticity and fracture phenomena. Modelling and Simulation in Materials Science and Engineering, 2015, 23, 015004.	0.8	117
24195	New Insights into the Formation of Hyperstoichiometric Plutonium Oxides. Journal of Physical Chemistry C, 2015, 119, 101-108.	1.5	26
24196	Interplay between Reaction Mechanism and Hydroxyl Species for Water Formation on Pt(111). ACS Catalysis, 2015, 5, 1068-1077.	5.5	24
24197	Selfâ€Regulation Mechanism for Charged Point Defects in Hybrid Halide Perovskites. Angewandte Chemie - International Edition, 2015, 54, 1791-1794.	7.2	484
24198	A modified embedded atom method potential for the titaniumâ€"oxygen system. Modelling and Simulation in Materials Science and Engineering, 2015, 23, 015006.	0.8	14
24199	ReaxFF molecular dynamics simulations on lithiated sulfur cathode materials. Physical Chemistry Chemical Physics, 2015, 17, 3383-3393.	1.3	143
24200	Pressure-induced metallization of dense (H2S)2H2 with high-Tc superconductivity. Scientific Reports, 2014, 4, 6968.	1.6	802
24201	Design Meets Nature: Tetrahedrite Solar Absorbers. Advanced Energy Materials, 2015, 5, 1401506.	10.2	45
24202	Modeling Ferro- and Antiferromagnetic Interactions in Metalâ€"Organic Coordination Networks. Journal of Physical Chemistry C, 2015, 119, 547-555.	1.5	23

#	Article	IF	Citations
24203	First-Principles Study of C₂ Oxygenates Synthesis Directly from Syngas over CoCu Bimetallic Catalysts. Journal of Physical Chemistry C, 2015, 119, 216-227.	1.5	47
24204	Multi-component solid solution and cluster hardening of Alâ€“Mnâ€“Si alloys. Materials Science & Engineering A: Structural Materials: Properties, Microstructure and Processing, 2015, 625, 153-157.	2.6	19
24205	Effects of strain on the band gap and effective mass in two-dimensional monolayer GaX (XÂ= S, Se, Te). RSC Advances, 2015, 5, 5788-5794.	1.7	75
24206	The ligand effect on the isomer stability of Au₂₄(SR)₂₀ clusters. Nanoscale, 2015, 7, 2225-2229.	2.8	61
24207	Spontaneous doping of two-dimensional NaCl films with Cr atoms: aggregation and electronic structure. Nanoscale, 2015, 7, 2366-2373.	2.8	15
24208	Poly(dimethyltin glutarate) as a Prospective Material for High Dielectric Applications. Advanced Materials, 2015, 27, 346-351.	11.1	64
24209	Strain-enhanced tunneling magnetoresistance in MgO magnetic tunnel junctions. Scientific Reports, 2014, 4, 6505.	1.6	36
24210	Gas-surface thermochemistry and kinetics for aluminum particle combustion. Proceedings of the Combustion Institute, 2015, 35, 2439-2446.	2.4	14
24211	The electronic, optical and ferroelectric properties of BiFeO3 during polarization reversal: A first principle study. Journal of Alloys and Compounds, 2015, 623, 393-400.	2.8	23
24212	Enhancing the performance of dye-sensitized solar cells: doping SnO₂photoanodes with Al to simultaneously improve conduction band and electron lifetime. Journal of Materials Chemistry A, 2015, 3, 3066-3073.	5.2	51
24213	Self-assembled 3D hierarchical sheaf-like Nb3O7(OH) nanostructures with enhanced photocatalytic activity. Nanoscale, 2015, 7, 1963-1969.	2.8	22
24214	How Much N-Doping Can Graphene Sustain?. Journal of Physical Chemistry Letters, 2015, 6, 106-112.	2.1	62
24215	Nondestructive atomic compositional analysis of BeMgZnO quaternary alloys using ion beam analytical techniques. Applied Surface Science, 2015, 327, 43-50.	3.1	15
24216	Stabilities and electronic properties of monolayer MoS₂ with one or two sulfur line vacancy defects. Physical Chemistry Chemical Physics, 2015, 17, 3813-3819.	1.3	37
24217	NO dissociation and reduction by H 2 on Pd(1 1 1): A first-principles study. Journal of Catalysis, 2015, 322, 73-83.	3.1	51
24218	Lattice Dynamics Modified by Excess Oxygen in Nd₂NiO_{4+Î´}: Triggering Low-Temperature Oxygen Diffusion. Journal of Physical Chemistry C, 2015, 119, 1557-1564.	1.5	43
24219	First-principles study of energy and atomic solubility of twinning-associated boundaries in hexagonal metals. Acta Materialia, 2015, 85, 144-154.	3.8	97
24220	A New Carbon Allotrope with Six-Fold Helical Chains in all-sp2 Bonding Networks. Scientific Reports, 2014, 4, 4339.	1.6	77

#	Article	IF	Citations
24221	Experimental Charge Density Evidence for Pnicogen Bonding in a Crystal of Ammonium Chloride. ChemPhysChem, 2015, 16, 676-681.	1.0	29
24222	Experimental and DFT studies of structure, optical and magnetic properties of (Zn1â^'2xCexCox)O nanopowders. Journal of Molecular Structure, 2015, 1084, 155-164.	1.8	4
24223	Adsorption thermodynamics of C1â€“C4 alcohols in H-FAU, H-MOR, H-ZSM-5, and H-ZSM-22. Journal of Catalysis, 2015, 322, 91-103.	3.1	35
24224	Circular test structure for the determination of piezoelectric constants of Sc x Al 1â^'x N thin films applying Laser Doppler Vibrometry and FEM simulations. Sensors and Actuators A: Physical, 2015, 222, 301-308.	2.0	30
24225	Molecular dynamics in finding nonadiabatic coupling for Î²-NaYF₄: Ce³⁺nanocrystals. Molecular Physics, 2015, 113, 385-391.	0.8	10
24226	First-principles study of native defects in LiTi2O4. Computational Materials Science, 2015, 96, 263-267.	1.4	6
24227	Spinel compounds as multivalent battery cathodes: a systematic evaluation based on ab initio calculations. Energy and Environmental Science, 2015, 8, 964-974.	15.6	430
24228	Vacancy-mediated ï‰-assisted Î±-phase formation mechanism in titaniumâ€“molybdenum alloy. Acta Materialia, 2015, 83, 499-506.	3.8	15
24229	Inelastic effects in low-energy electron reflectivity of two-dimensional materials. Journal of Vacuum Science and Technology B:Nanotechnology and Microelectronics, 2015, 33, 02B105.	0.6	7
24230	Structural and electronic properties of a single Si chain doped zigzag AlN nanoribbon. Physica E: Low-Dimensional Systems and Nanostructures, 2015, 68, 59-64.	1.3	1
24231	The origin of the â^¼274cmâ^'1 additional Raman mode induced by the incorporation of N dopants and a feasible route to achieve p-type ZnO:N thin films. Applied Surface Science, 2015, 327, 154-158.	3.1	32
24232	Comprehensive model of metadislocation movement in Al 13 Co 4. Scripta Materialia, 2015, 98, 24-27.	2.6	12
24233	Accelerating ab initio path integral molecular dynamics with multilevel sampling of potential surface. Journal of Computational Physics, 2015, 283, 299-311.	1.9	14
24234	Fundamentals of Methanol Synthesis on Metal Carbide Based Catalysts: Activation of CO2 and H2. Topics in Catalysis, 2015, 58, 159-173.	1.3	64
24235	Visible-Light Induced Photocatalytic Activity of Electrospun-TiO₂ in Arsenic(III) Oxidation. ACS Applied Materials & Interfaces, 2015, 7, 511-518.	4.0	42
24236	Photocatalytic reduction of CO 2 with water vapor on surface La-modified TiO 2 nanoparticles with enhanced CH 4 selectivity. Applied Catalysis B: Environmental, 2015, 168-169, 125-131.	10.8	99
24237	Design and performance characterization of electronic structure calculations on massively parallel supercomputers: a case study of GPAW on the Blue Gene/P architecture. Concurrency Computation Practice and Experience, 2015, 27, 69-93.	1.4	2
24238	Putting DFT to the Test: A First-Principles Study of Electronic, Magnetic, and Optical Properties of Co₃O₄. Journal of Chemical Theory and Computation, 2015, 11, 64-72.	2.3	93

#	Article	IF	Citations
24239	Thermodynamic modeling of the CaOâ€“CaF2â€“Al2O3 system aided by first-principles calculations. Calphad: Computer Coupling of Phase Diagrams and Thermochemistry, 2015, 48, 113-122.	0.7	11
24240	Tracking and Removing Br during the On-Surface Synthesis of a Graphene Nanoribbon. Journal of Physical Chemistry C, 2015, 119, 486-493.	1.5	77
24241	Mechanism of enhanced photocatalytic activities on N-doped La 2 Ti 2 O 7 : An insight from density-functional calculations. International Journal of Hydrogen Energy, 2015, 40, 980-989.	3.8	27
24242	Photocatalytic reactivity of {121} and {211} facets of brookite TiO₂ crystals. Journal of Materials Chemistry A, 2015, 3, 2331-2337.	5.2	54
24243	Structural heterogeneity and dynamics of dyes on TiO₂: implications for charge transfer across organicâ€“inorganic interfaces. Physical Chemistry Chemical Physics, 2015, 17, 3731-3740.	1.3	5
24244	Charge transfer tuning by chemical substitution and uniaxial pressure in the organic complex tetramethoxypyreneâ€“tetracyanoquinodimethane. Physical Chemistry Chemical Physics, 2015, 17, 4118-4126.	1.3	17
24245	The nature of the Feâ€“graphene interface at the nanometer level. Nanoscale, 2015, 7, 2450-2460.	2.8	44
24246	The interaction of hydrazine with an Rh(111) surface as a model for adsorption to rhodium nanoparticles: A dispersion-corrected DFT study. Applied Surface Science, 2015, 327, 462-469.	3.1	20
24247	Reductive Elimination of Hypersilyl Halides from Zinc(II) Complexes. Implications for Electropositive Metal Thin Film Growth. Inorganic Chemistry, 2015, 54, 7-9.	1.9	6
24248	Systematic pseudopotentials from reference eigenvalue sets for DFT calculations. Computational Materials Science, 2015, 98, 372-389.	1.4	57
24249	Effect of carbon types on the generation and morphology of GaN polycrystals grown using the Na flux method. CrystEngComm, 2015, 17, 1030-1036.	1.3	11
24250	Structures, stabilities, and magnetic properties of CoRu binary clusters. Chemical Physics, 2015, 446, 108-117.	0.9	5
24251	Understanding the Role of Metal-Modified Mo(110) Bimetallic Surfaces for Câ€“O/Câ•O and Câ€“C Bond Scission in C3 Oxygenates. ACS Catalysis, 2015, 5, 256-263.	5.5	9
24252	Adsorbate Diffusion on Transition Metal Nanoparticles. Nano Letters, 2015, 15, 629-634.	4.5	26
24253	Modulating the phase transition between metallic and semiconducting single-layer MoS₂ and WS₂ through size effects. Physical Chemistry Chemical Physics, 2015, 17, 1099-1105.	1.3	38
24254	Enabling electrochemical reduction of nitrogen to ammonia at ambient conditions through rational catalyst design. Physical Chemistry Chemical Physics, 2015, 17, 4909-4918.	1.3	246
24255	Spin-Dependent Transport and Optical Properties of Transparent Half-Metallic g-C₄N₃ Films. Journal of Physical Chemistry C, 2015, 119, 1859-1866.	1.5	16
24256	Chromium Tricarbonyl and Chromium Benzene Complexes of Graphene, Their Properties, Stabilities, and Interâ€Ring Haptotropic Rearrangements â€“ A DFT Investigation. European Journal of Inorganic Chemistry, 2015, 2015, 250-257.	1.0	14

#	Article	IF	Citations
24257	Multi-center semi-empirical quantum models for carbon under extreme thermodynamic conditions. Chemical Physics Letters, 2015, 622, 128-136.	1.2	14
24258	Edge reconstruction-mediated graphene fracture. Nanoscale, 2015, 7, 2716-2722.	2.8	24
24259	Energetics and defect clustering trends for trivalent rare earth cations substituted in UO2. Journal of Nuclear Materials, 2015, 457, 252-255.	1.3	8
24260	A theoretical study on the structural and physical properties of the ground-state CaC. Solid State Communications, 2015, 203, 10-15.	0.9	2
24261	Influences of interfacial terminations on electronic structure and magnetoelectric coupling in Fe/KNbO 3 superlattices. Chemical Physics Letters, 2015, 619, 163-168.	1.2	10
24262	A particle assembly/constrained expansion (PACE) model for the formation and structure of porous metal oxide deposits on nuclear fuel rods in pressurized light water reactors. Journal of Nuclear Materials, 2015, 457, 209-212.	1.3	4
24263	Phase stability and mechanical properties of sigma phase in Coâ€“Mo system by first principles calculations. Computational Materials Science, 2015, 98, 424-429.	1.4	10
24264	Responses of the topological surface states to Mn-covered on topological insulators Bi2Se3 film. Solid State Communications, 2015, 203, 46-50.	0.9	1
24265	Energy profiles of hydrogen migration in the early stages of lizardite dehydroxylation. Computational Materials Science, 2015, 98, 435-445.	1.4	0
24266	Constrained non-collinear magnetism in disordered Fe and Feâ€“Cr alloys. Annals of Nuclear Energy, 2015, 77, 246-251.	0.9	8
24267	Ab-initio study of the stability of the D8m-Nb5Sn2Ga and D8m-Ta5SnGa2 compounds. Journal of Alloys and Compounds, 2015, 625, 57-63.	2.8	3
24268	Effect of oxygen vacancy on the adsorption of O2 on anatase TiO2(001): A DFT-based study. Surface Science, 2015, 633, 38-45.	0.8	52
24269	Effective catalytic media using graphitic nitrogen-doped site in graphene for a non-aqueous Liâ€“O2 battery: A density functional theory study. Journal of Power Sources, 2015, 277, 222-227.	4.0	44
24270	Effects of structural relaxation on the generalized stacking fault energies of hexagonal-close-packed system from first-principles calculations. Computational Materials Science, 2015, 98, 405-409.	1.4	22
24271	A Gupta potential for magnesium in hcp phase. Computational Materials Science, 2015, 98, 328-332.	1.4	11
24272	Elastic properties and electronic structure of transition metal atoms in CeO2 solid solution: First principle studies. Computational Materials Science, 2015, 98, 459-465.	1.4	8
24273	Drawing Circuits with Carbon Nanotubes: Scratch-Induced Graphoepitaxial Growth of Carbon Nanotubes on Amorphous Silicon Oxide Substrates. Scientific Reports, 2014, 4, 5289.	1.6	11
24274	Spin-gapless semiconducting graphitic carbon nitrides: A theoretical design from first principles. Carbon, 2015, 84, 1-8.	5.4	72

#	Article	IF	Citations
24275	Parallel eigensolvers in plane-wave Density Functional Theory. Computer Physics Communications, 2015, 187, 98-105.	3.0	25
24276	DFT study of bio-oil decomposition mechanism on a Co stepped surface: Acetic acid as a model compound. International Journal of Hydrogen Energy, 2015, 40, 330-339.	3.8	47
24277	Chemical bonding in RFe6Ge4 (RÂ=ÂLi, Sc, Zr) and LuTi6Sn4 with rhombohedral LiFe6Ge4 type structure. Solid State Sciences, 2015, 39, 82-91.	1.5	4
24278	Surface energy-mediated construction of anisotropic semiconductor wires with selective crystallographic polarity. Scientific Reports, 2014, 4, 5680.	1.6	35
24279	Ultra-Flexibility and Unusual Electronic, Magnetic and Chemical Properties of Waved Graphenes and Nanoribbons. Scientific Reports, 2014, 4, 4198.	1.6	33
24280	Strain-induced phase transition and electron spin-polarization in graphene spirals. Scientific Reports, 2015, 4, 5699.	1.6	17
24281	Thermal Expansion Anomaly Regulated by Entropy. Scientific Reports, 2014, 4, 7043.	1.6	61
24282	Single adatom dynamics at monatomic steps of free-standing few-layer reduced graphene. Scientific Reports, 2014, 4, 6037.	1.6	10
24283	High-Performance Few-layer Mo-doped ReSe2 Nanosheet Photodetectors. Scientific Reports, 2014, 4, 5442.	1.6	82
24284	Strain-induced quantum spin Hall effect in methyl-substituted germanane GeCH3. Scientific Reports, 2014, 4, 7297.	1.6	68
24285	Massive Interfacial Reconstruction at Misfit Dislocations in Metal/Oxide Interfaces. Scientific Reports, 2014, 4, 6533.	1.6	34
24286	Revisiting the Al/Al2O3 Interface: Coherent Interfaces and Misfit Accommodation. Scientific Reports, 2014, 4, 4485.	1.6	78
24287	Experimental observation of defect pair separation triggering phase transitions. Scientific Reports, 2014, 4, 4110.	1.6	7
24288	High-pressure polymorphs of ZnCO3: Evolutionary crystal structure prediction. Scientific Reports, 2014, 4, 5172.	1.6	14
24289	Atomic-scale configurations of synchroshear-induced deformation twins in the ionic MnS crystal. Scientific Reports, 2015, 4, 5118.	1.6	7
24290	Impact of heterocirculene molecular symmetry upon two-dimensional crystallization. Scientific Reports, 2014, 4, 5415.	1.6	13
24291	Theoretical study on the role of dynamics on the unusual magnetic properties in MnBi. Scientific Reports, 2014, 4, 7222.	1.6	35
24292	Defect-Detriment to Graphene Strength Is Concealed by Local Probe: The Topological and Geometrical Effects. ACS Nano, 2015, 9, 401-408.	7.3	66

#	Article	IF	Citations
24293	Ab initio molecular dynamics simulation on stress reduction mechanism of Ti-doped diamond-like carbon films. Thin Solid Films, 2015, 584, 204-207.	0.8	10
24294	Solid State NMR Studies of Li₂MnO₃and Li-Rich Cathode Materials: Proton Insertion, Local Structure, and Voltage Fade. Journal of the Electrochemical Society, 2015, 162, A235-A243.	1.3	76
24295	Fundamental degradation mechanisms of layered oxide Li-ion battery cathode materials: Methodology, insights and novel approaches. Materials Science and Engineering B: Solid-State Materials for Advanced Technology, 2015, 192, 3-25.	1.7	357
24296	Unraveling the Catalytic Mechanism of Co₃O₄ for the Oxygen Evolution Reaction in a Liâ€“O₂ Battery. ACS Catalysis, 2015, 5, 73-81.	5.5	140
24297	Large-angle illumination STEM: Toward three-dimensional atom-by-atom imaging. Ultramicroscopy, 2015, 151, 122-129.	0.8	54
24299	Structure of palladium nanoparticles under oxidative conditions. Physical Chemistry Chemical Physics, 2015, 17, 2268-2273.	1.3	13
24300	Unravelling Orientation Distribution and Merging Behavior of Monolayer MoS₂ Domains on Sapphire. Nano Letters, 2015, 15, 198-205.	4.5	136
24301	What are the active carbon species during graphene chemical vapor deposition growth?. Nanoscale, 2015, 7, 1627-1634.	2.8	89
24302	Robust antiferromagnetism preventing superconductivity in pressurized (Ba0.61K0.39)Mn2Bi2. Scientific Reports, 2015, 4, 7342.	1.6	5
24303	First-principles investigation on crystal, electronic structures and Diffusion barriers of NaNi1/3Co1/3Mn1/3O2 for advanced rechargeable Na-ion batteries. Computational Materials Science, 2015, 98, 304-310.	1.4	37
24304	Pressure effect on stabilities of self-Interstitials in HCP-Zirconium. Scientific Reports, 2014, 4, 5735.	1.6	18
24305	A first principles study of H₂S adsorption and decomposition on a Ge(100) surface. RSC Advances, 2015, 5, 3825-3832.	1.7	7
24306	Hydrides of YPd 3 : Electronic structure and dynamic stability. International Journal of Hydrogen Energy, 2015, 40, 1071-1082.	3.8	4
24307	DFT and TD-DFT studies on the electronic and optical properties of explosive molecules adsorbed on boron nitride and graphene nano flakes. RSC Advances, 2015, 5, 4599-4608.	1.7	30
24308	Photocatalytic CO2 reduction in metalâ€“organic frameworks: A mini review. Journal of Molecular Structure, 2015, 1083, 127-136.	1.8	144
24309	Solubility of zirconium and silicon in molybdenum studied by first-principles calculations. Scripta Materialia, 2015, 97, 1-4.	2.6	10
24310	Thermodynamic description of the Biâ€“Cs and Biâ€“Tm system supported by first-principles calculations. Calphad: Computer Coupling of Phase Diagrams and Thermochemistry, 2015, 48, 72-78.	0.7	10
24311	Dynamics of Pd monomers and dimers adsorbed on the (001) surfaces of strongly correlated nickel oxides. Current Applied Physics, 2015, 15, 98-102.	1.1	7

#	Article	IF	Citations
24312	Combined computational and experimental investigation of the refractory properties of La2Zr2O7. Acta Materialia, 2015, 84, 275-282.	3.8	36
24313	Anisotropy in oxidation of zirconium surfaces from density functional theory calculations. Computational Materials Science, 2015, 98, 112-116.	1.4	15
24314	Multiscale analysis of prelithiated silicon nanowire for Li-ion battery. Computational Materials Science, 2015, 98, 99-104.	1.4	29
24315	Theoretical study of electronic structure, phase transition, elastic, and thermodynamic properties of ReN. Physica B: Condensed Matter, 2015, 458, 124-131.	1.3	6
24316	Hydrogen reduction of vanadium in vanadium-doped LiMnPO4. Materials Chemistry and Physics, 2015, 149-150, 209-215.	2.0	13
24317	Diamond polytypes under high pressure: A first-principles study. Computational Materials Science, 2015, 98, 129-135.	1.4	12
24318	Planar defects and dislocations in transition-metal disilicides. Intermetallics, 2015, 58, 43-49.	1.8	5
24319	Calorimetric measurements and first principles to study the (Ag-Li) liquid system. Journal of Chemical Thermodynamics, 2015, 82, 53-57.	1.0	7
24320	Small-Molecule Activation Driven by Confinement Effects. ACS Catalysis, 2015, 5, 215-224.	5.5	8
24321	Universality in surface mixing rule of adsorption strength for small adsorbates on binary transition metal alloys. Physical Chemistry Chemical Physics, 2015, 17, 3123-3130.	1.3	27
24322	A novel two-dimensional MgB₆ crystal: metal-layer stabilized boron kagome lattice. Physical Chemistry Chemical Physics, 2015, 17, 1093-1098.	1.3	38
24323	High-temperature miscibility of iron and rock during terrestrial planet formation. Earth and Planetary Science Letters, 2015, 410, 25-33.	1.8	55
24324	Water-Induced Oxidation and Dissociation of Small Cu Clusters on ZnO(101Ì…0). Journal of Physical Chemistry C, 2015, 119, 1382-1390.	1.5	3
24325	Spatial analysis of interactions at the silicene/Ag interface: first principles study. Journal of Physics Condensed Matter, 2015, 27, 015002.	0.7	23
24326	Transparent half metallic g-C4N3 nanotubes: potential multifunctional applications for spintronics and optical devices. Scientific Reports, 2015, 4, 6059.	1.6	31
24327	High-throughput prediction of activation energy for impurity diffusion in fcc metals of Group I and VIII. Journal of Alloys and Compounds, 2015, 624, 201-209.	2.8	8
24328	Strain effects on oxygen migration in perovskites. Physical Chemistry Chemical Physics, 2015, 17, 2715-2721.	1.3	70
24329	Orbital mixing in solids as a descriptor for materials mapping. Solid State Communications, 2015, 203, 31-34.	0.9	16

#	Article	IF	Citations
24330	Guaiacol Hydrodeoxygenation Mechanism on Pt(111): Insights from Density Functional Theory and Linear Free Energy Relations. ChemSusChem, 2015, 8, 315-322.	3.6	109
24331	Structural and electronic properties of transparent conducting delafossite: a comparison between the AgBO₂ and CuBO₂ families (BÂ= Al, Ga, In and Sc, Y). RSC Advances, 2015, 5, 1366-1377.	1.7	32
24332	First principles account for large changes in electronic structure and bonding from LaCu to LaCuMg and LaCuMg4. Computational Materials Science, 2015, 97, 231-236.	1.4	0
24333	Interface of Pt with SrTiO3(001); A combined theoretical and experimental study. Surface Science, 2015, 633, 8-16.	0.8	7
24334	External strain effect on the electronic and mechanical properties of the superconductor Nb2InC. Journal of Physics and Chemistry of Solids, 2015, 78, 28-34.	1.9	8
24335	Elasticity of superhydrous phase, B, Mg10Si3O14(OH)4. Physics of the Earth and Planetary Interiors, 2015, 238, 42-50.	0.7	15
24336	Crystal and chemical anisotropy effects in AE2ZnN2, (AEÂ=ÂCa, Sr, Ba) from ab initio. Solid State Sciences, 2015, 39, 10-14.	1.5	3
24337	A theoretical and experimental approach to shell-isolated nanoparticle-enhanced Raman spectroscopy of single-crystal electrodes. Surface Science, 2015, 631, 73-80.	0.8	30
24338	Charge carrier passivating nitrogenâ€“phosphorus defects in crystalline silicon. Computational Materials Science, 2015, 98, 220-225.	1.4	2
24339	Effects of Mn partitioning on nanoscale precipitation and mechanical properties of ferritic steels strengthened by NiAl nanoparticles. Acta Materialia, 2015, 84, 283-291.	3.8	108
24340	Ab initio phonon dynamics in the layered ternary diselenide KNi2Se2. Physics Letters, Section A: General, Atomic and Solid State Physics, 2015, 379, 183-186.	0.9	4
24341	Effects of the slab thickness on the crystal and electronic structures of In2O3(ZnO) revealed by first-principles calculations. Journal of Solid State Chemistry, 2015, 222, 25-36.	1.4	8
24342	Topological insulators based on 2D shape-persistent organic ligand complexes. Nanoscale, 2015, 7, 727-735.	2.8	46
24343	First principles study of van der Waals heterobilayers. Computational Condensed Matter, 2015, 2, 1-10.	0.9	33
24344	A density functional theory study of the tunable structure, magnetism and metal-insulator phase transition in VS2 monolayers induced by in-plane biaxial strain. Nano Research, 2015, 8, 1348-1356.	5.8	116
24345	Spintronic properties of Li1.5Mn0.5Z (Z=As, Sb) compounds in the Cu2Sb structure. Journal of Magnetism and Magnetic Materials, 2015, 377, 411-418.	1.0	3
24346	Topological crystalline insulator nanomembrane with strain-tunable band gap. Nano Research, 2015, 8, 967-979.	5.8	56
24347	Computational design of molecules for an all-quinone redox flow battery. Chemical Science, 2015, 6, 885-893.	3.7	341

#	Article	IF	Citations
24348	Electronic and magnetic properties of Fe(Mn)-doped Cd and Zn nitrides for spintronic applications: a first-principles study. Journal of Materials Science, 2015, 50, 1446-1456.	1.7	8
24349	Thickness dependence of spin polarization and electronic structure of ultra-thin films of MoS2 and related transition-metal dichalcogenides. Scientific Reports, 2014, 4, 6270.	1.6	36
24350	pentahexoctite: A new two-dimensional allotrope of carbon. Scientific Reports, 2014, 4, 7164.	1.6	85
24351	Fine precipitation scenarios of AlZnMg(Cu) alloys revealed by advanced atomic-resolution electron microscopy study Part II: Fine precipitation scenarios in AlZnMg(Cu) alloys. Materials Characterization, 2015, 99, 142-149.	1.9	50
24352	Propagation of Olefin Metathesis to Propene on WO₃ Catalysts: A Mechanistic and Kinetic Study. ACS Catalysis, 2015, 5, 59-72.	5.5	29
24353	Halfâ€Metallicity in Singleâ€Layered Manganese Dioxide Nanosheets by Defect Engineering. Angewandte Chemie - International Edition, 2015, 54, 1195-1199.	7.2	177
24354	Initial decomposition reaction of di-tetrazine-tetroxide (DTTO) from quantum molecular dynamics: implications for a promising energetic material. Journal of Materials Chemistry A, 2015, 3, 1972-1978.	5.2	38
24355	Electronic properties of PbX₃CH₃NH₃(X = Cl, Br, I) compounds for photovoltaic and photocatalytic applications. Physical Chemistry Chemical Physics, 2015, 17, 2199-2209.	1.3	52
24356	Predicting the voltage dependence of interfacial electrochemical processes at lithium-intercalated graphite edge planes. Physical Chemistry Chemical Physics, 2015, 17, 1637-1643.	1.3	68
24357	Ab initio investigations of electron correlation effect and phonon dynamics of orthorhombic uranium. Physica Status Solidi (B): Basic Research, 2015, 252, 521-531.	0.7	7
24358	Nitrogen concentration driving the hardness of rhenium nitrides. Scientific Reports, 2014, 4, 4797.	1.6	61
24359	Equilibrium coverage of halides on metal electrodes. Surface Science, 2015, 631, 17-22.	0.8	72
24360	A Highly Reversible Lithium Metal Anode. Scientific Reports, 2014, 4, 3815.	1.6	266
24361	Improved reversibility in lithium-oxygen battery: Understanding elementary reactions and surface charge engineering of metal alloy catalyst. Scientific Reports, 2014, 4, 4225.	1.6	133
24362	Ultrahigh-Gain Photodetectors Based on Atomically Thin Graphene-MoS2 Heterostructures. Scientific Reports, 2014, 4, 3826.	1.6	771
24363	First Principles Prediction of the Magnetic Properties of Fe-X6 (X = S, C, N, O, F) Doped Monolayer MoS2. Scientific Reports, 2014, 4, 3987.	1.6	78
24364	Elementary Process for CVD Graphene on Cu(110): Size-selective Carbon Clusters. Scientific Reports, 2014, 4, 4431.	1.6	30
24365	Gallium gradients in Cu(In,Ga)Se₂thin-film solar cells. Progress in Photovoltaics: Research and Applications, 2015, 23, 717-733.	4.4	122

#	Article	IF	Citations
24366	Exploring the structure as well as electrical and photovoltaic mechanism in PrFe0.5Ni0.5O3/GaAs heterojunction. Materials Science in Semiconductor Processing, 2015, 29, 206-212.	1.9	1
24367	Disorder-induced Room Temperature Ferromagnetism in Glassy Chromites. Scientific Reports, 2015, 4, 4686.	1.6	12
24368	Noble-metal-free plasmonic photocatalyst: hydrogen doped semiconductors. Scientific Reports, 2015, 4, 3986.	1.6	48
24369	Extraordinary role of Hg in enhancing the thermoelectric performance of p-type SnTe. Energy and Environmental Science, 2015, 8, 267-277.	15.6	347
24370	Layer-dependent Band Alignment and Work Function of Few-Layer Phosphorene. Scientific Reports, 2014, 4, 6677.	1.6	731
24371	Lattice structures and electronic properties of MO/MoSe2 interface from first-principles calculations. Physica E: Low-Dimensional Systems and Nanostructures, 2015, 66, 342-349.	1.3	7
24372	Band alignment of the hybrid halide perovskites CH₃NH₃PbCl₃, CH₃NH₃PbBr₃and CH₃NH₃PbI₃. Materials Horizons, 2015, 2, 228-231.	6.4	238
24373	Structural, elastic, thermal, and electronic responses of small-molecule-loaded metalâ€“organic framework materials. Journal of Materials Chemistry A, 2015, 3, 986-995.	5.2	42
24374	Ab-initio study of planar strain on electronic structure properties of graphene sheets with nanoholes. Indian Journal of Physics, 2015, 89, 23-29.	0.9	6
24375	Stability and diffusion properties of Ti atom on Î±-uranium surfaces: A first-principles study. Computational Materials Science, 2015, 97, 201-208.	1.4	3
24376	Allâ€Metallic Vertical Transistors Based on Stacked Dirac Materials. Advanced Functional Materials, 2015, 25, 68-77.	7.8	59
24377	Effect of lanthanide on the microstructure and structure of LnMn0.5Fe0.5O3 nanoparticles with Ln=La, Pr, Nd, Sm and Gd prepared by the polymer precursor method. Journal of Solid State Chemistry, 2015, 221, 325-333.	1.4	12
24378	The Materials Application Programming Interface (API): A simple, flexible and efficient API for materials data based on REpresentational State Transfer (REST) principles. Computational Materials Science, 2015, 97, 209-215.	1.4	322
24379	Mining for elastic constants of intermetallics from the charge density landscape. Physica B: Condensed Matter, 2015, 458, 1-7.	1.3	8
24380	Phase transitions, mechanical properties and electronic structures of novel boron phases under high-pressure: A first-principles study. Scientific Reports, 2014, 4, 6786.	1.6	15
24381	On the Electronic Structure of Organometallic Palladium Clusters of Medium and Large Size: A Theoretical Study. Journal of Cluster Science, 2015, 26, 41-51.	1.7	5
24382	Abnormal drop in electrical resistivity with impurity doping of single-crystal Ag. Scientific Reports, 2014, 4, 5450.	1.6	33
24383	Robust ferromagnetism in monolayer chromium nitride. Scientific Reports, 2014, 4, 5241.	1.6	61

#	Article	IF	Citations
24384	Organicâ€“inorganic halide perovskites: an ambipolar class of materials with enhanced photovoltaic performances. Journal of Materials Chemistry A, 2015, 3, 8981-8991.	5.2	109
24385	Metal-like fluorine-doped Î²-FeOOH nanorods grown on carbon cloth for scalable high-performance supercapacitors. Nano Energy, 2015, 11, 119-128.	8.2	184
24386	Elastic, phonon and thermodynamic properties of ZnAl2O4 and ZnAl2S4 compounds from firstâ€“principles calculations. Solid State Sciences, 2015, 40, 7-12.	1.5	4
24387	DFT study on the adsorption and dissociation of H2 on Pdn (n=4, 6, 13, 19, 55) clusters. Journal of Molecular Structure, 2015, 1080, 105-110.	1.8	32
24388	Reducing Mg Acceptor Activation-Energy in Al0.83Ga0.17N Disorder Alloy Substituted by Nanoscale (AlN)5/(GaN)1 Superlattice Using MgGa Î´-Doping: Mg Local-Structure Effect. Scientific Reports, 2015, 4, 6710.	1.6	11
24389	Comparative molecular dynamics study of fcc-Ni nanoplate stress corrosion in water. Surface Science, 2015, 633, 94-101.	0.8	30
24390	Stabilization of H3+ in the high pressure crystalline structure of HnCl (n = 2â€“7). Chemical Science, 2015, 6, 522-526.	3.7	28
24391	Electronic structure and optical properties of V- and Nb-doped ZnO from hybrid functional calculations. Journal of Alloys and Compounds, 2015, 621, 423-427.	2.8	11
24392	Oxygen vacancy and hole conduction in amorphous TiO₂. Physical Chemistry Chemical Physics, 2015, 17, 541-550.	1.3	194
24393	Chemical reduction of the elastic properties of zeolites: a comparison of the formation of carbonate species versus dealumination. Dalton Transactions, 2015, 44, 2703-2711.	1.6	8
24394	Formation of high-strength <mml:math xmlns:mml="http://www.w3.org/1998/Math/MathML" altimg="si4.gif" overflow="scroll"><mml:mrow><mml:msup><mml:mrow><mml:mi>Î²</mml:mi></mml:mrow><mml:mrow><mml:mo>â€²</mml:mo></ precipitates in Mgâ€“RE alloys: The role of the Mg/<mml:math xmlns:mml="http://www.w3.org/1998/Math/MathML" altimg="si3.gif" overflow="scroll"><mml:mrow><mml:msup><mml:mrow><mml:mi>Î²</mml:mi></mml:mrow><mml:mrow><mml:mo>â€³</mml:mo></	3.8	88
24395	A first principles molecular dynamics study of the relationship between atomic structure and elastic properties of Mgâ€“Znâ€“Ca amorphous alloys. Computational Materials Science, 2015, 96, 246-255.	1.4	19
24396	Structure and Stoichiometry Prediction of Surfaces Reacting with Multicomponent Gases. Advanced Materials, 2015, 27, 255-260.	11.1	15
24397	Molecular charge transfer by adsorbing TCNQ/TTF molecules via Ï€â€“Ï€ interaction: a simple and effective strategy to modulate the electronic and magnetic behaviors of zigzag SiC nanoribbons. Physical Chemistry Chemical Physics, 2015, 17, 941-950.	1.3	14
24398	Dimensionality of Intermolecular Interactions in Layered Crystals by Electronic-Structure Theory and Geometric Analysis. Inorganic Chemistry, 2015, 54, 956-962.	1.9	18
24399	Origin of the improved mobility and photo-bias stability in a double-channel metal oxide transistor. Scientific Reports, 2014, 4, 3765.	1.6	107
24400	Phosphorene nanoribbons: Passivation effect on bandgap and effective mass. Applied Surface Science, 2015, 324, 640-644.	3.1	30
24401	Impact of lattice distortion and electron doping on Î±-MoO3 electronic structure. Scientific Reports, 2014, 4, 7131.	1.6	107

#	Article	IF	Citations
24402	New ferromagnetic semiconductor double perovskites: La2FeMO6 (M= Co, Rh, and Ir). Journal of Alloys and Compounds, 2015, 622, 657-661.	2.8	29
24403	Formation mechanism of precipitate T1 in AlCuLi alloys. Journal of Alloys and Compounds, 2015, 624, 22-26.	2.8	71
24404	Theoretical study of defects Cu3SbSe4: Search for optimum dopants for enhancing thermoelectric properties. Journal of Alloys and Compounds, 2015, 625, 346-354.	2.8	51
24405	Origin of temperature-induced low friction of sputtered Si-containing amorphous carbon coatings. Acta Materialia, 2015, 82, 437-446.	3.8	43
24406	Enhancing Thermoelectric Performance of PbTe-Based Compounds by Substituting Elements: A First Principles Study. Journal of Electronic Materials, 2015, 44, 1460-1468.	1.0	22
24407	Planar amine-based dye features the rigidified O-bridged dithiophene Ï€-spacer: A potential high-efficiency sensitizer for dye-sensitized solar cells application. Journal of Power Sources, 2015, 275, 207-216.	4.0	45
24408	Density functional theory calculations on oxygen adsorption on the Cu2O surfaces. Applied Surface Science, 2015, 324, 53-60.	3.1	50
24409	The electronic and magnetic structure of p-element (C,N) doped rutile-TiO2; a hybrid DFT study. Computational Materials Science, 2015, 98, 42-50.	1.4	25
24410	Mechanism of negative thermal expansion in LaC2 from first-principles prediction. Physics Letters, Section A: General, Atomic and Solid State Physics, 2015, 379, 54-59.	0.9	10
24411	Ab initio study of adsorption properties of hazardous organic molecules on graphene: Phenol, phenyl azide, and phenylnitrene. Chemical Physics Letters, 2015, 618, 57-62.	1.2	26
24412	Influence of quantum well states on the formation of Auâ€“Pb alloy in ultra-thin Pb films. Surface Science, 2015, 632, 174-179.	0.8	5
24413	On the scaling factor in Debyeâ€“GrÃ¼neisen model: A case study of the Mgâ€“Zn binary system. Computational Materials Science, 2015, 98, 34-41.	1.4	31
24414	LDA+U/GGA+U calculations of structural and electronic properties of CdTe: Dependence on the effective U parameter. Computational Materials Science, 2015, 98, 18-23.	1.4	25
24415	Temperature-driven stabilization of fcc-ThH2 from first-principles theory coupled with lattice dynamics. Computational Materials Science, 2015, 98, 15-17.	1.4	8
24416	Bonding, charge rearrangement and interface dipoles of benzene, graphene, and PAH molecules on Au(1 1 1) and Cu(1 1 1). Carbon, 2015, 81, 620-628.	5.4	46
24417	A first-principles study of alkali-metal-decorated graphyne as oxygen-tolerant hydrogen storage media. Carbon, 2015, 81, 418-425.	5.4	29
24418	Thermodynamic modeling of the Caâ€“In and Caâ€“Sb systems supported with first-principles calculations. Calphad: Computer Coupling of Phase Diagrams and Thermochemistry, 2015, 48, 35-42.	0.7	8
24419	The influence of high grain boundary density on helium retention in tungsten. Journal of Nuclear Materials, 2015, 457, 80-87.	1.3	43

#	Article	IF	Citations
24420	Defect driven ferromagnetism in SnO₂: a combined study using density functional theory and positron annihilation spectroscopy. RSC Advances, 2015, 5, 1148-1152.	1.7	35
24421	Dispersion-corrected DFT study on the structure and absorption properties of crystalline 5-nitro-2,4-dihydro-1,2,4-triazole-3-one under compression. Structural Chemistry, 2015, 26, 477-484.	1.0	13
24422	Stable zinc-blende ZnO thin films: formation and physical properties. Journal of Materials Science, 2015, 50, 28-33.	1.7	13
24423	Some challenges in the first-principles modeling of structures and processes in electrochemical energy storage and transfer. Journal of Power Sources, 2015, 275, 531-538.	4.0	49
24424	The stability and electronic properties of novel three-dimensional graphene-MoS2 hybrid structure. Scientific Reports, 2014, 4, 7007.	1.6	45
24425	Can metal-free silicon-doped hexagonal boron nitride nanosheets and nanotubes exhibit activity toward CO oxidation?. Physical Chemistry Chemical Physics, 2015, 17, 888-895.	1.3	88
24426	Carbon-free and two-dimensional cathode structure based on silicene for lithiumâ€“oxygen batteries: A first-principles calculation. Journal of Power Sources, 2015, 275, 32-37.	4.0	37
24427	Novel metastable compounds in the Zrâ€“B system: an ab initio evolutionary study. Physical Chemistry Chemical Physics, 2015, 17, 1180-1188.	1.3	22
24428	Rational Design of a Bifunctional Catalyst for the Oxydehydration of Glycerol: A Combined Theoretical and Experimental Study. ACS Catalysis, 2015, 5, 82-94.	5.5	34
24429	From zeolite nets to sp³carbon allotropes: a topology-based multiscale theoretical study. Physical Chemistry Chemical Physics, 2015, 17, 1332-1338.	1.3	45
24430	Reaction mechanisms of aqueous monoethanolamine with carbon dioxide: a combined quantum chemical and molecular dynamics study. Physical Chemistry Chemical Physics, 2015, 17, 831-839.	1.3	95
24431	Vibrational spectrum of condensed H2O in hydrogen-bonding environment: anab initiosimulation study. Molecular Physics, 2015, 113, 63-68.	0.8	1
24432	Unraveling the Sinuous Grain Boundaries in Graphene. Advanced Functional Materials, 2015, 25, 367-373.	7.8	45
24433	Graphene Nanoribbons Under Mechanical Strain. Advanced Materials, 2015, 27, 303-309.	11.1	36
24434	Assessment of polyanion (BF₄^{â^'} and PF₆^{â^'}) substitutions in hybrid halide perovskites. Journal of Materials Chemistry A, 2015, 3, 9067-9070.	5.2	108
24435	Origins of the significant improvement in nanocrystalline Samariumâ€“Cobaltâ€™s magnetic properties when doping with Niobium. Journal of Alloys and Compounds, 2015, 622, 262-268.	2.8	11
24436	N2O dissociation on small Rh clusters: A density functional study. Computational Materials Science, 2015, 97, 32-35.	1.4	15
24437	First-principle calculations of the thermal properties of SrTiO 3 and SrO(SrTiO 3) n (n =1,2). Solid State Communications, 2015, 201, 25-30.	0.9	17

#	Article	IF	Citations
24438	Electronic structure and surface properties of PrMnO 3 (001): A density functional theory study. Solid State Communications, 2015, 201, 31-35.	0.9	17
24439	Adsorption and diffusion of oxygen on Î³-TiAl(0 0 1) and (1 0 0) surfaces. Computational Materials Science, 2015, 97, 55-63.	1.4	32
24440	Silicene on Ag(111): Geometric and electronic structures of a new honeycomb material of Si. Progress in Surface Science, 2015, 90, 1-20.	3.8	58
24441	Effect of Ce and Cu co-doping on the structural, morphological, and optical properties of ZnO nanocrystals and first principle investigation of their stability and magnetic properties. Physica E: Low-Dimensional Systems and Nanostructures, 2015, 66, 209-220.	1.3	28
24442	Halide perovskite materials for solar cells: a theoretical review. Journal of Materials Chemistry A, 2015, 3, 8926-8942.	5.2	1,114
24443	Correlation between the surface electronic structure and CO-oxidation activity of Pt alloys. Physical Chemistry Chemical Physics, 2015, 17, 4879-4887.	1.3	37
24444	Influence of carbon vacancy formation on the elastic constants and hardening mechanisms in transition metal carbides. Journal of the European Ceramic Society, 2015, 35, 95-103.	2.8	134
24445	First-principles study on the interfacial magnetic and electronic properties of Fe4N(0 0 1)/Si and Fe4N(1) Tj ETQq1 1 0.784314 rgBT /Ov	1.4	8
24446	Self-regulated growth and tunable properties of CuSbS2 solar absorbers. Solar Energy Materials and Solar Cells, 2015, 132, 499-506.	3.0	119
24447	Molecular dynamics simulations of the effects of vacancies on nickel self-diffusion, oxygen diffusion and oxidation initiation in nickel, using the ReaxFF reactive force field. Acta Materialia, 2015, 83, 102-112.	3.8	80
24448	Adsorption of organic molecules at the TiO2(110) surface: The effect of van der Waals interactions. Surface Science, 2015, 632, 142-153.	0.8	57
24449	Volcano-like Behavior of Au-Pd Core-shell Nanoparticles in the Selective Oxidation of Alcohols. Scientific Reports, 2014, 4, 5766.	1.6	73
24450	Ab-initio study of the structure and thermodynamic properties of Tiâ€“Siâ€“N at external pressure. Computational Materials Science, 2015, 96, 33-38.	1.4	5
24451	In situ photogenerated defects on surface-complex BiOCl (0 1 0) with high visible-light photocatalytic activity: A probe to disclose the charge transfer in BiOCl (0 1 0)/surface-complex system. Applied Catalysis B: Environmental, 2015, 163, 205-213.	10.8	60
24452	A possible critical temperature mechanism for H blistering nucleation/dissociation in metals. Solid State Communications, 2015, 201, 43-48.	0.9	5
24453	Induced Ferromagnetism at BiFeO3/YBa2Cu3O7 Interfaces. Scientific Reports, 2014, 4, 5368.	1.6	15
24454	Efficiently Enhancing Oxygen Reduction Electrocatalytic Activity of MnO₂ Using Facile Hydrogenation. Advanced Energy Materials, 2015, 5, 1400654.	10.2	78
24455	Ab initio study on the electronic origin of glass-forming ability in the binary Cuâ€“Zr and the ternary Cuâ€“Zrâ€“Al(Ag) metallic glasses. Journal of Alloys and Compounds, 2015, 619, 16-19.	2.8	26

#	Article	IF	Citations
24456	Overview of theoretical studies of Rashba effect in polar perovskite surfaces. Journal of Electron Spectroscopy and Related Phenomena, 2015, 201, 121-126.	0.8	6
24457	Stability of binary and ternary M23C6 carbides from first principles. Computational Materials Science, 2015, 96, 159-164.	1.4	52
24458	Electronic and dielectric properties of Ruddlesdenâ€“Popper type and MagnÃ©li type SrTiO3. Computational Materials Science, 2015, 96, 223-228.	1.4	15
24459	Polar and nonpolar structures of BiCrO3 from first-principles calculations. Computational Materials Science, 2015, 96, 219-222.	1.4	4
24460	Direct Observation of Ordered Oxygen Defects on the Atomic Scale in Li₂O₂ for Liâ€Ò₂ Batteries. Advanced Energy Materials, 2015, 5, 1400664.	10.2	32
24461	Metal Dichalcogenides Monolayers: Novel Catalysts for Electrochemical Hydrogen Production. Scientific Reports, 2014, 4, 5348.	1.6	151
24462	Geometric and Electronic Properties of Edge-decorated Graphene Nanoribbons. Scientific Reports, 2014, 4, 6038.	1.6	24
24463	Methylene migration and coupling on a non-reducible metal oxide: The reaction of dichloromethane on stoichiometric Î±-Cr2O3(0001). Surface Science, 2015, 632, 28-38.	0.8	4
24464	Mn4+ emission in pyrochlore oxides. Journal of Luminescence, 2015, 157, 69-73.	1.5	35
24465	Bubble formation and Kr distribution in Kr-irradiated UO2. Journal of Nuclear Materials, 2015, 456, 125-132.	1.3	29
24466	Au@Phenyacetylene organogold clusters: Direct spectroscopic evidence of goldâ€“carbon covalent band. Spectrochimica Acta - Part A: Molecular and Biomolecular Spectroscopy, 2015, 134, 96-100.	2.0	4
24467	Enhanced Thermoelectric Performance of Cu2CdSnSe4 by Mn Doping: Experimental and First Principles Studies. Scientific Reports, 2014, 4, 5774.	1.6	29
24468	The d-p band-inversion topological insulator in bismuth-based skutterudites. Scientific Reports, 2014, 4, 5131.	1.6	34
24469	SiH/TiO2 and GeH/TiO2 Heterojunctions: Promising TiO2-based Photocatalysts under Visible Light. Scientific Reports, 2014, 4, 4810.	1.6	43
24470	Anomalous phonon stiffening associated with the (1 1 1) antiphase boundary in L12 Ni3Al. Acta Materialia, 2015, 82, 287-294.	3.8	29
24471	Crystal structure and phase stability of AlSc in the near-equiatomic Alâ€“Sc alloy. Journal of Alloys and Compounds, 2015, 618, 192-196.	2.8	3
24472	Magnetic Exchange Coupling and Anisotropy of 3d Transition Metal Nanowires on Graphyne. Scientific Reports, 2014, 4, 4014.	1.6	56
24473	The effects of stepped sites and ruthenium adatom decoration on methanol dehydrogenation over platinum-based catalyst surfaces. Catalysis Today, 2015, 242, 230-239.	2.2	10

#	Article	IF	Citations
24474	Microstructural evolution of charged defects in the fatigue process of polycrystalline BiFeO3 thin films. Acta Materialia, 2015, 82, 190-197.	3.8	18
24475	Structural trends in hybrid perovskites [Me₂NH₂]M[HCOO]₃ (M =) Tj ETQq1 1 0.784314 rgBT /O 295-298.	1.3	29
24476	Arithmetic extraction of elastic constants of cubic crystals from first-principles calculations of stress. Computational Materials Science, 2015, 96, 117-123.	1.4	2
24477	First principles calculation of magnetic order in a low-temperature phase of the iron ludwigite. Journal of Magnetism and Magnetic Materials, 2015, 374, 148-152.	1.0	10
24478	First-principles-aided design of a new Ni-base superalloy: Influence of transition metal alloying elements on grain boundary and bulk cohesion. Acta Materialia, 2015, 82, 369-377.	3.8	119
24479	Tuning the Dirac cone of the topological insulator Bi2Te3 thin films by substitutional nonmagnetic atoms. Physica B: Condensed Matter, 2015, 456, 355-358.	1.3	3
24480	First-principles study of magnetic properties in Co-doped BiFeO3. Physica B: Condensed Matter, 2015, 457, 1-4.	1.3	17
24481	First principles investigations on the mechanical and vibrational properties for the selected B2-AgRE (RE=Sc, Y, La, Ce) intermetallics. Physica B: Condensed Matter, 2015, 457, 22-29.	1.3	1
24482	First principles study of N and H atoms adsorption and NH formation on Pd(111) and Pd3Ag(111) surfaces. Journal of Membrane Science, 2015, 474, 57-63.	4.1	12
24483	Elastic and electronic properties of partially ordered and disordered Zr(C1âˆ’N) solid solution compounds: A first principles calculation study. Journal of Alloys and Compounds, 2015, 619, 788-793.	2.8	23
24484	Experimental study and thermodynamic description of the erbiumâ€“hydrogenâ€“zirconium ternary system. Journal of Nuclear Materials, 2015, 456, 7-16.	1.3	1
24485	Amorphous Wâ€“Sâ€“N thin films: The atomic structure behind ultra-low friction. Acta Materialia, 2015, 82, 84-93.	3.8	31
24486	Phase stability of N substituted Li2âˆ’FeSiO4 electrode material: DFT calculations. Computational Materials Science, 2015, 96, 290-294.	1.4	9
24487	Oxidation of NO on Pt/M (M = Pt, Co, Fe, Mn): a first-principles density functional theory study. Catalysis Science and Technology, 2015, 5, 882-886.	2.1	11
24488	First-principles calculations on magnetic property of Cu-doped ZnO tuned by Na and Al dopants. Rare Metals, 2015, 34, 40-44.	3.6	0
24489	Engineering Topological Surface States and Giant Rashba Spin Splitting in BiTeI/Bi2Te3 Heterostructures. Scientific Reports, 2015, 4, 3841.	1.6	32
24490	Structural, electronic and magnetic properties of the Si chains doped zigzag AlN nanoribbons. Physica E: Low-Dimensional Systems and Nanostructures, 2015, 65, 114-119.	1.3	7
24491	Hydrogen-assisted phase transition in a trihydride MgNi2H3 synthesized at high H2 pressures: Thermodynamics, crystallographic and electronic structures. Acta Materialia, 2015, 82, 316-327.	3.8	24

#	Article	IF	Citations
24492	On the universality of Suzuki segregation in binary Mg alloys from first principles. Journal of Alloys and Compounds, 2015, 620, 38-41.	2.8	21
24493	Formation of Graphene Grain Boundaries on Cu(100) Surface and a Route Towards Their Elimination in Chemical Vapor Deposition Growth. Scientific Reports, 2014, 4, 6541.	1.6	21
24494	Statistical model and first-principles simulation on concentration of He V cluster and He bubble formation in Î±-Fe and W. Journal of Nuclear Materials, 2015, 456, 162-173.	1.3	20
24495	Atomic reconstruction of niobium (111) surfaces. Surface Science, 2015, 632, 60-63.	0.8	6
24496	Room temperature multiferroism in CaTcO3 by interface engineering. Computational Materials Science, 2015, 96, 171-177.	1.4	5
24497	Hydrogen adsorption and storage on palladium-decorated graphene with boron dopants and vacancy defects: A first-principles study. Physica E: Low-Dimensional Systems and Nanostructures, 2015, 66, 40-47.	1.3	29
24498	Theory of surface chemistry and reactivity of reducible oxides. Catalysis Today, 2015, 244, 63-84.	2.2	67
24499	Investigation of structural, surface morphological, optical properties and first-principles study on electronic and magnetic properties of (Ce, Fe)-co doped ZnO. Physica B: Condensed Matter, 2015, 456, 344-354.	1.3	28
24500	Homoatomic Clustering in T4Ga5 (T = Ta, Nb, Ta/Mo): A Story of Reluctant Intermetallics Crystallizing in a New Binary Structure Type. Inorganic Chemistry, 2015, 54, 821-831.	1.9	6
24501	A ternary Niâ€“Alâ€“W EAM potential for Ni-based single crystal superalloys. Physica B: Condensed Matter, 2015, 456, 283-292.	1.3	17
24502	Spinâ€“orbit Splitting and Magnetism of Icosahedral M@Ag12 Clusters (MÂ=Â3d and 4d atoms). Journal of Cluster Science, 2015, 26, 759-773.	1.7	12
24503	Coverage-dependent structural phase transformations in the adsorption of pentacene on an aperiodically modulated Cu film. Journal of Chemical Physics, 2016, 145, 154707.	1.2	1
24504	Oxygen Defect-Mediated Magnetism in Fe-C Codoped TiO₂. Advances in Materials Science and Engineering, 2016, 2016, 1-7.	1.0	3
24505	Comment on â€œHigh-pressure synthesis of orthorhombic SrIrO3 perovskite and its positive magnetoresistanceâ€•[J. Appl. Phys. 103, 103706 (2008)]. Journal of Applied Physics, 2016, 119, 086102.	1.1	6
24506	Ab-initio study on electronic and magnetic properties of (Ga,Co) co-doped ZnO. Journal of Physics: Conference Series, 2016, 743, 012002.	0.3	0
24507	Atomistically Informed Extended Gibbs Energy Description for Phase-Field Simulation of Tempering of Martensitic Steel. Materials, 2016, 9, 669.	1.3	6
24508	First-principles study of the structure of water layers on flat and stepped Pb electrodes. Beilstein Journal of Nanotechnology, 2016, 7, 533-543.	1.5	21
24509	Theoretical investigations of interactions between boron nitride nanotubes and drugs. , 2016, , 59-77.		9

#	Article	IF	Citations
24510	Fabrication of Semiconductor with Modified Microstructure for Efficient Photocatalytic Hydrogen Evolution Under Visible Light. , 0, , .		0
24511	Atomic Scale Simulations of Relationship between Macroscopic Mechanical Properties and Microscopic Defect Evolution in Ultrafine-grained Metals. Materials Transactions, 2016, 57, 1476-1481.	0.4	1
24512	Theoretical and Experimental Studies on the Crystal Structure, Electronic Structure and Optical Properties of SmTaO4. Materials, 2016, 9, 55.	1.3	20
24513	Mechanical Properties and Atomic Explanation of Plastic Deformation for Diamond-Like BC2. Materials, 2016, 9, 514.	1.3	3
24514	Effects of Aluminum on Hydrogen Solubility and Diffusion in Deformed Fe-Mn Alloys. Advances in Materials Science and Engineering, 2016, 2016, 1-9.	1.0	3
24515	Renormalized Phonon Microstructures at High Temperatures from First-Principles Calculations: Methodologies and Applications in Studying Strong Anharmonic Vibrations of Solids. Advances in Condensed Matter Physics, 2016, 2016, 1-11.	0.4	0
24516	Catalytic behavior of â€˜Pt-atomic chain encapsulated gold nanotubeâ€™: A density functional study. AIP Conference Proceedings, 2016, , .	0.3	0
24517	Electronic and Magnetic Properties Studies on Mn and Oxygen Vacancies Codoped Anatase TiO₂. Advances in Condensed Matter Physics, 2016, 2016, 1-7.	0.4	3
24518	Temperature-Dependent Generalized Planar Fault Energy and Twinnability of Mg Microalloyed with Er, Ho, Dy, Tb, and Gd: First-Principles Study. Advances in Materials Science and Engineering, 2016, 2016, 1-9.	1.0	3
24519	On the Electronic Effect of V, Fe, and Ni on MgO(100) and BaO(100) Surface: An Explanation from a Periodic Density Functional. Journal of Chemistry, 2016, 2016, 1-8.	0.9	1
24520	Thermodynamic properties and solidification kinetics of intermetallic Ni7Zr2 alloy investigated by electrostatic levitation technique and theoretical calculations. Journal of Applied Physics, 2016, 119, .	1.1	16
24521	Phonocatalysis. An ab initio simulation experiment. AIP Advances, 2016, 6, .	0.6	5
24522	Interfacial n-Doping Using an Ultrathin TiO₂ Layer for Contact Resistance Reduction in MoS₂. ACS Applied Materials & Interfaces, 2016, 8, 256-263.	4.0	117
24523	Cubic C3N: A New Superhard Phase of Carbon-Rich Nitride. Materials, 2016, 9, 840.	1.3	17
24524	Computational Chemistry of Zeolite Catalysis. , 2016, , 111-135.		3
24525	Aqueous Stability of Alkali Superionic Conductors from First-Principles Calculations. Frontiers in Energy Research, 2016, 4, .	1.2	19
24526	Charge Transfer Mechanism in Titanium-Doped Microporous Silica for Photocatalytic Water-Splitting Applications. Catalysts, 2016, 6, 34.	1.6	10
24527	Silicene Nanoribbons on Pb-Reconstructed Si(111) Surface. Condensed Matter, 2016, 1, 8.	0.8	11

#	Article	IF	Citations
24528	Interplay between Lattice Distortions, Vibrations and Phase Stability in NbMoTaW High Entropy Alloys. Entropy, 2016, 18, 403.	1.1	63
24529	Lattice Distortions in the FeCoNiCrMn High Entropy Alloy Studied by Theory and Experiment. Entropy, 2016, 18, 321.	1.1	151
24530	First-Principles Study of Mo Segregation in MoNi(111): Effects of Chemisorbed Atomic Oxygen. Materials, 2016, 9, 5.	1.3	15
24531	Energetic Study of Helium Cluster Nucleation and Growth in 14YWT through First Principles. Materials, 2016, 9, 17.	1.3	7
24532	Effect of Guest Atom Composition on the Structural and Vibrational Properties of the Type II Clathrate-Based Materials AxSi136, AxGe136 and AxSn136 (A = Na, K, Rb, Cs; 0 â‰¤ x â‰¤ 24). Materials, 2016, 9, 691.	1.3	6
24533	First Principles Study on the Interaction Mechanisms of Water Molecules on TiO2 Nanotubes. Materials, 2016, 9, 1018.	1.3	2
24534	Molecular Theory of Detonation Initiation: Insight from First Principles Modeling of the Decomposition Mechanisms of Organic Nitro Energetic Materials. Molecules, 2016, 21, 236.	1.7	61
24535	Photochemistry of the Î±-Al2O3-PETN Interface. Molecules, 2016, 21, 289.	1.7	8
24536	Pressure induced Ag2Te polymorphs in conjunction with topological non trivial to metal transition. AIP Advances, 2016, 6, 085003.	0.6	4
24537	Z method calculations to determine the melting curve of silica at high pressures. Journal of Physics: Conference Series, 2016, 720, 012032.	0.3	7
24538	The origin of the conductivity maximum in molten salts. II. SnCl2 and HgBr2. Journal of Chemical Physics, 2016, 145, 094504.	1.2	12
24539	Theoretical study of intrinsic defects in CdTe. Journal of Physics: Conference Series, 2016, 720, 012031.	0.3	5
24540	First-principles prediction of a rising star of solar energy material: SrTcO_3. Optics Express, 2016, 24, A1612.	1.7	1
24541	A New Superhard Phase and Physical Properties of ZrB3 from First-Principles Calculations. Materials, 2016, 9, 703.	1.3	21
24542	Magnetic Properties of Gadolinium-Doped ZnO Films and Nanostructures. , 2016, , .		3
24543	Hybrid functional study of Î±-uranium. AIP Conference Proceedings, 2016, , .	0.3	0
24544	Electronic and Optical Properties of O-Terminated Armchair Graphene Nanoribbons. Chinese Journal of Chemical Physics, 2016, 29, 205-211.	0.6	2
24545	Electronic Structures and Thermoelectric Properties of Two-Dimensional MoS2/MoSe2 Heterostructures. Chinese Journal of Chemical Physics, 2016, 29, 445-452.	0.6	9

#	Article	IF	Citations
24546	Alloying Effect Study on Thermodynamic Stability of MgH2 by First-principles Calculation. Chinese Journal of Chemical Physics, 2016, 29, 545-548.	0.6	2
24547	Adsorption and Decomposition of NH3 on Ni/Pt(111) and Ni/WC(001) Surfaces: A First-Principles Study. Chinese Journal of Chemical Physics, 2016, 29, 710-716.	0.6	3
24548	Radiation-Damage Resistance in Phyllosilicate Minerals From First Principles and Implications for Radiocesium and Strontium Retention in Soils. Clays and Clay Minerals, 2016, 64, 108-114.	0.6	6
24549	Electronic structures of nanocrystalline Fe90-xCuxSi10-yBy soft magnets. AIP Advances, 2016, 6, .	0.6	0
24550	EXAFS study of the structural properties of In and In + C implanted Ge. Journal of Physics: Conference Series, 2016, 712, 012102.	0.3	0
24551	The Magnetic Properties of Transition-Metal Atom Adsorbed Two Dimensional GaAs Nanosheet. , 2016, , .		0
24552	Silver-Antimony-Telluride: From First-Principles Calculations to Thermoelectric Applications. , 2016, , .		0
24553	Origin of the unidentified positive mobile ions causing the bias temperature instability in SiC MOSFETs and their diffusion process. Applied Physics Express, 2016, 9, 064301.	1.1	7
24554	Activation mechanisms of H 2 , O 2 , H 2 O, CO 2 , CO, CH 4 and C 2 H x on metallic Mo 2 C(001) as well as Mo/C terminated Mo 2 C(101) from density functional theory computations. Applied Catalysis A: General, 2016, 524, 223-236.	2.2	39
24555	Effect of Siâ€“Si Bonds in Silicon-Doped Î±-Phosphorene Bilayers: Two-Dimensional Layers and One-Dimensional Nanoribbons. Journal of Physical Chemistry C, 2016, 120, 17106-17114.	1.5	5
24556	Instability and Spontaneous Reconstruction of Few-Monolayer Thick GaN Graphitic Structures. Nano Letters, 2016, 16, 4849-4856.	4.5	51
24557	Reactivity of Hydrogen on and in Nanostructured Molybdenum Nitride: Crotonaldehyde Hydrogenation. ACS Catalysis, 2016, 6, 5797-5806.	5.5	44
24558	Structural transitions and electronic properties of sodium superoxide at high pressures. RSC Advances, 2016, 6, 67910-67915.	1.7	5
24559	Robust vanadium pentoxide electrodes for sodium and calcium ion batteries: thermodynamic and diffusion mechanical insights. Journal of Materials Chemistry A, 2016, 4, 12516-12525.	5.2	26
24560	Multiple Dirac cones in BN co-doped Î²-graphyne. Journal of Materials Chemistry C, 2016, 4, 7339-7344.	2.7	14
24561	Global structure search and physical properties of Os2C. Journal of Physics Condensed Matter, 2016, 28, 365502.	0.7	1
24562	Generation and the role of dislocations in single-crystalline phase-change In₂Se₃nanowires under electrical pulses. Nanotechnology, 2016, 27, 335704.	1.3	4
24563	First-principles modeling hydrogenation of bilayered boron nitride. Chinese Physics B, 2016, 25, 057301.	0.7	0

#	Article	IF	Citations
24564	Anisotropic elastic and vibrational properties of Ru₂B₃and Os₂B₃: a first-principles investigation. Materials Research Express, 2016, 3, 076501.	0.8	16
24565	<scp>DFT</scp> Predictions of Crystal Structure, Electronic Structure, Compressibility, and Elastic Properties of Hfâ€“Alâ€“C Carbides. Journal of the American Ceramic Society, 2016, 99, 3449-3457.	1.9	22
24566	Prediction of silicon-based room temperature quantum spin Hall insulator via orbital mixing. Europhysics Letters, 2016, 113, 67003.	0.7	6
24567	Does DFT+U mimic hybrid density functionals?. Theoretical Chemistry Accounts, 2016, 135, 1.	0.5	47
24568	Ab-initio search for cohesion-enhancing solute elements at grain boundaries in molybdenum and tungsten. International Journal of Refractory Metals and Hard Materials, 2016, 60, 75-81.	1.7	82
24569	Density functional theory-based derivation of an interatomic pair potential for helium impurities in nickel. Journal of Nuclear Materials, 2016, 479, 240-248.	1.3	20
24570	On the role of Sm in solidification of Al-Sm metallic glasses. Scripta Materialia, 2016, 124, 99-102.	2.6	30
24571	Tetrazoleâ€“Viologen-based Flexible Microporous Metalâ€“Organic Framework with High CO₂ Selective Uptake. Inorganic Chemistry, 2016, 55, 7335-7340.	1.9	48
24572	A comparative first-principles study of the lithiation, sodiation, and magnesiation of black phosphorus for Li-, Na-, and Mg-ion batteries. Physical Chemistry Chemical Physics, 2016, 18, 21391-21397.	1.3	73
24573	The cross-substitution effect of tantalum on the visible-light-driven water oxidation activity of BaNbO₂N crystals grown directly by an NH₃-assisted flux method. Journal of Materials Chemistry A, 2016, 4, 12807-12817.	5.2	50
24574	An interatomic potential for Wâ€“N interactions. Modelling and Simulation in Materials Science and Engineering, 2016, 24, 065007.	0.8	5
24575	Suppression of phononâ€mediated hot carrier relaxation in typeâ€II InAs/AlAs_xSb_{1 â^' x} quantum wells: a practical route to hot carrier solar cells. Progress in Photovoltaics: Research and Applications, 2016, 24, 591-599.	4.4	38
24576	Determination of the high pressure phases of CaWO₄ by CALYPSO and Xâ€ray diffraction studies. Physica Status Solidi (B): Basic Research, 2016, 253, 1947-1951.	0.7	8
24577	Mechanistic study of glycerol dehydration on BrÃ¸nsted acidic amorphous aluminosilicate. Journal of Catalysis, 2016, 341, 33-43.	3.1	46
24578	Point defect induced segregation of alloying solutes in Î±-Fe. Journal of Nuclear Materials, 2016, 479, 11-18.	1.3	5
24579	The role of minor yttrium in tailoring the failure resistance of surface oxide film formed on Mg alloys. Thin Solid Films, 2016, 615, 29-37.	0.8	11
24580	CO₂ Adsorption in Azobenzene Functionalized Stimuli Responsive Metalâ€“Organic Frameworks. Journal of Physical Chemistry C, 2016, 120, 16658-16667.	1.5	53
24581	Activating Catalytic Inert Basal Plane of Molybdenum Disulfide to Optimize Hydrogen Evolution Activity via Defect Doping and Strain Engineering. Journal of Physical Chemistry C, 2016, 120, 16761-16766.	1.5	138

#	Article	IF	Citations
24582	Structure Formation and Thermal Stability of Mono- and Multilayers of Ethylene Carbonate on Cu(111): A Model Study of the Electrode|Electrolyte Interface. Journal of Physical Chemistry C, 2016, 120, 16791-16803.	1.5	15
24583	Charge Transfer to LaAlO₃/SrTiO₃ Interfaces Controlled by Surface Water Adsorption and Proton Hopping. Advanced Functional Materials, 2016, 26, 5453-5459.	7.8	19
24584	Understanding the Structural Evolution and Redox Mechanism of a NaFeO₂â€“NaCoO₂ Solid Solution for Sodiumâ€ion Batteries. Advanced Functional Materials, 2016, 26, 6047-6059.	7.8	132
24585	Mechanical Isolation of Highly Stable Antimonene under Ambient Conditions. Advanced Materials, 2016, 28, 6332-6336.	11.1	444
24586	The Origin of Oxygen Vacancies Controlling La_{2/3}Sr_{1/3}MnO₃ Electronic and Magnetic Properties. Advanced Materials Interfaces, 2016, 3, 1500753.	1.9	73
24587	High On/Off Ratio Memristive Switching of Manganite/Cuprate Bilayer by Interfacial Magnetoelectricity. Advanced Materials Interfaces, 2016, 3, 1600086.	1.9	5
24588	Significant Roles of Intrinsic Point Defects in Mg₂X (X = Si, Ge, Sn) Thermoelectric Materials. Advanced Electronic Materials, 2016, 2, 1500284.	2.6	75
24589	Computational Design and Preparation of Cationâ€Disordered Oxides for Highâ€Energyâ€Density Liâ€ion Batteries. Advanced Energy Materials, 2016, 6, 1600488.	10.2	93
24590	Towards intrinsic phonon transport in singleâ€layer MoS₂. Annalen Der Physik, 2016, 528, 504-511.	0.9	65
24591	Mixed Boron(III) and Phosphorous(V) Complexes of mesoâ€Triaryl 25â€Oxasmaragdyrins. Chemistry - A European Journal, 2016, 22, 9699-9708.	1.7	5
24592	Enhanced Catalytic Activity in Liquidâ€Exfoliated FeOCl Nanosheets as a Fentonâ€Like Catalyst. Chemistry - A European Journal, 2016, 22, 9321-9329.	1.7	59
24593	Interplay of magnetic sublattices in langite Cu₄(OH)₆SO₄Â·2H₂O. New Journal of Physics, 2016, 18, 033020.	1.2	7
24594	Pressure induced phase transition and thermo-physical properties in LuX (X = N, P). Materials Research Express, 2016, 3, 046502.	0.8	3
24595	Thickness-dependent nanofriction of a rare gas monolayer sliding on Pb(111) ultrathin films. Europhysics Letters, 2016, 113, 46002.	0.7	1
24596	Electronic structure and magnetism of ThFeAsN. Europhysics Letters, 2016, 113, 67006.	0.7	16
24597	Stability of B₁₂(CN)₁₂^{2â^’}: Implications for Lithium and Magnesium Ion Batteries. Angewandte Chemie, 2016, 128, 3768-3772.	1.6	28
24598	A Singleâ€Material Logical Junction Based on 2D Crystal PdS₂. Advanced Materials, 2016, 28, 853-856.	11.1	85
24599	On the Quantum Spin Hall Gap of Monolayer 1Tâ€²â€WTe₂. Advanced Materials, 2016, 28, 4845-4851.	11.1	141

#	Article	IF	Citations
24600	Nanoscale Chemical and Valence Evolution at the Metal/Oxide Interface: A Case Study of Ti/SrTiO₃. Advanced Materials Interfaces, 2016, 3, 1600201.	1.9	25
24601	Operando Lithium Dynamics in the Liâ€Rich Layered Oxide Cathode Material via Neutron Diffraction. Advanced Energy Materials, 2016, 6, 1502143.	10.2	98
24602	Cyanoâ€Functionalized Triarylamines on Coinage Metal Surfaces: Interplay of Intermolecular and Moleculeâ€“Substrate Interactions. Chemistry - A European Journal, 2016, 22, 581-589.	1.7	30
24603	Interaction of Boron Nitride Nanosheets with Model Cell Membranes. ChemPhysChem, 2016, 17, 1573-1578.	1.0	20
24604	Superconductivity in Pd-intercalated charge-density-wave rare earth poly-tellurides RETe_n. Superconductor Science and Technology, 2016, 29, 065018.	1.8	10
24605	Structural phase transitions in boron carbide under stress. Modelling and Simulation in Materials Science and Engineering, 2016, 24, 015004.	0.8	17
24606	Dumbbell silicene: a strain-induced room temperature quantum spin Hall insulator. New Journal of Physics, 2016, 18, 043001.	1.2	24
24607	Electronegativity explanation on the efficiency-enhancing mechanism of the hybrid inorganicâ€“organic perovskite ABX ₃ from first-principles study. Chinese Physics B, 2016, 25, 027104.	0.7	21
24608	Effective band structure of Ru-doped BaFe₂As₂. Journal of Physics: Conference Series, 2016, 689, 012027.	0.3	6
24609	Coexistence of Ferroelectric Phases and Phonon Dynamics in Relaxor Ferroelectric Na_{0.5}Bi_{0.5}TiO₃ Based Single Crystals. Journal of the American Ceramic Society, 2016, 99, 2408-2414.	1.9	20
24610	Doping behaviors of adatoms adsorbed on phosphorene. Physica Status Solidi (B): Basic Research, 2016, 253, 1156-1166.	0.7	18
24611	Firstâ€principles prediction of a novel hexagonal phosphorene allotrope. Physica Status Solidi - Rapid Research Letters, 2016, 10, 563-565.	1.2	28
24612	Firstâ€principles calculations of oxygen adsorption on the Ti₃Al (0001) surface. Surface and Interface Analysis, 2016, 48, 1337-1340.	0.8	8
24613	Effects of Cr and W additions on the stability and migration of He in bcc Fe: A first-principles study. Computational Materials Science, 2016, 123, 85-92.	1.4	20
24614	Charge storage performances of micro-supercapacitor predominated by two-dimensional (2D) crystal structure. Nano Energy, 2016, 27, 58-67.	8.2	39
24615	CO Poisoning Effects on FeNC and CN_x ORR Catalysts: A Combined Experimentalâ€“Computational Study. Journal of Physical Chemistry C, 2016, 120, 15173-15184.	1.5	57
24616	Metallic VS₂ Monolayer Polytypes as Potential Sodium-Ion Battery Anode via ab Initio Random Structure Searching. ACS Applied Materials & Interfaces, 2016, 8, 18754-18762.	4.0	155
24617	Oxide Defect Engineering Enables to Couple Solar Energy into Oxygen Activation. Journal of the American Chemical Society, 2016, 138, 8928-8935.	6.6	840

#	Article	IF	Citations
24618	Valley polarization and p-/n-type doping of monolayer WTe₂ on top of Fe₃O₄(111). Physical Chemistry Chemical Physics, 2016, 18, 15039-15045.	1.3	32
24619	Nanostructured water and carbon dioxide inside collapsing carbon nanotubes at high pressure. Physical Chemistry Chemical Physics, 2016, 18, 19926-19932.	1.3	16
24620	Computational identification of promising thermoelectric materials among known quasi-2D binary compounds. Journal of Materials Chemistry A, 2016, 4, 11110-11116.	5.2	55
24621	In quest of cathode materials for Ca ion batteries: the CaMO₃ perovskites (M = Mo, Cr,) Tj ETQq1 1 0.784314 rgBT /Ove	1.3	64
24622	Predicted lithiumâ€“iron compounds under high pressure. RSC Advances, 2016, 6, 66721-66728.	1.7	4
24623	Insights on the atomistic origin of X and W photoluminescence lines inc-Si fromab initiosimulations. Journal Physics D: Applied Physics, 2016, 49, 075109.	1.3	10
24624	The electronic band structures of gadolinium chalcogenides: a first-principles prediction for neutron detecting. Journal of Physics Condensed Matter, 2016, 28, 185501.	0.7	0
24625	Phase equilibrium of Cd _{1â€“ x} Zn _x S alloys studied by first-principles calculations and Monte Carlo simulations. Chinese Physics B, 2016, 25, 013103.	0.7	0
24626	Energetics of carbon and nitrogen impurities and their interactions with vacancy in vanadium. Chinese Physics B, 2016, 25, 036104.	0.7	8
24627	First-principles study of strain effect on the formation and electronic structures of oxygen vacancy in SrFeO ₂. Chinese Physics B, 2016, 25, 057103.	0.7	1
24628	Investigation and calculation of positron lifetimes of monovacancies in crystals. Journal of Physics: Conference Series, 2016, 674, 012022.	0.3	1
24629	Effect of vanadium doping on the magnetic properties of LiMnPO₄. Physica Status Solidi (B): Basic Research, 2016, 253, 965-975.	0.7	10
24630	C-chain-doping induced band-state transition in armchair AlN nanoribbons. Physica Status Solidi (B): Basic Research, 2016, 253, 1643-1648.	0.7	2
24631	The direct observation of 2H-DPP metalation on Pd(111) and Cu/Pd(111) surface. Surface and Interface Analysis, 2016, 48, 237-242.	0.8	0
24632	A Firstâ€Principles Study on the Electronic, Vibrational, and Thermodynamic Properties of Jadeite and its Tentative Lowâ€Density Polymorph. Zeitschrift Fur Anorganische Und Allgemeine Chemie, 2016, 642, 590-596.	0.6	4
24633	Chloroform Hydrodechlorination over Palladiumâ€“Gold Catalysts: A Firstâ€Principles DFT Study. ChemCatChem, 2016, 8, 1739-1746.	1.8	12
24634	Origin of the Ability of Î±â€Fe₂O₃ Mesopores to Activate Câˆ’H Bonds in Methane. Chemistry - A European Journal, 2016, 22, 2046-2050.	1.7	7
24635	Coexistence of Three Ferroic Orders in the Multiferroic Compound [(CH₃)₄N][Mn(N₃)₃] with Perovskiteâ€Like Structure. Chemistry - A European Journal, 2016, 22, 7863-7870.	1.7	54

#	Article	IF	Citations
24636	Dehydrogenative Homocoupling of Alkyl Chains on Cu(110). Chemistry - A European Journal, 2016, 22, 1918-1921.	1.7	15
24637	Firstâ€Principles Study on Doping of SnSe₂ Monolayers. ChemPhysChem, 2016, 17, 375-379.	1.0	30
24638	Hybrid Density Functional Study on Monoâ€•and Codoped NaNbO₃ for Visibleâ€Light Photocatalysis. ChemPhysChem, 2016, 17, 489-499.	1.0	40
24639	Controlling the Electronic Structures of Perovskite Oxynitrides and their Solid Solutions for Photocatalysis. ChemSusChem, 2016, 9, 1027-1031.	3.6	14
24640	Density Functional Theory Calculation on the Dissociation Mechanism of Nitric Oxide Catalyzed by Cu₄ Cluster in ZSMâ€5 (Cu₄â€ZSMâ€5) and Bimetal Cu₃Fe in ZSMâ€5 (Cu₃Feâ€ZSMâ€5). Journal of the Chinese Chemical Society, 2016, 63, 499-505.	0.8	6
24641	First Principles Calculations of Structural and Elastic Properties of Perovskite Crystals: The Case of SrTiO₃. Journal of the Chinese Chemical Society, 2016, 63, 521-525.	0.8	2
24642	Theoretical and experimental investigation of optical absorption anisotropy in Î²-Ga₂O₃. Journal of Physics Condensed Matter, 2016, 28, 224005.	0.7	59
24643	Orbital-free density functional theory study of amorphous Liâ€“Si alloys and introduction of a simple density decomposition formalism. Modelling and Simulation in Materials Science and Engineering, 2016, 24, 035014.	0.8	4
24644	Tuning the energy gap of bilayer Î± -graphyne by applying strain and electric field. Chinese Physics B, 2016, 25, 023102.	0.7	15
24645	Structure and Composition of the 200â€…Kâ€Superconducting Phase of H₂S at Ultrahigh Pressure: The Perovskite (SH^{â^’})(H₃S⁺). Angewandte Chemie, 2016, 128, 3746-3748.	1.6	6
24646	Probing Absolute Electronic Energy Levels in Hgâ€Doped CdTe Semiconductor Nanocrystals by Electrochemistry and Density Functional Theory. ChemPhysChem, 2016, 17, 244-252.	1.0	7
24647	Dzyaloshinskii-Moriya interactions and magnetic texture in Fe films deposited on transition-metal dichalcogenides. Physica Status Solidi - Rapid Research Letters, 2016, 10, 218-221.	1.2	7
24649	Diffused Phase Transition Boosts Thermal Stability of Highâ€Performance Leadâ€Free Piezoelectrics. Advanced Functional Materials, 2016, 26, 1217-1224.	7.8	272
24650	The Swissâ€Armyâ€Knife Selfâ€Assembled Monolayer: Improving Electron Injection, Stability, and Wettability of Metal Electrodes with a Oneâ€Minute Process. Advanced Functional Materials, 2016, 26, 3172-3178.	7.8	27
24651	Colloidal Gold Nanocups with Orientationâ€Dependent Plasmonic Properties. Advanced Materials, 2016, 28, 6322-6331.	11.1	74
24652	Quasi 2D Ultrahigh Carrier Density in a Complex Oxide Brokenâ€Gap Heterojunction. Advanced Materials Interfaces, 2016, 3, 1500432.	1.9	32
24653	Optimized Temperature Effect of Liâ€Ion Diffusion with Layer Distance in Li(Ni_xMn_yCo_z)O₂ Cathode Materials for High Performance Liâ€Ion Battery. Advanced Energy Materials, 2016, 6, 1501309.	10.2	182
24654	Air Passivation of Chalcogen Vacancies in Twoâ€Dimensional Semiconductors. Angewandte Chemie, 2016, 128, 977-980.	1.6	15

#	Article	IF	Citations
24655	Air Passivation of Chalcogen Vacancies in Twoâ€Ðimensional Semiconductors. Angewandte Chemie - International Edition, 2016, 55, 965-968.	7.2	80
24656	First-principles Study on the Charge Transport Mechanism of Lithium Sulfide (Li2S) in Lithium-Sulfur Batteries. Chemistry - an Asian Journal, 2016, 11, 1288-1292.	1.7	27
24657	A new method applicable to study solid compounds with multiple polyhedral structures. Journal of Computational Chemistry, 2016, 37, 1476-1483.	1.5	10
24658	Prediction of Hostâ€“Guest Naâ€“Fe Intermetallics at High Pressures. Inorganic Chemistry, 2016, 55, 7026-7032.	1.9	8
24659	Layered-to-Tunnel Structure Transformation and Oxygen Redox Chemistry in LiRhO2 upon Li Extraction and Insertion. Inorganic Chemistry, 2016, 55, 7079-7089.	1.9	20
24660	A Theoretical Study on the Design, Structure, and Electronic Properties of Novel Forms of Graphynes. Journal of Physical Chemistry C, 2016, 120, 15153-15161.	1.5	54
24661	Valence and Conduction Band Densities of States of Metal Halide Perovskites: A Combined Experimentalâ€“Theoretical Study. Journal of Physical Chemistry Letters, 2016, 7, 2722-2729.	2.1	333
24662	Like Charges Attract?. Journal of Physical Chemistry Letters, 2016, 7, 2689-2695.	2.1	26
24663	Mesostructured Hf_xAl_yO₂ Thin Films as Reliable and Robust Gate Dielectrics with Tunable Dielectric Constants for High-Performance Graphene-Based Transistors. ACS Nano, 2016, 10, 6659-6666.	7.3	19
24664	Core electron excitations in U⁴⁺: modelling of the nd¹⁰5f²â†' nd⁹5f³transitions with n = 3, 4 and 5 by ligand field tools and density functional theory. Physical Chemistry Chemical Physics, 2016, 18, 19020-19031.	1.3	21
24665	Does the Dirac cone of germanene exist on metal substrates?. Physical Chemistry Chemical Physics, 2016, 18, 19451-19456.	1.3	39
24666	Tuning the Schottky contacts in the phosphorene and graphene heterostructure by applying strain. Physical Chemistry Chemical Physics, 2016, 18, 19918-19925.	1.3	62
24667	Switchable polarization in an unzipped graphene oxide monolayer. Physical Chemistry Chemical Physics, 2016, 18, 20443-20449.	1.3	16
24668	Electronic structures of p-type impurity in ZrS₂ monolayer. RSC Advances, 2016, 6, 58325-58328.	1.7	6
24669	Conversion of inert cryptomelane-type manganese oxide into a highly efficient oxygen evolution catalyst via limited Ir doping. Journal of Materials Chemistry A, 2016, 4, 12561-12570.	5.2	64
24670	Investigation of the elemental partitioning behaviour and site preference in ternary model nickel-based superalloys by atom probe tomography and first-principles calculations. Philosophical Magazine, 2016, 96, 2204-2218.	0.7	27
24671	Magnetic properties in BiFeO₃ doped with nonâ€metallic element: Firstâ€principles investigation. Physica Status Solidi (B): Basic Research, 2016, 253, 279-283.	0.7	10
24672	Atomic and electronic structures of a-ZnSnO3/a-SiO2interface byab initiomolecular dynamics simulations. Physica Status Solidi (B): Basic Research, 2016, 253, 1765-1770.	0.7	3

#	Article	IF	Citations
24673	Hydrogen on hybrid MoS₂/graphene nanostructures. Physica Status Solidi - Rapid Research Letters, 2016, 10, 453-457.	1.2	5
24674	Efficient simulation of large materials clusters using the jaguar quantum chemistry program: Parallelization and wavefunction initialization. International Journal of Quantum Chemistry, 2016, 116, 357-368.	1.0	5
24675	Neural network and ReaxFF comparison for Au properties. International Journal of Quantum Chemistry, 2016, 116, 979-987.	1.0	66
24676	Structural, electronic, and magnetic properties of 3d transition metal doped GaN nanosheet: A first-principles study. International Journal of Quantum Chemistry, 2016, 116, 1000-1005.	1.0	37
24677	<scp>GW</scp> method and Betheâ€“Salpeter equation for calculating electronic excitations. Wiley Interdisciplinary Reviews: Computational Molecular Science, 2016, 6, 532-550.	6.2	86
24678	An integrated first principles and experimental investigation of the relationship between structural rigidity and quantum efficiency in phosphors for solid state lighting. Journal of Luminescence, 2016, 179, 297-305.	1.5	24
24679	Formation mechanism of gas bubble superlattice in UMo metal fuels: Phase-field modeling investigation. Journal of Nuclear Materials, 2016, 479, 202-215.	1.3	54
24680	First principles study of thieno[2,3-b]indole-based organic dyes for dye-sensitized solar cells: Screen novel Ï€-linkers and explore the interface between photosensitizers and TiO2. Journal of Power Sources, 2016, 326, 193-202.	4.0	30
24681	First-Principle and Experiment Framework for Charge Distribution at the Interface of the Molybdenum Dichalcogenide Hybrid for Enhanced Electrochemical Hydrogen Generation. Journal of Physical Chemistry C, 2016, 120, 15096-15104.	1.5	21
24682	Growth mode and structures of magnetic Mn clusters on graphene. RSC Advances, 2016, 6, 64595-64604.	1.7	7
24683	Electronic structures and quantum capacitance of monolayer and multilayer graphenes influenced by Al, B, N and P doping, and monovacancy: Theoretical study. Carbon, 2016, 108, 7-20.	5.4	99
24684	CH₃NH₃CaI₃ Perovskite: Synthesis, Characterization, and First-Principles Studies. Journal of Physical Chemistry C, 2016, 120, 16393-16398.	1.5	67
24685	Single-Electron Activation of CO₂ on Graphene-Supported ZnO Nanoclusters: Effects of Doping in the Support. Journal of Physical Chemistry C, 2016, 120, 16732-16740.	1.5	14
24686	First-Principles Design of Graphene-Based Active Catalysts for Oxygen Reduction and Evolution Reactions in the Aprotic Liâ€“O₂ Battery. Journal of Physical Chemistry Letters, 2016, 7, 2803-2808.	2.1	52
24687	On the relationship between chemical expansion and hydration thermodynamics of proton conducting perovskites. Journal of Materials Chemistry A, 2016, 4, 5917-5924.	5.2	42
24688	The electronic structure and spinâ€“orbit-induced spin splitting in antimonene with vacancy defects. RSC Advances, 2016, 6, 66140-66146.	1.7	38
24689	A DFT Study of CO₂ Hydrogenation on Faujasiteâ€Supported Ir₄ Clusters: on the Role of Water for Selectivity Control. ChemCatChem, 2016, 8, 2500-2507.	1.8	17
24690	New developments in the multiscale hybrid energy density computational method. Chinese Physics B, 2016, 25, 013105.	0.7	0

#	Article	IF	Citations
24692	Fluorineâ€Doped and Partially Oxidized Tantalum Carbides as Nonprecious Metal Electrocatalysts for Methanol Oxidation Reaction in Acidic Media. Advanced Materials, 2016, 28, 2163-2169.	11.1	63
24693	Efficient Photocatalytic Hydrogen Production over Rhâ€Doped Inverse Spinel Zn₂TiO₄. ChemCatChem, 2016, 8, 2289-2295.	1.8	40
24694	Conversion Reactions of Solids: From a Surprising Threeâ€Step Mechanism towards Directed Product Formation. Chemistry - A European Journal, 2016, 22, 6333-6339.	1.7	5
24695	Critical Role of Dynamic Flexibility in Geâ€Containing Zeolites: Impact on Diffusion. Chemistry - A European Journal, 2016, 22, 10036-10043.	1.7	22
24696	Curvature-dependent adsorption of water inside and outside armchair carbon nanotubes. Journal of Computational Chemistry, 2016, 37, 1313-1320.	1.5	20
24697	Thermodynamic stability of mixed Pb:Sn methylâ€ammonium halide perovskites. Physica Status Solidi (B): Basic Research, 2016, 253, 1907-1915.	0.7	28
24698	HEOM-QUICK: a program for accurate, efficient, and universal characterization of strongly correlated quantum impurity systems. Wiley Interdisciplinary Reviews: Computational Molecular Science, 2016, 6, 608-638.	6.2	87
24699	First principles study of band line up at defective metal-oxide interface: oxygen point defects at Al/SiO₂interface. Journal Physics D: Applied Physics, 2016, 49, 095304.	1.3	15
24700	Tailoring Magnetic Properties of MAX Phases, a Theoretical Investigation of (Cr₂Ti)AlC₂ and Cr₂AlC. Journal of the American Ceramic Society, 2016, 99, 3371-3375.	1.9	14
24701	A first-principles study on the effect of phosphorus-doped palladium catalyst for formic acid dissociation. Applied Surface Science, 2016, 387, 221-227.	3.1	10
24702	Adsorption and dissociation of H2S on monometallic and monolayer bimetallic Ni/Pd(111) surfaces: A first-principles study. Applied Surface Science, 2016, 387, 301-307.	3.1	25
24703	The effects of copper doping on photocatalytic activity at (101) planes of anatase TiO2: A theoretical study. Applied Surface Science, 2016, 387, 682-689.	3.1	68
24704	First-principles study of vacancy, interstitial, noble gas atom interstitial and vacancy clusters in bcc-W. Computational Materials Science, 2016, 123, 121-130.	1.4	54
24705	First-principles derived complexion diagrams for phase boundaries in doped cemented carbides. Current Opinion in Solid State and Materials Science, 2016, 20, 299-307.	5.6	27
24706	Adsorption and diffusion of fluorine on Cr-doped Ni(111) surface: Fluorine-induced initial corrosion of non-passivated Ni-based alloy. Journal of Nuclear Materials, 2016, 478, 295-302.	1.3	14
24707	InBO3 and ScBO3 at high pressures: An ab initio study of elastic and thermodynamic properties. Journal of Physics and Chemistry of Solids, 2016, 98, 198-208.	1.9	8
24708	Maximum catalytic activity of Pt3M in Li-O2 batteries: M=group V transition metals. Nano Energy, 2016, 27, 1-7.	8.2	29
24709	In-situ TEM experiments and first-principles studies on the electrochemical and mechanical behaviors of Î±-MoO3 in Li-ion batteries. Nano Energy, 2016, 27, 95-102.	8.2	73

#	Article	IF	Citations
24710	Amorphous transitional metal borides as substitutes for Pt cocatalysts for photocatalytic water splitting. Nano Energy, 2016, 27, 103-113.	8.2	142
24711	Electronic structure and optical properties of boron suboxide B6O system: First-principles investigations. Solid State Communications, 2016, 244, 12-16.	0.9	10
24712	Structural and Electronic Properties of Interfaces in Graphene and Hexagonal Boron Nitride Lateral Heterostructures. Chemistry of Materials, 2016, 28, 5022-5028.	3.2	63
24713	X-ray Absorption Spectroscopic Quantification and Speciation Modeling of Sulfate Adsorption on Ferrihydrite Surfaces. Environmental Science & Technology, 2016, 50, 8067-8076.	4.6	96
24714	Turning a Nonreducible into a Reducible Oxide via Nanostructuring: Opposite Behavior of Bulk ZrO₂ and ZrO₂ Nanoparticles Toward H₂ Adsorption. Journal of Physical Chemistry C, 2016, 120, 15329-15337.	1.5	33
24715	Reactivity Enhancement and Fingerprints of Point Defects on a MoS₂ Monolayer Assessed by ab Initio Atomic Force Microscopy. Journal of Physical Chemistry C, 2016, 120, 17115-17126.	1.5	19
24716	Insight on the Interaction of Methanol-Selective Oxidation Intermediates with Au- or/and Pd-Containing Monometallic and Bimetallic Core@Shell Catalysts. Langmuir, 2016, 32, 7493-7502.	1.6	25
24717	Control of Electronic Structures and Phonon Dynamics in Quantum Dot Superlattices by Manipulation of Interior Nanospace. ACS Applied Materials & Interfaces, 2016, 8, 18321-18327.	4.0	8
24718	Unveil the Chemistry of Olivine FePO₄ as Magnesium Battery Cathode. ACS Applied Materials & Interfaces, 2016, 8, 18018-18026.	4.0	78
24719	Quantifying Uncertainty in Activity Volcano Relationships for Oxygen Reduction Reaction. ACS Catalysis, 2016, 6, 5251-5259.	5.5	70
24720	Hydrogen Doped Metal Oxide Semiconductors with Exceptional and Tunable Localized Surface Plasmon Resonances. Journal of the American Chemical Society, 2016, 138, 9316-9324.	6.6	201
24721	A multi-nuclear magnetic resonance and density functional theory investigation of epitaxially grown InGaP₂. Physical Chemistry Chemical Physics, 2016, 18, 21296-21304.	1.3	3
24722	A van der Waals density functional investigation of carboranethiol self-assembled monolayers on Au(111). Physical Chemistry Chemical Physics, 2016, 18, 12920-12927.	1.3	13
24723	Magnetism, structures and stabilities of cluster assembled TM@Si nanotubes (TM = Cr, Mn and Fe): a density functional study. Dalton Transactions, 2016, 45, 12432-12443.	1.6	18
24724	Acute mechano-electronic responses in twisted phosphorene nanoribbons. Nanoscale, 2016, 8, 14778-14784.	2.8	8
24725	Size induced modification of boron structural unit in YBO₃: systematic investigation by experimental and theoretical methods. RSC Advances, 2016, 6, 64065-64071.	1.7	7
24726	Insight into mechanism and selectivity of propane dehydrogenation over the Pd-doped Cu(111) surface. RSC Advances, 2016, 6, 65524-65532.	1.7	16
24727	Controlling armchair and zigzag edges in oxidative cutting of graphene. Journal of Materials Chemistry C, 2016, 4, 6539-6545.	2.7	8

#	Article	IF	Citations
24728	Effects of chemical substitution on the structural and optical properties of Î±-Ag_{2â^'2x}Ni_xWO₄ (0 â‰¤ x â‰¤ 0.08) solid solutions. Physical Chemistry Chemical Physics, 2016, 18, 21966-21975.	1.3	24
24729	Element-selective resonant state in M-doped SnTe (M = Ga, In, and Tl). Physical Chemistry Chemical Physics, 2016, 18, 20635-20639.	1.3	37
24730	Polymorphism and electronic structure of polyimine and its potential significance for prebiotic chemistry on Titan. Proceedings of the National Academy of Sciences of the United States of America, 2016, 113, 8121-8126.	3.3	35
24731	Precise control of Schottky barrier height in SrTiO₃/SrRuO₃heterojunctions using ultrathin interface polar layers. Journal Physics D: Applied Physics, 2016, 49, 255302.	1.3	5
24732	Vibrational and mechanical properties of single layer MXene structures: a first-principles investigation. Nanotechnology, 2016, 27, 335702.	1.3	226
24733	Stability of B₁₂(CN)₁₂^{2â^'}: Implications for Lithium and Magnesium Ion Batteries. Angewandte Chemie - International Edition, 2016, 55, 3704-3708.	7.2	72
24734	Skin Bond Electron Relaxation Dynamics of Germanium Manipulated by Interactions with H₂, O₂, H₂O, H₂O₂, HF, and Au. ChemPhysChem, 2016, 17, 310-316.	1.0	5
24735	Janus allâ€cisâ€1,2,3,4,5,6â€Hexafluorocyclohexane: A Molecular Motif for Aggregationâ€Induced Enhanced Polarization. ChemPhysChem, 2016, 17, 2373-2381.	1.0	29
24736	Templateâ€Based Engineering of Carbonâ€Doped Co₃O₄ Hollow Nanofibers as Anode Materials for Lithiumâ€Ion Batteries. Advanced Functional Materials, 2016, 26, 1428-1436.	7.8	404
24737	Enhancing Charge Separation in Metallic Photocatalysts: A Case Study of the Conducting Molybdenum Dioxide. Advanced Functional Materials, 2016, 26, 4445-4455.	7.8	154
24738	Understanding and Controlling the Work Function of Perovskite Oxides Using Density Functional Theory. Advanced Functional Materials, 2016, 26, 5471-5482.	7.8	127
24739	Ultrafast Discharge/Charge Rate and Robust Cycle Life for Highâ€Performance Energy Storage Using Ultrafine Nanocrystals on the Binderâ€Free Porous Graphene Foam. Advanced Functional Materials, 2016, 26, 5139-5148.	7.8	53
24740	Giant Rashbaâ€Type Spin Splitting in Ferroelectric GeTe(111). Advanced Materials, 2016, 28, 560-565.	11.1	155
24741	Highâ€Performance Phototransistor of Epitaxial PbS Nanoplateâ€Graphene Heterostructure with Edge Contact. Advanced Materials, 2016, 28, 6497-6503.	11.1	51
24742	Highâ€Temperature Neutron Diffraction, Raman Spectroscopy, and Firstâ€Principles Calculations of Ti₃SnC₂ and Ti₂SnC. Journal of the American Ceramic Society, 2016, 99, 2233-2242.	1.9	15
24743	Variation of Band Gap and Lattice Parameters of Î²â^'(Al_xGa_{1â^'x})₂O₃ Powder Produced by Solution Combustion Synthesis. Journal of the American Ceramic Society, 2016, 99, 2467-2473.	1.9	87
24744	Rock-salt structure lithium deuteride formation in liquid lithium with high-concentrations of deuterium: a first-principles molecular dynamics study. Nuclear Fusion, 2016, 56, 016020.	1.6	10
24745	First-principles investigation of ferroelectricity in LaBGeO5. Journal of Physics Condensed Matter, 2016, 28, 165901.	0.7	3

#	Article	IF	Citations
24746	Spin-exchange interaction between transition metals and metalloids in soft-ferromagnetic metallic glasses. Journal of Physics Condensed Matter, 2016, 28, 216003.	0.7	8
24747	Interplanar potential for tension-shear coupling at grain boundaries derived fromab initiocalculations. Modelling and Simulation in Materials Science and Engineering, 2016, 24, 015007.	0.8	5
24748	Tuning the band gap of silicene by functionalisation with naphthyl and anthracyl groups. Journal of Chemical Physics, 2016, 144, 114704.	1.2	6
24749	Transport properties of copper with excited electron subsystem. Journal of Physics: Conference Series, 2016, 774, 012103.	0.3	5
24750	Resistance switching behavior of atomic layer deposited SrTiO3 film through possible formation of Sr2Ti6O13 or Sr1Ti11O20 phases. Scientific Reports, 2016, 6, 20550.	1.6	17
24751	Positron annihilation spectroscopy of vacancy-related defects in CdTe:Cl and CdZnTe:Ge at different stoichiometry deviations. Scientific Reports, 2016, 6, 20641.	1.6	22
24752	Controlling microstructure, preferred orientation, and mechanical properties of Cr-Al-N by bombardment and alloying with Ta. Journal of Applied Physics, 2016, 119, .	1.1	20
24753	Predictions of point defect, surface, and interface properties in semiconductors using first-principles calculations. AIP Conference Proceedings, 2016, , .	0.3	1
24754	Mode-selective chemistry on metal surfaces: The dissociative chemisorption of CH4 on Pt(111). Journal of Chemical Physics, 2016, 144, 184709.	1.2	33
24755	Gate-tunable and thickness-dependent electronic and thermoelectric transport in few-layer MoS2. Journal of Applied Physics, 2016, 120, .	1.1	66
24756	DFT investigation on structure, electronic and magnetic properties of Crn (n=2-8) clusters. AIP Conference Proceedings, 2016, , .	0.3	1
24757	Gold deposited on a Ge(0â€‰0â€‰1) surface: DFT calculations. Journal of Physics Condensed Matter, 2016, 28, 435001.	0.7	0
24758	Modeling the melting of multicomponent systems: the case of MgSiO3 perovskite under lower mantle conditions. Scientific Reports, 2016, 6, 29830.	1.6	11
24759	Electromagnon dispersion probed by inelastic X-ray scattering in LiCrO2. Nature Communications, 2016, 7, 13547.	5.8	29
24760	Experimental and computational study of zero dimensional metallic behavior at the LaLuO3/SrTiO3 interface. Journal of Vacuum Science and Technology B:Nanotechnology and Microelectronics, 2016, 34, .	0.6	1
24761	Surface strain effects on the adsorption and the diffusion of Au atoms on MgO(001) surfaces. Journal of the Korean Physical Society, 2016, 69, 1776-1780.	0.3	5
24762	Magnetic Ordering in Sr3YCo4O10+x. Scientific Reports, 2016, 6, 19762.	1.6	9
24763	First-principles study of the structural and dynamic properties of the liquid and amorphous Liâ€“Si alloys. Journal of Chemical Physics, 2016, 144, 034502.	1.2	16

#	Article	IF	Citations
24764	Mechanical properties of bimetallic one-dimensional structures. Proceedings of SPIE, 2016, , .	0.8	0
24765	Modeling surface motion effects in N2 dissociation on W(110): Ab initio molecular dynamics calculations and generalized Langevin oscillator model. Journal of Chemical Physics, 2016, 144, 244708.	1.2	19
24766	Evaluation of Pt Alloys as Electrocatalysts for Oxalic Acid Oxidation: A Combined Experimental and Computational Study. Journal of the Electrochemical Society, 2016, 163, H787-H795.	1.3	4
24767	MoirÃ© superlattices at the topological insulator Bi2Te3. Scientific Reports, 2016, 6, 20278.	1.6	14
24768	Structural and electronic properties of UnOm (n=1-3,m=1-3n) clusters: A theoretical study using screened hybrid density functional theory. Journal of Chemical Physics, 2016, 144, 184304.	1.2	9
24769	Mechanism and modulation of terahertz generation from a semimetal - graphite. Scientific Reports, 2016, 6, 22798.	1.6	4
24770	Topological insulator behavior of WS2 monolayer with square-octagon ring structure. AIP Conference Proceedings, 2016, , .	0.3	1
24771	Newtype large Rashba splitting in quantum well states induced by spin chirality in metal/topological insulator heterostructures. NPG Asia Materials, 2016, 8, e332-e332.	3.8	6
24772	The enhancement of ferromagnetism in Ta-doped anatase TiO₂system by iron co-doping. Journal of Physics: Conference Series, 2016, 776, 012018.	0.3	5
24773	Modulation of electronic properties from stacking orders and spin-orbit coupling for 3R-type MoS2. Scientific Reports, 2016, 6, 24140.	1.6	23
24774	The incorporation site of Er in nanosized CaF2. Journal of Physics Condensed Matter, 2016, 28, 485301.	0.7	2
24775	High pressure and time resolved studies of optical properties of n-type doped GaN/AlN multi-quantum wells: Experimental and theoretical analysis. Journal of Applied Physics, 2016, 120, .	1.1	14
24776	Formation energies of intrinsic point defects in monoclinic VO2 studied by first-principles calculations. AIP Advances, 2016, 6, .	0.6	25
24777	Band Gap Insensitivity to Large Chemical Pressures in Ternary Bismuth Iodides for Photovoltaic Applications. Journal of Physical Chemistry C, 2016, 120, 28924-28932.	1.5	54
24778	Water adsorption on bimetallic PtRu/Pt(111) surface alloys. Proceedings of the Royal Society A: Mathematical, Physical and Engineering Sciences, 2016, 472, 20160618.	1.0	12
24779	Interface effects on the magnetic properties of layered Ni₂MnGa/Ni₂MnSn alloys: A first-principles investigation. Functional Materials Letters, 2016, 09, 1642010.	0.7	9
24780	Effects of Monoatomic Vacancies and Alloy Atoms on Hydrogen Diffusion at Al(111) Surfaces. Nippon Kinzoku Gakkaishi/Journal of the Japan Institute of Metals, 2016, 80, 570-574.	0.2	0
24781	Non-random walk diffusion enhances the sink strength of semicoherent interfaces. Nature Communications, 2016, 7, 10424.	5.8	81

#	Article	IF	Citations
24782	Low lattice thermal conductivity of stanene. Scientific Reports, 2016, 6, 20225.	1.6	161
24783	Polar Spinel-Perovskite Interfaces: an atomistic study of Fe3O4(111)/SrTiO3(111) structure and functionality. Scientific Reports, 2016, 6, 29724.	1.6	10
24784	Controlling Factors for the Formation of Guinier-Preston Zones in Al-Cu Alloys: An Atomistic Study. Nippon Kinzoku Gakkaishi/Journal of the Japan Institute of Metals, 2016, 80, 575-584.	0.2	8
24785	Fast hydrogen diffusion along the Î£7 grain boundary of Î±-Al2O3: A first-principles study. International Journal of Hydrogen Energy, 2016, 41, 22214-22220.	3.8	12
24786	The Enhancement of Surface Reactivity on CeO₂ (111) Mediated by Subsurface Oxygen Vacancies. Journal of Physical Chemistry C, 2016, 120, 27917-27924.	1.5	17
24787	In Situ Multitechnical Investigation into Capacity Fading of High-Voltage LiNi_{0.5}Co_{0.2}Mn_{0.3}O₂. ACS Applied Materials & Interfaces, 2016, 8, 35323-35335.	4.0	63
24788	Interplay of Chemical and Electronic Structure on the Single-Molecule Level in 2D Polymerization. ACS Nano, 2016, 10, 11511-11518.	7.3	35
24789	Designing high-performance layered thermoelectric materials through orbital engineering. Nature Communications, 2016, 7, 10892.	5.8	203
24790	Laser-induced phase separation of silicon carbide. Nature Communications, 2016, 7, 13562.	5.8	75
24791	Fluorinated benzalkylsilane molecular rectifiers. Scientific Reports, 2016, 6, 38092.	1.6	16
24792	Beyond the staple motif: a new order at the thiolateâ€“gold interface. Nanoscale, 2016, 8, 20103-20110.	2.8	32
24793	B₄CN₃and B₃CN₄monolayers as the promising candidates for metal-free spintronic materials. New Journal of Physics, 2016, 18, 093021.	1.2	27
24794	Site occupation, phase stability, crystal and electronic structures of the doped S phase (Al₂CuMg). International Journal of Modern Physics B, 2016, 30, 1650165.	1.0	4
24795	Electronic Structure and Magnetism of the Multiband New Superconductor CaRbFe₄As₄. Journal of the Physical Society of Japan, 2016, 85, 124714.	0.7	9
24796	Pseudodirect to Direct Compositional Crossover in Wurtzite GaP/In_xGa_{1â€“x}P Coreâ€“Shell Nanowires. Nano Letters, 2016, 16, 7930-7936.	4.5	19
24797	Magnetic Excitations and Electronic Interactions in <mml:math xmlns:mml="http://www.w3.org/1998/Math/MathML" display="inline"><mml:mrow><mml:msub><mml:mrow><mml:mi>Sr</mml:mi></mml:mrow><mml:mrow><mml:mn>2</mml:mn></mml:mrow></mml:msub><mml:mrow><mml:mi>Cu</mml:mi></mml:mrow><mml:msub><mml:mrow><mml:mi>O</mml:mi></mml:mrow><mml:mrow><mml:mn>3</mml:mn></mml:mrow></mml:msub></mml:mrow></mml:math> A Spin-<mml:math xmlns:mml="http://www.w3.org/1998/Math/MathML" display="inline"><mml:mrow><mml:mn>1</mml:mn><mml:mo>/</mml:mo><m. Physical Review Letters, 2016, 117, 237203.	2.9	36
24798	Resonant diffraction of synchrotron radiation: New possibilities. Crystallography Reports, 2016, 61, 768-778.	0.1	3
24799	Methylation of toluene with methanol over HZSM-5: A periodic density functional theory investigation. Chinese Journal of Catalysis, 2016, 37, 1882-1890.	6.9	18

#	Article	IF	Citations
24800	Quantum-chemical modeling of lithiation of a siliconâ€“silicon carbide composite. Russian Journal of Inorganic Chemistry, 2016, 61, 1423-1429.	0.3	4
24801	Nanoscale Charge-Balancing Mechanism in Alkali-Substituted Calciumâ€“Silicateâ€“Hydrate Gels. Journal of Physical Chemistry Letters, 2016, 7, 5266-5272.	2.1	47
24802	Temperature Dependence of the Energy Levels of Methylammonium Lead Iodide Perovskite from First-Principles. Journal of Physical Chemistry Letters, 2016, 7, 5247-5252.	2.1	100
24803	Magnetic effects in sulfur-decorated graphene. Scientific Reports, 2016, 6, 21460.	1.6	11
24804	Hexacoordinated nitrogen(V) stabilized by high pressure. Scientific Reports, 2016, 6, 36049.	1.6	10
24805	The atomic structures and electronic properties of potassium-doped phenanthrene from a first-principles study. Journal of Materials Chemistry C, 2016, 4, 11566-11571.	2.7	11
24806	Organometallic model complexes elucidate the active gallium species in alkane dehydrogenation catalysts based on ligand effects in Ga K-edge XANES. Catalysis Science and Technology, 2016, 6, 6339-6353.	2.1	90
24807	Edge effects on the characteristics of uranium diffusion on graphene and graphene nanoribbons. Chinese Physics B, 2016, 25, 086301.	0.7	1
24808	Diffusion in Ni-Based Single Crystal Superalloys with Density Functional Theory and Kinetic Monte Carlo Method. Communications in Computational Physics, 2016, 20, 603-618.	0.7	9
24809	Resonance Raman scattering and ab initio calculation of electron energy loss spectra of MoS 2 nanosheets. Physics Letters, Section A: General, Atomic and Solid State Physics, 2016, 380, 4057-4061.	0.9	3
24810	Searching for Highly Active Catalysts for Hydrogen Evolution Reaction Based on O-Terminated MXenes through a Simple Descriptor. Chemistry of Materials, 2016, 28, 9026-9032.	3.2	247
24811	Theoretical Investigation of Molecular and Electronic Structures of Buckminsterfullerene-Silicon Quantum Dot Systems. Journal of Physical Chemistry A, 2016, 120, 9767-9775.	1.1	2
24812	Energy Landscape and Crystal-to-Crystal Transition of Ternary Silicate Mg₂SiO₄. Journal of Physical Chemistry C, 2016, 120, 25110-25116.	1.5	7
24813	Synergistic Effects of Water and Oxygen Molecule Co-adsorption on (001) Surfaces of Tetragonal CH₃NH₃PbI₃: A First-Principles Study. Journal of Physical Chemistry C, 2016, 120, 28448-28455.	1.5	47
24814	Theoretical Study of the Structural, Energetic, and Electronic Properties of 55-Atom Metal Nanoclusters: A DFT Investigation within van der Waals Corrections, Spinâ€“Orbit Coupling, and PBE+U of 42 Metal Systems. Journal of Physical Chemistry C, 2016, 120, 28844-28856.	1.5	75
24815	Mapping the electrostatic force field of single molecules from high-resolution scanning probe images. Nature Communications, 2016, 7, 11560.	5.8	95
24816	Platinum single-atom and cluster catalysis of the hydrogen evolution reaction. Nature Communications, 2016, 7, 13638.	5.8	1,521
24817	Synthesis and DFT investigation of new bismuth-containing MAX phases. Scientific Reports, 2016, 6, 18829.	1.6	97

#	Article	IF	Citations
24818	High-pressure X-ray diffraction, Raman and computational studies of MgCl2 up to 1 Mbar: Extensive pressure stability of the Î²-MgCl2 layered structure. Scientific Reports, 2016, 6, 30631.	1.6	15
24819	Ultra-high electrochemical catalytic activity of MXenes. Scientific Reports, 2016, 6, 32531.	1.6	105
24820	Unraveling the Planar-Globular Transition in Gold Nanoclusters through Evolutionary Search. Scientific Reports, 2016, 6, 34974.	1.6	21
24821	Creating new layered structures at high pressures: SiS2. Scientific Reports, 2016, 6, 37694.	1.6	21
24822	A Density Functional Theory Study of a Calcium- Montmorillonite: A First Investigation for Medicine Application. Journal of Physics: Conference Series, 2016, 739, 012133.	0.3	3
24823	Structure of theAl13Co4(100) surface: Combination of surface x-ray diffraction andab initiocalculations. Physical Review B, 2016, 94, .	1.1	14
24824	Strain-induced quasi-one-dimensional rare-earth silicide structures on Si(111). Physical Review B, 2016, 94, .	1.1	9
24825	Pair potentials for warm dense matter and their application to x-ray Thomson scattering in aluminum and beryllium. Physical Review E, 2016, 94, 053211.	0.8	16
24826	Structural, electronic, sodium diffusion and elastic properties of Naâ€“P alloy anode for Na-ion batteries: Insight from first-principles calculations. Modern Physics Letters B, 2016, 30, 1650385.	1.0	5
24827	Metallic behavior of GaAs/BaTiO ₃ heterostructure. Europhysics Letters, 2016, 115, 16001.	0.7	4
24828	All The Catalytic Active Sites of MoS₂ for Hydrogen Evolution. Journal of the American Chemical Society, 2016, 138, 16632-16638.	6.6	664
24829	Metastable Layered Cobalt Chalcogenides from Topochemical Deintercalation. Journal of the American Chemical Society, 2016, 138, 16432-16442.	6.6	61
24830	Silicene nanomeshes: bandgap opening by bond symmetry breaking and uniaxial strain. Scientific Reports, 2016, 6, 20971.	1.6	16
24831	The thermal and electrical properties of the promising semiconductor MXene Hf2CO2. Scientific Reports, 2016, 6, 27971.	1.6	178
24832	Optimizing the Dopant and Carrier Concentration of Ca5Al2Sb6 for High Thermoelectric Efficiency. Scientific Reports, 2016, 6, 29550.	1.6	10
24833	Strain and electric-field tunable valley states in 2D van der Waals MoTe₂/WTe₂heterostructures. Journal of Physics Condensed Matter, 2016, 28, 505003.	0.7	13
24834	Structural, electronic, and magnetic properties of transition-metal atom adsorbed two-dimensional GaAs nanosheet. Chinese Physics B, 2016, 25, 097305.	0.7	3
24835	Electron and hole doping in the relativistic Mott insulator <mml:math xmlns:mml="http://www.w3.org/1998/Math/MathML"><mml:mrow><mml:msub><mml:mi mathvariant="bold">Sr</mml:mi><mml:mn mathvariant="bold">2</mml:mn></mml:msub><mml:msub><mml:mi mathvariant="bold">IrO</mml:mi><mml:mn mathvariant="bold">4</mml:mn></mml:msub></mml:mrow></mml:math> : A first-principles study using	1.1	27

#	Article	IF	Citations
24836	Integrating superconducting phase and topological crystalline quantum spin Hall effect in hafnium intercalated gallium film. Applied Physics Letters, 2016, 108, 253102.	1.5	4
24837	Two-dimensional topological nanomaterials and related Hall effects. , 2016, , .		0
24838	Quantum crystallographic charge density of urea. IUCrJ, 2016, 3, 237-246.	1.0	17
24839	Localised Ag+ vibrations at the origin of ultralow thermal conductivity in layered thermoelectric AgCrSe2. Scientific Reports, 2016, 6, 23415.	1.6	34
24840	Physics and Magnetism of Quaternary Heusler Alloys. Handbook of Magnetic Materials, 2016, , 1-66.	0.6	7
24841	Thermodynamics and kinetics of defects in Li2S. Applied Physics Letters, 2016, 108, .	1.5	15
24842	Perspective: Methods for large-scale density functional calculations on metallic systems. Journal of Chemical Physics, 2016, 145, 220901.	1.2	106
24843	Inherent instability by antibonding coupling in AgSbTe₂. Japanese Journal of Applied Physics, 2016, 55, 041801.	0.8	15
24844	Caesiumplatinidhydrid, 4â€‰Cs₂Ptâ‹…CsH: ein intermetallisches Doppelsalz mit Metallâ€Anionen. Angewandte Chemie, 2016, 128, 15059-15062.	1.6	0
24845	Ab-initio calculations on melting of thorium. AIP Conference Proceedings, 2016, , .	0.3	0
24846	Ab-initio study of thermal expansion in pure graphene. AIP Conference Proceedings, 2016, , .	0.3	2
24847	Strontium ruthenateâ€“anatase titanium dioxide heterojunctions from first-principles: Electronic structure, spin, and interface dipoles. Journal of Applied Physics, 2016, 120, 035302.	1.1	1
24848	First-principles studies of atomic dynamics in tetrahedrite thermoelectrics. APL Materials, 2016, 4, 104811.	2.2	13
24849	Stabilization of orthorhombic phase in single-crystal ZnSnN2 films. AIP Advances, 2016, 6, .	0.6	38
24850	Sn doped CdTe as candidate for intermediate-band solar cells: A first principles DFT+GW study. Journal of Physics: Conference Series, 2016, 720, 012033.	0.3	1
24851	Surface-hydrogen-induced metallization and rumpling in thin <mml:math xmlns:mml="http://www.w3.org/1998/Math/MathML"><mml:mrow><mml:mi>BaTi</mml:mi><mml:msub><mml:mi mathvariant="normal">O</mml:mi><mml:mn>3</mml:mn></mml:msub></mml:mrow></mml:math> films. Physical Review B, 2016, 94, .	1.1	3
24852	Two-dimensional silica: Structural, mechanical properties, and strain-induced band gap tuning. Journal of Applied Physics, 2016, 119, .	1.1	39
24853	Anisotropic electronic, mechanical, and optical properties of monolayer WTe2. Journal of Applied Physics, 2016, 119, .	1.1	76

#	Article	IF	Citations
24854	Manipulation of Optical Transmittance by Ordered-Oxygen-Vacancy in Epitaxial LaBaCo2O5.5+Î´ Thin Films. Scientific Reports, 2016, 6, 37496.	1.6	6
24855	Grain boundary and its hydrogenated effect in stanene. AIP Advances, 2016, 6, .	0.6	2
24856	Magnetism in alkali-metal-doped wurtzite semiconductor materials controlled by strain engineering. Journal of Applied Physics, 2016, 120, 125101.	1.1	2
24857	Pressure-induced structural transition of CdxZn1â^'xO alloys. Applied Physics Letters, 2016, 108, .	1.5	10
24858	On the structural and electronic properties of Ir-silicide nanowires on Si(001) surface. Journal of Applied Physics, 2016, 120, .	1.1	8
24859	Cartesian Decomposition of Infrared Spectra Reveals the Structure of Solution-Deposited, Self-Assembled Benzoate and Alkanoate Monolayers on Rutile (110). Journal of Physical Chemistry C, 2016, 120, 24866-24876.	1.5	4
24860	First-principle and experiment investigation of MoS2@SnO2 nano-heterogeneous structures with enhanced humidity sensing performance. Journal of Applied Physics, 2016, 119, .	1.1	13
24861	Stability, electronic structures and thermoelectric properties of binary Znâ€“Sb materials. Journal of Materials Chemistry C, 2016, 4, 11305-11312.	2.7	19
24862	Tunneling magnetoresistance and electroresistance in Fe/PbTiO3/Fe multiferroic tunnel junctions. Journal of Applied Physics, 2016, 120, 074102.	1.1	8
24863	Nonstoichiometry and Weyl fermionic behavior in TaAs. Physical Review B, 2016, 94, .	1.1	20
24864	Machine learning scheme for fast extraction of chemically interpretable interatomic potentials. AIP Advances, 2016, 6, .	0.6	49
24865	Topological Phase in Non-centrosymmetric Material NaSnBi. Chinese Physics Letters, 2016, 33, 127301.	1.3	11
24866	Interplay between strain, defect charge state, and functionality in complex oxides. Applied Physics Letters, 2016, 109, .	1.5	28
24867	Effects of interface oxygen vacancies on electronic bands of <mml:math xmlns:mml="http://www.w3.org/1998/Math/MathML"><mml:mrow><mml:mi>FeSe</mml:mi><mml:mo>/</mml:mo><mml:msub><m Physical Review B, 2016, 94, .	1.1	15
24868	Theoretical impurity-limited carrier mobility of monolayer black phosphorus. Applied Physics Letters, 2016, 108, .	1.5	14
24869	Surface enhanced single-molecule magnetism involving 4f spin. Applied Physics Letters, 2016, 108, 132407.	1.5	5
24870	Vibrational signatures in the THz spectrum of 1,3-DNB: A first-principles and experimental study. Europhysics Letters, 2016, 114, 37010.	0.7	1
24871	Perpendicular magnetic tunnel junction with a strained Mn-based nanolayer. Scientific Reports, 2016, 6, 30249.	1.6	48

#	Article	IF	Citations
24872	High applicability of two-dimensional phosphorous in Kagome lattice predicted from first-principles calculations. Scientific Reports, 2016, 6, 23151.	1.6	18
24873	Experimental and theoretical study of rotationally inelastic diffraction of H2(D2) from methyl-terminated Si(111). Journal of Chemical Physics, 2016, 145, 084705.	1.2	3
24874	A â€˜jump-to-coalescenceâ€™ mechanism during nanoparticle growth revealed byin situaberration-corrected transmission electron microscopy observations. Nanotechnology, 2016, 27, 205605.	1.3	24
24875	Anisotropy in layered half-metallic Heusler alloy superlattices. Journal of Applied Physics, 2016, 119, .	1.1	19
24876	Magnetic properties of bimetallic clusters composed of Gd and transition metals. Journal of Applied Physics, 2016, 119, 074301.	1.1	4
24877	A perfect wetting of Mg monolayer on Ag(111) under atomic scale investigation: First principles calculations, scanning tunneling microscopy, and Auger spectroscopy. Journal of Chemical Physics, 2016, 144, 194708.	1.2	1
24878	Pressure-induced phase transition of calcite and aragonite: A first principles study. Journal of Applied Physics, 2016, 120, 142118.	1.1	12
24879	Striking impact of Na insertion on structural and electronic properties of the electrode material Na2+xV6O16. Journal of Physics Condensed Matter, 2016, 28, 485501.	0.7	3
24880	Methane dissociation on Pt(111): Searching for a specific reaction parameter density functional. Journal of Chemical Physics, 2016, 144, 044702.	1.2	52
24881	Theoretical study on the top- and enclosed-contacted single-layer MoS2 piezotronic transistors. Applied Physics Letters, 2016, 108, 181603.	1.5	11
24882	Electronic properties of magnesium oxide - polyethylene interface. , 2016, , .		0
24883	Optical study of the band structure of wurtzite GaP nanowires. Journal of Applied Physics, 2016, 120, .	1.1	34
24884	Nitridation of GaN surface for power device application: A first-principles study. , 2016, , .		5
24885	Density functional theory simulations and experimental measurements of a-HfO<inf>2</inf>/a-Si<inf>3</inf>N<inf>4</inf>/SiGe, a-HfO<inf>2</inf>/SiO<inf>0.8</inf>N<inf>0.8</inf>/SiGe and a-HfO<inf>2</inf>/a-SiO/SiGe interfaces. , 2016, , .		0
24886	Complex optimization for big computational and experimental neutron datasets. Nanotechnology, 2016, 27, 484002.	1.3	3
24887	Predicting defect behavior in B2 intermetallics by merging ab initio modeling and machine learning. Npj Computational Materials, 2016, 2, .	3.5	90
24888	A fingerprint based metric for measuring similarities of crystalline structures. Journal of Chemical Physics, 2016, 144, 034203.	1.2	93
24889	Synthesis of heavy hydrocarbons at the core-mantle boundary. Scientific Reports, 2016, 5, 18382.	1.6	16

#	Article	IF	Citations
24890	H18 Carbon: A New Metallic Phase with sp2-sp3 Hybridized Bonding Network. Scientific Reports, 2016, 6, 21879.	1.6	57
24891	Isotope tracer investigation and ab-initio simulation of anisotropic hydrogen transport and possible multi-hydrogen centers in tin dioxide. Journal of Applied Physics, 2016, 119, 225704.	1.1	4
24892	Band gap anomaly and topological properties in lead chalcogenides. Chinese Physics B, 2016, 25, 037311.	0.7	8
24893	The modular approach enables a fullyab initiosimulation of the contacts between 3D and 2D materials. Journal of Physics Condensed Matter, 2016, 28, 395303.	0.7	6
24894	Effect of pressure on crystal structure and charge transport properties of 2,6-diphenylanthracene. Journal of Materials Research, 2016, 31, 3731-3744.	1.2	4
24895	Enhancement of piezoelectric constants induced by cation-substitution and two-dimensional strain effects on ZnO predicted by density functional perturbation theory. Journal of Applied Physics, 2016, 119, .	1.1	16
24896	Strain-controlled interfacial magnetization and orbital splitting in La2/3Sr1/3MnO3/tetragonal BiFeO3 heterostructures. Journal of Applied Physics, 2016, 120, 165303.	1.1	11
24897	Enhanced tunneling electroresistance in multiferroic tunnel junctions due to the reversible modulation of orbitals overlap. Applied Physics Letters, 2016, 109, .	1.5	11
24898	Lattice thermal expansion and anisotropic displacements in ?-sulfur from diffraction experiments and first-principles theory. Journal of Chemical Physics, 2016, 145, 234512.	1.2	19
24899	TCNQ Grown on Cu (001): Its Atomic and Electronic Structure Determination. Journal of Physical Chemistry C, 2016, 120, 26889-26898.	1.5	5
24900	Perspective: Role of structure prediction in materials discovery and design. APL Materials, 2016, 4, 053210.	2.2	114
24901	Strain-induced phase variation and dielectric constant enhancement of epitaxial Gd2O3. Journal of Applied Physics, 2016, 120, .	1.1	5
24902	Static electric field enhancement in nanoscale structures. Journal of Applied Physics, 2016, 120, .	1.1	19
24903	High-pressure structure and elastic properties of tantalum single crystal: First principles investigation. Chinese Physics B, 2016, 25, 126103.	0.7	9
24904	Influence of ambient gas pressure and carbon adsorption on dark current emission from a cathode. Journal of Vacuum Science and Technology B:Nanotechnology and Microelectronics, 2016, 34, .	0.6	4
24905	Mirror-symmetry protected non-TRIM surface state in the weak topological insulator Bi2TeI. Scientific Reports, 2016, 6, 20734.	1.6	27
24906	Chemical ordering in substituted fluorite oxides: a computational investigation of Ho2Zr2O7 and RE2Th2O7 (RE=Ho, Y, Gd, Nd, La). Scientific Reports, 2016, 6, 38772.	1.6	23
24907	Polymerization of defect states at dislocation cores in InAs. Journal of Applied Physics, 2016, 119, 045706.	1.1	8

#	Article	IF	Citations
24908	Ab initio study of electronic and magnetic properties in Ni-doped WS2 monolayer. AIP Advances, 2016, 6, .	0.6	22
24909	Strong piezoelectric response in stable TiZnN2, ZrZnN2, and HfZnN2 found by ab initio high-throughput approach. Journal of Applied Physics, 2016, 120, .	1.1	17
24910	Interaction of methanol and its dehydrogenation species with Pt-alloy surfaces. AIP Conference Proceedings, 2016, , .	0.3	1
24911	Ballistic thermal transport in monolayer transition-metal dichalcogenides: Role of atomic mass. Applied Physics Letters, 2016, 108, .	1.5	16
24912	Ab initio electronic structure of quasi-two-dimensional materials: A â€œnativeâ€•Gaussianâ€“plane wave approach. Journal of Chemical Physics, 2016, 144, 204122.	1.2	5
24913	Mechanism of oxidation protection of the Si(001) surface by sub-monolayer Sr template. Journal of Applied Physics, 2016, 120, .	1.1	17
24914	Diffusion mechanisms in Li0.5CoO2â€”A computational study. Applied Physics Letters, 2016, 108, 153902.	1.5	3
24915	Super-stretchable borophene. Europhysics Letters, 2016, 116, 36001.	0.7	22
24916	Early stage oxynitridation process of Si(001) surface by NO gas: Reactive molecular dynamics simulation study. Journal of Applied Physics, 2016, 119, .	1.1	6
24917	Theoretical insights into kesterite and stannite phases of Cu2(Sn1â€“XGeX)ZnSe4 based alloys: A prospective photovoltaic material. AIP Advances, 2016, 6, 125303.	0.6	5
24918	MÃ¶ssbauer parameters of Fe-related defects in group-IV semiconductors: First principles calculations. Journal of Applied Physics, 2016, 119, .	1.1	7
24919	Effective optical constants of silver nanofilms calculated in wide frequency range. Proceedings of SPIE, 2016, , .	0.8	1
24920	Quantum chemical modeling of nanostructured silicon Si n (n = 2â€”308). The snowball-type structures. Russian Chemical Bulletin, 2016, 65, 621-630.	0.4	5
24921	Pressure dependence of band-gap and phase transitions in bulk CuX (X = Cl, Br, I). AIP Conference Proceedings, 2016, , .	0.3	1
24922	Structure and optical properties of aSiAl and aSiAlHx magnetron sputtered thin films. APL Materials, 2016, 4, .	2.2	8
24923	Structural properties of Co2TiSi films on GaAs(001). Journal of Applied Physics, 2016, 120, .	1.1	1
24924	Anomalous domain periodicity observed in ferroelectric PbTiO3 nanodots having 180Â° stripe domains. Scientific Reports, 2016, 6, 26644.	1.6	10
24925	Mechanical properties of Liâ€“Sn alloys for Li-ion battery anodes: A first-principles perspective. AIP Advances, 2016, 6, .	0.6	23

#	Article	IF	Citations
24926	Experimental and theoretical investigation of Cr1-xScxN solid solutions for thermoelectrics. Journal of Applied Physics, 2016, 120, .	1.1	33
24927	Role of atomistic structure in the stochastic nature of conductivity in substoichiometric tantalum pentoxide. Journal of Applied Physics, 2016, 119, .	1.1	7
24928	Theoretical investigation of geometries, stabilities, electronic and optical properties for advanced Agn@(ZnO)42 (n=6-18) hetero-nanostructure. AIP Advances, 2016, 6, 075023.	0.6	1
24929	Unexpected Giant-Gap Quantum Spin Hall Insulator in Chemically Decorated Plumbene Monolayer. Scientific Reports, 2016, 6, 20152.	1.6	157
24930	CO adsorption on small Aun (n = 1â€“4) structures supported on hematite. II. Adsorption on the O-rich termination of Î±-Fe2O3(0001) surface. Journal of Chemical Physics, 2016, 144, 044705.	1.2	9
24931	Application of van der Waals functionals to the calculation of dissociative adsorption of N2 on W(110) for static and dynamic systems. Journal of Chemical Physics, 2016, 144, 084702.	1.2	12
24932	Research Update: The materials genome initiative: Data sharing and the impact of collaborative ab initio databases. APL Materials, 2016, 4, .	2.2	115
24933	Vibrational and elastic properties of As4O6 and As4O6Â·2He at high pressures: Study of dynamical and mechanical stability. Journal of Applied Physics, 2016, 120, .	1.1	8
24934	Standing and sitting adlayers in atomic layer deposition of ZnO. Journal of Vacuum Science and Technology A: Vacuum, Surfaces and Films, 2016, 34, .	0.9	20
24935	Mechanical and optical response of [100] lithium fluoride to multi-megabar dynamic pressures. Journal of Applied Physics, 2016, 120, 165901.	1.1	33
24936	A first principle study of the pressure dependent elastic properties of monazite LaPO4. AIP Conference Proceedings, 2016, , .	0.3	5
24937	Prediction of entropy stabilized incommensurate phases in the system MoS2â^'MoTe2. Journal of Applied Physics, 2016, 120, 155101.	1.1	4
24938	Features of structure and phase transitions in pure uranium and Uâ€“Mo alloys: atomistic simulation. Journal of Physics: Conference Series, 2016, 774, 012036.	0.3	2
24939	Vectorial mapping of noncollinear antiferromagnetic structure of semiconducting FeSe surface with spin-polarized scanning tunneling microscopy. Applied Physics Letters, 2016, 108, .	1.5	9
24940	Quantum molecular dynamics simulations of equation of state of warm dense ethane. Physics of Plasmas, 2016, 23, 092706.	0.7	0
24941	Orbital configuration in CaTiO3 films on NdGaO3. Applied Physics Letters, 2016, 109, .	1.5	7
24942	Configurations of nuclei in Au-catalyzed Si nanowire growth: a first-principles study. Proceedings of SPIE, 2016, , .	0.8	0
24943	Grain boundary stability and influence on ionic conductivity in a disordered perovskiteâ€”a first-principles investigation of lithium lanthanum titanate. MRS Communications, 2016, 6, 455-463.	0.8	11

#	Article	IF	Citations
24944	Crystallographic and optical properties and band structures of CuInSe₂, CuIn₃Se₅, and CuIn₅Se₈ phases in Cu-poor Cu₂Seâ€“In₂Se₃ pseudo-binary system. Japanese Journal of Applied Physics, 2016, 55, 04ES15.	0.8	59
24945	Tunable, broadband and high-efficiency Si/Ge hot luminescence with plasmonic nanocavity array. Journal of Applied Physics, 2016, 119, 223101.	1.1	0
24946	Synthesis of two-dimensional TlxBi1â^'x compounds and Archimedean encoding of their atomic structure. Scientific Reports, 2016, 6, 19446.	1.6	21
24947	First-principles determination of band-to-band electronic transition energies in cubic and hexagonal AlGaInN alloys. AIP Advances, 2016, 6, 085308.	0.6	4
24948	Structure and magnetism of new rare-earth-free intermetallic compounds: Fe3+xCo3â^'xTi2 (0 â‰¤ x â‰¤ 3). APL Materials, 2016, 4, .	2.2	8
24949	Domain overlap matrices from plane-wave-based methods of electronic structure calculation. Journal of Chemical Physics, 2016, 145, 154107.	1.2	20
24950	Origin of magnetic anisotropy in doped <mml:math xmlns:mml="http://www.w3.org/1998/Math/MathML"><mml:mrow><mml:msub><mml:mi mathvariant="bold">Ce</mml:mi><mml:mn>2</mml:mn></mml:msub><mml:msub><mml:mi mathvariant="bold">Co</mml:mi><mml:mn>17</mml:mn></mml:msub></mml:mrow></mml:math> alloys. Physical Review B, 2016, 94, .	1.1	15
24951	The moisture outgassing kinetics of a silica reinforced polydimethylsiloxane. Journal of Chemical Physics, 2016, 145, 114905.	1.2	8
24952	Theoretical Study of Carrier Mobility in Two-Dimensional Tetragonal Carbon Allotrope from Porous Graphene. Chinese Physics Letters, 2016, 33, 083101.	1.3	6
24953	First Principles Study of the Structure and Elastic Properties of Thorium Metal. MRS Advances, 2016, 1, 2447-2452.	0.5	0
24954	Understanding the Formation Mechanism of Two-Dimensional Atomic Islands on Crystal Surfaces by the Condensing Potential Model. Zeitschrift Fur Naturforschung - Section A Journal of Physical Sciences, 2016, 71, 321-324.	0.7	0
24955	CO adsorption on small Aun (n = 1â€“4) structures supported on hematite. I. Adsorption on iron terminated Î±-Fe2O3 (0001) surface. Journal of Chemical Physics, 2016, 144, 044704.	1.2	10
24956	Water adsorption on the LaMnO3 surface. Journal of Chemical Physics, 2016, 144, 064701.	1.2	5
24957	Exotic d magnetism in partial hydrogenated silicene. Applied Physics Letters, 2016, 108, .	1.5	19
24958	Structural and electronic properties of Fe(Al_xGa_{1â€“}_x)₃ system. Journal of Applied Physics, 2016, 120, 165102.	1.1	5
24959	Electrolyte decomposition on Li-metal surfaces from first-principles theory. Journal of Chemical Physics, 2016, 145, 204701.	1.2	30
24960	The effect of Al segregation on Schottky barrier height and effective work function in TiAl/TiN/HfO₂gate stacks. Journal Physics D: Applied Physics, 2016, 49, 275104.	1.3	3
24961	Surface- and strain-tuning of the optical dielectric function in epitaxially grown CaMnO3. Applied Physics Letters, 2016, 108, .	1.5	4

#	Article	IF	Citations
24962	Surface defect passivation of MoS2 by sulfur, selenium, and tellurium. Journal of Applied Physics, 2016, 119, .	1.1	15
24963	Multiporous carbon allotropes transformed from symmetry-matched carbon nanotubes. AIP Advances, 2016, 6, .	0.6	11
24964	The role of interstitial binding in radiation induced segregation in W-Re alloys. Journal of Applied Physics, 2016, 120, .	1.1	40
24965	Structural, thermodynamic, and transport properties of CH2 plasma in the two-temperature regime. Physics of Plasmas, 2016, 23, 102708.	0.7	5
24966	Atomic and electronic structure of CdTe/metal (Cu, Al, Pt) interfaces and their influence to the Schottky barrier. Journal of Applied Physics, 2016, 120, .	1.1	15
24967	Room-temperature dynamic correlation between methylammonium molecules in lead-iodine based perovskites: An ab initio molecular dynamics perspective. Physical Review B, 2016, 94, .	1.1	62
24968	Mesoscopic bar magnet based on Îµ-Fe2O3 hard ferrite. Scientific Reports, 2016, 6, 27212.	1.6	37
24969	Magnetic ordering and conduction mechanism of different electroactive regions in Lu2NiMnO6. Journal of Applied Physics, 2016, 120, .	1.1	18
24970	Two-Step Phase Transition in SnSe and the Origins of its High Power Factor from First Principles. Physical Review Letters, 2016, 117, 276601.	2.9	91
24971	Effects of line defects on spin-dependent electronic transport of zigzag MoS2 nanoribbons. AIP Advances, 2016, 6, 015015.	0.6	14
24972	Prediction of spin-dependent electronic structure in 3d-transition-metal doped antimonene. Applied Physics Letters, 2016, 109, .	1.5	49
24973	Observation of the anisotropic Dirac cone in the band dispersion of 112-structured iron-based superconductor Ca0.9La0.1FeAs2. Applied Physics Letters, 2016, 109, .	1.5	19
24974	Quantum spinâ€“quantum anomalous Hall effect with tunable edge states in Sb monolayer-based heterostructures. Physical Review B, 2016, 94, .	1.1	42
24975	Observation of Fermi arc and its connection with bulk states in the candidate type-II Weyl semimetal <mml:math xmlns:mml="http://www.w3.org/1998/Math/MathML"><mml:msub><mml:mi mathvariant="normal">WTe</mml:mi><mml:mn>2</mml:mn></mml:msub></mml:math>. Physical Review B, 2016, 94, .	1.1	182
24976	Synergistic Effects of Water and SO₂ on Degradation of MIL-125 in the Presence of Acid Gases. Journal of Physical Chemistry C, 2016, 120, 27230-27240.	1.5	79
24977	Temperature-driven topological quantum phase transitions in a phase-change material Ge2Sb2Te5. Scientific Reports, 2016, 6, 38799.	1.6	18
24978	The direct-to-indirect band gap crossover in two-dimensional van der Waals Indium Selenide crystals. Scientific Reports, 2016, 6, 39619.	1.6	150
24979	First-principles study of the electronic and optical properties of a new metallic MoAlB. Scientific Reports, 2016, 6, 39790.	1.6	68

#	Article	IF	Citations
24980	The LDA+U calculation of electronic band structure of GaAs. AIP Conference Proceedings, 2016, , .	0.3	2
24981	Tunable electronic properties of GeSe/phosphorene heterostructure from first-principles study. Applied Physics Letters, 2016, 109, .	1.5	87
24982	A computational ab initio study of surface diffusion of sulfur on the CdTe (111) surface. AIP Advances, 2016, 6, 085002.	0.6	1
24983	Elastic constants of polycrystals with generally anisotropic crystals. Journal of Applied Physics, 2016, 120, 165105.	1.1	78
24984	Theoretical and experimental investigation of defect formation / migration in Gd2Ti2O7: General rule of oxide-ion migration in A2B2O7 pyrochlore. AIP Advances, 2016, 6, .	0.6	21
24985	On the tautomerisation of porphycene on copper (111): Finding the subtle balance between van der Waals interactions and hybridisation. Journal of Chemical Physics, 2016, 145, 244701.	1.2	5
24986	Monoclinic high-pressure polymorph of AlOOH predicted from first principles. Physical Review B, 2016, 94, .	1.1	13
24987	First-principles study of the structural, elastic and electronic properties of Pt₃M alloys. Journal of Materials Research, 2016, 31, 2956-2963.	1.2	10
24988	Orientation Sensitivity of Oxygen Evolution Reaction on Hematite. Journal of Physical Chemistry C, 2016, 120, 28694-28700.	1.5	42
24989	Phonon anharmonicity, lifetimes, and thermal transport in <mml:math xmlns:mml="http://www.w3.org/1998/Math/MathML"><mml:mrow><mml:msub><mml:mi>CH</mml:mi><mml:mn>3</mml:mn></mml:msub></mml:mrow></mml:math> from many-body perturbation theory. Physical Review B, 2016, 94, .	1.1	131
24990	Spin-orbit driven Peierls transition and possible exotic superconductivity in<mml:math xmlns:mml="http://www.w3.org/1998/Math/MathML"><mml:mrow><mml:msub><mml:mi>CsW</mml:mi><mml:mn>2</mml:mn></mml:msub><mml:mi mathvariant="normal">O</mml:mi><mml:mn>6</mml:mn></mml:mrow></mml:math>. Physical Review B, 2016, 94, .	1.1	14
24991	Effect of Organic Cations on Hydrogen Oxidation Reaction of Carbon Supported Platinum. Journal of the Electrochemical Society, 2016, 163, F1503-F1509.	1.3	29
24992	A Database of the Structural and Electronic Properties of Prussian Blue, Prussian White, and Berlin Green Compounds through Density Functional Theory. Inorganic Chemistry, 2016, 55, 12851-12862.	1.9	92
24993	Ti₂CO₂ Nanotubes with Negative Strain Energies and Tunable Band Gaps Predicted from First-Principles Calculations. Journal of Physical Chemistry Letters, 2016, 7, 5280-5284.	2.1	37
24994	Enhancing Sodium Ion Battery Performance by Strongly Binding Nanostructured Sb₂S₃ on Sulfur-Doped Graphene Sheets. ACS Nano, 2016, 10, 10953-10959.	7.3	344
24995	Bond selectivity in electron-induced reaction due to directed recoil on an anisotropic substrate. Nature Communications, 2016, 7, 13690.	5.8	14
24996	Full-scale computation for all the thermoelectric property parameters of half-Heusler compounds. Scientific Reports, 2016, 6, 22778.	1.6	79
24997	Structural Phase Transition and Material Properties of Few-Layer Monochalcogenides. Physical Review Letters, 2016, 117, 246802.	2.9	101

#	Article	IF	Citations
24998	Magnetic characteristics of Auâ€“Mn nanowires. JETP Letters, 2016, 103, 593-597.	0.4	3
24999	Migration of lithium ions in a nonaqueous Nafion-based polymeric electrolyte: Quantum-chemical modeling. Russian Journal of Inorganic Chemistry, 2016, 61, 1545-1553.	0.3	10
25000	Core Level Shifts of Hydrogenated Pyridinic and Pyrrolic Nitrogen in the Nitrogen-Containing Graphene-Based Electrocatalysts: In-Plane vs Edge Defects. Journal of Physical Chemistry C, 2016, 120, 29225-29232.	1.5	123
25001	Polarization twist in perovskite ferrielectrics. Scientific Reports, 2016, 6, 32216.	1.6	26
25002	Strain-induced magnetism in ReS ₂ monolayer with defects. Chinese Physics B, 2016, 25, 117103.	0.7	6
25003	Coupling and competition between ferroelectricity, magnetism, strain, and oxygen vacancies in AMnO3 perovskites. MRS Communications, 2016, 6, 182-191.	0.8	62
25004	Ethanol Reaction on Co3O4(110) and Co(0001): A Microkinetic Model Analysis. Journal of Physical Chemistry C, 2016, 120, 28110-28124.	1.5	12
25005	Beyond Perturbation: Role of Vacancy-Induced Localized Phonon States in Thermal Transport of Monolayer MoS₂. Journal of Physical Chemistry C, 2016, 120, 29324-29331.	1.5	36
25006	Structural lubricity under ambient conditions. Nature Communications, 2016, 7, 12055.	5.8	93
25007	Nonmetallization and band inversion in beryllium dicarbide at high pressure. Scientific Reports, 2016, 6, 26398.	1.6	2
25008	Lattice structures and electronic properties of WZ-CuInS ₂ /WZ-CdS interface from first-principles calculations. Chinese Physics B, 2016, 25, 123101.	0.7	7
25009	Electrostatic Origin of Stabilization in MoS₂â€“Organic Nanocrystals. Journal of Physical Chemistry Letters, 2016, 7, 5162-5167.	2.1	14
25010	Atomic scale imaging of competing polar states in a Ruddlesdenâ€“Popper layered oxide. Nature Communications, 2016, 7, 12572.	5.8	26
25011	Electric-field-driven magnetization switching and nonlinear magnetoelasticity in Au/FeCo/MgO heterostructures. Scientific Reports, 2016, 6, 29815.	1.6	48
25012	Band Gap Engineering of Two-Dimensional Nitrogene. Scientific Reports, 2016, 6, 34177.	1.6	15
25013	Tinselenidene: a Two-dimensional Auxetic Material with Ultralow Lattice Thermal Conductivity and Ultrahigh Hole Mobility. Scientific Reports, 2016, 6, 19830.	1.6	155
25014	Electron beam-formed ferromagnetic defects on MoS2 surface along 1â€‰T phase transition. Scientific Reports, 2016, 6, 38730.	1.6	29
25015	Theoretical prediction of the band offsets at the ZnO/anatase TiO2 and GaN/ZnO heterojunctions using the self-consistent ab initio DFT/GGA-1/2 method. Journal of Chemical Physics, 2016, 144, 014704.	1.2	9

#	Article	IF	Citations
25016	A theoretical investigation of the structural and electronic properties of 55-atom nanoclusters: The examples of Yâ€“Tc and Pt. Journal of Chemical Physics, 2016, 144, 054310.	1.2	11
25017	Enhanced hydrogen storage by using lithium decoration on phosphorene. Journal of Applied Physics, 2016, 120, .	1.1	44
25018	Cluster-assembled cubic zirconia films with tunable and stable nanoscale morphology against thermal annealing. Journal of Applied Physics, 2016, 120, 055302.	1.1	56
25019	The dynamics of copper intercalated molybdenum ditelluride. Journal of Chemical Physics, 2016, 145, 194702.	1.2	8
25020	Negative magnetoresistance without well-defined chirality in the Weyl semimetal TaP. Nature Communications, 2016, 7, 11615.	5.8	429
25021	Atomic-level insights in optimizing reaction paths for hydroformylation reaction over Rh/CoO single-atom catalyst. Nature Communications, 2016, 7, 14036.	5.8	281
25022	Electrically controlled band gap and topological phase transition in two-dimensional multilayer germanane. Applied Physics Letters, 2016, 108, .	1.5	13
25023	Strain control of vibrational properties of few layer phosphorene. Journal of Applied Physics, 2016, 120, .	1.1	9
25024	Effects of intense optical phonon pumping on the structure and electronic properties of yttrium barium copper oxide. Physical Review B, 2016, 94, .	1.1	31
25025	Thickness characterization of atomically thin WSe2 on epitaxial graphene by low-energy electron reflectivity oscillations. Journal of Vacuum Science and Technology B:Nanotechnology and Microelectronics, 2016, 34, .	0.6	10
25026	Gallium vacancy complexes as a cause of Shockley-Read-Hall recombination in III-nitride light emitters. Applied Physics Letters, 2016, 108, .	1.5	91
25027	Tuning dissociation using isoelectronically doped graphene and hexagonal boron nitride: Water and other small molecules. Journal of Chemical Physics, 2016, 144, 154706.	1.2	20
25028	Effect of transition metal impurities on the strength of grain boundaries in vanadium. Journal of Applied Physics, 2016, 120, .	1.1	16
25029	A DFT+U study of the structural, electronic, magnetic, and mechanical properties of cubic and orthorhombic SmCoO3. Journal of Chemical Physics, 2016, 145, 224704.	1.2	15
25030	Atomic-Scale Visualization of Quasiparticle Interference on a Type-II Weyl Semimetal Surface. Physical Review Letters, 2016, 117, 266804.	2.9	56
25031	Gate-Controllable Magneto-optic Kerr Effect in Layered Collinear Antiferromagnets. Physical Review Letters, 2016, 117, 267203.	2.9	93
25032	First-principles study of roles of Cu and Cl in polycrystalline CdTe. Journal of Applied Physics, 2016, 119, .	1.1	44
25033	Magnetic and electronic properties of porphyrin-based molecular nanowires. AIP Advances, 2016, 6, 015216.	0.6	9

#	Article	IF	Citations
25034	Soft chemical synthesis of silicon nanosheets and their applications. Applied Physics Reviews, 2016, 3, .	5.5	38
25035	Band structure of germanium carbides for direct bandgap silicon photonics. Journal of Applied Physics, 2016, 120, .	1.1	25
25036	Electric field dependence of optical phonon frequencies in wurtzite GaN observed in GaN high electron mobility transistors. Journal of Applied Physics, 2016, 120, .	1.1	12
25037	Oxygen vacancy related distortions in rutile<mml:math xmlns:mml="http://www.w3.org/1998/Math/MathML"><mml:mrow><mml:mi>Ti</mml:mi><mml:msub><mml:mi mathvariant="normal">O</mml:mi><mml:mn>2</mml:mn></mml:msub></mml:mrow></mml:math>nanoparticles: A combined experimental and theoretical study. Physical Review B, 2016, 94, .	1.1	46
25038	Enhanced half-metallicity in orientationally misaligned graphene/hexagonal boron nitride lateral heterojunctions. Physical Review B, 2016, 94, .	1.1	17
25039	Lifshitz transition driven by spin fluctuations and spin-orbit renormalization inNaOsO3. Physical Review B, 2016, 94, .	1.1	34
25040	Electric field tuning of band offsets in transition metal dichalcogenides. Physical Review B, 2016, 94, .	1.1	24
25041	Electronic and optical properties of two-dimensional InSe from a DFT-parametrized tight-binding model. Physical Review B, 2016, 94, .	1.1	89
25042	The formation of H bubbles at small-angle tilt grain boundaries in W films. Physical Chemistry Chemical Physics, 2016, 18, 33103-33108.	1.3	6
25043	A DFT investigation of the adsorption of iodine compounds and water in H-, Na-, Ag-, and Cu- mordenite. Journal of Chemical Physics, 2016, 144, 244705.	1.2	61
25044	Elucidating dz2 orbital selective catalytic activity in brownmillerite Ca2Mn2O5. AIP Advances, 2016, 6, 095210.	0.6	6
25045	Band gap reduction in InNxSb1-x alloys: Optical absorption, k Â· P modeling, and density functional theory. Applied Physics Letters, 2016, 109, .	1.5	9
25046	Tunable electronic and magnetic properties of Cr2Mâ€²â€‰=â€‰Ti or V; Tâ€‰=â€‰O, OH or F). Applied Physics Letters, 2016, 109, .	1.5	81
25047	Visible-blind ultraviolet photodetector based on p-Cu2CdSnS4/n-ZnS heterojunction with a type-I band alignment. Journal of Applied Physics, 2016, 120, .	1.1	11
25048	Discharge, Relaxation, and Charge Model for the Lithium Trivanadate Electrode: Reactions, Phase Change, and Transport. Journal of the Electrochemical Society, 2016, 163, A2890-A2898.	1.3	17
25049	Insight into the effect of surface coverage and structure over different Co surfaces on the behaviors of H2 adsorption and activation. International Journal of Hydrogen Energy, 2016, 41, 23022-23032.	3.8	9
25050	A universal preconditioner for simulating condensed phase materials. Journal of Chemical Physics, 2016, 144, 164109.	1.2	46
25051	Monolayer borophene electrode for effective elimination of both the Schottky barrier and strong electric field effect. Applied Physics Letters, 2016, 109, .	1.5	26

#	Article	IF	Citations
25052	First-principles study of the optoelectronic properties and photovoltaic absorber layer efficiency of Cu-based chalcogenides. Journal of Applied Physics, 2016, 120, .	1.1	41
25053	A half-metallic half-Heusler alloy having the largest atomic-like magnetic moment at optimized lattice constant. AIP Advances, 2016, 6, .	0.6	13
25054	First-principles calculation of the elastic dipole tensor of a point defect: Application to hydrogen inÎ±-zirconium. Physical Review B, 2016, 94, .	1.1	24
25055	An efficient adaptive digital predistortion framework to achieve optimal linearization of power amplifier. , 2016, , .		2
25056	Magnetism and morphology in faceted B2-ordered FeRh nanoparticles. Europhysics Letters, 2016, 116, 27006.	0.7	8
25057	Raman signatures of inversion symmetry breaking and structural phase transition in type-II Weyl semimetal MoTe2. Nature Communications, 2016, 7, 13552.	5.8	118
25058	X-ray diffraction and density functional theory studies of R(Fe_{0.5}Co_{0.5})O₃ (R = Pr, Nd, Sm, Eu, Gd). Powder Diffraction, 2016, 31, 259-266.	0.4	5
25059	Strain-modulated ferromagnetism and band gap of Mn doped Bi2Se3. Scientific Reports, 2016, 6, 29161.	1.6	8
25060	Electrical and structural properties of In-implanted Si1âˆ’xGex alloys. Journal of Applied Physics, 2016, 119, .	1.1	2
25061	Ferroelectricity and tunneling electroresistance effect driven by asymmetric polar interfaces in all-oxide ferroelectric tunnel junctions. Applied Physics Letters, 2016, 108, .	1.5	61
25062	Ultralow lattice thermal conductivity in topological insulator TlBiSe2. Applied Physics Letters, 2016, 108, .	1.5	29
25063	Charge transport properties of graphene: Effects of Cu-based gate electrode. Journal of Applied Physics, 2016, 120, .	1.1	1
25064	Twinning in fcc lattice creates low-coordinated catalytically active sites in porous gold. Journal of Chemical Physics, 2016, 145, 084703.	1.2	16
25065	Dynamics of H2 dissociation on the close-packed (111) surface of the noblest metal: H2 + Au(111). Journal of Chemical Physics, 2016, 145, 144701.	1.2	22
25066	Effect of straining graphene on nanopore creation using Si cluster bombardment: A reactive atomistic investigation. Journal of Applied Physics, 2016, 120, .	1.1	15
25067	First-principles investigation on elastic and thermodynamic properties of Pnnm-CN under high pressure. AIP Advances, 2016, 6, 125040.	0.6	3
25068	Hybrid-density functional theory study on the band structures of tetradymite-Bi2Te3, Sb2Te3, Bi2Se3, and Sb2Se3 thermoelectric materials. Journal of the Korean Physical Society, 2016, 69, 1683-1687.	0.3	27
25069	The effect of absorbed hydrogen on the dissolution of steel. Heliyon, 2016, 2, e00209.	1.4	33

#	Article	IF	Citations
25070	Electronic Structure of Iron Porphyrin Adsorbed to the Pt(111) Surface. Journal of Physical Chemistry C, 2016, 120, 29173-29181.	1.5	13
25071	Experimental and Theoretical Studies on Oxidation of Cu-Au Alloy Surfaces: Effect of Bulk Au Concentration. Scientific Reports, 2016, 6, 31101.	1.6	33
25072	Heterostructures of phosphorene and transition metal dichalcogenides for excitonic solar cells: A first-principles study. Applied Physics Letters, 2016, 108, .	1.5	90
25073	Density functional study on the mechanism for the highly active palladium monolayer supported on titanium carbide for the oxygen reduction reaction. Journal of Chemical Physics, 2016, 144, 204703.	1.2	18
25074	Two-dimensional boron: Lightest catalyst for hydrogen and oxygen evolution reaction. Applied Physics Letters, 2016, 109, .	1.5	86
25075	Theoretical prediction of low-density hexagonal ZnO hollow structures. Journal of Applied Physics, 2016, 120, .	1.1	15
25076	Atomic displacement in the CrMnFeCoNi high-entropy alloy â€“ A scaling factor to predict solid solution strengthening. AIP Advances, 2016, 6, .	0.6	183
25077	Wide-band-gap wrinkled nanoribbon-like structures in a continuous metallic graphene sheet. Physical Review B, 2016, 94, .	1.1	7
25078	Ab initio simulations of phase stability and martensitic transitions in NiTi. Physical Review B, 2016, 94, .	1.1	40
25079	Unraveling the composition dependence of the martensitic transformation temperature: A first-principles study of Ti-Ta alloys. Physical Review B, 2016, 94, .	1.1	25
25080	Spin-orbit coupling and magnetic interactions in Si(111):{C,Si,Sn,Pb}. Physical Review B, 2016, 94, .	1.1	21
25081	Phonon transport properties of two-dimensional group-IV materials from ab initio calculations. Physical Review B, 2016, 94, .	1.1	164
25082	Mechanism for Solid-State Ion Exchange of Cu⁺ into Zeolites. Journal of Physical Chemistry C, 2016, 120, 29182-29189.	1.5	33
25083	Correlation of optical and structural properties of GaN/AlN multi-quantum wellsâ€”Ab initio and experimental study. Journal of Applied Physics, 2016, 119, 015703.	1.1	27
25084	Computational characterization of lightweight multilayer MXene Li-ion battery anodes. Applied Physics Letters, 2016, 108, .	1.5	79
25085	The electric field induced ferroelectric phase transition of AgNbO3. Journal of Applied Physics, 2016, 119, .	1.1	31
25086	Effects of Mg and Al doping on dislocation slips in GaN. Journal of Applied Physics, 2016, 119, .	1.1	11
25087	Optimum thickness of soft magnetic phase in FePt/FeCo permanent magnet superlattices with high energy product and large magnetic anisotropy energy. AIP Advances, 2016, 6, .	0.6	5

#	Article	IF	Citations
25088	A first-principles study on the mechanism of screening depolarizing field in two-dimensional BaTiO3 nanosheets. Journal of Applied Physics, 2016, 119, 104102.	1.1	1
25089	Intrinsic thermal conductivities and size effect of alloys of wurtzite AlN, GaN, and InN from first-principles. Journal of Applied Physics, 2016, 119, .	1.1	31
25090	Equiatomic quaternary Heusler alloys: A material perspective for spintronic applications. Applied Physics Reviews, 2016, 3, 031101.	5.5	242
25091	Calculations of oxide formation on low-index Cu surfaces. Journal of Chemical Physics, 2016, 145, 044711.	1.2	25
25092	Thermophysical properties of liquid Ni around the melting temperature from molecular dynamics simulation. Journal of Chemical Physics, 2016, 145, .	1.2	17
25093	Communication: Finite size correction in periodic coupled cluster theory calculations of solids. Journal of Chemical Physics, 2016, 145, 141102.	1.2	47
25094	Matildite versus schapbachite: First-principles investigation of the origin of photoactivity in<mml:math xmlns:mml="http://www.w3.org/1998/Math/MathML"><mml:mrow><mml:mi>AgBi</mml:mi><mml:msub><mml:mi mathvariant="normal">S</mml:mi><mml:mn>2</mml:mn></mml:msub></mml:mrow></mml:math>. Physical Review B, 2016, 94, .	1.1	39
25095	Quantum-chemical modeling of lithiationâ€“delithiation of infinite fibers [Si n C m] k (k = â^ž) for n = 12â€“16 and m = 8â€“19 and small silicon clusters. Russian Journal of Inorganic Chemistry, 2016, 61, 1677-1687.	0.3	6
25096	Heterogeneous Metal-Free Hydrogenation over Defect-Laden Hexagonal Boron Nitride. ACS Omega, 2016, 1, 1343-1354.	1.6	43
25097	Strain tunable magnetism in SnX2 (Xâ€‰=â€‰S, Se) monolayers by hole doping. Scientific Reports, 2016, 6, 39218.	1.6	36
25098	Triggering of spin-flipping-modulated exchange bias in FeCo nanoparticles by electronic excitation. Scientific Reports, 2016, 6, 39292.	1.6	7
25099	Tunable electronic and magnetism of SrTiO3/BiFeO3 (001) superlattice: For electrochemical applications. Applied Physics Letters, 2016, 108, 011602.	1.5	6
25100	Enhancement of thermoelectric properties by energy filtering: Theoretical potential and experimental reality in nanostructured ZnSb. Journal of Applied Physics, 2016, 119, .	1.1	31
25101	Cleaning graphene: A first quantum/classical molecular dynamics approach. Journal of Applied Physics, 2016, 119, 125309.	1.1	8
25102	Correlated structural and electronic phase transformations in transition metal chalcogenide under high pressure. Journal of Applied Physics, 2016, 119, .	1.1	5
25103	Electronic structure and thermoelectric properties of half-Heusler compounds with eight electron valence countâ€”KScX (Xâ€‰=â€‰C and Ge). Journal of Applied Physics, 2016, 119, .	1.1	31
25104	First-principles investigations on ionization and thermal conductivity of polystyrene for inertial confinement fusion applications. Physics of Plasmas, 2016, 23, .	0.7	40
25105	Influence of the â€œsecond gapâ€•on the transparency of transparent conducting oxides: An ab initio study. Applied Physics Letters, 2016, 108, .	1.5	19

#	Article	IF	Citations
25106	Enhanced hydrogen adsorption on Li-coated B12C6N6. Journal of Chemical Physics, 2016, 145, 164301.	1.2	25
25107	Perovskite-type oxyhydride with a two-dimensional electron system: First-principles prediction of KTiO2H. Applied Physics Letters, 2016, 109, .	1.5	3
25108	Domain-wall profiles in <mml:math xmlns:mml="http://www.w3.org/1998/Math/MathML"><mml:msub><mml:mrow><mml:mi>Co</mml:mi><mml:mo>/</mml:mo><mml:mi>Pt</mml:mi></mml:mrow><mml:m /Pt(111) ultrathin films: Influence of the Dzyaloshinskii-Moriya interaction. Physical Review B, 2016, 94, .	1.1	27
25109	Stability, electronic, and optical properties of wurtzite Cu2CdxZn1â^'xSnS4 alloys as photovoltaic materials: First-principles insight. Physical Review B, 2016, 94, .	1.1	9
25110	Revealing frustrated local moment model for pressurized hyperhoneycomb iridate: Paving the way toward a quantum spin liquid. Physical Review B, 2016, 94, .	1.1	28
25111	THE PROPERTIES OF HEAVY ELEMENTS IN GIANT PLANET ENVELOPES. Astrophysical Journal, 2016, 829, 14.	1.6	43
25112	Half-Metallic Ferromagnetism of Zn1-xMxO (M = Fe, Co) Thin Films: An ab-initio Study. Materials Today: Proceedings, 2016, 3, 4205-4208.	0.9	0
25113	Zr-Doped Mesoporous Ta₃N₅ Microspheres for Efficient Photocatalytic Water Oxidation. ACS Applied Materials & Interfaces, 2016, 8, 35407-35418.	4.0	57
25114	Interstitial oxygen as a source of p-type conductivity in hexagonal manganites. Nature Communications, 2016, 7, 13745.	5.8	61
25115	The origin of hyperferroelectricity in LiBO3 (Bâ€‰=â€‰V, Nb, Ta, Os). Scientific Reports, 2016, 6, 34085.	1.6	21
25116	Hubbard physics in the PAW GW approximation. Journal of Chemical Physics, 2016, 144, 244110.	1.2	2
25117	Quantum spin Hall phase in stanene-derived overlayers on passivated SiC substrates. Physical Review B, 2016, 94, .	1.1	18
25118	High-throughput computational design of cathode coatings for Li-ion batteries. Nature Communications, 2016, 7, 13779.	5.8	145
25119	Spin orientations of the spin-half Ir4+ ions in Sr3NiIrO6, Sr2IrO4, and Na2IrO3: Density functional, perturbation theory, and Madelung potential analyses. Journal of Chemical Physics, 2016, 144, 114706.	1.2	18
25120	Optical properties of group-3 metal hexaboride nanoparticles by first-principles calculations. Journal of Chemical Physics, 2016, 144, 234702.	1.2	18
25121	Band structure characterization of WS2 grown by chemical vapor deposition. Applied Physics Letters, 2016, 108, .	1.5	40
25122	Magnetism and magnetocrystalline anisotropy in single-layer PtSe2: Interplay between strain and vacancy. Journal of Applied Physics, 2016, 120, .	1.1	51
25123	The role of the cationic Pt sites in the adsorption properties of water and ethanol on the Pt4/Pt(111) and Pt4/CeO2(111) substrates: A density functional theory investigation. Journal of Chemical Physics, 2016, 145, 124709.	1.2	10

#	Article	IF	Citations
25124	Computational discovery and characterization of polymorphic two-dimensional IVâ€“V materials. Applied Physics Letters, 2016, 109, .	1.5	60
25125	Prospect for tunneling anisotropic magneto-resistance in ferrimagnets: Spin-orbit coupling effects in Mn3Ge and Mn3Ga. Applied Physics Letters, 2016, 109, .	1.5	9
25126	Raman scattering in the transition-metal dichalcogenides of <mml:math xmlns:mml="http://www.w3.org/1998/Math/MathML"><mml:mrow><mml:mn>1</mml:mn><mml:msup><mml:mi>T</mml:mi><mml:mo mathvariant="normal">e</mml:mi><mml:mn>2</mml:mn></mml:msub><mml:mo>,</mml:mo><mml:msub><mml:mi>T</mml:mi><mml:mi><mm mathvariant="normal">e</mml:mi><mml:mn>2</mml:mn><. Physical Review B, 2016, 94, .	1.1	66
25127	Error estimates for density-functional theory predictions of surface energy and work function. Physical Review B, 2016, 94, .	1.1	96
25128	Atomic-scale observation of structural and electronic orders in the layered compound Î±-RuCl3. Nature Communications, 2016, 7, 13774.	5.8	66
25129	Enhanced Absorption and Diffusion Properties of Lithium on B,N,VC-decorated Graphene. Scientific Reports, 2016, 6, 37911.	1.6	13
25130	Reduction mechanism of iron titanium based oxygen carriers with H₂for chemical looping applications â€“ a combined experimental and theoretical study. RSC Advances, 2016, 6, 106340-106346.	1.7	10
25131	Large-gap quantum spin Hall state in functionalized dumbbell stanene. Applied Physics Letters, 2016, 108, .	1.5	80
25132	Structural anisotropy results in strain-tunable electronic and optical properties in monolayer GeX and SnX (X = S, Se, Te). Journal of Chemical Physics, 2016, 144, 114708.	1.2	161
25133	Reactive Monte Carlo sampling with an ab initio potential. Journal of Chemical Physics, 2016, 144, 174109.	1.2	12
25134	Mechanism of electrochemical lithiation of a metal-organic framework without redox-active nodes. Journal of Chemical Physics, 2016, 144, 194702.	1.2	41
25135	Room temperature d0 ferromagnetism in ZnS nanocrystals. Journal of Applied Physics, 2016, 119, 223901.	1.1	18
25136	New structural and electronic properties of (TiO2)10. Journal of Chemical Physics, 2016, 144, 234312.	1.2	13
25137	Electronic structure and magnetism of Mn-doped GaSb for spintronic applications: A DFT study. Journal of Applied Physics, 2016, 120, .	1.1	33
25138	Topological states of nanoscale Bi2Se3 interfaced with AlN. Applied Physics Letters, 2016, 109, 131601.	1.5	5
25139	DFT simulations of inter-graphene-layer coupling with rotationally misaligned hBN tunnel barriers in graphene/hBN/graphene tunnel FETs. Journal of Applied Physics, 2016, 120, .	1.1	18
25140	Stable single-layer structure of group-V elements. Physical Review B, 2016, 94, .	1.1	108
25141	Electron-Beam Mapping of Vibrational Modes with Nanometer Spatial Resolution. Physical Review Letters, 2016, 117, 256101.	2.9	84

#	Article	IF	Citations
25142	Flux States and Topological Phases from Spontaneous Time-Reversal Symmetry Breaking in<mml:math xmlns:mml="http://www.w3.org/1998/Math/MathML" display="inline"><mml:mrow><mml:mi>CrSi</mml:mi><mml:mo stretchy="false">(</mml:mo><mml:mi>Ge</mml:mi><mml:mo) Tj ETQq0 0 0 rgBT /Overlock 10 Tf 50 732 Td (stretchy="false">)</mml:m Systems. Physical Review Letters, 2016, 117, 257201.	2.9	37
25143	Biaxially strained PtPb/Pt core/shell nanoplate boosts oxygen reduction catalysis. Science, 2016, 354, 1410-1414.	6.0	1,262
25144	A Crossover from High Stiffness to High Hardness: The Case of Osmium and Its Borides. Zeitschrift Fur Naturforschung - Section A Journal of Physical Sciences, 2016, 71, 831-836.	0.7	0
25145	The electronic, structural and magnetic properties of La1â"'1/3Sr1/3MnO3 film with oxygen vacancy: a first principles investigation. Scientific Reports, 2016, 6, 22422.	1.6	4
25146	High-Throughput Design of Two-Dimensional Electron Gas Systems Based on Polar/Nonpolar Perovskite Oxide Heterostructures. Scientific Reports, 2016, 6, 34667.	1.6	52
25147	Thermal equation of state of silicon carbide. Applied Physics Letters, 2016, 108, .	1.5	33
25148	Tuning conductivity and magnetism in isopolar oxide superlattices via compressive and tensile strain: A case study of SrVO3/SrMnO3 and SrCrO3/SrMnO3 heterostructure. Journal of Applied Physics, 2016, 119, .	1.1	5
25149	Tunable electronic structure of black phosphorus/blue phosphorus van der Waals p-n heterostructure. Applied Physics Letters, 2016, 108, .	1.5	109
25150	Effects of configurational disorder on the elastic properties of icosahedral boron-rich alloys based on B6O, B13C2, and B4C, and their mixing thermodynamics. Journal of Chemical Physics, 2016, 144, 134503.	1.2	18
25151	DFT-D2 simulations of water adsorption and dissociation on the low-index surfaces of mackinawite (FeS). Journal of Chemical Physics, 2016, 144, 174704.	1.2	33
25152	The impact of electron correlations on the energetics and stability of silicon nanoclusters. Journal of Chemical Physics, 2016, 145, 074313.	1.2	7
25153	Band alignments between SmTiO3, GdTiO3, and SrTiO3. Journal of Vacuum Science and Technology A: Vacuum, Surfaces and Films, 2016, 34, .	0.9	6
25154	Transfer processes in a metal with hot electrons excited by a laser pulse. JETP Letters, 2016, 104, 431-439.	0.4	23
25155	Room-temperature magnetic topological Weyl fermion and nodal line semimetal states in half-metallic Heusler Co2TiX (X=Si, Ge, or Sn). Scientific Reports, 2016, 6, 38839.	1.6	148
25156	High pressure structural, electronic, and optical properties of polymorphic InVO4 phases. Journal of Applied Physics, 2016, 119, 085702.	1.1	17
25157	Synthesis, crystal structure, and properties of a perovskite-related bismuth phase, (NH4)3Bi2I9. APL Materials, 2016, 4, .	2.2	106
25158	Preferred site occupation and magnetic properties of Ni-Fe-Ga-Co ferromagnetic shape memory alloys by first-principles calculations. AIP Advances, 2016, 6, 125007.	0.6	1
25159	Photo-induced athermal phase transitions of Hg X (X = S, Se, Te) by ab initio study. Chinese Physics B, 2016, 25, 076401.	0.7	0

#	Article	IF	Citations
25160	Synthesis and structure modeling of ZnS based quantum dots. Journal of Structural Chemistry, 2016, 57, 926-933.	0.3	3
25161	Plasmon-band subpeak and oxidation of solar-control LaB₆ nanoparticles. Journal of Materials Research, 2016, 31, 2780-2788.	1.2	8
25162	Robust Room-Temperature Quantum Spin Hall Effect in Methyl-functionalized InBi honeycomb film. Scientific Reports, 2016, 6, 23242.	1.6	25
25163	Direct-to-indirect bandgap transitions in âŸ¨110âŸ© silicon nanowires. Journal of Applied Physics, 2016, 119, .	1.1	18
25164	DFT+U study of ultrathin Î±-Fe2O3 nanoribbons from (110) and (104) surfaces. Journal of Applied Physics, 2016, 119, .	1.1	12
25165	Perspective: How good is DFT for water?. Journal of Chemical Physics, 2016, 144, 130901.	1.2	571
25166	Donor defects and small polarons on the TiO2(110) surface. Journal of Applied Physics, 2016, 119, .	1.1	51
25167	Inter-ribbon tunneling in graphene: An atomistic Bardeen approach. Journal of Applied Physics, 2016, 119, 214306.	1.1	9
25168	First-principles calculations of high-pressure phase transition of TiO2 during decompression: From baddeleyite-type TiO2 to Î±-PbO2-type TiO2. Journal of Applied Physics, 2016, 120, 142108.	1.1	5
25169	Mechanism of stabilization and magnetization of impurity-doped zigzag graphene nanoribbons. Journal of Applied Physics, 2016, 120, .	1.1	6
25170	Calcium Silicate Phases Explained by High-Temperature-Resistant Phosphate Probe Molecules. Langmuir, 2016, 32, 13577-13584.	1.6	13
25171	Stabilization of metastable phases in hafnia owing to surface energy effects. Applied Physics Letters, 2016, 108, .	1.5	108
25172	Quantum spin Hall insulator phase in monolayer WTe2 by uniaxial strain. AIP Advances, 2016, 6, .	0.6	31
25173	Interactions between Mn dopant and oxygen vacancy for insulation performance of BaTiO3. Journal of Applied Physics, 2016, 120, .	1.1	16
25174	Iron as a source of efficient Shockley-Read-Hall recombination in GaN. Applied Physics Letters, 2016, 109, .	1.5	64
25175	The impact of nitrogen content and vacancies on structure and mechanical properties of Moâ€“N thin films. Journal of Applied Physics, 2016, 120, .	1.1	55
25176	Effect of Î²-stabilizer elements on stacking faults energies and ductility of Î±-titanium using first-principles calculations. Journal of Applied Physics, 2016, 120, .	1.1	30
25177	Identification and properties of the non-cubic phases of Mg2Pb. AIP Advances, 2016, 6, 125108.	0.6	3

#	Article	IF	Citations
25178	Ab initio engineering of materials with stacked hexagonal tin frameworks. Scientific Reports, 2016, 6, 28369.	1.6	15
25179	Preferential site occupancy of alloying elements in TiAl-based phases. Journal of Applied Physics, 2016, 119, .	1.1	55
25180	A density functional theory study of the adsorption behaviour of CO2 on Cu2O surfaces. Journal of Chemical Physics, 2016, 145, 044709.	1.2	55
25181	High pressure structural, elastic and vibrational properties of green energetic oxidizer ammonium dinitramide. Journal of Chemical Physics, 2016, 145, .	1.2	18
25182	Strontium Cobalt Oxide Misfit Nanotubes. Chemistry of Materials, 2016, 28, 9150-9157.	3.2	9
25183	Identifying the Unique Properties of Î±-Bi₂Mo₃O₁₂ for the Activation of Propene. Journal of Physical Chemistry C, 2016, 120, 29233-29247.	1.5	9
25184	Thermally Stimulated Luminescence and First-Principle Study of Defect Configurations in the Perovskite-Type Hydrides LiMH₃:Eu²⁺ (M = Sr, Ba) and the Corresponding Deuterides. Journal of Physical Chemistry C, 2016, 120, 29414-29422.	1.5	19
25185	Penta-graphene: A Promising Anode Material as the Li/Na-Ion Battery with Both Extremely High Theoretical Capacity and Fast Charge/Discharge Rate. ACS Applied Materials & Interfaces, 2016, 8, 35342-35352.	4.0	174
25186	Suitable Fundamental Properties of Ta_{0.75}V_{0.25}ON Material for Visible-Light-Driven Photocatalysis: A DFT Study. ACS Omega, 2016, 1, 1041-1048.	1.6	14
25187	Site-selective local fluorination of graphene induced by focused ion beam irradiation. Scientific Reports, 2016, 6, 19719.	1.6	36
25188	Insights into enhanced visible-light photocatalytic activity of C₆₀ modified g-C₃N₄ hybrids: the role of nitrogen. Physical Chemistry Chemical Physics, 2016, 18, 33094-33102.	1.3	31
25189	First-principles calculations of Na and K impurities in CuInSe<inf>2</inf> and their effect on Cd incorporation. , 2016, , .		2
25190	Adsorption of Dimethyl Methylphosphonate on MoO₃: The Role of Oxygen Vacancies. Journal of Physical Chemistry C, 2016, 120, 29077-29088.	1.5	66
25191	Catalytic Mechanisms of Methanol Oxidation to Methyl Formate on Vanadiaâ€“Titania and Vanadiaâ€“Titaniaâ€“Sulfate Catalysts. Journal of Physical Chemistry C, 2016, 120, 29290-29301.	1.5	20
25192	Establishing and Understanding Adsorptionâ€“Energy Scaling Relations with Negative Slopes. Journal of Physical Chemistry Letters, 2016, 7, 5302-5306.	2.1	43
25193	Integrated Experimental and Theoretical Study of Shape-Controlled Catalytic Oxidative Coupling of Aromatic Amines over CuO Nanostructures. ACS Omega, 2016, 1, 1121-1138.	1.6	39
25194	Coexistence of multiple metastable polytypes in rhombohedral bismuth. Scientific Reports, 2016, 6, 20337.	1.6	16
25195	Structural and electronic features of binary Li2S-P2S5 glasses. Scientific Reports, 2016, 6, 21302.	1.6	100

#	Article	IF	Citations
25196	Optic phonons and anisotropic thermal conductivity in hexagonal Ge2Sb2Te5. Scientific Reports, 2016, 6, 37076.	1.6	44
25197	Exploring the coordination change of vanadium and structure transformation of metavanadate MgV2O6 under high pressure. Scientific Reports, 2016, 6, 38566.	1.6	25
25198	Direct evidence of interaction-induced Dirac cones in a monolayer silicene/Ag(111) system. Proceedings of the National Academy of Sciences of the United States of America, 2016, 113, 14656-14661.	3.3	76
25199	Phase transition of solid bismuth under high pressure. Chinese Physics B, 2016, 25, 108103.	0.7	10
25200	Native Point Defects in GaN: A Hybrid-Functional Study. Physical Review Applied, 2016, 6, .	1.5	57
25201	Pressure-induced phase transitions in the <mml:math xmlns:mml="http://www.w3.org/1998/Math/MathML"><mml:mrow><mml:mi>CdC</mml:mi><mml:msub><mml:mi mathvariant="normal">r</mml:mi><mml:mn>2</mml:mn></mml:msub><mml:mi mathvariant="normal">S</mml:mi><mml:msub><mml:mi mathvariant="normal">e</mml:mi><mml:mn>4</mml:mn></mml:msub></mml:mrow></mml:math> spinel.	1.1	16
25202	Raman spectroscopy of rare-earth orthoferrites <mml:math xmlns:mml="http://www.w3.org/1998/Math/MathML"><mml:mrow><mml:mi>R</mml:mi><mml:msub><mml:mi>FeO</mml:mi><mml:mn> (<mml:math xmlns:mml="http://www.w3.org/1998/Math/MathML"><mml:mi>R</mml:mi></mml:math>) Tj ETQq0 0 0 rgBT /Overlock 1	1.1	159
25203	Quantum anomalous Hall effect in stanene on a nonmagnetic substrate. Physical Review B, 2016, 94, .	1.1	31
25204	Evolution of electronic structure of few-layer phosphorene from angle-resolved photoemission spectroscopy of black phosphorous. Physical Review B, 2016, 94, .	1.1	44
25205	Ab initio study of oxygen vacancy effects on electronic and optical properties of NiO. MRS Advances, 2016, 1, 2617-2622.	0.5	9
25207	Energy band gap and spectroscopic studies in Mn1â^'xCuxWO4 (0 â‰¤ x â‰¤ 0.125). AIP Conference Proceedings, 2016, , .	0.3	0
25208	Theoretical modeling and experimental observations of the atomic layer deposition of SrO using a cyclopentadienyl Sr precursor. Journal of Chemical Physics, 2016, 145, 064701.	1.2	3
25209	Photoconductivities from band states and a dissipative electron dynamics: Si(111) without and with adsorbed Ag clusters. Journal of Chemical Physics, 2016, 144, 024107.	1.2	6
25210	Adsorption of oxygen on low-index surfaces of the TiAl3 alloy. Journal of Experimental and Theoretical Physics, 2016, 123, 991-1007.	0.2	13
25211	Enabling direct silicene integration in electronics: First principles study of silicene on NiSi2(111). Applied Physics Letters, 2016, 109, .	1.5	6
25212	Effect of metal-to-metal interface states on the electric-field modified magnetic anisotropy in MgO/Fe/non-magnetic metal. Journal of Applied Physics, 2016, 119, 133905.	1.1	9
25213	Investigating the effects of phosphorus in a binary-phase TiAl-Ti3Al alloy by first-principles: from site preference, interfacial energetics to mechanical properties. European Physical Journal B, 2016, 89, 1.	0.6	2
25214	Electronic Structure of Oxide Interfaces: A Comparative Analysis of GdTiO3/SrTiO3 and LaAlO3/SrTiO3 Interfaces. Scientific Reports, 2016, 5, 18647.	1.6	18

#	Article	IF	Citations
25215	Exploring the free energy surface using ab initio molecular dynamics. Journal of Chemical Physics, 2016, 144, 164101.	1.2	12
25216	Softening of phonon spectra in metallic glasses. Npj Computational Materials, 2016, 2, .	3.5	7
25217	Iterative diagonalization of the non-Hermitian transcorrelated Hamiltonian using a plane-wave basis set: Application to sp-electron systems with deep core states. Journal of Chemical Physics, 2016, 144, 104109.	1.2	13
25218	Strain-induced water dissociation on supported ultrathin oxide films. Scientific Reports, 2016, 6, 22853.	1.6	19
25219	Diffraction at GaAs/Fe3Si core/shell nanowires: The formation of nanofacets. AIP Advances, 2016, 6, .	0.6	2
25220	Theoretical investigation of the electronic and structural properties of AlN thin films. Russian Microelectronics, 2016, 45, 600-602.	0.1	1
25221	A co-crystal between benzene and ethane: a potential evaporite material for Saturn's moon Titan. IUCrJ, 2016, 3, 192-199.	1.0	26
25222	Anisotropy induced Kondo splitting in a mechanically stretched molecular junction: A first-principles based study. Journal of Chemical Physics, 2016, 144, 034101.	1.2	27
25223	First principles calculation of thermal expansion coefficients of pure and Cr doped Î±-alumina crystals. Journal of Applied Physics, 2016, 120, .	1.1	12
25224	Subsurface hydrogen bonds at the polar Zn-terminated ZnO(0001) surface. Physical Review B, 2016, 94, .	1.1	19
25225	Structures and magnetic properties of Ni n (n = 36-40) clusters from first-principles calculations. Journal of Structural Chemistry, 2016, 57, 868-874.	0.3	2
25226	Atomic-resolved depth profile of strain and cation intermixing around LaAlO3/SrTiO3 interfaces. Scientific Reports, 2016, 6, 28118.	1.6	26
25227	Spin-polarized, orbital-selected hole gas at the EuO/Pt interface. Journal of Applied Physics, 2016, 119, .	1.1	6
25228	Chebyshev polynomial filtered subspace iteration in the discontinuous Galerkin method for large-scale electronic structure calculations. Journal of Chemical Physics, 2016, 145, 154101.	1.2	28
25229	The effect of tantalum (Ta) doping on mechanical properties of tungsten (W): A first-principles study. Journal of Materials Research, 2016, 31, 3401-3408.	1.2	34
25230	Decoupled electron and phonon transports in hexagonal boron nitride-silicene bilayer heterostructure. Journal of Applied Physics, 2016, 119, .	1.1	29
25231	Optical spectroscopy and band gap analysis of hybrid improper ferroelectric Ca3Ti2O7. Applied Physics Letters, 2016, 108, .	1.5	25
25232	Two-way actuation of graphene oxide arising from quantum mechanical effects. Applied Physics Letters, 2016, 109, 143902.	1.5	4

#	Article	IF	Citations
25233	The nature of hydrogen-bonding interaction in the prototypic hybrid halide perovskite, tetragonal CH3NH3PbI3. Scientific Reports, 2016, 6, 21687.	1.6	123
25234	Three-Dimensional Carbon Allotropes Comprising Phenyl Rings and Acetylenic Chains in sp+sp2 Hybrid Networks. Scientific Reports, 2016, 6, 24665.	1.6	29
25235	Magnetism in transition metal-substituted germanane: A search for room temperature spintronic devices. Journal of Applied Physics, 2016, 119, .	1.1	46
25236	Availability of surface boron species in improved oxygen reduction activity of Pt catalysts: A first-principles study. Journal of Chemical Physics, 2016, 144, 144706.	1.2	7
25237	Synthesis of Functional Ionic Liquids and their Application for the Direct Saccharification of Cellulose. Journal of Chemical Engineering of Japan, 2016, 49, 466-474.	0.3	6
25238	Towards Translational Invariance of Total Energy with Finite Element Methods for Kohn-Sham Equation. Communications in Computational Physics, 2016, 19, 1-23.	0.7	3
25239	Study of optimization options for second generation solar cell materials by multilevel modeling. Modern Electronic Materials, 2016, 2, 66-69.	0.2	2
25240	Evaluating structure selection in the hydrothermal growth of FeS2 pyrite and marcasite. Nature Communications, 2016, 7, 13799.	5.8	67
25241	On the mean kinetic energy of the proton in strong hydrogen bonded systems. Journal of Chemical Physics, 2016, 144, 054302.	1.2	11
25242	Determination of the electronic, dielectric, and optical properties of sillenite Bi12TiO20 and perovskite-like Bi4Ti3O12 materials from hybrid first-principle calculations. Journal of Chemical Physics, 2016, 144, 134702.	1.2	45
25243	Effects of interfacial alignments on the stability of graphene on Ru(0001) substrate. Applied Physics Letters, 2016, 108, .	1.5	15
25244	Effect of intermixing at CdS/CdTe interface on defect properties. Applied Physics Letters, 2016, 109, 042105.	1.5	9
25245	First-principles predictions of electronic properties of GaAs1-x-yPyBix and GaAs1-x-yPyBix-based heterojunctions. Applied Physics Letters, 2016, 109, .	1.5	7
25246	Possible n/p-type conductivity of two-dimensional graphene oxide by boron and nitrogen doping: Evaluated via constrained excitation. Applied Physics Letters, 2016, 109, 203113.	1.5	5
25247	Persistence of polar distortion with electron doping in lone-pair driven ferroelectrics. Physical Review B, 2016, 94, .	1.1	50
25248	Gate-independent energy gap in noncovalently intercalated bilayer graphene on SiC(0001). Physical Review B, 2016, 94, .	1.1	4
25249	Tunable C2N Membrane for High Efficient Water Desalination. Scientific Reports, 2016, 6, 29218.	1.6	67
25250	Magnetic coupling in a hybrid Mn(<scp>ii</scp>) acetylene dicarboxylate. Physical Chemistry Chemical Physics, 2016, 18, 33329-33334.	1.3	4

#	Article	IF	Citations
25251	A search for manifestation of two types of collective excitations in dynamic structure of a liquid metal: Ab initio study of collective excitations in liquid Na. Journal of Chemical Physics, 2016, 144, 194501.	1.2	20
25252	Metastable phase transformation and hcp- Ï‰ transformation pathways in Ti and Zr under high hydrostatic pressures. Applied Physics Letters, 2016, 109, .	1.5	16
25253	Magnetism and electronic phase transitions in monoclinic transition metal dichalcogenides with transition metal atoms embedded. Journal of Applied Physics, 2016, 120, 064305.	1.1	10
25254	Charge compensation and electrostatic transferability in three entropy-stabilized oxides: Results from density functional theory calculations. Journal of Applied Physics, 2016, 120, .	1.1	100
25255	Safe and simple detection of sparse hydrogen by Pd-Au alloy/air based 1D photonic crystal sensor. Journal of Applied Physics, 2016, 120, 173102.	1.1	3
25256	Temperature effect on the structural stabilities and electronic properties of X22H28 (X=C, Si and Ge) nanocrystals: A first-principles study. AIP Advances, 2016, 6, 125112.	0.6	0
25257	Pressure effect on the spin-dependent electronic structure of Au intercalated h-BN/graphene/h-BN. Journal of Physics Condensed Matter, 2016, 28, 505004.	0.7	1
25258	Atomistic Modelling of Interfaces in Cold Welded Joints. Procedia CIRP, 2016, 54, 197-203.	1.0	0
25259	Experimental and first-principles studies on the elastic properties of Î±-hafnium metal under pressure. Journal of Applied Physics, 2016, 119, .	1.1	14
25260	A class of monolayer metal halogenides MX2: Electronic structures and band alignments. Applied Physics Letters, 2016, 108, .	1.5	49
25261	A first-principles study of the SnO2 monolayer with hexagonal structure. Journal of Chemical Physics, 2016, 145, 174702.	1.2	34
25262	Solute segregation and deviation from bulk thermodynamics at nanoscale crystalline defects. Science Advances, 2016, 2, e1601796.	4.7	56
25263	Comparative Computational Study of NP(V) and U(VI) Adsorption on (110) Edge Surfaces of Montmorillonite. Clays and Clay Minerals, 2016, 64, 438-451.	0.6	5
25264	Self-assembly of Carbon Vacancies in Sub-stoichiometric ZrC1â^'x. Scientific Reports, 2016, 5, 18098.	1.6	44
25265	A new type of vanadium carbide V5C3 and its hardening by tuning Fermi energy. Scientific Reports, 2016, 6, 21794.	1.6	22
25266	Suppress carrier recombination by introducing defects: The case of Si solar cell. Applied Physics Letters, 2016, 108, .	1.5	23
25267	Structure family and polymorphous phase transition in the compounds with soft sublattice: Cu2Se as an example. Journal of Chemical Physics, 2016, 144, 194502.	1.2	35
25268	Ab initio prediction of stable nanotwin double layers and 4O structure in <mml:math xmlns:mml="http://www.w3.org/1998/Math/MathML"><mml:mrow><mml:msub><mml:mi>Ni</mml:mi><mml:mn>12</mml:mn></mml:msub></mml:mrow></mml:math> Physical Review B, 2016, 94, .	1.1	28

#	Article	IF	Citations
25269	Large magnetic anisotropy predicted for rare-earth-free <mml:math xmlns:mml="http://www.w3.org/1998/Math/MathML"><mml:mrow><mml:mi mathvariant="normal">F</mml:mi><mml:msub><mml:mi mathvariant="normal">e</mml:mi><mml:mrow><mml:mn>16</mml:mn><mml:mo>â^'</mml:mo><mml:mi>x</mml:mi></mml:mrow><mml:mi mathvariant="normal">C</mml:mi><mml:msub><mml:mi mathvariant="normal">o</mml:mi><mml:mi>x</mml:mi></mml:msub><mml:msub><mml:mi mathvariant=	1.1	46
25270	Atomic and electronic structure of Lomer dislocations at CdTe bicrystal interface. Scientific Reports, 2016, 6, 27009.	1.6	35
25271	Predictions of thermal expansion coefficients of rare-earth zirconate pyrochlores: A quasi-harmonic approximation based on stable phonon modes. Journal of Applied Physics, 2016, 119, .	1.1	7
25272	Lattice dynamics, electronic structure, and optical properties of LiBeSb: A hexagonal ABC-type hyperferroelectrics. Journal of Applied Physics, 2016, 120, .	1.1	4
25273	Communication: Many-body stabilization of non-covalent interactions: Structure, stability, and mechanics of Ag3Co(CN)6 framework. Journal of Chemical Physics, 2016, 145, 241101.	1.2	11
25274	First principles calculations of point defect diffusion in CdS buffer layers: Implications for Cu(In,Ga)(Se,S)2 and Cu2ZnSn(Se,S)4-based thin-film photovoltaics. Journal of Applied Physics, 2016, 119, .	1.1	19
25275	Ferroelectricity and tunneling electroresistance effect in asymmetric ferroelectric tunnel junctions. Journal of Applied Physics, 2016, 119, 224104.	1.1	31
25276	Point defects stabilise cubic Mo-N and Ta-N. Journal Physics D: Applied Physics, 2016, 49, 375303.	1.3	64
25277	A polymer dataset for accelerated property prediction and design. Scientific Data, 2016, 3, 160012.	2.4	139
25278	Electronic hybridisation implications for the damage-tolerance of thin film metallic glasses. Scientific Reports, 2016, 6, 36556.	1.6	26
25279	Interactions between carbon species and Î²-spodumene by first principles calculation. RSC Advances, 2016, 6, 70284-70291.	1.7	0
25280	Density-functional theory molecular dynamics simulations of a-HfO2/Ge(100)(2 Ã— 1) and a-ZrO2/Ge(100)(2 Ã— 1) interface passivation. Journal of Chemical Physics, 2016, 144, 084704.	1.2	6
25281	Silicon-based chalcogenide: Unexpected quantum spin Hall insulator with sizable band gap. Applied Physics Letters, 2016, 109, 182109.	1.5	68
25282	Lattice dynamics and thermal conductivity of calcium fluoride via first-principles investigation. Journal of Applied Physics, 2016, 119, .	1.1	16
25283	Cohesive energy and structural parameters of binary oxides of groups IIA and IIIB from diffusion quantum Monte Carlo. Journal of Chemical Physics, 2016, 144, 174707.	1.2	36
25284	Two-dimensional electron gas in GaAs/SrHfO3 heterostructure. Journal of Applied Physics, 2016, 119, 235304.	1.1	6
25285	Effects of domain size on x-ray absorption spectra of boron nitride doped graphenes. Applied Physics Letters, 2016, 109, .	1.5	9
25286	Origin of Fast Ion Conduction in Li₁₀GeP₂S₁₂, a Superionic Conductor. Journal of Physical Chemistry C, 2016, 120, 29002-29010.	1.5	24

#	Article	IF	Citations
25287	Krypton oxides under pressure. Scientific Reports, 2016, 6, 18938.	1.6	15
25288	First-principle investigation on perovskite La _{1â˜' x} Eu _x GaO ₃. Chinese Physics B, 2016, 25, 123103.	0.7	0
25289	Hybrid crystals of cuprates and iron-based superconductors. Chinese Physics B, 2016, 25, 077402.	0.7	3
25290	On the structure of crystalline and molten cryolite: Insights from the ab initio molecular dynamics in NpT ensemble. Journal of Chemical Physics, 2016, 144, 064502.	1.2	18
25291	The interplay of covalency, hydrogen bonding, and dispersion leads to a long range chiral network: The example of 2-butanol. Journal of Chemical Physics, 2016, 144, 094703.	1.2	19
25292	Density-functional theory computer simulations of CZTS0.25Se0.75 alloy phase diagrams. Journal of Chemical Physics, 2016, 145, .	1.2	12
25293	Shock compression experiments on Lithium Deuteride (LiD) single crystals. Journal of Applied Physics, 2016, 120, .	1.1	11
25294	Quantum anomalous Hall effect in stable dumbbell stanene. Applied Physics Letters, 2016, 108, 082104.	1.5	13
25295	Monte Carlo modeling of phase separation in CuIn<inf>x</inf>Ga<inf>1â˜'x</inf>Se<inf>2</inf>. , 2016, , .		1
25296	Pressure-induced zircon to monazite phase transition in Y1â€"Ñ... La Ñ... PO4: First-principles calculations. Journal of Structural Chemistry, 2016, 57, 1513-1518.	0.3	5
25297	Density functional theory + U modeling of polarons in organohalide lead perovskites. AIP Advances, 2016, 6, .	0.6	25
25298	Band gap modulation in Î³ -graphyne by p-n codoping. Europhysics Letters, 2016, 115, 27009.	0.7	10
25299	Electronic structure and magnetic anisotropy of L1-FePt thin film studied by hard x-ray photoemission spectroscopy and first-principles calculations. Applied Physics Letters, 2016, 109, .	1.5	19
25300	Magnetism in molybdenum disulphide monolayer with sulfur substituted by 3d transition metals. Journal of Applied Physics, 2016, 120, 144305.	1.1	11
25301	Ferroelasticity and domain physics in two-dimensional transition metal dichalcogenide monolayers. Nature Communications, 2016, 7, 10843.	5.8	125
25302	Nontrivial contribution of FrÃ¶hlich electron-phonon interaction to lattice thermal conductivity of wurtzite GaN. Applied Physics Letters, 2016, 109, .	1.5	53
25303	Influence of the composition fluctuations and decomposition on the tunable direct gap and oscillator strength of Ge1-xSnx alloys. Applied Physics Letters, 2016, 108, 092101.	1.5	19
25304	First-principles simulations of 2-D semiconductor devices: Mobility, I-V characteristics, and contact resistance. , 2016, , .		20

#	Article	IF	Citations
25305	Oxygen vacancy effects on double perovskite Bi ₂ FeMnO ₆ : A first-principles study. Europhysics Letters, 2016, 116, 57002.	0.7	5
25306	The structure of water at a Pt(111) electrode and the potential of zero charge studied from first principles. Journal of Chemical Physics, 2016, 144, 194701.	1.2	127
25307	Analysis of local bond-orientational order for liquid gallium at ambient pressure: Two types of cluster structures. Journal of Chemical Physics, 2016, 145, 024506.	1.2	13
25308	Performance predictions of single-layer In-V double-gate n- and p-type field-effect transistors. , 2016, , .		1
25309	The local projection in the density functional theory plus U approach: A critical assessment. Journal of Chemical Physics, 2016, 144, 144106.	1.2	47
25310	Exploring Ag(111) Substrate for Epitaxially Growing Monolayer Stanene: A First-Principles Study. Scientific Reports, 2016, 6, 29107.	1.6	58
25311	Structure, electronic and magnetic properties of Mnn (n=2-8) clusters: A DFT investigation. AIP Conference Proceedings, 2016, , .	0.3	1
25312	Ab initio study of vacancy formation in cubic LaMnO3 and SmCoO3 as cathode materials in solid oxide fuel cells. Journal of Chemical Physics, 2016, 145, 014703.	1.2	25
25313	Degradation and annealing effects caused by oxygen in AlGaN/GaN high electron mobility transistors. Applied Physics Letters, 2016, 109, .	1.5	22
25314	First-Principles-Based Phonon Calculation and Raman Spectroscopy Measurement of RuGa₂ and RuAl₂ with High Thermoelectric Power Factors. Materials Transactions, 2016, 57, 1050-1054.	0.4	3
25315	Orbital Reconstruction Enhanced Exchange Bias in La0.6Sr0.4MnO3/Orthorhombic YMnO3 Heterostructures. Scientific Reports, 2016, 6, 24568.	1.6	10
25316	Variability of structural and electronic properties of bulk and monolayer Si2Te3. Applied Physics Letters, 2016, 109, .	1.5	24
25317	A single-volume approach for vacancy formation thermodynamics calculations. Europhysics Letters, 2016, 116, 16001.	0.7	4
25318	Investigations into the slip behavior of zirconium diboride. Journal of Materials Research, 2016, 31, 2749-2756.	1.2	11
25319	Suppression of lattice thermal conductivity by mass-conserving cation mutation in multi-component semiconductors. APL Materials, 2016, 4, 104809.	2.2	12
25320	Band gap engineering of ZnSnN2/ZnO (001) short-period superlattices via built-in electric field. Journal of Applied Physics, 2016, 120, .	1.1	11
25321	First-principles calculated decomposition pathways for LiBH4 nanoclusters. Scientific Reports, 2016, 6, 26056.	1.6	11
25322	First-principles based calculation of the macroscopic Î±/Î² interface in titanium. Journal of Applied Physics, 2016, 119, .	1.1	7

#	Article	IF	Citations
25323	From single molecules to water networks: Dynamics of water adsorption on Pt(111). Journal of Chemical Physics, 2016, 145, 094703.	1.2	18
25324	Pathway to oxide photovoltaics via band-structure engineering of SnO. APL Materials, 2016, 4, 106103.	2.2	28
25325	First-principles study on native point defects of cubic cuprite Ag2O. Journal of Applied Physics, 2016, 120, .	1.1	8
25326	Large influence of capping layers on tunnel magnetoresistance in magnetic tunnel junctions. Applied Physics Letters, 2016, 109, .	1.5	26
25327	Large magnetoresistance in LaBi: origin of field-induced resistivity upturn and plateau in compensated semimetals. New Journal of Physics, 2016, 18, 082002.	1.2	134
25328	Improved thermoelectric performance of (Fe,Co)Sb3-type skutterudites from first-principles. Journal of Applied Physics, 2016, 119, .	1.1	4
25329	First principles studies on the impact of point defects on the phase stability of (AlxCr1â^'x)2O3 solid solutions. AIP Advances, 2016, 6, .	0.6	18
25330	Theoretical and experimental study of metastable solid solutions and phase stability within the immiscible Ag-Mo binary system. Journal of Applied Physics, 2016, 119, .	1.1	14
25331	Elastic properties of AlAs-like and InSb-like strained interfaces in [InAs/AlSb] heterostructures. Applied Physics Letters, 2016, 109, .	1.5	2
25332	An efficient algorithm for finding the minimum energy path for cation migration in ionic materials. Journal of Chemical Physics, 2016, 145, 074112.	1.2	54
25333	Determination of the geometric structure of neutral niobium carbide clusters via infrared spectroscopy. Journal of Chemical Physics, 2016, 145, 164305.	1.2	7
25334	Nuclear quantum effects in a HIV/cancer inhibitor: The case of ellipticine. Journal of Chemical Physics, 2016, 145, 205102.	1.2	24
25335	Improper Inversion Symmetry Breaking and Piezoelectricity through Oxygen Octahedral Rotations in Layered Perovskite Family, LiRTiO₄ (R = Rare Earths). Advanced Electronic Materials, 2016, 2, 1500196.	2.6	28
25336	Density-Functional Study of the La₂Zr₂O₇ (001) and (011) Surfaces and Bulk. Journal of Physical Chemistry C, 2016, 120, 7522-7531.	1.5	11
25337	Lewis Acid Catalysis Confined in Zeolite Cages as a Strategy for Sustainable Heterogeneous Hydration of Epoxides. ACS Catalysis, 2016, 6, 2955-2964.	5.5	86
25338	Pd-Ag alloy hollow nanostructures with interatomic charge polarization for enhanced electrocatalytic formic acid oxidation. Nano Research, 2016, 9, 1590-1599.	5.8	102
25339	Construction of ternary Niâ€“Alâ€“Ta potential and its application in the effect of Ta on [1 1 0] edge dislocation slipping in Î³â€²(Ni3Al). Computational Materials Science, 2016, 118, 288-296.	1.4	4
25340	Adsorption of TCNQ and F4-TCNQ molecules on hydrogen-terminated Si(1 1 1) surface: van der Waals interactions included DFT study of the molecular orientations. Computational and Theoretical Chemistry, 2016, 1084, 179-187.	1.1	5

#	Article	IF	Citations
25341	Intimately coupled hybrid of graphitic carbon nitride nanoflakelets with reduced graphene oxide for supporting Pd nanoparticles: A stable nanocatalyst with high catalytic activity towards formic acid and methanol electrooxidation. Electrochimica Acta, 2016, 200, 131-141.	2.6	50
25342	Building compact dislocation cores in an elasto-plastic model of dislocation fields. International Journal of Plasticity, 2016, 82, 241-259.	4.1	10
25343	Interfacial effect on strengthening nanoscale metallic multilayers - a combined Hall-Petch relation and atomistic simulation study. Materials Science & Engineering A: Structural Materials: Properties, Microstructure and Processing, 2016, 663, 29-37.	2.6	9
25344	Structural Phase Transitions and Metallized Phenomena in Arsenic Telluride under High Pressure. Inorganic Chemistry, 2016, 55, 3907-3914.	1.9	17
25345	FeB₆ Monolayers: The Graphene-like Material with Hypercoordinate Transition Metal. Journal of the American Chemical Society, 2016, 138, 5644-5651.	6.6	219
25346	Carbene-mediated self-assembly of diamondoids on metal surfaces. Nanoscale, 2016, 8, 8966-8975.	2.8	20
25347	Effects of carbon vacancies on the structures, mechanical properties, and chemical bonding of zirconium carbides: a first-principles study. Physical Chemistry Chemical Physics, 2016, 18, 12299-12306.	1.3	53
25348	Critical Stresses for Twinning, Slip, and Transformation in Ti-Based Shape Memory Alloys. Shape Memory and Superelasticity, 2016, 2, 180-195.	1.1	36
25349	Electronic and optical properties of (U,Th)O 2 compound from screened hybrid density functional studies. Physics Letters, Section A: General, Atomic and Solid State Physics, 2016, 380, 1481-1486.	0.9	12
25350	Band-Gap Modulation in Single Bi³⁺-Doped Yttriumâ€“Scandiumâ€“Niobium Vanadates for Color Tuning over the Whole Visible Spectrum. Chemistry of Materials, 2016, 28, 2692-2703.	3.2	246
25351	Flexible 2D Crystals of Polycyclic Aromatics Stabilized by Static Distortion Waves. ACS Nano, 2016, 10, 6474-6483.	7.3	23
25352	The Critical Role of Substrate in Stabilizing Phosphorene Nanoflake: A Theoretical Exploration. Journal of the American Chemical Society, 2016, 138, 4763-4771.	6.6	72
25353	Magnetoelectric coupling and spin-induced electrical polarization in metalâ€“organic magnetic chains. Journal of Materials Chemistry C, 2016, 4, 4176-4185.	2.7	18
25354	From small fullerenes to the graphene limit: A harmonic forceâ€field method for fullerenes and a comparison to density functional calculations for <scp>G</scp>oldbergâ€“<scp>C</scp>oxeter fullerenes up to C₉₈₀. Journal of Computational Chemistry, 2016, 37, 10-17.	1.5	12
25355	Recent development of atomâ€pairwise van der waals corrections for density functional theory: From molecules to solids. International Journal of Quantum Chemistry, 2016, 116, 598-607.	1.0	19
25356	Abâ€initio study of germanium di -interstitial using a hybrid functional (HSE). Physica B: Condensed Matter, 2016, 480, 191-195.	1.3	16
25357	Ammonia Adsorption and Decomposition on Co(0001) in Relation to Fischerâ€“Tropsch Synthesis. Journal of Physical Chemistry C, 2016, 120, 3834-3845.	1.5	14
25358	Quantitative Structure of an Acetate Dye Molecule Analogue at the TiO₂â€“Acetic Acid Interface. Journal of Physical Chemistry C, 2016, 120, 7586-7590.	1.5	7

#	Article	IF	Citations
25359	Nitrogen-doped carbon nanotube as a potential metal-free catalyst for CO oxidation. Physical Chemistry Chemical Physics, 2016, 18, 12093-12100.	1.3	38
25360	Rare earth functionalization effect in optical response of ZnO nano clusters. European Physical Journal D, 2016, 70, 1.	0.6	4
25361	Optical properties of BN nanoribbons with H and F passivation. Optical and Quantum Electronics, 2016, 48, 1.	1.5	1
25362	Dissociative adsorption of methane on the Cu and Zn doped (111) surface of CeO2. Applied Catalysis B: Environmental, 2016, 197, 324-336.	10.8	49
25363	DFT study of the formation of Cdâ€“Ag surface alloys on Ag surfaces. Computational Materials Science, 2016, 118, 316-324.	1.4	2
25364	Electric field induced modification of magnetism in platinum tripod on pt (111) surface. Chemical Physics Letters, 2016, 648, 156-160.	1.2	1
25365	Secondary interactions in decachloro-closo-decaborates R2[B10Cl10] (R = Et3NH+, Ph4P+, and) Tj ETQq0 0 0 rgBT /Overlock 10 Tf 50 5	1.2	27
25366	The mechanism of hydrogen and oxygen evolution reactionÂinÂNiâ€“NiO/Î²-Ga2O3 photocatalyst. International Journal of Hydrogen Energy, 2016, 41, 5670-5681.	3.8	27
25367	Three-Parameter Crystal-Structure Prediction for sp-d-Valent Compounds. Chemistry of Materials, 2016, 28, 2550-2556.	3.2	26
25368	Electronic Structure and Bonding in Co-Based Single and Mixed Valence Oxides: A Quantum Chemical Perspective. Inorganic Chemistry, 2016, 55, 3307-3315.	1.9	40
25369	Structures and Electronic Properties of Ti_nV (n = 1â€“16) Clusters: First-Principles Calculations. Journal of Physical Chemistry A, 2016, 120, 2401-2407.	1.1	21
25370	Explicit Detection of the Mechanism of Platinum Nanoparticle Shape Control by Polyvinylpyrrolidone. Journal of Physical Chemistry C, 2016, 120, 7532-7542.	1.5	36
25371	Structural Characterization, Optical Properties, and Phase Transitions of In_{1â€“x}Sn_x Alloy Thin Films. Journal of Physical Chemistry C, 2016, 120, 7822-7828.	1.5	4
25372	Electronâ€“Vibron Coupling at Metalâ€“Organic Interfaces from Theory and Experiment. Journal of Physical Chemistry Letters, 2016, 7, 1422-1427.	2.1	14
25373	Mechanism of Dehydration of Phenols on Noble Metals via First-Principles Microkinetic Modeling. ACS Catalysis, 2016, 6, 3047-3055.	5.5	69
25374	Electric Field Induced Reversible Phase Transition in Li Doped Phosphorene: Shape Memory Effect and Superelasticity. Journal of the American Chemical Society, 2016, 138, 4772-4778.	6.6	26
25375	Dirac node arcs in PtSn4. Nature Physics, 2016, 12, 667-671.	6.5	223
25376	Understanding thermoelectric properties from high-throughput calculations: trends, insights, and comparisons with experiment. Journal of Materials Chemistry C, 2016, 4, 4414-4426.	2.7	193

#	Article	IF	Citations
25377	Pressure evolution of the potential barriers of phase transition of MoS₂, MoSe₂ and MoTe₂. Physical Chemistry Chemical Physics, 2016, 18, 12080-12085.	1.3	38
25378	Ni on the CeO₂(110) and (100) surfaces: adsorption vs. substitution effects on the electronic and geometric structures and oxygen vacancies. Physical Chemistry Chemical Physics, 2016, 18, 11139-11149.	1.3	38
25379	First-principles study of line-defect-embedded zigzag graphene nanoribbons: electronic and magnetic properties. Physical Chemistry Chemical Physics, 2016, 18, 12350-12356.	1.3	20
25380	Robust half-metallic ferromagnetism and curvature dependent magnetic coupling in fluorinated boron nitride nanotubes. Physical Chemistry Chemical Physics, 2016, 18, 12307-12311.	1.3	8
25381	Schottky potential barrier and spin polarization at Co/antimonene interfaces. RSC Advances, 2016, 6, 38746-38752.	1.7	9
25382	Origin of low sodium capacity in graphite and generally weak substrate binding of Na and Mg among alkali and alkaline earth metals. Proceedings of the National Academy of Sciences of the United States of America, 2016, 113, 3735-3739.	3.3	462
25383	Structural and optical properties of Ge60Te40: experimental and theoretical verification. Journal Physics D: Applied Physics, 2016, 49, 155105.	1.3	5
25384	Free energy model for solid high-pressure phases of carbon. Journal of Physics Condensed Matter, 2016, 28, 145401.	0.7	2
25385	Fast Photoresponse from 1T Tin Diselenide Atomic Layers. Advanced Functional Materials, 2016, 26, 137-145.	7.8	150
25386	Metal intercalation-induced selective adatom mass transport on graphene. Nano Research, 2016, 9, 1434-1441.	5.8	7
25387	Saturation of ion irradiation effects in MAX phase Cr2AlC. Acta Materialia, 2016, 110, 1-7.	3.8	51
25388	A comparative study of structural changes in lithium nickel cobalt manganese oxide as a function of Ni content during delithiation process. Journal of Power Sources, 2016, 315, 111-119.	4.0	122
25389	Anion Effects on Lanthanide(III) Tetrazole-1-acetate Dinuclear Complexes Showing Slow Magnetic Relaxation and Photofluorescent Emission. Inorganic Chemistry, 2016, 55, 3738-3749.	1.9	56
25390	Early Oxidation Processes on the Greigite Fe₃S₄(001) Surface by Water: A Density Functional Theory Study. Journal of Physical Chemistry C, 2016, 120, 8616-8629.	1.5	32
25391	Can Ice-Like Structures Form on Non-Ice-Like Substrates? The Example of the K-feldspar Microcline. Journal of Physical Chemistry C, 2016, 120, 6704-6713.	1.5	43
25392	Niâ€“Mâ€“O (M = Sn, Ti, W) Catalysts Prepared by a Dry Mixing Method for Oxidative Dehydrogenation of Ethane. ACS Catalysis, 2016, 6, 2852-2866.	5.5	120
25393	Quantum Electronic Transport of Topological Surface States in Î²-Ag₂Se Nanowire. ACS Nano, 2016, 10, 3936-3943.	7.3	24
25394	Chemically functionalized germanene for spintronic devices: a first-principles study. Physical Chemistry Chemical Physics, 2016, 18, 9809-9815.	1.3	20

#	Article	IF	Citations
25395	Structural and electronic properties of the heterointerfaces for Cu2ZnSnS4 photovoltaic cells: a density-functional theory study. Physical Chemistry Chemical Physics, 2016, 18, 12029-12034.	1.3	10
25396	Monolayer MXenes: promising half-metals and spin gapless semiconductors. Nanoscale, 2016, 8, 8986-8994.	2.8	380
25397	Ab initiostudy of tungsten defects near the surface. Modelling and Simulation in Materials Science and Engineering, 2016, 24, 045006.	0.8	12
25398	Magnetic and optical properties in the 1D TMâ€“O chain compounds Sr₂TMO₃ (TM = Ni, Co): A first-principle investigation. Modern Physics Letters B, 2016, 30, 1650119.	1.0	1
25399	First Principles Study of Structural and Electronic Properties of Pentagonal and Hexagonal Noble Metal Nanowires. Nano, 2016, 11, 1650069.	0.5	0
25400	Nanosecond Phase Transition Dynamics in Compressively Strained Epitaxial BiFeO₃. Advanced Electronic Materials, 2016, 2, 1500204.	2.6	6
25401	Influence of the tensile strain on CH4 dissociation on Cu(1 0 0) surface: A theoretical study. Applied Surface Science, 2016, 360, 826-832.	3.1	5
25402	First-principles investigation on the interface of transition metal dichalcogenide MX2 (M = Mo, W; X =) Tj ETQq1 1 0.784314 rgBT /Ov	1.4	16
25403	Positron annihilation lifetime characterization of oxygen ion irradiated rutile TiO2. Nuclear Instruments & Methods in Physics Research B, 2016, 379, 215-218.	0.6	33
25404	Resolving the Physical Origin of Octahedral Tilting in Halide Perovskites. Chemistry of Materials, 2016, 28, 4259-4266.	3.2	211
25405	Valence Band Splitting on Multilayer MoS₂: Mixing of Spinâ€“Orbit Coupling and Interlayer Coupling. Journal of Physical Chemistry Letters, 2016, 7, 2175-2181.	2.1	73
25406	Electronic structure, low-temperature transport and thermodynamic properties of polymorphic Î²-As₂Te₃. RSC Advances, 2016, 6, 52048-52057.	1.7	11
25407	Mn₂C monolayer: a 2D antiferromagnetic metal with high NÃ©el temperature and large spinâ€“orbit coupling. Nanoscale, 2016, 8, 12939-12945.	2.8	131
25408	A first-principles study of the diffusion coefficients of alloying elements in dilute Î±-Ti alloys. Physical Chemistry Chemical Physics, 2016, 18, 16870-16881.	1.3	39
25409	Electronic structure and quadrupole interactions in triple molybdates Li2M3Al(MoO4)4, M = Cs, Rb. Journal of Structural Chemistry, 2016, 57, 275-280.	0.3	2
25410	Electronic structure and formation energies of nonstoichiometric dichalcogenides M x X2â€“y (Đœ = Nb,) Tj ETQq1 1 0.784314 rgBT	0.3	2
25411	Insights into MoS2-coated LiVPO4F for lithium ion batteries: A first-principles investigation. Journal of Alloys and Compounds, 2016, 681, 253-259.	2.8	8
25412	Electronic and magnetic properties of X-doped (X=Ni, Pd, Pt) WS2 monolayer. Journal of Magnetism and Magnetic Materials, 2016, 414, 45-48.	1.0	28

#	Article	IF	Citations
25413	Stress induced phase transition on the medium-high carbon alloy steel hardfacing coating during the work hardening process: Experiments and first-principles calculation. Materials Science & Engineering A: Structural Materials: Properties, Microstructure and Processing, 2016, 670, 49-56.	2.6	3
25414	Finite-size effects on the molecular dynamics simulation of fast-ion conductors: A case study of lithium garnet oxide Li7La3Zr2O12. Solid State Ionics, 2016, 289, 143-149.	1.3	36
25415	Iodine adsorption on Ni(111): STM and DFT study. Surface Science, 2016, 651, 112-119.	0.8	9
25416	Adsorption and Oligomerization of 1,3-Phenylene Diisocyanide on Au(111). Journal of Physical Chemistry C, 2016, 120, 9270-9275.	1.5	5
25417	Disparate Strain Dependent Thermal Conductivity of Two-dimensional Penta-Structures. Nano Letters, 2016, 16, 3831-3842.	4.5	183
25418	Insight into both coverage and surface structure dependent CO adsorption and activation on different Ni surfaces from DFT and atomistic thermodynamics. Physical Chemistry Chemical Physics, 2016, 18, 17606-17618.	1.3	16
25419	Exploring crystal phase and morphology in the TiO 2 supporting materials used for visible-light driven plasmonic photocatalyst. Applied Catalysis B: Environmental, 2016, 198, 91-99.	10.8	20
25420	Ag diffusion in SiC high-energy grain boundaries: Kinetic Monte Carlo study with first-principle calculations. Computational Materials Science, 2016, 121, 248-257.	1.4	24
25421	Activating Mn3O4 by Morphology Tailoring for Oxygen Reduction Reaction. Electrochimica Acta, 2016, 205, 38-44.	2.6	65
25422	Modeling reaction pathways for hydrogen evolution and water dissociation on magnesium. Electrochimica Acta, 2016, 210, 261-270.	2.6	44
25423	Vacancies at LaAlO3 thin films: A 2D electron gas at the surface. Journal of Alloys and Compounds, 2016, 684, 544-548.	2.8	8
25424	Evolution of embedded lithium nanoclusters in lithium implanted alumina. Materials Chemistry and Physics, 2016, 179, 143-151.	2.0	4
25425	Chemisorption of oxygen and subsequent reactions on low index surfaces of Î²â€“Mo2C: Insights from first-principles thermodynamics and kinetics. Journal of Molecular Catalysis A, 2016, 417, 53-63.	4.8	12
25426	Fe(II)Ti(IV)O3 mixed oxide monolayer at rutile TiO2(011): Structures and reactivities. Surface Science, 2016, 653, 34-40.	0.8	4
25427	Interaction of Formaldehyde with the Rutile TiO₂(110) Surface: A Combined Experimental and Theoretical Study. Journal of Physical Chemistry C, 2016, 120, 12626-12636.	1.5	54
25428	Enhanced Kinetics of Hole Transfer and Electrocatalysis during Photocatalytic Oxygen Evolution by Cocatalyst Tuning. ACS Catalysis, 2016, 6, 4117-4126.	5.5	48
25429	Reactive force field development for magnesium chloride hydrates and its application for seasonal heat storage. Physical Chemistry Chemical Physics, 2016, 18, 15838-15847.	1.3	24
25430	Charge-transport anisotropy in black phosphorus: critical dependence on the number of layers. Physical Chemistry Chemical Physics, 2016, 18, 16345-16352.	1.3	17

#	Article	IF	Citations
25431	Temperature dependent terahertz properties of energetic materials. Proceedings of SPIE, 2016, , .	0.8	1
25432	MoS₂ Enhanced T-Phase Stabilization and Tunability Through Alloying. Journal of Physical Chemistry Letters, 2016, 7, 2304-2309.	2.1	54
25433	Decomposition and formation of magnesium borohydride. International Journal of Hydrogen Energy, 2016, 41, 11201-11224.	3.8	28
25434	Precipitation in a mixed Alâ€“Cuâ€“Mg/Alâ€“Znâ€“Mg alloy system. Journal of Alloys and Compounds, 2016, 684, 195-200.	2.8	22
25435	The Interplay between Homogeneous and Heterogeneous Phases of PdAu Catalysts for the Oxidation of Alcohols. ACS Catalysis, 2016, 6, 4135-4143.	5.5	30
25436	Nanotubes from Oxide-Based Misfit Family: The Case of Calcium Cobalt Oxide. ACS Nano, 2016, 10, 6248-6256.	7.3	23
25437	An ab initio molecular dynamics study of D2 dissociation on CO-precovered Ru(0001). Physical Chemistry Chemical Physics, 2016, 18, 21190-21201.	1.3	3
25438	A combined theoretical and experimental EXAFS study of the structure and dynamics of Au₁₄₇ nanoparticles. Catalysis Science and Technology, 2016, 6, 6879-6885.	2.1	26
25439	Alkali metals as efficient A-site acceptor dopants in proton conducting BaZrO₃. Journal of Materials Chemistry A, 2016, 4, 9229-9235.	5.2	24
25440	Driving forces for the phase transition of CuQ₂-TCNQ molecular crystals. CrystEngComm, 2016, 18, 5070-5073.	1.3	5
25441	Intra-chain superexchange couplings in quasi-1D 3dtransition-metal magnetic compounds. Journal of Physics Condensed Matter, 2016, 28, 276003.	0.7	8
25442	Strain-modulated electronic and thermal transport properties of two-dimensional O-silica. Nanotechnology, 2016, 27, 265706.	1.3	18
25443	Structural, electronic, elastic, optical, and vibrational properties of HfXSb (XÂ=ÂCo, Rh, Ru) half-Heusler compounds: an ab initio study. Indian Journal of Physics, 2016, 90, 1233-1241.	0.9	20
25444	On the adaptability of 1/1 cubic approximant structure in the Mgâ€“Alâ€“Zn system with the particular example of Mg 32 Al 12 Zn 37. Journal of Alloys and Compounds, 2016, 656, 159-165.	2.8	9
25445	First-principles study on band structures and electrical transports of doped-SnTe. Journal of Materiomics, 2016, 2, 158-164.	2.8	22
25446	A sublinear-scaling approach to density-functional-theory analysis of crystal defects. Journal of the Mechanics and Physics of Solids, 2016, 95, 530-556.	2.3	21
25447	Doping in controlling the type of conductivity in bulk and nanostructured thermoelectric materials. Journal of Solid State Chemistry, 2016, 240, 91-100.	1.4	8
25448	The structure phase transition in atom-wide Co wires on a vicinal Cu{111} surface. Materials Letters, 2016, 179, 69-72.	1.3	16

#	Article	IF	Citations
25449	Pressure-induced phase transformation in Î²-eucryptite: An X-ray diffraction and density functional theory study. Scripta Materialia, 2016, 122, 64-67.	2.6	10
25450	Delimiting the boron influence on the adsorptive properties of water and OH radicals on H-terminated Boron Doped Diamond catalysts: A Density Functional Theory analysis. Surface Science, 2016, 653, 27-33.	0.8	11
25451	Reactions of Molten LiI with I₂, H₂O, and O₂ Relevant to Halogen-Mediated Oxidative Dehydrogenation of Alkanes. Journal of Physical Chemistry C, 2016, 120, 4931-4936.	1.5	6
25452	Force Field Development from Periodic Density Functional Theory Calculations for Gas Separation Applications Using Metalâ€“Organic Frameworks. Journal of Physical Chemistry C, 2016, 120, 12590-12604.	1.5	95
25453	Quantitative Understanding of van der Waals Interactions by Analyzing the Adsorption Structure and Low-Frequency Vibrational Modes of Single Benzene Molecules on Silver. Journal of Physical Chemistry Letters, 2016, 7, 2228-2233.	2.1	6
25454	T-ZrS nanoribbons: structure and electronic properties. Philosophical Magazine, 2016, 96, 2074-2087.	0.7	8
25455	First-principles simulation on Seebeck coefficient in silicon and silicon carbide nanosheets. Japanese Journal of Applied Physics, 2016, 55, 06GJ07.	0.8	5
25456	Density Functional Theory. Graduate Texts in Physics, 2016, , 99-110.	0.1	1
25457	* Electronic Structure of Low-Dimensionality Systems. Graduate Texts in Physics, 2016, , 111-162.	0.1	2
25458	First-principles studying the properties of oxygen in vanadium: Thermodynamics and tensile/shear behavior. Computational Condensed Matter, 2016, 7, 7-13.	0.9	7
25459	Dielectric function and double absorption onset of monoclinic Cu 2 SnS 3 : Origin of experimental features explained by first-principles calculations. Solar Energy Materials and Solar Cells, 2016, 154, 121-129.	3.0	62
25460	The role of non-hydrostatic stresses in phase transitions in boron carbide. Computational Materials Science, 2016, 121, 106-112.	1.4	31
25461	Sr2SmNbO6 perovskite: Synthesis, characterization and density functional theory calculations. Materials Chemistry and Physics, 2016, 179, 55-64.	2.0	14
25462	Phonon spectral energy density analysis of solids: The <mml:math xmlns:mml="http://www.w3.org/1998/Math/MathML" altimg="si2.gif" overflow="scroll"><mml:mrow><mml:mi mathvariant="bold">k</mml:mi></mml:mrow></mml:math> point reduction in the first Brillouin zone of FCC crystals and a case study on solid argon. Computational Materials Science, 2016, 121, 97-105.	1.4	7
25463	Three dimensional atom probe and first-principles studies on spinodal decomposition of Cr in a Co-alloyed maraging stainless steel. Scripta Materialia, 2016, 121, 37-41.	2.6	22
25464	Optical-Vibrational Properties of the Cs₂SnX₆ (X = Cl, Br, I) Defect Perovskites and Hole-Transport Efficiency in Dye-Sensitized Solar Cells. Journal of Physical Chemistry C, 2016, 120, 11777-11785.	1.5	222
25465	Platy KTiNbO5 as a Selective Sr Ion Adsorbent: Crystal Growth, Adsorption Experiments, and DFT Calculations. Journal of Physical Chemistry C, 2016, 120, 11984-11992.	1.5	15
25466	Creating Two-Dimensional Electron Gas in Polar/Polar Perovskite Oxide Heterostructures: First-Principles Characterization of LaAlO₃/A⁺B⁵⁺O₃. ACS Applied Materials & Interfaces, 2016, 8, 13659-13668.	4.0	36

#	Article	IF	Citations
25467	Blue Phosphorene/MS₂ (M = Nb, Ta) Heterostructures As Promising Flexible Anodes for Lithium-Ion Batteries. ACS Applied Materials & Interfaces, 2016, 8, 13449-13457.	4.0	165
25468	Crystallographic Facet-Induced Toxicological Responses by Faceted Titanium Dioxide Nanocrystals. ACS Nano, 2016, 10, 6062-6073.	7.3	53
25469	Carbonation Competing Functionalization on Calcium-Silicate-Hydrates: Investigation of Four Promising Surface-Activation Techniques. ACS Sustainable Chemistry and Engineering, 2016, 4, 3985-3994.	3.2	14
25470	Electrochemical interfacial influences on deoxygenation and hydrogenation reactions in CO reduction on a Cu(100) surface. Physical Chemistry Chemical Physics, 2016, 18, 15304-15311.	1.3	6
25471	Ultra-small B₂O₃ nanocrystals grown in situ on highly porous carbon microtubes for lithiumâ€“iodine and lithiumâ€“sulfur batteries. Journal of Materials Chemistry A, 2016, 4, 8541-8547.	5.2	74
25472	Alloying Effects on the Phase Stability and Mechanical Properties of Doped Cu-Sn IMCs: A First-Principle Study. Journal of Electronic Materials, 2016, 45, 4018-4027.	1.0	15
25473	Inconsistencies in modelling interstitials in FeCr with empirical potentials. Computational Materials Science, 2016, 121, 204-208.	1.4	6
25474	Stability of Cuâ€“Nb layered nanocomposite from chemical bonding. Chemical Physics Letters, 2016, 655-656, 59-65.	1.2	5
25475	Single-layer cadmium chalcogenides: promising visible-light driven photocatalysts for water splitting. Physical Chemistry Chemical Physics, 2016, 18, 17029-17036.	1.3	75
25476	Structural, electronic and magnetic properties of metalâ€“organic-framework perovskites [AmH][Mn(HCOO)3]: a first-principles study. RSC Advances, 2016, 6, 48779-48787.	1.7	11
25477	Identification of vacancy defect complexes in transparent semiconducting oxides ZnO, In₂O₃ and SnO₂. Journal of Physics Condensed Matter, 2016, 28, 224002.	0.7	45
25478	Effect of Magnetic Transition Metal (TM = V, Cr, and Mn) Dopant on Characteristics of Copper Nitride. Journal of Superconductivity and Novel Magnetism, 2016, 29, 2351-2357.	0.8	11
25479	First-principles study of Ti doping in FeF3Â·0.33H2O. Current Applied Physics, 2016, 16, 905-913.	1.1	25
25480	Electronic structure of Mn 0.25 TaS 2. Journal of Electron Spectroscopy and Related Phenomena, 2016, 208, 74-77.	0.8	1
25481	Free energy landscape approach to aid pure phase synthesis of transition metal (X=Cr, Mn and Fe) doped bismuth titanate (Bi2Ti2O7). Journal of Crystal Growth, 2016, 444, 46-54.	0.7	16
25482	Electric field modulation of the band gap, dielectric constant and polarizability in SnS atomically thin layers. Physics Letters, Section A: General, Atomic and Solid State Physics, 2016, 380, 2227-2232.	0.9	19
25483	Direct Observation of Pressure-Driven Valence Electron Transfer in Ba₃BiRu₂O₉, Ba₃BiIr₂O₉, and Ba₄BiIr₃O₁₂. Inorganic Chemistry, 2016, 55, 5649-5654.	1.9	5
25484	Oxygen Adsorption on the Fe(110) Surface: The Old System â€“ New Structures. Journal of Physical Chemistry C, 2016, 120, 3807-3813.	1.5	7

#	Article	IF	Citations
25485	Properties of Ti/TiC Interfaces from Molecular Dynamics Simulations. Journal of Physical Chemistry C, 2016, 120, 12530-12538.	1.5	25
25486	Synthesis of Tellurium Fusiform Nanoarchitectures by Controlled Living Nanowire Modification. Journal of Physical Chemistry C, 2016, 120, 12305-12312.	1.5	9
25487	Shape and Size of Cobalt Nanoislands Formed Spontaneously on Cobalt Terraces during Fischerâ€“Tropsch Synthesis. Journal of Physical Chemistry Letters, 2016, 7, 1996-2001.	2.1	32
25488	Atomic structure of a peptide coated gold nanocluster identified using theoretical and experimental studies. Nanoscale, 2016, 8, 11454-11460.	2.8	16
25489	The charge states of Au on gold-substituted Ce1â^'xO2(111) surfaces with multiple oxygen vacancies. Physical Chemistry Chemical Physics, 2016, 18, 15884-15893.	1.3	16
25490	Optical and electronic properties of orthorhombic and trigonal AXO₃ (A=Cd, Zn; X=Sn,) Tj ETQq1 1 0.784314 rgBT /Ove	0.3	4
25491	Characterization of Nickel Aluminide Formed on Ni-Based Superalloy 690 Substrate, First-Principle Ni(Cr)/NiAl Interface Simulations and Stability of Aluminide in Aggressive Environment in Pre-oxidized State. Transactions of the Indian Institute of Metals, 2016, 69, 1889-1897.	0.7	2
25492	A QM/MM approach for low-symmetry defects in metals. Computational Materials Science, 2016, 118, 259-268.	1.4	14
25493	Thermal properties and thermoelasticity of L12 ordered Al3RE (RE=Er, Tm, Yb, Lu) phases: A first-principles study. Materials and Design, 2016, 102, 100-105.	3.3	17
25494	Tuning electrocatalytic activity of Pt monolayer shell by bimetallic Ir-M (M=Fe, Co, Ni or Cu) cores for the oxygen reduction reaction. Nano Energy, 2016, 29, 261-267.	8.2	61
25495	DFT modeling of plasma-assisted atomic layer deposition for Si(110) passivation: formation of boehmite-like chains as Î³-Al2O3 precursors. Theoretical Chemistry Accounts, 2016, 135, 1.	0.5	3
25496	Ab-initio study on the structural and spectral properties of Ce 3+ in strontium silicates phosphors. Journal of Luminescence, 2016, 177, 337-341.	1.5	3
25497	Thermodynamic optimization of the Liâ€“Pb system aided by first-principles calculations. Journal of Nuclear Materials, 2016, 477, 95-101.	1.3	15
25498	High-pressure crystal structures of TaAs from first-principles calculations. Solid State Communications, 2016, 240, 37-40.	0.9	8
25499	Promotional effects of chemisorbed oxygen and hydroxide in the activation of Câ€“H and Oâ€“H bonds over transition metal surfaces. Surface Science, 2016, 650, 210-220.	0.8	57
25500	One-dimensional nanoclustering of the Cu(100) surface under CO gas in the mbar pressure range. Surface Science, 2016, 651, 210-214.	0.8	32
25501	Chemical Tailoring of Band Offsets at the Interface of ZnSeâ€“CdS Heterostructures for Delocalized Photoexcited Charge Carriers. Journal of Physical Chemistry C, 2016, 120, 10118-10128.	1.5	17
25502	Topochemistry of Bowtie- and Star-Shaped Metal Dichalcogenide Nanoisland Formation. Nano Letters, 2016, 16, 3696-3702.	4.5	46

#	Article	IF	Citations
25503	Mechanisms for High Selectivity in the Hydrodeoxygenation of 5-Hydroxymethylfurfural over PtCo Nanocrystals. ACS Catalysis, 2016, 6, 4095-4104.	5.5	124
25504	Atomic-scale control of magnetic anisotropy via novel spinâ€“orbit coupling effect in La _{2/3} Sr _{1/3} MnO ₃ /SrIrO ₃ superlattices. Proceedings of the National Academy of Sciences of the United States of America, 2016, 113, 6397-6402.	3.3	108
25505	Spin friction between Co monolayer and Mn/W(110) surface: Ab Initio investigations. Tribology International, 2016, 95, 419-425.	3.0	9
25506	Adsorption toward Trivalent Rare Earth Element from Aqueous Solution by Zeolitic Imidazolate Frameworks. Industrial & Engineering Chemistry Research, 2016, 55, 6365-6372.	1.8	46
25507	Role of Tricoordinate Al Sites in CH₃ReO₃/Al₂O₃ Olefin Metathesis Catalysts. Journal of the American Chemical Society, 2016, 138, 6774-6785.	6.6	42
25508	Low-dimensional ScO₂with tunable electronic and magnetic properties: first-principles studies. Journal of Physics Condensed Matter, 2016, 28, 015004.	0.7	1
25509	In situgrowth of Ag nanoparticles onÎ±-Ag₂WO₄under electron irradiation: probing the physical principles. Nanotechnology, 2016, 27, 225703.	1.3	30
25510	Diverse Spectroscopic Studies and First-Principles Investigations of the Zinc Vacancy Mediated Ferromagnetism in Mn-Doped ZnO Nanoparticles. Crystal Growth and Design, 2016, 16, 3656-3668.	1.4	38
25511	Facilitating the Oxygen Evolution Reaction of Lithium Peroxide via Molecular Adsorption. Journal of Physical Chemistry C, 2016, 120, 10237-10243.	1.5	9
25512	Energy and Spectroscopic Line Shape of the Câ€“O Stretch Mode on Ir(111) in the Presence of Organic Molecules. Journal of Physical Chemistry C, 2016, 120, 11490-11497.	1.5	6
25513	Coexisting Honeycomb and Kagome Characteristics in the Electronic Band Structure of Molecular Graphene. Nano Letters, 2016, 16, 3519-3523.	4.5	41
25514	Controlled Sculpture of Black Phosphorus Nanoribbons. ACS Nano, 2016, 10, 5687-5695.	7.3	111
25515	Synergistic Effects in Bimetallic Palladiumâ€“Copper Catalysts Improve Selectivity in Oxygenate Coupling Reactions. Journal of the American Chemical Society, 2016, 138, 6805-6812.	6.6	94
25516	Disorder and polymorphism in Cu(<scp>II</scp>)-polyoxometalate complexes: [Cu_{1.5}(H₂O)_{7.5}PW₁₂O₄₀]Â·4.75H₂O, cis- & trans-[Cu₂(H₂O)₁₀SiW₁₂O₄₀]Â·6H₂O. CrystEngComm, 2016, 18, 5227-5232.	1.3	3
25517	Structural and Na-ion conduction characteristics of Na₃PS_xSe_{4â^'x}. Journal of Materials Chemistry A, 2016, 4, 9044-9053.	5.2	73
25518	Charge transfer induced activity of graphene for oxygen reduction. Nanotechnology, 2016, 27, 185402.	1.3	19
25519	Self-assembly of noble metal monolayers on transition metal carbide nanoparticle catalysts. Science, 2016, 352, 974-978.	6.0	495
25520	Mechanical properties of Î²â€³ precipitates containing Al and/or Cu in age hardening Al alloys. Journal of Materials Research, 2016, 31, 580-588.	1.2	6

#	Article	IF	Citations
25521	Assessment of the CSL and SU models for bcc-Fe grain boundaries from first principles. Computational Materials Science, 2016, 122, 22-29.	1.4	22
25522	Facile synthesis of tin phosphite nanosheets via exfoliated bulk crystals: Electronic structure and piezoelectric property. Journal of Colloid and Interface Science, 2016, 475, 192-195.	5.0	11
25523	Surface-Bulk Model for d⁰ Ferromagnetism in ZnS Quantum Dots and Wires. Journal of Physical Chemistry C, 2016, 120, 11253-11261.	1.5	14
25524	Understanding oxidative dehydrogenation of ethane on Co3O4 nanorods from density functional theory. Catalysis Science and Technology, 2016, 6, 6861-6869.	2.1	37
25525	Detailed Atomistic Modeling of Si(110) Passivation by Atomic Layer Deposition of Al2O3. , 2016, , 303-351.		0
25526	Periodic density functional theory study of ethylene hydrogenation over Co3O4 (1 1 1) surface: The critical role of oxygen vacancies. Applied Surface Science, 2016, 371, 61-66.	3.1	31
25527	Adsorption of oxygen atom on MoSi 2 (110) surface. Applied Surface Science, 2016, 382, 239-248.	3.1	37
25528	A comparative study on structural and electronic properties and formation energy of bulk Î±-Fe2O3 using first-principles calculations with different density functionals. Computational Materials Science, 2016, 113, 117-122.	1.4	15
25529	Prediction and Synthesis of a Non-Zintl Silicon Clathrate. Chemistry of Materials, 2016, 28, 3711-3717.	3.2	15
25530	Experimental and Computational Investigation of Lepidocrocite Anodes for Sodium-Ion Batteries. Chemistry of Materials, 2016, 28, 4284-4291.	3.2	20
25531	Coreâ€“Exciton Interaction in Sodium L_{2,3} edge Structure Investigated Using the Betheâ€“Salpeter Equation. Journal of Physical Chemistry C, 2016, 120, 9036-9042.	1.5	12
25532	Adsorbate-Induced Changes in Magnetic Interactions in Fe₂(dobdc) with Adsorbed Hydrocarbon Molecules. Journal of Physical Chemistry C, 2016, 120, 9933-9948.	1.5	15
25533	Elucidating Quantum Confinement in Graphene Oxide Dots Based On Excitation-Wavelength-Independent Photoluminescence. Journal of Physical Chemistry Letters, 2016, 7, 2087-2092.	2.1	143
25534	Structure Elucidation of Mixed-Linker Zeolitic Imidazolate Frameworks by Solid-State 1H CRAMPS NMR Spectroscopy and Computational Modeling. Journal of the American Chemical Society, 2016, 138, 7325-7336.	6.6	45
25535	Tuning Dirac points by strain in MoX₂nanoribbons (X = S, Se, Te) with a 1Tâ€² structure. Physical Chemistry Chemical Physics, 2016, 18, 16361-16366.	1.3	5
25536	Glycerol oxidehydration to pyruvaldehyde over silver-based catalysts for improved lactic acid production. Green Chemistry, 2016, 18, 4682-4692.	4.6	32
25537	Synthesis of two-dimensional titanium nitride Ti₄N₃(MXene). Nanoscale, 2016, 8, 11385-11391.	2.8	878
25538	Low-density superhard materials: computational study of Li-inserted B-substituted closo-carboranes LiBC₁₁ and Li₂B₂C₁₀. RSC Advances, 2016, 6, 52695-52699.	1.7	8

#	Article	IF	Citations
25539	A model for understanding the formation energies of nanolamellar phases in transition metal carbides and nitrides. Modelling and Simulation in Materials Science and Engineering, 2016, 24, 055004.	0.8	18
25540	Nanoporous PdZr surface alloy as highly active nonâ€“platinum electrocatalyst toward oxygen reduction reaction with unique structure stability and methanolâ€“tolerance. Journal of Power Sources, 2016, 316, 106-113.	4.0	17
25541	Flexible Self-Assembled Molecular Templates on Graphene. Journal of Physical Chemistry C, 2016, 120, 8772-8780.	1.5	37
25542	Synthesis, characterization and DFT studies of zinc-doped copper oxide nanocrystals for gas sensing applications. Journal of Materials Chemistry A, 2016, 4, 6527-6539.	5.2	157
25543	Chemical Pressure Schemes for the Prediction of Soft Phonon Modes: A Chemistâ€™s Guide to the Vibrations of Solid State Materials. Chemistry of Materials, 2016, 28, 3171-3183.	3.2	42
25544	The unexpectedly rich reconstructions of rutile TiO2(011)-(2 Ã— 1) surface and the driving forces behind their formation: an ab initio evolutionary study. Physical Chemistry Chemical Physics, 2016, 18, 19549-19556.	1.3	18
25545	Electric field control of the magnetic anisotropy energy of double-vacancy graphene decorated by iridium atoms. Physical Chemistry Chemical Physics, 2016, 18, 11550-11555.	1.3	10
25546	Phenomenological effets of tantalum incorporation into diamond films: Experimental and first principle studies. Applied Surface Science, 2016, 380, 83-90.	3.1	6
25547	Graphene monovacancies: Electronic and mechanical properties from large scale ab initio simulations. Carbon, 2016, 103, 200-208.	5.4	33
25548	The interaction of Pd clusters with the bulk and layered two-dimensional Silicalite-1 supports. Catalysis Today, 2016, 277, 108-117.	2.2	2
25549	Insights into the mechanism of nitrobenzene reduction to aniline over Pt catalyst and the significance of the adsorption of phenyl group on kinetics. Chemical Engineering Journal, 2016, 293, 337-344.	6.6	96
25550	Zirconium-peroxo embedded in non-stoichiometric yttria stabilized zirconia (110) from first-principles. Solid State Ionics, 2016, 285, 215-221.	1.3	2
25551	Nature, Strength, and Cooperativity of the Hydrogen-Bonding Network in Î±-Chitin. Biomacromolecules, 2016, 17, 996-1003.	2.6	57
25552	Two-Step Antiferromagnetic Transitions and Ferroelectricity in Spin-1 Triangular-Lattice Antiferromagnetic Sr₃NiTa₂O₉. Inorganic Chemistry, 2016, 55, 2709-2716.	1.9	14
25553	Electric Field Effects on Spin Splitting of Two-Dimensional van der Waals Arsenene/FeCl₂ Heterostructures. Journal of Physical Chemistry C, 2016, 120, 5613-5618.	1.5	46
25554	Ionothermal Synthesis of High-Voltage Alluaudite Na_{2+2x}Fe_{2-x}(SO₄)₃ Sodium Insertion Compound: Structural, Electronic, and Magnetic Insights. ACS Applied Materials & Interfaces, 2016, 8, 6982-6991.	4.0	66
25555	Unravelling the Effects of Grain Boundary and Chemical Doping on Electronâ€“Hole Recombination in CH₃NH₃PbI₃ Perovskite by Time-Domain Atomistic Simulation. Journal of the American Chemical Society, 2016, 138, 3884-3890.	6.6	333
25556	The O, OH and OOH-assisted selective coupling of methanol on Auâ€“Ag(111). Physical Chemistry Chemical Physics, 2016, 18, 9969-9978.	1.3	9

#	Article	IF	Citations
25557	Syntheses, structures, physical and electronic properties of quaternary semiconductors: Cs[RE₉Cd₄Se₁₈] (RE = Tbâ€“Tm). Dalton Transactions, 2016, 45, 5775-5782.	1.6	12
25558	A Ti-anchored Ti2CO2 monolayer (MXene) as a single-atom catalyst for CO oxidation. Journal of Materials Chemistry A, 2016, 4, 4871-4876.	5.2	242
25559	Robust room-temperature inversion-asymmetry topological transitions in functionalized HgSe monolayer. Journal of Materials Chemistry C, 2016, 4, 2243-2251.	2.7	22
25560	Controllable dissociations of PH₃molecules on Si(001). Nanotechnology, 2016, 27, 135704.	1.3	7
25561	Ab initiostudy of energetics and magnetism of sigma phase in Coâ€“Mo and Feâ€“Mo systems. Modelling and Simulation in Materials Science and Engineering, 2016, 24, 025009.	0.8	7
25562	Prediction of a new graphenelike<mml:math xmlns:mml="http://www.w3.org/1998/Math/MathML"><mml:mrow><mml:msub><mml:mi>Si</mml:mi><mml:mn>2</mml:mn></mml:msub></mml:mrow></mml:math>sheet with unusual Dirac cones: The<mml:math xmlns:mml="http://www.w3.org/1998/Math/MathML"><mml:mrow><mml:msub><mml:mi>Si</mml:mi><mml:mn>2</mml:mn></mml:msub></mml:mrow></mml:math>Bn monolayer. Physical Review B, 2016, 93, .	3.7	66
25563	Structure and Oxidizing Power of Single Layer Î±-V2O5. Topics in Catalysis, 2016, 59, 809-816.	1.3	6
25564	Pressure-induced variation of structural, elastic, vibrational, electronic, thermodynamic properties and hardness of Ruthenium Carbides. Journal of Physics and Chemistry of Solids, 2016, 94, 47-58.	1.9	2
25565	Thermodynamic Stability of Low- and High-Index Spinel LiMn₂O₄ Surface Terminations. ACS Applied Materials & Interfaces, 2016, 8, 11108-11121.	4.0	73
25566	Confined linear carbon chains as a route to bulkÂcarbyne. Nature Materials, 2016, 15, 634-639.	13.3	341
25567	Effect of Temperature on the Desorption of Lithium from Molybdenum(110) Surfaces: Implications for Fusion Reactor First Wall Materials. Journal of Physical Chemistry B, 2016, 120, 6110-6119.	1.2	15
25568	First-Principles Study on Nitrobenzene-Doped Graphene as a Metal-Free Electrocatalyst for Oxygen Reduction Reaction. Journal of Physical Chemistry C, 2016, 120, 8804-8812.	1.5	42
25569	Graphene Monoxide Bilayer As a High-Performance on/off Switching Media for Nanoelectronics. ACS Applied Materials & Interfaces, 2016, 8, 10477-10482.	4.0	10
25570	DFT Insights into the Competitive Adsorption of Sulfur- and Nitrogen-Containing Compounds and Hydrocarbons on Co-Promoted Molybdenum Sulfide Catalysts. ACS Catalysis, 2016, 6, 2904-2917.	5.5	66
25571	Investigation of magnetic and electronic properties of transition metal doped Sc₂CT₂(T = O, OH or F) using a first principles study. Physical Chemistry Chemical Physics, 2016, 18, 12914-12919.	1.3	70
25572	The electronic, optical, and thermodynamic properties of borophene from first-principles calculations. Journal of Materials Chemistry C, 2016, 4, 3592-3598.	2.7	333
25573	Properties of (Ga_{1â^'x}In_x)₂O₃ over the whole x range. Journal of Physics Condensed Matter, 2016, 28, 224001.	0.7	10
25574	QM/MM Methods for Crystalline Defects. Part 1: Locality of the Tight Binding Model. Multiscale Modeling and Simulation, 2016, 14, 232-264.	0.6	29

#	Article	IF	Citations
25575	dâ€AO spherical aromaticity in Ce₆O₈. Journal of Computational Chemistry, 2016, 37, 103-109.	1.5	32
25576	LOBSTER: A tool to extract chemical bonding from planeâ€wave based DFT. Journal of Computational Chemistry, 2016, 37, 1030-1035.	1.5	1,791
25577	Theoretical and experimental investigation of possible ferromagnetic ordering in wide band gap ZnO and related systems. Nuclear Instruments & Methods in Physics Research B, 2016, 379, 18-22.	0.6	7
25578	Atomic and Electronic Structures of WTe₂ Probed by High Resolution Electron Microscopy and ab Initio Calculations. Journal of Physical Chemistry C, 2016, 120, 8364-8369.	1.5	37
25579	Tuning the electronic and mechanical properties of penta-graphene via hydrogenation and fluorination. Physical Chemistry Chemical Physics, 2016, 18, 14191-14197.	1.3	103
25580	Graphene-like Two-Dimensional Ionic Boron with Double Dirac Cones at Ambient Condition. Nano Letters, 2016, 16, 3022-3028.	4.5	222
25581	Characterization of 'metal resist' for EUV lithography. Proceedings of SPIE, 2016, , .	0.8	8
25582	Ab initio molecular dynamics studies on effect of Zr on oxidation resistance of TiAlN coatings. Applied Surface Science, 2016, 378, 293-300.	3.1	19
25583	Density-functional study on the structural and magnetic properties of N-doped graphene oxide. Carbon, 2016, 102, 39-50.	5.4	15
25584	Alloying effect on the ideal tensile strength of ferromagnetic and paramagnetic bcc iron. Journal of Alloys and Compounds, 2016, 676, 565-574.	2.8	9
25585	Density functional theory insights into the structural stability and Li diffusion properties of monoclinic and orthorhombic Li 2 FeSiO 4 cathodes. Journal of Power Sources, 2016, 318, 136-145.	4.0	34
25586	Bismuthâ€“indium two-dimensional compounds on Si(111) surface. Surface Science, 2016, 651, 105-111.	0.8	19
25587	Catalysis in a Cage: Condition-Dependent Speciation and Dynamics of Exchanged Cu Cations in SSZ-13 Zeolites. Journal of the American Chemical Society, 2016, 138, 6028-6048.	6.6	588
25588	Generalization of first-principles thermodynamic model: Application to hexagonal close-packed <mml:math xmlns:mml="http://www.w3.org/1998/Math/MathML" altimg="si49.gif" overflow="scroll"><mml:mrow><mml:mi>Îµ</mml:mi></mml:mrow></mml:math>-Fe3N. Computational Materials Science, 2016, 117, 83-89.	1.4	4
25589	Three types of dislocation core structure in B2 alloys. Intermetallics, 2016, 73, 21-25.	1.8	6
25590	High pressure polyhydrides of molybdenum: A first-principles study. Solid State Communications, 2016, 239, 14-19.	0.9	15
25591	Fully Understanding the Photochemical Properties of Bi₂O₂(CO₃)_{1â€“x}S_x Nanosheets. Langmuir, 2016, 32, 3811-3819.	1.6	14
25592	Size-Dependent Penetration of Gold Nanoclusters through a Defect-Free, Nonporous NaCl Membrane. Nano Letters, 2016, 16, 3063-3070.	4.5	12

#	Article	IF	Citations
25593	Giant Mechanocaloric Effects in Fluorite-Structured Superionic Materials. Nano Letters, 2016, 16, 3124-3129.	4.5	39
25594	Single Precursor Mediated-Synthesis of Bi Semimetal Deposited N-Doped (BiO)₂CO₃ Superstructures for Highly Promoted Photocatalysis. ACS Sustainable Chemistry and Engineering, 2016, 4, 2969-2979.	3.2	64
25595	System-size dependent band alignment in lateral two-dimensional heterostructures. 2D Materials, 2016, 3, 025012.	2.0	18
25596	Effects of strain and interface on magnetic anisotropy of FeCo/FePt: A first principles study. Computational Materials Science, 2016, 117, 527-533.	1.4	3
25597	Simulation of hydrogen effect on equilibrium shape of gas bubbles in beryllium. Fusion Engineering and Design, 2016, 109-111, 1432-1436.	1.0	6
25598	Strong Infrared NLO Tellurides with Multifunction: CsX^{II}₄In₅Te₁₂ (X^{II} = Mn, Zn, Cd). Inorganic Chemistry, 2016, 55, 4470-4475.	1.9	47
25599	Width and Crystal Orientation Dependent Band Gap Renormalization in Substrate-Supported Graphene Nanoribbons. Journal of Physical Chemistry Letters, 2016, 7, 1526-1533.	2.1	47
25600	Molecular Origin of Properties of Organicâ€“Inorganic Hybrid Perovskites: The Big Picture from Small Clusters. Journal of Physical Chemistry Letters, 2016, 7, 1596-1603.	2.1	60
25601	Mobile Polaronic States in Î±-MoO₃: An ab Initio Investigation of the Role of Oxygen Vacancies and Alkali Ions. ACS Applied Materials & Interfaces, 2016, 8, 10911-10917.	4.0	49
25602	A First-Principle Study of Synergized O₂ Activation and CO Oxidation by Ag Nanoparticles on TiO₂(101) Support. ACS Applied Materials & Interfaces, 2016, 8, 10315-10323.	4.0	34
25603	The adsorption behaviours of Pt adatom on pristine and defective bilayer graphene. Molecular Physics, 2016, 114, 1898-1906.	0.8	3
25604	First-principles investigations of the structure and physical properties for new TcN crystal structure. Molecular Physics, 2016, 114, 1952-1959.	0.8	5
25605	Structural evolution and magnetic properties of L10-type Mn54.5Al45.5-xGax (xÂ=Â0.0, 15.0, 25.0, 35.0, 45.5) phase. Journal of Alloys and Compounds, 2016, 680, 14-19.	2.8	12
25606	Reducing the Schottky barrier height at the MoSe2/Mo(110) interface in thin-film solar cells: Insights from first-principles calculations. Thin Solid Films, 2016, 606, 143-147.	0.8	13
25607	Dispersion-Corrected Mean-Field Electronic Structure Methods. Chemical Reviews, 2016, 116, 5105-5154.	23.0	1,032
25608	Spectroscopy and Ultrafast Vibrational Dynamics of Strongly Hydrogen Bonded OH Species at the Î±-Al₂O₃(112l...0)/H₂O Interface. Journal of Physical Chemistry C, 2016, 120, 16153-16161.	1.5	42
25609	Density functional theory + U analysis of the electronic structure and defect chemistry of LSCF (La_{0.5}Sr_{0.5}Co_{0.25}Fe_{0.75}O_{3â^'Î´}). Physical Chemistry Chemical Physics, 2016, 18, 12260-12269.	1.3	39
25610	Tuning band gap and optical properties of SnX₂ nanosheets: Hybrid functional studies. Modern Physics Letters B, 2016, 30, 1650120.	1.0	3

#	Article	IF	Citations
25611	COMPARISON OF ELECTRONIC AND OPTICAL PROPERTIES OF GaN MONOLAYER AND BULK STRUCTURE: A FIRST PRINCIPLE STUDY. Surface Review and Letters, 2016, 23, 1650026.	0.5	5
25612	Structural study of the magnetocaloric material MnFePxAs1â^'x. Electronic Materials Letters, 2016, 12, 255-259.	1.0	3
25613	Electronic and magnetic properties of Ag-doped monolayer WS2 by stain. Journal of Alloys and Compounds, 2016, 680, 659-664.	2.8	19
25614	Conceptual design of tetraazaporphyrin- and subtetraazaporphyrin-based functional nanocarbon materials: electronic structures, topologies, optical properties, and methane storage capacities. Physical Chemistry Chemical Physics, 2016, 18, 13503-13518.	1.3	3
25615	First-principles investigations of electronic, magnetic and thermodynamic properties of Heusler alloy Co2Mn1â^'Ti Sn. Journal of Alloys and Compounds, 2016, 679, 74-79.	2.8	11
25616	First-principles studies of adsorption behavior for graphene nanosheet on Al-doped BiF3(111) surfaces. Materials Chemistry and Physics, 2016, 173, 291-297.	2.0	4
25617	Controlling Catalytic Properties of Pd Nanoclusters through Their Chemical Environment at the Atomic Level Using Isoreticular Metalâ€“Organic Frameworks. ACS Catalysis, 2016, 6, 3461-3468.	5.5	152
25618	Solar fuel photoanodes prepared by inkjet printing of copper vanadates. Journal of Materials Chemistry A, 2016, 4, 7483-7494.	5.2	56
25619	Electronic structure and magnetism of doped wurtzite InSb nanowire. Journal Physics D: Applied Physics, 2016, 49, 175303.	1.3	9
25620	A theoretical investigation on the magnetic and transport properties of the phosphorus nanoribbons with tetragons at the edges. Chemical Physics Letters, 2016, 652, 1-5.	1.2	7
25621	Adsorption and dissociation of H₂O on the (001) surface of uranium mononitride: energetics and mechanism from first-principles investigation. Physical Chemistry Chemical Physics, 2016, 18, 13255-13266.	1.3	17
25622	Experimental Part. Springer Theses, 2016, , 103-114.	0.0	0
25623	MEAMfit: A reference-free modified embedded atom method (RF-MEAM) energy and force-fitting code. Computer Physics Communications, 2016, 203, 354-355.	3.0	7
25624	Hydrogen effect on electronic and magnetic properties of Cd1â^'xMnxTe: Ab initio study. Solid State Communications, 2016, 239, 44-48.	0.9	4
25625	Nanoscale Solvation Leads to Spontaneous Formation of a Bicarbonate Monolayer on Rutile (110) under Ambient Conditions: Implications for CO₂ Photoreduction. Journal of Physical Chemistry C, 2016, 120, 9326-9333.	1.5	36
25626	Atomic structures and electronic properties of phosphorene grain boundaries. 2D Materials, 2016, 3, 025008.	2.0	49
25627	Strong dependence of flattening and decoupling of graphene on metals on the local distribution of intercalated oxygen atoms. Carbon, 2016, 101, 129-134.	5.4	18
25628	High catalytic activity of oxygen-induced (200) surface of Ta2O5 nanolayer towards durable oxygen evolution reaction. Nano Energy, 2016, 25, 60-67.	8.2	36

#	Article	IF	Citations
25629	The role of vdW interactions in coverage dependent adsorption energies of atomic adsorbates on Pt(111) and Pd(111). Surface Science, 2016, 650, 196-202.	0.8	5
25630	Computational Investigation of Feâ€“Cu Bimetallic Catalysts for CO₂ Hydrogenation. Journal of Physical Chemistry C, 2016, 120, 9364-9373.	1.5	49
25631	Charge density wave order in 1D mirror twin boundaries of single-layer MoSe2. Nature Physics, 2016, 12, 751-756.	6.5	209
25632	A theoretical study on the pH dependence of X-ray emission spectra for aqueous acetic acid. Chemical Physics Letters, 2016, 649, 156-161.	1.2	6
25633	Role of cation size for hydrogen carbonate stabilization and modification of the zeoliteâ€“CO2 interaction energy: Computational analysis in alkali Y zeolites. Microporous and Mesoporous Materials, 2016, 228, 182-195.	2.2	9
25634	Molybdenum Substituted Vanadyl Phosphate Îµ-VOPO₄ with Enhanced Two-Electron Transfer Reversibility and Kinetics for Lithium-Ion Batteries. Chemistry of Materials, 2016, 28, 3159-3170.	3.2	42
25635	Local and Extended Structures of <scp>d</scp>-(â^')-Tartaric Acid on Pd(111). Journal of Physical Chemistry C, 2016, 120, 2309-2319.	1.5	6
25636	D₂O Interaction with Planar ZnO(0001) Bilayer Supported on Au(111): Structures, Energetics and Influence of Hydroxyls. Journal of Physical Chemistry C, 2016, 120, 8157-8166.	1.5	12
25637	Correlation between Structure and Ferromagnetism in Nano-BiFeO₃. Journal of Physical Chemistry C, 2016, 120, 8411-8416.	1.5	37
25638	Reaction Network of Layer-to-Tunnel Transition of MnO₂. Journal of the American Chemical Society, 2016, 138, 5371-5379.	6.6	128
25639	Significantly enhanced oxygen reduction reaction performance of N-doped carbon by heterogeneous sulfur incorporation: synergistic effect between the two dopants in metal-free catalysts. Journal of Materials Chemistry A, 2016, 4, 7422-7429.	5.2	71
25640	Germanium and phosphorus co-doped carbon nanotubes with high electrocatalytic activity for oxygen reduction reaction. RSC Advances, 2016, 6, 33205-33211.	1.7	15
25641	Nanocrystals of CuCr₂S_{4â^'x}Se_x chalcospinels with tunable magnetic properties. Journal of Materials Chemistry C, 2016, 4, 3628-3639.	2.7	10
25642	A PRELIMINARY JUPITER MODEL. Astrophysical Journal, 2016, 820, 80.	1.6	105
25643	The role of metastable LPSO building block clusters in phase transformations of an Mg-Y-Zn alloy. Acta Materialia, 2016, 112, 171-183.	3.8	104
25644	Theoretical insights on the reaction pathways for oxygen reduction reaction on phosphorus doped graphene. Carbon, 2016, 105, 214-223.	5.4	57
25645	Cation synergies affect ammonia adsorption over VOX and (V,W)OX dispersed on Î±-Al2O3 (0001) and Î±-Fe2O3 (0001). Surface Science, 2016, 651, 41-50.	0.8	7
25646	An electron injection promoted highly efficient electrocatalyst of FeNi₃@GR@Fe-NiOOH for oxygen evolution and rechargeable metalâ€“air batteries. Journal of Materials Chemistry A, 2016, 4, 7762-7771.	5.2	70

#	Article	IF	Citations
25647	Magnetic Anisotropy of Small Irn Clusters (nÂ=Â2â€“5). Journal of Cluster Science, 2016, 27, 935-946.	1.7	7
25648	Predicting Coherency Loss of $$ gamma^{primeprime} $$ Precipitates in IN718 Superalloy. Metallurgical and Materials Transactions A: Physical Metallurgy and Materials Science, 2016, 47, 3235-3247.	1.1	46
25649	Degradation of polymer electrolyte membrane fuel cell by siloxane in biogas. Journal of Power Sources, 2016, 316, 44-52.	4.0	7
25650	Electronic structure and lattice dynamics of rhombohedral BiAlO 3 from first-principles. Materials Chemistry and Physics, 2016, 177, 405-412.	2.0	16
25651	Structural Evolution of Reversible Mg Insertion into a Bilayer Structure of V₂O₅Â·nH₂O Xerogel Material. Chemistry of Materials, 2016, 28, 2962-2969.	3.2	97
25652	Computational Prediction of High Thermoelectric Performance in Hole Doped Layered GeSe. Chemistry of Materials, 2016, 28, 3218-3226.	3.2	129
25653	Probing the Electronic Structure of Heterogeneous Metal Interfaces by Transition Metal Shelled Gold Nanoparticle-Enhanced Raman Spectroscopy. Journal of Physical Chemistry C, 2016, 120, 20684-20691.	1.5	28
25654	Stabilities and Reconstructions of Clean PbS and PbSe Surfaces: DFT Results and the Role of Dispersion Forces. Journal of Physical Chemistry C, 2016, 120, 8813-8820.	1.5	18
25655	Intrinsic Ferroelasticity and/or Multiferroicity in Two-Dimensional Phosphorene and Phosphorene Analogues. Nano Letters, 2016, 16, 3236-3241.	4.5	491
25656	Polar metals by geometric design. Nature, 2016, 533, 68-72.	13.7	262
25657	Adsorption of gas molecules and the induced magnetic properties of metal-decorated graphene. Integrated Ferroelectrics, 2016, 168, 97-106.	0.3	5
25658	Graphene on a metal surface with an h-BN buffer layer: gap opening and N-doping. Journal of the Korean Physical Society, 2016, 68, 833-838.	0.3	0
25659	Mechanistic Insight into the C₂ Hydrocarbons Formation from Syngas on fcc-Co(111) Surface: A DFT Study. Journal of Physical Chemistry C, 2016, 120, 9132-9147.	1.5	53
25660	Polymorphism of the azobenzene dye compound methyl yellow. CrystEngComm, 2016, 18, 3456-3461.	1.3	8
25661	Electronegative guests in CoSb₃. Energy and Environmental Science, 2016, 9, 2090-2098.	15.6	93
25662	Density functional studies on wurtzite piezotronic transistors: influence of different semiconductors and metals on piezoelectric charge distribution and Schottky barrier. Nanotechnology, 2016, 27, 205204.	1.3	12
25663	Two-Dimensional Halide Perovskites: Tuning Electronic Activities of Defects. Nano Letters, 2016, 16, 3335-3340.	4.5	94
25664	Misfit Stresses Caused by Atomic Size Mismatch: The Origin of Doping-Induced Destabilization of Dicalcium Silicate. Crystal Growth and Design, 2016, 16, 3124-3132.	1.4	31

#	Article	IF	Citations
25665	Reduction of CO₂ with Water on Pt-Loaded Rutile TiO₂(110) Modeled with Density Functional Theory. Journal of Physical Chemistry C, 2016, 120, 9160-9164.	1.5	29
25666	Preparation of Sn-doped CuAlS₂ films with an intermediate band and wide-spectrum solar response. RSC Advances, 2016, 6, 40806-40810.	1.7	21
25667	Bi-doped Sb₂S₃ for low effective mass and optimized optical properties. Journal of Materials Chemistry C, 2016, 4, 5081-5090.	2.7	23
25668	Theoretical insights on the catalytic activity and mechanism for oxygen reduction reaction at Fe and P codoped graphene. Physical Chemistry Chemical Physics, 2016, 18, 12675-12681.	1.3	22
25669	Controlling nucleation of monolayer WSe 2 during metal-organic chemical vapor deposition growth. 2D Materials, 2016, 3, 025015.	2.0	42
25670	High efficiency of Pt2+- CeO2 novel thin film catalyst as anode for proton exchange membrane fuel cells. Applied Catalysis B: Environmental, 2016, 197, 262-270.	10.8	52
25671	Mechanistic insights into the Cu(I) oxide-catalyzed conversion of CO 2 to fuels and chemicals: A DFT approach. Journal of CO2 Utilization, 2016, 15, 96-106.	3.3	35
25672	Hydrogenation induced structure and property changes in GdGa. Journal of Solid State Chemistry, 2016, 239, 184-191.	1.4	7
25673	Kinetic Regimes in Ethylene Hydrogenation over Transition-Metal Surfaces. ACS Catalysis, 2016, 6, 3277-3286.	5.5	43
25674	Mechanism of Electrochemical Hydrogen Storage for Î±-Fe₂O₃Particles as Anode Material for Aqueous Rechargeable Batteries. Journal of the Electrochemical Society, 2016, 163, H566-H569.	1.3	14
25675	Elastic anisotropy and phonon focusing for tetragonal crystals: Application to Î³-TiAl. Computational Materials Science, 2016, 118, 117-123.	1.4	9
25676	Mechanical properties and oxidation behavior of Ti-doped Nb4AlC3. Journal of the European Ceramic Society, 2016, 36, 1001-1008.	2.8	38
25677	Equation of state for technetium from Xâ€ray diffraction and first-principle calculations. Journal of Physics and Chemistry of Solids, 2016, 95, 6-11.	1.9	5
25678	Effect of N-Containing Functional Groups on CO₂ Adsorption of Carbonaceous Materials: A Density Functional Theory Approach. Journal of Physical Chemistry C, 2016, 120, 8087-8095.	1.5	114
25679	A van der Waals Density Functional Study of MoO₃ and Its Oxygen Vacancies. Journal of Physical Chemistry C, 2016, 120, 8959-8968.	1.5	91
25680	Stark Effect and Nonlinear Impedance of the Asymmetric Ag-CO-Ag Junction: An Optical Rectenna. Journal of Physical Chemistry C, 2016, 120, 20914-20921.	1.5	13
25681	Quantum spin Hall insulators in functionalized arsenene (AsX, X = F, OH and CH₃) monolayers with pronounced light absorption. Nanoscale, 2016, 8, 9657-9666.	2.8	63
25682	Tuning electronic transport in epitaxial graphene-based van der Waals heterostructures. Nanoscale, 2016, 8, 8947-8954.	2.8	21

#	Article	IF	Citations
25683	Well-structured bimetallic surface capable of molecular recognition for chemoselective nitroarene hydrogenation. Chemical Science, 2016, 7, 4476-4484.	3.7	75
25684	Comprehensive genetic algorithm forab initioglobal optimisation of clusters. Molecular Simulation, 2016, 42, 809-819.	0.9	88
25685	Impurity effect of Mg on the generalized planar fault energy of Al. Journal of Materials Science, 2016, 51, 6552-6568.	1.7	46
25686	Automating impurity-enhanced antiphase boundary energy calculations from ab initio Monte Carlo. Calphad: Computer Coupling of Phase Diagrams and Thermochemistry, 2016, 53, 20-24.	0.7	13
25687	Development of a second-nearest-neighbor modified embedded atom method potential for siliconâ€“phosphorus binary system. Computational Materials Science, 2016, 120, 1-12.	1.4	5
25688	Enhanced Exciton Binding Energy of ZnO by Long-Distance Perturbation of Doped Be Atoms. Journal of Physical Chemistry Letters, 2016, 7, 1484-1489.	2.1	25
25689	Exceptional photosensitivity of a polyoxometalate-based charge-transfer hybrid material. Chemical Communications, 2016, 52, 7394-7397.	2.2	97
25690	Markedly different adsorption behaviors of gas molecules on defective monolayer MoS₂: a first-principles study. Physical Chemistry Chemical Physics, 2016, 18, 15110-15117.	1.3	126
25691	First-principles study of thermal properties of borophene. Physical Chemistry Chemical Physics, 2016, 18, 14927-14932.	1.3	109
25692	Computer calculations across time and length scales in photovoltaic solar cells. Energy and Environmental Science, 2016, 9, 2197-2218.	15.6	27
25693	Electrochemically self-doped hierarchical TiO₂ nanotube arrays for enhanced visible-light photoelectrochemical performance: an experimental and computational study. RSC Advances, 2016, 6, 46871-46878.	1.7	20
25694	First-principles study of the effect of boron on grain boundary in NiAl. Computational Materials Science, 2016, 121, 1-5.	1.4	10
25695	Thorough investigations of the structural and electronic properties of AlxIn1-xN ternary compound via ab initio computations. Journal of Alloys and Compounds, 2016, 682, 338-344.	2.8	3
25696	Band structures in silicene on monolayer gallium phosphide substrate. Solid State Communications, 2016, 239, 32-36.	0.9	6
25697	Atomistic simulations of electrochemical metallization cells: mechanisms of ultra-fast resistance switching in nanoscale devices. Nanoscale, 2016, 8, 14037-14047.	2.8	22
25698	Stationary Full Li-Ion Batteries with Interlayer-Expanded V6O13 Cathodes and Lithiated Graphite Anodes. Electrochimica Acta, 2016, 203, 171-177.	2.6	42
25699	Chemisorption of Acetophenone on Si(111)-7 Ã— 7. Polar Aromatic Molecule on Electronically Complex Surface. Journal of Physical Chemistry C, 2016, 120, 9200-9206.	1.5	2
25700	A computational study of the interaction of graphene structures with biomolecular units. Physical Chemistry Chemical Physics, 2016, 18, 15312-15321.	1.3	18

#	Article	IF	Citations
25701	Electronic Structure Descriptor for the Discovery of Narrow-Band Red-Emitting Phosphors. Chemistry of Materials, 2016, 28, 4024-4031.	3.2	78
25702	Petascale Orbital-Free Density Functional Theory Enabled by Small-Box Algorithms. Journal of Chemical Theory and Computation, 2016, 12, 2950-2963.	2.3	41
25703	Detailed Atomic Reconstruction of Extended Line Defects in Monolayer MoS₂. ACS Nano, 2016, 10, 5419-5430.	7.3	161
25704	Electron dominated thermoelectric response in MNiSn (M: Ti, Zr, Hf) half-Heusler alloys. Physical Chemistry Chemical Physics, 2016, 18, 14017-14022.	1.3	25
25705	Pressure-induced structural and valence transition in AgO. Physical Chemistry Chemical Physics, 2016, 18, 15322-15326.	1.3	3
25706	Stability, electronic structure and magnetic properties of vacancy and nonmetallic atom-doped buckled arsenene: first-principles study. RSC Advances, 2016, 6, 43794-43801.	1.7	31
25707	Control of valence and conduction band energies in layered transition metal phosphates via surface functionalization. Physical Chemistry Chemical Physics, 2016, 18, 14122-14128.	1.3	5
25708	Effect of van der Waals corrections on DFT-computed metallic surface properties. Materials Research Express, 2016, 3, 046501.	0.8	28
25709	Theoretical Investigation of Stabilizing Mechanism by Boron in Body-Centered Cubic Iron Through (Fe,Cr)23(C,B)6 Precipitates. Metallurgical and Materials Transactions A: Physical Metallurgy and Materials Science, 2016, 47, 2487-2497.	1.1	37
25710	Lattice thermal conductivity of penta-graphene. Carbon, 2016, 105, 424-429.	5.4	120
25711	Nitrogen doping in acetylene bonded two dimensional carbon crystals: Ab-initio forecast of electrocatalytic activities vis-Ã-vis boron doping. Carbon, 2016, 105, 330-339.	5.4	27
25712	Exploring high-pressure FeB2: Structural and electronic properties predictions. Journal of Alloys and Compounds, 2016, 678, 109-112.	2.8	11
25713	Impact of Short-Range Forces on Defect Production from High-Energy Collisions. Journal of Chemical Theory and Computation, 2016, 12, 2871-2879.	2.3	49
25714	Impact of Point Defects on Proton Conduction in Strontium Cerate. Journal of Physical Chemistry C, 2016, 120, 9562-9568.	1.5	11
25715	Strain-Induced Electronic Structure Changes in Stacked van der Waals Heterostructures. Nano Letters, 2016, 16, 3314-3320.	4.5	122
25716	Unveiling the electrochemical mechanisms of Li₂Fe(SO₄)₂ polymorphs by neutron diffraction and density functional theory calculations. Physical Chemistry Chemical Physics, 2016, 18, 14509-14519.	1.3	20
25717	Role of various defects in the photoluminescence characteristics of nanocrystalline Nd₂Zr₂O₇: an investigation through spectroscopic and DFT calculations. Journal of Materials Chemistry C, 2016, 4, 4988-5000.	2.7	99
25718	Dependence of elastic and optical properties on surface terminated groups in two-dimensional MXene monolayers: a first-principles study. RSC Advances, 2016, 6, 35731-35739.	1.7	224

#	Article	IF	Citations
25719	Applications of Special Quasi-random Structures to High-Entropy Alloys. , 2016, , 333-368.		20
25720	Prediction of Structure and Phase Transformations. , 2016, , 267-298.		19
25721	Adsorption of gas molecules on Cu impurities embedded monolayer MoS 2 : A first- principles study. Applied Surface Science, 2016, 382, 280-287.	3.1	116
25722	Local structure study of tellurium corrosion of nickel alloy by X-ray absorption spectroscopy. Corrosion Science, 2016, 108, 169-172.	3.0	25
25723	Quasi-particle energies and optical excitations of wurtzite BeO and its nanosheet. Journal of Alloys and Compounds, 2016, 682, 254-262.	2.8	63
25724	Tuning electronic and magnetic properties of blue phosphorene by doping Al, Si, As and Sb atom: A DFT calculation. Solid State Communications, 2016, 242, 36-40.	0.9	72
25725	Pyramidal Structure Formation at the Interface between III/V Semiconductors and Silicon. Chemistry of Materials, 2016, 28, 3265-3275.	3.2	37
25726	Size- and Shape-Controlled Synthesis and Properties of Magneticâ€“Plasmonic Coreâ€“Shell Nanoparticles. Journal of Physical Chemistry C, 2016, 120, 10530-10546.	1.5	86
25727	Atomically Dispersed Pd, Ni, and Pt Species in Ceria-Based Catalysts: Principal Differences in Stability and Reactivity. Journal of Physical Chemistry C, 2016, 120, 9852-9862.	1.5	99
25728	High Chloride Doping Levels Stabilize the Perovskite Phase of Cesium Lead Iodide. Nano Letters, 2016, 16, 3563-3570.	4.5	247
25729	Efficient ambipolar transport properties in alternate stacking donorâ€“acceptor complexes: from experiment to theory. Physical Chemistry Chemical Physics, 2016, 18, 14094-14103.	1.3	81
25730	Mixed Ge/Pb perovskite light absorbers with an ascendant efficiency explored from theoretical view. Physical Chemistry Chemical Physics, 2016, 18, 14408-14418.	1.3	74
25731	Surface-induced spin state locking of the [Fe(H₂B(pz)₂)₂(bipy)] spin crossover complex. Journal of Physics Condensed Matter, 2016, 28, 206002.	0.7	50
25732	DFT MODELING OF BENZOYL PEROXIDE ADSORPTION ON Î±-Cr₂O₃ (0001) SURFACE. Surface Review and Letters, 2016, 23, 1650037.	0.5	1
25733	Phase diagram and polarization of stable phases of (Ga_{1â^’}) Tj ETQq0 0 0 rgBT /Overlock 10 Tf 50 182 Td (_xIn	1.1	124
25734	Valence charge density of multi-doped Mg2Si thermoelectric materials from maximum entropy method analysis. Journal of Alloys and Compounds, 2016, 681, 66-74.	2.8	2
25735	Structural and Electronic Effects on the Properties of Fe₂(dobdc) upon Oxidation with N₂O. Inorganic Chemistry, 2016, 55, 4924-4934.	1.9	15
25736	Stability and Polaronic Motion of Self-Trapped Holes in Silver Halides: Insight through DFT+U Calculations. Journal of Physical Chemistry C, 2016, 120, 8509-8524.	1.5	9

#	Article	IF	Citations
25737	Conduction and Surface Effects in Cathode Materials: Li₈ZrO₆ and Doped Li₈ZrO₆. Journal of Physical Chemistry C, 2016, 120, 9637-9649.	1.5	14
25738	Graphene Tunable Transparency to Tunneling Electrons: A Direct Tool To Measure the Local Coupling. ACS Nano, 2016, 10, 5131-5144.	7.3	23
25739	Evaluating silicene as a potential cathode host to immobilize polysulfides in lithiumâ€“sulfur batteries. Journal of Coordination Chemistry, 2016, 69, 2090-2105.	0.8	37
25740	Theoretical investigations on vibrational properties and thermal conductivities of ternary antimonides TiXSb, ZrXSb and HfXSb (X = Si, Ge). Philosophical Magazine, 2016, 96, 1712-1723.	0.7	10
25741	Analytical interactomic potential for a molybdenumâ€“erbium system. Modelling and Simulation in Materials Science and Engineering, 2016, 24, 045018.	0.8	2
25742	Understanding the interactions between lithium polysulfides and N-doped graphene using density functional theory calculations. Nano Energy, 2016, 25, 203-210.	8.2	347
25743	Role of Sodium Ion on TiO₂ Photocatalyst: Influencing Crystallographic Properties or Serving as the Recombination Center of Charge Carriers?. Journal of Physical Chemistry C, 2016, 120, 10390-10399.	1.5	28
25744	Metalâ€“Metal Bonding Stabilized Ground State Structure of Early Transition Metal Monoxide TMâ€“MO (TM = Ti, Hf, V, Ta). Journal of Physical Chemistry C, 2016, 120, 10009-10014.	1.5	10
25745	Nonradiative Relaxation of Photoexcited Black Phosphorus Is Reduced by Stacking with MoS₂: A Time Domain ab Initio Study. Journal of Physical Chemistry Letters, 2016, 7, 1830-1835.	2.1	36
25746	The surface stability and equilibrium crystal morphology of Ni₂P nanoparticles and nanowires from an ab initio atomistic thermodynamic approach. CrystEngComm, 2016, 18, 3808-3818.	1.3	17
25747	Direct Exfoliation of Graphite into Graphene by Pyrene-Based Molecules as Molecular-Level Wedges: A Tribological View. Tribology Letters, 2016, 62, 1.	1.2	7
25748	Magnetic BiMn-Î± phase synthesis prediction: First-principles calculation, thermodynamic modeling and nonequilibrium chemical partitioning. Computational Materials Science, 2016, 120, 117-126.	1.4	5
25749	Identifying the time-dependent predominance regimes of step and terrace sites for the Fischerâ€“Tropsch synthesis on ruthenium based catalysts. Catalysis Science and Technology, 2016, 6, 6495-6503.	2.1	10
25750	Hydrogen adsorption-mediated synthesis of concave Pt nanocubes and their enhanced electrocatalytic activity. Nanoscale, 2016, 8, 11559-11564.	2.8	39
25751	Electronic structure and topological features of tin-based binary nanosheets and their hydrogenated/fluorinated derivatives: A first-principles study. Applied Surface Science, 2016, 382, 1-9.	3.1	9
25752	van der Waals forces and confinement in carbon nanopores: Interaction between CH4, COOH, NH3, OH, SH and single-walled carbon nanotubes. Chemical Physics Letters, 2016, 652, 22-26.	1.2	4
25753	Activity and stability of cobalt phosphides for hydrogen evolution upon water splitting. Nano Energy, 2016, 29, 37-45.	8.2	166
25754	The detailed crystal and electronic structures of the cotunnite-type ZrO2. Solid State Communications, 2016, 239, 27-31.	0.9	3

#	Article	IF	Citations
25755	First-Principles Analysis on the Catalytic Role of Additives in Low-Temperature Synthesis of Transition Metal Diborides Using Nanolaminates. ACS Applied Materials & Interfaces, 2016, 8, 10995-11000.	4.0	6
25756	Achirality in the low temperature structure and lattice modes of tris(acetylacetonate)iron(iii). Dalton Transactions, 2016, 45, 8278-8283.	1.6	0
25757	Why host to dopant energy transfer is absent in the MgAl₂O₄:Eu³⁺ spinel? And exploring Eu³⁺ site distribution and local symmetry through its photoluminescence: interplay of experiment and theory. RSC Advances, 2016, 6, 42923-42932.	1.7	46
25758	Design of ternary alkaline-earth metal Sn(<scp>ii</scp>) oxides with potential good p-type conductivity. Journal of Materials Chemistry C, 2016, 4, 4592-4599.	2.7	29
25759	Understanding and Tuning the Hydrogen Evolution Reaction on Pt-Covered Tungsten Carbide Cathodes. Journal of the Electrochemical Society, 2016, 163, F629-F636.	1.3	15
25760	Multiscale description of carbon-supersaturated ferrite in severely drawn pearlitic wires. Acta Materialia, 2016, 111, 321-334.	3.8	35
25761	Correlating Lithium Hydroxyl Accumulation with Capacity Retention in V₂O₅ Aerogel Cathodes. ACS Applied Materials & Interfaces, 2016, 8, 11532-11538.	4.0	33
25762	Hydrostatic pressure effect on charge transport properties of phenacene organic semiconductors. Physical Chemistry Chemical Physics, 2016, 18, 13888-13896.	1.3	15
25763	A graphene-coupled Bi₂WO₆ nanocomposite with enhanced photocatalytic performance: a first-principles study. Physical Chemistry Chemical Physics, 2016, 18, 14113-14121.	1.3	27
25764	Band-gap modulation of C4H nanosheets by interlayer weak interaction and external electric field: a computational study. Theoretical Chemistry Accounts, 2016, 135, 1.	0.5	2
25765	Locating structures and evolution pathways of reconstructed rutile TiO2(011) using genetic algorithm aided density functional theory calculations. Journal of Molecular Modeling, 2016, 22, 114.	0.8	2
25766	An efficient ab-initio quasiharmonic approach for the thermodynamics of solids. Computational Materials Science, 2016, 120, 84-93.	1.4	65
25767	Doping-induced stability in vanadium-doped ZnO quantum well wires (QWW): Combination of DFT calculations within experimental measurements. Solid State Sciences, 2016, 57, 33-37.	1.5	2
25768	Detailed first-principles studies on surface energy and work function of hexagonal metals. Surface Science, 2016, 651, 137-146.	0.8	64
25769	Atomistic-Scale Analysis of Carbon Coating and Its Effect on the Oxidation of Aluminum Nanoparticles by ReaxFF-Molecular Dynamics Simulations. Journal of Physical Chemistry C, 2016, 120, 9464-9474.	1.5	116
25770	Electronic and Magnetic Properties of Transition-Metal-Doped Monolayer Black Phosphorus by Defect Engineering. Journal of Physical Chemistry C, 2016, 120, 9773-9779.	1.5	43
25771	Electronic Structure and Defect Chemistry of Tin(II) Complex Oxide SnNb₂O₆. Journal of Physical Chemistry C, 2016, 120, 9604-9611.	1.5	25
25772	Phase stability of the nanolaminates V2Ga2C and (Mo1â^'xVx)2Ga2C from first-principles calculations. Physical Chemistry Chemical Physics, 2016, 18, 12682-12688.	1.3	10

#	Article	IF	Citations
25773	Experimental and theoretical approach to account for green luminescence from Gd₂Zr₂O₇ pyrochlore: exploring the site occupancy and origin of host-dopant energy transfer in Gd₂Zr₂O₇:Eu³⁺. RSC Advances, 2016, 6, 44908-44920.	1.7	64
25774	The high-pressure semiconducting phase of LiBC. Europhysics Letters, 2016, 114, 16001.	0.7	8
25775	Strain and carrier-induced coexistence of topologically insulating and superconducting phase in iodized Si(111) films. Nano Research, 2016, 9, 1578-1589.	5.8	6
25776	Multi-scale analysis of an electrochemical model including coupled diffusion, stress, and nonideal solution in a silicon thin film anode. Journal of Power Sources, 2016, 307, 856-865.	4.0	27
25777	Effect of electron-electron correlation and site disorder on the magnetic moment and half-metallicity of Co 2 FeGa 1â^'x Si x alloys. Materials Chemistry and Physics, 2016, 177, 564-569.	2.0	5
25778	Theoretical investigation of surface states and energetics of PtSi surfaces. Surface Science, 2016, 649, 27-33.	0.8	4
25779	Single Atom (Pd/Pt) Supported on Graphitic Carbon Nitride as an Efficient Photocatalyst for Visible-Light Reduction of Carbon Dioxide. Journal of the American Chemical Society, 2016, 138, 6292-6297.	6.6	985
25780	Diverse anisotropy of phonon transport in two-dimensional group IVâ€“VI compounds: A comparative study. Nanoscale, 2016, 8, 11306-11319.	2.8	234
25781	Investigations of the band structures of edge-defect zigzag graphene nanoribbons using density functional theory. RSC Advances, 2016, 6, 39587-39594.	1.7	18
25782	Photocontrol of charge injection/extraction at electrode/semiconductor interfaces for high-photoresponsivity organic transistors. Journal of Materials Chemistry C, 2016, 4, 5289-5296.	2.7	29
25783	Band Anticrossing in Dilute Germanium Carbides Using Hybrid Density Functionals. Journal of Electronic Materials, 2016, 45, 2121-2126.	1.0	9
25784	Prediction of an ultrasoft graphene allotrope with Dirac cones. Carbon, 2016, 105, 323-329.	5.4	62
25785	First-principles molecular dynamics investigation on Na3AlF6 molten salt. Journal of Fluorine Chemistry, 2016, 185, 42-47.	0.9	31
25786	Electrochemical Lithiation Cycles of Gold Anodes Observed by In Situ High-Energy X-ray Diffraction. Chemistry of Materials, 2016, 28, 2941-2948.	3.2	38
25787	Effect of the Exchange-Correlation Potential on the Transferability of BrÃ¸nstedâ€“Evansâ€“Polanyi Relationships in Heterogeneous Catalysis. Journal of Chemical Theory and Computation, 2016, 12, 2121-2126.	2.3	20
25788	Exploring the Real Ground-State Structures of Molybdenum Dinitride. Journal of Physical Chemistry C, 2016, 120, 11060-11067.	1.5	39
25789	Electrochemical Surface Stress Development during CO and NO Oxidation on Pt. Journal of Physical Chemistry C, 2016, 120, 8674-8683.	1.5	22
25790	Coincidence Lattices of 2D Crystals: Heterostructure Predictions and Applications. Journal of Physical Chemistry C, 2016, 120, 10895-10908.	1.5	68

#	Article	IF	Citations
25791	CO oxidation by MoS₂-supported Au₁₉ nanoparticles: effects of vacancy formation and tensile strain. Physical Chemistry Chemical Physics, 2016, 18, 13232-13238.	1.3	14
25792	Catenation of carbon in LaC₂ predicted under high pressure. Physical Chemistry Chemical Physics, 2016, 18, 14286-14291.	1.3	5
25793	Theoretical characterization of the surface composition of ruthenium nanoparticles in equilibrium with syngas. Nanoscale, 2016, 8, 10974-10992.	2.8	43
25794	Tuning the work function of randomly oriented ZnO nanostructures by capping with faceted Au nanostructure and oxygen defects: enhanced field emission experiments and DFT studies. Nanotechnology, 2016, 27, 125701.	1.3	36
25795	Thermal conductivity and mechanical properties of nitrogenated holey graphene. Carbon, 2016, 106, 1-8.	5.4	118
25796	Thermodynamic properties of refractory high entropy alloys. Journal of Alloys and Compounds, 2016, 682, 773-777.	2.8	41
25797	Base tolerant polybenzimidazolium hydroxide membranes for solid alkaline-exchange membrane fuel cells. Journal of Membrane Science, 2016, 514, 398-406.	4.1	11
25798	Electronic structure and magnetic properties of oxygen deficient low-index surfaces of SnO2. Surface Science, 2016, 649, 112-119.	0.8	9
25799	Competing Pathways for Nucleation of the Double Perovskite Structure in the Epitaxial Synthesis of La₂MnNiO₆. Chemistry of Materials, 2016, 28, 3814-3822.	3.2	29
25800	First-Principles Study on the Effect of Pure and Oxidized Transition-Metal Buffers on Adhesion at the Alumina/Zinc Interface. Journal of Physical Chemistry C, 2016, 120, 9836-9844.	1.5	21
25801	Computational Approach for Epitaxial Polymorph Stabilization through Substrate Selection. ACS Applied Materials & Interfaces, 2016, 8, 13086-13093.	4.0	78
25802	Tri-s-triazine-Based Crystalline Graphitic Carbon Nitrides for Highly Efficient Hydrogen Evolution Photocatalysis. ACS Catalysis, 2016, 6, 3921-3931.	5.5	756
25803	Two-Dimensional Phosphorus Porous Polymorphs with Tunable Band Gaps. Journal of the American Chemical Society, 2016, 138, 7091-7098.	6.6	119
25804	Photochemical route for synthesizing atomically dispersed palladium catalysts. Science, 2016, 352, 797-800.	6.0	1,540
25805	Photocatalytic CO2 reduction highly enhanced by oxygen vacancies on Pt-nanoparticle-dispersed gallium oxide. Nano Research, 2016, 9, 1689-1700.	5.8	141
25806	Synergetic interplay between pressure and surface chemistry for the conversion of sp2-bonded carbon layers into sp3-bonded carbon films. Carbon, 2016, 106, 158-163.	5.4	15
25807	CO₂ Adsorption in M-IRMOF-10 (M = Mg, Ca, Fe, Cu, Zn, Ge, Sr, Cd, Sn, Ba). Journal of Physical Chemistry C, 2016, 120, 12819-12830.	1.5	21
25808	Carrier Self-trapping and Luminescence in Intrinsically Activated Scintillator: Cesium Hafnium Chloride (Cs₂HfCl₆). Journal of Physical Chemistry C, 2016, 120, 12187-12195.	1.5	85

#	Article	IF	Citations
25809	Band Gap Opening of Graphene by Forming Heterojunctions with the 2D Carbonitrides Nitrogenated Holey Graphene, g-C₃N₄, and g-CN: Electric Field Effect. Journal of Physical Chemistry C, 2016, 120, 11299-11305.	1.5	40
25810	Adsorption-Induced Surface Stresses of the Water/Quartz Interface: Ab Initio Molecular Dynamics Study. Langmuir, 2016, 32, 5259-5266.	1.6	18
25811	Diffusive nature of thermal transport in stanene. Physical Chemistry Chemical Physics, 2016, 18, 14257-14263.	1.3	34
25812	Thickness dependence of surface energy and contact angle of water droplets on ultrathin MoS₂ films. Physical Chemistry Chemical Physics, 2016, 18, 14449-14453.	1.3	37
25813	First principles study of nanoscale mechanism of oxygen adsorption on lanthanum zirconate surfaces. Physica E: Low-Dimensional Systems and Nanostructures, 2016, 83, 36-40.	1.3	4
25814	Adsorption-enhanced spinâ€“orbit coupling of buckled honeycomb silicon. Physica E: Low-Dimensional Systems and Nanostructures, 2016, 83, 141-145.	1.3	0
25815	Advanced polymeric dielectrics for high energy density applications. Progress in Materials Science, 2016, 83, 236-269.	16.0	286
25816	First-principles study on the magnetic and half-metallic properties in bulk and (001) surface of Ti2CoSn Heusler alloy. Thin Solid Films, 2016, 609, 19-24.	0.8	5
25817	Strain and Spinâ€“Orbital Coupling Effects on Electronic Structures and Magnetism of Semi-Hydrogenated Stanene. Journal of Physical Chemistry C, 2016, 120, 10622-10628.	1.5	34
25818	Structurally Accurate Model for the â€œ29â€•Structure of Cu_xO/Cu(111): A DFT and STM Study. Journal of Physical Chemistry C, 2016, 120, 10879-10886.	1.5	45
25819	Comparative DFT and DFT-D studies on structural, electronic, vibrational and absorption properties of crystalline ammonium perchlorate. RSC Advances, 2016, 6, 48489-48497.	1.7	11
25820	Germanium sulfide nanosheet: a universal anode material for alkali metal ion batteries. Journal of Materials Chemistry A, 2016, 4, 8905-8912.	5.2	188
25821	The induced nontrivialZ₂topological phase in graphene sandwiched by pnictogen bilayers. Journal of Physics Condensed Matter, 2016, 28, 235502.	0.7	0
25822	Fast Li-Ion Transport in Amorphous Li₂Si₂O₅: An Ab Initio Molecular Dynamics Simulation. Journal of the Electrochemical Society, 2016, 163, A1401-A1407.	1.3	17
25823	Concentration Effect of Reducing Agents on Green Synthesis of Gold Nanoparticles: Size, Morphology, and Growth Mechanism. Nanoscale Research Letters, 2016, 11, 230.	3.1	76
25824	Structure and magnetic order in Mn8Ga5. Acta Materialia, 2016, 113, 147-154.	3.8	7
25825	Stable and Metastable Structures in Compressed LiC₆: Dimensional Diversity. Journal of Physical Chemistry C, 2016, 120, 10137-10145.	1.5	11
25826	Ab initio molecular dynamics determination of competitive O₂vs. N₂ adsorption at open metal sites of M₂(dobdc). Physical Chemistry Chemical Physics, 2016, 18, 11528-11538.	1.3	28

#	Article	IF	Citations
25827	Highly efficient and ultrastable visible-light photocatalytic water splitting over ReS₂. Physical Chemistry Chemical Physics, 2016, 18, 14222-14227.	1.3	76
25828	Tailoring the germaneneâ€“substrate interactions by means of hydrogenation. Physical Chemistry Chemical Physics, 2016, 18, 15667-15672.	1.3	10
25829	First-principles study of the electronic structure of nonmetal-doped anatase TiO2. Journal of the Korean Physical Society, 2016, 68, 409-414.	0.3	8
25830	Application of ZnTiO3 in quantum-dot-sensitized solar cells and numerical simulations using first-principles theory. Journal of Alloys and Compounds, 2016, 681, 88-95.	2.8	34
25831	Effects of a TiC substrate on the catalytic activity of Pt for NO reduction. Physical Chemistry Chemical Physics, 2016, 18, 13304-13309.	1.3	17
25832	First-principles study of Ce-doped Y3Al5O12 with Siâ€“N incorporation: electronic structures and optical properties. Journal of Materials Chemistry C, 2016, 4, 5214-5221.	2.7	40
25833	The electronic structure of graphene tuned by hexagonal boron nitrogen layers: Semimetalâ€“semiconductor transition. Modern Physics Letters B, 2016, 30, 1650191.	1.0	6
25834	Topology-Driven Magnetic Quantum Phase Transition. Springer Theses, 2016, , 55-86.	0.0	0
25835	Thermodynamic Assessment of Zn-Fe-Nb Ternary System. Journal of Phase Equilibria and Diffusion, 2016, 37, 293-300.	0.5	3
25836	DFT-based microkinetic modeling of ethanol dehydration in H-ZSM-5. Journal of Catalysis, 2016, 339, 173-185.	3.1	69
25837	Ab initio investigation of helium in Y2Ti2O7: Mobility and effects on mechanical properties. Journal of Nuclear Materials, 2016, 477, 215-221.	1.3	14
25838	Energetics of a Li Atom adsorbed on B/N doped graphene with monovacancy. Journal of Solid State Chemistry, 2016, 240, 67-75.	1.4	22
25839	Optical Properties of Strained Wurtzite Gallium Phosphide Nanowires. Nano Letters, 2016, 16, 3703-3709.	4.5	40
25840	Ferromagnetism and Conductivity in Hydrogen Irradiated Co-Doped ZnO Thin Films. ACS Applied Materials & Interfaces, 2016, 8, 12925-12931.	4.0	25
25841	Phonon and thermal expansion properties in Weyl semimetals MX (M = Nb, Ta; X = P, As): ab initio studies. Physical Chemistry Chemical Physics, 2016, 18, 14503-14508.	1.3	14
25842	In-plane interfacing effects of two-dimensional transition-metal dichalcogenide heterostructures. Physical Chemistry Chemical Physics, 2016, 18, 15632-15638.	1.3	46
25843	Intrinsic quantum spin Hall and anomalous Hall effects in h-Sb/Bi epitaxial growth on a ferromagnetic MnO₂thin film. Nanoscale, 2016, 8, 11202-11209.	2.8	16
25844	Theoretical studies of the adsorption of hydroxymethylidyne (COH) on Pt-alloy surfaces using density functional theory. Physica Scripta, 2016, 91, 025803.	1.2	5

#	Article	IF	Citations
25845	First-principles study of the elastic and thermodynamic properties of thorium hydrides at high pressure. Chinese Physics B, 2016, 25, 057102.	0.7	1
25846	Study on nanophase iron oxyhydroxides in freshwater ferromanganese nodules from Green Bay, Lake Michigan, with implications for the adsorption of As and heavy metals. American Mineralogist, 2016, 101, 1986-1995.	0.9	26
25847	Study of fluorine doped (Nb,Ir)O2 solid solution electro-catalyst powders for proton exchange membrane based oxygen evolution reaction. Materials Science and Engineering B: Solid-State Materials for Advanced Technology, 2016, 212, 101-108.	1.7	18
25848	Lithium Extraction Mechanism in Li-Rich Li₂MnO₃ Involving Oxygen Hole Formation and Dimerization. Chemistry of Materials, 2016, 28, 6656-6663.	3.2	210
25849	Few-Layer Tin Sulfide: A New Black-Phosphorus-Analogue 2D Material with a Sizeable Band Gap, Oddâ€“Even Quantum Confinement Effect, and High Carrier Mobility. Journal of Physical Chemistry C, 2016, 120, 22663-22669.	1.5	130
25850	Understanding molecular self-assembly of a diol compound by considering competitive interactions. Physical Chemistry Chemical Physics, 2016, 18, 27390-27395.	1.3	6
25851	The role of the CeO₂/BiVO₄ interface in optimized Feâ€“Ce oxide coatings for solar fuels photoanodes. Journal of Materials Chemistry A, 2016, 4, 14356-14363.	5.2	19
25852	Toward a Unified Identification of Ti Location in the MFI Framework of High-Ti-Loaded TS-1: Combined EXAFS, XANES, and DFT Study. Journal of Physical Chemistry C, 2016, 120, 20114-20124.	1.5	45
25853	Hybridization Effects between Silicene/Silicene Oxides and Ag(111). Journal of Physical Chemistry C, 2016, 120, 20192-20198.	1.5	10
25854	First-principles study of the effect of oxygen vacancy and strain on the phase transition temperature of VO₂. RSC Advances, 2016, 6, 86872-86879.	1.7	32
25855	First-principles study of the magnetism of Ni-doped MoS₂ monolayer. Japanese Journal of Applied Physics, 2016, 55, 093001.	0.8	26
25856	Teâ€Doped Black Phosphorus Fieldâ€Effect Transistors. Advanced Materials, 2016, 28, 9408-9415.	11.1	241
25857	How Oxygen Vacancies Activate CO₂ Dissociation on TiO₂ Anatase (001). Journal of Physical Chemistry C, 2016, 120, 21659-21669.	1.5	141
25858	Density functional theory simulation of the adsorption of sulphur multilayers on Au(100). Physical Chemistry Chemical Physics, 2016, 18, 29987-29998.	1.3	4
25859	High catalytic activity for CO oxidation on single Fe atom stabilized in graphene vacancies. RSC Advances, 2016, 6, 93985-93996.	1.7	66
25860	Ligand-free nano-grain Cu₂SnS₃ as a potential cathode alternative for both cobalt and iodine redox electrolyte dye-sensitized solar cells. Journal of Materials Chemistry A, 2016, 4, 14865-14876.	5.2	21
25861	Type II band alignment in InAs zinc-blende/wurtzite heterostructured nanowires. Nanotechnology, 2016, 27, 415201.	1.3	5
25862	Predictive Control over Charge Density in the Two-Dimensional Electron Gas at the Polar-Nonpolar<mml:math xmlns:mml="http://www.w3.org/1998/Math/MathML" display="inline"><mml:mrow><mml:msub><mml:mrow><mml:mi>NdTiO</mml:mi></mml:mrow><mml:mn>3</mml:mn></mml:msub> Physical Review Letters, 2016, 117, 106803.	2.9	44

#	Article	IF	Citations
25863	Liâ€‰:â€‰Mg alloy with variable work function as highly efficient cathode for organic light-emitting devices. Physica Status Solidi (A) Applications and Materials Science, 2016, 213, 3245-3249.	0.8	4
25864	Cadmium Free Quantum Dots: Principal Attractions, Properties, and Applications. , 2016, , 437-471.		3
25865	Strong Li-Content Dependence of Li Diffusivity in TiO₂-B. Journal of Physical Chemistry C, 2016, 120, 22163-22168.	1.5	12
25866	Multiscale Investigation of Oxygen Vacancies in TiO₂ Anatase and Their Role in Memristorâ€™s Behavior. Journal of Physical Chemistry C, 2016, 120, 22045-22053.	1.5	24
25867	Enhancing the Hydrogen Activation Reactivity of Nonprecious Metal Substrates via Confined Catalysis Underneath Graphene. Nano Letters, 2016, 16, 6058-6063.	4.5	101
25868	Surface Chemical Tuning of Phonon and Electron Transport in Free-Standing Silicon Nanowire Arrays. Nano Letters, 2016, 16, 6364-6370.	4.5	16
25869	Elastic Properties, Defect Thermodynamics, Electrochemical Window, Phase Stability, and Li⁺ Mobility of Li₃PS₄: Insights from First-Principles Calculations. ACS Applied Materials & Interfaces, 2016, 8, 25229-25242.	4.0	114
25870	Mechanisms of Mo2C(101)-Catalyzed Furfural Selective Hydrodeoxygenation to 2-Methylfuran from Computation. ACS Catalysis, 2016, 6, 6790-6803.	5.5	51
25871	Experimental observation of topological Fermi arcs in type-II Weyl semimetal MoTe2. Nature Physics, 2016, 12, 1105-1110.	6.5	663
25872	Curvature, vacancy size and chirality effects of mono- to octa-vacancies in zigzag single-walled carbon nanotubes. New Journal of Chemistry, 2016, 40, 8625-8631.	1.4	1
25873	Band and bonding characteristics of N2+ ion-doped graphene. RSC Advances, 2016, 6, 84959-84964.	1.7	1
25874	Enhanced ideal strength of thermoelectric half-Heusler TiNiSn by sub-structure engineering. Journal of Materials Chemistry A, 2016, 4, 14625-14636.	5.2	48
25875	First-principles prediction of inversion-asymmetric topological insulator in hexagonal BiPbH monolayer. Journal of Materials Chemistry C, 2016, 4, 8750-8757.	2.7	10
25876	Hydrogenated borophene as a stable two-dimensional Dirac material with an ultrahigh Fermi velocity. Physical Chemistry Chemical Physics, 2016, 18, 27284-27289.	1.3	167
25877	The temperature-dependent dislocation properties of aluminum from the improved Peierlsâ€“Nabarro model and first-principles. Philosophical Magazine, 2016, 96, 2829-2852.	0.7	11
25878	Transport properties and metalâ€“insulator transition in oxygen deficient LaNiO₃: a density functional theory study. Materials Research Express, 2016, 3, 095701.	0.8	13
25879	Stabilization and strengthening effects of functional groups in two-dimensional titanium carbide. Physical Review B, 2016, 94, .	1.1	142
25880	Rareâ€Earth Dopant Effects on the Structural, Energetic, and Magnetic Properties of Alumina from First Principles. Journal of the American Ceramic Society, 2016, 99, 4007-4012.	1.9	8

#	Article	IF	Citations
25881	Theoretical aspects of methanol carbonylation on copper-containing zeolites. Petroleum Chemistry, 2016, 56, 259-266.	0.4	4
25882	Synthesis Strategies for Ultrastable Zeolite GIS Polymorphs as Sorbents for Selective Separations. Chemistry - A European Journal, 2016, 22, 16078-16088.	1.7	31
25883	Electronic and magnetic structures and bonding properties of Ce 2 CrN 3 and U 2 CrN 3 from first principles. Computational Condensed Matter, 2016, 9, 13-18.	0.9	3
25884	A promising two-dimensional solar cell donor: Black arsenicâ€“phosphorus monolayer with 1.54 eV direct bandgap and mobility exceeding 14,000 cm2Vâ^'1sâ^'1. Nano Energy, 2016, 28, 433-439.	8.2	212
25885	The strain effect on lithium ion migration in Li-Si alloys: A first-principles study. Solid State Communications, 2016, 247, 47-52.	0.9	4
25886	Determining a Structural Distortion and Anion Ordering in La2Si4N6C via Computation and Experiment. Inorganic Chemistry, 2016, 55, 9454-9460.	1.9	6
25887	Electric Field- and Strain-Induced Rashba Effect in Hybrid Halide Perovskites. Journal of Physical Chemistry Letters, 2016, 7, 3683-3689.	2.1	104
25888	Improving the photocatalytic activity of s-triazine based graphitic carbon nitride through metal decoration: an ab initio investigation. Physical Chemistry Chemical Physics, 2016, 18, 26466-26474.	1.3	16
25889	Crystal, electronic, and magnetic structures of M₂AgF₄ (M = Naâ€“Cs) phases as viewed from the DFT+U method. Dalton Transactions, 2016, 45, 16255-16261.	1.6	13
25890	Electronic and Magnetic Properties of Co- and Mn-codoped ZnO by Density Functional Theory. Chinese Physics Letters, 2016, 33, 097102.	1.3	7
25891	The role of interstitial native defects in the topological insulator Bi₂Se₃. Journal of Physics Condensed Matter, 2016, 28, 425801.	0.7	13
25892	Configurationally exhaustive first-principles study of a quaternary superalloy with a vast configuration space. Physical Review B, 2016, 94, .	1.1	6
25893	Quasi-One-Dimensional Metal-Insulator Transitions in Compound Semiconductor Surfaces. Physical Review Letters, 2016, 117, 116101.	2.9	5
25894	Organic crystal polymorphism: a benchmark for dispersion-corrected mean-field electronic structure methods. Acta Crystallographica Section B: Structural Science, Crystal Engineering and Materials, 2016, 72, 502-513.	0.5	53
25895	Toward Onâ€andâ€Off Magnetism: Reversible Electrochemistry to Control Magnetic Phase Transitions in Spinel Ferrites. Advanced Functional Materials, 2016, 26, 7507-7515.	7.8	69
25896	Molecular Dissociation on the SiC(0001) 3Ã—3 Surface. ChemPhysChem, 2016, 17, 3900-3906.	1.0	2
25897	Hydrogen adsorption on Li-decorated BN analogs of Î³-graphyne: A DFT study. Computational Materials Science, 2016, 125, 28-35.	1.4	29
25898	Activating basal-plane catalytic activity of two-dimensional MoS2 monolayer with remote hydrogen plasma. Nano Energy, 2016, 30, 846-852.	8.2	136

#	Article	IF	Citations
25899	First principles study on the structural, magnetic, electronic and optical properties of un-doped and La-doped BiFe0.75Mn0.125Ti0.125O3. Physics Letters, Section A: General, Atomic and Solid State Physics, 2016, 380, 3524-3529.	0.9	9
25900	Nâ€“Mg dual-acceptor co-doping in CuCrO2 studied by first-principles calculations. Physics Letters, Section A: General, Atomic and Solid State Physics, 2016, 380, 3861-3865.	0.9	10
25901	New R₃Pd₅ Compounds (R = Sc, Y, Gdâ€“Lu): Formation and Stability, Crystal Structure, and Antiferromagnetism. Crystal Growth and Design, 2016, 16, 6001-6015.	1.4	8
25902	Facet-Specific Stability of ZIF-8 in the Presence of Acid Gases Dissolved in Aqueous Solutions. Chemistry of Materials, 2016, 28, 6960-6967.	3.2	127
25903	Kondo Resonance of a Co Atom Exchange Coupled to a Ferromagnetic Tip. Nano Letters, 2016, 16, 6298-6302.	4.5	28
25904	Double Epitaxy as a Paradigm for Templated Growth of Highly Ordered Three-Dimensional Mesophase Crystals. ACS Nano, 2016, 10, 8670-8675.	7.3	2
25905	The possible formation of a magnetic FeS2 phase in the two-dimensional MoS2 matrix. Physical Chemistry Chemical Physics, 2016, 18, 26956-26959.	1.3	1
25906	Multistep atomic reaction enhanced by an atomic force microscope probe on Si(111) and Ge(111) surfaces. Physical Review B, 2016, 94, .	1.1	2
25907	Site preference and lattice relaxation around 4dand 5drefractory elements in Ni3Al. Journal of Synchrotron Radiation, 2016, 23, 286-292.	1.0	5
25908	Hydrogen Bonding and Stability of Hybrid Organicâ€“Inorganic Perovskites. ChemSusChem, 2016, 9, 2648-2655.	3.6	109
25909	Synergetic effects of blended materials for Lithium-ion batteries. Science China Technological Sciences, 2016, 59, 1370-1376.	2.0	5
25910	Iodine Anions beyond âˆ’1: Formation of LinI (n = 2â€“5) and Its Interaction with Quasiatoms. Inorganic Chemistry, 2016, 55, 9377-9382.	1.9	16
25911	Eight-Dimensional Quantum Dynamics Study of CH₄ and CD₄ Dissociation on Ni(100) Surface. Journal of Physical Chemistry C, 2016, 120, 20199-20205.	1.5	12
25912	Metallic and Magnetic 2D Materials Containing Planar Tetracoordinated C and N. Journal of Physical Chemistry C, 2016, 120, 21685-21690.	1.5	12
25913	Determination of surface and interface magnetic properties for the multiferroic heterostructure Co/BaTiO3using spleed and arpes. Journal of Physics Condensed Matter, 2016, 28, 436004.	0.7	1
25914	Positron surface state as a spectroscopic probe for characterizing surfaces of topological insulator materials. Physical Review B, 2016, 94, .	1.1	15
25916	Polyalanine Î±-helix microsolvation: assessing the energy of the peptide desolvation penalty with density functional theory. Theoretical Chemistry Accounts, 2016, 135, 1.	0.5	3
25917	Low charge overpotential of lithium-oxygen batteries with metallic Co encapsulated in single-layer graphene shell as the catalyst. Nano Energy, 2016, 30, 877-884.	8.2	67

#	Article	IF	Citations
25919	Competing Interfacial Reconstruction Mechanisms in La_{0.7}Sr_{0.3}MnO₃/SrTiO₃ Heterostructures. ACS Applied Materials & Interfaces, 2016, 8, 24192-24197.	4.0	24
25920	Reaction Pathways and Intermediates in Selective Ring Opening of Biomass-Derived Heterocyclic Compounds by Iridium. ACS Catalysis, 2016, 6, 7002-7009.	5.5	41
25921	Atomic Defects in Monolayer Titanium Carbide (Ti₃C₂T_x) MXene. ACS Nano, 2016, 10, 9193-9200.	7.3	785
25922	Steering the formation of supported Ptâ€“Sn nanoalloys by reactive metalâ€“oxide interaction. RSC Advances, 2016, 6, 85688-85697.	1.7	5
25923	Design of lateral heterostructure from arsenene and antimonene. 2D Materials, 2016, 3, 035017.	2.0	66
25924	Two-dimensional rectangular tantalum carbide halides TaCX (X = Cl, Br, I): novel large-gap quantum spin Hall insulators. 2D Materials, 2016, 3, 035018.	2.0	21
25925	Valley contrasting in epitaxial growth of In/Tl homoatomic monolayer with anomalous Nernst conductance. Physical Review B, 2016, 94, .	1.1	7
25926	Defect-induced magnetic structure of CuMnSb. Physical Review B, 2016, 94, .	1.1	8
25927	Electronic structure and magnetism of samarium and neodymium adatoms on free-standing graphene. Physical Review B, 2016, 94, .	1.1	22
25928	Theoretical Investigation on the Reaction Pathways of the Oxygen Reduction Reaction on Graphene Codoped with Manganese and Phosphorus as a Potential Nonprecious Metal Catalyst. ChemCatChem, 2016, 8, 3353-3360.	1.8	10
25929	Application of the Peierlsâ€“Nabarro Model to Symmetric Tilt Low-Angle Grain Boundary with Full <a> Dislocation in Pure Magnesium. Acta Metallurgica Sinica (English Letters), 2016, 29, 1053-1063.	1.5	0
25930	Versatile Titanium Silicide Monolayers with Prominent Ferromagnetic, Catalytic, and Superconducting Properties: Theoretical Prediction. Journal of Physical Chemistry Letters, 2016, 7, 3723-3729.	2.1	28
25931	Phosphine passivated gold clusters: how charge transfer affects electronic structure and stability. Physical Chemistry Chemical Physics, 2016, 18, 29686-29697.	1.3	18
25932	First-principles electronic structure calculations for the whole spinel oxide solid solution range Mn_xCo_{3â^'x}O₄ (0 â‰¤ x â‰¤ 3) and their comparison with experimental data. Physical Chemistry Chemical Physics, 2016, 18, 26166-26176.	1.3	11
25933	Tunable electronic structures in MPX₃ (M = Zn, Cd; X = S, Se) monolayers by strain engineering. RSC Advances, 2016, 6, 89901-89906.	1.7	19
25934	Quantum spin Hall state in cyanided dumbbell stanene. RSC Advances, 2016, 6, 86089-86094.	1.7	2
25935	Interfacial properties of staneneâ€“metal contacts. 2D Materials, 2016, 3, 035020.	2.0	26
25936	Electronic and magnetic properties of spiral spin-density-wave states in transition-metal chains. Physical Review B, 2016, 94, .	1.1	4

#	Article	IF	Citations
25937	Single-Layer Limit of Metallic Indium Overlayers on Si(111). Physical Review Letters, 2016, 117, 116102.	2.9	22
25938	Cyclic density functional theory: A route to the first principles simulation of bending in nanostructures. Journal of the Mechanics and Physics of Solids, 2016, 96, 605-631.	2.3	29
25939	An atomically thin ferromagnetic half-metallic pyrazine-fused Mn-porphyrin sheet: a slow spin relaxation system. Journal of Materials Chemistry C, 2016, 4, 9069-9077.	2.7	18
25940	Atomic and electronic structures evolution of the narrow band gap semiconductor Ag₂Se under high pressure. Journal of Physics Condensed Matter, 2016, 28, 385801.	0.7	9
25941	Exfoliated Metal Oxide Nanosheets as Effective and Applicable Substrates for Atomically Dispersed Metal Nanoparticles with Tailorable Functionalities. Advanced Materials Interfaces, 2016, 3, 1600661.	1.9	5
25942	Magnetic properties and stability of Cu3V2O8 compound in the different phases. Journal of Magnetism and Magnetic Materials, 2016, 417, 56-61.	1.0	3
25943	DFT-D3 Study of Molecular N₂ and H₂ Activation on Co₃Mo₃N Surfaces. Journal of Physical Chemistry C, 2016, 120, 21390-21398.	1.5	57
25944	Hydrogenation of Hydrogen Cyanide to Methane and Ammonia by a Metal Catalyst: Insight from First-Principles Calculations. Journal of Physical Chemistry C, 2016, 120, 22946-22956.	1.5	8
25945	Insight into CH x formation in Fischerâ€“Tropsch synthesis on the hexahedron Co catalyst: Effect of surface structure on the preferential mechanism and existence form. Applied Catalysis A: General, 2016, 525, 76-84.	2.2	18
25946	Interface characteristics in Co2MnSi/Ag/Co2MnSi trilayer. Applied Surface Science, 2016, 371, 296-300.	3.1	3
25947	Reaction mechanism of ethylene glycol decomposition on Pt model catalysts: A density functional theory study. Applied Surface Science, 2016, 390, 1015-1022.	3.1	2
25948	Thermodynamic description of the Cr-Mn-Si system. Calphad: Computer Coupling of Phase Diagrams and Thermochemistry, 2016, 55, 181-188.	0.7	6
25949	Ab initio phase stability of some cubic phases of ordered Ni-Fe alloys at high temperatures and pressures. Computational Materials Science, 2016, 125, 100-104.	1.4	7
25950	Robust diamond-like Fe-Si network in the zero-strain Na FeSiO4 cathode. Electrochimica Acta, 2016, 212, 934-940.	2.6	30
25951	The effect of titanium doping on carbon behavior in tungsten: A first-principles study. Fusion Engineering and Design, 2016, 112, 123-129.	1.0	5
25952	Synthesis and radiation tolerance of Lu2â^'Ce Ti2O7 pyrochlores. Journal of Nuclear Materials, 2016, 480, 182-188.	1.3	11
25953	Multiscale modelling of hydrogen behaviour on beryllium (0001) surface. Nuclear Materials and Energy, 2016, 9, 547-553.	0.6	10
25954	Work function reduction by a redox-active organometallic sandwich complex. Organic Electronics, 2016, 37, 263-270.	1.4	2

#	Article	IF	Citations
25955	The mechanism and process of spontaneous boron doping in graphene in the theoretical perspective. Physics Letters, Section A: General, Atomic and Solid State Physics, 2016, 380, 3384-3388.	0.9	2
25956	First-principles study of the crystal structures and physical properties of H18-BN and Rh6-BN. Physics Letters, Section A: General, Atomic and Solid State Physics, 2016, 380, 3891-3896.	0.9	16
25957	The electronic properties of bare and alkali metal adsorbed two-dimensional GeSi alloy sheet. Superlattices and Microstructures, 2016, 97, 250-257.	1.4	3
25958	Annealing effect on phase stability of doped zirconia using experimental and computational studies. Solid State Ionics, 2016, 297, 20-28.	1.3	7
25959	The Key Indicator for the Control of Metal Particle Sizes on Supports from First-Principles and Experimental Observation. Journal of Physical Chemistry C, 2016, 120, 21879-21887.	1.5	5
25960	Tunable Conductivity and Half Metallic Ferromagnetism in Monolayer Platinum Diselenide: A First-Principles Study. Journal of Physical Chemistry C, 2016, 120, 25030-25036.	1.5	38
25961	Charge Stripe Formation in Molecular Ferroelectric Organohalide Perovskites for Efficient Charge Separation. Journal of Physical Chemistry C, 2016, 120, 23969-23975.	1.5	14
25962	Optical phonons in methylammonium lead halide perovskites and implications for charge transport. Materials Horizons, 2016, 3, 613-620.	6.4	299
25963	Chemical instability leads to unusual chemical-potential-independent defect formation and diffusion in perovskite solar cell material CH₃NH₃PbI₃. Journal of Materials Chemistry A, 2016, 4, 16975-16981.	5.2	67
25964	A graphene-like Mg₃N₂monolayer: high stability, desirable direct band gap and promising carrier mobility. Physical Chemistry Chemical Physics, 2016, 18, 30379-30384.	1.3	29
25965	Origin of the wide band gap from 0.6 to 2.3 eV in photovoltaic material InN: quantum confinement from surface nanostructure. Journal of Materials Chemistry A, 2016, 4, 17412-17418.	5.2	6
25966	Formation of Sr adatom chains on SrTiO₃(1â€‰1â€‰0) surface determined by strain. Journal of Physics Condensed Matter, 2016, 28, 365003.	0.7	1
25967	Importance of inclusion of the effect of s electrons into bond-order potentials for transition bcc metals with d-band mediated bonding. Modelling and Simulation in Materials Science and Engineering, 2016, 24, 085001.	0.8	5
25968	Intrinsic magnetism in penta-hexa-graphene: A first-principles study. Physical Review B, 2016, 94, .	1.1	17
25969	Dynamic Surface Stress Response during Reversible Mg Electrodeposition and Stripping. Journal of the Electrochemical Society, 2016, 163, A2679-A2684.	1.3	9
25970	Insights into the Ringâ€Opening of Biomassâ€Derived Furanics over Carbonâ€Supported Ruthenium. ChemSusChem, 2016, 9, 3113-3121.	3.6	30
25971	Hydrogen and halide co-adsorption on Pt(111) in an electrochemical environment: a computational perspective. Electrochimica Acta, 2016, 216, 152-159.	2.6	66
25972	Electric field induced transitional magnetic coupling in (Ga, Cr)N/GaN magnetic tunnel junctions. Optik, 2016, 127, 8951-8955.	1.4	2

#	Article	IF	Citations
25973	Carrier-mediated antiferromagnetic interlayer exchange coupling in Ga co-doped (Zn, Ni)O-based multilayers. Optik, 2016, 127, 10705-10709.	1.4	1
25974	Impact of the substrate orientation on the N incorporation in GaAsN: Theoretical and experimental investigations. Journal of Alloys and Compounds, 2016, 687, 42-46.	2.8	5
25975	Influence of basicity on 1,3-butadiene formation from catalytic 2,3-butanediol dehydration over Î³-alumina. Journal of Catalysis, 2016, 344, 77-89.	3.1	23
25976	Depth of formation of CaSiO 3 -walstromite included in super-deep diamonds. Lithos, 2016, 265, 138-147.	0.6	55
25977	High thermoelectric performance of Weyl semimetal TaAs. Nano Energy, 2016, 30, 225-234.	8.2	47
25978	Hydrogen diffusion on Fe surface and into subsurface from first principles. Surface Science, 2016, 654, 48-55.	0.8	21
25979	Measurement of the dielectric function of Î±-Al2O3 by transmission electron microscopy â€“ Electron energy-loss spectroscopy without Cerenkov radiation effects. Ultramicroscopy, 2016, 169, 37-43.	0.8	3
25980	Radiation effects on two-dimensional materials. Physica Status Solidi (A) Applications and Materials Science, 2016, 213, 3065-3077.	0.8	48
25981	Growth and thermal stability of TiN/ZrAlN: Effect of internal interfaces. Acta Materialia, 2016, 121, 396-406.	3.8	44
25982	A DFT study of mechanical properties, thermal conductivity and electronic structures of Th-doped Gd2Zr2O7. Acta Materialia, 2016, 121, 299-309.	3.8	48
25983	Direct Evidence of Chelated Geometry of Catechol on TiO₂ by a Combined Solid-State NMR and DFT Study. Journal of Physical Chemistry C, 2016, 120, 23625-23630.	1.5	55
25984	Magnetic and Electronic Properties of Samarium-Doped Phenanthrene from First-Principles Study. Journal of Physical Chemistry C, 2016, 120, 22565-22570.	1.5	12
25985	Water Oxidation Catalyzed by Cobalt Oxide Supported on the Mattagamite Phase of CoTe₂. ACS Catalysis, 2016, 6, 7393-7397.	5.5	39
25986	Spectroscopic and theoretical studies on the counterion effect of Cu(<scp>ii</scp>) ion and graphene oxide interaction with titanium dioxide. Environmental Science: Nano, 2016, 3, 1361-1368.	2.2	77
25987	The growth modes of graphene in the initial stage of a chemical vapor-deposition process. RSC Advances, 2016, 6, 91157-91162.	1.7	4
25988	Thallium under extreme compression. Journal of Physics Condensed Matter, 2016, 28, 445401.	0.7	30
25989	Theoretical Analysis of Thermal Transport in Graphene Supported on Hexagonal Boron Nitride: The Importance of Strong Adhesion Due to<mml:math xmlns:mml="http://www.w3.org/1998/Math/MathML" display="inline"><mml:mi>Ï€</mml:mi></mml:math>-Bond Polarization. Physical Review Applied, 2016, 6, .	1.5	23
25990	Interplay between intercalated oxygen superstructures and monolayer<mml:math xmlns:mml="http://www.w3.org/1998/Math/MathML"><mml:mi>h</mml:mi></mml:math>-BN on Cu(100). Physical Review B, 2016, 94, .	1.1	16

#	Article	IF	Citations
25991	Isolated hydrogen configurations in zirconia as seen by muon spin spectroscopy andab initiocalculations. Physical Review B, 2016, 94, .	1.1	24
25992	Anomalous Enhancement of Liâ€O₂ Battery Performance with Li₂O₂ Films Assisted by NiFeO_x Nanofiber Catalysts: Insights into Morphology Control. Advanced Functional Materials, 2016, 26, 8290-8299.	7.8	47
25993	The effects of refractory elements on Ni-excesses and Ni-depletions at Î³(f.c.c.)/Î³â€²(L12) interfaces in model Ni-based superalloys: Atom-probe tomographic experiments and first-principles calculations. Acta Materialia, 2016, 121, 288-298.	3.8	45
25994	Time-temperature-transformation and continuous-heating-transformation diagrams of GeSb2Te4 from nanosecond-long ab initio molecular dynamics simulations. Acta Materialia, 2016, 121, 257-265.	3.8	13
25995	Theoretical study on the hydrogen storage mechanism of the Liâ€“Mgâ€“Nâ€“H system. International Journal of Hydrogen Energy, 2016, 41, 17506-17510.	3.8	5
25996	Study of adsorption and dissociation pathway of H 2 molecule on Mg n Rh (nÂ=Â1â€“10) clusters: A first principle investigation. International Journal of Hydrogen Energy, 2016, 41, 20113-20121.	3.8	59
25997	Lone-Pair-Electron-Driven Ionic Displacements in a Ferroelectric Metalâ€“Organic Hybrid. Inorganic Chemistry, 2016, 55, 10337-10342.	1.9	51
25998	Discovery of a Red-Emitting Li₃RbGe₈O₁₈:Mn⁴⁺ Phosphor in the Alkali-Germanate System: Structural Determination and Electronic Calculations. Inorganic Chemistry, 2016, 55, 10310-10319.	1.9	77
25999	Adsorption Behavior of Rare Earth Metal Cations in the Interlayer Space of Î³-ZrP. Langmuir, 2016, 32, 9993-9999.	1.6	5
26000	Adsorption of water and ethanol on noble and transition-metal substrates: a density functional investigation within van der Waals corrections. Physical Chemistry Chemical Physics, 2016, 18, 29526-29536.	1.3	30
26001	Surface and shape modification of mackinawite (FeS) nanocrystals by cysteine adsorption: a first-principles DFT-D2 study. Physical Chemistry Chemical Physics, 2016, 18, 32007-32020.	1.3	35
26002	High thermoelectric performance in Te-free (Bi,Sb)₂Se₃via structural transition induced band convergence and chemical bond softening. Energy and Environmental Science, 2016, 9, 3436-3447.	15.6	159
26003	Enhanced molecular adsorption of ethylene on reduced anatase TiO₂ (001): role of surface O-vacancies. RSC Advances, 2016, 6, 92241-92251.	1.7	13
26004	Macrocycles inserted in graphene: from coordination chemistry on graphene to graphitic carbon oxide. Nanoscale, 2016, 8, 17976-17983.	2.8	16
26005	Towards understanding the differences in irradiation effects of He, Ne and Ar plasma by investigating the physical origin of their clustering in tungsten. Nuclear Fusion, 2016, 56, 106002.	1.6	16
26006	Phase and structural stability in Ni-Al systems from first principles. Physical Review B, 2016, 94, .	1.1	36
26007	NV centers in<mml:math xmlns:mml="http://www.w3.org/1998/Math/MathML"><mml:mrow><mml:mn>3</mml:mn><mml:mi>C</mml:mi><mml:mo>,</mml:mo> and<mml:math xmlns:mml="http://www.w3.org/1998/Math/MathML"><mml:mrow><mml:mn>6</mml:mn><mml:mi>H</mml:mi></mml:mrow></mml:m carbide: A variable platform for solid-state qubits and nanosensors. Physical Review B, 2016, 94, .	1.1	75
26008	xmlns:mml="http://www.w3.org/1998/Math/MathML" display="inline"><mml:mrow><mml:msub><mml:mrow><mml:mi mathvariant="normal">H</mml:mi></mml:mrow><mml:mrow><mml:mn>2</mml:mn></mml:mrow></mml:msub><mml:mi mathvariant="normal">O</mml:mi></mml:mrow></mml:math>Ice. Physical Review Letters, 2016, 117, 135503.	2.9	53

#	Article	IF	Citations
26009	Exceptional Flux Growth and Chemical Transformation of Metastable Orthorhombic LiMnO2 Cuboids into Hierarchically-Structured Porous H1.6Mn1.6O4 Rods as Li Ion Sieves. Crystal Growth and Design, 2016, 16, 6178-6185.	1.4	17
26010	2D Covalent Metals: A New Materials Domain of Electrochemical CO₂ Conversion with Broken Scaling Relationship. Journal of Physical Chemistry Letters, 2016, 7, 4124-4129.	2.1	54
26011	Spontaneous Formation of Atomically Thin Stripes in Transition Metal Dichalcogenide Monolayers. Nano Letters, 2016, 16, 6982-6987.	4.5	48
26012	Systematic Approach To Calculate the Band Gap Energy of a Disordered Compound with a Low Symmetry and Large Cell Size via Density Functional Theory. ACS Omega, 2016, 1, 483-490.	1.6	14
26013	Nanostructural adsorption of vanadium oxide on functionalized graphene: a DFT study. Physical Chemistry Chemical Physics, 2016, 18, 29208-29217.	1.3	8
26014	Crystal structures and superconductivity of technetium hydrides under pressure. Physical Chemistry Chemical Physics, 2016, 18, 28791-28796.	1.3	15
26015	Unveiling the thermodynamic and kinetic properties of Na_xFe(SO₄)₂ (x = 0â€“2): toward a high-capacity and low-cost cathode material. Journal of Materials Chemistry A, 2016, 4, 17960-17969.	5.2	17
26016	Pressure-driven superconductivity in the transition-metal pentatelluride<mml:math xmlns:mml="http://www.w3.org/1998/Math/MathML"><mml:mrow><mml:mi>HfT</mml:mi><mml:msub><mml:mi mathvariant="normal">e</mml:mi><mml:mn>5</mml:mn></mml:msub></mml:mrow></mml:math>. Physical Review B, 2016, 94, .	1.1	46
26017	Chiral Weyl Pockets and Fermi Surface Topology of the Weyl Semimetal TaAs. Physical Review Letters, 2016, 117, 146401.	2.9	83
26018	Doping Mechanism in Transparent, Conducting Tantalum Doped ZnO Films Deposited Using Atomic Layer Deposition. Advanced Materials Interfaces, 2016, 3, 1600496.	1.9	15
26019	Selective Dehydrogenation of HCOOH on Zn-Decorated Pd(111) Surface Studied by First-Principles Calculations. Catalysis Letters, 2016, 146, 2348-2356.	1.4	6
26020	Theoretical insight into structure stability, elastic property and carrier mobility of monolayer arsenene under biaxial strains. Superlattices and Microstructures, 2016, 100, 324-334.	1.4	32
26021	Theory for Modeling of High Resolution Resonant and Nonresonant Raman Images. Journal of Chemical Theory and Computation, 2016, 12, 4986-4995.	2.3	24
26022	Epitaxial Strain-Induced Growth of CuO at Cu2O/ZnO Interfaces. Journal of Physical Chemistry C, 2016, 120, 23552-23558.	1.5	12
26023	Integrated High-Performance Infrared Phototransistor Arrays Composed of Nonlayered PbSâ€“MoS₂ Heterostructures with Edge Contacts. Nano Letters, 2016, 16, 6437-6444.	4.5	98
26024	Graphdiyne as a High-Efficiency Membrane for Separating Oxygen from Harmful Gases: A First-Principles Study. ACS Applied Materials & Interfaces, 2016, 8, 28166-28170.	4.0	68
26025	Structural Changes in 2D BiSe Bilayers as n Increases in (BiSe)_{1+Î´}(NbSe₂)_n (n = 1â€“4) Heterostructures. ACS Nano, 2016, 10, 9489-9499.	7.3	16
26026	Efficient Blue Electroluminescence Using Quantum-Confined Two-Dimensional Perovskites. ACS Nano, 2016, 10, 9720-9729.	7.3	299

#	Article	IF	Citations
26027	Purely substitutional nitrogen on graphene/Pt(111) unveiled by STM and first principles calculations. Nanoscale, 2016, 8, 17686-17693.	2.8	14
26028	Alkaline-earth metal-oxide overlayers on TiO₂: application toward CO₂ photoreduction. Catalysis Science and Technology, 2016, 6, 7885-7895.	2.1	29
26029	Environmental control of electronâ€“phonon coupling in barium doped graphene. 2D Materials, 2016, 3, 045003.	2.0	14
26030	Nitrogen-induced magnetism in stannates from first-principles calculations. International Journal of Modern Physics B, 2016, 30, 1650236.	1.0	1
26031	Ag@ZnO core-shell nanoparticles study by first principle: The structural, magnetic and optical properties. Journal of Solid State Chemistry, 2016, 244, 181-186.	1.4	14
26032	Li-atoms-induced structure changes of Guinierâ€“Prestonâ€“Bagaryatsky zones in AlCuLiMg alloys. Materials Characterization, 2016, 121, 207-212.	1.9	28
26033	La₃Li₃W₂O₁₂: Ionic Diffusion in a Perovskite with Lithium on both A- and B-Sites. Chemistry of Materials, 2016, 28, 7833-7851.	3.2	27
26034	Development of a ReaxFF Reactive Force Field for the Ptâ€“Ni Alloy Catalyst. Journal of Physical Chemistry A, 2016, 120, 8044-8055.	1.1	62
26035	Structure of Low and High Coverage Phases of Bromine on Pd(110). Journal of Physical Chemistry C, 2016, 120, 13523-13530.	1.5	2
26036	Block Copolymer-Assisted Solvothermal Synthesis of Hollow Bi₂MoO₆ Spheres Substituted with Samarium. Langmuir, 2016, 32, 10967-10976.	1.6	24
26037	Band Alignment for Rectification and Tunneling Effects in Al₂O₃ Atomic-Layer-Deposited on Back Contact for CdTe Solar Cell. ACS Applied Materials & Interfaces, 2016, 8, 28143-28148.	4.0	8
26038	Neural network molecular dynamics simulations of solidâ€“liquid interfaces: water at low-index copper surfaces. Physical Chemistry Chemical Physics, 2016, 18, 28704-28725.	1.3	141
26039	Insight into the mechanism about the initiation, growth and termination of the Câ€“C chain in syngas conversion on the Co(0001) surface: a theoretical study. Physical Chemistry Chemical Physics, 2016, 18, 27272-27283.	1.3	30
26040	First-principles studies of effects of interstitial boron and carbon on the structural, elastic, and electronic properties of Ni solution and Ni ₃ Al intermetallics. Chinese Physics B, 2016, 25, 107104.	0.7	5
26041	Higher-order elastic constants and megabar pressure effects of bcc tungsten:Ab initiocalculations. Physical Review B, 2016, 94, .	1.1	21
26042	Impact of anharmonic effects on the phase stability, thermal transport, and electronic properties of AlN. Physical Review B, 2016, 94, .	1.1	20
26043	Strong Intrinsic Spin Hall Effect in the TaAs Family of Weyl Semimetals. Physical Review Letters, 2016, 117, 146403.	2.9	164
26044	A first-principles study on the intrinsic phonon transport of Cu 2 GeSe 3. Europhysics Letters, 2016, 115, 26002.	0.7	6

#	Article	IF	Citations
26045	Indium-defect interactions in FCC and BCC metals studied using the modified embedded atom method. Hyperfine Interactions, 2016, 237, 1.	0.2	1
26046	Supercell design for first-principles simulations of solids and application to diamond, silica, and superionic water. High Energy Density Physics, 2016, 21, 8-15.	0.4	6
26047	Structure determination and stability for Pa-Si, Np-Si and U-X-Si (XÂ=ÂMo, Th, Np) phases from first-principles. Journal of Nuclear Materials, 2016, 479, 593-607.	1.3	4
26048	Controlled electronic and magnetic properties of WSe2 monolayers by doping transition-metal atoms. Superlattices and Microstructures, 2016, 100, 252-257.	1.4	16
26049	Fast Diffusivity of PF₆^{â€“} Anions in Graphitic Carbon for a Dual-Carbon Rechargeable Battery with Superior Rate Property. Journal of Physical Chemistry C, 2016, 120, 22887-22894.	1.5	82
26050	Formulation of Temperature-Dependent Thermal Conductivity of NaF, Î²-Na₃AlF₆, Na₅Al₃F₁₄, and Molten Na₃AlF₆ Supported by Equilibrium Molecular Dynamics and Density Functional Theory. Journal of Physical Chemistry C, 2016, 120, 22873-22886.	1.5	29
26051	A Novel Nanoporous Graphite Based on Graphynes: First-Principles Structure and Carbon Dioxide Preferential Physisorption. ACS Applied Materials & Interfaces, 2016, 8, 27996-28003.	4.0	31
26052	Real-space investigation of energy transfer in heterogeneous molecular dimers. Nature, 2016, 538, 364-367.	13.7	159
26053	Molecular simulations of nitrogen-doped hierarchical carbon adsorbents for post-combustion CO₂ capture. Physical Chemistry Chemical Physics, 2016, 18, 28747-28758.	1.3	21
26054	A first-principles study on the defective properties of MAX phase Cr₂AlC: the magnetic ordering and strong correlation effect. RSC Advances, 2016, 6, 84262-84268.	1.7	16
26055	Defects induced changes in the electronic structures of MgO and their correlation with the optical properties: a special case of electronâ€“hole recombination from the conduction band. RSC Advances, 2016, 6, 96398-96415.	1.7	78
26056	Modification of the electronic properties of hexagonal boron-nitride in BN/graphene vertical heterostructures. 2D Materials, 2016, 3, 045002.	2.0	10
26057	Electronic excitation-induced semiconductor-to-metal transition in monolayer<mml:math xmlns:mml="http://www.w3.org/1998/Math/MathML"><mml:msub><mml:mi>MoTe</mml:mi><mml:mn>2</mml:mn></mml:msub></m Physical Review B, 2016, 94, .	1.1	48
26058	Multiphase aluminum equations of state via density functional theory. Physical Review B, 2016, 94, .	1.1	70
26059	Phase diagram of<mml:math xmlns:mml="http://www.w3.org/1998/Math/MathML"><mml:mrow><mml:msub><mml:mi>Sr</mml:mi><mml:mrow><mml:mn>1</mml:mn></mml:mrow></mml:msub><mml:msub><mml:mi>Ir</mml:mi><mml:mn>1</mml:mn></mm a function of chemical doping, epitaxial strain, and external pressure. Physical Review B, 2016, 94, .	1.1	16
26060	H2 adsorption and dissociation on PdO(101) films supported on rutile TiO2 (110) facet: elucidating the support effect by DFT calculations. Journal of Molecular Modeling, 2016, 22, 204.	0.8	2
26061	Crystallographic facet-dependent stress responses by polyhedral lead sulfide nanocrystals and the potential â€œsafe-by-designâ€•approach. Nano Research, 2016, 9, 3812-3827.	5.8	14
26062	Mg/O₂ Battery Based on the Magnesiumâ€“Aluminum Chloride Complex (MACC) Electrolyte. Chemistry of Materials, 2016, 28, 7629-7637.	3.2	25

#	Article	IF	Citations
26063	Nanoscale Patterns on Polar Oxide Surfaces. Chemistry of Materials, 2016, 28, 7433-7443.	3.2	20
26064	CO Adsorption on the â€œ29â€•Cu_xO/Cu(111) Surface: An Integrated DFT, STM, and TPD Study. Journal of Physical Chemistry C, 2016, 120, 25387-25394.	1.5	24
26065	Substantial Band-Gap Tuning and a Strain-Controlled Semiconductor to Gapless/Band-Inverted Semimetal Transition in Rutile Lead/Stannic Dioxide. ACS Applied Materials & Interfaces, 2016, 8, 25667-25673.	4.0	18
26066	First-principles prediction of the softening of the silicon shock Hugoniot curve. Physical Review B, 2016, 94, .	1.1	39
26067	Pressure effect on hydrogen tunneling and vibrational spectrum in<mml:math xmlns:mml="http://www.w3.org/1998/Math/MathML"><mml:mi>Î±</mml:mi></mml:math>-Mn. Physical Review B, 2016, 94, .	1.1	7
26068	Mechanism of enhanced photocatalytic activities on tungsten trioxide doped with sulfur: Dopant-type effects. Modern Physics Letters B, 2016, 30, 1650340.	1.0	6
26069	Ab Initio Study of Deformation Influence on the Electronic Properties of Graphene Structures Containing One-Dimensional Topological Defects. Journal of Low Temperature Physics, 2016, 185, 712-716.	0.6	0
26070	Ionic Adsorbate Structures on Metal Electrodes Calculated from First-Principles. Industrial & Engineering Chemistry Research, 2016, 55, 11107-11113.	1.8	14
26071	Surface Energy as a Descriptor of Catalytic Activity. Journal of Physical Chemistry C, 2016, 120, 23698-23706.	1.5	83
26072	Electronic properties of Janus silicene: new direct band gap semiconductors. Journal Physics D: Applied Physics, 2016, 49, 445305.	1.3	51
26073	Stable monolayer honeycomb-like structures of<mml:math xmlns:mml="http://www.w3.org/1998/Math/MathML"><mml:mrow><mml:mtext>Ru</mml:mtext><mml:msub><mml:mi>X</mml:mi><mml:mn>3</mml:mn></mml:msub></mml:mrow></mml:math>(<mml:math xmlns:mml="http://www.w3.org/1998/Math/MathML"><mml:mo>(</mml:mo><mml:mrow><mml:mi>X</mml:mi><mml:mo>=</mml:mo> Physical Review B, 2016, 94, .	1.1	30
26074	A first principle hybrid functional calculation ofTmGe3+-VGedefect complexes in germanium. Computational Condensed Matter, 2016, 8, 31-35.	0.9	12
26075	Vibrational contributions to phase stability in the Mo-Ru system. Journal of Alloys and Compounds, 2016, 689, 969-976.	2.8	5
26076	Antiferromagnetic and semiconducting material CrNCN: Prediction from first-principles investigation. Journal of Physics and Chemistry of Solids, 2016, 98, 123-127.	1.9	0
26077	Structural stability, electronic, magnetic and optical properties of zincblende Zn 0.5 V 0.5 Te under pressure. Physics Letters, Section A: General, Atomic and Solid State Physics, 2016, 380, 3683-3689.	0.9	4
26078	Drastic changes of electronic structure and crystal chemistry upon oxidation of SnII2TiO4E2 into SnIV2TiO6: An ab initio study. Solid State Sciences, 2016, 59, 25-31.	1.5	2
26079	Ionic conductivity in Sm-doped ceria from first-principles non-equilibrium molecular dynamics. Solid State Ionics, 2016, 296, 47-53.	1.3	9
26080	Nonlinear Stark effect observed for carbon monoxide chemisorbed on gold core/palladium shell nanoparticle film electrodes, using in situ surface-enhanced Raman spectroscopy. Chinese Journal of Catalysis, 2016, 37, 1156-1165.	6.9	7

#	Article	IF	Citations
26081	DFT Perspective on the Thermochemistry of Carbon Nitride Synthesis. Journal of Physical Chemistry C, 2016, 120, 24542-24550.	1.5	21
26082	Mechanism of Isobutanalâ€“Isobutene Prins Condensation Reactions on Solid BrÃ¸nsted Acids. ACS Catalysis, 2016, 6, 7664-7684.	5.5	25
26083	Structural Diversity and Electron Confinement in Li₄N: Potential for 0-D, 2-D, and 3-D Electrides. Journal of the American Chemical Society, 2016, 138, 14108-14120.	6.6	59
26084	An atomistic mechanism study of GaN step-flow growth in vicinal m-plane orientations. Physical Chemistry Chemical Physics, 2016, 18, 29239-29248.	1.3	3
26085	Anomalous enhancement of Seebeck coefficients of the graphene/hexagonal boron nitride composites. Japanese Journal of Applied Physics, 2016, 55, 1102A9.	0.8	4
26086	Molecular Level Characterization of the Structure and Interactions in Peptideâ€Functionalized Metalâ€“Organic Frameworks. Chemistry - A European Journal, 2016, 22, 16531-16538.	1.7	27
26087	High-Throughput Computational Screening of Electrical and Phonon Properties of Two-Dimensional Transition Metal Dichalcogenides. Jom, 2016, 68, 2666-2672.	0.9	7
26088	Role of Organic Counterion in Lead- and Tin-Based Two-Dimensional Semiconducting Iodide Perovskites and Application in Planar Solar Cells. Chemistry of Materials, 2016, 28, 7781-7792.	3.2	228
26089	Highly Efficient Free Energy Calculations of the Fe Equation of State Using Temperature-Dependent Effective Potential Method. Journal of Physical Chemistry A, 2016, 120, 8761-8768.	1.1	6
26090	Visualization of Defect-Induced Excitonic Properties of the Edges and Grain Boundaries in Synthesized Monolayer Molybdenum Disulfide. Journal of Physical Chemistry C, 2016, 120, 24080-24087.	1.5	20
26091	Dense Hydrocarbon Structures at Megabar Pressures. Journal of Physical Chemistry Letters, 2016, 7, 4218-4222.	2.1	26
26092	Integrated Strategy toward Self-Powering and Selectivity Tuning of Semiconductor Gas Sensors. ACS Sensors, 2016, 1, 1256-1264.	4.0	28
26093	Cobalt carbide nanoprisms for direct production of lower olefins from syngas. Nature, 2016, 538, 84-87.	13.7	647
26094	First-principles study of relative stability of rutile and anatase TiO₂ using the random phase approximation. Physical Chemistry Chemical Physics, 2016, 18, 29914-29922.	1.3	51
26095	Prediction of flatness-driven quantum spin Hall effect in functionalized germanene and stanene. Physical Chemistry Chemical Physics, 2016, 18, 28134-28139.	1.3	21
26096	Global minimum of two-dimensional FeB₆and an oxidization induced negative Poisson's ratio: a new stable allotrope. Journal of Materials Chemistry C, 2016, 4, 9613-9621.	2.7	29
26097	Cubic scaling<mml:math xmlns:mml="http://www.w3.org/1998/Math/MathML"><mml:mrow><mml:mi>G</mml:mi><mml:mi>W</mml:mi></mml:mrow></mml:m Towards fast quasiparticle calculations. Physical Review B, 2016, 94, .	1.1	113
26098	Defect distribution and Schottky barrier at metal/Ge interfaces: Role of metal-induced gap states. Japanese Journal of Applied Physics, 2016, 55, 111302.	0.8	8

#	Article	IF	Citations
26099	Ferroelectric Control of Organic/Ferromagnetic Spinterface. Advanced Materials, 2016, 28, 10204-10210.	11.1	55
26100	Characteristics of n- and p-type dopants in 1T-HfS2 monolayer. Journal of Alloys and Compounds, 2016, 689, 302-306.	2.8	28
26101	The investigation of Ag/ZnO interface system by first principle: The structural, electronic and optical properties. Journal of Solid State Chemistry, 2016, 244, 175-180.	1.4	6
26102	Role of Hydrogen Abstraction Reaction in Photocatalytic Decomposition of High Energy Density Materials. Journal of Physical Chemistry C, 2016, 120, 24835-24846.	1.5	5
26103	Dimensionality and Valency Dependent Quantum Growth of Metallic Nanostructures: A Unified Perspective. Nano Letters, 2016, 16, 6628-6635.	4.5	4
26104	Photofragmentation Pathways for Gas-Phase Lanthanide Tris(isopropylcyclopentadienyl) Complexes. Organometallics, 2016, 35, 3461-3473.	1.1	14
26105	Characterization of Few-Layer 1Tâ€² MoTe₂ by Polarization-Resolved Second Harmonic Generation and Raman Scattering. ACS Nano, 2016, 10, 9626-9636.	7.3	148
26106	Nanoscale-Barrier Formation Induced by Low-Dose Electron-Beam Exposure in Ultrathin MoS₂ Transistors. ACS Nano, 2016, 10, 9730-9737.	7.3	26
26107	Reduced overpotentials for electrocatalytic water splitting over Fe- and Ni-modified BaTiO₃. Physical Chemistry Chemical Physics, 2016, 18, 29561-29570.	1.3	29
26108	C₂₀â^’Tcarbon: a novel superhardsp³carbon allotrope with large cavities. Journal of Physics Condensed Matter, 2016, 28, 475402.	0.7	30
26109	First-principles calculations for hydrogenation of acceptor defects in Li-doped SnO₂. Materials Research Express, 2016, 3, 105901.	0.8	3
26110	High-temperature large-gap quantum anomalous Hall insulating state in ultrathin double perovskite films. Physical Review B, 2016, 94, .	1.1	18
26111	Coexistence of Weyl fermion and massless triply degenerate nodal points. Physical Review B, 2016, 94, .	1.1	169
26112	The Phase Relations Studies of Mg-Zn-RE at 553ÂK Coupling with Diffusion Triple Technique and Frist Principle Calculations. Journal of Phase Equilibria and Diffusion, 2016, 37, 680-692.	0.5	0
26113	Predicting an alloying strategy for improving fracture toughness of C15 NbCr2 Laves phase: A first-principles study. Computational Materials Science, 2016, 123, 59-64.	1.4	13
26114	Selective hydrogenation of biomass-derived 2(5H)-furanone over Pt-Ni and Pt-Co bimetallic catalysts: From model surfaces to supported catalysts. Journal of Catalysis, 2016, 344, 148-156.	3.1	26
26115	Coexistence of Two Types of Lithium Motion in Monoclinic Li₂HfO₃: ^{6,7}Li NMR and Ab Initio Calculation Results. Journal of Physical Chemistry C, 2016, 120, 23911-23921.	1.5	10
26116	Layer dependent properties of <mml:math xmlns:mml="http://www.w3.org/1998/Math/MathML"><mml:msub><mml:mi mathvariant="bold">SnS</mml:mi><mml:mn>2</mml:mn></mml:msub></mml:math>and<mml:math xmlns:mml="http://www.w3.org/1998/Math/MathML"><mml:msub><mml:mi mathvariant="bold">SnSe</mml:mi><mml:mn>2</mml:mn></mml:msub></mml:math>two-dimensional materials. Physical Review B, 2016, 94, .	1.1	267

#	Article	IF	Citations
26117	Structural and electronic phase transitions of<mml:math xmlns:mml="http://www.w3.org/1998/Math/MathML"><mml:msub><mml:mi>ThS</mml:mi><mml:mn>2</mml:mn></mml:msub></mml first-principles calculations. Physical Review B, 2016, 94, .	1.1	15
26118	Brewster angle and reflectivity of optically nonuniform dense plasmas. Physical Review E, 2016, 94, 043202.	0.8	10
26119	Phase-controlled synthesis and comparative study of Î±- and Î²-WP 2 submicron particles as efficient electrocatalysts for hydrogen evolution. Electrochimica Acta, 2016, 216, 304-311.	2.6	17
26120	Toughening of Î±-Nb5Si3 by Ti. Journal of Alloys and Compounds, 2016, 689, 296-301.	2.8	36
26121	Polar phase transitions and physical properties in fresnoite A2TiSi2O8 (A= Ba, Sr) by first principles calculations. Journal of Solid State Chemistry, 2016, 242, 136-142.	1.4	4
26122	Yellow-green luminescence and extreme thermal quenching in the Sr6M2Al4O15:Eu2+ (MÂ=ÂY, Lu, Sc) phosphor series. Solid State Sciences, 2016, 60, 108-113.	1.5	9
26123	DFT Study on the Methane Synthesis from Syngas on a Cerium-Doped Ni(111) Surface. Journal of Physical Chemistry C, 2016, 120, 23030-23043.	1.5	19
26124	Co-decorated Cu alloy catalyst for C₂ oxygenate and ethanol formation from syngas on Cu-based catalyst: insight into the role of Co and Cu as well as the improved selectivity. Catalysis Science and Technology, 2016, 6, 8036-8054.	2.1	39
26125	A near-zero Poisson's ratio of Si with ordered nanopores. Physical Chemistry Chemical Physics, 2016, 18, 21949-21953.	1.3	2
26126	Skyrmions with Attractive Interactions in an Ultrathin Magnetic Film. Physical Review Letters, 2016, 117, 157205.	2.9	80
26127	Identifying the Distribution of Al³⁺ in LiNi_{0.8}Co_{0.15}Al_{0.05}O₂. Chemistry of Materials, 2016, 28, 8170-8180.	3.2	77
26128	Explicitly Unraveling the Roles of Counterions, Solvent Molecules, and Electron Correlation in Solution Phase Reaction Pathways. Journal of Physical Chemistry B, 2016, 120, 10797-10807.	1.2	13
26129	Insight into the Origin of Boosted Photosensitive Efficiency of Graphene from the Cooperative Experiment and Theory Study. Journal of Physical Chemistry C, 2016, 120, 27091-27103.	1.5	37
26130	Structure and Reducibility of CeO₂ Doped with Trivalent Cations. Journal of Physical Chemistry C, 2016, 120, 23430-23440.	1.5	66
26131	Strongly enhanced Rashba splittings in an oxide heterostructure: A tantalate monolayer onBaHfO3. Physical Review B, 2016, 94, .	1.1	12
26132	Engendering anion immunity in oxygen consuming cathodes based on Fe-Nx electrocatalysts: Spectroscopic and electrochemical advanced characterizations. Applied Catalysis B: Environmental, 2016, 198, 318-324.	10.8	53
26133	Revisiting thermodynamics and kinetic diffusivities of uraniumâ€“niobium with Bayesian uncertainty analysis. Calphad: Computer Coupling of Phase Diagrams and Thermochemistry, 2016, 55, 219-230.	0.7	46
26134	First principles study of AlH3 vacancy mediated mechanism in dehydriding of NaAlH4. International Journal of Hydrogen Energy, 2016, 41, 16966-16973.	3.8	1

#	Article	IF	Citations
26135	Stability of Prismatic and Octahedral Coordination in Layered Oxides and Sulfides Intercalated with Alkali and Alkaline-Earth Metals. Chemistry of Materials, 2016, 28, 7898-7904.	3.2	82
26136	Coexistence of Two Electronic Nano-Phases on a CH₃NH₃PbI_{3â€“x}Cl_x Surface Observed in STM Measurements. ACS Applied Materials & Interfaces, 2016, 8, 29110-29116.	4.0	21
26137	Li intercalation mechanisms in CaTi₅O₁₁, a bronze-B derived compound. Physical Chemistry Chemical Physics, 2016, 18, 32042-32049.	1.3	5
26138	Native defects as sources of optical transitions in MgAl₂O₄spinel. Materials Research Express, 2016, 3, 076202.	0.8	27
26139	Electronic Structures of Silicene Nanoribbons: Two-Edge-Chemistry Modification and First-Principles Study. Nanoscale Research Letters, 2016, 11, 371.	3.1	22
26140	Rb as an Alternative Cation for Templating Inorganic Lead-Free Perovskites for Solution Processed Photovoltaics. Chemistry of Materials, 2016, 28, 7496-7504.	3.2	249
26141	Tolerance Factors Revisited: Geometrically Designing the Ideal Environment for Perovskite Dopants. Journal of Physical Chemistry C, 2016, 120, 23293-23298.	1.5	20
26142	Auxetic Black Phosphorus: A 2D Material with Negative Poissonâ€™s Ratio. Nano Letters, 2016, 16, 6701-6708.	4.5	184
26143	Surface Morphology and Surface Stability against Oxygen Loss of the Lithium-Excess Li₂MnO₃ Cathode Material as a Function of Lithium Concentration. ACS Applied Materials & Interfaces, 2016, 8, 25595-25602.	4.0	38
26144	The interface of SrTiO ₃ and H ₂ O from density functional theory molecular dynamics. Proceedings of the Royal Society A: Mathematical, Physical and Engineering Sciences, 2016, 472, 20160293.	1.0	21
26145	Emergence of competing magnetic interactions induced by Ge doping in the semiconductorFeGa3. Physical Review B, 2016, 94, .	1.1	9
26146	Hydrodeoxygenation of butyric acid at multi-functional Nb2O5 catalyst: A density functional theory study. International Journal of Hydrogen Energy, 2016, 41, 18502-18508.	3.8	15
26147	Syntheses of six and twelve membered borophosphate ring structure with nonlinear optical activity. Journal of Solid State Chemistry, 2016, 243, 259-266.	1.4	11
26148	Selective dynamic separation of Xe and Kr in Co-MOF-74 through strong binding strength between Xe atom and unsaturated Co2+ site. Microporous and Mesoporous Materials, 2016, 236, 284-291.	2.2	52
26149	A first-principles study of transition metal doped arsenene. Superlattices and Microstructures, 2016, 100, 131-141.	1.4	26
26150	Fast-Dissolving, Prolonged Release, and Antibacterial Cyclodextrin/Limonene-Inclusion Complex Nanofibrous Webs via Polymer-Free Electrospinning. Journal of Agricultural and Food Chemistry, 2016, 64, 7325-7334.	2.4	92
26151	Uncloaking the Thermodynamics of the Studtite to Metastudtite Shear-Induced Transformation. Journal of Physical Chemistry C, 2016, 120, 16553-16560.	1.5	34
26152	Unraveling the Influence of Metal Substrates on Graphene Nucleation from First-Principles Study. Journal of Physical Chemistry C, 2016, 120, 23239-23245.	1.5	20

#	Article	IF	Citations
26153	Superhard Semiconducting Phase of Osmium Tetraboride Stabilizing at 11 GPa. Journal of Physical Chemistry C, 2016, 120, 23165-23171.	1.5	14
26154	Substrate-Induced Nanoscale Undulations of Borophene on Silver. Nano Letters, 2016, 16, 6622-6627.	4.5	155
26155	Quantum Mechanical Screening of Single-Atom Bimetallic Alloys for the Selective Reduction of CO₂ to C₁ Hydrocarbons. ACS Catalysis, 2016, 6, 7769-7777.	5.5	190
26156	Towards a comprehensive understanding of FeCo coated with N-doped carbon as a stable bi-functional catalyst in acidic media. NPG Asia Materials, 2016, 8, e312-e312.	3.8	82
26157	Promotion mechanism of pyridine N-doped carbocatalyst for SO₂ oxidation. RSC Advances, 2016, 6, 86316-86323.	1.7	17
26158	Strain controlled ferromagneticâ€“ferrimagnetic transition and vacancy formation energy of defective graphene. Nanotechnology, 2016, 27, 435206.	1.3	9
26159	Theoretical perspective on the electronic, magnetic and optical properties of Zn-doped monolayer SnS2. Applied Surface Science, 2016, 389, 484-490.	3.1	33
26160	First-principles phase diagram calculations for the carbonate quasibinary systems CaCO3-ZnCO3, CdCO3-ZnCO3, CaCO3-CdCO3 and MgCO3-ZnCO3. Chemical Geology, 2016, 443, 137-145.	1.4	11
26161	First-principles calculations on structure and properties of amorphous Li5P4O8N3 (LiPON). Journal of Power Sources, 2016, 331, 382-390.	4.0	33
26162	Screening of Copper Open Metal Site MOFs for Olefin/Paraffin Separations Using DFT-Derived Force Fields. Journal of Physical Chemistry C, 2016, 120, 23044-23054.	1.5	61
26163	Synthesis and Characterization of Ptâ€“Ag Alloy Nanocages with Enhanced Activity and Durability toward Oxygen Reduction. Nano Letters, 2016, 16, 6644-6649.	4.5	150
26164	Insight into the collective vibrational modes driving ultralow thermal conductivity of perovskite solar cells. Physical Review B, 2016, 94, .	1.1	52
26165	New mechanistic pathways for CO oxidation catalyzed by single-atom catalysts: Supported and doped Au1/ThO2. Nano Research, 2016, 9, 3868-3880.	5.8	68
26166	Heat treatment response of TiC-reinforced steel matrix composite. Metals and Materials International, 2016, 22, 935-941.	1.8	10
26167	Robust NdBa0.5Sr0.5Co1.5Fe0.5O5+Î´ cathode material and its degradation prevention operating logic for intermediate temperature-solid oxide fuel cells. Journal of Power Sources, 2016, 331, 495-506.	4.0	37
26168	Methylation of benzene with methanol over HZSM-11 and HZSM-5: A density functional theory study. Journal of Molecular Catalysis A, 2016, 424, 351-357.	4.8	30
26169	Structureâ€“Property Relationships in Î±-, Î²â€²-, and Î³-Modifications of Mn₃(PO₄)₂. Inorganic Chemistry, 2016, 55, 10692-10700.	1.9	15
26170	Substitution Boosts Charge Separation for High Solar-Driven Photocatalytic Performance. ACS Applied Materials & Interfaces, 2016, 8, 26783-26793.	4.0	39

#	Article	IF	Citations
26171	Rutile TiO₂(011)-2 Ã— 1 Reconstructed Surfaces with Optical Absorption over the Visible Light Spectrum. ACS Applied Materials & Interfaces, 2016, 8, 27403-27410.	4.0	18
26172	pH-Dependent Synthesis of Anisotropic Gold Nanostructures by Bioinspired Cysteine-Containing Peptides. ACS Omega, 2016, 1, 424-434.	1.6	25
26173	Promoting oxygen vacancy formation and p-type conductivity in SrTiO₃via alkali metal doping: a first principles study. Physical Chemistry Chemical Physics, 2016, 18, 28951-28959.	1.3	17
26174	High pressure-induced distortion in face-centered cubic phase of thallium. Proceedings of the National Academy of Sciences of the United States of America, 2016, 113, 11143-11147.	3.3	12
26175	Accurate prediction of band gaps and optical properties of HfO₂. Journal Physics D: Applied Physics, 2016, 49, 395301.	1.3	31
26176	Interface characteristics at an organic/metal junction: pentacene on Cu stepped surfaces. Journal of Physics Condensed Matter, 2016, 28, 445001.	0.7	2
26177	Novel cubic-phase pyrochlore Sb(III)2Sn(IV)2O7 transformed from Sn(II)2Sb(V)2O7: First-principles calculation-based prediction and experimental evidence. Materials and Design, 2016, 110, 207-213.	3.3	5
26178	Photoluminescence and Photocurrents of GaS_{1â€“x}Se_x Nanobelts. Chemistry of Materials, 2016, 28, 5811-5820.	3.2	28
26179	Alkali metalâ€“alkaline earth metal borate crystal LiBa₃(OH)(B₉O₁₆)[B(OH)₄] as a new deep-UV nonlinear optical material. Journal of Materials Chemistry C, 2016, 4, 8189-8196.	2.7	29
26180	Electronic properties of highly-active Ag₃AsO₄photocatalyst and its band gap modulation: an insight from hybrid-density functional calculations. Physical Chemistry Chemical Physics, 2016, 18, 23407-23411.	1.3	30
26181	Tuning the work function of graphene with the adsorbed organic molecules: first-principles calculations. Molecular Physics, 2016, 114, 2993-2998.	0.8	5
26182	Heterostructures based on graphene and MoS2layers decorated by C60fullerenes. Nanotechnology, 2016, 27, 365201.	1.3	11
26183	Ab initio Modeling of the Electronic Structures and Physical Properties of aâ€“Si_{1â^'x}Ge_xO₂ Glass (x = 0 to 1). Journal of the American Ceramic Society, 2016, 99, 3677-3684.	1.9	24
26184	Theoretical realization of half-metallicity in two-dimensional monolayered molybdenum dinitride by Mo vacancy tuning. Physics Letters, Section A: General, Atomic and Solid State Physics, 2016, 380, 2669-2673.	0.9	4
26185	Adsorption of H2, Cl2, and HCl molecules on Î±-Cr2O3(0001) surfaces: AÂdensity functional theory investigation. Surface Science, 2016, 653, 211-221.	0.8	11
26186	Water coordination and dehydration processes in defective UiO-66 type metal organic frameworks. CrystEngComm, 2016, 18, 7056-7069.	1.3	58
26187	van der Waals density functionals applied to corundum-type sesquioxides: bulk properties and adsorption of CH₃ and C₆H₆ on (0001) surfaces. Physical Chemistry Chemical Physics, 2016, 18, 23139-23146.	1.3	7
26188	Hybrid improper ferroelectricity in SrZrO₃/BaZrO₃ superlattice. Physical Chemistry Chemical Physics, 2016, 18, 24024-24032.	1.3	7

#	Article	IF	Citations
26189	Tuning the phase transition temperature, electrical and optical properties of VO₂ by oxygen nonstoichiometry: insights from first-principles calculations. RSC Advances, 2016, 6, 73070-73082.	1.7	42
26190	Dependence of high-order-harmonic generation on dipole moment in<mml:math xmlns:mml="http://www.w3.org/1998/Math/MathML"><mml:mrow><mml:mi>Si</mml:mi><mml:msub><mml:mi mathvariant="normal">O</mml:mi><mml:mn>2</mml:mn></mml:msub></mml:mrow></mml:math>crystals. Physical Review A, 2016, 94, .	1.0	70
26191	Magnetic, resonance, and optical properties of<mml:math xmlns:mml="http://www.w3.org/1998/Math/MathML"><mml:mrow><mml:msub><mml:mi>Cu</mml:mi><mml:mn>3</mml:mn></mml:msub><mml:msub><mml:mi mathvariant="normal">O</mml:mi><mml:mn>2</mml:mn></mml:msub><mml:msub><mml:mi>Cl</mml:mi></mml:mrow></mml:math>: A rare-earth francisite compound. Physical Review B, 2016, 94, .	1.1	30
26192	Effects of surface residual species in SBA-16 on encapsulated chiral (1S,2S)-DPEN-RuCl2(TPP)2 in asymmetric hydrogenation of acetophenone. Russian Journal of Physical Chemistry A, 2016, 90, 545-551.	0.1	1
26193	Boron Substituted Na₃V₂(P₁_{â^'x}B_xO₄)₃ Cathode Materials with Enhanced Performance for Sodiumâ€ion Batteries. Advanced Science, 2016, 3, 1600112.	5.6	88
26194	Theoretical study of coupling p-aminothiophenol to hydroazo- and azo-adducts on Au(111). Journal of Molecular Modeling, 2016, 22, 197.	0.8	0
26195	Dual-site oxygen reduction reaction mechanism on CoN4 and CoN2 embedded graphene: Theoretical insights. Carbon, 2016, 108, 541-550.	5.4	81
26196	Lattice dynamics and electronic structures of Ti3C2O2 and Mo2TiC2O2 (MXenes): The effect of Mo substitution. Computational Materials Science, 2016, 124, 8-14.	1.4	107
26197	Ferrous iron partitioning in the lower mantle. Physics of the Earth and Planetary Interiors, 2016, 257, 12-17.	0.7	23
26198	Strain engineering of magnetic state in vacancy-doped phosphorene. Physics Letters, Section A: General, Atomic and Solid State Physics, 2016, 380, 3270-3277.	0.9	26
26199	Ligancy-Driven Controlling of Covalency and Metallicity in a Ruthenium Two-Dimensional System. Chemistry of Materials, 2016, 28, 5784-5790.	3.2	3
26200	Promotional Effects of Cesium Promoter on Higher Alcohol Synthesis from Syngas over Cesium-Promoted Cu/ZnO/Al₂O₃ Catalysts. ACS Catalysis, 2016, 6, 5771-5785.	5.5	79
26201	Confining Sulfur Species in Cathodes of Lithiumâ€“Sulfur Batteries: Insight into Nonpolar and Polar Matrix Surfaces. ACS Energy Letters, 2016, 1, 481-489.	8.8	53
26202	Enhanced electrocatalytic CO2 reduction via field-induced reagent concentration. Nature, 2016, 537, 382-386.	13.7	1,429
26203	A first-principle study of the effect of OH^{â^'} doping on the elastic constants and electronic structure of HTB-FeF₃. RSC Advances, 2016, 6, 75766-75776.	1.7	9
26204	Particle size effects in the selective hydrogenation of cinnamaldehyde over supported palladium catalysts. RSC Advances, 2016, 6, 75541-75551.	1.7	66
26205	Stacking fault energy of face-centered cubic metals: thermodynamic andab initioapproaches. Journal of Physics Condensed Matter, 2016, 28, 395001.	0.7	43
26206	Giant gap quantum spin Hall effect and valley-polarized quantum anomalous Hall effect in cyanided bismuth bilayers. New Journal of Physics, 2016, 18, 083002.	1.2	18

#	Article	IF	Citations
26207	Crystalline and electronic structure of single-layer<mml:math xmlns:mml="http://www.w3.org/1998/Math/MathML"><mml:msub><mml:mi>TaS</mml:mi><mml:mn>2</mml:mn></mml:msub></mml Physical Review B, 2016, 94, .	1.1	25
26208	An Antimony Selenide Molecular Ink for Flexible Broadband Photodetectors. Advanced Electronic Materials, 2016, 2, 1600182.	2.6	31
26209	Thermodynamic Stability and Defect Chemistry of Bismuthâ€Based Leadâ€Free Double Perovskites. ChemSusChem, 2016, 9, 2628-2633.	3.6	273
26210	Computational study of metallic dopant segregation and embrittlement at molybdenum grain boundaries. Acta Materialia, 2016, 117, 91-99.	3.8	63
26211	Quantifying uncertainties in first-principles alloy thermodynamics using cluster expansions. Journal of Computational Physics, 2016, 323, 17-44.	1.9	17
26212	Phase equilibria in the U-Si system from first-principles calculations. Journal of Nuclear Materials, 2016, 479, 216-223.	1.3	68
26213	van der Waals Heteroepitaxy of Germanene Islands on Graphite. Journal of Physical Chemistry Letters, 2016, 7, 3246-3251.	2.1	42
26214	Novel room-temperature spin-valve-like magnetoresistance in magnetically coupled nano-column Fe₃O₄/Ni heterostructure. Nanoscale, 2016, 8, 15737-15743.	2.8	9
26215	Electronic and magnetic properties of the Co₂-based Heusler compounds under pressure: first-principles and Monte Carlo studies. Journal Physics D: Applied Physics, 2016, 49, 355004.	1.3	41
26216	First-Principles Calculation on Geometric, Electronic and Optical Properties of Fully Fluorinated Stanene: a Large-Gap Quantum Spin Hall Insulator. Chinese Physics Letters, 2016, 33, 067101.	1.3	5
26217	Metal versus insulator behavior in ultrathin<mml:math xmlns:mml="http://www.w3.org/1998/Math/MathML"><mml:msub><mml:mi mathvariant="normal">SrTiO</mml:mi><mml:mn>3</mml:mn></mml:msub></mml:math>-based heterostructures. Physical Review B, 2016, 94, .	1.1	2
26218	A wavelet-based Projector Augmented-WaveÂ(PAW) method: Reaching frozen-core all-electron precision with a systematic, adaptive and localized wavelet basis set. Computer Physics Communications, 2016, 208, 1-8.	3.0	18
26219	Ostwald ripening of faceted Si particles in an Al-Si-Cu melt. Materials Science & Engineering A: Structural Materials: Properties, Microstructure and Processing, 2016, 673, 307-320.	2.6	33
26220	Structural, Electronic, and Li Migration Properties of RE-Doped (RE = Ce, La) LiCoO₂for Li-ion Batteries: A First-Principles Investigation. Journal of Physical Chemistry C, 2016, 120, 18428-18434.	1.5	48
26221	Stabilization of Small Platinum Nanoparticles on Ptâ€“CeO₂Thin Film Electrocatalysts During Methanol Oxidation. Journal of Physical Chemistry C, 2016, 120, 19723-19736.	1.5	50
26222	Structural, Vibrational, and Electronic Study of Î±-As₂Te₃ under Compression. Journal of Physical Chemistry C, 2016, 120, 19340-19352.	1.5	37
26223	Moderate Humidity Delays Electronâ€“Hole Recombination in Hybrid Organicâ€“Inorganic Perovskites: Time-Domain Ab Initio Simulations Rationalize Experiments. Journal of Physical Chemistry Letters, 2016, 7, 3215-3222.	2.1	139
26224	Is the Surface Playing a Role during Pyridine-Catalyzed CO₂ Reduction on p-GaP Photoelectrodes?. ACS Energy Letters, 2016, 1, 464-468.	8.8	34

#	Article	IF	Citations
26225	Thermodynamic Control of Two-Dimensional Molecular Ionic Nanostructures on Metal Surfaces. ACS Nano, 2016, 10, 7821-7829.	7.3	8
26226	First-Principles Study of the Role of O₂ and H₂O in the Decoupling of Graphene on Cu(111). Journal of the American Chemical Society, 2016, 138, 10986-10994.	6.6	29
26227	Structural dependence of the photocatalytic properties of double perovskite compounds A₂InTaO₆ (A = Sr or Ba) doped with nickel. Physical Chemistry Chemical Physics, 2016, 18, 21491-21499.	1.3	35
26228	Doped graphenes as anodes with large capacity for lithium-ion batteries. Journal of Materials Chemistry A, 2016, 4, 13407-13413.	5.2	57
26229	Manifestation of nonlocal electron-electron interaction in graphene. Physical Review B, 2016, 94, .	1.1	14
26230	New family of Dirac and Weyl semimetals in XAuTe (X = Na, K, Rb) ternary honeycomb compounds. Science China: Physics, Mechanics and Astronomy, 2016, 59, 1.	2.0	5
26231	Calcium decorated two dimensional carbon allotropes for hydrogen storage: A first-principles study. Computational Materials Science, 2016, 124, 106-113.	1.4	25
26232	Development of a Modified Embedded Atom Force Field for Zirconium Nitride Using Multi-Objective Evolutionary Optimization. Journal of Physical Chemistry C, 2016, 120, 17475-17483.	1.5	23
26233	Could Borophene Be Used as a Promising Anode Material for High-Performance Lithium Ion Battery?. ACS Applied Materials & Interfaces, 2016, 8, 22175-22181.	4.0	138
26234	Feâ€“Si networks in Na₂FeSiO₄ cathode materials. Physical Chemistry Chemical Physics, 2016, 18, 23916-23922.	1.3	27
26235	Graphene layers on bimetallic Ni/Cu(111) surface and near surface alloys in controlled growth of graphene. RSC Advances, 2016, 6, 74973-74981.	1.7	5
26236	Lithium intercalation and diffusion in TiO₂ nanotubes: a first-principles investigation. Physical Chemistry Chemical Physics, 2016, 18, 24370-24376.	1.3	24
26237	Structural and Thermal Properties of BaTe₂O₆: Combined Variable-Temperature Synchrotron X-ray Diffraction, Raman Spectroscopy, and ab Initio Calculations. Inorganic Chemistry, 2016, 55, 8994-9005.	1.9	15
26238	CO₂ Binding and Induced Structural Collapse of a Surface-Supported Metalâ€“Organic Network. Journal of Physical Chemistry C, 2016, 120, 18622-18630.	1.5	12
26239	Electronic Structure of the (Undoped and Fe-Doped) NiOOH O₂ Evolution Electrocatalyst. Journal of Physical Chemistry C, 2016, 120, 18999-19010.	1.5	52
26240	Influence of sp³â€“sp² Carbon Nanodomains on Metal/Support Interaction, Catalyst Durability, and Catalytic Activity for the Oxygen Reduction Reaction. ACS Applied Materials & Interfaces, 2016, 8, 23260-23269.	4.0	95
26241	Calculation of positron annihilation characteristics of six main defects in<mml:math xmlns:mml="http://www.w3.org/1998/Math/MathML"><mml:mrow><mml:mn>6</mml:mn><mml:mi>H</mml:mi></mml:mrow></mml:m and the possibility to distinguish them experimentally. Physical Review B, 2016, 94, .	1.1	11
26242	Computational simulation of subatomic-resolution AFM and STM images for graphene/hexagonal boron nitride heterostructures with intercalated defects. Physical Review B, 2016, 94, .	1.1	5

#	Article	IF	Citations
26243	Effect of sputtering power on Cd/Zn atomic ratio and optical properties of Cu2ZnxCd1â^'xSnS4 thin films deposited by magnetron sputtering: An experimental and first-principle study. Chemical Physics Letters, 2016, 660, 132-135.	1.2	6
26244	Buckling of dislocation in graphene. Physica E: Low-Dimensional Systems and Nanostructures, 2016, 84, 340-347.	1.3	9
26245	Putting ScTGa5 (T = Fe, Co, Ni) on the Map: How Electron Counts and Chemical Pressure Shape the Stability Range of the HoCoGa5 Type. Crystal Growth and Design, 2016, 16, 5349-5358.	1.4	8
26246	Theoretical Prediction of the Intrinsic Half-Metallicity in Surface-Oxygen-Passivated Cr₂N MXene. Journal of Physical Chemistry C, 2016, 120, 18850-18857.	1.5	118
26247	Preventing Structural Rearrangements on Battery Cycling: A First-Principles Investigation of the Effect of Dopants on the Migration Barriers in Layered Li_{0.5}MnO₂. Journal of Physical Chemistry C, 2016, 120, 19521-19530.	1.5	14
26248	Two-Dimensional Y₂C Electride: A Promising Anode Material for Na-Ion Batteries. Journal of Physical Chemistry C, 2016, 120, 18473-18478.	1.5	81
26249	Mechanisms of H₂O and CO₂ Formation from Surface Oxygen Reduction on Co(0001). Journal of Physical Chemistry C, 2016, 120, 19265-19270.	1.5	25
26250	Dirac fermions in an antiferromagnetic semimetal. Nature Physics, 2016, 12, 1100-1104.	6.5	216
26251	The Tiâ€“Mn system revisited: experimental investigation and thermodynamic modelling. Physical Chemistry Chemical Physics, 2016, 18, 23326-23339.	1.3	16
26252	C-type related order in the defective fluorites La₂Ce₂O₇ and Nd₂Ce₂O₇ studied by neutron scattering and ab initio MD simulations. Physical Chemistry Chemical Physics, 2016, 18, 24070-24080.	1.3	18
26253	Electronic structure and optical property of metal-doped Ga₂O₃: a first principles study. RSC Advances, 2016, 6, 78322-78334.	1.7	68
26254	First-principles analysis on role of spinel (111) phase boundaries in Li_{4+3x}Ti₅O₁₂ Li-ion battery anodes. Physical Chemistry Chemical Physics, 2016, 18, 23383-23388.	1.3	17
26255	Multi-step reaction mechanism for F atom interactions with organosilicate glass and SiO_xfilms. Journal Physics D: Applied Physics, 2016, 49, 345203.	1.3	21
26256	First principles study of the electronic structure and magnetic properties of spin chain compounds: Ca3ZnMnO6and Ca3ZnCoO6. Journal of Physics Condensed Matter, 2016, 28, 375501.	0.7	6
26257	Intrinsic magnetic properties in<mml:math xmlns:mml="http://www.w3.org/1998/Math/MathML"><mml:mrow><mml:mi>R</mml:mi><mml:msub><mml:mrow><mml:mo>(</mml:		

#	Article	IF	Citations
26261	Nanosize stabilized Li-deficient Li2â^'xO2 through cathode architecture for high performance Li-O2 batteries. Nano Energy, 2016, 27, 577-586.	8.2	42
26262	DFT Studies of the Selective Câ€"O Hydrogenolysis and Ring-Opening of Biomass-Derived Tetrahydrofurfuryl Alcohol over Rh(111) surfaces. Journal of Physical Chemistry C, 2016, 120, 19124-19134.	1.5	17
26263	Effect of Chlorine Substitution on Lattice Distortion and Ferroelectricity of CH3NH3PbI3. Journal of Physical Chemistry C, 2016, 120, 17972-17977.	1.5	22
26264	Unveiling the atomic structure and electronic properties of atomically thin boron sheets on an Ag(111) surface. Nanoscale, 2016, 8, 16284-16291.	2.8	59
26265	New clathrates of Rb7.50(1)Tl0.50(1)Ge46and K7.62(1)Tl0.38(1)Ge45.34(3). RSC Advances, 2016, 6, 75269-75276.	1.7	2
26266	High pressure Î³-to-Î² phase transition in bulk and nanocrystalline In₂Se₃. High Pressure Research, 2016, 36, 549-556.	0.4	4
26267	Thermoelectric properties of monolayerMSe₂(M = Zr, Hf): low lattice thermal conductivity and a promising figure of merit. Nanotechnology, 2016, 27, 375703.	1.3	127
26268	Effects of quantum confinement on excited state properties of<mml:math xmlns:mml="http://www.w3.org/1998/Math/MathML"><mml:msub><mml:mi>SrTiO</mml:mi><mml:mn>3</mml:mn></mml:msub><mml:mi>Ab initio</mml:mi>many-body perturbation theory. Physical Review B, 2016, 94, .	1.1	14
26269	Phonon anharmonicity and negative thermal expansion in SnSe. Physical Review B, 2016, 94, .	1.1	90
26270	Designing substrates for silicene and germanene: First-principles calculations. Physical Review B, 2016, 94, .	1.1	50
26271	Thermally Driven Electronic Topological Transition in FeTi. Physical Review Letters, 2016, 117, 076402.	2.9	3
26272	Experimental and Computational Evaluation of a Sodium-Rich Anti-Perovskite for Solid State Electrolytes. Journal of the Electrochemical Society, 2016, 163, A2165-A2171.	1.3	43
26276	DFT-D2 Study of the Adsorption of Bio-Oil Model Compounds in HZSM-5: C1â€"C4 Carboxylic Acids. Catalysis Letters, 2016, 146, 2015-2024.	1.4	10
26277	Penetration of the first-two-row elements through mono-layer graphene. Carbon, 2016, 109, 117-123.	5.4	4
26278	First-principles study of sulfur atom doping and adsorption on Î±â€"Fe2O3 (0001) film. Physics Letters, Section A: General, Atomic and Solid State Physics, 2016, 380, 3149-3154.	0.9	7
26279	Charging single Co atoms on ultrathin NaCl films. Dalton Transactions, 2016, 45, 16566-16569.	1.6	1
26280	Influences of the Pb 6s² lone pair effect and quantum size effect on the diffusion of oxygen atoms on Pb(111) films. RSC Advances, 2016, 6, 78755-78761.	1.7	1
26281	Ab initioscaling laws for the formation energy of nanosized interstitial defect clusters in iron, tungsten, and vanadium. Physical Review B, 2016, 94, .	1.1	84

#	Article	IF	Citations
26282	Effect of lattice constant on pseudo Jahn-Teller polar distortion: Application to search for new multiferroic compounds. Physical Review B, 2016, 94, .	1.1	5
26283	Photoinduced Charge Transfer at Interfaces of Carbon Nanotube and Lead Selenide Nanowire. Journal of Physical Chemistry C, 2016, 120, 23197-23206.	1.5	13
26284	Energy Gap Tuning and Carrier Dynamics in Colloidal Ge_{1â€“x}Sn_x Quantum Dots. Journal of Physical Chemistry Letters, 2016, 7, 3295-3301.	2.1	23
26285	Single-Molecule Rotational Switch on a Dangling Bond Dimer Bearing. ACS Nano, 2016, 10, 8499-8507.	7.3	33
26286	Topological Phases in<mml:math xmlns:mml="http://www.w3.org/1998/Math/MathML" display="inline"><mml:msub><mml:mi>InAs</mml:mi><mml:mrow><mml:mn>1</mml:mn><mml:mo>â^’</mml:mo><mml:mi>x</mml:mi></mml:mrow></mml:msub></mml:math> From Novel Topological Semimetal to Majorana Wire. Physical Review Letters, 2016, 117, 076403.	2.9	89
26287	Electrophobic interaction induced impurity clustering in metals. Acta Materialia, 2016, 119, 1-8.	3.8	36
26288	Electronic structures of spinterface for thiophene molecule adsorbed at Co, Fe, and Ni electrode: First principles calculations. Applied Surface Science, 2016, 389, 916-920.	3.1	12
26289	Comparing the catalytic activity of the water gas shift reaction on Cu(3 2 1) and Cu(1 1 1) surfaces: Step sites do not always enhance the overall reactivity. Journal of Catalysis, 2016, 342, 75-83.	3.1	30
26290	Hydride-Based Electride Material, LnH₂ (Ln = La, Ce, or Y). Inorganic Chemistry, 2016, 55, 8833-8838.	1.9	60
26291	La₂SrCr₂O₇: Controlling the Tilting Distortions of n = 2 Ruddlesdenâ€“Popper Phases through A-Site Cation Order. Inorganic Chemistry, 2016, 55, 8951-8960.	1.9	21
26292	Growth, nanostructure, and optical properties of epitaxial VN_x/MgO(001) (0.80 â‰¤ x â‰¤ 1.00) layers deposited by reactive magnetron sputtering. Journal of Materials Chemistry C, 2016, 4, 7924-7938.	2.7	30
26293	Shuttle inhibition by chemical adsorption of lithium polysulfides in B and N co-doped graphene for Liâ€“S batteries. Physical Chemistry Chemical Physics, 2016, 18, 25241-25248.	1.3	87
26294	A modified embedded atom method potential for interstitial oxygen in titanium. Computational Materials Science, 2016, 124, 204-210.	1.4	14
26295	Application of silicene, germanene and stanene for Na or Li ion storage: A theoretical investigation. Electrochimica Acta, 2016, 213, 865-870.	2.6	245
26296	Na0.282V2O5: A high-performance cathode material for rechargeable lithium batteries and sodium batteries. Journal of Power Sources, 2016, 328, 241-249.	4.0	37
26297	Thieno[2,3-b]indole-based organic dyes for dye-sensitized solar cells: Effect of Ï€-linker on the performance of isolated dye and interface between dyes and TiO2. Organic Electronics, 2016, 38, 61-68.	1.4	23
26298	Theoretical and Experimental Insight on Ag₂CrO₄ Microcrystals: Synthesis, Characterization, and Photoluminescence Properties. Inorganic Chemistry, 2016, 55, 8961-8970.	1.9	31
26299	Coupled Electronic and Magnetic Phase Transition in the Infinite-Layer Phase LaSrNiRuO₄. Inorganic Chemistry, 2016, 55, 9012-9016.	1.9	22

#	Article	IF	Citations
26300	DFT Modeling of the Adsorption of Trimethylphosphine Oxide at the Internal and External Surfaces of Zeolite MFI. Journal of Physical Chemistry C, 2016, 120, 19097-19106.	1.5	24
26301	Competition between Pauli Exclusion and H-Bonding: H2O and NH3 on Silicene. Journal of Physical Chemistry C, 2016, 120, 19151-19159.	1.5	5
26302	Promoter effect of hydration on the nucleation of nanoparticles: direct observation for gold and copper on rutile TiO₂(110). Nanoscale, 2016, 8, 16475-16485.	2.8	5
26303	Effect of alloying elements on the ideal strength and charge redistribution of Î³â€²-Ni₃Al: a first-principles study of tensile deformation. RSC Advances, 2016, 6, 77489-77498.	1.7	17
26304	Crystal and electronic structure changes during the charge-discharge process of Na4Co3(PO4)2P2O7. Journal of Power Sources, 2016, 326, 220-225.	4.0	32
26305	Oxygen Evolution at Hematite Surfaces: The Impact of Structure and Oxygen Vacancies on Lowering the Overpotential. Journal of Physical Chemistry C, 2016, 120, 18201-18208.	1.5	107
26306	Structural Studies of Polyaramid Fibers: Solid-State NMR and First-Principles Modeling. Macromolecules, 2016, 49, 5548-5560.	2.2	12
26307	Tunable electronic structures of germanium monochalcogenide nanosheets via light non-metallic atom functionalization: a first-principles study. Physical Chemistry Chemical Physics, 2016, 18, 23080-23088.	1.3	18
26308	Fast self-diffusion of ions in CH₃NH₃PbI₃: the interstiticaly mechanism versus vacancy-assisted mechanism. Journal of Materials Chemistry A, 2016, 4, 13105-13112.	5.2	74
26309	Point defects in epitaxial silicene on Ag(111) surfaces. 2D Materials, 2016, 3, 025034.	2.0	35
26310	High-Temperature Quantum Anomalous Hall Effect in<mml:math xmlns:mml="http://www.w3.org/1998/Math/MathML" display="inline"><mml:mrow><mml:mi>n</mml:mi><mml:mtext>â^’</mml:mtext><mml:mi>p</mml:mi></mml:mrow></mml:math>Cod Topological Insulators. Physical Review Letters, 2016, 117, 056804.	2.9	71
26311	Nanostructured transition metal dichalcogenide electrocatalysts for CO ₂ reduction in ionic liquid. Science, 2016, 353, 467-470.	6.0	778
26312	Ab initio description of the thermoelectric properties of heterostructures in the diffusive limit of transport. Physica Status Solidi (A) Applications and Materials Science, 2016, 213, 672-683.	0.8	5
26313	2D Squaraineâ€Bridged Covalent Organic Polymers with Promising CO₂ Storage and Separation Properties. ChemistrySelect, 2016, 1, 533-538.	0.7	8
26314	Defect Physics of CH3NH3PbX3 (XÂ=ÂI, Br, Cl) Perovskites. , 2016, , 79-105.		19
26315	First-principles study of phase equilibrium in Tiâ€“V, Tiâ€“Nb, and Tiâ€“Ta alloys. Calphad: Computer Coupling of Phase Diagrams and Thermochemistry, 2016, 54, 125-133.	0.7	42
26316	Two-dimensional metallic MoS2: A DFT study. Computational Materials Science, 2016, 124, 49-53.	1.4	22
26317	Synthesis and structures of type-I clathrates: Rb6Na2Ge44.89(1), Cs6Na2Zn4Ge42 and Cs6.40(1)Na1.60(1)Ga8Ge38. Journal of Solid State Chemistry, 2016, 242, 155-161.	1.4	8

#	Article	IF	Citations
26318	First-principles investigation of high pressure Pbca phase of carbon mononitride. Physics Letters, Section A: General, Atomic and Solid State Physics, 2016, 380, 3217-3221.	0.9	4
26319	Refined Synthesis and Crystal Growth of Pb₂P₂Se₆ for Hard Radiation Detectors. Crystal Growth and Design, 2016, 16, 5100-5109.	1.4	12
26320	Dopants in Lanthanum Manganite: Insights from First-Principles Chemical Space Exploration. Journal of Physical Chemistry C, 2016, 120, 22126-22133.	1.5	11
26321	Surface Structure and Acidity Properties of Mesoporous Silica SBA-15 Modified with Aluminum and Titanium: First-Principles Calculations. Journal of Physical Chemistry C, 2016, 120, 18105-18114.	1.5	21
26322	Effect of Surface Chemistry on Water Interaction with Cu(111). Langmuir, 2016, 32, 8061-8070.	1.6	16
26323	Tuning the Morphology and Crystal Structure of Li₂O₂: A Graphene Model Electrode Study for Liâ€“O₂ Battery. ACS Applied Materials & Interfaces, 2016, 8, 21350-21357.	4.0	48
26324	Evolution of lattice dynamics in ferroelectric hexagonal REInO₃(RE = Ho, Dy, Tb, Gd, Eu,) Tj ETQq0 0 0 rgBT /Overlock 10 Tf	0.8	17
26325	Strain-induced structural instability in FeRh. Physical Review B, 2016, 94, .	1.1	40
26326	Multiple strain-induced phase transitions in<mml:math xmlns:mml="http://www.w3.org/1998/Math/MathML"><mml:mrow><mml:mi>LaNi</mml:mi><mml:msub><mml:mi mathvariant="normal">O</mml:mi><mml:mn>3</mml:mn></mml:msub></mml:mrow></mml:math>thin films. Physical Review B, 2016, 94, .	1.1	54
26327	Lattice dynamics of neodymium: Influence of<mml:math xmlns:mml="http://www.w3.org/1998/Math/MathML"><mml:mrow><mml:mn>4</mml:mn><mml:mi>f</mml:mi><mml:mrow></mml:mrow></mml:mrow></mml:m correlations. Physical Review B, 2016, 94, .	1.1	10
26328	Band structure and spin texture of<mml:math xmlns:mml="http://www.w3.org/1998/Math/MathML"><mml:mrow><mml:msub><mml:mi>Bi</mml:mi><mml:mn>21</mml:mn></mml:msub></mml:mrow></mml:m metal interface. Physical Review B, 2016, 94, .	1.1	58
26329	Single-spin manipulation by electric fields and adsorption of molecules. Physical Review B, 2016, 94, .	1.1	3
26330	Half-metallic Dirac cone in zigzag graphene nanoribbons on graphene. Physical Review B, 2016, 94, .	1.1	19
26331	Resistivity plateau and extremely large magnetoresistance in<mml:math xmlns:mml="http://www.w3.org/1998/Math/MathML"><mml:msub><mml:mi>NbAs</mml:mi><mml:mn>2</mml:mn></mml:msub></mml xmlns:mml="http://www.w3.org/1998/Math/MathML"><mml:msub><mml:mi>TaAs</mml:mi><mml:mn>2</mml:mn></mml:msub></ Physical Review B, 2016, 94, .	1.1	97
26332	Ab initiostudy of the effect of vacancies on the thermal conductivity of boron arsenide. Physical Review B, 2016, 94, .	1.1	65
26333	Electronic structure of hydrogenated diamond: Microscopical insight into surface conductivity. Physical Review B, 2016, 94, .	1.1	8
26334	Microscopic dielectric permittivities of graphene nanoribbons and graphene. Physical Review B, 2016, 94, .	1.1	42
26335	Inversion of Ferrimagnetic Magnetization by Ferroelectric Switching via a Novel Magnetoelectric Coupling. Physical Review Letters, 2016, 117, 037601.	2.9	36

#	Article	IF	Citations
26336	Adsorption of<mml:math xmlns:mml="http://www.w3.org/1998/Math/MathML" display="inline"><mml:mrow><mml:msub><mml:mrow><mml:mi mathvariant="normal">O</mml:mi></mml:mrow><mml:mrow><mml:mn>2</mml:mn></mml:mrow></mml:msub></mml:mrow></mml: Ag(111): Evidence of Local Oxide Formation. Physical Review Letters, 2016, 117, 056101.	2.9	28
26337	Surfaceâ€Energyâ€Driven Growth of ZnO Hexagonal Microtube Optical Resonators. Advanced Optical Materials, 2016, 4, 126-134.	3.6	19
26338	MnPSe₃ Monolayer: A Promising 2D Visibleâ€Light Photohydrolytic Catalyst with High Carrier Mobility. Advanced Science, 2016, 3, 1600062.	5.6	291
26339	Low Sound Velocity Contributing to the High Thermoelectric Performance of Ag₈SnSe₆. Advanced Science, 2016, 3, 1600196.	5.6	215
26340	Electronic structure and transport properties of filled skutterudites by first principles. Physica Status Solidi (A) Applications and Materials Science, 2016, 213, 750-757.	0.8	2
26341	Mo2C nanoparticles embedded within bacterial cellulose-derived 3D N-doped carbon nanofiber networks for efficient hydrogen evolution. NPG Asia Materials, 2016, 8, e288-e288.	3.8	153
26342	Stopping of Deuterium in Warm Dense Deuterium from Ehrenfest Timeâ€Dependent Density Functional Theory. Contributions To Plasma Physics, 2016, 56, 459-466.	0.5	19
26343	Tuning of electronic states and magnetic polarization in monolayered MoS2 by codoping with transition metals and nonmetals. Journal of Materials Science, 2016, 51, 9514-9525.	1.7	24
26344	Î±-Ferrous oxalate dihydrate: a simple coordination polymer featuring photocatalytic and photo-initiated Fenton oxidations. Science China Materials, 2016, 59, 574-580.	3.5	29
26345	Study of Mn absorption by complex oxide inclusions in Al Ti Mg killed steels. Acta Materialia, 2016, 118, 8-16.	3.8	54
26346	The atomistic simulation of pressure-induced phase transition in uranium mononitride. Journal of Nuclear Materials, 2016, 480, 7-14.	1.3	15
26347	Adsorption of Noble-Gas Atoms on the TiO₂(110) Surface: An Ab Initio-Assisted Study with van der Waals-Corrected DFT. Journal of Physical Chemistry C, 2016, 120, 18126-18139.	1.5	51
26348	Tunable Ambipolar Polarization-Sensitive Photodetectors Based on High-Anisotropy ReSe₂ Nanosheets. ACS Nano, 2016, 10, 8067-8077.	7.3	276
26349	Uncovering edge states and electrical inhomogeneity in MoS ₂ field-effect transistors. Proceedings of the National Academy of Sciences of the United States of America, 2016, 113, 8583-8588.	3.3	94
26350	Interactions between vacancies and prismatic Î£3 grain boundary in Î± -Al ₂ O ₃ : First principles study. Chinese Physics B, 2016, 25, 066804.	0.7	4
26351	Ab initiodiffuse-interface model for lithiated electrode interface evolution. Physical Review E, 2016, 94, 012802.	0.8	7
26352	Electronic structures and magnetic properties of the transition-metal atoms (Mn, Fe, Co and Ni) doped WS2: A first-principles study. Superlattices and Microstructures, 2016, 98, 148-157.	1.4	28
26353	Ab initiomodeling of quasielastic neutron scattering of hydrogen pipe diffusion in palladium. Physical Review B, 2016, 94, .	1.1	5

#	Article	IF	Citations
26354	Methodology for determining the electronic thermal conductivity of metals via direct nonequilibriumab initiomolecular dynamics. Physical Review B, 2016, 94, .	1.1	17
26355	Combined DFT and XPS investigation of iodine anions adsorption on the sulfur terminated (001) chalcopyrite surface. Applied Surface Science, 2016, 390, 412-421.	3.1	65
26356	Dissociation of N2O on anatase TiO2 (001) surface â€“ The effect of oxygen vacancy and presence of Ag cluster. Applied Surface Science, 2016, 389, 1220-1232.	3.1	13
26357	Stability of vacancy-oxygen complexes in bulk nickel: Atomistic and ab initio calculations. Computational Materials Science, 2016, 124, 428-437.	1.4	10
26358	Electrochemistry of Selenium with Sodium and Lithium: Kinetics and Reaction Mechanism. ACS Nano, 2016, 10, 8788-8795.	7.3	155
26359	Tunable donor and acceptor impurity states in a WSe₂ monolayer by adsorption of common gas molecules. RSC Advances, 2016, 6, 82793-82800.	1.7	43
26360	Hierarchically CuInS₂ Nanosheetâ€Constructed Nanowire Arrays for Photoelectrochemical Water Splitting. Advanced Materials Interfaces, 2016, 3, 1600494.	1.9	35
26361	Two-Dimensional Materials as Catalysts for Energy Conversion. Catalysis Letters, 2016, 146, 1917-1921.	1.4	58
26362	Structural and Electronic Properties of Sr2CoO2Cl2. Journal of Electronic Materials, 2016, 45, 4843-4846.	1.0	3
26363	A promising two-dimensional channel material: monolayer antimonide phosphorus. Science China Materials, 2016, 59, 648-656.	3.5	28
26364	Tuning the adsorption behaviors and conversions of CHx species on metal embedded graphene surfaces. Applied Surface Science, 2016, 390, 461-471.	3.1	4
26365	Ab-initio investigation of the finite-temperatures structural, elastic, and thermodynamic properties of Ti3AlC2 and Ti3SiC2. Computational Materials Science, 2016, 124, 420-427.	1.4	9
26366	LiNbO₃-Type InFeO₃: Room-Temperature Polar Magnet without Second-Order Jahnâ€“Teller Active Ions. Chemistry of Materials, 2016, 28, 6644-6655.	3.2	43
26367	Synthesis and Photoluminescence Properties of Ca₂Ga₂SiO₇:Eu³⁺ Red Phosphors with an Intense ⁵D₀ â†’ ⁷F₄ Transition. Inorganic Chemistry, 2016, 55, 9144-9146.	1.9	65
26368	DFT-D2 Study of the Adsorption and Dissociation of Water on Clean and Oxygen-Covered {001} and {011} Surfaces of Mackinawite (FeS). Journal of Physical Chemistry C, 2016, 120, 21441-21450.	1.5	34
26369	Defective Graphene and Graphene Allotropes as High-Capacity Anode Materials for Mg Ion Batteries. ACS Energy Letters, 2016, 1, 638-645.	8.8	73
26370	Optimizing Binding Energies of Key Intermediates for CO₂ Hydrogenation to Methanol over Oxide-Supported Copper. Journal of the American Chemical Society, 2016, 138, 12440-12450.	6.6	565
26371	A new topological crystalline insulator in two-dimensional PbPo with tunable large bulk gaps. Journal of Materials Chemistry C, 2016, 4, 8745-8749.	2.7	9

#	Article	IF	Citations
26372	Lattice modes and the Jahn-Teller ferroelectric transition of<mml:math xmlns:mml="http://www.w3.org/1998/Math/MathML"><mml:mrow><mml:msub><mml:mi>GaV</mml:mi><mml:mn>4</mml:mn></mml:msub><mml:mathvariant="normal">S</mml:mi><mml:mn>8</mml:mn></mml:msub></mml:mrow></mml:math>. Physical Review B, 2016, 94, .	1.1	30
26373	Strategic Preparation of Efficient and Durable NiCo Alloy Supported Nâ€Doped Porous Graphene as an Oxygen Evolution Electrocatalyst: A Theoretical and Experimental Investigation. Advanced Materials Interfaces, 2016, 3, 1600532.	1.9	50
26374	Highly active and selective nickel molybdenum catalysts for direct hydrazine fuel cell. Electrochimica Acta, 2016, 215, 420-426.	2.6	59
26375	Ab-initio simulations at the atomic scale of an exceptional experimental photoluminescence signal observed in Ce3+-doped Y2O3 sesquioxide system. Optik, 2016, 127, 10561-10568.	1.4	9
26376	Water dissociation on MnO(1 Ã— 1)/Ag(100). Physical Chemistry Chemical Physics, 2016, 18, 25355-25363.	1.3	7
26377	Enhancement of the spin transfer torque efficiency in magnetic STM junctions. Physical Review B, 2016, 94, .	1.1	5
26378	Toward the Intrinsic Limit of the Topological Insulator<mml:math xmlns:mml="http://www.w3.org/1998/Math/MathML" display="inline"><mml:mrow><mml:msub><mml:mrow><mml:mi>Bi</mml:mi></mml:mrow><mml:mrow><mml:mn>2</mml:mn></mml:mrow> Physical Review Letters, 2016, 117, 106401.	2.9	66
26379	Electronic Structure and Transport Properties of Doped Lead Chalcogenides from First Principles. MRS Advances, 2016, 1, 4003-4010.	0.5	1
26380	Piezoelectric properties of monolayer IIâ€“VI group oxides by firstâ€principles calculations. Physica Status Solidi (B): Basic Research, 2016, 253, 2534-2539.	0.7	43
26381	Highâ€Sulfurâ€Vacancy Amorphous Molybdenum Sulfide as a High Current Electrocatalyst in Hydrogen Evolution. Small, 2016, 12, 5530-5537.	5.2	177
26382	Quasi-particle energies and optical excitations of ZnS monolayer honeycomb structure. Applied Surface Science, 2016, 390, 377-384.	3.1	57
26383	Structure and electronic properties of palladium chains supported by NiAl(1 1 0): A first-principles study. Computational Materials Science, 2016, 124, 398-402.	1.4	5
26384	Strain-controlled boron and nitrogen doping of amorphous carbon layers for hard mask applications. Diamond and Related Materials, 2016, 69, 102-107.	1.8	9
26385	Transformation stress modeling in new Fe Mn Al Ni shape memory alloy. International Journal of Plasticity, 2016, 86, 93-111.	4.1	40
26386	Jahnâ€“Teller Assisted Na Diffusion for High Performance Na Ion Batteries. Chemistry of Materials, 2016, 28, 6575-6583.	3.2	135
26387	Defect properties of the two-dimensional (CH₃NH₃)₂Pb(SCN)₂I₂ perovskite: a density-functional theory study. Physical Chemistry Chemical Physics, 2016, 18, 25786-25790.	1.3	32
26388	Size-tunable synthesis of monolayer MoS₂nanoparticles and their applications in non-volatile memory devices. Nanoscale, 2016, 8, 16995-17003.	2.8	23
26389	Pressure-induced phase transitions of lead iodide. RSC Advances, 2016, 6, 84604-84609.	1.7	10

#	Article	IF	Citations
26390	Computational discovery of stable<mml:math xmlns:mml="http://www.w3.org/1998/Math/MathML"><mml:mrow><mml:msub><mml:mi>M</mml:mi><mml:mn>2</mml:mn></mml:msub></mml:mrow></mml:math> Physical Review B, 2016, 94, .	3.7	75
26391	Hybridization and spin-orbit coupling effects in the quasi-one-dimensional spin-12magnetBa3Cu3Sc4O12. Physical Review B, 2016, 94, .	1.1	10
26392	Electronic structure and exchange interactions of insulating double perovskite<mml:math xmlns:mml="http://www.w3.org/1998/Math/MathML"><mml:mrow><mml:msub><mml:mi>La</mml:mi><mml:mn>2</mml:mn></mml:msub></mml:mrow></mml:math> Physical Review B, 2016, 94, .	3.7	10
26393	Energetics of dislocation transformations in hcp metals. Acta Materialia, 2016, 119, 203-217.	3.8	52
26394	First-principles determination of grain boundary strengthening in tungsten: Dependence on grain boundary structure and metallic radius of solute. Acta Materialia, 2016, 120, 315-326.	3.8	143
26395	Evaluation of the tantalum-titanium phase diagram from ab-initio calculations. Acta Materialia, 2016, 120, 255-263.	3.8	29
26396	Exotic quantum spin Hall effect and anisotropic spin splitting in carbon based TMC 6 (TMÂ=ÂMo, W) kagome monolayers. Carbon, 2016, 109, 788-794.	5.4	10
26397	Stability and effects of carbon-induced surface reconstructions in cobalt Fischerâ€“Tropsch synthesis. Surface Science, 2016, 653, 82-87.	0.8	11
26398	Substituent Effects and Molecular Descriptors of Reactivity in Condensation and Esterification Reactions of Oxygenates on Acidâ€“Base Pairs at TiO₂ and ZrO₂ Surfaces. Journal of Physical Chemistry C, 2016, 120, 21589-21616.	1.5	44
26399	First-Principles Microkinetic Modeling of Methane Oxidation over Pd(100) and Pd(111). ACS Catalysis, 2016, 6, 6730-6738.	5.5	88
26400	Computationally designed tandem direct selective oxidation using molecular oxygen as oxidant without coreductant. RSC Advances, 2016, 6, 88189-88215.	1.7	2
26401	A scanning tunneling microscopy study of the electronic and spin states of bis(phthalocyaninato)terbium(<scp>iii</scp>) (TbPc₂) molecules on Ag(111). Dalton Transactions, 2016, 45, 16644-16652.	1.6	19
26402	The structure of the bulk and the (001) surface of V₂O₅. A DFT+U study. Materials Research Express, 2016, 3, 085005.	0.8	15
26403	Theoretical description of metal/oxide interfacial properties: The case of MgO/Ag(001). Applied Surface Science, 2016, 390, 578-582.	3.1	21
26404	Effects of strain and electric field on electronic structures and Schottky barrier in graphene and SnS hybrid heterostructures. Carbon, 2016, 109, 737-746.	5.4	106
26405	Electronic Structures of Germanene on MoS₂: Effect of Substrate and Molecular Adsorption. Journal of Physical Chemistry C, 2016, 120, 21691-21698.	1.5	40
26406	Dynamic Stereochemical Activity of the Sn²⁺ Lone Pair in Perovskite CsSnBr₃. Journal of the American Chemical Society, 2016, 138, 11820-11832.	6.6	217
26407	A multi-dimensional quasi-zeolite with 12 Ã— 10 Ã— 7-ring channels demonstrates high thermal stability and good gas adsorption selectivity. Chemical Science, 2016, 7, 3025-3030.	3.7	12

#	Article	IF	Citations
26408	DFT study of Rh-decorated pristine, B-doped and vacancy defected graphene for hydrogen adsorption. RSC Advances, 2016, 6, 83926-83941.	1.7	39
26409	Solvation and surface effects on polymorph stabilities at the nanoscale. Chemical Science, 2016, 7, 6617-6627.	3.7	128
26410	Porous BN with vacancy defects for selective removal of CO from H₂ feed gas in hydrogen fuel cells: a DFT study. Journal of Materials Chemistry A, 2016, 4, 15631-15637.	5.2	29
26411	Stability and accuracy control of k Â· p parameters. Semiconductor Science and Technology, 2016, 31, 105002.	1.0	11
26412	Thin-Film Photoluminescent Properties and the Atomistic Model of Mg2TiO4 as a Non-rare Earth Matrix Material for Red-Emitting Phosphor. Journal of Electronic Materials, 2016, 45, 6214-6221.	1.0	2
26413	Structural, electronic and magnetic properties of transition metal atom-doped ZnS dilute magnetic semiconductors: A first-principles study. Materials Chemistry and Physics, 2016, 183, 201-209.	2.0	13
26414	Crystal Phase Effects in Si Nanowire Polytypes and Their Homojunctions. Nano Letters, 2016, 16, 5694-5700.	4.5	38
26415	Effects of water molecules on the chemical stability of MAGeI₃ perovskite explored from a theoretical viewpoint. Physical Chemistry Chemical Physics, 2016, 18, 24526-24536.	1.3	22
26416	Structural, electronic, mechanical, and transport properties of phosphorene nanoribbons: Negative differential resistance behavior. Physical Review B, 2016, 94, .	1.1	57
26417	Tunable electronic structures and magnetism in arsenene nanosheets via transition metal doping. Journal of Materials Science, 2016, 51, 9504-9513.	1.7	46
26418	Electronic structure of FeAl alloy studied by resonant photoemission spectroscopy and Ab initio calculations. Journal of Alloys and Compounds, 2016, 688, 187-194.	2.8	18
26419	Ab initio and kinetic Monte Carlo study of lithium diffusion in LiSi, Li12Si7, Li13Si5 and Li15Si4. Journal of Power Sources, 2016, 328, 558-566.	4.0	18
26420	Pressure-Stabilized Ir3â€“in a Superconducting Potassium Iridide. Journal of Physical Chemistry C, 2016, 120, 20033-20039.	1.5	12
26421	Lateral Versus Vertical Growth of Two-Dimensional Layered Transition-Metal Dichalcogenides: Thermodynamic Insight into MoS₂. Nano Letters, 2016, 16, 5742-5750.	4.5	102
26422	Reconstructive Transitions from Rotations of Rigid Heteroanionic Polyhedra. Journal of the American Chemical Society, 2016, 138, 11882-11889.	6.6	13
26423	First-principles assessment of CO₂ capture mechanisms in aqueous piperazine solution. Physical Chemistry Chemical Physics, 2016, 18, 25296-25307.	1.3	26
26424	SnSe₂ 2D Anodes for Advanced Sodium Ion Batteries. Advanced Energy Materials, 2016, 6, 1601188.	10.2	243
26425	From the Superatom Model to a Diverse Array of Superâ€Elements: A Systematic Study of Dopant Influence on the Electronic Structure of Thiolateâ€Protected Gold Clusters. ChemPhysChem, 2016, 17, 3237-3244.	1.0	13

#	Article	IF	Citations
26426	How can we describe the adsorption of quinones on activated carbon surfaces?. Current Applied Physics, 2016, 16, 1437-1441.	1.1	7
26427	Structural and electronic properties of B2N3 planar nanostructure: A computational investigation. Chemical Physics Letters, 2016, 660, 244-249.	1.2	3
26428	Lattice dynamics, thermodynamics and elastic properties of C22-Zr6FeSn2 from first-principles calculations. Journal of Nuclear Materials, 2016, 479, 461-469.	1.3	12
26429	Three-dimensional porous structural MoP2 nanoparticles as a novel and superior catalyst for electrochemical hydrogen evolution. Journal of Power Sources, 2016, 328, 551-557.	4.0	88
26430	Realizing half-metallicity in K₂CoF₄ exfoliated nanosheets via defect engineering. Physical Chemistry Chemical Physics, 2016, 18, 15765-15773.	1.3	3
26431	Enhancement in the electrochemical performance of zirconium/phosphate bi-functional coatings on LiNi_{0.8}Co_{0.15}Mn_{0.05}O₂ by the removal of Li residuals. Physical Chemistry Chemical Physics, 2016, 18, 29076-29085.	1.3	69
26432	Modulation of doping and biaxial strain on the transition temperature of the charge density waveÂtransition in 1T-TiSe₂. RSC Advances, 2016, 6, 76972-76979.	1.7	20
26433	Mechanisms for <mml:math xmlns:mml="http://www.w3.org/1998/Math/MathML"><mml:mi>p</mml:mi></mml:math>-type behavior of ZnO,<mml:math xmlns:mml="http://www.w3.org/1998/Math/MathML"><mml:mrow><mml:msub><mml:mi>Zn</mml:mi><mml:mrow><mml:mn>1</mml:mn></mrow><mml:mi mathvariant="normal">O</mml:mi></mml:msub></mml:mrow></mml:math>, and related oxide semiconductors. Physical Review B, 2016, 94, .	1.1	7
26434	Layered Antiferromagnetic Ordering in the Most Active Perovskite Catalysts for the Oxygen Evolution Reaction. ChemCatChem, 2016, 8, 2968-2974.	1.8	61
26435	Atomic and Ionic Radii of Elements 1â€“96. Chemistry - A European Journal, 2016, 22, 14625-14632.	1.7	239
26436	Theoretical investigations of the interaction between transition-metal and benzoquinone: Metal dispersion and hydrogen storage. International Journal of Hydrogen Energy, 2016, 41, 11275-11283.	3.8	9
26437	Chemical Pressure-Driven Incommensurability in CaPd₅: Clues to High-Pressure Chemistry Offered by Complex Intermetallics. Inorganic Chemistry, 2016, 55, 6781-6793.	1.9	17
26438	First-Principles Thermodynamics Study of Spinel MgAl₂O₄ Surface Stability. Journal of Physical Chemistry C, 2016, 120, 19087-19096.	1.5	38
26439	Evaluation of sulfur spinel compounds for multivalent battery cathode applications. Energy and Environmental Science, 2016, 9, 3201-3209.	15.6	121
26440	Experimental and first-principles DFT study on the electrochemical reactivity of garnet-type solid electrolytes with carbon. Journal of Materials Chemistry A, 2016, 4, 14371-14379.	5.2	25
26441	Origins of phase separation in thermoelectric (Ti, Zr, Hf)NiSn half-Heusler alloys from first principles. Journal of Materials Chemistry A, 2016, 4, 13949-13956.	5.2	41
26442	Structure and magnetism of the<mml:math xmlns:mml="http://www.w3.org/1998/Math/MathML"><mml:mrow><mml:mo>(</mml:mo><mml:mn>2</mml:mn>×<mml:mo>Ã—</mml:mo> surface. Physical Review B, 2016, 94, .	1.1	7
26443	Dirac Node Lines in Pure Alkali Earth Metals. Physical Review Letters, 2016, 117, 096401.	2.9	174

#	Article	IF	Citations
26444	Lithium-Ion Cathode/Coating Pairs for Transition Metal Containment. Journal of the Electrochemical Society, 2016, 163, A2054-A2064.	1.3	14
26445	Exchange coupling and spin structure in cobalt-on-chromia thin films. Europhysics Letters, 2016, 115, 17003.	0.7	6
26446	Ab initio study of carrier mobility of few-layer InSe. Applied Physics Express, 2016, 9, 035203.	1.1	79
26447	Hosting of La3+ guest ions in type-I Ge clathrates: A first-principles characterization for thermoelectric applications. Computational Materials Science, 2016, 122, 46-56.	1.4	4
26448	Compression and phase diagram of lithium hydrides at elevated pressures and temperatures by first-principles calculation. Journal Physics D: Applied Physics, 2016, 49, 355305.	1.3	6
26449	Orbital hybridization mechanism for the enhanced photoluminescence in edge-functionalized sp 2 carbon clusters. Carbon, 2016, 109, 418-427.	5.4	8
26450	Understanding the Shape of GeTe Nanocrystals from First Principles. Chemistry of Materials, 2016, 28, 6682-6688.	3.2	16
26451	Surface Electronic Structure of Hybrid Organo Lead Bromide Perovskite Single Crystals. Journal of Physical Chemistry C, 2016, 120, 21710-21715.	1.5	58
26452	Electron anions and the glass transition temperature. Proceedings of the National Academy of Sciences of the United States of America, 2016, 113, 10007-10012.	3.3	15
26453	Quasi-ordered C₆₀molecular films grown on the pseudo-ten-fold (1 0 0) surface of the Al₁₃Co₄quasicrystalline approximant. Journal of Physics Condensed Matter, 2016, 28, 355001.	0.7	3
26454	Hydrogen intercalation in<mml:math xmlns:mml="http://www.w3.org/1998/Math/MathML"><mml:msub><mml:mi>MoS</mml:mi><mml:mn>2</mml:mn></mml:msub></mml:math>Physical Review B, 2016, 94, .	1.1	15
26455	Electronic Structure and N-Type Doping in Diamond from First Principles. MRS Advances, 2016, 1, 1093-1098.	0.5	20
26456	Modeling Off-Stoichiometry Materials with a High-Throughput Ab-Initio Approach. Chemistry of Materials, 2016, 28, 6484-6492.	3.2	78
26457	Electron States of 2D Metalâ€“Organic and Covalentâ€“Organic Honeycomb Frameworks: Ab Initio Results and a General Fitting Hamiltonian. Journal of Physical Chemistry C, 2016, 120, 19796-19803.	1.5	23
26458	Employing X-ray Photoelectron Spectroscopy for Determining Layer Homogeneity in Mixed Polar Self-Assembled Monolayers. Journal of Physical Chemistry Letters, 2016, 7, 2994-3000.	2.1	28
26459	The rapid growth of ADP single crystal. CrystEngComm, 2016, 18, 7530-7536.	1.3	24
26460	Pt₃₈cluster on OH- and COOH-functionalised graphene as a model for Pt/C-catalysts. Physical Chemistry Chemical Physics, 2016, 18, 25693-25704.	1.3	7
26461	Reduction enthalpy and charge distribution of substituted ferrites and doped ceria for thermochemical water and carbon dioxide splitting with DFT+U. Physical Chemistry Chemical Physics, 2016, 18, 23587-23595.	1.3	24

#	Article	IF	Citations
26462	Development of Xe and Kr empirical potentials for CeO₂, ThO₂, UO₂and PuO₂, combining DFT with high temperature MD. Journal of Physics Condensed Matter, 2016, 28, 405401.	0.7	29
26463	in<mml:math xmlns:mml="http://www.w3.org/1998/Math/MathML"><mml:mrow><mml:mn>4</mml:mn><mml:mi>f</mml:mi></mml:mrow></mml:m metal doped<mml:math xmlns:mml="http://www.w3.org/1998/Math/MathML"><mml:mrow><mml:mi mathvariant="normal">B</mml:mi><mml:msub><mml:mi mathvariant="normal">2</mml:mi><mml:mn>2</mml:mn></mml:msub><mml:mi mathvariant="normal">S	1.1	14
26464	Ferromagnetic origin of Na and Mn codoped CaZn2As2 diluted magnetic semiconductor: A first-principles study. JETP Letters, 2016, 103, 631-635.	0.4	4
26465	Nonlinear elastic response and anharmonic properties of MgO single crystal: First-principles investigation. Computational Materials Science, 2016, 124, 375-383.	1.4	8
26466	Light-element diffusion in Mg using first-principles calculations: Anisotropy and elastodiffusion. Physical Review B, 2016, 94, .	1.1	21
26467	Effects of strain on the stability of tetragonal<mml:math xmlns:mml="http://www.w3.org/1998/Math/MathML"><mml:msub><mml:mtext>ZrO</mml:mtext><mml:mn>2</mml:mn></mml:msub Physical Review B, 2016, 94, .	1.1	18
26468	Multi-scale simulations of metamagnetic martensite transition in NiCoMnIn. Journal of Alloys and Compounds, 2016, 689, 507-511.	2.8	5
26469	Stability of the M2 phase of vanadium dioxide induced by coherent epitaxial strain. Physical Review B, 2016, 94, .	1.1	62
26470	Biaxial Strain and Electric Field Dependent Conductivity of Monolayer WTe₂ on Top of Fe₃O₄(111). Advanced Materials Interfaces, 2016, 3, 1600581.	1.9	12
26471	Transition Metalâ€Promoted V₂CO₂ (MXenes): A New and Highly Active Catalyst for Hydrogen Evolution Reaction. Advanced Science, 2016, 3, 1600180.	5.6	279
26472	Influence of varying nitrogen partial pressures on microstructure, mechanical and optical properties of sputtered TiAlON coatings. Acta Materialia, 2016, 119, 26-34.	3.8	18
26473	Bulk and surface properties of magnesium peroxide MgO2. Applied Surface Science, 2016, 389, 1202-1207.	3.1	9
26474	Differences in the Existence States of Hydrogen in UO₂ and PuO₂ from DFT + U Calculations. Journal of Physical Chemistry C, 2016, 120, 18445-18451.	1.5	34
26475	Curvature-Dependent Selectivity of CO₂ Electrocatalytic Reduction on Cobalt Porphyrin Nanotubes. ACS Catalysis, 2016, 6, 6294-6301.	5.5	113
26476	Layer-Confined Excitonic Insulating Phase in Ultrathin Ta₂NiSe₅ Crystals. ACS Nano, 2016, 10, 8888-8894.	7.3	49
26477	Understanding sodium-ion diffusion in layered P2 and P3 oxides via experiments and first-principles calculations: a bridge between crystal structure and electrochemical performance. NPG Asia Materials, 2016, 8, e266-e266.	3.8	101
26478	Robust SierpiÅ„ski triangle fractals on symmetry-mismatched Ag(100). Chemical Communications, 2016, 52, 10578-10581.	2.2	50
26479	CoP for hydrogen evolution: implications from hydrogen adsorption. Physical Chemistry Chemical Physics, 2016, 18, 23864-23871.	1.3	84

#	Article	IF	Citations
26480	The influence of the electronic specific heat on swift heavy ion irradiation simulations of silicon. Journal of Physics Condensed Matter, 2016, 28, 395201.	0.7	23
26481	Finite-temperature elastic constants of paramagnetic materials within the disordered local moment picture fromab initiomolecular dynamics calculations. Physical Review B, 2016, 94, .	1.1	10
26482	New Ground-State Crystal Structure of Elemental Boron. Physical Review Letters, 2016, 117, 085501.	2.9	44
26483	Magnetostructural Transition Kinetics in Shocked Iron. Physical Review Letters, 2016, 117, 085701.	2.9	6
26484	Lightâ€Induced Ambient Degradation of Fewâ€Layer Black Phosphorus: Mechanism and Protection. Angewandte Chemie - International Edition, 2016, 55, 11437-11441.	7.2	514
26485	Structural, electronic and adsorption properties of Rh(111)/Mo(110) bimetallic catalyst: A DFT study. Applied Surface Science, 2016, 389, 1094-1103.	3.1	10
26486	Sodium ion storage in reduced graphene oxide. Electrochimica Acta, 2016, 214, 319-325.	2.6	49
26487	Enhancing Silicon Nanocrystal Photoluminescence through Temperature and Microstructure. Journal of Physical Chemistry C, 2016, 120, 18909-18916.	1.5	21
26488	Differential Permeability of Proton Isotopes through Graphene and Graphene Analogue Monolayer. Journal of Physical Chemistry Letters, 2016, 7, 3395-3400.	2.1	40
26489	Large dielectric constant, high acceptor density, and deep electron traps in perovskite solar cell material CsGeI₃. Journal of Materials Chemistry A, 2016, 4, 13852-13858.	5.2	148
26490	Anisotropic thermal motion in transition-metal carbonyls from experiments and ab initio theory. Dalton Transactions, 2016, 45, 13680-13685.	1.6	15
26491	Pressure-induced formation of hydrogen bonds in KNH₂ studied by first principles. RSC Advances, 2016, 6, 78678-78683.	1.7	1
26492	Magnetic properties of transition metal Mn, Fe and Co dimers on monolayer phosphorene. Nanotechnology, 2016, 27, 385701.	1.3	24
26493	Carbon-rich icosahedral boron carbides beyond<mml:math xmlns:mml="http://www.w3.org/1998/Math/MathML"><mml:mrow><mml:msub><mml:mi mathvariant="normal">B</mml:mi><mml:mn>4</mml:mn></mml:msub><mml:mi mathvariant="normal">C</mml:mi></mml:mrow></mml:math>and their thermodynamic stabilities at high temperature and pressure from first principles. Physical Review B, 2016, 94, .	1.1	21
26494	Fermi arc electronic structure and Chern numbers in the type-II Weyl semimetal candidate<mml:math xmlns:mml="http://www.w3.org/1998/Math/MathML"><mml:mrow><mml:msub><mml:mi>Mo</mml:mi><mml:mi>x</mml:mi></mml:m mathvariant="normal">W</mml:mi><mml:mrow><mml:mn>1</mml:mn><mml:mo>â^’</mml:mo><mml:mi>x</mml:mi></mml:mrow><mml:m Physical Review B, 2016, 94, .	1.1	115
26495	Firstâ€Principles Molecular Dynamics Study of Carbon Corrosion in PEFC Catalyst Materials. Fuel Cells, 2016, 16, 669-674.	1.5	12
26496	Organometallic Bonding in an Ullmann-Type On-Surface Chemical Reaction Studied by High-Resolution Atomic Force Microscopy. Small, 2016, 12, 5303-5311.	5.2	52
26497	Capturing Solvation Effects at a Liquid/Nanoparticle Interface by Ab Initio Molecular Dynamics: Pt₂₀₁ Immersed in Water. Small, 2016, 12, 5312-5319.	5.2	25

#	Article	IF	Citations
26498	Lithium Ion Disorder and Conduction Mechanism in LiCe(BH₄)₃Cl. Journal of Physical Chemistry C, 2016, 120, 19035-19042.	1.5	20
26499	How do random superficial defects influence the electro-oxidation of glycerol on Pt(111) surfaces?. Physical Chemistry Chemical Physics, 2016, 18, 25582-25591.	1.3	37
26500	Negative differential resistance in GeSi coreâ€“shell transport junctions: the role of local sp2hybridization. Nanoscale, 2016, 8, 16026-16033.	2.8	3
26501	Electronic structure and transport properties of antiferromagnetic double perovskite Y₂AlCrO₆. RSC Advances, 2016, 6, 80415-80423.	1.7	10
26502	Î²-Cyclodextrin modified graphitic carbon nitride for the removal of pollutants from aqueous solution: experimental and theoretical calculation study. Journal of Materials Chemistry A, 2016, 4, 14170-14179.	5.2	191
26503	Intrinsic ultralow lattice thermal conductivity of the unfilled skutterudite<mml:math xmlns:mml="http://www.w3.org/1998/Math/MathML"><mml:msub><mml:mi>FeSb</mml:mi><mml:mn>3</mml:mn></mml:msub></mml:math> Physical Review B, 2016, 94, .	1.1	22
26504	Optical properties of the organic-inorganic hybrid perovskite<mml:math xmlns:mml="http://www.w3.org/1998/Math/MathML"><mml:mrow><mml:mi mathvariant="normal">C</mml:mi><mml:msub><mml:mi mathvariant="normal">H</mml:mi><mml:mn>3</mml:mn></mml:msub><mml:mi mathvariant="normal">N</mml:mi><mml:msub><mml:mi mathvariant="normal">H</mml:mi><mml:mn>3</mml:mn></mml:msub><mml:mi>Pb</mml:mi><mml:msub><mml:mi	1.1	50
26505	Giant spin splitting, strong valley selective circular dichroism and valley-spin coupling induced in silicene. Physical Review B, 2016, 94, .	1.1	8
26506	Triple Point Topological Metals. Physical Review X, 2016, 6, .	2.8	273
26507	Lightâ€Induced Ambient Degradation of Fewâ€Layer Black Phosphorus: Mechanism and Protection. Angewandte Chemie, 2016, 128, 11609-11613.	1.6	78
26508	Towards Direct Synthesis of Alane: A Predicted Defectâ€Mediated Pathway Confirmed Experimentally. ChemSusChem, 2016, 9, 2358-2364.	3.6	5
26509	First principle investigation of crystal lattice structure, thermodynamics and mechanical properties in ZnZrAl2 intermetallic compound. Solid State Communications, 2016, 247, 82-87.	0.9	6
26510	Low Valence Cation Doping of Bulk Cr₂O₃: Charge Compensation and Oxygen Vacancy Formation. Journal of Physical Chemistry C, 2016, 120, 19160-19174.	1.5	59
26511	Group Additivity for Thermochemical Property Estimation of Lignin Monomers on Pt(111). Journal of Physical Chemistry C, 2016, 120, 19234-19241.	1.5	18
26512	New structures of bilayer germanium nanosheets predicted by a particle swarm optimization method. Nanoscale, 2016, 8, 16467-16474.	2.8	3
26513	Ab initio soluteâ€“interstitial impurity interactions in vanadium alloys: the roles of vacancy. RSC Advances, 2016, 6, 78621-78628.	1.7	11
26514	First principles study of a SnS₂/graphene heterostructure: a promising anode material for rechargeable Na ion batteries. Journal of Materials Chemistry A, 2016, 4, 14316-14323.	5.2	132
26515	Fermi Arcs and Their Topological Character in the Candidate Type-II Weyl Semimetal<mml:math xmlns:mml="http://www.w3.org/1998/Math/MathML" display="inline"><mml:mrow><mml:msub><mml:mrow><mml:mi>MoTe</mml:mi></mml:mrow><mml:mrow><mml:mn>2</mml:mn> Physical Review X, 2016, 6, .	2.8	154

#	Article	IF	Citations
26516	Oxygen Vacancy Formation on Î±-MoO₃ Slabs and Ribbons. Journal of Physical Chemistry C, 2016, 120, 19252-19264.	1.5	44
26517	Sensing Characteristics of Phosphorene Monolayers toward PH₃ and AsH₃ Gases upon the Introduction of Vacancy Defects. Journal of Physical Chemistry C, 2016, 120, 20428-20436.	1.5	71
26518	Strong dichroic emission in the pseudo one dimensional material ZrS₃. Nanoscale, 2016, 8, 16259-16265.	2.8	63
26519	Growth of Ba_{1âˆ’x}Sr_xZrO₃ (0 â‰¤ x â‰¤ 1) nanoparticles in supercritical water. RSC Advances, 2016, 6, 67525-67533.	1.7	13
26520	Hydrogenated group-IV binary monolayers: a new family of inversion-asymmetric topological insulators. RSC Advances, 2016, 6, 79452-79458.	1.7	3
26521	Theoretical prediction of long-range ferromagnetism in transition-metal atom-doped d⁰ dichalcogenide single layers SnS₂ and ZrS₂. Physical Chemistry Chemical Physics, 2016, 18, 25151-25160.	1.3	18
26522	A Cr₂CO₂ monolayer as a promising cathode for lithium and non-lithium ion batteries: a computational exploration. RSC Advances, 2016, 6, 81591-81596.	1.7	29
26523	Asymmetric mass acquisition in LaBi: Topological semimetal candidate. Physical Review B, 2016, 94, .	1.1	52
26524	Intermixing and Formation of Cu-Rich Secondary Phases at Sputtered CdS/CuInGaSe₂Heterojunctions. IEEE Journal of Photovoltaics, 2016, 6, 1308-1315.	1.5	7
26525	Electronic Structure and Site Occupancy of Lanthanide-Doped (Sr, Ca)3(Y, Lu)2Ge3O12 Garnets: A Spectroscopic and First-Principles Study. Journal of Physical Chemistry C, 2016, 120, 28743-28752.	1.5	22
26526	Comparative studies on the room-temperature ferrielectric and ferrimagnetic Ni3TeO6-type A2FeMoO6 compounds (Aâ€‰=â€‰Sc, Lu). Scientific Reports, 2016, 6, 20133.	1.6	10
26527	From Quasi-Planar B56 to Penta-Ring Tubular CaÂ©B56: Prediction of Metal-Stabilized CaÂ©B56 as the Embryo of Metal-Doped Boron Î±-Nanotubes. Scientific Reports, 2016, 6, 37893.	1.6	7
26528	Concurrent magnetic and structural reconstructions at the interface of (111)-oriented <mml:math xmlns:mml="http://www.w3.org/1998/Math/MathML"><mml:mrow><mml:mi mathvariant="normal">L</mml:mi><mml:msub><mml:mi mathvariant="normal">a</mml:mi><mml:mrow><mml:mn>0.7</mml:mn></mml:mrow></mml:msub><mml:mi mathvariant="normal">S</mml:mi><mml:msub><mml:mi mathvariant="normal">r</mml:mi><mml:mrow><mml:mn>0.3</mml:mn></mml:mrow></mml:msub><mml:mi>Mn</mml:mi><mml:msu	1.1	26
26529	Direct observation of incommensurate structure in Mo₃Si. Acta Crystallographica Section A: Foundations and Advances, 2016, 72, 660-666.	0.0	3
26530	Room temperatured⁰ferromagnetism in hole doped Y₂O₃: widening the choice of host to tailor DMS. Journal of Physics Condensed Matter, 2016, 28, 336001.	0.7	12
26531	Domain topology and domain switching kinetics in a hybrid improper ferroelectric. Nature Communications, 2016, 7, 11602.	5.8	46
26532	Static and Dynamical Properties of heavy actinide Monopnictides of Lutetium. Scientific Reports, 2016, 6, 29309.	1.6	20
26533	Interface Stability in Solid-State Batteries. Chemistry of Materials, 2016, 28, 266-273.	3.2	1,132

#	Article	IF	Citations
26534	High Electrocatalytic Hydrogen Evolution Activity of an Anomalous Ruthenium Catalyst. Journal of the American Chemical Society, 2016, 138, 16174-16181.	6.6	852
26535	Signature of coexistence of superconductivity and ferromagnetism in two-dimensional NbSe2 triggered by surface molecular adsorption. Nature Communications, 2016, 7, 11210.	5.8	85
26536	Ultrathin metalâ€“organic framework nanosheets for electrocatalytic oxygen evolution. Nature Energy, 2016, 1, .	19.8	1,979
26537	Ab initio molecular dynamic study of solid-state transitions of ammonium nitrate. Scientific Reports, 2016, 6, 18918.	1.6	5
26538	A new kind of 2D topological insulators BiCN with a giant gap and its substrate effects. Scientific Reports, 2016, 6, 30003.	1.6	10
26539	Stabilization of a Metastable Fibrous Bi21.2(1)(Mn1â€“xCox)20 Phase with Pseudo-Pentagonal Symmetry Prepared Using a Bi Self-Flux. Chemistry of Materials, 2016, 28, 8484-8488.	3.2	2
26540	Monopolar Magnetic MOF-74 with Hybrid Node Niâ€“Fe. Journal of Physical Chemistry C, 2016, 120, 26908-26914.	1.5	5
26541	New Mechanism for Photocatalytic Reduction of CO₂ on the Anatase TiO₂(101) Surface: The Essential Role of Oxygen Vacancy. Journal of the American Chemical Society, 2016, 138, 15896-15902.	6.6	256
26542	The influence of large cations on the electrochemical properties of tunnel-structured metal oxides. Nature Communications, 2016, 7, 13374.	5.8	180
26543	Phase transformation strengthening of high-temperature superalloys. Nature Communications, 2016, 7, 13434.	5.8	158
26544	Multiple unpinned Dirac points in group-Va single-layers with phosphorene structure. Npj Computational Materials, 2016, 2, .	3.5	57
26545	Two-dimensional Topological Crystalline Insulator Phase in Sb/Bi Planar Honeycomb with Tunable Dirac Gap. Scientific Reports, 2016, 6, 18993.	1.6	21
26546	First-Principle Electronic Properties of Dilute-P GaN1â^'xPx Alloy for Visible Light Emitters. Scientific Reports, 2016, 6, 24412.	1.6	15
26547	Role of Polar Phonons in the Photo Excited State of Metal Halide Perovskites. Scientific Reports, 2016, 6, 28618.	1.6	234
26548	In Situ and Ex Situ TEM Study of Lithiation Behaviours of Porous Silicon Nanostructures. Scientific Reports, 2016, 6, 31334.	1.6	43
26549	Topological phase transition and quantum spin Hall edge states of antimony few layers. Scientific Reports, 2016, 6, 33193.	1.6	38
26550	First-principles calculations of the electronic structure and bonding in metal clusterâ€“fullerene materials considered within the superatomic framework. Physical Chemistry Chemical Physics, 2016, 18, 32541-32550.	1.3	12
26551	Hydration in silica based mesoporous materials: a DFT model. Physical Chemistry Chemical Physics, 2016, 18, 32962-32972.	1.3	44

#	Article	IF	Citations
26552	Scaling relationships for nonadiabatic energy relaxation times in warm dense matter: toward understanding the equation of state. Physical Chemistry Chemical Physics, 2016, 18, 32466-32476.	1.3	14
26553	High-pressure phase of brucite stable at Earthâ€™s mantle transition zone and lower mantle conditions. Proceedings of the National Academy of Sciences of the United States of America, 2016, 113, 13971-13976.	3.3	35
26554	Scaling study and thermodynamic properties of the cubic helimagnet FeGe. Physical Review B, 2016, 94, .	1.1	34
26555	Impact of lattice dynamics on the phase stability of metamagnetic FeRh: Bulk and thin films. Physical Review B, 2016, 94, .	1.1	44
26556	Mechanism for strong magnetoelectric coupling in dilute magnetic ferroelectrics. Physical Review B, 2016, 94, .	1.1	7
26557	Metal-insulator transition in Ba3Fe1â^'xRu2+xO9 : Interplay between site disorder, chemical percolation, and electronic structure. Physical Review B, 2016, 94, .	1.1	9
26558	High-pressure synthesis of the layered iron oxyselenide BaFe2Se2O with strong magnetic anisotropy. Physical Review B, 2016, 94, .	1.1	11
26559	Electronic structure and stability of the <mml:math xmlns:mml="http://www.w3.org/1998/Math/MathML"><mml:mrow><mml:mi mathvariant="normal">C</mml:mi><mml:msub><mml:mi mathvariant="normal">H</mml:mi><mml:mn>3</mml:mn></mml:msub><mml:mi mathvariant="normal">N</mml:mi><mml:msub><mml:mi mathvariant="normal">H</mml:mi><mml:mn>3</mml:mn></mml:msub><mml:mi>PbB</mml:mi><mml:msub> <mml:mi	1.1	49
26560	Hybrid functionals with fixed mixing parameter perform no better than PBE for fundamental band gaps of nanoscale materials. Physical Review B, 2016, 94, .	1.1	6
26561	Electric-field tunable Dirac semimetal state in phosphorene thin films. Physical Review B, 2016, 94, .	1.1	36
26562	Large anomalous Hall effect driven by a nonvanishing Berry curvature in the noncolinear antiferromagnet Mn ₃ Ge. Science Advances, 2016, 2, e1501870.	4.7	561
26563	Firstâ€principles identification of defect levels in Erâ€doped GaN. Physica Status Solidi - Rapid Research Letters, 2016, 10, 915-918.	1.2	11
26564	Molecular Level Study of Graphene Networks Functionalized with Phenylenediamine Monomers for Supercapacitor Electrodes. Chemistry of Materials, 2016, 28, 9110-9121.	3.2	98
26565	Multiphysics Simulations of Lithiation-Induced Stress in Li_{1+x}Ti₂O₄ Electrode Particles. Journal of Physical Chemistry C, 2016, 120, 27871-27881.	1.5	8
26566	Electron-Hybridization-Induced Enhancement of Photoactivity in Indium-Doped Co₃O₄. Journal of Physical Chemistry C, 2016, 120, 28983-28991.	1.5	4
26567	The Bright Future for Electrode Materials of Energy Devices: Highly Conductive Porous Na-Embedded Carbon. Nano Letters, 2016, 16, 8029-8033.	4.5	50
26568	Schottky-Barrier-Free Contacts with Two-Dimensional Semiconductors by Surface-Engineered MXenes. Journal of the American Chemical Society, 2016, 138, 15853-15856.	6.6	444
26569	Magnetodielectric detection of magnetic quadrupole order in Ba(TiO)Cu4(PO4)4 with Cu4O12 square cupolas. Nature Communications, 2016, 7, 13039.	5.8	37

#	Article	IF	Citations
26570	Anomalously rotary polarization discovered in homochiral organic ferroelectrics. Nature Communications, 2016, 7, 13635.	5.8	129
26571	Orbital Delocalization and Enhancement of Magnetic Interactions in Perovskite Oxyhydrides. Scientific Reports, 2016, 6, 19653.	1.6	20
26572	Improved p-type conductivity in Al-rich AlGaN using multidimensional Mg-doped superlattices. Scientific Reports, 2016, 6, 21897.	1.6	49
26573	Electron work functionâ€“a promising guiding parameter for material design. Scientific Reports, 2016, 6, 24366.	1.6	55
26574	Investigating the adsorption mechanism of glycine in comparison with catechol on cristobalite surface using density functional theory for bio-adhesive materials. RSC Advances, 2016, 6, 114313-114319.	1.7	5
26575	Magnetic anisotropy energies of Mâ€“Fe wires (M = Vâ€“Co) on vicinal Cu(111). RSC Advances, 2016, 6, 108948-108954.	1.7	4
26576	Electronic structure of the high and low pressure polymorphs of MgSiN₂. Materials Research Express, 2016, 3, 085902.	0.8	13
26577	Revealing the hidden structural phases of FeRh. Physical Review B, 2016, 94, .	1.1	29
26578	Electronic and magnetic properties of <mml:math xmlns:mml="http://www.w3.org/1998/Math/MathML"><mml:mrow><mml:mn>2</mml:mn><mml:mi>H</mml:mi></mml:mrow><mml:m intercalated by <mml:math xmlns:mml="http://www.w3.org/1998/Math/MathML"><mml:mrow><mml:mn>3</mml:mn><mml:mi>d</mml:mi></mml:mrow></mml:r transition metals. Physical Review B, 2016, 94, .	1.1	35
26579	Fermi surface evolution of Na-doped PbTe studied through density functional theory calculations and Shubnikovâ€“de Haas measurements. Physical Review B, 2016, 94, .	1.1	14
26580	Origin of electron disproportionation in metallic sodium cobaltates. Physical Review B, 2016, 94, .	1.1	6
26581	High-Fidelity Bidirectional Nuclear Qubit Initialization in SiC. Physical Review Letters, 2016, 117, 220503.	2.9	16
26582	Temperature Effects in the Band Structure of Topological Insulators. Physical Review Letters, 2016, 117, 226801.	2.9	61
26583	Lithiationâ€“delithiation of infinite nanofibers of the Si n C m typeâ€”the possible promising anodic materials for lithium-ion batteries. Quantum-chemical modeling. Russian Journal of Electrochemistry, 2016, 52, 988-991.	0.3	5
26584	Ab initio modelling of Yâ€“O cluster formation in Î³â€Fe lattice. Physica Status Solidi (B): Basic Research, 2016, 253, 2136-2143.	0.7	4
26585	Observation and Analysis of Ordered and Disordered Structures on the ZnO(0001) Polar Surface. Journal of Physical Chemistry C, 2016, 120, 26915-26921.	1.5	9
26586	Generalized Surface Coordination Number as an Activity Descriptor for CO₂ Reduction on Cu Surfaces. Journal of Physical Chemistry C, 2016, 120, 28125-28130.	1.5	77
26587	Large enhancement of the photovoltaic effect in ferroelectric complex oxides through bandgap reduction. Scientific Reports, 2016, 6, 28313.	1.6	34

#	Article	IF	Citations
26588	Lazarevicite-type short-range ordering in ternary III-V nanowires. Physical Review B, 2016, 94, .	1.1	7
26589	Electronic, vibrational, Raman, and scanning tunneling microscopy signatures of two-dimensional boron nanomaterials. Physical Review B, 2016, 94, .	1.1	21
26590	Pressure induced elastic softening in framework aluminosilicate- albite (NaAlSi3O8). Scientific Reports, 2016, 6, 34815.	1.6	19
26591	High-throughput combinatorial study of the effect of<mml:math xmlns:mml="http://www.w3.org/1998/Math/MathML"><mml:mi>M</mml:mi></mml:math>site alloying on the solid solution behavior of<mml:math xmlns:mml="http://www.w3.org/1998/Math/MathML"><mml:mrow><mml:msub><mml:mi>M</mml:mi><mml:mn>2</mml:mn></mml:msub></mml:mrow></mml:math> phases. Physical Review B, 2016, 94, .	1.1	38
26592	Enhanced Photoelectrochemical Performance of the BiVO₄/Zn:BiVO₄ Homojunction for Water Oxidation. ChemCatChem, 2016, 8, 3279-3286.	1.8	33
26593	Nonlinear bandgap opening behavior of BN co-doped graphene. Carbon, 2016, 107, 857-864.	5.4	23
26594	Factors controlling oxygen migration barriers in perovskites. Solid State Ionics, 2016, 296, 71-77.	1.3	59
26595	Gold in the Layered Structures of R₃Au₇Sn₃: From Relativity to Versatility. Crystal Growth and Design, 2016, 16, 5657-5668.	1.4	18
26596	Double-Hole-Mediated Codoping on KNbO₃ for Visible Light Photocatalysis. Inorganic Chemistry, 2016, 55, 9620-9631.	1.9	30
26597	Synthesis, Optical, and Magnetic Properties of Ba₂Ni₃F₁₀ Nanowires. ACS Applied Materials & Interfaces, 2016, 8, 26213-26219.	4.0	4
26598	Effect of caffeic acid adsorption in controlling the morphology of gold nanoparticles: role of surface coverage and functional groups. Physical Chemistry Chemical Physics, 2016, 18, 27775-27783.	1.3	22
26599	Synergistic effect in B and N co-doped Ib-type diamond single crystal: A density function theory calculation. Canadian Journal of Physics, 2016, 94, 929-932.	0.4	4
26600	Semiconductive K₂MSbS₃(SH) (M = Zn, Cd) Featuring One-Dimensional _{âˆž}¹[M₂Sb₂S₆(SH₂)]^{4â€“} Chains. Inorganic Chemistry, 2016, 55, 9742-9747.	1.9	18
26601	Ferroelectric surface induced electron doping in a zigzag graphene nanoribbon. Journal of Physics Condensed Matter, 2016, 28, 435002.	0.7	7
26602	Role of valence states of adsorbates in inelastic electron tunneling spectroscopy: A study of nitric oxide on Cu(110) and Cu(001). Physical Review B, 2016, 94, .	1.1	12
26603	Low phonon conductivity of layered BiCuOS, BiCuOSe, and BiCuOTe from first principles. Physical Review B, 2016, 94, .	1.1	28
26604	Characterization of oxygen defects in diamond by means of density functional theory calculations. Physical Review B, 2016, 94, .	1.1	23
26605	Block antiferromagnetism and possible ferroelectricity in KFe₂Se₂. Physica Status Solidi - Rapid Research Letters, 2016, 10, 757-761.	1.2	6

#	Article	IF	Citations
26606	Contrasting room-temperature hydrogen sensing capabilities of Pt-SnO2 and Pt-TiO2 composite nanoceramics. Nano Research, 2016, 9, 3528-3535.	5.8	22
26607	Tunable Gravimetric and Volumetric Hydrogen Storage Capacities in Polyhedral Oligomeric Silsesquioxane Frameworks. ACS Applied Materials & Interfaces, 2016, 8, 25219-25228.	4.0	14
26608	Macroscale Superlubricity of Multilayer Polyethylenimine/Graphene Oxide Coatings in Different Gas Environments. ACS Applied Materials & Interfaces, 2016, 8, 27179-27187.	4.0	57
26609	Understanding the surface segregation behavior of transition metals on Ni(111): a first-principles study. Physical Chemistry Chemical Physics, 2016, 18, 26616-26622.	1.3	35
26610	A ZrNiAl related high-pressure modification of CeRuSn. Dalton Transactions, 2016, 45, 14216-14229.	1.6	6
26611	Nanotube-terminated zigzag edges of phosphorene formed by self-rolling reconstruction. Nanoscale, 2016, 8, 17940-17946.	2.8	39
26612	Physisorbed-precursor-assisted atomic layer deposition of reliable ultrathin dielectric films on inert graphene surfaces for low-power electronics. 2D Materials, 2016, 3, 035027.	2.0	15
26613	Polaronic contributions to oxidation and hole conductivity in acceptor-doped<mml:math xmlns:mml="http://www.w3.org/1998/Math/MathML"><mml:msub><mml:mi>BaZrO</mml:mi><mml:mn>3</mml:mn></mml:msub></m Physical Review B, 2016, 94, .	1.1	36
26614	Raman scattering study of large magnetoresistance semimetals<mml:math xmlns:mml="http://www.w3.org/1998/Math/MathML"><mml:msub><mml:mi>TaAs</mml:mi><mml:mn>2</mml:mn></mml:msub></mr xmlns:mml="http://www.w3.org/1998/Math/MathML"><mml:msub><mml:mi>NbAs</mml:mi><mml:mn>2</mml:mn></mml:msub></m Physical Review B, 2016, 94, .	1.1	10
26615	First-principles DFT+<mml:math xmlns:mml="http://www.w3.org/1998/Math/MathML"><mml:mi>U</mml:mi></mml:math>investigation of charged states of defects and fission gas atoms in<mml:math xmlns:mml="http://www.w3.org/1998/Math/MathML"><mml:msub><mml:mi>CeO</mml:mi><mml:mn>2</mml:mn></mml:msub></m Physical Review B, 2016, 94, .	1.1	23
26616	Distance- and spin-resolved spectroscopy of iridium atoms on an iron bilayer. Physical Review B, 2016, 94, .	1.1	2
26617	Observation of large topologically trivial Fermi arcs in the candidate type-II Weyl semimetal<mml:math xmlns:mml="http://www.w3.org/1998/Math/MathML"><mml:mrow><mml:mi>WT</mml:mi><mml:msub><mml:mi mathvariant="normal">e</mml:mi><mml:mn>2</mml:mn></mml:msub></mml:mrow></mml:math>. Physical Review B, 2016, 94, .	1.1	174
26618	Twin formation in hematite during dehydration of goethite. Physics and Chemistry of Minerals, 2016, 43, 749-757.	0.3	8
26619	An atomic-scale insight into the effects of hydrogen microalloying on the glass-forming ability and ductility of Zr-based bulk metallic glasses. Computational Materials Science, 2016, 125, 197-205.	1.4	11
26620	Direct Gap Semiconductors Pb₂BiS₂I₃, Sn₂BiS₂I₃, and Sn₂BiSI₅. Chemistry of Materials, 2016, 28, 7332-7343.	3.2	33
26621	Designing Fe-Based Oxygen Catalysts by Density Functional Theory Calculations. Chemistry of Materials, 2016, 28, 7058-7065.	3.2	43
26622	Complexation and Phase Evolution at Dimethylformamideâ€“Ag(111) Interfaces. Journal of Physical Chemistry C, 2016, 120, 22979-22988.	1.5	10
26623	Charge-Transfer in Silicon Governs the Pattern of Dissociative Attachment of Hydrogen Halides: HCl, HBr, and HI. Journal of Physical Chemistry C, 2016, 120, 22414-22420.	1.5	2

#	Article	IF	Citations
26624	Crystal Structure of AgBi₂I₇ Thin Films. Journal of Physical Chemistry Letters, 2016, 7, 3903-3907.	2.1	64
26625	High-Throughput Screening of Metalâ€“Organic Frameworks for CO₂ Capture in the Presence of Water. Langmuir, 2016, 32, 10368-10376.	1.6	124
26626	Degradation of Ethylene Carbonate Electrolytes of Lithium Ion Batteries via Ring Opening Activated by LiCoO₂ Cathode Surfaces and Electrolyte Species. ACS Applied Materials & Interfaces, 2016, 8, 26664-26674.	4.0	67
26627	Ferromagnetic and Half-Metallic FeC₂ Monolayer Containing C₂ Dimers. ACS Applied Materials & Interfaces, 2016, 8, 26207-26212.	4.0	58
26628	Nonlinear Rashba spin splitting in transition metal dichalcogenide monolayers. Nanoscale, 2016, 8, 17854-17860.	2.8	60
26629	Density functional theory study of high-energy metal (Al, Mg, Ti, and Zr)/CuO composites. RSC Advances, 2016, 6, 90206-90211.	1.7	7
26630	Photon energy storage materials with high energy densities based on diacetyleneâ€“azobenzene derivatives. Journal of Materials Chemistry A, 2016, 4, 16157-16165.	5.2	86
26631	Prediction of the quantum spin Hall effect in monolayers of transition-metal carbides MC (M = Ti, Zr,) Tj ETQq1 1 0.784314 rgBT /Ove	2.0	31
26632	Local structure in the disordered solid solution ofcis- andtrans-perinones. Acta Crystallographica Section B: Structural Science, Crystal Engineering and Materials, 2016, 72, 416-433.	0.5	12
26633	The Uncommon Channelâ€Based Lnâ€MOFs for Highly Selective Fe³⁺ Detection and Superior Rhodamineâ€…B Adsorption. Chemistry - A European Journal, 2016, 22, 16230-16235.	1.7	70
26634	Understanding the Atomic-Level Chemistry and Structure of Oxide Deposits on Fuel Rods in Light Water Nuclear Reactors Using First Principles Methods. Jom, 2016, 68, 2912-2921.	0.9	3
26635	Anisotropic electrical and lattice transport properties of ordered quaternary phases Cr2TiAlC2 and Mo2TiAlC2: A first principles study. Physics Letters, Section A: General, Atomic and Solid State Physics, 2016, 380, 3748-3755.	0.9	29
26636	A Joint Computational and Experimental Evaluation of CaMn₂O₄ Polymorphs as Cathode Materials for Ca Ion Batteries. Chemistry of Materials, 2016, 28, 6886-6893.	3.2	80
26637	Energies of Formation Reactions Measured for Adsorbates on Late Transition Metal Surfaces. Journal of Physical Chemistry C, 2016, 120, 25161-25172.	1.5	63
26638	Impact of Surface Point Defects on Electronic Properties and p-Type Doping of GaAs Nanowires. Journal of Physical Chemistry C, 2016, 120, 22088-22095.	1.5	13
26639	Reducing CO₂ to CO and H₂O on Ni(110): The Influence of Subsurface Hydrogen. Journal of Physical Chemistry C, 2016, 120, 23061-23068.	1.5	26
26640	Two Dimensional Antiferromagnetic Chern Insulator: NiRuCl₆. Nano Letters, 2016, 16, 6325-6330.	4.5	45
26641	Blue Phosphorene Oxide: Strain-Tunable Quantum Phase Transitions and Novel 2D Emergent Fermions. Nano Letters, 2016, 16, 6548-6554.	4.5	114

#	Article	IF	Citations
26642	About the Compatibility between High Voltage Spinel Cathode Materials and Solid Oxide Electrolytes as a Function of Temperature. ACS Applied Materials & Interfaces, 2016, 8, 26842-26850.	4.0	193
26643	In Situ Atomic Level Dynamics of Heterogeneous Nucleation and Growth of Graphene from Inorganic Nanoparticle Seeds. ACS Nano, 2016, 10, 9397-9410.	7.3	11
26644	Tuning of Thermal Stability in Layered Li(Ni_xMn_yCo_z)O₂. Journal of the American Chemical Society, 2016, 138, 13326-13334.	6.6	178
26645	Modelling the structure of Zr-rich Pb(Zr_{1âˆ'x}Ti_x)O₃, x = 0.4 by a multiphase approach. Physical Chemistry Chemical Physics, 2016, 18, 28316-28324.	1.3	9
26646	State-of-the-art Sn²⁺-based ternary oxides as photocatalysts for water splitting: electronic structures and optoelectronic properties. Catalysis Science and Technology, 2016, 6, 7656-7670.	2.1	45
26647	Superhalogens as building blocks of two-dimensional organicâ€“inorganic hybrid perovskites for optoelectronics applications. Nanoscale, 2016, 8, 17836-17842.	2.8	34
26648	Single layer PbI2: hydrogenation-driven reconstructions. RSC Advances, 2016, 6, 89708-89714.	1.7	10
26649	Half-metallicity in 2D organometallic honeycomb frameworks. Journal of Physics Condensed Matter, 2016, 28, 425301.	0.7	9
26650	Role of Metal-Lithium Oxide Interfaces in the Extra Lithium Capacity of Metal Oxide Lithium-Ion Battery Anode Materials. Journal of the Electrochemical Society, 2016, 163, A2172-A2178.	1.3	22
26651	Phase diagram and enthalpy of formation of Hf-Ni-Sn. Computational Materials Science, 2016, 125, 271-277.	1.4	10
26652	Electronic Structures and Li-Diffusion Properties of Group IVâ€“V Layered Materials: Hexagonal Germanium Phosphide and Germanium Arsenide. Journal of Physical Chemistry C, 2016, 120, 23842-23850.	1.5	41
26653	Dimensional Effects on the Charge Density Waves in Ultrathin Films of TiSe₂. Nano Letters, 2016, 16, 6331-6336.	4.5	61
26654	Atomically engineered ferroic layers yield a room-temperature magnetoelectric multiferroic. Nature, 2016, 537, 523-527.	13.7	275
26655	N₂ activation on Al metal clusters: catalyzing role of BN-doped graphene support. Physical Chemistry Chemical Physics, 2016, 18, 27721-27727.	1.3	36
26656	Experimental and theoretical evidence for competitive interactions of tetracycline and sulfamethazine with reduced graphene oxides. Environmental Science: Nano, 2016, 3, 1318-1326.	2.2	88
26657	Geometric structure, electronic structure and optical absorption properties of one-dimensional thiolate-protected gold clusters containing a quasi-face-centered-cubic (quasi-fcc) Au-core: a density-functional theoretical study. Nanoscale, 2016, 8, 17044-17054.	2.8	39
26658	A single-source precursor approach to solution processed indium arsenide thin films. Journal of Materials Chemistry C, 2016, 4, 6761-6768.	2.7	19
26659	Band offset formation at semiconductor heterojunctions through density-based minimization of interface energy. Physical Review B, 2016, 94, .	1.1	17

#	Article	IF	Citations
26660	Ab initiostudy of Cu impurity diffusion in bulk TiN. Physical Review B, 2016, 94, .	1.1	14
26661	Ideal tensile strength and shear strength of ZrO2(111)/Ni(111) ceramic-metal Interface: A first principle study. Materials and Design, 2016, 112, 254-262.	3.3	39
26662	Unraveling the different charge storage mechanism in T and H phases of MoS2. Electrochimica Acta, 2016, 217, 1-8.	2.6	37
26663	First-principles investigation of vacancies in LiTaO₃. Journal of Physics Condensed Matter, 2016, 28, 315501.	0.7	6
26664	Chemical disorder determines the deviation of the Slaterâ€“Pauling rule for Fe2MnSi-based Heusler alloys: evidences from neutron diffraction and density functional theory. Journal of Physics Condensed Matter, 2016, 28, 476002.	0.7	6
26665	Interplay between interstitial displacement and displacive lattice transformations. Physical Review B, 2016, 94, .	1.1	10
26666	First-principles study of O₂ and Cl₂ molecule adsorption on pristine doped boron nitride nanotubes. Canadian Journal of Physics, 2016, 94, 1071-1079.	0.4	6
26667	Mechanism of polysulfide immobilization on defective graphene sheets with N-substitution. Carbon, 2016, 110, 207-214.	5.4	92
26668	Lattice vibrational behavior and thermodynamic properties of uranium disilicide USi 2. Solid State Communications, 2016, 248, 47-52.	0.9	6
26669	Tuning the Thermoelectric Properties of Ca₉Zn_{4+x}Sb₉ by Controlled Doping on the Interstitial Structure. Chemistry of Materials, 2016, 28, 6917-6924.	3.2	41
26670	Detecting Important Intermediates in Pd Catalyzed Depolymerization of a Lignin Model Compound by a Combination of DFT Calculations and Constrained Minima Hopping. Journal of Physical Chemistry C, 2016, 120, 23469-23479.	1.5	8
26671	Corrosion of Concrete by Water-Induced Metalâ€“Proton Exchange. Journal of Physical Chemistry C, 2016, 120, 22455-22459.	1.5	18
26672	Tuning electronic structures of the stanene monolayer via defects and transition-metal-embedding: spinâ€“orbit coupling. Physical Chemistry Chemical Physics, 2016, 18, 28759-28766.	1.3	29
26673	Anisotropic etching of rhodium and gold as the onset of nanoparticle formation by cathodic corrosion. Faraday Discussions, 2016, 193, 207-222.	1.6	21
26674	Manipulating the magnetic moment in phosphorene by lanthanide atom doping: a first-principle study. RSC Advances, 2016, 6, 92048-92056.	1.7	26
26675	Crystal structures and dynamical properties of dense CO ₂. Proceedings of the National Academy of Sciences of the United States of America, 2016, 113, 11110-11115.	3.3	28
26676	First-principles investigation of magnetocrystalline anisotropy at theL21fullHeusler|MgOinterfaces and tunnel junctions. Physical Review B, 2016, 94, .	1.1	29
26677	Domain-dependent electronic structure and optical absorption property in hybrid organicâ€“inorganic perovskite. Physical Chemistry Chemical Physics, 2016, 18, 27358-27365.	1.3	10

#	Article	IF	Citations
26678	Molecular dynamics simulation of O₂ adsorption on Ag(110) from first principles electronic structure calculations. Physical Chemistry Chemical Physics, 2016, 18, 27366-27376.	1.3	14
26679	Assessing Hubbard-corrected AM05+U and PBEsol+U density functionals for strongly correlated oxides CeO₂ and Ce₂O₃. Physical Chemistry Chemical Physics, 2016, 18, 26816-26826.	1.3	25
26680	Regulating ancillary ligands of Ru(<scp>ii</scp>) complexes with square-planar quadridentate ligands for more efficient sensitizers in dye-sensitized solar cells: insights from theoretical investigations. Physical Chemistry Chemical Physics, 2016, 18, 29591-29599.	1.3	9
26681	Design of Li_{1+2x}Zn_{1â^'x}PS₄, a new lithium ion conductor. Energy and Environmental Science, 2016, 9, 3272-3278.	15.6	99
26682	Time dependent DFT investigation of the optical response in pristine and Gd doped Al2O3. RSC Advances, 2016, 6, 72537-72543.	1.7	1
26683	Tungsten oxide nanowire on copper surfaces: a DFT model. RSC Advances, 2016, 6, 88463-88468.	1.7	1
26684	Exploring the stability and electronic structure of beryllium and sulphur co-doped graphene: a first principles study. RSC Advances, 2016, 6, 88392-88402.	1.7	19
26685	Modulation of the band structures and optical properties of holey C₂N nanosheets by alloying with group IV and V elements. Journal of Materials Chemistry C, 2016, 4, 9294-9302.	2.7	24
26686	Mechanical responses of borophene sheets: a first-principles study. Physical Chemistry Chemical Physics, 2016, 18, 27405-27413.	1.3	149
26687	Stability of two-dimensional BN-Si structures. Physical Review B, 2016, 94, .	1.1	30
26688	First-principles study of the effect of lanthanum on the niobium diffusion in fcc Fe. International Journal of Modern Physics B, 2016, 30, 1650157.	1.0	1
26689	Ethylene Carbonate Reduction on Lithiated Surfaces of Hydroxylated Amorphous Silicon Dioxide. Journal of the Electrochemical Society, 2016, 163, A2197-A2202.	1.3	7
26690	Annealing-Induced Bi Bilayer on Bi₂Te₃ Investigated via Quasi-Particle-Interference Mapping. ACS Nano, 2016, 10, 8778-8787.	7.3	15
26691	Investigation of novel crystal structures of Biâ€“Sb binaries predicted using the minima hopping method. Physical Chemistry Chemical Physics, 2016, 18, 29771-29785.	1.3	37
26692	Mechanical properties of zigzag-shaped carbon nanotubes: the roles of the geometric parameters. RSC Advances, 2016, 6, 27999-28004.	1.7	0
26693	Borophene as an anode material for Ca, Mg, Na or Li ion storage: A first-principle study. Journal of Power Sources, 2016, 329, 456-461.	4.0	211
26694	Effects of the volume changes and elastic-strain energies on the phase transition in the Li-Sn battery. Journal of Power Sources, 2016, 330, 111-119.	4.0	24
26695	Many-Body Dispersion Correction Effects on Bulk and Surface Properties of Rutile and Anatase TiO₂. Journal of Physical Chemistry C, 2016, 120, 21552-21560.	1.5	11

#	Article	IF	Citations
26696	BiOX/BiOY (X, Y = F, Cl, Br, I) superlattices for visible light photocatalysis applications. RSC Advances, 2016, 6, 91508-91516.	1.7	41
26697	Magnetism in<mml:math xmlns:mml="http://www.w3.org/1998/Math/MathML"><mml:mrow><mml:msub><mml:mi>Sr</mml:mi><mml:mn>2</mml:mn></mml:msub></mml:mr A combinedab initioand model study. Physical Review B, 2016, 94, .	1.1	25
26698	Role of Oxide Reducibility in the Deoxygenation of Phenol on Ruthenium Clusters Supported on the Anatase Titania (1â€‰0â€‰1) Surface. ChemCatChem, 2016, 8, 2492-2499.	1.8	43
26699	How do you write and present research well? 17â€”Submit your manuscript to the journal you cite most. Canadian Journal of Chemical Engineering, 2016, 94, 2174-2178.	0.9	1
26700	Effect of Ca addition on interface formation in Al(Ca)/Al 2 O 3 composites prepared by gas pressure assisted infiltration. Materials and Design, 2016, 108, 618-623.	3.3	9
26701	Manipulation of electronic structure in WSe2 monolayer by strain. Solid State Communications, 2016, 245, 70-74.	0.9	19
26702	First-principles analysis of the spectroscopic limited maximum efficiency of photovoltaic absorber layers for CuAu-like chalcogenides and silicon. Physical Chemistry Chemical Physics, 2016, 18, 20542-20549.	1.3	54
26703	Theoretical study of electronic and mechanical properties of Fe₂B. RSC Advances, 2016, 6, 73576-73580.	1.7	13
26704	Phonon transport in the ground state of two-dimensional silicon and germanium. RSC Advances, 2016, 6, 69956-69965.	1.7	20
26705	Unexpected highly reversible topotactic CO₂ sorption/desorption capacity for potassium dititanate. Journal of Materials Chemistry A, 2016, 4, 12889-12896.	5.2	27
26706	Borophene as an extremely high capacity electrode material for Li-ion and Na-ion batteries. Nanoscale, 2016, 8, 15340-15347.	2.8	396
26707	Effect of multiple defects and substituted impurities on the band structure of graphene: a DFT study. Journal of Materials Science: Materials in Electronics, 2016, 27, 12669-12679.	1.1	13
26708	Electronic and optical properties of bilayer blue phosphorus. Computational Materials Science, 2016, 124, 23-29.	1.4	51
26709	First-principles study of intercalation of alkali ions in FeSe for solid-state batteries. Chemical Physics Letters, 2016, 659, 230-233.	1.2	18
26710	Effect of Anode Composition on Solid Electrolyte Interphase Formation. Electrochimica Acta, 2016, 213, 8-13.	2.6	7
26711	Crystal Structures, Surface Stability, and Water Adsorption Energies of La-BastnÃsite via Density Functional Theory and Experimental Studies. Journal of Physical Chemistry C, 2016, 120, 16767-16781.	1.5	28
26712	Structural Characterization of the EtOHâ€“TiCl₄â€“MgCl₂ Zieglerâ€“Natta Precatalyst. Journal of Physical Chemistry C, 2016, 120, 18075-18087.	1.5	28
26713	The Synergy between Metal Facet and Oxide Support Facet for Enhanced Catalytic Performance: The Case of Pdâ€“TiO₂. Nano Letters, 2016, 16, 5298-5302.	4.5	69

#	Article	IF	Citations
26714	First-Principles Prediction of Ultralow Lattice Thermal Conductivity of Dumbbell Silicene: A Comparison with Low-Buckled Silicene. ACS Applied Materials & Interfaces, 2016, 8, 20977-20985.	4.0	66
26715	The Importance of the Electrochemical Environment in the Electro-Oxidation of Methanol on Pt(111). ACS Catalysis, 2016, 6, 5575-5586.	5.5	117
26716	Discovery of the Pt-Based Superconductor LaPt₅As. Journal of the American Chemical Society, 2016, 138, 9927-9934.	6.6	11
26717	Precursor Triggering Synthesis of Self-Coupled Sulfide Polymorphs with Enhanced Photoelectrochemical Properties. Journal of the American Chemical Society, 2016, 138, 12913-12919.	6.6	90
26718	In situ TEM study of deformation-induced crystalline-to-amorphous transition in silicon. NPG Asia Materials, 2016, 8, e291-e291.	3.8	60
26719	Implication of the solvent effect, metal ions and topology in the electronic structure and hydrogen bonding of human telomeric G-quadruplex DNA. Physical Chemistry Chemical Physics, 2016, 18, 21573-21585.	1.3	41
26720	Density functional calculations of a staggered FeSe monolayer on aSrTiO3(110) surface. Physical Review B, 2016, 94, .	1.1	4
26721	Electric-field-induced structural changes in water confined between two graphene layers. Physical Review B, 2016, 94, .	1.1	36
26722	First-principles study of the cubic CaHfO3 (001) surface. International Journal of Modern Physics B, 2016, 30, 1650168.	1.0	5
26723	On the Nature of Support Effects of Metal Dioxides MO₂ (M = Ti, Zr, Hf, Ce, Th) in Single-Atom Gold Catalysts: Importance of Quantum Primogenic Effect. Journal of Physical Chemistry C, 2016, 120, 17514-17526.	1.5	120
26724	Surface directed reversible imidazole ligation to nickel(<scp>ii</scp>) octaethylporphyrin at the solution/solid interface: a single molecule level study. Physical Chemistry Chemical Physics, 2016, 18, 20819-20829.	1.3	23
26725	A new class of epitaxial porphyrin metalâ€“organic framework thin films with extremely high photocarrier generation efficiency: promising materials for all-solid-state solar cells. Journal of Materials Chemistry A, 2016, 4, 12739-12747.	5.2	75
26726	A first-principles study of the avalanche pressure of alpha zirconium. RSC Advances, 2016, 6, 72551-72558.	1.7	1
26727	Suppressing cation segregation on lanthanum-based perovskite oxides to enhance the stability of solid oxide fuel cell cathodes. RSC Advances, 2016, 6, 69782-69789.	1.7	41
26728	First-principles study on the electronic and magnetic properties of the Zn0.75Mo0.25M(M = S,Se,Te). Modern Physics Letters B, 2016, 30, 1650249.	1.0	5
26729	Thermal expansion and thermal diffusivity properties of Co-Si solid solutions and intermetallic compounds. Journal of Chemical Thermodynamics, 2016, 102, 1-8.	1.0	4
26730	Quantum mechanical study of CO2 and CO hydrogenation on Cu(111) surfaces doped with Ga, Mg, and Ti. Journal of Molecular Catalysis A, 2016, 423, 319-332.	4.8	25
26731	Experimental and ab Initio Study of Catena(bis(Î¼₂-iodo)-6-methylquinoline-copper(I)) under Pressure: Synthesis, Crystal Structure, Electronic, and Luminescence Properties. Inorganic Chemistry, 2016, 55, 7476-7484.	1.9	27

#	Article	IF	Citations
26732	Large anomalous Hall effect in a half-Heusler antiferromagnet. Nature Physics, 2016, 12, 1119-1123.	6.5	232
26733	Tunable schottky barrier in blue phosphorusâ€“graphene heterojunction with normal strain. Japanese Journal of Applied Physics, 2016, 55, 080306.	0.8	26
26734	Atomic scale behavior, growth morphology and magnetic properties of CoO on MgO(100) surface: a density functional study. Theoretical Chemistry Accounts, 2016, 135, 1.	0.5	0
26735	Formation and Migration of Oxygen Vacancies in SrCoO₃ and Their Effect on Oxygen Evolution Reactions. ACS Catalysis, 2016, 6, 5565-5570.	5.5	96
26736	Origins of Dirac cones and parity dependent electronic structures of Î±-graphyne derivatives and silagraphynes. Nanoscale, 2016, 8, 15223-15232.	2.8	24
26737	Solid state synthesis, structural characterization and ionic conductivity of bimetallic alkali-metal yttrium borohydrides MY(BH₄)₄ (M = Li and Na). Journal of Materials Chemistry A, 2016, 4, 8793-8802.	5.2	37
26738	Modelling of an ultra-thin silicatene/silicon-carbide hybrid film. Journal of Physics Condensed Matter, 2016, 28, 364005.	0.7	3
26739	Doping in the Valley of Hydrogen Solubility: A Route to Designing Hydrogen-Resistant Zirconium Alloys. Physical Review Applied, 2016, 5, .	1.5	32
26740	Phosphorus Diffusion Mechanisms and Deep Incorporation in Polycrystalline and Single-Crystalline CdTe. Physical Review Applied, 2016, 5, .	1.5	26
26741	Electronic Structure and Defect Physics of Tin Sulfides: SnS,<mml:math xmlns:mml="http://www.w3.org/1998/Math/MathML" display="inline"><mml:mrow><mml:msub><mml:mrow><mml:mi>Sn</mml:mi></mml:mrow><mml:mrow><mml:mn>2</mml:mn></mml:mrow></mml:msub></mml:mrow></mml:math>, and<mml:math xmlns:mml="http://www.w3.org/1998/Math/MathML" display="inline"><mml:mrow><mml:msub><mml:mi mathvariant="normal">S</mml:mi><mml:mrow><mml:mn>3</mml:mn></mml:mrow></mml:msub></mml:mrow></mml:math>. Physical Review Applied, 2016,	1.5	138
26742	Femtosecond-laser-driven molecular dynamics on surfaces: Photodesorption of molecular oxygen from Ag(110). Physical Review B, 2016, 93, .	1.1	42
26743	First-principles study of interface magnetic structure in Nd2Fe14B/(Fe,Co) exchange spring magnets. Physical Review B, 2016, 93, .	1.1	12
26744	Anatomy of electric field control of perpendicular magnetic anisotropy at Fe/MgO interfaces. Physical Review B, 2016, 93, .	1.1	59
26745	Dissociation products and structures of solid<mml:math xmlns:mml="http://www.w3.org/1998/Math/MathML"><mml:msub><mml:mi mathvariant="normal">H</mml:mi><mml:mn>2</mml:mn></mml:msub><mml:mi mathvariant="normal">S</mml:mi></mml:math>at strong compression. Physical Review B, 2016, 93, .	1.1	119
26746	Effect of magnetism on lattice dynamics in SrFe2As2 using high-resolution inelastic x-ray scattering. Physical Review B, 2016, 93, .	1.1	12
26747	Competing Jahn-Teller distortions and hydrostatic pressure effects in the quasi-one-dimensional quantum ferromagnet<mml:math xmlns:mml="http://www.w3.org/1998/Math/MathML"><mml:mrow><mml:msub><mml:mi>CuAs</mml:mi><mml:mn>2</mml:mn></mml:msub><mml:mi mathvariant="normal">O</mml:mi><mml:mn>4</mml:mn></mml:mrow></mml:math>. Physical Review B, 2016, 93, .	1.1	9
26748	Ionic conductivity in Gd-doped<mml:math xmlns:mml="http://www.w3.org/1998/Math/MathML"><mml:msub><mml:mi>CeO</mml:mi><mml:mn>2</mml:mn></mml:msub></mml:math>: ab initiocolor-diffusion nonequilibrium molecular dynamics study. Physical Review B, 2016, 93, .	1.1	15
26749	Structural, vibrational, and electrical study of compressed BiTeBr. Physical Review B, 2016, 93, .	1.1	25

#	Article	IF	Citations
26750	Exploring the impact of semicore level electronic relaxation on polaron dynamics: An adiabaticab initiostudy of<mml:math xmlns:mml="http://www.w3.org/1998/Math/MathML"><mml:msub><mml:mi>FePO</mml:mi><mml:mn>4</mml:mn></mml:msub></mml:math>. Physical Review B, 2016, 93, .	1.1	27
26751	Impact of oxygen doping and oxidation state of iron on the electronic and magnetic properties of<mml:math xmlns:mml="http://www.w3.org/1998/Math/MathML"><mml:msub><mml:mi>BaFeO</mml:mi><mml:mrow><mml:mn>3</mml:mn></mml:mrow></mml:msub></mml:math>. Physical Review B, 2016, 93, .	1.1	15
26752	Complex magnetic phase diagram and skyrmion lifetime in an ultrathin film from atomistic simulations. Physical Review B, 2016, 93, .	1.1	65
26753	Giant biquadratic interaction-induced magnetic anisotropy in the iron-based superconductor<mml:math xmlns:mml="http://www.w3.org/1998/Math/MathML"><mml:mrow><mml:msub><mml:mi>A</mml:mi><mml:mi>x</mml:mi></mml:msub><mml:msub><mml:mi mathvariant="normal">F</mml:mi><mml:mi>y</mml:mi></mml:msub><mml:msub><mml:mi mathvariant="normal">S</mml:mi><mml:mi>z</mml:mi></mml:msub></mml:mrow></mml:math>.	1.1	13
26754	42214 layered Fe-based superconductors: Anab initiostudy of their structural, magnetic, and electronic properties. Physical Review B, 2016, 93, .	1.1	3
26755	Accurate tight-binding Hamiltonian matrices fromab initiocalculations: Minimal basis sets. Physical Review B, 2016, 93, .	1.1	43
26756	Ab initiocalculation of ionization potential and electron affinity in solid-state organic semiconductors. Physical Review B, 2016, 93, .	1.1	26
26757	Topological states of non-Dirac electrons on a triangular lattice. Physical Review B, 2016, 93, .	1.1	40
26758	Pressure-induced phase transition and band-gap collapse in the wide-band-gap semiconductor<mml:math xmlns:mml="http://www.w3.org/1998/Math/MathML"><mml:mrow><mml:mi>InTa</mml:mi><mml:msub><mml:mi mathvariant="normal">O</mml:mi><mml:mn>4</mml:mn></mml:msub></mml:mrow></mml:math>. Physical Review B, 2016, 93, .	1.1	39
26759	Role of thermalizing and nonthermalizing walls in phonon heat conduction along thin films. Physical Review B, 2016, 93, .	1.1	12
26760	Exploring stereographic surface energy maps of cubic metals via an effective pair-potential approach. Physical Review B, 2016, 93, .	1.1	32
26761	Spilling of electronic states in Pb quantum wells. Physical Review B, 2016, 93, .	1.1	7
26762	Two-dimensional transition metal dichalcogenides with a hexagonal lattice: Room-temperature quantum spin Hall insulators. Physical Review B, 2016, 93, .	1.1	56
26763	Control of valley degeneracy in<mml:math xmlns:mml="http://www.w3.org/1998/Math/MathML"><mml:mrow><mml:mi>Mo</mml:mi><mml:msub><mml:mi mathvariant="normal">S</mml:mi><mml:mn>2</mml:mn></mml:msub></mml:mrow></mml:math>by layer thickness and electric field and its effect on thermoelectric properties. Physical Review B, 2016, 93, .	1.1	68
26764	Anomalous band inversion protected by symmetry in a topological insulator of the Kane-Mele model. Physical Review B, 2016, 93, .	1.1	4
26765	Observing spin excitations in<mml:math xmlns:mml="http://www.w3.org/1998/Math/MathML"><mml:mrow><mml:mn>3</mml:mn><mml:mi>d</mml:mi></mml:mrow></mml:math>adatoms on Pt(111) with inelastic scanning tunneling spectroscopy: A first-principles perspective. Physical Review B, 2016, 93, .	1.1	8
26766	Low-energy theory for the graphene twist bilayer. Physical Review B, 2016, 93, .	1.1	64
26767	Smooth gauge and Wannier functions for topological band structures in arbitrary dimensions. Physical Review B, 2016, 93, .	1.1	25

#	Article	IF	Citations
26768	Identifying different stacking sequences in few-layer CVD-grown<mml:math xmlns:mml="http://www.w3.org/1998/Math/MathML"><mml:mrow><mml:mi>Mo</mml:mi><mml:msub><mml:mi mathvariant="normal">S</mml:mi><mml:mn>2</mml:mn></mml:msub></mml:mrow></mml:math>by low-energy atomic-resolution scanning transmission electron microscopy. Physical Review B, 2016, 93, .	1.1	51
26769	Theoretical study of the cubic Rashba effect at the<mml:math xmlns:mml="http://www.w3.org/1998/Math/MathML"><mml:msub><mml:mi>SrTiO</mml:mi><mml:mn>3</mml:mn></mml:msub></mml:math>surfaces. Physical Review B, 2016, 93, .	1.1	28
26770	Semiclassical atom theory applied to solid-state physics. Physical Review B, 2016, 93, .	1.1	51
26771	Spin-density functional theories and their<mml:math xmlns:mml="http://www.w3.org/1998/Math/MathML"><mml:mrow><mml:mo>+</mml:mo><mml:mi>U</mml:mi></mml:mrow></mml:math><mml:math xmlns:mml="http://www.w3.org/1998/Math/MathML"><mml:mrow><mml:mo>+</mml:mo><mml:mi>J</mml:mi></mml:mrow></mml:math>A comparative study of transition metals and transition metal oxides. Physical Review B, 2016, 93, .	1.1	35
26772	Fully and partially iodinated germanane as a platform for the observation of the quantum spin Hall effect. Physical Review B, 2016, 93, .	1.1	18
26773	Quantum spin Hall effect in<mml:math xmlns:mml="http://www.w3.org/1998/Math/MathML"><mml:mi>Î±</mml:mi><mml:mo>â^'</mml:mo><mml:mi mathvariant="normal">Sn</mml:mi><mml:mo>/</mml:mo><mml:mtext>CdTe</mml:mtext><mml:mo>(</mml:mo><mml:mn>001</mml:mn>structures. Physical Review B, 2016, 93, .	1.1	8
26774	Self-ordered nanoporous lattice formed by chlorine atoms on Au(111). Physical Review B, 2016, 93, .	1.1	12
26775	Controlling adatom magnetism on bilayer graphene by external field. Physical Review B, 2016, 93, .	1.1	9
26776	High-pressure structural study of<mml:math xmlns:mml="http://www.w3.org/1998/Math/MathML"><mml:msub><mml:mi>MnF</mml:mi><mml:mn>2</mml:mn></mml:msub></mml:math>Physical Review B, 2016, 93, .	1.1	26
26777	Grand-canonical evolutionary algorithm for the prediction of two-dimensional materials. Physical Review B, 2016, 93, .	1.1	59
26778	Electronic and crystal structure changes induced by in-plane oxygen vacancies in multiferroic<mml:math xmlns:mml="http://www.w3.org/1998/Math/MathML"><mml:mrow><mml:mi>YMn</mml:mi><mml:msub><mml:mi mathvariant="normal">O</mml:mi><mml:mn>3</mml:mn></mml:msub></mml:mrow></mml:math>. Physical Review B, 2016, 93, .	1.1	28
26779	Magnetic exchange interactions and critical temperature of the nanolaminate<mml:math xmlns:mml="http://www.w3.org/1998/Math/MathML"><mml:mrow><mml:mi mathvariant="normal">M</mml:mi><mml:msub><mml:mi mathvariant="normal">n</mml:mi><mml:mn>2</mml:mn></mml:msub><mml:mi>GaC</mml:mi></mml:mrow></mml:math>from first-principles supercell methods. Physical Review B, 2016, 93, .	1.1	12
26780	Role of van der Waals forces in the diffraction of noble gases from metal surfaces. Physical Review B, 2016, 93, .	1.1	21
26781	<mml:math xmlns:mml="http://www.w3.org/1998/Math/MathML"><mml:msub><mml:mi>FeAs</mml:mi><mml:mn>2</mml:mn></mml:msub></mml:math>and electronic nematic ordering: Analysis in terms of structural transformations. Physical Review B, 2016, 93, .	1.1	6
26782	Raman phonons in the ferroelectric-like metal<mml:math xmlns:mml="http://www.w3.org/1998/Math/MathML"><mml:msub><mml:mi>LiOsO</mml:mi><mml:mn>3</mml:mn></mml:msub></mml:math>Physical Review B, 2016, 93, .	1.1	19
26783	Dual role of Fe dopants in enhancing stability and charge transfer in<mml:math xmlns:mml="http://www.w3.org/1998/Math/MathML"><mml:mrow><mml:mo>(</mml:mo><mml:msub><mml:mi>Li</mml:mi></mml:math>Physical Review B, 2016, 93, .	1.1	15
26784	Origins of<mml:math xmlns:mml="http://www.w3.org/1998/Math/MathML"><mml:mrow><mml:mo>â†'</mml:mo><mml:mo>â†'</mml:mo><mml:mo>â†"</mml:mo></mml:math>structure and ferroelectricity in multiferroic<mml:math xmlns:mml="http://www.w3.org/1998/Math/MathML"><mml:mrow><mml:msub><mml:mi>Lu</mml:mi><mml:mn>2</mml:mn></mml:math>Physical Review B, 2016, 93, .	1.1	20
26785	<mml:math xmlns:mml="http://www.w3.org/1998/Math/MathML"><mml:mrow><mml:mi mathvariant="normal">L</mml:mi><mml:msub><mml:mi mathvariant="normal">u</mml:mi><mml:mrow><mml:mn>1</mml:mn><mml:mo>â^'</mml:mo><mml:mi>x</mml:mi></mml:mrow></mml:msub><mml:mi mathvariant="normal">S</mml:mi><mml:msub><mml:mi mathvariant="normal">c</mml:mi><mml:mi>x</mml:mi></mml:msub><mml:mi>Fe</mml:mi><mml:msub><mml:mi mathvariant="normal">	1.1	60

#	Article	IF	Citations
26786	Structural investigations of<mml:math xmlns:mml="http://www.w3.org/1998/Math/MathML"><mml:mrow><mml:msub><mml:mi>Al</mml:mi><mml:mn>5</mml:mn></mml:m (100) surfaces: Influence of bonding strength and annealing temperature on surface terminations. Physical Review B, 2016, 93, .	1.1	8
26787	Low-coverage surface diffusion in complex periodic energy landscapes: Analytical solution for systems with symmetric hops and application to intercalation in topological insulators. Physical Review B, 2016, 93, .	1.1	11
26788	Topological fate of edge states of single Bi bilayer on Bi(111). Physical Review B, 2016, 93, .	1.1	26
26789	New family of graphene-based organic semiconductors: An investigation of photon-induced electronic structure manipulation in half-fluorinated graphene. Physical Review B, 2016, 93, .	1.1	5
26790	Role of surface termination in realizing well-isolated topological surface states within the bulk band gap in<mml:math xmlns:mml="http://www.w3.org/1998/Math/MathML"><mml:msub><mml:mi>TlBiSe</mml:mi><mml:mn>2</mml:mn></mml:msub></m xmlns:mml="http://www.w3.org/1998/Math/MathML"><mml:msub><mml:mi>TlBiTe</mml:mi><mml:mn>2</mml:mn></mml:msub></m Physical Review B, 2016, 93, .	1.1	12
26791	First-principles study of van der Waals interactions and lattice mismatch at<mml:math xmlns:mml="http://www.w3.org/1998/Math/MathML"><mml:msub><mml:mi>MoS</mml:mi><mml:mn>2</mml:mn></mml:msub><mml Physical Review B, 2016, 93, .	1.1	132
26792	Valence and conduction band structure of the quasi-two-dimensional semiconductor<mml:math xmlns:mml="http://www.w3.org/1998/Math/MathML"><mml:mrow><mml:mi>Sn</mml:mi><mml:msub><mml:mi mathvariant="normal">S</mml:mi><mml:mn>2</mml:mn></mml:msub></mml:mrow></mml:math>. Physical Review B, 2016, 93, .	1.1	11
26793	Two-dimensional magnetic boron. Physical Review B, 2016, 93, .	1.1	101
26794	Highly anisotropic thermal conductivity of arsenene: Anab initiostudy. Physical Review B, 2016, 93, .	1.1	114
26795	Node-surface and node-line fermions from nonsymmorphic lattice symmetries. Physical Review B, 2016, 93, .	1.1	231
26796	GaN: From three- to two-dimensional single-layer crystal and its multilayer van der Waals solids. Physical Review B, 2016, 93, .	1.1	139
26797	Depth dependence of vacancy formation energy at (100), (110), and (111) Al surfaces: A first-principles study. Physical Review B, 2016, 93, .	1.1	24
26798	Calculations of planar defect energies in substitutional alloys using the special-quasirandom-structure approach. Physical Review B, 2016, 93, .	1.1	12
26799	Stacking fault energetics ofÎ±â^'andÎ³-ceriuminvestigated withab initiocalculations. Physical Review B, 2016, 93, .	1.1	4
26800	High-pressure phases of<mml:math xmlns:mml="http://www.w3.org/1998/Math/MathML"><mml:mrow><mml:msub><mml:mi>Mg</mml:mi><mml:mn>2</mml:mn></mml:m first principles. Physical Review B, 2016, 93, .	1.1	26
26801	Effect of doping and strain on thermoelectric properties of<mml:math xmlns:mml="http://www.w3.org/1998/Math/MathML"><mml:msub><mml:mrow><mml:mo>(</mml:mo><mml:mi) Tj ETQq1 1 0.784314	1.1	17
26802	Unification of the low-energy excitation peaks in the heat capacity that appears in clathrates. Physical Review B, 2016, 93, .	1.1	7
26803	Direct evidence for minority spin gap in the<mml:math xmlns:mml="http://www.w3.org/1998/Math/MathML"><mml:mrow><mml:mi mathvariant="normal">C</mml:mi><mml:msub><mml:mi mathvariant="normal">o</mml:mi><mml:mn>2</mml:mn></mml:msub><mml:mi>MnSi</mml:mi></mml:mrow></mml:math>Heusle compound. Physical Review B, 2016, 93, .	1.1	65

#	Article	IF	Citations
26804	Spin density wave instabilities in the<mml:math xmlns:mml="http://www.w3.org/1998/Math/MathML"><mml:msub><mml:mi mathvariant="normal">NbS</mml:mi><mml:mn>2</mml:mn></mml:msub></mml:math>monolayer. Physical Review B, 2016, 93, .	1.1	23
26805	Estimates of the thermal conductivity and the thermoelectric properties of<mml:math xmlns:mml="http://www.w3.org/1998/Math/MathML"><mml:msub><mml:mi>PbTiO</mml:mi><mml:mn>3</mml:mn></mml:msub><mml:mr first principles. Physical Review B, 2016, 93, .	1.1	21
26806	Bismuth chalcohalides and oxyhalides as optoelectronic materials. Physical Review B, 2016, 93, .	1.1	82
26807	Antisite defects at oxide interfaces. Physical Review B, 2016, 93, .	1.1	13
26808	Pressure-induced structural transition in copper pyrazine dinitrate and implications for quantum magnetism. Physical Review B, 2016, 93, .	1.1	7
26809	Tailoring magnetic frustration in strained epitaxial FeRh films. Physical Review B, 2016, 93, .	1.1	22
26810	Synthesis and characterization of Fe-Ti-Sb intermetallic compounds: Discovery of a new Slater-Pauling phase. Physical Review B, 2016, 93, .	1.1	31
26811	Density functional theory study of skyrmion pinning by atomic defects in MnSi. Physical Review B, 2016, 93, .	1.1	18
26812	Photoinduced phase transitions in narrow-gap Mott insulators: The case of<mml:math xmlns:mml="http://www.w3.org/1998/Math/MathML"><mml:msub><mml:mi>VO</mml:mi><mml:mn>2</mml:mn></mml:msub></mml Physical Review B, 2016, 93, .	1.1	26
26813	Topological characters in<mml:math xmlns:mml="http://www.w3.org/1998/Math/MathML"><mml:mi mathvariant="normal">Fe</mml:mi><mml:mo>(</mml:mo><mml:mrow><mml:msub><mml:mi>Te</mml:mi><mml:mrow><mml:mn films. Physical Review B, 2016, 93, .	1.1	125
26814	Warm dense crystallography. Physical Review B, 2016, 93, .	1.1	10
26815	Interplay between electron correlations and polar displacements in metallicSrEuMo2O6. Physical Review B, 2016, 93, .	1.1	5
26816	Benchmarking density functional perturbation theory to enable high-throughput screening of materials for dielectric constant and refractive index. Physical Review B, 2016, 93, .	1.1	46
26817	Quasiparticle bands and spectra of<mml:math xmlns:mml="http://www.w3.org/1998/Math/MathML"><mml:mrow><mml:msub><mml:mi>Ga</mml:mi><mml:mn>2</mml:mn></mml:mr mathvariant="normal">O</mml:mi><mml:mn>3</mml:mn></mml:msub></mml:mrow></mml:math>polymorphs. Physical Review B, 2016, 93, .	1.1	165
26818	Optimizing spin-orbit splittings in InSb Majorana nanowires. Physical Review B, 2016, 93, .	1.1	16
26819	Strong charge density wave fluctuation and sliding state in PdTeI with quasi-one-dimensional PdTe chains. Physical Review B, 2016, 93, .	1.1	7
26820	Quantum oscillations and the Fermi surface topology of the Weyl semimetal NbP. Physical Review B, 2016, 93, .	1.1	64
26821	Tucker-tensor algorithm for large-scale Kohn-Sham density functional theory calculations. Physical Review B, 2016, 93, .	1.1	7

#	Article	IF	Citations
26822	Suppression of the charge density wave instability in<mml:math xmlns:mml="http://www.w3.org/1998/Math/MathML"><mml:mrow><mml:msub><mml:mi>R</mml:mi><mml:mn>2</mml:mn></mml:m mathvariant="normal">O</mml:mi><mml:mn>2</mml:mn></mml:msub><mml:mi>Bi</mml:mi></mml:mrow></mml:math>(<mml:math large spin-orbit coupling. Physical Review B, 2016, 93, .	1.1	18
26823	Phonovoltaic. II. Tuning band gap to optical phonon in graphite. Physical Review B, 2016, 93, .	1.1	9
26824	Bilayer<mml:math xmlns:mml="http://www.w3.org/1998/Math/MathML"><mml:msub><mml:mi>SnS</mml:mi><mml:mn>2</mml:mn></mml:msub></mm Tunable stacking sequence by charging and loading pressure. Physical Review B, 2016, 93, .	1.1	61
26825	Atomic size effects studied by transport in single silicide nanowires. Physical Review B, 2016, 93, .	1.1	14
26826	Direct band gaps in group IV-VI monolayer materials: Binary counterparts of phosphorene. Physical Review B, 2016, 93, .	1.1	156
26827	Hydrogen in vanadium: Site occupancy and isotope effects. Physical Review B, 2016, 93, .	1.1	12
26828	Two competing soft modes and an unusual phase transition in the stuffed tridymite-type oxide<mml:math xmlns:mml="http://www.w3.org/1998/Math/MathML"><mml:mrow><mml:msub><mml:mi>BaAl</mml:mi><mml:mn>2</mml:mn></mml:msub> mathvariant="normal">O</mml:mi><mml:mn>4</mml:mn></mml:msub></mml:mrow></mml:math>. Physical Review B, 2016, 93, .	1.1	13
26829	Ab initiostudy of the one-dimensional H-bonded ferroelectricCsH2PO4. Physical Review B, 2016, 93, .	1.1	17
26830	Theoretical study of negative optical mode splitting inLaAlO3. Physical Review B, 2016, 93, .	1.1	4
26831	Ferroelectricity in corundum derivatives. Physical Review B, 2016, 93, .	1.1	46
26832	Strong anisotropy and magnetostriction in the two-dimensional Stoner ferromagnet<mml:math xmlns:mml="http://www.w3.org/1998/Math/MathML"><mml:mrow><mml:msub><mml:mi>Fe</mml:mi><mml:mn>3</mml:mn></mml:msub></mml:m Physical Review B, 2016, 93, .	1.1	209
26833	Possible half-metallic antiferromagnetism in an iridium double-perovskite material. Physical Review B, 2016, 93, .	1.1	27
26834	Magnetically induced phonon splitting in<mml:math xmlns:mml="http://www.w3.org/1998/Math/MathML"><mml:mrow><mml:mi>A</mml:mi><mml:msub><mml:mtext>1</mml:mtext><mml:mtext>Cr</mml:mtext></mml:msub></mml:mrow><mml:mtext> from first principles. Physical Review B, 2016, 93, .	1.1	11
26835	xmlns:mml="http://www.w3.org/1998/Math/MathML"><mml:mrow><mml:mi>M</mml:mi><mml:msub><mml:mi mathvariant="normal">V</mml:mi><mml:mn>2</mml:mn></mml:msub><mml:mi mathvariant="normal">A</mml:mi><mml:msub><mml:mi mathvariant="normal">I</mml:mi><mml:mn>20</mml:mn></mml:msub><mml:mspace width="0.28em"		

#	Article	IF	Citations
26840	Anharmonicity effects in the frictionlike mode of graphite. Physical Review B, 2016, 93, .	1.1	1
26841	Efficient generation of generalized Monkhorst-Pack grids through the use of informatics. Physical Review B, 2016, 93, .	1.1	149
26842	Efficient and accurate approach to modeling the microstructure and defect properties of<mml:math xmlns:mml="http://www.w3.org/1998/Math/MathML"><mml:msub><mml:mtext>LaCoO</mml:mtext><mml:mn>3</mml:mn></mml:msub></mml:math> Physical Review B, 2016, 93, .	1.1	1
26843	Crystal structure and magnetism in<mml:math xmlns:mml="http://www.w3.org/1998/Math/MathML"><mml:mrow><mml:mi>Î±</mml:mi><mml:mo>â€²</mml:mo></mml:mrow></mml:math>-Na<mml:math xmlns:mml="http://www.w3.org/1998/Math/MathML"><mml:msub><mml:mi>Fe</mml:mi><mml:mn>2</mml:mn></mml:msub></mml:math>(<mml:math xmlns:mml="http://www.w3.org/1998/Math/MathML"><mml:msub><mml:mi>MoO</mml:mi><mml:mn>4</mml:mn></mml:msub></mml:math>)<mml:math xmlns:mml="http://www.w3.org/1998/Math/MathML"><mml:mn>3</mml:mn></mml:math>: Anab initiostudy. Physical Review B, 2016, 93, .	1.1	19
26844	Correlated electron behavior of metal-organic molecules: Insights from density functional theory combined with many-body effects using exact diagonalization. Physical Review B, 2016, 93, .	1.1	15
26845	van der Waals heterostructures of germanene, stanene, and silicene with hexagonal boron nitride and their topological domain walls. Physical Review B, 2016, 93, .	1.1	55
26846	Mermin-Wagner theorem, flexural modes, and degraded carrier mobility in two-dimensional crystals with broken horizontal mirror symmetry. Physical Review B, 2016, 93, .	1.1	78
26847	Topological nonsymmorphic ribbons out of symmorphic bulk. Physical Review B, 2016, 93, .	1.1	9
26848	Electronic correlations in the ferroelectric metallic state of<mml:math xmlns:mml="http://www.w3.org/1998/Math/MathML"><mml:msub><mml:mi>LiOsO</mml:mi><mml:mn>3</mml:mn></mml:msub></mml:math> Physical Review B, 2016, 93, .	1.1	29
26849	Active role of magnetic frustrations in magnetic interactions for double perovskite<mml:math xmlns:mml="http://www.w3.org/1998/Math/MathML"><mml:mrow><mml:mi mathvariant="normal">S</mml:mi><mml:msub><mml:mi mathvariant="normal">r</mml:mi><mml:mn>2</mml:mn></mml:msub><mml:mi>B</mml:mi><mml:mi>Os</mml:mi><mml:msub>		

#	Article	IF	Citations
26858	Multiferroic crossover in perovskite oxides. Physical Review B, 2016, 93, .	1.1	38
26859	Tunable topological states in electron-doped HTT-Pt. Physical Review B, 2016, 93, .	1.1	38
26860	Effects of molecule-insulator interaction on geometric property of a single phthalocyanine molecule adsorbed on an ultrathin NaCl film. Physical Review B, 2016, 93, .	1.1	21
26861	Tomonaga-Luttinger liquid theory for metallic fullurene polymers. Physical Review B, 2016, 93, .	1.1	5
26862	Band-gap engineering by Bi intercalation of graphene on Ir(111). Physical Review B, 2016, 93, .	1.1	30
26863	Structural transition in the magnetoelectric<mml:math xmlns:mml="http://www.w3.org/1998/Math/MathML"><mml:mrow><mml:mi>ZnC</mml:mi><mml:msub><mml:mi mathvariant="normal">r</mml:mi><mml:mn>2</mml:mn></mml:msub><mml:mi mathvariant="normal">S</mml:mi><mml:msub><mml:mi mathvariant="normal">e</mml:mi><mml:mn>4</mml:mn></mml:msub></mml:mrow></mml:math>spinel under pressure. Physical Review B, 2016, 93, .	1.1	16
26864	Multiferroic nature of intrinsic point defects in<mml:math xmlns:mml="http://www.w3.org/1998/Math/MathML"><mml:msub><mml:mi>BiFeO</mml:mi><mml:mn>3</mml:mn></mml:msub></mml:math>: A hybrid Hartree-Fock density functional study. Physical Review B, 2016, 93, .	1.1	39
26865	First-principles study of atomic and electronic structures of<mml:math xmlns:mml="http://www.w3.org/1998/Math/MathML"><mml:msup><mml:mn>60</mml:mn><mml:mo>â˜</mml:mo></mml:msup><mml:mn and<mml:math xmlns:mml="http://www.w3.org/1998/Math/MathML"><mml:msup><mml:mn>30</mml:mn><mml:mo>â˜</mml:mo></mml:msup><mml:mn glide dislocations in CdTe. Physical Review B, 2016, 93, .	1.1	20
26866	Evolution of the electronic and lattice structure with carrier injection inBiFeO3. Physical Review B, 2016, 93, .	1.1	13
26867	Nonlinear elastic response of strong solids: First-principles calculations of the third-order elastic constants of diamond. Physical Review B, 2016, 93, .	1.1	21
26868	Coherency effects on the mixing thermodynamics of cubic<mml:math xmlns:mml="http://www.w3.org/1998/Math/MathML"><mml:mrow><mml:msub><mml:mi>Ti</mml:mi><mml:mrow><mml:mn>1</mml:mn> mathvariant="normal">N</mml:mi><mml:mo>/</mml:mo><mml:mi>TiN</mml:mi></mml:mrow></mml:mrow></mml:math>(001) multilayers. Physical Review B, 2016, 93, .	1.1	10
26869	Anisotropic symmetric exchange as a new mechanism for multiferroicity. Physical Review B, 2016, 93, .	1.1	27
26870	Quasistatic magnetoelectric multipoles as order parameter for pseudogap phase in cuprate superconductors. Physical Review B, 2016, 93, .	1.1	39
26871	Probing the possibility of coexistence of martensite transition and half-metallicity in Ni and Co-based full-Heusler alloys: Anab initiocalculation. Physical Review B, 2016, 93, .	1.1	40
26872	Vibrational properties of<mml:math xmlns:mml="http://www.w3.org/1998/Math/MathML"><mml:mrow><mml:msub><mml:mi>LiNb</mml:mi><mml:mrow><mml:mn>1</mml:m mathvariant="normal">O</mml:mi><mml:mn>3</mml:mn></mml:msub></mml:mrow></mml:math>mixed crystals. Physical Review B, 2016, 93, .	1.1	26
26873	Collapse and control of theMnAu2spin-spiral state through pressure and doping. Physical Review B, 2016, 93, .	1.1	4
26874	Calculated impact of ferromagnetic substrate on the spin crossover in a<mml:math xmlns:mml="http://www.w3.org/1998/Math/MathML"><mml:msub><mml:mrow><mml:mi mathvariant="normal">Fe</mml:mi><mml:mo>(</mml:mo><mml:mn>1</mml:mn><mml:mo>,</mml:mo><mml:mn>1</mml:mn><mml:mn>10</mml:mn></mml:mrow><mml:mn Physical Review B, 2016, 93, .	1.1	22
26875	Electronic structure and the origin of the Dzyaloshinskii-Moriya interaction in MnSi. Physical Review B, 2016, 93, .	1.1	29

#	Article	IF	Citations
26876	Second-principles method for materials simulations including electron and lattice degrees of freedom. Physical Review B, 2016, 93, .	1.1	112
26877	Spin crossover in liquid (Mg,Fe)O at extreme conditions. Physical Review B, 2016, 93, .	1.1	17
26878	Strain-induced topological transition in<mml:math xmlns:mml="http://www.w3.org/1998/Math/MathML"><mml:mrow><mml:msub><mml:mi>SrRu</mml:mi><mml:mn>2</mml:mn></mml:msub><mml:msub><mml:mi mathvariant="normal">O</mml:mi><mml:mn>6</mml:mn></mml:msub></mml:mrow></mml:math>and<mml:math xmlns:mml="http://www.w3.org/1998/Math/MathML"><mml:mrow><mml:msub><mml:mi>CaOs</mml:mi><mml:mn>2</mml:mn></mml:msub><mml:msub><mml:mi mathvariant="normal">O</mml:mi><mml:mn>6</mml:mn></mml:msub></mml:mrow></mml:math>. Physical Review B, 2016, 93, .	1.1	14
26879	Spin polarization of two-dimensional electronic gas decoupled from structural asymmetry environment. Physical Review B, 2016, 93, .	1.1	9
26880	Rare-earth silicide thin films on the Si(111) surface. Physical Review B, 2016, 93, .	1.1	28
26881	Structural and electronic properties of Li-intercalated graphene on SiC(0001). Physical Review B, 2016, 93, .	1.1	44
26882	Structure and stability of ultrathin Fe films on W(110). Physical Review B, 2016, 93, .	1.1	6
26883	Hydrostatic pressure induced three-dimensional Dirac semimetal in black phosphorus. Physical Review B, 2016, 93, .	1.1	49
26884	Observation of topological nodal fermion semimetal phase in ZrSiS. Physical Review B, 2016, 93, .	1.1	309
26885	Role of excited states in Shockley-Read-Hall recombination in wide-band-gap semiconductors. Physical Review B, 2016, 93, .	1.1	89
26886	Comparative study of exchange-correlation functionals for accurate predictions of structural and magnetic properties of multiferroic oxides. Physical Review B, 2016, 93, .	1.1	10
26887	Effect of impurity substitution on band structure and mass renormalization of the correlatedFeTe0.5Se0.5superconductor. Physical Review B, 2016, 93, .	1.1	5
26888	Nematic antiferromagnetic states in bulk FeSe. Physical Review B, 2016, 93, .	1.1	22
26889	Configuration dependence of band-gap narrowing and localization in dilute<mml:math xmlns:mml="http://www.w3.org/1998/Math/MathML"><mml:mrow><mml:msub><mml:mi>GaAs</mml:mi><mml:mrow><mml:mn>1</mml:mn> Physical Review B, 2016, 93, .	1.1	31
26890	Influence of the optical-acoustic phonon hybridization on phonon scattering and thermal conductivity. Physical Review B, 2016, 93, .	1.1	55
26891	More realistic band gaps from meta-generalized gradient approximations: Only in a generalized Kohn-Sham scheme. Physical Review B, 2016, 93, .	1.1	182
26892	Orbital-frustration-induced ordering in semiconductor alloys. Physical Review B, 2016, 93, .	1.1	1
26893	Nonlinear elastic effects in phase field crystal and amplitude equations: Comparison toab initiosimulations of bcc metals and graphene. Physical Review B, 2016, 93, .	1.1	18

#	Article	IF	Citations
26894	Bond-order potential for magnetic body-centered-cubic iron and its transferability. Physical Review B, 2016, 93, .	1.1	14
26895	High-temperature- and high-pressure-induced formation of the Laves-phase compoundXeS2. Physical Review B, 2016, 93, .	1.1	12
26896	Phonon anharmonicity and components of the entropy in palladium and platinum. Physical Review B, 2016, 93, .	1.1	8
26897	First-principles calculation and experimental investigation of lattice dynamics in the rare-earth pyrochlores<mml:math xmlns:mml="http://www.w3.org/1998/Math/MathML"><mml:mrow><mml:msub><mml:mi>R</mml:mi><mml:mn>2</mml:mn></mml:m mathvariant="normal">O</mml:mi><mml:mn>7</mml:mn></mml:msub></mml:mrow></mml:math><mml:math		

#	Article	IF	Citations
26912	Stable Dirac semimetal in the allotropes of group-IV elements. Physical Review B, 2016, 93, .	1.1	13
26913	Topological semimetals with triply degenerate nodal points in<mml:math xmlns:mml="http://www.w3.org/1998/Math/MathML"><mml:mi>Î¸</mml:mi></mml:math>-phase tantalum nitride. Physical Review B, 2016, 93, .	1.1	242
26914	Electronic properties of<mml:math xmlns:mml="http://www.w3.org/1998/Math/MathML"><mml:mn>8</mml:mn><mml:mtext>â^'</mml:mtext><mml:mi mathvariant="italic">Pmmn</mml:mi></mml:math>borophene. Physical Review B, 2016, 93, .	1.1	128
26915	Energetic, spatial, and momentum character of the electronic structure at a buried interface: The two-dimensional electron gas between two metal oxides. Physical Review B, 2016, 93, .	1.1	29
26916	Rashba-Dresselhaus spin-splitting in the bulk ferroelectric oxide<mml:math xmlns:mml="http://www.w3.org/1998/Math/MathML"><mml:msub><mml:mi>BiAlO</mml:mi><mml:mn>3</mml:mn></mml:msub></m Physical Review B, 2016, 93, .	1.1	90
26917	Migration mechanisms and diffusion barriers of carbon and native point defects in GaN. Physical Review B, 2016, 93, .	1.1	62
26918	Semiconductor-topological insulator transition of two-dimensional SbAs induced by biaxial tensile strain. Physical Review B, 2016, 93, .	1.1	118
26919	Recognizing nitrogen dopant atoms in graphene using atomic force microscopy. Physical Review B, 2016, 93, .	1.1	12
26920	Quaternary phase diagrams of spinel<mml:math xmlns:mml="http://www.w3.org/1998/Math/MathML"><mml:mrow><mml:msub><mml:mi>Li</mml:mi><mml:mi>y</mml:mi></mml:m mathvariant="normal">O</mml:mi><mml:mn>4</mml:m. Physical Review B, 2016, 94, .	1.1	7
26921	Oxygen diffusion in hcp metals from first principles. Physical Review B, 2016, 94, .	1.1	16
26922	Effective interactions and atomic ordering in Ni-rich Ni-Re alloys. Physical Review B, 2016, 94, .	1.1	19
26923	Band alignment of two-dimensional semiconductors for designing heterostructures with momentum space matching. Physical Review B, 2016, 94, .	1.1	347
26924	Magnetic Dirac fermions and Chern insulator supported on pristine silicon surface. Physical Review B, 2016, 94, .	1.1	18
26925	Unconventional spin texture in a noncentrosymmetric quantum spin Hall insulator. Physical Review B, 2016, 94, .	1.1	22
26926	Manipulating superconductivity in ruthenates through Fermi surface engineering. Physical Review B, 2016, 94, .	1.1	26
26927	Alternative first-principles calculation of entropy for liquids. Physical Review E, 2016, 93, 042119.	0.8	2
26928	Probing Carrier Transport and Structure-Property Relationship of Highly Ordered Organic Semiconductors at the Two-Dimensional Limit. Physical Review Letters, 2016, 116, 016602.	2.9	220
26929	AbÂinitioPrediction of Martensitic and Intermartensitic Phase Boundaries in Ni-Mn-Ga. Physical Review Letters, 2016, 116, 025503.	2.9	57

#	Article	IF	Citations
26930	Carbon Tetragons as Definitive Spin Switches in Narrow Zigzag Graphene Nanoribbons. Physical Review Letters, 2016, 116, 026802.	2.9	51
26931	Ultralow-Frequency Collective Compression Mode and Strong Interlayer Coupling in Multilayer Black Phosphorus. Physical Review Letters, 2016, 116, 087401.	2.9	51
26932	Submolecular Resolution Imaging of Molecules by Atomic Force Microscopy: The Influence of the Electrostatic Force. Physical Review Letters, 2016, 116, 096102.	2.9	51
26933	Two-Dimensionalï€-Conjugated Covalent-Organic Frameworks as Quantum Anomalous Hall Topological Insulators. Physical Review Letters, 2016, 116, 096601.	2.9	75
26934	Origin of the Spin-Orbital Liquid State in a Nearly<mml:math xmlns:mml="http://www.w3.org/1998/Math/MathML" display="inline"><mml:mi>J</mml:mi><mml:mo>=</mml:mo><mml:mn>0</mml:mn></mml:math>Iridate<mml:math xmlns:mml="http://www.w3.org/1998/Math/MathML" display="inline"><mml:msub><mml:mi>Ba</mml:mi><mml:mn>3</mml:mn></mml:msub><mml:msub><mml:mi>ZnIr</mml:mi><mml:m mathvariant="normal">O</mml:mi><mml:mn>9</mml:mn></mml:msub></mml:math>. Physical Review Le	2.9	58
26935	EfficientAbÂinitioModeling of Random Multicomponent Alloys. Physical Review Letters, 2016, 116, 105501.	2.9	93
26936	Thermally Induced Graphene Rotation on Hexagonal Boron Nitride. Physical Review Letters, 2016, 116, 126101.	2.9	142
26937	Optical Coherence in Atomic-Monolayer Transition-Metal Dichalcogenides Limited by Electron-Phonon Interactions. Physical Review Letters, 2016, 116, 127402.	2.9	105
26938	Electric Field Cancellation on Quartz by Rb Adsorbate-Induced Negative Electron Affinity. Physical Review Letters, 2016, 116, 133201.	2.9	38
26939	Sparse Cyclic Excitations Explain the Low Ionic Conductivity of Stoichiometric<mml:math xmlns:mml="http://www.w3.org/1998/Math/MathML" display="inline"><mml:mrow><mml:msub><mml:mrow><mml:mi>Li</mml:mi></mml:mrow><mml:mrow><mml:mn>7</mml:mn></mml:m mathvariant="normal">O. Physical Review Letters, 2016, 116, 135901.	2.9	57
26940	Body-Centered Orthorhombic<mml:math xmlns:mml="http://www.w3.org/1998/Math/MathML" display="inline"><mml:mrow><mml:msub><mml:mrow><mml:mi mathvariant="normal">C</mml:mi></mml:mrow><mml:mrow><mml:mn>16</mml:mn></mml:mrow></mml:msub></mml:mrow></mm A Novel Topological Node-Line Semimetal. Physical Review Letters, 2016, 116, 195501.	2.9	170
26941	Strain Control of Fermiology and Many-Body Interactions in Two-Dimensional Ruthenates. Physical Review Letters, 2016, 116, 197003.	2.9	82
26942	Multiferroic Two-Dimensional Materials. Physical Review Letters, 2016, 116, 206803.	2.9	187
26943	Ideal Weyl Semimetals in the Chalcopyrites<mml:math xmlns:mml="http://www.w3.org/1998/Math/MathML" display="inline"><mml:mrow><mml:msub><mml:mrow><mml:mi>CuTlSe</mml:mi></mml:mrow><mml:mrow><mml:mn>2</mml:mn></mml:mr xmlns:mml="http://www.w3.org/1998/Math/MathML" display="inline"><mml:mrow><mml:msub><mml:mrow><mml:mi>AgTlTe</mml:mi></mml:mrow><mml:mrow><mml:mn>2</mml:mn></mml:mr xmlns:mml="http://www.w3.org/1998/Math. Physical Review Letters, 2016, 116, 226801.	2.9	116
26944	Unveiling the Room-Temperature Magnetoelectricity of Troilite FeS. Physical Review Letters, 2016, 116, 227601.	2.9	31
26945	Diffusion Barriers Block Defect Occupation on Reduced<mml:math xmlns:mml="http://www.w3.org/1998/Math/MathML" display="inline"><mml:mrow><mml:msub><mml:mrow><mml:mi>CeO</mml:mi></mml:mrow><mml:mrow><mml:mn>2</mml:mn></mml:mr stretchy="false">(</mml:mo><mml:mn>111</mml:mn><mml:mo) Tj ETQq1 1 0.784314 rgBT /Overlock 10 Tf 50 127 Td (stretchy="fa	2.9	25
26946	Intrinsic Charge Carrier Mobility in Single-Layer Black Phosphorus. Physical Review Letters, 2016, 116, 246401.	2.9	132
26947	Dzyaloshinskii-Moriya Interaction as a Consequence of a Doppler Shift due to Spin-Orbit-Induced Intrinsic Spin Current. Physical Review Letters, 2016, 116, 247201.	2.9	103

#	Article	IF	Citations
26948	Structural and Electronic Properties of Germanene on<mml:math xmlns:mml="http://www.w3.org/1998/Math/MathML" display="inline"><mml:msub><mml:mi>MoS</mml:mi><mml:mn>2</mml:mn></mml:msub></mml:math>. Physical Review Letters, 2016, 116, 256804.	2.9	329
26949	Evidence for Topological Edge States in a Large Energy Gap near the Step Edges on the Surface of<mml:math xmlns:mml="http://www.w3.org/1998/Math/MathML" display="inline"><mml:mrow><mml:msub><mml:mrow><mml:mi>ZrTe</mml:mi></mml:mrow><mml:mrow><mml:mn>5</mml:mn></mml:mrow> Physical Review X, 2016, 6, .	2.8	105
26950	Ab initiocalculation of thermodynamic potentials and entropies for superionic water. Physical Review E, 2016, 93, 022140.	0.8	47
26951	Electronic structure, ferroelectric properties, and phase stability of BiGaO3 under high pressure from first principles. Journal of Materials Science, 2016, 51, 9761-9770.	1.7	11
26952	Experimental and theoretical Raman study on the structure and microstructure of Li0.30La0.57TiO3 electrolyte prepared by the sol-gel method in acetic medium. Ceramics International, 2016, 42, 15414-15422.	2.3	23
26953	Ab initio energetics for modeling phase stability of the Np-U system. Journal of Nuclear Materials, 2016, 479, 260-270.	1.3	2
26954	Strain-Mediated Modification of Phagraphene Dirac Cones. Journal of Physical Chemistry C, 2016, 120, 17101-17105.	1.5	14
26955	Isolated Chromium(VI) Oxide Species Supported on Al-Modified Silica: A Molecular Description. Journal of Physical Chemistry C, 2016, 120, 17594-17603.	1.5	19
26956	Effect of Nanostructuring on the Reactivity of Zirconia: A DFT+U Study of Au Atom Adsorption. Journal of Physical Chemistry C, 2016, 120, 17604-17612.	1.5	13
26957	Tuning the electronic structures and magnetism of two-dimensional porous C₂N via transition metal embedding. Physical Chemistry Chemical Physics, 2016, 18, 22678-22686.	1.3	54
26958	Review on first-principles study of defect properties of CdTe as a solar cell absorber. Semiconductor Science and Technology, 2016, 31, 083002.	1.0	109
26959	Magnetoelectroelastic control of magnetism in an artificial multiferroic. Physical Review B, 2016, 94, .	1.1	17
26960	Magnetism from 2p states in K-doped ZnO monolayer: A density functional study. Europhysics Letters, 2016, 114, 47012.	0.7	10
26961	Interfacing BiVO 4 with Reduced Graphene Oxide for Enhanced Photoactivity: A Tale of Facet Dependence of Electron Shuttling. Small, 2016, 12, 5295-5302.	5.2	68
26962	Computational Investigation of Li Insertion in Li₃VO₄. Chemistry of Materials, 2016, 28, 5643-5651.	3.2	50
26963	Combined EXAFS, XRD, DRIFTS, and DFT Study of Nano Copper-Based Catalysts for CO₂ Hydrogenation. ACS Catalysis, 2016, 6, 5823-5833.	5.5	51
26964	Organics on oxidic metal surfaces: a first-principles DFT study of PMDA and ODA fragments on the pristine and mildly oxidized surfaces of Cu(111). Physical Chemistry Chemical Physics, 2016, 18, 21893-21902.	1.3	6
26965	Comparative studies of the electronic structure and thermoelectric properties in orthorhombic and tetragonal BaCu₂Se₂ by first-principles calculations. RSC Advances, 2016, 6, 60717-60722.	1.7	6

#	Article	IF	Citations
26966	Low-dimensional boron: searching for Dirac materials. Advances in Physics: X, 2016, 1, 412-424.	1.5	14
26967	Structure and dynamics of high-pressure Na close to the melting line: Anab initiomolecular dynamics study. Physical Review B, 2016, 94, .	1.1	16
26968	Thermoelasticity of Fe₇C₃ under inner core conditions. Journal of Geophysical Research: Solid Earth, 2016, 121, 5828-5837.	1.4	28
26969	First Principles Simulations of Cyclic Voltammograms on Stepped Pt(553) and Pt(533) Electrode Surfaces. ChemElectroChem, 2016, 3, 1609-1617.	1.7	47
26970	Computational Modelling as a Value Add in Energy Storage Materials. Nanostructure Science and Technology, 2016, , 481-513.	0.1	1
26971	Transition metal doped arsenene: A first-principles study. Applied Surface Science, 2016, 389, 594-600.	3.1	102
26972	Observation of graphene grain boundaries through selective adsorption of rhodamine B using fluorescence microscopy. Carbon, 2016, 108, 72-78.	5.4	3
26973	The half-metallic ferromagnetic characters of (001)-oriented thin films of the double perovskite Pb2FeMoO6. Thin Solid Films, 2016, 615, 318-323.	0.8	4
26974	Experimental Growth of New 6-fold Symmetry Patterned Microcrystals of AlN: Equilibrium Structures and Growth Mechanism. Crystal Growth and Design, 2016, 16, 5305-5311.	1.4	19
26975	Direct Câ€“C Coupling of CO₂ and the Methyl Group from CH₄ Activation through Facile Insertion of CO₂ into Znâ€“CH₃ Ïƒ-Bond. Journal of the American Chemical Society, 2016, 138, 10191-10198.	6.6	96
26976	Oxidation of the titanium(0001) surface: diffusion processes of oxygen from DFT. RSC Advances, 2016, 6, 71311-71318.	1.7	21
26977	Current emission from P-doped SiC nanowires with ultralow turn-on fields. Journal of Materials Chemistry C, 2016, 4, 7391-7396.	2.7	34
26978	Single and bilayer bismuthene: Stability at high temperature and mechanical and electronic properties. Physical Review B, 2016, 94, .	1.1	295
26979	Unconventional quantized edge transport in the presence of interedge coupling in intercalated graphene. Physical Review B, 2016, 94, .	1.1	1
26980	Magnetic Behavior of Volborthite<mml:math xmlns:mml="http://www.w3.org/1998/Math/MathML" display="inline"><mml:mrow><mml:mrow><mml:msub><mml:mrow><mml:mi>Cu</mml:mi></mml:mrow><mml:mrow><mml:mn>3</mml:mn></mml:mrow></mml:msub><mml:mo>(</mml:mo><mml:mrow><mml:msub><mml:mrow><mml:mi mathvariant="normal">V</mml:mi></mml:mrow><mml:mrow><mml:mn>2</mml:mn></mml:mrow></mml:msub></mml:mrow><mml:mo>)</mml:mo><mml:mrow><mml:msub><mml:mrow><mml:mi mathvariant="normal">O</mml:mi></mml:mrow><mml:mrow><mml:mn>7</mml:mn></mml:mrow></mml:msub></mml:mrow></mml:mrow></mml:mrow></mml:math>. Physical Review Letters, 2016, 117, 037206.	8.6	43
26981	Co spin state and magnetic structure in GdBaCo 2 O 5+x and Fe doped compounds: A first principles study. Current Applied Physics, 2016, 16, 1094-1099.	1.1	5
26982	Graphdiyne-supported single-atom Sc and Ti catalysts for high-efficient CO oxidation. Carbon, 2016, 108, 343-350.	5.4	114
26983	Stacking disorder in metastable NiSn4. Materials and Design, 2016, 109, 324-333.	3.3	11

#	Article	IF	Citations
26984	Density Functional Theory Studies of the Methanol Decomposition Reaction on Graphene-Supported Pt₁₃ Nanoclusters. Journal of Physical Chemistry C, 2016, 120, 17408-17417.	1.5	23
26985	Two-Dimensional Phosphorus Carbide: Competition between sp² and sp³ Bonding. Nano Letters, 2016, 16, 3247-3252.	4.5	137
26986	Highly Itinerant Atomic Vacancies in Phosphorene. Journal of the American Chemical Society, 2016, 138, 10199-10206.	6.6	134
26987	Pinning effect of reactive elements on adhesion energy and adhesive strength of incoherent Al₂O₃/NiAl interface. Physical Chemistry Chemical Physics, 2016, 18, 22864-22873.	1.3	19
26988	An assessment of silver copper sulfides for photovoltaic applications: theoretical and experimental insights. Journal of Materials Chemistry A, 2016, 4, 12648-12657.	5.2	42
26989	Strong covalent boron bonding induced extreme hardness of VB3. Journal of Alloys and Compounds, 2016, 688, 1101-1107.	2.8	14
26990	Martensitic transformation and magnetism in Ni and Fe-rich compositions of Ni-Fe-Ga shape memory alloys. Journal of Alloys and Compounds, 2016, 689, 199-207.	2.8	6
26991	Highly efficient metal halide substituted CH3NH3I(PbI2)1â^'X(CuBr2)X planar perovskite solar cells. Nano Energy, 2016, 27, 330-339.	8.2	106
26992	When the Grafting of Double Decker Phthalocyanines on Si(100)-2 Ã— 1 Partly Affects the Molecular Electronic Structure. Journal of Physical Chemistry C, 2016, 120, 14270-14276.	1.5	9
26993	An aminopyrimidine-functionalized cage-based metalâ€“organic framework exhibiting highly selective adsorption of C₂H₂ and CO₂ over CH₄. Dalton Transactions, 2016, 45, 13373-13382.	1.6	73
26994	Computational studies on the structural, electronic and optical properties of graphene-like MXenes (M₂CT₂, M = Ti, Zr, Hf; T = O, F, OH) and their potential applications as visible-light driven photocatalysts. Journal of Materials Chemistry A, 2016, 4, 12913-12920.	5.2	205
26995	Thermal Transition from a Disordered, 2D Network to a Regular, 1D, Fe(II)â€“DCNQI Coordination Network. Journal of Physical Chemistry C, 2016, 120, 16712-16721.	1.5	4
26996	Mechanism of Oxygen Reduction Reaction on Pt(111) in Alkaline Solution: Importance of Chemisorbed Water on Surface. Journal of Physical Chemistry C, 2016, 120, 15288-15298.	1.5	120
26997	Electronâ€“Rotor Interaction in Organicâ€“Inorganic Lead Iodide Perovskites Discovered by Isotope Effects. Journal of Physical Chemistry Letters, 2016, 7, 2879-2887.	2.1	79
26998	The structural evolution of hydrogenated silicon carbide nanocrystals: an approach from bond energy model, Wangâ€“Landau method and first-principles studies. Journal Physics D: Applied Physics, 2016, 49, 245305.	1.3	1
26999	Thermal stability of mulliteRMn₂O₅(Râ€‰â€‰=â€‰â€‰Bi, Y, Pr, Sm or Gd): combined density functional theory and experimental study. Journal of Physics Condensed Matter, 2016, 28, 125602.	0.7	17
27000	Graphene nanoribbons anchored to SiC substrates. Journal of Physics Condensed Matter, 2016, 28, 364001.	0.7	2
27001	Strain effects on borophene: ideal strength, negative Possionâ€™s ratio and phonon instability. New Journal of Physics, 2016, 18, 073016.	1.2	174

#	Article	IF	Citations
27002	Î³ - and Î± -Ce phase diagram: First-principle calculation. Chinese Physics B, 2016, 25, 033102.	0.7	1
27003	Efficient Computation of the Hartreeâ€“Fock Exchange in Real-Space with Projection Operators. Journal of Chemical Theory and Computation, 2016, 12, 3614-3622.	2.3	21
27004	Alternate to Molybdenum Disulfide: A 2D, Fewâ€Layer Transitionâ€Metal Thiophosphate and Its Hydrogen Evolution Reaction Activity over a Wide pH Range. ChemElectroChem, 2016, 3, 1392-1399.	1.7	44
27005	Calphad assessment of the Niâ€“Snâ€“Ti system. Calphad: Computer Coupling of Phase Diagrams and Thermochemistry, 2016, 54, 67-75.	0.7	18
27006	First-principles study of the stability and diffusion properties of hydrogen in zirconium carbide. Journal of Nuclear Materials, 2016, 479, 130-136.	1.3	14
27007	Density Functional Theory Study for Ni Diffusion on Ni(111) Surface under Solid Oxide Fuel Cell Operating Condition. Journal of Physical Chemistry C, 2016, 120, 16641-16648.	1.5	5
27008	Improved Electrochemical Performance of Lanthanum Silicide/Silicon Composite Electrode with Nickel Substitution for Lithium-Ion Batteries. Journal of Physical Chemistry C, 2016, 120, 16333-16339.	1.5	23
27009	Multiscale Analysis for Field-Effect Penetration through Two-Dimensional Materials. Nano Letters, 2016, 16, 5044-5052.	4.5	28
27010	Alloying ZnS in the hexagonal phase to create high-performing transparent conducting materials. Physical Chemistry Chemical Physics, 2016, 18, 22628-22635.	1.3	16
27011	Theoretical insights into the promotion effect of subsurface boron for the selective hydrogenation of CO to methanol over Pd catalysts. Physical Chemistry Chemical Physics, 2016, 18, 21720-21729.	1.3	30
27012	Towards an accurate specific reaction parameter density functional for water dissociation on Ni(111): RPBE versus PW91. Physical Chemistry Chemical Physics, 2016, 18, 21817-21824.	1.3	25
27013	A comparative study of Au_mRh_n (4 â‰¤ m + n â‰¤ 6) clusters in the gas phase versus those deposited on (100) MgO. Physical Chemistry Chemical Physics, 2016, 18, 22122-22128.	1.3	12
27014	Geometric, magnetic and electronic properties of folded graphene nanoribbons. RSC Advances, 2016, 6, 64852-64860.	1.7	10
27015	Direct quantitative identification of the â€œsurface trans-effectâ€• Chemical Science, 2016, 7, 5647-5656.	3.7	51
27016	Crystal structure and magnetic properties of new Fe₃Co₃X₂(Xâ€‰â€‰=â€‰â€‰Ti, Nb) intermetallic compounds. Journal Physics D: Applied Physics, 2016, 49, 175002.	1.3	11
27017	Characteristics of Li diffusion on silicene and zigzag nanoribbon. Chinese Physics B, 2016, 25, 017101.	0.7	5
27018	Discovery of robust in-plane ferroelectricity in atomic-thick SnTe. Science, 2016, 353, 274-278.	6.0	742
27019	Thermo-elastic and optical properties of molybdenum nitride. Canadian Journal of Physics, 2016, 94, 902-912.	0.4	11

#	Article	IF	Citations
27020	Strong deformation anisotropies of Ï‰-precipitates and strengthening mechanisms in Ti-10V-2Fe-3Al alloy micropillars: Precipitates shearing vs precipitates disordering. Acta Materialia, 2016, 117, 68-80.	3.8	78
27021	Tuning chemical bonding of MnO2 through transition-metal doping for enhanced CO oxidation. Journal of Catalysis, 2016, 341, 82-90.	3.1	132
27022	Structural, electronic and magnetic properties of the (Co, Ni) codoped ZnS: A first-principles study. Physics Letters, Section A: General, Atomic and Solid State Physics, 2016, 380, 2796-2802.	0.9	12
27023	Aliovalent Doping in Colloidal Quantum Dots and Its Manifestation on Their Optical Properties: Surface Attachment versus Structural Incorporation. Chemistry of Materials, 2016, 28, 5384-5393.	3.2	15
27024	High Energetic Polymeric Nitrogen Stabilized in the Confinement of Boron Nitride Nanotube at Ambient Conditions. Journal of Physical Chemistry C, 2016, 120, 16412-16417.	1.5	21
27025	Origin of Efficient Catalytic Combustion of Methane over Co₃O₄(110): Active Low-Coordination Lattice Oxygen and Cooperation of Multiple Active Sites. ACS Catalysis, 2016, 6, 5508-5519.	5.5	116
27026	Dipole-induced asymmetric conduction in tunneling junctions comprising self-assembled monolayers. RSC Advances, 2016, 6, 69479-69483.	1.7	31
27027	The symmetry-resolved electronic structure of 2H-WSe₂(0â€‰0â€‰0â€‰1). Journal of Physics Condensed Matter, 2016, 28, 345503.	0.7	7
27029	Highâ€Performance Ru₁/CeO₂ Singleâ€Atom Catalyst for CO Oxidation: A Computational Exploration. ChemPhysChem, 2016, 17, 3170-3175.	1.0	47
27030	Structure and Dynamics of Fluorophosphate Na-Ion Battery Cathodes. Chemistry of Materials, 2016, 28, 5450-5460.	3.2	72
27031	Stable Calcium Nitrides at Ambient and High Pressures. Inorganic Chemistry, 2016, 55, 7550-7555.	1.9	88
27032	DFT Calculations with van der Waals Interactions of Hydrated Calcium Carbonate Crystals CaCO₃Â·(H₂O, 6H₂O): Structural, Electronic, Optical, and Vibrational Properties. Journal of Physical Chemistry A, 2016, 120, 5752-5765.	1.1	31
27033	Interface and Doping Effect on the Electrochemical Property of Graphene/LiFePO₄. Journal of Physical Chemistry C, 2016, 120, 17165-17174.	1.5	21
27034	Tailoring Vacancies Far Beyond Intrinsic Levels Changes the Carrier Type and Optical Response in Monolayer MoSe_{2â^’x} Crystals. Nano Letters, 2016, 16, 5213-5220.	4.5	121
27035	Surface Proton Hopping and Fast-Kinetics Pathway of Water Oxidation on Co₃O₄ (001) Surface. ACS Catalysis, 2016, 6, 5610-5617.	5.5	83
27036	Synthesis and structure of ruthenium-fullerides. RSC Advances, 2016, 6, 69135-69148.	1.7	22
27037	Effect of strain on the electronic and magnetic properties of an Fe-doped WSe₂ monolayer. RSC Advances, 2016, 6, 69758-69763.	1.7	15
27038	The hydrogen-induced structural stability and promising electronic properties of molybdenum and tungsten dinitride nanosheets: a first-principles study. Journal of Materials Chemistry C, 2016, 4, 7485-7493.	2.7	35

#	Article	IF	Citations
27039	Scintillation Properties and Electronic Structures of the Intrinsic and Extrinsic Mixed Elpasolites<mml:math xmlns:mml="http://www.w3.org/1998/Math/MathML" display="inline"><mml:mrow><mml:msub><mml:mrow><mml:mi>Cs</mml:mi></mml:mrow><mml:mrow><mml:mn>2</mml:mn></mml:mrow></mml:msub><mml:mi mathvariant="normal">I</mml:mi></mml:mrow><mml:mrow><mml:mn>3</mml:m. Physical Review Applied, 2016, 5, .	1.5	12
27040	AbAInitioStudy of Water Adsorption and Reactivity on the (211) Surface of Anatase<mml:math xmlns:mml="http://www.w3.org/1998/Math/MathML" display="inline"><mml:mrow><mml:msub><mml:mrow><mml:mi>TiO</mml:mi></mml:mrow><mml:mrow><mml:mn>2</mml:mn></mml:mrow></mml:msub><mml:mi Physical Review Applied, 2016, 5, .	1.5	12
27041	Elastic and Thermodynamic Properties of Complex Mg-Al Intermetallic Compounds via Orbital-Free Density Functional Theory. Physical Review Applied, 2016, 5, .	1.5	30
27042	Superconductivity in two-dimensional boron allotropes. Physical Review B, 2016, 93, .	1.1	114
27043	Prediction of two-dimensional topological insulator by forming a surface alloy on Au/Si(111) substrate. Physical Review B, 2016, 93, .	1.1	27
27044	Ferroelectric instability and topological crystalline insulating nature in PbPo. Physical Review B, 2016, 93, .	1.1	4
27045	Metal-insulator transition in a spin-orbital-lattice coupled Mott system:<mml:math xmlns:mml="http://www.w3.org/1998/Math/MathML"><mml:mrow><mml:msub><mml:mi mathvariant="normal">K</mml:mi><mml:mn>2</mml:mn></mml:msub><mml:msub><mml:mi mathvariant="normal">V</mml:mi><mml:mn>8</mml:mn></mml:msub><mml:msub><mml:mi mathvariant="normal">O</mml:mi><mml:mn>16</mml:mn></mml:msub></mml:mrow></mml:math>. Physical Review B, 2016, 93, .	1.1	8
27046	Spin texture induced by oxygen vacancies in strontium perovskite (001) surfaces: A theoretical comparison between<mml:math xmlns:mml="http://www.w3.org/1998/Math/MathML"><mml:msub><mml:mi>SrTiO</mml:mi><mml:mn>3</mml:mn></mml:msub> xmlns:mml="http://www.w3.org/1998/Math/MathML"><mml:msub><mml:mi>SrHfO</mml:mi><mml:mn>3</mml:mn></mml:msub> Physical Review B, 2016, 93, .	1.1	18
27047	Effect of thermal lattice expansion on the stacking fault energies of fcc Fe and<mml:math xmlns:mml="http://www.w3.org/1998/Math/MathML"><mml:mrow><mml:msub><mml:mi>Fe</mml:mi><mml:mn>2</mml:mn></mml:msub> Physical Review B, 2016, 93, .	1.1	20
27048	Stability and magnetism of strongly correlated single-layer<mml:math xmlns:mml="http://www.w3.org/1998/Math/MathML"><mml:msub><mml:mi>VS</mml:mi><mml:mn>2</mml:mn></mml:msub> Physical Review B, 2016, 93, .	1.1	176
27049	First-principles equation of state calculations of warm dense nitrogen. Physical Review B, 2016, 93, .	1.1	53
27050	Ab initiostudy of the ferroelectric strain dependence and<mml:math xmlns:mml="http://www.w3.org/1998/Math/MathML"><mml:msup><mml:mn>180</mml:mn><mml:mo>â˜</mml:mo></mml:msup> walls in the barium metal fluorides<mml:math xmlns:mml="http://www.w3.org/1998/Math/MathML"><mml:msub><mml:mi>BaMgF</mml:mi><mml:mn>4</mml:mn></mml:msub> xmlns:mml="http://www.w3.org/1998/Math/MathML"><mml:msub><mml:mi>BaZnF</mml:mi><mml:mn>4</mml:mn></mml:msub> Physical Review B, 2016, 93, .	1.1	9
27051	A bespoke single-band Hubbard model material. Physical Review B, 2016, 93, .	1.1	6
27052	Layered structures of organic/inorganic hybrid halide perovskites. Physical Review B, 2016, 93, .	1.1	31
27053	Prediction model of band gap for inorganic compounds by combination of density functional theory calculations and machine learning techniques. Physical Review B, 2016, 93, .	1.1	252
27054	Splitting between bright and dark excitons in transition metal dichalcogenide monolayers. Physical Review B, 2016, 93, .	1.1	212
27055	Understanding topological phase transition in monolayer transition metal dichalcogenides. Physical Review B, 2016, 93, .	1.1	87
27056	Short-range phase coherence and origin of the<mml:math xmlns:mml="http://www.w3.org/1998/Math/MathML"><mml:mrow><mml:mn>1</mml:mn><mml:mi>T</mml:mi> density wave. Physical Review B, 2016, 93, .	1.1	47

#	Article	IF	Citations
27057	Density-functional study of atomic and electronic structures of multivacancies in silicon carbide. Physical Review B, 2016, 93, .	1.1	18
27058	Energy level alignment of self-assembled linear chains of benzenediamine on Au(111) from first principles. Physical Review B, 2016, 93, .	1.1	8
27059	Anomalous magnetotransport behavior in Fe-doped MnNiGe alloys. Physical Review B, 2016, 93, .	1.1	24
27060	Predicted phase diagram of boron-carbon-nitrogen. Physical Review B, 2016, 93, .	1.1	20
27061	Ferromagnetism and correlation strength in cubic barium ruthenate in comparison to strontium and calcium ruthenate: A dynamical mean-field study. Physical Review B, 2016, 93, .	1.1	26
27062	Submonolayer Ag films on Fe(100): A first-principles analysis of energetics controlling adlayer thermodynamics and kinetics. Physical Review B, 2016, 93, .	1.1	4
27063	Strong interlayer coupling mediated giant two-photon absorption in<mml:math xmlns:mml="http://www.w3.org/1998/Math/MathML"><mml:mrow><mml:mi>MoS</mml:mi><mml:msub><mml:mi mathvariant="normal">e</mml:mi><mml:mn>2</mml:mn></mml:msub></mml:mrow></mml:math>/graphene oxide heterostructure: Quenching of exciton bands. Physical Review B, 2016, 93, .	1.1	57
27064	Engineering charge ordering into multiferroicity. Physical Review B, 2016, 93, .	1.1	8
27065	Single-layer<mml:math xmlns:mml="http://www.w3.org/1998/Math/MathML"><mml:msub><mml:mtext>MoS</mml:mtext><mml:mn>2</mml:mn></mml:msub></mml:math>/Au(111): Band gap renormalization and substrate interaction. Physical Review B, 2016, 93, .	1.1	128
27066	Layer response theory: Energetics of layered materials from semianalytic high-level theory. Physical Review B, 2016, 93, .	1.1	11
27067	Origin of ferroelectric polarization in tetragonal tungsten-bronze-type oxides. Physical Review B, 2016, 93, .	1.1	44
27068	First-principles investigation of hydrogen interaction with TiC precipitates in<mml:math xmlns:mml="http://www.w3.org/1998/Math/MathML"><mml:mi>Î±</mml:mi></mml:math>-Fe. Physical Review B, 2016, 93, .	1.1	117
27069	STM and DFT study on formation and characterization of Ba-incorporated phases on a Ge(001) surface. Physical Review B, 2016, 93, .	1.1	7
27070	Pressure tuning the Fermi surface topology of the Weyl semimetal NbP. Physical Review B, 2016, 93, .	1.1	29
27071	High-throughput<mml:math xmlns:mml="http://www.w3.org/1998/Math/MathML"><mml:mrow><mml:mi>Z</mml:mi><mml:mi>T</mml:mi></mml:mrow></mml:ma of nanoporous bulk materials as next-generation thermoelectric materials: A material genome approach. Physical Review B, 2016, 93, .	1.1	33
27072	Green's function approach to edge states in transition metal dichalcogenides. Physical Review B, 2016, 93, .	1.1	16
27073	Potentially superhard hcp<mml:math xmlns:mml="http://www.w3.org/1998/Math/MathML"><mml:mrow><mml:mi>Cr</mml:mi><mml:msub><mml:mi mathvariant="normal">N</mml:mi><mml:mn>2</mml:mn></mml:msub></mml:mrow></mml:math>compound studied at high pressure. Physical Review B, 2016, 93, .	1.1	33
27074	Ab initioapproach to structural, electronic, and ferroelectric properties of antimony sulphoiodide. Physical Review B, 2016, 93, .	1.1	25

#	Article	IF	Citations
27075	Impact of local magnetism on stacking fault energies: A first-principles investigation for fcc iron. Physical Review B, 2016, 93, .	1.1	37
27076	Different effects of electronic excitation on metals and semiconductors. Physical Review B, 2016, 93, .	1.1	16
27077	Effects of electron correlation, electron-phonon coupling, and spin-orbit coupling on the isovalent Pd-substituted superconductor<mml:math xmlns:mml="http://www.w3.org/1998/Math/MathML"><mml:mrow><mml:msub><mml:mi>SrPt</mml:mi><mml:mn>3</mml:mn></mml:msub><mml:msub><mml:mi mathvariant="normal">P</mml:mi></mml:msub></mml:mrow></mml:math>. Physical Review B, 2016, 93, .	1.1	12
27078	Strong impact of lattice vibrations on electronic and magnetic properties of paramagnetic Fe revealed by disordered local moments molecular dynamics. Physical Review B, 2016, 93, .	1.1	43
27079	Correlation energy for the homogeneous electron gas: Exact Bethe-Salpeter solution and an approximate evaluation. Physical Review B, 2016, 93, .	1.1	80
27080	mBEEF-vdW: Robust fitting of error estimation density functionals. Physical Review B, 2016, 93, .	1.1	35
27081	Two-dimensional topological insulators in group-11 chalcogenide compounds:<mml:math xmlns:mml="http://www.w3.org/1998/Math/MathML"><mml:mrow><mml:msub><mml:mi>M</mml:mi><mml:mn>2</mml:mn></mml:msub><mml:mo>(</mml:mo><mml:mrow><mml:mi>M</mml:mi><mml:mo>=</mml:mo><mml:mi>Cu</mml:mi><mml:mo>,</mml:mo> width="0.28em" />	1.1	34
27082	Topological Dirac surface states and superconducting pairing correlations in<mml:math xmlns:mml="http://www.w3.org/1998/Math/MathML"><mml:msub><mml:mi>PbTaSe</mml:mi><mml:mn>2</mml:mn></mml:msub> Physical Review B, 2016, 93, .	1.1	79
27083	Electronic structure of interstitial hydrogen in lutetium oxide from<mml:math xmlns:mml="http://www.w3.org/1998/Math/MathML"><mml:mtext>DFT</mml:mtext><mml:mo>+</mml:mo><mml:mi>U</mml:mi> and comparison study with<mml:math xmlns:mml="http://www.w3.org/1998/Math/MathML"><mml:mrow><mml:mi>Î¼</mml:mi><mml:mi>SR</mml:mi></mml:mrow> Physical Review B, 2016, 94, .	1.1	21
27084	Direct evidence of metallic bands in a monolayer boron sheet. Physical Review B, 2016, 94, .	1.1	152
27085	Direct Observation of Electrostatically Driven Band Gap Renormalization in a Degenerate Perovskite Transparent Conducting Oxide. Physical Review Letters, 2016, 116, 027602.	2.9	100
27086	Weak Topological Insulators and Composite Weyl Semimetals:<mml:math xmlns:mml="http://www.w3.org/1998/Math/MathML"		

#	Article	IF	Citations
27093	<mml:math xmlns:mml="http://www.w3.org/1998/Math/MathML" display="inline"><mml:msub><mml:mi mathvariant="double-struck">Z</mml:mi><mml:mn>2</mml:mn></mml:msub></mml:math>Invariance of Germanene on<mml:math xmlns:mml="http://www.w3.org/1998/Math/MathML" display="inline"><mml:mrow><mml:msub><mml:mrow><mml:mi>MoS</mml:mi></mml:mrow><mml:mrow><mml:mn>2</mml:mn></mml:mrow></mml:msub></mml:mrow></mml:math>: First Principles. Physical Review Letters, 2016, 116, 256805.	2.9	35
27094	Correct Implementation of Polarization Constants in Wurtzite Materials and Impact on III-Nitrides. Physical Review X, 2016, 6, .	2.8	81
27095	Ab Initio Thermodynamics and Kinetics for Coalescence of Two-Dimensional Nanoislands and Nanopits on Metal (100) Surfaces. Journal of Physical Chemistry C, 2016, 120, 21617-21630.	1.5	24
27096	Cu₂ZnSnS₄ Nanocrystals as Highly Active and Stable Electrocatalysts for the Oxygen Reduction Reaction. Journal of Physical Chemistry C, 2016, 120, 24265-24270.	1.5	17
27097	Chemical Trends of Electronic Properties of Two-Dimensional Halide Perovskites and Their Potential Applications for Electronics and Optoelectronics. Journal of Physical Chemistry C, 2016, 120, 24682-24687.	1.5	41
27098	Unusual Multiferroic Phase Transitions in PbTiO₃ Nanowires. Nano Letters, 2016, 16, 6774-6779.	4.5	11
27099	Ferroelectricity in Covalently functionalized Two-dimensional Materials: Integration of High-mobility Semiconductors and Nonvolatile Memory. Nano Letters, 2016, 16, 7309-7315.	4.5	99
27100	Homologous Compounds ZnnIn2O3+n (n = 4, 5, and 7) Containing Laminated Functional Groups as Efficient Photocatalysts for Hydrogen Production. ACS Applied Materials & Interfaces, 2016, 8, 28700-28708.	4.0	24
27101	Revisiting the zero-temperature phase diagram of stoichiometric SrCoO₃ with first-principles methods. Physical Chemistry Chemical Physics, 2016, 18, 30686-30695.	1.3	14
27102	A copper-based sorbent with oxygen-vacancy defects from mechanochemical reduction for carbon disulfide absorption. Journal of Materials Chemistry A, 2016, 4, 17207-17214.	5.2	18
27103	Super-oxidation of silicon nanoclusters: magnetism and reactive oxygen species at the surface. Nanoscale, 2016, 8, 18616-18620.	2.8	13
27104	Breaking the icosahedra in boron carbide. Proceedings of the National Academy of Sciences of the United States of America, 2016, 113, 12012-12016.	3.3	31
27105	First-principles investigation of the effects of Sb doping on the LiNiO2. Journal of Solid State Chemistry, 2016, 244, 52-60.	1.4	18
27106	Unusual onset of p-element magnetization in a two dimensional structure. Solid State Sciences, 2016, 60, 55-58.	1.5	3
27107	Highly doped and exposed Cu(<scp>i</scp>)â€“N active sites within graphene towards efficient oxygen reduction for zincâ€“air batteries. Energy and Environmental Science, 2016, 9, 3736-3745.	15.6	374
27108	Catalyst and Process Design for the Continuous Manufacture of Rare Sugar Alcohols by Epimerizationâ€“Hydrogenation of Aldoses. ChemSusChem, 2016, 9, 3407-3418.	3.6	23
27109	Optical Identification of Topological Defect Types in Monolayer Arsenene by First-Principles Calculation. Journal of Physical Chemistry C, 2016, 120, 24917-24924.	1.5	24
27110	Can Pb-Free Halide Double Perovskites Support High-Efficiency Solar Cells?. ACS Energy Letters, 2016, 1, 949-955.	8.8	404

#	Article	IF	Citations
27111	Ab Initio Prediction of Adsorption Isotherms for Small Molecules in Metalâ€“Organic Frameworks. Journal of the American Chemical Society, 2016, 138, 14047-14056.	6.6	62
27112	Nickelâ€“vanadium monolayer double hydroxide for efficient electrochemical water oxidation. Nature Communications, 2016, 7, 11981.	5.8	808
27113	Metal-free photochemical silylations and transfer hydrogenations of benzenoid hydrocarbons and graphene. Nature Communications, 2016, 7, 12962.	5.8	58
27114	Multicolour synthesis in lanthanide-doped nanocrystals through cation exchange in water. Nature Communications, 2016, 7, 13059.	5.8	164
27115	Activity origin and catalyst design principles forÂelectrocatalytic hydrogen evolution on heteroatom-dopedÂgraphene. Nature Energy, 2016, 1, .	19.8	927
27116	Gold-supported cerium-doped NiOx catalysts for water oxidation. Nature Energy, 2016, 1, .	19.8	458
27117	Electronic structure and electron-phonon coupling in TiH2. Scientific Reports, 2016, 6, 28102.	1.6	21
27118	Distribution and self-assisted diffusion of Be and Mg impurities in ZnO. Physical Chemistry Chemical Physics, 2016, 18, 19631-19636.	1.3	5
27119	Atomic layer deposition of diisopropylaminosilane on WO3(001) and W(110): a density functional theory study. Physical Chemistry Chemical Physics, 2016, 18, 29139-29146.	1.3	3
27120	Fe doped LaGaO₃: good white light emitters. RSC Advances, 2016, 6, 100230-100238.	1.7	35
27121	Pressure-structure relationships in the 10â€‰K layered carbide halide superconductor Y₂C₂I₂. Journal of Physics Condensed Matter, 2016, 28, 375703.	0.7	2
27122	Strong anisotropic thermal conductivity of monolayer WTe ₂. 2D Materials, 2016, 3, 045010.	2.0	42
27123	Effect of spin-orbit and on-site Coulomb interactions on the electronic structure and lattice dynamics of uranium monocarbide. Physical Review B, 2016, 94, .	1.1	18
27124	Electron and phonon transport in shandite-structured <mml:math xmlns:mml="http://www.w3.org/1998/Math/MathML"><mml:mrow><mml:msub><mml:mi mathvariant="bold">Ni</mml:mi><mml:mn>3</mml:mn></mml:msub><mml:msub><mml:mi mathvariant="bold">Sn</mml:mi><mml:mn>2</mml:mn></mml:msub><mml:msub><mml:mi mathvariant="bold">S</mml:mi><mml:mn>2</mml:mn></mml:msub></mml:mrow></mml:math>. Physical Review B, 2016, 94, .	1.1	12
27125	Tunable Electronic Structures in Wrinkled 2D Transitionâ€Metalâ€Trichalcogenide (TMT) HfTe₃ Films. Advanced Electronic Materials, 2016, 2, 1600324.	2.6	9
27126	Ensemble-Average Representation of Pt Clusters in Conditions of Catalysis Accessed through GPU Accelerated Deep Neural Network Fitting Global Optimization. Journal of Chemical Theory and Computation, 2016, 12, 6213-6226.	2.3	106
27127	Photo-induced magnetization and first-principles calculations of a two-dimensional cyanide-bridged Coâ€“W bimetal assembly. Dalton Transactions, 2016, 45, 19249-19256.	1.6	14
27128	Proposing the prospects of Ti₃CN transition metal carbides (MXenes) as anodes of Li-ion batteries: a DFT study. Physical Chemistry Chemical Physics, 2016, 18, 32937-32943.	1.3	105

#	Article	IF	Citations
27129	Experimental and theoretical studies on a novel helical architecture driven by hydrogen and halogen bonding interactions. Journal of Chemical Sciences, 2016, 128, 1895-1904.	0.7	1
27130	Catalysis on solid acids: Mechanism and catalyst descriptors in oligomerization reactions of light alkenes. Journal of Catalysis, 2016, 344, 553-569.	3.1	80
27131	Effects of electron transfer in model catalysts composed of Pt nanoparticles on CeO2(1 1 1) surface. Journal of Catalysis, 2016, 344, 507-514.	3.1	41
27132	Modulating Carrier Density and Transport Properties of MoS₂ by Organic Molecular Doping and Defect Engineering. Chemistry of Materials, 2016, 28, 8611-8621.	3.2	105
27133	Thermodynamics of an Electrocyclic Ring-Closure Reaction on Au(111). Journal of Physical Chemistry C, 2016, 120, 21716-21721.	1.5	23
27134	Coexistence of Superconductivity and Superhardness in Beryllium Hexaboride Driven by Inherent Multicenter Bonding. Journal of Physical Chemistry Letters, 2016, 7, 4898-4904.	2.1	16
27135	Auxetic and Ferroelastic Borophane: A Novel 2D Material with Negative Possionâ€™s Ratio and Switchable Dirac Transport Channels. Nano Letters, 2016, 16, 7910-7914.	4.5	176
27136	Structure and Growth of Hexagonal Boron Nitride on Ir(111). ACS Nano, 2016, 10, 11012-11026.	7.3	93
27137	Carbon incorporation effects and reaction mechanism of FeOCl cathode materials for chloride ion batteries. Scientific Reports, 2016, 6, 19448.	1.6	43
27138	Intrinsic and Extrinsic Charge Transport in CH3NH3PbI3 Perovskites Predicted from First-Principles. Scientific Reports, 2016, 6, 19968.	1.6	119
27139	Giant electric-field-induced strain in lead-free piezoelectric materials. Scientific Reports, 2016, 6, 25346.	1.6	6
27140	Diverse Chemistry of Stable Hydronitrogens, and Implications for Planetary and Materials Sciences. Scientific Reports, 2016, 6, 25947.	1.6	27
27141	3d Transition Metal Adsorption Induced the valley-polarized Anomalous Hall Effect in Germanene. Scientific Reports, 2016, 6, 27830.	1.6	10
27142	Forming heterojunction: an effective strategy to enhance the photocatalytic efficiency of a new metal-free organic photocatalyst for water splitting. Scientific Reports, 2016, 6, 29327.	1.6	24
27143	Electronic structure of organometal halide perovskite CH3NH3BiI3 and optical absorption extending to infrared region. Scientific Reports, 2016, 6, 37425.	1.6	29
27144	An atomically thin layer of Ru/MoS2heterostructure: structural, electronic, and magnetic properties. Physical Chemistry Chemical Physics, 2016, 18, 32528-32533.	1.3	10
27145	Self-assembled monolayer structures of hexadecylamine on Cu surfaces: density-functional theory. Physical Chemistry Chemical Physics, 2016, 18, 32753-32761.	1.3	31
27146	Assessing exchange-correlation functional performance for structure and property predictions of oxyfluoride compounds from first principles. Physical Review B, 2016, 94, .	1.1	27

#	Article	IF	Citations
27147	Spin texture in type-II Weyl semimetal <mml:math xmlns:mml="http://www.w3.org/1998/Math/MathML"><mml:msub><mml:mi>WTe</mml:mi><mml:mn>2</mml:mn></mml:msub></mml:math> Physical Review B, 2016, 94, .	1.1	138
27148	Substrate-supported large-band-gap quantum spin Hall insulator based on III-V bismuth layers. Physical Review B, 2016, 94, .	1.1	4
27149	Strong spin-orbit splitting and magnetism of point defect states in monolayer <mml:math xmlns:mml="http://www.w3.org/1998/Math/MathML"><mml:msub><mml:mi>WS</mml:mi><mml:mn>2</mml:mn></mml:msub></mml:math> Physical Review B, 2016, 94, .	1.1	70
27150	The thermodynamic scale of inorganic crystalline metastability. Science Advances, 2016, 2, e1600225.	4.7	565
27151	Calculation of the electronic structure, lattice dynamics, and optical and magnetic properties of europium tetraborate EuB4O7. Physics of the Solid State, 2016, 58, 2300-2306.	0.2	1
27152	Activity coefficient and solubility of yttrium in Fe-Y dilute solid solution. Journal of Rare Earths, 2016, 34, 1168-1172.	2.5	14
27153	Relationship between acidity and catalytic reactivity of faujasite zeolite: A periodic DFT study. Journal of Catalysis, 2016, 344, 570-577.	3.1	72
27154	Elucidating Structureâ€“Compositionâ€“Property Relationships of the Î²-SiAlON:Eu²⁺ Phosphor. Chemistry of Materials, 2016, 28, 8622-8630.	3.2	50
27155	Construction of Electron Transfer Network by Self-Assembly of Self-n-Doped Fullerene Ammonium Iodide. Chemistry of Materials, 2016, 28, 8726-8731.	3.2	18
27156	Spinâ€“Lattice Coupling in [Ni(HF₂)(pyrazine)₂]SbF₆ Involving the HF₂^{â€“} Superexchange Pathway. Inorganic Chemistry, 2016, 55, 12172-12178.	1.9	7
27157	Design of Dipole-Allowed Direct Band Gaps in Ge/Sn Coreâ€“Shell Nanowires. Journal of Physical Chemistry C, 2016, 120, 28169-28175.	1.5	1
27158	Superconductivity in topologically nontrivial material Au2Pb. Npj Quantum Materials, 2016, 1, .	1.8	52
27159	Growth and Stress-induced Transformation of Zinc blende AlN Layers in Al-AlN-TiN Multilayers. Scientific Reports, 2016, 5, 18554.	1.6	25
27160	Spatial Electron-hole Separation in a One Dimensional Hybrid Organicâ€“Inorganic Lead Iodide. Scientific Reports, 2016, 6, 20626.	1.6	25
27161	Functionalized Thallium Antimony Films as Excellent Candidates for Large-Gap Quantum Spin Hall Insulator. Scientific Reports, 2016, 6, 21351.	1.6	27
27162	Prediction of Quantum Anomalous Hall Insulator in half-fluorinated GaBi Honeycomb. Scientific Reports, 2016, 6, 31317.	1.6	12
27163	Phosphorus K4 Crystal: A New Stable Allotrope. Scientific Reports, 2016, 6, 37528.	1.6	13
27164	Enlightening the ultrahigh electrical conductivities of doped double-wall carbon nanotube fibers by Raman spectroscopy and first-principles calculations. Nanoscale, 2016, 8, 19668-19676.	2.8	18

#	Article	IF	Citations
27165	Lattice dynamics of a quasi-2D layered TlCo2Se2 with a helical magnetic structure. RSC Advances, 2016, 6, 79121-79127.	1.7	2
27166	A novel p-type half-Heusler from high-throughput transport and defect calculations. Journal of Materials Chemistry C, 2016, 4, 11261-11268.	2.7	64
27167	Density functional theory study of bulk and single-layer magnetic semiconductor <mml:math xmlns:mml="http://www.w3.org/1998/Math/MathML"><mml:msub><mml:mi>CrPS</mml:mi><mml:mn>4</mml:mn></mml:msub></mml:mr Physical Review B, 2016, 94, .	3.1	53
27168	Electronic structure, lattice dynamics, and magnetoelectric properties of double perovskite La2CuTiO6. Physics of the Solid State, 2016, 58, 2294-2299.	0.2	9
27169	A many-electron perturbation theory study of the hexagonal boron nitride bilayer system*. European Physical Journal B, 2016, 89, 1.	0.6	11
27170	Self-healing in B₁₂P₂ through Mediated Defect Recombination. Chemistry of Materials, 2016, 28, 8415-8428.	3.2	9
27171	Local Structural Investigations, Defect Formation, and Ionic Conductivity of the Lithium Ionic Conductor Li₄P₂S₆. Chemistry of Materials, 2016, 28, 8764-8773.	3.2	111
27172	Adsorption of Methyl Acetoacetate at Ni{111}: Experiment and Theory. Journal of Physical Chemistry C, 2016, 120, 27490-27499.	1.5	17
27173	Structure and Failure Mechanism of the Thermoelectric CoSb₃/TiCoSb Interface. ACS Applied Materials & Interfaces, 2016, 8, 31968-31977.	4.0	13
27174	Biomass-Derived Porous Fe₃C/Tungsten Carbide/Graphitic Carbon Nanocomposite for Efficient Electrocatalysis of Oxygen Reduction. ACS Applied Materials & Interfaces, 2016, 8, 32307-32316.	4.0	88
27175	Performance of DFT+UApproaches in the Study of Catalytic Materials. ACS Catalysis, 2016, 6, 8370-8379.	5.5	135
27176	Facet Energy versus Enzyme-like Activities: The Unexpected Protection of Palladium Nanocrystals against Oxidative Damage. ACS Nano, 2016, 10, 10436-10445.	7.3	247
27177	Design and synthesis of the superionic conductor Na10SnP2S12. Nature Communications, 2016, 7, 11009.	5.8	246
27178	Oscillating edge states in one-dimensional MoS2 nanowires. Nature Communications, 2016, 7, 12904.	5.8	57
27179	Atomic and electronic structure of twin growth defects in magnetite. Scientific Reports, 2016, 6, 20943.	1.6	15
27180	Superconductivity of novel tin hydrides (SnnHm) under pressure. Scientific Reports, 2016, 6, 22873.	1.6	39
27181	Sn/Be Sequentially co-doped Hematite Photoanodes for Enhanced Photoelectrochemical Water Oxidation: Effect of Be2+ as co-dopant. Scientific Reports, 2016, 6, 23183.	1.6	75
27182	A new class of large band gap quantum spin hall insulators: 2D fluorinated group-IV binary compounds. Scientific Reports, 2016, 6, 26123.	1.6	17

#	Article	IF	Citations
27183	Bonding-restricted structure search for novel 2D materials with dispersed C2 dimers. Scientific Reports, 2016, 6, 29531.	1.6	14
27184	Interplay between surface and surface resonance states on height selective stability of fcc Dy(111) film at nanoscale. Physical Chemistry Chemical Physics, 2016, 18, 31238-31243.	1.3	2
27185	Proposed two-dimensional topological insulator in SiTe. Physical Review B, 2016, 94, .	1.1	45
27186	Lattice Vibrations Change the Solid Solubility of an Alloy at High Temperatures. Physical Review Letters, 2016, 117, 205502.	2.9	60
27187	Effect of Strain on the Physical Properties of Lanthanum Nickelate. , 0, , 247-252.		0
27188	Ab Initio Surface Phase Diagrams for Coadsorption of Aromatics and Hydrogen on the Pt(111) Surface. Journal of Physical Chemistry C, 2016, 120, 26249-26258.	1.5	22
27189	First-Principles Prediction of Two-Dimensional Electron Gas Driven by Polarization Discontinuity in Nonpolar/Nonpolar AHfO₃/SrTiO₃ (A = Ca, Sr, and Ba) Heterostructures. ACS Applied Materials & Interfaces, 2016, 8, 31959-31967.	4.0	24
27190	Quinary wurtzite Zn-Ga-Ge-N-O solid solutions and their photocatalytic properties under visible light irradiation. Scientific Reports, 2016, 6, 19060.	1.6	24
27191	A first-principles study on the phonon transport in layered BiCuOSe. Scientific Reports, 2016, 6, 21035.	1.6	52
27192	Theoretical perspective of energy harvesting properties of atomically thin BiI₃. Journal of Materials Chemistry A, 2016, 4, 19086-19094.	5.2	47
27193	<mml:math xmlns:mml="http://www.w3.org/1998/Math/MathML"><mml:msub><mml:mi mathvariant="normal">Ru</mml:mi><mml:mn>2</mml:mn></mml:msub><mml:mtext>NbGa</mml:mtext></mml:math> : A Heusler-type compound with semimetallic characteristics. Physical Review B, 2016, 94, .	n/a	18
27194	Paracrystalline Disorder from Phosphate Ion Orientation and Substitution in Synthetic Bone Mineral. Inorganic Chemistry, 2016, 55, 12290-12298.	1.9	17
27195	Solvent-Based Atomistic Theory for Doping Colloidal-Synthesized Quantum Dots via Cation Exchange. Journal of Physical Chemistry C, 2016, 120, 27085-27090.	1.5	6
27196	Superstrength through Nanotwinning. Nano Letters, 2016, 16, 7573-7579.	4.5	62
27197	Formation of Silicene Nanosheets on Graphite. ACS Nano, 2016, 10, 11163-11171.	7.3	84
27198	Interfacial control of oxygen vacancy doping and electrical conduction in thin film oxide heterostructures. Nature Communications, 2016, 7, 11892.	5.8	77
27199	Sub-molecular modulation of a 4f driven Kondo resonance by surface-induced asymmetry. Nature Communications, 2016, 7, 12785.	5.8	32
27200	How far away are iron carbide clusters from the bulk?. Physical Chemistry Chemical Physics, 2016, 18, 32944-32951.	1.3	12

#	Article	IF	Citations
27201	The electronic structure and spin states of 2D graphene/VX₂ (X = S, Se) heterostructures. Physical Chemistry Chemical Physics, 2016, 18, 33047-33052.	1.3	49
27202	Chemical vapor deposition-prepared sub-nanometer Zr clusters on Pd surfaces: promotion of methane dry reforming. Physical Chemistry Chemical Physics, 2016, 18, 31586-31599.	1.3	15
27203	Archimedean (4,8)-tessellation of haeckelite ultrathin nanosheets composed of boron and aluminum-group V binary materials. Nanoscale, 2016, 8, 19287-19301.	2.8	12
27204	Electron spin-polarization and spin-gapless states in an oxidized carbon nitride monolayer. RSC Advances, 2016, 6, 108280-108285.	1.7	0
27205	Stabilizing polysulfide-shuttle in a Liâ€“S battery using transition metal carbide nanostructures. RSC Advances, 2016, 6, 110301-110306.	1.7	40
27206	Magnetoelectric coupling in the type-I multiferroic ScFeO3. Physical Review B, 2016, 94, .	1.1	13
27207	Stability of single-layer and multilayer arsenene and their mechanical and electronic properties. Physical Review B, 2016, 94, .	1.1	93
27208	Optical properties of single-layer and bilayer arsenene phases. Physical Review B, 2016, 94, .	1.1	67
27209	Changes in work function due to <mml:math xmlns:mml="http://www.w3.org/1998/Math/MathML"><mml:msub><mml:mi>NO</mml:mi><mml:mn>2</mml:mn></mml:msub></mml adsorption on monolayer and bilayer epitaxial graphene on SiC(0001). Physical Review B, 2016, 94, .	1.1	16
27210	Electrochemical Stability of Magnesium Surfaces in an Aqueous Environment. Journal of Physical Chemistry C, 2016, 120, 26922-26933.	1.5	55
27211	The effect of oxygen vacancies on water wettability of transition metal based SrTiO₃ and rare-earth based Lu₂O₃. RSC Advances, 2016, 6, 109234-109240.	1.7	40
27212	Electron and magnetic properties of three-dimensional magnetic topological insulators Bi ₂ Se ₃ :Cr and Bi ₂ Se ₃ :Fe. Europhysics Letters, 2016, 115, 67004.	0.7	3
27213	Changing the chirality of single-wall carbon nanotubes during epitaxial growth : A density functional theory study. New Carbon Materials, 2016, 31, 525-531.	2.9	2
27214	Dynamic Processes of Formaldehyde at Terminal Ti Sites on the Rutile TiO₂(110) Surface. Journal of Physical Chemistry C, 2016, 120, 24287-24293.	1.5	16
27215	Modification of Charge Trapping at Particle/Particle Interfaces by Electrochemical Hydrogen Doping of Nanocrystalline TiO₂. Journal of the American Chemical Society, 2016, 138, 15956-15964.	6.6	45
27216	Spectral descriptors for bulk metallic glasses based on the thermodynamics of competing crystalline phases. Nature Communications, 2016, 7, 12315.	5.8	104
27217	Evolution of crystal and electronic structures of magnesium dicarbide at high pressure. Scientific Reports, 2016, 5, 17815.	1.6	11
27218	Prediction of novel stable compounds in the Mg-Si-O system under exoplanet pressures. Scientific Reports, 2016, 5, 18347.	1.6	43

#	Article	IF	Citations
27219	Atomic structures of a liquid-phase bonded metal/nitride heterointerface. Scientific Reports, 2016, 6, 22936.	1.6	20
27220	Mechanical properties and current-carrying capacity of Al reinforced with graphene/BN nanoribbons: a computational study. Nanoscale, 2016, 8, 20080-20089.	2.8	19
27221	Superhard BC ₂ N: an Orthogonal Crystal Obtained by Transversely Compressing (3,0)-CNTs and (3,0)-BNNTs. Chinese Physics Letters, 2016, 33, 106102.	1.3	8
27222	Giant perpendicular magnetic anisotropy energies in CoPt thin films: impact of reduced dimensionality and imperfections. Journal of Physics Condensed Matter, 2016, 28, 496002.	0.7	3
27223	Assessing the influence of van der Waals corrected exchange-correlation functionals on the anisotropic mechanical properties of coinage metals. Physical Review B, 2016, 94, .	1.1	19
27224	Structural and magnetic properties of Fe7â^'n Pt n with n = 0, 1, 2, . . . 7, bimetallic clusters. Journal of Nanoparticle Research, 2016, 18, 1.	0.8	2
27225	Structural stability and electronic properties of multi-functionalized two-dimensional chromium carbides. Thin Solid Films, 2016, 619, 131-136.	0.8	33
27226	Ultrafast Polarization Switching in a Biaxial Molecular Ferroelectric Thin Film: [Hdabco]ClO₄. Journal of the American Chemical Society, 2016, 138, 15784-15789.	6.6	107
27227	Switchable electric polarization and ferroelectric domains in a metal-organic-framework. Npj Quantum Materials, 2016, 1, .	1.8	103
27228	Suppression of radiation-induced point defects by rhenium and osmium interstitials in tungsten. Scientific Reports, 2016, 6, 36738.	1.6	28
27229	An anomalous interlayer exciton in MoS2. Scientific Reports, 2016, 6, 37075.	1.6	11
27230	Two-dimensional van der Waals nanocomposites as Z-scheme type photocatalysts for hydrogen production from overall water splitting. Journal of Materials Chemistry A, 2016, 4, 18892-18898.	5.2	108
27231	Doping of <mml:math xmlns:mml="http://www.w3.org/1998/Math/MathML"><mml:mrow><mml:msub><mml:mi>Ga</mml:mi><mml:mn>2</mml:mn></mml: mathvariant="normal">O</mml:mi><mml:mn>3</mml:mn></mml:msub></mml:mrow></mml:math> with transition metals. Physical Review B, 2016, 94, .	1.1	61
27232	Contradictory nature of Co doping in ferroelectricBaTiO3. Physical Review B, 2016, 94, .	1.1	8
27233	Structural, electronic and optical properties of the Zn0.5V0.5S in three phases. Modern Physics Letters B, 2016, 30, 1650356.	1.0	0
27236	Cesium Platinide Hydride 4Cs2Ptâ‹…CsH: An Intermetallic Double Salt Featuring Metal Anions. Angewandte Chemie - International Edition, 2016, 55, 14838-14841.	7.2	14
27237	Ideal shear strength and deformation behaviours of L10 TiAl from first-principles calculations. Bulletin of Materials Science, 2016, 39, 1411-1418.	0.8	2
27238	Interface electronic structure and Schottky-barrier height in Si/NiSi(010) and Si/PtSi(010) heterostructures: A first-principles theoretical study. Superlattices and Microstructures, 2016, 100, 808-817.	1.4	2

#	Article	IF	Citations
27239	Spin-Dependent Transport through Chiral Molecules Studied by Spin-Dependent Electrochemistry. Accounts of Chemical Research, 2016, 49, 2560-2568.	7.6	129
27240	Facile Preparation of Single MoS₂ Atomic Crystals with Highly Tunable Photoluminescence by Morphology and Atomic Structure. Crystal Growth and Design, 2016, 16, 7094-7101.	1.4	8
27241	Interaction of Black Phosphorus with Oxygen and Water. Chemistry of Materials, 2016, 28, 8330-8339.	3.2	436
27242	Defect and Substitution-Induced Silicene Sensor to Probe Toxic Gases. Journal of Physical Chemistry C, 2016, 120, 25256-25262.	1.5	81
27243	Unexpected Trend in Stability of Xeâ€“F Compounds under Pressure Driven by Xeâ€“Xe Covalent Bonds. Journal of Physical Chemistry Letters, 2016, 7, 4562-4567.	2.1	41
27244	Low-Temperature Methane Combustion over Pd/H-ZSM-5: Active Pd Sites with Specific Electronic Properties Modulated by Acidic Sites of H-ZSM-5. ACS Catalysis, 2016, 6, 8127-8139.	5.5	212
27245	Noncovalent Bonding Controls Selectivity in Heterogeneous Catalysis: Coupling Reactions on Gold. Journal of the American Chemical Society, 2016, 138, 15243-15250.	6.6	43
27246	Operando NMR spectroscopic analysis of proton transfer in heterogeneous photocatalytic reactions. Nature Communications, 2016, 7, 11918.	5.8	49
27247	Unusual lattice vibration characteristics in whiskers of the pseudo-one-dimensional titanium trisulfide TiS3. Nature Communications, 2016, 7, 12952.	5.8	69
27248	Surface energies of elemental crystals. Scientific Data, 2016, 3, 160080.	2.4	583
27249	Strong orbital interaction in a weak CH-Ï€ hydrogen bonding system. Scientific Reports, 2016, 6, 22304.	1.6	19
27250	Phononic Structure Engineering: the Realization of Einstein Rattling in Calcium Cobaltate for the Suppression of Thermal Conductivity. Scientific Reports, 2016, 6, 30530.	1.6	1
27251	Penta-BxNy sheet: a density functional theory study of two-dimensional material. Scientific Reports, 2016, 6, 31840.	1.6	65
27252	Heptagraphene: Tunable Dirac Cones in a Graphitic Structure. Scientific Reports, 2016, 6, 33220.	1.6	3
27253	Structures, Phase Transitions and Tricritical Behavior of the Hybrid Perovskite Methyl Ammonium Lead Iodide. Scientific Reports, 2016, 6, 35685.	1.6	440
27254	Unravelling the fundamentals of thermal and chemical expansion of BaCeO₃ from first principles phonon calculations. Physical Chemistry Chemical Physics, 2016, 18, 31296-31303.	1.3	14
27255	A computational study on the superionic behaviour of ThO₂. Physical Chemistry Chemical Physics, 2016, 18, 31494-31504.	1.3	17
27256	Predicted low thermal conductivities in antimony films and the role of chemical functionalization. Physical Chemistry Chemical Physics, 2016, 18, 30061-30067.	1.3	25

#	Article	IF	Citations
27257	Mechanisms of H- and OH-assisted CO activation as well as Câ€“C coupling on the flat Co(0001) surface â€“ revisited. Catalysis Science and Technology, 2016, 6, 8336-8343.	2.1	18
27258	Enhanced coking tolerance of a MgO-modified Ni cermet anode for hydrocarbon fueled solid oxide fuel cells. Journal of Materials Chemistry A, 2016, 4, 18031-18036.	5.2	45
27259	Adsorption and diffusion of Li with S on pristine and defected graphene. Physical Chemistry Chemical Physics, 2016, 18, 31268-31276.	1.3	9
27260	Voltage-gated spin-filtering properties and global minimum of planar MnB₆, and half-metallicity and room-temperature ferromagnetism of its oxide sheet. Journal of Materials Chemistry C, 2016, 4, 10866-10875.	2.7	26
27261	Controlling magnetic interfaces using ordered surface alloys. Physical Review B, 2016, 94, .	1.1	1
27262	Anomalous bulk modulus in vanadate spinels. Physical Review B, 2016, 94, .	1.1	9
27263	Disorder effect on the anisotropic resistivity of phosphorene determined by a tight-binding model. Physical Review B, 2016, 94, .	1.1	20
27264	Oxygen vacancy induced surface stabilization: (110) terminated magnetite. Physical Review B, 2016, 94, .	1.1	12
27265	Performance study of strained IIIâ€“V materials for ultra-thin body transistor applications. , 2016, , .		3
27266	NEMO5: Predicting MoS<inf>2</inf> heterojunctions. , 2016, , .		1
27267	Ab initio study of magnetic properties in the adsorption of transition-metal atoms on arsenene. JETP Letters, 2016, 104, 557-562.	0.4	11
27268	Investigating Robust Honeycomb Borophenes Sandwiching Manganese Layers in Manganese Diboride. Inorganic Chemistry, 2016, 55, 11140-11146.	1.9	31
27269	Enigmatic HCl + Au(111) Reaction: A Puzzle for Theory and Experiment. Journal of Physical Chemistry C, 2016, 120, 25760-25779.	1.5	48
27270	Realistic Surface Descriptions of Heterometallic Interfaces: The Case of TiWC Coated in Noble Metals. Journal of Physical Chemistry Letters, 2016, 7, 4475-4482.	2.1	24
27271	Layer-dependent quantum cooperation of electron and hole states in the anomalous semimetal WTe2. Nature Communications, 2016, 7, 10847.	5.8	96
27272	Engineering electrocatalytic activity in nanosized perovskite cobaltite through surface spin-state transition. Nature Communications, 2016, 7, 11510.	5.8	316
27273	Water-mediated cation intercalation of open-framework indium hexacyanoferrate with high voltage and fast kinetics. Nature Communications, 2016, 7, 11982.	5.8	90
27274	Non-equilibrium processing leads to record high thermoelectric figure of merit in PbTeâ€“SrTe. Nature Communications, 2016, 7, 12167.	5.8	498

#	Article	IF	Citations
27275	Enhanced hydrogenation activity and diastereomeric interactions of methyl pyruvate co-adsorbed with R-1-(1-naphthyl)ethylamine on Pd(111). Nature Communications, 2016, 7, 12380.	5.8	33
27276	Free-electron creation at the 60Â° twin boundary in Bi2Te3. Nature Communications, 2016, 7, 12449.	5.8	59
27277	Self-assembly of acetate adsorbates drives atomic rearrangement on the Au(110) surface. Nature Communications, 2016, 7, 13139.	5.8	23
27278	Protecting the properties of monolayer MoS2 on silicon based substrates with an atomically thin buffer. Scientific Reports, 2016, 6, 20890.	1.6	64
27279	Structural and electronic properties of epitaxial multilayer h-BN on Ni(111) for spintronics applications. Scientific Reports, 2016, 6, 23547.	1.6	80
27280	Electronic origins of photocatalytic activity in d0 metal organic frameworks. Scientific Reports, 2016, 6, 23676.	1.6	196
27281	Charge storage in oxygen deficient phases of TiO2: defect Physics without defects. Scientific Reports, 2016, 6, 28871.	1.6	48
27282	Role of vacancies, light elements and rare-earth metals doping in CeO2. Scientific Reports, 2016, 6, 31345.	1.6	40
27283	Anomalous Enhancement of Mechanical Properties in the Ammonia Adsorbed Defective Graphene. Scientific Reports, 2016, 6, 33810.	1.6	3
27284	Gas Protection of Two-Dimensional Nanomaterials from High-Energy Impacts. Scientific Reports, 2016, 6, 35532.	1.6	52
27285	Reactivity at the Cu₂O(100):Cuâ€“H₂O interface: a combined DFT and PES study. Physical Chemistry Chemical Physics, 2016, 18, 30570-30584.	1.3	21
27286	Investigation of helium at a Y₂Ti₂O₇ nanocluster embedded in a BCC Fe matrix. Physical Chemistry Chemical Physics, 2016, 18, 30128-30134.	1.3	6
27287	Epitaxial nucleation of CVD bilayer graphene on copper. Nanoscale, 2016, 8, 20001-20007.	2.8	8
27288	The polarization-dependent anisotropic Raman response of few-layer and bulk WTe₂under different excitation wavelengths. RSC Advances, 2016, 6, 103830-103837.	1.7	28
27289	Understanding the electrochemical properties of A₂MSiO₄ (A = Li and Na; M =) Tj ETQq0 0 0 rgBT /Overlock 1 calculations. Journal of Materials Chemistry A, 2016, 4, 17455-17463.	5.2	35
27290	Comprehensive structureâ€“function correlation of photoactive ionic Ï€-conjugated supermolecular assemblies: an experimental and computational study. Journal of Materials Chemistry C, 2016, 4, 10223-10239.	2.7	32
27291	Metastable cobalt nitride structures with high magnetic anisotropy for rare-earth free magnets. Physical Chemistry Chemical Physics, 2016, 18, 31680-31690.	1.3	28
27292	One-dimensional nanowires of pseudoboehmite (aluminum oxyhydroxide Î³-AlOOH). Proceedings of the National Academy of Sciences of the United States of America, 2016, 113, 11759-11764.	3.3	24

#	Article	IF	Citations
27293	Ab initio investigation of the anomalous phonon softening in FeSi. Physical Review B, 2016, 94, .	1.1	10
27294	Comparative study of phonon spectrum and thermal expansion of graphene, silicene, germanene, and blue phosphorene. Physical Review B, 2016, 94, .	1.1	80
27295	Resonant bonding driven giant phonon anharmonicity and low thermal conductivity of phosphorene. Physical Review B, 2016, 94, .	1.1	114
27296	Versatile van der Waals Density Functional Based on a Meta-Generalized Gradient Approximation. Physical Review X, 2016, 6, .	2.8	321
27297	Edge-selenated graphene nanoplatelets as durable metal-free catalysts for iodine reduction reaction in dye-sensitized solar cells. Science Advances, 2016, 2, e1501459.	4.7	88
27298	Van der Waals metal-semiconductor junction: Weak Fermi level pinning enables effective tuning of Schottky barrier. Science Advances, 2016, 2, e1600069.	4.7	446
27299	Plasmachemical and heterogeneous processes in ozonizers with oxygen activation by a dielectric barrier discharge. Plasma Physics Reports, 2016, 42, 956-969.	0.3	7
27300	Counterintuitive Reconstruction of the Polar O-Terminated ZnO Surface with Zinc Vacancies and Hydrogen. Journal of Physical Chemistry Letters, 2016, 7, 4483-4487.	2.1	19
27301	Salt concentration effects on mechanical properties of LiPF6/poly(propylene glycol) diacrylate solid electrolyte: Insights from reactive molecular dynamics simulations. Electrochimica Acta, 2016, 221, 115-123.	2.6	10
27302	Effects of Lattice Motion on Dissociative Chemisorption: Toward a Rigorous Comparison of Theory with Molecular Beam Experiments. Journal of Physical Chemistry Letters, 2016, 7, 4576-4584.	2.1	74
27303	Room-Temperature Activation of Methane and Dry Re-forming with CO₂ on Ni-CeO₂(111) Surfaces: Effect of Ce³⁺ Sites and Metalâ€“Support Interactions on Câ€“H Bond Cleavage. ACS Catalysis, 2016, 6, 8184-8191.	5.5	146
27304	Large elasto-optic effect and reversible electrochromism in multiferroic BiFeO3. Nature Communications, 2016, 7, 10718.	5.8	88
27305	Nucleation of amorphous shear bands at nanotwins in boron suboxide. Nature Communications, 2016, 7, 11001.	5.8	43
27306	Stacking orders induced direct band gap in bilayer MoSe2-WSe2 lateral heterostructures. Scientific Reports, 2016, 6, 31122.	1.6	39
27307	Electronic structures and enhanced optical properties of blue phosphorene/transition metal dichalcogenides van der Waals heterostructures. Scientific Reports, 2016, 6, 31994.	1.6	192
27308	Plasticity mechanisms in HfN at elevated and room temperature. Scientific Reports, 2016, 6, 34571.	1.6	7
27309	High-mobility two-dimensional electron gas in SrGeO₃- and BaSnO₃-based perovskite oxide heterostructures: an ab initio study. Physical Chemistry Chemical Physics, 2016, 18, 31924-31929.	1.3	29
27310	Technetium incorporation in scheelite: insights from first-principles. Dalton Transactions, 2016, 45, 18171-18176.	1.6	8

#	Article	IF	Citations
27311	Fabrication of nanocrystalline Î»-Ti₃O₅with tunable terahertz wave transmission properties across a temperature induced phase transition. Journal of Materials Chemistry C, 2016, 4, 10279-10285.	2.7	24
27312	On the Functionality of Complex Intermetallics: Frustration, Chemical Pressure Relief, and Potential Rattling Atoms in Y₁₁Ni₆₀C₆. Inorganic Chemistry, 2016, 55, 10397-10405.	1.9	14
27313	Hydration Structures of MgO, CaO, and SrO (001) Surfaces. Journal of Physical Chemistry C, 2016, 120, 24762-24769.	1.5	21
27314	Effect of Tin Coverage on Selectivity for Ethane Dehydrogenation over Platinumâ€“Tin Alloys. Journal of Physical Chemistry C, 2016, 120, 27307-27318.	1.5	50
27315	Three-Dimensional Covalently Linked Allotropic Structures of Phosphorus. Journal of Physical Chemistry C, 2016, 120, 26453-26458.	1.5	7
27316	Theoretical Insights into the Effects of Oxidation and Mo-Doping on the Structure and Stability of Ptâ€“Ni Nanoparticles. Nano Letters, 2016, 16, 7748-7754.	4.5	64
27317	Oxygen Vacancy Structure Associated Photocatalytic Water Oxidation of BiOCl. ACS Catalysis, 2016, 6, 8276-8285.	5.5	333
27318	Hydrogen bonding: a mechanism for tuning electronic and optical properties of hybrid organicâ€“inorganic frameworks. Npj Computational Materials, 2016, 2, .	3.5	32
27319	Highly Efficient Quantum Sieving in Porous Graphene-like Carbon Nitride for Light Isotopes Separation. Scientific Reports, 2016, 6, 19952.	1.6	45
27320	Unexpected electronic structure of the alloyed and doped arsenene sheets: First-Principles calculations. Scientific Reports, 2016, 6, 29114.	1.6	58
27321	First-principle study of CO adsorption influence on the properties of ferroelectric tunnel junctions. Physical Chemistry Chemical Physics, 2016, 18, 31115-31124.	1.3	0
27322	Electronic structure of the germanium phosphide monolayer and Li-diffusion in its bilayer. Physical Chemistry Chemical Physics, 2016, 18, 32458-32465.	1.3	32
27323	Oxygen vacancy promoted methane partial oxidation over iron oxide oxygen carriers in the chemical looping process. Physical Chemistry Chemical Physics, 2016, 18, 32418-32428.	1.3	88
27324	The effect of indium substitution on the structure and NLO properties of Ba₆Cs₂Ga₁₀Se₂₀Cl₄. Inorganic Chemistry Frontiers, 2016, 3, 952-958.	3.0	34
27325	Biaxial strain effect on electronic structure tuning in antimonene-based van der Waals heterostructures. RSC Advances, 2016, 6, 102724-102732.	1.7	32
27326	Energetics of Sn²⁺ isomorphic substitution into hydroxylapatite: first-principles predictions. RSC Advances, 2016, 6, 107286-107292.	1.7	2
27327	Local heterojunctions of atomic Pt clusters boost the oxygen reduction activity of Rucore@Pdshell nanocrystallites. Journal of Materials Chemistry A, 2016, 4, 17848-17856.	5.2	3
27328	Electronics and optoelectronics of lateral heterostructures within monolayer indium monochalcogenides. Journal of Materials Chemistry C, 2016, 4, 11253-11260.	2.7	49

#	Article	IF	Citations
27329	Subgap States near the Conduction-Band Edge Due to Undercoordinated Cations in Amorphous In-Ga-Zn-O and Zn-Sn-O Semiconductors. Physical Review Applied, 2016, 6, .	1.5	17
27330	Comparative study of thermal properties of group-VA monolayers with buckled and puckered honeycomb structures. Physical Review B, 2016, 94, .	1.1	56
27331	Possibility of combining ferroelectricity and Rashba-like spin splitting in monolayers of the<mml:math xmlns:mml="http://www.w3.org/1998/Math/MathML"><mml:mrow><mml:mn>1</mml:mn><mml:mi>T</mml:mi></mml:mrow></mml:m transition-metal dichalcogenides<mml:math		

#	Article	IF	Citations
27347	Periodic DFT Characterization of NO_x Adsorption in Cu-Exchanged SSZ-13 Zeolite Catalysts. Journal of Physical Chemistry C, 2016, 120, 27934-27943.	1.5	29
27348	Direct Conversion of Methane to Methanol by Metal-Exchanged ZSM-5 Zeolite (Metal = Fe, Co, Ni, Cu). ACS Catalysis, 2016, 6, 8321-8331.	5.5	141
27349	Atomic Structure and Spectroscopy of Single Metal (Cr, V) Substitutional Dopants in Monolayer MoS₂. ACS Nano, 2016, 10, 10227-10236.	7.3	96
27350	First-principles study of interface doping in ferroelectric junctions. Scientific Reports, 2016, 6, 24209.	1.6	6
27351	Rolling-induced Face Centered Cubic Titanium in Hexagonal Close Packed Titanium at Room Temperature. Scientific Reports, 2016, 6, 24370.	1.6	106
27352	Band engineering in a van der Waals heterostructure using a 2D polar material and a capping layer. Scientific Reports, 2016, 6, 27986.	1.6	5
27353	The atomistic structure of yttria stabilised zirconia at 6.7 mol%: an ab initio study. Physical Chemistry Chemical Physics, 2016, 18, 31277-31285.	1.3	15
27354	Monolayer MoS₂ film supported metal electrocatalysts: a DFT study. RSC Advances, 2016, 6, 107836-107839.	1.7	7
27355	First-principles study of the phase transition in Cd₂Ta₂O₇. Ferroelectrics, 2016, 502, 76-86.	0.3	0
27356	Effect of polaronic charge transfer on band alignment at the <mml:math xmlns:mml="http://www.w3.org/1998/Math/MathML"><mml:mi>Cu</mml:mi><mml:mo>/</mml:mo><mml:msub><mml:mi>TiO</mml:mi> interface. Physical Review B, 2016, 94, .	1.1	7
27357	Anion effects on electronic structure and electrodynamic properties of the Mott insulator<mml:math xmlns:mml="http://www.w3.org/1998/Math/MathML"><mml:mrow><mml:mi>Î</mml:mi><mml:mo>â^'</mml:mo><mml:msub><mml:m Physical Review B, 2016, 94, .	1.1	36
27358	Noncontact atomic force microscopy and density functional theory studies of the <mml:math xmlns:mml="http://www.w3.org/1998/Math/MathML"><mml:mo>(</mml:mo><mml:mrow><mml:mn>2</mml:mn><mml:mo>Ã— reconstructions of the polar AlN(0001) surface. Physical Review B, 2016, 94, .	1.1	4
27359	Ab initio prediction of superdense tetragonal and monoclinic polymorphs of carbon. Physical Review B, 2016, 94, .	1.1	18
27360	Oscillatory magnetic anisotropy and spin-reorientation induced by heavy-metal cap in Cu/FeCo/ M () Tj ETQq1 1 0.784314 rgBT /Over	1.1	6
27361	Model Hamiltonian approach to the magnetic anisotropy of iron phthalocyanine at solid surfaces. Physical Review B, 2016, 94, .	1.1	5
27362	Theoretical Investigation on the Reaction Pathways for Oxygen Reduction Reaction on Silicon Doped Graphene as Potential Metal-Free Catalyst. Journal of the Electrochemical Society, 2016, 163, F1496-F1502.	1.3	23
27363	The Influence of Pt Layers in Ag@Pt_{nL}(111) (n = 1 and 2) on Oxygen Reduction Reaction: A Theoretical Study. Journal of the Electrochemical Society, 2016, 163, F945-F951.	1.3	7
27364	Scanning tunneling microscopy study of the early stages of epitaxial growth of CoSi2 and CoSi films on Si(111) substrate: Surface and interface analysis. Thin Solid Films, 2016, 619, 153-159.	0.8	4

#	Article	IF	Citations
27365	A DFT Study and Microkinetic Simulation of Propylene Partial Oxidation on CuO (111) and CuO (100) Surfaces. Journal of Physical Chemistry C, 2016, 120, 27430-27442.	1.5	31
27366	Atomic Insight into the Origin of Various Operation Voltages of Cation-Based Resistance Switches. ACS Applied Materials & Interfaces, 2016, 8, 31978-31985.	4.0	8
27367	Decomposition Mechanism of Anisole on Pt(111): Combining Single-Crystal Experiments and First-Principles Calculations. ACS Catalysis, 2016, 6, 8166-8178.	5.5	34
27368	Suppressing molecular vibrations in organic semiconductors by inducing strain. Nature Communications, 2016, 7, 11156.	5.8	105
27369	Inversion of diffraction data for amorphous materials. Scientific Reports, 2016, 6, 33731.	1.6	47
27370	Lithium-Decorated Borospherene B40: A Promising Hydrogen Storage Medium. Scientific Reports, 2016, 6, 35518.	1.6	64
27371	Oxidation of InP nanowires: a first principles molecular dynamics study. Physical Chemistry Chemical Physics, 2016, 18, 31101-31106.	1.3	3
27372	Self-supported three-dimensional mesoporous semimetallic WP₂nanowire arrays on carbon cloth as a flexible cathode for efficient hydrogen evolution. Nanoscale, 2016, 8, 19779-19786.	2.8	84
27373	Continuous and ultrathin platinum films on graphene using atomic layer deposition: a combined computational and experimental study. Nanoscale, 2016, 8, 19829-19845.	2.8	39
27374	Paving a way to suppress hydrogen blistering by investigating the hydrogenâ€“beryllium interaction in tungsten. RSC Advances, 2016, 6, 103622-103631.	1.7	6
27375	Site-projected electronic structure of two-dimensional Ti₃C₂MXene: the role of the surface functionalization groups. Physical Chemistry Chemical Physics, 2016, 18, 30946-30953.	1.3	121
27376	The effects of biaxial strain and electric field on the electronic properties in stanene. Materials Research Express, 2016, 3, 105008.	0.8	15
27377	Surface Fermi arc connectivity in the type-II Weyl semimetal candidate<mml:math xmlns:mml="http://www.w3.org/1998/Math/MathML"><mml:msub><mml:mi>WTe</mml:mi><mml:mn>2</mml:mn></mml:msub></mm Physical Review B, 2016, 94, .	1.1	44
27378	Half-metallic Co-based quaternary Heusler alloys for spintronics: Defect- and pressure-induced transitions and properties. Physical Review B, 2016, 94, .	1.1	20
27379	Influence of out-of-plane response on optical properties of two-dimensional materials: First principles approach. Physical Review B, 2016, 94, .	1.1	80
27380	Design of a CO Oxidation Catalyst Based on Two-Dimensional MnO₂. Journal of Physical Chemistry C, 2016, 120, 24302-24306.	1.5	20
27381	Functional Independent Scaling Relation for ORR/OER Catalysts. Journal of Physical Chemistry C, 2016, 120, 24910-24916.	1.5	119
27382	Surface engineering of hierarchical platinum-cobalt nanowires for efficient electrocatalysis. Nature Communications, 2016, 7, 11850.	5.8	607

#	Article	IF	Citations
27383	One-dimensional Magnus-type platinum double salts. Nature Communications, 2016, 7, 11950.	5.8	34
27384	Intermediate stages of electrochemical oxidation of single-crystalline platinum revealed by in situ Raman spectroscopy. Nature Communications, 2016, 7, 12440.	5.8	175
27385	Spin-polarized surface resonances accompanying topological surface state formation. Nature Communications, 2016, 7, 13143.	5.8	71
27386	Facet-dependent photovoltaic efficiency variations in single grains of hybrid halideÂperovskite. Nature Energy, 2016, 1, .	19.8	308
27387	Extending the applicability of the Goldschmidt tolerance factor to arbitrary ionic compounds. Scientific Reports, 2016, 6, 23592.	1.6	119
27388	Electronic and magnetic properties of Co doped MoS2 monolayer. Scientific Reports, 2016, 6, 24153.	1.6	94
27389	MÃ¶ssbauer Spectroscopy of Iron Carbides: From Prediction to Experimental Confirmation. Scientific Reports, 2016, 6, 26184.	1.6	82
27390	Photochemical Copper Coating on 3D Printed Thermoplastics. Scientific Reports, 2016, 6, 31188.	1.6	17
27391	Self-organized Sr leads to solid state twinning in nano-scaled eutectic Si phase. Scientific Reports, 2016, 6, 31635.	1.6	34
27392	Reconciling Local Structure Disorder and the Relaxor State in (Bi1/2Na1/2)TiO3-BaTiO3. Scientific Reports, 2016, 6, 31739.	1.6	73
27393	Half-metallicity and ferromagnetism in penta-AlN2 nanostructure. Scientific Reports, 2016, 6, 33060.	1.6	33
27394	Room-Temperature All-solid-state Rechargeable Sodium-ion Batteries with a Cl-doped Na3PS4 Superionic Conductor. Scientific Reports, 2016, 6, 33733.	1.6	205
27395	Unravelling the Efficient Photocatalytic Activity of Boron-induced Ti3+ Species in the Surface Layer of TiO2. Scientific Reports, 2016, 6, 34765.	1.6	53
27396	Low viscosity and high attenuation in MgSiO3 post-perovskite inferred from atomic-scale calculations. Scientific Reports, 2016, 6, 34771.	1.6	22
27397	Lowered phase transition temperature and excellent solar heat shielding properties of well-crystallized VO₂ by W doping. Physical Chemistry Chemical Physics, 2016, 18, 28010-28017.	1.3	31
27398	Thermal conductivity switch: Optimal semiconductor/metal melting transition. Physical Review B, 2016, 94, .	1.1	21
27399	Prediction and control of spin polarization in a Weyl semimetallic phase of BiSb. Physical Review B, 2016, 94, .	1.1	41
27400	Electronic transitions induced by short-range structural order in amorphous<mml:math xmlns:mml="http://www.w3.org/1998/Math/MathML"><mml:msub><mml:mi>TiO</mml:mi><mml:mn>2</mml:mn></mml:msub></m Physical Review B, 2016, 94, .	1.1	37

#	Article	IF	Citations
27401	Oxygen dissociation on palladium and gold core/shell nanoparticles. International Journal of Quantum Chemistry, 2016, 116, 1486-1492.	1.0	12
27402	Effects of interlayer coupling on the electronic structures of antimonene/graphene van der Waals heterostructures. Superlattices and Microstructures, 2016, 100, 826-832.	1.4	27
27403	Structural Evolutions and Crystal Field Characterizations of Tm-Doped YAlO₃: New Theoretical Insights. ACS Applied Materials & Interfaces, 2016, 8, 30422-30429.	4.0	33
27404	Rational Design of Efficient Palladium Catalysts for Electroreduction of Carbon Dioxide to Formate. ACS Catalysis, 2016, 6, 8115-8120.	5.5	277
27405	Termination layer compensated tunnelling magnetoresistance in ferrimagnetic Heusler compounds with high perpendicular magnetic anisotropy. Nature Communications, 2016, 7, 10276.	5.8	72
27406	Efficient and stable perovskite solar cells prepared in ambient air irrespective of the humidity. Nature Communications, 2016, 7, 11105.	5.8	488
27407	Non-Radiative Carrier Recombination Enhanced by Two-Level Process: A First-Principles Study. Scientific Reports, 2016, 6, 21712.	1.6	74
27408	Correlating the Energetics and Atomic Motions of the Metal-Insulator Transition of M1 Vanadium Dioxide. Scientific Reports, 2016, 6, 26391.	1.6	8
27409	Enhancing Intrinsic Stability of Hybrid Perovskite Solar Cell by Strong, yet Balanced, Electronic Coupling. Scientific Reports, 2016, 6, 30305.	1.6	42
27410	Large gap Quantum Spin Hall Insulators of Hexagonal III-Bi monolayer. Scientific Reports, 2016, 6, 34861.	1.6	6
27411	Schottky barrier tuning of the single-layer MoS₂ on magnetic metal substrates through vacancy defects and hydrogenation. Physical Chemistry Chemical Physics, 2016, 18, 31027-31032.	1.3	7
27412	Ab Initiocalculations of thermomechanical properties and electronic structure of vitreloy<mml:math xmlns:mml="http://www.w3.org/1998/Math/MathML"><mml:mrow><mml:mi mathvariant="normal">Z</mml:mi><mml:msub><mml:mi mathvariant="normal">r</mml:mi><mml:mrow><mml:mn>41.2</mml:mn></mml:mrow></mml:msub><mml:mi mathvariant="normal">T</mml:mi><mml:msub><mml:mi mathvariant="normal">i</mml:mi><mml:mrow><mml:mn>13.8</mml:mn></mml:mrow></mml:msub><mml:mi	1.1	16
27413	Existence of topological nontrivial surface states in strained transition metals: W, Ta, Mo, and Nb. Physical Review B, 2016, 94, .	1.1	16
27414	Oxygen Evolution Reaction on Perovskite Electrocatalysts with Localized Spins and Orbital Rotation Symmetry. ChemCatChem, 2016, 8, 3762-3768.	1.8	35
27415	Optimizing the sputter deposition process of polymers for the Storing Matter technique using PMMA. Journal of Mass Spectrometry, 2016, 51, 889-899.	0.7	0
27416	Path integral Monte Carlo simulations of warm dense sodium. High Energy Density Physics, 2016, 21, 16-19.	0.4	11
27417	Design of a p-Type Electrode for Enhancing Electronic Conduction in High-Mn, Li-Rich Oxides. Chemistry of Materials, 2016, 28, 8201-8209.	3.2	24
27418	Density Functional Study of Stacking Structures and Electronic Behaviors of AnE-PV Copolymer. Journal of Physical Chemistry B, 2016, 120, 10854-10859.	1.2	4

#	Article	IF	Citations
27419	Effect of Ions on H-Bond Structure and Dynamics at the Quartz(101)â€“Water Interface. Langmuir, 2016, 32, 11353-11365.	1.6	41
27420	Polytypism and Unique Site Preference in LiZnSb: A Superior Thermoelectric Reveals Its True Colors. Journal of the American Chemical Society, 2016, 138, 14574-14577.	6.6	29
27421	Direct TEM observations of growth mechanisms of two-dimensional MoS2 flakes. Nature Communications, 2016, 7, 12206.	5.8	179
27422	A rhodium/silicon co-electrocatalyst design concept to surpass platinum hydrogen evolution activity at high overpotentials. Nature Communications, 2016, 7, 12272.	5.8	272
27423	A sulfur host based on titanium monoxide@carbon hollow spheres for advanced lithiumâ€“sulfur batteries. Nature Communications, 2016, 7, 13065.	5.8	590
27424	Spontaneous decays of magneto-elastic excitations in non-collinear antiferromagnet (Y,Lu)MnO3. Nature Communications, 2016, 7, 13146.	5.8	57
27425	Robust ultra-low-friction state of graphene via moirÃ© superlattice confinement. Nature Communications, 2016, 7, 13204.	5.8	116
27426	High-throughput ab-initio dilute solute diffusion database. Scientific Data, 2016, 3, 160054.	2.4	102
27427	Structures and Electronic Properties of Different CH3NH3PbI3/TiO2 Interface: A First-Principles Study. Scientific Reports, 2016, 6, 20131.	1.6	69
27428	Easily doped p-type, low hole effective mass, transparent oxides. Scientific Reports, 2016, 6, 20446.	1.6	60
27429	Spatial separation of photo-generated electron-hole pairs in BiOBr/BiOI bilayer to facilitate water splitting. Scientific Reports, 2016, 6, 32764.	1.6	53
27430	Mechanochemical route to the synthesis of nanostructured Aluminium nitride. Scientific Reports, 2016, 6, 33375.	1.6	32
27431	Thermal transport properties of antimonene: an ab initio study. Physical Chemistry Chemical Physics, 2016, 18, 31217-31222.	1.3	60
27432	Phase crossover in transition metal dichalcogenide nanoclusters. Nanoscale, 2016, 8, 19154-19160.	2.8	8
27433	Heavy Dirac fermions in a graphene/topological insulator hetero-junction. 2D Materials, 2016, 3, 034006.	2.0	18
27434	Giant tunneling electroresistance induced by ferroelectrically switchable two-dimensional electron gas at nonpolar<mml:math xmlns:mml="http://www.w3.org/1998/Math/MathML"><mml:mrow><mml:msub><mml:mi>BaTiO</mml:mi><mml:mn>3</mml:mn><m Physical Review B, 2016, 94, .	1.1	15
27435	Pressure dependence of the band-gap energy in BiTeI. Physical Review B, 2016, 94, .	1.1	11
27436	Unusual Dirac Fermions on the Surface of a Noncentrosymmetric <mml:math xmlns:mml="http://www.w3.org/1998/Math/MathML" display="inline"><mml:mi>Î±</mml:mi></mml:math> -BiPd Superconductor. Physical Review Letters, 2016, 117, 177001.	2.9	21

#	Article	IF	Citations
27437	Nanocluster-Assembled Materials. Series in Materials Science and Engineering, 2016, , 113-148.	0.1	3
27438	Catalytic Degradation of Benzene over Nanocatalysts containing Cerium and Manganese. ChemistryOpen, 2016, 5, 495-504.	0.9	10
27439	Structure, Vibrational Spectra and ¹¹B-NMR Chemical Shift of Na₈[AlSiO₄]₆(B(OH)₄)₂: Comparison of Theory and Experiment. Journal of Physical Chemistry A, 2016, 120, 7503-7509.	1.1	2
27440	CO Dissociation on Face-Centered Cubic and Hexagonal Close-Packed Nickel Catalysts: A First-Principles Study. Journal of Physical Chemistry C, 2016, 120, 24895-24903.	1.5	52
27441	Competition between Two High-Density Assemblies of Poly(phenyl)thiols on Au(111). Journal of Physical Chemistry C, 2016, 120, 25462-25472.	1.5	19
27442	Spectroscopic Identification of the Auâ€“C Bond Formation upon Electroreduction of an Aryl Diazonium Salt on Gold. Langmuir, 2016, 32, 11514-11519.	1.6	14
27443	Gasâ€“solid interfacial modification of oxygen activity in layered oxide cathodes for lithium-ion batteries. Nature Communications, 2016, 7, 12108.	5.8	531
27444	Room Temperature Quantum Spin Hall Insulator in Ethynyl-Derivative Functionalized Stanene Films. Scientific Reports, 2016, 6, 18879.	1.6	49
27445	Oxygen-Deficient Zirconia (ZrO2â^'x): A New Material for Solar Light Absorption. Scientific Reports, 2016, 6, 27218.	1.6	250
27446	Noble metal-free bifunctional oxygen evolution and oxygen reduction acidic media electro-catalysts. Scientific Reports, 2016, 6, 28367.	1.6	94
27447	Important Variation in Vibrational Properties of LiFePO4 and FePO4 Induced by Magnetism. Scientific Reports, 2016, 6, 33033.	1.6	8
27448	Predicting Global Minimum in Complex Beryllium Borate System for Deep-ultraviolet Functional Optical Applications. Scientific Reports, 2016, 6, 34839.	1.6	24
27449	Multilayer Dye Aggregation at Dye/TiO2 Interface via Ï€â€¦Ï€ Stacking and Hydrogen Bond and Its Impact on Solar Cell Performance: A DFT Analysis. Scientific Reports, 2016, 6, 35893.	1.6	30
27450	A general forcefield for accurate phonon properties of metalâ€“organic frameworks. Physical Chemistry Chemical Physics, 2016, 18, 29316-29329.	1.3	40
27451	A new understanding of the photocatalytic mechanism of the direct Z-scheme g-C₃N₄/TiO₂heterostructure. Physical Chemistry Chemical Physics, 2016, 18, 31175-31183.	1.3	459
27452	First-Principles Study of Properties of Strained PbTiO ₃ /KTaO ₃ Superlattice. Chinese Physics Letters, 2016, 33, 026302.	1.3	3
27453	Hypergeometric resummation of self-consistent sunset diagrams for steady-state electron-boson quantum many-body systems out of equilibrium. Physical Review B, 2016, 94, .	1.1	17
27454	Numerical simulation of the distribution of charge carrier in nanosized semiconductor heterostructures with account for polarization effects. Computational Mathematics and Mathematical Physics, 2016, 56, 161-172.	0.2	11

#	Article	IF	Citations
27455	Unravelling Local Atomic Order of the Anionic Sublattice in M(Al_{1â^'x}Ga_x)₄ with M=Sr and Ba by Using NMR Spectroscopy and Quantum Mechanical Modelling. Chemistry - A European Journal, 2016, 22, 17833-17842.	1.7	7
27456	Structural and compositional evolution of Al3(Zr,Y) precipitates in Al-Zr-Y alloy. Materials Characterization, 2016, 121, 195-198.	1.9	30
27457	Covalent Functionalization of Black Phosphorus from First-Principles. Journal of Physical Chemistry Letters, 2016, 7, 4540-4546.	2.1	71
27458	Prediction of a native ferroelectric metal. Nature Communications, 2016, 7, 11211.	5.8	71
27459	Group precipitation and age hardening of nanostructured Fe-based alloys with ultra-high strengths. Scientific Reports, 2016, 6, 21364.	1.6	44
27460	Surface degeneration of W crystal irradiated with low-energy hydrogen ions. Scientific Reports, 2016, 6, 23738.	1.6	8
27461	A study on the electron transport properties of ZnON semiconductors with respect to the relative anion content. Scientific Reports, 2016, 6, 24787.	1.6	38
27462	Band gap bowing in NixMg1â^'xO. Scientific Reports, 2016, 6, 31230.	1.6	43
27463	Spin-wave propagation steered by electric field modulated exchange interaction. Scientific Reports, 2016, 6, 31783.	1.6	6
27464	The stability and catalytic activity of W13@Pt42 core-shell structure. Scientific Reports, 2016, 6, 35464.	1.6	7
27465	Solvation free energies for periodic surfaces: comparison of implicit and explicit solvation models. Physical Chemistry Chemical Physics, 2016, 18, 31850-31861.	1.3	80
27466	First-principles study of pressure-induced structural phase transitions in MnF₂. Physical Chemistry Chemical Physics, 2016, 18, 33250-33263.	1.3	24
27467	First principles computational study on the adsorption mechanism of organic methyl iodide gas on triethylenediamine impregnated activated carbon. Physical Chemistry Chemical Physics, 2016, 18, 32050-32056.	1.3	32
27468	Extrinsic doping of the half-Heusler compounds. Nanotechnology, 2016, 27, 334002.	1.3	23
27469	Signatures of distinct impurity configurations in atomic-resolution valence electron-energy-loss spectroscopy: Application to graphene. Physical Review B, 2016, 94, .	1.1	8
27470	Quasi-freestanding epitaxial silicene on Ag(111) by oxygen intercalation. Science Advances, 2016, 2, e1600067.	4.7	138
27471	Visualizing weakly bound surface Fermi arcs and their correspondence to bulk Weyl fermions. Science Advances, 2016, 2, e1600709.	4.7	83
27473	Experimental Analysis of Real Crystal Surfaces. , 0, , 305-314.		0

#	Article	IF	Citations
27474	First-principles study on the thermal expansion of Ni-X binary alloys based on the quasi-harmonic Debye model. Metals and Materials International, 2016, 22, 1065-1072.	1.8	8
27475	Elucidating Oligomer-Surface and Oligomer-Oligomer Interactions at a Lithiated Silicon Surface. Electrochimica Acta, 2016, 220, 312-321.	2.6	9
27476	A heterogeneous mechanism for the catalytic decomposition of hydroperoxides and oxidation of alkanes over CeO2 nanoparticles: A combined theoretical and experimental study. Journal of Catalysis, 2016, 344, 334-345.	3.1	13
27477	Non-stoichiometry in U3Si2. Journal of Nuclear Materials, 2016, 482, 300-305.	1.3	64
27478	Defects and Oxide Ion Migration in the Solid Oxide Fuel Cell Cathode Material LaFeO₃. Chemistry of Materials, 2016, 28, 8210-8220.	3.2	95
27479	Stacking-Sequence Changes and Na Ordering in Layered Intercalation Materials. Chemistry of Materials, 2016, 28, 8640-8650.	3.2	66
27480	Two-Dimensional Fully Conjugated Polymeric Photosensitizers for Advanced Photodynamic Therapy. Chemistry of Materials, 2016, 28, 8651-8658.	3.2	47
27481	Improving Energy Density and Structural Stability of Manganese Oxide Cathodes for Na-Ion Batteries by Structural Lithium Substitution. Chemistry of Materials, 2016, 28, 9064-9076.	3.2	191
27482	Halogenâ˜Ï€ Interactions between Benzene and X2/CX4 (X = Cl, Br): Assessment of Various Density Functionals with Respect to CCSD(T). Journal of Physical Chemistry A, 2016, 120, 9305-9314.	1.1	32
27483	Comparative Theoretical Study of the Chemistry of Hydrogen Sulfide on Cu(100) and Au(100): Implications for Sulfur Tolerance of Water Gas Shift Nanocatalysts. Journal of Physical Chemistry C, 2016, 120, 25351-25360.	1.5	12
27484	H₂O Adsorption/Dissociation and H₂ Generation by the Reaction of H₂O with Al₂O₃ Materials: A First-Principles Investigation. Journal of Physical Chemistry C, 2016, 120, 21561-21570.	1.5	11
27485	Effects of the Interlayer Interaction and Electric Field on the Band Gap of Polar Bilayers: A Case Study of Sc₂CO₂. Journal of Physical Chemistry C, 2016, 120, 24857-24865.	1.5	42
27486	Chemisorption of Hydroxide on 2D Materials from DFT Calculations: Graphene versus Hexagonal Boron Nitride. Journal of Physical Chemistry Letters, 2016, 7, 4695-4700.	2.1	92
27487	Thermal selectivity of intermolecular versus intramolecular reactions on surfaces. Nature Communications, 2016, 7, 11002.	5.8	66
27488	Water electrolysis on La1â˜xSrxCoO3â˜Î´ perovskite electrocatalysts. Nature Communications, 2016, 7, 11053.	5.8	800
27489	An unforeseen polymorph of coronene by the application of magnetic fields during crystal growth. Nature Communications, 2016, 7, 11555.	5.8	68
27490	Van der Waals interactions and the limits of isolated atom models at interfaces. Nature Communications, 2016, 7, 11559.	5.8	111
27491	Two-dimensional shape memory graphene oxide. Nature Communications, 2016, 7, 11972.	5.8	33

#	Article	IF	Citations
27492	Atomic intercalation to measure adhesion of graphene on graphite. Nature Communications, 2016, 7, 13263.	5.8	35
27493	Dirac cone move and bandgap on/off switching of graphene superlattice. Scientific Reports, 2016, 6, 18869.	1.6	24
27494	Vacancy Structures and Melting Behavior in Rock-Salt GeSbTe. Scientific Reports, 2016, 6, 25453.	1.6	42
27495	Competing covalent and ionic bonding in Ge-Sb-Te phase change materials. Scientific Reports, 2016, 6, 25981.	1.6	35
27496	Gaseous NH3 Confers Porous Pt Nanodendrites Assisted by Halides. Scientific Reports, 2016, 6, 26196.	1.6	11
27497	A Synthetic Pseudo-Rh: NOx Reduction Activity and Electronic Structure of Pdâ€“Ru Solid-solution Alloy Nanoparticles. Scientific Reports, 2016, 6, 28265.	1.6	44
27498	Composition-dependent surface chemistry of colloidal Ba_xSr_{1â^'x}TiO₃ perovskite nanocrystals. Chemical Communications, 2016, 52, 13791-13794.	2.2	3
27499	First-principles prediction of a giant-gap quantum spin Hall insulator in Pb thin film. Physical Chemistry Chemical Physics, 2016, 18, 31862-31868.	1.3	23
27500	Thermoelectricity in transition metal compounds: the role of spin disorder. Physical Chemistry Chemical Physics, 2016, 18, 31777-31786.	1.3	27
27501	Graphene/nitrogen-functionalized graphene quantum dot hybrid broadband photodetectors with a buffer layer of boron nitride nanosheets. Nanoscale, 2016, 8, 19677-19683.	2.8	50
27502	Insights into the effect of Pt doping of Cu(110)/H2O for methanol decomposition: a density functional theory study. RSC Advances, 2016, 6, 109124-109131.	1.7	0
27503	Facet engineering of monodisperse PbS nanocrystals with shape- and facet-dependent photoresponse activity. RSC Advances, 2016, 6, 107151-107157.	1.7	22
27504	Characterizing hydrophobicity of amino acid side chains in a protein environment via measuring contact angle of a water nanodroplet on planar peptide network. Proceedings of the National Academy of Sciences of the United States of America, 2016, 113, 12946-12951.	3.3	87
27505	Vacancy-donor complexes in highlyn-type Ge doped with As, P and Sb. Journal of Physics Condensed Matter, 2016, 28, 335801.	0.7	13
27506	Ab initiosearch for cohesion-enhancing impurity elements at grain boundaries in molybdenum and tungsten. Modelling and Simulation in Materials Science and Engineering, 2016, 24, 085009.	0.8	57
27507	Statistical error in simulations of Poisson processes: Example of diffusion in solids. Physical Review B, 2016, 94, .	1.1	2
27508	First-principles approach to thin superconducting slabs and heterostructures. Physical Review B, 2016, 94, .	1.1	8
27509	Structural and magnetic properties of the Gd-based bulk metallic glasses<mml:math xmlns:mml="http://www.w3.org/1998/Math/MathML"><mml:msub><mml:mi>GdFe</mml:mi><mml:mn>2</mml:mn></mml:msub><mml:and<mml:math xmlns:mml="http://www.w3.org/1998/Math/MathML"><mml:msub><mml:mi>GdNi</mml:mi><mml:mn>2</mml:mn></mml:msub></mml:first principles. Physical Review B, 2016, 94, .	1.1	12

#	Article	IF	Citations
27510	Experimental observation and computational study of the spin-gap excitation in Ba3BiRu2O9. Physical Review B, 2016, 94, .	1.1	9
27511	Interaction-induced metallic state in graphene on hexagonal boron nitride. Physical Review B, 2016, 94, .	1.1	7
27512	Spin Orbit Coupling Gap and Indirect Gap in Strain-Tuned Topological Insulator-Antimonene. Nanoscale Research Letters, 2016, 11, 459.	3.1	26
27513	Efficient Decarbonylation of Furfural to Furan Catalyzed by Zirconiaâ€Supported Palladium Clusters with Low Atomicity. ChemSusChem, 2016, 9, 3441-3447.	3.6	47
27514	Modelling of Palladium Gold alloy- dielectric stratified loaded plasmonic waveguide for hydrogen detection at room temperature. Journal of Physics: Conference Series, 2016, 759, 012043.	0.3	1
27515	Growth of Single Element Quasicrystals. Materia Japan, 2016, 55, 259-266.	0.1	0
27516	Theoretical Investigation on Electronic and Magnetic Structures of FeRh. Journal of the Magnetics Society of Japan, 2016, 40, 77-80.	0.5	4
27518	Off-centering of rare-earth ion in (Ba,R)(Ti,Mg)O3(R= Gd, Dy). Japanese Journal of Applied Physics, 2016, 55, 10TC08.	0.8	2
27519	Prediction of B1 to B10 phase transition in LuN under pressure: An ab-initio investigation. AIP Conference Proceedings, 2016, , .	0.3	1
27520	Strong charge and spin fluctuations inLa2O3Fe2Se2. Physical Review B, 2016, 94, .	1.1	6
27521	Massively Parallel First-Principles Simulation of Electron Dynamics in Materials. , 2016, , .		5
27522	Electronic origin of strain effects on solute stabilities in iron. Journal of Applied Physics, 2016, 120, 075902.	1.1	2
27523	Strain-induced insulatorâ€“metal transition in ferroelectric BaTiO 3 (001) surface: First-principles study. Chinese Physics B, 2016, 25, 077302.	0.7	1
27524	The 7â€‰Ã—â€‰1 Fermi Surface Reconstruction in a Two-dimensional f -electron Charge Density Wave System: PrTe3. Scientific Reports, 2016, 6, 30318.	1.6	14
27525	Magnetic Properties Controlled by Interstitial or Interlayer Cations in Iron Chalcogenides. Scientific Reports, 2016, 6, 19031.	1.6	6
27526	Electronic structure and relaxation dynamics in a superconducting topological material. Scientific Reports, 2016, 6, 22557.	1.6	21
27527	Tunable one-dimensional electron gas carrier densities at nanostructured oxide interfaces. Scientific Reports, 2016, 6, 25452.	1.6	6
27528	Light-Induced Peroxide Formation in ZnO: Origin of Persistent Photoconductivity. Scientific Reports, 2016, 6, 35148.	1.6	28

#	Article	IF	Citations
27529	Hidden Order and Dimensional Crossover of the Charge Density Waves in TiSe2. Scientific Reports, 2016, 6, 37910.	1.6	40
27530	How does the spin-state of Co ions affect the insulator-metal transition in Bi2A2Co2O8 (Aâ€‰=â€‰Ca, Sr, Ba)?. Scientific Reports, 2016, 6, 38212.	1.6	6
27531	Condensed-matter equation of states covering a wide region of pressure studied experimentally. Scientific Reports, 2016, 6, 39212.	1.6	1
27532	Tuning high-harmonic generation by controlled deposition of ultrathin ionic layers on metal surfaces. Physical Review B, 2016, 94, .	1.1	3
27533	Theoretical and experimental studies of formation and migration of oxygen vacancies in BaM_xTi_{1â^'} _xO₃ (M = Zr, Ge). Japanese Journal of Applied Physics, 2016, 55, 10TB02.	0.8	8
27534	Vibration eigenmodes of the Au- <mml:math xmlns:mml="http://www.w3.org/1998/Math/MathML"><mml:mrow><mml:mo>(</mml:mo><mml:mn>5</mml:mn><mml:mo>Ã—</mml:mo> /Si(111) surface studied by Raman spectroscopy and first-principles calculations. Physical Review B, 2016, 94, .	1.1	16
27535	H-bonding of an NH3 gas molecule to H2O/Pt(111) â€" A barrier-free path. Journal of Chemical Physics, 2016, 144, 054701.	1.2	3
27536	Influence of optical non-uniformity on the reflectance of dense plasmas. Journal of Physics: Conference Series, 2016, 774, 012142.	0.3	0
27537	Electrical compensation via vacancyâ€"donor complexes in arsenic-implanted and laser-annealed germanium. Applied Physics Letters, 2016, 109, .	1.5	13
27538	Effects of guest atomic species on the lattice thermal conductivity of type-I silicon clathrate studied via classical molecular dynamics. Journal of Chemical Physics, 2016, 145, 064702.	1.2	4
27539	First-principles Calculations of Point Defects in Semiconductors. Materia Japan, 2016, 55, 221-224.	0.1	0
27540	Extent of hydrogen coverage of Si(001) under chemical vapor deposition conditions from ab initio approaches. Journal of Chemical Physics, 2016, 144, 204706.	1.2	10
27541	Magnetically launched flyer plate technique for probing electrical conductivity of compressed copper. Journal of Applied Physics, 2016, 119, 105902.	1.1	20
27542	Hydrogen-induced atomic structure evolution of the oxygen-chemisorbed Cu(110) surface. Journal of Chemical Physics, 2016, 145, 234704.	1.2	7
27543	A first-principles study on the negative thermal expansion material: Mn3(A0.5B0.5)N (A=Cu, Zn, Ag, or) Tj ETQq0 0 0 rgBT /Overlock 10	0.6	2
27544	Electronic properties of a new structured Sin/O superlattice. AIP Advances, 2016, 6, 115203.	0.6	0
27545	A comprehensive picture in the view of atomic scale on piezoelectricity of ZnO tunnel junctions: The first principles simulation. AIP Advances, 2016, 6, 065217.	0.6	1
27546	First-principles calculations of K-shell X-ray absorption spectra for warm dense nitrogen. Physics of Plasmas, 2016, 23, 053304.	0.7	2

#	Article	IF	Citations
27547	Local modification of intermolecular interactions at a sub-molecule level. Nanotechnology, 2016, 27, 415711.	1.3	2
27548	An improved d-band model of the catalytic activity of magnetic transition metal surfaces. Scientific Reports, 2016, 6, 35916.	1.6	164
27549	Giant Phonon Anharmonicity and Anomalous Pressure Dependence of Lattice Thermal Conductivity in Y2Si2O7 silicate. Scientific Reports, 2016, 6, 29801.	1.6	24
27550	First-principles study of He trapping in Î· -Fe ₂ C. Chinese Physics B, 2016, 25, 116801.	0.7	1
27551	Modelling of substitutional defects in the structure of Ti-bearing hibonite. Journal of Structural Chemistry, 2016, 57, 1369-1376.	0.3	1
27552	Robust and tunable itinerant ferromagnetism at the silicon surface of the antiferromagnet GdRh2Si2. Scientific Reports, 2016, 6, 24254.	1.6	29
27553	Computational Analysis of Coupled Anisotropic Chemical Expansion in Li2-XMnO3-Î´. MRS Advances, 2016, 1, 1037-1042.	0.5	4
27554	Driving force for martensitic transformation in<mml:math xmlns:mml="http://www.w3.org/1998/Math/MathML"><mml:msub><mml:mi>Ni</mml:mi><mml:mn>2</mml:mn></mml:msub><mm Physical Review B, 2016, 94, .	1.1	8
27555	Magnetic properties of intrinsic vacancies on the GaN $$(10ar 10)$$ surface: a density-functional-theory study. Journal of the Korean Physical Society, 2016, 68, 420-424.	0.3	2
27556	Site preferences for La and Pr in Nd2Fe14B permanent magnet: A first principles study. Journal of the Korean Physical Society, 2016, 69, 1564-1570.	0.3	4
27557	First-principles study of Cl-terminated silicon nanoribbons electronic properties. Journal of Physics: Conference Series, 2016, 758, 012002.	0.3	0
27558	First principles investigation of GaNbO4 as a photocatalytic material. AIP Conference Proceedings, 2016, , .	0.3	0
27559	The repopulation of electronic states upon vibrational excitation of niobium carbide clusters. Journal of Chemical Physics, 2016, 145, 024313.	1.2	7
27560	Structure of <mml:math xmlns:mml="http://www.w3.org/1998/Math/MathML"><mml:msub><mml:mi>TiO</mml:mi><mml:mn>2</mml:mn></mml:msub></m (011) revealed by photoelectron diffraction. Physical Review B, 2016, 94, .	1.1	6
27561	Communication: Energy transfer and reaction dynamics for DCl scattering on Au(111): An ab initio molecular dynamics study. Journal of Chemical Physics, 2016, 145, 011102.	1.2	32
27562	Thermal properties of layered oxychalcogenides BiCuOCh (Châ€‰=â€‰S, Se, and Te): A first-principles calculation. Journal of Applied Physics, 2016, 119, .	1.1	18
27563	Difficulty of carrier generation in orthorhombic PbO. Journal of Applied Physics, 2016, 119, .	1.1	14
27564	Electronically designed amorphous carbon and silicon. Physica Status Solidi (A) Applications and Materials Science, 2016, 213, 1653-1660.	0.8	10

#	Article	IF	Citations
27565	Thermodynamic parameters of Zr superconductor at â€“ structural phase transition. Physica Status Solidi (B): Basic Research, 2016, 253, 538-544.	0.7	2
27566	Hâ€bond and electric field correlations for water in highly hydrated crystals. International Journal of Quantum Chemistry, 2016, 116, 67-80.	1.0	14
27567	Stability of atomic oxygen chemisorption on Pt-alloy surfaces. Surface and Interface Analysis, 2016, 48, 181-185.	0.8	3
27569	Manipulation of Magnetic Properties by Oxygen Vacancies in Multiferroic YMnO₃. Advanced Functional Materials, 2016, 26, 3589-3598.	7.8	45
27570	Minimum Thermal Conductivity in Weak Topological Insulators with Bismuthâ€Based Stack Structure. Advanced Functional Materials, 2016, 26, 5360-5367.	7.8	29
27571	Extraordinarily Strong Interlayer Interaction in 2D Layered PtS₂. Advanced Materials, 2016, 28, 2399-2407.	11.1	415
27572	Employing Lead Thiocyanate Additive to Reduce the Hysteresis and Boost the Fill Factor of Planar Perovskite Solar Cells. Advanced Materials, 2016, 28, 5214-5221.	11.1	487
27573	Implementing Metalâ€toâ€Ligand Charge Transfer in Organic Semiconductor for Improved Visibleâ€Nearâ€Infrared Photocatalysis. Advanced Materials, 2016, 28, 6959-6965.	11.1	268
27574	CO₂ Hydrogenation over Oxideâ€Supported PtCo Catalysts: The Role of the Oxide Support in Determining the Product Selectivity. Angewandte Chemie - International Edition, 2016, 55, 7968-7973.	7.2	261
27575	Efficient Photocatalytic Oxygen Production over Nitrogenâ€Doped Sr₄Nb₂O₉ under Visibleâ€Light Irradiation. ChemCatChem, 2016, 8, 615-623.	1.8	45
27576	On the Importance of Regulating Hydroxyl Coverage on the Basal Plane of Graphene Oxide for Supercapacitors. ChemElectroChem, 2016, 3, 741-748.	1.7	6
27577	Photoluminescence and Photocatalytic Properties of Ag₃PO₄ Microcrystals: An Experimental and Theoretical Investigation. ChemPlusChem, 2016, 81, 202-212.	1.3	70
27578	Firstâ€principles prediction of fast migration channels of potassium ions in KAlSi₃O₈ hollandite: Implications for high conductivity anomalies in subduction zones. Geophysical Research Letters, 2016, 43, 6228-6233.	1.5	16
27579	Emergence of Negative Capacitance in Multidomain Ferroelectricâ€“Paraelectric Nanocapacitors at Finite Bias. Advanced Materials, 2016, 28, 335-340.	11.1	30
27580	Highâ€Performance Hydrogen Evolution from MoS_{2(1â€“x)}P_x Solid Solution. Advanced Materials, 2016, 28, 1427-1432.	11.1	309
27581	Dual Electricalâ€Behavior Regulation on Electrocatalysts Realizing Enhanced Electrochemical Water Oxidation. Advanced Materials, 2016, 28, 3326-3332.	11.1	145
27582	Ohmic Contacts to 2D Semiconductors through van der Waals Bonding. Advanced Electronic Materials, 2016, 2, 1500405.	2.6	91
27583	Nanoscale Elastic Changes in 2D Ti₃C₂T_x (MXene) Pseudocapacitive Electrodes. Advanced Energy Materials, 2016, 6, 1502290.	10.2	117

#	Article	IF	Citations
27584	Water Adsorption and Dissociation on Ceriaâ€Supported Singleâ€Atom Catalysts: A Firstâ€Principles DFT+U Investigation. Chemistry - A European Journal, 2016, 22, 2092-2099.	1.7	21
27585	Role of Oxygen Defects on the Photocatalytic Properties of Mgâ€Doped Mesoporous Ta₃N₅. ChemSusChem, 2016, 9, 1403-1412.	3.6	78
27586	Scattering strength of the scatterer inducing variability in graphene on silicon oxide. Journal of Physics Condensed Matter, 2016, 28, 115301.	0.7	3
27587	Density-functional investigation of the geometric and electronic structure of ethylene oxide adsorbed on Si(100). International Journal of Modern Physics B, 2016, 30, 1650116.	1.0	1
27588	Nature of Hydrogen Bonds and SÂ·Â·Â·S Interactions in the <scp>l</scp>-Cystine Crystal. Journal of Physical Chemistry A, 2016, 120, 4223-4230.	1.1	13
27589	The structural, electronic, magnetic and mechanical properties of quaternary Heusler alloys ZrTiCrZ(Zâ€‰â€‰=â€‰â€‰Al, Ga, In, Si, Ge, Sn): a first-principles study. Journal Physics D: Applied Physics, 2016, 49, 255002.	2.8	35
27590	First-principles analysis on Seebeck coefficient in zinc oxide nanowires for thermoelectric devices. IOP Conference Series: Materials Science and Engineering, 2016, 108, 012040.	0.3	4
27591	Density functional theory study of Li, Na, and Mg intercalation and diffusion in MoS₂with controlled interlayer spacing. Materials Research Express, 2016, 3, 064001.	0.8	100
27592	The lowest-energy charge-transfer state and its role in charge separation in organic photovoltaics. Physical Chemistry Chemical Physics, 2016, 18, 17546-17556.	1.3	17
27593	Modeling of metastable phase formation diagrams for sputtered thin films. Science and Technology of Advanced Materials, 2016, 17, 210-219.	2.8	27
27594	Electrons and phonons in amorphous semiconductors. Semiconductor Science and Technology, 2016, 31, 073002.	1.0	31
27595	Understanding the high p-type conductivity in Cu-excess CuAlS₂: A first-principles study. Applied Physics Express, 2016, 9, 031202.	1.1	5
27596	Comparative Study of Theoretical Partial Charges of Pristine and Doped GaAs Clusters Ga3As3, Ga7As7, AlGa2As3, and Al2Ga5As7. Journal of Cluster Science, 2016, 27, 551-561.	1.7	2
27597	Atomistic Mechanism of Pt Extraction at Oxidized Surfaces: Insights from DFT. Electrocatalysis, 2016, 7, 345-354.	1.5	41
27598	Slip Resistance of Ti-Based High-Temperature Shape Memory Alloys. Shape Memory and Superelasticity, 2016, 2, 50-61.	1.1	13
27599	Nanoindentation study of cementite size and temperature effects in nanocomposite pearlite: A molecular dynamics simulation. Current Applied Physics, 2016, 16, 1015-1025.	1.1	19
27600	The electronic and optical properties of Tungsten Disulfide under high pressure. Chemical Physics Letters, 2016, 651, 257-260.	1.2	6
27601	Origin of the strain glass transition in Ti50(Ni50â˜ÂD) alloys. Journal of Alloys and Compounds, 2016, 678, 325-328.	2.8	4

#	Article	IF	Citations
27602	Theoretical interpretation on lead adsorption behavior of new two-dimensional transition metal carbides and nitrides. Journal of Alloys and Compounds, 2016, 684, 504-509.	2.8	55
27603	Reduction of chromiaâ€“silica catalysts: A molecular picture. Journal of Catalysis, 2016, 340, 122-135.	3.1	42
27604	Effects of vacancies on valence stabilities of europium ions in Î²-Ca2SiO4: Eu phosphors. Journal of Luminescence, 2016, 178, 121-127.	1.5	15
27605	A comparative study on ferromagnetic C/O-implanted GaN films by positron annihilation spectroscopy. Nuclear Instruments & Methods in Physics Research B, 2016, 375, 107-111.	0.6	1
27606	Study of the electronic structure and half-metallicity of CaMnO3/BaTiO3 superlattice. Superlattices and Microstructures, 2016, 97, 116-124.	1.4	23
27607	Understanding the Phase Diagram of Self-Assembled Monolayers of Alkanethiolates on Gold. Journal of Physical Chemistry C, 2016, 120, 12059-12067.	1.5	27
27608	Unlocking the Origin of Superior Performance of a Siâ€“Ge Coreâ€“Shell Nanowire Quantum Dot Field Effect Transistor. Nano Letters, 2016, 16, 3995-4000.	4.5	14
27609	Preparation and methane adsorption of two-dimensional carbide Ti2C. Adsorption, 2016, 22, 915-922.	1.4	85
27610	Elastic Instability of the Orthorhombic Antiferromagnetic Phase of 122-Pnictides Under Pressure. Journal of Superconductivity and Novel Magnetism, 2016, 29, 685-689.	0.8	2
27611	Adsorption and decomposition of H2O on cobalt surfaces: A DFT study. Applied Surface Science, 2016, 384, 10-17.	3.1	32
27612	Liquid-liquid extraction of lithium using lipophilic dibenzo-14-crown-4 ether carboxylic acid in hydrophobic room temperature ionic liquid. Hydrometallurgy, 2016, 164, 362-371.	1.8	48
27613	Chemical Substitution - Alignment of the Surface Potentials for Efficient Charge Transport in Nanocrystalline TiO₂ Photocatalysts. Chemistry of Materials, 2016, 28, 4223-4230.	3.2	22
27614	Spin Frustration and Magnetic Ordering from One-Dimensional Stacking of Cr₃ Triangles in TiCrIr₂B₂. Inorganic Chemistry, 2016, 55, 5640-5648.	1.9	14
27615	Electrodeposition and ab Initio Studies of Metastable Orthorhombic Bi₂Se₃: A Novel Semiconductor with Bandgap for Photovoltaic Applications. Journal of Physical Chemistry C, 2016, 120, 11797-11806.	1.5	32
27616	Conjugation-Driven â€œReverse Marsâ€“van Krevelenâ€•Type Radical Mechanism for Low-Temperature Câ€“O Bond Activation. Journal of the American Chemical Society, 2016, 138, 8104-8113.	6.6	84
27617	Stable and metallic borophene nanoribbons from first-principles calculations. Journal of Materials Chemistry C, 2016, 4, 6380-6385.	2.7	75
27618	First-principle study of electronic structures and optical properties of chromium and carbon co-doped anatase TiO2. Ceramics International, 2016, 42, 13900-13908.	2.3	14
27619	Anatase TiO2 codoping with sulfur and acceptor IIB metals for water splitting. International Journal of Hydrogen Energy, 2016, 41, 13050-13057.	3.8	22

#	Article	IF	Citations
27620	GGA+U study of uranium mononitride: A comparison of the U-ramping and occupation matrix schemes and incorporation energies of fission products. Journal of Nuclear Materials, 2016, 478, 119-124.	1.3	39
27621	Exploring the sodium storage mechanism in disodium terephthalate as anode for organic battery using density-functional theory calculations. Journal of Power Sources, 2016, 324, 572-581.	4.0	51
27622	Fast Diffusion of Native Defects and Impurities in Perovskite Solar Cell Material CH₃NH₃PbI₃. Chemistry of Materials, 2016, 28, 4349-4357.	3.2	139
27623	Energy Landscape of Molecular Motion in Cubic Methylammonium Lead Iodide from First-Principles. Journal of Physical Chemistry C, 2016, 120, 12403-12410.	1.5	57
27624	Large-Scale Sublattice Asymmetry in Pure and Boron-Doped Graphene. Nano Letters, 2016, 16, 4535-4543.	4.5	55
27625	Tuning Catalytic Selectivity of Oxidative Catalysis through Deposition of Nonmetallic Atoms in Surface Lattice of Metal Oxide. ACS Catalysis, 2016, 6, 4218-4228.	5.5	32
27626	Cluster-Inspired Design of High-Capacity Anode for Li-Ion Batteries. ACS Energy Letters, 2016, 1, 202-208.	8.8	23
27627	Topological semimetals with helicoid surfaceÂstates. Nature Physics, 2016, 12, 936-941.	6.5	149
27628	Anodic performance of black phosphorus in magnesium-ion batteries: the significance of Mgâ€“P bond-synergy. Chemical Communications, 2016, 52, 8381-8384.	2.2	40
27629	Hydroxyapatite substituted by transition metals: experiment and theory. Physical Chemistry Chemical Physics, 2016, 18, 16457-16465.	1.3	91
27630	High-pressure phase transitions in rubidium and caesium hydroxides. Physical Chemistry Chemical Physics, 2016, 18, 16527-16534.	1.3	9
27631	Concentration of constitutional and thermal defects in UAl4. Journal of Nuclear Materials, 2016, 478, 74-82.	1.3	2
27632	Frontier Orbital Engineering of Metalâ€“Organic Frameworks with Extended Inorganic Connectivity: Porous Alkaline-Earth Oxides. Inorganic Chemistry, 2016, 55, 7265-7269.	1.9	13
27633	Intermolecular Hybridization Creating Nanopore Orbital in a Supramolecular Hydrocarbon Sheet. Nano Letters, 2016, 16, 4274-4281.	4.5	13
27634	CO₂ Activation on Ni/Î³â€“Al₂O₃ Catalysts by First-Principles Calculations: From Ideal Surfaces to Supported Nanoparticles. ACS Catalysis, 2016, 6, 4501-4505.	5.5	92
27635	Multi-scale theory and simulation of shape-selective nanocrystal growth. CrystEngComm, 2016, 18, 5410-5417.	1.3	30
27636	Double-hole codoped huge-gap semiconductor ZrO₂ for visible-light photocatalysis. Physical Chemistry Chemical Physics, 2016, 18, 17517-17524.	1.3	32
27637	Liquid self-diffusion of H₂O and DMF molecules in Co-MOF-74: molecular dynamics simulations and dielectric spectroscopy studies. Physical Chemistry Chemical Physics, 2016, 18, 19605-19612.	1.3	21

#	Article	IF	Citations
27638	Hydrogen influence on generalized stacking fault energies of Zr {0001} basal plane: a first-principles study. RSC Advances, 2016, 6, 54371-54376.	1.7	4
27639	Enhancement of anisotropic thermoelectric performance of tungsten disulfide by titanium doping. Journal of Materials Chemistry A, 2016, 4, 10159-10165.	5.2	29
27640	Exploring the mechanism of water-splitting reaction in NiO_x/Î²-Ga₂O₃ photocatalysts by first-principles calculations. Physical Chemistry Chemical Physics, 2016, 18, 11111-11119.	1.3	17
27641	Integrating cobalt phosphide and cobalt nitride-embedded nitrogen-rich nanocarbons: high-performance bifunctional electrocatalysts for oxygen reduction and evolution. Journal of Materials Chemistry A, 2016, 4, 10575-10584.	5.2	141
27642	Ground state structures of tantalum tetraboride and triboride: an ab initio study. Physical Chemistry Chemical Physics, 2016, 18, 18074-18080.	1.3	19
27643	A first-principles study on the magnetic properties of Sc, V, Cr and Mn-doped monolayer TiS₃. RSC Advances, 2016, 6, 55194-55202.	1.7	7
27644	Study on the crystal structure of (Gd_{2â^'x}Ce_x)Ti₂O₇(0â€‰â‰¤â€‰xâ€‰â‰¤â€‰ pyrochlore. Advances in Applied Ceramics, 2016, 115, 411-416.		
27645	A comparative investigation of the behaviors of H in Au and Ag from first principles. Modelling and Simulation in Materials Science and Engineering, 2016, 24, 045009.	0.8	4
27646	First principles study of the diffusional phenomena across the clean and Re-doped Î³ -Ni/ Î³ â€™-Ni ₃ Al interface of Ni-based single crystal superalloy. Chinese Physics B, 2016, 25, 067104.	0.7	6
27647	A comparative study on electrochemical cycling stability of lithium rich layered cathode materials Li 1.2 Ni 0.13 M 0.13 Mn 0.54 O 2 where MÂ=ÂFe or Co. Journal of Power Sources, 2016, 324, 462-474.	4.0	59
27648	Pressure-Induced Conductivity in a Neutral Nonplanar Spin-Localized Radical. Journal of the American Chemical Society, 2016, 138, 11517-11525.	6.6	38
27649	A DFT+U study on the contribution of 4f electrons to oxygen vacancy formation and migration in Ln-doped CeO₂. Physical Chemistry Chemical Physics, 2016, 18, 12938-12946.	1.3	43
27650	Tunneling spectra of graphene on copper unraveled. Physical Chemistry Chemical Physics, 2016, 18, 17081-17090.	1.3	2
27651	Antimonene: a monolayer material for ultraviolet optical nanodevices. Journal of Materials Chemistry C, 2016, 4, 6386-6390.	2.7	246
27652	Structural stability of calcium-manganate based CaO(CaMnO3)m (mÂ=Â1, 2, 3, â^ž) compounds for thermoelectric applications. Journal of Alloys and Compounds, 2016, 687, 562-569.	2.8	19
27653	Interfacial properties and electron structure of Al/B4C interface: A first-principles study. Journal of Nuclear Materials, 2016, 478, 227-235.	1.3	63
27654	First-principles study of size-, surface- and mechanical strain-dependent electronic properties of wurtzite and zinc-blende InSb nanowires. Physics Letters, Section A: General, Atomic and Solid State Physics, 2016, 380, 2678-2684.	0.9	3
27655	Extended homologous series of Snâ€“O layered systems: A first-principles study. Solid State Communications, 2016, 243, 36-43.	0.9	14

#	Article	IF	Citations
27656	Lone-Pair Stabilization in Transparent Amorphous Tin Oxides: A Potential Route to p-Type Conduction Pathways. Chemistry of Materials, 2016, 28, 4706-4713.	3.2	33
27657	Single-Component Conductors: A Sturdy Electronic Structure Generated by Bulky Substituents. Inorganic Chemistry, 2016, 55, 6036-6046.	1.9	22
27658	Spin rectification by orbital polarization in Bi-bilayer nanoribbons. Physical Chemistry Chemical Physics, 2016, 18, 8637-8642.	1.3	13
27659	First-principles investigation of the Schottky contact for the two-dimensional MoS₂ and graphene heterostructure. RSC Advances, 2016, 6, 60271-60276.	1.7	68
27660	Interactive exploration of atomic trajectories through relative-angle distribution and associated uncertainties. , 2016, , .		0
27661	First-principles study of nitrogen and carbon monoxide adsorptions on silicene. International Journal of Modern Physics B, 2016, 30, 1650176.	1.0	7
27662	First-principles simulation of oxygen vacancy migration in $$hbox {HfO}_{ x}$$, $$hbox {CeO}_{ x}$$, and at their interfaces for applications in resistive random-access memories. Journal of Computational Electronics, 2016, 15, 741-748.	1.3	2
27663	A first principles study of interactions of CO2 with surfaces of a Cu(benzeneâ€1,3,5â€tricarboxylate) metal organic framework. Applied Surface Science, 2016, 385, 578-586.	3.1	9
27664	Fabrication and band engineering of Cu-doped CdSe0.6Te0.4-alloyed quantum dots for solar cells. Solar Energy Materials and Solar Cells, 2016, 157, 161-170.	3.0	18
27665	Adsorption of gold subnano-structures on a magnetite(111) surface and their interaction with CO. Physical Chemistry Chemical Physics, 2016, 18, 18169-18179.	1.3	14
27666	Engineering magnetism and electronic properties of silicene by changing adsorption coverage. Applied Surface Science, 2016, 384, 65-72.	3.1	18
27667	A density functional theory study for the adsorption of various gases on a caesium-exchanged trapdoor chabazite. Computational Materials Science, 2016, 122, 307-313.	1.4	25
27668	The nucleation and growth of H blisters in dislocation loops in W{110}. Journal of Nuclear Materials, 2016, 478, 222-226.	1.3	3
27669	Structural and mechanical properties of nitrogen-deficient cubic Crâ€“Moâ€“N and Crâ€“Wâ€“N systems. Scripta Materialia, 2016, 123, 34-37.	2.6	23
27670	Silicon Framework-Based Lithium Silicides at High Pressures. ACS Applied Materials & Interfaces, 2016, 8, 16761-16767.	4.0	17
27671	A first-principles study of stable few-layer penta-silicene. Physical Chemistry Chemical Physics, 2016, 18, 18486-18492.	1.3	51
27672	SiTe monolayers: Si-based analogues of phosphorene. Journal of Materials Chemistry C, 2016, 4, 6353-6361.	2.7	54
27673	Discovering novel VC1â^' compounds through hybrid first-principles and evolutionary algorithms. Journal of the European Ceramic Society, 2016, 36, 3593-3599.	2.8	10

#	Article	IF	Citations
27674	Monoclinic sulfur cathode utilizing carbon for high-performance lithiumâ€“sulfur batteries. Journal of Power Sources, 2016, 325, 495-500.	4.0	28
27675	Nitrate reduction pathways on Cu single crystal surfaces: Effect of oxide and Clâ^'. Nano Energy, 2016, 29, 457-465.	8.2	124
27676	A comprehensive theoretical study of halide perovskites ABX3. Organic Electronics, 2016, 37, 61-73.	1.4	186
27677	Band gap modulation of transition-metal dichalcogenide MX 2 nanosheets by in-plane strain. Physica E: Low-Dimensional Systems and Nanostructures, 2016, 84, 216-222.	1.3	7
27678	Molecular Dynamics Simulations of Supported Pt Nanoparticles with a Hybrid Suttonâ€“Chen Potential. Journal of Physical Chemistry C, 2016, 120, 14883-14891.	1.5	11
27679	Atomically thin binary Vâ€“V compound semiconductor: a first-principles study. Journal of Materials Chemistry C, 2016, 4, 6581-6587.	2.7	126
27680	Bonding and electronic properties of the Cu₂ZnSnS₄â€‰/WZâ€“ZnO interface from first-principles calculations. Journal Physics D: Applied Physics, 2016, 49, 285107.	1.3	12
27681	First principles kinetic Monte Carlo study on the growth patterns of WSe ₂ monolayer. 2D Materials, 2016, 3, 025029.	2.0	59
27682	Structural and electrical study of the topological insulator SnBi2Te4 at high pressure. Journal of Alloys and Compounds, 2016, 685, 962-970.	2.8	28
27683	High-Throughput Computational Screening of Perovskites for Thermochemical Water Splitting Applications. Chemistry of Materials, 2016, 28, 5621-5634.	3.2	191
27684	Atomic Structural Evolution during the Reduction of Î±-Fe₂O₃ Nanowires. Journal of Physical Chemistry C, 2016, 120, 14854-14862.	1.5	37
27685	A Honeycomb BeN₂ Sheet with a Desirable Direct Band Gap and High Carrier Mobility. Journal of Physical Chemistry Letters, 2016, 7, 2664-2670.	2.1	100
27686	Methylation of olefins with ketene in zeotypes and its implications for the direct conversion of syngas to light olefins: a periodic DFT study. Catalysis Science and Technology, 2016, 6, 6644-6649.	2.1	36
27687	Adsorption and dissociation of dinitrogen on transition metal (Ta, W and Re) doped MgO surface. Computational and Theoretical Chemistry, 2016, 1090, 165-170.	1.1	1
27688	Pressure and temperature induced phase transition in WB4: A first principles study. Journal of Alloys and Compounds, 2016, 687, 579-585.	2.8	23
27689	Suppression of Jahnâ€“Teller Distortions and Origin of Piezochromism and Thermochromism in Cuâ€“Cl Hybrid Perovskite. Inorganic Chemistry, 2016, 55, 6817-6824.	1.9	24
27690	Transition Metal and Vacancy Defect Complexes in Phosphorene: A Spintronic Perspective. Journal of Physical Chemistry C, 2016, 120, 14991-15000.	1.5	59
27691	Mechanism of Hydrogen Evolution Reaction on 1T-MoS₂ from First Principles. ACS Catalysis, 2016, 6, 4953-4961.	5.5	678

#	Article	IF	Citations
27692	First-principles investigations of vanadium disulfide for lithium and sodium ion battery applications. RSC Advances, 2016, 6, 54874-54879.	1.7	55
27693	Monolayer Intermixed Oxide Surfaces: Fe, Ni, Cr, and V Oxides on Rutile TiO₂(011). Journal of Physical Chemistry C, 2016, 120, 14782-14794.	1.5	11
27694	Control of Triboelectrification by Engineering Surface Dipole and Surface Electronic State. ACS Applied Materials & Interfaces, 2016, 8, 18519-18525.	4.0	100
27695	Band Edge Engineering in BiVO₄/TiO₂ Heterostructure: Enhanced Photoelectrochemical Performance through Improved Charge Transfer. ACS Catalysis, 2016, 6, 5311-5318.	5.5	117
27696	Mechanism and microstructures in Ga₂O₃ pseudomartensitic solid phase transition. Physical Chemistry Chemical Physics, 2016, 18, 18563-18574.	1.3	12
27697	The origin of room temperature ferromagnetism mediated by Coâ€“V_{Zn} complexes in the ZnO grain boundary. RSC Advances, 2016, 6, 50818-50824.	1.7	32
27698	Manganous oxide nanoparticles encapsulated in few-layer carbon as an efficient electrocatalyst for oxygen reduction in alkaline media. Journal of Materials Chemistry A, 2016, 4, 11775-11781.	5.2	27
27699	Understanding the advantage of hexagonal WO₃as an efficient photoanode for solar water splitting: a first-principles perspective. Journal of Materials Chemistry A, 2016, 4, 11498-11506.	5.2	45
27700	Indirect-direct band gap transition in puckered arsenene through chemical doping of P, Sb and Bi: a computational study. Materials Technology, 2016, 31, 4-6.	1.5	9
27701	Structural, electronic, optical and elastic properties of the complex K₂PtCl₆-structure hydridesARuH₆(A= Mg, Ca, Sr and) Tj ETQq1 1 0.784314 rgBT /Overlock 10	1.7	37
27702	A computational study on the adsorption configurations and reactions of SiHx(x = 1-4) on clean and H-covered Si(100) surfaces. Applied Surface Science, 2016, 387, 546-556.	3.1	4
27703	Grain boundary and curvature enhanced lithium adsorption on carbon. Carbon, 2016, 107, 557-563.	5.4	17
27704	Predicted thermoelectric properties of natural superlattice structural compounds BaCu Ch F (Ch Â=ÂS,) Tj ETQq0 0 0 rgBT /Overlock 10	2.8	12
27705	Prediction of new stable structure, promising electronic and thermodynamic properties of MoS3: Ab initio calculations. Journal of Power Sources, 2016, 325, 246-251.	4.0	70
27706	Direct Observation of Lattice Aluminum Environments in Li Ion Cathodes LiNi_{1â€“yâ€“z}Co_yAl_zO₂ and Al-Doped LiNi_xMn_yCo_zO₂ via ²⁷Al MAS NMR Spectroscopy. ACS Applied Materials & Interfaces, 2016, 8, 16708-16717.	4.0	63
27707	Highly Active Au/Î´-MoC and Cu/Î´-MoC Catalysts for the Conversion of CO₂: The Metal/C Ratio as a Key Factor Defining Activity, Selectivity, and Stability. Journal of the American Chemical Society, 2016, 138, 8269-8278.	6.6	140
27708	A DFT study of planar vs. corrugated graphene-like carbon nitride (g-C₃N₄) and its role in the catalytic performance of CO₂ conversion. Physical Chemistry Chemical Physics, 2016, 18, 18507-18514.	1.3	125
27709	Polymer-free nanofibers from vanillin/cyclodextrin inclusion complexes: high thermal stability, enhanced solubility and antioxidant property. Food and Function, 2016, 7, 3141-3153.	2.1	87

#	Article	IF	Citations
27710	Doping enhanced ferromagnetism and induced half-metallicity in CrI ₃ monolayer. Europhysics Letters, 2016, 114, 47001.	0.7	146
27711	The nucleation and growth of borophene on the Ag (111) surface. Nano Research, 2016, 9, 2616-2622.	5.8	86
27712	Chiral vectors-tunable electronic property of MoS2 nanotubes. Physica E: Low-Dimensional Systems and Nanostructures, 2016, 84, 196-201.	1.3	6
27713	Preparation, Structure, and Surface Chemistry of Niâ€“Au Single Atom Alloys. Journal of Physical Chemistry C, 2016, 120, 13574-13580.	1.5	70
27714	Deposition Order Controls the First Stages of a Metalâ€“Organic Coordination Network on an Insulator Surface. Journal of Physical Chemistry C, 2016, 120, 14730-14735.	1.5	12
27715	Ionic Graphitization of Ultrathin Films of Ionic Compounds. Journal of Physical Chemistry Letters, 2016, 7, 2659-2663.	2.1	9
27716	Role of oxygen vacancies in crystalline WO₃. Journal of Materials Chemistry C, 2016, 4, 6641-6648.	2.7	95
27717	Unraveling the Intercalation Chemistry of Hexagonal Tungsten Bronze and Its Optical Responses. Chemistry of Materials, 2016, 28, 4528-4535.	3.2	47
27718	Toward Design Principles for Diffusionless Transformations: The Frustrated Formation of Coâ€“Co Bonds in a Low-Temperature Polymorph of GdCoSi₂. Inorganic Chemistry, 2016, 55, 6148-6160.	1.9	8
27719	Two-Dimensional Group IV Monochalcogenides: Anode Materials for Li-Ion Batteries. Journal of Physical Chemistry C, 2016, 120, 14522-14530.	1.5	120
27720	The interaction of molecular oxygen on LaO terminated surfaces of La₂NiO₄. Journal of Materials Chemistry A, 2016, 4, 13113-13124.	5.2	54
27721	First-principles study of Mg(0001)/MgO(1-11) interfaces. Modern Physics Letters B, 2016, 30, 1650152.	1.0	11
27722	Stability of Li- and Mn-Rich Layered-Oxide Cathodes within the First-Charge Voltage Plateau. Journal of the Electrochemical Society, 2016, 163, A1784-A1789.	1.3	11
27723	Transient existence of crystalline lithium disulfide Li2S2 in a lithium-sulfur battery. Journal of Power Sources, 2016, 325, 641-645.	4.0	57
27724	Transition-metal-decorated germanene as promising catalyst for removing CO contamination in H2. Materials and Design, 2016, 107, 82-89.	3.3	17
27725	Stability and hydrogen adsorption properties of Mg/TiMn2 interface by first principles calculation. Surface Science, 2016, 653, 22-26.	0.8	12
27726	Density functional theory study of the interaction of H2O, CO2 and CO with the ZrO2 (111), Ni/ZrO2 (111), YSZ (111) and Ni/YSZ (111) surfaces. Surface Science, 2016, 653, 153-162.	0.8	17
27727	Site Partition: Turning One Site into Two for Adsorbing CO₂. Journal of Physical Chemistry Letters, 2016, 7, 2568-2572.	2.1	17

#	Article	IF	Citations
27728	Dehalogenative Homocoupling of Terminal Alkynyl Bromides on Au(111): Incorporation of Acetylenic Scaffolding into Surface Nanostructures. ACS Nano, 2016, 10, 7023-7030.	7.3	150
27729	Structure and bonding in crystalline cesium uranyl tetrachloride under pressure. Physical Chemistry Chemical Physics, 2016, 18, 18398-18405.	1.3	7
27730	Ammonothermal Synthesis, Crystal Structure, and Properties of the Ytterbium(II) and Ytterbium(III) Amides and the First Two Rare-Earth-Metal Guanidinates, YbC(NH)₃ and Yb(CN₃H₄)₃. Inorganic Chemistry, 2016, 55, 6161-6168.	1.9	17
27731	Multifunctional Nitrogen-Doped Loofah Sponge Carbon Blocking Layer for High-Performance Rechargeable Lithium Batteries. ACS Applied Materials & Interfaces, 2016, 8, 15991-16001.	4.0	64
27732	First-principles study of the structural, electronic, and magnetic properties of double perovskite Sr 2 FeReO 6 containing various imperfections. Chinese Physics B, 2016, 25, 058102.	0.7	2
27733	Activating Inert Basal Planes of MoS₂ for Hydrogen Evolution Reaction through the Formation of Different Intrinsic Defects. Chemistry of Materials, 2016, 28, 4390-4396.	3.2	388
27734	First-Principles Predictions of Structureâ€“Function Relationships of Graphene-Supported Platinum Nanoclusters. Journal of Physical Chemistry C, 2016, 120, 11899-11909.	1.5	40
27735	Room temperature quantum spin Hall states in two-dimensional crystals composed of pentagonal rings and their quantum wells. NPG Asia Materials, 2016, 8, e264-e264.	3.8	65
27736	Dielsâ€“Alder attachment of a planar organic molecule to a dangling bond dimer on a hydrogenated semiconductor surface. Physical Chemistry Chemical Physics, 2016, 18, 16757-16765.	1.3	7
27737	Carrier-tunable magnetism in two dimensional graphene-like C₂N. RSC Advances, 2016, 6, 54027-54031.	1.7	28
27738	Quantum-chemical study of nitrogen and magnesium co-doping in Î±-Cr2O3. Modern Physics Letters B, 2016, 30, 1650219.	1.0	1
27739	Magnetic, magnetocaloric and structural properties of manganese based monoborides doped with iron and cobalt â€“ A candidate for thermomagnetic generators. Acta Materialia, 2016, 113, 213-220.	3.8	23
27740	Twin boundary activated Î±Â†'ÂÏ‰ phase transformation in titanium under shock compression. Acta Materialia, 2016, 115, 1-9.	3.8	28
27741	Mechanical properties of Wâ€“Ti alloys from first-principles calculations. Fusion Engineering and Design, 2016, 106, 34-39.	1.0	46
27742	Band engineering and rational design of high-performance thermoelectric materials by first-principles. Journal of Materiomics, 2016, 2, 114-130.	2.8	34
27743	Atomic structure and defect energetics of LiCoO2 grain boundary. Materials Research Bulletin, 2016, 82, 81-86.	2.7	11
27744	First-principles prediction of MgB2-like NaBC: A more promising high-temperature superconducting material than LiBC. Solid State Communications, 2016, 233, 30-34.	0.9	7
27745	Adsorption of formate species on Cu(h,k,l) low index surfaces. Surface Science, 2016, 653, 45-54.	0.8	25

#	Article	IF	Citations
27746	(TTF)Pb₂I₅: A Radical Cation-Stabilized Hybrid Lead Iodide with Synergistic Optoelectronic Signatures. Chemistry of Materials, 2016, 28, 3607-3611.	3.2	40
27747	Catalytic conversion of CHx and CO2 on non-noble metallic impurities in graphene. Physical Chemistry Chemical Physics, 2016, 18, 16998-17009.	1.3	6
27748	Strain enhancement of acoustic phonon limited mobility in monolayer TiS₃. Physical Chemistry Chemical Physics, 2016, 18, 14434-14441.	1.3	27
27749	Characterization of tungsten monomeric oxide species supported on hydroxylated silica; a DFT study. RSC Advances, 2016, 6, 39424-39432.	1.7	32
27750	Electric field induced insulator to metal transition in a buckled GaAs monolayer. RSC Advances, 2016, 6, 52920-52924.	1.7	18
27751	Effect of Sn Doping in (Bi0.25Sb0.75)2â^'x Sn x Te3 (0Ââ‰ÂxÂâ‰Â0.1) on Thermoelectric Performance. Journal of Electronic Materials, 2016, 45, 1441-1446.	1.0	3
27752	Complex Precipitation Sequences of Al-Cu-Li-(Mg) Alloys Characterized in Relation to Thermal Ageing Processes. Acta Metallurgica Sinica (English Letters), 2016, 29, 94-103.	1.5	34
27753	Theoretical investigations of the effects of ordered carbon vacancies in ZrC1â^'x on phase stability and thermo-mechanical properties. Acta Materialia, 2016, 111, 232-241.	3.8	32
27754	A computational study on the energetics and mechanisms for the dissociative adsorption of SiH (x=) Tj ETQq0 0 0 rgBT /Overlock 10 Tf 5	3.1	0
27755	Sp2 carbon embedded in Al-6061 and Al-7075 alloys in the form of crystalline graphene nanoribbons. Carbon, 2016, 107, 56-66.	5.4	28
27756	Adsorption and migration behaviours of Nbâ€“C atoms on clean diamond (0 0 1) surface: A first principles study. Computational Materials Science, 2016, 121, 159-166.	1.4	10
27757	Insight into the electronic and magnetic properties of TiO2 (1 0 1) surfaces with adsorbed water and ethanol molecules. Computational Materials Science, 2016, 121, 174-181.	1.4	4
27758	Point defects and Zn-doping in defective Laves phase C15 MgCu2: A first-principles study. Computational Materials Science, 2016, 122, 159-166.	1.4	10
27759	Activation Effect of Electrochemical Cycling on Gold Nanoparticles towards the Hydrogen Evolution Reaction in Sulfuric Acid. Electrochimica Acta, 2016, 209, 440-447.	2.6	32
27760	O2 adsorption on MO2 (M = Ru, Ir, Sn) films supported on rutile TiO2(1 1 0) by DFT calculations: Probing the nature of metal oxide-support interaction. Journal of Colloid and Interface Science, 2016, 473, 100-111.	5.0	10
27761	Comparing electrochemical performance of transition metal silicate cathodes and chevrel phase Mo6S8 in the analogous rechargeable Mg-ion battery system. Journal of Power Sources, 2016, 321, 76-86.	4.0	28
27762	Atomic and electronic structures of I-V-VI2 ternary chalcogenides. Journal of Science: Advanced Materials and Devices, 2016, 1, 51-56.	1.5	19
27763	Pre-Lithiation of Li(Ni_{1-x-y}Mn_xCo_y)O₂ Materials Enabling Enhancement of Performance for Li-Ion Battery. ACS Applied Materials & Interfaces, 2016, 8, 15361-15368.	4.0	32

#	Article	IF	Citations
27764	â€œGet in Touch and Keep in Contactâ€: Interface Effect on the Oxygen Reduction Reaction (ORR) Activity for Supported PtNi Nanoparticles. ACS Catalysis, 2016, 6, 4388-4393.	5.5	34
27765	Achieving Ultrafast Hole Transfer at the Monolayer MoS₂ and CH₃NH₃PbI₃ Perovskite Interface by Defect Engineering. ACS Nano, 2016, 10, 6383-6391.	7.3	130
27766	Ab initio calculations of X-ray magnetic circular dichroism spectra within the projector augmented wave method: An implementation into the VASP code. Computer Physics Communications, 2016, 207, 136-144.	3.0	8
27767	Theory of perpendicular magnetocrystalline anisotropy in Fe/MgO (001). Journal of Magnetism and Magnetic Materials, 2016, 414, 126-131.	1.0	18
27768	Direct time-domain observation of attosecond final-state lifetimes in photoemission from solids. Science, 2016, 353, 62-67.	6.0	181
27769	Surface relaxation of Pt(111) and Cu/Pt(111) revealed by DEPES. Applied Surface Science, 2016, 373, 32-37.	3.1	4
27770	Properties of two-dimensional insulators: A DFT study of bimetallic oxide CrW2O9 clusters adsorption on MgO ultrathin films. Applied Surface Science, 2016, 379, 213-222.	3.1	5
27771	Short-range effect at the semi-coherent metal/its native oxide interface. Applied Surface Science, 2016, 378, 451-459.	3.1	3
27772	Local property change of graphene induced by a Cu nanoparticle. Carbon, 2016, 98, 666-670.	5.4	6
27773	Ab initio X-ray absorption modeling of Cu-SAPO-34: Characterization of Cu exchange sites under different conditions. Catalysis Today, 2016, 267, 28-40.	2.2	10
27774	Structural, functional and mechanical properties of spark plasma sintered gadolinia (Gd 2 O 3). Ceramics International, 2016, 42, 1384-1391.	2.3	17
27775	C15 NbCr2 Laves phase with mechanical properties beyond Pughâ€™s criterion. Computational Materials Science, 2016, 121, 167-173.	1.4	24
27776	Chemical potential effects on polytypism in Au-catalyzed GaAs nanowire molecular beam epitaxy growth: A first-principles study. Chemical Physics Letters, 2016, 644, 147-151.	1.2	4
27777	Adsorption and Decomposition of Ethylene Carbonate on LiMn2O4 Cathode Surface. Electrochimica Acta, 2016, 210, 61-70.	2.6	10
27778	Structural, electronic and magnetic properties of Î·-carbides M3W3C (MÂ=ÂTi, V, Cr, Mn, Fe, Co, Ni). Journal of Alloys and Compounds, 2016, 681, 508-515.	2.8	23
27779	Theoretical assessment of bonaccordite formation in pressurized water reactors. Journal of Nuclear Materials, 2016, 474, 62-64.	1.3	5
27780	Thermodynamic assessment of the Pd Rh Ru system using calphad and first-principles methods. Journal of Nuclear Materials, 2016, 474, 163-173.	1.3	15
27781	High-temperature properties of thorium dioxide: A first-principles molecular dynamics study. Journal of Nuclear Materials, 2016, 478, 56-60.	1.3	9

#	Article	IF	Citations
27782	Structural phase transitions in EuNbO3 perovskite. Journal of Solid State Chemistry, 2016, 239, 192-199.	1.4	12
27783	NaV3(PO4)3/C nanocomposite as novel anode material for Na-ion batteries with high stability. Nano Energy, 2016, 26, 382-391.	8.2	69
27784	Hydrogen diffusion in bulk MgB2. Scripta Materialia, 2016, 117, 86-91.	2.6	6
27785	Lone electron pair (E) role on the crystal structures and the mechanism of high ionic conductivity of PbSnF 4 E 2 . Stereochemical and ab initio investigations. Solid State Sciences, 2016, 52, 29-36.	1.5	10
27786	Chemically selective formation of Siâ€“Oâ€“Al on SiGe(110) and (001) for ALD nucleation using H2O2(g). Surface Science, 2016, 652, 322-333.	0.8	7
27787	Dynamics of surface-migration: Electron-induced reaction of 1,2-dihaloethanes on Si(100). Surface Science, 2016, 652, 312-321.	0.8	8
27788	Au-induced deep groove nanowire structure on the Ge(001) surface: DFT calculations. Surface Science, 2016, 651, 164-174.	0.8	7
27789	Complexity of H-bonding between polar molecules on Si(100)-2 Ã— 1 and Ge(100)-2 Ã— 1 surfaces. Surface Science, 2016, 651, 187-194.	0.8	5
27790	The structure and electronic properties of Ge/SrZrO 3. Vacuum, 2016, 130, 165-173.	1.6	2
27791	First-principles studies on the charge density wave in uranium. Modelling and Simulation in Materials Science and Engineering, 2016, 24, 055011.	0.8	4
27792	Electronic and magnetic properties of 1T-HfS2 by doping transition-metal atoms. Applied Surface Science, 2016, 383, 151-158.	3.1	36
27793	Charge transfer of edge states in zigzag silicene nanoribbons with Stoneâ€“Wales defects from first-principles. Applied Surface Science, 2016, 383, 310-316.	3.1	9
27794	CO2 stability on the Ni low-index surfaces: van der Waals corrected DFT analysis. Catalysis Communications, 2016, 80, 33-38.	1.6	40
27795	Ab initio proposition of novel BCN3 hard material based on the intergrowth of wurtzite and pyrite-like motifs. Computational Condensed Matter, 2016, 7, 14-19.	0.9	2
27796	Adsorption of H 2 S on Î± -Cr 2 O 3 (0001) surfaces: A density functional theory investigation. Corrosion Science, 2016, 111, 1-12.	3.0	10
27797	NH3 adsorption on PtM (Fe, Co, Ni) surfaces: Cooperating effects of charge transfer, magnetic ordering and lattice strain. Chemical Physics Letters, 2016, 648, 166-169.	1.2	17
27798	Effect of electrolytes and soil minerals on nitrous oxide (N 2 O) hydrate formation kinetics. International Journal of Greenhouse Gas Control, 2016, 45, 34-42.	2.3	3
27799	Band structures and spatial carrier confinement in GaAs/GaP core-shell nanowires: Core/shell composition and size effects. Journal of Alloys and Compounds, 2016, 682, 571-578.	2.8	7

#	Article	IF	Citations
27800	Pressure-induced electron phase transitions of Î±-As2Te3. Journal of Alloys and Compounds, 2016, 685, 551-558.	2.8	13
27801	Insight into the promoting role of Rh doped on Pt(111) in methanol electro-oxidation. Journal of Electroanalytical Chemistry, 2016, 781, 24-29.	1.9	19
27802	First-principles search for efficient activators for LaI3. Journal of Luminescence, 2016, 176, 227-234.	1.5	11
27803	Reduction of thermal conductivity by low energy multi-Einstein optic modes. Journal of Materiomics, 2016, 2, 187-195.	2.8	53
27804	Exploring phase stability, electronic and mechanical properties of Ceâ€“Pb intermetallic compounds using first-principles calculations. Journal of Solid State Chemistry, 2016, 237, 385-393.	1.4	11
27805	Ab initio tensile tests of grain boundaries in the fcc crystals of Ni and Co with segregated sp-impurities. Materials Science & Engineering A: Structural Materials: Properties, Microstructure and Processing, 2016, 669, 218-225.	2.6	29
27806	Atomic-scale segregation behavior of Sn/Ti and O at Î£3[11Â¯0](111) grain boundary in niobium. Progress in Natural Science: Materials International, 2016, 26, 152-157.	1.8	1
27807	Enhanced interfacial proton migration on BaZr(Y)O3 by molten carbonate: A first principles study. Solid State Ionics, 2016, 289, 48-54.	1.3	7
27808	Rotation assisted diffusion of water trimers on Pd{111}. Surface Science, 2016, 648, 256-261.	0.8	1
27809	Oxygen Vacancies in CrO2: The Influences to Half Metallicity and the Formation Mode. IEEE Transactions on Magnetics, 2016, 52, 1-8.	1.2	3
27810	Bending rigidity of transition metal dichalcogenide monolayers from first-principles. Journal Physics D: Applied Physics, 2016, 49, 185301.	1.3	33
27811	Chiral vectors-tunable electronic property of MoS2 nanotubes. Physica E: Low-Dimensional Systems and Nanostructures, 2016, 83, 232-237.	1.3	6
27812	First-principles study of thermal expansion and thermomechanics of single-layer black and blue phosphorus. Physics Letters, Section A: General, Atomic and Solid State Physics, 2016, 380, 2098-2104.	0.9	60
27813	Revisiting Ir(CO)3Cl. Polyhedron, 2016, 103, 141-149.	1.0	11
27814	Tl(I) to Po(IV) 6s2 lone pairs in tetrahedral, triangular bipyramidal, square pyramidal, octahedral and hexahedral geometries: Crystal chemistry and ab initio visualizations and analyses. Progress in Solid State Chemistry, 2016, 44, 35-58.	3.9	9
27815	Synthesis and structure of a new halophosphate Sr 3 P 3 O 10 Cl with the flexible [P 3 O 10] 5â^' anions. Solid State Sciences, 2016, 55, 159-163.	1.5	7
27816	Surface morphology of orthorhombic Mo2C catalyst and high coverage hydrogen adsorption. Surface Science, 2016, 651, 195-202.	0.8	23
27817	Superlattice supertoughness of TiN/MN (M = V, Nb, Ta, Mo, and W): First-principles study. Thin Solid Films, 2016, 607, 59-66.	0.8	23

#	Article	IF	Citations
27818	Proteinâ€“Support Interactions for Rationally Designed Bilirubin Oxidase Based Cathode: A Computational Study. Journal of Physical Chemistry B, 2016, 120, 3634-3641.	1.2	24
27819	Structure of ZnCl₂ Melt. Part I: Raman Spectroscopy Analysis Driven by Ab Initio Methods. Journal of Physical Chemistry B, 2016, 120, 4174-4181.	1.2	20
27820	Incomplete Bilayer Termination of the Ice (0001) Surface. Journal of Physical Chemistry C, 2016, 120, 1097-1109.	1.5	15
27821	Effects of Chain Length on the Mechanism and Rates of Metal-Catalyzed Hydrogenolysis of n-Alkanes. Journal of Physical Chemistry C, 2016, 120, 8125-8138.	1.5	49
27822	Coadsorbed Species Explain the Mechanism of Methanol Temperature-Programmed Desorption on CeO₂(111). Journal of Physical Chemistry C, 2016, 120, 7241-7247.	1.5	14
27823	Describing the Diverse Geometries of Gold from Nanoclusters to Bulkâ€"A First-Principles-Based Hybrid Bond-Order Potential. Journal of Physical Chemistry C, 2016, 120, 13787-13800.	1.5	26
27824	Solution Deposition of Self-Assembled Benzoate Monolayers on Rutile (110): Effect of Ï€â€“Ï€ Interactions on Monolayer Structure. Journal of Physical Chemistry C, 2016, 120, 11581-11589.	1.5	12
27825	Modulation of Coordinate Bonds in Hydrogen-Bonded Trimesic Acid Molecular Networks on Highly Ordered Pyrolytic Graphite Surface. Journal of Physical Chemistry C, 2016, 120, 12605-12610.	1.5	23
27826	DFT+U Study of Chemical Impurities in PuO₂. Journal of Physical Chemistry C, 2016, 120, 13095-13102.	1.5	31
27827	Radiative/Nonradiative Recombination Affected by Defects and Electronâ€"Phone Coupling in CdWO₄ Nanorods. Journal of Physical Chemistry C, 2016, 120, 12218-12225.	1.5	28
27828	Insights into the Li Diffusion Dynamics and Nanostructuring of H₂Ti₁₂O₂₅ To Enhance Its Li Storage Performance. ACS Applied Materials & Interfaces, 2016, 8, 12186-12193.	4.0	8
27829	Strong Impact of Platinum Surface Structure on Primary and Secondary Alcohol Oxidation during Electro-Oxidation of Glycerol. ACS Catalysis, 2016, 6, 4491-4500.	5.5	156
27830	How Does the Surface Structure of Ptâ€"Ni Alloys Control Water and Hydrogen Peroxide Formation?. ACS Catalysis, 2016, 6, 5641-5650.	5.5	9
27831	Mechanistic Insight into the Interaction Between a Titanium Dioxide Photocatalyst and Pd Cocatalyst for Improved Photocatalytic Performance. ACS Catalysis, 2016, 6, 4239-4247.	5.5	50
27832	Tension-Enhanced Hydrogen Evolution Reaction on Vanadium Disulfide Monolayer. Nanoscale Research Letters, 2016, 11, 113.	3.1	37
27833	Ferromagnetism in Transitional Metal-Doped MoS2 Monolayer. Nanoscale Research Letters, 2016, 11, 154.	3.1	103
27834	Supercell program: a combinatorial structure-generation approach for the local-level modeling of atomic substitutions and partial occupancies in crystals. Journal of Cheminformatics, 2016, 8, 17.	2.8	292
27835	Plasmons of topological crystalline insulator SnTe with nanostructured patterns. RSC Advances, 2016, 6, 56042-56047.	1.7	1

#	Article	IF	Citations
27836	Interface properties of Ge on cubic SrHfO3 (001). Journal of Crystal Growth, 2016, 443, 66-74.	0.7	2
27837	Migration of helium-pair in metals. Journal of Nuclear Materials, 2016, 478, 13-25.	1.3	19
27838	Ab initio simulations of the structure, energetics and mobility of radiation-induced point defects in bcc Nb. Journal of Nuclear Materials, 2016, 478, 185-196.	1.3	21
27839	A Novel Small-Molecule Compound of Lithium Iodine and 3-Hydroxypropionitride as a Solid-State Electrolyte for Lithiumâ€“Air Batteries. Inorganic Chemistry, 2016, 55, 6504-6510.	1.9	15
27840	Interaction of Adatoms and Molecules with Single-Layer Arsenene Phases. Journal of Physical Chemistry C, 2016, 120, 14345-14355.	1.5	98
27841	Strain-Induced Isostructural and Magnetic Phase Transitions in Monolayer MoN₂. Nano Letters, 2016, 16, 4576-4582.	4.5	129
27842	Ultrafast charge-transfer in organic photovoltaic interfaces: geometrical and functionalization effects. Nanoscale, 2016, 8, 15902-15910.	2.8	9
27843	The structure-dependent enhancement of the oxygen reduction reaction performance of Co-based low Pt catalysts through Au addition. Journal of Materials Chemistry A, 2016, 4, 11023-11029.	5.2	15
27844	Two-dimensional polyaniline (C ₃ N) from carbonized organic single crystals in solid state. Proceedings of the National Academy of Sciences of the United States of America, 2016, 113, 7414-7419.	3.3	380
27845	Possible new metastable Mo2Ga2C and its phase transition under pressure: a density functional prediction. Journal of Materials Science, 2016, 51, 8452-8460.	1.7	8
27846	First-principles DFT +U calculations on the energetics of Ga in Pu, Pu2O3 and PuO2. Computational Materials Science, 2016, 122, 263-271.	1.4	29
27847	Rationalization of electrocatalysis of nickel phosphide nanowires for efficient hydrogen production. Nano Energy, 2016, 26, 496-503.	8.2	61
27848	Possible Formation of Graphyne on Transition Metal Surfaces: A Competition with Graphene from the Chemical Potential Point of View. Journal of Physical Chemistry C, 2016, 120, 14699-14705.	1.5	24
27849	Topologically Protected Metallic States Induced by a One-Dimensional Extended Defect in the Bulk of a 2D Topological Insulator. Nano Letters, 2016, 16, 4025-4031.	4.5	16
27850	Epitaxial-strain-induced polar-to-nonpolar transitions in layered oxides. Nature Materials, 2016, 15, 951-955.	13.3	94
27851	Energetics and kinetics of Cu atoms and clusters on the Si(111)-7 Ã— 7 surface: first-principles calculations. Physical Chemistry Chemical Physics, 2016, 18, 18549-18554.	1.3	3
27852	Two-dimensional BX (X = P, As, Sb) semiconductors with mobilities approaching graphene. Nanoscale, 2016, 8, 13407-13413.	2.8	122
27853	HÃgg carbide surfaces induced Pt morphological changes: a theoretical insight. Catalysis Science and Technology, 2016, 6, 6726-6738.	2.1	7

#	Article	IF	Citations
27854	Comparisons between adsorption and diffusion of alkali, alkaline earth metal atoms on silicene and those on silicane: Insight from first-principles calculations. Chinese Physics B, 2016, 25, 067103.	0.7	17
27855	On the stability and nature of adsorbed pentene in BrÃ¸nsted acid zeolite H-ZSM-5 at 323 K. Journal of Catalysis, 2016, 340, 227-235.	3.1	55
27856	Microkinetic model for the dry reforming of methane on Rh doped pyrochlore catalysts. Journal of Catalysis, 2016, 340, 196-204.	3.1	34
27857	Implications of sterically constrained n-butane oxidation reactions on the reaction mechanism and selectivity to 1-butanol. Surface Science, 2016, 653, 11-21.	0.8	5
27858	High-Pressure Crystal Structures of an Insensitive Energetic Crystal: 1,1-Diamino-2,2-dinitroethene. Journal of Physical Chemistry C, 2016, 120, 1218-1224.	1.5	42
27859	How molecular is the chemisorptive bond?. Physical Chemistry Chemical Physics, 2016, 18, 20868-20894.	1.3	41
27860	The plasticity of highly oriented nano-layered Zr/Nb composites. Acta Materialia, 2016, 115, 189-203.	3.8	60
27861	Point-defect kinetics in Î±- and Î³-MgH2. International Journal of Hydrogen Energy, 2016, 41, 5688-5692.	3.8	11
27862	Ab-initio study of half-metallic ferromagnetism in Co/Ni substituted Li2X (X=S, Se, Te) compounds. Journal of Magnetism and Magnetic Materials, 2016, 418, 148-157.	1.0	2
27863	Origin of the Orderâ€“Disorder Transition and the Associated Anomalous Change of Thermopower in AgBiS₂ Nanocrystals: A Combined Experimental and Theoretical Study. Inorganic Chemistry, 2016, 55, 6323-6331.	1.9	45
27864	Flexible Few-Layered Graphene for the Ultrafast Rechargeable Aluminum-Ion Battery. Journal of Physical Chemistry C, 2016, 120, 13384-13389.	1.5	164
27865	First-principles study of carbon segregation in bcc iron symmetrical tilt grain boundaries. Acta Materialia, 2016, 115, 259-268.	3.8	96
27866	Dumbbell Defects in FeSe Films: A Scanning Tunneling Microscopy and First-Principles Investigation. Nano Letters, 2016, 16, 4224-4229.	4.5	39
27867	Defect Tolerance to Intolerance in the Vacancy-Ordered Double Perovskite Semiconductors Cs₂SnI₆ and Cs₂TeI₆. Journal of the American Chemical Society, 2016, 138, 8453-8464.	6.6	415
27868	A generalized method for constructing hypothetical nanoporous materials of any net topology from graph theory. CrystEngComm, 2016, 18, 3777-3792.	1.3	104
27869	Self-healing properties of nanocrystalline materials: a first-principles analysis of the role of grain boundaries. Physical Chemistry Chemical Physics, 2016, 18, 17930-17940.	1.3	21
27870	Understanding divergent behaviors in the photocatalytic hydrogen evolution reaction on CdS and ZnS: a DFT based study. Physical Chemistry Chemical Physics, 2016, 18, 16862-16869.	1.3	36
27871	Enthalpies of formation of TMâ€“X compounds (X=Al, Ga, Si, Ge, Sn). Comparison of ab-initio values and experimental data. Calphad: Computer Coupling of Phase Diagrams and Thermochemistry, 2016, 54, 16-34.	0.7	12

#	Article	IF	Citations
27872	TRIQS/DFTTools: A TRIQS application for ab initio calculations of correlated materials. Computer Physics Communications, 2016, 204, 200-208.	3.0	113
27873	Magnetic, thermodynamic and transport properties of novel non-centrosymmetric RCoSi3 (R=Pr, Nd) Tj ETQq1 1 0.784314 rgBT /Ove	1.0	11
27874	Tolerance of non-platinum group metals cathodes proton exchange membrane fuel cells to air contaminants. Journal of Power Sources, 2016, 324, 556-571.	4.0	34
27875	Enhanced Hydrodeoxygenation of m-Cresol over Bimetallic Ptâ€“Mo Catalysts through an Oxophilic Metal-Induced Tautomerization Pathway. ACS Catalysis, 2016, 6, 4356-4368.	5.5	117
27876	Synthesis, antifungal evaluation and optical properties of silver molybdate microcrystals in different solvents: a combined experimental and theoretical study. Dalton Transactions, 2016, 45, 10736-10743.	1.6	49
27877	Electron and phonon properties and gas storage in carbon honeycombs. Nanoscale, 2016, 8, 12863-12868.	2.8	50
27878	Effect of the Local Atomic Ordering on the Stability of Î²-Spodumene. Inorganic Chemistry, 2016, 55, 6426-6434.	1.9	9
27879	Interaction between Monomeric Vanadium Oxide Clusters Supported on Titania and Its Influence on Their Reactivity. Journal of Physical Chemistry C, 2016, 120, 13610-13621.	1.5	10
27880	Tuning the Electronic Structure of the Metalâ€“Oxygen Group by Silicon Substitution in Lithium-Rich Manganese-Based Oxides for Superior Performance. Journal of Physical Chemistry C, 2016, 120, 13421-13426.	1.5	23
27881	Methane adsorption and dissociation on iron oxide oxygen carriers: the role of oxygen vacancies. Physical Chemistry Chemical Physics, 2016, 18, 16423-16435.	1.3	84
27882	A first-principles study of the tuning effect of a Fe₂O₃ cluster on the dehydrogenation properties of a LiBH₄ (001) surface. Dalton Transactions, 2016, 45, 10954-10959.	1.6	10
27883	Electronic, optical and thermoelectric properties of PrMO₃ (M = Al, Ga, In) from first-principles calculations. RSC Advances, 2016, 6, 59988-59997.	1.7	15
27884	The quantum mechanics derived atomistic mechanism underlying the acceleration of catalytic CO oxidation on Pt(110) by surface acoustic waves. Journal of Materials Chemistry A, 2016, 4, 12036-12045.	5.2	7
27885	Electronic and magnetic properties of SrRuO 3 with Ru-vacancy: First-principle calculations. Europhysics Letters, 2016, 113, 27001.	0.7	1
27886	Quantum and Classical Molecular Dynamics of Ionic Liquid Electrolytes for Na/Liâ€based Batteries: Molecular Origins of the Conductivity Behavior. ChemPhysChem, 2016, 17, 2473-2481.	1.0	29
27887	Platinumâ€Decorated Ultrafine Pd Nanoparticles Monodispersed on Pristine Graphene with Enhanced Electrocatalytic Performance. ChemPlusChem, 2016, 81, 172-175.	1.3	9
27888	Synthesis of the Singleâ€Crystalline Form and Firstâ€Principles Calculations of Photomagnetic Copper(II) Octacyanidomolybdate(IV). European Journal of Inorganic Chemistry, 2016, 2016, 1980-1988.	1.0	17
27889	Effects of an electric field on interaction of aromatic systems. Journal of Computational Chemistry, 2016, 37, 971-975.	1.5	7

#	Article	IF	Citations
27890	Modelling of measured optical properties of Pdâ€“Au alloy ultrathin film for room temperature hydrogen sensing. Physica Status Solidi (A) Applications and Materials Science, 2016, 213, 2406-2413.	0.8	1
27891	Reduction of lattice thermal conductivity of pseudogap intermetallic compound Al₃V. Physica Status Solidi (B): Basic Research, 2016, 253, 469-472.	0.7	5
27892	Site preference of manganese in Mn-alloyed cementite. Physica Status Solidi (B): Basic Research, 2016, 253, 1623-1628.	0.7	7
27893	Firstâ€principles study of the electronic structures and optical properties of Cr²⁺â€doped ZnSe as a function of impurity concentration. Physica Status Solidi (B): Basic Research, 2016, 253, 1133-1137.	0.7	13
27894	Indirect phase transition of TiC, ZrC, and HfC crystal structures. Physica Status Solidi (B): Basic Research, 2016, 253, 1177-1185.	0.7	12
27895	Binding energy shifts for nitrogenâ€containing grapheneâ€based electrocatalysts â€“ experiments and DFT calculations. Surface and Interface Analysis, 2016, 48, 293-300.	0.8	147
27896	The structural, electronic, and magnetic properties of the stoichiometric (001) surface of double perovskite <scp>Sr₂FeMoO₆</scp>. Surface and Interface Analysis, 2016, 48, 1040-1047.	0.8	3
27897	The Frontier of Molecular Spintronics Based on Multiple-Decker Phthalocyaninato Tb^{III}Single-Molecule Magnets. Chemical Record, 2016, 16, 987-1016.	2.9	37
27898	Computing optical properties of ultraâ€thin crystals. Wiley Interdisciplinary Reviews: Computational Molecular Science, 2016, 6, 351-368.	6.2	15
27899	Phase dependent structural and electronic properties of lanthanum orthophosphate (LaPO₄). Journal of Physics Condensed Matter, 2016, 28, 205501.	0.7	15
27900	First-principles study of lattice thermal conductivity of Tdâ€“WTe₂. New Journal of Physics, 2016, 18, 033017.	1.2	31
27901	Equations of State for Ablator Materials in Inertial Confinement Fusion Simulations. Journal of Physics: Conference Series, 2016, 717, 012082.	0.3	13
27902	Dopant Site Environment and Spectrum Blue Shift of Yellowâ€Emitting Solid Solution Phosphor Ba_{2â^'x}Sr_xMg(<scp>PO</scp>₄)₂:Eu²⁺. Journal of the American Ceramic Society, 2016, 99, 645-650.	3.4	9
27903	High coverage CO adsorption and dissociation on the Co(0001) and Co(100) surfaces from DFT and thermodynamics. Applied Catalysis A: General, 2016, 523, 209-220.	2.2	22
27904	A density functional theory study of propylene epoxidation on RuO2(110) surface. Applied Surface Science, 2016, 385, 99-105.	3.1	17
27905	Insight into the mechanism of Pt anchored graphene toward the CHx(xÂ=Â1Ââ¼Â4) reforming under H2 environments. International Journal of Hydrogen Energy, 2016, 41, 13197-13207.	3.8	5
27906	Strong interfacial coupling of MoS2/g-C3N4 van de Waals solids for highly active water reduction. Nano Energy, 2016, 27, 44-50.	8.2	96
27907	Reaction Mechanism of Ethanol on Model Cobalt Catalysts: DFT Calculations. Journal of Physical Chemistry C, 2016, 120, 14198-14208.	1.5	19

#	Article	IF	Citations
27908	Chemically Accurate Simulation of a Polyatomic Molecule-Metal Surface Reaction. Journal of Physical Chemistry Letters, 2016, 7, 2402-2406.	2.1	103
27909	Optimization of the Thermoelectric Figure of Merit in Crystalline C₆₀ with Intercalation Chemistry. Nano Letters, 2016, 16, 4203-4209.	4.5	10
27910	Aluminum Nitride Hydrolysis Enabled by Hydroxyl-Mediated Surface Proton Hopping. ACS Applied Materials & Interfaces, 2016, 8, 18550-18559.	4.0	21
27911	Ethanol Electro-oxidation on Palladium Revisited Using Polarization Modulation Infrared Reflection Absorption Spectroscopy (PM-IRRAS) and Density Functional Theory (DFT): Why Is It Difficult To Break the Câ€“C Bond?. ACS Catalysis, 2016, 6, 4894-4906.	5.5	109
27912	Catalyst Site Selection via Control over Noncovalent Interactions in Self-Assembled Monolayers. ACS Catalysis, 2016, 6, 5086-5094.	5.5	44
27913	First-principles study on the phase transition temperature of X-doped (X = Li, Na or K) VO₂. RSC Advances, 2016, 6, 64394-64399.	1.7	18
27914	Giant red shift of the absorption spectra due to nonstoichiometry in GdCoO3â€“Î´. JETP Letters, 2016, 103, 161-166.	0.4	1
27915	Structure and Properties of Cd₄P₂Cl₃, an Analogue of CdS. Journal of Physical Chemistry C, 2016, 120, 15063-15069.	1.5	13
27916	Anisotropic thermal transport in Weyl semimetal TaAs: a first principles calculation. Physical Chemistry Chemical Physics, 2016, 18, 16709-16714.	1.3	36
27917	Substrate-induced structures of bismuth adsorption on graphene: a first principles study. Physical Chemistry Chemical Physics, 2016, 18, 18978-18984.	1.3	7
27918	Introducing DDEC6 atomic population analysis: part 2. Computed results for a wide range of periodic and nonperiodic materials. RSC Advances, 2016, 6, 45727-45747.	1.7	351
27919	Interface effects for the hydrogenation of CO2 on Pt4/Î³-Al2O3. Applied Surface Science, 2016, 386, 196-201.	3.1	20
27920	Role of effective carrier mass in the photocatalytic efficiency of La-doped NaTaO3. Computational Materials Science, 2016, 123, 1-7.	1.4	20
27921	Lattice thermal conductivity of NiTiSn half-Heusler thermoelectric materials from first-principles calculations. Journal of Alloys and Compounds, 2016, 688, 248-252.	2.8	21
27922	Characterization of LSMO/C60 spinterface by first-principle calculations. Organic Electronics, 2016, 37, 55-60.	1.4	6
27923	Polymorphism of Water in Two Dimensions. Journal of Physical Chemistry C, 2016, 120, 13649-13655.	1.5	29
27924	First-Principles Characterization of the Unknown Crystal Structure and Ionic Conductivity of Li₇P₂S₈I as a Solid Electrolyte for High-Voltage Li Ion Batteries. Journal of Physical Chemistry Letters, 2016, 7, 2671-2675.	2.1	37
27925	Epitaxial Growth of Single Layer Blue Phosphorus: A New Phase of Two-Dimensional Phosphorus. Nano Letters, 2016, 16, 4903-4908.	4.5	609

#	Article	IF	Citations
27926	Introducing DDEC6 atomic population analysis: part 1. Charge partitioning theory and methodology. RSC Advances, 2016, 6, 47771-47801.	1.7	567
27927	Momentum-dependent band spin splitting in semiconducting MnO₂: a density functional calculation. Physical Chemistry Chemical Physics, 2016, 18, 13294-13303.	1.3	39
27928	Ground-State Structure and Physical Properties of NB 2 Predicted from First Principles. Chinese Physics Letters, 2016, 33, 036202.	1.3	5
27929	Emerging Parallel Dual 2D Composites: Natural Clay Mineral Hybridizing MoS₂ and Interfacial Structure. Advanced Functional Materials, 2016, 26, 2666-2675.	7.8	157
27930	CsPbX₃ Quantum Dots for Lighting and Displays: Roomâ€Temperature Synthesis, Photoluminescence Superiorities, Underlying Origins and White Lightâ€Emitting Diodes. Advanced Functional Materials, 2016, 26, 2435-2445.	7.8	2,055
27931	Trimetallic TriStar Nanostructures: Tuning Electronic and Surface Structures for Enhanced Electrocatalytic Hydrogen Evolution. Advanced Materials, 2016, 28, 2077-2084.	11.1	181
27932	Layer Engineering of 2D Semiconductor Junctions. Advanced Materials, 2016, 28, 5126-5132.	11.1	63
27933	High Performance of Planar Perovskite Solar Cells Produced from PbI₂(DMSO) and PbI₂(NMP) Complexes by Intramolecular Exchange. Advanced Materials Interfaces, 2016, 3, 1500768.	1.9	206
27934	Unraveling Selfâ€Doping Effects in Thermoelectric TiNiSn Halfâ€Heusler Compounds by Combined Theory and Highâ€Throughput Experiments. Advanced Electronic Materials, 2016, 2, 1500208.	2.6	26
27935	Onâ€Fabrication Solidâ€State Nâ€Doping of Graphene by an Electronâ€Transporting Metal Oxide Layer for Efficient Inverted Organic Solar Cells. Advanced Energy Materials, 2016, 6, 1600172.	10.2	46
27936	Effects of Ga doping on Pt/CeO₂â€Al₂O₃ catalysts for propane dehydrogenation. AICHE Journal, 2016, 62, 4365-4376.	1.8	79
27937	CO 2 Hydrogenation over Oxideâ€Supported PtCo Catalysts: The Role of the Oxide Support in Determining the Product Selectivity. Angewandte Chemie, 2016, 128, 8100-8105.	1.6	41
27938	Structure and Composition of the 200â€…Kâ€Superconducting Phase of H₂S at Ultrahigh Pressure: The Perovskite (SH^{â¯})(H₃S⁺). Angewandte Chemie - International Edition, 2016, 55, 3682-3684.	7.2	36
27939	The Unexpected Reactivity of the Carbon Sites on the Nanostructured Carbon Catalysts towards the Câ¯H Bond Activation from the Analysis of the Aromaticity. Chemistry - an Asian Journal, 2016, 11, 1668-1671.	1.7	10
27940	Computationally Probing the Performance of Hybrid, Heterogeneous, and Homogeneous Iridiumâ€Based Catalysts for Water Oxidation. ChemCatChem, 2016, 8, 1792-1798.	1.8	26
27941	Existence patterns of Dy in Î²-NiAl from first-principles calculations. Rare Metals, 2016, 35, 356-360.	3.6	2
27942	Computational Electrochemistry. Voltages of Lithium-Ion Battery Cathodes. Journal of Physical Chemistry B, 2016, 120, 1437-1439.	1.2	6
27943	Prediction of the crystal packing of diâ€tetrazineâ€tetroxide (DTTO) energetic material. Journal of Computational Chemistry, 2016, 37, 163-167.	1.5	24

#	Article	IF	Citations
27944	Analysis of Electronic and Structural Properties of Surfaces and Interfaces Based on LaAlO $$ _{3} $$ 3 and SrTiO $$ _{3}$$ 3. Journal of Low Temperature Physics, 2016, 185, 597-602.	0.6	6
27945	How to stabilize highly active Cu+ cations in a mixed-oxide catalyst. Catalysis Today, 2016, 263, 4-10.	2.2	11
27946	Enhancing the Photocatalytic Activity of BiVO₄ for Oxygen Evolution by Ce Doping: Ce³⁺ Ions as Hole Traps. Journal of Physical Chemistry C, 2016, 120, 2058-2063.	1.5	121
27947	Interfacial electronic effects control the reaction selectivity of platinum catalysts. Nature Materials, 2016, 15, 564-569.	13.3	548
27948	Spinâ€“orbit coupling effects on electronic structures in stanene nanoribbons. Physical Chemistry Chemical Physics, 2016, 18, 6534-6540.	1.3	42
27949	Tuning the surface electronic structure of a Pt₃Ti(111) electro catalyst. Nanoscale, 2016, 8, 13924-13933.	2.8	17
27950	The stability of B₆ octahedron in BaB₆ under high pressure. RSC Advances, 2016, 6, 18077-18081.	1.7	12
27951	Thickness-ultrathin and bismuth-rich strategies for BiOBr to enhance photoreduction of CO 2 into solar fuels. Applied Catalysis B: Environmental, 2016, 187, 281-290.	10.8	280
27952	Impurity-induced ferromagnetism and metallicity of WS2 monolayer. Ceramics International, 2016, 42, 2364-2369.	2.3	25
27953	Structural stability, mechanical properties and stacking fault energies of TiAl3 alloyed with Zn, Cu, Ag: First-principles study. Journal of Alloys and Compounds, 2016, 666, 185-196.	2.8	47
27954	A DFT study of atomic structure and adhesion at the Fe(BCC)/Fe3O4 interfaces. Surface Science, 2016, 647, 55-65.	0.8	12
27955	Synthesis and Reaction Mechanism of Novel Fluorinated Carbon Fiber as a High-Voltage Cathode Material for Rechargeable Na Batteries. Chemistry of Materials, 2016, 28, 1026-1033.	3.2	53
27956	Phenol-Modified Silicene: Preferred Substitution Site and Electronic Properties. Journal of Physical Chemistry C, 2016, 120, 6762-6770.	1.5	8
27957	Growth Mechanism and Morphology of Hexagonal Boron Nitride. Nano Letters, 2016, 16, 1398-1403.	4.5	123
27958	Lithiumâ€“Boron (Liâ€“B) Monolayers: First-Principles Cluster Expansion and Possible Two-Dimensional Superconductivity. ACS Applied Materials & Interfaces, 2016, 8, 2526-2532.	4.0	49
27959	Cathode Based on Molybdenum Disulfide Nanoflakes for Lithiumâ€“Oxygen Batteries. ACS Nano, 2016, 10, 2167-2175.	7.3	184
27960	Anomalous mechanical strengths and shear deformation paths of Al₂O₃ polymorphs with high ionicity. RSC Advances, 2016, 6, 12885-12892.	1.7	8
27961	Pressure-induced changes in structural and dynamic properties of liquid Fe close to the melting line. Anab initiostudy. Journal of Physics Condensed Matter, 2016, 28, 075101.	0.7	18

#	Article	IF	Citations
27962	Enhanced near-infrared shielding ability of (Li,K)-codoped WO₃for smart windows: DFT prediction validated by experiment. Nanotechnology, 2016, 27, 075203.	1.3	28
27963	A new family of sp 3 -hybridized carbon phases. Chinese Physics B, 2016, 25, 016103.	0.7	8
27964	A comparison of mechanical properties between Al and Al3Mg. International Journal of Modern Physics B, 2016, 30, 1550243.	1.0	7
27965	Interfacial structure, ferroelectric stability, and magnetoelectric effect of magnetoelectric junction FeCo/BaTiO3/FeCo with alloy electrode. Journal of Materials Science, 2016, 51, 3297-3302.	1.7	3
27966	The bulk and interfacial structures of the Î· (Al2Au) precipitate phase. Acta Materialia, 2016, 105, 284-293.	3.8	11
27967	Different spin textures in one-dimensional electronic bands on Si(553)-Au surface. Applied Surface Science, 2016, 373, 26-31.	3.1	17
27968	Site preference and diffusion of hydrogen during hydrogenation of Mg: A first-principles study. International Journal of Hydrogen Energy, 2016, 41, 3508-3516.	3.8	12
27969	A theoretical study of hydrogen atoms adsorption and diffusion on PuO2 (110) surface. Journal of Alloys and Compounds, 2016, 666, 287-291.	2.8	16
27970	CO2 hydrogenation on Pt, Pt/SiO2 and Pt/TiO2: Importance of synergy between Pt and oxide support. Journal of Catalysis, 2016, 343, 115-126.	3.1	250
27971	Investigation of metastable Na2FeSiO4 as a cathode material for Na-ion secondary battery. Materials Chemistry and Physics, 2016, 171, 45-49.	2.0	44
27972	First-principles study on electronic properties and lattice structures of WZ-ZnO/CdS interface. Materials Science in Semiconductor Processing, 2016, 45, 9-16.	1.9	23
27973	DFT calculations on atom-specific electronic properties of G/SiC(0001). Surface Science, 2016, 647, 39-44.	0.8	14
27974	Elucidating Structural Disorder and the Effects of Cu Vacancies on the Electronic Properties of Cu₂ZnSnS₄. Chemistry of Materials, 2016, 28, 864-869.	3.2	36
27975	Theoretical Study of Trimethylacetic Acid Adsorption on CeO₂(111) Surface. Journal of Physical Chemistry C, 2016, 120, 2655-2666.	1.5	12
27976	A Unified Understanding of the Thickness-Dependent Bandgap Transition in Hexagonal Two-Dimensional Semiconductors. Journal of Physical Chemistry Letters, 2016, 7, 597-602.	2.1	100
27977	Pressure-induced phase transition of SnH₄: a new layered structure. RSC Advances, 2016, 6, 10456-10461.	1.7	10
27978	A new approach for fabricating germanene with Dirac electrons preserved: a first principles study. Journal of Materials Chemistry C, 2016, 4, 1736-1740.	2.7	18
27979	Interface morphology and composition of Ga(NAsP) quantum well structures for monolithically integrated LASERs on silicon substrates. Journal Physics D: Applied Physics, 2016, 49, 075108.	1.3	18

#	Article	IF	Citations
27980	Surprising stability of neutral interstitial hydrogen in diamond and cubic BN. Journal of Physics Condensed Matter, 2016, 28, 06LT01.	0.7	7
27981	Lanthanide-doped LaSi 3 N 5 based phosphors: Ab initio study of electronic structures, band gaps, and energy level locations. Journal of Luminescence, 2016, 172, 83-91.	1.5	11
27982	Lower temperature deformation mechanisms in a Î³â€³-strengthened Ni-base superalloy. Scripta Materialia, 2016, 115, 108-112.	2.6	28
27983	Catalytic Activity of MS₂ Monolayer for Electrochemical Hydrogen Evolution. Journal of Physical Chemistry C, 2016, 120, 1623-1632.	1.5	75
27984	Activation of Cu(111) surface by decomposition into nanoclusters driven by CO adsorption. Science, 2016, 351, 475-478.	6.0	245
27985	Possible ferrimagnetism and ferroelectricity of half-substituted rare-earth titanate: A first-principles study on Y0.5La0.5TiO3. Frontiers of Physics, 2016, 11, 1.	2.4	5
27986	Microscopic study of gum-metal alloys: A role of trace oxygen for dislocation-free deformation. Acta Materialia, 2016, 105, 347-354.	3.8	24
27987	Surface composition of magnetron sputtered Pt-Co thin film catalyst for proton exchange membrane fuel cells. Applied Surface Science, 2016, 365, 245-251.	3.1	33
27988	Graphene-mediated highly-dispersed MoS2 nanosheets with enhanced triiodide reduction activity for dye-sensitized solar cells. Carbon, 2016, 100, 474-483.	5.4	100
27989	Ab initio thermodynamics of fcc H-Zr and formation of hydrides. Computational Materials Science, 2016, 114, 254-263.	1.4	9
27990	Molecular Dynamics Simulations on O 2 Permeation through Nafion Ionomer on Platinum Surface. Electrochimica Acta, 2016, 188, 767-776.	2.6	198
27991	Chemical partitioning for the Coâ€“Pr system: First-principles, experiments and energetic calculations to investigate the hard magnetic phase. Materials and Design, 2016, 90, 991-1004.	3.3	5
27992	N-heterocycles as corrosion inhibitors for mild steel in acid medium. Journal of Molecular Liquids, 2016, 216, 42-52.	2.3	94
27993	Comparison of Storage Mechanisms in RuO₂, SnO₂, and SnS₂for Lithium-Ion Battery Anode Materials. Journal of Physical Chemistry C, 2016, 120, 2036-2046.	1.5	54
27994	Fundamental insights into the electronic structure of zigzag MoS₂ nanoribbons. Physical Chemistry Chemical Physics, 2016, 18, 4675-4683.	1.3	16
27995	Adsorption of Helium Atoms on Two-Dimensional Substrates. Journal of Low Temperature Physics, 2016, 185, 392-398.	0.6	2
27996	Tuning the Nanofriction Between Two Graphene Layers by External Electric Fields: A Density Functional Theory Study. Tribology Letters, 2016, 61, 1.	1.2	15
27997	Ab initio calculations and experimental study of piezoelectric Y In1â^'N thin films deposited using reactive magnetron sputter epitaxy. Acta Materialia, 2016, 105, 199-206.	3.8	20

#	Article	IF	Citations
27998	Temperature dependent elastic and thermal expansion properties of W3Co3C, W6Co6C and W4Co2C ternary carbides. Journal of Alloys and Compounds, 2016, 666, 262-269.	2.8	22
27999	RESCU: A real space electronic structure method. Journal of Computational Physics, 2016, 307, 593-613.	1.9	89
28000	On the nature of the solvated electron in ice I_h. Physical Chemistry Chemical Physics, 2016, 18, 4652-4658.	1.3	6
28001	Amino acid modified copper electrodes for the enhanced selective electroreduction of carbon dioxide towards hydrocarbons. Energy and Environmental Science, 2016, 9, 1687-1695.	15.6	290
28002	The formation of the smallest fullerene-like carbon cages on metal surfaces. Nanoscale, 2016, 8, 2561-2567.	2.8	6
28003	Effects of nitrogen dopants on the atomic step kinetics and electronic structures of O-polar ZnO. Nanoscale, 2016, 8, 4381-4386.	2.8	5
28004	Contact-dependent mechanical properties of graphene nanoribbons: anab initiostudy. Nanotechnology, 2016, 27, 025702.	1.3	1
28005	Tuning thermoelectricity in a Bi₂Se₃topological insulator via varied film thickness. New Journal of Physics, 2016, 18, 015008.	1.2	47
28006	Correlation between crystallinity and oxygen vacancy formation in Inâ€“Gaâ€“Zn oxide. Japanese Journal of Applied Physics, 2016, 55, 021203.	0.8	19
28007	Increased photocatalytic activity of TiO2 mesoporous microspheres from codoping with transition metals and nitrogen. Ceramics International, 2016, 42, 3556-3562.	2.3	11
28008	Elasticity, ideal tensile strength and lattice dynamics of LuH 2 dihydride from first-principles investigations. International Journal of Hydrogen Energy, 2016, 41, 2720-2726.	3.8	3
28009	Adsorption of uranyl species on hydroxylated titanium carbide nanosheet: A first-principles study. Journal of Hazardous Materials, 2016, 308, 402-410.	6.5	115
28010	Luminescence Properties of SrZrO₃/Tb³⁺ Perovskite: Host-Dopant Energy-Transfer Dynamics and Local Structure of Tb³⁺. Inorganic Chemistry, 2016, 55, 1728-1740.	1.9	96
28011	Complex Magnetic Exchange Coupling between Co Nanostructures and Ni(111) across Epitaxial Graphene. ACS Nano, 2016, 10, 1101-1107.	7.3	27
28012	Cu₂Se and Cu Nanocrystals as Local Sources of Copper in Thermally Activated In Situ Cation Exchange. ACS Nano, 2016, 10, 2406-2414.	7.3	23
28013	Trimethylphosphine-Assisted Surface Fingerprinting of Metal Oxide Nanoparticle by ³¹P Solid-State NMR: A Zinc Oxide Case Study. Journal of the American Chemical Society, 2016, 138, 2225-2234.	6.6	83
28014	Interaction of Al, Ti, and Cu Atoms with Boron Nitride Nanotubes: A Computational Investigation. Journal of Physical Chemistry C, 2016, 120, 3509-3518.	1.5	12
28015	First-Principle Study of Adsorption and Desorption of Chlorine on Cu(111) Surface: Does Chlorine or Copper Chloride Desorb?. Journal of Physical Chemistry C, 2016, 120, 2829-2836.	1.5	13

#	Article	IF	Citations
28016	Quantum chemistry of the oxygen evolution reaction on cobalt(<scp>ii</scp>,<scp>iii</scp>) oxide â€“ implications for designing the optimal catalyst. Faraday Discussions, 2016, 188, 199-226.	1.6	18
28017	Nanoclusters of CaSe in calcium-doped Bi2Se3grown by molecular-beam epitaxy. Nanotechnology, 2016, 27, 085601.	1.3	3
28018	Oxygen vacancy induced metal-insulator transition in LaNiO3. European Physical Journal B, 2016, 89, 1.	0.6	16
28019	Mechanical properties of the interface structure of nanodiamond composite films: First-principles studies. Applied Surface Science, 2016, 363, 522-531.	3.1	2
28020	Do Au Atoms Titrate Ce³⁺ Ions at the CeO_{2â€“x}(111) Surface?. Journal of Physical Chemistry C, 2016, 120, 927-933.	1.5	14
28021	First-Principles Investigation of the Na⁺ Ion Transport Property in Oxyfluorinated Titanium(IV) Phosphate Na₃Ti₂P₂O₁₀F. Journal of Physical Chemistry C, 2016, 120, 1438-1445.	1.5	7
28022	Prediction of topological phase transition in X2â€“SiGe monolayers. Physical Chemistry Chemical Physics, 2016, 18, 3669-3674.	1.3	14
28023	Microstructure, mechanical and optical properties of TiAlON coatings sputter-deposited with varying oxygen partial pressures. Journal Physics D: Applied Physics, 2016, 49, 025307.	1.3	10
28024	Tuning band inversion symmetry of buckled III-Bi sheets by halogenation. Nanotechnology, 2016, 27, 055704.	1.3	42
28025	First-principles investigation on mechanical behaviors of Wâ€“Cr/Ti binary alloys. Journal of Nuclear Materials, 2016, 468, 105-112.	1.3	22
28026	Surface Segregation Entropy of Protons and Oxygen Vacancies in BaZrO₃. Chemistry of Materials, 2016, 28, 1363-1368.	3.2	42
28027	Kinetics of Topological Stoneâ€“Wales Defect Formation in Single-Walled Carbon Nanotubes. Journal of Physical Chemistry C, 2016, 120, 1989-1993.	1.5	17
28028	Biexciton Formation in Bilayer Tungsten Disulfide. ACS Nano, 2016, 10, 2176-2183.	7.3	57
28029	Phase diagrams for clathrate hydrates of methane, ethane, and propane from first-principles thermodynamics. Physical Chemistry Chemical Physics, 2016, 18, 3272-3279.	1.3	15
28030	Trigonal Cu₂-II-Sn-VI₄ (II = Ba, Sr and VI = S, Se) quaternary compounds for earth-abundant photovoltaics. Physical Chemistry Chemical Physics, 2016, 18, 4828-4834.	1.3	94
28031	Blockage of ultrafast and directional diffusion of Li atoms on phosphorene with intrinsic defects. Nanoscale, 2016, 8, 4001-4006.	2.8	84
28032	Thermal conductivity of monolayer MoS₂, MoSe₂, and WS₂: interplay of mass effect, interatomic bonding and anharmonicity. RSC Advances, 2016, 6, 5767-5773.	1.7	265
28033	Multiphysics Modeling of the Role of Iodine in Environmentally Assisted Cracking of Zirconium via Pellet-Clad Interaction. Corrosion, 2016, 72, 978-988.	0.5	3

#	Article	IF	Citations
28034	A DFT study of ethanol adsorption and decomposition on Î±-Al2O3(0001) surface. Applied Surface Science, 2016, 363, 636-643.	3.1	24
28035	Unusual dissociative adsorption of H2 over stoichiometric MgO thin film supported on molybdenum. Applied Surface Science, 2016, 366, 166-172.	3.1	15
28036	Dynamical properties of AlN nanostructures and heterogeneous interfaces predicted using COMB potentials. Computational Materials Science, 2016, 113, 80-87.	1.4	23
28037	Density functional theory calculations for estimation of gettering sites of C, H, intrinsic point defects and related complexes in Si wafers. Materials Science in Semiconductor Processing, 2016, 44, 13-17.	1.9	24
28038	Sr/Si(100)(1 Ã— 2) reconstruction as a template for the growth of crystalline high-k films on silicon: Atomic structure and reactivity. Surface Science, 2016, 646, 140-145.	0.8	7
28039	Ferromagnet-to-Topological Insulator Transition via Lithiation and Their Lateral Heterostructures within Intercalated Graphene: An ab Initio Study. Journal of Physical Chemistry C, 2016, 120, 2254-2259.	1.5	3
28040	Structure and Properties of Egyptian Blue Monolayer Family: XCuSi₄O₁₀ (X =) Tj ETQq0 0 0 rgBT /Overlock 10	2.1	24
28041	Probing the electrochemical capacitance of MXene nanosheets for high-performance pseudocapacitors. Physical Chemistry Chemical Physics, 2016, 18, 4460-4467.	1.3	65
28042	Metalâ€“semiconductorâ€“metal transition in zigzag carbon nanoscrolls. Nanoscale, 2016, 8, 2887-2891.	2.8	3
28043	Defect charge states in Si doped hexagonal boron-nitride monolayer. Journal of Physics Condensed Matter, 2016, 28, 055501.	0.7	13
28044	Thermodynamic modeling of Alâ€“Coâ€“Cr, Alâ€“Coâ€“Ni, Coâ€“Crâ€“Ni ternary systems towards a description for Alâ€“Coâ€“Crâ€“Ni. Calphad: Computer Coupling of Phase Diagrams and Thermochemistry, 2016, 52, 125-142.	0.7	60
28045	Identification of O-rich structures on platinum(111)-supported ultrathin iron oxide films. Surface Science, 2016, 652, 261-268.	0.8	27
28046	DFT modelling of hydrogen sulphide adsorption on Î±-Cr2O3 (0001) surface. Surface Science, 2016, 647, 78-83.	0.8	15
28047	Interfacial Oxygen Vacancies as a Potential Cause of Hysteresis in Perovskite Solar Cells. Chemistry of Materials, 2016, 28, 802-812.	3.2	128
28048	Insights into the synergistic role of metalâ€“lattice oxygen site pairs in four-centered Câ€“H bond activation of methane: the case of CuO. Catalysis Science and Technology, 2016, 6, 3984-3996.	2.1	59
28049	Diverse interface effects on ferroelectricity and magnetoelectric coupling in asymmetric multiferroic tunnel junctions: the role of the interfacial bonding structure. Physical Chemistry Chemical Physics, 2016, 18, 2850-2858.	1.3	14
28050	Substitutionally doped phosphorene: electronic properties and gas sensing. Nanotechnology, 2016, 27, 065708.	1.3	130
28051	Interfacial Study on Solid Electrolyte Interphase at Li Metal Anode: Implication for Li Dendrite Growth. Journal of the Electrochemical Society, 2016, 163, A592-A598.	1.3	180

#	Article	IF	Citations
28052	Description of the Zn/Br RFB System. SpringerBriefs in Energy, 2016, , 11-28.	0.2	3
28053	Revisiting Zinc-Side Electrochemistry. SpringerBriefs in Energy, 2016, , 29-43.	0.2	0
28054	Bromine-Side Electrode Functionality. SpringerBriefs in Energy, 2016, , 63-79.	0.2	1
28055	Solubility, permeation, and capturing of impurity oxygen in Au/Ag: A comparative investigation from first-principles. Computational Materials Science, 2016, 114, 79-85.	1.4	13
28056	Promotional effect of surface hydroxyls on electrochemical reduction of CO2 over SnO /Sn electrode. Journal of Catalysis, 2016, 343, 257-265.	3.1	113
28057	Two S = 1/2 one-dimensional barium copper phosphates showing antiferromagnetic and ferromagnetic intrachain interactions. Dalton Transactions, 2016, 45, 3319-3326.	1.6	1
28058	Large scale computational screening and experimental discovery of novel materials for high temperature CO₂ capture. Energy and Environmental Science, 2016, 9, 1346-1360.	15.6	61
28059	Electronic properties of MoS2 on monolayer, bilayer and bulk SiC: A density functional theory study. Journal of Alloys and Compounds, 2016, 666, 204-208.	2.8	16
28060	Ab Initio Structure Determination and Photoluminescent Properties of an Efficient, Thermally Stable Blue Phosphor, Ba₂Y₅B₅O₁₇:Ce³⁺. Chemistry of Materials, 2016, 28, 1121-1127.	3.2	78
28061	AuO: Evolving from Dis- to Comproportionation and Back Again. Inorganic Chemistry, 2016, 55, 1278-1286.	1.9	24
28062	Unraveling the Native Conduction of Trichalcogenides and Its Ideal Band Alignment for New Photovoltaic Interfaces. Journal of Physical Chemistry C, 2016, 120, 1390-1399.	1.5	55
28063	Nanoscale stabilization of zintl compounds: 1D ionic Liâ€“P double helix confined inside a carbon nanotube. Nanoscale, 2016, 8, 3454-3460.	2.8	14
28064	Electronic structure and thermoelectric properties of p-type half-Heusler compound NbFeSb: a first-principles study. RSC Advances, 2016, 6, 10507-10512.	1.7	42
28065	Effect of magnetism on surface segregation in FeNi alloys. Journal of Physics Condensed Matter, 2016, 28, 064003.	0.7	2
28066	Origin of weak magnetism in compounds with cubic laves structure. Journal of Physics Condensed Matter, 2016, 28, 065501.	0.7	2
28067	Solute clusters and GP zones in binary Mgâ€“RE alloys. Acta Materialia, 2016, 106, 260-271.	3.8	131
28068	Initial steps in reactions of aquathermolysis of cyclohexyl phenyl sulfide by means of ab initio calculations. Computational and Theoretical Chemistry, 2016, 1078, 138-145.	1.1	9
28069	Carbon adsorption on tungsten and electronic field emission. Surface Science, 2016, 645, 56-62.	0.8	11

#	Article	IF	Citations
28070	Interaction of CO with PtxAg1-x/Pt(111) surface alloys: More than dilution by Ag atoms. Surface Science, 2016, 650, 237-254.	0.8	11
28071	A Comprehensive Set of High-Quality Point Charges for Simulations of Metalâ€“Organic Frameworks. Chemistry of Materials, 2016, 28, 785-793.	3.2	140
28072	Experimental and Computational Investigation of Acetic Acid Deoxygenation over Oxophilic Molybdenum Carbide: Surface Chemistry and Active Site Identity. ACS Catalysis, 2016, 6, 1181-1197.	5.5	76
28073	Relativistic electronic structure and band alignment of BiSI and BiSeI: candidate photovoltaic materials. Journal of Materials Chemistry A, 2016, 4, 2060-2068.	5.2	127
28074	Oxygen character in the density of states as an indicator of the stability of Li-ion battery cathode materials. Solid State Ionics, 2016, 286, 83-89.	1.3	43
28075	Surface properties of NpO 2 and water reacting with stoichiometric and reduced NpO 2 (111), (110), and (100) surfaces from ab initio atomistic thermodynamics. Surface Science, 2016, 644, 153-164.	0.8	16
28076	Energy of Oxygen-Vacancy Formation on Oxide Surfaces: Role of the Spatial Distribution. Journal of Physical Chemistry C, 2016, 120, 2320-2323.	1.5	21
28077	Theory of Graphene Raman Scattering. ACS Nano, 2016, 10, 2803-2818.	7.3	94
28078	A first-principles study on the effect of oxygen content on the structural and electronic properties of silicon suboxide as anode material for lithium ion batteries. Journal of Power Sources, 2016, 307, 657-664.	4.0	32
28079	Electronic and magnetic behaviors of graphene with 5d series transition metal atom substitutions: A first-principles study. Physica E: Low-Dimensional Systems and Nanostructures, 2016, 80, 142-148.	1.3	56
28080	Stable Monolayer Transition Metal Dichalcogenide Ordered Alloys with Tunable Electronic Properties. Journal of Physical Chemistry C, 2016, 120, 2501-2508.	1.5	51
28081	Density Functional Theory Study for Catalytic Activation and Dissociation of CO₂ on Bimetallic Alloy Surfaces. Journal of Physical Chemistry C, 2016, 120, 3438-3447.	1.5	152
28082	Few-Layer MoS₂ p-Type Devices Enabled by Selective Doping Using Low Energy Phosphorus Implantation. ACS Nano, 2016, 10, 2128-2137.	7.3	315
28083	Organic-inorganic hybrid PtCo nanoparticle with high electrocatalytic activity and durability for oxygen reduction. NPG Asia Materials, 2016, 8, e237-e237.	3.8	57
28084	Precipitation in a Ag-Containing Mg-Y-Zn Alloy. Metallurgical and Materials Transactions A: Physical Metallurgy and Materials Science, 2016, 47, 927-940.	1.1	38
28085	Spin-polarized gapped Dirac spectrum of unsupported silicene. Applied Surface Science, 2016, 373, 45-50.	3.1	7
28086	Hydrogen and methoxy coadsorption in the computation of the catalytic conversion of methanol on the ceria (111) surface. Surface Science, 2016, 648, 242-249.	0.8	9
28087	Alloying and Defect Control within Chalcogenide Perovskites for Optimized Photovoltaic Application. Chemistry of Materials, 2016, 28, 821-829.	3.2	175

#	Article	IF	Citations
28088	Synergistic Resistive Switching Mechanism of Oxygen Vacancies and Metal Interstitials in Ta₂O₅. Journal of Physical Chemistry C, 2016, 120, 2456-2463.	1.5	34
28089	Anisotropy in lattice thermal conductivity tensor of bulk hexagonal-MT₂ (M = W, Mo and) Tj ETQq1 1 0.784314 rgBT /Ov	1.7	15
28090	Glide of dislocations in <1 1 1>{3 2 1} slip system: an atomistic study. Philosophical Magazine, 2016, 96, 71-83.	0.7	5
28091	Evolution of band structures in MoS₂-based homo- and heterobilayers. Journal Physics D: Applied Physics, 2016, 49, 065304.	1.3	8
28092	Thermal transport properties of MoS₂and MoSe₂monolayers. Nanotechnology, 2016, 27, 055703.	1.3	108
28093	Controlling Hydrogen Activation, Spillover, and Desorption with Pdâ€“Au Single-Atom Alloys. Journal of Physical Chemistry Letters, 2016, 7, 480-485.	2.1	169
28094	Monte Carlo simulation study of the halogenated MIL-47(V) frameworks: influence of functionalization on H2S adsorption and separation properties. Journal of Materials Science, 2016, 51, 2307-2319.	1.7	23
28095	TE Design Lab: A virtual laboratory for thermoelectric material design. Computational Materials Science, 2016, 112, 368-376.	1.4	98
28096	Charge distribution of Lithium-doped graphane/graphene hybrid system: Role of nearly-free electronic states. Solid State Communications, 2016, 229, 43-48.	0.9	5
28097	Three Dimensional Metallic Carbon from Distorting sp³-Bond. Crystal Growth and Design, 2016, 16, 1360-1365.	1.4	39
28098	Transition-Metal-Doped M-Li₈ZrO₆ (M = Mn, Fe, Co, Ni, Cu, Ce) as High-Specific-Capacity Li-Ion Battery Cathode Materials: Synthesis, Electrochemistry, and Quantum Mechanical Characterization. Chemistry of Materials, 2016, 28, 746-755.	3.2	30
28099	Coverage-Dependent N₂ Adsorption and Its Modification of Iron Surfaces Structures. Journal of Physical Chemistry C, 2016, 120, 2846-2854.	1.5	19
28100	Primary damage in tungsten using the binary collision approximation, molecular dynamic simulations and the density functional theory. Physica Scripta, 2016, T167, 014018.	1.2	16
28101	The effects of Sn-substitution on thermoelectric properties of In4â˜Sn Se3 ceramic. Ceramics International, 2016, 42, 5593-5599.	2.3	3
28102	Suppressing diborane production during the hydrogen release of metal borohydrides: The example of alloyed Al(BH 4) 3. International Journal of Hydrogen Energy, 2016, 41, 3571-3578.	3.8	9
28103	Computational Characterization of Defects in Metalâ€“Organic Frameworks: Spontaneous and Water-Induced Point Defects in ZIF-8. Journal of Physical Chemistry Letters, 2016, 7, 459-464.	2.1	119
28104	A Fundamental Relationship between Reaction Mechanism and Stability in Metal Oxide Catalysts for Oxygen Evolution. ACS Catalysis, 2016, 6, 1153-1158.	5.5	377
28105	Controlling phase transition for single-layer MTe₂ (M = Mo and W): modulation of the potential barrier under strain. Physical Chemistry Chemical Physics, 2016, 18, 4086-4094.	1.3	105

#	Article	IF	Citations
28106	Globally stable structures of Li_xZn (x = 1â€“4) compounds at high pressures. Physical Chemistry Chemical Physics, 2016, 18, 4437-4443.	1.3	8
28107	Hydrogen treated anatase TiO₂: a new experimental approach and further insights from theory. Journal of Materials Chemistry A, 2016, 4, 2670-2681.	5.2	117
28108	Effect of aluminum or zinc solute addition on enhancing impact fracture toughness in Mgâ€“Ca alloys. Acta Materialia, 2016, 104, 283-294.	3.8	55
28109	pH and Alkali Cation Effects on the Pt Cyclic Voltammogram Explained Using Density Functional Theory. Journal of Physical Chemistry C, 2016, 120, 457-471.	1.5	145
28110	Multiferroic Domain Walls in Ferroelectric PbTiO₃ with Oxygen Deficiency. Nano Letters, 2016, 16, 454-458.	4.5	44
28111	Unexpected photoluminescence properties from one-dimensional molecular chains. Nanoscale, 2016, 8, 1456-1461.	2.8	4
28112	Experimental and theoretical studies of structural phase transition in a novel polar perovskite-like [C₂H₅NH₃][Na_{0.5}Fe_{0.5}(HCOO)₃] formate. Dalton Transactions, 2016, 45, 2574-2583.	1.6	103
28113	Decomposition of activated CO2 species on Ni(110): Role of surface diffusion in the reaction mechanism. Catalysis Communications, 2016, 74, 65-70.	1.6	25
28114	The novel electronic and magnetic properties in 5d transition metal oxides system. Computational Materials Science, 2016, 112, 416-427.	1.4	9
28115	Lattice dynamics of bismuth-deficient BiFeO 3 from first principles. Computational Materials Science, 2016, 111, 374-379.	1.4	6
28116	Quercetin/Î²-cyclodextrin inclusion complex embedded nanofibres: Slow release and high solubility. Food Chemistry, 2016, 197, 864-871.	4.2	115
28117	Phase stability, mechanical properties and electronic structure of TiAl alloying with W, Mo, Sc and Yb: First-principles study. Journal of Alloys and Compounds, 2016, 658, 689-696.	2.8	53
28118	Improving the electrical conductivity and structural stability of the Li 2 MnO 3 cathode via P doping. Journal of Alloys and Compounds, 2016, 658, 818-823.	2.8	29
28119	Phosphorene ribbons as anode materials with superhigh rate and large capacity for Li-ion batteries. Journal of Power Sources, 2016, 302, 215-222.	4.0	46
28120	Density functional study on redox energetics of LaMO3 (M=Scâ€“Cu) perovskite-type oxides. Journal of Solid State Chemistry, 2016, 233, 62-66.	1.4	2
28121	Robust half-metallicity of hexagonal SrNiO3. Journal of Solid State Chemistry, 2016, 233, 438-443.	1.4	8
28122	The acidâ€“base and redox reactivity of CeO2 nanoparticles: Influence of the Hubbard U term in DFT + U studies. Surface Science, 2016, 648, 212-219.	0.8	18
28123	Effect of the Chalcogenide Element Doping on the Electronic Properties of Co2FeAl Heusler Alloys. Journal of Electronic Materials, 2016, 45, 1028-1034.	1.0	1

#	Article	IF	Citations
28124	Charge transfer induced negative thermal expansion in perovskite BiNiO3. Computational Materials Science, 2016, 113, 198-202.	1.4	10
28125	Blue-emitting Ca5(PO4)3Cl:Eu2+ phosphor for near-UV pumped light emitting diodes: Electronic structures, luminescence properties and LED fabrications. Journal of Alloys and Compounds, 2016, 663, 332-339.	2.8	39
28126	Synthesis, characterization and chemical stability of silicon dichalcogenides, Si(Se S1â^')2. Journal of Crystal Growth, 2016, 452, 151-157.	0.7	13
28127	Electroreduction of N₂ to Ammonia at Ambient Conditions on Mononitrides of Zr, Nb, Cr, and V: A DFT Guide for Experiments. ACS Catalysis, 2016, 6, 635-646.	5.5	317
28128	Transition metal carbides as novel materials for CO₂ capture, storage, and activation. Energy and Environmental Science, 2016, 9, 141-144.	15.6	155
28129	An investigation into the influence of grain boundary misorientation on the tensile strength of SiC bicrystals. Mechanics of Advanced Materials and Structures, 2016, 23, 494-502.	1.5	7
28130	Computational Studies of Bismuth-Doped Zinc Oxide Nanowires. Nanoscience and Technology, 2016, , 401-421.	1.5	1
28131	The ferrite/oxide interface and helium management in nano-structured ferritic alloys from the first principles. Acta Materialia, 2016, 103, 474-482.	3.8	68
28132	Study of Phase Transformation in BaTe2O6 by in Situ High-Pressure X-ray Diffraction, Raman Spectroscopy, and First-Principles Calculations. Inorganic Chemistry, 2016, 55, 227-238.	1.9	11
28133	Crystal Structures and Electronic Properties of Single-Layer, Few-Layer, and Multilayer GeH. Journal of Physical Chemistry C, 2016, 120, 793-800.	1.5	18
28134	Understanding and Tuning the Intrinsic Hydrophobicity of Rare-Earth Oxides: A DFT+U Study. ACS Applied Materials & Interfaces, 2016, 8, 152-160.	4.0	55
28135	Examining the Performance of Refractory Conductive Ceramics as Plasmonic Materials: A Theoretical Approach. ACS Photonics, 2016, 3, 43-50.	3.2	126
28136	Correlated metals as transparent conductors. Nature Materials, 2016, 15, 204-210.	13.3	291
28137	Counting electrons on supported nanoparticles. Nature Materials, 2016, 15, 284-288.	13.3	469
28138	Single-molecule insight into Wurtz reactions on metal surfaces. Physical Chemistry Chemical Physics, 2016, 18, 2730-2735.	1.3	31
28139	Quantum confinement and dielectric profiles of colloidal nanoplatelets of halide inorganic and hybrid organicâ€“inorganic perovskites. Nanoscale, 2016, 8, 6369-6378.	2.8	136
28140	Prospects of Spin Catalysis on Spin-Polarized Graphene Heterostructures. Australian Journal of Chemistry, 2016, 69, 753.	0.5	2
28141	Optimal Dopant Selection for Water Splitting with Cerium Oxides: Mining and Screening First Principles Data. Springer Series in Materials Science, 2016, , 157-171.	0.4	6

#	Article	IF	Citations
28142	Carbon dioxide adsorption on lanthanum zirconate nanostructured coating surface: a DFT study. Adsorption, 2016, 22, 159-163.	1.4	6
28143	Atomistic mechanism of nano-scale phase separation in fcc-based high entropy alloys. Journal of Alloys and Compounds, 2016, 663, 340-344.	2.8	16
28144	Tuning magnetism of monolayer GaN by vacancy and nonmagnetic chemical doping. Journal of Physics and Chemistry of Solids, 2016, 91, 1-6.	1.9	49
28145	Toward a Reliable Energetics of Adsorption at Solvated Mineral Surfaces: A Computational Study of Uranyl(VI) on 2:1 Clay Minerals. Journal of Physical Chemistry C, 2016, 120, 324-335.	1.5	18
28146	Epitaxial Stabilization between Intermetallic and Carbide Domains in the Structures of Mn₁₆SiC₄ and Mn₁₇Si₂C₄. Journal of the American Chemical Society, 2016, 138, 248-256.	6.6	20
28147	Computational insights into the reaction mechanism of methanol-to-olefins conversion in H-ZSM-5: nature of hydrocarbon pool. Catalysis Science and Technology, 2016, 6, 3279-3288.	2.1	55
28148	Interlayer interaction and related properties of bilayer hexagonal boron nitride: ab initio study. RSC Advances, 2016, 6, 6423-6435.	1.7	37
28149	Senary Refractory High-Entropy Alloy HfNbTaTiVZr. Metallurgical and Materials Transactions A: Physical Metallurgy and Materials Science, 2016, 47, 3333-3345.	1.1	83
28150	Effects of phase stability, lattice ordering, and electron density on plastic deformation in cubic TiWN pseudobinary transition-metal nitride alloys. Acta Materialia, 2016, 103, 823-835.	3.8	56
28151	Band engineering of ternary metal nitride system Ti_1-x Zr_xN for plasmonic applications. Optical Materials Express, 2016, 6, 29.	1.6	37
28152	Crystal structure, equation of state, and elasticity of hydrous aluminosilicate phase, topaz-OH (Al2SiO4(OH)2) at high pressures. Physics of the Earth and Planetary Interiors, 2016, 251, 24-35.	0.7	18
28153	Facet-dependent solar ammonia synthesis of BiOCl nanosheets via a proton-assisted electron transfer pathway. Nanoscale, 2016, 8, 1986-1993.	2.8	242
28154	Synthesis of urchin-like rutile titania carbon nanocomposites by iron-facilitated phase transformation of MXene for environmental remediation. Journal of Materials Chemistry A, 2016, 4, 489-499.	5.2	170
28155	Carbon Nanotubes Under Pressure. CISM International Centre for Mechanical Sciences, Courses and Lectures, 2016, , 99-134.	0.3	0
28156	Structure-sensitive electroreduction of acetaldehyde to ethanol on copper and its mechanistic implications for CO and CO 2 reduction. Catalysis Today, 2016, 262, 90-94.	2.2	132
28157	Magnetic reconstruction induced magnetoelectric coupling and spin-dependent tunneling in Ni/KNbO3/Ni multiferroic tunnel junctions. Journal of Magnetism and Magnetic Materials, 2016, 404, 1-6.	1.0	2
28158	High-Pressure Study of Mn(BH4)2 Reveals a Stable Polymorph with High Hydrogen Density. Chemistry of Materials, 2016, 28, 274-283.	3.2	17
28159	Anatomy and Giant Enhancement of the Perpendicular Magnetic Anisotropy of Cobaltâ€“Graphene Heterostructures. Nano Letters, 2016, 16, 145-151.	4.5	120

#	Article	IF	Citations
28160	Nanostructured BNâ€“Mg composites: features of interface bonding and mechanical properties. Physical Chemistry Chemical Physics, 2016, 18, 965-969.	1.3	12
28161	Geometric stability and adsorption property of hydroxyl group on graphene sheets. Composite Interfaces, 2016, 23, 65-73.	1.3	5
28162	Alloying effects on properties of Al 2 O 3 and TiO 2 in connection with oxidation resistance of TiAl. Intermetallics, 2016, 68, 57-62.	1.8	55
28163	Steam Reforming of Ethylene Glycol over MgAl₂O₄ Supported Rh, Ni, and Co Catalysts. ACS Catalysis, 2016, 6, 315-325.	5.5	45
28164	Density functional study on the hole doping of single-layer SnS₂ with metal element X (X) Tj ETQq0 0 0 rgBT /Overlock 10 T	1.3	43
28165	Tuning the Fermi level with topological phase transition by internal strain in a topological insulator Bi₂Se₃thin film. Nanoscale, 2016, 8, 741-751.	2.8	23
28166	Electronic and optical properties of single crystal SnS₂: an earth-abundant disulfide photocatalyst. Journal of Materials Chemistry A, 2016, 4, 1312-1318.	5.2	246
28167	Anti-precursor effect of Fe on martensitic transformation in TiNi alloys. Acta Materialia, 2016, 104, 18-24.	3.8	6
28168	Novel three dimensional topological nodal line semimetallic carbon. Carbon, 2016, 98, 468-473.	5.4	36
28169	Adsorption of polyiodobenzene molecules on the Pt(111) surface using van der Waals density functional theory. Surface Science, 2016, 644, 113-121.	0.8	6
28170	Structural Phase Transitions by Design in Monolayer Alloys. ACS Nano, 2016, 10, 289-297.	7.3	109
28171	Phononic and thermodynamic properties of the sulvanite compounds: A first-principles study. Computational Materials Science, 2016, 113, 275-279.	1.4	14
28172	Interfacial electronic structure and charge transfer of hybrid graphene quantum dot and graphitic carbon nitride nanocomposites: insights into high efficiency for photocatalytic solar water splitting. Physical Chemistry Chemical Physics, 2016, 18, 1050-1058.	1.3	57
28173	Broad temperature plateau for high ZTs in heavily doped p-type SnSe single crystals. Energy and Environmental Science, 2016, 9, 454-460.	15.6	396
28174	Efficient band structure tuning, charge separation, and visible-light response in ZrS₂-based van der Waals heterostructures. Energy and Environmental Science, 2016, 9, 841-849.	15.6	161
28175	Theoretical insights into a potential lead-free hybrid perovskite: substituting Pb²⁺with Ge²⁺. Nanoscale, 2016, 8, 1503-1512.	2.8	247
28176	First-principles study of the influence of doping elements on phase stability, crystal and electronic structure of Al 2 Cu (Î¸) phase. Computational Materials Science, 2016, 111, 328-333.	1.4	21
28177	Atomic investigation of alloying Cr, Ti, Y additions in a grain boundary of vanadium. Journal of Nuclear Materials, 2016, 468, 147-152.	1.3	14

#	Article	IF	Citations
28178	Adsorption of guaiacol on Fe (110) and Pd (111) from first principles. Surface Science, 2016, 648, 227-235.	0.8	36
28179	Automatized Parameterization of DFTB Using Particle Swarm Optimization. Journal of Chemical Theory and Computation, 2016, 12, 53-64.	2.3	55
28180	A combined computational and experimental investigation of Mg doped Î±-Fe₂O₃. Physical Chemistry Chemical Physics, 2016, 18, 781-791.	1.3	15
28181	High adsorption capacity of heavy metals on two-dimensional MXenes: an ab initio study with molecular dynamics simulation. Physical Chemistry Chemical Physics, 2016, 18, 228-233.	1.3	109
28182	Al-rich beta zeolites. Distribution of Al atoms in the framework and related protonic and metal-ion species. Journal of Catalysis, 2016, 333, 102-114.	3.1	86
28183	Kinetic Monte Carlo simulations of the water gas shift reaction on Cu(1 1 1) from density functional theory based calculations. Journal of Catalysis, 2016, 333, 217-226.	3.1	53
28184	Elongated Siliconâ€“Carbon Bonds at Graphene Edges. ACS Nano, 2016, 10, 142-149.	7.3	20
28185	Positional recurrence maps, a powerful tool to de-correlate static and dynamical disorder in distribution maps from molecular dynamics simulations: the case of Nd₂NiO_{4+d}. Physical Chemistry Chemical Physics, 2016, 18, 17398-17403.	1.3	14
28186	Discovery of elusive structures of multifunctional transition-metal borides. Nanoscale, 2016, 8, 1055-1065.	2.8	24
28187	Quaternary Al-Cu-Mg-Si Q Phase: Sample Preparation, Heat Capacity Measurement and First-Principles Calculations. Journal of Phase Equilibria and Diffusion, 2016, 37, 119-126.	0.5	12
28188	First-principles study of the origin of magnetism induced by intrinsic defects in monolayer MoS2. Applied Surface Science, 2016, 361, 199-205.	3.1	61
28189	Computational searching for new stable graphyne structures and their electronic properties. Carbon, 2016, 98, 404-410.	5.4	37
28190	Local structure investigation of (Co, Cu) co-doped ZnO nanocrystals and its correlation with magnetic properties. Journal of Physics and Chemistry of Solids, 2016, 90, 100-113.	1.9	29
28191	A first principles study of cohesive, elastic and electronic properties of binary Feâ€“Zr intermetallics. Computational Materials Science, 2016, 112, 52-66.	1.4	42
28192	First-Principles Analysis of Cation Diffusion in Mixed Metal Ferrite Spinels. Chemistry of Materials, 2016, 28, 214-226.	3.2	80
28193	Unraveling the origins of conduction band valley degeneracies in Mg2Si1â^'xSnx thermoelectrics. Physical Chemistry Chemical Physics, 2016, 18, 939-946.	1.3	12
28194	Solution synthesis of GeS and GeSe nanosheets for high-sensitivity photodetectors. Journal of Materials Chemistry C, 2016, 4, 479-485.	2.7	145
28195	Effects of Charging and Perpendicular Electric Field on Graphene Oxide. Nanoscience and Technology, 2016, , 261-290.	1.5	4

#	Article	IF	Citations
28196	First-principles study on the magnetism and electronic structure in 3d transition metal (X=Sc, V, Cr,) Tj ETQq0 0 0 rgBT /Overlock 10 Tf 5	1.3	6
28197	A Two-Dimensional Liquid Structure Explains the Elevated Melting Temperatures of Gallium Nanoclusters. Nano Letters, 2016, 16, 21-26.	4.5	18
28198	Neutron powder diffraction and theory-aided structure refinement of rubidium and cesium ureate. Zeitschrift Fur Naturforschung - Section B Journal of Chemical Sciences, 2016, 71, 431-438.	0.3	5
28199	First-principles study of defect formation in the photovoltaic semiconductor Cu2SnS3for comparison with Cu2ZnSnS4and CuInSe2. Japanese Journal of Applied Physics, 2016, 55, 04ES08.	0.8	9
28200	Magnetic properties in BiFeO3 doped with Cu and Zn first-principles investigation. Journal of Alloys and Compounds, 2016, 674, 463-469.	2.8	17
28201	Photovoltaic Properties of Two-Dimensional (CH₃NH₃)₂Pb(SCN)₂I₂ Perovskite: A Combined Experimental and Density Functional Theory Study. Journal of Physical Chemistry Letters, 2016, 7, 1213-1218.	2.1	135
28202	Spin Chains and Electron Transfer at Stepped Silicon Surfaces. Nano Letters, 2016, 16, 2698-2704.	4.5	34
28203	Facile synthesis of copper doped carbon dots and their application as a â€œturn-offâ€•fluorescent probe in the detection of Fe³⁺ ions. RSC Advances, 2016, 6, 28745-28750.	1.7	75
28204	Van der Waals heterostructure of phosphorene and hexagonal boron nitride: First-principles modeling. Chinese Physics B, 2016, 25, 037302.	0.7	9
28205	Density functional theory study of M-doped (MÂ=ÂB, C, N, Mg, Al) VO2 nanoparticles for thermochromic energy-saving foils. Journal of Alloys and Compounds, 2016, 662, 621-627.	2.8	39
28206	Structural analysis and atomic simulation of Ag/BN nanoparticle hybrids obtained by Ag ion implantation. Materials and Design, 2016, 98, 167-173.	3.3	16
28207	Crystal Structure and Band Gap Engineering in Polyoxometalate-Based Inorganicâ€“Organic Hybrids. Inorganic Chemistry, 2016, 55, 3364-3377.	1.9	27
28208	Periodic Pulay method for robust and efficient convergence acceleration of self-consistent field iterations. Chemical Physics Letters, 2016, 647, 31-35.	1.2	60
28209	First-principles calculation of formation energies and electronic structures of hydrogen defects at tetrahedral and octahedral interstitial sites in pyrochlore-type Y2Ti2O7 oxide. Journal of Alloys and Compounds, 2016, 678, 153-159.	2.8	13
28210	First-principles energetics of rare gases incorporation into uranium dioxide. Nuclear Instruments & Methods in Physics Research B, 2016, 373, 102-109.	0.6	8
28211	Segregation and Migration of the Oxygen Vacancies in the Î£3 (111) Tilt Grain Boundaries of Ceria. Journal of Physical Chemistry C, 2016, 120, 6625-6632.	1.5	11
28212	Role of Structural H₂O in Intercalation Electrodes: The Case of Mg in Nanocrystalline Xerogel-V₂O₅. Nano Letters, 2016, 16, 2426-2431.	4.5	194
28213	Synergistic effects towards H₂oxidation on the Cuâ€“CeO₂electrode: a combination study with DFT calculations and experiments. Journal of Materials Chemistry A, 2016, 4, 5745-5754.	5.2	24

#	Article	IF	Citations
28214	Heat conductivity of copper in two-temperature state. Applied Physics A: Materials Science and Processing, 2016, 122, 1.	1.1	22
28215	A density functional theory study of electronic properties of substitutional alloying of monolayer MoS 2 and CeS 2 surface models. Computational and Theoretical Chemistry, 2016, 1084, 98-102.	1.1	4
28216	Ab initio study of oxygen adsorption on the NiTi(1 1 0) surface and the surface phase diagram. Corrosion Science, 2016, 106, 137-146.	3.0	13
28217	Modular Approach for Metalâ€“Semiconductor Heterostructures with Very Large Interface Lattice Misfit: A First-Principles Perspective. Crystal Growth and Design, 2016, 16, 2328-2334.	1.4	7
28218	Tungsten Bronze Barium Neodymium Titanate (Ba_{6â€“3n}Nd_{8+2n}Ti₁₈O₅₄): An Intrinsic Nanostructured Material and Its Defect Distribution. Inorganic Chemistry, 2016, 55, 3338-3350.	1.9	17
28219	Raman Shifts in Electron-Irradiated Monolayer MoS₂. ACS Nano, 2016, 10, 4134-4142.	7.3	311
28220	Elucidating the Phase Transformation of Li₄Ti₅O₁₂ Lithiation at the Nanoscale. ACS Nano, 2016, 10, 4312-4321.	7.3	144
28221	Electronic structure and thermodynamic properties of platinumâ€“lead oxides PbPt₂O₄ and Pb₂PtO₄ by ab initio methods. Phase Transitions, 2016, 89, 1090-1102.	0.6	2
28222	Structure and Spin-Polarized Transport of Co Atomic Chains on Graphene with Topological Line Defects. Journal of Cluster Science, 2016, 27, 875-882.	1.7	3
28223	Thermodynamic reassessment of the Auâ€“Dy system supported by first-principles calculations. Calphad: Computer Coupling of Phase Diagrams and Thermochemistry, 2016, 53, 49-54.	0.7	4
28224	Local charge states in hexagonal boron nitride with Stoneâ€“Wales defects. Nanoscale, 2016, 8, 8210-8219.	2.8	43
28225	Polytypism and unexpected strong interlayer coupling in two-dimensional layered ReS₂. Nanoscale, 2016, 8, 8324-8332.	2.8	120
28226	Limitations of reactive atomistic potentials in describing defect structures in oxides. Modelling and Simulation in Materials Science and Engineering, 2016, 24, 035022.	0.8	5
28227	Interaction of VOCs with pyrene tetratopic ligands layered on ZnO nanorods under visible light. Journal of Photochemistry and Photobiology A: Chemistry, 2016, 324, 62-69.	2.0	17
28228	Charge-Transfer-Induced Magic Cluster Formation of Azaborine Heterocycles on Noble Metal Surfaces. Journal of Physical Chemistry C, 2016, 120, 6020-6030.	1.5	23
28229	Large Electronic Anisotropy and Enhanced Chemical Activity of Highly Rippled Phosphorene. Journal of Physical Chemistry C, 2016, 120, 6876-6884.	1.5	68
28230	Robust band gap of TiS₃ nanofilms. Physical Chemistry Chemical Physics, 2016, 18, 14805-14809.	1.3	40
28231	Mo₂C as a high capacity anode material: a first-principles study. Journal of Materials Chemistry A, 2016, 4, 6029-6035.	5.2	249

#	Article	IF	Citations
28232	Synthesis, characterization, and mechanism analysis of S = 2 quasi-one-dimensional ferromagnetic semiconductor Pb₂Mn(VO₄)₂(OH). Dalton Transactions, 2016, 45, 7022-7027.	1.6	7
28233	Halogenated arsenenes as Dirac materials. Applied Surface Science, 2016, 376, 286-289.	3.1	49
28234	First-principles studies on substitutional doping by group IV and VI atoms in the two-dimensional arsenene. Applied Surface Science, 2016, 378, 350-356.	3.1	36
28235	Magnetism in transition-metal-doped germanene: A first-principles study. Computational Materials Science, 2016, 118, 112-116.	1.4	69
28236	Understanding mechanisms of carbon dioxide conversion into methane for designing enhanced catalysts from first-principles. Computational and Theoretical Chemistry, 2016, 1083, 31-37.	1.1	17
28237	NO Reduction by H₂ on the Rh(111) and Rh(221) Surfaces: A Mechanistic and Kinetic Study. Journal of Physical Chemistry C, 2016, 120, 5410-5419.	1.5	28
28238	Fluorine-Terminated Diamond Surfaces as Dense Dipole Lattices: The Electrostatic Origin of Polar Hydrophobicity. Journal of the American Chemical Society, 2016, 138, 4018-4028.	6.6	47
28239	Oxygen vacancy formation characteristics in the bulk and across different surface terminations of La_(1â^'x)Sr_xFe_(1â^'y)Co_yO_(3â^'Î´) perovskite oxides for CO₂ conversion. Journal of Materials Chemistry A, 2016, 4, 5137-5148.	5.2	65
28240	Mode specificity for the dissociative chemisorption of H₂O on Cu(111): a quantum dynamics study on an accurately fitted potential energy surface. Physical Chemistry Chemical Physics, 2016, 18, 8537-8544.	1.3	33
28241	Surface Passivation in Empirical Tight Binding. IEEE Transactions on Electron Devices, 2016, 63, 954-958.	1.6	8
28242	Evidence for multi-polymorphic islands during epitaxial growth of ZnO on Ag(1â€‰1â€‰1). Journal of Physics Condensed Matter, 2016, 28, 224007.	0.7	9
28243	Pure H ^{â€“} conduction in oxyhydrides. Science, 2016, 351, 1314-1317.	6.0	155
28244	On the tetragonality of martensites in ferrous shape memory alloy Fe3Pt: A first-principles study. Acta Materialia, 2016, 111, 56-65.	3.8	5
28245	Water splitting and the band edge positions of TiO2. Electrochimica Acta, 2016, 199, 27-34.	2.6	64
28246	Electrochemical supercapacitor performance of SnO2 quantum dots. Electrochimica Acta, 2016, 203, 230-237.	2.6	93
28247	High-pressure, temperature elasticity of Fe- and Al-bearing MgSiO3: Implications for the Earth's lower mantle. Earth and Planetary Science Letters, 2016, 434, 264-273.	1.8	32
28248	A DFT study on the correlation between topology and Bader charges: Part IV, on the change of atomic charges in polymorphic transitions â€“ A case study on CaCl 2. Solid State Sciences, 2016, 52, 126-131.	1.5	2
28249	Effect and controlling mechanism of vanadium on Feâ€“Al interface reaction in Alâ€“Zn bath. Surface and Coatings Technology, 2016, 306, 408-417.	2.2	8

#	Article	IF	Citations
28250	Surface-Mediated Hydrogen Bonding of Proteinogenic Î±-Amino Acids on Silicon. Accounts of Chemical Research, 2016, 49, 942-951.	7.6	26
28251	Nonadiabatic Molecular Dynamics for Thousand Atom Systems: A Tight-Binding Approach toward PYXAID. Journal of Chemical Theory and Computation, 2016, 12, 1436-1448.	2.3	93
28252	Doping-Induced Room Temperature Stabilization of Metastable Î²-Ag₂WO₄ and Origin of Visible Emission in Î±- and Î²-Ag₂WO₄: Low Temperature Photoluminescence Studies. Journal of Physical Chemistry C, 2016, 120, 7265-7276.	1.5	46
28253	On-surface synthesis of two-dimensional imine polymers with a tunable band gap: a combined STM, DFT and Monte Carlo investigation. Nanoscale, 2016, 8, 8568-8574.	2.8	23
28254	Comprehensive electronic structure characterization of pristine and nitrogen/phosphorus doped carbon nanocages. Carbon, 2016, 103, 480-487.	5.4	23
28255	Magnetic and electronic properties of hard | soft magnetic interface in (YCo5 | Co)[0001] and (YFe5 | Co)[0001] superlattices. Journal of Magnetism and Magnetic Materials, 2016, 418, 92-98.	1.0	1
28256	Investigation of microstructure evolution during self-annealing in thin Cu films by combining mesoscale level set and ab initio modeling. Journal of the Mechanics and Physics of Solids, 2016, 90, 160-178.	2.3	24
28257	The impact of oxygen vacancies on lithium vacancy formation and diffusion in Li2-MnO3-. Solid State Ionics, 2016, 289, 87-94.	1.3	21
28258	Crystal Structure, Electronic Structure, and Photocatalytic Activity of Oxysulfides: La₂Ta₂ZrS₂O₈, La₂Ta₂TiS₂O₈, and La₂Nb₂TiS₂O₈. Inorganic Chemistry, 2016, 55, 3674-3679.	1.9	25
28259	Dissociative Adsorption of H₂ on PtRu Bimetallic Surfaces. Journal of Physical Chemistry C, 2016, 120, 7201-7212.	1.5	6
28260	Hexagonal Planar CdS Monolayer Sheet for Visible Light Photocatalysis. Journal of Physical Chemistry C, 2016, 120, 7052-7060.	1.5	132
28261	Origin of Indium Diffusion in High-k Oxide HfO₂. ACS Applied Materials & Interfaces, 2016, 8, 7595-7600.	4.0	28
28262	Role of the Support and Reaction Conditions on the Vapor-Phase Deoxygenation of m-Cresol over Pt/C and Pt/TiO₂ Catalysts. ACS Catalysis, 2016, 6, 2715-2727.	5.5	123
28263	Cuâ€“Sn Bimetallic Catalyst for Selective Aqueous Electroreduction of CO₂ to CO. ACS Catalysis, 2016, 6, 2842-2851.	5.5	380
28264	Two-dimensional self-assembly of benzotriazole on an inert substrate. Nanoscale, 2016, 8, 9167-9177.	2.8	15
28265	Effects of moisture on (La, A)MnO₃ (A = Ca, Sr, and Ba) solid oxide fuel cell cathodes: a first-principles and experimental study. Journal of Materials Chemistry A, 2016, 4, 5605-5615.	5.2	36
28266	Li₃Cs₂M₂B₃P₆O₂₄(M = Pb,) Tj ETQq0 0 0 rgBT /Overloc [BP₂O₈]^{3â^'}. Dalton Transactions, 2016, 45, 7124-7130.	1.6	17
28267	Carbon phosphide monolayers with superior carrier mobility. Nanoscale, 2016, 8, 8819-8825.	2.8	135

#	Article	IF	Citations
28268	The static and dynamic magnetic properties of monolayer iron dioxide and iron dichalcogenides. RSC Advances, 2016, 6, 31758-31761.	1.7	26
28269	Proton and hydrogen transport through two-dimensional monolayers. 2D Materials, 2016, 3, 025004.	2.0	64
28270	Phase Relationship and Ionic Conductivity in Naâ€“SrSiO₃ Ionic Conductor. Journal of the American Ceramic Society, 2016, 99, 324-331.	1.9	19
28271	Ab Initio Calculations on the Structural, Mechanical, Electronic, Dynamic, and Optical Properties of Semiconductor Half-Heusler Compound ZrPdSn. Zeitschrift Fur Naturforschung - Section A Journal of Physical Sciences, 2016, 71, 135-143.	0.7	2
28272	Highly spectrum-selective near-band-edge ultraviolet photodiode based on indium oxide with dipole-forbidden bandgap transition. Ceramics International, 2016, 42, 8017-8021.	2.3	5
28273	Understanding the enhanced catalytic activity of Cu1@Pd3(111) in formic acid dissociation, a theoretical perspective. Journal of Power Sources, 2016, 316, 8-16.	4.0	37
28274	Density functional theory study of nitrogen atoms and molecules interacting with Fe(1 1 1) surfaces. Nuclear Instruments & Methods in Physics Research B, 2016, 382, 105-109.	0.6	6
28275	Ultrahigh tensile transformation strains in new Ni50.5Ti36.2Hf13.3 shape memory alloy. Scripta Materialia, 2016, 118, 51-54.	2.6	23
28276	Heterogeneous Reduction Pathways for Hg(II) Species on Dry Aerosols: A First-Principles Computational Study. Journal of Physical Chemistry A, 2016, 120, 2106-2113.	1.1	10
28277	Band Structure Engineering: Insights from Defects, Band Gap, and Electron Mobility, from Study of Magnesium Tantalate. Journal of Physical Chemistry C, 2016, 120, 6930-6937.	1.5	26
28278	Understanding dislocation mechanics at the mesoscale using phase field dislocation dynamics. Philosophical Transactions Series A, Mathematical, Physical, and Engineering Sciences, 2016, 374, 20150166.	1.6	53
28279	The interfacial properties of SrRuO3/MoS2 heterojunction: a first-principles study. European Physical Journal B, 2016, 89, 1.	0.6	41
28280	A Simple and Nonâ€Destructive Method for Assessing the Incorporation of Bipyridine Dicarboxylates as Linkers within Metalâ€“Organic Frameworks. Chemistry - A European Journal, 2016, 22, 3713-3718.	1.7	28
28281	Automatized Parameterization of the Densityâ€functional Tightâ€binding Method. II. Twoâ€center Integrals. Journal of the Chinese Chemical Society, 2016, 63, 57-68.	0.8	13
28282	p-Type Co Interstitial Defects in Thermoelectric Skutterudite CoSb₃ Due to the Breakage of Sb₄-Rings. Chemistry of Materials, 2016, 28, 2172-2179.	3.2	28
28283	Maximizing the thermoelectric performance of topological insulator Bi₂Te₃films in the few-quintuple layer regime. Nanoscale, 2016, 8, 8855-8862.	2.8	53
28284	Highly-active Pdâ€“Cu electrocatalysts for oxidation of ubiquitous oxygenated fuels. Applied Catalysis B: Environmental, 2016, 191, 76-85.	10.8	61
28285	Investigation of fluorine adsorption on nitrogen doped MgAl 2 O 4 surface by first-principles. Applied Surface Science, 2016, 376, 97-104.	3.1	33

#	Article	IF	Citations
28286	An Unusual Crystal Growth Method of the Chalcohalide Semiconductor, Î²-Hg₃S₂Cl₂: A New Candidate for Hard Radiation Detection. Crystal Growth and Design, 2016, 16, 2678-2684.	1.4	16
28287	Combined Theoretical and in Situ Scattering Strategies for Optimized Discovery and Recovery of High-Pressure Phases: A Case Study of the GaNâ€“Nb₂O₅ System. Inorganic Chemistry, 2016, 55, 3384-3392.	1.9	4
28288	Chemically Driven Interfacial Coupling in Charge-Transfer Mediated Functional Superstructures. Nano Letters, 2016, 16, 2851-2859.	4.5	14
28289	Polymorphism driven optical properties of an anil dye. CrystEngComm, 2016, 18, 7249-7259.	1.3	29
28290	Direct and quasi-direct band gap silicon allotropes with remarkable stability. Physical Chemistry Chemical Physics, 2016, 18, 9682-9686.	1.3	49
28291	A quantum-chemical approach to Ni and Fe codoping in SnO2. Journal of Theoretical and Computational Chemistry, 2016, 15, 1650016.	1.8	1
28292	Thermal Boundary Conductance: A Materials Science Perspective. Annual Review of Materials Research, 2016, 46, 433-463.	4.3	185
28293	Vehement Competition of Multiple Superexchange Interactions and Peculiar Magnetically Disordered State in Cu(OH)F. Journal of the Physical Society of Japan, 2016, 85, 024709.	0.7	7
28294	Structural features and thermal properties of W/Cu compounds using tight-binding potential calculations. Journal of Materials Science, 2016, 51, 5948-5961.	1.7	18
28295	Crystal structure and tautomerism of Pigment Yellow 138 determined by X-ray powder diffraction and solid-state NMR. Dyes and Pigments, 2016, 131, 364-372.	2.0	20
28296	The electronic and magnetic properties of anion doped (C, N, S) GaFeO3; an ab initio DFT study. Computational Materials Science, 2016, 117, 380-389.	1.4	7
28297	Hindered Translator and Hindered Rotor Models for Adsorbates: Partition Functions and Entropies. Journal of Physical Chemistry C, 2016, 120, 9719-9731.	1.5	113
28298	Experimental realization of two-dimensional boron sheets. Nature Chemistry, 2016, 8, 563-568.	6.6	1,398
28299	The interaction of reactants, intermediates and products with Cu ions in Cu-SSZ-13 NH₃SCR catalysts: an energetic and ab initio X-ray absorption modeling study. Catalysis Science and Technology, 2016, 6, 5812-5829.	2.1	23
28300	Elastic properties of type-I clathrate K ₈ Zn ₄ Sn ₄₂ determined by inelastic X-ray scattering. Europhysics Letters, 2016, 113, 16001.	0.7	1
28301	First principles exploration of near-equiatomic NiFeCrCo high entropy alloys. Journal of Alloys and Compounds, 2016, 672, 510-520.	2.8	67
28302	Strong quantum confinement effect in Cu4SnS4 quantum dots synthesized via an improved hydrothermal approach. Journal of Alloys and Compounds, 2016, 672, 204-211.	2.8	21
28303	Surface binding energies of beryllium/tungsten alloys. Journal of Nuclear Materials, 2016, 472, 76-81.	1.3	16

#	Article	IF	Citations
28304	Tunable electronic structures and magnetic properties in two-dimensional stanene with hydrogenation. Materials Chemistry and Physics, 2016, 173, 246-254.	2.0	30
28305	Discovery of Fe₂P-Type Ti(Zr/Hf)₂O₆ Photocatalysts toward Water Splitting. Chemistry of Materials, 2016, 28, 1335-1342.	3.2	7
28306	Theoretical Limiting Potentials in Mg/O₂ Batteries. Chemistry of Materials, 2016, 28, 1390-1401.	3.2	42
28307	Multiferroic BaCoF₄ in Thin Film Form: Ferroelectricity, Magnetic Ordering, and Strain. ACS Applied Materials & Interfaces, 2016, 8, 2694-2703.	4.0	16
28308	Effects of Uniaxial and Biaxial Strain on Few-Layered Terrace Structures of MoS₂ Grown by Vapor Transport. ACS Nano, 2016, 10, 3186-3197.	7.3	83
28309	Heterointerface Screening Effects between Organic Monolayers and Monolayer Transition Metal Dichalcogenides. ACS Nano, 2016, 10, 2476-2484.	7.3	87
28310	Crossover from metal to insulator in dense lithium-rich compound CLi ₄. Proceedings of the National Academy of Sciences of the United States of America, 2016, 113, 2366-2369.	3.3	21
28311	Experimental and theoretical investigation of electronic structure of SrFeO_{3â^'} _xF_x epitaxial thin films prepared via topotactic reaction. Applied Physics Express, 2016, 9, 025801.	1.1	10
28312	Crystal structure predictions of Na C6O6 for sodium-ion batteries: First-principles calculations with an evolutionary algorithm. Electrochimica Acta, 2016, 195, 1-8.	2.6	30
28313	Strong coupling between magnetization and electric polarization in BC3 sheet adsorbed with Li, Na, K, and Ca. Solid State Communications, 2016, 226, 13-18.	0.9	3
28314	Light adatoms influences on electronic structures of the two-dimensional arsenene nanosheets. Solid State Communications, 2016, 230, 6-10.	0.9	24
28315	Determination of the Anisotropic Elastic Properties of Rocksalt Ge₂Sb₂Te₅ by XRD, Residual Stress, and DFT. Journal of Physical Chemistry C, 2016, 120, 5624-5629.	1.5	10
28316	Defect Luminescence from Wurtzite CuInS₂ Nanocrystals: Combined Experimental and Theoretical Analysis. Journal of Physical Chemistry C, 2016, 120, 5207-5212.	1.5	41
28317	Substrate-Sensitive Graphene Oxidation. Journal of Physical Chemistry Letters, 2016, 7, 867-873.	2.1	26
28318	Interface-Induced Renormalization of Electrolyte Energy Levels in Magnesium Batteries. Journal of Physical Chemistry Letters, 2016, 7, 874-881.	2.1	39
28319	Correlation of Methane Activation and Oxide Catalyst Reducibility and Its Implications for Oxidative Coupling. ACS Catalysis, 2016, 6, 1812-1821.	5.5	134
28320	Atomic and electronic structure transformations in SnS₂at high pressures: a joint single crystal X-ray diffraction and DFT study. Dalton Transactions, 2016, 45, 3798-3805.	1.6	39
28321	Super-ion inspired colorful hybrid perovskite solar cells. Journal of Materials Chemistry A, 2016, 4, 4728-4737.	5.2	84

#	Article	IF	Citations
28322	Determination of the microstructure, energy levels and magnetic dipole transition mechanism for Tm³⁺doped yttrium aluminum borate. Journal of Materials Chemistry C, 2016, 4, 1988-1995.	2.7	17
28323	Germanium monosulfide monolayer: a novel two-dimensional semiconductor with a high carrier mobility. Journal of Materials Chemistry C, 2016, 4, 2155-2159.	2.7	212
28324	Computational and experimental studies on structure and mechanical properties of Moâ€“Alâ€“N. Acta Materialia, 2016, 107, 273-278.	3.8	39
28325	The role of carboxylic acid in cobalt Fischer-Tropsch synthesis catalyst deactivation. Catalysis Today, 2016, 275, 127-134.	2.2	13
28326	Ferroelectric control of metalâ€“insulator transition. Solid State Communications, 2016, 229, 32-36.	0.9	1
28327	Long-Chain Polysulfide Retention at the Cathode of Liâ€“S Batteries. Journal of Physical Chemistry C, 2016, 120, 4296-4305.	1.5	85
28329	Real-Space Evidence of Rare Guanine Tautomer Induced by Water. ACS Nano, 2016, 10, 3776-3782.	7.3	23
28330	Engineering the electronic and magnetic properties of d⁰ 2D dichalcogenide materials through vacancy doping and lattice strains. Physical Chemistry Chemical Physics, 2016, 18, 7163-7168.	1.3	16
28331	First-principles analysis of seven novel phases of phosphorene with chirality. RSC Advances, 2016, 6, 22277-22284.	1.7	8
28332	Optoelectronic properties of atomically thin ReSSe with weak interlayer coupling. Nanoscale, 2016, 8, 5826-5834.	2.8	32
28333	Simultaneous tunability of the electronic and phononic gaps in SnS ₂ under normal compressive strain. 2D Materials, 2016, 3, 015009.	2.0	16
28334	On the early stages of precipitation in dilute Mgâ€“Nd alloys. Acta Materialia, 2016, 108, 367-379.	3.8	102
28335	Mechanism of adhesion of the diglycidyl ether of bisphenol A (DGEBA) to the Fe(100) surface. Composites Science and Technology, 2016, 126, 9-16.	3.8	32
28336	Microscopic Insight into the Activation of O₂ by Au Nanoparticles on ZnO(101) Support. Journal of Physical Chemistry C, 2016, 120, 4322-4328.	1.5	5
28337	Exchange Coupling of Spin-Crossover Molecules to Ferromagnetic Co Islands. Journal of Physical Chemistry Letters, 2016, 7, 900-904.	2.1	39
28338	Improved Endurance and Resistive Switching Stability in Ceria Thin Films Due to Charge Transfer Ability of Al Dopant. ACS Applied Materials & Interfaces, 2016, 8, 6127-6136.	4.0	78
28339	Reactivity and mechanism investigation of selective hydrogenation of 2,3,5-trimethylbenzoquinone on in situ generated metallic cobalt. Catalysis Science and Technology, 2016, 6, 4503-4510.	2.1	18
28340	Co-doping of magnesium with indium in nitrides: first principle calculation and experiment. RSC Advances, 2016, 6, 5111-5115.	1.7	13

#	Article	IF	Citations
28341	An experimental and computational study to resolve the composition of dolomitic lime. RSC Advances, 2016, 6, 16066-16072.	1.7	8
28342	New family of room temperature quantum spin Hall insulators in two-dimensional germanene films. Journal of Materials Chemistry C, 2016, 4, 2088-2094.	2.7	74
28343	Mechanical properties of metal dihydrides. Modelling and Simulation in Materials Science and Engineering, 2016, 24, 035005.	0.8	17
28344	Pressure-induced ferromagnetic half-metallicity in cobaltocene. Europhysics Letters, 2016, 113, 27005.	0.7	3
28345	A density functional study on properties of a Cu3Zn material and CO adsorption onto its surfaces. Applied Surface Science, 2016, 363, 128-139.	3.1	12
28346	First-principles study of transition metal (Ti, Nb)-doped NaAlH4. International Journal of Hydrogen Energy, 2016, 41, 3517-3526.	3.8	6
28347	First principles investigation of Î²â€²-short and Î²â€²-long in Mgâ€“Gd alloy. Journal of Alloys and Compounds, 2016, 671, 177-183.	2.8	18
28348	Methanol adsorption on monocrystalline ceria surfaces. Journal of Catalysis, 2016, 336, 116-125.	3.1	34
28349	Relationship between Site Symmetry, Spin State, and Doping Concentration for Co(II) or Co(III) in Î²-NaYF₄. Journal of Physical Chemistry C, 2016, 120, 7785-7794.	1.5	4
28350	Theoretical Study on the Mechanism of Photoreduction of CO₂ to CH₄ on the Anatase TiO₂(101) Surface. ACS Catalysis, 2016, 6, 2018-2025.	5.5	149
28351	Structural semiconductor-to-semimetal phase transition in two-dimensional materials induced by electrostatic gating. Nature Communications, 2016, 7, 10671.	5.8	318
28352	Hydrogen sensing characteristics from carbon nanotube field emissions. Nanoscale, 2016, 8, 5599-5604.	2.8	22
28353	Lithium-ion conductivity in Li₆Y(BO₃)₃: a thermally and electrochemically robust solid electrolyte. Journal of Materials Chemistry A, 2016, 4, 6972-6979.	5.2	13
28354	Constructingab initiomodels of ultra-thin Alâ€“AlO_xâ€“Al barriers. Molecular Simulation, 2016, 42, 542-548.	0.9	12
28355	Ab Initio Study of Carbon Impurities in Cu$_2$ ZnSnS$_4$. IEEE Journal of Photovoltaics, 2016, 6, 562-570.	1.5	3
28356	A new phase diagram of water under negative pressure: The rise of the lowest-density clathrate s-III. Science Advances, 2016, 2, e1501010.	4.7	92
28357	Black Phosphorus as a High-Capacity, High-Capability Negative Electrode for Sodium-Ion Batteries: Investigation of the Electrode/Electrolyte Interface. Chemistry of Materials, 2016, 28, 1625-1635.	3.2	238
28358	Theoretical Demonstration of the Ionic Barristor. Nano Letters, 2016, 16, 2090-2095.	4.5	9

#	Article	IF	Citations
28359	Predicting Single-Layer Technetium Dichalcogenides (TcX₂, X = S, Se) with Promising Applications in Photovoltaics and Photocatalysis. ACS Applied Materials & Interfaces, 2016, 8, 5385-5392.	4.0	100
28360	Anisotropic kinetics of solid phase transition from first principles: alphaâ€“omega phase transformation of Zr. Physical Chemistry Chemical Physics, 2016, 18, 4527-4534.	1.3	9
28361	Influence of carbon dopants on the structure, elasticity and lattice dynamics of Ti₅Si₃C_xNowotny phases. Modelling and Simulation in Materials Science and Engineering, 2016, 24, 025001.	0.8	8
28362	Reviewâ€”Defect Identification with Positron Annihilation Spectroscopy in Narrow Band Gap Semiconductors. ECS Journal of Solid State Science and Technology, 2016, 5, P3166-P3171.	0.9	7
28363	A DFT-based study of surface chemistries of rutile TiO2 and SnO2(110) toward formaldehyde and formic acid. Catalysis Today, 2016, 274, 103-108.	2.2	18
28364	Theoretical investigation of structural, electronic and magnetic properties for Pt Ni55â^' (n= 0â€“55) nanoparticles. Computational Materials Science, 2016, 117, 15-23.	1.4	8
28365	Effect of Cu doping on Ba0.5Sr0.5Fe1â^'xCuxO3â^'Î´ perovskites for solid oxide fuel cells: A first-principles study. Journal of Power Sources, 2016, 311, 13-20.	4.0	23
28366	Surface segregation phenomena in extended and nanoparticle surfaces of Cuâ€“Au alloys. Surface Science, 2016, 649, 39-45.	0.8	11
28367	Reconstruction of low-index graphite surfaces. Surface Science, 2016, 649, 60-65.	0.8	15
28368	Theoretical Study of the Dissociative Adsorption of Methane on Ir(111): The Role of Steps and Surface Distortions at High Temperatures. Journal of Physical Chemistry C, 2016, 120, 3946-3954.	1.5	26
28369	Understanding Chemical versus Electrostatic Shifts in X-ray Photoelectron Spectra of Organic Self-Assembled Monolayers. Journal of Physical Chemistry C, 2016, 120, 3428-3437.	1.5	125
28370	Intrinsic Two-Dimensional Organic Topological Insulators in Metalâ€“Dicyanoanthracene Lattices. Nano Letters, 2016, 16, 2072-2075.	4.5	81
28371	Quantitatively Predict the Potential of MnO₂ Polymorphs as Magnesium Battery Cathodes. ACS Applied Materials & Interfaces, 2016, 8, 4508-4515.	4.0	47
28372	Dual-doping to suppress cracking in spinel LiMn₂O₄: a joint theoretical and experimental study. Physical Chemistry Chemical Physics, 2016, 18, 6893-6900.	1.3	33
28373	Cyanophenyl vs. pyridine substituent: impact on the adlayer structure and formation on HOPG and Au(111). Physical Chemistry Chemical Physics, 2016, 18, 6668-6675.	1.3	4
28374	First-principles investigation of the effects of Ni and Y co-doped on destabilized MgH₂. RSC Advances, 2016, 6, 23110-23116.	1.7	21
28375	Quantitative determination of occupation sites of trace Co substituted for multiple Fe sites in M-type hexagonal ferrite using statistical beam-rocking TEM-EDXS analysis. Microscopy (Oxford, England), 2016, 65, 127-137.	0.7	9
28376	Quantum Anomalous Hall Effect in a Perovskite and Inverse-Perovskite Sandwich Structure. Journal of the Physical Society of Japan, 2016, 85, 014706.	0.7	5

#	Article	IF	Citations
28377	Density functional investigation of the electronic structure and charge transfer excited states of a multichromophoric antenna. Chemical Physics, 2016, 469-470, 1-8.	0.9	3
28378	On the formation of two-dimensional alloys of Sn and Pb co-adsorbed on Ru(0001). Journal of Alloys and Compounds, 2016, 672, 317-323.	2.8	2
28379	High-Pressure Phase Stability and Superconductivity of Pnictogen Hydrides and Chemical Trends for Compressed Hydrides. Chemistry of Materials, 2016, 28, 1746-1755.	3.2	68
28380	Electronic and magnetic properties of SnSe monolayers doped by Ga, In, As, and Sb: a first-principles study. Physical Chemistry Chemical Physics, 2016, 18, 8158-8164.	1.3	42
28381	Interlayer Interactions in van der Waals Heterostructures: Electron and Phonon Properties. ACS Applied Materials & Interfaces, 2016, 8, 6286-6292.	4.0	63
28382	Black phosphorene/monolayer transition-metal dichalcogenides as two dimensional van der Waals heterostructures: a first-principles study. Physical Chemistry Chemical Physics, 2016, 18, 7381-7388.	1.3	101
28383	Shuffling-controlled versus strain-controlled deformation twinning: The case for HCP Mg twin nucleation. International Journal of Plasticity, 2016, 82, 32-43.	4.1	71
28384	Preferential activation of CO near hydrocarbon chains during Fischerâ€“Tropsch synthesis on Ru. Journal of Catalysis, 2016, 337, 91-101.	3.1	54
28385	The Hakoniwa method, an approach to predict material properties based on statistical thermodynamics and ab initio calculations. Materials Science in Semiconductor Processing, 2016, 43, 209-213.	1.9	11
28386	Phase Stability, Crystal Structure, and Thermoelectric Properties of Cu₁₂Sb₄S_{13â€“x}Se_x Solid Solutions. Chemistry of Materials, 2016, 28, 1781-1786.	3.2	89
28387	Fundamental properties of GaN(0001) films grown directly on $$hbox {Gd} _{2}hbox {O} _{3}(0001)$$ Gd 2 O 3 (0001) platforms: abÂinitio structural simulations. Optical and Quantum Electronics, 2016, 48, 1.	1.5	2
28388	Synthesis and phase transformation mechanism of Nb2C carbide phases. Journal of Alloys and Compounds, 2016, 671, 424-434.	2.8	30
28389	Structural, electronic and magnetic properties of 3d transition metals embedded graphene-like carbon nitride sheet: A DFT + U study. Physics Letters, Section A: General, Atomic and Solid State Physics, 2016, 380, 1373-1377.	0.9	20
28390	Intrinsic magnetic properties of ZnO nanoislands: Insight from first-principles study. Physics Letters, Section A: General, Atomic and Solid State Physics, 2016, 380, 1324-1328.	0.9	4
28391	Tunable and Energetically Robust PbS Nanoplatelets for Optoelectronic Applications. Chemistry of Materials, 2016, 28, 1888-1896.	3.2	35
28392	Bonding and Electron Energy-Level Alignment at Metal/TiO₂ Interfaces: A Density Functional Theory Study. Journal of Physical Chemistry C, 2016, 120, 5549-5556.	1.5	45
28393	Ionic Mixed Hydride Fluoride Compounds: Stabilities Predicted by DFT, Synthesis, and Luminescence of Divalent Europium. Journal of Physical Chemistry C, 2016, 120, 10506-10511.	1.5	19
28394	Design of Nanostructured Heterogeneous Solid Ionic Coatings through a Multiscale Defect Model. ACS Applied Materials & Interfaces, 2016, 8, 5687-5693.	4.0	53

#	Article	IF	Citations
28395	Structural prediction of ultrahard semi-titanium boride (Ti₂B) using the frozen-phonon method. Physical Chemistry Chemical Physics, 2016, 18, 7927-7931.	1.3	16
28396	Manipulation of n and p type dope black phosphorene layer: A first principles study. Current Applied Physics, 2016, 16, 506-514.	1.1	12
28397	High mobility n-type conductive ultrananocrystalline diamond and graphene nanoribbon hybridized carbon films. Carbon, 2016, 98, 671-680.	5.4	32
28398	Study on the electronic structures and optical absorption of F center in the SrO crystal with G 0 W 0 â€“BSE. Computational and Theoretical Chemistry, 2016, 1080, 79-83.	1.1	6
28399	Ru55 nanoparticles catalyze the dissociation of H2O monomerÂandÂdimer to produce hydrogen: A comparative DFTÂstudy. International Journal of Hydrogen Energy, 2016, 41, 3844-3853.	3.8	6
28400	Insights from methane decomposition on nanostructured palladium. Journal of Catalysis, 2016, 337, 111-121.	3.1	38
28401	Atomic-Scale Structure and Local Chemistry of CoFeBâ€“MgO Magnetic Tunnel Junctions. Nano Letters, 2016, 16, 1530-1536.	4.5	85
28402	Two-dimensional tricycle arsenene with a direct band gap. Physical Chemistry Chemical Physics, 2016, 18, 8723-8729.	1.3	27
28403	Two-dimensional transition-metal oxide monolayers as cathode materials for Li and Na ion batteries. Physical Chemistry Chemical Physics, 2016, 18, 7527-7534.	1.3	54
28404	Two-dimensional germanane and germanane ribbons: density functional calculation of structural, electronic, optical and transport properties and the role of defects. RSC Advances, 2016, 6, 28298-28307.	1.7	18
28405	Prediction of Pressure-Induced Structural Transition and Mechanical Properties of MgY from First-Principles Calculations. Communications in Theoretical Physics, 2016, 65, 92-98.	1.1	5
28406	Facile preparation of semimetallic WP₂ as a novel photocatalyst with high photoactivity. RSC Advances, 2016, 6, 15724-15730.	1.7	23
28407	Electronic and magnetic properties of n-type and p-doped MoS₂ monolayers. RSC Advances, 2016, 6, 16772-16778.	1.7	54
28408	Multi-scale computation methods: Their applications in lithium-ion battery research and development. Chinese Physics B, 2016, 25, 018212.	0.7	449
28409	HAXPES Applications to Advanced Materials. Springer Series in Surface Sciences, 2016, , 467-531.	0.3	1
28410	Insight into the Relationship Between Structural and Electronic Properties of Bimetallic RhnPt55â^'n (nÂ=ÂÂ0â€“55) Clusters with Cuboctahedral Structure: DFT Approaches. Journal of Cluster Science, 2016, 27, 895-911.	1.7	5
28411	Adsorption and dissociation of O2 on Ni-doped (5, 5) SWCNT: A DFT study. Applied Surface Science, 2016, 370, 6-10.	3.1	13
28412	Synthesis and ionic transport mechanisms of Î±-LiAlO2. Solid State Ionics, 2016, 286, 122-134.	1.3	33

#	Article	IF	Citations
28413	Supramolecular clusters and chains of 2,6-dimethylpyridine on Cu(110): Observation of dynamic configuration change with real-space surface science techniques and DFT calculations. Surface Science, 2016, 652, 82-90.	0.8	1
28414	Defect Physics and Chemistry in Layered Mixed Transition Metal Oxide Cathode Materials: (Ni,Co,Mn) vs (Ni,Co,Al). Chemistry of Materials, 2016, 28, 1325-1334.	3.2	78
28415	Persistent Luminescence Hole-Type Materials by Design: Transition-Metal-Doped Carbon Allotrope and Carbides. ACS Applied Materials & Interfaces, 2016, 8, 5439-5444.	4.0	14
28416	Long-Life and High-Areal-Capacity Liâ€“S Batteries Enabled by a Light-Weight Polar Host with Intrinsic Polysulfide Adsorption. ACS Nano, 2016, 10, 4111-4118.	7.3	376
28417	Thermodynamic Constraints in Using AuM (M = Fe, Co, Ni, and Mo) Alloys as N₂ Dissociation Catalysts: Functionalizing a Plasmon-Active Metal. ACS Nano, 2016, 10, 2940-2949.	7.3	40
28418	Possible light-induced superconductivity in K3C60 at high temperature. Nature, 2016, 530, 461-464.	13.7	572
28419	Microscopic origin of chiral shape induction in achiral crystals. Nature Chemistry, 2016, 8, 326-330.	6.6	68
28420	Seamless growth of a supramolecular carpet. Nature Communications, 2016, 7, 10653.	5.8	13
28421	Polarization effects on the interfacial conductivity in LaAlO₃/SrTiO₃heterostructures: a first-principles study. Physical Chemistry Chemical Physics, 2016, 18, 6831-6838.	1.3	34
28422	Selective hydrogenation of acetylene over TiO₂-supported PdAg cluster: carbon species effect. RSC Advances, 2016, 6, 14593-14601.	1.7	12
28423	Interplay between surface chemistry and performance of rutile-type catalysts for halogen production. Chemical Science, 2016, 7, 2996-3005.	3.7	21
28424	Square planar Cu(<scp>i</scp>) stabilized by a pyridinediimine ligand. Chemical Communications, 2016, 52, 4156-4159.	2.2	22
28425	U(<scp>v</scp>) in metal uranates: a combined experimental and theoretical study of MgUO₄, CrUO₄, and FeUO₄. Dalton Transactions, 2016, 45, 4622-4632.	1.6	45
28426	Towards rational catalyst design: a general optimization framework. Philosophical Transactions Series A, Mathematical, Physical, and Engineering Sciences, 2016, 374, 20150078.	1.6	22
28427	Kinetic and Theoretical Insights into the Mechanism of Alkanol Dehydration on Solid BrÃ¸nsted Acid Catalysts. Journal of Physical Chemistry C, 2016, 120, 3371-3389.	1.5	42
28428	Origins of Large Voltage Hysteresis in High-Energy-Density Metal Fluoride Lithium-Ion Battery Conversion Electrodes. Journal of the American Chemical Society, 2016, 138, 2838-2848.	6.6	212
28429	Incorrect DFT-GGA predictions of the stability of non-stoichiometric/polar dielectric surfaces: the case of Cu₂O(111). Physical Chemistry Chemical Physics, 2016, 18, 6729-6733.	1.3	46
28430	Enhancing the cycling stability of Na-ion batteries by bonding SnS₂ultrafine nanocrystals on amino-functionalized graphene hybrid nanosheets. Energy and Environmental Science, 2016, 9, 1430-1438.	15.6	312

#	Article	IF	Citations
28431	Spin-polarized Dirac cones and topological nontriviality in a metalâ€“organic framework Ni₂C₂₄S₆H₁₂. Physical Chemistry Chemical Physics, 2016, 18, 8059-8064.	1.3	48
28432	First-principles study on the elastic properties of Cu ₂ GeSe ₃. Europhysics Letters, 2016, 113, 26001.	0.7	22
28433	Electronic and optical properties of novel carbon allotropes. Carbon, 2016, 101, 77-85.	5.4	98
28434	Low temperature transport and thermodynamic properties of the Zintl compound Yb11AlSb9: A new Kondo lattice semiconductor. Journal of Alloys and Compounds, 2016, 669, 60-65.	2.8	5
28435	Electronic and magnetic properties of nonmetal atoms doped blue phosphorene: First-principles study. Journal of Magnetism and Magnetic Materials, 2016, 408, 121-126.	1.0	43
28436	Grain growth in Uâ€“7Mo alloy: A combined first-principles and phase field study. Journal of Nuclear Materials, 2016, 473, 300-308.	1.3	32
28437	LiNbO₃-Type Oxide (Tl_{1â€“x}Sc_x)ScO₃: High-Pressure Synthesis, Crystal Structure, and Electronic Properties. Inorganic Chemistry, 2016, 55, 1940-1945.	1.9	6
28438	Interaction of CO₂ and CH₄ with Functionalized Periodic Mesoporous Phenyleneâ€“Silica: Periodic DFT Calculations and Gas Adsorption Measurements. Journal of Physical Chemistry C, 2016, 120, 3863-3875.	1.5	41
28439	Surface-Controlled Mono/Diselective ortho Câ€“H Bond Activation. Journal of the American Chemical Society, 2016, 138, 2809-2814.	6.6	120
28440	Exceptional H₂ sorption characteristics in a Mg²⁺-based metalâ€“organic framework with small pores: insights from experimental and theoretical studies. Physical Chemistry Chemical Physics, 2016, 18, 1786-1796.	1.3	24
28441	Molecular structure and vibrations of NTCDA monolayers on Ag(111) from density-functional theory and infrared absorption spectroscopy. Physical Chemistry Chemical Physics, 2016, 18, 6316-6328.	1.3	24
28442	Intrinsic defect processes and O migration in PrBa(Co/Fe)₂O_{5.5}. Journal of Materials Chemistry A, 2016, 4, 3560-3564.	5.2	6
28443	Kohnâ€“Sham density functional theory prediction of fracture in silicon carbide under mixed mode loading. Modelling and Simulation in Materials Science and Engineering, 2016, 24, 035004.	0.8	7
28444	Towards Next Generation Lithium-Sulfur Batteries: Non-Conventional Carbon Compartments/Sulfur Electrodes and Multi-Scale Analysis. Journal of the Electrochemical Society, 2016, 163, A730-A741.	1.3	43
28445	Prediction of the band structures of Bi2Te3-related binary and Sb/Se-doped ternary thermoelectric materials. Journal of the Korean Physical Society, 2016, 68, 115-120.	0.3	30
28446	First principles study of the behavior of hydrogen atoms in a W monovacancy. Journal of Materials Science, 2016, 51, 1445-1455.	1.7	14
28447	The effect of structural ordering on the magnetic, electronic, and optical properties of the LaPbMnSbO6 double perovskite. Journal of Alloys and Compounds, 2016, 671, 184-191.	2.8	15
28448	Effect of phosphorus doping on electronic structure and photocatalytic performance of g-C3N4: Insights from hybrid density functional calculation. Journal of Alloys and Compounds, 2016, 672, 271-276.	2.8	110

#	Article	IF	Citations
28449	Flux-mediated syntheses, structural characterization and low-temperature polymorphism of the p-type semiconductor Cu2Ta4O11. Journal of Solid State Chemistry, 2016, 236, 10-18.	1.4	14
28450	Understanding the Structure of Cationic Sites in Alkali Metal-Grafted USY Zeolites. Journal of Physical Chemistry C, 2016, 120, 4954-4960.	1.5	11
28451	Electronic Structure and Phase Stability of PdPt Nanoparticles. Journal of Physical Chemistry Letters, 2016, 7, 736-740.	2.1	40
28452	Two-Dimensional Disorder in Black Phosphorus and Monochalcogenide Monolayers. Nano Letters, 2016, 16, 1704-1712.	4.5	96
28453	Common electronic origin of superconductivity in (Li,Fe)OHFeSe bulk superconductor and single-layer FeSe/SrTiO3 films. Nature Communications, 2016, 7, 10608.	5.8	164
28454	Al atom on MoO₃(010) surface: adsorption and penetration using density functional theory. Physical Chemistry Chemical Physics, 2016, 18, 7359-7366.	1.3	14
28455	Magnetostructural phase transition assisted by temperature in Agâ€“Î±MnO₂: a density functional theory study. Physical Chemistry Chemical Physics, 2016, 18, 7442-7448.	1.3	6
28456	Lattice vibrations of the charge-transfer salt<mml:math xmlns:mml="http://www.w3.org/1998/Math/MathML"><mml:mi>Î¹</mml:mi><mml:mo>â”</mml:mo><mml:mo>(</mml:mo><mml:m Comprehensive explanation of the electrodynamic response in a spin-liquid compound. Physical Review B, 2016, 93, .	1.1	43
28457	O₂ activation at the Au/MgO(001) interface boundary facilitates CO oxidation. Physical Chemistry Chemical Physics, 2016, 18, 5486-5490.	1.3	13
28458	â€˜Ferroelectricâ€™ metals reexamined: fundamental mechanisms and design considerations for new materials. Journal of Materials Chemistry C, 2016, 4, 4000-4015.	2.7	119
28459	Titanium induced polarity inversion in ordered (In,Ga)N/GaN nanocolumns. Nanotechnology, 2016, 27, 065705.	1.3	16
28460	Anisotropic and temperature-dependent growth mechanism of S-phase precipitates in Alâ€“Cuâ€“Mg alloy in relation with GPB zones. Transactions of Nonferrous Metals Society of China, 2016, 26, 1-11.	1.7	23
28461	Reactivity of metal oxide nanocluster modified rutile and anatase TiO2: Oxygen vacancy formation and CO2 interaction. Applied Catalysis A: General, 2016, 521, 240-249.	2.2	51
28462	Migration behaviour of carbon atoms on clean diamond (0 0 1) surface: A first principle study. Applied Surface Science, 2016, 362, 387-393.	3.1	3
28463	Structural, electronic and optical properties of TcX2 (X = S, Se, Te) from first principles calculations. Computational Materials Science, 2016, 115, 177-183.	1.4	18
28464	Origin of the Ni/Mn ordering in high-voltage spinel LiNi0.5Mn1.5O4: The role of oxygen vacancies and cation doping. Computational Materials Science, 2016, 115, 109-116.	1.4	57
28465	Insight into CO Activation over Cu(100) under Electrochemical Conditions. Electrochimica Acta, 2016, 190, 446-454.	2.6	19
28466	DFT studies of the methanol decomposition mechanism on the H 2 O/Cu(110) and OH pre-adsorbed H 2 O/Cu(110) interfaces: ComparisonÂwith the clean Cu(110) surface. International Journal of Hydrogen Energy, 2016, 41, 2411-2423.	3.8	15

#	Article	IF	Citations
28467	Influence of alloying elements on the stability and dehydrogenation properties on Y(BH4)3 by first principles calculations. International Journal of Hydrogen Energy, 2016, 41, 1662-1671.	3.8	2
28468	Cation ordering/disordering effects upon photocatalytic activity of CrNbO4, CrTaO4, Sr2CrNbO6 and Sr2CrTaO6. International Journal of Hydrogen Energy, 2016, 41, 1550-1558.	3.8	30
28469	Influence of Ti, V and Cr substitution on the electronic structure and magnetic properties of Li2O: An ab-initio study. Journal of Alloys and Compounds, 2016, 665, 311-318.	2.8	2
28470	Improved superconducting properties of La3Co4Sn13 with indium substitution. Journal of Alloys and Compounds, 2016, 665, 333-338.	2.8	8
28471	On the electrochemical behavior of formamidine disulfide on gold electrodes in acid media. Journal of Electroanalytical Chemistry, 2016, 764, 79-87.	1.9	6
28472	Structure-dependent photocatalytic decomposition of formic acid on the anatase TiO2(101) surface and strategies to increase its reaction rate. Journal of Power Sources, 2016, 306, 208-212.	4.0	17
28473	Cathode reaction mechanism on the h-BN/Ni (111) heterostructure for the lithium-oxygen battery. Journal of Power Sources, 2016, 307, 379-384.	4.0	18
28474	Polytype distributions in low-defect zeolite beta crystals synthesized without an organic structure-directing agent. Microporous and Mesoporous Materials, 2016, 225, 210-215.	2.2	14
28475	Electronic and optical properties of the O-terminated AlN nanoribbons: First-principles study. Superlattices and Microstructures, 2016, 91, 31-36.	1.4	5
28476	An Insight into the Various Defects-Induced Emission in MgAl₂O₄ and Their Tunability with Phase Behavior: Combined Experimental and Theoretical Approach. Journal of Physical Chemistry C, 2016, 120, 4016-4031.	1.5	100
28477	Ni₉Te₆(PEt₃)₈C₆₀ Is a Superatomic Superalkali Superparamagnetic Cluster Assembled Material (S³-CAM). Journal of the American Chemical Society, 2016, 138, 1916-1921.	6.6	42
28478	New quantum spin Hall insulator in two-dimensional MoS₂with periodically distributed pores. Nanoscale, 2016, 8, 4915-4921.	2.8	20
28479	Thermodynamic properties of pure and doped (B,ÂN) graphene. RSC Advances, 2016, 6, 12158-12168.	1.7	33
28480	Manipulation of carbon nanotube magnetism with metal-rich iron nanoparticles. Journal of Materials Chemistry C, 2016, 4, 1215-1227.	2.7	7
28481	Enhanced piezoelectricity and half-metallicity of fluorinated AlN nanosheets and nanoribbons: a first-principles study. Journal of Materials Chemistry C, 2016, 4, 1517-1526.	2.7	19
28482	The transformation pathways for vitual long period stacking-ordered Mg: First-principles study. Computational Materials Science, 2016, 114, 1-12.	1.4	2
28483	Effects of S and N doping on the structural, magnetic and electronic properties of rutile CrO2. Journal of Magnetism and Magnetic Materials, 2016, 405, 253-258.	1.0	3
28484	Ab initio study of the trapping of polonium on noble metals. Journal of Nuclear Materials, 2016, 472, 35-42.	1.3	6

#	Article	IF	Citations
28485	Augmenting the sensing aptitude of hydrogenated graphene by crafting with defects and dopants. Sensors and Actuators B: Chemical, 2016, 228, 317-321.	4.0	44
28486	Acid Dissociation of 3-Mercaptopropionic Acid Coated CdSeâ€“CdS/Cd_{0.5}Zn_{0.5}S/ZnS Coreâ€“Multishell Quantum Dot and Strong Ionic Interaction with Ca²⁺ Ion. Journal of Physical Chemistry C, 2016, 120, 3519-3529.	1.5	15
28487	Potential Application of Metal Dichalcogenides Double-Layered Heterostructures as Anode Materials for Li-Ion Batteries. Journal of Physical Chemistry C, 2016, 120, 4779-4788.	1.5	92
28488	Nonradiative Electronâ€“Hole Recombination Rate Is Greatly Reduced by Defects in Monolayer Black Phosphorus: Ab Initio Time Domain Study. Journal of Physical Chemistry Letters, 2016, 7, 653-659.	2.1	99
28489	Dielectric Enhancement in Graphene/Barium Titanate Nanocomposites. ACS Applied Materials & Interfaces, 2016, 8, 3340-3348.	4.0	47
28490	Influence of Coadsorbed Water and Alcohol Molecules on Isopropyl Alcohol Dehydration on Î³-Alumina: Multiscale Modeling of Experimental Kinetic Profiles. ACS Catalysis, 2016, 6, 1905-1920.	5.5	43
28491	Tuning the hydrogen evolution activity of MS₂ (M = Mo or Nb) monolayers by strain engineering. Physical Chemistry Chemical Physics, 2016, 18, 9388-9395.	1.3	60
28492	Thermodynamic and kinetic studies of LiNi_{0.5}Co_{0.2}Mn_{0.3}O₂ as a positive electrode material for Li-ion batteries using first principles. Physical Chemistry Chemical Physics, 2016, 18, 6799-6812.	1.3	126
28493	The conversion of CO₂ to methanol on orthorhombic Î²-Mo₂C and Cu/Î²-Mo₂C catalysts: mechanism for admetal induced change in the selectivity and activity. Catalysis Science and Technology, 2016, 6, 6766-6777.	2.1	101
28494	Nano-scale polarâ€“nonpolar oxide heterostructures for photocatalysis. Nanoscale, 2016, 8, 6057-6063.	2.8	14
28495	Band gap and work function tailoring of SnO₂for improved transparent conducting ability in photovoltaics. Journal of Materials Chemistry C, 2016, 4, 1467-1475.	2.7	189
28496	First principles calculations on the hydrogen atom passivation of TiO₂ nanotubes. RSC Advances, 2016, 6, 19190-19198.	1.7	3
28497	Methanol dissociation on bimetallic surfaces: validity of the general BrÃ¸nstedâ€“Evansâ€“Polanyi relationship for Oâ€“H bond cleavage. RSC Advances, 2016, 6, 18695-18702.	1.7	10
28498	First-principles study of structural and work function properties for nitrogen-doped single-walled carbon nanotubes. Applied Surface Science, 2016, 368, 477-482.	3.1	17
28499	The effects of Br dopant on the photo-catalytic properties of Bi2WO6. Materials Science and Engineering B: Solid-State Materials for Advanced Technology, 2016, 206, 79-84.	1.7	24
28500	Identification of Auâ€“S complexes on Au(100). Physical Chemistry Chemical Physics, 2016, 18, 4891-4901.	1.3	20
28501	Theoretical study on the influence of a secondary metal on the Cu(110) surface in the presence of H₂O for methanol decomposition. RSC Advances, 2016, 6, 15127-15136.	1.7	5
28502	Bandgap engineering of MoS₂/MX₂ (MX₂ = WS₂,) Tj ETQq1 1 0.784314 rgBT /O compressive strain. RSC Advances, 2016, 6, 18319-18325.	1.7	39

#	Article	IF	Citations
28503	Effects of interlayer coupling and electric fields on the electronic structures of graphene and MoS₂heterobilayers. Journal of Materials Chemistry C, 2016, 4, 1776-1781.	2.7	114
28504	First-principles simulations on the new hybrid phases of germanene with alkali metal atoms coverage. Applied Surface Science, 2016, 360, 707-714.	3.1	21
28505	Li₂S Film Formation on Lithium Anode Surface of Liâ€“S batteries. ACS Applied Materials & Interfaces, 2016, 8, 4700-4708.	4.0	70
28506	Band engineering and improved thermoelectric performance in M-doped SnTe (M = Mg, Mn, Cd, and Hg). Physical Chemistry Chemical Physics, 2016, 18, 7141-7147.	1.3	86
28507	First-principles investigation on vibrational, anisotropic elastic and thermodynamic properties for L1₂ structure of Al₃Er and Al₃Yb under high pressure. Philosophical Magazine, 2016, 96, 320-348.	0.7	18
28508	Deposition Morphology and Magnetism of Co, Pt Adatoms and Small CoPt Adclusters on Ni(100) Substrate. Journal of Cluster Science, 2016, 27, 947-964.	1.7	2
28509	Atomistic modelling of zirconium and silicon segregation at twist and tilt grain boundaries in molybdenum. Journal of Materials Science, 2016, 51, 1873-1881.	1.7	15
28510	Thermodynamic stability of Mgâ€“Yâ€“Zn ternary alloys through first-principles. Intermetallics, 2016, 72, 25-29.	1.8	15
28511	Comparative theoretical study of adsorption of lithium polysulfides (Li2Sx) on pristine and defective graphene. Journal of Power Sources, 2016, 308, 166-171.	4.0	70
28512	The Carbocation Rearrangement Mechanism, Clarified. Journal of Organic Chemistry, 2016, 81, 1410-1415.	1.7	21
28513	Mechanistic Study of Selective Catalytic Reduction of NO with NH₃ on W-Doped CeO₂ Catalysts: Unraveling the Catalytic Cycle and the Role of Oxygen Vacancy. Journal of Physical Chemistry C, 2016, 120, 2271-2283.	1.5	97
28514	Amorphous ZnO-Based Compounds as Thermoelectrics. Journal of Physical Chemistry C, 2016, 120, 2529-2535.	1.5	19
28515	Potential-Dependent Generation of O₂^{â€“} and LiO₂ and Their Critical Roles in O₂ Reduction to Li₂O₂ in Aprotic Liâ€“O₂ Batteries. Journal of Physical Chemistry C, 2016, 120, 3690-3698.	1.5	149
28516	Evaluating bulk Nb2O2F3 for Li-battery electrode applications. Physical Chemistry Chemical Physics, 2016, 18, 3530-3535.	1.3	0
28517	Effect of carbon ion irradiation on Ag diffusion in SiC. Journal of Nuclear Materials, 2016, 471, 220-232.	1.3	11
28518	Oxygen transport in epitaxial La0.875Sr0.125CoO3-Î´ thin-film cathodes for solid oxide fuel cells: Roles of anisotropic strain. Scripta Materialia, 2016, 115, 141-144.	2.6	4
28519	Structural evolution of TaN-alloyed Crâ€“Alâ€“Yâ€“N coatings. Surface and Coatings Technology, 2016, 288, 203-210.	2.2	11
28520	Layered-to-Rock-Salt Transformation in Desodiated Na_xCrO₂ (x) Tj ETQq1 1 0.784314 rgBT /O	3.2	120

#	Article	IF	Citations
28521	Beyond Graphitic Carbon Nitride: Nitrogen-Rich Penta-CN₂ Sheet. Journal of Physical Chemistry C, 2016, 120, 3993-3998.	1.5	167
28522	Depopulation of Single-Phthalocyanine Molecular Orbitals upon Pyrrolic-Hydrogen Abstraction on Graphene. ACS Nano, 2016, 10, 2010-2016.	7.3	22
28523	Atomic-Scale Picture of the Composition, Decay, and Oxidation of Two-Dimensional Radioactive Films. ACS Nano, 2016, 10, 2152-2158.	7.3	5
28524	Interface control by chemical and dimensional matching in an oxide heterostructure. Nature Chemistry, 2016, 8, 347-353.	6.6	53
28525	Effects of Mo/W codoping on the visible-light photocatalytic activity of monoclinic BiVO₄ within the GGA + U framework. RSC Advances, 2016, 6, 12290-12297.	1.7	44
28526	Explaining stability of transition metal carbides â€“ and why TcC does not exist. RSC Advances, 2016, 6, 16197-16202.	1.7	37
28527	YCuTe₂: a member of a new class of thermoelectric materials with CuTe₄-based layered structure. Journal of Materials Chemistry A, 2016, 4, 2461-2472.	5.2	52
28528	Metal oxide nanocluster-modified TiO₂as solar activated photocatalyst materials. Journal of Physics Condensed Matter, 2016, 28, 074006.	0.7	22
28529	Impact of magnetic fluctuations on lattice excitations in fcc nickel. Journal of Physics Condensed Matter, 2016, 28, 076002.	0.7	15
28530	Identification of Microscopic Hole-Trapping Mechanisms in Nitride Semiconductors. IEEE Electron Device Letters, 2016, 37, 154-156.	2.2	7
28531	A phase diagram for band inversion of topological materials as a function of interactions between two involved bands. Europhysics Letters, 2016, 113, 17008.	0.7	4
28532	All-graphene edge contacts: Electrical resistance of graphene T-junctions. Carbon, 2016, 101, 101-106.	5.4	10
28533	Novel structures and superconductivities of calciumâ€“lithium alloys at high pressures: A first-principles study. Journal of Alloys and Compounds, 2016, 669, 101-107.	2.8	4
28534	Synthesis, electronic structure and luminescence properties of color-controllable Dy3+/Eu3+-codoped CaWO4 phosphors. Journal of Luminescence, 2016, 173, 192-198.	1.5	43
28535	Application of a Parallel Genetic Algorithm to the Global Optimization of Gas-Phase and Supported Goldâ€“Iridium Sub-Nanoalloys. Journal of Physical Chemistry C, 2016, 120, 3759-3765.	1.5	24
28536	Effects of Si Codoping on Optical Properties of Ce-Doped Ca₆BaP₄O₁₇: Insights from First-Principles Calculations. Journal of Physical Chemistry C, 2016, 120, 3999-4006.	1.5	22
28537	Spin Unrestricted Excited State Relaxation Study of Vanadium(IV)-Doped Anatase. Journal of Physical Chemistry C, 2016, 120, 5890-5905.	1.5	19
28538	High Catalytic Activity and Chemoselectivity of Sub-nanometric Pd Clusters on Porous Nanorods of CeO₂ for Hydrogenation of Nitroarenes. Journal of the American Chemical Society, 2016, 138, 2629-2637.	6.6	387

#	Article	IF	Citations
28539	Hot-Carrier Degradation in GaN HEMTs Due to Substitutional Iron and Its Complexes. IEEE Transactions on Electron Devices, 2016, 63, 1486-1494.	1.6	27
28540	The Impact of Specifically Adsorbed Ions on the Copper-Catalyzed Electroreduction of CO₂. Journal of the Electrochemical Society, 2016, 163, F477-F484.	1.3	92
28541	First principles investigation on the electronic, magnetic and optical properties of Bi0.8M0.2Fe0.9Co0.1O3 (M = La, Gd, Er, Lu). Computational and Theoretical Chemistry, 2016, 1084, 36-42.	1.1	27
28542	Buckminsterfullerene's movability on the Fe(001) surface. Journal of Magnetism and Magnetic Materials, 2016, 410, 41-46.	1.0	3
28543	Revealing the Intrinsic Li Mobility in the Li₂MnO₃ Lithium-Excess Material. Chemistry of Materials, 2016, 28, 2081-2088.	3.2	59
28544	Monolayer Phosphoreneâ€“Metal Contacts. Chemistry of Materials, 2016, 28, 2100-2109.	3.2	199
28545	Interplay of Orbital and Relativistic Effects in Bismuth Oxyhalides: BiOF, BiOCl, BiOBr, and BiOI. Chemistry of Materials, 2016, 28, 1980-1984.	3.2	291
28546	Influence of Electron Correlation on the Electronic Structure and Magnetism of Transition-Metal Phthalocyanines. Journal of Chemical Theory and Computation, 2016, 12, 1772-1785.	2.3	54
28547	Theoretical and experimental investigations of the Li storage capacity in single-walled carbon nanotube bundles. RSC Advances, 2016, 6, 27260-27266.	1.7	9
28548	Tuning the electronic properties of monolayer and bilayer PtSe₂via strain engineering. Journal of Materials Chemistry C, 2016, 4, 3106-3112.	2.7	96
28549	Formation mechanism of the Nb2C phase in the Nbâ€“1Zrâ€“0.1C (wt.%) alloy and interrelation between Î³, Î² and Î±-Nb2C carbide phases. Acta Materialia, 2016, 108, 186-196.	3.8	24
28550	Effects of alloying elements and temperature on the elastic properties of W-based alloys by first-principles calculations. Journal of Alloys and Compounds, 2016, 671, 267-275.	2.8	33
28551	Thermoelectric Performance of the MXenes M₂CO₂ (M = Ti, Zr, or Hf). Chemistry of Materials, 2016, 28, 1647-1652.	3.2	132
28552	Point Defects in Layer-Structured Cathode Materials for Lithium-Ion Batteries. Journal of Physical Chemistry C, 2016, 120, 4173-4182.	1.5	24
28553	The Surface Structure of Cu₂O(100). Journal of Physical Chemistry C, 2016, 120, 4373-4381.	1.5	46
28554	Octahedral Rotation Preferences in Perovskite Iodides and Bromides. Journal of Physical Chemistry Letters, 2016, 7, 918-922.	2.1	115
28555	Ab Initio Prediction and Characterization of Mo₂C Monolayer as Anodes for Lithium-Ion and Sodium-Ion Batteries. Journal of Physical Chemistry Letters, 2016, 7, 937-943.	2.1	334
28556	Reactivity of atomically dispersed Pt²⁺ species towards H₂: model Ptâ€“CeO₂ fuel cell catalyst. Physical Chemistry Chemical Physics, 2016, 18, 7672-7679.	1.3	61

#	Article	IF	Citations
28557	Impact of van der Waalâ€™s interaction in the hybrid bilayer of silicene/SiC. RSC Advances, 2016, 6, 21948-21953.	1.7	11
28558	A theoretical study of the stability of anionic defects in cubic ZrO2 at extreme conditions. Journal of Materials Science, 2016, 51, 4845-4855.	1.7	8
28559	memory device. Chemical Research in Chinese Universities, 2016, 32, 76-81.	1.3	4
28560	Enhanced band gap opening in germanene by organic molecule adsorption. Materials Chemistry and Physics, 2016, 173, 379-384.	2.0	39
28561	Assessing the potential of Mg-doped Cr₂O₃as a novelp-type transparent conducting oxide. Journal of Physics Condensed Matter, 2016, 28, 125501.	0.7	21
28562	Interaction between phosphorene and the surface of a substrate. Materials Research Express, 2016, 3, 025013.	0.8	10
28563	Adsorption mechanisms of lithium oxides (LixO2) on N-doped graphene: a density functional theory study with implications for lithiumâ€“air batteries. Theoretical Chemistry Accounts, 2016, 135, 1.	0.5	22
28564	The Composite Structure and Two-Peak Emission Behavior of a Ca_{1.5}Ba_{0.5}Si₅O₃N₆:Eu²⁺ Phosphor. Inorganic Chemistry, 2016, 55, 2534-2543.	1.9	24
28565	Structure of V₂O₅Â·nH₂O Xerogels. Journal of Physical Chemistry C, 2016, 120, 3986-3992.	1.5	68
28566	Computational Design of a CeO₂-Supported Pd-Based Bimetallic Nanorod for CO Oxidation. Journal of Physical Chemistry C, 2016, 120, 5557-5564.	1.5	42
28567	Ab Initio Determined Phase Diagram of Clean and Solvated Muscovite Mica Surfaces. Langmuir, 2016, 32, 1027-1033.	1.6	9
28568	Thermal Stability and Reactivity of Cathode Materials for Li-Ion Batteries. ACS Applied Materials & Interfaces, 2016, 8, 7013-7021.	4.0	93
28569	Effects of adatoms and physisorbed molecules on the physical properties of antimonene. Physical Review B, 2016, 93, .	1.1	84
28570	Large-scale ab initio simulations based on systematically improvable atomic basis. Computational Materials Science, 2016, 112, 503-517.	1.4	61
28571	Density function theory study of water gas shift reaction on 2Cu/ZnO<mml:math xmlns:mml="http://www.w3.org/1998/Math/MathML" altimg="si1.gif" overflow="scroll"><mml:mrow><mml:mo		

#	Article	IF	Citations
28575	Unconventional properties of nanometric FeO(111) films on Ru(0001): stoichiometry and surface structure. Journal of Materials Chemistry C, 2016, 4, 1850-1859.	2.7	24
28576	Interface-Induced Spin Polarization in Graphene on Chromia. IEEE Magnetics Letters, 2016, 7, 1-4.	0.6	14
28577	Thermal conductivity of bulk and monolayer MoS ₂. Europhysics Letters, 2016, 113, 36002.	0.7	117
28578	The role of silicon, vacancies, and strain in carbon distribution in low temperature bainite. Journal of Alloys and Compounds, 2016, 673, 289-294.	2.8	10
28579	The structural, electronic and magnetic properties of quaternary Heusler alloy TiZrCoIn. Solid State Communications, 2016, 231-232, 64-67.	0.9	36
28580	CO adsorption on a silica bilayer supported on Ru(0001). Surface Science, 2016, 648, 2-9.	0.8	29
28581	How Guest Molecules Stabilize the Narrow Pore Phase of Soft Porous Crystals: Structural and Mechanical Properties of MIL-53(Al)âŠƒH2O. Journal of Physical Chemistry C, 2016, 120, 5059-5066.	1.5	14
28582	Ferroelectric polarization switching with a remarkably high activation energy in orthorhombic GaFeO3 thin films. NPG Asia Materials, 2016, 8, e242-e242.	3.8	72
28583	Promising electron mobility and high thermal conductivity in Sc₂CT₂(T = F,) Tj ETQq0 0 0 rgBT /Overlock 10 T	2.8	205
28584	Magnetic structure of (C5H12N)CuBr3: origin of the uniform Heisenberg chain behavior and the magnetic anisotropy of the Cu2+(S = 1/2) ions. RSC Advances, 2016, 6, 22722-22727.	1.7	4
28585	Changes in the magnetization hysteresis direction and structure-driven magnetoresistance of a chalcopyrite-based magnetic semiconductor. Journal Physics D: Applied Physics, 2016, 49, 125007.	1.3	10
28586	Development of a pair potential for Niâ€“He. Journal of Nuclear Materials, 2016, 472, 105-109.	1.3	10
28587	Magnetic anisotropy of metal functionalized phthalocyanine 2D networks. Journal of Solid State Chemistry, 2016, 238, 41-45.	1.4	5
28588	The effect of lithium adsorption on the formation of 1T-MoS2 phase based on first-principles calculation. Physics Letters, Section A: General, Atomic and Solid State Physics, 2016, 380, 1767-1771.	0.9	16
28589	Hybrid Organicâ€“Inorganic Coordination Complexes as Tunable Optical Response Materials. Inorganic Chemistry, 2016, 55, 3393-3400.	1.9	31
28590	Reactivity of the Fe₂O₃(0001) Surface for Methane Oxidation: A GGA + U Study. Journal of Physical Chemistry C, 2016, 120, 6642-6650.	1.5	51
28591	Bulk electronic, elastic, structural, and dielectric properties of the Weyl semimetal TaAs. Physical Review B, 2016, 93, .	1.1	42
28592	Reviewâ€”Properties of Intrinsic Point Defects in Si and Ge Assessed by Density Functional Theory. ECS Journal of Solid State Science and Technology, 2016, 5, P3176-P3195.	0.9	16

#	Article	IF	Citations
28593	Computational Studies of Silicene on Silver Surfaces. Springer Series in Materials Science, 2016, , 203-213.	0.4	1
28594	Theoretical Studies of Functionalised Silicene. Springer Series in Materials Science, 2016, , 107-127.	0.4	1
28595	A novel fullerene-like B30N30 structure: Stability and electronic property. Carbon, 2016, 102, 273-278.	5.4	18
28596	A density functional theory study of uranium-doped thoria and uranium adatoms on the major surfaces of thorium dioxide. Journal of Nuclear Materials, 2016, 473, 99-111.	1.3	28
28597	Two Dimensional Ice from First Principles: Structures and Phase Transitions. Physical Review Letters, 2016, 116, 025501.	2.9	167
28598	Oxygen adsorption and diffusion on an Al(111) surface and subsurface: a theoretical study. Canadian Journal of Chemistry, 2016, 94, 541-546.	0.6	6
28599	Scaling Relationships for Molecular Adsorption and Dissociation in Lewis Acid Zeolites. Journal of Physical Chemistry C, 2016, 120, 6714-6722.	1.5	31
28600	The Stable or Metastable Phases in Compressed Zn-O Systems. Chinese Physics Letters, 2016, 33, 026104.	1.3	6
28601	Structure of periodic crystals and quasicrystals in ultrathin films of Ba-Ti-O. Physical Review B, 2016, 93, 0201011-201014.	1.1	17
28602	xmlns:mml="http://www.w3.org/1998/Math/MathML"><mml:mrow><mml:mi>Z</mml:mi><mml:mi>T</mml:mi></mml:mrow></mml:ma xmlns:mml="http://www.w3.org/1998/Math/MathML"><mml:mrow><mml:mi mathvariant="normal">B</mml:mi><mml:msub><mml:mi mathvariant="normal">i</mml:mi><mml:mn>2</mml:mn></mml:msub><mml:mi	1.1	15
28603	Ca-decorated novel boron sheet: A potential hydrogen storage medium. International Journal of Hydrogen Energy, 2016, 41, 5276-5283.	3.8	76
28604	Classical molecular dynamics and quantum ab-initio studies on lithium-intercalation in interconnected hollow spherical nano-spheres of amorphous silicon. Journal of Alloys and Compounds, 2016, 665, 165-172.	2.8	5
28605	Density Functional Theory Study of Iron Phthalocyanine Porous Layer Deposited on Graphene Substrate: A Pt-Free Electrocatalyst for Hydrogen Fuel Cells. Journal of Physical Chemistry C, 2016, 120, 5384-5391.	1.5	41
28606	Silicon- and carbon-based anode materials: Quantum-chemical modeling. Russian Journal of Inorganic Chemistry, 2016, 61, 48-54.	0.3	11
28607	Structural, electronic and optical properties of copper, silver and gold sulfide: a DFT study. Theoretical Chemistry Accounts, 2016, 135, 1.	0.5	35
28608	Tuning the work function of VO2(1 0 0) surface by Ag adsorption and incorporation: Insights from first-principles calculations. Applied Surface Science, 2016, 367, 507-517.	3.1	31
28609	Suppression of irreversible capacity loss in Li-rich layered oxide by fluorine doping. Journal of Power Sources, 2016, 313, 65-72.	4.0	91
28610	Thermodynamics, Kinetics and Structural Evolution of Îµ-LiVOPO4 over Multiple Lithium Intercalation. Chemistry of Materials, 2016, 28, 1794-1805.	3.2	64

#	Article	IF	Citations
28611	Solution Combustion Synthesis, Characterization, and Photoelectrochemistry of CuNb₂O₆ and ZnNb₂O₆ Nanoparticles. Journal of Physical Chemistry C, 2016, 120, 16024-16034.	1.5	56
28612	Preparation and characterization of a possible topological insulator BiYO₃: experiment versus theory. Physical Chemistry Chemical Physics, 2016, 18, 8205-8211.	1.3	6
28613	Band modification of graphene by using slow Cs⁺ ions. RSC Advances, 2016, 6, 9106-9111.	1.7	5
28614	Calculation of dopant solubilities and phase diagrams of Xâ€“Pbâ€“Se (X = Br, Na) limited to defects with localized charge. Journal of Materials Chemistry C, 2016, 4, 1769-1775.	2.7	12
28615	Rationally designed donorâ€“acceptor scheme based molecules for applications in opto-electronic devices. Physical Chemistry Chemical Physics, 2016, 18, 9133-9147.	1.3	17
28616	Ï€-Bonding-dominated energy gaps in graphene oxide. RSC Advances, 2016, 6, 24458-24463.	1.7	10
28617	A comprehensive first-principles study of pure elements: Vacancy formation and migration energies and self-diffusion coefficients. Acta Materialia, 2016, 109, 128-141.	3.8	117
28618	Stability of pseudotwins in D03-type alloys calculated from first principles. Acta Materialia, 2016, 109, 82-89.	3.8	3
28619	Size effect on the magnetic and electronic properties of the monolayer lateral hetero-junction WS2-MoS2 nanoribbon. Applied Surface Science, 2016, 371, 376-382.	3.1	26
28620	A computational study of adsorption and activation of CO 2 and H 2 over Fe(1 0 0) surface. Journal of CO2 Utilization, 2016, 15, 107-114.	3.3	38
28621	A density functional theory study of the structure of pure-silica and aluminium-substituted MFI nanosheets. Journal of Solid State Chemistry, 2016, 237, 192-203.	1.4	28
28622	Unusual electronic and mechanical properties of sodium chlorides at high pressures. Physics Letters, Section A: General, Atomic and Solid State Physics, 2016, 380, 1556-1561.	0.9	2
28623	Structural and Electrochemical Consequences of Al and Ga Cosubstitution in Li₇La₃Zr₂O₁₂ Solid Electrolytes. Chemistry of Materials, 2016, 28, 2384-2392.	3.2	258
28624	Self-Organized Supported Clusters of l-Methionine. Journal of Physical Chemistry C, 2016, 120, 6534-6542.	1.5	2
28625	Structure and Proton-Transfer Mechanism in One-Dimensional Chains of Benzimidazoles. Journal of Physical Chemistry C, 2016, 120, 5804-5809.	1.5	8
28626	Response of Metal Sites toward Water Effects on Postcombustion CO₂ Capture in Metalâ€“Organic Frameworks. ACS Sustainable Chemistry and Engineering, 2016, 4, 2387-2394.	3.2	24
28627	Two-sided effects of strong hydrogen bonding on the stability of dihydroxylammonium 5,5â€²-bistetrazole-1,1â€²-diolate (TKX-50). CrystEngComm, 2016, 18, 2258-2267.	1.3	60
28628	The formation of H₂S on metal-modified graphene under hydrogen environments. Composite Interfaces, 2016, 23, 423-432.	1.3	3

#	Article	IF	Citations
28629	Catalytic methyl mercaptan coupling to ethylene in chabazite: DFT study of the first C C bond formation. Applied Catalysis B: Environmental, 2016, 187, 195-203.	10.8	13
28630	Elastic, lattice dynamical, thermal stabilities and thermodynamic properties of BiF3-type Mg3RE compounds from first-principles calculations. Journal of Alloys and Compounds, 2016, 663, 565-573.	2.8	29
28631	First-principles evaluation of the inherent stabilities of pure Li x MPO 4 (M=Mn, Fe, Co,) and mixed binary Li x Fe y Mâ€² 1-y PO 4 (M'=Mn, Co) olivine phosphates. Materials Chemistry and Physics, 2016, 174, 54-58.	2.0	7
28632	Adsorption Behavior of Nonplanar Phthalocyanines: Competition of Different Adsorption Conformations. Journal of Physical Chemistry C, 2016, 120, 6869-6875.	1.5	10
28633	Bridging the g-C₃N₄ Interlayers for Enhanced Photocatalysis. ACS Catalysis, 2016, 6, 2462-2472.	5.5	869
28634	Visualizing Redox Dynamics of a Single Ag/AgCl Heterogeneous Nanocatalyst at Atomic Resolution. ACS Nano, 2016, 10, 3738-3746.	7.3	61
28635	Gold as a 6p-Element in Dense Lithium Aurides. Journal of the American Chemical Society, 2016, 138, 4046-4052.	6.6	101
28636	Control of electronic properties of 2D carbides (MXenes) by manipulating their transition metal layers. Nanoscale Horizons, 2016, 1, 227-234.	4.1	394
28637	Ab initio simulations of defect-based magnetism: the case of CoSi nanowires. RSC Advances, 2016, 6, 23634-23639.	1.7	2
28638	Na₂M₂(SO₄)₃ (M = Fe, Mn, Co and Ni): towards high-voltage sodium battery applications. Physical Chemistry Chemical Physics, 2016, 18, 9658-9665.	1.3	40
28639	Magnetism of Asymmetrically Terminated FeRh(001) Thin Films: A First-Principle Study. IEEE Transactions on Magnetics, 2016, 52, 1-3.	1.2	0
28640	The nature of strong BrÃ¸nsted acidity of Ni-SMM clay. Applied Catalysis B: Environmental, 2016, 191, 62-75.	10.8	14
28641	Blue-shift of spectrum and enhanced luminescent properties of YAG: Ce3+ phosphor induced by small amount of La3+ incorporation. Journal of Alloys and Compounds, 2016, 674, 93-97.	2.8	44
28642	Cu(II)-Silsesquioxanes as Secondary Building Units for Construction of Coordination Polymers: A Case Study of Cesium-Containing Compounds. Crystal Growth and Design, 2016, 16, 1968-1977.	1.4	24
28643	Ethylene Epoxidation Catalyzed by a Cu₃₈ Nanoparticle: A Computational Study. Journal of Physical Chemistry C, 2016, 120, 7646-7652.	1.5	8
28644	The 90Â° partial dislocation in semiconductor silicon: An investigation from the lattice Pâ€“N theory and the first principle calculation. Acta Materialia, 2016, 109, 187-201.	3.8	16
28645	Effect of geometrical defects on the tensile properties of graphene. Carbon, 2016, 103, 125-133.	5.4	40
28646	Influence of pressure on the properties of GaN/AlN multi-quantum wells â€“ Ab initio study. Journal of Physics and Chemistry of Solids, 2016, 93, 100-117.	1.9	8

#	Article	IF	Citations
28647	Hydrogenation-Induced Structure and Property Changes in the Rare-Earth Metal Gallide NdGa: Evolution of a [GaH]^{2â€“} Polyanion Containing Peierls-like Gaâ€“H Chains. Inorganic Chemistry, 2016, 55, 345-352.	1.9	15
28648	Insight into the Vibrational and Thermodynamic Properties of Layered Lithium Transition-Metal Oxides LiMO₂(M = Co, Ni, Mn): A First-Principles Study. Journal of Physical Chemistry C, 2016, 120, 5876-5882.	1.5	28
28649	Electronic Structure of Zn⁺-Modified Zeolite: A Density Functional Theory Study of Ferrierite. Journal of Physical Chemistry C, 2016, 120, 6031-6038.	1.5	10
28650	Highly Efficient and Stable Vanadiaâ€“Titaniaâ€“Sulfate Catalysts for Methanol Oxidation to Methyl Formate: Synthesis and Mechanistic Study. Journal of Physical Chemistry C, 2016, 120, 6591-6600.	1.5	22
28651	Transition-Metal Mixing and Redox Potentials in Li_x(M_{1â€“y}Mâ€²_y)PO₄ (M, Mâ€² = Mn, Fe) Tj ETQq0 0 0 rgBT 5932-5939.	1.5	29
28652	Insights into the Performance Limits of the Li₇P₃S₁₁ Superionic Conductor: A Combined First-Principles and Experimental Study. ACS Applied Materials & Interfaces, 2016, 8, 7843-7853.	4.0	169
28653	Structures of seven molybdenum surfaces and their coverage dependent hydrogen adsorption. Physical Chemistry Chemical Physics, 2016, 18, 6005-6012.	1.3	23
28654	Investigations on Nb₂C monolayer as promising anode material for Li or non-Li ion batteries from first-principles calculations. RSC Advances, 2016, 6, 27467-27474.	1.7	147
28655	SiC₇siligraphene: a novel donor material with extraordinary sunlight absorption. Nanoscale, 2016, 8, 6994-6999.	2.8	70
28656	Prediction of large magnetoelectric coupling in Fe₄N/BaTiO₃ and MnFe₃N/BaTiO₃ junctions from a first-principles study. RSC Advances, 2016, 6, 29504-29511.	1.7	5
28657	Synthesis, structure and ionic conductivities of novel Li-ion conductor A3Li Ta6â‚Zr Si4O26 (A= Sr and) Tj ETQq0 0 0 rgBT /Overlock 10	1.3	1
28658	Luminescence Mechanistic Study of BaLaGa₃O₇:Nd Using Density Functional Theory Calculations. Inorganic Chemistry, 2016, 55, 2855-2863.	1.9	15
28659	First-Principles Study of the Î±â€“Î² Phase Transition of Ferroelectric Poly(vinylidene difluoride): Observation of Multiple Transition Pathways. Journal of Physical Chemistry B, 2016, 120, 3240-3249.	1.2	21
28660	Viability of Lead-Free Perovskites with Mixed Chalcogen and Halogen Anions for Photovoltaic Applications. Journal of Physical Chemistry C, 2016, 120, 6435-6441.	1.5	72
28661	Thermodynamic Origin of Photoinstability in the CH₃NH₃Pb(I_{1â€“x}Br_x)₃ Hybrid Halide Perovskite Alloy. Journal of Physical Chemistry Letters, 2016, 7, 1083-1087.	2.1	298
28662	Enhancement of oxygen reduction reaction activities by Pt nanoclusters decorated on ordered mesoporous porphyrinic carbons. Journal of Materials Chemistry A, 2016, 4, 5869-5876.	5.2	17
28663	Understanding and controlling water stability of MOF-74. Journal of Materials Chemistry A, 2016, 4, 5176-5183.	5.2	155
28664	Bismuth oxyhalides: synthesis, structure and photoelectrochemical activity. Chemical Science, 2016, 7, 4832-4841.	3.7	252

#	Article	IF	Citations
28665	Novel synthesis of N-doped graphene as an efficient electrocatalyst towards oxygen reduction. Nano Research, 2016, 9, 808-819.	5.8	81
28666	Multiaxial stressâ€“strain response and displacive transformations in NiTi alloy from first principles. Acta Materialia, 2016, 109, 223-229.	3.8	6
28667	Ball-milling synthesis of ZnO@sulphur/carbon nanotubes and Ni(OH)2@sulphur/carbon nanotubes composites for high-performance lithium-sulphur batteries. Electrochimica Acta, 2016, 196, 369-376.	2.6	77
28668	Computational design of smallest nanotube junctions in 0.3 nm diameter. Materials and Design, 2016, 95, 641-647.	3.3	9
28669	Stability of Solid Electrolyte Interphase Components on Lithium Metal and Reactive Anode Material Surfaces. Journal of Physical Chemistry C, 2016, 120, 6302-6313.	1.5	139
28670	Interface Magnetoelectric Coupling in Co/Pb(Zr,Ti)O₃. ACS Applied Materials & Interfaces, 2016, 8, 7553-7563.	4.0	19
28671	Effect of Phosphorus-Doping on Electrochemical Performance of Silicon Negative Electrodes in Lithium-Ion Batteries. ACS Applied Materials & Interfaces, 2016, 8, 7125-7132.	4.0	93
28672	Tuning Ionic Transport in Memristive Devices by Graphene with Engineered Nanopores. ACS Nano, 2016, 10, 3571-3579.	7.3	139
28673	Lithium storage on carbon nitride, graphenylene and inorganic graphenylene. Physical Chemistry Chemical Physics, 2016, 18, 14205-14215.	1.3	93
28674	Mechanistic and microkinetic analysis of CO₂ hydrogenation on ceria. Physical Chemistry Chemical Physics, 2016, 18, 7987-7996.	1.3	34
28675	In search of non-conventional surface oxidic motifs of Cu on Au(111). Physical Chemistry Chemical Physics, 2016, 18, 7349-7358.	1.3	7
28676	Effects of oxygen coverage, catalyst size, and core composition on Pt-alloy coreâ€“shell nanoparticles for oxygen reduction reaction. Catalysis Science and Technology, 2016, 6, 5168-5177.	2.1	22
28677	Transition voltages respond to synthetic reorientation of embedded dipoles in self-assembled monolayers. Chemical Science, 2016, 7, 781-787.	3.7	46
28678	Thermally stable coherent domain boundaries in complex-structured Cr₂Nb intermetallics. Philosophical Magazine, 2016, 96, 58-70.	0.7	10
28679	Effect of MgO/Fe Interface Oxidation State on Electric-Field Modulation of Interfacial Magnetic Anisotropy. Journal of Electronic Materials, 2016, 45, 3162-3166.	1.0	5
28680	Configuration- and concentration-dependent electronic properties of hydrogenated graphene. Carbon, 2016, 103, 84-93.	5.4	21
28681	Lithium diffusion in graphene and graphite: Effect of edge morphology. Carbon, 2016, 103, 209-216.	5.4	53
28682	Effect of edge-hydrogen passivation and nanometer size on the electronic properties of phagraphene ribbons. Computational Materials Science, 2016, 117, 279-285.	1.4	13

#	Article	IF	Citations
28683	Electron Counting and a Large Family of Two-Dimensional Semiconductors. Chemistry of Materials, 2016, 28, 1994-1999.	3.2	52
28684	Thermal Conductivity Comparison of Indium Gallium Zinc Oxide Thin Films: Dependence on Temperature, Crystallinity, and Porosity. Journal of Physical Chemistry C, 2016, 120, 7467-7475.	1.5	31
28685	Large Spatial Spin Polarization at Benzene/La_{2/3}Sr_{1/3}MnO₃ Spinterface: Toward Organic Spintronic Devices. Journal of Physical Chemistry C, 2016, 120, 6156-6164.	1.5	28
28686	Colossal magnetoresistance in amino-functionalized graphene quantum dots at room temperature: manifestation of weak anti-localization and doorway to spintronics. Nanoscale, 2016, 8, 8245-8254.	2.8	6
28687	Ab initio study of PbCr_(1â^'x)S_xO₄ solid solution: an inside look at Van Gogh Yellow degradation. Chemical Science, 2016, 7, 4197-4203.	3.7	16
28688	NO adsorption on Cu(110) and O(2 Ã— 1)/Cu(110) surfaces from density functional theory calculations. Physical Chemistry Chemical Physics, 2016, 18, 9476-9483.	1.3	8
28689	Towards stable single-atom catalysts: strong binding of atomically dispersed transition metals on the surface of nanostructured ceria. Catalysis Science and Technology, 2016, 6, 6806-6813.	2.1	92
28690	Ab initiocalculations of grain boundaries in bcc metals. Modelling and Simulation in Materials Science and Engineering, 2016, 24, 035013.	0.8	113
28691	Quasiparticle interference of the Fermi arcs and surface-bulk connectivity of a Weyl semimetal. Science, 2016, 351, 1184-1187.	6.0	156
28692	Ferromagnetism in zigzag GaN nanoribbons with tunable half-metallic gap. Computational Materials Science, 2016, 117, 300-305.	1.4	13
28693	Reforming and oxidative dehydrogenation of ethane with CO2 as a soft oxidant over bimetallic catalysts. Journal of Catalysis, 2016, 343, 168-177.	3.1	115
28694	First-principles study on magnetism and half-metallicity in bulk and various (001) surfaces of Heusler alloy Zr2VSn with Hg2CuTi-type structure. Journal of Magnetism and Magnetic Materials, 2016, 409, 28-33.	1.0	14
28695	Accelerated Removal of Fe-Antisite Defects while Nanosizing Hydrothermal LiFePO₄ with Ca²⁺. Nano Letters, 2016, 16, 2692-2697.	4.5	52
28696	Heterovalent Pb-substitution in ferroelectric bismuth silicate Bi₂SiO₅. Journal of Materials Chemistry C, 2016, 4, 3168-3174.	2.7	15
28697	Nanoscale characterization of oxidized ultrathin Co-films by ballistic electron emission microscopy. Materials Research Express, 2016, 3, 015001.	0.8	0
28698	Interaction of octahedral Mg(II) and tetrahedral Al(III) substitutions in aluminium-rich dioctahedral smectites. Theoretical Chemistry Accounts, 2016, 135, 1.	0.5	8
28699	Efficient visible light photocatalytic oxidation of NO with hierarchical nanostructured 3D flower-like BiOClxBr1â^'x solid solutions. Journal of Alloys and Compounds, 2016, 671, 318-327.	2.8	66
28700	Ruddlesdenâ€“Popper perovskite sulfides A3B2S7: A new family of ferroelectric photovoltaic materials for the visible spectrum. Nano Energy, 2016, 22, 507-513.	8.2	66

#	Article	IF	Citations
28701	Formaldehyde adsorption and decomposition on rutile (110): A first-principles study. Surface Science, 2016, 652, 156-162.	0.8	18
28702	Dynamic Structural Evolution of Metalâ€“Metal Bonding Network in Monolayer WS₂. Chemistry of Materials, 2016, 28, 2308-2314.	3.2	37
28703	Thin-Film Deposition and Characterization of a Sn-Deficient Perovskite Derivative Cs₂SnI₆. Chemistry of Materials, 2016, 28, 2315-2322.	3.2	329
28704	Thermodynamic Properties of Molecular Crystals Calculated within the Quasi-Harmonic Approximation. Journal of Physical Chemistry A, 2016, 120, 2022-2034.	1.1	48
28705	Investigating Orientational Defects in Energetic Material RDX Using First-Principles Calculations. Journal of Physical Chemistry A, 2016, 120, 1917-1924.	1.1	8
28706	Water Durable Electride Y₅Si₃: Electronic Structure and Catalytic Activity for Ammonia Synthesis. Journal of the American Chemical Society, 2016, 138, 3970-3973.	6.6	217
28707	Amount of tungsten dopant influencing the photocatalytic water oxidation activity of LaTiO₂N crystals grown directly by an NH₃-assisted flux method. Catalysis Science and Technology, 2016, 6, 5389-5396.	2.1	25
28708	Dehydrogenation of methanol to formaldehyde catalyzed by pristine and defective ceria surfaces. Physical Chemistry Chemical Physics, 2016, 18, 9990-9998.	1.3	9
28709	Predicting high thermoelectric performance of ABX ternary compounds NaMgX (X = P, Sb, As) with weak electronâ€“phonon coupling and strong bonding anharmonicity. Journal of Materials Chemistry C, 2016, 4, 3281-3289.	2.7	43
28710	Structural morphology of carbon nanofibers grown on different substrates. Carbon, 2016, 98, 343-351.	5.4	25
28711	Ab initio molecular dynamics simulations of the O2/Pt(1 1 1) interaction. Catalysis Today, 2016, 260, 60-65.	2.2	23
28712	Thermodynamic properties of LiD under compression with different pseudopotentials for lithium. Computational Materials Science, 2016, 114, 128-134.	1.4	24
28713	Ab initio structure determination of kidney stone potassium quadriurate from synchrotron powder diffraction data, a 150 year problem solved. Comptes Rendus Chimie, 2016, 19, 1535-1541.	0.2	10
28714	Ab-initio study of electronic structure and thermodynamic properties of aurates BaAu2O4 and SrAu2O4. Solid State Communications, 2016, 229, 10-15.	0.9	2
28715	Mechanisms of Si and Ge diffusion on surfactant terminated (111) silicon and germanium surfaces. Surface Science, 2016, 647, 12-16.	0.8	3
28716	Nitrogenated, phosphorated and arsenicated monolayer holey graphenes. Physical Chemistry Chemical Physics, 2016, 18, 3144-3150.	1.3	57
28717	Thermal exfoliation of stoichiometric single-layer silica from the stishovite phase: insight from first-principles calculations. Nanoscale, 2016, 8, 10598-10606.	2.8	7
28718	Low frequency noise and photo-enhanced field emission from ultrathin PbBi₂Se₄ nanosheets. Journal of Materials Chemistry C, 2016, 4, 1096-1103.	2.7	14

#	Article	IF	Citations
28719	Engineering Coexposed {001} and {101} Facets in Oxygen-Deficient TiO₂ Nanocrystals for Enhanced CO₂ Photoreduction under Visible Light. ACS Catalysis, 2016, 6, 1097-1108.	5.5	529
28720	Germanene on Al(111): Interface Electronic States and Charge Transfer. Journal of Physical Chemistry C, 2016, 120, 1580-1585.	1.5	58
28721	Defects in metalâ€“organic frameworks: a compromise between adsorption and stability?. Dalton Transactions, 2016, 45, 4352-4359.	1.6	140
28722	Elastic Properties of the Solid Electrolyte Li₇La₃Zr₂O₁₂(LLZO). Chemistry of Materials, 2016, 28, 197-206.	3.2	445
28723	Atomic-Level Understanding toward a High-Capacity and High-Power Silicon Oxide (SiO) Material. Journal of Physical Chemistry C, 2016, 120, 886-892.	1.5	105
28724	Defect-engineered graphene chemical sensors with ultrahigh sensitivity. Physical Chemistry Chemical Physics, 2016, 18, 14198-14204.	1.3	110
28725	Interlayer coupling of a direct van der Waals epitaxial MoS₂/graphene heterostructure. RSC Advances, 2016, 6, 323-330.	1.7	42
28726	Porous graphene for high capacity lithium ion battery anode material. Applied Surface Science, 2016, 363, 318-322.	3.1	19
28727	Theoretical study of the migration behaviour of Y-C atoms on diamond (001) surface. Diamond and Related Materials, 2016, 61, 102-108.	1.8	6
28728	More Cu, more problems: Decreased CO2 conversion ability by Cu-doped La0.75Sr0.25FeO3 perovskite oxides. Surface Science, 2016, 648, 92-99.	0.8	34
28729	Shear-Induced Structural Transformation for Tetragonal BC₄. Journal of Physical Chemistry C, 2016, 120, 581-586.	1.5	3
28730	Role of Branching on the Rate and Mechanism of Câ€“C Cleavage in Alkanes on Metal Surfaces. ACS Catalysis, 2016, 6, 469-482.	5.5	40
28731	New routes for improving adhesion at the metal/Î±-Al₂O₃(0001) interface. Physical Chemistry Chemical Physics, 2016, 18, 3032-3039.	1.3	16
28732	Structure prediction of the solid forms of methanol: an ab initio random structure searching approach. Physical Chemistry Chemical Physics, 2016, 18, 2736-2746.	1.3	15
28733	The variation of PbTiO₃bandgap at ferroelectric phase transition. Journal of Physics Condensed Matter, 2016, 28, 025501.	0.7	21
28734	Methane formation mechanism in methanol to hydrocarbon process: A periodic density functional theory study. Catalysis Communications, 2016, 75, 45-49.	1.6	14
28735	Metalâ€“support interaction effects on chemoâ€“regioselectivity: Hydrogenation of crotonaldehyde on Pt 13 /CeO 2 (1 1 1). Journal of Catalysis, 2016, 334, 68-78.	3.1	31
28736	Computational and Experimental Investigations of Na-Ion Conduction in Cubic Na₃PSe₄. Chemistry of Materials, 2016, 28, 252-258.	3.2	108

#	Article	IF	Citations
28737	Mechanisms for Engineering Highly Anisotropic Conductivity in a Layered Covalent-Organic Framework. Journal of Physical Chemistry C, 2016, 120, 174-178.	1.5	24
28738	Adsorption of water at the SrO surface ofÂruthenates. Nature Materials, 2016, 15, 450-455.	13.3	63
28739	Structural and electronic properties of ZnO/GaN heterostructured nanowires from first-principles study. Physical Chemistry Chemical Physics, 2016, 18, 3097-3102.	1.3	18
28740	Cation doping size effect for methane activation on alkaline earth metal doping of the CeO2 (111) surface. Catalysis Science and Technology, 2016, 6, 3544-3558.	2.1	20
28741	Interlayer electronic hybridization leads to exceptional thickness-dependent vibrational properties in few-layer black phosphorus. Nanoscale, 2016, 8, 2740-2750.	2.8	153
28742	A user guide for SLUSCHI: Solid and Liquid in Ultra Small Coexistence with Hovering Interfaces. Calphad: Computer Coupling of Phase Diagrams and Thermochemistry, 2016, 52, 88-97.	0.7	23
28743	First-principles study of transition-metal nitrides as diffusion barriers against Al. Journal of Nuclear Materials, 2016, 471, 208-213.	1.3	6
28744	Metallosupramolecular Assembly of Cr and p-Terphenyldinitrile by Dissociation of Metal Carbonyls on Au(111). Journal of Physical Chemistry C, 2016, 120, 1049-1055.	1.5	6
28745	Nanostructured SnS with inherent anisotropic optical properties for high photoactivity. Nanoscale, 2016, 8, 2293-2303.	2.8	123
28746	Luminescence of undoped and Eu³⁺ doped nanocrystalline SrWO₄ scheelite: time resolved fluorescence complimented by DFT and positron annihilation spectroscopic studies. RSC Advances, 2016, 6, 3792-3805.	1.7	57
28747	Theoretical Investigations on the Elastic and Thermodynamic Properties of Rhenium Phosphide. Zeitschrift Fur Naturforschung - Section A Journal of Physical Sciences, 2016, 71, 1-8.	0.7	2
28748	New insights into the thermal reduction of graphene oxide: Impact of oxygen clustering. Carbon, 2016, 100, 90-98.	5.4	94
28749	Carbon nanoribbons and nanotubes based on Î´-graphyne: A first-principles study. Physica E: Low-Dimensional Systems and Nanostructures, 2016, 78, 19-24.	1.3	12
28750	Insights into Intrinsic Defects and the Incorporation of Na and K in the Cu₂ZnSnSe₄ Thin-Film Solar Cell Material from Hybrid-Functional Calculations. Journal of Physical Chemistry C, 2016, 120, 2064-2069.	1.5	18
28751	Lattice-Polarity-Driven Epitaxy of Hexagonal Semiconductor Nanowires. Nano Letters, 2016, 16, 1328-1334.	4.5	35
28752	Engineering of hydrogenated two-dimensional h-BN/C superlattices as electrostatic substrates. Physical Chemistry Chemical Physics, 2016, 18, 974-981.	1.3	5
28753	Density functional studies of olivine-type LiFePO4 and NaFePO4 as positive electrode materials for rechargeable lithium and sodium ion batteries. Solid State Ionics, 2016, 286, 40-44.	1.3	53
28754	Density functional theory study of Oâ€“H and Câ€“H bond scission of methanol catalyzed by a chemisorbed oxygen layer on Cu(111). Surface Science, 2016, 646, 288-297.	0.8	16

#	Article	IF	Citations
28755	Probing Spinâ€“Orbit Coupling and Interlayer Coupling in Atomically Thin Molybdenum Disulfide Using Hydrostatic Pressure. ACS Nano, 2016, 10, 1619-1624.	7.3	47
28756	Magnetic and magnetocaloric properties of iron substituted holmium chromite and dysprosium chromite. RSC Advances, 2016, 6, 9475-9483.	1.7	42
28757	Computational and experimental study on the cation distribution of Laâ€“Cu substituted barium hexaferrites. Journal of Alloys and Compounds, 2016, 664, 406-410.	2.8	28
28758	Strengthening effect of nano-scale precipitates in a die-cast Mgâ€“4Alâ€“5.6Smâ€“0.3Mn alloy. Journal of Alloys and Compounds, 2016, 665, 240-250.	2.8	52
28759	An ab initio study on electronic and magnetic properties of Cr, V doped Cd and Zn nitrides for spintronic applications. Journal of Magnetism and Magnetic Materials, 2016, 406, 48-59.	1.0	11
28760	A hybrid functional calculation of Tm3+ defects in germanium (Ge). Materials Science in Semiconductor Processing, 2016, 43, 129-133.	1.9	15
28762	Electron Transfer and Catalytic Mechanism of Organic Molecule-Adsorbed Graphene Nanoribbons as Efficient Catalysts for Oxygen Reduction and Evolution Reactions. Journal of Physical Chemistry C, 2016, 120, 2166-2175.	1.5	42
28763	Toward the Ultimate Limit of Connectivity in Quantum Dots with High Mobility and Clean Gaps. ACS Nano, 2016, 10, 606-614.	7.3	23
28764	Extreme compressibility in LnFe(CN)6 coordination framework materials via molecular gears and torsion springs. Nature Chemistry, 2016, 8, 270-275.	6.6	71
28765	Giant tunnel magneto-resistance in graphene based molecular tunneling junction. Nanoscale, 2016, 8, 3432-3438.	2.8	30
28766	Amorphous carbon nanotubes as potent sorbents for removal of a phenolic derivative compound and arsenic: theoretical support of experimental findings. RSC Advances, 2016, 6, 8913-8922.	1.7	17
28767	Sulphur diffusion inÎ²-NiAl and effect of Pt additive: anab initiostudy. Journal Physics D: Applied Physics, 2016, 49, 055306.	1.3	4
28768	Novel hetero-bilayered materials for photovoltaics. Applied Materials Today, 2016, 2, 24-31.	2.3	23
28769	How Big Does a Si Nanocluster Favor Bulk Bonding Geometry?. Journal of Physical Chemistry C, 2016, 120, 1966-1970.	1.5	7
28770	Realizing diverse electronic and magnetic properties in hybrid zigzag BNC nanoribbons via hydrogenation. Physical Chemistry Chemical Physics, 2016, 18, 1326-1340.	1.3	9
28771	High resistivity in undoped CdTe: carrier compensation of Te antisites and Cd vacancies. Journal Physics D: Applied Physics, 2016, 49, 035101.	1.3	21
28772	First-principles investigation of helium in Y₂O₃. Journal Physics D: Applied Physics, 2016, 49, 065301.	1.3	11
28773	Molecular modeling of the proton density distribution in a water-filled slab-like nanopore bounded by Pt oxide and ionomer. Catalysis Today, 2016, 262, 133-140.	2.2	25

#	Article	IF	Citations
28774	Ab initio investigations of the phase stability in group IVB and VB transition metal carbides. Computational Materials Science, 2016, 112, 318-326.	1.4	77
28775	Structural and Energetic Trends of Ethylene Hydrogenation over Transition Metal Surfaces. Journal of Physical Chemistry C, 2016, 120, 995-1003.	1.5	39
28776	Interaction of a Self-Assembled Ionic Liquid Layer with Graphite(0001): A Combined Experimental and Theoretical Study. Journal of Physical Chemistry Letters, 2016, 7, 226-233.	2.1	68
28777	Electron stimulated hydroxylation of a metal supported silicate film. Physical Chemistry Chemical Physics, 2016, 18, 3755-3764.	1.3	33
28778	Dependence on size of supported Rh nanoclusters for CO adsorption. RSC Advances, 2016, 6, 3830-3839.	1.7	12
28779	First-principles calculations of transition metal solute interactions with hydrogen in tungsten. Nuclear Fusion, 2016, 56, 026004.	1.6	33
28780	A search for the ground state structure and the phase stability of tantalum pentoxide. Journal of Physics Condensed Matter, 2016, 28, 035801.	0.7	27
28781	Study on the electronic structure of Î±-U2N3 by XPS and first principles. Journal of Alloys and Compounds, 2016, 664, 745-749.	2.8	20
28782	Density-functional theory study of high hydrogen content complex hydrides Mg(BH 4) 2 at low temperature. Renewable Energy, 2016, 90, 114-119.	4.3	16
28783	QSTEM-based HAADF-STEM image analysis of Mo/V distribution in MoVTeTaO M1 phase and their correlations with surface reactivity. Applied Catalysis A: General, 2016, 512, 27-35.	2.2	14
28784	New High-Pressure Gallium Borate Ga₂B₃O₇(OH) with Photocatalytic Activity. Inorganic Chemistry, 2016, 55, 676-681.	1.9	36
28785	CuO Surfaces and CO₂ Activation: A Dispersion-Corrected DFT+U Study. Journal of Physical Chemistry C, 2016, 120, 2198-2214.	1.5	165
28786	Rationalizing the Hydrogen and Oxygen Evolution Reaction Activity of Two-Dimensional Hydrogenated Silicene and Germanene. ACS Applied Materials & Interfaces, 2016, 8, 1536-1544.	4.0	69
28787	High thermoelectric performance from optimization of hole-doped CuInTe₂. Physical Chemistry Chemical Physics, 2016, 18, 5925-5931.	1.3	36
28788	Adsorption of proline, hydroxyproline and glycine on anatase (001) surface: a first-principle study. Theoretical Chemistry Accounts, 2016, 135, 1.	0.5	8
28789	Fast and Huge Anisotropic Diffusion of Cu (Ag) and Its Resistance on the Sn Self-diffusivity in Solid Î²â€“Sn. Journal of Materials Science and Technology, 2016, 32, 121-128.	5.6	18
28790	First-Principles Design of New Electrodes for Proton-Conducting Solid-Oxide Electrochemical Cells: A-Site Doped Sr₂Fe_{1.5}Mo_{0.5}O_{6â˜Î´} Perovskite. Chemistry of Materials, 2016, 28, 490-500.	3.2	86
28791	Predicted Unusual Catalytic Activity of One-Dimensional Pt-Induced Atomic Nanowires on Ge(001) Surface. Journal of Physical Chemistry C, 2016, 120, 402-406.	1.5	2

#	Article	IF	Citations
28792	Prediction of Giant Thermoelectric Efficiency in Crystals with Interlaced Nanostructure. Nano Letters, 2016, 16, 121-125.	4.5	4
28793	Ligand ordering determines the catalytic response of hybrid palladium nanoparticles in hydrogenation. Catalysis Science and Technology, 2016, 6, 1621-1631.	2.1	45
28794	Dissociation of O₂ and its reactivity on O/S doped graphene. RSC Advances, 2016, 6, 7015-7021.	1.7	18
28795	Pressure-induced structural and magnetic transitions in the infinite-chains iron oxide Sr2FeO3: a first-principle investigation. Journal Physics D: Applied Physics, 2016, 49, 055303.	1.3	3
28796	Graphene/phosphorene bilayer: High electron speed, optical property and semiconductor-metal transition with electric field. Current Applied Physics, 2016, 16, 318-323.	1.1	27
28797	Half metallicity and magnetism in graphene containing monovacancies decorated with Carbon/Nitrogen adatom. Journal of Alloys and Compounds, 2016, 663, 100-106.	2.8	14
28798	Novel superhard Bâ€“Câ€“O phases predicted from first principles. Physical Chemistry Chemical Physics, 2016, 18, 1859-1863.	1.3	44
28799	Covalent pathways in engineering h-BN supported graphene. Carbon, 2016, 98, 449-456.	5.4	8
28800	Structural and magnetocaloric properties of novel gadolinium borohydrides. Journal of Alloys and Compounds, 2016, 664, 378-384.	2.8	45
28801	Theoretical investigation of Chevrel phase materials for cathodes accommodating Ca2+ ions. Journal of Power Sources, 2016, 306, 431-436.	4.0	58
28802	Stability and nucleation of Ir n (n = 1â€“5) clusters on different Î³ -Al 2 O 3 surfaces: A density functional theory study. Physics Letters, Section A: General, Atomic and Solid State Physics, 2016, 380, 718-725.	0.9	8
28803	Complete Series of Alkali-Metal M(BH₃NH₂BH₂NH₂BH₃) Hydrogen-Storage Salts Accessed via Metathesis in Organic Solvents. Inorganic Chemistry, 2016, 55, 37-45.	1.9	24
28804	Confinement of the Pt(111) Surface State in Graphene Nanoislands. Journal of Physical Chemistry C, 2016, 120, 345-349.	1.5	9
28805	Structural Transformation of MXene (V₂C, Cr₂C, and Ta₂C) with O Groups during Lithiation: A First-Principles Investigation. ACS Applied Materials & Interfaces, 2016, 8, 74-81.	4.0	159
28806	Ligand Addition Energies and the Stoichiometry of Colloidal Nanocrystals. ACS Nano, 2016, 10, 1462-1474.	7.3	33
28807	Understanding and solving disorder in the substitution pattern of amino functionalized MIL-47(V). Dalton Transactions, 2016, 45, 4309-4315.	1.6	5
28808	Carbon nanobuds based on carbon nanotube caps: a first-principles study. Nanoscale, 2016, 8, 2343-2349.	2.8	13
28809	Theoretical study of the NO, NO2, CO, SO2, and NH3adsorptions on multi-diameter single-wall MoS2nanotube. Journal Physics D: Applied Physics, 2016, 49, 045106.	1.3	22

#	Article	IF	Citations
28810	Periodic density functional theory study of the high-pressure behavior of crystalline l-serine-l-ascorbic acid. Journal of Molecular Modeling, 2016, 22, 19.	0.8	10
28811	Electronic structure, magnetic and optical properties of Cr-doped GaAs using hybrid density functional. Computational Materials Science, 2016, 113, 75-79.	1.4	7
28812	Theoretical investigation of hydrogen absorption properties of rhodiumâ€“silver alloys. Journal of Alloys and Compounds, 2016, 662, 404-408.	2.8	5
28813	Non-equilibrium properties of interatomic potentials in cascade simulations in tungsten. Journal of Nuclear Materials, 2016, 470, 119-127.	1.3	63
28814	Initial stages of water solvation of stepped platinum surfaces. Physical Chemistry Chemical Physics, 2016, 18, 3416-3422.	1.3	32
28815	Electronic structure, photovoltage, and photocatalytic hydrogen evolution with p-CuBi₂O₄ nanocrystals. Journal of Materials Chemistry A, 2016, 4, 2936-2942.	5.2	158
28816	Ce 3+ -doped Li 4 Ti 5 O 12 with CeO 2 surface modification by a sol-gel method for high-performance lithium-ion batteries. Electrochimica Acta, 2016, 189, 147-157.	2.6	66
28817	Tetrahedral tilting and ferroelectricity in Bi2AO5 (A=Si, Ge) from first principles calculations. Journal of Solid State Chemistry, 2016, 235, 68-75.	1.4	33
28818	Using degrees of rate control to improve selective n-butane oxidation over model MOF-encapsulated catalysts: sterically-constrained Ag₃Pd(111). Faraday Discussions, 2016, 188, 21-38.	1.6	15
28819	High thermoelectric performance can be achieved in black phosphorus. Journal of Materials Chemistry C, 2016, 4, 991-998.	2.7	59
28820	A DFT study of hydrogen storage in Zr(Cr 0.5 Ni 0.5) 2 Laves phase. International Journal of Hydrogen Energy, 2016, 41, 2700-2710.	3.8	19
28821	Thermophysical properties of titanium and vanadium nitrides: Thermodynamically self-consistent approach coupled with density functional theory. Journal of Alloys and Compounds, 2016, 662, 240-251.	2.8	21
28822	Charge storage in KCu7S4 as redox active material for a flexible all-solid-state supercapacitor. Nano Energy, 2016, 19, 363-372.	8.2	77
28823	A theoretical study on the electronic property of a new two-dimensional material molybdenum dinitride. Physics Letters, Section A: General, Atomic and Solid State Physics, 2016, 380, 768-772.	0.9	27
28824	Interaction between oxygen interstitials and deformation twins in alpha-titanium. Acta Materialia, 2016, 105, 44-51.	3.8	31
28825	Strong room-temperature blue-violet photoluminescence of multiferroic BaMnF₄. Physical Chemistry Chemical Physics, 2016, 18, 2054-2058.	1.3	6
28826	Effect of temperature on the distribution and inhomogeneity degree of Se-S atoms in CuIn(Se1â^'xSx)2alloys. Journal Physics D: Applied Physics, 2016, 49, 025101.	1.3	3
28827	Tailoring the substitution on the surface of Fe13/Pt42 coreâ€“shell nanoparticles by Au atoms. Materials and Design, 2016, 92, 794-801.	3.3	1

#	Article	IF	Citations
28828	Adsorption of Water on the Fe₃O₄(111) Surface: Structures, Stabilities, and Vibrational Properties Studied by Density Functional Theory. Journal of Physical Chemistry C, 2016, 120, 1056-1065.	1.5	71
28829	Creating Two-Dimensional Electron Gas in Nonpolar/Nonpolar Oxide Interface via Polarization Discontinuity: First-Principles Analysis of CaZrO₃/SrTiO₃ Heterostructure. ACS Applied Materials & Interfaces, 2016, 8, 390-399.	4.0	45
28830	Atomistic Insights into the Oriented Attachment of Tunnel-Based Oxide Nanostructures. ACS Nano, 2016, 10, 539-548.	7.3	66
28831	Nb and Ta layer doping effects on the interfacial energetics and electronic properties of LaAlO₃/SrTiO₃ heterostructure: first-principles analysis. Physical Chemistry Chemical Physics, 2016, 18, 2379-2388.	1.3	21
28832	Unexpectedly large impact of van der Waals interactions on the description of heterogeneously catalyzed reactions: the water gas shift reaction on Cu(321) as a case example. Physical Chemistry Chemical Physics, 2016, 18, 2792-2801.	1.3	22
28833	Quasi one-dimensional band dispersion and surface metallization in long-range ordered polymeric wires. Nature Communications, 2016, 7, 10235.	5.8	91
28834	Association of defects in doped non-stoichiometric ceria from first principles. Physical Chemistry Chemical Physics, 2016, 18, 3804-3811.	1.3	35
28835	New Polymorph of Dehydroepiandrosterone Obtained via Cryomodification. Crystal Growth and Design, 2016, 16, 1088-1095.	1.4	11
28836	Al₂C Monolayer Sheet and Nanoribbons with Unique Direction-Dependent Acoustic-Phonon-Limited Carrier Mobility and Carrier Polarity. Journal of Physical Chemistry Letters, 2016, 7, 302-307.	2.1	30
28837	Characterization of Phosphate Species on Hydrated Anatase TiO2 Surfaces. Langmuir, 2016, 32, 997-1008.	1.6	18
28838	Two-Dimensional SiS Layers with Promising Electronic and Optoelectronic Properties: Theoretical Prediction. Nano Letters, 2016, 16, 1110-1117.	4.5	149
28839	Nanoporous PdCr alloys as highly active electrocatalysts for oxygen reduction reaction. Physical Chemistry Chemical Physics, 2016, 18, 4166-4173.	1.3	25
28840	The capacity fading mechanism and improvement of cycling stability in MoS₂-based anode materials for lithium-ion batteries. Nanoscale, 2016, 8, 2918-2926.	2.8	168
28841	Implications of boron doping on electrocatalytic activities of graphyne and graphdiyne families: a first principles study. Physical Chemistry Chemical Physics, 2016, 18, 2949-2958.	1.3	59
28842	Pyridine intercalated Bi2Se3heterostructures: controlling the topologically protected states. Nanotechnology, 2016, 27, 035704.	1.3	2
28843	Hydroxylated graphyne and graphdiyne: First-principles study. Applied Surface Science, 2016, 361, 206-212.	3.1	22
28844	A modeling approach for new CrSi2 based alloys: Application to metastable Cr1-xZrxSi2 as a potential thermoelectric material. Journal of Alloys and Compounds, 2016, 662, 150-156.	2.8	15
28845	Tuning structural stability and lithium-storage properties by d -orbital hybridization substitution in full tetrahedron Li 2 FeSiO 4 nanocrystal. Nano Energy, 2016, 20, 117-125.	8.2	44

#	Article	IF	Citations
28846	Geometry and Electronic Properties of Glycerol Adsorbed on Bare and Transition-Metal Surface-Alloyed Au(111): A Density Functional Theory Study. Journal of Physical Chemistry C, 2016, 120, 1749-1757.	1.5	18
28847	Complex Stoichiometry-Dependent Reordering of 3,4,9,10-Perylenetetracarboxylic Dianhydride on Ag(111) upon K Intercalation. ACS Nano, 2016, 10, 2365-2374.	7.3	22
28848	Production of Highly Monolayer Enriched Dispersions of Liquid-Exfoliated Nanosheets by Liquid Cascade Centrifugation. ACS Nano, 2016, 10, 1589-1601.	7.3	365
28849	Chemical bonding-induced rich electronic properties of oxygen adsorbed few-layer graphenes. Physical Chemistry Chemical Physics, 2016, 18, 4000-4007.	1.3	5
28850	Solar energy conversion properties and defect physics of ZnSiP₂. Energy and Environmental Science, 2016, 9, 1031-1041.	15.6	49
28851	A universal chemical potential for sulfur vapours. Chemical Science, 2016, 7, 1082-1092.	3.7	44
28852	Adsorption mechanism of graphene-like ZnO monolayer towards CO₂molecules: enhanced CO₂capture. Nanotechnology, 2016, 27, 015502.	1.3	69
28853	Diffusion coefficients of alloying elements in dilute Mg alloys: A comprehensive first-principles study. Acta Materialia, 2016, 103, 573-586.	3.8	169
28854	Surface segregation and oxidation of Pt3Ni(1 1 1) alloys under oxygen environment. Catalysis Today, 2016, 260, 3-7.	2.2	26
28855	Prediction of structures and properties of 2,4,6-triamino-1,3,5-triazine-1,3,5-trioxide (MTO) and 2,4,6-trinitro-1,3,5-triazine-1,3,5-trioxide (MTO3N) green energetic materials from DFT and ReaxFF molecular modeling. Journal of Materials Chemistry A, 2016, 4, 1264-1276.	5.2	17
28856	Elastic Properties of Alkali Superionic Conductor Electrolytes from First Principles Calculations. Journal of the Electrochemical Society, 2016, 163, A67-A74.	1.3	265
28857	Energetics of antiphase boundaries in Î³â€² Co3(Al,W)-based superalloys. Acta Materialia, 2016, 103, 57-62.	3.8	40
28858	Hybrid functional study on optical properties of Sr 2 M 2 O 7â^'x N x (MÂ=ÂNb,ÂTa) photocatalysts with perovskite-slab structures. Current Applied Physics, 2016, 16, 1-7.	1.1	13
28859	Bandgap engineering of different stacking WS2 bilayer under an external electric field. Solid State Communications, 2016, 225, 32-37.	0.9	27
28860	Synergetic interplay between metal (Pt) and nonmetal (C) species in codoped TiO 2 : A DFT+U study. Computational Materials Science, 2016, 111, 513-524.	1.4	18
28861	Soluteâ€“grain boundary interaction and segregation formation in Al: First principles calculations and molecular dynamics modeling. Computational Materials Science, 2016, 112, 18-26.	1.4	32
28862	Structural, electronic and optical properties of Zn0.5Cr0.5S from first-principles. Computational Materials Science, 2016, 112, 39-43.	1.4	11
28863	Ab initio calculations of the atomic and electronic structures of crystalline PEO3:LiCF3SO3 electrolytes. Computational Materials Science, 2016, 112, 170-174.	1.4	9

#	Article	IF	Citations
28864	Electron tunneling in Fe/KNbO3/Fe multiferroic tunnel junctions. Computational Materials Science, 2016, 112, 257-262.	1.4	3
28865	Adsorption and dissociation of H2 on PuO2 (110) surface: A density functional theory study. Journal of Alloys and Compounds, 2016, 654, 567-573.	2.8	16
28866	Intrinsic defect-mediated magnetism in Feâ€“N codoped TiO 2. Journal of Alloys and Compounds, 2016, 657, 372-378.	2.8	18
28867	Investigations on the origin of ferromagnetism in Ga 1â^'x Cr x N and Si-doped Ga 1â^'x Cr x N films: Experiments and theory. Journal of Alloys and Compounds, 2016, 658, 800-805.	2.8	1
28868	Competitive adsorption of nitrogen and sulphur compounds on a multisite model of NiMoS catalyst: A theoretical study. Journal of Catalysis, 2016, 333, 78-93.	3.1	52
28869	Structure and magnetism of Mn, Fe, or Co adatoms on monolayer and bilayer black phosphorus. Journal of Magnetism and Magnetic Materials, 2016, 401, 706-710.	1.0	16
28870	Distortion induced magnetic phase transition in cubic BaFeO 3. Journal of Magnetism and Magnetic Materials, 2016, 401, 1097-1105.	1.0	7
28871	Hydrogen isotope dissolution, diffusion, and permeation in Er2O3. Journal of Power Sources, 2016, 303, 168-174.	4.0	13
28872	Theoretical investigations of the ternary compound LaUN3. Journal of Solid State Chemistry, 2016, 233, 484-491.	1.4	1
28873	Geometrical and orientational investigations on the electronic structure of graphene with adsorbed aluminium or silicon. Materials and Design, 2016, 89, 27-35.	3.3	6
28874	Crystal structure and band gap studies of sodalite: experimental and calculated results. Journal of Molecular Structure, 2016, 1106, 59-63.	1.8	9
28875	Insights into enhanced visible-light photocatalytic activity of CeO 2 doped with nonmetal impurity from the first principles. Materials Science in Semiconductor Processing, 2016, 41, 200-208.	1.9	44
28876	Comparative Raman spectroscopic study of phase stability and anharmonic effects in AZr2(PO4)3 (A=K,) Tj ETQq0 0 0 rgBT /Overlock 10	2.0	8
28877	Energy band gaps in periodic bent graphene. Solid State Communications, 2016, 225, 22-26.	0.9	4
28878	Na Deposition on MnO(100). Surface Science, 2016, 645, 23-29.	0.8	11
28879	A high-spin nickel(ii) borohydride complex in dehalogenation. Inorganic Chemistry Frontiers, 2016, 3, 157-163.	3.0	12
28880	Interatomic Potentials Including Chemistry. Springer Series in Materials Science, 2016, , 107-194.	0.4	1
28881	Mechanism of boron and nitrogen in situ doping during graphene chemical vapor deposition growth. Carbon, 2016, 98, 633-637.	5.4	16

#	Article	IF	Citations
28882	Chirality and vacancy effect on phonon dispersion of MoS 2 with strain. Physics Letters, Section A: General, Atomic and Solid State Physics, 2016, 380, 745-752.	0.9	13
28883	Predicting electrochemical properties and ionic diffusion in Na_{2+2x}Mn_{2â^'x}(SO₄)₃: crafting a promising high voltage cathode material. Journal of Materials Chemistry A, 2016, 4, 451-457.	5.2	21
28884	Energetic analysis of He and monovacancies in Cu/W metallic interfaces. Materials and Design, 2016, 91, 171-179.	3.3	30
28885	First-principles study of the binding preferences and diffusion behaviors of solutes in vanadium alloys. Journal of Alloys and Compounds, 2016, 660, 55-61.	2.8	31
28886	Pressure-induced anomalies in structure, charge density and transport properties of Bi 2 Te 3 : A first principles study. Journal of Alloys and Compounds, 2016, 661, 428-434.	2.8	32
28887	Energetics and the magnetic state of Mn2 adsorbed on Au(111): Dimer bond distance dependence. Journal of Magnetism and Magnetic Materials, 2016, 403, 172-180.	1.0	4
28888	Energetic stability, oxidation states, and electronic structure of Bi-doped NaTaO₃: a first-principles hybrid functional study. Physical Chemistry Chemical Physics, 2016, 18, 857-865.	1.3	15
28889	WO₃ with surface oxygen vacancies as an anode buffer layer for high performance polymer solar cells. Journal of Materials Chemistry A, 2016, 4, 894-900.	5.2	68
28890	Ab initio derived reaction mechanism for the dry reforming of methane on Rh doped pyrochlore catalysts. Journal of Catalysis, 2016, 333, 59-70.	3.1	31
28891	Possibility of martensite transition in Ptâ€“Yâ€“Ga (Y=Cr, Mn, and Fe) system: An ab-initio calculation of the bulk mechanical, electronic and magnetic properties. Journal of Magnetism and Magnetic Materials, 2016, 401, 929-937.	1.0	30
28892	Electronic characterization of a single dangling bond on n- and p-type Si(001)-(2 Ã— 1):H. Surface Science, 2016, 645, 88-92.	0.8	17
28893	Predicting a new phase (Tâ€²â€²) of two-dimensional transition metal di-chalcogenides and strain-controlled topological phase transition. Nanoscale, 2016, 8, 4969-4975.	2.8	50
28894	Interactions of hydrogen with the iron and iron carbide interfaces: a ReaxFF molecular dynamics study. Physical Chemistry Chemical Physics, 2016, 18, 761-771.	1.3	61
28895	Structural, energetic, and electronic properties of gyroidal graphene nanostructures. Carbon, 2016, 96, 998-1007.	5.4	9
28896	Quantized phenomena in graphene nanoripples. Carbon, 2016, 96, 1175-1180.	5.4	4
28897	Understanding the thermodynamic pathways of SnO-to-SnO x phase transition. Computational Materials Science, 2016, 111, 359-365.	1.4	22
28898	Temperature dependence of elastic properties of L1 2 -Al 3 Sc: A first-principles study. Computational Materials Science, 2016, 111, 424-429.	1.4	9
28899	First-principles investigation of the magnetic structures and pressure-induced magnetic phase transition in magnetocaloric MnRhAs. Computational Materials Science, 2016, 112, 34-38.	1.4	3

#	Article	IF	Citations
28900	The effects of uniaxial and biaxial strain on the electronic structure of germanium. Computational Materials Science, 2016, 112, 263-268.	1.4	16
28901	Study of interaction between transition metal atoms and bigraphene monovacancy by means of quantum chemistry. Computational Materials Science, 2016, 112, 269-275.	1.4	1
28902	CO₂ adsorption of three isostructural metalâ€“organic frameworks depending on the incorporated highly polarized heterocyclic moieties. Dalton Transactions, 2016, 45, 190-197.	1.6	47
28903	Effect of surface doping on the band structure of graphene: a DFT study. Journal of Materials Science: Materials in Electronics, 2016, 27, 2728-2740.	1.1	16
28904	Effect of strain on the optical properties of LaNiO3: A first-principle study. Computational Materials Science, 2016, 112, 113-119.	1.4	21
28905	Surface elasticity revisited in the context of second strain gradient theory. Mechanics of Materials, 2016, 93, 220-237.	1.7	21
28906	Synthesis of olive-green few-layered BiOI for efficient photoreduction of CO2 into solar fuels under visible/near-infrared light. Solar Energy Materials and Solar Cells, 2016, 144, 732-739.	3.0	120
28907	Facet Dependence of CO₂ Reduction Paths on Cu Electrodes. ACS Catalysis, 2016, 6, 219-229.	5.5	420
28908	Prediction of two planar carbon allotropes with large meshes. Physical Chemistry Chemical Physics, 2016, 18, 1172-1177.	1.3	12
28909	Ru catalysts for levulinic acid hydrogenation with formic acid as a hydrogen source. Green Chemistry, 2016, 18, 2014-2028.	4.6	126
28910	Does p-type ohmic contact exist in WSe₂â€“metal interfaces?. Nanoscale, 2016, 8, 1179-1191.	2.8	166
28911	Structure and residual stress evolution of Ti/Al, Cr/Al or W/Al co-doped amorphous carbon nanocomposite films: Insights from ab initio calculations. Materials and Design, 2016, 89, 1123-1129.	3.3	23
28912	Tuning Zr₆ Metalâ€“Organic Framework (MOF) Nodes as Catalyst Supports: Site Densities and Electron-Donor Properties Influence Molecular Iridium Complexes as Ethylene Conversion Catalysts. ACS Catalysis, 2016, 6, 235-247.	5.5	150
28913	Ultrahigh power factor and thermoelectric performance in hole-doped single-crystal SnSe. Science, 2016, 351, 141-144.	6.0	1,594
28914	Structure and quantum well states in silicene nanoribbons on Ag(110). Surface Science, 2016, 645, 74-79.	0.8	27
28915	An experimental and theoretical investigation of the anisotropic branching in gold nanocrosses. Nanoscale, 2016, 8, 543-552.	2.8	90
28916	Manipulating Thermal Conductivity by Interfacial Modification of Misfit-Layered Cobaltites Ca3Co4O9. Journal of Electronic Materials, 2016, 45, 1217-1226.	1.0	12
28917	Importance of surface carbide formation on the activity and selectivity of Pd surfaces in the selective hydrogenation of acetylene. Surface Science, 2016, 646, 45-49.	0.8	45

#	Article	IF	Citations
28918	On the chemistry of the carbides in a molybdenum base Mo-Hf-C alloy produced by powder metallurgy. Journal of Alloys and Compounds, 2016, 654, 445-454.	2.8	19
28919	Electronic and magnetic properties of Sr2MoBO6 (B=W, RE, Os): Investigation of possible half metal. Journal of Magnetism and Magnetic Materials, 2016, 399, 72-76.	1.0	8
28920	Slip nucleation in single crystal FeNiCoCrMn high entropy alloy. Scripta Materialia, 2016, 112, 54-57.	2.6	114
28921	Direct atomic-scale evidence for shearâ€“dilatation correlation in metallic glasses. Scripta Materialia, 2016, 112, 37-41.	2.6	28
28922	Two-body potential model based on cosine series expansion for ionic materials. Computational Materials Science, 2016, 111, 54-63.	1.4	1
28923	Nickel sulfides for electrocatalytic hydrogen evolution under alkaline conditions: a case study of crystalline NiS, NiS₂, and Ni₃S₂ nanoparticles. Catalysis Science and Technology, 2016, 6, 1077-1084.	2.1	408
28924	Structural and electrical properties of selenium nanotubes. Physics Letters, Section A: General, Atomic and Solid State Physics, 2016, 380, 238-241.	0.9	5
28925	Oxygen orders differently under graphene: new superstructures on Ir(111). Nanoscale, 2016, 8, 1932-1943.	2.8	25
28926	Entropy and Diffuse Scattering: Comparison of NbTiVZr and CrMoNbV. Metallurgical and Materials Transactions A: Physical Metallurgy and Materials Science, 2016, 47, 3306-3311.	1.1	24
28927	DFT study of the water gas shift reaction on Ni(111), Ni(100) and Ni(110) surfaces. Surface Science, 2016, 644, 53-63.	0.8	84
28928	Multi-scale simulation of the experimental response of ion-irradiated zirconium carbide: Role of interstitial clustering. Acta Materialia, 2016, 102, 79-87.	3.8	22
28929	Molecular dynamics simulation of surface step reconstruction and irreversibility under cyclic loading. Acta Materialia, 2016, 102, 149-161.	3.8	11
28930	High-throughput computational search for strengthening precipitates in alloys. Acta Materialia, 2016, 102, 125-135.	3.8	83
28931	First-principles study of point defects in C14 MgZn2 Laves phase. Journal of Alloys and Compounds, 2016, 654, 475-481.	2.8	16
28932	Self doping promoted photocatalytic removal of no under visible light with bi2moo6: Indispensable role of superoxide ions. Applied Catalysis B: Environmental, 2016, 182, 316-325.	10.8	157
28933	Theoretical and experimental determination of the major thermo-mechanical properties of RE 2 SiO 5 (RE = Tb, Dy, Ho, Er, Tm, Yb, Lu, and Y) for environmental and thermal barrier coating applications. Journal of the European Ceramic Society, 2016, 36, 189-202.	2.8	171
28934	Reconstructive Phase Transition in Ultrashort Peptide Nanostructures and Induced Visible Photoluminescence. Langmuir, 2016, 32, 2847-2862.	1.6	74
28935	Interface Schottky barrier engineering via strain in metalâ€“semiconductor composites. Nanoscale, 2016, 8, 1352-1359.	2.8	45

#	Article	IF	Citations
28936	Understanding gate adsorption behaviour of CO₂ on elastic layer-structured metalâ€“organic framework-11. Dalton Transactions, 2016, 45, 4193-4202.	1.6	43
28937	Spin and orbital magnetic moments and spin anisotropy energies of light rare earth atoms embedded in graphene: A first-principles study. Physica E: Low-Dimensional Systems and Nanostructures, 2016, 75, 169-173.	1.3	15
28938	Deep HDS of FCC gasoline over alumina supported CoMoS catalyst: Inhibiting effects of carbon monoxide and water. Applied Catalysis B: Environmental, 2016, 183, 317-327.	10.8	28
28939	First principles study of enhanced CO 2 adsorption on MOF-253 by salt-insertion. Computational Materials Science, 2016, 111, 79-85.	1.4	7
28940	A systematic fitting procedure for accurate force field models to reproduce ab initio phonon spectra of nanostructures. Computer Physics Communications, 2016, 200, 27-36.	3.0	4
28941	Phase equilibria and solidification characteristics of the Alâ€“Scâ€“Si alloys. Journal of Materials Science, 2016, 51, 1644-1658.	1.7	13
28942	An object oriented Python interface for atomistic simulations. Computer Physics Communications, 2016, 198, 230-237.	3.0	1
28943	The diffusion of point defects in uranium mononitride: Combination of DFT and atomistic simulation with novel potential. Journal of Alloys and Compounds, 2016, 658, 385-394.	2.8	25
28944	Electronic and optical properties of Mg-, F-doped and Mgâ^–F-codoped M 1 -VO 2 via hybrid density functional calculations. Journal of Alloys and Compounds, 2016, 658, 569-575.	2.8	30
28945	Electronic structures, magnetic properties, half-metallicity and optical properties of the zincblende Zn 1â^'x Mo x S. Journal of Magnetism and Magnetic Materials, 2016, 401, 746-750.	1.0	4
28946	Dirac-like fermions and node-loop features in bilayer BC 3 sheet sandwiching a triangular alkaline metal layer. Physics Letters, Section A: General, Atomic and Solid State Physics, 2016, 380, 475-479.	0.9	1
28947	Effects of A 3+ cations on hydration in A 2 M 3 O 12 family materials: A first-principles study. Computational Materials Science, 2016, 111, 28-33.	1.4	14
28948	A mechanistic DFT study of low temperature SCR of NO with NH₃ on MnCe_{1â^'x}O₂(111). Catalysis Science and Technology, 2016, 6, 2120-2128.	2.1	55
28949	First-principles study of structural, elastic and electronic properties of Î±-, Î²- and Î³-graphyne. Carbon, 2016, 96, 879-887.	5.4	235
28950	Critical stress for the bccâ€“hcp martensite nucleation in Tiâ€“6.25at.%Ta and Tiâ€“6.25at.%Nb alloys. Computational Materials Science, 2016, 111, 157-162.	1.4	19
28951	Nexus: A modular workflow management system for quantum simulation codes. Computer Physics Communications, 2016, 198, 154-168.	3.0	62
28952	On the hydrogen adsorption and dissociation on Cu surfaces and nanorows. Surface Science, 2016, 646, 221-229.	0.8	37
28953	Charge modulation of magnetization in X-doped MgO nanotube clusters (X=C, N). Physica E: Low-Dimensional Systems and Nanostructures, 2016, 76, 135-139.	1.3	9

#	Article	IF	Citations
28954	Influence of trap connectivity on H diffusion: Vacancy trapping. Acta Materialia, 2016, 103, 334-340.	3.8	38
28955	CALYPSO structure prediction method and its wide application. Computational Materials Science, 2016, 112, 406-415.	1.4	138
28956	The valence band electronic structure of rhombohedral-like and tetragonal-like BiFeO 3 thin films from hard X-ray photoelectron spectroscopy and first-principles theory. Journal of Electron Spectroscopy and Related Phenomena, 2016, 208, 63-66.	0.8	14
28957	Multilayer heterostructures of magnetic Heusler and binary compounds from first principles. Journal of Magnetism and Magnetic Materials, 2016, 401, 138-143.	1.0	2
28958	First-principles study on doping effect of Sn in BiF 3 as cathode materials for Li-ion battery. Current Applied Physics, 2016, 16, 12-19.	1.1	2
28959	Long-range intercluster interactions of solute nanoprecipitates in Mgâ€“Y alloys: A first-principles study. Journal of Alloys and Compounds, 2016, 657, 662-670.	2.8	14
28960	Experimental and first principles investigation of the multiferroics BiFeO3 and Bi0.9Ca0.1FeO3: Structure, electronic, optical and magnetic properties. Physica B: Condensed Matter, 2016, 481, 45-52.	1.3	42
28961	Adsorption of SO2 molecule on doped (8, 0) boron nitride nanotube: A first-principles study. Physica E: Low-Dimensional Systems and Nanostructures, 2016, 76, 47-51.	1.3	31
28962	Quantum emission from hexagonal boron nitride monolayers. Nature Nanotechnology, 2016, 11, 37-41.	15.6	1,006
28963	Electrically conducting palladium selenide (Pd₄Se, Pd₁₇Se₁₅,) Tj ETQq1 1 0.784314 rgBT /Ove Chemical Communications, 2016, 52, 206-209.	2.2	75
28964	Effect of NaBH 4 on properties of nanoscale zero-valent iron and its catalytic activity for reduction of p -nitrophenol. Applied Catalysis B: Environmental, 2016, 182, 541-549.	10.8	229
28965	The excitonic photoluminescence mechanism and lasing action in band-gap-tunable CdS_{1â^'x}Se_x nanostructures. Nanoscale, 2016, 8, 804-811.	2.8	22
28966	Properties of armchair ZnTe nanotubes: A density functional study. Computational Materials Science, 2016, 112, 1-7.	1.4	3
28967	Novel crystal structures for lithiumâ€“silicon alloy predicted by minima hopping method. Journal of Alloys and Compounds, 2016, 655, 147-154.	2.8	21
28968	Co-adsorption and mutual interaction of nCO +mH2 on the Fe(1 1 0) and Fe(1 1 1) surfaces. Catalysis Today, 2016, 261, 82-92.	2.2	17
28969	Ab initio prediction of threshold displacement energies in ZrC. Journal of Nuclear Materials, 2016, 471, 214-219.	1.3	14
28970	Invisible growth of microstructural defects in graphene chemical vapor deposition on copper foil. Carbon, 2016, 96, 237-242.	5.4	43
28971	Growth of nitrogen-doped graphene on copper: Multiscale simulations. Surface Science, 2016, 644, 102-108.	0.8	7

#	Article	IF	Citations
28972	First-principles study on surface stability of tantalum carbides. Surface Science, 2016, 644, 24-28.	0.8	16
28973	Theoretical insight on reactivity trends in CO₂ electroreduction across transition metals. Catalysis Science and Technology, 2016, 6, 1042-1053.	2.1	57
28974	Investigation of microstructure changes in ODS-EUROFER after hydrogen loading. Journal of Nuclear Materials, 2016, 468, 355-359.	1.3	6
28975	Preparation of porous carbons based on polyvinylidene fluoride for CO 2 adsorption: A combined experimental and computational study. Microporous and Mesoporous Materials, 2016, 219, 59-65.	2.2	28
28976	Electronic structure, optical dielectric constant and born effective charge of EuAlO. Journal of Physics and Chemistry of Solids, 2016, 88, 1-7.	1.9	9
28977	Half-metallic and magnetic properties of full-Heusler alloys Zr2CrZ (Z=Ga, In) with Hg2CuTi-type structure: A first-principles study. Journal of Magnetism and Magnetic Materials, 2016, 397, 120-124.	1.0	33
28978	High-Entropy Alloys in Hexagonal Close-Packed Structure. Metallurgical and Materials Transactions A: Physical Metallurgy and Materials Science, 2016, 47, 3322-3332.	1.1	158
28979	Electronic and magnetic properties of Co 2 Fe(Ga 1â^'x Si x) and Co 2 Fe(Al 1â^'y Si y) Heusler alloys with high Curie temperature. Journal of Magnetism and Magnetic Materials, 2016, 398, 7-12.	1.0	20
28980	Interaction of carboxylic acids with rutile TiO2(110): IR-investigations of terephthalic and benzoic acid adsorbed on a single crystal substrate. Surface Science, 2016, 643, 117-123.	0.8	39
28981	Partitioning of Cr and Si between cementite and ferrite derived from first-principles thermodynamics. Acta Materialia, 2016, 102, 241-250.	3.8	17
28982	Dimorphic HT- and LT-TbTiGe: Electronic and magnetic structures and bonding properties from first principles. Journal of Magnetism and Magnetic Materials, 2016, 397, 275-280.	1.0	0
28983	Adsorption and transformations of ethene on hydrogenated rhodium clusters in faujasite-type zeolite. A computational study. Catalysis Science and Technology, 2016, 6, 1726-1736.	2.1	5
28984	Magnetic properties of sulfur-doped graphene. Journal of Magnetism and Magnetic Materials, 2016, 401, 70-76.	1.0	25
28985	Electronic Structure Change in DNA Caused by Base Pair Motions and Its Effect on Charge Transfer in DNA Chains. Australian Journal of Chemistry, 2016, 69, 300.	0.5	1
28986	Electronic and magnetic properties of X-doped (XÂ=ÂTi, Zr, Hf) tungsten disulphide monolayer. Journal of Alloys and Compounds, 2016, 654, 574-579.	2.8	45
28987	Computational screening of alloying elements for the development of sustainable V-based hydrogen separation membranes. Journal of Membrane Science, 2016, 497, 270-281.	4.1	7
28988	First-principles study on the magnetic and half-metallic properties of the Heusler alloy Ti 2 CoSn (110) surface. Surface Science, 2016, 644, 109-112.	0.8	9
28989	Exfoliating biocompatible ferromagnetic Cr-trihalide monolayers. Physical Chemistry Chemical Physics, 2016, 18, 8777-8784.	1.3	273

#	Article	IF	Citations
28990	A First-Principles Theoretical Study on the Thermoelectric Properties of the Compound Cu5AlSn2S8. Journal of Electronic Materials, 2016, 45, 1453-1458.	1.0	6
28991	Solid solution strengthening of hexagonal titanium alloys: Restoring forces and stacking faults calculated from first principles. Acta Materialia, 2016, 102, 304-314.	3.8	113
28992	Interfacial insight in multi-junction metal oxide photoanodes for water-splitting applications. Nano Energy, 2016, 19, 415-427.	8.2	45
28993	The size-dependent site composition of FCC cobalt nanocrystals. Catalysis Today, 2016, 261, 48-59.	2.2	123
28994	Molecular entrapment of volatile organic compounds (VOCs) by electrospun cyclodextrin nanofibers. Chemosphere, 2016, 144, 736-744.	4.2	75
28995	Initial oxidation of Cr 2 Nb (1 1 1) surface: A density functional study. Computational Materials Science, 2016, 111, 7-11.	1.4	2
28996	TiC₂: a new two-dimensional sheet beyond MXenes. Nanoscale, 2016, 8, 233-242.	2.8	161
28997	Facile synthesis of silver@carbon nanocable-supported platinum nanoparticles as high-performing electrocatalysts for glycerol oxidation in direct glycerol fuel cells. Green Chemistry, 2016, 18, 386-391.	4.6	23
28998	Morphology control of K2O promoter on HÃgg carbide (Ï‡-Fe5C2) under Fischerâ€“Tropsch synthesis condition. Catalysis Today, 2016, 261, 93-100.	2.2	35
28999	Room-Temperature Magnetism of Ceria Nanocubes by Inductively Transferring Electrons to Ce Atoms from Nearby Oxygen Vacancy. Nano-Micro Letters, 2016, 8, 13-19.	14.4	23
29000	Adsorption of prototypical amino acids on silica: Influence of the pre-adsorbed water multilayer. Surface Science, 2016, 646, 239-246.	0.8	10
29001	Extending the cluster scaling technique to ruthenium clusters with hcp structures. Surface Science, 2016, 643, 156-163.	0.8	10
29002	CO adsorption over Pd nanoparticles: A general framework for IR simulations on nanoparticles. Surface Science, 2016, 646, 210-220.	0.8	65
29003	Exploring pure and RE co-doped (Eu3+, Tb3+ and Dy3+) gadolinium scandate: Luminescence behaviour and dynamics of energy transfer. Chemical Engineering Journal, 2016, 283, 114-126.	6.6	51
29004	Ab initio prediction of giant magnetostriction and spin-reorientation in strained Au/FeCo/MgO heterostructure. Journal of Magnetism and Magnetic Materials, 2016, 400, 262-265.	1.0	1
29005	Reaction mechanism of methyl nitrite dissociation during co catalytic coupling to dimethyl oxalate: A density functional theory study. Chinese Journal of Chemical Engineering, 2016, 24, 132-139.	1.7	19
29006	Quantum dynamics of polyatomic dissociative chemisorption on transition metal surfaces: mode specificity and bond selectivity. Chemical Society Reviews, 2016, 45, 3621-3640.	18.7	140
29007	Tailoring physical properties of graphene: Effects of hydrogenation, oxidation, and grain boundaries by atomistic simulations. Computational Materials Science, 2016, 112, 527-546.	1.4	14

#	Article	IF	Citations
29008	Organic linkers on oxide surfaces: Adsorption and chemical bonding of phthalic anhydride on MgO(100). Surface Science, 2016, 646, 90-100.	0.8	7
29009	Understanding the structure of salicyl hydrazone metallocomplexes: crystal structure, AIM and Hirshfeld surface analysis of trichloro-(N-salicylidenebenzoylhydrazinato-N,O,Oâ€²)-tin(IV). Structural Chemistry, 2016, 27, 25-36.	1.0	6
29010	Composition, structure and stability of surfaces formed by Ni deposition on Pd(111). Surface Science, 2016, 646, 56-64.	0.8	7
29011	Synthesis, crystal structure, spectral characterization, and theoretical study of glycolato peroxido complexes of vanadium(V). Structural Chemistry, 2016, 27, 605-615.	1.0	5
29012	Enhanced Electrical Activation in In-Implanted Si_{0.35}Ge_{0.65} by C Co-Doping. Materials Research Letters, 2017, 5, 29-34.	4.1	1
29013	Electrochemical synthesis of ammonia via Mars-van Krevelen mechanism on the (111) facets of group IIIâ€“VII transition metal mononitrides. Catalysis Today, 2017, 286, 78-84.	2.2	117
29014	Surface composition changes of CuNi-ZrO2 during methane decomposition: An operando NAP-XPS and density functional study. Catalysis Today, 2017, 283, 134-143.	2.2	48
29015	First Principles Calculations of Palladium Nanoparticle XANES Spectra. Topics in Catalysis, 2017, 60, 283-288.	1.3	28
29016	Exploring structure and reactivity of Cu sites in functionalized UiO-67 MOFs. Catalysis Today, 2017, 283, 89-103.	2.2	50
29017	Periodic density functional theory study of the highâ€pressure behavior of crystalline 7,2â€²â€anhydroâ€Î²â€<scp>d</scp>â€arabinosylorotidine. Journal of Physical Organic Chemistry, 2017, 30, e3590.	0.9	7
29018	Giant Anisotropic Raman Response of Encapsulated Ultrathin Black Phosphorus by Uniaxial Strain. Advanced Functional Materials, 2017, 27, 1600986.	7.8	100
29019	Photocatalytic hydrogen production over solid solutions between BiFeO 3 and SrTiO 3. Applied Surface Science, 2017, 391, 535-541.	3.1	58
29020	Synthesis of Mn-doped ZnS microspheres with enhanced visible light photocatalytic activity. Applied Surface Science, 2017, 391, 557-564.	3.1	76
29021	Endurance and Cycle-to-cycle Uniformity Improvement in Tri-Layered CeO2/Ti/CeO2 Resistive Switching Devices by Changing Top Electrode Material. Scientific Reports, 2017, 7, 39539.	1.6	81
29022	A density functional theory based approach for predicting melting points of ionic liquids. Physical Chemistry Chemical Physics, 2017, 19, 4114-4124.	1.3	22
29023	Highly-dispersive spin gapless semiconductors in rare-earth-element contained quaternary Heusler compounds. Journal Physics D: Applied Physics, 2017, 50, 105003.	1.3	14
29024	The Structure of Glycine Dihydrate: Implications for the Crystallization of Glycine from Solution and Its Structure in Outer Space. Angewandte Chemie - International Edition, 2017, 56, 2030-2034.	7.2	35
29025	Effects of applied strain and electric field on small-molecule sensing by stanene monolayers. Journal of Materials Science, 2017, 52, 5083-5096.	1.7	36

#	Article	IF	Citations
29026	Effects of iron and chromium on the dynamic properties of oxygen in liquid leadâ€“bismuth eutectic alloy. Corrosion Science, 2017, 118, 1-11.	3.0	20
29027	Syntheses, Crystal Structures, and Optical and Photocatalytic Properties of Four Small-Amine-Molecule-Directed Mâ€“Snâ€“Q (M = Zn, Ag; Q = S, Se) Compounds. Crystal Growth and Design, 2017, 17, 1235-1244.	1.4	38
29028	Kinetics on NiZn Bimetallic Catalysts for Hydrogen Evolution via Selective Dehydrogenation of Methylcyclohexane to Toluene. ACS Catalysis, 2017, 7, 1592-1600.	5.5	59
29029	Chemical Insights into the Design and Development of Face-Centered Cubic Ruthenium Catalysts for Fischerâ€“Tropsch Synthesis. Journal of the American Chemical Society, 2017, 139, 2267-2276.	6.6	147
29030	Adatom surface diffusion of catalytic metals on the anatase TiO₂(101) surface. Physical Chemistry Chemical Physics, 2017, 19, 4541-4552.	1.3	28
29031	Electromechanical scale-bridging model for piezoelectric nanostructures. Applied Physics Letters, 2017, 110, 013104.	1.5	4
29032	Uranium Redox Transformations after U(VI) Coprecipitation with Magnetite Nanoparticles. Environmental Science & Technology, 2017, 51, 2217-2225.	4.6	112
29033	Theoretical Investigation of the Interfaces and Mechanisms of Induced Spin Polarization of 1D Narrow Zigzag Graphene- and h-BN Nanoribbons on a SrO-Terminated LSMO(001) Surface. Journal of Physical Chemistry A, 2017, 121, 680-689.	1.1	1
29034	Oxygen Binding to Active Sites of Feâ€“Nâ€“C ORR Electrocatalysts Observed by Ambient-Pressure XPS. Journal of Physical Chemistry C, 2017, 121, 2836-2843.	1.5	135
29035	Electronic, Optical, and Mechanical Properties of Diamond Nanowires Encapsulated in Carbon Nanotubes: A First-Principles View. Journal of Physical Chemistry C, 2017, 121, 3661-3672.	1.5	3
29036	Double-Layer Graphene Outperforming Monolayer as Catalyst on Silicon Photocathode for Hydrogen Production. ACS Applied Materials & Interfaces, 2017, 9, 3570-3580.	4.0	20
29037	NASICON-Type Mg_{0.5}Ti₂(PO₄)₃ Negative Electrode Material Exhibits Different Electrochemical Energy Storage Mechanisms in Na-Ion and Li-Ion Batteries. ACS Applied Materials & Interfaces, 2017, 9, 4709-4718.	4.0	47
29038	Mechanochemistry of One-Dimensional Boron: Structural and Electronic Transitions. Journal of the American Chemical Society, 2017, 139, 2111-2117.	6.6	41
29039	Semi-Dirac semimetal in silicene oxide. Physical Chemistry Chemical Physics, 2017, 19, 3820-3825.	1.3	40
29040	Achieving tunable sensitivity in composite high-energy density materials. AIP Conference Proceedings, 2017, , .	0.3	0
29041	Equation of state and transport properties of warm dense aluminum by ab initio and chemical model simulations. Physics of Plasmas, 2017, 24, .	0.7	8
29042	The potential for fast van der Waals computations for layered materials using a Lifshitz model. 2D Materials, 2017, 4, 025005.	2.0	6
29043	Effects of boron on the mechanical properties of the TiAlâ€“Ti3AlÂalloy:ÂA first-principles investigation. Modern Physics Letters B, 2017, 31, 1750002.	1.0	0

#	Article	IF	Citations
29044	Magnetic Moments and Ordered States in Pyrochlore Iridates Nd₂Ir₂O₇ and Sm₂Ir₂O₇ Studied by Muon-Spin Relaxation. Journal of the Physical Society of Japan, 2017, 86, 024705.	0.7	15
29045	Firstâ€principle calculations of optical properties of monolayer arsenene and antimonene allotropes. Annalen Der Physik, 2017, 529, 1600152.	0.9	129
29046	Organisation von Metalloxidâ€NanowÃ¼rfeln durch Hydroxylierung. Angewandte Chemie, 2017, 129, 1428-1432.	1.6	0
29047	Sc and Nb dopants in SrCoO3 modulate electronic and vacancy structures for improved water splitting and SOFC cathodes. Energy Storage Materials, 2017, 9, 229-234.	9.5	31
29048	Investigations on molybdenum dinitride as a promising anode material for Na-ion batteries from first-principle calculations. Journal of Alloys and Compounds, 2017, 701, 875-881.	2.8	17
29049	Effects of intrinsic defects on the electronic structure and magnetic properties of CoFe 2 O 4 : A first-principles study. Journal of Magnetism and Magnetic Materials, 2017, 429, 263-269.	1.0	20
29050	Using the 18-Electron Rule To Understand the Nominal 19-Electron Half-Heusler NbCoSb with Nb Vacancies. Chemistry of Materials, 2017, 29, 1210-1217.	3.2	93
29051	Exploring Structural Diversity and Fluxionality of Pt_n (n = 10â€“13) Clusters from First-Principles. Journal of Physical Chemistry C, 2017, 121, 10796-10802.	1.5	42
29052	Electrocatalyst Design for Direct Borohydride Oxidation Guided by First Principles. Journal of Physical Chemistry C, 2017, 121, 2872-2881.	1.5	13
29053	Effects of Defects on Photocatalytic Activity of Hydrogen-Treated Titanium Oxide Nanobelts. ACS Catalysis, 2017, 7, 1742-1748.	5.5	173
29054	Improper electric polarization in simple perovskite oxides with two magnetic sublattices. Nature Communications, 2017, 8, 14025.	5.8	53
29055	Decomposition mechanisms in metal borohydrides and their ammoniates. Journal of Materials Chemistry A, 2017, 5, 4084-4092.	5.2	15
29056	Vacancies at the Cuâ€“Nb semicoherent interface. Modelling and Simulation in Materials Science and Engineering, 2017, 25, 025012.	0.8	5
29057	Potential of Titania-covered Ag Catalysts for NO_x Reduction: A DFT Study. Chemistry Letters, 2017, 46, 456-459.	0.7	15
29058	Excitons in scintillator materials: Optical properties and electron-energy loss spectra of NaI, LaBr₃, BaI₂, and SrI₂. Journal of Materials Research, 2017, 32, 56-63.	1.2	6
29059	Calcium as a nonradiative recombination center in InGaN. Applied Physics Express, 2017, 10, 021001.	1.1	19
29060	Ultrasmall CuCo₂S₄ Nanocrystals: Allâ€inâ€One Theragnosis Nanoplatform with Magnetic Resonance/Nearâ€Infrared Imaging for Efficiently Photothermal Therapy of Tumors. Advanced Functional Materials, 2017, 27, 1606218.	7.8	106
29061	Chemisorption of a Strained but Flexible Molecule: Cyclooctyne on Si(001). Chemistry - A European Journal, 2017, 23, 5459-5466.	1.7	20

#	Article	IF	Citations
29062	Potassium promotion on CO hydrogenation on the Ï‡-Fe 5 C 2 (111) surface with carbon vacancy. Applied Catalysis A: General, 2017, 534, 22-29.	2.2	16
29063	A simulation study of the distribution of Î²â€² precipitates in a crept Mg-Gd-Zr alloy. Computational Materials Science, 2017, 130, 152-164.	1.4	15
29064	The effects of metalloid elements (P, C, B) on the properties of Co-based amorphous alloys studied by ab initio molecular dynamics simulations. Computational Materials Science, 2017, 130, 76-83.	1.4	6
29065	Phase transformations, detwinning and superelasticity of shape-memory NiTi from MEAM with practical capability. Computational Materials Science, 2017, 130, 138-143.	1.4	24
29066	Atomic and electronic structures of thermochromic VO2 with Sb-doping. Computational Materials Science, 2017, 130, 103-108.	1.4	12
29067	Prediction of a new ice clathrate with record low density: A potential candidate as ice XIX in guest-free form. Chemical Physics Letters, 2017, 671, 186-191.	1.2	36
29068	Synthesis of Durable Small-sized Bilayer Au@Pt Nanoparticles for High Performance PEMFC Catalysts. Electrochimica Acta, 2017, 228, 389-397.	2.6	18
29069	The effects of interstitial impurities on the mechanical properties of vanadium alloys: A first-principles study. Journal of Alloys and Compounds, 2017, 701, 975-980.	2.8	17
29070	First principles electronic structure and magnetic properties of inverse Heusler alloys X 2 YZ(X=Cr;) Tj ETQq0 0 0 rgBT /Overlock 10 Tf 50	1.0	27
29071	Structural and magnetic studies on (Fe, Cu) co-doped ZnO nanocrystals. Journal of Physics and Chemistry of Solids, 2017, 104, 198-206.	1.9	11
29072	AgBiI₄ as a Lead-Free Solar Absorber with Potential Application in Photovoltaics. Chemistry of Materials, 2017, 29, 1538-1549.	3.2	102
29073	Nanoscale Voltage Enhancement at Cathode Interfaces in Li-Ion Batteries. Chemistry of Materials, 2017, 29, 1218-1229.	3.2	5
29074	Dual Substitution Strategy to Enhance Li⁺ Ionic Conductivity in Li₇La₃Zr₂O₁₂ Solid Electrolyte. Chemistry of Materials, 2017, 29, 1769-1778.	3.2	169
29075	Ab Initio Thermodynamics of Surface Oxide Structures under Controlled Growth Conditions. Journal of Physical Chemistry C, 2017, 121, 2228-2233.	1.5	11
29076	Computational Search for Novel Hard Chromium-Based Materials. Journal of Physical Chemistry Letters, 2017, 8, 755-764.	2.1	62
29077	High-Dimensional Atomistic Neural Network Potentials for Moleculeâ€“Surface Interactions: HCl Scattering from Au(111). Journal of Physical Chemistry Letters, 2017, 8, 666-672.	2.1	94
29078	Hybridization of Zinc Oxide Tetrapods for Selective Gas Sensing Applications. ACS Applied Materials & Interfaces, 2017, 9, 4084-4099.	4.0	135
29079	Facile Synthesis of Vanadium-Doped Ni₃S₂ Nanowire Arrays as Active Electrocatalyst for Hydrogen Evolution Reaction. ACS Applied Materials & Interfaces, 2017, 9, 5959-5967.	4.0	196

#	Article	IF	Citations
29080	Electrochemical Window of the Li-Ion Solid Electrolyte Li₇La₃Zr₂O₁₂. ACS Energy Letters, 2017, 2, 462-468.	8.8	255
29081	Strong Adlayerâ€"Substrate Interactions â€œBreakâ€•the Patching Growth of h-BN onto Graphene on Re(0001). ACS Nano, 2017, 11, 1807-1815.	7.3	27
29082	Chemical Functionalization of Pentagermanene Leads to Stabilization and Tunable Electronic Properties by External Tensile Strain. ACS Omega, 2017, 2, 171-180.	1.6	15
29083	Design of Lead-Free Inorganic Halide Perovskites for Solar Cells via Cation-Transmutation. Journal of the American Chemical Society, 2017, 139, 2630-2638.	6.6	714
29084	Doping with Graphitic Nitrogen Triggers Ferromagnetism in Graphene. Journal of the American Chemical Society, 2017, 139, 3171-3180.	6.6	202
29085	Resonant level-induced high thermoelectric response in indium-doped GeTe. NPG Asia Materials, 2017, 9, e343-e343.	3.8	170
29086	Anisotropic hydrogen diffusion in Î±-Zr and Zircaloy predicted by accelerated kinetic Monte Carlo simulations. Scientific Reports, 2017, 7, 41033.	1.6	33
29087	Structural metatransition of energetically tangled crystalline phases. Physical Chemistry Chemical Physics, 2017, 19, 4560-4566.	1.3	23
29088	Centrosymmetric to noncentrosymmetric structural transformation of new quaternary selenides induced by isolated dimeric [Sn₂Se₄] units: from Ba₈Ga₂Sn₇Se₁₈to Ba₁₀Ga₂Sn₉Se₂₂. RSC Advances, 2017, 7, 8082-8089.	1.7	9
29089	Modulation of silicene properties by AsSb with van der Waals interaction. RSC Advances, 2017, 7, 5827-5835.	1.7	10
29090	Screening novel candidates for mid-IR nonlinear optical materials from I₃â€"Vâ€"VI₄compounds. Journal of Materials Chemistry C, 2017, 5, 1963-1972.	2.7	32
29091	Evolution of structural and magnetic properties in LaxCe2-xCo16Ti for 0Ââ‰¤xÂâ‰¤Â2. Journal of Alloys and Compounds, 2017, 695, 2266-2272.	2.8	5
29092	Intrasurface electron transition contribution to energy of adsorption of silicon at the SiC(0001) surface â€" A density functional theory (DFT) study. Journal of Crystal Growth, 2017, 468, 870-873.	0.7	2
29093	First principles investigation of SiC/AlGaN(0001) band offset. Journal of Crystal Growth, 2017, 468, 758-760.	0.7	2
29094	The direct exchange mechanism of induced spin polarization of low-dimensional Ï€-conjugated carbon- and h-BN fragments at LSMO(001) MnO-terminated interfaces. Journal of Magnetism and Magnetic Materials, 2017, 440, 23-29.	1.0	2
29095	Ab-initio molecular dynamics study of lanthanides in liquid sodium. Journal of Nuclear Materials, 2017, 484, 98-102.	1.3	12
29096	Fission gas in thoria. Journal of Nuclear Materials, 2017, 485, 47-55.	1.3	13
29097	Synthesis, crystal structure and electronic structure of the binary phase Rh2Cd5. Journal of Solid State Chemistry, 2017, 246, 302-308.	1.4	5

#	Article	IF	Citations
29098	Waved graphene: Unique structure for the adsorption of small molecules. Materials Chemistry and Physics, 2017, 189, 111-117.	2.0	22
29099	Ab initio study of He-He interactions in homogeneous electron gas. Nuclear Instruments & Methods in Physics Research B, 2017, 393, 140-143.	0.6	2
29100	A theoretical study on the charge transport properties of DNA. Organic Electronics, 2017, 42, 244-255.	1.4	7
29101	Raman active high energy excitations in URu2Si2. Physica B: Condensed Matter, 2017, 506, 19-22.	1.3	4
29102	Adsorption of C 20 on two-dimensional materials. Physica E: Low-Dimensional Systems and Nanostructures, 2017, 87, 166-170.	1.3	2
29103	n s 2 n p 4 (n Â=Â4, 5) lone pair triplets whirling in M*F 2 E 3 (M*Â=ÂKr, Xe): Stereochemistry and ab initio analyses. Solid State Sciences, 2017, 64, 114-124.	1.5	5
29104	Lattice dynamics and thermal conductivity of cesium chloride via first-principles investigation. Solid State Communications, 2017, 254, 31-36.	0.9	13
29105	Effect of intrinsic point defects on ferroelectric polarization behavior of <mml:math xmlns:mml="http://www.w3.org/1998/Math/MathML"><mml:msub><mml:mi>SrTiO</mml:mi><mml:mn>3</mml:mn></mml:msub><m Physical Review B, 2017, 95, .	3.7	37
29106	Intralayered Ostwald Ripening to Ultrathin Nanomesh Catalyst with Robust Oxygenâ€Evolving Performance. Advanced Materials, 2017, 29, 1604765.	11.1	283
29107	Electronic characteristics of p-type transparent SnO monolayer with high carrier mobility. Applied Surface Science, 2017, 401, 114-119.	3.1	36
29108	Oxygen-Vacancy-Induced Midgap States Responsible for the Fluorescence and the Long-Lasting Phosphorescence of the Inverse Spinel Mg(Mg,Sn)O₄. Chemistry of Materials, 2017, 29, 1069-1075.	3.2	36
29109	Polymorphism of Two-Dimensional Halogen Bonded Supramolecular Networks on a Graphene/Iridium(111) Surface. Journal of Physical Chemistry C, 2017, 121, 2201-2210.	1.5	13
29110	Titanium Trisulfide Monolayer as a Potential Thermoelectric Material: A First-Principles-Based Boltzmann Transport Study. ACS Applied Materials & Interfaces, 2017, 9, 2509-2515.	4.0	99
29111	De Novo Discovery of [Hdabco]BF₄ Molecular Ferroelectric Thin Film for Nonvolatile Low-Voltage Memories. Journal of the American Chemical Society, 2017, 139, 1319-1324.	6.6	88
29112	Hardness of cubic solid solutions. Scientific Reports, 2017, 7, 40276.	1.6	14
29113	Electronic, magnetic and spectroscopic properties of doped Mn_(1â^'x)A_xWO₄(Aâ€‰â€‰=â€‰â€‰Co, Cu, Ni and Fe) multiferroic: an experimental and DFT study. Journal of Physics Condensed Matter, 2017, 29, 075901.	2.7	17
29114	Ab initiostudy of the nature and stability of the defects and multi-vacancies in TaN. Comparison with TiN. Journal of Physics Condensed Matter, 2017, 29, 075501.	0.7	3
29115	Strain-engineered optoelectronic properties of 2D transition metal dichalcogenide lateral heterostructures. 2D Materials, 2017, 4, 021016.	2.0	72

#	Article	IF	Citations
29116	Magnetic properties of bilayer <mml:math xmlns:mml="http://www.w3.org/1998/Math/MathML"><mml:mrow><mml:msub><mml:mi mathvariant="bold">Sr</mml:mi><mml:mn>3</mml:mn></mml:msub><mml:msub><mml:mi mathvariant="bold">Ir</mml:mi><mml:mn>2</mml:mn></mml:msub><mml:msub><mml:mi mathvariant="bold">O</mml:mi><mml:mn>7</mml:mn></mml:msub></mml:mrow></mml:math> : Role of epitaxial strain and oxygen vacancies. Physical Review B, 2017, 95, .	1.1	15
29117	Principles and simulations of high-resolution STM imaging with a flexible tip apex. Physical Review B, 2017, 95, .	1.1	76
29118	Effects of Contact Placement and Intra/Interlayer Interaction in Current Distribution of Black Phosphorus Sub-10-nm FET. IEEE Transactions on Electron Devices, 2017, 64, 579-586.	1.6	5
29119	Theoretical insights into the activation of O2 by Pt single atom and Pt4 nanocluster on functionalized graphene support: Critical role of Pt positive polarized charges. Carbon, 2017, 115, 11-17.	5.4	125
29120	Reduction of HCHO with OHâ˜ on Pt loading anatase TiO2 (001) surface: A DFT calculation. Catalysis Communications, 2017, 92, 23-26.	1.6	18
29121	Anomalous packing state in Ce-Ga-Cu bulk metallic glasses. Intermetallics, 2017, 84, 25-29.	1.8	16
29122	New method for calculations of nanostructure kinetic stability at high temperature. Journal of Magnetism and Magnetic Materials, 2017, 440, 167-170.	1.0	1
29123	A First-Principles Study on Proton Conductivity of Acceptor-Doped Tin Pyrophosphate. Journal of Physical Chemistry C, 2017, 121, 1578-1584.	1.5	11
29124	Discovery of high-performance low-cost n-type Mg3Sb2-based thermoelectric materials with multi-valley conduction bands. Nature Communications, 2017, 8, 13901.	5.8	415
29125	Complex Roles of Solution Chemistry on Graphene Oxide Coagulation onto Titanium Dioxide: Batch Experiments, Spectroscopy Analysis and Theoretical Calculation. Scientific Reports, 2017, 7, 39625.	1.6	27
29126	Intrinsic Origins of Crack Generation in Ni-rich LiNi0.8Co0.1Mn0.1O2 Layered Oxide Cathode Material. Scientific Reports, 2017, 7, 39669.	1.6	225
29127	Engineering magnetic anisotropy and magnetization switching in multilayers by strain. Physical Chemistry Chemical Physics, 2017, 19, 4125-4130.	1.3	7
29128	First-principles study of the initial oxygen reduction reaction on stoichiometric and reduced CeO₂ (111) surfaces as a cathode catalyst for lithiumâ€“oxygen batteries. Journal of Materials Chemistry A, 2017, 5, 3320-3329.	5.2	35
29129	Weak d ⁰ ferromagnetism: Zn vacancy condensation in ZnS nanocrystals. Journal of Physics Condensed Matter, 2017, 29, 025803.	0.7	3
29130	Adsorption-induced surface stress on ac(4â€‰â€‰Ã—â€‰â€‰2) adatom surface by an alkanethiol. Materials Research Express, 2017, 4, 015020.	0.8	1
29131	Oxygen evolution from olivine <mml:math xmlns:mml="http://www.w3.org/1998/Math/MathML"><mml:mrow><mml:mi mathvariant="normal">M</mml:mi><mml:msub><mml:mi mathvariant="normal">n</mml:mi><mml:mrow><mml:mn>1</mml:mn><mml:mo>â˜’</mml:mo><mml:mi>x</mml:mi></mml:mrow></mml:msub><mml:mi mathvariant="normal">x</mml:mi></mml:msub><mml:mi mathvariant="normal">P</mml:mi><mml:msub><mml:mi mathvariant="normal">O</mml:mi><mml:mn>4</mml:mn></mml:msub></mml:mrow></mml:math>	1.1	3
29132	Morphology evolution and nanostructure of chemical looping transition metal oxide materials upon redox processes. Acta Materialia, 2017, 124, 568-578.	3.8	32
29133	Grown-in beryllium diffusion in indium gallium arsenide: An ab initio, continuum theory and kinetic Monte Carlo study. Acta Materialia, 2017, 125, 455-464.	3.8	3

#	Article	IF	Citations
29134	Local Bi ordering in MOVPE grown Ga(As,Bi) investigated by high resolution scanning transmission electron microscopy. Applied Materials Today, 2017, 6, 22-28.	2.3	21
29135	CO oxidation on PdO catalysts with perfect and defective rutile-TiO2 as supports: Elucidating the role of oxygen vacancy in support by DFT calculations. Applied Surface Science, 2017, 401, 49-56.	3.1	9
29136	Ferromagnetic orderings in Co Cu Zn1â^'(+)O by GGA and GGA+U formalisms within density functional theory. Computational Materials Science, 2017, 126, 344-350.	1.4	5
29137	Computational investigation of interstitial neon diffusion in pure hematite. Computational Materials Science, 2017, 128, 67-74.	1.4	11
29138	Influence of oxygen vacancy on electric structure and optical properties of pure and N-doped Sr2M2O7(M = Nb, Ta). Computational Materials Science, 2017, 127, 180-186.	1.4	6
29139	Band offset engineering in C-functionalized boronitrene. Computational Materials Science, 2017, 128, 373-378.	1.4	9
29140	Ab initio insight into graphene nanofibers to destabilize hydrazine borane for hydrogen release. Chemical Physics Letters, 2017, 669, 110-114.	1.2	3
29141	Data files for ab initio calculations of the lattice parameter and elastic stiffness coefficients of bcc Fe with solutes. Data in Brief, 2017, 10, 147-150.	0.5	4
29142	Comments on â€œGeometry and fast diffusion of AlCl 4 cluster intercalated in graphite [Electrochim. Acta 195 (2016) 158â€“165]â€• Electrochimica Acta, 2017, 223, 135-136.	2.6	16
29143	Influence of anions on the adsorption of uranyl on hydroxylated Î±-SiO2(001): A first-principles study. Green Energy and Environment, 2017, 2, 30-41.	4.7	13
29144	Versatile Optimization of Chemical Ordering in Bimetallic Nanoparticles. Journal of Physical Chemistry C, 2017, 121, 10803-10808.	1.5	29
29145	First-principles study of tantalum-arsenic binary compounds. Journal of Applied Physics, 2017, 121, 015101.	1.1	3
29146	Localized defect states in MoS₂monolayers: Electronic and optical properties. Physica Status Solidi (B): Basic Research, 2017, 254, 1600645.	0.7	30
29147	A general model for thermal and electrical conductivity of binary metallic systems. Acta Materialia, 2017, 126, 272-279.	3.8	17
29148	XAS and XES studies of carbonate and bicarbonate ions in aqueous solutions. Journal of Electron Spectroscopy and Related Phenomena, 2017, 220, 96-100.	0.8	3
29149	Impact of non-metal dopants on band-gap engineering and photocatalytic ability of Î»-Ta2O5 from a hybrid density functional study. Journal of Alloys and Compounds, 2017, 700, 1-11.	2.8	7
29150	The Tynode: A new vacuum electron multiplier. Nuclear Instruments and Methods in Physics Research, Section A: Accelerators, Spectrometers, Detectors and Associated Equipment, 2017, 847, 148-161.	0.7	14
29151	DFT study of the molecular and crystal structure and vibrational analysis of cisplatin. Spectrochimica Acta - Part A: Molecular and Biomolecular Spectroscopy, 2017, 176, 58-66.	2.0	28

#	Article	IF	Citations
29152	Modular Design with 2D Topological-Insulator Building Blocks: Optimized Synthesis and Crystal Growth and Crystal and Electronic Structures of Bi_xTeI (x = 2, 3). Chemistry of Materials, 2017, 29, 1321-1337.	3.2	23
29153	DFT Global Optimization of Gas-Phase Subnanometer Ruâ€“Pt Clusters. Journal of Physical Chemistry C, 2017, 121, 10773-10780.	1.5	44
29154	Vacancies and Vacancy-Mediated Self Diffusion in Cr₂O₃: A First-Principles Study. Journal of Physical Chemistry C, 2017, 121, 1817-1831.	1.5	24
29155	High Performance Electrocatalytic Reaction of Hydrogen and Oxygen on Ruthenium Nanoclusters. ACS Applied Materials & Interfaces, 2017, 9, 3785-3791.	4.0	108
29156	Activating lattice oxygen redox reactions in metal oxides to catalyse oxygen evolution. Nature Chemistry, 2017, 9, 457-465.	6.6	1,409
29157	Asymmetric interaction of point defects and heterophase interfaces in ZrN/TaN multilayered nanofilms. Scientific Reports, 2017, 7, 40044.	1.6	9
29158	Layered structure of the near-surface region of oxidized chalcopyrite (CuFeS₂): hard X-ray photoelectron spectroscopy, X-ray absorption spectroscopy and DFT+U studies. Physical Chemistry Chemical Physics, 2017, 19, 2749-2759.	1.3	21
29159	Engineering the electronic and optoelectronic properties of InX (X = S, Se, Te) monolayers via strain. Physical Chemistry Chemical Physics, 2017, 19, 4855-4860.	1.3	71
29160	A comparative study of hydrogen evolution reaction on pseudo-monolayer WS₂ and PtS₂: insights based on the density functional theory. Catalysis Science and Technology, 2017, 7, 687-692.	2.1	51
29161	Predicting point defect equilibria across oxide hetero-interfaces: model system of ZrO₂/Cr₂O₃. Physical Chemistry Chemical Physics, 2017, 19, 3869-3883.	1.3	28
29162	Electric field tunable half-metallic characteristic at Fe₃O₄/BaTiO₃ interfaces. Physical Chemistry Chemical Physics, 2017, 19, 4330-4336.	1.3	4
29163	Computational prediction of high thermoelectric performance in p-type half-Heusler compounds with low band effective mass. Physical Chemistry Chemical Physics, 2017, 19, 4411-4417.	1.3	88
29164	B₄₀cluster stability, reactivity, and its planar structural precursor. Nanoscale, 2017, 9, 1805-1810.	2.8	33
29165	All-carbon-based porous topological semimetal for Li-ion battery anode material. Proceedings of the National Academy of Sciences of the United States of America, 2017, 114, 651-656.	3.3	125
29166	The role of the alkali and chalcogen atoms on the stability of the layered chalcogenide $mathbf{{{A}_{2}}{{M}^{II}}M_{3}^{,IV}{{Q}_{8}}}$ (Aâ€‰â€‰=â€‰â€‰alkali-metal; Mâ€‰â€‰=â€‰â€‰metal-cations; Qâ€ compounds: a density functional theory investigation within van der Waals corrections. Journal of Physics Condensed Matter, 2017, 29, 035402.	0.7	7
29167	Optical and fundamental band gaps disparity in transparent conducting oxides: new findings for the $mathbf{I}{{mathbf{n}}_{mathbf{2}}}{{mathbf{O}}_{mathbf{3}}}$ and $mathbf{S}{{mathbf{n}}_{{}}}{{mathbf{O}}_{mathbf{2}}}$ systems. Journal of Physics Condensed Matter, 2017, 29, 085501.	0.7	9
29168	Effects of K-Doping on Thermoelectric Properties of Bi1â^'x K x CuOTe. Journal of Electronic Materials, 2017, 46, 2717-2723.	1.0	7
29169	Oxygen-suppressed selective growth of monolayer hexagonal boron nitride on copper twin crystals. Nano Research, 2017, 10, 826-833.	5.8	12

#	Article	IF	Citations
29170	Unintentional doping effects in black phosphorus by native vacancies in h-BN supporting layer. Applied Surface Science, 2017, 402, 175-181.	3.1	14
29171	Direct observation of grain boundaries in chemical vapor deposited graphene. Carbon, 2017, 115, 147-153.	5.4	22
29172	An interatomic potential for simulation of Zr-Nb system. Computational Materials Science, 2017, 129, 259-272.	1.4	38
29173	Spin filter type transformation in Sn-phthalocyanine. Organic Electronics, 2017, 43, 47-54.	1.4	7
29174	Hydrogen-Bond Bridged Water Oxidation on {001} Surfaces of Anatase TiO₂. Journal of Physical Chemistry C, 2017, 121, 2251-2257.	1.5	50
29175	High Defect Tolerance in Lead Halide Perovskite CsPbBr₃. Journal of Physical Chemistry Letters, 2017, 8, 489-493.	2.1	899
29176	Fe on Sb(111): Potential Two-Dimensional Ferromagnetic Superstructures. ACS Nano, 2017, 11, 2143-2149.	7.3	9
29177	Adsorbate-induced lattice deformation in IRMOF-74 series. Nature Communications, 2017, 8, 13945.	5.8	34
29178	Differentiation of the Câ€“O and Câ€“C bond scission mechanisms of 1-hexadecanol on Pt(111) and Ru(0001): a first principles analysis. Catalysis Science and Technology, 2017, 7, 743-760.	2.1	18
29179	Tuning chemical compositions of bimetallic AuPd catalysts for selective catalytic hydrogenation of halogenated quinolines. Journal of Materials Chemistry A, 2017, 5, 3260-3266.	5.2	40
29180	Na_{3+x}M_xP_{1â^'x}S₄(M = Ge⁴⁺,) Tj ETQq0 0 0 rgBT /Overlock 10 Tf 50 3 Na_{2+2Î´}Fe_{2â^'Î´}(SO₄)₃ | Na_{3+x}M_xP_{1â^'x}S<su Journal of Materials Chemistry A, 2017, 5, 3377-3388.	5.2	62
29181	Tetragonal-structured anisotropic 2D metal nitride monolayers and their halides with versatile promises in energy storage and conversion. Journal of Materials Chemistry A, 2017, 5, 2870-2875.	5.2	42
29182	Fermi-level pinning and intrinsic surface states of Al1â^'xInxN(101Â¯) surfaces. Applied Physics Letters, 2017, 110, .	1.5	5
29183	Domain walls and ferroelectric reversal in corundum derivatives. Physical Review B, 2017, 95, .	1.1	14
29184	Large-scale all-electron density functional theory calculations using an enriched finite-element basis. Physical Review B, 2017, 95, .	1.1	37
29185	Atomistic Modelingâ€Based Design of Novel Materials. Advanced Engineering Materials, 2017, 19, 1600688.	1.6	14
29186	Elasticity, Flexibility, and Ideal Strength of Borophenes. Advanced Functional Materials, 2017, 27, 1605059.	7.8	237
29187	Ruddlesden-Popper compounds in the double-perovskite family Sr2FeTaO6(SrO)n (n = 0, 1 and 2) and their photocatalytic properties. Applied Catalysis B: Environmental, 2017, 206, 35-43.	10.8	33

#	Article	IF	Citations
29188	Chemically accurate simulation of dissociative chemisorption of D2 on Pt(1 1 1). Chemical Physics Letters, 2017, 683, 329-335.	1.2	37
29189	First-principles study of mechanical and thermodynamic properties of Ti-Ga intermetallic compounds. Journal of Alloys and Compounds, 2017, 700, 208-214.	2.8	17
29190	The New Semiconductor Cs₄Cu₃Bi₉S₁₇. Chemistry of Materials, 2017, 29, 1744-1751.	3.2	13
29191	Facile Syntheses of Ba₂[B₄O₇(OH)₂] and Na[B₅O₇(OH)₂](H₂O) Borate Salts Exhibiting Nonlinear Optical Activity in the Ultraviolet. Inorganic Chemistry, 2017, 56, 1340-1348.	1.9	43
29192	Performance of Cu-Alloyed Pd Single-Atom Catalyst for Semihydrogenation of Acetylene under Simulated Front-End Conditions. ACS Catalysis, 2017, 7, 1491-1500.	5.5	374
29193	Magnetocaloric Behavior in Ternary Europium Indides EuT₅In: Probing the Design Capability of First-Principles-Based Methods on the Multifaceted Magnetic Materials. Chemistry of Materials, 2017, 29, 2599-2614.	3.2	29
29194	Potential Functional Embedding Theory at the Correlated Wave Function Level. 2. Error Sources and Performance Tests. Journal of Chemical Theory and Computation, 2017, 13, 1081-1093.	2.3	16
29195	Development of a Classical Interatomic Potential for MAPbBr₃. Journal of Physical Chemistry C, 2017, 121, 3724-3733.	1.5	31
29196	Theoretical Investigation of Ta₂O₅, TaON, and Ta₃N₅: Electronic Band Structures and Absolute Band Edges. Journal of Physical Chemistry C, 2017, 121, 3241-3251.	1.5	49
29197	Modeling Segregation on AuPd(111) Surfaces with Density Functional Theory and Monte Carlo Simulations. Journal of Physical Chemistry C, 2017, 121, 3479-3487.	1.5	48
29198	Cs₂InAgCl₆: A New Lead-Free Halide Double Perovskite with Direct Band Gap. Journal of Physical Chemistry Letters, 2017, 8, 772-778.	2.1	752
29199	Revisiting CO Activation on Co Catalysts: Impact of Step and Kink Sites from DFT. ACS Catalysis, 2017, 7, 1984-1992.	5.5	64
29200	Water-evaporation-induced electricity with nanostructured carbon materials. Nature Nanotechnology, 2017, 12, 317-321.	15.6	747
29201	Catalytic behavior of metal catalysts in high-temperature RWGS reaction: In-situ FT-IR experiments and first-principles calculations. Scientific Reports, 2017, 7, 41207.	1.6	57
29202	EuNi₅InH_{1.5â^'x} (x = 0â€“1.5): hydrogen induced structural and magnetic transitions. Journal of Materials Chemistry C, 2017, 5, 2994-3006.	2.7	10
29203	Electrochemical reduction of CO₂ into CO on Cu(100): a new insight into the Câ€“O bond breaking mechanism. Chemical Communications, 2017, 53, 2594-2597.	2.2	39
29204	Ideal strength and elastic instability in single-layer 8-Pmmn borophene. RSC Advances, 2017, 7, 8654-8660.	1.7	53
29205	Thermodynamic properties and phase transitions of Î³ and liquid uranium: QMD and classical MD modeling. AIP Conference Proceedings, 2017, , .	0.3	1

#	Article	IF	Citations
29206	A first-principles model of copperâ€“boron interactions in Si: implications for the light-induced degradation of solar Si. Journal of Physics Condensed Matter, 2017, 29, 065701.	0.7	0
29207	A Theoretical Investigation on CO Oxidation by Singleâ€Atom Catalysts M₁/Î³â€Al₂O₃ (M=Pd, Fe, Co, and Ni). ChemCatChem, 2017, 9, 1222-1229.	1.8	76
29208	Multi-Cell Monte Carlo Relaxation method for predicting phase stability of alloys. Scripta Materialia, 2017, 132, 9-12.	2.6	24
29209	Ligand Influence on Local Magnetic Moments in Fe-Based Metalâ€“Organic Networks. Journal of Physical Chemistry C, 2017, 121, 4253-4260.	1.5	12
29210	Tunable Structural, Electronic, and Optical Properties of Layered Two-Dimensional C₂N and MoS₂ van der Waals Heterostructure as Photovoltaic Material. Journal of Physical Chemistry C, 2017, 121, 3654-3660.	1.5	233
29211	Comparison Studies of Interfacial Electronic and Energetic Properties of LaAlO₃/TiO₂ and TiO₂/LaAlO₃ Heterostructures from First-Principles Calculations. ACS Applied Materials & Interfaces, 2017, 9, 7682-7690.	4.0	11
29212	Influence of magnetic ordering and Jahnâ€“Teller distortion on the lithiation process of LiMn₂O₄. Physical Chemistry Chemical Physics, 2017, 19, 6481-6486.	1.3	46
29213	Tailored synthesis of nonlinear optical quaternary chalcohalides: Ba₄Ge₃S₉Cl₂, Ba₄Si₃Se₉Cl₂ and Ba₄Ge₃Se₉Cl₂. Dalton Transactions, 2017, 46, 2715-2721.	1.6	42
29214	Pressure-induced structural, magnetic and transport transitions in Sr2FeO3from first-principles. AIP Advances, 2017, 7, 055703.	0.6	0
29215	Atomic-scale imaging of few-layer black phosphorus and its reconstructed edge. Journal Physics D: Applied Physics, 2017, 50, 084003.	1.3	42
29216	Metastable phases of 2D boron sheets on Ag(1â€‰1â€‰1). Journal of Physics Condensed Matter, 2017, 29, 095002.	0.7	78
29217	Modulation of band gap by normal strain and an applied electric field in SiC-based heterostructures. JETP Letters, 2017, 105, 114-118.	0.4	0
29218	First-principles study of structural, elastic and thermodynamic properties of Niâ€“Snâ€“P intermetallics. Journal of Materials Research, 2017, 32, 512-521.	1.2	4
29219	Equilibrium Fractionation of Non-traditional Isotopes: a Molecular Modeling Perspective. Reviews in Mineralogy and Geochemistry, 2017, 82, 27-63.	2.2	71
29220	Structural, electronic, and magnetic properties in transition-metal-doped arsenene: Ab initio study. Japanese Journal of Applied Physics, 2017, 56, 015201.	0.8	5
29221	Ringâ€Opening Reaction of Furfural and Tetrahydrofurfuryl Alcohol on Hydrogenâ€Predosed Iridium(1â€‰1â€‰1) and Cobalt/Iridium(1â€‰1â€‰1) Surfaces. ChemCatChem, 2017, 9, 1701-1707.	1.8	34
29222	Effects of alloying elements (Sn, Fe, Cr, Nb) on mechanical properties of zirconium: Generalized stacking-fault energies from first-principles calculations. Computational Condensed Matter, 2017, 10, 22-24.	0.9	18
29223	First principles study on structural, electronic and optical properties of 3d transition metals-substituted CuGaSe2. Optik, 2017, 135, 346-352.	1.4	12

#	Article	IF	Citations
29224	Band gap tuning of 1T-MoS2/SiC bilayers with normal strain: A density functional study. Optik, 2017, 135, 79-84.	1.4	2
29225	Network Formation by Condensed Tetrahedral [Au₃Al] Units in Na₂Au₃Al: Crystal and Electronic Structure, Spectroscopic Investigations, and Physical Properties of an Ordered Ternary Auride. Inorganic Chemistry, 2017, 56, 1919-1931.	1.9	10
29226	Thermodynamic, Spectroscopic, and Computational Studies of f-Element Complexation by N-Hydroxyethyl-diethylenetriamine-N,Nâ€²,Nâ€³,Nâ€³-tetraacetic Acid. Inorganic Chemistry, 2017, 56, 1722-1733.	1.9	19
29227	Modulating Electronic and Optical Properties of Monolayer MoS₂ Using Nonbonded Phthalocyanine Molecules. Journal of Physical Chemistry C, 2017, 121, 2959-2967.	1.5	53
29228	Redox Active Cation Intercalation/Deintercalation in Two-Dimensional Layered MnO₂ Nanostructures for High-Rate Electrochemical Energy Storage. ACS Applied Materials & Interfaces, 2017, 9, 6282-6291.	4.0	80
29229	Structural phase transitions of (Bi_{1âˆ’x}Sb_x)₂(Te_{1âˆ’y}Se_y)₃ compounds under high pressure and the influence of the atomic radius on the compression processes of tetradymites. Physical Chemistry Chemical Physics, 2017, 19, 2207-2216.	1.3	18
29230	Enhanced photovoltaic performance of polymer-filled nanoporous Si hybrid structures. Physical Chemistry Chemical Physics, 2017, 19, 5121-5126.	1.3	4
29231	Dehydrogenation of goethite in Earthâ€™s deep lower mantle. Proceedings of the National Academy of Sciences of the United States of America, 2017, 114, 1498-1501.	3.3	83
29232	Electronic structure of AlCrN films investigated using various photoelectron spectroscopies andab initiocalculations. Journal of Physics Condensed Matter, 2017, 29, 085502.	0.7	8
29233	Ab initio study of hydrogenic effective mass impurities in Si nanowires. Journal of Physics Condensed Matter, 2017, 29, 095303.	0.7	1
29234	A study of adatom ripening on an Al (1 1 1) surface with machine learning force fields. Computational Materials Science, 2017, 129, 332-335.	1.4	33
29235	Effects of vacancies on the mechanical properties of zirconium: An ab initio investigation. Materials and Design, 2017, 119, 30-37.	3.3	33
29236	M₄Mg₄(P₂O₇)₃ (M = K, Rb): Structural Engineering of Pyrophosphates for Nonlinear Optical Applications. Chemistry of Materials, 2017, 29, 1845-1855.	3.2	187
29237	Tetrel Bonds in Infinite Molecular Chains by Electronic Structure Theory and Their Role for Crystal Stabilization. Journal of Physical Chemistry A, 2017, 121, 1381-1387.	1.1	15
29238	A strong diffusive ion mode in dense ionized matter predicted by Langevin dynamics. Nature Communications, 2017, 8, 14125.	5.8	30
29239	Determining crystal phase purity in c-BP through X-ray absorption spectroscopy. Physical Chemistry Chemical Physics, 2017, 19, 8174-8187.	1.3	7
29240	Pressure-driven phase transition mechanisms revealed by quantum chemistry: <scp>l</scp>-serine polymorphs. Physical Chemistry Chemical Physics, 2017, 19, 6671-6676.	1.3	26
29241	Influences of the adsorption of different elements on the electronic structures of a tin sulfide monolayer. Physical Chemistry Chemical Physics, 2017, 19, 5423-5429.	1.3	17

#	Article	IF	Citations
29242	Simultaneous improvement of power factor and thermal conductivity via Ag doping in p-type Mg₃Sb₂ thermoelectric materials. Journal of Materials Chemistry A, 2017, 5, 4932-4939.	5.2	105
29243	Influence of phase transitions and defect associates on the oxygen migration in the ion conductor Na_{1/2}Bi_{1/2}TiO₃. Journal of Materials Chemistry A, 2017, 5, 4368-4375.	5.2	45
29244	Neural network predictions of oxygen interactions on a dynamic Pd surface. Molecular Simulation, 2017, 43, 346-354.	0.9	58
29245	High-pressure structural, elastic, and thermodynamic properties of zircon-type HoPO₄and TmPO₄. Journal of Physics Condensed Matter, 2017, 29, 095401.	0.7	43
29246	Oxidation of free-standing and supported borophene. 2D Materials, 2017, 4, 025025.	2.0	31
29247	Automated firstâ€principles mapping for phaseâ€change materials. Journal of Computational Chemistry, 2017, 38, 620-628.	1.5	9
29248	Fundamental Structural, Electronic, and Chemical Properties of Carbon Nanostructures: Graphene, Fullerenes, Carbon Nanotubes, and Their Derivatives. , 2017, , 1175-1258.		2
29249	Molecular Dynamics Simulation: From â€œAb Initioâ€•to â€œCoarse Grainedâ€• , 2017, , 337-396.		2
29250	Role of nitrogen-related complex in stabilizing ferromagnetic ordering in a rare-earth and nitrogen codoped ZnO. Ceramics International, 2017, 43, 6013-6018.	2.3	8
29251	The structural, electronic and magnetic properties of a novel quaternary Heusler alloy TiZrCoSn. Journal of Physics and Chemistry of Solids, 2017, 105, 9-15.	1.9	42
29252	Variations of thermoelectric performance by electric fields in bilayer MX₂ (M = W, Mo; X) Tj ETQq0 0 0 rgBT /Overlock 10 T	1.3	19
29253	Electrochemical properties and structural evolution of O3-type layered sodium mixed transition metal oxides with trivalent nickel. Journal of Materials Chemistry A, 2017, 5, 4596-4606.	5.2	63
29254	Alumina-supported sub-nanometer Pt₁₀ clusters: amorphization and role of the support material in a highly active CO oxidation catalyst. Journal of Materials Chemistry A, 2017, 5, 4923-4931.	5.2	72
29255	First-principles study of Zrâ€“N crystalline phases: phase stability, electronic and mechanical properties. RSC Advances, 2017, 7, 4697-4703.	1.7	45
29256	An in situ photoelectroreduction approach to fabricate Bi/BiOCl heterostructure photocathodes: understanding the role of Bi metal for solar water splitting. Journal of Materials Chemistry A, 2017, 5, 4894-4903.	5.2	96
29257	Hydrogen functionalisation of transition metal dichalcogenide monolayers from first principles. Molecular Simulation, 2017, 43, 379-383.	0.9	6
29258	The prospects of phosphorene as an anode material for high-performance lithium-ion batteries: a fundamental study. Nanotechnology, 2017, 28, 075401.	1.3	48
29259	Quasiâ€“solid state rechargeable Na-CO ₂ batteries with reduced graphene oxide Na anodes. Science Advances, 2017, 3, e1602396.	4.7	193

#	Article	IF	Citations
29260	A New Type of Scaling Relations to Assess the Accuracy of Computational Predictions of Catalytic Activities Applied to the Oxygen Evolution Reaction. ChemCatChem, 2017, 9, 1261-1268.	1.8	75
29261	Characters of group V and VII atoms doped WSe 2 monolayer. Journal of Alloys and Compounds, 2017, 699, 291-296.	2.8	14
29262	Tuning the electronic and magnetic properties of germanene by surface adsorption of small nitrogen-based molecules. Physica E: Low-Dimensional Systems and Nanostructures, 2017, 88, 237-242.	1.3	18
29263	CO₂ Electroreduction Performance of Phthalocyanine Sheet with Mn Dimer: A Theoretical Study. Journal of Physical Chemistry C, 2017, 121, 3963-3969.	1.5	95
29264	First-Principles Study of Novel Two-Dimensional (C₄H₉NH₃)₂PbX₄ Perovskites for Solar Cell Absorbers. Journal of Physical Chemistry Letters, 2017, 8, 876-883.	2.1	61
29265	Salt-Templated Synthesis of 2D Metallic MoN and Other Nitrides. ACS Nano, 2017, 11, 2180-2186.	7.3	359
29266	Piezoelectric scattering limited mobility of hybrid organic-inorganic perovskites CH3NH3PbI3. Scientific Reports, 2017, 7, 41860.	1.6	31
29267	The electronic properties of the stanene/MoS₂ heterostructure under strain. RSC Advances, 2017, 7, 9176-9181.	1.7	34
29268	Edge states of hydrogen terminated monolayer materials: silicene, germanene and stanene ribbons. Journal of Physics Condensed Matter, 2017, 29, 115302.	0.7	22
29269	Grain boundary segregation of elements of groups 14 and 15 and its consequences for intergranular cohesion of ferritic iron. Journal of Materials Science, 2017, 52, 5822-5834.	1.7	11
29270	The structure, electronic, magnetic and optical properties of the Mn doped and Mn-X (XÂ=ÂF, Cl, Br, I and) Tj ETQq0 0 0 rgBT /Overlock 138-145.	2.8	28
29271	Self-assembled nanostructures of a di-carbonitrile molecule on copper single-crystal surfaces. RSC Advances, 2017, 7, 1771-1775.	1.7	0
29272	Regulating Li deposition at artificial solid electrolyte interphases. Journal of Materials Chemistry A, 2017, 5, 3483-3492.	5.2	258
29273	The oxygen reduction reaction mechanism on Sn doped graphene as an electrocatalyst in fuel cells: a DFT study. RSC Advances, 2017, 7, 729-734.	1.7	27
29274	Three-dimensional organic Dirac-line materials due to nonsymmorphic symmetry: A data mining approach. Physical Review B, 2017, 95, .	1.1	29
29275	Effect of terminal substituents on self-assembly behavior of porphyrin molecules on Ag(110). Surface and Interface Analysis, 2017, 49, 140-144.	0.8	0
29276	Thermodynamic modelling of Ti-Zr-N system. Calphad: Computer Coupling of Phase Diagrams and Thermochemistry, 2017, 56, 102-107.	0.7	22
29277	Rupture of polymers by chain scission. Extreme Mechanics Letters, 2017, 13, 17-24.	2.0	86

#	Article	IF	Citations
29278	Doping and vacancy effects of graphyne on SO2 adsorption. Journal of Colloid and Interface Science, 2017, 493, 123-129.	5.0	30
29279	Structural and Vibrational Properties of the TiOPc Monolayer on Ag(111). Journal of Physical Chemistry C, 2017, 121, 1608-1617.	1.5	20
29280	Ab Initio Simulations To Understand the Leaf-Shape Crystal Morphology of ZIF-L with Two-Dimensional Layered Network. Journal of Physical Chemistry C, 2017, 121, 2221-2227.	1.5	35
29281	Formation of Zintl Ions and Their Configurational Change during Sodiation in Naâ€“Sn Battery. Nano Letters, 2017, 17, 679-686.	4.5	32
29282	Enhanced selective oxidation of h-BN nanosheet through a substrate-mediated localized charge effect. Physical Chemistry Chemical Physics, 2017, 19, 4435-4439.	1.3	10
29283	Estimating carrier relaxation times in the Ba₈Ga₁₆Ge₃₀ clathrate in the extrinsic regime. Physical Chemistry Chemical Physics, 2017, 19, 3010-3018.	1.3	11
29284	Potential for high thermoelectric performance in n-type Zintl compounds: a case study of Ba doped KAlSb₄. Journal of Materials Chemistry A, 2017, 5, 4036-4046.	5.2	55
29285	Widely tunable and anisotropic charge carrier mobility in monolayer tin(<scp>ii</scp>) selenide using biaxial strain: a first-principles study. Journal of Materials Chemistry C, 2017, 5, 1247-1254.	2.7	104
29286	Zintl layer formation during perovskite atomic layer deposition on Ge (001). Journal of Chemical Physics, 2017, 146, 052817.	1.2	11
29287	Unravelling the interplay of geometrical, magnetic and electronic properties of metal-doped graphene nanomeshes. Journal of Physics Condensed Matter, 2017, 29, 055301.	0.7	7
29288	Graphene as a flexible template for controlling magnetic interactions between metal atoms. Journal of Physics Condensed Matter, 2017, 29, 085001.	0.7	1
29289	Spectrum-splitting approach for Fermi-operator expansion in all-electron Kohn-Sham DFT calculations. Physical Review B, 2017, 95, .	1.1	11
29290	Electronic and Optical Properties of a Semiconducting Spinel (Fe₂CrO₄). Advanced Functional Materials, 2017, 27, 1605040.	7.8	23
29291	Bodyâ€Centered Tetragonal C₁₆: A Novel Topological Nodeâ€Line Semimetallic Carbon Composed of Tetrarings. Small, 2017, 13, 1602894.	5.2	65
29292	Enhanced CO2 electroreduction on armchair graphene nanoribbons edge-decorated with copper. Nano Research, 2017, 10, 1641-1650.	5.8	35
29293	Systematic ab initio investigation of the elastic modulus in quaternary transition metal nitride alloys and their coherent multilayers. Acta Materialia, 2017, 127, 124-132.	3.8	44
29294	Spontaneous formation of graphene on diamond (111) driven by B-doping induced surface reconstruction. Carbon, 2017, 115, 388-393.	5.4	18
29295	Elementary steps in acetone condensation reactions catalyzed by aluminosilicates with diverse void structures. Journal of Catalysis, 2017, 346, 134-153.	3.1	73

#	Article	IF	Citations
29296	A possible new family of unconventional high temperature superconductors. Science Bulletin, 2017, 62, 212-217.	4.3	15
29297	Electronic and magnetic properties of TM atoms adsorption on 2D silicon carbide by first-principles calculations. Solid State Communications, 2017, 252, 1-5.	0.9	20
29298	Understanding the Structural and Electronic Effect of Zr⁴⁺-Doped KNb(Zr)O₃ Perovskite for Enhanced Photoactivity: A Combined Experimental and Computational Study. Journal of Physical Chemistry C, 2017, 121, 2597-2604.	1.5	9
29299	Novel Two-Dimensional Silicon Dioxide with in-Plane Negative Poissonâ€™s Ratio. Nano Letters, 2017, 17, 772-777.	4.5	184
29300	A Ternary Alloy Substrate to Synthesize Monolayer Graphene with Liquid Carbon Precursor. ACS Nano, 2017, 11, 1371-1379.	7.3	21
29301	Inter-Layer Coupling Induced Valence Band Edge Shift in Mono- to Few-Layer MoS2. Scientific Reports, 2017, 7, 40559.	1.6	32
29302	Defect interactions and the role of complexes in the CdTe solar cell absorber. Journal of Materials Chemistry A, 2017, 5, 3503-3513.	5.2	69
29303	The Adsorption Geometry and Electronic Structure of Organic Dye Molecule on TiO2(101) Surface from First Principles Calculations. MATEC Web of Conferences, 2017, 88, 03002.	0.1	0
29304	Optical properties of Cu2ZnSn(SxSe1-x)4 solar absorbers: Spectroscopic ellipsometry and ab initio calculations. Applied Physics Letters, 2017, 110, .	1.5	16
29305	Electronic properties of LaAlO₃/SrTiO₃n-type interfaces: a GGA+Ustudy. Journal of Physics Condensed Matter, 2017, 29, 095501.	0.7	20
29306	Ab initiostudy of doping effects in the 42214 compounds: A new family of layered iron-based superconductors. Physical Review B, 2017, 95, .	1.1	2
29307	Elastic anharmonicity of bcc Fe and Fe-based random alloys from first-principles calculations. Physical Review B, 2017, 95, .	1.1	4
29308	Ab initio investigation of the surface properties of austenitic Fe-Ni-Cr alloys in aqueous environments. Applied Surface Science, 2017, 402, 108-113.	3.1	8
29309	Presentation of the PyDEF post-treatment Python software to compute publishable charts for defect energy formation. Chemical Physics Letters, 2017, 671, 124-130.	1.2	37
29310	Initial stages of CO₂ adsorption on CaO: a combined experimental and computational study. Physical Chemistry Chemical Physics, 2017, 19, 4231-4242.	1.3	47
29311	Insights into the mechanism of electrochemical ozone production via water splitting on the Ni and Sb doped SnO₂ catalyst. Physical Chemistry Chemical Physics, 2017, 19, 3800-3806.	1.3	18
29312	First-principles prediction of a low energy edge-reconstruction for zigzag phosphorene nanoribbons. Journal Physics D: Applied Physics, 2017, 50, 065304.	1.3	6
29313	The Phase Stability, Ductility and Hardness of MoN and NbN: First-Principles Study. Journal of Electronic Materials, 2017, 46, 1914-1925.	1.0	8

#	Article	IF	Citations
29314	Unraveling the facet-dependent and oxygen vacancy role for ethylene hydrogenation on Co3O4 (110) surface: A DFT+U study. Applied Surface Science, 2017, 401, 241-247.	3.1	36
29315	Strengthening materials by changing the number of valence electrons. Computational Materials Science, 2017, 129, 252-258.	1.4	7
29316	Prediction on technetium triboride from first-principles calculations. Solid State Communications, 2017, 252, 40-45.	0.9	20
29317	Density Functional Theory and Microkinetic Studies of Bio-oil Decomposition on a Cobalt Surface: Formic Acid as a Model Compound. Energy & Fuels, 2017, 31, 1866-1873.	2.5	12
29318	Extension of the ReaxFF Combustion Force Field toward Syngas Combustion and Initial Oxidation Kinetics. Journal of Physical Chemistry A, 2017, 121, 1051-1068.	1.1	204
29319	Elucidation of high sensitivity of Î´-HMX: New insight from first principles simulations. AIP Conference Proceedings, 2017, , .	0.3	1
29320	Topological, Valleytronic, and Optical Properties of Monolayer PbS. Advanced Materials, 2017, 29, 1604788.	11.1	26
29321	Design of a Hole Trapping Ligand. Nano Letters, 2017, 17, 909-914.	4.5	24
29322	Strain Concentration at the Boundaries in 5-Fold Twins of Diamond and Silicon. ACS Applied Materials & Interfaces, 2017, 9, 4253-4258.	4.0	19
29323	First-principles study of interfacial interaction between carbon nanotube and Al2O3(0001). Journal of Applied Physics, 2017, 121, 025304.	1.1	7
29324	Effects of high pressure sintering on the microstructure and thermoelectric properties of BiCuSeO. High Pressure Research, 2017, 37, 36-45.	0.4	7
29325	Transition metal substitution for H in graphane: a high-throughput study. Journal of Physics Condensed Matter, 2017, 29, 085302.	0.7	0
29326	Spinâ€“exciton interaction and related micro-photoluminescence spectra of ZnSe:Mn DMS nanoribbon. Nanotechnology, 2017, 28, 105202.	1.3	29
29327	Interplay of composition, structure, and electron density of states in W-Os cathode materials and relationship with thermionic emission. Journal of Vacuum Science and Technology A: Vacuum, Surfaces and Films, 2017, 35, 021601.	0.9	4
29328	ZrO2 Nanoparticles: a density functional theory study of structure, properties and reactivity. Rendiconti Lincei, 2017, 28, 19-27.	1.0	15
29329	Photocatalytic improvement of Mn-adsorbed g-C3N4. Applied Catalysis B: Environmental, 2017, 206, 271-281.	10.8	118
29330	Establishment of half-metallicity, ferrimagnetic ordering and double exchange interactions in Ni-doped BiFeO3 â€“ A first-principles study. Computational Materials Science, 2017, 130, 84-90.	1.4	13
29331	First-principles understanding of durable titanium nitride (TiN) electrocatalyst supports. Journal of Industrial and Engineering Chemistry, 2017, 49, 69-75.	2.9	34

#	Article	IF	Citations
29332	Understanding the emission redshift in Sr 2 Si 5 N 8 :Eu 2+ with increasing Eu doping concentration from density functional calculations. Journal of Luminescence, 2017, 185, 187-191.	1.5	9
29333	Investigating fold structures of 2D materials by quantitative transmission electron microscopy. Micron, 2017, 95, 16-22.	1.1	2
29334	High-efficient physical adsorption and detection of formaldehyde using Sc- and Ti-decorated graphdiyne. Physics Letters, Section A: General, Atomic and Solid State Physics, 2017, 381, 879-885.	0.9	42
29335	MgF 2 monolayer as an anti-reflecting material. Solid State Communications, 2017, 252, 22-28.	0.9	27
29336	Polymorphism Controlled Singlet Fission in TIPS-Anthracene: Role of Stacking Orientation. Journal of Physical Chemistry C, 2017, 121, 1412-1420.	1.5	60
29337	Tandem Site- and Size-Controlled Pd Nanoparticles for the Directed Hydrogenation of Furfural. ACS Catalysis, 2017, 7, 2266-2274.	5.5	113
29338	Electronic and spinâ€“orbit properties of the kagome MOF family M₃(1,2,5,6,9,) Tj ETQq0 0 0 rgBT /Overlock 10 Tf 50 507 2017, 29, 09LT01.	0.7	11
29339	Novel hybrid C/BN two-dimensional heterostructures. Nanotechnology, 2017, 28, 085205.	1.3	8
29340	Tradeâ€Offs in Thin Film Solar Cells with Layered Chalcostibite Photovoltaic Absorbers. Advanced Energy Materials, 2017, 7, 1601935.	10.2	58
29341	Strain Mediated Bandgap Reduction, Light Spectrum Broadening, and Carrier Mobility Enhancement of Methylammonium Lead/Tin Iodide Perovskites. Particle and Particle Systems Characterization, 2017, 34, 1600288.	1.2	13
29342	Ab initioprediction of a new allotrope of two-dimensional silicon. Physica Status Solidi - Rapid Research Letters, 2017, 11, 1600422.	1.2	9
29343	A blended NPT/NVT scheme for simulating metallic glasses. Computational Materials Science, 2017, 130, 130-137.	1.4	5
29344	Structural, electronic, magnetic and optical properties of Zn 1-x Ni x O from first-principles. Journal of Physics and Chemistry of Solids, 2017, 104, 267-275.	1.9	5
29345	Doping optimization of organic-inorganic hybrid perovskite CH 3 NH 3 PbI 3 for high thermoelectric efficiency. Synthetic Metals, 2017, 225, 108-114.	2.1	34
29346	DFT-Based Method for More Accurate Adsorption Energies: An Adaptive Sum of Energies from RPBE and vdW Density Functionals. Journal of Physical Chemistry C, 2017, 121, 4937-4945.	1.5	80
29347	Crystal Structure and Li-Ion Transport in Li₂CoPO₄F High-Voltage Cathode Material for Li-Ion Batteries. Journal of Physical Chemistry C, 2017, 121, 3194-3202.	1.5	37
29348	Hydroxyl-Induced Partial Charge States of Single Porphyrins on Titania Rutile. Journal of Physical Chemistry C, 2017, 121, 3607-3614.	1.5	23
29349	Atomistic Origins of Surface Defects in CH₃NH₃PbBr₃ Perovskite and Their Electronic Structures. ACS Nano, 2017, 11, 2060-2065.	7.3	123

#	Article	IF	Citations
29350	Donorâ€“Acceptor Interaction Determines the Mechanism of Photoinduced Electron Injection from Graphene Quantum Dots into TiO₂: Ï€-Stacking Supersedes Covalent Bonding. Journal of the American Chemical Society, 2017, 139, 2619-2629.	6.6	132
29351	Characterizing Substrateâ€“Surface Interactions on Alumina-Supported Metal Catalysts by Dynamic Nuclear Polarization-Enhanced Double-Resonance NMR Spectroscopy. Journal of the American Chemical Society, 2017, 139, 2702-2709.	6.6	59
29352	Surface reconstructions and related local properties of a BiFeO3 thin film. Scientific Reports, 2017, 7, 39698.	1.6	13
29353	Magnetic modification of GaSe monolayer by absorption of single Fe atom. RSC Advances, 2017, 7, 4285-4290.	1.7	10
29354	Density-functional based tight-binding for the study of CO₂/MOF interactions: the case of Zn(ADC)Â·DMSO. Molecular Simulation, 2017, 43, 428-438.	0.9	8
29355	Anomalously low electronic thermal conductivity in metallic vanadium dioxide. Science, 2017, 355, 371-374.	6.0	307
29356	Theoretical Study of Impact of Internal and External Stresses on Thermal Equilibrium Concentrations of Intrinsic Point Defects in Doped Si Crystals. ECS Journal of Solid State Science and Technology, 2017, 6, P78-P99.	0.9	4
29357	Band structures for short-period (InAs)_n(GaSb)_nsuperlattices calculated by the quasiparticle self-consistent GW method. Japanese Journal of Applied Physics, 2017, 56, 021201.	0.8	9
29358	Adsorption and decomposition of dimethyl methylphosphonate on pristine and mono-vacancy defected graphene: A first principles study. Applied Surface Science, 2017, 418, 318-327.	3.1	9
29359	Magnetism and magnetocrystalline anisotropy in vacancy doped and (non)metal adsorbed single-layer PtSe2. Computational Materials Science, 2017, 129, 171-177.	1.4	14
29360	First-principles investigations on structure stability, elastic properties, anisotropy and Debye temperature of tetragonal LiFeAs and NaFeAs under pressure. Journal of Physics and Chemistry of Solids, 2017, 104, 243-251.	1.9	30
29361	Calculations of Oxygen Adsorption-Induced Surface Reconstruction and Oxide Formation on Cu(100). Chemistry of Materials, 2017, 29, 1472-1484.	3.2	12
29362	Influence of Anion/Cation Substitution (Sr²⁺ â†' Ba²⁺, Al³⁺ â†') Tj ETQq0 0 0 rgBT /Overlock 10 Properties of Ba₃Si₆O₁₅:Eu²⁺ Phosphors. Chemistry of Materials, 2017, 29, 1813-1829.	3.2	118
29363	Electronic Origin of the Stability of Transition-Metal-Doped B₁₄ Drum-Shaped Boron Clusters and Their Assembly into a Nanotube. Journal of Physical Chemistry C, 2017, 121, 10728-10742.	1.5	19
29364	Prediction of Co nanoparticle morphologies stabilized by ligands: towards a kinetic model. Physical Chemistry Chemical Physics, 2017, 19, 4636-4647.	1.3	5
29365	Transition metal-substituted lead halide perovskite absorbers. Journal of Materials Chemistry A, 2017, 5, 3578-3588.	5.2	62
29366	Synthesized MoSe2/TiO2 heterogeneous structure as the promising photocatalytic material: Studies from theory to experiment. Journal of Applied Physics, 2017, 121, .	1.1	19
29367	First-principles study on structural, thermal, mechanical and dynamic stability of Tâ€™-MoS₂. Journal of Physics Condensed Matter, 2017, 29, 095702.	0.7	14

#	Article	IF	Citations
29368	First-principles study on the dielectric and transport properties of the LiNbO₃-type CdPbO₃. International Journal of Modern Physics B, 2017, 31, 1750032.	1.0	0
29369	Does the Sâ^'H Bond Always Break after Adsorption of an Alkylthiol on Au(111)?. Chemistry - A European Journal, 2017, 23, 1402-1408.	1.7	23
29370	Reliable and efficient reaction path and transition state finding for surface reactions with the growing string method. Journal of Computational Chemistry, 2017, 38, 645-658.	1.5	40
29371	Metal-embedded nitrogen-doped graphene for H2O molecule dissociation. Carbon, 2017, 115, 773-780.	5.4	50
29372	Spatially resolving and energy splitting of edge state in zigzag edged triangle graphene quantum dots on Cu(111) surface. Physica E: Low-Dimensional Systems and Nanostructures, 2017, 89, 10-14.	1.3	2
29373	Surface Reaction of CO on Carbide-Modified Mo(110). Journal of Physical Chemistry C, 2017, 121, 3133-3142.	1.5	1
29374	Raman signature and phonon dispersion of atomically thin boron nitride. Nanoscale, 2017, 9, 3059-3067.	2.8	141
29375	Effect of Ag and Pd promotion on CH₄selectivity in Fe(100) Fischerâ€"TrÃ¶psch catalysis. Physical Chemistry Chemical Physics, 2017, 19, 5495-5503.	1.3	4
29376	Fineâ€Tuning the Properties of Doped Multifunctional Materials by Controlled Reduction of Dopants. Chemistry - A European Journal, 2017, 23, 2998-3001.	1.7	6
29377	Theoretical insights into the relationship between structures and properties in tri-metallic Pd 13â^'n Ni n @Pt 42 (n = 0â€"13) nanoparticles. Computational and Theoretical Chemistry, 2017, 1107, 94-101.	1.1	12
29378	Tuning Electronic Properties and Band Alignments of Phosphorene Combined With MoSe₂ and WSe₂. Journal of Physical Chemistry C, 2017, 121, 3862-3869.	1.5	55
29379	Is the Metallic Phosphorus Carbide (Î²₀-PC) Monolayer Stable? An Answer from a Theoretical Perspective. Journal of Physical Chemistry Letters, 2017, 8, 747-754.	2.1	47
29380	Charge Carrier Trapping at Surface Defects of Perovskite Solar Cell Absorbers: A First-Principles Study. Journal of Physical Chemistry Letters, 2017, 8, 742-746.	2.1	228
29381	Ab initio study of several static and dynamic properties of bulk liquid Ni near melting. Journal of Chemical Physics, 2017, 146, 034501.	1.2	16
29382	First principles study of structural and magnetic properties of transition metal nitrides TMN (TM =) Tj ETQq0 0 0 rgBT /Overlock 10 Tf 50	0.6	9
29383	An Î±-CrPO₄-type NaV₃(PO₄)₃ anode for sodium-ion batteries with excellent cycling stability and the exploration of sodium storage behavior. Journal of Materials Chemistry A, 2017, 5, 3839-3847.	5.2	24
29384	Conformational adaptation and manipulation of manganese tetra(4-pyridyl)porphyrin molecules on Cu(111). Journal of Chemical Physics, 2017, 146, .	1.2	15
29385	Direct Evidence of Dirac Signature in Bilayer Germanene Islands on Cu(111). Advanced Materials, 2017, 29, 1606046.	11.1	111

#	Article	IF	Citations
29386	Charge Transfer and Interface Engineering of the Pentacene and MoS₂ Monolayer Complex. Advanced Materials Interfaces, 2017, 4, 1601083.	1.9	31
29387	Antiperovskite Nitridophosphate Oxide Ho3[PN4]O by High-Pressure Metathesis. European Journal of Inorganic Chemistry, 2017, 2017, 1930-1937.	1.0	15
29388	Influences of Orientation on Magnetoelectric Coupling at La1â^'x Sr x MnO3/BaTiO3 Interface from Ab Initio Calculations. Journal of Electronic Materials, 2017, 46, 3808-3814.	1.0	3
29389	Electronic structure, optical properties and band edges of layered MoO3: A first-principles investigation. Computational Materials Science, 2017, 130, 242-248.	1.4	76
29390	Estimation of graphene surface stability against the adsorption of environmental and technological chemical agents. Physica Status Solidi (B): Basic Research, 2017, 254, 1600702.	0.7	5
29391	A simple method to approximate electrode potential-dependent activation energies using density functional theory. Catalysis Today, 2017, 288, 63-73.	2.2	77
29392	Towards understanding the dissolving behaviors of oxygen at finite temperature in Au and Ag: First-principles total energy and phonon spectrum calculations. Chinese Journal of Physics, 2017, 55, 218-229.	2.0	0
29393	The electronic structure, optical absorption and photocatalytic water splitting of (FeÂ+ÂNi)-codoped TiO2: A DFT +U study. International Journal of Hydrogen Energy, 2017, 42, 4966-4976.	3.8	22
29394	Two-dimensional ferromagnetism and spin filtering in Cr and Mn-doped graphdiyne. Journal of Physics and Chemistry of Solids, 2017, 105, 61-65.	1.9	20
29395	Ideal Strength and Deformation Mechanism in High-Efficiency Thermoelectric SnSe. Chemistry of Materials, 2017, 29, 2382-2389.	3.2	50
29396	Insight into the topological defects and dopants in metal-free holey graphene for triiodide reduction in dye-sensitized solar cells. Journal of Materials Chemistry A, 2017, 5, 5952-5960.	5.2	49
29397	Communication: Band bending at the interface in polyethylene-MgO nanocomposite dielectric. Journal of Chemical Physics, 2017, 146, 051101.	1.2	29
29398	Electronic and optical properties of antiferromagnetic iron doped NiO â€“ A first principles study. AIP Advances, 2017, 7, .	0.6	12
29399	Controlled formation of nanostructures on MoS2 layers by focused laser irradiation. Applied Physics Letters, 2017, 110, 083101.	1.5	19
29400	The elastic constants of rubrene determined by Brillouin scattering and density functional theory. Applied Physics Letters, 2017, 110, .	1.5	15
29401	Understanding dislocation slip in stoichiometric rocksalt transition metal carbides and nitrides. Journal of Materials Science, 2017, 52, 6235-6248.	1.7	44
29402	The migration behavior of the fourth period transition metals in liquid Al: An ab initio molecular dynamics study. Computational Materials Science, 2017, 130, 183-190.	1.4	7
29403	Insights on the extraordinary tolerance to alcohols of Fe-N-C cathode catalysts in highly performing direct alcohol fuel cells. Nano Energy, 2017, 34, 195-204.	8.2	113

#	Article	IF	Citations
29404	Ab-initio study on the stability, electronic and mechanical properties of transition metal nitrides under external pressure. Solid State Sciences, 2017, 66, 16-22.	1.5	4
29405	Control of Surface and Edge Oxidation on Phosphorene. ACS Applied Materials & Interfaces, 2017, 9, 9126-9135.	4.0	135
29406	Cooperative Electronâ€“Phonon Coupling and Buckled Structure in Germanene on Au(111). ACS Nano, 2017, 11, 3553-3559.	7.3	75
29407	Understanding and reducing deleterious defects in the metastable alloy GaAsBi. NPG Asia Materials, 2017, 9, e345-e345.	3.8	24
29408	Enhanced oxidation resistance of active nanostructures via dynamic size effect. Nature Communications, 2017, 8, 14459.	5.8	51
29409	Room temperature organic magnets derived from sp3 functionalized graphene. Nature Communications, 2017, 8, 14525.	5.8	112
29410	The â€œelectron crystalâ€•behavior in copper chalcogenides Cu₂X (X = Se, S). Journal of Materials Chemistry A, 2017, 5, 5098-5105.	5.2	81
29411	Design Principles for Covalent Organic Frameworks as Efficient Electrocatalysts in Clean Energy Conversion and Green Oxidizer Production. Advanced Materials, 2017, 29, 1606635.	11.1	167
29412	Spectroscopic Observation of a Hydrogenated CO Dimer Intermediate During CO Reduction on Cu(100) Electrodes. Angewandte Chemie - International Edition, 2017, 56, 3621-3624.	7.2	366
29413	The investigation of adsorption and dissociation of H 2 O on Li 2 O (111) by ab initio theory. Applied Surface Science, 2017, 407, 44-51.	3.1	11
29414	Structural and electronic properties of solid-state (LiMPO4âˆ£Î³-Li3PO4)[010] electrochemical interface (M= Fe and Co). Applied Surface Science, 2017, 418, 17-21.	3.1	1
29415	A van der Waals Inclusive Density Functional Theory Study of the Nature of Bonding for Thiophene Adsorption on Ni(100) and Cu(100) Surfaces. Journal of Physical Chemistry C, 2017, 121, 6090-6103.	1.5	19
29416	Impact of Isovalent and Aliovalent Doping on Mechanical Properties of Mixed Phase BiFeO₃. ACS Nano, 2017, 11, 2805-2813.	7.3	23
29417	Quantum Effects and Phase Tuning in Epitaxial Hexagonal and Monoclinic MoTe₂ Monolayers. ACS Nano, 2017, 11, 3282-3288.	7.3	46
29418	Product selectivity in plasmonic photocatalysis for carbon dioxide hydrogenation. Nature Communications, 2017, 8, 14542.	5.8	348
29419	Emergence of topological nodal loops in alkaline-earth hexaborides XB₆(X = Ca, Sr, and) Tj ETQq1 1 0.784314 rgBT /Ove	1.3	19
29420	Evidence of a strong effect of defect-free metal oxide supports on Pt nanoparticles. Nanoscale, 2017, 9, 4478-4485.	2.8	7
29421	Influence of defects and dopants on the photovoltaic performance of Bi₂S₃: first-principles insights. Journal of Materials Chemistry A, 2017, 5, 6200-6210.	5.2	97

#	Article	IF	Citations
29422	Trivalent cerium-preponderant CeO₂/graphene sandwich-structured nanocomposite with greatly enhanced catalytic activity for the oxygen reduction reaction. Journal of Materials Chemistry A, 2017, 5, 6656-6663.	5.2	66
29423	Structure and luminescence properties of a Nd³⁺doped Bi₄Ge₃O₁₂scintillation crystal: new insights from a comprehensive study. Journal of Materials Chemistry C, 2017, 5, 3079-3087.	2.7	27
29424	The Remarkable Amphoteric Nature of Defective UiOâ€66 in Catalytic Reactions. ChemCatChem, 2017, 9, 2203-2210.	1.8	46
29425	Structural, electrical, phonon, and optical properties of Ti- and V-doped two-dimensional MoS2. Chemical Physics Letters, 2017, 674, 157-163.	1.2	33
29426	X-ray photoelectron spectroscopic study and electronic structure of double-perovskites A 2 SmTaO 6 (A= Ba, Sr, Ca). Solid State Sciences, 2017, 67, 114-118.	1.5	8
29427	Uniform Atomic Layer Deposition of Al₂O₃ on Graphene by Reversible Hydrogen Plasma Functionalization. Chemistry of Materials, 2017, 29, 2090-2100.	3.2	64
29428	Structural, Electronic, and Optical Properties of K2Sn3O7 with an Offset Hollandite Structure. Inorganic Chemistry, 2017, 56, 2914-2918.	1.9	5
29429	Spinâ€“Orbit Coupling Effects on Ligand-Free Icosahedral Matryoshka Superatoms. Journal of Physical Chemistry A, 2017, 121, 2420-2428.	1.1	6
29430	Anion Disorder in K₃BH₄B₁₂H₁₂ and Its Effect on Cation Mobility. Journal of Physical Chemistry C, 2017, 121, 5503-5514.	1.5	18
29431	Two-Dimensional Excitonic Photoluminescence in Graphene on a Cu Surface. ACS Nano, 2017, 11, 3207-3212.	7.3	11
29432	Rosin-enabled ultraclean and damage-free transfer of graphene for large-area flexible organic light-emitting diodes. Nature Communications, 2017, 8, 14560.	5.8	184
29433	Films based on group IVâ€“Vâ€“VI elements for the design of a large-gap quantum spin Hall insulator with tunable Rashba splitting. RSC Advances, 2017, 7, 11636-11643.	1.7	6
29434	Structure-property relationships in cubic cuprous iodide: A novel view on stability, chemical bonding, and electronic properties. Journal of Chemical Physics, 2017, 146, 064706.	1.2	24
29435	Energy level alignment at molecule-metal interfaces from an optimally tuned range-separated hybrid functional. Journal of Chemical Physics, 2017, 146, .	1.2	59
29436	Assessment of dispersion correction methods within density functional theory for energetic materials. Molecular Simulation, 2017, 43, 568-574.	0.9	27
29437	Hydrogen release at metal-oxide interfaces: A first principle study of hydrogenated Al/SiO 2 interfaces. Applied Surface Science, 2017, 406, 128-135.	3.1	16
29438	A new stable antiferromagnetic semiconductor: The case of inverse Heusler compound Ti 2 CrSn. Intermetallics, 2017, 85, 149-155.	1.8	3
29439	Zinc oxide for gas sensing of formaldehyde: Density functional theory modelling of the effect of nanostructure morphology and gas concentration on the chemisorption reaction. Materials Chemistry and Physics, 2017, 193, 274-284.	2.0	23

#	Article	IF	Citations
29440	The impact of Pd on the light harvesting in hybrid organic-inorganic perovskite for solar cells. Nano Energy, 2017, 34, 141-154.	8.2	28
29441	Unique Optoelectronic Structure and Photoreduction Properties of Sulfur-Doped Lead Chromates Explaining Their Instability in Paintings. Analytical Chemistry, 2017, 89, 3326-3334.	3.2	11
29442	Investigation of Structural Evolution of Li_{1.1}V₃O₈ by In Situ X-ray Diffraction and Density Functional Theory Calculations. Chemistry of Materials, 2017, 29, 2364-2373.	3.2	40
29443	Interfacial and Alloying Effects on Activation of Ethanol from First-Principles. Journal of Physical Chemistry C, 2017, 121, 5603-5611.	1.5	24
29444	Anatase (101)-like Structural Model Revealed for Metastable Rutile TiO₂(011) Surface. ACS Applied Materials & Interfaces, 2017, 9, 7891-7896.	4.0	29
29445	High-throughput screening of inorganic compounds for the discovery of novel dielectric and optical materials. Scientific Data, 2017, 4, 160134.	2.4	140
29446	Prediction of thermodynamically stable Liâ€“B compounds at ambient pressure. Physical Chemistry Chemical Physics, 2017, 19, 8471-8477.	1.3	8
29447	Computational study of phononic resonators and waveguides in monolayer transition metal dichalcogenides. Physical Chemistry Chemical Physics, 2017, 19, 8082-8090.	1.3	5
29448	Geometric distortion and spin-dependent electronic structure of C6H6-adsorbed Fe3O4(001): A first-principles study. Journal of Applied Physics, 2017, 121, .	1.1	10
29449	Equation of state and shock compression of warm dense sodiumâ€”A first-principles study. Journal of Chemical Physics, 2017, 146, 074505.	1.2	29
29450	Irradiation-induced void evolution in iron: A phase-field approach with atomistic derived parameters. Chinese Physics B, 2017, 26, 026102.	0.7	6
29451	Equilibrium crystal shape of BaZrO3 and space charge formation in the (011) surface by using ab-initio thermodynamics. Journal of the Korean Physical Society, 2017, 70, 75-80.	0.3	6
29452	Recurring polyhedral motifs in the amorphous indium gallium zinc oxide network. Physica Status Solidi (A) Applications and Materials Science, 2017, 214, 1600471.	0.8	4
29453	Ab initio simulations of liquid carbon monoxide at high pressure. High Energy Density Physics, 2017, 22, 41-45.	0.4	8
29454	High-pressure phases of AlxIn1â^'xN compounds: First principles calculations. Journal of Alloys and Compounds, 2017, 704, 160-169.	2.8	9
29455	Strong trapping and slow diffusion of helium in a tungsten grain boundary. Journal of Nuclear Materials, 2017, 487, 158-166.	1.3	38
29456	Magnetic engineering in 3d transition metals on phosphorene by strain. Physics Letters, Section A: General, Atomic and Solid State Physics, 2017, 381, 1236-1240.	0.9	16
29457	First-Principles Study of InVO₄ under Pressure: Phase Transitions from CrVO₄- to AgMnO₄-Type Structure. Inorganic Chemistry, 2017, 56, 2697-2711.	1.9	25

#	Article	IF	Citations
29458	Reconstruction of the Wet Chemical Synthesis Process: The Case of Fe₅C₂ Nanoparticles. Journal of Physical Chemistry C, 2017, 121, 5154-5160.	1.5	24
29459	Highly Efficient and Exceptionally Durable CO₂ Photoreduction to Methanol over Freestanding Defective Single-Unit-Cell Bismuth Vanadate Layers. Journal of the American Chemical Society, 2017, 139, 3438-3445.	6.6	508
29460	Crystal shape controlled H2 storage rate in nanoporous carbon composite with ultra-fine Pt nanoparticle. Scientific Reports, 2017, 7, 42438.	1.6	6
29461	Large scale in silico screening of materials for carbon capture through chemical looping. Energy and Environmental Science, 2017, 10, 818-831.	15.6	67
29462	Anionâ€“Ï€ recognition between [M(CN)₆]^{3â^'} complexes and HAT(CN)₆: structural matching and electronic charge density modification. Dalton Transactions, 2017, 46, 3482-3491.	1.6	20
29463	Temperature effect on lattice and electronic structures of WTe2 from first-principles study. Journal of Applied Physics, 2017, 121, .	1.1	11
29464	Tunable band gap of MoS2-SiC van der Waals heterostructures under normal strain and an external electric field. AIP Advances, 2017, 7, 015116.	0.6	8
29465	The effect of oxygen vacancies on the hyperfine properties of metal-doped SnO₂. Journal Physics D: Applied Physics, 2017, 50, 115103.	1.3	8
29466	Theoretical Investigation of 2D Layered Materials as Protective Films for Lithium and Sodium Metal Anodes. Advanced Energy Materials, 2017, 7, 1602528.	10.2	196
29467	Superlight and Superflexible Threeâ€Dimensional Semiconductor Frameworks A(Xâ‰¡Y)₄ (A=Si,) Tj ETQq1 1 0.784314 rgB Chemistry - an Asian Journal, 2017, 12, 804-810.	1.7	3
29468	Silverâ€Promoted Dehydroaromatization of Ethylene over ZSMâ€5 Catalysts. ChemCatChem, 2017, 9, 1675-1682.	1.8	31
29469	Formation of Organometallic Intermediate States in Onâ€Surface Ullmann Couplings. Chemistry - A European Journal, 2017, 23, 6190-6197.	1.7	36
29470	Improved Finnis-Sinclair potential for vanadium-rich Vâ€“Tiâ€“Cr ternary alloys. Journal of Alloys and Compounds, 2017, 705, 369-375.	2.8	14
29471	Anisotropic phonon transport and lattice thermal conductivities in tin dichalcogenides SnS₂ and SnSe₂. RSC Advances, 2017, 7, 8098-8105.	1.7	50
29472	Band gap scaling laws in group IV nanotubes. Nanotechnology, 2017, 28, 115202.	1.3	8
29473	Anisotropic mechanical and optical response and negative Poissonâ€™s ratio in Mo₂C nanomembranes revealed by first-principles simulations. Nanotechnology, 2017, 28, 115705.	1.3	57
29474	Band Structure and Optical Properties of Kesterite Type Compounds: first principle calculations. IOP Conference Series: Materials Science and Engineering, 2017, 175, 012014.	0.3	1
29475	High-temperature intrinsic quantum anomalous Hall effect in rare Earth monohalide. 2D Materials, 2017, 4, 021014.	2.0	28

#	Article	IF	Citations
29476	Ab initio calculations of uranium and thorium storage in CaSiO₃-perovskite in the Earthâ€™s lower mantle. American Mineralogist, 2017, 102, 321-326.	0.9	5
29477	Dependence of Ion Transport on the Electronegativity of the Constituting Atoms in Ionic Crystals. ChemPhysChem, 2017, 18, 965-969.	1.0	4
29478	Identification and visualization of the intellectual structure and the main research lines in nanoscience and nanotechnology at the worldwide level. Journal of Nanoparticle Research, 2017, 19, 62.	0.8	32
29479	Magnetic coupling between 3d transition metal adatoms on graphene supported by metallic substrates. Carbon, 2017, 116, 599-605.	5.4	14
29480	Self-limiting CVD of a passivating SiO x control layer on InGaAs(001)-(2x4) with the prevention of III-V oxidation. Surface Science, 2017, 660, 31-38.	0.8	0
29481	Highly Efficient and Anomalous Charge Transfer in van der Waals Trilayer Semiconductors. Nano Letters, 2017, 17, 1623-1628.	4.5	78
29482	Strain-Modulated Electronic Structure and Infrared Light Adsorption in Palladium Diselenide Monolayer. Scientific Reports, 2017, 7, 39995.	1.6	39
29483	A DFT and MD study of aqueous-phase dehydrogenation of glycerol on Pt(1 1 1): comparing chemical accuracy versus computational expense in different methods for calculating aqueous-phase system energies. Molecular Simulation, 2017, 43, 370-378.	0.9	19
29484	Interface effects between germanene and Au(1â€†1â€†1) from first principles. Journal Physics D: Applied Physics, 2017, 50, 115301.	1.3	8
29485	Geometrically induced Ï€ -band splitting in graphene superlattices. Chinese Physics B, 2017, 26, 028103.	0.7	1
29486	Temperature-dependent structure evolution in liquid gallium. Acta Materialia, 2017, 128, 304-312.	3.8	57
29487	Theoretical insight into the distinct photocatalytic activity between NiOx and CoOx loaded Ta3N5 photocatalyst. Applied Surface Science, 2017, 405, 289-297.	3.1	14
29488	Impact of Mo on the Ï‰ o phase in Î² -solidifying TiAl alloys: An experimental and computational approach. Intermetallics, 2017, 85, 26-33.	1.8	21
29489	Thermodynamic stability, magnetism and half-metallicity of various (100) surfaces of Heusler alloy Ti2FeSn. Materials Chemistry and Physics, 2017, 192, 253-259.	2.0	15
29490	First-principles calculations on elastic and entropy properties in FeRh alloys. Materials Letters, 2017, 195, 156-158.	1.3	6
29491	Interaction between Post-Graphene Group-IV Honeycomb Monolayers and Metal Substrates: Implication for Synthesis and Structure Control. Journal of Physical Chemistry C, 2017, 121, 5123-5129.	1.5	21
29492	Study of Grains and Boundaries of Molybdenum Diselenide and Tungsten Diselenide Using Liquid Crystal. Nano Letters, 2017, 17, 1474-1481.	4.5	24
29493	Synthesis of Nanoflower-Shaped MXene Derivative with Unexpected Catalytic Activity for Dehydrogenation of Sodium Alanates. ACS Applied Materials & Interfaces, 2017, 9, 7611-7618.	4.0	64

#	Article	IF	Citations
29494	Quantum-state-resolved reactivity of overtone excited CH4 on Ni(111): Comparing experiment and theory. Journal of Chemical Physics, 2017, 146, 054701.	1.2	6
29495	Structural, electronic, and magnetic properties of transition metal doped ReS2 monolayer. JETP Letters, 2017, 105, 255-259.	0.4	7
29496	Exceptionally High Ionic Conductivity in Na₃P_{0.62}As_{0.38}S₄ with Improved Moisture Stability for Solidâ€State Sodiumâ€Ion Batteries. Advanced Materials, 2017, 29, 1605561.	11.1	164
29497	Effect of Atomic Vacancies on the Structure and the Electrocatalytic Activity of Ptâ€rich/C Nanoparticles: A Combined Experimental and Density Functional Theory Study. ChemCatChem, 2017, 9, 2324-2338.	1.8	23
29498	Effects of metals doping on the removal of Hg and H2S over ceria. Applied Surface Science, 2017, 403, 500-508.	3.1	8
29499	Enhanced thermoelectric properties and electronic structures of p -type BiCu 1â^'x Ag x SeO ceramics. Ceramics International, 2017, 43, 6117-6123.	2.3	5
29500	Competition between insertion of Li + and Mg 2+ : An example of TiO 2 -B nanowires for Mg rechargeable batteries and Li + /Mg 2+ hybrid-ion batteries. Journal of Power Sources, 2017, 346, 134-142.	4.0	70
29501	Nitrogen non-stoichiometric stabilization of UN 2. Solid State Communications, 2017, 254, 21-25.	0.9	4
29502	Cation Substitution Effect on a Molecular Analogue of Perovskite Manganites. Journal of Physical Chemistry C, 2017, 121, 10893-10898.	1.5	3
29503	Theoretical design of a new family of two-dimensional topological insulators. Physical Chemistry Chemical Physics, 2017, 19, 7481-7485.	1.3	12
29504	Impact of surface strain on the spin dynamics of deposited Co nanowires. Journal of Applied Physics, 2017, 121, 014306.	1.1	3
29505	Graphene contacts to a HfSe2/SnS2 heterostructure. Journal of Chemical Physics, 2017, 146, 064701.	1.2	8
29506	Giant interfacial perpendicular magnetic anisotropy in MgO/CoFe/capping layer structures. Applied Physics Letters, 2017, 110, .	1.5	73
29507	Experimental and Firstâ€Principles Evidence for Interfacial Activity of Ru/TiO₂ for the Direct Conversion of mâ€Cresol to Toluene. ChemCatChem, 2017, 9, 2642-2651.	1.8	42
29508	TNUâ€9 Zeolite: Aluminum Distribution and Extraâ€Framework Sites of Divalent Cations. Chemistry - A European Journal, 2017, 23, 8857-8870.	1.7	15
29509	Movement of Dirac points and band gaps in graphyne under rotating strain. Nano Research, 2017, 10, 2005-2020.	5.8	15
29510	Origin of excellent rate and cycle performance of Na + -solvent cointercalated graphite vs. poor performance of Li + -solvent case. Nano Energy, 2017, 34, 456-462.	8.2	75
29511	Adsorption of CO on Low-Energy, Low-Symmetry Pt Nanoparticles: Energy Decomposition Analysis and Prediction via Machine-Learning Models. Journal of Physical Chemistry C, 2017, 121, 5612-5619.	1.5	58

#	Article	IF	Citations
29512	Charge Transfer in Iridate-Manganite Superlattices. Nano Letters, 2017, 17, 2126-2130.	4.5	53
29513	Pressureâ€“Temperature Phase Diagram of Vanadium Dioxide. Nano Letters, 2017, 17, 2512-2516.	4.5	65
29514	Field Effect in Graphene-Based van der Waals Heterostructures: Stacking Sequence Matters. Nano Letters, 2017, 17, 2660-2666.	4.5	21
29515	Covalently Connected Carbon Nanotubes as Electrocatalysts for Hydrogen Evolution Reaction through Band Engineering. ACS Catalysis, 2017, 7, 2676-2684.	5.5	41
29516	Role of relativity in high-pressure phase transitions of thallium. Scientific Reports, 2017, 7, 42983.	1.6	4
29517	The conflicting role of buckled structure in phonon transport of 2D group-IV and group-V materials. Nanoscale, 2017, 9, 7397-7407.	2.8	131
29518	Molecular and dissociative adsorption of water and hydrogen sulfide at perfect and defective Cu(110) surfaces. Physical Chemistry Chemical Physics, 2017, 19, 8111-8120.	1.3	20
29519	Superconductivity of monolayer Mo2C: The key role of functional groups. Journal of Chemical Physics, 2017, 146, 034705.	1.2	61
29520	Dimensionality-strain phase diagram of strontium iridates. Physical Review B, 2017, 95, .	1.1	37
29521	Atomic and electronic structure of perfect dislocations in the solar absorber materials <mml:math xmlns:mml="http://www.w3.org/1998/Math/MathML"><mml:msub><mml:mi mathvariant="normal">CuInSe</mml:mi><mml:mn>2</mml:mn></mml:msub></mml:math> and <mml:math xmlns:mml="http://www.w3.org/1998/Math/MathML"><mml:msub><mml:mi mathvariant="normal">CuGaSe</mml:mi><mml:mn>2</mml:mn></mml:msub></mml:math> studied by first-principles calculations. Physical Review B, 2017, 95, .	1.1	6
29522	Electronic Stopping of Slow Protons in Transition and Rare Earth Metals: Breakdown of the Free Electron Gas Concept. Physical Review Letters, 2017, 118, 103401.	2.9	52
29523	Topology-Scaling Identification of Layered Solids and Stable Exfoliated 2D Materials. Physical Review Letters, 2017, 118, 106101.	2.9	262
29524	Tailoring magnetic behavior of CoFeMnNiX (XÂ= Al, Cr, Ga, and Sn) high entropy alloys by metal doping. Acta Materialia, 2017, 130, 10-18.	3.8	220
29525	Influence of electron correlation on the electronic and magnetic structures of nitric-oxide-adsorbed manganese phthalocyanine. Chemical Physics Letters, 2017, 675, 15-19.	1.2	3
29526	Density-functional study of plutonium monoxide monohydride. Journal of Nuclear Materials, 2017, 485, 181-188.	1.3	4
29527	First principles study of inert-gas (helium, neon, and argon) interactions with hydrogen in tungsten. Journal of Nuclear Materials, 2017, 487, 128-134.	1.3	17
29528	Ligand-Induced Variations in Symmetry and Structural Dimensionality of Lead Oxide Carboxylates. Crystal Growth and Design, 2017, 17, 1574-1582.	1.4	11
29529	Template-Free Vapor-Phase Growth of PatrÃ³nite by Atomic Layer Deposition. Chemistry of Materials, 2017, 29, 2864-2873.	3.2	37

#	Article	IF	Citations
29530	Long-Range Order in [(SnSe)_{1.2}]₁[TiSe₂]₁ Prepared from Designed Precursors. Inorganic Chemistry, 2017, 56, 3499-3505.	1.9	10
29531	Ab Initio Molecular Dynamics Study of Dissociative Chemisorption and Scattering of CO₂ on Ni(100): Reactivity, Energy Transfer, Steering Dynamics, and Lattice Effects. Journal of Physical Chemistry C, 2017, 121, 5594-5602.	1.5	41
29532	Isolation of Cu Atoms in Pd Lattice: Forming Highly Selective Sites for Photocatalytic Conversion of CO₂ to CH₄. Journal of the American Chemical Society, 2017, 139, 4486-4492.	6.6	455
29533	Al-Doped CoP nanoarray: a durable water-splitting electrocatalyst with superhigh activity. Nanoscale, 2017, 9, 4793-4800.	2.8	268
29534	On-surface manipulation of atom substitution between cobalt phthalocyanine and the Cu(111) substrate. RSC Advances, 2017, 7, 13827-13835.	1.7	40
29535	Bismuth based half-Heusler alloys with giant thermoelectric figures of merit. Journal of Materials Chemistry A, 2017, 5, 6131-6139.	5.2	52
29536	Hybrid n-type Sn_{1â^'x}Ta_xO₂ nanowalls bonded with graphene-like layers as high performance electrocatalysts for flexible energy conversion devices. Journal of Materials Chemistry A, 2017, 5, 6884-6892.	5.2	8
29537	Geometrically frustrated <mml:math xmlns:mml="http://www.w3.org/1998/Math/MathML"><mml:msub><mml:mi>GdInO</mml:mi><mml:mn>3</mml:mn></mml:msub><m : An exotic system to study negative thermal expansion and spin-lattice coupling. Physical Review B, 2017, 95, .	1.1	12
29538	Abnormal volumetric thermal expansion in the hourglass fermion materials KHgAs and KHgSb. Physical Review B, 2017, 95, .	1.1	8
29539	â€œAb initioâ€•synthesis of zeolites for preestablished catalytic reactions. Science, 2017, 355, 1051-1054.	6.0	204
29540	Experimental and first-principles studies of high-pressure effects on the structural, electronic, and optical properties of semiconductors and lanthanide doped solids. Japanese Journal of Applied Physics, 2017, 56, 05FA02.	0.8	7
29541	Semiconductorâ€toâ€Metal Transition and Quasiparticle Renormalization in Doped Graphene Nanoribbons. Advanced Electronic Materials, 2017, 3, 1600490.	2.6	33
29542	NO and NO 2 adsorption on subsurface doped MgO (100) and BaO (100) surfaces. A density functional study. Applied Surface Science, 2017, 404, 216-229.	3.1	12
29543	Interfacial strengthening between graphene and polymer through Stone-Thrower-Wales defects: Ab initio and molecular dynamics simulations. Carbon, 2017, 118, 66-77.	5.4	68
29544	Significantly reduced thermal conductivity and enhanced thermoelectric properties of single- and bi-layer graphene nanomeshes with sub-10 nm neck-width. Nano Energy, 2017, 35, 26-35.	8.2	90
29545	Intrinsic Conductivity in Magnesiumâ€“Oxygen Battery Discharge Products: MgO and MgO₂. Chemistry of Materials, 2017, 29, 3152-3163.	3.2	46
29546	Phonon-Mode Calculation, Far- and Mid-Infrared, and Raman Spectra of an Îµ-Ga_{0.5}Fe_{1.5}O₃ Magnet. Journal of Physical Chemistry C, 2017, 121, 5812-5819.	1.5	9
29547	Dynamic Phase Engineering of Bendable Transition Metal Dichalcogenide Monolayers. Nano Letters, 2017, 17, 2473-2481.	4.5	41

#	Article	IF	Citations
29548	Giant Electronâ€“Hole Interactions in Confined Layered Structures for Molecular Oxygen Activation. Journal of the American Chemical Society, 2017, 139, 4737-4742.	6.6	243
29549	Selective hydrogenation of acetylene over Cu(211), Ag(211) and Au(211): Horiutiâ€“Polanyi mechanism vs. non-Horiutiâ€“Polanyi mechanism. Catalysis Science and Technology, 2017, 7, 1508-1514.	2.1	43
29550	Effects of Mgâ€“Zr codoping on the photoelectrochemical properties of a Ta₃N₅semiconductor: a theoretical insight. Journal of Materials Chemistry A, 2017, 5, 6966-6973.	5.2	19
29551	Gas adsorption on monolayer blue phosphorus: implications for environmental stability and gas sensors. Nanotechnology, 2017, 28, 175708.	1.3	81
29552	Quantum interference effects in molecular spin hybrids. Physical Review B, 2017, 95, .	1.1	11
29553	Atomistic Origin of Deformation Twinning in Biomineral Aragonite. Physical Review Letters, 2017, 118, 105501.	2.9	25
29554	Controlling the stability of a Feâ€“Ni reforming catalyst: Structural organization of the active components. Applied Catalysis B: Environmental, 2017, 209, 405-416.	10.8	89
29555	DFT study of the hexagonal high-entropy alloy fission product system. Journal of Nuclear Materials, 2017, 488, 70-74.	1.3	18
29556	Intervalley scattering by acoustic phonons in two-dimensional MoS2 revealed by double-resonance Raman spectroscopy. Nature Communications, 2017, 8, 14670.	5.8	196
29557	Commensurability effect on the electronic structure of carbon nanostructures: Impact on supercell calculations in nanotubes. Europhysics Letters, 2017, 117, 27005.	0.7	2
29558	Density functional theory study of stable configurations of substitutional and interstitial C and Sn atoms in Si and Ge crystals. Journal of Crystal Growth, 2017, 463, 110-115.	0.7	3
29559	Generation of phonon density of states and thermal scattering law using ab initio molecular dynamics. Progress in Nuclear Energy, 2017, 101, 461-467.	1.3	9
29560	Interplay between Methanol and Anatase TiO₂(101) Surface: The Effect of Subsurface Oxygen Vacancy. Journal of Physical Chemistry C, 2017, 121, 6072-6080.	1.5	29
29561	Atomically Precise Lateral Modulation of a Two-Dimensional Electron Liquid in Anatase TiO₂ Thin Films. Nano Letters, 2017, 17, 2561-2567.	4.5	28
29562	Anisotropic layered Bi2Te3-In2Te3 composites: control of interface density for tuning of thermoelectric properties. Scientific Reports, 2017, 7, 43611.	1.6	18
29563	Defects in crystalline PVDF: a density functional theory-density functional tight binding study. Physical Chemistry Chemical Physics, 2017, 19, 7560-7567.	1.3	8
29564	Vastly enhancing the chemical stability of phosphorene by employing an electric field. Nanoscale, 2017, 9, 4219-4226.	2.8	22
29565	Enhancement of magnetoelectric operating temperature in compressed Cr2O3 under hydrostatic pressure. Applied Physics Letters, 2017, 110, .	1.5	19

#	Article	IF	Citations
29566	Using gapped topological surface states of Bi2Se3 films in a field effect transistor. Journal of Applied Physics, 2017, 121, .	1.1	16
29567	Band Gap Adjustment of SiC Honeycomb Structure through Hydrogenation and Fluorination. Chinese Physics Letters, 2017, 34, 017302.	1.3	5
29568	Atypically small temperature-dependence of the direct band gap in the metastable semiconductor copper nitride<mml:math xmlns:mml="http://www.w3.org/1998/Math/MathML"><mml:mrow><mml:msub><mml:mi>Cu</mml:mi><mml:mn>3</mml:mn></mml:msub><mml:mathvariant="normal">N</mml:mi></mml:mrow></mml:math>. Physical Review B, 2017, 95, .	1.1	35
29569	Investigation of Î±-phase and liquid uranium by the method of quantum molecular dynamics. High Temperature, 2017, 55, 40-46.	0.1	6
29570	Low conductance of nickel atomic junctions in hydrogen atmosphere. Frontiers of Physics, 2017, 12, 1.	2.4	5
29571	Tuning the electronic and magnetic properties of porous graphene-like carbon nitride through 3d transition-metal doping. Carbon, 2017, 117, 120-125.	5.4	52
29572	Seebeck Coefficients of Layered BiCuSeO Phases: Analysis of Their Hole-Density Dependence and Quantum Confinement Effect. Chemistry of Materials, 2017, 29, 2348-2354.	3.2	27
29573	Structural Tuning and Piezoluminescence Phenomenon in Trithiocyanuric Acid. Journal of Physical Chemistry C, 2017, 121, 1870-1875.	1.5	6
29574	Reinvestigation of Mechanical Properties and Shear-Induced Atomic Deformation of Tetragonal Superhard Semiconducting OsB4. Journal of Physical Chemistry C, 2017, 121, 6290-6299.	1.5	7
29575	Computational Predictions of Catalytic Activity of Zincblende (110) Surfaces of Metal Nitrides for Electrochemical Ammonia Synthesis. Journal of Physical Chemistry C, 2017, 121, 6141-6151.	1.5	99
29576	A comparative study of surface energies and water adsorption on Ce-bastnÃsite, La-bastnÃsite, and calcite via density functional theory and water adsorption calorimetry. Physical Chemistry Chemical Physics, 2017, 19, 7820-7832.	1.3	30
29577	Strong enhancement of spinâ€“orbit splitting induced by Ïƒâ€“Ï€ coupling in Pb-decorated silicene. RSC Advances, 2017, 7, 11761-11767.	1.7	1
29578	First-principles calculations on slip system activation in the rock salt structure: electronic origin of ductility in silver chloride. Philosophical Magazine, 2017, 97, 1281-1310.	0.7	15
29579	Another selective instability in the kagome ironarsenides <mml:math xmlns:mml="http://www.w3.org/1998/Math/MathML"><mml:mrow><mml:msub><mml:mi>Cu</mml:mi><mml:mn>3</mml:mn></mml:msub><mml:mathvariant="normal">Bi</mml:mi></mml:mrow></mml:math>. Physical Review B, 2017, 95, .	1.1	25
29580	Elastic and thermodynamic properties of the Ti₂AlNb orthorhombic phase from firstâ€principles calculations. Physica Status Solidi (B): Basic Research, 2017, 254, 1600634.	0.7	16
29581	A possible highly active supported Ni dimer catalyst for O2 dissociation: A first-principles study. Applied Surface Science, 2017, 402, 168-174.	3.1	4
29582	Electronic, dielectric and optical properties of orthorhombic lanthanum gallate perovskite. Journal of Alloys and Compounds, 2017, 708, 187-193.	2.8	16
29583	Energetics of NiTi allotropes under uniaxial compression. Scripta Materialia, 2017, 133, 92-95.	2.6	4

#	Article	IF	Citations
29584	Significant band-gap opening in graphene and Pd-doped graphene via the adsorption of ionized methane. Superlattices and Microstructures, 2017, 104, 341-348.	1.4	4
29585	Macroscopic, Spectroscopic, and Theoretical Investigation for the Interaction of Phenol and Naphthol on Reduced Graphene Oxide. Environmental Science & Technology, 2017, 51, 3278-3286.	4.6	207
29586	Cluster Size Effects in Ethylene Hydrogenation over Palladium. Journal of Physical Chemistry C, 2017, 121, 10870-10875.	1.5	15
29587	Benign Interfacial Iodine Vacancies in Perovskite Solar Cells. Journal of Physical Chemistry C, 2017, 121, 5905-5913.	1.5	36
29588	CO Dissociation Mechanism on Pd-Doped Fe(100): Comparison with Cu/Fe(100). Journal of Physical Chemistry C, 2017, 121, 6820-6834.	1.5	8
29589	A-Site and B-Site Charge Orderings in an sâ€“d Level Controlled Perovskite Oxide PbCoO₃. Journal of the American Chemical Society, 2017, 139, 4574-4581.	6.6	52
29590	Precise tuning in platinum-nickel/nickel sulfide interface nanowires for synergistic hydrogen evolution catalysis. Nature Communications, 2017, 8, 14580.	5.8	648
29591	Spin-dependent quantum interference in photoemission process from spin-orbit coupled states. Nature Communications, 2017, 8, 14588.	5.8	34
29592	Biaxial strain effect induced electronic structure alternation and trimeron recombination in Fe3O4. Scientific Reports, 2017, 7, 43403.	1.6	14
29593	Ab initio study of aspirin adsorption on single-walled carbon and carbon nitride nanotubes. Physical Chemistry Chemical Physics, 2017, 19, 8076-8081.	1.3	21
29594	Steam methane reforming on a Ni-based bimetallic catalyst: density functional theory and experimental studies of the catalytic consequence of surface alloying of Ni with Ag. Catalysis Science and Technology, 2017, 7, 1713-1725.	2.1	55
29595	An insight into methanol oxidation mechanisms on RuO₂(100) under an aqueous environment by DFT calculations. Physical Chemistry Chemical Physics, 2017, 19, 7476-7480.	1.3	15
29596	Novel bonding patterns and optoelectronic properties of the two-dimensional Si_xC_ymonolayers. Journal of Materials Chemistry C, 2017, 5, 3561-3567.	2.7	41
29597	The staging mechanism of AlCl₄ intercalation in a graphite electrode for an aluminium-ion battery. Physical Chemistry Chemical Physics, 2017, 19, 7980-7989.	1.3	144
29598	Vibrational and thermal properties of Î²-HMX and TATB from dispersion corrected density functional theory. AIP Conference Proceedings, 2017, , .	0.3	12
29599	Water dissociation on Ni(100), Ni(110), and Ni(111) surfaces: Reaction path approach to mode selectivity. Journal of Chemical Physics, 2017, 146, 074705.	1.2	28
29600	Dopant activation mechanism of Bi wire-Î´-doping into Si crystal, investigated with wavelength dispersive fluorescence x-ray absorption fine structure and density functional theory. Journal of Physics Condensed Matter, 2017, 29, 155001.	0.7	3
29601	Site preference of ternary alloying elements in Ni3Al-X (Xâ€‰â€‰=â€‰â€‰Co,Nb): a first-principles calculations in combination with XPS study. Materials Research Express, 2017, 4, 025016.	0.8	3

#	Article	IF	Citations
29602	First-principles and Monte Carlo studies of the Ni₂(Mn,Cr)Ga Heusler alloys electronic and magnetic properties. Materials Research Express, 2017, 4, 026105.	0.8	10
29603	Aligning the Band Structures of Polymorphic Molybdenum Oxides and Organic Emitters in Light-Emitting Diodes. Physical Review Applied, 2017, 7, .	1.5	19
29604	Stratified construction of neural network based interatomic models for multicomponent materials. Physical Review B, 2017, 95, .	1.1	67
29605	High thermopower and potential thermoelectric properties of crystalline LiH and NaH. Physical Review B, 2017, 95, .	1.1	26
29606	Phase stability and large in-plane resistivity anisotropy in the 112-type iron-based superconductor <mml:math xmlns:mml="http://www.w3.org/1998/Math/MathML"><mml:mrow><mml:msub><mml:mi mathvariant="bold">Ca</mml:mi><mml:mrow><mml:mn>1</mml:mn><mml:mo>â^'</mml:mo><mml:mi>x</mml:mi></mml:mrow></m mathvariant="bold">La</mml:mi><mml:mi>x</mml:mi></mml:msub><mml:msub><mml:mi>FeAs</mml:mi><mml:mn>2</mml:mn></m Physical Review B, 2017, 95, .	1.1	18
29607	Pressure-stabilized hafnium nitrides and their properties. Physical Review B, 2017, 95, .	1.1	85
29608	First-principles study of the effect of (111) strain on octahedral rotations and structural phases of<mml:math xmlns:mml="http://www.w3.org/1998/Math/MathML"><mml:mrow><mml:mi>LaAl</mml:mi><mml:msub><mml:mi mathvariant="normal">O</mml:mi><mml:mn>3</mml:mn></mml:msub></mml:mrow></mml:math>. Physical Review B, 2017, 95, .	1.1	17
29609	Thermodynamic stability and properties of boron subnitrides from first principles. Physical Review B, 2017, 95, .	1.1	13
29610	A comparative study of electronic, structural, and magnetic properties of<mml:math xmlns:mml="http://www.w3.org/1998/Math/MathML"><mml:mi>Î±</mml:mi></mml:math>-,<mml:math xmlns:mml="http://www.w3.org/1998/Math/MathML"><mml:mi>Î²</mml:mi></mml:math>-, and<mml:math xmlns:mml="http://www.w3.org/1998/Math/MathML"><mml:mrow><mml:mi>Î³</mml:mi><mml:mo>â^'</mml:mo><mml:msub><mml:mi mathvariant="normal">V</mml:mi><mml:mn>2</mml:mn></mml:msub><mml:msub><mml:mi ma. Physical Review B, 2017, 95, .	1.1	25
29611	Strain-induced indirect-to-direct band-gap transition in bulk <mml:math xmlns:mml="http://www.w3.org/1998/Math/MathML"><mml:msub><mml:mi>SnS</mml:mi><mml:mn>2</mml:mn></mml:msub></m Physical Review B, 2017, 95, .	1.1	49
29612	Choosing the correct hybrid for defect calculations: A case study on intrinsic carrier trapping in <mml:math xmlns:mml="http://www.w3.org/1998/Math/MathML"><mml:mrow><mml:mi>Î²</mml:mi><mml:mo>â^'</mml:mo><mml:mi mathvariant="normal">G</mml:mi><mml:msub><mml:mi mathvariant="normal">a</mml:mi><mml:mn>2</mml:mn></mml:msub><mml:msub><mml:mi mathvariant="normal">O</mml:mi><mml:mn>3</mml:mn></mml:msub></mml:mrow></mml:math>. Physi	1.1	184
29613	Robust dual topological character with spin-valley polarization in a monolayer of the Dirac semimetal <mml:math xmlns:mml="http://www.w3.org/1998/Math/MathML"><mml:mrow><mml:msub><mml:mi>Na</mml:mi><mml:mn>3</mml:mn></mml:msub></mml:mrow></mml:math> Physical Review B, 2017, 95, .	1.1	34
29614	Magnetism in a graphene- 4fâ^'3d hybrid system. Physical Review B, 2017, 95, .	1.1	22
29615	Two-dimensional topological crystalline quantum spin Hall effect in transition metal intercalated compounds. Physical Review B, 2017, 95, .	1.1	10
29616	Local resilience of the <mml:math xmlns:mml="http://www.w3.org/1998/Math/MathML"><mml:mrow><mml:mn>1</mml:mn><mml:mi>T</mml:mi></mml:mrow></mml:math>-<mml:mtext>Ti</mml:mtext>â^'<mml:mi charge density wave to Ti self-doping. Physical Review B, 2017, 95, .	1.1	15
29617	Rehabilitation of the Perdew-Burke-Ernzerhof generalized gradient approximation for layered materials. Physical Review B, 2017, 95, .	1.1	91
29618	Electronic properties of single-layer antimony: Tight-binding model, spin-orbit coupling, and the strength of effective Coulomb interactions. Physical Review B, 2017, 95, .	1.1	33
29619	<mml:math xmlns:mml="http://www.w3.org/1998/Math/MathML"><mml:msub><mml:mi>BaSn</mml:mi><mml:mn>2</mml:mn></mml:msub></mml:math> : A wide-gap strong topological insulator. Physical Review B, 2017, 95, .	1.1	15

#	Article	IF	Citations
29620	Rapidly convergent cluster expansion and application to lithium ion battery materials. Physical Review B, 2017, 95, .	1.1	6
29621	Control of the dipole layer of polar organic molecules adsorbed on metal surfaces via different charge-transfer channels. Physical Review B, 2017, 95, .	1.1	8
29622	Half Layer By Half Layer Growth of a Blue Phosphorene Monolayer on a GaN(001) Substrate. Physical Review Letters, 2017, 118, 046101.	2.9	149
29623	Charge-Order-Induced Ferroelectricity in<mml:math xmlns:mml="http://www.w3.org/1998/Math/MathML" display="inline"><mml:mrow><mml:mrow><mml:msub><mml:mrow><mml:mi>LaVO</mml:mi></mml:mrow><mml:mrow><mml:mn>3</mml:mn> Physical Review Letters, 2017, 118, 087602.	2.9	29
29624	Efficient oxygen reduction catalysis by subnanometer Pt alloy nanowires. Science Advances, 2017, 3, e1601705.	4.7	330
29625	Crystal structure of Î·â€²-Fe3Al8; low-temperature phase of Î·-Fe2Al5 accompanied by an ordered arrangement of Al atoms of full occupancy in the c-axis chain sites. Acta Materialia, 2017, 129, 290-299.	3.8	50
29626	Characterization of hexagonal boron nitride layers on nickel surfaces by low-energy electron microscopy. Surface Science, 2017, 659, 31-42.	0.8	20
29627	Density Functional Study on the Intercalation of Fullerenes into AnE-PV Copolymer Layers. Journal of Physical Chemistry B, 2017, 121, 2202-2206.	1.2	1
29628	Prediction of Two-Dimensional Phase of Boron with Anisotropic Electric Conductivity. Journal of Physical Chemistry Letters, 2017, 8, 1224-1228.	2.1	41
29629	Understanding Active Sites in the Waterâ€“Gas Shift Reaction for Ptâ€“Re Catalysts on Titania. ACS Catalysis, 2017, 7, 2597-2606.	5.5	34
29630	An sd2hybridized transition-metal monolayer with a hexagonal lattice: reconstruction between the Dirac and kagome bands. Physical Chemistry Chemical Physics, 2017, 19, 8046-8054.	1.3	5
29631	An origin of unintentional doping in transition metal dichalcogenides: the role of hydrogen impurities. Nanoscale, 2017, 9, 4265-4271.	2.8	21
29632	Structure and stability of CaH₂surfaces: on the possibility of electron-rich surfaces in metal hydrides for catalysis. Journal of Materials Chemistry A, 2017, 5, 5550-5558.	5.2	21
29633	Sulfur-alloyed Cr₂O₃: a new p-type transparent conducting oxide host. RSC Advances, 2017, 7, 4453-4459.	1.7	9
29634	A modified Wenzel model for water wetting on van der Waals layered materials with topographic surfaces. Nanoscale, 2017, 9, 3843-3849.	2.8	12
29635	Photocatalytic oxygen evolution from low-bandgap conjugated microporous polymer nanosheets: a combined first-principles calculation and experimental study. Nanoscale, 2017, 9, 4090-4096.	2.8	126
29636	Accuracy of first-principles interatomic interactions and predictions of ferroelectric phase transitions in perovskite oxides: Energy functional and effective Hamiltonian. Physical Review B, 2017, 95, .	1.1	51
29637	Pressure-induced low-lying phonon modes softening and enhanced thermal resistance in<mml:math xmlns:mml="http://www.w3.org/1998/Math/MathML"><mml:mrow><mml:mi>I²</mml:mi><mml:mtext>a¯</mml:mtext><mml:mi mathvariant="normal">M</mml:mi><mml:msub><mml:mi mathvariant="normal">g</mml:mi><mml:mn>2</mml:mn></mml:msub><mml:mi mathvariant="normal">A</mml:mi><mml:msub><mml:mi mathvariant="normal">l</mml:mi><mml:mn>4</mml:mn></mml:msub><mml:mi mathvariant="normal">	1.1	5

#	Article	IF	Citations
29638	Strong correlations and the search for high- <mml:math xmlns:mml="http://www.w3.org/1998/Math/MathML"><mml:msub><mml:mi>T</mml:mi><mml:mi>c</mml:mi></mml:msub></mml:ma superconductivity in chromium pnictides and chalcogenides. Physical Review B, 2017, 95, .	1.1	18
29639	Planar heterostructures of single-layer transition metal dichalcogenides: Composite structures, Schottky junctions, tunneling barriers, and half metals. Physical Review B, 2017, 95, .	1.1	20
29640	High-Precision Shock Wave Measurements of Deuterium: Evaluation of Exchange-Correlation Functionals at the Molecular-to-Atomic Transition. Physical Review Letters, 2017, 118, 035501.	2.9	68
29641	Reaction Pathways for the Deoxygenation of Biomassâ€Pyrolysisâ€Derived Bioâ€oil on Ru: A DFT Study using Furfural as a Model Compound. ChemCatChem, 2017, 9, 2828-2838.	1.8	39
29642	Equiatomic AEAuX (AE=Caâ^'Ba, X=Alâ^'In) Intermetallics: A Systematic Study of their Electronic Structure and Spectroscopic Properties. Chemistry - A European Journal, 2017, 23, 4187-4196.	1.7	12
29643	Divalent-doped Na3Zr2Si2PO12 natrium superionic conductor: Improving the ionic conductivity via simultaneously optimizing the phase and chemistry of the primary and secondary phases. Journal of Power Sources, 2017, 347, 229-237.	4.0	122
29644	Substitution Patterns Understood through Chemical Pressure Analysis: Atom/Dumbbell and Ru/Co Ordering in Derivatives of YCo₅. Crystal Growth and Design, 2017, 17, 1610-1619.	1.4	16
29645	Functionalization of Single-Layer Nitrogene by Vacancy, Adatoms, and Molecules. Journal of Physical Chemistry C, 2017, 121, 6329-6338.	1.5	16
29646	Modulation of the electronic and mechanical properties of phagraphene via hydrogenation and fluorination. Physical Chemistry Chemical Physics, 2017, 19, 11771-11777.	1.3	35
29647	Chiral segregation driven by a dynamical response of the adsorption footprint to the local adsorption environment: bitartrate on Cu(110). Physical Chemistry Chemical Physics, 2017, 19, 7617-7623.	1.3	10
29648	Puzzle of magnetic moments of Ni clusters revisited using quantum Monte Carlo method. Journal of Chemical Physics, 2017, 146, 084313.	1.2	3
29649	Intermediate states and structure evolution in the free-falling process of the dislocation in graphene. Philosophical Magazine, 2017, 97, 759-774.	0.7	2
29650	Multiferroic properties of the PbTiO₃/La_{2/3}Sr_{1/3}MnO₃interface studied from first principles. Journal of Physics Condensed Matter, 2017, 29, 175801.	0.7	5
29651	Temperature and isotope effects on the thermoelectric properties in SnTe. Journal of Physics Condensed Matter, 2017, 29, 175701.	0.7	4
29652	Magnetism and Faraday Rotation in Oxygen-Deficient Polycrystalline and Single-Crystal Iron-Substituted Strontium Titanate. Physical Review Applied, 2017, 7, .	1.5	16
29653	Dislocations near elastic instability in high-pressure body-centered-cubic magnesium. Physical Review B, 2017, 95, .	1.1	4
29654	Influence of site occupancy on diffusion of hydrogen in vanadium. Physical Review B, 2017, 95, .	1.1	8
29655	Insulating phases of vanadium dioxide are Mott-Hubbard insulators. Physical Review B, 2017, 95, .	1.1	57

#	Article	IF	Citations
29656	Probing Intermolecular Coupled Vibrations between Two Molecules. Physical Review Letters, 2017, 118, 036801.	2.9	22
29657	Dirac Fermions in Borophene. Physical Review Letters, 2017, 118, 096401.	2.9	353
29658	Crystal structure and spin-trimer magnetism of Rb_{2.3}(H₂O)_{0.8}Mn₃[B₄P₆O₂₄(OH)<sub> Dalton Transactions, 2017, 46, 2957-2965.	4.6	7
29659	Iron incorporation affecting the structure and boosting catalytic activity of Î²-Co(OH)₂: exploring the reaction mechanism of ultrathin two-dimensional carbon-free Fe₃O₄-decorated Î²-Co(OH)₂nanosheets as efficient oxygen evolution electrocatalysts. Journal of Materials Chemistry A, 2017, 5, 6849-6859.	5.2	67
29660	2D MoS₂/polyaniline heterostructures with enlarged interlayer spacing for superior lithium and sodium storage. Journal of Materials Chemistry A, 2017, 5, 5383-5389.	5.2	102
29661	First principles investigation of copper and silver intercalated molybdenum disulfide. Journal of Applied Physics, 2017, 121, .	1.1	23
29662	Transmutation ofABO4compounds incorporating technetium-99 and caesium-137. Modelling and Simulation in Materials Science and Engineering, 2017, 25, 025011.	0.8	6
29663	Hydrogen passivation of vacancies in diamond: Electronic structure and stability from ab initio calculations. MRS Advances, 2017, 2, 309-314.	0.5	7
29664	Firstâ€•order Raman scattering in threeâ€•layered Moâ€•based ternaries: MoAlB, Mo₂Ga₂C and Mo₂GaC. Journal of Raman Spectroscopy, 2017, 48, 631-638.	1.2	37
29665	Prediction and characterization of the marcasite phase of iron pernitride under high pressure. Journal of Alloys and Compounds, 2017, 702, 132-137.	2.8	20
29666	Carbonation of Hydrous Materials at the Molecular Level: A Time of Flight-Secondary Ion Mass Spectrometry, Raman and Density Functional Theory Study. Crystal Growth and Design, 2017, 17, 1036-1044.	1.4	16
29667	Fast Diffusion of O₂ on Nitrogen-Doped Graphene to Enhance Oxygen Reduction and Its Application for High-Rate Znâ€“Air Batteries. ACS Applied Materials & Interfaces, 2017, 9, 7125-7130.	4.0	52
29668	Graphite to Diamond: Origin for Kinetics Selectivity. Journal of the American Chemical Society, 2017, 139, 2545-2548.	6.6	51
29669	Formulating the bonding contribution equation in heterogeneous catalysis: a quantitative description between the surface structure and adsorption energy. Physical Chemistry Chemical Physics, 2017, 19, 5063-5069.	1.3	15
29670	The Structure of Glycine Dihydrate: Implications for the Crystallization of Glycine from Solution and Its Structure in Outer Space. Angewandte Chemie, 2017, 129, 2062-2066.	1.6	14
29671	An integrated flow microcalorimetry, infrared spectroscopy and density functional theory approach to the study of chromate complexation on hematite and ferrihdyrite. Chemical Geology, 2017, 464, 23-33.	1.4	26
29672	Half-metallicity in hole-doped nitrogenated honey graphene: A first-principles study. Physics Letters, Section A: General, Atomic and Solid State Physics, 2017, 381, 1097-1101.	0.9	8
29673	Investigating the Intercalation Chemistry of Alkali Ions in Fluoride Perovskites. Chemistry of Materials, 2017, 29, 1561-1568.	3.2	44

#	Article	IF	Citations
29674	Modeling Ironâ€“Gold Nanoparticles Using a Dedicated Semi-Empirical Potential: Application to the Stability of Coreâ€“Shell Structures. Journal of Physical Chemistry C, 2017, 121, 4680-4691.	1.5	16
29675	Direct Pathway to Molecular Photodissociation on Metal Surfaces Using Visible Light. Journal of the American Chemical Society, 2017, 139, 3115-3121.	6.6	60
29676	Asymmetric response of ferroelectric/metal oxide heterojunctions for catalysis arising from interfacial chemistry. Physical Chemistry Chemical Physics, 2017, 19, 5870-5879.	1.3	11
29677	Aluminium and magnesium insertion in sulfur-based spinels: a first-principles study. Physical Chemistry Chemical Physics, 2017, 19, 6076-6081.	1.3	33
29678	Direct observation of site-selective hydrogenation and spin-polarization in hydrogenated hexagonal boron nitride on Ni(111). Nanoscale, 2017, 9, 2369-2375.	2.8	17
29679	The origin of the enhanced photocatalytic activity of carbon nitride nanotubes: a first-principles study. Journal of Materials Chemistry A, 2017, 5, 4827-4834.	5.2	50
29680	Covalent surface modification with electron-donating/accepting Ï€-conjugated chains to effectively tune the electronic and magnetic properties of zigzag SiC nanoribbons. Journal of Materials Chemistry C, 2017, 5, 2022-2032.	2.7	7
29681	A first-principles investigation of a new hard multi-layered MnB₂ structure. RSC Advances, 2017, 7, 10559-10563.	1.7	10
29682	The indirectâ€“direct band gap tuning in armchair MoS₂ nanoribbon by edge passivation. Journal Physics D: Applied Physics, 2017, 50, 095102.	1.3	20
29683	Effects of Mechanical Strain on Ionic Conductivity in the Interface between LiPON and Ni-Mn Spinel. Journal of the Electrochemical Society, 2017, 164, A594-A599.	1.3	2
29684	Structure-Function Correlation of Photoactive Ionic pi-Conjugated Binary Porphyrin Assemblies. MRS Advances, 2017, 2, 2267-2273.	0.5	0
29685	Metal-metal bond excitation in colloidal solution of NbS 3. Spectrochimica Acta - Part A: Molecular and Biomolecular Spectroscopy, 2017, 179, 46-50.	2.0	4
29686	New two-dimensional boron nitride allotropes with attractive electronic and optical properties. Solid State Communications, 2017, 253, 51-56.	0.9	53
29687	The Role of Low-Coordinated Sites on the Adsorption of Glycerol on Defected Pt_n/Pt(111) Substrates: A Density Functional Investigation within the D3 van der Waals Correction. Journal of Physical Chemistry C, 2017, 121, 3445-3454.	1.5	14
29688	Strong Interaction at the Perovskite/TiO₂ Interface Facilitates Ultrafast Photoinduced Charge Separation: A Nonadiabatic Molecular Dynamics Study. Journal of Physical Chemistry C, 2017, 121, 3797-3806.	1.5	69
29689	High temperature ferromagnetism in Ï€-conjugated two-dimensional metalâ€“organic frameworks. Chemical Science, 2017, 8, 2859-2867.	3.7	86
29690	A computational assessment of the electronic, thermoelectric, and defect properties of bournonite (CuPbSbS₃) and related substitutions. Physical Chemistry Chemical Physics, 2017, 19, 6743-6756.	1.3	47
29691	Challenges in calculating the bandgap of triazine-based carbon nitride structures. Journal of Materials Chemistry A, 2017, 5, 5115-5122.	5.2	34

#	Article	IF	Citations
29692	Hydrogen weakens interlayer bonding in layered transition metal sulfide Fe_{1+x}S. Journal of Materials Chemistry A, 2017, 5, 5030-5035.	5.2	11
29693	Non-conventional fluorescent biogenic and synthetic polymers without aromatic rings. Polymer Chemistry, 2017, 8, 1722-1727.	1.9	152
29694	Epitaxial strain controlled magnetocrystalline anisotropy in ultrathin FeRh/MgO bilayers. AIP Advances, 2017, 7, 055914.	0.6	7
29695	Full atomistic reaction mechanism with kinetics for CO reduction on Cu(100) from ab initio molecular dynamics free-energy calculations at 298 K. Proceedings of the National Academy of Sciences of the United States of America, 2017, 114, 1795-1800.	3.3	414
29696	Ferromagnetic contact between Ni and MoX ₂ (Xâ€‰â€‰=â€‰â€‰S, Se, or Te) with Fermi-level pinning. 2D Materials, 2017, 4, 024006.	2.0	28
29697	Application of dual descriptor to understand the activity of C u/Z r O 2 catalysts in the water gas shift reaction. Journal of Molecular Modeling, 2017, 23, 34.	0.8	6
29698	Diffusion of single Au, Ag and Cu atoms inside Si(111)-(7Ã—7) half unit cells: A comparative study. Applied Surface Science, 2017, 401, 225-231.	3.1	7
29699	Selectivity for CO2 over CH4 on a functionalized periodic mesoporous phenylene-silica explained by transition state theory. Chemical Physics Letters, 2017, 671, 161-164.	1.2	13
29700	A physical model of thermal vacancies within the CALPHAD approach. Scripta Materialia, 2017, 133, 5-8.	2.6	12
29701	Factors Favoring Ferroelectricity in Hafnia: A First-Principles Computational Study. Journal of Physical Chemistry C, 2017, 121, 4139-4145.	1.5	158
29702	Influence of Surface Adsorption on the Oxygen Evolution Reaction on IrO₂(110). Journal of the American Chemical Society, 2017, 139, 3473-3479.	6.6	269
29703	Towards highly active Pd/CeO₂for alkene hydrogenation by tuning Pd dispersion and surface properties of the catalysts. Nanoscale, 2017, 9, 3140-3149.	2.8	35
29704	Tuning the hydrogen evolution activity of Î²-Mo₂C nanoparticles via control of their growth conditions. Nanoscale, 2017, 9, 3252-3260.	2.8	38
29705	Solvent-controlled syntheses of mixed-alkali-metal borates exhibiting UV nonlinear optical properties. Inorganic Chemistry Frontiers, 2017, 4, 692-700.	3.0	21
29706	2D lateral heterostructures of monolayer and bilayer phosphorene. Journal of Materials Chemistry C, 2017, 5, 2291-2300.	2.7	25
29707	Fluorine impurities at CeO2(111): Effects on oxygen vacancy formation, molecular adsorption, and surface re-oxidation. Journal of Chemical Physics, 2017, 146, 044703.	1.2	17
29708	A Density Functional Theory Investigation of Ni_n, Pd_n, and Pt_n Clusters (n=1â€“4) Adsorbed on Buckminsterfullerene. ChemPhysChem, 2017, 18, 1376-1384.	1.0	2
29709	Structures and Mechanical and Electronic Properties of the Ti2CO2 MXene Incorporated with Neighboring Elements (Sc, V, B and N). Journal of Electronic Materials, 2017, 46, 2460-2466.	1.0	68

#	Article	IF	Citations
29710	Thermodynamic stability of Al 11 RE 3 intermetallic compounds from first-principles calculations. Computational Materials Science, 2017, 131, 28-34.	1.4	19
29711	Structural stability and Li-ion transport property of LiFePO4 under high-pressure. Solid State Ionics, 2017, 301, 133-137.	1.3	25
29712	Epitaxial NiWO4 films on Ni(110): Experimental and theoretical study of surface stability. Surface Science, 2017, 659, 20-30.	0.8	12
29713	Using Machine Learning To Identify Factors That Govern Amorphization of Irradiated Pyrochlores. Chemistry of Materials, 2017, 29, 2574-2583.	3.2	33
29714	Metal-like Boronic-Organic Frameworks: A Design and Computation. Inorganic Chemistry, 2017, 56, 2490-2495.	1.9	3
29715	Lattice Transparency of Graphene. Nano Letters, 2017, 17, 1711-1718.	4.5	35
29716	Substrate-Mediated Câ€“C and Câ€“H Coupling after Dehalogenation. Journal of the American Chemical Society, 2017, 139, 3669-3675.	6.6	39
29717	Origins of Ripples in CVD-Grown Few-layered MoS2 Structures under Applied Strain at Atomic Scales. Scientific Reports, 2017, 7, 40862.	1.6	9
29718	Schottky barrier at graphene/metal oxide interfaces: insight from first-principles calculations. Scientific Reports, 2017, 7, 41771.	1.6	23
29719	Strategies Based on Nitride Materials Chemistry to Stabilize Li Metal Anode. Advanced Science, 2017, 4, 1600517.	5.6	185
29720	Ultrasensitive Ironâ€Triggered Nanosized Feâ€“CoOOH Integrated with Graphene for Highly Efficient Oxygen Evolution. Advanced Energy Materials, 2017, 7, 1602148.	10.2	216
29721	Abâ€…Initio Simulation of the Acid Sites at the External Surface of Zeolite Beta. ChemCatChem, 2017, 9, 2176-2185.	1.8	32
29722	Strong thermal transport along polycrystalline transition metal dichalcogenides revealed by multiscale modeling for MoS 2. Applied Materials Today, 2017, 7, 67-76.	2.3	35
29723	Insights on the Mechanism of Na-Ion Storage in Soft Carbon Anode. Chemistry of Materials, 2017, 29, 2314-2320.	3.2	177
29724	Electronic Structure and Comparative Properties of LiNi_xMn_yCo_zO₂ Cathode Materials. Journal of Physical Chemistry C, 2017, 121, 6002-6010.	1.5	147
29725	Molecular Seesaw: Intricate Dynamics and Versatile Chemistry of Heteroaromatics on Metal Surfaces. Journal of Physical Chemistry Letters, 2017, 8, 1235-1240.	2.1	6
29726	Enhanced Average Thermoelectric Figure of Merit of the PbTeâ€“SrTeâ€“MnTe Alloy. ACS Applied Materials & Interfaces, 2017, 9, 8729-8736.	4.0	38
29727	Atomic Structure and Dynamics of Single Platinum Atom Interactions with Monolayer MoS₂. ACS Nano, 2017, 11, 3392-3403.	7.3	126

#	Article	IF	Citations
29728	Realization of a spin-<mml:math xmlns:mml="http://www.w3.org/1998/Math/MathML"><mml:mfrac><mml:mn>1</mml:mn><mml:mn>2</mml:mn></mml:mfrac></mml anisotropic square lattice in a quasi-two-dimensional quantum antiferromagnet<mml:math		

#	Article	IF	Citations
29747	Magnetic properties and spin-driven ferroelectricity in multiferroic skyrmion host GaV4S8. Physical Review B, 2017, 95, .	1.1	13
29748	Thermal transport in novel carbon allotropes with <mml:math xmlns:mml="http://www.w3.org/1998/Math/MathML"><mml:mrow><mml:mi>s</mml:mi><mml:msup><mml:mi>p</mml:mi><mml:m> or <mml:math xmlns:mml="http://www.w3.org/1998/Math/MathML"><mml:mrow><mml:mi>s</mml:mi><mml:msup><mml:mi>p</mml:mi><mml:m> hybridization: An ab initio study. Physical Review B, 2017, 95, .	1.1	42
29749	Ultrafast Structure Switching through Nonlinear Phononics. Physical Review Letters, 2017, 118, 054101.	2.9	76
29750	Itinerant Antiferromagnetism in <mml:math xmlns:mml="http://www.w3.org/1998/Math/MathML" display="inline"><mml:mrow><mml:msub><mml:mrow><mml:mi>RuO</mml:mi></mml:mrow><mml:mrow><mml:mn>2</mml:mn></mml:mrow> Physical Review Letters, 2017, 118, 077201.	8.9	89
29751	Layer-stacking effect on electronic structures of bilayer arsenene. Europhysics Letters, 2017, 117, 27002.	0.7	17
29752	Topological Quantum Phase Transition and Superconductivity Induced by Pressure in the Bismuth Tellurohalide BiTeI. Advanced Materials, 2017, 29, 1605965.	11.1	51
29753	Firstâ€principles study of surface segregation in bimetallic Ni₃M (Mâ€‰=â€‰Mo, Co, Fe) alloys with chemisorbed atomic oxygen. Physica Status Solidi (B): Basic Research, 2017, 254, 1600810.	0.7	8
29754	Origin of enhanced visible-light photocatalytic activity of transition-metal (Fe, Cr and Co)-doped CeO2: effect of 3d orbital splitting. Applied Physics A: Materials Science and Processing, 2017, 123, 1.	1.1	37
29755	Stability, electronic and thermodynamic properties of aluminene from first-principles calculations. Applied Surface Science, 2017, 409, 85-90.	3.1	72
29756	Gamma (Î³)-ray irradiated multi-walled carbon nanotubes (MWCNTs) for hydrogen storage. Applied Surface Science, 2017, 418, 49-55.	3.1	41
29757	Experimental investigation and thermodynamic assessment of the Li-Sb system. Calphad: Computer Coupling of Phase Diagrams and Thermochemistry, 2017, 57, 28-36.	0.7	8
29758	Ab initio study of effect of Co substitution on the magnetic properties of Ni and Pt-based Heusler alloys. Physics Letters, Section A: General, Atomic and Solid State Physics, 2017, 381, 1449-1456.	0.9	8
29759	Controlling n-Type Doping in MoO₃. Chemistry of Materials, 2017, 29, 2563-2567.	3.2	74
29760	Prediction of Single-Wall Boron Nanotube Structures and the Effects of Hydrogenation. Journal of Physical Chemistry C, 2017, 121, 5841-5847.	1.5	9
29761	Changes in the Electronic States of Low-Temperature Solid n-Tetradecane: Decrease in the HOMOâ€“LUMO Gap. ACS Omega, 2017, 2, 618-625.	1.6	25
29762	Detection of defect populations in superhard semiconductor boron subphosphide B₁₂P₂ through X-ray absorption spectroscopy. Journal of Materials Chemistry A, 2017, 5, 5737-5749.	5.2	7
29763	Angle resolved vibrational properties of anisotropic transition metal trichalcogenide nanosheets. Nanoscale, 2017, 9, 4175-4182.	2.8	64
29764	Computational investigation of CO₂ electroreduction on tin oxide and predictions of Ti, V, Nb and Zr dopants for improved catalysis. Journal of Materials Chemistry A, 2017, 5, 11756-11763.	5.2	44

#	Article	IF	Citations
29765	From tunneling to contact in a magnetic atom: The non-equilibrium Kondo effect. Journal of Chemical Physics, 2017, 146, 092309.	1.2	20
29766	Atomic force microscope manipulation of Ag atom on the Si(111) surface. Physical Review B, 2017, 95, .	1.1	7
29767	Lattice dynamics and thermal transport in multiferroic<mml:math xmlns:mml="http://www.w3.org/1998/Math/MathML"><mml:msub><mml:mi mathvariant="bold">CuCrO</mml:mi><mml:mn>2</mml:mn></mml:msub></mml:math>. Physical Review B, 2017, 95, .	1.1	19
29768	Free energy calculation of mechanically unstable but dynamically stabilized bcc titanium. Physical Review B, 2017, 95, .	1.1	40
29769	Metal-insulator transition and the role of electron correlation in FeO2. Physical Review B, 2017, 95, .	1.1	33
29770	<mml:math xmlns:mml="http://www.w3.org/1998/Math/MathML"><mml:mi>h</mml:mi><mml:mtext>-AlN-</mml:mtext><mml:mtext>Mg</mml:mtext> van der Waals bilayer heterostructure: Tuning the excitonic characteristics. Physical Review B, 2017, 95, .	1.1	20
29771	Influence of misorientation on graphene MoirÃ© patterns. Physical Review B, 2017, 95, .	1.1	12
29772	Prediction of superstrong Ï„ -boron carbide phase from quantum mechanics. Physical Review B, 2017, 95, .	1.1	14
29773	Impact of strain on the electronic properties of InAs/GaSb quantum well systems. Physical Review B, 2017, 95, .	1.1	6
29774	Structural and electronic properties of monolayer group III monochalcogenides. Physical Review B, 2017, 95, .	1.1	294
29775	Kinetic path towards the passivation of threading dislocations in GaN by oxygen impurities. Physical Review B, 2017, 95, .	1.1	5
29776	Tuning the Solid Electrolyte Interphase for Selective Liâ€•and Naâ€‐Ion Storage in Hard Carbon. Advanced Materials, 2017, 29, 1606860.	11.1	157
29777	Enhancing sampling in atomistic simulations of solid-state materials for batteries: a focus on olivine $$hbox {NaFePO}_4$$ NaFePO 4. Theoretical Chemistry Accounts, 2017, 136, 1.	0.5	10
29778	Nitrogen-doped graphene-wrapped iron nanofragments for high-performance oxygen reduction electrocatalysts. Journal of Nanoparticle Research, 2017, 19, 1.	0.8	36
29779	First-principles investigation on thermal properties and infrared spectra of imperfect graphene. Applied Thermal Engineering, 2017, 116, 456-462.	3.0	11
29780	Electric field tunable electronic structure in two dimensional van der Waals g-C2N/XSe2(XÂ=ÂMo, W) heterostructures. Carbon, 2017, 117, 393-398.	5.4	36
29781	Adsorption manners of hydrogen on Pt(1 0 0), (1 1 0) and (1 1 1) surfaces at high coverage. Computational and Theoretical Chemistry, 2017, 1106, 43-49.	1.1	31
29782	Structural and elastic properties of zinc-blende and wurtzite InN1-Bi alloys. Journal of Alloys and Compounds, 2017, 708, 323-327.	2.8	5

#	Article	IF	Citations
29783	Structure stability and magnetism in graphene impurity complexes with embedded V and Nb atoms. Journal of Magnetism and Magnetic Materials, 2017, 433, 109-115.	1.0	10
29784	Electric-field tunable electronic structure in WSe 2 /arsenene van der Waals heterostructure. Superlattices and Microstructures, 2017, 104, 518-524.	1.4	17
29785	Excited-State N₂ Dissociation Pathway on Fe-Functionalized Au. Journal of the American Chemical Society, 2017, 139, 4390-4398.	6.6	76
29786	Alkaline-earth metal (Mg) polynitrides at high pressure as possible high-energy materials. Physical Chemistry Chemical Physics, 2017, 19, 9246-9252.	1.3	77
29787	One-atom-thick 2D copper oxide clusters on graphene. Nanoscale, 2017, 9, 3980-3985.	2.8	32
29788	Structural evolution of FeH₄ under high pressure. RSC Advances, 2017, 7, 12570-12575.	1.7	20
29789	Coupled modeling of the competitive gettering of transition metals and impact on performance of lifetime sensitive devices. Journal of Applied Physics, 2017, 121, 095702.	1.1	4
29790	Neural network potentials for dynamics and thermodynamics of gold nanoparticles. Journal of Chemical Physics, 2017, 146, 084314.	1.2	46
29791	Importance of bulk states for the electronic structure of semiconductor surfaces: implications for finite slabs. Journal of Physics Condensed Matter, 2017, 29, 145502.	0.7	11
29792	Type-II Dirac surface states in topological crystalline insulators. Physical Review B, 2017, 95, .	1.1	40
29793	Tuning the conductivity along atomic chains by selective chemisorption. Physical Review B, 2017, 95, .	1.1	22
29794	Exact Model of Vacancy-Mediated Solute Transport in Magnesium. Physical Review Letters, 2017, 118, 105901.	2.9	26
29795	Crystalline Electric-Field Randomness in the Triangular Lattice Spin-Liquid <mml:math xmlns:mml="http://www.w3.org/1998/Math/MathML" display="inline"><mml:mrow><mml:msub><mml:mrow><mml:mi>YbMgGaO</mml:mi></mml:mrow><mml:mrow><mml:mn>4</mml:m Physical Review Letters, 2017, 118, 107202.	2.9	139
29796	Heavy Weyl Fermion State in <mml:math xmlns:mml="http://www.w3.org/1998/Math/MathML" display="inline"><mml:mrow><mml:msub><mml:mrow><mml:mi>CeRu</mml:mi></mml:mrow><mml:mrow><mml:mn>4</mml:mn> Physical Review X, 2017, 7, .	2.8	38
29797	Vibrational properties of anhydrous and partially hydrated uranyl fluoride. Journal of Chemical Physics, 2017, 146, 024502.	1.2	10
29798	Water graphene contact surface investigated by pairwise potentials from force-matching PAW-PBE with dispersion correction. Journal of Chemical Physics, 2017, 146, 054702.	1.2	28
29799	Piezoelectricity of 2D nanomaterials: characterization, properties, and applications. Semiconductor Science and Technology, 2017, 32, 043006.	1.0	49
29800	First-principles study of the Cu-Pd phase diagram. Calphad: Computer Coupling of Phase Diagrams and Thermochemistry, 2017, 56, 224-229.	0.7	13

#	Article	IF	Citations
29801	Investigation of structural, elastic, electronic, optical and vibrational properties of silver chromate spinels: Normal (CrAg2O4) and inverse (Ag2CrO4). Journal of Alloys and Compounds, 2017, 704, 101-108.	2.8	26
29802	Mechanistic analysis of the role of metal oxophilicity in the hydrodeoxygenation of anisole. Journal of Catalysis, 2017, 347, 102-115.	3.1	107
29803	First-principles calculation of atomic configurations of carbon and tin near the surface of a silicon thin film used for solar cells. Materials Science in Semiconductor Processing, 2017, 63, 45-51.	1.9	2
29804	Surface ferromagnetism in<mml:math xmlns:mml="http://www.w3.org/1998/Math/MathML" altimg="si0064.gif" overflow="scroll"><mml:msub subscriptshift="65%"><mml:mrow><mml:mi>HfO</mml:mi></mml:mrow><mml:mrow><mml:mn>2</mml:mn></mml:mrow></mml:msub></mml:math> by excess oxygen. Solid State Communications, 2017, 252, 33-39.	0.9	5
29805	Periodic domain boundary ordering in a dense molecular adlayer: Sub-saturation carbon monoxide on Pd(111). Surface Science, 2017, 658, 46-54.	0.8	1
29806	Thermodynamics of the Flexible Metalâ€“Organic Framework Material MIL-53(Cr) From First-Principles. Journal of Physical Chemistry C, 2017, 121, 4312-4317.	1.5	40
29807	Lithiation mechanisms and lithium storage capacity of reduced graphene oxide nanoribbons: a first-principles study. Journal of Materials Chemistry A, 2017, 5, 4912-4922.	5.2	22
29809	Hypothetical planar and nanotubular crystalline structures with five interatomic bonds of Kepler nets type. AIP Advances, 2017, 7, 025202.	0.6	14
29810	Antimony Diffusion in CdTe. IEEE Journal of Photovoltaics, 2017, 7, 870-873.	1.5	11
29811	Width-dependent structural stability and magnetic properties ofÂmonolayer zigzag MoS₂ nanoribbons. Modern Physics Letters B, 2017, 31, 1750017.	1.0	12
29812	Tunable Magnetic Interaction of Co-Doped SiC Monolayer Under Electric Field: Ab Initio Study. Journal of Superconductivity and Novel Magnetism, 2017, 30, 1269-1273.	0.8	6
29813	Length dependent stability of single-walled carbon nanotubes and how it affects their growth. Carbon, 2017, 116, 443-447.	5.4	14
29814	Is borophene a suitable anode material for sodium ion battery?. Journal of Alloys and Compounds, 2017, 704, 152-159.	2.8	62
29815	Halogen-Bond-Based Molecular Self-Assembly on Graphene Surface: A First-Principles Study. Journal of Physical Chemistry C, 2017, 121, 4451-4461.	1.5	17
29816	Structural, electronic and catalytic performances of single-atom Fe stabilized by divacancy-nitrogen-doped graphene. RSC Advances, 2017, 7, 7920-7928.	1.7	36
29817	Tuning Pt and Cu sites population inside functionalized UiO-67 MOF by controlling activation conditions. Faraday Discussions, 2017, 201, 265-286.	1.6	31
29818	The local electronic properties of individual Pt atoms adsorbed on TiO₂(110) studied by Kelvin probe force microscopy and first-principles simulations. Nanoscale, 2017, 9, 5812-5821.	2.8	16
29819	Mechanistic Insights into Ethylene Transformations on Ir(111) by Density Functional Calculations and Microkinetic Modeling. ChemPhysChem, 2017, 18, 906-916.	1.0	10

#	Article	IF	Citations
29820	Surface termination dependent atomic relaxation of RT5 ultra-thin slabs (R= Y, Ce, Sm and T= Fe, Co, Ni) and their electronic and magnetic properties. Applied Surface Science, 2017, 418, 291-295.	3.1	0
29821	Novel (1 Ã— 1)-reconstructions and native defects of TiO2 anatase (101) surface. Applied Surface Science, 2017, 405, 205-208.	3.1	5
29822	Enhanced visible light absorption in ZnO/GaN heterostructured nanofilms. Journal of Alloys and Compounds, 2017, 704, 478-483.	2.8	12
29823	Defect Chemistry as a Crystal Structure Design Parameter: Intrinsic Point Defects and Ga Substitution in InMnO₃. Chemistry of Materials, 2017, 29, 2425-2434.	3.2	31
29824	A Simple Computational Proxy for Screening Magnetocaloric Compounds. Chemistry of Materials, 2017, 29, 1613-1622.	3.2	58
29825	Self-Diffusion of Surface Defects at Copperâ€“Water Interfaces. Journal of Physical Chemistry C, 2017, 121, 4368-4383.	1.5	31
29826	New Method to Determine the Schottky Barrier in Few-Layer Black Phosphorus Metal Contacts. ACS Applied Materials & Interfaces, 2017, 9, 7873-7877.	4.0	15
29827	A zero-thermal-quenching phosphor. Nature Materials, 2017, 16, 543-550.	13.3	748
29828	An efficient and pH-universal ruthenium-based catalyst for the hydrogen evolution reaction. Nature Nanotechnology, 2017, 12, 441-446.	15.6	1,271
29829	Stabilization of carbocations CH₃⁺, C₂H₅⁺, i-C₃H₇⁺, tert-Bu⁺, and cyclo-pentyl⁺in solid phases: experimental data versus calculations. Physical Chemistry Chemical Physics, 2017, 19, 7270-7279.	1.3	10
29830	Rational design of super-alkalis and their role in CO₂activation. Nanoscale, 2017, 9, 4891-4897.	2.8	58
29831	Splitting methanol on ultra-thin MgO(100) films deposited on a Mo substrate. Physical Chemistry Chemical Physics, 2017, 19, 7245-7251.	1.3	10
29832	p-Type transition-metal doping of large-area MoS₂thin films grown by chemical vapor deposition. Nanoscale, 2017, 9, 3576-3584.	2.8	75
29833	Prediction of tunable quantum spin Hall effect in methyl-functionalized tin film. Journal of Materials Chemistry C, 2017, 5, 2656-2661.	2.7	16
29834	Comparing van der Waals DFT methods for water on NaCl(001) and MgO(001). Journal of Chemical Physics, 2017, 146, 064703.	1.2	29
29835	A first-principles model for anomalous segregation in dilute ternary tungsten-rhenium-vacancy alloys. Journal of Physics Condensed Matter, 2017, 29, 145403.	0.7	49
29836	The role of water in the elastic properties of aluminosilicate zeolites: DFT investigation. Journal of Molecular Modeling, 2017, 23, 68.	0.8	11
29837	Revisiting the conversion reaction voltage and the reversibility of the CuF2 electrode in Li-ion batteries. Nano Research, 2017, 10, 4232-4244.	5.8	55

#	Article	IF	Citations
29838	Influence of Step and Island Edges on Local Adsorption Properties: Hydrogen Adsorption on Pt Monolayer Island Modified Ru(0001) Electrodes. Electrocatalysis, 2017, 8, 530-539.	1.5	9
29839	Self-healing Pd3Au@Pt/C core-shell electrocatalysts with substantially enhanced activity and durability towards oxygen reduction. Applied Catalysis B: Environmental, 2017, 206, 666-674.	10.8	14
29840	Thermodynamic stability of cobalt oxide's low-index surfaces from density functional theory calculations. Surface and Coatings Technology, 2017, 320, 18-22.	2.2	5
29841	Spin polarization properties of thiophene molecule adsorbed to the edge of zigzag graphene nanoribbon. Synthetic Metals, 2017, 226, 46-49.	2.1	11
29842	Chemical Vapor-Deposited Hexagonal Boron Nitride as a Scalable Template for High-Performance Organic Field-Effect Transistors. Chemistry of Materials, 2017, 29, 2341-2347.	3.2	52
29843	Influence of a ZrO₂ Support and Its Surface Structures on the Stability and Nucleation of Pt_n (n = 1â€“5) Clusters: A Density Functional Theory Study. Journal of Physical Chemistry B, 2017, 121, 2132-2141.	1.2	25
29844	Water Adsorption on AnO₂ {111}, {110}, and {100} Surfaces (An = U and Pu): A Density Functional Theory + U Study. Journal of Physical Chemistry C, 2017, 121, 1675-1682.	1.5	48
29845	Advanced rechargeable aluminium ion battery with a high-quality natural graphite cathode. Nature Communications, 2017, 8, 14283.	5.8	453
29846	Chemical and entropic control on the molecular self-assembly process. Nature Communications, 2017, 8, 14463.	5.8	51
29847	Composition dependent band offsets of ZnO and its ternary alloys. Scientific Reports, 2017, 7, 41567.	1.6	42
29848	Adsorption dynamics of molecular nitrogen at an Fe(111) surface. Physical Chemistry Chemical Physics, 2017, 19, 7370-7379.	1.3	9
29849	Quantum spin Hall phase transitions in two-dimensional SbBi alloy films. Journal of Materials Chemistry C, 2017, 5, 2649-2655.	2.7	8
29850	Probing the electronic structures of Co_n (n = 1â€“5) clusters on Î³-Al₂O₃ surfaces using first-principles calculations. Physical Chemistry Chemical Physics, 2017, 19, 3679-3687.	1.3	18
29851	Atomistic understanding of the lateral growth of graphene from the edge of an h-BN domain: towards a sharp in-plane junction. Nanoscale, 2017, 9, 3585-3592.	2.8	19
29852	Diffusion of tellurium at nickel grain boundaries: a first-principles study. RSC Advances, 2017, 7, 8421-8428.	1.7	17
29853	The design and preparation of the thermally stable, Mn⁴⁺ ion activated, narrow band, red emitting fluoride Na₃GaF₆:Mn⁴⁺ for warm WLED applications. Journal of Materials Chemistry C, 2017, 5, 2910-2918.	2.7	138
29854	Topologically insulating states in ternary transition metal dichalcogenides. Journal of Applied Physics, 2017, 121, 024303.	1.1	5
29855	Strain and water effects on the electronic structure and chemical activity of in-plane graphene/silicene heterostructure. Journal of Physics Condensed Matter, 2017, 29, 095302.	0.7	25

#	Article	IF	Citations
29856	Fundamental mechanisms responsible for the temperature coefficient of resonant frequency in microwave dielectric ceramics. Journal of the American Ceramic Society, 2017, 100, 1508-1516.	1.9	16
29857	Firstâ€Principles Modeling of Point Defects and Complexes in Thinâ€Film Solarâ€Cell Absorber CuInSe₂. Advanced Electronic Materials, 2017, 3, 1600353.	2.6	32
29858	Unexpected Geâ€“Ge Contacts in the Twoâ€Dimensional Ge₄Se₃Te Phase and Analysis of Their Chemical Cause with the Density of Energy (DOE) Function. Angewandte Chemie - International Edition, 2017, 56, 10204-10208.	7.2	64
29859	Structural Defectâ€Induced Bandgap Narrowing in Dopantâ€Free Anodic TiO₂ Nanotubes. ChemElectroChem, 2017, 4, 1227-1235.	1.7	15
29860	Fibrous Hybrid of Graphene and Sulfur Nanocrystals for High-Performance Lithiumâ€“Sulfur Batteries. Springer Theses, 2017, , 57-74.	0.0	1
29861	Design lithium storage materials by lithium adatoms adsorption at the edges of zigzag silicene nanoribbon: A first principle study. Applied Surface Science, 2017, 406, 161-169.	3.1	20
29862	Ab initio molecular dynamics simulation on the glass forming ability of Ni-metalloid amorphous alloys. Journal of Non-Crystalline Solids, 2017, 461, 87-92.	1.5	2
29863	Computational Study of Nb-Doped-SnO₂/Pt Interfaces: Dopant Segregation, Electronic Transport, and Catalytic Properties. Chemistry of Materials, 2017, 29, 1641-1649.	3.2	12
29864	First-Principles Study of the Charge Transport Mechanisms in Lithium Superoxide. Chemistry of Materials, 2017, 29, 2202-2210.	3.2	30
29865	Why Porous Materials Have Selective Adsorptions: A Rational Aspect from Electrodynamics. Inorganic Chemistry, 2017, 56, 2614-2620.	1.9	12
29866	Tuning Electronic Properties of Monolayer Hexagonal Boron Phosphide with Group IIIâ€“IVâ€“V Dopants. Journal of Physical Chemistry C, 2017, 121, 4583-4592.	1.5	49
29867	Identifying and Visualizing the Edge Terminations of Single-Layer MoSe₂ Island Epitaxially Grown on Au(111). ACS Nano, 2017, 11, 1689-1695.	7.3	48
29868	Exfoliation of natural van der Waals heterostructures to a single unit cell thickness. Nature Communications, 2017, 8, 14410.	5.8	93
29869	Selective sulfur dioxide adsorption on crystal defect sites on an isoreticular metal organic framework series. Nature Communications, 2017, 8, 14457.	5.8	133
29870	Strain Gated Bilayer Molybdenum Disulfide Field Effect Transistor with Edge Contacts. Scientific Reports, 2017, 7, 41593.	1.6	17
29871	Enhanced adsorption of CO₂ at steps of ultrathin ZnO: the importance of Znâ€“O geometry and coordination. Physical Chemistry Chemical Physics, 2017, 19, 5296-5303.	1.3	10
29872	Charge transfer induced polymerization of EDOT confined between 2D titanium carbide layers. Journal of Materials Chemistry A, 2017, 5, 5260-5265.	5.2	142
29873	Ab-initio study of the structural, electronic, elastic and vibrational properties of HfX (X = Rh, Ru and) Tj ETQq1 1 0.784314 rgBT /Overl	0.5	11

#	Article	IF	Citations
29874	Adsorption and migration of single metal atoms on the calcite (10.4) surface. Journal of Physics Condensed Matter, 2017, 29, 135001.	0.7	7
29875	Structural changes and anomalous selfâ€diffusion of oxygen in liquid iron at high pressure. Geophysical Research Letters, 2017, 44, 3526-3534.	1.5	15
29876	Lattice Dislocations Enhancing Thermoelectric PbTe in Addition to Band Convergence. Advanced Materials, 2017, 29, 1606768.	11.1	365
29877	Uniaxial pressure induced compensated half metal in Crâ€substituted iron(II) fluoride. Physica Status Solidi - Rapid Research Letters, 2017, 11, 1700052.	1.2	2
29878	Gallium bismuth halide GaBi-X2 (X = I, Br, Cl) monolayers with distorted hexagonal framework: Novel room-temperature quantum spin Hall insulators. Nano Research, 2017, 10, 2168-2180.	5.8	18
29879	Segregation effects of Y, Ti, Cr and Si on the intergranular fracture of niobium. Journal of Alloys and Compounds, 2017, 711, 637-642.	2.8	17
29880	Electronic structure and phase transition in polar ScFeO3 from first principles calculations. Journal of Alloys and Compounds, 2017, 713, 187-193.	2.8	8
29881	Stability, bonding and electronic structures of halogenated MoS 2 monolayer: A first-principles study. Physica E: Low-Dimensional Systems and Nanostructures, 2017, 91, 8-14.	1.3	9
29882	Photophysical Properties of SrTaO₂N Thin Films and Influence of Anion Ordering: A Joint Theoretical and Experimental Investigation. Chemistry of Materials, 2017, 29, 3989-3998.	3.2	37
29883	Roles of Zeolite Confinement and Cuâ€“Oâ€“Cu Angle on the Direct Conversion of Methane to Methanol by [Cu₂(Î¼-O)]²⁺-Exchanged AEI, CHA, AFX, and MFI Zeolites. ACS Catalysis, 2017, 7, 3741-3751.	5.5	129
29884	Light-assisted delithiation of lithium iron phosphate nanocrystals towards photo-rechargeable lithium ion batteries. Nature Communications, 2017, 8, 14643.	5.8	179
29885	Resonant electron tunnelling assisted by charged domain walls in multiferroic tunnel junctions. Nature Nanotechnology, 2017, 12, 655-662.	15.6	92
29886	Towards accurate quantum simulations of large systems with small computers. Scientific Reports, 2017, 7, 41263.	1.6	0
29887	Geometrical and electronic structures of small Coâ€“Mo nanoclusters. RSC Advances, 2017, 7, 4933-4940.	1.7	6
29888	Redox-mediated conversion of atomically dispersed platinum to sub-nanometer particles. Journal of Materials Chemistry A, 2017, 5, 9250-9261.	5.2	11
29889	First-principles study of defect formation in the photovoltaic semiconductors Cu₂GeS₃and Cu₂ZnGeS₄for comparison with Cu₂SnS₃, Cu₂ZnSnS₄, and CuInSe₂. Japanese Journal of Applied Physics, 2017, 56, 04CS08.	0.8	14
29890	Regulating Topâ€Surface Multilayer/Singleâ€Crystal Graphene Growth by â€œGetteringâ€•Carbon Diffusion at Backside of the Copper Foil. Advanced Functional Materials, 2017, 27, 1700121.	7.8	35
29891	Fewâ€Layer Black Phosphorus Carbide Fieldâ€Effect Transistor via Carbon Doping. Advanced Materials, 2017, 29, 1700503.	11.1	133

#	Article	IF	Citations
29892	Two-dimensional semiconductors XY 2 (XÂ=ÂGe,Sn;YÂ=ÂS,Se) with promising piezoelectric properties. Computational Condensed Matter, 2017, 11, 33-39.	0.9	10
29893	Sequestration of carbon dioxide in coal: Energetics and bonding from first-principles calculations. Computational Materials Science, 2017, 133, 145-151.	1.4	5
29894	Understanding the graphene-based electric double layer from dielectric perspective: A density functional study. Chemical Physics Letters, 2017, 677, 137-142.	1.2	13
29895	Experimental and thermodynamic investigation of Al-Cu-Nd ternary system. Materials Chemistry and Physics, 2017, 195, 94-104.	2.0	3
29896	Correlating Local Compositions and Structures with the Macroscopic Optical Properties of Ce³⁺-Doped CaSc₂O₄, an Efficient Green-Emitting Phosphor. Chemistry of Materials, 2017, 29, 3538-3546.	3.2	66
29897	High Thermoelectric Performance in n-Doped Silicon-Based Chalcogenide Si₂Te₃. Chemistry of Materials, 2017, 29, 3723-3730.	3.2	34
29898	Modified Anion Packing of Na₂B₁₂H₁₂ in Close to Room Temperature Superionic Conductors. Inorganic Chemistry, 2017, 56, 5006-5016.	1.9	55
29899	Preparation-Dependent Composition and O/F Ordering in NbO₂F and TaO₂F. Inorganic Chemistry, 2017, 56, 5219-5232.	1.9	17
29900	QM/MD Simulations on Graphene Hydrogenation/Deuteration: C_xH/D Formation Mechanism and Isotope Effect. Journal of Physical Chemistry C, 2017, 121, 8480-8489.	1.5	2
29901	Light, Catalyst, Activation: Boosting Catalytic Oxygen Activation Using a Light Pretreatment Approach. ACS Catalysis, 2017, 7, 3644-3653.	5.5	20
29902	Exceptional Oxygen Reduction Reaction Activity and Durability of Platinumâ€“Nickel Nanowires through Synthesis and Post-Treatment Optimization. ACS Omega, 2017, 2, 1408-1418.	1.6	53
29903	The role of halogens in on-surface Ullmann polymerization. Faraday Discussions, 2017, 204, 453-469.	1.6	54
29904	Seeing the invisible plasma with transient phonons in cuprous oxide. Physical Chemistry Chemical Physics, 2017, 19, 1151-1157.	1.3	1
29905	Traction curves for the decohesion of covalent crystals. Applied Physics Letters, 2017, 110, .	1.5	6
29906	From Twoâ€•to Threeâ€Ðimensional Structures of a Supertetrahedral Boran Using Density Functional Calculations. Angewandte Chemie - International Edition, 2017, 56, 10118-10122.	7.2	24
29907	Error estimation in high-throughput density functional theory calculation for material property: elastic constants of cubic binary alloy case. Computational Materials Science, 2017, 134, 190-200.	1.4	6
29908	Structure and surface energy of Au 55 nanoparticles: An ab initio study. Computational Materials Science, 2017, 134, 137-144.	1.4	16
29909	The structural stability and the strain-induced electronic properties of Î±-Si 1 C 7 -graphyne like monolayer. Computational Materials Science, 2017, 135, 9-17.	1.4	7

#	Article	IF	Citations
29910	Ideal strength, phonon stability and thermodynamics of the CrB-type CaX IV (X IV Â=ÂSi, Ge, and Sn) binary compounds. Journal of Alloys and Compounds, 2017, 712, 296-302.	2.8	4
29911	Pt surface segregation in L1 0 -FePt nano-grains. Scripta Materialia, 2017, 135, 88-91.	2.6	12
29912	Controlled nucleation assisted restricted volume solvent annealing for stable perovskite solar cells. Solar Energy Materials and Solar Cells, 2017, 167, 70-86.	3.0	39
29913	Reduction of the Work Function of Gold by N-Heterocyclic Carbenes. Chemistry of Materials, 2017, 29, 3403-3411.	3.2	76
29914	Promoted Electrochemical Performance of Î²-MnO₂ through Surface Engineering. ACS Applied Materials & Interfaces, 2017, 9, 15176-15181.	4.0	18
29915	Multiscale structural and electronic control of molybdenum disulfide foam for highly efficient hydrogen production. Nature Communications, 2017, 8, 14430.	5.8	488
29916	Atomic structure and electronic properties of MgO grain boundaries in tunnelling magnetoresistive devices. Scientific Reports, 2017, 7, 45594.	1.6	35
29917	Electrochemical reduction of CO₂ on graphene supported transition metals â€“ towards single atom catalysts. Physical Chemistry Chemical Physics, 2017, 19, 11436-11446.	1.3	86
29918	Modeling single molecule junction mechanics as a probe of interface bonding. Journal of Chemical Physics, 2017, 146, .	1.2	11
29919	A first-principles study of the formation of Î¸â€²â€² phase in Alâ€“Cu alloys. Philosophical Magazine Letters, 2017, 97, 197-205.	0.5	5
29920	A density functional theory study of the influence of exchange-correlation functionals on the properties of FeAs. Journal of Physics Condensed Matter, 2017, 29, 215604.	0.7	5
29921	Hydrogen-Induced Oxygen Vacancy Bistability and Its Impact on RRAM Device Operation. IEEE Electron Device Letters, 2017, 38, 728-731.	2.2	10
29922	Novel electronic properties of a new MoS 2 /TiO 2 heterostructure and potential applications in solar cells and photocatalysis. Applied Surface Science, 2017, 414, 34-40.	3.1	36
29923	Prediction of huge magnetic anisotropy in organometallic molecules. Computational Materials Science, 2017, 135, 18-21.	1.4	1
29924	Probing the dynamics of complexed local anesthetics via neutron scattering spectroscopy and DFT calculations. International Journal of Pharmaceutics, 2017, 524, 397-406.	2.6	14
29925	Thermal stabilities, electronic structures and optical properties of intrinsic defects and dopant cerium in Ca4F2Si2O7. Journal of Alloys and Compounds, 2017, 713, 28-37.	2.8	6
29926	First-principles molecular dynamics modeling of UCl 3 in LiCl-KCl eutectic. Journal of Molecular Liquids, 2017, 234, 279-286.	2.3	43
29927	Bond Polarizability Model for Sum Frequency Generation at the Al₂O₃(0001)â€“H₂O Interface. Journal of Physical Chemistry A, 2017, 121, 3045-3055.	1.1	16

#	Article	IF	Citations
29928	Nanoscale Conductance in Lead Phthalocyanine Thin Films: Influence of Molecular Packing and Humidity. Journal of Physical Chemistry C, 2017, 121, 9249-9259.	1.5	13
29929	Toward Rational Design of Oxide-Supported Single-Atom Catalysts: Atomic Dispersion of Gold on Ceria. Journal of the American Chemical Society, 2017, 139, 6190-6199.	6.6	333
29930	Synthesis, crystal and electronic structures, physical properties and121Sb and151Eu MÃ¶ssbauer spectroscopy of the alumo-antimonide Zintl-phase Eu5Al2Sb6. Materials Chemistry Frontiers, 2017, 1, 1563-1572.	3.2	17
29931	2D Supramolecular networks of dibenzonitrilediacetylene on Ag(111) stabilized by intermolecular hydrogen bonding. Physical Chemistry Chemical Physics, 2017, 19, 10602-10610.	1.3	6
29932	Magnetic properties and martensitic transformation of Niâ€“Mnâ€“Ge Heusler alloys from first-principles and Monte Carlo studies. Journal Physics D: Applied Physics, 2017, 50, 195001.	1.3	8
29933	Thermodynamics and crystal chemistry of rhomboclase, (H₅O₂)Fe(SO₄)₂Â·2H₂O, and the phase (H₃O)Fe(SO₄)₂and implications for acid mine drainage. American Mineralogist, 2017, 102, 643-654.	0.9	5
29934	First-principles study on magnetic tunneling junctions with semiconducting CuInSe₂and CuGaSe₂barriers. Japanese Journal of Applied Physics, 2017, 56, 020306.	0.8	9
29935	Au/Ni12P5 core/shell single-crystal nanoparticles as oxygen evolution reaction catalyst. Nano Research, 2017, 10, 3103-3112.	5.8	48
29936	PdZn intermetallic on a CN@ZnO hybrid as an efficient catalyst for the semihydrogenation of alkynols. Journal of Catalysis, 2017, 350, 13-20.	3.1	51
29937	Electronic physics and possible superconductivity in layered orthorhombic cobalt oxychalcogenides. Science Bulletin, 2017, 62, 563-571.	4.3	7
29938	Pressure-Induced Stable Beryllium Peroxide. Inorganic Chemistry, 2017, 56, 5233-5238.	1.9	17
29939	Microscopic Properties of Mg in Li and Nb Sites of LiNbO₃ by First-Principle Hybrid Functional: Formation and Related Optical Properties. Journal of Physical Chemistry C, 2017, 121, 8968-8975.	1.5	21
29940	Acceptor doping in the proton conductor SrZrO₃. Physical Chemistry Chemical Physics, 2017, 19, 11485-11491.	1.3	23
29941	Negative thermal expansion properties in tetragonal NbPO5 from the first principles studies. AIP Advances, 2017, 7, 035202.	0.6	2
29942	Diffusion Pathways and Activation Energies in Crystalline Lithium-Ion Conductors. Zeitschrift Fur Physikalische Chemie, 2017, 231, 1279-1302.	1.4	9
29943	MoSe₂â€Covered N,Pâ€Doped Carbon Nanosheets as a Longâ€Life and Highâ€Rate Anode Material for Sodiumâ€Ion Batteries. Advanced Functional Materials, 2017, 27, 1700522.	7.8	454
29944	Potassiumâ€Promoted Molybdenum Carbide as a Highly Active and Selective Catalyst for CO₂ Conversion to CO. ChemSusChem, 2017, 10, 2408-2415.	3.6	65
29945	Interfacial instability of amorphous LiPON against lithium: A combined Density Functional Theory and spectroscopic study. Journal of Power Sources, 2017, 354, 124-133.	4.0	49

#	Article	IF	Citations
29946	Tuning electronic structure and optical properties of SrTiO 3 by site-specific doping by Nb with N/B from hybrid functional calculations. Materials Chemistry and Physics, 2017, 195, 170-175.	2.0	4
29947	Channel-Assisted Proton Conduction Behavior in Hydroxyl-Rich Lanthanide-Based Magnetic Metalâ€“Organic Frameworks. Inorganic Chemistry, 2017, 56, 4956-4965.	1.9	73
29948	From Permeation to Cluster Arrays: Graphene on Ir(111) Exposed to Carbon Vapor. Nano Letters, 2017, 17, 3105-3112.	4.5	20
29949	Determining Atomic-Scale Structure and Composition of Organo-Lead Halide Perovskites by Combining High-Resolution X-ray Absorption Spectroscopy and First-Principles Calculations. ACS Energy Letters, 2017, 2, 1183-1189.	8.8	23
29950	Elucidation of crystal and electronic structures within highly strained BiFeO3 by transmission electron microscopy and first-principles simulation. Scientific Reports, 2017, 7, 46498.	1.6	15
29951	Giant magnetic anisotropy of rare-earth adatoms and dimers adsorbed by graphene oxide. Physical Chemistry Chemical Physics, 2017, 19, 13245-13251.	1.3	22
29952	MoS ₂ edges and heterophase interfaces: energy, structure and phase engineering. 2D Materials, 2017, 4, 025080.	2.0	16
29953	Unusual magnetic properties of Auâ€“Mn nanowires on copper and silicon substrates. Physica Status Solidi (B): Basic Research, 2017, 254, 1600850.	0.7	2
29954	Exploring from ab initio calculations the structural and electronic properties of supported metal linear atomic chains on the NiAl (110) surface. Theoretical Chemistry Accounts, 2017, 136, 1.	0.5	3
29955	Transformation of monolayer MoS2 into multiphasic MoTe2: Chalcogen atom-exchange synthesis route. Nano Research, 2017, 10, 2761-2771.	5.8	13
29956	Two-dimensional scandium-based carbides (MXene): Band gap modulation and optical properties. Journal of Alloys and Compounds, 2017, 712, 752-759.	2.8	68
29957	Microstructure and property evolution of Fe-N ferrite undergoing early-stages of precipitation. Materials Science & Engineering A: Structural Materials: Properties, Microstructure and Processing, 2017, 696, 198-207.	2.6	10
29958	Tunable Schottky Barrier at MoSe₂/Metal Interfaces with a Buffer Layer. Journal of Physical Chemistry C, 2017, 121, 9305-9311.	1.5	45
29959	A Simple Descriptor to Rapidly Screen CO Oxidation Activity on Rare-Earth Metal-Doped CeO2: From Experiment to First-Principles. ACS Applied Materials & Interfaces, 2017, 9, 15449-15458.	4.0	59
29960	Theoretical Investigation of the Acid Catalyzed Formation of Oxymethylene Dimethyl Ethers from Trioxane and Dimethoxymethane. ACS Catalysis, 2017, 7, 3615-3621.	5.5	37
29961	Bi1Te1 is a dual topological insulator. Nature Communications, 2017, 8, 14976.	5.8	66
29962	First-principles investigation of Zr-O compounds, their crystal structures, and mechanical properties. Journal of Applied Physics, 2017, 121, .	1.1	18
29963	Antibacterial electrospun zein nanofibrous web encapsulating thymol/cyclodextrin-inclusion complex for food packaging. Food Chemistry, 2017, 233, 117-124.	4.2	179

#	Article	IF	Citations
29964	Lattice distortion induced site dependent carbon gettering at twin boundaries in silicon. Journal of Alloys and Compounds, 2017, 712, 599-604.	2.8	21
29965	Perpendicular Magnetic Anisotropy Preserved by Orbital Oscillation in Strained Tetragonal Fe₄N/BiFeO₃ Bilayers. ACS Applied Materials & Interfaces, 2017, 9, 15887-15892.	4.0	21
29966	The effect of atomic arrangement on photoabsorption of freestanding double-layer honeycomb sheets of zinc selenide. Journal of Materials Chemistry C, 2017, 5, 4505-4510.	2.7	8
29967	Electronic structures of rutile (011)(2 Ã— 1) surfaces: A many-body perturbation theory study. Journal of Chemical Physics, 2017, 146, 124702.	1.2	6
29968	Inversion domain boundaries in Mn and Al dualâ€doped ZnO: Atomic structure and electronic properties. Journal of the American Ceramic Society, 2017, 100, 4252-4262.	1.9	17
29969	Long life rechargeable Li-O2 batteries enabled by enhanced charge transfer in nanocable-like Fe@N-doped carbon nanotube catalyst. Science China Materials, 2017, 60, 415-426.	3.5	26
29970	Characterization of titanate nanotubes for energy applications. Journal of Energy Storage, 2017, 12, 66-77.	3.9	20
29971	Low rank factorization of the Coulomb integrals for periodic coupled cluster theory. Journal of Chemical Physics, 2017, 146, 124105.	1.2	60
29972	Radiation Tolerant Interfaces: Influence of Local Stoichiometry at the Misfit Dislocation on Radiation Damage Resistance of Metal/Oxide Interfaces. Advanced Materials Interfaces, 2017, 4, 1700037.	1.9	10
29973	Balancing Mechanical Properties and Sustainability in the Search for Superhard Materials. Integrating Materials and Manufacturing Innovation, 2017, 6, 1-8.	1.2	25
29974	Yin and Yang Dual Characters of CuO_x Clusters for Câ€“C Bond Oxidation Driven by Visible Light. ACS Catalysis, 2017, 7, 3850-3859.	5.5	103
29975	Highly Oriented Low-Dimensional Tin Halide Perovskites with Enhanced Stability and Photovoltaic Performance. Journal of the American Chemical Society, 2017, 139, 6693-6699.	6.6	723
29976	Redox-controlled potassium intercalation into two polyaromatic hydrocarbon solids. Nature Chemistry, 2017, 9, 644-652.	6.6	32
29977	Platinum-nickel alloy excavated nano-multipods with hexagonal close-packed structure and superior activity towards hydrogen evolution reaction. Nature Communications, 2017, 8, 15131.	5.8	364
29978	Mechanistic origin of low polarization in aprotic Naâ€“O₂ batteries. Physical Chemistry Chemical Physics, 2017, 19, 12375-12383.	1.3	24
29979	Thermal conductivity of Bi₂Te₃ nanowires: how size affects phonon scattering. Nanoscale, 2017, 9, 6741-6747.	2.8	41
29980	Ferroelectric fatigue in layered perovskites from self-energy corrected density functional theory. RSC Advances, 2017, 7, 21856-21868.	1.7	19
29981	Effects of Cr-doping on the adsorption and dissociation of S, SO, and SO2 on Ni(111) surfaces. Journal of Chemical Physics, 2017, 146, 154701.	1.2	5

#	Article	IF	Citations
29982	A first-principles study of NbSe₂monolayer as anode materials for rechargeable lithium-ion and sodium-ion batteries. Journal Physics D: Applied Physics, 2017, 50, 235501.	1.3	69
29983	Effects of strain on mechanical and electronic properties of borophene. Materials Research Express, 2017, 4, 045020.	0.8	11
29984	Topological Insulators: Electronic Band Structure and Spectroscopy. IOP Conference Series: Materials Science and Engineering, 2017, 175, 012004.	0.3	5
29985	Synergic effects of VLi and Ti doping on hydrogen desorption on LiBH4 (010) surface: A first-principles investigation. International Journal of Hydrogen Energy, 2017, 42, 18442-18451.	3.8	4
29986	Effect of oxygen and magnesium vacancies on the d 0 magnetism of C-monodoped MgO using ab initio method. Journal of Alloys and Compounds, 2017, 712, 526-534.	2.8	11
29987	Elastic moduli tensors, ideal strength, and morphology of stanene based on an enhanced continuum model and first principles. Mechanics of Materials, 2017, 110, 1-15.	1.7	18
29988	An atomic-scale modeling and experimental study of <mml:math xmlns:mml="http://www.w3.org/1998/Math/MathML" altimg="si0029.gif" overflow="scroll"><mml:mrow><mml:mo stretchy="false">ã€ˆ</mml:mo><mml:mi>c</mml:mi><mml:mo>+</mml:mo><mml:mi>a</mml:mi><mml:mo stretchy="false">ã€‰</mml:mo></mml:mrow></mml:math> dislocations in Mg. Materials Science & Engineering A: Structural Materials: Properties, Microstructure and Processing, 2017, 695, 270-278.	2.6	32
29989	Stages of Se adsorption on Au(111): A combined XPS, LEED, TOF-DRS, and DFT study. Surface Science, 2017, 662, 113-122.	0.8	3
29990	Charge Transfer and Functionalization of Monolayer InSe by Physisorption of Small Molecules for Gas Sensing. Journal of Physical Chemistry C, 2017, 121, 10182-10193.	1.5	83
29991	Tetra-silicene: A Semiconducting Allotrope of Silicene with Negative Poissonâ€™s Ratios. Journal of Physical Chemistry C, 2017, 121, 9627-9633.	1.5	57
29992	Pressure-induced structural and spin transitions of Fe3S4. Scientific Reports, 2017, 7, 46334.	1.6	10
29993	Low thermal conductivity of monolayer ZnO and its anomalous temperature dependence. Physical Chemistry Chemical Physics, 2017, 19, 12882-12889.	1.3	55
29994	Acoustic phonon softening and reduced thermal conductivity in Mg2Si1â^'xSnx solid solutions. Applied Physics Letters, 2017, 110, .	1.5	21
29996	From Twoâ€•to Threeâ€Dimensional Structures of a Supertetrahedral Boran Using Density Functional Calculations. Angewandte Chemie, 2017, 129, 10252-10256.	1.6	2
29997	A microscopic continuum model for defect dynamics in metallic glasses. Journal of the Mechanics and Physics of Solids, 2017, 104, 1-11.	2.3	5
29998	Two-Dimensional Metal-Free Organic Multiferroic Material for Design of Multifunctional Integrated Circuits. Journal of Physical Chemistry Letters, 2017, 8, 1973-1978.	2.1	64
29999	Ab initio investigation of Jahnâ€“Teller-distortion-tuned Li-ion migration in Î»-MnO₂. Journal of Materials Chemistry A, 2017, 5, 9618-9626.	5.2	23
30000	Defect-mediated leakage in lithium intercalated bilayer graphene. AIP Advances, 2017, 7, .	0.6	5

#	Article	IF	Citations
30001	(110) Facet of rutile-structured GeO₂: anab initioinvestigation. Molecular Physics, 2017, 115, 1598-1605.	0.8	4
30002	Adsorption and spin-related properties of multi-Co atoms assembled in the half unit cells of Si(111)-(7 Ã— Tj ETQq1 1 0.784314 rgBT /C	1.2	3
30003	Proton conduction across and along BaOâ€“ and ZrO2â€“terminated (001) BaZrO3 surfaces using density functional theory. Solid State Ionics, 2017, 306, 137-141.	1.3	7
30004	Atomistic Insights into Nitrogen-Cycle Electrochemistry: A Combined DFT and Kinetic Monte Carlo Analysis of NO Electrochemical Reduction on Pt(100). ACS Catalysis, 2017, 7, 3869-3882.	5.5	201
30005	Atomic structures of twin boundaries in hexagonal close-packed metallic crystals with particular focus on Mg. Npj Computational Materials, 2017, 3, .	3.5	28
30006	Carbon-bearing silicate melt at deep mantle conditions. Scientific Reports, 2017, 7, 848.	1.6	30
30007	An approximate full-dimensional quantum dynamics study of the mode specificity in the dissociative chemisorption of D₂O on rigid Cu(111). Physical Chemistry Chemical Physics, 2017, 19, 11960-11967.	1.3	9
30008	Directional electron delivery via a vertical channel between g-C₃N₄ layers promotes photocatalytic efficiency. Journal of Materials Chemistry A, 2017, 5, 9358-9364.	5.2	159
30009	Superhalogen-based lithium superionic conductors. Journal of Materials Chemistry A, 2017, 5, 13373-13381.	5.2	55
30010	Tailoring magnetic insulator proximity effects in graphene: first-principles calculations. 2D Materials, 2017, 4, 025074.	2.0	121
30011	Chipâ€Scale Mass Manufacturable Highâ€Q Silicon Microdisks. Advanced Materials Technologies, 2017, 2, 1600299.	3.0	11
30012	Synthesis, Crystal Structures, and Properties of Zeoliteâ€Like T₃(H₃O)₂[M(CN)₆]₂Â·uH₂O (T = Co, Zn; M = Ru, Os). European Journal of Inorganic Chemistry, 2017, 2017, 2980-2989.	1.0	13
30013	The dependence on ammonia pretreatment of Nâ^'O activation by Co(II) sites in zeolites: a DFT and ab initio molecular dynamics study. Journal of Molecular Modeling, 2017, 23, 160.	0.8	6
30014	Genetic algorithm approach to global optimization of the full-dimensional potential energy surface for hydrogen atom at fcc-metal surfaces. Chemical Physics Letters, 2017, 683, 286-290.	1.2	19
30015	Activity and electrochemical stability of a chromium modified nickel catalyst for oxygen reduction reaction. Electrochimica Acta, 2017, 236, 260-272.	2.6	10
30016	Luminescence and theoretical calculations of novel red-emitting NaYPO 4 F:Eu 3+ phosphor for LED applications. Journal of Alloys and Compounds, 2017, 712, 225-232.	2.8	28
30017	Defect-Controlled Electronic Structure and Phase Stability in Thermoelectric Skutterudite CoSb₃. Chemistry of Materials, 2017, 29, 3999-4007.	3.2	17
30018	Mechanism of Methanol Decomposition on the Pt₃Ni(111) Surface: DFT Study. Journal of Physical Chemistry C, 2017, 121, 9348-9360.	1.5	46

#	Article	IF	Citations
30019	Computational Modeling of Novel Bulk Materials for the Intermediate-Band Solar Cells. ACS Omega, 2017, 2, 1454-1462.	1.6	26
30020	Waterâ€“Ice Analogues of Polycyclic Aromatic Hydrocarbons: Water Nanoclusters on Cu(111). Journal of the American Chemical Society, 2017, 139, 6403-6410.	6.6	32
30021	3D lattice distortions and defect structures in ion-implanted nano-crystals. Scientific Reports, 2017, 7, 45993.	1.6	96
30022	Size and strain tunable band alignment of blackâ€“blue phosphorene lateral heterostructures. Physical Chemistry Chemical Physics, 2017, 19, 12466-12472.	1.3	25
30023	A small bandgap semiconductor, p-type MnV₂O₆, active for photocatalytic hydrogen and oxygen production. Dalton Transactions, 2017, 46, 10657-10664.	1.6	32
30024	Designing 3D topological insulators by 2D-Xene (X = Ge, Sn) sheet functionalization in GaGeTe-type structures. Journal of Materials Chemistry C, 2017, 5, 4752-4762.	2.7	21
30025	Investigating anomalous thermal expansion of copper halides by inelastic neutron scattering and ab initio phonon calculations. Physical Chemistry Chemical Physics, 2017, 19, 12107-12116.	1.3	9
30026	DFT investigation into the underperformance of sulfide materials in photovoltaic applications. Journal of Materials Chemistry A, 2017, 5, 9132-9140.	5.2	19
30027	Influence of Si substitution on structural, electronic and magnetic properties of Fe2MnGa Heusler compound. European Physical Journal B, 2017, 90, 1.	0.6	2
30028	Ab initio modelling of solute segregation energies to a general grain boundary. Acta Materialia, 2017, 132, 138-148.	3.8	42
30029	Pressure-Driven Isostructural Phase Transition in InNbO₄: In Situ Experimental and Theoretical Investigations. Inorganic Chemistry, 2017, 56, 5420-5430.	1.9	29
30030	First-Principles Study on CO Removing Mechanism on Pt-Decorated Oxygen-Rich Anode Surfaces (Pt2/o-MO2(110), M = Ru and Ir) in DMFC. Journal of Physical Chemistry C, 2017, 121, 9825-9832.	1.5	14
30031	Synergistic Effect of Hydrogenation and Thiocyanate Treatments on Ag-Loaded TiO₂ Nanoparticles for Solar-to-Hydrogen Conversion. Journal of Physical Chemistry C, 2017, 121, 9681-9690.	1.5	17
30032	Electron transport and visible light absorption in a plasmonic photocatalyst based on strontium niobate. Nature Communications, 2017, 8, 15070.	5.8	64
30033	Magnetism in the p-type Monolayer II-VI semiconductors SrS and SrSe. Scientific Reports, 2017, 7, 45869.	1.6	17
30034	Insights into the thermoelectric properties of SnSe from ab initio calculations. Physical Chemistry Chemical Physics, 2017, 19, 12804-12815.	1.3	42
30035	Gismondine cobalt phosphate (CoPO₄) as a monovalent-ion battery cathode material: a first-principles study. Journal of Materials Chemistry A, 2017, 5, 9287-9292.	5.2	4
30036	Phosphorus-Mo₂C@carbon nanowires toward efficient electrochemical hydrogen evolution: composition, structural and electronic regulation. Energy and Environmental Science, 2017, 10, 1262-1271.	15.6	379

#	Article	IF	Citations
30037	Ferrimagnetic half-metallic properties of Cr/Fe Î´ doped MoS₂ monolayer. RSC Advances, 2017, 7, 20116-20122.	1.7	12
30038	Superionic and electronic conductivity in monolayer W₂C: ab initio predictions. Journal of Materials Chemistry A, 2017, 5, 11094-11099.	5.2	51
30039	Magnetic and electronic properties of La₃ MO₇ and possible polaron formation in hole-doped La₃ MO₇ (Mâ€‰â€‰=â€‰â€‰Ru and Os). Journal of Physics Condensed Matter, 2017, 29, 095803.	2.1	2
30040	Enhanced carbon tolerance on Ni-based reforming catalyst with Ir alloying: A DFT study. Applied Surface Science, 2017, 419, 678-682.	3.1	11
30041	Accurate classical short-range forces for the study of collision cascades in Feâ€“Niâ€“Cr. Computer Physics Communications, 2017, 219, 11-19.	3.0	39
30042	Interpreting radiation-induced segregation and enhanced radiation tolerance of single-phase concentrated solid-solution alloys from first principles. Materials Letters, 2017, 202, 120-122.	1.3	6
30043	Emergence of Novel Polynitrogen Molecule-like Species, Covalent Chains, and Layers in Magnesiumâ€“Nitrogen Mg_xN_y Phases under High Pressure. Journal of Physical Chemistry C, 2017, 121, 11037-11046.	1.5	76
30044	Chemical Vapor Deposition Synthesis and Optical Properties of Nb₂O₅ Thin Films with Hybrid Functional Theoretical Insight into the Band Structure and Band Gaps. ACS Applied Materials & Interfaces, 2017, 9, 18031-18038.	4.0	54
30045	â€œElectron/Ion Spongeâ€•Like V-Based Polyoxometalate: Toward High-Performance Cathode for Rechargeable Sodium Ion Batteries. ACS Nano, 2017, 11, 6911-6920.	7.3	95
30046	A Kinetic Pathway toward High-Density Ordered N Doping of Epitaxial Graphene on Cu(111) Using C₅NCl₅ Precursors. Journal of the American Chemical Society, 2017, 139, 7196-7202.	6.6	16
30047	Tunable and low-loss correlated plasmons in Mott-like insulating oxides. Nature Communications, 2017, 8, 15271.	5.8	42
30048	Oxygen diffusion in ceria doped with rare-earth elements. Physical Chemistry Chemical Physics, 2017, 19, 13723-13730.	1.3	17
30049	Structural and electronic properties of defects at grain boundaries in CuInSe₂. Physical Chemistry Chemical Physics, 2017, 19, 14770-14780.	1.3	16
30050	Reducibility of ZrO₂/Pt₃Zr and ZrO₂/Pt 2D films compared to bulk zirconia: a DFT+U study of oxygen removal and H₂adsorption. Nanoscale, 2017, 9, 6866-6876.	2.8	19
30051	Direct quantitative measurement of the Câ•Oâ‹…â‹…â‹…Hâ€“C bond by atomic force microscopy. Science Advances, 2017, 3, e1603258.	4.7	80
30052	Structural and electronic properties of lead sulfide quantum dots from screened hybrid density functional calculations including spinâ€“orbit coupling effects. Theoretical Chemistry Accounts, 2017, 136, 1.	0.5	3
30053	Functionalization of Î³-graphyne by transition metal adatoms. Carbon, 2017, 120, 63-70.	5.4	81
30054	Mechanism on the Improved Performance of Lithium Sulfur Batteries with MXene-Based Additives. Journal of Physical Chemistry C, 2017, 121, 11047-11054.	1.5	118

#	Article	IF	Citations
30055	Mechanically-Controlled Reversible Spin Crossover of Single Fe-Porphyrin Molecules. ACS Nano, 2017, 11, 6295-6300.	7.3	29
30056	Tuning of Interlayer Coupling in Large-Area Graphene/WSe₂ van der Waals Heterostructure via Ion Irradiation: Optical Evidences and Photonic Applications. ACS Photonics, 2017, 4, 1531-1538.	3.2	75
30057	Dark trions and biexcitons in WS2 and WSe2 made bright by e-e scattering. Scientific Reports, 2017, 7, 45998.	1.6	48
30058	Phosphorene: A Promising Candidate for Highly Sensitive and Selective SF₆ Decomposition Gas Sensors. IEEE Electron Device Letters, 2017, 38, 963-966.	2.2	132
30059	Thermo-elastic behavior of grossular garnet at high pressures and temperatures. American Mineralogist, 2017, 102, 851-859.	0.9	38
30060	SGO: A fast engine for ab initio atomic structure global optimization by differential evolution. Computer Physics Communications, 2017, 219, 35-44.	3.0	14
30061	The effects of metal-cluster on electronic transport of graphene with vacancy studied by first-principles. Superlattices and Microstructures, 2017, 109, 47-53.	1.4	3
30062	Improved Ductility of B₁₂ Icosahedra-based Superhard Materials through Icosahedral Slip. Journal of Physical Chemistry C, 2017, 121, 11831-11838.	1.5	13
30063	Isolated Single-Atom Pd Sites in Intermetallic Nanostructures: High Catalytic Selectivity for Semihydrogenation of Alkynes. Journal of the American Chemical Society, 2017, 139, 7294-7301.	6.6	354
30064	Intrinsic ferromagnetism and quantum anomalous Hall effect in a CoBr₂monolayer. Physical Chemistry Chemical Physics, 2017, 19, 13432-13437.	1.3	34
30065	Luminescence properties and site occupancy of Ce³⁺ in Ba₂SiO₄: a combined experimental and ab initio study. RSC Advances, 2017, 7, 25685-25693.	1.7	20
30066	Insight from first principles into the stability and magnetism of alkali-metal superoxide nanoclusters. Journal of Chemical Physics, 2017, 146, 184301.	1.2	1
30067	Direct growth of MoS ₂ single crystals on polyimide substrates. 2D Materials, 2017, 4, 021028.	2.0	39
30068	Mechanical, Dynamical and Thermodynamic Properties of Al-3wt%Mg from First Principles. Zeitschrift Fur Naturforschung - Section A Journal of Physical Sciences, 2017, 72, 527-534.	0.7	1
30069	Additional Sodium Insertion into Polyanionic Cathodes for Higherâ€Energy Naâ€Ion Batteries. Advanced Energy Materials, 2017, 7, 1700514.	10.2	157
30070	Inducing Complexity in Intermetallics through Electronâ€“Hole Matching: The Structure of Fe 14 Pd 17 Al 69. Angewandte Chemie - International Edition, 2017, 56, 10145-10150.	7.2	8
30071	Bimetallic Nickelâ€Substituted Cobaltâ€Borate Nanowire Array: An Earthâ€Abundant Water Oxidation Electrocatalyst with Superior Activity and Durability at Near Neutral pH. Small, 2017, 13, 1700394.	5.2	95
30072	The evolution of the deformation substructure in a Ni-Co-Cr equiatomic solid solution alloy. Acta Materialia, 2017, 132, 35-48.	3.8	357

#	Article	IF	Citations
30073	Ionization Energy as a Stability Criterion for Halide Perovskites. Journal of Physical Chemistry C, 2017, 121, 11977-11984.	1.5	42
30074	Defect Antiperovskite Compounds Hg₃Q₂I₂ (Q = S, Se, and Te) for Room-Temperature Hard Radiation Detection. Journal of the American Chemical Society, 2017, 139, 7939-7951.	6.6	45
30075	Tunable electronic structure and magnetic moment in C2N nanoribbons with different edge functionalization atoms. Physical Chemistry Chemical Physics, 2017, 19, 15021-15029.	1.3	10
30076	Charge separation in a nanostep structured perovskite-type photocatalyst induced by successive surface heterojunctions. Journal of Materials Chemistry A, 2017, 5, 10442-10449.	5.2	34
30077	Anisotropic thermal expansion of SnSe from first-principles calculations based on GrÃ¼neisen's theory. Physical Chemistry Chemical Physics, 2017, 19, 15187-15193.	1.3	35
30078	Metal-free spin and spin-gapless semiconducting heterobilayers: monolayer boron carbonitrides on hexagonal boron nitride. Physical Chemistry Chemical Physics, 2017, 19, 14801-14810.	1.3	6
30079	Mechanical properties of a gallium fumarate metalâ€“organic framework: a joint experimental-modelling exploration. Journal of Materials Chemistry A, 2017, 5, 11047-11054.	5.2	27
30080	Thermoelectric phase diagram of the SrTiO3â€“SrNbO3 solid solution system. Journal of Applied Physics, 2017, 121, .	1.1	22
30081	Elastic, electronic, and dielectric properties of bulk and monolayer ZrS₂, ZrSe₂, HfS₂, HfSe₂ from van der Waals densityâ€functional theory. Physica Status Solidi (B): Basic Research, 2017, 254, 1700033.	0.7	110
30082	Niâ€Fe Nitride Nanoplates on Nitrogenâ€Doped Graphene as a Synergistic Catalyst for Reversible Oxygen Evolution Reaction and Rechargeable Znâ€Air Battery. Small, 2017, 13, 1700099.	5.2	151
30083	Prediction of two-dimensional d-block elemental materials with normal honeycomb, triangular-dodecagonal, and square-octagonal structures from first principles. Applied Surface Science, 2017, 419, 484-496.	3.1	6
30084	Tunable gap opening and spin polarization of two dimensional graphene/hafnene van der Waals heterostructures. Carbon, 2017, 120, 121-127.	5.4	32
30085	Simultaneous enhanced performance of electrical conductivity and Seebeck coefficient in Bi2â^'Sn S3 by solvothermal and microwave sintering. Journal of Alloys and Compounds, 2017, 717, 177-182.	2.8	15
30086	An experimental and theoretical study on soft chemically grown CuS thin film for photosensor application. Materials Science in Semiconductor Processing, 2017, 67, 62-68.	1.9	47
30087	Theoretical study on the poly(m-phenylene) derivatives with lower HOMOâ€“LUMO gaps. Synthetic Metals, 2017, 229, 16-21.	2.1	5
30088	Predicting the Thermodynamic Stability of Solids Combining Density Functional Theory and Machine Learning. Chemistry of Materials, 2017, 29, 5090-5103.	3.2	217
30089	Converting Carbohydrates to Carbon-Based Photocatalysts for Environmental Treatment. Environmental Science & Technology, 2017, 51, 7076-7083.	4.6	107
30090	First-Principles Study of High Temperature CO₂ Electrolysis on Transition Metal Electrocatalysts. Industrial & Engineering Chemistry Research, 2017, 56, 6155-6163.	1.8	16

#	Article	IF	Citations
30091	A-Site Cation Bulk and Surface Diffusion in A-Site-Deficient BaZrO₃ and SrZrO₃ Perovskites. Journal of Physical Chemistry C, 2017, 121, 12220-12229.	1.5	11
30092	On-Surface Heck Reaction of Aryl Bromides with Alkene on Au(111) with Palladium as Catalyst. Organic Letters, 2017, 19, 2801-2804.	2.4	22
30093	Effective and Highly Selective CO Generation from CO₂ Using a Polycrystalline Î±-Mo₂C Catalyst. ACS Catalysis, 2017, 7, 4323-4335.	5.5	108
30094	Quantitative Coordinationâ€“Activity Relations for the Design of Enhanced Pt Catalysts for CO Electro-oxidation. ACS Catalysis, 2017, 7, 4355-4359.	5.5	45
30095	First-principles prediction on bismuthylene monolayer as a promising quantum spin Hall insulator. Nanoscale, 2017, 9, 8207-8212.	2.8	26
30096	Experimental and computational study of the magnetic properties of ZrMn2â^'xCoxGe4O12. Dalton Transactions, 2017, 46, 6921-6933.	1.6	7
30097	Two excellent phase-matchable infrared nonlinear optical materials based on 3D diamond-like frameworks: RbGaSn₂Se₆ and RbInSn₂Se₆. Dalton Transactions, 2017, 46, 7714-7721.	1.6	30
30098	Potential energyâ€“driven spin manipulation via a controllable hydrogen ligand. Science Advances, 2017, 3, e1602060.	4.7	13
30099	A Model for Estimating Chemical Potentials in Ternary Semiconductor Compounds: the Case of InGaAs. MRS Advances, 2017, 2, 2909-2914.	0.5	3
30100	Density Functional Theory Evaluated for Structural and Electronic Properties of 1T-Li _x TiS₂ and Lithium Ion Migration in 1T-Li_{0.94}TiS₂. Zeitschrift Fur Physikalische Chemie, 2017, 231, 1263-1278.	1.4	4
30101	Theoretical Insights to Bulk Activity Towards Oxygen Evolution in Oxyhydroxides. Catalysis Letters, 2017, 147, 1533-1539.	1.4	43
30102	Tuning the Adsorption of Polysulfides in Lithiumâ€“Sulfur Batteries with Metalâ€“Organic Frameworks. Chemistry of Materials, 2017, 29, 4932-4939.	3.2	98
30103	A comprehensive understanding of water photooxidation on Ag₃PO₄ surfaces. RSC Advances, 2017, 7, 23994-24003.	1.7	13
30104	Interface optimization of ZnO nanorod/CdS quantum dots heterostructure by a facile two-step low-temperature thermal treatment for improved photoelectrochemical water splitting. Chemical Engineering Journal, 2017, 325, 151-159.	6.6	65
30105	Density Functional Theory Calculations of Atomic Configurations and Bandgaps of C-, Ge-, and Sn-Doped Si Crystals for Solar Cells. ECS Journal of Solid State Science and Technology, 2017, 6, P326-P331.	0.9	1
30106	Prediction of New Structure, Phase Transition, Mechanical, and Thermodynamic Properties of Nb3Si. Advanced Engineering Materials, 2017, 19, 1700099.	1.6	22
30107	Novel Hybrid Catalyst for the Oxidation of Organic Acids: Pd Nanoparticles Supported on Mnâ€Nâ€3Dâ€Graphene Nanosheets. ChemElectroChem, 2017, 4, 2336-2344.	1.7	5
30108	Enhancing the Acylation Activity of Acetic Acid by Formation of an Intermediate Aromatic Ester. ChemSusChem, 2017, 10, 2823-2832.	3.6	20

#	Article	IF	Citations
30109	In-operando elucidation of bimetallic CoNi nanoparticles during high-temperature CH4/CO2 reaction. Applied Catalysis B: Environmental, 2017, 213, 177-189.	10.8	88
30110	Synergistic effect of nitrogen and sulfur co-doped graphene as efficient metal-free counter electrode for dye-sensitized solar cells: A first-principle study. Computational Materials Science, 2017, 136, 44-51.	1.4	32
30111	Neutron diffraction study of superconductingLa3Ni2B112N3â˜Î´. Journal of Alloys and Compounds, 2017, 716, 251-258.	2.8	0
30112	Negative thermal expansion of quartz glass at low temperatures: An ab initio simulation study. Journal of Non-Crystalline Solids, 2017, 468, 82-91.	1.5	7
30113	Thermoelectric Performance and Defect Chemistry in n-Type Zintl KGaSb₄. Chemistry of Materials, 2017, 29, 4523-4534.	3.2	59
30114	Effect of Transition Metal Cations on Stability Enhancement for Molybdate-Based Hybrid Supercapacitor. ACS Applied Materials & Interfaces, 2017, 9, 17977-17991.	4.0	82
30115	Nanotubular Gamma Alumina with High-Energy External Surfaces: Synthesis and High Performance for Catalysis. ACS Catalysis, 2017, 7, 4083-4092.	5.5	41
30116	Atomic-level energy storage mechanism of cobalt hydroxide electrode for pseudocapacitors. Nature Communications, 2017, 8, 15194.	5.8	250
30117	Self-assembly of glycine on Cu(001): the effect of temperature and polarity. RSC Advances, 2017, 7, 4116-4123.	1.7	3
30118	Phase evolution of lithium intercalation dynamics in 2H-MoS₂. Nanoscale, 2017, 9, 7533-7540.	2.8	83
30119	Diffusion coefficients of transition metals in fcc cobalt. Acta Materialia, 2017, 132, 467-478.	3.8	65
30120	Preparation of Ti 3 C 2 and Ti 2 C MXenes by fluoride salts etching and methane adsorptive properties. Applied Surface Science, 2017, 416, 781-789.	3.1	407
30121	Pressure-induced electronic topological transitions in the charge-density-wave material In4Se3. Journal of Alloys and Compounds, 2017, 715, 237-241.	2.8	5
30122	Prediction of the mechanical properties of MoSi 2 doped with Cr, Nb and W from first-principles calculations. Journal of Alloys and Compounds, 2017, 714, 459-466.	2.8	34
30123	A new metallic carbon allotrope with high stability and potential for lithium ion battery anode material. Nano Energy, 2017, 38, 263-270.	8.2	77
30124	Bond length variation in Zn substituted NiO studied from extended X-ray absorption fine structure. Solid State Communications, 2017, 259, 40-44.	0.9	10
30125	Metallic Hydrogen in Atomically Precise Gold Nanoclusters. Chemistry of Materials, 2017, 29, 4840-4847.	3.2	70
30126	Copper Cluster Size Effect in Methanol Synthesis from CO₂. Journal of Physical Chemistry C, 2017, 121, 10406-10412.	1.5	144

#	Article	IF	Citations
30127	Computational Screening for Design of Optimal Coating Materials to Suppress Gas Evolution in Li-Ion Battery Cathodes. ACS Applied Materials & Interfaces, 2017, 9, 17822-17834.	4.0	32
30128	A hybrid organic-inorganic perovskite dataset. Scientific Data, 2017, 4, 170057.	2.4	112
30129	Pressure-induced insulator-to-metal transitions for enhancing thermoelectric power factor in bismuth telluride-based alloys. Physical Chemistry Chemical Physics, 2017, 19, 12784-12793.	1.3	23
30130	The preparation, and structural and multiferroic properties of B-site ordered double-perovskite Bi₂FeMnO₆. Journal of Materials Chemistry C, 2017, 5, 5494-5500.	2.7	28
30131	Nanotwins soften boron-rich boron carbide (B13C2). Applied Physics Letters, 2017, 110, .	1.5	30
30132	Anisotropic features in the electronic structure of the two-dimensional transition metal trichalcogenide TiS ₃ : electron doping and plasmons. 2D Materials, 2017, 4, 025085.	2.0	24
30133	Tunneling Spintronics across MgO Driven by Double Oxygen Vacancies. Advanced Electronic Materials, 2017, 3, 1600390.	2.6	11
30134	Enhanced atomic oxygen adsorption on defective nickel surfaces: An ab initio study. Surface Science, 2017, 663, 62-70.	0.8	5
30135	Searching for â€œDefect-Tolerantâ€•Photovoltaic Materials: Combined Theoretical and Experimental Screening. Chemistry of Materials, 2017, 29, 4667-4674.	3.2	275
30136	Active Tetrahedral Iron Sites of Î³-Fe₂O₃ Catalyzing NO Reduction by NH₃. Environmental Science and Technology Letters, 2017, 4, 246-250.	3.9	47
30137	Spectroscopic Fingerprints of Carbon Monomers and Dimers on Ir(111): Experiment and Theory. Journal of Physical Chemistry C, 2017, 121, 11335-11345.	1.5	9
30138	Surface-Engineering of Ultrathin Gold Nanowires: Tailored Self-Assembly and Enhanced Stability. Langmuir, 2017, 33, 5456-5463.	1.6	22
30139	Understanding the Thermal Stability of Palladiumâ€“Platinum Coreâ€“Shell Nanocrystals by In Situ Transmission Electron Microscopy and Density Functional Theory. ACS Nano, 2017, 11, 4571-4581.	7.3	53
30140	Photoresponse of Natural van der Waals Heterostructures. ACS Nano, 2017, 11, 6024-6030.	7.3	44
30141	Efficient hydrogen isotopologues separation through a tunable potential barrier: The case of a C2N membrane. Scientific Reports, 2017, 7, 1483.	1.6	21
30142	Influence of interface interaction on the moirÃ© superstructures of graphene on transition-metal substrates. RSC Advances, 2017, 7, 12179-12184.	1.7	10
30143	Strain engineering of electronic structures and photocatalytic responses of MXenes functionalized by oxygen. Physical Chemistry Chemical Physics, 2017, 19, 14738-14744.	1.3	60
30144	Size-dependent plastic deformation of twinned nanopillars in body-centered cubic tungsten. Journal of Applied Physics, 2017, 121, .	1.1	30

#	Article	IF	Citations
30145	Novel magnetic properties of CoTe nanorods and diversified CoTe₂ nanostructures obtained at different NaOH concentrations. Science and Technology of Advanced Materials, 2017, 18, 325-333.	2.8	29
30146	A Computational Study of a Singleâ€Walled Carbonâ€Nanotubeâ€Based Ultrafast Highâ€Capacity Aluminum Battery. Chemistry - an Asian Journal, 2017, 12, 1944-1951.	1.7	20
30147	Noncovalent Interactions between Dopamine and Regular and Defective Graphene. ChemPhysChem, 2017, 18, 2065-2080.	1.0	27
30148	First-principle studies of radioactive fission productions Cs/Sr/Ag/I adsorption on chromeâ€“molybdenum steel in Chinese 200ÂMW HTR-PM. Nuclear Science and Techniques/Hewuli, 2017, 28, 1.	1.3	3
30149	Synthesis and characterization of mixed alkali borophosphate with a new 1D chain: Li3Cs2BP4O14. Inorganica Chimica Acta, 2017, 466, 174-179.	1.2	9
30150	New metastable phases in an oxyborate compound obtained by an evolutionary algorithm and Density Functional Theory. Journal of Magnetism and Magnetic Materials, 2017, 435, 33-39.	1.0	4
30151	In-situ mass-electrochemical study of surface redox potential and interfacial chemical reactions of Li(Na)FePO 4 nanocrystals for Li(Na)-ion batteries. Nano Energy, 2017, 37, 90-97.	8.2	20
30152	A New Split Charge Equilibration Model and REPEAT Electrostatic Potential Fitted Charges for Periodic Frameworks with a Net Charge. Journal of Chemical Theory and Computation, 2017, 13, 2858-2869.	2.3	12
30153	Zinc Promotion of Platinum for Catalytic Light Alkane Dehydrogenation: Insights into Geometric and Electronic Effects. ACS Catalysis, 2017, 7, 4173-4181.	5.5	168
30154	Epitaxial growth and intrinsic nature of molybdenum disulfide on graphite. Applied Physics Express, 2017, 10, 055201.	1.1	3
30155	Adsorption and decomposition of HMX and CLâ€20 on Al(111) surface by DFT investigation. Surface and Interface Analysis, 2017, 49, 441-449.	0.8	9
30156	Bonding characteristics and electronic structures of the contact interfaces between group 13 metals and carbon nanotubes. Carbon, 2017, 119, 365-370.	5.4	3
30157	First-principles study on the magnetic and electronic properties of Al or P doped armchair silicene nanoribbons. Physics Letters, Section A: General, Atomic and Solid State Physics, 2017, 381, 2097-2102.	0.9	33
30158	Structural, Electronic, and Magnetic Properties of Iron Disulfide Fe_nS₂^{0/Â±} (n = 1â€“6) Clusters. Journal of Physical Chemistry A, 2017, 121, 3768-3780.	1.1	6
30159	Adsorption and Decomposition of a Lignin Î²-O-4 Linkage Model, 2-Phenoxyethanol, on Pt(111): Combination of Experiments and First-Principles Calculations. Journal of Physical Chemistry C, 2017, 121, 9889-9900.	1.5	16
30160	Inverse Magnetoresistance in Polymer Spin Valves. ACS Applied Materials & Interfaces, 2017, 9, 15644-15651.	4.0	35
30161	Growth of Quasi-Free-Standing Single-Layer Blue Phosphorus on Tellurium Monolayer Functionalized Au(111). ACS Nano, 2017, 11, 4943-4949.	7.3	109
30162	Ab initio assessment of Bi_{1â^'x}RE_xCuOS (RE = La, Gd, Y, Lu) solid solutions as a semiconductor for photochemical water splitting. Physical Chemistry Chemical Physics, 2017, 19, 12321-12330.	1.3	21

#	Article	IF	Citations
30163	D-Type Anti-Ferromagnetic Ground State in Ca ₂ Mn ₂ O ₅. Chinese Physics Letters, 2017, 34, 027101.	1.3	2
30164	Atomic motions in the layered copper pseudochalcogenide CuNCN indicative of a quantum spin-liquid scenario. Journal of Physics Condensed Matter, 2017, 29, 235701.	0.7	5
30165	Local structure of the Mg_xNi_xCo_xCu_xZn_xO(x=0.2) entropyâ€stabilized oxide: An EXAFS study. Journal of the American Ceramic Society, 2017, 100, 2732-2738.	3.9	168
30166	Temperature induced transitions in La 4 (Co 1â^'x Ni x) 3 O 10+Î´ ; oxygen stoichiometry and mobility. Solid State Ionics, 2017, 305, 7-15.	1.3	10
30167	Interaction of Acid Gases SO₂ and NO₂ with Coordinatively Unsaturated Metal Organic Frameworks: M-MOF-74 (M = Zn, Mg, Ni, Co). Chemistry of Materials, 2017, 29, 4227-4235.	3.2	99
30168	Persistence of Mixed and Non-intermediate Valence in the High-Pressure Structure of Silver(I,III) Oxide, AgO: A Combined Raman, X-ray Diffraction (XRD), and Density Functional Theory (DFT) Study. Inorganic Chemistry, 2017, 56, 5804-5812.	1.9	19
30169	Enabling the Electrochemical Activity in Sodium Iron Metaphosphate [NaFe(PO₃)₃] Sodium Battery Insertion Material: Structural and Electrochemical Insights. Inorganic Chemistry, 2017, 56, 5918-5929.	1.9	29
30170	Adsorption Study of a Water Molecule on Vacancy-Defected Nonpolar CdS Surfaces. Journal of Physical Chemistry C, 2017, 121, 9815-9824.	1.5	8
30171	DFT-based Monte Carlo Simulations of Impurity Clustering at CeO₂(111). Journal of Physical Chemistry C, 2017, 121, 15127-15134.	1.5	9
30172	Surface Reconstruction-Induced Site-Specific Charge Separation and Photocatalytic Reaction on Anatase TiO₂(001) Surface. Journal of Physical Chemistry C, 2017, 121, 9991-9999.	1.5	37
30173	Lattice Defects and the Mechanical Anisotropy of Borophene. Journal of Physical Chemistry C, 2017, 121, 10224-10232.	1.5	112
30174	Controlling Oriented Attachment and in Situ Functionalization of TiO₂ Nanoparticles During Hydrothermal Synthesis with APTES. Journal of Physical Chemistry C, 2017, 121, 11897-11906.	1.5	26
30175	Near-Perfect Spin Filtering and Negative Differential Resistance in an Fe(II)S Complex. Journal of Physical Chemistry Letters, 2017, 8, 2189-2194.	2.1	12
30176	Purely one-dimensional bands with a giant spin-orbit splitting: Pb nanoribbons on Si(553) surface. Scientific Reports, 2017, 7, 46215.	1.6	26
30177	Structural stability and intriguing electronic properties of two-dimensional transition metal dichalcogenide alloys. Physical Chemistry Chemical Physics, 2017, 19, 13846-13854.	1.3	46
30178	Atomic structure and formation mechanism of sub-nanometer pores in 2D monolayer MoS₂. Nanoscale, 2017, 9, 6417-6426.	2.8	54
30179	Heterogeneous Cuâ€“Pd binary interface boosts stability and mass activity of atomic Pt clusters in the oxygen reduction reaction. Nanoscale, 2017, 9, 7207-7216.	2.8	21
30180	Impurity-induced deep centers in Tl6SI4. Journal of Applied Physics, 2017, 121, 145102.	1.1	9

#	Article	IF	Citations
30181	Pressure-induced boron nitride nanotube derivatives: 3D metastable allotropes. Journal of Applied Physics, 2017, 121, .	1.1	25
30182	Tunable Schottky barrier in van der Waals heterostructures of graphene and g-GaN. Applied Physics Letters, 2017, 110, .	1.5	166
30183	Stability of bound species during alkene reactions on solid acids. Proceedings of the National Academy of Sciences of the United States of America, 2017, 114, E3900-E3908.	3.3	52
30184	The atomic size effect on hybrid inorganicâ€“organic perovskite CH₃NH₃B₃ (B = Pb, Sn) from first-principles study. Modern Physics Letters B, 2017, 31, 1750139.	1.0	2
30185	Cu Diffusionâ€Driven Dynamic Modulation of the Electrical Properties of Amorphous Oxide Semiconductors. Advanced Functional Materials, 2017, 27, 1700336.	7.8	8
30186	The Unique Electronic Structure of Mg₂Si: Shaping the Conduction Bands of Semiconductors with Multicenter Bonding. Angewandte Chemie - International Edition, 2017, 56, 10135-10139.	7.2	18
30187	Evaluating Solvent Effects at the Aqueous/Pt(111) Interface. ChemPhysChem, 2017, 18, 2171-2190.	1.0	53
30188	Engineering a tubular mesoporous silica nanocontainer with well-preserved clay shell from natural halloysite. Nano Research, 2017, 10, 2782-2799.	5.8	71
30189	Adsorption and dissociation of H 2 O and CO 2 on the clean and O-pre-covered Ru(0001) surface. Applied Catalysis A: General, 2017, 540, 31-36.	2.2	8
30190	On the influence of junction structures on the mechanical and thermal properties of carbon honeycombs. Carbon, 2017, 119, 278-286.	5.4	56
30191	Ordered yttrium concentration effects on barium zirconate structure, proton binding sites and transition states. Solid State Ionics, 2017, 304, 126-134.	1.3	10
30192	Influence of trivalent doping on point and Frenkel defect formation in bulk chromium (III) oxide. Solid State Ionics, 2017, 307, 51-64.	1.3	7
30193	Effect of Water on the CO₂ Adsorption Capacity of Amine-Functionalized Carbon Sorbents. Industrial & Engineering Chemistry Research, 2017, 56, 6317-6325.	1.8	18
30194	Subsurface Polaron Concentration As a Factor in the Chemistry of Reduced TiO₂ (110) Surfaces. Journal of Physical Chemistry C, 2017, 121, 11325-11334.	1.5	16
30195	Study of NaFâ€“AlF₃ Melts by Coupling Molecular Dynamics, Density Functional Theory, and NMR Measurements. Journal of Physical Chemistry C, 2017, 121, 10289-10297.	1.5	29
30196	Enhanced Photovoltaic Properties Induced by Ferroelectric Domain Structures in Organometallic Halide Perovskites. Journal of Physical Chemistry C, 2017, 121, 11151-11158.	1.5	44
30197	Hydroxyl-Dependent Evolution of Oxygen Vacancies Enables the Regeneration of BiOCl Photocatalyst. ACS Applied Materials & Interfaces, 2017, 9, 16620-16626.	4.0	176
30198	The Two-Dimensional A_xCd_xBi_{4â€“x}Q₆ (A = K, Rb, Cs; Q =) Tj ETQq1 1 0.784314 rgB Society, 2017, 139, 6978-6987.	6.6	18

#	Article	IF	Citations
30199	Interface engineering of 3D BiVO₄/Fe-based layered double hydroxide core/shell nanostructures for boosting photoelectrochemical water oxidation. Journal of Materials Chemistry A, 2017, 5, 9952-9959.	5.2	134
30200	Strong ferroelectric polarization of CH₃NH₃GeI₃ with high-absorption and mobility transport anisotropy: theoretical study. Journal of Materials Chemistry C, 2017, 5, 5356-5364.	2.7	101
30201	Li₂TiSiO₅: a low potential and large capacity Ti-based anode material for Li-ion batteries. Energy and Environmental Science, 2017, 10, 1456-1464.	15.6	93
30202	Prediction on the light-assisted exfoliation of multilayered arsenene by the photo-isomerization of azobenzene. Nanoscale, 2017, 9, 7006-7011.	2.8	40
30203	Carbon dioxide capture in 2-aminoethanol aqueous solution from ab initio molecular dynamics simulations. Journal of Chemical Physics, 2017, 146, .	1.2	9
30204	Density functional investigation of the adsorption effects of PH3 and SH2 on the structure stability of the Au55 and Pt55 nanoclusters. Journal of Chemical Physics, 2017, 146, 164304.	1.2	9
30205	Tunable electronic properties of monolayer silicane via fluorine doping: a first-principles study. Journal of Physics Condensed Matter, 2017, 29, 265501.	0.7	0
30206	Tunable structural and electrical properties of zigzag CdS nanotubes: A density functional study. Physica Status Solidi (B): Basic Research, 2017, 254, 1700038.	0.7	5
30207	Theoretical study of the adsorption of substituted guaiacol and catechol radicals on a graphite surface. Electrochimica Acta, 2017, 242, 66-72.	2.6	6
30208	Morphology and location manipulation of Fe nanoparticles on carbon nanofibers as catalysts for ammonia decomposition to generate hydrogen. International Journal of Hydrogen Energy, 2017, 42, 17466-17475.	3.8	20
30209	Fabrication of MoSe2 nanoribbons via an unusual morphological phase transition. Nature Communications, 2017, 8, 15135.	5.8	70
30210	Surfaces and morphologies of covellite (CuS) nanoparticles by means of ab initio atomistic thermodynamics. CrystEngComm, 2017, 19, 3078-3084.	1.3	38
30211	A direct four-electron process on Feâ€“N₃ doped graphene for the oxygen reduction reaction: a theoretical perspective. RSC Advances, 2017, 7, 23812-23819.	1.7	33
30212	Electric field control of magnetic anisotropy in bilayer contacts with Rashba-type spinâ€“orbit interaction. Journal Physics D: Applied Physics, 2017, 50, 235001.	1.3	0
30213	Electron-counting in intermetallics made easy: the 18-n rule and isolobal bonds across the Osâ€“Al system. Zeitschrift Fur Kristallographie - Crystalline Materials, 2017, 232, 487-496.	0.4	8
30214	Performance of Cu^{II}â€, Pb^{II}â€, and Hg^{II}â€Exchanged Mordenite in the Adsorption of I₂, ICH₃, H₂O, CO, ClCH₃, and Cl₂: A Density Functional Study. ChemPhysChem, 2017, 18, 1642-1652.	1.0	23
30215	Flat borophene films as anode materials for Mg, Na or Li-ion batteries with ultra high capacities: A first-principles study. Applied Materials Today, 2017, 8, 60-67.	2.3	122
30216	Theoretical study on in situ synthesis of Pt/Ni Al hydroxide composites by etching of Pt Ni nanoparticles. Chemical Physics Letters, 2017, 679, 200-206.	1.2	3

#	Article	IF	Citations
30217	Intrinsic Origin of Superior Catalytic Properties of Tungsten-based Catalysts in Dye-sensitized Solar Cells. Electrochimica Acta, 2017, 242, 390-399.	2.6	73
30218	Fast Prediction of CO Binding Energy via the Local Structure Effect on PtCu Alloy Surfaces. Langmuir, 2017, 33, 8700-8706.	1.6	24
30219	Wide bandgap BaSnO3 films with room temperature conductivity exceeding 104 S cmâˆ'1. Nature Communications, 2017, 8, 15167.	5.8	175
30220	Hallmarks of Hunds coupling in the Mott insulator Ca2RuO4. Nature Communications, 2017, 8, 15176.	5.8	66
30221	Effects of the capping ligands, linkers and oxide surface on the electron injection mechanism of copper sulfide quantum dot-sensitized solar cells. Physical Chemistry Chemical Physics, 2017, 19, 14580-14587.	1.3	12
30222	Single- and few-layer BiOI as promising photocatalysts for solar water splitting. RSC Advances, 2017, 7, 24446-24452.	1.7	59
30223	Dynamics of carbon monoxide dissociation on Co(112Ì„0). Physical Chemistry Chemical Physics, 2017, 19, 12826-12837.	1.3	9
30224	Compressive strain induced enhancement in thermoelectric-power-factor in monolayer MoS₂nanosheet. Journal of Physics Condensed Matter, 2017, 29, 225501.	0.7	38
30225	Phosphorus Nanostripe Arrays on Cu(110): A Case Study to Understand the Substrate Effect on the Phosphorus thin Film Growth. Advanced Materials Interfaces, 2017, 4, 1601167.	1.9	18
30226	Singleâ€Domain Ferromagnet of Noncentrosymmetric Uniaxial Magnetic Ions and Magnetoelectric Interaction. Angewandte Chemie - International Edition, 2017, 56, 10196-10199.	7.2	0
30227	Boron Nitrideâ€supported Subâ€nanometer Pd 6 Clusters for Formic Acid Decomposition: A DFT Study. ChemCatChem, 2017, 9, 1610-1620.	1.8	23
30228	Analysis of the Magnetic Entropy in Oxygen Reduction Reactions Catalysed by Manganite Perovskites. ChemCatChem, 2017, 9, 3358-3363.	1.8	22
30229	Selfâ€Standing CoP Nanosheets Array: A Threeâ€Dimensional Bifunctional Catalyst Electrode for Overall Water Splitting in both Neutral and Alkaline Media. ChemElectroChem, 2017, 4, 1840-1845.	1.7	345
30230	First-principles study of Pd-skin/Pd3Fe(111) electrocatalyst for oxygen reduction reaction. Journal of Applied Electrochemistry, 2017, 47, 747-754.	1.5	8
30231	Electronic and magnetic properties of 4d series transition metal substituted graphene: A first-principles study. Carbon, 2017, 120, 265-273.	5.4	135
30232	Strengthening mechanism of Ï‰-Zr. Computational Materials Science, 2017, 135, 134-140.	1.4	5
30233	Ab initio calculations of structural and magnetic properties of Ni-Co-Mn-Cr-Sn supercell. Intermetallics, 2017, 87, 55-60.	1.8	11
30234	Age-hardening in a two component immiscible nanolaminate metal system. Scripta Materialia, 2017, 136, 33-36.	2.6	1

#	Article	IF	Citations
30235	The structural, electronic, magnetic, elastic properties of new Heusler alloys Hf 2 CrZ (Z=Al, Ga, In): A first-principles study. Solid State Communications, 2017, 259, 1-6.	0.9	11
30236	Structural, phononic and electronic properties of Ge-doped Î³-graphynes: A first-principles study. Solid State Communications, 2017, 258, 38-44.	0.9	11
30237	H2O and CO coadsorption on Co (0001): The effect of intermolecular hydrogen bond. Surface Science, 2017, 663, 56-61.	0.8	9
30238	Local Structure of Disordered Bi_{0.5}K_{0.5}TiO₃ Investigated by Pair Distribution Function Analysis and First-Principles Calculations. Chemistry of Materials, 2017, 29, 4244-4252.	3.2	51
30239	Probing the Li Insertion Mechanism of ZnFe₂O₄ in Li-Ion Batteries: A Combined X-Ray Diffraction, Extended X-Ray Absorption Fine Structure, and Density Functional Theory Study. Chemistry of Materials, 2017, 29, 4282-4292.	3.2	62
30240	Li⁺ Defects in a Solid-State Li Ion Battery: Theoretical Insights with a Li₃OCl Electrolyte. Chemistry of Materials, 2017, 29, 4330-4340.	3.2	80
30241	Hexagonal BC₃ Electrode for a High-Voltage Al-Ion Battery. Journal of Physical Chemistry C, 2017, 121, 9748-9756.	1.5	37
30242	Borophane as a Benchmate of Graphene: A Potential 2D Material for Anode of Li and Na-Ion Batteries. ACS Applied Materials & Interfaces, 2017, 9, 16148-16158.	4.0	142
30243	Concerted Chemoselective Hydrogenation of Acrolein on Secondary Phosphine Oxide Decorated Gold Nanoparticles. ACS Catalysis, 2017, 7, 3949-3954.	5.5	59
30244	Molecular Arrangement and Charge Transfer in C₆₀/Graphene Heterostructures. ACS Nano, 2017, 11, 4686-4693.	7.3	60
30245	Electric-Field-Driven Direct Desulfurization. ACS Nano, 2017, 11, 4703-4709.	7.3	43
30246	Control of Charge Carriers Trapping and Relaxation in Hematite by Oxygen Vacancy Charge: Ab Initio Non-adiabatic Molecular Dynamics. Journal of the American Chemical Society, 2017, 139, 6707-6717.	6.6	132
30247	Two-dimensional Mo1.33C MXene with divacancy ordering prepared from parent 3D laminate with in-plane chemical ordering. Nature Communications, 2017, 8, 14949.	5.8	525
30248	Electronegativity determination of individual surface atoms by atomic force microscopy. Nature Communications, 2017, 8, 15155.	5.8	46
30249	Induced perpendicular magnetization in a Cu layer inserted between Co and Pt layers revealed by x-ray magnetic circular dichroism. Scientific Reports, 2017, 7, 46132.	1.6	16
30250	Tuning the electronic properties of monolayer and bilayer transition metal dichalcogenide compounds under direct out-of-plane compression. Physical Chemistry Chemical Physics, 2017, 19, 13333-13340.	1.3	20
30251	DFT-D3 study of H₂ and N₂ chemisorption over cobalt promoted Ta₃N₅-(100), (010) and (001) surfaces. Physical Chemistry Chemical Physics, 2017, 19, 11968-11974.	1.3	22
30252	A van der Waals DFT study of chain length dependence of alkanethiol adsorption on Au(111): physisorption vs. chemisorption. Physical Chemistry Chemical Physics, 2017, 19, 13756-13766.	1.3	23

#	Article	IF	Citations
30253	Tuning electronic states of catalytic sites enhances SCR activity of hexagonal WO3by Mo framework substitution. Catalysis Science and Technology, 2017, 7, 2467-2473.	2.1	8
30254	Magnetic structure and properties of centrosymmetric twisted-melilite K2CoP2O7. Dalton Transactions, 2017, 46, 6409-6416.	1.6	10
30255	Negative thermal expansion of pure and doped graphene. RSC Advances, 2017, 7, 22378-22387.	1.7	52
30256	NiX₂(X = Cl and Br) sheets as promising spin materials: a first-principles study. RSC Advances, 2017, 7, 22541-22547.	1.7	25
30257	Compatibility issues between electrodes and electrolytes in solid-state batteries. Energy and Environmental Science, 2017, 10, 1150-1166.	15.6	267
30258	Design of efficient mono-aminosilane precursors for atomic layer deposition of SiO₂ thin films. RSC Advances, 2017, 7, 22672-22678.	1.7	16
30259	Effect of metal adatoms on hydrogen adsorption properties of phosphorene. Materials Research Express, 2017, 4, 045503.	0.8	6
30260	Measurement andab initiocalculation of the structural parameters and physical properties of 3dtransition intermetallics TiMP (Mâ€‰â€‰=â€‰â€‰Cr, Mn, Fe, Co, or Ni). Materials Research Express, 2017, 4, 046505.	0.8	4
30261	A Vacancy-Interstitial Defect Pair Model for Positive-Bias Temperature Stress-Induced Electron Trapping Transformation in the High- $kappa $ Gate n-MOSFET. IEEE Transactions on Electron Devices, 2017, 64, 2505-2511.	1.6	4
30262	Inner-shell chemistry under high pressure. Japanese Journal of Applied Physics, 2017, 56, 05FA10.	0.8	11
30263	Enhanced Electrocatalysis for Energyâ€Efficient Hydrogen Production over CoP Catalyst with Nonelectroactive Zn as a Promoter. Advanced Energy Materials, 2017, 7, 1700020.	10.2	519
30264	Density Functional Theory and ab Initio Molecular Dynamics Investigation of Hydronium Interactions with Graphene. Energy Procedia, 2017, 110, 518-522.	1.8	4
30265	Accurate Neural Network Description of Surface Phonons in Reactive Gasâ€“Surface Dynamics: N₂ + Ru(0001). Journal of Physical Chemistry Letters, 2017, 8, 2131-2136.	2.1	126
30266	A type-II GeSe/SnS heterobilayer with a suitable direct gap, superior optical absorption and broad spectrum for photovoltaic applications. Journal of Materials Chemistry A, 2017, 5, 13400-13410.	5.2	138
30267	Observation of crystalline changes of titanium dioxide during lithium insertion by visible spectrum analysis. Physical Chemistry Chemical Physics, 2017, 19, 13140-13146.	1.3	10
30268	Edge-functionalization of armchair graphene nanoribbons with pentagonal-hexagonal edge structures. Journal of Physics Condensed Matter, 2017, 29, 245301.	0.7	2
30269	Epitaxial growth of a graphene single crystal on the Ni(111) surface. JETP Letters, 2017, 105, 185-188.	0.4	9
30270	Allâ€Silicon Switchable Magnetoelectric Effect through Interlayer Exchange Coupling. ChemPhysChem, 2017, 18, 1916-1920.	1.0	1

#	Article	IF	Citations
30271	Software Platforms for Electronic/Atomistic/Mesoscopic Modeling: Status and Perspectives. Integrating Materials and Manufacturing Innovation, 2017, 6, 92-110.	1.2	6
30272	Sodium Iron(II) Pyrosilicate Na2Fe2Si2O7: A Potential Cathode Material in the Na2O-FeO-SiO2 System. Chemistry of Materials, 2017, 29, 4361-4366.	3.2	19
30273	A Novel Polymerization of Nitrogen in Beryllium Tetranitride at High Pressure. Journal of Physical Chemistry C, 2017, 121, 9766-9772.	1.5	67
30274	Catalytic Directional Cutting of Hexagonal Boron Nitride: The Roles of Interface and Etching Agents. Nano Letters, 2017, 17, 3208-3214.	4.5	26
30275	Five low energy phosphorene allotropes constructed through gene segments recombination. Scientific Reports, 2017, 7, 46431.	1.6	31
30276	Crystal packing of cubane and its nitryl-derivatives: a case of the discrete dependence of packing densities on substituent quantities. CrystEngComm, 2017, 19, 2644-2652.	1.3	18
30277	Exploration of crystal structures and phase transitions in Hf3N4. CrystEngComm, 2017, 19, 2608-2613.	1.3	5
30278	Thermally induced age hardening in tough Ta-Al-N coatings via spinodal decomposition. Journal of Applied Physics, 2017, 121, .	1.1	14
30279	Interatomic potential to study plastic deformation in tungsten-rhenium alloys. Journal of Applied Physics, 2017, 121, .	1.1	38
30280	Charge optimized many body (COMB) potentials for Pt and Au. Journal of Physics Condensed Matter, 2017, 29, 225901.	0.7	12
30281	Fundamental limits on the electron mobility ofÎ²-Ga₂O₃. Journal of Physics Condensed Matter, 2017, 29, 234001.	0.7	99
30282	MoirÃ© superlattice-level stick-slip instability originated from geometrically corrugated graphene on a strongly interacting substrate. 2D Materials, 2017, 4, 025079.	2.0	33
30283	Effects of hole doping and strain on magnetism in buckled phosphorene and arsenene. 2D Materials, 2017, 4, 025107.	2.0	40
30284	Optical identification of sulfur vacancies: Bound excitons at the edges of monolayer tungsten disulfide. Science Advances, 2017, 3, e1602813.	4.7	213
30285	Engineering Efficient pâ€Type TMD/Metal Contacts Using Fluorographene as a Buffer Layer. Advanced Electronic Materials, 2017, 3, 1600318.	2.6	9
30286	Multiscale modelling of the morphology and spatial distribution of Î¸â€² precipitates in Al-Cu alloys. Acta Materialia, 2017, 132, 611-626.	3.8	64
30287	The bi-layered precipitate phase Î¶ in the Al-Ag alloy system. Acta Materialia, 2017, 132, 525-537.	3.8	14
30288	The role of water on the selective decarbonylation of 5-hydroxymethylfurfural over Pd/Al 2 O 3 catalyst: Experimental and DFT studies. Applied Catalysis B: Environmental, 2017, 212, 15-22.	10.8	29

#	Article	IF	Citations
30289	First-principles investigations of metal (V, Nb, Ta)-doped monolayer MoS2: Structural stability, electronic properties and adsorption of gas molecules. Applied Surface Science, 2017, 419, 522-530.	3.1	104
30290	Towards a metal-semiconductor transition in two dimensions. Chemical Physics Letters, 2017, 679, 127-131.	1.2	4
30291	Pressure-induced electronic, magnetic, half-metallic, and mechanical properties of half-Heusler compound CoCrBi. Journal of Magnetism and Magnetic Materials, 2017, 438, 5-11.	1.0	18
30292	First-principles study of noble gas stability in ThO 2. Journal of Nuclear Materials, 2017, 490, 181-187.	1.3	13
30293	Theoretical Investigations of Pt₁@CeO₂ Single-Atom Catalyst for CO Oxidation. Journal of Physical Chemistry C, 2017, 121, 11281-11289.	1.5	138
30294	Methyl Formate Formation during Methanol Conversion over the (111) Ceria Surface. Journal of Physical Chemistry C, 2017, 121, 9920-9928.	1.5	4
30295	Orientation Selection during Heterogeneous Nucleation: Implications for Heterogeneous Catalysis. Journal of Physical Chemistry C, 2017, 121, 10027-10037.	1.5	13
30296	Ground-State Structure of YN₂ Monolayer Identified by Global Search. Journal of Physical Chemistry C, 2017, 121, 10258-10264.	1.5	38
30297	Nanoscale Characterization of Back Surfaces and Interfaces in Thin-Film Kesterite Solar Cells. ACS Applied Materials & Interfaces, 2017, 9, 17024-17033.	4.0	18
30298	Origin of Outstanding Phase and Moisture Stability in a Na₃P_{1â€“x}As_xS₄ Superionic Conductor. ACS Applied Materials & Interfaces, 2017, 9, 16261-16269.	4.0	46
30299	Building an Electronic Bridge via Ag Decoration To Enhance Kinetics of Iron Fluoride Cathode in Lithium-Ion Batteries. ACS Applied Materials & Interfaces, 2017, 9, 19852-19860.	4.0	54
30300	Reduction and oxidation of Au adatoms on the CeO₂(111) surface â€“ DFT+U versus hybrid functionals. Physical Chemistry Chemical Physics, 2017, 19, 12546-12558.	1.3	12
30301	First principles study of bimetallic Ni13â^’nAgn nano-clusters (n = 0â€“13): Structural, mixing, electronic, and magnetic properties. Journal of Chemical Physics, 2017, 146, 164301.	1.2	28
30302	HCl dissociating on a rigid Au(111) surface: A six-dimensional quantum mechanical study on a new potential energy surface based on the RPBE functional. Journal of Chemical Physics, 2017, 146, 164706.	1.2	20
30303	Effects of edge reconstruction on the common groups terminated zigzag phosphorene nanoribbon. Journal Physics D: Applied Physics, 2017, 50, 195301.	1.3	5
30304	The application of tailor-made force fields and molecular dynamics for NMR crystallography: a case study of free base cocaine. IUCrJ, 2017, 4, 175-184.	1.0	10
30305	The origin of negative stacking fault energies and nano-twin formation in face-centered cubic high entropy alloys. Scripta Materialia, 2017, 130, 96-99.	2.6	223
30306	Siteâ€Specific Reactivity of Ethylene at Distorted Danglingâ€Bond Configurations on Si(001). ChemPhysChem, 2017, 18, 357-365.	1.0	22

#	Article	IF	Citations
30307	Diamondâ€™s third-order elastic constants: ab initio calculations and experimental investigation. Journal of Materials Science, 2017, 52, 3447-3456.	1.7	16
30308	Effect of twin boundary on crack propagation behavior in magnesium binary alloys; Experimental and calculation studies. Scripta Materialia, 2017, 130, 114-118.	2.6	28
30309	The role of oxygen defects in a bismuth doped ScVO₄ matrix: tuning luminescence by hydrogen treatment. Journal of Materials Chemistry C, 2017, 5, 314-321.	2.7	15
30310	Isopropanol Dehydration on Amorphous Silicaâ€“Alumina: Synergy of BrÃ¸nsted and Lewis Acidities at Pseudoâ€Bridging Silanols. Angewandte Chemie - International Edition, 2017, 56, 230-234.	7.2	47
30311	Nonâ€centrosymmetric Selenides AZn₄In₅Se₁₂ (A=Rb, Cs): Synthesis, Characterization and Nonlinear Optical Properties. Chemistry - an Asian Journal, 2017, 12, 453-458.	1.7	41
30312	New carbazole-based dyes with asymmetric butterfly structure for dye-sensitized solar cells: Design and properties studies. Dyes and Pigments, 2017, 139, 148-156.	2.0	28
30313	Multiscale modeling of doping processes in advanced semiconductor devices. Materials Science in Semiconductor Processing, 2017, 62, 49-61.	1.9	12
30314	Anomalous radial and angular strain relaxation around dilute p-, isoelectronic-, and n-type dopants in Si crystal. Physica B: Condensed Matter, 2017, 506, 198-204.	1.3	0
30315	Stacking-dependent transport properties in few-layers graphene. Solid State Communications, 2017, 250, 70-74.	0.9	10
30316	2D MXenes: A New Family of Promising Catalysts for the Hydrogen Evolution Reaction. ACS Catalysis, 2017, 7, 494-500.	5.5	825
30317	Facet Effect of Single-Crystalline Pd Nanocrystals for Aerobic Oxidation of 5-Hydroxymethyl-2-furfural. ACS Catalysis, 2017, 7, 421-432.	5.5	85
30318	Straintronics in two-dimensional in-plane heterostructures of transition-metal dichalcogenides. Physical Chemistry Chemical Physics, 2017, 19, 663-672.	1.3	56
30319	Syntheses, structures, and properties of sulfides constructed by SbS₄teeter-totter polyhedra: Ba₃La₄Ga₂Sb₂S₁₅and BaLa₃GaSb₂S₁₀. Inorganic Chemistry Frontiers, 2017, 4, 123-130.	3.0	10
30320	Controlling of the electronic properties of WS₂ and graphene oxide heterostructures from first-principles calculations. Journal of Materials Chemistry C, 2017, 5, 201-207.	2.7	16
30321	Formation of Zn- and O- vacancy clusters in ZnO through deuterium annealing. Materials Science in Semiconductor Processing, 2017, 69, 23-27.	1.9	14
30322	The mechanism of H₂ and H₂O desorption from bridging hydroxyls of a TiO₂(110) surface. Catalysis Science and Technology, 2017, 7, 251-264.	2.1	13
30323	Magnetism in Yttrium Intermetallics: Ab Initio Study. Journal of Superconductivity and Novel Magnetism, 2017, 30, 1003-1018.	0.8	3
30324	First-principles study on codoping effect to enhance photocatalytic activity of anatase TiO₂. International Journal of Modern Physics B, 2017, 31, 1750036.	1.0	3

#	Article	IF	Citations
30325	Ammonothermal Synthesis of Novel Nitrides: Case Study on CaGaSiN₃. Chemistry - A European Journal, 2017, 23, 2583-2590.	1.7	42
30326	Effect of carbon and alloying solute atoms on helium behaviors in Î± -Fe. Journal of Nuclear Materials, 2017, 484, 103-109.	1.3	9
30327	Phase stability of nickel and zirconium stannides. Journal of Physics and Chemistry of Solids, 2017, 103, 40-48.	1.9	11
30328	Isopropanol Dehydration on Amorphous Silica-Alumina: Synergy of BrÃ¸nsted and Lewis Acidities at Pseudo-Bridging Silanols. Angewandte Chemie, 2017, 129, 236-240.	1.6	10
30329	Catalytically Triggered Energy Release from Strained Organic Molecules: The Surface Chemistry of Quadricyclane and Norbornadiene on Pt(111). Chemistry - A European Journal, 2017, 23, 1613-1622.	1.7	31
30330	Bionanofiber Assisted Decoration of Fewâ€Layered MoSe₂ Nanosheets on 3D Conductive Networks for Efficient Hydrogen Evolution. Small, 2017, 13, 1602866.	5.2	67
30331	Conductive graphene oxide-polyacrylic acid (GOPAA) binder for lithium-sulfur battery. Nano Energy, 2017, 31, 568-574.	8.2	147
30332	Effect of strain on electronic and magnetic properties of n-type Cr-doped WSe 2 monolayer. Physica E: Low-Dimensional Systems and Nanostructures, 2017, 87, 6-9.	1.3	18
30333	Bottom-up Design of Three-Dimensional Carbon-Honeycomb with Superb Specific Strength and High Thermal Conductivity. Nano Letters, 2017, 17, 179-185.	4.5	95
30334	High intrinsic catalytic activity of two-dimensional boron monolayers for the hydrogen evolution reaction. Nanoscale, 2017, 9, 533-537.	2.8	116
30335	A Ruâ€“Ru pair housed in ruthenium phthalocyanine: the role of a â€œcageâ€•architecture in the molecule coupling with the Ag(111) surface. Physical Chemistry Chemical Physics, 2017, 19, 1449-1457.	1.3	7
30336	CO oxidation on Rh-doped hexadecagold clusters. Catalysis Science and Technology, 2017, 7, 75-83.	2.1	15
30337	DFT study of Ag and La codoped BaTiO 3. Journal of Physics and Chemistry of Solids, 2017, 102, 136-141.	1.9	24
30338	Water-Gas Shift Activity of Atomically Dispersed Cationic Platinum versus Metallic Platinum Clusters on Titania Supports. ACS Catalysis, 2017, 7, 301-309.	5.5	78
30339	Understanding Structure-Dependent Catalytic Performance of Nickel Selenides for Electrochemical Water Oxidation. ACS Catalysis, 2017, 7, 310-315.	5.5	155
30340	Structural, mechanical, dynamical and electronic properties and high-pressure behavior of Mo2GeC: A first-principles study. Computational Materials Science, 2017, 137, 306-313.	1.4	7
30341	Quantification and modeling of nanomechanical properties of chlorpropamide Î±, Î², and Î³ conformational polymorphs. European Journal of Pharmaceutical Sciences, 2017, 110, 109-116.	1.9	9
30342	First-principle investigation on electronic structure, magnetism and multiferroicity of BiMn 3 Fe 4 O 12. Journal of Magnetism and Magnetic Materials, 2017, 441, 296-302.	1.0	3

#	Article	IF	Citations
30343	Band gap engineering and visible light response for GaS monolayer by isovalent anion-cation codoping. Materials Chemistry and Physics, 2017, 198, 275-282.	2.0	19
30344	Exploring the high entropy alloy concept in (AlTiVNbCr)N. Thin Solid Films, 2017, 636, 346-352.	0.8	27
30345	First-Principles Prediction of a Stable Hexagonal Phase of CH₃NH₃PbI₃. Chemistry of Materials, 2017, 29, 6003-6011.	3.2	62
30346	Canonical, Deprotonated, or Zwitterionic? A Computational Study on Amino Acid Interaction with the TiO₂ (101) Anatase Surface. Journal of Physical Chemistry C, 2017, 121, 14156-14165.	1.5	28
30347	Anchoring Small Au Clusters on the Dehydroxylated and Hydroxylated SiO2 Î±-Quartz (001) Surface via Ti-Alloying. Journal of Physical Chemistry C, 2017, 121, 14717-14724.	1.5	9
30348	Tunability of the Quantum Spin Hall Effect in Bi(110) Films: Effects of Electric Field and Strain Engineering. ACS Applied Materials & Interfaces, 2017, 9, 21515-21523.	4.0	32
30349	Intrinsically low thermal conductivity from a quasi-one-dimensional crystal structure and enhanced electrical conductivity network via Pb doping in SbCrSe3. NPG Asia Materials, 2017, 9, e387-e387.	3.8	37
30350	CO adsorption, oxidation and carbonate formation mechanisms on Fe₃O₄ surfaces. Physical Chemistry Chemical Physics, 2017, 19, 17287-17299.	1.3	34
30351	Defect segregation to grain boundaries in BaZrO₃ from first-principles free energy calculations. Journal of Materials Chemistry A, 2017, 5, 13421-13429.	5.2	30
30352	Impact of air exposure and surface chemistry on Liâ€“Li₇La₃Zr₂O₁₂ interfacial resistance. Journal of Materials Chemistry A, 2017, 5, 13475-13487.	5.2	300
30353	Cu metal embedded in oxidized matrix catalyst to promote CO ₂ activation and CO dimerization for electrochemical reduction of CO ₂. Proceedings of the National Academy of Sciences of the United States of America, 2017, 114, 6685-6688.	3.3	322
30354	Low temperature ferromagnetic properties of CdS and CdTe thin films. Chinese Physics B, 2017, 26, 067503.	0.7	10
30355	Identifying Ferroelectric Switching Pathways in HfO2: First Principles Calculations under Electric Fields. , 2017, , .		10
30356	Simulation of hydrogen diffusion in TiH x structures. Physics of Metals and Metallography, 2017, 118, 28-38.	0.3	14
30357	Effect of Cr addition on Î³â€“Î³â€² cobalt-based Coâ€“Moâ€“Alâ€“Ta class of superalloys: a combined experimental and computational study. Journal of Materials Science, 2017, 52, 11036-11047.	1.7	61
30358	Electronic and optical properties of Zn-doped InGaAs emission layer with vacancy defects: A DFT study. Optik, 2017, 143, 135-141.	1.4	6
30359	On the phase stability of CaCu5-type compounds. Journal of Alloys and Compounds, 2017, 722, 549-554.	2.8	4
30360	Localized defects related to the 14N+ ion irradiation-induced magnetism in SiC. Physica E: Low-Dimensional Systems and Nanostructures, 2017, 93, 6-11.	1.3	2

#	Article	IF	Citations
30361	Possible Mechanism for Hole Conductivity in Cuâ€“Asâ€“Te Thermoelectric Glasses: A XANES and EXAFS Study. Journal of Physical Chemistry C, 2017, 121, 14045-14050.	1.5	24
30362	Nitrogen-Doped Graphene on Transition Metal Substrates as Efficient Bifunctional Catalysts for Oxygen Reduction and Oxygen Evolution Reactions. ACS Applied Materials & Interfaces, 2017, 9, 22578-22587.	4.0	128
30363	Surface restructuring of Cu-based single-atom alloy catalysts under reaction conditions: the essential role of adsorbates. Physical Chemistry Chemical Physics, 2017, 19, 18010-18017.	1.3	53
30364	Exploring surface landscapes with molecules: rotationally induced diffraction of H₂ on LiF(001) under fast grazing incidence conditions. Physical Chemistry Chemical Physics, 2017, 19, 16317-16322.	1.3	8
30365	Structural stability and stabilization of Li₂MoO₃. Physical Chemistry Chemical Physics, 2017, 19, 17538-17543.	1.3	20
30366	Computational characterization of monolayer C3N: A two-dimensional nitrogen-graphene crystal. Journal of Materials Research, 2017, 32, 2993-3001.	1.2	110
30367	Software tools for high-throughput CALPHAD from first-principles data. Calphad: Computer Coupling of Phase Diagrams and Thermochemistry, 2017, 58, 70-81.	0.7	57
30368	Vibrational Excitation of H₂ Scattering from Cu(111): Effects of Surface Temperature and of Allowing Energy Exchange with the Surface. Journal of Physical Chemistry C, 2017, 121, 13617-13633.	1.5	26
30369	Understanding the Charge Transfer at the Interface of Electron Donors and Acceptors: TTFâ€“TCNQ as an Example. ACS Applied Materials & Interfaces, 2017, 9, 27266-27272.	4.0	21
30370	First-principles study of structure sensitivity of chain growth and selectivity in Fischerâ€“Tropsch synthesis using HCP cobalt catalysts. Catalysis Science and Technology, 2017, 7, 2967-2977.	2.1	30
30371	Preparation and temperature-dependent photoluminescence properties of ScF₃:Eu³⁺submicroparticles. New Journal of Chemistry, 2017, 41, 7915-7923.	1.4	15
30372	CoN₃ embedded graphene, a potential catalyst for the oxygen reduction reaction from a theoretical perspective. Physical Chemistry Chemical Physics, 2017, 19, 17670-17676.	1.3	41
30373	A reconstructed anatase (001)-1 Ã— 4 surface and its reactivity. Physical Chemistry Chemical Physics, 2017, 19, 16615-16620.	1.3	9
30374	First-principles study of decomposition mechanisms of Mg(BH₄)₂Â·2NH₃ and LiMg(BH₄)₃Â·2NH₃. RSC Advances, 2017, 7, 31027-31032.	1.7	9
30375	Electronic and transport properties of fluorite structure of La2Ce2O7. AIP Conference Proceedings, 2017, , .	0.3	1
30376	Sn2Se3: A conducting crystalline mixed valent phase change memory compound. Journal of Applied Physics, 2017, 121, .	1.1	9
30377	Study of Niobium Diffusion and Clusterization in hcp Zr-Nb Dilute Alloys. Defect and Diffusion Forum, 2017, 375, 167-174.	0.4	1
30378	Revealing the Microstates of Body-Centered-Cubic (BCC) Equiatomic High Entropy Alloys. Journal of Phase Equilibria and Diffusion, 2017, 38, 404-415.	0.5	21

#	Article	IF	Citations
30379	Conditions for magnetic and electronic properties of ultrathin Niâ€“Fe hydroxide nanosheets as catalysts: a DFT+U study. Science China Materials, 2017, 60, 664-673.	3.5	7
30380	Adsorption behavior of formaldehyde on ZnO<mml:math xmlns:mml="http://www.w3.org/1998/Math/MathML" altimg="si8.gif" overflow="scroll"><mml:mrow><mml:mrow><mml:mo		

#	Article	IF	Citations
30397	Protective molecular passivation of black phosphorus. Npj 2D Materials and Applications, 2017, 1, .	3.9	52
30398	Structural stability and the electronic properties of a (SiH)₂O-formed siloxene sheet: a computational study. Physical Chemistry Chemical Physics, 2017, 19, 18030-18035.	1.3	7
30399	Oxidation of the hexagonal Mo₂C(101) surface by H₂O dissociative adsorption. Catalysis Science and Technology, 2017, 7, 2789-2797.	2.1	6
30400	Novel optical and magnetic properties of Li-doped quasi-2D manganate Ca₃Mn₂O₇ particles. Journal of Materials Chemistry C, 2017, 5, 7011-7019.	2.7	18
30401	Two-dimensional honeycomb hafnene monolayer: stability and magnetism by structural transition. Nanoscale, 2017, 9, 10038-10043.	2.8	6
30402	The Unique Electronic Structure of Mg₂Si: Shaping the Conduction Bands of Semiconductors with Multicenter Bonding. Angewandte Chemie, 2017, 129, 10269-10273.	1.6	3
30403	Thermodynamic assessment of the Al-C-Fe system. Calphad: Computer Coupling of Phase Diagrams and Thermochemistry, 2017, 58, 34-49.	0.7	41
30404	The geometric and electronic transitions in body-centered-tetragonal C8: A first principle study. Carbon, 2017, 120, 89-94.	5.4	17
30405	Porous RuO2 nanosheet/CNT electrodes for DMSO-based Li-O2 and Li ion O2 batteries. Energy Storage Materials, 2017, 8, 110-118.	9.5	36
30406	Quantum Monte Carlo Calculations on a Benchmark Moleculeâ€“Metal Surface Reaction: H₂ + Cu(111). Journal of Chemical Theory and Computation, 2017, 13, 3208-3219.	2.3	35
30407	Enhancing Dissociative Adsorption of Water on Cu(111) via Chemisorbed Oxygen. Journal of Physical Chemistry C, 2017, 121, 12117-12126.	1.5	17
30408	An Efficient Scheme for Crystal Structure Prediction Based on Structural Motifs. Journal of Physical Chemistry C, 2017, 121, 11891-11896.	1.5	7
30409	Systematic Investigation into Mg²⁺/Li⁺ Dual-Cation Transport in Chevrel Phases Using Computational and Experimental Approaches. Journal of Physical Chemistry C, 2017, 121, 12617-12623.	1.5	14
30410	Understanding the Dual Active Sites of the FeO/Pt(111) Interface and Reaction Kinetics: Density Functional Theory Study on Methanol Oxidation to Formaldehyde. ACS Catalysis, 2017, 7, 4281-4290.	5.5	50
30411	Defect-Mediated Electronâ€“Hole Separation in One-Unit-Cell ZnIn₂S₄ Layers for Boosted Solar-Driven CO₂ Reduction. Journal of the American Chemical Society, 2017, 139, 7586-7594.	6.6	764
30412	Optical determination of crystal phase in semiconductor nanocrystals. Nature Communications, 2017, 8, 14849.	5.8	29
30413	Theoretical perspectives on the structure, electronic, and optical properties of titanosilicates Li₂M₄[(TiO)Si₄O₁₂] (M = K⁺,) Tj ETQq0 0 0 rgBT /Overlock 10 Tf 50 9	1.6	
30414	Powder diffraction and crystal structure prediction identify four new coumarin polymorphs. Chemical Science, 2017, 8, 4926-4940.	3.7	97

#	Article	IF	Citations
30415	External electric field driving the ultra-low thermal conductivity of silicene. Nanoscale, 2017, 9, 7227-7234.	2.8	69
30416	Exploring new phases of Fe_{3â"x}Co_xC for rare-earth-free magnets. Journal Physics D: Applied Physics, 2017, 50, 215005.	1.3	11
30417	Glass-like energy and property landscape of Pt nanoclusters. Nano Research, 2017, 10, 2721-2731.	5.8	5
30418	First-principles thermoelasticity and stability of pyrite-type FeO 2 under high pressure and temperature. Journal of Alloys and Compounds, 2017, 719, 42-46.	2.8	10
30419	Enhanced optical absorption and photocatalytic activity of anatase TiO 2 through C Nd-codoped: A DFT+ U calculations. Journal of Physics and Chemistry of Solids, 2017, 109, 70-77.	1.9	6
30420	Cleavage of rutile SiO 2 hemi-crystals: Insights from first-principles investigations. Solid State Sciences, 2017, 67, 119-124.	1.5	5
30421	The Third Ambient Aspirin Polymorph. Crystal Growth and Design, 2017, 17, 3562-3566.	1.4	73
30422	Importance of Solvation for the Accurate Prediction of Oxygen Reduction Activities of Pt-Based Electrocatalysts. Journal of Physical Chemistry Letters, 2017, 8, 2243-2246.	2.1	85
30423	Solid frustrated-Lewis-pair catalysts constructed by regulations on surface defects of porous nanorods of CeO2. Nature Communications, 2017, 8, 15266.	5.8	272
30424	Porphyrin-based metal-organic frameworks for solar fuel synthesis photocatalysis: band gap tuning via iron substitutions. Journal of Materials Chemistry A, 2017, 5, 11894-11904.	5.2	84
30425	Highly active and durable nitrogen doped-reduced graphene oxide/double perovskite bifunctional hybrid catalysts. Journal of Materials Chemistry A, 2017, 5, 13019-13031.	5.2	45
30426	First-principles investigation of intrinsic defects and self-diffusion in ordered phases of V₂C. Journal of Physics Condensed Matter, 2017, 29, 245403.	0.7	21
30427	The nitridoborate nitrides Mg₃[BN₂]N and Ca₃[BN₂]N â€" electronic structure and chemical bonding. Zeitschrift Fur Naturforschung - Section B Journal of Chemical Sciences, 2017, 72, 433-439.	0.3	4
30428	Feasibility of N₂ Binding and Reduction to Ammonia on Feâ€Deposited MoS₂ 2D Sheets: A DFT Study. Chemistry - A European Journal, 2017, 23, 8275-8279.	1.7	173
30429	Bonding analyses of unconventional carbon allotropes. Carbon, 2017, 121, 154-162.	5.4	19
30430	Surface Reactions of Ethylene Carbonate and Propylene Carbonate on the Li(001) Surface. Electrochimica Acta, 2017, 243, 320-330.	2.6	26
30431	Superhydrophobic Ptâ€"Pd/Al 2 O 3 catalyst coating for hydrogen mitigation system of nuclear power plant. International Journal of Hydrogen Energy, 2017, 42, 14829-14840.	3.8	12
30432	Reaction mechanisms of methanol synthesis from CO/CO 2 hydrogenation on Cu 2 O(111): Comparison with Cu(111). Journal of CO2 Utilization, 2017, 20, 59-65.	3.3	60

#	Article	IF	Citations
30433	Optimization of self-interstitial clusters in 3C-SiC with genetic algorithm. Journal of Nuclear Materials, 2017, 492, 62-73.	1.3	10
30434	Density functional theory study of the zeolite-mediated tautomerization of phenol and catechol. Molecular Catalysis, 2017, 433, 334-345.	1.0	14
30435	Effect of Surface Coverage and Composition on the Stability and Interfacial Dipole of Functionalized Silicon. Journal of Physical Chemistry C, 2017, 121, 11312-11318.	1.5	13
30436	Tuning Adhesion at Metal/Oxide Interfaces by Surface Hydroxylation. Journal of Physical Chemistry C, 2017, 121, 11464-11471.	1.5	28
30437	Exceptional bi-step switching of quadratic nonlinear optical properties in a one-dimensional channel compound. Chemical Communications, 2017, 53, 7669-7672.	2.2	27
30438	Highly active Au/Î´-MoC and Au/Î²-Mo₂C catalysts for the low-temperature water gas shift reaction: effects of the carbide metal/carbon ratio on the catalyst performance. Catalysis Science and Technology, 2017, 7, 5332-5342.	2.1	39
30439	LaTiO2Nâ€“LaCrO3: continuous solid solutions towards enhanced photocatalytic H2 evolution under visible-light irradiation. Dalton Transactions, 2017, 46, 10685-10693.	1.6	6
30440	Intrinsic valley polarization of magnetic VSe₂ monolayers. Journal of Physics Condensed Matter, 2017, 29, 255501.	0.7	73
30441	LSDA+ U study on the electronic and anti-ferromagnetic properties of Ni-doped CuO and Cu-doped NiO. Chinese Journal of Catalysis, 2017, 38, 767-773.	6.9	14
30442	On nearsightedness in metallic systems for <mml:math xmlns:mml="http://www.w3.org/1998/Math/MathML" altimg="si21.gif" overflow="scroll"><mml:mrow><mml:mi mathvariant="script">O</mml:mi><mml:mo stretchy="false">(</mml:mo><mml:mi>N</mml:mi><mml:mo) Tj ETQq1 1 0.784314 rgBT /Overlock 10 Tf 50 372 Td (stretchy="false">) case study on aluminum. Chemical Physics Letters, 2017, 679, 146-151.	1.2	21
30443	Exploration of CoSi-based alloys promising for thermoelectricity. Intermetallics, 2017, 88, 46-54.	1.8	7
30444	First-principles study of noble gas atoms in bcc Fe. Journal of Nuclear Materials, 2017, 492, 134-141.	1.3	15
30445	Influence of Cu 2 S, SnS and Cu 2 ZnSnSe 4 on optical properties of Cu 2 ZnSnS 4. Materials Letters, 2017, 202, 70-72.	1.3	22
30446	Competition and Cooperation of Hydrogenation and Deoxygenation Reactions during Hydrodeoxygenation of Phenol on Pt(111). Journal of Physical Chemistry C, 2017, 121, 12249-12260.	1.5	57
30447	Origin of cooperativity in hydrogen bonding. Physical Chemistry Chemical Physics, 2017, 19, 15256-15263.	1.3	47
30448	Energetics of intrinsic point defects in aluminium via orbital-free density functional theory. Philosophical Magazine, 2017, 97, 2164-2181.	0.7	18
30449	The effect of point defect on mechanical properties of MoSi₂. International Journal of Modern Physics B, 2017, 31, 1744081.	1.0	3
30450	Chapter 9 Memories of Shock Wave Research at Sandia. Shock Wave and High Pressure Phenomena, 2017, , 275-594.	0.1	1

#	Article	IF	Citations
30451	First-principles study of nickel complex with 1,3-dithiole-2-thione-4,5-dithiolate ligands as model photosensitizers. Theoretical Chemistry Accounts, 2017, 136, 1.	0.5	7
30452	Theoretical investigation of solid solution states of Ti1â^'V H2. Acta Materialia, 2017, 134, 274-282.	3.8	4
30453	Nonmagnetic Quantum Emitters in Boron Nitride with Ultranarrow and Sideband-Free Emission Spectra. ACS Nano, 2017, 11, 6652-6660.	7.3	105
30454	Ti₂CO₂MXene: a highly active and selective photocatalyst for CO₂reduction. Journal of Materials Chemistry A, 2017, 5, 12899-12903.	5.2	221
30455	Effect of water on the effective Goldschmidt tolerance factor and photoelectric conversion efficiency of organicâ€“inorganic perovskite: insights from first-principles calculations. Physical Chemistry Chemical Physics, 2017, 19, 14955-14960.	1.3	10
30456	Oneâ€Step Synthesis of Highly Oxygenâ€Deficient Lithium Titanate Oxide with Conformal Amorphous Carbon Coating as Anode Material for Lithium Ion Batteries. Advanced Materials Interfaces, 2017, 4, 1700329.	1.9	38
30457	Improving Thermoelectric Performance of Î±â€MgAgSb by Theoretical Band Engineering Design. Advanced Energy Materials, 2017, 7, 1700076.	10.2	46
30458	Hydrogenated Coreâ€“Shell MAX@K₂Ti₈O₁₇ Pseudocapacitance with Ultrafast Sodium Storage and Longâ€Term Cycling. Advanced Energy Materials, 2017, 7, 1700700.	10.2	54
30459	Prediction of Tâ€•and Hâ€Phase Twoâ€Dimensional Transitionâ€Metal Carbides/Nitrides and Their Semiconductingâ€“Metallic Phase Transition. ChemPhysChem, 2017, 18, 1897-1902.	1.0	30
30460	Change of local structures for 0.5Li2MnO3â€“0.5LiMn1/3Ni1/3Co1/3O2 in first charge process of different rates. Journal of Materials Science, 2017, 52, 8630-8649.	1.7	10
30461	DFT study of methanol adsorption on PtCo(111). Applied Surface Science, 2017, 420, 383-389.	3.1	21
30462	Discovery of intrinsic quantum anomalous Hall effect in organic Mn-DCA lattice. Applied Physics Letters, 2017, 110, .	1.5	61
30463	Interplay between quantum confinement and surface effects in thickness selective stability of thin Ag and Eu films. Journal of Physics Condensed Matter, 2017, 29, 185504.	0.7	4
30464	Nickeloceneâ€Precursorâ€Facilitated Fast Growth of Graphene/hâ€BN Vertical Heterostructures and Its Applications in OLEDs. Advanced Materials, 2017, 29, 1701325.	11.1	54
30465	Structural, electronic, and magnetic properties of double perovskite Pb₂ FeReO₆ thin films with (001) orientation and three possible terminations. Surface and Interface Analysis, 2017, 49, 960-966.	0.8	1
30466	Synthesis of novel hydride Li 3 AlFeH 8 at high temperature and pressure. International Journal of Hydrogen Energy, 2017, 42, 22489-22495.	3.8	8
30467	Cobalt based nanostructured alloys: Versatile high performance robust hydrogen evolution reaction electro-catalysts for electrolytic and photo-electrochemical water splitting. International Journal of Hydrogen Energy, 2017, 42, 17049-17062.	3.8	35
30468	Effects of the evolution of electronic properties on twin-boundary segregation energies of zirconium from first-principles calculations. Materials Letters, 2017, 204, 112-114.	1.3	4

#	Article	IF	Citations
30469	Van der Waals bilayer antimonene: A promising thermophotovoltaic cell material with 31% energy conversion efficiency. Nano Energy, 2017, 38, 561-568.	8.2	92
30470	Size effect on brittle and ductile fracture of two-dimensional interlinked carbon nanotube network. Physica B: Condensed Matter, 2017, 520, 82-88.	1.3	6
30471	Unraveling the Complex Delithiation and Lithiation Mechanisms of the High Capacity Cathode Material V₆O₁₃. Chemistry of Materials, 2017, 29, 5513-5524.	3.2	35
30472	R₃Au₉Pn (R = Y, Gdâ€“Tm; Pn = Sb, Bi): A Link between Cu₁₀Sn₃ and Gd₁₄Ag₅₁. Inorganic Chemistry, 2017, 56, 7247-7256.	1.9	10
30473	Impact of Mg-Doping Site Control in the Performance of Li₄Ti₅O₁₂ Li-Ion Battery Anode: First-Principles Predictions and Experimental Verifications. Journal of Physical Chemistry C, 2017, 121, 14994-15001.	1.5	15
30474	Molecular Dynamics Simulations of the Interfacial Region between Boehmite and Gibbsite Basal Surfaces and High Ionic Strength Aqueous Solutions. Journal of Physical Chemistry C, 2017, 121, 13692-13700.	1.5	18
30475	Quantum Spin Hall Effect and Tunable Spin Transport in As-Graphane. Nano Letters, 2017, 17, 4359-4364.	4.5	15
30476	Facile CO₂ Electro-Reduction to Formate via Oxygen Bidentate Intermediate Stabilized by High-Index Planes of Bi Dendrite Catalyst. ACS Catalysis, 2017, 7, 5071-5077.	5.5	263
30477	Elucidating the Copperâ€“HÃgg Iron Carbide Synergistic Interactions for Selective CO Hydrogenation to Higher Alcohols. ACS Catalysis, 2017, 7, 5500-5512.	5.5	82
30478	Methionine as a Friction Modifier for Tungsten Carbide-Functionalized Surfaces via in Situ Tribo-Chemical Reactions. ACS Sustainable Chemistry and Engineering, 2017, 5, 7030-7039.	3.2	6
30479	Boosting the Thermoelectric Performance of (Na,K)-Codoped Polycrystalline SnSe by Synergistic Tailoring of the Band Structure and Atomic-Scale Defect Phonon Scattering. Journal of the American Chemical Society, 2017, 139, 9714-9720.	6.6	168
30480	Origin of fast ion diffusion in super-ionic conductors. Nature Communications, 2017, 8, 15893.	5.8	570
30481	New quaternary half-metallic ferromagnets with large Curie temperatures. Scientific Reports, 2017, 7, 1803.	1.6	119
30482	First Principles Theory of the hcp-fcc Phase Transition in Cobalt. Scientific Reports, 2017, 7, 3778.	1.6	92
30483	Designing a molecular magnetic button based on 4d and 5d transition-metal phthalocyanines. Scientific Reports, 2017, 7, 3647.	1.6	4
30484	On the interaction of toxic Heavy Metals (Cd, Hg, Pb) with graphene quantum dots and infinite graphene. Scientific Reports, 2017, 7, 3934.	1.6	94
30485	Ultra-high electrocatalytic activity of VS₂ nanoflowers for efficient hydrogen evolution reaction. Journal of Materials Chemistry A, 2017, 5, 15080-15086.	5.2	189
30486	Graph Theoretical Representation, Analysis and Synthesis of Amorphous Metal Oxide Networks. MRS Advances, 2017, 2, 2639-2644.	0.5	0

#	Article	IF	Citations
30487	Superconductivity Induced by Oxygen Doping in Y 2 O 2 Bi. Angewandte Chemie, 2017, 129, 10257-10260.	1.6	1
30488	Defective Tungsten Oxide Hydrate Nanosheets for Boosting Aerobic Coupling of Amines: Synergistic Catalysis by Oxygen Vacancies and BrÃ¸nsted Acid Sites. Small, 2017, 13, 1701354.	5.2	62
30489	Theoretical study of metal-doped Î²-Ga2O3 photocatalysts for overall water splitting. Theoretical Chemistry Accounts, 2017, 136, 1.	0.5	12
30490	Mechanistic insights into tunable luminescence and persistent luminescence of the full-color-emitting BCNO phosphors. Carbon, 2017, 122, 176-184.	5.4	18
30491	Modulation effect on the effective mass of free carriers induced by multicomponent elements in In2O3-based transparent conducting oxides. Computational Materials Science, 2017, 137, 332-339.	1.4	1
30492	Methanol adsorption and dissociation on LaMnO3 and Sr doped LaMnO3 (001) surfaces. Surface Science, 2017, 664, 155-161.	0.8	4
30493	Scaling Relations and Kinetic Monte Carlo Simulations To Bridge the Materials Gap in Heterogeneous Catalysis. ACS Catalysis, 2017, 7, 5054-5061.	5.5	74
30494	Computational Study of MoS₂/HfO₂ Defective Interfaces for Nanometer-Scale Electronics. ACS Omega, 2017, 2, 2827-2834.	1.6	16
30495	Lattice-Hydride Mechanism in Electrocatalytic CO₂ Reduction by Structurally Precise Copper-Hydride Nanoclusters. Journal of the American Chemical Society, 2017, 139, 9728-9736.	6.6	261
30496	Aromatic stacking â€“ a key step in nucleation. Chemical Communications, 2017, 53, 7905-7908.	2.2	70
30497	Atomistic dynamics of sulfur-deficient high-symmetry grain boundaries in molybdenum disulfide. Nanoscale, 2017, 9, 10312-10320.	2.8	18
30498	Composition design, optical gap and stability investigations of lead-free halide double perovskite Cs₂AgInCl₆. Journal of Materials Chemistry A, 2017, 5, 15031-15037.	5.2	319
30499	Atomic-layered Au clusters on Î±-MoC as catalysts for the low-temperature water-gas shift reaction. Science, 2017, 357, 389-393.	6.0	534
30500	Recent Progress in the Development of Semiconductorâ€Based Photocatalyst Materials for Applications in Photocatalytic Water Splitting and Degradation of Pollutants. Advanced Sustainable Systems, 2017, 1, 1700006.	2.7	144
30501	Abnormal polar nanoregion evolution in (Bi_{0.09}Ba_{0.91})(Zn_{0.045}Ti_{0.955})O₃ (9BZTâ€BT) ceramic. Physica Status Solidi (B): Basic Research, 2017, 254, 1700012.	0.7	4
30502	Modeling resistive switching materials and devices across scales. Journal of Electroceramics, 2017, 39, 39-60.	0.8	19
30503	Substrate induced reconstruction and activation of platinum clusters: A systematic DFT study. Applied Surface Science, 2017, 422, 1075-1081.	3.1	8
30504	Opto-electronic and interfacial charge transfer properties of azobenzene dyes on anatase TiO 2 (001) surface â€“ The effect of anchoring group. Journal of Photochemistry and Photobiology A: Chemistry, 2017, 346, 372-381.	2.0	10

#	Article	IF	Citations
30505	Complex investigation of structural and magnetic properties of the Ni-Mn-(Ga, Ge) alloys within ab initio approach. Materials Today: Proceedings, 2017, 4, 4616-4620.	0.9	0
30506	Solution Deposition of Phenylphosphinic Acid Leads to Highly Ordered, Covalently Bound Monolayers on TiO₂ (110) Without Annealing. Journal of Physical Chemistry C, 2017, 121, 14213-14221.	1.5	14
30507	Insight into Electronic and Structural Reorganizations for Defect-Induced VO₂ Metalâ€“Insulator Transition. Journal of Physical Chemistry Letters, 2017, 8, 3129-3132.	2.1	24
30508	Mechanical properties of atomically thin boron nitride and the role of interlayer interactions. Nature Communications, 2017, 8, 15815.	5.8	576
30509	Compressed few-layer black phosphorus nanosheets from semiconducting to metallic transition with the highest symmetry. Nanoscale, 2017, 9, 10741-10749.	2.8	16
30510	Emergence of intrinsic half-metallicity in MoS2 nano-crystals : A first principles study. AIP Conference Proceedings, 2017, , .	0.3	0
30511	Defects in Na-, K-, and Cd-Doped CuInSe$_2$: Canonical Thermodynamics Based on Ab Initio Calculations. IEEE Journal of Photovoltaics, 2017, 7, 1143-1152.	1.5	5
30512	Pressure-induced insulatorâ€“metal transition in EuMnO₃. Journal of Physics Condensed Matter, 2017, 29, 305801.	0.7	11
30513	Dynamics of the Lithiation and Sodiation of Silicon Allotropes: From the Bulk to the Surface. Journal of the Electrochemical Society, 2017, 164, A1644-A1650.	1.3	6
30514	DFT Study on the Li Mobility in Li-Ion-Based Solid-State Electrolytes. MRS Advances, 2017, 2, 3277-3282.	0.5	5
30515	Metal Immiscibility Route to Synthesis of Ultrathin Carbides, Borides, and Nitrides. Advanced Materials, 2017, 29, 1700364.	11.1	61
30516	Ultrafast Growth of Highâ€Quality Monolayer WSe₂ on Au. Advanced Materials, 2017, 29, 1700990.	11.1	139
30517	Group of Quantum Bits Acting as a Bit Using a Singleâ€Domain Ferromagnet of Uniaxial Magnetic Ions. ChemPhysChem, 2017, 18, 2147-2150.	1.0	1
30518	Intensified Biobutanol Recovery by using Zeolites with Complementary Selectivity. ChemSusChem, 2017, 10, 2968-2977.	3.6	30
30519	High NOx Reduction Activity of an Ultrathin Zirconia Film Covering a Cu Surface: A DFT Study. Catalysis Letters, 2017, 147, 1827-1833.	1.4	18
30520	Superelasticity and Shape Memory Behavior of NiTiHf Alloys. Shape Memory and Superelasticity, 2017, 3, 168-187.	1.1	30
30521	Ab initio study of beryllium surfaces with different hydrogen coverages. Acta Materialia, 2017, 134, 81-92.	3.8	10
30522	Vacancy mediated alloying strengthening effects on Î³/Î³â€² interface of Ni-based single crystal superalloys: A first-principles study. Acta Materialia, 2017, 135, 25-34.	3.8	61

#	Article	IF	Citations
30523	First-principles prediction of the stacking fault energy of gold at finite temperature. Acta Materialia, 2017, 135, 88-95.	3.8	16
30524	Two-dimensional germanium monochalcogenides for photocatalytic water splitting with high carrier mobility. Applied Catalysis B: Environmental, 2017, 217, 275-284.	10.8	197
30525	Photocatalytic hydrogen production over Aurivillius compound Bi3TiNbO9 and its modifications by Cr/Nb co-doping. Applied Catalysis B: Environmental, 2017, 217, 342-352.	10.8	62
30526	Theoretical investigation of the crystal structure of AlOF. Chemical Physics, 2017, 491, 112-117.	0.9	5
30527	First-principles study of fission product stability and clustering in ThO2. Computational Materials Science, 2017, 137, 186-194.	1.4	3
30528	Conversion of toluene into benzyl radical on anatase TiO 2 (0 0 1) surface. Computational and Theoretical Chemistry, 2017, 1115, 13-21.	1.1	1
30529	Effect of external strain on the charge transfer: Adsorption of gas molecules on monolayer GaSe. Materials Chemistry and Physics, 2017, 198, 49-56.	2.0	15
30530	Nitrogen-doped Ti 3 C 2 T x MXene electrodes for high-performance supercapacitors. Nano Energy, 2017, 38, 368-376.	8.2	528
30531	Effect of interactions between elements on the diffusion of solutes in Ni X Y systems and Î³â€²-coarsening in model Ni-based superalloys. Scripta Materialia, 2017, 138, 100-104.	2.6	30
30532	The electronic structure of GeSe monolayer with light nonmetallic elements decoration. Superlattices and Microstructures, 2017, 109, 829-840.	1.4	13
30533	31P MAS NMR spectroscopy with 93Nb decoupling and DFT calculations: AÂstructural characterization of defects in a niobium-phosphate phase. Solid State Nuclear Magnetic Resonance, 2017, 84, 210-215.	1.5	9
30534	Revisiting Hollandites: Channels Filling by Main-Group Elements Together with Transition Metals in Bi2â€“yVyV8O16. Chemistry of Materials, 2017, 29, 5558-5565.	3.2	4
30535	Tunable Optical Properties and Increased Thermal Quenching in the Blue-Emitting Phosphor Series: Ba₂(Y_{1â€“x}Lu_x)₅B₅O₁₇:Ce³⁺ (x = 0â€“1). Chemistry of Materials, 2017, 29, 5267-5275.	8.2	163
30536	Impact of Hydrogen Bonding in the Binding Site between Capsid Protein and MS2 Bacteriophage ssRNA. Journal of Physical Chemistry B, 2017, 121, 6321-6330.	1.2	30
30537	High-Pressure Effects on Hofmann-Type Clathrates: Promoted Release and Restricted Insertion of Guest Molecules. Journal of Physical Chemistry Letters, 2017, 8, 2745-2750.	2.1	13
30538	Computational Dissection of Two-Dimensional Rectangular Titanium Mononitride TiN: Auxetics and Promises for Photocatalysis. Nano Letters, 2017, 17, 4466-4472.	4.5	104
30539	Theoretical Insights and the Corresponding Construction of Supported Metal Catalysts for Highly Selective CO₂ to CO Conversion. ACS Catalysis, 2017, 7, 4613-4620.	5.5	104
30540	TlSn₂I₅, a Robust Halide Antiperovskite Semiconductor for Î³-Ray Detection at Room Temperature. ACS Photonics, 2017, 4, 1805-1813.	3.2	33

#	Article	IF	Citations
30541	Accelerated discovery of two crystal structure types in a complex inorganic phase field. Nature, 2017, 546, 280-284.	13.7	61
30542	Multiferroic Phases and Transitions in Ferroelectric Lead Titanate Nanodots. Scientific Reports, 2017, 7, 45373.	1.6	7
30543	Density functional theory calculations for the band gap and formation energy of Pr_{4â^'x}Ca_xSi₁₂O_{3+x}N_{18â^'x}; a highly disordered compound with low symmetry and a large cell size. Physical Chemistry Chemical Physics, 2017, 19, 16702-16712.	1.3	17
30544	Direct versus ligand-exchange synthesis of [PtAg₂₈(BDT)₁₂(TPP)₄]^{4â^'}nanoclusters: effect of a single-atom dopant on the optoelectronic and chemical properties. Nanoscale, 2017, 9, 9529-9536.	2.8	62
30545	Toward understanding the adsorption mechanism of large size organic corrosion inhibitors on an Fe(110) surface using the DFTB method. RSC Advances, 2017, 7, 29042-29050.	1.7	170
30546	Drastically enhanced hydrogen evolution activity by 2D to 3D structural transition in anion-engineered molybdenum disulfide thin films for efficient Si-based water splitting photocathodes. Journal of Materials Chemistry A, 2017, 5, 15534-15542.	5.2	69
30547	Phase diagram of waterâ€“methane by first-principles thermodynamics: discovery of MH-IV and MH-V hydrates. Physical Chemistry Chemical Physics, 2017, 19, 15996-16002.	1.3	12
30548	The mechanism of anomalous hardening in transition-metal monoborides. Nanoscale, 2017, 9, 9112-9118.	2.8	21
30549	Silicene growth through island migration and coalescence. Nanoscale, 2017, 9, 10186-10192.	2.8	15
30550	Atomistic insight into the electrode reaction mechanism of the cathode in molten carbonate fuel cells. Journal of Materials Chemistry A, 2017, 5, 13763-13768.	5.2	18
30551	Non-metallic dopant modulation of conductivity in substoichiometric tantalum pentoxide: A first-principles study. Journal of Applied Physics, 2017, 121, .	1.1	2
30552	Band offsets of Ag2ZnSnSe4/CdS heterojunction: An experimental and first-principles study. Journal of Applied Physics, 2017, 121, .	1.1	22
30553	Phase transformations upon doping in WO3. Journal of Chemical Physics, 2017, 146, 214504.	1.2	25
30554	Hydrogen anion and subgap states in amorphous Inâ€“Gaâ€“Znâ€“O thin films for TFT applications. Applied Physics Letters, 2017, 110, .	1.5	121
30555	Effects of pressure on structural, electronic, and mechanical properties of Î± , Î² , and Î³ uranium. Chinese Physics B, 2017, 26, 066104.	0.7	7
30556	The effect of irradiation-induced point defects on energetics and kinetics of hydrogen in 3C-SiC in a fusion environment. Nuclear Fusion, 2017, 57, 066031.	1.6	11
30557	Ohmic contact in monolayer InSe-metal interface. 2D Materials, 2017, 4, 025116.	2.0	60
30558	New allotropic forms of carbon based on Đ¡60 and Đ¡20 fullerenes with specific mechanical characteristics. JETP Letters, 2017, 105, 419-425.	0.4	3

#	Article	IF	Citations
30559	Experimental investigation and ab initio calculation of the properties of Sc-, in-doped bismuth titanates with the pyrochlore type structure. Physics of the Solid State, 2017, 59, 495-503.	0.2	10
30560	Trapping of helium atom by vacancy in tungsten: a density functional theory study. European Physical Journal B, 2017, 90, 1.	0.6	19
30561	A Lithium Amideâ€Borohydride Solidâ€State Electrolyte with Lithiumâ€Ion Conductivities Comparable to Liquid Electrolytes. Advanced Energy Materials, 2017, 7, 1700294.	10.2	95
30562	Crystal Structures of CaB₃N₃ at High Pressures. Inorganic Chemistry, 2017, 56, 7449-7453.	1.9	2
30563	Ground-State Crystal Structure of Strontium Peroxide Predicted from First Principles. Inorganic Chemistry, 2017, 56, 7545-7549.	1.9	7
30564	Promotion of the Inactive Iron Sulfide to an Efficient Hydrodesulfurization Catalyst. ACS Catalysis, 2017, 7, 4805-4816.	5.5	63
30565	Adsorption Energy Correlations at the Metalâ€“Support Boundary. ACS Catalysis, 2017, 7, 4707-4715.	5.5	49
30566	Controlling the spin and valley degeneracy splitting in monolayer MnPSe₃ by atom doping. Physical Chemistry Chemical Physics, 2017, 19, 15388-15393.	1.3	21
30567	First-principles equation-of-state table of beryllium based on density-functional theory calculations. Physics of Plasmas, 2017, 24, 062702.	0.7	20
30568	Electronic and thermoelectric properties of Mg ₂ Ge _x Sn _{1â^' x} (x = 0.25, 0.50, 0.75) solid solutions by first-principles calculations. Chinese Physics B, 2017, 26, 066103.	0.7	5
30569	Zweidimensionales Haeckelitâ€NbS₂ â€“ ein diamagnetischer Halbleiter mit Nb⁴⁺â€Ionen und hoher LadungstrÃgermobilitÃt. Angewandte Chemie, 2017, 129, 10348-10352.	1.6	0
30570	Enhanced adsorption of carbonyl molecules on graphene via Ï€-Li-Ï€ interaction: a first-principle study. Science China Materials, 2017, 60, 674-680.	3.5	12
30571	Orbital rearrangement mechanism and half-metallicity transition in strained Fe3O4/BaTiO3 interfaces. Computational Materials Science, 2017, 137, 243-248.	1.4	1
30572	FCC metal-like deformation behaviour of Ir3Nb with the L12 structure. International Journal of Plasticity, 2017, 97, 145-158.	4.1	10
30573	Oxygen defects formation and optical identification in monolayer borophene. Materials Chemistry and Physics, 2017, 198, 346-353.	2.0	9
30574	Monolayer Bismuthene-Metal Contacts: A Theoretical Study. ACS Applied Materials & Interfaces, 2017, 9, 23128-23140.	4.0	73
30575	Adsorption differences between low coverage enantiomers of alanine on the chiral Cu{421}^R surface. Physical Chemistry Chemical Physics, 2017, 19, 13562-13570.	1.3	6
30576	Optical polarization in mono and bilayer MoS2. Current Applied Physics, 2017, 17, 1153-1157.	1.1	7

#	Article	IF	Citations
30577	First principles study of Cr poisoning in solid oxide fuel cell cathodes: Application to (La,Sr) CoO3. Computational Materials Science, 2017, 137, 6-9.	1.4	4
30578	Exploring electronic and optical properties of CH 3 NH 3 GeI 3 perovskite: Insights from the first principles. Computational and Theoretical Chemistry, 2017, 1114, 20-24.	1.1	14
30579	Quasi-particle energies and optical excitations of novel porous graphene phases from first-principles many-body calculations. Diamond and Related Materials, 2017, 77, 35-40.	1.8	25
30580	Resistance against water and acid water (pHÂ=Â4.0) via Al-doped ZnO thin films for environmentally friendly glass panels. Journal of Alloys and Compounds, 2017, 719, 271-280.	2.8	13
30581	Uncovering the Thermo-Kinetic Origins of Phase Ordering in Mixed-Valence Antimony Tetroxide by First-Principles Modeling. Inorganic Chemistry, 2017, 56, 6545-6550.	1.9	3
30582	Competing Gap Opening Mechanisms of Monolayer Graphene and Graphene Nanoribbons on Strong Topological Insulators. Nano Letters, 2017, 17, 4013-4018.	4.5	41
30583	Acidâ€“Base Reactivity of Perovskite Catalysts Probed via Conversion of 2-Propanol over Titanates and Zirconates. ACS Catalysis, 2017, 7, 4423-4434.	5.5	81
30584	A computational study of the electronic properties, ionic conduction, and thermal expansion of Sm_{1â^'x}A_xCoO₃and Sm_{1â^'x}A_xCoO_{3â^'x/2}(A = Ba²⁺, Ca²⁺,) Tj ETQq1 1 0.784314 rgBT /Overlock 10 Tf 50 Chemical Physics, 2017, 19, 13960-13969.	1.3	14
30585	GaS_{0.5}Te_{0.5} monolayer as an efficient water splitting photocatalyst. Physical Chemistry Chemical Physics, 2017, 19, 15394-15402.	1.3	17
30586	Phosphomolybdic acid supported atomically dispersed transition metal atoms (M = Fe, Co, Ni, Cu, Ru,) Tj ETQq1 1 0.784314 rgBT /Overlock 10 Tf 50 Advances, 2017, 7, 24925-24932.	1.7	23
30587	Porphyrinâ€“graphene oxide frameworks for long life sodium ion batteries. Journal of Materials Chemistry A, 2017, 5, 13204-13211.	5.2	40
30588	Gauge invariant theory for super high resolution Raman images. Journal of Chemical Physics, 2017, 146, 194106.	1.2	12
30589	Perfect Spin Filter in a Tailored Zigzag Graphene Nanoribbon. Nanoscale Research Letters, 2017, 12, 357.	3.1	15
30590	Interfacial void segregation of Cl in Cu-Sn micro-connects. Electronic Materials Letters, 2017, 13, 307-312.	1.0	6
30591	Electronic structure and electrical conduction by polaron hopping mechanism in A2LuTaO6 (A= Ba, Sr,) Tj ETQq0 0 0 rgBT /Overlock 10 Tf 50	2.3	31
30592	Response of the physical properties of Î´-Y 6 WO 12 and Y 6 UO 12 to pressure. Computational Materials Science, 2017, 134, 201-205.	1.4	5
30593	Ab initio DFT studies of adsorption characteristics of benzene on close-packed surfaces of transition metals. Computational Materials Science, 2017, 137, 10-19.	1.4	9
30594	Nanoscale reactivity of Zn x Mg 20â^'x investigated by structural and electronic indicators. Corrosion Science, 2017, 124, 35-45.	3.0	6

#	Article	IF	Citations
30595	First-principles study on surface properties of t-LiFeSO4F: Showing a potential way to enhance electronic conductivity. Chemical Physics Letters, 2017, 684, 177-185.	1.2	1
30596	Theoretical study of direct versus oxygen-assisted water dissociation on Co(0 0 0 1) surface. Chemical Physics Letters, 2017, 681, 29-35.	1.2	8
30597	Partitioning and diffusion of transition metal solutes in ternary model Ni-based single crystal superalloys. Materials and Design, 2017, 130, 157-165.	3.3	46
30598	Elasticity of phase-Pi (Al3Si2O7(OH)3) â€“ A hydrous aluminosilicate phase. Physics of the Earth and Planetary Interiors, 2017, 269, 91-97.	0.7	8
30599	Electronic and magnetic properties tuning of armchair BC 2 N nanoribbons by edge modification. Solid State Communications, 2017, 257, 27-31.	0.9	1
30600	Theoretical investigations on helium trapping in the Zr/Ti 2 AlC interface. Surface and Coatings Technology, 2017, 322, 19-24.	2.2	17
30601	Postsynthetic Route for Modifying the Metalâ€”Insulator Transition of VO₂ by Interstitial Dopant Incorporation. Chemistry of Materials, 2017, 29, 5401-5412.	3.2	36
30602	Structures and Magnetic Properties of MoS₂ Grain Boundaries with Antisite Defects. Journal of Physical Chemistry C, 2017, 121, 12261-12269.	1.5	63
30603	Stretching-Induced Conductance Variations as Fingerprints of Contact Configurations in Single-Molecule Junctions. Journal of the American Chemical Society, 2017, 139, 8286-8294.	6.6	29
30604	para-Azaquinodimethane: A Compact Quinodimethane Variant as an Ambient Stable Building Block for High-Performance Low Band Gap Polymers. Journal of the American Chemical Society, 2017, 139, 8355-8363.	6.6	65
30605	First-principles study of the structural stability and electrochemical properties of Na₂MSiO₄ (M = Mn, Fe, Co and Ni) polymorphs. Physical Chemistry Chemical Physics, 2017, 19, 14462-14470.	1.3	31
30606	Predicting photon cascade emission in Pr3+doped fluorides. Physical Chemistry Chemical Physics, 2017, 19, 15503-15511.	1.3	4
30607	Substrate-mediated growth of vanadium carbide with controllable structure as high performance electrocatalysts for dye-sensitized solar cells. RSC Advances, 2017, 7, 26710-26716.	1.7	15
30608	Exotic thermoelectric behavior in nitrogenated holey graphene. RSC Advances, 2017, 7, 25803-25810.	1.7	25
30609	Wavelengthâ€Tunability and Multiband Emission from Singleâ€Site Mn²⁺ Doped CaO Through Antiferromagnetic Coupling and Tailored Superexchange Reactions. Advanced Optical Materials, 2017, 5, 1700070.	3.6	40
30610	Local Bonding Influence on the Band Edge and Band Gap Formation in Quaternary Chalcopyrites. Advanced Science, 2017, 4, 1700080.	5.6	35
30611	Enhanced CO2 photocatalytic reduction on alkali-decorated graphitic carbon nitride. Applied Catalysis B: Environmental, 2017, 216, 146-155.	10.8	127
30612	Dynamics of adsorbate rotation in electron-induced reaction. Chemical Physics Letters, 2017, 683, 443-447.	1.2	1

#	Article	IF	Citations
30613	Cathode Properties of Perovskite-type NaMF3 (M= Fe, Mn, and Co) Prepared by Mechanical Ball Milling for Sodium-ion Battery. Electrochimica Acta, 2017, 245, 424-429.	2.6	24
30614	Periodic DFT Study of Rutile IrO₂: Surface Reactivity and Catechol Adsorption. Journal of Physical Chemistry C, 2017, 121, 13135-13143.	1.5	32
30615	Tuning the Morphology of Li₂O₂ by Noble and 3d metals: A Planar Model Electrode Study for Liâ€“O₂ Battery. ACS Applied Materials & Interfaces, 2017, 9, 19800-19806.	4.0	39
30616	Achieving Remarkable Activity and Durability toward Oxygen Reduction Reaction Based on Ultrathin Rh-Doped Pt Nanowires. Journal of the American Chemical Society, 2017, 139, 8152-8159.	6.6	265
30617	Novel magnesium borides and their superconductivity. Physical Chemistry Chemical Physics, 2017, 19, 14486-14494.	1.3	10
30618	Theoretical investigation of energy gap bowing in CdSxSe1â^'x alloy quantum dots. Physical Chemistry Chemical Physics, 2017, 19, 14495-14502.	1.3	3
30619	Formation and structures of Auâ€“Rh bimetallic nanoclusters supported on a thin film of Al2O3/NiAl(100). Physical Chemistry Chemical Physics, 2017, 19, 14566-14579.	1.3	5
30620	Strain induced quantum spin Hall insulator in monolayer Î²-BiSb from first-principles study. RSC Advances, 2017, 7, 27816-27822.	1.7	26
30621	Nontrivial Berry phase in magnetic BaMnSb ₂ semimetal. Proceedings of the National Academy of Sciences of the United States of America, 2017, 114, 6256-6261.	3.3	71
30622	First-principles study of water reacting with the (110) surface of uranium mononitride. Journal of Nuclear Materials, 2017, 492, 244-252.	1.3	6
30623	Enhancing Enantiomeric Separation with Strain: The Case of Serine on Cu(531). Journal of the American Chemical Society, 2017, 139, 8167-8173.	6.6	12
30624	Complex magnetic orders in small cobaltâ€“benzene molecules. Physical Chemistry Chemical Physics, 2017, 19, 14854-14860.	1.3	6
30625	Fe/Ni core/shell nanowires and nanorods: a combined first-principles and atomistic simulation study. Physical Chemistry Chemical Physics, 2017, 19, 16267-16275.	1.3	7
30626	Tailoring lanthanide doping in perovskite CaTiO₃ for luminescence applications. Physical Chemistry Chemical Physics, 2017, 19, 16189-16197.	1.3	22
30627	Exploring ion migration in Li₂MnSiO₄ for Li-ion batteries through strain effects. RSC Advances, 2017, 7, 26089-26096.	1.7	15
30628	Asymmetric passivation of edges: a route to make magnetic graphene nanoribbons. RSC Advances, 2017, 7, 27932-27937.	1.7	2
30629	Cd and In-doping in thin film SnO2. Journal of Applied Physics, 2017, 121, 195303.	1.1	7
30630	Ab initio study on the anisotropy of mechanical behavior and deformation mechanism for boron carbide. Chinese Physics B, 2017, 26, 047101.	0.7	9

#	Article	IF	Citations
30631	Double Dirac point semimetal in 2D material: Ta ₂ Se ₃. 2D Materials, 2017, 4, 025111.	2.0	18
30632	Hexakis [60]Fullerene Adductâ€Mediated Covalent Assembly of Ruthenium Nanoparticles and Their Catalytic Properties. Chemistry - A European Journal, 2017, 23, 13379-13386.	1.7	22
30633	Effect of Pd doping on CH 4 reactivity over Co 3 O 4 catalysts from density-functional theory calculations. Chinese Journal of Catalysis, 2017, 38, 813-820.	6.9	13
30634	Indirect phase transition of refractory nitrides compounds of: TiN, ZrN and HfN crystal structures. Computational Materials Science, 2017, 137, 75-84.	1.4	10
30635	Using density functional theory to increase the accuracy of experimental crystal structures: The case of potassium peroxocarbonate. Journal of Molecular Structure, 2017, 1146, 1-4.	1.8	1
30636	Effect of structural disorder on the ground state properties of Co 2 CrAl Heusler alloy. Physica B: Condensed Matter, 2017, 519, 82-89.	1.3	16
30637	Strain- and Fluorination-Induced Quantum Spin Hall Insulators in Blue Phosphorene: A First-Principles Study. Journal of Physical Chemistry C, 2017, 121, 12945-12952.	1.5	36
30638	Direct Imaging of Kinetic Pathways of Atomic Diffusion in Monolayer Molybdenum Disulfide. Nano Letters, 2017, 17, 3383-3390.	4.5	34
30639	Tailoring Active Sites via Synergy between Graphitic and Pyridinic N for Enhanced Catalytic Efficiency of a Carbocatalyst. ACS Applied Materials & Interfaces, 2017, 9, 19861-19869.	4.0	62
30640	Enhanced Energy-Storage Density and High Efficiency of Lead-Free CaTiO₃â€“BiScO₃ Linear Dielectric Ceramics. ACS Applied Materials & Interfaces, 2017, 9, 19963-19972.	4.0	145
30641	Interface-driven formation of a two-dimensional dodecagonal fullerene quasicrystal. Nature Communications, 2017, 8, 15367.	5.8	16
30642	Monolayer AgBiP₂Se₆: an atomically thin ferroelectric semiconductor with out-plane polarization. Nanoscale, 2017, 9, 8427-8434.	2.8	97
30643	Properties of hydrogen, helium, and silicon dioxide mixtures in giant planet interiors. Physics of Plasmas, 2017, 24, .	0.7	52
30644	Spherical harmonics based descriptor for neural network potentials: Structure and dynamics of Au147 nanocluster. Journal of Chemical Physics, 2017, 146, 204301.	1.2	48
30645	Finite temperature properties of NiTi from first principles simulations: Structure, mechanics, and thermodynamics. Journal of Applied Physics, 2017, 121, .	1.1	35
30646	Defect levels and hyperfine constants of hydrogen in beryllium oxide from hybrid-functional calculations and muonium spectroscopy. Philosophical Magazine, 2017, 97, 2108-2128.	0.7	13
30647	Electronic and optical properties of strained graphene and other strained 2D materials: a review. Reports on Progress in Physics, 2017, 80, 096501.	8.1	383
30648	K0.4TaO2.4F0.6 Nanocubes as Highly Efficient Noble Metal-Free Electrocatalysts for Hydrogen Evolution Reaction in Acidic Media. Electrochimica Acta, 2017, 245, 193-200.	2.6	6

#	Article	IF	Citations
30649	Comprehensive theoretical and experimental study of electrical transport mechanism on BiFeO 3 multiferroic nanoparticles. Journal of Alloys and Compounds, 2017, 720, 47-53.	2.8	10
30650	Comparative studies about CO methanation over Ni(211) and Zr-modified Ni(211) surfaces: Qualitative insight into the effect of surface structure and composition. Molecular Catalysis, 2017, 438, 1-14.	1.0	19
30651	Theoretical and experimental investigations of the thermoelectric properties of Al-, Bi- and Sn-doped ZnO. Materials Science in Semiconductor Processing, 2017, 66, 247-252.	1.9	35
30652	Adsorption of benzene on low index surfaces of platinum in the presence of van der Waals interactions. Surface Science, 2017, 664, 8-15.	0.8	7
30653	Mechanistic Insight into Câ€“C Coupling over Feâ€“Cu Bimetallic Catalysts in CO₂ Hydrogenation. Journal of Physical Chemistry C, 2017, 121, 13164-13174.	1.5	91
30654	Effect of Point Defects on Optical Properties of Graphene Fluoride: A First-Principles Study. Journal of Physical Chemistry C, 2017, 121, 12855-12862.	1.5	30
30655	Large-Gap Magnetic Topological Heterostructure Formed by Subsurface Incorporation of a Ferromagnetic Layer. Nano Letters, 2017, 17, 3493-3500.	4.5	129
30656	Shuttlecock-Shaped Molecular Rectifier: Asymmetric Electron Transport Coupled with Controlled Molecular Motion. Nano Letters, 2017, 17, 4061-4066.	4.5	13
30657	Ultra-stiff metallic glasses through bond energy density design. Journal of Physics Condensed Matter, 2017, 29, 265502.	0.7	11
30658	An improved method to predict the Wulff shape: An example for Li2CoSiO4. Computational Materials Science, 2017, 137, 113-118.	1.4	8
30659	van Hove singularities and tight-binding model in high-temperature superconductor H 3 Se. Physics Letters, Section A: General, Atomic and Solid State Physics, 2017, 381, 2526-2530.	0.9	4
30660	Crystal Structure Induced Preferential Surface Alloying of Sb on Wurtzite/Zinc Blende GaAs Nanowires. Nano Letters, 2017, 17, 3634-3640.	4.5	14
30661	Pressure-induced structural change in liquid GaIn eutectic alloy. Scientific Reports, 2017, 7, 1139.	1.6	17
30662	Structureâ€“reactivity relationship in isolated Zr sites present in Zr-zeolite and ZrO₂ for the Meerweinâ€“Ponndorfâ€“Verley reaction. Catalysis Science and Technology, 2017, 7, 2865-2873.	2.1	52
30663	Novel structural phases and the electrical properties of Si3B under high pressure. Physical Chemistry Chemical Physics, 2017, 19, 16206-16212.	1.3	9
30664	Dirac node lines in two-dimensional Lieb lattices. Nanoscale, 2017, 9, 8740-8746.	2.8	46
30665	First-principles study of electronic and optical properties of boron and nitrogen doped graphene. AIP Conference Proceedings, 2017, , .	0.3	3
30666	Thermodynamic investigation of the Zr-Fe-Nb system and its applications. Intermetallics, 2017, 88, 91-100.	1.8	27

#	Article	IF	Citations
30667	Growth and polarized Raman spectroscopy investigations of single crystal CdSiP 2 : Experimental measurements and ab initio calculations. Journal of Crystal Growth, 2017, 473, 28-33.	0.7	8
30668	Mechanical, electronic and thermodynamic properties of hexagonal and orthorhombic U 2 Mo: A first-principle calculation. Progress in Nuclear Energy, 2017, 99, 110-118.	1.3	9
30669	Computational Evidence for Lewis Base-Promoted CO₂ Hydrogenation to Formic Acid on Gold Surfaces. ACS Catalysis, 2017, 7, 4519-4526.	5.5	42
30670	First-principles computational studies on layered Na₂Mn₃O₇ as a high-rate cathode material for sodium ion batteries. Journal of Materials Chemistry A, 2017, 5, 12752-12756.	5.2	39
30671	Low energy bands and transport properties of chromium arsenide. Journal of Physics Condensed Matter, 2017, 29, 224004.	0.7	12
30672	High Tunnel Magnetoresistance in Mo/CoFe/MgO Magnetic Tunnel Junction: A First-Principles Study. IEEE Transactions on Magnetics, 2017, 53, 1-4.	1.2	4
30673	Significant modification of perpendicular magnetic anisotropy of W/Fe(001) multilayer by controlling in-plane lattice constant. Applied Physics Express, 2017, 10, 063005.	1.1	4
30674	First principles study of electronic, phonon and elastic properties of rock-salt-phase MTe (MÂ=ÂMg, Ca,) Tj ETQq1 1 0.784314 rgBT /Ove	0.9	2
30675	The high hydrogen storage capacities of Li-decorated borophene. Computational Materials Science, 2017, 137, 119-124.	1.4	73
30676	Enhanced defect-mediated ferromagnetism in Cu2O by Co doping. Journal of Magnetism and Magnetic Materials, 2017, 441, 374-386.	1.0	16
30677	Exploring the PbSâ€“Bi₂S₃ Series for Next Generation Energy Conversion Materials. Chemistry of Materials, 2017, 29, 5156-5167.	3.2	32
30678	Tunable Magnetism and Transport Properties in Nitride MXenes. ACS Nano, 2017, 11, 7648-7655.	7.3	276
30679	Ab initio mechanical and thermal properties of FeMnP1â^'xGaxcompounds as refrigerant for room-temperature magnetic refrigeration. RSC Advances, 2017, 7, 27454-27463.	1.7	5
30680	MgFeSiO₄ as a potential cathode material for magnesium batteries: ion diffusion rates and voltage trends. Journal of Materials Chemistry A, 2017, 5, 13161-13167.	5.2	51
30681	Electronic and magnetic properties of transition metal doped graphyne. AIP Conference Proceedings, 2017, , .	0.3	2
30682	Pressure-induced phase transition and electronic properties of MgB2C2. Journal of Applied Physics, 2017, 121, 195102.	1.1	3
30683	Molybdenum Carbide: A Stable Topological Semimetal with Line Nodes and Triply Degenerate Points. Chinese Physics Letters, 2017, 34, 027102.	1.3	14
30684	Adsorption of 3d, 4d, and 5dtransition metal atoms onÎ²₁₂â€"Borophene. Journal of Physics Condensed Matter, 2017, 29, 305302.	0.7	16

#	Article	IF	Citations
30685	First-principle study of the structural, electronic, and optical properties of SiC nanowires. Chinese Physics B, 2017, 26, 057103.	0.7	3
30686	Twoâ€Dimensional Haeckelite NbS₂: A Diamagnetic Highâ€Mobility Semiconductor with Nb⁴⁺ Ions. Angewandte Chemie - International Edition, 2017, 56, 10214-10218.	7.2	32
30687	Magnetic phases at the molecular scale: the case of cylindrical Co nanoparticles. Journal of Nanoparticle Research, 2017, 19, 1.	0.8	1
30688	Ba₆Zn₇Ga₂S₁₆: A Wide Band Gap Sulfide with Phase-Matchable Infrared NLO Properties. Chemistry of Materials, 2017, 29, 5259-5266.	3.2	97
30689	The Hydration Effect and Selectivity of Alkali Metal Ions on Poly(ethylene glycol) Models in Cyclic and Linear Topology. Journal of Physical Chemistry A, 2017, 121, 4721-4731.	1.1	32
30690	Advancements in the Synthesis of Building Block Materials: Experimental Evidence and Modeled Interpretations of the Effect of Na and K on Imogolite Synthesis. Journal of Physical Chemistry C, 2017, 121, 12658-12668.	1.5	18
30691	Ag-Modified BiOCl Single-Crystal Nanosheets: Dependence of Photocatalytic Performance on the Region-Selective Deposition of Ag Nanoparticles. Journal of Physical Chemistry C, 2017, 121, 13191-13201.	1.5	106
30692	Honeycomb Boron Allotropes with Dirac Cones: A True Analogue to Graphene. Journal of Physical Chemistry Letters, 2017, 8, 2647-2653.	2.1	57
30693	Can CF₃-Functionalized La@C₆₀ Be Isolated Experimentally and Become Superconducting?. Nano Letters, 2017, 17, 3402-3408.	4.5	22
30694	Coherent Interlayer Tunneling and Negative Differential Resistance with High Current Density in Double Bilayer Grapheneâ€“WSe₂ Heterostructures. Nano Letters, 2017, 17, 3919-3925.	4.5	53
30695	Biphenylene and Phagraphene as Lithium Ion Battery Anode Materials. ACS Applied Materials & Interfaces, 2017, 9, 20577-20584.	4.0	122
30696	Dodecahedral W@WC Composite as Efficient Catalyst for Hydrogen Evolution and Nitrobenzene Reduction Reactions. ACS Applied Materials & Interfaces, 2017, 9, 20594-20602.	4.0	28
30697	A novel borophene featuring heptagonal holes: a common precursor of borospherenes. Physical Chemistry Chemical Physics, 2017, 19, 19890-19895.	1.3	12
30698	Structural, electronic and lattice dynamical properties of perovskite CaZrO3 under high pressure. AIP Conference Proceedings, 2017, , .	0.3	3
30699	Electronic and optical properties of Cu2XSnS4 (Xâ€‰=â€‰Be, Mg, Ca, Mn, Fe, and Ni) and the impact of native defect pairs. Journal of Applied Physics, 2017, 121, .	1.1	31
30700	Coexistence of Strong Second Harmonic Generation Response and Wide Band Gap in AZn₄Ga₅S₁₂ (A=K, Rb, Cs) with 3D Diamondâ€like Frameworks. Chemistry - A European Journal, 2017, 23, 10407-10412.	1.7	53
30701	Microscopic analysis of AgCl polymorphism. Theoretical Chemistry Accounts, 2017, 136, 1.	0.5	0
30702	Mechanical stability and superconductivity of PbO-type phase of thorium monocarbide at high pressure. Computational Materials Science, 2017, 136, 238-242.	1.4	8

#	Article	IF	Citations
30703	Intermediate phases in sodium intercalation into MoS2 nanosheets and their implications for sodium-ion batteries. Nano Energy, 2017, 38, 342-349.	8.2	151
30704	Glycerol adsorption on a defected Pt6/Pt(100) substrate: a density functional theory investigation within the D3 van der Waals correction. RSC Advances, 2017, 7, 17122-17127.	1.7	5
30705	A scheme for the generation of Feâ€“P networks to search for low-energy LiFePO4 crystal structures. Journal of Materials Chemistry A, 2017, 5, 14611-14618.	5.2	9
30706	Topologically nontrivial electronic states in CaSn3. Journal of Applied Physics, 2017, 121, .	1.1	14
30707	Identification of ground-state spin ordering in antiferromagnetic transition metal oxides using the Ising model and a genetic algorithm. Science and Technology of Advanced Materials, 2017, 18, 246-252.	2.8	17
30708	libvdwxc: a library for exchangeâ€“correlation functionals in the vdW-DF family. Modelling and Simulation in Materials Science and Engineering, 2017, 25, 065004.	0.8	28
30709	Unveiling the controversial mechanism of reversible Na storage in TiO2 nanotube arrays: Amorphous versus anatase TiO2. Nano Research, 2017, 10, 2891-2903.	5.8	90
30710	Electronic evidence of temperature-induced Lifshitz transition and topological nature in ZrTe5. Nature Communications, 2017, 8, 15512.	5.8	190
30711	Temperature-regulated guest admission and release in microporous materials. Nature Communications, 2017, 8, 15777.	5.8	60
30712	Synthesis, structure and photocatalytic activity of layered LaOInS₂. Journal of Materials Chemistry A, 2017, 5, 14270-14277.	5.2	30
30713	Novel phase diagram behavior and materials design in heterostructural semiconductor alloys. Science Advances, 2017, 3, e1700270.	4.7	46
30714	Bis-chlorinated aromatics adsorption in Faujasites investigated by molecular simulation-influence of Na + cation. Microporous and Mesoporous Materials, 2017, 251, 83-93.	2.2	6
30715	Diffusion of point defects near stacking faults in 3C-SiC via first-principles calculations. Scripta Materialia, 2017, 139, 1-4.	2.6	24
30716	Understanding effects of Cr content on the slurry erosion behavior of high-Cr cast irons through local property mapping and computational analysis. Wear, 2017, 376-377, 587-594.	1.5	17
30717	Polar Magnets in Double Corundum Oxides. Chemistry of Materials, 2017, 29, 5447-5457.	3.2	46
30718	Binary Compound Bilayer and Multilayer with Vertical Polarizations: Two-Dimensional Ferroelectrics, Multiferroics, and Nanogenerators. ACS Nano, 2017, 11, 6382-6388.	7.3	301
30719	Very Large-Sized Transition Metal Dichalcogenides Monolayers from Fast Exfoliation by Manual Shaking. Journal of the American Chemical Society, 2017, 139, 9019-9025.	6.6	109
30720	Hafniumâ€”an optical hydrogen sensor spanning six orders in pressure. Nature Communications, 2017, 8, 15718.	5.8	41

#	Article	IF	Citations
30721	Intrinsically patterned two-dimensional materials for selective adsorption of molecules andÂnanoclusters. Nature Materials, 2017, 16, 717-721.	13.3	150
30722	First-principles study on structural, electronic, vibrational and thermodynamic properties of Sr₁₀(PO₄)₆X₂(X = F, Cl, Br). RSC Advances, 2017, 7, 30310-30319.	1.7	6
30723	Identifying the bottleneck of water oxidation by ab initio analysis of in situ optical absorbance spectrum. Physical Chemistry Chemical Physics, 2017, 19, 17278-17286.	1.3	25
30724	K-doped Sr₂Fe_{1.5}Mo_{0.5}O_{6â^Î´} predicted as a bifunctional catalyst for air electrodes in proton-conducting solid oxide electrochemical cells. Journal of Materials Chemistry A, 2017, 5, 12735-12739.	5.2	21
30725	Electronic structures of solids made of C20 clusters. AIP Advances, 2017, 7, 025103.	0.6	1
30726	High-pressure structures of yttrium hydrides. Journal of Physics Condensed Matter, 2017, 29, 325401.	0.7	17
30727	Stability of Sulphur Dimers (S₂) in Cometary Ices. Astrophysical Journal, 2017, 835, 134.	1.6	9
30728	DDT Polymorphism and the Lethality of Crystal Forms. Angewandte Chemie - International Edition, 2017, 56, 10165-10169.	7.2	46
30729	An Experimental Study on the Reduction Kinetics of Iron Titanium Based Oxygen Carriers with CO Validated by First Principle Calculations. ChemistrySelect, 2017, 2, 274-278.	0.7	1
30730	CO2 Activation and Hydrogenation: A Comparative DFT Study of Ru10/TiO2 and Cu10/TiO2 Model Catalysts. Catalysis Letters, 2017, 147, 1871-1881.	1.4	25
30731	The dynamic behavior of the exohedral transition metal complexes of $$mathrm{B}_{40}: {upeta}^{6}$$ B 40 : Î· 6 - and $${upeta}^{7}$$ Î· 7 - $$mathrm{B}_{40}hbox {Cr(CO)}_{3}$$ B 40 Cr(CO) 3 and $$hbox {Cr(CO)}_{3}$$ Cr(CO) 3 - $${upeta}^{7}$$ Î· 7 - $$hbox {B}_{40}$$ B 40 - $${upeta}^{7}$$ Î· 7 - $$hbox {Cr(CO)}_{3}$$ Cr(CO) 3. Journal of Chemical Sciences, 2017, 129, 1061-1067.	0.7	2
30732	Interfacial electronic and structural properties of SiO2(010)/BaTiO3(001) from first-principles calculations. Ceramics International, 2017, 43, 12988-12991.	2.3	4
30733	Many-body mechanism of Guinier-Preston zones stabilization in Alâ€“Cu alloys. Scripta Materialia, 2017, 138, 130-133.	2.6	17
30734	Selective and Efficient Removal of Volatile Organic Compounds by Channel-type Gamma-Cyclodextrin Assembly through Inclusion Complexation. Industrial & Engineering Chemistry Research, 2017, 56, 7345-7354.	1.8	25
30735	Electrocatalytic Activity and Design Principles of Heteroatom-Doped Graphene Catalysts for Oxygen-Reduction Reaction. Journal of Physical Chemistry C, 2017, 121, 14434-14442.	1.5	49
30736	Adsorption, Assembly, and Oligomerization of Aspartic Acid on Pd(111). Journal of Physical Chemistry C, 2017, 121, 13239-13248.	1.5	3
30737	Structure, Bonding, and Catalytic Properties of Defect Graphene Coordinated Pdâ€“Ni Nanoparticles. Journal of Physical Chemistry C, 2017, 121, 14668-14677.	1.5	11
30738	Parity-Forbidden Transitions and Their Impact on the Optical Absorption Properties of Lead-Free Metal Halide Perovskites and Double Perovskites. Journal of Physical Chemistry Letters, 2017, 8, 2999-3007.	2.1	441

#	Article	IF	Citations
30739	Epitaxial Templating of Two-Dimensional Metal Chloride Nanocrystals on Monolayer Molybdenum Disulfide. ACS Nano, 2017, 11, 6404-6415.	7.3	20
30740	Mechanism of mechanically induced optoelectronic and spintronic phase transitions in 1D graphene spirals: insight into the role of interlayer coupling. Nanoscale, 2017, 9, 9693-9700.	2.8	14
30741	Theoretical investigation of the electronic structure and luminescence properties for Nd_xY_{1â^'x}Al₃(BO₃)₄nonlinear laser crystal. Journal of Materials Chemistry C, 2017, 5, 7174-7181.	2.7	30
30742	Stable sandwich structures of two-dimensional iron borides FeB_xalloy: a first-principles calculation. RSC Advances, 2017, 7, 30320-30326.	1.7	7
30743	Two-dimensional arsenene oxide: A realistic large-gap quantum spin Hall insulator. Applied Physics Letters, 2017, 110, .	1.5	123
30744	Effect of oxygen vacancies and strain on the phonon spectrum of HfO2 thin films. Journal of Applied Physics, 2017, 121, .	1.1	10
30745	Experimental and DFT study of nitrogen atoms interactions with SiOCH low-Îº films. European Physical Journal D, 2017, 71, 1.	0.6	7
30746	First-principles study of the structures and fundamental electronic properties of two-dimensional P_{0.5}As_{0.5}alloy. Physica Status Solidi (B): Basic Research, 2017, 254, 1700157.	0.7	6
30747	Unexpected elastic isotropy in a black phosphorene/TiC2 van der Waals heterostructure with flexible Li-ion battery anode applications. Nano Research, 2017, 10, 3136-3150.	5.8	67
30748	Catalytic growth of diamond-like carbon on Fe3C-containing carburized layer through a single-step plasma-assisted carburizing process. Carbon, 2017, 122, 1-8.	5.4	49
30749	First-principles study of the adsorption properties of atoms and molecules on UN2 (001) surface. Journal of Nuclear Materials, 2017, 493, 124-131.	1.3	3
30750	Template-Grown MoS₂ Nanowires Catalyze the Hydrogen Evolution Reaction: Ultralow Kinetic Barriers with High Active Site Density. ACS Catalysis, 2017, 7, 5097-5102.	5.5	78
30751	Nanophase Segregation of Self-Assembled Monolayers on Gold Nanoparticles. ACS Nano, 2017, 11, 7371-7381.	7.3	35
30752	Methane Oxidation to Methanol Catalyzed by Cu-Oxo Clusters Stabilized in NU-1000 Metalâ€“Organic Framework. Journal of the American Chemical Society, 2017, 139, 10294-10301.	6.6	282
30753	The enhanced oxygen reduction reaction performance on PtSn nanowires: the importance of segregation energy and morphological effects. Journal of Materials Chemistry A, 2017, 5, 14355-14364.	5.2	23
30754	Piezoelectricity in two-dimensional covalent organic frameworks. Journal of Applied Physics, 2017, 121, 225112.	1.1	0
30755	Electronic properties and lattice configurations ofÂAu/CH3NH3PbI3 interface. Modern Physics Letters B, 2017, 31, 1750199.	1.0	3
30756	Revisit the electromigration effect: In situ synchrotron X-ray and scanning electron microscopy and ab initio calculations. , 2017, , .		0

#	Article	IF	Citations
30757	B₁₂(SCN)₁₂^{â€“}: An Ultrastable Weakly Coordinating Dianion. Journal of Physical Chemistry C, 2017, 121, 7697-7702.	1.5	31
30758	Double-layer ice from first principles. Physical Review B, 2017, 95, .	1.1	29
30759	CO Adsorption on (110)-(1 Ã— 2) Missing-Row Reconstructed Surfaces of Pd, Au, and Pd₃Au: Electronic Structures and Vibrational Frequencies. Journal of the Physical Society of Japan, 2017, 86, 044712.	0.7	3
30760	Deriving phosphorus atomic chains from few-layer black phosphorus. Nano Research, 2017, 10, 2519-2526.	5.8	26
30761	First principles investigations on the electronic properties of Cr doped Î±-Ca(BH4)2. Chinese Journal of Physics, 2017, 55, 870-875.	2.0	1
30762	Ab initio study on hydrogen interaction with calcium decorated silicon carbide nanotube. International Journal of Hydrogen Energy, 2017, 42, 11452-11460.	3.8	21
30763	The order-disorder transition in Cu 2 ZnSnS 4 : A theoretical and experimental study. Journal of Solid State Chemistry, 2017, 250, 140-144.	1.4	24
30764	Heat-Induced Solidâ€“Solid Phase Transformation of TKX-50. Journal of Physical Chemistry C, 2017, 121, 8262-8271.	1.5	42
30765	Preferential CH₃NH₃⁺ Alignment and Octahedral Tilting Affect Charge Localization in Cubic Phase CH₃NH₃PbI₃. Journal of Physical Chemistry C, 2017, 121, 8319-8326.	1.5	24
30766	Thermoelectric and phonon transport properties of two-dimensional IVâ€“VI compounds. Scientific Reports, 2017, 7, 506.	1.6	224
30767	The role of excess Sn in Cu₄Sn₇S₁₆ for modification of the band structure and a reduction in lattice thermal conductivity. Journal of Materials Chemistry C, 2017, 5, 4206-4213.	2.7	22
30768	Stability and strength of atomically thin borophene from first principles calculations. Materials Research Letters, 2017, 5, 399-407.	4.1	172
30769	First principles study of methane decomposition on B5 step-edge type site of Ru surface. Journal of Physics Condensed Matter, 2017, 29, 184001.	0.7	8
30770	Graphene Nanoribbon Based Thermoelectrics: Controllable Selfâ€•Doping and Longâ€Range Disorder. Advanced Science, 2017, 4, 1600467.	5.6	5
30771	Superconductivity Induced by Oxygen Doping in Y₂O₂Bi. Angewandte Chemie - International Edition, 2017, 56, 10123-10126.	7.2	11
30772	Amorphous phase stability and the interplay between electronic structure and topology. Acta Materialia, 2017, 131, 131-140.	3.8	12
30773	Formation of and interaction between Î²â€² F and Î²â€² phases in a Mgâ€'Gd alloy. Journal of Alloys and Compounds, 2017, 712, 334-344.	2.8	48
30774	Visible-light-induced Fe-doped BiVO4 photocatalyst for contaminated water treatment. Molecular Catalysis, 2017, 432, 220-231.	1.0	99

#	Article	IF	Citations
30775	Low-Dimensional Oxygen Vacancy Ordering and Diffusion in SrCrO_{3â˜Î´}. Journal of Physical Chemistry Letters, 2017, 8, 1757-1763.	2.1	15
30776	An intrinsic growth instability in isotropic materials leads to quasi-two-dimensional nanoplatelets. Nature Materials, 2017, 16, 743-748.	13.3	193
30777	High electron mobility and quantum oscillations in non-encapsulated ultrathin semiconducting Bi2O2Se. Nature Nanotechnology, 2017, 12, 530-534.	15.6	507
30778	Assessment of van der Waals inclusive density functional theory methods for layered electroactive materials. Physical Chemistry Chemical Physics, 2017, 19, 10133-10139.	1.3	43
30779	Electrical property effect of oxygen vacancies in the heterojunction of LaGaO ₃ / SrTiO ₃. Chinese Physics B, 2017, 26, 037101.	0.7	4
30781	Study of Structure and Deformation Pathways in Ti-7Al Using Atomistic Simulations, Experiments, and Characterization. Metallurgical and Materials Transactions A: Physical Metallurgy and Materials Science, 2017, 48, 2222-2236.	1.1	19
30782	On the structure and role of <mml:math xmlns:mml="http://www.w3.org/1998/Math/MathML" altimg="si1.gif" overflow="scroll"><mml:msubsup><mml:mtext>Î²</mml:mtext><mml:mtext>F</mml:mtext><mml:mtext>â€²</mml:mtext></mml:msu in Î²1 precipitation in Mgâ€“Nd alloys. Acta Materialia, 2017, 133, 408-426.	3.8	59
30783	Lithiation-enhanced charge transfer and sliding strength at the silicon-graphene interface: A first-principles study. Acta Mechanica Solida Sinica, 2017, 30, 254-262.	1.0	9
30784	The (2Ã—2) reconstructions on the surface of cobalt silicides: Atomic configuration at the annealed Co/Si(111) interface. Surface Science, 2017, 662, 6-11.	0.8	6
30785	Lattice thermal conductivity of borophene from first principle calculation. Scientific Reports, 2017, 7, 45986.	1.6	60
30786	Deformation mechanisms in high-efficiency thermoelectric layered Zintl compounds. Journal of Materials Chemistry A, 2017, 5, 9050-9059.	5.2	31
30787	High pressure band gap modification of LiCaAlF6. Applied Physics Letters, 2017, 110, .	1.5	15
30788	Radiation-induced alloy rearrangement in InxGa1â˜xN. Applied Physics Letters, 2017, 110, .	1.5	11
30789	Ab initioexplanation of disorder and off-stoichiometry in Fe-Mn-Al-C<mml:math xmlns:mml="http://www.w3.org/1998/Math/MathML"><mml:mi>Îº</mml:mi></mml:math>carbides. Physical Review B, 2017, 95, .	1.1	29
30790	Firstâ€principles investigation of chemical stability and proton conductivity of Mâ€doped BaZrO₃ (M=K, Rb, and Cs). Journal of the American Ceramic Society, 2017, 100, 2997-3003.	1.9	19
30791	Ferromagnetism in the unusual low-valence layered material LaSrNiRuO ₄. Europhysics Letters, 2017, 117, 37005.	0.7	4
30792	Synthesis, Structure, and Properties of Clathrate Si_{30.3(8)}P_{15.7(8)}Se_{7.930(3)}. Chemistry - A European Journal, 2017, 23, 9505-9516.	1.7	3
30793	Sc₂C as a Promising Anode Material with High Mobility and Capacity: A Firstâ€Principles Study. ChemPhysChem, 2017, 18, 1627-1634.	1.0	88

#	Article	IF	Citations
30794	Peculiarity of self-assembled cubic nanolamellae in the TiN/AlN system: Epitaxial self-stabilization by element deficiency/excess. Acta Materialia, 2017, 131, 391-399.	3.8	28
30795	Curvature dependence of single-walled carbon nanotubes for SO 2 adsorption and oxidation. Applied Surface Science, 2017, 404, 364-369.	3.1	23
30796	DFT study of oxygen adsorption on Mo 2 C(001) and (201) surfaces at different conditions. Applied Surface Science, 2017, 411, 394-399.	3.1	6
30797	Ferromagnetism of Na 0.5 Bi 0.5 TiO 3 (1 0 0) surface with O 2 adsorption. Applied Surface Science, 2017, 412, 77-84.	3.1	7
30798	Stability of defects in monolayer MoS 2 and their interaction with O 2 molecule: A first-principles study. Applied Surface Science, 2017, 412, 385-393.	3.1	72
30799	First-principles study on segregation of ternary additions for MoSi2/Mo5Si3 interface. Calphad: Computer Coupling of Phase Diagrams and Thermochemistry, 2017, 56, 150-153.	0.7	2
30800	The study of defect structure in tungsten: Rotation and migration property for the self-interstitial atoms. Fusion Engineering and Design, 2017, 124, 1122-1126.	1.0	6
30801	Structural dependence of photocatalytic hydrogen production over La/Cr co-doped perovskite compound ATiO 3 (A = Ca, Sr and Ba). International Journal of Hydrogen Energy, 2017, 42, 23539-23547.	3.8	39
30802	Functionalised hybrid Poly(ether ether ketone) containing MnO2: Investigation of operative conditions for hydrogen sorption. International Journal of Hydrogen Energy, 2017, 42, 10089-10098.	3.8	6
30803	Massively parallel first-principles simulation of electron dynamics in materials. Journal of Parallel and Distributed Computing, 2017, 106, 205-214.	2.7	42
30804	Local and average structure of Mn- and La-substituted BiFeO3. Journal of Solid State Chemistry, 2017, 250, 75-82.	1.4	21
30805	Ab-initio study on the stability, electronic and mechanical properties of transition metal nitrides under external pressure. Solid State Sciences, 2017, 67, 13-18.	1.5	4
30806	A room-temperature-operated Si LED with Î²-FeSi2 nanocrystals in the active layer: Î¼W emission power at 1.5â€‰Î¼m. Journal of Applied Physics, 2017, 121, .	1.1	13
30807	Ab initio study on interlayer exchange coupling in (Zn,Ni)O multilayers. Ferroelectrics, 2017, 506, 111-117.	0.3	1
30808	Effect of exchange-correlation and GW approximations on electrical property of cubic, tetragonal and orthorhombic CH3NH3PbI3. Integrated Ferroelectrics, 2017, 177, 1-9.	0.3	2
30809	Coulomb interactions and screening effects in few-layer black phosphorus: a tight-binding consideration beyond the long-wavelength limit. 2D Materials, 2017, 4, 025064.	2.0	28
30810	Fast and accurate approximate quasiparticle band structure calculations of ZnO, CdO, and MgO polymorphs. Physical Review B, 2017, 95, .	1.1	23
30811	Role of Composition and Size of Cobalt Ferrite Nanocrystals in the Oxygen Evolution Reaction. ChemCatChem, 2017, 9, 2988-2995.	1.8	74

#	Article	IF	Citations
30812	Nonadiabatic charge dynamics in novel solar cell materials. Wiley Interdisciplinary Reviews: Computational Molecular Science, 2017, 7, e1305.	6.2	71
30813	Adsorption of precious and coinage metals on Rh (111), Ru (0001) and W (110) surfaces. Applied Surface Science, 2017, 410, 282-290.	3.1	4
30814	Bandgap nature of chalcopyrite ZnXP2 (X = Si, Ge, Sn). Computational Materials Science, 2017, 133, 152-158.	1.4	16
30815	Unexpected Oddâ€“Even Oscillation in the Enhanced Chemical Activities of the Ru_n (n = 2â€“14) Nanoclusters for H₂O Splitting. Journal of Physical Chemistry C, 2017, 121, 7188-7198.	1.5	7
30816	Schottky Barriers in Bilayer Phosphorene Transistors. ACS Applied Materials & Interfaces, 2017, 9, 12694-12705.	4.0	94
30817	Interlayer resistance of misoriented MoS₂. Physical Chemistry Chemical Physics, 2017, 19, 10406-10412.	1.3	12
30818	Grand canonical electronic density-functional theory: Algorithms and applications to electrochemistry. Journal of Chemical Physics, 2017, 146, 114104.	1.2	211
30819	Ordering effect on the mechanical, electronic and magnetic properties of the Î²-based non-canonical approximant phases: Î²-Al50Cu33Fe17, Î·-Al50Cu44Fe6 and Ît-Al47.5Cu49.5Fe3. Philosophical Magazine, 2017, 97, 1024-1046.	0.7	1
30820	Hybrid phosphorene/graphene nanocomposite as an anode material for Na-ion batteries: a first-principles study. Journal Physics D: Applied Physics, 2017, 50, 165501.	1.3	31
30821	Construction of crystal structure prototype database: methods and applications. Journal of Physics Condensed Matter, 2017, 29, 165901.	0.7	31
30822	Direct mapping of spin and orbital entangled wave functions under interband spin-orbit coupling of giant Rashba spin-split surface states. Physical Review B, 2017, 95, .	1.1	33
30823	Band splitting and Weyl nodes in trigonal tellurium studied by angle-resolved photoemission spectroscopy and density functional theory. Physical Review B, 2017, 95, .	1.1	56
30824	Active sites for CO ₂ hydrogenation to methanol on Cu/ZnO catalysts. Science, 2017, 355, 1296-1299.	6.0	1,180
30825	Systematic Density Functional Theory Investigation of Stability of Dopant Atoms in Ge Ultra-Thin Film Grown on Si Substrate. ECS Journal of Solid State Science and Technology, 2017, 6, P154-P160.	0.9	1
30826	Evidence and Effect of Photogenerated Charge Transfer for Enhanced Photocatalysis in WO₃/TiO₂ Heterojunction Films: A Computational and Experimental Study. Advanced Functional Materials, 2017, 27, 1605413.	7.8	115
30827	Effect of the modulation ratio on the interface structure of TiAlN/TiN and TiAlN/ZrN multilayers: First-principles and experimental investigations. Acta Materialia, 2017, 130, 281-288.	3.8	88
30828	High-pressure induced phase transition of FeS2: Electronic, mechanical and thermoelectric properties. Journal of Alloys and Compounds, 2017, 710, 267-273.	2.8	13
30829	Investigation of half-metallic ferromagnetism in Heusler compounds Co2VZ (Z = Ga, Ge, As, Se). Journal of Magnetism and Magnetic Materials, 2017, 442, 80-86.	1.0	11

#	Article	IF	Citations
30830	Structure and electronic properties of graphene on ferroelectric LiNbO 3 surface. Physics Letters, Section A: General, Atomic and Solid State Physics, 2017, 381, 1749-1752.	0.9	12
30831	Effect of strain on electronic and magnetic properties of Fe-doped monolayer SnS 2. Physics Letters, Section A: General, Atomic and Solid State Physics, 2017, 381, 1732-1737.	0.9	19
30832	Adsorbate Entropies with Complete Potential Energy Sampling in Microkinetic Modeling. Journal of Physical Chemistry C, 2017, 121, 7199-7207.	1.5	70
30833	Mechanisms of Hydrogen-Assisted CO₂ Reduction on Nickel. Journal of the American Chemical Society, 2017, 139, 4663-4666.	6.6	63
30835	A theoretical simulation of small-molecules sensing on an S-vacancy SnS₂ monolayer. Physical Chemistry Chemical Physics, 2017, 19, 10470-10480.	1.3	52
30836	ZnO powders as multi-facet single crystals. Physical Chemistry Chemical Physics, 2017, 19, 10622-10628.	1.3	12
30837	Metalâ€“organic and covalent organic frameworks as single-site catalysts. Chemical Society Reviews, 2017, 46, 3134-3184.	18.7	861
30838	Interface engineering for a rational design of poison-free bimetallic CO oxidation catalysts. Nanoscale, 2017, 9, 5244-5253.	2.8	28
30839	The atomic simulation environmentâ€”a Python library for working with atoms. Journal of Physics Condensed Matter, 2017, 29, 273002.	0.7	1,933
30840	Effect of P impurity on NiAlÎ£5 grain boundary from first-principles study. Chinese Physics B, 2017, 26, 023101.	0.7	1
30841	Unified explanation of chemical ordering, the Slater-Pauling rule, and half-metallicity in full Heusler compounds. Physical Review B, 2017, 95, .	1.1	49
30842	Unified band-theoretic description of structural, electronic, and magnetic properties of vanadium dioxide phases. Physical Review B, 2017, 95, .	1.1	40
30843	Nature of monovacancies on quasi-hexagonal structure of reconstructed Au(100) surface. Applied Surface Science, 2017, 407, 345-352.	3.1	12
30844	Investigation of the structural anisotropy in a self-assembling glycinate layer on Cu(100) by scanning tunneling microscopy and density functional theory calculations. Applied Surface Science, 2017, 409, 111-116.	3.1	1
30845	A DFT study of molecular adsorption on titania-supported AuRh nanoalloys. Computational and Theoretical Chemistry, 2017, 1107, 142-151.	1.1	17
30846	Temperature-dependent dissolution and diffusion of H isotopes in iron for nuclear energy applications: First-principles and vibration spectrum predictions. International Journal of Hydrogen Energy, 2017, 42, 11560-11573.	3.8	11
30847	Strong effect of compressive strain on Ni-doped monolayer WSe 2. Physica E: Low-Dimensional Systems and Nanostructures, 2017, 90, 85-89.	1.3	6
30848	First-principles study on the thermodynamic stability, magnetism, and half-metallicity of full-Heusler alloy Ti2FeGe (001) surface. Physics Letters, Section A: General, Atomic and Solid State Physics, 2017, 381, 1592-1597.	0.9	11

#	Article	IF	Citations
30849	PdAu Alloy Nanoparticle Catalysts: Effective Candidates for Nitrite Reduction in Water. ACS Catalysis, 2017, 7, 3268-3276.	5.5	89
30850	Structures, mobility and electronic properties of point defects in arsenene, antimonene and an antimony arsenide alloy. Journal of Materials Chemistry C, 2017, 5, 4159-4166.	2.7	72
30851	Nb-H system at high pressures and temperatures. Physical Review B, 2017, 95, .	1.1	32
30852	High Pâ€“T experiments and first principles calculations of the diffusion of Si and Cr in liquid iron. Geochimica Et Cosmochimica Acta, 2017, 203, 323-342.	1.6	16
30853	The origin of palladium particle size effects in the direct synthesis of H2O2: Is smaller better?. Journal of Catalysis, 2017, 349, 30-40.	3.1	98
30854	Spectroelectrochemical detection of specifically adsorbed cyanurate anions at gold electrodes with (111) orientation in contact with cyanate and cyanuric acid neutral solutions. Journal of Electroanalytical Chemistry, 2017, 800, 167-175.	1.9	8
30855	Linker Functionalization in MIL-47(V)-R Metalâ€“Organic Frameworks: Understanding the Electronic Structure. Journal of Physical Chemistry C, 2017, 121, 8014-8022.	1.5	10
30856	Photoinduced Single- and Multiple-Electron Dynamics Processes Enhanced by Quantum Confinement in Lead Halide Perovskite Quantum Dots. Journal of Physical Chemistry Letters, 2017, 8, 3032-3039.	2.1	52
30857	Critical Role of Oxygen in Silver-Catalyzed Glaserâ€“Hay Coupling on Ag(100) under Vacuum and in Solution on Ag Particles. ACS Catalysis, 2017, 7, 3113-3120.	5.5	8
30858	High-Performance Rh₂P Electrocatalyst for Efficient Water Splitting. Journal of the American Chemical Society, 2017, 139, 5494-5502.	6.6	343
30859	A comparative first-principles study of the structural and electronic properties of the liquid Liâ€“Si and Liâ€“Ge alloys. Journal of Chemical Physics, 2017, 146, 064502.	1.2	2
30860	Defect mechanisms of coloration in Fe-doped SrTiO3 from first principles. Applied Physics Letters, 2017, 110, .	1.5	47
30861	Phase diagram of boron carbide with variable carbon composition. Physical Review B, 2017, 95, .	1.1	9
30862	Low-temperature features in the heat capacity of unary metals and intermetallics for the example of bulk aluminum and<mml:math xmlns:mml="http://www.w3.org/1998/Math/MathML"><mml:msub><mml:mi>Al</mml:mi><mml:mn>3</mml:mn></mml:msub><mml:mi mathvariant="normal">Sc</mml:mi></mml:math>. Physical Review B, 2017, 95, .	1.1	12
30863	Correlation corrected phonon vibration in YTiO 3 and its effect on electronic properties. Europhysics Letters, 2017, 117, 27004.	0.7	2
30864	Atomic-scale understanding of stress-induced phase transformation in cold-rolled Hf. Acta Materialia, 2017, 131, 271-279.	3.8	98
30865	First-principles study of fission gas incorporation and migration in zirconium nitride. Computational Materials Science, 2017, 133, 175-184.	1.4	5
30866	Embedded atom method interatomic potentials fitted upon density functional theory calculations for the simulation of binary Pt Ni nanoparticles. Computational Materials Science, 2017, 133, 185-193.	1.4	4

#	Article	IF	Citations
30867	Electronic structure of substitutionally doped diamond: Spin-polarized, hybrid density functional theory analysis. Diamond and Related Materials, 2017, 75, 146-151.	1.8	30
30868	Theoretical insights into the interaction between Ru n Pt 13-n (n = 4, 7 and 9) clusters and [BMIM] + based ionic liquids: Effect of anion. Journal of Molecular Graphics and Modelling, 2017, 74, 117-124.	1.3	2
30869	Core structures and mobility of âŸ¨câŸ© dislocations in magnesium. Scripta Materialia, 2017, 135, 37-40.	2.6	21
30870	First-Principles Calculations That Clarify Energetics and Reactions of Oxygen Adsorption and Carbon Desorption on 4H-SiC (112ì…0) Surface. Journal of Physical Chemistry C, 2017, 121, 3920-3928.	1.5	8
30871	Translating XPS Measurement Procedure for Band Alignment into Reliable Ab Initio Calculation Method. Journal of Physical Chemistry C, 2017, 121, 7139-7143.	1.5	11
30872	Computationally predicted energies and properties of defects in GaN. Npj Computational Materials, 2017, 3, .	3.5	196
30873	Engineering Topological Surface State of Cr-doped Bi2Se3 under external electric field. Scientific Reports, 2017, 7, .	1.6	4
30874	New carbon allotropes with metallic conducting properties: a first-principles prediction. RSC Advances, 2017, 7, 17417-17426.	1.7	45
30875	Origin of the Tetragonal Ground State of Heusler Compounds. Physical Review Applied, 2017, 7, .	1.5	134
30876	Phonons and elasticity of cementite through the Curie temperature. Physical Review B, 2017, 95, .	1.1	8
30877	Phase Transition, Dielectric Properties, and Ionic Transport in the [(CH₃)₂NH₂]PbI₃ Organicâ€“Inorganic Hybrid with 2H-Hexagonal Perovskite Structure. Inorganic Chemistry, 2017, 56, 4918-4927.	1.9	58
30878	Structure and Properties of Some Layered U₂O₅ Phases: A Density Functional Theory Study. Inorganic Chemistry, 2017, 56, 4468-4473.	1.9	16
30879	First-Principles Predictions of Phase Transition and Mechanical Properties of Tungsten Diboride under Pressure. Journal of Physical Chemistry C, 2017, 121, 7397-7403.	1.5	15
30880	Ferroelectricity, Antiferroelectricity, and Ultrathin 2D Electron/Hole Gas in Multifunctional Monolayer MXene. Nano Letters, 2017, 17, 3290-3296.	4.5	184
30881	Two-Dimensional Large Gap Topological Insulators with Tunable Rashba Spin-Orbit Coupling in Group-IV films. Scientific Reports, 2017, 7, 45923.	1.6	19
30882	Effect of pressure on two polymorphs of tolazamide: why no interconversion?. CrystEngComm, 2017, 19, 2243-2252.	1.3	27
30883	Composition-directed Fe_XMo_{2â^'X}P bimetallic catalysts for hydrodeoxygenation reactions. Catalysis Science and Technology, 2017, 7, 1857-1867.	2.1	48
30884	Comparison of Li, Na, Mg and Al-ion insertion in vanadium pentoxides and vanadium dioxides. RSC Advances, 2017, 7, 18643-18649.	1.7	66

#	Article	IF	Citations
30885	Understanding the Li-storage in few layers graphene with respect to bulk graphite: experimental, analytical and computational study. Journal of Materials Chemistry A, 2017, 5, 8662-8679.	5.2	70
30886	Landscape of DNA-like inorganic metal free double helical semiconductors and potential applications in photocatalytic water splitting. Journal of Materials Chemistry A, 2017, 5, 8484-8492.	5.2	22
30887	Surface intermixing by atomic scale roughening in Sb-terminated InAs. Journal of Applied Physics, 2017, 121, 095301.	1.1	2
30888	How strongly do hydrogen and water molecules stick to carbon nanomaterials?. Journal of Chemical Physics, 2017, 146, .	1.2	38
30889	Degradation of CH3NH3PbI3 perovskite due to soft x-ray irradiation as analyzed by an x-ray photoelectron spectroscopy time-dependent measurement method. Journal of Applied Physics, 2017, 121, .	1.1	34
30890	Communication: Calculations of the (2 Ã— 1)-O reconstruction kinetics on Cu(110). Journal of Chemical Physics, 2017, 146, 111101.	1.2	8
30891	Structure of oxidised silver (1â€‰1â€‰1) and (1â€‰1â€‰0) surfaces. Molecular Simulation, 2017, 43, 355-369.	0.9	2
30892	Structural and magnetic properties of transition-metal adsorbed ReS₂monolayer. Japanese Journal of Applied Physics, 2017, 56, 055701.	0.8	7
30893	Exploring the electronic and optical properties of Cu₂Sn_{1â^'x}Ge_xS₃ and Cu₂Sn_{1â^'x}Si_xS₃ (xâ€‰=â€‰0, 0.5, and 1). Physica Status Solidi (B): Basic Research, 2017, 254, 1700111.	0.7	10
30894	Effect of the Ni size on CH 4 /CO 2 reforming over Ni/MgO catalyst: A DFT study. Chinese Journal of Chemical Engineering, 2017, 25, 1442-1448.	1.7	22
30895	Thermodynamic Origin of Irreversible Magnesium Trapping in Chevrel Phase Mo₆S₈: Importance of Magnesium and Vacancy Ordering. Chemistry of Materials, 2017, 29, 3731-3739.	3.2	59
30896	Adsorbate Pairing on Oxide Surfaces: Influence on Reactivity and Dependence on Oxide, Adsorbate Pair, and Density Functional. Journal of Physical Chemistry C, 2017, 121, 8390-8398.	1.5	12
30897	Stability of V₂O₅ Supported on Titania in the Presence of Water, Bulk Oxygen Vacancies, and Adsorbed Oxygen Atoms. Journal of Physical Chemistry C, 2017, 121, 8444-8451.	1.5	13
30898	Ab Initio Molecular Dynamic Simulations on Pd Clusters Confined in UiO-66-NH₂. Journal of Physical Chemistry C, 2017, 121, 8857-8863.	1.5	27
30899	Strain-Induced Optimization of Nanoelectromechanical Energy Harvesting and Nanopiezotronic Response in a MoS₂ Monolayer Nanosheet. Journal of Physical Chemistry C, 2017, 121, 9181-9190.	1.5	50
30900	Evidence of a Cu²⁺â€“Alkane Interaction in Cu-Zeolite Catalysts Crucial for the Selective Catalytic Reduction of NO_x with Hydrocarbons. ACS Catalysis, 2017, 7, 3501-3509.	5.5	28
30901	Competition between Hydrogen Bonds and Coordination Bonds Steered by the Surface Molecular Coverage. ACS Nano, 2017, 11, 3727-3732.	7.3	60
30902	Tunability of the Adsorbate Binding on Bimetallic Alloy Nanoparticles for the Optimization of Catalytic Hydrogenation. Journal of the American Chemical Society, 2017, 139, 5538-5546.	6.6	96

#	Article	IF	Citations
30903	Prediction of intrinsic two-dimensional ferroelectrics in In2Se3 and other III2-VI3 van der Waals materials. Nature Communications, 2017, 8, 14956.	5.8	830
30904	First-principles identification of novel double perovskites for water-splitting applications. Journal of Materials Science, 2017, 52, 8518-8525.	1.7	10
30905	Effect of the structure distortion on the high photocatalytic performance of C 60 /g-C 3 N 4 composite. Applied Surface Science, 2017, 414, 124-130.	3.1	74
30906	Elastic, electronic and optical properties of stable pentagonal ZnO 2. Physica E: Low-Dimensional Systems and Nanostructures, 2017, 91, 82-87.	1.3	26
30907	Mapping Charge Distribution in Single PbS Core â€“ CdS Arm Nano-Multipod Heterostructures by Off-Axis Electron Holography. Nano Letters, 2017, 17, 2778-2787.	4.5	10
30908	Ru-Catalyzed Steam Methane Reforming: Mechanistic Study from First Principles Calculations. ACS Omega, 2017, 2, 1295-1301.	1.6	17
30909	Cu₃N and its analogs: a new class of electrodes for lithium ion batteries. Journal of Materials Chemistry A, 2017, 5, 8762-8768.	5.2	29
30910	Edge dominated electronic properties of MoS₂/graphene hybrid 2D materials: edge state, electron coupling and work function. Journal of Materials Chemistry C, 2017, 5, 4845-4851.	2.7	28
30911	Spectroscopic Observation of a Hydrogenated CO Dimer Intermediate During CO Reduction on Cu(100) Electrodes. Angewandte Chemie, 2017, 129, 3675-3678.	1.6	112
30912	Magnetoelectricity in Fe/PbTiO 3 /Fe superlattices. Current Applied Physics, 2017, 17, 675-678.	1.1	3
30913	A theoretical method to predict novel organic electrode materials for Na-ion batteries. Computational Materials Science, 2017, 134, 42-47.	1.4	14
30914	Direct observation of solute interstitials and their clusters in Mg alloys. Materials Characterization, 2017, 128, 226-231.	1.9	10
30915	Density functional theory study of ethanol synthesis from dimethyl ether and syngas over cobalt catalyst. Molecular Catalysis, 2017, 432, 115-124.	1.0	6
30916	Direct observation of vast off-stoichiometric defects in single crystalline SnSe. Nano Energy, 2017, 35, 321-330.	8.2	101
30917	Enhanced CO catalytic oxidation by Sr reconstruction on the surface of La x Sr 1â˜' x CoO 3â˜' Î´. Science Bulletin, 2017, 62, 658-664.	4.3	38
30918	Pressure-induced metallization and superconducting phase in ReS 2. Npj Quantum Materials, 2017, 2, .	1.8	53
30919	Formation of novel transition metal hydride complexes with ninefold hydrogen coordination. Scientific Reports, 2017, 7, 44253.	1.6	32
30920	Mechanistic insights into the remarkable catalytic activity of nanosized Co@C composites for hydrogen desorption from the LiBH4â€“2LiNH2 system. Catalysis Science and Technology, 2017, 7, 1838-1847.	2.1	10

#	Article	IF	Citations
30921	Highly-ordered wide bandgap materials for quantized anomalous Hall and magnetoelectric effects. 2D Materials, 2017, 4, 025082.	2.0	195
30922	MoS2-graphene in-plane contact for high interfacial thermal conduction. Nano Research, 2017, 10, 2944-2953.	5.8	59
30923	First-principles investigation on the geometries, stabilities and defective properties of fluoride surfaces. Computational Materials Science, 2017, 133, 159-166.	1.4	8
30924	Phenolic Polymer Solvation in Water and Ethylene Glycol, II: Ab Initio Computations. Journal of Physical Chemistry B, 2017, 121, 2852-2863.	1.2	2
30925	Binary Approach to Ternary Cluster Expansions: NOâ€“Oâ€“Vacancy System on Pt(111). Journal of Physical Chemistry C, 2017, 121, 7344-7354.	1.5	21
30926	Nitrogen-Terminated Diamond (111) Surface for Room-Temperature Quantum Sensing and Simulation. Nano Letters, 2017, 17, 2294-2298.	4.5	65
30927	Defects Mediated Corrosion in Graphene Coating Layer. ACS Applied Materials & Interfaces, 2017, 9, 11902-11908.	4.0	48
30928	Ethylene Dehydrogenation on Pt_{4,7,8} Clusters on Al₂O₃: Strong Cluster Size Dependence Linked to Preferred Catalyst Morphologies. ACS Catalysis, 2017, 7, 3322-3335.	5.5	124
30929	Coordination Characteristics of Uranyl BBP Complexes: Insights from an Electronic Structure Analysis. ACS Omega, 2017, 2, 1055-1062.	1.6	6
30930	Computational design of cobalt-free mixed protonâ€“electron conductors for solid oxide electrochemical cells. Journal of Materials Chemistry A, 2017, 5, 11825-11833.	5.2	57
30931	Electric-field-induced widely tunable direct and indirect band gaps in hBN/MoS₂ van der Waals heterostructures. Journal of Materials Chemistry C, 2017, 5, 4426-4434.	2.7	29
30932	Mechanistic study of graphitic carbon layer and nanosphere formation on the surface of T-ZnO. Inorganic Chemistry Frontiers, 2017, 4, 978-985.	3.0	12
30933	Ab initio and experimental studies of polarization and polarization related fields in nitrides and nitride structures. AIP Advances, 2017, 7, .	0.6	23
30934	Tuning Cd adsorption behaviours on graphene by introducing defects: a first-principles study. Materials Technology, 2017, 32, 840-844.	1.5	8
30935	Platinum atomic contacts: From tunneling to contact. Physical Review B, 2017, 95, .	1.1	8
30936	Efficient photocatalytic hydrogen production over La/Rh co-doped Ruddlesden-Popper compound Sr 2 TiO 4. Applied Catalysis B: Environmental, 2017, 210, 149-159.	10.8	45
30937	First-principle investigation on multiferroicity in cubic perovskite LaMn3Fe4O12 compound. Computational Materials Science, 2017, 133, 116-121.	1.4	0
30938	Bonding interactions in Li/Na oxides, peroxides and superoxides and their implication to the performance of the Li/Na-air batteries. Solid State Ionics, 2017, 303, 24-28.	1.3	3

#	Article	IF	Citations
30939	Hydrogen Transfer in Energetic Materials from ReaxFF and DFT Calculations. Journal of Physical Chemistry A, 2017, 121, 3019-3027.	1.1	19
30940	Fast MAS ¹H NMR Study of Water Adsorption and Dissociation on the (100) Surface of Ceria Nanocubes: A Fully Hydroxylated, Hydrophobic Ceria Surface. Journal of Physical Chemistry C, 2017, 121, 7450-7465.	1.5	26
30941	Growth of Carbon Nanostructures on Cu Nanocatalysts. Journal of Physical Chemistry C, 2017, 121, 7232-7239.	1.5	5
30942	Defect-Induced Band-Edge Reconstruction of a Bismuth-Halide Double Perovskite for Visible-Light Absorption. Journal of the American Chemical Society, 2017, 139, 5015-5018.	6.6	288
30943	Ab initio calculation of the attempt frequency of oxygen diffusion in pure and samarium doped ceria. Physical Chemistry Chemical Physics, 2017, 19, 9957-9973.	1.3	58
30944	A new Dirac cone material: a graphene-like Be₃C₂ monolayer. Nanoscale, 2017, 9, 5577-5582.	2.8	85
30945	Observation of variable hybridized-band gaps in Eu-intercalated graphene. Nanotechnology, 2017, 28, 205201.	1.3	16
30946	Solid-State NMR Spectroscopy Study of Cation Dynamics in Layered Na₂Ti₃O₇ and Li₂Ti₃O₇. Zeitschrift Fur Physikalische Chemie, 2017, 231, 1243-1262.	1.4	4
30947	Surface structure of novel semimetal WTe₂. Applied Physics Express, 2017, 10, 045702.	1.1	9
30948	Methanol Oxidation on Pt(111) from First-Principles in Heterogeneous and Electrocatalysis. Electrocatalysis, 2017, 8, 577-586.	1.5	26
30949	The role of negatively charged oxygen vacancies upon Î²-MnO2 conductivity. Acta Materialia, 2017, 131, 88-97.	3.8	13
30950	A DFT study of Cu nanoparticles adsorbed on defective graphene. Applied Surface Science, 2017, 412, 146-151.	3.1	20
30951	Microscopic theory of the refractive index. Optik, 2017, 140, 62-85.	1.4	9
30952	Geometric and electronic effects of bimetallic Niâ€“Re catalysts for selective deoxygenation of m-cresol to toluene. Journal of Catalysis, 2017, 349, 84-97.	3.1	112
30953	Wide-range ideal 2D Rashba electron gas with large spin splitting in Bi2Se3/MoTe2 heterostructure. Npj Computational Materials, 2017, 3, .	3.5	25
30954	Long-range charge transfer and oxygen vacancy interactions in strontium ferrite. Journal of Materials Chemistry A, 2017, 5, 4493-4506.	5.2	69
30955	Layer-independent and layer-dependent nonlinear optical properties of two-dimensional GaX (X = S, Se,) Tj ETQq0 0 0 rgBT /Overlock 10	1.3	40
30956	Electronic structure and multi-scale behaviour for the dislocationâ€“doping complex in the gamma phase of nickel-base superalloys. RSC Advances, 2017, 7, 19124-19135.	1.7	7

#	Article	IF	Citations
30957	The structure and unconventional dihydrogen bonding of a pressure-stabilized hydrogen-rich (NH3BH3)(H2)x (x = 1.5) compound. Journal of Materials Chemistry A, 2017, 5, 7111-7117.	5.2	4
30958	Structural design principles for low hole effective mass s-orbital-based p-type oxides. Journal of Materials Chemistry C, 2017, 5, 5772-5779.	2.7	56
30959	Adsorption and diffusion of mono, di, and trivalent ions on two-dimensional TiS₂. Nanotechnology, 2017, 28, 175401.	1.3	124
30960	Band engineering of the MoS₂/stanene heterostructure: strain and electrostatic gating. Nanotechnology, 2017, 28, 195702.	1.3	44
30961	Magnetic phase transitions and magnetoelastic coupling in S=12 Heisenberg antiferromagnets. Physical Review B, 2017, 95, .	1.1	5
30962	Realization of quantum anomalous Hall effect in graphene from <mml:math xmlns:mml="http://www.w3.org/1998/Math/MathML"><mml:mrow><mml:mi>n</mml:mi><mml:mo>â^'</mml:mo><mml:mi>1</mml:mi></mml:mrow></mml:math> codoping-induced stable atomic adsorption. Physical Review B, 2017, 95, .	1.1	13
30963	Firstâ€Principles Investigation of the Relevant Surfaces Exposed by Polycrystalline LaFeO₃. ChemCatChem, 2017, 9, 2383-2389.	1.8	10
30964	Enhancing visible light photocatalytic activity of KNbO $$_{3}$$ 3 by Nâ€“F passivated co-doping for hydrogen generation by water splitting. Journal of Materials Science, 2017, 52, 5333-5344.	1.7	7
30965	Study of butanol conversion to butenes over H-ZSM-5: Effect of chemical structure on activity, selectivity and reaction pathways. Applied Catalysis A: General, 2017, 539, 1-12.	2.2	37
30966	Thermodynamic assessment of Feâ€“Tiâ€“S ternary phase diagram. Calphad: Computer Coupling of Phase Diagrams and Thermochemistry, 2017, 57, 62-77.	0.7	5
30967	Enabling accurate first-principle calculations of electronic properties with a corrected <mml:math xmlns:mml="http://www.w3.org/1998/Math/MathML" altimg="si3.gif" overflow="scroll"><mml:mrow><mml:mi mathvariant="bold">k</mml:mi><mml:mo>Â·</mml:mo><mml:mi mathvariant="bold">p</mml:mi></mml:mrow></mml:math> scheme. Computational Materials Science, 2017, 134, 17-24.	1.4	13
30968	The novel structure and superconductivity of zirconium hydride. Computational Materials Science, 2017, 134, 38-41.	1.4	5
30969	Benzene co-reaction with methanol and dimethyl ether over zeolite and zeotype catalysts: Evidence of parallel reaction paths to toluene and diphenylmethane. Journal of Catalysis, 2017, 349, 136-148.	3.1	70
30970	Investigation of the Optical and Excitonic Properties of the Visible Light-Driven Photocatalytic BiVO₄ Material. Chemistry of Materials, 2017, 29, 3380-3386.	3.2	38
30971	Probing Evolution of Twist-Angle-Dependent Interlayer Excitons in MoSe₂/WSe₂ van der Waals Heterostructures. ACS Nano, 2017, 11, 4041-4050.	7.3	227
30972	Imaging Successive Intermediate States of the On-Surface Ullmann Reaction on Cu(111): Role of the Metal Coordination. ACS Nano, 2017, 11, 4183-4190.	7.3	71
30973	Cr_{0.5}Nb_{24.5}O₆₂ Nanowires with High Electronic Conductivity for High-Rate and Long-Life Lithium-Ion Storage. ACS Nano, 2017, 11, 4217-4224.	7.3	121
30974	Semimetallic carbon allotrope with a topological nodal line in mixed sp2-sp3 bonding networks. NPG Asia Materials, 2017, 9, e361-e361.	3.8	18

#	Article	IF	Citations
30975	Graphene-like nanoribbons periodically embedded with four- and eight-membered rings. Nature Communications, 2017, 8, 14924.	5.8	139
30976	A high-throughput framework for determining adsorption energies on solid surfaces. Npj Computational Materials, 2017, 3, .	3.5	70
30977	Chemical states of 3d transition metal impurities in a liquid leadâ€“bismuth eutectic analyzed using first principles calculations. Physical Chemistry Chemical Physics, 2017, 19, 9945-9956.	1.3	16
30978	Self-assembled nitrogen-doped fullerenes and their catalysis for fuel cell and rechargeable metalâ€“air battery applications. Nanoscale, 2017, 9, 7373-7379.	2.8	56
30979	Electronic and defect properties of (CH₃NH₃)₂Pb(SCN)₂I₂analogues for photovoltaic applications. Journal of Materials Chemistry A, 2017, 5, 7845-7853.	5.2	43
30980	The dissociative chemisorption of CO2 on Ni(100): A quantum dynamics study. Journal of Chemical Physics, 2017, 146, 074704.	1.2	23
30981	Quantum behavior of water nano-confined in beryl. Journal of Chemical Physics, 2017, 146, 124307.	1.2	18
30982	Multiferroic <mml:math xmlns:mml="http://www.w3.org/1998/Math/MathML"><mml:msub><mml:mi>Bi</mml:mi><mml:mn>2</mml:mn></mml:msub><mml:m mathvariant="normal">NiMnO</mml:mi><mml:mn>6</mml:mn></mml:msub></mml:math> thin films: A computational prediction. Physical Review B, 2017, 95, .	1.1	9
30983	Ternary rhombohedral Laves phases RE ₂Rh₃Ga (REâ€‰=â€‰Y, Laâ€“Nd, Sm,) Tj ETQq0 0 0 rg	0.3	26
30984	Al₄SiC₄ vibrational properties: density functional theory calculations compared to Raman and infrared spectroscopy measurements. Journal of Raman Spectroscopy, 2017, 48, 891-896.	1.2	5
30985	Electronic structure and magnetism of RbGd2Fe4As4O2. Journal of Alloys and Compounds, 2017, 708, 392-396.	2.8	7
30986	Characterization of Mn-doped electrospun LiNbO3 nanofibers by Raman spectroscopy. Materials Characterization, 2017, 127, 209-213.	1.9	7
30987	First-principles investigation of metal-doped cubic BaTiO 3. Materials Research Bulletin, 2017, 96, 372-378.	2.7	39
30988	Enhanced Electrocatalytic Activity of Carbon-Supported Ordered Intermetallic Palladiumâ€“Lead (Pd₃Pb) Nanoparticles toward Electrooxidation of Formic Acid. Chemistry of Materials, 2017, 29, 2906-2913.	3.2	73
30989	Simulation of First-Charge Oxygen-Dimerization and Mn-Migration in Li-Rich Layered Oxides xLi₂MnO₃Â·(1 â€“ x)LiMO₂ and Implications for Voltage Fade. Journal of Physical Chemistry C, 2017, 121, 6492-6499.	1.5	26
30990	Surface Stabilizes Ceria in Unexpected Stoichiometry. Journal of Physical Chemistry C, 2017, 121, 6844-6851.	1.5	40
30991	Oxidation Resistance of Monolayer Group-IV Monochalcogenides. ACS Applied Materials & Interfaces, 2017, 9, 12013-12020.	4.0	118
30992	Electronic properties of reduced molybdenum oxides. Physical Chemistry Chemical Physics, 2017, 19, 9232-9245.	1.3	171

#	Article	IF	Citations
30993	Structural formation and charge storage mechanisms for intercalated two-dimensional carbides MXenes. Physical Chemistry Chemical Physics, 2017, 19, 9509-9518.	1.3	19
30994	Spin splitting and reemergence of charge compensation in monolayer WTe₂by 3d transition-metal adsorption. Physical Chemistry Chemical Physics, 2017, 19, 7721-7727.	1.3	15
30995	Artificial neural network for the configuration problem in solids. Journal of Chemical Physics, 2017, 146, 064103.	1.2	10
30996	Evenly transferred single-layered graphene membrane assisted by strong substrate adhesion. Nanotechnology, 2017, 28, 145706.	1.3	2
30997	New ternary superconducting compound LaRu ₂ As ₂ : Physical properties from density functional theory calculations. Chinese Physics B, 2017, 26, 037103.	0.7	39
30998	Chemical ordering patterns and magnetism of NiAl nanoclusters. Materials Research Express, 2017, 4, 015010.	0.8	5
30999	Electronic Properties, Screening, and Efficient Carrier Transport in<mml:math xmlns:mml="http://www.w3.org/1998/Math/MathML" display="inline"><mml:mrow><mml:msub><mml:mrow><mml:mi>NaSbS</mml:mi></mml:mrow><mml:mrow><mml:mn>2</mml:mn></mml:mrow> Physical Review Applied, 2017, 7, .	1.5	36
31000	Zn vacancy as a polaronic hole trap in ZnO. Physical Review B, 2017, 95, .	1.1	71
31001	Electronic structure of tetraphenylporphyrin layers on Ag(100). Physical Review B, 2017, 95, .	1.1	9
31002	Piezoelectricity in two-dimensional materials: Comparative study between lattice dynamics andab initiocalculations. Physical Review B, 2017, 95, .	1.1	36
31003	Unexpected Xe anions in XeLi n intermetallic compounds. Europhysics Letters, 2017, 117, 26002.	0.7	14
31004	The Influence of Water on the Performance of Molybdenum Carbide Catalysts in Hydrodeoxygenation Reactions: A Combined Theoretical and Experimental Study. ChemCatChem, 2017, 9, 1985-1991.	1.8	29
31005	Spin selection at organic spinterface by anchoring group. Applied Surface Science, 2017, 409, 60-64.	3.1	10
31006	Adsorption of arginine, glycine and aspartic acid on Mg and Mg-based alloy surfaces: A first-principles study. Applied Surface Science, 2017, 409, 149-155.	3.1	22
31007	Ultra-thin ZnSe: Anisotropic and flexible crystal structure. Applied Surface Science, 2017, 409, 426-430.	3.1	8
31008	Ultra high stiffness and thermal conductivity of graphene like C3N. Carbon, 2017, 118, 25-34.	5.4	235
31009	An embedded atom method interatomic potential for the zirconium-iron system. Computational Materials Science, 2017, 133, 6-13.	1.4	5
31010	Influence of alloying elements on stability and adhesion ability of TiAl/TiO 2 interface by first-principles calculations. Intermetallics, 2017, 85, 80-89.	1.8	31

#	Article	IF	Citations
31011	Giant enhancement of ultraviolet near-band-edge emission from a wide-bandgap oxide with dipole-forbidden bandgap transition. Journal of Alloys and Compounds, 2017, 705, 492-496.	2.8	5
31012	Missing Linkers: An Alternative Pathway to UiO-66 Electronic Structure Engineering. Chemistry of Materials, 2017, 29, 3006-3019.	3.2	176
31013	Defect Coupling and Sub-Angstrom Structural Distortions in W_{1â€“x}Mo_xS₂ Monolayers. Nano Letters, 2017, 17, 2802-2808.	4.5	42
31014	Manganese mono-boride, an inexpensive room temperature ferromagnetic hard material. Scientific Reports, 2017, 7, 43759.	1.6	47
31015	Highly effective Ir-based catalysts for benzoic acid hydrogenation: experiment- and theory-guided catalyst rational design. Green Chemistry, 2017, 19, 1766-1774.	4.6	27
31016	Lateral heterostructures of monolayer group-IV monochalcogenides: band alignment and electronic properties. Journal of Materials Chemistry C, 2017, 5, 3788-3795.	2.7	94
31017	Thermoelectric enhancement in sliver tantalate via strain-induced band modification and chemical bond softening. RSC Advances, 2017, 7, 8460-8466.	1.7	8
31018	Comparative study of crystallization process in metallic melts usingab initiomolecular dynamics simulations. Journal of Physics Condensed Matter, 2017, 29, 185401.	0.7	6
31019	Atomistic modeling of dislocation interactions with twin boundaries in Ti. Modelling and Simulation in Materials Science and Engineering, 2017, 25, 045003.	0.8	23
31020	Geometric stability and electronic structure of infinite and finite phosphorus atomic chains. Chinese Physics B, 2017, 26, 036803.	0.7	11
31021	Brittle failure of Î²- and Ï„-boron: Amorphization under high pressure. Physical Review B, 2017, 95, .	1.1	8
31022	Effect of intervalley interaction on band topology of commensurate graphene/EuO heterostructures. Physical Review B, 2017, 95, .	1.1	26
31023	First-principles study on the effect and magnetism of iron segregation in Cu grain boundary. Journal of Materials Science, 2017, 52, 4309-4322.	1.7	8
31024	Simulation study of temperature-dependent diffusion behaviors of Ag/Ag(001) at low substrate temperature. Applied Surface Science, 2017, 406, 277-284.	3.1	7
31025	Thermodynamic modelling of the Cr-Nb-Sn system. Calphad: Computer Coupling of Phase Diagrams and Thermochemistry, 2017, 57, 37-45.	0.7	14
31026	Luminescence of VO 4 3â^' centers in LiMgPO 4 and LiMgVO 4 : Effect of [PO 4] 3â^' /[VO 4] 3â^' substitution on the structure and optical properties. Journal of Alloys and Compounds, 2017, 709, 1-7.	2.8	15
31027	Determination of Crystal Structure of Graphitic Carbon Nitride: Ab Initio Evolutionary Search and Experimental Validation. Chemistry of Materials, 2017, 29, 2694-2707.	3.2	83
31028	Structural, Electronic, and Optical Properties of Cu₂NiSnS₄: A Combined Experimental and Theoretical Study toward Photovoltaic Applications. Chemistry of Materials, 2017, 29, 3133-3142.	3.2	90

#	Article	IF	Citations
31029	Reaction Mechanism for the Conversion of Î³-Valerolactone (GVL) over a Ru Catalyst: A First-Principles Study. Industrial & Engineering Chemistry Research, 2017, 56, 3217-3222.	1.8	12
31030	Counterintuitive Adsorption of [PW₁₁O₃₉]^{7â€“} on Au(100). Inorganic Chemistry, 2017, 56, 3961-3969.	1.9	18
31031	Water Oxidation on Oxygen-Deficient Barium Titanate: A First-Principles Study. Journal of Physical Chemistry C, 2017, 121, 8378-8389.	1.5	34
31032	Multiferroic Dislocations in Ferroelectric PbTiO₃. Nano Letters, 2017, 17, 2674-2680.	4.5	27
31033	High-Throughput Survey of Ordering Configurations in MXene Alloys Across Compositions and Temperatures. ACS Nano, 2017, 11, 4407-4418.	7.3	146
31034	Molybdenum Carbide-Embedded Nitrogen-Doped Porous Carbon Nanosheets as Electrocatalysts for Water Splitting in Alkaline Media. ACS Nano, 2017, 11, 3933-3942.	7.3	367
31035	Tuning the wettability of carbon nanotube arrays for efficient bifunctional catalysts and Znâ€“air batteries. Journal of Materials Chemistry A, 2017, 5, 7103-7110.	5.2	62
31036	Adsorption of small inorganic molecules on a defective MoS₂monolayer. Physical Chemistry Chemical Physics, 2017, 19, 9485-9499.	1.3	68
31037	The mechanism of hydrogen adsorption on transition metal dichalcogenides as hydrogen evolution reaction catalyst. Physical Chemistry Chemical Physics, 2017, 19, 10125-10132.	1.3	126
31038	Intrinsic defects and their effects on the optical properties in the nonlinear optical crystal CdSiP₂: a first-principles study. Physical Chemistry Chemical Physics, 2017, 19, 9558-9565.	1.3	14
31039	Orbitally driven low thermal conductivity of monolayer gallium nitride (GaN) with planar honeycomb structure: a comparative study. Nanoscale, 2017, 9, 4295-4309.	2.8	155
31040	Optimizing CdTeâ€“metal interfaces for high performance solar cells. Journal of Materials Chemistry A, 2017, 5, 7118-7124.	5.2	18
31041	Insight into the role of oxygen in the phase-change material GeTe. Journal of Materials Chemistry C, 2017, 5, 3592-3599.	2.7	18
31042	Size dependent tunnel diode effects in gold tipped CdSe nanodumbbells. Journal of Chemical Physics, 2017, 146, 054703.	1.2	1
31043	Conductivity of graphene affected by metal adatoms. AIP Advances, 2017, 7, .	0.6	6
31044	Lattice dynamics and ferroelectric properties of the nitride perovskite <mml:math xmlns:mml="http://www.w3.org/1998/Math/MathML"><mml:msub><mml:mi>LaWN</mml:mi><mml:mn>3</mml:mn></mml:msub><mml:m Physical Review B, 2017, 95, .	1.1	18
31045	Fully converged plane-wave-based self-consistent<mml:math xmlns:mml="http://www.w3.org/1998/Math/MathML"><mml:mrow><mml:mi>G</mml:mi><mml:mi>W</mml:mi></mml:mrow></mml:m of periodic solids. Physical Review B, 2017, 95, .	1.1	17
31046	Self-consistent mapping: Effect of local environment on formation of magnetic moment in <mml:math xmlns:mml="http://www.w3.org/1998/Math/MathML"><mml:mrow><mml:mi>Î±</mml:mi><mml:mo>â^’</mml:mo><mml:mi>Mn</mml:mi></mml:mrow></mml:m Physical Review B, 2017, 95, .	1.1	16

#	Article	IF	Citations
31047	Stacking fault energies of nondilute binary alloys using special quasirandom structures. Physical Review B, 2017, 95, .	1.1	9
31048	First Principles Calculations of Transition Metal Binary Alloys: Phase Stability and Surface Effects. Journal of Electronic Materials, 2017, 46, 3776-3783.	1.0	13
31049	Interfacial structure evolution of the growing composite precipitates in Al-Cu-Li alloys. Acta Materialia, 2017, 129, 352-360.	3.8	72
31050	Elastic anisotropy and thermodynamic properties of superhard c -C 3 N under pressure. Diamond and Related Materials, 2017, 74, 132-137.	1.8	4
31051	Controlling Li2CuO2 single phase transition to preserve cathode capacity and cyclability in Li-ion batteries. Solid State Ionics, 2017, 303, 89-96.	1.3	19
31052	Reaction pathway of CH 4 /CO 2 reforming over Ni8/MgO(100). Surface Science, 2017, 660, 22-30.	0.8	13
31053	Influence of Rb/Cs Cation-Exchange on Inorganic Sn Halide Perovskites: From Chemical Structure to Physical Properties. Chemistry of Materials, 2017, 29, 3181-3188.	3.2	89
31054	Pressure-Stabilized Superconductive Ionic Tantalum Hydrides. Inorganic Chemistry, 2017, 56, 3901-3908.	1.9	41
31055	Semihydrogenation of Acetylene on Al₅Co₂ Surfaces. Journal of Physical Chemistry C, 2017, 121, 4958-4969.	1.5	16
31056	Size-Selective Reactivity of Subnanometer Ag₄ and Ag₁₆ Clusters on a TiO₂ Surface. Journal of Physical Chemistry C, 2017, 121, 6614-6625.	1.5	21
31057	First-Principles Study: Tuning the Redox Behavior of Lithium-Rich Layered Oxides by Chlorine Doping. Journal of Physical Chemistry C, 2017, 121, 7155-7163.	1.5	41
31058	Structural Complexity and Phonon Physics in 2D Arsenenes. Journal of Physical Chemistry Letters, 2017, 8, 1375-1380.	2.1	41
31059	Enhancing CO2 electrolysis through synergistic control of non-stoichiometry and doping to tune cathode surface structures. Nature Communications, 2017, 8, 14785.	5.8	215
31060	High-throughput search of ternary chalcogenides for p-type transparent electrodes. Scientific Reports, 2017, 7, 43179.	1.6	46
31061	Solution of an elusive pigment crystal structure from a thin film: a combined X-ray diffraction and computational study. CrystEngComm, 2017, 19, 1902-1911.	1.3	15
31062	Perspective: Explicitly correlated electronic structure theory for complex systems. Journal of Chemical Physics, 2017, 146, 080901.	1.2	51
31063	AlM₂B₂(Mâ€‰â€‰=â€‰â€‰Cr, Mn, Fe, Co, Ni): a group of nanolaminated materials. Journal of Physics Condensed Matter, 2017, 29, 155402.	0.7	72
31064	Impact of <mml:math xmlns:mml="http://www.w3.org/1998/Math/MathML"><mml:mi>d</mml:mi></mml:math> -band filling on the dislocation properties of bcc transition metals: The case of tantalum-tungsten alloys investigated by density-functional theory. Physical Review B, 2017, 95, .	1.1	23

#	Article	IF	Citations
31065	Efficient systematic scheme to construct second-principles lattice dynamical models. Physical Review B, 2017, 95, .	1.1	23
31066	Density Functional Theory Study on Formation Energy and Diffusion Path of Metal Atom near Dopant in Si Crystals. ECS Journal of Solid State Science and Technology, 2017, 6, P125-P131.	0.9	6
31067	3D Synergistically Active Carbon Nanofibers for Improved Oxygen Evolution. Advanced Energy Materials, 2017, 7, 1602928.	10.2	120
31068	MoTe2 is a good match for GeI by preserving quantum spin Hall phase. Nano Research, 2017, 10, 2823-2832.	5.8	7
31069	First principles prediction of two-dimensional tungsten carbide (W2C) monolayer and its Li storage capability. Computational Condensed Matter, 2017, 10, 35-38.	0.9	17
31070	Self-Consistent Charge Density-Functional Tight-Binding Parametrization for Ptâ€“Ru Alloys. Journal of Physical Chemistry A, 2017, 121, 2497-2502.	1.1	23
31071	HLE17: An Improved Local Exchangeâ€“Correlation Functional for Computing Semiconductor Band Gaps and Molecular Excitation Energies. Journal of Physical Chemistry C, 2017, 121, 7144-7154.	1.5	66
31072	Negative Linear Compressibility Due to Layer Sliding in a Layered Metalâ€“Organic Framework. Journal of Physical Chemistry Letters, 2017, 8, 1436-1441.	2.1	36
31073	Accurate, Large-Scale Density Functional Melting of Hg: Relativistic Effects Decrease Melting Temperature by 160 K. Journal of Physical Chemistry Letters, 2017, 8, 1407-1412.	2.1	21
31074	Trends in the Surface and Catalytic Chemistry of Transition-Metal Ceramics in the Deoxygenation of a Woody Biomass Pyrolysis Model Compound. ACS Catalysis, 2017, 7, 3169-3180.	5.5	32
31075	Nanostructured Bulk-Heterojunction Solar Cells Based on Amorphous Carbon. ACS Energy Letters, 2017, 2, 882-888.	8.8	3
31076	Tailoring the electronic and magnetic properties of monolayer SnO by B, C, N, O and F adatoms. Scientific Reports, 2017, 7, 44568.	1.6	21
31077	Modulation of electronic and optical properties in mixed halide perovskites CsPbCl3xBr3(1-x) and CsPbBr3xI3(1-x). Applied Physics Letters, 2017, 110, .	1.5	28
31078	Stability of Ar(H ₂) ₂ to 358 GPa. Proceedings of the National Academy of Sciences of the United States of America, 2017, 114, 3596-3600.	3.3	23
31079	Intrinsic air stability mechanisms of two-dimensional transition metal dichalcogenide surfaces: basal versus edge oxidation. 2D Materials, 2017, 4, 025050.	2.0	87
31080	Effects of biaxial strain on the improper multiferroicity inhâ^'LuFeO3films studied using the restrained thermal expansion method. Physical Review B, 2017, 95, .	1.1	14
31081	Interlayer states arising from anionic electrons in the honeycomb-lattice-based compounds AeAlSi () Tj ETQq0 0 0 rgBT /Overlock 10 Tf 5	1.1	8
31082	Density-functional calculations of transport properties in the nondegenerate limit and the role of electron-electron scattering. Physical Review E, 2017, 95, 033203.	0.8	52

#	Article	IF	Citations
31083	Neutron filter efficiency of beryllium and magnesium fluorides. Journal of Applied Crystallography, 2017, 50, 441-450.	1.9	4
31084	Significantly Increased Raman Enhancement on MoX₂ (X = S, Se) Monolayers upon Phase Transition. Advanced Functional Materials, 2017, 27, 1606694.	7.8	158
31085	Effects of Ti and Mn Co-substitution on P4mm BiFeO3: An Ab Initio Calculation. Journal of Superconductivity and Novel Magnetism, 2017, 30, 2471-2479.	0.8	1
31086	First-principles modeling of anisotropic anodic dissolution of metals and alloys in corrosive environments. Acta Materialia, 2017, 130, 137-146.	3.8	129
31087	Strong p -magnetism in carbon suboxide C 2 O devised from first principles. Chemical Physics Letters, 2017, 674, 115-119.	1.2	4
31088	Structural, electronic and magnetic properties of Ti-doped polar and nonpolar GaN surfaces. Journal of Crystal Growth, 2017, 467, 12-17.	0.7	6
31089	A DFT study on the correlation between topology and Bader charges: Part V, on the correlation between interatomic distances and Bader charges in the structures of Ti n O m compounds â€“ A comment on the â€œcharge and size conceptâ€•in crystal chemistry. Solid State Sciences, 2017, 67, 85-92.	1.5	3
31090	Revealing the Electronic Structure of Silicon Intercalated Armchair Graphene Nanoribbons by Scanning Tunneling Spectroscopy. Nano Letters, 2017, 17, 2197-2203.	4.5	92
31091	Phase diagram, stability and electronic properties of an Feâ€“P system under high pressure: a first principles study. RSC Advances, 2017, 7, 15986-15991.	1.7	23
31092	Sandwiched graphene inserted with graphene-encapsulated yolkâ€“shell Î³-Fe2O3 nanoparticles for efficient lithium ion storage. Journal of Materials Chemistry A, 2017, 5, 7035-7042.	5.2	42
31093	Metastable cubic tin sulfide: A novel phonon-stable chiral semiconductor. APL Materials, 2017, 5, 036101.	2.2	51
31094	Interplay of electronic, structural and magnetic properties as the driving feature of high-entropy CoCrFeNiPd alloys. Journal Physics D: Applied Physics, 2017, 50, 185002.	1.3	16
31095	Aggregation of BiTe monolayer on Bi2Te3 (111) induced by diffusion of intercalated atoms in the van der Waals gap. Physical Review B, 2017, 95, .	1.1	3
31096	Structural phase transition, electronic, elastic, and vibrational properties of LiAl intermetallic compound: insights from first-principles calculations. Canadian Journal of Physics, 2017, 95, 691-698.	0.4	4
31097	3D Hierarchically Porous Graphitic Carbon Nitride Modified Grapheneâ€Pt Hybrid as Efficient Methanol Oxidation Catalysts. Advanced Materials Interfaces, 2017, 4, 1601219.	1.9	27
31098	Microstructure-Based Multiscale Analysis of Hot Rolling of Duplex Stainless Steel Using Various Simulation Software. Integrating Materials and Manufacturing Innovation, 2017, 6, 69-82.	1.2	7
31099	Effect of Ti addition on the thermal expansion anisotropy of Mo5Si3. Acta Materialia, 2017, 132, 25-34.	3.8	12
31100	A DFT study and micro-kinetic analysis of acetylene selective hydrogenation on Pd-doped Cu(111) surfaces. Applied Surface Science, 2017, 410, 154-165.	3.1	42

#	Article	IF	Citations
31101	First-principles study of H, O, and N adsorption on metal embedded carbon nanotubes. Applied Surface Science, 2017, 403, 645-651.	3.1	6
31102	Observation of reduced phase transition temperature in N-doped thermochromic film of monoclinic VO2. Applied Surface Science, 2017, 410, 363-372.	3.1	43
31103	Carbon-rich carbon nitride monolayers with Dirac cones: Dumbbell C4N. Carbon, 2017, 118, 285-290.	5.4	40
31104	The effect of yttrium on the generalized stacking fault energies in Mg. Computational Materials Science, 2017, 133, 1-5.	1.4	15
31105	SPARC: Accurate and efficient finite-difference formulation and parallel implementation of Density Functional Theory: Extended systems. Computer Physics Communications, 2017, 216, 109-125.	3.0	109
31106	Diffusion of Lithium Ions in Amorphous and Crystalline Poly(ethylene oxide)3:LiCF3SO3 Polymer Electrolytes. Electrochimica Acta, 2017, 235, 122-128.	2.6	32
31107	The large absorption coefficient and photoconductivity of oP12-FeB2 high hard material: A first-principles study. Optik, 2017, 138, 160-165.	1.4	2
31108	Competing rhombohedral and monoclinic crystal structures in <mml:math xmlns:mml="http://www.w3.org/1998/Math/MathML" altimg="si1.gif" overflow="scroll"><mml:mrow><mml:msub><mml:mrow><mml:mtext>MnPn</mml:mtext></mml:mrow><mml:mn>2</mml:mn></mml compounds: An ab-initio study. Journal of Alloys and Compounds, 2017, 709, 172-178.	2.8	58
31109	The influence of silicon atom doping phagraphene nanoribbons on the electronic and magnetic properties. Materials Science and Engineering B: Solid-State Materials for Advanced Technology, 2017, 220, 30-36.	1.7	11
31110	Density functional theory study of defects in unalloyed Î´-Pu. Scripta Materialia, 2017, 134, 57-60.	2.6	12
31111	Atomistic modeling study of a strain-free stress driven grain boundary migration mechanism. Scripta Materialia, 2017, 134, 52-56.	2.6	10
31112	Prediction of Stable Ground-State Lithium Polyhydrides under High Pressures. Inorganic Chemistry, 2017, 56, 3867-3874.	1.9	20
31113	Quantum Mechanical Study of N-Heterocyclic Carbene Adsorption on Au Surfaces. Journal of Physical Chemistry A, 2017, 121, 2674-2682.	1.1	29
31114	First-Principles Calculations on the Crystal/Electronic Structure and Phase Stability of H-Doped SrFeO₂. Journal of Physical Chemistry C, 2017, 121, 7478-7484.	1.5	1
31115	Thickness-Dependent Adsorption of Melamine on Cu/Au(111) Films. Journal of Physical Chemistry C, 2017, 121, 7977-7984.	1.5	15
31116	Complex Ion Dynamics in Carbonate Lithium-Ion Battery Electrolytes. Journal of Physical Chemistry C, 2017, 121, 6589-6595.	1.5	16
31117	Efficient Lanthanide Catalyzed Debromination and Oligomeric Length-Controlled Ullmann Coupling of Aryl Halides. Journal of Physical Chemistry C, 2017, 121, 8033-8041.	1.5	22
31118	Quartic Dispersion, Strong Singularity, Magnetic Instability, and Unique Thermoelectric Properties in Two-Dimensional Hexagonal Lattices of Group-VA Elements. Nano Letters, 2017, 17, 2589-2595.	4.5	33

#	Article	IF	Citations
31119	Functional electronic inversion layers at ferroelectric domain walls. Nature Materials, 2017, 16, 622-627.	13.3	127
31120	Structural, electronic and mechanical properties of sp³-hybridized BN phases. Physical Chemistry Chemical Physics, 2017, 19, 9923-9933.	1.3	9
31121	First-principles study of structural stability, dynamical and mechanical properties of Li₂FeSiO₄ polymorphs. RSC Advances, 2017, 7, 16843-16853.	1.7	32
31122	Intrinsic point defects in buckled and puckered arsenene: a first-principles study. Physical Chemistry Chemical Physics, 2017, 19, 9862-9871.	1.3	38
31123	Large gap two dimensional topological insulators: the bilayer triangular lattice TlM (M = N, P, As, Sb). Journal of Materials Chemistry C, 2017, 5, 4268-4274.	2.7	6
31124	Nitrile versus isonitrile adsorption at interstellar grains surfaces. Astronomy and Astrophysics, 2017, 598, A18.	2.1	25
31125	Efficient noble metal nanocatalysts supported on HfC(001) for O2 dissociation. AIP Advances, 2017, 7, .	0.6	6
31126	Tunable dynamics of a flake on graphene: Libration frequency. Physical Review B, 2017, 95, .	1.1	7
31127	n- and p-type dopants in the InSe monolayer via substitutional doping. Journal of Materials Science, 2017, 52, 7207-7214.	1.7	48
31128	Temperature and coverage effects on the stability of epitaxial silicene on Ag(111) surfaces. Applied Surface Science, 2017, 409, 97-101.	3.1	13
31129	Experimental study and thermodynamic modeling of the Al-Sc-Zr system. Computational Materials Science, 2017, 133, 82-92.	1.4	18
31130	Enhanced optical absorption and photocatalytic H2 production activity of g-C3N4/TiO2 heterostructure by interfacial coupling: A DFT+U study. International Journal of Hydrogen Energy, 2017, 42, 9903-9913.	3.8	50
31131	Magnetic evolution of itinerant ferromagnetism and interlayer antiferromagnetism in cerium doped LaCo 2 P 2 crystals. Physica B: Condensed Matter, 2017, 512, 75-80.	1.3	3
31132	Hydrogen bubble nucleation in Î±-iron. Scripta Materialia, 2017, 134, 105-109.	2.6	34
31133	Molecule-decorated rutile-type ZnF 2 (110): A periodic DFT study. Surface Science, 2017, 662, 34-41.	0.8	5
31134	New AuN (N = 27â€“30) Lowest Energy Clusters Obtained by Means of an Improved DFTâ€“Genetic Algorithm Methodology. Journal of Physical Chemistry C, 2017, 121, 10982-10991.	1.5	41
31135	Strain Controlled Ferromagnetic-Antiferromagnetic Transformation in Mn-Doped Silicene for Information Transformation Devices. Journal of Physical Chemistry Letters, 2017, 8, 1484-1488.	2.1	55
31136	Heterogeneous Pyrolysis: A Route for Epitaxial Growth of hBN Atomic Layers on Copper Using Separate Boron and Nitrogen Precursors. Nano Letters, 2017, 17, 2404-2413.	4.5	21

#	Article	IF	Citations
31137	Atomistic Insights into Nucleation and Formation of Hexagonal Boron Nitride on Nickel from First-Principles-Based Reactive Molecular Dynamics Simulations. ACS Nano, 2017, 11, 3585-3596.	7.3	55
31138	Optimizing Charge Injection across Transition Metal Dichalcogenide Heterojunctions: Theory and Experiment. ACS Nano, 2017, 11, 3904-3910.	7.3	29
31139	Immobilization of sulfur by constructing three-dimensional nitrogen rich carbons for long life lithiumâ€“sulfur batteries. Journal of Materials Chemistry A, 2017, 5, 8360-8366.	5.2	26
31140	Interlayer locking and atomic-scale friction in commensurate small-diameter boron nitride nanotubes. Physical Review B, 2017, 95, .	1.1	5
31141	Electronic structure and magnetic properties in <mml:math xmlns:mml="http://www.w3.org/1998/Math/MathML"><mml:msub><mml:mi>T</mml:mi><mml:mn>2</mml:mn></mml:msub><mml:m mathvariant="normal">AlB</mml:mi><mml:mn>2</mml:mn></mml:msub></mml:math> (<mml:math) Tj ETQq0 0 0 rgBT /Overlock 10 T	1.1	4
31142	Investigation of the structural, optical and electronic properties of Cu₂Zn(Sn,Si/Ge)(S/Se)₄ alloys for solar cell applications. Physica Status Solidi (B): Basic Research, 2017, 254, 1700084.	0.7	11
31143	Layer effect on catalytic activity of Pd-Cu bimetal for CO oxidation. Applied Catalysis A: General, 2017, 538, 66-73.	2.2	8
31144	Effect of nanostructuring of ZnO for gas sensing of nitrogen dioxide. Computational Materials Science, 2017, 132, 104-115.	1.4	23
31145	Effect of flue gas components on the adsorption of sulfur oxides on CaO(1 0 0). Fuel, 2017, 197, 541-550.	3.4	19
31146	Strain engineering and photocatalytic application of single-layer ReS2. International Journal of Hydrogen Energy, 2017, 42, 161-167.	3.8	30
31147	Vanadium sulfide sub-microspheres: A new near-infrared-driven photocatalyst. Journal of Colloid and Interface Science, 2017, 498, 442-448.	5.0	35
31148	The adsorption and activation of formic acid on different anatase TiO 2 surfaces. Journal of Energy Chemistry, 2017, 26, 738-742.	7.1	6
31149	Low-temperature hydrogen production from water and methanol using Pt/Î±-MoC catalysts. Nature, 2017, 544, 80-83.	13.7	1,090
31150	Two-dimensional germanium monochalcogenide photocatalyst for water splitting under ultraviolet, visible to near-infrared light. Nanoscale, 2017, 9, 8608-8615.	2.8	124
31151	Firstâ€Principles Calculations and Optical Absorption Spectrum of a Lightâ€Colored Aluminumâ€Substituted Îµâ€Iron Oxide Magnet. European Journal of Inorganic Chemistry, 2017, 2017, 531-534.	1.0	4
31152	First-principles investigation of point defect and atomic diffusion in Al 2 Ca. Journal of Physics and Chemistry of Solids, 2017, 103, 6-12.	1.9	8
31153	Efficient electron transfer kuramite Cu3SnS4 nanosheet thin film towards platinum-free cathode in dye-sensitized solar cells. Journal of Power Sources, 2017, 341, 60-67.	4.0	39
31154	Theoretical insight into Cobalt subnano-clusters adsorption on Î±-Al2O3 (0001). Journal of Solid State Chemistry, 2017, 246, 176-185.	1.4	5

#	Article	IF	Citations
31155	Defect-induced magnetism in two-dimensional NbSe2. Superlattices and Microstructures, 2017, 101, 349-353.	1.4	7
31156	Atomic-Scale Structural Evolution of Rh(110) during Catalysis. ACS Catalysis, 2017, 7, 664-674.	5.5	20
31157	Why conclusions from platinum model surfaces do not necessarily lead to enhanced nanoparticle catalysts for the oxygen reduction reaction. Chemical Science, 2017, 8, 2283-2289.	3.7	173
31158	New insight into Li/Ni disorder in layered cathode materials for lithium ion batteries: a joint study of neutron diffraction, electrochemical kinetic analysis and first-principles calculations. Journal of Materials Chemistry A, 2017, 5, 1679-1686.	5.2	73
31159	Zigzag double-chain Câ€“Be nanoribbon featuring planar pentacoordinate carbons and ribbon aromaticity. Journal of Materials Chemistry C, 2017, 5, 408-414.	2.7	10
31160	X-ray diffraction data-assisted structure searches. Computer Physics Communications, 2017, 213, 40-45.	3.0	30
31161	Elastic properties of cubic K2B12H12 from theoretical calculations. Journal of Alloys and Compounds, 2017, 695, 2916-2922.	2.8	16
31162	Solution-processable exfoliation and photoelectric properties of two-dimensional layered MoS2 photoelectrodes. Journal of Colloid and Interface Science, 2017, 490, 287-293.	5.0	25
31163	Structure and ionic conductivity of the solid electrolyte interphase layer on tin anodes in Na-ion batteries. Journal of Power Sources, 2017, 341, 107-113.	4.0	28
31164	Li ion diffusion dynamics on Li oxides and peroxides surfaces. Materials Letters, 2017, 188, 208-211.	1.3	2
31165	Solid state DFT modeling and vibrational characterisation of butylenediammonium and hexylenediammonium hexafluorosilicate, NH3(CH2)nNH3SiF6 (n=4 and 6). Vibrational Spectroscopy, 2017, 88, 83-93.	1.2	11
31166	Competing Structural Instabilities in the Ruddlesdenâ€“Popper Derivatives HRTiO₄ (R = Rare) Tj ETQq1 1 0.784314 rgBT /O Centrosymmetricity. Chemistry of Materials, 2017, 29, 656-665.	3.2	22
31167	Effect of Ablation Rate on the Microstructure and Electrochromic Properties of Pulsed-Laser-Deposited Molybdenum Oxide Thin Films. Langmuir, 2017, 33, 19-33.	1.6	35
31168	Solution-Synthesized Chevron Graphene Nanoribbons Exfoliated onto H:Si(100). Nano Letters, 2017, 17, 170-178.	4.5	49
31169	Atomistic Mechanisms Underlying Selectivities in C₁ and C₂ Products from Electrochemical Reduction of CO on Cu(111). Journal of the American Chemical Society, 2017, 139, 130-136.	6.6	320
31170	The Formation Time of Tiâ€“O^{â€¢} and Tiâ€“O^{â€¢}â€“Ti Radicals at the n-SrTiO₃/Aqueous Interface during Photocatalytic Water Oxidation. Journal of the American Chemical Society, 2017, 139, 1830-1841.	6.6	76
31171	Effect of doping and chemical ordering on the optoelectronic properties of complex oxides: Fe₂O₃â€“V₂O₃ solid solutions and hetero-structures. Physical Chemistry Chemical Physics, 2017, 19, 1097-1107.	1.3	4
31172	Novel multiferroic state and ME enhancement by breaking the AFM frustration in LuMn1â^'xO3. Physical Chemistry Chemical Physics, 2017, 19, 1335-1341.	1.3	10

#	Article	IF	Citations
31173	Topological insulating states in 2D transition metal dichalcogenides induced by defects and strain. Nanoscale, 2017, 9, 562-569.	2.8	28
31174	Two-dimensional hydrogenated molybdenum and tungsten dinitrides MN₂H₂(M = Mo, W) as novel quantum spin hall insulators with high stability. Nanoscale, 2017, 9, 1007-1013.	2.8	15
31175	Softening and hardening of yield stress by hydrogenâ€“solute interactions. Philosophical Magazine, 2017, 97, 400-418.	0.7	34
31176	First-Principles Investigations on Structural, Elastic, Dynamical, and Thermal Properties of Earth-Abundant Nitride Semiconductor CaZn₂N₂ under Pressure. Zeitschrift Fur Naturforschung - Section A Journal of Physical Sciences, 2017, 72, 39-49.	0.7	8
31177	Ab Initio Study of Electronic Structure, Elastic and Transport Properties of Fluoroperovskite LiBeF3. Journal of Electronic Materials, 2017, 46, 2205-2210.	1.0	19
31178	Bandgap Engineering of Barium Bismuth Niobate Double Perovskite for Photoelectrochemical Water Oxidation. Advanced Energy Materials, 2017, 7, 1602260.	10.2	67
31179	MÃ¶ssbauer spectroscopy evidence of intrinsic nonâ€stoichiometry in iron telluride single crystals. Annalen Der Physik, 2017, 529, 1600241.	0.9	3
31180	Ab-initio study of surface segregation in aluminum alloys. Applied Surface Science, 2017, 399, 351-358.	3.1	3
31181	Identifying the significance of proton-electron transfer in CH4 production on Cu (100) in CO2 electro-reduction. Journal of Electroanalytical Chemistry, 2017, 793, 184-187.	1.9	10
31182	Determination of Bulk and Surface Atomic Arrangement in Niâ€“Zn Î³-Brass Phase at Different Ni to Zn Ratios. Chemistry of Materials, 2017, 29, 504-512.	3.2	17
31183	Using Force Matching To Determine Reactive Force Fields for Water under Extreme Thermodynamic Conditions. Journal of Chemical Theory and Computation, 2017, 13, 135-146.	2.3	24
31184	A Close Look at the Structure of the TiO₂-APTES Interface in Hybrid Nanomaterials and Its Degradation Pathway: An Experimental and Theoretical Study. Journal of Physical Chemistry C, 2017, 121, 430-440.	1.5	123
31185	Photoelectrochemical Properties and Behavior of Î±-SnWO₄ Photoanodes Synthesized by Hydrothermal Conversion of WO₃ Films. ACS Applied Materials & Interfaces, 2017, 9, 1459-1470.	4.0	42
31186	Nanopatterning of Group V Elements for Tailoring the Electronic Properties of Semiconductors by Monolayer Doping. ACS Applied Materials & Interfaces, 2017, 9, 1922-1928.	4.0	9
31187	Chemical Vapor Deposition Growth of Few-Layer MoTe₂ in the 2H, 1Tâ€², and 1T Phases: Tunable Properties of MoTe₂ Films. ACS Nano, 2017, 11, 900-905.	7.3	173
31188	Auâ€“Ge MEAM potential fitted to the binary phase diagram. Modelling and Simulation in Materials Science and Engineering, 2017, 25, 025004.	0.8	5
31189	The structural, elastic, electronic and dynamical properties of chalcopyrite semiconductor BeGeAs2 from first-principles calculations. Applied Physics A: Materials Science and Processing, 2017, 123, 1.	1.1	3
31190	Structures of Bimetallic Copperâ€“Ruthenium Nanoparticles: Incoherent Interface and Surface Active Sites for Catalytic Nitric Oxide Dissociation. Journal of Physical Chemistry C, 2017, 121, 300-307.	1.5	15

#	Article	IF	Citations
31191	Correlation between Uniaxial Negative Thermal Expansion and Negative Linear Compressibility in Ag₃[Co(CN)₆]. Journal of Physical Chemistry C, 2017, 121, 333-341.	1.5	28
31192	Effect of Elasticity of the MoS₂ Surface on Li Atom Bouncing and Migration: Mechanism from Ab Initio Molecular Dynamic Investigations. Journal of Physical Chemistry C, 2017, 121, 1329-1338.	1.5	3
31193	Can a Photosensitive Oxide Catalyze Decomposition of Energetic Materials?. Journal of Physical Chemistry C, 2017, 121, 1153-1161.	1.5	12
31194	Solid-State Polymerization of CO₂ from Catalytic Photoexcitation: An Ab Initio Molecular Dynamics Study. Journal of Physical Chemistry C, 2017, 121, 115-122.	1.5	2
31195	High-Mobility Transport Anisotropy in Few-Layer MoO₃ and Its Origin. ACS Applied Materials & Interfaces, 2017, 9, 1702-1709.	4.0	51
31196	Hydrogenâ€“vacancyâ€“dislocation interactions inÎ±-Fe. Modelling and Simulation in Materials Science and Engineering, 2017, 25, 025001.	0.8	28
31197	Hydroxylation Induced Alignment of Metal Oxide Nanocubes. Angewandte Chemie - International Edition, 2017, 56, 1407-1410.	7.2	19
31198	First-principles calculations of the structural, mechanical, electronic and bonding properties of (CrB) Tj ETQq1 1 0.784314 rgBT /Overlo	2.8	29
31199	Theory and Applications of Generalized Pipekâ€“Mezey Wannier Functions. Journal of Chemical Theory and Computation, 2017, 13, 460-474.	2.3	32
31200	Time-Domain ab Initio Modeling of Electronâ€“Phonon Relaxation in High-Temperature Cuprate Superconductors. Journal of Physical Chemistry Letters, 2017, 8, 193-198.	2.1	20
31201	Interfacial engineering of phthalocyanine molecules on graphitic and metal substrates. Molecular Simulation, 2017, 43, 384-393.	0.9	2
31202	Quasimolecules in Compressed Lithium. Angewandte Chemie, 2017, 129, 992-995.	1.6	16
31203	Ab initio study of interaction of helium with edge and screw dislocations in tungsten. Nuclear Instruments & Methods in Physics Research B, 2017, 393, 150-154.	0.6	17
31204	Earth-Abundant and Non-Toxic SiX (X = S, Se) Monolayers as Highly Efficient Thermoelectric Materials. Journal of Physical Chemistry C, 2017, 121, 123-128.	1.5	41
31205	First-Principles Investigation of the Epitaxial Stabilization of Oxide Polymorphs: TiO₂ on (Sr,Ba)TiO₃. ACS Applied Materials & Interfaces, 2017, 9, 4106-4118.	4.0	17
31206	Band gap opening in stanene induced by patterned Bâ€“N doping. Physical Chemistry Chemical Physics, 2017, 19, 3660-3669.	1.3	50
31207	A new quaternary semiconductor compound (Ba2Sb4GeS10): Ab initio study. Philosophical Magazine, 2017, 97, 549-560.	0.7	5
31208	Energy gap of extended states in SiC-doped graphene nanoribbon: Ab initio calculations. Applied Surface Science, 2017, 400, 1-5.	3.1	5

#	Article	IF	Citations
31209	Electron transport determines the electrochemical properties of tetrahedral amorphous carbon (ta-C) thin films. Electrochimica Acta, 2017, 225, 1-10.	2.6	49
31210	Magnetic doping in two-dimensional transition-metal dichalcogenide zirconium diselenide. Journal of Alloys and Compounds, 2017, 698, 611-616.	2.8	28
31211	Computational Design of Rare-Earth-Free Magnets with the Ti₃Co₅B₂-Type Structure. Chemistry of Materials, 2017, 29, 2535-2541.	3.2	24
31212	Design of van der Waals Two-Dimensional Heterostructures from Facially Polarized Janus All-Cis 1,2,3,4,5,6-Hexafluorocyclohexane (C6H6F6). Journal of Physical Chemistry C, 2017, 121, 1752-1762.	1.5	18
31213	A novel Mn⁴⁺â€activated red phosphor for use in light emitting diodes, K₃SiF₇:Mn⁴⁺. Journal of the American Ceramic Society, 2017, 100, 1044-1050.	1.9	45
31214	Electric Dipoles and Ionic Conductivity in a Na⁺Glass Electrolyte. Journal of the Electrochemical Society, 2017, 164, A207-A213.	1.3	26
31215	Experimental and theoretical investigation of the chromiumâ€“vanadiumâ€“antimony system. Zeitschrift Fur Kristallographie - Crystalline Materials, 2017, 232, 235-244.	0.4	0
31216	Interfacial interaction in monolayer transition metal dichalcogenide/metal oxide heterostructures and its effects on electronic and optical properties: The case of MX₂/CeO₂. Applied Physics Express, 2017, 10, 011201.	1.1	11
31217	Activating Basal Planes and Sâ€Terminated Edges of MoS₂ toward More Efficient Hydrogen Evolution. Advanced Functional Materials, 2017, 27, 1604943.	7.8	131
31218	Metamorphosis in carbon network: From penta-graphene to biphenylene under uniaxial tension. FlatChem, 2017, 1, 65-73.	2.8	46
31219	Ab initio study of He trapping, diffusion and clustering in Y2O3. Nuclear Instruments & Methods in Physics Research B, 2017, 393, 82-87.	0.6	6
31220	Identification of Second Shell Coordination in Transition Metal Species Using Theoretical XANES: Example of Tiâ€“Oâ€“(C, Si, Ge) Complexes. Journal of Physical Chemistry A, 2017, 121, 162-167.	1.1	7
31221	Split-Charge Equilibration Parameters for Generating Rapid Partial Atomic Charges in Metalâ€“Organic Frameworks and Porous Polymer Networks for High-Throughput Screening. Journal of Physical Chemistry C, 2017, 121, 903-910.	1.5	12
31222	Strong Localization of Anionic Electrons at Interlayer for Electrical and Magnetic Anisotropy in Two-Dimensional Y₂C Electride. Journal of the American Chemical Society, 2017, 139, 615-618.	6.6	71
31223	The Fine Line between a Twoâ€Phase and Solidâ€Solution Phase Transformation and Highly Mobile Phase Interfaces in Spinel Li₄₊_xTi₅O₁₂. Advanced Energy Materials, 2017, 7, 1601781.	10.2	33
31224	Adsorption and Dissociation of H2 on Cluster Al6N. Journal of Cluster Science, 2017, 28, 1335-1344.	1.7	3
31225	Tunable band structure and effective mass of disordered chalcopyrite. Frontiers of Physics, 2017, 12, 1.	2.4	2
31226	Theoretical stability and materials synthesis of a chemically ordered MAX phase, Mo2ScAlC2, and its two-dimensional derivate Mo2ScC2 MXene. Acta Materialia, 2017, 125, 476-480.	3.8	185

#	Article	IF	Citations
31227	Multi-fidelity machine learning models for accurate bandgap predictions of solids. Computational Materials Science, 2017, 129, 156-163.	1.4	235
31228	First-principles study on hydrogen adsorption on nitrogen doped graphene. Physica E: Low-Dimensional Systems and Nanostructures, 2017, 88, 115-124.	1.3	67
31229	Yield anomaly in L12 Co3AlxW1â^'x vis-Ã-vis Ni3Al. Scripta Materialia, 2017, 130, 269-273.	2.6	22
31230	Manifestations of two-dimensional electron gas in molecular crystals. Surface Science, 2017, 657, 20-27.	0.8	1
31231	Engineering and Probing Topological Properties of Dirac Semimetal Films by Asymmetric Charge Transfer. Nano Letters, 2017, 17, 963-972.	4.5	14
31232	Contrasting Structural Reconstructions, Electronic Properties, and Magnetic Orderings along Different Edges of Zigzag Transition Metal Dichalcogenide Nanoribbons. Nano Letters, 2017, 17, 1097-1101.	4.5	75
31233	Covalent Functionalization by Cycloaddition Reactions of Pristine Defect-Free Graphene. ACS Nano, 2017, 11, 627-634.	7.3	69
31234	A structural insight into mechanical strength of graphene-like carbon and carbon nitride networks. Nanotechnology, 2017, 28, 055707.	1.3	32
31235	Polydopamineâ€Inspired, Dual Heteroatomâ€Doped Carbon Nanotubes for Highly Efficient Overall Water Splitting. Advanced Energy Materials, 2017, 7, 1602068.	10.2	319
31236	Methanol decomposition on low index and stepped CeO 2 surfaces from GGA+ U. Applied Surface Science, 2017, 394, 509-518.	3.1	8
31237	Theoretical study on influence of CaO and MgO on the reduction of FeO by CO. Applied Surface Science, 2017, 399, 630-637.	3.1	13
31238	Electronic and magnetic properties of Re-doped single-layer MoS2: A DFT study. Computational Materials Science, 2017, 128, 287-293.	1.4	39
31239	Influence of point defects on optical properties of GaN-based materials by first principle study. Computational Materials Science, 2017, 129, 49-54.	1.4	14
31240	Density functional theory study on the effect of OH and Cl adsorption on the surface structure of Î±-Fe2O3. Computational and Theoretical Chemistry, 2017, 1100, 91-101.	1.1	22
31241	Functionality-Directed Screening of Pb-Free Hybrid Organicâ€“Inorganic Perovskites with Desired Intrinsic Photovoltaic Functionalities. Chemistry of Materials, 2017, 29, 524-538.	3.2	135
31242	Anion Ordering in CaTaO₂N: Structural Impact on the Photocatalytic Activity. Insights from First-Principles. Chemistry of Materials, 2017, 29, 539-545.	3.2	52
31243	CuTaS₃: Intermetal dâ€“d Transitions Enable High Solar Absorption. Chemistry of Materials, 2017, 29, 2594-2598.	3.2	21
31244	Multifunctional Materials: A Case Study of the Effects of Metal Doping on ZnO Tetrapods with Bismuth and Tin Oxides. Advanced Functional Materials, 2017, 27, 1604676.	7.8	140

#	Article	IF	Citations
31245	Theoretical study of the impact of stress and interstitial oxygen on the behavior of intrinsic point defects in growing Czochralski Si crystals. Journal of Crystal Growth, 2017, 474, 89-95.	0.7	8
31246	Simulation of natural dyes adsorbed on TiO2 for photovoltaic applications. Solar Energy, 2017, 142, 215-223.	2.9	17
31247	Spin Orientation of Two-Dimensional Electrons Driven by Temperature-Tunable Competition of Spinâ€“Orbit and Exchangeâ€“Magnetic Interactions. Nano Letters, 2017, 17, 811-820.	4.5	28
31248	Topological phase transition and evolution of edge states in In-rich InGaN/GaN quantum wells under hydrostatic pressure. Journal of Physics Condensed Matter, 2017, 29, 055702.	0.7	8
31249	CO Oxidation on Au Nanoparticles Supported on ZrO₂: Role of Metal/Oxide Interface and Oxide Reducibility. ChemCatChem, 2017, 9, 1119-1127.	1.8	54
31250	The Solvation Structure of Lithium Ions in an Ether Based Electrolyte Solution from First-Principles Molecular Dynamics. Journal of Physical Chemistry B, 2017, 121, 180-188.	1.2	41
31251	Rational Design of Two-Dimensional Metallic and Semiconducting Spintronic Materials Based on Ordered Double-Transition-Metal MXenes. Journal of Physical Chemistry Letters, 2017, 8, 422-428.	2.1	165
31252	Tunable Positive to Negative Magnetoresistance in Atomically Thin WTe₂. Nano Letters, 2017, 17, 878-885.	4.5	92
31253	Investigation of intrinsic defect magnetic properties in wurtzite ZnO materials. Journal of Magnetism and Magnetic Materials, 2017, 440, 5-9.	1.0	19
31254	Density Functional Theory Study of Ni Clusters Supported on the ZrO₂(111) Surface. Fuel Cells, 2017, 17, 125-131.	1.5	16
31255	A new carbon allotrope: Penta-graphene as a metal-free catalyst for CO oxidation. Carbon, 2017, 114, 465-472.	5.4	91
31256	Single Pd atoms supported by graphitic carbon nitride, a potential oxygen reduction reaction catalyst from theoretical perspective. Carbon, 2017, 114, 619-627.	5.4	78
31257	Structural and luminescent properties of solid-solution phosphor Ba Sr1-Al2O4: Eu2+. Journal of Luminescence, 2017, 191, 46-50.	1.5	4
31258	Thermophysical properties of Ni-containing single-phase concentrated solid solution alloys. Materials and Design, 2017, 117, 185-192.	3.3	96
31259	Prediction of electronic structure of van der Waals interfaces: Benzene adsorbed monolayer MoS 2 , WS 2 and WTe 2. Physica E: Low-Dimensional Systems and Nanostructures, 2017, 88, 87-96.	1.3	8
31260	Single-layer ZnS supported on Au(111): A combined XPS, LEED, STM and DFT study. Surface Science, 2017, 658, 9-14.	0.8	20
31261	Probing the Release and Uptake of Water in Î±-MnO₂Â·xH₂O. Chemistry of Materials, 2017, 29, 1507-1517.	3.2	31
31262	Variations of Local Motifs around Ge Atoms in Amorphous GeTe Ultrathin Films. Journal of Physical Chemistry C, 2017, 121, 1122-1128.	1.5	7

#	Article	IF	Citations
31263	Thermodynamic Stability of BiFeO₃ (0001) Surfaces from ab Initio Theory. ACS Applied Materials & Interfaces, 2017, 9, 3168-3177.	4.0	31
31264	Catalytic selectivity of Rh/TiO₂catalyst in syngas conversion to ethanol: probing into the mechanism and functions of TiO₂support and promoter. Catalysis Science and Technology, 2017, 7, 1073-1085.	2.1	31
31265	Onset potentials for different reaction mechanisms of nitrogen activation to ammonia on transition metal nitride electro-catalysts. Catalysis Today, 2017, 286, 69-77.	2.2	164
31266	Controlled Growth of Ceria Nanoarrays on Anatase Titania Powder: A Bottom-up Physical Picture. Nano Letters, 2017, 17, 348-354.	4.5	29
31267	The work function of few-layer graphene. Journal of Physics Condensed Matter, 2017, 29, 035003.	0.7	56
31268	From Activeâ€Site Models to Real Catalysts: Importance of the Material Gap in the Design of Pd Catalysts for Methane Oxidation. ChemCatChem, 2017, 9, 1594-1600.	1.8	15
31269	Induced magnetism in transition metal-doped 1T-ZrS2. Journal of Alloys and Compounds, 2017, 695, 2048-2053.	2.8	27
31270	Magnetic Structures of Heterometallic M(II)â€“M(III) Formate Compounds. Inorganic Chemistry, 2017, 56, 197-207.	1.9	33
31271	Machine Learning Force Fields: Construction, Validation, and Outlook. Journal of Physical Chemistry C, 2017, 121, 511-522.	1.5	368
31272	van der Waals Stacking-Induced Topological Phase Transition in Layered Ternary Transition Metal Chalcogenides. Nano Letters, 2017, 17, 467-475.	4.5	67
31273	Tailoring the Edge Structure of Molybdenum Disulfide toward Electrocatalytic Reduction of Carbon Dioxide. ACS Nano, 2017, 11, 453-460.	7.3	208
31274	Li-ion site disorder driven superionic conductivity in solid electrolytes: a first-principles investigation of Î²-Li₃PS₄. Journal of Materials Chemistry A, 2017, 5, 1153-1159.	5.2	50
31275	Dramatically enhanced thermoelectric performance of MoS₂ by introducing MoO₂ nanoinclusions. Journal of Materials Chemistry A, 2017, 5, 2004-2011.	5.2	66
31276	Carbon adsorption on and diffusion through the Fe(110) surface and in bulk: Developing a new strategy for the use of empirical potentials in complex material setâ€ups. Physica Status Solidi (B): Basic Research, 2017, 254, 1600408.	0.7	15
31277	Hydrodeoxygenation of acrylic acid using Mo2C/Al2O3. Applied Catalysis A: General, 2017, 531, 69-78.	2.2	22
31278	Mechanistic study for enhanced CO oxidation activity on (Mn,Fe) co-doped CeO 2 (111). Catalysis Today, 2017, 293-294, 82-88.	2.2	32
31279	New insight of the Mars-van Krevelen mechanism of the CO oxidation by gold catalyst on the ZnO(101) surface. Computational and Theoretical Chemistry, 2017, 1100, 28-33.	1.1	7
31280	Electronic and vibrational properties of transition metal-oxides: Comparison of GGA, GGA + U, and hybrid approaches. Chemical Physics Letters, 2017, 669, 1-8.	1.2	19

#	Article	IF	Citations
31281	Atomic and Local Electronic Structures of Ca₂AlMnO_{5+Î´} as an Oxygen Storage Material. Chemistry of Materials, 2017, 29, 648-655.	3.2	12
31282	Lattice thermal conductivities and thermoelectric performances of binary tin-based sheets: A computational study. Applied Surface Science, 2017, 396, 1164-1169.	3.1	6
31283	The role of strain on the quantum spin hall effect and band inversion in stanene. Computational Condensed Matter, 2017, 10, 1-9.	0.9	2
31284	Theoretical study on the electronic structure properties of a PbS quantum dot adsorbed on TiO2 substrates and their role on solid-state devices. Computational and Theoretical Chemistry, 2017, 1100, 83-90.	1.1	0
31285	A first-principles study of Sc-decorated graphene with pyridinic-N defects for hydrogen storage. International Journal of Hydrogen Energy, 2017, 42, 3106-3113.	3.8	47
31286	Experimental and theoretical assessment of the mechanism and site requirements for ketonization of carboxylic acids on oxides. Journal of Catalysis, 2017, 345, 183-206.	3.1	95
31287	First-principles investigation of the energetics of point defects at a grain boundary in tungsten. Nuclear Instruments & Methods in Physics Research B, 2017, 393, 144-149.	0.6	18
31288	Layered Structures and Disordered Polyanionic Nets in the Cation-Poor Polar Intermetallics CsAu1.4Ga2.8 and CsAu2Ga2.6. Crystal Growth and Design, 2017, 17, 693-700.	1.4	4
31289	Micro-kinetic simulations of the catalytic decomposition of hydrazine on the Cu(111) surface. Faraday Discussions, 2017, 197, 41-57.	1.6	14
31290	Room Temperature Electricâ€Field Control of Magnetism in Layered Oxides with Cation Order. Advanced Functional Materials, 2017, 27, 1604312.	7.8	22
31291	Dualâ€Functional N Dopants in Edges and Basal Plane of MoS₂ Nanosheets Toward Efficient and Durable Hydrogen Evolution. Advanced Energy Materials, 2017, 7, 1602086.	10.2	286
31292	The Role of Ruthenium on Carbonâ€Supported PtRu Catalysts for Electrocatalytic Glycerol Oxidation under Acidic Conditions. ChemCatChem, 2017, 9, 1683-1690.	1.8	56
31293	Calculations in Li-Ion Battery Materials. , 2017, , 313-328.		2
31294	PtPd alloy embedded in nitrogen-rich graphene nanopores: High-performance bifunctional electrocatalysts for hydrogen evolution and oxygen reduction. Carbon, 2017, 114, 740-748.	5.4	94
31295	Creating nanoporous graphene with swift heavy ions. Carbon, 2017, 114, 511-518.	5.4	52
31296	DFT study of the role of N- and B-doping on structural, elastic and electronic properties of Î±-, Î²- and Î³-graphyne. Carbon, 2017, 114, 301-310.	5.4	71
31297	The structures, stabilities, electronic and magnetic properties of fully and partially hydrogenated germanene nanoribbons: A first-principles investigation. Physica E: Low-Dimensional Systems and Nanostructures, 2017, 87, 27-36.	1.3	14
31298	Polyiodide-Doped Graphene. Journal of Physical Chemistry C, 2017, 121, 609-615.	1.5	23

#	Article	IF	Citations
31299	Symmetry, Dynamics, and Defects in Methylammonium Lead Halide Perovskites. Journal of Physical Chemistry Letters, 2017, 8, 61-66.	2.1	75
31300	BN-schwarzite: novel boron nitride spongy crystals. Physical Chemistry Chemical Physics, 2017, 19, 1167-1173.	1.3	8
31301	Reaction of CO, H₂O, H₂ and CO₂ on the clean as well as O, OH and H precovered Fe(100) and Fe(111) surfaces. Catalysis Science and Technology, 2017, 7, 427-440.	2.1	22
31302	Doping anatase TiO₂ with group V-b and VI-b transition metal atoms: a hybrid functional first-principles study. Physical Chemistry Chemical Physics, 2017, 19, 1945-1952.	1.3	21
31303	Alâ€Doped Black Phosphorus pâ€“n Homojunction Diode for High Performance Photovoltaic. Advanced Functional Materials, 2017, 27, 1604638.	7.8	145
31304	Well-defined linear Au n (nâ€‰=â€‰2â€“4) chains encapsulated in SWCNTs: a DFT study. Journal of Molecular Modeling, 2017, 23, 19.	0.8	0
31305	Interatomic potential that describes martensitic phase transformations in pure lithium. Computational Materials Science, 2017, 129, 202-210.	1.4	10
31306	A coupled experimental and thermodynamic study of the Al-Cr and Al-Cr-Mg systems. Journal of Alloys and Compounds, 2017, 698, 1038-1057.	2.8	26
31307	Highly active and stable single iron site confined in graphene nanosheets for oxygen reduction reaction. Nano Energy, 2017, 32, 353-358.	8.2	234
31308	Li₃Y(PS₄)₂ and Li₅PS₄Cl₂: New Lithium Superionic Conductors Predicted from Silver Thiophosphates using Efficiently Tiered Ab Initio Molecular Dynamics Simulations. Chemistry of Materials, 2017, 29, 2474-2484.	3.2	85
31309	Screening of Oxygen-Reduction-Reaction-Efficient Electrocatalysts Based on Agâ€“M (M = 3d, 4d, and 5d) Tj ETQq0 0 0 rgBT /Overlock 1 1874-1881.	2.5	13
31310	Self-Consistent-Charge Density-Functional Tight-Binding (SCC-DFTB) Parameters for Ceria in 0D to 3D. Journal of Physical Chemistry C, 2017, 121, 4593-4607.	1.5	21
31311	Understanding Size-Dependent Morphology Transition of Triangular MoS₂ Nanoclusters: The Role of Metal Substrate and Sulfur Chemical Potential. Journal of Physical Chemistry C, 2017, 121, 1809-1816.	1.5	11
31312	Ti3C2 MXene co-catalyst on metal sulfide photo-absorbers for enhanced visible-light photocatalytic hydrogen production. Nature Communications, 2017, 8, 13907.	5.8	1,496
31313	A niobium and tantalum co-doped perovskite cathode for solid oxide fuel cells operating below 500â€‰Â°C. Nature Communications, 2017, 8, 13990.	5.8	180
31314	Hydrogen diffusion into the subsurfaces of model metal catalysts from first principles. Physical Chemistry Chemical Physics, 2017, 19, 3557-3564.	1.3	21
31315	Promoting the oxygen reduction reaction with gold at step/edge sites of Ni@AuPt coreâ€“shell nanoparticles. Catalysis Science and Technology, 2017, 7, 596-606.	2.1	27
31316	Stability and electronic properties of two-dimensional indium iodide. Physical Review B, 2017, 95, .	1.1	10

#	Article	IF	Citations
31317	A Simple Ansatz to Predict the Structure of Li₄Ti₅O₁₂. Journal of the Electrochemical Society, 2017, 164, A221-A225.	1.3	13
31318	Onâ€Surface Dualâ€Response Structural Transformations of Guanine Molecules and Fe Atoms. Chemistry - A European Journal, 2017, 23, 2356-2362.	1.7	16
31319	Predicting core level binding energies shifts: Suitability of the projector augmented wave approach as implemented in VASP. Journal of Computational Chemistry, 2017, 38, 518-522.	1.5	47
31320	Dataset on the structure and thermodynamic and dynamic stability of Mo 2 ScAlC 2 from experiments and first-principles calculations. Data in Brief, 2017, 10, 576-582.	0.5	3
31321	Dynamic Fluctuation of U³⁺ Coordination Structure in the Molten LiClâ€“KCl Eutectic via First Principles Molecular Dynamics Simulations. Journal of Physical Chemistry A, 2017, 121, 571-578.	1.1	41
31322	Low Density of Conduction and Valence Band States Contribute to the High Open-Circuit Voltage in Perovskite Solar Cells. Journal of Physical Chemistry C, 2017, 121, 1455-1462.	1.5	57
31323	Stability of Sulfur Nitrides: A First-Principles Study. Journal of Physical Chemistry C, 2017, 121, 1515-1520.	1.5	30
31324	The Role of Intrinsic Defects in Electrocatalytic Activity of Monolayer VS₂ Basal Planes for the Hydrogen Evolution Reaction. Journal of Physical Chemistry C, 2017, 121, 1530-1536.	1.5	93
31325	ZnTe Alloying Effect on Enhanced Thermoelectric Properties of p-Type PbTe. ACS Applied Materials & Interfaces, 2017, 9, 3766-3773.	4.0	23
31326	Adsorbing the 3d-transition metal atoms to effectively modulate the electronic and magnetic behaviors of zigzag SiC nanoribbons. Physical Chemistry Chemical Physics, 2017, 19, 3694-3705.	1.3	9
31327	Water-gas-shift reaction on reduced gold-substituted Ce1âˆ’xO2(111) surfaces: the role of Au charge. Physical Chemistry Chemical Physics, 2017, 19, 2201-2206.	1.3	10
31328	Two-dimensional C₁₂Mn₂/C₁₂Cr₂ as a room-temperature half metal/antiferromagnetic semiconductor: a systematic study. Physical Chemistry Chemical Physics, 2017, 19, 3394-3404.	1.3	4
31329	Ultrahigh energy storage and ultrafast ion diffusion in borophene-based anodes for rechargeable metal ion batteries. Journal of Materials Chemistry A, 2017, 5, 2328-2338.	5.2	134
31330	Intrinsic localized mode and low thermal conductivity of PbSe. Physical Review B, 2017, 95, .	1.1	84
31331	Two-dimensional lateral GaN/SiC heterostructures: First-principles studies of electronic and magnetic properties. Physical Review B, 2017, 95, .	1.1	22
31332	Stripe and Short Range Order in the Charge Density Wave of <mml:math xmlns:mml="http://www.w3.org/1998/Math/MathML" display="inline"><mml:mrow><mml:mn>1</mml:mn><mml:mi>T</mml:mi><mml:mtext>âˆ’</mml:mtext><mml:msub><mml:mrow><m Physical Review Letters, 2017, 118, 017002.	2.0	49
31333	Interface Engineered W_xC@WS₂ Nanostructure for Enhanced Hydrogen Evolution Catalysis. Advanced Functional Materials, 2017, 27, 1605802.	7.8	122
31334	Catalytic conversion of ethanol to 1,3-butadiene on MgO: A comprehensive mechanism elucidation using DFT calculations. Journal of Catalysis, 2017, 346, 78-91.	3.1	70

#	Article	IF	Citations
31335	Si/Fe flux ratio influence on growth and physical properties of polycrystalline Î²-FeSi2 thin films on Si(100) surface. Journal of Magnetism and Magnetic Materials, 2017, 440, 144-152.	1.0	17
31336	First-principles calculations on the structural and electronic properties of cubic KCaF 3 and NaCaF 3 (001) surfaces. Physics Letters, Section A: General, Atomic and Solid State Physics, 2017, 381, 890-895.	0.9	11
31337	Impact of Vacancies on the Mechanical Properties of Ultraincompressible, Hard Rhenium Subnitrides: Re₂N and Re₃N. Chemistry of Materials, 2017, 29, 2542-2549.	3.2	17
31338	Structural Stabilities and Electronic Properties of High-Angle Grain Boundaries in Perovskite Cesium Lead Halides. Journal of Physical Chemistry C, 2017, 121, 1715-1722.	1.5	99
31339	Ultra-high capacity hydrogen storage in a Li decorated two-dimensional C₂N layer. Journal of Materials Chemistry A, 2017, 5, 2821-2828.	5.2	127
31340	Influence of heavy metal materials on magnetic properties of Pt/Co/heavy metal tri-layered structures. Applied Physics Letters, 2017, 110, .	1.5	26
31341	Microstructure, mechanical and corrosion behaviors of AlCoCuFeNi-(Cr,Ti) high entropy alloys. Materials and Design, 2017, 116, 438-447.	3.3	167
31342	Determination of Krypton Diffusion Coefficients in Uranium Dioxide Using Atomic Scale Calculations. Inorganic Chemistry, 2017, 56, 125-137.	1.9	30
31343	First-principles modeling of metal (ii) ferrocyanide: electronic property, magnetism, bulk moduli, and the role of Câ€‰â€‰â‰¡â€‰â€‰N^{â^'}defect. Journal Physics D: Applied Physics, 2017, 50, 035004.	1.3	3
31344	AlN/BP Heterostructure Photocatalyst for Water Splitting. IEEE Electron Device Letters, 2017, 38, 145-148.	2.2	68
31345	Twoâ€Dimensional Singleâ€Layer Organicâ€“Inorganic Hybrid Perovskite Semiconductors. Advanced Energy Materials, 2017, 7, 1601731.	10.2	93
31346	Unveiling the Unique Phase Transformation Behavior and Sodiation Kinetics of 1D van der Waals Sb₂S₃ Anodes for Sodium Ion Batteries. Advanced Energy Materials, 2017, 7, 1602149.	10.2	152
31347	Experimental and DFT high pressure study of fluorinated graphite (C2F)n. Carbon, 2017, 114, 690-699.	5.4	20
31348	Band structure diagram paths based on crystallography. Computational Materials Science, 2017, 128, 140-184.	1.4	457
31349	A first-principle study of the structural, elastic, lattice dynamical and thermodynamic properties of <mml:math xmlns:mml="http://www.w3.org/1998/Math/MathML" altimg="si4.gif" overflow="scroll"><mml:mrow><mml:msup><mml:mrow><mml:mi>Î±</mml:mi></mml:mrow><mml:mrow><mml:mo>â€³</mml:mo><mathvariant="italic">Fe</mml:mi></mml:mrow><mml:mrow><mml:mn>16</mml:mn></mml:mrow></mml:msub><mml:msub><mml:m Computational Materials Science, 2017, 128, 278-286.	1.4	19
31350	Atomic self-diffusion anisotropy of HCP metals from first-principles calculations. Computational Materials Science, 2017, 128, 236-242.	1.4	12
31351	CPA descriptions of random Cu-Au alloys in comparison with SQS approach. Computational Materials Science, 2017, 128, 302-309.	1.4	21
31352	Crystal structure and bonding characteristics of transformation products of bcc Î² in Ti-Mo alloys. Journal of Alloys and Compounds, 2017, 705, 769-781.	2.8	25

#	Article	IF	Citations
31353	Canted Antiferromagnetism in Two-Dimensional Silver(II) Bis[pentafluoridooxidotungstate(VI)]. Inorganic Chemistry, 2017, 56, 224-233.	1.9	10
31354	Activation of surface oxygen sites on an iridium-based model catalyst for the oxygen evolution reaction. Nature Energy, 2017, 2, .	19.8	435
31355	Electrolyte-controlled discharge product distribution of Naâ€“O₂batteries: a combined computational and experimental study. Physical Chemistry Chemical Physics, 2017, 19, 2940-2949.	1.3	14
31356	Solution-based synthesis and processing of Sn- and Bi-doped Cu₃SbSe₄nanocrystals, nanomaterials and ring-shaped thermoelectric generators. Journal of Materials Chemistry A, 2017, 5, 2592-2602.	5.2	73
31357	Anisotropic intrinsic lattice thermal conductivity of borophane from first-principles calculations. Physical Chemistry Chemical Physics, 2017, 19, 2843-2849.	1.3	40
31358	Electronic and optical properties of oxygen vacancies in amorphous Ta₂O₅from first principles. Nanoscale, 2017, 9, 1120-1127.	2.8	45
31359	How covalence breaks adsorption-energy scaling relations and solvation restores them. Chemical Science, 2017, 8, 124-130.	3.7	145
31360	Band alignment of two-dimensional lateral heterostructures. 2D Materials, 2017, 4, 015038.	2.0	80
31361	Ferromagnetism at Room Temperature Induced by Spin Structure Change in BiFe_{1â^'}_xCo_xO₃ Thin Films. Advanced Materials, 2017, 29, 1603131.	11.1	45
31362	The synergetic effect of V and Fe-co-doping in TiO 2 studied from the DFT + U first-principle calculation. Applied Surface Science, 2017, 399, 654-662.	3.1	43
31363	A comparison of Redlich-Kister polynomial and cubic spline representations of the chemical potential in phase field computations. Computational Materials Science, 2017, 128, 127-139.	1.4	17
31364	Effect of temperature and branching on the nature and stability of alkene cracking intermediates in H-ZSM-5. Journal of Catalysis, 2017, 345, 53-69.	3.1	92
31365	DFT investigation of electronic structures and magnetic properties of halides family MeHal3 (Me=Ti,) Tj ETQq0 0 0 rgBT /Overlock 10 Tf 2017, 440, 93-96.	1.0	4
31366	Prediction of a Mobile Solid State in Dense Hydrogen under High Pressures. Journal of Physical Chemistry Letters, 2017, 8, 223-228.	2.1	12
31367	Partial-Redox-Promoted Mn Cycling of Mn(II)-Doped Heterogeneous Catalyst for Efficient H₂O₂-Mediated Oxidation. ACS Applied Materials & Interfaces, 2017, 9, 371-380.	4.0	31
31368	Support Effects in Single-Atom Platinum Catalysts for Electrochemical Oxygen Reduction. ACS Catalysis, 2017, 7, 1301-1307.	5.5	363
31369	Sm³⁺ and Eu³⁺ codoped SrBi₂B₂O₇: a red-emitting phosphor with improved thermal stability. RSC Advances, 2017, 7, 1146-1153.	1.7	43
31370	Quasimolecules in Compressed Lithium. Angewandte Chemie - International Edition, 2017, 56, 972-975.	7.2	32

#	Article	IF	Citations
31371	First principles modeling and simulation of Zr-Si-B-C-N ceramics: Developing hard and oxidation resistant coatings. Acta Materialia, 2017, 125, 246-254.	3.8	12
31372	Molecular and dissociative adsorption of water at a defective Cu(110) surface. Surface Science, 2017, 658, 1-8.	0.8	15
31373	GeSe Thin-Film Solar Cells Fabricated by Self-Regulated Rapid Thermal Sublimation. Journal of the American Chemical Society, 2017, 139, 958-965.	6.6	238
31374	First-principles study of thermal transport in nitrogenated holey graphene. Nanotechnology, 2017, 28, 045709.	1.3	29
31375	The Role of Surfactants in the Stability of NiO Nanofluids: An Experimental and DFT Study. ChemPhysChem, 2017, 18, 346-356.	1.0	8
31376	Defect character at grain boundary facet junctions: Analysis of an asymmetric Î£Â=Â5 grain boundary in Fe. Acta Materialia, 2017, 124, 383-396.	3.8	49
31377	High-Throughput Screening of Extrinsic Point Defect Properties in Si and Ge: Database and Applications. Chemistry of Materials, 2017, 29, 975-984.	3.2	10
31378	Strain-Enhanced Oxygen Dynamics and Redox Reversibility in Topotactic SrCoO_{3-Î´} (0 < Î´ â‰¤) Tj ETQq1 1 0.784314 rg	3.2	49
31379	Electric-Field Switchable Second-Harmonic Generation in Bilayer MoS₂ by Inversion Symmetry Breaking. Nano Letters, 2017, 17, 392-398.	4.5	71
31380	Electronic properties of layered phosphorus heterostructures. Physical Chemistry Chemical Physics, 2017, 19, 1229-1235.	1.3	10
31381	New insights into the stability and structural evolution of some gold nanoclusters. Nanoscale, 2017, 9, 856-861.	2.8	15
31382	Î´-Phosphorene: a two dimensional material with a highly negative Poisson's ratio. Nanoscale, 2017, 9, 850-855.	2.8	150
31383	Passivation of Black Phosphorus via Selfâ€Assembled Organic Monolayers by van der Waals Epitaxy. Advanced Materials, 2017, 29, 1603990.	11.1	113
31384	The Influence of Isomer Purity on Trap States and Performance of Organic Thinâ€Film Transistors. Advanced Electronic Materials, 2017, 3, 1600294.	2.6	37
31385	The Interplay of Long Range Interactions and Electron Density Distributions in Polar and Strongly Correlated Materials. Journal of Superconductivity and Novel Magnetism, 2017, 30, 91-96.	0.8	4
31386	Aluminum nitride nanotubes. Chemical Papers, 2017, 71, 881-893.	1.0	51
31387	Synergistic Effect of Alloying Atoms on Intrinsic Stacking-Fault Energy in Austenitic Steels. Acta Metallurgica Sinica (English Letters), 2017, 30, 272-279.	1.5	7
31388	Breaking surface states causes transformation from metallic to semi-conducting behavior in carbon foam nanowires. Carbon, 2017, 111, 867-877.	5.4	20

#	Article	IF	Citations
31389	Origin of Blue-Green Emission in Î±-Zn₂P₂O₇ and Local Structure of Ln³⁺ Ion in Î±-Zn₂P₂O₇:Ln³⁺ (Ln = Sm,) Tj ETQq0 0 0 rgBT /Overloc 167-178.	1.9	53
31390	Al₂O₃ Surface Complexation for Photocatalytic Organic Transformations. Journal of the American Chemical Society, 2017, 139, 269-276.	6.6	64
31391	Structure, fragmentation patterns, and magnetic properties of small nickel oxide clusters. Physical Chemistry Chemical Physics, 2017, 19, 3366-3383.	1.3	12
31392	Second-order nonlinear optical properties of bulk GeC polytypes, g-GeC and corresponding nanotubes: first-principles calculations. Physical Chemistry Chemical Physics, 2017, 19, 2235-2244.	1.3	17
31393	Physical and chemical properties of Cu(<scp>i</scp>) compounds with O and/or H. Dalton Transactions, 2017, 46, 529-538.	1.6	9
31394	Adsorption and dehydrogenation of ethane, propane and butane on Rh13 clusters supported on unzipped graphene oxide and TiO2(110) â€“ a DFT study. Physical Chemistry Chemical Physics, 2017, 19, 4989-4996.	1.3	11
31395	Electronic structures and transport properties of a MoS₂â€“NbS₂ nanoribbon lateral heterostructure. Physical Chemistry Chemical Physics, 2017, 19, 1303-1310.	1.3	30
31396	Searching for promising new perovskite-based photovoltaic absorbers: the importance of electronic dimensionality. Materials Horizons, 2017, 4, 206-216.	6.4	553
31397	Competing antiferromagnetism in a quasi-2D itinerant ferromagnet: Fe ₃ GeTe ₂. 2D Materials, 2017, 4, 011005.	2.0	123
31398	Double Nanoporous Structure with Nanoporous PtFe Embedded in Graphene Nanopores: Highly Efficient Bifunctional Electrocatalysts for Hydrogen Evolution and Oxygen Reduction. Advanced Materials Interfaces, 2017, 4, 1601029.	1.9	36
31399	Characteristics of Interlayer Tunneling Field-Effect Transistors Computed by a â€œDFT-Bardeenâ€•Method. Journal of Electronic Materials, 2017, 46, 1378-1389.	1.0	5
31400	Dioxygen molecule adsorption and oxygen atom diffusion on clean and defective aluminum(111) surface using first principles calculations. Surface Science, 2017, 657, 79-89.	0.8	16
31401	First-Principles Modeling of Mn(II) Migration above and Dissolution from Li_xMn₂O₄ (001) Surfaces. Chemistry of Materials, 2017, 29, 2550-2562.	3.2	87
31402	On the Preferred Active Sites of Promoted MoS₂ for Hydrodesulfurization with Minimal Organonitrogen Inhibition. ACS Catalysis, 2017, 7, 501-509.	5.5	78
31403	What will freestanding borophene nanoribbons look like? An analysis of their possible structures, magnetism and transport properties. Physical Chemistry Chemical Physics, 2017, 19, 1054-1061.	1.3	32
31404	Mechanism of coverage dependent CO adsorption and dissociation on the Mo(100) surface. Physical Chemistry Chemical Physics, 2017, 19, 2186-2192.	1.3	11
31405	Magnetic moment and spin state transition on rare monovalent iron ion in nitridoferrate Ca₆Li_{0.5}Fe_{0.5}Te₂N₃. Journal of Materials Chemistry C, 2017, 5, 733-737.	2.7	1
31406	Effect of cation dopants in zirconia on interfacial properties in nickel/zirconia systems: an atomistic modeling study. Journal of Physics Condensed Matter, 2017, 29, 045001.	0.7	5

#	Article	IF	Citations
31407	First-principles study of the mechanism of wettability transition of defective graphene. Nanotechnology, 2017, 28, 064003.	1.3	11
31408	Hybrid Palladium Nanoparticles for Direct Hydrogen Peroxide Synthesis: The Key Role of the Ligand. Angewandte Chemie, 2017, 129, 1801-1805.	1.6	36
31409	Hybrid Palladium Nanoparticles for Direct Hydrogen Peroxide Synthesis: The Key Role of the Ligand. Angewandte Chemie - International Edition, 2017, 56, 1775-1779.	7.2	78
31410	Electronic structure of the Heusler compound Fe₂VAl and its point defects by ab initio calculations. Physica Status Solidi (B): Basic Research, 2017, 254, 1600441.	0.7	26
31411	Structural, electronic and optical properties of famatinite and enargite Cu₃SbS₄ under pressure: A theoretical investigation. Physica Status Solidi (B): Basic Research, 2017, 254, 1600608.	0.7	6
31412	First-principles and thermodynamic analysis of trimethylgallium (TMG) decomposition during MOVPE growth of GaN. Journal of Crystal Growth, 2017, 468, 950-953.	0.7	8
31413	Modeling the Photochromism of S-Doped Sodalites Using DFT, TD-DFT, and SAC-CI Methods. Inorganic Chemistry, 2017, 56, 414-423.	1.9	18
31414	Structural, elastic, electronic, and optical properties of the tricycle-like phosphorene. Physical Chemistry Chemical Physics, 2017, 19, 2245-2251.	1.3	42
31415	New insight into the structural evolution of PbTiO₃: an unbiased structure search. Physical Chemistry Chemical Physics, 2017, 19, 1420-1424.	1.3	5
31416	Tracking motion trajectories of individual nanoparticles using time-resolved current traces. Chemical Science, 2017, 8, 1854-1861.	3.7	127
31417	Formation and migration of hydride ions in BaTiO_{3â˜'x}H_x oxyhydride. Journal of Materials Chemistry A, 2017, 5, 1050-1056.	5.2	28
31418	Defect chemistry and enhancement of thermoelectric performance in Ag-doped Sn_{1+Î´â˜'x}Ag_xTe. Journal of Materials Chemistry A, 2017, 5, 2235-2242.	5.2	54
31419	Negative thermal expansion in 2H CuScO₂ originating from the cooperation of transverse thermal vibrations of Cu and O atoms. Physical Chemistry Chemical Physics, 2017, 19, 2067-2072.	1.3	11
31420	Surface functionalization of molybdenum dinitride nanosheets by halogen and alkali atoms: a first-principles study. Journal of Materials Chemistry C, 2017, 5, 683-689.	2.7	10
31421	On-Surface Synthesis and Characterization of Honeycombene Oligophenylene Macrocycles. ACS Nano, 2017, 11, 134-143.	7.3	39
31422	Room-temperature ferromagnetism in the two-dimensional layered Cu₂MoS₄ nanosheets. Physical Chemistry Chemical Physics, 2017, 19, 1735-1739.	1.3	12
31423	Computational search for two-dimensional intrinsic half-metals in transition-metal dinitrides. Journal of Materials Chemistry C, 2017, 5, 727-732.	2.7	61
31424	Bonding Structures of ZrH_x Thin Films by X-ray Spectroscopy. Journal of Physical Chemistry C, 2017, 121, 25750-25758.	1.5	16

#	Article	IF	Citations
31425	Visualizing Type-II Weyl Points in Tungsten Ditelluride by Quasiparticle Interference. ACS Nano, 2017, 11, 11459-11465.	7.3	37
31426	Activating MoS₂ for pH-Universal Hydrogen Evolution Catalysis. Journal of the American Chemical Society, 2017, 139, 16194-16200.	6.6	164
31427	Multifaceted Modularity: A Key for Stepwise Building of Hierarchical Complexity in Actinide Metalâ€“Organic Frameworks. Journal of the American Chemical Society, 2017, 139, 16852-16861.	6.6	107
31428	Two-dimensional transition-metal dichalcogenides-based ferromagnetic van der Waals heterostructures. Nanoscale, 2017, 9, 17585-17592.	2.8	53
31429	Space-confinement and chemisorption co-involved in encapsulation of sulfur for lithiumâ€“sulfur batteries with exceptional cycling stability. Journal of Materials Chemistry A, 2017, 5, 24602-24611.	5.2	24
31430	Petascale supercomputing to accelerate the design of high-temperature alloys. Science and Technology of Advanced Materials, 2017, 18, 828-838.	2.8	17
31431	Impact of Transition Metal Cations on the 29Si NMR Signal in Metal Oxide Glasses: A DFT Case Study of Hafnia Silica Glass. Journal of Physical Chemistry C, 2017, 121, 24152-24158.	1.5	3
31432	Structural and Electronic Features of Nb-Doped SrCoO₃: Insight from First-Principles Calculations. Journal of Physical Chemistry C, 2017, 121, 24987-24993.	1.5	4
31433	Unraveling the Mechanism of the Initiation Reaction of the Methanol to Olefins Process Using ab Initio and DFT Calculations. ACS Catalysis, 2017, 7, 7987-7994.	5.5	118
31434	Control of Fullerene Crystallization from 2D to 3D through Combined Solvent and Template Effects. Journal of the American Chemical Society, 2017, 139, 16732-16740.	6.6	35
31435	Tuning methane decomposition on stepped Ni surface: The role of subsurface atoms in catalyst design. Scientific Reports, 2017, 7, 13963.	1.6	41
31436	Interaction of solid and polymeric lithium electrolytes with composites based on carbon fibers and silicon nanoclusters: Quantum-chemical modeling. Russian Journal of Inorganic Chemistry, 2017, 62, 1360-1365.	0.3	3
31437	Origin of ferromagnetism in Cu doped rutile TiO 2 - An ab-initio approach. Computational Condensed Matter, 2017, 13, 127-130.	0.9	21
31438	Hydrogen adsorption, dissociation and diffusion on two-dimensional Ti2C monolayer. International Journal of Hydrogen Energy, 2017, 42, 27214-27219.	3.8	27
31439	Promising thermoelectric performance in van der Waals layered SnSe2. Materials Today Physics, 2017, 3, 127-136.	2.9	95
31440	C₂ Oxygenate Synthesis via Fischerâ€“Tropsch Synthesis on Co₂C and Co/Co₂C Interface Catalysts: How To Control the Catalyst Crystal Facet for Optimal Selectivity. ACS Catalysis, 2017, 7, 8285-8295.	5.5	81
31441	Entropies of defect association in ceria from first principles. Physical Chemistry Chemical Physics, 2017, 19, 29625-29628.	1.3	3
31442	Potential of transition metal atoms embedded in buckled monolayer g-C₃N₄ as single-atom catalysts. Physical Chemistry Chemical Physics, 2017, 19, 30069-30077.	1.3	78

#	Article	IF	Citations
31443	Design of new photovoltaic systems based on two-dimensional group-IV monochalcogenides for high performance solar cells. Journal of Materials Chemistry A, 2017, 5, 24145-24152.	5.2	64
31444	Seeking the Dirac cones in the MoS2/WSe2 van der Waals heterostructure. Applied Physics Letters, 2017, 111, 171602.	1.5	31
31445	Stability and carrier mobility of organic-inorganic hybrid perovskite CH3NH3PbI3 in two-dimensional limit. Journal of Chemical Physics, 2017, 147, 164703.	1.2	16
31446	First-Principles Research on the Structural and Electric Properties of the Graphene-Like Alkali-Metal Absorbed InSe-M. IOP Conference Series: Materials Science and Engineering, 2017, 250, 012018.	0.3	0
31447	Electronic Structure of the Metastable Epitaxial Rock-Salt SnSe <mml:math xmlns:mml="http://www.w3.org/1998/Math/MathML" display="inline"><mml:mrow><mml:mo stretchy="false">{</mml:mo><mml:mn>111</mml:mn><mml:mo stretchy="false">}</mml:mo></mml:mrow></mml:math> Topological Crystalline Insulator. Physical Review X, 2017, 7, .	2.8	17
31448	Experimental and Theoretical Investigation of the Anti-Ferromagnetic Coupling of Cr^{III} Ions through Diamagnetic â”Oâ€“Nb^Vâ€“Oâ€“ Bridges. Inorganic Chemistry, 2017, 56, 6879-6889.	1.9	16
31449	Prediction of topological crystalline insulators and topological phase transitions in two-dimensional PbTe films. Physical Chemistry Chemical Physics, 2017, 19, 29647-29652.	1.3	8
31450	A two-dimensional TiB₄monolayer exhibits planar octacoordinate Ti. Nanoscale, 2017, 9, 17983-17990.	2.8	50
31451	Evolution of hydrogen by few-layered black phosphorus under visible illumination. Journal of Materials Chemistry A, 2017, 5, 24874-24879.	5.2	45
31452	Spin transport through a junction entirely consisting of molecules from first principles. Applied Physics Letters, 2017, 111, .	1.5	18
31453	Exploring the Crystal Structure Space of CoFe₂P by Using Adaptive Genetic Algorithm Methods. IEEE Transactions on Magnetics, 2017, 53, 1-5.	1.2	3
31454	Thermodynamic modeling of phase equilibria and defect chemistry in the Zn-S system. Calphad: Computer Coupling of Phase Diagrams and Thermochemistry, 2017, 59, 171-181.	0.7	8
31455	Ultrahigh power factors in P-type 1T-ZrX2 (Xâ€¯=â€¯S, Se) single layers. Science Bulletin, 2017, 62, 1530-1537.	4.3	25
31456	Role of Point Defects in Spinel Mg Chalcogenide Conductors. Chemistry of Materials, 2017, 29, 9657-9667.	3.2	56
31457	Competitive Adsorption-Assisted Formation of One-Dimensional Cobalt Nanochains with High CO Hydrogenation Activity. Journal of Physical Chemistry C, 2017, 121, 24588-24593.	1.5	8
31458	Distorted Carbon Nitride Structure with Substituted Benzene Moieties for Enhanced Visible Light Photocatalytic Activities. ACS Applied Materials & Interfaces, 2017, 9, 40360-40368.	4.0	80
31459	Mechanocaloric effects in superionic thin films from atomistic simulations. Nature Communications, 2017, 8, 963.	5.8	47
31460	First-principles study of the high-pressure behavior of crystalline benzoic acid. International Journal of Modern Physics C, 2017, 28, 1750125.	0.8	6

#	Article	IF	Citations
31461	Dependence of the constitution, microstructure and electrochemical behaviour of magnetron sputtered Liâ€“Niâ€“Mnâ€“Coâ€“O thin film cathodes for lithium-ion batteries on the working gas pressure and annealing conditions. International Journal of Materials Research, 2017, 108, 879-886.	0.1	3
31462	Computational Design of Perovskite Ba_xSr_{1â€“x}SnO₃ Alloys as Transparent Conductors and Photocatalysts. Journal of Physical Chemistry C, 2017, 121, 26446-26456.	1.5	14
31463	Promising Approach for High-Performance MoS₂ Nanodevice: Doping the BN Buffer Layer to Eliminate the Schottky Barriers. ACS Applied Materials & Interfaces, 2017, 9, 40940-40948.	4.0	22
31464	High-throughput DFT calculations of formation energy, stability and oxygen vacancy formation energy of ABO3 perovskites. Scientific Data, 2017, 4, 170153.	2.4	259
31465	Spin-dependent electron transport in C and Ge doped BN monolayers. Physical Chemistry Chemical Physics, 2017, 19, 30370-30380.	1.3	7
31466	First-principles calculation of the structure and electronic properties of Fe-substituted Bi₂Ti₂O₇. Semiconductor Science and Technology, 2017, 32, 125007.	1.0	7
31467	The structural, magnetic and electronic properties of p-type and n-type doped monolayer WS 2 systems. Superlattices and Microstructures, 2017, 112, 619-627.	1.4	14
31468	Construction of Novel Cyclic Tetrads by Axial Coordination of Thiaporphyrins to Tin(IV) Porphyrin. Inorganic Chemistry, 2017, 56, 13913-13929.	1.9	4
31469	Stretching Epitaxial La_{0.6}Sr_{0.4}CoO_{3â^Î´} for Fast Oxygen Reduction. Journal of Physical Chemistry C, 2017, 121, 25651-25658.	1.5	38
31470	The Role of Water in the Reversible Optoelectronic Degradation of Hybrid Perovskites at Low Pressure. Journal of Physical Chemistry C, 2017, 121, 25659-25665.	1.5	19
31471	Evolution of Graphene Growth on Pt(111): From Carbon Clusters to Nanoislands. Journal of Physical Chemistry C, 2017, 121, 25074-25078.	1.5	7
31472	Giant Piezoelectric Effects in Monolayer Group-V Binary Compounds with Honeycomb Phases: A First-Principles Prediction. Journal of Physical Chemistry C, 2017, 121, 25576-25584.	1.5	78
31473	Ab Initio Predictions of Hexagonal Zr(B,C,N) Polymorphs for Coherent Interface Design. Journal of Physical Chemistry C, 2017, 121, 26007-26018.	1.5	9
31474	Effect of Mn in Li₃V_{2â€“x}Mn_x(PO₄)₃ as High Capacity Cathodes for Lithium Batteries. ACS Applied Materials & Interfaces, 2017, 9, 40307-40316.	4.0	30
31475	Atmospheric pressure chemical vapor deposition of methylammonium bismuth iodide thin films. Journal of Materials Chemistry A, 2017, 5, 24728-24739.	5.2	41
31476	Effects of impurity adsorption on topological surface states of Bi 2 Te 3. Europhysics Letters, 2017, 119, 47001.	0.7	3
31477	First-principles investigation of Pd3Bi as a catalyst for the oxygen reduction reaction. International Journal of Hydrogen Energy, 2017, 42, 30359-30363.	3.8	4
31478	Experimental and theoretical assessment of the mechanism of hydrogen transfer in alkane-alkene coupling on solid acids. Journal of Catalysis, 2017, 354, 287-298.	3.1	7

#	Article	IF	Citations
31479	Effect of alloying elements on grain boundary sliding in magnesium binary alloys: Experimental and numerical studies. Materials Science & Engineering A: Structural Materials: Properties, Microstructure and Processing, 2017, 708, 267-273.	2.6	32
31480	Reversible conversion of MoS2 upon sodium extraction. Nano Energy, 2017, 41, 217-224.	8.2	60
31481	First-principles insight into the structural fundamental of super ionic conducting in NASICON MTi2(PO4)3 (M = Li, Na) materials for rechargeable batteries. Nano Energy, 2017, 41, 626-633.	8.2	67
31482	Role of metal impurity in hydrogen diffusion from surface into bulk magnesium: A theoretical study. Physics Letters, Section A: General, Atomic and Solid State Physics, 2017, 381, 3696-3700.	0.9	5
31483	Topological Dirac States beyond Ï€-Orbitals for Silicene on SiC(0001) Surface. Nano Letters, 2017, 17, 6195-6202.	4.5	36
31484	Degradation Mechanism of Dimethyl Carbonate (DMC) Dissociation on the LiCoO₂ Cathode Surface: A First-Principles Study. ACS Applied Materials & Interfaces, 2017, 9, 36377-36384.	4.0	10
31485	Spinel-Structured ZnCr₂O₄ with Excess Zn Is the Active ZnO/Cr₂O₃ Catalyst for High-Temperature Methanol Synthesis. ACS Catalysis, 2017, 7, 7610-7622.	5.5	109
31486	Enhancing the solar energy conversion efficiency of solution-deposited Bi₂S₃ thin films by annealing in sulfur vapor at elevated temperature. Sustainable Energy and Fuels, 2017, 1, 2134-2144.	2.5	25
31487	Strain and pH facilitated artificial photosynthesis in monolayer MoS₂ nanosheets. Journal of Materials Chemistry A, 2017, 5, 22265-22276.	5.2	40
31488	Hole polarons and p -type doping in boron nitride polymorphs. Physical Review B, 2017, 96, .	1.1	18
31489	Polaron-Driven Surface Reconstructions. Physical Review X, 2017, 7, .	2.8	32
31490	First-principles investigations of the electronic and magnetic structures and the bonding properties of uranium nitride fluoride (UNF). Zeitschrift Fur Naturforschung - Section B Journal of Chemical Sciences, 2017, 72, 725-730.	0.3	1
31491	Diverse carrier mobility of monolayer BNC_x: a combined density functional theory and Boltzmann transport theory study. Journal of Physics Condensed Matter, 2017, 29, 455305.	0.7	1
31492	Photoluminescence characterization of the grain boundary thermal stability in chemical vapor deposition grown WS₂. Materials Research Express, 2017, 4, 106202.	0.8	8
31493	Compressed tetragonal phase in XFe2As2 (X=Na , K, Rb, Cs) and in the alloy Na0.5K0.5Fe2As2. Physical Review B, 2017, 95, .	1.1	6
31494	Implications of the <mml:math xmlns:mml="http://www.w3.org/1998/Math/MathML"><mml:mrow><mml:mi mathvariant="normal">DFT</mml:mi><mml:mo>+</mml:mo><mml:mi>U</mml:mi></mml:mrow></mml:math> method on polaron properties in energy materials. Physical Review B, 2017, 96, .	1.1	30
31495	Identification of Distinct Copper Species in Cu-CHA Samples Using NO as Probe Molecule. A Combined IR Spectroscopic and DFT Study. Topics in Catalysis, 2017, 60, 1653-1663.	1.3	19
31496	Weak binding mode of CH 4 on rutile crystallites from density functional theory calculations. Computational and Theoretical Chemistry, 2017, 1121, 11-28.	1.1	3

#	Article	IF	Citations
31497	Introducing DDEC6 atomic population analysis: part 3. Comprehensive method to compute bond orders. RSC Advances, 2017, 7, 45552-45581.	1.7	327
31498	Insight into sulfur vacancy-induced insulator to metal transition of Li₂S. Functional Materials Letters, 2017, 10, 1750067.	0.7	19
31499	Level Alignment as Descriptor for Semiconductor/Catalyst Systems in Water Splitting: The Case of Hematite/Cobalt Hexacyanoferrate Photoanodes. ChemSusChem, 2017, 10, 4552-4560.	3.6	33
31500	Trends in Adsorption Energies of the Oxygenated Species on Single Platinum Atom Embedded in Carbon Nanotubes. Catalysis Letters, 2017, 147, 2689-2696.	1.4	10
31501	Screening Divalent Metals for A- and B-Site Dopants in LaFeO₃. Chemistry of Materials, 2017, 29, 8147-8157.	3.2	50
31502	Reconstruction of the Al₁₃Ru₄(010) Approximant Surface Leading to Anisotropic Molecular Adsorption. Journal of Physical Chemistry C, 2017, 121, 22067-22072.	1.5	3
31503	Interaction of Alkylamines with Cu Surfaces: A Metalâ€“Organic Many-Body Force Field. Journal of Physical Chemistry C, 2017, 121, 22531-22541.	1.5	24
31504	Flexible and Anisotropic Properties of Monolayer MX₂ (M = Tc and Re; X = S, Se). Journal of Physical Chemistry C, 2017, 121, 23744-23751.	1.5	35
31505	NanoVelcro: Theory of Guided Folding in Atomically Thin Sheets with Regions of Complementary Doping. Nano Letters, 2017, 17, 6708-6714.	4.5	8
31506	Rationally Designed Probe for Reversible Sensing of Zinc and Application in Cells. ACS Omega, 2017, 2, 6201-6210.	1.6	20
31507	Cs2AgBiBr6 single-crystal X-ray detectors with a low detection limit. Nature Photonics, 2017, 11, 726-732.	15.6	984
31508	A new layered titanate Na₂Li₂Ti₅O₁₂as a high-performance intercalation anode for sodium-ion batteries. Journal of Materials Chemistry A, 2017, 5, 22208-22215.	5.2	18
31509	Embedding for bulk systems using localized atomic orbitals. Journal of Chemical Physics, 2017, 147, 034110.	1.2	17
31510	Ab initio study of lattice instabilities of zinc chalcogenides ZnX (X=O, S, Se, Te) induced by ultrafast intense laser irradiation. AIP Advances, 2017, 7, 095021.	0.6	5
31511	Li-rich antiperovskite superionic conductors based on cluster ions. Proceedings of the National Academy of Sciences of the United States of America, 2017, 114, 11046-11051.	3.3	107
31512	Hydrostatic pressure effects on the structural, elastic and thermodynamic properties of the complex transition metal hydrides A₂OsH₆ (Aâ€‰=â€‰Mg, Ca, Sr and Ba). High Pressure Research, 2017, 37, 558-578.	0.4	13
31513	Topological crystalline antiferromagnetic state in tetragonal FeS. Physical Review B, 2017, 96, .	1.1	10
31514	Face-to-face crosslinking of graphdiyne and related carbon sheets toward integrated graphene nanoribbon arrays. Carbon, 2017, 125, 536-543.	5.4	19

#	Article	IF	Citations
31515	Benzene-like N₆rings in a Be₂N₆monolayer: a stable 2D semiconductor with high carrier mobility. Journal of Materials Chemistry C, 2017, 5, 11515-11521.	2.7	15
31516	First-principles study of Ga-vacancy induced magnetism in Î²-Ga₂O₃. Physical Chemistry Chemical Physics, 2017, 19, 28928-28935.	1.3	17
31517	Local structural distortions in strained <mml:math xmlns:mml="http://www.w3.org/1998/Math/MathML"><mml:mrow><mml:msub><mml:mi>Ba</mml:mi><mml:mrow><mml:mn>0.5</mml:mn> thin films. Physical Review B, 2017, 96, .	1.1	2
31518	Coupling of quantum well states and phonons in thin multilayer Pb films on Si(111). Physical Review B, 2017, 96, .	1.1	6
31519	Magnetic and structural properties of <mml:math xmlns:mml="http://www.w3.org/1998/Math/MathML"><mml:mrow><mml:mi>FeC</mml:mi><mml:msub><mml:mi mathvariant="normal">O</mml:mi><mml:mn>3</mml:mn></mml:msub></mml:mrow></mml:math> at high pressures. Physical Review B, 2017, 96, .	1.1	13
31520	Electrically Driven Reversible Phase Changes in Layered In₂Se₃ Crystalline Film. Advanced Materials, 2017, 29, 1703568.	11.1	77
31521	First-principles study of copper nanoclusters for enhanced electrochemical CO2 reduction to CH4. Computational and Theoretical Chemistry, 2017, 1120, 84-90.	1.1	25
31522	Metal Borohydrides as Electrolytes for Solid-State Li, Na, Mg, and Ca Batteries: A First-Principles Study. Chemistry of Materials, 2017, 29, 9308-9319.	3.2	115
31523	Effect of Molecular Guest Binding on the dâ€“d Transitions of Ni²⁺ of CPO-27-Ni: A Combined UVâ€“Vis, Resonant-Valence-to-Core X-ray Emission Spectroscopy, and Theoretical Study. Inorganic Chemistry, 2017, 56, 14408-14425.	1.9	22
31524	Thermoelectric properties of Se and Zn/Cd/Sn double substituted Co₄Sb₁₂ skutterudite compounds. Physical Chemistry Chemical Physics, 2017, 19, 28116-28126.	1.3	10
31525	Atom-scale dispersed palladium in a conductive Pd_{0.1}TaS₂ lattice with a unique electronic structure for efficient hydrogen evolution. Journal of Materials Chemistry A, 2017, 5, 22618-22624.	5.2	23
31526	First-principles study of helium clustering at initial stage in ThO 2. Chinese Physics B, 2017, 26, 097101.	0.7	5
31527	Structures and electronic properties of germanium-doped Ni n clusters, n = 13â€“23. Russian Journal of Physical Chemistry A, 2017, 91, 2180-2187.	0.1	0
31528	Theory and Neutrons Combine To Reveal a Family of Layered Perovskites without Inversion Symmetry. Chemistry of Materials, 2017, 29, 9489-9497.	3.2	36
31529	Hydrogen Evolution Reaction Catalyzed by Transition-Metal Nitrides. Journal of Physical Chemistry C, 2017, 121, 24036-24045.	1.5	108
31530	Remarkably Strong Chemisorption of Nitric Oxide on Insulating Oxide Films Promoted by Hybrid Structure. Journal of Physical Chemistry C, 2017, 121, 21482-21490.	1.5	10
31531	VS₂/Graphene Heterostructures as Promising Anode Material for Li-Ion Batteries. Journal of Physical Chemistry C, 2017, 121, 24179-24184.	1.5	73
31532	Optically and Electrically Controllable Adatom Spinâ€“orbital Dynamics in Transition Metal Dichalcogenides. Nano Letters, 2017, 17, 6721-6726.	4.5	4

#	Article	IF	Citations
31533	Cobalt Hexacyanoferrate on BiVO₄ Photoanodes for Robust Water Splitting. ACS Applied Materials & Interfaces, 2017, 9, 37671-37681.	4.0	109
31534	A₂MnXO₄ Family (A = Li, Na, Ag; X = Si, Ge): Structural and Magnetic Properties. Inorganic Chemistry, 2017, 56, 14023-14039.	1.9	19
31535	Partial Oxidation of Methane on Anatase and Rutile Defective TiO₂ Supported Rh₄ Cluster: A Density Functional Theory Study. Journal of Physical Chemistry C, 2017, 121, 26308-26320.	1.5	20
31536	Capture of Iodine Species in MIL-53(Al), MIL-120(Al), and HKUST-1(Cu) Periodic DFT and Ab-Initio Molecular Dynamics Studies. Journal of Physical Chemistry C, 2017, 121, 25283-25291.	1.5	26
31537	Complete Separation of Carriers in the GeS/SnS Lateral Heterostructure by Uniaxial Tensile Strain. ACS Applied Materials & Interfaces, 2017, 9, 40969-40977.	4.0	34
31538	Structureâ€“activity relationship of surface hydroxyl groups during NO₂ adsorption and transformation on TiO₂ nanoparticles. Environmental Science: Nano, 2017, 4, 2388-2394.	2.2	49
31539	Nonâ€Rareâ€Earth K₂XF₇:Mn⁴⁺ (X = Ta, Nb): A Highlyâ€Efficient Narrowâ€Band Red Phosphor Enabling the Application in Wideâ€Colorâ€Gamut LCD. Laser and Photonics Reviews, 2017, 11, 1700148.	4.4	120
31540	Structure and stability of hcp iron carbide precipitates: A first-principles study. Heliyon, 2017, 3, e00408.	1.4	6
31541	Enhanced Photoelectrochemical Water Oxidation Efficiency of CuWO₄ Photoanodes by Surface Modification with Ag₂NCN. Journal of Physical Chemistry C, 2017, 121, 26265-26274.	1.5	36
31542	Ultrathin Lanthanum Tantalate Perovskite Nanosheets Modified by Nitrogen Doping for Efficient Photocatalytic Water Splitting. ACS Nano, 2017, 11, 11441-11448.	7.3	96
31543	Universal Dynamics of Molecular Reorientation in Hybrid Lead Iodide Perovskites. Journal of the American Chemical Society, 2017, 139, 16875-16884.	6.6	129
31544	The role of Ï€-blocking hydride ligands in a pressure-induced insulator-to-metal phase transition in SrVO2H. Nature Communications, 2017, 8, 1217.	5.8	47
31545	Chemically induced large-gap quantum anomalous Hall insulator states in III-Bi honeycombs. Npj Computational Materials, 2017, 3, .	3.5	15
31546	Encapsulation of cathode in lithium-sulfur batteries with a novel two-dimensional carbon allotrope: DHP-graphene. Scientific Reports, 2017, 7, 14948.	1.6	32
31547	Investigating the crystal structures of alkali and alkaline-earth metal salts of 2,5-(dianilino)terephthalic acid. CrystEngComm, 2017, 19, 6787-6796.	1.3	5
31548	Compressive strain induced dynamical stability of monolayer 1T-MX2 (Mâ€°â€°=â€°â€°Mo, W; Xâ€°â€°=â€°â€°S, Se). Ma Research Express, 2017, 4, 115018.	0.8	13
31549	Soft phonon mode dynamics in Aurivillius-type structures. Physical Review B, 2017, 96, .	1.1	17
31550	Divergent synthesis routes and superconductivity of ternary hydride<mml:math xmlns:mml="http://www.w3.org/1998/Math/MathML"><mml:msub><mml:mi>MgSiH</mml:mi><mml:mn>6</mml:mn></mml:msub> high pressure. Physical Review B, 2017, 96, .	1.1	67

#	Article	IF	Citations
31551	Extremely large magnetoresistance and Kohler's rule in <mml:math xmlns:mml="http://www.w3.org/1998/Math/MathML"><mml:msub><mml:mi>PdSn</mml:mi><mml:mn>4</mml:mn></mml:msub></mml: : A complete study of thermodynamic, transport, and band-structure properties. Physical Review B, 2017, 96, .	1.1	69
31552	Defect physics in intermediate-band materials: Insights from an optimized hybrid functional. Physical Review B, 2017, 96, .	1.1	13
31553	Giant interfacial perpendicular magnetic anisotropy in Fe/CuIn1â^'xGaxSe2 beyond Fe/MgO. Physical Review B, 2017, 96, .	1.1	14
31554	Electronic properties and bonding in <mml:math xmlns:mml="http://www.w3.org/1998/Math/MathML"><mml:mrow><mml:mi>Zr</mml:mi><mml:msub><mml:mi mathvariant="normal">H</mml:mi><mml:mi>x</mml:mi></mml:msub></mml:mrow></mml:math> thin films investigated by valence-band x-ray photoelectron spectroscopy. Physical Review B, 2017, 96, .	1.1	9
31555	Structural evolution of Bi thin films on Au(111) revealed by scanning tunneling microscopy. Physical Review B, 2017, 96, .	1.1	20
31556	Electronic-Structure Origin of Cation Disorder in Transition-Metal Oxides. Physical Review Letters, 2017, 119, 176402.	2.9	135
31557	Interatomic Spin Coupling in Manganese Clusters Registered on Graphene. Physical Review Letters, 2017, 119, 176806.	2.9	20
31558	Noncollinear Magnetic Structure and Multipolar Order in Eu2Ir2O7. Physical Review Letters, 2017, 119, 187203.	2.9	18
31559	Ab initio theory and modeling of water. Proceedings of the National Academy of Sciences of the United States of America, 2017, 114, 10846-10851.	3.3	340
31560	Local structure and oxide-ion conduction mechanism in apatite-type lanthanum silicates. Science and Technology of Advanced Materials, 2017, 18, 644-653.	2.8	6
31561	Segregation ofsp-impurities at grain boundaries and surfaces: comparison of fcc cobalt and nickel. Modelling and Simulation in Materials Science and Engineering, 2017, 25, 085004.	0.8	12
31562	Enhanced thermoelectric properties of penta-graphene by strain effects process. Materials Research Express, 2017, 4, 105031.	0.8	12
31563	Electronic and vibrational properties of <mml:math xmlns:mml="http://www.w3.org/1998/Math/MathML"><mml:mrow><mml:msub><mml:mi>Pu</mml:mi><mml:mn>3</mml:mn></mml:msub></mml:mrow></mml: : A theoretical explanation for the phonon softening observed in Pu-Ga alloys. Physical Review B, 2017, 96, .	1.1	4
31564	Segregation-induced ordered superstructures at general grain boundaries in a nickel-bismuth alloy. Science, 2017, 358, 97-101.	6.0	130
31565	Oxidation Effect for the Carbon Related Defect Formation in SiC/SiO₂ Interface by First Principles Calculation. Materials Science Forum, 2017, 897, 131-134.	0.3	5
31566	Density Functional Theory on NV Center in 4H SiC. Materials Science Forum, 0, 897, 269-274.	0.3	1
31567	Solid Aluminum Borohydrides for Prospective Hydrogen Storage. ChemSusChem, 2017, 10, 4725-4734.	3.6	24
31568	Epitaxial Growth of ZnGa₂O₄: A New, Deep Ultraviolet Semiconductor Candidate. Crystal Growth and Design, 2017, 17, 6071-6078.	1.4	61

#	Article	IF	Citations
31569	K_{1â€“x}Mo₃P₂O₁₄ as Support for Single-Atom Catalysts. Journal of Physical Chemistry C, 2017, 121, 22895-22900.	1.5	12
31570	Strain induced atomic structure at the Ir-doped LaAlO₃/SrTiO₃ interface. Physical Chemistry Chemical Physics, 2017, 19, 28676-28683.	1.3	7
31571	Identification of activity trends for CO oxidation on supported transition-metal single-atom catalysts. Catalysis Science and Technology, 2017, 7, 5860-5871.	2.1	69
31572	Layered tetragonal zinc chalcogenides for energy-related applications: from photocatalysts for water splitting to cathode materials for Li-ion batteries. Nanoscale, 2017, 9, 17303-17311.	2.8	29
31573	Strain-induced thermoelectric performance enhancement of monolayer ZrSe₂. RSC Advances, 2017, 7, 47243-47250.	1.7	70
31574	Indole-based conjugated macromolecules as a redox-mediated electrolyte for an ultrahigh power supercapacitor. Energy and Environmental Science, 2017, 10, 2441-2449.	15.6	68
31575	Benchmarking a first-principles thermal neutron scattering law for water ice with a diffusion experiment. EPJ Web of Conferences, 2017, 146, 13004.	0.1	7
31576	Chiral phase transition at 180Â° domain walls in ferroelectric PbTiO3 driven by epitaxial compressive strains. Journal of Applied Physics, 2017, 122, .	1.1	9
31577	Iron disulfide compound: a promising thermoelectric material. Materials Research Express, 2017, 4, 105907.	0.8	7
31578	Assessing Density Functionals Using Many Body Theory for Hybrid Perovskites. Physical Review Letters, 2017, 119, 145501.	2.9	65
31579	A highly selective and stable ZnO-ZrO ₂ solid solution catalyst for CO ₂ hydrogenation to methanol. Science Advances, 2017, 3, e1701290.	4.7	683
31580	Ba2+ Doped CH3NH3PbI3 to Tune the Energy State and Improve the Performance of Perovskite Solar Cells. Electrochimica Acta, 2017, 254, 165-171.	2.6	44
31581	Non-adiabatic effects in elementary reaction processes at metal surfaces. Progress in Surface Science, 2017, 92, 317-340.	3.8	79
31582	Improved Crystal Growth of Tl₆SeI₄ for Î³-Ray Detection Material by Oxide Impurity Removal. Crystal Growth and Design, 2017, 17, 6096-6104.	1.4	6
31583	Exceptional Thermoelectric Properties of Layered GeAs₂. Chemistry of Materials, 2017, 29, 9300-9307.	3.2	80
31584	Interaction of Sulfur Dioxide and Near-Ambient Pressures of Water Vapor with Cuprous Oxide Surfaces. Journal of Physical Chemistry C, 2017, 121, 24011-24024.	1.5	11
31585	Density Functional Theory Modeling the Interfacial Chemistry of the LiNO₃ Additive for Lithiumâ€“Sulfur Batteries by Means of Simulated Photoelectron Spectroscopy. Journal of Physical Chemistry C, 2017, 121, 23324-23332.	1.5	27
31586	Phases and thermoelectric properties of SnTe with (Ge, Mn) co-doping. Physical Chemistry Chemical Physics, 2017, 19, 28749-28755.	1.3	31

#	Article	IF	Citations
31587	The interaction of halogen atoms and molecules with borophene. Physical Chemistry Chemical Physics, 2017, 19, 28963-28969.	1.3	28
31588	Structural evolution and atomic diffusion behavior in the Ce70Al10Cu20 melt under compression: A theoretical study using ab-initio molecular dynamics simulations. Journal of Applied Physics, 2017, 122, .	1.1	3
31589	Prediction for electronic, vibrational and thermoelectric properties of chalcopyrite AgX(X=In,Ga)Te ₂ : PBEâ€‰+â€‰U approach. Royal Society Open Science, 2017, 4, 170750.	1.1	17
31590	Aragonite-II and CaCO₃-VII: New High-Pressure, High-Temperature Polymorphs of CaCO₃. Crystal Growth and Design, 2017, 17, 6291-6296.	1.4	61
31591	Revealing the Conversion Mechanism of Transition Metal Oxide Electrodes during Lithiation from First-Principles. Chemistry of Materials, 2017, 29, 9011-9022.	3.2	60
31592	Hot carrier-enhanced interlayer electronâ€“hole pair multiplication in 2D semiconductor heterostructure photocells. Nature Nanotechnology, 2017, 12, 1134-1139.	15.6	74
31593	Rare-Earth Free Self-Activated Graphene Quantum Dots and Copper-Cysteamine Phosphors for Enhanced White Light-Emitting-Diodes under Single Excitation. Scientific Reports, 2017, 7, 12872.	1.6	44
31594	A novel explanation for the increased conductivity in annealed Al-doped ZnO: an insight into migration of aluminum and displacement of zinc. Physical Chemistry Chemical Physics, 2017, 19, 27866-27877.	1.3	37
31595	Anisotropic ultrahigh hole mobility in two-dimensional penta-SiC₂ by strain-engineering: electronic structure and chemical bonding analysis. RSC Advances, 2017, 7, 45705-45713.	1.7	28
31596	New Wang-Landau approach to obtain phase diagrams for multicomponent alloys. Physical Review B, 2017, 96, .	1.1	6
31597	Charged defects in two-dimensional semiconductors of arbitrary thickness and geometry: Formulation and application to few-layer black phosphorus. Physical Review B, 2017, 96, .	1.1	28
31598	The Nextâ€Generation of Nonlinear Optical Materials: Rb₃Ba₃Li₂Al₄B₆O₂₀Fâ€”Synthesis, Characterization, and Crystal Growth. Advanced Optical Materials, 2017, 5, 1700840.	3.6	68
31599	A superhard sp3 microporous carbon with direct bandgap. Chemical Physics Letters, 2017, 689, 68-73.	1.2	39
31600	Tuned thermoelectric transport properties of Co2.0Sb1.6Se2.4 and Co2.0Sb1.5M0.1Se2.4 (M=Zn, Sn): Compounds with high phonon scattering. Journal of Alloys and Compounds, 2017, 729, 303-312.	2.8	5
31601	Growth Mechanism of Pine-leaf-like Nanostructure from the Backbone of SrCO₃ Nanorods using LaMerâ€™s Surface Diffusion: Impact of Higher Surface Energy (Î³ = 38.9) Tj ETQq0 0 0 rgBT /Overlock 10 Tf 50 182 Td Calculations. Crystal Growth and Design, 2017, 17, 6394-6406.	1.4	5
31602	Selective Hydrogenation of Acetylene over Pd-In/Al₂O₃ Catalyst: Promotional Effect of Indium and Composition-Dependent Performance. ACS Catalysis, 2017, 7, 7835-7846.	5.5	194
31603	Tuning the electrical transport of type II Weyl semimetal WTe2 nanodevices by Ga+ ion implantation. Scientific Reports, 2017, 7, 12688.	1.6	10
31604	N-Functionalized MXenes: ultrahigh carrier mobility and multifunctional properties. Physical Chemistry Chemical Physics, 2017, 19, 28710-28717.	1.3	48

#	Article	IF	Citations
31605	A unified understanding of the direct coordination of NO to first-transition-row metal centers in metalâ€“ligand complexes. Physical Chemistry Chemical Physics, 2017, 19, 28098-28104.	1.3	4
31606	Model creation and electronic structure calculation of amorphous hydrogenated boron carbide: a classical/ab initio hybrid approach. RSC Advances, 2017, 7, 46788-46795.	1.7	2
31607	Low temperature diffusivity of self-interstitial defects in tungsten. New Journal of Physics, 2017, 19, 073024.	1.2	45
31608	Interaction of C and Mn in a â^3 grain boundary of bcc iron. IOP Conference Series: Materials Science and Engineering, 2017, 219, 012044.	0.3	8
31609	Excellent valleytronic properties and nontrivial topological phase in germanene heterostructure. Materials Research Express, 2017, 4, 105032.	0.8	2
31610	Photoemission study of the electronic structure of valence band convergent SnSe. Physical Review B, 2017, 96, .	1.1	30
31611	Cleavage tendency of anisotropic two-dimensional materials:<mml:math xmlns:mml="http://www.w3.org/1998/Math/MathML"><mml:mrow><mml:mi>Re</mml:mi><mml:msub><mml:mi>X</mml:mi><mml:mr and<mml:math xmlns:mml="http://www.w3.org/1998/Math/MathML"><mm. Physical Review B, 2017, 96, .	1.1	36
31612	Atomic oxygen adsorption on Pb(1 0 0). European Physical Journal B, 2017, 90, 1.	0.6	0
31613	Guided Molecular Assembly on a Locally Reactive 2D Material. Advanced Materials, 2017, 29, 1703929.	11.1	7
31614	Thermal Conductivity of Compounds Present in the Side Ledge in Aluminium Electrolysis Cells. Jom, 2017, 69, 2412-2417.	0.9	8
31615	Monolayer Sc₂CO₂: A Promising Candidate as a SO₂ Gas Sensor or Capturer. Journal of Physical Chemistry C, 2017, 121, 24077-24084.	1.5	126
31616	Structural phase transition in monolayer MoTe2 driven by electrostatic doping. Nature, 2017, 550, 487-491.	13.7	548
31617	Surface phase diagram prediction from a minimal number of DFT calculations: redox-active adsorbates on zinc oxide. Physical Chemistry Chemical Physics, 2017, 19, 28731-28748.	1.3	4
31618	Exploiting a single intramolecular conformational switching Ni-TPP molecule to probe charge transfer dynamics at the nanoscale on bare Si(100)-2 Ã— 1. Physical Chemistry Chemical Physics, 2017, 19, 28982-28992.	1.3	2
31619	First-principles study on the initial decomposition process of CH3NH3PbI3. Journal of Chemical Physics, 2017, 147, 124702.	1.2	10
31620	Blue and red shifted temperature dependence of implicit phonon shifts in graphene. Materials Research Express, 2017, 4, 075038.	0.8	3
31621	Switching from pyroelectric to ferroelectric order in Ni-doped <mml:math xmlns:mml="http://www.w3.org/1998/Math/MathML"><mml:mrow><mml:mi>CaBaC</mml:mi><mml:msub><mml:mi mathvariant="normal">o</mml:mi><mml:mn>4</mml:mn></mml:msub><mml:msub><mml:mi mathvariant="normal">O</mml:mi><mml:mn>7</mml:mn></mml:msub></mml:mrow></mml:math>. Physical Review B, 2017, 96, .	1.1	12
31622	Elastic properties of noncarbon nanotubes as compared to carbon nanotubes. Physical Review B, 2017, 96, .	1.1	26

#	Article	IF	Citations
31623	Multiband <mml:math xmlns:mml="http://www.w3.org/1998/Math/MathML"><mml:mrow><mml:mi mathvariant="bold">k</mml:mi><mml:mo>Â·</mml:mo><mml:mi mathvariant="bold">p</mml:mi></mml:mrow></mml:math> theory of monolayer <mml:math xmlns:mml="http://www.w3.org/1998/Math/MathML"><mml:mrow><mml:mi>X</mml:mi><mml:mi>Se</mml:mi></mml:mrow></mml:m		

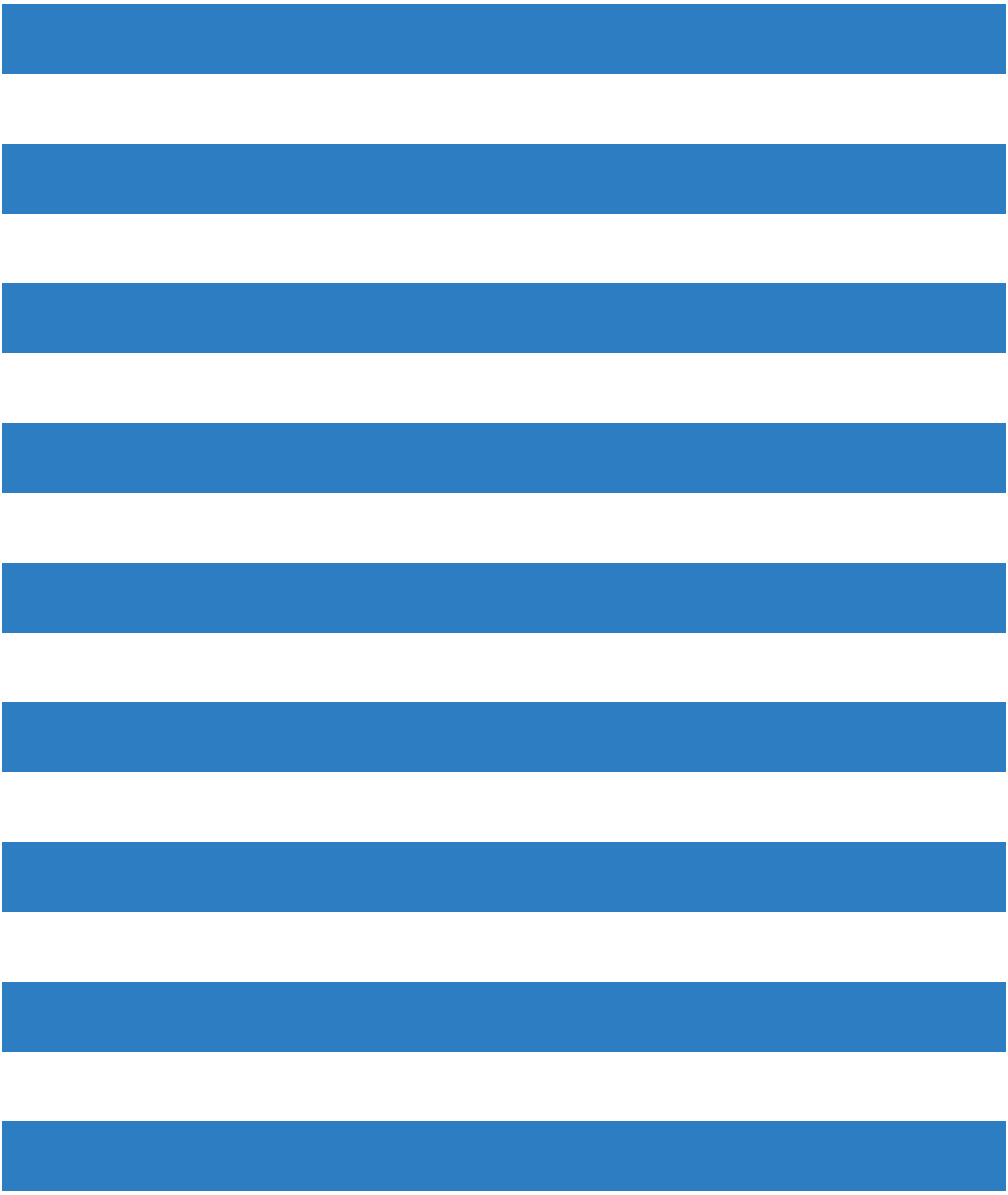

#	Article	IF	Citations
31641	Effect of hydrogen passivation on the decoupling of graphene on SiC(0001) substrate: First-principles calculations. Scientific Reports, 2017, 7, 8461.	1.6	4
31642	Dimension-dependent band alignment and excitonic effects in graphitic carbon nitride: a many-body perturbation and time-dependent density functional theory study. RSC Advances, 2017, 7, 44997-45002.	1.7	6
31643	A two-dimensional layered CdS/C₂N heterostructure for visible-light-driven photocatalysis. Physical Chemistry Chemical Physics, 2017, 19, 28216-28224.	1.3	75
31644	A nonmagnetic topological Weyl semimetal in quaternary Heusler compound CrAlTiV. Applied Physics Letters, 2017, 111, .	1.5	6
31645	Cs diffusion in SiC high-energy grain boundaries. Journal of Applied Physics, 2017, 122, 105901.	1.1	3
31646	Magnetic fluctuations and superconducting properties of <mml:math xmlns:mml="http://www.w3.org/1998/Math/MathML"><mml:mrow><mml:msub><mml:mi>CaKFe</mml:mi><mml:mn>4</mml:mn><mml:mi>As</mml:mi><mml:mn>4</mml:mn></mml:msub></mml:mrow></mml:math> studied by <mml:math xmlns:mml="http://www.w3.org/1998/Math/MathML"><mml:mmultiscripts><mml:mi>As</mml:mi><mml:mprescripts /><mml:none /><mml:mn>75</mml:mn></mml:mmultiscripts></mml:math> NMR. Physical Review B, 2017, 96, .	1.1	40
31647	Quantum-chemical modeling of lithium removal from lithiumâ€“siliconâ€“silicon carbide composite. Russian Journal of Inorganic Chemistry, 2017, 62, 1182-1190.	0.3	3
31648	High-Coverage H₂ Adsorption on the Reconstructed Cu₂O(111) Surface. Journal of Physical Chemistry C, 2017, 121, 22081-22091.	1.5	50
31649	Chemisorption of Pentacene on Pt(111) with a Little Molecular Distortion. Journal of Physical Chemistry C, 2017, 121, 22797-22805.	1.5	17
31650	Computational Screening of Rutile Oxides for Electrochemical Ammonia Formation. ACS Sustainable Chemistry and Engineering, 2017, 5, 10327-10333.	3.2	115
31651	Structural and transport properties of ammonia along the principal Hugoniot. Scientific Reports, 2017, 7, 12338.	1.6	7
31652	Effect of lithium-trapping on nitrogen-doped graphene as an anchoring material for lithiumâ€“sulfur batteries: a density functional theory study. Physical Chemistry Chemical Physics, 2017, 19, 28189-28194.	1.3	56
31653	Enhanced piezoelectricity of monolayer phosphorene oxides: a theoretical study. Physical Chemistry Chemical Physics, 2017, 19, 27508-27515.	1.3	27
31654	Ab initio coverage-dependent microkinetic modeling of benzene hydrogenation on Pd(111). Catalysis Science and Technology, 2017, 7, 5267-5283.	2.1	19
31655	Charge injection driven switching between ferromagnetism and antiferromagnetism in transitional metal-doped MoS2 materials. Journal Physics D: Applied Physics, 2017, 50, 465006.	1.3	4
31656	Electronic structure and magnetism of epitaxial Niâ€“Mnâ€“Ga(-Co) thin films with partial disorder: a view across the phase transition. Journal Physics D: Applied Physics, 2017, 50, 465005.	1.3	10
31657	Non-enzymatic glucose sensing properties of MoO3 nanorods: experimental and density functional theory investigations. Journal Physics D: Applied Physics, 2017, 50, 475401.	1.3	15
31658	Bilayers of Ni₃C₁₂S₁₂and Pt₃C₁₂S₁₂: graphene-like 2D topological insulators tunable by electric fields. Journal of Physics Condensed Matter, 2017, 29, 465502.	0.7	8

#	Article	IF	Citations
31659	Magnetic properties of strained multiferroic <mml:math xmlns:mml="http://www.w3.org/1998/Math/MathML"><mml:mrow><mml:mi>CoC</mml:mi><mml:msub><mml:mi mathvariant="normal">r</mml:mi><mml:mn>2</mml:mn></mml:msub><mml:msub><mml:mi mathvariant="normal">O</mml:mi><mml:mn>4</mml:mn></mml:msub></mml:mrow></mml:math> : A soft x-ray study. Physical Review B, 2017, 95, .	1.1	19
31660	Tuning magnetoresistance in molybdenum disulphide and graphene using a molecular spin transition. Nature Communications, 2017, 8, 677.	5.8	20
31661	Epitaxial thin films of pyrochlore iridate Bi2+xIr2-yO7-Î´: structure, defects and transport properties. Scientific Reports, 2017, 7, 7740.	1.6	29
31662	Electric field control of magnetism in nickel with coaxial cylinder structure at room temperature by electric double layer gating. Journal of Materials Chemistry C, 2017, 5, 10609-10614.	2.7	3
31663	Electronic structure of heavy fermion system CePt ₂ In ₇ from angle-resolved photoemission spectroscopy. Chinese Physics B, 2017, 26, 077401.	0.7	5
31664	Magnetic properties of AlN monolayer doped with group 1A or 2A nonmagnetic element: First-principles study. Chinese Physics B, 2017, 26, 097503.	0.7	3
31665	Semiconductive Copper(I)â€“Organic Frameworks for Efficient Lightâ€Driven Hydrogen Generation Without Additional Photosensitizers and Cocatalysts. Angewandte Chemie, 2017, 129, 14829-14833.	1.6	26
31666	Semiconductive Copper(I)â€“Organic Frameworks for Efficient Lightâ€Driven Hydrogen Generation Without Additional Photosensitizers and Cocatalysts. Angewandte Chemie - International Edition, 2017, 56, 14637-14641.	7.2	248
31667	Solute segregation at the Al/Î¸â€²-Al2Cu interface in Al-Cu alloys. Acta Materialia, 2017, 141, 327-340.	3.8	121
31668	Magnetic, electrochemical and thermoelectric properties of <mml:math xmlns:mml="http://www.w3.org/1998/Math/MathML" altimg="si1.gif" overflow="scroll"><mml:mrow><mml:mtext>P</mml:mtext><mml:mn>2</mml:mn><mml:mo>-</mml:mo><mml:msub><mml:mrow>		

#	Article	IF	Citations
31677	Hybrid-DFTâ€‰â€‰+â€‰â€‰V_w method for band structure calculation of semiconducting transition metal compounds: the case of cerium dioxide. Journal of Physics Condensed Matter, 2017, 29, 454002.	0.7	5
31678	Topological Dirac line nodes and superconductivity coexist in SnSe at high pressure. Physical Review B, 2017, 96, .	1.1	35
31679	Doping-controlled phase transitions in single-layer <mml:math xmlns:mml="http://www.w3.org/1998/Math/MathML"><mml:msub><mml:mi>MoS</mml:mi><mml:mn>2</mml:mn></mml:msub></mm Physical Review B, 2017, 96, .	1.1	62
31680	First-principles investigations of the atomic structure and magnetic properties of Ni and Co films on Cu substrate. Lobachevskii Journal of Mathematics, 2017, 38, 940-943.	0.1	1
31681	Thermodynamics of concentrated solid solution alloys. Current Opinion in Solid State and Materials Science, 2017, 21, 238-251.	5.6	142
31682	Dopants Promoting Ferroelectricity in Hafnia: Insights from a comprehensive Chemical Space Exploration. Chemistry of Materials, 2017, 29, 9102-9109.	3.2	139
31683	Designing High-Efficiency Nanostructured Two-Phase Heusler Thermoelectrics. Chemistry of Materials, 2017, 29, 9386-9398.	3.2	19
31684	First Principle Study on the Adsorption of Hydrocarbon Chains Involved in Fischerâ€“Tropsch Synthesis over Iron Carbides. Journal of Physical Chemistry C, 2017, 121, 25052-25063.	1.5	16
31685	Intragranular Phase Proton Conduction in Crystalline Sn_{1â€“x}In_xP₂O₇ (x = 0 and 0.1). Journal of Physical Chemistry C, 2017, 121, 23896-23905.	1.5	15
31686	MoirÃ© Superstructure and Dimensional Crossover of 2D Electronic States on Nanoscale Lead Quantum Films. Scientific Reports, 2017, 7, 12735.	1.6	4
31687	Oscillatory electrostatic potential on graphene induced by group IV element decoration. Scientific Reports, 2017, 7, 13152.	1.6	4
31688	CO₂adsorption and separation in covalent organic frameworks with interlayer slipping. CrystEngComm, 2017, 19, 6950-6963.	1.3	51
31689	Band-edge engineering via molecule intercalation: a new strategy to improve stability of few-layer black phosphorus. Physical Chemistry Chemical Physics, 2017, 19, 29232-29236.	1.3	10
31690	Electrical compensation mechanism in fluorine-doped SnO2. Applied Physics Letters, 2017, 111, .	1.5	8
31691	Improved prediction of heat of mixing and segregation in metallic alloys using tunable mixing rule for embedded atom method. Modelling and Simulation in Materials Science and Engineering, 2017, 25, 085011.	0.8	16
31692	Topological Hopf and Chain Link Semimetal States and Their Application to <mml:math xmlns:mml="http://www.w3.org/1998/Math/MathML" display="inline"><mml:mrow><mml:mrow><mml:msub><mml:mrow><mml:mi>Co</mml:mi></mml:mrow><mml:mrow><mml:mn>2</mml:mn> Physical Review Letters, 2017, 119, 156401.	2.9	183
31693	Geometrical eigen-subspace framework based molecular conformation representation for efficient structure recognition and comparison. Journal of Chemical Physics, 2017, 146, 154108.	1.2	16
31694	Stability and electronic properties of hybrid SnO bilayers: SnO/graphene and SnO/BN. Nanotechnology, 2017, 28, 475708.	1.3	8

#	Article	IF	Citations
31695	Role of electrodes materials in determining the interfacial and magnetoelectric properties in BaTiO3-based multiferroic tunnel junctions. European Physical Journal B, 2017, 90, 1.	0.6	14
31696	Computational modeling of high-entropy alloys: Structures, thermodynamics and elasticity. Journal of Materials Research, 2017, 32, 3627-3641.	1.2	56
31697	Onâ€Surface Synthesis of Adenine Oligomers via Ullmann Reaction. ChemPhysChem, 2017, 18, 3544-3547.	1.0	2
31698	Magnetic coupling constants for MnO as calculated using hybrid density functional theory. Chemical Physics Letters, 2017, 690, 47-53.	1.2	5
31699	Jahnâ€“Teller distortion affected Li ion migration in spinel TiO2. Solid State Ionics, 2017, 312, 17-20.	1.3	2
31700	Exploring Emerging Photovoltaic Materials Beyond Perovskite: The Case of Skutterudite. Chemistry of Materials, 2017, 29, 9429-9435.	3.2	16
31701	Defect Genome of Cubic Perovskites for Fuel Cell Applications. Journal of Physical Chemistry C, 2017, 121, 26637-26647.	1.5	24
31702	Foreign In³⁺ treatment improving the photoelectrochemical performance of a hematite nanosheet array for water splitting. Nanoscale, 2017, 9, 17513-17523.	2.8	22
31703	Development of low temperature stoichiometric solution combustion derived transparent conductive ternary zinc tin co-doped indium oxide electrodes. RSC Advances, 2017, 7, 48253-48262.	1.7	19
31704	Structural stability and electronic property in K₂S under pressure. RSC Advances, 2017, 7, 7424-7430.	1.7	13
31705	First-principles investigation of competing magnetic interactions in <mml:math xmlns:mml="http://www.w3.org/1998/Math/MathML"><mml:mrow><mml:mo>(</mml:mo><mml:mi>Mn</mml:mi><mml:mo>,</mml:m Heusler solid solutions. Physical Review B, 2017, 96, .	1.1	7
31706	Planetary Ices and the Linear Mixing Approximation. Astrophysical Journal, 2017, 848, 67.	1.6	54
31708	First-principles study of gas adsorption on Î³-graphyne. Chemical Physics Letters, 2017, 689, 185-189.	1.2	30
31709	Alkylation of toluene with cyclohexene over phosphotungstic acid: A combined experimental and computational study. Journal of Catalysis, 2017, 355, 145-155.	3.1	10
31710	First-Principles Screening of Lead-Free Methylammonium Metal Iodine Perovskites for Photovoltaic Application. Journal of Physical Chemistry C, 2017, 121, 24359-24364.	1.5	25
31711	Selective Hybridization of a Terpyridine-Based Molecule with a Noble Metal. Journal of Physical Chemistry C, 2017, 121, 23574-23581.	1.5	4
31712	Simulations of a Graphene Nanoflake as a Nanovector To Improve ZnPc Phototherapy Toxicity: From Vacuum to Cell Membrane. ACS Applied Materials & Interfaces, 2017, 9, 37554-37562.	4.0	20
31713	Anomalous Kondo resonance mediated by semiconducting graphene nanoribbons in a molecular heterostructure. Nature Communications, 2017, 8, 946.	5.8	16

#	Article	IF	Citations
31714	Two-dimensional metallic tantalum disulfide as a hydrogen evolution catalyst. Nature Communications, 2017, 8, 958.	5.8	191
31715	Location, distribution and acidity of Al substitution in ZSM-5 with different Si/Al ratios â€“ a periodic DFT computation. Catalysis Science and Technology, 2017, 7, 5694-5708.	2.1	30
31716	Theoretical prediction of MXene-like structured Ti₃C₄as a high capacity electrode material for Na ion batteries. Physical Chemistry Chemical Physics, 2017, 19, 29106-29113.	1.3	51
31717	Stabilization of Au Monatomic-High Islands on the <mml:math xmlns:mml="http://www.w3.org/1998/Math/MathML" display="inline"><mml:mrow><mml:mo stretchy="false">(</mml:mo><mml:mrow><mml:mn>2</mml:mn><mml:mo>Ã—</mml:mo><mml:mn>2</mml:mn></mml:mrow><mml	1.5	1
31718	Non-Fermi surface nesting driven commensurate magnetic ordering in Fe-doped <mml:math xmlns:mml="http://www.w3.org/1998/Math/MathML"><mml:mrow><mml:mi mathvariant="normal">S</mml:mi><mml:msub><mml:mi mathvariant="normal">r</mml:mi><mml:mn>2</mml:mn></mml:msub><mml:mi>Ru</mml:mi><mml:msub><mml:mi mathvariant="normal">O</mml:mi><mml:mn>4</mml:mn></mml:msub></mml:mrow></mml:math>. Physical Review B, 2017, 95, .	1.1	4
31719	Phase stability, ordering tendencies, and magnetism in single-phase fcc Au-Fe nanoalloys. Physical Review B, 2017, 96, .	1.1	11
31720	Pressure-induced anomalous enhancement of insulating state and isosymmetric structural transition in quasi-one-dimensional <mml:math xmlns:mml="http://www.w3.org/1998/Math/MathML"><mml:mrow><mml:mi>Ti</mml:mi><mml:msub><mml:mi mathvariant="normal">S</mml:mi><mml:mn>3</mml:mn></mml:msub></mml:mrow></mml:math>. Physical Review B, 2017, 96, .	1.1	12
31721	Optical properties of highly compressed polystyrene: An ab initio study. Physical Review B, 2017, 96, .	1.1	22
31722	Interplay between breathing mode distortion and magnetic order in rare-earth nickelates <mml:math xmlns:mml="http://www.w3.org/1998/Math/MathML"><mml:mrow><mml:mi>R</mml:mi><mml:msub><mml:mi>NiO</mml:mi><mml:m within <mml:math xmlns:mml="http://www.w3.org/1998/Math/MathML"><mml:mrow><mml:mi>DFT</mml:mi><mml:mo>+</mml:mo><mml:mi>U</mml:mi></mml: Physical Review B, 2017, 96, .	1.1	37
31723	Quantum anomalous Hall insulator phase in asymmetrically functionalized germanene. Physical Review B, 2017, 96, .	1.1	18
31725	Electronicâ€Reconstructionâ€Enhanced Tunneling Conductance at Terrace Edges of Ultrathin Oxide Films. Advanced Materials, 2017, 29, 1702001.	11.1	7
31726	Unexpected Competition between Antiferromagnetic and Ferromagnetic States in Hf₂MnRu₅B₂: Predicted and Realized. Inorganic Chemistry, 2017, 56, 12674-12677.	1.9	10
31727	Boron-Doped Graphene as a Promising Anode Material for Potassium-Ion Batteries with a Large Capacity, High Rate Performance, and Good Cycling Stability. Journal of Physical Chemistry C, 2017, 121, 24418-24424.	1.5	118
31728	Three-Dimensionally Hierarchical Ni/Ni₃S₂/S Cathode for Lithiumâ€“Sulfur Battery. ACS Applied Materials & Interfaces, 2017, 9, 38477-38485.	4.0	60
31729	Stress-Mediated Enhancement of Ionic Conductivity in Fast-Ion Conductors. ACS Applied Materials & Interfaces, 2017, 9, 38773-38783.	4.0	29
31730	Enhanced Solar Water Oxidation Performance of TiO₂ via Band Edge Engineering: A Tale of Sulfur Doping and Earth-Abundant CZTS Nanoparticles Sensitization. ACS Catalysis, 2017, 7, 8077-8089.	5.5	39
31731	Structure and Electronic Properties of Interface-Confined Oxide Nanostructures. ACS Nano, 2017, 11, 11449-11458.	7.3	23
31732	Surface Modification of Perfect and Hydroxylated TiO₂ Rutile (110) and Anatase (101) with Chromium Oxide Nanoclusters. ACS Omega, 2017, 2, 6795-6808.	1.6	18

#	Article	IF	Citations
31733	c-T phase diagram and Landau free energies of (AgAu)55 nanoalloy via neural-network molecular dynamic simulations. Journal of Chemical Physics, 2017, 147, 154303.	1.2	14
31734	Vanadium supersaturated silicon system: a theoretical and experimental approach. Journal Physics D: Applied Physics, 2017, 50, 495101.	1.3	10
31735	Modulating the electronic and optical properties of monolayer arsenene phases by organic molecular doping. Nanotechnology, 2017, 28, 495202.	1.3	22
31736	Fragment approach to the electronic structure of <mml:math xmlns:mml="http://www.w3.org/1998/Math/MathML"><mml:mrow><mml:mi>Ï„</mml:mi><mml:mtext>-boron</mml:mtext></mml:mro allotrope. Physical Review B, 2017, 95, .	1.1	6
31737	Double-stage nematic bond ordering above double stripe magnetism: Application to <mml:math xmlns:mml="http://www.w3.org/1998/Math/MathML"><mml:mrow><mml:msub><mml:mi>BaTi</mml:mi><mml:mn>2</mmn></mm mathvariant="normal">O</mml:mi></mml:mrow></mml:math>. Physical Review B, 2017, 95, .	1.1	20
31738	Dependence of the structure and dynamics of liquid silicon on the choice of density functional approximation. Physical Review B, 2017, 96, .	1.1	26
31739	Pressure-induced half-collapsed-tetragonal phase in <mml:math xmlns:mml="http://www.w3.org/1998/Math/MathML"><mml:mrow><mml:msub><mml:mi>CaKFe</mml:mi><mml:mn>4</mml:mn></mml:mn></m Physical Review B, 2017, 96, .	1.1	36
31740	Investigation of melting at the uranium Î³ phase by quantum and classical molecular dynamics methods. High Temperature, 2017, 55, 711-717.	0.1	5
31741	Hybrid organicâ€“inorganic CH₃NH₃PbI₃ perovskite building blocks: Revealing ultraâ€strong hydrogen bonding and mulliken inner complexes and their implications in materials design. Journal of Computational Chemistry, 2017, 38, 2802-2818.	1.5	32
31742	Insights from first principles graphene/g-C2N bilayer: gap opening, enhanced visible light response and electrical field tuning band structure. Applied Physics A: Materials Science and Processing, 2017, 123, 1.	1.1	18
31743	Computational and Experimental Investigation of the Electrochemical Stability and Li-Ion Conduction Mechanism of LiZr₂(PO₄)₃. Chemistry of Materials, 2017, 29, 8983-8991.	3.2	68
31744	Improving Sensing of Sulfur-Containing Gas Molecules with ZnO Monolayers by Implanting Dopants and Defects. Journal of Physical Chemistry C, 2017, 121, 24365-24375.	1.5	35
31745	Gate-Tunable Electronic Structure of Black Phosphorus/HfS₂ Pâ€“N van der Waals Heterostructure with Uniformly Anisotropic Band Dispersion. Journal of Physical Chemistry C, 2017, 121, 24845-24852.	1.5	15
31746	Grand Canonical Quantum Mechanical Study of the Effect of the Electrode Potential on N-Heterocyclic Carbene Adsorption on Au Surfaces. Journal of Physical Chemistry C, 2017, 121, 24618-24625.	1.5	12
31747	Unconventional Current Scaling and Edge Effects for Charge Transport through Molecular Clusters. Nano Letters, 2017, 17, 7350-7357.	4.5	14
31748	Ligand-Induced Energy Shift and Localization of Kondo Resonances in Cobalt-Based Complexes on Cu(111). Nano Letters, 2017, 17, 7146-7151.	4.5	18
31749	Effective Trapping of Lithium Polysulfides Using a Functionalized Carbon Nanotube-Coated Separator for Lithiumâ€“Sulfur Cells with Enhanced Cycling Stability. ACS Applied Materials & Interfaces, 2017, 9, 38445-38454.	4.0	82
31750	Half-Metallicity in Co-Doped WSe₂ Nanoribbons. ACS Applied Materials & Interfaces, 2017, 9, 38796-38801.	4.0	17

#	Article	IF	Citations
31751	Cp-Graphyne: A Low-Energy Graphyne Polymorph with Double Distorted Dirac Points. ACS Omega, 2017, 2, 6822-6830.	1.6	41
31752	Experimental realization of two-dimensional Dirac nodal line fermions in monolayer Cu2Si. Nature Communications, 2017, 8, 1007.	5.8	219
31753	CO2 reduction catalysis by tunable square-planar transition-metal complexes: a theoretical investigation using nitrogen-substituted carbon nanotube models. Physical Chemistry Chemical Physics, 2017, 19, 29068-29076.	1.3	6
31754	Facile Synthesis of Ru-Based Octahedral Nanocages with Ultrathin Walls in a Face-Centered Cubic Structure. Chemistry of Materials, 2017, 29, 9227-9237.	3.2	55
31755	Coadsorption of Butadiene and Hydrogen on the (111) Surfaces of Pt and Pt2Sn Surface Alloy: Understanding the Cohabitation from First-Principles Calculations. Journal of Physical Chemistry C, 2017, 121, 25152-25163.	1.5	14
31756	Quenching of the Resonant States of Single Carbon Vacancies in Graphene/Pt(111). Journal of Physical Chemistry C, 2017, 121, 24641-24647.	1.5	4
31757	New Features and Uncovered Benefits of Polycrystalline Magnetite as Reusable Catalyst in Reductive Chemical Conversion. Journal of Physical Chemistry C, 2017, 121, 25195-25205.	1.5	15
31758	Molecular analogue of the perovskite repeating unit and evidence for direct MnIII-CeIV-MnIII exchange coupling pathway. Nature Communications, 2017, 8, 500.	5.8	28
31759	Superelasticity and cryogenic linear shape memory effects of CaFe2As2. Nature Communications, 2017, 8, 1083.	5.8	22
31760	Structure and lattice dynamics of the wide band gap semiconductors MgSiN2 and MgGeN2. Journal of Applied Physics, 2017, 122, .	1.1	17
31761	Density-Functional-Theory Modeling of Cation Diffusion in Bulk <mml:math xmlns:mml="http://www.w3.org/1998/Math/MathML" display="inline"><mml:mrow><mml:msub><mml:mrow><mml:mi>La</mml:mi></mml:mrow><mml:mrow><mml:mn>1</mml:mn><mm Physical Review Applied, 2017, 8, .	1.5	11
31762	Structural and electronic changes of pentacene induced by potassium doping. Physical Review B, 2017, 95, .	1.1	4
31763	Epicycle method for elasticity limit calculations. Physical Review B, 2017, 95, .	1.1	11
31764	Calculation of spin states of photoelectrons emitted from spin-polarized surface states of Bi(111) surfaces with a mirror symmetry. Physical Review B, 2017, 95, .	1.1	7
31765	Ru doping in iron-based pnictides: The â€œunfoldedâ€•dominant role of structural effects for superconductivity. Physical Review B, 2017, 95, .	1.1	11
31766	Electronic properties, low-energy Hamiltonian, and superconducting instabilities in <mml:math xmlns:mml="http://www.w3.org/1998/Math/MathML"><mml:mrow><mml:msub><mml:mi>CaKFe</mml:mi><mml:mn>4</mml:mn><mml:mn><m Physical Review B, 2017, 96, .	1.1	28
31767	Anisotropic field-induced gap in the quasi-one-dimensional antiferromagnet <mml:math xmlns:mml="http://www.w3.org/1998/Math/MathML"><mml:mrow><mml:msub><mml:mi>KCuMoO</mml:mi><mml:mn>4</mml:mn></mml:mn><< Physical Review B, 2017, 96, .	1.1	7
31768	Closure of the Mott gap and formation of a superthermal metal in the FrÃ¶hlich-type nonequilibrium polaron Bose-Einstein condensate in UO2+x. Physical Review B, 2017, 96, .	1.1	5

#	Article	IF	Citations
31769	Self-compensation in phosphorus-doped CdTe. Physical Review B, 2017, 96, .	1.1	13
31770	Magnetic diversity in stable and metastable structures of CrAs. Physical Review B, 2017, 96, .	1.1	9
31771	Ab initio nonadiabatic molecular dynamics investigation on the dynamics of photogenerated spin hole current in Cu-doped <mml:math xmlns:mml="http://www.w3.org/1998/Math/MathML"><mml:mrow><mml:mi>Mo</mml:mi><mml:msub><mml:mi mathvariant="normal">S</mml:mi><mml:mn>2</mml:mn></mml:msub></mml:mrow></mml:math>. Physical Review B, 2017, 96, .	1.1	32
31772	Computing energy barriers for rare events from hybrid quantum/classical simulations through the virtual work principle. Physical Review B, 2017, 96, .	1.1	13
31773	Spin reorientation in <mml:math xmlns:mml="http://www.w3.org/1998/Math/MathML"><mml:msub><mml:mrow><mml:mtext>NdFe</mml:mtext></mml:mrow><mml:m mathvariant="normal">O</mml:mi></mml:mrow><mml:mn>3</mml:mn></mml:msub></mml:math> : Neutron scattering and ab initio study. Physical Review B, 2017, 96, .	1.1	12
31774	First-principles study of lateral atom manipulation assisted by structural relaxation of a scanning tip apex. Physical Review B, 2017, 96, .	1.1	2
31775	Thinning <mml:math xmlns:mml="http://www.w3.org/1998/Math/MathML"><mml:mrow><mml:msub><mml:mi>CsPb</mml:mi><mml:mn>2</mml:mn> perovskite down to monolayers: Cs-dependent stability. Physical Review B, 2017, 96, .	1.1	26
31776	Band Filling Control of the Dzyaloshinskii-Moriya Interaction in Weakly Ferromagnetic Insulators. Physical Review Letters, 2017, 119, 167201.	2.9	42
31777	Statistics-Based Analysis of the Evolution of Structural and Electronic Properties of Realistic Amorphous Alumina During the Densification Process: Insights from First-Principles Approach. Journal of Physical Chemistry C, 2017, 121, 24745-24758.	1.5	4
31778	Localizing Holes as Polarons and Predicting Band Gaps, Defect Levels, and Delithiation Energies of Solid-State Materials with a Local Exchange-Correlation Functional. Journal of Physical Chemistry C, 2017, 121, 23955-23963.	1.5	18
31779	Optical Transmittance Enhancement of Flexible Copper Film Electrodes with a Wetting Layer for Organic Solar Cells. ACS Applied Materials & Interfaces, 2017, 9, 38695-38705.	4.0	44
31780	Proximity Effect Induced Spin Injection in Phosphorene on Magnetic Insulator. ACS Applied Materials & Interfaces, 2017, 9, 38999-39010.	4.0	22
31781	Band-gap engineering of porous BiVO₄ nanoshuttles by Fe and Mo co-doping for efficient photocatalytic water oxidation. Inorganic Chemistry Frontiers, 2017, 4, 2045-2054.	3.0	59
31782	Ordering tendencies and electronic properties in quaternary Heusler derivatives. Physical Review B, 2017, 96, .	1.1	29
31783	Crystal-Chemical Composition of Dicoctahedral Smectites: An Energy-Based Assessment of Empirical Relations. ACS Earth and Space Chemistry, 2017, 1, 629-636.	1.2	6
31784	Robust Bain distortion in the premartensite phase of a platinum-substituted Ni2MnGa magnetic shape memory alloy. Nature Communications, 2017, 8, 1006.	5.8	26
31785	Transmutation effects on long-term Cs retention in phyllosilicate minerals from first principles. Physical Chemistry Chemical Physics, 2017, 19, 27007-27014.	1.3	4
31786	Structures, electron density and characterization of novel photocatalysts, (BaTaO₂N)_{1â”'x}(SrWO₂N)_xsolid solutions. Dalton Transactions, 2017, 46, 14947-14956.	1.6	16

#	Article	IF	Citations
31787	Single Ni atom incorporated with pyridinic nitrogen graphene as an efficient catalyst for CO oxidation: first-principles investigation. RSC Advances, 2017, 7, 48819-48824.	1.7	49
31788	Electricâ€Fieldâ€Controlled Phase Transformation in WO₃ Thin Films through Hydrogen Evolution. Advanced Materials, 2017, 29, 1703628.	11.1	79
31789	Evolution of the electronic and magnetic properties of zigzag silicene nanoribbon used for hydrogen storage material. International Journal of Hydrogen Energy, 2017, 42, 27184-27205.	3.8	14
31790	Strain effects on oxygen vacancy formation energy in perovskites. Solid State Ionics, 2017, 311, 105-117.	1.3	36
31791	Theoretical Design of Robust Ferromagnetism and Bipolar Semiconductivity in Graphene-Based Nanoroads. Journal of Physical Chemistry C, 2017, 121, 24824-24830.	1.5	5
31792	Effect of the Hydrofluoroether Cosolvent Structure in Acetonitrile-Based Solvate Electrolytes on the Li⁺ Solvation Structure and Liâ€“S Battery Performance. ACS Applied Materials & Interfaces, 2017, 9, 39357-39370.	4.0	58
31793	Dissociation mechanism of H₂ molecule on the Li₂O/hydrogenated-Li₂O (111) surface from first principles calculations. RSC Advances, 2017, 7, 35239-35250.	1.7	10
31794	An intrinsic representation of atomic structure: From clusters to periodic systems. Journal of Chemical Physics, 2017, 147, 144106.	1.2	9
31795	First principle study of edge topological defect-modulated electronic and magnetic properties in zigzag graphene nanoribbons. Chinese Physics B, 2017, 26, 103103.	0.7	5
31796	Controlling the Surface Reactivity of Titania via Electronic Tuning of Self-Assembled Monolayers. ACS Catalysis, 2017, 7, 8351-8357.	5.5	30
31797	Hydrogen functionalization induced two-dimensional ferromagnetic semiconductor in Mn di-halide systems. Physical Chemistry Chemical Physics, 2017, 19, 29516-29524.	1.3	9
31798	Band edge tuned Zn_xCd_{1â^'x}S solid solution nanopowders for efficient solar photocatalysis. Physical Chemistry Chemical Physics, 2017, 19, 29998-30009.	1.3	16
31799	An excellent cyan-emitting orthosilicate phosphor for NUV-pumped white LED application. Journal of Materials Chemistry C, 2017, 5, 12365-12377.	2.7	203
31800	Abiotic production of sugar phosphates and uridine ribonucleoside in aqueous microdroplets. Proceedings of the National Academy of Sciences of the United States of America, 2017, 114, 12396-12400.	3.3	166
31801	Hydrogenation-driven phase transition in single-layer TiSe₂. Nanotechnology, 2017, 28, 495709.	1.3	6
31802	Adsorption properties of chloroform molecule on graphene: Experimental and first-principles calculations. Modern Physics Letters B, 2017, 31, 1750335.	1.0	4
31803	Interplay between Halogen and Hydrogen Bonds in 2D Self-Assembly on the Gold Surface: A First-Principles Investigation. Journal of Physical Chemistry C, 2017, 121, 24707-24720.	1.5	11
31804	Photosystem II Acts as a Spin-Controlled Electron Gate during Oxygen Formation and Evolution. Journal of the American Chemical Society, 2017, 139, 16604-16608.	6.6	52

#	Article	IF	Citations
31805	Structure- and Potential-Dependent Cation Effects on CO Reduction at Copper Single-Crystal Electrodes. Journal of the American Chemical Society, 2017, 139, 16412-16419.	6.6	289
31806	Effects of line defects on the electronic and optical properties of strain-engineered WO₃ thin films. Journal of Materials Chemistry C, 2017, 5, 11694-11699.	2.7	25
31807	Growth and characterization of BaZnGa. Philosophical Magazine, 2017, 97, 3317-3324.	0.7	0
31808	Molecular dynamics investigation of the thermal conductivity of ternary siliconâ€“germaniumâ€“tin alloys. Journal Physics D: Applied Physics, 2017, 50, 494001.	1.3	12
31809	The structural, electronic, magnetic and elastic properties of the binary Heusler alloys Mn₂Z (Zâ€‰â€‰=â€‰â€‰As, Sb, Bi): a first-principles study. Materials Research Express, 2017, 4, 116501.	0.8	11
31810	Adsorption of oxygen on low-index surfaces of Ti3Al alloy. Physics of the Solid State, 2017, 59, 1852-1866.	0.2	9
31811	Tunable Fluorescence Properties Due to Carbon Incorporation in Zinc Oxide Nanowires. Advanced Optical Materials, 2017, 5, 1700381.	3.6	10
31812	Enhancing Charge Carrier Lifetime in Metal Oxide Photoelectrodes through Mild Hydrogen Treatment. Advanced Energy Materials, 2017, 7, 1701536.	10.2	104
31813	The comparative study on bulk-PtSe2 and 2D 1-Layer-PtSe2 under high pressure via first-principle calculations. Theoretical Chemistry Accounts, 2017, 136, 1.	0.5	4
31814	Mechanical characteristics of FeAl2O4 and AlFe2O4 spinel phases in coatings â€“ A study combining experimental evaluation and first-principles calculations. Ceramics International, 2017, 43, 16094-16100.	2.3	19
31815	DynaPhoPy: A code for extracting phonon quasiparticles from molecular dynamics simulations. Computer Physics Communications, 2017, 221, 221-234.	3.0	105
31816	Synthesis of TiO2@g-C3N4 core-shell nanorod arrays with Z-scheme enhanced photocatalytic activity under visible light. Journal of Colloid and Interface Science, 2017, 508, 419-425.	5.0	61
31817	Influence of Inversion on Mg Mobility and Electrochemistry in Spinels. Chemistry of Materials, 2017, 29, 7918-7930.	3.2	75
31818	Atomic Structure of Submonolayer NaCl Grown on Ag(110) Surface. Journal of Physical Chemistry C, 2017, 121, 20272-20278.	1.5	9
31819	Control of Multiple Exciton Generation and Electronâ€“Phonon Coupling by Interior Nanospace in Hyperstructured Quantum Dot Superlattice. ACS Applied Materials & Interfaces, 2017, 9, 32080-32088.	4.0	5
31820	Effect of Surface Structure of TiO₂ Nanoparticles on CO₂ Adsorption and SO₂ Resistance. ACS Sustainable Chemistry and Engineering, 2017, 5, 9295-9306.	3.2	49
31821	Au₆S₂monolayer sheets: metallic and semiconducting polymorphs. Materials Horizons, 2017, 4, 1085-1091.	6.4	26
31822	Perovskites decorated with oxygen vacancies and Feâ€“Ni alloy nanoparticles as high-efficiency electrocatalysts for the oxygen evolution reaction. Journal of Materials Chemistry A, 2017, 5, 19836-19845.	5.2	141

#	Article	IF	Citations
31823	Investigation of superconductivity in compressed vanadium hydrides. Physical Chemistry Chemical Physics, 2017, 19, 26280-26284.	1.3	18
31824	Interface effect on electronic and optical properties of antimonene/GaAs van der Waals heterostructures. Journal of Materials Chemistry C, 2017, 5, 9687-9693.	2.7	29
31825	Lattice thermal expansion and anisotropic displacements in urea, bromomalonic aldehyde, pentachloropyridine, and naphthalene. Journal of Chemical Physics, 2017, 147, 074112.	1.2	16
31826	An all-carbon vdW heterojunction composed of penta-graphene and graphene: Tuning the Schottky barrier by electrostatic gating or nitrogen doping. Applied Physics Letters, 2017, 111, .	1.5	30
31827	The origin of lattice instability in bcc tungsten under triaxial loading. Philosophical Magazine, 2017, 97, 2971-2984.	0.7	9
31828	Prediction of huge magnetic anisotropies in 5dtransition metallocenes. Journal of Physics Condensed Matter, 2017, 29, 435802.	0.7	4
31829	Interface phenomena in magnetron sputtered Cu₂O/ZnO heterostructures. Journal of Physics Condensed Matter, 2017, 29, 435002.	0.7	5
31830	Electronic transport properties of graphene doped by gallium. Nanotechnology, 2017, 28, 415203.	1.3	14
31831	Properties of in-plane graphene/MoS ₂ heterojunctions. 2D Materials, 2017, 4, 045001.	2.0	34
31832	New phases of osmium carbide from evolutionary algorithm andab initiocomputations. Materials Research Express, 2017, 4, 096503.	0.8	0
31833	Lack of quantum confinement in <mml:math xmlns:mml="http://www.w3.org/1998/Math/MathML"><mml:mrow><mml:msub><mml:mi>Ga</mml:mi><mml:mn>2</mml:mn></mml: mathvariant="normal">O</mml:mi><mml:mn>3</mml:mn></mml:msub></mml:mrow></mml:math> nanolayers. Physical Review B, 2017, 96, .	1.1	36
31834	On/off switchable electronic conduction in intercalated metal-organic frameworks. Science Advances, 2017, 3, e1603103.	4.7	56
31835	Raman Spectra of Polycrystalline CeO₂: A Density Functional Theory Study. Journal of Physical Chemistry C, 2017, 121, 20834-20849.	1.5	278
31836	Superstrengthening <mml:math xmlns:mml="http://www.w3.org/1998/Math/MathML"> display="inline"><mml:mrow><mml:msub><mml:mrow><mml:mi>Bi</mml:mi></mml:mrow><mml:mn>2</mml:mn></mml:msub><mml:m through Nanotwinning. Physical Review Letters, 2017, 119, 085501.	2.9	58
31837	Enhanced Stability and Electrochemical Performance of Carbonâ€Coated Ti³⁺ Selfâ€Doped TiO₂â€Reduced Graphene Oxide Hollow Nanostructureâ€Supported Ptâ€Catalyzed Fuel Cell Electrodes. Advanced Materials Interfaces, 2017, 4, 1700564.	1.9	15
31838	Insights into the radiation behavior of Ln2TiO5 (Ln = La-Y) from defect energetics. Computational Materials Science, 2017, 139, 295-300.	1.4	9
31839	Modulating the Band Gap of the FeS₂ by O and Se Doping. Journal of Physical Chemistry C, 2017, 121, 19334-19340.	1.5	18
31840	Oxygen Scrambling of CO₂ Adsorbed on CaO(001). Journal of Physical Chemistry C, 2017, 121, 18625-18634.	1.5	12

#	Article	IF	Citations
31841	Spin filtering of a termination-controlled LSMO/Alq₃ heterojunction for an organic spin valve. Journal of Materials Chemistry C, 2017, 5, 9128-9137.	2.7	9
31842	MoS₂-supported gold nanoparticle for CO hydrogenation. Journal of Physics Condensed Matter, 2017, 29, 415201.	0.7	12
31843	Embedded-atom method potential for modeling hydrogen and hydrogen-defect interaction in tungsten. Journal of Physics Condensed Matter, 2017, 29, 435401.	0.7	26
31844	Visualizing redox orbitals and their potentials in advanced lithium-ion battery materials using high-resolution x-ray Compton scattering. Science Advances, 2017, 3, e1700971.	4.7	24
31845	Î'â€Doping Effects on Electronic and Energetic Properties of LaAlO₃/SrTiO₃ Heterostructure: Firstâ€Principles Analysis of 23 Transitionâ€Metal Dopants. Advanced Materials Interfaces, 2017, 4, 1700579.	1.9	8
31846	Gateâ€Voltage Control of Borophene Structure Formation. Angewandte Chemie, 2017, 129, 15623-15628.	1.6	18
31847	First-principles/Phase-field modeling of Î¸â€² precipitation in Al-Cu alloys. Acta Materialia, 2017, 140, 344-354.	3.8	75
31848	Thermoelectric power factor of Bi-Sb-Te and Bi-Te-Se alloys and doping strategy: First-principles study. Journal of Alloys and Compounds, 2017, 727, 1067-1075.	2.8	16
31849	Water Adsorption and Insertion in MOF-5. ACS Omega, 2017, 2, 4921-4928.	1.6	59
31850	Surface effects on converse piezoelectricity of crystals. Physical Chemistry Chemical Physics, 2017, 19, 24724-24734.	1.3	7
31851	Understanding CO2 capture mechanisms in aqueous hydrazine via combined NMR and first-principles studies. Physical Chemistry Chemical Physics, 2017, 19, 24067-24075.	1.3	12
31852	Ab initio molecular dynamics study of collective dynamics in liquid Tl: Thermo-viscoelastic analysis. EPJ Web of Conferences, 2017, 151, 02001.	0.1	0
31853	White-light emission of blue-luminescent graphene quantum dots by europium (III) complex incorporation. Carbon, 2017, 124, 479-485.	5.4	36
31854	Switching charge transfer of C3N4/W18O49 from type-II to Z-scheme by interfacial band bending for highly efficient photocatalytic hydrogen evolution. Nano Energy, 2017, 40, 308-316.	8.2	346
31855	First principles studies on the selectivity of dimethoxymethane and methyl formate in methanol oxidation over V₂O₅/TiO₂-based catalysts. Physical Chemistry Chemical Physics, 2017, 19, 19393-19406.	1.3	9
31856	Room temperature quantum spin Hall insulator: Functionalized stanene on layered PbI2 substrate. Applied Physics Letters, 2017, 111, .	1.5	12
31857	Electronic transport in partially ionized water plasmas. Physics of Plasmas, 2017, 24, 092306.	0.7	24
31858	Strain broadening of the 1042-nm zero phonon line of the <mml:math xmlns:mml="http://www.w3.org/1998/Math/MathML"><mml:msup><mml:mrow><mml:mi>NV</mml:mi></mml:mrow><mml:mo>â˜	1.1	18

#	Article	IF	Citations
31859	DFTÂ+ U and ab initio atomistic thermodynamics approache for mixed transitional metallic oxides: A case study of CoCu 2 O 3 surface terminations. Materials Chemistry and Physics, 2017, 201, 241-250.	2.0	13
31860	Modulation of electronic structures of MoSe2/WSe2 van der Waals heterostructure by external electric field. Solid State Communications, 2017, 266, 11-15.	0.9	10
31861	Theoretical Investigation of Methane Hydroxylation over Isoelectronic [FeO]²⁺- and [MnO]⁺-Exchanged Zeolites Activated by N₂O. Inorganic Chemistry, 2017, 56, 10370-10380.	1.9	32
31862	Acetylene and Ethylene Adsorption on a Î²-Mo₂C(100) Surface: A Periodic DFT Study on the Role of C- and Mo-Terminations for Bonding and Hydrogenation Reactions. Journal of Physical Chemistry C, 2017, 121, 19786-19795.	1.5	22
31863	Spatial Heterogeneities and Onset of Passivation Breakdown at Lithium Anode Interfaces. Journal of Physical Chemistry C, 2017, 121, 20188-20196.	1.5	48
31864	Route to Stable Lead-Free Double Perovskites with the Electronic Structure of CH₃NH₃PbI₃: A Case for Mixed-Cation [Cs/CH₃NH₃/CH(NH₂)₂]₂InBiBr₆. Journal of Physical Chemistry Letters, 2017, 8, 3917-3924.	2.1	82
31865	Gap maximum of graphene nanoflakes: a first-principles study combined with the Monte Carlo tree search method. RSC Advances, 2017, 7, 37881-37886.	1.7	5
31866	Novel two-dimensional ferroelectric PbTe under tension: A first-principles prediction. Journal of Applied Physics, 2017, 122, .	1.1	30
31867	Large magnetoelectric effect in the strained CoPt/SrTiO3 junction. Journal of Applied Physics, 2017, 122, 065302.	1.1	0
31868	Orientation-dependent properties of epitaxially strained perovskite oxide thin films: Insights from first-principles calculations. Physical Review B, 2017, 95, .	1.1	22
31869	Revealing the Nitridation Effects on GaN Surface by First-Principles Calculation and X-Ray/Ultraviolet Photoemission Spectroscopy. IEEE Transactions on Electron Devices, 2017, 64, 4036-4043.	1.6	25
31870	Gateâ€Voltage Control of Borophene Structure Formation. Angewandte Chemie - International Edition, 2017, 56, 15421-15426.	7.2	44
31871	Dense CO Adlayers as Enablers of CO Hydrogenation Turnovers on Ru Surfaces. Journal of the American Chemical Society, 2017, 139, 11789-11802.	6.6	54
31872	Direct Observation of Double Hydrogen Transfer via Quantum Tunneling in a Single Porphycene Molecule on a Ag(110) Surface. Journal of the American Chemical Society, 2017, 139, 12681-12687.	6.6	49
31873	Pressure-induced abnormal insulating state in triangular layered cobaltite Li_xCoO₂ (x = 0.9). Journal of Materials Chemistry A, 2017, 5, 19390-19397.	5.2	9
31874	Two-dimensional graphene-directed formation of cylindrical iron carbide nanocapsules for Fischerâ€“Tropsch synthesis. Catalysis Science and Technology, 2017, 7, 4609-4621.	2.1	56
31875	New phases of 3d-transition metalâ€“cerium binary compounds: an extensive structural search. RSC Advances, 2017, 7, 40486-40498.	1.7	10
31876	Surface structures and compositions of Auâ€“Rh bimetallic nanoclusters supported on thin-film Al2O3/NiAl(100) probed with CO. Journal of Chemical Physics, 2017, 147, 044704.	1.2	4

#	Article	IF	Citations
31877	Polar ordering and structural distortion in electronic domain-wall properties of BiFeO3. Journal of Applied Physics, 2017, 122, 075103.	1.1	9
31878	Redox properties of birnessite from a defect perspective. Proceedings of the National Academy of Sciences of the United States of America, 2017, 114, 9523-9528.	3.3	50
31879	Theoretical study of the thickness dependence of the metal-insulator transition in <mml:math xmlns:mml="http://www.w3.org/1998/Math/MathML"><mml:mrow><mml:msub><mml:mi>Bi</mml:mi><mml:mn>2</mml:mn></mml:n mathvariant="normal">O</mml:mi><mml:mn>8</mml:mn></mml:msub></mml:mrow></mml:math> nanosheets. Physical Review B, 2017, 96, .	1.1	1
31880	MoirÃ©-regulated self-assembly of cesium adatoms on epitaxial graphene. Physical Review B, 2017, 96, .	1.1	12
31881	Towards Highly scalable Ab Initio Molecular Dynamics (AIMD) Simulations on the Intel Knights Landing Manycore Processor. , 2017, , .		12
31882	Plane-Wave DFT Methods for Chemistry. Annual Reports in Computational Chemistry, 2017, 13, 185-228.	0.9	17
31883	Nitrogen and oxygen dual-doped hollow carbon nanospheres derived from catechol/polyamine as sulfur hosts for advanced lithium sulfur batteries. Carbon, 2017, 124, 23-33.	5.4	79
31884	Optical characteristic study of monolayer VS2 based on first-principles calculations. Solid State Communications, 2017, 266, 26-29.	0.9	9
31885	Strong Effect of Anionic Boron-Induced Bonding in LiBSi2. Inorganic Chemistry, 2017, 56, 10815-10823.	1.9	2
31886	Mechanistic Study of Selective Catalytic Reduction of NO_x with NH₃ over Mn-TiO₂: A Combination of Experimental and DFT Study. Journal of Physical Chemistry C, 2017, 121, 19859-19871.	1.5	47
31887	Hydrogen-Bond Symmetrization Breakdown and Dehydrogenation Mechanism of FeO₂H at High Pressure. Journal of the American Chemical Society, 2017, 139, 12129-12132.	6.6	34
31888	Magnetism and spin entropy in Ru doped Na0.5CoO2. Physical Chemistry Chemical Physics, 2017, 19, 23425-23430.	1.3	7
31889	Structure and photoluminescence study of silicon based two-dimensional Si2Te3 nanostructures. Journal of Applied Physics, 2017, 122, .	1.1	23
31890	Bias voltage effects on tunneling magnetoresistance in Fe/ <mml:math xmlns:mml="http://www.w3.org/1998/Math/MathML"><mml:msub><mml:mi mathvariant="normal">MgAl</mml:mi><mml:mn>2</mml:mn></mml:msub><mml:msub><mml:mi mathvariant="normal">O</mml:mi><mml:mn>4</mml:mn></mml:msub><mml:mo>/</mml:mo><mml:mi mathvariant="normal">Fe</mml:mi><mml:mo>(</mml:mo><mml:mn>001</mml:mn><mml:mo>)</mml:mo></mml:math> junctions: Comparative study with Fe/MgO/Fe(001) junctions. Physical Review B, 2017, 96, .	1.1	17
31891	Theoretical study of the pressure-induced topological phase transition in LaSb. Physical Review B, 2017, 96, .	1.1	27
31892	Topâ€Down Synthesis of Hollow Graphene Nanostructures for Use in Resistive Switching Memory Devices. Advanced Electronic Materials, 2017, 3, 1700264.	2.6	7
31893	Energetics of halogen impurities in thorium dioxide. Journal of Nuclear Materials, 2017, 495, 192-201.	1.3	5
31894	Pt skin coated hollow Ag-Pt bimetallic nanoparticles with high catalytic activity for oxygen reduction reaction. Journal of Power Sources, 2017, 365, 17-25.	4.0	25

#	Article	IF	Citations
31895	Catalytic Activity and Product Selectivity Trends for Carbon Dioxide Electroreduction on Transition Metal-Coated Tungsten Carbides. Journal of Physical Chemistry C, 2017, 121, 20306-20314.	1.5	35
31896	Surface Reaction Barriometry: Methane Dissociation on Flat and Stepped Transition-Metal Surfaces. Journal of Physical Chemistry Letters, 2017, 8, 4177-4182.	2.1	75
31897	Atomically Abrupt Topological pâ€“n Junction. ACS Nano, 2017, 11, 9671-9677.	7.3	26
31898	Considering the spinâ€“orbit coupling effect on the photocatalytic performance of AlN/MX₂ nanocomposites. Journal of Materials Chemistry C, 2017, 5, 9412-9420.	2.7	36
31899	Rotational superstructure in van der Waals heterostructure of self-assembled C₆₀ monolayer on the WSe₂ surface. Nanoscale, 2017, 9, 13245-13256.	2.8	23
31900	Li states on a Câ€“H vacancy in graphane: a first-principles study. RSC Advances, 2017, 7, 39748-39757.	1.7	7
31901	Transition metal partially supported graphene: Magnetism and oscillatory electrostatic potentials. Journal of Applied Physics, 2017, 122, .	1.1	2
31902	General procedure for the calculation of accurate defect excitation energies from DFT-1/2 band structures: The case of the <mml:math xmlns:mml="http://www.w3.org/1998/Math/MathML"><mml:msup><mml:mrow><mml:mi>NV</mml:mi></mml:mrow><mml:mo>â˜	1.1	19
31903	Creation of half-metallic <mml:math xmlns:mml="http://www.w3.org/1998/Math/MathML"><mml:mi>f</mml:mi></mml:math> -orbital Dirac fermion with superlight elements in orbital-designed molecular lattice. Physical Review B, 2017, 96, .	1.1	10
31904	Stacking in incommensurate graphene/hexagonal-boron-nitride heterostructures based on ab initio study of interlayer interaction. Physical Review B, 2017, 96, .	1.1	23
31905	Polymer-modified halide perovskite films for efficient and stable planar heterojunction solar cells. Science Advances, 2017, 3, e1700106.	4.7	588
31906	Application of the weighted-density approximation to the accurate description of electron-positron correlation effects in materials. Physical Review B, 2017, 96, .	1.1	7
31907	Tunable and laser-reconfigurable 2D heterocrystals obtained by epitaxial stacking of crystallographically incommensurate Bi ₂ Se ₃ and MoS ₂ atomic layers. Science Advances, 2017, 3, e1601741.	4.7	39
31908	Modelling oxygen defects in orthorhombic LaMnO₃ and its low index surfaces. Physical Chemistry Chemical Physics, 2017, 19, 24636-24646.	1.3	25
31909	The adsorption of Cu on the CeO₂(110) surface. Physical Chemistry Chemical Physics, 2017, 19, 27191-27203.	1.3	17
31910	Magnetic domain configuration of (111)-oriented LaFeO3 epitaxial thin films. APL Materials, 2017, 5, .	2.2	7
31911	Hybrid-Functional Calculations of the Copper Impurity in Silicon. Physical Review Applied, 2017, 8, .	1.5	13
31912	Tetrahedral bonding in twisted bilayer graphene by carbon intercalation. European Physical Journal B, 2017, 90, 1.	0.6	0

#	Article	IF	Citations
31913	Mechanical bending induced catalytic activity enhancement of monolayer 1ÂTâ€™-MoS2 for hydrogen evolution reaction. Journal of Nanoparticle Research, 2017, 19, 1.	0.8	12
31914	Surface Reactivity of the Vanadium Phosphate Catalyst for the Oxidation of Methane. Topics in Catalysis, 2017, 60, 1698-1708.	1.3	4
31915	Exploring an effective oxygen reduction reaction catalyst via 4eâ^' process based on waved-graphene. Science China Materials, 2017, 60, 739-746.	3.5	11
31916	Band gap modulation and indirect to direct band gap transition in ZnS/Si and Si/ZnS core/shell nanowires. Physica B: Condensed Matter, 2017, 524, 163-172.	1.3	11
31917	First-Principles Simulation of the (Liâ€“Niâ€“Vacancy)O Phase Diagram and Its Relevance for the Surface Phases in Ni-Rich Li-Ion Cathode Materials. Chemistry of Materials, 2017, 29, 7840-7851.	3.2	79
31918	Initial-Stage Oxidation of Ni₃Al(100) and -(110) from Ab Initio Thermodynamics. Journal of Physical Chemistry C, 2017, 121, 19191-19200.	1.5	12
31919	In Situ Spectroscopy and Mechanistic Insights into CO Oxidation on Transition-Metal-Substituted Ceria Nanoparticles. ACS Catalysis, 2017, 7, 6843-6857.	5.5	78
31920	Steam Reforming of Acetic Acid over Co-Supported Catalysts: Coupling Ketonization for Greater Stability. ACS Sustainable Chemistry and Engineering, 2017, 5, 9136-9149.	3.2	25
31921	First principles study of the Mn-doping effect on the physical and chemical properties of mullite-family Al₂SiO₅. Physical Chemistry Chemical Physics, 2017, 19, 24991-25001.	1.3	5
31922	Low-temperature-flux syntheses of ultraviolet-transparent borophosphates Na₄MB₂P₃O₁₃(M = Rb, Cs) exhibiting a second-harmonic generation response. Dalton Transactions, 2017, 46, 12605-12611.	1.6	17
31923	Electronic structures of hybrid graphane/boron nitride nanoribbons with hydrogen vacancies. AIP Advances, 2017, 7, .	0.6	1
31924	Correlation between local structure and glass forming ability enhanced by similar element substitution in (La-Ce)-Co-Al bulk metallic glasses. Journal of Applied Physics, 2017, 122, 085103.	1.1	3
31925	Half-metallic properties of CoS₂, doped CoN_{0.25}S_{1.75}and CoP_{0.25}S_{1.75}. Materials Research Express, 2017, 4, 086306.	0.8	4
31926	Ab initio calculation of spin-orbit coupling for an NV center in diamond exhibiting dynamic Jahn-Teller effect. Physical Review B, 2017, 96, .	1.1	68
31927	Quantum Dot Self-Assembly Driven by a Surfactant-Induced Morphological Instability. Physical Review Letters, 2017, 119, 086101.	2.9	18
31928	Adsorption of self-assembled monolayer on Cu(111): First-principles study. Modern Physics Letters B, 2017, 31, 1750198.	1.0	0
31929	Structural, mechanical and electronic properties of CaB ₂ C ₂ at high pressure. Europhysics Letters, 2017, 118, 66001.	0.7	2
31930	Geometric, electronic and optical properties of undoped and cerium-doped La5(Si2+B1â^')(O13â^'N) solid solutions: A theoretical investigation. Journal of Luminescence, 2017, 192, 1026-1032.	1.5	2

#	Article	IF	Citations
31931	Pressure-induced stable BeN 4 as a high-energy density material. Journal of Power Sources, 2017, 365, 155-161.	4.0	43
31932	Revisiting the Siâ€“Te System: SiTe₂ Finally Found by Means of Experimental and Quantum-Chemical Techniques. Inorganic Chemistry, 2017, 56, 11398-11405.	1.9	21
31933	Quantum Chemical Investigation of the Selenite Incorporation into the Calcite (101Ì…4) Surface. Journal of Physical Chemistry C, 2017, 121, 20217-20228.	1.5	12
31934	Intrinsic Defect Physics in Indium-based Lead-free Halide Double Perovskites. Journal of Physical Chemistry Letters, 2017, 8, 4391-4396.	2.1	71
31935	A first-principles study on zigzag phosphorene nanoribbons passivated by iron-group atoms. Physical Chemistry Chemical Physics, 2017, 19, 25441-25445.	1.3	11
31936	Pressure-induced superconductivity up to 13.1 K in the pyrite phase of palladium diselenide <mml:math xmlns:mml="http://www.w3.org/1998/Math/MathML"><mml:mrow><mml:mi>PdS</mml:mi><mml:msub><mml:mi mathvariant="normal">e</mml:mi><mml:mn>2</mml:mn></mml:msub></mml:mrow></mml:math>. Physical Review B, 2017, 96, .	1.1	66
31937	Design of ultrathin Pt-Mo-Ni nanowire catalysts for ethanol electrooxidation. Science Advances, 2017, 3, e1603068.	4.7	224
31938	Prediction and synthesis of a family of atomic laminate phases with KagomÃ©-like and in-plane chemical ordering. Science Advances, 2017, 3, e1700642.	4.7	156
31939	Enhanced photovoltaic performance and stability with a new type of hollow 3D perovskite {en}FASnI ₃. Science Advances, 2017, 3, e1701293.	4.7	325
31940	Subnanometric Hybrid Pd-M(OH)2, MÂ= Ni, Co, Clusters in Zeolites as Highly Efficient Nanocatalysts for Hydrogen Generation. CheM, 2017, 3, 477-493.	5.8	212
31941	Finding and characterization of an energetically favorable cubic Ce0.75Zr0.25O2 solid solution using genetic algorithm and density functional theory. Computational Materials Science, 2017, 138, 219-224.	1.4	5
31942	An experimental and first-principles investigation of noncentrosymmetric cubic Re3W. Journal of Alloys and Compounds, 2017, 728, 984-991.	2.8	3
31943	Computational Study of Halide Perovskite-Derived A₂BX₆ Inorganic Compounds: Chemical Trends in Electronic Structure and Structural Stability. Chemistry of Materials, 2017, 29, 7740-7749.	3.2	215
31944	(C₆H₅C₂H₄NH₃)₂GeI₄: A Layered Two-Dimensional Perovskite with Potential for Photovoltaic Applications. Journal of Physical Chemistry Letters, 2017, 8, 4402-4406.	2.1	98
31945	Toward a Comprehensive Understanding of Enhanced Photocatalytic Activity of the Bimetallic PdAu/TiO₂ Catalyst for Selective Oxidation of Methanol to Methyl Formate. ACS Applied Materials & Interfaces, 2017, 9, 31825-31833.	4.0	36
31946	Beta transmutations in apatites with ferric iron as an electron acceptor â€“ implication for nuclear waste form development. Physical Chemistry Chemical Physics, 2017, 19, 25487-25497.	1.3	7
31947	Geometric and electronic properties of ultrathin anatase TiO₂(001) films. Physical Chemistry Chemical Physics, 2017, 19, 25456-25462.	1.3	15
31948	Electronic band structures and excitonic properties of delafossites: A GW-BSE study. Journal of Applied Physics, 2017, 122, 085104.	1.1	22

#	Article	IF	Citations
31949	First-principles and molecular dynamics study of thermoelectric transport properties of N-type silicon-based superlattice-nanocrystalline heterostructures. Journal of Applied Physics, 2017, 122, 085105.	1.1	12
31950	Effects of the Hubbard U on density functional-based predictions of BiFeO₃properties. Journal of Physics Condensed Matter, 2017, 29, 445501.	0.7	25
31951	The structural phases and vibrational properties of Mo _{1â^'x} W _x Te ₂ alloys. 2D Materials, 2017, 4, 045008.	2.0	65
31952	Ab initio study of ceria films for resistive switching memory applications. Materials Research Express, 2017, 4, 106301.	0.8	11
31953	Geometric and electronic structure of the Cs-doped <mml:math xmlns:mml="http://www.w3.org/1998/Math/MathML"><mml:mrow><mml:msub><mml:mi>Bi</mml:mi><mml:mn>2</mml:mn></mml:msub></mml:mrow></mml:math> (0001) surface. Physical Review B, 2017, 95, .	3.8	8
31954	Band Gaps and Band Offsets of Monolayer <mml:math xmlns:mml="http://www.w3.org/1998/Math/MathML" display="inline"><mml:mrow><mml:mi>Ïf</mml:mi><mml:mtext>â^'</mml:mtext><mml:mi>Ï€</mml:mi></mml:mrow></mml:math> Interband Scattering in <mml:math xmlns:mml="http://www.w3.org/1998/Math/MathML" display="inline"><mml:mrow><mml:msub><mml:mrow><mml:mi>MgB</mml:mi></mml:mrow><mml:mrow><mml:mn>2</mml:mn></mml:mrow></mml:msub></mml:mrow></mml:math>. Physical Review Letters, 2017, 119, 097002.	2.9	16
31955	Investigation of cobalt doped tin dioxide structure and defects: Density functional theory and empirical force fields. Journal of Contemporary Physics, 2017, 52, 227-233.	0.1	8
31956	Probing the Unique Role of Gallium in Amorphous Oxide Semiconductors through Structureâ€“Property Relationships. Advanced Electronic Materials, 2017, 3, 1700189.	2.6	32
31957	Strengthening and strain hardening mechanisms in a precipitation-hardened high-Mn lightweight steel. Acta Materialia, 2017, 140, 258-273.	3.8	179
31958	Surface Chemistry Mechanism of Ultra-Low Interfacial Resistance in the Solid-State Electrolyte Li₇La₃Zr₂O₁₂. Chemistry of Materials, 2017, 29, 7961-7968.	3.2	612
31959	Probing Biomolecular Interactions with Gold Nanoparticle-Decorated Single-Walled Carbon Nanotubes. Journal of Physical Chemistry C, 2017, 121, 20813-20820.	1.5	9
31960	Electronic excitation induced hydrogen-bond adjustment and lattice control in organicâ€“inorganic hybrid cubic perovskites: a fixed occupation molecular dynamics study. Physical Chemistry Chemical Physics, 2017, 19, 26164-26168.	1.3	2
31961	First-principles study of conducting behavior of warm dense neon. Physics of Plasmas, 2017, 24, 082709.	0.7	2
31962	First principles investigation of carbon-screw dislocation interactions in body-centered cubic metals. Modelling and Simulation in Materials Science and Engineering, 2017, 25, 084001.	0.8	26
31963	Hopping processes explain linear rise in temperature of thermal conductivity in thermoelectric clathrates with off-center guest atoms. Physical Review B, 2017, 96, .	1.1	15
31964	Raman spectroscopy and x-ray diffraction of <mml:math xmlns:mml="http://www.w3.org/1998/Math/MathML"><mml:mrow><mml:msup><mml:mrow><mml:mi mathvariant="italic">sp</mml:mi></mml:mrow><mml:mn>3</mml:mn></mml:msup><mml:mspace width="4pt" /><mml:mi>CaC</mml:mi><mml:msub><mml:mi mathvariant="normal">O</mml:mi><mml:mn>3</mml:mn></mml:msub></mml:mrow></mml:math> at lower mantle pressures. Physical Review B, 2017, 96, .	1.1	54
31965	Low-energy transmission electron diffraction and imaging of large-area graphene. Science Advances, 2017, 3, e1603231.	4.7	35
31966	Scaling reducibility of metal oxides. Theoretical Chemistry Accounts, 2017, 136, 1.	0.5	67

#	Article	IF	Citations
31967	Electronic and optical properties of the wurtzite-ZnO/CH3NH3PbI3 interface: first-principles calculations. Journal of Materials Science, 2017, 52, 13841-13851.	1.7	10
31968	Solute-induced solid-solution softening and hardening in bcc tungsten. Acta Materialia, 2017, 141, 304-316.	3.8	88
31969	Low pressure hydrogen sensing based on carbon nanotube field emission: Mechanism of atomic adsorption induced work function effects. Carbon, 2017, 124, 669-674.	5.4	13
31970	First-principles calculations on the stacking fault energy, surface energy and dislocation properties of NbCr2 and HfCr2. Computational Materials Science, 2017, 140, 334-343.	1.4	13
31971	Active learning of linearly parametrized interatomic potentials. Computational Materials Science, 2017, 140, 171-180.	1.4	360
31972	Effects of boron and carbon on the ideal strength of Ni solution and Ni3Al intermetallics: A first-principles study of tensile deformation. Computational Materials Science, 2017, 140, 140-147.	1.4	15
31973	A crystal plasticity model incorporating the effects of precipitates in superalloys: Application to tensile, compressive, and cyclic deformation of Inconel 718. International Journal of Plasticity, 2017, 99, 162-185.	4.1	127
31974	Electronic structural, optical and phonon lattice dynamical properties of pure- and La-doped SrTiO 3 : An ab initio thermodynamics study. Journal of Solid State Chemistry, 2017, 256, 239-251.	1.4	32
31975	Enormous excitonic effects in bulk, mono- and bi- layers of cuprous halides using many-body perturbation technique. Solid State Communications, 2017, 265, 41-46.	0.9	3
31976	Ferromagnetic properties of Mn-doped HfS 2 monolayer under strain. Solid State Communications, 2017, 268, 15-19.	0.9	6
31977	Fundamental Semiconducting Properties of Perovskite Oxynitride SrNbO₂N: Epitaxial Growth and Characterization. Chemistry of Materials, 2017, 29, 7697-7703.	3.2	17
31978	Ionic Conductivity in Ti-Doped KFeO₂: Experiment and Mathematical Modeling. Journal of Physical Chemistry C, 2017, 121, 21128-21135.	1.5	16
31979	Anomalous Frictional Behaviors of Ir and Au Tips Sliding on Graphene/Ni(111) Substrate: Density Functional Theory Calculations. Journal of Physical Chemistry C, 2017, 121, 21397-21404.	1.5	16
31980	A Novel Intrinsic Interface State Controlled by Atomic Stacking Sequence at Interfaces of SiC/SiO₂. Nano Letters, 2017, 17, 6458-6463.	4.5	36
31981	LiMn₂O₄ Surface Chemistry Evolution during Cycling Revealed by in Situ Auger Electron Spectroscopy and X-ray Photoelectron Spectroscopy. ACS Applied Materials & Interfaces, 2017, 9, 33968-33978.	4.0	37
31982	Highly Controllable and Efficient Synthesis of Mixed-Halide CsPbX₃ (X = Cl, Br, I) Perovskite QDs toward the Tunability of Entire Visible Light. ACS Applied Materials & Interfaces, 2017, 9, 33020-33028.	4.0	132
31983	The Positive Role of Hydrogen on the Dehydrogenation of Propane on Pt(111). ACS Catalysis, 2017, 7, 7495-7508.	5.5	95
31984	Significance of Surface Formate Coverage on the Reaction Kinetics of Methanol Synthesis from CO₂ Hydrogenation over Cu. ACS Catalysis, 2017, 7, 7187-7195.	5.5	83

#	Article	IF	Citations
31985	Multicontrol Over Grapheneâ€“Molecule Hetereojunctions. ACS Omega, 2017, 2, 5824-5830.	1.6	2
31986	Highly Efficient and Stable Narrow-Band Red Phosphor Cs₂SiF₆:Mn⁴⁺ for High-Power Warm White LED Applications. ACS Photonics, 2017, 4, 2556-2565.	3.2	177
31987	Direct observation of multiple rotational stacking faults coexisting in freestanding bilayer MoS2. Scientific Reports, 2017, 7, 8323.	1.6	15
31988	First-principles study of crystallographic slip modes in Ï‰-Zr. Scientific Reports, 2017, 7, 8932.	1.6	10
31989	Carrier scattering in quasi-free standing graphene on hexagonal boron nitride. Nanoscale, 2017, 9, 15934-15944.	2.8	7
31990	Origin of the optical anisotropy and the electronic structure of Ru-based double perovskite oxides: DFT and XPS studies. RSC Advances, 2017, 7, 43531-43539.	1.7	8
31991	Two-dimensional VS₂ monolayers as potential anode materials for lithium-ion batteries and beyond: first-principles calculations. Journal of Materials Chemistry A, 2017, 5, 21370-21377.	5.2	176
31992	Intrinsic magnetism and electronic structure of graphene-like Be₃C₂ nanoribbons and their Si, Ge analogues: a computational study. Journal of Materials Chemistry C, 2017, 5, 10728-10736.	2.7	11
31993	A topological study of chemical bonds under pressure: solid hydrogen as a model case. Physical Chemistry Chemical Physics, 2017, 19, 26381-26395.	1.3	7
31994	First principles studies of CO₂ and O₂ chemisorption on La₂O₃ surfaces. Physical Chemistry Chemical Physics, 2017, 19, 26799-26811.	1.3	21
31995	Surface chemistry of MgO/SiO₂ catalyst during the ethanol catalytic conversion to 1,3-butadiene: in-situ DRIFTS and DFT study. Catalysis Science and Technology, 2017, 7, 4648-4668.	2.1	58
31996	Hierarchical cobaltâ€“nitride and â€“oxide co-doped porous carbon nanostructures for highly efficient and durable bifunctional oxygen reaction electrocatalysts. Nanoscale, 2017, 9, 15846-15855.	2.8	29
31997	Epitaxial fabrication of two-dimensional NiSe2 on Ni(111) substrate. Applied Physics Letters, 2017, 111, .	1.5	29
31998	Magnetic two-dimensional organic topological insulator: Auâ€“1,3,5-triethynylbenzene framework. Journal of Chemical Physics, 2017, 147, 104704.	1.2	9
31999	Defects and oxidation of group-III monochalcogenide monolayers. Journal of Chemical Physics, 2017, 147, 104709.	1.2	35
32000	Oriented tuning the photovoltaic properties ofÎ³-RbGeX₃by strain-induced electron effective mass mutation. Journal Physics D: Applied Physics, 2017, 50, 465101.	1.3	50
32001	Nucleation and growth of WSe ₂ : enabling large grain transition metal dichalcogenides. 2D Materials, 2017, 4, 045019.	2.0	96
32002	AbÂinitio Surface Phase Diagram of Sn/Cu(001) : Reconciling Experiments with Theory. Physical Review Applied, 2017, 8, .	1.5	2

#	Article	IF	Citations
32003	Three-dimensional topological critical Dirac semimetal in <mml:math xmlns:mml="http://www.w3.org/1998/Math/MathML"><mml:mrow><mml:mi>A</mml:mi><mml:mi>MgBi</mml:mi></mml:mrow><mm width="0.16em" /><mml:mo>(</mml:mo><mml:mrow><mml:mi>A</mml:mi><mml:mo>=</mml:mo></mml:mrow></mml:math>) Tj ETQq0 0 0 rgBT /Ov	1.1	39
32004	Unexpected Large Hole Effective Masses in SnSe Revealed by Angle-Resolved Photoemission Spectroscopy. Physical Review Letters, 2017, 119, 116401.	2.9	47
32005	Multiple structural transitions driven by spin-phonon couplings in a perovskite oxide. Science Advances, 2017, 3, e1700288.	4.7	42
32006	First-principles study on electronic properties of stanene/WS₂ monolayer. Modern Physics Letters B, 2017, 31, 1750271.	1.0	7
32007	<i>Ab Initio</i> Based Modelling of Diffusion and Phase Stability of Alloys. , 0, 12, 1-22.		1
32008	Characterization of Edge Contact: Atomically Resolved Semiconductorâ€“Metal Lateral Boundary in MoS₂. Advanced Materials, 2017, 29, 1702931.	11.1	14
32009	Adaptive Simulation Selection for the Discovery of the Ground State Line of Binary Alloys with a Limited Computational Budget. Fields Institute Communications, 2017, , 185-211.	0.6	6
32010	Screw dislocation mediated solution strengthening of substitutional Î±-Ti alloys - First principles investigation. Acta Materialia, 2017, 141, 405-418.	3.8	26
32011	First-principles study of the heavy metal atoms X (X=Au, Hg, Tl or Pb) doped monolayer WS 2. Superlattices and Microstructures, 2017, 112, 224-229.	1.4	5
32012	Pressure-Induced Stable Li₅P for High-Performance Lithium-Ion Batteries. Journal of Physical Chemistry C, 2017, 121, 21199-21205.	1.5	36
32013	Effect of Embedding Platinum Clusters in Alumina on Sintering, Coking, and Activity. Journal of Physical Chemistry C, 2017, 121, 21527-21534.	1.5	9
32014	A universal strategy for the creation of machine learning-based atomistic force fields. Npj Computational Materials, 2017, 3, .	3.5	188
32015	Mechanistic study of Na-ion diffusion and small polaron formation in KrÃ¶hnkite Na₂Fe(SO₄)₂Â·2H₂O based cathode materials. Journal of Materials Chemistry A, 2017, 5, 21726-21739.	5.2	18
32016	Exact location of dopants below the Si(001):H surface from scanning tunneling microscopy and density functional theory. Physical Review B, 2017, 95, .	1.1	10
32017	Importance of elastic finite-size effects: Neutral defects in ionic compounds. Physical Review B, 2017, 96, .	1.1	22
32018	Magnetic field-temperature phase diagram of multiferroic <mml:math xmlns:mml="http://www.w3.org/1998/Math/MathML"><mml:mrow><mml:mrow><mml:mo>[</mml:mo><mml:msub><mml:mrow><mml:mrow><mm Physical Review B, 2017, 96, .	1.1	24
32022	Conformation-based signal transfer and processing at the single-molecule level. Nature Nanotechnology, 2017, 12, 1071-1076.	15.6	37
32023	Dissociative iodomethane adsorption on Ag-MOR and the formation of AgI clusters: an ab initio molecular dynamics study. Physical Chemistry Chemical Physics, 2017, 19, 27530-27543.	1.3	41

#	Article	IF	Citations
32024	Computational prediction of a simple cubic carbon allotrope consisting of C12 clusters. Journal of Chemical Physics, 2017, 147, 064512.	1.2	6
32025	Manipulation of ionized impurity scattering for achieving high thermoelectric performance in n-type Mg ₃ Sb ₂ -based materials. Proceedings of the National Academy of Sciences of the United States of America, 2017, 114, 10548-10553.	3.3	267
32026	Atomically inspired<mml:math xmlns:mml="http://www.w3.org/1998/Math/MathML"><mml:mrow><mml:mi>k</mml:mi><mml:mo>Â·</mml:mo><mml:mi>p</mml:mi></mml:mi> and valley Zeeman effect in transition metal dichalcogenide monolayers. Physical Review B, 2017, 95, .	1.1	96
32027	Mechanism of nucleation and incipient growth of Re clusters in irradiated W-Re alloys from kinetic Monte Carlo simulations. Physical Review B, 2017, 96, .	1.1	48
32028	Dynamic simulation of structural phase transitions in magnetic iron. Physical Review B, 2017, 96, .	1.1	36
32029	Towards understanding MgO/Fe interface formation: Adsorption of O and Mg atoms on an Fe(001) surface. Physical Review B, 2017, 96, .	1.1	6
32030	Enthalpies of formation of layered LiNixMnxCo1â€“2xO2 (0 â‰¤ x â‰¤ 0.5) compounds as lithium ion battery cathode materials. International Journal of Materials Research, 2017, 108, 869-878.	0.1	16
32031	Strain engineering effect on surprising magnetic semiconducting behavior in zigzag arsenene nanoribbons. Computational Materials Science, 2017, 139, 185-190.	1.4	9
32032	Prediction of stable ground-state and pressure-induced phase transition of molybdenum monosulfide. Materials Science and Engineering B: Solid-State Materials for Advanced Technology, 2017, 226, 114-119.	1.7	0
32033	Identifying the Ground State Geometry of a MoN₂ Sheet through a Global Structure Search and Its Tunable p-Electron Half-Metallicity. Chemistry of Materials, 2017, 29, 8588-8593.	3.2	44
32034	Optimal Size of a Cylindrical Pore for Post-Combustion CO₂ Capture. Journal of Physical Chemistry C, 2017, 121, 22025-22030.	1.5	9
32035	Adsorption and Diffusion of Fluids in Defective Carbon Nanotubes: Insights from Molecular Simulations. Langmuir, 2017, 33, 11834-11844.	1.6	9
32036	Formation and Characterization of Hydrogen Boride Sheets Derived from MgB₂ by Cation Exchange. Journal of the American Chemical Society, 2017, 139, 13761-13769.	6.6	157
32037	Toward rational nanoparticle synthesis: predicting surface intermixing in bimetallic alloy nanocatalysts. Nanoscale, 2017, 9, 15005-15017.	2.8	24
32038	Topological semimetal in honeycomb lattice LnSI. Proceedings of the National Academy of Sciences of the United States of America, 2017, 114, 10596-10600.	3.3	42
32039	Simultaneous Deep Tunneling and Classical Hopping for Hydrogen Diffusion on Metals. Physical Review Letters, 2017, 119, 126001.	2.9	46
32040	Highâ€Efficiency Photovoltaic Conversion at Selective Electron Tunneling Heterointerfaces. Advanced Electronic Materials, 2017, 3, 1700211.	2.6	5
32041	Hydrogen Chemisorption on Singly Vanadiumâ€Doped Aluminum Clusters. Chemistry - A European Journal, 2017, 23, 15638-15643.	1.7	24

#	Article	IF	Citations
32042	Structural Optimization of (Au_mâ€Ag_nâ€Pd_oâ€Pt_p) (m=10) Tj ETQq0 0 0 rgBT /Ove Approach. ChemistrySelect, 2017, 2, 8063-8071.	0.7	1
32043	Effect of oxygen vacancy and surface plasmon resonance: a photocatalytic activity study on Ag/Bi4Ti3O12 nanocomposites. Journal of Materials Science: Materials in Electronics, 2017, 28, 17896-17907.	1.1	9
32044	Study of reaction mechanism of methane conversion over Ni-based oxygen carrier in chemical looping reforming. Fuel, 2017, 210, 866-872.	3.4	37
32045	Quantitative evaluation of hydrogen atoms trapped at single vacancies in tungsten using positron annihilation lifetime measurements: Experiments and theoretical calculations. Journal of Nuclear Materials, 2017, 496, 9-17.	1.3	12
32046	Bismuth Silver Oxysulfide for Photoconversion Applications: Structural and Optoelectronic Properties. Chemistry of Materials, 2017, 29, 8679-8689.	3.2	28
32047	Ion Dynamics and CO₂ Absorption Properties of Nb-, Ta-, and Y-Doped Li₂ZrO₃ Studied by Solid-State NMR, Thermogravimetry, and First-Principles Calculations. Journal of Physical Chemistry C, 2017, 121, 21877-21886.	1.5	17
32048	Reversibility of the Hydrogen Transfer in TKX-50 and Its Influence on Impact Sensitivity: An Exceptional Case from Common Energetic Materials. Journal of Physical Chemistry C, 2017, 121, 21252-21261.	1.5	26
32049	Electronic Interactions of Size-Selected Oxide Clusters on Metallic and Thin Film Oxide Supports. Journal of Physical Chemistry C, 2017, 121, 22234-22247.	1.5	12
32050	Two-Dimensional Magnetic Semiconductor in Feroxyhyte. ACS Applied Materials & Interfaces, 2017, 9, 35368-35375.	4.0	14
32051	Atomistic Origins of High Capacity and High Structural Stability of Polymer-Derived SiOC Anode Materials. ACS Applied Materials & Interfaces, 2017, 9, 35001-35009.	4.0	34
32052	Origin of Spectral Blue Shift of Lu³⁺-Codoped YAG:Ce³⁺ Phosphor: First-Principles Study. ACS Omega, 2017, 2, 5935-5941.	1.6	24
32053	Picoscale materials engineering. Nature Reviews Materials, 2017, 2, .	23.3	42
32054	Hydrodeoxygenation of water-insoluble bio-oil to alkanes using a highly dispersed Pdâ€“Mo catalyst. Nature Communications, 2017, 8, 591.	5.8	110
32055	Prediction of superconducting ternary hydride MgGeH₆: from divergent high-pressure formation routes. Physical Chemistry Chemical Physics, 2017, 19, 27406-27412.	1.3	40
32056	Machine learnt bond order potential to model metalâ€“organic (Coâ€“C) heterostructures. Nanoscale, 2017, 9, 18229-18239.	2.8	11
32057	Characterization of defects in copper antimony disulfide. Journal of Materials Chemistry A, 2017, 5, 21986-21993.	5.2	33
32058	Half-metallic TiF₃: a potential anode material for Li-ion spin batteries. Journal of Materials Chemistry A, 2017, 5, 21486-21490.	5.2	16
32059	Earth-abundant elements doping for robust and stable solar-driven water splitting by FeOOH. Journal of Materials Chemistry A, 2017, 5, 21478-21485.	5.2	54

#	Article	IF	Citations
32060	First-principles study of enhanced magnetic anisotropies in transition-metal atoms doped WS₂monolayer. Journal of Physics Condensed Matter, 2017, 29, 475803.	0.7	4
32061	Two-dimensional metal phosphorus trisulfide nanosheet with solar hydrogen-evolving activity. Nano Energy, 2017, 40, 673-680.	8.2	91
32062	Theoretical insights on the reaction pathways of the oxygen reduction reaction on yttrium doped graphene as a catalyst in fuel cells. Synthetic Metals, 2017, 232, 131-137.	2.1	1
32063	Ag₂S Quantum Dot-Sensitized Solar Cells by First Principles: The Effect of Capping Ligands and Linkers. Journal of Physical Chemistry A, 2017, 121, 7290-7296.	1.1	17
32064	Robust and Pristine Topological Dirac Semimetal Phase in Pressured Two-Dimensional Black Phosphorus. Journal of Physical Chemistry C, 2017, 121, 20931-20936.	1.5	18
32065	Catalytic Activity Control via Crossover between Two Different Microstructures. Journal of the American Chemical Society, 2017, 139, 13740-13748.	6.6	39
32066	Energy-free machine learning force field for aluminum. Scientific Reports, 2017, 7, 8512.	1.6	50
32067	Theoretical study on geometric, electronic and catalytic performances of Fe dopant pairs in graphene. Physical Chemistry Chemical Physics, 2017, 19, 26369-26380.	1.3	9
32068	On the viability of Mg extraction in MgMoN₂: a combined experimental and theoretical approach. Physical Chemistry Chemical Physics, 2017, 19, 26435-26441.	1.3	11
32069	Influence of oxygen partial pressure on the adsorption and diffusion during oxide growth: ZnO(0001) surface. Physical Review B, 2017, 96, .	1.1	6
32070	Hydrogen Clathrate Structures in Rare Earth Hydrides at High Pressures: Possible Route to Room-Temperature Superconductivity. Physical Review Letters, 2017, 119, 107001.	2.9	591
32071	Electronic structure, magnetic properties, and mixed valence character of Ce₂Ni₃Si₅ from first principles calculations. Journal of Computational Chemistry, 2017, 38, 2475-2480.	1.5	3
32072	Adsorption patterns of aromatic amino acids on monolayer MoS 2 and Au-modified MoS 2 surfaces: A first-principles study. Computational and Theoretical Chemistry, 2017, 1118, 115-122.	1.1	22
32073	Perovskite-Type InCoO3 with Low-Spin Co3+: Effect of Inâ€“O Covalency on Structural Stabilization in Comparison with Rare-Earth Series. Inorganic Chemistry, 2017, 56, 11113-11122.	1.9	7
32074	Design of Two-Dimensional Graphene-like Dirac Materials Î²₁₂-XBeB₅ (X = H, F,) Tj ETQq0 0 0 rgBT /Overlock 1 4594-4599.	2.1	23
32075	Revealing and exploiting hierarchical material structure through complex atomic networks. Npj Computational Materials, 2017, 3, .	3.5	19
32076	Inhomogeneous strain-induced half-metallicity in bent zigzag graphene nanoribbons. Npj Computational Materials, 2017, 3, .	3.5	33
32077	Structure and crystallization of SiO₂and B₂O₃doped lithium disilicate glasses from theory and experiment. Physical Chemistry Chemical Physics, 2017, 19, 25298-25308.	1.3	0

#	Article	IF	Citations
32078	Influence of antisite defects and stacking faults on the magnetocrystalline anisotropy of FePt. Physical Review B, 2017, 96, .	1.1	10
32079	Recipe for generating Weyl semimetals with extended topologically protected features. Physical Review B, 2017, 96, .	1.1	6
32080	Interface-engineered MoS2/C nanosheet heterostructure arrays for ultra-stable sodium-ion batteries. Chemical Engineering Science, 2017, 174, 104-111.	1.9	60
32081	First principles study on HenV clusters in Î±-Fe bulk and grain boundaries. Computational Materials Science, 2017, 139, 419-429.	1.4	5
32082	A comparison study of decomposition mechanisms of single-cation and double-cations (Li, Al) ammine borohydrides. International Journal of Hydrogen Energy, 2017, 42, 24861-24867.	3.8	1
32083	After-glow, luminescent thermal quenching, and energy band structure of Ce-doped yttrium aluminum-gallium garnets. Journal of Luminescence, 2017, 192, 1278-1287.	1.5	44
32084	Computational Discovery of Nickel-Based Catalysts for CO₂ Reduction to Formic Acid. Journal of Physical Chemistry C, 2017, 121, 20865-20870.	1.5	39
32085	Tip-Induced Switch of Germanene Atomic Structure. Journal of Physical Chemistry Letters, 2017, 8, 4587-4593.	2.1	21
32086	Long-Range Orientational Self-Assembly, Spatially Controlled Deprotonation, and Off-Centered Metalation of an Expanded Porphyrin. Journal of the American Chemical Society, 2017, 139, 14129-14136.	6.6	23
32087	Evaluation of the concentration of point defects in GaN. Scientific Reports, 2017, 7, 9297.	1.6	55
32088	Excellent thermoelectric properties induced by different contact geometries in phenalenyl-based single-molecule devices. Scientific Reports, 2017, 7, 10842.	1.6	19
32089	An unsaturated metal site-promoted approach to construct strongly coupled noble metal/HNb₃O₈ nanosheets for efficient thermo/photo-catalytic reduction. Nanoscale, 2017, 9, 14654-14663.	2.8	30
32090	Electronic and excitonic properties of two-dimensional and bulk InN crystals. RSC Advances, 2017, 7, 42455-42461.	1.7	34
32091	An unmodified graphene foam chemical sensor based on SVM for discrimination of chemical molecules with broad selectivity. RSC Advances, 2017, 7, 43560-43566.	1.7	3
32092	Characterization and formation of NV centers in <mml:math xmlns:mml="http://www.w3.org/1998/Math/MathML"><mml:mrow><mml:mn>3</mml:mn><mml:mi>C</mml:mi></mml:mrow><mml:m , and <mml:math xmlns:mml="http://www.w3.org/1998/Math/MathML"><mml:mrow><mml:mn>6</mml:mn><mml:mi>H</mml:mi></mml:mrow></mml:m SiC: An ab initio study. Physical Review B, 2017, 96, .	1.1	45
32093	Elastic Properties, Phonon Focusing and Electronic Structures of Typical Long-Period Superstructures Al₅Ti₂ and Al₁₁Ti₅. Materials Science Forum, 0, 898, 1026-1035.	0.3	1
32094	Constrained Ab Initio Thermodynamics: Transferring the Concept of Surface Pourbaix Diagrams in Electrocatalysis to Electrode Materials in Lithiumâ€ion Batteries. ChemElectroChem, 2017, 4, 3231-3237.	1.7	27
32095	Codoping of Ni and Fe in tetragonal BaTiO 3. Computational Condensed Matter, 2017, 13, 49-54.	0.9	6

#	Article	IF	Citations
32096	Study of the stability of small AuRh clusters found by a Genetic Algorithm methodology. Computational and Theoretical Chemistry, 2017, 1119, 51-58.	1.1	18
32097	Migration properties of mono-vacancy in W-4d/5d transition metal alloys. Journal of Alloys and Compounds, 2017, 728, 363-367.	2.8	6
32098	Electronic, optical and thermal properties of Cr 3 AlB 4 by first-principles calculations. Vacuum, 2017, 145, 234-240.	1.6	17
32099	Semiconducting Pavonites CdMBi₄Se₈ (M = Sn and Pb) and Their Thermoelectric Properties. Chemistry of Materials, 2017, 29, 8494-8503.	3.2	18
32100	Overview of the Oxygen Behavior in the Degradation of Li₂MnO₃ Cathode Material. Journal of Physical Chemistry C, 2017, 121, 21118-21127.	1.5	30
32101	An Ultrathin Single Crystalline Relaxor Ferroelectric Integrated on a High Mobility Semiconductor. Nano Letters, 2017, 17, 6248-6257.	4.5	11
32102	Phase-Field Based Multiscale Modeling of Heterogeneous Solid Electrolytes: Applications to Nanoporous Li₃PS₄. ACS Applied Materials & Interfaces, 2017, 9, 33341-33350.	4.0	21
32103	Understanding of Electrochemical Mechanisms for CO₂ Capture and Conversion into Hydrocarbon Fuels in Transition-Metal Carbides (MXenes). ACS Nano, 2017, 11, 10825-10833.	7.3	359
32104	Emergence of charge density waves and a pseudogap in single-layer TiTe2. Nature Communications, 2017, 8, 516.	5.8	90
32105	Surface reconstruction of InAs (001) depending on the pressure and temperature examined by density functional thermodynamics. Scientific Reports, 2017, 7, 10691.	1.6	14
32106	Ordering and phase separation in Gd-doped ceria: a combined DFT, cluster expansion and Monte Carlo study. Physical Chemistry Chemical Physics, 2017, 19, 26606-26620.	1.3	23
32107	Hydrogen assisted synthesis of branched nickel nanostructures: a combined theoretical and experimental study. Physical Chemistry Chemical Physics, 2017, 19, 26718-26727.	1.3	13
32108	BP ₅ monolayer with multiferroicity and negative Poissonâ€™s ratio: a prediction by global optimization method. 2D Materials, 2017, 4, 045020.	2.0	83
32109	Multiscale Examination of Strain Effects in Nd-Fe-B Permanent Magnets. Physical Review Applied, 2017, 8, .	1.5	15
32110	Subatomic electronic feature from dynamic motion of Si dimer defects in Bi nanolines on Si(001). Physical Review B, 2017, 96, .	1.1	2
32111	Cu-Sb dumbbell arrangement in the spin-orbital liquid candidate <mml:math xmlns:mml="http://www.w3.org/1998/Math/MathML"><mml:mrow><mml:msub><mml:mi>Ba</mml:mi><mml:mn>3</mml:mn></mml:msub><mml:msub><mml:mi mathvariant="normal">O</mml:mi><mml:mn>9</mml:mn></mml:msub></mml:mrow></mml:math>. Physical Review B, 2017, 96, .	1.1	4
32112	Hybrid density functional theory insight into the stability and microscopic properties of Bi-doped <mml:math xmlns:mml="http://www.w3.org/1998/Math/MathML"><mml:msub><mml:mi>LiNbO</mml:mi><mml:mn>3</mml:mn></mml:msub></m : Lone electron pair effect. Physical Review B, 2017, 96, .	1.1	20
32113	Dirac semimetal phase in hexagonal LiZnBi. Physical Review B, 2017, 96, .	1.1	26

#	Article	IF	Citations
32114	Realizing double Dirac particles in the presence of electronic interactions. Physical Review B, 2017, 96, .	1.1	23
32115	Firstâ€Principles Calculations of Quantum Efficiency for Point Defects in Semiconductors: The Example of Yellow Luminance by GaN: C_N+O_N and GaN:C_N. Advanced Optical Materials, 2017, 5, 1700404.	3.6	33
32116	A-Site Ordered Double Perovskite CaMnTi₂O₆ as a Multifunctional Piezoelectric and Ferroelectricâ€“Photovoltaic Material. Inorganic Chemistry, 2017, 56, 11854-11861.	1.9	54
32117	Density Functional Studies on Layered Perovskite Oxyhalide Bi₄MO₈X Photocatalysts (M = Nb and Ta, X = Cl, Br, and I). Journal of Physical Chemistry C, 2017, 121, 20662-20672.	1.5	24
32118	Catalysis at the Rim: A Mechanism for Low Temperature CO Oxidation over Pt₃Sn. ACS Catalysis, 2017, 7, 7431-7441.	5.5	32
32119	Prediction of Green Phosphorus with Tunable Direct Band Gap and High Mobility. Journal of Physical Chemistry Letters, 2017, 8, 4627-4632.	2.1	101
32120	Novel Au Catalysis Strategy for the Synthesis of Au@Pt Coreâ€“Shell Nanoelectrocatalyst with Self-Controlled Quasi-Monolayer Pt Skin. ACS Applied Materials & Interfaces, 2017, 9, 32688-32697.	4.0	23
32121	Origin of the emergence of higher T c than bulk in iron chalcogenide thin films. Scientific Reports, 2017, 7, 9994.	1.6	24
32122	3D Foam Strutted Graphene Carbon Nitride with Highly Stable Optoelectronic Properties. Advanced Functional Materials, 2017, 27, 1703711.	7.8	87
32123	Endohedral metallofullerenes (M@C60) as efficient catalysts for highly active hydrogen evolution reaction. Journal of Catalysis, 2017, 354, 231-235.	3.1	84
32124	On grain boundary segregation in molybdenum materials. Materials and Design, 2017, 135, 204-212.	3.3	46
32125	The analysis of the stress corrosion effects for H atom in the symmetrical tilt Ni Î£ 5 (012) grain boundary structure. Materials Today: Proceedings, 2017, 4, 7011-7017.	0.9	0
32126	Bismuthâ€“Indiumâ€“Sodium two-dimensional compounds on Si(111) surface. Surface Science, 2017, 666, 64-69.	0.8	4
32127	Large Area Atomically Flat Surfaces via Exfoliation of Bulk Bi₂Se₃ Single Crystals. Chemistry of Materials, 2017, 29, 8472-8477.	3.2	8
32128	Embedded Cluster Model for Al₂O₃ and AlPO₄ Surfaces Using Point Charges and Periodic Electrostatic Potential. Journal of Physical Chemistry C, 2017, 121, 20242-20253.	1.5	7
32129	Influence of Hubbard U Parameter in Simulating Adsorption and Reactivity on CuO: Combined Theoretical and Experimental Study. Journal of Physical Chemistry C, 2017, 121, 21343-21353.	1.5	35
32130	Spontaneous Octahedral Tilting in the Cubic Inorganic Cesium Halide Perovskites CsSnX₃ and CsPbX₃ (X = F, Cl, Br, I). Journal of Physical Chemistry Letters, 2017, 8, 4720-4726.	2.1	186
32131	Theoretical Discovery of a Superconducting Two-Dimensional Metalâ€“Organic Framework. Nano Letters, 2017, 17, 6166-6170.	4.5	86

#	Article	IF	Citations
32132	Theoretical Prediction of Surface Stability and Morphology of LiNiO₂ Cathode for Li Ion Batteries. ACS Applied Materials & Interfaces, 2017, 9, 33257-33266.	4.0	65
32133	Uric Acid as an Electrochemically Active Compound for Sodium-Ion Batteries: Stepwise Na⁺-Storage Mechanisms of Ï€-Conjugation and Stabilized Carbon Anion. ACS Applied Materials & Interfaces, 2017, 9, 33934-33940.	4.0	13
32134	Fully Atomistic Understanding of the Electronic and Optical Properties of a Prototypical Doped Charge-Transfer Interface. ACS Nano, 2017, 11, 10495-10508.	7.3	20
32135	Finite Size Effects in Submonolayer Catalysts Investigated by CO Electrosorption on Pt_{sML}/Pd(100). Journal of the American Chemical Society, 2017, 139, 13676-13679.	6.6	23
32136	A rechargeable iodine-carbon battery that exploits ion intercalation and iodine redox chemistry. Nature Communications, 2017, 8, 527.	5.8	176
32137	Superior Electronic Structure in Two-Dimensional MnPSe 3 /MoS2 van der Waals Heterostructures. Scientific Reports, 2017, 7, 9504.	1.6	28
32138	Facile microwave synthesis of ScPO₄Â·2H₂O flowerlike superstructures: morphology control, electronic structure and multicolor tunable luminescent properties. CrystEngComm, 2017, 19, 5787-5796.	1.3	8
32139	Insulator-to-metal transition of lithiumâ€“sulfur battery. RSC Advances, 2017, 7, 44326-44332.	1.7	18
32140	The influence of lattice dynamics on the electronic spectrum of CoSb₃skutterudite. Journal of Materials Chemistry C, 2017, 5, 10185-10190.	2.7	4
32141	Perovskites beyond photovoltaics: field emission from morphology-tailored nanostructured methylammonium lead triiodide. Physical Chemistry Chemical Physics, 2017, 19, 26708-26717.	1.3	10
32142	Periodic DFT+U investigation of the bulk and surface properties of marcasite (FeS2). Physical Chemistry Chemical Physics, 2017, 19, 27478-27488.	1.3	32
32143	Interface and interaction of graphene layers on SiC(0001Ì„) covered with TiC(111) intercalation. Physical Chemistry Chemical Physics, 2017, 19, 26765-26775.	1.3	1
32144	A computational study on hydrogen storage in potential wells using K-intercalated graphite oxide. RSC Advances, 2017, 7, 33953-33960.	1.7	0
32145	Tuning the p-type Schottky barrier in 2D metal/semiconductor interface:boron-sheet on MoSe2, and WSe2. Journal of Physics Condensed Matter, 2017, 29, 405002.	0.7	3
32146	Structural and electronic phase transitions of MoTe 2 induced by Li ionic gating. 2D Materials, 2017, 4, 045012.	2.0	9
32147	Local inversion symmetry breaking and spin-phonon coupling in the perovskite <mml:math xmlns:mml="http://www.w3.org/1998/Math/MathML"><mml:msub><mml:mi>GdCrO</mml:mi><mml:mn>3</mml:mn></mml:msub> Physical Review B, 2017, 96, .	1.1	43
32148	First-principles calculations on the origin of ferromagnetism in transition-metal doped Ge. Physical Review B, 2017, 96, .	1.1	10
32149	Influence of hydrogen in silicon nitride films on the surface reactions during hydrofluorocarbon plasma etching. Journal of Vacuum Science and Technology A: Vacuum, Surfaces and Films, 2017, 35, .	0.9	26

#	Article	IF	Citations
32150	Magnetoresistance and Shubnikov-de Haas oscillation in YSb. Europhysics Letters, 2017, 119, 17002.	0.7	28
32151	Transport properties and electronic structure of Na0.28PtSi. Japanese Journal of Applied Physics, 2017, 56, 075801.	0.8	5
32152	Ethers on Si(001): A Prime Example for the Common Ground between Surface Science and Molecular Organic Chemistry. Angewandte Chemie - International Edition, 2017, 56, 15150-15154.	7.2	26
32153	Strain-phonon coupling in (111)-oriented perovskite oxides. Physical Review B, 2017, 96, .	1.1	7
32154	Spin-reorientation transitions in the Cairo pentagonal magnet Bi4Fe5O13F. Physical Review B, 2017, 96, .	1.1	15
32155	Theoretical study of stability and superconductivity of<mml:math xmlns:mml="http://www.w3.org/1998/Math/MathML"><mml:msub><mml:mi>ScH</mml:mi><mml:mi>n</mml:mi></mml:msub></mml:math> at high pressure. Physical Review B, 2017, 96, .	1.1	44
32156	Coherent generation of symmetry-forbidden phonons by light-induced electron-phonon interactions in magnetite. Physical Review B, 2017, 96, .	1.1	14
32157	Sequential insulator-metal-insulator phase transitions of <mml:math xmlns:mml="http://www.w3.org/1998/Math/MathML"><mml:mrow><mml:mi mathvariant="normal">V</mml:mi><mml:msub><mml:mi mathvariant="normal">O</mml:mi><mml:mn>2</mml:mn></mml:msub></mml:mrow></mml:math>	1.1	53
32158	Structural and electronic properties of <mml:math xmlns:mml="http://www.w3.org/1998/Math/MathML"><mml:mi>Î±</mml:mi></mml:math> -(BEDT-TTF) <mml:math xmlns:mml="http://www.w3.org/1998/Math/MathML"><mml:mrow><mml:msub><mml:mrow /><mml:mn>2</mml:mn></mml:msub><mml:msub><mml:mi mathvariant="normal">I</mml:mi><mml:mn>3</mml:mn></mml:msub></mml:mrow></mml:math> , <mml:math xmlns:mml="http://www.w3.org/1998/Math/MathML"><mml:mi>Î²</mml:mi></mml:math>		

#	Article	IF	Citations
32168	Layered nanostructured ferroelectric perovskite Bi₅FeTi₃O₁₅ for visible light photodegradation of antibiotics. Journal of Materials Chemistry A, 2017, 5, 21275-21290.	5.2	88
32169	Single orthorhombic b axis orientation and antiferromagnetic ordering type in multiferroic CaMnO3 thin film with La0.67Ca0.33MnO3 buffer layer. Applied Physics Letters, 2017, 111, .	1.5	6
32170	On the First Principles Calculation of Redox Potential in Molten LiCl-KCl Eutectic Based on Adiabatic Substitution. Journal of the Electrochemical Society, 2017, 164, H846-H853.	1.3	10
32171	The Ternary Postâ€transition Metal Carbodiimide SrZn(NCN)₂. Zeitschrift Fur Anorganische Und Allgemeine Chemie, 2017, 643, 1456-1461.	0.6	15
32172	Quantum Many-Body Effects in Defective Transition-Metal-Oxide Superlattices. Journal of Chemical Theory and Computation, 2017, 13, 5604-5609.	2.3	7
32173	Projected Commutator DIIS Method for Accelerating Hybrid Functional Electronic Structure Calculations. Journal of Chemical Theory and Computation, 2017, 13, 5458-5467.	2.3	21
32174	A First-Principles Study of O₂ Dissociation on Platinum Modified Titanium Carbide: A Possible Efficient Catalyst for the Oxygen Reduction Reaction. Journal of Physical Chemistry C, 2017, 121, 21333-21342.	1.5	18
32175	Origin of Structural Degradation During Cycling and Low Thermal Stability of Ni-Rich Layered Transition Metal-Based Electrode Materials. Journal of Physical Chemistry C, 2017, 121, 22628-22636.	1.5	199
32176	Supertetrahedral Aluminum â€“ A New Allotropic Ultralight Crystalline Form of Aluminum. Journal of Physical Chemistry C, 2017, 121, 22187-22190.	1.5	11
32177	Alchemical Predictions for Computational Catalysis: Potential and Limitations. Journal of Physical Chemistry Letters, 2017, 8, 5002-5007.	2.1	48
32178	Operando Phonon Studies of the Protonation Mechanism in Highly Active Hydrogen Evolution Reaction Pentlandite Catalysts. Journal of the American Chemical Society, 2017, 139, 14360-14363.	6.6	53
32179	Electron work function â€“ a probe for interfacial diagnosis. Scientific Reports, 2017, 7, 9673.	1.6	20
32180	Simultaneous increase in strength and ductility by decreasing interface energy between Zn and Al phases in cast Al-Zn-Cu alloy. Scientific Reports, 2017, 7, 12195.	1.6	7
32181	Band gap opening of graphene by forming a graphene/PtSe₂ van der Waals heterojunction. RSC Advances, 2017, 7, 45393-45399.	1.7	60
32182	Band structure and photoconductivity of blue-green light absorbing AlTiN films. Journal of Materials Chemistry A, 2017, 5, 20824-20832.	5.2	10
32183	Curved-line search algorithm for abÂinitio atomic structure relaxation. Physical Review B, 2017, 96, .	1.1	3
32184	Exploitation of the Largeâ€Area Basal Plane of MoS₂ and Preparation of Bifunctional Catalysts through Onâ€Surface Selfâ€Assembly. Advanced Science, 2017, 4, 1700356.	5.6	9
32185	Ab Initio Modeling of Structure and Properties of Single and Mixed Alkali Silicate Glasses. Journal of Physical Chemistry A, 2017, 121, 7697-7708.	1.1	44

#	Article	IF	Citations
32186	Solvation and Dynamics of Sodium and Potassium in Ethylene Carbonate from ab Initio Molecular Dynamics Simulations. Journal of Physical Chemistry C, 2017, 121, 21913-21920.	1.5	152
32187	Catalytic Descriptors for the Design of Zieglerâ€“Natta Catalysts Revealed by the Investigation of the Clâ€“Ti(0001) Interaction by Density of States Calculations. Journal of Physical Chemistry C, 2017, 121, 20871-20876.	1.5	1
32188	Interactions of Water with the (111) and (100) Surfaces of Ceria. Journal of Physical Chemistry C, 2017, 121, 21571-21578.	1.5	33
32189	Exploiting Diffusion Barrier and Chemical Affinity of Metalâ€“Organic Frameworks for Efficient Hydrogen Isotope Separation. Journal of the American Chemical Society, 2017, 139, 15135-15141.	6.6	125
32190	Oxygen evolution on Fe-doped NiO electrocatalysts deposited via microplasma. Nanoscale, 2017, 9, 15070-15082.	2.8	60
32191	Unexpected stable stoichiometries and superconductivity of potassium-rich sulfides. RSC Advances, 2017, 7, 44884-44889.	1.7	5
32192	Finite-temperature H behaviors in tungsten and molybdenum: first-principles total energy and vibration spectrum calculations. Nuclear Fusion, 2017, 57, 126024.	1.6	8
32193	Multi-scale model for point defects behaviour in uranium mononitride. Journal of Physics: Conference Series, 2017, 781, 012044.	0.3	1
32194	Atomic defects and dopants in ternary Z-phase transition-metal nitrides <mml:math xmlns:mml="http://www.w3.org/1998/Math/MathML"><mml:mrow><mml:mi mathvariant="bold">Cr</mml:mi><mml:mi mathvariant="bold-italic">M</mml:mi><mml:mi mathvariant="bold">N</mml:mi></mml:mrow></mml:math> with <mml:math xmlns:mml="http://www.w3.org/1998/Math/MathML"><mml:mrow><mml:mi mathvariant="bold-italic">M</mml:mi><mml:mo>=</mml:mo><mml:mi mathvariant="bold">V</mml:mi><mml:	1.1	5
32195	Cu Diffusion in Amorphous Ta₂O₅ Studied with a Simplified Neural Network Potential. Journal of the Physical Society of Japan, 2017, 86, 104004.	0.7	29
32196	Role of Disproportionation in the Dissolution of Mn from Lithium Manganate Spinel. Journal of Physical Chemistry C, 2017, 121, 22049-22053.	1.5	41
32197	A comparative study of the mechanical and thermal properties of defective ZrC, TiC and SiC. Scientific Reports, 2017, 7, 9344.	1.6	34
32198	Designing functionality in perovskite thin films using ion implantation techniques: Assessment and insights from first-principles calculations. Scientific Reports, 2017, 7, 11166.	1.6	5
32199	Stability and optical properties of plutonium monoxide from first-principle calculation. Scientific Reports, 2017, 7, 12167.	1.6	13
32200	Crystal structures of Fe4C vs. Fe4N analysed by DFT calculations: Fcc-based interstitial superstructures explored. Acta Materialia, 2017, 140, 433-442.	3.8	25
32201	Intergranular fracture of tungsten containing phosphorus impurities: A first principles investigation. Computational Materials Science, 2017, 139, 368-378.	1.4	12
32202	Ab initio study of the likely orientation relationships of interphase and homophase interfaces in a two-phase HCP + BCC Mg-Li alloy. Computational Materials Science, 2017, 139, 406-411.	1.4	10
32203	Ruddlesden-Popper compounds (SrO)(LaFeO3)n (n = 1 and 2) as p-type semiconductors for photocatalytic hydrogen production. Electrochimica Acta, 2017, 252, 138-146.	2.6	29

#	Article	IF	Citations
32204	Tetragonal-prism-like Guinierâ€“Prestonâ€“Bagaryatsky zones in an AlCuMg alloy. Materials Characterization, 2017, 132, 139-144.	1.9	20
32205	Peering into the Mechanism of Low-Temperature Synthesis of Bronze-type TiO₂ in Ionic Liquids. Crystal Growth and Design, 2017, 17, 5586-5601.	1.4	21
32206	First-principles calculations of X-ray absorption spectra for warm dense methane. Physics of Plasmas, 2017, 24, 092705.	0.7	1
32207	Submolecular resolution in scanning probe images of Sn-phthalocyanines on Cu(1â€‰0â€‰0) using metal tips. Journal of Physics Condensed Matter, 2017, 29, 394004.	0.7	2
32208	Low-temperature thermal transport and thermopower of monolayer transition metal dichalcogenide semiconductors. Journal of Physics Condensed Matter, 2017, 29, 405701.	0.7	5
32209	Conditions for T2 resistivity from electron-electron scattering. European Physical Journal B, 2017, 90, 1.	0.6	12
32210	Nitrogen-vacancy diamond sensor: novel diamond surfaces from ab initio simulations. MRS Communications, 2017, 7, 551-562.	0.8	25
32211	Ferroelectricity Tailored Valley Splitting in Monolayer WTe₂/YMnO₃ Heterostructures: A Route toward Electrically Controlled Valleytronics. Advanced Electronic Materials, 2017, 3, 1700245.	2.6	19
32212	Performance evaluation of catalysts in the dry reforming reaction of methane via the ratings concept. Reaction Kinetics, Mechanisms and Catalysis, 2017, 122, 53-68.	0.8	8
32213	Tuning electronic and magnetic properties in monolayer MoSe2 by metal adsorption. Chemical Physics Letters, 2017, 687, 54-59.	1.2	12
32214	Effect of atomic-layer-deposited TiO 2 on carbon-supported Ni catalysts for electrocatalytic glycerol oxidation in alkaline media. Electrochemistry Communications, 2017, 83, 46-50.	2.3	33
32215	Habituation based synaptic plasticity and organismic learning in a quantum perovskite. Nature Communications, 2017, 8, 240.	5.8	84
32216	Fast kinetics of magnesium monochloride cations in interlayer-expanded titanium disulfide for magnesium rechargeable batteries. Nature Communications, 2017, 8, 339.	5.8	304
32217	Structure sensitive photocatalytic reduction of nitroarenes over TiO 2. Scientific Reports, 2017, 7, 8783.	1.6	173
32218	Structure and magnetic properties of icosahedral PdxAg13â^'x (x = 0â€“13) clusters. Scientific Reports, 2017, 7, 9539.	1.6	3
32219	Lead and selenite adsorption at waterâ€“goethite interfaces from first principles. Journal of Physics Condensed Matter, 2017, 29, 365101.	0.7	8
32220	Properties of hydrogen doped Cu nanowires and nanocontacts: a density-functional theory study. Materials Research Express, 2017, 4, 095010.	0.8	3
32221	Gauge-including projector augmented-wave NMR chemical shift calculations with DFT+ <mml:math xmlns:mml="http://www.w3.org/1998/Math/MathML"><mml:mi>U</mml:mi></mml:math>. Physical Review B, 2017, 96, .	1.1	7

#	Article	IF	Citations
32222	Water-resistance of macromolecules adsorbed on CH3NH3PbI3 surfaces: A first-principles study. Chemical Physics Letters, 2017, 686, 203-211.	1.2	7
32223	The effect of lattice stability determination on the computational phase diagrams of intermetallic alloys. Journal of Alloys and Compounds, 2017, 728, 314-321.	2.8	6
32224	First principle and tight-binding study of strained SnC. Journal of Physics and Chemistry of Solids, 2017, 111, 458-463.	1.9	23
32225	Pressure effects on the electronic properties in CeCoIn 5 : A first-principle study. Physica C: Superconductivity and Its Applications, 2017, 542, 18-22.	0.6	0
32226	First-principle study of pressure-induced phase transitions and electronic properties of electride Y2C. Solid State Communications, 2017, 266, 34-38.	0.9	5
32227	Computational prediction of new auxetic materials. Nature Communications, 2017, 8, 323.	5.8	105
32228	Enhanced optical absorption via cation doping hybrid lead iodine perovskites. Scientific Reports, 2017, 7, 7843.	1.6	61
32229	Thickness-controlled electronic structure and thermoelectric performance of ultrathin SnS2 nanosheets. Scientific Reports, 2017, 7, 8914.	1.6	34
32230	One-dimensional water channels in lanthanum sulfate: a first-principles study. Journal of Materials Chemistry A, 2017, 5, 20188-20194.	5.2	7
32231	Theoretical study of solvent effects on the decomposition of formic acid over a Co(111) surface. International Journal of Hydrogen Energy, 2017, 42, 24726-24736.	3.8	16
32232	A new insight for ohmic contacts to MoS₂: by tuning MoS₂ affinity energies but not metal work-functions. Physical Chemistry Chemical Physics, 2017, 19, 26151-26157.	1.3	18
32233	Novel boron channel-based structure of boron carbide at high pressures. Journal of Physics Condensed Matter, 2017, 29, 455401.	0.7	1
32234	Adsorption properties of oxygen atom on the surface of Ti2AlNb by first principles calculations. Computational Materials Science, 2017, 139, 412-418.	1.4	27
32235	Catching the electron in action in real space inside a Geâ€“Si coreâ€“shell nanowire transistor. Nanoscale, 2017, 9, 13425-13431.	2.8	9
32236	Comparison of approximations in density functional theory calculations: Energetics and structure of binary oxides. Physical Review B, 2017, 96, .	1.1	85
32237	Raman study of electron-phonon coupling in thin films of the spinel oxide superconductor <mml:math xmlns:mml="http://www.w3.org/1998/Math/MathML"><mml:mrow><mml:msub><mml:mi>LiTi</mml:mi><mml:mn>2</mml:mn></mml:msub><mathvariant="normal">O</mml:mi><mml:mn>4</mml:mn></mml:msub></mml:mrow></mml:math>. Physical Review B, 2017, 96, .	1.1	6
32238	Strain Modulation of Electronic and Heat Transport Properties of Bilayer Boronitrene. International Journal of Thermophysics, 2017, 38, 1.	1.0	2
32239	Predicting the morphologies of Î³Ê¹ precipitates in cobalt-based superalloys. Acta Materialia, 2017, 141, 273-284.	3.8	70

#	Article	IF	Citations
32240	Theoretical realization of Mo2P; a novel stable 2D material with superionic conductivity and attractive optical properties. Applied Materials Today, 2017, 9, 292-299.	2.3	43
32241	Tuning magnetic properties of Cr2M2C3T2 (M = Ti and V) using extensile strain. Computational Materials Science, 2017, 139, 313-319.	1.4	40
32242	Rational design of carbon-doped TiO2 modified g-C3N4 via in-situ heat treatment for drastically improved photocatalytic hydrogen with excellent photostability. Nano Energy, 2017, 41, 1-9.	8.2	170
32243	First-principles calculations of the structural, elastic and thermodynamic properties of mackinawite (FeS) and pyrite (FeS 2). Physica B: Condensed Matter, 2017, 525, 119-126.	1.3	28
32244	Stress reduction mechanism of diamond-like carbon films incorporated with different Cu contents. Thin Solid Films, 2017, 640, 45-51.	0.8	28
32245	Computational Screening of Functionalized UiO-66 Materials for Selective Contaminant Removal from Air. Journal of Physical Chemistry C, 2017, 121, 20396-20406.	1.5	28
32246	Point defect formation in M2AlC (Mâ€‰=â€‰Zr,Cr) MAX phases and their tendency to disorder and amorphize. Scientific Reports, 2017, 7, 9667.	1.6	13
32247	A first principles study of spinel ZnFe₂O₄ for electrode materials in lithium-ion batteries. Physical Chemistry Chemical Physics, 2017, 19, 26322-26329.	1.3	45
32248	The structural, electronic and catalytic properties of Au_n (n = 1â€“4) nanoclusters on monolayer MoS₂. RSC Advances, 2017, 7, 42529-42540.	1.7	10
32249	Designing transition metal and nitrogen-codoped SrTiO₃(001) perovskite surfaces as efficient photocatalysts for water splitting. Sustainable Energy and Fuels, 2017, 1, 1968-1980.	2.5	15
32250	AC stress and electronic effects on SET switching of HfO2 RRAM. Applied Physics Letters, 2017, 111, 093502.	1.5	1
32251	Semimetallic behavior in Heusler-type Ru2TaAl and thermoelectric performance improved by off-stoichiometry. Physical Review B, 2017, 96, .	1.1	19
32252	Ultrahigh mobility and efficient charge injection in monolayer organic thin-film transistors on boron nitride. Science Advances, 2017, 3, e1701186.	4.7	146
32253	Nonaqueous LiNafion-based polymeric electrolyte: quantum-chemical modeling. Russian Journal of Inorganic Chemistry, 2017, 62, 1051-1057.	0.3	4
32254	Support Interaction Effect of Platinum Nanoparticles on Nonâ€Yâ€Ceâ€Doped Anatase and Its Implication on the ORR in Acid and Alkaline Media. ChemElectroChem, 2017, 4, 3264-3275.	1.7	24
32255	Elecreoreduction of CO2 to formic acid on Cu: Role of water bilayer in modeling electrochemical interface. Applied Catalysis A: General, 2017, 547, 214-218.	2.2	9
32256	Hydrogen adsorption and dissociation on the TM-doped (TM=Ti, Nb) Mg55 nanoclusters: A DFT study. International Journal of Hydrogen Energy, 2017, 42, 24797-24810.	3.8	31
32257	Oxygen adsorption at heterophase boundaries of the oxygenated Cu(110). Surface Science, 2017, 666, 28-43.	0.8	11

#	Article	IF	Citations
32258	Defects Slow Down Nonradiative Electronâ€“Hole Recombination in TiS₃ Nanoribbons: A Time-Domain Ab Initio Study. Journal of Physical Chemistry Letters, 2017, 8, 4522-4529.	2.1	16
32259	Capture of organic iodides from nuclear waste by metal-organic framework-based molecular traps. Nature Communications, 2017, 8, 485.	5.8	171
32260	Stable reconstruction of the (110) surface and its role in pseudocapacitance of rutile-like RuO2. Scientific Reports, 2017, 7, 10357.	1.6	30
32261	Origins of Dirac cone formation in AB3 and A3B (A, Bâ€‰=â€‰C, Si, and Ge) binary monolayers. Scientific Reports, 2017, 7, 10546.	1.6	32
32262	Effect of Cr-doping on the electronic structure and work function of Î±-Fe2O3 thin films. Physical Chemistry Chemical Physics, 2017, 19, 26248-26254.	1.3	5
32263	Investigation of high oxygen reduction reaction catalytic performance on Mn-based mullite SmMn₂O₅. Journal of Materials Chemistry A, 2017, 5, 20922-20931.	5.2	39
32264	Tuning the surface structure and conductivity of niobium-doped rutile TiO₂ single crystals via thermal reduction. Physical Chemistry Chemical Physics, 2017, 19, 30339-30350.	1.3	9
32265	General promoting effect of polydopamine on supported noble metal catalysts. Journal of Materials Chemistry A, 2017, 5, 20789-20796.	5.2	26
32266	First-principles analysis of solute diffusion in dilute bcc Fe- <mml:math xmlns:mml="http://www.w3.org/1998/Math/MathML"><mml:mi mathvariant="italic">X</mml:mi></mml:math> alloys. Physical Review B, 2017, 96, .	1.1	63
32267	Synergy of van der Waals and self-interaction corrections in transition metal monoxides. Physical Review B, 2017, 96, .	1.1	50
32268	Fundamental Resolution of Difficulties in the Theory of Charged Point Defects in Semiconductors. Physical Review Letters, 2017, 119, 105501.	2.9	25
32269	Theoretical Study of Nitrogen Absorption in Metals. Journal of Physical Chemistry C, 2017, 121, 17016-17028.	1.5	5
32270	Immobilization of single argon atoms in nano-cages of two-dimensional zeolite model systems. Nature Communications, 2017, 8, 16118.	5.8	29
32271	Mechanical properties and electronic structure of edge-doped graphene nanoribbons with F, O, and Cl atoms. Physical Chemistry Chemical Physics, 2017, 19, 21474-21480.	1.3	2
32272	Native defects and substitutional impurities in two-dimensional monolayer InSe. Nanoscale, 2017, 9, 11619-11624.	2.8	32
32273	The tunable effect of nitrogen and boron dopants on a single walled carbon nanotube support on the catalytic properties of a single gold atom catalyst: a first principles study of CO oxidation. Journal of Materials Chemistry A, 2017, 5, 16653-16662.	5.2	58
32274	Electronic structure and switching behavior of the metastable silicene domain boundary. Applied Physics Letters, 2017, 110, 263112.	1.5	10
32275	Native point defects on hydrogen-passivated 4Hâ€“SiC (0001) surface and the effects on metal adsorptions. Journal of Chemical Physics, 2017, 147, 024707.	1.2	6

#	Article	IF	Citations
32276	A fast hybrid methodology based on machine learning, quantum methods, and experimental measurements for evaluating material properties. Modelling and Simulation in Materials Science and Engineering, 2017, 25, 065014.	0.8	3
32277	First-principles equation of state and shock compression predictions of warm dense hydrocarbons. Physical Review E, 2017, 96, 013204.	0.8	37
32278	Orientation-dependent behaviors of H dissolution and diffusion near W surfaces: A first-principles study. International Journal of Modern Physics C, 2017, 28, 1750090.	0.8	4
32279	Insights into the Li Intercalation and SEI Formation on LiSi Nanoclusters. Journal of the Electrochemical Society, 2017, 164, E3457-E3464.	1.3	10
32280	Narrowing of antiferromagnetic domain wall in corundum-type Cr₂O₃ by lattice strain. Applied Physics Express, 2017, 10, 013002.	1.1	19
32281	Facile Hydrothermal Synthesis of MnWO₄ Nanorods for Nonâ€Enzymatic Glucose Sensing and Supercapacitor Properties with Insights from Density Functional Theory Simulations. ChemistrySelect, 2017, 2, 5707-5715.	0.7	26
32282	Different catalytic behaviors of Pd and Pt metals in decalin dehydrogenation to naphthalene. Catalysis Science and Technology, 2017, 7, 3728-3735.	2.1	38
32283	Transparent conducting n-type ZnO:Sc â€“ synthesis, optoelectronic properties and theoretical insight. Journal of Materials Chemistry C, 2017, 5, 7585-7597.	2.7	46
32284	Stability and electronic structure of defect complexes in Gd-doped GaN: First-principles calculations. Journal of Applied Physics, 2017, 122, 023901.	1.1	3
32285	Accurate calculation free energies of the <mml:math xmlns:mml="http://www.w3.org/1998/Math/MathML"><mml:mrow><mml:mn>3</mml:mn><mml:mi mathvariant="italic">d</mml:mi><mml:mo>,</mml:mo><mml:mn>4</mml:mn><mml:mi mathvariant="italic">d</mml:mi></mml:mrow></mml:math> , and <mml:math xmlns:mml="http://www.w3.org/1998/Math/MathML"><mml:mrow><mml:mn>5</mml:mn><mml:mi mathvariant="italic">d</mml:mi></mml:mrow></mml:math> transition metals at high temperatures. Ph	1.1	70
32286	Colossal Stability of Gasâ€Phase Trianions: Superâ€Pnictogens. Angewandte Chemie, 2017, 129, 13606-13610.	1.6	6
32287	Colossal Stability of Gasâ€Phase Trianions: Superâ€Pnictogens. Angewandte Chemie - International Edition, 2017, 56, 13421-13425.	7.2	23
32288	Spinâ€singlet Quantum Ground State in Zigzag Spin Ladder Cu(CF₃COO)₂. ChemPhysChem, 2017, 18, 2482-2486.	1.0	6
32289	A first-principles study of bulk and surface Sn-doped LiFePO₄ : The role of intermediate valence component in the multivalent doping. Physica Status Solidi (B): Basic Research, 2017, 254, 1700041.	0.7	10
32290	Effect of two identical 3d transition-metal atoms M doping (Mâ€‰=â€‰V, Cr, Mn, Fe, Co, and Ni) on the structural, electronic, and magnetic properties of ZnO. Physica Status Solidi (B): Basic Research, 2017, 254, 1700098.	0.7	11
32291	Exploring the stability and reactivity of Ni2P and Mo2C catalysts using ab initio atomistic thermodynamics and conceptual DFT approaches. Biomass Conversion and Biorefinery, 2017, 7, 377-383.	2.9	3
32292	Hydrogen enhances the radiation resistance of amorphous silicon oxycarbides. Acta Materialia, 2017, 136, 415-424.	3.8	12
32293	Identification of a ternary Î¼-phase in the Co-Ti-W system â€“ An advanced correlative thin-film and bulk combinatorial materials investigation. Acta Materialia, 2017, 138, 100-110.	3.8	12

#	Article	IF	Citations
32294	The effect of the adsorbate layer on the work function reduction of gold substrates under external electric fields. Applied Surface Science, 2017, 425, 776-780.	3.1	1
32295	A DFT study of hydrogen electroadsorption on the missing row Pt(1 1 0)-(1<mml:math) Tj ETQq1 1 0.784314 rgBT /Overlock 10 Tf 50 7 Computational Materials Science, 2017, 138, 295-301.	1.4	10
32296	Oxygen Ion Transport and Effects of Doping in Ba₃Ti₃O₆(BO₃)₂. Chemistry of Materials, 2017, 29, 6425-6433.	3.2	6
32297	Water Adsorption and Dissociation on Copper/Nickel Bimetallic Surface Alloys: Effect of Surface Temperature on Reactivity. Journal of Physical Chemistry C, 2017, 121, 16351-16365.	1.5	58
32298	DFT Study on Reaction Mechanism of Nitric Oxide to Ammonia and Water on a Hydroxylated Rutile TiO₂(110) Surface. Journal of Physical Chemistry C, 2017, 121, 16373-16380.	1.5	11
32299	Improving the Carrier Lifetime of Tin Sulfide via Prediction and Mitigation of Harmful Point Defects. Journal of Physical Chemistry Letters, 2017, 8, 3661-3667.	2.1	22
32300	Molybdenum Carbide Modified Nanocarbon Catalysts for Alkane Dehydrogenation Reactions. ACS Catalysis, 2017, 7, 5820-5827.	5.5	55
32301	CO diffusion as a re-orientation mechanism in the NaY zeolite. Physical Chemistry Chemical Physics, 2017, 19, 20930-20940.	1.3	5
32302	Atomic-scale computational design of hydrophobic RE surface-doped Al2O3 and TiO2. Physical Chemistry Chemical Physics, 2017, 19, 21119-21126.	1.3	7
32303	In- and Ga-based inorganic double perovskites with direct bandgaps for photovoltaic applications. Physical Chemistry Chemical Physics, 2017, 19, 21691-21695.	1.3	37
32304	Efficient ³He/⁴He separation in a nanoporous graphenylene membrane. Physical Chemistry Chemical Physics, 2017, 19, 21522-21526.	1.3	9
32305	Defect induced charge trapping in C-doped Î±-Al2O3. Journal of Applied Physics, 2017, 122, 025702.	1.1	6
32306	Substitutional carbon doping of free-standing and Ru-supported BN sheets: a first-principles study. Journal of Physics Condensed Matter, 2017, 29, 415301.	0.7	5
32307	Predicted novel insulating electride compound between alkali metals lithium and sodium under high pressure. Chinese Physics B, 2017, 26, 056102.	0.7	14
32308	Quantum anomalous Hall phase and half-metallic phase in ferromagnetic (111) bilayers of 4d and 5d transition metal perovskites. Physical Review B, 2017, 95, .	1.1	13
32309	Design principles for radiation-resistant solid solutions. Physical Review B, 2017, 95, .	1.1	15
32310	Optical and structural study of the pressure-induced phase transition of <mml:math xmlns:mml="http://www.w3.org/1998/Math/MathML"><mml:msub><mml:mi>CdWO</mml:mi><mml:mn>4</mml:mn></mml:msub></r Physical Review B, 2017, 95, .	1.1	23
32311	Molecular detection on a defective MoS2 monolayer by simultaneous conductance and force simulations. Physical Review B, 2017, 95, .	1.1	2

#	Article	IF	Citations
32312	First-principles prediction of stabilities and instabilities of compounds and alloys in the ternary B-As-P system. Physical Review B, 2017, 96, .	1.1	18
32313	Impurity band effects on transport and thermoelectric properties of Fe2â^'xNixVAl. Physical Review B, 2017, 96, .	1.1	26
32314	First-principles simulations of warm dense lithium fluoride. Physical Review E, 2017, 95, 043205.	0.8	27
32316	On Ternary Intermetallic Aurides: CaAu₂Al₂, SrAu_{2â€“x}Al_{2+x} and Ba₃Au_{5+x}Al_{6â€“x}. Zeitschrift Fur Anorganische Und Allgemeine Chemie, 2017, 643, 1379-1390.	0.6	7
32317	High coverage water adsorption on the CuO(111) surface. Applied Surface Science, 2017, 425, 803-810.	3.1	50
32318	Effect of Interfacial Lithium Insertion on the Stability and Electronic Structure of Graphene/LiFePO4. Electrochimica Acta, 2017, 247, 1030-1037.	2.6	15
32319	Zn vacancy ferromagnetism in ZnS nanocrystals. Journal of Magnetism and Magnetic Materials, 2017, 443, 9-12.	1.0	1
32320	Theoretical and experimental study of ethanol adsorption and dissociation on Î²-Mo 2 C surfaces. Molecular Catalysis, 2017, 439, 163-170.	1.0	10
32321	Phase stability of the Cu-Sn-S system and optimal growth conditions for earth-abundant Cu2SnS3 solar materials. Solar Energy, 2017, 155, 745-757.	2.9	29
32322	Magnetic Moment Controlling Desorption Temperature in Hydrogen Storage: A Case of Zirconium-Doped Graphene as a High Capacity Hydrogen Storage Medium. Journal of Physical Chemistry C, 2017, 121, 16721-16730.	1.5	59
32323	Chemical Bond Modification upon Phase Transformation of TiO₂ Nanoribbons Revealed by Nanoscale X-ray Linear Dichroism. Journal of Physical Chemistry C, 2017, 121, 17038-17042.	1.5	12
32324	Using heterostructural alloying to tune the structure and properties of the thermoelectric Sn_{1â^'x}Ca_xSe. Journal of Materials Chemistry A, 2017, 5, 16873-16882.	5.2	19
32325	Intermediate bands in type-II silicon clathrate with Cu and Ag guest atoms. Physical Review B, 2017, 95, .	1.1	0
32326	Efficient and accurate machine-learning interpolation of atomic energies in compositions with many species. Physical Review B, 2017, 96, .	1.1	228
32327	Antiferroelectric Topological Insulators in Orthorhombic <mml:math xmlns:mml="http://www.w3.org/1998/Math/MathML" display="inline"><mml:mrow><mml:mi>A</mml:mi><mml:mi>MgBi</mml:mi></mml:mrow></mml:math> Compounds (<mml:math xmlns:mml="http://www.w3.org/1998/Math/MathML") Tj ETQq0 0 0 rgBT /Overlock 10 Tf 50 172 Td (display=	2.9	30
32328	Engineering the Electronic and Magnetic Properties of Sc₂CF₂ MXene Material through Vacancy Doping and Lattice Straining. Materials Science Forum, 0, 900, 61-64.	0.3	1
32329	Reduction in Modulus of Suspended Subâ€¢2 nm Single Crystalline Silicon Nanomembranes. Advanced Materials Interfaces, 2017, 4, 1700529.	1.9	3
32330	Phonon transport properties of bulk and monolayer GaN from first-principles calculations. Computational Materials Science, 2017, 138, 419-425.	1.4	39

#	Article	IF	Citations
32331	Bimetallic Ions Codoped Nanocrystals: Doping Mechanism, Defect Formation, and Associated Structural Transition. Journal of Physical Chemistry Letters, 2017, 8, 3249-3255.	2.1	18
32332	Structures, phase transitions, and magnetic properties of Co3Si from first-principles calculations. Physical Review B, 2017, 96, .	1.1	8
32333	Spin-polarized two-dimensional electron gas at <mml:math xmlns:mml="http://www.w3.org/1998/Math/MathML"><mml:mrow><mml:mi>GdTi</mml:mi><mml:msub><mml:mi mathvariant="normal">O</mml:mi><mml:mn>3</mml:mn></mml:msub><mml:mo>/</mml:mo><mml:mi>SrTi</mml:mi><mml:msub><mml:mi mathvariant="normal">O</mml:mi><mml:mn>3</mml:mn></mml:msub></mml:mrow></mml:math> interfaces: Insight from first-principles calculations. Physical Review B, 2017, 96, .	1.1	22
32334	Multiscale Modeling of Uranium Mononitride: Point Defects Diffusion, Self-Diffusion, Phase Composition. Defect and Diffusion Forum, 0, 375, 101-113.	0.4	5
32335	Unusual Metallic Multiferroic Transitions in Electronâ€Doped PbTiO₃. Advanced Electronic Materials, 2017, 3, 1700134.	2.6	11
32336	Nitrogenâ€doped C₆₀ as a robust catalyst for CO oxidation. Journal of Computational Chemistry, 2017, 38, 2041-2046.	1.5	47
32337	Effects of single metal atom (Pt, Pd, Rh and Ru) adsorption on the photocatalytic properties of anatase TiO 2. Applied Surface Science, 2017, 426, 639-646.	3.1	99
32338	Anomalous behavior of rutile GeO2 facets: A computational study. Materials Chemistry and Physics, 2017, 199, 552-556.	2.0	2
32339	First-principle studies of radioactive fission productions of Cs/Sr/Ag/I adsorption on silicon carbide in HTGR. Progress in Nuclear Energy, 2017, 100, 164-170.	1.3	5
32340	Impact of Cl Doping on Electrochemical Performance in Orthosilicate (Li₂FeSiO₄): A Density Functional Theory Supported Experimental Approach. ACS Applied Materials & Interfaces, 2017, 9, 26885-26896.	4.0	37
32341	Donorâ€“Acceptor Properties of a Single-Molecule Altered by On-Surface Complex Formation. ACS Nano, 2017, 11, 8413-8420.	7.3	30
32342	Pressure-induced structural transformations and polymerization in ThC2. Scientific Reports, 2017, 7, 45872.	1.6	13
32343	CH4 and H2S reforming to CH3SH and H2 catalyzed by metal-promoted Mo6S8 clusters: a first-principles micro-kinetic study. Catalysis Science and Technology, 2017, 7, 3546-3554.	2.1	10
32344	The effect of potassium on steam-methane reforming on the Ni₄/Al₂O₃ surface: a DFT study. Catalysis Science and Technology, 2017, 7, 3613-3625.	2.1	32
32345	Theoretical evaluation of the structureâ€“activity relationship in graphene-based electrocatalysts for hydrogen evolution reactions. RSC Advances, 2017, 7, 27033-27039.	1.7	21
32346	Tuning electronic structures of Sc₂CO₂/MoS₂ polarâ€“nonpolar van der Waals heterojunctions: interplay of internal and external electric fields. Journal of Materials Chemistry C, 2017, 5, 8128-8134.	2.7	8
32347	Intrinsic magnetism of graphdiyne. Applied Physics Letters, 2017, 111, .	1.5	45
32348	Topological Nodal Line Semimetal in Non-Centrosymmetric PbTaS${}_{2}$. Chinese Physics Letters, 2017, 34, 077101.	1.3	7

#	Article	IF	Citations
32349	Electric-field noise from carbon-adatom diffusion on a Au(110) surface: First-principles calculations and experiments. Physical Review A, 2017, 95, .	1.0	20
32350	Polar instability under electrostatic doping in tetragonal <mml:math xmlns:mml="http://www.w3.org/1998/Math/MathML"><mml:mrow><mml:mi>SnTi</mml:mi><mml:msub><mml:mi mathvariant="normal">O</mml:mi><mml:mn>3</mml:mn></mml:msub></mml:mrow></mml:math>. Physical Review B, 2017, 96, .	1.1	14
32351	Critical point and mechanism of the fluidâ€“fluid phase transition in warm dense hydrogen. Doklady Physics, 2017, 62, 294-298.	0.2	15
32352	Pd nanoparticles encaged within amine-functionalized metal-organic frameworks: Catalytic activity and reaction mechanism in the hydrogenation of 2,3,5-trimethylbenzoquinone. Chemical Engineering Journal, 2017, 328, 977-987.	6.6	37
32353	Synthesis, crystal structure and optical properties of K2Cu2GeS4. Journal of Alloys and Compounds, 2017, 725, 557-562.	2.8	9
32354	Decohesion models informed by first-principles calculations: The ab initio tensile test. Journal of the Mechanics and Physics of Solids, 2017, 107, 494-508.	2.3	18
32355	Extra long electronâ€“hole diffusion lengths in CH₃NH₃PbI_{3âˆ’x}Cl_x perovskite single crystals. Journal of Materials Chemistry C, 2017, 5, 8431-8435.	2.7	91
32356	Improper Ferroelectricity in Stuffed Aluminate Sodalites for Pyroelectric Energy Harvesting. Physical Review Applied, 2017, 7, .	1.5	22
32357	Metric for strong intrinsic fourth-order phonon anharmonicity. Physical Review B, 2017, 95, .	1.1	26
32358	Ternary Weyl semimetal <mml:math xmlns:mml="http://www.w3.org/1998/Math/MathML"><mml:msub><mml:mi>NbIrTe</mml:mi><mml:mn>4</mml:mn></mml:msub></mml:math> proposed from first-principles calculation. Physical Review B, 2017, 96, .	1.1	18
32359	Orbital Contributions to the Electron <mml:math xmlns:mml="http://www.w3.org/1998/Math/MathML" display="inline"><mml:mrow><mml:mi>g</mml:mi></mml:mrow></mml:math> Factor in Semiconductor Nanowires. Physical Review Letters, 2017, 119, 037701.	2.9	51
32360	Significantly enhanced photocatalytic activity of visible light responsive AgBr/Bi 2 Sn 2 O 7 heterostructured composites. Applied Surface Science, 2017, 426, 1173-1181.	3.1	42
32361	Electronic, optical and thermal properties of highly stretchable 2D carbon Ene-yne graphyne. Carbon, 2017, 123, 344-353.	5.4	46
32362	Effect of processing strain rate and temperature on interfacial segregation of zinc in a magnesium alloy. Materials Science & Engineering A: Structural Materials: Properties, Microstructure and Processing, 2017, 703, 54-67.	2.6	8
32363	Chemical Tuning of Carrier Type and Concentration in a Homologous Series of Crystalline Chalcogenides. Chemistry of Materials, 2017, 29, 6749-6757.	3.2	18
32364	Redox Potentials from Ab Initio Molecular Dynamics and Explicit Entropy Calculations: Application to Transition Metals in Aqueous Solution. Journal of Chemical Theory and Computation, 2017, 13, 3432-3441.	2.3	18
32365	Design of Ruddlesdenâ€“Popper Oxides with Optimal Surface Oxygen Exchange Properties for Oxygen Reduction and Evolution. ACS Catalysis, 2017, 7, 5912-5920.	5.5	32
32366	Hydrogen Transfer versus Methylation: On the Genesis of Aromatics Formation in the Methanol-To-Hydrocarbons Reaction over H-ZSM-5. ACS Catalysis, 2017, 7, 5773-5780.	5.5	102

#	Article	IF	Citations
32367	High performance platinum single atom electrocatalyst for oxygen reduction reaction. Nature Communications, 2017, 8, 15938.	5.8	569
32368	Fluorination-enriched electronic and magnetic properties in graphene nanoribbons. Physical Chemistry Chemical Physics, 2017, 19, 20667-20676.	1.3	18
32369	Universal two-dimensional characteristics in perovskite-type oxyhydrides ATiO2H (A = Li, Na, K, Rb, Cs). Journal of Chemical Physics, 2017, 147, 034507.	1.2	1
32370	First-principles calculations of hydrogen interactions with nickel containing a monovacancy and divacancies. Materials Research Express, 2017, 4, 076505.	0.8	5
32371	Compositional phase stability of strongly correlated electron materials within DFT+ <mml:math xmlns:mml="http://www.w3.org/1998/Math/MathML"><mml:mi>U</mml:mi></mml:math>. Physical Review B, 2017, 95, .	1.1	11
32372	Two-dimensional electron systems in <mml:math xmlns:mml="http://www.w3.org/1998/Math/MathML"><mml:mrow><mml:mi>A</mml:mi><mml:msub><mml:mi>TiO</mml:mi><mml:mn perovskites (<mml:math) Tj ETQq1 1 0.784314 rgBT /Overlock 10 Tf 50 537 Td (xmlns:mml="http://www.w3.org/1998/Math/MathML	1.1	11
32373	Equation of state, phonons, and lattice stability of ultrafast warm dense matter. Physical Review E, 2017, 95, 043201.	0.8	19
32374	Electric-Field-Controlled Interface Exchange Coupling in Cobaltâ€“Chromia Thin Films. IEEE Transactions on Magnetics, 2017, 53, 1-4.	1.2	1
32375	First-principles study of the stability, magnetic and electronic properties of Fe and Co monoatomic chains encapsulated into copper nanotube. European Physical Journal B, 2017, 90, 1.	0.6	0
32376	Equilibrium composition variation of Q-phase precipitates in aluminum alloys. Acta Materialia, 2017, 138, 150-160.	3.8	32
32377	First principles study on the adsorption of Au dimer on metal-oxide surfaces: The implications for Au growing. Applied Surface Science, 2017, 426, 554-561.	3.1	13
32378	THD-graphene used for a selective gas detector. Materials Chemistry and Physics, 2017, 200, 50-56.	2.0	15
32379	Predicting Selectivity for Ethane Dehydrogenation and Coke Formation Pathways over Model Ptâ€“M Surface Alloys with ab Initio and Scaling Methods. Journal of Physical Chemistry C, 2017, 121, 17882-17892.	1.5	42
32380	Spin Unrestricted Nonradiative Relaxation Dynamics of Cobalt-Doped Anatase Nanowire. Journal of Physical Chemistry C, 2017, 121, 16110-16125.	1.5	8
32381	Solvent Effect Inside the Nanocage of Zeolite Catalysts: A Combined Solid-State NMR Approach and Multiscale Simulation. Journal of Physical Chemistry C, 2017, 121, 16921-16931.	1.5	8
32382	DFT-Assisted Polymorph Identification from Lattice Raman Fingerprinting. Journal of Physical Chemistry Letters, 2017, 8, 3690-3695.	2.1	42
32383	Surface configuration and wettability of nickel(oxy)hydroxides: a first-principles investigation. Physical Chemistry Chemical Physics, 2017, 19, 22659-22669.	1.3	31
32384	Electrons on the surface of 2D materials: from layered electrides to 2D electrenes. Journal of Materials Chemistry C, 2017, 5, 11196-11213.	2.7	45

#	Article	IF	Citations
32385	Hybrid density functional theory modeling of Ca, Zn, and Al ion batteries using the Chevrel phase Mo₆S₈ cathode. Physical Chemistry Chemical Physics, 2017, 19, 20684-20690.	1.3	41
32386	Thickness dependent semiconductor-to-metal transition of two-dimensional polyaniline with unique work functions. Nanoscale, 2017, 9, 12025-12031.	2.8	24
32387	Thermal conductivity of hexagonal Si and hexagonal Si nanowires from first-principles. Applied Physics Letters, 2017, 111, .	1.5	21
32388	Crossover from band-like to thermally activated charge transport in organic transistors due to strain-induced traps. Proceedings of the National Academy of Sciences of the United States of America, 2017, 114, E6739-E6748.	3.3	77
32389	Quantum confinement: A route to enhance the Curie temperature of Mn doped GaAs. Physical Review B, 2017, 96, .	1.1	1
32390	Comparative first-principles studies of prototypical ferroelectric materials by LDA, GGA, and SCAN meta-GGA. Physical Review B, 2017, 96, .	1.1	156
32391	Properties at the interface of graphene and <mml:math xmlns:mml="http://www.w3.org/1998/Math/MathML"><mml:mrow><mml:msub><mml:mi>Ti</mml:mi><mml:mn>2</mml:mn></mml:msub><mml:m mathvariant="normal">C</mml:mi></mml:mrow></mml:math> MXene. Physical Review B, 2017, 96, .	1.1	20
32392	Site preference, structural and magnetic properties of La3Co29â^'Ni Si4B10 predicted by first-principles calculations. Computational Materials Science, 2017, 138, 412-418.	1.4	1
32393	Structural evolution in liquid calcium under pressure. Journal of Non-Crystalline Solids, 2017, 472, 25-30.	1.5	3
32394	Ferroelectricity in Pb_{1+Î´}ZrO₃ Thin Films. Chemistry of Materials, 2017, 29, 6544-6551.	3.2	32
32395	Prediction of Novel High-Pressure Structures of Magnesium Niobium Dihydride. ACS Applied Materials & Interfaces, 2017, 9, 26169-26176.	4.0	16
32396	Ion-selective copper hexacyanoferrate with an open-framework structure enables high-voltage aqueous mixed-ion batteries. Journal of Materials Chemistry A, 2017, 5, 16740-16747.	5.2	74
32397	Comparing contribution of flexural and planar modes to thermodynamic properties. AIP Conference Proceedings, 2017, , .	0.3	0
32398	Influence of Antisite Defects on the Thermoelectric Properties of Fe₂VAl. Nanoscale and Microscale Thermophysical Engineering, 2017, 21, 237-246.	1.4	16
32399	Ab initio calculation of magnetic properties in B, Al, C, Si, N, P and As-doped rutile TiO₂. International Journal of Modern Physics B, 2017, 31, 1750227.	1.0	32
32400	Hierarchical VS₂ Nanosheet Assemblies: A Universal Host Material for the Reversible Storage of Alkali Metal Ions. Advanced Materials, 2017, 29, 1702061.	11.1	320
32401	Towards a Comprehensive Understanding of the Reaction Mechanisms Between Defective MoS₂ and Thiol Molecules. Angewandte Chemie - International Edition, 2017, 56, 10501-10505.	7.2	88
32402	Cage disorder and gas encapsulation as routes to tailor properties of inorganic clathrates. Acta Materialia, 2017, 131, 475-481.	3.8	6

#	Article	IF	Citations
32403	Ab initio investigations of the phase stability in group IVB and VB transition metal nitrides. Computational Materials Science, 2017, 138, 333-345.	1.4	33
32404	Tuning Charge Carrier Types, Superior Mobility and Absorption in Lead-free Perovskite CH3NH3GeI3: Theoretical Study. Electrochimica Acta, 2017, 247, 891-898.	2.6	56
32405	Facile synthesis of FeSi4P4 and its Sodium Ion Storage Performance. Electrochimica Acta, 2017, 247, 820-825.	2.6	11
32406	First principles study of the electronic structure and magnetic properties of YFeO3 oxide. Journal of Magnetism and Magnetic Materials, 2017, 442, 255-264.	1.0	22
32407	Rational design of freestanding MoS2 monolayers for hydrogen evolution reaction. Nano Energy, 2017, 39, 409-417.	8.2	107
32408	Thermodynamic Routes to Novel Metastable Nitrogen-Rich Nitrides. Chemistry of Materials, 2017, 29, 6936-6946.	3.2	121
32409	Insight into the Role of Metalâ€“Oxygen Bond and O 2p Hole in High-Voltage Cathode LiNi_xMn_{2â€“x}O₄. Journal of Physical Chemistry C, 2017, 121, 16079-16087.	1.5	50
32410	Ductility in Crystalline Boron Subphosphide (B₁₂P₂) for Large Strain Indentation. Journal of Physical Chemistry C, 2017, 121, 16644-16649.	1.5	18
32411	Structure of Supported and Unsupported Catalytic Rh Nanoparticles: Effects on Nucleation of Single-Walled Carbon Nanotubes. Langmuir, 2017, 33, 11109-11119.	1.6	1
32412	Competing Annulene and Radialene Structures in a Single Anti-Aromatic Molecule Studied by High-Resolution Atomic Force Microscopy. ACS Nano, 2017, 11, 8122-8130.	7.3	64
32413	Electric field control of magnetization direction across the antiferromagnetic to ferromagnetic transition. Scientific Reports, 2017, 7, 5366.	1.6	21
32414	Catalytic role of vacancy diffusion in ceria supported atomic gold catalyst. Chemical Communications, 2017, 53, 9125-9128.	2.2	18
32415	The adsorption and diffusion behavior of noble metal adatoms (Pd, Pt, Cu, Ag and Au) on a MoS₂ monolayer: a first-principles study. Physical Chemistry Chemical Physics, 2017, 19, 20713-20722.	1.3	135
32416	New allotropes of Li₂MnO₃ as cathode materials with better cycling performance predicted in high pressure synthesis. Journal of Materials Chemistry A, 2017, 5, 16936-16943.	5.2	17
32417	Assembling phosphorene flexagons for 2D electron-density-guided nanopatterning and nanofabrication. Nanoscale, 2017, 9, 10465-10474.	2.8	1
32418	Methane dissociation on Ni(111): A seven-dimensional to nine-dimensional quantum dynamics study. Journal of Chemical Physics, 2017, 147, 024702.	1.2	8
32419	Exchange interactions in transition metal oxides: the role of oxygen spin polarization. Journal of Physics Condensed Matter, 2017, 29, 335801.	0.7	30
32420	Carrier-Induced Band-Gap Variation and Point Defects in <mml:math xmlns:mml="http://www.w3.org/1998/Math/MathML" display="inline"><mml:mrow><mml:msub><mml:mrow><mml:mi>Zn</mml:mi></mml:mrow><mml:mrow><mml:mi mathvariant="normal">N</mml:mi></mml:mrow></mml:msub></mml:mrow></mml:math> from First Principles. Physical Review Applied, 2017, 8, .	1.6	28

#	Article	IF	Citations
32421	Representation of compounds for machine-learning prediction of physical properties. Physical Review B, 2017, 95, .	1.1	220
32422	Identify the topological nodal-line semimetal phase in <mml:math xmlns:mml="http://www.w3.org/1998/Math/MathML"><mml:mrow><mml:mi>ZrSi</mml:mi><mml:mi>X</mml:mi></mml:mrow></mml:math>		

#	Article	IF	Citations
32439	Electronic, magnetic properties of transition metal doped Tl 2 S: First-principles study. Applied Surface Science, 2017, 425, 393-399.	3.1	9
32440	Thermal recovery mechanisms of UO2 lattices by defect annihilation. Journal of Alloys and Compounds, 2017, 724, 841-850.	2.8	4
32441	Probing the (110)-Oriented plane of rutile ZnF2: A DFT investigation. Journal of Physics and Chemistry of Solids, 2017, 111, 63-69.	1.9	3
32442	(CaO) IrO2 (n = 1, 2, 4) family: Chemical scissors effects of CaO on structural characteristics correlated to physical properties. Ab initio study. Journal of Solid State Chemistry, 2017, 255, 82-88.	1.4	10
32443	Structural, magnetic and electronic properties of Ni-Mn-Ga-Cr Heusler alloys: ab initio and Monte Carlo studies. Materials Today: Proceedings, 2017, 4, 4621-4625.	0.9	1
32444	Anisotropy of magnetic interactions and spin filter behavior in hexagonal (Ga,Mn)As nanoribbons. Physica E: Low-Dimensional Systems and Nanostructures, 2017, 93, 291-294.	1.3	1
32445	Stereochemistry and ab initio topology analyses of electron lone pair triplets and twins in interhalogen compounds and halogen suboxides. Progress in Solid State Chemistry, 2017, 47-48, 1-18.	3.9	3
32446	Interface-induced electronic structure toughening of nitride superlattices. Surface and Coatings Technology, 2017, 325, 410-416.	2.2	34
32447	Vacancy-driven extended stability of cubic metastable Ta-Al-N and Nb-Al-N phases. Surface and Coatings Technology, 2017, 326, 37-44.	2.2	15
32448	Computational Prediction and Evaluation of Solid-State Sodium Superionic Conductors Na₇P₃X₁₁ (X = O, S, Se). Chemistry of Materials, 2017, 29, 7475-7482.	3.2	56
32449	Experimental and Theoretical Evidence for the Reactivity of Bound Intermediates in Ketonization of Carboxylic Acids and Consequences of Acidâ€“Base Properties of Oxide Catalysts. Journal of Physical Chemistry C, 2017, 121, 18030-18046.	1.5	33
32450	Probing Franckâ€“Condon-like Excitations in Anchoring of Phthalocyanine Molecules on Au(111). Journal of Physical Chemistry C, 2017, 121, 17402-17408.	1.5	4
32451	Why is sodium-intercalated graphite unstable?. RSC Advances, 2017, 7, 36550-36554.	1.7	194
32452	The electronic and diffusion properties of metal adatoms on graphene sheets: a first-principles study. RSC Advances, 2017, 7, 33208-33218.	1.7	12
32453	Non-classical behaviour of higher valence dopants in chromium (III) oxide by a Cr vacancy compensation mechanism. Journal of Physics Condensed Matter, 2017, 29, 415501.	0.7	2
32454	Few-layer MoS₂as nitrogen protective barrier. Nanotechnology, 2017, 28, 415706.	1.3	6
32455	Valley-Polarized Quantum Anomalous Hall Effect in Ferrimagnetic Honeycomb Lattices. Physical Review Letters, 2017, 119, 046403.	2.9	64
32456	Bandgap engineering of SrTiO₃ /NaTaO₃ heterojunction for visible light photocatalysis. International Journal of Quantum Chemistry, 2017, 117, e25424.	1.0	17

#	Article	IF	Citations
32457	Boron-/Fe-codoped graphene as high-activity single-atom catalyst. Theoretical Chemistry Accounts, 2017, 136, 1.	0.5	5
32458	Fabrication of poly(ethylene glycol) hydrogels containing vertically and horizontally aligned graphene using dielectrophoresis: An experimental and modeling study. Carbon, 2017, 123, 460-470.	5.4	24
32459	Effect of Ti content and nitrogen on the high-temperature oxidation behavior of (Mo,Ti)5Si3. Intermetallics, 2017, 90, 103-112.	1.8	18
32460	Structural stability and the alloying effect of TiB polymorphs in TiAl alloys. Intermetallics, 2017, 90, 97-102.	1.8	35
32461	A parallel orbital-updating based plane-wave basis method for electronic structure calculations. Journal of Computational Physics, 2017, 348, 482-492.	1.9	5
32462	A combined DFT and molecular dynamics study of U(VI)/calcite interaction in aqueous solution. Science Bulletin, 2017, 62, 1064-1073.	4.3	30
32463	Comprehensive View of the Ligandâ€“Gold Interface from First Principles. Chemistry of Materials, 2017, 29, 6908-6915.	3.2	59
32464	Role of Transient Co-Subcarbonyls in Ostwald Ripening Sintering of Cobalt Supported on Î³-Alumina Surfaces. Journal of Physical Chemistry C, 2017, 121, 16739-16753.	1.5	22
32465	Temperature Dependence of Electronâ€“Phonon Interactions in Gold Films Rationalized by Time-Domain Ab Initio Analysis. Journal of Physical Chemistry C, 2017, 121, 17488-17497.	1.5	21
32466	Atomic-Level Design of Water-Resistant Hybrid Perovskites for Solar Cells by Using Cluster Ions. Journal of Physical Chemistry Letters, 2017, 8, 3726-3733.	2.1	15
32467	Two-Dimensional Intrinsic Half-Metals With Large Spin Gaps. Nano Letters, 2017, 17, 5251-5257.	4.5	172
32468	Evidence for Ultralow-Energy Vibrations in Large Organic Molecules. Nano Letters, 2017, 17, 4929-4933.	4.5	11
32469	Nanosheet Supported Single-Metal Atom Bifunctional Catalyst for Overall Water Splitting. Nano Letters, 2017, 17, 5133-5139.	4.5	395
32470	Stress-Induced Cubic-to-Hexagonal Phase Transformation in Perovskite Nanothin Films. Nano Letters, 2017, 17, 5148-5155.	4.5	26
32471	Chemically Functionalized Phosphorene: Two-Dimensional Multiferroics with Vertical Polarization and Mobile Magnetism. Journal of the American Chemical Society, 2017, 139, 11506-11512.	6.6	119
32472	Giant magnetoresistance and perfect spin filter effects in manganese phthalocyanine based molecular junctions. Nanoscale, 2017, 9, 12684-12689.	2.8	41
32473	Structural and magnetic properties and DFT analysis of ZnO:(Al,Er) nanoparticles. RSC Advances, 2017, 7, 32931-32941.	1.7	28
32474	A CNH monolayer: a direct gap 2D semiconductor with anisotropic electronic and optical properties. Journal of Materials Chemistry C, 2017, 5, 8498-8503.	2.7	13

#	Article	IF	Citations
32475	Metal-doped ceria nanoparticles: stability and redox processes. Physical Chemistry Chemical Physics, 2017, 19, 21729-21738.	1.3	30
32476	Gate induced monolayer behavior in twisted bilayer black phosphorus. 2D Materials, 2017, 4, 035025.	2.0	18
32477	Accurate and precise ab initio anharmonic free-energy calculations for metallic crystals: Application to hcp Fe at high temperature and pressure. Physical Review B, 2017, 96, .	1.1	25
32478	Direct and Selective Synthesis of Hydrogen Peroxide over Palladiumâ€“Tellurium Catalysts at Ambient Pressure. ChemSusChem, 2017, 10, 3342-3346.	3.6	57
32479	Experimental investigation and thermodynamic assessment of Alâ€“Caâ€“Ni ternary system. Journal of Materials Science, 2017, 52, 12409-12426.	1.7	12
32480	Electric field tunable band-gap crossover in black(blue) phosphorus/g-ZnO van der Waals heterostructures. RSC Advances, 2017, 7, 34584-34590.	1.7	34
32481	Charging assisted structural phase transitions in monolayer InSe. Physical Chemistry Chemical Physics, 2017, 19, 22502-22508.	1.3	6
32482	Hydrogenation of silicene on Ag(111) and formation of half-silicane. Journal of Materials Chemistry A, 2017, 5, 18128-18137.	5.2	18
32483	The stabilization of the rocksalt structured tantalum nitride. Journal of Applied Physics, 2017, 122, .	1.1	9
32484	Thermal expansion coefficient of WRe alloys from first principles. Physical Review B, 2017, 96, .	1.1	17
32485	First-principles investigation of magnetic properties and metamagnetic transition of NiCoMnZ(ZÂ=ÂIn,) Tj ETQq0 0 0 rgBT /Overlock 10	1.8	18
32486	Doping effects on the electronic properties of armchair phosphorene nanoribbons: A first-principles study. Physica E: Low-Dimensional Systems and Nanostructures, 2017, 94, 53-58.	1.3	12
32487	A First-Principles Study of Hydrogen Diffusivity and Dissociation on Î´-Pu (100) and (111) Surfaces. Journal of Physical Chemistry C, 2017, 121, 17950-17957.	1.5	21
32488	Reduction of Hydrogenated ZrO₂ Nanoparticles by Water Desorption. ACS Omega, 2017, 2, 3878-3885.	1.6	14
32489	Boron Switch for Selectivity of Catalytic Dehydrogenation on Size-Selected Pt Clusters on Al₂O₃. Journal of the American Chemical Society, 2017, 139, 11568-11575.	6.6	103
32490	Realizing Haldane model in Fe-based honeycomb ferromagnetic insulators. Npj Quantum Materials, 2017, 2, .	1.8	32
32491	Spin splitting and electric field modulated electron-hole pockets in antimonene nanoribbons. Npj Quantum Materials, 2017, 2, .	1.8	14
32492	Interfacial chemical bonding-mediated ionic resistive switching. Scientific Reports, 2017, 7, 1264.	1.6	6

#	Article	IF	Citations
32493	Chiral magnetoresistance in the Weyl semimetal NbP. Scientific Reports, 2017, 7, 43394.	1.6	71
32494	The effect of defects on the catalytic activity of single Au atom supported carbon nanotubes and reaction mechanism for CO oxidation. Physical Chemistry Chemical Physics, 2017, 19, 22344-22354.	1.3	38
32495	Comparison of the polymorphs of VOPO₄ as multi-electron cathodes for rechargeable alkali-ion batteries. Journal of Materials Chemistry A, 2017, 5, 17421-17431.	5.2	46
32496	A planar C₃Ca₂ film: a novel 2p Dirac half metal. Journal of Materials Chemistry C, 2017, 5, 8504-8508.	2.7	37
32497	Deep donor state of the copper acceptor as a source of green luminescence in ZnO. Applied Physics Letters, 2017, 111, 042101.	1.5	26
32498	Single-layer group IV-V and group V-IV-III-VI semiconductors: Structural stability, electronic structures, optical properties, and photocatalysis. Physical Review B, 2017, 96, .	1.1	56
32499	A DFT+U study of the catalytic activity of lanthanum nickelate. European Physical Journal B, 2017, 90, 1.	0.6	2
32500	Tiered Electron Anions in Multiple Voids of LaScSi and Their Applications to Ammonia Synthesis. Advanced Materials, 2017, 29, 1700924.	11.1	85
32501	Dynamic covalent bond from first principles: Diarylbibenzofuranone structural, electronic, and oxidation studies. Journal of Computational Chemistry, 2017, 38, 2675-2679.	1.5	3
32502	Influence of adsorbate and defect on structural and electronic properties of ultrathin silver nanotube. Journal of Physics and Chemistry of Solids, 2017, 111, 135-141.	1.9	1
32503	Theoretical Design of Highly Efficient CO₂/N₂ Separation Membranes Based on Electric Quadrupole Distinction. Journal of Physical Chemistry C, 2017, 121, 17925-17931.	1.5	15
32504	Self-optimizing, highly surface-active layeredÂmetal dichalcogenide catalysts for hydrogen evolution. Nature Energy, 2017, 2, .	19.8	336
32505	Initial Growth Mechanism of Blue Phosphorene on Au(111) Surface. Journal of Physical Chemistry C, 2017, 121, 17893-17899.	1.5	48
32506	Interaction of Cobalt Atoms, Dimers, and Co₄ Clusters with Circumcoronene: A Theoretical Study. Journal of Physical Chemistry C, 2017, 121, 18900-18908.	1.5	12
32507	Adsorption of Metallic, Metalloidic, and Nonmetallic Adatoms on Two-Dimensional C₃N. Journal of Physical Chemistry C, 2017, 121, 18575-18583.	1.5	111
32508	Structural Dependence of the Sulfur Reduction Mechanism in Carbon-Based Cathodes for Lithiumâ€“Sulfur Batteries. Journal of Physical Chemistry C, 2017, 121, 18369-18377.	1.5	17
32509	Dynamic Disorder and Potential Fluctuation in Two-Dimensional Perovskite. Journal of Physical Chemistry Letters, 2017, 8, 3875-3880.	2.1	31
32510	Chemical Reactivity Descriptor for the Oxide-Electrolyte Interface in Li-Ion Batteries. Journal of Physical Chemistry Letters, 2017, 8, 3881-3887.	2.1	104

#	Article	IF	Citations
32511	Excess Li-Ion Storage on Reconstructed Surfaces of Nanocrystals To Boost Battery Performance. Nano Letters, 2017, 17, 6018-6026.	4.5	53
32512	Janus Monolayer Transition-Metal Dichalcogenides. ACS Nano, 2017, 11, 8192-8198.	7.3	1,001
32513	Extending the Ïƒ-Hole Concept to Metals: An Electrostatic Interpretation of the Effects of Nanostructure in Gold and Platinum Catalysis. Journal of the American Chemical Society, 2017, 139, 11012-11015.	6.6	136
32514	Full picture discovery for mixed-fluorine anion effects on high-voltage spinel lithium nickel manganese oxide cathodes. NPG Asia Materials, 2017, 9, e398-e398.	3.8	22
32515	Impact of interfacial molecular orientation on radiative recombination and charge generation efficiency. Nature Communications, 2017, 8, 79.	5.8	198
32516	Disentangling the intricate atomic short-range order and electronic properties in amorphous transition metal oxides. Scientific Reports, 2017, 7, 2044.	1.6	19
32517	Giant Rashba effect at the topological surface of PrGe revealing antiferromagnetic spintronics. Scientific Reports, 2017, 7, 4120.	1.6	11
32518	A kinetic Monte Carlo simulation method of van der Waals epitaxy for atomistic nucleation-growth processes of transition metal dichalcogenides. Scientific Reports, 2017, 7, 2977.	1.6	72
32519	The electromigration effect revisited: non-uniform local tensile stress-driven diffusion. Scientific Reports, 2017, 7, 3082.	1.6	30
32520	One-dimensional electron gas in strained lateral heterostructures of single layer materials. Scientific Reports, 2017, 7, 4316.	1.6	4
32521	Thermal conductivities of phosphorene allotropes from first-principles calculations: a comparative study. Scientific Reports, 2017, 7, 4623.	1.6	36
32522	Electronic structure of SrSn2As2 near the topological critical point. Scientific Reports, 2017, 7, 6133.	1.6	19
32523	Unconventional band inversion and intrinsic quantum spin Hall effect in functionalized group-V binary films. Scientific Reports, 2017, 7, 6126.	1.6	16
32524	On the stochastic phase stability of Ti2AlC-Cr2AlC. Scientific Reports, 2017, 7, 5138.	1.6	16
32525	Theoretical study of superionic phase transition in Li2S. Scientific Reports, 2017, 7, 5873.	1.6	10
32526	Heteroborospherene clusters Ninâ€‰â^â€‰B40 (nâ€‰=â€‰1â€“4) and heteroborophene monolayers Ni2â€‰â^â€‰B14 with pla heptacoordinate transition-metal centers in Î·7-B7 heptagons. Scientific Reports, 2017, 7, 5701.	1.6	16
32527	Electronic Structure of Polyethylene: Role of Chemical, Morphological and Interfacial Complexity. Scientific Reports, 2017, 7, 6128.	1.6	53
32528	Design of new Mott multiferroics via complete charge transfer: promising candidates for bulk photovoltaics. Scientific Reports, 2017, 7, 6142.	1.6	19

#	Article	IF	Citations
32529	Effects of Ni doping on various properties of NbH phases: A first-principles investigation. Scientific Reports, 2017, 7, 6535.	1.6	7
32530	Impact of isovalent and aliovalent substitution on the mechanical and thermal properties of Gd2Zr2O7. Scientific Reports, 2017, 7, 6399.	1.6	17
32531	Transition metal alloying effect on the phosphoric acid adsorption strength of Pt nanoparticles: an experimental and density functional theory study. Scientific Reports, 2017, 7, 7186.	1.6	17
32532	Hydrogen physisorption based on the dissociative hydrogen chemisorption at the sulphur vacancy of MoS2 surface. Scientific Reports, 2017, 7, 7152.	1.6	32
32533	Electronic structure and its external electric field modulation of PbPdO2 ultrathin slabs with (002) and (211) preferred orientations. Scientific Reports, 2017, 7, 6898.	1.6	9
32534	Model representations of kerogen structures: An insight from density functional theory calculations and spectroscopic measurements. Scientific Reports, 2017, 7, 7068.	1.6	19
32535	Improved electrochemical properties of LiNi0.91Co0.06Mn0.03O2 cathode material via Li-reactive coating with metal phosphates. Scientific Reports, 2017, 7, 7151.	1.6	68
32536	Room temperature ferroelectricity in fluoroperovskite thin films. Scientific Reports, 2017, 7, 7182.	1.6	19
32537	Observation of nodal line in non-symmorphic topological semimetal InBi. New Journal of Physics, 2017, 19, 065007.	1.2	51
32538	Liquid-to-liquid crossover in the GaIn eutectic alloy. Physical Review B, 2017, 95, .	1.1	21
32539	Magnetic properties of the CrMnFeCoNi high-entropy alloy. Physical Review B, 2017, 96, .	1.1	124
32540	Role of Ordered Ni Atoms in Li Layers for Liâ€Rich Layered Cathode Materials. Advanced Functional Materials, 2017, 27, 1700982.	7.8	36
32541	Towards a Comprehensive Understanding of the Reaction Mechanisms Between Defective MoS₂ and Thiol Molecules. Angewandte Chemie, 2017, 129, 10637-10641.	1.6	4
32542	Selfâ€Templating Construction of Hollow Amorphous CoMoS₄ Nanotube Array towards Efficient Hydrogen Evolution Electrocatalysis at Neutral pH. Chemistry - A European Journal, 2017, 23, 12718-12723.	1.7	48
32543	Theoretical prediction of robust and intrinsic half-metallicity in Ni 2 N MXene with different types of surface terminations. Applied Surface Science, 2017, 426, 804-811.	3.1	35
32544	Accurate representation of formation energies of crystalline alloys with many components. Computational Materials Science, 2017, 139, 26-30.	1.4	40
32545	Optical Transitions and Excitonic Properties of Ge_{1â€“x}Sn_x Alloy Quantum Dots. Journal of Physical Chemistry C, 2017, 121, 18299-18306.	1.5	11
32546	Ru-Sn/AC for the Aqueous-Phase Reduction of Succinic Acid to 1,4-Butanediol under Continuous Process Conditions. ACS Catalysis, 2017, 7, 6207-6219.	5.5	44

#	Article	IF	Citations
32547	Ultrathin TiO₂-B nanowires as an anode material for Mg-ion batteries based on a surface Mg storage mechanism. Nanoscale, 2017, 9, 12934-12940.	2.8	42
32548	A critical role of catalyst morphology in low-temperature synthesis of carbon nanotubeâ€“transition metal oxide nanocomposite. Nanoscale, 2017, 9, 12416-12424.	2.8	14
32549	Collaborative design of Liâ€“S batteries using 3D N-doped graphene aerogel as a sulfur host and graphitic carbon nitride paper as an interlayer. Sustainable Energy and Fuels, 2017, 1, 1759-1765.	2.5	35
32550	The mechanism for the formation of OH radicals in condensed-phase water under ultraviolet irradiation. Physical Chemistry Chemical Physics, 2017, 19, 21453-21460.	1.3	21
32551	Shape control in concave metal nanoparticles by etching. Nanoscale, 2017, 9, 13089-13094.	2.8	60
32552	Magnetic anisotropy energy of ferromagnetic shape memory alloys Ni2X(X=Fe, Co)Ga by first-principles calculations. AIP Advances, 2017, 7, 075001.	0.6	6
32553	Using strain to control molecule chemisorption on silicene. Journal of Chemical Physics, 2017, 147, 044705.	1.2	8
32554	Modeling of the interface formation during CuO deposition on Al(111) substrate: linking material design and elaboration process parameters through multi-levels approach. Modelling and Simulation in Materials Science and Engineering, 2017, 25, 064005.	0.8	1
32555	Ultrathin ternary semiconductor TlGaSe ₂ phototransistors with broad-spectral response. 2D Materials, 2017, 4, 035021.	2.0	22
32556	Thermomechanical stabilization of electron small polarons in <mml:math xmlns:mml="http://www.w3.org/1998/Math/MathML"><mml:mrow><mml:mi>SrTi</mml:mi><mml:msub><mml:mi mathvariant="normal">O</mml:mi><mml:mn>3</mml:mn></mml:msub></mml:mrow></mml:math> assessed by the quasiharmonic approximation. Physical Review B, 2017, 95, .	1.1	14
32557	Equation of state for charge-doping-induced deformation and hardening in cubic crystals. Physical Review B, 2017, 96, .	1.1	0
32558	Manipulation of type-I and type-II Dirac points in <mml:math xmlns:mml="http://www.w3.org/1998/Math/MathML"><mml:msub><mml:mi>PdTe</mml:mi><mml:mn>2</mml:mn></mml:msub></ superconductor by external pressure. Physical Review B, 2017, 96, .	1.1	62
32559	In Situ Electrochemical Activation of Atomic Layer Deposition Coated MoS₂ Basal Planes for Efficient Hydrogen Evolution Reaction. Advanced Functional Materials, 2017, 27, 1701825.	7.8	87
32560	An investigation of the in-plane chemically ordered atomic laminates (Mo_{2/3}Sc_{1/3})₂AlC and (Mo_{2/3}Y_{1/3})₂AlC from first principles. Physical Chemistry Chemical Physics, 2017, 19, 21595-21603.	1.3	22
32561	Hole doping, hybridization gaps, and electronic correlation in graphene on a platinum substrate. Nanoscale, 2017, 9, 11498-11503.	2.8	8
32562	A strain-induced new phase diagram and unusually high Curie temperature in manganites. Journal of Materials Chemistry C, 2017, 5, 7813-7819.	2.7	6
32563	Two-dimensional GaGeTe film: a promising graphene-like material with tunable band structure and high carrier mobility. Journal of Materials Chemistry C, 2017, 5, 8847-8853.	2.7	26
32564	Novel 3D metallic boron nitride containing only sp²bonds. Journal Physics D: Applied Physics, 2017, 50, 385302.	1.3	10

#	Article	IF	Citations
32565	Characterization of the liquid Li-solid Mo (1â€‰1â€‰0) interface from classical molecular dynamics for plasma-facing applications. Nuclear Fusion, 2017, 57, 116036.	1.6	7
32566	Anomalous vibrational modes in few layer WTe ₂ revealed by polarized Raman scattering and first-principles calculations. 2D Materials, 2017, 4, 035024.	2.0	27
32567	Fundamental properties of Ti₆Si₂Bâ€”a new ternary phase in the Tiâ€“Siâ€“B system. Materials Research Express, 2017, 4, 076508.	0.8	2
32568	Ab initiosimulations of the dynamic ion structure factor of warm dense lithium. Physical Review B, 2017, 95, .	1.1	25
32569	Mechanism of the high transition temperature for the 1111-type iron-based superconductors <mml:math xmlns:mml="http://www.w3.org/1998/Math/MathML"><mml:mrow><mml:mi>R</mml:mi><mml:mi>FeAsO</mml:mi></mml:mrow></m <mml:math xmlns:mml="http://www.w3.org/1998/Math/MathML"><mml:mo>(</mml:mo><mml:mrow><mml:mi>R</mml:mi><mml:mo>=	1.1	8
32570	Synergisti Phonon properties of copper oxide phases from first principles. Physical Review B, 2017, 96, .	1.1	9
32571	Singlet Orbital Ordering in Bilayer <mml:math xmlns:mml="http://www.w3.org/1998/Math/MathML" display="inline"><mml:mrow><mml:msub><mml:mrow><mml:mi>Sr</mml:mi></mml:mrow><mml:mrow><mml:mn>3</mml:mn></mml:mrow></mm mathvariant="normal">O</mml:mi></mml:mrow><mml:mrow><mml:mn>7</mml:mn></mml:mrow></mml:msub></mml:mrow></mml: Physical Review Letters, 2017, 118, 207207.	2.9	12
32572	Mechanical failure of metal/ceramic interfacial regions under shear loading. Acta Materialia, 2017, 138, 224-236.	3.8	53
32573	Structural, electronic and optical properties of layered GaSe1âˆ’xAs. Computational Materials Science, 2017, 139, 31-38.	1.4	17
32574	The LDA-1/2 method implemented in the excitingÂcode. Computer Physics Communications, 2017, 220, 263-268.	3.0	7
32575	Electronic and magnetic properties of zigzag C2N-h2D nanoribbons: Edge and width effects. Chemical Physics Letters, 2017, 685, 363-370.	1.2	11
32576	Towards the calculations of redox potentials in molten LiCl-KCl eutectic by ensemble averages based on first principles molecular dynamics. Electrochimica Acta, 2017, 248, 462-469.	2.6	17
32577	The effect of titanium(Ti) doping on hydrogen incorporation in tungsten(W)ï¼šFirst-principles calculations. Fusion Engineering and Design, 2017, 121, 227-234.	1.0	16
32578	Hydrogen storage of Al-Li bimetal alloy nanostructures. Journal of Alloys and Compounds, 2017, 725, 388-392.	2.8	6
32579	Preferential growth of boron layer in magnesium diboride (MgB2) by Mg diffusion method. Journal of Alloys and Compounds, 2017, 725, 526-535.	2.8	12
32580	Improvement of power factor of n-type Bi2Te3 by dispersed nanosized Ga2Te3 precipitates. Journal of Alloys and Compounds, 2017, 726, 578-586.	2.8	5
32581	Effects of solute concentration on the stacking fault energy in copper alloys at finite temperatures. Journal of Alloys and Compounds, 2017, 726, 601-607.	2.8	36
32582	Giant ferroelectric polarization and electric reversal of strong spontaneous magnetization in multiferroic Bi 2 FeMoO 6. Journal of Magnetism and Magnetic Materials, 2017, 441, 497-502.	1.0	9

#	Article	IF	Citations
32583	A comprehensive study of magnetic exchanges in the layered oxychalcogenides Sr3Fe2O5Cu2Q2 (Q= S,) Tj ETQq0 0 0 rgBT /Overlock 1	1.0	4
32584	Exchange bias and spin glass transition in quaternary MnCuNiSn Heusler alloy. Journal of Magnetism and Magnetic Materials, 2017, 444, 61-67.	1.0	5
32585	Diffusion of yttrium in bcc-iron studied by kinetic Monte Carlo simulations. Journal of Nuclear Materials, 2017, 494, 157-164.	1.3	14
32586	First-principles investigation on the composition of Ni-Si precipitates formed in irradiated stainless steels. Journal of Nuclear Materials, 2017, 494, 354-360.	1.3	8
32587	Solubility, diffusivity, and permeability of hydrogen at PdCu phases. Journal of Membrane Science, 2017, 542, 24-30.	4.1	34
32588	Gaseous swelling of U3Si2 during steady-state LWR operation: A rate theory investigation. Nuclear Engineering and Design, 2017, 322, 336-344.	0.8	42
32589	Band offsets in La2O3/InN heterostructures. Solid State Communications, 2017, 265, 19-22.	0.9	0
32590	The effect of silicon on spangle size in hot-dipped 55 wt%Al-Zn coatings. Surface and Coatings Technology, 2017, 327, 110-117.	2.2	5
32591	Reaction mechanisms of acetylene hydrochlorination catalyzed by AuCl3/C catalysts: A density functional study. Catalysis Communications, 2017, 101, 120-124.	1.6	11
32592	Peculiar hydrogenation reactivity of Niâ€“NiÎ´+ clusters stabilized by ceria in reducing nitrobenzene to azoxybenzene. Journal of Catalysis, 2017, 353, 107-115.	3.1	36
32593	Bandgap Engineering of the g-ZnO Nanosheet via Cationicâ€“Anionic Passivated Codoping for Visible-Light-Driven Photocatalysis. Journal of Physical Chemistry C, 2017, 121, 18534-18543.	1.5	33
32594	Insights into the Câ€“H Bond Activation on NiO Surfaces: The Role of Nickel and Oxygen Vacancies and of Low Valent Dopants on the Reactivity and Energetics. Journal of Physical Chemistry C, 2017, 121, 17969-17981.	1.5	44
32595	On the shuttling mechanism of a chlorine atom in a chloroaluminum phthalocyanine based molecular switch. Physical Chemistry Chemical Physics, 2017, 19, 22401-22405.	1.3	11
32596	The interaction of CO molecules on Auâ€“Rh bimetallic nanoclusters supported on a thin film of Al₂O₃/NiAl(100). RSC Advances, 2017, 7, 13362-13371.	1.7	6
32597	Strain-driven diffusion process during silicon oxidation investigated by coupling density functional theory and activation relaxation technique. Journal of Chemical Physics, 2017, 147, 054701.	1.2	6
32598	Optical, electronic, and elastic properties of some A⁵B⁶C⁷ferroelectrics (A=Sb, Bi; B=S, Se; C=I, Br, Cl): First principle calculation. Ferroelectrics, 2017, 511, 22-34.	0.3	13
32599	Application of the Lanyâ€“Zunger polaron correction for calculating surface charge trapping. Journal of Physics Condensed Matter, 2017, 29, 394001.	0.7	11
32600	Rules and mechanisms governing octahedral tilts in perovskites under pressure. Physical Review B, 2017, 96, .	1.1	45

#	Article	IF	Citations
32601	Simple way to apply nonlocal van der Waals functionals within all-electron methods. Physical Review B, 2017, 96, .	1.1	16
32602	Creating anisotropic spin-split surface states in momentum space by molecular adsorption. Physical Review B, 2017, 96, .	1.1	6
32603	Theoretical investigation of phase separation in thermoelectric AgSbTe2. Japanese Journal of Applied Physics, 2017, 56, 081201.	0.8	1
32604	DDT Polymorphism and the Lethality of Crystal Forms. Angewandte Chemie, 2017, 129, 10299-10303.	1.6	21
32605	optPBE-vdW density functional theory study of liquid water and pressure-induced structural evolution in ice Ih. Canadian Journal of Chemistry, 2017, 95, 1205-1211.	0.6	6
32606	Firstâ€principles prediction of Siâ€doped Fe carbide as one of the possible constituents of Earth's inner core. Geophysical Research Letters, 2017, 44, 8776-8784.	1.5	9
32607	Coexistence of Normal and Auxetic Behavior in a Thermally and Chemically Stable sp³ Nanothread: Poly[5]asterane. Chemistry - A European Journal, 2017, 23, 12917-12923.	1.7	12
32608	Powerful recombination centers resulting from reactions of hydrogen with carbonâ€“oxygen defects in nâ€type Czochralskiâ€grown silicon. Physica Status Solidi - Rapid Research Letters, 2017, 11, 1700133.	1.2	13
32609	Short-Range Order in High Entropy Alloys: Theoretical Formulation and Application to Mo-Nb-Ta-V-W System. Journal of Phase Equilibria and Diffusion, 2017, 38, 391-403.	0.5	102
32610	Bromination-induced stability enhancement with a multivalley optical response signature in guanidinium [C(NH₂)₃]⁺-based hybrid perovskite solar cells. Journal of Materials Chemistry A, 2017, 5, 18561-18568.	5.2	8
32611	Optical properties of <mml:math xmlns:mml="http://www.w3.org/1998/Math/MathML"><mml:mrow><mml:msub><mml:mi>Ti</mml:mi><mml:mi>x</mml:mi></mml:ms mathvariant="normal">O</mml:mi><mml:mn>2</mml:mn></mml:msub></mml:mrow></mml:math> solid solutions. Physical Review B, 2017, 95, .	1.1	9
32612	Singleâ€Domain Ferromagnet of Noncentrosymmetric Uniaxial Magnetic Ions and Magnetoelectric Interaction. Angewandte Chemie, 2017, 129, 10330-10333.	1.6	1
32613	Revealing the Nature of Bonding in Rareâ€Earth Transitionâ€Metal Tellurides by Means of Methods Based on First Principles. European Journal of Inorganic Chemistry, 2017, 2017, 3395-3400.	1.0	19
32614	Edge magnetism modulation of graphene nanoribbons via planar tetrahedral coordinated atoms embedding. Journal of Materials Science, 2017, 52, 12307-12313.	1.7	3
32615	Ab Initio Investigation on Structural, Elastic and Electronic Properties of Î·-Phase Cu4.5Ni1Au0.5Sn5 and Cu5Ni1Sn4.5In0.5 Intermetallic Compounds. Journal of Electronic Materials, 2017, 46, 5684-5692.	1.0	1
32616	The Structure, Electronic, Magnetic and Optical Properties of the Mn-X (XÂ=ÂB, C, N and O) Co-Doped Monolayer WS2. Journal of Electronic Materials, 2017, 46, 6544-6552.	1.0	5
32617	TGMin: A global-minimum structure search program based on a constrained basin-hopping algorithm. Nano Research, 2017, 10, 3407-3420.	5.8	97
32618	Shear-strain gradient induced polarization reversal in ferroelectric <mml:math xmlns:mml="http://www.w3.org/1998/Math/MathML"><mml:msub><mml:mi mathvariant="bold">BaTiO</mml:mi><mml:mn>3</mml:mn></mml:msub></mml:math> thin films: A first-principles total-energy study. Physical Review B, 2017, 95, .	1.1	9

#	Article	IF	Citations
32619	Recent Advances in Understanding the Structure and Properties of Amorphous Oxide Semiconductors. Advanced Electronic Materials, 2017, 3, 1700082.	2.6	124
32620	Inducing Complexity in Intermetallics through Electronâ€“Hole Matching: The Structure of Fe 14 Pd 17 Al 69. Angewandte Chemie, 2017, 129, 10279-10284.	1.6	0
32621	On The Density Functional Theory Treatment of Lanthanide Coordination Compounds: A Comparative Study in a Series of Cuâ€“Ln (Ln = Gd, Tb, Lu) Binuclear Complexes. Inorganic Chemistry, 2017, 56, 9474-9485.	1.9	22
32622	Dramatic Drop of d⁰ Ferromagnetism with ZnO Nanocrystal Size in Vacuum and Air. Journal of Physical Chemistry C, 2017, 121, 19401-19406.	1.5	7
32623	Electrical Contacts in Monolayer Arsenene Devices. ACS Applied Materials & Interfaces, 2017, 9, 29273-29284.	4.0	76
32624	In situ atomic-scale observation of oxygen-driven core-shell formation in Pt3Co nanoparticles. Nature Communications, 2017, 8, 204.	5.8	102
32625	Occurrence of spintronics behaviour (half-metallicity, spin gapless semiconductor and bipolar) Tj ETQq0 0 0 rgBT /Overlock 10 Tf 50 507 _{0.17} O ₃. Royal Society Open Science, 2017, 4, 170273.	1.1	9
32626	Electron interactions, spin-orbit coupling, and intersite correlations in pyrochlore iridates. Physical Review B, 2017, 95, .	1.1	27
32627	Strain-induced quantum topological phase transitions in Na3Bi. Physical Review B, 2017, 96, .	1.1	37
32628	First-principles equation-of-state table of silicon and its effects on high-energy-density plasma simulations. Physical Review E, 2017, 95, 043210.	0.8	17
32629	Ab initio study of new sp3 silicon and germanium allotropes predicted from the zeolite topologies. European Physical Journal B, 2017, 90, 1.	0.6	8
32630	Effect of chemical and hydrostatic pressure on electronic structure of BiPd2O4: A first-principles study. Journal of Alloys and Compounds, 2017, 726, 737-750.	2.8	3
32631	Molybdenum-doped ZnS sheets with dominant {1 1 1} facets for enhanced visible light photocatalytic activities. Journal of Colloid and Interface Science, 2017, 507, 200-208.	5.0	10
32632	Site preference of transition-metal elements additions on mechanical and electronic properties of B2 DyCu-based alloys. Materials and Design, 2017, 133, 476-486.	3.3	29
32633	Liquid-like Ionic Diffusion in Solid Bismuth Oxide Revealed by Coherent Quasielastic Neutron Scattering. Chemistry of Materials, 2017, 29, 7408-7415.	3.2	23
32634	Hole Transfer in Dye-Sensitized Cesium Lead Halide Perovskite Photovoltaics: Effect of Interfacial Bonding. Journal of Physical Chemistry C, 2017, 121, 20113-20125.	1.5	14
32635	Electronic Structures and Photoanodic Properties of Ilmenite-type MTiO₃ Epitaxial Films (M = Mn, Fe, Co, Ni). Journal of Physical Chemistry C, 2017, 121, 18717-18724.	1.5	26
32636	Time-Disordered Crystal Structure of AlPO₄-5. Journal of Physical Chemistry C, 2017, 121, 18762-18770.	1.5	4

#	Article	IF	Citations
32637	Transition-metal doping induces the transition of electronic and magnetic properties in armchair MoS₂ nanoribbons. Physical Chemistry Chemical Physics, 2017, 19, 24594-24604.	1.3	24
32638	Hysteresis and bonding reconstruction in the pressure-induced B3â€“B1 phase transition of 3C-SiC. Physical Chemistry Chemical Physics, 2017, 19, 22887-22894.	1.3	8
32639	Stable and metallic two-dimensional TaC₂as an anode material for lithium-ion battery. Journal of Materials Chemistry A, 2017, 5, 18698-18706.	5.2	75
32640	Structural and electrical analysis of epitaxial 2D/3D vertical heterojunctions of monolayer MoS2 on GaN. Applied Physics Letters, 2017, 111, .	1.5	27
32641	Quantum-mechanical study of tensorial elastic and high-temperature thermodynamic properties of grain boundary states in superalloy-phase Ni3Al. IOP Conference Series: Materials Science and Engineering, 2017, 219, 012019.	0.3	6
32642	Ab-initio modeling of self-heating in single-layer MoS<inf>2</inf> transistors. , 2017, , .		0
32643	Computational Verification of So-Called Perovskite Solar Cells as PbI₆^{4â^'}-Aligned Solar Cells. Journal of the Electrochemical Society, 2017, 164, E3598-E3605.	1.3	3
32644	First-principles study on adsorption structure and electronic state of stanene on Î±-alumina surface. Japanese Journal of Applied Physics, 2017, 56, 095701.	0.8	7
32645	Giant Enhancement of Luminescence from Phosphors through Oxygenâ€Vacancyâ€Mediated Chemical Pressure Relaxation. Advanced Optical Materials, 2017, 5, 1700448.	3.6	21
32646	Ab initio triangle maps for new insights into the crystal wave functions of carbon allotropes. Carbon, 2017, 123, 708-716.	5.4	3
32647	Adsorption of chloroform on N-doped and Al-doped graphene: A first-principle study. Chemical Physics Letters, 2017, 685, 344-348.	1.2	19
32648	First principles investigations of the magnetic properties and martensitic transformation in Mn2NiB Heusler alloy. Journal of Magnetism and Magnetic Materials, 2017, 444, 43-48.	1.0	2
32649	Enhanced Pseudocapacitance of MoO₃-Reduced Graphene Oxide Hybrids with Insight from Density Functional Theory Investigations. Journal of Physical Chemistry C, 2017, 121, 18992-19001.	1.5	51
32650	van der Waals Bonded Co/h-BN Contacts to Ultrathin Black Phosphorus Devices. Nano Letters, 2017, 17, 5361-5367.	4.5	48
32651	Universal Surface Engineering of Transition Metals for Superior Electrocatalytic Hydrogen Evolution in Neutral Water. Journal of the American Chemical Society, 2017, 139, 12283-12290.	6.6	207
32652	Electric-field-controlled phase transition in a 2D molecular layer. Scientific Reports, 2017, 7, 7357.	1.6	26
32653	Monitoring and manipulating single molecule rotors on the Bi(111) surface by the scanning tunneling microscopy. RSC Advances, 2017, 7, 34262-34266.	1.7	1
32654	Diffusion quantum Monte Carlo calculations of SrFeO3 and LaFeO3. Journal of Chemical Physics, 2017, 147, 034701.	1.2	27

#	Article	IF	Citations
32655	Electric field modulations of band alignments in arsenene/Ca(OH)₂heterobilayers for multi-functional device applications. Journal Physics D: Applied Physics, 2017, 50, 415304.	1.3	12
32656	Rhenium doping induced structural transformation in mono-layered MoS₂ with improved catalytic activity for hydrogen evolution reaction. Journal Physics D: Applied Physics, 2017, 50, 405303.	1.3	23
32657	Convergence of separate orbits for enhanced thermoelectric performance of layered ZrS₂. New Journal of Physics, 2017, 19, 073036.	1.2	24
32658	Interplay of phase sequence and electronic structure in the modulated martensites of <mml:math xmlns:mml="http://www.w3.org/1998/Math/MathML"><mml:mrow><mml:msub><mml:mi>Mn</mml:mi><mml:mn>2</mml:mn></mml:msub></mml:mrow></mml:math> from first-principles calculations. Physical Review B, 2017, 96, .	1.1	19
32659	Type-II nodal loops: Theory and material realization. Physical Review B, 2017, 96, .	1.1	158
32660	Theoretical Investigation of Strain and Doping on the Raman Spectra of Monolayer MoS₂. Physica Status Solidi (B): Basic Research, 2017, 254, 1700184.	0.7	49
32661	Ab-Initio Calculations and Thermodynamic Description of the Yb-Cd and Yb-Sn Systems. Journal of Phase Equilibria and Diffusion, 2017, 38, 665-675.	0.5	0
32662	Facile synthesis of Fe-modified manganese oxide with high content of oxygen vacancies for efficient airborne ozone destruction. Applied Catalysis A: General, 2017, 546, 79-86.	2.2	69
32663	First-principles study of hydrogen behavior in vanadium-based binary alloy membranes for hydrogen separation. International Journal of Hydrogen Energy, 2017, 42, 22925-22932.	3.8	24
32664	Analysis of single and composite structural defects in pure amorphous silicon: A first-principles study. Journal of Non-Crystalline Solids, 2017, 473, 64-73.	1.5	2
32665	Mechanistic Insights into Alkane Metathesis Catalyzed by Silica-Supported Tantalum Hydrides: A DFT Study. Inorganic Chemistry, 2017, 56, 10458-10473.	1.9	14
32666	Homologous Series of 2D Chalcogenides Csâ€“Agâ€“Biâ€“Q (Q = S, Se) with Ion-Exchange Properties. Journal of the American Chemical Society, 2017, 139, 12601-12609.	6.6	22
32667	Giant lattice expansion by quantum stress and universal atomic forces in semiconductors under instant ultrafast laser excitation. Physical Chemistry Chemical Physics, 2017, 19, 24735-24741.	1.3	7
32668	Electronic structures and band alignments of monolayer metal trihalide semiconductors MX₃. Journal of Materials Chemistry C, 2017, 5, 9066-9071.	2.7	45
32669	Potential thermoelectric material open framework Si24 from a first-principles study. Journal Physics D: Applied Physics, 2017, 50, 425501.	1.3	15
32670	First-principles study of thermoelectric transport properties of monolayer gallium chalcogenides. Journal Physics D: Applied Physics, 2017, 50, 405301.	1.3	16
32671	Structural prediction of two-dimensional materials under strain. 2D Materials, 2017, 4, 045009.	2.0	19
32672	Comparative investigation of electronic transport across three-dimensional nanojunctions. Physical Review B, 2017, 95, .	1.1	2

#	Article	IF	Citations
32673	Oxygen-vacancy driven electron localization and itinerancy in rutile-based <mml:math xmlns:mml="http://www.w3.org/1998/Math/MathML"><mml:msub><mml:mi>TiO</mml:mi><mml:mn>2</mml:mn></mml:msub></mml Physical Review B, 2017, 95, .	1.1	59
32674	Ab initio molecular dynamics study of the structural and electronic transition in <mml:math xmlns:mml="http://www.w3.org/1998/Math/MathML"><mml:msub><mml:mi>VO</mml:mi><mml:mn>2</mml:mn></mml:msub></mml Physical Review B, 2017, 96, .	1.1	11
32675	Germanium aluminum nitride thin films for piezo-MEMS devices. , 2017, , .		4
32676	Computational Studies of Solubilities of LiO₂and Li₂O₂in Aprotic Solvents. Journal of the Electrochemical Society, 2017, 164, E3696-E3701.	1.3	26
32677	Tunable electronic structure in stained two dimensional van der Waals g-C2N/XSe2 (X = Mo, W) heterostructures. Physica E: Low-Dimensional Systems and Nanostructures, 2017, 94, 148-152.	1.3	8
32678	Dopant Induced Impurity Bands and Carrier Concentration Control for Thermoelectric Enhancement in p-Type Cr₂Ge₂Te₆. Chemistry of Materials, 2017, 29, 7401-7407.	3.2	53
32679	An Exceptionally Narrow Band-Gap (â¼4 eV) Silicate Predicted in the Cubic Perovskite Structure: BaSiO₃. Inorganic Chemistry, 2017, 56, 10535-10542.	1.9	16
32680	Behavior of Methylammonium Dipoles in MAPbX₃ (X = Br and I). Journal of Physical Chemistry Letters, 2017, 8, 4113-4121.	2.1	103
32681	A computational approach towards understanding hydrogen gas adsorption in Coâ€“MIL-88A. RSC Advances, 2017, 7, 39583-39593.	1.7	7
32682	Significant enhancement of the selectivity of propylene epoxidation for propylene oxide: a molecular oxygen mechanism. Physical Chemistry Chemical Physics, 2017, 19, 25129-25139.	1.3	31
32683	Shallow trapping vs. deep polarons in a hybrid lead halide perovskite, CH₃NH₃PbI₃. Physical Chemistry Chemical Physics, 2017, 19, 27184-27190.	1.3	18
32684	First-principles investigation of quantum emission from hBN defects. Nanoscale, 2017, 9, 13575-13582.	2.8	167
32685	Tuning the electronic and magnetic properties of penta-graphene using a hydrogen atom: a theoretical study. RSC Advances, 2017, 7, 40200-40207.	1.7	34
32686	First-principles prediction of interstitial carbon, nitrogen, and oxygen effects on the helium behavior in nickel. Journal of Applied Physics, 2017, 122, .	1.1	5
32687	Narrow-band anisotropic electronic structure of <mml:math xmlns:mml="http://www.w3.org/1998/Math/MathML"><mml:msub><mml:mi>ReS</mml:mi><mml:mn>2</mml:mn></mml:msub></mml Physical Review B, 2017, 96, .	1.1	89
32688	Tunable magnetic interaction by an applied electric field in a Co-adsorbed SiC monolayer. JETP Letters, 2017, 106, 258-261.	0.4	2
32689	Covalent-bonding to irreducible SiO2 leads to high-loading and atomically dispersed metal catalysts. Journal of Catalysis, 2017, 353, 315-324.	3.1	47
32690	Highly Efficient Performance and Conversion Pathway of Photocatalytic NO Oxidation on SrO-Clusters@Amorphous Carbon Nitride. Environmental Science & Technology, 2017, 51, 10682-10690.	4.6	203

#	Article	IF	Citations
32691	Two-Dimensional TiO₂ Nanosheets for Photo and Electro-Chemical Oxidation of Water: Predictions of Optimal Dopant Species from First-Principles. Journal of Physical Chemistry C, 2017, 121, 19201-19208.	1.5	14
32692	Chemical Origin of Termination-Functionalized MXenes: Ti₃C₂T₂ as a Case Study. Journal of Physical Chemistry C, 2017, 121, 19254-19261.	1.5	194
32693	Nonacene Generated by On-Surface Dehydrogenation. ACS Nano, 2017, 11, 9321-9329.	7.3	107
32694	Large magnetic anisotropy and strain induced enhancement of magnetic anisotropy in monolayer TaTe₂. Physical Chemistry Chemical Physics, 2017, 19, 24341-24347.	1.3	48
32695	Two-dimensional hexagonal M₃C₂ (M = Zn, Cd and Hg) monolayers: novel quantum spin Hall insulators and Dirac cone materials. Journal of Materials Chemistry C, 2017, 5, 9181-9187.	2.7	34
32696	Hard templating ultrathin polycrystalline hematite nanosheets: effect of nano-dimension on CO₂ to CO conversion via the reverse water-gas shift reaction. Nanoscale, 2017, 9, 12984-12995.	2.8	36
32697	On the ab initio calculation of vibrational formation entropy of point defect: the case of the silicon vacancy. EPJ Photovoltaics, 2017, 8, 85505.	0.8	4
32698	Structural transformations and adsorption properties of PtNi nanoalloy thin film electrocatalysts prepared by magnetron co-sputtering. Electrochimica Acta, 2017, 251, 427-441.	2.6	15
32699	First-principles study of the phase stability and elastic properties of Ti-X alloys (XÂ=ÂMo, Nb, Al, Sn, Zr,) Tj ETQq0 0 0 rgBT /Overlock 10 T	2.8	59
32700	Davydov Collective Vibrational Modes and Infrared Spectrum Features in Aniline Crystal: Influence of Geometry Change Induced by van der Waals Interactions. Journal of Physical Chemistry C, 2017, 121, 18867-18875.	1.5	1
32701	Intricate Resonant Raman Response in Anisotropic ReS₂. Nano Letters, 2017, 17, 5897-5907.	4.5	66
32702	Conjugated-Backbone Effect of Organic Small Molecules for n-Type Thermoelectric Materials with ZT over 0.2. Journal of the American Chemical Society, 2017, 139, 13013-13023.	6.6	215
32703	Single-Layer Tl₂O: A Metal-Shrouded 2D Semiconductor with High Electronic Mobility. Journal of the American Chemical Society, 2017, 139, 11694-11697.	6.6	72
32704	Enhanced photoelectrochemical performance of anatase TiO₂ for water splitting via surface codoping. RSC Advances, 2017, 7, 39877-39884.	1.7	25
32705	5,6-Di(2-fluoro-2,2-dinitroethoxy)furazano[3,4-b]pyrazine: a high performance melt-cast energetic material and its polycrystalline properties. RSC Advances, 2017, 7, 38844-38852.	1.7	15
32706	Enhancing the thermoelectric performance of Cu₃SnS₄-based solid solutions through coordination of the Seebeck coefficient and carrier concentration. Journal of Materials Chemistry A, 2017, 5, 18808-18815.	5.2	39
32707	Strong interfacial interaction and enhanced optical absorption in graphene/InAs and MoS₂/InAs heterostructures. Journal of Materials Chemistry C, 2017, 5, 9429-9438.	2.7	32
32708	Two-dimensional GeP₃ as a high capacity electrode material for Li-ion batteries. Physical Chemistry Chemical Physics, 2017, 19, 25886-25890.	1.3	81

#	Article	IF	Citations
32709	Strain and electric field tunable electronic structure of buckled bismuthene. RSC Advances, 2017, 7, 39546-39555.	1.7	53
32710	Structural, mechanical and electronic properties of Nb₂C: first-principles calculations. RSC Advances, 2017, 7, 33402-33407.	1.7	14
32711	Candidate photoferroic absorber materials for thin-film solar cells from naturally occurring minerals: enargite, stephanite, and bournonite. Sustainable Energy and Fuels, 2017, 1, 1339-1350.	2.5	32
32712	An organic-inorganic perovskite ferroelectric with large piezoelectric response. Science, 2017, 357, 306-309.	6.0	744
32713	Direct atomic-level insight into the active sites of a high-performance PGM-free ORR catalyst. Science, 2017, 357, 479-484.	6.0	1,273
32714	Dynamic multinuclear sites formed by mobilized copper ions in NO _x selective catalytic reduction. Science, 2017, 357, 898-903.	6.0	667
32715	Adatom doping-enriched geometric and electronic properties of pristine graphene: a method to modify the band gap. Structural Chemistry, 2017, 28, 1311-1318.	1.0	3
32716	A density functional study of chalcopyrite MgGeSb2. Indian Journal of Physics, 2017, 91, 1487-1492.	0.9	0
32717	AELAS: Automatic ELAStic property derivations via high-throughput first-principles computation. Computer Physics Communications, 2017, 220, 403-416.	3.0	84
32718	Positron annihilation analysis of the atomic scale changes in oxidized Zircaloy-4 samples. Journal of Nuclear Materials, 2017, 495, 172-180.	1.3	12
32719	Effect of pressure on structural, elastic and mechanical properties of transition metal hydrides Mg7TMH16 (TMÂ=ÂSc, Ti, V, Y, Zr and Nb): First-principles investigation. Journal of Physics and Chemistry of Solids, 2017, 111, 229-237.	1.9	7
32720	Unveiling photophysical properties of phenanthro[9,10-d]imidazole derivatives for organic light-emitting diodes. Organic Electronics, 2017, 50, 220-227.	1.4	7
32721	Strain modulations of magnetism in Fe-doped InSe monolayer. Physica E: Low-Dimensional Systems and Nanostructures, 2017, 94, 153-157.	1.3	4
32722	Electronic and Optical Properties of TiO₂ Solid-Solution Nanosheets for Bandgap Engineering: A Hybrid Functional Study. Journal of Physical Chemistry C, 2017, 121, 18683-18691.	1.5	5
32723	Fast Lithium Ion Migration in Room Temperature LiBH₄. Journal of Physical Chemistry C, 2017, 121, 17773-17779.	1.5	12
32724	A first principles study of p-type defects in LaCrO₃. Physical Chemistry Chemical Physics, 2017, 19, 22870-22876.	1.3	18
32725	Understanding the catalytic activity of nanoporous gold: Role of twinning in fcc lattice. Journal of Chemical Physics, 2017, 147, 044713.	1.2	17
32726	A comprehensive study of piezomagnetic response in CrPS₄monolayer: mechanical, electronic properties and magnetic ordering under strains. Journal of Physics Condensed Matter, 2017, 29, 405801.	0.7	28

#	Article	IF	Citations
32727	Origin of the abnormal diffusion of transition metal atoms in rutile. Physical Review B, 2017, 95, .	1.1	5
32728	Temperatureâ€Triggered Sulfur Vacancy Evolution in Monolayer MoS₂/Graphene Heterostructures. Small, 2017, 13, 1602967.	5.2	77
32729	Ab initio investigation on the slip preference of ã€ˆaã€‰-dislocations in hexagonal metals and alloys. Computational Materials Science, 2017, 139, 209-215.	1.4	4
32730	Puckered Arsenene: A Promising Room-Temperature Thermoelectric Material from First-Principles Prediction. Journal of Physical Chemistry C, 2017, 121, 19080-19086.	1.5	56
32731	Kinetically-Driven Phase Transformation during Lithiation in Copper Sulfide Nanoflakes. Nano Letters, 2017, 17, 5726-5733.	4.5	67
32732	Theoretical understanding on the selectivity of acrolein hydrogenation over silver surfaces: the non-Horiutiâ€“Polanyi mechanism is the key. Catalysis Science and Technology, 2017, 7, 4024-4033.	2.1	19
32733	A machine learning approach to graph-theoretical cluster expansions of the energy of adsorbate layers. Journal of Chemical Physics, 2017, 147, 054106.	1.2	31
32734	Electronic properties of lithiated SnO-based anode materials. Journal of Applied Physics, 2017, 122, 055105.	1.1	2
32735	Electronic structures and optical properties of Al, Cu, and Ag in zero, two, and three dimensional structures. Journal of Applied Physics, 2017, 122, 063104.	1.1	5
32736	Continuum Lowering and Fermi-Surface Rising in Strongly Coupled and Degenerate Plasmas. Physical Review Letters, 2017, 119, 065001.	2.9	55
32737	First principles studies of hydrogen insertion effects on magnetic properties, bonding and structure reordering of UZr 2. Computational Condensed Matter, 2017, 12, 19-24.	0.9	3
32738	Diffusion of a Single Platinum Atom on Light-Element-Doped Graphene. Journal of Physical Chemistry C, 2017, 121, 17787-17795.	1.5	21
32739	First-Principles Study on O2 Adsorption and Dissociation Processes over Rh(100) and Rh(111) Surfaces. Langmuir, 2017, 33, 11156-11163.	1.6	8
32740	Interfacial properties of borophene contacts with two-dimensional semiconductors. Physical Chemistry Chemical Physics, 2017, 19, 23982-23989.	1.3	42
32741	First-principles investigation on Au_n@(ZnO)₄₂ (n = 6â€“16) core-shell nanoparticles: structure stability and catalytic activity. Journal of Physics Condensed Matter, 2017, 29, 435701.	0.7	1
32742	Observation of magnetoelastic effects in a quasi-one-dimensional spiral magnet. Physical Review B, 2017, 96, .	1.1	6
32743	Gaseous Nanocarvingâ€Mediated Carbon Framework with Spontaneous Metal Assembly for Structureâ€Tunable Metal/Carbon Nanofibers. Advanced Materials, 2017, 29, 1702958.	11.1	13
32744	Design of Optimally Stable Molecular Coatings for Fe-Based Nanoparticles in Aqueous Environments. ACS Omega, 2017, 2, 4480-4487.	1.6	3

#	Article	IF	Citations
32745	Valence-band offsets of CoTiSb/In0.53Ga0.47As and CoTiSb/In0.52Al0.48As heterojunctions. Applied Physics Letters, 2017, 111, .	1.5	8
32746	Next generation extended Lagrangian first principles molecular dynamics. Journal of Chemical Physics, 2017, 147, 054103.	1.2	27
32747	Electrical conductivity of SiO ₂ at extreme conditions and planetary dynamos. Proceedings of the National Academy of Sciences of the United States of America, 2017, 114, 9009-9013.	3.3	33
32748	Uniaxial strain-modulated electronic structures of Cd X (X = S, Se, Te) from first-principles calculations: A comparison between bulk and nanowires. Chinese Physics B, 2017, 26, 087103.	0.7	1
32749	Effect of Pt substitution on the magnetocrystalline anisotropy of <mml:math xmlns:mml="http://www.w3.org/1998/Math/MathML"><mml:msub><mml:mi>Ni</mml:mi><mml:mn>2</mml:mn></mml:msub><mml:n : A competition between chemistry and elasticity. Physical Review B, 2017, 96, .	1.1	22
32750	Electronic origin of the spin-phonon coupling effect in transition-metal perovskites. Physical Review B, 2017, 96, .	1.1	2
32751	Enhancing the perpendicular magnetic anisotropy of 1T-FeCl2 monolayer by applying strain: first-principles study. Journal of Magnetism and Magnetic Materials, 2017, 444, 184-189.	1.0	25
32752	First-principle investigation 3,4-ethylenedioxythiophene molecule adsorption on Cu(110)-(2 â€Ã—â€ 1)O surface. Surface Science, 2017, 665, 83-88.	0.8	2
32753	Spectroscopic and Computational Investigation of Room-Temperature Decomposition of a Chemical Warfare Agent Simulant on Polycrystalline Cupric Oxide. Chemistry of Materials, 2017, 29, 7483-7496.	3.2	48
32754	Reorientational Hydrogen Dynamics in Complex Hydrides with Enhanced Li+ Conduction. Journal of Physical Chemistry C, 2017, 121, 17693-17702.	1.5	11
32755	Dissociative adsorption dynamics of nitrogen on a Fe(111) surface. Physical Chemistry Chemical Physics, 2017, 19, 24626-24635.	1.3	9
32756	First-principles study of charged steps on 180Â° domain walls in ferroelectric PbTiO3. Journal of Applied Physics, 2017, 122, .	1.1	9
32757	Electronic and optical properties of BaTiO3 across tetragonal to cubic phase transition: An experimental and theoretical investigation. Journal of Applied Physics, 2017, 122, .	1.1	95
32758	A key role of tensile strain and surface termination in formation and properties of La0.7Sr0.3MnO3 composites with carbon nanotubes. Computational Materials Science, 2017, 139, 125-131.	1.4	1
32759	Atomate: A high-level interface to generate, execute, and analyze computational materials science workflows. Computational Materials Science, 2017, 139, 140-152.	1.4	223
32760	Mechanism of ethylene oxychlorination over ruthenium oxide. Journal of Catalysis, 2017, 353, 171-180.	3.1	12
32761	Alloyed surfaces: New substrates for graphene growth. Surface Science, 2017, 665, 28-31.	0.8	2
32762	Understanding Chemical Ordering in Intermetallic Clathrates from Atomic Scale Simulations. Chemistry of Materials, 2017, 29, 7554-7562.	3.2	19

#	Article	IF	Citations
32763	Metaheuristics-Assisted Combinatorial Screening of Eu²⁺-Doped Caâ€“Srâ€“Baâ€“Liâ€“Mgâ€“Alâ€“Siâ€“Geâ€“N Compositional Space in Search of a Narrow-Band Green Emitting Phosphor and Density Functional Theory Calculations. Inorganic Chemistry, 2017, 56, 9814-9824.	1.9	23
32764	Modulation of the Local Density of States of Carbon Nanotubes by Encapsulation of Europium Nanowires As Observed by Scanning Tunneling Microscopy and Spectroscopy. Journal of Physical Chemistry C, 2017, 121, 18195-18201.	1.5	2
32765	Investigation of the Reversible Intercalation/Deintercalation of Al into the Novel Li₃VO₄@C Microsphere Composite Cathode Material for Aluminum-Ion Batteries. ACS Applied Materials & Interfaces, 2017, 9, 28486-28494.	4.0	98
32766	Self-compensation in arsenic doping of CdTe. Scientific Reports, 2017, 7, 4563.	1.6	59
32767	Data Mining for Three-Dimensional Organic Dirac Materials: Focus on Space Group 19. Scientific Reports, 2017, 7, 7298.	1.6	25
32768	Lone pair-Ï€ interaction-induced generation of photochromic coordination networks with photoswitchable conductance. Chemical Communications, 2017, 53, 9701-9704.	2.2	75
32769	Does increasing pressure always accelerate the condensed material decay initiated through bimolecular reactions? A case of the thermal decomposition of TKX-50 at high pressures. Physical Chemistry Chemical Physics, 2017, 19, 23309-23317.	1.3	12
32770	Structural and electronic properties of Sn substituted Cun (n=10, 13) clusters: A first principles study. AIP Conference Proceedings, 2017, , .	0.3	0
32771	Modulating the properties of monolayer C ₂ N: A promising metal-free photocatalyst for water splitting. Chinese Physics B, 2017, 26, 087301.	0.7	12
32772	Effect of oxygen vacancy segregation in Au or Pt/oxide hetero-interfaces on electronic structures. RSC Advances, 2017, 7, 36034-36037.	1.7	2
32773	Ionic conductivity of acceptor doped sodium bismuth titanate: influence of dopants, phase transitions and defect associates. Journal of Materials Chemistry C, 2017, 5, 8958-8965.	2.7	65
32774	The prediction of a family group of two-dimensional node-line semimetals. Nanoscale, 2017, 9, 13112-13118.	2.8	58
32775	Extension of the Hugoniot and analytical release model of Î±-quartz to 0.2â€“3 TPa. Journal of Applied Physics, 2017, 122, .	1.1	40
32776	Wannier Koopman method calculations of the band gaps of alkali halides. Applied Physics Letters, 2017, 111, .	1.5	10
32777	Mechanical properties of non-centrosymmetric CePt3Si and CePt3B. Journal of Physics Condensed Matter, 2017, 29, 185402.	0.7	5
32778	Structural characterization of water-metal interfaces. Physical Review B, 2017, 96, .	1.1	5
32779	Theory versus experiment for a family of single-layer compounds with a similar atomic arrangement: <mml:math		

#	Article	IF	Citations
32781	New multifunctional tungsten nitride with energetic N ₆ and extreme hardness predicted from first principles. Europhysics Letters, 2017, 118, 46001.	0.7	23
32782	Ironâ€Doped BaMnO₃ for Hybrid Water Splitting and Syngas Generation. ChemSusChem, 2017, 10, 3402-3408.	3.6	46
32783	The electronic and mechanical properties of tetragonal YB2C as explored by first-principles methods. Journal of Alloys and Compounds, 2017, 726, 173-178.	2.8	8
32784	Selective coordination of N3â^' and tuning of luminescence in garnet (Y1â^'x,Lax)3(Al,Si)5(O,N)12: Ce3+ phosphors. Journal of Alloys and Compounds, 2017, 726, 658-663.	2.8	18
32785	Van der Waals Interaction Really Matters: Energetics of Benzoic Acid on TiO₂ Rutile Surfaces. Journal of Physical Chemistry C, 2017, 121, 17207-17214.	1.5	14
32786	SBH10: A Benchmark Database of Barrier Heights on Transition Metal Surfaces. Journal of Physical Chemistry C, 2017, 121, 19807-19815.	1.5	89
32787	MoS₂@VS₂ Nanocomposite as a Superior Hybrid Anode Material. ACS Applied Materials & Interfaces, 2017, 9, 29942-29949.	4.0	74
32788	How Nitrogen-Doped Graphene Quantum Dots Catalyze Electroreduction of CO₂ to Hydrocarbons and Oxygenates. ACS Catalysis, 2017, 7, 6245-6250.	5.5	129
32789	Discovery and ramifications of incidental MagnÃ©li phase generation and release from industrial coal-burning. Nature Communications, 2017, 8, 194.	5.8	44
32790	Proton Transfer in Molten Lithium Carbonate: Mechanism and Kinetics by Density Functional Theory Calculations. Scientific Reports, 2017, 7, 7381.	1.6	7
32791	Ab initio study of Li, Mg and Al insertion into rutile VO₂: fast diffusion and enhanced voltages for multivalent batteries. Physical Chemistry Chemical Physics, 2017, 19, 22538-22545.	1.3	38
32792	Double-ring tubular (B2O2)nclusters (n = 6â€“42) rolled up from the most stable BO double-chain ribbon in boron monoxides. Physical Chemistry Chemical Physics, 2017, 19, 23213-23217.	1.3	3
32793	Effect of Ti doping on mechanical and optical properties of super-hard I2d-CN2 materials. RSC Advances, 2017, 7, 37943-37951.	1.7	3
32794	Challenges in bimetallic multilayer structure formation: Pt growth on Cu monolayers on Ru(0001). Physical Chemistry Chemical Physics, 2017, 19, 24100-24114.	1.3	3
32795	Anisotropic carrier mobility in two-dimensional materials with tilted Dirac cones: theory and application. Physical Chemistry Chemical Physics, 2017, 19, 23942-23950.	1.3	69
32796	Insight into the preferred formation mechanism of long-chain hydrocarbons in Fischerâ€“Tropsch synthesis on Hcp Co(10â^'11) surfaces from DFT and microkinetic modeling. Catalysis Science and Technology, 2017, 7, 3758-3776.	2.1	39
32797	Carrier providers or killers: The case of Cu defects in CdTe. Applied Physics Letters, 2017, 111, 042106.	1.5	22
32798	Orbital electronic occupation effect on metalâ€“insulator transition in Ti x V1â^'x O2. Journal of Physics Condensed Matter, 2017, 29, 355402.	0.7	6

#	Article	IF	Citations
32799	Polyamorphic Transformations in Feâ€Niâ€C Liquids: Implications for Chemical Evolution of Terrestrial Planets. Journal of Geophysical Research: Solid Earth, 2017, 122, 9745-9754.	1.4	10
32800	Modern level for properties prediction of iodine-containing organic compounds: the halogen bonds formed by iodine. Russian Chemical Bulletin, 2017, 66, 1345-1356.	0.4	20
32801	Strain induced band inversion and topological phase transition in methyl-decorated stanene film. Scientific Reports, 2017, 7, 17089.	1.6	9
32802	Amorphous chalcogenides as random octahedrally bonded solids: I. Implications for the first sharp diffraction peak, photodarkening, and Boson peak. Journal of Chemical Physics, 2017, 147, 114505.	1.2	9
32803	Study of Li atom diffusion in amorphous Li3PO4 with neural network potential. Journal of Chemical Physics, 2017, 147, 214106.	1.2	108
32804	Lattice stability and the effect of Co and Re on the ideal strength of Ni: First-principles study of uniaxial tensile deformation. Chinese Physics B, 2017, 26, 093106.	0.7	4
32805	Cr doped topological insulator Bi2Se3 under external electric field: A first-principle study. Journal of Physics: Conference Series, 2017, 864, 012039.	0.3	1
32806	Atomistic spin dynamics simulations of the MnAl <mml:math xmlns:mml="http://www.w3.org/1998/Math/MathML"><mml:mi>Ï„</mml:mi></mml:math> -phase and its antiphase boundary. Physical Review B, 2017, 96, .	1.1	18
32807	Reversible electric-field manipulation of the adsorption morphology and magnetic anisotropy of small Fe and Co clusters on graphene. Physical Review B, 2017, 96, .	1.1	10
32808	JDFTx: Software for joint density-functional theory. SoftwareX, 2017, 6, 278-284.	1.2	238
32809	Giant barocaloric effects over a wide temperature range in superionic conductor AgI. Nature Communications, 2017, 8, 1851.	5.8	95
32810	Designing flexible 2D transition metal carbides with strain-controllable lithium storage. Proceedings of the National Academy of Sciences of the United States of America, 2017, 114, E11082-E11091.	3.3	51
32811	Atomic structure of a decagonal Al-Pd-Mn phase. Physical Review B, 2017, 96, .	1.1	3
32812	Annealing of ion-irradiated hexagonal boron nitride on Ir(111). Physical Review B, 2017, 96, .	1.1	17
32813	First-Principles Study of Alkoxides Adsorbed on Au(111) and Au(110) Surfaces: Assessing the Roles of Noncovalent Interactions and Molecular Structures in Catalysis. Journal of Physical Chemistry C, 2017, 121, 27905-27914.	1.5	12
32814	Thiophene Derivatives on Gold and Molecular Dissociation Processes. Journal of Physical Chemistry C, 2017, 121, 27923-27935.	1.5	29
32815	Dissociation reaction of B₂H₆ on TiN surfaces during atomic layer deposition: first-principles study. RSC Advances, 2017, 7, 55750-55755.	1.7	11
32816	Hybrid density functional study of bandgaps for 27 new proposed half-Heusler semiconductors. Journal of Applied Physics, 2017, 122, .	1.1	28

#	Article	IF	Citations
32817	Appearance and disappearance of ferromagnetism in ultrathin <mml:math xmlns:mml="http://www.w3.org/1998/Math/MathML"><mml:msub><mml:mi>LaMnO</mml:mi><mml:mn>3</mml:mn></mml:msub></ on <mml:math xmlns:mml="http://www.w3.org/1998/Math/MathML"><mml:msub><mml:mi>SrTiO</mml:mi><mml:mn>3</mml:mn></mml:msub></m substrate: A viewpoint from first principles. Physical Review B, 2017, 96, .	1.1	27
32818	First principles, thermal stability and thermodynamic assessment of the binary Niâ€“W system. International Journal of Materials Research, 2017, 108, 1025-1035.	0.1	17
32819	Atomic-scale investigation of nuclear quantum effects of surface water: Experiments and theory. Progress in Surface Science, 2017, 92, 203-239.	3.8	29
32820	Hourglass Dirac chain metal in rhenium dioxide. Nature Communications, 2017, 8, 1844.	5.8	116
32821	Predicted High Thermoelectric Performance of Quasi-Two-Dimensional Compound GeAs Using First-Principles Calculations *. Chinese Physics Letters, 2017, 34, 117202.	1.3	3
32822	Stability, electronic and phononic properties ofÎ²and 1T structures of SiTe_x(x= 1, 2) and their vertical heterostructures. Journal of Physics Condensed Matter, 2017, 29, 395504.	0.7	6
32823	Computational methods for 2D materials: discovery, property characterization, and application design. Journal of Physics Condensed Matter, 2017, 29, 473001.	0.7	55
32824	Efficient approach to compute melting properties fully from ab initio with application to Cu. Physical Review B, 2017, 96, .	1.1	53
32825	Weyl node assisted conductivity switch in interfacial phase-change memory with van der Waals interfaces. Physical Review B, 2017, 96, .	1.1	16
32826	Off-plane polarization ordering in metal chalcogen diphosphates from bulk to monolayer. Physical Review B, 2017, 96, .	1.1	60
32827	Exploring the subsurface atomic structure of the epitaxially grown phase-change material <mml:math xmlns:mml="http://www.w3.org/1998/Math/MathML"><mml:mrow><mml:msub><mml:mi mathvariant="bold">Ge</mml:mi><mml:mn>2</mml:mn></mml:msub><mml:msub><mml:mi mathvariant="bold">Sb</mml:mi><mml:mn>2</mml:mn></mml:msub><mml:msub><mml:mi mathvariant="bold">Te</mml:mi><mml:mn>5</mml:mn></mml:msub></mml:mrow></mml:math>. Physical Review B, 2017, 96, .	1.1	10
32828	Hydrogen-induced <mml:math xmlns:mml="http://www.w3.org/1998/Math/MathML"><mml:mrow><mml:mi>s</mml:mi><mml:msup><mml:mi>p</mml:mi><mml:mn> rehybridization in epitaxial silicene. Physical Review B, 2017, 96, .	1.1	14
32829	Atomic-Scale Quantification of Interfacial Binding between Peptides and Inorganic Crystals: The Case of Calcium Carbonate Binding Peptide on Aragonite. Journal of Physical Chemistry C, 2017, 121, 28354-28363.	1.5	24
32830	In-plane magnetization-induced quantum anomalous Hall effect in atomic crystals of group-V elements. Physical Review B, 2017, 96, .	1.1	25
32831	Li(Ni,Co,Al)O₂ Cathode Delithiation: A Combination of Topological Analysis, Density Functional Theory, Neutron Diffraction, and Machine Learning Techniques. Journal of Physical Chemistry C, 2017, 121, 28293-28305.	1.5	41
32832	Theoretical study on the photophysical properties of boron-fused double helicenes. RSC Advances, 2017, 7, 56543-56549.	1.7	5
32833	Mechanism of Magnetic Coupling in Carrier-Doped SnO Nanosheets. Physical Review Applied, 2017, 8, .	1.5	13
32834	Two-dimensional hyperferroelectric metals: A different route to ferromagnetic-ferroelectric multiferroics. Physical Review B, 2017, 96, .	1.1	113

#	Article	IF	Citations
32835	Large anomalous Nernst and spin Nernst effects in the noncollinear antiferromagnets <mml:math xmlns:mml="http://www.w3.org/1998/Math/MathML"><mml:mrow><mml:msub><mml:mi>Mn</mml:mi><mml:mn>3</mml:mn></mml: (<mml:math) Tj ETQq0 0 0 rgBT /Overlock 10 Tf 50 737 Td (xmlns:mml="http://www.w3.org/1998/Math/MathML"><mml:mrow><mml:n	1.1	68
32836	Ab initio study on nonmetal and nonmagnetic metal atoms doped arsenene. JETP Letters, 2017, 106, 434-439.	0.4	7
32837	Atomistic simulations of the equation of state and hybridization of liquid carbon at a temperature of 6000 K in the pressure range of 1â€“25 GPa. Journal of Chemical Physics, 2017, 147, 214302.	1.2	16
32838	A first-principles study of impurity effects on monolayer MoS₂: bandgap dominated by donor impurities. Materials Research Express, 2017, 4, 126301.	0.8	10
32839	Type-II Dirac cone and Dirac cone protected by nonsymmorphic symmetry in the carbon-lithium compound <mml:math xmlns:mml="http://www.w3.org/1998/Math/MathML"><mml:mrow><mml:msub><mml:mi mathvariant="normal">C</mml:mi><mml:mn>4</mml:mn></mml:msub><mml:mi>Li</mml:mi></mml:mrow></mml:math>. Physical Review B, 2017, 96, .	1.1	4
32840	Effect of solid electrolyte interphase on the reactivity of polysulfide over lithium-metal anode. Electrochimica Acta, 2017, 258, 1320-1328.	2.6	13
32841	Mechanical properties of Fe rich Feâ€“Si alloys:ab initiolocal bulk-modulus viewpoint. Materials Research Express, 2017, 4, 116518.	0.8	9
32842	Thermal conductivity of type-I, type-II, and type-VIII pristine silicon clathrates: A first-principles study. Physical Review B, 2017, 96, .	1.1	14
32843	Tackling the Defect Conundrum in UiO-66: A Mixed-Linker Approach to Engineering Missing Linker Defects. Chemistry of Materials, 2017, 29, 10478-10486.	3.2	102
32844	Structural Stability of Iodide Perovskite: A Combined Cluster Expansion Method and First-Principles Study. Journal of Physical Chemistry C, 2017, 121, 27797-27804.	1.5	23
32845	Deciphering the Electrocatalytic Activity of Nitrogen-Doped Carbon Embedded with Cobalt Nanoparticles and the Reaction Mechanism of Triiodide Reduction in Dye-Sensitized Solar Cells. Journal of Physical Chemistry C, 2017, 121, 27332-27343.	1.5	18
32846	Oxygen Evolution via the Bridging Inequivalent Dual-Site Reaction: First-Principles Study of a Quadruple-Perovskite Oxide Catalyst. Journal of Physical Chemistry C, 2017, 121, 28403-28411.	1.5	29
32847	Formation of intrinsic and silicon defects in MoO3 under varied oxygen partial pressure and temperature conditions: an ab initio DFT investigation. RSC Advances, 2017, 7, 53810-53821.	1.7	18
32848	Anomalous phase behavior of first-order fluid-liquid phase transition in phosphorus. Journal of Chemical Physics, 2017, 147, 204501.	1.2	5
32849	Research on c-HfO2 (0 0 1)/Î±-Al2O3 (1 -1 0 2) interface in CTM devices based on first principle theory. AIP Advances, 2017, 7, 125001.	0.6	6
32850	Development of density-functional tight-binding repulsive potentials for bulk zirconia using particle swarm optimization algorithm. AIP Conference Proceedings, 2017, , .	0.3	3
32851	Surface magnetism of gallium arsenide nanofilms. Physical Review B, 2017, 96, .	1.1	1
32852	Viologen-Based Photochromic Coordination Polymers for Inkless and Erasable Prints. Inorganic Chemistry, 2017, 56, 14926-14935.	1.9	90

#	Article	IF	Citations
32853	Halogen versus Pseudo-Halogen Induced Perovskite for Planar Heterojunction Solar Cells: Some New Physical Insights. Journal of Physical Chemistry C, 2017, 121, 28443-28453.	1.5	13
32854	Deeply Repairing Surface States with Wet Chemistry Methods: Enhanced Performance in TiO₂ Nanowire Arraysâ€Based Optoelectronic Device. ChemistrySelect, 2017, 2, 10971-10978.	0.7	10
32855	From Multiple Nodal Chain to Dirac/Weyl Semimetal and Topological Insulator in Ternary Hexagonal Materials. Journal of Physical Chemistry C, 2017, 121, 28587-28593.	1.5	21
32856	Symmetry, Shape, and Energy Variations in Frontier Molecular Orbitals at Organic/Metal Interfaces: The Case of F₄TCNQ. Journal of Physical Chemistry C, 2017, 121, 28412-28419.	1.5	7
32857	Unusual Protonation of the Hydroxylammonium Cation Leading to the Low Thermal Stability of Hydroxylammonium-Based Salts. Journal of Physical Chemistry C, 2017, 121, 27874-27885.	1.5	35
32858	Novel Surface Molecular Functionalization Route To Enhance Environmental Stability of Tellurium-Containing 2D Layers. ACS Applied Materials & Interfaces, 2017, 9, 44625-44631.	4.0	15
32859	First-principles investigation of the orientation influenced He dissolution and diffusion behaviors onÂW surfaces. RSC Advances, 2017, 7, 25789-25795.	1.7	12
32860	Orientation dependence of the work function for metal nanocrystals. Journal of Chemical Physics, 2017, 147, 214301.	1.2	21
32861	Structural superlubricity of platinum on graphite under ambient conditions: The effects of chemistry and geometry. Applied Physics Letters, 2017, 111, .	1.5	23
32862	Photocatalytic Behavior of Fluorinated Rutile TiO₂(110) Surface: Understanding from the Band Model. Solar Rrl, 2017, 1, 1700183.	3.1	17
32863	Tuning the Physical and Chemical Properties of 2D InSe with Interstitial Boron Doping: A First-Principles Study. Journal of Physical Chemistry C, 2017, 121, 28312-28316.	1.5	11
32864	Toward a Mechanistic Understanding of Vertical Growth of van der Waals Stacked 2D Materials: A Multiscale Model and Experiments. ACS Nano, 2017, 11, 12780-12788.	7.3	89
32865	Enabling the high capacity of lithium-rich anti-fluorite lithium iron oxide by simultaneous anionic and cationic redox. Nature Energy, 2017, 2, 963-971.	19.8	140
32866	Hidden Magnetic States Emergent Under Electric Field, In A Room Temperature Composite Magnetoelectric Multiferroic. Scientific Reports, 2017, 7, 15460.	1.6	25
32867	Crystal phase transition of urea: what governs the reaction kinetics in molecular crystal phase transitions. Physical Chemistry Chemical Physics, 2017, 19, 32125-32131.	1.3	10
32868	Theoretical prediction of fracture conditions for delithiation in silicon anode of lithium ion battery. APL Materials, 2017, 5, .	2.2	13
32869	Phase stability and mechanical properties of Mo1-xNx with 0 â‰ x â‰ 1. Journal of Applied Physics, 2017, 122, .	1.1	39
32870	Renewable acrylonitrile production. Science, 2017, 358, 1307-1310.	6.0	122

#	Article	IF	Citations
32871	Design and Synthesis of Heteroleptic Iridium(III) Phosphors for Efficient Organic Light-Emitting Devices. Inorganic Chemistry, 2017, 56, 15304-15313.	1.9	20
32872	Properties of Highly Oriented Pyrolytic Graphite Supported TaSi₁₆ Clusters: A Density Functional Investigation. Journal of Physical Chemistry C, 2017, 121, 28490-28497.	1.5	9
32873	Investigation of Ligand-Stabilized Gold Clusters on Defect-Rich Titania. Journal of Physical Chemistry C, 2017, 121, 28007-28016.	1.5	20
32874	Structure, Stability, and Kinetics of Vacancy Defects in Monolayer PtSe2: A First-Principles Study. ACS Omega, 2017, 2, 8640-8648.	1.6	40
32875	Alloy-assisted deposition of three-dimensional arrays of atomic gold catalyst for crystal growth studies. Nature Communications, 2017, 8, 2014.	5.8	21
32876	Controlled spin switching in a metallocene molecular junction. Nature Communications, 2017, 8, 1974.	5.8	60
32877	First-principles investigation of oxygen-excess defects in amorphous silica. AIP Advances, 2017, 7, 105118.	0.6	10
32878	Electronic field emission models beyond the Fowler-Nordheim one. Journal of Applied Physics, 2017, 122, .	1.1	31
32879	Effects of magnetic dopants in <mml:math xmlns:mml="http://www.w3.org/1998/Math/MathML"><mml:mrow><mml:mo>(</mml:mo><mml:msub><mml:mi>Li</mml:mi><mml:mn		

#	Article	IF	Citations
32889	Polyhedral gold nanocrystals/polyelectrolyte composite film: One-pot synthesis via interfacial liquid plasma polymerization. Composites Science and Technology, 2017, 153, 198-208.	3.8	2
32890	Formic Acid Dissociative Adsorption on NiO(111): Energetics and Structure of Adsorbed Formate. Journal of Physical Chemistry C, 2017, 121, 28001-28006.	1.5	9
32891	Dehydrogenation Selectivity of Ethanol on Close-Packed Transition Metal Surfaces: A Computational Study of Monometallic, Pd/Au, and Rh/Au Catalysts. Journal of Physical Chemistry C, 2017, 121, 27504-27510.	1.5	96
32892	Magnetically Ordered Transition-Metal-Intercalated WSe₂. ACS Omega, 2017, 2, 7985-7990.	1.6	20
32893	First-principles screening of structural properties of intermetallic compounds on martensitic transformation. Npj Computational Materials, 2017, 3, .	3.5	12
32894	Spin-orbit coupling, optical transitions, and spin pumping in monolayer and few-layer InSe. Physical Review B, 2017, 96, .	1.1	31
32895	Enhanced Strength Through Nanotwinning in the Thermoelectric Semiconductor InSb. Physical Review Letters, 2017, 119, 215503.	2.9	45
32896	Strain effect on electronic structure of two-dimensional Î³-InSe nanosheets. Applied Physics Express, 2017, 10, 125202.	1.1	8
32897	Carbon adsorption on doped cementite surfaces for effective catalytic growth of diamond-like carbon: a first-principles study. Physical Chemistry Chemical Physics, 2017, 19, 32341-32348.	1.3	13
32898	The crystal structure and sodium disorder of high-temperature polymorph Î²-Na₃PS₄. Journal of Materials Chemistry A, 2017, 5, 25025-25030.	5.2	46
32899	Surface, final state, and spin effects in the valence-band photoemission spectra ofLaCoO3(001). Physical Review B, 2017, 96, .	1.1	4
32900	Gas Separation through Bilayer Silica, the Thinnest Possible Silica Membrane. ACS Applied Materials & Interfaces, 2017, 9, 43061-43071.	4.0	34
32901	Atomic-Scale Origin of the Quasi-One-Dimensional Metallic Conductivity in Strontium Niobates with Perovskite-Related Layered Structures. ACS Nano, 2017, 11, 12519-12525.	7.3	8
32902	Regio- and Chemoselective Hydrogenation of Dienes to Monoenes Governed by a Well-Structured Bimetallic Surface. Journal of the American Chemical Society, 2017, 139, 18231-18239.	6.6	48
32903	Structural, electronic, magnetic, half-metallic, mechanical, and thermodynamic properties of the quaternary Heusler compound FeCrRuSi: A first-principles study. Scientific Reports, 2017, 7, 16183.	1.6	59
32904	Reversible switching of the spin state in a manganese phthalocyanine molecule by atomic nitrogen. Physical Chemistry Chemical Physics, 2017, 19, 32655-32662.	1.3	7
32905	Valence band modification of Cr₂O₃by Ni-doping: creating a high figure of merit p-type TCO. Journal of Materials Chemistry C, 2017, 5, 12610-12618.	2.7	36
32906	A look into atomic carbon and oxygen adsorption on 1Tâ€²-MoS2monolayer: density functional theory calculations. Materials Research Express, 2017, 4, 125026.	0.8	3

#	Article	IF	Citations
32907	Universality of scanning tunneling microscopy in cuprate superconductors. Physical Review B, 2017, 96, .	1.1	13
32908	<mml:math xmlns:mml="http://www.w3.org/1998/Math/MathML"><mml:mrow><mml:msub><mml:mi mathvariant="normal">H</mml:mi><mml:mn>2</mml:mn></mml:msub><mml:mo>/</mml:mo><mml:mi>LiF</mml:mi><mml:mrow> diffractive scattering under fast grazing incidence using a DFT-based potential energy surface. Physical Review B, 2017, 96, .	1.1	7
32909	Isochoric, isobaric, and ultrafast conductivities of aluminum, lithium, and carbon in the warm dense matter regime. Physical Review E, 2017, 96, 053206.	0.8	18
32910	Molecular insights into the enhanced rate of CO2 absorption to produce bicarbonate in aqueous 2-amino-2-methyl-1-propanol. Physical Chemistry Chemical Physics, 2017, 19, 32116-32124.	1.3	16
32911	MoirÃ©-pattern interlayer potentials in van der Waals materials in the random-phase approximation. Physical Review B, 2017, 96, .	1.1	19
32912	Uniaxial Negative Thermal Expansion, Negative Linear Compressibility, and Negative Poissonâ€™s Ratio Induced by Specific Topology in Zn[Au(CN)₂]₂. Inorganic Chemistry, 2017, 56, 15101-15109.	1.9	25
32913	MgTaO₂N Photocatalysts: Perovskite versus Ilmenite Structure. A Theoretical Investigation. Journal of Physical Chemistry C, 2017, 121, 27813-27821.	1.5	13
32914	Surface Reactivity of Li₂MnO₃: First-Principles and Experimental Study. ACS Applied Materials & Interfaces, 2017, 9, 44222-44230.	4.0	20
32915	Room-Temperature Activation of CO2 by Dual Defect-Stabilized Nanoscale Hematite (Fe2â‹Î´O3â€“ν): Concurrent Role of Fe and O Vacancies. ACS Omega, 2017, 2, 8407-8413.	1.6	8
32916	Scaling relationships and theory for vibrational frequencies of adsorbates on transition metal surfaces. Nature Communications, 2017, 8, 1842.	5.8	23
32917	Work function and surface stability of tungsten-based thermionic electron emission cathodes. APL Materials, 2017, 5, .	2.2	52
32918	Hydrogen accumulation around dislocation loops and edge dislocations: from atomistic to mesoscopic scales in BCC tungsten. Physica Scripta, 2017, T170, 014073.	1.2	15
32919	First-principles Green's-function method for surface calculations: A pseudopotential localized basis set approach. Physical Review B, 2017, 96, .	1.1	211
32920	Large nonsaturating magnetoresistance and pressure-induced phase transition in the layered semimetal <mml:math xmlns:mml="http://www.w3.org/1998/Math/MathML"><mml:msub><mml:mi>HfTe</mml:mi><mml:mn>2</mml:mn></mml:msub></ Physical Review B, 2017, 96, .	1.1	34
32921	Role of square planar coordination in the magnetic properties of Na4IrO4. Physical Review B, 2017, 96, .	1.1	16
32922	First-principles study of the giant magnetic anisotropy energy in bulk Na4IrO4. Physical Review B, 2017, 96, .	1.1	11
32923	Intrinsic Dirac half-metal and quantum anomalous Hall phase in a hexagonal metal-oxide lattice. Physical Review B, 2017, 96, .	1.1	161
32924	Electrical and Thermal Characteristics of the Insulatorâ€“Metal Transition in Crystalline $$hbox {V}_{2}hbox {O}_{5}$$ V 2 O 5. International Journal of Thermophysics, 2017, 38, 1.	1.0	1

#	Article	IF	Citations
32925	A combined experimental and computational study of water-gas shift reaction over rod-shaped Ce0.75M0.25O2 (Mâ€¯=â€¯Ti, Zr, and Mn) supported Cu catalysts. International Journal of Hydrogen Energy, 2017, 42, 30086-30097.	3.8	14
32926	Facet-Dependent Selective Adsorption of Mn-Doped Î±-Fe₂O₃ Nanocrystals toward Heavy-Metal Ions. Chemistry of Materials, 2017, 29, 10198-10205.	3.2	82
32927	Efficient Construction of Free Energy Profiles of Breathing Metalâ€“Organic Frameworks Using Advanced Molecular Dynamics Simulations. Journal of Chemical Theory and Computation, 2017, 13, 5861-5873.	2.3	45
32928	Disparity in Photoexcitation Dynamics between Vertical and Lateral MoS₂/WSe₂ Heterojunctions: Time-Domain Simulation Emphasizes the Importance of Donorâ€“Acceptor Interaction and Band Alignment. Journal of Physical Chemistry Letters, 2017, 8, 5771-5778.	2.1	52
32929	Nanocomposite Phosphor Consisting of CaI₂:Eu²⁺ Single Nanocrystals Embedded in Crystalline SiO₂. ACS Applied Materials & Interfaces, 2017, 9, 41405-41412.	4.0	2
32930	Catalytically Active Boron Nitride in Acetylene Hydrochlorination. ACS Catalysis, 2017, 7, 8572-8577.	5.5	54
32931	Two-Dimensional Semiconducting Boron Monolayers. Journal of the American Chemical Society, 2017, 139, 17233-17236.	6.6	57
32932	Large Piezoelectric Effect in a Lead-Free Molecular Ferroelectric Thin Film. Journal of the American Chemical Society, 2017, 139, 18071-18077.	6.6	160
32933	Optically-controlled long-term storage and release of thermal energy in phase-change materials. Nature Communications, 2017, 8, 1446.	5.8	210
32934	Deposition of topological silicene, germanene and stanene on graphene-covered SiC substrates. Scientific Reports, 2017, 7, 15700.	1.6	36
32935	Novel penta-graphene nanotubes: strain-induced structural and semiconductorâ€“metal transitions. Nanoscale, 2017, 9, 19310-19317.	2.8	18
32936	Volatility of the catalytic hydrogenation products of 1,4 bis(phenylethynyl)benzene. Journal of Chemical Physics, 2017, 147, 194701.	1.2	11
32937	Structural properties of transition-metal clusters via force-biased Monte Carlo and ab initio calculations: A comparative study. Physical Review B, 2017, 96, .	1.1	6
32938	Catalytic molten metals for the direct conversion of methane to hydrogen and separable carbon. Science, 2017, 358, 917-921.	6.0	306
32939	High-Pressure Behavior of Silver Fluorides up to 40 GPa. Inorganic Chemistry, 2017, 56, 14651-14661.	1.9	26
32940	Ab Initio Study of Interfacial Structure Transformation of Amorphous Carbon Catalyzed by Ti, Cr, and W Transition Layers. ACS Applied Materials & Interfaces, 2017, 9, 41115-41119.	4.0	19
32941	Effect of Amidogen Functionalization on Quantum Spin Hall Effect in Bi/Sb(111) Films. ACS Applied Materials & Interfaces, 2017, 9, 41443-41453.	4.0	139
32942	New Insights into the Electronic Structure and Photoelectrochemical Properties of Nitrogen-Doped HNb3O8 via a Combined in Situ Experimental and DFT Investigation. ACS Applied Materials & Interfaces, 2017, 9, 42751-42760.	4.0	7

#	Article	IF	Citations
32943	Thermal expansion of Pd-based metallic glasses by ab initio methods and high energy X-ray diffraction. Scientific Reports, 2017, 7, 15744.	1.6	14
32944	Facile synthesis and heteroepitaxial growth mechanism of Au@Cu coreâ€“shell bimetallic nanocubes probed by first-principles studies. CrystEngComm, 2017, 19, 7287-7297.	1.3	10
32945	Phonon coupling and transport in individual polyethylene chains: a comparison study with the bulk crystal. Nanoscale, 2017, 9, 18022-18031.	2.8	57
32946	3d transition metal doping-induced electronic structures and magnetism in 1T-HfSe₂ monolayers. RSC Advances, 2017, 7, 52747-52754.	1.7	15
32947	Silicene spintronics: Fe(111)/silicene system for efficient spin injection. Applied Physics Letters, 2017, 111, .	1.5	9
32948	Magnetic coupling in nonmagnetic metal adsorption on arsenene monolayer: Ab initio study. AIP Advances, 2017, 7, .	0.6	13
32949	Effect of Fe and Co substitution on the martensitic stability and the elastic, electronic, and magnetic properties of<mml:math xmlns:mml="http://www.w3.org/1998/Math/MathML"><mml:mrow><mml:msub><mml:mi>Mn</mml:mi><mml:mn>2</mml:mn></mml: Insights fromab initiocalculations. Physical Review B, 2017, 96, .	1.1	15
32950	First-principles-based Landau-Devonshire potential for <mml:math xmlns:mml="http://www.w3.org/1998/Math/MathML"><mml:msub><mml:mi>BiFeO</mml:mi><mml:mn>3</mml:mn></mml:msub><mml:mi>m Physical Review B, 2017, 96, .	1.1	18
32951	Relaxation of dynamically disordered tetragonal platelets in the relaxor ferroelectric <mml:math xmlns:mml="http://www.w3.org/1998/Math/MathML"><mml:mrow><mml:mn>0.964</mml:mn><mml:msub><mml:mi>Na</mml:mi><mml:mi><m Physical Review B, 2017, 96, .	1.1	8
32952	Multiple Types of Topological Fermions in Transition Metal Silicides. Physical Review Letters, 2017, 119, 206402.	2.9	298
32953	Efficiency Analysis of Intel and AMD x86_64 Architectures for Ab Initio Calculations: A Case Study of VASP. Communications in Computer and Information Science, 2017, , 430-441.	0.4	6
32954	Prediction of new metastable $$hbox {HfO}_{2}$$ HfO 2 phases: toward understanding ferro- and antiferroelectric films. Journal of Computational Electronics, 2017, 16, 1227-1235.	1.3	44
32955	Thermodynamic Modeling of B-Ta and B-C-Ta Systems. Journal of Phase Equilibria and Diffusion, 2017, 38, 874-886.	0.5	13
32956	A promising alkali-metal ion battery anode material: 2D metallic phosphorus carbide (Î²0-PC). Electrochimica Acta, 2017, 258, 582-590.	2.6	40
32957	Theoretical Study on Rotational Controllability of Organic Cations in Organicâ€“Inorganic Hybrid Perovskites: Hydrogen Bonds and Halogen Substitution. Journal of Physical Chemistry C, 2017, 121, 26188-26195.	1.5	19
32958	Inorganic Lattice Fluctuation Induces Charge Separation in Lead Iodide Perovskites: Theoretical Insights. Journal of Physical Chemistry C, 2017, 121, 26648-26654.	1.5	10
32959	Halide Perovskite Heteroepitaxy: Bond Formation and Carrier Confinement at the PbSâ€“CsPbBr₃ Interface. Journal of Physical Chemistry C, 2017, 121, 27351-27356.	1.5	40
32960	Signatures of a time-reversal symmetric Weyl semimetal with only four Weyl points. Nature Communications, 2017, 8, 942.	5.8	98

#	Article	IF	Citations
32961	Precise control of alloying sites of bimetallic nanoclusters via surface motif exchange reaction. Nature Communications, 2017, 8, 1555.	5.8	122
32962	Tunable electronic and magnetic properties of arsenene nanoribbons. RSC Advances, 2017, 7, 51935-51943.	1.7	8
32963	Unveiling orbital coupling at the CoPc/Bi(111) surface by ab initio calculations and photoemission spectroscopy. RSC Advances, 2017, 7, 52143-52150.	1.7	1
32964	Emergence of ferrimagnetic half-metallicity in two-dimensional MXene Mo3N2F2. Applied Physics Letters, 2017, 111, .	1.5	30
32965	Biaxial strain-induced enhancement in the thermoelectric performance of monolayer WSe ₂. Chinese Physics B, 2017, 26, 117202.	0.7	5
32966	Quasiparticle interference in ZrSiS: Strongly band-selective scattering depending on impurity lattice site. Physical Review B, 2017, 96, .	1.1	18
32967	Magnetic properties of a Na-doped WS2 monolayer in the presence of an isotropic strain. JETP Letters, 2017, 106, 672-676.	0.4	4
32968	Chemical Sensitivity of Valence-to-Core X-ray Emission Spectroscopy Due to the Ligand and the Oxidation State: A Computational Study on Cu-SSZ-13 with Multiple H₂O and NH₃ Adsorption. Journal of Physical Chemistry C, 2017, 121, 25759-25767.	1.5	12
32969	Nature of Highly Active Electrocatalytic Sites for the Hydrogen Evolution Reaction at Pt Electrodes in Acidic Media. ACS Omega, 2017, 2, 8141-8147.	1.6	46
32970	Molecular Scaffolding Strategy with Synergistic Active Centers To Facilitate Electrocatalytic CO₂ Reduction to Hydrocarbon/Alcohol. Journal of the American Chemical Society, 2017, 139, 18093-18100.	6.6	439
32971	Adsorption and diffusion of hydrogen and oxygen in FCC-Co: a first-principles study. Physical Chemistry Chemical Physics, 2017, 19, 32404-32411.	1.3	11
32972	High-pressure versus isoelectronic doping effect on the honeycomb iridate <mml:math xmlns:mml="http://www.w3.org/1998/Math/MathML"><mml:mrow><mml:msub><mml:mi>Na</mml:mi><mml:mn>2</mml:mn></mml: Physical Review B, 2017, 96, .	1.1	27
32973	Segregation of Native Defects to the Grain Boundaries in Methylammonium Lead Iodide Perovskite. Journal of Physical Chemistry Letters, 2017, 8, 5935-5942.	2.1	56
32974	Defect Engineering in MoSe₂ for the Hydrogen Evolution Reaction: From Point Defects to Edges. ACS Applied Materials & Interfaces, 2017, 9, 42688-42698.	4.0	171
32975	Type-I Ca(OH)₂/Î±-MoTe₂ vdW heterostructure for ultraviolet optoelectronic device applications: electric field effects. Journal of Materials Chemistry C, 2017, 5, 12629-12634.	2.7	25
32976	Estimation of electric field effects on the adsorption of molecular superoxide species on Au based on density functional theory. Physical Chemistry Chemical Physics, 2017, 19, 32626-32635.	1.3	8
32977	Highâ€Pressure Î³â€CaMgSi₂O₆: Does Pentaâ€Coordinated Silicon Exist in the Earth's Mantle?. Geophysical Research Letters, 2017, 44, 11,340.	1.5	18
32978	Features of Electronic, Mechanical, and Electromechanical Properties of Fluorinated Diamond Films of Nanometer Thickness. Journal of Physical Chemistry C, 2017, 121, 28484-28489.	1.5	29

#	Article	IF	Citations
32979	Modeling the Complex Adsorption Dynamics of Large Organic Molecules: Cyclooctyne on Si(001). Journal of Physical Chemistry C, 2017, 121, 26840-26850.	1.5	11
32980	Monitoring Local Strain Vector in Atomic-Layered MoSe₂ by Second-Harmonic Generation. Nano Letters, 2017, 17, 7539-7543.	4.5	128
32981	Hydrogen-bearing iron peroxide and the origin of ultralow-velocity zones. Nature, 2017, 551, 494-497.	13.7	113
32982	Oxidation behavior of graphene-coated copper at intrinsic graphene defects of different origins. Nature Communications, 2017, 8, 1549.	5.8	60
32983	Two-Dimensional Co2S2 monolayer with robust ferromagnetism. Scientific Reports, 2017, 7, 15993.	1.6	23
32984	Strongly Coupled Magnetic and Electronic Transitions in Multivalent Strontium Cobaltites. Scientific Reports, 2017, 7, 16066.	1.6	13
32985	The cohesive energy of superheavy element copernicium determined from accurate relativistic coupled-cluster theory. Physical Chemistry Chemical Physics, 2017, 19, 32286-32295.	1.3	15
32986	Computational design of enhanced photocatalytic activity of two-dimensional cadmium iodide. RSC Advances, 2017, 7, 53653-53657.	1.7	12
32987	BInGaN alloys nearly lattice-matched to GaN for high-power high-efficiency visible LEDs. Applied Physics Letters, 2017, 111, .	1.5	26
32988	Mono- and Bilayer ZnSnN₂ Sheets for Visible-Light Photocatalysis: First-Principles Predictions. Journal of Physical Chemistry C, 2017, 121, 26063-26068.	1.5	19
32989	Role of Metal Lattice Expansion and Molecular Ï€-Conjugation for the Magnetic Hardening at Cuâ€“Organics Interfaces. Journal of Physical Chemistry C, 2017, 121, 23777-23787.	1.5	4
32990	Toward the Realization of 2D Borophene Based Gas Sensor. Journal of Physical Chemistry C, 2017, 121, 26869-26876.	1.5	148
32991	Selective Activation of Methane on Single-Atom Catalyst of Rhodium Dispersed on Zirconia for Direct Conversion. Journal of the American Chemical Society, 2017, 139, 17694-17699.	6.6	297
32992	Carbon vacancies in Ti₂CT₂MXenes: defects or a new opportunity?. Physical Chemistry Chemical Physics, 2017, 19, 31773-31780.	1.3	81
32993	Engineering an Insulating Ferroelectric Superlattice with a Tunable Band Gap from Metallic Components. Physical Review Letters, 2017, 119, 177603.	2.9	16
32994	Amphoteric Be in GaN: Experimental Evidence for Switching between Substitutional and Interstitial Lattice Sites. Physical Review Letters, 2017, 119, 196404.	2.9	44
32995	Structural â€œ Î´ Dopingâ€•to Control Local Magnetization in Isovalent Oxide Heterostructures. Physical Review Letters, 2017, 119, 197204.	2.9	28
32996	Pressure Driven Enhancement of Ideal Shear Strength in bc8-Carbon and Diamond. Journal of Physical Chemistry C, 2017, 121, 26457-26464.	1.5	9

#	Article	IF	Citations
32997	Anisotropic attosecond charge carrier dynamics and layer decoupling in quasi-2D layered SnS2. Nature Communications, 2017, 8, 1369.	5.8	27
32998	Functional Group Effects on the Photoelectronic Properties of MXene (Sc2CT2, T = O, F, OH) and Their Possible Photocatalytic Activities. Scientific Reports, 2017, 7, 15095.	1.6	74
32999	Weak interlayer dependence of lattice thermal conductivity on stacking thickness of penta-graphene. Applied Physics Letters, 2017, 111, .	1.5	20
33000	Germanene nanomeshes: Cooperative effects of degenerate perturbation and uniaxial strain on tuning bandgap. Chinese Physics B, 2017, 26, 108101.	0.7	3
33001	Theoretical prediction of two-dimensional functionalized MXene nitrides as topological insulators. Physical Review B, 2017, 96, .	1.1	83
33002	Coexistence of type-II Dirac point and weak topological phase in <mml:math xmlns:mml="http://www.w3.org/1998/Math/MathML"><mml:mrow><mml:msub><mml:mi>Pt</mml:mi><mml:mn>3</mml:mn></mml:msub></mml:mrow></mml:math> Physical Review B, 2017, 96, .	1.1	5
33003	Origin of polymorphism of the two-dimensional group-IV monochalcogenides. Physical Review B, 2017, 96, .	1.1	19
33004	Interaction-driven quantum anomalous Hall effect in halogenated hematite nanosheets. Physical Review B, 2017, 96, .	1.1	13
33005	MoirÃ© excitons: From programmable quantum emitter arrays to spin-orbitâ€“coupled artificial lattices. Science Advances, 2017, 3, e1701696.	4.7	427
33006	Thermodynamic considerations of the vapor phase reactions in IIIâ€“nitride metal organic vapor phase epitaxy. Japanese Journal of Applied Physics, 2017, 56, 04CJ04.	0.8	17
33007	Oxidation Mechanism and Protection Strategy of Ultrathin Indium Selenide: Insight from Theory. Journal of Physical Chemistry Letters, 2017, 8, 4368-4373.	2.1	62
33008	High-fraction brookite films from amorphous precursors. Scientific Reports, 2017, 7, 15232.	1.6	56
33009	Impurity states in InSe monolayers doped with group II and IV elements. Journal of Applied Physics, 2017, 122, 185702.	1.1	5
33010	Machine learning reveals orbital interaction in materials. Science and Technology of Advanced Materials, 2017, 18, 756-765.	2.8	78
33011	Absence of quantum anomalous Hall state in <mml:math xmlns:mml="http://www.w3.org/1998/Math/MathML"><mml:mrow><mml:mn>4</mml:mn><mml:mi>d</mml:mi></mml:mrow></mml:math> transition-metal-doped <mml:math xmlns:mml="http://www.w3.org/1998/Math/MathML"><mml:mrow><mml:mi mathvariant="normal">B</mml:mi><mml:msub><mml:mi mathvariant="normal">I</mml:mi><mml:mn>2</mml:mn></mml:msub><mml:mi mathvariant="normal">S	1.1	3
33012	Force-matched empirical potential for martensitic transitions and plastic deformation in Ti-Nb alloys. Physical Review B, 2017, 96, .	1.1	15
33013	Phonon thermal conductivity of scandium nitride for thermoelectrics from first-principles calculations and thin-film growth. Physical Review B, 2017, 96, .	1.1	30
33014	Critical Role of the Exchange Interaction for the Electronic Structure and Charge-Density-Wave Formation in <mml:math xmlns:mml="http://www.w3.org/1998/Math/MathML" display="inline"><mml:mrow><mml:msub><mml:mrow><mml:mi>TiSe</mml:mi></mml:mrow><mml:mrow><mml:mn>2</mml:mn> Physical Review Letters, 2017, 119, 176401.	2.9	55

#	Article	IF	Citations
33015	Electronic structures and magneto-transport properties of co-based Heusler alloy based magneto-resistance junctions. Journal of Shanghai Jiaotong University (Science), 2017, 22, 530-535.	0.5	0
33016	Toward an Understanding of Selective Alkyne Hydrogenation on Ceria: On the Impact of O Vacancies on H₂ Interaction with CeO₂(111). Journal of the American Chemical Society, 2017, 139, 17608-17616.	6.6	120
33017	Cooperative Bond Scission in a Soft Porous Crystal Enables Discriminatory Gate Opening for Ethylene over Ethane. Journal of the American Chemical Society, 2017, 139, 18313-18321.	6.6	72
33018	Iced photochemical reduction to synthesize atomically dispersed metals by suppressing nanocrystal growth. Nature Communications, 2017, 8, 1490.	5.8	322
33019	Large voltage-controlled magnetic anisotropy in the SrTiO3/Fe/Cu structure. Applied Physics Letters, 2017, 111, 152403.	1.5	16
33020	Large exchange anisotropy in quasi-one-dimensional spin- <mml:math xmlns:mml="http://www.w3.org/1998/Math/MathML"><mml:mfrac><mml:mn>1</mml:mn><mml:mn>2</mml:mn></mml:mfrac></mml fluoride antiferromagnets with a <mml:math xmlns:mml="http://www.w3.org/1998/Math/MathML"><mml:mrow><mml:mi>d</mml:mi><mml:msup><mml:mrow><mml:mo>(</mml ground state. Physical Review B, 2017, 96, .	1.1	15
33021	Discovery and Characterization of a Pourbaix-Stable, 1.8 eV Direct Gap Bismuth Manganate Photoanode. Chemistry of Materials, 2017, 29, 10027-10036.	3.2	17
33022	First-Principles Analysis of Li Intercalation in VO₂(B). Chemistry of Materials, 2017, 29, 10075-10087.	3.2	28
33023	Computational Screening of Useful Holeâ€“Electron Dopants in SnO₂. Chemistry of Materials, 2017, 29, 10095-10103.	3.2	12
33024	Fe-Cluster Compounds of Chalcogenides: Candidates for Rare-Earth-Free Permanent Magnet and Magnetic Nodal-Line Topological Material. Inorganic Chemistry, 2017, 56, 14577-14583.	1.9	4
33025	Ab Initio Investigation of the Role of CO Adsorption on the Physical Properties of 55-Atom PtCo Nanoalloys. Journal of Physical Chemistry C, 2017, 121, 27721-27732.	1.5	12
33026	Electronic Structure Reconfiguration toward Pyrite NiS₂ via Engineered Heteroatom Defect Boosting Overall Water Splitting. ACS Nano, 2017, 11, 11574-11583.	7.3	310
33027	Investigations on structural determination of semi-transition-metal borides. Physical Chemistry Chemical Physics, 2017, 19, 31592-31598.	1.3	17
33028	Twisted MX₂/MoS₂heterobilayers: effect of van der Waals interaction on the electronic structure. Nanoscale, 2017, 9, 19131-19138.	2.8	43
33029	Robust indirect band gap and anisotropy of optical absorption in B-doped phosphorene. Physical Chemistry Chemical Physics, 2017, 19, 31796-31803.	1.3	18
33030	Strain engineering of phonon thermal transport properties in monolayer 2H-MoTe₂. Physical Chemistry Chemical Physics, 2017, 19, 32072-32078.	1.3	78
33031	Metalâ€“semiconductor transition of two-dimensional Mg₂C monolayer induced by biaxial tensile strain. Physical Chemistry Chemical Physics, 2017, 19, 32086-32090.	1.3	16
33032	Computational insights into charge transfer across functionalized semiconductor surfaces. Science and Technology of Advanced Materials, 2017, 18, 681-692.	2.8	12

#	Article	IF	Citations
33033	Alternative long-ranged charge optimized many-body potential for aluminium. Journal of Physics Condensed Matter, 2017, 29, 485401.	0.7	0
33034	An empirical potential for simulating vacancy clusters in tungsten. Journal of Physics Condensed Matter, 2017, 29, 505501.	0.7	45
33035	Microscopic origin of the mobility enhancement at a spinel/perovskite oxide heterointerface revealed by photoemission spectroscopy. Physical Review B, 2017, 96, .	1.1	32
33036	Magnon-phonon relaxation in yttrium iron garnet from first principles. Physical Review B, 2017, 96, .	1.1	22
33037	Magnetism and superconductivity in the layered hexagonal transition metal pnictides. Physical Review B, 2017, 96, .	1.1	14
33038	Visualization of Room-Temperature Ferroelectricity and Polarization Rotation in the Thin Film of Quinuclidinium Perrhenate. Physical Review Letters, 2017, 119, 207602.	2.9	50
33039	ChIMES: A Force Matched Potential with Explicit Three-Body Interactions for Molten Carbon. Journal of Chemical Theory and Computation, 2017, 13, 6222-6229.	2.3	54
33040	High-Throughput Study of Compositions and Optical Properties in Heavily Co-Doped Silicon Nanoparticles. Journal of Physical Chemistry C, 2017, 121, 27741-27750.	1.5	11
33041	Strong Influence of Ti Adhesion Layer on Electronâ€“Phonon Relaxation in Thin Gold Films: Ab Initio Nonadiabatic Molecular Dynamics. ACS Applied Materials & Interfaces, 2017, 9, 43343-43351.	4.0	25
33042	Identifying â€œOptimalâ€•Electrocatalysts: Impact of Operating Potential and Charge Transfer Model. ACS Catalysis, 2017, 7, 8641-8652.	5.5	21
33043	A mechanism for the selective epimerization of the glucose mannose pair by Mo-based compounds: towards catalyst optimization. Green Chemistry, 2017, 19, 5932-5939.	4.6	14
33044	Metal phosphides as potential thermoelectric materials. Journal of Materials Chemistry C, 2017, 5, 12441-12456.	2.7	53
33045	Enhancing the thermoelectric performance of Ce_xBi₂S₃ by optimizing the carrier concentration combined with band engineering. Journal of Materials Chemistry C, 2017, 5, 12492-12499.	2.7	39
33046	Magnetic structure of the mixed antiferromagnet <mml:math xmlns:mml="http://www.w3.org/1998/Math/MathML"><mml:mrow><mml:msub><mml:mi>NdMn</mml:mi><mml:mrow><mml:mn>0.8</mml:mn> mathvariant="normal">O</mml:mi><mml:mn>3</mml:mn></mml:msub></mml:mrow></mml:math>. Physical Review B, 2017, 96, .	1.1	7
33047	Striped magnetic ground state of the kagome lattice in <mml:math xmlns:mml="http://www.w3.org/1998/Math/MathML"><mml:mrow><mml:msub><mml:mi>Fe</mml:mi><mml:mn>4</mml:mn></mml:mn></mml:r mathvariant="normal">O</mml:mi><mml:mn>16</mml:mn></mml:msub></mml:mrow></mml:math>. Physical Review B, 2017, 96, .	1.1	7
33048	Role of defects in enhanced Fermi level pinning at interfaces between metals and transition metal dichalcogenides. Physical Review B, 2017, 96, .	1.1	26
33049	Charge density waves and the Coulomb correlation effects in <mml:math xmlns:mml="http://www.w3.org/1998/Math/MathML"><mml:mrow><mml:msub><mml:mi>Na</mml:mi><mml:mn>2</mml:mn></mml:mn></mml:		

#	Article	IF	Citations
33051	Identification of Si-vacancy related room-temperature qubits in <mml:math xmlns:mml="http://www.w3.org/1998/Math/MathML"><mml:mrow><mml:mn>4</mml:mn><mml:mi>H</mml:mi></mml:mrow></mml:math> silicon carbide. Physical Review B, 2017, 96, .	1.1	74
33052	Evaluation of energy band offset of Si1â^'xSnxsemiconductors by numerical calculation using density functional theory. Japanese Journal of Applied Physics, 2017, 56, 04CR10.	0.8	3
33053	Rattling of Oxygen Ions in a Sub-Nanometer-Sized Cage Converts Terahertz Radiation to Visible Light. ACS Nano, 2017, 11, 12358-12364.	7.3	12
33054	Sub-band-gap absorption in Ga2O3. Applied Physics Letters, 2017, 111, .	1.5	44
33055	Charge-transfer modified embedded atom method dynamic charge potential for Liâ€“Coâ€“O system. Journal of Physics Condensed Matter, 2017, 29, 475903.	0.7	3
33056	Effects of the Be ₂₂ W phase formation on hydrogen retention and blistering in mixed Be/W systems. Chinese Physics B, 2017, 26, 076801.	0.7	0
33057	Ferromagnetic Weyl semimetal phase in a tetragonal structure. Physical Review B, 2017, 96, .	1.1	48
33058	Localized Control of Curie Temperature in Perovskite Oxide Film by Capping-Layer-Induced Octahedral Distortion. Physical Review Letters, 2017, 119, 177203.	2.9	31
33059	Bonding Frustration in the 9.5â€‰GPa fcc Polymeric C₆₀. Physica Status Solidi - Rapid Research Letters, 2017, 11, 1700343.	1.2	6
33060	Barium disilicide as a promising thin-film photovoltaic absorber: structural, electronic, and defect properties. Journal of Materials Chemistry A, 2017, 5, 25293-25302.	5.2	68
33061	Galvanic-replacement mediated synthesis of copperâ€“nickel nitrides as electrocatalyst for hydrogen evolution reaction. Journal of Materials Chemistry A, 2017, 5, 24850-24858.	5.2	88
33062	First principles prediction of CH₄ reactivities with Co₃O₄ nanocatalysts of different morphologies. Physical Chemistry Chemical Physics, 2017, 19, 30874-30882.	1.3	12
33063	Enhanced electrochemical water oxidation: the impact of nanoclusters and nanocavities. Physical Chemistry Chemical Physics, 2017, 19, 31300-31305.	1.3	6
33064	Two-dimensional multilayer M₂CO₂(M = Sc, Zr, Hf) as photocatalysts for hydrogen production from water splitting: a first principles study. Journal of Materials Chemistry A, 2017, 5, 24972-24980.	5.2	90
33065	Investigation of chloride ion adsorption onto Ti₂C MXene monolayers by first-principles calculations. Journal of Materials Chemistry A, 2017, 5, 24720-24727.	5.2	57
33066	Stable monolayer Î±-phase of CdTe: strain-dependent properties. Journal of Materials Chemistry C, 2017, 5, 12249-12255.	2.7	9
33067	Longitudinal sound velocities, elastic anisotropy, and phase transition of high-pressure cubic <mml:math xmlns:mml="http://www.w3.org/1998/Math/MathML"><mml:mrow><mml:msub><mml:mi mathvariant="normal">H</mml:mi><mml:mn>2</mml:mn></mml:msub><mml:mi mathvariant="normal">O</mml:mi></mml:mrow></mml:math> ice to 82 GPa. Physical Review B, 2017, 96, .	1.1	22
33068	Topological surface electronic states in candidate nodal-line semimetal CaAgAs. Physical Review B, 2017, 96, .	1.1	51

#	Article	IF	Citations
33069	Theory of the carbon vacancy in <mml:math xmlns:mml="http://www.w3.org/1998/Math/MathML"><mml:mrow><mml:mn>4</mml:mn><mml:mi>H</mml:mi></mml:mrow></mml:math> -SiC: Crystal field and pseudo-Jahn-Teller effects. Physical Review B, 2017, 96, .	1.1	32
33070	Structural, electronic, magnetic, and transport properties of the equiatomic quaternary Heusler alloy CoRhMnGe: Theory and experiment. Physical Review B, 2017, 96, .	1.1	54
33071	Tunable band structures in digital oxides with layered crystal habits. Physical Review B, 2017, 96, .	1.1	0
33072	Effective Zeeman splitting in bent lateral heterojunctions of graphene and hexagonal boron nitride: A new mechanism towards half-metallicity. Physical Review B, 2017, 96, .	1.1	14
33073	First principle investigations of the Pbnm phaseÂBiFeO3, BiFe0.875Mn0.125O3 and Bi0.875X0.125Fe0.875Mn0.125O3 (XBFM) (X = Ce, Gd, Lu). Modern Physics Letters B, 2017, 31, 1750304.	1.0	5
33074	Unusual Twisting Phonons and Breathing Modes in Tubeâ€Terminated Phosphorene Nanoribbons and Their Effects on Thermal Conductivity. Advanced Functional Materials, 2017, 27, 1702776.	7.8	21
33075	First-principles calculations and thermodynamic modeling of the Yb-Ni binary system. Calphad: Computer Coupling of Phase Diagrams and Thermochemistry, 2017, 59, 207-217.	0.7	10
33076	Orientational Glass Formation in Substituted Hybrid Perovskites. Chemistry of Materials, 2017, 29, 10168-10177.	3.2	36
33077	High Photocatalytic Activity of Heptazine-Based g-C₃N₄/SnS₂ Heterojunction and Its Origin: Insights from Hybrid DFT. Journal of Physical Chemistry C, 2017, 121, 25827-25835.	1.5	142
33078	Tension-Tailored Electronic and Magnetic Switching of 2D Ti₂NO₂. Journal of Physical Chemistry C, 2017, 121, 25729-25735.	1.5	33
33079	Synthesis of Multilayer Silicene on Si(111)â^š3 Ã— â^š3-Ag. Journal of Physical Chemistry C, 2017, 121, 27182-27190.	1.5	34
33080	Dominant Kinetic Pathways of Graphene Growth in Chemical Vapor Deposition: The Role of Hydrogen. Journal of Physical Chemistry C, 2017, 121, 25949-25955.	1.5	61
33081	Observation of Effective Pseudospin Scattering in ZrSiS. Nano Letters, 2017, 17, 7213-7217.	4.5	29
33082	Constructing Ultrahigh-Capacity Zincâ€“Nickelâ€“Cobalt Oxide@Ni(OH)₂ Coreâ€“Shell Nanowire Arrays for High-Performance Coaxial Fiber-Shaped Asymmetric Supercapacitors. Nano Letters, 2017, 17, 7552-7560.	4.5	231
33083	On-Surface Cyclization of ortho-Dihalotetracenes to Four- and Six-Membered Rings. Journal of the American Chemical Society, 2017, 139, 17617-17623.	6.6	68
33084	Free surfaces recast superconductivity in few-monolayer MgB2: Combined first-principles and ARPES demonstration. Scientific Reports, 2017, 7, 14458.	1.6	27
33085	Single parabolic band transport in p-type EuZn₂Sb₂ thermoelectrics. Journal of Materials Chemistry A, 2017, 5, 24185-24192.	5.2	38
33086	Superatomic states in nickel clusters: Revising the prospects for transition metal based superatoms. Journal of Chemical Physics, 2017, 147, 154307.	1.2	8

#	Article	IF	Citations
33087	A quantum chemical analysis of Zn and Sb doping and co-doping in SnO2. AIP Advances, 2017, 7, .	0.6	11
33088	Stable ultra-thin CdTe crystal: a robust direct gap semiconductor. Journal of Physics Condensed Matter, 2017, 29, 485302.	0.7	4
33089	Two- and three-dimensional topological phases in <mml:math xmlns:mml="http://www.w3.org/1998/Math/MathML"><mml:mrow><mml:mi>BiTe</mml:mi><mml:mi>X</mml:mi></mml:mrow></mml compounds. Physical Review B, 2017, 96, .	1.1	14
33090	Carrier-driven coupling in ferromagnetic oxide heterostructures. Physical Review B, 2017, 96, .	1.1	5
33091	<mml:math xmlns:mml="http://www.w3.org/1998/Math/MathML"><mml:mrow><mml:msub><mml:mi mathvariant="normal">C</mml:mi><mml:mn>4</mml:mn></mml:msub><mml:msub><mml:mi mathvariant="normal">N</mml:mi><mml:mn>3</mml:mn></mml:msub><mml:mi mathvariant="normal">H</mml:mi></mml:mrow></mml:math> monolayer: A two-dimensional organic Dirac material with high Fermi velocity. Physical Review B, 2017, 96, .	1.1	15
33092	Thickness-dependent energetics for Pb adatoms on low-index Pb nanofilm surfaces: First-principles calculations. Physical Review B, 2017, 96, .	1.1	13
33093	Adsorption of Water onto SrTiO₃ from Periodic MÃ¸llerâ€“Plesset Second-Order Perturbation Theory. Journal of Chemical Theory and Computation, 2017, 13, 6301-6307.	2.3	1
33094	Improving Adhesion at the Alumina/Zinc Interface by Stainless Steel Buffers. Journal of Physical Chemistry C, 2017, 121, 25143-25151.	1.5	13
33095	I, N-Codoping Modification of TiO₂ for Enhanced Photoelectrochemical H₂O Splitting in Visible-Light Region. Journal of Physical Chemistry C, 2017, 121, 26202-26208.	1.5	11
33096	Ferroelectric Domains May Lead to Two-Dimensional Confinement of Holes, but not of Electrons, in CH₃NH₃PbI₃ Perovskite. Journal of Physical Chemistry C, 2017, 121, 26698-26705.	1.5	11
33097	Designing Two-Dimensional Dirac Heterointerfaces of Few-Layer Graphene and Tetradymite-Type Sb₂Te₃ for Thermoelectric Applications. ACS Applied Materials & Interfaces, 2017, 9, 42050-42057.	4.0	14
33098	Biphase-Interface Enhanced Sodium Storage and Accelerated Charge Transfer: Flower-Like Anatase/Bronze TiO₂/C as an Advanced Anode Material for Na-Ion Batteries. ACS Applied Materials & Interfaces, 2017, 9, 43648-43656.	4.0	63
33099	New avenues for the large-scale harvesting of blue energy. Nature Reviews Chemistry, 2017, 1, .	13.8	383
33100	Dissociative chemisorption of methane on Ni(111) using a chemically accurate fifteen dimensional potential energy surface. Physical Chemistry Chemical Physics, 2017, 19, 30540-30550.	1.3	40
33101	Stanene based gas sensors: effect of spinâ€“orbit coupling. Physical Chemistry Chemical Physics, 2017, 19, 31325-31334.	1.3	51
33102	An insight into intrinsic interfacial properties between Li metals and Li₁₀GeP₂S₁₂ solid electrolytes. Physical Chemistry Chemical Physics, 2017, 19, 31436-31442.	1.3	49
33103	Cluster-Expansion Model for Complex Quinary Alloys: Application to Alnico Permanent Magnets. Physical Review Applied, 2017, 8, .	1.5	7
33104	Shear-induced mechanical failure of <mml:math xmlns:mml="http://www.w3.org/1998/Math/MathML"><mml:mrow><mml:mi>Î²</mml:mi><mml:mtext>â^'</mml:mtext><mml:mi mathvariant="normal">G</mml:mi><mml:msub><mml:mi mathvariant="normal">a</mml:mi><mml:mn>2</mml:mn></mml:msub><mml:msub><mml:mi mathvariant="normal">O</mml:mi><mml:mn>3</mml:mn></mml:msub></mml:mrow></mml:math> from quantum mechanics simulations. Physical Review B, 2017, 96, .	1.1	6

#	Article	IF	Citations
33105	Hydride Transfer versus Deprotonation Kinetics in the Isobutaneâ€“Propene Alkylation Reaction: A Computational Study. ACS Catalysis, 2017, 7, 8613-8627.	5.5	49
33106	Mechanistic Insights for Low-Overpotential Electroreduction of CO₂ to CO on Copper Nanowires. ACS Catalysis, 2017, 7, 8578-8587.	5.5	106
33107	Interplay between Localized and Free Charge Carriers Can Explain Hot Fluorescence in the CH3NH3PbBr3 Perovskite: Time-Domain Ab Initio Analysis. Journal of the American Chemical Society, 2017, 139, 17327-17333.	6.6	70
33108	Hydrogenation of CO to Methanol on Ni(110) through Subsurface Hydrogen. Journal of the American Chemical Society, 2017, 139, 17582-17589.	6.6	35
33109	Charge doping in graphene on thermodynamically preferred BiFeO3(0001) polar surfaces. Physical Chemistry Chemical Physics, 2017, 19, 31352-31361.	1.3	12
33110	Tunable Dirac cones in two-dimensional covalent organic materials: C2N6S3 and its analogs. RSC Advances, 2017, 7, 52065-52070.	1.7	9
33111	Ab-initio study of charged oxygen defects in Gd2Zr2O7. AIP Conference Proceedings, 2017, , .	0.3	1
33112	Defect induced visible-light-activated near-infrared emissions in Gd3â^'xâ^'yâ^'zYbxBiyErzGa5O12. Journal of Applied Physics, 2017, 122, .	1.1	4
33113	Alloying strategy for two-dimensional GaN optical emitters. Physical Review B, 2017, 96, .	1.1	15
33114	Competing magnetic interactions in a spin- <mml:math xmlns:mml="http://www.w3.org/1998/Math/MathML"><mml:mfrac><mml:mn>1</mml:mn><mml:mn>2</mml:mn></mml:mfrac></mml square lattice: Hidden order in <mml:math xmlns:mml="http://www.w3.org/1998/Math/MathML"><mml:mrow><mml:msub><mml:mi>Sr</mml:mi><mml:mn>2</mml:mn></mml Physical Review B, 2017, 96, .	1.1	8
33115	Layer-by-Layer Degradation of Methylammonium Lead Tri-iodide Perovskite Microplates. Joule, 2017, 1, 548-562.	11.7	199
33116	Chemisorption of a hydrogen adatom on metal doped Î± -Zr (0Â0Â0Â1) surfaces in a vacuum and an implicit solvation environment. Nuclear Materials and Energy, 2017, 13, 28-34.	0.6	6
33117	Theoretical investigation of structural, mechanical and electronic properties of GaAs1-N alloys under ambient and high pressure. Physica B: Condensed Matter, 2017, 526, 1-6.	1.3	5
33118	Fixed-Point Iteration. , 0, , 631-642.		1
33119	Evolution of the Magnetic and Optical Properties in CocoreAushell and (CoRh)coreAushell Coreâ€“Shell Nanoparticles. Journal of Physical Chemistry C, 2017, 121, 24798-24803.	1.5	3
33120	Extrapolating Energetics on Clusters and Single-Crystal Surfaces to Nanoparticles by Machine-Learning Scheme. Journal of Physical Chemistry C, 2017, 121, 26397-26405.	1.5	41
33121	Conductive Copper Benzenehexathiol Coordination Polymer as a Hydrogen Evolution Catalyst. ACS Applied Materials & Interfaces, 2017, 9, 40752-40759.	4.0	129
33122	Micro- and Macromechanical Properties of Thermoelectric Lead Chalcogenides. ACS Applied Materials & Interfaces, 2017, 9, 40488-40496.	4.0	45

#	Article	IF	Citations
33123	Bimetallic Effect of Single Nanocatalysts Visualized by Super-Resolution Catalysis Imaging. ACS Central Science, 2017, 3, 1189-1197.	5.3	65
33124	Copper-Based Intermetallic Electride Catalyst for Chemoselective Hydrogenation Reactions. Journal of the American Chemical Society, 2017, 139, 17089-17097.	6.6	90
33125	A theoretical prediction on the shear-induced phase transformation of TKX-50. Physical Chemistry Chemical Physics, 2017, 19, 31054-31062.	1.3	14
33126	Order parameters for symmetry-breaking structural transitions: The tetragonal-monoclinic transition in <mml:math xmlns:mml="http://www.w3.org/1998/Math/MathML"><mml:msub><mml:mi>ZrO</mml:mi><mml:mn>2</mml:mn></mml:msub></m Physical Review B, 2017, 96, .	1.1	12
33127	Observation of the topological surface state in the nonsymmorphic topological insulator KHgSb. Physical Review B, 2017, 96, .	1.1	21
33128	Coexistence of polar distortion and metallicity in <mml:math xmlns:mml="http://www.w3.org/1998/Math/MathML"><mml:mrow><mml:msub><mml:mi>PbTi</mml:mi><mml:mrow><mml:mn>1< mathvariant="normal">O</mml:mi><mml:mn>3</mml:mn></mml:msub></mml:mrow></mml:math>. Physical Review B, 2017, 96, .	1.1	34
33129	Electronic Stopping of Slow Protons in Oxides: Scaling Properties. Physical Review Letters, 2017, 119, 163401.	2.9	34
33130	Lattice Thermal Conductivity of Polyethylene Molecular Crystals from First-Principles Including Nuclear Quantum Effects. Physical Review Letters, 2017, 119, 185901.	2.9	51
33131	Mechanical and Structural Degradation of LiNi_xMn_yCo_zO₂Cathode in Li-Ion Batteries: An Experimental Study. Journal of the Electrochemical Society, 2017, 164, A3333-A3341.	1.3	134
33132	Methane Adsorption in Zr-Based MOFs: Comparison and Critical Evaluation of Force Fields. Journal of Physical Chemistry C, 2017, 121, 25309-25322.	1.5	34
33133	Valence band splitting in bulk dilute bismides. Applied Physics Letters, 2017, 111, 182103.	1.5	7
33136	Relationship between the crystal structures of LiMn1.5Ni0.5O4 and LiMn1.5Ni0.45Fe0.05O4 and their internal resistances as cathode materials for lithium ion batteries. Journal of Solid State Electrochemistry, 2017, 21, 3301-3314.	1.2	4
33137	The role of emerging grain boundary at iron surface, temperature and hydrogen on metal dusting initiation. Acta Materialia, 2017, 135, 340-347.	3.8	12
33138	Steering the interlayer energy barrier and charge flow via bioriented transportation channels in g-C3N4: Enhanced photocatalysis and reaction mechanism. Journal of Catalysis, 2017, 352, 351-360.	3.1	173
33139	The exploration of nonlinear elasticity and its efficient parameterization for crystalline materials. Journal of the Mechanics and Physics of Solids, 2017, 107, 76-95.	2.3	36
33140	First principles study of the structural and magnetic properties of Fe(Rh, Pd) and Fe(Rh, Ni) alloys. Materials Today: Proceedings, 2017, 4, 4642-4646.	0.9	11
33141	Anomalous in-plane anisotropic Raman response of monoclinic semimetal 1â€‰TÂ´-MoTe 2. Scientific Reports, 2017, 7, 1758.	1.6	47
33142	DFT study of Î²-d-glucose adsorption on single-walled carbon nanotubes decorated with platinum. A bonding analysis. Applied Surface Science, 2017, 423, 542-548.	3.1	7

#	Article	IF	Citations
33143	Polystyrene-template-assisted synthesis of Li3VO4/C/rGO ternary composite with honeycomb-like structure for durable high-rate lithium ion battery anode materials. Electrochimica Acta, 2017, 247, 771-778.	2.6	40
33144	Experimental investigation and theoretical exploration of single-atom electrocatalysis in hybrid photovoltaics: The powerful role of Pt atoms in triiodide reduction. Nano Energy, 2017, 39, 1-8.	8.2	25
33145	Precipitation of (Si2â˜xAlx)Hf in an Alâ€“Siâ€“Mgâ€“Hf Alloy. Microscopy and Microanalysis, 2017, 23, 724-729.	0.2	2
33146	Unraveling the Magnesium-Ion Intercalation Mechanism in Vanadium Pentoxide in a Wet Organic Electrolyte by Structural Determination. Inorganic Chemistry, 2017, 56, 7668-7678.	1.9	63
33147	First-Principles and Molecular Dynamics on Aâ€“D(Î)â€“A Type Sensitizers for Dye-Sensitized Solar Cells: Effects of Various Anchoring Groups on Electronic Coupling and Dye Aggregation. Journal of Physical Chemistry C, 2017, 121, 14019-14026.	1.5	18
33148	Divulging the Hidden Capacity and Sodiation Kinetics of Na_xC₆Cl₄O₂: A High Voltage Organic Cathode for Sodium Rechargeable Batteries. Journal of Physical Chemistry C, 2017, 121, 14027-14036.	1.5	19
33149	Density Functional Analysis of Fluorite-Structured (Ce, Zr)O₂/CeO₂ Interfaces. Journal of Physical Chemistry C, 2017, 121, 14678-14687.	1.5	12
33150	Alkali-created rich properties in grapheme nanoribbons: Chemical bondings. Scientific Reports, 2017, 7, 1722.	1.6	3
33151	Modeling cooperative effects in halogen-bonded infinite linear chains. Physical Chemistry Chemical Physics, 2017, 19, 18529-18538.	1.3	9
33152	Schottky barrier and band edge engineering via the interfacial structure and strain for the Pt/TiO₂ heterostructure. Physical Chemistry Chemical Physics, 2017, 19, 18750-18756.	1.3	18
33153	Nearest-neighbor sp3s* tight-binding parameters based on the hybrid quasi-particle self-consistent GW method verified by modeling of type-II superlattices. Journal of Applied Physics, 2017, 121, .	1.1	14
33154	Increased magnetic damping in ultrathin films of Co2FeAl with perpendicular anisotropy. Applied Physics Letters, 2017, 110, .	1.5	20
33155	On the nature of the (de)coupling of the magnetostructural transition in Er5 Si4. Physica Status Solidi (B): Basic Research, 2017, 254, 1700143.	0.7	1
33156	Water dissociation on multimetallic catalysts. Applied Catalysis B: Environmental, 2017, 218, 199-207.	10.8	14
33157	The structural and electronic properties of metal atoms adsorbed on graphene. Physica E: Low-Dimensional Systems and Nanostructures, 2017, 93, 265-270.	1.3	9
33158	From Linear Molecular Chains to Extended Polycyclic Networks: Polymerization of Dicyanoacetylene. Chemistry of Materials, 2017, 29, 6706-6718.	3.2	9
33159	Stabilities of Bimetallic Nanoparticles for Chirality-Selective Carbon Nanotube Growth and the Effect of Carbon Interstitials. Journal of Physical Chemistry C, 2017, 121, 15430-15436.	1.5	3
33160	Excitation-dependent local symmetry reversal in single host lattice Ba₂A(BO₃)₂:Eu³⁺ [A = Mg and Ca] phosphors with tunable emission colours. Physical Chemistry Chemical Physics, 2017, 19, 17383-17395.	1.3	11

#	Article	IF	Citations
33161	Twinborn TiO₂â€“TiN heterostructures enabling smooth trappingâ€“diffusionâ€“conversion of polysulfides towards ultralong life lithiumâ€“sulfur batteries. Energy and Environmental Science, 2017, 10, 1694-1703.	15.6	884
33162	Novel III-Teâ€“graphene van der Waals heterojunctions for optoelectronic devices. RSC Advances, 2017, 7, 32383-32390.	1.7	8
33163	A first-principles study of carbon-related energy levels in GaN. I. Complexes formed by substitutional/interstitial carbons and gallium/nitrogen vacancies. Journal of Applied Physics, 2017, 121, .	1.1	77
33164	A first-principles study of carbon-related energy levels in GaN. II. Complexes formed by carbon and hydrogen, silicon or oxygen. Journal of Applied Physics, 2017, 121, 195702.	1.1	34
33165	First-principles study of MnAl for its application in MgO-based perpendicular magnetic tunnel junctions. Applied Physics Letters, 2017, 110, .	1.5	19
33166	Thermal transport in monolayer InSe. Journal of Physics Condensed Matter, 2017, 29, 335702.	0.7	37
33167	Reliable Piezoelectricity in Bilayer WSe₂ for Piezoelectric Nanogenerators. Advanced Materials, 2017, 29, 1606667.	11.1	158
33168	Temperature effects on the friction-like mode of graphite. Theoretical Chemistry Accounts, 2017, 136, 1.	0.5	0
33169	Substrate-mediated single-atom isolation: dispersion of Ni and La on Î³-graphyne. Theoretical Chemistry Accounts, 2017, 136, 1.	0.5	14
33170	Structural and Magnetic Properties of Transition Metal-Adsorbed MoS2 Monolayer. Journal of Superconductivity and Novel Magnetism, 2017, 30, 2849-2854.	0.8	10
33171	Cr3+ and Nb5+ co-doped Ti2Nb10O29 materials for high-performance lithium-ion storage. Journal of Power Sources, 2017, 360, 470-479.	4.0	85
33172	Strontium manganese vanadates from hydrothermal brines: Synthesis and structure of Sr2Mn2(V3O10)(VO4), Sr3Mn(V2O7)2, and Sr2Mn(VO4)2(OH). Journal of Solid State Chemistry, 2017, 255, 225-233.	1.4	10
33173	Semimetallic Two-Dimensional TiB₁₂: Improved Stability and Electronic Properties Tunable by Biaxial Strain. Chemistry of Materials, 2017, 29, 5922-5930.	3.2	41
33174	Highly Efficient CO₂ Electrolysis on Cathodes with Exsolved Alkaline Earth Oxide Nanostructures. ACS Applied Materials & Interfaces, 2017, 9, 25350-25357.	4.0	47
33175	Atomic Structure and Dynamics of Defects in 2D MoS₂ Bilayers. ACS Omega, 2017, 2, 3315-3324.	1.6	32
33176	Two prospective Li-based half-Heusler alloys for spintronic applications based on structural stability and spinâ€“orbit effect. Journal of Applied Physics, 2017, 122, 013901.	1.1	11
33177	Superconductivity and unexpected chemistry of germanium hydrides under pressure. Physical Review B, 2017, 95, .	1.1	16
33178	Adsorption and migration behavior of Si atoms on the hydrogen-terminated diamond (001) surface: A first principles study. Applied Surface Science, 2017, 420, 542-549.	3.1	20

#	Article	IF	Citations
33179	Atomically dispersed Co atoms on MoS 2 monolayer: A promising high-activity catalyst for CO oxidation. Applied Surface Science, 2017, 425, 478-483.	3.1	29
33180	A DFT study of transition metal (Fe, Co, Ni, Cu, Ag, Au, Rh, Pd, Pt and Ir)-embedded monolayer MoS2 for gas adsorption. Computational Materials Science, 2017, 138, 255-266.	1.4	195
33181	Speciation of magnesium in monohydrocalcite: XANES, ab initio and geochemical modeling. Geochimica Et Cosmochimica Acta, 2017, 213, 457-474.	1.6	19
33182	Role of Lone Pair Cations in Ferroelectric Tungsten Bronzes. Chemistry of Materials, 2017, 29, 6414-6424.	3.2	20
33183	Globally-Optimized Local Pseudopotentials for (Orbital-Free) Density Functional Theory Simulations of Liquids and Solids. Journal of Chemical Theory and Computation, 2017, 13, 3684-3695.	2.3	18
33184	Effect of Alkali Metal Atom Doping on the CuInSe₂-Based Solar Cell Absorber. Journal of Physical Chemistry C, 2017, 121, 15516-15528.	1.5	125
33185	Impact of Carbonyl Formation on Cobalt Ripening over Titania Surface. Journal of Physical Chemistry C, 2017, 121, 15880-15887.	1.5	3
33186	Reduction of Electrolyte Components on a Coated Si Anode of Lithium-Ion Batteries. Journal of Physical Chemistry Letters, 2017, 8, 3404-3408.	2.1	13
33187	Effects of Nonhydrostatic Stress on Structural and Optoelectronic Properties of Methylammonium Lead Bromide Perovskite. Journal of Physical Chemistry Letters, 2017, 8, 3457-3465.	2.1	53
33188	Macroporous Inverse Opal-like Mo_xC with Incorporated Mo Vacancies for Significantly Enhanced Hydrogen Evolution. ACS Nano, 2017, 11, 7527-7533.	7.3	102
33189	Three-dimensional buckled honeycomb boron lattice with vacancies as an intermediate phase on the transition pathway from Î±-B to Î³-B. NPG Asia Materials, 2017, 9, e400-e400.	3.8	4
33190	Revealing the influence of Cyano in Anchoring Groups of Organic Dyes on Adsorption Stability and Photovoltaic Properties for Dye-Sensitized Solar Cells. Scientific Reports, 2017, 7, 4979.	1.6	30
33191	Evolution of the topologically protected surface states in superconductorÎ²-Bi2Pd from the three-dimensional to the two-dimensional limit. Journal of Physics Condensed Matter, 2017, 29, 325501.	0.7	14
33192	Electronic and magnetic properties of low-dimensional system Co₂TeO₃Cl₂. Journal of Physics Condensed Matter, 2017, 29, 395801.	0.7	4
33193	Synthesis, magnetic properties and electronic structure of theSâ€‰â€‰=â€‰â€‰Â½ uniform spin chain system InCuPO5. Materials Research Express, 2017, 4, 076103.	0.8	1
33194	The role of molybdenum in suppressing cold dwell fatigue in titanium alloys. Proceedings of the Royal Society A: Mathematical, Physical and Engineering Sciences, 2017, 473, 20170189.	1.0	10
33195	<mml:math xmlns:mml="http://www.w3.org/1998/Math/MathML"><mml:mrow><mml:msub><mml:mrow><mml:mo>(</mml:mo><mml:msub><mm as a model system for unconventional charge transfer and polar metallicity. Physical Review B, 2017, 95, .	1.1	11
33196	Structural and electronic phase transitions in ferromagnetic monolayer <mml:math xmlns:mml="http://www.w3.org/1998/Math/MathML"><mml:msub><mml:mi>VS</mml:mi><mml:mn>2</mml:mn></mml:msub></mml induced by charge doping. Physical Review B, 2017, 95, .	1.1	50

#	Article	IF	Citations
33197	Premelting hcp to bcc Transition in Beryllium. Physical Review Letters, 2017, 118, 145702.	2.9	32
33198	DFT study of the structural and electronic properties of crystalline 2-benzylidene-1-indanone under different hydrostatic pressures. International Journal of Modern Physics C, 2017, 28, 1750072.	0.8	1
33199	Magnetism and energetics for vacancy and helium impurity in Fe-9Cr alloy: A first-principles study. Computational Materials Science, 2017, 138, 267-276.	1.4	10
33200	Os/Si nanocomposites as excellent hydrogen evolution electrocatalysts with thermodynamically more favorable hydrogen adsorption free energy than platinum. Nano Energy, 2017, 39, 284-290.	8.2	40
33201	Irradiation effect on infrared spectra of LiF:OH crystals: Theoretical modeling. Physica B: Condensed Matter, 2017, 521, 258-263.	1.3	5
33202	Strain effect on SnS2 nanoribbons: Robust direct bandgap of zigzag-edge and sensitive indirect semiconductor with armchair-edge states. Superlattices and Microstructures, 2017, 111, 480-486.	1.4	5
33203	High coverage water adsorption on CuO(011) surface. Physical Chemistry Chemical Physics, 2017, 19, 18652-18659.	1.3	19
33204	Monolayer germanium monochalcogenides (GeS/GeSe) as cathode catalysts in nonaqueous Liâ€“O₂batteries. Physical Chemistry Chemical Physics, 2017, 19, 20457-20462.	1.3	36
33205	Electronic structure & yield strength prediction for dislocationâ€“Mo complex in the Î³ phase of nickel-based superalloys. Chinese Physics B, 2017, 26, 076104.	0.7	1
33206	Density functional theory investigation of carbon monoxide adsorption on the kaolinite (001) surface. Chinese Physics B, 2017, 26, 079101.	0.7	4
33207	Trapping of hydrogen and helium at dislocations in tungsten: anab initiostudy. Nuclear Fusion, 2017, 57, 126040.	1.6	42
33208	Surface-bound states in nanodiamonds. Physical Review B, 2017, 95, .	1.1	13
33209	Electronic properties of superconducting FeS. Physical Review B, 2017, 95, .	1.1	10
33210	First-principles investigation of phase stability in the Mg-Sc binary alloy. Physical Review B, 2017, 95, .	1.1	27
33211	Ideal strength and ductility in metals from second- and third-order elastic constants. Physical Review B, 2017, 96, .	1.1	31
33212	Semimetallic bands derived from interlayer electrons in the quasi-two-dimensional electride <mml:math xmlns:mml="http://www.w3.org/1998/Math/MathML"><mml:mrow><mml:msub><mml:mi mathvariant="normal">Y</mml:mi><mml:mn>2</mml:mn></mml:msub><mml:mi mathvariant="normal">C</mml:mi></mml:mrow></mml:math>. Physical Review B, 2017, 96, .	1.1	17
33213	Electronic properties of thin BaSi₂ films with different orientations. Japanese Journal of Applied Physics, 2017, 56, 05DA03.	0.8	12
33214	The effects of stacking patterns and interlayer coupling on electronic and optical properties of bilayer BiI3. Journal of Materials Science, 2017, 52, 11513-11523.	1.7	3

#	Article	IF	Citations
33215	Twinnability of Alâ€“Mg alloys: A first-principles interpretation. Transactions of Nonferrous Metals Society of China, 2017, 27, 1313-1318.	1.7	3
33216	Manipulation of Dirac cones in intercalated epitaxial graphene. Carbon, 2017, 123, 93-98.	5.4	25
33217	Superhard three-dimensional carbon with metallic conductivity. Carbon, 2017, 123, 311-317.	5.4	61
33218	almaBTE : A solver of the spaceâ€“time dependent Boltzmann transport equation for phonons in structured materials. Computer Physics Communications, 2017, 220, 351-362.	3.0	193
33219	Direct Observation of â€œPac-Manâ€•Coarsening. Nano Letters, 2017, 17, 4661-4664.	4.5	3
33220	Systematic First-Principles Study of Binary Metal Hydrides. ACS Combinatorial Science, 2017, 19, 513-523.	3.8	26
33221	Revealing the Role of Interfacial Properties on Catalytic Behaviors by in Situ Surface-Enhanced Raman Spectroscopy. Journal of the American Chemical Society, 2017, 139, 10339-10346.	6.6	127
33222	Helium Irradiation and Implantation Effects on the Structure of Amorphous Silicon Oxycarbide. Scientific Reports, 2017, 7, 3900.	1.6	28
33223	The structural and electronic properties of reduced amorphous titania. Physical Chemistry Chemical Physics, 2017, 19, 18671-18684.	1.3	31
33224	Au cluster adsorption on perfect and defective MoS₂ monolayers: structural and electronic properties. Physical Chemistry Chemical Physics, 2017, 19, 20735-20748.	1.3	103
33225	Synthesis of methanol from CO₂hydrogenation promoted by dissociative adsorption of hydrogen on a Ga₃Ni₅(221) surface. Physical Chemistry Chemical Physics, 2017, 19, 18539-18555.	1.3	43
33226	Tuning band gaps and optical absorption of BiOCl through doping and strain: insight form DFT calculations. Physical Chemistry Chemical Physics, 2017, 19, 20968-20973.	1.3	34
33227	Improved cyclic redox reactivity of lanthanum modified iron-based oxygen carriers in carbon monoxide chemical looping combustion. Journal of Materials Chemistry A, 2017, 5, 20153-20160.	5.2	38
33228	The effect of Dâ€“[D_eâ€“Ï€â€“A]_n (n = 1, 2, 3) type dyes on the overall performance of DSSCs: a theoretical investigation. Journal of Materials Chemistry C, 2017, 5, 7510-7520.	2.7	22
33229	Mechanical properties of thermoelectric lanthanum telluride from quantum mechanics. Journal Physics D: Applied Physics, 2017, 50, 274002.	1.3	12
33230	Equation of state for warm dense lithium: A first principles investigation. Chinese Physics B, 2017, 26, 065101.	0.7	0
33231	Magnetism induced by Ga vacancy in rare earth R(R=Gd,Eu,Tm)doped GaN. Journal of Physics: Conference Series, 2017, 827, 012016.	0.3	0
33232	High-pressure studies on the properties of <mml:math xmlns:mml="http://www.w3.org/1998/Math/MathML"><mml:msub><mml:mi>FeGa</mml:mi><mml:mn>3</mml:mn></mml:msub></mml: : Role of on-site Coulomb correlation. Physical Review B, 2017, 95, .	1.1	7

#	Article	IF	Citations
33233	Type-II Dirac semimetals in the <mml:math xmlns:mml="http://www.w3.org/1998/Math/MathML"><mml:mrow><mml:msub><mml:mi>YPd</mml:mi><mml:mn>2</mml:mn></mml class. Physical Review B, 2017, 95, .	1.1	43
33234	First-principles modeling of the Invar effect in <mml:math xmlns:mml="http://www.w3.org/1998/Math/MathML"><mml:mrow><mml:msub><mml:mi>Fe</mml:mi><mml:mn>65</mml:mn></ by the spin-wave method. Physical Review B, 2017, 95, .	1.1	22
33235	Adsorption and desorption of hydrogen at nonpolar <mml:math xmlns:mml="http://www.w3.org/1998/Math/MathML"><mml:mrow><mml:mi>GaN</mml:mi><mml:mo>(</mml:mo><mml:mn>1</mml: surfaces: Kinetics and impact on surface vibrational and electronic properties. Physical Review B, 2017, 95, .	1.1	15
33236	Anomalously temperature-dependent thermal conductivity of monolayer GaN with large deviations from the traditional <mml:math xmlns:mml="http://www.w3.org/1998/Math/MathML"><mml:mn>1</mml:mn><mml:mo>/</mml:mo><mml:mi>T</mml:mi></mml:ma law. Physical Review B, 2017, 95, .	1.1	101
33237	Longitudinal, transverse, and single-particle dynamics in liquid Zn:Ab initiostudy and theoretical analysis. Physical Review B, 2017, 95, .	1.1	26
33238	Quasi-freestanding, striped WS2 monolayer with an invariable band gap on Au(001). Nano Research, 2017, 10, 3875-3884.	5.8	13
33239	Titania-Modified Silver Electrocatalyst for Selective CO₂ Reduction to CH₃OH and CH₄ from DFT Study. Journal of Physical Chemistry C, 2017, 121, 16275-16282.	1.5	47
33240	Enhancement of Friction by Water Intercalated between Graphene and Mica. Journal of Physical Chemistry Letters, 2017, 8, 3482-3487.	2.1	57
33241	Large In-Plane and Vertical Piezoelectricity in Janus Transition Metal Dichalchogenides. ACS Nano, 2017, 11, 8242-8248.	7.3	599
33242	First-Principles Study of Sodium Intercalation in Crystalline Na x Si24 (0â€‰â‰â€‰xâ€‰â‰â€‰4) as Anode Material for Na-ion Batteries. Scientific Reports, 2017, 7, 5350.	1.6	31
33243	Fluorine substituted (Mn,Ir)O₂:F high performance solid solution oxygen evolution reaction electro-catalysts for PEM water electrolysis. RSC Advances, 2017, 7, 17311-17324.	1.7	53
33244	Enhancing the oxygen vacancy formation and migration in bulk chromium(<scp>iii</scp>) oxide by alkali metal doping: a change from isotropic to anisotropic oxygen diffusion. Journal of Materials Chemistry A, 2017, 5, 15613-15630.	5.2	36
33245	Self-assembly of melem on Au(111) and Ag(111): the origin of two different hydrogen bonding configurations. Physical Chemistry Chemical Physics, 2017, 19, 18704-18708.	1.3	10
33246	Decouple electronic and phononic transport in nanotwinned structures: a new strategy for enhancing the figure-of-merit of thermoelectrics. Nanoscale, 2017, 9, 9987-9996.	2.8	31
33247	Electronic and protonic conduction in LaFeO₃. Journal of Materials Chemistry A, 2017, 5, 15367-15379.	5.2	48
33248	Ba₆Li₂CdSn₄S₁₆: lithium substitution simultaneously enhances band gap and SHG intensity. Journal of Materials Chemistry C, 2017, 5, 7067-7074.	2.7	38
33249	Topological phase transition coupled with spin-valley physics in ferroelectric oxide heterostructures. Physical Review B, 2017, 95, .	1.1	9
33250	Magnetic and electronic crossovers in graphene nanoflakes. Physical Review B, 2017, 95, .	1.1	24

#	Article	IF	Citations
33251	Robustness of the cluster expansion: Assessing the roles of relaxation and numerical error. Physical Review B, 2017, 96, .	1.1	29
33252	New group-V elemental bilayers: A tunable structure model with four-, six-, and eight-atom rings. Physical Review B, 2017, 96, .	1.1	15
33253	Nonisovalent Si-III-V and Si-II-VI alloys: Covalent, ionic, and mixed phases. Physical Review B, 2017, 96, .	1.1	2
33254	Critical Temperature for the Conversion from Wurtzite to Zincblende of the Optical Emission of InAs Nanowires. Journal of Physical Chemistry C, 2017, 121, 16650-16656.	1.5	2
33255	Mechanisms of Lithium Intercalation and Conversion Processes in Organicâ€“Inorganic Halide Perovskites. ACS Energy Letters, 2017, 2, 1818-1824.	8.8	111
33256	Ultra low lattice thermal conductivity and high carrier mobility of monolayer SnS₂and SnSe₂: a first principles study. Physical Chemistry Chemical Physics, 2017, 19, 20677-20683.	1.3	166
33257	Lead-free and stable antimonyâ€“silver-halide double perovskite (CH₃NH₃)₂AgSbI₆. RSC Advances, 2017, 7, 35175-35180.	1.7	75
33258	Partially planar BP₃with high electron mobility as a phosphorene analog. Journal of Materials Chemistry C, 2017, 5, 11267-11274.	2.7	37
33259	Exploring the driving forces behind the structural assembly of biphenylthiolates on Au(111). Journal of Chemical Physics, 2017, 147, 024706.	1.2	8
33260	Magnetic subunits within a single moleculeâ€“surface hybrid. New Journal of Physics, 2017, 19, 053016.	1.2	12
33261	Inelastic x-ray investigation of the ferroelectric transition in SnTe. Physical Review B, 2017, 95, .	1.1	32
33262	Doping-induced spin-orbit splitting in Bi-doped ZnO nanowires. Physical Review B, 2017, 95, .	1.1	8
33263	Structural simplicity as a restraint on the structure of amorphous silicon. Physical Review B, 2017, 95, .	1.1	18
33264	Stable charge density wave phase in a <mml:math xmlns:mml="http://www.w3.org/1998/Math/MathML"><mml:mrow><mml:mn>1</mml:mn><mml:mi>T</mml:mi><mml:mo>â€“</mml:mo> monolayer. Physical Review B, 2017, 95, .	1.1	56
33265	Electronic structure, lattice dynamics, and optical properties of a novel van der Waals semiconductor heterostructure: <mml:math xmlns:mml="http://www.w3.org/1998/Math/MathML"><mml:msub><mml:mi>InGaSe</mml:mi><mml:mn>2</mml:mn></mml:msub></ Physical Review B, 2017, 96, .	1.1	13
33266	Three-Dimensional Electronic Structure of the Type-II Weyl Semimetal <mml:math xmlns:mml="http://www.w3.org/1998/Math/MathML" display="inline"><mml:mrow><mml:msub><mml:mrow><mml:mi>WTe</mml:mi></mml:mrow><mml:mrow><mml:mn>2</mml:mn> Physical Review Letters, 2017, 119, 026403.	2.9	55
33267	First-principles study of phosphorus embrittlement in austenitic steels with Î³-carbide precipitates. Computational Materials Science, 2017, 138, 105-110.	1.4	1
33268	Tailoring catalytic activities of transition metal disulfides for water splitting. FlatChem, 2017, 4, 68-80.	2.8	24

#	Article	IF	Citations
33269	Flexible Force Field Parameterization through Fitting on the Ab Initio-Derived Elastic Tensor. Journal of Chemical Theory and Computation, 2017, 13, 3722-3730.	2.3	13
33270	Structural, Vibrational, and Elastic Properties of Yttrium Orthoaluminate Nanoperovskite at High Pressures. Journal of Physical Chemistry C, 2017, 121, 15353-15367.	1.5	13
33271	Giant Optical Second Harmonic Generation in Two-Dimensional Multiferroics. Nano Letters, 2017, 17, 5027-5034.	4.5	137
33272	Genetic algorithm prediction of two-dimensional group-IV dioxides for dielectrics. Physical Review B, 2017, 95, .	1.1	23
33273	Tunable hyperbolic dispersion and negative refraction in natural electride materials. Physical Review B, 2017, 95, .	1.1	56
33274	Cycloidal magnetism driven ferroelectricity in double tungstate LiFe(WO4)2. Physical Review B, 2017, 95, .	1.1	20
33275	First-principles investigation of strain effects on the stacking fault energies, dislocation core structure, and Peierls stress of magnesium and its alloys. Physical Review B, 2017, 95, .	1.1	36
33276	Warm Dense Matter Demonstrating Non-Drude Conductivity from Observations of Nonlinear Plasmon Damping. Physical Review Letters, 2017, 118, 225001.	2.9	68
33277	Investigation on formation mechanism of T1 precipitate in an Al-Cu-Li alloy. Journal of Alloys and Compounds, 2017, 723, 661-666.	2.8	72
33278	Ab initiodensity functional theory calculation of La₅Ti₂Cu_{1â^'x}Ag_xS₅O₇solid solution semiconductor photocatalysts for water splitting. Journal Physics D: Applied Physics, 2017,	1.3	3
33279	Pressure-driven phase transition from antiferromagnetic semiconductor to nonmagnetic metal in the two-leg ladders <mml:math xmlns:mml="http://www.w3.org/1998/Math/MathML"><mml:mrow><mml:mi>A</mml:mi><mml:msub><mml:mi>Fe</mml:mi><mml:mr		

#	Article	IF	Citations
33287	Rationalizing the formation of binary mixed thiol self-assembled monolayers. Materials Today Chemistry, 2017, 5, 34-42.	1.7	13
33288	QPHT-graphene: A new two-dimensional metallic carbon allotrope. Physics Letters, Section A: General, Atomic and Solid State Physics, 2017, 381, 2845-2849.	0.9	32
33289	Comparative study on structural, elastic, dynamical, and thermodynamic properties of Weyl semimetals MX (M = Ta or Nb; X = As or P). Solid State Communications, 2017, 263, 10-18.	0.9	14
33290	Effects of Iron Doping on the Physical Properties of Quaternary Ferromagnetic Sulfide: Ba2Fe0.6V1.4S6. Inorganic Chemistry, 2017, 56, 8302-8310.	1.9	1
33291	The Role of Connectivity on Electronic Properties of Lead Iodide Perovskite-Derived Compounds. Inorganic Chemistry, 2017, 56, 8408-8414.	1.9	83
33292	Density Functional Theory Study of Interface Interactions in Hydroxyapatite/Rutile Composites for Biomedical Applications. Journal of Physical Chemistry C, 2017, 121, 15687-15695.	1.5	16
33293	Poor Photovoltaic Performance of Cs₃Bi₂I₉: An Insight through First-Principles Calculations. Journal of Physical Chemistry C, 2017, 121, 17062-17067.	1.5	121
33294	First-Principles Calculation of Pt Surface Energies in an Electrochemical Environment: Thermodynamic Driving Forces for Surface Faceting and Nanoparticle Reconstruction. Langmuir, 2017, 33, 7043-7052.	1.6	31
33295	Kinetics and Mechanism of Methanol Conversion over Anatase Titania Nanoshapes. ACS Catalysis, 2017, 7, 5345-5356.	5.5	31
33296	Atomic and electronic basis for the serrations of refractory high-entropy alloys. Npj Computational Materials, 2017, 3, .	3.5	64
33297	Dramatic band gap reduction incurred by dopant coordination rearrangement in Co-doped nanocrystals of CeO2. Scientific Reports, 2017, 7, 4715.	1.6	25
33298	Density functional study of structure and dynamics in liquid antimony and Sbn clusters. Journal of Chemical Physics, 2017, 146, 194502.	1.2	15
33299	Distinguishing attosecond electronâ€“electron scattering and screening in transition metals. Proceedings of the National Academy of Sciences of the United States of America, 2017, 114, E5300-E5307.	3.3	55
33300	Local structure of the crystalline and amorphous states of<mml:math xmlns:mml="http://www.w3.org/1998/Math/MathML"><mml:mrow><mml:msub><mml:mi>Ga</mml:mi><mml:mn>2</mml:mn></mml	1.1	14
33301	Superlattice-induced oscillations of interplanar distances and strain effects in the CrN/AlN system. Physical Review B, 2017, 95, .	1.1	13
33302	Phase-field study of ripening and rearrangement of precipitates under chemomechanical coupling. Physical Review B, 2017, 95, .	1.1	14
33303	Superconductivity in a new intermetallic structure type based on endohedral <mml:math xmlns:mml="http://www.w3.org/1998/Math/MathML"><mml:mrow><mml:mi>Ta</mml:mi><mml:mo>@</mml:mo><mml:mi mathvariant="normal">I</mml:mi><mml:msub><mml:mi mathvariant="normal">r</mml:mi><mml:mn>7</mml:mn></mml:msub><mml:mi mathvariant="normal">G</mml:mi><mml:msub><mml:mi mathvariant="normal">e</mml:mi><mml:mn>4</mml:mn></mml:msub></mml:mrow></mml:math> cluste	1.1	16
33304	Ab initio based empirical potential applied to tungsten at high pressure. Physical Review B, 2017, 95, .	1.1	11

#	Article	IF	Citations
33305	First-principles investigation of local structure deformation induced by x-ray irradiation in <mml:math xmlns:mml="http://www.w3.org/1998/Math/MathML"><mml:mrow><mml:mi>Î¹</mml:mi><mml:mo>â^'</mml:mo><mml:msub><mml:m		

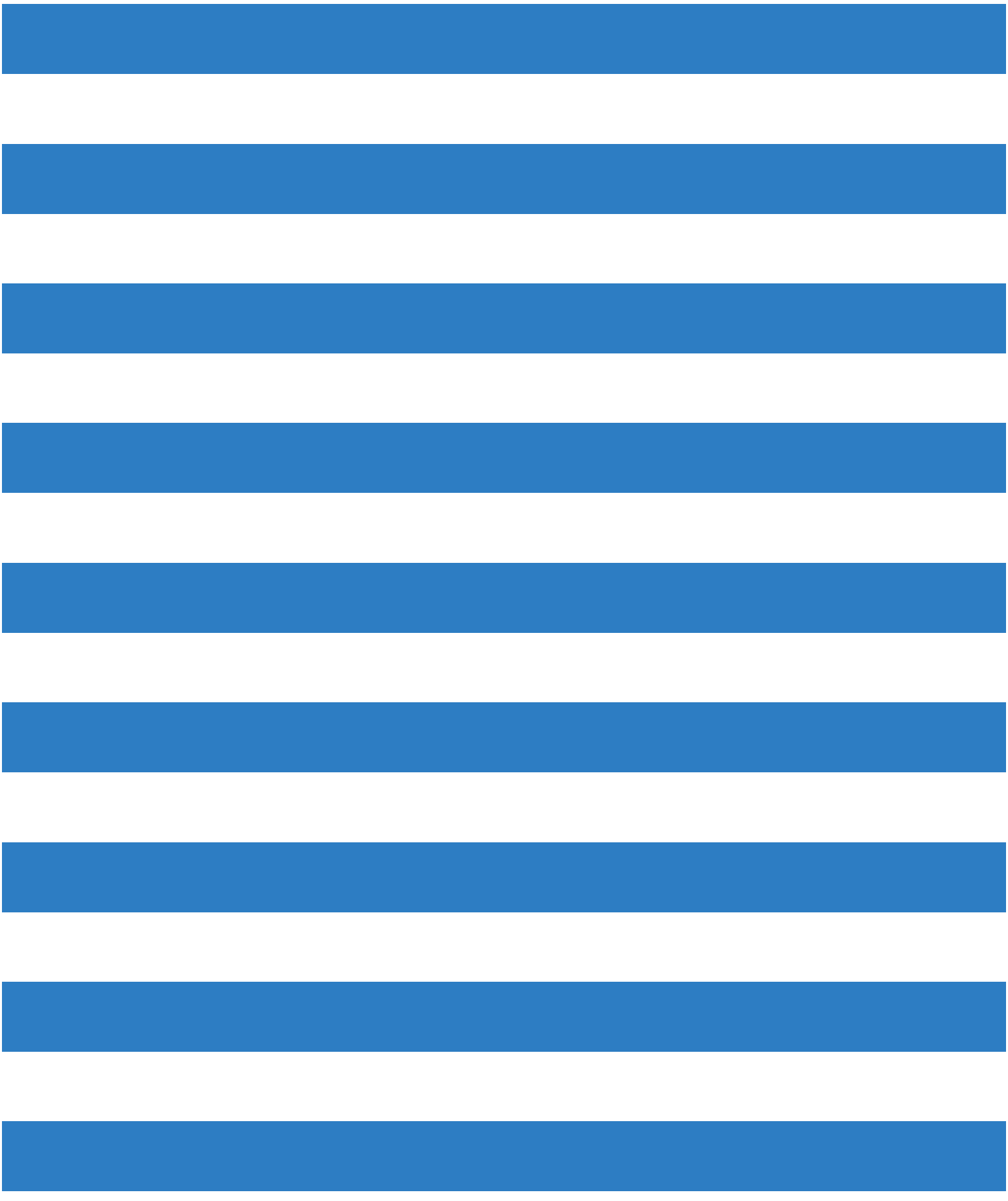

#	Article	IF	Citations
33323	Prediction of two-dimensional electron gas mediated magnetoelectric coupling at ferroelectric <mml:math xmlns:mml="http://www.w3.org/1998/Math/MathML"><mml:mrow><mml:msub><mml:mi>PbTiO</mml:mi><mml:mn>3</mml:mn></m heterostructures. Physical Review B, 2017, 95, .	1.1	22
33324	Phonon thermal transport in transition-metal and rare-earth nitride semiconductors from first principles. Physical Review B, 2017, 95, .	1.1	11
33325	Computational design of a robust two-dimensional antiferromagnetic semiconductor. Physical Review B, 2017, 96, .	1.1	20
33326	Effect of interstitial carbon distribution and nickel substitution on the tetragonality of martensite: A first-principles study. Intermetallics, 2017, 89, 92-99.	1.8	30
33327	Two-dimensional metallicity and ferromagnetic ordering in monoatomic-thick Ce layer on Si(111). Materials Chemistry and Physics, 2017, 199, 225-229.	2.0	1
33328	GeAs₂: A IVâ€“V Group Two-Dimensional Semiconductor with Ultralow Thermal Conductivity and High Thermoelectric Efficiency. Chemistry of Materials, 2017, 29, 6261-6268.	3.2	80
33329	Temperature and Eu²⁺-Doping Induced Phase Selection in NaAlSiO₄ Polymorphs and the Controlled Yellow/Blue Emission. Chemistry of Materials, 2017, 29, 6552-6559.	3.2	79
33330	Spatially Confined Liâ€“Oxygen Interaction in the Tunnel of Î±-MnO₂ Catalyst for Liâ€“Air Battery: A First-Principles Study. Journal of Physical Chemistry C, 2017, 121, 16193-16200.	1.5	15
33331	Revealing Surface Elemental Composition and Dynamic Processes Involved in Facet-Dependent Oxidation of Pt₃Co Nanoparticles via in Situ Transmission Electron Microscopy. Nano Letters, 2017, 17, 4683-4688.	4.5	71
33332	Optimizing Interfacial Cross-Linking in Graphene-Derived Materials, Which Balances Intralayer and Interlayer Load Transfer. ACS Applied Materials & Interfaces, 2017, 9, 24830-24839.	4.0	31
33333	Nanoscale Bandgap Tuning across an Inhomogeneous Ferroelectric Interface. ACS Applied Materials & Interfaces, 2017, 9, 24704-24710.	4.0	14
33334	Toward a More Rational Design of the Direct Synthesis of Aniline: A Density Functional Theory Study. ACS Omega, 2017, 2, 3214-3227.	1.6	1
33335	Lattice Effects on the Formation of Oxygen Vacancies in Perovskite Thin Films. Physical Review Applied, 2017, 7, .	1.5	36
33336	Finite-temperature properties of nonmagnetic transition metals: Comparison of the performance of constraint-based semilocal and nonlocal functionals. Physical Review B, 2017, 95, .	1.1	35
33337	Ionic and superionic phases in ammonia dihydrate <mml:math xmlns:mml="http://www.w3.org/1998/Math/MathML"><mml:mrow><mml:mi mathvariant="normal">N</mml:mi><mml:msub><mml:mi mathvariant="normal">H</mml:mi><mml:mn>3</mml:mn></mml:msub><mml:mo>Â·</mml:mo><mml:mn>2</mml:mn><mml:msub><mml:mi mathvariant="normal">H</mml:mi><mml:mn>2</mml:mn></mml:msub><mml:mi display="inline"><mml:mrow><mml:msub><mml:mrow><mml:mi>PdSe</mml:mi></mml:mrow><mml:mn>2</mml:mn></mml:msub>	1.1	21
33338	Two-Dimensional Phase Driven by Interlayer Fusion in Layered <mml:math xmlns:mml="http://www.w3.org/1998/Math/MathML" display="inline"><mml:mrow><mml:msub><mml:mrow><mml:mi>PdSe</mml:mi></mml:mrow></mml:msub>, Physical Review Letters, 2017, 119, 016101.	2.9	111
33339	First-Principles Prediction of Spin-Polarized Multiple Dirac Rings in Manganese Fluoride. Physical Review Letters, 2017, 119, 016403.	2.9	84
33340	Reactive pathways of hydrogen and carbon removal from organosilicate glass low-Îº films by F atoms. European Physical Journal D, 2017, 71, 1.	0.6	7

#	Article	IF	Citations
33341	Element-specific amorphization of vacancy-ordered GeSbTe for ternary-state phase change memory. Acta Materialia, 2017, 136, 242-248.	3.8	30
33342	First-principles based analysis of the piezoelectric response in <mml:math xmlns:mml="http://www.w3.org/1998/Math/MathML" altimg="si1.gif" overflow="scroll"><mml:mrow><mml:mi>Î±</mml:mi></mml:mrow></mml:math>-LiIO3. Computational Materials Science, 2017, 138, 199-203.	1.4	5
33343	Electronic structure and chemical hydrogen storage of a porous sp3 tetragonal BC2N compound. Journal of Alloys and Compounds, 2017, 724, 229-233.	2.8	12
33344	A Combined Probe-Molecule, MÃ¶ssbauer, Nuclear Resonance Vibrational Spectroscopy, and Density Functional Theory Approach for Evaluation of Potential Iron Active Sites in an Oxygen Reduction Reaction Catalyst. Journal of Physical Chemistry C, 2017, 121, 16283-16290.	1.5	75
33345	Cationâ€“Eutectic Transition via Sublattice Melting in CuInP₂S₆/In_{4/3}P₂S₆ van der Waals Layered Crystals. ACS Nano, 2017, 11, 7060-7073.	7.3	54
33346	Emerging novel electronic structure in hydrogen-Arsenene-halogen nanosheets: A computational study. Scientific Reports, 2017, 7, 4773.	1.6	9
33347	Hole density and acceptor-type defects in MBE-grown GaSb_{1-x}â€‰Bi_x. Journal Physics D: Applied Physics, 2017, 50, 295102.	1.3	12
33348	Lithiation of Silicon Nanoclusters. Physical Review Applied, 2017, 7, .	1.5	9
33349	Interface-driven noncollinear magnetic structure and phase transition of Fe thin films. Physical Review B, 2017, 95, .	1.1	6
33350	Lattice thermal conductivity evaluated using elastic properties. Physical Review B, 2017, 95, .	1.1	114
33351	Effects of partial La filling and Sb vacancy defects on <mml:math xmlns:mml="http://www.w3.org/1998/Math/MathML"><mml:mrow><mml:mi>CoS</mml:mi><mml:msub><mml:mi mathvariant="normal">b</mml:mi><mml:mn>3</mml:mn></mml:msub></mml:mrow></mml:math> skutterudites. Physical Review B, 2017, 95, .	1.1	26
33352	Prospective high thermoelectric performance of the heavily <mml:math xmlns:mml="http://www.w3.org/1998/Math/MathML"><mml:mi mathvariant="bold-italic">p</mml:mi></mml:math> -doped half-Heusler compound CoVSn. Physical Review B, 2017, 95, .	1.1	37
33353	Phosphorus allotropes: Stability of black versus red phosphorus re-examined by means of the van der Waals inclusive density functional method. Physical Review B, 2017, 95, .	1.1	30
33354	First-principles study on <mml:math xmlns:mml="http://www.w3.org/1998/Math/MathML"><mml:mrow><mml:msub><mml:mi>Ni</mml:mi><mml:mn>3</mml:mn></mml:msub></mml:mrow></mml:math> antiphase boundary with Ti and Hf impurities. Physical Review B, 2017, 95, .	1.1	22
33355	Nontrivial topology of cubic alkali bismuthides. Physical Review B, 2017, 95, .	1.1	4
33356	Rocksalt versus layered ordering in double perovskites: A case study with <mml:math xmlns:mml="http://www.w3.org/1998/Math/MathML"><mml:mrow><mml:msub><mml:mi>La</mml:mi><mml:mn>2</mml:mn></mml:msub></mml:mrow></mml:math> and <mml:math xmlns:mml="http://www.w3.org/1998/Math/MathML"><mml:mrow><mml:msub><mml:mi>La</mml:mi><mml:mn>2</mml:mn></mml:msub></mml:mrow></mml:math> Physical Review B, 2017, 95, .	1.1	15
33357	First-principles description of van der Waals bonded spin-polarized systems using the vdW-DF+ <mml:math xmlns:mml="http://www.w3.org/1998/Math/MathML"><mml:mi>U</mml:mi></mml:math> method: Application to solid oxygen at low pressure. Physical Review B, 2017, 95, .	1.1	6
33358	Tunable correlated-electron phases in (111) <mml:math xmlns:mml="http://www.w3.org/1998/Math/MathML"><mml:mrow><mml:msub><mml:mi>LaAlO</mml:mi><mml:mn>3</mml:mn></mml:msub></mml:mrow></mml:math> band insulator heterostructures. Physical Review B, 2017, 95, .	1.1	6

#	Article	IF	Citations
33359	Ab initio prediction of the high-pressure phase diagram of BaBiO3. Physical Review B, 2017, 96, .	1.1	8
33360	Isolated Spin Qubits in SiC with a High-Fidelity Infrared Spin-to-Photon Interface. Physical Review X, 2017, 7, .	2.8	125
33361	Effect of saddle point anisotropy of point defects on their absorption by dislocations and cavities. Acta Materialia, 2017, 136, 323-334.	3.8	47
33362	Effect of structural phase transformations under pressure on electronic and optical properties of CuInS 2. Current Applied Physics, 2017, 17, 1564-1569.	1.1	3
33363	Are metals made from molecules?. Structural Chemistry, 2017, 28, 1409-1417.	1.0	5
33364	Fe Oxides on Ag Surfaces: Structure and Reactivity. Topics in Catalysis, 2017, 60, 492-502.	1.3	10
33365	Spin filtering in transition-metal phthalocyanine molecules from first principles. Frontiers of Physics, 2017, 12, 1.	2.4	13
33366	Structural, Electronic, and Optical Properties of Superhard Materials tP10-FeB4 and I4 1 /acd-FeB4. Journal of Electronic Materials, 2017, 46, 2506-2511.	1.0	1
33367	Two-dimensional square transition metal dichalcogenides with lateral heterostructures. Nano Research, 2017, 10, 3909-3919.	5.8	17
33368	Electronic properties of a graphene/periodic porous graphene heterostructure. Carbon, 2017, 122, 281-286.	5.4	27
33369	AFLUX: The LUX materials search API for the AFLOW data repositories. Computational Materials Science, 2017, 137, 362-370.	1.4	56
33370	Phonon spectrum and thermodynamic properties of LaCoO 3 based on first-principles theory. Computational Materials Science, 2017, 136, 191-197.	1.4	12
33371	Ab initio calculations of pressure-dependence of high-order elastic constants using finite deformations approach. Computer Physics Communications, 2017, 220, 20-30.	3.0	12
33372	Crystal structure of and displacive phase transition in tungsten nitride WN. Journal of Alloys and Compounds, 2017, 722, 517-524.	2.8	17
33373	Synergistically optimizing thermoelectric transport properties of n-type PbTe via Se and Sn co-alloying. Journal of Alloys and Compounds, 2017, 724, 208-221.	2.8	59
33374	A newly designed porous oxynitride photoanode with enhanced charge carrier mobility. Nano Energy, 2017, 39, 172-182.	8.2	21
33375	Rare earth interstitial-complexes in Ge: Hybrid density functional studies. Nuclear Instruments & Methods in Physics Research B, 2017, 409, 9-13.	0.6	4
33376	Rare earth substitutional impurities in germanium: A hybrid density functional theory study. Nuclear Instruments & Methods in Physics Research B, 2017, 409, 31-35.	0.6	3

#	Article	IF	Citations
33377	Layer-controlled band alignment, work function and optical properties of few-layer GeSe. Physica B: Condensed Matter, 2017, 519, 90-94.	1.3	27
33378	Effects of Embedded Dipole Layers on Electrostatic Properties of Alkanethiolate Self-Assembled Monolayers. Journal of Physical Chemistry C, 2017, 121, 15815-15830.	1.5	45
33379	Elucidating the Origin of Hydrogen Evolution Reaction Activity in Mono- and Bimetallic Metal- and Nitrogen-Doped Carbon Catalysts (Meâ€“Nâ€“C). ACS Applied Materials & Interfaces, 2017, 9, 25184-25193.	4.0	32
33380	Single-Atomic Ruthenium Catalytic Sites on Nitrogen-Doped Graphene for Oxygen Reduction Reaction in Acidic Medium. ACS Nano, 2017, 11, 6930-6941.	7.3	435
33381	High Tolerance to Iron Contamination in Lead Halide Perovskite Solar Cells. ACS Nano, 2017, 11, 7101-7109.	7.3	90
33382	Direct Neutron Spectroscopy Observation of Cerium Hydride Species on a Cerium Oxide Catalyst. Journal of the American Chemical Society, 2017, 139, 9721-9727.	6.6	138
33383	Exsolution trends and co-segregation aspects of self-grown catalyst nanoparticles in perovskites. Nature Communications, 2017, 8, 15967.	5.8	305
33384	Computationally-driven engineering of sublattice ordering in a hexagonal AlHfScTiZr high entropy alloy. Scientific Reports, 2017, 7, 2209.	1.6	71
33385	Characterization of Thin Film Materials using SCAN meta-GGA, an Accurate Nonempirical Density Functional. Scientific Reports, 2017, 7, 44766.	1.6	54
33386	Prediction of metallic nanotube reactivity for H2O activation. Physical Chemistry Chemical Physics, 2017, 19, 19188-19195.	1.3	1
33387	ORR viability of alumina-supported platinum nanocluster: exploring oxidation behaviour by DFT. Physical Chemistry Chemical Physics, 2017, 19, 19308-19315.	1.3	15
33388	Enhanced current rectification and self-powered photoresponse in multilayer p-MoTe₂/n-MoS₂ van der Waals heterojunctions. Nanoscale, 2017, 9, 10733-10740.	2.8	75
33389	Improved thermoelectric power factor and conversion efficiency of perovskite barium stannate. RSC Advances, 2017, 7, 32703-32709.	1.7	34
33390	Two-step model for ultrafast interfacial electron transfer: limitations of Fermiâ€™s golden rule revealed by quantum dynamics simulations. Chemical Science, 2017, 8, 5979-5991.	3.7	17
33391	Electric field-tunable electronic structures of 2D alkaline-earth metal hydroxideâ€“graphene heterostructures. Journal of Materials Chemistry C, 2017, 5, 7230-7235.	2.7	21
33392	Anionic ancillary ligands in cyclometalated Ru(<scp>ii</scp>) complex sensitizers improve photovoltaic efficiency of dye-sensitized solar cells: insights from theoretical investigations. Journal of Materials Chemistry A, 2017, 5, 15567-15577.	5.2	33
33393	Photoluminescence excitation spectroscopy of SiV^{â^'}and GeV^{â^'}color center in diamond. New Journal of Physics, 2017, 19, 063036.	1.2	75
33394	2D halide perovskite-based van der Waals heterostructures: contact evaluation and performance modulation. 2D Materials, 2017, 4, 035009.	2.0	23

#	Article	IF	Citations
33395	Theoretical study of the interaction between hydrogen and 4d alloying atom in nickel. Nuclear Science and Techniques/Hewuli, 2017, 28, 1.	1.3	6
33396	New methods for prediction of elastic constants based on density functional theory combined with machine learning. Computational Materials Science, 2017, 138, 135-148.	1.4	17
33397	Tunable electronic properties of MoS2/ReS2 van der Waals heterostructure from first-principles study. Optik, 2017, 144, 334-339.	1.4	10
33398	Precipitation in simultaneously nitrided and aged Mo-containing maraging steel. Materials Characterization, 2017, 131, 21-30.	1.9	13
33399	Quantifying van der Waals Interactions in Layered Transition Metal Dichalcogenides from Pressure-Enhanced Valence Band Splitting. Nano Letters, 2017, 17, 4982-4988.	4.5	53
33400	A Density Functional +UAssessment of Oxygen Evolution Reaction Mechanisms on Î²-NiOOH. ACS Catalysis, 2017, 7, 5329-5339.	5.5	110
33401	Electronic structures and physical properties of Na2O doped silicate glass. Journal of Applied Physics, 2017, 121, .	1.1	29
33402	Theoretical investigation on radiation tolerance of ${{oldsymbol{M}}}_{{oldsymbol{n}}+1}{{oldsymbol{AX}}}_{{oldsymbol{n}}}$ phases. Chinese Physics B, 2017, 26, 060703.	0.7	1
33403	Covalent versus localized nature of <mml:math xmlns:mml="http://www.w3.org/1998/Math/MathML"><mml:mrow><mml:mn>4</mml:mn><mml:mi>f</mml:mi></mml:mrow></mml:m electrons in ceria: Resonant angle-resolved photoemission spectroscopy and density functional theory. Physical Review B, 2017, 95, .	1.1	13
33404	Two-dimensional van der Waals p-n junction of InSe/phosphorene. Physical Review B, 2017, 95, .	1.1	68
33405	Graphene-supported small transition-metal clusters: A density functional theory investigation within van der Waals corrections. Physical Review B, 2017, 95, .	1.1	49
33406	Migration mechanisms and diffusion barriers of vacancies in <mml:math xmlns:mml="http://www.w3.org/1998/Math/MathML"><mml:mrow><mml:msub><mml:mi>Ga</mml:mi><mml:mn>2</mml:mn></mml mathvariant="normal">O</mml:mi><mml:mn>3</mml:mn></mml:msub></mml:mrow></mml:math>. Physical Review B, 2017, 95, .	1.1	107
33407	Comment on â€œNew Ground-State Crystal Structure of Elemental Boronâ€• Physical Review Letters, 2017, 118, 159601.	2.9	4
33408	Comment on â€œLinear Scaling of the Exciton Binding Energy versus the Band Gap of Two-Dimensional Materialsâ€• Physical Review Letters, 2017, 118, 209701.	2.9	8
33409	Structural transformations on an oxidized Ag(111) surface. JETP Letters, 2017, 105, 292-296.	0.4	6
33410	Effects of Cr on H and He trapping and vacancy complexes in V in a fusion environment: a first-principles study. European Physical Journal B, 2017, 90, 1.	0.6	2
33411	Fluorine atoms interaction with the nanoporous materials: experiment and DFT simulation. European Physical Journal D, 2017, 71, 1.	0.6	12
33412	The Third-Order Elastic Moduli and Debye Temperature of SrFe2As2 and BaFe2As2: a First-Principles Study. Journal of Superconductivity and Novel Magnetism, 2017, 30, 1749-1756.	0.8	10

#	Article	IF	Citations
33413	Can uranyl complexes encapsulate to carbon nanotubes? A periodic DFT study. Journal of Chemical Sciences, 2017, 129, 783-790.	0.7	2
33414	Magnetic interactions and electronic structure of $$hbox {Pt}_{2}hbox {Mn}_{1-x}hbox {Y}_{x} hbox {Ga (Y = Cr and Fe)}$$ Pt 2 Mn 1 - x Y x Ga (Y = Cr and Fe) system: An ab-initio calculation. Pramana - Journal of Physics, 2017, 89, 1.	0.9	2
33415	First-principles calculations of stacking fault energies in Mg-Y, Mg-Al and Mg-Zn alloys and implications for <mml:math xmlns:mml="http://www.w3.org/1998/Math/MathML" altimg="si1.gif" overflow="scroll"><mml:mrow><mml:mo>â€ˆ</mml:mo><mml:mi mathvariant="bold">c</mml:mi><mml:mo>+</mml:mo><mml:mi mathvariant="bold">a</mml:mi><mml:mo>â€‰</mml:mo></mml:mrow></mml:math> activity. Acta Materialia, 2017, 136, 249-261.	3.8	84
33416	Design of lithium selective crown ethers: Synthesis, extraction and theoretical binding studies. Chemical Engineering Journal, 2017, 326, 921-933.	6.6	78
33417	Electrical resistivity of solid and liquid Cu up to 5ÂGPa: Decrease along the melting boundary. Journal of Physics and Chemistry of Solids, 2017, 110, 386-393.	1.9	30
33418	Electronic structure in 1T-ZrS2 monolayer by strain. Physica E: Low-Dimensional Systems and Nanostructures, 2017, 93, 87-91.	1.3	12
33419	Enhanced photocatalytic performance of anatase TiO 2 substitutionally co-doped with La and N. Solar Energy Materials and Solar Cells, 2017, 170, 233-238.	3.0	12
33420	Towards the directional transport of molecules on surfaces. Tetrahedron, 2017, 73, 4858-4863.	1.0	3
33421	Borophene as Efficient Sulfur Hosts for Lithiumâ€“Sulfur Batteries: Suppressing Shuttle Effect and Improving Conductivity. Journal of Physical Chemistry C, 2017, 121, 15549-15555.	1.5	97
33422	Doped Amorphous Ti Oxides To Deoptimize Oxygen Reduction Reaction Catalysis. Journal of Physical Chemistry C, 2017, 121, 16825-16830.	1.5	19
33423	Enhanced Nonenzymatic Glucose-Sensing Properties of Electrodeposited NiCo₂O₄â€“Pd Nanosheets: Experimental and DFT Investigations. ACS Applied Materials & Interfaces, 2017, 9, 23894-23903.	4.0	97
33424	Effects of Fluorine Doping on the Electrical Performance of ZnON Thin-Film Transistors. ACS Applied Materials & Interfaces, 2017, 9, 24688-24695.	4.0	21
33425	Single-molecule quantum dot as a Kondo simulator. Nature Communications, 2017, 8, 16012.	5.8	77
33426	Relationship between structural order and water-like anomalies in metastable liquid silicon: Ab initio molecular dynamics. Scientific Reports, 2017, 7, 39952.	1.6	9
33427	Nanoclusters and nanolines: the effect of molybdenum oxide substrate stoichiometry on iron self-assembly. Nanotechnology, 2017, 28, 205602.	1.3	1
33428	First-principles study of exchange interactions of yttrium iron garnet. Physical Review B, 2017, 95, .	1.1	66
33429	Conduction electrons mediating the evolution from antiferromagnetic to ferromagnetic ordering inGd(Co1â^'yFey)2Zn20(0â‰¤yâ‰¤1). Physical Review B, 2017, 95, .	1.1	7
33430	Phonon-induced topological transition to a type-II Weyl semimetal. Physical Review B, 2017, 95, .	1.1	18

#	Article	IF	Citations
33431	Surface electron states on the quasi-two-dimensional excess-electron compounds<mml:math xmlns:mml="http://www.w3.org/1998/Math/MathML"><mml:mrow><mml:msub><mml:mi>Ca</mml:mi><mml:mn>2</mml:mn></mml:mrow><mml:mrow><mml:mi mathvariant="normal">N</mml:mi></mml:mrow></mml:math>and<mml:math xmlns:mml="http://www.w3.org/1998/Math/MathML"><mml:mrow><mml:msub><mml:mi mathvariant="normal">Y</mml:mi><mml:mn>2</mml:mn></mml:msub><mml:msub><mml:mi mathvariant="normal">C</mml:mi></mml:msub></mml:mrow></mml:math>. Physical Review B, 2017, 95, .	1.1	21
33432	[redacted]		

#	Article	IF	Citations
33449	Oxidative dehydrogenation of methanol at ceria-supported vanadia oligomers. Journal of Catalysis, 2017, 352, 382-387.	3.1	28
33450	Catalytic diversity conferred by confinement of protons within porous aluminosilicates in Prins condensation reactions. Journal of Catalysis, 2017, 352, 415-435.	3.1	20
33451	Gigantic perpendicular magnetic anisotropy of heavy transition metal cappings on Fe/MgO(0 0 1). Journal of Magnetism and Magnetic Materials, 2017, 442, 183-188.	1.0	5
33452	Electrochemical properties and lithium ion diffusion in Li4FeSbO6 studied by first principle. Journal of Solid State Chemistry, 2017, 254, 132-137.	1.4	5
33453	Structural characterization and cytotoxicity studies of different forms of a combretastatin A4 analogue. Journal of Molecular Structure, 2017, 1147, 226-234.	1.8	10
33454	Impurity characteristics of group V and VII element-doped two-dimensional ZrSe2 monolayer. Physica E: Low-Dimensional Systems and Nanostructures, 2017, 93, 279-283.	1.3	16
33455	A Yellow-Emitting Homoleptic Iridium(III) Complex Constructed from a Multifunctional Spiro Ligand for Highly Efficient Phosphorescent Organic Light-Emitting Diodes. Inorganic Chemistry, 2017, 56, 8397-8407.	1.9	23
33456	Photoinduced Charge Transfer versus Fragmentation Pathways in Lanthanum Cyclopentadienyl Complexes. Journal of Chemical Theory and Computation, 2017, 13, 4281-4296.	2.3	26
33457	Constrained-Orbital Density Functional Theory. Computational Method and Applications to Surface Chemical Processes. Journal of Chemical Theory and Computation, 2017, 13, 3561-3574.	2.3	19
33458	Defect Interactions in the CeO₂â€“ZrO₂â€“Y₂O₃ Solid Solution. Journal of Physical Chemistry C, 2017, 121, 15078-15084.	1.5	17
33459	Structural Evolution of Flower Defects and Effects on the Electronic Structures of Epitaxial Graphene. Journal of Physical Chemistry C, 2017, 121, 15282-15287.	1.5	10
33460	Atomic Layer Deposition of Stable LiAlF₄ Lithium Ion Conductive Interfacial Layer for Stable Cathode Cycling. ACS Nano, 2017, 11, 7019-7027.	7.3	276
33461	High-performance thermal sensitive VO₂(B) thin films prepared by sputtering with TiO₂(A) buffer layer and first-principles calculations study. RSC Advances, 2017, 7, 29496-29504.	1.7	23
33462	The formation mechanism of the initial Câ€“C chain in ethanol synthesis on Î³-AlOOH(100). Physical Chemistry Chemical Physics, 2017, 19, 19300-19307.	1.3	14
33463	The transition metal surface dependent methane decomposition in graphene chemical vapor deposition growth. Nanoscale, 2017, 9, 11584-11589.	2.8	76
33464	Experimental and theoretical investigation of pressure-dependent Raman spectra of triaminotrinitrobenzene (TATB) at high pressures. AIP Conference Proceedings, 2017, , .	0.3	4
33465	Pressure dependent Raman spectra used to validate DFT EOS of hexanitrostilbene (HNS). AIP Conference Proceedings, 2017, , .	0.3	2
33466	Properties of Ar at extreme compression. AIP Conference Proceedings, 2017, , .	0.3	0

#	Article	IF	Citations
33467	MD simulation of steady shock-wave fronts with phase transition in single-crystal iron. AIP Conference Proceedings, 2017, , .	0.3	12
33468	Dehydrogenation of methanol on Cu2O(100) and (111). Journal of Chemical Physics, 2017, 146, 244702.	1.2	23
33469	From two-dimensional nano-sheets to roll-up structures: expanding the family of nanoscroll. Nanotechnology, 2017, 28, 385704.	1.3	24
33470	Bismuthene on a SiC substrate: A candidate for a high-temperature quantum spin Hall material. Science, 2017, 357, 287-290.	6.0	803
33471	Large perpendicular exchange bias and high blocking temperature in Al-doped Cr₂O₃/Co thin film systems. Applied Physics Express, 2017, 10, 073003.	1.1	10
33472	Electronic and gap properties of lead-free perfect and mixed hybrid halide perovskites: An ab-initio study. Computational Materials Science, 2017, 138, 92-98.	1.4	24
33473	Phase separation in the half-Heusler thermoelectric materials (Hf,Ti,Zr)NiSn. Scripta Materialia, 2017, 139, 122-125.	2.6	18
33474	Periodic Arrays of Phosphorene Nanopores as Antidot Lattices with Tunable Properties. ACS Nano, 2017, 11, 7494-7507.	7.3	42
33475	Two-dimensional Penta-BP5 Sheets: High-stability, Strain-tunable Electronic Structure and Excellent Mechanical Properties. Scientific Reports, 2017, 7, 2404.	1.6	52
33476	Strengthening Mg by self-dispersed nano-lamellar faults. Materials Research Letters, 2017, 5, 415-425.	4.1	17
33477	Manipulating the mechanical properties of <mml:math xmlns:mml="http://www.w3.org/1998/Math/MathML"><mml:mrow><mml:msub><mml:mi>Ti</mml:mi><mml:mn>2</mml:mn></mml:m mathvariant="normal">C</mml:mi></mml:mrow></mml:math> MXene: Effect of substitutional doping. Physical Review B, 2017, 95, .	1.1	65
33478	Highly responsive ground state of <mml:math xmlns:mml="http://www.w3.org/1998/Math/MathML"><mml:msub><mml:mi>PbTaSe</mml:mi><mml:mn>2</mml:mn></mml:msub></ : Structural phase transition and evolution of superconductivity under pressure. Physical Review B, 2017, 95, .	1.1	13
33479	Tricritical behavior of the two-dimensional intrinsically ferromagnetic semiconductor <mml:math xmlns:mml="http://www.w3.org/1998/Math/MathML"><mml:msub><mml:mi mathvariant="bold">CrGeTe</mml:mi><mml:mn>3</mml:mn></mml:msub></mml:math>. Physical Review B, 2017, 95, .	1.1	103
33480	Ab initio phonon scattering by dislocations. Physical Review B, 2017, 95, .	1.1	49
33481	Nonlinear Electron-Phonon Coupling in Doped Manganites. Physical Review Letters, 2017, 118, 247601.	2.9	32
33482	Crystalline hydrates of calix[4]arene-para-sulfonic acid with n (n = 6â€“16) water molecules: a structure modeling. Russian Chemical Bulletin, 2017, 66, 62-69.	0.4	3
33483	Tunable electronic and magnetic properties from structure phase transition of layered vanadium diselenide. Journal Wuhan University of Technology, Materials Science Edition, 2017, 32, 574-578.	0.4	9
33484	An ab initio investigation of phosphorene/hexagonal boron nitride heterostructures with defects for high performance photovoltaic applications. Applied Surface Science, 2017, 423, 1003-1011.	3.1	9

#	Article	IF	Citations
33485	Hydroxyurea electrooxidation at gold electrodes. In situ infrared spectroelectrochemical and DFT characterization of adsorbed intermediates. Electrochimica Acta, 2017, 246, 951-962.	2.6	8
33486	Pristine and Se-/In-doped TlAsS2 enhance the solar energy-driven water splitting for hydrogen generation. International Journal of Hydrogen Energy, 2017, 42, 15464-15470.	3.8	12
33487	Nature of active sites on UiO-66 and beneficial influence of water in the catalysis of Fischer esterification. Journal of Catalysis, 2017, 352, 401-414.	3.1	172
33488	High-Performance Low-Cost n-Type Se-Doped Mg₃Sb₂-Based Zintl Compounds for Thermoelectric Application. Chemistry of Materials, 2017, 29, 5371-5383.	3.2	148
33489	Synthesis and Structural Characterization of a CHA-type AlPO4 Molecular Sieve with Penta-Coordinated Framework Aluminum Atoms. Inorganic Chemistry, 2017, 56, 8504-8512.	1.9	11
33490	Ï˜-Graphene: A New Metallic Allotrope of Planar Carbon with Potential Applications as Anode Materials for Lithium-Ion Batteries. Journal of Physical Chemistry Letters, 2017, 8, 3234-3241.	2.1	205
33491	Structure- and Coverage-Sensitive Mechanism of NO Reduction on Platinum Electrodes. ACS Catalysis, 2017, 7, 4660-4667.	5.5	118
33492	Superconductivity in Alkaline Earth Metal-Filled Skutterudites Ba_xIr₄X₁₂ (X = As, P). Journal of the American Chemical Society, 2017, 139, 8106-8109.	6.6	13
33493	Î´-Doping of oxygen vacancies dictated by thermodynamics in epitaxial SrTiO3 films. AIP Advances, 2017, 7, .	0.6	9
33494	Frontier molecular orbitals of a single molecule adsorbed on thin insulating films supported by a metal substrate: electron and hole attachment energies. Journal of Physics Condensed Matter, 2017, 29, 355002.	0.7	12
33495	Effect of Strain on Polaron Hopping and Electronic Conductivity in Bulk <mml:math xmlns:mml="http://www.w3.org/1998/Math/MathML" display="inline"><mml:mrow><mml:msub><mml:mrow><mml:mi>LiCoO</mml:mi></mml:mrow><mml:mrow><mml:mn>2</mml:mn></ Physical Review Applied, 2017, 7, .	1.5	12
33496	Localization of Electronic States in III-V Semiconductor Alloys: A Comparative Study. Physical Review Applied, 2017, 7, .	1.5	22
33497	Band alignment of semiconductors and insulators using dielectric-dependent hybrid functionals: Toward high-throughput evaluation. Physical Review B, 2017, 95, .	1.1	59
33498	Tuning deep dopants to shallow ones in 2D semiconductors by substrate screening: The case of <mml:math xmlns:mml="http://www.w3.org/1998/Math/MathML"><mml:msub><mml:mi mathvariant="normal">X</mml:mi><mml:mi mathvariant="normal">S</mml:mi></mml:msub></mml:math> (X = Cl, Br, I) in <mml:math xmlns:mml="http://www.w3.org/1998/Math/MathML"><mml:msub><mml:mi>MoS</mml:mi><mml:mn>2</mml:mn></mml:msub></ Physical Review B, 2017, 95, .	1.1	18
33499	Strain induced enhancement of perpendicular magnetic anisotropy in Co/graphene and Co/BN heterostructures. Physical Review B, 2017, 95, .	1.1	89
33500	Palladium-based ferroelectrics and multiferroics: Theory and experiment. Physical Review B, 2017, 95, .	1.1	23
33501	Relativistic coupled-cluster and density-functional studies of argon at high pressure. Physical Review B, 2017, 95, .	1.1	19
33502	Role of the <mml:math xmlns:mml="http://www.w3.org/1998/Math/MathML"><mml:mi>A</mml:mi></mml:math> -site cation in determining the properties of the hybrid perovskite <mml:math xmlns:mml="http://www.w3.org/1998/Math/MathML"><mml:mrow><mml:msub><mml:mi mathvariant="bold">CH</mml:mi><mml:mn>3</mml:mn></mml:msub><mml:msub><mml:mi mathvariant="bold">NH</mml:mi><mml:mn>3</mml:mn></mml:msub><mml:mi mathvariant=	1.1	10

#	Electronic and optical properties of the monolayer group-IV monochalcogenides <mml:math xmlns:mml="http://www.w3.org/1998/Math/MathML"><mml:mrow><mml:mi>M</mml:mi><mml:mi>X</mml:mi></mml:mrow></mml:m	IF	Citations
33503			

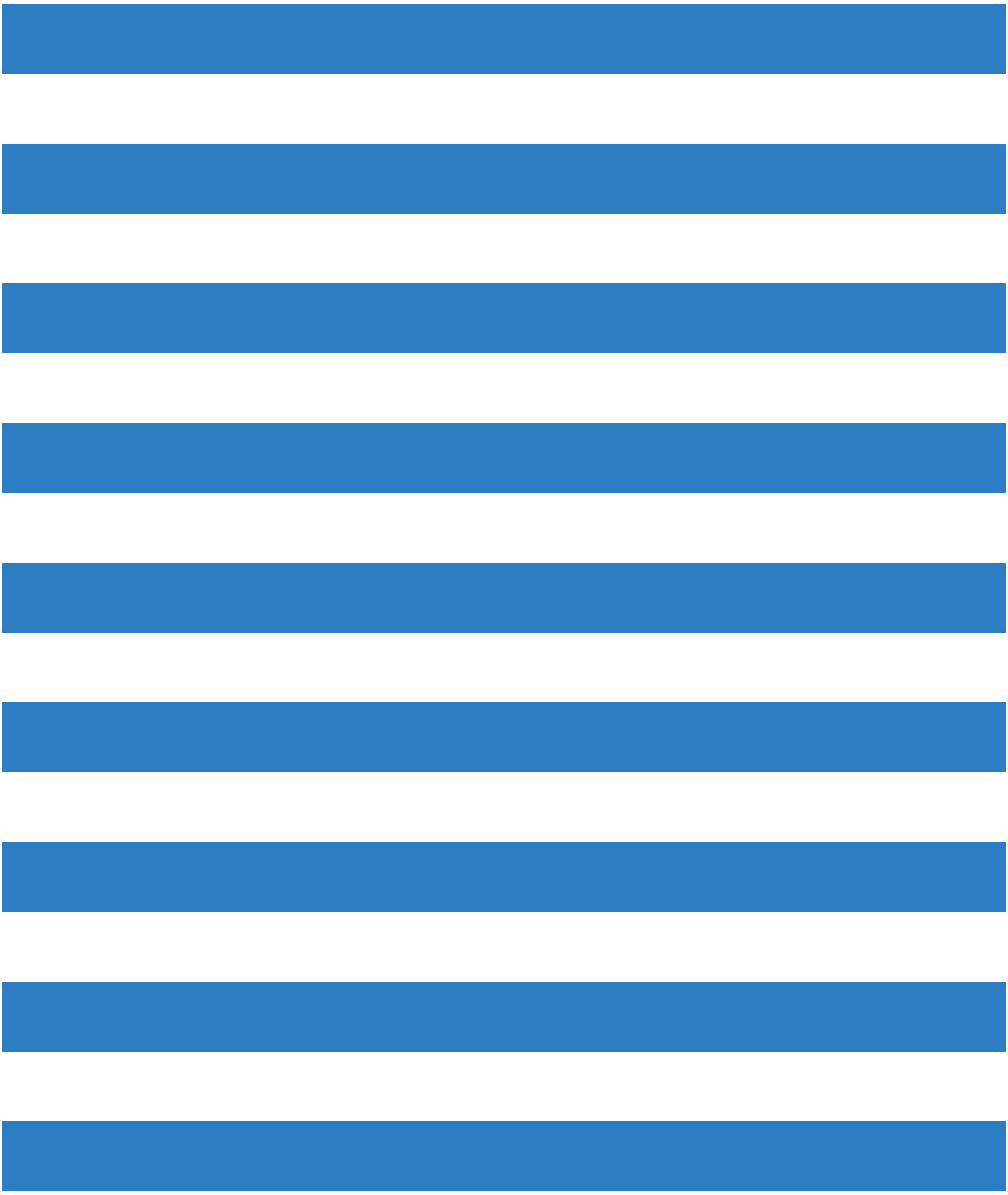

#	Article	IF	Citations
33521	Brittle Fracture of 2D MoSe₂. Advanced Materials, 2017, 29, 1604201.	11.1	138
33522	3D Macroporous Nitrogenâ€Enriched Graphitic Carbon Scaffold for Efficient Bioelectricity Generation in Microbial Fuel Cells. Advanced Energy Materials, 2017, 7, 1601364.	10.2	146
33523	A computational high-throughput search for new ternary superalloys. Acta Materialia, 2017, 122, 438-447.	3.8	70
33524	First principles study of adsorption and oxidation mechanism of elemental mercury by HCl over MoS 2 (1 0 0) surface. Chemical Engineering Journal, 2017, 308, 1225-1232.	6.6	31
33525	A high-performance anode material based on FeMnO3/graphene composite. Journal of Alloys and Compounds, 2017, 695, 1223-1230.	2.8	34
33526	Î±-Fe₂O₃/TiO₂3D hierarchical nanostructures for enhanced photoelectrochemical water splitting. Nanoscale, 2017, 9, 134-142.	2.8	97
33527	DFT study of the structural transformations and absorption properties of crystalline 2,6-dimethyl-4-(diphenylmethylene)-2,5-cyclohexadienone under hydrostatic compression. International Journal of Modern Physics C, 2017, 28, 1750027.	0.8	3
33528	Theoretical study of Sn adsorbed on the Au(1 1 1) surface. Computational Materials Science, 2017, 127, 48-59.	1.4	11
33529	Conetronics in 2D metal-organic frameworks: double/half Dirac cones and quantum anomalous Hall effect. 2D Materials, 2017, 4, 015015.	2.0	41
33530	Highâ€Performance Photothermal Conversion of Narrowâ€Bandgap Ti₂O₃ Nanoparticles. Advanced Materials, 2017, 29, 1603730.	11.1	766
33531	Ab Initio Study of Electronic and Magnetic Properties in TM-Doped Germanene. Journal of Superconductivity and Novel Magnetism, 2017, 30, 1019-1024.	0.8	7
33532	Flexible highly-effective energy harvester via crystallographic and computational control of nanointerfacial morphotropic piezoelectric thin film. Nano Research, 2017, 10, 437-455.	5.8	86
33533	New candidate for the simple cubic carbon sample shock-synthesized by compression of the mixture of carbon black and tetracyanoethylene. Carbon, 2017, 112, 91-96.	5.4	27
33534	Adsorption of As(III) and As(V) compounds on Fe3O4(0 0 1) surfaces: A first principle study. Computational Materials Science, 2017, 127, 110-120.	1.4	18
33535	Strength and ductility of niobium alloys with nonmetallic elements: A first-principles study. Materials Letters, 2017, 189, 310-312.	1.3	21
33536	Electrochemical Reduction of N₂ under Ambient Conditions for Artificial N₂ Fixation and Renewable Energy Storage Using N₂/NH₃ Cycle. Advanced Materials, 2017, 29, 1604799.	11.1	969
33537	Coincidence Lattices and Interlayer Twist in van der Waals Heterostructures: Application of the Coincidence Lattice Method on $$hbox {hBN/MoSe}_2$$ hBN/MoSe 2 Heterobilayer Systems. Journal of Electronic Materials, 2017, 46, 3910-3916.	1.0	9
33538	Methylammonium cation deficient surface for enhanced binding stability at TiO2/CH3NH3PbI3 interface. Nano Research, 2017, 10, 483-490.	5.8	8

#	Article	IF	Citations
33539	Tunable Rashba spin splitting in quantum-spin Hall-insulator AsF bilayers. Nano Research, 2017, 10, 491-502.	5.8	16
33540	Ti/Al co-doping induced residual stress reduction and bond structure evolution of amorphous carbon films: An experimental and ab initio study. Carbon, 2017, 111, 467-475.	5.4	39
33541	Adsorption of small molecules on the [Zn-Zn]2+ linkage in zeolite. A DFT study of ferrierite. Surface Science, 2017, 656, 115-125.	0.8	5
33542	Bending-induced extension in two-dimensional crystals. Acta Mechanica Sinica/Lixue Xuebao, 2017, 33, 71-76.	1.5	8
33543	A new superhard carbon allotrope: tetragonal C64. Journal of Materials Science, 2017, 52, 2385-2391.	1.7	52
33544	High-performance thermal sensitive W-doped VO2(B) thin film and its identification by first-principles calculations. Applied Surface Science, 2017, 397, 30-39.	3.1	27
33545	Na_{2.32}Co_{1.84}(SO₄)₃ as a new member of the alluaudite family of high-voltage sodium battery cathodes. Dalton Transactions, 2017, 46, 55-63.	1.6	52
33546	Interwoven MXene Nanosheet/Carbonâ€Nanotube Composites as Liâ€“S Cathode Hosts. Advanced Materials, 2017, 29, 1603040.	11.1	606
33547	[Ag(OH₂)₂][Ag(SO₄)₂]: A Hydrate of a Silver(II) Salt. Chemistry - A European Journal, 2017, 23, 1805-1813.	1.7	6
33548	Firstâ€principles Studies of the Electronic and Thermoelectric Properties of Misfit Layered Phases of Calcium Cobaltite. Israel Journal of Chemistry, 2017, 57, 522-528.	1.0	2
33549	Validity of Rigid-Band Approximation in the Study of Thermoelectric Properties of p-Type FeNbSb-Based Half-Heusler Compounds. Journal of Electronic Materials, 2017, 46, 3030-3035.	1.0	20
33550	Theoretical insights into the energetics and electronic properties of MPt12 (M = Fe, Co, Ni, Cu, and Pd) nanoparticles supported by N-doped defective graphene. Applied Surface Science, 2017, 397, 199-205.	3.1	25
33551	Adsorption of formaldehyde molecule on the pristine and transition metal doped graphene: First-principles study. Applied Surface Science, 2017, 396, 1020-1025.	3.1	72
33552	Global structural optimization and growth mechanism of cobalt oxide nanoclusters by genetic algorithm with spin-polarized DFT. Journal of Alloys and Compounds, 2017, 695, 2513-2518.	2.8	4
33553	Structure of a model TiO2Âphotocatalytic interface. Nature Materials, 2017, 16, 461-466.	13.3	234
33554	Adsorption of CO molecules on the Si(111)-(7Ã—7) surface. Surface Science, 2017, 656, 33-38.	0.8	5
33555	First principles calculations of beryllium stability in zirconium surfaces. Acta Materialia, 2017, 122, 359-368.	3.8	9
33556	Influence of grain boundaries on the radiation-induced defects and hydrogen in nanostructured and coarse-grained tungsten. Acta Materialia, 2017, 122, 277-286.	3.8	69

#	Article	IF	Citations
33557	Tuning the band gap and optical spectra of silicon-doped graphene: Many-body effects and excitonic states. Journal of Alloys and Compounds, 2017, 693, 1185-1196.	2.8	119
33558	DFT and spectroelectrochemical study of cyanate adsorption on gold single crystal electrodes in neutral medium. Journal of Electroanalytical Chemistry, 2017, 793, 147-156.	1.9	9
33559	Effect of Ti/Cr additive on helium diffusion and segregation in dilute vanadium alloys. Nuclear Instruments & Methods in Physics Research B, 2017, 393, 130-134.	0.6	10
33560	Engineering Valence Band Dispersion for High Mobility p-Type Semiconductors. Chemistry of Materials, 2017, 29, 2402-2413.	3.2	66
33561	Bubble growth from clustered hydrogen and helium atoms in tungsten under a fusion environment. Nuclear Fusion, 2017, 57, 016006.	1.6	23
33562	Confined chemical and structural states at dislocations in Fe-9wt%Mn steels: A correlative TEM-atom probe study combined with multiscale modelling. Acta Materialia, 2017, 124, 305-315.	3.8	73
33563	A first-principles study of the preventive effects of Al and Mg doping on the degradation in LiNi_{0.8}Co_{0.1}Mn_{0.1}O₂ cathode materials. Physical Chemistry Chemical Physics, 2017, 19, 1762-1769.	1.3	172
33564	Adjusting band gap and charge transfer of organometallic complex adsorbed on MoS₂monolayer using vertical electric-field: a first-principles investigation. Journal of Physics Condensed Matter, 2017, 29, 015003.	0.7	2
33565	A Comprehensive Approach toward Stable Lithiumâ€“Sulfur Batteries with High Volumetric Energy Density. Advanced Energy Materials, 2017, 7, 1601630.	10.2	277
33566	Understanding the Reaction Mechanism of Glycerol Hydrogenolysis over a CuCr₂O₄ Catalyst. ChemSusChem, 2017, 10, 442-454.	3.6	13
33567	Black Phosphorus Nâ€Type Fieldâ€Effect Transistor with Ultrahigh Electron Mobility via Aluminum Adatoms Doping. Small, 2017, 13, 1602909.	5.2	61
33568	Strain induced polymorphism and band structure modulation in low-temperature 2,7-dioctyl[1]benzothieno[3,2-b][1]benzothiophene single crystal. Science China Chemistry, 2017, 60, 275-283.	4.2	4
33569	Dirac cones and highly anisotropic electronic structure of super-graphyne. Carbon, 2017, 113, 40-45.	5.4	34
33570	Quantum-chemical prediction of the effects of Ni-loading on the hydrogenation and water-splitting efficiency of TiO2 nanoparticles with an experimental test. Chemical Physics Letters, 2017, 667, 278-283.	1.2	4
33571	First-principles structure optimization of scandium and lutetium trihydrides. Journal of Alloys and Compounds, 2017, 696, 96-101.	2.8	0
33572	Mechanical properties of refractory high-entropy alloys: Experiments and modeling. Journal of Alloys and Compounds, 2017, 696, 1139-1150.	2.8	307
33573	One-step electrodeposited 3D-ternary composite of zirconia nanoparticles, rGO and polypyrrole with enhanced supercapacitor performance. Nano Energy, 2017, 31, 225-232.	8.2	86
33574	New ultra-incompressible phases of NbB4 predicted from first principles. Physics Letters, Section A: General, Atomic and Solid State Physics, 2017, 381, 362-367.	0.9	7

#	Article	IF	Citations
33575	Two single-layer porous gallium nitride nanosheets: A first-principles study. Solid State Communications, 2017, 250, 18-22.	0.9	28
33576	Metallic NiPS₃@NiOOH Coreâ€“Shell Heterostructures as Highly Efficient and Stable Electrocatalyst for the Oxygen Evolution Reaction. ACS Catalysis, 2017, 7, 229-237.	5.5	233
33577	A DFT Investigation of the Mechanism of Propene Ammoxidation over Î±-Bismuth Molybdate. ACS Catalysis, 2017, 7, 161-176.	5.5	26
33578	Composition- and temperature-dependent liquid structures in Alâ€“Cu alloys: anab initiomolecular dynamics and x-ray diffraction study. Journal of Physics Condensed Matter, 2017, 29, 035101.	0.7	13
33579	Rare Earth Interstitials in Ge: A Hybrid Density Functional Theory Study. Journal of Electronic Materials, 2017, 46, 1022-1029.	1.0	8
33580	A DFT study of the interaction between large PAHs and atomic chlorine or hydrogen chloride molecule: Toward a modelling of the influence of chlorinated species on the trapping of water by soot. Chemical Physics, 2017, 483-484, 46-55.	0.9	3
33581	Quantum molecular dynamics: Accelerating diffusion via parallel replica method.. Computational Materials Science, 2017, 128, 1-7.	1.4	2
33582	A theoretical study of the effects of sp-elements on hydrogen in nickel-based alloys. Computational Materials Science, 2017, 128, 37-41.	1.4	3
33583	Density functional theory model of amorphous zinc oxide (a-ZnO) and a-X0.375Z0.625O (X= Al, Ga and) Tj ETQq0 0 0 rgBT /Overlock 10	1.5	10
33584	The helium effect at grain boundaries in Fe-Cr alloys: A first-principles study. Nuclear Instruments & Methods in Physics Research B, 2017, 393, 118-121.	0.6	2
33585	First-principles investigation of mechanical properties of silicene, germanene and stanene. Physica E: Low-Dimensional Systems and Nanostructures, 2017, 87, 228-232.	1.3	158
33586	Electric field modulation of the band structure in MoS2/WS2 van der waals heterostructure. Solid State Communications, 2017, 250, 9-13.	0.9	34
33587	Reduction of Fermi level pinning at Auâ€“MoS ₂ interfaces by atomic passivation on Au surface. 2D Materials, 2017, 4, 015019.	2.0	40
33588	Comparative study on hydrogenation of propanal on Ni(111) and Cu(111) from density functional theory. Applied Surface Science, 2017, 394, 333-339.	3.1	22
33589	Controlling nucleation, growth, and orientation of metal halide perovskite thin films with rationally selected additives. Journal of Materials Chemistry A, 2017, 5, 113-123.	5.2	115
33590	The Gaussian distribution of lattice size and atomic level heterogeneity in high entropy alloys. Extreme Mechanics Letters, 2017, 11, 84-88.	2.0	36
33591	First-principles calculations of Ti 3 SiC 2 and Ti 3 AlC 2 with hydrogen interstitial. Journal of Nuclear Materials, 2017, 488, 261-266.	1.3	14
33592	Precipitation in a copper matrix modeled byab initiocalculations and atomistic kinetic Monte Carlo simulations. Physica Status Solidi (B): Basic Research, 2017, 254, 1600407.	0.7	7

#	Article	IF	Citations
33593	Quaternary non-centrosymmetric sulfide Y 4 GaSbS 9 : Syntheses, structures, optical properties and theoretical studies. Journal of Solid State Chemistry, 2017, 245, 110-114.	1.4	13
33594	Mechanical alloying as a new synthesis route for metastable silicon clathrates. Materials Letters, 2017, 187, 1-3.	1.3	3
33595	Does aluminum play well with others? Intrinsic Al-A alloying behavior in 211/312 MAX phases. Materials Research Letters, 2017, 5, 170-178.	4.1	20
33596	Reduced work function of graphene by metal adatoms. Applied Surface Science, 2017, 394, 98-107.	3.1	36
33597	Sn(II)-Containing Phosphates as Optoelectronic Materials. Chemistry of Materials, 2017, 29, 2459-2465.	3.2	17
33598	Metalâ€Free Dual Modal Contrast Agents Based on Fluorographene Quantum Dots. Particle and Particle Systems Characterization, 2017, 34, 1600221.	1.2	25
33599	Theory and Analysis of XAFS. , 2017, , 13-50.		2
33600	A lightweight single-phase AlTiVCr compositionally complex alloy. Acta Materialia, 2017, 123, 115-124.	3.8	151
33601	Energy Level Shifts at the Silica/Ru(0001) Heterojunction Driven by Surface and Interface Dipoles. Topics in Catalysis, 2017, 60, 481-491.	1.3	32
33602	Passivation for Cu 2 ZnSnS 4 /WZ-ZnO interface states: From the first principles calculations. Applied Surface Science, 2017, 394, 58-62.	3.1	6
33603	A comparative study of magnetic and optical properties of Mn-, Gd-, and Nd-doped ZnO nanowires. International Journal of Modern Physics B, 2017, 31, 1650241.	1.0	3
33604	Creating the Smallest BN Nanotube from Bilayer hâ€BN. Advanced Functional Materials, 2017, 27, 1603897.	7.8	28
33605	Hierarchical Chemical Bonds Contributing to the Intrinsically Low Thermal Conductivity in Î±â€MgAgSb Thermoelectric Materials. Advanced Functional Materials, 2017, 27, 1604145.	7.8	195
33606	Tuning the magnetic properties of pure hafnium by high pressure torsion. Acta Materialia, 2017, 123, 206-213.	3.8	14
33607	Ab initio calculations of the lattice parameter and elastic stiffness coefficients of bcc Fe with solutes. Computational Materials Science, 2017, 126, 503-513.	1.4	36
33608	Tunable magnetism in 2D silicon carbide doped with Co and Fe dopants: Ab initio study. Optik, 2017, 130, 589-593.	1.4	8
33609	Structural, magnetic and electronic properties of single Iron atom at graphene edges. Physica E: Low-Dimensional Systems and Nanostructures, 2017, 86, 243-247.	1.3	2
33610	Energetics of cobalt alloys and compounds and soluteâ€“vacancy binding in fcc cobalt: A first-principles database. Acta Materialia, 2017, 124, 1-8.	3.8	18

#	Article	IF	Citations
33611	Vibrational spectrum and entropy in simulation of melting. Computational Materials Science, 2017, 127, 42-47.	1.4	15
33612	Determination of calcium carbonate and sodium carbonate melting curves up to Earth's transition zone pressures with implications for the deep carbon cycle. Earth and Planetary Science Letters, 2017, 457, 395-402.	1.8	50
33613	The role of H ₂ O and O ₂ molecules and phosphorus vacancies in the structure instability of phosphorene. 2D Materials, 2017, 4, 015010.	2.0	101
33614	First-Principles Study on Lattice Structures and Bonding Character of CoSb3/Ti Interface. Journal of Electronic Materials, 2017, 46, 2929-2935.	1.0	1
33615	Comprehensive first-principles study of stable stacking faults in hcp metals. Acta Materialia, 2017, 123, 223-234.	3.8	139
33616	DFT +U studies of triclinic phase of BiNiO3 and La-substituted BiNiO3. Computational Materials Science, 2017, 126, 407-417.	1.4	6
33617	High pressure synthesis, structure and thermoelectric properties of BiCuChO (Ch = S, Se, Te). Journal of the European Ceramic Society, 2017, 37, 1541-1546.	2.8	39
33618	2Flux growth and characterization of Ce-substituted <mml:math xmlns:mml="http://www.w3.org/1998/Math/MathML" altimg="si0047.gif" overflow="scroll"><mml:mrow><mml:msub><mml:mrow><mml:mi>Nd</mml:mi></mml:mrow><mml:mrow><mml:mn>2</mml:mn></mml:mrow></mml:msub><mml:mrow><mml:mi mathvariant="normal">B</mml:mi></mml:mrow></mml:math> single crystals. Journal of Magnetism and Magnetic Materials, 2017, 434, 1-9.	1.0	36
33619	Helium diffusion in pure hematite (Î±-Fe2O3) for thermochronometric applications: A theoretical multi-scale study. Computational and Theoretical Chemistry, 2017, 1099, 21-28.	1.1	23
33620	Electronic structure of RMn2Si2 (RÂ=ÂY, La) intermetallics: DFT and XPS studies. Journal of Alloys and Compounds, 2017, 695, 1663-1671.	2.8	9
33621	Doping induced dimensionality reduction of the magnetic order in DyFe1-In O3. Journal of Alloys and Compounds, 2017, 695, 1699-1705.	2.8	2
33622	Evolutionary algorithm based structure search and first-principles study of B12C3 polytypes. Journal of Alloys and Compounds, 2017, 695, 2023-2034.	2.8	10
33623	Precursor States of Organic Adsorbates on Semiconductor Surfaces are Chemisorbed and Immobile. ChemPhysChem, 2017, 18, 34-38.	1.0	24
33624	Local variation in Bi crystal sites of epitaxial GaAsBi studied by photoelectron spectroscopy and first-principles calculations. Applied Surface Science, 2017, 396, 688-694.	3.1	5
33625	Tantalum surface oxidation: Bond relaxation, energy entrapment, and electron polarization. Applied Surface Science, 2017, 396, 177-184.	3.1	9
33626	Investigations on the origin of ferromagnetism of Cu doped anatase TiO 2 nanotubes. Materials Research Bulletin, 2017, 86, 287-294.	2.7	11
33627	Magnetization and Spin Polarization of Heusler Alloys Co $_{2}$TiSn and Co$_{2}$ TiGa$_{0.5}$Sn $_{0.5}$. IEEE Magnetics Letters, 2017, 8, 1-4.	0.6	4
33628	Structural, electronic and magnetic properties of RE3+-doping in CoFe2O4: A first-principles study. Journal of Magnetism and Magnetic Materials, 2017, 421, 300-305.	1.0	28

#	Article	IF	Citations
33629	Robust ruthenium catalysts for the selective conversion of stearic acid to diesel-range alkanes. Applied Catalysis B: Environmental, 2017, 201, 137-149.	10.8	60
33630	A density functional theory investigation of oxalate and Fe(II) adsorption onto the (010) goethite surface with implications for ligand- and reduction-promoted dissolution. Chemical Geology, 2017, 464, 14-22.	1.4	41
33631	Calcium Doping of Lithium Titanium Oxide Nanospheres: A Combined Firstâ€Principles and Experimental Study. Energy Technology, 2017, 5, 539-543.	1.8	14
33632	Size-dependence of carbon nanotube confinement in catalysis. Chemical Science, 2017, 8, 278-283.	3.7	53
33633	Magnetism of coherent Co and Ni thin films on Cu(111) and Au(111) substrates: An ab initio study. Journal of Magnetism and Magnetic Materials, 2017, 424, 394-401.	1.0	1
33634	Sublattice dependent magnetic response of dual Cr doped graphene monolayer: a full potential approach. Indian Journal of Physics, 2017, 91, 43-51.	0.9	6
33635	Versatile two-dimensional stanene-based membrane for hydrogen purification. International Journal of Hydrogen Energy, 2017, 42, 5577-5583.	3.8	13
33636	Predicting the structural and electronic properties of transition metal monoxides from bulk to surface morphology. Catalysis Today, 2017, 282, 96-104.	2.2	6
33637	Mechanisms of removal of three widespread pharmaceuticals by two clay materials. Journal of Hazardous Materials, 2017, 323, 575-583.	6.5	66
33638	First-principles study of the Hf-based Heusler alloys: Hf2CoGa and Hf2CoIn. Journal of Magnetism and Magnetic Materials, 2017, 421, 1-6.	1.0	15
33639	Modulating the phases of iron carbide nanoparticles: from a perspective of interfering with the carbon penetration of Fe@Fe₃O₄ by selectively adsorbed halide ions. Chemical Science, 2017, 8, 473-481.	3.7	105
33640	High halogenated nitrobenzene hydrogenation selectivity over nano Ir particles. Chinese Journal of Chemical Engineering, 2017, 25, 306-312.	1.7	20
33641	Thermoelectric transport properties of tetradymite-type Pb1-Sn Bi2Te4 compounds. Journal of Alloys and Compounds, 2017, 690, 966-970.	2.8	7
33642	Efficient photocatalytic hydrogen production over solid solutions Sr1-xBixTi1-xFexO3 (0 â‰¤ x â‰¤ 0.5). Applied Catalysis B: Environmental, 2017, 200, 412-419.	10.8	67
33643	Combined effect of Mg and vacancy on the generalized planar fault energy of Al. Journal of Alloys and Compounds, 2017, 690, 841-850.	2.8	21
33644	Hydrogenated and halogenated blue phosphorene as Dirac materials: A first principles study. Applied Surface Science, 2017, 392, 46-50.	3.1	64
33645	Design of Mg alloys: The effects of Li concentration on the structure and elastic properties in the Mg-Li binary system by first principles calculations. Journal of Alloys and Compounds, 2017, 691, 15-25.	2.8	41
33646	First-principles study on the solubility of iron in dilute Cu-Fe-X alloys. Journal of Alloys and Compounds, 2017, 691, 992-996.	2.8	24

#	Article	IF	Citations
33647	Vibrational monitor of early demineralization in tooth enamel after in vitro exposure to phosphoridic liquid. Spectrochimica Acta - Part A: Molecular and Biomolecular Spectroscopy, 2017, 173, 19-33.	2.0	22
33648	Orientational order controls crystalline andÂamorphous thermal transport in superatomicÂcrystals. Nature Materials, 2017, 16, 83-88.	13.3	94
33649	Structural, Electronic, and Magnetic Properties of Bimetallic Ni m Nb n (m + n â‰¤ 8) Clusters: First Principle Study. Journal of Superconductivity and Novel Magnetism, 2017, 30, 251-260.	0.8	3
33650	Phase formation of Nb2AlC investigated by combinatorial thin film synthesis and ab initio calculations. Journal of the European Ceramic Society, 2017, 37, 35-41.	2.8	7
33651	Data-Driven First-Principles Methods for the Study and Design of Alkali Superionic Conductors. Chemistry of Materials, 2017, 29, 281-288.	3.2	190
33652	Discovery of a Novel Sn(II)â€Based Oxide Î²â€²SnMoO₄ for Daylightâ€Driven Photocatalysis. Advanced Science, 2017, 4, 1600246.	5.6	22
33653	Lithium ion adsorption and diffusion on black phosphorene nanotube: A first-principles study. Applied Surface Science, 2017, 392, 88-94.	3.1	32
33654	Dispersion-corrected DFT study on the structural transformations and absorption properties of crystalline 3â€²-Amino-3â€²-deoxyadenosine. Journal of Molecular Structure, 2017, 1128, 151-161.	1.8	4
33655	N2O formation and dissociation during ammonia combustion: A combined DFT and experimental study. Proceedings of the Combustion Institute, 2017, 36, 637-644.	2.4	5
33656	Structural, mechanical, electronic, and thermodynamic properties of dense B₃N₄ under high pressure predicted from first principles. Physica Status Solidi (B): Basic Research, 2017, 254, 1600312.	0.7	1
33657	Ab initio study of electronic and magnetic properties in TM-doped 2D silicon carbide. Physica E: Low-Dimensional Systems and Nanostructures, 2017, 85, 280-284.	1.3	16
33658	Adsorption of transition metal adatoms on h-BN/Rh(111): Implications for nanocluster self-assembly. Catalysis Today, 2017, 280, 220-231.	2.2	15
33659	Role of grain boundary character on oxygen and hydrogen segregation-induced embrittlement in polycrystalline Ni. Journal of Materials Science, 2017, 52, 30-45.	1.7	30
33660	Simulated Temperature Programmed Desorption of Acetaldehyde on CeO2(111): Evidence for the Role of Oxygen Vacancy and Hydrogen Transfer. Topics in Catalysis, 2017, 60, 446-458.	1.3	15
33661	Characterizing chemical stability and proton conductivity of B-site doped barium hafnate (BaHfO3) and barium stannate (BaSnO3) with first principles modeling. Journal of Alloys and Compounds, 2017, 693, 738-743.	2.8	22
33662	A planar carbon allotrope with linear bipentagon-octagon and hexagon arrangement. Physica E: Low-Dimensional Systems and Nanostructures, 2017, 87, 107-111.	1.3	7
33663	Bulk modulus and thermodynamic properties of L21 Ni2 XY (XÂ=ÂMn, Fe, Co, YÂ=ÂGa, In) compounds studied by first-principles calculations. Journal of Materials Science, 2017, 52, 1149-1155.	1.7	2
33664	Magnetic behavior of superatomic-fullerene assemblies. Physical Chemistry Chemical Physics, 2017, 19, 996-1002.	1.3	5

#	Article	IF	Citations
33665	Electronic charge transfer contribution in adsorption of silicon at the SiC(0001) surfaceâ€"A density functional theory (DFT) study. Applied Surface Science, 2017, 393, 168-179.	3.1	8
33666	Geometric, electronic, magnetic and catalytic properties of carbon deposited on metal embedded graphene. Computational Materials Science, 2017, 126, 74-81.	1.4	2
33667	Stereochemistry of nitrogen E lone pair in NH3E, NOFE, N2O3E2, AgNO2E, and NCl3E. Comptes Rendus Chimie, 2017, 20, 446-459.	0.2	8
33668	Temperature-dependent stable phase domains of Zrâ€"Câ€"N (Zrâ€"ZrCâ€"ZrC0.96â€"Zr(C1â^'N)â^'ZrN, xÂ=Â0.1â€"0.9) systems from ab initio calculations and experimental results. Journal of Alloys and Compounds, 2017, 692, 997-1003.	2.8	9
33669	Thermodynamic reassessment of the Niâ€"Siâ€"Ti system using a four-sublattice model for ordered/disordered fcc phases supported by first-principles calculations. Journal of Alloys and Compounds, 2017, 693, 344-356.	2.8	21
33670	First-principles calculations and thermodynamic modeling of the S-Se system and implications for chalcogenide alloys. Journal of Alloys and Compounds, 2017, 694, 510-521.	2.8	7
33671	Ab initio studies on electronic and magnetic properties of X2PtGa (X=Cr, Mn, Fe, Co) Heusler alloys. Journal of Magnetism and Magnetic Materials, 2017, 423, 395-404.	1.0	28
33672	Effect of Au clustering on ferromagnetism in Au doped TiO2 films: theory and experiments investigation. Journal of Physics and Chemistry of Solids, 2017, 100, 71-77.	1.9	12
33673	The catalytic oxidation of NH3 on Co3O4(110): A theoretical study. Proceedings of the Combustion Institute, 2017, 36, 4365-4373.	2.4	15
33674	Elastic properties of the sigma W-Re phase: A first principles investigation. Scripta Materialia, 2017, 128, 45-48.	2.6	18
33675	Unusual Feâ€"H bonding associated with oxygen vacancies at the (001) surface of Fe3O4. Surface Science, 2017, 655, 25-30.	0.8	31
33676	Tuning Crystal Structures and Thermoelectric Properties through Al Doping in ReSi_{1.75}. European Journal of Inorganic Chemistry, 2017, 2017, 47-55.	1.0	6
33677	Stacking fault energy of C-alloyed steels: The effect of magnetism. Acta Materialia, 2017, 122, 72-81.	3.8	30
33678	Insight into chemoselectivity of nitroarene hydrogenation: A DFT-D3 study of nitroarene adsorption on metal surfaces under the realistic reaction conditions. Applied Surface Science, 2017, 392, 456-471.	3.1	25
33679	Carbon nanohoops as attractive toughening and lubricant agents in TiN porous films. Applied Surface Science, 2017, 393, 60-66.	3.1	10
33680	Nitrogen coordinated silicon-doped graphene as a potential alternative metal-free catalyst for CO oxidation. Carbon, 2017, 111, 448-458.	5.4	97
33681	Unusually high electron density in an intermolecular non-bonding region: Role of metal substrate. Chinese Chemical Letters, 2017, 28, 759-764.	4.8	11
33682	Parallel 3-dim fast Fourier transforms with load balancing of the plane waves. Computer Physics Communications, 2017, 211, 54-60.	3.0	7

#	Article	IF	Citations
33683	Enhancing the dehydriding properties of perovskite-type NaMgH3 by introducing potassium as dopant. International Journal of Hydrogen Energy, 2017, 42, 3716-3722.	3.8	18
33684	Density functional theory investigations into the structures and acidity properties of Ti-doped SSZ-13 zeolite. Microporous and Mesoporous Materials, 2017, 237, 132-139.	2.2	14
33685	Strain-Controlled Transport Mechanism in Strongly Correlated LaNiO3. Journal of Electronic Materials, 2017, 46, 150-157.	1.0	9
33686	Theoretical study of high-pressure phase stability of NaZr2(PO4)3 via elastic constants and equation of state. Indian Journal of Physics, 2017, 91, 277-286.	0.9	1
33687	Atomic-resolution evaluation of microsegregation and degree of atomic order at antiphase boundaries in Ni50Mn20In30 Heusler alloy. Acta Materialia, 2017, 122, 166-177.	3.8	14
33688	The effects of nonmetal dopants on the electronic, optical and chemical performances of monolayer gâ€“C3N4 by first-principles study. Applied Surface Science, 2017, 392, 966-974.	3.1	106
33689	Structural, energetic and dynamical properties of ordered and disordered bcc Fe25at.%Ni alloys: A first-principles study. Computational Materials Science, 2017, 126, 82-89.	1.4	4
33690	First-principles study on the adhesive properties of Al/TiC interfaces: Revisited. Computational Materials Science, 2017, 126, 108-120.	1.4	23
33691	Benchmark problems for numerical implementations of phase field models. Computational Materials Science, 2017, 126, 139-151.	1.4	57
33692	Absence of Dirac cones in monolayer silicene and multilayer Si films on Ag(111). Journal of Electron Spectroscopy and Related Phenomena, 2017, 219, 2-8.	0.8	18
33693	High-pressure lattice-dynamics of NdVO4. Journal of Physics and Chemistry of Solids, 2017, 100, 126-133.	1.9	24
33694	Interaction of O2 with monolayer MoS2: Effect of doping and hydrogenation. Materials and Design, 2017, 113, 1-8.	3.3	28
33695	First-principles investigation on slip systems and twinnability of TiC. Computational Materials Science, 2017, 126, 103-107.	1.4	14
33696	Electrochemical Effects at Surfactantâ€“Platinum Nanoparticle Interfaces Boost Catalytic Performance. ChemCatChem, 2017, 9, 604-609.	1.8	14
33697	Hydrogenation of o-cresol on platinum catalyst: Catalytic experiments and first-principles calculations. Applied Surface Science, 2017, 393, 212-220.	3.1	23
33698	Doping effect of copper zinc tin sulphide counter electrode for dye-sensitized solar cells. Computational Materials Science, 2017, 126, 160-169.	1.4	6
33699	A first-principles study on the origin of magnetism induced by intrinsic defects in monolayer SnS2. Computational Materials Science, 2017, 126, 52-58.	1.4	31
33700	Interplay of Cation Ordering and Ferroelectricity in Perovskite Tin Iodides: Designing a Polar Halide Perovskite for Photovoltaic Applications. Inorganic Chemistry, 2017, 56, 26-32.	1.9	37

#	Article	IF	Citations
33701	Interfacial acidity in ligand-modified ruthenium nanoparticles boosts the hydrogenation of levulinic acid to gamma-valerolactone. Green Chemistry, 2017, 19, 2361-2370.	4.6	58
33702	Computational investigation of the kinetics and mechanism of the initial steps of the Fischerâ€“Tropsch synthesis on cobalt. Faraday Discussions, 2017, 197, 117-151.	1.6	37
33703	Temperature dependent phase stability of Ti(C1â^'N) solid solutions using first-principles calculations. Ceramics International, 2017, 43, 650-657.	2.3	16
33704	An Ab Initio Study of Carbon-Induced Ordering in Austenitic Fe-Mn-Al-C Alloys. Steel Research International, 2017, 88, 1600292.	1.0	14
33705	Empirical Evidence for Aâ€Site Order in Perovskites. Journal of the American Ceramic Society, 2017, 100, 429-442.	1.9	5
33706	Adsorption and Dimerization of Late Transition Metal Atoms on the Regular and Defective Quartz (001) Surface. Topics in Catalysis, 2017, 60, 459-470.	1.3	13
33707	Ab-initio study of C and N point defects in the C14-Fe2Nb phase. Journal of Alloys and Compounds, 2017, 693, 1315-1322.	2.8	6
33708	Dissociation and reconstruction of double-decker bis(phthalocyaninato) terbium(III) complex (TbPc2) on Pd(001): A theoretical investigation. Surface Science, 2017, 655, 12-16.	0.8	4
33709	Adsorption of hydrogen on stable and metastable Ir(100) surfaces. Surface Science, 2017, 656, 66-76.	0.8	9
33710	Adsorption sensitivity of metal atom decorated bilayer graphene toward toxic gas molecules (CO, NO,) Tj ETQq1 1 0.784314 rgBT /Ov	4.0	105
33711	A periodic-DFT study of retro-aldol fragmentation of fuctose on MoO3. Applied Catalysis A: General, 2017, 530, 75-82.	2.2	6
33712	First-principles study of codoping TiO2 systems capable of improving the specific surface area and the dissociation of H2O to generate H2 and O2. Computational Materials Science, 2017, 127, 204-210.	1.4	7
33713	Influence of alloying elements on stability and electronic structures of Cu6Sn5(0 1 0) surface by first principles calculations. Computational Materials Science, 2017, 127, 230-235.	1.4	2
33714	Highly optimized embedding atom method potential for Pt-Cu alloys. Journal of Alloys and Compounds, 2017, 696, 470-480.	2.8	5
33715	Density functional theory study of dopant effect on formation energy of intrinsic point defects in germanium crystals. Journal of Crystal Growth, 2017, 474, 104-109.	0.7	4
33716	Spin transport properties in silicene-based heterojunctions with different edge hydrogenation. Organic Electronics, 2017, 41, 333-339.	1.4	12
33717	Synthesis, X-ray structure, spectroscopic (IR, NMR) analysis and DFT modeling of a new polymeric Zinc(II) complex of cystamine, [Zn(Cym-Cym)Cl2]. Polyhedron, 2017, 122, 105-115.	1.0	5
33718	The properties of isolated dangling bonds on hydrogenated 2H-SiC surfaces. Surface Science, 2017, 656, 109-114.	0.8	5

#	Article	IF	Citations
33719	LEED â€“ IV and DFT study of the co-adsorption of chlorine and water on Cu(100). Surface Science, 2017, 657, 51-57.	0.8	4
33720	First-principles studies of the structural, elastic, and lattice dynamical properties of ZrMo₂ and HfMo₂. Phase Transitions, 2017, 90, 598-609.	0.6	21
33721	Thermal response in van der Waals heterostructures. Journal of Physics Condensed Matter, 2017, 29, 035504.	0.7	4
33722	Metalated graphene nanoplatelets and their uses as anode materials for lithium-ion batteries. 2D Materials, 2017, 4, 014002.	2.0	15
33723	Nobleâ€Metalâ€Free Hybrid Membranes for Highly Efficient Hydrogen Evolution. Advanced Materials, 2017, 29, 1603617.	11.1	73
33724	Reprint of â€œTheoretical description of metal/oxide interfacial properties: The case of MgO/Ag(001)â€• Applied Surface Science, 2017, 396, 1850-1854.	3.1	0
33725	Van-der-Waals-gap tunneling spectroscopy for single-wall carbon nanotubes. Carbon, 2017, 113, 237-242.	5.4	9
33726	Surface excess elasticity of gold: Ab initio coefficients and impact on the effective elastic response of nanowires. Acta Materialia, 2017, 124, 468-477.	3.8	32
33727	Gentle way to build reduced titanium dioxide nanodots integrated with graphite-like carbon spheres: From DFT calculation to experimental measurement. Applied Catalysis B: Environmental, 2017, 204, 283-295.	10.8	45
33728	Half-metallicity and high spin-filtering effect of magnetic atoms embedded zigzag 6, 6, 12-graphyne nanoribbon. Carbon, 2017, 113, 170-175.	5.4	24
33729	Thermal equilibrium concentration of intrinsic point defects in heavily doped silicon crystals - Theoretical study of formation energy and formation entropy in area of influence of dopant atoms-. Journal of Crystal Growth, 2017, 474, 110-120.	0.7	4
33730	Dependence of improper ferroelectricity on the preferred orientation of Mn3 spins in CaMn 7 O 12. Journal of Magnetism and Magnetic Materials, 2017, 424, 314-322.	1.0	5
33731	Tuning the Schottky barrier in the arsenene/graphene van der Waals heterostructures by electric field. Physica E: Low-Dimensional Systems and Nanostructures, 2017, 88, 6-10.	1.3	37
33732	Electronic and magnetic properties of Mn-doped WSe 2 monolayer under strain. Physica E: Low-Dimensional Systems and Nanostructures, 2017, 88, 11-17.	1.3	13
33733	Edge passivation induced single-edge ferromagnetism of zigzag MoS2 nanoribbons. Physics Letters, Section A: General, Atomic and Solid State Physics, 2017, 381, 301-306.	0.9	15
33734	Computational investigations on band structure and electronic features of chromium-based carbides and nitride Cr3PX (XÂ=ÂC and N) through the FP-APW+LO approach. Superlattices and Microstructures, 2017, 109, 1-12.	1.4	10
33735	Non-reactively sputtered ultra-high temperature Hf-C and Ta-C coatings. Surface and Coatings Technology, 2017, 309, 436-444.	2.2	35
33736	Spatial manipulating spin-polarization and tunneling patterns in graphene spirals via periphery structural modification. Carbon, 2017, 113, 325-333.	5.4	12

#	Article	IF	Citations
33737	First-principles study of coherent interfaces of Laves-phase MgZn2 and stability of thin MgZn2 layers in Mg-Zn alloys. Journal of Alloys and Compounds, 2017, 696, 109-117.	2.8	25
33738	Ab initio study of interstitial cluster interaction with Re, Os, and TaÂinÂW. Journal of Nuclear Materials, 2017, 484, 30-41.	1.3	42
33739	Identifying anthropogenic uranium compounds using soft X-ray near-edge absorption spectroscopy. Spectrochimica Acta, Part B: Atomic Spectroscopy, 2017, 127, 20-27.	1.5	7
33740	Tunable magneto-optical effects in hole-doped group-IIIA metal-monochalcogenide monolayers. 2D Materials, 2017, 4, 015017.	2.0	47
33741	Comparison of performance of van der Waals-corrected exchange-correlation functionals for interlayer interaction in graphene and hexagonal boron nitride. Computational Materials Science, 2017, 128, 45-58.	1.4	72
33742	On the photophysics and speciation of actinide ion in MgAl2O4 spinel using photoluminescence spectroscopy and first principle calculation: A case study with uranium. Journal of Alloys and Compounds, 2017, 695, 337-343.	2.8	16
33743	Theory-Driven Insight into the Crystal Packing of Trialkylsilylethynyl Pentacenes. Chemistry of Materials, 2017, 29, 2502-2512.	3.2	30
33744	Xâ€“H Bond Activation on Cr(III),O Sites (X = R, H): Key Steps in Dehydrogenation and Hydrogenation Processes. Organometallics, 2017, 36, 234-244.	1.1	51
33745	Shape, electronic structure and steric effects of organometallic nanocatalysts: relevant tools to improve the synergy between theory and experiment. Dalton Transactions, 2017, 46, 378-395.	1.6	17
33746	Two-dimensional hexagonal CrN with promising magnetic and optical properties: A theoretical prediction. Nanoscale, 2017, 9, 621-630.	2.8	66
33747	Density functional theory-based cluster expansion to simulate thermal annealing in FeCrW alloys. Philosophical Magazine, 2017, 97, 299-317.	0.7	11
33748	First-principles phase diagram calculations for the rocksalt-structure quasibinary systems TiNâ€“ZrN, TiNâ€“HfN and ZrNâ€“HfN. Journal of Physics Condensed Matter, 2017, 29, 035401.	0.7	33
33749	An ab initio investigation of Bi₂Se₃ topological insulator deposited on amorphous SiO₂. Journal of Physics Condensed Matter, 2017, 29, 045302.	0.7	3
33750	A unified description of ordering in HCP Mg-RE alloys. Acta Materialia, 2017, 124, 620-632.	3.8	45
33751	Entropic contributions enhance polarity compensation for CeO2(100) surfaces. Nature Materials, 2017, 16, 328-334.	13.3	88
33752	Thermoelectric properties of SnSe₂monolayer. Journal of Physics Condensed Matter, 2017, 29, 015001.	0.7	84
33753	About copper promotion in CH 4 formation from CO hydrogenation on Fe(100): A density functional theory study. Applied Catalysis A: General, 2017, 530, 83-92.	2.2	16
33754	First-principles study of stability, electronic structure and magnetic properties of Be 2 C nanoribbons. Applied Surface Science, 2017, 394, 315-322.	3.1	1

#	Article	IF	Citations
33755	Screening of active metals for reactive adsorption desulfurization adsorbent using density functional theory. Applied Surface Science, 2017, 399, 440-450.	3.1	31
33756	Unsupported trimetallic Ni(Co)-Mo-W sulphide catalysts prepared from mixed oxides: Characterisation and catalytic tests for simultaneous tetralin HDA and dibenzothiophene HDS reactions. Catalysis Today, 2017, 292, 84-96.	2.2	21
33757	Vacancy-enhanced mechanism for helium diffusion along Î£7 grain boundary in Î±-Al2O3: A first principle study. Nuclear Instruments & Methods in Physics Research B, 2017, 393, 88-92.	0.6	5
33758	Bifunctional Oxygen Reaction Catalysis of Quadruple Manganese Perovskites. Advanced Materials, 2017, 29, 1603004.	11.1	148
33759	Surfaceâ€Chargeâ€Mediated Formation of Hâ€TiO₂@Ni(OH)₂ Heterostructures for Highâ€Performance Supercapacitors. Advanced Materials, 2017, 29, 1604164.	11.1	203
33760	Highâ€Electronâ€Mobility and Airâ€Stable 2D Layered PtSe₂ FETs. Advanced Materials, 2017, 29, 1604230.	11.1	502
33761	Crystal facet-dependent reactivity of Î±-Mn2O3 microcrystalline catalyst for soot combustion. Applied Catalysis B: Environmental, 2017, 204, 374-384.	10.8	141
33762	Enhanced CO 2 capture on graphene via N, S dual-doping. Applied Surface Science, 2017, 399, 420-425.	3.1	53
33763	Two-dimensional As 1-x P x binary compounds: Highly tunable electronic structure and optical properties. Current Applied Physics, 2017, 17, 186-191.	1.1	14
33764	Influence of phonon and electron excitations on the free energy of defect clusters in solids: A first-principles study. Computational Materials Science, 2017, 127, 284-294.	1.4	8
33765	SPARC: Accurate and efficient finite-difference formulation and parallel implementation of Density Functional Theory: Isolated clusters. Computer Physics Communications, 2017, 212, 189-204.	3.0	71
33766	Formation of cyanuric acid from cyanate adsorbed at gold electrodes. Electrochemistry Communications, 2017, 74, 1-4.	2.3	5
33767	Interatomic potential to study the formation of NiCr clusters in high Cr ferritic steels. Journal of Nuclear Materials, 2017, 484, 42-50.	1.3	20
33768	Alloying effect on the elastic properties of refractory high-entropy alloys. Materials and Design, 2017, 114, 243-252.	3.3	85
33769	Gd-doping-induced insulator-metal transition in SrTiO3. Solid State Communications, 2017, 250, 1-4.	0.9	3
33770	Magnetic control of single transition metal doped MoS2 through H/F chemical decoration. Journal of Magnetism and Magnetic Materials, 2017, 422, 243-248.	1.0	7
33771	Energetics, electronic and optical properties of X (XÂ=ÂSi, Ge, Sn, Pb) doped VO2(M) from first-principles calculations. Journal of Alloys and Compounds, 2017, 693, 211-220.	2.8	24
33772	Electronic properties of Cr-, B-doped and codoped SrTiO3. Journal of Physics and Chemistry of Solids, 2017, 100, 1-8.	1.9	15

#	Article	IF	Citations
33773	Polar Nature of (CH₃NH₃)₃Bi₂I₉ Perovskite-Like Hybrids. Inorganic Chemistry, 2017, 56, 33-41.	1.9	58
33774	Atomistic investigations of Î²-carbide precipitation in austenitic Fe-Mn-Al-C lightweight steels and the effect of Mo addition. Scripta Materialia, 2017, 127, 97-101.	2.6	80
33775	First-principles study on the multiferroic BiFeO3 (0001) polar surfaces. Applied Surface Science, 2017, 392, 135-143.	3.1	28
33776	Equilibrium Born-Oppenheimer molecular-dynamics exploration of the lattice thermal conductivity of silicon clathrates. Computational Materials Science, 2017, 126, 1-6.	1.4	9
33777	Ionization and diffusion of metal atoms under electric field at metal/insulator interfaces; First-principles study. Materials Science in Semiconductor Processing, 2017, 70, 78-82.	1.9	5
33778	Atomic Ordering and Sn Segregation in Ptâ€“Sn Nanoalloys Supported on CeO2 Thin Films. Topics in Catalysis, 2017, 60, 522-532.	1.3	11
33779	Strainâ€engineered atomicâ€layer movements and valenceâ€band maximum shifts in a twoâ€dimensional single quintuple film of Bi₂Te₃. Physica Status Solidi (B): Basic Research, 2017, 254, 1600362.	0.7	2
33780	Alloying element's substitution in titanium alloy with improved oxidation resistance and enhanced magnetic properties. Journal of Magnetism and Magnetic Materials, 2017, 422, 20-24.	1.0	4
33781	CO adsorption on Pd(111) at 0.5ML: A first principles study. Surface Science, 2017, 655, 7-11.	0.8	12
33782	Theoretical Aspects of Infrared and Raman Spectroscopies. Developments in Clay Science, 2017, 8, 6-33.	0.3	1
33783	Hydrogen-Bond Symmetrization of Î´ -AlOOH. Chinese Physics Letters, 2017, 34, 108301.	1.3	8
33784	High-pressure behavior of the Feâ€“S system and composition of the Earth's inner core. Physics-Uspekhi, 2017, 60, 1025-1032.	0.8	13
33785	First-principles study on the magnetic properties of ordered Nd6(Fe,Ga)14 alloys. Journal of Applied Physics, 2017, 122, 243904.	1.1	8
33786	Study of the orpiment and anorpiment phases of As2S3 under pressure. Journal of Physics: Conference Series, 2017, 950, 042018.	0.3	4
33787	First-principles simulation on Seebeck coefficient in silicon nanowires. Japanese Journal of Applied Physics, 2017, 56, 06GH04.	0.8	0
33788	Alloy Systems and Compounds Containing Rare Earth Metals and Carbon. Fundamental Theories of Physics, 2017, , 1-263.	0.1	9
33789	First-principles calculations of structure and elasticity of hydrous fayalite under high pressure. Chinese Physics B, 2017, 26, 126103.	0.7	7
33790	Tuning electronic properties of the S 2 /graphene heterojunction by strains from density functional theory. Chinese Physics B, 2017, 26, 127101.	0.7	1

#	Article	IF	Citations
33791	Tunable electronic and optical properties of gas molecules adsorbed monolayer graphitic ZnO: Implications for gas sensor and environment monitoring. Journal of Applied Physics, 2017, 122, .	1.1	11
33792	When water meets iron at Earth's coreâ€“mantle boundary. National Science Review, 2017, 4, 870-878.	4.6	75
33793	Aqueous Electrochemical Activity of the Mg Surface: The Role of Group 14 and 15 Microalloying Elements. Journal of the Electrochemical Society, 2017, 164, C918-C929.	1.3	18
33794	Potentiality of Density-Functional Theory in Analyzing the Devices Containing Graphene-Crystalline Solid Interfaces: A Review. IEEE Transactions on Electron Devices, 2017, 64, 4738-4745.	1.6	8
33795	Unexpected Trend Deviation in Isoelectronic Transition Metal Borides A₃T₅B₂ (A = group 4, T = group 9): Ti₃Co₅B₂â€•vs. Perovskiteâ€Type Studied by Experiments and DFT Calculations. Zeitschrift Fur Anorganische Und Allgemeine Chemie, 2017, 643, 1551-1556.	0.6	7
33797	The structural, magnetic and optical properties of TMn@(ZnO)42 (TMâ€‰=â€‰Fe, Co and Ni) hetero-nanostructure. Scientific Reports, 2017, 7, 16485.	1.6	12
33798	Dynamic instabilities in strongly correlated <mml:math xmlns:mml="http://www.w3.org/1998/Math/MathML"><mml:msub><mml:mtext>VSe</mml:mtext><mml:mn>2</mml:mn></mml:msub monolayers and bilayers. Physical Review B, 2017, 96, .	1.1	91
33799	Prediction of a mobile two-dimensional electron gas at the <mml:math xmlns:mml="http://www.w3.org/1998/Math/MathML"><mml:mrow><mml:mi>LaSc</mml:mi><mml:msub><mml:mi mathvariant="normal">O</mml:mi><mml:mn>3</mml:mn></mml:msub></mml:mrow><mml:mo>/</mml:mo><mml:mrow><mml:mi>Ba mathvariant="normal">O</mml:mi><mml:mn>3</mml:mn></mml:msub></mml:mrow></mml:math> (001) interface. Physical Review B, 2017, 96, .	1.1	22
33800	Modification of electronic structure, magnetic structure, and topological phase of bismuthene by point defects. Physical Review B, 2017, 96, .	1.1	54
33801	Mottness Collapse in <mml:math xmlns:mml="http://www.w3.org/1998/Math/MathML" display="inline"><mml:mrow><mml:mn>1</mml:mn><mml:mi mathvariant="normal">T</mml:mi><mml:mtext>â€“</mml:mtext><mml:msub><mml:mrow><mml:mi>TaS</mml:mi></mml:mrow><mml:m Transition-Metal Dichalcogenide: An Interplay between Localized. Physical Review X, 2017, 7, .	2.8	53
33802	Second harmonic generation property of monolayer TMDCs and its potential application in producing terahertz radiation. Journal of Chemical Physics, 2017, 147, 244701.	1.2	19
33803	Weakly-Correlated Nature of Ferromagnetism in Nonsymmorphic <mml:math xmlns:mml="http://www.w3.org/1998/Math/MathML" display="inline"><mml:mrow><mml:msub><mml:mrow><mml:mi>CrO</mml:mi></mml:mrow><mml:mrow><mml:mn>2</mml:mn></mml:mrow><m Revealed by Bulk-Sensitive Soft-X-Ray ARPES. Physical Review X, 2017, 7, .	2.8	19
33804	ReS2-based interlayer tunnel field effect transistor. Journal of Applied Physics, 2017, 122, .	1.1	7
33805	First principles electronic and elastic properties of fresnoite Ba₂TiSi₂O₈. Materials Research Express, 2017, 4, 125904.	0.8	5
33806	Prediction of the High Thermoelectric Performance of Pnictogen Dichalcogenide Layered Compounds with Quasi-One-Dimensional Gapped Dirac-like Band Dispersion. Physical Review Applied, 2017, 8, .	1.5	16
33807	Triply degenerate nodal points and topological phase transitions in <mml:math xmlns:mml="http://www.w3.org/1998/Math/MathML"><mml:mrow><mml:msub><mml:mi>NaCu</mml:mi><mml:mn>3</mml:mn></mml:m Physical Review B, 2017, 96, .	1.1	23
33808	Periodic modeling of zeolite Ti-LTA. Journal of Chemical Physics, 2017, 147, 074701.	1.2	11
33809	Intrinsic optical conductivity of a ${{m{C}}}_{2v}$ symmetric topological insulator. Semiconductor Science and Technology, 2017, 32, 075013.	1.0	1

#	Article	IF	Citations
33810	Molecular Adsorption, Hindered Rotation, and Species Separation of H₂/SrTiO₃(001). Journal of the Physical Society of Japan, 2017, 86, 073601.	0.7	3
33811	Multiphase modelling of Pb(Zr1-xTix)O3 structure. Ferroelectrics, 2017, 520, 1-9.	0.3	2
33812	Quasiparticle and hybrid density functional methods in defect studies: An application to the nitrogen vacancy in GaN. Physical Review B, 2017, 96, .	1.1	18
33813	Prediction of Ideal Topological Semimetals with Triply Degenerate Points in the<mml:math xmlns:mml="http://www.w3.org/1998/Math/MathML" display="inline"><mml:mrow><mml:msub><mml:mrow><mml:mi>NaCu</mml:mi></mml:mrow><mml:mrow><mml:mn>3</mml:mn></ Physical Review Letters, 2017, 119, 256402.	2.9	36
33814	Frustration-driven C 4 symmetric order in a naturally-heterostructured superconductor Sr2VO3FeAs. Nature Communications, 2017, 8, 2167.	5.8	13
33815	Competing magnetostructural phases in a semiclassical system. Npj Quantum Materials, 2017, 2, .	1.8	5
33816	A Universal 3D Voxel Descriptor for Solid-State Material Informatics with Deep Convolutional Neural Networks. Scientific Reports, 2017, 7, 16991.	1.6	51
33817	Magnetism and spin-driven ferroelectricity in the multiferroic material <mml:math xmlns:mml="http://www.w3.org/1998/Math/MathML"><mml:mrow><mml:mi>Î±</mml:mi><mml:mo>â^'</mml:mo><mml:msub><mml:mi mathvariant="normal">V</mml:mi><mml:mn>2</mml:mn></mml:msub><mml:msub><mml:mi mathvariant="normal">O</mml:mi><mml:mn>7</mml:mn></mml:msub></mml:mrow></mml:math>. Physical Review B, 2017, 96, .	1.1	9
33818	Strain-induced negative differential resistance in ultrasmall carbon nanotube. Modern Physics Letters B, 2017, 31, 1750217.	1.0	1
33819	Theoretical Investigations of the Electrochemical Reduction of CO on Single Metal Atoms Embedded in Graphene. ACS Central Science, 2017, 3, 1286-1293.	5.3	54
33820	Hydrogen motion in rutile TiO2. Scientific Reports, 2017, 7, 17065.	1.6	15
33821	Magneto-transport and electronic structures of BaZnBi₂. New Journal of Physics, 2017, 19, 123044.	1.2	12
33822	Uncovering a reconstructive solidâ€“solid phase transition in a metalâ€“organic framework. Royal Society Open Science, 2017, 4, 171355.	1.1	7
33823	Intrinsic damping phenomena from quantum to classical magnets: An ab initio study of Gilbert damping in a Pt/Co bilayer. Physical Review B, 2017, 96, .	1.1	15
33824	Magnetic order induces symmetry breaking in the single-crystalline orthorhombic CuMnAs semimetal. Physical Review B, 2017, 96, .	1.1	22
33825	Electronic coupling between Bi nanolines and the Si(001) substrate: An experimental and theoretical study. Physical Review B, 2017, 96, .	1.1	2
33826	Two-photon absorption spectrum of liquid water and the effect of nondiagonal self-energy elements in the self-consistent <mml:math xmlns:mml="http://www.w3.org/1998/Math/MathML"><mml:mrow><mml:mi>G</mml:mi><mml:mi>W</mml:mi></mml:mrow></mml:m approach on the band gap. Physical Review B, 2017, 96, .	1.1	3
33827	Probing a divergent van Hove singularity of graphene with a <mml:math xmlns:mml="http://www.w3.org/1998/Math/MathML"><mml:mrow><mml:msub><mml:mi>Ca</mml:mi><mml:mn>2</mml:mn></mml:mr mathvariant="normal">N</mml:mi></mml:mrow></mml:math> support: A layered electride as a solid-state dopant. Physical Review B, 2017, 96, .	1.1	13

#	Article	IF	Citations
33828	Coupling Molecular Dynamics and Finite Element Simulations to Investigate the Nearest Neighbor Dependence of Field Evaporation. Microscopy and Microanalysis, 2017, 23, 646-647.	0.2	1
33829	Oxygen Packing Fraction and the Structure of Silicon and Germanium Oxide Glasses. Journal of Physical Chemistry B, 2017, 121, 10726-10732.	1.2	23
33830	Prediction of Mechanical Twinning in Magnesium Silicate Post-Perovskite. Scientific Reports, 2017, 7, 17640.	1.6	5
33831	Correlation between the electronic structure, topologic structure and dynamic properties of liquid cerium. Physical Chemistry Chemical Physics, 2017, 19, 30498-30503.	1.3	6
33832	Absence of static magnetic order in nonsuperconducting FeSe thin films on SrTiO3 (001) revealed by the magnetism of Se vacancies. Physical Review B, 2017, 96, .	1.1	4
33833	Refined phase diagram of the H-S system with high- Tc superconductivity. Physical Review B, 2017, 96, .	1.1	25
33834	Giant enhancement of the intrinsic spin Hall conductivity in <mml:math xmlns:mml="http://www.w3.org/1998/Math/MathML"><mml:mi>Î²</mml:mi></mml:math> -tungsten via substitutional doping. Physical Review B, 2017, 96, .	1.1	58
33835	Exploring dissociative water adsorption on isoelectronically BN doped graphene using alchemical derivatives. Journal of Chemical Physics, 2017, 147, 164113.	1.2	25
33836	Polaronic transport in Ag-based quaternary chalcogenides. Journal of Applied Physics, 2017, 122, .	1.1	20
33837	Temperature dependence of the effective mass of the hybrid organic-inorganic perovskites CH3NH3PbI3. Applied Physics Letters, 2017, 111, .	1.5	11
33838	Insights into the thermoelectric properties of the Cu 2 Ge(S 1-x Se x) 3 solid solutions. Materials Today: Proceedings, 2017, 4, 12349-12359.	0.9	8
33839	Magnetic Frustration Driven by Itinerancy in Spinel CoV2O4. Scientific Reports, 2017, 7, 17129.	1.6	24
33840	Superconductivity in two-dimensional ferromagnetic MnB. Scientific Reports, 2017, 7, 17101.	1.6	11
33841	Control of interlayer physics in 2H transition metal dichalcogenides. Journal of Applied Physics, 2017, 122, .	1.1	21
33842	Doping stability and charge-density-wave transition of strained 1T-TiSe ₂. Europhysics Letters, 2017, 120, 17006.	0.7	6
33843	First principles study of oxidation of Si-segregated Î±-Ti(0001) surfaces. Japanese Journal of Applied Physics, 2017, 56, 125701.	0.8	10
33844	Stacking stability and sliding mechanism in weakly bonded 2D transition metal carbides by van der Waals force. RSC Advances, 2017, 7, 55912-55919.	1.7	53
33845	Characterizing the geometric and electronic structure of defects in the â€œ29â€•copper surface oxide. Journal of Chemical Physics, 2017, 147, 224706.	1.2	9

#	Article	IF	Citations
33846	Electrochemically Stable Coating Materials for Li, Na, and Mg Metal Anodes in Durable High Energy Batteries. Journal of the Electrochemical Society, 2017, 164, A3582-A3589.	1.3	25
33847	Coverage-dependent essential properties of halogenated graphene: A DFT study. Scientific Reports, 2017, 7, 17858.	1.6	32
33848	Rapid prediction of molecule arrangements on metal surfaces via Bayesian optimization. Applied Physics Express, 2017, 10, 065502.	1.1	30
33849	Effects of Mn dopant locations on the electronic bandgap of PbS quantum dots. Applied Physics Letters, 2017, 111, .	1.5	8
33850	Atomic layer reversal on CeO2 (100) surface. Science China Materials, 2017, 60, 903-908.	3.5	17
33851	Effect of Si on the oxidation reaction of Î±-Ti(0â€‰0â€‰0â€‰1) surface: ab initio molecular dynamics study. Science and Technology of Advanced Materials, 2017, 18, 998-1004.	2.8	8
33852	Prediction and characterization of an Mg-Al intermetallic compound with potentially improved ductility via orbital-free and Kohn-Sham density functional theory. Modelling and Simulation in Materials Science and Engineering, 2017, 25, 075002.	0.8	11
33853	Versatile electronic and magnetic properties of chemically doped 2D platinum diselenide monolayers: A first-principles study. AIP Advances, 2017, 7, 125126.	0.6	4
33854	Identifying the structure of 4-chlorophenyl isocyanide adsorbed on Au(111) and Pt(111) surfaces by first-principles simulations of Raman spectra. Physical Chemistry Chemical Physics, 2017, 19, 32389-32397.	1.3	12
33855	Anomalous thermal expansion, negative linear compressibility, and high-pressure phase transition in ZnAu2(CN)4 : Neutron inelastic scattering and lattice dynamics studies. Physical Review B, 2017, 96, .	1.1	13
33856	Structural, electronic, and thermodynamic properties of curium dioxide: Density functional theory calculations. Physical Review B, 2017, 96, .	1.1	36
33857	First-principles study on the electronic, optical, and transport properties of monolayer <mml:math xmlns:mml="http://www.w3.org/1998/Math/MathML"><mml:mi>Î±</mml:mi></mml:math> - and <mml:math xmlns:mml="http://www.w3.org/1998/Math/MathML"><mml:mi>Î²</mml:mi></mml:math> -GeSe. Physical Review B, 2017, 96, .	1.1	81
33858	Dimensionality-Driven Metal-Insulator Transition in Spin-Orbit-Coupled <mml:math xmlns:mml="http://www.w3.org/1998/Math/MathML" display="inline"><mml:mrow><mml:msub><mml:mrow><mml:mi>SrIrO</mml:mi></mml:mrow><mml:mrow><mml:mn>3</mml:mn></	2.9	81
	Physical Review Letters, 2017, 119, 256404.		
33859	Prediction of a low-temperature N ₂ dissociation catalyst exploiting near-IRâ€“toâ€“visible light nanoplasmonics. Science Advances, 2017, 3, eaao4710.	4.7	74
33860	Haeckelite and N-Doped Haeckelite as Catalysts for Oxygen Reduction Reaction: Theoretical Studies. Journal of Physical Chemistry C, 2017, 121, 28339-28347.	1.5	8
33861	Phase-field modeling and electronic structural analysis of flexoelectric effect at 180Â° domain walls in ferroelectric PbTiO3. Journal of Applied Physics, 2017, 122, .	1.1	15
33862	Exploring the electronic structure and optical properties of double perovskite Ba₂RESbO₆ (RE = Ho, Er) from first-principles calculations. Ferroelectrics, 2017, 518, 163-170.	0.3	2
33863	Microstructural characterization of the Î·-Ni₃(Ti, Al) phase in a long-term-aged Ni-based superalloy. Philosophical Magazine Letters, 2017, 97, 442-449.	0.5	5

#	Article	IF	Citations
33864	Aggregation-induced emission in lamellar solids of colloidal perovskite quantum wells. Science Advances, 2017, 3, eaaq0208.	4.7	65
33865	Robust ferromagnetism and half-metallicity in fluorinated two-dimensional BeN2 sheets. Applied Physics Letters, 2017, 111, .	1.5	8
33866	Stability and mechanical properties of various Hfâ€“H phases: A density-functional theory study. Chinese Physics B, 2017, 26, 106103.	0.7	1
33867	Spin-induced ferroelectricity in a triangular-lattice antiferromagnet studied by magnetoelectric coupling tensors. Physical Review B, 2017, 96, .	1.1	8
33868	Electronic and spin dynamics in the insulating iron pnictide<mml:math xmlns:mml="http://www.w3.org/1998/Math/MathML"><mml:mrow><mml:msub><mml:mi>NaFe</mml:mi><mml:mrow><mml:mn>0.5< Physical Review B, 2017, 96, .	1.1	4
33869	Electronic and Optical Properties of GaAs Bilayer. Macromolecular Symposia, 2017, 376, 1600208.	0.4	1
33870	Investigations of the Optical Properties of GaNAs Alloys by First-Principle. Scientific Reports, 2017, 7, 17285.	1.6	7
33871	Two-dimensional semiconductors ZrNCl and HfNCl: Stability, electric transport, and thermoelectric properties. Scientific Reports, 2017, 7, 17330.	1.6	30
33872	Strong bonding and high spin-polarization of lanthanide atoms on vacancies in graphene. AIP Advances, 2017, 7, .	0.6	7
33873	Effect of ionic substitutions on the magnetic properties of strontium hexaferrite: A first principles study. AIP Advances, 2017, 7, 115209.	0.6	15
33874	Structural stabilities and electronic properties of Mg28-nAln clusters: A first-principles study. AIP Advances, 2017, 7, 095023.	0.6	7
33875	Ab initio molecular dynamics study of fluid H2O-CO2 mixture in broad pressure-temperature range. AIP Advances, 2017, 7, .	0.6	6
33876	Inelastic electron tunneling mediated by a molecular quantum rotator. Physical Review B, 2017, 96, .	1.1	5
33877	Features of the electronic spectrum and optical absorption of ultrathin Bi2Se3 films. JETP Letters, 2017, 106, 422-428.	0.4	4
33878	Thermoelectric Properties of 2D Ni₃(hitp)₂and 3D Cu₃(btc)₂MOFs: First-Principles Studies. ECS Journal of Solid State Science and Technology, 2017, 6, N236-N242.	0.9	7
33879	Ordered and Disordered Phases in Mo1â^'xWxS2 Monolayer. Scientific Reports, 2017, 7, 15124.	1.6	21
33880	Peculiar electronic, strong in-plane and out-of-plane second harmonic generation and piezoelectric properties of atom-thick Î±-M₂X₃ (M = Ga, In; X = S, Se): role of spontaneous electric dipole orientations. RSC Advances, 2017, 7, 55034-55043.	1.7	66
33881	Prediction of TiRhAs as a Dirac nodal line semimetal via first-principles calculations. Physical Review B, 2017, 96, .	1.1	4

#	Article	IF	Citations
33882	Substrate-induced semiconductor-to-metal transition in monolayer <mml:math xmlns:mml="http://www.w3.org/1998/Math/MathML"><mml:msub><mml:mi>WS</mml:mi><mml:mn>2</mml:mn></mml:msub></mml:math> Physical Review B, 2017, 96, .	1.1	33
33883	Class of diatomic ferroelectrics with multifunctional properties: IV-VI compounds in the distorted NiAs-type structure. Physical Review B, 2017, 96, .	1.1	4
33884	Effective scheme to determine accurate defect formation energies and charge transition levels of point defects in semiconductors. Physical Review B, 2017, 96, .	1.1	10
33885	Defects and magnetic structure of CuMnSb. Journal of Physics: Conference Series, 2017, 903, 012034.	0.3	0
33886	A Density Functional Theory Study of Adsorption States of Hydrogen Molecules on Ice Surfaces. Journal of the Vacuum Society of Japan, 2017, 60, 249-255.	0.3	2
33887	Symmetry Breaking-induced Band-splitting in GaAs Thin Film by First-principles Calculations. Journal of the Vacuum Society of Japan, 2017, 60, 445-449.	0.3	3
33889	Titaniaâ€Supported Singleâ€Atom Platinum Catalyst for Waterâ€Gas Shift Reaction. Chemie-Ingenieur-Technik, 2017, 89, 1343-1349.	0.4	22
33890	Polarization Dependent Bulk-sensitive Valence Band Photoemission Spectroscopy and Density Functional Theory Calculations: Part I. 3dTransition Metals. Journal of the Physical Society of Japan, 2017, 86, 124706.	0.7	17
33891	Filament-to-dielectric band alignments in $$hbox {TiO}_{2}$$ TiO 2 and $$hbox {HfO}_{2}$$ HfO. Journal of Computational Electronics, 2017, 16, 1057-1065.	1.3	7
33892	Thermal neutron scattering law calculations using ab initio molecular dynamics. EPJ Web of Conferences, 2017, 146, 13002.	0.1	10
33893	The electronic structure of ultrathin [111]-oriented tin nanowire with hydrogen passivation. AIP Conference Proceedings, 2017, , .	0.3	0
33894	Influence of heavy metal materials on magnetic properties of Pt/Co/heavy metal tri-layered structures. , 2017, , .		1
33895	Investigation of the charge distribution in small cluster ions Ar 13 + and Ar 19 +. Moscow University Physics Bulletin (English Translation of Vestnik Moskovskogo Universiteta, Fizika), 2017, 72, 470-473.	0.1	0
33896	The Pressure Dependence of Structural, Electronic, Mechanical, Vibrational, and Thermodynamic Properties of Palladium-Based Heusler Alloys. Zeitschrift Fur Naturforschung - Section A Journal of Physical Sciences, 2017, 72, 843-853.	0.7	4
33897	First Principles Investigation of the Magnetic, Magnetoelectric, and Optical Properties of Double Perovskites Containing Ions of Transition Metals LaPbTSbO6 (T = Fe, Co, Ni). Journal of Experimental and Theoretical Physics, 2017, 125, 1116-1126.	0.2	0
33898	Quantum confinement effects on electronic photomobilities at nanostructured semiconductor surfaces: Si(111) without and with adsorbed Ag clusters. Journal of Chemical Physics, 2017, 147, 224703.	1.2	12
33899	Energy loss and surface temperature effects in ab initio molecular dynamics simulations: N adsorption on Ag(111) as a case study. Physical Review B, 2017, 96, .	1.1	19
33900	First-Principle Study of the Electronic Structure and Stability of Reconstructed AgInSe2 (112) Polar Surfaces. IEEE Journal of Photovoltaics, 2017, 7, 1781-1788.	1.5	4

#	Article	IF	Citations
33901	Graphdiyne nanoribbons with open hexagonal rings: Existence of topological unprotected edge states. Physics Letters, Section A: General, Atomic and Solid State Physics, 2017, 381, 3337-3341.	0.9	12
33902	A posteriori metadata from automated provenance tracking: integration of AiiDA and TCOD. Journal of Cheminformatics, 2017, 9, 56.	2.8	24
33903	Advances in the understanding of microscopic switching mechanisms in ReRAM devices (Invited paper). , 2017, , .		3
33904	Defect Chemistry and Basic Properties of Non-Stoichiometric PuO₂. Defect and Diffusion Forum, 0, 375, 57-70.	0.4	11
33905	Strain and defects engineering of phosphorene. , 2017, , .		1
33906	Effect of Mo on the thermal stability, oxidation resistance, and tribo-mechanical properties of arc evaporated Ti-Al-N coatings. Journal of Vacuum Science and Technology A: Vacuum, Surfaces and Films, 2017, 35, .	0.9	18
33907	Possible effect of static surface disorder on diffractive scattering of H2 from Ru(0001): Comparison between theory and experiment. Journal of Chemical Physics, 2017, 147, 244705.	1.2	10
33908	Structural and electronic properties transitions induced by different pressures in crystalline nalidixic acid. International Journal of Modern Physics C, 2017, 28, 1750147.	0.8	3
33909	Abnormal behavior of potassium adsorbed phosphorene. International Journal of Computational Materials Science and Engineering, 2017, 06, 1850002.	0.5	0
33910	Pressureâ€Induced Phase Transition in Weyl Semimetallic WTe₂. Small, 2017, 13, 1701887.	5.2	37
33911	N-type lithium-nitrogen codoping in diamond from first principles. , 2017, , .		0
33912	Origin of 6-fold coordinated aluminum at (010)-type pyrophyllite edges. AIP Advances, 2017, 7, 055211.	0.6	6
33913	Novel electronic properties of 2D MoS2/TiO2van der Waals heterostructure. Semiconductor Science and Technology, 2017, 32, 105011.	1.0	13
33914	Origin of Electrical Instabilities in Self-Aligned Amorphous Inâ€“Gaâ€“Znâ€“O Thin-Film Transistors. IEEE Transactions on Electron Devices, 2017, 64, 4965-4973.	1.6	28
33915	Antimonene: A promising candidate for acetone sensors with high selectivity and sensitivity. , 2017, , .		5
33916	Comparison of basis sets for efficient Ab-initio modeling of semiconductors. , 2017, , .		0
33917	Modeling of black phosphorus vertical TFETs without chemical doping for drain. , 2017, , .		0
33918	Effect of B on Growth of Recrystallized Grain of Ti-added Ultra-low Carbon Cold-rolled Steel Sheets. Tetsu-To-Hagane/Journal of the Iron and Steel Institute of Japan, 2017, 103, 221-229.	0.1	2

#	Article	IF	Citations
33919	Development of a compact bushing for NBI. AIP Conference Proceedings, 2017, , .	0.3	4
33920	g-C3N4/SnS2 Heterostructure: a Promising Water Splitting Photocatalyst. Chinese Journal of Chemical Physics, 2017, 30, 36-42.	0.6	25
33921	Theoretical Simulations of Irradiation-Induced Sputtering at Tungsten Surface. Chinese Journal of Chemical Physics, 2017, 30, 77-82.	0.6	3
33922	First-Principles Study on Magnetism of Manganese Dithiolene-diamine and Dihydroxyl-diamine Nanosheets. Chinese Journal of Chemical Physics, 2017, 30, 529-537.	0.6	1
33923	Enhanced Water Oxidation Activity on Ni, Co-Doped Fe2O3 (0001) Surface. Chinese Journal of Chemical Physics, 2017, 30, 553-558.	0.6	3
33924	Quasiparticle Band Structures of Defects in Anatase TiO2 Bulk. Chinese Journal of Chemical Physics, 2017, 30, 771-775.	0.6	6
33925	Interaction of O_{2i} Dimers with Ga in Si and Implications for a Comprehensive Model of Light- Induced Degradation. , 2017, , .		0
33926	The Optical Phenomena of Interplay between Nanobio Complexes: A Theoretical Insight into Their Biomedical Applications. , 0, , .		2
33927	First-Principles Modeling of Alkali Metal Post Deposition Treatment Effects in CIGS Solar Cells. , 2017, , .		0
33928	Diffusion of Formaldehyde on Rutile TiO2(110) Assisted by Surface Hydroxyl Groups. Chinese Journal of Chemical Physics, 2017, 30, 253-258.	0.6	3
33929	The Reactivity of Anatase TiO2 (211) Surface and the Bond- Charge Counting Model. , 2017, , .		2
33930	First-Principles Study of Phase Stability and Solubility in Fe-RE (Y, La, Ce) Alloys. Rare Metal Materials and Engineering, 2017, 46, 3188-3192.	0.8	8
33931	Electronic Structure and Thermoelectric Properties of Pseudogap Intermetallic Compound Al₅Co₂. Nippon Kinzoku Gakkaishi/Journal of the Japan Institute of Metals, 2017, 81, 55-59.	0.2	1
33932	Comparison of Ab-initio Solute-Boundary Binding Energies and Experimental Recrystallization Data in Austenite for Solute Nb and Other Elements. ISIJ International, 2017, 57, 1847-1850.	0.6	5
33933	Effects of Oxygen Vacancy on the Adsorption of Formaldehyde on Rutile TiO2(110) Surface. Chinese Journal of Chemical Physics, 2017, 30, 312-318.	0.6	4
33934	Bulk quadrupole contribution to second harmonic generation from classical oscillator model in silicon. Optics Express, 2017, 25, 26567.	1.7	7
33935	Optical readout of hydrogen storage in films of Au and Pd. Optics Express, 2017, 25, 24081.	1.7	24
33936	Î±-Silicene as oxidation-resistant ultra-thin coating material. Beilstein Journal of Nanotechnology, 2017, 8, 1808-1814.	1.5	3

#	Article	IF	Citations
33937	Adsorption of iron tetraphenylporphyrin on (111) surfaces of coinage metals: a density functional theory study. Beilstein Journal of Nanotechnology, 2017, 8, 2484-2491.	1.5	3
33938	Si- and Sn-containing SiOCN-based nanocomposites as anode materials for lithium ion batteries: synthesis, thermodynamic characterization and modeling. International Journal of Materials Research, 2017, 108, 920-932.	0.1	8
33939	Intercalation of Si between MoS₂ layers. Beilstein Journal of Nanotechnology, 2017, 8, 1952-1960.	1.5	27
33940	Structural model of silicene-like nanoribbons on a Pb-reconstructed Si(111) surface. Beilstein Journal of Nanotechnology, 2017, 8, 1836-1843.	1.5	7
33941	Crystal structure of cobalt hydroxide carbonate Co₂CO₃(OH)₂: density functional theory and X-ray diffraction investigation. Acta Crystallographica Section B: Structural Science, Crystal Engineering and Materials, 2017, 73, 868-873.	0.5	12
33942	Synthesis, Crystal Structure, Polymorphism, and Magnetism of Eu(CN3H4)2 and First Evidence of EuC(NH)3. Inorganics, 2017, 5, 10.	1.2	17
33943	First-Principles Study of Vacancies in Ti3SiC2 and Ti3AlC2. Materials, 2017, 10, 103.	1.3	29
33944	Exploring the Mechanical Anisotropy and Ideal Strengths of Tetragonal B4CO4. Materials, 2017, 10, 128.	1.3	20
33945	A Practical Approach to Evaluate Lattice Thermal Conductivity in Two-Phase Thermoelectric Alloys for Energy Applications. Materials, 2017, 10, 386.	1.3	9
33946	Formation of Surface and Quantum-Well States in Ultra Thin Pt Films on the Au(111) Surface. Materials, 2017, 10, 1409.	1.3	5
33947	The Role of Î²-Carbides as Hydrogen Traps in High-Mn Steels. Metals, 2017, 7, 264.	1.0	27
33948	Revisiting Mgâ€“Mg2Ni System from Electronic Perspective. Metals, 2017, 7, 489.	1.0	5
33949	Computational Predictions for Single Chain Chalcogenide-Based One-Dimensional Materials. Nanomaterials, 2017, 7, 115.	1.9	13
33950	Regulation of the Electroanalytical Performance of Ultrathin Titanium Dioxide Nanosheets toward Lead Ions by Non-Metal Doping. Nanomaterials, 2017, 7, 327.	1.9	14
33951	Surface states and positron annihilation spectroscopy: results and prospects from a first-principles approach. Journal of Physics: Conference Series, 2017, 791, 012036.	0.3	1
33952	Adsorption structure of Bi on the fivefold surface of i-Ag-In-Yb quasicrystal. Journal of Physics: Conference Series, 2017, 809, 012018.	0.3	3
33953	Understanding electronic and optical properties of strontium titanate at both PBE and HSE06 levels. IOP Conference Series: Materials Science and Engineering, 2017, 167, 012010.	0.3	8
33954	Impact of Alloying on Stacking Fault Energies in Î³-TiAl. Applied Sciences (Switzerland), 2017, 7, 1193.	1.3	25

#	Article	IF	Citations
33955	Theoretical Prediction of Electronic Structures and Phonon Dispersion of Ce2XN2 (X = S, Se, and Te) Ternary. Computation, 2017, 5, 29.	1.0	2
33956	Ab Initio Study of the Elastic and Mechanical Properties of B19 TiAl. Crystals, 2017, 7, 39.	1.0	35
33957	Site Identity and Importance in Cosubstituted Bixbyite In2O3. Crystals, 2017, 7, 47.	1.0	3
33958	First-Principles Investigations on Structural and Elastic Properties of Orthorhombic TiAl under Pressure. Crystals, 2017, 7, 111.	1.0	27
33959	First Principles Study on Structure Stability and Mechanical Properties of YNi2B2C and LuNi2B2C under Pressure. Crystals, 2017, 7, 173.	1.0	3
33960	First-Principles Study of the Nonlinear Elasticity of Rare-Earth Hexaborides REB6 (RE = La, Ce). Crystals, 2017, 7, 320.	1.0	5
33961	High-Pressure Reactivity of Kr and F2â€"Stabilization of Krypton in the +4 Oxidation State. Crystals, 2017, 7, 329.	1.0	4
33962	Enthalpy of Mixing in Alâ€"Tb Liquid. Entropy, 2017, 19, 290.	1.1	2
33963	Insertion of Mono- vs. Bi- vs. Trivalent Atoms in Prospective Active Electrode Materials for Electrochemical Batteries: An ab Initio Perspective. Energies, 2017, 10, 2061.	1.6	10
33964	Experimental and Theoretical Investigation of the Elastic Moduli of Silicate Glasses and Crystals. Frontiers in Materials, 2017, 4, .	1.2	13
33965	Nonlinear Elasticity of Borocarbide Superconductor YNi₂B₂C: A First-Principles Study. Advances in Materials Science and Engineering, 2017, 2017, 1-8.	1.0	0
33966	Density Functional Theory Investigation into the B and Ga Doped Clean and Water Covered Î³-Alumina Surfaces. Journal of Chemistry, 2017, 2017, 1-7.	0.9	4
33967	Spectroscopic Characterization of Omeprazole and Its Salts. Journal of Spectroscopy, 2017, 2017, 1-11.	0.6	5
33968	Properties of Hydrogenated Nanoporous SiC: An Ab Initio Study. Journal of Nanomaterials, 2017, 2017, 1-6.	1.5	5
33969	Toward lead halide perovskite-based intermediate band absorbers. , 2017, , .		0
33970	Ab Initio Study of Electronic Transport in Cubic-HfO2 Grain Boundaries. Journal of Nanomaterials, 2017, 2017, 1-9.	1.5	3
33971	Vibrational Spectroscopy of Binary Titanium Borides: First-Principles and Experimental Studies. Advances in Condensed Matter Physics, 2017, 2017, 1-9.	0.4	13
33972	First-Principles Study of Properties of Alpha Uranium Crystal and Seven Alpha Uranium Surfaces. Journal of Chemistry, 2017, 2017, 1-7.	0.9	6

#	Article	IF	Citations
33973	Hybrid Perovskite, CH₃NH₃PbI₃, for Solar Applications: An Experimental and Theoretical Analysis of Substitution in A and B Sites. Journal of Nanomaterials, 2017, 2017, 1-10.	1.5	8
33974	Atomic-Scale Structural Analysis of Metal/Nitride Interfaces Using Advanced Atomic-Resolution Analytical Electron Microscopy. Nihon Kessho Gakkaishi, 2017, 59, 246-251.	0.0	0
33975	Diffusion Behaviors of Hydrogen Isotopes in Incoloy 800H: A First-Principles Study. Science and Technology of Nuclear Installations, 2017, 2017, 1-6.	0.3	2
33976	Adsorption Behaviors of Cobalt on the Graphite and SiC Surface: A First-Principles Study. Science and Technology of Nuclear Installations, 2017, 2017, 1-8.	0.3	3
33977	Adsorption and diffusion characteristics of lithium on hydrogenated Î±- and Î²-silicene. Beilstein Journal of Nanotechnology, 2017, 8, 1742-1748.	1.5	1
33978	Atomistic study of comblike structure on the MoO2/Mo(110) surface by scanning tunneling microscopy and density functional theory calculations. Japanese Journal of Applied Physics, 2017, 56, 095501.	0.8	2
33979	Insight into the Mechanism of CO Oxidation on WO3(001) Surfaces for Gas Sensing: A DFT Study. Sensors, 2017, 17, 1898.	2.1	20
33980	Alane adsorption and dissociation on the Si(0â€‰0â€‰1) surface. Journal of Physics Condensed Matter, 2017, 29, 395001.	0.7	3
33981	Design and Control of Cooperativity in Spin-Crossover in Metalâ€“Organic Complexes: A Theoretical Overview. Inorganics, 2017, 5, 47.	1.2	30
33982	Quantum-trajectory analysis for charge transfer in solid materials induced by strong laser fields. Journal of Physics Condensed Matter, 2017, 29, 275702.	0.7	16
33983	X-ray Powder Diffraction. , 2017, , 45-73.		3
33984	Organic materials database: An open-access online database for data mining. PLoS ONE, 2017, 12, e0171501.	1.1	65
33985	A full understanding of oxygen reduction reaction mechanism on Au(1â€‰1â€‰1) surface. Journal of Physics Condensed Matter, 2017, 29, 365201.	0.7	7
33986	Possibility of Metal-Oxide-Nitride-Oxide-Semiconductor Memories for Long Lifespan Archive Memories. IEICE Transactions on Electronics, 2017, E100.C, 928-933.	0.3	0
33987	High magnesium mobility in ternary spinel chalcogenides. Nature Communications, 2017, 8, 1759.	5.8	212
33988	Exploration of pyrazine-embedded antiaromatic polycyclic hydrocarbons generated by solution and on-surface azomethine ylide homocoupling. Nature Communications, 2017, 8, 1948.	5.8	88
33989	Phonon broadening in high entropy alloys. Npj Computational Materials, 2017, 3, .	3.5	100
33990	Electride and superconductivity behaviors in Mn5Si3-type intermetallics. Npj Quantum Materials, 2017, 2, .	1.8	47

#	Article	IF	Citations
33991	Investigations of Vacancy Structures Related to Their Growth in h-BN Sheet. Nanoscale Research Letters, 2017, 12, 445.	3.1	23
33992	First-Principles Study on the Stability and STM Image of Borophene. Nanoscale Research Letters, 2017, 12, 514.	3.1	19
33993	Defects on the Surface of Ti-Doped MgAl2O4 Nanophosphor. Nanoscale Research Letters, 2017, 12, 536.	3.1	1
33994	Large change of magnetic moment in Ni<inf>13</inf>Co<inf>3</inf>Mn<inf>13</inf>Sn<inf>3</inf> and Ni<inf>13</inf>Co<inf>3</inf>Mn<inf>13</inf>Sn<inf>2</inf>Al<inf>1</inf> Heusler alloys at martensitic transitions: Investigation from first principles. , 2017, , .		0
33995	Discovering charge density functionals and structure-property relationships with PROPhet: A general framework for coupling machine learning and first-principles methods. Scientific Reports, 2017, 7, 1192.	1.6	98
33996	Linear magnetoelectric effect in gÃ¶thite, Î±-FeOOH. Scientific Reports, 2017, 7, 16410.	1.6	7
33998	Effects of multiple atom doping in graphene. , 2017, , .		0
33999	Synthesis and First-principle Calculation of TiO2 Rutile Nanowire Electrodes for Dye-sensitized Solar Cells. International Journal of Electrochemical Science, 2017, 12, 9725-9735.	0.5	4
34000	Vibrational and Thermodynamic Properties of Layered LiM0.5Ni0.5O2 (M=Mn, Co) Cathode Materials for Li Ion Batteries. International Journal of Electrochemical Science, 2017, , 2963-2972.	0.5	1
34001	Bandgap Engineering of Black Phosphorus-Based Nano structures. , 2017, , .		0
34002	Electronic and magnetic properties of SnS 2 monolayer doped with 4 d transition metals. Journal of Magnetism and Magnetic Materials, 2017, 438, 152-162.	1.0	35
34003	First-principles simulation on thermoelectric properties in Bi-Sb System. Journal of Physics: Conference Series, 2017, 939, 012019.	0.3	2
34004	Validation of missed space-group symmetry in X-ray powder diffraction structures with dispersion-corrected density functional theory. Acta Crystallographica Section B: Structural Science, Crystal Engineering and Materials, 2017, 73, 756-766.	0.5	2
34005	Au55, a stable glassy cluster: results of ab initio calculations. Beilstein Journal of Nanotechnology, 2017, 8, 2221-2229.	1.5	6
34006	Theoretical Studies of the Adsorption and Migration Behavior of Boron Atoms on Hydrogen-Terminated Diamond (001) Surface. Coatings, 2017, 7, 57.	1.2	8
34007	First-Principles Calculation for the Half Metallic Properties of La 2 NbMnO 6. Chinese Physics Letters, 2017, 34, 107101.	1.3	3
34009	ZnO-polyethylene interface: Band alignment. , 2017, , .		1
34010	First-Principles Calculations of Ti₂N and Ti₂NT₂ (T = O, F, OH) Monolayers as Potential Anode Materials for Lithium-Ion Batteries and Beyond. Journal of Physical Chemistry C, 2017, 121, 13025-13034.	1.5	151

#	Article	IF	Citations
34011	New tetrahedral polymorphs of the group-14 elements. Journal of Physics: Conference Series, 2017, 950, 042010.	0.3	0
34012	Notice of Removal Antimony diffusion in CdTe. , 2017, , .		0
34013	A thermal neutron scattering law for yttrium hydride. EPJ Web of Conferences, 2017, 146, 13005.	0.1	13
34014	Cluster assembly route to a novel octagonal two-dimensional ZnO monolayer. Journal of Physics Condensed Matter, 2017, 29, 335501.	0.7	11
34015	Methanol Desorption from Cu-ZSM-5 Studied by In Situ Infrared Spectroscopy and First-Principles Calculations. Journal of Physical Chemistry C, 2017, 121, 27389-27398.	1.5	23
34016	Ab initiostudies of isolated boron substitutional defects ingraphane. Journal of Physics: Conference Series, 2017, 905, 012032.	0.3	0
34017	Unexpected robustness of the band gaps of TiO2 under high pressures. Journal of Physics Communications, 2017, 1, 055014.	0.5	3
34018	Prediction of Fundamental Properties of Semiconductors and Materials Exploration Using First-Principles Calculations. Materia Japan, 2017, 56, 554-559.	0.1	0
34019	Infrared Spectroscopic and Computational Studies on Li₄FeH₆ with High Gravimetric Hydrogen Density. Materials Transactions, 2017, 58, 157-159.	0.4	4
34020	A Computational Study of the Combustion of Hydrazine with Dinitrogen Tetroxide. Journal of Nanotoxicology and Nanomedicine, 2017, 2, 12-30.	0.7	2
34021	Discretization error cancellation in electronic structure calculation: toward a quantitative study. ESAIM: Mathematical Modelling and Numerical Analysis, 2017, 51, 1617-1636.	0.8	8
34022	Novel band structures in germanene on aluminium nitride substrate. Japanese Journal of Applied Physics, 2017, 56, 095201.	0.8	2
34023	First-Principles Density Functional Theory Calculation of Metal-Substituted Lead Halide Perovskite. , 2017, , .		0
34024	Interface engineering: The Ni(OH) 2 /MoS 2 heterostructure for highly efficient alkaline hydrogen evolution. Nano Energy, 2017, 37, 74-80.	8.2	436
34025	First principles application for mechanical properties of Ti-doped W particles enhanced U matrix composite. Rare Metals, 2018, 37, 815-822.	3.6	4
34026	Gas sensing and capturing based on twoâ€dimensional layered materials: Overview from theoretical perspective. Wiley Interdisciplinary Reviews: Computational Molecular Science, 2018, 8, e1361.	6.2	101
34027	Dependence of hydrogen-absorption and -desorption characteristics on density of lithiumâ€“zirconium oxides exposed in air at room temperature. Acta Materialia, 2018, 148, 185-192.	3.8	5
34028	High coverage H2 adsorption and dissociation on fcc Co surfaces from DFT and thermodynamics. International Journal of Hydrogen Energy, 2018, 43, 5576-5590.	3.8	23

#	Article	IF	Citations
34029	Stability and elasticity of metastable solid solutions and superlattices in the MoNâ€“TaN system: First-principles calculations. Materials and Design, 2018, 144, 310-322.	3.3	29
34030	Anisotropic carrier mobility in single- and bi-layer C 3 N sheets. Physica B: Condensed Matter, 2018, 537, 314-319.	1.3	38
34031	Oxygen evolution reaction in nanoconfined carbon nanotubes. Physica E: Low-Dimensional Systems and Nanostructures, 2018, 99, 1-5.	1.3	9
34032	Lewis Base Passivation of Hybrid Halide Perovskites Slows Electronâ€“Hole Recombination: Time-Domain Ab Initio Analysis. Journal of Physical Chemistry Letters, 2018, 9, 1164-1171.	2.1	90
34033	>1000-Fold Lifetime Extension of a Nickel Electromechanical Contact Device via Graphene. ACS Applied Materials & Interfaces, 2018, 10, 9085-9093.	4.0	23
34034	Suppression of Cation Segregation in (La,Sr)CoO_{3â^'Î´} by Elastic Energy Minimization. ACS Applied Materials & Interfaces, 2018, 10, 8057-8065.	4.0	44
34035	Surface Adatom Mediated Structural Transformation in Bromoarene Monolayers: Precursor Phases in Surface Ullmann Reaction. ACS Nano, 2018, 12, 2267-2274.	7.3	49
34036	Bulk and surface properties of metal carbides: implications for catalysis. Physical Chemistry Chemical Physics, 2018, 20, 6905-6916.	1.3	82
34037	Depolymerization of sodium polyphosphates on an iron oxide surface at high temperature. Physical Chemistry Chemical Physics, 2018, 20, 7819-7835.	1.3	15
34038	Tuning mobility and stability of lithium ion conductors based on lattice dynamics. Energy and Environmental Science, 2018, 11, 850-859.	15.6	158
34039	Anti-perovskite cathodes for lithium batteries. Journal of Materials Chemistry A, 2018, 6, 5185-5192.	5.2	39
34040	Highly polarization sensitive photodetectors based on quasi-1D titanium trisulfide (TiS₃). Nanotechnology, 2018, 29, 184002.	1.3	67
34041	Strong anti-strain capacity of CoFeB/MgO interface on electronic structure and state coupling. Chinese Physics B, 2018, 27, 017502.	0.7	1
34042	Elastic, mechanical, and thermodynamic properties of Bi-Sb binaries: Effect of spin-orbit coupling. Physical Review B, 2018, 97, .	1.1	76
34043	Two-dimensional ferroelectric topological insulators in functionalized atomically thin bismuth layers. Physical Review B, 2018, 97, .	1.1	37
34044	Structural and optical properties of Ni atoms and $$hbox {Ni}_{55}$$ Ni 55 cluster adsorbed on a rutile $$hbox {TiO}_{2}$$. Theoretical Chemistry Accounts, 2018, 137, 1.	0.5	2
34045	Adsorption of Carbohydrazide on Au(111) and Au3Ni(111) Surfaces. Catalysis Letters, 2018, 148, 1073-1079.	1.4	4
34046	Insight into solid-solution strengthened bulk and stacking faults properties in Ti alloys: a comprehensive first-principles study. Journal of Materials Science, 2018, 53, 7493-7505.	1.7	17

#	Article	IF	Citations
34047	First-principles investigation of quantum transport in GeP3 nanoribbon-based tunneling junctions. Frontiers of Physics, 2018, 13, 1.	2.4	6
34048	Structural, dynamical and thermodynamic properties of CdXP2 (XÂ=ÂSi, Ge) from first principles. Indian Journal of Physics, 2018, 92, 315-323.	0.9	5
34049	Tuning the magnetic properties of DyNiO3 by high-pressures. Computational Materials Science, 2018, 146, 213-219.	1.4	2
34050	Improved stability of Ni-rich cathode by the substitutive cations with stronger bonds. Electrochimica Acta, 2018, 268, 41-48.	2.6	62
34051	Structural analysis and electrical characterization of cation-substituted lithium ion conductors Li1â^'Ti1â^'MOPO4 (Mâ€¯=â€¯Nb, Ta, Sb). Solid State Ionics, 2018, 319, 170-179.	1.3	4
34052	DFT-Computed Trends in the Properties of Bimetallic Precious Metal Nanoparticles with Core@Shell Segregation. Journal of Physical Chemistry C, 2018, 122, 5721-5730.	1.5	19
34053	Influence of Strain on the Surfaceâ€“Oxygen Interaction and the Oxygen Evolution Reaction of SrIrO₃. Journal of Physical Chemistry C, 2018, 122, 4359-4364.	1.5	39
34054	C-Methylation of Alcohols, Ketones, and Indoles with Methanol Using Heterogeneous Platinum Catalysts. ACS Catalysis, 2018, 8, 3091-3103.	5.5	85
34055	Hybrid Dionâ€“Jacobson 2D Lead Iodide Perovskites. Journal of the American Chemical Society, 2018, 140, 3775-3783.	6.6	686
34056	Route to high-energy density polymeric nitrogen t-N via Heâ^'N compounds. Nature Communications, 2018, 9, 722.	5.8	131
34057	Probing the impact of magnetic interactions on the lattice dynamics of two-dimensional Ti₂X (X = C, N) MXenes. Physical Chemistry Chemical Physics, 2018, 20, 7754-7763.	1.3	27
34058	Two-dimensional GeSe for high performance thin-film solar cells. Journal of Materials Chemistry A, 2018, 6, 5032-5039.	5.2	83
34059	The graphene/n-Ge(110) interface: structure, doping, and electronic properties. Nanoscale, 2018, 10, 6088-6098.	2.8	28
34060	Room-temperature relaxor ferroelectricity and photovoltaic effects in tin titanate directly deposited on a silicon substrate. Physical Review B, 2018, 97, .	1.1	28
34061	First-principles investigation of magnetocrystalline anisotropy oscillations in <mml:math xmlns:mml="http://www.w3.org/1998/Math/MathML"><mml:mrow><mml:msub><mml:mi>Co</mml:mi><mml:mn>2</mml:mn></mml:msub></mml: heterostructures. Physical Review B, 2018, 97, .	1.1	10
34062	DEPENDENCE OF HOMOâ€“LUMO GAP OF DNA BASE PAIR STEPS ON TWIST ANGLE: A DENSITY FUNCTIONAL APPROACH. Journal of Biological Systems, 2018, 26, 23-40.	0.5	2
34063	Graphite as Cointercalation Electrode for Sodiumâ€ion Batteries: Electrode Dynamics and the Missing Solid Electrolyte Interphase (SEI). Advanced Energy Materials, 2018, 8, 1702724.	10.2	191
34064	First-principles study of the structural, elastic and electronic properties of SbXI (X=S, Se, Te) crystals. Journal of Molecular Modeling, 2018, 24, 66.	0.8	23

#	Article	IF	Citations
34065	Enhanced carbon monoxide sensing properties of TiO2 with exposed (0 0 1) facet: A combined first-principle and experimental study. Applied Surface Science, 2018, 442, 507-516.	3.1	85
34066	An ab initio study of mechanical and dynamical stability of MoSi2. Journal of Alloys and Compounds, 2018, 746, 720-728.	2.8	17
34067	2D Hydrogenated graphene-like borophene as a high capacity anode material for improved Li/Na ion batteries: A first principles study. Materials Today Energy, 2018, 8, 22-28.	2.5	93
34068	Investigation on structure, electronic and magnetic properties of Cr doped (ZnO)12 clusters: First-principles calculations. Physica E: Low-Dimensional Systems and Nanostructures, 2018, 99, 51-57.	1.3	2
34069	Role of Structural Defects in the Water Adsorption Properties of MOF-801. Journal of Physical Chemistry C, 2018, 122, 5545-5552.	1.5	68
34070	Effect of glycine functionalization of 2D titanium carbide (MXene) on charge storage. Journal of Materials Chemistry A, 2018, 6, 4617-4622.	5.2	103
34071	Deep defect level engineering: a strategy of optimizing the carrier concentration for high thermoelectric performance. Energy and Environmental Science, 2018, 11, 933-940.	15.6	188
34072	Structural and electronic properties of hydrogenated GaBi and InBi honeycomb monolayers with point defects. RSC Advances, 2018, 8, 7022-7028.	1.7	9
34073	A C20 fullerene-based sheet with ultrahigh thermal conductivity. Nanoscale, 2018, 10, 6099-6104.	2.8	12
34074	Promoting sulfur adsorption using surface Cu sites in metalâ€“organic frameworks for lithium sulfur batteries. Journal of Materials Chemistry A, 2018, 6, 4811-4821.	5.2	85
34075	Quantum tunneling in real space: Tautomerization of single porphycene molecules on the (111) surface of Cu, Ag, and Au. Journal of Chemical Physics, 2018, 148, 102330.	1.2	29
34076	xNiâ€“yCuâ€“ZrO₂ catalysts for the hydrogenation of levulinic acid to gamma valorlactone. Journal of Lithic Studies, 2018, 4, 12-23.	0.1	9
34077	On the thermal expansion in MgSiN₂. Journal Physics D: Applied Physics, 2018, 51, 105108.	1.3	5
34078	New two-dimensional V-V binary compounds with a honeycomb-like structure: a first-principles study. Materials Research Express, 2018, 5, 035903.	0.8	34
34079	Strain relaxation induced coexistence of ferromagnetism and antiferromagnetism in (110)-oriented <mml:math xmlns:mml="http://www.w3.org/1998/Math/MathML"><mml:msub><mml:mi>LuMnO</mml:mi><mml:mn>3</mml:mn></mml:msub></ thin films on <mml:math xmlns:mml="http://www.w3.org/1998/Math/MathML"><mml:msub><mml:mi>YAlO</mml:mi><mml:mn>3</mml:mn></mml:msub></mr : A first-principles study. Physical Review B, 2018, 97, .	1.1	7
34080	First-Order Interfacial Transformations with a Critical Point: Breaking the Symmetry at a Symmetric Tilt Grain Boundary. Physical Review Letters, 2018, 120, 085702.	2.9	43
34081	Kinetics and Atomic Mechanisms of Structural Phase Transformations in Photoexcited Monolayer TMDCs. MRS Advances, 2018, 3, 345-350.	0.5	0
34082	Exploring Critical Factors Affecting Strain Distribution in 1D Siliconâ€Based Nanostructures for Lithiumâ€Ion Battery Anodes. Advanced Materials, 2018, 30, e1705430.	11.1	113

#	Article	IF	Citations
34083	Bandgap Engineering of Stable Leadâ€Free Oxide Double Perovskites for Photovoltaics. Advanced Materials, 2018, 30, e1705901.	11.1	57
34084	Internal Polarization Modulation in Bi₂MoO₆ for Photocatalytic Performance Enhancement under Visibleâ€Light Illumination. ChemSusChem, 2018, 11, 1521-1532.	3.6	55
34085	Spin polarization properties of benzene/graphene with transition metals as dopants: First principles calculations. Applied Surface Science, 2018, 439, 1158-1162.	3.1	14
34086	Vibrational and thermodynamic properties of LiBH 4 polymorphs from first-principles calculations. International Journal of Hydrogen Energy, 2018, 43, 6625-6631.	3.8	11
34087	VSC-doping and VSU-doping of Na3V2-xTix(PO4)2F3 compounds for sodium ion battery cathodes: Analysis of electrochemical performance and kinetic properties. Nano Energy, 2018, 47, 340-352.	8.2	113
34088	Instability of the layered orthorhombic post-perovskite phase of SrTiO3 and other candidate orthorhombic phases under pressure. Solid State Communications, 2018, 274, 27-30.	0.9	5
34089	New Iron-Based Intercalation Host for Lithium-Ion Batteries. Chemistry of Materials, 2018, 30, 1956-1964.	3.2	20
34090	Barrierless On-Surface Metal Incorporation in Phthalocyanine-Based Molecules. Journal of Physical Chemistry C, 2018, 122, 6678-6683.	1.5	11
34091	Direct n- to p-Type Channel Conversion in Monolayer/Few-Layer WS₂ Field-Effect Transistors by Atomic Nitrogen Treatment. ACS Nano, 2018, 12, 2506-2513.	7.3	107
34092	Reactivity ofÂHe withÂionic compounds under high pressure. Nature Communications, 2018, 9, 951.	5.8	59
34093	Black hybrid iodobismuthate containing linear anionic chains. New Journal of Chemistry, 2018, 42, 6354-6363.	1.4	30
34094	InSe: a two-dimensional material with strong interlayer coupling. Nanoscale, 2018, 10, 7991-7998.	2.8	102
34095	Hierarchical MoS₂/Carbon microspheres as long-life and high-rate anodes for sodium-ion batteries. Journal of Materials Chemistry A, 2018, 6, 5668-5677.	5.2	128
34096	Complementary evaluation of structure stability of perovskite oxides using bond-valence and density-functional-theory calculations. Science and Technology of Advanced Materials, 2018, 19, 101-107.	2.8	38
34097	Suppression of material transfer at contacting surfaces: the effect of adsorbates on Al/TiN and Cu/diamond interfaces from first-principles calculations. Journal of Physics Condensed Matter, 2018, 30, 105001.	0.7	7
34098	Carbon diffusion in molten uranium: anab initiomolecular dynamics study. Modelling and Simulation in Materials Science and Engineering, 2018, 26, 035013.	0.8	4
34099	Modulation of electronic and magnetic properties in InSe nanoribbons: edge effect. Nanotechnology, 2018, 29, 205708.	1.3	15
34100	Atomic structure of a metal-supported two-dimensional germania film. Physical Review B, 2018, 97, .	1.1	16

#	Article	IF	Citations
34101	Shock compression of strongly correlated oxides: A liquid-regime equation of state for cerium(IV) oxide. Physical Review B, 2018, 97, .	1.1	17
34102	Tip-induced local strain on <mml:math xmlns:mml="http://www.w3.org/1998/Math/MathML"><mml:mrow><mml:mi>Mo</mml:mi><mml:msub><mml:mi mathvariant="normal">S</mml:mi><mml:mn>2</mml:mn></mml:msub><mml:mo>/</mml:mo><mml:mi>graphite</mml:mi></mml:mr detected by inelastic electron tunneling spectroscopy. Physical Review B, 2018, 97, .	1.1	6
34103	Encapsulating Various Sulfur Allotropes within Graphene Nanocages for Longâ€Lasting Lithium Storage. Advanced Functional Materials, 2018, 28, 1706443.	7.8	60
34104	The oxidation of methanol on hydroxylated m-ZrO2(â^'Â1 1 1): a first-principles study. Theoretical Chemistry Accounts, 2018, 137, 1.	0.5	2
34105	Water Dissociative Adsorption on Î±-Al₂O₃(112Ì…0) Is Controlled by Surface Site Undercoordination, Density, and Topology. Journal of Physical Chemistry C, 2018, 122, 6573-6584.	1.5	17
34106	Molecular Photophysics under Shock Compression: Ab Initio Nonadiabatic Molecular Dynamics of Rhodamine Dye. Journal of Physical Chemistry C, 2018, 122, 13600-13607.	1.5	4
34107	Combined Experimental and Theoretical Study of Methyl Acetoacetate Adsorption on Ni{100}. Journal of Physical Chemistry C, 2018, 122, 6186-6194.	1.5	6
34108	Switch in Relative Stability between cis and trans 2-Butene on Pt(111) as a Function of Experimental Conditions: A Density Functional Theory Study. ACS Catalysis, 2018, 8, 3067-3075.	5.5	8
34109	Operando spectroscopy study of the carbon dioxide electro-reduction by iron species on nitrogen-doped carbon. Nature Communications, 2018, 9, 935.	5.8	182
34110	Batch production of 6-inch uniform monolayer molybdenum disulfide catalyzed by sodium in glass. Nature Communications, 2018, 9, 979.	5.8	338
34111	An atomic-scale view of single-site Pt catalysis for low-temperature CO oxidation. Nature Catalysis, 2018, 1, 192-198.	16.1	292
34112	Materials discovery by chemical analogy: role of oxidation states in structure prediction. Faraday Discussions, 2018, 211, 553-568.	1.6	22
34113	Thin-film topological insulators for continuously tunable terahertz absorption. Applied Physics Letters, 2018, 112, .	1.5	8
34114	Coreâ€“Shell NiO@Niâ€P Hybrid Nanosheet Array for Synergistically Enhanced Oxygen Evolution Electrocatalysis: Experimental and Theoretical Insights. Chemistry - an Asian Journal, 2018, 13, 944-949.	1.7	9
34115	Computational analysis of the competitive bonding and reactivity pattern of a bifunctional cyclooctyne on Si(001). Theoretical Chemistry Accounts, 2018, 137, 1.	0.5	16
34116	Selective synthesis of higher manganese silicides: a new Mn17Si30 phase, its electronic, transport, and optical properties in comparison with Mn4Si7. Journal of Materials Science, 2018, 53, 7571-7594.	1.7	3
34117	The Structural Stability and Mechanical Properties of $$hbox {Cu}_{2}hbox {MnAl}$$ Cu 2 MnAl and $$hbox {Cu}_{2}hbox {MnIn}. Journal of Electronic Materials, 2018, 47, 3005-3017.	1.0	2
34118	Mechanical properties in thermoelectric oxides: Ideal strength, deformation mechanism, and fracture toughness. Acta Materialia, 2018, 149, 341-349.	3.8	25

#	Article	IF	Citations
34119	The surface stability and morphology of tobermorite 11â€˜Ã… from first principles. Applied Surface Science, 2018, 444, 287-292.	3.1	15
34120	Magnetic properties and thermal stability of N-doped CrO2 (100) films. Ceramics International, 2018, 44, 9664-9670.	2.3	5
34121	Mn promoted Co catalysts for Fischer-Tropsch production of light olefins â€“ An experimental and theoretical study. Journal of Catalysis, 2018, 361, 23-32.	3.1	62
34122	On the origin of vibrational properties of calcium manganate based thermoelectric compounds. Nano Energy, 2018, 47, 451-462.	8.2	19
34123	Tailoring the electrocatalytic activity of bimetallic nickel-iron diselenide hollow nanochains for water oxidation. Nano Energy, 2018, 47, 275-284.	8.2	116
34124	Thickness-dependent surface energies of few-layered arsenene and antimonene films in Î± and Î² phases. Physica E: Low-Dimensional Systems and Nanostructures, 2018, 101, 38-43.	1.3	8
34125	Understanding the Formation of the Truncated Morphology of High-Voltage Spinel LiNi_{0.5}Mn_{1.5}O₄ via Direct Atomic-Level Structural Observations. Chemistry of Materials, 2018, 30, 2174-2182.	3.2	38
34126	Oxygen Vacancy Formation and Water Adsorption on Reduced AnO₂{111}, {110}, and {100} Surfaces (An = U, Pu): A Computational Study. Journal of Physical Chemistry C, 2018, 122, 7149-7165.	1.5	45
34127	Electronic Origin and Kinetic Feasibility of the Lattice Oxygen Participation During the Oxygen Evolution Reaction on Perovskites. Journal of Physical Chemistry Letters, 2018, 9, 1473-1479.	2.1	62
34128	Origins of the Stokes Shift in PbS Quantum Dots: Impact of Polydispersity, Ligands, and Defects. ACS Nano, 2018, 12, 2838-2845.	7.3	50
34129	Metal-Free Oxygen Evolution and Oxygen Reduction Reaction Bifunctional Electrocatalyst in Alkaline Media: From Mechanisms to Structureâ€“Catalytic Activity Relationship. ACS Sustainable Chemistry and Engineering, 2018, 6, 4973-4980.	3.2	62
34130	Dielectric properties of hexagonal boron nitride and transition metal dichalcogenides: from monolayer to bulk. Npj 2D Materials and Applications, 2018, 2, .	3.9	563
34131	Vertically co-oriented two dimensional metal-organic frameworks for packaging enhanced supercapacitive performance. Communications Chemistry, 2018, 1, .	2.0	73
34132	Hydride ion (H^{â^’}) transport behavior in barium hydride under high pressure. Physical Chemistry Chemical Physics, 2018, 20, 8917-8923.	1.3	17
34133	Effect of cation substitution on the pseudocapacitive performance of spinel cobaltite MCo₂O₄ (M = Mn, Ni, Cu, and Co). Journal of Materials Chemistry A, 2018, 6, 10674-10685.	5.2	266
34134	A high-throughput exploration of magnetic materials by using structure predicting methods. Journal of Applied Physics, 2018, 123, .	1.1	9
34135	Transition-metal-doped group-IV monochalcogenides: a combination of two-dimensional triferroics and diluted magnetic semiconductors. Nanotechnology, 2018, 29, 215703.	1.3	41
34136	Theoretical study on electronic structure and thermoelectric properties of PbS _x Te _{1â^’ x} (x = 0.25, 0.5, and 0.75) solid solution. Chinese Physics B, 2018, 27, 026103.	0.7	4

#	Article	IF	Citations
34137	Prediction of manganese trihalides as two-dimensional Dirac half-metals. Physical Review B, 2018, 97, .	1.1	107
34138	Observation of gapless Dirac surface states in ZrGeTe. Physical Review B, 2018, 97, .	1.1	34
34139	Perovskite <mml:math xmlns:mml="http://www.w3.org/1998/Math/MathML"><mml:msub><mml:mi mathvariant="bold">ThTaN</mml:mi><mml:mn mathvariant="bold">3</mml:mn></mml:msub></mml:math> : A large-thermopower topological crystalline insulator. Physical Review B, 2018, 97, .	1.1	17
34140	Quartic Anharmonicity of Rattlers and Its Effect on Lattice Thermal Conductivity of Clathrates from First Principles. Physical Review Letters, 2018, 120, 105901.	2.9	130
34141	Theoretical Insights into the Effect of the Framework on the Initiation Mechanism of the MTO Process. Catalysis Letters, 2018, 148, 1246-1253.	1.4	46
34142	Temperature-induced structural evolution in liquid Sn85Zn15 eutectic alloy. Scripta Materialia, 2018, 148, 68-72.	2.6	11
34143	Changes in Electronic Structure upon Li Deintercalation from LiCoPO₄ Derivatives. Chemistry of Materials, 2018, 30, 1898-1906.	3.2	26
34144	An Earth-Abundant Tungstenâ€“Nickel Alloy Electrocatalyst for Superior Hydrogen Evolution. ACS Applied Nano Materials, 2018, 1, 1228-1235.	2.4	57
34145	Interlocking Mechanism between Molecular Gears Attached to Surfaces. ACS Nano, 2018, 12, 3020-3029.	7.3	21
34146	Theoretical study of tetrahedral site occupation by hydrogen in Pd nanoparticles. Journal of Chemical Physics, 2018, 148, 034705.	1.2	18
34147	First principles study of LiAlO₂: new dense monoclinic phase under high pressure. Journal of Physics Condensed Matter, 2018, 30, 115401.	0.7	4
34148	On-surface synthesis on a bulk insulator surface. Journal of Physics Condensed Matter, 2018, 30, 133001.	0.7	7
34149	Giant magnetic anisotropy and robust quantum anomalous Hall effect in boron-doped graphene with Re-adsorption. Journal of Physics Condensed Matter, 2018, 30, 145001.	0.7	1
34150	One dimensional metallic edges in atomically thin WSe ₂ induced by air exposure. 2D Materials, 2018, 5, 025017.	2.0	47
34151	Comparison of mechanical and thermodynamic properties of fcc and bcc titanium under high pressure. Materials Research Express, 2018, 5, 026527.	0.8	1
34152	Efficient evaluation of nonlocal operators in density functional theory. Physical Review B, 2018, 97, .	1.1	5
34153	Correlation matrix renormalization theory for correlated-electron materials with application to the crystalline phases of atomic hydrogen. Physical Review B, 2018, 97, .	1.1	7
34154	Extremely large magnetoresistance and electronic structure of TmSb. Physical Review B, 2018, 97, .	1.1	23

#	Article	IF	Citations
34155	Electronic and magnetic properties of two dimensional cluster-assembled materials based on TM@Si12 (TMâ€¯=â€¯3d transition metal) clusters. Computational Materials Science, 2018, 146, 134-142.	1.4	12
34156	Effects of alloying elements on the stability and mechanical properties of Fe3Al from first-principles calculations. Computational Materials Science, 2018, 146, 303-309.	1.4	11
34157	Anisotropic magnetocaloric response in AlFe2B2. Journal of Alloys and Compounds, 2018, 745, 505-512.	2.8	49
34158	Study on the thermoelectric performance of polycrystal SnSe with Se vacancies. Journal of Alloys and Compounds, 2018, 745, 513-518.	2.8	27
34159	Mechanistic study of the catalytic conversion of 2,3-butanediol to butenes. Journal of Catalysis, 2018, 360, 221-239.	3.1	15
34160	Coralloid Carbon Fiber-Based Composite Lithium Anode for Robust Lithium Metal Batteries. Joule, 2018, 2, 764-777.	11.7	609
34161	Crystal facet-dependent p-type and n-type sensing responses of TiO 2 nanocrystals. Sensors and Actuators B: Chemical, 2018, 263, 557-567.	4.0	48
34162	Effect of structural defects on electronic and magnetic properties of ZrS 2 monolayer. Superlattices and Microstructures, 2018, 116, 164-170.	1.4	14
34163	Bismuth titanate pyrochlores doped by alkaline earth elements: First-principles calculations and experimental study. Solid State Ionics, 2018, 317, 183-189.	1.3	17
34164	A New Effective Approach to Prevent the Degradation of Black Phosphorus: The Scandium Transition Metal Doping. Journal of Physical Chemistry C, 2018, 122, 9654-9662.	1.5	20
34165	A theoretical study on the mechanism of hydrogen evolution on non-precious partially oxidized nickel-based heterostructures for fuel cells. Physical Chemistry Chemical Physics, 2018, 20, 7968-7973.	1.3	15
34166	Stability and electronic structure of hydrogen vacancies in ADP: hybrid DFT with vdW correction. RSC Advances, 2018, 8, 6931-6939.	1.7	11
34167	Stability and mobility of supported Nin (nÂ= 1â€“10) clusters on ZrO2(111) and YSZ(111) surfaces: a density functional theory study. Faraday Discussions, 2018, 208, 87-104.	1.6	7
34168	Electronic properties and surface reactivity of SrO-terminated SrTiO₃ and SrO-terminated iron-doped SrTiO₃. Science and Technology of Advanced Materials, 2018, 19, 221-230.	2.8	31
34169	Novel elastic, lattice dynamics and thermodynamic properties of metallic single-layer transition metal phosphides: 2H-M₂P (Mo₂P, W₂P, Nb₂P and) Tj ETQq0 0 0 rgBT /Overlock 1		
34170	A theoretical insight into H accumulation and bubble formation by applying isotropic strain on the Wâ€“H system under a fusion environment. Nuclear Fusion, 2018, 58, 046014.	1.6	1
34171	Theoretical investigation of the band alignment of graphene on a polar <mml:math xmlns:mml="http://www.w3.org/1998/Math/MathML"><mml:mrow><mml:mi>SrTi</mml:mi><mml:msub><mml:mi mathvariant="normal">O</mml:mi><mml:mn>3</mml:mn></mml:msub></mml:mrow></mml:math> (111) surface. Physical Review B, 2018, 97, .	1.1	11
34172	Comment on â€œComparative study of ab initio nonradiative recombination rate calculations under different formalismsâ€• Physical Review B, 2018, 97, .	1.1	11

#	Article	IF	Citations
34173	Electronic bulk and domain wall properties in <mml:math xmlns:mml="http://www.w3.org/1998/Math/MathML"><mml:mi>B</mml:mi></mml:math> -site doped hexagonal <mml:math xmlns:mml="http://www.w3.org/1998/Math/MathML"><mml:msub><mml:mi>ErMnO</mml:mi><mml:mn>3</mml:mn></mml:msub></r Physical Review B, 2018, 97, .	1.1	34
34174	First-Principles Study of the Effect of Cr Content on Interstitial Oxygen Solution Behavior in Nb-Cr Alloys. Materials Science Forum, 2018, 913, 582-588.	0.3	0
34175	Polarity identification of ZnO(0001) surface by reflection high-energy electron diffraction. Japanese Journal of Applied Physics, 2018, 57, 045701.	0.8	0
34176	In Situ Hydrogenation and Crystal Chemistry Studies of Co₂Si Type Compounds MgPd₂ and Pd₂Zn. Zeitschrift Fur Anorganische Und Allgemeine Chemie, 2018, 644, 367-375.	0.6	1
34177	A strain-controlled C2N monolayer membrane for gas separation in PEMFC application. Applied Surface Science, 2018, 441, 408-414.	3.1	33
34178	Manganese deception on graphene and implications in catalysis. Carbon, 2018, 132, 623-631.	5.4	54
34179	Description of light-element magnetic systems via density functional theory plus U with an example system of fluorinated boron nitride: An efficient alternative to hybrid functional approach. Computational Materials Science, 2018, 146, 84-89.	1.4	2
34180	Atomic-scale understanding of non-stoichiometry effects on the electrochemical performance of Ni-rich cathode materials. Journal of Power Sources, 2018, 378, 750-758.	4.0	20
34181	Phase-field modeling of stress generation in polycrystalline LiCoO2. Solid State Ionics, 2018, 319, 209-217.	1.3	23
34182	Structure and Energetics of (111) Surface of Î³-Al₂O₃: Insights from DFT Including Periodic Boundary Approach. ACS Omega, 2018, 3, 1881-1888.	1.6	34
34183	Remarkable charge-transfer mobility from [6] to [10]phenacene as a high performance p-type organic semiconductor. Physical Chemistry Chemical Physics, 2018, 20, 8658-8667.	1.3	11
34184	Molecules ionization at phase transition in warm dense hydrogen. Journal of Physics: Conference Series, 2018, 946, 012121.	0.3	0
34185	A density functional theory study of the role of functionalized graphene particles as effective additives in power cable insulation. Royal Society Open Science, 2018, 5, 170772.	1.1	8
34186	CRSS of Mg-X(X=Zn, Y) Binary Solid Solution via First-Principles Study. Materials Science Forum, 2018, 913, 614-619.	0.3	2
34187	A Combined Experimental and Computational Study of Gas Sensing by Cu₃SnS₄ Nanoparticulate Film: High Selectivity, Stability, and Reversibility for Room Temperature H₂S Sensing. Advanced Materials Interfaces, 2018, 5, 1701492.	1.9	18
34188	Design of Pd-Pb Catalysts for Glycerol and Ethylene Glycol Electrooxidation in Alkaline Medium. Electrocatalysis, 2018, 9, 480-485.	1.5	20
34189	P-doping Li 2 CoSiO 4 /C cathode material: A joint experimental and theoretical study. Electrochimica Acta, 2018, 264, 166-172.	2.6	11
34190	First principles study of surface stability and segregation of PdRuRh ternary metal alloy system. Surface Science, 2018, 671, 51-59.	0.8	6

#	Article	IF	Citations
34191	Molecule-Adsorbed Topological Insulator and Metal Surfaces: A Comparative First-Principles Study. Chemistry of Materials, 2018, 30, 1849-1855.	3.2	10
34192	Inverse Band Structure Design via Materials Database Screening: Application to Square Planar Thermoelectrics. Chemistry of Materials, 2018, 30, 1540-1546.	3.2	29
34193	Point Defect Effects on Photoelectronic Properties of the Potential Metal-Free C₂N Photocatalysts: Insight from First-Principles Computations. Journal of Physical Chemistry C, 2018, 122, 5291-5302.	1.5	47
34194	Direct Determination of Atomic Structure and Magnetic Coupling of Magnetite Twin Boundaries. ACS Nano, 2018, 12, 2662-2668.	7.3	30
34195	Two spin-canting textures in the antiferromagnetic phase AF1 of MnWO₄based on the new polar atomistic model inP2. Journal of Physics Condensed Matter, 2018, 30, 135802.	0.7	1
34196	Origins of <mml:math xmlns:mml="http://www.w3.org/1998/Math/MathML"><mml:mi>n</mml:mi></mml:math> -type doping difficulties in perovskite stannates. Physical Review B, 2018, 97, .	1.1	41
34197	Synergistic Nanotubular Copperâ€Doped Nickel Catalysts for Hydrogen Evolution Reactions. Small, 2018, 14, e1704137.	5.2	111
34198	Single layer of carbon phosphide as an efficient material for optoelectronic devices. Journal of Materials Science, 2018, 53, 8314-8327.	1.7	41
34199	Computational Screening of Hydration Reactions for Thermal Energy Storage: New Materials and Design Rules. Chemistry of Materials, 2018, 30, 2006-2017.	3.2	45
34200	Size and Shape Effects on Charge Recombination Dynamics of TiO₂ Nanoclusters. Journal of Physical Chemistry C, 2018, 122, 5201-5208.	1.5	39
34201	Mechanisms of Formaldehyde and C₂ Formation from Methylene Reacting with CO₂ Adsorbed on Ni(110). Journal of Physical Chemistry C, 2018, 122, 13827-13833.	1.5	6
34202	Adsorption of Li on single-layer silicene for anodes of Li-ion batteries. Physical Chemistry Chemical Physics, 2018, 20, 8887-8896.	1.3	62
34203	Is ReO₃ a mixed ionicâ€“electronic conductor? A DFT study of defect formation and migration in a B^{VI}O₃ perovskite-type oxide. Physical Chemistry Chemical Physics, 2018, 20, 8008-8015.	1.3	16
34204	Different effects of water molecules on CO oxidation with different reaction mechanisms. Physical Chemistry Chemical Physics, 2018, 20, 8341-8348.	1.3	13
34205	Reassignment of â€˜magic numbersâ€™ for Au clusters of decahedral and FCC structural motifs. Nanoscale, 2018, 10, 5124-5132.	2.8	23
34206	Computational modeling of the effect of varying aqueous solutions on Ni(OH)2 precipitates. AIP Advances, 2018, 8, .	0.6	6
34207	Ground State Structures of Boron-Rich Rhodium Boride: An Ab Initio Study. Chinese Physics Letters, 2018, 35, 016401.	1.3	3
34208	Band structure and unconventional electronic topology of CoSi. Journal of Physics Condensed Matter, 2018, 30, 135501.	0.7	53

#	Article	IF	Citations
34209	Inducing and manipulating magnetization in 2D zincâ€“oxide by strain and external voltage. Journal of Physics Condensed Matter, 2018, 30, 145802.	0.7	0
34210	Strain-induced tunable negative differential resistance in triangle graphene spirals. Nanotechnology, 2018, 29, 205202.	1.3	6
34211	Single-layer 1 T â€²-MoS ₂ under electron irradiation from ab initio molecular dynamics. 2D Materials, 2018, 5, 025022.	2.0	13
34212	The electronic structures and optical properties of light-element atom adsorbed SnSe monolayers. Materials Research Express, 2018, 5, 035013.	0.8	4
34213	Electronic Structure, Mechanical and Dynamical Stability of Hexagonal Subcarbides M2C (M = Tc, Ru,) Tj ETQq0 0 0 rgBT /Overlock 10 Tf	0.2	18
34214	Crown oxygen-doping graphene with embedded main-group metal atoms. European Physical Journal B, 2018, 91, 1.	0.6	3
34215	Radioactive Iodine-129 Capture in Mixed Cation Sodalites: ab initio Modelling. MRS Advances, 2018, 3, 1105-1110.	0.5	2
34216	Epitaxial Growth of Honeycomb Monolayer CuSe with Dirac Nodal Line Fermions. Advanced Materials, 2018, 30, e1707055.	11.1	110
34217	Density Functional Theory Simulations of Water Adsorption and Activation on the (â^'201) Î²â€Ga₂O₃ Surface. Chemistry - A European Journal, 2018, 24, 7445-7455.	1.7	11
34218	Charge-doping and chemical composition-driven magnetocrystalline anisotropy in CoPt core-shell alloy clusters. Journal of Nanoparticle Research, 2018, 20, 1.	0.8	2
34219	Atomic-scale distorted lattice in chemically disordered equimolar complex alloys. Acta Materialia, 2018, 150, 182-194.	3.8	89
34220	Orthorhombic carbon oC24: A novel topological nodal line semimetal. Carbon, 2018, 133, 39-43.	5.4	48
34221	Enhance the fluorination activity of graphene via the interfacial interaction from Ni(1â€¯1â€¯1) substrate. Computational Materials Science, 2018, 147, 28-33.	1.4	7
34222	Surface thermodynamic stability, electronic and magnetic properties in various (001) surfaces of Zr2CoSn Heusler alloy. Superlattices and Microstructures, 2018, 117, 82-91.	1.4	8
34223	Diboryne Nanostructures Stabilized by Multitopic N-Heterocyclic Carbenes: A Computational Study. Inorganic Chemistry, 2018, 57, 3931-3940.	1.9	9
34224	Charge-Transfer-Promoted High Oxygen Evolution Activity of Co@Co₉S₈ Coreâ€“Shell Nanochains. ACS Applied Materials & Interfaces, 2018, 10, 11565-11571.	4.0	46
34225	Activating Layered Perovskite Compound Sr₂TiO₄ via La/N Codoping for Visible Light Photocatalytic Water Splitting. ACS Catalysis, 2018, 8, 3209-3221.	5.5	82
34226	First-principles investigation of polarization and ion conduction mechanisms in hydroxyapatite. Physical Chemistry Chemical Physics, 2018, 20, 8744-8752.	1.3	20

#	Article	IF	Citations
34227	Enhanced hydrogen permeability of hafnium nitride nanocrystalline membranes by interfacial hydride conduction. Journal of Materials Chemistry A, 2018, 6, 2730-2741.	5.2	16
34228	Revealing the correlation between real-space structure and chiral magnetic order at the atomic scale. Physical Review B, 2018, 97, .	1.1	7
34229	Spin friction in two-dimensional antiferromagnetic crystals. Physical Review B, 2018, 97, .	1.1	7
34230	Atomically thin gallium layers from solid-melt exfoliation. Science Advances, 2018, 4, e1701373.	4.7	157
34231	Structure, fragmentation patterns, and electronic properties of small indium oxide clusters. Theoretical Chemistry Accounts, 2018, 137, 1.	0.5	2
34232	Theoretical insight into methanol steam reforming on indium oxide with different coordination environments. Science China Chemistry, 2018, 61, 336-343.	4.2	20
34233	Evolution of amorphous carbon across densities: An inferential study. Carbon, 2018, 131, 168-174.	5.4	49
34234	Effect of nitrogen doping on electronic and optical properties of ZnO sheet: DFT+U study. Computational Condensed Matter, 2018, 15, 1-6.	0.9	11
34235	Active sites speciation of supported CoMoS phase probed by NO molecule: A combined IR and DFT study. Journal of Catalysis, 2018, 361, 62-72.	3.1	20
34236	Engineering phosphorus-doped LaFeO3-Î´ perovskite oxide as robust bifunctional oxygen electrocatalysts in alkaline solutions. Nano Energy, 2018, 47, 199-209.	8.2	202
34237	High performance Al₃Sc alloy doped Al₃Scâ€“Sb₂Te chalcogenides for phase change memory application. Journal of Materials Chemistry C, 2018, 6, 4177-4182.	2.7	19
34238	Structural, thermodynamic, and electronic properties of Laves-phase <mml:math xmlns:mml="http://www.w3.org/1998/Math/MathML"><mml:msub><mml:mi>NbMn</mml:mi><mml:mn>2</mml:mn></mml:msub><m from first principles, x-ray diffraction, and calorimetric experiments. Physical Review B, 2018, 97, .	1.1	6
34239	Standard Enthalpy of Formation of the Bimolecular Crystal of CL-20 with Tris-Oxadiazolo-Azepine and Its Thermal Stability. Combustion, Explosion and Shock Waves, 2018, 54, 89-96.	0.3	2
34240	Half-metallic ferromagnetism prediction in MoS₂-based two-dimensional superlattice from first-principles. Modern Physics Letters B, 2018, 32, 1850098.	1.0	4
34241	A first-principle study on the electronic properties of substitutionally Cu (I, II)-doped LiNbO₃. Journal of Advanced Dielectrics, 2018, 08, 1820002.	1.5	18
34242	Quantum Crystallography: Current Developments and Future Perspectives. Chemistry - A European Journal, 2018, 24, 10881-10905.	1.7	108
34243	Reversible K⁺-Insertion/Deinsertion and Concomitant Na⁺-Redistribution in Pâ€²3-Na_{0.52}CrO₂ for High-Performance Potassium-Ion Battery Cathodes. Chemistry of Materials, 2018, 30, 2049-2057.	3.2	76
34244	Palladium Carbide and Hydride Formation in the Bulk and at the Surface of Palladium Nanoparticles. Journal of Physical Chemistry C, 2018, 122, 12029-12037.	1.5	61

#	Article	IF	Citations
34245	Rational Surface Modification of Two-Dimensional Layered Black Phosphorus: Insights from First-Principles Calculations. ACS Omega, 2018, 3, 2445-2451.	1.6	10
34246	Lewisâ€“BrÃ¸nsted Acid Pairs in Ga/H-ZSM-5 To Catalyze Dehydrogenation of Light Alkanes. Journal of the American Chemical Society, 2018, 140, 4849-4859.	6.6	198
34247	Structural, electronic and adhesion characteristics of zinc/silica interfaces: ab initio study on zinc/Î²-cristobalite. Physical Chemistry Chemical Physics, 2018, 20, 6254-6263.	1.3	6
34248	Popgraphene: a new 2D planar carbon allotrope composed of 5â€“8â€“5 carbon rings for high-performance lithium-ion battery anodes from bottom-up programming. Journal of Materials Chemistry A, 2018, 6, 6815-6821.	5.2	212
34249	Exploring the formation and electronic structure properties of the g-C₃N₄nanoribbon with density functional theory. Journal of Physics Condensed Matter, 2018, 30, 155303.	0.7	11
34250	First-principles calculations on elastic, magnetoelastic, and phonon properties of Ni ₂ FeGa magnetic shape memory alloys. Chinese Physics B, 2018, 27, 016201.	0.7	2
34251	First-principles study of crystal structure, elastic stiffness constants, piezoelectric constants, and spontaneous polarization of orthorhombicPna2₁-M₂O₃(M) Tj ETQq0 0 0 rgBT /Overlock	0.8	10
34252	Detection of sub-MeV dark matter with three-dimensional Dirac materials. Physical Review D, 2018, 97, .	1.6	142
34253	Noble Metal Nanocluster Formation in Epitaxial Perovskite Thin Films. ACS Omega, 2018, 3, 2169-2173.	1.6	15
34254	Multi-objective Optimization for Materials Discovery via Adaptive Design. Scientific Reports, 2018, 8, 3738.	1.6	94
34255	Versatile two-dimensional silicon diphosphide (SiP₂) for photocatalytic water splitting. Nanoscale, 2018, 10, 6369-6374.	2.8	51
34256	Clathrate ice sL: a new crystalline phase of ice with ultralow density predicted by first-principles phase diagram computations. Physical Chemistry Chemical Physics, 2018, 20, 8333-8340.	1.3	23
34257	A bond-order potential for the Alâ€“Cuâ€“H ternary system. New Journal of Chemistry, 2018, 42, 5215-5228.	1.4	14
34258	First-Principles Study of Helium Trapping in Carbide Precipitates (Cr23C6) in Ferritic-Martensitic Steels. Fusion Science and Technology, 2018, 74, 177-185.	0.6	5
34259	Density functional theory computational study of ferroelectricity and piezoelectricity in BaTiO₃/PbTiO₃(0â€‰1â€‰1) superlattices. Journal of Physics Condensed Matter, 2018, 30, 155401.	0.7	1
34260	Electronic and mechanical properties of half-metallic half-Heusler compounds CoCr Z (Z = S, Se, and) Tj ETQq1 1 0.784314 rgBT /Overlo	0.7	8
34261	Multi- <mml:math xmlns:mml="http://www.w3.org/1998/Math/MathML" display="inline"><mml:mi>q</mml:mi></mml:math> Mesoscale Magnetism in <mml:math xmlns:mml="http://www.w3.org/1998/Math/MathML" display="inline"><mml:mrow><mml:msub><mml:mrow><mml:mi>CeAuSb</mml:mi></mml:mrow><mml:mrow><mml:mn>2</mml:mn> Physical Review Letters, 2018, 120, 097201.	2.9	34
34262	Pressure-induced phase transition in titanium alloys. International Journal of Modern Physics B, 2018, 32, 1850141.	1.0	1

#	Article	IF	Citations
34263	Resonant enhancement of band-to-band tunneling in in-plane MoS₂/WS₂heterojunctions. Japanese Journal of Applied Physics, 2018, 57, 04FP03.	0.8	5
34264	Substrateâ€Induced Phase of a Benzothiophene Derivative Detected by Midâ€Infrared and Lattice Phonon Raman Spectroscopy. ChemPhysChem, 2018, 19, 993-1000.	1.0	8
34265	Inâ€Plane Heterostructures Enable Internal Stress Assisted Strain Engineering in 2D Materials. Small, 2018, 14, e1703512.	5.2	9
34266	Direct Covalent Chemical Functionalization of Unmodified Two-Dimensional Molybdenum Disulfide. Chemistry of Materials, 2018, 30, 2112-2128.	3.2	93
34267	Understanding of Selective H₂ Generation from Hydrazine Decomposition on Ni(111) Surface. Journal of Physical Chemistry C, 2018, 122, 5443-5451.	1.5	26
34268	Engineering the Electronic Structure of Tin Sulfide Nanoribbons: A Computational Study. Journal of Physical Chemistry C, 2018, 122, 5731-5741.	1.5	18
34269	Effect of Sn-Doping on Behavior of Li-Intercalation in V₂O₅ Cathode Materials of Li-Ion Batteries: A Computational Perspective. Journal of Physical Chemistry C, 2018, 122, 5896-5907.	1.5	24
34270	Enhanced CO₂ Conversion to CO by Silica-Supported Perovskite Oxides at Low Temperatures. ACS Catalysis, 2018, 8, 3021-3029.	5.5	87
34271	A Linear Scaling Relation for CO Oxidation on CeO₂-Supported Pd. Journal of the American Chemical Society, 2018, 140, 4580-4587.	6.6	126
34272	Non-catalytic hydrogenation of VO2 in acid solution. Nature Communications, 2018, 9, 818.	5.8	87
34273	Nitrogen-doped tungsten carbide nanoarray as an efficient bifunctional electrocatalyst for water splitting in acid. Nature Communications, 2018, 9, 924.	5.8	571
34274	The reaction mechanism and selectivity of acetylene hydrogenation over Niâ€“Ga intermetallic compound catalysts: a density functional theory study. Dalton Transactions, 2018, 47, 4198-4208.	1.6	38
34275	Uncovering reaction sequences on surfaces through graphical methods. Physical Chemistry Chemical Physics, 2018, 20, 7721-7729.	1.3	10
34276	Synthesis of ultrathin Ni nanosheets for semihydrogenation of phenylacetylene to styrene under mild conditions. Nanoscale, 2018, 10, 6936-6944.	2.8	26
34277	Influence of lanthanides on spin-relaxation and spin-structure in a family of Fe₇Ln₄ single molecule magnets. Journal of Materials Chemistry C, 2018, 6, 2862-2872.	2.7	16
34278	Observation of soft phonon mode in <mml:math xmlns:mml="http://www.w3.org/1998/Math/MathML"><mml:mrow><mml:msub><mml:mi>TbFe</mml:mi><mml:mn>3</mml:mn></ by inelastic neutron scattering. Physical Review B, 2018, 97, .	1.1	1
34279	Strain-driven electric control of magnetization reversal at multiferroic interfaces. Physical Review B, 2018, 97, .	1.1	17
34280	Temperature Measurement by a Nanoscale Electron Probe Using Energy Gain and Loss Spectroscopy. Physical Review Letters, 2018, 120, 095901.	2.9	97

#	Article	IF	Citations
34281	The Oxygen Reduction Reaction Mechanism on FeN₃Doped Divacancy Graphene: A Theoretical Perspective. Journal of the Electrochemical Society, 2018, 165, F145-F151.	1.3	18
34282	Learning from the past: Are catalyst design principles transferrable between hydrodesulfurization and deoxygenation?. AIChE Journal, 2018, 64, 3121-3133.	1.8	9
34283	Where Does the Sulphur Go? Deactivation of a Low Temperature CO Oxidation Catalyst by Sulphur Poisoning. Catalysis Letters, 2018, 148, 1445-1450.	1.4	3
34284	Extended Hallâ€"Petch Relationships for Yield, Cleavage and Intergranular Fracture Strengths of bcc Steel and Its Deformation and Fracture Behaviors. Metals and Materials International, 2018, 24, 265-281.	1.8	21
34285	Structures of WxNy Crystals and Their Intrinsic Properties: First-Principles Calculations. Crystal Growth and Design, 2018, 18, 2270-2278.	1.4	20
34286	Crystal Structures and Electronic Properties of Oxygen-rich Titanium Oxides at High Pressure. Inorganic Chemistry, 2018, 57, 3254-3260.	1.9	19
34287	Projection-Based Correlated Wave Function in Density Functional Theory Embedding for Periodic Systems. Journal of Chemical Theory and Computation, 2018, 14, 1928-1942.	2.3	70
34288	Ternary Bismuthide SrPtBi₂: Computation and Experiment in Synergism to Explore Solid-State Materials. Journal of Physical Chemistry C, 2018, 122, 5057-5063.	1.5	4
34289	Enhanced Hydrogen Production from Methanol Photolysis on a Formate-Modified Rutile-TiO₂(110) Surface. Journal of Physical Chemistry C, 2018, 122, 13774-13781.	1.5	7
34290	Layered Insulator/Molecule/Metal Heterostructures with Molecular Functionality through Porphyrin Intercalation. ACS Nano, 2018, 12, 2677-2684.	7.3	14
34291	The kinetics of chirality assignment in catalytic single-walled carbon nanotube growth and the routes towards selective growth. Chemical Science, 2018, 9, 3056-3061.	3.7	41
34292	Sulfur film sandwiched between few-layered MoS₂ electrocatalysts and conductive reduced graphene oxide as a robust cathode for advanced lithiumâ€"sulfur batteries. Journal of Materials Chemistry A, 2018, 6, 5899-5909.	5.2	95
34293	Quantumâ€mechanical condensed matter simulations with CRYSTAL. Wiley Interdisciplinary Reviews: Computational Molecular Science, 2018, 8, e1360.	6.2	1,277
34294	The role of dopant charge state on defect chemistry and grain growth of doped UO2. Acta Materialia, 2018, 150, 403-413.	3.8	51
34295	Atomic-scale observation and analysis of chemical ordering in M3B2 and M5B3 borides. Acta Materialia, 2018, 149, 274-284.	3.8	37
34296	Site dependent enhancement of magnetic anisotropy in 4d and 5d impurity doped Î±â€³-Fe 16 N 2 : A first principles study. Current Applied Physics, 2018, 18, 526-533.	1.1	8
34297	Spontaneous antiferromagnetic order and strain effect on electronic properties of Î±-graphyne. Carbon, 2018, 131, 223-228.	5.4	19
34298	Electronic structure of Li+@C60: Photoelectron spectroscopy of the Li+@C60[PF6â^'] salt and STM of the single Li+@C60 molecules on Cu(111). Carbon, 2018, 133, 23-30.	5.4	17

#	Article	IF	Citations
34299	Mechanism of ferroelectric properties of (BaCa)(ZrTi)O3 from first-principles calculations. Ceramics International, 2018, 44, 9684-9688.	2.3	10
34300	Effect of alloying elements on mechanical, electronic and magnetic properties of Fe2B by first-principles investigations. Computational Materials Science, 2018, 147, 322-330.	1.4	23
34301	First-principles investigation of surface properties and adsorption of oxygen on Ni-22Cr and the role of molybdenum. Corrosion Science, 2018, 134, 103-111.	3.0	37
34302	A comparison study of the structural, electronic, magnetic and optical properties of yttrium-based Heusler alloys Y 3 Si, Y 2 CrSi and ScYCrSi. Materials Chemistry and Physics, 2018, 211, 283-294.	2.0	7
34303	Importance of van der Waals interaction on structural, vibrational, and thermodynamic properties of NaCl. Solid State Communications, 2018, 273, 11-16.	0.9	16
34304	Structural electronic and mechanical properties of YM2 (M=Mn, Fe, Co) laves phase compounds: First principle calculations analyzed with datamining approach. Solid State Communications, 2018, 274, 9-20.	0.9	8
34305	Understanding the Improved Kinetics and Cyclability of a Li₂MnSiO₄ Cathode with Calcium Substitution. Inorganic Chemistry, 2018, 57, 3223-3231.	1.9	14
34306	Tunable Band Gaps of In_xGa_{1â€“x}N Alloys: From Bulk to Two-Dimensional Limit. Journal of Physical Chemistry C, 2018, 122, 6930-6942.	1.5	35
34307	Structural behaviour of copper chloride catalysts during the chlorination of CO to phosgene. Faraday Discussions, 2018, 208, 67-85.	1.6	3
34308	A general representation scheme for crystalline solids based on Voronoi-tessellation real feature values and atomic property data. Science and Technology of Advanced Materials, 2018, 19, 231-242.	2.8	24
34309	Magnetic and electronic properties of single-walled Mo₂C nanotube: a first-principles study. Journal of Physics Condensed Matter, 2018, 30, 155305.	0.7	6
34310	Structural and electronic properties of the V-V compounds isoelectronic to GaN and isostructural to gray arsenic. Materials Research Express, 2018, 5, 035904.	0.8	2
34311	Supraâ€monolayer coverages on small metal clusters and their effects on H₂ chemisorption particle size estimates. AICHE Journal, 2018, 64, 3109-3120.	1.8	24
34312	Suppression of the Verwey Transition by Charge Trapping. Annalen Der Physik, 2018, 530, 1700363.	0.9	6
34313	First-principles study on the structure and electronic property of gas molecules adsorption on Ge2Li2 monolayer. Applied Surface Science, 2018, 442, 390-397.	3.1	4
34314	Enhanced chemical activity and wettability at adjacent BrÃ¸nsted acid sites in HZSM-5. Catalysis Today, 2018, 312, 44-50.	2.2	20
34315	Molecular-Level Insight into How Hydroxyl Groups Boost Catalytic Activity in CO2 Hydrogenation into Methanol. CheM, 2018, 4, 613-625.	5.8	110
34316	On the chemical effects in molten Ni1â^'xMx alloy. Computational Materials Science, 2018, 146, 158-175.	1.4	4

#	Article	IF	Citations
34317	Cubic diamondlike BC7 predicted from first principles as a superhard material. Computational Materials Science, 2018, 147, 238-242.	1.4	2
34318	Electrochemical and DFT studies of laser-alloyed TiB2/TiC/Al coatings on aluminium alloy. Corrosion Science, 2018, 136, 18-27.	3.0	21
34319	The PseudoDojo: Training and grading a 85 element optimized norm-conserving pseudopotential table. Computer Physics Communications, 2018, 226, 39-54.	3.0	1,001
34320	Iodate in calcite, aragonite and vaterite CaCO3: Insights from first-principles calculations and implications for the I/Ca geochemical proxy. Geochimica Et Cosmochimica Acta, 2018, 236, 351-360.	1.6	52
34321	Near-IR luminescence characteristics of monovalent bismuth in Bi-doped pure silica optical fiber: First-principle study. Journal of Luminescence, 2018, 198, 384-388.	1.5	21
34322	Ferroelectric engineering of two-dimensional group-IV monochalcogenides: The effects of alloying and strain. Journal of Materiomics, 2018, 4, 139-143.	2.8	21
34323	The defect chemistry of <mml:math xmlns:mml="http://www.w3.org/1998/Math/MathML" altimg="si1.gif" overflow="scroll"><mml:mrow><mml:mi mathvariant="normal">U</mml:mi><mml:msub><mml:mi mathvariant="normal">O</mml:mi><mml:mrow><mml:mn>2</mml:mn><mml:mo>Â±</mml:mo><mml:mi>x</mml:mi></mml:mrow></ from atomistic simulations. Journal of Nuclear Materials, 2018, 504, 251-260.	1.3	45
34324	Influence of surface termination on formaldehyde oxidation by Mn-doped ceria: A density function theory study. Molecular Catalysis, 2018, 448, 30-37.	1.0	8
34325	High-selective sensitive NH 3 gas sensor: A density functional theory study. Sensors and Actuators B: Chemical, 2018, 263, 502-507.	4.0	43
34326	Origin of enhanced catalytic activity of oxygen reduction reaction on zirconium oxynitrides: A first-principle study. Solid State Ionics, 2018, 317, 15-20.	1.3	6
34327	Imaging Catalytic Activation of CO₂ on Cu₂O (110): A First-Principles Study. Chemistry of Materials, 2018, 30, 1912-1923.	3.2	56
34328	Interfacial Interaction between Boron Cluster and Metal Oxide Surface and Its Effects: A Case Study of B₂₀/Ag₃PO₄ van der Waals Heterostructure. Journal of Physical Chemistry C, 2018, 122, 6151-6158.	1.5	7
34329	Tunable Electronic and Optical Properties of Monolayer and Multilayer Janus MoSSe as a Photocatalyst for Solar Water Splitting: A First-Principles Study. Journal of Physical Chemistry C, 2018, 122, 6209-6216.	1.5	233
34330	The intrinsic interface properties of the top and edge 1T/2H MoS2 contact: A first-principles study. Journal of Applied Physics, 2018, 123, .	1.1	19
34331	Stable iridium dinuclear heterogeneous catalysts supported on metal-oxide substrate for solar water oxidation. Proceedings of the National Academy of Sciences of the United States of America, 2018, 115, 2902-2907.	3.3	229
34332	Strain-engineering stabilization of <mml:math xmlns:mml="http://www.w3.org/1998/Math/MathML"><mml:mrow><mml:mi>BaTi</mml:mi><mml:msub><mml:mi mathvariant="normal">O</mml:mi><mml:mn>3</mml:mn></mml:msub></mml:mrow></mml:math> -based polar metals. Physical Review B, 2018, 97, .	1.1	26
34333	High Coke Resistance of a TiO₂ Anatase (001) Catalyst Surface during Dry Reforming of Methane. Journal of Physical Chemistry C, 2018, 122, 9389-9396.	1.5	7
34334	Thermally Induced Transformation of Nonhexagonal Carbon Rings in Graphene-like Nanoribbons. Journal of Physical Chemistry C, 2018, 122, 9586-9592.	1.5	14

#	Article	IF	Citations
34335	Electrooxidation of Glycerol on Gold in Acidic Medium: A Combined Experimental and DFT Study. Journal of Physical Chemistry C, 2018, 122, 10489-10494.	1.5	32
34336	Doubly Screened Hybrid Functional: An Accurate First-Principles Approach for Both Narrow- and Wide-Gap Semiconductors. Journal of Physical Chemistry Letters, 2018, 9, 2338-2345.	2.1	37
34337	Improving Olefin Purification Using Metal Organic Frameworks with Open Metal Sites. ACS Applied Materials & Interfaces, 2018, 10, 16911-16917.	4.0	25
34338	Understanding the deformation mechanism and mechanical characteristics of cementitious mineral analogues from first principles and reactive force field molecular dynamics. Physical Chemistry Chemical Physics, 2018, 20, 13920-13933.	1.3	6
34339	Electronic and optical properties of boron phosphide/blue phosphorus heterostructures. Physical Chemistry Chemical Physics, 2018, 20, 12053-12060.	1.3	53
34340	Aqueous solution-processed off-stoichiometric Cuâ€“Inâ€“S QDs and their application in quantum dot-sensitized solar cells. Journal of Materials Chemistry A, 2018, 6, 9629-9641.	5.2	40
34341	Metalâ€“organic framework-derived integrated nanoarrays for overall water splitting. Journal of Materials Chemistry A, 2018, 6, 9009-9018.	5.2	74
34342	Two-dimensional GeAs with a visible range band gap. Journal of Materials Chemistry A, 2018, 6, 9089-9098.	5.2	55
34343	Titanium-related color centers in diamond: a density functional theory prediction. Journal of Materials Chemistry C, 2018, 6, 5261-5268.	2.7	26
34344	Substrate-molecule decoupling induced by self-assemblyâ€”Implications for graphene nanoribbon fabrication. AIP Advances, 2018, 8, 045117.	0.6	2
34345	Study of electronic and magnetic properties of h-BN on Ni surfaces: A DFT approach. AIP Conference Proceedings, 2018, , .	0.3	0
34346	Valence electron concentration as an indicator for mechanical properties in rocksalt structure nitrides, carbides and carbonitrides. Acta Materialia, 2018, 152, 175-185.	3.8	178
34347	Planar metallic carbon allotrope from graphene-like nanoribbons. Carbon, 2018, 135, 21-28.	5.4	55
34348	The structural, electronic, magnetic and elastic properties of Ge doped half-Heusler compounds Mn2GexAs1â^'x (xâ€¯=â€¯0.25, 0.50, 0.75, 1.00). Journal of Magnetism and Magnetic Materials, 2018, 460, 461-470.	1.0	10
34349	New Insights into the Crystal Structures of Plutonium Hydrides from First-Principles Calculations. Journal of Physical Chemistry C, 2018, 122, 10103-10112.	1.5	15
34350	g-C₃N₄/Ti₃C₂T_x (MXenes) composite with oxidized surface groups for efficient photocatalytic hydrogen evolution. Journal of Materials Chemistry A, 2018, 6, 9124-9131.	5.2	233
34351	Configurational forces in electronic structure calculations using Kohn-Sham density functional theory. Physical Review B, 2018, 97, .	1.1	14
34352	Multimode Jahn-Teller effect in bulk systems: A case of the <mml:math xmlns:mml="http://www.w3.org/1998/Math/MathML"><mml:mrow><mml:mi mathvariant="normal">N</mml:mi><mml:msup><mml:mrow><mml:mi mathvariant="normal">V</mml:mi></mml:mrow><mml:mn>0</mml:mn></mml:msup></mml:mrow></mml:math> center in diamond. Physical Review B, 2018, 97, .	1.1	7

#	Article	IF	Citations
34353	Bound nuclear spin states of H2 in an anisotropic potential induced by a stepped metal surface. Journal of Vacuum Science and Technology A: Vacuum, Surfaces and Films, 2018, 36, 030601.	0.9	5
34354	Improving visible-light-driven photocatalytic NO oxidation over BiOBr nanoplates through tunable oxygen vacancies. Chinese Journal of Catalysis, 2018, 39, 779-789.	6.9	57
34355	Evaluation of dry reforming reaction catalysts via computational screening. Catalysis Today, 2018, 312, 23-34.	2.2	8
34356	Inducing skyrmions in ultrathin Fe films by hydrogen exposure. Nature Communications, 2018, 9, 1571.	5.8	40
34357	Toxicity assessment and mechanistic investigation of engineered monoclinic VO₂nanoparticles. Nanoscale, 2018, 10, 9736-9746.	2.8	14
34358	First-principles investigation of diffusion and defect properties of Fe and Ni in Cr2O3. Journal of Applied Physics, 2018, 123, .	1.1	10
34359	Epitaxial engineering of polar Îµ-Ga2O3 for tunable two-dimensional electron gas at the heterointerface. Applied Physics Letters, 2018, 112, .	1.5	77
34360	Effect on electronic and optical properties of Frenkel and Schottky defects in HfS2 monolayer. AIP Conference Proceedings, 2018, , .	0.3	5
34361	Tuning the Electronic, Optical, and Magnetic Properties of Monolayer GaSe with a Vertical Electric Field. Physical Review Applied, 2018, 9, .	1.5	38
34362	Highly Reversible Oxygenâ€Redox Chemistry at 4.1 V in Na_{4/7â˜}_x[â–¡_{1/7}Mn_{6/7}]O₂ (â–¡: Mn) Tj ET Q q 1 1 0.784314 g	1.5	734
34363	Oxygen reduction reaction on Pt(1â€¯1â€¯1), Pt(2â€¯2â€¯1), and Ni/Au1Pt3(2â€¯2â€¯1) surfaces: Probing scaling relationships of reaction energetics and interfacial composition. Chemical Engineering Science, 2018, 184, 239-250.	1.9	16
34364	Investigation of impurity induced twinning in MgO from first principles calculations. Computational Materials Science, 2018, 150, 390-396.	1.4	3
34365	First-principles study of the optical properties of YPO 4 crystal with oxygen vacancies. Journal of Physics and Chemistry of Solids, 2018, 120, 1-5.	1.9	5
34366	Kinetic theory for the formation of diamond nanothreads with desired configurations: a strainâ€“temperature controlled phase diagram. Nanoscale, 2018, 10, 9664-9672.	2.8	13
34367	Atomically thin transition metal layers: Atomic layer stabilization and metal-semiconductor transition. Journal of Applied Physics, 2018, 123, 154301.	1.1	8
34368	Simplified DFT methods for consistent structures and energies of large systems. Journal of Physics Condensed Matter, 2018, 30, 213001.	0.7	42
34369	Typeâ€Ⅱ Transition Metal Dichalcogenides Lateral Homojunctions: Layer Thickness and External Electric Field Effects. Small, 2018, 14, e1800365.	5.2	41
34370	The role of iron-oxide aerosols and sunlight in the atmospheric reduction of Hg(II) species: A DFT+U study. Applied Catalysis B: Environmental, 2018, 234, 347-356.	10.8	10

#	Article	IF	Citations
34371	Elastic properties of long periodic stacking ordered phases in Mg-Gd-Al alloys: A first-principles study. Intermetallics, 2018, 98, 18-27.	1.8	21
34372	Surface structure analysis of Eu Zintl template on Ge(001). Surface Science, 2018, 674, 94-102.	0.8	9
34373	Understanding Ionic Diffusion through SEI Components for Lithium-Ion and Sodium-Ion Batteries: Insights from First-Principles Calculations. Chemistry of Materials, 2018, 30, 3315-3322.	3.2	88
34374	Synthesis and Optical Properties of Colloidal M₃Bi₂I₉ (M = Cs, Rb) Perovskite Nanocrystals. Journal of Physical Chemistry C, 2018, 122, 10643-10649.	1.5	95
34375	Molecular-Level Insight into Selective Catalytic Reduction of NO_x with NH₃ to N₂ over a Highly Efficient Bifunctional V_a-MnO_x Catalyst at Low Temperature. ACS Catalysis, 2018, 8, 4937-4949.	5.5	103
34376	Heterogeneous Fe3 single-cluster catalyst for ammonia synthesis via an associative mechanism. Nature Communications, 2018, 9, 1610.	5.8	409
34377	Quantum anomalous/valley Hall effect and tunable quantum state in hydrogenated arsenene decorated with a transition metal. Physical Chemistry Chemical Physics, 2018, 20, 12138-12148.	1.3	5
34378	Optoelectronics and defect levels in hydroxyapatite by first-principles. Journal of Chemical Physics, 2018, 148, 154706.	1.2	54
34379	Metal-nonmetal oscillations in doped blue phosphorene: a first-principles study. Materials Research Express, 2018, 5, 055007.	0.8	6
34380	Allotropes of Phosphorus with Remarkable Stability and Intrinsic Piezoelectricity. Physical Review Applied, 2018, 9, .	1.5	16
34381	Defects and Low-Frequency Noise in Irradiated Black Phosphorus MOSFETs With HfO₂ Gate Dielectrics. IEEE Transactions on Nuclear Science, 2018, 65, 1227-1238.	1.2	39
34382	A One-Dimensional Model for Photoemission Calculations from Plane-Wave Band Structure Codes. E-Journal of Surface Science and Nanotechnology, 2018, 16, 49-52.	0.1	1
34383	Structural Analysis of Self-Assembled Platinum-Silicide Nanostructures on Si(001) Using Ion Scattering Spectroscopy. E-Journal of Surface Science and Nanotechnology, 2018, 16, 66-71.	0.1	0
34384	Predicting Surface Energies and Particle Morphologies of Boehmite (Î³-AlOOH) from Density Functional Theory. Journal of Physical Chemistry C, 2018, 122, 10400-10412.	1.5	26
34385	Effect of LiFSI Concentrations To Form Thickness- and Modulus-Controlled SEI Layers on Lithium Metal Anodes. Journal of Physical Chemistry C, 2018, 122, 9825-9834.	1.5	131
34386	Two-Dimensional MoS₂ Confined Co(OH)₂ Electrocatalysts for Hydrogen Evolution in Alkaline Electrolytes. ACS Nano, 2018, 12, 4565-4573.	7.3	302
34387	A Two-Dimensional â€˜Zigzagâ€™ Silica Polymorph on a Metal Support. Journal of the American Chemical Society, 2018, 140, 6164-6168.	6.6	14
34388	Prediction of Novel pâ€Type Transparent Conductors in Layered Double Perovskites: A Firstâ€Principles Study. Advanced Functional Materials, 2018, 28, 1800332.	7.8	49

#	Article	IF	Citations
34389	Metallic Contact between MoS₂ and Ni via Au Nanoglue. Small, 2018, 14, e1704526.	5.2	32
34390	Facile preparation of novel hydrophobic sponges coated by Cu2O with different crystal facet structure for selective oil absorption and oil/water separation. Journal of Materials Science, 2018, 53, 10025-10038.	1.7	15
34391	New two-dimensional allotrope of single layer IV-V semiconductor XBi (Xâ€¯=â€¯Si, Ge, Sn). Computational Materials Science, 2018, 150, 314-320.	1.4	8
34392	Growth of Dihydrotetraazapentacene Layers on Cu(110). Journal of Physical Chemistry C, 2018, 122, 10828-10834.	1.5	5
34393	Effect of Solvent and Substrate on the Surface Binding Mode of Carboxylate-Functionalized Aromatic Molecules. Journal of Physical Chemistry C, 2018, 122, 10846-10856.	1.5	5
34394	One-Dimensional Organicâ€“Inorganic Hybrid Perovskite Incorporating Near-Infrared-Absorbing Cyanine Cations. Journal of Physical Chemistry Letters, 2018, 9, 2438-2442.	2.1	22
34395	Precise Control of Local Spin States in an Adsorbed Magnetic Molecule with an STM Tip: Theoretical Insights from First-Principles-Based Simulation. Journal of Physical Chemistry Letters, 2018, 9, 2418-2425.	2.1	32
34396	Lone-Pair Electrons Do Not Necessarily Lead to Low Lattice Thermal Conductivity: An Exception of Two-Dimensional Penta-CN₂. Journal of Physical Chemistry Letters, 2018, 9, 2474-2483.	2.1	38
34397	Two-Dimensional AuMX2 (M = Al, Ga, In; X = S, Se) Monolayers Featuring Intracrystalline Aurophilic Interactions with Novel Electronic and Optical Properties. ACS Applied Materials & Interfaces, 2018, 10, 16739-16746.	4.0	11
34398	Ab Initio Predictions of Strong Interfaces in Transition-Metal Carbides and Nitrides for Superhard Nanocomposite Coating Applications. ACS Applied Nano Materials, 2018, 1, 2029-2035.	2.4	17
34399	Strain-Tuning Atomic Substitution in Two-Dimensional Atomic Crystals. ACS Nano, 2018, 12, 4853-4860.	7.3	75
34400	TiC₃ Monolayer with High Specific Capacity for Sodium-Ion Batteries. Journal of the American Chemical Society, 2018, 140, 5962-5968.	6.6	244
34401	Dopant driven tuning of the hydrogen oxidation mechanism at the pore/nickel/zirconia triple phase boundary. Physical Chemistry Chemical Physics, 2018, 20, 12574-12588.	1.3	4
34402	A first-principles study of hydrogen storage capacity based on Liâ€“Na-decorated silicene. Physical Chemistry Chemical Physics, 2018, 20, 13903-13908.	1.3	19
34403	Effects of oxygen chemical potential on the anisotropy of the adsorption properties of Zr surfaces. Physical Chemistry Chemical Physics, 2018, 20, 14410-14419.	1.3	7
34404	A potential material for hydrogen storage: a Li decorated graphitic-CN monolayer. Physical Chemistry Chemical Physics, 2018, 20, 13473-13477.	1.3	59
34405	Nitrogen electroreduction and hydrogen evolution on cubic molybdenum carbide: a density functional study. Physical Chemistry Chemical Physics, 2018, 20, 14679-14687.	1.3	55
34406	Theoretical investigation of the strengthening mechanism and precipitation evolution in high strength Alâ€“Znâ€“Mg alloys. Physical Chemistry Chemical Physics, 2018, 20, 13616-13622.	1.3	5

#	Article	IF	Citations
34407	Quantum spin Hall insulator BiXH (XH = OH, SH) monolayers with a large bulk band gap. Physical Chemistry Chemical Physics, 2018, 20, 13632-13636.	1.3	14
34408	The role of the solid electrolyte interphase layer in preventing Li dendrite growth in solid-state batteries. Energy and Environmental Science, 2018, 11, 1803-1810.	15.6	304
34409	Bipolar magnetic semiconductors among intermediate states during the conversion from Sc₂C(OH)₂to Sc₂CO₂MXene. Nanoscale, 2018, 10, 8763-8771.	2.8	27
34410	The effect of octahedral distortions on the electronic properties and magnetic interactions in O3 NaTMO₂ compounds (TM = Tiâ€“Ni & Zrâ€“Pd). RSC Advances, 2018, 8, 13842-13849.	1.7	18
34411	Analysis on the energetics, magnetism and electronic properties in a 45Â° ZnO grain boundary doped with Gd. RSC Advances, 2018, 8, 13850-13856.	1.7	10
34412	Ionic conduction in sodium azide under high pressure: Experimental and theoretical approaches. Applied Physics Letters, 2018, 112, 173903.	1.5	12
34413	Energetics of He and H Atoms in Wâ€“Ta Alloys: First-Principle Calculations. Chinese Physics Letters, 2018, 35, 047102.	1.3	4
34414	Probing ionization potential, electron affinity and self-energy effect on the spectral shape and exciton binding energy of quantum liquid water with self-consistent many-body perturbation theory and the Betheâ€“Salpeter equation. Journal of Physics Condensed Matter, 2018, 30, 215502.	0.7	8
34415	Topological Weyl semimetals in <mml:math xmlns:mml="http://www.w3.org/1998/Math/MathML"><mml:mrow><mml:msub><mml:mi>Bi</mml:mi><mml:mrow><mml:mn>1</mml:mn><mml:mo>−</mml:mo><mml:mi>x</mml:mi></mml:mrow></mml:msub><mml:msub><mml:mi>Sb</mml:mi><mml:mi>x</mml:mi></mml:msub></mml:mrow></mml:math> alloys. Physical Review B, 2018, 97, .	1.1	17
34416	Hourglass Dirac chain metal and the topological nodal-line transition in <mml:math xmlns:mml="http://www.w3.org/1998/Math/MathML"><mml:mrow><mml:mi>CaAg</mml:mi><mml:mo>(</mml:mo><mml:msub><mml:mi>Sb</mml:mi><mml:mi>x</mml:mi></mml:msub><mml:msub><mml:mi>Bi</mml:mi><mml:mrow><mml:mn>1</mml:mn><mml:mo>−</mml:mo><mml:mi>x</mml:mi></mml:mrow></mml:msub><mml:mo>)</mml:mo></mml:mrow></mml:math> Physical Review B, 2018, 97, .	1.1	25
34417	The Interaction between Cu and Fe in P2-Type Na_xTMO₂Cathodes for Advanced Battery Performance. Journal of the Electrochemical Society, 2018, 165, A1184-A1192.	1.3	32
34418	The Effect of Oxygen Adsorption for Vacancy-Induced d0 Magnetism in HfO2 (110) Surface. Journal of Superconductivity and Novel Magnetism, 2018, 31, 3361-3370.	0.8	1
34419	High-pressure polymorphs of LiPN2: A first-principles study. Frontiers of Physics, 2018, 13, 1.	2.4	5
34420	Ultralow Lattice Thermal Conductivity and Significantly Enhanced Near-Room-Temperature Thermoelectric Figure of Merit in Î±-Cu₂Se through Suppressed Cu Vacancy Formation by Overstoichiometric Cu Addition. Chemistry of Materials, 2018, 30, 3276-3284.	3.2	58
34421	Cobalt Molybdenum Oxide Derived High-Performance Electrocatalyst for the Hydrogen Evolution Reaction. ACS Catalysis, 2018, 8, 5062-5069.	5.5	124
34422	Refined description of liquid and supercooled silicon from ab initio simulations. Physical Review B, 2018, 97, .	1.1	9
34423	First-principles study on the electronic structure and elastic properties of Mo₂NiB₂doped with V. Modern Physics Letters B, 2018, 32, 1850065.	1.0	7
34424	High Capacity, Dendriteâ€Free Growth, and Minimum Volume Change Na Metal Anode. Small, 2018, 14, e1703717.	5.2	104

#	Article	IF	Citations
34425	Sbâ€Doped SnO₂ Nanorods Underlayer Effect to the Î±â€Fe₂O₃ Nanorods Sheathed with TiO₂ for Enhanced Photoelectrochemical Water Splitting. Small, 2018, 14, e1703860.	5.2	69
34426	Modeling of EPR Parameters for Cu(II): Application to the Selective Reduction of NOx Catalyzed by Cu-Zeolites. Topics in Catalysis, 2018, 61, 810-832.	1.3	26
34427	Tunable electronic and magnetic properties of antimonene system via Fe doping and defect complex: A first-principles perspective. Applied Surface Science, 2018, 448, 281-287.	3.1	24
34428	Synergistic electrocatalytic oxygen reduction reactions of Pd/B4C for ultra-stable Zn-air batteries. Energy Storage Materials, 2018, 15, 226-233.	9.5	45
34429	Stability of X-C-vacancy complexes (X=H, He) in vanadium from first principles investigations. Journal of Nuclear Materials, 2018, 505, 119-126.	1.3	12
34430	Toupinâ€“Mindlin first strain gradient theory revisited for cubic crystals of hexoctahedral class: Analytical expression of the material parameters in terms of the atomic force constants and evaluation via ab initio DFT. Mechanics of Materials, 2018, 123, 19-29.	1.7	16
34431	Siligraphene as a promising anode material for lithium-ion batteries predicted from first-principles calculations. Nano Energy, 2018, 49, 67-76.	8.2	95
34432	First-principles study of Au-decorated carbon nanotubes. Physica E: Low-Dimensional Systems and Nanostructures, 2018, 101, 273-277.	1.3	3
34433	A new superhard carbon allotrope: Orthorhombic C20. Physics Letters, Section A: General, Atomic and Solid State Physics, 2018, 382, 1685-1689.	0.9	32
34434	The structural, electronic, magnetic and optical properties of the half-metallic binary alloys ZCl 3 (Z=Be, Mg, Ca, Sr): A first-principles study. Superlattices and Microstructures, 2018, 118, 230-241.	1.4	9
34435	Asymmetric electric field screening in van der Waals heterostructures. Nature Communications, 2018, 9, 1271.	5.8	38
34436	Synergetic optimization of electronic and thermal transport for high-performance thermoelectric GeSeâ€“AgSbTe₂ alloy. Journal of Materials Chemistry A, 2018, 6, 8215-8220.	5.2	38
34437	Adsorbing the magnetic superhalogen MnCl₃ to realize intriguing half-metallic and spin-gapless-semiconducting behavior in zigzag or armchair SiC nanoribbon. RSC Advances, 2018, 8, 13167-13177.	1.7	6
34438	Embedded atom method potential for studying mechanical properties of binary Cuâ€“Au alloys. Modelling and Simulation in Materials Science and Engineering, 2018, 26, 055006.	0.8	17
34439	Hybrid <mml:math xmlns:mml="http://www.w3.org/1998/Math/MathML"><mml:mrow><mml:mi mathvariant="bold">k</mml:mi><mml:mo>Â·</mml:mo><mml:mi mathvariant="bold">p</mml:mi></mml:mrow></mml:math> tight-binding model for intersubband optics in atomically thin InSe films. Physical Review B, 2018, 97, .	1.1	16
34440	Identifying Active Sites of Nitrogenâ€Doped Carbon Materials for the CO₂ Reduction Reaction. Advanced Functional Materials, 2018, 28, 1800499.	7.8	244
34441	Realâ€Time Observation of Orderâ€Disorder Transformation of Organic Cations Induced Phase Transition and Anomalous Photoluminescence in Hybrid Perovskites. Advanced Materials, 2018, 30, e1705801.	11.1	60
34442	Coadsorbateâ€Induced Reversal of Solidâ€“Liquid Interface Dynamics. Angewandte Chemie, 2018, 130, 6173-6176.	1.6	6

#	Article	IF	Citations
34443	Computational screening for selective catalysts: Cleaving the C C bond during ethanol electro-oxidation reaction. Electrochimica Acta, 2018, 274, 274-278.	2.6	26
34444	First-principles investigation of aluminum intercalation and diffusion in TiO2 materials: Anatase versus rutile. Journal of Power Sources, 2018, 384, 249-255.	4.0	29
34445	Stoichiometric Effects on the Photoelectric Properties of LiInSe₂ Crystals for Neutron Detection. Crystal Growth and Design, 2018, 18, 2864-2870.	1.4	16
34446	Comparative Investigation of MgMnSiO₄ and Olivine-Type MgMnSiS₄ as Cathode Materials for Mg Batteries. Journal of Physical Chemistry C, 2018, 122, 9356-9362.	1.5	28
34447	Mechanism of Phosphorus Transport Through Silicon Oxide During Phosphonic Acid Monolayer Doping. Journal of Physical Chemistry C, 2018, 122, 10088-10095.	1.5	16
34448	Novel Conductive Metalâ€“Organic Framework for a High-Performance Lithiumâ€“Sulfur Battery Host: 2D Cu-Benzenehexathial (BHT). ACS Applied Materials & Interfaces, 2018, 10, 15012-15020.	4.0	105
34449	Effects of Controlled Crystalline Surface of Hydroxyapatite on Methane Oxidation Reactions. ACS Catalysis, 2018, 8, 4493-4507.	5.5	30
34450	Entrapped Single Tungstate Site in Zeolite for Cooperative Catalysis of Olefin Metathesis with BrÃ¸nsted Acid Site. Journal of the American Chemical Society, 2018, 140, 6661-6667.	6.6	71
34451	Asymmetric twins in boron rich boron carbide. Physical Chemistry Chemical Physics, 2018, 20, 13340-13347.	1.3	4
34452	Insights into the electronic properties and reactivity of graphene-like BC₃ supported metal catalysts. New Journal of Chemistry, 2018, 42, 11299-11311.	1.4	4
34453	Investigating the dynamics of excitons in monolayer WSe₂ before and after organic super acid treatment. Nanoscale, 2018, 10, 9346-9352.	2.8	12
34454	A comprehensive study on carrier mobility and artificial photosynthetic properties in group VI B transition metal dichalcogenide monolayers. Journal of Materials Chemistry A, 2018, 6, 8693-8704.	5.2	204
34455	Phase diagram and oxygenâ€“vacancy ordering in the CeO₂â€“Gd₂O₃ system: a theoretical study. Physical Chemistry Chemical Physics, 2018, 20, 11805-11818.	1.3	26
34456	Photogenerated-carrier separation along edge dislocation of WO₃single-crystal nanoflower photoanode. Journal of Materials Chemistry A, 2018, 6, 8604-8611.	5.2	51
34457	Electronic implications of organic nitrogen lone pairs in lead iodide perovskites. Journal of Materials Chemistry C, 2018, 6, 4765-4768.	2.7	1
34458	First principles study of pressure induced polymorphic phase transition in trimethylamine. AIP Conference Proceedings, 2018, , .	0.3	3
34459	gâ€₃N₄ Loading Black Phosphorus Quantum Dot for Efficient and Stable Photocatalytic H₂ Generation under Visible Light. Advanced Functional Materials, 2018, 28, 1800668.	7.8	257
34460	Impact of High Valence State Cation Ti/Ta Surface Doping on the Stabilization of Spinel LiNi_{0.5}Mn_{1.5}O₄ Cathode Materials: A Systematic Density Functional Theory Investigation. Advanced Materials Interfaces, 2018, 5, 1800077.	1.9	25

#	Article	IF	Citations
34461	On the Balance of Intercalation and Conversion Reactions in Battery Cathodes. Advanced Energy Materials, 2018, 8, 1800379.	10.2	43
34462	Electrochemical and density functional theory investigation on the differential behaviors of core-ring structured NiCo 2 O 4 nanoplatelets toward heavy metal ions. Analytica Chimica Acta, 2018, 1022, 37-44.	2.6	39
34463	In pursuit of bifunctional catalytic activity in PdS2 pseudo-monolayer through reaction coordinate mapping. Nano Energy, 2018, 49, 283-289.	8.2	44
34464	Heteroatoms dual-doped hierarchical porous carbon-selenium composite for durable Liâ€“Se and Naâ€“Se batteries. Nano Energy, 2018, 49, 137-146.	8.2	158
34465	Electronic properties of g-C3N4/CdS heterojunction from the first-principles. Physica E: Low-Dimensional Systems and Nanostructures, 2018, 103, 459-463.	1.3	26
34466	Ethane oxidative dehydrogenation mechanism on MoO3(010) surface: A first-principle study using on-site Coulomb correction. Surface Science, 2018, 674, 45-50.	0.8	9
34467	Vanadium Oxide Oligomers and Ordered Monolayers Supported on CeO₂(111): Structure and Stability Studied by Density Functional Theory. Journal of Physical Chemistry C, 2018, 122, 9101-9110.	1.5	19
34468	Single-Crystal Antimonene Films Prepared by Molecular Beam Epitaxy: Selective Growth and Contact Resistance Reduction of the 2D Material Heterostructure. ACS Applied Materials & Interfaces, 2018, 10, 15058-15064.	4.0	43
34469	Role of Lattice Oxygen Participation in Understanding Trends in the Oxygen Evolution Reaction on Perovskites. ACS Catalysis, 2018, 8, 4628-4636.	5.5	339
34470	Field-effect transistors made from solution-grown two-dimensional tellurene. Nature Electronics, 2018, 1, 228-236.	13.1	591
34471	Active learning with non-ab initio input features toward efficient CO₂ reduction catalysts. Chemical Science, 2018, 9, 5152-5159.	3.7	82
34472	Atomically flat and thermally stable graphene on Si(111) with preserved intrinsic electronic properties. Nanoscale, 2018, 10, 8377-8384.	2.8	4
34473	A lead-free perovskite-like hybrid with above-room-temperature switching of quadratic nonlinear optical properties. Chemical Communications, 2018, 54, 5614-5617.	2.2	37
34474	Silicon compatible Sn-based resistive switching memory. Nanoscale, 2018, 10, 9441-9449.	2.8	24
34475	Inner edge magnetisms in carbon honeycombs. Journal of Applied Physics, 2018, 123, 144301.	1.1	1
34476	Ab-initio study of pressure evolution of structural, mechanical and magnetic properties of cementite (Fe3C) phase. AIP Conference Proceedings, 2018, , .	0.3	0
34477	Anti-site defected MoS2 sheet for catalytic application. AIP Conference Proceedings, 2018, , .	0.3	1
34478	Work function tunability of borophene via doping: A first principle study. AIP Conference Proceedings, 2018, , .	0.3	1

#	Article	IF	Citations
34479	Magnetocrystalline anisotropy in cobalt based magnets: a choice of correlation parameters and the relativistic effects. Journal of Physics Condensed Matter, 2018, 30, 195801.	0.7	21
34480	Gallenene epitaxially grown on Si(1â€‰1â€‰1). 2D Materials, 2018, 5, 035009.	2.0	42
34481	Influence of defects and doping on phonon transport properties of monolayer MoSe ₂. 2D Materials, 2018, 5, 031008.	2.0	30
34482	Single-atom heterogeneous catalysts based on distinct carbon nitride scaffolds. National Science Review, 2018, 5, 642-652.	4.6	132
34483	Probing quasi-one-dimensional band structures by plasmon spectroscopy. Physical Review B, 2018, 97, .	1.1	19
34484	Hydrophobic Properties of Al₂O₃ Doped with Rareâ€Earth Metals: Ab Initio Modeling Studies. Physica Status Solidi (A) Applications and Materials Science, 2018, 215, 1700895.	0.8	4
34485	Identification of local structures around Ce3+ centers in potassium magnesium fluoride. Journal of Luminescence, 2018, 201, 24-30.	1.5	3
34486	Influence of Cr 3+ doping on the enhanced dielectric and nonlinear optical features of pyroelectric Pb 5 Ge 3 O 11 single crystals. Materials Chemistry and Physics, 2018, 213, 461-471.	2.0	15
34487	Tunable magnetic properties of double perovskite La2Fe2-xCoxO6. Physica B: Condensed Matter, 2018, 540, 33-37.	1.3	10
34488	An Effective Purification Process for the Nuclear Radiation Detector Tl₆SeI₄. Crystal Growth and Design, 2018, 18, 3484-3493.	1.4	9
34489	Direct Observation of Chemical Conversion from Fe₃O₄ to Îµ-Fe₂O₃ by a Nanosize Wet Process. Chemistry of Materials, 2018, 30, 2888-2894.	3.2	24
34490	Filling the Gap in Extended Metal Atom Chains: Ferromagnetic Interactions in a Tetrairon(II) String Supported by Oligo-Î±-pyridylamido Ligands. Inorganic Chemistry, 2018, 57, 5438-5448.	1.9	16
34491	Electronâ€“Phonon Coupling in Luminescent Europium-Doped Hydride Perovskites Studied by Luminescence Spectroscopy, Inelastic Neutron Scattering, and First-Principles Calculations. Journal of Physical Chemistry C, 2018, 122, 10501-10509.	1.5	26
34492	Local Environment Sensitivity of the Cu K-Edge XANES Features in Cu-SSZ-13: Analysis from First-Principles. Journal of Physical Chemistry Letters, 2018, 9, 3035-3042.	2.1	34
34493	Correlated High-Pressure Phase Sequence of VO₂ under Strong Compression. Journal of Physical Chemistry Letters, 2018, 9, 2388-2393.	2.1	20
34494	A Rigorous Method of Calculating Exfoliation Energies from First Principles. Nano Letters, 2018, 18, 2759-2765.	4.5	207
34495	Surface Vacancy-Induced Switchable Electric Polarization and Enhanced Ferromagnetism in Monolayer Metal Trihalides. Nano Letters, 2018, 18, 2943-2949.	4.5	157
34496	Highly Stable Thin-Film Transistors Based on Indium Oxynitride Semiconductor. ACS Applied Materials & Interfaces, 2018, 10, 15873-15879.	4.0	14

#	Article	IF	Citations
34497	Mechanistic Understanding of Alloy Effect and Water Promotion for Pd-Cu Bimetallic Catalysts in CO₂ Hydrogenation to Methanol. ACS Catalysis, 2018, 8, 4873-4892.	5.5	171
34498	Revealing the Janus Character of the Coke Precursor in the Propane Direct Dehydrogenation on Pt Catalysts from a kMC Simulation. ACS Catalysis, 2018, 8, 4694-4704.	5.5	85
34499	Artificial two-dimensional polar metal at room temperature. Nature Communications, 2018, 9, 1547.	5.8	61
34500	An ab initio study of Cu-based delafossites as an alternative to nickel oxide in photocathodes: effects of Mg-doping and surface electronic features. Physical Chemistry Chemical Physics, 2018, 20, 14082-14089.	1.3	26
34501	Unveiling the atomistic mechanisms for oxygen intercalation in a strongly interacting grapheneâ€“metal interface. Physical Chemistry Chemical Physics, 2018, 20, 13370-13378.	1.3	12
34502	Quantum oscillation in carrier transport in two-dimensional junctions. Nanoscale, 2018, 10, 7912-7917.	2.8	5
34503	Water dissociating on rigid Ni(100): A quantum dynamics study on a full-dimensional potential energy surface. Journal of Chemical Physics, 2018, 148, 144705.	1.2	20
34504	Designing superhard metals: The case of low borides. AIP Advances, 2018, 8, 045305.	0.6	14
34505	Perovskite solar cells: must lead be replaced â€“ and can it be done?. Science and Technology of Advanced Materials, 2018, 19, 425-442.	2.8	151
34506	Magnetism by embedding 3d transition metal atoms into germanene. Journal Physics D: Applied Physics, 2018, 51, 225006.	1.3	6
34507	Voltage-induced switching of an antiferromagnetically ordered topological Dirac semimetal. Physical Review B, 2018, 97, .	1.1	7
34508	<mml:math xmlns:mml="http://www.w3.org/1998/Math/MathML"><mml:mi>A</mml:mi></mml:math> -cation control of magnetoelectric quadrupole order in <mml:math xmlns:mml="http://www.w3.org/1998/Math/MathML"><mml:mrow><mml:mi>A</mml:mi><mml:msub><mml:mrow><mml:mo>(</mml:mo> Physical Review B, 2018, 97, .	1.1	21
34509	Mechanisms of ultralow and anisotropic thermal expansion in cordierite Mg₂Al₄Si₅O₁₈: Insight from phonon behaviors. Journal of the American Ceramic Society, 2018, 101, 4708-4718.	1.9	9
34510	First Principle and Experimental Study for Site Preferences of Formability Improved Alloying Elements in Mg Crystal. Metals and Materials International, 2018, 24, 830-839.	1.8	3
34511	Dual Electrostatic Assembly of Graphene Encapsulated Nanosheetâ€Assembled ZnOâ€Mnâ€€ Hollow Microspheres as a Lithium Ion Battery Anode. Advanced Functional Materials, 2018, 28, 1707433.	7.8	83
34512	Electronic Structure and Stability of Lead-free Hybrid Halide Perovskites: A Density Functional Theory Study. Journal of Shanghai Jiaotong University (Science), 2018, 23, 202-208.	0.5	2
34513	Crystal structures and thermodynamic stabilities of two new CaGe2 polymorphs. Acta Materialia, 2018, 151, 347-355.	3.8	13
34514	Cobalt-modified molybdenum carbide as a selective catalyst for hydrodeoxygenation of furfural. Applied Catalysis B: Environmental, 2018, 233, 160-166.	10.8	64

#	Article	IF	Citations
34515	Density-functional theory molecular dynamics simulations of a-HfO2/a-SiO2/SiGe and a-HfO2/a-SiO2/Ge with a-SiO2 and a-SiO suboxide interfacial layers. Applied Surface Science, 2018, 443, 644-654.	3.1	11
34516	Applying isotropic strain on Mo to predict H solution behaviors for nuclear energy application: Temperature dependence. International Journal of Hydrogen Energy, 2018, 43, 3750-3760.	3.8	7
34517	Electronic structures and optical properties of ZrS2 monolayer by n- and p-type doping. Journal of Alloys and Compounds, 2018, 748, 798-803.	2.8	22
34518	Dominant role of orbital splitting in determining cathode potential in O3 NaTMO2 compounds. Journal of Power Sources, 2018, 388, 1-4.	4.0	12
34519	Identifying the tuning key of disproportionation redox reaction in terephthalate: A Li-based anode for sustainable organic batteries. Nano Energy, 2018, 47, 301-308.	8.2	17
34520	Contrastive thermoelectric properties of strained SnSe crystals from the first-principles calculations. Physica B: Condensed Matter, 2018, 539, 8-13.	1.3	9
34521	Electronic and magnetic properties of transition metal decorated monolayer GaS. Physica E: Low-Dimensional Systems and Nanostructures, 2018, 101, 131-138.	1.3	5
34522	Understanding the Electrochemical Mechanisms Induced by Gradient Mg²⁺ Distribution of Na-Rich Na_{3+x}V_{2â€“x}Mg_x(PO₄)₃/C for Sodium Ion Batteries. Chemistry of Materials, 2018, 30, 2498-2505.	3.2	102
34523	Shape-, Size-, and Composition-Controlled Thallium Lead Halide Perovskite Nanowires and Nanocrystals with Tunable Band Gaps. Chemistry of Materials, 2018, 30, 2973-2982.	3.2	28
34524	Ba₄B₈TeO₁₉: A UV Nonlinear Optical Material. Inorganic Chemistry, 2018, 57, 4771-4776.	1.9	31
34525	Competitive Binding of Ethylene, Water, and Carbon Monoxide in Metalâ€“Organic Framework Materials with Open Cu Sites. Journal of Physical Chemistry C, 2018, 122, 8960-8966.	1.5	35
34526	On-Demand Final State Control of a Surface-Bound Bistable Single Molecule Switch. Nano Letters, 2018, 18, 2950-2956.	4.5	11
34527	Poly-Amide Modified Copper Foam Electrodes for Enhanced Electrochemical Reduction of Carbon Dioxide. ACS Catalysis, 2018, 8, 4132-4142.	5.5	165
34528	Computational Comparison of Late Transition Metal (100) Surfaces for the Electrocatalytic Reduction of CO to C₂ Species. ACS Energy Letters, 2018, 3, 1062-1067.	8.8	103
34529	Enhanced Photocatalytic Performance through Magnetic Field Boosting Carrier Transport. ACS Nano, 2018, 12, 3351-3359.	7.3	190
34530	Multistep Lithiation of Tin Sulfide: An Investigation Using in Situ Electron Microscopy. ACS Nano, 2018, 12, 3638-3645.	7.3	50
34531	Growth of Ni nanoclusters on irradiated graphene: a molecular dynamics study. Physical Chemistry Chemical Physics, 2018, 20, 16347-16353.	1.3	5
34532	Designing lateral spintronic devices with giant tunnel magnetoresistance and perfect spin injection efficiency based on transition metal dichalcogenides. Physical Chemistry Chemical Physics, 2018, 20, 10286-10291.	1.3	22

#	Article	IF	Citations
34533	KCl-mediated dual electronic channels in layered g-C₃N₄ for enhanced visible light photocatalytic NO removal. Nanoscale, 2018, 10, 8066-8074.	2.8	126
34534	Metastable electronic states in uranium tetrafluoride. Physical Chemistry Chemical Physics, 2018, 20, 10384-10395.	1.3	5
34535	Assessing the role of hydrogen in Fermi-level pinning in chalcopyrite and kesterite solar absorbers from first-principles calculations. Journal of Applied Physics, 2018, 123, .	1.1	14
34536	Atomistic models of Cu diffusion in CuInSe2 under variations in composition. Journal of Applied Physics, 2018, 123, 115116.	1.1	2
34537	Experimental and ab initio study of Mg doping in the intrinsic ferromagnetic semiconductor GdN. Journal of Applied Physics, 2018, 123, .	1.1	5
34538	Local corrugation and persistent charge density wave in ZrTe3 with Ni intercalation. Physical Review B, 2018, 97, .	1.1	16
34539	Importance of the van Hove singularity in superconducting <mml:math xmlns:mml="http://www.w3.org/1998/Math/MathML"><mml:msub><mml:mi>PdTe</mml:mi><mml:mn>2</mml:mn></mml:msub></mml:math> Physical Review B, 2018, 97, .	1.1	36
34540	Trends on band alignments: Validity of Anderson's rule in<mml:math xmlns:mml="http://www.w3.org/1998/Math/MathML"><mml:msub><mml:mi>SnS</mml:mi><mml:mn>2</mml:mn></mml:msub></mml:math> and<mml:math xmlns:mml="http://www.w3.org/1998/Math/MathML"><mml:msub><mml:mi>SnSe</mml:mi><mml:mn>2</mml:mn></mml:msub></mml:math> van der Waals heterostructures. Physical Review B, 2018, 97, .	1.1	57
34541	Revealing the Contribution of Individual Factors to Hydrogen Evolution Reaction Catalytic Activity. Advanced Materials, 2018, 30, e1706076.	11.1	86
34542	Oxidized Laserâ€Induced Graphene for Efficient Oxygen Electrocatalysis. Advanced Materials, 2018, 30, e1707319.	11.1	94
34543	Scalable Waterâ€Based Production of Highly Conductive 2D Nanosheets with Ultrahigh Volumetric Capacitance and Rate Capability. Advanced Energy Materials, 2018, 8, 1800227.	10.2	26
34544	Kineticsâ€Controlled Degradation Reactions at Crystalline LiPON/Li_xCoO₂ and Crystalline LiPON/Liâ€Metal Interfaces. ChemSusChem, 2018, 11, 1956-1969.	3.6	32
34545	Synergistic effect between undercoordinated platinum atoms and defective nickel hydroxide on enhanced hydrogen evolution reaction in alkaline solution. Nano Energy, 2018, 48, 590-599.	8.2	76
34546	A covalent heterostructure of monodisperse Ni2P immobilized on N, P-co-doped carbon nanosheets for high performance sodium/lithium storage. Nano Energy, 2018, 48, 510-517.	8.2	139
34547	Structures and Electronic Properties of Au Clusters Encapsulated ZIF-8 and ZIF-90. Journal of Physical Chemistry C, 2018, 122, 8901-8909.	1.5	20
34548	Growth Analysis of Single-Walled Carbon Nanotubes Based on Interatomic Potentials by Molecular Dynamics Simulation. Journal of Physical Chemistry C, 2018, 122, 9648-9653.	1.5	7
34549	Adsorption and Diffusion of CO on Clean and CO₂-Precovered ZnO(101Ì…0). Journal of Physical Chemistry C, 2018, 122, 8919-8924.	1.5	18
34550	Searching for Photoactive Polymorphs of CsNbQ₃ (Q = O, S, Se, Te) with Enhanced Optical Properties and Intrinsic Thermodynamic Stabilities. Journal of Physical Chemistry C, 2018, 122, 8814-8821.	1.5	11

#	Article	IF	Citations
34551	Novel Sulfur Host Composed of Cobalt and Porous Graphitic Carbon Derived from MOFs for the High-Performance Liâ€“S Battery. ACS Applied Materials & Interfaces, 2018, 10, 13499-13508.	4.0	54
34552	Chirality, Rigidity, and Conjugation: A First-Principles Study of the Key Molecular Aspects of Lignin Depolymerization on Ni-Based Catalysts. ACS Catalysis, 2018, 8, 4230-4240.	5.5	24
34553	Mediating both valence and conduction bands of TiO₂ by anionic dopants for visible- and infrared-light photocatalysis. Physical Chemistry Chemical Physics, 2018, 20, 12785-12790.	1.3	20
34554	Oriented attachment growth of hundred-nanometer-size LaTaON₂ single crystals in molten salts for enhanced photoelectrochemical water splitting. Journal of Materials Chemistry A, 2018, 6, 7706-7713.	5.2	26
34555	Grain boundary phases in bcc metals. Nanoscale, 2018, 10, 8253-8268.	2.8	55
34556	2D lateral heterostructures of group-III monochalcogenide: Potential photovoltaic applications. Applied Physics Letters, 2018, 112, .	1.5	66
34557	Tuning the magnetism of the top-layer FeAs on BaFe2As2 (001): First-principles study. Physical Review B, 2018, 97, .	1.1	1
34558	Preserving half-metallic surface states in CrO2 : Insights into surface reconstruction rules. Physical Review B, 2018, 97, .	1.1	3
34559	Magnetic and Electronic Properties of h-BN Nanosheets with Nonmetal Atoms Adsorbed: an Ab Initio Study. JETP Letters, 2018, 107, 163-167.	0.4	5
34560	Large Oblate Hemispheroidal Ruthenium Particles Supported on Calcium Amide as Efficient Catalysts for Ammonia Decomposition. Chemistry - A European Journal, 2018, 24, 7976-7984.	1.7	34
34561	Pressure-induced phase transition of KTa1/2Nb1/2O3 solid solutions: A first-principles study. Chemical Physics Letters, 2018, 699, 80-84.	1.2	3
34562	Development of a Multicenter Density Functional Tight Binding Model for Plutonium Surface Hydriding. Journal of Chemical Theory and Computation, 2018, 14, 2652-2660.	2.3	27
34563	Tuning the Deoxygenation of Bulk-Dissolved Oxygen in Copper. Journal of Physical Chemistry C, 2018, 122, 8254-8261.	1.5	15
34564	Augmented Pairwise Additive Interaction Model for Lateral Adsorbate Interactions: The NOâ€“CO Reaction System on Rh(100) and Rh(111). Langmuir, 2018, 34, 5174-5183.	1.6	7
34565	Statistical variances of diffusional properties from ab initio molecular dynamics simulations. Npj Computational Materials, 2018, 4, .	3.5	240
34566	Influence of shell effects on thermodynamic properties of matter at high pressures. Journal of Physics: Conference Series, 2018, 946, 012083.	0.3	1
34567	Determination of Magneto-crystalline Anisotropy Energy (MAE) Of ordered L10CoPt and FePt nanoparticles. IOP Conference Series: Materials Science and Engineering, 2018, 305, 012017.	0.3	3
34568	Epitaxial phase diagrams of SrTiO3,ÂCaTiO3 , and SrHfO3 : Computational investigation including the role of antiferrodistortive and A -site displacement modes. Physical Review B, 2018, 97, .	1.1	5

#	Article	IF	Citations
34569	1Tâ€²â€Mo_{1â^'x}W_xS₂/CdS Heterostructure Enabling Robust Photocatalytic Water Splitting: Unveiling the Interfacial Charge Polarization. Solar Rrl, 2018, 2, 1800032.	3.1	27
34570	Hydrogenâ€Bonding Strategy to Optimize Charge Distribution of PC₇₁BM and Enable a High Efficiency of 12.45% for Organic Solar Cells. Solar Rrl, 2018, 2, 1800038.	3.1	22
34571	Effect of Intrinsic Defects on Electronic and Magnetic Properties in Tm-Doped GaN: First-Principles Calculations. Journal of Superconductivity and Novel Magnetism, 2018, 31, 3911-3917.	0.8	3
34572	First-principles study on the Poisson's ratio of transition-metal dichalcogenides. Current Applied Physics, 2018, 18, 799-802.	1.1	5
34573	Structure and thermodynamic properties of zirconium hydrides by structure search method and first principles calculations. Computational Materials Science, 2018, 150, 77-85.	1.4	34
34574	Crystal structures of CsSi6 at high pressures. Computational Materials Science, 2018, 150, 144-148.	1.4	8
34575	Ethylene versus ethane: A DFT-based selectivity descriptor for efficient catalyst screening. Journal of Catalysis, 2018, 362, 18-24.	3.1	52
34576	Towards understanding the mechanism of rhenium and osmium precipitation in tungsten and its implication for tungsten-based alloys. Journal of Nuclear Materials, 2018, 505, 30-43.	1.3	29
34577	First-principles study of solvent-solute mixed dumbbells in body-centered-cubic tungsten crystals. Journal of Nuclear Materials, 2018, 505, 15-21.	1.3	18
34578	The structural, elastic and electronic properties of marcasite FeS 2 under pressure. Journal of Physics and Chemistry of Solids, 2018, 118, 88-94.	1.9	6
34579	A first principles theoretical study of the adsorption of SF6 decomposition gases on a cassiterite (110) surface. Materials Chemistry and Physics, 2018, 212, 453-460.	2.0	27
34580	Hydrogen Evolution Reaction at Anion Vacancy of Two-Dimensional Transition-Metal Dichalcogenides: Ab Initio Computational Screening. Journal of Physical Chemistry Letters, 2018, 9, 2049-2055.	2.1	98
34581	Structural prediction of host-guest structure in lithium at high pressure. Scientific Reports, 2018, 8, 5278.	1.6	21
34582	Significant enhancement of the performance of hydrogen evolution reaction through shape-controlled synthesis of hierarchical dendrite-like platinum. Journal of Materials Chemistry A, 2018, 6, 8068-8077.	5.2	46
34583	Gaussian approximation potential modeling of lithium intercalation in carbon nanostructures. Journal of Chemical Physics, 2018, 148, 241714.	1.2	71
34584	Doping and band gap control at poly(vinylidene fluoride)/graphene interface. Journal Physics D: Applied Physics, 2018, 51, 195303.	1.3	4
34585	Microscopic study of thermoelectric In-doped SnTe. Nanotechnology, 2018, 29, 26LT01.	1.3	11
34586	Multiple shock reverberation compression of dense Ne up to the warm dense regime: Evaluating the theoretical models. Physical Review B, 2018, 97, .	1.1	10

#	Article	IF	Citations
34587	<mml:math xmlns:mml="http://www.w3.org/1998/Math/MathML"><mml:mrow><mml:mn>2</mml:mn><mml:mi>p</mml:mi></mml:mrow></mml:r -insulator heterointerfaces: Creation of half-metallicity and anionogenic ferromagnetism via double exchange. Physical Review B, 2018, 97, .	1.1	2
34588	Theoretical insight into the effects of nitrogen and vacancy defects on the behavior of helium in tungsten. Applied Physics Express, 2018, 11, 015801.	1.1	5
34589	Mechanistic understanding of methanol carbonylation: Interfacing homogeneous and heterogeneous catalysis via carbon supported Ir La. Journal of Catalysis, 2018, 361, 414-422.	3.1	28
34590	The vertical growth of MoS2 layers at the initial stage of CVD from first-principles. Journal of Chemical Physics, 2018, 148, 134704.	1.2	18
34591	Origin of the monolayer Raman signature in hexagonal boron nitride: a first-principles analysis. Journal of Physics Condensed Matter, 2018, 30, 185701.	0.7	3
34592	Morphologyâ€Dependent Magnetism in Nanographene: Beyond Nanoribbons. Advanced Functional Materials, 2018, 28, 1800592.	7.8	5
34593	Coadsorbateâ€Induced Reversal of Solidâ€“Liquid Interface Dynamics. Angewandte Chemie - International Edition, 2018, 57, 6065-6068.	7.2	25
34594	Adsorption of organic molecules on mineral surfaces studied by first-principle calculations: A review. Advances in Colloid and Interface Science, 2018, 256, 230-241.	7.0	52
34595	Mesoscale simulations of radiation damage effects in Materials: A SEAKMC perspective. Computational Materials Science, 2018, 150, 180-189.	1.4	9
34596	Low-energy 3D sp²carbons with versatile properties beyond graphite and graphene. Dalton Transactions, 2018, 47, 6233-6239.	1.6	7
34597	Firstâ€principles study in an interâ€granular glassy film model of silicon nitride. Journal of the American Ceramic Society, 2018, 101, 2673-2688.	1.9	23
34598	Engineering giant magnetic anisotropy in single-molecule magnets by dimerizing heavy transition-metal atoms. Applied Physics Express, 2018, 11, 055201.	1.1	5
34599	Insight of Diversified Reactivity and Theoretical Study of Mixedâ€Phase Titanium Dioxide for the Photoactivation of Small Molecules. ChemistrySelect, 2018, 3, 3659-3663.	0.7	11
34600	Computational investigations of Cu-embedded MoS2 sheet for CO oxidation catalysis. Journal of Materials Science, 2018, 53, 9578-9588.	1.7	23
34601	Comprehensive first-principles study of transition-metal substitution in the Î³ phase of nickel-based superalloys. Calphad: Computer Coupling of Phase Diagrams and Thermochemistry, 2018, 61, 41-49.	0.7	6
34602	Mechanical and thermodynamic properties of plutonium dihydride. Journal of Alloys and Compounds, 2018, 750, 258-264.	2.8	9
34603	Anions induced evolution of Co3X4 (Xâ€¯=â€¯O, S, Se) as sodium-ion anodes: The influences of electronic structure, morphology, electrochemical property. Nano Energy, 2018, 48, 617-629.	8.2	227
34604	Synthesis of N-phosphorylated sydnone imines and their functionalization via 4-Li derivatives. Novel bicyclic sydnone imines. Tetrahedron, 2018, 74, 2693-2702.	1.0	11

#	Article	IF	Citations
34605	Six New Members of the A₂M^{II}M^{IV}₃Q₈ Family and Their Structural Relationship. Crystal Growth and Design, 2018, 18, 3124-3131.	1.4	20
34606	Reaction Pathways and Microkinetic Modeling of n-Butane Oxidation to 1-Butanol on Cu, Cu₃Pd, Pd, Ag₃Pd, and PdZn (111) Surfaces. Industrial & Engineering Chemistry Research, 2018, 57, 5580-5590.	1.8	6
34607	Lithiation and Delithiation Processes in Lithiumâ€“Sulfur Batteries from Ab Initio Molecular Dynamics Simulations. Journal of Physical Chemistry C, 2018, 122, 8769-8779.	1.5	28
34608	Observation of Quasi-Two-Dimensional Polar Domains and Ferroelastic Switching in a Metal, Ca₃Ru₂O₇. Nano Letters, 2018, 18, 3088-3095.	4.5	62
34609	Enhanced Activity Promoted by CeO_x on a CoO_x Electrocatalyst for the Oxygen Evolution Reaction. ACS Catalysis, 2018, 8, 4257-4265.	5.5	151
34610	CO Adsorption on Metal-Decorated Phosphorene. ACS Omega, 2018, 3, 3957-3965.	1.6	32
34611	Room-temperature ductile inorganic semiconductor. Nature Materials, 2018, 17, 421-426.	13.3	262
34612	Quantitative assessment of intermolecular interactions by atomic force microscopy imaging using copper oxide tips. Nature Nanotechnology, 2018, 13, 371-375.	15.6	67
34613	Proton transfer ferroelectricity/multiferroicity in rutile oxyhydroxides. Nanoscale, 2018, 10, 9509-9515.	2.8	13
34614	Ab initio calculation of electronic structure and magnetic properties of R2Fe14BNx (R = Pr,Nd). AIP Advances, 2018, 8, .	0.6	4
34615	First-principles study of perpendicular magnetic anisotropy in ferrimagnetic D022-Mn3X (X = Ga, Ge) on MgO and SrTiO3. Applied Physics Letters, 2018, 112, 142403.	1.5	22
34616	Structural analysis of LaVO3 thin films under epitaxial strain. APL Materials, 2018, 6, .	2.2	19
34617	Boron monosulfide: Equation of state and pressure-induced phase transition. Journal of Applied Physics, 2018, 123, .	1.1	13
34618	Strain and ferroelectric soft-mode induced superconductivity in strontium titanate. Physical Review B, 2018, 97, .	1.1	31
34619	Probing the Fermi surface and magnetotransport properties of <mml:math xmlns:mml="http://www.w3.org/1998/Math/MathML"><mml:msub><mml:mi>MoAs</mml:mi><mml:mn>2</mml:mn></mml:msub></m Physical Review B, 2018, 97, .	1.1	16
34620	Converting topological insulators into topological metals within the tetradymite family. Physical Review B, 2018, 97, .	1.1	4
34621	Temperature-driven evolution of critical points, interlayer coupling, and layer polarization in bilayer <mml:math xmlns:mml="http://www.w3.org/1998/Math/MathML"><mml:mrow><mml:mi>Mo</mml:mi><mml:msub><mml:mi mathvariant="normal">S</mml:mi><mml:mn>2</mml:mn></mml:msub></mml:mrow></mml:math>. Physical Review B, 2018, 97, .	1.1	23
34622	Wâ€Based Atomic Laminates and Their 2D Derivative W_{1.33}C MXene with Vacancy Ordering. Advanced Materials, 2018, 30, e1706409.	11.1	240

#	Article	IF	Citations
34623	Metalâ€Free Artificial Photosynthesis of Carbon Monoxide Using Nâ€Doped ZnTe Nanorod Photocathode Decorated with Nâ€Doped Carbon Electrocatalyst Layer. Advanced Energy Materials, 2018, 8, 1702636.	10.2	42
34624	Sodiumâ€Doped Tin Sulfide Single Crystal: A Nontoxic Earthâ€Abundant Material with High Thermoelectric Performance. Advanced Energy Materials, 2018, 8, 1800087.	10.2	80
34625	The structural, elastic, electronic, magnetic and optical properties of the Zn0.75V0.25X (Xâ€‰=â€‰S, Se or Te). Journal of Materials Science: Materials in Electronics, 2018, 29, 10190-10203.	1.1	0
34626	Utilizing SO2 as self-installing gate to regulate the separation properties of porous graphenes. Carbon, 2018, 134, 145-152.	5.4	3
34627	First-principles study of hydrogen segregation at the MgZn2 precipitate in Al-Mg-Zn alloys. Computational Materials Science, 2018, 148, 301-306.	1.4	51
34628	Electronic structure and hydrogen storage properties of Liâ€“decorated single layer blue phosphorus. International Journal of Hydrogen Energy, 2018, 43, 8415-8425.	3.8	18
34629	Surface Terminationâ€”A Key Factor to Influence Electronic and Optical Properties of CsSnI3. Journal of Physical Chemistry C, 2018, 122, 9275-9282.	1.5	50
34630	First-Principles Insights into Ammonia Decomposition Catalyzed by Ru Clusters Anchored on Carbon Nanotubes: Size Dependence and Interfacial Effects. Journal of Physical Chemistry C, 2018, 122, 9091-9100.	1.5	35
34631	Two-body SchrÃ¶dinger wave functions in a plane-wave basis via separation of dimensions. Journal of Chemical Physics, 2018, 148, 104101.	1.2	10
34632	Strength and texture of sodium chloride to 56â€‰GPa. Journal of Applied Physics, 2018, 123, 135901.	1.1	10
34633	On compensation in Si-doped AlN. Applied Physics Letters, 2018, 112, .	1.5	97
34634	Magnetism of a Co monolayer on Pt(111) capped by overlayers of <mml:math xmlns:mml="http://www.w3.org/1998/Math/MathML"><mml:mrow><mml:mn>5</mml:mn><mml:mi>d</mml:mi></mml:mrow></mml:math> elements: A spin-model study. Physical Review B, 2018, 97, .	1.1	28
34635	Tunable ferroelectricity and anisotropic electric transport in monolayer <mml:math xmlns:mml="http://www.w3.org/1998/Math/MathML"><mml:mi>Î²</mml:mi></mml:math> -GeSe. Physical Review B, 2018, 97, .	1.1	72
34636	Colloquium : Strong-field phenomena in periodic systems. Reviews of Modern Physics, 2018, 90, .	16.4	192
34637	Direct IR Spectroscopic Detection of a Lowâ€Lying Electronic State in a Metal Carbide Cluster. ChemPhysChem, 2018, 19, 1424-1427.	1.0	5
34638	Structure, mechanical, electronic and thermodynamic properties of Mo5Si3 from first-principles calculations. Ceramics International, 2018, 44, 12357-12362.	2.3	92
34639	Experimental investigation and thermodynamic modelling of LiF-NdF3-DyF3 system. Journal of Alloys and Compounds, 2018, 753, 388-394.	2.8	9
34640	Tunable phase transition in single-layer TiSe2 via electric field. Journal of Solid State Chemistry, 2018, 262, 309-312.	1.4	4

#	Article	IF	Citations
34641	Complex reactions on a convertible catalyst surface: A study of the S-O-Cu system. Surface Science, 2018, 678, 228-233.	0.8	2
34642	Lanthanum-induced quasi-one-dimensional reconstructions on Si(111). Surface Science, 2018, 674, 40-44.	0.8	6
34643	Synergetic Influence of Alkali-Metal and Lone-Pair Cations on Frameworks of Tellurites. Inorganic Chemistry, 2018, 57, 5406-5412.	1.9	13
34644	Bonding Properties and Oxidation States of Plutonium in Pu₂O_n (n = 1â€“8) Molecules Studied by Using Screened Hybrid Density Functional Theory. Journal of Physical Chemistry A, 2018, 122, 4085-4091.	1.1	6
34645	Electrocapillary Coupling at Metal Surfaces from First Principles: On the Impact of Excess Charge on Surface Stress and Relaxation. Langmuir, 2018, 34, 4920-4928.	1.6	5
34646	Enhanced Electrochemical and Thermal Transport Properties of Graphene/MoS₂ Heterostructures for Energy Storage: Insights from Multiscale Modeling. ACS Applied Materials & Interfaces, 2018, 10, 14614-14621.	4.0	56
34647	Reducing Coercive-Field Scaling in Ferroelectric Thin Films via Orientation Control. ACS Nano, 2018, 12, 4736-4743.	7.3	47
34648	Reversible Mn2+/Mn4+ double redox in lithium-excess cathode materials. Nature, 2018, 556, 185-190.	13.7	525
34649	Rapid and damage-free outgassing of implanted helium from amorphous silicon oxycarbide. Scientific Reports, 2018, 8, 5009.	1.6	13
34650	Boosting the hydrogen evolution performance of ruthenium clusters through synergistic coupling with cobalt phosphide. Energy and Environmental Science, 2018, 11, 1819-1827.	15.6	350
34651	Phonons, phase transitions and thermal expansion in LiAlO₂: an ab initio density functional study. Physical Chemistry Chemical Physics, 2018, 20, 12248-12259.	1.3	9
34652	Fullerene/layered antiferromagnetic reconstructed spinterface: Subsurface layer dominates molecular orbitalsâ€™ spin-split and large induced magnetic moment. Journal of Chemical Physics, 2018, 148, 114704.	1.2	3
34653	Light controllable catalytic activity of Au clusters decorated with photochromic molecules. Nanotechnology, 2018, 29, 245705.	1.3	5
34654	Janus single layers of <mml:math xmlns:mml="http://www.w3.org/1998/Math/MathML"><mml:msub><mml:mi>In</mml:mi><mml:mn>2</mml:mn></mml:msub> : A first-principles study. Physical Review B, 2018, 97, .	1.7	27
34655	Superconducting Open-Framework Allotrope of Silicon at Ambient Pressure. Physical Review Letters, 2018, 120, 157001.	2.9	39
34656	Theoretical Insights into Oxidation States of Transition Metals at (001) and (111) LiNi0.5Mn1.5O4Spinel Surfaces. Journal of the Electrochemical Society, 2018, 165, A1099-A1103.	1.3	14
34657	Hydration of Concrete: The First Steps. Chemistry - A European Journal, 2018, 24, 8603-8608.	1.7	13
34658	Plasma phase transition in warm dense hydrogen. Contributions To Plasma Physics, 2018, 58, 122-127.	0.5	9

#	Article	IF	Citations
34659	First principles computational studies of spontaneous reduction reaction of Eu(III) in eutectic LiCl-KCl molten salt. International Journal of Energy Research, 2018, 42, 2757-2765.	2.2	14
34660	Computational Screening of 2D Materials and Rational Design of Heterojunctions for Water Splitting Photocatalysts. Small Methods, 2018, 2, 1700359.	4.6	151
34661	The effect of oxygen vacancies on the properties of polar and nonpolar (0â€¯0â€¯1) LaAlO3/SrTiO3 heterostructures. Applied Surface Science, 2018, 450, 260-264.	3.1	4
34662	The intrinsic low lattice thermal conductivity in the rock salt SnSe. Computational Materials Science, 2018, 148, 54-59.	1.4	16
34663	A theoretical investigation of structural, electronic and optical properties of bulk copper nitrides. Journal of Alloys and Compounds, 2018, 753, 576-585.	2.8	8
34664	Magnetic anisotropy of ultrathin Pd 4 Co(111) film by first-principles calculations. Journal of Science: Advanced Materials and Devices, 2018, 3, 243-253.	1.5	1
34665	Hybrid Density Functional Study of the Local Structures and Energy Levels of CaAl₂O₄:Ce³⁺. Journal of Physical Chemistry A, 2018, 122, 4306-4312.	1.1	5
34666	Pressure-Induced Topological Phase Transitions in CdGeSb₂ and CdSnSb₂. Journal of Physical Chemistry Letters, 2018, 9, 2202-2207.	2.1	14
34667	High-Pressure Evolution of Crystal Bonding Structures and Properties of FeOOH. Journal of Physical Chemistry Letters, 2018, 9, 2181-2185.	2.1	69
34668	Inhibition of Surface Chemical Moieties by Tris(hydroxymethyl)aminomethane: A Key to Understanding Oxygen Reduction on Ironâ€“Nitrogenâ€“Carbon Catalysts. ACS Applied Energy Materials, 2018, 1, 1942-1949.	2.5	18
34669	Role of Hyper-Reduced States in Hydrogen Evolution Reaction at Sulfur Vacancy in MoS₂. ACS Catalysis, 2018, 8, 4508-4515.	5.5	45
34670	Magnetically-driven phase transformation strengthening in high entropy alloys. Nature Communications, 2018, 9, 1363.	5.8	263
34671	Tuning Ising superconductivity with layer and spinâ€“orbit coupling in two-dimensional transition-metal dichalcogenides. Nature Communications, 2018, 9, 1427.	5.8	230
34672	Out-of-plane interface dipoles and anti-hysteresis in graphene-strontium titanate hybrid transistor. Npj 2D Materials and Applications, 2018, 2, .	3.9	13
34673	Synthesis of submillimeter SnSe_xS_{2â^'x} (0 < x < 1) two-dimensional alloy and photoinduced reversible transformation between Schottky and Ohmic contact behaviors in devices. Journal of Materials Chemistry C, 2018, 6, 4985-4993.	2.7	9
34674	Red-shifting and blue-shifting OH groups on metal oxide surfaces â€“ towards a unified picture. Physical Chemistry Chemical Physics, 2018, 20, 12678-12687.	1.3	12
34675	Enhanced interface interaction between modified carbon nanotubes and magnesium matrix. Composite Interfaces, 2018, 25, 1101-1114.	1.3	6
34676	Multichannel high-order harmonic generation from solids. Physical Review A, 2018, 97, .	1.0	33

#	Article	IF	Citations
34677	Electron-Mediated Phonon-Phonon Coupling Drives the Vibrational Relaxation of CO on Cu(100). Physical Review Letters, 2018, 120, 156804.	2.9	26
34678	Bottom-up synthesis of multifunctional nanoporous graphene. Science, 2018, 360, 199-203.	6.0	429
34679	Oxygen concentration dependence of silicon oxide dynamical properties. Japanese Journal of Applied Physics, 2018, 57, 06KD01.	0.8	2
34680	Synergistic Effect of B and N Dopants in Catalytic Transfer Hydrogenation. Asian Journal of Organic Chemistry, 2018, 7, 1107-1112.	1.3	7
34681	Hydride Shuttle Formation and Reaction with CO₂ on GaP(110). ChemSusChem, 2018, 11, 1558-1566.	3.6	19
34682	Excitation-driven non-thermal conversion of few-layer graphenes into sp3-bonded carbon nanofilms. Chemical Physics Letters, 2018, 694, 23-28.	1.2	1
34684	Impact of isotropic strain on electronic and magnetic properties of O-adsorbed SiC monolayer. Materials Science in Semiconductor Processing, 2018, 83, 27-32.	1.9	4
34685	MnSb₂S₄ Monolayer as an Anode Material for Metal-Ion Batteries. Chemistry of Materials, 2018, 30, 3208-3214.	3.2	74
34686	Unveiling Charge-Density Wave, Superconductivity, and Their Competitive Nature in Two-Dimensional NbSe₂. Nano Letters, 2018, 18, 2924-2929.	4.5	130
34687	Photocatalytic Cleavage of Câ€“C Bond in Lignin Models under Visible Light on Mesoporous Graphitic Carbon Nitride through Ï€â€“Ï€ Stacking Interaction. ACS Catalysis, 2018, 8, 4761-4771.	5.5	205
34688	New design for highly durable infrared-reflective coatings. Light: Science and Applications, 2018, 7, 17175-17175.	7.7	37
34689	Structural, magnetic, and electronic properties of Fe82Si4B10P4 metallic glass. Scientific Reports, 2018, 8, 5680.	1.6	15
34690	Highly negative Poisson's ratio in a flexible two-dimensional tungsten carbide monolayer. Physical Chemistry Chemical Physics, 2018, 20, 18924-18930.	1.3	42
34691	Self-powered photogalvanic phosphorene photodetectors with high polarization sensitivity and suppressed dark current. Nanoscale, 2018, 10, 7694-7701.	2.8	49
34692	Chemical vapor deposition and phase stability of pyrite on SiO₂. Journal of Materials Chemistry C, 2018, 6, 4753-4759.	2.7	9
34693	Modulation of magnetism in transition-metal-doped two-dimensional GeS. Journal Physics D: Applied Physics, 2018, 51, 225001.	1.3	2
34694	Electronic properties of two-dimensional in-plane heterostructures of WS₂/WSe₂/MoS₂. Materials Research Express, 2018, 5, 046307.	0.8	18
34695	Pressure effects on the electronic properties of the undoped superconductor ThFeAsN. Physical Review B, 2018, 97, .	1.1	8

#	Article	IF	Citations
34696	Multiple heteroatom substitution to graphene nanoribbon. Science Advances, 2018, 4, eaar7181.	4.7	151
34697	Transformation of Perovskite BaBiO₃ into Layered BaBiO_{2.5} Crystals Featuring Unusual Chemical Bonding and Luminescence. Chemistry - A European Journal, 2018, 24, 8875-8882.	1.7	1
34698	Interfacial Engineering of Hierarchical Transition Metal Oxide Heterostructures for Highly Sensitive Sensing of Hydrogen Peroxide. Small, 2018, 14, e1703713.	5.2	40
34699	Formic acid electrooxidation activity of Pt and Pt/Au catalysts: Effects of surface physical properties and irreversible adsorption of Bi. Electrochimica Acta, 2018, 273, 307-317.	2.6	28
34700	Active Site Ensembles Enabled Câ€“C Coupling of CO₂ and CH₄ for Acetone Production. Journal of Physical Chemistry C, 2018, 122, 9570-9577.	1.5	17
34701	Effects of graphene/BN encapsulation, surface functionalization and molecular adsorption on the electronic properties of layered InSe: a first-principles study. Physical Chemistry Chemical Physics, 2018, 20, 12939-12947.	1.3	27
34702	Synthesis, electronic structures, and photoluminescence properties of an efficient and thermally stable red-emitting phosphor Ca₃ZrSi₂O₉:Eu³⁺,Bi³⁺ for deep UV-LEDs. RSC Advances, 2018, 8, 13054-13060.	1.7	13
34703	Local structure of Ge2Sb2Te5 during crystallization under pressure. Applied Physics Letters, 2018, 112, .	1.5	6
34704	Local spin structure of the <mml:math xmlns:mml="http://www.w3.org/1998/Math/MathML"><mml:mrow><mml:mi>Î±</mml:mi><mml:mo>â^'</mml:mo><mml:mn> honeycomb-lattice magnet observed via muon spin rotation/relaxation. Physical Review B, 2018, 97, .	1.1	10
34705	Bursting at the seams: Rippled monolayer bismuth on NbSe ₂. Science Advances, 2018, 4, eaaq0330.	4.7	28
34706	Highly Inâ€Plane Optical and Electrical Anisotropy of 2D Germanium Arsenide. Advanced Functional Materials, 2018, 28, 1707379.	7.8	121
34707	New Insight on Tuning Electrical Transport Properties via Chalcogen Doping in nâ€type Mg₃Sb₂â€Based Thermoelectric Materials. Advanced Energy Materials, 2018, 8, 1702776.	10.2	85
34708	Anisotropic Thermal and Guestâ€Induced Responses of an Ultramicroporous Framework with Rigid Linkers. Chemistry - A European Journal, 2018, 24, 4774-4779.	1.7	3
34709	First-Principles Calculations of Stacking Fault Energies in Quinary High-Entropy Alloy Systems. Minerals, Metals and Materials Series, 2018, , 661-667.	0.3	0
34710	Theoretical investigations of electrical transport properties in CoSb3 skutterudites under hydrostatic loadings. Rare Metals, 2018, 37, 316-325.	3.6	8
34711	Band structure engineering and efficient charge transport in oxygen substituted g-C3N4 for superior photocatalytic hydrogen evolution. Applied Catalysis B: Environmental, 2018, 230, 115-124.	10.8	143
34712	Confined electron and hole states in semiconducting carbon nanotube sub-10â€¯nm artificial quantum dots. Carbon, 2018, 132, 304-311.	5.4	5
34713	A metallic peanut-shaped carbon nanotube and its potential for CO2 capture. Carbon, 2018, 132, 249-256.	5.4	13

#	Article	IF	Citations
34714	Nitrogen-doped penta-graphene as a superior catalytic activity for CO oxidation. Carbon, 2018, 132, 257-262.	5.4	51
34715	Thermodynamic modeling of LiF-NaF-KF-CrF3 system. Journal of Fluorine Chemistry, 2018, 209, 6-13.	0.9	15
34716	First-principles study of electronic and optical properties of lead-free double perovskites Cs2NaBX6 (B) Tj ETQq0 0 0 rgBT /Overlock 10 T	1.9	129
34717	The structural, electronic and magnetic properties of CoS 2 under pressure. Solid State Communications, 2018, 273, 60-65.	0.9	7
34718	Mechanism of Ethylene Oxychlorination on Ceria. ACS Catalysis, 2018, 8, 2651-2663.	5.5	22
34719	Solution-Grown Sodium Bismuth Dichalcogenides: Toward Earth-Abundant, Biocompatible Semiconductors. Journal of the American Chemical Society, 2018, 140, 3736-3742.	6.6	41
34720	Novel Chern insulators with half-metallic edge states. NPG Asia Materials, 2018, 10, e467-e467.	3.8	20
34721	Chemisorption of polysulfides through redox reactions with organic molecules for lithiumâ€“sulfur batteries. Nature Communications, 2018, 9, 705.	5.8	207
34722	The High-Pressure Superconducting Phase of Arsenic. Scientific Reports, 2018, 8, 3026.	1.6	16
34723	A self-template synthesis of defect-rich WS₂ as a highly efficient electrocatalyst for the hydrogen evolution reaction. Chemical Communications, 2018, 54, 2631-2634.	2.2	79
34724	Oxocarbon-functionalized graphene as a lithium-ion battery cathode: a first-principles investigation. Physical Chemistry Chemical Physics, 2018, 20, 7447-7456.	1.3	15
34725	Atomistic mechanisms of ReRAM cell operation and reliability. Materials Research Express, 2018, 5, 014005.	0.8	2
34726	Theoretical investigations of the anisotropic optical properties of distorted <mml:math xmlns:mml="http://www.w3.org/1998/Math/MathML"><mml:mrow><mml:mn>1</mml:mn><mml:mi>T</mml:mi><mml:mspace width="0.16em" /><mml:msub><mml:mi>ReS</mml:mi><mml:mn>2</mml:mn></mml:msub></mml:mrow></mml:math> and <mml:math xmlns:mml="http://www.w3.org/1998/Math/MathML"><mml:msub><mml:mi>ReSe</mml:mi><mml:mn>2</mml:mn></mml:msub></mml:mr	1.1	53
34727	Stabilization of <mml:math xmlns:mml="http://www.w3.org/1998/Math/MathML"><mml:mi>E</mml:mi></mml:math> -type magnetic order caused by epitaxial strain in perovskite manganites. Physical Review B, 2018, 97, .	1.1	12
34728	Imaging the dynamics of an individual hydrogen atom intercalated between two graphene sheets. Physical Review B, 2018, 97, .	1.1	7
34729	Topological states in a two-dimensional metal alloy in Si surface: BiAg/Si(111)- <mml:math xmlns:mml="http://www.w3.org/1998/Math/MathML"><mml:mrow><mml:mn>4</mml:mn><mml:mo>Ã—</mml:mo><mml:mn>4</mml:mn></mml:mr surface. Physical Review B, 2018, 97, .	1.1	10
34730	Sensing of CO and NO on Cu-Doped MoS₂Monolayer-Based Single Electron Transistor: A First Principles Study. IEEE Sensors Journal, 2018, 18, 2853-2860.	2.4	72
34731	Experimental and Theoretical Studies of the Metallic Conductivity in Cubic PbVO₃ under High Pressure. Journal of the Physical Society of Japan, 2018, 87, 024801.	0.7	24

#	Article	IF	Citations
34732	Binding maps for the study and prediction of bimetallic catalyst surface reactions: The case of methanol oxidation. International Journal of Quantum Chemistry, 2018, 118, e25606.	1.0	3
34733	DFT study of stabilization effects on N-doped graphene for ORR catalysis. Catalysis Today, 2018, 312, 118-125.	2.2	81
34734	Stability, electronic and magnetic properties of small M-doped rhodium clusters. Journal of Alloys and Compounds, 2018, 745, 497-504.	2.8	8
34735	Ternary interfacial superstructure enabling extraordinary hydrogen evolution electrocatalysis. Materials Today, 2018, 21, 602-610.	8.3	48
34736	Role of the H-containing groups on the structural dynamics of Ti 3 C 2 T x MXene. Physica B: Condensed Matter, 2018, 537, 155-161.	1.3	17
34737	Self-Assembled Binuclear Cu(II)â€“Histidine Complex for Absolute Configuration and Enantiomeric Excess Determination of Naproxen by Tandem Mass Spectrometry. Analytical Chemistry, 2018, 90, 4089-4097.	3.2	15
34738	The Mystery of the AuIn 1:1 Phase and Its Incommensurate Structural Variations. Inorganic Chemistry, 2018, 57, 2791-2796.	1.9	4
34739	On-Surface Polymerization of 1,6-Dibromo-3,8-diiodpyreneâ€”A Comparative Study on Au(111) Versus Ag(111) by STM, XPS, and NEXAFS. Journal of Physical Chemistry C, 2018, 122, 5967-5977.	1.5	29
34740	High-Throughput Computational Approach to Li/Vacancy Configurations and Structural Evolution during Delithiation: The Case of Li₂MnO₃ Surface. Journal of Physical Chemistry C, 2018, 122, 5496-5508.	1.5	4
34741	Tuning the optical bandgap in multi-cation compound transparent conducting-oxides: The examples of In2ZnO4 and In4Sn3O12. Journal of Applied Physics, 2018, 123, .	1.1	3
34742	Benchmarking several van der Waals dispersion approaches for the description of intermolecular interactions. Journal of Chemical Physics, 2018, 148, 064112.	1.2	37
34743	Nuclear quantum effect with pure anharmonicity and the anomalous thermal expansion of silicon. Proceedings of the National Academy of Sciences of the United States of America, 2018, 115, 1992-1997.	3.3	68
34744	Comparative Study of Electronic Structure and Magnetic Properties of Osmate Double Perovskites: Ca₂FeOsO₆versus Ca₂Co(Ni)OsO₆. Journal of the Physical Society of Japan, 2018, 87, 041007.	0.7	7
34745	Centimeterâ€Sized Cs₄PbBr₆ Crystals with Embedded CsPbBr₃ Nanocrystals Showing Superior Photoluminescence: Nonstoichiometry Induced Transformation and Lightâ€Emitting Applications. Advanced Functional Materials, 2018, 28, 1706567.	7.8	251
34746	First principles calculations of optical properties of the armchair SiC nanoribbons with O, F and H termination. Pramana - Journal of Physics, 2018, 90, 1.	0.9	4
34747	Electrically tunable band gap of the 1T-MoS2 based heterostructure: A first-principles calculation. Optik, 2018, 159, 222-228.	1.4	4
34748	Enhancing thermoelectric properties of BiCuSeO via uniaxial compressive strain: First-principles calculations. Journal of Alloys and Compounds, 2018, 743, 610-617.	2.8	13
34749	Modulation of band gap by an applied electric field in BN-based heterostructures. Solid State Communications, 2018, 273, 44-49.	0.9	9

#	Article	IF	Citations
34750	Experimental and Theoretical Insights into the Potential of V₂O₃ Surface Coatings for Hydrogen Permeable Vanadium Membranes. Journal of Physical Chemistry C, 2018, 122, 3488-3496.	1.5	13
34751	A computational study of high pressure polymorphic transformations in monazite-type LaPO₄. Physical Chemistry Chemical Physics, 2018, 20, 7621-7634.	1.3	8
34752	The electronic properties of Au clusters on CeO₂ (110) surface with and without O-defects. Faraday Discussions, 2018, 208, 123-145.	1.6	12
34753	Tuning the catalytic activity of colloidal noble metal nanocrystals by using differently charged surfactants. Nanoscale, 2018, 10, 5607-5616.	2.8	14
34754	Double negatively charged carbon vacancy at the h- and k-sites in 4H-SiC: Combined Laplace-DLTS and DFT study. Journal of Applied Physics, 2018, 123, .	1.1	36
34755	Structure, electronic properties, and oxygen incorporation/diffusion characteristics of the Î£5 TiN(310)[001] tilt grain boundary. Journal of Applied Physics, 2018, 123, .	1.1	18
34756	Photoinduced reversible lattice expansion in W-doped TiO2through the change of its electronic structure. Applied Physics Letters, 2018, 112, 061904.	1.5	4
34757	Magnetism and piezoelectricity of hexagonal boron nitride with triangular vacancy. Chinese Physics B, 2018, 27, 016301.	0.7	13
34758	Quaternary Ammonium Cation Specific Adsorption on Platinum Electrodes: A Combined Experimental and Density Functional Theory Study. Journal of the Electrochemical Society, 2018, 165, F114-F121.	1.3	26
34759	Highly efficient direct Z-scheme WO3/CdS-diethylenetriamine photocatalyst and its enhanced photocatalytic H2 evolution under visible light irradiation. Applied Surface Science, 2018, 442, 20-29.	3.1	137
34760	Attractive interaction between interstitial solutes and screw dislocations in bcc iron from first principles. Computational Materials Science, 2018, 148, 21-26.	1.4	40
34761	The effect of oxygenâ€“containing functional groups on the H2 adsorption of grapheneâ€“based nanomaterials: experiment and theory. International Journal of Hydrogen Energy, 2018, 43, 5668-5679.	3.8	31
34762	Cluster-assisted nucleation mechanism of titanium oxides in Fe-Ti supercooled alloys. Journal of Alloys and Compounds, 2018, 744, 797-800.	2.8	6
34763	Mining Unexplored Chemistries for Phosphors for High-Color-Quality White-Light-Emitting Diodes. Joule, 2018, 2, 914-926.	11.7	97
34764	Mechanical behavior, electronic and phonon properties of ZrB 12 under pressure. Journal of Physics and Chemistry of Solids, 2018, 117, 173-179.	1.9	12
34765	Pd-Doped WO₃ Nanostructures as Potential Glucose Sensor with Insight from Electronic Structure Simulations. Journal of Physical Chemistry B, 2018, 122, 2737-2746.	1.2	47
34766	Epitaxial Growth of Flat Antimonene Monolayer: A New Honeycomb Analogue of Graphene. Nano Letters, 2018, 18, 2133-2139.	4.5	219
34767	Electronic and optical properties of hydrogenated group-IV multilayer materials. Physical Chemistry Chemical Physics, 2018, 20, 8112-8118.	1.3	12

#	Article	IF	Citations
34768	Effects of Grain Boundary Characteristics on Its Capability to Trap Point Defects in Tungsten. Chinese Physics Letters, 2018, 35, 026101.	1.3	15
34769	Tracking the ultrafast XUV optical properties of x-ray free-electron-laser heated matter with high-order harmonics. Physical Review A, 2018, 97, .	1.0	16
34770	Ab Initio Study of Electronic and Magnetic Properties of Germanene with Different Nonmagnetic Metal Adatoms. Journal of Superconductivity and Novel Magnetism, 2018, 31, 3193-3199.	0.8	2
34771	Boosting photocatalytic water oxidation reactions over strontium tantalum oxynitride by structural laminations. Applied Catalysis B: Environmental, 2018, 228, 10-18.	10.8	62
34772	Tunable Schottky barrier and electronic properties in borophene/g-C2N van der Waals heterostructures. Applied Surface Science, 2018, 440, 42-46.	3.1	26
34773	Modified embedded-atom method interatomic potentials for pure Zn and Mg-Zn binary system. Calphad: Computer Coupling of Phase Diagrams and Thermochemistry, 2018, 60, 200-207.	0.7	26
34774	Unique adsorption behaviors of NO and O2 at hydrogenated anatase TiO2(101). Chinese Chemical Letters, 2018, 29, 765-768.	4.8	15
34775	Electrochemical properties of stanene as an efficient anode material for Na-ion batteries. Computational Condensed Matter, 2018, 14, 84-88.	0.9	9
34776	The effect of pressure on structural, electronic, elastic, vibration and optical properties of ScXSb (X=Ni, Pd, Pt) compounds. Computational Condensed Matter, 2018, 14, 176-185.	0.9	16
34777	Mechanical responses of two-dimensional MoTe2; pristine 2H, 1T and 1Tâ€² and 1Tâ€²/2H heterostructure. Extreme Mechanics Letters, 2018, 20, 65-72.	2.0	34
34778	Correlating electrocatalytic oxygen reduction activity with d-band centers of metallic nanoparticles. Energy Storage Materials, 2018, 13, 189-198.	9.5	40
34779	Robust mechanical stability, electronic structure, magnetism and thermoelectric properties of CoFeMnSb quaternary Heusler alloy: AÂfirst principle study. Journal of Alloys and Compounds, 2018, 742, 903-909.	2.8	16
34780	On the mechanism of the electrochemical conversion of ammonia to dinitrogen on Pt(1â€¯0â€¯0) in alkaline environment. Journal of Catalysis, 2018, 359, 82-91.	3.1	62
34781	Hydrodeoxygenation of m-cresol over bimetallic NiFe alloys: Kinetics and thermodynamics insight into reaction mechanism. Journal of Catalysis, 2018, 359, 272-286.	3.1	95
34782	Vacancy formation enthalpies of high-entropy FeCoCrNi alloy via first-principles calculations and possible implications to its superior radiation tolerance. Journal of Materials Science and Technology, 2018, 34, 355-364.	5.6	87
34783	Conductive nitrides: Growth principles, optical and electronic properties, and their perspectives in photonics and plasmonics. Materials Science and Engineering Reports, 2018, 123, 1-55.	14.8	180
34784	A quaternary sodium superionic conductor - Na10.8Sn1.9PS11.8. Nano Energy, 2018, 47, 325-330.	8.2	55
34785	Electronic structure of grapheneâ€“ and BNâ€“supported phosphorene. Physica B: Condensed Matter, 2018, 534, 63-67.	1.3	36

#	Article	IF	Citations
34786	Biological hydrogen peroxide detection with aryl boronate and benzil BODIPY-based fluorescent probes. Sensors and Actuators B: Chemical, 2018, 262, 750-757.	4.0	35
34787	Adsorption, hydrogenation and dehydrogenation of C 2 H on a CoCu bimetallic layer. Surface Science, 2018, 671, 36-42.	0.8	8
34788	Thermodynamic study of the Al-Sc-Y system. Thermochimica Acta, 2018, 661, 147-159.	1.2	4
34789	Stability and band offsets of nonpolar (11<mml:math) Tj ETQq1 1 0.784314 rgBT /Overlock 10 Tf 50 637 Td (xmlns:mml= http://www.w ZnO on (001) LaAlO 3. Vacuum, 2018, 150, 29-34.	1.6	10
34790	Thermodynamics and Kinetics of Graphene Growth on Ni(111) and the Origin of Triangular Shaped Graphene Islands. Journal of Physical Chemistry C, 2018, 122, 3334-3340.	1.5	10
34791	Theoretical Evaluation on Terahertz Source Generators from Ternary Metal Chalcogenides of PbM₆Te₁₀ (M = Ga, In). Journal of Physical Chemistry C, 2018, 122, 4557-4564.	1.5	21
34792	Coexistence of Type-I and Type-II Weyl Points in the Weyl-Semimetal OsC₂. Journal of Physical Chemistry C, 2018, 122, 3533-3538.	1.5	23
34793	MBene (MnB): a new type of 2D metallic ferromagnet with high Curie temperature. Nanoscale Horizons, 2018, 3, 335-341.	4.1	183
34794	Understanding the ionic conductivity maximum in doped ceria: trapping and blocking. Physical Chemistry Chemical Physics, 2018, 20, 14291-14321.	1.3	116
34795	Strain-induced modulations of electronic structure and electronâ€“phonon coupling in dense H₃S. Physical Chemistry Chemical Physics, 2018, 20, 5952-5957.	1.3	15
34796	Optically adjustable valley Hall current in single-layer transition metal dichalcogenides. Journal of Applied Physics, 2018, 123, 054301.	1.1	2
34797	First-principles study of charge and magnetic ordering in monolayer <mml:math xmlns:mml="http://www.w3.org/1998/Math/MathML"><mml:msub><mml:mi>NbSe</mml:mi><mml:mn>2</mml:mn></mml:msub></mml Physical Review B, 2018, 97, .	1.1	38
34798	Mechanism for selective growth in electrical steel. Metals and Materials International, 2018, 24, 216-220.	1.8	0
34799	The role of Ag, Ca, Zr and Al in strengthening effects of ZK series alloys by altering G.P. zones stability. Acta Materialia, 2018, 147, 42-50.	3.8	15
34800	Effects of alloying elements on vacancies and vacancy-hydrogen clusters at coherent twin boundaries in nickel alloys. Acta Materialia, 2018, 148, 9-17.	3.8	36
34801	Photogenerated charge transfer via interfacial internal electric field for significantly improved photocatalysis in direct Z-scheme oxygen-doped carbon nitrogen/CoAl-layered double hydroxide heterojunction. Applied Catalysis B: Environmental, 2018, 227, 530-540.	10.8	219
34802	DFT study on bimetallic Pt/Cu(1â€¯1â€¯1) as efficient catalyst for H2 dissociation. Applied Surface Science, 2018, 441, 23-28.	3.1	9
34803	Hydrogen production from organic fatty acids using carbon-doped TiO2 nanoparticles under visible light irradiation. International Journal of Hydrogen Energy, 2018, 43, 4335-4346.	3.8	20

#	Article	IF	Citations
34804	Strain and electric field induced metallization in the GaX (Xâ€¯=â€¯N, P, As & Sb) monolayer. Physica E: Low-Dimensional Systems and Nanostructures, 2018, 99, 236-243.	1.3	24
34805	TiO₂(B) and Anatase Angstrom-Scale Wires: A Theoretical Study. Journal of Physical Chemistry C, 2018, 122, 3363-3370.	1.5	4
34806	Tuning Electronic Structure of Single Layer MoS₂ through Defect and Interface Engineering. ACS Nano, 2018, 12, 2569-2579.	7.3	203
34807	Acidâ€“Base Control of Valency within Carboranedithiol Self-Assembled Monolayers: Molecules Do the Can-Can. ACS Nano, 2018, 12, 2211-2221.	7.3	23
34808	Photocarrier generation from interlayer charge-transfer transitions in WS ₂ -graphene heterostructures. Science Advances, 2018, 4, e1700324.	4.7	160
34809	Extension of the QuickFF force field protocol for an improved accuracy of structural, vibrational, mechanical and thermal properties of metalâ€“organic frameworks. Journal of Computational Chemistry, 2018, 39, 999-1011.	1.5	59
34810	Martensitic transition in Fe via Bain path at finite temperatures: A comprehensive first-principles study. Acta Materialia, 2018, 147, 261-276.	3.8	44
34811	A CALPHAD assessment of the Alâ€“Mnâ€“C system supported by ab initio calculations. Calphad: Computer Coupling of Phase Diagrams and Thermochemistry, 2018, 60, 231-239.	0.7	10
34812	Thermodynamic modeling of the Al-C-Mn system supported by ab initio calculations. Calphad: Computer Coupling of Phase Diagrams and Thermochemistry, 2018, 60, 222-230.	0.7	11
34813	DFT study on phase transition behavior and mechanical properties of HgSe polymorphs under high pressure. Current Applied Physics, 2018, 18, 424-436.	1.1	7
34814	First-principles study of the atomic and electronic properties of (1â€¯0â€¯0) stacking faults in BaSnO3 crystal. Chemical Physics Letters, 2018, 694, 65-69.	1.2	1
34815	Aggregation and ordering of helium in thoria. Journal of Alloys and Compounds, 2018, 743, 196-202.	2.8	4
34816	Ruddlesden-Popper compound Sr2TiO4 co-doped with La and Fe for efficient photocatalytic hydrogen production. Journal of Catalysis, 2018, 359, 112-121.	3.1	42
34817	Strong electronic metal-support interaction of Pt/CeO2 enables efficient and selective hydrogenation of quinolines at room temperature. Journal of Catalysis, 2018, 359, 101-111.	3.1	146
34818	Symmetrical metallic and magnetic edge states of nanoribbon from semiconductive monolayer PtS2. Physics Letters, Section A: General, Atomic and Solid State Physics, 2018, 382, 776-780.	0.9	12
34819	Defect thermodynamics and interfacial instability of crystalline Li4P2S6. Solid State Ionics, 2018, 319, 53-60.	1.3	9
34820	Predictive Design and Experimental Realization of InAs/GaAs Superlattices with Tailored Thermal Conductivity. Journal of Physical Chemistry C, 2018, 122, 4054-4062.	1.5	14
34821	Insights into the Stability of Zeolitic Imidazolate Frameworks in Humid Acidic Environments from First-Principles Calculations. Journal of Physical Chemistry C, 2018, 122, 4339-4348.	1.5	55

#	Article	IF	Citations
34822	High Hydrides of Scandium under Pressure: Potential Superconductors. Journal of Physical Chemistry C, 2018, 122, 6298-6309.	1.5	83
34823	Transition Metal-Doped Tin Monoxide Monolayer: A First-Principles Study. Journal of Physical Chemistry C, 2018, 122, 4651-4661.	1.5	33
34824	Atomically dispersed Ni(i) as the active site for electrochemical CO2 reduction. Nature Energy, 2018, 3, 140-147.	19.8	1,594
34825	Direct observation of a two-dimensional hole gas at oxide interfaces. Nature Materials, 2018, 17, 231-236.	13.3	151
34826	Support effects on adsorption and catalytic activation of O₂ in single atom iron catalysts with graphene-based substrates. Physical Chemistry Chemical Physics, 2018, 20, 7333-7341.	1.3	64
34827	Spin splitting and p-/n-type doping of two-dimensional WSe2/BiIrO3(111) heterostructures. Physical Chemistry Chemical Physics, 2018, 20, 6100-6107.	1.3	7
34828	A theoretical study on the electronic properties of in-plane CdS/ZnSe heterostructures: type-II band alignment for water splitting. Journal of Materials Chemistry A, 2018, 6, 4161-4166.	5.2	99
34829	Theoretical prediction of sandwiched two-dimensional phosphide binary compound sheets with tunable bandgaps and anisotropic physical properties. Nanotechnology, 2018, 29, 095703.	1.3	6
34830	Development of a machine learning potential for graphene. Physical Review B, 2018, 97, .	1.1	142
34831	Synergistic Effect of Graphene Oxide for Impeding the Dendritic Plating of Li. Advanced Functional Materials, 2018, 28, 1705917.	7.8	92
34832	Electronic Properties of Csâ€Based Halide Perovskites: An Ab Initio Study. Physica Status Solidi (A) Applications and Materials Science, 2018, 215, 1700941.	0.8	6
34833	Solute segregation in Cu: DFT vs. Experiment. Acta Materialia, 2018, 147, 122-132.	3.8	45
34834	Nanotwinning and amorphization of boron suboxide. Acta Materialia, 2018, 147, 195-202.	3.8	23
34835	Investigations of the microstructure evolution and tensile deformation behavior of austenitic Fe-Mn-Al-C lightweight steels and the effect of Mo addition. Acta Materialia, 2018, 147, 226-235.	3.8	87
34836	O 2 activation and CO oxidation on n-p codoped h-BN single-atom catalysts. Computational and Theoretical Chemistry, 2018, 1127, 31-36.	1.1	14
34837	Conductive Nb25O62 and Nb12O29 anode materials for use in high-performance lithium-ion storage. Electrochimica Acta, 2018, 266, 202-211.	2.6	39
34838	Structure and reactivity of oxalate surface complexes on lepidocrocite derived from infrared spectroscopy, DFT-calculations, adsorption, dissolution and photochemical experiments. Geochimica Et Cosmochimica Acta, 2018, 226, 244-262.	1.6	37
34839	First principles study on elastic and electronic properties of bialkali alanates M2Mâ€²AlH6. International Journal of Hydrogen Energy, 2018, 43, 3862-3870.	3.8	15

#	Article	IF	Citations
34840	Tunable magnetism in the LaAlO 3 /SrTiO 3 heterostructure: Insights from first-principles calculations. Physica E: Low-Dimensional Systems and Nanostructures, 2018, 98, 120-124.	1.3	6
34841	Experimental realization of honeycomb borophene. Science Bulletin, 2018, 63, 282-286.	4.3	397
34842	Zintl Ions within Framework Channels: The Complex Structure and Low-Temperature Transport Properties of Na4Ge13. Inorganic Chemistry, 2018, 57, 2002-2012.	1.9	7
34843	Structural and Bonding Characteristics of Potassium-Doped p-Terphenyl Superconductors. Journal of Physical Chemistry C, 2018, 122, 3801-3808.	1.5	36
34844	Decomposition Mechanism of Zinc Ammine Borohydride: A First-Principles Calculation. Journal of Physical Chemistry C, 2018, 122, 4241-4249.	1.5	6
34845	First-Principles Study on Layered C₂Nâ€“Metal Interfaces. Langmuir, 2018, 34, 2647-2653.	1.6	12
34846	High-Capacity and Long-Cycle Life Aqueous Rechargeable Lithium-Ion Battery with the FePO₄ Anode. ACS Applied Materials & Interfaces, 2018, 10, 7061-7068.	4.0	34
34847	Microkinetics of alcohol reforming for H2 production from a FAIR density functional theory database. Nature Communications, 2018, 9, 526.	5.8	38
34848	Chemistry through cocrystals: pressure-induced polymerization of C₂H₂Â·C₆H₆to an extended crystalline hydrocarbon. Physical Chemistry Chemical Physics, 2018, 20, 7282-7294.	1.3	15
34849	Expedite random structure searching using objects from Wyckoff positions. Journal of Chemical Physics, 2018, 148, 054101.	1.2	4
34850	Strain Effects on Properties of Phosphorene and Phosphorene Nanoribbons: a DFT and Tight Binding Study. Chinese Physics Letters, 2018, 35, 017302.	1.3	7
34851	Quasiparticle scattering in type-II Weyl semimetal MoTe2. Journal of Physics Condensed Matter, 2018, 30, 105703.	0.7	7
34852	Hydrogen-assisted post-growth substitution of tellurium into molybdenum disulfide monolayers with tunable compositions. Nanotechnology, 2018, 29, 145603.	1.3	17
34853	Dy adsorption and penetration on defected graphene by first-principles calculations. Materials Research Express, 2018, 5, 025022.	0.8	8
34854	Strong magnetization and Chern insulators in compressed <mml:math xmlns:mml="http://www.w3.org/1998/Math/MathML"><mml:msub><mml:mrow><mml:mi>graphene</mml:mi><mml:mtext>/26</mml:mtext></mml:mrow></mml:msub></mml:math> van der Waals heterostructures. Physical Review B, 2018, 97, .	1.1	26
34855	Comparison of the periodic slab approach with the finite cluster description of metalâ€“organic interfaces at the example of PTCDA on Ag(110). Journal of Computational Chemistry, 2018, 39, 844-852.	1.5	17
34856	Hydrogen adatom interaction on graphene: A first principles study. Carbon, 2018, 131, 137-141.	5.4	16
34857	Proximity effect induced spin filtering and gap opening in graphene by half-metallic monolayer Cr2C ferromagnet. Carbon, 2018, 132, 25-31.	5.4	39

#	Article	IF	Citations
34858	A theoretical study on reaction mechanisms and kinetics of thiophene hydrodesulfurization over MoS2 catalysts. Catalysis Today, 2018, 312, 158-167.	2.2	25
34859	Room-Temperature Aluminum-Sulfur Batteries with a Lithium-Ion-Mediated Ionic Liquid Electrolyte. CheM, 2018, 4, 586-598.	5.8	127
34860	Electronic and gap properties of Sb and Bi based halide perovskites: An ab-initio study. Computational Condensed Matter, 2018, 14, 161-166.	0.9	14
34861	Phonon thermal transport in monolayer FeB2 from first principles. Computational Materials Science, 2018, 147, 132-136.	1.4	13
34862	Predicting the structural and electronic properties of two-dimensional single layer boron nitride sheets. Chemical Physics Letters, 2018, 694, 102-106.	1.2	32
34863	Density functional theory study of inter-layer coupling in bulk tin selenide. Chemical Physics Letters, 2018, 695, 200-204.	1.2	24
34864	Role of S-S interlayer spacing on the hydrogen storage mechanism of MoS 2. International Journal of Hydrogen Energy, 2018, 43, 3087-3091.	3.8	74
34865	Ca and K decorated germanene as hydrogen storage: An ab initio study. International Journal of Hydrogen Energy, 2018, 43, 4393-4400.	3.8	54
34866	Preparation and the superior oxygen permeability of a new CO2-resistant Ruddlesdenâ€“Popper composite oxide Pr2Ni0.9Mo0.1O4+. Journal of Alloys and Compounds, 2018, 742, 966-976.	2.8	13
34867	Relative cooling power enhancement by tuning magneto-structural stability in Ni-Mn-In Heusler alloys. Journal of Alloys and Compounds, 2018, 744, 785-790.	2.8	17
34868	Dy3Al2(AlO4)3 ceramic nanogarnets: Sol-gel auto-combustion synthesis, characterization and joint experimental and computational structural analysis for electrochemical hydrogen storage performances. Journal of Alloys and Compounds, 2018, 744, 574-582.	2.8	30
34869	First-principles investigation of Cr-doped Fe2B: Structural, mechanical, electronic and magnetic properties. Journal of Magnetism and Magnetic Materials, 2018, 456, 150-159.	1.0	14
34870	Basal-plane stacking-fault energies of Mg alloys: A first-principles study of metallic alloying effects. Journal of Materials Science and Technology, 2018, 34, 1773-1780.	5.6	62
34871	A first-principle study of the electronic, mechanical and optical properties of inorganic perovskite Cs2SnI6 for intermediate-band solar cells. Materials Letters, 2018, 218, 233-236.	1.3	61
34872	Intrinsic defects and spectral characteristics of SrZrO 3 perovskite. Physica B: Condensed Matter, 2018, 534, 105-112.	1.3	9
34873	First-principles study of intrinsic phononic thermal transport in monolayer C3N. Physica E: Low-Dimensional Systems and Nanostructures, 2018, 99, 194-201.	1.3	58
34874	Electronic and magnetic properties of SnS2 monolayer doped with non-magnetic elements. Physica E: Low-Dimensional Systems and Nanostructures, 2018, 99, 182-188.	1.3	9
34875	High-Pressure Synthesis of CeOCl Crystals and Investigation of Their Photoluminescence and Compressibility Properties. Crystal Growth and Design, 2018, 18, 1843-1847.	1.4	5

#	Article	IF	Citations
34876	Selective Hydride Occupation in BaVO_{3â€“x}H_x (0.3 â‰¤ x â‰¤ 0.8) with Face- and Corner-Shared Octahedra. Chemistry of Materials, 2018, 30, 1566-1574.	3.2	25
34877	Extreme Sensitivity of a Topochemical Reaction to Cation Substitution: SrVO₂H versus SrV_{1â€“x}Ti_xO_{1.5}H_{1.5}. Inorganic Chemistry, 2018, 57, 2890-2898.	1.9	14
34878	Effects of Spinâ€“Orbit Coupling on Nonequilibrium Quantum Transport Properties of Hybrid Halide Perovskites. Journal of Physical Chemistry C, 2018, 122, 4150-4155.	1.5	8
34879	Formation of Multilayer Cu Islands Embedded beneath the Surface of Graphite: Characterization and Fundamental Insights. Journal of Physical Chemistry C, 2018, 122, 4454-4469.	1.5	27
34880	Changing the Usual Interpretation of the Structure and Ground State of Cu²⁺-Layered Perovskites. Journal of Physical Chemistry C, 2018, 122, 5071-5082.	1.5	51
34881	Iron Superhydrides FeH₅ and FeH₆: Stability, Electronic Properties, and Superconductivity. Journal of Physical Chemistry C, 2018, 122, 4731-4736.	1.5	48
34882	Design Strategy for the Molecular Functionalization of Semiconductor Photoelectrodes: A Case Study of p-Si(111) Photocathodes for H₂ Generation. Langmuir, 2018, 34, 2959-2966.	1.6	2
34883	Plasmon-Enhanced Catalysis: Distinguishing Thermal and Nonthermal Effects. Nano Letters, 2018, 18, 1714-1723.	4.5	251
34884	Highly Surface-Active Ca(OH)₂ Monolayer as a CO₂ Capture Material. Nano Letters, 2018, 18, 1786-1793.	4.5	24
34885	Effect of Bromine Substitution on the Ion Migration and Optical Absorption in MAPbI₃ Perovskite Solar Cells: The First-Principles Study. ACS Applied Energy Materials, 2018, 1, 1374-1380.	2.5	46
34886	Investigating the Role of Copper Oxide in Electrochemical CO₂ Reduction in Real Time. ACS Applied Materials & Interfaces, 2018, 10, 8574-8584.	4.0	207
34887	Modulating Reactivity and Selectivity of 2-Pyrone-Derived Bicyclic Lactones through Choice of Catalyst and Solvent. ACS Catalysis, 2018, 8, 2450-2463.	5.5	14
34888	Two-Dimensional Fluorinated Boron Sheets: Mechanical, Electronic, and Thermal Properties. ACS Omega, 2018, 3, 1815-1822.	1.6	53
34889	Anti-fouling graphene-based membranes for effective water desalination. Nature Communications, 2018, 9, 683.	5.8	197
34890	Solid-state electron spin lifetime limited by phononic vacuum modes. Nature Materials, 2018, 17, 313-317.	13.3	53
34891	Theoretical aspects in structural distortion and the electronic properties of lithium peroxide under high pressure. Physical Chemistry Chemical Physics, 2018, 20, 9488-9497.	1.3	4
34892	Metamagnetism stabilized giant magnetoelectric coupling in ferroelectric xBaTiO3â€“(1 â^’ x)BiCoO3 solid solution. Physical Chemistry Chemical Physics, 2018, 20, 7021-7032.	1.3	8
34893	Reaction mechanisms and sensitivity of silicon nitrocarbamate and related systems from quantum mechanics reaction dynamics. Journal of Materials Chemistry A, 2018, 6, 5082-5097.	5.2	8

#	Article	IF	Citations
34894	Tuning the electronic and magnetic properties of InSe nanosheets by transition metal doping. Physical Chemistry Chemical Physics, 2018, 20, 7532-7537.	1.3	15
34895	High-throughput theoretical optimization of the hydrogen evolution reaction on MXenes by transition metal modification. Journal of Materials Chemistry A, 2018, 6, 4271-4278.	5.2	198
34896	Atomic structure and electronic properties of A₂B₂XY (A = Siâ€“Pb, B = Clâ€“I,) Tj ETQq0 0 0 rgBT /Overlock 1 Chemical Physics, 2018, 20, 10060-10068.	1.3	4
34897	Improved power factor in low thermal conductive Fe2VAl-based full-Heusler thin films by composition-control with off-axis sputtering method. Applied Physics Letters, 2018, 112, .	1.5	8
34898	Structure formation and surface chemistry of ionic liquids on model electrode surfacesâ€”Model studies for the electrode | electrolyte interface in Li-ion batteries. Journal of Chemical Physics, 2018, 148, 193821.	1.2	17
34899	<mml:math xmlns:mml="http://www.w3.org/1998/Math/MathML"><mml:mrow><mml:msub><mml:mi>Ba</mml:mi><mml:mn>3</mml:mn></mml:msub><mml:msub><mml:mi mathvariant="normal">O</mml:mi><mml:mn>9</mml:mn></mml:msub></mml:mrow></mml:math> hexagonal perovskites in the light of spin-orbit coupling and local structural distortions. Physical Review B, 2018, 97, .	1.1	17
34900	Saddle-like topological surface states on the <mml:math xmlns:mml="http://www.w3.org/1998/Math/MathML"><mml:mrow><mml:mi>T</mml:mi><mml:msup><mml:mi>T</mml:mi><mml:mo>		

#	Article	IF	Citations
34912	An Aqueous Inorganic Polymer Binder for High Performance Lithiumâ€“Sulfur Batteries with Flame-Retardant Properties. ACS Central Science, 2018, 4, 260-267.	5.3	147
34913	Geometric isotope effect of deuteration in a hydrogen-bonded hostâ€“guest crystal. Nature Communications, 2018, 9, 481.	5.8	76
34914	Monolayer PdSe2: A promising two-dimensional thermoelectric material. Scientific Reports, 2018, 8, 2764.	1.6	133
34915	A DFT study of chlorine coverage over late transition metals and its implication on 1,2-dichloroethane hydrodechlorination. Catalysis Science and Technology, 2018, 8, 1555-1563.	2.1	16
34916	Gold fillings unravel the vacancy role in the phase transition of GeTe. Applied Physics Letters, 2018, 112, 071902.	1.5	10
34917	Stability, elastic and electronic properties of a novel BN2 sheet with extended hexagons with Nâ€“N bonds. Journal of Physics Condensed Matter, 2018, 30, 135002.	0.7	3
34918	A new series of two-dimensional silicon crystals with versatile electronic properties. 2D Materials, 2018, 5, 025013.	2.0	8
34919	Meta-screening and permanence of polar distortion in metallized ferroelectrics. Physical Review B, 2018, 97, .	1.1	39
34920	Harmonizing Energy and Power Density toward 2.7 V Asymmetric Aqueous Supercapacitor. Advanced Energy Materials, 2018, 8, 1702630.	10.2	201
34921	Impact of Polar Edge Terminations of the Transition Metal Dichalcogenide Monolayers during Vapor Growth. Journal of Physical Chemistry C, 2018, 122, 3575-3581.	1.5	6
34922	Efficient MOF-based degradation of organophosphorus compounds in non-aqueous environments. Journal of Materials Chemistry A, 2018, 6, 3038-3045.	5.2	42
34923	Bending energy of 2D materials: graphene, MoS₂ and imogolite. RSC Advances, 2018, 8, 4577-4583.	1.7	26
34924	Ab initio calculations of ideal strength and lattice instability in W-Ta and W-Re alloys. Physical Review B, 2018, 97, .	1.1	11
34925	Tuning the ferroelectric-to-paraelectric transition temperature and dipole orientation of group-IV monochalcogenide monolayers. Physical Review B, 2018, 97, .	1.1	79
34926	Energetics of oxygen-octahedra rotations in perovskite oxides from first principles. Physical Review B, 2018, 97, .	1.1	32
34927	Descriptors for Machine Learning of Materials Data. , 2018, , 3-23.		45
34928	Disentangling the Effects of Inter- and Intra-octahedral Distortions on the Electronic Structure in Binary Metal Trioxides. Journal of Physical Chemistry C, 2018, 122, 3558-3566.	1.5	14
34929	First-Principles Investigation of Titanium Nanoparticle Oxidation. Journal of Physical Chemistry C, 2018, 122, 3107-3114.	1.5	5

#	Article	IF	Citations
34930	High Anisotropy in Tubular Layered Exfoliated KP₁₅. ACS Nano, 2018, 12, 1712-1719.	7.3	24
34931	Hydrogen bonding effect between active site and protein environment on catalysis performance in H₂-producing [NiFe] hydrogenases. Physical Chemistry Chemical Physics, 2018, 20, 6735-6743.	1.3	15
34932	Topologically protected hybrid states in grapheneâ€“staneneâ€“graphene heterojunctions. Journal of Materials Chemistry C, 2018, 6, 1920-1925.	2.7	9
34933	Emergent property of high hardness for C-rich ruthenium carbides: partial covalent Ruâ€“Ru bonds. Physical Chemistry Chemical Physics, 2018, 20, 6108-6115.	1.3	5
34934	Theoretical investigations on diamondoids (CnHm, n = 10â€“41): Nomenclature, structural stabilities, and gap distributions. Journal of Chemical Physics, 2018, 148, 014306.	1.2	4
34935	Advances in modelling switchable mechanically interlocked molecular architectures. International Reviews in Physical Chemistry, 2018, 37, 1-82.	0.9	10
34936	Comparative study of perovskite-type scintillator materials CsCaI₃ and KCaI₃ via first-principles calculations. Journal Physics D: Applied Physics, 2018, 51, 065303.	1.3	18
34937	Investigating the Reactivity of Single Atom Alloys Using Density Functional Theory. Topics in Catalysis, 2018, 61, 462-474.	1.3	117
34938	Isotope- and Thickness-Dependent Friction of Water Layers Intercalated Between Graphene and Mica. Tribology Letters, 2018, 66, 1.	1.2	24
34939	Interfacial Cation-Defect Charge Dipoles in Stacked TiO₂/Al₂O₃ Gate Dielectrics. ACS Applied Materials & Interfaces, 2018, 10, 5140-5146.	4.0	10
34940	Accelerating evaluation of converged lattice thermal conductivity. Npj Computational Materials, 2018, 4, .	3.5	50
34941	Natural Intermediate Band in I 2 -II-IV-VI4 Quaternary Chalcogenide Semiconductors. Scientific Reports, 2018, 8, 1604.	1.6	15
34942	Pressure-induced phase transition of 4-aminobenzonitrile: the formation and enhancement of Nâ€“Hâ‹¯N weak hydrogen bonds. RSC Advances, 2018, 8, 4588-4594.	1.7	2
34943	Band structure and thermoelectric properties of half-Heusler semiconductors from many-body perturbation theory. Physical Review B, 2018, 97, .	1.1	43
34944	Orbital Physics of Perovskites for the Oxygen Evolution Reaction. Topics in Catalysis, 2018, 61, 267-275.	1.3	16
34945	Efficient Transition State Optimization of Periodic Structures through Automated Relaxed Potential Energy Surface Scans. Journal of Chemical Theory and Computation, 2018, 14, 981-990.	2.3	47
34946	First-Principle Study of Li-Ion Storage of Functionalized Ti₂C Monolayer with Vacancies. ACS Applied Materials & Interfaces, 2018, 10, 6369-6377.	4.0	89
34947	Liquid-Phase Modeling in Heterogeneous Catalysis. ACS Catalysis, 2018, 8, 2188-2194.	5.5	101

#	Article	IF	Citations
34948	Highly Dual-Heteroatom-Doped Ultrathin Carbon Nanosheets with Expanded Interlayer Distance for Efficient Energy Storage. ACS Sustainable Chemistry and Engineering, 2018, 6, 3143-3153.	3.2	38
34949	Evidence of local structural influence on the shape driven magnetic anisotropy in electronically excited Ni nanoparticles embedded in SiO2 matrix. Scientific Reports, 2018, 8, 1040.	1.6	3
34950	Electronic Structure and Band Gap Engineering of Two-Dimensional Octagon-Nitrogene. Scientific Reports, 2018, 8, 1674.	1.6	23
34951	Non-metal atom anchored BC₃ sheet: a promising low-cost and high-activity catalyst for CO oxidation. New Journal of Chemistry, 2018, 42, 3770-3780.	1.4	14
34952	Towards enhanced sodium storage by investigation of the Li ion doping and rearrangement mechanism in Na₃V₂(PO₄)₃ for sodium ion batteries. Journal of Materials Chemistry A, 2018, 6, 4209-4218.	5.2	54
34953	Anisotropic suppression of octahedral breathing distortion with the fully strained BaBiO3/BaCeO3 heterointerface. APL Materials, 2018, 6, 016107.	2.2	9
34954	Consistent interpretation of experimental data for expanded liquid tungsten near the liquid-gas coexistence curve. Physical Review B, 2018, 97, .	1.1	33
34955	Oxygen vacancy formation in the SrTiO 3 Î£5 [001] twist grain boundary from firstâ€principles. Journal of the American Ceramic Society, 2018, 101, 3118-3129.	1.9	3
34956	Anionâ€“Cation Double Substitution in Transition Metal Dichalcogenide to Accelerate Water Dissociation Kinetic for Electrocatalysis. Advanced Energy Materials, 2018, 8, 1702139.	10.2	70
34957	Metal Templates and Boron Sources Controlling Borophene Structures: An Ab Initio Study. Journal of Physical Chemistry C, 2018, 122, 2268-2274.	1.5	20
34958	Intercorrelated In-Plane and Out-of-Plane Ferroelectricity in Ultrathin Two-Dimensional Layered Semiconductor In₂Se₃. Nano Letters, 2018, 18, 1253-1258.	4.5	509
34959	Measuring Dipole Inversion in Self-Assembled Nano-Dielectric Molecular Layers. ACS Applied Materials & Interfaces, 2018, 10, 6484-6490.	4.0	4
34960	Monolayered Silicon and Germanium Monopnictide Semiconductors: Excellent Stability, High Absorbance, and Strain Engineering of Electronic Properties. ACS Applied Materials & Interfaces, 2018, 10, 5133-5139.	4.0	89
34961	Pressure-induced superconductivity and topological quantum phase transitions in a quasi-one-dimensional topological insulator: Bi4I4. Npj Quantum Materials, 2018, 3, .	1.8	34
34962	Bimodal hole transport in bulk BiVO₄ from computation. Journal of Materials Chemistry A, 2018, 6, 3714-3723.	5.2	20
34963	CO₂abatement using two-dimensional MXene carbides. Journal of Materials Chemistry A, 2018, 6, 3381-3385.	5.2	152
34964	Ferromagnetism induced by point defect in Janus monolayer MoSSe regulated by strain engineering. Journal Physics D: Applied Physics, 2018, 51, 105004.	1.3	33
34965	Completely flat 2D Zn3O2 monolayer with triangle and pentangle coordinated networks. Journal of Physics Condensed Matter, 2018, 30, 095301.	0.7	1

#	Article	IF	Citations
34966	Ab-initiocalculation and experimental observation of room temperature ferromagnetism in 50 keV nitrogen implanted rutile TiO2. Materials Research Express, 2018, 5, 026104.	0.8	13
34967	Structural phases arising from reconstructive and isostructural transitions in high-melting-point oxides under hydrostatic pressure: A first-principles study. Physical Review B, 2018, 97, .	1.1	19
34968	Oxygen self-diffusion mechanisms in monoclinic <mml:math xmlns:mml="http://www.w3.org/1998/Math/MathML"><mml:mrow><mml:mi>Zr</mml:mi><mml:msub><mml:mi mathvariant="normal">O</mml:mi><mml:mn>2</mml:mn></mml:msub></mml:mrow></mml:math> revealed and quantified by density functional theory, random walk analysis, and kinetic Monte Carlo calculations. Physical Review B, 2018, 97, .	1.1	20
34969	Design of nâ€Type Transparent Conducting Oxides: The Case of Transition Metal Doping in In₂O₃. Advanced Electronic Materials, 2018, 4, 1700553.	2.6	58
34970	Enhanced Adsorption of p-Arsanilic Acid from Water by Amine-Modified UiO-67 as Examined Using Extended X-ray Absorption Fine Structure, X-ray Photoelectron Spectroscopy, and Density Functional Theory Calculations. Environmental Science & Technology, 2018, 52, 3466-3475.	4.6	148
34971	Evaluation of the Giant Ferromagnetic Ï€â€“d Interaction in Iron-Phthalocyanine Molecule. Journal of Physical Chemistry A, 2018, 122, 1678-1690.	1.1	6
34972	Lithographically Patterned Functional Polymerâ€“Graphene Hybrids for Nanoscale Electronics. ACS Nano, 2018, 12, 1928-1933.	7.3	10
34973	Neutralizing the Charge Imbalance Problem in Eu³⁺-Activated BaAl₂O₄ Nanophosphors: Theoretical Insights and Experimental Validation Considering K⁺ Codoping. ACS Omega, 2018, 3, 788-800.	1.6	47
34974	Role of fluorine in two-dimensional dichalcogenide of SnSe 2. Scientific Reports, 2018, 8, 1645.	1.6	9
34975	X-ray absorption near edge structure and first-principles spectral investigations of cationic disorder in MgAl₂O₄ induced by swift heavy ions. Physical Chemistry Chemical Physics, 2018, 20, 4962-4969.	1.3	7
34976	Lithium doping on 2D squaraine-bridged covalent organic polymers for enhancing adsorption properties: a theoretical study. Physical Chemistry Chemical Physics, 2018, 20, 6487-6499.	1.3	15
34977	Novel two-dimensional ferromagnetic semiconductors: Ga-based transition-metal trichalcogenide monolayers. Physical Chemistry Chemical Physics, 2018, 20, 6374-6382.	1.3	39
34978	An efficient synthetic strategy for uniform perovskite coreâ€“shell nanocubes NaMgF₃:Mn²⁺,Yb³⁺@NaMgF₃:Yb³⁺ with enhanced near infrared upconversion luminescence. Journal of Materials Chemistry C, 2018, 6, 2342-2350.	2.7	6
34979	Gold nanoparticles decorated on BaTiO₃as photocatalyst: effect of SPR and ferroelectricity. Materials Research Express, 2018, 5, 025505.	0.8	14
34980	Conduction-band valley spin splitting in single-layer H- <mml:math xmlns:mml="http://www.w3.org/1998/Math/MathML"><mml:mrow><mml:mi mathvariant="normal">T</mml:mi><mml:msub><mml:mi mathvariant="normal">I</mml:mi><mml:mn>2</mml:mn></mml:msub><mml:mi mathvariant="normal">O</mml:mi></mml:mrow></mml:math>. Physical Review B, 2018, 97, .	1.1	41
34981	Topologically invariant double Dirac states in bismuth-based perovskites: Consequence of ambivalent charge states and covalent bonding. Physical Review B, 2018, 97, .	1.1	15
34982	Highâ€Efficiency Fullerene Solar Cells Enabled by a Spontaneously Formed Mesostructured CuSCNâ€Nanowire Heterointerface. Advanced Science, 2018, 5, 1700980.	5.6	19
34983	First-principle-based computational doping of SrTiO $$_{3}$$ 3 using combinatorial genetic algorithms. Bulletin of Materials Science, 2018, 41, 1.	0.8	24

#	Article	IF	Citations
34984	Shedding Light on the Protonation States and Location of Protonated N Atoms of Adenine in Metalâ€“Organic Frameworks. Inorganic Chemistry, 2018, 57, 1888-1900.	1.9	21
34985	Enhancement of the selectivity of MXenes (M₂C, M = Ti, V, Nb, Mo) via oxygen-functionalization: promising materials for gas-sensing and -separation. Physical Chemistry Chemical Physics, 2018, 20, 6073-6082.	1.3	99
34986	Effect of annealing temperature on the phase transition, band gap and thermoelectric properties of Cu₂SnSe₃. Journal of Materials Chemistry C, 2018, 6, 1780-1788.	2.7	30
34987	First-principles study of theÎ±-Ï‰phase transformation in Ti and Zr coupled to slip modes. Journal of Applied Physics, 2018, 123, 045903.	1.1	6
34988	Raman scattering study of the ferroelectric phase transition in <mml:math xmlns:mml="http://www.w3.org/1998/Math/MathML"><mml:mrow><mml:mi>BaT</mml:mi><mml:msub><mml:mi mathvariant="normal">i</mml:mi><mml:mn>2</mml:mn></mml:msub><mml:msub><mml:mi mathvariant="normal">O</mml:mi><mml:mn>5</mml:mn></mml:msub></mml:mrow></mml:math>. Physical Review B, 2018, 97, .	1.1	24
34989	Transport of Sodium in TiB2 Materials Investigated by a Laboratory Test and DFT Calculations. Minerals, Metals and Materials Series, 2018, , 1321-1328.	0.3	2
34990	Exploring Polaronic, Excitonic Structures and Luminescence in Cs₄PbBr₆/CsPbBr₃. Journal of Physical Chemistry Letters, 2018, 9, 830-836.	2.1	122
34991	Ionic to Electronic Transport in Ba₃Ti₃O₆(BO₃)₂ under Reducing Atmosphere. ACS Applied Energy Materials, 2018, 1, 510-521.	2.5	7
34992	Interface Engineering of Earth-Abundant Transition Metals Using Boron Nitride for Selective Electroreduction of CO₂. ACS Applied Materials & Interfaces, 2018, 10, 6694-6700.	4.0	52
34993	Structural Changes as a Function of Thickness in [(SnSe)1+Î´]mTiSe2 Heterostructures. ACS Nano, 2018, 12, 1285-1295.	7.3	11
34994	Defect-Free Graphene Synthesized Directly at 150 Â°C via Chemical Vapor Deposition with No Transfer. ACS Nano, 2018, 12, 2008-2016.	7.3	55
34995	Net W monolayer: A high-performance electrode material for Li-ion batteries. Applied Physics Letters, 2018, 112, .	1.5	29
34996	Iron and intrinsic deep level states in Ga2O3. Applied Physics Letters, 2018, 112, .	1.5	196
34997	First Principles Study on the Magnetism of Rectangular Nanosilicenes. Chinese Physics Letters, 2018, 35, 017301.	1.3	0
34998	Bismuth oxide film: a promising room-temperature quantum spin Hall insulator. Journal of Physics Condensed Matter, 2018, 30, 105303.	0.7	4
34999	Metastable state in a tensile-strained <mml:math xmlns:mml="http://www.w3.org/1998/Math/MathML"><mml:mrow><mml:mi>Cu</mml:mi><mml:mspace width="0.16em" /><mml:mi mathvariant="normal">Î£</mml:mi><mml:mn>5</mml:mn></mml:mrow></mml:math>grain boundary: A first principles study. Physical Review B, 2018, 97, .	1.1	6
35000	Ab initio calculations of the concentration dependent band gap reduction in dilute nitrides. Physical Review B, 2018, 97, .	1.1	9
35001	Coupled quantum mechanics/molecular mechanics modeling of metallic materials: Theory and applications. Journal of Materials Research, 2018, 33, 796-812.	1.2	4

#	Article	IF	Citations
35002	Semiclassical transport properties of IrGa₃: a promising thermoelectric material. Journal of Physics Condensed Matter, 2018, 30, 085701.	0.7	7
35003	Determination of latent hardening response for FeNiCoCrMn for twin-twin interactions. Acta Materialia, 2018, 147, 149-164.	3.8	43
35004	The structural and electronic properties of Pt-Cu alloy clusters: Embedding atom method combined with density functional theory study. Journal of Alloys and Compounds, 2018, 741, 604-609.	2.8	9
35005	Abnormal phase transition between two-dimensional high-density liquid crystal and low-density crystalline solid phases. Nature Communications, 2018, 9, 198.	5.8	9
35006	Topological behaviour of ternary non-symmorphic crystals KZnX (X = P, As, Sb) under pressure and strain: a first principles study. Physical Chemistry Chemical Physics, 2018, 20, 5084-5102.	1.3	9
35007	Rational construction of an ssa-type of MOF through pre-organizing the ligand's conformation and its exceptional gas adsorption properties. Dalton Transactions, 2018, 47, 2444-2452.	1.6	31
35008	Borophene hydride: a stiff 2D material with high thermal conductivity and attractive optical and electronic properties. Nanoscale, 2018, 10, 3759-3768.	2.8	109
35009	Efficient evaluation of atom tunneling combined with electronic structure calculations. Journal of Chemical Physics, 2018, 148, 102334.	1.2	23
35010	Magnetocrystalline anisotropy of Îµ-Fe2O3. AIP Advances, 2018, 8, .	0.6	10
35011	N-doped ZnO nanosheets: towards high performance two dimensional catalysts. Nanotechnology, 2018, 29, 105707.	1.3	4
35012	Realization of a half-metallic state on bilayer WSe₂ using doping transition metals (Cr,) Tj ETQq0 0 0 rgBT /Overlock 10 Tf 5	1.3	20
35013	First principles predictions of magneto-optical data for semiconductor point defect identification: the case of divacancy defects in 4Hâ€“SiC. New Journal of Physics, 2018, 20, 023035.	1.2	39
35014	Nonsymmorphic-symmetry-protected hourglass Dirac loop, nodal line, and Dirac point in bulk and monolayer <mml:math xmlns:mml="http://www.w3.org/1998/Math/MathML"><mml:mrow><mml:msub><mml:mi>X</mml:mi><mml:mn>3</mml:mn></mml:msub></mml:m (<mml:math xmlns:mml="http://www.w3.org/1998/Math/MathML"><mml:mi>X</mml:mi></mml:math> =) Tj ETQq0 0 0 rgBT /Overlock	3.1	115
35015	How and Why Does Helium Permeate Nonporous Arsenolite Under High Pressure?. ChemPhysChem, 2018, 19, 857-864.	1.0	10
35016	Effect of vacancy defect on optoelectronic properties of monolayer tungsten diselenide. Optical and Quantum Electronics, 2018, 50, 1.	1.5	105
35017	An algorithm to use higher order invariants for modelling potential energy surface of nanoclusters. Chemical Physics Letters, 2018, 693, 152-158.	1.2	4
35018	Delimited Polyacenes: Edge Topology as a Tool To Modulate Carbon Nanoribbon Structure, Conjugation, and Mobility. Chemistry of Materials, 2018, 30, 947-957.	3.2	21
35019	Quantum Capacitance of Silicene-Based Electrodes from First-Principles Calculations. Journal of Physical Chemistry C, 2018, 122, 1903-1912.	1.5	39

#	Article	IF	Citations
35020	Theoretical potential for low energy consumption phase change memory utilizing electrostatically-induced structural phase transitions in 2D materials. Npj Computational Materials, 2018, 4, .	3.5	40
35021	A computational study of energy barriers of structural transformations and hydrogen transfer in boehmite. RSC Advances, 2018, 8, 2377-2384.	1.7	8
35022	Band gap engineering of SnS₂ nanosheets by anionâ€“anion codoping for visible-light photocatalysis. RSC Advances, 2018, 8, 3304-3311.	1.7	31
35023	Strength of FePd/MgO and FePt/MgO interfaces from first principles. Modelling and Simulation in Materials Science and Engineering, 2018, 26, 035002.	0.8	3
35024	Electronic and magnetic properties of 3D transition-metal atom adsorbed arsenene. Nanotechnology, 2018, 29, 095203.	1.3	17
35025	Engineering the Kondo state in two-dimensional semiconducting phosphorene. Physical Review B, 2018, 97, .	1.1	4
35026	Lowâ€Bandgap Methylammoniumâ€Rubidium Cation Snâ€Rich Perovskites for Efficient Ultravioletâ€“Visibleâ€“Near Infrared Photodetectors. Advanced Functional Materials, 2018, 28, 1706068.	7.8	70
35027	DFT study of the adsorption and dissociation of 5-hydroxy-3-butanedithiol-1,4-naphthaquinone (Jug-C4-thiol) on Au(111) surface. Adsorption, 2018, 24, 191-201.	1.4	4
35028	DFT study of interaction of additives with Cu(111) surface relevant to Cu electrodeposition. Journal of Applied Electrochemistry, 2018, 48, 211-219.	1.5	15
35029	Electronic and magnetic properties of magnetoelectric compound Ca2CoSi2O7: An ab initio study. Journal of Magnetism and Magnetic Materials, 2018, 453, 114-117.	1.0	5
35030	Is Subsurface Oxygen Necessary for the Electrochemical Reduction of CO₂ on Copper?. Journal of Physical Chemistry Letters, 2018, 9, 601-606.	2.1	118
35031	Why Does CuFeS₂ Resemble Gold?. Journal of Physical Chemistry Letters, 2018, 9, 696-701.	2.1	31
35032	Shear-Induced Brittle Failure along Grain Boundaries in Boron Carbide. ACS Applied Materials & Interfaces, 2018, 10, 5072-5080.	4.0	21
35033	Hydrogen Evolution Reaction on Hybrid Catalysts of Vertical MoS₂ Nanosheets and Hydrogenated Graphene. ACS Catalysis, 2018, 8, 1828-1836.	5.5	180
35034	Substrate engineering of graphene reactivity: towards high-performance graphene-based catalysts. Npj 2D Materials and Applications, 2018, 2, .	3.9	86
35035	On-surface synthesis: a promising strategy toward the encapsulation of air unstable ultra-thin 2D materials. Nanoscale, 2018, 10, 3799-3804.	2.8	18
35036	Introducing DDEC6 atomic population analysis: part 4. Efficient parallel computation of net atomic charges, atomic spin moments, bond orders, and more. RSC Advances, 2018, 8, 2678-2707.	1.7	129
35037	Adsorption of an Au atom and dimer on a thin Î¸-Al₂O₃/NiAl(100) film: dependence on the thickness of the Î¸-Al₂O₃ film. RSC Advances, 2018, 8, 2642-2652.	1.7	6

#	Article	IF	Citations
35038	Comprehensive resistive switching behavior of hybrid polyvinyl alcohol and TiO₂ nanotube nanocomposites identified by combining experimental and density functional theory studies. Journal of Materials Chemistry C, 2018, 6, 1971-1979.	2.7	30
35039	New carbon allotropes in sp + sp³ bonding networks consisting of C₈ cubes. Physical Chemistry Chemical Physics, 2018, 20, 7962-7967.	1.3	33
35040	Tuning the pure monoclinic phase of WO3 and WO3-Ag nanostructures for non-enzymatic glucose sensing application with theoretical insight from electronic structure simulations. Journal of Applied Physics, 2018, 123, .	1.1	44
35041	Magnitude of the current in 2D interlayer tunneling devices. Journal of Physics Condensed Matter, 2018, 30, 055703.	0.7	2
35042	Phase transformation pathways of ultrafast-laser-irradiated <mml:math xmlns:mml="http://www.w3.org/1998/Math/MathML"><mml:mrow><mml:msub><mml:mi>Ln</mml:mi><mml:mn>2</mml:mn></mml:r mathvariant="normal">O</mml:mi><mml:mn>3</mml:mn></mml:msub></mml:mrow><mml:mspace width="4pt" /><mml:mo>(</mml:mo><mml:mrow><mml:mi>Ln</mml:mi><mml:mo>=</mml:mo><mml:mi>Er</mml:mi><mml:mo>â€“</mml:mo><r Physical Review B, 2018, 97, .	1.1	4
35043	Nature of the octahedral tilting phase transitions in perovskites: A case study of <mml:math xmlns:mml="http://www.w3.org/1998/Math/MathML"><mml:msub><mml:mi>CaMnO</mml:mi><mml:mn>3</mml:mn></mml:msub> Physical Review B, 2018, 97, .	1.1	36
35044	Sequential structural and antiferromagnetic transitions in <mml:math xmlns:mml="http://www.w3.org/1998/Math/MathML"><mml:mrow><mml:msub><mml:mi>BaFe</mml:mi><mml:mn>2</mml:mn></mml:msub> under pressure. Physical Review B, 2018, 97, .	1.1	46
35045	Charge density wave states in tantalum dichalcogenides. Physical Review B, 2018, 97, .	1.1	35
35046	KVP₂O₇ as a Robust Highâ€Energy Cathode for Potassiumâ€Ion Batteries: Pinpointed by a Full Screening of the Inorganic Registry under Specific Search Conditions. Advanced Energy Materials, 2018, 8, 1703099.	10.2	154
35047	Bandgap engineering in CsSnxPb(1â^'x)I3 and their influence on light absorption. Materials Letters, 2018, 218, 253-256.	1.3	11
35048	Quaternary Pavonites A_{1+x}Sn_{2â€“x}Bi_{5+x}S₁₀ (A⁺ = Li⁺, Na⁺): Site Occupancy Disorder Defines Electronic Structure. Inorganic Chemistry, 2018, 57, 2260-2268.	1.9	12
35049	Adsorption Conformation and Lateral Registry of Cobalt Porphine on Cu(111). Journal of Physical Chemistry C, 2018, 122, 5452-5461.	1.5	14
35050	Density Functional Theory-Based Adsorption Isotherms for Pure and Flue Gas Mixtures on Mg-MOF-74. Application in CO₂ Capture Swing Adsorption Processes. Journal of Physical Chemistry C, 2018, 122, 3945-3957.	1.5	38
35051	Predicting Two-Dimensional C₃B/C₃N van der Waals pâ€“n Heterojunction with Strong Interlayer Electron Coupling and Enhanced Photocurrent. Journal of Physical Chemistry Letters, 2018, 9, 858-862.	2.1	74
35052	Electron Pair Repulsion Responsible for the Peculiar Edge Effects and Surface Chemistry of Black Phosphorus. Journal of Physical Chemistry Letters, 2018, 9, 947-953.	2.1	15
35053	Grain Boundaries Softening Thermoelectric Oxide BiCuSeO. ACS Applied Materials & Interfaces, 2018, 10, 6772-6777.	4.0	10
35054	Boosting Formate Production in Electrocatalytic CO₂ Reduction over Wide Potential Window on Pd Surfaces. Journal of the American Chemical Society, 2018, 140, 2880-2889.	6.6	310
35055	Influence of chromium hyperdoping on the electronic structure of CH3NH3PbI3 perovskite: a first-principles insight. Scientific Reports, 2018, 8, 2511.	1.6	13

#	Article	IF	Citations
35056	Unusual strain response of thermal transport in dimerized three-dimensional graphene. Nanoscale, 2018, 10, 5229-5238.	2.8	22
35057	Extended band anti-crossing model for dilute bismides. Applied Physics Letters, 2018, 112, .	1.5	8
35058	Surface oxidation: an effective way to induce piezoelectricity in 2D black phosphorus. Journal Physics D: Applied Physics, 2018, 51, 12LT01.	1.3	11
35059	First-principles study of Cs/Rb co-doped FAPbI₃ stability and degradation in the presence of water and oxygen. Materials Research Express, 2018, 5, 026203.	0.8	4
35060	Selective Solvent-Induced Stabilization of Polar Oxide Surfaces in an Electrochemical Environment. Physical Review Letters, 2018, 120, 066101.	2.9	20
35061	Finely Controlled Stepwise Engineering of Pore Environments and Mechanistic Elucidation of Waterâ€Stable, Flexible 2D Porous Coordination Polymers. Chemistry - A European Journal, 2018, 24, 6412-6417.	1.7	16
35062	Unique Zigzag-Shaped Buckling Zn₂C Monolayer with Strain-Tunable Band Gap and Negative Poisson Ratio. Inorganic Chemistry, 2018, 57, 1958-1963.	1.9	22
35063	Quantum-Confined Electronic States Arising from the MoirÃ© Pattern of MoS₂â€“WSe₂ Heterobilayers. Nano Letters, 2018, 18, 1849-1855.	4.5	91
35064	Thin and Dense Solid-solid Heterojunction Formation Promoted by Crystal Growth in Flux on a Substrate. Scientific Reports, 2018, 8, 96.	1.6	3
35065	Boron-phil and boron-phob structure units in novel borides Ni3Zn2B and Ni2ZnB: experiment and first principles calculations. Dalton Transactions, 2018, 47, 3303-3320.	1.6	8
35066	Formation of a large gap quantum spin Hall phase in a 2D trigonal lattice with three p-orbitals. Nanoscale, 2018, 10, 5496-5502.	2.8	13
35067	Oxygen redox in hexagonal layered Na_xTMO₃ (TM = 4d elements) for high capacity Na ion batteries. Journal of Materials Chemistry A, 2018, 6, 3747-3753.	5.2	24
35068	Electric field analyses on monolayer semiconductors: the example of InSe. Physical Chemistry Chemical Physics, 2018, 20, 6945-6950.	1.3	46
35069	Friction induced structural transformations of water monolayers at graphene/Cu interfaces. Physical Chemistry Chemical Physics, 2018, 20, 4137-4143.	1.3	8
35070	Novel stable structure of Li3PS4 predicted by evolutionary algorithm under high-pressure. AIP Advances, 2018, 8, .	0.6	8
35071	A sp2+sp3 hybridized carbon allotrope transformed from AB stacking graphyne and THD-graphene. AIP Advances, 2018, 8, 015028.	0.6	10
35072	Collapsed tetragonal phase as a strongly covalent and fully nonmagnetic state: Persistent magnetism with interlayer Asâ€“As bond formation in Rh-doped <mml:math xmlns:mml="http://www.w3.org/1998/Math/MathML"><mml:mrow><mml:msub><mml:mi mathvariant="bold">Ca</mml:mi><mml:mrow><mml:mn mathvariant="bold">0</mml:mn><mml:mo>.</mml:mo><mml:mn mathvariant="bold">8</mml:mn></mml:mrow></mml:msub><mml:msub><mml:mi mathvariant="bold">S	1.1	6
35073	Magnetic Properties of SiC Monolayer with Different Nonmagnetic Metal Dopants. Journal of Superconductivity and Novel Magnetism, 2018, 31, 3277-3282.	0.8	8

#	Article	IF	Citations
35074	Phosphorus Dimerization in Gallium Phosphide at High Pressure. Inorganic Chemistry, 2018, 57, 2432-2437.	1.9	9
35075	CO oxidative coupling to dimethyl oxalate over Pdâ€“Me (Me = Cu, Al) catalysts: a combined DFT and kinetic study. Physical Chemistry Chemical Physics, 2018, 20, 7317-7332.	1.3	22
35076	XANES spectra of forsterite in crystal, surface, and amorphous states. AIP Advances, 2018, 8, .	0.6	11
35077	Compositional partitioning during the spinodal decomposition in Cuâ€“Niâ€“Sn alloy. Philosophical Magazine, 2018, 98, 1204-1216.	0.7	6
35078	Metallic MoN layer and its application as anode for lithium-ion batteries. Nanotechnology, 2018, 29, 165402.	1.3	15
35079	Atomicâ€Scale Insight into Structure and Interface of Al₂Y Phase in an Mgâ€“Alâ€“Y Alloy. Advanced Engineering Materials, 2018, 20, 1701015.	1.6	9
35080	Decomposition Mechanisms of Anti-wear Lubricant Additive Tricresyl Phosphate on Iron Surfaces Using DFT and Atomistic Thermodynamic Studies. Tribology Letters, 2018, 66, 1.	1.2	20
35081	Unusual Negative Formation Enthalpies and Atomic Ordering in Isovalent Alloys of Transition Metal Dichalcogenide Monolayers. Chemistry of Materials, 2018, 30, 1547-1555.	3.2	20
35082	Chemical Vapor Deposition of Photocatalytically Active Pure Brookite TiO₂ Thin Films. Chemistry of Materials, 2018, 30, 1353-1361.	3.2	79
35083	A computational study of supported Cu-based bimetallic nanoclusters for CO oxidation. Physical Chemistry Chemical Physics, 2018, 20, 7508-7513.	1.3	17
35084	Electronic structure, polaron formation, and functional properties in transition-metal tungstates. RSC Advances, 2018, 8, 4191-4196.	1.7	33
35085	A comprehensive study of g-factors, elastic, structural and electronic properties of III-V semiconductors using hybrid-density functional theory. Journal of Applied Physics, 2018, 123, .	1.1	23
35086	The oxygen reduction reaction on graphitic carbon nitride supported single Ce atom and CexPt6-x cluster catalysts from first-principles. Carbon, 2018, 130, 636-644.	5.4	30
35087	Carbon chain-based spintronic devices: Tunable single-spin Seebeck effect, negative differential resistance and giant rectification effects. Organic Electronics, 2018, 55, 170-176.	1.4	9
35088	Adsorption of 3d transition metal atoms on graphene-like gallium nitride monolayer: A first-principles study. Superlattices and Microstructures, 2018, 115, 108-115.	1.4	32
35089	Atomic-Scale Understanding of Catalyst Activation: Carboxylic Acid Solutions, but Not the Acid Itself, Increase the Reactivity of Anatase (001) Faceted Nanocatalysts. Journal of Physical Chemistry C, 2018, 122, 4307-4314.	1.5	14
35090	First stages of oxide growth on Al(1â€¯1â€¯0) and core-level shifts from density functional theory calculations. Applied Surface Science, 2018, 441, 174-186.	3.1	11
35091	Stability and charge separation of different CH3NH3SnI3/TiO2 interface: A first-principles study. Applied Surface Science, 2018, 441, 394-400.	3.1	18

#	Article	IF	Citations
35092	Charged vacancy defects in an AlN nanosheet: A first-principles DFT study. Computational Condensed Matter, 2018, 14, 153-160.	0.9	10
35093	The reaction pathways of the oxygen reduction reaction on IrN 4 doped divacancy graphene: A theoretical study. Journal of Molecular Graphics and Modelling, 2018, 80, 293-298.	1.3	11
35094	Diffusion mechanism in the superionic conductor Li4PS4I studied by first-principlesÂcalculations. Solid State Ionics, 2018, 319, 83-91.	1.3	23
35095	Crystal Structure and Band-Gap Engineering of a Semiconducting Coordination Polymer Consisting of Copper(I) Bromide and a Bridging Acceptor Ligand. Inorganic Chemistry, 2018, 57, 2373-2376.	1.9	21
35096	Fast Oxidation of Porous Cu Induced by Nano-Twinning. Inorganic Chemistry, 2018, 57, 2908-2916.	1.9	6
35097	Adsorption Mechanisms of Lithium Polysulfides on Graphene-Based Interlayers in Lithium Sulfur Batteries. ACS Applied Energy Materials, 2018, 1, 455-463.	2.5	28
35098	2D MoS2 as an efficient protective layer for lithium metal anodes in high-performance Liâ€“S batteries. Nature Nanotechnology, 2018, 13, 337-344.	15.6	624
35099	Activation of the surface dark-layer to enhance upconversion in a thermal field. Nature Photonics, 2018, 12, 154-158.	15.6	270
35100	Magnetism of coupled spin tetrahedra in ilinskite-type KCu5O2(SeO3)2Cl3. Scientific Reports, 2018, 8, 2379.	1.6	17
35101	Cluster assemblies as superatomic solids: a first principles study of bonding & electronic structure. Physical Chemistry Chemical Physics, 2018, 20, 6167-6175.	1.3	8
35102	Rational Design of Multifunctional Fe@Î³â€Fe₂O₃@Hâ€TiO₂ Nanocomposites with Enhanced Magnetic and Photoconversion Effects for Wide Applications: From Photocatalysis to Imagingâ€Guided Photothermal Cancer Therapy. Advanced Materials, 2018, 30, e1706747.	11.1	102
35103	Broadband Photodetectors Enabled by Localized Surface Plasmonic Resonance in Doped Iron Pyrite Nanocrystals. Advanced Optical Materials, 2018, 6, 1701241.	3.6	32
35104	Ab Initio Study on Structure, Elastic, and Mechanical Properties of Lanthanide Sesquioxides. Physica Status Solidi (B): Basic Research, 2018, 255, 1700668.	0.7	21
35105	A first-principles and experimental study of helium diffusion in periclase MgO. Physics and Chemistry of Minerals, 2018, 45, 641-654.	0.3	2
35106	First-principles calculations of thermal properties of the mechanically unstable phases of the PtTi and NiTi shape memory alloys. Acta Materialia, 2018, 147, 296-303.	3.8	26
35107	Segregation of alloying elements to planar faults in <mml:math xmlns:mml="http://www.w3.org/1998/Math/MathML" altimg="si1.gif" overflow="scroll"><mml:mrow><mml:mi>Î³</mml:mi><mml:mo>'</mml:mo></mml:mrow></mml:math>-Ni3Al. Acta Materialia, 2018, 148, 173-184.	3.8	70
35108	Peierls stresses estimated via the Peierls-Nabarro model using ab-initio Î³-surface and their comparison with experiments. Acta Materialia, 2018, 148, 355-362.	3.8	51
35109	Transformation stress of shape memory alloy CuZnAl: Non-Schmid behavior. Acta Materialia, 2018, 149, 220-234.	3.8	19

#	Article	IF	Citations
35110	Fabrication of carbon bridged g-C3N4 through supramolecular self-assembly for enhanced photocatalytic hydrogen evolution. Applied Catalysis B: Environmental, 2018, 229, 114-120.	10.8	128
35111	First-principles studies on 3d transition metal atom adsorbed twin graphene. Applied Surface Science, 2018, 441, 647-653.	3.1	30
35112	Mono- and bimetallic nanoparticles decorated KTaO3 photocatalysts with improved Vis and UVâ€“Vis light activity. Applied Surface Science, 2018, 441, 993-1011.	3.1	26
35113	Hydrogen storage in N- and B-doped graphene decorated by small platinum clusters: A computational study. Applied Surface Science, 2018, 441, 607-612.	3.1	42
35114	Electronic and magnetic properties of MoSe 2 armchair nanoribbons controlled by the different edge structures. Superlattices and Microstructures, 2018, 115, 30-39.	1.4	11
35115	Theoretical Analysis of Oxidative Carbonylation of Methanol: Saegusaâ€™s Scheme of Dimethylcarbonate Synthesis over Binuclear Cationic Oxo-Clusters in CuNaX Zeolite. Journal of Physical Chemistry C, 2018, 122, 5366-5375.	1.5	5
35116	Structure and Gas Transport at the Polymerâ€“Zeolite Interface: Insights from Molecular Dynamics Simulations. ACS Applied Materials & Interfaces, 2018, 10, 5992-6005.	4.0	50
35117	Rhombohedral to Cubic Conversion of GeTe via MnTe Alloying Leads to Ultralow Thermal Conductivity, Electronic Band Convergence, and High Thermoelectric Performance. Journal of the American Chemical Society, 2018, 140, 2673-2686.	6.6	307
35118	Promising half-metallicity in ductile NbF₃: a first-principles prediction. Physical Chemistry Chemical Physics, 2018, 20, 4781-4786.	1.3	10
35119	Molecular dynamics of the halloysite nanotubes. Physical Chemistry Chemical Physics, 2018, 20, 5841-5849.	1.3	39
35120	An experimental and theoretical study of adenine adsorption on Au(111). Physical Chemistry Chemical Physics, 2018, 20, 4688-4698.	1.3	13
35121	Influence of the number of layers on ultrathin CsSnI₃ perovskite: from electronic structure to carrier mobility. Journal Physics D: Applied Physics, 2018, 51, 105101.	1.3	35
35122	Electronic structure and optical properties of Ag-MoS₂ composite systems. Journal Physics D: Applied Physics, 2018, 51, 085303.	1.3	16
35123	Formation energies of substitutional NAs and split interstitial complexes in dilute GaAsN alloys with different growth orientations. Applied Physics A: Materials Science and Processing, 2018, 124, 1.	1.1	2
35124	Comparative Study on the Charge-Ordered and Mixed-Valence Phases of LuFe2O4 via First-Principles Calculations. Journal of Superconductivity and Novel Magnetism, 2018, 31, 2915-2923.	0.8	0
35125	A Comparative Study of Hydrodeoxygenation of Furfural Over Fe/Pt(111) and Fe/Mo2C Surfaces. Topics in Catalysis, 2018, 61, 439-445.	1.3	13
35126	Insight into the C C chain growth in Fischer-Tropsch synthesis on HCP Co(10-10) surface: The effect of crystal facets on the preferred mechanism. Computational Materials Science, 2018, 145, 263-279.	1.4	16
35127	Hunting the Correlation between Fe₅C₂ Surfaces and Their Activities on CO: The Descriptor of Bond Valence. Journal of Physical Chemistry C, 2018, 122, 2806-2814.	1.5	26

#	Article	IF	Citations
35128	A Facile Space-Confined Solid-Phase Sulfurization Strategy for Growth of High-Quality Ultrathin Molybdenum Disulfide Single Crystals. Nano Letters, 2018, 18, 2021-2032.	4.5	42
35129	Stability and anisotropy of (FexNi1â^'x)2O under high pressure and implications in Earthâ€™s and super-Earthsâ€™ core. Scientific Reports, 2018, 8, 236.	1.6	8
35130	Time-resolved operando studies of carbon supported Pd nanoparticles under hydrogenation reactions by X-ray diffraction and absorption. Faraday Discussions, 2018, 208, 187-205.	1.6	47
35131	Tunable dipole and carrier mobility for a few layer Janus MoSSe structure. Journal of Materials Chemistry C, 2018, 6, 1693-1700.	2.7	164
35132	Zr₂Si: an antiferromagnetic Dirac MXene. Physical Chemistry Chemical Physics, 2018, 20, 3946-3952.	1.3	19
35133	Solid, liquid, and interfacial properties of TiAl alloys: parameterization of a new modified embedded atom method model. Journal of Physics Condensed Matter, 2018, 30, 075002.	0.7	5
35134	First-principles study of defect formation in a photovoltaic semiconductor Cu₂ZnGeSe₄. Japanese Journal of Applied Physics, 2018, 57, 02CE06.	0.8	5
35135	A review on fabricating heterostructures from layered double hydroxides for enhanced photocatalytic activities. Catalysis Science and Technology, 2018, 8, 1207-1228.	2.1	89
35136	Path integral Monte Carlo simulations of dense carbon-hydrogen plasmas. Journal of Chemical Physics, 2018, 148, 102318.	1.2	33
35137	Accurate identification of layer number for few-layer WS₂and WSe₂via spectroscopic study. Nanotechnology, 2018, 29, 124001.	1.3	52
35138	High-pressure phases of VO2 from the combination of Raman scattering and ab initio structural search. Physical Review B, 2018, 97, .	1.1	9
35139	How Methylammonium Cations and Chlorine Dopants Heal Defects in Lead Iodide Perovskites. Advanced Energy Materials, 2018, 8, 1702754.	10.2	86
35140	Spin-dependent electronic transport characteristics in Fe4N/BiFeO3/Fe4N perpendicular magnetic tunnel junctions. Journal of Applied Physics, 2018, 123, .	1.1	13
35141	Silicene-terminated surface of calcium and strontium disilicides: properties and comparison with bulk structures by computational methods. Philosophical Magazine, 2018, 98, 1131-1150.	0.7	4
35142	Firstâ€Principles Characterization of Equilibrium Vacancy Concentration in Metamagnetic Shape Memory Alloys: An Example of Ni₂MnGa. Physica Status Solidi (B): Basic Research, 2018, 255, 1700523.	0.7	6
35143	Water distribution in the lower mantle: Implications for hydrolytic weakening. Earth and Planetary Science Letters, 2018, 484, 363-369.	1.8	18
35144	Electronic and optical performances of (Cu, N) codoped TiO2/g-C3N4 heterostructure photocatalyst: A spin-polarized DFTâ€+â€U study. Solar Energy, 2018, 162, 306-316.	2.9	23
35145	Electron-Hopping Brings Lattice Strain and High Catalytic Activity in the Low-Temperature Oxidative Coupling of Methane in an Electric Field. Journal of Physical Chemistry C, 2018, 122, 2089-2096.	1.5	26

#	Article	IF	Citations
35146	Ternary intermetallic LaCoSi as a catalyst for N2 activation. Nature Catalysis, 2018, 1, 178-185.	16.1	221
35147	Tuning electronic and magnetic properties of monolayer Î±-RuCl₃ by in-plane strain. Journal of Materials Chemistry C, 2018, 6, 2019-2025.	2.7	47
35148	On the feasibility of p-type Ga2O3. Applied Physics Letters, 2018, 112, .	1.5	208
35149	Accurate modeling of defects in graphene transport calculations. Physical Review B, 2018, 97, .	1.1	18
35150	Soft antiphase tilt of oxygen octahedra in the hybrid improper multiferroic <mml:math xmlns:mml="http://www.w3.org/1998/Math/MathML"><mml:mrow><mml:msub><mml:mi>Ca</mml:mi><mml:mn>3</mml:mn></mml: mathvariant="normal">O</mml:mi><mml:mn>7</mml:mn></mml:msub></mml:mrow></mml:math>. Physical Review B, 2018, 97, .	1.1	27
35151	Vanadium Diboride (VB₂) Synthesized at High Pressure: Elastic, Mechanical, Electronic, and Magnetic Properties and Thermal Stability. Inorganic Chemistry, 2018, 57, 1096-1105.	1.9	64
35152	Realizing Large-Scale, Electronic-Grade Two-Dimensional Semiconductors. ACS Nano, 2018, 12, 965-975.	7.3	172
35153	Posner molecules: from atomic structure to nuclear spins. Physical Chemistry Chemical Physics, 2018, 20, 12373-12380.	1.3	29
35154	Visualization and manipulation of magnetic domains in the quasi-two-dimensional material <mml:math xmlns:mml="http://www.w3.org/1998/Math/MathML"><mml:mrow><mml:mi mathvariant="normal">F</mml:mi><mml:msub><mml:mi mathvariant="normal">e</mml:mi><mml:mn>3</mml:mn></mml:msub><mml:mi>GeT</mml:mi><mml:msub><mml:mi mathvariant="normal">e</mml:mi><mml:mn>2</mml:mn></mml:msub></mml:mrow></mml:math>. Physical Review B, 2018, 97, .	1.1	74
35155	Tunneling anisotropic magnetoresistance via molecular Ï€ orbitals of Pb dimers. Physical Review B, 2018, 97, .	1.1	4
35156	Dopantâ€“dopant interactions in beryllium doped indium gallium arsenide: An ab initio study. Journal of Materials Research, 2018, 33, 401-413.	1.2	4
35157	Reaction Pathway Dependence in Plasmonic Catalysis: Hydrogenation as a Model Molecular Transformation. Chemistry - A European Journal, 2018, 24, 12330-12339.	1.7	33
35158	Magneto-Spinâ€“Orbit Graphene: Interplay between Exchange and Spinâ€“Orbit Couplings. Nano Letters, 2018, 18, 1564-1574.	4.5	32
35159	Methane Partial Oxidation over [Cu₂(Î¼-O)]²⁺ and [Cu₃(Î¼-O)₃]²⁺ Active Species in Large-Pore Zeolites. ACS Catalysis, 2018, 8, 1500-1509.	5.5	104
35160	Strong Fe3+-O(H)-Pt Interfacial Interaction Induced Excellent Stability of Pt/NiFe-LDH/rGO Electrocatalysts. Scientific Reports, 2018, 8, 1359.	1.6	26
35161	Simultaneous drug delivery and cellular imaging using graphene oxide. Biomaterials Science, 2018, 6, 813-819.	2.6	59
35162	Origin of the overpotentials for HCOO^{â^'} and CO formation in the electroreduction of CO₂ on Cu(211): the reductive desorption processes decide. Physical Chemistry Chemical Physics, 2018, 20, 5756-5765.	1.3	19
35163	Structural phase transition and bonding properties of high-pressure polymeric CaN3. RSC Advances, 2018, 8, 4314-4320.	1.7	14

#	Article	IF	Citations
35164	Symmetry-dependent topological phase transitions in PbTe layers. Materials Research Express, 2018, 5, 015051.	0.8	7
35165	Interstitial Moâ€Assisted Photovoltaic Effect in Multilayer MoSe₂ Phototransistors. Advanced Materials, 2018, 30, e1705542.	11.1	48
35166	Directly Assembled 3D Molybdenum Disulfide on Silicon Wafer for Efficient Photoelectrochemical Water Reduction. Advanced Sustainable Systems, 2018, 2, 1700142.	2.7	36
35167	First-principles molecular dynamics simulations of anorthite (CaAl2Si2O8) glass at high pressure. Physics and Chemistry of Minerals, 2018, 45, 575-587.	0.3	20
35168	Machine learning properties of binary wurtzite superlattices. Journal of Materials Science, 2018, 53, 6652-6664.	1.7	24
35169	Benchmark First-Principles Calculations of Adsorbate Free Energies. ACS Catalysis, 2018, 8, 1945-1954.	5.5	43
35170	Metallic Ti₃C₂T_x MXene Gas Sensors with Ultrahigh Signal-to-Noise Ratio. ACS Nano, 2018, 12, 986-993.	7.3	1,153
35171	Temperature-driven topological transition in 1T'-MoTe2. Npj Quantum Materials, 2018, 3, .	1.8	36
35172	CO adsorption and oxygen activation on group 11 nanoparticles â€“ a combined DFT and high level CCSD(T) study about size effects and activation processes. Faraday Discussions, 2018, 208, 105-121.	1.6	16
35173	Prediction of topological property in TlPBr₂ monolayer with appreciable Rashba effect. Physical Chemistry Chemical Physics, 2018, 20, 4308-4316.	1.3	5
35174	Band alignments and heterostructures of monolayer transition metal trichalcogenides MX₃ (M = Zr, Hf; X = S, Se) and dichalcogenides MX₂ (M = Tc, Re; X=S, Se) for solar applications. Nanoscale, 2018, 10, 3547-3555.	2.8	70
35175	Affordable and accurate large-scale hybrid-functional calculations on GPU-accelerated supercomputers. Journal of Physics Condensed Matter, 2018, 30, 095901.	0.7	16
35176	Ab initio calculation of the migration free energy of oxygen diffusion in pure and samarium-doped ceria. Physical Review B, 2018, 97, .	1.1	26
35177	Reduced interface spin polarization by antiferromagnetically coupled Mn segregated to the <mml:math xmlns:mml="http://www.w3.org/1998/Math/MathML"><mml:mrow><mml:mi mathvariant="normal">C</mml:mi><mml:msub><mml:mi mathvariant="normal">o</mml:mi><mml:mn>2</mml:mn></mml:msub><mml:mi>MnSi</mml:mi></mml:mrow></mml:math> /GaAs (001) interface. Physical Review B, 2018, 97, .	1.1	10
35178	Approximate quasiparticle correction for calculations of the energy gap in two-dimensional materials. Physical Review B, 2018, 97, .	1.1	20
35179	Mechanistic origin and prediction of enhanced ductility in magnesium alloys. Science, 2018, 359, 447-452.	6.0	432
35180	Theoretical study of phase stability, crystal and electronic structure of MeMgN2 (MeÂ=ÂTi, Zr, Hf) compounds. Journal of Materials Science, 2018, 53, 4294-4305.	1.7	15
35181	Unraveling the Mechanisms of Visible Light Photocatalytic NO Purification on Earth-Abundant Insulator-Based Coreâ€“Shell Heterojunctions. Environmental Science & Technology, 2018, 52, 1479-1487.	4.6	192

#	Article	IF	Citations
35182	Band-Gap Tuning in Ferroelectric Bi₂FeCrO₆ Double Perovskite Thin Films. Journal of Physical Chemistry C, 2018, 122, 1070-1077.	1.5	34
35183	High-Pressure Phase Diagram and Superionicity of Alkaline Earth Metal Difluorides. Journal of Physical Chemistry C, 2018, 122, 1267-1279.	1.5	23
35184	Biogas Upgrading by Transition Metal Carbides. ACS Applied Energy Materials, 2018, 1, 43-47.	2.5	22
35185	Chlorine-Incorporation-Induced Formation of the Layered Phase for Antimony-Based Lead-Free Perovskite Solar Cells. Journal of the American Chemical Society, 2018, 140, 1019-1027.	6.6	241
35186	Encapsulation of camphor in cyclodextrin inclusion complex nanofibers via polymer-free electrospinning: enhanced water solubility, high temperature stability, and slow release of camphor. Journal of Materials Science, 2018, 53, 5436-5449.	1.7	28
35187	The Effect of Platinum on Î²-NiAl/Î±-Al2O3 Interfacial Tensile Stress: A Combined Ab Initio DFT and Mechanics-Based Model Study. Oxidation of Metals, 2018, 90, 65-82.	1.0	3
35188	Oxygen adatoms and vacancies on the (110) surface of CeO2. Science China Technological Sciences, 2018, 61, 135-139.	2.0	14
35189	Spontaneous ferroelectricity in strained low-temperature monoclinic Fe3O4: A first-principles study. Frontiers of Physics, 2018, 13, 1.	2.4	4
35190	Alkali (Li, K and Na) and alkali-earth (Be, Ca and Mg) adatoms on SiC single layer. Applied Surface Science, 2018, 435, 338-345.	3.1	20
35191	A computational thermodynamic and kinetic study of chlorine binding to the Zr(0001) surface. Colloids and Surfaces A: Physicochemical and Engineering Aspects, 2018, 539, 92-100.	2.3	7
35192	Divacancy-nitrogen/boron-codoped graphene as a metal-free catalyst for high-efficient CO oxidation. Materials Chemistry and Physics, 2018, 207, 11-22.	2.0	29
35193	Simulating Charge, Spin, and Orbital Ordering: Application to Jahnâ€“Teller Distortions in Layered Transition-Metal Oxides. Chemistry of Materials, 2018, 30, 607-618.	3.2	35
35194	Shaping the Magnetic Properties of BaFeO₃ Perovskite-Type by Alkaline-Earth Doping. Journal of Physical Chemistry C, 2018, 122, 2983-2989.	1.5	23
35195	Anomalous Dependence of the Reactivity on the Presence of Steps: Dissociation of D₂ on Cu(211). Journal of Physical Chemistry Letters, 2018, 9, 170-175.	2.1	27
35196	A computational study of CO oxidation reactions on metal impurities in graphene divacancies. Physical Chemistry Chemical Physics, 2018, 20, 2284-2295.	1.3	52
35197	Magnetic coupling properties of two-dimensional SiC with nonmetal atoms adsorbed: Density functional calculations. Japanese Journal of Applied Physics, 2018, 57, 021301.	0.8	1
35198	High-throughput estimation of planar fault energies in A3B compounds with L12 structure. Acta Materialia, 2018, 145, 532-542.	3.8	19
35199	Segregation of Mg, Cu and their effects on the strength of Al Î£5 (210)[001] symmetrical tilt grain boundary. Acta Materialia, 2018, 145, 235-246.	3.8	101

#	Article	IF	Citations
35200	DFT calculation for stability and strength of iron borides. Computational Materials Science, 2018, 144, 147-153.	1.4	3
35201	The Mineral StÃ¼tzite: a Zintl-Phase or Polar Intermetallic? A Case Study Using Experimental and Quantum-Chemical Techniques. Inorganic Chemistry, 2018, 57, 412-421.	1.9	17
35202	Elucidating the Formation Mechanisms of Silver Nanoparticles from a Comprehensive Simulation Based on First-Principles Calculations. Journal of Physical Chemistry C, 2018, 122, 1333-1344.	1.5	3
35203	Interlaminar Anionic Transport in Layered Double Hydroxides: Estimation of Diffusion Coefficients. Journal of Physical Chemistry C, 2018, 122, 171-176.	1.5	9
35204	Diborane Interactions with Pt₇/Alumina: Preparation of Size-Controlled Borated Pt Model Catalysts. Journal of Physical Chemistry C, 2018, 122, 1631-1644.	1.5	17
35205	Thermodynamic Stability of Molybdenum Oxycarbides Formed from Orthorhombic Mo₂C in Oxygen-Rich Environments. Journal of Physical Chemistry C, 2018, 122, 1223-1233.	1.5	33
35206	Rediscovering the MP₁₅ Family (M = Li, Na, and K) as an Anisotropic Layered Semiconducting Material. Journal of Physical Chemistry Letters, 2018, 9, 732-738.	2.1	15
35207	Adsorption of Carbon on Partially Oxidized Low-Index Cu Surfaces. Langmuir, 2018, 34, 1311-1320.	1.6	2
35208	The structural, electronic and magnetic properties of Co1â^'xFexS2. Materials Research Express, 2018, 5, 016507.	0.8	5
35209	MoTe₂: A Promising Candidate for SF₆ Decomposition Gas Sensors With High Sensitivity and Selectivity. IEEE Electron Device Letters, 2018, 39, 292-295.	2.2	74
35210	Metalâ€“Insulator Transition of Geâ€“Sbâ€“Te Superlattice: An Electron Counting Model Study. IEEE Nanotechnology Magazine, 2018, 17, 140-146.	1.1	31
35211	CO oxidation on inverse Ce6O12/Cu(111) catalyst: role of copperâ€“ceria interactions. Journal of Molecular Modeling, 2018, 24, 20.	0.8	4
35212	Role of Zr in strengthening MoSi2 from density functional theory calculations. Acta Materialia, 2018, 145, 470-476.	3.8	17
35213	The cluster-plus-glue-atom models of solid solution CuNi alloys: A first-principles study. Computational Materials Science, 2018, 143, 439-445.	1.4	5
35214	Y6Mg9Co2 and Y9Mg30Co2: Novel magnesium-rich compounds representing new structure types. Journal of Alloys and Compounds, 2018, 737, 613-622.	2.8	6
35215	Exploration work function and optical properties of monolayer SnSe allotropes. Superlattices and Microstructures, 2018, 114, 251-258.	1.4	57
35216	Peierls instability as the insulating origin of the Na/Si(111)-(3â€²â€²Ã—â€²â€²1) surface with a Na coverage of 2/3 monolayers. Surface Science, 2018, 669, 130-132.	0.8	0
35217	Ternary Iodido Bismuthates and the Special Role of Copper. Inorganic Chemistry, 2018, 57, 633-640.	1.9	29

#	Article	IF	Citations
35218	Development of Embedded and Performance of Density Functional Methods for Molecular Crystals. Journal of Physical Chemistry A, 2018, 122, 708-713.	1.1	22
35219	The Role of Composition of Uniform and Highly Dispersed Cobalt Vanadium Iron Spinel Nanocrystals for Oxygen Electrocatalysis. ACS Catalysis, 2018, 8, 1259-1267.	5.5	101
35220	Mechanical and thermal properties of grain boundary in a planar heterostructure of graphene and hexagonal boron nitride. Nanoscale, 2018, 10, 3497-3508.	2.8	47
35221	Manipulation of cation combinations and configurations of halide double perovskites for solar cell absorbers. Journal of Materials Chemistry A, 2018, 6, 1809-1815.	5.2	85
35222	Photoinduced dynamics to photoluminescence in Ln³⁺ (Ln = Ce, Pr) doped Î²-NaYF₄ nanocrystals computed in basis of non-collinear spin DFT with spin-orbit coupling. Molecular Physics, 2018, 116, 697-707.	0.8	8
35223	Optical fiber-based in situ spectroscopic characterization of supported TiO₂ in photocatalytic dye degradation. Materials Research Express, 2018, 5, 015010.	0.8	2
35224	Bipolar Magnetic Materials Based on 2D Ni[TCNE] Metalâ€“Organic Coordination Networks. Advanced Electronic Materials, 2018, 4, 1700323.	2.6	17
35225	Revealing Pseudocapacitive Mechanisms of Metal Dichalcogenide SnS₂/Grapheneâ€CNT Aerogels for Highâ€Energy Na Hybrid Capacitors. Advanced Energy Materials, 2018, 8, 1702488.	10.2	135
35226	Multifunctional Interlayer Based on Molybdenum Diphosphide Catalyst and Carbon Nanotube Film for Lithiumâ€“Sulfur Batteries. Small, 2018, 14, 1702853.	5.2	142
35227	Synergistic Interlayer and Defect Engineering in VS₂ Nanosheets toward Efficient Electrocatalytic Hydrogen Evolution Reaction. Small, 2018, 14, 1703098.	5.2	180
35228	Degradable rhenium trioxide nanocubes with high localized surface plasmon resonance absorbance like gold for photothermal theranostics. Biomaterials, 2018, 159, 68-81.	5.7	52
35229	Probing the edge effect on the ORR activity using platinum nanorods: A DFT study. Catalysis Today, 2018, 312, 126-131.	2.2	12
35230	CO oxidation on Al Au nano-composite systems. Chemical Physics, 2018, 502, 18-26.	0.9	2
35231	Thermal decomposition of energetic MOFs nickel hydrazine nitrate crystals from an ab initio molecular dynamics simulation. Computational Materials Science, 2018, 143, 170-181.	1.4	4
35232	Chemical doping in pnictides superconductors: The case ofCa(Fe1-xXx)2As2, Xâ€¯=â€¯Co, Ni, Pt. Journal of Magnetism and Magnetic Materials, 2018, 452, 179-183.	1.0	2
35233	Lattice dynamics, elasticity and magnetic abnormality in ordered crystalline alloys Fe3Pt at high pressures. Journal of Magnetism and Magnetic Materials, 2018, 453, 67-77.	1.0	7
35234	A new observation of strain-induced grain boundary serration and its underlying mechanism in a Niâ€“20Cr binary model alloy. Materials Characterization, 2018, 135, 146-153.	1.9	13
35235	Strain tuned magnetocrystalline anisotropy in ferromagnetic H-FeCl2 monolayer. Solid State Communications, 2018, 271, 66-70.	0.9	17

#	Article	IF	Citations
35236	Quasi-2D silicon structures based on ultrathin Me2Si (Meâ€¯=â€¯Mg, Ca, Sr, Ba) films. Surface Science, 2018, 670, 51-57.	0.8	11
35237	Structural Characterization of the Li-Ion Battery Cathode Materials LiTi_xMn_{2â€“x}O₄ (0.2 â‰¤ x â‰¤ 1.5): A Combined Experimental ⁷Li NMR and First-Principles Study. Chemistry of Materials, 2018, 30, 817-829.	3.2	27
35238	Deducing the Adsorption Geometry of Rhodamine 6G from the Surface-Induced Mode Renormalization in Surface-Enhanced Raman Spectroscopy. Journal of Physical Chemistry C, 2018, 122, 465-473.	1.5	19
35239	Roles of Pseudo-Closed s² Orbitals for Different Intrinsic Hole Generation between Tlâ€“Bi and Inâ€“Bi Bromide Double Perovskites. Journal of Physical Chemistry Letters, 2018, 9, 258-262.	2.1	27
35240	First-principles energy and vibration spectrum simulations of Cr/V interacting with H in W-based alloy in a fusion reactor. Journal of Nuclear Science and Technology, 2018, 55, 123-137.	0.7	1
35241	Alloying in an Intercalation Host: Metal Titanium Niobates as Anodes for Rechargeable Alkaliâ€Ion Batteries. Chemistry - an Asian Journal, 2018, 13, 299-310.	1.7	4
35242	A Chemical View on Xâ€ray Photoelectron Spectroscopy: the ESCA Molecule and Surfaceâ€toâ€Bulk XPS Shifts. ChemPhysChem, 2018, 19, 169-174.	1.0	24
35243	Exploring the relevance of thiophene rings as bridge unit in acceptorâ€bridgeâ€donor dyes on selfâ€aggregation and performance in DSSCs. Journal of Computational Chemistry, 2018, 39, 685-698.	1.5	10
35244	Properties of Y2TiO5 and Y2Ti2O7 crystals: Development of novel interatomic potentials. Journal of Alloys and Compounds, 2018, 739, 1037-1047.	2.8	12
35245	Preferential oxidation of CO in H2 on Cu and Cu/CeOx catalysts studied by in situ UVâ€“Vis and mass spectrometry and DFT. Journal of Catalysis, 2018, 357, 176-187.	3.1	25
35246	Controlling Oxygen-Based Electrochemical Reactions through Spin Orientation. Journal of Physical Chemistry C, 2018, 122, 894-901.	1.5	14
35247	Exploring the transposition effects on the electronic and optical properties of Cs₂AgSbCl₆via a combined computational-experimental approach. Journal of Materials Chemistry A, 2018, 6, 2346-2352.	5.2	100
35248	Nanoporous carbon foam structures with excellent electronic properties predicted by first-principles studies. Carbon, 2018, 129, 809-818.	5.4	23
35249	Magnetic properties of rhenium disulfide (ReS2) monolayer doped with different nonmetal atoms. Optik, 2018, 158, 291-296.	1.4	3
35250	Mechanical, optoelectronic and transport properties of single-layer Ca2N and Sr2N electrides. Journal of Alloys and Compounds, 2018, 739, 643-652.	2.8	14
35251	Menthol/cyclodextrin inclusion complex nanofibers: Enhanced water-solubility and high-temperature stability of menthol. Journal of Food Engineering, 2018, 224, 27-36.	2.7	82
35252	Atomic-scale simulations of the local structures of molten Ni1-xCox and Ni1-xFex. Journal of Non-Crystalline Solids, 2018, 481, 470-478.	1.5	5
35253	Tunable electronic structure and spin splitting in single and multiple Fe-adsorbed g-C2N with different layers: A first-principles study. Journal of Physics and Chemistry of Solids, 2018, 115, 221-227.	1.9	10

#	Article	IF	Citations
35254	Study on the intrinsic defects in tin oxide with first-principles method. Journal of Physics and Chemistry of Solids, 2018, 115, 228-232.	1.9	4
35255	Evaluation of magnesium ion migration in inorganic oxides by the bond valence site energy method. Solid State Ionics, 2018, 315, 111-115.	1.3	34
35256	Clarification of the interaction between Au atoms and the anatase TiO2 (112) surface using density functional theory. Surface Science, 2018, 670, 23-32.	0.8	16
35257	Liquid-Phase Multicomponent Adsorption and Separation of Xylene Mixtures by Flexible MIL-53 Adsorbents. Journal of Physical Chemistry C, 2018, 122, 386-397.	1.5	52
35258	Superposed Redox Chemistry of Fused Carbon Rings in Cyclooctatetraene-Based Organic Molecules for High-Voltage and High-Capacity Cathodes. ACS Applied Materials & Interfaces, 2018, 10, 2496-2503.	4.0	12
35259	Ab-initio calculation of the magnetic properties of P and As doped SnO 2. Computational Condensed Matter, 2018, 14, 36-39.	0.9	17
35260	New predicted ground state and high pressure phases of TcB3 and TcB4: First-principles. Computational Materials Science, 2018, 144, 154-160.	1.4	4
35261	Tetragon-based carbon allotropes T-C8 and its derivatives: A theoretical investigation. Computational Materials Science, 2018, 144, 170-175.	1.4	17
35262	Carbon and Mo transformations during the synthesis of mesoporous Mo2C/carbon catalysts by carbothermal hydrogen reduction. Journal of Solid State Chemistry, 2018, 258, 818-824.	1.4	27
35263	Evolution of Water Structures on Stepped Platinum Surfaces. Journal of Physical Chemistry C, 2018, 122, 604-611.	1.5	6
35264	High Stability and Reactivity of Single-Metal Atom Catalysts Supported on Yttria-Stabilized Zirconia: The Role of the Surface Oxygen Vacancy. Journal of Physical Chemistry C, 2018, 122, 1622-1630.	1.5	8
35265	Atomic-Scale Understanding of Gold Cluster Growth on Different Substrates and Adsorption-Induced Structural Change. Journal of Physical Chemistry C, 2018, 122, 1753-1760.	1.5	18
35266	Influence of chalcogen composition on the structural transition and on the electronic and optical properties of the monolayer titanium trichalcogenide ordered alloys. Physical Chemistry Chemical Physics, 2018, 20, 1431-1439.	1.3	9
35267	In situ observation of atomic movement in a ferroelectric film under an external electric field and stress. Nano Research, 2018, 11, 3824-3832.	5.8	7
35268	Island shape, size and interface dependency on electronic and magnetic properties of graphene hexagonal-boron nitride (h-BN) in-plane hybrids. Journal of Physics and Chemistry of Solids, 2018, 115, 187-198.	1.9	10
35269	One-dimensional coordination polymers of whole row rare earth tris-pivalates. Journal of Solid State Chemistry, 2018, 258, 876-884.	1.4	17
35270	Computational and experimental analysis on Te-doped ZnSb thermoelectric material. Materials Research Bulletin, 2018, 101, 90-99.	2.7	11
35271	Protons in cubic yttria-stabilized zirconia: Binding sites and migration pathways. Solid State Ionics, 2018, 315, 116-125.	1.3	9

#	Article	IF	Citations
35272	Two-Dimensional Metalâ€“Organic Half-metallic Antiferromagnet: CoFePz. Journal of Physical Chemistry C, 2018, 122, 1846-1851.	1.5	24
35273	First-Principle Study of Phosphine Adsorption on Si(001)-2 Ã— 1â€“Cl. Journal of Physical Chemistry C, 2018, 122, 1741-1745.	1.5	21
35274	Molybdenum sulfide clusters immobilized on defective graphene: a stable catalyst for the hydrogen evolution reaction. Journal of Materials Chemistry A, 2018, 6, 2289-2294.	5.2	44
35275	Nanostructured mullite steam oxidation resistant coatings for silicon carbide deposited via atomic layer deposition. Journal of the American Ceramic Society, 2018, 101, 2493-2505.	1.9	11
35276	Nanosizing Ammonia Borane with Nickel: A Path toward the Direct Hydrogen Release and Uptake of Bï£¿Nï£¿H Systems. Advanced Sustainable Systems, 2018, 2, 1700122.	2.7	17
35277	Recovery of edge states of graphene nanoislands on an iridium substrate by silicon intercalation. Nano Research, 2018, 11, 3722-3729.	5.8	10
35278	Density-functional theory based molecular dynamics simulation of tetrahedrite thermoelectrics: Effect of cell size and basis sets. Computational Materials Science, 2018, 144, 315-321.	1.4	1
35279	Structural, mechanical and electronic properties of two-dimensional structure of III-arsenide (1 1 1) binary compounds: An ab-initio study. Computational Materials Science, 2018, 144, 285-293.	1.4	10
35280	Atomic mechanical properties of structure and diffusion in the MoO3 anode materials during lithiation. Computational Materials Science, 2018, 145, 8-13.	1.4	7
35281	Activation of oxygen on (NH3Cu NH3)+ in NH3-SCR over Cu-CHA. Journal of Catalysis, 2018, 358, 179-186.	3.1	91
35282	Investigating the impact of the defect dynamic characteristics on the PBTI in the high-Î² gate device. Microelectronics Reliability, 2018, 80, 24-28.	0.9	1
35283	The structural, magnetic, electronic and optical properties of the cluster Fe-X6 (X=S, N, O or F) doped monolayer WS2. Superlattices and Microstructures, 2018, 114, 274-283.	1.4	6
35284	Thermodynamic assessment of the Mo-S system and its application in thermal decomposition of MoS 2. Thermochimica Acta, 2018, 660, 44-55.	1.2	10
35285	Electronic structure, metamagnetism and thermopower of LaSiFe₁₂and interstitially doped LaSiFe₁₂. Journal Physics D: Applied Physics, 2018, 51, 034003.	1.3	18
35286	Charged dopants in neutral supercells through substitutional donor (acceptor): nitrogen donor charging of the nitrogen-vacancy center in diamond. New Journal of Physics, 2018, 20, 023002.	1.2	14
35287	Mechanical and half-metallic properties of half-Heusler CoCrSn. Modern Physics Letters B, 2018, 32, 1850006.	1.0	6
35288	Triangular lattice atomic layer of Sn(1 Ã— 1) at graphene/SiC(0001) interface. Applied Physics Express, 2018, 11, 015202.	1.1	15
35289	Highly Defective Layered Double Perovskite Oxide for Efficient Energy Storage via Reversible Pseudocapacitive Oxygenâ€Anion Intercalation. Advanced Energy Materials, 2018, 8, 1702604.	10.2	99

#	Article	IF	Citations
35290	Structural, optical, and thermal properties of MAX-phase Cr2AlB2. Frontiers of Physics, 2018, 13, 1.	2.4	10
35291	Spontaneous Growth of 3D Framework Carbon from Sodium Citrate for High Energyâ€and Powerâ€Density and Longâ€Life Sodiumâ€Ion Hybrid Capacitors. Advanced Energy Materials, 2018, 8, 1702409.	10.2	221
35292	Effect of Material Structure on Photoluminescence of ZnO/MgO Coreâ€Shell Nanowires. ChemNanoMat, 2018, 4, 291-300.	1.5	5
35293	Theoretical insights on the oxygen-reduction reaction mechanism of LaN4-embedded graphene. Journal of Molecular Modeling, 2018, 24, 14.	0.8	5
35294	Magnetic and Electronic Properties of BN Nanosheets with Different Nonmagnetic Metal Dopants: a First-Principles Study. Journal of Superconductivity and Novel Magnetism, 2018, 31, 2211-2216.	0.8	3
35295	A FirstPrinciple Study on the Magnetic Properties of Ag, Al, Li, Mg, and NaDoped ReS2 Monolayers. Journal of Superconductivity and Novel Magnetism, 2018, 31, 2431-2436.	0.8	2
35296	Optimal water adsorption on phosphorene. Journal of Alloys and Compounds, 2018, 737, 365-371.	2.8	13
35297	Developing porous carbon with dihydrogen phosphate groups as sulfur host for high performance lithium sulfur batteries. Journal of Power Sources, 2018, 378, 40-47.	4.0	42
35298	High Seebeck Coefficient and Unusually Low Thermal Conductivity Near Ambient Temperatures in Layered Compound Yb_{2â€“x}Eu_xCdSb₂. Chemistry of Materials, 2018, 30, 484-493.	3.2	45
35299	Deeper Understanding of Interstitial Boron-Doped Anatase Thin Films as A Multifunctional Layer Through Theory and Experiment. Journal of Physical Chemistry C, 2018, 122, 714-726.	1.5	16
35300	Fluoroethylene Carbonate as a Directing Agent in Amorphous Silicon Anodes: Electrolyte Interface Structure Probed by Sum Frequency Vibrational Spectroscopy and Ab Initio Molecular Dynamics. Nano Letters, 2018, 18, 1145-1151.	4.5	59
35301	Perovskite nickelates as electric-field sensors in salt water. Nature, 2018, 553, 68-72.	13.7	146
35302	Mechanisms of the oxygen reduction reaction on B- and/or N-doped carbon nanomaterials with curvature and edge effects. Nanoscale, 2018, 10, 1129-1134.	2.8	81
35303	Siteâ€Selective In Situ Electrochemical Doping for Mnâ€Rich Layered Oxide Cathode Materials in Lithiumâ€Ion Batteries. Advanced Energy Materials, 2018, 8, 1702514.	10.2	57
35304	Atomic adsorption on pristine graphene along the Periodic Table of Elements â€“ From PBE to non-local functionals. Applied Surface Science, 2018, 436, 433-440.	3.1	61
35305	Structural and magnetic properties of Fe-membranes embedded in hexagonal graphene nanoholes. Computational Materials Science, 2018, 143, 374-383.	1.4	2
35306	Tunable magnetic coupling of BN nanosheets with different nonmetal dopants: A first-principles study. Optik, 2018, 156, 797-802.	1.4	6
35307	Understanding the incorporating effect of Co2+/Co3+ in NiFe-layered double hydroxide for electrocatalytic oxygen evolution reaction. Journal of Catalysis, 2018, 358, 100-107.	3.1	194

#	Article	IF	Citations
35308	Strontium-free rare earth perovskite ferrites with fast oxygen exchange kinetics: Experiment and theory. Journal of Solid State Chemistry, 2018, 259, 57-66.	1.4	21
35309	Role of Lead Vacancies for Optoelectronic Properties of Lead-Halide Perovskites. Journal of Physical Chemistry C, 2018, 122, 5216-5226.	1.5	20
35310	First-Principles Study of Manipulating the Phonon Transport of Molybdenum Disulfide by Sodium Intercalating. Journal of Physical Chemistry C, 2018, 122, 2632-2640.	1.5	6
35311	Enhanced Switchable Ferroelectric Photovoltaic Effects in Hexagonal Ferrite Thin Films via Strain Engineering. ACS Applied Materials & Interfaces, 2018, 10, 1846-1853.	4.0	47
35312	Oxygen-induced degradation of the electronic properties of thin-layer InSe. Physical Chemistry Chemical Physics, 2018, 20, 2238-2250.	1.3	23
35313	Tunable Schottky contacts in MSe₂/NbSe₂ (M = Mo and W) heterostructures and promising application potential in field-effect transistors. Physical Chemistry Chemical Physics, 2018, 20, 1897-1903.	1.3	17
35314	Negative Poisson's ratio and high-mobility transport anisotropy in SiC₆siligraphene. Nanoscale, 2018, 10, 2108-2114.	2.8	51
35315	Nuclear quantum effects of light and heavy water studied by all-electron first principles path integral simulations. Journal of Chemical Physics, 2018, 148, 102324.	1.2	21
35316	Electronic and optical properties of bilayer PbI2: a first-principles study. Journal Physics D: Applied Physics, 2018, 51, 035301.	1.3	9
35317	$sqrt{3} {imes} sqrt{3} $ germanene on Al(111) grown at nearly room temperature. Applied Physics Express, 2018, 11, 015502.	1.1	20
35318	Anatase (101) Reconstructed Surface with Novel Functionalities: Desired Bandgap for Visible Light Absorption and High Chemical Reactivity. Advanced Functional Materials, 2018, 28, 1705529.	7.8	9
35319	Surface-adsorbed ions on TiO2 nanosheets for selective photocatalytic CO2 reduction. Nano Research, 2018, 11, 3362-3370.	5.8	44
35320	First-principles study of crystal structure and stability of T1 precipitates in Al-Li-Cu alloys. Acta Materialia, 2018, 145, 337-346.	3.8	39
35321	Coexistence of rhombohedral and orthorhombic phases in ultrathin BiFeO3 films driven by interfacial oxygen octahedral coupling. Acta Materialia, 2018, 145, 220-226.	3.8	29
35322	Hidden spin polarization in the 1 T -phase layered transition-metal dichalcogenides MX 2 (M â€¯=â€¯Zr, Hf; X) Tj ETQq0 0 0 rgBT /Overlo	4.3	25
35323	Adiabatic and Nonadiabatic Charge Transport in Liâ€“S Batteries. Chemistry of Materials, 2018, 30, 915-928.	3.2	30
35324	Structure Transformation and Cerium-Substituted Optical Response across the Carbonitridosilicate Solid Solution (La_{Î´}Y_{1â^'Î´})₂Si₄N₆C (Î´ = 0â€“0.5). Inorganic Chemistry, 2018, 57, 519-527.	1.9	1
35325	Role of Surface Chemistry on Catalyst/Ionomer Interactions for Transition Metalâ€“Nitrogenâ€“Carbon Electrocatalysts. ACS Applied Energy Materials, 2018, 1, 68-77.	2.5	44

#	Article	IF	Citations
35326	Câ€“C Coupling on Single-Atom-Based Heterogeneous Catalyst. Journal of the American Chemical Society, 2018, 140, 954-962.	6.6	142
35327	Intrinsic origin of intra-granular cracking in Ni-rich layered oxide cathode materials. Physical Chemistry Chemical Physics, 2018, 20, 9045-9052.	1.3	70
35328	Strain effects on the magnetism of transition metal-doped MoTe2 monolayer. Journal of Materials Science, 2018, 53, 5114-5124.	1.7	20
35329	An efficient method for hybrid density functional calculation with spinâ€“orbit coupling. Computer Physics Communications, 2018, 224, 90-97.	3.0	5
35330	SQDFT: Spectral Quadrature method for large-scale parallel <mml:math xmlns:mml="http://www.w3.org/1998/Math/MathML" id="mml10" display="inline" overflow="scroll" altimg="si10.gif"><mml:mi mathvariant="script">O</mml:mi><mml:mrow><mml:mo>(</mml:mo><mml:mi>N</mml:mi><mml:mo>)</mml:mo></mml:mrow></mm Kohnâ€“Sham calculations at high temperature. Computer Physics Communications, 2018, 224, 288-298.	3.0	42
35331	First principles study of the structural phase stability and magnetic order in various structural phases of Mn2FeGa. Intermetallics, 2018, 93, 209-216.	1.8	17
35332	Energetics of small helium clusters near tungsten surface by ab initio calculations. Journal of Nuclear Materials, 2018, 499, 539-545.	1.3	10
35333	Al-based composites reinforced with AlB2, AlN and BN phases: Experimental and theoretical studies. Materials and Design, 2018, 141, 88-98.	3.3	69
35334	Thermodynamic and Kinetic Study on Carbon Dioxide Hydrogenation to Methanol over a Ga₃Ni₅(111) Surface: The Effects of Step Edge. Journal of Physical Chemistry C, 2018, 122, 315-330.	1.5	26
35335	Dissociation Mechanism of Water Molecules on the PuO₂(110) Surface: An Ab Initio Molecular Dynamics Study. Journal of Physical Chemistry C, 2018, 122, 371-376.	1.5	24
35336	Identifying the Thermal Decomposition Mechanism of Guaiacol on Pt(111): An Integrated X-ray Photoelectron Spectroscopy and Density Functional Theory Study. Journal of Physical Chemistry C, 2018, 122, 4261-4273.	1.5	5
35337	Different Topological Quantum States in Ternary Zintl compounds: BaCaX (X = Si, Ge, Sn and Pb). Journal of Physical Chemistry C, 2018, 122, 705-713.	1.5	14
35338	Ambipolar Half-Metallicity in One-Dimensional Metalâ€“(1,2,4,5-Benzenetetramine) Coordination Polymers via Carrier Doping. Journal of Physical Chemistry C, 2018, 122, 989-994.	1.5	27
35339	Halogen-Adatom Mediated Phase Transition of Two-Dimensional Molecular Self-Assembly on a Metal Surface. Langmuir, 2018, 34, 553-560.	1.6	18
35340	Molecular Simulation Insights on Xe/Kr Separation in a Set of Nanoporous Crystalline Membranes. ACS Applied Materials & Interfaces, 2018, 10, 582-592.	4.0	44
35341	Local Electronic Structure of a Single-Layer Porphyrin-Containing Covalent Organic Framework. ACS Nano, 2018, 12, 385-391.	7.3	68
35342	Three dimensional porous SiC for lithium polysulfide trapping. Physical Chemistry Chemical Physics, 2018, 20, 4005-4011.	1.3	10
35343	Understanding the activity and selectivity of single atom catalysts for hydrogen and oxygen evolution via ab initial study. Catalysis Science and Technology, 2018, 8, 996-1001.	2.1	94

#	Article	IF	Citations
35344	Microscopic evidence for the dissociation of water molecules on cleaved GaN(11Ì„00). Physical Chemistry Chemical Physics, 2018, 20, 1261-1266.	1.3	6
35345	Hybrid density functional study on the photocatalytic properties of AlN/MoSe₂, AlN/WS₂, and AlN/WSe₂heterostructures. Journal Physics D: Applied Physics, 2018, 51, 025109.	1.3	35
35346	Phonon-driven electron scattering and magnetothermoelectric effect in two-dimensional tin selenide. Journal of Physics Condensed Matter, 2018, 30, 055301.	0.7	7
35347	Tuning electronic and optical properties of arsenene/C₃N van der Waals heterostructure by vertical strain and external electric field. Nanotechnology, 2018, 29, 075201.	1.3	89
35348	Effect of boron on the hydrogen-induced grain boundary embrittlement in Î±-Fe. International Journal of Hydrogen Energy, 2018, 43, 1909-1925.	3.8	22
35349	Selective adsorption of a supramolecular structure on flat and stepped gold surfaces. Surface Science, 2018, 670, 44-50.	0.8	3
35350	Stabilization of Metastable Thermoelectric Crystalline Phases by Tuning the Glass Composition in the Cuâ€“Asâ€“Te System. Inorganic Chemistry, 2018, 57, 754-767.	1.9	14
35351	Crystallographic Facet Dependence of the Hydrogen Evolution Reaction on CoPS: Theory and Experiments. ACS Catalysis, 2018, 8, 1143-1152.	5.5	71
35352	Adsorbate-Induced Modification of the Confining Barriers in a Quantum Box Array. ACS Nano, 2018, 12, 768-778.	7.3	6
35353	Nanocorrugation-Induced Forces between Electrically Neutral Metallic Objects. ACS Nano, 2018, 12, 804-812.	7.3	2
35354	Kinetic Monte Carlo Study of Li Intercalation in LiFePO₄. ACS Nano, 2018, 12, 844-851.	7.3	47
35355	Multiscale Computational Design of Functionalized Photocathodes for H₂ Generation. Journal of the American Chemical Society, 2018, 140, 50-53.	6.6	14
35356	The synergic effects at the molecular level in CoS₂ for selective hydrogenation of nitroarenes. Green Chemistry, 2018, 20, 671-679.	4.6	54
35357	The origin of excellent rate and cycle performance of Sn₄P₃ binary electrodes for sodium-ion batteries. Journal of Materials Chemistry A, 2018, 6, 1772-1779.	5.2	42
35358	Tunable electronic and magnetic properties of graphene-like XYBe₃ (XY = BN, AlN, SiC, GeC) nanosheets with carrier doping: a first-principles study. Physical Chemistry Chemical Physics, 2018, 20, 6830-6837.	1.3	9
35359	Simulations of hydrogen, carbon dioxide, and small hydrocarbon sorption in a nitrogen-rich rht-metalâ€“organic framework. Physical Chemistry Chemical Physics, 2018, 20, 1761-1777.	1.3	15
35360	Hybrid Structures and Strain-Tunable Electronic Properties of Carbon Nanothreads. Journal of Physical Chemistry C, 2018, 122, 3101-3106.	1.5	15
35361	Solution-Processed n-Type Graphene Doping for Cathode in Inverted Polymer Light-Emitting Diodes. ACS Applied Materials & Interfaces, 2018, 10, 4874-4881.	4.0	24

#	Article	IF	Citations
35362	Largely Tunable Band Structures of Few-Layer InSe by Uniaxial Strain. ACS Applied Materials & Interfaces, 2018, 10, 3994-4000.	4.0	84
35363	Mechanism of CO₂ Reduction at Copper Surfaces: Pathways to C₂ Products. ACS Catalysis, 2018, 8, 1490-1499.	5.5	608
35364	Evaluating the Risk of Câ€“C Bond Formation during Selective Hydrogenation of Acetylene on Palladium. ACS Catalysis, 2018, 8, 1662-1671.	5.5	65
35365	Graphene analogue in (111)-oriented BaBiO3 bilayer heterostructures for topological electronics. Scientific Reports, 2018, 8, 555.	1.6	6
35366	Potassium associated manganese vacancy in birnessite-type manganese dioxide for airborne formaldehyde oxidation. Catalysis Science and Technology, 2018, 8, 1799-1812.	2.1	117
35367	Equation of state and optical properties of warm dense helium. Physics of Plasmas, 2018, 25, .	0.7	18
35368	Experimental and theoretical comparison of Sb, As, and P diffusion mechanisms and doping in CdTe. Journal Physics D: Applied Physics, 2018, 51, 075102.	1.3	51
35369	Ferromagnetism in CVT grown tungsten diselenide single crystals with nickel doping. Nanotechnology, 2018, 29, 115701.	1.3	31
35370	Superconductivity proximate to antiferromagnetism in a copper-oxide monolayer grown on Bi2Sr2CaCu2O8+Î´. Physical Review B, 2018, 97, .	1.1	5
35371	Gapped electronic structure of epitaxial stanene on InSb(111). Physical Review B, 2018, 97, .	1.1	91
35372	Lattice dynamics of ultrathin FeSe films on <mml:math xmlns:mml="http://www.w3.org/1998/Math/MathML"><mml:msub><mml:mi>SrTiO</mml:mi><mml:mn>3</mml:mn></mml:msub></m Physical Review B, 2018, 97, .	1.1	26
35373	Observation of a two-dimensional Fermi surface and Dirac dispersion in <mml:math xmlns:mml="http://www.w3.org/1998/Math/MathML"><mml:msub><mml:mi>YbMnSb</mml:mi><mml:mn>2</mml:mn></mml:msub> Physical Review B, 2018, 97, .	1.1	54
35374	Unraveling Hidden Mgâ€“Mnâ€“H Phase Relations at High Pressures and Temperatures by in Situ Synchrotron Diffraction. Inorganic Chemistry, 2018, 57, 1614-1622.	1.9	9
35375	Hydrogen-Bond Relations for Surface OH Species. Journal of Physical Chemistry C, 2018, 122, 4849-4858.	1.5	9
35376	Directing Oxygen Vacancy Channels in SrFeO_{2.5} Epitaxial Thin Films. ACS Applied Materials & Interfaces, 2018, 10, 4831-4837.	4.0	43
35377	Designing half-metallic ferromagnetism by a new strategy: an example of superhalogen modified graphitic C₃N₄. Journal of Materials Chemistry C, 2018, 6, 1709-1714.	2.7	21
35378	Influence of impurities on the high temperature conductivity of SrTiO3. Applied Physics Letters, 2018, 112, .	1.5	28
35379	Elucidating the phase transitions and temperature-dependent photoluminescence of MAPbBr₃ single crystal. Journal Physics D: Applied Physics, 2018, 51, 045105.	1.3	54

#	Article	IF	Citations
35380	Electronic, Magnetic, and Transport Properties of Polyacrylonitrile-Based Carbon Nanofibers of Various Widths: Density-Functional Theory Calculations. Physical Review Applied, 2018, 9, .	1.5	8
35381	First-Principles Prediction of New Electrides with Nontrivial Band Topology Based on One-Dimensional Building Blocks. Physical Review Letters, 2018, 120, 026401.	2.9	58
35382	Topological Nodal-Net Semimetal in a Graphene Network Structure. Physical Review Letters, 2018, 120, 026402.	2.9	93
35383	Magnetic Behaviors of 3d Transition Metal-Doped Silicane: a First-Principle Study. Journal of Superconductivity and Novel Magnetism, 2018, 31, 2789-2795.	0.8	81
35384	Origin of the Phase Transition in Lithium Garnets. Journal of Physical Chemistry C, 2018, 122, 1963-1972.	1.5	46
35385	Size Dependence of Vapor Phase Hydrodeoxygenation of m-Cresol on Ni/SiO₂ Catalysts. ACS Catalysis, 2018, 8, 1672-1682.	5.5	171
35386	Theoretical prediction of a charge-transfer phase transition. Scientific Reports, 2018, 8, 63.	1.6	26
35387	A first-principles study of a real energetically stable MoN₂ nanosheet and its tunable electronic structure. Journal of Materials Chemistry C, 2018, 6, 2245-2251.	2.7	23
35388	A review of Ga2O3 materials, processing, and devices. Applied Physics Reviews, 2018, 5, .	5.5	1,816
35389	Tutorial: Novel properties of defects in semiconductors revealed by their vibrational spectra. Journal of Applied Physics, 2018, 123, .	1.1	41
35390	First-principles study of alloying effects on fluorine incorporation in Al_xGa_{1â^'x}N alloys. Journal Physics D: Applied Physics, 2018, 51, 065108.	1.3	10
35391	Confinement-driven electronic and topological phases in corundum-derived <mml:math xmlns:mml="http://www.w3.org/1998/Math/MathML"><mml:mrow><mml:mn>3</mml:mn><mml:mi>d</mml:mi></mml:mrow></mm -oxide honeycomb lattices. Physical Review B, 2018, 97, .	1.1	14
35392	Tunable magnetism and spin-polarized electronic transport in graphene mediated by molecular functionalization of extended defects. Physical Review B, 2018, 97, .	1.1	9
35393	Ultrahighâ€Pressure Phase Transitions in FeS₂ and FeO₂: Implications for Superâ€Earths' Deep Interior. Journal of Geophysical Research: Solid Earth, 2018, 123, 277-284.	1.4	10
35394	Inclusion of aggregation effect to evaluate the performance of organic dyes in dye-sensitized solar cells. Applied Surface Science, 2018, 439, 160-167.	3.1	6
35395	Pressure dependent mechanical properties of calcium carbides. Ceramics International, 2018, 44, 7429-7434.	2.3	2
35396	Accelerating exploitation of Co-Al-based superalloys from theoretical study. Materials and Design, 2018, 142, 139-148.	3.3	29
35397	Thickness Control of the Spin-Polarized Two-Dimensional Electron Gas in LaAlO3/BaTiO3 Superlattices. Scientific Reports, 2018, 8, 467.	1.6	7

#	Article	IF	Citations
35398	Reduced sintering of mass-selected Au clusters on SiO₂by alloying with Ti: an aberration-corrected STEM and computational study. Nanoscale, 2018, 10, 2363-2370.	2.8	14
35399	The effect of Pd ensemble structure on the O2 dissociation and CO oxidation mechanisms on Auâ€”Pd(100) surface alloys. Journal of Chemical Physics, 2018, 148, 024701.	1.2	15
35400	Empirical optimization of DFTâ€‰â€‰+â€‰â€‰U and HSE for the band structure of ZnO. Journal of Physics Condensed Matter, 2018, 30, 065501.	0.7	26
35401	Vibrational properties of the Au-(<mml:math) Tj ETQq1 1 0.784314 rgBT /Overlock 10 Tf 50 627 Td (xmlns:mml="http://www.w3.org/1	1.1	10
35402	Oxygenâ€Vacancy Abundant Ultrafine Co₃O₄/Graphene Composites for Highâ€Rate Supercapacitor Electrodes. Advanced Science, 2018, 5, 1700659.	5.6	392
35403	The role of rareâ€“earth dopants in tailoring the magnetism and magnetic anisotropy in Fe4N. Journal of Physics and Chemistry of Solids, 2018, 116, 7-14.	1.9	6
35404	Tunable Valley and Spin Polarizations in BiXO₃/BiIrO₃ (X = Fe, Mn) Ferroelectric Superlattices. ACS Applied Materials & Interfaces, 2018, 10, 3822-3829.	4.0	16
35405	Cu₂I₂Se₆: A Metalâ€“Inorganic Framework Wide-Bandgap Semiconductor for Photon Detection at Room Temperature. Journal of the American Chemical Society, 2018, 140, 1894-1899.	6.6	19
35406	Strain control of oxygen kinetics in the Ruddlesden-Popper oxide La1.85Sr0.15CuO4. Nature Communications, 2018, 9, 92.	5.8	38
35407	Synthesis of Wurtzite Cu2ZnSnS4 Nanosheets with Exposed High-Energy (002) Facets for Fabrication of Efficient Pt-Free Solar Cell Counter Electrodes. Scientific Reports, 2018, 8, 248.	1.6	30
35408	Spin-coupling-induced Improper Polarizations and Latent Magnetization in Multiferroic BiFeO3. Scientific Reports, 2018, 8, 405.	1.6	5
35409	Excellent room temperature deformability in high strain rate regimes of magnesium alloy. Scientific Reports, 2018, 8, 656.	1.6	37
35410	Electrodynamic properties of an artificial heterostructured superconducting cuprate. Physical Review B, 2018, 97, .	1.1	4
35411	Origamiâ€Inspired 3D Interconnected Molybdenum Carbide Nanoflakes. Advanced Materials Interfaces, 2018, 5, 1701113.	1.9	13
35412	Highâ€Efficiency Thinâ€Film Superlattice Thermoelectric Cooler Modules Enabled by Low Resistivity Contacts. Advanced Electronic Materials, 2018, 4, 1700381.	2.6	9
35413	A Dualâ€Insertion Type Sodiumâ€Ion Full Cell Based on Highâ€Quality Ternaryâ€Metal Prussian Blue Analogs. Advanced Energy Materials, 2018, 8, 1702856.	10.2	143
35414	Origin of pseudoelasticity by twinning in D03-type Fe3Ga. Computational Materials Science, 2018, 145, 154-162.	1.4	0
35415	Transition metal decorated covalent triazine-based frameworks as a capacity hydrogen storage medium. International Journal of Hydrogen Energy, 2018, 43, 2823-2830.	3.8	27

#	Article	IF	Citations
35416	Experimental and first principle calculation study on titanium, zirconium and aluminum oxides in promoting ferrite nucleation. Journal of Alloys and Compounds, 2018, 742, 112-122.	2.8	18
35417	A first principle study of hydrogenated graphdiyne. Physics Letters, Section A: General, Atomic and Solid State Physics, 2018, 382, 662-666.	0.9	14
35418	Electrochemical Intercalation of Calcium and Magnesium in TiS₂: Fundamental Studies Related to Multivalent Battery Applications. Chemistry of Materials, 2018, 30, 847-856.	3.2	105
35419	First-Principles Study on Stability and HER Activity of Noble Metal Single Atoms on TiO₂: The Effect of Loading Density. Journal of Physical Chemistry C, 2018, 122, 2546-2553.	1.5	27
35420	Janus Structures of Transition Metal Dichalcogenides as the Heterojunction Photocatalysts for Water Splitting. Journal of Physical Chemistry C, 2018, 122, 3123-3129.	1.5	246
35421	New Mechanism for Ferroelectricity in the Perovskite Ca_{2â€“x}Mn_xTi₂O₆ Synthesized by Spark Plasma Sintering. Journal of the American Chemical Society, 2018, 140, 2214-2220.	6.6	32
35422	Active Site Revealed for Water Oxidation on Electrochemically Induced Î´-MnO₂: Role of Spinel-to-Layer Phase Transition. Journal of the American Chemical Society, 2018, 140, 1783-1792.	6.6	95
35423	Evaluating differences in the active-site electronics of supported Au nanoparticle catalysts using Hammett and DFT studies. Nature Chemistry, 2018, 10, 268-274.	6.6	78
35424	Reconfiguring crystal and electronic structures of MoS2 by substitutional doping. Nature Communications, 2018, 9, 199.	5.8	128
35425	Thermodynamic insight into stimuli-responsive behaviour of soft porous crystals. Nature Communications, 2018, 9, 204.	5.8	104
35426	Chemically accurate adsorption energies for methane and ethane monolayers on the MgO(001) surface. Physical Chemistry Chemical Physics, 2018, 20, 9760-9769.	1.3	26
35427	Polymerizable ionic liquid as a precursor for N, P co-doped carbon toward the oxygen reduction reaction. Catalysis Science and Technology, 2018, 8, 1142-1150.	2.1	44
35428	Earth abundant perovskite oxides for low temperature CO₂conversion. Energy and Environmental Science, 2018, 11, 648-659.	15.6	93
35429	Work function of bismuth telluride: First-principles approach. Journal of the Korean Physical Society, 2018, 72, 122-128.	0.3	16
35430	Enhanced photochemical performance of hexagonal WO3 by metal-assisted Sâ€“O coupling for solar-driven water splitting. Science China Materials, 2018, 61, 91-100.	3.5	4
35431	Low temperature synthesis and characterization of zinc gallate quantum dots for optoelectronic applications. Journal of Alloys and Compounds, 2018, 740, 567-573.	2.8	29
35432	Effects of methylating agent and BrÃ¸nsted acidity on methylation activity of olefins in CHA-structured zeolites: A periodic DFT study. Molecular Catalysis, 2018, 446, 106-114.	1.0	4
35433	Fundamental effects of Ag alloying on hydrogen behaviors in PdCu. Journal of Membrane Science, 2018, 550, 230-237.	4.1	14

#	Article	IF	Citations
35434	Role of Hydrogen in High-Yield Growth of Boron Nitride Nanotubes at Atmospheric Pressure by Induction Thermal Plasma. ACS Nano, 2018, 12, 884-893.	7.3	66
35435	A new phase of the two-dimensional ReS₂ sheet with tunable magnetism. Journal of Materials Chemistry C, 2018, 6, 1248-1254.	2.7	35
35436	Theoretical prediction of high electron mobility in multilayer MoS2 heterostructured with MoSe2. Journal of Chemical Physics, 2018, 148, 014704.	1.2	15
35437	Transition-metal alloying of <mml:math xmlns:mml="http://www.w3.org/1998/Math/MathML"><mml:mrow><mml:msup><mml:mi>Î³</mml:mi><mml:mo>â€²</mml:mo></m : Effects on the ideal uniaxial compressive strength from first-principles calculations. Physical Review B, 2018, 97, .	1.1	21
35438	Observation of spin-orbit magnetoresistance in metallic thin films on magnetic insulators. Science Advances, 2018, 4, eaao3318.	4.7	32
35439	Work functions of metal hexaborides: Density functional study. Modern Physics Letters B, 2018, 32, 1850007.	1.0	6
35440	An Unusual Strong Visibleâ€Light Absorption Band in Red Anatase TiO₂ Photocatalyst Induced by Atomic Hydrogenâ€Occupied Oxygen Vacancies. Advanced Materials, 2018, 30, 1704479.	11.1	231
35441	Stabilization of Oxidized Copper Nanoclusters in Confined Spaces. Topics in Catalysis, 2018, 61, 419-427.	1.3	13
35442	Shape Control in Gold Nanoparticles by N-Containing Ligands: Insights from Density Functional Theory and Wulff Constructions. Topics in Catalysis, 2018, 61, 412-418.	1.3	10
35443	Carbon ene-yne graphyne monolayer as an outstanding anode material for Li/Na ion batteries. Applied Materials Today, 2018, 10, 115-121.	2.3	44
35444	Highly conductive and transparent films of HAuCl4-doped single-walled carbon nanotubes for flexible applications. Carbon, 2018, 130, 448-457.	5.4	68
35445	Heliumâ€“vacancy interactions in vanadium and tantalum. Computational Materials Science, 2018, 145, 197-207.	1.4	8
35446	First-principles study for strain effects on oxygen migration in zirconium. Computational Materials Science, 2018, 144, 345-354.	1.4	7
35447	On the abnormal fast diffusion of solute atoms in Î±-Ti: A first-principles investigation. Journal of Alloys and Compounds, 2018, 740, 156-166.	2.8	28
35448	Study on the Electrochemical Oxidation Desulfurization Behavior of Model Diesel on Anodic Alumina Oxide and Ceria Nanotubes. Energy & Fuels, 2018, 32, 2612-2621.	2.5	16
35449	Synthesis, Structure, and Optical Properties of Antiperovskite-Derived Ba₂MQ₃X (M = As, Sb; Q = S, Se; X = Cl, Br, I) Chalcohalides. Inorganic Chemistry, 2018, 57, 1449-1454.	1.9	18
35450	Structure and Properties of Boron-Very-Rich Boron Carbides: B₁₂ Icosahedra Linked through Bent CBB Chains. Journal of Physical Chemistry C, 2018, 122, 2448-2453.	1.5	15
35451	Pt/Cu single-atom alloys as coke-resistant catalysts for efficient Câ€“H activation. Nature Chemistry, 2018, 10, 325-332.	6.6	472

#	Article	IF	Citations
35452	Electronic characterization of silicon intercalated chevron graphene nanoribbons on Au(111). Chemical Communications, 2018, 54, 1619-1622.	2.2	19
35453	Large valley polarization in monolayer MoTe₂ on a magnetic substrate. Physical Chemistry Chemical Physics, 2018, 20, 3805-3812.	1.3	46
35454	Strain-tunable electronic and optical properties of BC₃monolayer. RSC Advances, 2018, 8, 1686-1692.	1.7	24
35455	A novel electrically controllable volatile memory device based on few-layer black phosphorus. Journal of Materials Chemistry C, 2018, 6, 2460-2466.	2.7	15
35456	Enhanced vibronic interaction caused by local lattice symmetry lowering in the (Fe, Mg)As2 ternary system. Journal of Applied Physics, 2018, 123, .	1.1	0
35457	Ab initio molecular dynamics study of the Eley-Rideal reaction of H + Clâ€“Au(111) â†' HCl + Au(111): Impact of energy dissipation to surface phonons and electron-hole pairs. Journal of Chemical Physics, 2018, 148, 014702.	1.2	25
35458	New structures of Fe₃S for rare-earth-free permanent magnets. Journal Physics D: Applied Physics, 2018, 51, 075001.	1.3	4
35459	Covalency and spin-orbit coupling driven magnetism in the double-perovskite iridates <mml:math xmlns:mml="http://www.w3.org/1998/Math/MathML"><mml:mrow><mml:msub><mml:mi>Sr</mml:mi><mml:mn>2</mml:mn></mml: (<mml:math) Tj ETQq1 1 0.784314 rgBT /Overlock 10 Tf 50 457 Td (xmlns:mml="http://www.w3.org/1998/Math/MathML"><mml:mr	1.1	15
35460	The structural, electronic, magnetic and optical properties of the new promising spintronic material Bi0.92Tb0.08FeO3: A first-principles approach. Computational Materials Science, 2018, 145, 244-251.	1.4	4
35461	Design of highly efficient Ni-based water-electrolysis catalysts by a third transition metal addition into Ni 3 Mo. Intermetallics, 2018, 94, 99-105.	1.8	7
35462	Possibility of a ferromagnetic and conducting metal-organic network. Journal of Magnetism and Magnetic Materials, 2018, 453, 48-52.	1.0	12
35463	Structural and electronic properties of CdSe/ZnS and ZnS/CdSe core/shell nanowires via first principles study. Journal of Physics and Chemistry of Solids, 2018, 116, 37-42.	1.9	5
35464	How grain boundary chemistry controls the fracture mode of molybdenum. Materials and Design, 2018, 142, 36-43.	3.3	52
35465	Theoretical Approach to the Sulfidation of the BaTiO₃(001) Surfaces and Its Effect on the H₂ Oxidation Reaction and CH₄ Sequential Dissociation. Journal of Physical Chemistry C, 2018, 122, 1437-1446.	1.5	3
35466	Elucidating the Vibrational Fingerprint of the Flexible Metalâ€“Organic Framework MIL-53(Al) Using a Combined Experimental/Computational Approach. Journal of Physical Chemistry C, 2018, 122, 2734-2746.	1.5	70
35467	Massless Dirac Fermions in ZrTe₂ Semimetal Grown on InAs(111) by van der Waals Epitaxy. ACS Nano, 2018, 12, 1696-1703.	7.3	82
35468	BN nanoparticle/Ag hybrids with enhanced catalytic activity: theory and experiments. Catalysis Science and Technology, 2018, 8, 1652-1662.	2.1	23
35469	The S-functionalized Ti₃C₂ Mxene as a high capacity electrode material for Na-ion batteries: a DFT study. Nanoscale, 2018, 10, 3385-3392.	2.8	139

#	Article	IF	Citations
35470	Influence of Flexibility on the Separation of Chiral Isomers in STWâ€Type Zeolite. Chemistry - A European Journal, 2018, 24, 4121-4132.	1.7	14
35471	First-principles surface interaction studies of aluminum-copper and aluminum-copper-magnesium secondary phases in aluminum alloys. Applied Surface Science, 2018, 439, 910-918.	3.1	20
35472	Electron donation mechanism of superior Cs-supported oxides for catalytic soot combustion. Chemical Engineering Journal, 2018, 337, 654-660.	6.6	39
35473	Fabrication of TiCâ€“ZrCâ€“Co composites with refined microstructure using ultrafine TiCâ€“ZrC mixture powders. Journal of Alloys and Compounds, 2018, 740, 82-87.	2.8	7
35474	Atomic scale analysis of Hf-containing precipitates in an Al-Si-Mg-Hf alloy. Journal of Alloys and Compounds, 2018, 741, 1070-1079.	2.8	4
35475	First principles study of the elastic properties of magnesium and iron based bio-resorbable alloys. Materials Science and Engineering B: Solid-State Materials for Advanced Technology, 2018, 230, 20-23.	1.7	9
35476	Few-layer Tellurium: one-dimensional-like layered elementary semiconductor with striking physical properties. Science Bulletin, 2018, 63, 159-168.	4.3	207
35477	Mechanistic Effects of Water on the Fe-Catalyzed Hydrodeoxygenation of Phenol. The Role of BrÃ¸nsted Acid Sites. ACS Catalysis, 2018, 8, 2200-2208.	5.5	50
35478	Weakly perturbative imaging of interfacial water with submolecular resolution by atomic force microscopy. Nature Communications, 2018, 9, 122.	5.8	105
35479	Three-component fermions with surface Fermi arcs in tungsten carbide. Nature Physics, 2018, 14, 349-354.	6.5	109
35480	The importance of grand-canonical quantum mechanical methods to describe the effect of electrode potential on the stability of intermediates involved in both electrochemical CO₂ reduction and hydrogen evolution. Physical Chemistry Chemical Physics, 2018, 20, 2549-2557.	1.3	53
35481	Molecular dynamics of reactions between (4,0) zigzag carbon nanotube and hydrogen peroxide under extreme conditions. Molecular Physics, 2018, 116, 708-716.	0.8	4
35482	Mechanism of fast lattice diffusion of hydrogen in palladium: Interplay of quantum fluctuations and lattice strain. Physical Review B, 2018, 97, .	1.1	30
35483	Volkov basis for simulation of interaction of strong laser pulses and solids. Physical Review B, 2018, 97, .	1.1	9
35484	Structural distortions in monolayers of binary semiconductors. Physical Review B, 2018, 97, .	1.1	6
35485	Large valley splitting in monolayer <mml:math xmlns:mml="http://www.w3.org/1998/Math/MathML"><mml:msub><mml:mi mathvariant="bold">WS</mml:mi><mml:mn mathvariant="bold">2</mml:mn></mml:msub></mml:math> by proximity coupling to an insulating antiferromagnetic substrate. Physical Review B, 2018, 97, .	1.1	134
35486	Dangling bond defects in SiC: An ab initio study. Physical Review B, 2018, 97, .	1.1	9
35487	Material Discovery and Design Principles for Stable, High Activity Perovskite Cathodes for Solid Oxide Fuel Cells. Advanced Energy Materials, 2018, 8, 1702708.	10.2	125

#	Article	IF	Citations
35488	Highly Stable, New, Organicâ€Inorganic Perovskite (CH₃NH₃)₂PdBr₄: Synthesis, Structure, and Physical Properties. Chemistry - A European Journal, 2018, 24, 4991-4998.	1.7	25
35489	Ultrathin Bismuth Nanosheets as a Highly Efficient CO₂ Reduction Electrocatalyst. ChemSusChem, 2018, 11, 848-853.	3.6	116
35490	Origins and dissociation of pyramidal <cÂ+Âa> dislocations in magnesium and its alloys. Acta Materialia, 2018, 146, 265-272.	3.8	82
35491	Phase stability and transformation in a light-weight high-entropy alloy. Acta Materialia, 2018, 146, 280-293.	3.8	131
35492	Core structure and solute strengthening of second-order pyramidal <mml:math xmlns:mml="http://www.w3.org/1998/Math/MathML" altimg="si1.gif" overflow="scroll"><mml:mrow><mml:mo>â€ˆ</mml:mo><mml:mi>c</mml:mi><mml:mo>+</mml:mo><mml:mi>a</mml:mi><mml:mo> dislocations in Mg-Y alloys. Acta Materialia, 2018, 147, 1-9.	3.8	42
35493	Significant band gap induced by uniaxial strain in graphene/blue phosphorene bilayer. Carbon, 2018, 130, 120-126.	5.4	31
35494	Transparency enhancement for SrVO3 by SrTiO3 mixing: A first-principles study. Computational Materials Science, 2018, 144, 139-146.	1.4	13
35495	Generalized stacking fault energies and ideal strengths of MC systems (MÂ=ÂTi, Zr, Hf) doped with Si/Al using first principles calculations. Journal of Alloys and Compounds, 2018, 739, 431-438.	2.8	14
35496	AuPb₂I₇: A Narrow Bandgap Au³⁺ Iodide Semiconductor. Inorganic Chemistry, 2018, 57, 804-810.	1.9	3
35497	Nature of Cu Active Centers in Cu-SSZ-13 and Their Responses to SO₂ Exposure. ACS Catalysis, 2018, 8, 1325-1337.	5.5	172
35498	MXenes/graphene heterostructures for Li battery applications: a first principles study. Journal of Materials Chemistry A, 2018, 6, 2337-2345.	5.2	173
35499	On the H₂ interactions with transition metal adatoms supported on graphene: a systematic density functional study. Physical Chemistry Chemical Physics, 2018, 20, 3819-3830.	1.3	22
35500	Metalâ€“Organic Frameworkâ€Derived ZnO/ZnS Heteronanostructures for Efficient Visibleâ€Lightâ€Driven Photocatalytic Hydrogen Production. Advanced Science, 2018, 5, 1700590.	5.6	169
35501	Combining nitrogen substitutional defects and oxygen intercalation to control the graphene corrugation and doping level. Carbon, 2018, 130, 362-368.	5.4	8
35502	Electronic structure of transitional metal doped two dimensional 1T-TaS2: A first-principles study. Journal of Alloys and Compounds, 2018, 739, 723-728.	2.8	18
35503	Efficiently enhanced photoluminescence in Eu3+-doped Lu2(MoO4)3 by Gd3+ substituting. Materials Research Bulletin, 2018, 100, 97-101.	2.7	27
35504	Tunable Catalytic Performance of Single Pt Atom on Doped Graphene in Direct Dehydrogenation of Propane by Rational Doping: A Density Functional Theory Study. Journal of Physical Chemistry C, 2018, 122, 1570-1576.	1.5	52
35505	Comparison of the Performance of van der Waals Dispersion Functionals in the Description of Water and Ethanol on Transition Metal Surfaces. Journal of Physical Chemistry C, 2018, 122, 1577-1588.	1.5	36

#	Article	IF	Citations
35506	Modeling Polaron-Coupled Li Cation Diffusion in V₂O₅ Cathode Material. Journal of Physical Chemistry C, 2018, 122, 150-157.	1.5	26
35507	Adsorption and Structure of Chiral Epoxides on Pd(111): Propylene Oxide and Glycidol. Journal of Physical Chemistry C, 2018, 122, 1215-1222.	1.5	1
35508	Self-Supported Ternary Niâ€“Sâ€“Se Nanorod Arrays as Highly Active Electrocatalyst for Hydrogen Generation in Both Acidic and Basic Media: Experimental Investigation and DFT Calculation. ACS Applied Materials & Interfaces, 2018, 10, 2430-2441.	4.0	83
35509	Active Site Identification and Modification of Electronic States by Atomic-Scale Doping To Enhance Oxide Catalyst Innovation. ACS Catalysis, 2018, 8, 1399-1404.	5.5	42
35510	Effect of n-Butanol Cofeeding on the Methanol to Aromatics Conversion over Ga-Modified Nano H-ZSM-5 and Its Mechanistic Interpretation. ACS Catalysis, 2018, 8, 1352-1362.	5.5	88
35511	Epitaxial Synthesis of Molybdenum Carbide and Formation of a Mo₂C/MoS₂ Hybrid Structure via Chemical Conversion of Molybdenum Disulfide. ACS Nano, 2018, 12, 338-346.	7.3	148
35512	Anisotropic Ordering in 1Tâ€² Molybdenum and Tungsten Ditelluride Layers Alloyed with Sulfur and Selenium. ACS Nano, 2018, 12, 894-901.	7.3	52
35513	Hydrophobic CuO Nanosheets Functionalized with Organic Adsorbates. Journal of the American Chemical Society, 2018, 140, 1824-1833.	6.6	59
35514	Defects controlled hole doping and multivalley transport in SnSe single crystals. Nature Communications, 2018, 9, 47.	5.8	95
35515	Theoretical investigations on the unsymmetrical effect of Î²-link Znâ€“porphyrin sensitizers on the performance for dye-sensitized solar cells. Physical Chemistry Chemical Physics, 2018, 20, 3741-3751.	1.3	24
35516	Predicted detonation properties at the Chapmanâ€“Jouguet state for proposed energetic materials (MTO) Tj ETQq0 0 0 rgBT /Overlock 1 Chemical Physics, 2018, 20, 3953-3969.	1.3	21
35517	Novel titanium nitride halide TiNX (X = F, Cl, Br) monolayers: potential materials for highly efficient excitonic solar cells. Journal of Materials Chemistry A, 2018, 6, 2073-2080.	5.2	75
35518	First-principles simulation of local response in transition metal dichalcogenides under electron irradiation. Nanoscale, 2018, 10, 2388-2397.	2.8	34
35519	Tuning transport performance in two-dimensional metal-organic framework semiconductors: Role of the metal d band. Applied Physics Letters, 2018, 112, .	1.5	53
35520	Assessing the performance of the Tranâ€“Blaha modified Beckeâ€“Johnson exchange potential for optical constants of semiconductors in the ultravioletâ€“visible light region. Journal of Applied Physics, 2018, 123, .	1.1	21
35521	Abiotic synthesis of purine and pyrimidine ribonucleosides in aqueous microdroplets. Proceedings of the National Academy of Sciences of the United States of America, 2018, 115, 36-40.	3.3	98
35522	A density functional theory parameterised neural network model of zirconia. Molecular Simulation, 2018, 44, 623-630.	0.9	20
35523	Collective-Goldstone-mode-induced ultralow lattice thermal conductivity in Sn-filled skutterudite <mml:math xmlns:mml="http://www.w3.org/1998/Math/MathML"><mml:mrow><mml:msub><mml:mi>SnFe</mml:mi><mml:mn>4</mml:mn></ Physical Review B, 2018, 97, .	1.1	11

#	Article	IF	Citations
35524	Enhanced Stability of Black Phosphorus Fieldâ€Effect Transistors via Hydrogen Treatment. Advanced Electronic Materials, 2018, 4, 1700455.	2.6	19
35525	Improved Photoactivity of Pyroxene Silicates by Cation Substitutions. ChemPhysChem, 2018, 19, 943-953.	1.0	2
35526	Exotic ferromagnetism in the two-dimensional quantum material C3N. Frontiers of Physics, 2018, 13, 1.	2.4	9
35527	Stability of the Fe12O12 cluster. Nano Research, 2018, 11, 3574-3581.	5.8	18
35528	Formic acid decomposition on Pt1/Cu (111) single platinum atom catalyst: Insights from DFT calculations and energetic span model analysis. Applied Surface Science, 2018, 436, 631-638.	3.1	30
35529	The electronic structure and room temperature ferromagnetism in non-magnetic element X (Xâ€¯=â€¯Al, Mg) Tj ETQq1 1 0.784314 rg BT 102-108.	1.4	8
35530	Schottky barrier tuning of the graphene/SnS2 van der Waals heterostructures through electric field. Solid State Communications, 2018, 271, 56-61.	0.9	18
35531	Systematic Doping of Cobalt into Layered Manganese Oxide Sheets Substantially Enhances Water Oxidation Catalysis. Inorganic Chemistry, 2018, 57, 557-564.	1.9	43
35532	First-Principles Computational Screening of Highly Active Pyrites Catalysts for Hydrogen Evolution Reaction through a Universal Relation with a Thermodynamic Variable. Journal of Physical Chemistry C, 2018, 122, 2107-2112.	1.5	18
35533	3R TaS₂ Surpasses the Corresponding 1T and 2H Phases for the Hydrogen Evolution Reaction. Journal of Physical Chemistry C, 2018, 122, 2382-2390.	1.5	38
35534	Charge Balance Controls the (100) Surface Structure of the Ba8Au5.25Ge40.75 Clathrate. Journal of Physical Chemistry C, 2018, 122, 2215-2220.	1.5	6
35535	Constructing High-Dimensional Neural Network Potential Energy Surfaces for Gasâ€“Surface Scattering and Reactions. Journal of Physical Chemistry C, 2018, 122, 1761-1769.	1.5	78
35536	Anchoring of Iron Oxyhydroxide Clusters at H and L Ferritin Subunits. ACS Biomaterials Science and Engineering, 2018, 4, 483-490.	2.6	5
35537	Momentum-resolved observations of the phonon instability driving geometric improper ferroelectricity in yttrium manganite. Nature Communications, 2018, 9, 15.	5.8	30
35538	Tailoring electronic properties of multilayer phosphorene by siliconization. Physical Chemistry Chemical Physics, 2018, 20, 2075-2083.	1.3	25
35539	Effects of adatom and gas molecule adsorption on the physical properties of tellurene: a first principles investigation. Physical Chemistry Chemical Physics, 2018, 20, 4058-4066.	1.3	87
35540	Role of non-metallic atoms in enhancing the catalytic activity of nickel-based compounds for hydrogen evolution reaction. Chemical Science, 2018, 9, 1822-1830.	3.7	46
35541	A Janus MoSSe monolayer: a potential wide solar-spectrum water-splitting photocatalyst with a low carrier recombination rate. Journal of Materials Chemistry A, 2018, 6, 2295-2301.	5.2	387

#	Article	IF	Citations
35542	Atomic resolution on the (111)B surface of mercury cadmium telluride by scanning tunneling microscopy. Physical Review B, 2018, 97, .	1.1	2
35543	Electrical tuning of spin splitting in Bi-doped ZnO nanowires. Physical Review B, 2018, 97, .	1.1	7
35544	Residual Li Reactive Coating with Co₃O₄for Superior Electrochemical Properties of LiNi_{0.91}Co_{0.06}Mn_{0.03}O₂Cathode Material. Journal of the Electrochemical Society, 2018, 165, A79-A85.	1.3	58
35545	A mild one-step method for enhancing optical absorption of amine-functionalized metal-organic frameworks. Applied Catalysis B: Environmental, 2018, 227, 190-197.	10.8	72
35546	Layered oxides-LiNi1/3Co1/3Mn1/3O2 as anode electrode for symmetric rechargeable lithium-ion batteries. Journal of Power Sources, 2018, 378, 516-521.	4.0	24
35547	Improving electron transport in the hybrid perovskite solar cells using CaMnO3-based buffer layer. Nano Energy, 2018, 45, 287-297.	8.2	19
35548	Pressure-induced structural phase transformation and superconducting properties of titanium mononitride. Solid State Communications, 2018, 271, 16-20.	0.9	3
35549	Optical Properties of Ce-Doped Li₄SrCa(SiO₄)₂: A Combined Experimental and Theoretical Study. Inorganic Chemistry, 2018, 57, 1116-1124.	1.9	26
35550	Oxidation Protection with Amorphous Surface Oxides: Thermodynamic Insights from Ab Initio Simulations on Aluminum. ACS Applied Materials & Interfaces, 2018, 10, 3039-3045.	4.0	50
35551	Enhancing Thermoelectric Performances of Bismuth Antimony Telluride via Synergistic Combination of Multiscale Structuring and Band Alignment by FeTe₂ Incorporation. ACS Applied Materials & Interfaces, 2018, 10, 3689-3698.	4.0	66
35552	Effect of charging on silicene with alkali metal atom adsorption. Journal Physics D: Applied Physics, 2018, 51, 075302.	1.3	3
35553	Double-Weyl Phonons in Transition-Metal Monosilicides. Physical Review Letters, 2018, 120, 016401.	2.9	240
35554	1D SbSeI, SbSI, and SbSBr With High Stability and Novel Properties for Microelectronic, Optoelectronic, and Thermoelectric Applications. Advanced Theory and Simulations, 2018, 1, 1700005.	1.3	65
35555	Possible Origin of Ferromagnetism in Transition Metal Doped Zirconia. Journal of Superconductivity and Novel Magnetism, 2018, 31, 2559-2565.	0.8	7
35556	Oxygen vacancy engineering of Bi2O3/Bi2O2CO3 heterojunctions: Implications of the interfacial charge transfer, NO adsorption and removal. Applied Catalysis B: Environmental, 2018, 231, 357-367.	10.8	203
35557	Oxygen vacancies driven size-dependent d0 room temperature ferromagnetism in well-dispersed dopant-free ZnO nanoparticles and density functional theory calculation. Journal of Alloys and Compounds, 2018, 739, 1080-1088.	2.8	54
35558	First-principles study on the phase transitions, crystal stabilities and thermodynamic properties of TiN under high pressure. Physics Letters, Section A: General, Atomic and Solid State Physics, 2018, 382, 656-661.	0.9	7
35559	The effects of the impurity distribution on the electrical and optical properties of Cr2+:ZnSe nanowires: First-principles study. Results in Physics, 2018, 8, 628-632.	2.0	10

#	Article	IF	Citations
35560	Lateral and Vertical Heterostructures of Transition Metal Dichalcogenides. Journal of Physical Chemistry C, 2018, 122, 1547-1555.	1.5	26
35561	Calculations of CO Oxidation over a Au/TiO₂ Catalyst: A Study of Active Sites, Catalyst Deactivation, and Moisture Effects. ACS Catalysis, 2018, 8, 1376-1383.	5.5	64
35562	Oxygen vacancy and doping atom effect on electronic structure and optical properties of Cd₂SnO₄. RSC Advances, 2018, 8, 640-646.	1.7	20
35563	Coexistence of open and closed type nodal line topological semimetals in two dimensional B₂C. Journal of Materials Chemistry C, 2018, 6, 1206-1214.	2.7	68
35564	A DFT study of the adsorption of short peptides on Mg and Mg-based alloy surfaces. Physical Chemistry Chemical Physics, 2018, 20, 3602-3607.	1.3	16
35565	Methane dissociation on the steps and terraces of Pt(211) resolved by quantum state and impact site. Journal of Chemical Physics, 2018, 148, 014701.	1.2	50
35566	Enhancing magnetic properties in <mml:math xmlns:mml="http://www.w3.org/1998/Math/MathML"><mml:mrow><mml:msub><mml:mi>Mn</mml:mi><mml:mn>3</mml:mn></mml: thin films by doping. Physical Review B, 2018, 97, .	1.3	4
35567	A Combined Density Functional Theory and Monte Carlo Investigation of the Competitive Adsorption of Atomic Oxygen and Chlorine to the Ni (111) Surface. Journal of the Electrochemical Society, 2018, 165, C302-C309.	1.3	10
35568	Controllable Phase Stabilities in Transition Metal Dichalcogenides through Curvature Engineering: First-Principles Calculations and Continuum Prediction. Advanced Theory and Simulations, 2018, 1, 1800003.	1.3	5
35569	2â€Electron Reduction of CO₂ by Graphene Supported Ru Complexes â€“ on the Role of Electron Donation.. ChemElectroChem, 2018, 5, 2105-2112.	1.7	10
35570	The rise of twoâ€dimensional van der Waals ferroelectrics. Wiley Interdisciplinary Reviews: Computational Molecular Science, 2018, 8, e1365.	6.2	127
35571	Photoinduced pure spin-current in triangulene-based nano-devices. Carbon, 2018, 137, 1-5.	5.4	37
35572	Intercalation and Conversion Reactions of Nanosized Î²-MnO₂ Cathode in the Secondary Zn/MnO₂ Alkaline Battery. Journal of Physical Chemistry C, 2018, 122, 11177-11185.	1.5	56
35573	Identification of the Active and Selective Sites over a Single Pt Atom-Alloyed Cu Catalyst for the Hydrogenation of 1,3-Butadiene: A Combined DFT and Microkinetic Modeling Study. Journal of Physical Chemistry C, 2018, 122, 10883-10891.	1.5	58
35574	Crystal Facet Effects on Nanomagnetism of Co₃O₄. ACS Applied Materials & Interfaces, 2018, 10, 19235-19247.	4.0	47
35575	Insight into Room-Temperature Catalytic Oxidation of Nitric oxide by Cr₂O₃: A DFT Study. ACS Catalysis, 2018, 8, 5415-5424.	5.5	32
35576	Insight into the structure and morphology of Run clusters on Co(111) and Co(311) surfaces. Catalysis Science and Technology, 2018, 8, 2728-2739.	2.1	7
35577	Canted antiferromagnet superimposed on a buckled kagomÃ© network in RbMn₄(PO₄)₃. Acta Crystallographica Section C, Structural Chemistry, 2018, 74, 641-649.	0.2	6

#	Article	IF	Citations
35578	Real-space and real-time observation of a plasmon-induced chemical reaction of a single molecule. Science, 2018, 360, 521-526.	6.0	224
35579	Metal-Free Half-Metallicity in B-Doped gh-C3N4 Systems. Nanoscale Research Letters, 2018, 13, 57.	3.1	23
35580	The Ideal Strengths of Superconducting MgCNi3 and CdCNi3. Journal of Superconductivity and Novel Magnetism, 2018, 31, 2355-2361.	0.8	2
35581	Effect of Coverage on Catalytic Selectivity and Activity on Metallic and Alloy Catalysts; Vinyl Acetate Monomer Synthesis. Topics in Catalysis, 2018, 61, 722-735.	1.3	10
35582	Synthesis and thermoelectric properties of Rashba semiconductor BiTeBr with intensive texture. Rare Metals, 2018, 37, 274-281.	3.6	20
35583	Origin of the moirÃ© superlattice scale lateral force modulation of graphene on a transition metal substrate. Nanoscale, 2018, 10, 10576-10583.	2.8	14
35584	Thermodynamics of inversion-domain boundaries in aluminum nitride: Interplay between interface energy and electric dipole potential energy. Journal of Applied Physics, 2018, 123, .	1.1	3
35585	Electrical and material properties of hydrothermally grown single crystal (111) UO2. European Physical Journal B, 2018, 91, 1.	0.6	6
35586	Hydrogen diffusion in titanium dihydrides from first principles. Acta Materialia, 2018, 153, 250-256.	3.8	15
35587	Helium behavior in different oxides inside ODS steels: A comparative ab initio study. Journal of Nuclear Materials, 2018, 507, 101-111.	1.3	14
35588	First-principles study of mechanical and magnetic properties of transition metal (M) nitrides in the cubic M4N structure. Journal of Physics and Chemistry of Solids, 2018, 120, 197-206.	1.9	41
35589	Synthesis, characterization, DFT calculations and antimicrobial studies of cadmium(II) sulfate complexes of thioureas and 2-mercaptopyridine; X-ray structures of polymeric diaqua(N,Nâ€²-dimethylthiourea) sulfatocadmium(II) and bis(2-mercaptopyridine)sulfatocadmium(II). Polyhedron, 2018, 149, 126-133.	1.0	3
35590	Universal Scaling Relationship To Screen an Efficient Metallic Adsorbent for Adsorptive Removal of Iodine Gas under Humid Conditions: First-Principles Study. Journal of Physical Chemistry C, 2018, 122, 11799-11806.	1.5	7
35591	Thermal Conductivity of Solids from First-Principles Molecular Dynamics Calculations. Journal of Physical Chemistry C, 2018, 122, 10682-10690.	1.5	16
35592	Reaction Pathways for Solvent Decomposition on Magnesium Anodes. Journal of Physical Chemistry C, 2018, 122, 10714-10724.	1.5	28
35593	Effect of Cyano Substitution on the Step-Edge Adsorption of Copper Phthalocyanine on Au(111). Journal of Physical Chemistry C, 2018, 122, 11848-11854.	1.5	7
35594	Structure and Dynamic Behavior of the Naâ€“Crown Ether Complex in the Graphite Layers Studied by DFT and ¹H NMR. Journal of Physical Chemistry C, 2018, 122, 10963-10970.	1.5	12
35595	Buildup of the Solid Electrolyte Interphase on Lithium-Metal Anodes: Reactive Molecular Dynamics Study. Journal of Physical Chemistry C, 2018, 122, 10783-10791.	1.5	44

#	Article	IF	Citations
35596	Magic Clusters of MoS₂ by Edge S₂ Interdimer Spacing Modulation. Journal of Physical Chemistry Letters, 2018, 9, 2697-2702.	2.1	2
35597	Polyelectrolyte-Assisted Oxygen Vacancies: A New Route to Defect Engineering in Molybdenum Oxide. Langmuir, 2018, 34, 6296-6306.	1.6	35
35598	Anomalous diffusion of water molecules at grain boundaries in ice I_h. Physical Chemistry Chemical Physics, 2018, 20, 13944-13951.	1.3	15
35599	Shock compression behavior of a mixture of cubic and hexagonal boron nitride. Journal of Applied Physics, 2018, 123, .	1.1	9
35600	Inversion symmetry breaking induced triply degenerate points in orderly arranged PtSeTe family materials. Journal of Physics Condensed Matter, 2018, 30, 245502.	0.7	5
35601	A High-Temperature Î² -Phase NaMnO ₂ Stabilized by Cu Doping and Its Na Storage Properties. Chinese Physics Letters, 2018, 35, 048801.	1.3	18
35602	Theoretical approach to embed nanocrystallites into a bulk crystalline matrix and the embedding influence on the electronic band structure and optical properties of the resulting heterostructures. Journal of Physics Condensed Matter, 2018, 30, 245301.	0.7	0
35603	Atomic-scale defects and electronic properties of a transferred synthesized MoS₂ monolayer. Nanotechnology, 2018, 29, 305703.	1.3	22
35604	Evidence for a pressure-induced spin transition in olivine-type LiFePO4 triphylite. Physical Review B, 2018, 97, .	1.1	6
35605	Theoretical prediction of a two-dimensional intrinsic double-metal ferromagnetic semiconductor MnCoO4. Applied Surface Science, 2018, 450, 422-428.	3.1	3
35606	Room temperature ferromagnetism in naphthalene. Carbon, 2018, 136, 125-129.	5.4	10
35607	La doping inhibits stress production at the grain boundaries in Niâ€“WC coating. Journal of Alloys and Compounds, 2018, 753, 688-694.	2.8	11
35608	Role of Co in formation of Ni-Ti clusters in maraging stainless steel. Journal of Materials Science and Technology, 2018, 34, 1671-1675.	5.6	26
35609	Ultralow Thermal Conductivity in Diamond-Like Semiconductors: Selective Scattering of Phonons from Antisite Defects. Chemistry of Materials, 2018, 30, 3395-3409.	3.2	28
35610	Surface Properties of Fluorite in Presence of Water: An Atomistic Investigation. Journal of Physical Chemistry B, 2018, 122, 6829-6836.	1.2	39
35611	Ptâ€“Ni Subsurface Alloy Catalysts: An Improved Performance toward CH₄ Dissociation. Journal of Physical Chemistry C, 2018, 122, 10857-10870.	1.5	37
35612	Interlocking Molecular Gear Chains Built on Surfaces. Journal of Physical Chemistry Letters, 2018, 9, 2611-2619.	2.1	17
35613	Quantitative Attachment of Bimetal Combinations of Transition-Metal Ions to the Surface of TiO₂ Nanorods. Langmuir, 2018, 34, 5422-5434.	1.6	5

#	Article	IF	Citations
35614	Crystal Orientation-Dependent Reactivity of Oxide Surfaces in Contact with Lithium Metal. ACS Applied Materials & Interfaces, 2018, 10, 17471-17479.	4.0	9
35615	Specific Metalâ€“Support Interactions between Nanoparticle Layers for Catalysts with Enhanced Methanol Oxidation Activity. ACS Catalysis, 2018, 8, 5391-5398.	5.5	63
35616	Combining CO₂ Reduction with Ethane Oxidative Dehydrogenation by Oxygen-Modification of Molybdenum Carbide. ACS Catalysis, 2018, 8, 5374-5381.	5.5	58
35617	The Principal Hugoniot of Forsterite to 950 GPa. Geophysical Research Letters, 2018, 45, 3865-3872.	1.5	31
35618	Half-metallicity in a honeycombâ€“kagome-lattice Mg₃C₂ monolayer with carrier doping. Physical Chemistry Chemical Physics, 2018, 20, 14166-14173.	1.3	19
35619	Feâ€“Si networks and charge/discharge-induced phase transitions in Li₂FeSiO₄ cathode materials. Physical Chemistry Chemical Physics, 2018, 20, 14557-14563.	1.3	12
35620	Stabilization of planar tetra-coordinate silicon in a 2D-layered extended system and design of a high-capacity anode material for Li-ion batteries. Nanoscale, 2018, 10, 10450-10458.	2.8	41
35621	Alkaline earth metal oxide nanocluster modification of rutile TiO₂ (110) promotes water activation and CO₂ chemisorption. Journal of Materials Chemistry A, 2018, 6, 9451-9466.	5.2	24
35622	Thermoelectric transport properties of rock-salt SnSe: first-principles investigation. Journal of Materials Chemistry C, 2018, 6, 12016-12022.	2.7	43
35623	Decomposition of methanol-d₄ on Auâ€“Rh bimetallic nanoclusters on a thin film of Al₂O₃/NiAl(100). Physical Chemistry Chemical Physics, 2018, 20, 11260-11272.	1.3	6
35624	Quasi-self-trapped Frenkel-exciton near-UV luminescence with large Stokes shift in wide-bandgap Cs4PbCl6 nanocrystals. Applied Physics Letters, 2018, 112, .	1.5	24
35625	In pursuit of barrierless transition metal dichalcogenides lateral heterojunctions. Nanotechnology, 2018, 29, 295202.	1.3	6
35626	Band-Gap Engineering in ZnO Thin Films: A Combined Experimental and Theoretical Study. Physical Review Applied, 2018, 9, .	1.5	25
35627	Using first-principles calculations to screen for fragile magnetism: Case study of <mml:math xmlns:mml="http://www.w3.org/1998/Math/MathML"><mml:mrow><mml:msub><mml:mi mathvariant="normal">LaCrGe</mml:mi><mml:mn>3</mml:mn></mml:msub></mml:mrow></mml:math> and <mml:math xmlns:mml="http://www.w3.org/1998/Math/MathML"><mml:mrow><mml:msub><mml:mi mathvariant="normal">LaCrSb</mml:mi><mml:mn>3</mml:mn></mml:msub></mml:mrow></mml:math>. Physical Review B, 2018, 97, .	1.1	6
35628	First-principle calculations of electronic structures and polar properties of (Î°,Îµ)-Ga₂O₃. Applied Physics Express, 2018, 11, 061101.	1.1	53
35629	Development of Fe-C interatomic potential for carbon impurities in Î±-iron. Computational Materials Science, 2018, 150, 510-516.	1.4	13
35630	Quantum chemical calculations to determine partitioning coefficients for HgCl2 on iron-oxide aerosols. Science of the Total Environment, 2018, 636, 580-587.	3.9	9
35631	Over-Stoichiometry in Heavy Metal Oxides: The Case of Iono-Covalent Tantalum Trioxides. Inorganic Chemistry, 2018, 57, 6057-6064.	1.9	6

#	Article	IF	Citations
35632	Oxygen Vacancy-Modified B-/N-Codoped ZnGa₂O₄ Nanospheres with Enhanced Photocatalytic Hydrogen Evolution Performance in the Absence of a Pt Cocatalyst. Journal of Physical Chemistry C, 2018, 122, 10737-10748.	1.5	19
35633	Transferable Self-Consistent Charge Density Functional Tight-Binding Parameters for Liâ€“Metal and Li-Ions in Inorganic Compounds and Organic Solvents. Journal of Physical Chemistry C, 2018, 122, 10755-10764.	1.5	22
35634	Monitoring the Doping and Diffusion Characteristics of Mn Dopants in Cesium Lead Halide Perovskites. Journal of Physical Chemistry C, 2018, 122, 11543-11549.	1.5	15
35635	Metastable States in Pressurized Bulk and Mesoporous Germanium. Journal of Physical Chemistry C, 2018, 122, 10929-10938.	1.5	6
35636	Interfacial Engineered Polyaniline/Sulfur-Doped TiO₂ Nanotube Arrays for Ultralong Cycle Lifetime Fiber-Shaped, Solid-State Supercapacitors. ACS Applied Materials & Interfaces, 2018, 10, 18390-18399.	4.0	56
35637	Double Indirect Interlayer Exciton in a MoSe₂/WSe₂ van der Waals Heterostructure. ACS Nano, 2018, 12, 4719-4726.	7.3	160
35638	Pressure-induced strong ferroelectric polarization in tetra-phase perovskite CsPbBr₃. Physical Chemistry Chemical Physics, 2018, 20, 14718-14724.	1.3	71
35639	Efficient nitrogen fixation to ammonia on MXenes. Physical Chemistry Chemical Physics, 2018, 20, 14504-14512.	1.3	82
35640	First-principles study of lattice thermal conductivity in ZrTe5 and HfTe5. Journal of Applied Physics, 2018, 123, .	1.1	19
35641	Functionalization of group-14 two-dimensional materials. Journal of Physics Condensed Matter, 2018, 30, 233003.	0.7	23
35642	Directional Forces by Momentumless Excitation and Order-to-Order Transition in Peierls-Distorted Solids: The Case of GeTe. Physical Review Letters, 2018, 120, 185701.	2.9	38
35643	AFLOW-SYM: platform for the complete, automatic and self-consistent symmetry analysis of crystals. Acta Crystallographica Section A: Foundations and Advances, 2018, 74, 184-203.	0.0	44
35644	Shearâ€induced brittle failure of titanium carbide from quantum mechanics simulations. Journal of the American Ceramic Society, 2018, 101, 4184-4192.	1.9	7
35645	Tunable Ultraviolet Photorefractive Effect in LiNbO₃/TiO₂â€X (Xâ€‰=â€‰Pd or N): Theoretically Prediction and Experimental Validation. Physica Status Solidi (A) Applications and Materials Science, 2018, 215, 1700646.	0.8	1
35646	Co on the H-passivated Si(001) surface: Density-functional calculations. Physica B: Condensed Matter, 2018, 542, 44-50.	1.3	1
35647	Incorporation Modes of Iodate in Calcite. Environmental Science & Technology, 2018, 52, 5902-5910.	4.6	31
35648	Water Oxidation Catalysis via Size-Selected Iridium Clusters. Journal of Physical Chemistry C, 2018, 122, 9965-9972.	1.5	20
35649	Stability, Electronic and Optical Properties of M₄Mâ€²₂X₄ (M = Ga or In, Mâ€² = Si,) Tj ETQq1 1 0.784314 rgB 10360-10364.	1.5	7

#	Article	IF	Citations
35650	Efficient Green Emission from Wurtzite Al_xIn_{1â€“x}P Nanowires. Nano Letters, 2018, 18, 3543-3549.	4.5	16
35651	Ultrathin Bismuth Film on 1T-TaS₂: Structural Transition and Charge-Density-Wave Proximity Effect. Nano Letters, 2018, 18, 3235-3240.	4.5	28
35652	Orbital Redistribution Enhanced Perpendicular Magnetic Anisotropy of CoFe₃N Nitrides by Adsorbing Organic Molecules. ACS Applied Materials & Interfaces, 2018, 10, 16674-16680.	4.0	17
35653	Bioinspired Interfacial Chelating-like Reinforcement Strategy toward Mechanically Enhanced Lamellar Materials. ACS Nano, 2018, 12, 4269-4279.	7.3	40
35654	Auto-optimizing Hydrogen Evolution Catalytic Activity of ReS₂ through Intrinsic Charge Engineering. ACS Nano, 2018, 12, 4486-4493.	7.3	111
35655	Reaction Mechanism and Kinetics for Ammonia Synthesis on the Fe(111) Surface. Journal of the American Chemical Society, 2018, 140, 6288-6297.	6.6	126
35656	Nanocrystalline Iron Monosulfides Near Stoichiometry. Scientific Reports, 2018, 8, 6591.	1.6	11
35657	Superconductivity in two-dimensional phosphorus carbide (Î²₀-PC). Physical Chemistry Chemical Physics, 2018, 20, 12362-12367.	1.3	40
35658	Naturally abundant high-performance rechargeable aluminum/iodine batteries based on conversion reaction chemistry. Journal of Materials Chemistry A, 2018, 6, 9984-9996.	5.2	58
35659	Physics-informed machine learning for inorganic scintillator discovery. Journal of Chemical Physics, 2018, 148, 241729.	1.2	28
35660	Passivation of carbon dimer defects in amorphous SiO ₂ /4Hâ€“SiC (0001) interface: A first-principles study. Chinese Physics B, 2018, 27, 047103.	0.7	11
35661	Generalization of soft phonon modes. Physical Review B, 2018, 97, .	1.1	7
35662	Magnetic properties of Co-doped Nb clusters. Physical Review B, 2018, 97, .	1.1	6
35663	High-pressure phase transitions of nitinol NiTi to a semiconductor with an unusual topological structure. Physical Review B, 2018, 97, .	1.1	6
35664	Structural and spectroscopic properties of the polar antiferromagnet <mml:math xmlns:mml="http://www.w3.org/1998/Math/MathML"><mml:mrow><mml:mi mathvariant="normal">N</mml:mi><mml:msub><mml:mi mathvariant="normal">i</mml:mi><mml:mn>2</mml:mn></mml:msub><mml:mi>MnTe</mml:mi><mml:msub><mml:mi mathvariant="normal">O</mml:mi><mml:mn>6</mml:mn></mml:msub></mml:mrow></mml:math>. Physical Review B, 2018, 97, .	1.1	11
35665	Quasiparticle interference of Fermi arc states in the type-II Weyl semimetal candidate <mml:math xmlns:mml="http://www.w3.org/1998/Math/MathML"><mml:mrow><mml:mi>WT</mml:mi><mml:msub><mml:mi mathvariant="normal">e</mml:mi><mml:mn>2</mml:mn></mml:msub></mml:mrow></mml:math>. Physical Review B, 2018, 97, .	1.1	14
35666	Linear Hyperfine Tuning of Donor Spins in Silicon Using Hydrostatic Strain. Physical Review Letters, 2018, 120, 167701.	2.9	34
35667	Enabling Generalized Coordination Numbers to Describe Strain Effects. ChemSusChem, 2018, 11, 1824-1828.	3.6	57

#	Article	IF	Citations
35668	Exploring the work function variability and structural stability of VO2(1â€¯1â€¯0) surface upon noble metal (Ag, Au, Pt) adsorption and incorporation. Applied Surface Science, 2018, 450, 318-327.	3.1	14
35669	Theoretical investigation of dephosphorylation of phosphate monoesters on CeO2(111). Catalysis Today, 2018, 312, 141-148.	2.2	16
35670	Computational predictive design for metal-decorated-graphene size-specific subnanometer to nanometer ORR catalysts. Catalysis Today, 2018, 312, 105-117.	2.2	13
35671	Fabrication and theoretical investigation of MoS2-Co3S4 hybrid hollow structure as electrode material for lithium-ion batteries and supercapacitors. Chemical Engineering Journal, 2018, 347, 607-617.	6.6	81
35672	Modeling pseudo-elastic behavior in small-scale ThCr2Si2-type crystals. Computational Materials Science, 2018, 150, 86-95.	1.4	4
35673	Energy storage properties of selectively functionalized Cr-group MXenes. Computational Materials Science, 2018, 150, 236-243.	1.4	18
35674	DFT study of M-doped (Mâ€=â€P, As, Bi) VO2 for thermochromic energy-saving materials. Computational Materials Science, 2018, 150, 337-345.	1.4	12
35675	Î³-Graphyne analogues based on As and Sb elements. Computational Materials Science, 2018, 150, 325-328.	1.4	0
35676	Computational study of the electronic, optical and photocatalytic properties of single-layer hexagonal zinc chalcogenides. Computational Materials Science, 2018, 150, 432-438.	1.4	24
35677	On real-space Density Functional Theory for non-orthogonal crystal systems: Kronecker product formulation of the kinetic energy operator. Chemical Physics Letters, 2018, 700, 156-162.	1.2	9
35678	A new orthorhombic ground-state phase and mechanical strengths of ternary B2CO compound. Chemical Physics Letters, 2018, 701, 86-92.	1.2	10
35679	The influence of nitrogen pressure on formation of niobium nitride by thermal processing. Journal of Alloys and Compounds, 2018, 746, 370-376.	2.8	6
35680	Self-assembled supramolecular system PDINH on TiO2 surface enhances hydrogen production. Journal of Colloid and Interface Science, 2018, 525, 136-142.	5.0	20
35681	Material-genome perspective towards tunable thermal expansion of rare-earth di-silicates. Journal of the European Ceramic Society, 2018, 38, 3547-3554.	2.8	27
35682	First principles study of the structural, electronic, and optical properties of Sn2+-doped ZnOâ€“P2O5 glasses. Journal of Non-Crystalline Solids, 2018, 492, 108-114.	1.5	6
35683	Effect of anti-site point defects on the mechanical and thermodynamic properties of MgZn2, MgCu2 Laves phases: A first-principle study. Journal of Solid State Chemistry, 2018, 263, 18-23.	1.4	13
35684	Eu2P7X and Ba2As7X (Xâ€=â€Br, I): Chiral double-Zintl salts containing heptapnictotricyclane clusters. Journal of Solid State Chemistry, 2018, 263, 195-202.	1.4	3
35685	Nanoindentation-induced phase transformation between SiC polymorphs. Materials Letters, 2018, 220, 152-155.	1.3	5

#	Article	IF	Citations
35686	Enhancing CO2 electrolysis performance with vanadium-doped perovskite cathode in solid oxide electrolysis cell. Nano Energy, 2018, 50, 43-51.	8.2	158
35687	Precursor controlled synthesis of graphene oxide supported iron catalysts for Fischerâ€“Tropsch synthesis. Catalysis Science and Technology, 2018, 8, 2883-2893.	2.1	21
35688	Unusually low thermal conductivity of atomically thin 2D tellurium. Nanoscale, 2018, 10, 12997-13003.	2.8	141
35689	Predicting multiple Dirac-cones and ultrahigh Fermi velocity in perovskiteR3Ì„cphase LaCuO₃. Journal of Materials Chemistry C, 2018, 6, 6132-6137.	2.7	21
35690	Energy shifts in photoemission lines during the tetragonal- to cubic-phase transition in BaTiO3 single crystals and systems with CoFe2O4 and NiFe2O4 overlayers. Journal of Physics Condensed Matter, 2018, 30, 205401.	0.7	2
35691	Role of zero-point effects in stabilizing the ground state structure of bulk Fe₂P. Journal of Physics Condensed Matter, 2018, 30, 215401.	0.7	6
35692	Brightened spin-triplet interlayer excitons and optical selection rules in van der Waals heterobilayers. 2D Materials, 2018, 5, 035021.	2.0	107
35693	Theoretical Study on Magnetic Tunneling Junctions with Semiconductor Barriers CuInSe₂ and CuGaSe₂ Including a Detailed Analysis of Band-Resolved Transmittances. Journal of the Magnetics Society of Japan, 2018, 42, 37-40.	0.5	2
35694	Interpolating DFT Data for 15D Modeling of Methane Dissociation on an fcc Metal. International Journal of Chemical Kinetics, 2018, 50, 285-293.	1.0	3
35695	Thermoelectric Properties of Topological Insulators. Physica Status Solidi (B): Basic Research, 2018, 255, 1800020.	0.7	37
35696	Pointâ€Defectâ€induced Half Metal in CrCl 3 Monolayer. Physica Status Solidi - Rapid Research Letters, 2018, 12, 1800105.	1.2	14
35697	W and X Photoluminescence Centers in Crystalline Si: Chasing Candidates at Atomic Level Through Multiscale Simulations. Journal of Electronic Materials, 2018, 47, 5045-5049.	1.0	7
35698	Insights into the Sm/Zr co-doping effects on N2 selectivity and SO2 resistance of a MnOx-TiO2 catalyst for the NH3-SCR reaction. Chemical Engineering Journal, 2018, 347, 27-40.	6.6	233
35699	Thermodynamic stabilities in the Fe-Fe16C2 system: Influence of carbon-carbon interactions studied by DFT. Computational Materials Science, 2018, 150, 524-534.	1.4	6
35700	Ab initio study of ferroelectric BiAlO3 (0â€¯0â€¯0â€¯1) polar surfaces. Computational Materials Science, 2018, 150, 448-453.	1.4	9
35701	Substituting Cs for MA on the surface of MAPbI3 perovskite: A first-principles study. Computational Materials Science, 2018, 150, 411-417.	1.4	18
35702	Site preference and diffusion behaviors of H influenced by the implanted-He in 3C-Î² SiC. Journal of Alloys and Compounds, 2018, 742, 226-231.	2.8	4
35703	A first principle study of the phase stability, ion transport and substitution strategy for highly ionic conductive sodium antipervoskite as solid electrolyte for sodium ion batteries. Journal of Power Sources, 2018, 390, 61-70.	4.0	31

#	Article	IF	Citations
35704	Strain effects on structural and magnetic properties of SrIrO3/SrTiO3 superlattice. Materials Today Physics, 2018, 4, 43-49.	2.9	16
35705	Functionalization of silicon surface by thiadiazole molecule: A DFT study. Surface Science, 2018, 674, 87-93.	0.8	7
35706	Low-Temperature Hydrogen Production via Water Conversion on Pt/TiO₂. Journal of Physical Chemistry C, 2018, 122, 10956-10962.	1.5	29
35707	Interface Engineering of Monolayer MoS₂/GaN Hybrid Heterostructure: Modified Band Alignment for Photocatalytic Water Splitting Application by Nitridation Treatment. ACS Applied Materials & Interfaces, 2018, 10, 17419-17426.	4.0	214
35708	Tuning the Dynamic Interfacial Structure of Copperâ€“Ceria Catalysts by Indium Oxide during CO Oxidation. ACS Catalysis, 2018, 8, 5261-5275.	5.5	100
35709	Ultrathin WO₃Â·0.33H₂O Nanotubes for CO₂ Photoreduction to Acetate with High Selectivity. Journal of the American Chemical Society, 2018, 140, 6474-6482.	6.6	233
35710	Momentum-space indirect interlayer excitons in transition-metal dichalcogenide van der Waals heterostructures. Nature Physics, 2018, 14, 801-805.	6.5	229
35711	A universal principle for a rational design of single-atom electrocatalysts. Nature Catalysis, 2018, 1, 339-348.	16.1	1,214
35712	Electronic effects and fundamental physics studied in molecular interfaces. Chemical Communications, 2018, 54, 5508-5517.	2.2	5
35713	Tuning the adsorption and interaction of CO and O₂ on graphene-like BC₃-supported non-noble metal atoms. Physical Chemistry Chemical Physics, 2018, 20, 14040-14052.	1.3	16
35714	Lattice thermal conductivity of monolayer AsP from first-principles molecular dynamics. Physical Chemistry Chemical Physics, 2018, 20, 14024-14030.	1.3	34
35715	Half-metallicity and enhanced ferromagnetism in Li-adsorbed ultrathin chromium triiodide. Journal of Materials Chemistry C, 2018, 6, 5716-5720.	2.7	71
35716	Structural and dynamical properties of water adsorption on PtO₂(001). RSC Advances, 2018, 8, 15078-15086.	1.7	7
35717	Dynamical and electronic properties of rare-earth aluminides. AIP Conference Proceedings, 2018, , .	0.3	0
35718	Designing Hybrids of Graphene Oxide and Gold Nanoparticles for Nonlinear Optical Response. Physical Review Applied, 2018, 9, .	1.5	41
35719	Ion-ion dynamic structure factor, acoustic modes, and equation of state of two-temperature warm dense aluminum. Physical Review E, 2018, 97, 043210.	0.8	20
35720	Investigation of the GaN/Al₂O₃ Interface by First Principles Calculations. Physica Status Solidi (B): Basic Research, 2018, 255, 1700323.	0.7	14
35721	Dislocation dissociations in C11b MoSi2 and their impact on its plastic deformation. Intermetallics, 2018, 97, 34-41.	1.8	2

#	Article	IF	Citations
35722	Predicting thermoelectric performance of eco-friendly intermetallic compound p-type CaMgSi from first-principles investigation. Journal of Alloys and Compounds, 2018, 752, 85-92.	2.8	8
35723	Dipole effect on ethylene epoxidation: Influence of alkali metals and chlorine. Journal of Catalysis, 2018, 363, 18-25.	3.1	41
35724	Insight into lead-free organic-inorganic hybrid perovskites for photovoltaics and optoelectronics: A first-principles study. Organic Electronics, 2018, 59, 99-106.	1.4	123
35725	The structural, elastic, electronic and optical properties of orthorhombic FeX 2 (X=S, Se, Te). Superlattices and Microstructures, 2018, 119, 201-211.	1.4	12
35726	Microstructure and properties investigation of garnet structured Li7La3Zr2O12 as electrolyte for all-solid-state batteries. Solid State Ionics, 2018, 321, 126-134.	1.3	32
35727	Quantitative Observation of Threshold Defect Behavior in Memristive Devices with Operando X-ray Microscopy. ACS Nano, 2018, 12, 4938-4945.	7.3	12
35728	Topologically guided tuning of Zr-MOF pore structures for highly selective separation of C6 alkane isomers. Nature Communications, 2018, 9, 1745.	5.8	251
35729	Bayesian-Driven First-Principles Calculations for Accelerating Exploration of Fast Ion Conductors for Rechargeable Battery Application. Scientific Reports, 2018, 8, 5845.	1.6	77
35730	Boosting the thermoelectric performance of PbSe through dynamic doping and hierarchical phonon scattering. Energy and Environmental Science, 2018, 11, 1848-1858.	15.6	163
35731	Theoretical insight into the catalytic activities of oxygen reduction reaction on transition metalâ€“N₄ doped graphene. New Journal of Chemistry, 2018, 42, 9620-9625.	1.4	21
35732	Mechanism of phosphorus passivation of near-interface oxide traps in 4Hâ€“SiC MOS devices investigated by CCDLTS and DFT calculation. Semiconductor Science and Technology, 2018, 33, 065005.	1.0	7
35733	Electronic structure and magnetic properties of the strong-rung spin-1 ladder compound Rb3Ni2(NO3)7. Physical Review B, 2018, 97, .	1.1	4
35734	Ab initio calculations of ionic hydrocarbon compounds with heptacoordinate carbon. Journal of Molecular Modeling, 2018, 24, 116.	0.8	10
35735	Three-dimensional N- and S-codoped graphene hydrogel with in-plane pores for high performance supercapacitor. Microporous and Mesoporous Materials, 2018, 268, 260-267.	2.2	39
35736	Force Field for Water over Pt(111): Development, Assessment, and Comparison. Journal of Chemical Theory and Computation, 2018, 14, 3238-3251.	2.3	38
35737	One Oxygen Vacancy, Two Charge States: Characterization of Reduced Î±-MoO₃(010) through Theoretical Methods. Journal of Physical Chemistry Letters, 2018, 9, 2568-2573.	2.1	43
35738	First-Principle Study of the Optical Properties of Dilute-P GaN1â^'xPx Alloys. Scientific Reports, 2018, 8, 6025.	1.6	6
35739	Icosahedra clustering and short range order in Ni-Nb-Zr amorphous membranes. Scientific Reports, 2018, 8, 6084.	1.6	13

#	Article	IF	Citations
35740	Microporosity as a new property control factor in graphene-like 2D allotropes. Journal of Materials Chemistry A, 2018, 6, 10348-10353.	5.2	18
35741	Properties and Potential Applications of Quasi-Two-Dimensional Molybdenum Disulfide for Nanoelectronic Elements. Inorganic Materials: Applied Research, 2018, 9, 175-183.	0.1	4
35742	Thermodynamic limit for synthesis of metastable inorganic materials. Science Advances, 2018, 4, eaaq0148.	4.7	212
35743	Readily accessible shape-memory effect in a porous interpenetrated coordination network. Science Advances, 2018, 4, eaaq1636.	4.7	61
35744	Stanene nanomeshes as anode materials for Na-ion batteries. Journal of Materials Chemistry A, 2018, 6, 7933-7941.	5.2	72
35745	CO oxidation on Ruâ€“Pt bimetallic nanoclusters supported on TiO2(101): The effect of charge polarization. Journal of Chemical Physics, 2018, 148, 124701.	1.2	14
35746	Anisotropic Negative Differential Resistance in Monolayer Black Phosphorus. IOP Conference Series: Earth and Environmental Science, 2018, 108, 022046.	0.2	0
35747	Theoretical and experimental investigation of conjugation of 1,6-hexanedithiol on MoS₂. Materials Research Express, 2018, 5, 036415.	0.8	9
35748	Sulfur-vacancy-dependent geometric and electronic structure of bismuth adsorbed on <mml:math xmlns:mml="http://www.w3.org/1998/Math/MathML"><mml:mrow><mml:mi>Mo</mml:mi><mml:msub><mml:mi mathvariant="normal">S</mml:mi><mml:mn>2</mml:mn></mml:msub></mml:mrow></mml:math>. Physical Review B, 2018, 97, .	1.1	4
35749	From node-line semimetals to large-gap quantum spin Hall states in a family of pentagonal group-IVA chalcogenide. Physical Review B, 2018, 97, .	1.1	22
35750	Moleculeâ€Doped Nickel Oxide: Verified Charge Transfer and Planar Inverted Mixed Cation Perovskite Solar Cell. Advanced Materials, 2018, 30, e1800515.	11.1	287
35751	An insight into the dopant selection for CeO2-based resistive-switching memory system: a DFT and experimental study. Applied Nanoscience (Switzerland), 2018, 8, 839-851.	1.6	16
35752	Insights into the surface-defect dependence of molecular oxygen activation over birnessite-type MnO2. Applied Catalysis B: Environmental, 2018, 233, 184-193.	10.8	194
35753	Plasmon-Mediated Electron Injection from Au Nanorods into MoS2: Traditional versus Photoexcitation Mechanism. CheM, 2018, 4, 1112-1127.	5.8	71
35754	Embedded atom method potentials for Ce-Ni binary alloy. Computational Materials Science, 2018, 150, 1-8.	1.4	5
35755	Highly dispersed and COad-tolerant Ptshell-Pdcore catalyst for ethanol oxidation reaction: Catalytic activity and long-term durability. International Journal of Hydrogen Energy, 2018, 43, 11335-11344.	3.8	6
35756	Principles determining the activity of magnetic oxides for electron transfer reactions. Journal of Catalysis, 2018, 361, 331-338.	3.1	105
35757	Effects of anion and cation doping on the thermoelectric properties of n-type PbS. Journal of the European Ceramic Society, 2018, 38, 3512-3517.	2.8	19

#	Article	IF	Citations
35758	ENDF/B-VIII.0: The 8 th Major Release of the Nuclear Reaction Data Library with CIELO-project Cross Sections, New Standards and Thermal Scattering Data. Nuclear Data Sheets, 2018, 148, 1-142.	0.7	1,324
35759	First principles calculations of the electronic structure and magnetic properties of Y(Fe,M) 9.2 and Y(Fe,M) 9.2 C (M= Si, Ga, Zr). Physica B: Condensed Matter, 2018, 538, 207-212.	1.3	1
35760	Structural Disorder and Coherence across the Phase Transitions of Lead-Free Piezoelectric Bi_{0.5}K_{0.5}TiO₃. Chemistry of Materials, 2018, 30, 2631-2640.	3.2	24
35761	Cs2Ge3In6Se14: A Structure Transformation Driven by the Size Preference and Its Properties. Inorganic Chemistry, 2018, 57, 4667-4672.	1.9	7
35762	Density Functional Theory Modeling of MnO₂ Polymorphs as Cathodes for Multivalent Ion Batteries. Journal of Physical Chemistry C, 2018, 122, 8788-8795.	1.5	70
35763	Iron-Based Perovskites for Catalyzing Oxygen Evolution Reaction. Journal of Physical Chemistry C, 2018, 122, 8445-8454.	1.5	106
35764	The Pentagonal Nature of Self-Assembled Silicon Chains and Magic Clusters on Ag(110). Nano Letters, 2018, 18, 2937-2942.	4.5	52
35765	Role of Carbonaceous Aerosols in Catalyzing Sulfate Formation. ACS Catalysis, 2018, 8, 3825-3832.	5.5	59
35766	F-Doped carbon nano-onion films as scaffold for highly efficient and stable Li metal anodes: a novel laser direct-write process. Nanoscale, 2018, 10, 7630-7638.	2.8	20
35767	Defects and impurities induced structural and electronic changes in pyrite CoS₂: first principles studies. Physical Chemistry Chemical Physics, 2018, 20, 11649-11655.	1.3	5
35768	Ethane dehydrogenation on pristine and AlO_x decorated Pt stepped surfaces. Catalysis Science and Technology, 2018, 8, 2159-2174.	2.1	18
35769	Compositional descriptor-based recommender system for the materials discovery. Journal of Chemical Physics, 2018, 148, 241719.	1.2	33
35770	The ground state of two-dimensional silicon. 2D Materials, 2018, 5, 035010.	2.0	25
35771	Phonon-assisted optical absorption in <mml:math xmlns:mml="http://www.w3.org/1998/Math/MathML"><mml:mi>BaSnO</mml:mi><mml:msub><mml:mrow /><mml:mn>3</mml:mn></mml:msub></mml:math> from first principles. Physical Review B, 2018, 97, .	1.1	26
35772	Magnetic excitations of the <mml:math xmlns:mml="http://www.w3.org/1998/Math/MathML"><mml:msup><mml:mrow><mml:mi>Cu</mml:mi></mml:mrow><mml:mrow><m quantum spin chain in <mml:math xmlns:mml="http://www.w3.org/1998/Math/MathML"><mml:mrow><mml:msub><mml:mi>Sr</mml:mi><mml:mn>3</mml:mn></mml:r	1.1	8
35773	Physical Review B, 2018, 97, . Local real-space view of the Achiral <mml:math xmlns:mml="http://www.w3.org/1998/Math/MathML" display="inline"><mml:mrow><mml:mn>1</mml:mn><mml:mi>T</mml:mi><mml:mtext>â^'</mml:mtext><mml:msub><mml:mrow><m <mml:math xmlns:mml="http://www.w3.org/1998/Math/MathML" display="inline"><mml:mrow><mml:mn>2</mml:mn><mml:mo>Ã—</mml:mo><mml:mrow><mml:mn>2</mml:mn><mml:mo>Ã—</m Physical Review Letters, 2018, 120, 136404.	2.9	29
35774	Influence of the core-hole effect on optical properties of magnesium oxide (MgO) near the MgL-edge region. Journal of Synchrotron Radiation, 2018, 25, 771-776.	1.0	5
35775	Interfacial segregation and fracture in Mg-based binary alloys: Experimental and first-principles perspective. Acta Materialia, 2018, 151, 78-86.	3.8	74

#	Article	IF	Citations
35776	Understanding zeolite-catalyzed benzene methylation reactions by methanol and dimethyl ether at operating conditions from first principle microkinetic modeling and experiments. Catalysis Today, 2018, 312, 35-43.	2.2	28
35777	Highly uranium elimination by crab shells-derived porous graphitic carbon nitride: Batch, EXAFS and theoretical calculations. Chemical Engineering Journal, 2018, 346, 406-415.	6.6	64
35778	Electronic and optical properties of vanadium oxides from first principles. Computational Materials Science, 2018, 146, 310-318.	1.4	54
35779	A comparison study of the structural and mechanical properties of cubic, tetragonal, monoclinic, and three orthorhombic phases of ZrO2. Journal of Alloys and Compounds, 2018, 749, 283-292.	2.8	46
35780	Understanding the anisotropic strain effects on lithium diffusion in graphite anodes: A first-principles study. Physica B: Condensed Matter, 2018, 539, 66-71.	1.3	15
35781	Intrinsic Role of Excess Electrons in Surface Reactions on Rutile TiO₂ (110): Using Water and Oxygen as Probes. Journal of Physical Chemistry C, 2018, 122, 8270-8276.	1.5	12
35782	New Types of CZTS Î£3 {112} Grain Boundaries: Algorithms to Passivation. Journal of Physical Chemistry C, 2018, 122, 7759-7770.	1.5	11
35783	Sn2+â€”Stabilization in MASnI3 perovskites by superhalide incorporation. Journal of Chemical Physics, 2018, 148, 124111.	1.2	19
35784	Saturation and negative temperature coefficient of electrical resistivity in liquid iron-sulfur alloys at high densities from first-principles calculations. Physical Review B, 2018, 97, .	1.1	18
35785	Selfâ€Limited Epitaxial Growth of Ultrathin Nonlayered CdS Flakes for Highâ€Performance Photodetectors. Advanced Functional Materials, 2018, 28, 1800181.	7.8	86
35786	Correlation between Geometrically Induced Oxygen Octahedral Tilts and Multiferroic Behaviors in BiFeO₃ Films. Advanced Functional Materials, 2018, 28, 1800839.	7.8	21
35787	Bismuth Microparticles as Advanced Anodes for Potassiumâ€Ion Battery. Advanced Energy Materials, 2018, 8, 1703496.	10.2	306
35788	Effects of Molybdenum Addition on Hydrogen Desorption of TiC Precipitation-Hardened Steel. Metals and Materials International, 2018, 24, 532-536.	1.8	17
35789	Structural stability, electronic structures and enhanced photocatalytic properties of BiF3 nanowires: A first-principles study. Ceramics International, 2018, 44, 9623-9632.	2.3	5
35790	Mechanical strength and origin of the strengthening effect of tantalum in superhard W 0.5 Ta 0.5 B monoboride. Ceramics International, 2018, 44, 10463-10469.	2.3	20
35791	A systematic study of the microstructure and laser characteristics of Pr3+-doped lithium lutetium fluoride. Journal of Alloys and Compounds, 2018, 749, 391-398.	2.8	7
35792	High-performance solar-blind flexible deep-UV photodetectors based on quantum dots synthesized by femtosecond-laser ablation. Nano Energy, 2018, 48, 551-559.	8.2	74
35793	Theoretical research on novel orthorhombic tungsten dinitride from first principles calculations. RSC Advances, 2018, 8, 9272-9276.	1.7	4

#	Article	IF	Citations
35794	Effects of ligand functionalization on the photocatalytic properties of titanium-based MOF: A density functional theory study. AIP Advances, 2018, 8, .	0.6	35
35795	Origin of photoluminescence in <mml:math xmlns:mml="http://www.w3.org/1998/Math/MathML"><mml:mrow><mml:mi>Î²</mml:mi><mml:mo>â^'</mml:mo><mml:mi mathvariant="normal">G</mml:mi><mml:msub><mml:mi mathvariant="normal">a</mml:mi><mml:mn>2</mml:mn></mml:msub><mml:msub><mml:mi mathvariant="normal">O</mml:mi><mml:mn>3</mml:mn></mml:msub></mml:mrow></mml:math>. Physical Review B, 2018, 97.	1.1	104
35796	An Openâ€Structured Matrix as Oxygen Cathode with High Catalytic Activity and Large Li₂O₂ Accommodations for Lithiumâ€“Oxygen Batteries. Advanced Energy Materials, 2018, 8, 1800089.	10.2	88
35797	Modeling palladium surfaces with density functional theory, neural networks and molecular dynamics. Catalysis Today, 2018, 312, 132-140.	2.2	15
35798	Convolutional neural networks for atomistic systems. Computational Materials Science, 2018, 149, 134-142.	1.4	39
35799	The role of boundary conditions in tuning the electronic properties of the (0â€²0â€²1) LaAlO3/SrTiO3 interface. Computational Materials Science, 2018, 149, 354-359.	1.4	5
35800	Adsorption of 3d transition-metal atom on InSe monolayer: A first-principles study. Computational Materials Science, 2018, 150, 33-41.	1.4	38
35801	A linear response approach to determine Hubbard U and its application to evaluate properties of Y2B2O7, Bâ€²=â€²transition metals 3d, 4d and 5d. Journal of Alloys and Compounds, 2018, 749, 909-925.	2.8	24
35802	Theoretical study of YFe2H (xâ€²=â€²0â€“5): A comparison between cubic and orthorhombic phases. Journal of Magnetism and Magnetic Materials, 2018, 460, 61-68.	1.0	13
35803	High pressure in solid state chemistry: Combined experimental and modeling approaches for assessing and predicting properties. Solid State Sciences, 2018, 80, 178-195.	1.5	1
35804	Narrowing of band gap at source/drain contact scheme of nanoscale InAsâ€“nMOS. Solid-State Electronics, 2018, 142, 31-35.	0.8	1
35805	A Family of Layered Phosphates Crystallizing in a Rare Geometrical Isomer of the Phosphuranylite Topology: Synthesis, Characterization, and Computational Modeling of A₄[(UO₂)₃O₂(PO₄)₂] (A =) Tj ETQq1 1 0.784314 rgBT /(	1.9	20
35806	Na₂(UO₂)(BO₃): An All-Uranium(V) Borate Synthesized under Mild Hydrothermal Conditions. Inorganic Chemistry, 2018, 57, 4244-4247.	1.9	14
35807	Evidence of Charge Transfer to Atomic and Molecular Adsorbates on ZnO/X(111) (X = Cu, Ag, Au) Ultrathin Films. Relevance for Cu/ZnO Catalysts. ACS Catalysis, 2018, 8, 4110-4119.	5.5	36
35808	Niâ€“Sn-Supported ZrO₂ Catalysts Modified by Indium for Selective CO₂ Hydrogenation to Methanol. ACS Omega, 2018, 3, 3688-3701.	1.6	130
35809	Non-Dirac Chern insulators with large band gaps and spin-polarized edge states. Nanoscale, 2018, 10, 8569-8577.	2.8	17
35810	The phonon confinement effect in two-dimensional nanocrystals of black phosphorus with anisotropic phonon dispersions. Nanoscale, 2018, 10, 8704-8711.	2.8	21
35811	Rare earth indates (RE: Laâ€“Yb): influence of the synthesis route and heat treatment on the crystal structure. Dalton Transactions, 2018, 47, 6787-6799.	1.6	12

#	Article	IF	Citations
35812	Doping-stabilized two-dimensional black phosphorus. Nanoscale, 2018, 10, 7898-7904.	2.8	20
35813	First principles study of ceramic materials (IVB group carbides) under ultrafast laser irradiation. Chinese Physics B, 2018, 27, 036301.	0.7	1
35814	The adsorption properties of CHx species on metal modified graphene. International Journal of Modern Physics B, 2018, 32, 1850153.	1.0	0
35815	Stability of Excess Oxygen Atoms near Oxide Precipitate and Oxygen Solubility in Silicon Crystal. ECS Journal of Solid State Science and Technology, 2018, 7, P102-P108.	0.9	5
35816	Prediction of Quantum Anomalous Hall Effect in MBi and MSb (M:Ti, Zr, and Hf) Honeycombs. Nanoscale Research Letters, 2018, 13, 43.	3.1	12
35817	Influence of H-Content on Thermo-Mechanical Properties of NiAl Alloys. Materials Science Forum, 0, 915, 224-228.	0.3	0
35818	First principles study of the effect of hydrogen annealing on SiC MOSFETs. Japanese Journal of Applied Physics, 2018, 57, 04FR05.	0.8	0
35819	Momentâ€Volume Coupling in La(Fe_{1â”x}Si_x)₁₃. Physica Status Solidi (B): Basic Research, 2018, 255, 1700465.	0.7	14
35820	Nanoporous ZnO: Structural and electronic study under biaxial strain. Computational Materials Science, 2018, 149, 91-97.	1.4	0
35821	Ab initio description of the different phases in the Al-Fe-V system: Structure, magnetism and thermodynamics. Computational Materials Science, 2018, 149, 28-36.	1.4	5
35822	Enhanced photoelectrochemical performance of TiO2 through controlled Ar+ ion irradiation: A combined experimental and theoretical study. International Journal of Hydrogen Energy, 2018, 43, 6936-6944.	3.8	11
35823	A Highly Efficient Multi-phase Catalyst Dramatically Enhances the Rate of Oxygen Reduction. Joule, 2018, 2, 938-949.	11.7	221
35824	Low-Symmetry Rhombohedral GeTe Thermoelectrics. Joule, 2018, 2, 976-987.	11.7	402
35825	Hollow Mo-doped CoP nanoarrays for efficient overall water splitting. Nano Energy, 2018, 48, 73-80.	8.2	608
35826	The surface energy and stress of metals. Surface Science, 2018, 674, 51-68.	0.8	68
35827	Ab Initio Investigation of the Role of Atomic Radius in the Structural Formation of Pt_nTM_{55â€“n} (TM = Y, Zr, Nb, Mo, and Tc) Nanoclusters. Journal of Physical Chemistry C, 2018, 122, 7444-7454.	1.5	21
35828	Atomic and Electronic Structure of Two-Dimensional Inorganic Halide Perovskites A_{n+1}M_nX_{3n+1} (n = 1â€“6, A = Cs, M = Pb) Tj ETQq0 0 0 rgBT /Overl 122, 7464-7473.	1.5	31
35829	Computational Study of Structural and Electronic Properties of Lead-Free CsMI₃ Perovskites (M = Ge, Sn, Pb, Mg, Ca, Sr, and Ba). Journal of Physical Chemistry C, 2018, 122, 7838-7848.	1.5	62

#	Article	IF	Citations
35830	Identifying the Emission Centers and Probing the Mechanism for Highly Efficient and Thermally Stable Luminescence in the La₃Si₆N₁₁:Ce³⁺ Phosphor. Journal of Physical Chemistry C, 2018, 122, 7849-7858.	1.5	43
35831	Interaction of Boron Nitride Nanotubes with Aluminum: A Computational Study. Journal of Physical Chemistry C, 2018, 122, 15226-15240.	1.5	6
35832	Computational Study of Chemical and Electrochemical Intercalation of Li Into Li1+xTi2O4 Spinel Structures. Journal of Physical Chemistry C, 2018, 122, 7779-7789.	1.5	3
35833	Electronic Properties of van der Waals Heterostructure of Black Phosphorus and MoS₂. Journal of Physical Chemistry C, 2018, 122, 7027-7032.	1.5	82
35834	Investigation of the Water Adsorption Properties and Structural Stability of MIL-100(Fe) with Different Anions. Langmuir, 2018, 34, 4180-4187.	1.6	33
35835	Engineering Crystal Facet of Î±-MnO₂ Nanowire for Highly Efficient Catalytic Oxidation of Carcinogenic Airborne Formaldehyde. ACS Catalysis, 2018, 8, 3435-3446.	5.5	485
35836	Opening Magnesium Storage Capability of Two-Dimensional MXene by Intercalation of Cationic Surfactant. ACS Nano, 2018, 12, 3733-3740.	7.3	208
35837	Heterostructures of MXenes and N-doped graphene as highly active bifunctional electrocatalysts. Nanoscale, 2018, 10, 10876-10883.	2.8	215
35838	Mechanism of Na accumulation at extended defects in Si from first-principles. Journal of Applied Physics, 2018, 123, 161560.	1.1	12
35839	First-principles study of magnetic properties of ultra-thin MoSi2 films. Journal of Applied Physics, 2018, 123, 104304.	1.1	5
35840	First-principles simulations of binding energies of alloying elements to the ferrite-austenite interface in iron. Journal of Applied Physics, 2018, 123, .	1.1	19
35841	Intrinsic point defects in Î²-In2S3 studied by means of hybrid density-functional theory. Journal of Applied Physics, 2018, 123, .	1.1	22
35842	Shock interactions with heterogeneous energetic materials. Journal of Applied Physics, 2018, 123, .	1.1	32
35843	Clustering and Dissolution of Small Helium Clusters in Bulk Tungsten. Chinese Physics Letters, 2018, 35, 027102.	1.3	4
35844	First-principles study of pollutant molecules absorbed on polymeric adsorbents using the vdW-DF2 functional. Materials Research Express, 2018, 5, 035516.	0.8	4
35845	Magnetism on a Boron-doped Si(111)- $$sqrt 3 imes sqrt 3 $$ 3 Ã— 3 Surface. Journal of the Korean Physical Society, 2018, 72, 577-581.	0.3	0
35846	Electrochemical CO₂ Reduction with Atomic Ironâ€Dispersed on Nitrogenâ€Doped Graphene. Advanced Energy Materials, 2018, 8, 1703487.	10.2	369
35847	Single Pd atom and Pd dimer embedded graphene catalyzed formic acid dehydrogenation: AÂfirst-principles study. International Journal of Hydrogen Energy, 2018, 43, 6997-7006.	3.8	36

#	Article	IF	Citations
35848	Electrochemically active and robust cobalt doped copper phosphosulfide electro-catalysts for hydrogen evolution reaction in electrolytic and photoelectrochemical water splitting. International Journal of Hydrogen Energy, 2018, 43, 7855-7871.	3.8	37
35849	Origin of the sensitivity in modeling the glide behaviour of dislocations. International Journal of Plasticity, 2018, 106, 48-56.	4.1	11
35850	Electronic and magnetic properties of Fe-, Co-, and Ni-decorated BC 3 : A first-principles study. Physics Letters, Section A: General, Atomic and Solid State Physics, 2018, 382, 1395-1400.	0.9	3
35851	Compressibility of Cs 2 SnBr 6 by X-ray diffraction and Raman spectroscopy. Solid State Communications, 2018, 275, 68-72.	0.9	24
35852	Ultrathin silica films on Pd(111): Structure and adsorption properties. Surface Science, 2018, 678, 118-123.	0.8	25
35853	Tailoring the Crystal Structure of Nanoclusters Unveiled High Photoluminescence via Ion Pairing. Chemistry of Materials, 2018, 30, 2719-2725.	3.2	76
35854	CsFe_{4â˜Î´}Se₄: A Compound Closely Related to Alkali-Intercalated FeSe Superconductors. Inorganic Chemistry, 2018, 57, 4502-4509.	1.9	8
35855	Toward Effective Utilization of Methane: Machine Learning Prediction of Adsorption Energies on Metal Alloys. Journal of Physical Chemistry C, 2018, 122, 8315-8326.	1.5	140
35856	Temperature-Dependent and Gate-Tunable Rectification in a Black Phosphorus/WS₂ van der Waals Heterojunction Diode. ACS Applied Materials & Interfaces, 2018, 10, 13150-13157.	4.0	61
35857	Large Perpendicular Magnetocrystalline Anisotropy at the Fe/Pb(001) Interface. ACS Applied Materials & Interfaces, 2018, 10, 13181-13186.	4.0	10
35858	CO Adsorption Site Preference on Platinum: Charge Is the Essence. ACS Catalysis, 2018, 8, 3770-3774.	5.5	51
35859	Computer predictions on Rh-based double perovskites with unusual electronic and magnetic properties. Npj Quantum Materials, 2018, 3, .	1.8	11
35860	A density functional study on the oxygen reduction reaction mechanism on FeN₂-doped graphene. New Journal of Chemistry, 2018, 42, 6873-6879.	1.4	41
35861	Adsorption of 3d, 4d, and 5d transition-metal atoms on single-layer boron nitride. Journal of Applied Physics, 2018, 123, .	1.1	15
35862	Engineering magnetic anisotropy in two-dimensional magnetic materials. Advances in Physics: X, 2018, 3, 1432415.	1.5	28
35863	Density functional theory study of electronic structure of defects and the role on the strain relaxation behavior of MoS2 bilayer structures. Journal of Materials Science, 2018, 53, 9064-9075.	1.7	6
35864	Phase Equilibria and Thermodynamic Descriptions of Ag-Ge and Ag-Ge-Ni Systems. Journal of Electronic Materials, 2018, 47, 3666-3677.	1.0	6
35865	First-principles investigation of grain boundary morphology effects on helium solutions in tungsten. Computational Materials Science, 2018, 148, 224-230.	1.4	19

#	Article	IF	Citations
35866	Ab initio molecular dynamics simulation on interfacial reaction behavior of Fe-Cr-Ni stainless steel in high temperature water. Computational Materials Science, 2018, 149, 143-152.	1.4	6
35867	Structural and electronic properties of 90Â° dislocations in silicon nanorods: A first-principles calculation. Computational Materials Science, 2018, 149, 243-249.	1.4	1
35868	Effects of atom arrangement and thickness of Pt atomic layers on Pd nanocrystals for electrocatalysis. Electrochimica Acta, 2018, 271, 519-525.	2.6	6
35869	Comparative investigation of the molybdenum sulphide doped with cobalt and selenium towards hydrogen evolution reaction. Electrochimica Acta, 2018, 271, 211-219.	2.6	30
35870	Superior Na-ion storage achieved by Ti substitution in Na3V2(PO4)3. Energy Storage Materials, 2018, 15, 108-115.	9.5	100
35871	First-principles study the phase stability and mechanical properties of binary W-Mo alloys. Fusion Engineering and Design, 2018, 130, 56-61.	1.0	35
35872	First-principles analysis of ferroelectric transition in MnSnO3 and MnTiO3 perovskites. Journal of Solid State Chemistry, 2018, 262, 251-255.	1.4	7
35873	Strain induced anisotropic mechanical and electronic properties of 2D-SiC. Mechanics of Materials, 2018, 120, 43-52.	1.7	25
35874	Insights into the Microstructure and Transition Mechanism for Nd³⁺-Doped Bi₄Si₃O₁₂: A Promising Near-Infrared Laser Material. Inorganic Chemistry, 2018, 57, 4563-4570.	1.9	11
35875	Al₃ (A = As, Sb) Single Layers and Their vdW Heterostructure for Photocatalysis and Solar Cell Applications. Journal of Physical Chemistry C, 2018, 122, 7656-7663.	1.5	34
35876	Topological Phase Transition with Nanoscale Inhomogeneity in (Bi_{1â€“x}In_x)₂Se₃. Nano Letters, 2018, 18, 2677-2682.	4.5	7
35877	First-Principles Study of Oxyhydride Hâ€“ Ion Conductors: Toward Facile Anion Conduction in Oxide-Based Materials. ACS Applied Energy Materials, 2018, 1, 1626-1634.	2.5	26
35878	Engineering Cobalt Defects in Cobalt Oxide for Highly Efficient Electrocatalytic Oxygen Evolution. ACS Catalysis, 2018, 8, 3803-3811.	5.5	430
35879	Drying-induced atomic structural rearrangements in sodium-based calcium-alumino-silicate-hydrate gel and the mitigating effects of ZrO₂ nanoparticles. Physical Chemistry Chemical Physics, 2018, 20, 8593-8606.	1.3	11
35880	Indium selenide monolayer: a two-dimensional material with strong second harmonic generation. CrystEngComm, 2018, 20, 2573-2582.	1.3	16
35881	Application of 3D hierarchical monoclinic-type structural Sb-doped WO₃ towards NO₂ gas detection at low temperature. Nanoscale, 2018, 10, 7440-7450.	2.8	54
35882	Pd₂Se₃monolayer: a novel two-dimensional material with excellent electronic, transport, and optical properties. Journal of Materials Chemistry C, 2018, 6, 4494-4500.	2.7	36
35883	Structure prediction of boron-doped graphene by machine learning. Journal of Chemical Physics, 2018, 148, 241716.	1.2	46

#	Article	IF	Citations
35884	Non-parametric correlative uncertainty quantification and sensitivity analysis: Application to a Langmuir bimolecular adsorption model. AIP Advances, 2018, 8, .	0.6	8
35885	Experimental studies of thorium ion implantation from pulse laser plasma into thin silicon oxide layers. Laser Physics Letters, 2018, 15, 056101.	0.6	13
35886	Thermally induced coloration of KBr at high pressures. Physical Review B, 2018, 97, .	1.1	7
35887	Accurate critical pressures for structural phase transitions of group IV, III-V, and II-VI compounds from the SCAN density functional. Physical Review B, 2018, 97, .	1.1	100
35888	Predicting the ground-state structure of sodium boride. Physical Review B, 2018, 97, .	1.1	26
35889	Robust spin-valley polarization in commensurate <mml:math xmlns:mml="http://www.w3.org/1998/Math/MathML"><mml:mrow><mml:mi>Mo</mml:mi><mml:msub><mml:mi mathvariant="normal">S</mml:mi><mml:mn>2</mml:mn></mml:msub></mml:mrow></mml:math> /graphene heterostructures. Physical Review B, 2018, 97, .	1.1	27
35890	Highâ€Voltage Lithiumâ€Metal Batteries Enabled by Localized Highâ€Concentration Electrolytes. Advanced Materials, 2018, 30, e1706102.	11.1	761
35891	Catalytic methane combustion over Pd/ZrO2 catalysts: Effects of crystalline structure and textural properties. Applied Catalysis B: Environmental, 2018, 232, 544-552.	10.8	86
35892	Using BrÃ¸nsted-Evans-Polanyi relations to predict electrode potential-dependent activation energies. Catalysis Today, 2018, 312, 82-91.	2.2	36
35893	Preparation and characterization of Na3PS4â€“Na4GeS4 glass and glass-ceramic electrolytes. Solid State Ionics, 2018, 320, 193-198.	1.3	16
35894	Universal Descriptor for Large-Scale Screening of High-Performance MXene-Based Materials for Energy Storage and Conversion. Chemistry of Materials, 2018, 30, 2687-2693.	3.2	71
35895	Theoretical Investigation of CO₂ Adsorption and Dissociation on Low Index Surfaces of Transition Metals. Journal of Physical Chemistry C, 2018, 122, 8306-8314.	1.5	104
35896	Optimum Particle Size for Gold-Catalyzed CO Oxidation. Journal of Physical Chemistry C, 2018, 122, 8327-8340.	1.5	45
35897	A Comparative Ab Initio Study of Anhydrous Dehydrogenation of Linear-Chain Alcohols on Cu(110). Journal of Physical Chemistry C, 2018, 122, 7806-7815.	1.5	18
35898	Actinium Hydrides AcH₁₀, AcH₁₂, and AcH₁₆ as High-Temperature Conventional Superconductors. Journal of Physical Chemistry Letters, 2018, 9, 1920-1926.	2.1	100
35899	Computational Screening of Near-Surface Alloys for CO₂ Electroreduction. ACS Catalysis, 2018, 8, 3885-3894.	5.5	79
35900	First-principles study on thermodynamic stability of the hybrid interfacial structure of LiMn₂O₄ cathode and carbonate electrolyte in Li-ion batteries. Physical Chemistry Chemical Physics, 2018, 20, 11592-11597.	1.3	19
35901	A study of the density of states of ZnCoO:H from resistivity measurements. RSC Advances, 2018, 8, 9895-9900.	1.7	3

#	Article	IF	Citations
35902	Synthesis and crystal structure of solvent-free dodecahydro closo-dodecaborate of nickel, NiB₁₂H₁₂. Dalton Transactions, 2018, 47, 5843-5849.	1.6	14
35903	High thermoelectric performance in Bi_{0.46}Sb_{1.54}Te₃ nanostructured with ZnTe. Energy and Environmental Science, 2018, 11, 1520-1535.	15.6	239
35904	Quantum anomalous Hall effect in a stable 1T-YN₂monolayer with a large nontrivial bandgap and a high Chern number. Nanoscale, 2018, 10, 8153-8161.	2.8	35
35905	Tune the chemical activity of graphene via the transition metal substrate. RSC Advances, 2018, 8, 11807-11812.	1.7	4
35906	Electronic, magnetic, catalytic, and electrochemical properties of two-dimensional Janus transition metal chalcogenides. Journal of Materials Chemistry A, 2018, 6, 8021-8029.	5.2	53
35907	Phosphorene oxides as a promising cathode material for sealed non-aqueous Liâ€“oxygen batteries. Journal of Materials Chemistry A, 2018, 6, 7815-7826.	5.2	20
35908	Insight into fast Li diffusion in Li-excess spinel lithium manganese oxide. Journal of Materials Chemistry A, 2018, 6, 9893-9898.	5.2	51
35909	Maximally resolved anharmonic OH vibrational spectrum of the water/ZnO(101Â¯0) interface from a high-dimensional neural network potential. Journal of Chemical Physics, 2018, 148, 241720.	1.2	28
35910	Density functional theory study of atomic and electronic properties of defects in reduced anatase TiO2 nanocrystals. AIP Advances, 2018, 8, .	0.6	22
35911	Thermal transport in phosphorene and phosphorene-based materials: A review on numerical studies. Chinese Physics B, 2018, 27, 036501.	0.7	23
35912	Probing lattice dynamics and electron-phonon coupling in the topological nodal-line semimetal ZrSiS. Physical Review B, 2018, 97, .	1.1	25
35913	Zn vacancy-donor impurity complexes in ZnO. Physical Review B, 2018, 97, .	1.1	39
35914	Electronic confining effects in SierpiÅ„ski triangle fractals. Physical Review B, 2018, 97, .	1.1	14
35915	Coupling effect of topological states and Chern insulators in two-dimensional triangular lattices. Physical Review B, 2018, 97, .	1.1	25
35916	First-Principles Study of Charge Diffusion between Proximate Solid-State Qubits and Its Implications on Sensor Applications. Physical Review Letters, 2018, 120, 136401.	2.9	16
35917	Interstitial-atom-induced phase transformation upon hydrogenation in vanadium. Journal of Alloys and Compounds, 2018, 750, 33-41.	2.8	7
35918	Quantum chemical modeling of solid-state B 4 X structures containing tetrahedral B 4 units with X = B, C, Al, Si. Mendeleev Communications, 2018, 28, 173-175.	0.6	4
35919	C3N monolayers as promising candidates for NO2 sensors. Sensors and Actuators B: Chemical, 2018, 266, 664-673.	4.0	172

#	Article	IF	Citations
35920	Lowest-Energy Crystalline Polymorphs of P3HT. Journal of Physical Chemistry C, 2018, 122, 9141-9151.	1.5	18
35921	Thermodynamics Study of Dehydriding Reaction on the PuO₂(110) Surface from First Principles. Journal of Physical Chemistry C, 2018, 122, 7790-7794.	1.5	13
35922	Halide Composition Controls Electronâ€“Hole Recombination in Cesiumâ€“Lead Halide Perovskite Quantum Dots: A Time Domain Ab Initio Study. Journal of Physical Chemistry Letters, 2018, 9, 1872-1879.	2.1	103
35923	Mechanism of Chemical Reactions between SiO₂ and CO₂ under Mantle Conditions. ACS Earth and Space Chemistry, 2018, 2, 548-555.	1.2	12
35924	Density functional theory modeling of chromate adsorption onto ferrihydrite nanoparticles. Geochemical Transactions, 2018, 19, 8.	1.8	26
35925	The Global Optimization of Pt13 Cluster Using the First-Principle Molecular Dynamics with the Quenching Technique. Journal of Statistical Physics, 2018, 171, 427-433.	0.5	1
35926	N-doped graphitic carbon materials hybridized with transition metals (compounds) for hydrogen evolution reaction: Understanding the synergistic effect from atomistic level. Carbon, 2018, 133, 260-266.	5.4	100
35927	An atomistic building block description of C-S-H - Towards a realistic C-S-H model. Cement and Concrete Research, 2018, 107, 221-235.	4.6	78
35928	First principles study of trirutile magnesium bismuth oxide: Ideal bandgap for photovoltaics, strain-mediated band-inversion and semiconductor-to-semimetal transition. Computational Materials Science, 2018, 149, 158-161.	1.4	9
35929	Density functional theory calculations and analysis for the reduction of NO by H2 on Pd6/TiO2. Computational Materials Science, 2018, 149, 182-190.	1.4	8
35930	Assessing exchange-correlation functionals for elasticity and thermodynamics of <mml:math xmlns:mml="http://www.w3.org/1998/Math/MathML" altimg="si2.gif" overflow="scroll"><mml:mrow><mml:mi>Î±</mml:mi></mml:mrow></mml:math>-<mml:math xmlns:mml="http://www.w3.org/1998/Math/MathML" altimg="si27.gif" overflow="scroll"><mml:mrow><mml:msub><mml:mrow><mml:mtext>ZrW</mml:mtext></mml:mrow><mml:mrow><mml:mn>2</mml:mn> Chemical Physics Letters, 2018, 698, 195-199.	1.2	9
35931	Three-dimensional carbon frameworks enabling MoS2 as anode for dual ion batteries with superior sodium storage properties. Energy Storage Materials, 2018, 15, 22-30.	9.5	125
35932	Half-metallic ferromagnetism and metalâ€“insulator transition in Sn-doped SrRuO3 perovskite oxides. Journal of Magnetism and Magnetic Materials, 2018, 460, 54-60.	1.0	13
35933	First-principles predictions on structural, elastic and half-metallic properties of Fe 2 LiAs Heusler compound. Journal of Magnetism and Magnetic Materials, 2018, 458, 235-240.	1.0	6
35934	First-principles calculations of electronic, acoustic and anharmonic properties of Mn 2 RuZ (Zâ€¯=â€¯Si and) Tj ETQq0 0 0 rgBT /Overlock	1.0	11
35935	Infrared Light-Driven CO2 Overall Splitting at Room Temperature. Joule, 2018, 2, 1004-1016.	11.7	258
35936	Theoretical investigation of electronic, bonding and optical properties of nanolaminated boride WAlB. Materials Chemistry and Physics, 2018, 212, 122-130.	2.0	5
35937	A first-principle investigation of the Li diffusion mechanism in the super-ionic conductor lithium orthothioborate Li3BS3 structure. Materials Letters, 2018, 219, 186-189.	1.3	9

#	Article	IF	Citations
35938	Simultaneous multi-wavelength ultraviolet excited single-phase white light emitting phosphor Ba1-x(Zr,Ti)Si3O9:xEu. Optical Materials, 2018, 79, 53-62.	1.7	6
35939	First-principle study of single TM atoms X (X=Fe, Ru or Os) doped monolayer WS2 systems. Superlattices and Microstructures, 2018, 117, 155-162.	1.4	14
35940	Fermi-Level Characteristics of Potential Chalcogenide Superconductors. Chemistry of Materials, 2018, 30, 2251-2261.	3.2	15
35941	First-Principles Study of Spinel MgTiS₂ as a Cathode Material. Chemistry of Materials, 2018, 30, 2436-2442.	3.2	20
35942	First-Principles Screening of All-Inorganic Lead-Free ABX₃ Perovskites. Journal of Physical Chemistry C, 2018, 122, 7670-7675.	1.5	98
35943	Construction of Polarized Carbonâ€“Nickel Catalytic Surfaces for Potent, Durable, and Economic Hydrogen Evolution Reactions. ACS Nano, 2018, 12, 4148-4155.	7.3	121
35944	Mechanistic Insights into Photocatalyzed Hydrogen Desorption from Palladium Surfaces Assisted by Localized Surface Plasmon Resonances. ACS Nano, 2018, 12, 3512-3522.	7.3	62
35945	Insight into point defects and impurities in titanium from first principles. Npj Computational Materials, 2018, 4, .	3.5	62
35946	A valence balanced rule for discovery of 18-electron half-Heuslers with defects. Energy and Environmental Science, 2018, 11, 1480-1488.	15.6	105
35947	Relative stability of FeS₂polymorphs with the random phase approximation approach. Journal of Materials Chemistry A, 2018, 6, 6606-6616.	5.2	23
35948	Stable narrowband red emission in fluorotellurate KTeF₅:Mn⁴⁺viaMn⁴⁺noncentral-site occupation. Journal of Materials Chemistry C, 2018, 6, 4418-4426.	2.7	47
35949	Robust half-metallicities and perfect spin transport properties in 2D transition metal dichlorides. Journal of Materials Chemistry C, 2018, 6, 4087-4094.	2.7	73
35950	Magnetic moment and magnetic anisotropy of Ge3Mn5 thinfilms on Ge(111) substrate: A density functional study. Journal of Chemical Physics, 2018, 148, 074701.	1.2	3
35951	Quantum anomalous Hall effect and topological phase transition in two-dimensional antiferromagnetic Chern insulator NiOsCl6. Journal of Physics Condensed Matter, 2018, 30, 185501.	0.7	0
35952	Spin-polarized two-dimensional <mml:math xmlns:mml="http://www.w3.org/1998/Math/MathML"><mml:msub><mml:mi>t</mml:mi><mml:mrow><mml:mn>2</mml:mn><mml:mi electron gas: Ab initio study of EuO interface with oxygen-deficient <mml:math xmlns:mml="http://www.w3.org/1998/Math/MathML"><mml:mrow><mml:mi>SrTi</mml:mi><mml:msub><mml:mi mathvariant="normal">O</mml:mi><mml:mn>3</mml:mn></mml:msub></mml:mrow></mml:math>. Physical Review B, 2018, 97, .	1.1	9
35953	Molecular Modelling of the H₂â€Adsorptive Properties of Tetrazolateâ€Based Metalâ€“Organic Frameworks: From the Cluster Approach to Periodic Simulations. ChemPhysChem, 2018, 19, 1349-1357.	1.0	6
35954	Preparation and surface characteristics of Re3W matrix scandate cathode: An experimental and theoretical study. Applied Surface Science, 2018, 440, 763-769.	3.1	18
35955	Adsorption and diffusion of H and O on an Ni(1 1 1) surface containing different amounts of Cr. Applied Surface Science, 2018, 445, 217-228.	3.1	18

#	Article	IF	Citations
35956	Electronic structure and optical properties of SrTiO3 codoped by W/Mo on different cationic sites with C/N from hybrid functional calculations. Computational Materials Science, 2018, 146, 150-157.	1.4	11
35957	Structural and electronic properties of PdS 2 nanoribbons. Journal of Magnetism and Magnetic Materials, 2018, 458, 310-316.	1.0	10
35958	Polypyrrole on graphene: A density functional theory study. Surface Science, 2018, 674, 1-5.	0.8	13
35959	Thermal Stability Enhanced Tetraethylenepentamine/Silica Adsorbents for High Performance CO2 Capture. Industrial & Engineering Chemistry Research, 2018, 57, 4632-4639.	1.8	46
35960	Methane Adsorption and Separation in Slipped and Functionalized Covalent Organic Frameworks. Industrial & Engineering Chemistry Research, 2018, 57, 4767-4778.	1.8	36
35961	Intermediate Band Material of Titanium-Doped Tin Disulfide for Wide Spectrum Solar Absorption. Inorganic Chemistry, 2018, 57, 3956-3962.	1.9	35
35962	CaP₃: A New Two-Dimensional Functional Material with Desirable Band Gap and Ultrahigh Carrier Mobility. Journal of Physical Chemistry Letters, 2018, 9, 1728-1733.	2.1	112
35963	Operando tribochemical formation of onion-like-carbon leads to macroscale superlubricity. Nature Communications, 2018, 9, 1164.	5.8	199
35964	An effective method to screen sodium-based layered materials for sodium ion batteries. Npj Computational Materials, 2018, 4, .	3.5	77
35965	Silicene and germanene on InSe substrates: structures and tunable electronic properties. Physical Chemistry Chemical Physics, 2018, 20, 11369-11377.	1.3	44
35966	A first principle comparative study of the ionic diffusivity in LiAlO2 and NaAlO2 polymorphs for solid-state battery applications. Physical Chemistry Chemical Physics, 2018, 20, 9824-9832.	1.3	16
35967	Bubble-wrap carbon: an integration of graphene and fullerenes. Nanoscale, 2018, 10, 11328-11334.	2.8	15
35968	Two-dimensional graphitic C₃N₅ materials: promising metal-free catalysts and CO₂ adsorbents. Journal of Materials Chemistry A, 2018, 6, 7168-7174.	5.2	58
35969	Critical point and mechanism of the phase transition in warm dense hydrogen. Journal of Physics: Conference Series, 2018, 946, 012122.	0.3	0
35970	Investigation on preferably oriented abnormal growth of CdSe nanorods along (0002) plane synthesized by henna leaf extract-mediated green synthesis. Royal Society Open Science, 2018, 5, 171430.	1.1	19
35971	Finite-temperature lattice dynamics and superionic transition in ceria from first principles. Physical Review B, 2018, 97, .	1.1	12
35972	Pressure effect on the magnetic properties of the half-metallic Heusler alloy <mml:math xmlns:mml="http://www.w3.org/1998/Math/MathML"><mml:mrow><mml:msub><mml:mi>Co</mml:mi><mml:mn>2</mml:mn></mml:msub></mml:mrow></mml:math> Physical Review B, 2018, 97, .	1.1	27
35973	Coherent Electron Transfer at the <mml:math xmlns:mml="http://www.w3.org/1998/Math/MathML" display="inline"><mml:mrow><mml:mrow><mml:mi>Ag</mml:mi><mml:mo>/</mml:mo></mml:mrow><mml:mi>Graphite</mml:mi></mml:mrow></mml:math> Heterojunction Interface. Physical Review Letters, 2018, 120, 126801.	2.9	47

#	Article	IF	Citations
35974	Black Silicon IR Photodiode Supersaturated With Nitrogen by Femtosecond Laser Irradiation. IEEE Sensors Journal, 2018, 18, 3595-3601.	2.4	25
35975	Solute strengthening of basal slip in Mg alloys. Acta Materialia, 2018, 151, 56-66.	3.8	87
35976	Triggering superior sodium ion adsorption on (2â€¯0â€¯0) facet of mesoporous WO3 nanosheet arrays for enhanced supercapacitance. Chemical Engineering Journal, 2018, 345, 165-173.	6.6	39
35977	Electronic and magnetic properties of structural defects in pristine ZrSe2 monolayer. Computational Materials Science, 2018, 146, 36-41.	1.4	16
35978	Cations controlled growth of Î²-MnO2 crystals with tunable facets for electrochemical energy storage. Nano Energy, 2018, 48, 301-311.	8.2	56
35979	Self-compensation induced vacancies for significant phonon scattering in InSb. Nano Energy, 2018, 48, 189-196.	8.2	30
35980	Understanding slow-growing alumina scale mediated by reactive elements: Perspective via local metal-oxygen bonding strength. Scripta Materialia, 2018, 150, 139-142.	2.6	26
35981	Tuning electronic properties of silicane layers by tensile strain and external electric field: A first-principles study. Thin Solid Films, 2018, 654, 107-115.	0.8	36
35982	Identification of Intermediates during the Hydration of Na₈[AlSiO₄]₆(BH₄)₂: A Combined Theoretical and Experimental Approach. Journal of Physical Chemistry A, 2018, 122, 3293-3300.	1.1	1
35983	Potential Dependence of the Buckling Structure of the Interfacial Water Bilayer on a Graphene Electrode. Journal of Physical Chemistry C, 2018, 122, 7795-7800.	1.5	4
35984	Surprising Stability of Cubane under Extreme Pressure. Journal of Physical Chemistry Letters, 2018, 9, 2031-2037.	2.1	12
35985	Anharmonicity and Disorder in the Black Phases of Cesium Lead Iodide Used for Stable Inorganic Perovskite Solar Cells. ACS Nano, 2018, 12, 3477-3486.	7.3	546
35986	Bismuth and antimony-based oxyhalides and chalcohalides as potential optoelectronic materials. Npj Computational Materials, 2018, 4, .	3.5	86
35987	Direct synthesis and in situ characterization of monolayer parallelogrammic rhenium diselenide on gold foil. Communications Chemistry, 2018, 1, .	2.0	58
35988	An accurate first-principles treatment of doping-dependent electronic structure of high-temperature cuprate superconductors. Communications Physics, 2018, 1, .	2.0	94
35989	Superior electronic structure of two-dimensional 3d transition metal dicarbides for applications in spintronics. Journal of Materials Chemistry C, 2018, 6, 4290-4299.	2.7	23
35990	A first-principles study on the adsorption of small molecules on antimonene: oxidation tendency and stability. Journal of Materials Chemistry C, 2018, 6, 4308-4317.	2.7	68
35991	Tuning the optoelectronic characteristics of ionic organic crystalline assemblies. Journal of Materials Chemistry C, 2018, 6, 4041-4056.	2.7	15

#	Article	IF	Citations
35992	Is RuAs2 a candidate for high temperature thermoelectric applications?. Physical Chemistry Chemical Physics, 2018, 20, 9930-9937.	1.3	3
35993	Quantum spin Hall effect in two-dimensional hydrogenated SnPb alloy films. Physical Chemistry Chemical Physics, 2018, 20, 9610-9615.	1.3	2
35994	Tuning charge transfer in the LaTiO3/RO/LaNiO3 (Râ€‰=â€‰rare-earth) superlattices by the rare-earth oxides interfaces from a first-principles calculation. Journal of Applied Physics, 2018, 123, .	1.1	2
35995	Structural, vibrational, and electronic topological transitions of Bi1.5Sb0.5Te1.8Se1.2 under pressure. Journal of Applied Physics, 2018, 123, .	1.1	14
35996	Efficient Discovery of Optimal N-Layered TMDC Hetero-Structures. MRS Advances, 2018, 3, 397-402.	0.5	5
35997	Direct inversion of the iterative subspace (DIIS) convergence accelerator for crystalline solids employing Gaussian basis sets. Theoretical Chemistry Accounts, 2018, 137, 1.	0.5	17
35998	Biodegradable, electro-active chitin nanofiber films for flexible piezoelectric transducers. Nano Energy, 2018, 48, 275-283.	8.2	101
35999	Pathways of phase transformation in Î²-phase-stabilized Ïƒ/Î³-TiAl alloys subjected to two-step heat treatments. Scripta Materialia, 2018, 149, 70-74.	2.6	17
36000	Oxygen Species on Nitrogen-Doped Carbon Nanosheets as Efficient Active Sites for Multiple Electrocatalysis. ACS Applied Materials & Interfaces, 2018, 10, 11678-11688.	4.0	58
36001	Microwave-assisted hydrothermal synthesis of cobalt phosphide nanostructures for advanced supercapacitor electrodes. CrystEngComm, 2018, 20, 2413-2420.	1.3	30
36002	Metallic VO₂ monolayer as an anode material for Li, Na, K, Mg or Ca ion storage: a first-principle study. RSC Advances, 2018, 8, 10848-10854.	1.7	51
36003	A unified model of Grignard reagent formation. Physical Chemistry Chemical Physics, 2018, 20, 11100-11108.	1.3	6
36004	Ab initio magnesium-solute transport database using exact diffusion theory. Acta Materialia, 2018, 150, 339-350.	3.8	35
36005	Dependence of H2 and CO2 selectivity on Cu oxidation state during partial oxidation of methanol on Cu/ZnO. Applied Catalysis A: General, 2018, 556, 64-72.	2.2	34
36006	Effect of hydrogen coverage on hydrogenation of o-cresol on Pt(111). Applied Surface Science, 2018, 443, 575-580.	3.1	11
36007	Prediction of fully compensated ferrimagnetic and nonmagnetic semiconductors with promising thermoelectric properties through the Mo substitution of Cr for Ti 2 CrZ (Z=Ge, Sn) Heusler alloys. Intermetallics, 2018, 96, 72-78.	1.8	4
36008	Mechanical exfoliation of two-dimensional materials. Journal of the Mechanics and Physics of Solids, 2018, 115, 248-262.	2.3	143
36009	Hydrogen trapping in carbon supersaturated Î±â€˜iron and its decohesion effect in martensitic steel. Scripta Materialia, 2018, 149, 79-83.	2.6	40

#	Article	IF	Citations
36010	Exploring the methanol decomposition mechanism on the Pt₃Ni(100) surface: a periodic density functional theory study. Physical Chemistry Chemical Physics, 2018, 20, 10132-10141.	1.3	8
36011	A theoretical perspective of the enhanced photocatalytic properties achieved by forming tetragonal ZnS/ZnSe hetero-bilayer. Physical Chemistry Chemical Physics, 2018, 20, 9950-9956.	1.3	14
36012	Hindered rotation and nuclear spin isomers separation of molecularly chemisorbed H2 on Pd(210). Journal of Applied Physics, 2018, 123, .	1.1	5
36013	Catalyst design by scanning probe block copolymer lithography. Proceedings of the National Academy of Sciences of the United States of America, 2018, 115, 3764-3769.	3.3	40
36014	A First-Principles Study on the Vibrational and Electronic Properties of Zr-C MXenes. Communications in Theoretical Physics, 2018, 69, 336.	1.1	15
36015	Electrically active induced energy levels and metastability of B and N vacancy-complexes in 4Hâ€“SiC. Journal of Physics Condensed Matter, 2018, 30, 185702.	0.7	4
36016	Electric field effect on the electronic structure of 2D Y 2 C electride. 2D Materials, 2018, 5, 035005.	2.0	14
36017	Strain mapping in single-layer two-dimensional crystals via Raman activity. Physical Review B, 2018, 97, .	1.1	43
36018	First-principles study of electronic structure modulations in graphene on Ru(0001) by Au intercalation. Physical Review B, 2018, 97, .	1.1	2
36019	Dislocation-driven growth of two-dimensional lateral quantum-well superlattices. Science Advances, 2018, 4, eaap9096.	4.7	38
36020	Trapping of volatile fission products by C60. Carbon, 2018, 132, 477-485.	5.4	16
36021	The origin of cycling enhanced capacity of Ni/NiO species confined on nitrogen doped carbon nanotubes for lithium-ion battery anodes. Journal of Alloys and Compounds, 2018, 750, 17-22.	2.8	12
36022	The structural, electronic, elastic, thermodynamic, magnetic, and optical properties of the yttrium-based full-Heusler alloys Y 2 CrZ (Z=Si, Ge, Sn). Journal of Physics and Chemistry of Solids, 2018, 119, 71-79.	1.9	21
36023	A New Anisotropic Dirac Cone Material: A B₂S Honeycomb Monolayer. Journal of Physical Chemistry Letters, 2018, 9, 1815-1820.	2.1	96
36024	Degradation Chemistry and Stabilization of Exfoliated Few-Layer Black Phosphorus in Water. Journal of the American Chemical Society, 2018, 140, 7561-7567.	6.6	273
36025	Lanthanide atom substitutionally doped blue phosphorene: electronic and magnetic behaviors. Physical Chemistry Chemical Physics, 2018, 20, 11003-11012.	1.3	27
36026	Effect of Al-distribution on oxygen activation over Cuâ€“CHA. Catalysis Science and Technology, 2018, 8, 2131-2136.	2.1	47
36027	Co-mixing hydrogen and methane may double the energy storage capacity. Journal of Materials Chemistry A, 2018, 6, 8916-8922.	5.2	22

#	Article	IF	Citations
36028	Point Defects and <mml:math xmlns:mml="http://www.w3.org/1998/Math/MathML" display="inline"><mml:mi>p</mml:mi></mml:math> -Type Doping in ScN from First Principles. Physical Review Applied, 2018, 9, .	1.5	33
36029	First principles investigation of the unipolar resistive switching mechanism in an interfacial phase change memory based on a GeTe/Sb₂Te₃superlattice. Japanese Journal of Applied Physics, 2018, 57, 04FE08.	0.8	7
36030	Thermodynamic analysis of trimethylgallium decomposition during GaN metal organic vapor phase epitaxy. Japanese Journal of Applied Physics, 2018, 57, 04FJ03.	0.8	12
36031	Rich interfacial chemistry and properties of carbon-doped hexagonal boron nitride nanosheets revealed by electronic structure calculations. Japanese Journal of Applied Physics, 2018, 57, 04FL11.	0.8	3
36032	Spectroscopic Studies of Photochemical Transformations of Cymantrenylquinazolinone Derivatives. European Journal of Inorganic Chemistry, 2018, 2018, 1945-1952.	1.0	4
36033	Fine speciation of active sites in zeolites by a CO probe: Dynamics and IR frequencies. International Journal of Quantum Chemistry, 2018, 118, e25625.	1.0	5
36034	First-principles study of lithium-ion diffusion in Î² -Li 3 PS 4 for solid-state electrolytes. Current Applied Physics, 2018, 18, 541-545.	1.1	18
36035	Synthesis of Atomically Thin Transition Metal Ditelluride Films by Rapid Chemical Transformation in Solution Phase. Chemistry of Materials, 2018, 30, 2463-2473.	3.2	25
36036	Exploring Defect-Induced Emission in ZnAl₂O₄: An Exceptional Color-Tunable Phosphor Material with Diverse Lifetimes. Inorganic Chemistry, 2018, 57, 3963-3982.	1.9	72
36037	High voltage structural evolution and enhanced Na-ion diffusion in P2-Na_{2/3}Ni_{1/3â^'x}Mg_xMn_{2/3}O₂ (0 â‰¤ x) Tj ETQq1 1 0.7843 Environmental Science, 2018, 11, 1470-1479.	15.6	148
36038	Ferroelectric critical size and vortex domain structures of PbTiO3 nanodots: A density functional theory study. Journal of Applied Physics, 2018, 123, .	1.1	11
36039	Synchrotron-based ambient pressure X-ray photoelectron spectroscopy of hydrogen and helium. Applied Physics Letters, 2018, 112, .	1.5	13
36040	Two-dimensional <mml:math xmlns:mml="http://www.w3.org/1998/Math/MathML"><mml:mi>n</mml:mi></mml:math> -InSe/ <mml:math xmlns:mml="http://www.w3.org/1998/Math/MathML"><mml:mi>p</mml:mi></mml:math> -GeSe(SnS) van der Waals heterojunctions: High carrier mobility and broadband performance. Physical Review B, 2018, 97, .	1.1	113
36041	Nonequilibrium BN-ZnO: Optical properties and excitonic effects from first principles. Physical Review B, 2018, 97, .	1.1	9
36042	AbÂInitio Calculation of the Miscibility Diagram for Hydrogen-Helium Mixtures. Physical Review Letters, 2018, 120, 115703.	2.9	70
36043	First-principles study of interaction between vacancies and nitrogen atoms in fcc iron. Computational Materials Science, 2018, 149, 65-72.	1.4	8
36044	High electrical transport properties performance enhanced by anti-site defects in single crystalline SnSe. Journal of Alloys and Compounds, 2018, 748, 80-86.	2.8	13
36045	Exotic chemical arrangements and magnetic moment evolution of <mml:math xmlns:mml="http://www.w3.org/1998/Math/MathML" altimg="si1.gif" overflow="scroll"><mml:mrow><mml:msub><mml:mrow><mml:mtext>Ni</mml:mtext></mml:mrow><mml:mrow><mml:mi>x</mml:mi>		

#	Article	IF	Citations
36046	Prediction of optimal structural water concentration for maximized performance in tunnel manganese oxide electrodes. Physical Chemistry Chemical Physics, 2018, 20, 9480-9487.	1.3	12
36047	Defects controlling electrical and optical properties of electrodeposited Bi doped Cu2O. Journal of Applied Physics, 2018, 123, .	1.1	21
36048	Exploring the effect of nanoholes on arsenene: a density functional theory study. Journal of Physics Condensed Matter, 2018, 30, 195305.	0.7	3
36049	Effect of multicomponent alloying with Ni, Mn and Mo on phase stability of bcc Fe-Cr alloys. Acta Materialia, 2018, 150, 117-129.	3.8	23
36050	Mechanistic insight into the quantitative synthesis of acetic acid by direct conversion of CH4 and CO2: An experimental and theoretical approach. Applied Catalysis B: Environmental, 2018, 229, 237-248.	10.8	59
36051	The promotion effects of graphitic and pyridinic N combinational doping on graphene for ORR. Applied Surface Science, 2018, 445, 398-403.	3.1	71
36052	A rational design of hole-transport small molecules based on fluorene with different modified groups for organic lead-halide perovskite solar cells. Dyes and Pigments, 2018, 154, 275-281.	2.0	25
36053	Exploring pristine and Li-doped Mg2NiH4 compounds with potential lithium-storage properties: Ab initio insight. Journal of Alloys and Compounds, 2018, 746, 140-146.	2.8	8
36054	The stability of vacancy clusters and their effect on helium behaviors in 3C-SiC. Journal of Nuclear Materials, 2018, 503, 271-278.	1.3	29
36055	Acid-base bifunctional catalyst: Carboxyl ionic liquid immobilized on MIL-101-NH2 for rapid synthesis of propylene carbonate from CO2 and propylene oxide under facile solvent-free conditions. Microporous and Mesoporous Materials, 2018, 267, 84-92.	2.2	59
36056	Dopant-Dependent SFG Response of Rhenium CO₂ Reduction Catalysts Chemisorbed on SrTiO₃ (100) Single Crystals. Journal of Physical Chemistry C, 2018, 122, 13944-13952.	1.5	10
36057	Latent Order in High-Angle Grain Boundary of GaN. Scientific Reports, 2018, 8, 4647.	1.6	2
36058	Lithium adsorption and migration in group IVâ€“VI compounds and GeS/graphene heterostructures: a comparative study. Physical Chemistry Chemical Physics, 2018, 20, 9865-9871.	1.3	14
36059	Stability and band offsets between c-plane ZnO semiconductor and LaAlO3 gate dielectric. Journal of Applied Physics, 2018, 123, .	1.1	2
36060	Constructing first-principles phase diagrams of amorphous LixSi using machine-learning-assisted sampling with an evolutionary algorithm. Journal of Chemical Physics, 2018, 148, 241711.	1.2	121
36061	Observations of non-linear plasmon damping in dense plasmas. Physics of Plasmas, 2018, 25, .	0.7	29
36062	Forces and electronic transport in a contact formed by a graphene tip and a defective MoS₂monolayer: a theoretical study. Nanotechnology, 2018, 29, 225704.	1.3	2
36063	Methanol Oxidation to Formaldehyde Promoted at the Step Sites of Ultrathin ZnO. Topics in Catalysis, 2018, 61, 499-508.	1.3	11

#	Article	IF	Citations
36064	Interfacial properties of black phosphorus/transition metal carbide van der Waals heterostructures. Frontiers of Physics, 2018, 13, 1.	2.4	19
36065	Atomistic origins of the differences in anisotropic fracture behaviour of LiTaO3 and LiNbO3 single crystals. Acta Materialia, 2018, 150, 373-380.	3.8	17
36066	The activation of reactants and intermediates promotes the selective photocatalytic NO conversion on electron-localized Sr-intercalated g-C3N4. Applied Catalysis B: Environmental, 2018, 232, 69-76.	10.8	125
36067	An improved interatomic potential function for thermoelectric Mg2Si: A combination study of ab-initio and molecular dynamics method. Computational Materials Science, 2018, 149, 49-56.	1.4	7
36068	Photoresponse enhancement in SnO2-based ultraviolet photodetectors via coupling with surface plasmons of Ag particles. Journal of Alloys and Compounds, 2018, 748, 398-403.	2.8	27
36069	Cycloketone condensation catalyzed by zirconia: Origin of reactant selectivity. Journal of Catalysis, 2018, 361, 186-192.	3.1	12
36070	The complexity of non-Schmid behavior in the CuZnAl shape memory alloy. Journal of the Mechanics and Physics of Solids, 2018, 114, 238-257.	2.3	15
36071	Na2MnO3 as cathode materials for Na ion batteries: From first-principles investigations. Solid State Ionics, 2018, 320, 210-214.	1.3	31
36072	Stability of Tetrabutylphosphonium Beidellite Organoclay. Journal of Physical Chemistry C, 2018, 122, 8380-8389.	1.5	10
36073	Passivated Codoping Can Improve the Solar-to-Hydrogen Efficiency of Graphitic Carbon Nitride. Journal of Physical Chemistry C, 2018, 122, 7296-7302.	1.5	20
36074	Local Fluxionality of Surface-Deposited Cluster Catalysts: The Case of Pt₇ on Al₂O₃. Journal of Physical Chemistry Letters, 2018, 9, 1696-1702.	2.1	69
36075	Band Engineering of Carbon Nitride Monolayers by N-Type, P-Type, and Isoelectronic Doping for Photocatalytic Applications. ACS Applied Materials & Interfaces, 2018, 10, 11143-11151.	4.0	92
36076	Carbon Capture by Metal Oxides: Unleashing the Potential of the (111) Facet. Journal of the American Chemical Society, 2018, 140, 4736-4742.	6.6	83
36077	ZnO/MoX₂ (X = S, Se) composites used for visible light photocatalysis. RSC Advances, 2018, 8, 10828-10835.	1.7	36
36078	First-principles investigation of the Lewis acidâ€“base adduct formation at the methylammonium lead iodide surface. Physical Chemistry Chemical Physics, 2018, 20, 11183-11195.	1.3	9
36079	Stronger-than-Pt hydrogen adsorption in a Au₂₂ nanocluster for the hydrogen evolution reaction. Journal of Materials Chemistry A, 2018, 6, 7532-7537.	5.2	63
36080	Exploring new two-dimensional monolayers: pentagonal transition metal borides/carbides (penta-TMB/Cs). Journal of Materials Chemistry A, 2018, 6, 10226-10232.	5.2	77
36081	The effect of ionic composition on acoustic phonon speeds in hybrid perovskites from Brillouin spectroscopy and density functional theory. Journal of Materials Chemistry C, 2018, 6, 3861-3868.	2.7	23

#	Article	IF	Citations
36082	First-Principle Calculations on the Structural, Mechanical, and Electronic Properties of Mn2RuSi and Mn2RuGe Under Pressure. Journal of Superconductivity and Novel Magnetism, 2018, 31, 3667-3677.	0.8	4
36083	Ab initio study of two-dimensional PdPS as an ideal light harvester and promising catalyst for hydrogen evolution reaction. Materials Today Energy, 2018, 7, 136-140.	2.5	24
36084	Nature of Photoinduced Quenching Traps in Methylammonium Lead Triiodide Perovskite Revealed by Reversible Photoluminescence Decline. ACS Photonics, 2018, 5, 2034-2043.	3.2	42
36085	Efficient first-principles prediction of solid stability: Towards chemical accuracy. Npj Computational Materials, 2018, 4, .	3.5	157
36086	Hydrodeoxygenation of guaiacol over bimetallic Fe-alloyed (Ni, Pt) surfaces: reaction mechanism, transition-state scaling relations and descriptor for predicting Câ€“O bond scission reactivity. Catalysis Science and Technology, 2018, 8, 2146-2158.	2.1	56
36087	Stacking sequences of black phosphorous allotropes and the corresponding few-layer phosphorenes. Physical Chemistry Chemical Physics, 2018, 20, 10185-10192.	1.3	8
36088	Reaction paths of alane dissociation on the Si(0â€‰0â€‰1) surface. Journal of Physics Condensed Matter, 2018, 30, 105002.	0.7	1
36089	Interface passivation and trap reduction via hydrogen fluoride for molybdenum disulfide on silicon oxide back-gate transistors. Semiconductor Science and Technology, 2018, 33, 045005.	1.0	7
36090	Thermoelectric properties of two-dimensional hexagonal indium-VA. Chinese Physics B, 2018, 27, 026802.	0.7	11
36091	Frustrated magnetism in the tetragonal CoSe analog of superconducting FeSe. Physical Review B, 2018, 97, .	1.1	35
36092	Quantum-Chemical Modeling of the Surface Contact of Superionic Conductor Li10GeP2S12 with Different Materials. Russian Journal of Inorganic Chemistry, 2018, 63, 69-77.	0.3	0
36093	First-Principles Lattice Dynamics Method for Strongly Anharmonic Crystals. Journal of the Physical Society of Japan, 2018, 87, 041015.	0.7	93
36094	How Low Nucleation Density of Graphene on CuNi Alloy is Achieved. Advanced Science, 2018, 5, 1700961.	5.6	25
36095	Healable Structure Triggered by Thermal/Electrochemical Force in Layered GeSe₂ for High Performance Liâ€ion Batteries. Advanced Energy Materials, 2018, 8, 1703635.	10.2	59
36096	Sulfur/Oxygen Codoped Porous Hard Carbon Microspheres for Highâ€Performance Potassiumâ€ion Batteries. Advanced Energy Materials, 2018, 8, 1800171.	10.2	363
36097	Selective Semihydrogenation of Phenylacetylene to Styrene Catalyzed by Alloyed Palladium/Gold Catalysts Anchored on Cerium Oxide. ChemNanoMat, 2018, 4, 472-476.	1.5	11
36098	Theoretical design of sandwich two-dimensional structures for photocatalysts and nano-optoelectronic devices. Journal of Materials Science, 2018, 53, 8274-8284.	1.7	7
36099	Ab initio simulation of hydrogen-induced decohesion in cementite-containing microstructures. Acta Materialia, 2018, 150, 53-58.	3.8	40

#	Article	IF	Citations
36100	Detailed mechanism of the NOâ€¯+â€¯CO reaction on Rh(1 0 0) and Rh(1 1 1): A first-principles study. Applied Surface Science, 2018, 444, 276-286.	3.1	20
36101	Few-layer MoS2 nanosheets-deposited on Bi2MoO6 microspheres: A Z-scheme visible-light photocatalyst with enhanced activity. Catalysis Today, 2018, 315, 67-78.	2.2	74
36102	Electrochemical measurements and atomistic simulations of Clâ¯-induced passivity breakdown on a Cu2O film. Corrosion Science, 2018, 136, 119-128.	3.0	31
36103	In situ growth of iron-nickel nitrides on carbon nanotubes with enhanced stability and activity for oxygen evolution reaction. Electrochimica Acta, 2018, 267, 8-14.	2.6	45
36104	Enhancement in thermoelectric properties of Te-embedded Bi2Te3 by preferential phonon scattering in heterostructure interface. Nano Energy, 2018, 47, 374-384.	8.2	101
36105	Influence of carbon deficiency on phase formation and thermal stability of super-hard TaCy thin films. Scripta Materialia, 2018, 149, 150-154.	2.6	25
36106	CH3Br adsorption on MgO/Mo ultrathin films: A DFT study. Surface Science, 2018, 672-673, 1-6.	0.8	3
36107	High-Throughput Description of Infinite Compositionâ€“Structureâ€“Propertyâ€“Performance Relationships of Lithiumâ€“Manganese Oxide Spinel Cathodes. Chemistry of Materials, 2018, 30, 2287-2298.	3.2	20
36108	Nonadiabatic Molecular Dynamics Simulation of Charge Separation and Recombination at a WS₂/QD Heterojunction. Journal of Physical Chemistry C, 2018, 122, 7041-7050.	1.5	16
36109	Photocatalytic Activity of Phosphorene Derivatives: Coverage, Electronic, Optical, and Excitonic Properties. Journal of Physical Chemistry C, 2018, 122, 7194-7202.	1.5	9
36110	Rapid Decoherence Suppresses Charge Recombination in Multi-Layer 2D Halide Perovskites: Time-Domain Ab Initio Analysis. Nano Letters, 2018, 18, 2459-2466.	4.5	114
36111	Rational Design of Dithienopicenocarbazole-Based Dyes and a Prediction of Their Energy-Conversion Efficiency Characteristics for Dye-Sensitized Solar Cells. ACS Applied Energy Materials, 2018, 1, 1435-1444.	2.5	36
36112	High Interfacial Charge Storage Capability of Carbonaceous Cathodes for Mg Batteries. ACS Nano, 2018, 12, 2998-3009.	7.3	26
36113	A Universal Method to Engineer Metal Oxideâ€“Metalâ€“Carbon Interface for Highly Efficient Oxygen Reduction. ACS Nano, 2018, 12, 3042-3051.	7.3	125
36114	Switchable Polarization in Mn Embedded Graphene. Scientific Reports, 2018, 8, 4538.	1.6	4
36115	Methanol decomposition reactions over a boron-doped graphene supported Ruâ€“Pt catalyst. Physical Chemistry Chemical Physics, 2018, 20, 9355-9363.	1.3	25
36116	Engineering of charge carriersviaa two-dimensional heterostructure to enhance the thermoelectric figure of merit. Nanoscale, 2018, 10, 7077-7084.	2.8	76
36117	Identifying key descriptors in surface binding: interplay of surface anchoring and intermolecular interactions for carboxylates on Au(110). Chemical Science, 2018, 9, 3759-3766.	3.7	11

#	Article	IF	Citations
36118	Finite-temperature property-maps of Liâ€“Mnâ€“Niâ€“O cathode materials from ab initio calculations. Journal of Materials Chemistry A, 2018, 6, 5687-5694.	5.2	3
36119	Anisotropic vacancy-mediated phonon mode softening in Sm and Gd doped ceria. Physical Chemistry Chemical Physics, 2018, 20, 10048-10059.	1.3	10
36120	Construction of hierarchical Niâ€“Coâ€“P hollow nanobricks with oriented nanosheets for efficient overall water splitting. Energy and Environmental Science, 2018, 11, 872-880.	15.6	773
36121	Two-dimensional ferroelectricity and switchable spin-textures in ultra-thin elemental Te multilayers. Materials Horizons, 2018, 5, 521-528.	6.4	96
36122	Ordered three-fold symmetric graphene oxide/buckled graphene/graphene heterostructures on MgO(111) by carbon molecular beam epitaxy. Journal of Materials Chemistry C, 2018, 6, 4225-4233.	2.7	1
36123	2D carbon sheets with negative Gaussian curvature assembled from pentagonal carbon nanoflakes. Physical Chemistry Chemical Physics, 2018, 20, 9123-9129.	1.3	6
36124	First-principles insights into tin-based two-dimensional hybrid halide perovskites for photovoltaics. Journal of Materials Chemistry A, 2018, 6, 5652-5660.	5.2	71
36125	First-principles investigations on elastic, thermodynamic and lattice thermal conductivity of topological insulator LaAs. Philosophical Magazine, 2018, 98, 1900-1918.	0.7	11
36126	Graphene-like monolayer InSeâ€“X: several promising half-metallic nanosheets in spintronics. Journal of Physics Condensed Matter, 2018, 30, 155306.	0.7	6
36127	Efficient band structure modulations in two-dimensional MnPSe₃/CrSiTe₃ van der Waals heterostructures. Nanotechnology, 2018, 29, 214001.	1.3	14
36128	First-principles study of polarization and piezoelectricity behavior in tetragonal PbTiO ₃ -based superlattices. Chinese Physics B, 2018, 27, 027701.	0.7	2
36129	The high-pressure stability of Ni2In-type structure of ZrO2 with respect to OII and Fe2P-type phases: A first-principles study. IOP Conference Series: Materials Science and Engineering, 2018, 305, 012016.	0.3	4
36130	The effect of surface reconstruction on the minimum-energy grain boundary fracture path: a first-principles study. Materials Research Express, 2018, 5, 036525.	0.8	1
36131	Nodal surface semimetals: Theory and material realization. Physical Review B, 2018, 97, .	1.1	248
36132	Applicability of Kerker preconditioning scheme to the self-consistent density functional theory calculations of inhomogeneous systems. Physical Review E, 2018, 97, 033305.	0.8	14
36133	Point defect concentrations of L12-Al3X(Sc, Zr, Er). Rare Metals, 2018, 37, 699-706.	3.6	11
36134	Defect induced room temperature ferromagnetism in lead-free ferroelectric Bi 0.5 K 0.5 TiO 3 materials. Physica B: Condensed Matter, 2018, 532, 108-114.	1.3	24
36135	Mechanistic Study of Nitric Oxide Reduction by Hydrogen on Pt(100) (I): A DFT Analysis of the Reaction Network. Journal of Physical Chemistry B, 2018, 122, 432-443.	1.2	29

#	Article	IF	Citations
36136	Computational predictions of zinc oxide hollow structures. Physica B: Condensed Matter, 2018, 532, 15-19.	1.3	9
36137	Interfacial microstructure and nucleating mechanism of melt-spun CeB 6 /Al composite inoculant. Applied Surface Science, 2018, 431, 202-206.	3.1	15
36138	Metal-organic framework-derived porous shuttle-like vanadium oxides for sodium-ion battery application. Nano Research, 2018, 11, 449-463.	5.8	108
36139	Superior catalytic performance of Mn-Mullite over Mn-Perovskite for NO oxidation. Catalysis Today, 2018, 310, 195-201.	2.2	52
36140	Selectivity shifts in hydrogenation of cinnamaldehyde on electron-deficient ruthenium nanoparticles. Comptes Rendus Chimie, 2018, 21, 346-353.	0.2	29
36141	Adsorption of H 2 O, H 2 , O 2 , CO, NO, and CO 2 on graphene/g-C 3 N 4 nanocomposite investigated by density functional theory. Applied Surface Science, 2018, 430, 125-136.	3.1	56
36142	Effect of pressure on the Raman-active modes of zircon (ZrSiO4): a first-principles study. Physics and Chemistry of Minerals, 2018, 45, 173-184.	0.3	12
36143	Tunable Magnetic Interaction of Mn-Doped MoS2/SiC van der Waals Heterostructures Under Normal Strain. Journal of Superconductivity and Novel Magnetism, 2018, 31, 449-453.	0.8	1
36144	Strain and different edge terminations modulated electronic and magnetic properties of armchair AlN/SiC nanoribbons: first-principles study. Canadian Journal of Physics, 2018, 96, 30-35.	0.4	0
36145	A first principles study of energetics and electronic structural responses of uranium-based coordination polymers to Np incorporation. Radiochimica Acta, 2018, 106, 1-13.	0.5	5
36146	New understanding of photocatalytic properties of zigzag and armchair g-C 3 N 4 nanotubes from electronic structures and carrier effective mass. Applied Surface Science, 2018, 430, 348-354.	3.1	40
36147	Surface Termination of Fe₃O₄(111) Films Studied by CO Adsorption Revisited. Journal of Physical Chemistry B, 2018, 122, 527-533.	1.2	46
36148	Trends of Alkane Activation on Doped Cobalt (II,â€…III) Oxide from First Principles. ChemCatChem, 2018, 10, 244-249.	1.8	25
36149	Matildite Contact with Media: First-Principles Study of AgBiS₂ Surfaces and Nanoparticle Morphology. Journal of Physical Chemistry B, 2018, 122, 521-526.	1.2	15
36150	General Effect of van der Waals Interactions on the Stability of Alkoxy Intermediates on Metal Surfaces. Journal of Physical Chemistry B, 2018, 122, 555-560.	1.2	17
36151	Native point defects in MoS 2 and their influences on optical properties by first principles calculations. Physica B: Condensed Matter, 2018, 532, 184-194.	1.3	11
36152	A pyridine vapor sensor based on metal-organic framework-modified quartz crystal microbalance. Sensors and Actuators B: Chemical, 2018, 254, 872-877.	4.0	27
36153	Three-layer phosphorene-metal interfaces. Nano Research, 2018, 11, 707-721.	5.8	72

#	Article	IF	Citations
36154	Density functional theory calculation of monolayer WTe 2 transition metal dichalcogenides doped with H, Li and Be. Physica B: Condensed Matter, 2018, 535, 167-170.	1.3	1
36155	Density functional theory study for the enhanced sulfur tolerance of Ni catalysts by surface alloying. Applied Surface Science, 2018, 429, 87-94.	3.1	26
36156	Two-dimensional boron on Pb (1 1 0) surface. FlatChem, 2018, 7, 34-41.	2.8	7
36157	Dry Dehydrogenation of Ethanol on Ptâ€“Cu Single Atom Alloys. Topics in Catalysis, 2018, 61, 328-335.	1.3	49
36158	Interaction of Pd single atoms with different CeO 2 crystal planes: A first-principles study. Applied Surface Science, 2018, 433, 1036-1048.	3.1	17
36159	Heterolytic dissociative adsorption state of dihydrogen favored by interfacial defects. Applied Surface Science, 2018, 433, 862-868.	3.1	9
36160	Computational study of phase engineered transition metal dichalcogenides heterostructures. Computational Materials Science, 2018, 142, 129-134.	1.4	11
36161	Giant permittivity and low dielectric loss of Fe doped BaTiO3 ceramics: Experimental and first-principles calculations. Journal of the European Ceramic Society, 2018, 38, 1562-1568.	2.8	54
36162	Spin ordering in oxide nanoclusters without magnetic element atoms. Journal of Magnetism and Magnetic Materials, 2018, 459, 272-275.	1.0	1
36163	Enhancement of photocatalytic decarboxylation on TiO2 by water-induced change in adsorption-mode. Applied Catalysis B: Environmental, 2018, 224, 376-382.	10.8	33
36164	Segregation and mechanical properties of Si, Fe and Ti on the Al/Al2.5X0.5Zr (X = Cu, Zn, Ag) coherent interfaces: First-principles calculations. Computational Materials Science, 2018, 141, 325-340.	1.4	6
36165	Electronic structure, vibronic properties and enhanced magnetic anisotropy induced by tetragonal symmetry in ternary iron nitrides: A first-principles study. Computational Materials Science, 2018, 142, 145-152.	1.4	17
36166	Strain rate-induced plasticity in bcc Î²-Ti alloy single crystal micropillars containing brittle Ï‰-precipitates. Materials and Design, 2018, 137, 404-413.	3.3	18
36167	A theoretical investigation and synthesis of layered ternary carbide system U-Al-C. Ceramics International, 2018, 44, 1646-1652.	2.3	11
36168	Mechanical switching of ferroelectric domains beyond flexoelectricity. Journal of the Mechanics and Physics of Solids, 2018, 111, 43-66.	2.3	37
36169	A first-principles study of gas adsorption on monolayer AlN sheet. Vacuum, 2018, 147, 18-23.	1.6	43
36170	ELSI: A unified software interface for Kohnâ€“Sham electronic structure solvers. Computer Physics Communications, 2018, 222, 267-285.	3.0	78
36171	Hard three-dimensional BN framework with one-dimensional metallicity. Journal of Alloys and Compounds, 2018, 731, 364-368.	2.8	27

#	Article	IF	Citations
36172	A first-principles study on Pd modified ZSM-12 zeolites. Microporous and Mesoporous Materials, 2018, 260, 227-234.	2.2	10
36173	New metallic carbon: Three dimensionally carbon allotropes comprising ultrathin diamond nanostripes. Carbon, 2018, 126, 601-610.	5.4	36
36174	Structural, magnetic and thermodynamic properties of Mn3-X-C (X = Ga, Sn) compounds: ab initio study. Physica B: Condensed Matter, 2018, 549, 94-97.	1.3	1
36175	Structure Sensitivity of Acrolein Hydrogenation by Platinum Nanoparticles on Ba x Sr 1â^' x TiO 3 Nanocuboids. ChemCatChem, 2018, 10, 632-641.	1.8	8
36176	Magnetism induced by 3d transition metal atom doping in InSe monolayer. Journal of Materials Science, 2018, 53, 3500-3508.	1.7	14
36177	CO adsorption, dissociation and coupling formation mechanisms on Fe2C(001) surface. Applied Surface Science, 2018, 434, 464-472.	3.1	29
36178	An insight into the structures, stabilities and magnetic properties of Fe2Bn (nÂ=Â1â€“10) clusters. Materials Chemistry and Physics, 2018, 205, 1-8.	2.0	15
36179	Support effects and reaction mechanism of acetylene trimerization over silica-supported Cu 4 clusters: A DFT study. Surface Science, 2018, 668, 125-133.	0.8	9
36180	Antioxidant electrospun zein nanofibrous web encapsulating quercetin/cyclodextrin inclusion complex. Journal of Materials Science, 2018, 53, 1527-1539.	1.7	70
36181	Role of size, composition and substrate in controlling the reactivity of Î±(0001)-Al 2 O 3 supported Ag n Au m (n+m = 2 â^' 4) alloy clusters for CO-oxidation: A comprehensive density functional study. Applied Surface Science, 2018, 433, 756-764.	3.1	1
36182	Trivalent ions modification for high-silica mordenite: A first principles study. Applied Surface Science, 2018, 433, 627-638.	3.1	15
36183	Modulation of band gap by normal strain in SiC-based heterostructures. Optik, 2018, 154, 634-639.	1.4	1
36184	Magnetic properties of nonmetal doped SiC monolayer: Density functional calculations. Optik, 2018, 154, 763-768.	1.4	1
36185	Effect of structural defects on electronic and magnetic properties in pristine and Cr-doped HfS2 monolayer. Journal of Alloys and Compounds, 2018, 731, 303-309.	2.8	15
36186	Spontaneous magnetization-induced phonons stability in Î³â€²-Fe4N crystalline alloys and high-pressure new phase. Journal of Magnetism and Magnetic Materials, 2018, 451, 87-95.	1.0	4
36187	Dinuclear Iron(II) Spinâ€Crossover Compounds: A Theoretical Study. Chemistry - A European Journal, 2018, 24, 5183-5190.	1.7	20
36188	Coverage evolution of the unoccupied Density of States in sulfur superstructures on Ru(0001). Applied Surface Science, 2018, 433, 300-305.	3.1	3
36189	Two-dimensional siligraphenes as cathode catalysts for nonaqueous lithium-oxygen batteries. Carbon, 2018, 126, 580-587.	5.4	40

#	Article	IF	Citations
36190	Promoting mechanism of N-doped single-walled carbon nanotubes for O2 dissociation and SO2 oxidation. Applied Surface Science, 2018, 434, 382-388.	3.1	7
36191	Effect of Al2O3 on phase formation and thermal expansion of a BaO-SrO-ZnO-SiO2 glass ceramic. Ceramics International, 2018, 44, 2098-2108.	2.3	7
36192	Atomic structure, stability and electronic properties of S(Al2CuMg)/Al interface: A first-principles study. Intermetallics, 2018, 93, 329-337.	1.8	31
36193	Role of organic cations on hybrid halide perovskite CH3NH3PbI3 surfaces. Journal of Solid State Chemistry, 2018, 258, 488-494.	1.4	10
36194	Robust valley polarization of helium ion modified atomically thin MoS ₂. 2D Materials, 2018, 5, 011007.	2.0	55
36195	Interaction of tantalum, titanium and phosphorus at 1070ÂK: Phase diagram and structural chemistry. Journal of Alloys and Compounds, 2018, 732, 777-783.	2.8	3
36196	The Ti₃AlC₂ MAX Phase as an Efficient Catalyst for Oxidative Dehydrogenation of nâ€Butane. Angewandte Chemie, 2018, 130, 1501-1506.	1.6	25
36197	Single Cr atom catalytic growth of graphene. Nano Research, 2018, 11, 2405-2411.	5.8	41
36198	DFT investigation on two-dimensional GeS/WS2 van der Waals heterostructure for direct Z-scheme photocatalytic overall water splitting. Applied Surface Science, 2018, 434, 365-374.	3.1	128
36199	Thermoelectric power factor of La 0.9 M 0.1 FeO 3 (MÂ=ÂCa and Ba) system: Structural, band gap and electrical transport evaluations. Physica B: Condensed Matter, 2018, 529, 1-8.	1.3	13
36200	The Ti₃AlC₂ MAX Phase as an Efficient Catalyst for Oxidative Dehydrogenation of nâ€Butane. Angewandte Chemie - International Edition, 2018, 57, 1485-1490.	7.2	61
36201	Role of oxygen vacancies in photocatalytic water oxidation on ceria oxide: Experiment and DFT studies. Applied Catalysis B: Environmental, 2018, 224, 101-108.	10.8	197
36202	Tailoring the thermostability and hydrogen storage capacity of Li decorated carbon materials by heteroatom doping. Applied Surface Science, 2018, 435, 1065-1071.	3.1	29
36203	Magnetism in Boron Nitride Monolayer Induced by Cobalt or Nickel Doping. Journal of Superconductivity and Novel Magnetism, 2018, 31, 1559-1565.	0.8	18
36204	Chemical bonding in carbide MXene nanosheets. Journal of Electron Spectroscopy and Related Phenomena, 2018, 224, 27-32.	0.8	64
36205	Phonon instability and charge density wave in U2Ti. Journal of Alloys and Compounds, 2018, 730, 36-41.	2.8	3
36206	Pressure-induced influence on the crystal structure, electronic structure and thermoelectric properties of NaB3: A first-principles study. Journal of Alloys and Compounds, 2018, 731, 323-331.	2.8	6
36207	Elucidating the unintentional p-type nature of spinel Co3O4: A defect study using ab-initio calculation. Journal of the European Ceramic Society, 2018, 38, 629-635.	2.8	10

#	Article	IF	Citations
36208	Examining the rudimentary steps of the oxygen reduction reaction on single-atomic Pt using Ti-based non-oxide supports. Journal of Industrial and Engineering Chemistry, 2018, 58, 208-215.	2.9	14
36209	Energy paths of twin-related lattice reorientation in hexagonal metals via ab initio calculations. Journal of Materials Science and Technology, 2018, 34, 700-707.	5.6	7
36210	Investigation of structural, electronic, anisotropic elastic, and lattice dynamical properties of MAX phases borides: An Ab-initio study on hypothetical MAB (MÂ=ÂTi, Zr, Hf; AÂ=ÂAl, Ga, In) compounds. Materials Chemistry and Physics, 2018, 203, 106-117.	2.0	93
36211	Strongly reduced Ehrlichâ€“Schwoebel barriers at the Cu (111) stepped surface with In and Pb surfactants. Surface Science, 2018, 667, 13-16.	0.8	5
36212	High Temperature Stability of BaZrO₃: An Ab Initio Thermodynamic Study. Physica Status Solidi (B): Basic Research, 2018, 255, 1700398.	0.7	4
36213	Transition metal substitution in Fe2P-based MnFe0.95P0.50Si0.50 magnetocaloric compounds. Journal of Alloys and Compounds, 2018, 730, 392-398.	2.8	28
36214	Elastic, mechanical, electronic, and defective properties of Zrâ€“Alâ€“C nanolaminates from first principles. Journal of the American Ceramic Society, 2018, 101, 756-772.	1.9	13
36215	Probing Structural and Magnetic Instabilities and Hysteresis in Heuslers by Density Functional Theory Calculations. Physica Status Solidi (B): Basic Research, 2018, 255, 1700296.	0.7	11
36216	Design of high-activity single-atom catalysts via n-p codoping. Applied Surface Science, 2018, 433, 60-65.	3.1	10
36217	Experimental and theoretical study on the structural, electrical and optical properties of tantalum-doped ZnO nanoparticles prepared via sol-gel acetate route. Ceramics International, 2018, 44, 703-711.	2.3	16
36218	Interface structures of ZnO/MoO3 and their effect on workfunction of ZnO surfaces from first principles calculations. Computational Materials Science, 2018, 141, 162-169.	1.4	10
36219	The atomistic mechanism for Sb segregation and As displacement of Sb in InSb(001) surfaces. Surface Science, 2018, 667, 45-53.	0.8	4
36220	A new insight into the theoretical design of highly dispersed and stable ceria supported metal nanoparticles. Journal of Colloid and Interface Science, 2018, 512, 775-783.	5.0	8
36221	Fluorination of Lithiumâ€Excess Transition Metal Oxide Cathode Materials. Advanced Energy Materials, 2018, 8, 1701533.	10.2	115
36222	Adsorption and reaction of CO and H2O on WC(0001) surface: A first-principles investigation. Applied Surface Science, 2018, 428, 579-585.	3.1	8
36223	Computational study of Mn-doped GaN polar and non-polar surfaces. Computational Materials Science, 2018, 141, 68-74.	1.4	8
36224	Synthesis, crystal structure and DFT studies of a novel dinuclear copper(I) complex with triphenylphosphine and 2-mercaptonicotinic acid. Journal of Molecular Structure, 2018, 1153, 179-186.	1.8	3
36225	Metastable precipitate phases in Mgâ€“9.8Âwt%Sn alloy. Acta Materialia, 2018, 144, 590-600.	3.8	54

#	Article	IF	Citations
36226	Light impurity atoms as the probes for the electronic structures of actinide dioxides. Computational Materials Science, 2018, 142, 25-31.	1.4	15
36227	Enhancement of the optical absorption of carbon group elements doped ZnS in the visible light range. Renewable Energy, 2018, 117, 22-27.	4.3	30
36228	Two superstructures of Ce3Rh4Ge4. Zeitschrift Fur Kristallographie - Crystalline Materials, 2018, 233, 81-95.	0.4	2
36229	Magnetocaloric effect in Ni-Co-Mn-(Sn, Al) Heusler alloys: Theoretical study. Journal of Magnetism and Magnetic Materials, 2018, 459, 295-300.	1.0	9
36230	Radiation-Induced Charge Trapping and Low-Frequency Noise of Graphene Transistors. IEEE Transactions on Nuclear Science, 2018, 65, 156-163.	1.2	15
36231	Defect structure of oxygen-vacancy clusters in O18 and self ion implanted Fe(100) crystal by ion channeling and ab-initio study. Acta Materialia, 2018, 143, 198-204.	3.8	2
36232	Oxygen termination of homoepitaxial diamond surface by ozone and chemical methods: An experimental and theoretical perspective. Applied Surface Science, 2018, 433, 408-418.	3.1	40
36233	Spin-dependent electrochemistry: A novel paradigm. Current Opinion in Electrochemistry, 2018, 7, 36-41.	2.5	25
36234	Recent theoretical progress in the development of perovskite photovoltaic materials. Journal of Energy Chemistry, 2018, 27, 637-649.	7.1	48
36235	Effects of an electric field on the adsorption of water molecules on the Cd(0001) surface. Surface Science, 2018, 668, 1-6.	0.8	3
36236	Strain-Dependent Electronic and Magnetic of Mg-Doped Monolayer of WS2. Journal of Superconductivity and Novel Magnetism, 2018, 31, 1637-1642.	0.8	2
36237	WannierTools: An open-source software package for novel topological materials. Computer Physics Communications, 2018, 224, 405-416.	3.0	1,557
36238	Equation of state of FeO2. Journal of Magnetism and Magnetic Materials, 2018, 459, 280-281.	1.0	2
36239	Chromium-vacancy clusters in dilute bcc Fe-Cr alloys: An ab initio study. Journal of Nuclear Materials, 2018, 499, 613-621.	1.3	12
36240	Understanding and manipulating luminescence in carbon nanodots. Carbon, 2018, 126, 58-64.	5.4	29
36241	Oxidation of half-Heusler NiTiSn materials: Implications for thermoelectric applications. Intermetallics, 2018, 92, 62-71.	1.8	25
36242	Site occupation and spectroscopic properties of Ce3+ in Y3Si5N9O from first-principles calculations. Journal of Alloys and Compounds, 2018, 730, 57-61.	2.8	3
36243	The role of the anionic and cationic pt sites in the adsorption site preference of water and ethanol on defected Pt4/Pt(111) substrates: A density functional theory investigation within the D3 van der waals corrections. Surface Science, 2018, 667, 84-91.	0.8	6

#	Article	IF	Citations
36244	Strong electron-polarized atom chain in amorphous phase-change memory Ge Sb Te alloy. Acta Materialia, 2018, 143, 102-106.	3.8	24
36245	Computation of entropies and phase equilibria in refractory V-Nb-Mo-Ta-W high-entropy alloys. Acta Materialia, 2018, 143, 88-101.	3.8	55
36246	Topological materials discovery using electron filling constraints. Nature Physics, 2018, 14, 55-61.	6.5	39
36247	Oxygen vacancy chain and conductive filament formation in hafnia. Journal of Applied Physics, 2018, 123, .	1.1	34
36248	Physical Properties of Superhard Diamond-Like BC5 from a First-Principles Study. Journal of Electronic Materials, 2018, 47, 272-284.	1.0	5
36249	Simultaneous Detection and Removal of Formaldehyde at Room Temperature: Janus Au@ZnO@ZIF-8 Nanoparticles. Nano-Micro Letters, 2018, 10, 4.	14.4	84
36250	Layered heterostructures based on graphene, hexagonal zinc oxide and molybdenum disulfide: Modeling of geometry and electronic properties. Computational Materials Science, 2018, 142, 32-37.	1.4	7
36251	First-principles study of native defects in bulk Sm2CuO4 and its (001) surface structure. Journal of Applied Physics, 2018, 123, .	1.1	2
36252	Influence of Alloying Elements and Effect of Stress on Anisotropic Hydrogen Diffusion in Zr-Based Alloys Predicted by Accelerated Kinetic Monte Carlo Simulations. Minerals, Metals and Materials Series, 2018, , 599-610.	0.3	0
36253	Real-time decay of fluorinated fullerene molecules on Cu(001) surface controlled by initial coverage. Nano Research, 2018, 11, 2069-2082.	5.8	13
36254	Anionâ€“Anion Coâ€Đoped Monolayer MoS₂ for Visible Light Photocatalysis. Physica Status Solidi (B): Basic Research, 2018, 255, 1700413.	0.7	9
36255	The stability of titaniaâ€silica interface. International Journal of Quantum Chemistry, 2018, 118, e25495.	1.0	10
36256	Enhanced photocatalytic activity induced by sp3 to sp2 transition of carbon dopants in BiOCl crystals. Applied Catalysis B: Environmental, 2018, 221, 467-472.	10.8	58
36257	The possible magnetoelectric coupling induced by adsorption in SnTe films. Applied Surface Science, 2018, 428, 89-93.	3.1	6
36258	Effects of dopant separation on electronic states and magnetism in monolayer MoS2. Applied Surface Science, 2018, 428, 226-232.	3.1	16
36259	Experimental and computational investigation of graphene/SAMs/n-Si Schottky diodes. Applied Surface Science, 2018, 428, 1010-1017.	3.1	11
36260	First-principles investigation of platinum monolayer adsorption on the BiFeO3 (0001) polar surfaces. Applied Surface Science, 2018, 428, 964-971.	3.1	6
36261	Structural, electronic, elastic, optical and vibrational properties of MAl2O4 (M = Co and Mn) aluminate spinels. Ceramics International, 2018, 44, 310-316.	2.3	17

#	Article	IF	Citations
36262	First-principles optical spectra for the oxygen vacancy in YAlO3 crystal. Computational Materials Science, 2018, 141, 127-132.	1.4	14
36263	Ab initio study of the magnetic behavior of metal hydrides: A comparison with the Slater-Pauling curve. Computational Materials Science, 2018, 141, 122-126.	1.4	4
36264	Asymmetric hydrogenation-induced ferromagnetism in stanene nanoribbons considering electric field and strain effects. Journal of Materials Science, 2018, 53, 657-666.	1.7	3
36265	Enhancement of Thermoelectric Properties in SnTe with (Ag, In) Co-Doping. Journal of Electronic Materials, 2018, 47, 205-211.	1.0	28
36266	Magnetic Properties in Nonmagnetic Metal Atom Adsorption on SiC Monolayer: First-Principles Study. Journal of Superconductivity and Novel Magnetism, 2018, 31, 1235-1240.	0.8	13
36267	A DFT based method for calculating the surface energies of asymmetric MoP facets. Applied Surface Science, 2018, 427, 357-362.	3.1	81
36268	Electronic structure and relative stability of the coherent and semi-coherent HfO2/III-V interfaces. Applied Surface Science, 2018, 427, 243-252.	3.1	6
36269	First-principles calculations of high-pressure iron-bearing monoclinic dolomite and single-cation carbonates with internally consistent Hubbard U. Physics and Chemistry of Minerals, 2018, 45, 293-302.	0.3	11
36270	Modulating the gas sensing properties of nitrogen coordinated dopants in graphene sheets: A first-principles study. Applied Surface Science, 2018, 427, 376-386.	3.1	17
36271	The location of excess electrons on H₂O/TiO₂(110) surface and its role in the surface reactions. Molecular Physics, 2018, 116, 171-178.	0.8	7
36272	Structure and stability of bilayer borophene: The roles of hexagonal holes and interlayer bonding. FlatChem, 2018, 7, 48-54.	2.8	58
36273	An adaptive FEM with ITP approach for steady SchrÃ¶dinger equation. International Journal of Computer Mathematics, 2018, 95, 187-201.	1.0	4
36274	Theoretical and experimental investigations of mercury adsorption on hematite surfaces. Journal of the Air and Waste Management Association, 2018, 68, 39-53.	0.9	13
36275	Tunable Rashba spin splitting in two-dimensional graphene/As-I heterostructures. Applied Surface Science, 2018, 427, 10-14.	3.1	7
36276	Influences of Electrode Potential on Mechanism of Oxygen Reduction Reaction on Pd-Skin/Pd3Fe(111) Electrocatalyst: Insights from DFT-Based Calculations. Electrocatalysis, 2018, 9, 10-21.	1.5	4
36277	Sulfur Atoms Adsorbed on Cu(100) at Low Coverage: Characterization and Stability against Complexation. Journal of Physical Chemistry B, 2018, 122, 963-971.	1.2	15
36278	Efficient defect-controlled photocatalytic hydrogen generation based on near-infrared Cu-In-Zn-S quantum dots. Nano Research, 2018, 11, 1379-1388.	5.8	41
36279	Oxidation mechanism of chalcopyrite revealed by X-ray photoelectron spectroscopy and first principles studies. Applied Surface Science, 2018, 427, 233-241.	3.1	46

#	Article	IF	Citations
36280	Realizing p-Type MoS₂ with Enhanced Thermoelectric Performance by Embedding VMo₂S₄ Nanoinclusions. Journal of Physical Chemistry B, 2018, 122, 713-720.	1.2	44
36281	Theoretical Evidence behind Bifunctional Catalytic Activity in Pristine and Functionalized Al₂C Monolayers. ChemPhysChem, 2018, 19, 148-152.	1.0	11
36282	From Surface ZrO₂ Coating to Bulk Zr Doping by High Temperature Annealing of Nickelâ€Rich Lithiated Oxides and Their Enhanced Electrochemical Performance in Lithium Ion Batteries. Advanced Energy Materials, 2018, 8, 1701682.	10.2	443
36283	First principles hybrid functional study of small polarons in doped SrCeO3 perovskite: towards computation design of materials with tailored polaron. Ionics, 2018, 24, 1139-1151.	1.2	12
36284	Electrically tunable polarizer based on 2D orthorhombic ferrovalley materials. 2D Materials, 2018, 5, 011001.	2.0	46
36285	Self-supported CoMoS4 nanosheet array as an efficient catalyst for hydrogen evolution reaction at neutral pH. Nano Research, 2018, 11, 2024-2033.	5.8	147
36286	Hierarchical cobalt poly-phosphide hollow spheres as highly active and stable electrocatalysts for hydrogen evolution over a wide pH range. Applied Surface Science, 2018, 427, 800-806.	3.1	37
36287	The effect of oxygen molecule adsorption on lead iodide perovskite surface by first-principles calculation. Applied Surface Science, 2018, 428, 140-147.	3.1	39
36288	Phase transformations in the relaxor Na_{1/2}Bi_{1/2}TiO₃ studied by means of density functional theory calculations. Journal of the American Ceramic Society, 2018, 101, 472-482.	1.9	10
36289	Electronic, magnetic and structural properties of Co3O4 (100) surface: a DFT+U study. Applied Surface Science, 2018, 427, 1090-1095.	3.1	17
36290	In situ transformation of Cu2O@MnO2 to Cu@Mn(OH)2 nanosheet-on-nanowire arrays for efficient hydrogen evolution. Nano Research, 2018, 11, 1798-1809.	5.8	37
36291	Effects of alloying elements on relative phase stability and elastic properties of L12 Co3V from first-principles calculations. Journal of Materials Science, 2018, 53, 1204-1216.	1.7	8
36292	Bismuth spheres assembled on graphene oxide: Directional charge transfer enhances plasmonic photocatalysis and in situ DRIFTS studies. Applied Catalysis B: Environmental, 2018, 221, 482-489.	10.8	92
36293	Modelling the aqueous and nonaqueous interfaces for CO2 electro-reduction over Sn catalysts. Applied Surface Science, 2018, 428, 514-519.	3.1	3
36294	Ab initio predicted elastic and thermodynamic properties of Imm 2-BN under high pressure. Chinese Journal of Physics, 2018, 56, 423-431.	2.0	2
36295	Chromium and hydrogen doping effects on magnetic and electronic properties of ZnO. Journal of Magnetism and Magnetic Materials, 2018, 446, 192-199.	1.0	11
36296	Enhanced catalytic performance by oxygen vacancy and active interface originated from facile reduction of OMS-2. Chemical Engineering Journal, 2018, 331, 626-635.	6.6	100
36297	Improving the efficiency and environmental stability of inverted planar perovskite solar cells via silver-doped nickel oxide hole-transporting layer. Applied Surface Science, 2018, 427, 782-790.	3.1	93

#	Article	IF	Citations
36298	Nickelâ€“Copper Alloy Encapsulated in Graphitic Carbon Shells as Electrocatalysts for Hydrogen Evolution Reaction. Advanced Energy Materials, 2018, 8, 1701759.	10.2	225
36299	CH4 dissociation in the early stage of graphene growth on Feâ€“Cu(100) surface: Theoretical insights. Applied Surface Science, 2018, 427, 953-960.	3.1	11
36300	First principles computational study on hydrolysis of hazardous chemicals phosphorus trichloride and oxychloride (PCl3 and POCl3) catalyzed by molecular water clusters. Journal of Hazardous Materials, 2018, 341, 457-463.	6.5	13
36301	Prediction on electronic structure of CH 3 NH 3 PbI 3 /Fe 3 O 4 interfaces. Solid State Communications, 2018, 269, 90-95.	0.9	3
36302	Synthesis and characterization of rhodium nanoclusters on TiO2(110) surface using organometallic compounds. Surface Science, 2018, 667, 38-44.	0.8	2
36303	High Lithium Insertion Voltage Singleâ€Crystal H₂Ti₁₂O₂₅ Nanorods as a Highâ€Capacity and Highâ€Rate Lithiumâ€Ion Battery Anode Material. ChemSusChem, 2018, 11, 299-310.	3.6	18
36304	Fluorine-graphite intercalation compound (C4F)n at high pressure: Experimental and theoretical study. Carbon, 2018, 127, 384-391.	5.4	12
36305	Prediction of novel stable Fe-V-Si ternary phase. Journal of Alloys and Compounds, 2018, 732, 567-572.	2.8	4
36306	Geometric structure and photovoltaic properties of mixed halide germanium perovskites from theoretical view. Organic Electronics, 2018, 53, 50-56.	1.4	74
36307	Non-equilibrium solid solution of molybdenum and sodium: Atomic scale experimental and first principles studies. Acta Materialia, 2018, 144, 700-706.	3.8	6
36308	Mechanistic insight into the synergetic catalytic effect of Pd and MnO2 for high-performance Liâ€“O2 cells. Energy Storage Materials, 2018, 12, 8-16.	9.5	23
36309	Tuning the electronic properties of bilayer group-IV monochalcogenides by stacking order, strain and an electric field: a computational study. Physical Chemistry Chemical Physics, 2018, 20, 214-220.	1.3	32
36310	XANES study of vanadium and nitrogen dopants in photocatalytic TiO₂ thin films. Physical Chemistry Chemical Physics, 2018, 20, 221-231.	1.3	17
36311	Defect-mediated, thermally-activated encapsulation of metals at the surface of graphite. Carbon, 2018, 127, 305-311.	5.4	24
36312	First principles calculations for iodine atom diffusion in SiC with point defects. Computational Materials Science, 2018, 142, 427-436.	1.4	3
36313	Theoretical and experimental investigation of highly photocatalytic performance of CuInZnS nanoporous structure for removing the NO gas. Journal of Catalysis, 2018, 357, 100-107.	3.1	214
36314	Theoretical study on the photocatalytic properties of graphene oxide with single Au atom adsorption. Surface Science, 2018, 669, 71-78.	0.8	18
36315	Reactivity of CO ₂ on the surfaces of magnetite (Fe ₃ O ₄), greigite (Fe ₃ S ₄) and mackinawite (FeS). Philosophical Transactions Series A, Mathematical, Physical, and Engineering Sciences, 2018, 376, 20170065.	1.6	27

#	Article	IF	Citations
36316	Discovery of 2D Anisotropic Dirac Cones. Advanced Materials, 2018, 30, 1704025.	11.1	91
36317	First-Principles Study on the Tensile Properties and Failure Mechanism of the CoSb3/Ti Interface. Journal of Electronic Materials, 2018, 47, 3210-3217.	1.0	3
36318	Crystal structure of Th2B2C3 with unique mixed B-C structural units. Acta Materialia, 2018, 144, 484-495.	3.8	7
36319	C3B monolayer as an anchoring material for lithium-sulfur batteries. Carbon, 2018, 129, 38-44.	5.4	105
36320	Effects of rare-earth doping on the ionic conduction of CeO2 in solid oxide fuel cells. Ceramics International, 2018, 44, 3707-3711.	2.3	30
36321	The effect of B on solid solution structure and preferred orientation of vapor-deposited Al-B thin film: A first-principles study. Computational Materials Science, 2018, 142, 325-331.	1.4	4
36322	Thermal stability and mechanical properties of Ti-Al-B-N thin films. International Journal of Refractory Metals and Hard Materials, 2018, 71, 320-324.	1.7	16
36323	Impact of bi-axial strain on the structural, electronic and optical properties of photo-catalytic bulk bismuth oxyhalides. Physical Chemistry Chemical Physics, 2018, 20, 103-111.	1.3	18
36324	Tuning to the band gap by complex defects engineering: insights from hybrid functional calculations in CuInS₂. Journal Physics D: Applied Physics, 2018, 51, 025105.	1.3	10
36325	Highâ€Pressureâ€Induced Comminution and Recrystallization of CH₃NH₃PbBr₃ Nanocrystals as Large Thin Nanoplates. Advanced Materials, 2018, 30, 1705017.	11.1	89
36326	Chemisorbed Oxygen at Pt(111): a DFT Study of Structural and Electronic Surface Properties. Electrocatalysis, 2018, 9, 370-379.	1.5	25
36327	Monoclinic C16: sp-sp hybridized nodal-line semimetal protected by PT-symmetry. Carbon, 2018, 127, 527-532.	5.4	32
36328	The influence of hydrogen on transition metal - Catalysed graphene nucleation. Carbon, 2018, 128, 215-223.	5.4	11
36329	Ab initio study of structural and electronic properties of copper and nickel tungstate. Computational Materials Science, 2018, 143, 301-307.	1.4	9
36330	Spin-orbit coupling effect on structural and magnetic properties of Co Rh13â^' (nâ€¯=â€¯0â€“13) clusters. Journal of Magnetism and Magnetic Materials, 2018, 451, 360-367.	1.0	11
36331	Alloyed monolayers of Cu, Ag, Au and Pt in hexagonal phase: A comprehensive first principles study. Materials Science and Engineering B: Solid-State Materials for Advanced Technology, 2018, 228, 84-90.	1.7	17
36332	Graphene Oxide Epoxy (GOâ€xy): GO as Epoxy Adhesive by Interfacial Reaction of Functionalities. Advanced Materials Interfaces, 2018, 5, 1700657.	1.9	19
36333	Unexpected ground-state structures and properties of carbon nitride C3N at ambient and high pressures. Materials and Design, 2018, 140, 45-53.	3.3	3

#	Article	IF	Citations
36334	A two-dimensional tetragonal yttrium nitride monolayer: a ferroelastic semiconductor with switchable anisotropic properties. Nanoscale, 2018, 10, 215-221.	2.8	62
36335	Hollow CaTiO3 cubes modified by La/Cr co-doping for efficient photocatalytic hydrogen production. Applied Catalysis B: Environmental, 2018, 225, 139-147.	10.8	106
36336	Strain-modulated magnetic behavior in Li-doped WS2 monolayer. Optik, 2018, 157, 827-832.	1.4	2
36337	Revisiting intrinsic brittleness and deformation behavior of B2 NiAl intermetallic compound: A first-principles study. Journal of Materials Science and Technology, 2018, 34, 620-626.	5.6	16
36338	Dynamic imaging of metastable reaction pathways in lithiated cobalt oxide electrodes. Nano Energy, 2018, 44, 15-22.	8.2	24
36339	Adsorption of thiophene on transition metal surfaces with the inclusion of van der Waals effects. Surface Science, 2018, 669, 121-129.	0.8	25
36340	Origin of enhanced BrÃ¸nsted acidity of NiF-modified synthetic micaâ€“montmorillonite clay. Catalysis Science and Technology, 2018, 8, 244-251.	2.1	8
36341	Deterministic Phonon Transport Predictions of Thermal Conductivity in Uranium Dioxide With Xenon Impurities. Journal of Heat Transfer, 2018, 140, .	1.2	6
36342	Highly enhanced visible light photocatalysis and in situ FT-IR studies on Bi metal@defective BiOCl hierarchical microspheres. Applied Catalysis B: Environmental, 2018, 225, 218-227.	10.8	238
36343	Confined Li ion migration in the silicon-graphene complex system: An ab initio investigation. Applied Surface Science, 2018, 436, 505-510.	3.1	14
36344	Invited paper: Reconciling SGTE and ab initio enthalpies of the elements. Calphad: Computer Coupling of Phase Diagrams and Thermochemistry, 2018, 60, 1-6.	0.7	18
36345	Investigation of the conditions required for the formation of V(C,N) during carburization of vanadium or carbothermal reduction of V2O5 under nitrogen. Ceramics International, 2018, 44, 2847-2855.	2.3	11
36346	Structural, electronic and photocatalytic properties of atomic defective BiI3 monolayers. Chemical Physics Letters, 2018, 691, 341-346.	1.2	13
36347	Hydrogen adsorption and dissociation on nickel-adsorbed and -substituted Mg17Al12 (100) surface: A density functional theory study. International Journal of Hydrogen Energy, 2018, 43, 793-800.	3.8	20
36348	Experimental and theoretical studies on the NLO properties of two quaternary non-centrosymmetric chalcogenides: BaAg₂GeS₄and BaAg₂SnS₄. Dalton Transactions, 2018, 47, 429-437.	1.6	55
36349	Formation of defects and their effects on hydride ion transport properties in a series of K₂NiF₄-type oxyhydrides. Journal of Materials Chemistry A, 2018, 6, 1454-1461.	5.2	19
36350	Theoretical design and exploration of novel high energy density materials based on silicon. Journal of Energetic Materials, 2018, 36, 291-301.	1.0	4
36351	Co-doped phosphorene: Enhanced sensitivity of CO gas sensing. International Journal of Modern Physics B, 2018, 32, 1850068.	1.0	10

#	Article	IF	Citations
36352	Computational Screening of Doped Î±â€MnO₂ Catalysts for the Oxygen Evolution Reaction. ChemSusChem, 2018, 11, 629-637.	3.6	40
36353	Mapping the relationship among composition, stacking fault energy and ductility in Nb alloys: A first-principles study. Acta Materialia, 2018, 144, 853-861.	3.8	32
36354	The role of Ga in the acetylene adsorption on PdGa intermetallic. Applied Surface Science, 2018, 435, 568-573.	3.1	13
36355	Influence of nearest neighbor atoms and coordination polyhedron on atomic volume of sigma phases. Computational Materials Science, 2018, 143, 308-315.	1.4	3
36356	Brush-Like Cobalt Nitride Anchored Carbon Nanofiber Membrane: Current Collector-Catalyst Integrated Cathode for Long Cycle Liâ€“O₂ Batteries. ACS Nano, 2018, 12, 128-139.	7.3	230
36357	Pressure-Induced Polymerization of CO₂ in Lithiumâ€“Carbon Dioxide Phases. Journal of the American Chemical Society, 2018, 140, 413-422.	6.6	11
36358	Recycling of zincite (ZnO) via uptake of hydrogen halides. Physical Chemistry Chemical Physics, 2018, 20, 1221-1230.	1.3	26
36359	Role of surface adsorption in tuning the properties of black phosphorus. Physical Chemistry Chemical Physics, 2018, 20, 112-117.	1.3	17
36360	Ultrafast interfacial charge transfer from the LUMO+1 in ruthenium(<scp>ii</scp>) polypyridyl quinoxaline-sensitized solar cells. Dalton Transactions, 2018, 47, 561-576.	1.6	12
36361	Two-dimensional stoichiometric boron carbides with unexpected chemical bonding and promising electronic properties. Journal of Materials Chemistry C, 2018, 6, 1651-1658.	2.7	35
36362	Remarkable enhancement in thermoelectric performance of BiCuSeO through biaxial strain modulation. Physica E: Low-Dimensional Systems and Nanostructures, 2018, 97, 392-400.	1.3	11
36363	Intrinsic sources of high thermal conductivity of CdSiP₂ determined by first-principle anharmonic calculations. Physical Chemistry Chemical Physics, 2018, 20, 1568-1574.	1.3	8
36364	Ab initiomodeling of MAX phase solid solutions using the special quasirandom structure approach. Physical Chemistry Chemical Physics, 2018, 20, 1173-1180.	1.3	15
36365	Site occupancy, composition and magnetic structure dependencies of martensitic transformation in Mn2Ni1 +xSn1â^'x. Journal of Physics Condensed Matter, 2018, 30, 015401.	0.7	5
36366	Oxygen Reduction Reaction on Ag(111) in Alkaline Solution: A Combined Density Functional Theory and Kinetic Monte Carlo Study. ChemCatChem, 2018, 10, 540-549.	1.8	18
36367	Support effects in single atom iron catalysts on adsorption characteristics of toxic gases (NO2, NH3,) Tj ETQq1 1 0.784314 rgBT /Ove	3.1	81
36368	Ab initio dynamical stability of tungsten at high pressures and high temperatures. Computational Materials Science, 2018, 144, 32-35.	1.4	10
36369	Ab initio study of growth mechanism of omega precipitates in Al-Cu-Mg-Ag alloy and similar systems. Journal of Alloys and Compounds, 2018, 737, 207-212.	2.8	15

#	Article	IF	Citations
36370	Stability and electronic structure of two-dimensional arsenic phosphide monolayer. Materials Science and Engineering B: Solid-State Materials for Advanced Technology, 2018, 228, 206-212.	1.7	21
36371	Two-dimensional silicon crystals with sizable band gaps and ultrahigh carrier mobility. Nanoscale, 2018, 10, 1265-1271.	2.8	28
36372	Bandgap engineering and charge separation in two-dimensional GaS-based van der Waals heterostructures for photocatalytic water splitting. Applied Surface Science, 2018, 439, 374-379.	3.1	36
36373	Investigation of the interstitial oxygen behaviors in vanadium alloy: A first-principles study. Current Applied Physics, 2018, 18, 183-190.	1.1	12
36374	Magnetic moment changed by interlayer charge transfer in vertical graphene/C-doped hexagonal boron nitride heterostructure. Chemical Physics Letters, 2018, 692, 81-87.	1.2	2
36375	Characterization of lattice defects in metallic materials by positron annihilation spectroscopy: A review. Journal of Materials Science and Technology, 2018, 34, 577-598.	5.6	127
36376	Debye temperature for binary alloys and its relationship with cohesive energy. Physica B: Condensed Matter, 2018, 531, 95-101.	1.3	9
36377	Chemical Origin of Sodium Phosphate Interactions on Iron and Iron Oxide Surfaces by First Principle Calculations. Journal of Physical Chemistry C, 2018, 122, 635-647.	1.5	29
36378	Influence of the Fe:Ni Ratio and Reaction Temperature on the Efficiency of (Fe_xNi_{1â€“x})₉S₈ Electrocatalysts Applied in the Hydrogen Evolution Reaction. ACS Catalysis, 2018, 8, 987-996.	5.5	134
36379	Luminescence properties and the thermal quenching mechanism of Mn²⁺ doped Zn₂GeO₄ long persistent phosphors. Dalton Transactions, 2018, 47, 1303-1311.	1.6	67
36380	Multiscale simulations of ligand adsorption and exchange on gold nanoparticles. Physical Chemistry Chemical Physics, 2018, 20, 1381-1394.	1.3	25
36381	The electronic and optical properties of the sulvanite compounds: a many-body perturbation and time-dependent density functional theory study. Journal of Physics Condensed Matter, 2018, 30, 035502.	0.7	6
36382	Discovering chemical site occupancy- modulus correlations in Ni based intermetallics via statistical learning methods. Computational Condensed Matter, 2018, 14, 8-14.	0.9	3
36383	A DFT study of the stability of SIAs and small SIA clusters in the vicinity of solute atoms in Fe. Journal of Nuclear Materials, 2018, 500, 92-109.	1.3	24
36384	Electronic structure engineering in silicene via atom substitution and a new two-dimensional Dirac structure Si 3 C. Physica E: Low-Dimensional Systems and Nanostructures, 2018, 98, 39-44.	1.3	11
36385	Ferromagnetism and antiferromagnetism coexistence in Sr1-xLaxRuO3 induced by La-doping. Solid State Communications, 2018, 270, 119-123.	0.9	7
36386	The Rich Solid-State Phase Behavior of dl-Aminoheptanoic Acid: Five Polymorphic Forms and Their Phase Transitions. Crystal Growth and Design, 2018, 18, 242-252.	1.4	11
36387	Evaluating the Energetic Driving Force for Cocrystal Formation. Crystal Growth and Design, 2018, 18, 892-904.	1.4	145

#	Article	IF	Citations
36388	Probing Solidâ€“Solid Interfacial Reactions in All-Solid-State Sodium-Ion Batteries with First-Principles Calculations. Chemistry of Materials, 2018, 30, 163-173.	3.2	150
36389	Enhancing Ferroelectric Dipole Ordering in Organicâ€“Inorganic Hybrid Perovskite CH₃NH₃PbI₃: Strain and Doping Engineering. Journal of Physical Chemistry C, 2018, 122, 177-184.	1.5	35
36390	Band Structure Engineering of Cs₂AgBiBr₆ Perovskite through Orderâ€“Disordered Transition: A First-Principle Study. Journal of Physical Chemistry Letters, 2018, 9, 31-35.	2.1	121
36391	Tunneling Hot Spots in Ferroelectric SrTiO₃. Nano Letters, 2018, 18, 491-497.	4.5	30
36392	Manipulation of Origin of Life Molecules: Recognizing Single-Molecule Conformations in Î²-Carotene and Chlorophyll-a/Î²-Carotene Clusters. ACS Nano, 2018, 12, 217-225.	7.3	4
36393	Superior non-enzymatic glucose sensing properties of Ag-/Au-NiCo₂O₄ nanosheets with insight from electronic structure simulations. Analyst, The, 2018, 143, 571-579.	1.7	35
36394	One-dimensional cadmium sulphide nanotubes for photocatalytic water splitting. Physical Chemistry Chemical Physics, 2018, 20, 1904-1913.	1.3	31
36395	Modelling complete methane oxidation over palladium oxide in a porous catalyst using first-principles surface kinetics. Catalysis Science and Technology, 2018, 8, 508-520.	2.1	17
36396	Controlling magnetism via transition metal exchange in the series of intermetallics Eu(T1,T2)5In (T =) Tj ETQq0 0 0 rgBT /Overlock 10 Tf	2.7	1
36397	Exploring the charge localization and band gap opening of borophene: a first-principles study. Nanoscale, 2018, 10, 1403-1410.	2.8	77
36398	Influence of a Confined Methanol Solvent on the Reactivity of Active Sites in UiOâ€66. ChemPhysChem, 2018, 19, 420-429.	1.0	17
36399	Electronic Structure and Thermoelectric Properties of Transition Metal Monosilicides. Journal of Electronic Materials, 2018, 47, 3277-3281.	1.0	16
36400	Thermal vacancy formation enthalpy of random solid solutions: The FePt case. Computational Materials Science, 2018, 143, 206-211.	1.4	5
36401	Influence of surface stoichiometry and quantum confinement on the electronic structure of small diameter InxGa1-xAs nanowires. Materials Chemistry and Physics, 2018, 206, 35-39.	2.0	2
36402	First-Principles Study of the Voltage Profile and Mobility of Mg Intercalation in a Chromium Oxide Spinel. Chemistry of Materials, 2018, 30, 153-162.	3.2	53
36403	Potential Semiconducting and Superconducting Metastable Si₃C Structures under Pressure. Chemistry of Materials, 2018, 30, 421-427.	3.2	5
36404	Molecular Building Block-Based Electronic Charges for High-Throughput Screening of Metalâ€“Organic Frameworks for Adsorption Applications. Journal of Chemical Theory and Computation, 2018, 14, 365-376.	2.3	18
36405	Density Functional Theory Study of the Formaldehyde Catalytic Oxidation Mechanism on a Au-Doped CeO2(111) Surface. Journal of Physical Chemistry C, 2018, 122, 438-448.	1.5	22

#	Article	IF	Citations
36406	Formation of Ag nanoparticles under electron beam irradiation: Atomistic origins from firstâ€principles calculations. International Journal of Quantum Chemistry, 2018, 118, e25551.	1.0	21
36407	In situ surface stress measurement and computational analysis examining the oxygen reduction reaction on Pt and Pd. Electrochimica Acta, 2018, 260, 400-406.	2.6	14
36408	First-principles investigation on stability and diffusion mechanism of helium impurities in 4H-SiC. Journal of Nuclear Materials, 2018, 499, 168-174.	1.3	6
36409	First principle calculation of helium in La2Zr2O7: Effects on structural, electronic properties and radiation tolerance. Journal of Nuclear Materials, 2018, 500, 72-80.	1.3	18
36410	Theoretical and experimental researches on NiS2 nanocubes with uniform reactive exposure facets. Materials Chemistry and Physics, 2018, 207, 194-202.	2.0	10
36411	Unusual Ferroelectricity in Two-Dimensional Perovskite Oxide Thin Films. Nano Letters, 2018, 18, 595-601.	4.5	41
36412	Ultralow and anisotropic thermal conductivity in semiconductor As₂Se₃. Physical Chemistry Chemical Physics, 2018, 20, 1809-1816.	1.3	16
36413	Orthorhombic Ti₂O₃: A Polymorphâ€Dependent Narrowâ€Bandgap Ferromagnetic Oxide. Advanced Functional Materials, 2018, 28, 1705657.	7.8	36
36414	Phase, hardness, and deformation slip behavior in mixed HfxTa1-xC. Acta Materialia, 2018, 145, 142-153.	3.8	81
36415	CALPHAD modeling and ab initio calculations of the Np-U-Zr system. Computational Materials Science, 2018, 143, 505-514.	1.4	6
36416	Phase Boundary Mapping to Obtain n-type Mg3Sb2-Based Thermoelectrics. Joule, 2018, 2, 141-154.	11.7	274
36417	Cocrystals Help Break the â€œRulesâ€•of Isostructurality: Solid Solutions and Polymorphism in the Malic/Tartaric Acid System. Crystal Growth and Design, 2018, 18, 855-863.	1.4	27
36418	Diffusion Kinetics of Gold and Copper Atoms on Pristine and Reduced Rutile TiO₂ (110) Surfaces. Journal of Physical Chemistry C, 2018, 122, 3824-3837.	1.5	12
36419	Enhancing Intermolecular Interaction by Cyano Substitution in Copper Phthalocyanine. Journal of Physical Chemistry C, 2018, 122, 429-437.	1.5	8
36420	Controllable dissociation of H₂O on a CeO₂(111) surface. Physical Chemistry Chemical Physics, 2018, 20, 1575-1582.	1.3	10
36421	Atomic-scale mechanisms of defect- and light-induced oxidation and degradation of InSe. Journal of Materials Chemistry C, 2018, 6, 518-525.	2.7	43
36422	A combined theoretical and experimental approach of a new ternary metal oxide in molybdate composite for hybrid energy storage capacitors. APL Materials, 2018, 6, .	2.2	26
36423	First-principles study of SnS electronic properties using LDA, PBE and HSE06 functionals. Philosophical Magazine, 2018, 98, 710-726.	0.7	16

#	Article	IF	Citations
36424	Local Builtâ€In Electric Field Enabled in Carbonâ€Doped Co₃O₄ Nanocrystals for Superior Lithiumâ€Ion Storage. Advanced Functional Materials, 2018, 28, 1705951.	7.8	128
36425	Highly efficient catalytic scavenging of oxygen free radicals with graphene-encapsulated metal nanoshields. Nano Research, 2018, 11, 2821-2835.	5.8	31
36426	Design lateral heterostructure of monolayer ZrS2 and HfS2 from first principles calculations. Applied Surface Science, 2018, 436, 919-926.	3.1	33
36427	Validation of inter-atomic potential for WS2 and WSe2 crystals through assessment of thermal transport properties. Computational Materials Science, 2018, 144, 92-98.	1.4	36
36428	Predicting two-dimensional carbon phosphide compouds: C2P4 by the global optimization method. Computational Materials Science, 2018, 144, 70-75.	1.4	21
36429	Studies of O18 impurity trapping at interstitial dislocation loops in ion implanted Fe (1â€¯1â€¯0) by ion channeling and ab initio calculations. Nuclear Instruments & Methods in Physics Research B, 2018, 414, 141-145.	0.6	1
36430	Exploring the properties of carbazole-based derivatives as hole transport materials from first principle and MD simulation. Organic Electronics, 2018, 54, 14-20.	1.4	18
36431	Origin of n-type conductivity in two-dimensional InSe: In atoms from surface adsorption and van der Waals gap. Physica E: Low-Dimensional Systems and Nanostructures, 2018, 98, 66-73.	1.3	8
36432	Comparative DFT+U and HSE Study of the Oxygen Evolution Electrocatalysis on Perovskite Oxides. Journal of Physical Chemistry C, 2018, 122, 1135-1147.	1.5	46
36433	Carboxylic Acid Group-Induced Oxygen Vacancy Migration on an Anatase (101) Surface. Langmuir, 2018, 34, 546-552.	1.6	11
36434	A new pnictidehalide with van der Waals hostâ€“guest interactions exhibiting both geometric spin frustration and resistive humidity sensitivity. New Journal of Chemistry, 2018, 42, 1787-1795.	1.4	1
36435	Electronic properties of topological insulator candidate CaAgAs. Journal of Physics Condensed Matter, 2018, 30, 045501.	0.7	18
36436	Stable structures of exohedrally decorated C60-fullerenes. Carbon, 2018, 129, 847-853.	5.4	27
36437	Understanding All-Solid Frustrated-Lewis-Pair Sites on CeO₂ from Theoretical Perspectives. ACS Catalysis, 2018, 8, 546-554.	5.5	135
36438	The truth is out there: the metal-Ï€ interactions in crystal of Cr(CO)₃(pcp) as revealed by the study of vibrational smearing of electron density. Zeitschrift Fur Kristallographie - Crystalline Materials, 2018, 233, 317-336.	0.4	7
36439	First-principles studies on the electronic and optical properties of Fe-doped potassium dihydrogen phosphate crystal. Computational Materials Science, 2018, 143, 398-402.	1.4	16
36440	First principles study on interface between dual-channel anchorable organic dyes and TiO2 for dye-sensitized solar cells. Dyes and Pigments, 2018, 149, 908-914.	2.0	22
36441	Atomistic simulation of cubic and tetragonal phases of U-Mo alloy: Structure and thermodynamic properties. Journal of Nuclear Materials, 2018, 499, 451-463.	1.3	47

#	Article	IF	Citations
36442	Hybrid density functional study on the mechanism for the enhanced photocatalytic properties of the ultrathin hybrid layered nanocomposite g-C3N4/BiOCl. Applied Surface Science, 2018, 435, 1351-1360.	3.1	50
36443	Charge and strain induced magnetism in monolayer MoS2 with S vacancy. Journal of Magnetism and Magnetic Materials, 2018, 451, 520-525.	1.0	23
36444	Edge orientations of mechanically exfoliated anisotropic two-dimensional materials. Journal of the Mechanics and Physics of Solids, 2018, 112, 157-168.	2.3	22
36445	Solute â€“ ã€ˆ111ã€‰ interstitial loop interaction in Î±-Fe: A DFT study. Journal of Nuclear Materials, 2018, 499, 582-594.	1.3	34
36446	Screening of rare-earth-lean intermetallic 1-11 and 1-11-X compounds of YNi9In2-type for hard-magnetic applications. Scripta Materialia, 2018, 154, 295-299.	2.6	14
36447	Combined crystal chemistry and DFT studies of ThNCl and Th 2 N 2 X (X:Âchalcogen) behaving as pseudo-binaries. Solid State Sciences, 2018, 76, 1-7.	1.5	0
36448	Correlation of grain boundary extra free volume with vacancy and solute segregation at grain boundaries: a case study for Al. Philosophical Magazine, 2018, 98, 464-483.	0.7	38
36449	Electric field tuned MoS₂/metal interface for hydrogen evolution catalyst from first-principles investigations. Nanotechnology, 2018, 29, 03LT01.	1.3	16
36450	Electronic and thermoelectric properties of atomically thin C₃Si₃/C and C₃Ge₃/C superlattices. Nanotechnology, 2018, 29, 045402.	1.3	5
36451	Large area planar stanene epitaxially grown on Ag(1â€‰1â€‰1). 2D Materials, 2018, 5, 025002.	2.0	164
36452	Mapping deformation mechanisms in lamellar titanium aluminide. Acta Materialia, 2018, 144, 835-843.	3.8	27
36453	Tuning the Schottky rectification in graphene-hexagonal boron nitride-molybdenum disulfide heterostructure. Journal of Colloid and Interface Science, 2018, 513, 677-683.	5.0	34
36454	Computer-aided design of metal chalcohalide semiconductors: from chemical composition to crystal structure. Chemical Science, 2018, 9, 1022-1030.	3.7	54
36455	The mixing effect of organic cations on the structural, electronic and optical properties of FA_xMA_{1âˆ’x}PbI₃perovskites. Physical Chemistry Chemical Physics, 2018, 20, 941-950.	1.3	24
36456	Van der Waals heterojunction diode composed of WS₂flake placed on p-type Si substrate. Nanotechnology, 2018, 29, 045201.	1.3	21
36457	Structural Basis for Metastability in Amorphous Calcium Barium Carbonate (ACBC). Advanced Functional Materials, 2018, 28, 1704202.	7.8	22
36458	Energetic and Electronic Properties of (0001) Inversion Domain Boundaries in ZnO. Physica Status Solidi (B): Basic Research, 2018, 255, 1700429.	0.7	7
36459	Enhanced Performance of MoS₂ Photodetectors by Inserting an ALDâ€Processed TiO₂ Interlayer. Small, 2018, 14, 1703176.	5.2	51

#	Article	IF	Citations
36460	Electrochemical properties and first-principle analysisof Na x [M y Mn1â˜'y]O2 (Mâ€‰=â€‰Fe, Ni) cathode. Journal of Solid State Electrochemistry, 2018, 22, 1079-1089.	1.2	24
36461	Mechanistic Insights into Hydration of Solid Oxides. Chemistry of Materials, 2018, 30, 138-144.	3.2	26
36462	Square transition-metal carbides MC₆ (M = Mo, W) as stable two-dimensional Dirac cone materials. Physical Chemistry Chemical Physics, 2018, 20, 732-737.	1.3	13
36463	Atomic adsorption on graphene with a single vacancy: systematic DFT study through the periodic table of elements. Physical Chemistry Chemical Physics, 2018, 20, 858-865.	1.3	81
36464	TiS₃ sheet based van der Waals heterostructures with a tunable Schottky barrier. Nanoscale, 2018, 10, 807-815.	2.8	26
36465	Room-temperature fabrication of a delafossite CuCrO₂hole transport layer for perovskite solar cells. Journal of Materials Chemistry A, 2018, 6, 469-477.	5.2	91
36466	Convergence of calculated dislocation core structures in hexagonal close packed titanium. Modelling and Simulation in Materials Science and Engineering, 2018, 26, 014003.	0.8	12
36467	Charge Density and Band Offsets at Heterovalent Semiconductor Interfaces. Advanced Theory and Simulations, 2018, 1, 1700001.	1.3	20
36468	Recovery Mechanism of Degraded Black Phosphorus Fieldâ€Effect Transistors by 1,2â€Ethanedithiol Chemistry and Extended Device Stability. Small, 2018, 14, 1703194.	5.2	23
36469	Electrochemical Pourbaix diagrams of Ni Ti alloys from first-principles calculations and experimental aqueous states. Computational Materials Science, 2018, 143, 431-438.	1.4	25
36470	Strengthening effects of alloying elements W and Re on Ni3Al: A first-principles study. Computational Materials Science, 2018, 144, 23-31.	1.4	27
36471	Defect engineering of mesoporous nickel ferrite and its application for highly enhanced water oxidation catalysis. Journal of Catalysis, 2018, 358, 1-7.	3.1	68
36472	Magnetic states of Ni2MnZ and Ni2CrZ (Zâ€¯=â€¯Al, As, Bi, Ga, Ge, In, P, Pb, Sb, Si, Sn, Tl) Heusler alloys. Journal of Magnetism and Magnetic Materials, 2018, 459, 78-83.	1.0	11
36473	Ab initio calculations of elastic properties of alloys with mechanical instability: Application to BCC Ti-V alloys. Materials and Design, 2018, 140, 357-365.	3.3	19
36474	An Active Alkali-Exchanged Faujasite Catalyst for p-Xylene Production via the One-Pot Dielsâ€“Alder Cycloaddition/Dehydration Reaction of 2,5-Dimethylfuran with Ethylene. ACS Catalysis, 2018, 8, 760-769.	5.5	54
36475	Passivation of Hydrated Cement. ACS Sustainable Chemistry and Engineering, 2018, 6, 727-737.	3.2	12
36476	Electronic and magnetic properties of monolayer Î±-RuCl₃: a first-principles and Monte Carlo study. Physical Chemistry Chemical Physics, 2018, 20, 997-1004.	1.3	57
36477	Direct n-octanol amination by ammonia on supported Ni and Pd catalysts: activity is enhanced by â€œspectatorâ€•ammonia adsorbates. Catalysis Science and Technology, 2018, 8, 611-621.	2.1	26

#	Article	IF	Citations
36478	Stabilizing benzene-like planar N₆rings to form a single atomic honeycomb BeN₃sheet with high carrier mobility. Nanoscale, 2018, 10, 949-957.	2.8	18
36479	Atomic layer doping of Mn magnetic impurities from surface chains at a Ge/Si hetero-interface. Nanoscale, 2018, 10, 295-301.	2.8	4
36480	Crystal structure and anti-site boundary defect characterisation of Cu₂ZnSnSe₄. Journal of Materials Chemistry A, 2018, 6, 189-197.	5.2	11
36481	Nonplanar core structure of the screw dislocations in tantalum from the improved Peierlsâ€“Nabarro theory. Philosophical Magazine, 2018, 98, 484-516.	0.7	17
36482	Pressure-induced metallization in layered ReSe₂. Journal of Physics Condensed Matter, 2018, 30, 035401.	0.7	12
36483	Synthesis and thermal decomposition of potassium tetraamidoboranealuminate, K[Al(NH2BH3)4]. International Journal of Hydrogen Energy, 2018, 43, 311-321.	3.8	13
36484	Study of the Al-T-Si (T = Fe, Co, Ni) alloys in the solid, liquid and as-quenched states. Materials Characterization, 2018, 138, 315-324.	1.9	6
36485	Active site structure of a lithium phosphate catalyst for the isomerization of 2,3-epoxybutane to 3-buten-2-ol. Molecular Catalysis, 2018, 445, 133-141.	1.0	0
36486	Modulating the Hysteresis of an Electronic Transition: Launching Alternative Transformation Pathways in the Metalâ€“Insulator Transition of Vanadium(IV) Oxide. Chemistry of Materials, 2018, 30, 214-224.	3.2	20
36487	Grain boundaries in bcc-Fe: a density-functional theory and tight-binding study. Modelling and Simulation in Materials Science and Engineering, 2018, 26, 025008.	0.8	37
36488	Onion-like carbon as dopant/modification-free electrocatalyst for [VO]2+/[VO2]+ redox reaction: Performance-control mechanism. Carbon, 2018, 127, 31-40.	5.4	11
36489	Revisiting the diffusion mechanism of helium in UO2: A DFT+U study. Journal of Nuclear Materials, 2018, 498, 373-377.	1.3	15
36490	Electrochemical behavior of LiV3O8 positive electrode in hybrid Li,Naâ€“ion batteries. Journal of Power Sources, 2018, 373, 1-10.	4.0	15
36491	Structural properties of small Li_n (n = 5â€“8) atomic clusters via ab initio random structure searching: A look into the role of different implementations of long-range dispersion corrections. International Journal of Modern Physics B, 2018, 32, 1850009.	1.0	2
36492	Multiâ€site Cooperativity in Alkaliâ€Metalâ€Exchanged Faujasites for the Production of Biomassâ€Derived Aromatics. ChemPhysChem, 2018, 19, 446-458.	1.0	21
36493	Ce0.3Zr0.7O1.88N0.12 solid solution as a stable photocatalyst for visible light driven water splitting. Applied Catalysis B: Environmental, 2018, 224, 733-739.	10.8	4
36494	Atomistic simulation of Si-Au melt crystallization with novel interatomic potential. Computational Materials Science, 2018, 142, 303-311.	1.4	22
36495	Structural and electronic properties of MnSi under high pressure: A first-principles calculation. Computational Materials Science, 2018, 142, 285-289.	1.4	7

#	Article	IF	Citations
36496	First-principles study of the surface properties of U-Mo system. Computational Materials Science, 2018, 142, 355-360.	1.4	18
36497	Pressure-induced structural transitions and electronic topological transition of Cu2Se. Journal of Alloys and Compounds, 2018, 732, 280-285.	2.8	11
36498	Water adsorption on the stoichiometric and defected Fe(110) surfaces. Surface Science, 2018, 668, 144-149.	0.8	15
36499	A highly efficient double-hierarchical sulfur host for advanced lithiumâ€“sulfur batteries. Chemical Science, 2018, 9, 666-675.	3.7	97
36500	Room-temperature ferromagnetism in alkaline-earth-metal doped AlP: First-principle calculations. Computational Materials Science, 2018, 142, 338-345.	1.4	9
36501	Enhanced activity of ethanol oxidation reaction on PtM (M=Au, Ag and Sn): The importance of oxophilicity and surface oxygen containing species. Electrochimica Acta, 2018, 259, 733-741.	2.6	21
36502	Efficient cold cathode emission in crystalline-amorphous hybrid: Study on carbon nanotube-cadmium selenide system. Physica E: Low-Dimensional Systems and Nanostructures, 2018, 97, 162-169.	1.3	5
36503	Charge and Discharge Processes and Sodium Storage in Disodium Pyridineâ€2,5â€Dicarboxylate Anodeâ€”Insights from Experiments and Theory. Advanced Energy Materials, 2018, 8, 1701572.	10.2	40
36504	Effect of Strain on Magnetic Coupling in Ga-Doped WS2 Monolayer: Ab Initio Study. Journal of Superconductivity and Novel Magnetism, 2018, 31, 1801-1805.	0.8	3
36505	Experimental and theoretical study of hydrogen desorption process from Mn(BH4)2. Journal of Alloys and Compounds, 2018, 735, 277-284.	2.8	6
36506	Electronic and magnetic properties of zigzag GaN nanoribbons with hydrogenation and fluorination. Physica E: Low-Dimensional Systems and Nanostructures, 2018, 97, 144-150.	1.3	11
36507	Quasiharmonic calculations of thermodynamic properties for La3â^'xTe4 system. Computational Materials Science, 2018, 142, 417-426.	1.4	6
36508	Optimum Cu nanoparticle catalysts for CO2 hydrogenation towards methanol. Nano Energy, 2018, 43, 200-209.	8.2	133
36509	STRUCTURAL AND ELECTRONIC PROPERTIES OF Pd AND Au MONOLAYERS ADSORBED ON MoS₂: A COMPARATIVE STUDY FROM DFT CALCULATIONS. Surface Review and Letters, 2018, 25, 1850117.	0.5	0
36510	Influencing factors of atomic order in the binary sigma phase. Intermetallics, 2018, 93, 6-19.	1.8	8
36511	Reduction, sintering and mechanical properties of rhenium-tungsten compounds. Journal of Alloys and Compounds, 2018, 735, 2685-2693.	2.8	24
36512	Hydrogen generation due to water splitting on SiÂ-Âterminated 4H-Sic(0001) surfaces. Surface Science, 2018, 668, 68-72.	0.8	2
36513	Influence of transition group elements on the stability of theÎ´- andÎ·-phase in nickelbase alloys. Modelling and Simulation in Materials Science and Engineering, 2018, 26, 015005.	0.8	6

#	Article	IF	Citations
36514	Unconventional thermal transport enhancement with large atom mass: a comparative study of 2D transition dichalcogenides. 2D Materials, 2018, 5, 015022.	2.0	12
36515	Mechanical Properties in Metalâ€“Organic Frameworks: Emerging Opportunities and Challenges for Device Functionality and Technological Applications. Advanced Materials, 2018, 30, e1704124.	11.1	165
36516	Solution Adsorption Formation of a Ï€â€Conjugated Polymer/Graphene Composite for Highâ€Performance Fieldâ€Effect Transistors. Advanced Materials, 2018, 30, 1705377.	11.1	48
36517	Elucidating the Impact of Chalcogen Content on the Photovoltaic Properties of Oxychalcogenide Perovskites: NaMO_{3â”x}Q_x (M=Nb, Ta; Q=S, Se, Te). ChemPhysChem, 2018, 19, 703-714.	1.0	17
36518	Investigation of CHx (xâ€‰=â€‰2â€“4) Adsorption on Mo2C and Mo4C2 Sites Incorporated in ZSM-5 Zeolite Using Periodic-DFT Approach. Catalysis Letters, 2018, 148, 68-78.	1.4	9
36519	Metal adsorption on monolayer blue phosphorene: A first principles study. Physics Letters, Section A: General, Atomic and Solid State Physics, 2018, 382, 205-209.	0.9	20
36520	Electronic structure of monolayer 1Tâ€²-MoTe2 grown by molecular beam epitaxy. APL Materials, 2018, 6, .	2.2	44
36521	Thermal transport through Ge-rich Ge/Si superlattices grown on Ge(0â€‰0â€‰1). Journal Physics D: Applied Physics, 2018, 51, 014001.	1.3	22
36522	Morphology control and its effect on the electrochemical performance of Na2Li2Ti6O14 anode materials for lithium ion battery application. Electrochimica Acta, 2018, 259, 855-864.	2.6	24
36523	On the stability and mobility of di-vacancies in tungsten. Nuclear Fusion, 2018, 58, 026004.	1.6	27
36524	Modeling Kinetics of Water Adsorption on the Rutile TiO₂ (110) Surface: Influence of Exchangeâ€Correlation Functional. Physica Status Solidi (B): Basic Research, 2018, 255, 1700344.	0.7	5
36525	Electronic and Magnetic Properties of Monolayer and Bilayer Phosphorene Doped with Transitionâ€Metal Atoms. Physica Status Solidi (B): Basic Research, 2018, 255, 1700370.	0.7	9
36526	Non-uniformly functionalized titanium carbide-based MXenes as an anchoring material for Li-S batteries: A first-principles calculation. Applied Surface Science, 2018, 435, 210-215.	3.1	51
36527	Optimal sample formulations for DNP SENS: The importance of radical-surface interactions. Current Opinion in Colloid and Interface Science, 2018, 33, 9-18.	3.4	42
36528	Visible-light-induced charge transfer pathway and photocatalysis mechanism on Bi semimetal@defective BiOBr hierarchical microspheres. Journal of Catalysis, 2018, 357, 41-50.	3.1	246
36529	Structural, electronic, magnetic and optical properties of semiconductor Zn 1â^'x Mo x Te compound. Journal of Physics and Chemistry of Solids, 2018, 114, 240-245.	1.9	17
36530	Mechanistic Insights into Solution-Phase Oxidative Esterification of Primary Alcohols on Pd(111) from First-Principles Microkinetic Modeling. ACS Catalysis, 2018, 8, 272-282.	5.5	8
36531	Role of Stoichiometry in the Growth of Large Pb₂P₂Se₆ Crystals for Nuclear Radiation Detection. ACS Photonics, 2018, 5, 566-573.	3.2	15

#	Article	IF	Citations
36532	Coupled electron-ion Monte Carlo simulation of hydrogen molecular crystals. Journal of Chemical Physics, 2018, 148, 102314.	1.2	38
36533	Magnetic order multilayering in FeRh thin films by He-Ion irradiation. Materials Research Letters, 2018, 6, 106-112.	4.1	36
36534	Insights into Nitrate Reduction over Indium-Decorated Palladium Nanoparticle Catalysts. ACS Catalysis, 2018, 8, 503-515.	5.5	188
36535	Enhanced Activity for CO₂ Electroreduction on a Highly Active and Stable Ternary Au-CDots-C₃N₄ Electrocatalyst. ACS Catalysis, 2018, 8, 188-197.	5.5	94
36536	Organicâ"Inorganicâ€Hybridâ€Derived Molybdenum Carbide Nanoladders: Impacts of Surface Oxidation for Hydrogen Evolution Reaction. ChemNanoMat, 2018, 4, 194-202.	1.5	23
36537	Elastic, electronic structure, and optical properties of orthorhombic Na3AlF6: a first-principles study. Ionics, 2018, 24, 1377-1383.	1.2	9
36538	Chemical intuition for high thermoelectric performance in monolayer black phosphorus, Î±-arsenene and aW-antimonene. Journal of Materials Chemistry A, 2018, 6, 2018-2033.	5.2	80
36539	Atomic Vacancies Control of Pdâ€Based Catalysts for Enhanced Electrochemical Performance. Advanced Materials, 2018, 30, 1704171.	11.1	102
36540	Electrocatalysts for Hydrogen Evolution in Alkaline Electrolytes: Mechanisms, Challenges, and Prospective Solutions. Advanced Science, 2018, 5, 1700464.	5.6	1,022
36541	Verifying the Rechargeability of Liâ€CO₂ Batteries on Working Cathodes of Ni Nanoparticles Highly Dispersed on Nâ€Doped Graphene. Advanced Science, 2018, 5, 1700567.	5.6	159
36542	First-Principles Calculations of Acoustic and Anharmonic Properties of Ferromagnetic Cu2MnZ (Z =) Tj ETQq0 0 0 rgBT /Overlock 10 Tf 5	0.8	5
36543	New insights into mercury removal mechanism on CeO2-based catalysts: A first-principles study. Frontiers of Environmental Science and Engineering, 2018, 12, 1.	3.3	4
36544	Lattice dynamics and thermomechanical properties of zirconium(IV) chloride: Evidence for low-temperature negative thermal expansion. Chemical Physics Letters, 2018, 691, 98-102.	1.2	5
36545	First principles investigation of the electronic properties of graphitic carbon nitride with different building block and sheet staggered arrangement. Journal of Alloys and Compounds, 2018, 735, 131-139.	2.8	40
36546	Inducement of nanoscale Cuâ€"BTC on nanocomposite of PPyâ€"rGO and its performance in ammonia sensing. Materials Research Bulletin, 2018, 99, 152-160.	2.7	46
36547	Thermoelectric properties of thin film topological insulators: A first-principles study. Solid State Communications, 2018, 270, 22-25.	0.9	6
36548	Warming Up Density Functional Theory. , 2018, , 249-271.		15
36549	Formation mechanism of stable NbC carbide phase in Nb-1Zr-0.1C (wt.%) alloy. Acta Materialia, 2018, 144, 470-483.	3.8	23

#	Article	IF	Citations
36550	Adsorption mechanism of H2O molecule on the Li4SiO4 (0â€¯1â€¯0) surface from first principles. Chemical Physics Letters, 2018, 691, 1-7.	1.2	17
36551	Magnetocrystalline anisotropy of cementite pseudo single crystal fabricated under a rotating magnetic field. Journal of Magnetism and Magnetic Materials, 2018, 451, 1-4.	1.0	16
36552	Temperature dependent structural evolution in liquid Ag₅₀Ga₅₀ alloy. Journal of Physics Condensed Matter, 2018, 30, 015402.	0.7	6
36553	Tunable thermal properties in yttrium silicates switched by anharmonicity of low-frequency phonons. Journal of the European Ceramic Society, 2018, 38, 2043-2052.	2.8	16
36554	Enhanced scintillation of Ba3In(B3O6)3 based on nitrogen doping. Journal of Solid State Chemistry, 2018, 258, 351-357.	1.4	9
36555	Strain-induced enhancement of thermoelectric performance of TiS₂monolayer based on first-principles phonon and electron band structures. Nanotechnology, 2018, 29, 015204.	1.3	56
36556	Lithium halide monolayer sheets: First-principles many-body calculations. Computational Materials Science, 2018, 143, 103-111.	1.4	26
36557	Robust electronic and mechanical properties to layer number in 2D wide-gap X(OH)₂ (Xâ€‰â€‰=â€‰â€‰Mg, Ca). Journal Physics D: Applied Physics, 2018, 51, 015107.	1.3	7
36558	Selfâ€Established Rapid Magnesiation/Deâ€Magnesiation Pathways in Binary Seleniumâ€“Copper Mixtures with Significantly Enhanced Mgâ€Ion Storage Reversibility. Advanced Functional Materials, 2018, 28, 1701718.	7.8	71
36559	Monte Carlo Simulations of Thermal Hysteresis in Niâ€Mnâ€Based Heusler Alloys. Physica Status Solidi (B): Basic Research, 2018, 255, 1700265.	0.7	3
36560	Impact of Co and Fe Doping on the Martensitic Transformation and the Magnetic Properties in Niâ€Mnâ€Based Heusler Alloys. Physica Status Solidi (B): Basic Research, 2018, 255, 1700455.	0.7	14
36561	Niâ€Nanocluster Modified Black TiO₂ with Dual Active Sites for Selective Photocatalytic CO₂ Reduction. Small, 2018, 14, 1702928.	5.2	116
36562	Point defects at the <mml:math xmlns:mml="http://www.w3.org/1998/Math/MathML" altimg="si1.gif" overflow="scroll"><mml:mrow><mml:mtext>Î£</mml:mtext><mml:mn>5</mml:mn></mml:mrow></mml:math>(012)[100] grain boundary in TiN and the early stages of Cu diffusion: An ab initio study. Acta Materialia, 2018, 144, 496-504.	3.8	20
36563	Magnetic switching in Cr (xâ€²=â€²2â€“8) and its oxide cluster series. Journal of Magnetism and Magnetic Materials, 2018, 451, 32-37.	1.0	4
36564	The behaviors of helium atoms in tantalum, rhenium and osmium. Journal of Nuclear Materials, 2018, 499, 1-8.	1.3	13
36565	Crystallochemical tools in the search for cathode materials of rechargeable Na-ion batteries and analysis of their transport properties. Solid State Ionics, 2018, 314, 129-140.	1.3	51
36566	Oxygen Vacancies Confined in Nickel Molybdenum Oxide Porous Nanosheets for Promoted Electrocatalytic Urea Oxidation. ACS Catalysis, 2018, 8, 1-7.	5.5	372
36567	Development of a reactive force field for the Feâ€“C interaction to investigate the carburization of iron. Physical Chemistry Chemical Physics, 2018, 20, 775-783.	1.3	14

#	Article	IF	Citations
36568	A hybrid functional study of native point defects in Cu₂SnS₃: implications for reducing carrier recombination. Physical Chemistry Chemical Physics, 2018, 20, 256-261.	1.3	12
36569	Carbon segregation at Î£3 {1â€¯1â€¯2} grain boundaries in silicon. Computational Materials Science, 2018, 143, 80-86.	1.4	13
36570	Thickness-dependent stabilization of tetragonal ZrO2 in oxidized zirconium. Scripta Materialia, 2018, 145, 95-98.	2.6	13
36571	Trends and Control in the Nitridation of Transition-Metal Surfaces. ACS Catalysis, 2018, 8, 63-68.	5.5	19
36572	Ethanol synthesis from syngas over Cu(Pd)-doped Fe(100): a systematic theoretical investigation. Physical Chemistry Chemical Physics, 2018, 20, 2492-2507.	1.3	21
36573	Strain-Induced Tunable Magnetic Interaction in (Mo,Co)S2/(Si,Co)C Heterostructure. Journal of Superconductivity and Novel Magnetism, 2018, 31, 597-601.	0.8	3
36574	Photocatalytic activity enhancement of core-shell structure g-C3N4@TiO2 via controlled ultrathin g-C3N4 layer. Applied Catalysis B: Environmental, 2018, 220, 337-347.	10.8	357
36575	Adsorption of Prototypical Asphaltenes on Silica: First-Principles DFT Simulations Including Dispersion Corrections. Journal of Physical Chemistry B, 2018, 122, 618-624.	1.2	21
36576	Layered material GeSe and vertical GeSe/MoS2 p-n heterojunctions. Nano Research, 2018, 11, 420-430.	5.8	74
36577	Insights into the activation mechanism of calcium ions on the sericite surface: A combined experimental and computational study. Applied Surface Science, 2018, 427, 162-168.	3.1	31
36578	Effects of rhenium on graphene grown on SiC(0001). Journal of Electron Spectroscopy and Related Phenomena, 2018, 222, 117-121.	0.8	1
36579	Integrated investigation of the Li4Ti5O12 phase stability. Ionics, 2018, 24, 707-713.	1.2	9
36580	Emission and evaporation properties of 75 at.% Re-25 at.% W mixed matrix impregnated cathode. Applied Surface Science, 2018, 427, 874-882.	3.1	20
36581	Effect of carbon on behavior of helium in vanadium: A first-principles investigation. International Journal of Modern Physics B, 2018, 32, 1750269.	1.0	0
36582	Supported Ru Metalloporphyrins for Electrocatalytic CO₂ Conversion. ChemCatChem, 2018, 10, 1814-1820.	1.8	12
36583	Combined plane wave and localized orbital electronic structure calculation: Adsorption energy of hydrogen on Pd(111). International Journal of Quantum Chemistry, 2018, 118, e25452.	1.0	5
36584	Microkinetic modeling of H2SO4 formation on Pt based diesel oxidation catalysts. Applied Catalysis B: Environmental, 2018, 220, 348-355.	10.8	4
36585	Electric field induced spin polarization oscillation in nonmagnetic benzene/Cu(100) interface: First principles calculations. Applied Surface Science, 2018, 427, 156-161.	3.1	9

#	Article	IF	Citations
36586	Effects of shell thickness on Ag-Cu 2 O core-shell nanoparticles with bumpy structures for enhancing photocatalytic activity and stability. Catalysis Today, 2018, 303, 313-319.	2.2	41
36587	First-Principles Study of BCC/FCC Phase Transition Promoted by Interstitial Carbon in Iron. Materials Transactions, 2018, 59, 870-875.	0.4	16
36588	The nature of the band gap of GeSn alloys. , 2018, , .		2
36589	Structural stability of Pr-related defects in diamond and electronic structure single photon source: A first-principles study. AIP Advances, 2018, 8, .	0.6	6
36590	Multiscale energy density algorithm and application to surface structure of Ni matrix of superalloy. Chinese Physics B, 2018, 27, 097105.	0.7	0
36591	Ab initio simulations of superionic H2O, H2O2, and H9O4 compounds. AIP Conference Proceedings, 2018, , .	0.3	1
36592	Reaction Mechanisms and Solidâ€“Gas Phase Reactions: Theory and Density Functional Theory Simulations. Reviews in Mineralogy and Geochemistry, 2018, 84, 85-101.	2.2	6
36593	Atomistic study of SiN based ReRAM with high program/erase cycle endurance. IEICE Electronics Express, 2018, 15, 20180868-20180868.	0.3	0
36594	Thermodynamic Stability of Mg-Based Laves Phases. Materials Transactions, 2018, 59, 890-896.	0.4	5
36595	Systematic analysis for triple points in all magnetic symmorphic systems and symmetry-allowed coexistence of Dirac points and triple points. New Journal of Physics, 2018, 20, 123002.	1.2	5
36596	Transport Properties of the Layered Transition Metal Oxypnictide Sr₂ScCo_{1â^'x}Fe_xPO₃with Fe-doped Co_{1â^'x}Fe_xP layers. Journal of Physics: Conference Series, 2018, 969, 012032.	0.3	0
36597	Directional detection of light dark matter with polar materials. Physical Review D, 2018, 98, .	1.6	90
36598	First-principles calculations of orientation dependence of Si thermal oxidation based on Si emission model. Japanese Journal of Applied Physics, 2018, 57, 04FB06.	0.8	3
36599	Effect of P impurity on mechanical properties of NiAl Î£5 grain boundary: From perspectives of stress and energy. Chinese Physics B, 2018, 27, 037105.	0.7	1
36600	Simulation of Solar Cells Employing 2 Dimensional Transition Metal Dichalcogenide â€“ Silicon Front Surfaces. , 2018, , .		2
36601	Ab Initio Simulation of Magnesium Surface Oxidation. Bulletin of the Lebedev Physics Institute, 2018, 45, 311-313.	0.1	0
36602	First-Principles Investigation of Atomic Hydrogen Adsorption and Diffusion on/into Mo-doped Nb (100) Surface. Applied Sciences (Switzerland), 2018, 8, 2466.	1.3	11
36603	Creep Property of Boron Added 9Cr Heat Resistant Steels after Welding. Materials Science Forum, 2018, 941, 340-345.	0.3	0

#	Article	IF	Citations
36604	Intermolecular Interactions in Crystals of the Photosensitive Coordination Compounds of Zinc(II). Russian Journal of Coordination Chemistry/Koordinatsionnaya Khimiya, 2018, 44, 733-737.	0.3	11
36605	Unintentionally doped hydrogen removal mechanism in Li doped ZnO. AIP Advances, 2018, 8, .	0.6	6
36606	First-Principles Study of Magnetic Properties of TM 13 and TM 13 @Au 32 Clusters (TM=Mn, Co). Chinese Physics Letters, 2018, 35, 103601.	1.3	2
36607	Electronâ€“phonon coupling in semiconductors within the GW approximation. New Journal of Physics, 2018, 20, 123008.	1.2	68
36608	Stability of charges in titanium compounds and charge transfer to oxygen in titanium dioxide. Journal of Physics: Conference Series, 2018, 1136, 012017.	0.3	12
36609	Structure and Stability of Intermediate (Fe, Cr)₇C₃ Carbides. Solid State Phenomena, 0, 284, 634-639.	0.3	1
36610	HOD on Ni(111): Ab Initio molecular dynamics prediction of molecular beam experiments. Journal of Chemical Physics, 2018, 149, 244706.	1.2	12
36611	The interaction between lithium acceptors and gallium donors in zinc oxide. Journal of Applied Physics, 2018, 124, 245702.	1.1	1
36612	Material-Dependent Screening of Coulomb Interaction in Single-Layer Cuprates. Journal of the Physical Society of Japan, 2018, 87, 114701.	0.7	9
36613	Quantum dynamics studies of the dissociative chemisorption of CH4 on the steps and terraces of Ni(211). Journal of Chemical Physics, 2018, 149, 244704.	1.2	13
36614	Vibrational properties and lattice specific heat of KFeS2. AIP Conference Proceedings, 2018, , .	0.3	3
36615	Vibrational properties and lattice specific heat of RbFeS2. AIP Conference Proceedings, 2018, , .	0.3	0
36616	Interaction of Chloride Anions With Copper Surfaces. , 2018, , 166-181.		6
36617	Chemical bonding in initial building blocks of semiconductors: Geometrical structures and optical absorption spectra of isolated CdSe2+ and Cd2Se2+ species. Journal of Chemical Physics, 2018, 149, 244308.	1.2	7
36618	Strain Tunable Bandgap and High Carrier Mobility in SiAs and SiAs2 Monolayers from First-Principles Studies. Nanoscale Research Letters, 2018, 13, 404.	3.1	17
36619	A Universal Strategy for Constructing Seamless Graphdiyne on Metal Oxides to Stabilize the Electrochemical Structure and Interface. Advanced Materials, 2019, 31, e1806272.	11.1	59
36620	Hydrogen Storage in All-Metal and Nonmetal Aromatic Clusters. , 2018, , 329-362.		0
36621	BaTiO3 polar surface in ultrahigh vacuum calculated by local density functional theory with a large supercell. Ferroelectrics, 2018, 534, 183-189.	0.3	1

#	Article	IF	Citations
36622	From Bulk CeO2 to Transition-Metal Clusters Supported on the CeO2(111) Surface: A Critical Discussion. , 2018, , 452-459.		0
36623	Atomistic Insights of Multiple Stacking Faults in CdTe Thin-Film Photovoltaics: A DFT Study. , 2018, , .		4
36624	Electronic, mechanical, and optical properties of Ruddlesden-Popper perovskite sulfides: First principle calculation. Ferroelectrics, 2018, 535, 142-151.	0.3	2
36625	Modification of a Shockley-Type Surface State on Pt(111) upon Deposition of Gold Thin Layers. Materials, 2018, 11, 2569.	1.3	1
36626	Surface Strain Effects on the Adsorption of Au Adatoms on MgO(001) Surfaces with Surface O Vacancies. Journal of the Korean Physical Society, 2018, 73, 1324-1328.	0.3	0
36627	P-T Phase Diagram of LuFe2O4. Crystals, 2018, 8, 184.	1.0	2
36628	Synthesis, Crystal Structure, and Chemical-Bonding Analysis of BaZn(NCN)2. Inorganics, 2018, 6, 1.	1.2	27
36629	A Computational Study of AlF3 and ACF Surfaces. Inorganics, 2018, 6, 124.	1.2	4
36630	Electronic, Thermal Expanding, and Optical Absorption Properties of Transition Metal Dichalcogenides: A First-principles Study. Journal Wuhan University of Technology, Materials Science Edition, 2018, 33, 1355-1359.	0.4	0
36631	First-principle calculations of the exchange interaction characteristics for multilayer magnetic structures. EPJ Web of Conferences, 2018, 185, 03007.	0.1	2
36632	Multiscale Simulation of Precipitation in Copper-Alloyed Pipeline Steels and in Cu-Ni-Si Alloys. , 2018, , 1-41.		0
36633	Optimization Problems of Nanosized Semiconductor Heterostructures. Russian Microelectronics, 2018, 47, 583-588.	0.1	3
36634	Charge self-consistent many-body corrections using optimized projected localized orbitals. Journal of Physics Condensed Matter, 2018, 30, 475901.	0.7	36
36635	Study of Local Mechanical Properties of Fe₇₈Al₂₂ Alloy. Key Engineering Materials, 2018, 784, 27-32.	0.4	1
36636	In Silico Screening and Design of Coating Materials for PEMFC Bipolar Plates. Coatings, 2018, 8, 386.	1.2	4
36637	Valence charge distribution in homogenous silicon-aluminium thin-films. Journal of Physics Condensed Matter, 2018, 30, 335502.	0.7	2
36638	Polymeric Nitrogen A7 Layers Stabilized in the Confinement of a Multilayer BN Matrix at Ambient Conditions. Scientific Reports, 2018, 8, 13758.	1.6	8
36639	Self-passivating (Re,Al)B2 coatings synthesized by magnetron sputtering. Scientific Reports, 2018, 8, 15570.	1.6	5

#	Article	IF	Citations
36640	Room temperature d0 ferromagnetism in PbS films: nonuniform distribution of Pb vacancies. Physical Chemistry Chemical Physics, 2018, 20, 29804-29810.	1.3	4
36641	Large magnetic anisotropy and its strain modulation in two-dimensional intrinsic ferromagnetic monolayer RuO₂ and OsO₂. Physical Chemistry Chemical Physics, 2018, 20, 28162-28168.	1.3	26
36642	Electronic structure and optical properties of novel monolayer gallium nitride and boron phosphide heterobilayers. Physical Chemistry Chemical Physics, 2018, 20, 28124-28134.	1.3	58
36643	Two dimensional allotropes of arsenene with a wide range of high and anisotropic carrier mobility. Physical Chemistry Chemical Physics, 2018, 20, 29939-29950.	1.3	86
36644	Efficient light-driven CO₂ hydrogenation on Ru/CeO₂ catalysts. Catalysis Science and Technology, 2018, 8, 6503-6510.	2.1	18
36645	Eco-friendly synthesis of N,S co-doped hierarchical nanocarbon as a highly efficient metal-free catalyst for the reduction of nitroarenes. Nanoscale, 2018, 10, 21764-21771.	2.8	24
36646	Impact of trace extrinsic defect formation on the local symmetry transition in spinel LiNi_{0.5}Mn_{1.5}O_{4â˜Î´} systems and their electrochemical characteristics. Journal of Materials Chemistry A, 2018, 6, 22749-22757.	5.2	10
36647	Colloidal Niâ€“Coâ€“Sn nanoparticles as efficient electrocatalysts for the methanol oxidation reaction. Journal of Materials Chemistry A, 2018, 6, 22915-22924.	5.2	85
36648	Piezoelectric and polarized enhancement by hydrofluorination of penta-graphene. Physical Chemistry Chemical Physics, 2018, 20, 26288-26296.	1.3	26
36649	A density functional theory study of propylene epoxidation mechanism on Ag₂O(001) surface. Physical Chemistry Chemical Physics, 2018, 20, 26681-26687.	1.3	13
36650	Ostwald's rule of stages and metastable transitions in the hydrogenâ€“water system at high pressure. Physical Chemistry Chemical Physics, 2018, 20, 26853-26858.	1.3	8
36651	PAW-mediated ab initio simulations on linear response phonon dynamics of anisotropic black phosphorous monolayer for thermoelectric applications. Physical Chemistry Chemical Physics, 2018, 20, 26688-26695.	1.3	7
36652	Hybrid functional calculations of electronic and thermoelectric properties of GaS, GaSe, and GaTe monolayers. Physical Chemistry Chemical Physics, 2018, 20, 28575-28582.	1.3	65
36653	Effect of the degree of inversion on optical properties of spinel ZnFe₂O₄. Physical Chemistry Chemical Physics, 2018, 20, 28267-28278.	1.3	88
36654	Phonon mode contributions to thermal conductivity of pristine and defective Î²-Ga₂O₃. Physical Chemistry Chemical Physics, 2018, 20, 29236-29242.	1.3	25
36655	Mixed-dimensional 2D/3D heterojunctions between MoS₂ and Si(100). Physical Chemistry Chemical Physics, 2018, 20, 25240-25245.	1.3	7
36656	Protecting quantum anomalous Hall state from thermal fluctuation via the giant magnetic anisotropy of Os-based dimers. Physical Chemistry Chemical Physics, 2018, 20, 28169-28175.	1.3	11
36657	Electronâ€“phonon interaction and superconductivity in the high-pressure cI16 phase of lithium from first principles. Physical Chemistry Chemical Physics, 2018, 20, 27125-27130.	1.3	12

#	Article	IF	Citations
36658	The role of Andersonâ€™s rule in determining electronic, optical and transport properties of transition metal dichalcogenide heterostructures. Physical Chemistry Chemical Physics, 2018, 20, 30351-30364.	1.3	47
36659	Negative/zero thermal expansion in black phosphorus nanotubes. Physical Chemistry Chemical Physics, 2018, 20, 28726-28731.	1.3	11
36660	Interfacial barriers to gas transport in zeolites: distinguishing internal and external resistances. Physical Chemistry Chemical Physics, 2018, 20, 26386-26395.	1.3	32
36661	Tuning the electronic properties of van der Waals heterostructures composed of black phosphorus and graphitic SiC. Physical Chemistry Chemical Physics, 2018, 20, 29333-29340.	1.3	17
36662	Theoretical evaluation of thermal decomposition of dichlorosilane for plasma-enhanced atomic layer deposition of silicon nitride: the important role of surface hydrogen. Physical Chemistry Chemical Physics, 2018, 20, 29152-29158.	1.3	9
36663	Tunable band offsets in the BP/P₄O₁₀ van der Waals heterostructure: first-principles calculations. Physical Chemistry Chemical Physics, 2018, 20, 29931-29938.	1.3	7
36664	First-principles study of rocksalt early transition-metal carbides as potential catalysts for Liâ€“O₂ batteries. Physical Chemistry Chemical Physics, 2018, 20, 30231-30238.	1.3	9
36665	A predictive modeling study of the impact of chemical doping on the strength of a Ag/ZnO interface. Journal of Applied Physics, 2018, 124, .	1.1	3
36666	Dispersion-mediated steering of organic adsorbates on a precovered silicon surface. Beilstein Journal of Organic Chemistry, 2018, 14, 2715-2721.	1.3	5
36667	Single-site point defects in semimetal WTe₂: A density functional theory study. AIP Advances, 2018, 8, 125323.	0.6	8
36668	Transparent Amorphous Oxide Semiconductor as Excellent Thermoelectric Materials. Coatings, 2018, 8, 462.	1.2	13
36669	Spectroscopic characterization of a highly selective NiCu₃/C hydrodeoxygenation catalyst. Catalysis Science and Technology, 2018, 8, 6100-6108.	2.1	9
36670	Ligand-functionalized Pt nanoparticles as asymmetric heterogeneous catalysts: molecular reaction control by ligandâ€“reactant interactions. Catalysis Science and Technology, 2018, 8, 6062-6075.	2.1	19
36671	The effect of electrostatic field on the catalytic properties of platinum clusters confined in zeolite for hydrogenation. Catalysis Science and Technology, 2018, 8, 6384-6395.	2.1	18
36672	Disorder induced polymorphic transitions in the high hydrogen density compound Sr(BH₄)₂(NH₃BH₃)₂. Dalton Transactions, 2018, 47, 16737-16746.	1.6	5
36673	Significantly enhanced magnetoresistance in monolayer WTe2via heterojunction engineering: a first-principles study. Nanoscale, 2018, 10, 22231-22236.	2.8	11
36674	Structural characterization of heterogeneous RhAu nanoparticles from a microwave-assisted synthesis. Nanoscale, 2018, 10, 22520-22532.	2.8	15
36675	Discovery of a novel spin-polarized nodal ring in a two-dimensional HK lattice. Nanoscale, 2018, 10, 20748-20753.	2.8	54

#	Article	IF	Citations
36676	Anisotropic ultraviolet-plasmon dispersion in black phosphorus. Nanoscale, 2018, 10, 21918-21927.	2.8	18
36677	Controlled p-type substitutional doping in large-area monolayer WSe₂crystals grown by chemical vapor deposition. Nanoscale, 2018, 10, 21374-21385.	2.8	58
36678	Super-alkalis as building blocks of one-dimensional hierarchical electrides. Nanoscale, 2018, 10, 22963-22969.	2.8	13
36679	Remote homoepitaxy of ZnO microrods across graphene layers. Nanoscale, 2018, 10, 22970-22980.	2.8	33
36680	Janus monolayer of WSeTe, a new structural phase transition material driven by electrostatic gating. Nanoscale, 2018, 10, 21629-21633.	2.8	68
36681	Strain and screening effects on field emission properties of armchair graphene nanoribbon arrays: a first-principles study. RSC Advances, 2018, 8, 22625-22634.	1.7	3
36682	Discovery of zirconium dioxides for the design of better oxygen-ion conductors using efficient algorithms beyond data mining. RSC Advances, 2018, 8, 25534-25545.	1.7	18
36683	Effect of pressure on the structural, electronic and mechanical properties of ultraincompressible W₂B. RSC Advances, 2018, 8, 35664-35671.	1.7	9
36684	Coupled magneticâ€“elastic and metalâ€“insulator transition in epitaxially strained SrMnO₃/BaMnO₃ superlattices. RSC Advances, 2018, 8, 36407-36411.	1.7	1
36685	Retention and diffusion of transmutation H and He atoms in Be₁₂Ti: first-principles calculations. RSC Advances, 2018, 8, 35735-35743.	1.7	12
36686	Stability of theÂV and Co atomic wires: a first-principles study. RSC Advances, 2018, 8, 41552-41560.	1.7	0
36687	The influences ofÂV and Gd dopants on the structures and electrical and magnetic properties of PbPdO₂ thin films. RSC Advances, 2018, 8, 38751-38757.	1.7	4
36688	Synergistic coreâ€“shell interactions enable ultra-low overpotentials for enhanced CO₂ electro-reduction activity. Journal of Materials Chemistry A, 2018, 6, 21120-21130.	5.2	10
36689	Synthesis, crystal structure, and ionic conductivity of hydride ion-conducting Ln₂LiHO₃ (Ln = La, Pr, Nd) oxyhydrides. Journal of Materials Chemistry A, 2018, 6, 23457-23463.	5.2	31
36690	Thermal and thermoelectric properties of monolayer indium triphosphide (InP₃): a first-principles study. Journal of Materials Chemistry A, 2018, 6, 21532-21541.	5.2	91
36691	Dynamical stabilization in delafossite nitrides for solar energy conversion. Journal of Materials Chemistry A, 2018, 6, 20852-20860.	5.2	19
36692	Potential of one-dimensional blue phosphorene nanotubes as a water splitting photocatalyst. Journal of Materials Chemistry A, 2018, 6, 21087-21097.	5.2	37
36693	Atomic layer deposition and first principles modeling of glassy Li₃BO₃â€“Li₂CO₃ electrolytes for solid-state Li metal batteries. Journal of Materials Chemistry A, 2018, 6, 19425-19437.	5.2	48

#	Article	IF	Citations
36694	First-principles characterization of two-dimensional (CH₃(CH₂)₃NH₃)₂(CH₃NH₃)_nâ^'1</s perovskite. Journal of Materials Chemistry A, 2018, 6, 24389-24396.	5.2	58
36695	Low lattice thermal conductivity and promising thermoelectric figure of merit of Zintl type TlInTe₂. Journal of Materials Chemistry C, 2018, 6, 13269-13274.	2.7	30
36696	Promising photovoltaic and solid-state-lighting materials: two-dimensional Ruddlesdenâ€“Popper type lead-free halide double perovskites Cs_{n+1}In_{n/2}Sb_{n/2}I_{3n+1}(n= 3) and Cs_{n+1}In_{n/2}Sb_{n/2}Cl_{3n+1}/Cs_{m+1}Cu_{m/2}Bi_{m/2}	2.7	19
36697	Hexagonal M₂C₃ (M = As, Sb, and Bi) monolayers: new functional materials with desirable band gaps and ultrahigh carrier mobility. Journal of Materials Chemistry C, 2018, 6, 12689-12697.	2.7	42
36698	Synthesis and the physical properties of layered copper oxytellurides Sr₂TMCu₂Te₂O₂ (TM = Mn, Co, Zn). Journal of Materials Chemistry C, 2018, 6, 12260-12266.	2.7	15
36699	Geometric structures and electronic properties of the Bi₂X₂Y (X, Y = O, S, Se,) Tj ETQq1 1 0.784314 rgBT /O 13241-13249.	2.7	23
36700	Fabrication of a high performance ZnIn₂S₄/Si heterostructure photodetector array for weak signal detection. Journal of Materials Chemistry C, 2018, 6, 12928-12939.	2.7	25
36701	Antiphase boundaries in truncated octahedron-shaped Zn-doped magnetite nanocrystals. Journal of Materials Chemistry C, 2018, 6, 12800-12807.	2.7	9
36702	Structure stabilization effect of configuration entropy in cubic WN. Physical Chemistry Chemical Physics, 2018, 20, 29243-29248.	1.3	3
36703	An efficient cluster model to describe the oxygen reduction reaction activity of metal catalysts: a combined theoretical and experimental study. Physical Chemistry Chemical Physics, 2018, 20, 26675-26680.	1.3	10
36704	Atomistic determination of the surface structure of Cu₂O(111): experiment and theory. Physical Chemistry Chemical Physics, 2018, 20, 27456-27463.	1.3	33
36705	DFT exploration of active site motifs in methane hydroxylation by Ni-ZSM-5 zeolite. Catalysis Science and Technology, 2018, 8, 5875-5885.	2.1	30
36706	Optimising the magnetic performance of Co ferrite nanoparticles via organic ligand capping. Nanoscale, 2018, 10, 21244-21253.	2.8	35
36707	Crystal structures of transition metal pernitrides predicted from first principles. RSC Advances, 2018, 8, 36412-36421.	1.7	15
36708	Preferential proton conduction along a three-dimensional dopant network in yttrium-doped barium zirconate: a first-principles study. Journal of Materials Chemistry A, 2018, 6, 22721-22730.	5.2	37
36709	Room temperature methoxylation in zeolite H-ZSM-5: an operando DRIFTS/mass spectrometric study. Chemical Communications, 2018, 54, 12875-12878.	2.2	25
36710	Theoretical description of alkali metal closo-boranes â€“ towards the crystal structure of MgB₁₂H₁₂. Physical Chemistry Chemical Physics, 2018, 20, 30140-30149.	1.3	8
36711	Tracking down the origin of peculiar vibrational spectra of aromatic self-assembled thiolate monolayers. Physical Chemistry Chemical Physics, 2018, 20, 29918-29930.	1.3	6

#	Article	IF	Citations
36712	Chemically driven surface effects in polar intermetallic topological insulators A3Bi. Physical Chemistry Chemical Physics, 2018, 20, 26372-26385.	1.3	4
36713	Comparison of different machine learning models for the prediction of forces in copper and silicon dioxide. Physical Chemistry Chemical Physics, 2018, 20, 30006-30020.	1.3	23
36714	The first stages of oxide growth at the low index Al surfaces (100), (110), (111): clusters and stripes vs. homogeneous growth. Physical Chemistry Chemical Physics, 2018, 20, 29549-29557.	1.3	7
36715	C₂N: an excellent catalyst for the hydrogen evolution reaction. Physical Chemistry Chemical Physics, 2018, 20, 27970-27974.	1.3	37
36716	Oxygen-defect-dependent ferromagnetism and strain modulation in free-standing two-dimensional TiO₂ monolayers. Physical Chemistry Chemical Physics, 2018, 20, 27176-27184.	1.3	7
36717	Bareversusprotected tetrairidium clusters by density functional theory. Physical Chemistry Chemical Physics, 2018, 20, 29480-29492.	1.3	4
36718	How robust is the metallicity of two dimensional gallium?. Physical Chemistry Chemical Physics, 2018, 20, 27668-27674.	1.3	14
36719	Determination of possible configurations for Li_{0.5}CoO₂delithiated Li-ion battery cathodesviaDFT calculations coupled with a multi-objective non-dominated sorting genetic algorithm (NSGA-III). Physical Chemistry Chemical Physics, 2018, 20, 26405-26413.	1.3	20
36720	Structural search for stable Mgâ€“Ca alloys accelerated with a neural network interatomic model. Physical Chemistry Chemical Physics, 2018, 20, 27545-27557.	1.3	19
36721	Operando investigations of lithiation and delithiation processes in a BiVO₄ anode material. Physical Chemistry Chemical Physics, 2018, 20, 29798-29803.	1.3	15
36722	Phase transition and superconductivity in ReS2, ReSe2 and ReTe2. Physical Chemistry Chemical Physics, 2018, 20, 29472-29479.	1.3	15
36723	First principles study on 2Hâ€“1Tâ€² transition in MoS₂ with copper. Physical Chemistry Chemical Physics, 2018, 20, 26986-26994.	1.3	39
36724	A comparative study of the structure, stability and energetic performance of 5,5â€²-bitetrazole-1,1â€²-diolate based energetic ionic salts: future high energy density materials. Physical Chemistry Chemical Physics, 2018, 20, 29693-29707.	1.3	34
36725	Ab initio electronic structure calculations of entire blue copper azurins. Physical Chemistry Chemical Physics, 2018, 20, 30392-30402.	1.3	19
36726	Mechanistic study of the ceria supported, re-catalyzed deoxydehydration of vicinal OH groups. Catalysis Science and Technology, 2018, 8, 5750-5762.	2.1	24
36727	Surface defects enhance the adsorption affinity and selectivity of Mg(OH)₂ towards As(<scp>v</scp>) and Cr(<scp>vi</scp>) oxyanions: a combined theoretical and experimental study. Environmental Science: Nano, 2018, 5, 2570-2578.	2.2	27
36728	Onset of vertical bonds in new GaN multilayers: beyond van der Waals solids. Nanoscale, 2018, 10, 21842-21850.	2.8	13
36729	Interlayer interactions in 2D WS₂/MoS₂ heterostructures monolithically grown by in situ physical vapor deposition. Nanoscale, 2018, 10, 22927-22936.	2.8	62

#	Article	IF	Citations
36730	Prediction of high-temperature Chern insulator with half-metallic edge states in asymmetry-functionalized stanene. Nanoscale, 2018, 10, 20226-20233.	2.8	102
36731	Overall reaction mechanism for a full atomic layer deposition cycle ofÂW films on TiN surfaces: first-principles study. RSC Advances, 2018, 8, 39039-39046.	1.7	6
36732	Inorganic molecule (O₂, NO) adsorption on nitrogen- and phosphorus-doped MoS₂ monolayer using first principle calculations. RSC Advances, 2018, 8, 38656-38666.	1.7	21
36733	The roles of oxygen vacancies, electrolyte composition, lattice structure, and doping density on the electrochemical reactivity of MagnÃ©li phase TiO₂anodes. Journal of Materials Chemistry A, 2018, 6, 23828-23839.	5.2	35
36734	Interaction of SrO-terminated SrTiO₃ surface with oxygen, carbon dioxide, and water. Journal of Materials Chemistry A, 2018, 6, 22662-22672.	5.2	24
36735	First-principles calculations and experimental studies of XYZ₂ thermoelectric compounds: detailed analysis of van der Waals interactions. Journal of Materials Chemistry A, 2018, 6, 19502-19519.	5.2	20
36736	Molybdenum carbide chemical sensors with ultrahigh signal-to-noise ratios and ambient stability. Journal of Materials Chemistry A, 2018, 6, 23408-23416.	5.2	35
36737	Experimental and computational phase boundary mapping of Co₄Sn₆Te₆. Journal of Materials Chemistry A, 2018, 6, 24175-24185.	5.2	26
36738	Two-dimensional few-layer group-III metal monochalcogenides as effective photocatalysts for overall water splitting in the visible range. Journal of Materials Chemistry A, 2018, 6, 22768-22777.	5.2	90
36739	New insight into the structure of PuGaO₃ from ab initio particle-swarm optimization methodology. Journal of Materials Chemistry A, 2018, 6, 22798-22808.	5.2	16
36740	Emergence of high piezoelectricity along with robust electron mobility in Janus structures in semiconducting Group IVB dichalcogenide monolayers. Journal of Materials Chemistry A, 2018, 6, 24885-24898.	5.2	127
36741	Theoretical study on cation codoped SrTiO₃ photocatalysts for water splitting. Journal of Materials Chemistry A, 2018, 6, 24342-24349.	5.2	20
36742	Two-dimensional Î²-phase group-VA binary compounds for versatile electronic and optical properties. Journal of Materials Chemistry C, 2018, 6, 11694-11700.	2.7	28
36743	Bipolar magnetism in a two-dimensional NbS₂ semiconductor with high Curie temperature. Journal of Materials Chemistry C, 2018, 6, 11401-11406.	2.7	35
36744	Synthesis of a novel strontium-based wide-bandgap semiconductor via X-ray photochemistry under extreme conditions. Journal of Materials Chemistry C, 2018, 6, 12473-12478.	2.7	11
36745	The competition between mechanical stability and charge carrier mobility in MA-based hybrid perovskites: insight from DFT. Journal of Materials Chemistry C, 2018, 6, 12252-12259.	2.7	42
36746	Geometric structure and electronic properties of wurtzite GaN/HfO2 interface: A first-principles study. Journal of Applied Physics, 2018, 124, 245703.	1.1	2
36747	Strongly inhomogeneous distribution of spectral properties of silicon-vacancy color centers in nanodiamonds. New Journal of Physics, 2018, 20, 115002.	1.2	52

#	Article	IF	Citations
36748	Interface Local Magnetic Moment and Its Near Periodic Modulation in Oxide SrRuO₃|LaAlO₃ Heterojunctions: An <italic>Ab Initio</italic> Investigation. IEEE Transactions on Magnetics, 2018, 54, 1-7.	1.2	1
36749	Ab-Initio Modeling of Lubricant Reactions with a Metal Al (111) Surface. , 2018, , .		0
36750	Atomic Displacement and Strength Properties in Equiatomic High Entropy Alloys with the FCC Structure. Materia Japan, 2018, 57, 312-316.	0.1	1
36751	Acceleration of metal-atom diffusion in electric field at metal/insulator interfaces: First-principles study. Japanese Journal of Applied Physics, 2018, 57, 04FB05.	0.8	8
36752	Charge-governed phase manipulation of few-layer tellurium. Nanoscale, 2018, 10, 22263-22269.	2.8	28
36753	The stability and unexpected chemistry of oxide clusters. Physical Chemistry Chemical Physics, 2018, 20, 30437-30444.	1.3	11
36754	Allotropes of tellurium from first-principles crystal structure prediction calculations under pressure. RSC Advances, 2018, 8, 39650-39656.	1.7	9
36755	New insight into Na intercalation with Li substitution on alkali site and high performance of O3-type layered cathode material for sodium ion batteries. Journal of Materials Chemistry A, 2018, 6, 22731-22740.	5.2	21
36756	Nanoporous PdCe bimetallic nanocubes with high catalytic activity towards ethanol electro-oxidation and the oxygen reduction reaction in alkaline media. Journal of Materials Chemistry A, 2018, 6, 23560-23568.	5.2	38
36757	PNTCDA: a promising versatile organic electrode material for alkali-metal ion batteries. Journal of Materials Chemistry A, 2018, 6, 24869-24876.	5.2	11
36758	Out of plane stacking of InSe-based heterostructures towards high performance electronic and optoelectronic devices using a graphene electrode. Journal of Materials Chemistry C, 2018, 6, 12509-12517.	2.7	28
36759	Carrier Transport Properties of MoS2 Asymmetric Gas Sensor Under Charge Transfer-Based Barrier Modulation. Nanoscale Research Letters, 2018, 13, 265.	3.1	6
36760	Ultralow Interlayer Friction of Layered Electride Ca2N: A Potential Two-Dimensional Solid Lubricant Material. Materials, 2018, 11, 2462.	1.3	15
36761	Strengthening Mechanisms of Powder Metallurgy Extruded CP Titanium Materials with Zirconium and Oxygen Solid Solution via Decomposition of ZrO₂ Additives in Sintering. Funtai Oyobi Fummatsu Yakin/Journal of the Japan Society of Powder and Powder Metallurgy, 2018, 65, 746-755.	0.1	2
36762	Tunable Electric Properties of Bilayer Î±-GeTe with Different Interlayer Distances and External Electric Fields. Nanoscale Research Letters, 2018, 13, 400.	3.1	25
36763	Influence of Functional Groups and Modification Sites of Metal-Organic Frameworks on CO2/CH4 Separation: A Monte Carlo Simulation Study. Chinese Journal of Chemical Physics, 2018, 31, 52-60.	0.6	3
36764	Combination Effect of Cation Vacancies and O2 Adsorption on Ferromagnetism of Na0.5Bi0.5TiO3(100) Surface: ab initio Study. Chinese Journal of Chemical Physics, 2018, 31, 177-183.	0.6	2
36765	Enhanced oxygen reduction on graphene via Y5Si3 electride substrate: A first-principles study. Chinese Journal of Chemical Physics, 2018, 31, 649-654.	0.6	6

#	Article	IF	Citations
36766	Theoretical study of adsorption and dehydrogenation of C2H4 on Cu(410). Chinese Journal of Chemical Physics, 2018, 31, 485-491.	0.6	5
36767	Origins of the High Reactivity of Au Nanostructures Deduced from the Structure and Properties of Model Surfaces. , 0, , .		1
36768	Au Atom Diffusions on Reduced and Cl-Adsorbed Rutile TiO₂(110) Surfaces: A DFT + <i>U</i> Study. E-Journal of Surface Science and Nanotechnology, 2018, 16, 267-273.	0.1	3
36769	Evaluation of Vacancy Formation and Migration Enthalpies in CoCrFeMnNi High-entropy Alloy using Positron Lifetime Measurements and Firstprinciples Calculations. Materia Japan, 2018, 57, 323-327.	0.1	0
36770	Electronic structures and optical properties of Ga doped single-layer indium nitride. Chinese Journal of Chemical Physics, 2018, 31, 313-317.	0.6	4
36771	First principles study of the structural, stability properties and lattice thermal conductivity of bulk ReSe2. Materials Today: Proceedings, 2018, 5, 10424-10430.	0.9	8
36772	First-Principles Calculations of the Electronic and Optical Properties of CH 3 NH 3 PbI 3 for Photovoltaic Applications. Materials Today: Proceedings, 2018, 5, 10570-10576.	0.9	7
36773	Roles of spin-orbit coupling in tetragonal hybrid halide perovskite for photovoltaics light-absorber. Materials Today: Proceedings, 2018, 5, 14857-14861.	0.9	6
36774	Effect of transition metal (TM) doping on structural and magnetic properties in hexagonal YMn0.917TM0.083O3 systems. Heliyon, 2018, 4, e00993.	1.4	3
36775	Structures of liquid selenium at high pressures. Journal of Physics: Conference Series, 2018, 946, 012101.	0.3	2
36776	Clusters of Local Bond-Orientational Order in Liquid Gallium: Studies of ab initio and Classical MD Simulations. Journal of Physics: Conference Series, 2018, 1136, 012016.	0.3	0
36777	Quantum molecular dynamics simulation of structural and thermodynamic properties of NiAl. Journal of Physics: Conference Series, 2018, 946, 012090.	0.3	0
36778	Ab initio simulation of liquid Mo and W near the liquidâ€“gas coexistence curve. Journal of Physics: Conference Series, 2018, 946, 012093.	0.3	5
36779	Emergence of magnetism in silicene by introducing carbon atom as foreign atom in all possible ways. Integrated Ferroelectrics, 2018, 194, 53-59.	0.3	0
36780	Effect of dispersion corrections on ab initio predictions of graphite and diamond properties under pressure. Physical Review B, 2018, 98, .	1.1	24
36781	Oxygen vacancies in the bulk and at neutral domain walls in hexagonal <mml:math xmlns:mml="http://www.w3.org/1998/Math/MathML"><mml:msub><mml:mi>YMnO</mml:mi><mml:mn>3</mml:mn></mml:msub></mml:math> Physical Review B, 2018, 98, .	1.1	22
36782	Advantages of the Surface Structuration of KBr Materials for Spectrometry and Sensors. Sensors, 2018, 18, 3013.	2.1	15
36783	Ab Initio Evaluation of Henry Coefficients Using Importance Sampling. Journal of Chemical Theory and Computation, 2018, 14, 6359-6369.	2.3	12

#	Article	IF	Citations
36784	Coupled LiPF₆ Decomposition and Carbonate Dehydrogenation Enhanced by Highly Covalent Metal Oxides in High-Energy Li-Ion Batteries. Journal of Physical Chemistry C, 2018, 122, 27368-27382.	1.5	127
36785	Extremely High Mobilities in Two-Dimensional Group-VA Binary Compounds with Large Conversion Efficiency for Solar Cells. Journal of Physical Chemistry C, 2018, 122, 27590-27596.	1.5	17
36786	Stacking-Dependent Magnetism in Bilayer CrI₃. Nano Letters, 2018, 18, 7658-7664.	4.5	475
36787	Chemical bonding origin of the unexpected isotropic physical properties in thermoelectric Mg3Sb2 andÂrelated materials. Nature Communications, 2018, 9, 4716.	5.8	102
36788	Unusually complex phase of dense nitrogen at extreme conditions. Nature Communications, 2018, 9, 4717.	5.8	28
36789	Bilayer MoS2 quantum dots with tunable magnetism and spin. AIP Advances, 2018, 8, 115103.	0.6	2
36790	Ground-state crystal structures of superconducting Nb3Al and the phase transformation under high pressures. Journal of Applied Physics, 2018, 124, 173902.	1.1	7
36791	Giant direct and inverse electrocaloric effects in multiferroic thin films. Physical Review B, 2018, 98, .	1.1	22
36792	Mirror protected multiple nodal line semimetals and material realization. Physical Review B, 2018, 98, .	1.1	24
36793	Unique Gap Structure and Symmetry of the Charge Density Wave in Single-Layer <mml:math xmlns:mml="http://www.w3.org/1998/Math/MathML" display="inline"><mml:mrow><mml:msub><mml:mrow><mml:mi>VSe</mml:mi></mml:mrow><mml:mrow><mml:mn>2</mml:mn></mml:mrow></mml:msub></mml:mrow></mml:math>. Physical Review Letters, 2018, 121, 196402.	2.9	139
36794	Band Alignment and the Built-in Potential of Solids. Physical Review Letters, 2018, 121, 196802.	2.9	27
36795	Exploring the High-Pressure Materials Genome. Physical Review X, 2018, 8, .	2.8	15
36796	Influence of the Thickness of Nonmagnetic Spacer on the Magnetic Properties of Fe/Cu Multilayered Nanowires. Key Engineering Materials, 2018, 787, 93-98.	0.4	0
36797	Dramatically Enhanced Stability of Silver Passivated Dicalcium Nitride Electride: Ag-Ca₂N. Chemistry of Materials, 2018, 30, 7803-7812.	3.2	9
36798	First-principle atomistic thermodynamic study on the early-stage corrosion of NiCr alloy under fluoride salt environment. Physical Chemistry Chemical Physics, 2018, 20, 28832-28839.	1.3	11
36799	Strain-engineering the electronic properties and anisotropy of GeSe₂ monolayers. RSC Advances, 2018, 8, 33445-33450.	1.7	9
36800	Rare earth doping and effective band-convergence in SnTe for improved thermoelectric performance. Applied Physics Letters, 2018, 113, .	1.5	25
36801	Optimizing special quasirandom structure (SQS) models for accurate functional property prediction in disordered 2D alloys. Journal of Physics Condensed Matter, 2018, 30, 485402.	0.7	4

#	Article	IF	Citations
36802	A Multiscale Model for Electrochemical Reactions in LSCF Based Solid Oxide Cells. Journal of the Electrochemical Society, 2018, 165, F1232-F1241.	1.3	14
36803	Strain Engineered Band Gaps and Electronic Properties in PbPdO2 and PbPd0.75Co0.25O2 Slabs. Materials, 2018, 11, 2002.	1.3	4
36804	Atomistic Simulations of Pure Tin Based on a New Modified Embedded-Atom Method Interatomic Potential. Metals, 2018, 8, 900.	1.0	22
36805	Two-Dimensional Titanium Carbonitride Mxene for High-Performance Sodium Ion Batteries. ACS Applied Nano Materials, 2018, 1, 6854-6863.	2.4	71
36806	Evidence for a quantum spin Hall phase in graphene decorated with Bi ₂ Te ₃ nanoparticles. Science Advances, 2018, 4, eaau6915.	4.7	36
36807	Highâ€Pressure Behavior of Lead Cyanamide PbNCN. Zeitschrift Fur Anorganische Und Allgemeine Chemie, 2018, 644, 1881-1885.	0.6	5
36808	Nucleation of Cu_n (n = 1â€“5) Clusters and Equilibrium Morphology of Cu Particles Supported on CeO₂ Surface: A Density Functional Theory Study. Journal of Physical Chemistry C, 2018, 122, 27402-27411.	1.5	15
36809	Developing ReaxFF to Visit CO Adsorption and Dissociation on Iron Surfaces. Journal of Physical Chemistry C, 2018, 122, 27582-27589.	1.5	15
36810	Perpendicular Optical Reversal of the Linear Dichroism and Polarized Photodetection in 2D GeAs. ACS Nano, 2018, 12, 12416-12423.	7.3	157
36811	Defect identification based on first-principles calculations for deep level transient spectroscopy. Applied Physics Letters, 2018, 113, .	1.5	51
36812	The effect of hydrogen on the electronic, mechanical and phonon properties of LaMgNi4 and its hydrides for hydrogen storage applications. International Journal of Hydrogen Energy, 2018, 43, 23397-23408.	3.8	40
36813	Janus Group-III Chalcogenide Monolayers and Derivative Type-II Heterojunctions as Water-Splitting Photocatalysts with Strong Visible-Light Absorbance. Journal of Physical Chemistry C, 2018, 122, 27795-27802.	1.5	73
36814	Synergetic Effect of B and O Dopants for Aerobic Oxidative Coupling of Amines to Imines. ACS Sustainable Chemistry and Engineering, 2018, 6, 17410-17418.	3.2	25
36815	Localized surface plasmon resonance on two-dimensional HfSe2 and ZrSe2. Semiconductor Science and Technology, 2018, 33, 124014.	1.0	8
36816	Band engineering of double-wall Mo-based hybrid nanotubes. Chinese Physics B, 2018, 27, 076104.	0.7	4
36817	Trimer bonding states on the surface of the transition-metal dichalcogenide <mml:math xmlns:mml="http://www.w3.org/1998/Math/MathML"><mml:mrow><mml:mi>TaT</mml:mi><mml:msub><mml:mi mathvariant="normal">e</mml:mi><mml:mn>2</mml:mn></mml:msub></mml:mrow></mml:math>. Physical Review B, 2018, 98, .	1.1	19
36818	An Ab Initio Study of Connections between Tensorial Elastic Properties and Chemical Bonds in Î£5(210) Grain Boundaries in Ni3Si. Materials, 2018, 11, 2263.	1.3	4
36819	High performance thermoelectric materials based on metal organic coordination polymers through firstâ€principles band engineering. Journal of Computational Chemistry, 2018, 39, 2582-2588.	1.5	12

#	Article	IF	Citations
36820	Two-Dimensional, Ordered, Double Transition Metal Carbides (MXenes): A New Family of Promising Catalysts for the Hydrogen Evolution Reaction. Journal of Physical Chemistry C, 2018, 122, 28113-28122.	1.5	104
36821	Origin of the Ï€â€“Ï€ Spacing Change upon Doping of Semiconducting Polymers. Journal of Physical Chemistry C, 2018, 122, 27983-27990.	1.5	25
36822	Tunable auxetic properties in group-IV monochalcogenide monolayers. Physical Review B, 2018, 98, .	1.1	42
36823	Structural stability and energy levels of carbon-related defects in amorphous SiO₂ and its interface with SiC. Japanese Journal of Applied Physics, 2018, 57, 125701.	0.8	15
36824	Experimental investigation and thermodynamic calculation of the B-Fe-W ternary system. Calphad: Computer Coupling of Phase Diagrams and Thermochemistry, 2018, 63, 212-219.	0.7	8
36825	Transformation of the Anion Sublattice in the Cation-Exchange Synthesis of Au2S from Cu2â€“xS Nanocrystals. Chemistry of Materials, 2018, 30, 8843-8851.	3.2	17
36826	V₂Te₂O: A Two-Dimensional van der Waals Correlated Metal. Inorganic Chemistry, 2018, 57, 14617-14623.	1.9	8
36827	Diversity of Adsorbed Hydrogen on the TiC(001) Surface at High Coverages. Journal of Physical Chemistry C, 2018, 122, 28013-28020.	1.5	17
36828	Highly Promoted Carrier Mobility and Intrinsic Stability by Rolling Up Monolayer Black Phosphorus into Nanoscrolls. Journal of Physical Chemistry Letters, 2018, 9, 6847-6852.	2.1	20
36829	Unravelling the Role of Topological Defects on Catalytic Unzipping of Single-Walled Carbon Nanotubes by Single Transition Metal Atom. Journal of Physical Chemistry Letters, 2018, 9, 6801-6807.	2.1	7
36830	Layered-Structure SbPO₄/Reduced Graphene Oxide: An Advanced Anode Material for Sodium Ion Batteries. ACS Nano, 2018, 12, 12869-12878.	7.3	87
36831	Lead-Free Direct Band Gap Double-Perovskite Nanocrystals with Bright Dual-Color Emission. Journal of the American Chemical Society, 2018, 140, 17001-17006.	6.6	399
36832	Two-dimensional tessellation by molecular tiles constructed from halogenâ€“halogen and halogenâ€“metal networks. Nature Communications, 2018, 9, 4871.	5.8	38
36833	Pressure-induced superconductivity in topological semimetal NbAs2. Npj Quantum Materials, 2018, 3, .	1.8	25
36834	High-throughput first-principles-calculations based estimation of lithium ion storage in monolayer rhenium disulfide. Communications Chemistry, 2018, 1, .	2.0	22
36835	Octahedral coupling in (111)- and (001)-oriented La2/3Sr1/3MnO3/SrTiO3 heterostructures. Journal of Applied Physics, 2018, 124, .	1.1	5
36836	Oxidation effect on the shear strength of graphene on aluminum and titanium surfaces. Physical Review B, 2018, 98, .	1.1	16
36837	Prediction of novel high-pressure H2O -NaCl and carbon oxide compounds with a symmetry-driven structure search algorithm. Physical Review B, 2018, 98, .	1.1	5

#	Article	IF	Citations
36838	Repulsive forces between neutral surfaces induced by adatoms. Physical Review B, 2018, 98, .	1.1	1
36839	Covalency-driven collapse of strong spin-orbit coupling in face-sharing iridium octahedra. Physical Review B, 2018, 98, .	1.1	15
36840	Realization of flat band with possible nontrivial topology in electronic Kagome lattice. Science Advances, 2018, 4, eaau4511.	4.7	131
36841	Reversible superdense ordering of lithium between two graphene sheets. Nature, 2018, 564, 234-239.	13.7	178
36842	Magnetic origin of phase stability in cubic Î³-MoN. Applied Physics Letters, 2018, 113, 221901.	1.5	6
36843	Strain-driven magnetic phase transitions from an antiferromagnetic to a ferromagnetic state in perovskite <mml:math xmlns:mml="http://www.w3.org/1998/Math/MathML"><mml:mrow><mml:mi>R</mml:mi><mml:msub><mml:mi>MnO</mml:mi><mml: films. Physical Review B, 2018, 98, .	1.1	17
36844	Pseudo Dirac nodal sphere semimetal. Physical Review B, 2018, 98, .	1.1	29
36845	Origin of the deep band-gap state in <mml:math xmlns:mml="http://www.w3.org/1998/Math/MathML"><mml:msub><mml:mi>TiO</mml:mi><mml:mn>2</mml:mn></mml:msub></m (110): <mml:math xmlns:mml="http://www.w3.org/1998/Math/MathML"><mml:mrow><mml:mi>d</mml:mi><mml:mi>d</mml:mi><mml:mi>Ïƒ</mml:m bonds between Ti-Ti pairs. Physical Review B, 2018, 98, .	1.1	14
36846	Spin Polarization Properties of Pentagonal PdSe2 Induced by 3D Transition-Metal Doping: First-Principles Calculations. Materials, 2018, 11, 2339.	1.3	12
36847	Pressure Effect of the Vibrational and Thermodynamic Properties of Chalcopyrite-Type Compound AgGaS2: A First-Principles Investigation. Materials, 2018, 11, 2370.	1.3	6
36848	Electronic structure, defect properties, and hydrogen storage capacity of 2H-WS2: A first-principles study. International Journal of Hydrogen Energy, 2018, 43, 23126-23134.	3.8	12
36849	Quasi-Chemical Theory with Cluster Sampling from Ab Initio Molecular Dynamics: Fluoride (F^{â€“}) Anion Hydration. Journal of Physical Chemistry A, 2018, 122, 9806-9812.	1.1	12
36850	High-Pressure Evolution of Unexpected Chemical Bonding and Promising Superconducting Properties of YB₆. Journal of Physical Chemistry C, 2018, 122, 27820-27828.	1.5	23
36851	New Insights into the Anchoring Mechanism of Polysulfides inside Nanoporous Covalent Organic Frameworks for Lithiumâ€“Sulfur Batteries. ACS Applied Materials & Interfaces, 2018, 10, 43896-43903.	4.0	35
36852	Strain-Tuned Topological Insulator and Rashba-Induced Anisotropic Momentum-Locked Dirac Cones in Two-Dimensional SeTe Monolayers. ACS Applied Materials & Interfaces, 2018, 10, 43962-43969.	4.0	5
36853	Breaking H₂ with CeO₂: Effect of Surface Termination. ACS Omega, 2018, 3, 16063-16073.	1.6	47
36854	QM-Mechanism-Based Hierarchical High-Throughput in Silico Screening Catalyst Design for Ammonia Synthesis. Journal of the American Chemical Society, 2018, 140, 17702-17710.	6.6	32
36855	The AFLOW Fleet for Materials Discovery. , 2018, , 1-28.		9

#	Article	IF	Citations
36856	Synthesis, Structure, and Properties of the Layered Oxide Chalcogenides Sr₂CuO₂Cu₂S₂ and Sr₂CuO₂Cu₂Se₂. Inorganic Chemistry, 2018, 57, 15379-15388.	1.9	15
36857	Finding Order in the Disordered Hydration Shell of Rapidly Exchanging Water Molecules around the Heaviest Alkali Cs⁺ and Fr⁺. Journal of Physical Chemistry B, 2018, 122, 12067-12076.	1.2	16
36858	Two-Stage Solid-Phase Transition of Cubic Ice to Hexagonal Ice: Structural Origin and Kinetics. Journal of Physical Chemistry C, 2018, 122, 29009-29016.	1.5	15
36859	Experimental Identification of Critical Condition for Drastically Enhancing Thermoelectric Power Factor of Two-Dimensional Layered Materials. Nano Letters, 2018, 18, 7538-7545.	4.5	72
36860	Solid-Phase Epitaxial Growth of an Alumina Layer Having a Stacking-Mismatched Domain Structure of the Intermediate Î³-Phase. ACS Applied Materials & Interfaces, 2018, 10, 41487-41496.	4.0	4
36861	Adsorption and diffusion of sulfur on the (111), (100), (110), and (211) surfaces of FCC metals: Density functional theory calculations. Journal of Chemical Physics, 2018, 149, 204701.	1.2	25
36862	Effects of Electric Field on the Electronic Structures of Broken-gap Phosphorene/ <mml:math xmlns:mml="http://www.w3.org/1998/Math/MathML" display="inline" overflow="scroll"><mml:mi>Sn</mml:mi><mml:msub><mml:mi>X</mml:mi><mml:mn>2</mml:mn></mml:msub></mml:math>		

#	Source	IF	Citations
36874	Superconductivity in the metastable <mml:math xmlns:mml="http://www.w3.org/1998/Math/MathML"><mml:mrow><mml:mn>1</mml:mn><mml:msup><mml:mi>T</mml:mi><mml:mo and <mml:math xmlns:mml="http://www.w3.org/1998/Math/MathML"><mml:mrow><mml:mn>1</mml:mn><mml:msup><mml:mi>T</mml:mi><mml:mn phases of <mml:math xmlns:mml="http://www.w3.org/1998/Math/MathML"><mml:mrow><mml:mi>Mo</mml:mi><m. Physical Review, 2018, 97, 214513.	0.7	29
36875	Ozone Adsorption and Release by Hexagonal Manganese Clusters (MnAkBi)m Â· nH2O (A, B = O, SO4,) Tj ETQq1 1 0.784314 rgBT /Ov Chemistry, 2018, 63, 1461-1471.	0.3	1
36876	The origin of low bandgap and ferroelectricity of a co-doped BaTiO ₃. Europhysics Letters, 2018, 124, 27005.	0.7	8
36877	Effects of alloying elements (Al, Mn, Ru) on desorption plateau pressures of vanadium hydrides: An experimental and first-principles study. International Journal of Hydrogen Energy, 2018, 43, 21441-21450.	3.8	11
36878	Exploring a Novel Atomic Layer with Extremely Low Lattice Thermal Conductivity: ZnPSe₃ and Its Thermoelectrics. Journal of Physical Chemistry C, 2018, 122, 27917-27924.	1.5	18
36879	Abnormal subsurface hydrogen diffusion behaviors in heterogeneous hydrogenation reactions. Journal of Chemical Physics, 2018, 149, 174704.	1.2	10
36880	High-accuracy large-scale DFT calculations using localized orbitals in complex electronic systems: the case of grapheneâ€“metal interfaces. Journal of Physics Condensed Matter, 2018, 30, 505901.	0.7	9
36881	Detrimental Effects of Doping Al and Ba on the Thermoelectric Performance of GeTe. Materials, 2018, 11, 2237.	1.3	33
36882	Interlayer-Decoupled Sc-Based Mxene with High Carrier Mobility and Strong Light-Harvesting Ability. Journal of Physical Chemistry Letters, 2018, 9, 6915-6920.	2.1	49
36883	Dopant Control of Electronâ€“Hole Recombination in Cesiumâ€“Titanium Halide Double Perovskite by Time Domain Ab Initio Simulation: Codoping Supersedes Monodoping. Journal of Physical Chemistry Letters, 2018, 9, 6907-6914.	2.1	24
36884	Pulsed axial epitaxy of colloidal quantum dots in nanowires enables facet-selective passivation. Nature Communications, 2018, 9, 4947.	5.8	22
36885	Mechanism of large tunable thermal transport in graphene with oxygen functional groups. Journal of Applied Physics, 2018, 124, 175108.	1.1	4
36886	A Computational Study on P2-Type Nax[Ni1/3Ti2/3]O2as Bi-Functional Electrode Material for Na-Ion Batteries. Journal of the Electrochemical Society, 2018, 165, A3586-A3594.	1.3	5
36887	Optical Properties of Graphene/MoS2 Heterostructure: First Principles Calculations. Nanomaterials, 2018, 8, 962.	1.9	64
36888	DFT Calculations of Hydrogenation of 2(5H)-Furanone over Ni-, Rh-, Pd-, and Pt-Metal Surfaces Considering the Effects of Subsurface H Atoms. Journal of Physical Chemistry C, 2018, 122, 28182-28191.	1.5	5
36889	Graphene-Based Nanocomposites for Efficient Photocatalytic Hydrogen Evolution: Insight into the Interface toward Separation of Photogenerated Charges. ACS Applied Materials & Interfaces, 2018, 10, 43760-43767.	4.0	42
36890	High-entropy high-hardness metal carbides discovered by entropy descriptors. Nature Communications, 2018, 9, 4980.	5.8	604
36891	Theoretical Design of an InSe/GaTe vdW Heterobilayer: A Potential Visible-Light Photocatalyst for Water Splitting. Journal of Physical Chemistry C, 2018, 122, 27803-27810.	1.5	55

#	Article	IF	Citations
36892	Extraordinary Magnetoresistance in Janus Monolayer MoTeB₂: A Theoretical Prediction. Journal of Physical Chemistry C, 2018, 122, 28423-28430.	1.5	6
36893	Synthesis and Anisotropic Electrocatalytic Activity of Covellite Nanoplatelets with Fixed Thickness and Tunable Diameter. ACS Applied Materials & Interfaces, 2018, 10, 42417-42426.	4.0	10
36894	Crystalline structure, electronic and lattice-dynamics properties of NbTe2. Scientific Reports, 2018, 8, 16984.	1.6	26
36895	Carbon network evolution from dimers to sheets in superconducting ytrrium dicarbide under pressure. Communications Chemistry, 2018, 1, .	2.0	8
36896	Stability line of liquid molecular nitrogen based on the SCAN meta- <mml:math xmlns:mml="http://www.w3.org/1998/Math/MathML"><mml:mrow><mml:mi>G</mml:mi><mml:mi>G</mml:mi><mml:mi>A</mml:mi> density functional. Physical Review B, 2018, 98, .	3.7	11
36897	Catalytic de-halogenation of alkyl halides by copper surfaces. Journal of Environmental Chemical Engineering, 2018, 6, 7214-7224.	3.3	5
36898	Wet NH₃-Triggered NH₂-MIL-125(Ti) Structural Switch for Visible Fluorescence Immunoassay Impregnated on Paper. Analytical Chemistry, 2018, 90, 14121-14125.	3.2	182
36899	Rapid Phase Screening via Hydride Route: A Discovery of K8â€“xZn18+3xSb16. Chemistry of Materials, 2018, 30, 8707-8715.	3.2	19
36900	Dispersion-Corrected Modified Embedded-Atom Method Bond Order Interatomic Potential for Sulfur. Journal of Physical Chemistry A, 2018, 122, 9572-9578.	1.1	4
36901	Ba8Au5.25Ge40.75(110): A Nano-Caged Surface Electronically Controlled by Barium and Gold Adatoms. Journal of Physical Chemistry C, 2018, 122, 29298-29306.	1.5	5
36902	Flexoelectricity in Monolayer Transition Metal Dichalcogenides. Journal of Physical Chemistry Letters, 2018, 9, 6841-6846.	2.1	51
36903	Calculations of the pH-Dependent Onset Potential for CO Electrooxidation on Au(111). Langmuir, 2018, 34, 15268-15275.	1.6	18
36904	Recipe for Dirac Phonon States with a Quantized Valley Berry Phase in Two-Dimensional Hexagonal Lattices. Nano Letters, 2018, 18, 7755-7760.	4.5	54
36905	One-Dimensional Porous Hybrid Structure of Mo₂C-CoP Encapsulated in N-Doped Carbon Derived from MOF: An Efficient Electrocatalyst for Hydrogen Evolution Reaction over the Entire pH Range. ACS Applied Materials & Interfaces, 2018, 10, 42335-42347.	4.0	101
36906	Unusual Enhancement of the Adsorption Energies of Sodium and Potassium in Sulfurâ^'Nitrogen and Siliconâ^'Boron Codoped Graphene. ACS Omega, 2018, 3, 15821-15828.	1.6	15
36907	Tuning the balance between dispersion and entropy to design temperature-responsive flexible metal-organic frameworks. Nature Communications, 2018, 9, 4899.	5.8	90
36908	Predicting accurate cathode properties of layered oxide materials using the SCAN meta-GGA density functional. Npj Computational Materials, 2018, 4, .	3.5	99
36909	Oxygen containing Siâ€“H nanoparticles: a potential electrode for Liâ€“ion battery. EPJ Applied Physics, 2018, 83, 10401.	0.3	0

#	Article	IF	Citations
36910	A transferable artificial neural network model for atomic forces in nanoparticles. Journal of Chemical Physics, 2018, 149, 194101.	1.2	9
36911	On the calculation of the stress tensor in real-space Kohn-Sham density functional theory. Journal of Chemical Physics, 2018, 149, 194104.	1.2	9
36912	On the work function of the surface Mo(0â€‰0â€‰1) and its temperature dependence: an ab initio molecular dynamics study. Journal of Physics Condensed Matter, 2018, 30, 505001.	0.7	3
36913	Nanoskyrmion engineering with sp -electron materials: Sn monolayer on a SiC(0001) surface. Physical Review B, 2018, 98, .	1.1	7
36914	Shear instability in twisted bilayer graphene. Physical Review B, 2018, 98, .	1.1	31
36915	The Infrared spectrum of very large (periodic) systems: global versus fragment strategiesâ€”the case of three defects in diamond. Theoretical Chemistry Accounts, 2018, 137, 1.	0.5	10
36916	Shear-Assisted Formation of Cation-Disordered Rocksalt NaMO₂ (M = Fe or Mn). Chemistry of Materials, 2018, 30, 8811-8821.	3.2	17
36917	Enhanced Carrier Transport and Bandgap Reduction in Sulfur-Modified BiVO₄ Photoanodes. Chemistry of Materials, 2018, 30, 8630-8638.	3.2	39
36918	Enabling Electrocatalytic N₂ Reduction to NH₃ by Y₂O₃ Nanosheet under Ambient Conditions. Industrial & Engineering Chemistry Research, 2018, 57, 16622-16627.	1.8	39
36919	Visualizing Reversible Two-Dimensional Phase Transitions in Oxygen Chemisorbed Layers. Journal of Physical Chemistry C, 2018, 122, 28233-28244.	1.5	7
36920	Electrochemical surface passivation of LiCoO2 particles at ultrahigh voltage and its applications in lithium-based batteries. Nature Communications, 2018, 9, 4918.	5.8	260
36921	Comparison of the electronic and thermoelectric properties of three layered phases Bi2Te3, PbBi2Te4 and PbBi4Te7: LEGO thermoelectrics. AIP Advances, 2018, 8, .	0.6	11
36922	Point defects and dopants of boron arsenide from first-principles calculations: Donor compensation and doping asymmetry. Applied Physics Letters, 2018, 113, .	1.5	33
36923	Cluster Magnetism of Ba4NbMn3O12: Localized Electrons or Molecular Orbitals?. JETP Letters, 2018, 108, 686-690.	0.4	12
36924	Electronic exchange-correlation, many-body effect issues on first-principles calculations of bulk SiC polytypes. International Journal of Modern Physics B, 2018, 32, 1850328.	1.0	2
36925	Enhanced Stability of Single-Layer w-Gallenene through Hydrogenation. Journal of Physical Chemistry C, 2018, 122, 28302-28309.	1.5	25
36926	Cobalt Phosphate Nanostructures for Non-Enzymatic Glucose Sensing at Physiological pH. ACS Applied Materials & Interfaces, 2018, 10, 42786-42795.	4.0	64
36927	Higher Strength and Ductility than Diamond: Nanotwinned Diamond/Cubic Boron Nitride Multilayer. ACS Applied Materials & Interfaces, 2018, 10, 42804-42811.	4.0	19

#	Article	IF	Citations
36928	Edge-Functionalized Graphene Nanoribbon Chemical Sensor: Comparison with Carbon Nanotube and Graphene. ACS Applied Materials & Interfaces, 2018, 10, 42905-42914.	4.0	41
36929	Guiding Synthesis of Polymorphs of Materials Using Nanometric Phase Diagrams. Journal of the American Chemical Society, 2018, 140, 17290-17296.	6.6	15
36930	First-principles study of electric field effect and spin-polarization transport properties of zigzag Î±-2 graphyne nanoribbons. Journal of Applied Physics, 2018, 124, .	1.1	32
36931	Interaction of sodium atoms with stacking faults in silicon with different Fermi levels. Applied Physics Express, 2018, 11, 061303.	1.1	5
36932	Understanding Synergism of Cobalt Metal and Copper Oxide toward Highly Efficient Electrocatalytic Oxygen Evolution. ACS Catalysis, 2018, 8, 12030-12040.	5.5	60
36933	X-ray-activated long persistent phosphors featuring strong UVC afterglow emissions. Light: Science and Applications, 2018, 7, 88.	7.7	159
36934	Enhanced strength and ductility in a high-entropy alloy via ordered oxygen complexes. Nature, 2018, 563, 546-550.	13.7	988
36935	Monitoring Mechanical, Electronic, and Catalytic Trends in a Titanium Metal Organic Framework Under the Influence of Guest-Molecule Encapsulation Using Density Functional Theory. Scientific Reports, 2018, 8, 16651.	1.6	12
36936	Highly Improved Solar Energy Harvesting for Fuel Production from CO2 by a Newly Designed Graphene Film Photocatalyst. Scientific Reports, 2018, 8, 16741.	1.6	21
36937	GGA-1/2 self-energy correction for accurate band structure calculations: the case of resistive switching oxides. Journal of Physics Communications, 2018, 2, 105005.	0.5	70
36938	Counterpropagating topological interface states in graphene patchwork structures with regular arrays of nanoholes. Physical Review B, 2018, 98, .	1.1	11
36939	Evidence of Incoherent Carriers Associated with Resonant Impurity Levels and Their Influence on Superconductivity in the Anomalous Superconductor <mml:math xmlns:mml="http://www.w3.org/1998/Math/MathML" display="inline"><mml:mrow><mml:msub><mml:mrow><mml:mi>Pb</mml:mi></mml:mrow><mml:mrow><mml:mn>1</mml:mn><mml:mn>m</mml:mn> Physical Review Letters, 2018, 121, 207001.	2.9	12
36940	Applicability of the Strongly Constrained and Appropriately Normed Density Functional to Transition-Metal Magnetism. Physical Review Letters, 2018, 121, 207201.	2.9	118
36941	Ab initio molecular dynamics simulation of irradiation particles behavior in tungsten. European Physical Journal B, 2018, 91, 1.	0.6	0
36942	Hydrogen storage on cation-decorated biphenylene carbon and nitrogenated holey graphene. International Journal of Hydrogen Energy, 2018, 43, 22966-22975.	3.8	33
36943	Atomic scale insights into structure instability and decomposition pathway of methylammonium lead iodide perovskite. Nature Communications, 2018, 9, 4807.	5.8	161
36944	Theoretical study of fluorine-induced surface segregation of Cr in non-passivated Ni-based alloys. Journal of Applied Physics, 2018, 124, .	1.1	8
36945	Ab initio study of electronic properties of graphene/MoS2 heterostructure under biaxial deformations. AIP Conference Proceedings, 2018, , .	0.3	3

#	Article	IF	Citations
36946	Discrete Superconducting Phases in FeSe-Derived Superconductors. Physical Review Letters, 2018, 121, 207003.	2.9	49
36947	Negative differential conductivity in liquid aluminum from real-time quantum simulations. European Physical Journal B, 2018, 91, 1.	0.6	18
36948	Design strategy for ferroelectric-based polar metals with dimensionality-tunable electronic states. Science China: Physics, Mechanics and Astronomy, 2018, 61, 1.	2.0	8
36949	Understanding the Stability of Salt-Inclusion Phases for Nuclear Waste-forms through Volume-based Thermodynamics. Scientific Reports, 2018, 8, 15294.	1.6	8
36950	High-throughput ab initio calculations on dielectric constant and band gap of non-oxide dielectrics. Scientific Reports, 2018, 8, 14794.	1.6	16
36951	Assessing the performance of the recent meta-GGA density functionals for describing the lattice constants, bulk moduli, and cohesive energies of alkali, alkaline-earth, and transition metals. Journal of Chemical Physics, 2018, 149, 164703.	1.2	35
36952	1D tungsten oxide nanostructures on a Cu(1â€‰1â€‰0) surface. Journal of Physics Condensed Matter, 2018, 30, 465001.	0.7	1
36953	Ab Initio Spin-Strain Coupling Parameters of Divacancy Qubits in Silicon Carbide. Physical Review Applied, 2018, 10, .	1.5	23
36954	Imaging empty states on the Ge(100) surface at 12 K. Physical Review B, 2018, 98, .	1.1	2
36955	Origin of the Low Magnetic Moment in Fe2AlTi: An Ab Initio Study. Materials, 2018, 11, 1732.	1.3	19
36956	Direct Visualization of Li Dendrite Effect on LiCoO₂ Cathode by In Situ TEM. Small, 2018, 14, e1803108.	5.2	34
36957	Most facile synthesis of Zn-Al:LDHs nanosheets at room temperature via environmentally friendly process and their high power generation by flexoelectricity. Materials Today Energy, 2018, 10, 254-263.	2.5	14
36958	First-principles investigation of Ag-, Co-, Cr-, Cu-, Fe-, Mn-, Ni-, Pd- and Rh-hexaaminobenzene 2D metal-organic frameworks. Materials Today Energy, 2018, 10, 336-342.	2.5	18
36959	Tuning Binding Tendencies of Small Molecules in Metalâ€“Organic Frameworks with Open Metal Sites by Metal Substitution and Linker Functionalization. Journal of Physical Chemistry C, 2018, 122, 27486-27494.	1.5	34
36960	Opto-Mechanics Driven Fast Martensitic Transition in Two-Dimensional Materials. Nano Letters, 2018, 18, 7794-7800.	4.5	38
36961	Hole-Doped 2D InSe for Spintronic Applications. ACS Applied Nano Materials, 2018, 1, 6656-6665.	2.4	41
36962	Mechanistic Origin of the High Performance of Yolk@Shell Bi₂S₃@N-Doped Carbon Nanowire Electrodes. ACS Nano, 2018, 12, 12597-12611.	7.3	213
36963	Density functional theory study of cerium deuterides. AIP Conference Proceedings, 2018, , .	0.3	3

#	Article	IF	Citations
36964	The electronic structures and optical properties of B, C or N doped BaTiO3. AIP Advances, 2018, 8, .	0.6	12
36965	Ionicity of bonding in elemental solids. Journal of Physics Communications, 2018, 2, 115009.	0.5	3
36966	The Interactions between High Temperature Water and Fe3O4(111) by First-Principles Molecular Dynamics Simulation. International Journal of Electrochemical Science, 2018, 13, 2430-2440.	0.5	6
36967	Strength and Brittleness of Interfaces in Fe-Al Superalloy Nanocomposites under Multiaxial Loading: An ab initio and Atomistic Study. Nanomaterials, 2018, 8, 873.	1.9	22
36968	Theoretical Insights into Perovskite Compounds MAPb_{1â^'Î±}X_{Î±}I_{3â^'Î²}Y_{Î²} (X = Ge, Sn; Y = Cl, Br): An Exploration for Superior Optical Performance. Journal of Physical Chemistry C, 2018, 122, 27205-27213.	1.5	7
36969	Adsorption of Molecular Hydrogen on Lithiumâ€“Phosphorus Double-Helices. Journal of Physical Chemistry C, 2018, 122, 27941-27946.	1.5	7
36970	Graphene Nucleation Preference at CuO Defects Rather Than Cu₂O on Cu(111): A Combination of DFT Calculation and Experiment. ACS Applied Materials & Interfaces, 2018, 10, 43156-43165.	4.0	16
36971	Single Nickel Atoms Anchored on Nitrogen-Doped Graphene as a Highly Active Cocatalyst for Photocatalytic H₂ Evolution. ACS Catalysis, 2018, 8, 11863-11874.	5.5	183
36972	Efficient and stable emission of warm-white light from lead-free halide double perovskites. Nature, 2018, 563, 541-545.	13.7	1,451
36973	Self-structuring in Zr1â^'xAlxN films as a function of composition and growth temperature. Scientific Reports, 2018, 8, 16327.	1.6	9
36974	A theoretical investigation of the glide dislocations in the sphalerite ZnS. Journal of Applied Physics, 2018, 124, .	1.1	8
36975	Hydrogen adsorption on Pt(111) revisited from random phase approximation. Journal of Chemical Physics, 2018, 149, 164702.	1.2	24
36976	Six-dimensional quantum dynamics for the dissociative chemisorption of HCl on rigid Ag(111) on three potential energy surfaces with different density functionals. Journal of Chemical Physics, 2018, 149, 174702.	1.2	7
36977	Role of oxygen and chlorine impurities in <mml:math xmlns:mml="http://www.w3.org/1998/Math/MathML"><mml:mrow><mml:mi>Î²</mml:mi><mml:mo>â^'</mml:mo><mml:msub><mml:mi mathvariant="normal">S</mml:mi><mml:mn>3</mml:mn></mml:msub></mml:mrow></mml:math> : A first-principles study. Physical Review B, 2018, 98, .	1.1	7
36978	Optical Properties of Silicene and Related Materials from First Principles. Nanoscience and Technology, 2018, , 73-98.	1.5	6
36979	Extrinsic Defects in Crystalline MoO₃: Solubility and Effect on the Electronic Structure. Journal of Physical Chemistry C, 2018, 122, 27241-27249.	1.5	7
36980	Selective Hydrogenation of Cinnamaldehyde over Co-Based Intermetallic Compounds Derived from Layered Double Hydroxides. ACS Catalysis, 2018, 8, 11749-11760.	5.5	106
36981	Electrochemically-mediated selective capture of heavy metal chromium and arsenic oxyanions from water. Nature Communications, 2018, 9, 4701.	5.8	193

#	Article	IF	Citations
36982	Anisotropic Dirac Fermions in BaMnBi2 and BaZnBi2. Scientific Reports, 2018, 8, 15322.	1.6	14
36983	The quantum mechanics-based polarizable force field for water simulations. Journal of Chemical Physics, 2018, 149, 174502.	1.2	27
36984	Reexploring the cation ordering and magnetic cation substitution effects on the elastic anisotropy of aluminum spinels. Journal of Applied Physics, 2018, 124, 175901.	1.1	7
36985	Modifying spin current filtering and magnetoresistance in a molecular spintronic device. RSC Advances, 2018, 8, 41587-41593.	1.7	4
36986	Active learning for accelerated design of layered materials. Npj Computational Materials, 2018, 4, .	3.5	107
36987	Characterization of scrutinyite SnO₂ and investigation of the transformation with ¹¹⁹Sn NMR and complex impedance method. AIP Advances, 2018, 8, 125226.	0.6	2
36988	Theoretical investigation of Ti and Ni co-doping on the anti-disproportionation ability of ZrCo alloy. Materials Research Express, 2018, 5, 105501.	0.8	9
36989	First Principles Study of Tritium Diffusion in Li2TiO3 Crystal with Lithium Vacancy. Materials, 2018, 11, 2383.	1.3	16
36990	Ab Initio Study of Optoelectronic and Magnetic Properties of Ternary Chromium Chalcogenides. Advances in Materials Science and Engineering, 2018, 2018, 1-6.	1.0	2
36991	Cage-like $ext{N}_{10}^{6-}$ salt with N-N single bonds. Europhysics Letters, 2018, 124, 67004.	0.7	3
36992	Metaheuristic Ab Initio Optimum Search for Doping Effects in Nanocarbons. Materials Science Forum, 2018, 941, 2356-2359.	0.3	1
36993	Ultralow thermal conductivity in a two-dimensional material due to surface-enhanced resonant bonding. Materials Today Physics, 2018, 7, 89-95.	2.9	12
36994	Are dispersion corrections accurate outside equilibrium? A case study on benzene. Beilstein Journal of Organic Chemistry, 2018, 14, 1181-1191.	1.3	15
36995	Atomistic Simulations of Hydrogen Effects on Lattice Defects in Alpha Iron. , 2018, , 1-18.		2
36996	Rheological properties of super critical CO2 with CuO: Multi-scale computational modeling. Journal of Chemical Physics, 2018, 149, 224702.	1.2	12
36997	Theoretical and Experimental Evidence for a Post-Cotunnite Phase Transition in Hafnia at High Pressures. Journal of Superhard Materials, 2018, 40, 374-383.	0.5	5
36998	Impact of Nano-Scale Distribution of Atoms on Electronic and Magnetic Properties of Phases in Fe-Al Nanocomposites: An Ab Initio Study. Nanomaterials, 2018, 8, 1059.	1.9	15
36999	Electronâ€“Hole Pairs in Surface Dynamics. , 2018, , 356-365.		1

#	Article	IF	Citations
37000	First-principles study of thermal conductivities of uranium aluminides. Materialia, 2018, 4, 449-456.	1.3	8
37001	Magnetically driven orbital-selective insulatorâ€“metal transition in double perovskite oxides. Npj Quantum Materials, 2018, 3, .	1.8	16
37002	Structural and electronic effects of adatoms on metallic atomic chains in Si(111)5â€‰Ã—â€‰2-Au. Scientific Reports, 2018, 8, 15537.	1.6	9
37003	Study of the crystal structure and mechanical properties of ZrTi₂ under pressure. Journal of Physics: Conference Series, 2018, 1119, 012010.	0.3	3
37004	Nonequilibrium Greenâ€™s function method: Transport and band tail predictions in transition metal dichalcogenides. , 2018, , .		0
37005	Application Performance on the Newest Processors and GPUs. , 2018, , .		11
37006	Ab initio calculation of the spin lattice relaxation time <mml:math xmlns:mml="http://www.w3.org/1998/Math/MathML"><mml:msub><mml:mi>T</mml:mi><mml:mn>1</mml:mn></mml:msub></mml:m for nitrogen-vacancy centers in diamond. Physical Review B, 2018, 98, .	1.1	16
37007	Damping and antidamping phenomena in metallic antiferromagnets: An ab initio study. Physical Review B, 2018, 98, .	1.1	13
37008	Temperature dependence of the stacking-fault Gibbs energy for Al, Cu, and Ni. Physical Review B, 2018, 98, .	1.1	61
37009	Effects of electron-phonon coupling on absorption spectrum: <mml:math xmlns:mml="http://www.w3.org/1998/Math/MathML"><mml:mi>K</mml:mi></mml:math> edge of hexagonal boron nitride. Physical Review B, 2018, 98, .	1.1	26
37010	Layer <mml:math xmlns:mml="http://www.w3.org/1998/Math/MathML"><mml:mi>k</mml:mi></mml:math> -projection and unfolding electronic bands at interfaces. Physical Review B, 2018, 98, .	1.1	64
37011	Electronic and optical properties of bilayer SnS with different stacking orders: A first principles study. Journal of Applied Physics, 2018, 124, .	1.1	7
37012	Perpendicular magnetic anisotropy at the <mml:math xmlns:mml="http://www.w3.org/1998/Math/MathML"><mml:mrow><mml:mi>Fe</mml:mi><mml:mo>/</mml:mo><mml:msub><mml:m mathvariant="normal">O</mml:mi><mml:mn>4</mml:mn></mml:msub></mml:mrow></mml:math> interface: Comparative first-principles study with Fe/MgO. Physical Review B, 2018, 98, .	1.1	26
37013	Ab initio investigation of the formation of ZrO2-like structures upon the adsorption of Zrn on the CeO2(111) surface. Journal of Chemical Physics, 2018, 149, 244702.	1.2	7
37014	Materials informatics for dielectric materials. Japanese Journal of Applied Physics, 2018, 57, 11UB01.	0.8	10
37015	Hybrid Density Functional Study of Au2Cs2I6, Ag2GeBaS4, Ag2ZnSnS4, and AgCuPO4 for the Intermediate Band Solar Cells. Energies, 2018, 11, 3457.	1.6	5
37016	Ab initio inspection of thermophysical experiments for molybdenum near melting. AIP Advances, 2018, 8, 125012.	0.6	18
37017	Improved thermoelectric property of Ti0.75HfMo0.25CrGe by doping Ti2CrGe Heusler alloy with Hf and Mo: Confirmation of entropy â€œengineâ€•in thermoelectric materials design. Journal of Applied Physics, 2018, 124, .	1.1	5

#	Article	IF	Citations
37018	Electronic and magnetic properties of Al-doped WS₂ monolayer under strain. Ferroelectrics, 2018, 531, 114-121.	0.3	5
37019	Electron and phonon transport properties of layered Bi₂O₂Se and Bi₂O₂Te from first-principles calculations. New Journal of Physics, 2018, 20, 123014.	1.2	50
37020	Subcycle interference in high-order harmonic generation from solids. Physical Review A, 2018, 98, .	1.0	27
37021	Induced valley splitting in monolayer <mml:math xmlns:mml="http://www.w3.org/1998/Math/MathML"><mml:mrow><mml:mi>Mo</mml:mi><mml:msub><mml:mi mathvariant="normal">S</mml:mi><mml:mn>2</mml:mn></mml:msub></mml:mrow></mml:math> by an antiferromagnetic insulating CoO(111) substrate. Physical Review B, 2018, 98, .	1.1	35
37022	First-principles prediction of one-dimensional giant Rashba splittings in Bi-adsorbed In atomic chains. Physical Review B, 2018, 98, .	1.1	10
37023	Extrinsic doping on the atomic scale: Tuning metallicity in atomic Au chains. Physical Review B, 2018, 98, .	1.1	17
37024	Magnesium-Sodium Hybrid Battery With High Voltage, Capacity and Cyclability. Frontiers in Chemistry, 2018, 6, 611.	1.8	15
37025	Spin-orbit coupling driven insulating state in hexagonal iridates <mml:math xmlns:mml="http://www.w3.org/1998/Math/MathML"><mml:mrow><mml:mi mathvariant="normal">S</mml:mi><mml:msub><mml:mi mathvariant="normal">r</mml:mi><mml:mn>3</mml:mn></mml:msub><mml:mi>M</mml:mi><mml:mi>Ir</mml:mi><mml:msub><m		

#	Article	IF	Citations
37036	Computational Study of Methane Activation on Î³-Al₂O₃. ACS Omega, 2018, 3, 18242-18250.	1.6	30
37037	Broadband Emission in Hybrid Organicâ€“Inorganic Halides of Group 12 Metals. ACS Omega, 2018, 3, 18791-18802.	1.6	70
37038	Thermoelastic Properties of Aluminous Phases in MORB from Firstâ€principles Calculation: Implications for Earth's Lower Mantle. Journal of Geophysical Research: Solid Earth, 2018, 123, 10,583.	1.4	4
37039	Novel phases in ammonia-water mixtures under pressure. Journal of Chemical Physics, 2018, 149, 234501.	1.2	22
37040	Acceptor levels of the carbon vacancy in 4H-SiC: Combining Laplace deep level transient spectroscopy with density functional modeling. Journal of Applied Physics, 2018, 124, 245701.	1.1	19
37041	First-principles investigation of Sc-III/IV under high pressure. Physical Review B, 2018, 98, .	1.1	12
37042	Establishing characteristic behavior of voltage control of magnetic anisotropy by ionic migration. Physical Review B, 2018, 98, .	1.1	16
37043	Impact of Different Ratios of Fluorine, Oxygen, and Hydroxyl Surface Terminations on Ti3C2T<inf>x</inf> MXene as Ammonia Sensor: A First-Principles Study. , 2018, , .		18
37044	Interfacial Interaction between Carbon Nanotube and Stoichio- and Nonstoichiometric Ceramic Surfaces by <i>Ab-Initio</i> Calculations. Materials Transactions, 2018, 59, 1684-1690.	0.4	3
37045	Ir-Ni Bimetallic OER Catalysts Prepared by Controlled Ni Electrodeposition on Irpoly and Ir(111). Surfaces, 2018, 1, 165-186.	1.0	17
37046	Phonon and Thermodynamic Properties in YNi2B2C and LuNi2B2C from First-Principles Study. Journal of Superconductivity and Novel Magnetism, 2018, 31, 1925-1931.	0.8	1
37047	Anomalous diffusion along metal/ceramic interfaces. Nature Communications, 2018, 9, 5251.	5.8	51
37048	Spin-filter state of Au-Co nanowires. EPJ Web of Conferences, 2018, 185, 01019.	0.1	1
37049	Surface-Induced Enhancement of Piezoelectricity in ZnO Nanowires. Chinese Physics Letters, 2018, 35, 127701.	1.3	3
37050	First-principles study on the negative- <mml:math xmlns:mml="http://www.w3.org/1998/Math/MathML" display="inline" overflow="scroll"><mml:mi>U</mml:mi></mml:math> behavior of <mml:math xmlns:mml="http://www.w3.org/1998/Math/MathML" display="inline" overflow="scroll"><mml:mi>K</mml:mi></mml:math> centers in amorphous <mml:math xmlns:mml="http://www.w3.org/1998/Math/MathML" display="inline" overflow="scroll"><mml:msub><mml:mi>Si</mml:mi><mml:mn>3</mml:mn></mml:msub><mml:msub><mml:mrow><mml:mrow><mm	1.5	7
37051	Structural Deformations During Cycling of the Conversion Cathode Nanocomposite Based on FeF3. Journal of Structural Chemistry, 2018, 59, 1719-1725.	0.3	0
37052	Enhanced oxygen reduction with single-atomic-site iron catalysts for a zinc-air battery and hydrogen-air fuel cell. Nature Communications, 2018, 9, 5422.	5.8	696
37053	First-principles calculations of the ultralow thermal conductivity in two-dimensional group-IV selenides. Physical Review B, 2018, 98, .	1.1	98

#	Article	IF	Citations
37054	Rare Helium-Bearing Compound <mml:math xmlns:mml="http://www.w3.org/1998/Math/MathML" display="inline"><mml:mrow><mml:mrow><mml:msub><mml:mrow><mml:mi>FeO</mml:mi></mml:mrow><mml:mrow><mml:mn>2</mml:mn></mml:mrow></mml:msub></mml:mrow></mml:mrow></mml:math> Stabilized at Deep-Earth Conditions. Physical Review Letters, 2018, 121, 255703.	2.9	68
37055	Pressure-induced structural change and nucleation in liquid aluminum. Journal of Applied Physics, 2018, 124, 225903.	1.1	2
37056	Partially replacing Pb2+ by Mn2+ in hybrid metal halide perovskites: Structural and electronic properties. APL Materials, 2018, 6, .	2.2	15
37057	Xanes Specroscopic Diagnostics of the 3D Local Atomic Structure of Nanostructured Materials. Journal of Structural Chemistry, 2018, 59, 1691-1706.	0.3	5
37058	New Cr-Ni-Base Alloy for High-Temperature Applications Designed on the Basis of First Principles Calculations. Advances in Condensed Matter Physics, 2018, 2018, 1-8.	0.4	13
37059	Switching excitonic recombination and carrier trapping in cesium lead halide perovskites by air. Communications Physics, 2018, 1, .	2.0	59
37060	Two-Dimensional Mechanical Metamaterials with Unusual Poisson Ratio Behavior. Physical Review Applied, 2018, 10, .	1.5	17
37061	Phase transition systematics in <mml:math xmlns:mml="http://www.w3.org/1998/Math/MathML"><mml:msub><mml:mi>BiVO</mml:mi><mml:mn>4</mml:mn></mml:msub></mml:math> by means of high-pressureâ€“high-temperature Raman experiments. Physical Review B, 2018, 98, .	1.1	24
37062	Semiconducting defect-free polymorph of borophene: Peierls distortion in two dimensions. Physical Review B, 2018, 98, .	1.1	16
37063	Connecting the Simpler Structures to Topologically Close-Packed Phases. Physical Review Letters, 2018, 121, 255701.	2.9	20
37064	A Computational Study on the Variation of Bandgap Due to Native Defects in Non-Stoichiometric NiO and Pd, Pt Doping in Stoichiometric NiO. Condensed Matter, 2018, 3, 46.	0.8	10
37065	Toward the Design of New Suitable Materials for Solar Water Splitting Using Density Functional Theory. ACS Omega, 2018, 3, 18117-18123.	1.6	15
37066	Alkali-metal-adsorbed g-GaN monolayer: ultralow work functions and optical properties. Nanoscale Research Letters, 2018, 13, 207.	3.1	79
37067	First-principles calculations and thermodynamic modelling of long periodic stacking ordered (LPSO) phases in Mg-Al-Gd. Materialia, 2018, 4, 192-202.	1.3	8
37068	An improved static corrugation model. Journal of Chemical Physics, 2018, 149, 234702.	1.2	13
37069	Atomistic mechanisms for chemical defects formation in polyethylene. Journal of Chemical Physics, 2018, 149, 234902.	1.2	11
37070	Revealing the role of nitrogen on hydride nucleation and stability in pure niobium using first-principles calculations. Superconductor Science and Technology, 2018, 31, 115007.	1.8	19
37071	Enhancing the Thermoelectric Properties of Layered Bi2O2Q (Q = S, Se): the Effect of Mixed Chalcogen Net. Journal of the Korean Physical Society, 2018, 73, 1684-1689.	0.3	4

#	Article	IF	Citations
37072	Magnetism in Î±-RuCl3: Dependence on Coulomb Interaction and Hundâ€™s Coupling. Journal of the Korean Physical Society, 2018, 73, 1691-1697.	0.3	1
37073	Peculiar magnetic properties of NC6 and NC12 layered compounds from first principles. Journal of Theoretical and Applied Physics, 2018, 12, 209-217.	1.4	0
37074	Reaction energetics of hydrogen on Si(100) surface: A periodic many-electron theory study. Journal of Chemical Physics, 2018, 149, 244105.	1.2	11
37075	First-order nonadiabatic couplings in extended systems by time-dependent density functional theory. Journal of Chemical Physics, 2018, 149, 244103.	1.2	8
37076	Design Guidelines and Limitations of Multilayer Two-dimensional Vertical Tunneling FETs for UltraLow Power Logic Applications. , 2018, , .		0
37077	First-Principles Study of Point Defects in GaAs/AlAs Superlattice: the Phase Stability and the Effects on the Band Structure and Carrier Mobility. Nanoscale Research Letters, 2018, 13, 301.	3.1	29
37078	Unravelling the Potential of Density Functional Theory through Integrated Computational Environments: Recent Applications of the Vienna Ab Initio Simulation Package in the MedeAÂ® Software. Computation, 2018, 6, 63.	1.0	7
37079	Ab Initio Thermodynamics of Iridium Surface Oxidation and Oxygen Evolution Reaction. Journal of Physical Chemistry C, 2018, 122, 29350-29358.	1.5	28
37080	Ab Initio Prediction of Proton Exchange Barriers for Alkanes at BrÃ¸nsted Sites of Zeolite H-MFI. Journal of the American Chemical Society, 2018, 140, 18151-18161.	6.6	50
37081	Porous platinumâ€“silver bimetallic alloys: surface composition and strain tunability toward enhanced electrocatalysis. Nanoscale, 2018, 10, 21703-21711.	2.8	20
37082	Enhancement of thermoelectric properties by lattice softening and energy band gap control in Te-deficient InTe1â^'Î´. AIP Advances, 2018, 8, .	0.6	24
37083	Pressure-induced multiple phase transformations of the BaBi3 superconductor. Physical Review B, 2018, 98, .	1.1	8
37084	Characterization of topological band structures away from the Fermi level by the anomalous Nernst effect. Physical Review B, 2018, 98, .	1.1	37
37085	Cu-Doped TiO2: Visible Light Assisted Photocatalytic Antimicrobial Activity. Applied Sciences (Switzerland), 2018, 8, 2067.	1.3	149
37088	Reversible and selective ion intercalation through the top surface of few-layer MoS2. Nature Communications, 2018, 9, 5289.	5.8	119
37089	Four-spin ring interaction as a source of unconventional magnetic orders in orthorhombic perovskite manganites. Physical Review B, 2018, 98, .	1.1	6
37090	Liquid Structure of Shock-Compressed Hydrocarbons at Megabar Pressures. Physical Review Letters, 2018, 121, 245501.	2.9	16
37091	Firstâ€Principles Study of Aziridinium Lead Iodide Perovskite for Photovoltaics. ChemPhysChem, 2019, 20, 602-607.	1.0	8

#	Article	IF	Citations
37092	Tailoring properties of hybrid perovskites by domain-width engineering with charged walls. Npj Computational Materials, 2018, 4, .	3.5	15
37093	Remarkable negative differential resistance and perfect spin-filtering effects of the indium triphosphide (InP₃) monolayer tuned by electric and optical ways. Physical Chemistry Chemical Physics, 2018, 20, 29440-29445.	1.3	13
37094	Resistive switching in Si₂Te₃ nanowires. AIP Advances, 2018, 8, 125008.	0.6	13
37095	Anomalous K-Point Phonons in Noble Metal/Graphene Heterostructure Activated by Localized Surface Plasmon Resonance. ACS Nano, 2018, 12, 12733-12740.	7.3	10
37096	Zigzag sp² Carbon Chains Passing through an sp³ Framework: A Driving Force toward Room-Temperature Ferromagnetic Graphene. ACS Nano, 2018, 12, 12847-12859.	7.3	19
37097	Dielectric Behavior as a Screen in Rational Searches for Electronic Materials: Metal Pnictide Sulfosalts. Journal of the American Chemical Society, 2018, 140, 18058-18065.	6.6	69
37098	Three-dimensional atomic scale electron density reconstruction of octahedral tilt epitaxy in functional perovskites. Nature Communications, 2018, 9, 5220.	5.8	32
37099	Expansion and Fragmentation of a Liquid-Metal Droplet by a Short Laser Pulse. Physical Review Applied, 2018, 10, .	1.5	31
37100	Ab initio thermal conductivity of thermoelectric <mml:math xmlns:mml="http://www.w3.org/1998/Math/MathML"><mml:mrow><mml:msub><mml:mi>Mg</mml:mi><mml:mn>3</mml:mn></mml: : Evidence for dominant extrinsic effects. Physical Review B, 2018, 98, .	1.1	22
37101	Visualizing topological edge states of single and double bilayer Bi supported on multibilayer Bi(111) films. Physical Review B, 2018, 98, .	1.1	40
37102	Polarization Direction Dependence of Thermodynamic Stability of Ferroelectric BiAlO3(0001) Polar Surfaces. Journal of Physical Chemistry C, 2018, 122, 29220-29227.	1.5	11
37103	High-Temperature Superconductivity in a Thâ€“H System under Pressure Conditions. ACS Applied Materials & Interfaces, 2018, 10, 43809-43816.	4.0	95
37104	Size and strain effects on mechanical and electronic properties of green phosphorene nanoribbons. AIP Advances, 2018, 8, .	0.6	4
37105	Prediction of two-dimensional organic topological insulator in metal-DCB lattices. Applied Physics Letters, 2018, 113, .	1.5	12
37106	Topological crystalline insulator states in the <mml:math xmlns:mml="http://www.w3.org/1998/Math/MathML"><mml:mrow><mml:msub><mml:mi>Ca</mml:mi><mml:mn>2</mml:mn></mml:msub></mml: family. Physical Review B, 2018, 98, .	1.1	28
37107	Decoupling Carrier Concentration and Electron-Phonon Coupling in Oxide Heterostructures Observed with Resonant Inelastic X-Ray Scattering. Physical Review Letters, 2018, 121, 236802.	2.9	22
37108	Extremely Light Carrierâ€Effective Mass in a Distorted Simple Metal Oxide. Advanced Electronic Materials, 2019, 5, 1800504.	2.6	2
37109	High Thermoelectric Figure of Merit via Tunable Valley Convergence Coupled Low Thermal Conductivity in AIIBIVC2VChalcopyrites. Journal of Physical Chemistry C, 2018, 122, 29150-29157.	1.5	25

#	Article	IF	Citations
37110	Minimising oxygen contamination through a liquid copper-aided group IV metal production process. Scientific Reports, 2018, 8, 17391.	1.6	4
37111	Auxiliary-field quantum Monte Carlo calculations of the structural properties of nickel oxide. Journal of Chemical Physics, 2018, 149, 164102.	1.2	24
37112	High Curie temperature CoSi nanowires by Mn-doping. Journal of Applied Physics, 2018, 124, .	1.1	1
37113	Phonon thermodynamics and elastic behavior of GaN at high temperatures and pressures. Physical Review B, 2018, 98, .	1.1	10
37114	Relaxation and domain formation in incommensurate two-dimensional heterostructures. Physical Review B, 2018, 98, .	1.1	177
37115	Free-radical gases on two-dimensional transition-metal disulfides (XS₂, X = Mo/W): robust half-metallicity for efficient nitrogen oxide sensors. Beilstein Journal of Nanotechnology, 2018, 9, 1641-1646.	1.5	8
37116	Data set for diffusion coefficients and relative creep rate ratios of 26 dilute Ni-X alloy systems from first-principles calculations. Data in Brief, 2018, 20, 1537-1551.	0.5	24
37117	Stable 1T Tungsten Disulfide Monolayer and Its Junctions: Growth and Atomic Structures. ACS Nano, 2018, 12, 12080-12088.	7.3	74
37118	Excellent thermal stability and thermoelectric properties of Pnma -phase SnSe in middle temperature aerobic environment. Chinese Physics B, 2018, 27, 118105.	0.7	12
37119	Effect of hydration and ammonization on the thermal expansion behavior of ZrW2O8 : Ab initio lattice dynamical perspective. Physical Review B, 2018, 98, .	1.1	2
37120	Dihedral-angle-corrected registry-dependent interlayer potential for multilayer graphene structures. Physical Review B, 2018, 98, .	1.1	41
37121	Order Parameter and Band Gap of ZnSnN2. , 2018, , .		1
37122	Cation Exchange as a Mechanism To Engineer Polarity in Layered Perovskites. Chemistry of Materials, 2018, 30, 8915-8924.	3.2	25
37123	Persistence of the R3m Phase in Powder GeTe at High Pressure and High Temperature. Journal of Physical Chemistry C, 2018, 122, 28460-28465.	1.5	6
37124	Systematic Study of Descriptors for Oxygen Evolution Reaction Catalysis in Perovskite Oxides. Journal of Physical Chemistry C, 2018, 122, 27885-27892.	1.5	103
37125	Theoretical Approaches to Describing the Oxygen Reduction Reaction Activity of Single-Atom Catalysts. Journal of Physical Chemistry C, 2018, 122, 29307-29318.	1.5	68
37126	Visualizing Elementary Reactions of Methanol by Electrons and Holes on TiO₂(110) Surface. Journal of Physical Chemistry C, 2018, 122, 28805-28814.	1.5	17
37127	Single-Crystal Nitrogen-Rich Two-Dimensional Mo₅N₆ Nanosheets for Efficient and Stable Seawater Splitting. ACS Nano, 2018, 12, 12761-12769.	7.3	317

#	Article	IF	Citations
37128	Charge density wave in LuP2In (P=Pt , Pd) induced by electron-phonon interaction. Physical Review B, 2018, 98, .	1.1	5
37129	Reproduction of the Charge Density Wave Phase Diagram in <mml:math xmlns:mml="http://www.w3.org/1998/Math/MathML" display="inline"><mml:mrow><mml:mn>1</mml:mn><mml:mi>T</mml:mi><mml:mtext>â^'</mml:mtext><mml:msub><mml:mrow><m Exposes its Excitonic Character. Physical Review Letters, 2018, 121, 226602.	2.9	49
37130	Ultrathin Films of Superconducting Metals as a Platform for Topological Superconductivity. Physical Review Letters, 2018, 121, 227701.	2.9	20
37131	Isostructural metal-insulator transition in VO ₂. Science, 2018, 362, 1037-1040.	6.0	158
37132	Calcination Atmosphere Regulated Morphology and Catalytic Performance of Pt/SiO₂ in Gasâ€phase Oxidative Dehydrogenation of KAâ€oil. ChemCatChem, 2018, 10, 5689-5697.	1.8	3
37133	Designing band engineering for thermoelectrics starting from the periodic table of elements. Materials Today Physics, 2018, 7, 35-44.	2.9	75
37134	Super-Ionic Conduction in Solid-State Li₇P₃S₁₁-Type Sulfide Electrolytes. Chemistry of Materials, 2018, 30, 8764-8770.	3.2	43
37135	Graphene-Supported Monometallic and Bimetallic Dimers for Electrochemical CO2 Reduction. Journal of Physical Chemistry C, 2018, 122, 28629-28636.	1.5	27
37136	Crystal Facet Dependence for the Selectivity of C₂ Species over Co₂C Catalysts in the Fischerâ€“Tropsch Synthesis. Journal of Physical Chemistry C, 2018, 122, 29249-29258.	1.5	22
37137	Density Functional Theory Calculations of Oxygen Vacancy Formation and Subsequent Molecular Adsorption on Oxide Surfaces. Journal of Physical Chemistry C, 2018, 122, 29435-29444.	1.5	103
37138	Jahn-Teller Splitting in Single Adsorbed Molecules Revealed by Isospin-Flip Excitations. Physical Review Letters, 2018, 121, 226402.	2.9	8
37139	Nodeless High- <mml:math xmlns:mml="http://www.w3.org/1998/Math/MathML" display="inline"><mml:msub><mml:mi>T</mml:mi><mml:mi>c</mml:mi></mml:msub></mml:math> Superconductivity in the Highly Overdoped <mml:math xmlns:mml="http://www.w3.org/1998/Math/MathML" display="inline"><mml:mrow><mml:msub><mml:mrow><mml:mi>CuO</mml:mi></mml:mrow><mml:mrow><mml:mn>2</mml:mn></mml:mrow> Monolayer. Physical Review Letters, 2018, 121, 227002.	2.9	31
37140	Polymeric vanadyl species determine the low-temperature activity of V-based catalysts for the SCR of NO _x with NH ₃. Science Advances, 2018, 4, eaau4637.	4.7	206
37141	An Ab Initio Study of Thermodynamic and Mechanical Stability of Heusler-Based Fe2AlCo Polymorphs. Materials, 2018, 11, 1543.	1.3	12
37142	Amorphization as a Pathway to Fast Charging Kinetics in Atomic Layer Deposition-Derived Titania Films for Lithium Ion Batteries. Chemistry of Materials, 2018, 30, 8871-8882.	3.2	22
37143	Novel Single-Crystal Hollandite K1.46Fe0.8Ti7.2O16 Microrods: Synthesis, Double Absorption, and Magnetism. Inorganic Chemistry, 2018, 57, 15187-15197.	1.9	18
37144	Difluorophosphorane-Flattened Phosphorene through Difluorination. Journal of Physical Chemistry Letters, 2018, 9, 6963-6966.	2.1	7
37145	Reactive Molecular Dynamics Simulations of Thermal Film Growth from Di-tert-butyl Disulfide on an Fe(100) surface. Langmuir, 2018, 34, 15681-15688.	1.6	12

#	Article	IF	Citations
37146	Garnet Electrolyte Surface Degradation and Recovery. ACS Applied Energy Materials, 2018, 1, 7244-7252.	2.5	81
37147	Quasi-1D TiS₃ Nanoribbons: Mechanical Exfoliation and Thickness-Dependent Raman Spectroscopy. ACS Nano, 2018, 12, 12713-12720.	7.3	77
37148	Controlling Topological States in Topological/Normal Insulator Heterostructures. ACS Omega, 2018, 3, 15900-15906.	1.6	10
37149	Spontaneous Frenkel pair formation in zirconium carbide. Physical Review B, 2018, 98, .	1.1	10
37150	Theoretical Study on the Quantum Capacitance Origin of Graphene Cathodes in Lithium Ion Capacitors. Catalysts, 2018, 8, 444.	1.6	21
37151	Molecular Insight into Fatty Acid Adsorption on Bare and Hydrated (111) Fluorite Surface. Journal of Physical Chemistry B, 2018, 122, 12403-12410.	1.2	45
37152	Successive Dissociation of CO, CH₄, C₂H₆, and CH₃CHO on Fe(110): Retrosynthetic Understanding of FTS Mechanism. Journal of Physical Chemistry C, 2018, 122, 28846-28855.	1.5	11
37153	Elucidating CO₂ Chemisorption in Diamine-Appended Metalâ€“Organic Frameworks. Journal of the American Chemical Society, 2018, 140, 18016-18031.	6.6	107
37154	Design Principles for Trap-Free CsPbX₃ Nanocrystals: Enumerating and Eliminating Surface Halide Vacancies with Softer Lewis Bases. Journal of the American Chemical Society, 2018, 140, 17760-17772.	6.6	446
37155	Charge transfer drives anomalous phase transition in ceria. Nature Communications, 2018, 9, 5063.	5.8	48
37156	Structural, electronic and magnetic properties of MnxGa/Co2MnSi (xâ€‰=â€‰1, 3) bilayers. Scientific Reports, 2018, 8, 16530.	1.6	10
37157	Atomic and electronic structure of the Si(331)-(12 Ã— 1) surface. Journal of Chemical Physics, 2018, 149, 204702.	1.2	8
37158	Effect of stacking faults and surface roughness on the thermal conductivity of InAs nanowires. Journal of Applied Physics, 2018, 124, 205101.	1.1	3
37159	Lattice dynamics and coupled quadrupole-phonon excitations in CeAuAl3. Physical Review B, 2018, 98, .	1.1	6
37160	Surface vibrations in the <mml:math xmlns:mml="http://www.w3.org/1998/Math/MathML"><mml:msub><mml:mi mathvariant="normal">T</mml:mi><mml:mn>4</mml:mn></mml:msub></mml:math> and <mml:math xmlns:mml="http://www.w3.org/1998/Math/MathML"><mml:msub><mml:mi mathvariant="normal">H</mml:mi><mml:mn>3</mml:mn></mml:msub></mml:math> Pb phases on Si(111). Physical Review B, 2018, 98, .	1.1	4
37161	Dirac semimetal in type-IV magnetic space groups. Physical Review B, 2018, 98, .	1.1	97
37162	High-Pressure Synthesis, Crystal Structure, Chemical Bonding, and Ferroelectricity of LiNbO₃-Type LiSbO₃. Inorganic Chemistry, 2018, 57, 15462-15473.	1.9	19
37163	STM and DFT Study of Chlorine Adsorption on the Ag(111)-p(4 Ã— 4)â€“O Surface. Journal of Physical Chemistry C, 2018, 122, 28862-28867.	1.5	8

#	Article	IF	Citations
37164	Oscillatory Tunnel Magnetoresistance in a Carbon Nanotube Based Three-Terminal Magnetic Tunnel Junction. Journal of Physical Chemistry C, 2018, 122, 29062-29068.	1.5	3
37165	High-Yield Formation of Graphdiyne Macrocycles through On-Surface Assembling and Coupling Reaction. ACS Nano, 2018, 12, 12612-12618.	7.3	35
37166	First-Principles Structural, Mechanical, and Thermodynamic Calculations of the Negative Thermal Expansion Compound Zr2(WO4)(PO4)2. ACS Omega, 2018, 3, 15780-15788.	1.6	8
37167	Predicting Dirac semimetals based on sodium ternary compounds. Npj Computational Materials, 2018, 4, .	3.5	14
37168	Tuning structure and mechanical properties of Ta-C coatings by N-alloying and vacancy population. Scientific Reports, 2018, 8, 17669.	1.6	27
37169	Enhancement of photoluminescence efficiency in GeSe ultrathin slab by thermal treatment and annealing: experiment and first-principles molecular dynamics simulations. Scientific Reports, 2018, 8, 17671.	1.6	10
37170	Molecular tunneling in large tubes of 3D nitrogenated micropore materials. Journal of Applied Physics, 2018, 124, 194303.	1.1	22
37171	Anharmonic stabilization and lattice heat transport in rocksalt Î²-GeTe. Applied Physics Letters, 2018, 113, .	1.5	39
37172	Oxygen reduction reaction of FeN4 center embedded in graphene and carbon nanotube: Density functional calculations. AIP Advances, 2018, 8, .	0.6	17
37173	Competing adsorption mechanisms of pyridine on Cu, Ag, Au, and Pt(110) surfaces. Journal of Chemical Physics, 2018, 149, 214703.	1.2	9
37174	Angle-dependent magnetoresistance as a sensitive probe of the charge density wave in quasi-one-dimensional semimetal Ta2NiSe7. Applied Physics Letters, 2018, 113, .	1.5	5
37175	Exploring configurational degrees of freedom in disordered solids. AIP Conference Proceedings, 2018, , .	0.3	0
37176	DFT-guided design of catalysts for methane activation. AIP Conference Proceedings, 2018, , .	0.3	0
37177	Evaluation of exchange-correlation functionals with multiple-shock conductivity measurements in hydrogen and deuterium at the molecular-to-atomic transition. Physical Review B, 2018, 98, .	1.1	17
37178	Impact of interface structure on magnetic exchange coupling in <mml:math xmlns:mml="http://www.w3.org/1998/Math/MathML"><mml:mrow><mml:mi>MnBi</mml:mi><mml:mo>/</mml:mo><mml:mi> bilayers. Physical Review B, 2018, 98, .	1.1	5
37179	Noncollinear spin density of an adatom on a magnetic surface. Physical Review B, 2018, 98, .	1.1	4
37180	Excitonic effects in two-dimensional <mml:math xmlns:mml="http://www.w3.org/1998/Math/MathML"><mml:msub><mml:mi>TiSe</mml:mi><mml:mn>2</mml:mn></mml:msub> from hybrid density functional theory. Physical Review B, 2018, 98, .	1.1	23
37181	A DFT Screening of M-HKUST-1 MOFs for Nitrogen-Containing Compounds Adsorption. Nanomaterials, 2018, 8, 958.	1.9	13

#	Article	IF	Citations
37182	Nitrogen Tuned Charge Redistribution and Orbital Reconfiguration in Fe/MgO Interface for Significant Interfacial Magnetism Tunability. Advanced Functional Materials, 2019, 29, 1806677.	7.8	10
37183	Revealing Activity Trends of Metal Diborides Toward pHâ€Universal Hydrogen Evolution Electrocatalysts with Ptâ€Like Activity. Advanced Energy Materials, 2019, 9, 1803369.	10.2	111
37184	Charge state switching of the divacancy defect in <mml:math xmlns:mml="http://www.w3.org/1998/Math/MathML"><mml:mn>4</mml:mn><mml:mi>H</mml:mi></mml:math> -SiC. Physical Review B, 2018, 98, .	1.1	7
37185	Vibrational properties and magnetic specific heat of the covalent chain antiferromagnet RbFeSe2. Physical Review B, 2018, 98, .	1.1	5
37186	Influence of organic cations on the structural anisotropy in cubic lead halide perovskites. , 2018, , .		0
37187	The vacancy ordering produces a new cubic monocarbide: ReC. Materials Today Physics, 2018, 7, 54-60.	2.9	12
37188	Atomic Structure and Magnetic Properties of the Fe78B13Si9 Amorphous Alloy Surface. Journal of Physical Chemistry C, 2018, 122, 28613-28618.	1.5	6
37189	Predicting the structure and stability of titanium oxide electrides. Npj Computational Materials, 2018, 4, .	3.5	25
37190	Exploring the synergy of 2D MXene-supported black phosphorus quantum dots in hydrogen and oxygen evolution reactions. Journal of Materials Chemistry A, 2018, 6, 21255-21260.	5.2	151
37191	Carbon dioxide capture in 2,2â€²-iminodiethanol aqueous solution fromab initiomolecular dynamics simulations. Journal of Chemical Physics, 2018, 149, 224103.	1.2	7
37192	Role of dilution on the electronic structure and magnetic ordering of spinel cobaltites. Physical Review B, 2018, 98, .	1.1	17
37193	Effect of Electron-phonon Scattering on the Thermal Conductivity of Si Nanowires. , 2018, , .		0
37194	Origin of Two-Dimensional Vertical Ferroelectricity in WTe₂ Bilayer and Multilayer. Journal of Physical Chemistry Letters, 2018, 9, 7160-7164.	2.1	168
37195	Air-stable phosphorus-doped molybdenum nitride for enhanced electrocatalytic hydrogen evolution. Communications Chemistry, 2018, 1, .	2.0	36
37196	Dissociation of CHD3 on Cu(111), Cu(211), and single atom alloys of Cu(111). Journal of Chemical Physics, 2018, 149, 224701.	1.2	17
37197	Density Functional Theory Calculations Applied to Nuclear Fuels. , 2018, , 1-20.		1
37198	Combined theoretical and experimental studies of CO oxidation on PdRu nanoalloys. Applied Catalysis A: General, 2018, 568, 176-182.	2.2	4
37199	Formation and structural growth of two dimensional layer of hafnene on Ir(1â€¯1â€¯1) surface. Chemical Physics Letters, 2018, 712, 60-65.	1.2	3

#	Article	IF	Citations
37200	Effect of disorder on magnetic properties and martensitic transformation of Co-doped Ni-Mn-Al Heusler alloy. Intermetallics, 2018, 102, 132-139.	1.8	12
37201	Magnetic and electronic properties of Î±-U2N3 and its role in preventing uranium from oxidation: First-principles studies. Journal of Nuclear Materials, 2018, 512, 72-78.	1.3	4
37202	First-Principles Comparison of Proton and Divalent Copper Cation Exchange Energy Landscapes in SSZ-13 Zeolite. Journal of Physical Chemistry C, 2018, 122, 23564-23573.	1.5	35
37203	Theoretical Prediction of Janus MoSSe as a Potential Anode Material for Lithium-Ion Batteries. Journal of Physical Chemistry C, 2018, 122, 23899-23909.	1.5	56
37204	Computational Study of NaVOPO₄ Polymorphs as Cathode Materials for Na-Ion Batteries: Diffusion, Electronic Properties, and Cation-Doping Behavior. Journal of Physical Chemistry C, 2018, 122, 25829-25836.	1.5	36
37205	Structure and Reactivity of Methanol Adsorbed on Rutile TiO₂(011) Surface. Journal of Physical Chemistry C, 2018, 122, 24202-24208.	1.5	2
37206	A Potassium Metal-Organic Framework based on Perylene-3,4,9,10-tetracarboxylate as Sensing Layer for Humidity Actuators. Scientific Reports, 2018, 8, 14414.	1.6	27
37207	Healing detrimental defects in two-dimensional semiconductors through strain engineering. Semiconductor Science and Technology, 2018, 33, 075005.	1.0	0
37208	Approaching the forbidden fruit of reaction dynamics: Aiming reagent at selected impact parameters. Science Advances, 2018, 4, eaau2821.	4.7	13
37209	Structure Sensitivity of Formic Acid Electrooxidation on Transition Metal Surfaces: A First-Principles Study. Journal of the Electrochemical Society, 2018, 165, J3109-J3121.	1.3	39
37210	Optimized Pt-Based Catalysts for Oxygen Reduction Reaction in Alkaline Solution: A First Principle Study. Journal of the Electrochemical Society, 2018, 165, J3090-J3094.	1.3	13
37211	The Effects of Carbon Content on the Anisotropic Deformation Mechanism of Boron Carbide. Materials, 2018, 11, 1861.	1.3	7
37212	Stable Silicene in Graphene/Silicene Van der Waals Heterostructures. Advanced Materials, 2018, 30, e1804650.	11.1	86
37213	Anionic Redox Activity in a Newly Znâ€Doped Sodium Layered Oxide P2â€Na_{2/3}Mn_{1â^'}_yZn_yO₂ (0 <	11.1	1027
37214	Effects of hydrogen insertion on electronic, magnetic and optical properties of Co-doped ZnO: A theoretical investigation. Computational Condensed Matter, 2018, 17, e00343.	0.9	0
37215	On the role of intermolecular interactions in stabilizing AuNP@Ampicillin nano-antibiotics. Materialia, 2018, 4, 297-309.	1.3	4
37216	First-principles study of plutonium and cerium solubility in Gd2Sn2O7 pyrochlore. Nuclear Instruments & Methods in Physics Research B, 2018, 436, 211-216.	0.6	4
37217	Strain-tunable magnetic anisotropy in monolayer <mml:math xmlns:mml="http://www.w3.org/1998/Math/MathML"><mml:msub><mml:mi>CrCl</mml:mi><mml:mn>3</mml:mn></mml:msub></mml:math>, <mml:math xmlns:mml="http://www.w3.org/1998/Math/MathML"><mml:msub><mml:mi>CrBr</mml:mi><mml:mn>3</mml:mn></mml:msub></mml:math>, and <mml:math xmlns:mml="http://www.w3.org/1998/Math/MathML"><mml:msub><mml:mi>CrI</mml:mi><mml:mn>3</mml:mn></mml:msub></mml:math>	1.1	405

#	Article	IF	Citations
37218	Strain-Induced Quantum Spin Hall Effect in Two-Dimensional Methyl-Functionalized Silicene SiCH3. Nanomaterials, 2018, 8, 698.	1.9	4
37219	First-principles Investigations of Magnetic Semiconductors: An example of Transition Metal Decorated Two-dimensional SnS Monolayer. Nanomaterials, 2018, 8, 789.	1.9	12
37220	Stable, Efficient Red Perovskite Lightâ€Emitting Diodes by (Î±, Î´)â€CsPbI₃ Phase Engineering. Advanced Functional Materials, 2018, 28, 1804285.	7.8	105
37221	Electronic structure of Pr₂MnNiO₆from x-ray photoemission, absorption and density functional theory. Journal of Physics Condensed Matter, 2018, 30, 435603.	0.7	8
37222	Ab initio study of H/O trapping and clustering on U/Al interface. Chinese Physics B, 2018, 27, 097303.	0.7	3
37223	Dynamics and superconductivity in compressed lanthanum superhydride. Physical Review B, 2018, 98, .	1.1	85
37224	Bond ordering and phase transitions in Na2IrO3 under high pressure. Physical Review B, 2018, 98, .	1.1	17
37225	Infrared spectroscopic studies of the topological properties in <mml:math xmlns:mml="http://www.w3.org/1998/Math/MathML"><mml:msub><mml:mi>CaMnSb</mml:mi><mml:mn>2</mml:mn></mml:msub> Physical Review B, 2018, 98, .	1.1	10
37226	Topological phases in the <mml:math xmlns:mml="http://www.w3.org/1998/Math/MathML"><mml:msub><mml:mi>TaSe</mml:mi><mml:mn>3</mml:mn></mml:msub></mml:math> compound. Physical Review B, 2018, 98, .	1.1	44
37227	Ferroelectric Problem beyond the Conventional Scaling Law. Physical Review Letters, 2018, 121, 135702.	2.9	10
37228	Quantum-Mechanical Modeling of the Elastic Properties of Aluminum-Based Metal-Organic Frameworks. Russian Journal of Physical Chemistry A, 2018, 92, 1940-1946.	0.1	3
37229	Temperature Effects on the Elastic Constants, Stacking Fault Energy and Twinnability of Ni3Si and Ni3Ge: A First-Principles Study. Crystals, 2018, 8, 364.	1.0	3
37230	Boosting Potassium Storage Capacity Based on Stressâ€Induced Sizeâ€Dependent Solidâ€Solution Behavior. Advanced Energy Materials, 2018, 8, 1802175.	10.2	28
37231	Simulating heterogeneous catalysis on metallic nanoparticles: From under-coordinated sites to extended facets. Frontiers of Nanoscience, 2018, , 101-128.	0.3	1
37232	Atomistic Insight into the Redox Reactions in Fe/Oxide Coreâ€“Shell Nanoparticles. Chemistry of Materials, 2018, 30, 7306-7312.	3.2	28
37233	Crystal Chemistry, Opticalâ€“Electronic Properties, and Electronic Structure of Cd_{1â€“x}In_{2+2x/3}S₄ Compounds (0 â‰¤ x â‰¤ 1), Potential Buffer in CIGS-Based Thin-Film Solar Cells. Inorganic Chemistry, 2018, 57, 12624-12631.	1.9	9
37234	Cluster-Assembled Semiconductor CdO Polymorph with Good Ductility, High Carrier Mobility, and Promising Optical Properties. Journal of Physical Chemistry C, 2018, 122, 24287-24294.	1.5	6
37235	Band Structures of Periodic Porphyrin Nanostructures. Journal of Physical Chemistry C, 2018, 122, 23790-23798.	1.5	21

#	Article	IF	Citations
37236	Layer-Coupled States Facilitate Ultrafast Charge Transfer in a Transition Metal Dichalcogenide Trilayer Heterostructure. Journal of Physical Chemistry Letters, 2018, 9, 5970-5978.	2.1	16
37237	High magnetoresistance in ultra-thin two-dimensional Cr-based MXenes. Nanoscale, 2018, 10, 19492-19497.	2.8	26
37238	The nickel battery positive electrode revisited: stability and structure of the Î²-NiOOH phase. Journal of Materials Chemistry A, 2018, 6, 19256-19265.	5.2	27
37239	Efficient lattice constants and energy bandgaps for condensed systems from a meta-GGA level screened range-separated hybrid functional. Journal of Chemical Physics, 2018, 149, 094105.	1.2	14
37240	Characterizing self-assembled molecular layers on weakly interacting substrates: the role of van der Waals and the chemical interactions. Nano Futures, 2018, 2, 045002.	1.0	2
37241	Role of the orbital moment in a series of isostructural weak ferromagnets. Physical Review B, 2018, 98, .	1.1	7
37242	Strong spin-orbit coupling in the noncentrosymmetric Kondo lattice. Physical Review B, 2018, 98, .	1.1	16
37243	Electronic Structure, Optical Properties, and Pressure Behavior of the CdB4O7 and HgB4O7 Compounds. Physics of the Solid State, 2018, 60, 1704-1711.	0.2	0
37244	EvaluaciÃ³n de caminos de difusiÃ³n de Al en UAl4. Revista Materia, 2018, 23, .	0.1	0
37245	Possible Origin of the Absence of Magnetic Order in LiOsO₃: Spinâ€“Orbit Coupling Controlled Ground State. Physica Status Solidi - Rapid Research Letters, 2018, 12, 1800396.	1.2	6
37246	Role of Oxygen Vacancies on Oxygen Evolution Reaction Activity: Î²-Ga₂O₃ as a Case Study. Chemistry of Materials, 2018, 30, 7714-7726.	3.2	43
37247	Dominant Role of Entropy in Stabilizing Sugar Isomerization Transition States within Hydrophobic Zeolite Pores. Journal of the American Chemical Society, 2018, 140, 14244-14266.	6.6	83
37248	Theoretical Insight into Gate-Opening Adsorption Mechanism and Sigmoidal Adsorption Isotherm into Porous Coordination Polymer. Journal of the American Chemical Society, 2018, 140, 13958-13969.	6.6	48
37249	Structural stability and electronic properties of alkaline-earth metal induced Si(111)-(3 Ã— 2) surfaces. Physical Chemistry Chemical Physics, 2018, 20, 25235-25239.	1.3	6
37250	Kinetic pathways towards mass production of single crystalline stanene on topological insulator substrates. Nanoscale, 2018, 10, 18988-18994.	2.8	8
37251	Optimized symmetry functions for machine-learning interatomic potentials of multicomponent systems. Journal of Chemical Physics, 2018, 149, 124106.	1.2	19
37252	Type-I and type-II nodal lines coexistence in the antiferromagnetic monolayer <mml:math xmlns:mml="http://www.w3.org/1998/Math/MathML"><mml:msub><mml:mi>CrAs</mml:mi><mml:mn>2</mml:mn></mml:msub></mml:math> Physical Review B, 2018, 98, .	1.1	37
37253	Electronic fingerprints of Cr and V dopants in the topological insulator <mml:math xmlns:mml="http://www.w3.org/1998/Math/MathML"><mml:mrow><mml:msub><mml:mi>Sb</mml:mi><mml:mn>2</mml:mn></mml:msub></mml:mrow></mml:math> Physical Review B, 2018, 98, .	1.1	19

#	Article	IF	Citations
37254	Density functional theory study of the point defect energetics in Î³-LiAlO2, Li2ZrO3 and Li2TiO3 materials. Journal of Nuclear Materials, 2018, 511, 375-389.	1.3	18
37255	Influence of deposition temperature on the properties of sputtered films grown from a Cu2O CdO TeO2 composite target: Electronic properties of CdTe2O5. Superlattices and Microstructures, 2018, 123, 403-413.	1.4	1
37256	Phonons and Thermal Expansion Behavior of NiSi and NiGe. Frontiers in Chemistry, 2018, 6, 331.	1.8	6
37257	Dynamic Electronic Doping for Correlated Oxides by a Triboelectric Nanogenerator. Advanced Materials, 2018, 30, e1803580.	11.1	20
37258	Orbital Interactions in Biâ€Sn Bimetallic Electrocatalysts for Highly Selective Electrochemical CO₂ Reduction toward Formate Production. Advanced Energy Materials, 2018, 8, 1802427.	10.2	259
37259	Insight into the Role of Additives in Catalytic Synthesis of Cyclohexylamine from Nitrobenzene. Chinese Journal of Chemistry, 2018, 36, 1191-1196.	2.6	24
37260	Ru/Al2O3 catalyzed CO2 hydrogenation: Oxygen-exchange on metal-support interfaces. Journal of Catalysis, 2018, 367, 194-205.	3.1	74
37261	Photocatalytic properties of intrinsically defective undoped bismuth vanadate (BiVO4) photocatalyst: A DFT study. Journal of Electroanalytical Chemistry, 2018, 828, 97-101.	1.9	5
37262	Constructing tunable dual active sites on two-dimensional C3N4@MoN hybrid for electrocatalytic hydrogen evolution. Nano Energy, 2018, 53, 690-697.	8.2	175
37263	Two-Dimensional Janus Transition Metal Oxides and Chalcogenides: Multifunctional Properties for Photocatalysts, Electronics, and Energy Conversion. ACS Applied Materials & Interfaces, 2018, 10, 35289-35295.	4.0	135
37264	CO Adsorption on Pt(111): From Isolated Molecules to Ordered High-Coverage Structures. ACS Catalysis, 2018, 8, 10225-10233.	5.5	38
37265	Gallium nitride nanowire as a linker of molybdenum sulfides and silicon for photoelectrocatalytic water splitting. Nature Communications, 2018, 9, 3856.	5.8	87
37266	Complex strain evolution of polar and magnetic order in multiferroic BiFeO3 thin films. Nature Communications, 2018, 9, 3764.	5.8	40
37267	Tunable ideal strength of ZrSe2 monolayer by charge doping. Journal of Applied Physics, 2018, 124, .	1.1	5
37268	Tuning Thermal Transport in <mml:math xmlns:mml="http://www.w3.org/1998/Math/MathML" display="inline" overflow="scroll"><mml:msub><mml:mrow><mml:mrow><mml:mi mathvariant="normal">C</mml:mi></mml:mrow></mml:mrow><mml:mn>3</mml:mn></mml:msub><mml:mrow><mml:mi mathvariant="normal">N</mml:mi></mml:mrow></mml:math> Monolayers by Adding and Removing Carbon Atoms. Physical Review Applied, 2018, 10, .	1.5	25
37269	Electric Control of the Edge Magnetization in Zigzag Stanene Nanoribbons from First Principles. Physical Review Applied, 2018, 10, .	1.5	14
37270	Enhanced thermoelectric performance of <mml:math xmlns:mml="http://www.w3.org/1998/Math/MathML"><mml:mrow><mml:msub><mml:mi>Mg</mml:mi><mml:mn>2</mml:mn></mml:msub></mml:mrow></mml:math> codoped with Bi and Cr. Physical Review B, 2018, 98, .	1.1	17
37271	Large magneto-optical Kerr effect and magnetic anisotropy energy in two-dimensional <mml:math xmlns:mml="http://www.w3.org/1998/Math/MathML"><mml:msub><mml:mrow><mml:mi mathvariant="normal">Cr</mml:mi></mml:mrow><mml:mn>2</mml:mn></mml:msub><mml:msub><mml:mrow><mml:mi mathvariant="normal">Ge</mml:mi></mml:mrow><mml:mn>2</mml:mn></mml:msub><mml:msub><mml:mrow><mml:mi mathvariant="normal">Te</mml:mi></mml:mrow><mml:mn>6</mml:mn></mml:msub></mml:math>. Physical Review B, 2018, 98, .	1.1	119

#	Article	IF	Citations
37272	Anomalous Phonon Lifetime Shortening in Paramagnetic CrN Caused by Spin-Lattice Coupling: A Combined Spin and AbÂInitio Molecular Dynamics Study. Physical Review Letters, 2018, 121, 125902.	2.9	53
37273	Active basal plane in ZT-phased MX2 (M = Mo, W; X = S, Se, Te) catalysts for the hydrogen evolution reaction: A theoretical study. International Journal of Hydrogen Energy, 2018, 43, 19432-19437.	3.8	15
37274	Electronic and optical properties of strained noble metals: Implications for applications based on LSPR. Nano Energy, 2018, 53, 932-939.	8.2	45
37275	Liquid-phase exfoliated ultrathin Bi nanosheets: Uncovering the origins of enhanced electrocatalytic CO2 reduction on two-dimensional metal nanostructure. Nano Energy, 2018, 53, 808-816.	8.2	247
37276	High-Throughput Screening of Magnetic Antiperovskites. Chemistry of Materials, 2018, 30, 6983-6991.	3.2	34
37277	Intercalation Mechanisms of Fe Atoms underneath A Graphene Monolayer on Ru(0001). Journal of Physical Chemistry C, 2018, 122, 22903-22910.	1.5	7
37278	Novel Phase of AlN₄ as a Possible Superhard Material. Journal of Physical Chemistry C, 2018, 122, 22660-22666.	1.5	17
37279	Mechanisms governing metal vacancy formation in BaTiO3 and SrTiO3. Journal of Applied Physics, 2018, 124, .	1.1	42
37280	Ptâ€“Graphene Contacts Fabricated by Plasma Functionalization and Atomic Layer Deposition. Advanced Materials Interfaces, 2018, 5, 1800268.	1.9	9
37281	High-Power Li-Metal Anode Enabled by Metal-Organic Framework Modified Electrolyte. Joule, 2018, 2, 2117-2132.	11.7	227
37282	Few-layered ReS₂ nanosheets vertically aligned on reduced graphene oxide for superior lithium and sodium storage. Journal of Materials Chemistry A, 2018, 6, 20267-20276.	5.2	61
37283	Catalytic CO oxidation on B-doped and BN co-doped penta-graphene: a computational study. Physical Chemistry Chemical Physics, 2018, 20, 26414-26421.	1.3	31
37284	The impact of substrate surface defects on the properties of two-dimensional van der Waals heterostructures. Nanoscale, 2018, 10, 19212-19219.	2.8	10
37285	Cystamine-configured lead halide based 2D hybrid molecular crystals: Synthesis and photoluminescence systematics. APL Materials, 2018, 6, 114204.	2.2	13
37286	Multiscale approach for determining hydrogen diffusivity in zirconium. Modelling and Simulation in Materials Science and Engineering, 2018, 26, 085002.	0.8	7
37287	Reverse-engineering of graphene on metal surfaces: a case study of embedded ruthenium. Nanotechnology, 2018, 29, 505601.	1.3	22
37288	Borderline Magnetism: How Adding <mml:math xmlns:mml="http://www.w3.org/1998/Math/MathML" display="inline" overflow="scroll"><mml:mi>Mg</mml:mi></mml:math> to Paramagnetic <mml:math xmlns:mml="http://www.w3.org/1998/Math/MathML" display="inline" overflow="scroll"><mml:mi>Ce</mml:mi><mml:msub><mml:mi>Co</mml:mi><mml:mn>3</mml:mn></mml:msub></mml:math> Makes <mml:math xmlns:mml="http://www.w3.org/1998/Math/MathML" display="inline" overflow="scroll"><mml:mi>Y</mml:mi><mml:msub><mml:mi mathvariant="normal">b</mml:mi><mml:mn>5</mml:mn></mml:msub><mml:mi mathvariant="normal">S</mml:mi><mml:msub><mml:mi mathvariant="normal">o</mml:mi><mml:mn>3</mml:mn></mml:msub></mml:mrow></mml:math>. Physical Review Applied, 2018, 10, .	1.5	14
37289		1.1	30

#	Article	IF	Citations
37290	Tb₃Pd₂, Er₃Pd₂ and Er₆Co_{5â€“x}: structural variations and bonding in rare-earth-richer binary intermetallics. Acta Crystallographica Section C, Structural Chemistry, 2018, 74, 991-996.	0.2	2
37291	Novel 2D Germanene Dioxide Monolayers: Mechanical Properties, Holeâ€Mobility Values, and Carrier Mobility. Annalen Der Physik, 2018, 530, 1800214.	0.9	3
37292	A Complex Zeolite Containing Multiple Ring Sizes in a Single Channel: Oneâ€Dimensional Zeolite UZMâ€55. Chemistry - A European Journal, 2018, 24, 17779-17787.	1.7	7
37293	Direct inversion of the iterative subspace with contracted planewave basis functions. Journal of Computational Chemistry, 2018, 39, 1890-1901.	1.5	2
37294	Hydrogen storage in MgX (X = Cu and Ni) systems - is there still news?. Journal of Power Sources, 2018, 402, 394-401.	4.0	17
37295	Solidâ€“Liquid Interfacial Reaction Trigged Propagation of Phase Transition from Surface into Bulk Lattice of Ni-Rich Layered Cathode. Chemistry of Materials, 2018, 30, 7016-7026.	3.2	80
37296	Grain Boundary Facilitates Photocatalytic Reaction in Rutile TiO₂ Despite Fast Charge Recombination: A Time-Domain ab Initio Analysis. Journal of Physical Chemistry Letters, 2018, 9, 5884-5889.	2.1	27
37297	Understanding the Impact of Surface Reconstruction of Perovskite Catalysts on CH₄ Activation and Combustion. ACS Catalysis, 2018, 8, 10306-10315.	5.5	50
37298	Precise Control of Pt Particle Size for Surface Structureâ€“Reaction Activity Relationship. Journal of Physical Chemistry C, 2018, 122, 23451-23459.	1.5	8
37299	Roles of Chenodeoxycholic Acid Coadsorbent in Anthracene-Based Dye-Sensitized Solar Cells: A Density Functional Theory Study. Journal of Physical Chemistry C, 2018, 122, 23280-23287.	1.5	18
37300	Simple Scheme to Predict Transition-State Energies of Dehydration Reactions in Zeolites with Relevance to Biomass Conversion. Journal of Physical Chemistry C, 2018, 122, 23062-23067.	1.5	14
37301	New Universal Type of Interface in the Magnetic Insulator/Topological Insulator Heterostructures. Nano Letters, 2018, 18, 6521-6529.	4.5	51
37302	Strongly Enhanced Thermoelectric Performance over a Wide Temperature Range in Topological Insulator Thin Films. ACS Applied Energy Materials, 0, , .	2.5	4
37303	Crystalline and oxide phases revealed and formed on InSb(111)B. Scientific Reports, 2018, 8, 14382.	1.6	11
37304	Ab initio study of the structure, isotope effects, and vibrational properties in KDP crystals. Physical Review B, 2018, 98, .	1.1	19
37305	Design of phosphorene/graphene heterojunctions for high and tunable interfacial thermal conductance. Nanoscale, 2018, 10, 19854-19862.	2.8	38
37306	Ab initio study of <mml:math xmlns:mml="http://www.w3.org/1998/Math/MathML"><mml:mrow><mml:mi>A</mml:mi><mml:msub><mml:mi>BiO</mml:mi><mml:m (<mml:math) Tj ETQq0 0 0 rgBT /Overlock 10 Tf 50 97 Td (xmlns:mml="http://www.w3.org/1998/Math/MathML"><mml:mrow><mml:m	1.1	3
37307	Deorbitalized meta-GGA exchange-correlation functionals in solids. Physical Review B, 2018, 98, .	1.1	59

#	Article	IF	Citations
37308	2D layered transition metal dichalcogenides (MoS2): Synthesis, applications and theoretical aspects. Applied Materials Today, 2018, 13, 242-270.	2.3	139
37309	Discovery of a new quantum spin Hall phase in bilayer plumbene. Chemical Physics Letters, 2018, 712, 78-82.	1.2	20
37310	Effect of metal doping on carbon monoxide adsorption on phosphorene: A first-principles study. Superlattices and Microstructures, 2018, 124, 168-175.	1.4	25
37311	Interface dominated cooperative nanoprecipitation in interstitial alloys. Nature Communications, 2018, 9, 4017.	5.8	12
37312	Sulfone-containing covalent organic frameworks for photocatalytic hydrogen evolution from water. Nature Chemistry, 2018, 10, 1180-1189.	6.6	883
37313	Effects of thermostatting in molecular dynamics on anharmonic properties of crystals: Application to fcc Al at high pressure and temperature. Journal of Chemical Physics, 2018, 149, 124109.	1.2	16
37314	Local environment dependence of Mn magnetism in bcc iron-manganese alloys: A first-principles study. Physical Review B, 2018, 98, .	1.1	23
37315	Route to achieving giant magnetoelectric coupling in <mml:math xmlns:mml="http://www.w3.org/1998/Math/MathML"><mml:mrow><mml:msub><mml:mi>BaTiO</mml:mi><mml:mn>3</mml:mn><mml:mi mathvariant="normal">F</mml:mi></mml:msub></mml:mrow></mml:math> perovskite heterostructures. Physical Review B, 2018, 98, .	1.1	9
37316	Size-Controllable Synthesis of Zeolitic Imidazolate Framework/Carbon Nanotube Composites. Crystals, 2018, 8, 367.	1.0	23
37317	Synthesis and Mechanical Characterization of Binary and Ternary Intermetallic Alloys Based on Fe-Ti-Al by Resonant Ultrasound Vibrational Methods. Materials, 2018, 11, 746.	1.3	9
37318	Sodium, Potassium, and Calcium in Europa: An Atomic Journey through Water Ice. Astrophysical Journal Letters, 2018, 865, L16.	3.0	6
37319	Saddleâ€Point Excitons and Their Extraordinary Light Absorption in 2D Î²â€Phase Groupâ€IV Monochalcogenides. Advanced Functional Materials, 2018, 28, 1804581.	7.8	23
37320	Thermodynamic Assessment of the Ag-Se System Aided by First-Principles Calculations. Journal of Phase Equilibria and Diffusion, 2018, 39, 870-881.	0.5	2
37321	A mixed anion hydroborate/carba-hydroborate as a room temperature Na-ion solid electrolyte. Journal of Power Sources, 2018, 404, 7-12.	4.0	72
37322	Insight into the Mechanism of the Ionic Conductivity for Ln-Doped Ceria (Ln = La, Pr, Nd, Pm, Sm, Gd, Tb,) Tj ETQq0 0 0 rgBT /Overlock 1	1.9	33
37323	Crystal Chemistry and Phonon Heat Capacity in Quaternary Honeycomb Delafossites: Cu[Li_{1/3}Sn_{2/3}]O₂ and Cu[Na_{1/3}Sn_{2/3}]O₂. Inorganic Chemistry, 2018, 57, 12709-12717.	1.9	13
37324	Novel Two-Dimensional Semiconductor SnP₃ with High Carrier Mobility, Good Light Absorption, and Strong Interlayer Quantum Confinement. Journal of Physical Chemistry C, 2018, 122, 24359-24367.	1.5	42
37325	Atomic and Molecular Adsorption on the Bi(111) Surface: Insights into Catalytic CO₂ Reduction. Journal of Physical Chemistry C, 2018, 122, 23084-23090.	1.5	48

#	Article	IF	Citations
37326	Insight into the Photocatalytic Mechanism of Tin Dioxide/Polyaniline Nanocomposites for NO Degradation under Solar Light. ACS Applied Nano Materials, 2018, 1, 5786-5794.	2.4	39
37327	Ab Initio Investigation of Water Adsorption and Hydrogen Evolution on Co₉S₈ and Co₃S₄ Low-Index Surfaces. ACS Omega, 2018, 3, 12215-12228.	1.6	17
37328	Hydrogen solubility in donor-doped SrTiO3 from first principles. Applied Physics Letters, 2018, 113, .	1.5	12
37329	Cu₂Teâ€“Ag₂Te lateral topological insulator heterojunction: stability and properties. Nanotechnology, 2018, 29, 505711.	1.3	2
37330	Effect of Oxygen on the Quantum, Magnetic, and Thermodynamic Properties of Co Nanowires on the Reconstructed Anisotropic (1 Ã— 2)/Au(110) and (1 Ã— 2)/Pt(110) Surfaces: Ab Initio Approach. Journal of Experimental and Theoretical Physics, 2018, 127, 179-188.	0.2	4
37331	Fracture Toughness of the Feâ€“Zn Intermetallic Compounds Measured by Bend Testing of Chevron-Notched Single-Crystal Microbeams. ISIJ International, 2018, 58, 1569-1577.	0.6	10
37332	Tuning optical and electronic properties in novel carbazole photosensitizers for p-type dye-sensitized solar cells. Electrochimica Acta, 2018, 292, 805-816.	2.6	67
37333	Tunable Electronic Structures of Hydrogenated Zigzag and Armchair Dumbbell Silicene Nanosheets: A Computational Study. Journal of Physical Chemistry C, 2018, 122, 23208-23216.	1.5	9
37334	Microwave-Assisted Synthesis of Classically Immiscible Agâ€“Ir Alloy Nanoparticle Catalysts. ACS Catalysis, 2018, 8, 11386-11397.	5.5	57
37335	Identifying Charge Transfer Mechanisms across Semiconductor Heterostructures via Surface Dipole Modulation and Multiscale Modeling. Journal of the American Chemical Society, 2018, 140, 13223-13232.	6.6	19
37336	Phonon transport properties of two-dimensional electride Ca2Nâ€”A first-principles study. Applied Physics Letters, 2018, 113, .	1.5	11
37337	Electronic structure based descriptor for characterizing local atomic environments. Physical Review B, 2018, 98, .	1.1	15
37338	Ferrimagnetic cluster formation due to oxygen vacancies in <mml:math xmlns:mml="http://www.w3.org/1998/Math/MathML"><mml:mrow><mml:msub><mml:mi>CaFe</mml:mi><mml:mn>2</mml:mn></mml:msub><mml:mi mathvariant="normal">O</mml:mi><mml:mrow><mml:mn>4</mml:mn><mml:mo>â^’</mml:mo><mml:mi>Î´</mml:mi></mml:mrow></ Physical Review B, 2018, 98, .	1.1	8
37339	Two dimensional XAs (X = Si, Ge, Sn) monolayers as promising photocatalysts for water splitting hydrogen production with high carrier mobility. Applied Materials Today, 2018, 13, 276-284.	2.3	51
37340	Engineering the band gap of armchair MoSe2 nanoribbon with edge passivation. Superlattices and Microstructures, 2018, 124, 62-71.	1.4	3
37341	Impact of Surface Energy on the Formation of Composite Metal Oxide Nanoparticles. Journal of Physical Chemistry C, 2018, 122, 24350-24358.	1.5	9
37342	Structure and Vibrational Properties of Potassium-Promoted Tungsten Oxide Catalyst Monomeric Sites Supported on Alumina (K2O/WO3/Al2O3) Characterized Using Periodic Density Functional Theory. Journal of Physical Chemistry C, 2018, 122, 24190-24201.	1.5	11
37343	DFT Study of the Oxygen Reduction Reaction on Carbon-Coated Iron and Iron Carbide. ACS Catalysis, 2018, 8, 10521-10529.	5.5	46

#	Article	IF	Citations
37344	Metal-Free Single Atom Catalyst for N₂ Fixation Driven by Visible Light. Journal of the American Chemical Society, 2018, 140, 14161-14168.	6.6	742
37345	Comparing the Descriptors for Investigating the Influence of Lattice Dynamics on Ionic Transport Using the Superionic Conductor Na₃PS_{4â€“x}Se_x. Journal of the American Chemical Society, 2018, 140, 14464-14473.	6.6	122
37346	First-principles study of interaction energies of atomic defects in bcc ferromagnetic iron. Physical Review B, 2018, 98, .	1.1	13
37347	Anharmonic effect driven topological phase transition in PbO2 predicted by first-principles calculations. Physical Review B, 2018, 98, .	1.1	7
37348	Interfacial Electron Transfer of Ni₂Pâ€“NiP₂ Polymorphs Inducing Enhanced Electrochemical Properties. Advanced Materials, 2018, 30, e1803590.	11.1	298
37349	PyDEF 2.0: An Easy to Use Postâ€treatment Software for Publishable Charts Featuring a Graphical User Interface. Journal of Computational Chemistry, 2018, 39, 2251-2261.	1.5	27
37350	Optical properties of photovoltaic materials: Organic-inorganic mixed halide perovskites CH3NH3Pb(I1-yXy)3 (Xâ€¯=â€¯Cl, Br). Computational and Theoretical Chemistry, 2018, 1144, 1-8.	1.1	12
37351	Dopant solubility in ceria: alloy thermodynamics combined with the DFT+U calculations. Solid State Ionics, 2018, 325, 258-264.	1.3	1
37352	Direct in Situ Observation and Analysis of the Formation of Palladium Nanocrystals with High-Index Facets. Nano Letters, 2018, 18, 7004-7013.	4.5	42
37353	Rhombohedral Lanthanum Manganite: A New Class of Dirac Half-Metal with Promising Potential in Spintronics. ACS Applied Materials & Interfaces, 2018, 10, 36088-36093.	4.0	43
37354	Intrinsic Carrier Mobility of Cesium Lead Halide Perovskites. Physical Review Applied, 2018, 10, .	1.5	59
37355	Monodisperse water clusters grown on the semimetallic Bi(111) surface. Physical Review B, 2018, 98, .	1.1	4
37356	Direct electric field imaging of graphene defects. Nature Communications, 2018, 9, 3878.	5.8	74
37357	Langmuirâ€“Blodgett artificial solid-electrolyte interphases for practical lithium metal batteries. Nature Energy, 2018, 3, 889-898.	19.8	347
37358	Anisotropic polarization-induced conductance at a ferroelectricâ€“insulator interface. Nature Nanotechnology, 2018, 13, 1132-1136.	15.6	53
37359	D-carbon: Ab initio study of a novel carbon allotrope. Journal of Chemical Physics, 2018, 149, 114702.	1.2	33
37360	MonteCoffee: A programmable kinetic Monte Carlo framework. Journal of Chemical Physics, 2018, 149, 114101.	1.2	26
37361	Quantum transport in a compensated semimetal <mml:math xmlns:mml="http://www.w3.org/1998/Math/MathML"><mml:mrow><mml:msub><mml:mi mathvariant="normal">W</mml:mi><mml:mn>2</mml:mn></mml:msub><mml:msub><mml:mi>As</mml:mi><mml:mn>3</mml:mn></mml:msub></mml:mrow></mml:math> with nontrivial <mml:math xmlns:mml="http://www.w3.org/1998/Math/MathML"><mml:msub><mml:mi>Z</mml:mi><mml:mn>2</mml:mn></mml:msub></mml:math> indices. Physical Review B, 2018, 98, .	1.1	8

#	Article	IF	Citations
37362	Modeling of electron transport in nanoribbon devices using Bloch waves. , 2018, , .		0
37363	Spin Polarization of Mn5Ge3 in the Bulk and Thin Films. JETP Letters, 2018, 107, 422-425.	0.4	0
37364	Moderate Energy for Charging Liâ€Ion Batteries Determined by Firstâ€Principles Calculations. Batteries and Supercaps, 2018, 1, 209-214.	2.4	20
37365	Density Functional Theory Investigation of Carbon Dots as Holeâ€transport Material in Perovskite Solar Cells. ChemPhysChem, 2018, 19, 3018-3023.	1.0	18
37366	DFT modeling of metallic nanoparticles. Frontiers of Nanoscience, 2018, 12, 239-293.	0.3	8
37367	Cobalt polyoxometalate-derived CoWO4 oxygen-evolving catalysts for efficient electrochemical and photoelectrochemical water oxidation. Journal of Catalysis, 2018, 367, 212-220.	3.1	44
37368	Predicting a new class of metal-organic frameworks as efficient catalyst for bi-functional oxygen evolution/reduction reactions. Journal of Catalysis, 2018, 367, 206-211.	3.1	61
37369	Thermoelectric properties of n-type transition metal-doped PbSe. Materials Today Physics, 2018, 6, 45-52.	2.9	23
37370	Efficient near ultraviolet to near infrared downconversion photoluminescence of La2GeO5: Bi3+, Nd3+ phosphor for silicon-based solar cells. Optical Materials, 2018, 85, 523-530.	1.7	23
37371	Computational Discovery of Liâ€“Mâ€“O Ion Exchange Materials for Lithium Extraction from Brines. Chemistry of Materials, 2018, 30, 6961-6968.	3.2	23
37372	Behavior of Photogenerated Electronâ€“Hole Pair for Water Splitting on TiO₂(110). Journal of Physical Chemistry C, 2018, 122, 22930-22938.	1.5	27
37373	From Reticular Chemistry Design to Density Functional Theory Modeling for New Zeolitic Imidazolate Framework Topologies: Mechanical Stability, Electronic Structure, and CO₂ Selectivity. Journal of Physical Chemistry C, 2018, 122, 23543-23553.	1.5	4
37374	Unusual Ferroelectricity of Trans-Unitcell Ion-Displacement and Multiferroic Soliton in Sodium and Potassium Hydroxides. ACS Applied Materials & Interfaces, 2018, 10, 35361-35366.	4.0	10
37375	Orbital-Engineering-Based Screening of Ï€-Conjugated d⁸ Transition-Metal Coordination Polymers for High-Performance n-Type Thermoelectric Applications. ACS Applied Materials & Interfaces, 2018, 10, 35306-35315.	4.0	32
37376	An orbitally derived single-atom magnetic memory. Nature Communications, 2018, 9, 3904.	5.8	34
37377	Electrical conductivity and magnetic dynamos in magma oceans of Super-Earths. Nature Communications, 2018, 9, 3883.	5.8	48
37378	A hexadecanuclear silver alkynyl cluster based NbO framework with triple emissions from the visible to near-infrared II region. Chemical Communications, 2018, 54, 11905-11908.	2.2	35
37379	Large tunneling magnetoresistance in magnetic tunneling junctions based on two-dimensional CrX₃ (X = Br, I) monolayers. Nanoscale, 2018, 10, 22196-22202.	2.8	44

#	Article	IF	Citations
37380	Photogalvanic effect induced fully spin polarized current and pure spin current in zigzag SiC nanoribbons. Physical Chemistry Chemical Physics, 2018, 20, 26744-26751.	1.3	42
37381	An atomistic model for the charge distribution in layered MoS2. Journal of Chemical Physics, 2018, 149, 124102.	1.2	5
37382	The contribution of distinct response characteristics of Fe atoms to switching of magnetic anisotropy in Fe4N/MgO heterostructures. Applied Physics Letters, 2018, 113, .	1.5	26
37383	The tunable bandgap effect of SnS films. Journal of Physics Condensed Matter, 2018, 30, 465302.	0.7	7
37384	Role of temperature and Coulomb correlation in the stabilization of the CsCl-type phase in FeS under pressure. Physical Review B, 2018, 98, .	1.1	9
37385	Berry curvature dipole current in the transition metal dichalcogenides family. Physical Review B, 2018, 98, .	1.1	121
37386	Antiferromagnetic ground state of <mml:math xmlns:mml="http://www.w3.org/1998/Math/MathML"><mml:mrow><mml:msub><mml:mi>La</mml:mi><mml:mn>12</mml:mn></mml:msub></mml:r : A parameter-free ab initio description. Physical Review B, 2018, 98, .	1.1	80
37387	Structural and electrochemical properties of Na2FeSiO4 polymorphs for sodium-ion batteries. Electrochimica Acta, 2018, 292, 190-198.	2.6	17
37388	Building Fluorinated Hybrid Crystals: Understanding the Role of Noncovalent Interactions. Crystal Growth and Design, 2018, 18, 6901-6910.	1.4	14
37389	Factors Controlling Oxygen Interstitial Diffusion in the Ruddlesdenâ€“Popper Oxide La_{2â€“x}Sr_xNiO_{4+Î´}. Chemistry of Materials, 2018, 30, 7166-7177.	3.2	28
37390	Bi_{2+2n}O_{2+2n}Cu_{2â^'Î´}Se_{2+nâ€“Î´}X_{Î´} (X = Cl, Br): A Three-Anion Homologous Series. Inorganic Chemistry, 2018, 57, 12489-12500.	1.9	15
37391	Tailoring the Electronic Structure and Chemical Activity of Iron via Confining into Two-Dimensional Materials. Journal of Physical Chemistry C, 2018, 122, 24037-24045.	1.5	5
37392	Systematic analysis of electron energy-loss near-edge structures in Li-ion battery materials. Physical Chemistry Chemical Physics, 2018, 20, 25052-25061.	1.3	18
37393	Transition metal modification and carbon vacancy promoted Cr₂CO₂ (MXenes): a new opportunity for a highly active catalyst for the hydrogen evolution reaction. Journal of Materials Chemistry A, 2018, 6, 20956-20965.	5.2	74
37394	Elastic properties of single crystal hydrogen sulfide: A Brillouin scattering study under high pressure-temperature. Journal of Applied Physics, 2018, 124, 125901.	1.1	2
37395	Subsurface reconstruction and saturation of surface bonds. Science Bulletin, 2018, 63, 1570-1575.	4.3	16
37396	From Transition Metals to Lanthanides to Actinides: Metal-Mediated Tuning of Electronic Properties of Isostructural Metalâ€“Organic Frameworks. Inorganic Chemistry, 2018, 57, 13246-13251.	1.9	80
37397	Engineering Defect Transition-Levels through the van der Waals Heterostructure. Journal of Physical Chemistry C, 2018, 122, 24475-24480.	1.5	27

#	Article	IF	Citations
37398	Polarity Control within One Monolayer at ZnO/GaN Heterointerface: (0001) Plane Inversion Domain Boundary. ACS Applied Materials & Interfaces, 2018, 10, 37651-37660.	4.0	5
37399	Exceptional catalytic effects of black phosphorus quantum dots in shuttling-free lithium sulfur batteries. Nature Communications, 2018, 9, 4164.	5.8	304
37400	Robust ferromagnetism in hydrogenated graphene mediated by spin-polarized pseudospin. Scientific Reports, 2018, 8, 13940.	1.6	5
37401	CO₂ neutral fuels. EPJ Web of Conferences, 2018, 189, 00010.	0.1	14
37402	Theoretical investigation of the Ag filament morphology in conductive bridge random access memories. Journal of Applied Physics, 2018, 124, .	1.1	17
37403	Communication: First-principles evaluation of alkali ion adsorption and ion exchange in pure silica LTA zeolite. Journal of Chemical Physics, 2018, 149, 131102.	1.2	9
37404	Epitaxy of <mml:math xmlns:mml="http://www.w3.org/1998/Math/MathML" display="inline" overflow="scroll"><mml:mo stretchy="false">(</mml:mo><mml:mi>Ga</mml:mi><mml:mrow><mml:mrow><mml:mi) Tj ETQq0 0 0 rgBT /Overlock 10 Tf 50 507 Td (		

#	Article	IF	Citations
37416	Organicâ€“Organic Hybrid g-C₃N₄/Ethanediamine Nanosheets for Photocatalytic H₂ Evolution. Journal of Physical Chemistry C, 2018, 122, 24725-24731.	1.5	15
37417	Effect of Interface Structure on the Mechanical Properties of Graphene Nanosheets Reinforced Copper Matrix Composites. ACS Applied Materials & Interfaces, 2018, 10, 37586-37601.	4.0	99
37418	Computation-Aided Design of Single-Atom Catalysts for One-Pot CO₂ Capture, Activation, and Conversion. ACS Applied Materials & Interfaces, 2018, 10, 36866-36872.	4.0	70
37419	Carbon Excess C₃N: A Potential Candidate as Li-Ion Battery Material. ACS Applied Materials & Interfaces, 2018, 10, 37135-37141.	4.0	44
37420	Low threshold and efficient multiple exciton generation in halide perovskite nanocrystals. Nature Communications, 2018, 9, 4197.	5.8	110
37421	Low-temperature anomalies in disordered solids: a cold case of contested relics?. Advances in Physics: X, 2018, 3, 1510296.	1.5	9
37422	First principles global optimization of metal clusters and nanoalloys. Advances in Physics: X, 2018, 3, S100009.	1.5	23
37423	Mechanical and Dynamic Stability of Complete and Nonstoichiometric 3C-SixCy from Ab Initio Calculations. Physics of the Solid State, 2018, 60, 2012-2018.	0.2	0
37424	Computational prediction of two-dimensional monolayer B₆C₂P₂ by the global optimization method. Modern Physics Letters B, 2018, 32, 1850370.	1.0	3
37425	Probing the Physical Origin of Anisotropic Thermal Transport in Black Phosphorus Nanoribbons. Advanced Materials, 2018, 30, e1804928.	11.1	50
37426	High-Throughput Identification of Electrides from All Known Inorganic Materials. Chemistry of Materials, 2018, 30, 7521-7526.	3.2	63
37427	Computational Insights into Morphology and Interface of Zeolite Catalysts: a Case Study of K-LTL Zeolite with Different Si/Al Ratios. Journal of Physical Chemistry C, 2018, 122, 24843-24850.	1.5	3
37428	Two-Dimensional WS₂@Nitrogen-Doped Graphite for High-Performance Lithium Ion Batteries: Experiments and Molecular Dynamics Simulations. ACS Applied Materials & Interfaces, 2018, 10, 37928-37936.	4.0	28
37429	Activity Trend for Low-Concentration NO Oxidation at Room Temperature on Rutile-Type Metal Oxides. ACS Catalysis, 2018, 8, 10864-10870.	5.5	26
37430	Emissions at Perovskite Quantum Dot/Film Interface with Halide Anion Exchange. ACS Photonics, 2018, 5, 4504-4512.	3.2	17
37431	Activation of the Basal Plane in Two Dimensional Transition Metal Chalcogenide Nanostructures. Journal of the American Chemical Society, 2018, 140, 13663-13671.	6.6	38
37432	Investigation of structural and magnetic properties of Fe-Rh-(Z) (Z = Co, Pt) alloys by first principles method. EPJ Web of Conferences, 2018, 185, 05005.	0.1	1
37433	Intrinsic Defect Properties in Halide Double Perovskites for Optoelectronic Applications. Physical Review Applied, 2018, 10, .	1.5	109

#	Article	IF	Citations
37434	Structural, electronic, vibrational, and elastic properties of graphene/ <mml:math xmlns:mml="http://www.w3.org/1998/Math/MathML"><mml:msub><mml:mi>MoS</mml:mi><mml:mn>2</mml:mn></mml:msub></mml bilayer heterostructures. Physical Review B, 2018, 98, .	3.7	82
37435	First principles phase diagram calculation for the 2D TMD system WS2â^'WTe2. Calphad: Computer Coupling of Phase Diagrams and Thermochemistry, 2018, 63, 142-147.	0.7	3
37436	The influence of a chloride-based supporting electrolyte on electrodeposited zinc in zinc/bromine flow batteries. Electrochimica Acta, 2018, 292, 903-913.	2.6	9
37437	Role of lattice oxygen content and Ni geometry in the oxygen evolution activity of the Ba-Ni-O system. Journal of Power Sources, 2018, 404, 56-63.	4.0	15
37438	Layer-Dependent Rashba Band Splitting in 2D Hybrid Perovskites. Chemistry of Materials, 2018, 30, 8538-8545.	3.2	92
37439	Isomerization of N2O4in Solid N2H4and Its Implication for the Explosion of N2O4â€“N2H4Solid Mixtures. Journal of Physical Chemistry C, 2018, 122, 23501-23505.	1.5	8
37440	Hybrid Density-Functional Theory Calculations of Electronic and Optical Properties of Mercaptocarboxylic Acids on ZnO(101Ì…0) Surfaces. Journal of Physical Chemistry C, 2018, 122, 24838-24842.	1.5	3
37441	Adsorption of CO₂ on Heterostructures of Bi₂O₃ Nanocluster-Modified TiO₂ and the Role of Reduction in Promoting CO₂ Activation. ACS Omega, 2018, 3, 13117-13128.	1.6	20
37442	Electrocatalytic Study of the Oxygen Reduction Reaction at Gold Nanoparticles in the Absence and Presence of Interactions with SnO_x Supports. Journal of the American Chemical Society, 2018, 140, 13775-13785.	6.6	42
37443	Single-Crystal Electrochemistry Reveals Why Metal Nanowires Grow. Journal of the American Chemical Society, 2018, 140, 14740-14746.	6.6	76
37444	Synthesis of Pure NiTiSn by Mechanical Alloying: An Investigation of the Optimal Experimental Conditions Supported by First Principles Calculations. Metals, 2018, 8, 835.	1.0	8
37445	A density functional theory study of reactions of relevance to catalytic hydrocarbon synthesis and combustion. Theoretical Chemistry Accounts, 2018, 137, 1.	0.5	3
37446	Control of Charge Recombination in Perovskites by Oxidation State of Halide Vacancy. Journal of the American Chemical Society, 2018, 140, 15753-15763.	6.6	129
37447	The Shape of Native Plant Cellulose Microfibrils. Scientific Reports, 2018, 8, 13983.	1.6	86
37448	Complex Low Energy Tetrahedral Polymorphs of Group IV Elements from First Principles. Physical Review Letters, 2018, 121, 175701.	2.9	95
37449	Ab Initio Modeling of the Local Violation of a Peierls Transition at the Sb(111) Surface. JETP Letters, 2018, 107, 780-784.	0.4	2
37450	First-Principles Determination of Active Sites of Ni Metal-Based Electrocatalysts for Hydrogen Evolution Reaction. ACS Applied Materials & Interfaces, 2018, 10, 39624-39630.	4.0	41
37451	Breaking the scaling relationship via thermally stable Pt/Cu single atom alloys for catalytic dehydrogenation. Nature Communications, 2018, 9, 4454.	5.8	451

#	Article	IF	Citations
37452	Atomistic insights toward strengthening of GeTe phase change material by impurity doping and grain boundary engineering. Journal of Applied Physics, 2018, 124, .	1.1	3
37453	Optical vs electronic gap of hafnia by ab initio Bethe-Salpeter equation. Applied Physics Letters, 2018, 113, .	1.5	13
37454	Tunability of vortex-like patterns on 180^o domain walls in ferroelectric PbTiO₃. Philosophical Magazine Letters, 2018, 98, 266-271.	0.5	1
37455	First-principles investigation of activity and solubility of Si in Mo solid solution. International Journal of Modern Physics B, 2018, 32, 1850305.	1.0	4
37456	Pressure effect on the mechanical and electronic properties of orthorhombic-C20. Modern Physics Letters B, 2018, 32, 1850380.	1.0	1
37457	Cyclodextrin-assisted low-metal Ni-Pd/Al2O3 bimetallic catalysts for the direct amination of aliphatic alcohols. Journal of Catalysis, 2018, 368, 172-189.	3.1	23
37458	Evidence of Ferrimagnetism in Fe-Doped CdSe Quantum Dots. Chemistry of Materials, 2018, 30, 8446-8456.	3.2	11
37459	Finite Temperature Coupled Cluster Theories for Extended Systems. Journal of Chemical Theory and Computation, 2018, 14, 6505-6514.	2.3	26
37460	Impact of iodine antisite (IPb) defects on the electronic properties of the (110) CH3NH3PbI3 surface. Journal of Chemical Physics, 2018, 149, 164704.	1.2	17
37461	A First Principles Study on the Electronic, Optical and Hole Effective Mass Properties of Mg-Doped CuAlO2 and AgAlO2. MRS Advances, 2018, 3, 3315-3321.	0.5	4
37462	Ultimate Control over Hydrogen Bond Formation and Reaction Rates for Scalable Synthesis of Highly Crystalline vdW MOF Nanosheets with Large Aspect Ratio. Advanced Materials, 2018, 30, e1802497.	11.1	30
37463	Transition state optimization of periodic systems using delocalized internal coordinates. Theoretical Chemistry Accounts, 2018, 137, 1.	0.5	12
37464	KAgSe: A New Two-Dimensional Efficient Photovoltaic Material with Layer-Independent Behaviors. ACS Applied Materials & Interfaces, 2018, 10, 41670-41677.	4.0	41
37465	A Coupled Density Functional Theoryâ€“Microkinetic Modeling for the Hydrodeoxygenation of Glycerol to Propylene on MoO₃. ACS Sustainable Chemistry and Engineering, 2018, 6, 16169-16178.	3.2	15
37466	Alleviating oxygen evolution from Li-excess oxide materials through theory-guided surface protection. Nature Communications, 2018, 9, 4597.	5.8	56
37467	Perpendicular magnetic anisotropy in bulk and thin-film CuMnAs for antiferromagnetic memory applications. Applied Physics Letters, 2018, 113, .	1.5	5
37468	High-pressure spectroscopic investigation of multiferroic <mml:math xmlns:mml="http://www.w3.org/1998/Math/MathML"><mml:mrow><mml:msub><mml:mi>Ni</mml:mi><mml:mn>3</mml:mn></mml:r Physical Review B, 2018, 98, .	1.1	4
37469	Numerical investigation for lithium isotope effect in ionic superconductor. Fusion Engineering and Design, 2018, 136, 205-209.	1.0	8

#	Article	IF	Citations
37470	Heat capacity of Mg3Sb2, Mg3Bi2, and their alloys at high temperature. Materials Today Physics, 2018, 6, 83-88.	2.9	87
37471	Mutual interactions in a ternary protein/bioprotectant/water system. Vibrational Spectroscopy, 2018, 99, 190-195.	1.2	1
37472	Record-Low and Anisotropic Thermal Conductivity of a Quasi-One-Dimensional Bulk ZrTe₅ Single Crystal. ACS Applied Materials & Interfaces, 2018, 10, 40740-40747.	4.0	33
37473	Defect properties of Na and K in Cu2ZnSnS4 from hybrid functional calculation. Journal of Applied Physics, 2018, 124, 165701.	1.1	14
37474	First-principles study on charged vacancies in MoS₂. Japanese Journal of Applied Physics, 2018, 57, 125202.	0.8	4
37475	Benchmarking the performance of plane-wave vs. localized orbital basis set methods in DFT modeling of metal surface: a case study for Fe-(110). Journal of Computational Science, 2018, 29, 163-167.	1.5	9
37476	Uncovering a Stable Phase in Group V Transition-metal Dinitride (MN₂, M = Ta, Nb, V) Nanosheets and Their Electronic Properties via First-principles Investigations. Journal of Physical Chemistry C, 2018, 122, 26748-26755.	1.5	32
37477	Density-Functional and Tight-Binding Theory of Silicene and Silicane. Nanoscience and Technology, 2018, , 23-41.	1.5	0
37478	New Quadratic Self-Assembly of Double-Decker Phthalocyanine on Gold(111) Surface: From Macroscopic to Microscopic Scale. Journal of Physical Chemistry C, 2018, 122, 26480-26488.	1.5	6
37479	To Be or Not To Be Protonated: cyclo-N₅^{â€“} in Crystal and Solvent. Journal of Physical Chemistry Letters, 2018, 9, 7137-7145.	2.1	12
37480	Wafer-Scale Fabrication of Two-Dimensional PtS₂/PtSe₂ Heterojunctions for Efficient and Broad band Photodetection. ACS Applied Materials & Interfaces, 2018, 10, 40614-40622.	4.0	110
37481	Controlling reaction pathways of selective Câ€“O bond cleavage of glycerol. Nature Communications, 2018, 9, 4612.	5.8	54
37482	Epitaxial growth of ultraflat stanene with topological band inversion. Nature Materials, 2018, 17, 1081-1086.	13.3	267
37483	Ferroelectrically tunable magnetic skyrmions in ultrathin oxide heterostructures. Nature Materials, 2018, 17, 1087-1094.	13.3	265
37484	Properties of Novel Non-Silicon Materials for Photovoltaic Applications: A First-Principle Insight. Materials, 2018, 11, 2006.	1.3	11
37485	Pressure Effect on Elastic Constants and Related Properties of Ti3Al Intermetallic Compound: A First-Principles Study. Materials, 2018, 11, 2015.	1.3	46
37486	First-Principles Calculations on Structural Property and Anisotropic Elasticity of Î³1-Ti4Nb3Al9 under Pressure. Materials, 2018, 11, 2025.	1.3	2
37487	Predicting the strain-mediated topological phase transition in 3D cubic ThTaN₃. Beilstein Journal of Nanotechnology, 2018, 9, 1399-1404.	1.5	2

#	Article	IF	Citations
37488	Electronic Structure of Polymer Dielectrics: The Role of Chemical and Morphological Complexity. Chemistry of Materials, 2018, 30, 7699-7706.	3.2	26
37489	Graphene Oxide-Supported Transition Metal Catalysts for Di-Nitrogen Reduction. Journal of Physical Chemistry C, 2018, 122, 25441-25446.	1.5	24
37490	Linear Alkane Polymerization on Au-Covered Ag(110) Surfaces. Journal of Physical Chemistry C, 2018, 122, 24209-24214.	1.5	7
37491	Alkali Metal Cation Effects in Structuring Pt, Rh, and Au Surfaces through Cathodic Corrosion. ACS Applied Materials & Interfaces, 2018, 10, 39363-39379.	4.0	50
37492	Obtaining Intrinsically Occupied Free-Space Superatom States in an Encapsulated Ca2N Nanotube. ACS Omega, 2018, 3, 11966-11971.	1.6	3
37493	Hybrid Improper Ferroelectricity in (Sr,Ca)₃Sn₂O₇ and Beyond: Universal Relationship between Ferroelectric Transition Temperature and Tolerance Factor in n = 2 Ruddlesdenâ€“Popper Phases. Journal of the American Chemical Society, 2018, 140, 15690-15700.	6.6	74
37494	Band gap tuning of layered III-Te materials. Journal of Applied Physics, 2018, 124, .	1.1	7
37495	Adsorption and diffusion of F 2 molecules on pristine graphene. Chinese Physics B, 2018, 27, 106801.	0.7	6
37496	Mixing A -type and G -type B -site antiferromagnetism in AMn1â^'xFexO3(A=La,Nd). Physical Review B, 2018, 98, .	1.1	3
37497	The role of coâ€dopants on the luminescent properties of Îµâ€Al₂O₃:Mn⁴⁺ and BaMgAl₁₀O₁₇:Mn⁴⁺. Journal of the American Ceramic Society, 2019, 102, 2737-2744.	1.9	22
37498	Synergistic Effect of Doping and Compositing on Photocatalytic Efficiency: A Case Study of La₂Ti₂O₇. ACS Applied Materials & Interfaces, 2018, 10, 39327-39335.	4.0	17
37499	Studies on Catalytic Activity of Hydrogen Peroxide Generation according to Au Shell Thickness of Pd/Au Nanocubes. ACS Applied Materials & Interfaces, 2018, 10, 38109-38116.	4.0	32
37500	Rhombohedralâ€“Orthorhombic Ferroelectric Morphotropic Phase Boundary Associated with a Polar Vortex in BiFeO₃ Films. ACS Nano, 2018, 12, 11098-11105.	7.3	57
37501	Sesame-style decomposition of KS-DFT molecular dynamics for direct interrogation of nuclear models. AIP Conference Proceedings, 2018, , .	0.3	1
37502	Photoluminescence, infrared, and Raman spectra of co-doped Si nanoparticles from first principles. Journal of Chemical Physics, 2018, 149, 154702.	1.2	6
37503	Stability and electronic properties of planar defects in quaternary I2-II-IV-VI4 semiconductors. Journal of Applied Physics, 2018, 124, 165705.	1.1	5
37504	Theoretical Investigation of Surface Oxidation of NiO/Au Core-Shell Catalyst. E-Journal of Surface Science and Nanotechnology, 2018, 16, 242-246.	0.1	5
37505	Mechanical and Thermal Conductivity Properties of Enhanced Phases in Mg-Zn-Zr System from First Principles. Materials, 2018, 11, 2010.	1.3	8

#	Article	IF	Citations
37506	KCrS₂ Cathode with Considerable Cyclability and High Rate Performance: The First K⁺ Stoichiometric Layered Compound for Potassiumâ€ion Batteries. Small, 2018, 14, e1803495.	5.2	33
37507	Synthetic routes, structure and catalytic activity of Ag/BN nanoparticle hybrids toward CO oxidation reaction. Journal of Catalysis, 2018, 368, 217-227.	3.1	18
37508	New Theoretical Strategy for the Correlation of Oxygen Evolution Performance and Metal Catalysts Adsorption at BiVO₄ Surfaces. Journal of Physical Chemistry C, 2018, 122, 25195-25203.	1.5	10
37509	Screening and Design of Novel 2D Ferromagnetic Materials with High Curie Temperature above Room Temperature. ACS Applied Materials & Interfaces, 2018, 10, 39032-39039.	4.0	167
37510	Enhancing the Photocatalytic Performance of MXenes via Stoichiometry Engineering of Their Electronic and Optical Properties. ACS Applied Materials & Interfaces, 2018, 10, 39879-39889.	4.0	37
37511	Synthesis, Crystal Structure, UVâ€“Vis Adsorption Properties, Photoelectric Behavior, and DFT Computational Study of All-Inorganic and Lead-Free Copper Halide Salt K₂Cu₂Cl₆. ACS Omega, 2018, 3, 14021-14026.	1.6	17
37512	Testing topological protection of edge states in hexagonal quantum spin Hall candidate materials. Physical Review B, 2018, 98, .	1.1	32
37513	Theoretical confirmation of the polaron model for the Mg acceptor in Î²-Ga2O3. Journal of Applied Physics, 2018, 124, .	1.1	34
37514	Brittle failure of orthorhombic borides from first-principles simulations. Physical Review B, 2018, 98, .	1.1	0
37515	Synthesis of Ni2H3 at high temperatures and pressures. Physical Review B, 2018, 98, .	1.1	14
37516	Superconductivity of Bi-III phase of elemental bismuth: Insights from muon-spin rotation and density functional theory. Physical Review B, 2018, 98, .	1.1	12
37517	Emphanitic anharmonicity in PbSe at high temperature and anomalous electronic properties in the PbQ(Q=S,Se,Te) system. Physical Review B, 2018, 98, .	1.1	23
37518	Uranium polyhydrides at moderate pressures: Prediction, synthesis, and expected superconductivity. Science Advances, 2018, 4, eaat9776.	4.7	82
37520	Insight into the catalytic activity of MXenes for hydrogen evolution reaction. Science Bulletin, 2018, 63, 1397-1403.	4.3	61
37521	First-principles identification of spinel CaCo2O4 as a promising cathode material for Ca-ion batteries. Solid State Ionics, 2018, 326, 145-149.	1.3	13
37522	Phase Evolution and Degradation Modes of R3Ì…m Li_xNi_{1â€“yâ€“z}Co_yAl_zO₂ Electrodes Cycled Near Complete Delithiation. Chemistry of Materials, 2018, 30, 7545-7574.	8.2	30
37523	Insight into the Solvation Structure of Tetraglyme-Based Electrolytes via First-Principles Molecular Dynamics Simulation. Journal of Physical Chemistry B, 2018, 122, 10014-10022.	1.2	12
37524	Lithium Intercalation in Grapheneâ€“MoS₂ Heterostructures. Journal of Physical Chemistry C, 2018, 122, 24535-24541.	1.5	41

#	Article	IF	Citations
37525	Characterization of Mechanical Degradation in Perfluoropolyether Film for Its Application to Antifingerprint Coatings. ACS Applied Materials & Interfaces, 2018, 10, 37498-37506.	4.0	12
37526	A novel class of oxynitrides stabilized by nitrogen dimer formation. Scientific Reports, 2018, 8, 14471.	1.6	6
37527	Water desorption from rapidly-heated metal oxide surfacesâ€"first principles, molecular dynamics, and the Temkin isotherm. Journal of Physics Condensed Matter, 2018, 30, 465002.	0.7	16
37528	Nearly triple nodal point topological phase in half-metallic GdN. Physical Review B, 2018, 98, .	1.1	17
37529	Hybrid density functional study on the electronic structures and properties of P3HTâ€PbS and P3HTâ€CdS hybrid interface for photovoltaic applications. Journal of Computational Chemistry, 2018, 39, 1990-1999.	1.5	1
37530	Investigation of Conductivity and Ionic Transport of VO₂(M) and VO₂(R) via Electrochemical Study. Chemistry of Materials, 2018, 30, 7535-7544.	3.2	5
37531	Energetics of Lithium Insertion into Magnetite, Defective Magnetite, and Maghemite. Chemistry of Materials, 2018, 30, 7922-7937.	3.2	26
37532	Monolayer to Bulk Properties of Hexagonal Boron Nitride. Journal of Physical Chemistry C, 2018, 122, 25524-25529.	1.5	134
37533	High-Throughput Screening and Automated Processing toward Novel Topological Insulators. Journal of Physical Chemistry Letters, 2018, 9, 6224-6231.	2.1	24
37534	Stable GaSe-Like Phosphorus Carbide Monolayer with Tunable Electronic and Optical Properties from Ab Initio Calculations. Materials, 2018, 11, 1937.	1.3	13
37535	An Unusual Red Carbon Nitride to Boost the Photoelectrochemical Performance of Wide Bandgap Photoanodes. Advanced Functional Materials, 2018, 28, 1805698.	7.8	94
37536	Surface Tuning of Solid Oxide Fuel Cell Cathode by Atomic Layer Deposition. Advanced Energy Materials, 2018, 8, 1802506.	10.2	48
37537	Hollow Bimetallic Zinc Cobalt Phosphosulfides for Efficient Overall Water Splitting. Chemistry - A European Journal, 2019, 25, 621-626.	1.7	29
37538	Bonding Hierarchy Gives Rise to High Thermoelectric Performance in Layered Zintl Compound BaAu2P4. Chemistry of Materials, 2018, 30, 7760-7768.	3.2	28
37539	Tuning On-Surface Synthesis of Graphene Nanoribbons by Noncovalent Intermolecular Interactions. Journal of Physical Chemistry C, 2018, 122, 24415-24420.	1.5	6
37540	Changes in Catalytic and Adsorptive Properties of 2 nm Pt₃Mn Nanoparticles by Subsurface Atoms. Journal of the American Chemical Society, 2018, 140, 14870-14877.	6.6	121
37541	Solvent Tunes the Selectivity of Hydrogenation Reaction over Î±-MoC Catalyst. Journal of the American Chemical Society, 2018, 140, 14481-14489.	6.6	167
37542	Phase-selective synthesis of 1Tâ€² MoS2 monolayers and heterophase bilayers. Nature Materials, 2018, 17, 1108-1114.	13.3	348

#	Article	IF	Citations
37543	Water oxidation on a mononuclear manganese heterogeneous catalyst. Nature Catalysis, 2018, 1, 870-877.	16.1	244
37544	Interface properties and built-in potential profile of a <mml:math xmlns:mml="http://www.w3.org/1998/Math/MathML"><mml:mrow><mml:mrow><mml:mspace width="4pt" /><mml:mi>LaCr</mml:mi></mml:mrow><mml:msub><mml:mi mathvariant="normal">O</mml:mi><mml:mn>3</mml:mn></mml:msub><mml:mo>/</mml:mo><mml:mi>SrTi</mml:mi><mml:msub><mml:mi mathvariant="normal">O</mml:mi><mml:mn>3</mml:mn></mml:msub></mml:mrow></mml:math> superlattice determined by standing-wave excited photoemission spectroscopy. Physical Review B, 2018,	1.1	22
37545	Impact of Intergrain Spin-Transfer Torques Due to Huge Thermal Gradients in Heat-Assisted Magnetic Recording. IEEE Transactions on Magnetics, 2018, 54, 1-11.	1.2	11
37546	On the Structure of Ultrathin FeO Films on Ag(111). Nanomaterials, 2018, 8, 828.	1.9	9
37547	Electronic Structure and Transport Properties of La₂Zr₂O₇ Pyrochlore from First Principles. Solid State Phenomena, 0, 281, 767-773.	0.3	3
37548	Mesoscale modeling of irradiation damage evolution in bcc iron and vanadium: A comparative study. Fusion Engineering and Design, 2018, 137, 303-311.	1.0	8
37549	Effect of Curvature on the Hydrogen Evolution Reaction of Graphene. Journal of Physical Chemistry C, 2018, 122, 25331-25338.	1.5	33
37550	Unusual Electronic and Optical Properties of Two-Dimensional Ga₂O₃ Predicted by Density Functional Theory. Journal of Physical Chemistry C, 2018, 122, 24592-24599.	1.5	58
37551	Rutile Alloys in the Mnâ€“Sbâ€“O System Stabilize Mn³⁺ To Enable Oxygen Evolution in Strong Acid. ACS Catalysis, 2018, 8, 10938-10948.	5.5	97
37552	Superconductivity at 3.5 K and/or 7.2 K in potassium-doped triphenylbismuth. Journal of Chemical Physics, 2018, 149, 144502.	1.2	16
37553	Parity-breaking in single-element phases: ferroelectric-like elemental polar metals. Journal of Physics Condensed Matter, 2018, 30, 415504.	0.7	5
37554	Anomalous pressure effect on the thermal conductivity of ZnO, GaN, and AlN from first-principles calculations. Physical Review B, 2018, 98, .	1.1	42
37555	Interplay of alternation and further neighbor interaction in S=12 spin chains: A case study of Cs2CuAl4O8. Physical Review B, 2018, 98, .	1.1	5
37556	Relative energies and electronic structures of CoO polymorphs through ab initio diffusion quantum Monte Carlo. Physical Review B, 2018, 98, .	1.1	18
37557	Grain-Boundary Shear-Migration Coupling in Al Bicrystals. Atomistic Modeling. Physics of the Solid State, 2018, 60, 1916-1923.	0.2	5
37558	Effect of a Rare-Earth Ion on the Structural Instability in RFe3(BO3)4 Crystals. JETP Letters, 2018, 108, 116-120.	0.4	3
37559	Physical Properties and Photovoltaic Application of Semiconducting Pd2Se3 Monolayer. Nanomaterials, 2018, 8, 832.	1.9	16
37560	Carbon Nitride Nanofibres with Exceptional Lithium Storage Capacity: From Theoretical Prediction to Experimental Implementation. Advanced Functional Materials, 2018, 28, 1803972.	7.8	77

#	Article	IF	Citations
37561	First-principles study of dissociation processes of O2 molecular on the Al (111) surface. Current Applied Physics, 2018, 18, 1528-1533.	1.1	7
37562	Investigation on structural, electronic, optical and elastic properties of thallium phosphide and gallium phosphide binary compounds and their ternary alloys and superlattices. Computational Condensed Matter, 2018, 17, e00344.	0.9	7
37563	In-situ growth of metallic nanoparticles on perovskite parent as a hydrogen electrode for solid oxide cells. Journal of Power Sources, 2018, 405, 114-123.	4.0	45
37564	Bariumâ€"Nitrogen Phases Under Pressure: Emergence of Structural Diversity and Nitrogen-Rich Compounds. Chemistry of Materials, 2018, 30, 7623-7636.	3.2	70
37565	Quantifying Support Interactions and Reactivity Trends of Single Metal Atom Catalysts over TiO₂. Journal of Physical Chemistry C, 2018, 122, 25274-25289.	1.5	31
37566	Enhancing Visible Light Absorption for Ferroelectric Sn₂P₂S₆ by Se Anion Substitution. Journal of Physical Chemistry C, 2018, 122, 25565-25572.	1.5	7
37567	Significantly Enhanced Emission Stability of CsPbBr₃ Nanocrystals via Chemically Induced Fusion Growth for Optoelectronic Devices. ACS Applied Nano Materials, 2018, 1, 6091-6098.	2.4	42
37568	Ligand-Capped Ru Nanoparticles as Efficient Electrocatalyst for the Hydrogen Evolution Reaction. ACS Catalysis, 2018, 8, 11094-11102.	5.5	70
37569	Tunable Ultrafast Nonlinear Optical Properties of Graphene/MoS₂ van der Waals Heterostructures and Their Application in Solid-State Bulk Lasers. ACS Nano, 2018, 12, 11376-11385.	7.3	113
37570	Effects of annealing with CO and CO2 molecules on oxygen vacancy defect density in amorphous SiO2 formed by thermal oxidation of SiC. Journal of Applied Physics, 2018, 124, 135701.	1.1	8
37571	Structural stability and electro-elastic property of YCOB crystal annealed in harsh environment. Applied Physics Letters, 2018, 113, .	1.5	15
37572	Structural and electronic properties of wurtzite, zincblende and rocksalt Al1â€‰â^'â€‰xInxN ternary alloys at ambient and high pressure. Phase Transitions, 2018, 91, 1232-1245.	0.6	1
37573	Ab initio calculations of carbon and boron nitride allotropes and their structural phase transitions using periodic coupled cluster theory. Physical Review B, 2018, 98, .	1.1	28
37574	Accuracy of the Heyd-Scuseria-Ernzerhof hybrid functional to describe many-electron interactions and charge localization in semiconductors. Physical Review B, 2018, 98, .	1.1	13
37575	Ultrathin Ti₂Nb₂O₉ Nanosheets with Pseudocapacitive Properties as Superior Anode for Sodiumâ€Ion Batteries. Advanced Materials, 2018, 30, e1804378.	11.1	117
37576	Nanoarchitectured Grapheneâ€Organic Frameworks (GOFs): Synthetic Strategies, Properties, and Applications. Chemistry - an Asian Journal, 2018, 13, 3561-3574.	1.7	56
37577	Prevalence of trans-Alkenes in Hydrogenation Processes on Metal Surfaces: A Density Functional Theory Study. Journal of Physical Chemistry C, 2018, 122, 25339-25348.	1.5	4
37578	How Does the Flexibility of Molecules Affect the Performance of Molecular Rotors?. Journal of Physical Chemistry C, 2018, 122, 25067-25074.	1.5	15

#	Article	IF	Citations
37579	Possible High-T_C Layered Ferromagnetic Insulator Sr₂NiRuO₄: An Ab Initio Study. Journal of Physical Chemistry C, 2018, 122, 25589-25594.	1.5	2
37580	Ultrathin Bismuth Film on High-Temperature Cuprate Superconductor Bi2Sr2CaCu2O8+Î´ as a Candidate of a Topological Superconductor. ACS Nano, 2018, 12, 10977-10983.	7.3	15
37581	CHD3 dissociation on Pt(111): A comparison of the reaction dynamics based on the PBE functional and on a specific reaction parameter functional. Journal of Chemical Physics, 2018, 149, 044701.	1.2	16
37582	Total dose effect of Al₂O₃-based metalâ€“oxideâ€“semiconductor structures and its mechanism under gamma-ray irradiation. Semiconductor Science and Technology, 2018, 33, 115010.	1.0	13
37583	Photoactivity and Stability Coâ€Enhancement: When Localized Plasmons Meet Oxygen Vacancies in MgO. Small, 2018, 14, e1803233.	5.2	28
37584	Dynamic Field Modulation of the Octahedral Framework in Metal Oxide Heterostructures. Advanced Materials, 2018, 30, e1804775.	11.1	13
37585	Charge Density Waves Driven by Peierls Instability at the Interface of Twoâ€Dimensional Lateral Heterostructures. Small, 2018, 14, e1803040.	5.2	2
37586	Discerning Chemical Pressure amidst Weak Potentials: Vibrational Modes and Dumbbell/Atom Substitution in Intermetallic Aluminides. Journal of Physical Chemistry A, 2018, 122, 8412-8426.	1.1	31
37587	Ice Nucleation on a Corrugated Surface. Journal of the American Chemical Society, 2018, 140, 15804-15811.	6.6	30
37588	A robust fuel cell operated on nearly dry methane at 500 Â°C enabled by synergistic thermal catalysis and electrocatalysis. Nature Energy, 2018, 3, 1042-1050.	19.8	230
37589	Detection of catalytic intermediates at an electrode surface during carbon dioxide reduction by an earth-abundant catalyst. Nature Catalysis, 2018, 1, 952-959.	16.1	59
37590	Behaviors of Ce, Pr, and Nd in liquid cesium by ab initio molecular dynamics simulations. Journal of Applied Physics, 2018, 124, 135102.	1.1	2
37591	The interaction of ethylene with free gold cluster cations: infrared photodissociation spectroscopy combined with electronic and vibrational structure calculations. Journal of Physics Condensed Matter, 2018, 30, 504001.	0.7	12
37592	Magnetoelectric multipoles in metals. Philosophical Transactions Series A, Mathematical, Physical, and Engineering Sciences, 2018, 376, 20170450.	1.6	33
37593	Sr3Ir2O7F2 : Topochemical conversion of a relativistic Mott state into a spin-orbit driven band insulator. Physical Review B, 2018, 98, .	1.1	3
37594	Beyond the quasiparticle approximation: Fully self-consistent <mml:math xmlns:mml="http://www.w3.org/1998/Math/MathML"><mml:mrow><mml:mi>G</mml:mi><mml:mi>W</mml:mi></mml:mrow></mml:m calculations. Physical Review B, 2018, 98, .	1.1	56
37595	Strong coupling and periodic potential at the Pb/Sb(111) interface. Physical Review B, 2018, 98, .	1.1	2
37596	Hydrogenation-driven formation of local magnetic moments in <mml:math xmlns:mml="http://www.w3.org/1998/Math/MathML"><mml:mrow><mml:msub><mml:mi>FeO</mml:mi><mml:mn>2</mml:mn></ mathvariant="normal">H</mml:mi><mml:mi>x</mml:mi></mml:msub></mml:mrow></mml:math>. Physical Review B, 2018, 98, .	1.1	11

#	Article	IF	Citations
37597	Theoretical paradigm for the quantum spin Hall effect at high temperatures. Physical Review B, 2018, 98, .	1.1	55
37598	Extended X-Ray Absorption Fine Structure of ZrW2O8: Theory vs. Experiment. Frontiers in Chemistry, 2018, 6, 356.	1.8	8
37599	Electronic Detection of Oxygen Adsorption and Sizeâ€Specific Doping of Fewâ€Atom Gold Clusters on Graphene. Advanced Materials Interfaces, 2018, 5, 1801274.	1.9	11
37600	Epitaxial Synthesis of Blue Phosphorene. Small, 2018, 14, e1804066.	5.2	114
37601	Using Ion-Beam-Assisted Deposition and Ion Implantation for the Rational Control of Nanomagnetism in Thin Film and Nanostructured Systems. Solid State Physics, 2018, 69, 1-45.	1.3	8
37602	Elasticity, lattice dynamics and ideal strengths of USi3 and U3Si via first principles calculations. Journal of Nuclear Materials, 2018, 512, 407-416.	1.3	7
37603	Inelastic electron tunneling spectroscopy by STM of phonons at solid surfaces and interfaces. Progress in Surface Science, 2018, 93, 131-145.	3.8	8
37604	Assessing High-Throughput Descriptors for Prediction of Transparent Conductors. Chemistry of Materials, 2018, 30, 8375-8389.	3.2	60
37605	Theoretical Insights into Vinyl Derivatives Adsorption on a Cu(100) Surface. Journal of Physical Chemistry C, 2018, 122, 27301-27313.	1.5	6
37606	Direct Observation of Transition from Solid-State to Molecular-Like Optical Properties in Ultrasmall Silicon Carbide Nanoparticles. Journal of Physical Chemistry C, 2018, 122, 26713-26721.	1.5	7
37607	Effect of Water Adsorption on the Interfacial Structure and Band Edge Alignment of Anatase TiO₂(001)/Water by First-Principles Molecular Dynamics. Journal of Physical Chemistry C, 2018, 122, 26965-26973.	1.5	22
37608	Improving the Electrocatalytic Activity and Durability of the La_{0.6}Sr_{0.4}Co_{0.2}Fe_{0.8}O_{3â˜Î´} Cathode by Surface Modification. ACS Applied Materials & Interfaces, 2018, 10, 39785-39793.	4.0	71
37609	Online Kinetics Study of Oxidative Coupling of Methane over La₂O₃ for Methane Activation: What Is Behind the Distinguished Light-off Temperatures?. ACS Catalysis, 2018, 8, 11761-11772.	5.5	60
37610	Chemoselective Lactonization of Renewable Succinic Acid with Heterogeneous Nanoparticle Catalysts. ACS Sustainable Chemistry and Engineering, 2018, 6, 16341-16351.	3.2	10
37611	Tunable magnetic topological insulating phases in monolayer <mml:math xmlns:mml="http://www.w3.org/1998/Math/MathML"><mml:msub><mml:mi mathvariant="normal">CrI</mml:mi><mml:mn>3</mml:mn></mml:msub></mml:math>. Physical Review B, 2018, 98, .	1.1	33
37612	29Si NMR Chemical Shifts in Crystalline and Amorphous Silicon Nitrides. Materials, 2018, 11, 1646.	1.3	7
37613	Synthesis of metastable B2-type Feâ€“Sn alloy epitaxial films and study of their magnetic properties. Japanese Journal of Applied Physics, 2018, 57, 120302.	0.8	9
37614	Generation and transformation of ROS on g-C3N4 for efficient photocatalytic NO removal: A combined in situ DRIFTS and DFT investigation. Chinese Journal of Catalysis, 2018, 39, 1695-1703.	6.9	18

#	Article	IF	Citations
37615	Consequences of Acid Strength and Diffusional Constraints for Alkane Isomerization and Î²-Scission Turnover Rates and Selectivities on Bifunctional Metal-Acid Catalysts. Journal of Physical Chemistry C, 2018, 122, 25475-25497.	1.5	34
37616	Controlling the Electrochemical Properties of Spinel Intercalation Compounds. ACS Applied Energy Materials, 2018, 1, 6833-6839.	2.5	13
37617	Thermoelectric Transport Properties of Cd_xBi_yGe_{1â€“xâ€“y}Te Alloys. ACS Applied Materials & Interfaces, 2018, 10, 39904-39911.	4.0	41
37618	Surface Termination and Composition Control of Activity of the Co_xNi_{1â€“x}Fe₂O₄(001) Surface for Water Oxidation: Insights from DFT+U Calculations. ACS Catalysis, 2018, 8, 11773-11782.	5.5	59
37619	Interfacing nickel nitride and nickel boosts both electrocatalytic hydrogen evolution and oxidation reactions. Nature Communications, 2018, 9, 4531.	5.8	410
37620	Systematic investigation of the deformation mechanisms of a Î³-TiAl single crystal. Scientific Reports, 2018, 8, 15200.	1.6	27
37621	Multiscale in modelling and validation for solar photovoltaics. EPJ Photovoltaics, 2018, 9, 10.	0.8	6
37622	Computational predictions of stable phase for antiperovskite Na3OCl via tilting of Na6O octahedra. Journal of Applied Physics, 2018, 124, .	1.1	13
37623	Ferromagnetism and magnetostructural coupling in V-doped MnNiGe alloys. Chinese Physics B, 2018, 27, 107502.	0.7	5
37624	Lattice expansion and local lattice distortion in Nb- and La-doped <mml:math xmlns:mml="http://www.w3.org/1998/Math/MathML"><mml:mrow><mml:mi>SrTi</mml:mi><mml:msub><mml:mi mathvariant="normal">O</mml:mi><mml:mn>3</mml:mn></mml:msub></mml:mrow></mml:math> single crystals investigated by x-ray diffraction and first-principles calculations. Physical Review B,	1.1	23
37625	Frustrated Structural Instability in Superconducting Quasi-One-Dimensional <mml:math xmlns:mml="http://www.w3.org/1998/Math/MathML" display="inline"><mml:mrow><mml:msub><mml:mrow><mml:mi mathvariant="normal">K</mml:mi></mml:mrow><mml:mrow><mml:mn>2</mml:mn></mml:mrow></mml:msub></mml:mrow><mml:m Physical Review Letters, 2018, 121, 187002.	2.9	16
37626	Generalized Stacking Fault Energies of Aluminum Alloysâ€“Density Functional Theory Calculations. Metals, 2018, 8, 823.	1.0	47
37627	Synthesis of 1,2,3,4â€Tetrazine 1,3â€Dioxides Annulated with 1,3â€‰a,4,6â€‰aâ€Tetraazapentalene Systems. Asian Journal of Organic Chemistry, 2018, 7, 2534-2543.	1.3	18
37628	Strain-Induced Band Structure Modulation in Hexagonal Boron Phosphide/Blue Phosphorene vdW Heterostructure. Journal of Physical Chemistry C, 2018, 122, 26120-26129.	1.5	28
37629	Selective Capture of Phenol from Biofuel Using Protonated Faujasite Zeolites with Different Si/Al Ratios. Journal of Physical Chemistry C, 2018, 122, 26419-26429.	1.5	41
37630	Polaron States in Fullerene Adducts Modeled by Coarse-Grained Molecular Dynamics and Tight Binding. Journal of Physical Chemistry Letters, 2018, 9, 6616-6623.	2.1	10
37631	Lead Vacancy Can Explain the Suppressed Nonradiative Electronâ€“Hole Recombination in FAPbI₃ Perovskite under Iodine-Rich Conditions: A Time-Domain Ab Initio Study. Journal of Physical Chemistry Letters, 2018, 9, 6489-6495.	2.1	29
37632	P3Cl2: A Unique Post-Phosphorene 2D Material with Superior Properties against Oxidation. Journal of Physical Chemistry Letters, 2018, 9, 6568-6575.	2.1	16

#	Article	IF	Citations
37633	Dipolar couplings in solid polypeptides probed by 14N NMR spectroscopy. Communications Chemistry, 2018, 1, .	2.0	10
37634	First-principles prediction of two hexagonal silicon crystals as potential absorbing layer materials for solar-cell application. Journal of Applied Physics, 2018, 124, .	1.1	10
37635	Phase transition and electronic structure evolution of <mml:math xmlns:mml="http://www.w3.org/1998/Math/MathML"><mml:msub><mml:mi>MoTe</mml:mi><mml:mn>2</mml:mn></mml:msub></m induced by W substitution. Physical Review B, 2018, 98, .	1.1	9
37636	Effect of covalent bonding on the superconducting critical temperature of the H-S-Se system. Physical Review B, 2018, 98, .	1.1	54
37637	Ultrafast disordering of vanadium dimers in photoexcited VO ₂. Science, 2018, 362, 572-576.	6.0	159
37638	Paths to Stabilizing Electronically Aberrant Compounds: A Defect-Stabilized Polymorph and Constrained Atomic Motion in PtGa2. Inorganic Chemistry, 2018, 57, 13880-13894.	1.9	7
37639	Design of Efficient Catalysts for CO Oxidation on Titanium Carbide-Supported Platinum via Computational Study. Journal of Physical Chemistry C, 2018, 122, 25974-25982.	1.5	10
37640	Solving the Puzzle of the Coexistence of Different Adsorption Geometries of Graphene on Ni(111). Journal of Physical Chemistry C, 2018, 122, 26105-26110.	1.5	9
37641	Intercalated metalâ€“organic frameworks with high electronic conductivity as negative electrode materials for hybrid capacitors. Communications Chemistry, 2018, 1, .	2.0	22
37642	First-principle electronic properties of dilute-P AlNP deep ultraviolet semiconductor. AIP Advances, 2018, 8, .	0.6	4
37643	Electrical properties and structural transition of Ge2Sb2Te5 adjusted by rare-earth element Gd for nonvolatile phase-change memory. Journal of Applied Physics, 2018, 124, .	1.1	15
37644	Hoâ€Mediated Alkyne Reactions at Low Temperatures on Ag(111). Chemistry - A European Journal, 2018, 24, 16126-16135.	1.7	9
37645	Surface Modifications of Ti₂CO₂ for Obtaining High Hydrogen Evolution Reaction Activity and Conductivity: A Computational Approach. ChemPhysChem, 2018, 19, 3380-3387.	1.0	20
37646	CO Oxidation at SnO2/Pt3Sn(111) Interfaces. Topics in Catalysis, 2018, 61, 1458-1464.	1.3	4
37647	Photo-Driven Syngas Conversion to Lower Olefins over Oxygen-Decorated Fe5C2 Catalyst. CheM, 2018, 4, 2917-2928.	5.8	62
37648	Toward Heterogeneously Catalyzed Detoxification of Phosphotriesters: Insights from Kinetics and Theoretical Calculations. Journal of Physical Chemistry C, 2018, 122, 25530-25538.	1.5	3
37649	Molecular structure of the substrate-induced thin-film phase of tetracene. Journal of Chemical Physics, 2018, 149, 144701.	1.2	23
37650	Tuning hydrogen adsorption on pure and doped ZnO (000 1 Â¯) surfaces by a simple electron counting model. Journal of Applied Physics, 2018, 124, 155302.	1.1	2

#	Article	IF	Citations
37651	Ab initio investigation on the experimental observation of metallic hydrogen. Physical Review B, 2018, 98, .	1.1	12
37652	Density Functional Perturbation Theory to Predict Piezoelectric Properties. , 0, , .		2
37653	Effect of Hf additions on phase stability and mechanical properties of binary W-Hf alloys: A first-principles study. Fusion Engineering and Design, 2018, 137, 295-302.	1.0	12
37654	Temperature-dependent structural transformation and friction behavior of nanocomposite VCN-(Ag) coatings. Materials and Design, 2018, 160, 964-973.	3.3	29
37655	Monofluorophosphates: A New Source of Deep-Ultraviolet Nonlinear Optical Materials. Chemistry of Materials, 2018, 30, 7823-7830.	3.2	166
37656	Theoretical Descriptors of Electrides. Journal of Physical Chemistry A, 2018, 122, 9371-9391.	1.1	63
37657	Insight into the Superior Catalytic Activity of MnO₂ for Low-Content NO Oxidation at Room Temperature. Journal of Physical Chemistry C, 2018, 122, 25365-25373.	1.5	22
37658	Selective Electrocatalytic Mechanism of CO₂ Reduction Reaction to CO on Silver Electrodes: A Unique Reaction Intermediate. Journal of Physical Chemistry C, 2018, 122, 25447-25455.	1.5	37
37659	How One-Dimensional Are Atomic Gold Chains on a Substrate?. Journal of Physical Chemistry C, 2018, 122, 25580-25588.	1.5	22
37660	Rational Design of High-Efficiency Organic Dyes in Dye-Sensitized Solar Cells by Multiscale Simulations. Journal of Physical Chemistry C, 2018, 122, 25219-25228.	1.5	32
37661	Mechanical Properties and Chemical Reactivity of Li_xSiO_y Thin Films. ACS Applied Materials & Interfaces, 2018, 10, 38558-38564.	4.0	21
37662	First-Principles Study on the Thermoelectric Properties of FeAsS. ACS Omega, 2018, 3, 13630-13635.	1.6	8
37663	TiO₂ and NaTaO₃ Decorated by Trimetallic Au/Pd/Pt Coreâ€“Shell Nanoparticles as Efficient Photocatalysts: Experimental and Computational Studies. ACS Sustainable Chemistry and Engineering, 2018, 6, 16665-16682.	3.2	38
37664	Contact properties of a vdW heterostructure composed of penta-graphene and penta-BN2 sheets. Journal of Applied Physics, 2018, 124, .	1.1	16
37665	Two-dimensional MoS2-MoSe2 lateral superlattice with minimized lattice thermal conductivity. Journal of Applied Physics, 2018, 124, .	1.1	32
37666	Nature of the magnetic interactions in <mml:math xmlns:mml="http://www.w3.org/1998/Math/MathML"><mml:mrow><mml:msub><mml:mi>Sr</mml:mi><mml:mn>2</mml:mn></mml:msub><mml:mi>Ir</mml:mi><mml:mn>1</mml:mn></mml:mrow></mml:math> Physical Review B, 2018, 98, .	1.1	9
37667	High-throughput search for potential potassium ion conductors: A combination of geometrical-topological and density functional theory approaches. Solid State Ionics, 2018, 326, 188-199.	1.3	37
37668	Unveiling the First Nucleation and Growth Steps of Inorganic Solid Electrolyte Interphase Components. Journal of Physical Chemistry C, 2018, 122, 25858-25868.	1.5	6

#	Article	IF	Citations
37669	Identifying an efficient, thermally robust inorganic phosphor host via machine learning. Nature Communications, 2018, 9, 4377.	5.8	228
37670	A rhombohedral ferroelectric phase in epitaxially strained Hf0.5Zr0.5O2 thin films. Nature Materials, 2018, 17, 1095-1100.	13.3	324
37671	Local structure of stoichiometric and oxygen-deficient A2Ti6O13 (Aâ€‰=â€‰Li, Na, and K) studied by X-ray absorption spectroscopy and first-principles calculations. Journal of Applied Physics, 2018, 124, 155101.	1.1	11
37672	Prediction of ideal triple degenerate points in HfIrAs and HfIrBi. Physical Review B, 2018, 98, .	1.1	7
37673	Universality of electronic characteristics and photocatalyst applications in the two-dimensional Janus transition metal dichalcogenides. Physical Review B, 2018, 98, .	1.1	229
37674	Investigation, using density function theory, of coverage of the kaolinite (001) surface during hydrogen adsorption. Clay Minerals, 2018, 53, 393-402.	0.2	2
37675	Adsorption of Transition Metals on Black Phosphorene: a First-Principles Study. Nanoscale Research Letters, 2018, 13, 282.	3.1	79
37676	Material Properties for the Interiors of Massive Giant Planets and Brown Dwarfs. Astronomical Journal, 2018, 156, 149.	1.9	18
37677	Early stages of growth of Pb, Sn and Ge on Ru(0001): A comparative density functional theory study. Thin Solid Films, 2018, 665, 123-130.	0.8	0
37678	Lattice relaxations in disordered Fe-based materials in the paramagnetic state from first principles. Physical Review B, 2018, 98, .	1.1	18
37679	Grain Boundary Segregation in Pd-Cu-Ag Alloys for High Permeability Hydrogen Separation Membranes. Membranes, 2018, 8, 81.	1.4	7
37680	Structural and Compositional Factors That Control the Li-Ion Conductivity in LiPON Electrolytes. Chemistry of Materials, 2018, 30, 7077-7090.	3.2	105
37681	Lithium Transport in Li4.4M0.4Mâ€²0.6S4 (M = Al3+, Ga3+, and Mâ€² = Ge4+, Sn4+): Combined Crystallographic, Conductivity, Solid State NMR, and Computational Studies. Chemistry of Materials, 2018, 30, 7183-7200.	3.2	28
37682	First-Principles Study of Substitutional Impurity Segregation in Zirconia, Hafnia, and Yttria-Stabilized-Zirconia Grain Boundaries. , 2018, , .		0
37683	Quantum-chemical modeling of the charge transport properties of the ammonium form of Nafion. Solid State Ionics, 2018, 325, 214-220.	1.3	2
37684	Cause for the Orbital Ordering of Cs₂AgF₄ and Its Effect on Thermoelectric Properties. Inorganic Chemistry, 2018, 57, 11895-11900.	1.9	7
37685	Interface Engineering of Metal Oxynitride Lateral Heterojunctions for Photocatalytic and Optoelectronic Applications. Journal of Physical Chemistry C, 2018, 122, 22504-22511.	1.5	6
37686	Design of Effective Catalysts for Selective Alkyne Hydrogenation by Doping of Ceria with a Single-Atom Promotor. Journal of the American Chemical Society, 2018, 140, 12964-12973.	6.6	204

#	Article	IF	Citations
37687	Magnetic field-induced ferroelectricity in Sâ€‰=â€‰1/2 kagome staircase compound PbCu3TeO7. Npj Quantum Materials, 2018, 3, .	1.8	25
37688	Fluid-enhanced surface diffusion controls intraparticle phase transformations. Nature Materials, 2018, 17, 915-922.	13.3	104
37689	Single atom alloy catalyst for SO₃ decomposition: enhancement of platinum catalyst's performance by Ag atom embedding. Nanoscale, 2018, 10, 20599-20610.	2.8	24
37690	Vapor-phase hydrothermal transformation of a nanosheet array structure Ni(OH)₂ into ultrathin Ni₃S₂ nanosheets on nickel foam for high-efficiency overall water splitting. Journal of Materials Chemistry A, 2018, 6, 19201-19209.	5.2	47
37691	Structural, magnetic and electronic properties of CrO₂ at multimegabar pressures. RSC Advances, 2018, 8, 24561-24570.	1.7	10
37692	Octahedral connectivity and its role in determining the phase stabilities and electronic structures of low-dimensional, perovskite-related iodoplumbates. APL Materials, 2018, 6, .	2.2	23
37693	First-principles study of electronic properties of Cu doped Ag₂S. Journal of Physics Condensed Matter, 2018, 30, 425502.	0.7	10
37694	Anti-PbO-type CoSe film: a possible analog to FeSe superconductors. Superconductor Science and Technology, 2018, 31, 115011.	1.8	6
37695	Quantum spin Hall insulators in chemically functionalized As (110) and Sb (110) films. Chinese Physics B, 2018, 27, 087305.	0.7	1
37696	Computational discovery of a new rhombohedral diamond phase. Physical Review B, 2018, 98, .	1.1	22
37697	Binary Two-Dimensional Honeycomb Lattice with Strong Spin-Orbit Coupling and Electron-Hole Asymmetry. Physical Review Letters, 2018, 121, 126801.	2.9	33
37698	Effects of point defects on the mechanical response of LaRu2P2. Acta Materialia, 2018, 160, 224-234.	3.8	7
37699	Atomistic simulations of PdTi high-temperature shape-memory alloys. Intermetallics, 2018, 102, 46-57.	1.8	3
37700	Microstructure engineering beyond SnSe1-xSx solid solution for high thermoelectric performance. Journal of Materiomics, 2018, 4, 321-328.	2.8	18
37701	Lattice thermodynamic behavior in nuclear fuel ThO2 from first principles. Journal of Nuclear Materials, 2018, 511, 11-17.	1.3	20
37702	Enhanced electrical transport properties via Pb vacancies in single crystalline PbTe prepared by Te-flux method. Physica B: Condensed Matter, 2018, 550, 9-14.	1.3	1
37703	Na1/2Bi1/2VO3 and K1/2Bi1/2VO3: New Lead-Free Tetragonal Perovskites with Moderate c/a Ratios. Chemistry of Materials, 2018, 30, 6728-6736.	3.2	8
37704	Anhydrous Methanol and Ethanol Dehydrogenation at Cu(111) Step Edges. Journal of Physical Chemistry C, 2018, 122, 21952-21962.	1.5	21

#	Article	IF	Citations
37705	Strong Topological States and High Charge Carrier Mobility in Tetraoxa[8]circulene Nanosheets. Journal of Physical Chemistry C, 2018, 122, 22216-22222.	1.5	25
37706	Formation, Structural Variety, and Impact of Antiphase Boundaries on Li Diffusion in LiCoO₂ Thin-Film Cathodes. Journal of Physical Chemistry Letters, 2018, 9, 5515-5520.	2.1	17
37707	Stability of Hydrogen Hydrates from Second-Order MÃ¸llerâ€“Plesset Perturbation Theory. Journal of Physical Chemistry Letters, 2018, 9, 5624-5629.	2.1	7
37708	Direct Z-Scheme Water Splitting Photocatalyst Based on Two-Dimensional Van Der Waals Heterostructures. Journal of Physical Chemistry Letters, 2018, 9, 5419-5424.	2.1	114
37709	Pentacene/TiO₂ Anatase Hybrid Interface Study by Scanning Probe Microscopy and First Principles Calculations. ACS Applied Materials & Interfaces, 2018, 10, 34718-34726.	4.0	3
37710	How Chain Length and Branching Influence the Alkene Cracking Reactivity on H-ZSM-5. ACS Catalysis, 2018, 8, 9579-9595.	5.5	70
37711	First-Principles Analysis of Radiative Recombination in Lead-Halide Perovskites. ACS Energy Letters, 2018, 3, 2329-2334.	8.8	81
37712	High-Density Ultra-small Clusters and Single-Atom Fe Sites Embedded in Graphitic Carbon Nitride (g-C₃N₄) for Highly Efficient Catalytic Advanced Oxidation Processes. ACS Nano, 2018, 12, 9441-9450.	7.3	455
37713	Theoretical Studies on the Electronic and Optical Properties of Honeycomb BC₃ monolayer: A Promising Candidate for Metal-free Photocatalysts. ACS Omega, 2018, 3, 10517-10525.	1.6	50
37714	Synergistic Boron Doping of Semiconductor and Dielectric Layers for High-Performance Metal Oxide Transistors: Interplay of Experiment and Theory. Journal of the American Chemical Society, 2018, 140, 12501-12510.	6.6	43
37715	Two-Dimensional MoxW1â^'xS2 Graded Alloys: Growth and Optical Properties. Scientific Reports, 2018, 8, 12889.	1.6	24
37716	CO₂ formation mechanism in Fischerâ€“Tropsch synthesis over iron-based catalysts: a combined experimental and theoretical study. Catalysis Science and Technology, 2018, 8, 5288-5301.	2.1	45
37717	The dielectric response and electronic properties of GaS monolayer: A first-principles study. AIP Conference Proceedings, 2018, , .	0.3	1
37718	Theoretical study of bismuth-doped CdTe. Journal of Physics: Conference Series, 2018, 1043, 012044.	0.3	1
37719	Electronic structure of electron-irradiated graphene and effects of hydrogen passivation. Materials Research Express, 2018, 5, 115603.	0.8	9
37720	Two-Dimensional Photogalvanic Spin-Battery. Physical Review Applied, 2018, 10, .	1.5	64
37721	Uncovering the Mechanism of the Impurity-Selective Mott Transition in Paramagnetic <mml:math xmlns:mml="http://www.w3.org/1998/Math/MathML" display="inline"><mml:mrow><mml:msub><mml:mrow><mml:mi mathvariant="normal">V</mml:mi></mml:mrow><mml:mrow><mml:mn>2</mml:mn></mml:mrow></mml:msub><mml:msub><mml:mi mathvariant="normal">O</mml:mi></mml:mrow><mml:mrow><mml:mn>3</mml:mn></mml:mrow></mml:msub></mml:mrow></mml:	2.9	21
37722	Dirac, Weyl Semimetals, Coexistence of Dirac and Weyl Fermions in Polar Hexagonal <mml:math xmlns:mml="http://www.w3.org/1998/Math/MathML" display="inline"><mml:mi>A</mml:mi><mml:mi>B</mml:mi><mml:mi>C</mml:mi></mml:math> Crystals. Physical Review Letters, 2018, 121, 106404.	2.9	50

#	Article	IF	Citations
37723	Stability of Cu-Precipitates in Al-Cu Alloys. Applied Sciences (Switzerland), 2018, 8, 1003.	1.3	8
37724	Ultrathin Metal Crystals: Growth on Supported Graphene Surfaces and Applications. Small, 2018, 14, e1801529.	5.2	7
37725	One-step hydrogen extraction and storage in plasma generated palladium nanoparticles. Journal of Nanoparticle Research, 2018, 20, 1.	0.8	5
37726	A new porous metallic silicon dicarbide for highly efficient Li-ion battery anode identified by targeted structure search. Carbon, 2018, 140, 680-687.	5.4	25
37727	Analysis of the variables that modify the robustness of Ti-SiO2 catalysts for alkene epoxidation: Role of silylation, deactivation and potential solutions. Molecular Catalysis, 2018, 459, 55-60.	1.0	9
37728	Relating Interfacial Order to Sum Frequency Generation with Ab Initio Simulations of the Aqueous Al₂O₃(0001) and (112Ì…0) Interfaces. Journal of Physical Chemistry C, 2018, 122, 21284-21294.	1.5	30
37729	Armchair MoS2 nanoribbons turned into half metals through deposition of transition-metal and Si atomic chains. Scientific Reports, 2018, 8, 13307.	1.6	5
37730	High-symmetry tubular Ta@B₁₈^{3â^'}, Ta₂@B₁₈, and Ta₂@B₂₇⁺ as embryos of Î±-boronanotubes with a transition-metal wire coordinated inside. Physical Chemistry Chemical Physics, 2018, 20, 25009-25015.	1.3	9
37731	Superconductivity and phase stability of potassium-doped biphenyl. Physical Chemistry Chemical Physics, 2018, 20, 25217-25223.	1.3	31
37732	Geometries, electronic properties and stability of molybdenum and tungsten nitrides low-index surfaces. Materials Research Express, 2018, 5, 126402.	0.8	8
37733	Phonons and anomalous thermal expansion behavior of <mml:math xmlns:mml="http://www.w3.org/1998/Math/MathML"><mml:mrow><mml:msub><mml:mi mathvariant="normal">H</mml:mi><mml:mn>2</mml:mn></mml:msub><mml:mi mathvariant="normal">O</mml:mi></mml:mrow></mml:math> and <mml:math xmlns:mml="http://www.w3.org/1998/Math/MathML"><mml:mrow><mml:msub><mml:mi mathvariant="normal">D</mml:mi><mml:mn>2</mml:mn></mml:msub><mml:mi mathvariant="normal">	1.1	8
37734	Topological phase transitions driven by strain in monolayer tellurium. Physical Review B, 2018, 98, .	1.1	34
37735	Mosaicâ€Structured Cobalt Nickel Thiophosphate Nanosheets Incorporated Nâ€doped Carbon for Efficient and Stable Electrocatalytic Water Splitting. Advanced Functional Materials, 2018, 28, 1805075.	7.8	57
37736	Lightâ€Induced Spin Transitions in Copperâ€Nitroxideâ€Based Switchable Molecular Magnets: Insights from Periodic DFT+U Calculations. Chemistry - A European Journal, 2018, 24, 18988-18997.	1.7	3
37737	First-principles study of the nanotubes from the TiO2 hexagonal sheet. Journal of Materials Science, 2018, 53, 15530-15540.	1.7	4
37738	Surface decorated cobalt sulfide as efficient catalyst for oxygen evolution reaction and its intrinsic activity. Journal of Catalysis, 2018, 367, 43-52.	3.1	39
37739	Computational simulation of He bubble evolution in fcc Cu with Î£3 twin boundary using object kinetic Monte Carlo method. Nuclear Instruments & Methods in Physics Research B, 2018, 436, 22-28.	0.6	0
37740	Thermodynamical Stability of Plutonium Monoxide with Carbon Substitution. Journal of Physical Chemistry C, 2018, 122, 22821-22828.	1.5	9

#	Article	IF	Citations
37741	Mechanical and Chemical Stability of Monolayer Black Phosphorous Studied by Density Functional Theory Simulations. Journal of Physical Chemistry C, 2018, 122, 22366-22373.	1.5	15
37742	Multifunctionality of Partially Reduced Graphene Oxideâ€“CrVO₄Nanocomposite: Electrochemical and Photocatalytic Studies with Theoretical Insight from Density Functional Theory. Journal of Physical Chemistry C, 2018, 122, 21140-21150.	1.5	25
37743	Two-Dimensional Titania: Structures and Properties Predicted by First Principle Calculation. Journal of Physical Chemistry C, 2018, 122, 22911-22919.	1.5	12
37744	Correlating DFT Calculations with CO Oxidation Reactivity on Ga-Doped Pt/CeO₂ Single-Atom Catalysts. Journal of Physical Chemistry C, 2018, 122, 22460-22468.	1.5	91
37745	Predicting New Two-Dimensional Pd₃(PS₄)₂ as an Efficient Photocatalyst for Water Splitting. Journal of Physical Chemistry C, 2018, 122, 21927-21932.	1.5	26
37746	Rhodium Nanoparticles/F-Doped Graphene Composites as Multifunctional Electrocatalyst Superior to Pt/C for Hydrogen Evolution and Formic Acid Oxidation Reaction. ACS Applied Materials & Interfaces, 2018, 10, 33153-33161.	4.0	63
37747	Unexpected stable phases of tungsten borides. Physical Chemistry Chemical Physics, 2018, 20, 24665-24670.	1.3	30
37748	Methane on a stepped surface: Dynamical insights on the dissociation of CHD3 on Pt(111) and Pt(211). Journal of Chemical Physics, 2018, 149, 094701.	1.2	15
37749	Theory of the optical spin-polarization loop of the nitrogen-vacancy center in diamond. Physical Review B, 2018, 98, .	1.1	59
37750	Stripe order and magnetic anisotropy in the <mml:math xmlns:mml="http://www.w3.org/1998/Math/MathML"><mml:mrow><mml:mi>S</mml:mi><mml:mo>=</mml:mo><mml:mn>1</mml:mn> antiferromagnet <mml:math xmlns:mml="http://www.w3.org/1998/Math/MathML"><mml:mrow><mml:msub><mml:mi>BaMoP</mml:mi><mml:mn>2</mml:mn> mathvariant="normal">O</mml:mi><mml:mn>8</mml:mn></mml:msub></mml:mrow></mml:math>. Physical Review B, 2018, 98, .	1.1	7
37751	Theoretical studies of electronic transport in monolayer and bilayer phosphorene: A critical overview. Physical Review B, 2018, 98, .	1.1	78
37752	Magnetization-direction tunable nodal-line and Weyl phases. Physical Review B, 2018, 98, .	1.1	16
37753	Growth of a predicted two-dimensional topological insulator based on InBi-Si(111)- <mml:math xmlns:mml="http://www.w3.org/1998/Math/MathML"><mml:mrow><mml:msqrt><mml:mn>7</mml:mn></mml:msqrt><mml:mo>Ã—</ Physical Review B, 2018, 98, .	1.1	22
37754	Thermodynamic Evaluation of Trace-Amount Transition-Metal-Ion Doping in NiOOH Films. Journal of the Electrochemical Society, 2018, 165, F907-F913.	1.3	7
37755	The Magnetic, Electronic, and Thermodynamic Properties of High Entropy Alloy CrMnFeCoNi: A Firstâ€Principles Study. Physica Status Solidi (B): Basic Research, 2018, 255, 1800306.	0.7	19
37756	Optical properties of anatase TiO2: synergy between transition metal doping and oxygen vacancies. Journal of Molecular Modeling, 2018, 24, 276.	0.8	8
37757	Activating Aromatic Rings as Na-Ion Storage Sites to Achieve High Capacity. CheM, 2018, 4, 2463-2478.	5.8	82
37758	The mechanical properties of high entropy (-like) alloy Wx(TaTiVCr)1-x via first-principles calculations. Fusion Engineering and Design, 2018, 137, 35-42.	1.0	26

#	Article	IF	Citations
37759	Suppressing heating rate-dependent martensitic stabilization in ductile Cu-Al-Mn shape memory alloys by Ni addition: An experimental and first-principles study. Materials Characterization, 2018, 145, 381-388.	1.9	9
37760	Insight into the oxidation mechanism of Nb3Si(111) surface: First-principles calculations. Materials Research Bulletin, 2018, 107, 484-491.	2.7	42
37761	STM studies of photochemistry and plasmon chemistry on metal surfaces. Progress in Surface Science, 2018, 93, 163-176.	3.8	21
37762	Spin phonon interactions and magneto-thermal transport behavior in p-Si. Solid State Communications, 2018, 283, 37-42.	0.9	10
37763	Lattice dynamics, transport and superconducting properties of Ba-substituted Sr3SnO. Solid State Communications, 2018, 284-286, 14-19.	0.9	2
37764	Efficiency Improvement of Sb₂Se₃ Solar Cells via Grain Boundary Inversion. ACS Energy Letters, 2018, 3, 2335-2341.	8.8	112
37765	When the Surface Matters: Prebiotic Peptideâ€Bond Formation on the TiO₂ (101) Anatase Surface through Periodic DFTâ€Đ2 Simulations. Chemistry - A European Journal, 2018, 24, 16292-16301.	1.7	23
37767	Structural disorder in fused silica with ODC(I) defect. Applied Physics A: Materials Science and Processing, 2018, 124, 1.	1.1	6
37768	Pressures Tuning the Band Gap of Organicâ€“Inorganic Trihalide Perovskites (MAPbBr3): A First-Principles Study. Journal of Electronic Materials, 2018, 47, 7204-7211.	1.0	12
37769	Pressure effect on the electronic structure and thermoelectric properties of Î±-MgAgSb. Computational Materials Science, 2018, 155, 450-456.	1.4	9
37770	Modeling the Adsorption of NO and NH₃ on Fe-SSZ-13 from First-Principles: A DFT Study. Industrial & Engineering Chemistry Research, 2018, 57, 13396-13405.	1.8	16
37771	CeO_x-Decorated NiFe-Layered Double Hydroxide for Efficient Alkaline Hydrogen Evolution by Oxygen Vacancy Engineering. ACS Applied Materials & Interfaces, 2018, 10, 35145-35153.	4.0	156
37772	Steps Control the Dissociation of CO₂ on Cu(100). Journal of the American Chemical Society, 2018, 140, 12974-12979.	6.6	70
37773	Control of coordinatively unsaturated Zr sites in ZrO2 for efficient Câ€“H bond activation. Nature Communications, 2018, 9, 3794.	5.8	133
37774	Deep neural networks for accurate predictions of crystal stability. Nature Communications, 2018, 9, 3800.	5.8	178
37775	Water printing of ferroelectric polarization. Nature Communications, 2018, 9, 3809.	5.8	75
37776	The surface and catalytic chemistry of the first row transition metal phosphides in deoxygenation. Catalysis Science and Technology, 2018, 8, 5302-5314.	2.1	21
37777	Narrow bandgap semiconductor decorated wood membrane for high-efficiency solar-assisted water purification. Journal of Materials Chemistry A, 2018, 6, 18839-18846.	5.2	208

#	Article	IF	Citations
37778	Modulating the electronic properties of perovskite via Ïƒâ€“Ï€ interfacial interactions: A computational study. APL Materials, 2018, 6, .	2.2	6
37779	Tellurium cluster (Te8) induced tuned electronic properties of boron nitride sheet: A first principle study. AIP Conference Proceedings, 2018, , .	0.3	0
37780	CO-tip manipulation using repulsive interactions. Nanotechnology, 2018, 29, 495701.	1.3	5
37781	New antiferromagnetic order with pressure-induced superconductivity in <mml:math xmlns:mml="http://www.w3.org/1998/Math/MathML"><mml:mrow><mml:msub><mml:mi>EuFe</mml:mi><mml:mn>2</mml:mn></mml:msub><mml:mn></mml:mn> Physical Review B, 2018, 98, .	1.1	6
37782	Lattice contraction with boron doping in fully strained SiGe epitaxial layers. Japanese Journal of Applied Physics, 2018, 57, 065504.	0.8	4
37783	Why Tinâ€Doping Enhances the Efficiency of Hematite Photoanodes for Water Splittingâ€”The Full Picture. Advanced Functional Materials, 2018, 28, 1804472.	7.8	53
37784	Boosted Electrocatalytic N₂ Reduction to NH₃ by Defectâ€Rich MoS₂ Nanoflower. Advanced Energy Materials, 2018, 8, 1801357.	10.2	482
37785	Anisotropic plastic deformation of single crystals of the MAX phase compound Ti3SiC2 investigated by micropillar compression. Acta Materialia, 2018, 161, 161-170.	3.8	66
37786	Telluride-Based Atomically Thin Layers of Ternary Two-Dimensional Transition Metal Dichalcogenide Alloys. Chemistry of Materials, 2018, 30, 7262-7268.	3.2	37
37787	First-Principles Analysis of Site- and Condition-Dependent Fe Speciation in SSZ-13 and Implications for Catalyst Optimization. ACS Catalysis, 2018, 8, 10119-10130.	5.5	41
37788	H₂ Oxidation over Supported Au Nanoparticle Catalysts: Evidence for Heterolytic H₂ Activation at the Metalâ€“Support Interface. Journal of the American Chemical Society, 2018, 140, 16469-16487.	6.6	113
37789	Absolute timing of the photoelectric effect. Nature, 2018, 561, 374-377.	13.7	77
37790	Enhanced interlayer neutral excitons and trions in trilayer van der Waals heterostructures. Npj 2D Materials and Applications, 2018, 2, .	3.9	44
37791	Spin signatures in the electrical response of graphene nanogaps. Nanoscale, 2018, 10, 18169-18177.	2.8	10
37792	High-performance Na ion cathodes based on the ubiquitous and reversible O redox reaction. Journal of Materials Chemistry A, 2018, 6, 24120-24127.	5.2	5
37793	Formation of hollow MoO₃/SnS₂ heterostructured nanotubes for efficient light-driven hydrogen peroxide production. Journal of Materials Chemistry A, 2018, 6, 20304-20312.	5.2	106
37794	Accurate lattice geometrical parameters and bulk moduli from a semilocal density functional. AIP Advances, 2018, 8, .	0.6	15
37795	Old puzzle of incommensurate crystal structure of calaverite AuTe ₂ and predicted stability of novel AuTe compound. Proceedings of the National Academy of Sciences of the United States of America, 2018, 115, 9945-9950.	3.3	14

#	Article	IF	Citations
37796	First-principles study on the structures and electronic properties of graphene-supported Ni_n (nâ€‰=â€‰1â€“6) clusters. Molecular Simulation, 2018, 44, 1529-1538.	0.9	7
37797	High-throughput screening of chalcogenide single perovskites by first-principles calculations for photovoltaics. Journal Physics D: Applied Physics, 2018, 51, 474003.	1.3	50
37798	Transformation of 2D group-III selenides to ultra-thin nitrides: enabling epitaxy on amorphous substrates. Nanotechnology, 2018, 29, 47LT02.	1.3	6
37799	Surface Electrochemical Stability and Strainâ€Tunable Lithium Storage of Highly Flexible 2D Transition Metal Carbides. Advanced Functional Materials, 2018, 28, 1804867.	7.8	33
37800	Effects of Charge, Size, and Shape of Transition States, Bound Intermediates, and Confining Voids in Reactions of Alkenes on Solid Acids. ChemCatChem, 2018, 10, 4028-4037.	1.8	27
37801	Transition from the twinning induced plasticity to the Î³-Îµ transformation induced plasticity in a high manganese steel. Acta Materialia, 2018, 161, 273-284.	3.8	17
37802	Atomistic simulation study on the shear behavior of Ag/MgO interface. Computational Materials Science, 2018, 155, 116-128.	1.4	10
37803	Oxygen vacancy induced strong anisotropy of the thermoelectric properties of strontium barium niobate. Computational Materials Science, 2018, 155, 393-399.	1.4	6
37804	Efficient design principle for interfacial charge separation in hydrogen-intercalated nonstoichiometric oxides. Nano Energy, 2018, 53, 887-897.	8.2	27
37805	Inch-Scale Grain Boundary Free Organic Crystals Developed by Nucleation Seed-Controlled Shearing Method. ACS Applied Materials & Interfaces, 2018, 10, 35395-35403.	4.0	48
37806	Facile Electrodeposition of Niâ€“Cuâ€“P Dendrite Nanotube Films with Enhanced Hydrogen Evolution Reaction Activity and Durability. ACS Applied Materials & Interfaces, 2018, 10, 35224-35233.	4.0	74
37807	Essential Role of Spinel ZnFe₂O₄ Surfaces during Lithiation. ACS Applied Materials & Interfaces, 2018, 10, 35623-35630.	4.0	24
37808	In Situ Tuning of Catalytic Activity by Thermoelectric Effect for Ethylene Oxidation. ACS Catalysis, 2018, 8, 10164-10172.	5.5	20
37809	Identifying the Non-Identical Outermost Selenium Atoms and Invariable Band Gaps across the Grain Boundary of Anisotropic Rhenium Diselenide. ACS Nano, 2018, 12, 10095-10103.	7.3	25
37810	Discovery of topological nodal-line fermionic phase in a magnetic material GdSbTe. Scientific Reports, 2018, 8, 13283.	1.6	70
37811	Unraveling the structureâ€“sensitivity of the photocatalytic decomposition of N₂O on CeO₂: a DFT+U study. Journal of Materials Chemistry A, 2018, 6, 19241-19255.	5.2	12
37812	Halogen bond shortens and strengthens the bridge bond of [1.1.1]propellane and the open form of [2.2.2]propellane. Physical Chemistry Chemical Physics, 2018, 20, 25792-25798.	1.3	15
37813	Holey single-walled carbon nanotubes for ultra-fast broadband bolometers. Nanoscale, 2018, 10, 18665-18671.	2.8	29

#	Article	IF	Citations
37814	Band gap engineering of a MoS₂ monolayer through oxygen alloying: an ab initio study. Nanotechnology, 2018, 29, 505701.	1.3	8
37815	Site preferences of alloying transition metal elements in Ni-based superalloy: A first-principles study. Chinese Physics B, 2018, 27, 097102.	0.7	3
37816	Size and temperature transferability of direct and local deep neural networks for atomic forces. Physical Review B, 2018, 98, .	1.1	16
37817	Pressure-induced structural modulations in coesite. Physical Review B, 2018, 98, .	1.1	4
37818	Investigation of Charge-Transfer Interaction in Mixed Stack Donorâ€“Acceptor Cocrystals Toward Tunable Solid-State Emission Characteristics. Crystal Growth and Design, 2018, 18, 6001-6008.	1.4	51
37819	Computational Prediction and Experimental Realization of p-Type Carriers in the Wide-Band-Gap Oxide SrZn_{1â€“x}Li_xO₂. Inorganic Chemistry, 2018, 57, 11874-11883.	1.9	6
37820	Kinetically Determined Phase Transition from Stage II (LiC₁₂) to Stage I (LiC₆) in a Graphite Anode for Li-Ion Batteries. Journal of Physical Chemistry Letters, 2018, 9, 5567-5573.	2.1	74
37821	One-Pot Pyrolysis Method to Fabricate Carbon Nanotube Supported Ni Single-Atom Catalysts with Ultrahigh Loading. ACS Applied Energy Materials, 0, , .	2.5	19
37822	Activity and Selectivity Control in CO₂ Electroreduction to Multicarbon Products over CuO_x Catalysts via Electrolyte Design. ACS Catalysis, 2018, 8, 10012-10020.	5.5	173
37823	Ultrathin Gold Nanowires with the Polytetrahedral Structure of Bulk Manganese. ACS Nano, 2018, 12, 9521-9531.	7.3	21
37824	Biotemplating Growth of Nepenthes-like N-Doped Graphene as a Bifunctional Polysulfide Scavenger for Liâ€“S Batteries. ACS Nano, 2018, 12, 10240-10250.	7.3	146
37825	Large intrinsic anomalous Hall effect in half-metallic ferromagnet Co3Sn2S2 with magnetic Weyl fermions. Nature Communications, 2018, 9, 3681.	5.8	446
37826	The polymerization of nitrogen in Li2N2 at high pressures. Scientific Reports, 2018, 8, 13144.	1.6	4
37827	Spinâ€“orbit coupling induced spin polarized valley states in SrRuO₃/BiIrO₃ heterostructures. Physical Chemistry Chemical Physics, 2018, 20, 24768-24774.	1.3	0
37828	Critical conditions for the formation of p-type ZnO with Li doping. RSC Advances, 2018, 8, 30868-30874.	1.7	18
37829	Computational investigation of gas detection and selectivity on TiS3 nanoflakes supported by experimental evidence. Physical Chemistry Chemical Physics, 2018, 20, 25458-25466.	1.3	3
37830	Pressure dependence on electronic structures, charge distribution and bond orders of solid nitromethane using nonlocal DFT functional. Molecular Simulation, 2018, 44, 1454-1460.	0.9	2
37831	Quantum-accurate spectral neighbor analysis potential models for Ni-Mo binary alloys and fcc metals. Physical Review B, 2018, 98, .	1.1	65

#	Article	IF	Citations
37832	Tunable electronic and magneto-optical properties of monolayer arsenene: From <mml:math xmlns:mml="http://www.w3.org/1998/Math/MathML"><mml:mrow><mml:mi mathvariant="normal">G</mml:mi><mml:msub><mml:mi mathvariant="normal">W</mml:mi><mml:mn>0</mml:mn></mml:msub></mml:mrow></mml:math> approximation to large-scale tight-binding propagation simulations. Physical Review B, 2018, 98, .	1.1	9
37833	Study of the New Two-Dimensional Compound CoC. JETP Letters, 2018, 108, 13-17.	0.4	9
37834	Environmental Stimuliâ€Responsive Longâ€Term Radical Scavenging of 2D Transition Metal Dichalcogenides through Defectâ€Mediated Hydrogen Atom Transfer in Aqueous Media. Advanced Functional Materials, 2018, 28, 1802737.	7.8	9
37835	Role of Aluminum Doping in Anataseâ€toâ€Rutile Transformation from Thermodynamic View Point. Physica Status Solidi - Rapid Research Letters, 2018, 12, 1800234.	1.2	4
37836	Quantum chemical studies on anion specificity of CÎ±NN motif in functional proteins. Journal of Computer-Aided Molecular Design, 2018, 32, 929-936.	1.3	0
37837	Shearing of Î³â€™ particles in Co-base and Co-Ni-base superalloys. Acta Materialia, 2018, 161, 99-109.	3.8	45
37838	Atomic Ordering of Two Neighboring Transition Metalsâ€”Cu and Zn from Binary CuZn to Ternary Cu3ZnSb. Inorganic Chemistry, 2018, 57, 11970-11977.	1.9	7
37839	AFLOW-CHULL: Cloud-Oriented Platform for Autonomous Phase Stability Analysis. Journal of Chemical Information and Modeling, 2018, 58, 2477-2490.	2.5	69
37840	One-Dimensional Atomic Segregation at Semiconductorâ€“Metal Interfaces of Polymorphic Transition Metal Dichalcogenide Monolayers. Nano Letters, 2018, 18, 6157-6163.	4.5	4
37841	Dry Reforming of Methane on Single-Site Ni/MgO Catalysts: Importance of Site Confinement. ACS Catalysis, 2018, 8, 9821-9835.	5.5	156
37842	Active learning across intermetallics to guide discovery of electrocatalysts for CO2 reduction and H2 evolution. Nature Catalysis, 2018, 1, 696-703.	16.1	497
37843	Tin(<scp>ii</scp>) oxide carbodiimide and its relationship to SnO. Dalton Transactions, 2018, 47, 13378-13383.	1.6	17
37844	Magnetization dynamics induced by the Rashba effect in ferromagnetic films. Nanoscale, 2018, 10, 18728-18733.	2.8	1
37845	Assessing the SCAN functional for itinerant electron ferromagnets. Physical Review B, 2018, 98, .	1.1	64
37846	Direct Magnetization-Polarization Coupling in <mml:math xmlns:mml="http://www.w3.org/1998/Math/MathML" display="inline"><mml:mrow><mml:msub><mml:mrow><mml:mi>BaCuF</mml:mi></mml:mrow><mml:mrow><mml:mn>4</mml:mn></mml:mrow> Physical Review Letters, 2018, 121, 117601.	2.9	18
37847	Influence of CO molecule on structure stability and electronic properties of silver nanotube. Chinese Journal of Physics, 2018, 56, 1999-2005.	2.0	0
37848	Three-dimensional pentagonal silicon: Stability and properties. Computational Materials Science, 2018, 155, 373-377.	1.4	8
37849	Novel structure of AgInS2 compound under high pressure: First principles calculations. Solid State Communications, 2018, 284-286, 20-24.	0.9	4

#	Article	IF	Citations
37850	Two-Dimensional CsAg₅Te_{3â€“x}S_x Semiconductors: Multi-anion Chalcogenides with Dynamic Disorder and Ultralow Thermal Conductivity. Chemistry of Materials, 2018, 30, 7245-7254.	3.2	15
37851	Rb₃SiF₇:Mn⁴⁺ and Rb₂CsSiF₇:Mn⁴⁺ Red-Emitting Phosphors with a Faster Decay Rate. Chemistry of Materials, 2018, 30, 6936-6944.	3.2	81
37852	Hydrogenated Na₂Ti₃O₇ Epitaxially Grown on Flexible N-Doped Carbon Sponge for Potassium-Ion Batteries. ACS Applied Materials & Interfaces, 2018, 10, 37974-37980.	4.0	45
37853	Selective SnO_x Atomic Layer Deposition Driven by Oxygen Reactants. ACS Applied Materials & Interfaces, 2018, 10, 33335-33342.	4.0	28
37854	Spin-Dependent O2 Binding to Hemoglobin. ACS Omega, 2018, 3, 9241-9245.	1.6	9
37855	Na1â^'xSn2P2 as a new member of van der Waals-type layered tin pnictide superconductors. Scientific Reports, 2018, 8, 12852.	1.6	22
37856	Suppression by Pt of CO adsorption and dissociation and methane formation on Fe5C2(100) surfaces. Physical Chemistry Chemical Physics, 2018, 20, 25246-25255.	1.3	9
37857	Cation vacancy repair for the enhancement of orange-yellow luminescence in Sr₉Mg_{1.5â^'x}K_x(PO₄)₇:Eu²⁺ phosphors. Journal of Materials Chemistry C, 2018, 6, 10723-10729.	2.7	41
37858	Large piezoelectric response of van der Waals layered solids. Journal of Materials Chemistry C, 2018, 6, 11035-11044.	2.7	19
37859	Bi₂OS₂: a direct-gap two-dimensional semiconductor with high carrier mobility and surface electron states. Materials Horizons, 2018, 5, 1058-1064.	6.4	45
37860	Engineering of the resistive switching properties in V2O5 thin film by atomic structural transition: Experiment and theory. Journal of Applied Physics, 2018, 124, .	1.1	3
37861	Electronic structure and migration of interstitial hydrogen in the rutile phase of TiO2. Journal of Physics Condensed Matter, 2018, 30, 425503.	0.7	8
37862	Electrically tunable optical properties of few-layer black arsenic phosphorus. Nanotechnology, 2018, 29, 484001.	1.3	28
37863	Optical properties of In₂O₃ from experiment and first-principles theory: influence of lattice screening. New Journal of Physics, 2018, 20, 053016.	1.2	20
37864	Magnetism and exchange-bias effect at the MnN/Fe interface. Physical Review B, 2018, 98, .	1.1	5
37865	Electrical control of excitons in van der Waals heterostructures with type-II band alignment. Physical Review B, 2018, 98, .	1.1	21
37866	Leadâ€Free Highly Efficient Blueâ€Emitting Cs₃Cu₂I₅ with 0D Electronic Structure. Advanced Materials, 2018, 30, e1804547.	11.1	477
37867	Molecular dynamics study of hydrogen-vacancy interactions in Î±-zirconium. Journal of Nuclear Materials, 2018, 511, 341-352.	1.3	16

#	Article	IF	Citations
37868	Metalâ€“Oxygen Hybridization Determined Activity in Spinel-Based Oxygen Evolution Catalysts: A Case Study of ZnFe_{2â€“x}Cr_xO₄. Chemistry of Materials, 2018, 30, 6839-6848.	3.2	65
37869	Auâ€“Rh Surface Structures on Rh(111): DFT Insights into the Formation of an Ordered Surface Alloy. Journal of Physical Chemistry C, 2018, 122, 22435-22447.	1.5	5
37870	Structural Evolutions of the Self-Assembled N-Decyldecanamide on Au(111). Journal of Physical Chemistry C, 2018, 122, 22538-22543.	1.5	1
37871	Structure and Activity Transition from Oxidized to Metallic Tungsten for Catalytic Hydrogenation: A Density Functional Theory Study. Journal of Physical Chemistry C, 2018, 122, 23053-23061.	1.5	4
37872	Simple Route to Metal cyclo-N₅^{â€“} Salt: High-Pressure Synthesis of CuN₅. Journal of Physical Chemistry C, 2018, 122, 22339-22344.	1.5	46
37873	Ligand Effects on the Selective Hydrogenation of Nitrobenzene to Cyclohexylamine Using Ruthenium Nanoparticles as Catalysts. ACS Applied Nano Materials, 2018, 1, 5885-5894.	2.4	26
37874	Metal-Free Nitrogen- and Boron-Codoped Mesoporous Carbons for Primary Amides Synthesis from Primary Alcohols via Direct Oxidative Dehydrogenation. ACS Catalysis, 2018, 8, 9936-9944.	5.5	59
37875	Sheet-membrane Mn-doped nickel hydroxide encapsulated via heterogeneous Ni₃S₂ nanoparticles for efficient alkaline batteryâ€“supercapacitor hybrid devices. Journal of Materials Chemistry A, 2018, 6, 19020-19029.	5.2	55
37876	The effect of surface coverage on N₂, NO and N₂O formation over Pt(111). Physical Chemistry Chemical Physics, 2018, 20, 25314-25323.	1.3	13
37877	Eutectic solvent-mediated selective synthesis of Cuâ€“Sbâ€“S-based nanocrystals: combined experimental and theoretical studies toward highly efficient water splitting. Journal of Materials Chemistry A, 2018, 6, 19798-19809.	5.2	11
37878	Dimethyl methylphosphonate adsorption and decomposition on MoO₂ as studied by ambient pressure x-ray photoelectron spectroscopy and DFT calculations. Journal of Physics Condensed Matter, 2018, 30, 134005.	0.7	19
37879	Unraveling the complex magnetic structure of multiferroic pyroxene <mml:math xmlns:mml="http://www.w3.org/1998/Math/MathML"><mml:mrow><mml:msub><mml:mi>NaFeGe</mml:mi><mml:mn>2</mml:mn></ mathvariant="normal">O</mml:mi><mml:mn>6</mml:mn></mml:msub></mml:mrow></mml:math> : A combined experimental and theoretical study. Physical Review B, 2018, 98, .	1.1	10
37880	Finite-temperature phase diagram of (111) nickelate bilayers. Physical Review B, 2018, 98, .	1.1	6
37881	Electronic structures and unusually robust bandgap in an ultrahigh-mobility layered oxide semiconductor, Bi ₂ O ₂ Se. Science Advances, 2018, 4, eaat8355.	4.7	167
37882	Spin-Order-Induced Ferroelectricity and Magnetoelectric Effect in <mml:math xmlns:mml="http://www.w3.org/1998/Math/MathML" display="inline" overflow="scroll"><mml:mi>Li</mml:mi><mml:mi>Cu</mml:mi><mml:msub><mml:mi>Fe</mml:mi><mml:mn>2</mml:mn></mml:msub stretchy="false">(</mml:mo><mml:msub><mml:mi>VO</mml:mi><mml:mn>4</mml:mn></mml:msub><mml:msub><mml:mo) Tj ETQq 2018, 10, .	1.5	8
37883	Interplay of lattice, electronic, and spin degrees of freedom in detwinned <mml:math xmlns:mml="http://www.w3.org/1998/Math/MathML"><mml:mrow><mml:msub><mml:mi>BaFe</mml:mi><mml:mn>2</mml:mn></ : A Raman scattering study. Physical Review B, 2018, 98, .	1.1	15
37884	Wannier-Koopmans method calculations of organic molecule crystal band gaps. Europhysics Letters, 2018, 123, 37002.	0.7	3
37885	Electron Transport from Quantum Kinetic Monte Carlo Simulations. Journal of Physical Chemistry C, 2018, 122, 20550-20554.	1.5	4

#	Article	IF	Citations
37886	Electrochemical Atomic Force Microscopy and First-Principles Calculations of Ferriprotoporphyrin Adsorption and Polymerization. Langmuir, 2018, 34, 11335-11346.	1.6	0
37887	Room-Temperature Bound Exciton with Long Lifetime in Monolayer GaN. ACS Photonics, 2018, 5, 4081-4088.	3.2	30
37888	Modulation of Water Vapor Sorption by a Fourth-Generation Metalâ€“Organic Material with a Rigid Framework and Self-Switching Pores. Journal of the American Chemical Society, 2018, 140, 12545-12552.	6.6	42
37889	Distinct spinâ€“lattice and spinâ€“phonon interactions in monolayer magnetic CrI₃. Physical Chemistry Chemical Physics, 2018, 20, 23546-23555.	1.3	84
37890	Step-like band alignment and stacking-dependent band splitting in trilayer TMD heterostructures. Physical Chemistry Chemical Physics, 2018, 20, 25000-25008.	1.3	13
37891	OPGs: promising anode materials with high specific capacity and rate capability for Li/Na ion batteries. Nanoscale, 2018, 10, 17942-17948.	2.8	16
37892	Insights into the mechanism of the enhanced visible-light photocatalytic activity of black phosphorus/BiVO₄ heterostructure: a first-principles study. Journal of Materials Chemistry A, 2018, 6, 19167-19175.	5.2	86
37893	Adsorption of common solvent molecules on graphene and MoS2 from first-principles. Journal of Chemical Physics, 2018, 149, 094702.	1.2	17
37894	From one to three, exploring the rungs of Jacobâ€™s ladder in magnetic alloys. European Physical Journal B, 2018, 91, 1.	0.6	15
37895	Data-driven design of inorganic materials with the Automatic Flow Framework for Materials Discovery. MRS Bulletin, 2018, 43, 670-675.	1.7	35
37896	A Review of Current Development of Graphene Mechanics. Crystals, 2018, 8, 357.	1.0	68
37897	In Situ Observations of Early Stage Oxidation of Ni-Cr and Ni-Cr-Mo Alloys. Corrosion, 2018, 74, 939-946.	0.5	39
37898	Clarification of the Molecular Doping Mechanism in Organic Singleâ€Crystalline Semiconductors and their Application in Colorâ€Tunable Lightâ€Emitting Devices. Advanced Materials, 2018, 30, e1801078.	11.1	53
37899	Properties Design: Prediction and Experimental Validation of the Luminescence Properties of a New Eu^{II}â€Based Phosphor. Chemistry - A European Journal, 2018, 24, 16276-16281.	1.7	11
37900	Materials Informatics for Dark Matter Detection. Physica Status Solidi - Rapid Research Letters, 2018, 12, 1800293.	1.2	30
37901	Atomicâ€Scale Valence State Distribution inside Ultrafine CeO₂ Nanocubes and Its Size Dependence. Small, 2018, 14, e1802915.	5.2	77
37902	One-pot synthesized porous Ti-doped MoO2 anode material for high energy density lithium ion batteries. Journal of Materials Science: Materials in Electronics, 2018, 29, 17571-17579.	1.1	5
37903	Distinct magnetic responses under hydrostatic pressure in Mn-Ga phase with variant crystallographic structure. Intermetallics, 2018, 102, 72-77.	1.8	1

#	Article	IF	Citations
37904	Chemically Functionalized Penta-stanene Monolayers for Light Harvesting with High Carrier Mobility. Journal of Physical Chemistry C, 2018, 122, 21763-21769.	1.5	18
37905	Molecularly thin two-dimensional hybrid perovskites with tunable optoelectronic properties due to reversible surface relaxation. Nature Materials, 2018, 17, 908-914.	13.3	295
37906	Electrical half-wave rectification at ferroelectric domain walls. Nature Nanotechnology, 2018, 13, 1028-1034.	15.6	77
37907	Li-decorated carbon eneâ€“yne as a potential high-capacity hydrogen storage medium. Physical Chemistry Chemical Physics, 2018, 20, 24011-24018.	1.3	7
37908	First-principles study of magnetization reorientation and large perpendicular magnetic anisotropy in <mml:math xmlns:mml="http://www.w3.org/1998/Math/MathML"><mml:mi>Cu</mml:mi><mml:mrow><mml:msub><mml:mi>Fe</mml:mi><mml:mn>4</mml:mn></mml:msub></mml:mrow><mml:mo>/</mml:mo><mml:mi>MgO</mml:mi><mml:msub><mml:mi mathvariant="normal">O</mml:mi><mml:mn>4</mml:mn></mml:msub></mml:mrow><mml:mo>/</mml:mo><mml:mi>MgO</mml:mi> heterostructures. Physical Review B, 2018, 98, .	1.1	14
37909	Laser/Electron Irradiation on Indium Phosphide (InP) Semiconductor: Promising Pathways to In Situ Formation of Indium Nanoparticles. Particle and Particle Systems Characterization, 2018, 35, 1800237.	1.2	12
37910	Controlled Airâ€Etching Synthesis of Porousâ€Carbon Nanotube Aerogels with Ultrafast Charging at 1000 A g^{â^'1}. Small, 2018, 14, e1802394.	5.2	37
37911	Lattice thermal conductivity and bandgap engineering of a three-dimensional <mml:math xmlns:mml="http://www.w3.org/1998/Math/MathML" altimg="si21.gif" overflow="scroll"><mml:mrow><mml:msup><mml:mrow><mml:mi mathvariant="italic">sp</mml:mi></mml:mrow><mml:mrow><mml:mn>2</mml:mn></mml:mrow></mml:msup></mml:mrow></mml:m Dirac carbon material. HS-C18. Computational Materials Science, 2018, 155, 293-297.	1.4	9
37912	Metalâ€toâ€Semiconductor Transition and Electronic Dimensionality Reduction of Ca₂N Electride under Pressure. Advanced Science, 2018, 5, 1800666.	5.6	36
37913	Electronic Structure and Optical Properties of LiBiO3 Doped with V, Nb, and Ta. Journal Wuhan University of Technology, Materials Science Edition, 2018, 33, 863-870.	0.4	1
37914	In-situ investigation of pressure effect on structural evolution and conductivity of Na3SbS4 superionic conductor. Journal of Power Sources, 2018, 401, 111-116.	4.0	26
37915	Structural, thermodynamic, electronic and magnetic properties of Sr3Sn1â^'xYxO (Yâ€¯=â€¯V, Fe) from first-principles study. Results in Physics, 2018, 11, 283-290.	2.0	5
37916	Modeling the Phase-Change Memory Material, Ge₂Sb₂Te₅, with a Machine-Learned Interatomic Potential. Journal of Physical Chemistry B, 2018, 122, 8998-9006.	1.2	102
37917	Low toxic Cu2GeS3/InP quantum dot sensitized infrared solar cells. Journal of Renewable and Sustainable Energy, 2018, 10, .	0.8	9
37918	Far-infrared reflectivity spectra of nanotwinned GaV₄Se₈. Phase Transitions, 2018, 91, 942-952.	0.6	1
37919	First principle study of structural, electronic, mechanical, dynamic and optical properties of half-Heusler compound LiScSi under pressure. Phase Transitions, 2018, 91, 1206-1222.	0.6	37
37920	Ultrathin MXene Nanosheets Decorated with TiO₂ Quantum Dots as an Efficient Sulfur Host toward Fast and Stable Liâ€“S Batteries. Small, 2018, 14, e1802443.	5.2	125
37921	Colorimetric oxygen sensor based on nano-sized black TiO2 catalysts: DFT modeling and experiments. Molecular Catalysis, 2018, 459, 16-20.	1.0	1

#	Article	IF	Citations
37922	First-principles calculations of the electronic properties of SiC-based bilayer and trilayer heterostructures. Physical Chemistry Chemical Physics, 2018, 20, 24726-24734.	1.3	77
37923	Self-scrolling MoS₂ metallic wires. Nanoscale, 2018, 10, 18178-18185.	2.8	83
37924	High energetic polymeric nitrogen sheet confined in a graphene matrix. RSC Advances, 2018, 8, 30912-30918.	1.7	14
37925	Self-trapped holes in BaTiO3. Journal of Applied Physics, 2018, 124, .	1.1	12
37926	Pressure-induced structural and electronic transitions in kesterite-type Cu2ZnSnS4. Journal of Applied Physics, 2018, 124, 085905.	1.1	7
37927	Dynamics of liquid crystal on hexagonal lattice. 2D Materials, 2018, 5, 045021.	2.0	5
37928	Clustering of hydrogen, phosphorus, and vacancies in diamond: A density functional theory analysis. Physical Review B, 2018, 98, .	1.1	22
37929	Dynamics and fragmentation mechanism of (C₅H₄CH₃)Pt(CH₃)₃ on SiO₂ surfaces. Beilstein Journal of Nanotechnology, 2018, 9, 711-720.	1.5	10
37930	End-member compounds of a 4-sublattice model of multicomponent BCC solid solutions. Data in Brief, 2018, 20, 1018-1022.	0.5	2
37931	Morphology control of Co2C nanostructures via the reduction process for direct production of lower olefins from syngas. Journal of Catalysis, 2018, 366, 289-299.	3.1	52
37932	High-Throughput Computational Screening of Vertical 2D van der Waals Heterostructures for High-efficiency Excitonic Solar Cells. ACS Applied Materials & Interfaces, 2018, 10, 32142-32150.	4.0	75
37933	The dimensional and hydrogenating effect on the electronic properties of ZnSe nanomaterials: a computational investigation. Physical Chemistry Chemical Physics, 2018, 20, 24453-24464.	1.3	4
37934	Double-atom catalysts: transition metal dimer-anchored C₂N monolayers as N₂ fixation electrocatalysts. Journal of Materials Chemistry A, 2018, 6, 18599-18604.	5.2	224
37935	Nontrivial topology and topological phase transition in two-dimensional monolayer Tl. Physical Chemistry Chemical Physics, 2018, 20, 24790-24795.	1.3	8
37936	Monitoring the effect of asymmetrical vertical strain on Janus single layers of MoSSe via vibrational spectrum. Journal of Chemical Physics, 2018, 149, 084707.	1.2	13
37937	Energetics and kinetics of vacancy defects in 4H -SiC. Physical Review B, 2018, 98, .	1.1	26
37938	Valence band inversion and spin-orbit effects in the electronic structure of monolayer GaSe. Physical Review B, 2018, 98, .	1.1	47
37939	Quadratic contact point semimetal: Theory and material realization. Physical Review B, 2018, 98, .	1.1	57

#	Article	IF	Citations
37940	Computational exploration of two-dimensional silicon diarsenide and germanium arsenide for photovoltaic applications. Beilstein Journal of Nanotechnology, 2018, 9, 1247-1253.	1.5	14
37941	Limits on the Contribution of Endogenic Radiolysis to the Presence of Molecular Oxygen in Comet 67P/Churyumovâ€“Gerasimenko. Astrophysical Journal, 2018, 864, 9.	1.6	3
37942	Micropillar compression deformation of single crystals of Mo5SiB2 with the tetragonal D8 structure. Acta Materialia, 2018, 159, 416-428.	3.8	29
37943	Mechanical-pressure induced response of the MOF Al-MIL-53-TDC. Polyhedron, 2018, 155, 144-148.	1.0	17
37944	Superconductivity in Anti-ThCr2Si2-type Er2O2Bi Induced by Incorporation of Excess Oxygen with CaO Oxidant. Inorganic Chemistry, 2018, 57, 10587-10590.	1.9	14
37945	Developing an interatomic potential for martensitic phase transformations in zirconium by machine learning. Npj Computational Materials, 2018, 4, .	3.5	79
37946	Atomically sharp interlayer stacking shifts at anti-phase grain boundaries in overlapping MoS₂ secondary layers. Nanoscale, 2018, 10, 16692-16702.	2.8	22
37947	High-performance photodetectors based on two-dimensional tin(<scp>ii</scp>) sulfide (SnS) nanoflakes. Journal of Materials Chemistry C, 2018, 6, 10036-10041.	2.7	54
37948	High-temperature Dirac half-metal PdCl₃: a promising candidate for realizing quantum anomalous Hall effect. Journal of Materials Chemistry C, 2018, 6, 10284-10291.	2.7	52
37949	Two-dimensional transitional metal dihydride crystals with anisotropic and spin-polarized Fermi Dirac cones. Journal of Materials Chemistry C, 2018, 6, 11243-11247.	2.7	7
37950	Effect of oxygen vacancy on antisite disorder in LaFeO3/LaMnO3 heterostructure: A first-principles study. AIP Conference Proceedings, 2018, , .	0.3	0
37951	Pressure-induced reversible phase transition on Mo2Ga2C. Journal of Applied Physics, 2018, 124, .	1.1	7
37952	Azulene revisited: solid-state structure, invariom modeling and lattice-energy minimization of a classical example of disorder. Acta Crystallographica Section B: Structural Science, Crystal Engineering and Materials, 2018, 74, 416-426.	0.5	25
37953	Thicknessâ€Dependent Carrier Transport Characteristics of a New 2D Elemental Semiconductor: Black Arsenic. Advanced Functional Materials, 2018, 28, 1802581.	7.8	125
37954	Tunable Electronic and Magnetic Properties of Grapheneâ€Embedded Transition Metalâ€N₄ Complexes: Insightâ€‰From Firstâ€Principles Calculations. Chemistry - an Asian Journal, 2018, 13, 3239-3245.	1.7	18
37955	Mixedâ€valence Compounds: AuO₂ and AuS. ChemPhysChem, 2018, 19, 2989-2994.	1.0	7
37956	Performance of Elbrus Processors forÂComputational Materials Science Codes and Fast Fourier Transform. Communications in Computer and Information Science, 2018, , 92-103.	0.4	0
37957	Theoretical analysis of band alignment and charge carriers migration in mixed-phase TiO2 systems. Journal of Computational Electronics, 2018, 17, 1505-1514.	1.3	9

#	Article	IF	Citations
37958	PRISMS: An Integrated, Open-Source Framework for Accelerating Predictive Structural Materials Science. Jom, 2018, 70, 2298-2314.	0.9	30
37959	On the interfacial phase growth and vacancy evolution during accelerated electromigration in Cu/Sn/Cu microjoints. Acta Materialia, 2018, 160, 185-198.	3.8	35
37960	Lattice distortion in a strong and ductile refractory high-entropy alloy. Acta Materialia, 2018, 160, 158-172.	3.8	325
37961	The role of Ni in modifying the order of the phase transition of La(Fe,Ni,Si)13. Acta Materialia, 2018, 160, 137-146.	3.8	45
37962	Nature of localized phonon modes of tilt grain boundaries in graphene. Carbon, 2018, 140, 250-258.	5.4	18
37963	Origin of low Young modulus of multicomponent, biomedical Ti alloys - Seeking optimal elastic properties through a first principles investigation. Journal of the Mechanical Behavior of Biomedical Materials, 2018, 88, 352-361.	1.5	15
37964	13C NMR spectrum of crystalline [Rh(Acac) (CO)2]: A contribution to the discussion on [Rh(Acac) (CO)2] molecular structure in the solid state. Journal of Organometallic Chemistry, 2018, 874, 70-73.	0.8	0
37965	Ultraviolet-light-driven charge carriers tunability mechanism in graphene. Materials and Design, 2018, 159, 232-239.	3.3	8
37966	Czochralski Growth and Characterization of a Novel Nonlinear Optical Crystal Te2P2O9. Crystal Growth and Design, 2018, 18, 5919-5926.	1.4	20
37967	New Class of 3.7 V Fe-Based Positive Electrode Materials for Na-Ion Battery Based on Cation-Disordered Polyanion Framework. Chemistry of Materials, 2018, 30, 6346-6352.	3.2	23
37968	Why Some Noncentrosymmetric Borates Do Not Make Good Nonlinear Optical Materials: A Case Study with K₃B₅O₈(OH)₂. Inorganic Chemistry, 2018, 57, 11801-11808.	1.9	17
37969	Adsorption of Acetone on Rutile TiO₂: A DFT and FTIRS Study. Journal of Physical Chemistry C, 2018, 122, 19481-19490.	1.5	23
37970	First-Principles Based Microkinetic Modeling of CO₂ Reduction at the Ni/SDC Cathode of a Solid Oxide Electrolysis Cell. Journal of Physical Chemistry C, 2018, 122, 21151-21161.	1.5	43
37971	Polytypism in Hexagonal Tungsten Trioxide: Insights from Ab Initio Molecular Dynamics Simulations. Journal of Physical Chemistry C, 2018, 122, 21644-21650.	1.5	7
37972	Adsorption of Monocyclic Aromatics on Transition Metal Surfaces: Insight into Variation of Binding Strength from First-Principles. Journal of Physical Chemistry C, 2018, 122, 21897-21909.	1.5	39
37973	Evaluating the Stability of Single-Atom Catalysts with High Chemical Activity. Journal of Physical Chemistry C, 2018, 122, 21919-21926.	1.5	20
37974	Robust Half-Metallic Magnetism in Two-Dimensional Fe/MoS₂. Journal of Physical Chemistry C, 2018, 122, 21617-21622.	1.5	18
37975	Concerted Metal Cation Desorption and Proton Transfer on Deprotonated Silica Surfaces. Journal of Physical Chemistry Letters, 2018, 9, 5379-5385.	2.1	19

#	Article	IF	Citations
37976	Tuning Local Electrical Conductivity via Fine Atomic Scale Structures of Two-Dimensional Interfaces. Nano Letters, 2018, 18, 6030-6036.	4.5	22
37977	Electron Density Optimization and the Anisotropic Thermoelectric Properties of Ti Self-Intercalated Ti_{1+x}S₂ Compounds. ACS Applied Materials & Interfaces, 2018, 10, 32344-32354.	4.0	23
37978	Heterogeneous Nanostructure Design Based on the Epitaxial Growth of Spongy MoS_x on 2D Co(OH)₂ Nanoflakes for Triple-Enzyme Mimetic Activity: Experimental and Density Functional Theory Studies on the Dramatic Activation Mechanism. ACS Applied Materials & Interfaces, 2018, 10, 32567-32578.	4.0	32
37979	Surface Adsorption Affects the Performance of Alkaline Anion-Exchange Membrane Fuel Cells. ACS Catalysis, 2018, 8, 9429-9439.	5.5	55
37980	Quantitative Analysis of Calcium Phosphate Nanocluster Growth Using Time-of-Flight Medium-Energy-Ion-Scattering Spectroscopy. ACS Central Science, 2018, 4, 1253-1260.	5.3	5
37981	Modulation of Hydrogen Evolution Catalytic Activity of Basal Plane in Monolayer Platinum and Palladium Dichalcogenides. ACS Omega, 2018, 3, 10058-10065.	1.6	46
37982	Single Cobalt Atoms Anchored on Porous N-Doped Graphene with Dual Reaction Sites for Efficient Fenton-like Catalysis. Journal of the American Chemical Society, 2018, 140, 12469-12475.	6.6	1,044
37983	Cationic Ordering Coupled to Reconstruction of Basic Building Units during Synthesis of High-Ni Layered Oxides. Journal of the American Chemical Society, 2018, 140, 12484-12492.	6.6	113
37984	Color-stable highly luminescent sky-blue perovskite light-emitting diodes. Nature Communications, 2018, 9, 3541.	5.8	536
37985	Mapping the elastic properties of two-dimensional MoS2 via bimodal atomic force microscopy and finite element simulation. Npj Computational Materials, 2018, 4, .	3.5	61
37986	Tetrahedral honeycomb surface reconstructions of quartz, cristobalite and stishovite. Scientific Reports, 2018, 8, 11947.	1.6	12
37987	Visualizing Degradation of Black Phosphorus Using Liquid Crystals. Scientific Reports, 2018, 8, 12966.	1.6	10
37988	Strong electronâ€“phonon interaction retarding phonon transport in superconducting hydrogen sulfide at high pressures. Physical Chemistry Chemical Physics, 2018, 20, 24222-24226.	1.3	7
37989	Tuning coreâ€“shell interactions in tungsten carbideâ€“Pt nanoparticles for the hydrogen evolution reaction. Physical Chemistry Chemical Physics, 2018, 20, 23262-23271.	1.3	11
37990	Tunable interlayer coupling and Schottky barrier in graphene and Janus MoSSe heterostructures by applying an external field. Physical Chemistry Chemical Physics, 2018, 20, 24109-24116.	1.3	86
37991	n- and p-type ohmic contacts at monolayer gallium nitrideâ€“metal interfaces. Physical Chemistry Chemical Physics, 2018, 20, 24239-24249.	1.3	13
37992	Structural and electronic properties Te62+ and Te82+: A DFT study. AIP Conference Proceedings, 2018, , .	0.3	0
37993	Nontrivial superconductivity in topological MoTe2â^'xSx crystals. Proceedings of the National Academy of Sciences of the United States of America, 2018, 115, 9503-9508.	3.3	65

#	Article	IF	Citations
37994	PtSe₂/graphene hetero-multilayer: gate-tunable Schottky barrier height and contact type. Nanotechnology, 2018, 29, 465707.	1.3	22
37995	Midinfrared one-dimensional photonic crystal constructed from two-dimensional electride material. Physical Review B, 2018, 98, .	1.1	10
37996	Characterization of epitaxial silicene with Raman spectroscopy. Physical Review B, 2018, 98, .	1.1	7
37997	Gate-dependent vacancy diffusion in graphene. Physical Review B, 2018, 98, .	1.1	10
37998	Electronic properties of a Ï€-conjugated Cairo pentagonal lattice: Direct band gap, ultrahigh carrier mobility, and slanted Dirac cones. Physical Review B, 2018, 98, .	1.1	22
37999	Two-dimensional imaging of energy bands from crystal orientation dependent higher-order harmonic spectra in <mml:math xmlns:mml="http://www.w3.org/1998/Math/MathML"><mml:mrow><mml:mi>h</mml:mi><mml:mo>â^'</mml:mo><mml:mi>BN</mml:mi></mml:mr Physical Review B, 2018, 98, .	1.1	65
38000	Comparative study of electronic and magnetic properties of iron and cobalt phthalocyanine molecules physisorbed on two-dimensional <mml:math xmlns:mml="http://www.w3.org/1998/Math/MathML"><mml:msub><mml:mi>MoS</mml:mi><mml:mn>2</mml:mn></mml:msub></mm and graphene. Physical Review B, 2018, 98, .	1.1	24
38001	Ab initio study of transition metals impurities and stability of complexes in germanium (Ge). Ife Journal of Science, 2018, 20, 433.	0.1	0
38002	Enthalpies of formation of rare-earth borides from first principles. Comparison with experimental values. Calphad: Computer Coupling of Phase Diagrams and Thermochemistry, 2018, 62, 49-60.	0.7	11
38003	Screened Coulomb hybrid density functional investigation of oxygen point defects on ZnO nanowires. Computational Condensed Matter, 2018, 16, e00307.	0.9	2
38004	Hydrogen trapping in helium-implanted W and W-Ta alloy: First-principles approach. Journal of Nuclear Materials, 2018, 508, 249-256.	1.3	12
38005	Surface phase diagrams of titanium in Oxygen, Nitrogen and Hydrogen environments: A first principles analysis. Surface Science, 2018, 677, 18-25.	0.8	20
38006	Abnormal band bowing effects in phase instability crossover region of GaSe1-xTe x nanomaterials. Nature Communications, 2018, 9, 1927.	5.8	20
38007	Extremely stable graphene electrodes doped with macromolecular acid. Nature Communications, 2018, 9, 2037.	5.8	96
38008	Efficient charge separation and visible-light response in bilayer HfS₂-based van der Waals heterostructures. RSC Advances, 2018, 8, 18889-18895.	1.7	20
38009	Determining ideal strength and failure mechanism of thermoelectric CuInTe2 through quantum mechanics. Journal of Materials Chemistry A, 2018, 6, 11743-11750.	5.2	10
38010	Morphology control of anatase TiO2 for well-defined surface chemistry. Physical Chemistry Chemical Physics, 2018, 20, 14362-14373.	1.3	25
38011	Photocarrier dynamics in monolayer phosphorene and bulk black phosphorus. Nanoscale, 2018, 10, 11307-11313.	2.8	29

#	Article	IF	Citations
38012	Global minimum beryllium hydride sheet with novel negative Poisson's ratio: first-principles calculations. RSC Advances, 2018, 8, 19432-19436.	1.7	7
38013	High-pressure chemistry of hydrocarbons relevant to planetary interiors and inertial confinement fusion. Physics of Plasmas, 2018, 25, .	0.7	24
38014	Predicting the thermodynamic stability of double-perovskite halides from density functional theory. APL Materials, 2018, 6, .	2.2	42
38015	A tungsten-rhenium interatomic potential for point defect studies. Journal of Applied Physics, 2018, 123, .	1.1	22
38016	Point-Defect Nature of the Ultraviolet Absorption Band in AlN. Physical Review Applied, 2018, 9, .	1.5	41
38017	Cu Metal/Mn Phthalocyanine Organic Spinterfaces atop Co with High Spin Polarization at Room Temperature. Advanced Functional Materials, 2018, 28, 1707123.	7.8	9
38018	Few Layered N, P Dualâ€Doped Carbonâ€Encapsulated Ultrafine MoP Nanocrystal/MoP Cluster Hybrids on Carbon Cloth: An Ultrahigh Active and Durable 3D Selfâ€Supported Integrated Electrode for Hydrogen Evolution Reaction in a Wide pH Range. Advanced Functional Materials, 2018, 28, 1801527.	7.8	142
38019	Electrochemical Ammonia Synthesis via Nitrogen Reduction Reaction on a MoS₂ Catalyst: Theoretical and Experimental Studies. Advanced Materials, 2018, 30, e1800191.	11.1	697
38020	Structural and Electronic Properties of Inorganic Mixed Halide Perovskites. Physica Status Solidi - Rapid Research Letters, 2018, 12, 1800193.	1.2	19
38021	Construction of bilayer PdSe2 on epitaxial graphene. Nano Research, 2018, 11, 5858-5865.	5.8	84
38022	CaFe2O4 oxygen carrier characterization during the partial oxidation of coal in the chemical looping gasification application. Applied Energy, 2018, 224, 708-716.	5.1	38
38023	Catalytic activity of Î³-AlOOH (0â€¯0â€¯1) surface in syngas conversion: Probing into the mechanism of carbon chain growth. Applied Surface Science, 2018, 455, 123-131.	3.1	14
38024	Thermodynamic modeling of the La-Te system aided by first-principles calculations. Calphad: Computer Coupling of Phase Diagrams and Thermochemistry, 2018, 61, 227-236.	0.7	4
38025	High chemisorption abilities of hydrogen and oxygen on ultrasmall iron clusters: A first-principles study. Chemical Physics Letters, 2018, 705, 59-64.	1.2	3
38026	Synthesis and characterization of monodisperse yttrium aluminum garnet (YAG) micro-crystals with rhombic dodecahedron. Journal of Alloys and Compounds, 2018, 762, 537-547.	2.8	6
38027	ns2 lone pair (E) and structural evolution of trichlorides M*Cl3E (M*Â= N, P, As, Sb and Bi) series. Stereochemistry and ab initio topology of Cl electron pair triplets. Solid State Sciences, 2018, 82, 44-51.	1.5	2
38028	Significant Dzyaloshinskiiâ€“Moriya interaction at grapheneâ€“ferromagnet interfaces due to the Rashba effect. Nature Materials, 2018, 17, 605-609.	13.3	188
38029	Phase transition in metalâ€“organic complex trans-PtCl₂(PEt₃)₂ under pressure: insights into the molecular and crystal structure. CrystEngComm, 2018, 20, 3728-3740.	1.3	5

#	Article	IF	Citations
38030	Directed self-assembly pathways of three-dimensional Pt/Pd nanocrystal superlattice electrocatalysts for enhanced methanol oxidationÂreaction. Journal of Materials Chemistry A, 2018, 6, 12759-12767.	5.2	31
38031	Oxide-ion conduction via interstitials in scheelite-type LaNbO₄: a first-principles study. Journal of Materials Chemistry A, 2018, 6, 12004-12011.	5.2	20
38032	Enhanced doping effect on tuning structural phases of monolayer antimony. Applied Physics Letters, 2018, 112, 213104.	1.5	13
38033	The nature of the Pt(111)/Î±-Fe2O3(0001) interfaces revealed by DFT calculations. Journal of Chemical Physics, 2018, 148, 204701.	1.2	8
38034	Proximity exchange induced gap opening and topological feature in graphene/1Tâ€²-MX₂ (Mâ€‰â€‰=â€‰â€‰Mo,W; Xâ€‰â€‰=â€‰â€‰S,Se,Te) Dirac heterostructures. Journal of Physics Condensed Matter, 2018, 30,	0.7	3
38035	First-principles study of plutonium adsorption on perfect and defective graphene and hexagonal boron nitride. Materials Research Express, 2018, 5, 055041.	0.8	3
38036	New Possible Structure of Silicide Mg2Si under Pressure. Physics of the Solid State, 2018, 60, 865-869.	0.2	0
38037	First-principles study on the mechanism of lithium intercalation in cubic CoN. Modern Physics Letters B, 2018, 32, 1850184.	1.0	2
38038	Anchoring effects of S-terminated Ti2C MXene for lithium-sulfur batteries: A first-principles study. Applied Surface Science, 2018, 455, 522-526.	3.1	134
38039	First principle study of tritium trapping at oxygen vacancies in Li4SiO4. Journal of Nuclear Materials, 2018, 508, 257-264.	1.3	7
38040	Structural, electronic, and magnetic properties of gas molecules on Mo-, Si-, and Pt-doped BC3 sheets. Journal of Physics and Chemistry of Solids, 2018, 121, 247-255.	1.9	8
38041	Spectroscopic Limited Practical Efficiency (SLPE) model for organometal halide perovskites solar cells evaluation. Organic Electronics, 2018, 59, 389-398.	1.4	6
38042	A novel superhard tungsten nitride predicted by machine-learning accelerated crystal structure search. Science Bulletin, 2018, 63, 817-824.	4.3	102
38043	Identifying Few-Molecule Water Clusters with High Precision on Au(111) Surface. ACS Nano, 2018, 12, 6452-6457.	7.3	25
38044	Hydrogen adsorption engineering by intramolecular proton transfer on 2D nanosheets. NPG Asia Materials, 2018, 10, 441-454.	3.8	16
38045	Transition metal atoms absorbed on MoS₂/h-BN heterostructure: stable geometries, band structures and magnetic properties. Physical Chemistry Chemical Physics, 2018, 20, 17387-17392.	1.3	12
38046	Achieving half-metallicity in zigzag MoS₂ nanoribbon with a sulfur vacancy by edge passivation. Journal Physics D: Applied Physics, 2018, 51, 265005.	1.3	5
38047	A type-I van der Waals heterobilayer of WSe₂/MoTe₂. Nanotechnology, 2018, 29, 335203.	1.3	24

#	Article	IF	Citations
38048	Performance of various density-functional approximations for cohesive properties of 64 bulk solids. New Journal of Physics, 2018, 20, 063020.	1.2	185
38049	Metal-substitution strategy to control the conductive path in titanium dioxide: ab initio calculations. European Physical Journal B, 2018, 91, 1.	0.6	4
38050	Ultrahigh Tunneling-Magnetoresistance Ratios in Nitride-Based Perpendicular Magnetic Tunnel Junctions from First Principles. Physical Review Applied, 2018, 9, .	1.5	22
38051	Sum-frequency ionic Raman scattering. Physical Review B, 2018, 97, .	1.1	55
38052	Biaxial strain engineering of charge ordering and orbital ordering in HoNiO3. Physical Review B, 2018, 97, .	1.1	5
38053	Single-crystal study of the charge density wave metal <mml:math xmlns:mml="http://www.w3.org/1998/Math/MathML"><mml:mtext>LuNiC</mml:mtext><mml:msub><mml:mrow /><mml:mn>2</mml:mn></mml:msub></mml:math>. Physical Review B, 2018, 97, .	1.1	17
38054	Phonon-coupled ultrafast interlayer charge oscillation at van der Waals heterostructure interfaces. Physical Review B, 2018, 97, .	1.1	81
38055	Applying the Coupled-Cluster Ansatz to Solids and Surfaces in the Thermodynamic Limit. Physical Review X, 2018, 8, .	2.8	80
38056	Enhancement of photoluminescence and hole mobility in 1- to 5-layer InSe due to the top valence-band inversion: strain effect. Nanoscale, 2018, 10, 11441-11451.	2.8	58
38057	Hydrogen plasma reduced potassium titanate as a high power and ultralong lifespan anode material for sodium-ion batteries. Journal of Materials Chemistry A, 2018, 6, 22037-22042.	5.2	18
38058	Transition metal intercalated bilayer silicene. AIP Conference Proceedings, 2018, , .	0.3	1
38059	n-type Rashba spin splitting in a bilayer inorganic halide perovskite with external electric field. Journal of Physics Condensed Matter, 2018, 30, 265501.	0.7	6
38060	Antidamping-Torque-Induced Switching in Biaxial Antiferromagnetic Insulators. Physical Review Letters, 2018, 120, 207204.	2.9	246
38061	Characterization and Modeling of Deformation Mechanisms in Ni-Base Superalloy 718. Minerals, Metals and Materials Series, 2018, , 319-338.	0.3	3
38062	First principle study of chain termination reactions during Fischer-Tropsch Synthesis on Ï‡ -Fe 5 C 2 (010). Molecular Catalysis, 2018, 453, 55-63.	1.0	8
38063	Insights into the Li+ storage mechanism of TiC@C-TiO2 core-shell nanostructures as high performance anodes. Nano Energy, 2018, 50, 25-34.	8.2	53
38064	Atomic rearrangement from disordered to ordered Pd-Fe nanocatalysts with trace amount of Pt decoration for efficient electrocatalysis. Nano Energy, 2018, 50, 70-78.	8.2	66
38065	High-Pressure-Induced Phase Transition in 2,5-Diketopiperazine: The Anisotropic Compression of Nâ€“HÂ·Â·Â·O Hydrogen-Bonded Tapes. Journal of Physical Chemistry C, 2018, 122, 11747-11753.	1.5	7

#	Article	IF	Citations
38066	Highly Sensitive Electromechanical Piezoresistive Pressure Sensors Based on Large-Area Layered PtSe₂ Films. Nano Letters, 2018, 18, 3738-3745.	4.5	125
38067	SnO₂/Reduced Graphene Oxide Interlayer Mitigating the Shuttle Effect of Liâ€“S Batteries. ACS Applied Materials & Interfaces, 2018, 10, 18665-18674.	4.0	129
38068	Strain induced electronic structure variation in methyl-ammonium lead iodide perovskite. Scientific Reports, 2018, 8, 7760.	1.6	53
38069	Computational screening of high-performance optoelectronic materials using OptB88vdW and TB-mBJ formalisms. Scientific Data, 2018, 5, 180082.	2.4	79
38070	3D charge and 2D phonon transports leading to high out-of-plane ZT in n-type SnSe crystals. Science, 2018, 360, 778-783.	6.0	859
38071	CO ₂ electroreduction to ethylene via hydroxide-mediated copper catalysis at an abrupt interface. Science, 2018, 360, 783-787.	6.0	1,638
38073	Weak Electron Phonon Coupling and Deep Level Impurity for High Thermoelectric Performance Pb_{1â^'}_xGa_xTe. Advanced Energy Materials, 2018, 8, 1800659.	10.2	111
38074	Highâ€Pressure Synthesis of a Nitrogenâ€Rich Inclusion Compound ReN₈â‹…xâ€‰N₂ with Conjugated Polymeric Nitrogen Chains. Angewandte Chemie - International Edition, 2018, 57, 9048-9053.	7.2	70
38075	BoltzTraP2, a program for interpolating band structures and calculating semi-classical transport coefficients. Computer Physics Communications, 2018, 231, 140-145.	3.0	730
38076	Chemical and substitutional doping, and anti-site and vacancy formation in monolayer AlN and GaN. Physical Chemistry Chemical Physics, 2018, 20, 16077-16091.	1.3	45
38077	Tuning the electrocatalytic activity of Pt by structurally ordered PdFe/C for the hydrogen oxidation reaction in alkaline media. Journal of Materials Chemistry A, 2018, 6, 11346-11352.	5.2	41
38078	Interplay of cation and anion redox in Li ₄ Mn ₂ O ₅ cathode material and prediction of improved Li ₄ (Mn,M) ₂ O ₅ electrodes for Li-ion batteries. Science Advances, 2018, 4, eaao6754.	4.7	58
38079	Local spatial charge separation and proton activation induced by surface hydroxylation promoting photocatalytic hydrogen evolution of polymeric carbon nitride. Nano Energy, 2018, 50, 383-392.	8.2	226
38080	Atomically Resolved Observation of Continuous Interfaces between an As-Grown MoS₂ Monolayer and a WS₂/MoS₂ Heterobilayer on SiO₂. ACS Applied Nano Materials, 2018, 1, 2041-2048.	2.4	13
38081	Large quantum-spin-Hall gap in single-layer 1Tâ€² WSe2. Nature Communications, 2018, 9, 2003.	5.8	117
38082	Lithiation-induced amorphization of Pd3P2S8 for highly efficient hydrogen evolution. Nature Catalysis, 2018, 1, 460-468.	16.1	247
38083	Modified MXene: promising electrode materials for constructing Ohmic contacts with MoS₂for electronic device applications. Physical Chemistry Chemical Physics, 2018, 20, 16551-16557.	1.3	44
38084	Theoretical modeling of tip-enhanced resonance Raman images of switchable azobenzene molecules on Au(111). Nanoscale, 2018, 10, 11850-11860.	2.8	12

#	Article	IF	Citations
38085	Coherent control of thermal phonon transport in van der Waals superlattices. Nanoscale, 2018, 10, 14432-14440.	2.8	13
38086	Theoretical design of blue phosphorene/arsenene lateral heterostructures with superior electronic properties. Journal Physics D: Applied Physics, 2018, 51, 255304.	1.3	28
38087	Phase transition studies of Na₃Bi system under uniaxial strain. Journal of Physics Condensed Matter, 2018, 30, 125502.	0.7	7
38088	Evidence of large spin-orbit coupling effects in quasi-free-standing graphene on Pb/Ir(1â€‰1â€‰1). 2D Materials, 2018, 5, 035029.	2.0	33
38089	Exfoliation of single layer BiTeI flakes. 2D Materials, 2018, 5, 031013.	2.0	34
38090	Magnesium acceptor in gallium nitride. II. Koopmans-tuned Heyd-Scuseria-Ernzerhof hybrid functional calculations of its dual nature and optical properties. Physical Review B, 2018, 97, .	1.1	16
38091	Reversible Sodium and Lithium Insertion in Iron Fluoride Perovskites. Advanced Functional Materials, 2018, 28, 1802057.	7.8	33
38092	Tunable electronic structure and magnetic coupling in strained two-dimensional semiconductor MnPSe3. Frontiers of Physics, 2018, 13, 1.	2.4	30
38093	Lone-pair electrons induced anomalous enhancement of thermal transport in strained planar two-dimensional materials. Nano Energy, 2018, 50, 425-430.	8.2	55
38094	A comparison study of the Born effective charges and dielectric properties of the cubic, tetragonal, monoclinic, ortho-I, ortho-II and ortho-III phases of zirconia. Solid State Sciences, 2018, 81, 58-65.	1.5	8
38095	Precisely Geometry Controlled Microsupercapacitors for Ultrahigh Areal Capacitance, Volumetric Capacitance, and Energy Density. Chemistry of Materials, 2018, 30, 3979-3990.	3.2	52
38096	A-Site Cation in Inorganic A₃Sb₂I₉ Perovskite Influences Structural Dimensionality, Exciton Binding Energy, and Solar Cell Performance. Chemistry of Materials, 2018, 30, 3734-3742.	3.2	134
38097	Chemical Activity of the Peroxide/Oxide Redox Couple: Case Study of Ba₅Ru₂O₁₁ in Aqueous and Organic Solvents. Chemistry of Materials, 2018, 30, 3882-3893.	3.2	8
38098	Negative Thermal Expansion Properties and the Role of Guest Alkali Atoms in LnFe(CN)₆ (Ln) Tj ETQq1 1 0.784314 rgBT	1.5	7
38099	High-pressure-assisted X-ray-induced damage as a new route for chemical and structural synthesis. Physical Chemistry Chemical Physics, 2018, 20, 18949-18956.	1.3	14
38100	Intrinsic composition and electronic effects of multicomponent platinum nanocatalysts with high activity and selectivity for ethanol oxidation reaction. Journal of Materials Chemistry A, 2018, 6, 11270-11280.	5.2	38
38101	Effects of surface hydroxylation on adhesion at zinc/silica interfaces. Physical Chemistry Chemical Physics, 2018, 20, 15581-15588.	1.3	6
38102	A systematic evaluation of the role of lanthanide elements in functional complex oxides; implications for energy conversion devices. Journal of Materials Chemistry A, 2018, 6, 11819-11829.	5.2	21

#	Article	IF	Citations
38103	Thermodynamic Evaluation of the Co-Al-C System by Coupling Ab Initio Calculations and CALPHAD Approach. Journal of Phase Equilibria and Diffusion, 2018, 39, 538-548.	0.5	4
38104	A mechanistic study on the decomposition of a model bio-oil compound for hydrogen production over a stepped Ni surface: Formic acid. Applied Surface Science, 2018, 452, 87-95.	3.1	18
38105	Initial oxidation of Cu(100) studied by X-ray photo-electron spectroscopy and density functional theory calculations. Surface Science, 2018, 675, 64-69.	0.8	17
38106	Tolerance Factor and Cooperative Tilting Effects in Vacancy-Ordered Double Perovskite Halides. Chemistry of Materials, 2018, 30, 3909-3919.	3.2	105
38107	Interfacial Properties of Monolayer SnSâ€“Metal Contacts. Journal of Physical Chemistry C, 2018, 122, 12322-12331.	1.5	15
38108	Surface (Electro)chemistry of CO₂ on Pt Surface: An in Situ Surface-Enhanced Infrared Absorption Spectroscopy Study. Journal of Physical Chemistry C, 2018, 122, 12341-12349.	1.5	19
38109	First-Principles Investigation of Native Interstitial Diffusion in Cr₂O₃. Journal of Physical Chemistry C, 2018, 122, 12984-12993.	1.5	19
38110	Enhancement of CO₂ binding and mechanical properties upon diamine functionalization of M₂(dobpdc) metalâ€“organic frameworks. Chemical Science, 2018, 9, 5197-5206.	3.7	39
38111	Towards an atomistic understanding of disordered carbon electrode materials. Chemical Communications, 2018, 54, 5988-5991.	2.2	84
38112	Molecular and dissociative O₂ adsorption on the Cu₂O(111) surface. Physical Chemistry Chemical Physics, 2018, 20, 20352-20362.	1.3	26
38113	How many ritonavir cases are there still out there?. Faraday Discussions, 2018, 211, 441-458.	1.6	44
38114	Atomic scale origins of sub-band gap optical absorption in gold-hyperdoped silicon. AIP Advances, 2018, 8, 055014.	0.6	18
38115	Structural transitions in hybrid improper ferroelectric <mml:math xmlns:mml="http://www.w3.org/1998/Math/MathML"><mml:mrow><mml:mi mathvariant="normal">C</mml:mi><mml:msub><mml:mi mathvariant="normal">a</mml:mi><mml:mn>3</mml:mn></mml:msub><mml:mi mathvariant="normal">T</mml:mi><mml:msub><mml:mi mathvariant="normal">i</mml:mi><mml:mn>2</mml:mn></mml:msub><mml:msub><mml:mi mathvariant	1.1	18
38116	Synthesis and Characterization of the Nano-TiO2 Visible Light Photocatalysts: Vanadium Surface Doping Modification. Journal of the Korean Physical Society, 2018, 72, 1214-1220.	0.3	2
38117	Groupâ€…IV Monochalcogenides MX (M=Ge, Sn; X=S, Se) as Chemical Anchors of Polysulfides for Lithiumâ€“Sulfur Batteries. Chemistry - A European Journal, 2018, 24, 11193-11199.	1.7	28
38118	Adsorption of Hydrogen Sulfide, Hydrosulfide and Sulfide at Cu(110) â€•Polarizability and Cooperativity Effects. First Stages of Formation of a Sulfide Layer.. ChemPhysChem, 2018, 19, 2159-2168.	1.0	13
38119	Strong Coupling of MoS₂ Nanosheets and Nitrogenâ€Doped Graphene for Highâ€Performance Pseudocapacitance Lithium Storage. Small, 2018, 14, e1704410.	5.2	89
38120	Evolution of crystal structures and electronic properties for TiS2 at high pressure. Journal of Alloys and Compounds, 2018, 757, 448-454.	2.8	18

#	Article	IF	Citations
38121	First-Principles-Derived Force Fields for CH₄ Adsorption and Diffusion in Siliceous Zeolites. Journal of Physical Chemistry C, 2018, 122, 12880-12891.	1.5	25
38122	Barium in High Oxidation States in Pressure-Stabilized Barium Fluorides. Journal of Physical Chemistry C, 2018, 122, 12448-12453.	1.5	22
38123	Controlling the Reaction Steps of Bifunctional Molecules 1,5-Dibromo-2,6-dimethylnaphthalene on Different Substrates. Journal of Physical Chemistry C, 2018, 122, 13001-13008.	1.5	21
38124	Multifunctional Binary Monolayers Ge_xP_y: Tunable Band Gap, Ferromagnetism, and Photocatalyst for Water Splitting. ACS Applied Materials & Interfaces, 2018, 10, 19897-19905.	4.0	48
38125	Mechanistic investigations of the Au catalysed Câ€“H bond activations in on-surface synthesis. Physical Chemistry Chemical Physics, 2018, 20, 15901-15906.	1.3	9
38126	Understanding the quenching nature of Mn⁴⁺in wide band gap inorganic compounds: design principles for Mn⁴⁺phosphors with higher efficiency. Physical Chemistry Chemical Physics, 2018, 20, 16992-16999.	1.3	30
38127	Transition metal anchored C₂N monolayers as efficient bifunctional electrocatalysts for hydrogen and oxygen evolution reactions. Journal of Materials Chemistry A, 2018, 6, 11446-11452.	5.2	223
38128	A super hygroscopic hydrogel for harnessing ambient humidity for energy conservation and harvesting. Energy and Environmental Science, 2018, 11, 2179-2187.	15.6	134
38129	Temperature-induced band shift in bulk Î³-InSe by angle-resolved photoemission spectroscopy. AIP Advances, 2018, 8, 055123.	0.6	5
38130	Infrared and Raman spectroscopy of Î±â€ŽZrW₂O₈: A comprehensive density functional perturbation theory and experimental study. Journal of Raman Spectroscopy, 2018, 49, 1373-1384.	1.2	18
38131	Density Functional Theory Investigation of the Role of Cocatalytic Water in Methane Steam Reforming over Anatase TiO₂ (101). Industrial & Engineering Chemistry Research, 2018, 57, 8131-8143.	1.8	8
38132	Adsorption of Polychlorinated Aromatics in EMT-Type Zeolites: A Combined Experimental-Simulation Approach. Journal of Physical Chemistry C, 2018, 122, 12731-12741.	1.5	4
38133	Appearance of Lithium-Ion Conduction in a Laâ€“Liâ€“Coâ€“O Band Insulator: Possible Route to Oxide Electrolyte. ACS Applied Energy Materials, 2018, 1, 2546-2554.	2.5	8
38134	Synthesis of Ru Icosahedral Nanocages with a Face-Centered-Cubic Structure and Evaluation of Their Catalytic Properties. ACS Catalysis, 2018, 8, 6948-6960.	5.5	66
38135	Creating Cavities at Palladiumâ€“Phosphine Interfaces for Enhanced Selectivity in Heterogeneous Biomass Conversion. ACS Catalysis, 2018, 8, 6138-6145.	5.5	19
38136	Elemental Identification by Combining Atomic Force Microscopy and Kelvin Probe Force Microscopy. ACS Nano, 2018, 12, 5274-5283.	7.3	37
38137	Conductivity Enhancement of Nickel Oxide by Copper Cation Codoping for Hybrid Organic-Inorganic Light-Emitting Diodes. ACS Photonics, 2018, 5, 3389-3398.	3.2	12
38138	Absence of Nanostructuring in NaPb_mSbTe_{m+2}: Solid Solutions with High Thermoelectric Performance in the Intermediate Temperature Regime. Journal of the American Chemical Society, 2018, 140, 7021-7031.	6.6	27

#	Article	IF	Citations
38139	Two-dimensional nitrides as highly efficient potential candidates for CO₂ capture and activation. Physical Chemistry Chemical Physics, 2018, 20, 17117-17124.	1.3	55
38140	Electronic and optical properties of CH3NH3Pb1-xAgxI3from the first-principles calculations. Journal of Renewable and Sustainable Energy, 2018, 10, 033504.	0.8	4
38141	Superior ionic and electronic properties of ReN₂ monolayers for Na-ion battery electrodes. Nanotechnology, 2018, 29, 325401.	1.3	17
38142	A theoretical study on metal atom-modified BC3 sheets for effects of gas molecule adsorptions. Applied Physics A: Materials Science and Processing, 2018, 124, 1.	1.1	24
38143	A novel hybrid sp-sp2 metallic carbon allotrope. Frontiers of Physics, 2018, 13, 1.	2.4	36
38144	Structures and energetics of point defects with charge states in zircon: A first-principles study. Journal of Alloys and Compounds, 2018, 759, 60-69.	2.8	4
38145	The crystal facet-dependent electrochemical performance of TiO2 nanocrystals for heavy metal detection: Theoretical prediction and experimental proof. Sensors and Actuators B: Chemical, 2018, 271, 195-202.	4.0	31
38146	Photoinduced Localized Hole Delays Nonradiative Electronâ€“Hole Recombination in Cesiumâ€“Lead Halide Perovskites: A Time-Domain Ab Initio Analysis. Journal of Physical Chemistry Letters, 2018, 9, 3021-3028.	2.1	22
38147	Origin of magnetic properties in carbon implanted ZnO nanowires. Scientific Reports, 2018, 8, 7758.	1.6	40
38148	Carbonate-mediated Marsâ€“van Krevelen mechanism for CO oxidation on cobalt-doped ceria catalysts: facet-dependence and coordination-dependence. Physical Chemistry Chemical Physics, 2018, 20, 16045-16059.	1.3	54
38149	Enhancement of the spin polarization of an Fe₃O₄(100) surface by nitric oxide adsorption. Physical Chemistry Chemical Physics, 2018, 20, 15871-15875.	1.3	5
38150	Novel phases and superconductivity of tin sulfide compounds. Journal of Chemical Physics, 2018, 148, 194701.	1.2	17
38151	Uniaxial stress induced band structure changes in h-SiB. AIP Conference Proceedings, 2018, , .	0.3	0
38152	Highâ€Pressure Synthesis of a Nitrogenâ€Rich Inclusion Compound ReN₈â‹…xâ€‰N₂ with Conjugated Polymeric Nitrogen Chains. Angewandte Chemie, 2018, 130, 9186-9191.	1.6	16
38153	Energetics of native defects, solute partitioning, and interfacial energy of Q precipitate in Al-Cu-Mg-Si alloys. Acta Materialia, 2018, 154, 207-219.	3.8	13
38154	Mechanistic roles of catalyst surface coating in nitrobenzene selective reduction: A first-principles study. Applied Catalysis B: Environmental, 2018, 236, 509-517.	10.8	19
38155	Tuning the electronic property of two dimensional SiSe monolayer by in-plane strain. Chemical Physics Letters, 2018, 705, 12-18.	1.2	13
38156	Theoretical insights into dehydrogenative chemisorption of alkylaromatics on Pt(1â€¯0â€¯0) and Ni(1â€¯0â€¯0). Journal of Catalysis, 2018, 363, 197-203.	3.1	3

#	Article	IF	Citations
38157	Gd(Co 1-x Ga x) 2 : Synthesis, crystal structures, and investigation of structural transformations and magnetic properties. Journal of Solid State Chemistry, 2018, 264, 68-76.	1.4	3
38158	Large positive linear magnetoresistance in the two-dimensional t 2g electron gas at the EuO/SrTiO3 interface. Scientific Reports, 2018, 8, 7721.	1.6	40
38159	Screening effects on the field enhancement factor of zigzag graphene nanoribbon arrays: a first-principles study. Physical Chemistry Chemical Physics, 2018, 20, 14627-14634.	1.3	6
38160	Intrinsic charge-mobility in benzothieno[3,2-b][1]benzothiophene (BTBT) organic semiconductors is enhanced with long alkyl side-chains. Physical Chemistry Chemical Physics, 2018, 20, 15970-15979.	1.3	21
38161	Surface termination effects on the oxygen reduction reaction rate at fuel cell cathodes. Journal of Materials Chemistry A, 2018, 6, 11929-11940.	5.2	38
38162	Predicting the stability of ternary intermetallics with density functional theory and machine learning. Journal of Chemical Physics, 2018, 148, 241728.	1.2	30
38163	Structural models of increasing complexity for icosahedral boron carbide with compositions throughout the single-phase region from first principles. Physical Review B, 2018, 97, .	1.1	9
38164	Highly Efficient Blueâ€Emitting Biâ€Doped Cs₂SnCl₆ Perovskite Variant: Photoluminescence Induced by Impurity Doping. Advanced Functional Materials, 2018, 28, 1801131.	7.8	358
38165	Tetrahexcarbon: A two-dimensional allotrope of carbon. Carbon, 2018, 137, 266-273.	5.4	91
38166	Bandgap engineering of Janus MoSSe monolayer implemented by Se vacancy. Computational Materials Science, 2018, 152, 20-27.	1.4	46
38168	Graphene Oxideâ€Template Controlled Cuboidâ€Shaped Highâ€Capacity VS₄ Nanoparticles as Anode for Sodiumâ€Ion Batteries. Advanced Functional Materials, 2018, 28, 1801806.	7.8	125
38169	Ferroelectric Sr₃Zr₂O₇: Competition between Hybrid Improper Ferroelectric and Antiferroelectric Mechanisms. Advanced Functional Materials, 2018, 28, 1801856.	7.8	89
38170	Tunable Photocatalytic Properties of GaNâ€Based Twoâ€Dimensional Heterostructures. Physica Status Solidi (B): Basic Research, 2018, 255, 1800133.	0.7	21
38171	Ab initio study of adsorption behaviors of molecular adsorbates on the surface and at the edge of MoS 2. Current Applied Physics, 2018, 18, 1013-1019.	1.1	18
38172	CO oxidation on Ni doped and Ni-M (Mâ€¯=â€¯Ca, Sc, V, Cu) bimetal-doped graphene: A first-principles study. Computational Materials Science, 2018, 151, 189-195.	1.4	9
38173	Activation of hydrogen iodide on silver tetramers: Role of confinement. Chemical Physics Letters, 2018, 705, 71-77.	1.2	2
38174	Influence of surface relaxation on solute atoms positioning within atom probe tomography reconstructions. Materials Characterization, 2018, 146, 324-335.	1.9	21
38175	Temperature dependence of NiTi martensite structures: Density functional theory calculations. Scripta Materialia, 2018, 154, 134-138.	2.6	15

#	Article	IF	Citations
38176	Oxygen Evolution Reaction on Pristine and Oxidized TiC (100) Surface in Liâ€“O₂ Battery. Journal of Physical Chemistry C, 2018, 122, 12665-12672.	1.5	27
38177	Effects of Catalyst Model and High Adsorbate Coverages in ab Initio Studies of Alkane Hydrogenolysis. ACS Catalysis, 2018, 8, 6375-6387.	5.5	21
38178	Electronic Structure of Visible Light-Driven Photocatalyst Î´-Bi₁₁VO₁₉ Nanoparticles Synthesized by Thermal Plasma. ACS Omega, 2018, 3, 5853-5864.	1.6	18
38179	Efficient Oxygen Electrocatalysis by Nanostructured Mixed-Metal Oxides. Journal of the American Chemical Society, 2018, 140, 8128-8137.	6.6	49
38180	Enhanced electronic and optical properties of three TMD heterobilayers. Physical Chemistry Chemical Physics, 2018, 20, 16604-16614.	1.3	23
38181	Tailoring the hexagonal boron nitride nanomesh on Rh(111) with gold. Physical Chemistry Chemical Physics, 2018, 20, 15473-15485.	1.3	17
38182	Density functional study of the phase stability and Raman spectra of Yb₂O₃, Yb₂SiO₅ and Yb₂Si₂O₇ under pressure. Physical Chemistry Chemical Physics, 2018, 20, 16518-16527.	1.3	30
38183	First crystal structures of oxo-bridged [Cr^{III}Ta^V] dinuclear complexes: spectroscopic, magnetic and theoretical investigations of the Crâ€“Oâ€“Ta core. New Journal of Chemistry, 2018, 42, 10912-10921.	1.4	8
38184	Enhancing the low temperature NH₃-SCR activity of FeTiO_x catalysts via Cu doping: a combination of experimental and theoretical study. RSC Advances, 2018, 8, 19301-19309.	1.7	10
38185	Rhombohedral R3c to orthorhombic Pnma phase transition induced by Y-doping in BiFeO₃. Journal of Physics Condensed Matter, 2018, 30, 285701.	0.7	11
38186	Phonon mode softening and elastic properties of hafnium under pressure. Physical Review B, 2018, 97, .	1.1	4
38187	Dirac Electrons at the Source: Breaking the 60-mV/Decade Switching Limit. IEEE Transactions on Electron Devices, 2018, 65, 2736-2743.	1.6	62
38188	AFLOW-ML: A RESTful API for machine-learning predictions of materials properties. Computational Materials Science, 2018, 152, 134-145.	1.4	72
38189	Tailoring the stability of <mml:math xmlns:mml="http://www.w3.org/1998/Math/MathML" altimg="si1.gif" overflow="scroll"><mml:mrow><mml:mo stretchy="false">{</mml:mo><mml:mn>1</mml:mn><mml:mspace width="0.12em" /><mml:mn>0</mml:mn><mml:mspace width="0.12em" /><mml:mover accent="true"><mml:mrow><mml:mn>1</mml:mn></mml:mrow><mml:mrow><mml:mo>Â¯</mml:mo></mml:mrow></mml:mover><mml:mspace width="0.12em" /><mml:mn>2</mml:mn><mml:mo stretchy="false">}	1.4	7
38190	Molybdenum substitution induced luminescence enhancement in Gd2W1-Mo O6:Eu3+ phosphors for near ultraviolet based solid-state lighting. Journal of Luminescence, 2018, 202, 97-106.	1.5	26
38191	Thermoelectric Properties of Doped-Cu₃SbSe₄ Compounds: A First-Principles Insight. Inorganic Chemistry, 2018, 57, 7321-7333.	1.9	36
38192	Understanding Chemical Bonding in Alloys and the Representation in Atomistic Simulations. Journal of Physical Chemistry C, 2018, 122, 14996-15009.	1.5	30
38193	Indirect-to-Direct Band Gap Transition of Si Nanosheets: Effect of Biaxial Strain. Journal of Physical Chemistry C, 2018, 122, 15297-15303.	1.5	8

#	Article	IF	Citations
38194	Improved thermoelectric performance of solid solution Cu4Sn7.5S16 through isoelectronic substitution of Se for S. Scientific Reports, 2018, 8, 8202.	1.6	11
38195	Phonon Instability and Broken Long-Ranged <mml:math xmlns:mml="http://www.w3.org/1998/Math/MathML" display="inline"><mml:mi>p</mml:mi></mml:math> Bond in Ge-Sb-Te Phase-Change Materials from First Principles. Physical Review Applied, 2018, 9, .	1.5	6
38196	Universal link of magnetic exchange and structural behavior under pressure in chromium spinels. Physical Review B, 2018, 97, .	1.1	24
38197	Origin of the extremely large magnetoresistance in topological semimetal <mml:math xmlns:mml="http://www.w3.org/1998/Math/MathML"><mml:mrow><mml:mi>PtS</mml:mi><mml:msub><mml:mi mathvariant="normal">n</mml:mi><mml:mn>4</mml:mn></mml:msub></mml:mrow></mml:math>. Physical Review B, 2018, 97, .	1.1	21
38198	TCNQ Physisorption on the Topological Insulator Bi 2 Se 3. ChemPhysChem, 2018, 19, 2405-2410.	1.0	6
38199	A study of the most condensed configuration of oxocarbon molecule adsorption on graphene surface: A first-principle investigation. Applied Surface Science, 2018, 455, 216-220.	3.1	3
38200	The local structure in heavily boron-doped diamond and the effect this has on its electrochemical properties. Carbon, 2018, 137, 333-342.	5.4	44
38201	Molybdenum substitution simultaneously induced band structure modulation and luminescence enhancement in LiLaMg(W, Mo)O6: Eu3+ red-emitting phosphor for near ultraviolet excited white light diodes. Journal of Alloys and Compounds, 2018, 763, 278-288.	2.8	25
38202	Isomerization and Î²-scission reactions of alkanes on bifunctional metal-acid catalysts: Consequences of confinement and diffusional constraints on reactivity and selectivity. Journal of Catalysis, 2018, 368, 389-410.	3.1	104
38203	On the Nature of Trapped-Hole States in CdS Nanocrystals and the Mechanism of Their Diffusion. Journal of Physical Chemistry Letters, 2018, 9, 3532-3537.	2.1	24
38204	Ethylene Carbonate-Based Electrolyte Decomposition and Solidâ€“Electrolyte Interphase Formation on Ca Metal Anodes. Journal of Physical Chemistry Letters, 2018, 9, 3295-3300.	2.1	29
38205	Tracking the Chemical and Structural Evolution of the TiS₂ Electrode in the Lithium-Ion Cell Using Operando X-ray Absorption Spectroscopy. Nano Letters, 2018, 18, 4506-4515.	4.5	51
38206	L-Phenylalanine-Templated Platinum Catalyst with Enhanced Performance for Oxygen Reduction Reaction. ACS Applied Materials & Interfaces, 2018, 10, 21321-21327.	4.0	15
38207	CO Oxidation on a Au/TiO₂ Nanoparticle Catalyst via the Au-Assisted Marsâ€“van Krevelen Mechanism. ACS Catalysis, 2018, 8, 6513-6525.	5.5	103
38208	Sulfur dioxide gas-sensitive materials based on zeolitic imidazolate framework-derived carbon nanotubes. Journal of Materials Chemistry A, 2018, 6, 12115-12124.	5.2	45
38209	Au147 nanoparticles: Ordered or amorphous?. Journal of Chemical Physics, 2018, 148, 204308.	1.2	22
38210	<tt>QMCPACK</tt>: an open sourceab initioquantum Monte Carlo package for the electronic structure of atoms, molecules and solids. Journal of Physics Condensed Matter, 2018, 30, 195901.	0.7	187
38211	Study of the solubility of Pb, Bi and Sn in aluminum by mixed CALPHAD/DFT methods: Applicability to aluminum machining alloys. Calphad: Computer Coupling of Phase Diagrams and Thermochemistry, 2018, 61, 275-287.	0.7	7

#	Article	IF	Citations
38212	The electronic, magnetic and optical properties of Co doped marcasite FeS2. Journal of Physics and Chemistry of Solids, 2018, 121, 285-291.	1.9	4
38213	Quaternary rare-earth selenides Ba2REGaSe5 and Ba2REInSe5. Journal of Solid State Chemistry, 2018, 265, 167-175.	1.4	5
38214	Preparation of nano-Fe0 modified coal fly-ash composite and its application for U(VI) sequestration. Journal of Molecular Liquids, 2018, 266, 824-833.	2.3	21
38215	New Tungsten Borides, Their Stability and Outstanding Mechanical Properties. Journal of Physical Chemistry Letters, 2018, 9, 3470-3477.	2.1	61
38216	Flue gas adsorption on periodic mesoporous phenylene-silica: a DFT approach. Physical Chemistry Chemical Physics, 2018, 20, 16686-16694.	1.3	15
38217	1T phase as an efficient hole injection layer to TMDs transistors: a universal approach to achieve p-type contacts. 2D Materials, 2018, 5, 031012.	2.0	27
38218	Insights into the selective catalytic reduction of NO by NH3 over Mn3O4(110): a DFT study coupled with microkinetic analysis. Science China Chemistry, 2018, 61, 457-467.	4.2	26
38219	Promotion of catalytic selectivity on transition metal oxide through restructuring surface lattice. Applied Catalysis B: Environmental, 2018, 237, 957-969.	10.8	20
38220	On the diversity in the thermal transport properties of graphene: A first-principles-benchmark study testing different exchange-correlation functionals. Computational Materials Science, 2018, 151, 153-159.	1.4	34
38221	Electronic band structure and magnetic properties of I vacancy and nonmetallic atoms doped single layer PbI2. Journal of Magnetism and Magnetic Materials, 2018, 463, 36-43.	1.0	8
38222	Defect Engineering of Earth-Abundant Solar Absorbers BiSI and BiSeI. Chemistry of Materials, 2018, 30, 3827-3835.	3.2	68
38223	Photoexcitation Dynamics in Janus-MoSSe/WSe₂ Heterobilayers: Ab Initio Time-Domain Study. Journal of Physical Chemistry Letters, 2018, 9, 2797-2802.	2.1	89
38224	Prediction of Enhanced Catalytic Activity for Hydrogen Evolution Reaction in Janus Transition Metal Dichalcogenides. Nano Letters, 2018, 18, 3943-3949.	4.5	267
38225	The role of metal/oxide interfaces for long-range metal particle activation during CO oxidation. Nature Materials, 2018, 17, 519-522.	13.3	136
38226	The effect of hydration number on the interfacial transport of sodium ions. Nature, 2018, 557, 701-705.	13.7	205
38227	A general synthetic approach for hexagonal phase tungsten nitride composites and their application in the hydrogen evolution reaction. Journal of Materials Chemistry A, 2018, 6, 10967-10975.	5.2	62
38228	In situ vibrational spectroscopy of adsorbed nitrogen in porous carbon materials. Physical Chemistry Chemical Physics, 2018, 20, 15411-15418.	1.3	7
38229	Cu atomic chains supported on Î²-borophene sheets for effective CO₂electroreduction. Nanoscale, 2018, 10, 11064-11071.	2.8	50

#	Article	IF	Citations
38230	Coke-resistant defect-confined Ni-based nanosheet-like catalysts derived from halloysites for CO₂ reforming of methane. Nanoscale, 2018, 10, 10528-10537.	2.8	67
38231	Effect of tensile strain on the band structure and carrier transport of germanium monosulphide monolayer: a firstâ€principles study. Micro and Nano Letters, 2018, 13, 600-605.	0.6	14
38232	Fate of the open-shell singlet ground state in the experimentally accessible acenes: A quantum Monte Carlo study. Journal of Chemical Physics, 2018, 148, 134112.	1.2	24
38233	Effect of alkaline metal cations on the ionic structure of cryolite melts: Ab-initio NpT MD study. Journal of Chemical Physics, 2018, 148, 064501.	1.2	8
38234	A DFT study of pure and lithium doped gold clusters. AIP Conference Proceedings, 2018, , .	0.3	0
38235	Versatile mechanical properties of novel g-SiC _x monolayers from graphene to silicene: a first-principles study. Nanotechnology, 2018, 29, 315701.	1.3	19
38236	Growth of MoS₂ Nanoflowers with Expanded Interlayer Distance onto Nâ€Doped Graphene for Reversible Lithium Storage. ChemElectroChem, 2018, 5, 2263-2270.	1.7	24
38237	First-principles study of adsorption and diffusion of oxygen on surfaces of TiN, ZrN and HfN. Applied Surface Science, 2018, 452, 457-462.	3.1	37
38238	Effect of Nb Promoter on the Structure and Performance of Iron Titanate Catalysts for the Selective Catalytic Reduction of NO with NH₃. Industrial & Engineering Chemistry Research, 2018, 57, 7802-7810.	1.8	26
38239	Stability, Elastic Properties, and Deformation of LiBN2: A Potential High-Energy Material. Inorganic Chemistry, 2018, 57, 6333-6339.	1.9	0
38240	Mechanisms of Formation of H, HO, and Water and of Water Desorption in the Early Stages of Cellulose Pyrolysis. Journal of Physical Chemistry C, 2018, 122, 12168-12176.	1.5	16
38241	Three-Dimensional Spin Texture in Hybrid Perovskites and Its Impact on Optical Transitions. Journal of Physical Chemistry Letters, 2018, 9, 2903-2908.	2.1	50
38242	Similarity Between Amorphous and CrystallineÂPhases: TheÂCaseÂofÂTiO₂. Journal of Physical Chemistry Letters, 2018, 9, 2985-2990.	2.1	78
38243	Thermodynamics of Alkanethiol Self-Assembled Monolayer Assembly on Pd Surfaces. Langmuir, 2018, 34, 6346-6357.	1.6	13
38244	Preferential Pt Nanocluster Seeding at Grain Boundary Dislocations in Polycrystalline Monolayer MoS₂. ACS Nano, 2018, 12, 5626-5636.	7.3	27
38245	Intercalation of aromatic amine for the 2Hâ€“1Tâ€² phase transition of MoS₂ by experiments and calculations. Nanoscale, 2018, 10, 11349-11356.	2.8	54
38246	Sustainable p-type copper selenide solar material with ultra-large absorption coefficient. Chemical Science, 2018, 9, 5405-5414.	3.7	20
38247	Truncated hexagonal bi-pyramidal gallium ferrite nanocrystals: integration of structural details with visible-light photo-activity and self-cleaning properties. Journal of Materials Chemistry A, 2018, 6, 13031-13040.	5.2	9

#	Article	IF	Citations
38248	Theoretical studies of optoelectronic, magnetization and heat transport properties of conductive metal adatoms adsorbed on edge chlorinated nanographenes. RSC Advances, 2018, 8, 17723-17731.	1.7	1
38249	Performance of exchange-correlation functionals in density functional theory calculations for liquid metal: A benchmark test for sodium. Journal of Chemical Physics, 2018, 148, 144501.	1.2	5
38250	Auger losses in dilute InAsBi. Applied Physics Letters, 2018, 112, .	1.5	9
38251	Ab-initio study of electronic and magnetic properties of Co-doped Mo2C monolayer. AIP Conference Proceedings, 2018, , .	0.3	7
38252	Cubic phase stability, optical and magnetic properties of Cu-stabilized zirconia nanocrystals. Journal Physics D: Applied Physics, 2018, 51, 225304.	1.3	8
38253	Two-dimensional PdSe ₂ -Pd ₂ Se ₃ junctions can serve as nanowires. 2D Materials, 2018, 5, 035025.	2.0	18
38254	Lattice anharmonicity, phonon dispersion, and thermal conductivity of PbTe studied by the phonon quasiparticle approach. Physical Review B, 2018, 97, .	1.1	42
38255	Unexpected magnetic coupling oscillations for <mml:math xmlns:mml="http://www.w3.org/1998/Math/MathML"><mml:mrow><mml:mi>L</mml:mi><mml:msub><mml:mn>1</mml:mn> films induced by quantum wells. Physical Review B, 2018, 97, .	1.1	12
38256	Continuous Sound Velocity Measurements along the Shock Hugoniot Curve of Quartz. Physical Review Letters, 2018, 120, 215703.	2.9	15
38257	Excitonic Instability and Pseudogap Formation in Nodal Line Semimetal ZrSiS. Physical Review Letters, 2018, 120, 216401.	2.9	40
38258	Structure and energetics of ultrathin Cu adlayers on Ru(1â€¯0â€¯1Â¯â€¯0). Applied Surface Science, 2018, 454, 319-326.	3.1	1
38259	A new molecular pathway allows the chemoselective reduction of nitroaromatics on non-noble metal catalysts. Journal of Catalysis, 2018, 364, 19-30.	3.1	57
38260	2D metalâ€“organic-framework array-derived hierarchical network architecture of cobalt oxide flakes with tunable oxygen vacancies towards efficient oxygen evolution reaction. Journal of Catalysis, 2018, 364, 48-56.	3.1	56
38261	First-principles study on structural, mechanical and electronic properties of thorium dichalcogenides under high pressure. Journal of Nuclear Materials, 2018, 508, 147-153.	1.3	0
38262	Computational study of lithium nucleation tendency in Li7La3Zr2O12 (LLZO) and rational design of interlayer materials to prevent lithium dendrites. Journal of Power Sources, 2018, 392, 79-86.	4.0	144
38263	Hydrogen titanate nanotubes for dye sensitized solar cells applications: Experimental and theoretical study. Materials Research Bulletin, 2018, 106, 40-48.	2.7	16
38264	Ab-initio study of Seebeck coefficient of p-doped PbTe. Materials Today: Proceedings, 2018, 5, 10235-10239.	0.9	0
38265	Elastic properties of face-centered cubic, body-centered cubic and hexagonal high entropy alloys by MaxEnt approach. Materials Research Express, 2018, 5, 076503.	0.8	4

#	Article	IF	Citations
38266	The effect of stretching or buckling behavior on the charge distribution of C, Si, P and S single atom chains. Journal of Physics Communications, 2018, 2, 065004.	0.5	2
38267	Impact of thermal atomic displacements on the Curie temperature of <mml:math xmlns:mml="http://www.w3.org/1998/Math/MathML"><mml:mrow><mml:mn>3</mml:mn><mml:mi>d</mml:mi></mml:mrow></mml transition metals. Physical Review B, 2018, 97, .	1.1	21
38268	Tuning transport properties of nickel-doped zinc oxide for thermoelectric applications. MRS Communications, 2018, 8, 858-864.	0.8	2
38269	Deep Level Defects in 4H-SiC Epitaxial Layers. Materials Science Forum, 2018, 924, 225-228.	0.3	1
38270	Spin-flip effect enhanced photocatalytic activity in Fe and single-electron-trapped oxygen vacancy co-doped TiO2. Applied Surface Science, 2018, 457, 633-643.	3.1	12
38271	Spin-orbit coupling induced band splitting in bulk ferroelectric BiAlO3 with tetragonal phase. Journal of Alloys and Compounds, 2018, 765, 1003-1007.	2.8	0
38272	The influence of crystal orientation on corrosion behavior of iron in liquid PbLi. Journal of Nuclear Materials, 2018, 509, 212-217.	1.3	10
38273	On the nexus between atom probe microscopy and density functional theory simulations. Materials Characterization, 2018, 146, 347-358.	1.9	19
38274	Phase Diagram of Methane Hydrates and Discovery of MH-VI Hydrate. Journal of Physical Chemistry A, 2018, 122, 6007-6013.	1.1	5
38275	Water Molecular Beam Scattering at Î±-Al₂O₃(0001): An Ab Initio Molecular Dynamics Study. Journal of Physical Chemistry C, 2018, 122, 15494-15504.	1.5	4
38276	Influence of Tight Confinement on Selective Oxidative Dehydrogenation of Ethane on MoVTeNb Mixed Oxides. ACS Catalysis, 2018, 8, 7051-7067.	5.5	59
38277	Refining Defect States in W₁₈O₄₉ by Mo Doping: A Strategy for Tuning N₂ Activation towards Solar-Driven Nitrogen Fixation. Journal of the American Chemical Society, 2018, 140, 9434-9443.	6.6	722
38278	MXene nanoribbons as electrocatalysts for the hydrogen evolution reaction with fast kinetics. Physical Chemistry Chemical Physics, 2018, 20, 19390-19397.	1.3	74
38279	Unveiling the multifunctional roles of hitherto known capping ligand oleic acid as blue emitter and sensitizer in tuning the emission colour to white in red-emitting phosphors. Physical Chemistry Chemical Physics, 2018, 20, 19087-19097.	1.3	4
38280	Introduction of newly synthesized Schiff base molecules as efficient corrosion inhibitors for mild steel in 1 M HCl medium: an experimental, density functional theory and molecular dynamics simulation study. Materials Chemistry Frontiers, 2018, 2, 1674-1691.	3.2	101
38281	Half-metallicity and spin-valley coupling in 5d transition metal substituted monolayer MnPSe₃. Journal of Materials Chemistry C, 2018, 6, 8092-8098.	2.7	23
38282	Comparative study of electronic structure and microscopic model of SrMn3P4O14 and Sr3Cu3(PO4)4. AIP Conference Proceedings, 2018, , .	0.3	0
38283	Physical realization of 2D spin liquid state by ab initio design and strain engineering in FeX₃. Journal of Physics Condensed Matter, 2018, 30, 325801.	0.7	4

#	Article	IF	Citations
38284			

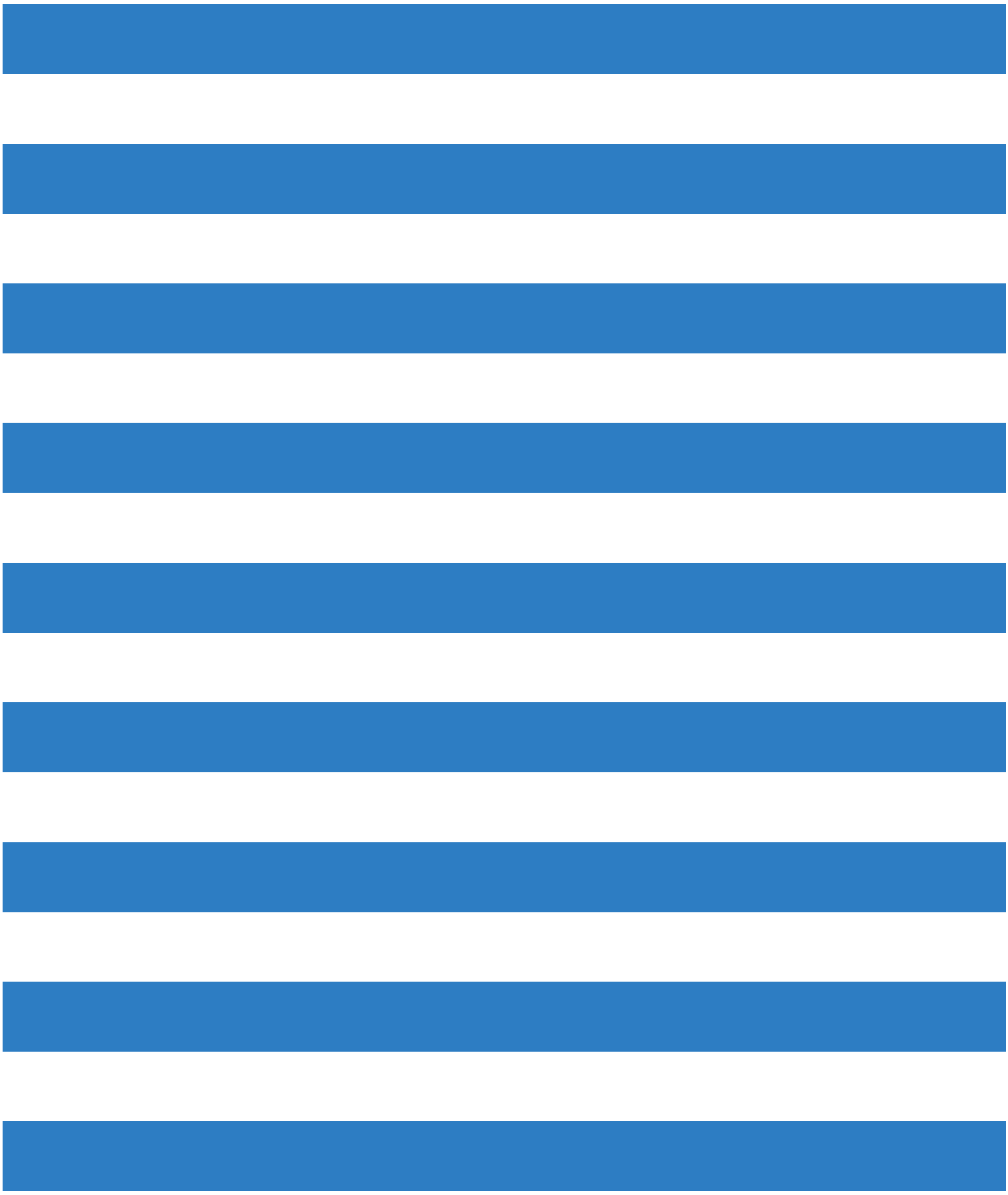

#	Article	IF	Citations
38302	Adsorption of Maleic Acid Monomer on the Surface of Hydroxyapatite and TiO2: A Pathway toward Biomaterial Composites. ACS Applied Materials & Interfaces, 2018, 10, 24382-24391.	4.0	11
38303	Electric-field control of magnetism in a few-layered van der Waals ferromagnetic semiconductor. Nature Nanotechnology, 2018, 13, 554-559.	15.6	466
38304	Interaction trends between single metal atoms and oxide supports identified with density functional theory and statistical learning. Nature Catalysis, 2018, 1, 531-539.	16.1	269
38305	Safe and high-rate supercapacitors based on an â€œacetonitrile/water in saltâ€•hybrid electrolyte. Energy and Environmental Science, 2018, 11, 3212-3219.	15.6	297
38306	Electronic structure, pore size distribution, and sorption characterization of an unusual MOF, {[Ni(dpbz)][Ni(CN)4]}n, dpbz = 1,4-bis(4-pyridyl)benzene. Journal of Applied Physics, 2018, 123, 245105.	1.1	9
38307	Density functional theory calculations for magnetic properties of Co3W systems. Journal of Chemical Physics, 2018, 149, 014303.	1.2	2
38308	Facile in situ construction of mediator-free direct Z-scheme g-C₃N₄/CeO₂ heterojunctions with highly efficient photocatalytic activity. Journal Physics D: Applied Physics, 2018, 51, 275302.	1.3	110
38309	Superior structural, elastic and electronic properties of 2D titanium nitride MXenes over carbide MXenes: a comprehensive first principles study. 2D Materials, 2018, 5, 045004.	2.0	171
38310	Ab initio calculations of the mechanical and acoustic properties of Ti2-based Heusler alloys under pressures. European Physical Journal B, 2018, 91, 1.	0.6	10
38311	C-, N-, S-, and F-Doped Anatase TiO₂ (101) with Oxygen Vacancies: Photocatalysts Active in the Visible Region. International Journal of Photoenergy, 2018, 2018, 1-12.	1.4	18
38312	Carrier-induced absorption as a mechanism for electrochromism in tungsten trioxide. MRS Communications, 2018, 8, 926-931.	0.8	9
38313	New Ironâ€Cobalt Oxide Catalysts Promoting BiVO₄ Films for Photoelectrochemical Water Splitting. Advanced Functional Materials, 2018, 28, 1802685.	7.8	248
38314	Sn[B₂O₃F₂]â€”The First Tin Fluorooxoborate as Possible NLO Material. Advanced Optical Materials, 2018, 6, 1800497.	3.6	89
38315	Monolayer AsTe₂: Stable Robust Metal in 2D, 1D and 0D. ChemPhysChem, 2018, 19, 2176-2182.	1.0	3
38316	Allâ€Optical Detection of Periodic Structure of Chalcogenide Superlattice Using Coherent Folded Acoustic Phonons. Physica Status Solidi - Rapid Research Letters, 2018, 12, 1800246.	1.2	0
38317	Ab initio study of energetics and structures of heterophase interfaces: From coherent to semicoherent interfaces. Acta Materialia, 2018, 156, 20-30.	3.8	26
38318	Promoting effect of cerium on MoVTeNb mixed oxide catalyst for oxidative dehydrogenation of ethane to ethylene. Applied Catalysis B: Environmental, 2018, 237, 554-562.	10.8	56
38319	Lattice-matched heterojunctions between blue phosphorene and MXene Y2CX2 (Xâ€¯=â€¯F, O, and Yâ€¯=â€¯Zr, Hf). Computational Materials Science, 2018, 152, 256-261.	1.4	6

#	Article	IF	Citations
38320	Experimental and theoretical investigations of unusual enhancement of room temperature ferromagnetism in nickel-cobalt codoped CeO2 nanostructures. Journal of Magnetism and Magnetic Materials, 2018, 465, 756-761.	1.0	6
38321	Constructive effects of the interfacial properties: A strategy to design hole transport materials for high performance perovskite solar cells. Organic Electronics, 2018, 62, 591-597.	1.4	22
38322	Elucidation of Li_xNi_{0.8}Co_{0.15}Al_{0.05}O₂ Redox Chemistry by Operando Raman Spectroscopy. Chemistry of Materials, 2018, 30, 4694-4703.	3.2	76
38323	Experimental and Theoretical Studies on Î±-In₂Se₃ at High Pressure. Inorganic Chemistry, 2018, 57, 8241-8252.	1.9	46
38324	Calculation of strained BaTiO3 with different exchange correlation functionals examined with criterion by Ginzburg-Landau theory, uncovering expressions by crystallographic parameters. Journal of Chemical Physics, 2018, 148, 194702.	1.2	9
38325	Stepping Stone Mechanism: Carrier-Free Long-Range Magnetism Mediated by Magnetized Cation States in Quintuple Layer. Chinese Physics Letters, 2018, 35, 017502.	1.3	6
38326	Roadmap on finding chiral valleys: screening 2D materials for valleytronics. Nano Futures, 2018, 2, 032001.	1.0	58
38327	Topological surface Fermi arcs in the magnetic Weyl semimetal <mml:math xmlns:mml="http://www.w3.org/1998/Math/MathML"><mml:mrow><mml:msub><mml:mi>Co</mml:mi><mml:mn>3</mml:mn></mml:msub><mml:mi mathvariant="normal">S</mml:mi><mml:mn>2</mml:mn></mml:mrow></mml:math>. Physical Review B, 2018, 97, .	1.1	159
38328	Firstâ€Principles Calculations on the Groupâ€IIIA Elements Xâ€Doped (Xâ€‰=â€‰Ga, In, Tl) VO₂. Physica Status Solidi (B): Basic Research, 2018, 255, 1800138.	0.7	3
38329	Tuning the optical properties of phosphorene by adsorption of alkali metals and halogens. Optical and Quantum Electronics, 2018, 50, 1.	1.5	14
38330	Bismuth vacancy mediated single unit cell Bi2WO6 nanosheets for boosting photocatalytic oxygen evolution. Applied Catalysis B: Environmental, 2018, 238, 119-125.	10.8	173
38331	The effect of solutes on the precipitate/matrix interface properties in the Vanadium alloys: A first-principles study. Computational Materials Science, 2018, 153, 113-118.	1.4	5
38332	Direct-gap semiconducting tri-layer silicene with 29% photovoltaic efficiency. Nano Energy, 2018, 51, 489-495.	8.2	46
38333	Solute Sn-induced formation of composite Î²â€²/Î²â€³ precipitates in Al-Mg-Si alloy. Scripta Materialia, 2018, 155, 68-72.	2.6	42
38334	The Influence of Local Distortions on Proton Mobility in Acceptor Doped Perovskites. Chemistry of Materials, 2018, 30, 4919-4925.	3.2	40
38335	Efficient Carrier Separation and Band Structure Tuning of Two-Dimensional C₂N/GaTe van der Waals Heterostructure. Journal of Physical Chemistry C, 2018, 122, 15892-15902.	1.5	55
38336	Pressure Impact on the Crystal Structure, Optical, and Transport Properties in Layered Oxychalcogenides BiCuChO (Ch = S, Se). Journal of Physical Chemistry C, 2018, 122, 15929-15936.	1.5	15
38337	Enhanced electrical properties of antimony doped tin oxide thin films deposited via aerosol assisted chemical vapour deposition. Journal of Materials Chemistry C, 2018, 6, 7257-7266.	2.7	97

#	Article	IF	Citations
38338	Doping stability of nonphotorefractive ions in stoichiometric and congruent LiNbO₃. Physical Chemistry Chemical Physics, 2018, 20, 17477-17486.	1.3	9
38339	Pure CO₂ electrolysis over an Ni/YSZ cathode in a solid oxide electrolysis cell. Journal of Materials Chemistry A, 2018, 6, 13661-13667.	5.2	77
38340	Structural and electronic properties of a-edge dislocations along âŸ¨1-100âŸ© in GaN. Journal of Applied Physics, 2018, 123, .	1.1	6
38341	Electronic and magnetic properties of semihydrogenated, fully hydrogenated monolayer and bilayer MoN ₂ sheets. Chinese Physics B, 2018, 27, 060306.	0.7	4
38342	Critical curvature localization in graphene. I. Quantum-flexoelectricity effect. Proceedings of the Royal Society A: Mathematical, Physical and Engineering Sciences, 2018, 474, 20180054.	1.0	15
38343	Gradient-level and nonlocal density functional descriptions of Cu-Au intermetallic compounds. European Physical Journal B, 2018, 91, 1.	0.6	5
38344	Enhancing ROS generation and suppressing toxic intermediate production in photocatalytic NO oxidation on O/Ba co-functionalized amorphous carbon nitride. Applied Catalysis B: Environmental, 2018, 237, 938-946.	10.8	134
38345	Initial stage of C60 cation formation in superacids. Chemical Physics, 2018, 513, 13-16.	0.9	0
38346	Ab initio study of Be and Be12Ti for fusion applications. Intermetallics, 2018, 100, 163-170.	1.8	25
38347	High-efficient and defect tolerant Co2MnSb ternary Heusler alloy for spintronic application. Journal of Alloys and Compounds, 2018, 765, 1055-1060.	2.8	19
38348	Ab-initio based search for late blooming phase compositions in iron alloys. Journal of Nuclear Materials, 2018, 509, 225-236.	1.3	14
38349	Mechanical anisotropy and ideal strength of ThBC. Journal of Physics and Chemistry of Solids, 2018, 122, 203-209.	1.9	5
38350	First-principles studies of polar perovskite KTaO₃surfaces: structural reconstruction, charge compensation, and stability diagram. Physical Chemistry Chemical Physics, 2018, 20, 18515-18527.	1.3	35
38351	Tunable Quasiâ€Oneâ€Dimensional Ribbon Enhanced Light Absorption in Sb₂Se₃ Thinâ€film Solar Cells Grown by Closeâ€Space Sublimation. Solar Rrl, 2018, 2, 1800128.	3.1	64
38352	First principles investigation of the structural and bonding properties of hydrated actinide (IV) oxalates, An(C2O4)2·6H2O (Anâ€=â€U, Pu). Computational Materials Science, 2018, 153, 146-152.	1.4	7
38353	Adsorption and Activation of Methane on the (110) Surface of Rutile-type Metal Dioxides. Journal of Physical Chemistry C, 2018, 122, 15359-15381.	1.5	85
38354	Intrinsic Defects Drive Persistent Luminescence in Monoclinic SrAl₂O₄:Eu²⁺. Journal of Physical Chemistry C, 2018, 122, 16309-16314.	1.5	46
38355	DFT Study on the H₂ Storage Properties of Sc-Decorated Covalent Organic Frameworks Based on Adamantane Units. Journal of Physical Chemistry C, 2018, 122, 16853-16865.	1.5	6

#	Article	IF	Citations
38356	Ultrahigh Conductivity in Two-Dimensional InSe via Remote Doping at Room Temperature. Journal of Physical Chemistry Letters, 2018, 9, 3897-3903.	2.1	23
38357	Grain Boundaries Are Benign and Suppress Nonradiative Electronâ€“Hole Recombination in Monolayer Black Phosphorus: A Time-Domain Ab Initio Study. Journal of Physical Chemistry Letters, 2018, 9, 3856-3862.	2.1	54
38358	High-performance bifunctional porous non-noble metal phosphide catalyst for overall water splitting. Nature Communications, 2018, 9, 2551.	5.8	812
38359	Ab initio design of light absorption through silver atomic cluster decoration of TiO₂. Physical Chemistry Chemical Physics, 2018, 20, 19110-19119.	1.3	31
38360	Synthesis of amine-functionalized ZIF-8 with 3-amino-1,2,4-triazole by postsynthetic modification for efficient CO₂-selective adsorbents and beyond. Journal of Materials Chemistry A, 2018, 6, 18912-18919.	5.2	87
38361	Excellent ZT achieved in Cu_{1.8}S thermoelectric alloys through introducing rare-earth trichlorides. Journal of Materials Chemistry A, 2018, 6, 14440-14448.	5.2	39
38362	Research Update: Ca doping effect on the Li-ion conductivity in NASICON-type solid electrolyte LiZr2(PO4)3: A first-principles molecular dynamics study. APL Materials, 2018, 6, .	2.2	31
38363	Prediction of a metallic phase for Cs3Pentacene compound. Materials Research Express, 2018, 5, 066554.	0.8	2
38364	Interplay of covalency, spin-orbit coupling, and geometric frustration in the <mml:math xmlns:mml="http://www.w3.org/1998/Math/MathML"><mml:msup><mml:mi>d</mml:mi><mml:mrow><mml:mn>3.5</mml:mn></mml: system <mml:math xmlns:mml="http://www.w3.org/1998/Math/MathML"><mml:mrow><mml:msub><mml:mi>Ba</mml:mi><mml:mn>3</mml:mn></mml:m mathvariant="normal">O</mml:mi><mml:mn>9</mml:mn></mml:msub></mml:mrow><. Physical Review	1.1	9
38365	Self-modulation doping effect in the high-mobility layered semiconductor <mml:math xmlns:mml="http://www.w3.org/1998/Math/MathML"><mml:mrow><mml:msub><mml:mi>Bi</mml:mi><mml:mn>2</mml:mn></mml:m mathvariant="normal">O</mml:mi><mml:mn>2</mml:mn></mml:msub><mml:mi>Se</mml:mi></mml:mrow></mml:math>. Physical Review B, 2018, 97, .	1.1	63
38366	Topological nodal line semimetal in an orthorhombic graphene network structure. Physical Review B, 2018, 97, .	1.1	29
38367	Almost ideal nodal-loop semimetal in monoclinic <mml:math xmlns:mml="http://www.w3.org/1998/Math/MathML"><mml:msub><mml:mi mathvariant="bold">CuTeO</mml:mi><mml:mn>3</mml:mn></mml:msub></mml:math> material. Physical Review B, 2018, 97, .	1.1	30
38368	An examination of the structural, electronic, elastic, vibrational and thermodynamic properties of Ru2YGa (Yâ€“â€“Sc, Ti and V) Heusler alloys. Chinese Journal of Physics, 2018, 56, 1772-1780.	2.0	11
38369	The property of surface heterojunction performed by crystal facets for photogenerated charge separation. Computational Materials Science, 2018, 153, 28-35.	1.4	13
38370	The computational probing of carrier transport in MAPbI3â^'xClx. Computational and Theoretical Chemistry, 2018, 1138, 135-139.	1.1	2
38371	Insights into the plasticity of Ag3Sn from density functional theory. International Journal of Plasticity, 2018, 110, 57-73.	4.1	6
38372	â€œDeep Ultra-Strengthâ€•Induced Band Structure Evolution in Silicon Nanowires. Journal of Physical Chemistry C, 2018, 122, 15780-15785.	1.5	5
38373	Linearized machine-learning interatomic potentials for non-magnetic elemental metals: Limitation of pairwise descriptors and trend of predictive power. Journal of Chemical Physics, 2018, 148, 234106.	1.2	20

#	Article	IF	Citations
38374	A perturbation theory for equation of state of hydrogen in warm and hot dense regimes. Physics of Plasmas, 2018, 25, 062710.	0.7	0
38375	Atomistic simulation of phosphorus segregation to Î£3 (111) symmetrical tilt grain boundary in Î±-iron. Modelling and Simulation in Materials Science and Engineering, 2018, 26, 065005.	0.8	5
38376	Interfacial coupling induced direct Z-scheme water splitting in metal-free photocatalyst: C₃N/g-C₃N₄ heterojunctions. Nanotechnology, 2018, 29, 365401.	1.3	39
38377	First-Principles Calculations of the Structure Stability and Mechanical Properties of LiFeAs and NaFeAs under Pressure. Advances in Materials Science and Engineering, 2018, 2018, 1-9.	1.0	5
38378	Molecular Vibration Theoretical Analysis of Two-Dimensional Photoelectric Conversion Material WSe₂. Key Engineering Materials, 2018, 765, 16-23.	0.4	0
38379	Interlayerâ€Spacingâ€Regulated VOPO₄ Nanosheets with Fast Kinetics for Highâ€Capacity and Durable Rechargeable Magnesium Batteries. Advanced Materials, 2018, 30, e1801984.	11.1	171
38380	A comparative study of the dissolubility of pure and silicon substituted hydroxyapatite from density functional theory calculations. Journal of Molecular Modeling, 2018, 24, 168.	0.8	3
38381	First principles study of phase stability and ferroelectric properties of Bi1â^'xRExFeO3 (REâ€¯=â€¯Y, La) solid solutions. Computational Materials Science, 2018, 152, 183-191.	1.4	5
38382	Exotic high-pressure behavior of double nitride CuPN2. Computational Materials Science, 2018, 152, 217-222.	1.4	0
38383	Structural stability of FeO2 in the pressure range of lower mantle. Journal of Alloys and Compounds, 2018, 765, 271-277.	2.8	6
38384	Mg3X2 (XÂ= C, Si) monolayer in a honeycomb-kagome lattice: A global minimum structure. Journal of Alloys and Compounds, 2018, 765, 969-976.	2.8	6
38385	Three-dimensional hexagonal boron nitride foam containing both <mml:math xmlns:mml="http://www.w3.org/1998/Math/MathML" altimg="si1.gif" overflow="scroll"><mml:mrow><mml:mi>s</mml:mi><mml:msup><mml:mi>p</mml:mi><mml:mn>2</mml:mn></mml:msup></mml:mr and <mml:math xmlns:mml="http://www.w3.org/1998/Math/MathML" altimg="si2.gif" overflow="scroll"><mml:mrow><mml:mi>s</mml:mi><mml:msup><mml:mi>p</mml:mi><mml:mn>3</mml:mn></mml:msup></mml:mr hybridized bonds. Materials Chemistry and Physics, 2018, 217, 5-10.	2.0	5
38386	Enhancement of photo-electrochemical reactions in MAPbI3/Au. Materials Today Energy, 2018, 9, 303-310.	2.5	7
38387	Electric-field control of Li-doping induced phase transition in VO2 film with crystal facet-dependence. Nano Energy, 2018, 51, 300-307.	8.2	40
38388	First-principles predictions of the geometries and electronic structures of tungsten ditelluride nanoribbons. Physics Letters, Section A: General, Atomic and Solid State Physics, 2018, 382, 2754-2758.	0.9	6
38389	Twin-like fault in Mgâ€“9.8â€¯wt%Sn alloy. Scripta Materialia, 2018, 155, 89-93.	2.6	15
38390	Iron Dissolution from Goethite (Î±-FeOOH) Surfaces in Water by Ab Initio Enhanced Free-Energy Simulations. Journal of Physical Chemistry C, 2018, 122, 16086-16091.	1.5	33
38391	Biohybridization of Supported Gold Nanoassemblies on Silicon. Journal of Physical Chemistry C, 2018, 122, 16113-16121.	1.5	4

#	Article	IF	Citations
38392	Mechanisms and Active Sites for Câ€“O Bond Rupture within 2-Methyltetrahydrofuran over Ni, Ni₁₂P₅, and Ni₂P Catalysts. ACS Catalysis, 2018, 8, 7141-7157.	5.5	29
38393	Structureâ€“performance descriptors and the role of Lewis acidity in the methanol-to-propylene process. Nature Chemistry, 2018, 10, 804-812.	6.6	221
38394	A heterogeneous single-atom palladium catalyst surpassing homogeneous systems for Suzuki coupling. Nature Nanotechnology, 2018, 13, 702-707.	15.6	471
38395	The structural, electronic, and optical properties of organicâ€“inorganic mixed halide perovskites CH		

#	Article	IF	Citations
38410	Understanding crystallization pathways leading to manganese oxide polymorph formation. Nature Communications, 2018, 9, 2553.	5.8	98
38411	A multi-electron transfer ferrocene derivative positive redox moiety with improved solubility and potential. Chemical Communications, 2018, 54, 8419-8422.	2.2	18
38412	Tunable spin states in the two-dimensional magnet CrI₃. Nanoscale, 2018, 10, 14298-14303.	2.8	136
38413	Hexagonal Co₃O₄ anchored reduced graphene oxide sheets for high-performance supercapacitors and non-enzymatic glucose sensing. Journal of Materials Chemistry A, 2018, 6, 14367-14379.	5.2	118
38414	Hexagonal Boron Nitrideâ€“Metal Junction: Removing the Schottky Barriers by Grain Boundary. Advanced Theory and Simulations, 2018, 1, 1800045.	1.3	5
38415	A Density Functional Theory Study of the Mechanism of Direct Glucose Dehydration to 5â€Hydroxymethylfurfural on Anatase Titania. ChemCatChem, 2018, 10, 4084-4089.	1.8	27
38416	Preparation and adsorption performance of a NiO/MgF2 composite adsorbent. Journal of Radioanalytical and Nuclear Chemistry, 2018, 317, 287-295.	0.7	1
38417	Adsorption of CH3I on Ag(1â€¯1â€¯1) and Ag2O(1â€¯1â€¯1) surface: A density functional theory study. Chemical Physics, 2018, 513, 35-40.	0.9	4
38418	Achieving the dehydriding reversibility and elevating the equilibrium pressure of YFe2 alloy by partial Y substitution with Zr. International Journal of Hydrogen Energy, 2018, 43, 14541-14549.	3.8	19
38419	Electronic properties of porous graphene and its hydrogen storage potentials. Journal of Alloys and Compounds, 2018, 766, 104-111.	2.8	9
38420	Origin of ligand-driven selectivity in alkyne semihydrogenation over silica-supported copper nanoparticles. Journal of Catalysis, 2018, 364, 437-445.	3.1	21
38421	High-pressure structures of helium and carbon dioxide from first-principles calculations. Solid State Communications, 2018, 283, 9-13.	0.9	3
38422	Native Defects in Li₁₀GeP₂S₁₂ and Their Effect on Lithium Diffusion. Chemistry of Materials, 2018, 30, 4995-5004.	3.2	33
38423	Pressure-Induced Conformer Modifications and Electronic Structural Changes in 1,3,5-Triamino-2,4,6-trinitrobenzene (TATB) up to 20 GPa. Journal of Physical Chemistry C, 2018, 122, 15861-15867.	1.5	16
38424	Spinâ€“phonon couplings in transition metal complexes with slow magnetic relaxation. Nature Communications, 2018, 9, 2572.	5.8	93
38425	Effect of transition-metal-ion dopants on the oxygen evolution reaction on NiOOH(0001). Physical Chemistry Chemical Physics, 2018, 20, 19525-19531.	1.3	33
38426	Effect of mixed surface terminations on the structural and electrochemical properties of two-dimensional Ti₃C₂T₂ and V₂CT₂ MXenes multilayers. Nanoscale, 2018, 10, 13520-13530.	2.8	143
38427	Origin of the stability of two-dimensional perovskites: a first-principles study. Journal of Materials Chemistry A, 2018, 6, 14949-14955.	5.2	79

#	Article	IF	Citations
38428	MoS₂ nanosheets vs. nanowires: preparation and a theoretical study of highly stable and efficient nanofluids for concentrating solar power. Journal of Materials Chemistry A, 2018, 6, 14919-14929.	5.2	24
38429	Effect of Ag Doping on the Electronic Structure and Optical Properties of ZnO(0001) Surface. MATEC Web of Conferences, 2018, 142, 01008.	0.1	0
38430	First-principles study of the properties for crystal Ge2Sb2Te5 with Ge vacancy. AIP Advances, 2018, 8, .	0.6	4
38431	New nickel-based hybrid organic/inorganic metal halide for photovoltaic applications. Journal of Chemical Physics, 2018, 148, 244703.	1.2	5
38432	Carrier density control of magnetism and Berry phases in doped EuTiO3. APL Materials, 2018, 6, .	2.2	24
38433	Effects of strain on electronic properties of Delta nitrogen-doped graphene nanoribbons. Ferroelectrics, 2018, 530, 1-10.	0.3	1
38434	MoS2/Phosphorene Heterostructure for Optical Absorption in Visible Region. IEEE Journal of Quantum Electronics, 2018, 54, 1-6.	1.0	25
38435	Morphological Growth and Theoretical Understanding of Gold and Other Noble Metal Nanoplates. Chemistry - A European Journal, 2018, 24, 15589-15595.	1.7	9
38436	Structural, electronic and magnetic properties in bulk and various (0â€¯0â€¯1) surfaces of X2CoIn (Xâ€¯=â€¯Ti, Zr) Heusler alloy. Applied Surface Science, 2018, 457, 403-410.	3.1	8
38437	First-principles study of adsorption of 3d and 4d transition metal atoms on aluminene. Computational Condensed Matter, 2018, 16, e00319.	0.9	6
38438	Impact of correlative defects induced by double Re-addition on the ideal shear strength of Î³â€²-Ni3Al phases. Computational Materials Science, 2018, 152, 408-416.	1.4	19
38439	Atomic Structures of Pt Nanoclusters Supported on Graphene Grown on Pt(111). Journal of Physical Chemistry C, 2018, 122, 16132-16141.	1.5	5
38440	Defect Evolution Enhanced Visible-Light Photocatalytic Activity in Nitrogen-Doped Anatase TiO₂ Thin Films. Journal of Physical Chemistry C, 2018, 122, 16600-16606.	1.5	19
38441	Maneuvering the Physical Properties and Spin States To Enhance the Activity of Laâ€“Srâ€“Coâ€“Feâ€“O Perovskite Oxide Nanoparticles in Electrochemical Water Oxidation. ACS Applied Energy Materials, 2018, 1, 3342-3350.	2.5	29
38442	Multistates and Polyamorphism in Phase-Change K₂Sb₈Se₁₃. Journal of the American Chemical Society, 2018, 140, 9261-9268.	6.6	12
38443	Excited-state vibrational dynamics toward the polaron in methylammonium lead iodide perovskite. Nature Communications, 2018, 9, 2525.	5.8	129
38444	On the possibility of an Eleyâ€“Rideal mechanism for ammonia synthesis on Mn₆N_{5+x} (x = 1)-(111) surfaces. Physical Chemistry Chemical Physics, 2018, 20, 18729-18736.	1.3	6
38445	Growth of boron nitride nanotubes from magnesium diboride catalysts. Nanoscale, 2018, 10, 13895-13901.	2.8	28

#	Article	IF	Citations
38446	Phase stability, electronic structures and elastic properties of (U,Np)O2 and (Th,Np)O2 mixed oxides. Physical Chemistry Chemical Physics, 2018, 20, 18707-18717.	1.3	9
38447	Mechanism for amorphization of boron carbide under complex stress conditions. Materials Research Express, 2018, 5, 055204.	0.8	14
38448	Temperature dependence of the Gibbs energy of vacancy formation of fcc Ni. Physical Review B, 2018, 97, .	1.1	45
38449	Ab Initio Study of the Structural, Magnetic, Electronic, and Thermodynamic Properties of Pd2MnZ (Z =) Tj ETQq1 1 0.784314 rgBT /Ov	0.2	8
38450	Enhanced Photocatalytic Properties by Forming Tetragonal ZnX/PbO (X = S, Se) Heteroâ€Bilayers: A Computational Prediction. Advanced Theory and Simulations, 2018, 1, 1800046.	1.3	9
38451	How different are Te clustersâ€”a first-principles study. Journal of Nanoparticle Research, 2018, 20, 1.	0.8	3
38452	The role of electronic and crystal structure in the effect of volumetric band convergence. Computational Materials Science, 2018, 153, 141-145.	1.4	0
38453	Electrospinning preparation of Sn4+-doped BiFeO3 nanofibers as efficient visible-light-driven photocatalyst for O2 evolution. Journal of Alloys and Compounds, 2018, 766, 274-283.	2.8	37
38454	Crystal structure prediction of uranium hydrides at high pressure: A new hydrogen-rich phase. Physics Letters, Section A: General, Atomic and Solid State Physics, 2018, 382, 2959-2964.	0.9	11
38455	Proton transfer in barium zirconate: Lattice reorganization, Landau-Zener curve-crossing approach. Solid State Ionics, 2018, 323, 172-202.	1.3	17
38456	Oxygen vacancies induced ferromagnetic behaviors in Co3O4â€“: An experimental and first-principles study. Thin Solid Films, 2018, 660, 287-293.	0.8	9
38457	Graphene Oxide/Perovskite Interfaces For Photovoltaics. Journal of Physical Chemistry C, 2018, 122, 16715-16726.	1.5	22
38458	Anomalous Pressure Characteristics of Defects in Hexagonal Boron Nitride Flakes. ACS Nano, 2018, 12, 7127-7133.	7.3	51
38459	Insights into the Impact of Native Defects on the Conductivity of CuVO₃ Material for Photovoltaic Application: A First-Principles Computational Study. ACS Omega, 2018, 3, 6605-6610.	1.6	3
38460	Materials informatics for self-assembly of functionalized organic precursors on metal surfaces. Nature Communications, 2018, 9, 2469.	5.8	13
38461	2D transition metal dichalcogenides with glucan multivalency for antibody-free pathogen recognition. Nature Communications, 2018, 9, 2549.	5.8	44
38462	Semi-metals as potential thermoelectric materials. Scientific Reports, 2018, 8, 9876.	1.6	71
38463	Tuning the Pd-catalyzed electroreduction of CO₂to CO with reduced overpotential. Catalysis Science and Technology, 2018, 8, 3894-3900.	2.1	24

#	Article	IF	Citations
38464	The Flexible Unit Structure Engine (FUSE) for probe structure-based composition prediction. Faraday Discussions, 2018, 211, 117-131.	1.6	9
38465	Large-scaleab initiocalculations of Raman scattering spectra within time-dependent density functional perturbation theory. Journal of Chemical Physics, 2018, 148, 244103.	1.2	5
38466	First-principles calculations of iron-hydrogen reactions in silicon. Journal of Applied Physics, 2018, 123, .	1.1	3
38467	Defect physics in complex energy materials. Journal of Physics Condensed Matter, 2018, 30, 293001.	0.7	29
38468	Band-edge levels of the NaCl(100) surface: Self-consistent hybrid density functional theory compared to many-body perturbation theory. Physical Review B, 2018, 97, .	1.1	11
38469	Nodal line fermions in magnetic oxides. Physical Review B, 2018, 97, .	1.1	24
38470	van der Waals screening by graphenelike monolayers. Physical Review B, 2018, 97, .	1.1	17
38471	Single atom accelerates ammonia photosynthesis. Science China Chemistry, 2018, 61, 1187-1196.	4.2	107
38472	Tuning the structures of two-dimensional cuprous oxide confined on Au(111). Nano Research, 2018, 11, 5957-5967.	5.8	8
38473	Aluminum- and vanadium-free titanium alloys for application in medical engineering. , 2018, , 477-492.		4
38474	DFT modelling of ethanol on BaTiO3 (0â€¯0â€¯1) surface. Applied Surface Science, 2018, 456, 276-289.	3.1	18
38475	Strong affinity of mineral dusts for sulfur dioxide and catalytic mechanisms towards acid rain formation. Catalysis Communications, 2018, 114, 79-83.	1.6	16
38476	Theoretical and experimental investigations on high temperature mechanical and thermal properties of BaZrO3. Ceramics International, 2018, 44, 16475-16482.	2.3	56
38477	Effect of solutes on the lattice parameters and elastic stiffness coefficients of body-centered tetragonal Fe. Computational Materials Science, 2018, 152, 308-323.	1.4	15
38478	Tunable magnetic and electronic properties in 3d transition-metal adsorbed Î²12 and Ï‡3 borophene. Computational Materials Science, 2018, 153, 10-15.	1.4	31
38479	Structural, electronic, dynamical and thermodynamic properties of Ca10(PO4)6(OH)2 and Sr10(PO4)6(OH)2: First-principles study. International Journal of Hydrogen Energy, 2018, 43, 13639-13648.	3.8	11
38480	First-principles GGAÂ+ÂU calculation investigating the hydriding and diffusion properties of hydrogen in PuH2+, 0Ââ‰xâ‰Â1. International Journal of Hydrogen Energy, 2018, 43, 13632-13638.	3.8	17
38481	Third-order elastic constants and anharmonic properties of three fcc high-entropy alloys from first-principles. Journal of Alloys and Compounds, 2018, 764, 906-912.	2.8	11

#	Article	IF	Citations
38482	Selective hydrogenation of phenol to cyclohexanone by SiO2-supported rhodium nanoparticles under mild conditions. Journal of Catalysis, 2018, 364, 354-365.	3.1	57
38483	Modelling of dislocation-solute interaction in ODS steels: Analytic bond-order potential for the iron-yttrium system. Journal of Nuclear Materials, 2018, 509, 102-113.	1.3	5
38484	A current collector covering nanostructured villous oxygen-deficient NiO fabricated by rapid laser-scan for Li-O2 batteries. Nano Energy, 2018, 51, 83-90.	8.2	54
38485	Strain effects on the Schottky contacts of graphene and MoSe2 heterobilayers. Physica E: Low-Dimensional Systems and Nanostructures, 2018, 103, 284-288.	1.3	17
38486	Nano-laminated thin film metallic glass design for outstanding mechanical properties. Scripta Materialia, 2018, 155, 73-77.	2.6	23
38487	Hierarchical Materials as Tailored Nuclear Waste Forms: A Perspective. Chemistry of Materials, 2018, 30, 4475-4488.	3.2	98
38488	High-Efficiency Production of Graphene by Supercritical CO₂ Exfoliation with Rapid Expansion. Langmuir, 2018, 34, 7797-7804.	1.6	20
38489	Modulations in martensitic Heusler alloys originate from nanotwin ordering. Scientific Reports, 2018, 8, 8489.	1.6	47
38490	2D SnSe-based vdW heterojunctions: tuning the Schottky barrier by reducing Fermi level pinning. Nanoscale, 2018, 10, 13767-13772.	2.8	32
38491	Spontaneous valley splitting and valley pseudospin field effect transistors of monolayer VAgP₂Se₆. Nanoscale, 2018, 10, 13986-13993.	2.8	50
38493	High n-type and p-type thermoelectric performance of two-dimensional SiTe at high temperature. RSC Advances, 2018, 8, 21280-21287.	1.7	11
38494	Computational realization of Dirac nodal point and Dirac nodal loop fermions in novel Î²-graphyne analogues. Journal of Materials Chemistry C, 2018, 6, 7626-7634.	2.7	20
38495	Novel compounds of cerium binary alloys from high-throughput first-principles calculations. Journal of Applied Physics, 2018, 123, .	1.1	3
38496	Descriptor-based crystal structure prediction of magnetic transition metals: Orbital-spin occupancy rule. AIP Advances, 2018, 8, .	0.6	5
38497	Interplay between p â^'â€‰â€‰and d â^'â€‰â€‰orbitals yields multiple Dirac states in one- and two-dimensional CrB ₄. 2D Materials, 2018, 5, 035041.	2.0	23
38498	Comparative study of the properties of ionic solids from density functionals. Materials Research Express, 2018, 5, 076302.	0.8	8
38499	Screened hybrid functionals applied to ceria: Effect of Fock exchange. Physical Review B, 2018, 97, .	1.1	23
38500	Mechanism of the Interaction between F Atoms and SiCF3 Groups on the Low-Î² Dielectric Surface. Journal of Surface Investigation, 2018, 12, 535-539.	0.1	3

#	Article	IF	Citations
38501	Realization of N-Type Semiconducting of Phosphorene through Surface Metal Doping and Work Function Study. Journal of Nanomaterials, 2018, 2018, 1-9.	1.5	9
38502	Role of zirconium in direct CO2 hydrogenation to lower olefins on oxide/zeolite bifunctional catalysts. Journal of Catalysis, 2018, 364, 382-393.	3.1	174
38503	Structures and thermodynamic stability of cobalt molybdenum oxide (CoMoO4-II). Surface Science, 2018, 677, 52-59.	0.8	9
38504	Suppressed topological phase transitions due to nonsymmorphism in SnTe stacking. Scientific Reports, 2018, 8, 9452.	1.6	4
38505	Investigation of n-type doping strategies for Mg₃Sb₂. Journal of Materials Chemistry A, 2018, 6, 13806-13815.	5.2	80
38506	Structural and electronic optimization of graphene encapsulating binary metal for highly efficient water oxidation. Nano Energy, 2018, 52, 494-500.	8.2	145
38507	First principles study of point defect effects on iodine diffusion in zirconium. Nuclear Materials and Energy, 2018, 16, 238-244.	0.6	1
38508	Pd₂Se₃ Monolayer: A Promising Two-Dimensional Thermoelectric Material with Ultralow Lattice Thermal Conductivity and High Power Factor. Chemistry of Materials, 2018, 30, 5639-5647.	3.2	119
38509	Modeling Oxygen Ion Migration in the CeO₂â€“ZrO₂â€“Y₂O₃ Solid Solution. Journal of Physical Chemistry C, 2018, 122, 18809-18817.	1.5	19
38510	Theoretical Insights into the Interaction of Oxygenated Organic Molecules and Cobalt(II) Precursor with Î³-Al₂O₃Surfaces. Journal of Physical Chemistry C, 2018, 122, 19560-19574.	1.5	8
38511	Understanding W Doping in Wurtzite ZnO. Journal of Physical Chemistry C, 2018, 122, 19082-19089.	1.5	4
38512	Calcium Phosphate Deposition on Planar and Stepped (101) Surfaces of Anatase TiO₂: Introducing an Interatomic Potential for the TiO₂/Ca-PO₄/Water Interface. Langmuir, 2018, 34, 10144-10152.	1.6	5
38513	Insight into the NH₃-Assisted Selective Catalytic Reduction of NO on Î²-MnO₂(110): Reaction Mechanism, Activity Descriptor, and Evolution from a Pristine State to a Steady State. ACS Catalysis, 2018, 8, 9269-9279.	5.5	76
38514	Multicomponent electrocatalyst with ultralow Pt loading and high hydrogen evolution activity. Nature Energy, 2018, 3, 773-782.	19.8	542
38515	Giant anomalous Hall effect in a ferromagnetic kagome-lattice semimetal. Nature Physics, 2018, 14, 1125-1131.	6.5	876
38516	Optimizing edges and defects of supported MoS₂ catalysts for hydrogen evolution via an external electric field. Physical Chemistry Chemical Physics, 2018, 20, 26083-26090.	1.3	25
38517	Phosphomolybdic acid supported single-metal-atom catalysis in CO oxidation: first-principles calculations. Physical Chemistry Chemical Physics, 2018, 20, 20661-20668.	1.3	34
38518	Elucidating lithium-ion and proton dynamics in anti-perovskite solid electrolytes. Energy and Environmental Science, 2018, 11, 2993-3002.	15.6	95

#	Article	IF	Citations
38519	Robust half-metallicity in transition metal tribromide nanowires. Nanoscale, 2018, 10, 15545-15552.	2.8	16
38520	Cu dimer anchored on C₂N monolayer: low-cost and efficient Bi-atom catalyst for CO oxidation. Nanoscale, 2018, 10, 15696-15705.	2.8	68
38521	A hidden symmetry-broken phase of MoS₂ revealed as a superior photovoltaic material. Journal of Materials Chemistry A, 2018, 6, 16087-16093.	5.2	16
38522	Self-diffusion barriers: possible descriptors for dendrite growth in batteries?. Energy and Environmental Science, 2018, 11, 3400-3407.	15.6	247
38523	Electronic and optical properties of Î±â€MoO₃/TiO₂ heterostructures: A DFT study. International Journal of Quantum Chemistry, 2018, 118, e25681.	1.0	6
38524	The Electronic Structure of Cu3BiS3 for Use as a PV Absorber. Springer Theses, 2018, , 139-173.	0.0	0
38525	Theoretical and experimental studies on the influence of Cr incorporation on the structural, optical, and magnetic properties of Bi0.5K0.5TiO3 materials. Journal of Sol-Gel Science and Technology, 2018, 87, 528-536.	1.1	17
38526	Prediction on elastic and thermal properties of defective L12â€“Al3Li intermetallics. Indian Journal of Physics, 2018, 92, 1083-1089.	0.9	3
38527	Theory-guided metal-decoration of nanoporous carbon for hydrogen storage applications. Surface and Coatings Technology, 2018, 351, 42-49.	2.2	16
38528	Effect of Ag Doping on Electronic Structure of Cluster Compounds Ag_xMo₉Se₁₁ (x = 3.4, 3.9). ACS Applied Energy Materials, 2018, 1, 4032-4039.	2.5	8
38529	Combined Structural, Chemometric, and Electrochemical Investigation of Vertically Aligned TiO₂ Nanotubes for Na-ion Batteries. ACS Omega, 2018, 3, 8440-8450.	1.6	86
38530	Dirac semimetal in Î² -CuI without surface Fermi arcs. Proceedings of the National Academy of Sciences of the United States of America, 2018, 115, 8311-8315.	3.3	30
38531	Elastic constants of the IIâ€“IV nitride semiconductors MgSiN₂, MgGeN₂and MgSnN₂. Journal Physics D: Applied Physics, 2018, 51, 375101.	1.3	8
38532	Local atomic geometry and Ti <mml:math xmlns:mml="http://www.w3.org/1998/Math/MathML"><mml:mrow><mml:mn>1</mml:mn><mml:mi>s</mml:mi></mml:mrow></mml:m near-edge spectra in <mml:math xmlns:mml="http://www.w3.org/1998/Math/MathML"><mml:msub><mml:mi>PbTiO</mml:mi><mml:mn>3</mml:mn></mml:msub> and <mml:math xmlns:mml="http://www.w3.org/1998/Math/MathML"><mml:msub><mml:mi>SrTiO</mml:mi><mml:mn>3</mml:mn></mml:msub>	1.1	12
38533	Enhanced efficiency in lead-free bismuth iodide with post treatment based on a hole-conductor-free perovskite solar cell. Nano Research, 2018, 11, 6283-6293.	5.8	72
38534	General trends between solute segregation tendency and grain boundary character in aluminum - An ab inito study. Acta Materialia, 2018, 158, 257-268.	3.8	49
38535	Structural stability and electronic properties of the (0â€¯0â€¯0â€¯1) inversion domain boundary in III-nitrides. Computational Materials Science, 2018, 154, 152-158.	1.4	1
38536	A route towards understanding the kinetic processes of bis(trifluoromethanesulfonyl) imide anion intercalation into graphite for dual-ion batteries. Electrochimica Acta, 2018, 284, 669-680.	2.6	41

#	Article	IF	Citations
38537	Highly-efficient sensitizer with zinc porphyrin as building block: Insights from DFT calculations. Solar Energy, 2018, 173, 283-290.	2.9	27
38538	Layer-Number-Dependent Exciton Recombination Behaviors of MoS₂ Determined by Fluorescence-Lifetime Imaging Microscopy. Journal of Physical Chemistry C, 2018, 122, 18651-18658.	1.5	21
38539	Synergistically Enhanced Oxygen Evolution Reaction Catalysis for Multielement Transition-Metal Oxides. ACS Applied Energy Materials, 2018, 1, 3711-3721.	2.5	53
38540	Distinct multiple fermionic states in a single topological metal. Nature Communications, 2018, 9, 3002.	5.8	16
38541	Bandgap tuning in MoSSe bilayers: synergistic effects of dipole moment and interlayer distance. Physical Chemistry Chemical Physics, 2018, 20, 20919-20926.	1.3	46
38542	Multiple states and roles of hydrogen in p-type SnS semiconductors. Physical Chemistry Chemical Physics, 2018, 20, 20952-20956.	1.3	10
38543	Role of the Mn substituent in Na₃V₂(PO₄)₃ for high-rate sodium storage. Journal of Materials Chemistry A, 2018, 6, 16627-16637.	5.2	58
38544	Pressure-induced enhancement in the thermoelectric properties of monolayer and bilayerÂSnSe ₂. Royal Society Open Science, 2018, 5, 171827.	1.1	13
38545	Effects of Bi on band gap bowing in InP₁₋xBix alloys. Optical Materials Express, 2018, 8, 1184.	1.6	13
38546	Nearest-neighbor sp³d⁵s* tight-binding parameters based on the hybrid quasi-particle self-consistent GW method verified by modeling of type-II superlattices. Optical Materials Express, 2018, 8, 1569.	1.6	11
38547	Optical properties and applications for MoS₂-Sb₂Te₃-MoS₂heterostructure materials. Photonics Research, 2018, 6, 220.	3.4	141
38548	Significant Strainâ€Induced Orbital Reconstruction and Strong Interfacial Magnetism in TiNi(Nb)/Ferromagnet/Oxide Heterostructures via Oxygen Manipulation. Advanced Functional Materials, 2018, 28, 1803335.	7.8	30
38549	The Use of Photoemission Spectroscopies for the Characterisation and Identification of Cu2ZnSnS4 and its Secondary Phases. Springer Theses, 2018, , 215-306.	0.0	0
38550	Defect Sites in Ultrathin Pd Nanowires Facilitate the Highly Efficient Electrochemical Hydrodechlorination of Pollutants by H*_{ads}. Environmental Science & Technology, 2018, 52, 9992-10002.	4.6	137
38551	Generating Sub-nanometer Pores in Single-Layer MoS₂ by Heavy-Ion Bombardment for Gas Separation: A Theoretical Perspective. ACS Applied Materials & Interfaces, 2018, 10, 28909-28917.	4.0	37
38552	Two dimensional monolayer rhombic silicene on the diamond (111) surface. Physical Chemistry Chemical Physics, 2018, 20, 21699-21704.	1.3	5
38553	Two-dimensional zigzag-shaped Cd₂C monolayer with a desirable bandgap and high carrier mobility. Journal of Materials Chemistry C, 2018, 6, 9175-9180.	2.7	19
38554	Electron localization in niobium doped CaMnO3 due to the energy difference of electronic states of Mn and Nb. Physical Chemistry Chemical Physics, 2018, 20, 20571-20574.	1.3	6

#	Article	IF	Citations
38555	Ionic vs. van der Waals layered materials: identification and comparison of elastic anisotropy. Journal of Materials Chemistry A, 2018, 6, 15828-15838.	5.2	22
38556	Reconstruction of release isentropes based on first-principle simulations. Journal of Physics: Conference Series, 2018, 946, 012089.	0.3	4
38557	Computational and Experimental Investigations of Defect Interaction and Ionic Conductivity in Doped Zirconia. Physical Review Applied, 2018, 10, .	1.5	6
38558	Determining the vibrational entropy change in the giant magnetocaloric material <mml:math xmlns:mml="http://www.w3.org/1998/Math/MathML"><mml:msub><mml:mrow><mml:mi mathvariant="normal">LaFe</mml:mi></mml:mrow><mml:mrow><mml:mn>11.6</mml:mn></mml:mrow></mml:msub><mml:msub><mml:mi mathvariant="normal">Si</mml:mi></mml:mrow><mml:mrow><mml:mn>1.4</mml:mn></mml:mrow></mml:msub></mml:math> by nuclear resonant inelastic x-ray scattering. Physical Review B, 2018, 98, .	1.1	14
38559	Spin-strain interaction in nitrogen-vacancy centers in diamond. Physical Review B, 2018, 98, .	1.1	77
38560	Nature of the Positron State in CdSe Quantum Dots. Physical Review Letters, 2018, 121, 057401.	2.9	7
38561	Microsecond Valley Lifetime of Defect-Bound Excitons in Monolayer <mml:math xmlns:mml="http://www.w3.org/1998/Math/MathML" display="inline"><mml:mrow><mml:msub><mml:mrow><mml:mi>WSe</mml:mi></mml:mrow><mml:mn>2</mml:mn></mml:msub></ Physical Review Letters, 2018, 121, 057403.	2.9	114
38562	Defect engineering by synchrotron radiation X-rays in CeO₂ nanocrystals. Journal of Synchrotron Radiation, 2018, 25, 1395-1399.	1.0	7
38563	In situ XPS study on atomic layer etching of Fe thin film using Cl2 and acetylacetone. Journal of Vacuum Science and Technology A: Vacuum, Surfaces and Films, 2018, 36, .	0.9	20
38564	Translational Inelasticity of NO and CO in Scattering from Ultrathin Metallic Films of Ag/Au(111). Journal of Physical Chemistry C, 2018, 122, 18942-18948.	1.5	9
38565	In Silico Optimization of Organicâ€“Inorganic Hybrid Perovskites for Photocatalytic Hydrogen Evolution Reaction in Acidic Solution. Journal of Physical Chemistry C, 2018, 122, 20918-20922.	1.5	6
38566	Metal-to-insulator transition in two-dimensional ferromagnetic monolayer induced by substrate. Chinese Physics B, 2018, 27, 077106.	0.7	1
38567	Hydrogen bubble nucleation by self-clustering: density functional theory and statistical model studies using tungsten as a model system. Nuclear Fusion, 2018, 58, 096021.	1.6	34
38568	A first-principles study of 2D antimonene electrodes for Li ion storage. Applied Surface Science, 2018, 462, 270-275.	3.1	39
38569	Sodium ions pre-intercalation stabilized tunnel structure of Na2Mn8O16 nanorods for supercapacitors with long cycle life. Chemical Engineering Journal, 2018, 354, 1050-1057.	6.6	48
38570	Theoretical prediction of two-dimensional CrOF sheet as a ferromagnetic semiconductor or a half-metal. Chemical Physics, 2018, 513, 182-187.	0.9	25
38571	Simulations of Hâ€“He mixtures using the van der Waals density functional. Journal of Plasma Physics, 2018, 84, .	0.7	4
38572	Coordination of Atomic Coâ€“Pt Coupling Species at Carbon Defects as Active Sites for Oxygen Reduction Reaction. Journal of the American Chemical Society, 2018, 140, 10757-10763.	6.6	464

#	Article	IF	Citations
38573	Cs₂PbI₂Cl₂, All-Inorganic Two-Dimensional Ruddlesdenâ€“Popper Mixed Halide Perovskite with Optoelectronic Response. Journal of the American Chemical Society, 2018, 140, 11085-11090.	6.6	167
38574	Self-assembly directed one-step synthesis of [4]radialene on Cu(100) surfaces. Nature Communications, 2018, 9, 3113.	5.8	41
38575	Borophene's tryst with stability: exploring 2D hydrogen boride as an electrode for rechargeable batteries. Physical Chemistry Chemical Physics, 2018, 20, 22008-22016.	1.3	45
38576	Room-temperature surface-assisted reactivity of a melanin precursor: silver metalâ€“organic coordination versus covalent dimerization on gold. Nanoscale, 2018, 10, 16721-16729.	2.8	23
38577	Discovery of asymmetric NaXBi (X= Sn /Pb) monolayers with non-trivial topological properties. RSC Advances, 2018, 8, 27995-28001.	1.7	1
38578	The effects of combining alloying elements on the elastic properties of Î³ -Ni in Ni-based superalloy: High-throughput first-principles calculations. Chinese Physics B, 2018, 27, 077104.	0.7	6
38579	Unraveling the structure and bonding evolution of the newly discovered iron oxide <mml:math xmlns:mml="http://www.w3.org/1998/Math/MathML"><mml:msub><mml:mi>FeO</mml:mi><mml:mn>2</mml:mn></mml:msub></mml Physical Review B, 2018, 98, .	1.1	62
38580	Strain engineering of antimonene by a first-principles study: Mechanical and electronic properties. Physical Review B, 2018, 98, .	1.1	82
38581	Efficient Capacitive Deionization Using Thin Film Sodium Manganese Oxide. Journal of the Electrochemical Society, 2018, 165, A2330-A2339.	1.3	12
38583	Janus MoSSe Nanotubes: Tunable Band Gap and Excellent Optical Properties for Surface Photocatalysis. Advanced Theory and Simulations, 2018, 1, 1800082.	1.3	35
38584	Metallic Octahedral CoSe₂ Threaded by Nâ€Doped Carbon Nanotubes: A Flexible Framework for Highâ€Performance Potassiumâ€Ion Batteries. Advanced Science, 2018, 5, 1800782.	5.6	198
38585	Localization of Yttrium Segregation within YSZ Grain Boundary Dislocation Cores. Physica Status Solidi (A) Applications and Materials Science, 2018, 215, 1800349.	0.8	10
38586	The Electronic Structure of CuSbS2 for Use as a PV Absorber. Springer Theses, 2018, , 99-138.	0.0	0
38587	Low-temperature direct synthesis of high quality WS2 thin films by plasma-enhanced atomic layer deposition for energy related applications. Applied Surface Science, 2018, 459, 596-605.	3.1	42
38588	The role of metal-oxo intermediate to oxygen reduction reaction catalysis: A theoretical investigation using nitrogen-substituted carbon nanotube models. Surface Science, 2018, 677, 301-305.	0.8	2
38589	Investigating C₂H₂ Sorption in Î±-[M₃(O₂CH)₆] (M = Mg, Mn) Through Theoretical Studies. Crystal Growth and Design, 2018, 18, 5342-5352.	1.4	2
38590	Structural Origin of the Midgap Electronic States and the Urbach Tail in Pnictogen-Chalcogenide Glasses. Journal of Physical Chemistry B, 2018, 122, 8082-8097.	1.2	6
38591	Hydrogen Spillover to Copper Clusters on Hydroxylated Î³-Al₂O₃. Journal of Physical Chemistry C, 2018, 122, 18445-18455.	1.5	44

#	Article	IF	Citations
38592	Tinâ€“Selenium Compounds at Ambient and High Pressures. Journal of Physical Chemistry C, 2018, 122, 18274-18281.	1.5	13
38593	Increased Lattice Stiffness Suppresses Nonradiative Charge Recombination in MAPbI₃ Doped with Larger Cations: Time-Domain Ab Initio Analysis. ACS Energy Letters, 2018, 3, 2070-2076.	8.8	68
38594	Giant Electronâ€“Phonon Coupling and Deep Conduction Band Resonance in Metal Halide Double Perovskite. ACS Nano, 2018, 12, 8081-8090.	7.3	190
38595	Discovery of High-Performance Thermoelectric Chalcogenides through Reliable High-Throughput Material Screening. Journal of the American Chemical Society, 2018, 140, 10785-10793.	6.6	134
38596	Energy dissipation to tungsten surfaces upon hot-atom and Eleyâ€“Rideal recombination of H₂. Physical Chemistry Chemical Physics, 2018, 20, 21334-21344.	1.3	7
38597	Structure and properties of a novel boride: ThNi₁₂B₆. Dalton Transactions, 2018, 47, 12933-12943.	1.6	1
38598	Zero-strain K_{0.6}Mn₁F_{2.7} hollow nanocubes for ultrastable potassium ion storage. Energy and Environmental Science, 2018, 11, 3033-3042.	15.6	87
38599	Penta-Pt₂N₄: an ideal two-dimensional material for nanoelectronics. Nanoscale, 2018, 10, 16169-16177.	2.8	58
38600	An amorphous tin-based nanohybrid for ultra-stable sodium storage. Journal of Materials Chemistry A, 2018, 6, 18920-18927.	5.2	22
38601	Redox inactive ion meliorated BaCo0.4Fe0.4Zr0.1Y0.1O3â^Î´ perovskite oxides as efficient electrocatalysts for the oxygen evolution reaction. Journal of Materials Chemistry A, 2018, 6, 17288-17296.	5.2	28
38602	Acceleration of oxidation process of iron in supercritical water containing dissolved oxygen by the formation of H2O2. AIP Advances, 2018, 8, 085104.	0.6	1
38603	Electronic structure theory of strained two-dimensional materials with hexagonal symmetry. Physical Review B, 2018, 98, .	1.1	57
38604	Role of oxygen vacancy in the spin-state change and magnetic ordering in <mml:math xmlns:mml="http://www.w3.org/1998/Math/MathML"><mml:msub><mml:mi>SrCoO</mml:mi><mml:mrow><mml:mn>3</mml:mn><m Physical Review B, 2018, 98, .	1.1	28
38605	Adsorption and Diffusion Properties of a Single Iron Atom on Light-Element-Doped Graphene. E-Journal of Surface Science and Nanotechnology, 2018, 16, 193-200.	0.1	3
38606	Elasticity of high-entropy alloys from ab initio theory. Journal of Materials Research, 2018, 33, 2938-2953.	1.2	38
38607	A Search for Two Types of Transverse Excitations in Liquid Polyvalent Metals at Ambient Pressure: An Ab Initio Molecular Dynamics Study of Collective Excitations in Liquid Al, Tl, and Ni. Frontiers in Physics, 2018, 6, .	1.0	16
38608	Effects of substrate and environmental adsorbates on the electronic properties and structural stability of antimonene. Journal of Materials Science, 2018, 53, 15559-15568.	1.7	11
38609	PdCu nanoalloy immobilized in ZIF-derived N-doped carbon/graphene nanosheets: Alloying effect on catalysis. Chemical Engineering Journal, 2018, 353, 311-318.	6.6	52

#	Article	IF	Citations
38610	The first principle calculations of structural, vibrational, elastic, thermodynamic and electronic properties of MgX (XÂ= La, Nd, Sm) intermetallics. Computational Condensed Matter, 2018, 16, e00324.	0.9	6
38611	Enhanced hydrogen storage properties of MgH 2 catalyzed with carbon-supported nanocrystalline TiO 2. Journal of Power Sources, 2018, 398, 183-192.	4.0	176
38612	Carbon dioxide electroreduction over imidazolate ligands coordinated with Zn(II) center in ZIFs. Nano Energy, 2018, 52, 345-350.	8.2	121
38613	Nonequivalent Spin Exchanges of the Hexagonal Spin Lattice Affecting the Low-Temperature Magnetic Properties of RInO₃ (R = Gd, Tb, Dy): Importance of Spinâ€“Orbit Coupling for Spin Exchanges between Rare-Earth Cations with Nonzero Orbital Moments. Inorganic Chemistry, 2018, 57, 9260-9265.	1.9	11
38614	Investigating Reaction Mechanisms for Furfural Hydrodeoxygenation on Ni and the Effect of Boron Doping on the Activity and Selectivity of the Catalyst. Journal of Physical Chemistry C, 2018, 122, 18383-18394.	1.5	32
38615	Tunable Out-of-Plane Piezoelectricity in Thin-Layered MoTe₂ by Surface Corrugation-Mediated Flexoelectricity. ACS Applied Materials & Interfaces, 2018, 10, 27424-27431.	4.0	44
38616	Resolving the Amorphous Structure of Lithium Phosphorus Oxynitride (Lipon). Journal of the American Chemical Society, 2018, 140, 11029-11038.	6.6	99
38617	Atomic-level insight into super-efficient electrocatalytic oxygen evolution on iron and vanadium co-doped nickel (oxy)hydroxide. Nature Communications, 2018, 9, 2885.	5.8	669
38618	Theoretical investigation on the interaction between Rh^{III} octaethylporphyrin and a graphite basal surface: a comparison study of DFT, DFT-D, and AFM. Physical Chemistry Chemical Physics, 2018, 20, 20235-20246.	1.3	14
38619	OH formation and H₂ adsorption at the liquid waterâ€“Pt(111) interface. Chemical Science, 2018, 9, 6912-6921.	3.7	76
38620	Optimizing the thermoelectric transport properties of BiCuSeO via doping with the rare-earth variable-valence element Yb. Journal of Materials Chemistry C, 2018, 6, 8479-8487.	2.7	26
38621	Enhancing sodium ionic conductivity in tetragonal-Na₃PS₄by halogen doping: a first principles investigation. Physical Chemistry Chemical Physics, 2018, 20, 20525-20533.	1.3	41
38622	Two-dimensional carbon dioxide with high stability, a negative Poisson's ratio and a huge band gap. Physical Chemistry Chemical Physics, 2018, 20, 20615-20621.	1.3	13
38623	Multiporous sp²-hybridized boron nitride (d-BN): stability, mechanical properties, lattice thermal conductivity and promising application in energy storage. Physical Chemistry Chemical Physics, 2018, 20, 20726-20731.	1.3	19
38624	Electronic and magneto-optical properties of ZnO:Co. EPJ Web of Conferences, 2018, 185, 06012.	0.1	0
38625	Experimental and Computational Study on the Interaction of an Ionic Liquid Monolayer with Lithium on Pristine and Lithiated Graphite. Journal of Physical Chemistry C, 2018, 122, 18968-18981.	1.5	14
38626	Intermediate Bands in Zero-Dimensional Antimony Halide Perovskites. Journal of Physical Chemistry Letters, 2018, 9, 4652-4656.	2.1	27
38627	Bifunctional Hybrid a-SiO_x(Mo) Layer for Hole-Selective and Interface Passivation of Highly Efficient MoO_x/a-SiO_x(Mo)/n-Si Heterojunction Photovoltaic Device. ACS Applied Materials & Interfaces, 2018, 10, 27454-27464.	4.0	28

#	Article	IF	Citations
38628	A rational method to kinetically control the rate-determining step to explore efficient electrocatalysts for the oxygen evolution reaction. NPG Asia Materials, 2018, 10, 659-669.	3.8	66
38629	Hybridization induced metallic and magnetic edge states in noble transition-metal-dichalcogenides of PtX₂ (X = S, Se) nanoribbons. Physical Chemistry Chemical Physics, 2018, 20, 21441-21446.	1.3	13
38630	Monte-Carlo study of electronic transport in non-Ïƒh-symmetric two-dimensional materials: Silicene and germanene. Journal of Applied Physics, 2018, 124, .	1.1	28
38631	Reverse-martensitic hcp-to-fcc transformation in technetium under shock compression. Journal of Applied Physics, 2018, 124, .	1.1	5
38632	Structural transformation, Griffiths phase and metal-insulator transition in polycrystalline Nd_{2â^'x}Sr_xNiMnO₆ (xâ€‰â€‰=â€‰â€‰0, 0.2, 0.4, 0.5 and 1) compound. Journal of Physics Condensed Matter, 2018, 30, 355401.	1.7	51
38633	Anisotropic elastic properties and ideal uniaxial compressive strength of TiB 2 from first principles calculations. Chinese Physics B, 2018, 27, 077103.	0.7	3
38634	Flexible polarization rotation at the ferroelectric/metal interface as a seed for domain nucleation. Physical Review B, 2018, 98, .	1.1	14
38635	Formation and dynamics of small polarons on the rutile <mml:math xmlns:mml="http://www.w3.org/1998/Math/MathML"><mml:msub><mml:mi>TiO</mml:mi><mml:mn>2</mml:mn></mml:msub></m (110) surface. Physical Review B, 2018, 98, .	1.1	67
38636	A Defect-Driven Metal-free Electrocatalyst for Oxygen Reduction in Acidic Electrolyte. CheM, 2018, 4, 2345-2356.	5.8	292
38637	Can an element form a two-dimensional nanosheet of type 15 pentagons?. Computational Materials Science, 2018, 154, 37-40.	1.4	34
38638	A comparative first-principles study of tetragonal TiAl and Ti4Nb3Al9 intermetallic compounds. Intermetallics, 2018, 101, 72-80.	1.8	13
38639	Structural, electronic and magnetic properties and pressure-induced half metallicity in double perovskite Ca2AOsO6 (Aâ€¯=â€¯Cr, Mo). Journal of Magnetism and Magnetic Materials, 2018, 467, 145-149.	1.0	7
38640	A promising high-efficiency photovoltaic alternative non-silicon material: A first-principle investigation. Scripta Materialia, 2018, 156, 134-137.	2.6	2
38641	Quantum Confinement in Oxide Heterostructures: Room-Temperature Intersubband Absorption in SrTiO₃/LaAlO₃ Multiple Quantum Wells. ACS Nano, 2018, 12, 7682-7689.	7.3	15
38642	Communication: Fingerprints of reaction mechanisms in product distributions: Eley-Rideal-type reactions between D and CD3/Cu(111). Journal of Chemical Physics, 2018, 149, 031101.	1.2	16
38643	Structural, vibrational, and electronic properties of single-layer hexagonal crystals of group IV and V elements. Physical Review B, 2018, 98, .	1.1	102
38644	First-Principles Study of the Structure and Magnetic Properties of Fe8Rh8 â€“ xZx (Z = Mn, Pt, Co; x = 1,) Tj ETQq0 0 0 rgBT /Overlock 10	0.2	1
38645	First principles study of the electronic and optical properties of crystalline and liquid Sb₂Te₃: Phase-transition-induced changes in optical properties. Japanese Journal of Applied Physics, 2018, 57, 09SD01.	0.8	2

#	Article	IF	Citations
38646	H2S adsorption and dissociation on Rh(110) surface: a first-principles study. Adsorption, 2018, 24, 563-574.	1.4	8
38647	Elucidating mechanisms of Li plating on Li anodes of lithium-based batteries. Electrochimica Acta, 2018, 284, 485-494.	2.6	19
38648	Stability and hydrogen adsorption properties of Mg/Mg2Ni interface: A first principles study. International Journal of Hydrogen Energy, 2018, 43, 16598-16608.	3.8	22
38649	Extraordinary thermoelectric performance in n-type manganese doped Mg3Sb2 Zintl: High band degeneracy, tuned carrier scattering mechanism and hierarchical microstructure. Nano Energy, 2018, 52, 246-255.	8.2	188
38650	CO₂ and H₂ Adsorption and Reaction at Ni_n/YSZ(111) Interfaces: A Density Functional Theory Study. Journal of Physical Chemistry C, 2018, 122, 19463-19472.	1.5	15
38651	Germanene Growth on Al(111): A Case Study of Interface Effect. Journal of Physical Chemistry C, 2018, 122, 18669-18681.	1.5	17
38652	Equilibrium Auâ€“Pd(100) Surface Structures under CO Pressure: Energetic Stabilities and Phase Diagrams. Journal of Physical Chemistry C, 2018, 122, 18922-18932.	1.5	2
38653	Metallic Metalâ€“Organic Frameworks Predicted by the Combination of Machine Learning Methods and Ab Initio Calculations. Journal of Physical Chemistry Letters, 2018, 9, 4562-4569.	2.1	84
38654	The diffusion behavior of Ti atoms in pure nanocrystalline Fe by first principles calculations. Materials Research Express, 2018, 5, 095010.	0.8	6
38655	Modulation of Ionic Current Limitations by Doping Graphite Anodes. Journal of the Electrochemical Society, 2018, 165, A2233-A2238.	1.3	8
38656	Optical absorption coefficient red shift effect of iodine vacancy in MAPbI3. Computational Materials Science, 2018, 154, 138-142.	1.4	0
38657	Hierarchical mesoporous flower-like ZnCo2O4@NiO nanoflakes grown on nickel foam as high-performance electrodes for supercapacitors. Electrochimica Acta, 2018, 284, 128-141.	2.6	47
38658	High-temperature mechanical and thermodynamic properties of silicon carbide polytypes. Journal of Alloys and Compounds, 2018, 768, 722-732.	2.8	34
38659	The search for high entropy alloys: A high-throughput ab-initio approach. Acta Materialia, 2018, 159, 364-383.	3.8	142
38660	A molecular dynamics framework to explore the structure and dynamics of layered double hydroxides. Applied Clay Science, 2018, 163, 164-177.	2.6	27
38661	PASTA: Python Algorithms for Searching Transition stAtes. Computer Physics Communications, 2018, 233, 261-268.	3.0	15
38662	Truncated cobalt hexacyanoferrate nanocubes threaded by carbon nanotubes as a high-capacity and high-rate cathode material for dual-ion rechargable aqueous batteries. Journal of Power Sources, 2018, 399, 1-7.	4.0	35
38663	Oxygen Vacancy Enhanced Gas-Sensing Performance of CeO₂/Graphene Heterostructure at Room Temperature. Analytical Chemistry, 2018, 90, 9821-9829.	3.2	77

#	Article	IF	Citations
38664	Chloride Flux Growth of Idiomorphic AWO₄ (A = Sr, Ba) Single Microcrystals. Crystal Growth and Design, 2018, 18, 5301-5310.	1.4	8
38665	Evaluation of Gas-to-Liquid 17O Chemical Shift of Water: A Test Case for Molecular and Periodic Approaches. Journal of Chemical Theory and Computation, 2018, 14, 4041-4051.	2.3	2
38666	Machine-Learning Approach for the Development of Structureâ€“Energy Relationships of ZnO Nanoparticles. Journal of Physical Chemistry C, 2018, 122, 18621-18639.	1.5	12
38667	Role of Oxygen Vacancy Defects in the Electrocatalytic Activity of Substoichiometric Molybdenum Oxide. Journal of Physical Chemistry C, 2018, 122, 18212-18222.	1.5	63
38668	Structural, Spectroscopic, and Computational Characterization of the Concomitant Polymorphs of the Natural Semiconductor Indigo. Journal of Physical Chemistry C, 2018, 122, 18422-18431.	1.5	22
38669	Mechanisms of Covalent Coupling Reaction of Dibromofluoranthene on Au(111). Journal of Physical Chemistry C, 2018, 122, 17756-17763.	1.5	3
38670	Screening Surface Structure of MXenes by High-Throughput Computation and Vibrational Spectroscopic Confirmation. Journal of Physical Chemistry C, 2018, 122, 18501-18509.	1.5	130
38671	Two-Dimensional Materials Inserted at the Metal/Semiconductor Interface: Attractive Candidates for Semiconductor Device Contacts. Nano Letters, 2018, 18, 4878-4884.	4.5	34
38672	Nanoalloying MgO-Deposited Pt Clusters with Si To Control the Selectivity of Alkane Dehydrogenation. ACS Catalysis, 2018, 8, 8346-8356.	5.5	32
38673	Co6Se8(PEt3)6 superatoms as tunable chemical dopants for two-dimensional semiconductors. Npj Computational Materials, 2018, 4, .	3.5	20
38674	Calibrating the Extended HÃ¼ckel Method to Quantitatively Screen the Electronic Properties of Materials. Scientific Reports, 2018, 8, 10530.	1.6	3
38675	Dislocation driven spiral and non-spiral growth in layered chalcogenides. Nanoscale, 2018, 10, 15023-15034.	2.8	24
38676	Atomic insight into the structural transformation and anionic/cationic redox reactions of VS₂ nanosheets in sodium-ion batteries. Journal of Materials Chemistry A, 2018, 6, 15985-15992.	5.2	33
38677	Scanning tunneling microscopy investigations of unoccupied surface states in two-dimensional semiconducting Î²-â^š3 Ã— â^š3-Bi/Si(111) surface. Physical Chemistry Chemical Physics, 2018, 20, 20188-20193.	1.3	8
38678	Water dissociation on K₂O-pre-adsorbed transition metals: a systematic theoretical study. Physical Chemistry Chemical Physics, 2018, 20, 19850-19859.	1.3	7
38679	Identification and modulation of electronic band structures of single-phase Î²-(AlxGa1â^'x)2O3 alloys grown by laser molecular beam epitaxy. Applied Physics Letters, 2018, 113, .	1.5	43
38680	Linear scanning tunneling spectroscopy over a large energy range in black phosphorus. Journal of Applied Physics, 2018, 124, .	1.1	4
38681	Robust quantum spin Hall state and quantum anomalous Hall state in graphenelike BC3 with adatoms. New Journal of Physics, 2018, 20, 073047.	1.2	2

#	Article	IF	Citations
38682	Extremely large magnetoresistance and the complete determination of the Fermi surface topology in the semimetal ScSb. Physical Review B, 2018, 98, .	1.1	20
38683	Triply degenerate nodal points in <mml:math xmlns:mml="http://www.w3.org/1998/Math/MathML"><mml:mrow><mml:mi>R</mml:mi><mml:msub><mml:mi>Rh</mml:mi><mml:mn width="4pt" /><mml:mo>(</mml:mo><mml:mi>R</mml:mi><mml:mo>=</mml:mo><mml:mtext>Y</mml:mtext><mml:mo>,</mml:mo><mml:mtext> Physical Review B, 2018, 98, .	1.1	12
38684	Microscopic theory of refractive index applied to metamaterials: effective current response tensor corresponding to standard relation n2 = Îµeffî¼eff. European Physical Journal B, 2018, 91, 1.	0.6	2
38685	First-Principles Study on the Structural and Electronic Properties of Monolayer MoS2 with S-Vacancy under Uniaxial Tensile Strain. Nanomaterials, 2018, 8, 74.	1.9	55
38686	First-principles studies on the interface between light-absorbing layer and Mo back electrode in Cu(In,Ga)Se₂, Cu₂ZnSn(S,Se)₄, and Cu₂SnS₃ solar cells. Japanese Journal of Applied Physics, 2018, 57, 08RC17.	0.8	7
38687	Enhanced oxidation resistance of NaBH4-treated mackinawite (FeS): Application to Cr(VI) and As(III) removal. Chemical Engineering Journal, 2018, 353, 890-899.	6.6	36
38688	New gallium chalcogenides/arsenene van der Waals heterostructures promising for photocatalytic water splitting. International Journal of Hydrogen Energy, 2018, 43, 15995-16004.	3.8	49
38689	Azobenzene Adsorption on the MoS₂(0001) Surface: A Density Functional Investigation within van der Waals Corrections. Journal of Physical Chemistry C, 2018, 122, 18895-18901.	1.5	15
38690	Microscopic Origins of the Variability of Water Contact Angle with Adsorbed Contaminants on Layered Materials. Journal of Physical Chemistry C, 2018, 122, 18520-18527.	1.5	7
38691	Selective Oxidation of Methane to Formaldehyde Catalyzed by Phosphates: Kinetic Description by Bond Strengths and Specific Total Acidities. ACS Catalysis, 2018, 8, 8263-8272.	5.5	10
38692	Phase transformation, ionic diffusion, and charge transfer mechanisms of KVOPO₄ in potassium ion batteries: first-principles calculations. Journal of Materials Chemistry A, 2018, 6, 16228-16234.	5.2	50
38693	Invited Article: Mode-locked waveguide lasers modulated by rhenium diselenide as a new saturable absorber. APL Photonics, 2018, 3, .	3.0	44
38694	Tunable direct-indirect band gaps of ZrSe2 nanoribbons. Journal of Applied Physics, 2018, 124, .	1.1	7
38695	Electronic response of aluminum-bearing minerals. Journal of Chemical Physics, 2018, 149, 024502.	1.2	11
38696	Two-dimensional multiferroic semiconductors with coexisting ferroelectricity and ferromagnetism. Applied Physics Letters, 2018, 113, .	1.5	114
38697	Realizing robust large-gap quantum spin Hall state in 2D HgTe monolayer on insulating substrate. 2D Materials, 2018, 5, 045012.	2.0	3
38698	Theoretical study of the atomistic behavior of O vacancy complexes with N and H atoms in the SiO2 layer of a metalâ€“oxideâ€“nitrideâ€“oxideâ€“semiconductor memory: Physical origin of the irreversible threshold voltage shift observed in metalâ€“oxideâ€“nitrideâ€“oxideâ€–semiconductor memories. Japanese Journal of Applied Physics, 2018, 57, 081101.	0.8	2
38699	Exploring triazine and heptazine based self assembled molecular materials through first principles investigations. Journal of Molecular Modeling, 2018, 24, 217.	0.8	5

#	Article	IF	Citations
38700	Strain and interlayer coupling tailored magnetic properties and valley splitting in layered ferrovalley 2H-VSe2. Applied Surface Science, 2018, 458, 191-197.	3.1	46
38701	Promoted methane activation on doped ceria via occupation of Pr(4f) states. Applied Surface Science, 2018, 458, 397-404.	3.1	9
38702	Synthesis and properties of (Hf1-xTax)C solid solution carbides. Ceramics International, 2018, 44, 19247-19253.	2.3	19
38703	First-principles study of the products of CO2 dissociation on nickel-based alloys: Trends in energetics with alloying element. Surface Science, 2018, 677, 219-231.	0.8	10
38704	IodideÂ·Â·Â·Ï€ Interactions of Perhalogenated Quinoid Rings in Co-crystals with Organic Bases. Crystal Growth and Design, 2018, 18, 5182-5193.	1.4	19
38705	Structural and Chemical Features Giving Rise to Defect Tolerance of Binary Semiconductors. Chemistry of Materials, 2018, 30, 5583-5592.	3.2	36
38706	Determination of the Intrinsic Defect at the Origin of Poor H₂ Evolution Performance of the Monoclinic BiVO₄ Photocatalyst Using Density Functional Theory. Journal of Physical Chemistry C, 2018, 122, 18204-18211.	1.5	28
38707	Phase Exploration and Identification of Multinary Transition-Metal Selenides as High-Efficiency Oxygen Evolution Electrocatalysts through Combinatorial Electrodeposition. ACS Catalysis, 2018, 8, 8273-8289.	5.5	76
38708	Evaluation of thermodynamic equations of state across chemistry and structure in the materials project. Npj Computational Materials, 2018, 4, .	3.5	32
38709	Computational screening of organic polymer dielectrics for novel accelerator technologies. Scientific Reports, 2018, 8, 9258.	1.6	4
38710	Achieving ultrahigh carrier mobilities and opening the band gap in two-dimensional Si₂BN. Physical Chemistry Chemical Physics, 2018, 20, 21716-21723.	1.3	30
38711	Band gap temperature-dependence and exciton-like state in copper antimony sulphide, CuSbS2. APL Materials, 2018, 6, .	2.2	14
38712	Effect of electrons scattered by optical phonons on superconductivity in <mml:math xmlns:mml="http://www.w3.org/1998/Math/MathML"><mml:mrow><mml:mi>M</mml:mi><mml:msub><mml:mi mathvariant="normal">H</mml:mi><mml:mn>3</mml:mn></mml:msub></mml:mrow></mml:math> () Tj ETQq0 0 0 rgBT /Overlock 10	1.1	17
38713	Molecular and Selfâ€Trapped Excitonic Contributions to the Broadband Luminescence in Diamineâ€Based Lowâ€Dimensional Hybrid Perovskite Systems. Advanced Optical Materials, 2018, 6, 1800751.	3.6	43
38714	Properties and Decomposition of Heusler Alloys. Energy Technology, 2018, 6, 1478-1490.	1.8	24
38715	Electronic properties of NiO (1â€¯1â€¯0)/CH3NH3PbI3 (1â€¯0â€¯0) interface from the first-principles calculations. Chemical Physics Letters, 2018, 707, 133-139.	1.2	7
38716	Tuning nitrogen reduction reaction activity via controllable Fe magnetic moment: A computational study of single Fe atom supported on defective graphene. Electrochimica Acta, 2018, 284, 392-399.	2.6	148
38717	Mechanisms of hydroxyl radicals production from pyrite oxidation by hydrogen peroxide: Surface versus aqueous reactions. Geochimica Et Cosmochimica Acta, 2018, 238, 394-410.	1.6	66

#	Article	IF	Citations
38718	A new complex ternary phase in the Al-Cr-Sc push-pull alloy. Journal of Alloys and Compounds, 2018, 768, 230-239.	2.8	3
38719	The role of Cr on the electronic and optical properties of InCrN: A first principles study. Journal of Crystal Growth, 2018, 499, 13-17.	0.7	4
38720	Thickness effect on magnetocrystalline anisotropy of MnPt(0â€¯0â€¯1) film. Journal of Magnetism and Magnetic Materials, 2018, 467, 69-73.	1.0	3
38721	Effect of High Pressure on the Crystal Structure and Vibrational Properties of Olivine-Type LiNiPO₄. Inorganic Chemistry, 2018, 57, 10265-10276.	1.9	16
38722	Influence of AlN(0001) Surface Reconstructions on the Wettability of an Al/AlN System: A First-Principle Study. Materials, 2018, 11, 775.	1.3	9
38723	First-Principles Investigation on the Electronic and Mechanical Properties of Cs-Doped CH3NH3PbI3. Materials, 2018, 11, 1141.	1.3	18
38724	The Effect of U Atom Adsorption on the Structural, Electronic and Magnetic Properties of Single-Walled Carbon Nanotubes. Journal of Electronic Materials, 2018, 47, 5810-5815.	1.0	1
38725	Role of surface oxidation for thickness-driven insulator-to-metal transition in epitaxial MoO2 films. Applied Surface Science, 2018, 459, 92-97.	3.1	9
38726	Improved LDA-1/2 method for band structure calculations in covalent semiconductors. Computational Materials Science, 2018, 153, 493-505.	1.4	63
38727	The mechanism of ethanol steam reforming on the Co0 and Co2+ sites: A DFT study. Journal of Catalysis, 2018, 365, 391-404.	3.1	33
38728	From the Nonexistent Polar Intermetallic Pt₃Pr₄ via Pt_{2â€“x}Pr₃ to Pt/Sn/Pr Ternaries. Inorganic Chemistry, 2018, 57, 9949-9961.	1.9	10
38729	Interaction of HCl with a CeO₂(111) Layer Supported on Ru(0001): A Theory and Experiment Combined Study. Journal of Physical Chemistry C, 2018, 122, 19584-19592.	1.5	6
38730	Raman Spectra and Strain Effects in Bismuth Oxychalcogenides. Journal of Physical Chemistry C, 2018, 122, 19970-19980.	1.5	76
38731	Identifying Influential Parameters of Octahedrally Coordinated Cations in Spinel ZnMn_xCo_{2â€“x}O₄ Oxides for the Oxidation Reaction. ACS Catalysis, 2018, 8, 8568-8577.	5.5	68
38732	The Spatially Oriented Charge Flow and Photocatalysis Mechanism on Internal van der Waals Heterostructures Enhanced g-C₃N₄. ACS Catalysis, 2018, 8, 8376-8385.	5.5	219
38733	The effect of strain and functionalization on the optical properties of borophene. Physical Chemistry Chemical Physics, 2018, 20, 21043-21050.	1.3	45
38734	Tunable photoluminescence in a van der Waals heterojunction built from a MoS₂ monolayer and a PTCDA organic semiconductor. Nanoscale, 2018, 10, 16107-16115.	2.8	39
38735	Temperature effect on the nucleation of graphene on Cu (111). RSC Advances, 2018, 8, 27825-27831.	1.7	3

#	Article	IF	Citations
38736	Insight into lithium-ion mobility in Li₂La(TaTi)O₇. Journal of Materials Chemistry A, 2018, 6, 22152-22160.	5.2	16
38737	Three-dimensional quantum anomalous Hall effect in ferromagnetic insulators. Physical Review B, 2018, 98, .	1.1	25
38738	Raman spectrum of <mml:math xmlns:mml="http://www.w3.org/1998/Math/MathML"><mml:msub><mml:mi>CrI</mml:mi><mml:mn>3</mml:mn></mml:msub></mml: : An <mml:math xmlns:mml="http://www.w3.org/1998/Math/MathML"><mml:mrow><mml:mi mathvariant="italic">ab</mml:mi><mml:mspace width="0.28em" /><mml:mi mathvariant="italic">initio</mml:mi></mml:mrow></mml:math> study. Physical Review B, 2018, 98, .	1.1	51
38739	Ultrafast Relaxation Dynamics of the Antiferrodistortive Phase in Ca Doped <mml:math xmlns:mml="http://www.w3.org/1998/Math/MathML" display="inline"><mml:mrow><mml:msub><mml:mrow><mml:mi>SrTiO</mml:mi></mml:mrow><mml:mrow><mml:mn>3</mml:mn></ Physical Review Letters, 2018, 121, 055701.	2.9	20
38740	Role of Cation-Anion Organic Ligands for Optical Properties of Fully Inorganic Perovskite Quantum Dots. MRS Advances, 2018, 3, 3255-3261.	0.5	8
38741	Thermal Transport of Bulk Semiconductors in the KCM. Springer Theses, 2018, , 75-100.	0.0	0
38742	Long-range interactions in Mg-Al-rare earth alloys with 10H-type long-period stacking ordered structure. Computational Materials Science, 2018, 153, 297-302.	1.4	3
38743	An experimental and theoretical study of the hydrogen resistance of Ti3SiC2 and Ti3AlC2. Corrosion Science, 2018, 142, 295-304.	3.0	10
38744	A new tetragonal superhard metallic carbon allotrope. Journal of Alloys and Compounds, 2018, 769, 347-352.	2.8	38
38745	Strain-induced insulating ferromagnetism in LaMnO3 thin films from first-principles investigations. Journal of Magnetism and Magnetic Materials, 2018, 466, 406-410.	1.0	9
38746	Role of nanosize icosahedral quasicrystal of Mg-Al and Mg-Ca alloys in avoiding crystallization of liquid Mg: Ab initio molecular dynamics study. Journal of Non-Crystalline Solids, 2018, 499, 173-182.	1.5	8
38747	Hydrogen Bonding Controls the Structural Evolution in Perovskite-Related Hybrid Platinum(IV) Iodides. Inorganic Chemistry, 2018, 57, 10375-10382.	1.9	40
38748	New Calcium Hydrides with Mixed Atomic and Molecular Hydrogen. Journal of Physical Chemistry C, 2018, 122, 19370-19378.	1.5	38
38749	In-Plane Optical Anisotropy and Linear Dichroism in Low-Symmetry Layered TlSe. ACS Nano, 2018, 12, 8798-8807.	7.3	64
38750	Non-covalent interactions for carbonaceous materials: impacts of doping, curving and their combination. Physical Chemistry Chemical Physics, 2018, 20, 22228-22240.	1.3	3
38751	Tuning Schottky barriers for monolayer GaSe FETs by exploiting a weak Fermi level pinning effect. Physical Chemistry Chemical Physics, 2018, 20, 21732-21738.	1.3	19
38752	First-principles database driven computational neural network approach to the discovery of active ternary nanocatalysts for oxygen reduction reaction. Physical Chemistry Chemical Physics, 2018, 20, 24539-24544.	1.3	37
38753	Assessing the performance of the Tao-Mo semilocal density functional in the projector-augmented-wave method. Journal of Chemical Physics, 2018, 149, 044120.	1.2	50

#	Article	IF	Citations
38754	Compensation and hydrogen passivation of magnesium acceptors in Î²-Ga2O3. Applied Physics Letters, 2018, 113, .	1.5	77
38755	Functionalization of the electronic and magnetic properties of silicene by halogen atoms unilateral adsorption: a first-principles study. Journal of Physics Condensed Matter, 2018, 30, 365001.	0.7	5
38756	Acoustic deformation potentials of <mml:math xmlns:mml="http://www.w3.org/1998/Math/MathML"><mml:mi>n</mml:mi></mml:math> -type PbTe from first principles. Physical Review B, 2018, 98, .	1.1	17
38757	Effect of B on Growth of Recrystallized Grain of Ti-added Ultra-low Carbon Cold-rolled Steel Sheets. ISIJ International, 2018, 58, 1901-1909.	0.6	4
38758	Revisit to the Impacts of Rattlers on Thermal Conductivity of Clathrates. Frontiers in Energy Research, 2018, 6, .	1.2	14
38759	Effect of an Al-adlayer in the c-plane ZnO/AlN heterostructure. Europhysics Letters, 2018, 122, 26003.	0.7	2
38760	Using Applications and Tools to Visualize ab initio Calculations Performed in VASP. Lecture Notes in Computer Science, 2018, , 489-496.	1.0	1
38761	Thermodynamic assessment of the Fe-Te system. Part II: Thermodynamic modeling. Journal of Alloys and Compounds, 2018, 767, 883-893.	2.8	13
38762	Carbon interstitial defects causing emission red shift in YAG:Ce phosphor: First-principles calculation. Journal of Rare Earths, 2018, 36, 1239-1244.	2.5	6
38763	Surface Orientation Dependent Water Dissociation on Rutile Ruthenium Dioxide. Journal of Physical Chemistry C, 2018, 122, 17802-17811.	1.5	44
38764	Accuracy of Density Functional Theory for Predicting Kinetics of Methanol Synthesis from CO and CO₂ Hydrogenation on Copper. Journal of Physical Chemistry C, 2018, 122, 17942-17953.	1.5	31
38765	Principles of Design for Substrate-Supported Molecular Switches Based on Physisorbed and Chemisorbed States. ACS Applied Materials & Interfaces, 2018, 10, 26772-26780.	4.0	15
38766	Mechanistic Study of the Direct Hydrodeoxygenation of m-Cresol over WO_x-Decorated Pt/C Catalysts. ACS Catalysis, 2018, 8, 7749-7759.	5.5	87
38767	Tunable double-Weyl Fermion semimetal state in the SrSi2 materials class. Scientific Reports, 2018, 8, 10540.	1.6	30
38768	Single-atom iron catalyst with single-vacancy graphene-based substrate as a novel catalyst for NO oxidation: a theoretical study. Catalysis Science and Technology, 2018, 8, 4159-4168.	2.1	76
38769	Monolayer GeS as a potential candidate for NO₂ gas sensors and capturers. Journal of Materials Chemistry C, 2018, 6, 8082-8091.	2.7	86
38770	Mapping conditions for the formation of high-performance scandate cathodes: New insights into the role of sc. , 2018, , .		0
38771	The dipole model at the atomic scale: Explaining variations in work function due to configurational and compositional changes in Ba/Sc/O adsorbates on W (001), (110), and (112). , 2018, , .		0

#	Article	IF	Citations
38772	Bipolar Resistive Switching Characteristics of Thermally Evaporated V₂O₅ Thin Films. IEEE Electron Device Letters, 2018, 39, 1290-1293.	2.2	4
38773	The Electronic and Elastic Properties of Si Atom Doping in TiN: A First-Principles Calculation. Coatings, 2018, 8, 4.	1.2	3
38774	Electronic Structure Characterization of Hydrogen Terminated n-type Silicon Passivated by Benzoquinone-Methanol Solutions. Coatings, 2018, 8, 108.	1.2	1
38775	First Principles Study of Topochemical Effects and Electronic Structure Relationships between ANCl and A2N2Se (A = Zr, Ce) Assimilated to Pseudo-Binaries: {AN}Cl and {A2N2}Se. Computation, 2018, 6, 30.	1.0	1
38776	Theoretical and Experimental Investigations into Novel Oxynitride Discovery in the GaN-TiO2 System at High Pressure. Crystals, 2018, 8, 15.	1.0	5
38777	Structure of the Basal Edge Dislocation in ZnO. Crystals, 2018, 8, 127.	1.0	5
38778	Rhombohedral Distortion of the Cubic MgCu2-Type Structure in Ca2Pt3Ga and Ca2Pd3Ga. Crystals, 2018, 8, 186.	1.0	4
38779	Lu5Pd4Ge8 and Lu3Pd4Ge4: Two More Germanides among Polar Intermetallics. Crystals, 2018, 8, 205.	1.0	13
38780	The Crystal Orbital Hamilton Population (COHP) Method as a Tool to Visualize and Analyze Chemical Bonding in Intermetallic Compounds. Crystals, 2018, 8, 225.	1.0	199
38781	Boron Monochalcogenides; Stable and Strong Two-Dimensional Wide Band-Gap Semiconductors. Energies, 2018, 11, 1573.	1.6	32
38782	Thermodynamic optimization of Si-Zr-N system using Calphad approach coupled with ab initio methods. Calphad: Computer Coupling of Phase Diagrams and Thermochemistry, 2018, 62, 148-153.	0.7	4
38783	Clarifying the capacity deterioration mechanism sheds light on the design of ultra-long-life hydrogen storage alloys. Chemical Engineering Journal, 2018, 352, 325-332.	6.6	22
38784	Composition effect of oxygen reduction reaction on PtSn nanorods: An experimental and computational study. International Journal of Hydrogen Energy, 2018, 43, 14427-14438.	3.8	22
38785	Enhanced gas-sensing performance of graphene by doping transition metal atoms: A first-principles study. Physics Letters, Section A: General, Atomic and Solid State Physics, 2018, 382, 2965-2973.	0.9	34
38786	Development of activityâ€“descriptor relationships for supported metal ion hydrogenation catalysts on silica. Polyhedron, 2018, 152, 73-83.	1.0	11
38787	The melilite-type compound(Sr1-x,Ax)2MnGe2S6O(A â€¯=â€¯K, La) being a room temperature ferromagnetic semiconductor. Science Bulletin, 2018, 63, 887-891.	4.3	6
38788	Interaction between hydrogen and gallium vacancies in Î²-Ga2O3. Scientific Reports, 2018, 8, 10142.	1.6	30
38789	The Siâ€“Ge substitutional series in the chiral STW zeolite structure type. Journal of Materials Chemistry A, 2018, 6, 15110-15122.	5.2	33

#	Article	IF	Citations
38790	Effect of chemical ordering on optical properties of Fe3Si epitaxial films. EPJ Web of Conferences, 2018, 185, 03014.	0.1	2
38791	Dependence of phonon transport properties with stacking thickness in layered ZnO. Journal Physics D: Applied Physics, 2018, 51, 315303.	1.3	9
38792	Stability enhancement of Cu₂S against Cu vacancy formation by Ag alloying. Journal of Physics Condensed Matter, 2018, 30, 165701.	0.7	10
38793	Doping SnO2 crystal with increasing concentrations of Zn and Sb atoms: a quantum chemical analysis. Physica Scripta, 2018, 93, 095801.	1.2	5
38794	Understanding shear-induced <mml:math xmlns:mml="http://www.w3.org/1998/Math/MathML"><mml:mrow><mml:mi>s</mml:mi><mml:msup><mml:mi>p</mml:mi><mml:mn> -to- <mml:math xmlns:mml="http://www.w3.org/1998/Math/MathML"><mml:mrow><mml:mi>s</mml:mi><mml:msup><mml:mi>p</mml:mi><mml:mn> phase transitions in glassy carbon at low pressure using first-principles calculations. Physical Review B, 2018, 98, .	1.1	8
38795	Exploring the correlation between MoS2 nanosheets and 3D graphene-based nanostructures for reversible lithium storage. Applied Surface Science, 2018, 459, 98-104.	3.1	11
38796	The elastic behaviors and theoretical tensile strength of <mml:math xmlns:mml="http://www.w3.org/1998/Math/MathML" altimg="si1.gif" overflow="scroll"><mml:mi>Î³</mml:mi></mml:math>-TiAl alloy from the first principles calculations. Intermetallics, 2018, 101, 1-7.	1.8	30
38797	SnS nanoribbon/graphene mixed-dimensional heterostructures: Group VII passivation and quantum size effects. Journal of Alloys and Compounds, 2018, 766, 215-220.	2.8	2
38798	Long persistent phosphor SrZrO3:Yb3+ with dual emission in NUV and NIR region: A combined experimental and first-principles methods. Journal of Alloys and Compounds, 2018, 766, 663-671.	2.8	12
38799	Enhanced Thermoelectric Properties in a New Silicon Crystal Si₂₄ with Intrinsic Nanoscale Porous Structure. Nano Letters, 2018, 18, 4748-4754.	4.5	15
38800	Pressure-induced enhancement of non-polar to polar transition temperature in metallic LiOsO3. Applied Physics Letters, 2018, 113, .	1.5	21
38801	First-principle high-throughput calculations of carrier effective masses of two-dimensional transition metal dichalcogenides. Journal of Semiconductors, 2018, 39, 072001.	2.0	18
38802	Magnetic Transitions in K-Doped Biphenyl and ${p}$ -Terphenyl. IEEE Transactions on Magnetics, 2018, 54, 1-5.	1.2	3
38803	Immobilization of a Full Photosystem in the Largeâ€Pore MILâ€101 Metalâ€“Organic Framework for CO₂ reduction. ChemSusChem, 2018, 11, 3315-3322.	3.6	57
38804	Highly conductive CrNb11O29 nanorods for use in high-energy, safe, fast-charging and stable lithium-ion batteries. Journal of Power Sources, 2018, 397, 231-239.	4.0	48
38805	Preparation and electron correlation effects of the perovskite La0.8Ca0.1Pb0.1Fe1â^'Co O3 (0â€¯â‰¤â€¯xâ€¯â‰¤â€¯0.20). Solid State Ionics, 2018, 324, 157-162.	1.3	7
38806	Reaction Mechanism with Thermodynamic Structural Screening for Electrochemical Hydrogen Evolution on Monolayer 1Tâ€² Phase MoS₂. Chemistry of Materials, 2018, 30, 5404-5411.	3.2	33
38807	Existence of an Electrochemically Inert CO Population on Cu Electrodes in Alkaline pH. ACS Catalysis, 2018, 8, 7507-7516.	5.5	176

#	Article	IF	Citations
38808	Temperature coefficient of redox potential of LixFePO4. AIP Advances, 2018, 8, 065021.	0.6	5
38809	The prediction of a new high-pressure phase of hafnia using first-principles computations. IOP Conference Series: Materials Science and Engineering, 2018, 305, 012006.	0.3	5
38810	Local probe of irradiation-induced structural changes and orbital magnetism in <mml:math xmlns:mml="http://www.w3.org/1998/Math/MathML"><mml:mrow><mml:msub><mml:mi mathvariant="normal">Fe</mml:mi><mml:mn>60</mml:mn></mml:msub><mml:msub><mml:mi>Al</mml:mi><mml:mn>40</mml:mn> thin films via an order-disorder phase transition. Physical Review B, 2018, 98, .	1.1	14
38811	Deciphering complex features in STM images of O adatoms on Ag(110). Physical Review B, 2018, 98, .	1.1	6
38812	The lanthanide hydride oxides SmHO and HoHO. Zeitschrift Fur Naturforschung - Section B Journal of Chemical Sciences, 2018, 73, 535-538.	0.3	13
38813	Chromiteen: A New 2D Oxide Magnetic Material from Natural Ore. Advanced Materials Interfaces, 2018, 5, 1800549.	1.9	36
38814	Crystal-plane-dependent metal oxide-support interaction in CeO2/g-C3N4 for photocatalytic hydrogen evolution. Applied Catalysis B: Environmental, 2018, 238, 111-118.	10.8	178
38815	Stability and electronic properties of sulfur terminated two-dimensional early transition metal carbides and nitrides (MXene). Computational Materials Science, 2018, 153, 303-308.	1.4	46
38816	Two-dimensional III2-VI3 materials: Promising photocatalysts for overall water splitting under infrared light spectrum. Nano Energy, 2018, 51, 533-538.	8.2	213
38817	Effects of the Aqueous Environment on the Stability and Chemistry of Î²-NiOOH Surfaces. Chemistry of Materials, 2018, 30, 5205-5219.	3.2	41
38818	Synthesis, Crystal and Topological Electronic Structures of New Bismuth Tellurohalides Bi₂TeBr and Bi₃TeBr. Chemistry of Materials, 2018, 30, 5272-5284.	3.2	10
38819	Revealing the Effects of Electrode Crystallographic Orientation on Battery Electrochemistry via the Anisotropic Lithiation and Sodiation of ReS₂. ACS Nano, 2018, 12, 7875-7882.	7.3	28
38820	Eu²⁺ Site Preferences in the Mixed Cation K₂BaCa(PO₄)₂ and Thermally Stable Luminescence. Journal of the American Chemical Society, 2018, 140, 9730-9736.	6.6	428
38821	Tuning anisotropic ion transport in mesocrystalline lithium orthosilicate nanostructures with preferentially exposed facets. NPG Asia Materials, 2018, 10, 606-617.	3.8	18
38822	Substrate-induced enhancement of the chemical reactivity in metal-supported graphene. Physical Chemistry Chemical Physics, 2018, 20, 19492-19499.	1.3	10
38823	Contributions of the lead-bromine weighted bands to the occupied density of states of the hybrid tri-bromide perovskites. Applied Physics Letters, 2018, 113, 022101.	1.5	6
38824	Orbitronic effect on the magnetic reconstruction of monocell SrMnO3 on ferroelectric BaTiO3 substrate. Journal of Applied Physics, 2018, 124, 014101.	1.1	0
38825	Optical and dielectric properties of Î²-Ta₂O₅. Journal of Physics: Conference Series, 2018, 1043, 012036.	0.3	3

#	Article	IF	Citations
38826	Van der Waals interfaces in epitaxial vertical metal/2D/3D semiconductor heterojunctions of monolayer MoS₂and GaN. 2D Materials, 2018, 5, 045016.	2.0	21
38827	Negative thermal expansion behavior in <mml:math xmlns:mml="http://www.w3.org/1998/Math/MathML"><mml:mrow><mml:mi>M</mml:mi><mml:mi>Zr</mml:mi><mml:msub><mml:mi mathvariant="normal">F</mml:mi><mml:mn>6</mml:mn></mml:msub></mml:mrow><mml:mspace width="4pt" /><mml:mo>(</mml:mo><mml:mrow><mml:mi>M</mml:mi><mml:mo>=</mml:mo><mml:mi>Ca</mml:mi><mml:mo>,</mml:mo><mml:mn : Ab initio lattice dynamical stud. Physical Review B, 2018, 98, .	1.1	13
38828	Intrinsic Origin of Enhancement of Ferroelectricity in SnTe Ultrathin Films. Physical Review Letters, 2018, 121, 027601.	2.9	55
38829	Enhancement of Perpendicular Magnetic Anisotropy Through Fe Insertion at the CoFe/W Interface. IEEE Transactions on Magnetics, 2018, 54, 1-5.	1.2	6
38830	Bond Insertion at Distorted Si(001) Subsurface Atoms. Inorganics, 2018, 6, 17.	1.2	9
38831	DFT Study on Intermetallic Pdâ€“Cu Alloy with Cover Layer Pd as Efficient Catalyst for Oxygen Reduction Reaction. Materials, 2018, 11, 33.	1.3	24
38832	The Electronic Properties of O-Doped Pure and Sulfur Vacancy-Defect Monolayer WS2: A First-Principles Study. Materials, 2018, 11, 218.	1.3	32
38833	Optoelectronic Properties of X-Doped (X = O, S, Te) Photovoltaic CSe with Puckered Structure. Materials, 2018, 11, 431.	1.3	11
38834	Polycyclic Aromatic Hydrocarbons Adsorption onto Graphene: A DFT and AIMD Study. Materials, 2018, 11, 726.	1.3	41
38835	Electrochemical and Electronic Charge Transport Properties of Ni-Doped LiMn2O4 Spinel Obtained from Polyol-Mediated Synthesis. Materials, 2018, 11, 806.	1.3	19
38836	Interaction of Model Inhibitor Compounds with Minimalist Cluster Representations of Hydroxyl Terminated Metal Oxide Surfaces. Metals, 2018, 8, 81.	1.0	3
38837	Linking Ab Initio Data on Hydrogen and Carbon in Steel to Statistical and Continuum Descriptions. Metals, 2018, 8, 219.	1.0	6
38838	Magnetic Isotropy/Anisotropy in Layered Metal Phosphorous Trichalcogenide MPS3 (M = Mn, Fe)Single Crystals. Micromachines, 2018, 9, 292.	1.4	26
38839	Monitoring Reaction Paths Using Vibrational Spectroscopies: The Case of the Dehydrogenation of Propane toward Propylene on Pd-Doped Cu(111) Surface. Molecules, 2018, 23, 126.	1.7	7
38840	Magnetic Properties of Metalâ€“Organic Coordination Networks Based on 3d Transition Metal Atoms. Molecules, 2018, 23, 964.	1.7	9
38841	The Band-Gap Modulation of Graphyne Nanoribbons by Edge Quantum Entrapment. Nanomaterials, 2018, 8, 92.	1.9	2
38842	Tunable Electronic and Topological Properties of Germanene by Functional Group Modification. Nanomaterials, 2018, 8, 145.	1.9	19
38843	Hybrid Density Functional Study on the Photocatalytic Properties of Two-dimensional g-ZnO Based Heterostructures. Nanomaterials, 2018, 8, 374.	1.9	15

#	Article	IF	Citations
38844	Tailoring Bandgap of Perovskite BaTiO3 by Transition Metals Co-Doping for Visible-Light Photoelectrical Applications: A First-Principles Study. Nanomaterials, 2018, 8, 455.	1.9	42
38845	TiC MXene High Energy Density Cathode for Lithiumâ€“Air Battery. Advanced Theory and Simulations, 2018, 1, 1800059.	1.3	21
38846	Spectroscopic Fingerprints of Intermolecular Hâ€Bonding Interactions in Carbon Nitride Model Compounds. Chemistry - A European Journal, 2018, 24, 14198-14206.	1.7	17
38847	Locating Si atoms in Si-doped boron carbide: A route to understand amorphization mitigation mechanism. Acta Materialia, 2018, 157, 106-113.	3.8	42
38848	A novel hydrogen storage medium of Ca-coated B40: First principles study. International Journal of Hydrogen Energy, 2018, 43, 15338-15347.	3.8	30
38849	Multi-electric field modulation for photocatalytic oxygen evolution: Enhanced charge separation by coupling oxygen vacancies with faceted heterostructures. Nano Energy, 2018, 51, 764-773.	8.2	88
38850	Hydration Mechanisms and Proton Conduction in the Mixed Ionicâ€“Electronic Conductors Ba₄Nb₂O₉ and Ba₄Ta₂O₉. Chemistry of Materials, 2018, 30, 4949-4958.	3.2	12
38851	Quaternary Chalcogenide Semiconductors with 2D Structures: Rb2ZnBi2Se5 and Cs6Cd2Bi8Te17. Inorganic Chemistry, 2018, 57, 9403-9411.	1.9	10
38852	Fast Magnesium Ion Transport in the Bi/Mg₃Bi₂ Two-Phase Electrode. Journal of Physical Chemistry C, 2018, 122, 17643-17649.	1.5	24
38853	Lithium Borocarbide LiBC as an Anode Material for Rechargeable Li-Ion Batteries. Journal of Physical Chemistry C, 2018, 122, 18231-18236.	1.5	16
38854	Effect of Surface Termination on Charge Doping in Graphene/BiFeO₃(0001) Hybrid Structure. Journal of Physical Chemistry C, 2018, 122, 17250-17260.	1.5	19
38855	Ferroelectric Polarization in CsPbI₃/CsSnI₃ Perovskite Heterostructure. Journal of Physical Chemistry C, 2018, 122, 17820-17824.	1.5	11
38856	Adsorption, Dissociation, and Spillover of Hydrogen over Au/TiO₂ Catalysts: The Effects of Cluster Size and Metalâ€“Support Interaction from DFT. Journal of Physical Chemistry C, 2018, 122, 17895-17916.	1.5	44
38857	Machine Learning Directed Search for Ultraincompressible, Superhard Materials. Journal of the American Chemical Society, 2018, 140, 9844-9853.	6.6	215
38858	Doping-Enhanced Short-Range Order of Perovskite Nanocrystals for Near-Unity Violet Luminescence Quantum Yield. Journal of the American Chemical Society, 2018, 140, 9942-9951.	6.6	548
38859	Influence of atomic site-specific strain on catalytic activity of supported nanoparticles. Nature Communications, 2018, 9, 2722.	5.8	102
38860	Fe-N system at high pressure reveals a compound featuring polymeric nitrogen chains. Nature Communications, 2018, 9, 2756.	5.8	153
38861	Non-flammable electrolyte enables Li-metal batteries with aggressive cathode chemistries. Nature Nanotechnology, 2018, 13, 715-722.	15.6	964

#	Article	IF	Citations
38862	Direct observation of noble metal nanoparticles transforming to thermally stable single atoms. Nature Nanotechnology, 2018, 13, 856-861.	15.6	741
38863	Novel triadius-like N4 specie of iron nitride compounds under high pressure. Scientific Reports, 2018, 8, 10670.	1.6	36
38864	CO₂ interaction with violarite (FeNi₂S₄) surfaces: a dispersion-corrected DFT study. Physical Chemistry Chemical Physics, 2018, 20, 20439-20446.	1.3	15
38865	Robust two-dimensional bipolar magnetic semiconductors by defect engineering. Journal of Materials Chemistry C, 2018, 6, 8435-8443.	2.7	26
38866	Ternary phase diagram of Ni-Mn-Ga: insights from ab initio calculations. EPJ Web of Conferences, 2018, 185, 05012.	0.1	1
38867	Precipitation strengthening in Cuâ€“Niâ€“Si alloys modeled with ab initio based interatomic potentials. Journal of Chemical Physics, 2018, 149, 024701.	1.2	5
38868	Ab initio molecular dynamics simulation of self-diffusion in Alâ€“Si binary melts. Modelling and Simulation in Materials Science and Engineering, 2018, 26, 065006.	0.8	12
38869	Structural and electronic properties of 5,5â€²-Hydrazinebistetrazole under high pressure: A DFT study. IOP Conference Series: Materials Science and Engineering, 2018, 377, 012107.	0.3	0
38870	Multiple topologically nontrivial bands in noncentrosymmetric YSn2. Physical Review B, 2018, 98, .	1.1	4
38871	Exfoliation energy, quasiparticle band structure, and excitonic properties of selenium and tellurium atomic chains. Physical Review B, 2018, 98, .	1.1	33
38872	Conductivity Maximum in 3D Graphene Foams. Small, 2018, 14, e1801458.	5.2	25
38873	Electronic and mechanical properties of stiff rhenium carbide monolayers: A first-principles investigation. Applied Surface Science, 2018, 458, 762-768.	3.1	8
38874	Ba Sc O on W (0 0 1), (1 1 0), and (1 1 2) in scandate cathodes: Connecting to experiment via <mml:math xmlns:mml="http://www.w3.org/1998/Math/MathML" altimg="si13.gif" overflow="scroll"><mml:mrow><mml:msub><mml:mrow><mml:mi>ï¼</mml:mi></mml:mrow><mml:mrow><mml:mi>O</mml:mi></m and equilibrium crystal shape. Applied Surface Science, 2018, 458, 827-838.	3.1	30
38875	Tailoring Pt locations in KL zeolite by improved atomic layer deposition for excellent performance in n-heptane aromatization. Journal of Catalysis, 2018, 365, 163-173.	3.1	34
38876	Surface Reorganization Leads to Enhanced Photocatalytic Activity in Defective BiOCl. Chemistry of Materials, 2018, 30, 5128-5136.	3.2	55
38877	Crystal Structure, Thermal Behavior, and Photocatalytic Activity of NaBiO₃Â·nH₂O. Inorganic Chemistry, 2018, 57, 8903-8908.	1.9	26
38878	Synthesis, Structure, and Electrical Properties of the Single Crystal Ba₈Cu₁₆As₃₀. Inorganic Chemistry, 2018, 57, 9327-9334.	1.9	7
38879	Torsional Potentials of Glyoxal, Oxalyl Halides, and Their Thiocarbonyl Derivatives: Challenges for Popular Density Functional Approximations. Journal of Chemical Theory and Computation, 2018, 14, 4806-4817.	2.3	10

#	Article	IF	Citations
38880	Theoretical Modeling of Electronic Excitations of Gas-Phase and Solvated TiO₂ Nanoclusters and Nanoparticles of Interest in Photocatalysis. Journal of Chemical Theory and Computation, 2018, 14, 4391-4404.	2.3	24
38881	New Route for â€œCold-Passivationâ€•of Defects in Tin-Based Oxides. Journal of Physical Chemistry C, 2018, 122, 17612-17620.	1.5	15
38882	Revealing the Role of Oxygen Debris and Functional Groups on the Water Flux and Molecular Separation of Graphene Oxide Membrane: A Combined Experimental and Theoretical Study. Journal of Physical Chemistry C, 2018, 122, 17507-17517.	1.5	32
38883	Stabilizing Lead-Free All-Inorganic Tin Halide Perovskites by Ion Exchange. Journal of Physical Chemistry C, 2018, 122, 17660-17667.	1.5	68
38884	Assignment of the Raman Spectrum of Benzylic Amide [2]Catenane: Raman Microscopy Experiments and First-Principles Calculations. Journal of Physical Chemistry C, 2018, 122, 18102-18109.	1.5	4
38885	Origin of Chemically Ordered Atomic Laminates (i-MAX): Expanding the Elemental Space by a Theoretical/Experimental Approach. ACS Nano, 2018, 12, 7761-7770.	7.3	99
38886	Direct Formation of Câ€“C Double-Bonded Structural Motifs by On-Surface Dehalogenative Homocoupling of gem-Dibromomethyl Molecules. ACS Nano, 2018, 12, 7959-7966.	7.3	24
38887	Robust large gap quantum spin Hall insulators in methyl and ethynyl functionalized TlSb buckled honeycombs. Journal of Applied Physics, 2018, 124, .	1.1	5
38888	Strain-induced dimensional phase change of graphene-like boron nitride monolayers. Nanotechnology, 2018, 29, 405201.	1.3	7
38889	Promising electronic structure of double perovskite Sr2TiMoO6: Spin-polarized DFT+U approach. IOP Conference Series: Materials Science and Engineering, 2018, 382, 022025.	0.3	0
38890	Structural, electronic and thermodynamic properties of bulk and surfaces of terbium dioxide (TbO₂). Materials Research Express, 2018, 5, 085901.	0.8	9
38891	Novel high-pressure calcium carbonates. Physical Review B, 2018, 98, .	1.1	32
38892	Stability and mechanical properties of high-La content Laâ€“Ni phases by first-principles study. International Journal of Modern Physics B, 2018, 32, 1850242.	1.0	2
38893	Effects of Scandium Addition on the Structural Stability and Ideal Strengths of Magnesium-Lithium Alloys. Zeitschrift Fur Naturforschung - Section A Journal of Physical Sciences, 2018, 73, 947-956.	0.7	1
38894	Hydrogen storage in Zr0.9Ti0.1(Ni0.5Cr0.5-xVx)2 Laves phase, with xÂ=Â0, 0.125, 0.25, 0.375, 0.5. A theoretical approach. International Journal of Hydrogen Energy, 2018, 43, 16085-16091.	3.8	10
38895	A strategy for designing new AB 4.5 -type hydrogen storage alloys with high capacity and long cycling life. Journal of Power Sources, 2018, 398, 42-48.	4.0	26
38896	Theoretical Prediction of Blue Phosphorene/Borophene Heterostructure as a Promising Anode Material for Lithium-Ion Batteries. Journal of Physical Chemistry C, 2018, 122, 18294-18303.	1.5	59
38897	New monolayer ternary In-containing sesquichalcogenides BiInSe₃, SbInSe₃, BiInTe₃, and SbInTe₃ with high stability and extraordinary piezoelectric properties. Physical Chemistry Chemical Physics, 2018, 20, 19177-19187.	1.3	38

#	Article	IF	Citations
38898	First-principles study of elastic and slip properties of non-canonical Î²-based Alâ€“Cuâ€“Fe approximants. Philosophical Magazine, 2018, 98, 2135-2150.	0.7	0
38899	Thickness-dependent magneto-optical effects in hole-doped GaS and GaSe multilayers: a first-principles study. New Journal of Physics, 2018, 20, 043048.	1.2	14
38900	Towards understanding the influence of Re on H dissolution and retention in W by investigating the interaction between dispersed/aggregated-Re and H. Nuclear Fusion, 2018, 58, 096026.	1.6	16
38901	Bifunctional Separator Coated with Hexachlorocyclotriphosphazene/Reduced Graphene Oxide for Enhanced Performance of Lithiumâ€“Sulfur Batteries. Chemistry - A European Journal, 2018, 24, 13582-13588.	1.7	12
38902	Amorphous germanium as a promising anode material for sodium ion batteries: a first principle study. Journal of Materials Science, 2018, 53, 14423-14434.	1.7	23
38903	The adsorption and diffusion properties of scandium atom on the surfaces of tungsten and noble metals. Applied Surface Science, 2018, 457, 1057-1063.	3.1	5
38904	The effect of binary sulfides precursors with different value states on CZTS thin films. Ceramics International, 2018, 44, 18408-18412.	2.3	5
38905	Atomically dispersed Au1 catalyst towards efficient electrochemical synthesis of ammonia. Science Bulletin, 2018, 63, 1246-1253.	4.3	225
38906	First-principles study of hydrogen retention and diffusion behaviors in 4H-SiC. Superlattices and Microstructures, 2018, 122, 362-370.	1.4	1
38907	Insights into the Charge-Transfer Stabilization of Heterostructure Components with Unstable Bulk Analogs. Chemistry of Materials, 2018, 30, 4738-4747.	3.2	12
38908	Improved Nonenzymatic Glucose Sensing Properties of Pd/MnO₂ Nanosheets: Synthesis by Facile Microwave-Assisted Route and Theoretical Insight from Quantum Simulations. Journal of Physical Chemistry B, 2018, 122, 7636-7646.	1.2	28
38909	Chemisorption of NH₃ on Monomeric Vanadium Oxide Supported on Anatase TiO₂: A Combined DRIFT and DFT Study. Journal of Physical Chemistry C, 2018, 122, 16674-16682.	1.5	36
38910	Resolving Deep Quantum-Well States in Atomically Thin 2H-MoTe₂ Flakes by Nanospot Angle-Resolved Photoemission Spectroscopy. Nano Letters, 2018, 18, 4664-4668.	4.5	13
38911	Accordion Strain Accommodation Mechanism within the Epitaxially Constrained Electrode. ACS Energy Letters, 2018, 3, 1848-1853.	8.8	5
38912	Fine-grained optimization method for crystal structure prediction. Npj Computational Materials, 2018, 4, .	3.5	20
38913	Suppression of surfaces states at cubic perovskite (001) surfaces by CO2 adsorption. Physical Chemistry Chemical Physics, 2018, 20, 18828-18836.	1.3	13
38914	Substrate-induced magnetism and topological phase transition in silicene. Nanoscale, 2018, 10, 14667-14677.	2.8	10
38915	Ni and Se co-doping increases the power factor and thermoelectric performance of CoSbS. Journal of Materials Chemistry A, 2018, 6, 15123-15131.	5.2	20

#	Article	IF	Citations
38916	Structural and magnetic properties of heusler alloys Pd2MnZ (Z=Ga, Ge, As): AB INITIO study. EPJ Web of Conferences, 2018, 185, 05007.	0.1	3
38917	Direct observation of ferroelectricity in Ca3Mn2O7 and its prominent light absorption. Applied Physics Letters, 2018, 113, .	1.5	51
38918	Indexing of grazing-incidence X-ray diffraction patterns: the case of fibre-textured thin films. Acta Crystallographica Section A: Foundations and Advances, 2018, 74, 373-387.	0.0	19
38919	Improved Cycling Stability of Li[Ni_{0.90}Co_{0.05}Mn_{0.05}]O₂ Through Microstructure Modification by Boron Doping for Liâ€ion Batteries. Advanced Energy Materials, 2018, 8, 1801202.	10.2	336
38920	Electrical tree inhibition by SiO2/XLPE nanocomposites: insights from first-principles calculations. Journal of Molecular Modeling, 2018, 24, 200.	0.8	11
38921	Recursive alloy Hamiltonian construction and its application to the Ni-Al-Cr system. Acta Materialia, 2018, 159, 257-265.	3.8	9
38922	Electronic structure of heterojunction MoO2/g-C3N4 catalyst for oxidative desulfurization. Applied Catalysis B: Environmental, 2018, 238, 263-273.	10.8	178
38923	The role of interface charge transfer on Pt based catalysts for water splitting. International Journal of Hydrogen Energy, 2018, 43, 15225-15233.	3.8	11
38924	Enhanced Visible-Light-Driven Hydrogen Production of Carbon Nitride by Band Structure Tuning. Journal of Physical Chemistry C, 2018, 122, 17261-17267.	1.5	23
38925	Electrically Conductive Copper Coreâ€“Shell Nanowires through Benzenethiol-Directed Assembly. Nano Letters, 2018, 18, 4900-4907.	4.5	8
38926	Copper Nanoflower Assembled by Sub-2 nm Rough Nanowires for Efficient Oxygen Reduction Reaction: High Stability and Poison Resistance and Density Functional Calculations. ACS Applied Materials & Interfaces, 2018, 10, 26233-26240.	4.0	9
38927	Unraveling the Mechanism of Photoinduced Charge-Transfer Process in Bilayer Heterojunction. ACS Applied Materials & Interfaces, 2018, 10, 25401-25408.	4.0	29
38928	Amorphous graphene: a constituent part of low density amorphous carbon. Physical Chemistry Chemical Physics, 2018, 20, 19546-19551.	1.3	25
38929	Nitrogen-rich 1Tâ€²-MoS₂ layered nanostructures using alkyl amines for high catalytic performance toward hydrogen evolution. Nanoscale, 2018, 10, 14726-14735.	2.8	39
38930	Performance-improved Li-O₂ batteries by tailoring the phases of Mo_xC porous nanorods as an efficient cathode. Nanoscale, 2018, 10, 14877-14884.	2.8	28
38931	Understanding the loss of electrochemical activity of nanosized LiMn₂O₄particles: a combined experimental andab initioDFT study. Journal of Materials Chemistry A, 2018, 6, 14967-14974.	5.2	13
38932	Photocatalytic activity and the radiative lifetimes of excitons via an ab initio approach. Journal of Materials Chemistry A, 2018, 6, 15027-15032.	5.2	12
38933	Effects of oxygen vacancies on the electronic structure of the (LaVO₃)₆/SrVO₃ superlattice: a computational study. New Journal of Physics, 2018, 20, 073011.	1.2	5

#	Article	IF	Citations
38934	Environment-dependent and anion-vacancy-controlled reversible phase transition of MoS ₂ synthesized by chemical vapor deposition. 2D Materials, 2018, 5, 041002.	2.0	1
38935	Hydrogen as a source of flux noise in SQUIDs. Physical Review B, 2018, 98, .	1.1	11
38936	First-Principles Study of the Calcium Insertion in Layered and Non-Layered Phases of Vanadia. MRS Advances, 2018, 3, 3507-3512.	0.5	4
38937	A Decade of Computational Surface Catalysis. , 2018, , 1-11.		0
38938	Nickel-catalyzed preparation of self-bonded SiC refractories with improved microstructure and properties. Journal of the European Ceramic Society, 2018, 38, 5219-5227.	2.8	19
38939	Hydrogenation of Cyclohexene on the M/Pt(111) and Pt/M/Pt(111) (M = Fe, Co, Ni, and Cu) Surfaces from a Systematic DFT Study. Journal of Physical Chemistry C, 2018, 122, 16692-16703.	1.5	9
38940	Improved Prediction of Nanoalloy Structures by the Explicit Inclusion of Adsorbates in Cluster Expansions. Journal of Physical Chemistry C, 2018, 122, 18040-18047.	1.5	19
38941	Transition-Metal Dihydride Monolayers: A New Family of Two-Dimensional Ferromagnetic Materials with Intrinsic Room-Temperature Half-Metallicity. Journal of Physical Chemistry Letters, 2018, 9, 4260-4266.	2.1	118
38942	Tuning BrÃ¸nsted Acid Strength by Altering Site Proximity in CHA Framework Zeolites. ACS Catalysis, 2018, 8, 7842-7860.	5.5	41
38943	Effect of Passivation on Stability and Electronic Structure of Bulk-like ZnO Clusters. ACS Omega, 2018, 3, 7692-7702.	1.6	1
38944	Gold with +4 and +6 Oxidation States in AuF₄ and AuF₆. Journal of the American Chemical Society, 2018, 140, 9545-9550.	6.6	80
38945	Sub-molecular spectroscopy and temporary molecular charging of Ni-phthalocyanine on graphene with STM. Physical Chemistry Chemical Physics, 2018, 20, 19507-19514.	1.3	7
38946	Tunable electronic structures and magnetic properties of zigzag C₃N nanoribbons. Journal Physics D: Applied Physics, 2018, 51, 345301.	1.3	9
38947	Elastic properties of bulk and low-dimensional materials using van der Waals density functional. Physical Review B, 2018, 98, .	1.1	88
38948	Critical behavior in the itinerant ferromagnet <mml:math xmlns:mml="http://www.w3.org/1998/Math/MathML"><mml:mrow><mml:mi>AsNC</mml:mi><mml:msub><mml:mi mathvariant="normal">r</mml:mi><mml:mn>3</mml:mn></mml:msub></mml:mrow></mml:math> with tetragonal-antiperovskite structure. Physical Review B, 2018, 98, .	1.1	18
38949	Unusual Pressure-Induced Periodic Lattice Distortion in <mml:math xmlns:mml="http://www.w3.org/1998/Math/MathML" display="inline"><mml:mrow><mml:msub><mml:mrow><mml:mi>SnSe</mml:mi></mml:mrow><mml:mrow><mml:mn>2</mml:mn></mml:mrow> Physical Review Letters, 2018, 121, 027003.	2.9	24
38950	Metal-free three-dimensional perovskite ferroelectrics. Science, 2018, 361, 151-155.	6.0	570
38951	Monolayered semiconducting GeAsSe and SnSbTe with ultrahigh hole mobility. Frontiers of Physics, 2018, 13, 1.	2.4	11

#	Article	IF	Citations
38952	Favourable band edge alignment and increased visible light absorption in Î²-MoO3/Î±-MoO3 oxide heterojunction for enhanced photoelectrochemical performance. International Journal of Hydrogen Energy, 2018, 43, 15773-15783.	3.8	26
38953	Orbital Alignment for High Performance Thermoelectric YbCd₂Sb₂ Alloys. Chemistry of Materials, 2018, 30, 5339-5345.	3.2	50
38954	Single Molybdenum Atom Anchored on N-Doped Carbon as a Promising Electrocatalyst for Nitrogen Reduction into Ammonia at Ambient Conditions. Journal of Physical Chemistry C, 2018, 122, 16842-16847.	1.5	223
38955	Electronic Origin of Optically-Induced Sub-Picosecond Lattice Dynamics in MoSe₂ Monolayer. Nano Letters, 2018, 18, 4653-4658.	4.5	16
38956	Boron-Doped Graphene Nanoribbons: Electronic Structure and Raman Fingerprint. ACS Nano, 2018, 12, 7571-7582.	7.3	38
38957	WO₃ as a nucleating agent for BaO/SrO/ZnO/SiO₂ glasses â€“ experiments and simulations. CrystEngComm, 2018, 20, 4565-4574.	1.3	10
38958	Influence of the lattice constant on defects in cerium oxide. Physical Chemistry Chemical Physics, 2018, 20, 19792-19799.	1.3	7
38959	Model of dielectric breakdown in hafnia-based ferroelectric capacitors. Journal of Applied Physics, 2018, 124, .	1.1	20
38960	Simulating electronically driven structural changes in silicon with two-temperature molecular dynamics. Physical Review B, 2018, 98, .	1.1	18
38961	Surface-modulated palladium-nickel icosahedra as high-performance non-platinum oxygen reduction electrocatalysts. Science Advances, 2018, 4, eaap8817.	4.7	94
38962	Room temperature in-plane ferroelectricity in van der Waals In ₂ Se ₃. Science Advances, 2018, 4, eaar7720.	4.7	224
38963	Van der Waals Density Functional Theory Study of Molecular Adsorbates on MoX2(X = S, Se or Te). Journal of the Korean Physical Society, 2018, 73, 100-104.	0.3	14
38964	Ab initio study of impact of nitridation at amorphous-SiN _x /GaN interface. Applied Physics Express, 2018, 11, 081003.	1.1	9
38965	First-Principles Study on Hydrogen Diffusivity in BCC, FCC, and HCP Iron. Metallurgical and Materials Transactions A: Physical Metallurgy and Materials Science, 2018, 49, 5015-5022.	1.1	63
38966	A comprehensive first-principles study of solute elements in dilute Ni alloys: Diffusion coefficients and their implications to tailor creep rate. Acta Materialia, 2018, 157, 126-141.	3.8	49
38967	Ab initio study of the lattice dynamical and thermodynamic properties of SbXI (X= S, Se, Te) compounds. Computational Condensed Matter, 2018, 16, e00320.	0.9	7
38968	Catalyzing Cubic-to-Hexagonal Phase Transition in NaYF₄ via Ligand Enhanced Surface Ordering. Crystal Growth and Design, 2018, 18, 5080-5088.	1.4	25
38969	Promotion Effect of Methane Activation on Cu(111) by the Surface-Active Oxygen Species: A Combination of DFT and ReaxFF Study. Journal of Physical Chemistry C, 2018, 122, 17338-17346.	1.5	23

#	Article	IF	Citations
38970	Lead free halide perovskite Cs₃Bi₂I₉ bulk crystals grown by a low temperature solution method. CrystEngComm, 2018, 20, 4935-4941.	1.3	60
38971	First-principles study on the lattice plane and termination dependence of the electronic properties of the NiO/CH₃NH₃PbI₃ interfaces. Journal of Materials Chemistry C, 2018, 6, 8226-8233.	2.7	10
38972	Inducing regioselective chemical reactivity in graphene with alkali metal intercalation. Physical Chemistry Chemical Physics, 2018, 20, 19987-19994.	1.3	6
38973	Two-dimensional Au-1,3,5 triethynylbenzene organometallic lattice: Structure, half-metallicity, and gas sensing. Journal of Chemical Physics, 2018, 149, 024702.	1.2	5
38974	Structural evolution and magnetic properties of anionic clusters Cr₂Ge_n (nâ€‰â€‰=â€‰â€‰3â€“14): photoelectron spectroscopy and density functional theory computation. Journal of Physics Condensed Matter, 2018, 30, 335501.	2.7	20
38975	Potential thermoelectric material Sr2TiMoO6 from ab initio calculations. IOP Conference Series: Materials Science and Engineering, 2018, 382, 022024.	0.3	2
38976	Tuning the morphology of chevron-type graphene nanoribbons by choice of annealing temperature. Nano Research, 2018, 11, 6190-6196.	5.8	20
38977	The mechanism and kinetics of methyl isobutyl ketone synthesis from acetone over ion-exchanged hydroxyapatite. Journal of Catalysis, 2018, 365, 174-183.	3.1	25
38978	Toward a Reliable Description of the Lattice Vibrations in Organic Molecular Crystals: The Impact of van der Waals Interactions. Journal of Chemical Theory and Computation, 2018, 14, 4380-4390.	2.3	26
38979	Predicted Binary Compounds of Tin and Sulfur. Journal of Physical Chemistry C, 2018, 122, 17067-17072.	1.5	6
38980	Thermodynamic Properties, MÃ¶ssbauer Study, and First-Principles Calculations of TlFe(MoO₄)₂. Journal of Physical Chemistry C, 2018, 122, 19746-19755.	1.5	4
38981	Pressure-Induced Topological Nontrivial Phase and Tunable Optical Properties in All-Inorganic Halide Perovskites. Journal of Physical Chemistry C, 2018, 122, 17718-17725.	1.5	40
38982	Mechanistic Complexity of Methane Oxidation with H₂O₂ by Single-Site Fe/ZSM-5 Catalyst. ACS Catalysis, 2018, 8, 7961-7972.	5.5	98
38983	Significantly Improving Lithium-Ion Transport via Conjugated Anion Intercalation in Inorganic Layered Hosts. ACS Nano, 2018, 12, 8670-8677.	7.3	54
38984	Ab initio study of methanol and ethanol adsorption on BrÃ¸nsted sites in zeolite H-MFI. Physical Chemistry Chemical Physics, 2018, 20, 19964-19970.	1.3	29
38985	C₂N-graphene supported single-atom catalysts for CO₂ electrochemical reduction reaction: mechanistic insight and catalyst screening. Nanoscale, 2018, 10, 15262-15272.	2.8	156
38986	Oxygen vacancy-originated highly active electrocatalysts for the oxygen evolution reaction. Journal of Materials Chemistry A, 2018, 6, 15102-15109.	5.2	67
38987	In situ study of nucleation and growth dynamics of Au nanoparticles on MoS₂nanoflakes. Nanoscale, 2018, 10, 15809-15818.	2.8	38

#	Article	IF	Citations
38988	Combined computational and experimental investigation of the La ₂ CuO _{4â€“ x} S _x (0 â‰¤ x â‰¤ 4) quaternary system. Proceedings of the National Academy of Sciences of the United States of America, 2018, 115, 7890-7895.	3.3	8
38989	Density Functional Theory Study of Structural and Electronic Properties ofÎ³'-Ni₃Al andÎ³"-Ni₃Nb. IOP Conference Series: Materials Science and Engineering, 2018, 338, 012041.	0.3	1
38990	Induced ferromagnetism and metal-insulator transition due to a charge transfer effect in silver nanoparticle decorated <mml:math xmlns:mml="http://www.w3.org/1998/Math/MathML"><mml:mrow><mml:mi>Mo</mml:mi><mml:msub><mml:mi mathvariant="normal">S</mml:mi><mml:mn>2</mml:mn></mml:msub></mml:mrow></mml:math>. Physical Review B, 2018, 98, .	1.1	10
38991	Observation of Double Weyl Phonons in Parity-Breaking FeSi. Physical Review Letters, 2018, 121, 035302.	2.9	137
38992	Wallpaper fermions and the nonsymmorphic Dirac insulator. Science, 2018, 361, 246-251.	6.0	125
38993	Fully Ab-Initio Determination of the Thermoelectric Properties of Half-Heusler NiTiSn: Crucial Role of Interstitial Ni Defects. Materials, 2018, 11, 868.	1.3	31
38994	Hydrogenated and halogenated MB (M=As, Sb and Bi) monolayers: Structural, electronic, optical and topological properties by first principles calculations. Journal of Alloys and Compounds, 2018, 767, 552-558.	2.8	8
38995	Structural Diversity and Electronic Properties of 3d Transition Metal Tetraphosphides, TMP₄ (TM = V, Cr, Mn, and Fe). Inorganic Chemistry, 2018, 57, 9385-9392.	1.9	21
38996	Introducing Quantum Chemistry in Chemical Engineering Curriculum. Journal of Chemical Education, 2018, 95, 1562-1571.	1.1	6
38997	Microscopic mechanism of biphasic interface relaxation in lithium iron phosphate after delithiation. Nature Communications, 2018, 9, 2863.	5.8	27
38998	Unraveling reaction networks behind the catalytic oxidation of methane with H₂O₂ over a mixed-metal MIL-53(Al,Fe) MOF catalyst. Chemical Science, 2018, 9, 6765-6773.	3.7	67
38999	Few-layered Î±-MoTe₂ Schottky junction for a high sensitivity chemical-vapour sensor. Journal of Materials Chemistry C, 2018, 6, 10714-10722.	2.7	25
39000	Mechanistic insights into hydrodeoxygenation of phenol on bimetallic phosphide catalysts. Catalysis Science and Technology, 2018, 8, 4083-4096.	2.1	31
39001	Local atomic structure correlating to phase selection in undercooled liquid Ni-Zr peritectic alloy. Journal of Applied Physics, 2018, 124, .	1.1	20
39002	Optoelectronic properties of calcium cobalt oxide misfit nanotubes. Applied Physics Letters, 2018, 113, .	1.5	7
39003	Electron-donor doping enhanced Li storage in electride Ca₂N monolayer: a first-principles study. Journal of Physics Condensed Matter, 2018, 30, 345501.	0.7	6
39004	Density functional theory study of the magnetic moment of solute Mn in bcc Fe. Physical Review B, 2018, 98, .	1.1	14
39005	Spin-orbital entangled two-dimensional electron gas at the <mml:math xmlns:mml="http://www.w3.org/1998/Math/MathML"><mml:mrow><mml:msub><mml:mi>LaAlO</mml:mi><mml:mn>3</mml:mn></mml:msub></mml:mrow></mml:math> interface. Physical Review B, 2018, 98, .	1.1	8

#	Article	IF	Citations
39006	Molecular Deformation, Charge Flow, and Spongelike Behavior in Anionâ€“Ï€ {[M(CN)₄]^{2â^'};[HAT(CN)₆]}_{âˆž} (M=Ni, Pd, Pt) Supramolecular Stacks. Chemistry - A European Journal, 2018, 24, 16302-16314.	1.7	10
39007	Crystal structure, energetics, and phase stability of strengthening precipitates in Mg alloys: A first-principles study. Acta Materialia, 2018, 158, 65-78.	3.8	35
39008	Noble metal-free modified ultrathin carbon nitride with promoted molecular oxygen activation for photocatalytic formaldehyde oxidization and DFT study. Applied Surface Science, 2018, 458, 59-69.	3.1	62
39009	Theoretical and experimental investigations on H2 sensing properties of flower-like titanium dioxide. Materials Research Bulletin, 2018, 107, 139-146.	2.7	18
39010	Intrinsic Properties Affecting the Catalytic Activity of 3d Transition-Metal Carbides in Liâ€“O₂ Battery. Journal of Physical Chemistry C, 2018, 122, 17812-17819.	1.5	23
39011	Self-assembled alloy nanoparticles in a layered double perovskite as a fuel oxidation catalyst for solid oxide fuel cells. Journal of Materials Chemistry A, 2018, 6, 15947-15953.	5.2	77
39012	Enhanced superconductivity upon weakening of charge density wave transport in <mml:math xmlns:mml="http://www.w3.org/1998/Math/MathML"><mml:mrow><mml:mn>2</mml:mn><mml:mi>H</mml:mi><mml:msub> in the two-dimensional limit. Physical Review B, 2018, 98, .	3.7	81
39013	First-Principles Calculations on the Wettability of Li Atoms on the (111) Surfaces of W and Mo Substrates. Plasma Physics Reports, 2018, 44, 692-701.	0.3	4
39014	Mechanical Properties and Stability of Body-Centered-Tetragonal C8 at High Pressures. Zeitschrift Fur Naturforschung - Section A Journal of Physical Sciences, 2018, 73, 939-945.	0.7	5
39015	Stability, Electronic Structure, and Dehydrogenation Properties of Pristine and Doped 2D MgH2 by the First Principles Study. Metals, 2018, 8, 482.	1.0	6
39016	Ultralow Overpotential of Hydrogen Evolution Reaction using Feâ€Đoped Defective Graphene: A Density Functional Study. ChemCatChem, 2018, 10, 4450-4455.	1.8	22
39017	The role of Bi-doping in promoting electron transfer and catalytic performance of Pt/3DOM-Ce1â^'Bi O2â^'Î´. Journal of Catalysis, 2018, 365, 292-302.	3.1	59
39018	First principles, microkinetic, and experimental analysis of Lewis acid site speciation during ethanol dehydration on Sn-Beta zeolites. Journal of Catalysis, 2018, 365, 261-276.	3.1	49
39019	Boosting electrocatalytic oxygen evolution by synergistically coupling layered double hydroxide with MXene. Nano Energy, 2018, 44, 181-190.	8.2	458
39020	Nontrivial thermoelectric behavior in cubic SnSe driven by spin-orbit coupling. Nano Energy, 2018, 51, 649-655.	8.2	37
39021	Microscopic Mechanism of the Helix-to-Layer Transformation in Elemental Group VI Solids. Nano Letters, 2018, 18, 4908-4913.	4.5	19
39022	Ultrathin Silver Film Electrodes with Ultralow Optical and Electrical Losses for Flexible Organic Photovoltaics. ACS Applied Materials & Interfaces, 2018, 10, 27510-27520.	4.0	80
39023	Visible light induced electron transfer from a semiconductor to an insulator enables efficient photocatalytic activity on insulator-based heterojunctions. Nanoscale, 2018, 10, 15513-15520.	2.8	53

#	Article	IF	Citations
39024	Vanadium oxide nanoparticles supported on cubic carbon nanoboxes as highly active catalyst precursors for hydrogen storage in MgH₂. Journal of Materials Chemistry A, 2018, 6, 16177-16185.	5.2	113
39025	Influence of interfaces on the phonon density of states of nanoscale metallic multilayers: Phonon confinement and localization. Physical Review B, 2018, 98, .	1.1	11
39026	Raman Signatures of Broken Inversion Symmetry and Inâ€Plane Anisotropy in Typeâ€II Weyl Semimetal Candidate TaIrTe₄. Advanced Materials, 2018, 30, e1706402.	11.1	54
39027	Interstitial Occupancy by Extrinsic Alkali Cations in Perovskites and Its Impact on Ion Migration. Advanced Materials, 2018, 30, e1707350.	11.1	233
39028	Three-dimensional phase field simulation of intragranular void formation and thermal conductivity in irradiated Î±-Fe. Journal of Materials Science, 2018, 53, 11002-11014.	1.7	15
39029	Single-layer graphdiyne-covered Pt(111) surface: improved catalysis confined under two-dimensional overlayer. Journal of Nanoparticle Research, 2018, 20, 1.	0.8	9
39030	Synthesis of nitrogen and sulfur co-doped reduced graphene oxide as efficient metal-free cocatalyst for the photo-activity enhancement of CdS. Applied Catalysis B: Environmental, 2018, 236, 212-221.	10.8	68
39031	Imeall: A computational framework for the calculation of the atomistic properties of grain boundaries. Computer Physics Communications, 2018, 232, 256-263.	3.0	8
39032	Theoretical study of ZrCoH3 and the anti-disproportionation ability of alloying elements. International Journal of Hydrogen Energy, 2018, 43, 10410-10419.	3.8	25
39033	Rhenium-promoted selective CO2 methanation on Ni-based catalyst. Journal of CO2 Utilization, 2018, 26, 8-18.	3.3	49
39034	Theoretical exploration of the abnormal trend in lattice thermal conductivity for monosilicates RE2SiO5 (REâ€“Dy, Ho, Er, Tm, Yb and Lu). Journal of the European Ceramic Society, 2018, 38, 3539-3546.	2.8	49
39035	Rational design of metal-free organic D-Ï€-A dyes in dye-sensitized solar cells: Insight from density functional theory (DFT) and time-dependent DFT (TD-DFT) investigations. Organic Electronics, 2018, 59, 131-139.	1.4	28
39036	An Ultrahigh CO₂-Loaded Silicalite-1 Zeolite: Structural Stability and Physical Properties at High Pressures and Temperatures. Inorganic Chemistry, 2018, 57, 6447-6455.	1.9	19
39037	Effect of halogen dopants on the properties of Li₂O₂: is chloride special?. Physical Chemistry Chemical Physics, 2018, 20, 16924-16931.	1.3	9
39038	Face-centered cubic MoS₂: a novel superconducting three-dimensional crystal more stable than layered T-MoS₂. Journal of Materials Chemistry C, 2018, 6, 6046-6051.	2.7	11
39039	Imaging the ordering of a weakly adsorbed two-dimensional condensate: ambient-pressure microscopy and spectroscopy of CO₂ molecules on rutile TiO₂(110). Physical Chemistry Chemical Physics, 2018, 20, 13122-13126.	1.3	9
39040	First-principles study of polarization and piezoelectric properties of PbZrO3. AIP Conference Proceedings, 2018, , .	0.3	2
39041	Critical vaporization of MgSiO ₃. Proceedings of the National Academy of Sciences of the United States of America, 2018, 115, 5371-5376.	3.3	23

#	Article	IF	Citations
39042	Stability, structure, and suppression of the martensitic transition temperature by B19â€² compound twins in NiTi: ab initio and classical simulations. Acta Materialia, 2018, 154, 182-189.	3.8	18
39043	Enhanced methane conversion in chemical looping partial oxidation systems using a copper doping modification. Applied Catalysis B: Environmental, 2018, 235, 143-149.	10.8	103
39044	Insight into the role of the promoters Pt, Ru and B in inhibiting the deactivation of Co catalysts in Fischer-Tropsch synthesis. Applied Surface Science, 2018, 453, 309-319.	3.1	16
39045	N-graphdiyne two-dimensional nanomaterials: Semiconductors with low thermal conductivity and high stretchability. Carbon, 2018, 137, 57-67.	5.4	82
39046	Accurate and efficient band-offset calculations from density functional theory. Computational Materials Science, 2018, 151, 174-180.	1.4	56
39047	Helium trapping and clustering in ThO2. Journal of Nuclear Materials, 2018, 507, 288-296.	1.3	6
39048	Density Functional Theory Investigation of the Role of Cocatalytic Water in the Water Gas Shift Reaction over Anatase TiO₂ (101). Industrial & Engineering Chemistry Research, 2018, 57, 6830-6841.	1.8	8
39049	Theoretical Prediction and Synthesis of (Cr_{2/3}Zr_{1/3})₂AlC i-MAX Phase. Inorganic Chemistry, 2018, 57, 6237-6244.	1.9	59
39050	Selective and Stable Electroreduction of CO₂ to CO at the Copper/Indium Interface. ACS Catalysis, 2018, 8, 6571-6581.	5.5	175
39051	Synergistic Effect of Molecular-Type Electrocatalysts with Ultrahigh Pore Volume Carbon Microspheres for Lithiumâ€“Sulfur Batteries. ACS Nano, 2018, 12, 6013-6022.	7.3	100
39052	Experimental and Theoretical Structural Investigation of AuPt Nanoparticles Synthesized Using a Direct Electrochemical Method. Journal of the American Chemical Society, 2018, 140, 6249-6259.	6.6	33
39053	Origin of anisotropic negative Poisson's ratio in graphene. Nanoscale, 2018, 10, 10365-10370.	2.8	43
39054	Delithiated states of layered cathode materials: doping and dispersion interaction effects on the structure. EPJ Web of Conferences, 2018, 177, 02001.	0.1	3
39055	Stability and magnetic properties of SnSe monolayer doped by transition metal atom (Mn, Fe, and Co): a first-principles study. Journal Physics D: Applied Physics, 2018, 51, 245004.	1.3	18
39056	Thermodynamic consideration and ground-state search of icosahedral boron subselenide B12(B1â^'xSex)2 from a first-principles cluster expansion. Physical Review B, 2018, 97, .	1.1	2
39057	Electronic structure and surface properties of <mml:math xmlns:mml="http://www.w3.org/1998/Math/MathML"><mml:msub><mml:mi>MgB</mml:mi><mml:mn>2</mml:mn></mml:msub></mml:math> (0001) upon oxygen adsorption. Physical Review B, 2018, 97, .	1.1	13
39058	Structural, phase transition, mechanical and thermodynamic properties of TMNs under external pressures: A first-principles study. International Journal of Modern Physics B, 2018, 32, 1850181.	1.0	4
39059	Ordered Phases in Fe-Si Alloys: A First-Principles Study. Journal of the Korean Physical Society, 2018, 72, 737-740.	0.3	4

#	Article	IF	Citations
39060	Effect of incorporation of nitrogen atoms in Al₂O₃gate dielectric of wide-bandgap-semiconductor MOSFET on gate leakage current and negative fixed charge. Applied Physics Express, 2018, 11, 061501.	1.1	17
39062	First Full Structural Characterization of Chloro Formamidinium Salts. Zeitschrift Fur Anorganische Und Allgemeine Chemie, 2018, 644, 1485-1491.	0.6	1
39063	First-principles simulation on thermoelectric propertiesof transition metal dichalcogenide monolayers. Japanese Journal of Applied Physics, 2018, 57, 06HE04.	0.8	4
39064	Electronic conductivity of solid and liquid (Mg, Fe)O computed from first principles. Earth and Planetary Science Letters, 2018, 490, 11-19.	1.8	18
39065	Transition metal doping of Pd(1 1 1) for the NOâ€¯+â€¯CO reaction. Journal of Catalysis, 2018, 363, 154-163.	3.1	34
39066	Large and realistic models of amorphous silicon. Journal of Non-Crystalline Solids, 2018, 492, 27-32.	1.5	22
39067	Defect Design of Two-Dimensional MoS₂ Structures by Using a Graphene Layer and Potato Stamp Concept. Journal of Physical Chemistry C, 2018, 122, 11911-11917.	1.5	13
39068	Transition state redox during dynamical processes in semiconductors and insulators. NPG Asia Materials, 2018, 10, 45-51.	3.8	3
39069	Interfacial magnetic-phase transition mediated large perpendicular magnetic anisotropy in FeRh/MgO by a heavy transition-metal capping. Scientific Reports, 2018, 8, 6900.	1.6	17
39070	Enhanced Photocatalytic Hydrogen Evolution by Loading Cd0.5Zn0.5S QDs onto Ni2P Porous Nanosheets. Nanoscale Research Letters, 2018, 13, 31.	3.1	30
39071	Dirac Signature in Germanene on Semiconducting Substrate. Advanced Science, 2018, 5, 1800207.	5.6	59
39072	Computational study on the half-metallicity in transition metalâ€”oxide-incorporated 2D g-C3N4 nanosheets. Frontiers of Physics, 2018, 13, 1.	2.4	11
39073	Optical Properties of a Single Carbon Chain-Doped Silicene Nanoribbon. Journal of Electronic Materials, 2018, 47, 4585-4593.	1.0	2
39074	A Nanoindentation Study of the Plastic Deformation and Fracture Mechanisms in Single-Crystalline CaFe2As2. Jom, 2018, 70, 1074-1080.	0.9	4
39075	Thio-olivine Mn2SiS4 thin films by reactive magnetron sputtering: Structural and optical properties with insights from first principles calculations. Materials and Design, 2018, 152, 110-118.	3.3	4
39076	Benzene Adsorption on Rh(111): A New Perspective on Intermolecular Interactions and Molecular Ordering. Journal of Physical Chemistry C, 2018, 122, 11890-11904.	1.5	3
39077	Stable Metallic State of a Neutral-Radical Single-Component Conductor at Ambient Pressure. Journal of the American Chemical Society, 2018, 140, 6998-7004.	6.6	48
39078	Atomic origins of water-vapour-promoted alloy oxidation. Nature Materials, 2018, 17, 514-518.	13.3	106

#	Article	IF	Citations
39079	Study of oxygen evolution reaction on amorphous Au₁₃@Ni₁₂₀P₅₀ nanocluster. Physical Chemistry Chemical Physics, 2018, 20, 14545-14556.	1.3	7
39080	Evolutionary structure prediction of two-dimensional IrB₁₄: a promising gas sensor material. Journal of Materials Chemistry C, 2018, 6, 5803-5811.	2.7	13
39081	ROY revisited, again: the eighth solved structure. Faraday Discussions, 2018, 211, 477-491.	1.6	55
39082	Impact of Thickness on Contact Issues for Pinning Effect in Black Phosphorus Fieldâ€Effect Transistors. Advanced Functional Materials, 2018, 28, 1801398.	7.8	39
39083	Theoryâ€Guided Synthesis of a Metastable Leadâ€Free Piezoelectric Polymorph. Advanced Materials, 2018, 30, 1800559.	11.1	6
39084	Impact of Hydroxylation and Hydration on the Reactivity of Îºâ€Fe 2 O 3 (0001) and (102) Surfaces under Environmental and Electrochemical Conditions. Advanced Energy Materials, 2018, 8, 1800545.	10.2	9
39085	Density functional theory study of <mml:math xmlns:mml="http://www.w3.org/1998/Math/MathML" altimg="si1.gif" overflow="scroll"><mml:mrow><mml:mo stretchy="false">{</mml:mo><mml:mn>1</mml:mn><mml:mspace width="0.12em" /><mml:mn>0</mml:mn><mml:mspace width="0.12em" /><mml:mover accent="true"><mml:mrow><mml:mn>1</mml:mn></mml:mrow><mml:mrow><mml:mo>Â¯</mml:mo></mml:mrow></mml:mover><m stretchy="false">}</mml:mo></mml:mrow></mml:math> twin boundaries of Zn under high pressure. C	1.4	5
39086	Nonempirical Meta-Generalized Gradient Approximations for Modeling Chemisorption at Metal Surfaces. Journal of Chemical Theory and Computation, 2018, 14, 3083-3090.	2.3	20
39087	Nonmetallic FeH₆ under High Pressure. Journal of Physical Chemistry C, 2018, 122, 12022-12028.	1.5	29
39088	Electronic structure and microscopic model of CoNb2O6. AIP Conference Proceedings, 2018, , .	0.3	1
39089	Cooperative Couplings between Octahedral Rotations and Ferroelectricity in Perovskites and Related Materials. Physical Review Letters, 2018, 120, 197602.	2.9	43
39090	Separation of enantiomers by their enantiospecific interaction with achiral magnetic substrates. Science, 2018, 360, 1331-1334.	6.0	283
39091	Theoretical study of the influence of surface effects on GaN-based chemical sensors. Applied Surface Science, 2018, 452, 75-86.	3.1	12
39092	DFT study on water oxidation on nitrogen-doped ceria oxide. Applied Surface Science, 2018, 452, 423-428.	3.1	17
39093	Tuning the electronic and magnetic properties of graphyne by hydrogenation. Applied Surface Science, 2018, 452, 181-189.	3.1	13
39094	Facet effect on CO2 adsorption, dissociation and hydrogenation over Fe catalysts: Insight from DFT. Journal of CO2 Utilization, 2018, 26, 160-170.	3.3	35
39095	Soft-phonon dynamics of the thermoelectric Î² -SnSe at high temperatures. Physics Letters, Section A: General, Atomic and Solid State Physics, 2018, 382, 1937-1941.	0.9	10
39096	Experimental and first-principles study of defect structure of topological insulator Bi2Se3 single crystal. Superlattices and Microstructures, 2018, 120, 48-53.	1.4	4

#	Article	IF	Citations
39097	Structure and electronic properties of Si-doped CeO2 (111) surface by the first principle method. Solid State Communications, 2018, 277, 45-49.	0.9	11
39098	In Silico Discovery of New Dopants for Fe-Doped Ni Oxyhydroxide (Ni_{1â€“x}Fe_xOOH) Catalysts for Oxygen Evolution Reaction. Journal of the American Chemical Society, 2018, 140, 6745-6748.	6.6	274
39099	Evidence of radical chemistry in catalytic methane oxybromination. Nature Catalysis, 2018, 1, 363-370.	16.1	41
39100	Deconstructing collagen piezoelectricity using alanine-hydroxyproline-glycine building blocks. Nanoscale, 2018, 10, 9653-9663.	2.8	36
39101	First-principles study of thermoelectric properties of Mg2Siâ€“Mg2Pb semiconductor materials. RSC Advances, 2018, 8, 17168-17175.	1.7	15
39102	Electron-rich graphite-like electrode: stability vs.Âvoltage for Al batteries. Journal of Materials Chemistry A, 2018, 6, 10776-10786.	5.2	27
39103	Boronâ€“graphdiyne: a superstretchable semiconductor with low thermal conductivity and ultrahigh capacity for Li, Na and Ca ion storage. Journal of Materials Chemistry A, 2018, 6, 11022-11036.	5.2	104
39104	Colloidal Ni_{2â^'x}Co_xP nanocrystals for the hydrogen evolution reaction. Journal of Materials Chemistry A, 2018, 6, 11453-11462.	5.2	57
39105	Role of electron-phonon coupling and thermal expansion on band gaps, carrier mobility, and interfacial offsets in kesterite thin-film solar cells. Applied Physics Letters, 2018, 112, .	1.5	19
39106	Phase-transition temperature suppression to achieve cubic GeTe and high thermoelectric performance by Bi and Mn codoping. Proceedings of the National Academy of Sciences of the United States of America, 2018, 115, 5332-5337.	3.3	183
39107	Superconductivity in non-centrosymmetric sulfide Y _x S ₄. Europhysics Letters, 2018, 121, 57001.	0.7	2
39109	Combining batch technique with theoretical calculation studies to analyze the highly efficient enrichment of U(VI) and Eu(III) on magnetic MnFe2O4 nanocubes. Chemical Engineering Journal, 2018, 349, 347-357.	6.6	82
39110	Lithium ionic conduction in composites of Li(BH4)0.75I0.25 and amorphous 0.75Li2SÂ·0.25P2S5 for battery applications. Electrochimica Acta, 2018, 278, 332-339.	2.6	35
39111	On the formation and stability of precipitate phases in a near lamellar Î³-TiAl based alloy during creep. Intermetallics, 2018, 98, 115-125.	1.8	15
39112	Tunable twin stability and an accurate magnesium interatomic potential for dislocation-twin interactions. Materials and Design, 2018, 153, 232-241.	3.3	16
39113	Thermodynamic Stabilities, Electronic Properties, and Optical Transitions of Intrinsic Defects and Lanthanide Ions (Ce³⁺, Eu²⁺, and Eu³⁺) in Li₂SrSiO₄. Inorganic Chemistry, 2018, 57, 6142-6151.	1.9	20
39114	First-Principles Insight into Electrocatalytic Reduction of CO₂ to CH₄ on a Copper Nanoparticle. Journal of Physical Chemistry C, 2018, 122, 11392-11398.	1.5	56
39115	Spin valley and giant quantum spin Hall gap of hydrofluorinated bismuth nanosheet. Scientific Reports, 2018, 8, 7436.	1.6	8

#	Article	IF	Citations
39116	Transformation Paths from Cubic to Low-Symmetry Structures in Heusler Ni2MnGa Compound. Scientific Reports, 2018, 8, 7275.	1.6	23
39117	Electric field effects on the optical properties of buckled GaAs monolayer. AIP Conference Proceedings, 2018, , .	0.3	0
39118	Strain induced optical properties of BaReO3. AIP Conference Proceedings, 2018, , .	0.3	2
39119	Superconductivity in solid benzene molecular crystal. Journal of Physics Condensed Matter, 2018, 30, 245703.	0.7	5
39120	Vacancy assisted He-interstitial clustering and their elemental interaction at fcc-bcc semicoherent metallic interface. Scientific Reports, 2018, 8, 3844.	1.6	19
39121	Synthesis of inverse ringwoodite sheds light on the subduction history of Tibetan ophiolites. Scientific Reports, 2018, 8, 5457.	1.6	20
39122	Scalability assessment of Group-IV mono-chalcogenide based tunnel FET. Scientific Reports, 2018, 8, 5993.	1.6	27
39123	Accurate estimation of a phase diagram from a single STM image. Scientific Reports, 2018, 8, 6841.	1.6	4
39124	Electron injection study of photoexcitation effects on supported subnanometer Pt clusters for CO2 photoreduction. Physical Chemistry Chemical Physics, 2018, 20, 15926-15938.	1.3	7
39125	Single-layer ZnMN₂ (M = Si, Ge, Sn) zinc nitrides as promising photocatalysts. Physical Chemistry Chemical Physics, 2018, 20, 14619-14626.	1.3	17
39126	DFT insight into the effect of potassium on the adsorption, activation and dissociation of CO₂ over Fe-based catalysts. Physical Chemistry Chemical Physics, 2018, 20, 14694-14707.	1.3	40
39127	Tl₂S: a metal-shrouded two-dimensional semiconductor. Physical Chemistry Chemical Physics, 2018, 20, 14778-14784.	1.3	11
39128	Synthesis, PtS-type structure, and anomalous mechanics of the Cd(CN)₂ precursor Cd(NH₃)₂[Cd(CN)₄]. Dalton Transactions, 2018, 47, 7263-7271.	1.6	9
39129	Monolayer tellureneâ€“metal contacts. Journal of Materials Chemistry C, 2018, 6, 6153-6163.	2.7	81
39130	Pressure-induced structural and semiconductor-semiconductor transitions in <mml:math xmlns:mml="http://www.w3.org/1998/Math/MathML"><mml:mrow><mml:mi mathvariant="normal">C</mml:mi><mml:msub><mml:mi mathvariant="normal">o</mml:mi><mml:mrow><mml:mn>0.5</mml:mn></mml:mrow></mml:msub><mml:mi mathvariant="normal">M</mml:mi><mml:msub><mml:mi	1.1	20
39131	Observation of a nodal chain with Dirac surface states in <mml:math xmlns:mml="http://www.w3.org/1998/Math/MathML"><mml:mrow><mml:mi>Ti</mml:mi><mml:msub><mml:mi mathvariant="normal">B</mml:mi><mml:mn>2</mml:mn></mml:msub></mml:mrow></mml:math>. Physical Review B, 2018, 97, .	1.1	44
39132	Toward tailoring Majorana bound states in artificially constructed magnetic atom chains on elemental superconductors. Science Advances, 2018, 4, eaar5251.	4.7	233
39133	Theoretical prediction of honeycomb carbon as Li-ion batteries anode material. European Physical Journal B, 2018, 91, 1.	0.6	11

#	Article	IF	Citations
39134	Room temperature <mml:math xmlns:mml="http://www.w3.org/1998/Math/MathML"><mml:msup><mml:mi>d</mml:mi><mml:mn>0</mml:mn></mml:msup></mml:m ferromagnetism in carbon-doped <mml:math xmlns:mml="http://www.w3.org/1998/Math/MathML"><mml:mrow><mml:msub><mml:mi mathvariant="normal">Y</mml:mi><mml:mn>2</mml:mn></mml:msub><mml:msub><mml:mi mathvariant="normal">O</mml:mi><mml:mn>3</mml:mn></mml:msub></mml:mrow></mml:math> for s	1.1	22
39135	Influence of point defects on the thermal conductivity in FeSi. Physical Review B, 2018, 97, .	1.1	21
39136	Ferromagnetism and Charge Order from a Frozen Electron Configuration in Strained Epitaxial <mml:math xmlns:mml="http://www.w3.org/1998/Math/MathML" display="inline"><mml:mrow><mml:msub><mml:mrow><mml:mi>LaCoO</mml:mi></mml:mrow><mml:mrow><mml:mn>3</mml:mn></mml:m Physical Review Letters, 2018, 120, 197201.	2.9	26
39137	Probing Surface Chemistry Changes Using LiCoO₂-only Electrodes in Li-Ion Batteries. Journal of the Electrochemical Society, 2018, 165, A1377-A1387.	1.3	46
39138	Atomicâ€Scale Core/Shell Structure Engineering Induces Precise Tensile Strain to Boost Hydrogen Evolution Catalysis. Advanced Materials, 2018, 30, e1707301.	11.1	148
39139	NiFeâ€Based Metalâ€“Organic Framework Nanosheets Directly Supported on Nickel Foam Acting as Robust Electrodes for Electrochemical Oxygen Evolution Reaction. Advanced Energy Materials, 2018, 8, 1800584.	10.2	442
39140	Effect of solutes on ideal shear resistance and electronic properties of magnesium: A first-principles study. Acta Materialia, 2018, 153, 327-335.	3.8	21
39141	First-principles investigation on diffusion mechanism of alloying elements in dilute Zr alloys. Acta Materialia, 2018, 154, 161-171.	3.8	38
39142	A novel strategy to develop non-noble metal catalyst for CO2 electroreduction: Hybridization of metal-organic polymer. Applied Catalysis B: Environmental, 2018, 236, 154-161.	10.8	43
39143	High-throughput screening for superhard carbon and boron nitride allotropes with superior stiffness and strength. Carbon, 2018, 137, 156-164.	5.4	22
39144	Diffusion of helium, hydrogen and deuterium in diamond: Experiment, theory and geochemical applications. Geochimica Et Cosmochimica Acta, 2018, 232, 206-224.	1.6	11
39145	Formation enthalpy of Ga-Li intermetallic phases. Experiment vs. calculations. Journal of Chemical Thermodynamics, 2018, 124, 101-106.	1.0	7
39146	Evidence for a Dirac nodal-line semimetal in SrAs3. Science Bulletin, 2018, 63, 535-541.	4.3	34
39147	Efficient Automatized Density-Functional Tight-Binding Parametrizations: Application to Group IV Elements. Journal of Chemical Theory and Computation, 2018, 14, 2947-2954.	2.3	18
39148	Band Gap Modulated by Electronic Superlattice in Blue Phosphorene. ACS Nano, 2018, 12, 5059-5065.	7.3	92
39149	Inversion symmetry and bulk Rashba effect in methylammonium lead iodide perovskite single crystals. Nature Communications, 2018, 9, 1829.	5.8	189
39150	A theoretical study on the structures and electronic and magnetic properties of new boron nitride composite nanosystems by depositing superhalogen Al13on the surface of nanosheets/nanoribbons. Physical Chemistry Chemical Physics, 2018, 20, 15424-15433.	1.3	3
39151	Non-covalent interactions in electrochemical reactions and implications in clean energy applications. Physical Chemistry Chemical Physics, 2018, 20, 15680-15686.	1.3	53

#	Article	IF	Citations
39152	First-principles analysis of a molecular piezoelectric meta-nitroaniline. RSC Advances, 2018, 8, 16991-16996.	1.7	8
39153	Strain induced structural and electronic properties of BaReO3: A DFT study. AIP Conference Proceedings, 2018, , .	0.3	2
39154	Fast Rotational Diffusion of Water Molecules in a 2D Hydrogen Bond Network at Cryogenic Temperatures. Physical Review Letters, 2018, 120, 196001.	2.9	10
39155	Electronic Structure Investigation of the Bulk Properties of Uraniumâ€“Plutonium Mixed Oxides (U,) Tj ETQq1 1 0.784314 rgBT /Over	1.9	22
39156	Incident Angle Dependence of CHD₃ Dissociation on the Stepped Pt(211) Surface. Journal of Physical Chemistry C, 2018, 122, 19652-19660.	1.5	18
39157	Drastic Improvement in Gas-Sensing Characteristics of Phosphorene Nanosheets under Vacancy Defects and Elemental Functionalization. Journal of Physical Chemistry C, 2018, 122, 20186-20193.	1.5	60
39158	Stable Covalent Organic Frameworks as Efficient Adsorbents for High and Selective Removal of an Aryl-Organophosphorus Flame Retardant from Water. ACS Applied Materials & Interfaces, 2018, 10, 30265-30272.	4.0	138
39159	Anisotropic Surface Modulation of Pt Catalysts for Highly Reversible Liâ€“O₂ Batteries: High Index Facet as a Critical Descriptor. ACS Catalysis, 2018, 8, 9006-9015.	5.5	68
39160	Ultralong 1D Vacancy Channels for Rapid Atomic Migration during 2D Void Formation in Monolayer MoS₂. ACS Nano, 2018, 12, 7721-7730.	7.3	54
39161	Tuning Band Gap and Work Function Modulations in Monolayer hBN/Cu(111) Heterostructures with MoirÃ© Patterns. ACS Nano, 2018, 12, 9355-9362.	7.3	33
39162	Defect generation in TiO₂ nanotube anodes via heat treatment in various atmospheres for lithium-ion batteries. Physical Chemistry Chemical Physics, 2018, 20, 22537-22546.	1.3	29
39163	Tuning the phase stability of Mo-based TMD monolayers through coupled vacancy defects and lattice strain. Journal of Materials Chemistry C, 2018, 6, 9561-9568.	2.7	52
39164	Vibration analysis of hydrogen, deuterium and tritium in metals: consequences on the isotope effect. Journal of Physics Condensed Matter, 2018, 30, 335402.	0.7	12
39165	Magnetic and energetic properties of transition metal doped alumina. Journal of Physics Condensed Matter, 2018, 30, 395801.	0.7	5
39166	Ultrashort Pulse Generation in Ce:LiCAF Ultraviolet Laser. , 0, , .		0
39167	Tailoring the photocatalytic activity of WO3 by Nb-F codoping from first-principles calculations. Chinese Journal of Physics, 2018, 56, 2285-2290.	2.0	2
39168	Direct band gap tunability of the LiYF4 crystal through high-pressure applications. Computational Materials Science, 2018, 153, 431-437.	1.4	6
39169	Binding Characteristics of Anticancer Drug Doxorubicin with Two-Dimensional Graphene and Graphene Oxide: Insights from Density Functional Theory Calculations and Fluorescence Spectroscopy. Journal of Physical Chemistry C, 2018, 122, 21031-21038.	1.5	41

#	Article	IF	Citations
39170	Boron-Doped C₃N Monolayer as a Promising Metal-Free Oxygen Reduction Reaction Catalyst: A Theoretical Insight. Journal of Physical Chemistry C, 2018, 122, 20312-20322.	1.5	78
39171	High-Pressure Studies of Hydrogen-Bonded Energetic Material 3,6-Dihydrazino-s-tetrazine Using DFT. ACS Omega, 2018, 3, 9388-9399.	1.6	19
39172	Ductile deformation mechanism in semiconductor Î±-Ag2S. Npj Computational Materials, 2018, 4, .	3.5	54
39173	Type-II InSe/MoSe₂(WSe₂) van der Waals heterostructures: vertical strain and electric field effects. Journal of Materials Chemistry C, 2018, 6, 10010-10019.	2.7	59
39174	Giant magnetic anisotropy of a two-dimensional metalâ€“dicyanoanthracene framework. Nanoscale, 2018, 10, 17335-17340.	2.8	8
39175	Anisotropic Diffusion of a Charged Tritium Interstitial in <mml:math xmlns:mml="http://www.w3.org/1998/Math/MathML" display="inline" overflow="scroll"><mml:msub><mml:mi>Li</mml:mi><mml:mn>2</mml:mn></mml:msub><mml:mi>Ti</mml:mi><mml:msub><mml:mrow><mml:mi mathvariant="normal">O</mml:mi></mml:mrow><mml:mn>3</mml:mn></mml:msub></mml:math> from First-Principles Calculations. Physical Review Applied, 2018, 10, .	4.6	12
39176	First-Principles Study of Charge Carrier Dynamics with Explicit Treatment of Momentum Dispersion on Si Nanowires along <211> crystallographic Directions. MRS Advances, 2018, 3, 3477-3482.	0.5	6
39177	Ab-initio Study of Physical Properties of MgO/FeOx/Fe(001) Interfaces. Journal of the Korean Physical Society, 2018, 73, 320-324.	0.3	5
39178	Origin of Nb₂O₅ Lewis Acid Catalysis for Activation of Carboxylic Acids in the Presence of a Hard Base. ChemPhysChem, 2018, 19, 2848-2857.	1.0	28
39179	High Tolerance of Double-Decker Phthalocyanine toward Molecular Oxygen. Journal of Physical Chemistry C, 2018, 122, 20244-20251.	1.5	3
39180	Adsorption and Decomposition of Formic Acid on Cobalt(0001). Journal of Physical Chemistry C, 2018, 122, 20279-20288.	1.5	16
39181	Effect of Intrinsic Properties of Anions on the Electrocatalytic Activity of NiCo₂O₄ and NiCo₂O_xS_{4â€“x} Grown by Chemical Bath Deposition. ACS Omega, 2018, 3, 9066-9074.	1.6	17
39182	First principles mechanistic study of self-limiting oxidative adsorption of remote oxygen plasma during the atomic layer deposition of alumina. Physical Chemistry Chemical Physics, 2018, 20, 22783-22795.	1.3	14
39183	A new carbon allotrope with orthorhombic symmetry formed via graphitic sheet buckling. Physical Chemistry Chemical Physics, 2018, 20, 22762-22767.	1.3	9
39184	Oxygen vacancies induced structural distortions, valence fluctuations and enhanced optical properties in BiFe_{0.83}Ni_{0.17}O₃. Semiconductor Science and Technology, 2018, 33, 115009.	1.0	0
39185	Structural evolutions and electronic properties of Au n Gd (n = 6â€“15) small clusters: A first principles study. Chinese Physics B, 2018, 27, 083601.	0.7	3
39186	High quality PdTe2 thin films grown by molecular beam epitaxy. Chinese Physics B, 2018, 27, 086804.	0.7	39
39187	Accumulation of beryllium and its effects on hydrogen retention in tungsten divertor. Nuclear Fusion, 2018, 58, 106015.	1.6	2

#	Article	IF	Citations
39188	Polyanionic Goldâ€“Tin Bonding and Crystal Structure Preference in REAu_{1.5}Sn_{0.5} (RE = La, Ce, Pr, Nd). Inorganic Chemistry, 2018, 57, 10736-10743.	1.9	4
39189	Dual Functions of Water in Stabilizing Metal-Pentazolate Hydrates [M(N₅)₂(H₂O)₄]Â·4H₂O (M = Mn, Fe, Co,) Tj ET Q q 1 1 0.784314 rg BT	2.1	14
39190	Non-phase-separated 2D Bâ€“Câ€“N alloys via molecule-like carbon doping in 2D BN: atomic structures and optoelectronic properties. Physical Chemistry Chemical Physics, 2018, 20, 23106-23111.	1.3	6
39191	Direct Z-scheme photocatalytic overall water splitting on 2D CdS/InSe heterostructures. Journal Physics D: Applied Physics, 2018, 51, 395501.	1.3	51
39192	Nonlinear Spectroscopy with X-Ray Two-Photon Absorption in Metallic Copper. Physical Review Letters, 2018, 121, 083901.	2.9	38
39193	Broadband Terahertz Generation via the Interface Inverse Rashba-Edelstein Effect. Physical Review Letters, 2018, 121, 086801.	2.9	118
39194	First-Principles Study of the Structures and Electronic Properties of Ninâ€“1Al (n = 2-20) Clusters. Journal of Structural Chemistry, 2018, 59, 520-528.	0.3	0
39195	Effect of impurity carbon and oxygen atoms on the behavior of hydrogen in vanadium in a fusion environment: A first-principles study. International Journal of Modern Physics B, 2018, 32, 1850232.	1.0	1
39196	Enhancement of the Magnetic Anisotropy in Rare-Earth-Free Multilayer Fe16N2/Ag/Fe16N2 and Fe16N2/Au/Fe16N2. Journal of the Korean Physical Society, 2018, 72, 1343-1349.	0.3	1
39197	Yellow Emission from Low Coordination Site of Sr₂SiO₄:Eu²⁺, Ce³⁺: Influence of Lanthanide Dopants on the Electron Density and Crystallinity in Crystal Site Engineering Approach. Chemistry - A European Journal, 2018, 24, 16149-16159.	1.7	20
39198	Tailoring the electronic structure of Mn-doped SnTe via strain. Journal of Materials Science, 2018, 53, 15995-16000.	1.7	6
39199	Interface reaction processes and reactive properties of Al/CuO nanothermite: An ab initio molecular dynamics simulation. Applied Surface Science, 2018, 459, 835-844.	3.1	16
39200	Steering reduction and decomposition of peroxide compounds by interface interactions between MgO thin film and transition-metal support. Applied Surface Science, 2018, 459, 812-821.	3.1	8
39201	Thermodynamic modeling of the Moâ€“Ni system. Calphad: Computer Coupling of Phase Diagrams and Thermochemistry, 2018, 62, 215-222.	0.7	6
39202	Two-dimensional sheet of germanium selenide as an anode material for sodium and potassium ion batteries: First-principles simulation study. Computational Materials Science, 2018, 154, 204-211.	1.4	74
39203	Spin-dependent electrochemistry: Enantio-selectivity driven by chiral-induced spin selectivity effect. Electrochimica Acta, 2018, 286, 271-278.	2.6	35
39204	First-principles screening visible-light active delafossite ABO2 structures for photocatalytic application. International Journal of Hydrogen Energy, 2018, 43, 17271-17282.	3.8	11
39205	First-principles calculations of interaction between solutes and dislocations in tungsten. Nuclear Materials and Energy, 2018, 16, 221-225.	0.6	13

#	Article	IF	Citations
39206	Synergistic Coupling of Metallic Cobalt Nitride Nanofibers and IrO_x Nanoparticle Catalysts for Stable Oxygen Evolution. Chemistry of Materials, 2018, 30, 5941-5950.	3.2	57
39207	Corrosion protection of Al(111) by 8-hydroxyquinoline: a comprehensive DFT study. Physical Chemistry Chemical Physics, 2018, 20, 21474-21486.	1.3	10
39208	Hydrogen adsorption and desorption from Cu(111) and Cu(211). Physical Chemistry Chemical Physics, 2018, 20, 22477-22488.	1.3	26
39209	A 2D ferromagnetic semiconductor in monolayer Cr-trihalide and its Janus structures. Physical Chemistry Chemical Physics, 2018, 20, 21755-21763.	1.3	38
39210	Improving the activity of gold nanoparticles for the water-gas shift reaction using TiO₂â€“Y₂O₃: an example of catalyst design. Physical Chemistry Chemical Physics, 2018, 20, 22076-22083.	1.3	8
39211	Theoretical discovery of novel two-dimensional V^A-N binary compounds with auxiticity. Physical Chemistry Chemical Physics, 2018, 20, 22027-22037.	1.3	52
39212	Discovering minimum energy pathways via distortion symmetry groups. Physical Review B, 2018, 98, .	1.1	14
39213	Relativistic Theory and Ab Initio Simulations of Electroweak Decay Spectra in Mediumâ€Heavy Nuclei and of Atomic and Molecular Electronic Structure. Advanced Theory and Simulations, 2018, 1, 1800086.	1.3	2
39214	New interatomic potential for simulation of pure magnesium and magnesium hydrides. Computational Materials Science, 2018, 154, 295-302.	1.4	17
39215	A first-principle study of NaMPO4 (M = Mn, Fe, Co, Ni) possible novel structures as cathode materials for sodium-ion batteries: Structural and electrochemical characterisation. Materials Chemistry and Physics, 2018, 219, 212-221.	2.0	14
39216	Insights into Antibonding Induced Energy Density Enhancement and Exotic Electronic Properties for Germanium Nitrides at Modest Pressures. Inorganic Chemistry, 2018, 57, 10416-10423.	1.9	4
39217	Unravelling the Effects of A-Site Cations on Nonradiative Electronâ€“Hole Recombination in Lead Bromide Perovskites: Time-Domain ab Initio Analysis. Journal of Physical Chemistry Letters, 2018, 9, 4834-4840.	2.1	24
39218	Understanding the apparent fractional charge of protons in the aqueous electrochemical double layer. Nature Communications, 2018, 9, 3202.	5.8	47
39219	Atomically thin semiconducting penta-PdP₂ and PdAs₂ with ultrahigh carrier mobility. Journal of Materials Chemistry C, 2018, 6, 9055-9059.	2.7	39
39220	Hydraulic Power Manufacturing for Highly Scalable and Stable 2D Nanosheet Dispersions and Their Film Electrode Application. Advanced Functional Materials, 2018, 28, 1802952.	7.8	24
39221	Optothermoplasmonic Nanolithography for Onâ€Demand Patterning of 2D Materials. Advanced Functional Materials, 2018, 28, 1803990.	7.8	35
39222	Phase stability and mechanical properties of ternary transition elements X(Xâ€¯=â€¯Cu,Zn,Ag) in Al3Hf intermetallic from first-principles calculations. Computational Materials Science, 2018, 154, 266-275.	1.4	3
39223	Atomic layer deposited Pt-Co bimetallic catalysts for selective hydrogenation of Î±, Î²-unsaturated aldehydes to unsaturated alcohols. Journal of Catalysis, 2018, 366, 61-69.	3.1	61

#	Article	IF	Citations
39224	Understanding the underlying mechanism of improved selectivity in pd1 single-atom catalyzed hydrogenation reaction. Journal of Catalysis, 2018, 366, 70-79.	3.1	70
39225	Density functional theory study of tunable electronic and magnetic properties of monolayer BeO with intrinsic vacancy and transition metal substitutional doping. Journal of Magnetism and Magnetic Materials, 2018, 468, 252-258.	1.0	22
39226	Mechanical softening of thermoelectric semiconductor Mg2Si from nanotwinning. Scripta Materialia, 2018, 157, 90-94.	2.6	13
39227	Ion-Transport Engineering of Alkaline-Earth Hydrides for Hydride Electrolyte Applications. Chemistry of Materials, 2018, 30, 5878-5885.	3.2	15
39228	Modeling the Chemical Mechanism of the Thermal Atomic Layer Etch of Aluminum Oxide: A Density Functional Theory Study of Reactions during HF Exposure. Chemistry of Materials, 2018, 30, 5912-5922.	3.2	39
39229	Scalable Synthesis of a Ruthenium-Based Electrocatalyst as a Promising Alternative to Pt for Hydrogen Evolution Reaction. ACS Applied Materials & Interfaces, 2018, 10, 32171-32179.	4.0	33
39230	Tuning the electrolyte network structure to invoke quasi-solid state sulfur conversion and suppress lithium dendrite formation in Liâ€“S batteries. Nature Energy, 2018, 3, 783-791.	19.8	421
39231	Low temperature a/b nanotwins in Ni50Mn25+xGa25â^'x Heusler alloys. Scientific Reports, 2018, 8, 11943.	1.6	14
39232	Spin polarization and spin channel reversal in graphitic carbon nitrides on top of an Î±-Fe₂O₃(0001) surface. Physical Chemistry Chemical Physics, 2018, 20, 22489-22497.	1.3	5
39233	Synthesis of self-assembled PtPdAg nanostructures with a high catalytic activity for oxygen reduction reactions. Nanoscale, 2018, 10, 17140-17147.	2.8	11
39234	Low-temperature activation of methane on doped single atoms: descriptor and prediction. Physical Chemistry Chemical Physics, 2018, 20, 22909-22914.	1.3	62
39235	Prediction of an extremely long exciton lifetime in a Janus-MoSTe monolayer. Nanoscale, 2018, 10, 19310-19315.	2.8	93
39236	Phase polymorphism and electronic structures of TeSe₂. Journal of Materials Chemistry C, 2018, 6, 10218-10225.	2.7	12
39237	Electronic properties of fluorides by efficient approximated quasiparticle DFT-1/2 and PSIC methods: BaF₂, CaF₂and CdF₂as test cases. Journal of Physics Condensed Matter, 2018, 30, 365501.	0.7	16
39238	Ab initio determination of anharmonic phonon peaks. Physical Review B, 2018, 98, .	1.1	24
39239	Electron doping in Sr3Ir2O7 : Collapse of band gap and magnetic order. Physical Review B, 2018, 98, .	1.1	3
39240	A simple method for the prediction of the orientation of H₂O molecules in ionic crystals. Journal of Applied Crystallography, 2018, 51, 1116-1124.	1.9	7
39241	Controlling Chemical Reactions in Confined Environments: Water Dissociation in MOF-74. Applied Sciences (Switzerland), 2018, 8, 270.	1.3	10

#	Article	IF	Citations
39242	Molecular Orientations Change Reaction Kinetics and Mechanism: A Review on Catalytic Alcohol Oxidation in Gas Phase and Liquid Phase on Size-Controlled Pt Nanoparticles. Catalysts, 2018, 8, 226.	1.6	16
39243	Pseudo-Jahnâ€“Teller effects in two-dimensional silicene, germanene and stanene: a crystal orbital vibronic coupling density analysis. Bulletin of Materials Science, 2018, 41, 1.	0.8	5
39244	Reinforced photocatalytic reduction of CO2 to fuel by efficient S-TiO2: Significance of sulfur doping. International Journal of Hydrogen Energy, 2018, 43, 17682-17695.	3.8	43
39245	Planar perovskite FAxMA1-xPbI3 solar cell by two-step deposition method in air ambient. Optical Materials, 2018, 85, 55-60.	1.7	16
39246	Adsorption of Surfactants on Î±-Fe₂O₃(0001): A Density Functional Theory Study. Journal of Physical Chemistry C, 2018, 122, 20817-20826.	1.5	39
39247	Theoretical Investigation of the Interaction of the CuInSe₂ Absorber Material with Oxygen, Hydrogen, and Water. Journal of Physical Chemistry C, 2018, 122, 21202-21209.	1.5	8
39248	Chemical Bond Formation and Rupture Processes: An Application of DFTâ€“Chemical Pressure Approach. Journal of Physical Chemistry C, 2018, 122, 21216-21225.	1.5	9
39249	Atomic engineering of high-density isolated Co atoms on graphene with proximal-atom controlled reaction selectivity. Nature Communications, 2018, 9, 3197.	5.8	146
39250	Phosphorus doped SnO₂ thin films for transparent conducting oxide applications: synthesis, optoelectronic properties and computational models. Chemical Science, 2018, 9, 7968-7980.	3.7	33
39251	Destabilization of pseudo-Jahnâ€“Teller distortion in cesium-doped hexagonal tungsten bronzes. Journal of Applied Physics, 2018, 124, .	1.1	19
39252	Theory-assisted determination of nano-rippling and impurities in atomic resolution images of angle-mismatched bilayer graphene. 2D Materials, 2018, 5, 041008.	2.0	5
39253	Surface symmetry breaking and disorder effects on superconductivity in perovskite BaBi3 epitaxial films. Physical Review B, 2018, 98, .	1.1	1
39254	Theoretical and experimental investigation of the equation of state of boron plasmas. Physical Review E, 2018, 98, 023205.	0.8	23
39255	Efficient Calculation of the Negative Thermal Expansion in ZrW2O8. Frontiers in Chemistry, 2018, 6, 296.	1.8	13
39256	Abnormal Nearâ€Infrared Absorption in 2D Black Phosphorus Induced by Ag Nanoclusters Surface Functionalization. Advanced Materials, 2018, 30, e1801931.	11.1	43
39257	A topologically substituted boron nitride hybrid aerogel for highly selective CO2 uptake. Nano Research, 2018, 11, 6325-6335.	5.8	14
39258	Molecular Identification of Cr(VI) Removal Mechanism on Vivianite Surface. Environmental Science & Technology, 2018, 52, 10647-10656.	4.6	53
39259	Structureâ€“Property Relations in Multiferroic [(CH₃)₂NH₂]M(HCOO)₃ (M = Mn, Co, Ni). Inorganic Chemistry, 2018, 57, 11569-11577.	1.9	15

#	Article	IF	Citations
39260	Observation of topologically protected states at crystalline phase boundaries in single-layer WSe2. Nature Communications, 2018, 9, 3401.	5.8	107
39261	Giant magnetoelectric effect at the graphone/ferroelectric interface. Scientific Reports, 2018, 8, 12448.	1.6	5
39262	Controlling Dzyaloshinskii-Moriya Interaction via Chirality Dependent Atomic-Layer Stacking, Insulator Capping and Electric Field. Scientific Reports, 2018, 8, 12356.	1.6	153
39263	Pressure dependence of spin canting in ammonium metal formate antiferromagnets. Physical Chemistry Chemical Physics, 2018, 20, 24465-24476.	1.3	7
39264	Thermoelectric properties of two-dimensional selenene and tellurene from group-VI elements. Physical Chemistry Chemical Physics, 2018, 20, 24250-24256.	1.3	73
39265	Non-monotonic thickness dependence of Curie temperature and ferroelectricity in two-dimensional SnTe film. Applied Physics Letters, 2018, 113, .	1.5	7
39266	Impurity resonant state p-doping layer for high-efficiency nitride-based light-emitting diodes. Semiconductor Science and Technology, 2018, 33, 114004.	1.0	4
39267	Trends in pressure-induced layer-selective half-collapsed tetragonal phases in the iron-based superconductor family <mml:math xmlns:mml="http://www.w3.org/1998/Math/MathML"><mml:mrow><mml:mi>A</mml:mi><mml:mi>e</mml:mi><mml:mrow /><mml:mi>A</mml:mi><mml:msub><mml:mi>Fe</mml:mi><mml:mn>4</mml:mn></mml:msub><mml:msub><mml:mi>As</mml:mi> Physical Review B, 2018, 98, .	1.1	18
39268	Electronic and vibrational properties of PbI2 : From bulk to monolayer. Physical Review B, 2018, 98, .	1.1	49
39269	First-Cycle Simulation for Li-Rich Layered Oxide Cathode MaterialxLi2MnO3â‹…(1-x)LiMO2(x= 0.4). Journal of the Electrochemical Society, 2018, 165, A2667-A2674.	1.3	10
39270	Structural, electronic and magnetic properties of hydrogenated BC2N. Physics Letters, Section A: General, Atomic and Solid State Physics, 2018, 382, 3120-3124.	0.9	5
39271	Unexpected Semimetallic BiS₂ at High Pressure and High Temperature. Journal of Physical Chemistry Letters, 2018, 9, 5785-5791.	2.1	12
39272	<mml:math xmlns:mml="http://www.w3.org/1998/Math/MathML"><mml:mrow><mml:msub><mml:mi>MgTa</mml:mi><mml:mn>2</mml:mn></mml mathvariant="normal">N</mml:mi><mml:mn>3</mml:mn></mml:msub></mml:mrow></mml:math> : A reference Dirac semimetal. Physical Review B, 2018, 98, .	1.1	16
39273	Unravelling the New Roles of Na and Mn Promoter in CO₂ Hydrogenation over Fe₃O₄â€Based Catalysts for Enhanced Selectivity to Light Î±â€Olefins. ChemCatChem, 2018, 10, 4718-4732.	1.8	122
39274	Possible doping of single-layer MoS2 with Pt: A DFT study. Applied Surface Science, 2018, 462, 409-416.	3.1	21
39275	Candidate replacements for lead in CH3NH3PbI3 from first principles calculations. Computational Materials Science, 2018, 155, 69-73.	1.4	7
39276	Interface relationship between TiN and Ti substrate by first-principles calculation. Computational Materials Science, 2018, 155, 36-47.	1.4	25
39277	First Principles Insight into H₂ Activation and Hydride Species on TiO₂ Surfaces. Journal of Physical Chemistry C, 2018, 122, 20323-20328.	1.5	44

#	Article	IF	Citations
39278	Insights into Different Products of Nitrosobenzene and Nitrobenzene Hydrogenation on Pd(111) under Realistic Reaction Conditions. Journal of Physical Chemistry C, 2018, 122, 20337-20350.	1.5	37
39279	CO Direct versus H-Assisted Dissociation on Hydrogen Coadsorbed Ï‡-Fe₅C₂ Fischerâ€“Tropsch Catalysts. Journal of Physical Chemistry C, 2018, 122, 20907-20917.	1.5	23
39280	Single atom detachment from Cu clusters, and diffusion and trapping on CeO₂(111): implications in Ostwald ripening and atomic redispersion. Nanoscale, 2018, 10, 17893-17901.	2.8	47
39281	Correlation of structure with UV-visible spectra by varying SH composition in Au-SH nanoclusters. Journal of Chemical Physics, 2018, 149, 074307.	1.2	2
39282	Six-dimensional potential energy surfaces of the dissociative chemisorption of HCl on Ag(111) with three density functionals. Journal of Chemical Physics, 2018, 149, 054702.	1.2	15
39283	Multiple triple-point fermions in Heusler compounds. Journal of Physics Condensed Matter, 2018, 30, 375702.	0.7	8
39284	In Situ Spectroscopic Insights on the Molecular Structure of the MgO/SiO₂ Catalytic Active Sites during Ethanol Conversion to 1,3-Butadiene. Journal of Physical Chemistry C, 2018, 122, 20894-20906.	1.5	30
39285	Wafer-Scale Black Arsenicâ€“Phosphorus Thin-Film Synthesis Validated with Density Functional Perturbation Theory Predictions. ACS Applied Nano Materials, 2018, 1, 4737-4745.	2.4	42
39286	Giant spin-valley polarization and multiple Hall effect in functionalized bismuth monolayers. Npj Quantum Materials, 2018, 3, .	1.8	44
39287	Zeolite framework functionalisation by tuneable incorporation of various metals into the IPC-2 zeolite. Inorganic Chemistry Frontiers, 2018, 5, 2746-2755.	3.0	17
39288	Interlayer coupling and external electric field tunable electronic properties of a 2D type-I Î±-tellurene/MoS₂ heterostructure. Journal of Materials Chemistry C, 2018, 6, 10256-10262.	2.7	56
39289	Air molecules in XPbI3 (X=MA, FA, Cs) perovskite: A degradation mechanism based on first-principles calculations. Journal of Applied Physics, 2018, 124, .	1.1	15
39290	Vibrational enhancement in the dynamics of ammonia dissociative chemisorption on Ru(0001). Journal of Chemical Physics, 2018, 149, 044703.	1.2	15
39291	Hourglasslike nodal net semimetal in <mml:math xmlns:mml="http://www.w3.org/1998/Math/MathML"><mml:mrow><mml:msub><mml:mi>Ag</mml:mi><mml:mn>2</mml:mn></mml:msub></mml Physical Review B, 2018, 98, .	1.1	38
39292	Flatbands and Emergent Ferromagnetic Ordering in <mml:math xmlns:mml="http://www.w3.org/1998/Math/MathML" display="inline"><mml:mrow><mml:msub><mml:mrow><mml:mi>Fe</mml:mi></mml:mrow><mml:mrow><mml:mn>3</mml:mn></mml:mrow></mml Kagome Lattices. Physical Review Letters, 2018, 121, 096401.	2.9	221
39293	Triiodide Organic Salts: Photoelectrochemistry at the Border between Insulators and Semiconductors. ChemElectroChem, 2018, 5, 3486-3497.	1.7	8
39294	On the Role of Ferromagnetic Interactions in Highly Active Moâ€Based Catalysts for Ammonia Synthesis. ChemPhysChem, 2018, 19, 2843-2847.	1.0	16
39295	Phosphorusâ€Doped CdS Nanowires Showing nâ€Type Behavior. Physica Status Solidi (B): Basic Research, 2018, 255, 1800294.	0.7	0

#	Article	IF	Citations
39296	The high reactive site and the unusually short Scâ€€ bond of the scandium phosphinoalkylidene complex, an explanation from firstâ€principles calculation. International Journal of Quantum Chemistry, 2018, 118, e25691.	1.0	0
39297	Asymmetric quantum confinement-induced energetically and spatially splitting Dirac rings in graphene/phosphorene/graphene heterostructure. Carbon, 2018, 140, 164-170.	5.4	25
39298	Effect of neon on the hydrogen behaviors in tungsten: AÂfirst-principles study. Journal of Nuclear Materials, 2018, 510, 492-498.	1.3	3
39299	The structural, electronic, magnetic and optical properties of the Zn0.75V0.25Te alloy under pressure. Materials Chemistry and Physics, 2018, 220, 66-74.	2.0	0
39300	Magnetic and electronic properties of zigzag boron nitride nanoribbons with nonmetallic atom terminations from first-principles. Physica E: Low-Dimensional Systems and Nanostructures, 2018, 104, 297-301.	1.3	3
39301	Spontaneous Direct Band Gap, High Hole Mobility, and Huge Exciton Energy in Atomic-Thin TiO₂ Nanosheet. Chemistry of Materials, 2018, 30, 6449-6457.	3.2	50
39302	Activity Trends for Catalytic CO and NO Co-Oxidation at Low Temperature Diesel Emission Conditions. Industrial & Engineering Chemistry Research, 2018, 57, 12715-12725.	1.8	13
39303	Controlled Crystal Growth of Indium Selenide, In₂Se₃, and the Crystal Structures of Î±-In₂Se₃. Inorganic Chemistry, 2018, 57, 11775-11781.	1.9	97
39304	Theoretical Study on the Electronic Structures and Charge Transport Properties of a Series of Rubrene Derivatives. Journal of Physical Chemistry C, 2018, 122, 21226-21238.	1.5	16
39305	Construction of graphene oxide based mixed matrix membranes with CO₂-philic sieving gas-transport channels through strong Ï€â€“Ï€ interactions. Journal of Materials Chemistry A, 2018, 6, 17854-17860.	5.2	35
39306	The electric double layer at metal-water interfaces revisited based on a charge polarization scheme. Journal of Chemical Physics, 2018, 149, 084705.	1.2	128
39307	Manipulating the mechanical properties of Ti2C MXene: Effect of substitutional doping. AIP Conference Proceedings, 2018, , .	0.3	0
39308	Anomalous Hall effect in Weyl semimetal half-Heusler compounds RPtBi (R = Gd and Nd). Proceedings of the National Academy of Sciences of the United States of America, 2018, 115, 9140-9144.	3.3	126
39309	Observation of intrinsic dark exciton in Janus-MoSSe heterosturcture induced by intrinsic electric field. Journal of Physics Condensed Matter, 2018, 30, 395001.	0.7	14
39310	Multiferroic and Ferroic Topological Order in Ligand-Functionalized Germanene and Arsenene. Physical Review Applied, 2018, 10, .	1.5	31
39311	High-pressure investigations on the semi-Heusler compound CuMnSb. Physical Review B, 2018, 98, .	1.1	4
39312	Influence of substitutional atoms on the diffusion of oxygen in dilute iron alloys. Physical Review B, 2018, 98, .	1.1	13
39313	Fully spin-polarized current in gated bilayer silicene. Physical Review B, 2018, 98, .	1.1	18

#	Article	IF	Citations
39314	Realizing an intrinsic excitonic insulator by decoupling exciton binding energy from the minimum band gap. Physical Review B, 2018, 98, .	1.1	25
39315	Novel 2-D Materials for Tunneling FETs: an Ab-initio Study. , 2018, , .		0
39316	Structure and Properties of New High-Pressure Phases of Fe7N3. JETP Letters, 2018, 107, 379-383.	0.4	5
39317	Mode-specific and bond-selective dissociative chemisorption of CHD3 and CH2D2 on Ni(111) revisited using a new potential energy surface. Science China Chemistry, 2018, 61, 1134-1142.	4.2	5
39318	Long triple carbon chains formation by heat treatment of graphene nanoribbon: Molecular dynamics study with revised Brenner potential. Carbon, 2018, 140, 543-556.	5.4	13
39319	First-principles study of phase-transition temperature and optical properties of alkaline earth metal (Be, Mg, Ca, Sr or Ba)-doped VO2. Ceramics International, 2018, 44, 20814-20820.	2.3	18
39320	A DFT study of H solubility and diffusion in the Fe-Cr system. Computational Materials Science, 2018, 154, 243-250.	1.4	5
39321	Expanding the Iâ€“IIâ€“V Phase Space: Soft Synthesis of Polytypic Ternary and Binary Zinc Antimonides. Chemistry of Materials, 2018, 30, 6173-6182.	3.2	15
39322	Multiferroism in Iron-Based Oxyfluoride Perovskites. Inorganic Chemistry, 2018, 57, 10616-10624.	1.9	13
39323	Low-Frequency Phonon Driven Negative Thermal Expansion in Cubic GaFe(CN)₆ Prussian Blue Analogues. Inorganic Chemistry, 2018, 57, 10918-10924.	1.9	32
39324	X-ray Absorption Near-Edge Spectroscopy Calculations on Pristine and Modified Chalcopyrite Surfaces. Journal of Physical Chemistry C, 2018, 122, 20200-20209.	1.5	8
39325	In-Situ Atomic-Scale Phase Transformation of Mg under Hydrogen Conditions. Journal of Physical Chemistry C, 2018, 122, 19532-19539.	1.5	5
39326	New Pathway for Hot Electron Relaxation in Two-Dimensional Heterostructures. Nano Letters, 2018, 18, 6057-6063.	4.5	49
39327	New Insight for Surface Chemistries in Ultra-thin Self-assembled Monolayers Modified High-voltage Spinel Cathodes. Scientific Reports, 2018, 8, 11771.	1.6	11
39328	Microstructure and oxidation resistance of relaxed epitaxial nickel thin films grown on (100)- and (110)-SrTiO₃ substrates by pulsed laser deposition. CrystEngComm, 2018, 20, 5061-5073.	1.3	2
39329	Tuning transition metal carbide activity by surface metal alloying: a case study on CO₂capture and activation. Physical Chemistry Chemical Physics, 2018, 20, 22179-22186.	1.3	12
39330	Olefin methylation and cracking reactions in H-SSZ-13 investigated with ab initio and DFT calculations. Catalysis Science and Technology, 2018, 8, 4420-4429.	2.1	26
39331	Interfacial coupling between noble metal nanoparticles and metalâ€“organic frameworks for enhanced catalytic activity. Nanoscale, 2018, 10, 16425-16430.	2.8	46

#	Article	IF	Citations
39332	Synthesis of silver sulfide nanoparticles and their photodetector applications. RSC Advances, 2018, 8, 28447-28452.	1.7	29
39333	Strongly correlated perovskite lithium ion shuttles. Proceedings of the National Academy of Sciences of the United States of America, 2018, 115, 9672-9677.	3.3	55
39334	Interlayer excitons in transition-metal dichalcogenide heterostructures with type-II band alignment. Journal of Physics Condensed Matter, 2018, 30, 374002.	0.7	9
39335	Switchable Rashba effect by dipole moment switching in an Ag₂Te monolayer. Journal of Physics Condensed Matter, 2018, 30, 385502.	0.7	4
39336	Formation mechanism of multivacancies on H-passivated and Si-reconstructed surfaces of 6Hâ€“SiC (0001): a DFT calculation. Materials Research Express, 2018, 5, 105901.	0.8	2
39337	Two-dimensional ferroelastic topological insulators in single-layer Janus transition metal dichalcogenides <mml:math xmlns:mml="http://www.w3.org/1998/Math/MathML"><mml:mrow><mml:mi>M</mml:mi><mml:mi>SSe</mml:mi><mml:mo>(</mml:mo> Physical Review B, 2018, 98, .	3.7	68
39338	Substrate-Induced Liquid Layering: A New Insight into the Heterogeneous Nucleation of Liquid Metals. Metals, 2018, 8, 521.	1.0	14
39339	Ionic Modulation of the Interfacial Magnetism in a Bilayer System Comprising a Heavy Metal and a Magnetic Insulator for Voltageâ€Tunable Spintronic Devices. Advanced Materials, 2018, 30, e1802902.	11.1	22
39340	High-temperature superconductivity as viewed from the maximum hardness principle. Journal of Molecular Modeling, 2018, 24, 233.	0.8	2
39341	Chemical state and atomic scale environment of nickel in the corrosion layer of irradiated Zircaloy-2 at a burn-up around 45â€‰MWd/kg. Corrosion Science, 2018, 143, 200-211.	3.0	6
39342	First principles study of helium cluster induced local strain effects near the oxygen-enriched nanoclusters in Fe-based alloys. Journal of Nuclear Materials, 2018, 510, 270-276.	1.3	0
39343	Electronic structure and thermophysical properties of U3Si2: A systematic first principle study. Journal of Nuclear Materials, 2018, 510, 360-365.	1.3	15
39344	First-principles study of the structural and electronic properties of CoX0.25S1.75 (X = F, Cl, or Br). Journal of Physics and Chemistry of Solids, 2018, 123, 284-293.	1.9	0
39345	Electronic and Polar Properties of Vanadate Compounds Stabilized by Epitaxial Strain. Chemistry of Materials, 2018, 30, 5870-5877.	3.2	8
39346	Size-Induced Phase Evolution of MoSe₂ Nanoflakes Revealed by Density Functional Theory. Journal of Physical Chemistry C, 2018, 122, 20483-20488.	1.5	17
39347	Mineralâ€“Water Interface Structure of Xenotime (YPO4) {100}. Journal of Physical Chemistry C, 2018, 122, 20232-20243.	1.5	10
39348	Soft phonon modes from off-center Ge atoms lead to ultralow thermal conductivity and superior thermoelectric performance in n-type PbSeâ€“GeSe. Energy and Environmental Science, 2018, 11, 3220-3230.	15.6	115
39349	Unravelling the electrochemical mechanisms for nitrogen fixation on single transition metal atoms embedded in defective graphitic carbon nitride. Journal of Materials Chemistry A, 2018, 6, 21941-21948.	5.2	161

#	Article	IF	Citations
39350	Rapid and durable electrochemical storage behavior enabled by V₄Nb₁₈O₅₅ beaded nanofibers: a joint theoretical and experimental study. Journal of Materials Chemistry A, 2018, 6, 17389-17400.	5.2	24
39351	Structures and magnetic properties of iron silicide from adaptive genetic algorithm and first-principles calculations. Journal of Applied Physics, 2018, 124, .	1.1	6
39352	Electronic structure probed with positronium: Theoretical viewpoint. AIP Conference Proceedings, 2018, , .	0.3	0
39353	Discovery of Two-Dimensional Quantum Spin Hall Effect in Triangular Transition-Metal Carbides. Chinese Physics Letters, 2018, 35, 087303.	1.3	6
39354	Ground-state structures, physical properties and phase diagram of carbon-rich nitride C₅N. Journal of Physics Condensed Matter, 2018, 30, 385402.	0.7	9
39355	Magnetic properties and electronic state of Mo x Fe3â˜'x O4 ferrites. Materials Research Express, 2018, 5, 086103.	0.8	0
39356	Graphite under compression: shift of layer breathing and shear modes frequencies with interlayer spacing. Journal of Physics Communications, 2018, 2, 045004.	0.5	5
39357	Advances in Ti-Based Systems as High Temperature Shape Memory Alloys. Key Engineering Materials, 2018, 770, 230-238.	0.4	2
39358	Triboelectric Series of 2D Layered Materials. Advanced Materials, 2018, 30, e1801210.	11.1	179
39359	Rational design of new phases of tin monosulfide by first-principles structure searches. Science China: Physics, Mechanics and Astronomy, 2018, 61, 1.	2.0	15
39360	DFT study of [BH4]â˜' rotation in pressure-driven phase transition of MBH4. Computational Materials Science, 2018, 154, 143-146.	1.4	1
39361	The effects of Fe@C nanoparticles on the lithium storage performance of VS4 anode. Journal of Alloys and Compounds, 2018, 768, 938-943.	2.8	11
39362	Enhanced thermoelectric performance of two dimensional MS2 (MÂ=ÂMo, W) through phase engineering. Journal of Materiomics, 2018, 4, 329-337.	2.8	21
39363	Modifying Disordered Sites with Rational Cations to Regulate Band-Gaps and Second Harmonic Generation Responses Markedly: Ba₆Li₂ZnSn₄S₁₆ vs Ba₆Ag₂ZnSn₄S₁₆ vs Ba₆Li_{2.67}Sn_{4.33}S₁₆. Crystal Growth and Design, 2018, 18, 5609-5616.	1.4	21
39364	Light-Activated Hybrid Nanocomposite Film for Water and Oxygen Sensing. ACS Applied Materials & Interfaces, 2018, 10, 31745-31754.	4.0	12
39365	Facile Doping in Two-Dimensional Transition-Metal Dichalcogenides by UV Light. ACS Applied Materials & Interfaces, 2018, 10, 29893-29901.	4.0	18
39366	Programming ORR Activity of Ni/NiO_x@Pd Electrocatalysts via Controlling Depth of Surface-Decorated Atomic Pt Clusters. ACS Omega, 2018, 3, 8733-8744.	1.6	27
39367	Ab initio description of highly correlated states in defects for realizing quantum bits. Npj Quantum Materials, 2018, 3, .	1.8	60

#	Article	IF	Citations
39368	Effect of cobalt content on the electrochemical properties and structural stability of NCA type cathode materials. Physical Chemistry Chemical Physics, 2018, 20, 22805-22817.	1.3	27
39369	Simultaneous introduction of oxygen vacancies and Bi metal onto the {001} facet of Bi₃O₄Cl woven nanobelts for synergistically enhanced photocatalysis. Nanoscale, 2018, 10, 16928-16934.	2.8	41
39370	Hydrogen transfer through different crystal phases of nickel oxy/hydroxide. Physical Chemistry Chemical Physics, 2018, 20, 25169-25178.	1.3	10
39371	Effects of the erosion zone of magnetron sputtering targets on the spatial distribution of structural and electrical properties of transparent conductive Al-doped ZnO polycrystalline films. Journal of Applied Physics, 2018, 124, 065304.	1.1	10
39372	Emergent magnetism at the 3d-5d interface: SrMnO3/SrIrO3. AIP Conference Proceedings, 2018, , .	0.3	4
39373	Static and dynamic structure of Pu³⁺ in molten LiCl-KCl eutectic revealed by first-principles molecular dynamics simulations. Molecular Simulation, 2018, 44, 1353-1361.	0.9	5
39374	Atomistic Insight into the Formation of Metal-Graphene One-Dimensional Contacts. Physical Review Applied, 2018, 10, .	1.5	8
39375	Strain-induced tuning of the electronic Coulomb interaction in <mml:math xmlns:mml="http://www.w3.org/1998/Math/MathML"><mml:mrow><mml:mn>3</mml:mn><mml:mi>d</mml:mi></mml:mrow></mml:math> transition metal oxide perovskites. Physical Review B, 2018, 98, .	1.1	18
39376	Synergy of TiO₂/Na_{0.23}TiO₂ Heterojunction for Enhanced Photocatalysis. Crystal Research and Technology, 2018, 53, 1700153.	0.6	6
39377	Effects of Nd doping on the mechanical properties and electronic structures of Gd2Zr2O7: a first-principles-based study. Journal of Materials Science, 2018, 53, 16423-16438.	1.7	21
39378	Two-dimensional group-VA porous crystals: Diverse electronic structures and photocatalytic properties. Computational Materials Science, 2018, 154, 459-463.	1.4	4
39379	Enhanced thermoelectric performance in Ca-substituted Sr3SnO. Journal of Physics and Chemistry of Solids, 2018, 123, 318-326.	1.9	10
39380	Ab initio modelling of the Y, O, and Ti solute interaction in fcc-Fe matrix. Nuclear Instruments & Methods in Physics Research B, 2018, 433, 106-110.	0.6	3
39381	First Principle Study of Ti₅₀Al₅₀ Alloys. Key Engineering Materials, 2018, 770, 224-229.	0.4	0
39382	Realistic Largeâ€Scale Modeling of Rashba and Induced Spinâ€“Orbit Effects in Graphene/Highâ€Zâ€Metal Systems. Advanced Theory and Simulations, 2018, 1, 1800063.	1.3	11
39383	Local Charge Distribution Engineered by Schottky Heterojunctions toward Urea Electrolysis. Advanced Energy Materials, 2018, 8, 1801775.	10.2	266
39384	Effect of N-doping on hard carbon nano-balls as anode for Li-ion battery: improved hydrothermal synthesis and volume expansion study. Journal of Solid State Electrochemistry, 2018, 22, 3443-3455.	1.2	23
39385	Pressure-induced superconducting ternary hydride H3SXe: A theoretical investigation. Frontiers of Physics, 2018, 13, 1.	2.4	29

#	Article	IF	Citations
39386	Modeling the Effect of the Electrolyte on Standard Reduction Potentials of Polyoxometalates. Journal of Physical Chemistry C, 2018, 122, 18545-18553.	1.5	3
39387	Two-Dimensional Organometallic Kondo Lattice with Long-Range Antiferromagnetic Order. Journal of Physical Chemistry C, 2018, 122, 20046-20054.	1.5	14
39388	Photo-oxidative Degradation and Protection Mechanism of Black Phosphorus: Insights from Ultrafast Dynamics. Journal of Physical Chemistry Letters, 2018, 9, 5034-5039.	2.1	45
39389	Ultralow Defect Density at Sub-0.5 nm HfO₂/SiGe Interfaces via Selective Oxygen Scavenging. ACS Applied Materials & Interfaces, 2018, 10, 30794-30802.	4.0	31
39390	MoirÃ© Phonons in Twisted Bilayer MoS₂. ACS Nano, 2018, 12, 8770-8780.	7.3	149
39391	Diacetylene Linked Anthracene Oligomers Synthesized by One-Shot Homocoupling of Trimethylsilyl on Cu(111). ACS Nano, 2018, 12, 8791-8797.	7.3	41
39392	Hexagonal Ti₂B₂ monolayer: a promising anode material offering high rate capability for Li-ion and Na-ion batteries. Physical Chemistry Chemical Physics, 2018, 20, 22168-22178.	1.3	96
39393	Discovery of a high-pressure phase of rutile-like CoO₂ and its potential as a cathode material. Journal of Materials Chemistry A, 2018, 6, 18449-18457.	5.2	9
39394	Correlation-Driven Dimerization and Topological Gap Opening in Isotropically Strained Graphene. Physical Review Letters, 2018, 121, 066402.	2.9	34
39395	Lattice Energetics and Correlation-Driven Metal-Insulator Transitions: The Case of <mml:math xmlns:mml="http://www.w3.org/1998/Math/MathML" display="inline"><mml:mrow><mml:msub><mml:mrow><mml:mi>Ca</mml:mi></mml:mrow><mml:mrow><mml:mn>2</mml:mn></ Physical Review Letters, 2018, 121, 067601.	2.9	35
39396	Nextâ€Generation Narrowâ€Band Greenâ€Emitting RbLi(Li₃SiO₄)₂:Eu²⁺ Phosphor for Backlight Display Application. Advanced Materials, 2018, 30, e1802489.	11.1	407
39397	Energyâ€Efficient Nitrogen Reduction to Ammonia at Low Overpotential in Aqueous Electrolyte under Ambient Conditions. ChemSusChem, 2018, 11, 3416-3422.	3.6	140
39398	Coupling Phenomena in Magnetocaloric Materials. Energy Technology, 2018, 6, 1429-1447.	1.8	15
39399	Using local softness to reveal oxygen participation in redox processes in cathode materials. Journal of Molecular Modeling, 2018, 24, 227.	0.8	5
39400	Influence of surface strain on activity and selectivity of Pd-based catalysts for the hydrogenation of acetylene: A DFT study. Chinese Journal of Catalysis, 2018, 39, 1493-1499.	6.9	19
39401	Carbon doped hexagonal BN as a highly efficient metal-free base catalyst for Knoevenagel condensation reaction. Applied Catalysis B: Environmental, 2018, 239, 254-259.	10.8	102
39402	Effect of functional group position change of pyridinesulfonic acid as interface-modified layer on perovskite solar cell. Applied Surface Science, 2018, 462, 517-525.	3.1	18
39403	Efficient extraction of multivalent cations from aqueous solutions into sitinakite-based sorbents. Chemical Engineering Journal, 2018, 354, 727-739.	6.6	17

#	Article	IF	Citations
39404	First-principles prediction of ferromagnetism in transition-metal doped monolayer AlN. Superlattices and Microstructures, 2018, 122, 171-180.	1.4	18
39405	Dioxygen Activation on Cu-MOR Zeolite: Theoretical Insights into the Formation of Cu₂O and Cu₃O₃ Active Species. Inorganic Chemistry, 2018, 57, 10146-10152.	1.9	37
39406	Effects of Oxidation State on Charge Carrier Lifetimes in B,N Codoped Graphene Oxide Quantum Dots. Journal of Physical Chemistry C, 2018, 122, 18818-18828.	1.5	9
39407	Edge Defect Engineering of Nitrogen-Doped Carbon for Oxygen Electrocatalysts in Znâ€“Air Batteries. ACS Applied Materials & Interfaces, 2018, 10, 29448-29456.	4.0	110
39408	Role of Ionic Liquid [EMIM]⁺[SCN]^{â^'} in the Adsorption and Diffusion of Gases in Metalâ€“Organic Frameworks. ACS Applied Materials & Interfaces, 2018, 10, 29694-29704.	4.0	38
39409	Theoretical Insights into 1D Transition-Metal Nanoalloys Grown on the NiAl(110) Surface. ACS Omega, 2018, 3, 8819-8828.	1.6	3
39410	Anomalous isoelectronic chalcogen rejection in 2D anisotropic vdW TiS_{3(1â^'x)}Se_{3x} trichalcogenides. Nanoscale, 2018, 10, 15654-15660.	2.8	6
39411	Dynamic process of the resonant phonon scattering in fully filled skutterudites. Physical Review B, 2018, 98, .	1.1	10
39412	The Mechanism of the Transition of Solid Hydrogen to the Conducting State at High Pressures. Doklady Physics, 2018, 63, 272-275.	0.2	5
39413	Effect of defects on adsorption characteristics of AlN monolayer towards SO2 and NO2: Ab initio exposure. Applied Surface Science, 2018, 462, 615-622.	3.1	42
39414	Density functional theory-based ab initio molecular dynamics simulation of ionic conduction in N-/F-doped ZrO2 under epitaxial strain. Computational Materials Science, 2018, 154, 91-96.	1.4	3
39415	Structural, electronic and magnetic properties of the H- passivated armchair MoSe2 nanoribbons with the periodic vacancy. Superlattices and Microstructures, 2018, 122, 203-215.	1.4	1
39416	Hydrogen Bond-Driven Self-Assembly between Single-Layer MoS₂ and Alkyldiamine Molecules. Crystal Growth and Design, 2018, 18, 5116-5123.	1.4	18
39417	Tunable Optical and Photocatalytic Properties of Low-Dimensional Copper(I)-Iodide Hybrids Using Coordinating Organic Ligands. Crystal Growth and Design, 2018, 18, 5406-5416.	1.4	16
39418	Monte Carlo Potential Energy Sampling for Molecular Entropy in Zeolites. Journal of Physical Chemistry C, 2018, 122, 20351-20357.	1.5	27
39419	Understanding the Role of Minor Molybdenum Doping in LiNi_{0.5}Co_{0.2}Mn_{0.3}O₂ Electrodes: from Structural and Surface Analyses and Theoretical Modeling to Practical Electrochemical Cells. ACS Applied Materials & Interfaces, 2018, 10, 29608-29621.	4.0	97
39420	A novel WS₂/NbSe₂ vdW heterostructure as an ultrafast charging and discharging anode material for lithium-ion batteries. Journal of Materials Chemistry A, 2018, 6, 17040-17048.	5.2	53
39421	Development of a ReaxFF reactive force field for lithium ion conducting solid electrolyte Li_{1+x}Al_xTi_{2â^'x}(PO₄)₃ (LATP). Physical Chemistry Chemical Physics, 2018, 20, 22134-22147.	1.3	30

#	Article	IF	Citations
39422	Influences of vacancy and doping on electronic and magnetic properties of monolayer SnS. Journal of Applied Physics, 2018, 124, .	1.1	31
39423	Î¼SR study of spin freezing and persistent spin dynamics in NaCaNi₂F₇. Journal of Physics Condensed Matter, 2018, 30, 385802.	0.7	3
39424	Electronic properties of silicene in BN/silicene van der Waals heterostructures. Chinese Physics B, 2018, 27, 077302.	0.7	9
39425	Spin-orbit coupling driven crossover from a starfruitlike nodal semimetal to Dirac and Weyl semimetal state in CaAuAs. Physical Review B, 2018, 98, .	1.1	29
39426	Tunable band inversion in half-Heusler topological LuAuSn/LuPtBi superlattices. Applied Physics Express, 2018, 11, 095701.	1.1	3
39427	Curvature induced improvement of Li storage in Ca2N nanotubes. Applied Surface Science, 2018, 459, 406-410.	3.1	5
39428	Ab initio based interionic potential for silver iodide. Solid State Ionics, 2018, 325, 102-111.	1.3	4
39429	Optical absorption enhancement of Hg-doped ZnX (X= S, Se) for hydrogen production from water splitting driven by solar energy. Vacuum, 2018, 157, 36-44.	1.6	5
39430	Nitrogen-Doped Carbon Nanomaterials as Highly Active and Specific Peroxidase Mimics. Chemistry of Materials, 2018, 30, 6431-6439.	3.2	236
39431	First-Principles Study of the Adsorption and Depolymerization Mechanisms of Sodium Silicate on Iron Surfaces at High Temperature. Journal of Physical Chemistry C, 2018, 122, 20827-20840.	1.5	18
39432	Physical Origins of the Transient Absorption Spectra and Dynamics in Thin-Film Semiconductors: The Case of BiVO₄. Journal of Physical Chemistry C, 2018, 122, 20642-20652.	1.5	53
39433	Room-temperature mechanocaloric effects in lithium-based superionic materials. Nature Communications, 2018, 9, 3337.	5.8	21
39434	The adsorption of alcohols on strained Pt₃Ni(111) substrates: a density functional investigation within the D3 van der Waals correction. Physical Chemistry Chemical Physics, 2018, 20, 24210-24221.	1.3	14
39435	Ideal inert substrates for planar antimonene: h-BN and hydrogenated SiC(0001). Physical Chemistry Chemical Physics, 2018, 20, 23397-23402.	1.3	2
39436	Phase-transitionâ€“induced p-n junction in single halide perovskite nanowire. Proceedings of the National Academy of Sciences of the United States of America, 2018, 115, 8889-8894.	3.3	48
39437	Dirac states from p_{x,y} orbitals in the buckled honeycomb structures: A tight-binding model and first-principles combined study. Chinese Physics B, 2018, 27, 087101.	0.7	4
39438	Half-metallicity in two-dimensional Co ₂ Se ₃ monolayer with superior mechanical flexibility. 2D Materials, 2018, 5, 045026.	2.0	29
39439	Role of Multiple Charge States of <mml:math xmlns:mml="http://www.w3.org/1998/Math/MathML" display="inline" overflow="scroll"><mml:mi>Ce</mml:mi></mml:math> in the Scintillation of <mml:math xmlns:mml="http://www.w3.org/1998/Math/MathML" display="inline" overflow="scroll"><mml:mi mathvariant="italic">AB</mml:mi><mml:msub><mml:mrow><mml:mrow><mml:mi mathvariant="normal">O</mml:mi></mml:mrow></mml:mrow><mml:mn>3</mml:mn></mml:msub></mml:math>	1.5	15

#	Article	IF	Citations
39440	Electronic and structural response to pressure in the hyperkagome-lattice <mml:math xmlns:mml="http://www.w3.org/1998/Math/MathML"><mml:mrow><mml:msub><mml:mi>Na</mml:mi><mml:mn>3</mml:mn></mml:msub><mml:mathvariant="normal">O</mml:mi><mml:mn>8</mml:mn></mml:msub></mml:mrow></mml:math>. Physical Review B, 2018, 98, .	1.1	10
39441	Strain-tunable p-type Ag doping in the native n-type InSe monolayer. Applied Surface Science, 2018, 462, 387-392.	3.1	6
39442	Graphene layer effect on protecting the refined surface of transition metal substrate Re(0â€˜0â€˜1): A first-principles study. Applied Surface Science, 2018, 462, 502-507.	3.1	1
39443	Strain dependent electronic and optical properties of PtS2 monolayer. Chemical Physics Letters, 2018, 709, 65-70.	1.2	53
39444	Strain effect on the electronic properties of Ce-doped SnS2 monolayer. Physica B: Condensed Matter, 2018, 547, 1-5.	1.3	11
39445	A Zero-Dimensional Mixed-Anion Hybrid Halogenobismuthate(III) Semiconductor: Structural, Optical, and Photovoltaic Properties. Inorganic Chemistry, 2018, 57, 10576-10586.	1.9	26
39446	Oxygen Vacancy in Wurtzite ZnO and Metal-Supported ZnO/M(111) Bilayer Films (M = Cu, Ag and Au). Journal of Physical Chemistry C, 2018, 122, 20880-20887.	1.5	18
39447	Atomistic Sodiation Mechanism of a Phosphorene/Graphene Heterostructure for Sodium-Ion Batteries Determined by First-Principles Calculations. Journal of Physical Chemistry C, 2018, 122, 20653-20660.	1.5	35
39448	Theoretical Study of Propylene Epoxidation over Cu₂O(111) Surface: Activity of O^{2â€“}, O^{â€“}, and O₂^{â€“} Species. Journal of Physical Chemistry C, 2018, 122, 21500-21513.	1.5	34
39449	Site-Specific Positioning and Patterning of MoS₂ Monolayers: The Role of Au Seeding. ACS Nano, 2018, 12, 8970-8976.	7.3	50
39450	Nickel Adatoms Induced Tautomeric Dehydrogenation of Thymine Molecules on Au(111). ACS Nano, 2018, 12, 9033-9039.	7.3	14
39451	Three-dimensional atomic-scale observation of structural evolution of cathode material in a working all-solid-state battery. Nature Communications, 2018, 9, 3341.	5.8	60
39452	Comparative study of structural and electronic properties of GaSe and InSe polytypes. Journal of Chemical Physics, 2018, 149, 054106.	1.2	35
39453	Electronic structure and thermoelectric properties of monolayers of group V atoms. AIP Conference Proceedings, 2018, , .	0.3	5
39454	Study of magnetic and multiferroic properties of Î±-copper pyrovanadate. AIP Conference Proceedings, 2018, , .	0.3	0
39455	A multi-scale model for stresses, strains and swelling of reactor components under irradiation. Nuclear Fusion, 2018, 58, 126002.	1.6	61
39456	Density functional based tight-binding parametrization of hafnium oxide: Simulations of amorphous structures. Physical Review B, 2018, 98, .	1.1	6
39457	Interaction of water with stepped Co(0001): how is it different from flat Co(0001)?. European Physical Journal B, 2018, 91, 1.	0.6	2

#	Article	IF	Citations
39458	The Unified Electrochemical Band Diagram Framework: Understanding the Driving Forces of Materials Electrochemistry. Advanced Functional Materials, 2018, 28, 1803439.	7.8	8
39459	A Universal Strategy to Metal Wavy Nanowires for Efficient Electrochemical Water Splitting at pHâ€Universal Conditions. Advanced Functional Materials, 2018, 28, 1803722.	7.8	71
39460	Theoretical investigations of HCOOH decomposition on ordered Cu-Pd alloy surfaces. Applied Surface Science, 2018, 462, 649-658.	3.1	13
39461	H2O adsorption on the Au and Pd single atom catalysts supported on ceria: A first-principles study. Applied Surface Science, 2018, 462, 399-408.	3.1	7
39462	Efficiency of Generalized Regular <mml:math xmlns:mml="http://www.w3.org/1998/Math/MathML" altimg="si1.gif" overflow="scroll"><mml:mrow><mml:mi mathvariant="bold">k</mml:mi></mml:mrow></mml:math>-point grids. Computational Materials Science, 2018, 153, 424-430.	1.4	26
39463	Thermodynamic properties of Pb3U11O36. Journal of Nuclear Materials, 2018, 510, 38-42.	1.3	0
39464	Tribological properties of AZ31 alloy pre-deformed at low and high strain rates via the work function. Wear, 2018, 414-415, 126-135.	1.5	11
39465	Chemistry of Solvated Electrons in Molten Alkali Chloride Salts. Journal of Physical Chemistry C, 2018, 122, 19603-19612.	1.5	11
39466	Photo-generated dinuclear {Eu(II)}2 active sites for selective CO2 reduction in a photosensitizing metal-organic framework. Nature Communications, 2018, 9, 3353.	5.8	195
39467	A possible candidate for triply degenerate point fermions in trigonal layered PtBi2. Nature Communications, 2018, 9, 3249.	5.8	55
39468	Interfacing with silica boosts the catalysis of copper. Nature Communications, 2018, 9, 3367.	5.8	159
39469	Exposure of mass-selected bimetallic Ptâ€“Ti nanoalloys to oxygen explored using scanning transmission electron microscopy and density functional theory. RSC Advances, 2018, 8, 27276-27282.	1.7	6
39470	Improvement of thermoelectric performance of copper-deficient compounds Cu_{2.5+Î´}In_{4.5}Te₈ (Î´ = 0â€“0.15) due to a degenerate impurity band and ultralow lattice thermal conductivity. RSC Advances, 2018, 8, 27163-27170.	1.7	4
39471	Spin Hall effect emerging from a noncollinear magnetic lattice without spinâ€“orbit coupling. New Journal of Physics, 2018, 20, 073028.	1.2	65
39472	High throughput screening for two-dimensional topological insulators. 2D Materials, 2018, 5, 045023.	2.0	25
39473	Effects of Mn and Al addition on structural and magnetic properties of FeCoNi-based high entropy alloys. Materials Research Express, 2018, 5, 106511.	0.8	16
39474	Enhanced Carrier Concentration and Electronic Transport by Inserting Graphene into van der Waals Heterostructures of Transition-Metal Dichalcogenides. Physical Review Applied, 2018, 10, .	1.5	19
39475	Correlation length and dimensional crossover in a quasi-one-dimensional surface system. Physical Review B, 2018, 98, .	1.1	2

#	Article	IF	Citations
39476	Computational Predictions and Microwave Plasma Synthesis of Superhard Boron-Carbon Materials. Materials, 2018, 11, 1279.	1.3	9
39477	Atomic-scale forces induced by a hydrogen molecule trapped in a tunneling junction. Surface Science, 2018, 678, 189-193.	0.8	4
39478	Densityâ€Pressure Profiles of Feâ€Bearing MgSiO₃ Liquid: Effects of Valence and Spin States, and Implications for the Chemical Evolution of the Lower Mantle. Geophysical Research Letters, 2018, 45, 3959-3966.	1.5	22
39479	Operando monitoring the lithium spatial distribution of lithium metal anodes. Nature Communications, 2018, 9, 2152.	5.8	96
39480	Inherent orbital spin textures in Rashba effect and their implications in spinâ€“orbitronics. Journal of Physics Condensed Matter, 2018, 30, 285502.	0.7	3
39481	Ferromagnetic Weyl fermions in CrO2. Physical Review B, 2018, 97, .	1.1	20
39482	Effect of oxygen vacancies on intrinsic dielectric permittivity of strontium titanate ceramics. Journal of the Ceramic Society of Japan, 2018, 126, 263-268.	0.5	22
39483	Segregation and Phase Transformations Along Superlattice Intrinsic Stacking Faults in Ni-Based Superalloys. Metallurgical and Materials Transactions A: Physical Metallurgy and Materials Science, 2018, 49, 4186-4198.	1.1	45
39484	Electric field effects on electronic structure of tantalum dichalcogenides van der Waals TaS2/TaSe2 and TaSe2/TaTe2 heterostructures. Applied Surface Science, 2018, 455, 963-969.	3.1	9
39485	Revealing the local lattice strains and strengthening mechanisms of Ti alloys. Computational Materials Science, 2018, 152, 169-177.	1.4	29
39486	Structural, electronic and optical properties of bandgap-tunable Cu 2 ZnSi x Sn 1â˜' x Se 4 alloys. Chemical Physics Letters, 2018, 705, 92-96.	1.2	4
39487	Site Occupation of Eu²⁺ in Ba_{2â€“x}Sr_xSiO₄ (x = 0â€“1.9) and Origin of Improved Luminescence Thermal Stability in the Intermediate Composition. Inorganic Chemistry, 2018, 57, 7090-7096.	1.9	42
39488	Insights on the Synthesis, Crystal and Electronic Structures, and Optical and Thermoelectric Properties of Sr_{1â€“x}Sb_xHfSe₃ Orthorhombic Perovskite. Inorganic Chemistry, 2018, 57, 7402-7411.	1.9	20
39489	Achieving High-Performance Surface-Enhanced Raman Scattering through One-Step Thermal Treatment of Bulk MoS₂. Journal of Physical Chemistry C, 2018, 122, 14467-14473.	1.5	25
39490	Origin of H₂ Formation on Perfect SrTiO₃ (001) Surface: A First-principles Study. Journal of Physical Chemistry C, 2018, 122, 12951-12955.	1.5	1
39491	Design of Nickel-Based Cation-Disordered Rock-Salt Oxides: The Effect of Transition Metal (M = V, Ti,) Tj ETQq1 1 0.784314 rgBT /Ove Materials & Interfaces, 2018, 10, 21957-21964.	4.0	37
39492	Insight into the Near-Conduction Band States at the Crystallized Interface between GaN and SiN_x Grown by Low-Pressure Chemical Vapor Deposition. ACS Applied Materials & Interfaces, 2018, 10, 21721-21729.	4.0	24
39493	Suppressing Voltage Decay of a Lithium-Rich Cathode Material by Surface Enrichment with Atomic Ruthenium. ACS Applied Materials & Interfaces, 2018, 10, 21349-21355.	4.0	36

#	Article	IF	Citations
39494	Structures and Stability of Iron Halides at the Earthâ€™s Mantle and Core Pressures: Implications for the Missing Halogen Paradox. ACS Earth and Space Chemistry, 2018, 2, 711-719.	1.2	8
39495	Electron delocalization and charge mobility as a function of reduction in a metalâ€“organic framework. Nature Materials, 2018, 17, 625-632.	13.3	255
39496	Giant magnetic response of a two-dimensional antiferromagnet. Nature Physics, 2018, 14, 806-810.	6.5	44
39497	Anatomy of interfacial spin-orbit coupling in Co/Pd multilayers using X-ray magnetic circular dichroism and first-principles calculations. Scientific Reports, 2018, 8, 8303.	1.6	33
39498	An insight into the effects of transition metals on the thermal expansion of complex perovskite compounds: an experimental and density functional theory investigation. Physical Chemistry Chemical Physics, 2018, 20, 17781-17789.	1.3	4
39499	Nitrogen-promoted molybdenum dioxide nanosheets for electrochemical hydrogen generation. Journal of Materials Chemistry A, 2018, 6, 12532-12540.	5.2	34
39500	Design of two-dimensional electron gas systems via polarization discontinuity from large-scale first-principles calculations. Journal of Materials Chemistry C, 2018, 6, 6680-6690.	2.7	16
39501	Tin and germanium based two-dimensional Ruddlesdenâ€“Popper hybrid perovskites for potential lead-free photovoltaic and photoelectronic applications. Nanoscale, 2018, 10, 11314-11319.	2.8	73
39502	New optimization scheme to obtain interaction potentials for oxide glasses. Journal of Chemical Physics, 2018, 148, 194504.	1.2	60
39503	Intrinsic and anisotropic Rashba spin splitting in Janus transition-metal dichalcogenide monolayers. Physical Review B, 2018, 97, .	1.1	228
39504	Extremely large magnetoresistance in the topologically trivial semimetal <mml:math xmlns:mml="http://www.w3.org/1998/Math/MathML"><mml:mrow><mml:mi>Î±</mml:mi><mml:mo>â^’</mml:mo><mml:mn>1</mml:mn><mml:msub><mml:r Physical Review B, 2018, 97, .	1.1	41
39505	Design and exploration of semiconductors from first principles: A review of recent advances. Applied Physics Express, 2018, 11, 060101.	1.1	109
39506	Bifunctionally active and durable hierarchically porous transition metal-based hybrid electrocatalyst for rechargeable metal-air batteries. Applied Catalysis B: Environmental, 2018, 239, 677-687.	10.8	64
39507	Fundamental mechanisms of fracture and its suppression in Ni-rich layered cathodes: Mechanics-based multiscale approaches. Extreme Mechanics Letters, 2018, 22, 98-105.	2.0	17
39508	Metalâ€“Insulator Transition and Heterostructure Formation by Glycines Self-Assembled on Defect-Patterned Graphene. Journal of Physical Chemistry C, 2018, 122, 14598-14605.	1.5	28
39509	A remarkable two-dimensional membrane for multifunctional gas separation: halogenated metal-free fused-ring polyphthalocyanine. Physical Chemistry Chemical Physics, 2018, 20, 18931-18937.	1.3	7
39510	Water adsorption on the Fe₃O₄(111) surface: dissociation and network formation. Physical Chemistry Chemical Physics, 2018, 20, 15764-15774.	1.3	26
39511	Polyhedral perspectives on the capacity limit of cathode compounds for lithium-ion batteries: a case study for Li₆CoO₄. Physical Chemistry Chemical Physics, 2018, 20, 20363-20370.	1.3	13

#	Article	IF	Citations
39512	Ab initio theory of noble gas atoms in bcc transition metals. Physical Chemistry Chemical Physics, 2018, 20, 17048-17058.	1.3	9
39513	Anharmonic contribution to the stabilization of Mg(OH)2 from first principles. Physical Chemistry Chemical Physics, 2018, 20, 17799-17808.	1.3	10
39514	Highly anisotropic solar-blind UV photodetector based on large-size two-dimensional Î± -MoO ₃ atomic crystals. 2D Materials, 2018, 5, 035033.	2.0	49
39515	Finite temperature stability of single-layer black and blue phosphorus adsorbed on Au(1â€‰1â€‰1): a first-principles study. 2D Materials, 2018, 5, 035044.	2.0	14
39516	Spectroscopic and theoretical investigation of the electronic states of layered perovskite oxyfluoride <mml:math xmlns:mml="http://www.w3.org/1998/Math/MathML"><mml:mrow><mml:mi mathvariant="normal">S</mml:mi><mml:msub><mml:mi mathvariant="normal">r</mml:mi><mml:mn>2</mml:mn></mml:msub><mml:mi>Ru</mml:mi><mml:msub><mml:mi mathvariant="normal">O</mml:mi><mml:mn>3</mml:mn></mml:msub><mml:msub><mml:mi mathvariant="normal">F</mml:mi><mml:mn>2</mml:mn></mml:msub></mml:mrow></mml:math> thin fi	1.1	6
39517	DFT simulation of stacking faults defects in 4H-SiC. , 2018, , .		2
39518	Ensemble Monte Carlo simulation of 4H-SiC for electrons mobility calculation. , 2018, , .		2
39519	First-principles investigation of neutron-irradiation-induced point defects in B4C, a neutron absorber for sodium-cooled fast nuclear reactors. Japanese Journal of Applied Physics, 2018, 57, 055801.	0.8	14
39520	High Thermoelectric Performance in Supersaturated Solid Solutions and Nanostructured nâ€Type PbTeâ€“GeTe. Advanced Functional Materials, 2018, 28, 1801617.	7.8	92
39521	Enhancement of Solar Energy Absorption and Optoelectronic Properties of SrCuSbS₃ by Lead Doping. Solar Rrl, 2018, 2, 1800021.	3.1	9
39522	Hydrogenation of CO on Ni(110) by Energetic Deuterium. Journal of Physical Chemistry C, 2018, 122, 14671-14677.	1.5	2
39523	Graphdiyne as an ideal monolayer coating material for lithium-ion battery cathodes with ultralow areal density and ultrafast Li penetration. Journal of Materials Chemistry A, 2018, 6, 12630-12636.	5.2	24
39524	Porous Molybdenum Carbide Nanorods as Novel â€œBifunctionalâ€•Cathode Material for Liâ€S Batteries. Chemistry - A European Journal, 2018, 24, 14154-14161.	1.7	35
39525	Improvement of Thermoelectricity Through Magnetic Interactions in Layered Cr₂Ge₂Te₆. Physica Status Solidi - Rapid Research Letters, 2018, 12, 1800172.	1.2	9
39526	Metal dopants adjusted perovskite stannates: Conductivity and optical properties. Ceramics International, 2018, 44, 16051-16057.	2.3	14
39527	Enhanced stability and induced magnetic moments of silicene by substitutional doping of nickel. Chemical Physics Letters, 2018, 706, 202-207.	1.2	13
39528	The synergistic effect of Ni promoter on Mo-S/CNT catalyst towards hydrodesulfurization and hydrogen evolution reactions. Fuel, 2018, 232, 36-44.	3.4	30
39529	Water activation by single Pt atoms supported on a Cu2O thin film. Journal of Catalysis, 2018, 364, 166-173.	3.1	18

#	Article	IF	Citations
39530	3D long-range magnetic ordering in (C2H5NH3)2CuCl4 compound revealed by internal magnetic field from muon spin rotation and first principal calculation. Physica B: Condensed Matter, 2018, 545, 76-79.	1.3	4
39531	Electronic Structure and Magnetic Interactions in the Radical Salt [BEDT-TTF]₂[CuCl₄]. Inorganic Chemistry, 2018, 57, 7077-7089.	1.9	5
39532	Controlling Heterogeneous Catalysis of Water Dissociation Using Cuâ€“Ni Bimetallic Alloy Surfaces: A Quantum Dynamics Study. Journal of Physical Chemistry A, 2018, 122, 5698-5709.	1.1	20
39533	Highly Active Surface Structure in Nanosized Spinel Cobalt-Based Oxides for Electrocatalytic Water Splitting. Journal of Physical Chemistry C, 2018, 122, 14447-14458.	1.5	24
39534	Acetylene Adsorption on Pdâ€“Ag Alloys: Evidence for Limited Island Formation and Strong Reverse Segregation from Monte Carlo Simulations. Journal of Physical Chemistry C, 2018, 122, 15456-15463.	1.5	35
39535	Water Dissociation on Clean and Potassium Preadsorbed Transition Metals: A Systematic Theoretical Study. Journal of Physical Chemistry C, 2018, 122, 15474-15484.	1.5	16
39536	Mechanistic Insight into Enhanced Hydrogen Evolution Reaction Activity of Ultrathin Hexagonal Boron Nitride-Modified Pt Electrodes. ACS Catalysis, 2018, 8, 6636-6644.	5.5	63
39537	A Reduction in Particle Size Generally Causes Body-Centered-Cubic Metals to Expand but Face-Centered-Cubic Metals to Contract. ACS Nano, 2018, 12, 7246-7252.	7.3	17
39538	Robust band gaps in the graphene/oxide heterostructure: SnO/graphene/SnO. Physical Chemistry Chemical Physics, 2018, 20, 17983-17989.	1.3	25
39539	Efficient and stable photocatalytic NO removal on C self-doped g-C₃N₄: electronic structure and reaction mechanism. Catalysis Science and Technology, 2018, 8, 3387-3394.	2.1	60
39540	Mesoporous cobalt/manganese oxide: a highly selective bifunctional catalyst for amineâ€“imine transformations. Green Chemistry, 2018, 20, 3180-3185.	4.6	34
39541	Selecting electrode materials for monolayer ReS₂ with an Ohmic contact. Journal of Materials Chemistry C, 2018, 6, 6764-6770.	2.7	34
39542	Magnetic properties of X-C2N (X=Cl, Br and I) monolayers: A first-principles study. AIP Advances, 2018, 8, 055333.	0.6	4
39543	Diffusion quantum Monte Carlo and density functional calculations of the structural stability of bilayer arsenene. Journal of Chemical Physics, 2018, 148, 214706.	1.2	23
39544	Solidification behaviour of Alâ€“Si based alloys with controlled additions of Eu and P. International Journal of Cast Metals Research, 2018, 31, 319-331.	0.5	18
39545	Investigation of iron spin crossover pressure in Fe-bearing MgO using hybrid functional. Journal of Physics Condensed Matter, 2018, 30, 155403.	0.7	5
39546	Origin of metallicity in 2D multilayer nickel bis(dithiolene) sheets. 2D Materials, 2018, 5, 035027.	2.0	5
39547	<italic>Ab Initio</italic> Simulation of Band-to-Band Tunneling FETs With Single- and Few-Layer 2-D Materials as Channels. IEEE Transactions on Electron Devices, 2018, 65, 4180-4187.	1.6	23

#	Article	IF	Citations
39548	Structural, elastic, electronic and thermodynamic properties of ZrB₂ under high-pressure: First-principle study. International Journal of Modern Physics B, 2018, 32, 1850200.	1.0	3
39549	Amine group induced high activity of highly torn amine functionalized nitrogen-doped graphene as the metal-free catalyst for hydrogen evolution reaction. Carbon, 2018, 138, 169-178.	5.4	46
39550	Anisotropic antiferromagnetic order in the spin-orbit coupled trigonal-lattice <mml:math xmlns:mml="http://www.w3.org/1998/Math/MathML"><mml:mrow><mml:msub><mml:mi>Ca</mml:mi><mml:mn>2</mml:mn></mml:msub> Physical Review B, 2018, 97, .	1.1	6
39551	First-Principles Approach to Model Electrochemical Reactions: Understanding the Fundamental Mechanisms behind Mg Corrosion. Physical Review Letters, 2018, 120, 246801.	2.9	71
39552	Structural Investigations of (Ni,Cu) Coâ€“Doped ZnO Nanocrystals by Xâ€ray Absorption Spectroscopy. ChemistrySelect, 2018, 3, 5644-5651.	0.7	4
39553	Activation of formyl C H and hydroxyl O H bonds in HMF by the CuO(1â€¯1â€¯1) and Co3O4(1â€¯1â€¯0) surfaces: A DFT study. Applied Surface Science, 2018, 456, 174-183.	3.1	39
39554	Theoretical study on the reaction mechanism of carbon dioxide reforming of methane on La and La2O3 modified Ni(1â€¯1â€¯1) surface. Journal of Catalysis, 2018, 364, 248-261.	3.1	30
39555	Three-dimensional-networked Ni2P/Ni3S2 heteronanoflake arrays for highly enhanced electrochemical overall-water-splitting activity. Nano Energy, 2018, 51, 26-36.	8.2	378
39556	Observation of superconductivity in structure-selected Ti2O3 thin films. NPG Asia Materials, 2018, 10, 522-532.	3.8	43
39557	Selective hydrogenation of 1,3-butadiene catalyzed by a single Pd atom anchored on graphene: the importance of dynamics. Chemical Science, 2018, 9, 5890-5896.	3.7	55
39558	Minimal effect of stacking number on intrinsic cleavage and shear behavior of Tin+1AlCn and Tan+1AlCn MAX phases. Journal of Applied Physics, 2018, 123, .	1.1	3
39559	Structural, electronic and phononic properties of PtSe₂: from monolayer to bulk. Semiconductor Science and Technology, 2018, 33, 085002.	1.0	82
39560	Interconversion of intrinsic defects in <mml:math xmlns:mml="http://www.w3.org/1998/Math/MathML"><mml:mrow><mml:mi>SrTi</mml:mi><mml:msub><mml:mi mathvariant="normal">O</mml:mi><mml:mn>3</mml:mn></mml:msub><mml:mrow><mml:mo>(</mml:mo><mml:mn>001</mml:mn> Physical Review B, 2018, 97, .	1.1	19
39561	Layer and doping tunable ferromagnetic order in two-dimensional <mml:math xmlns:mml="http://www.w3.org/1998/Math/MathML"><mml:mrow><mml:mi>Cr</mml:mi><mml:msub><mml:mi mathvariant="normal">S</mml:mi><mml:mn>2</mml:mn></mml:msub></mml:mrow></mml:math> layers. Physical Review B, 2018, 97, .	1.1	96
39562	AbÂInitio Magneto-Optical Spectrum of Group-IV Vacancy Color Centers in Diamond. Physical Review X, 2018, 8, .	2.8	104
39563	Dirac-source field-effect transistors as energy-efficient, high-performance electronic switches. Science, 2018, 361, 387-392.	6.0	226
39564	Theoretical Study of Ultrafast Electron Injection into a Dye/TiO2 System in Dye-Sensitized Solar Cells. Journal of the Korean Physical Society, 2018, 72, 1307-1312.	0.3	8
39565	Hysteresis Design of Magnetocaloric Materialsâ€”From Basic Mechanisms to Applications. Energy Technology, 2018, 6, 1397-1428.	1.8	79

#	Article	IF	Citations
39566	First-principles molecular dynamics study of ionic structure and transport properties of LiF-NaF-AlF3 molten salt. Chemical Physics Letters, 2018, 706, 237-242.	1.2	31
39567	Facile preparation of biomass-derived bifunctional electrocatalysts for oxygen reduction and evolution reactions. International Journal of Hydrogen Energy, 2018, 43, 8611-8622.	3.8	64
39568	Nanoscale Control of Oxygen Defects and Metalâ€“Insulator Transition in Epitaxial Vanadium Dioxides. ACS Nano, 2018, 12, 7159-7166.	7.3	41
39569	Carbon nitride supported Fe2 cluster catalysts with superior performance for alkene epoxidation. Nature Communications, 2018, 9, 2353.	5.8	278
39570	A combined DFT and experimental study on the nucleation mechanism of NiO nanodots on graphene. Journal of Materials Chemistry A, 2018, 6, 13717-13724.	5.2	17
39571	Fitting electron density as a physically sound basis for the development of interatomic potentials of complex alloys. Physical Chemistry Chemical Physics, 2018, 20, 18647-18656.	1.3	2
39572	Theoretical investigation of zirconium carbide MXenes as prospective high capacity anode materials for Na-ion batteries. Journal of Materials Chemistry A, 2018, 6, 13652-13660.	5.2	111
39573	Factors driving stable growth of He clusters in W: first-principles study. Nuclear Fusion, 2018, 58, 076024.	1.6	2
39574	Bandgap modulation of partially chlorinated graphene (C4Cl) nanosheets via biaxial strain and external electric field: a computational study. Applied Physics A: Materials Science and Processing, 2018, 124, 1.	1.1	20
39575	Three-dimensional C60 polymers with ordered binary-alloy-type structures. Carbon, 2018, 137, 511-518.	5.4	12
39576	Localized High-Concentration Sulfone Electrolytes for High-Efficiency Lithium-Metal Batteries. CheM, 2018, 4, 1877-1892.	5.8	628
39577	Mono and bi-layer germanene as prospective anode material for Li-ion batteries: A first-principles study. Computational Condensed Matter, 2018, 16, e00314.	0.9	25
39578	Dopant segregation and CO adsorption on doped Fe3O4 (1â€¯1â€¯1) surfaces: A first-principle study. Journal of Catalysis, 2018, 364, 291-296.	3.1	22
39579	Boosting hot electron flux and catalytic activity at metalâ€“oxide interfaces of PtCo bimetallic nanoparticles. Nature Communications, 2018, 9, 2235.	5.8	80
39580	Tunable quantum order in bilayer Bi2Te3: Stacking dependent quantum spin Hall states. Applied Physics Letters, 2018, 112, 243103.	1.5	6
39581	Nature of Localized Excitons in <mml:math xmlns:mml="http://www.w3.org/1998/Math/MathML" display="inline"><mml:mrow><mml:mi>CsMg</mml:mi><mml:msub><mml:mrow><mml:mi>X</mml:mi></mml:mrow><mml:mrow><mml:m (<mml:math xmlns:mml="http://www.w3.org/1998/Math/MathML") Tj ETQq1 1 0.784314 rgBT /Overlock 10 Tf 50 142 Td (display="in	1.5	8
39582	Review Applied, 2018, 9, Chemicalâ€Strain Induced Tilted Dirac Nodes in (BEDTâ€TTF)₂X₃ (Xâ€‰=â€‰I, Cl, Br, F) Based Chargeâ€Transfer Salts. Physica Status Solidi - Rapid Research Letters, 2018, 12, 1800081.	1.2	9
39583	Elucidating the dominant reaction mechanism of methanol-to-olefins conversion in H-SAPO-18: A first-principles study. Chinese Journal of Catalysis, 2018, 39, 1272-1279.	6.9	14

#	Article	IF	Citations
39584	The adsorption characteristics of mercury species on single atom iron catalysts with different graphene-based substrates. Applied Surface Science, 2018, 455, 940-951.	3.1	50
39585	Coupled cluster and density functional investigation of the neutral sodium-benzene and potassium-benzene complexes. Chemical Physics Letters, 2018, 706, 343-347.	1.2	11
39586	Origin of storage capacity enhancement by replacing univalent ion with multivalent ion for energy storage. Electrochimica Acta, 2018, 282, 30-37.	2.6	11
39587	Correlation between structure and glass-forming ability in Al86Ni14-xLax(xâ€¯=â€¯3,5,9) alloys: An ab initio molecular dynamics study. Journal of Alloys and Compounds, 2018, 763, 392-398.	2.8	14
39588	Anisotropic mechanical properties and strain tuneable band-gap in single-layer SiP, SiAs, GeP and GeAs. Physica E: Low-Dimensional Systems and Nanostructures, 2018, 103, 273-278.	1.3	45
39589	A possible family of Ni-based high temperature superconductors. Science Bulletin, 2018, 63, 957-963.	4.3	12
39590	Investigation of the initial reactions of lithium oxides on the graphitic carbon nitrides (g-C3N4) for catalyst in non-aqueous lithium - air batteries: A first-principles calculations. Thin Solid Films, 2018, 660, 186-190.	0.8	6
39591	Unexplored photoluminescence from bulk and mechanically exfoliated few layers of Bi2Te3. Scientific Reports, 2018, 8, 9205.	1.6	15
39592	First-principles description of oxygen self-diffusion in rutile TiO₂: assessment of uncertainties due to enthalpy and entropy contributions. Physical Chemistry Chemical Physics, 2018, 20, 17448-17457.	1.3	12
39593	Entropy optimized phase transitions and improved thermoelectric performance in n-type liquid-like Ag9GaSe6 materials. Materials Today Physics, 2018, 5, 20-28.	2.9	70
39594	Electronic structures and optical properties of P and Cl atoms adsorbed/substitutionally doped monolayer MoS 2. Solid State Communications, 2018, 280, 6-12.	0.9	22
39595	Degree of Geometric Tilting Determines the Activity of FeO₆Octahedra for Water Oxidation. Chemistry of Materials, 2018, 30, 4313-4320.	3.2	54
39596	Electronic Structure Analysis of the Dielsâ€“Alder Cycloaddition Catalyzed by Alkali-Exchanged Faujasites. Journal of Physical Chemistry C, 2018, 122, 14733-14743.	1.5	23
39597	Transition Metal Induced the Contraction of Tungsten Carbide Lattice as Superior Hydrogen Evolution Reaction Catalyst. ACS Applied Materials & Interfaces, 2018, 10, 22094-22101.	4.0	64
39598	Tuning Noncollinear Spin Structure and Anisotropy in Ferromagnetic Nitride MXenes. ACS Nano, 2018, 12, 6319-6325.	7.3	101
39599	Vibrational and electrical properties of Cu2â^'xTe films: experimental data and first principle calculations. Scientific Reports, 2018, 8, 8093.	1.6	42
39600	Structure and properties of DOTA-chelated radiopharmaceuticals within the²²⁵Ac decay pathway. MedChemComm, 2018, 9, 1155-1163.	3.5	11
39601	Semiconducting edges and flake-shape evolution of monolayer GaSe: role of edge reconstructions. Nanoscale, 2018, 10, 12133-12140.	2.8	10

#	Article	IF	Citations
39602	Significantly improved thermal stability and thermoelectric performance of Cu-deficient Cu_{4â^'Î´}Ga₄Te₈ (<i>Î´</i> = 1.12) chalcogenides through addition of Sb. Journal of Materials Chemistry A, 2018, 6, 12672-12681.	5.2	5
39603	Ab-initio study of boron incorporation and compositional limits at GaN and AlN (0001) surfaces. AIP Advances, 2018, 8, .	0.6	10
39604	Thermoelectric transport of GaAs, InP, and PbTe: Hybrid functional with kÂ·pÌƒ interpolation versus scissor-corrected generalized gradient approximation. Journal of Applied Physics, 2018, 123, .	1.1	16
39605	Copper interstitial recombination centers in <mml:math xmlns:mml="http://www.w3.org/1998/Math/MathML"><mml:mrow><mml:msub><mml:mi>Cu</mml:mi><mml:mn>3</mml:mn></mm mathvariant="normal">N</mml:mi></mml:mrow></mml:math>. Physical Review B, 2018, 97, .	1.3	18
39606	Breakdown of Magnetic Order in the Pressurized Kitaev Iridate <mml:math xmlns:mml="http://www.w3.org/1998/Math/MathML" display="inline"><mml:mrow><mml:mi>Î²</mml:mi><mml:mtext>â^'</mml:mtext><mml:msub><mml:mrow><mml:mi>Li</mml:mi></m Physical Review Letters, 2018, 120, 237202.	2.9	57
39607	Photoinduced Nonequilibrium Topological States in Strained Black Phosphorus. Physical Review Letters, 2018, 120, 237403.	2.9	80
39608	Structure and Thermodynamic Characteristics of Impurity Centers in Lithium-Doped Cadmium Oxide: an Ab Initio Paw-Study. Journal of Structural Chemistry, 2018, 59, 253-260.	0.3	2
39609	Structural and magneto-transport properties of Mn1+Co1â^'Sn (xâ€‰=â€‰0.0â€"1.0) alloys. Journal of Magnetism and Magnetic Materials, 2018, 465, 360-364.	1.0	11
39610	Understanding the effects of Cr doping in rutile TiO2 by DFT calculations and X-ray spectroscopy. Scientific Reports, 2018, 8, 8740.	1.6	16
39611	Antisite-disorder engineering in La-based oxide heterostructures via oxygen vacancy control. Physical Chemistry Chemical Physics, 2018, 20, 17871-17880.	1.3	7
39612	Combinatorial alloying improves bismuth vanadate photoanodes <i>via</i> reduced monoclinic distortion. Energy and Environmental Science, 2018, 11, 2444-2457.	15.6	21
39613	Theoretical design of porphyrin sensitizers with different acceptors for application in dye-sensitized solar cells. RSC Advances, 2018, 8, 19804-19810.	1.7	10
39614	Influence of Cu and Na incorporation on the thermodynamic stability and electronic properties of Î²-In₂S₃. Journal of Materials Chemistry C, 2018, 6, 7226-7231.	2.7	14
39615	Pressure-induced structural and electronic transitions, metallization, and enhanced visible-light responsiveness in layered rhenium disulphide. Physical Review B, 2018, 97, .	1.1	35
39616	The effect of alloying of transition metals (MÂ= Fe, Co, Ni) with palladium catalysts on the electrocatalytic activity for the oxygen reduction reaction in alkaline media. Electrochimica Acta, 2018, 283, 1045-1052.	2.6	30
39617	Two-dimensional MTe2 (M = Co, Fe, Mn, Sc, Ti) transition metal tellurides as sodium ion battery anode materials: Density functional theory calculations. Physics Letters, Section A: General, Atomic and Solid State Physics, 2018, 382, 2781-2786.	0.9	21
39618	Effect of illumination and Se vacancies on fast oxidation of ultrathin gallium selenide. Nanoscale, 2018, 10, 12180-12186.	2.8	37
39619	Origin of photovoltage in perovskite solar cells probed by first-principles calculations. Applied Physics Letters, 2018, 112, .	1.5	1

#	Article	IF	Citations
39620	Effects of vacancy defects on Fe properties incorporated in MgO. Journal of Physics Condensed Matter, 2018, 30, 295701.	0.7	1
39621	Crystal structure analysis of a star-shaped triazine compound: a combination of single-crystal three-dimensional electron diffraction and powder X-ray diffraction. Acta Crystallographica Section B: Structural Science, Crystal Engineering and Materials, 2018, 74, 287-294.	0.5	1
39622	Ab Initio Study of the Polarization, Electronic, Magnetic, and Optical Properties of Perovskite SrMO3 (M = Fe, Mn) Crystals and Thin Films Containing Magnetic Ions. Journal of Experimental and Theoretical Physics, 2018, 126, 497-505.	0.2	8
39623	Black Arsenic: A Layered Semiconductor with Extreme Inâ€Plane Anisotropy. Advanced Materials, 2018, 30, e1800754.	11.1	161
39624	Stabilizing and Organizing Bi3 Cu4 and Bi7 Cu12 Nanoclusters in Two-Dimensional Metal-Organic Networks. Angewandte Chemie, 2018, 130, 4707-4711.	1.6	5
39625	Mechanistic study of bio-oil catalytic steam reforming for hydrogen production: Acetic acid decomposition. International Journal of Hydrogen Energy, 2018, 43, 13212-13224.	3.8	26
39626	Structural and magnetic properties of MoS 2 monolayer zigzag nanoribbon doped by Ti, V, Cr, and Mn. Physics Letters, Section A: General, Atomic and Solid State Physics, 2018, 382, 2354-2360.	0.9	14
39627	Layered Hexagonal Oxycarbides, Mn+1AO2Xn (M = Sc, Y, La, Cr, and Mo; A = Ca; X = C): Unexpected Photovoltaic Ceramics. Journal of Physical Chemistry C, 2018, 122, 14240-14247.	1.5	3
39628	Stability Trend of Tilted Perovskites. Journal of Physical Chemistry C, 2018, 122, 15214-15219.	1.5	30
39629	Deprotonation-Induced Phase Evolutions in Co-Assembled Molecular Structures. Langmuir, 2018, 34, 7852-7858.	1.6	19
39630	High-Performance and Industrially Feasible Ni-Rich Layered Cathode Materials by Integrating Coherent Interphase. ACS Applied Materials & Interfaces, 2018, 10, 20599-20610.	4.0	75
39631	Defective Mesocrystal ZnO-Supported Gold Catalysts: Facilitating CO Oxidation via Vacancy Defects in ZnO. ACS Catalysis, 2018, 8, 6862-6869.	5.5	88
39632	In situ atomistic insight into the growth mechanisms of single layer 2D transition metal carbides. Nature Communications, 2018, 9, 2266.	5.8	125
39633	Steering post-Câ€“C coupling selectivity enables high efficiency electroreduction of carbon dioxide to multi-carbon alcohols. Nature Catalysis, 2018, 1, 421-428.	16.1	537
39634	Bilayers of Janus WSSe: monitoring the stacking type via the vibrational spectrum. Physical Chemistry Chemical Physics, 2018, 20, 17380-17386.	1.3	56
39635	Mechanistic study of dry reforming of ethane by CO₂ on a bimetallic PtNi(111) model surface. Catalysis Science and Technology, 2018, 8, 3748-3758.	2.1	24
39636	Discovery of highly spin-polarized conducting surface states in the strong spin-orbit coupling semiconductor Sb2Se3. Physical Review B, 2018, 97, .	1.1	6
39637	Epitaxial Growth of Singleâ€Layer Niobium Selenides with Controlled Stoichiometric Phases. Advanced Materials Interfaces, 2018, 5, 1800429.	1.9	13

#	Article	IF	Citations
39638	Understanding the Effect of Iodide Ions on the Morphology of Gold Nanorods. Particle and Particle Systems Characterization, 2018, 35, 1800051.	1.2	6
39639	Optical Properties of Cu₂ZnSn(S_xSe_{1â€x})₄ by Firstâ€Principles Calculations. Physica Status Solidi (A) Applications and Materials Science, 2018, 215, 1700945.	0.8	4
39640	Performance of Modified La_xSr_{1â€“x}MnO₃ Perovskite Catalysts for NH₃ Oxidation: TPD, DFT, and Kinetic Studies. Environmental Science & Technology, 2018, 52, 7443-7449.	4.6	67
39641	Noble-Metal-Supported GeS Monolayer as Promising Single-Atom Catalyst for CO Oxidation. Journal of Physical Chemistry C, 2018, 122, 14488-14498.	1.5	35
39642	Comprehensive Phase Diagrams of MoS₂ Edge Sites Using Dispersion-Corrected DFT Free Energy Calculations. Journal of Physical Chemistry C, 2018, 122, 15318-15329.	1.5	18
39643	Mechanisms of CO Activation, Surface Oxygen Removal, Surface Carbon Hydrogenation, and Câ€“C Coupling on the Stepped Fe(710) Surface from Computation. Journal of Physical Chemistry C, 2018, 122, 15505-15519.	1.5	12
39644	Adsorption Induced Indirect-to-Direct Band Gap Transition in Monolayer Blue Phosphorus. Journal of Physical Chemistry C, 2018, 122, 15792-15798.	1.5	10
39645	Strain Control of Giant Magnetic Anisotropy in Metallic Perovskite SrCoO3â^Î´ Thin Films. ACS Applied Materials & Interfaces, 2018, 10, 22348-22355.	4.0	19
39646	In-Situ Formed Hydroxide Accelerating Water Dissociation Kinetics on Co₃N for Hydrogen Production in Alkaline Solution. ACS Applied Materials & Interfaces, 2018, 10, 22102-22109.	4.0	54
39647	Hierarchical MoO₃/SnS₂ coreâ€“shell nanowires with enhanced electrochemical performance for lithium-ion batteries. Physical Chemistry Chemical Physics, 2018, 20, 17171-17179.	1.3	32
39648	Two-dimensional pentagonal CrX (X = S, Se or Te) monolayers: antiferromagnetic semiconductors for spintronics and photocatalysts. Physical Chemistry Chemical Physics, 2018, 20, 18348-18354.	1.3	26
39649	Magnetoelectric Ïµ-Fe2O3: DFT study of a potential candidate for electrode material in photoelectrochemical cells. Journal of Chemical Physics, 2018, 148, 214707.	1.2	10
39650	Molecular dynamics simulation of the solid-liquid interface migration in terbium. Journal of Chemical Physics, 2018, 148, 214705.	1.2	17
39651	Electronâ^'hole separation in ferroelectric oxides for efficient photovoltaic responses. Proceedings of the National Academy of Sciences of the United States of America, 2018, 115, 6566-6571.	3.3	40
39652	Effects of trigonal deformation on electronic structure and thermoelectric properties of bismuth. Journal of Physics Condensed Matter, 2018, 30, 285504.	0.7	17
39653	Stability of SnSe_{1â^'x}S_x solid solutions revealed by first-principles cluster expansion. Journal of Physics Condensed Matter, 2018, 30, 29LT01.	0.7	14
39654	Adaptive modulation in the <mml:math xmlns:mml="http://www.w3.org/1998/Math/MathML"><mml:mrow><mml:mi mathvariant="normal">N</mml:mi><mml:msub><mml:mi mathvariant="normal">i</mml:mi><mml:mn>2</mml:mn></mml:msub><mml:mi mathvariant="normal">M</mml:mi><mml:msub><mml:mi mathvariant="normal">n</mml:mi><mml:mrow><mml:mn>1.4</mml:mn></mml:mrow></mml:msub><mml:mi	1.1	18
39655	Layer-dependent band alignment of few layers of blue phosphorus and their van der Waals heterostructures with graphene. Physical Review B, 2018, 97, .	1.1	45

#	Article	IF	Citations
39656	What Drives Metal-Surface Step Bunching in Graphene Chemical Vapor Deposition?. Physical Review Letters, 2018, 120, 246101.	2.9	52
39657	Origin of efficient oxygen reduction reaction on Pd monolayer supported on Pd-M (M=Ni, Fe) intermetallic alloy. Electrochimica Acta, 2018, 282, 680-686.	2.6	26
39658	Stability of FeVO₄ under Pressure: An X-ray Diffraction and First-Principles Study. Inorganic Chemistry, 2018, 57, 7860-7876.	1.9	27
39659	High energy-density and reversibility of iron fluoride cathode enabled via an intercalation-extrusion reaction. Nature Communications, 2018, 9, 2324.	5.8	136
39660	On-surface synthesis of poly(p-phenylene ethynylene) molecular wires via in situ formation of carbon-carbon triple bond. Nature Communications, 2018, 9, 2322.	5.8	51
39661	Giant photovoltaic response in band engineered ferroelectric perovskite. Scientific Reports, 2018, 8, 8005.	1.6	36
39662	Density functional theory study of thermodynamic and kinetic isotope effects of H2/D2 dissociative adsorption on transition metals. Catalysis Science and Technology, 2018, 8, 3321-3335.	2.1	26
39663	Double transition metal MXenes with wide band gaps and novel magnetic properties. Nanoscale, 2018, 10, 11962-11968.	2.8	88
39664	Valley-selective circular dichroism and high carrier mobility of graphene-like BC₆N. Nanoscale, 2018, 10, 13179-13186.	2.8	37
39665	First-principles study of structural, electronic, and optical properties of surface defects in GaAs(001) - Î²2(2x4). AIP Advances, 2018, 8, .	0.6	12
39666	Ab-Initio Calculation of Spectral Absorption Coefficients in Molten Fluoride Salts with Metal Impurities. Nuclear Technology, 2018, 204, 59-65.	0.7	7
39667	Effects of overlayer capping and lattice strain on perpendicular magnetic anisotropy of TM|FePt|MgO heterostructures. Scientific Reports, 2018, 8, 9429.	1.6	5
39668	Lattice dynamics and metastability of fcc metals in the hcp structure and the crucial role of spin-orbit coupling in platinum. Physical Review B, 2018, 97, .	1.1	16
39669	Ab initio density functional theory study of the electronic, dynamic, and thermoelectric properties of the crystalline pseudobinary chalcogenide <mml:math xmlns:mml="http://www.w3.org/1998/Math/MathML"><mml:msub><mml:mrow><mml:mtext>(GeTe)</mml:mtext></mml:mrow><mml:mn width="0.. Physical Review B, 2018, 97, .	1.1	18
39670	Effective lattice Hamiltonian for monolayer tin disulfide: Tailoring electronic structure with electric and magnetic fields. Physical Review B, 2018, 97, .	1.1	5
39671	Theoretical study of strain-induced modulation of the bandgap in SiC. Japanese Journal of Applied Physics, 2018, 57, 071301.	0.8	11
39672	Entropy Contributions to Transition State Modeling. , 2018, , 189-228.		5
39673	Room-Temperature Methane Conversion by Graphene-Confined Single Iron Atoms. CheM, 2018, 4, 1902-1910.	5.8	350

#	Article	IF	Citations
39674	Understanding the Effect of Local Short-Range Ordering on Lithium Diffusion in Li1.3Nb0.3Mn0.4O2 Single-Crystal Cathode. CheM, 2018, 4, 2108-2123.	5.8	80
39675	Interfacial properties of high-order aggregation of organic dyes: A combination of static and dynamic properties. Energy, 2018, 158, 537-545.	4.5	15
39676	On the role of water in selective hydrogenation of cinnamaldehyde to cinnamyl alcohol on PtFe catalysts. Journal of Catalysis, 2018, 364, 192-203.	3.1	87
39677	Dioxygen activation routes in Mars-van Krevelen redox cycles catalyzed by metal oxides. Journal of Catalysis, 2018, 364, 228-247.	3.1	36
39678	Design rules of heteroatom-doped graphene to achieve high performance lithiumâ€“sulfur batteries: Both strong anchoring and catalysing based on first principles calculation. Journal of Colloid and Interface Science, 2018, 529, 426-431.	5.0	50
39679	Theoretical understanding of SnS monolayer as Li ion battery anode material. Journal of Physics and Chemistry of Solids, 2018, 121, 261-265.	1.9	22
39680	Bethe-Salpeter Equation calculations of nitrogen-vacancy defects in diamond. Journal of Physics and Chemistry of Solids, 2018, 122, 87-93.	1.9	3
39681	Substoichiometry and tantalum dependent thermal stability of Î±-structured W-Ta-B thin films. Scripta Materialia, 2018, 155, 5-10.	2.6	38
39682	Understanding the Effects of Cd and Ag Doping in Cu₂ZnSnS₄ Solar Cells. Chemistry of Materials, 2018, 30, 4543-4555.	3.2	76
39683	Designing and Discovering a New Family of Semiconducting Quaternary Heusler Compounds Based on the 18-Electron Rule. Chemistry of Materials, 2018, 30, 4978-4985.	3.2	57
39684	Thickness-Dependent Reactivity of O₂ on Cu Layers Grown on Ru(0001) Surfaces. Journal of Physical Chemistry C, 2018, 122, 15529-15538.	1.5	8
39685	Designing Optoelectronic Properties by On-Surface Synthesis: Formation and Electronic Structure of an Ironâ€“Terpyridine Macromolecular Complex. ACS Nano, 2018, 12, 6545-6553.	7.3	13
39686	The stabilization mechanism and size effect of nonpolar-to-polar crystallography facet tailored ZnO nano/micro rods via a top-down strategy. Physical Chemistry Chemical Physics, 2018, 20, 18455-18462.	1.3	3
39687	A first-principles study of the electrically tunable band gap in few-layer penta-graphene. Physical Chemistry Chemical Physics, 2018, 20, 18110-18116.	1.3	14
39688	An electron compensation mechanism for the polymorphism of boron monolayers. Nanoscale, 2018, 10, 13410-13416.	2.8	19
39689	Electronic structure, bonding characteristics, and mechanical properties in (W_{2/3}Sc_{1/3})₂AlC and (W_{2/3}Y_{1/3})₂AlC i-MAX phases from first-principles calculations. Journal of Physics Condensed Matter, 2018, 30, 305502.	0.7	9
39690	Native point defects and impurities in hexagonal boron nitride. Physical Review B, 2018, 97, .	1.1	200
39691	Strong anomalous Nernst effect in collinear magnetic Weyl semimetals without net magnetic moments. Physical Review B, 2018, 97, .	1.1	34

#	Article	IF	Citations
39692	Substrate-determined exchange interactions between an STM tip and an adatom. Physical Review B, 2018, 97, .	1.1	0
39693	Multiple water layers on AnO2 {111}, {110}, and {100} surfaces (An = U, Pu): A computational study. Journal of Vacuum Science and Technology A: Vacuum, Surfaces and Films, 2018, 36, .	0.9	9
39694	Highâ€Mobility pâ€Type and nâ€Type Copper Nitride Semiconductors by Direct Nitriding Synthesis and In Silico Doping Design. Advanced Materials, 2018, 30, e1801968.	11.1	30
39695	Revisiting the Phase Stability in Ni-X (X=Mo, Ti, In) Systems Using Ab Initio Calculations. Journal of Phase Equilibria and Diffusion, 2018, 39, 584-591.	0.5	2
39696	Molecular Perspective of Gasâ€“Liquid Interfaces. , 2018, , 1-40.		1
39697	Control of surface potential and hydroxyapatite formation on TiO2 scales containing nitrogen-related defects. Acta Materialia, 2018, 155, 379-385.	3.8	9
39698	First-principles prediction of oxygen diffusivity near the <mml:math xmlns:mml="http://www.w3.org/1998/Math/MathML" altimg="si1.gif" overflow="scroll"><mml:mrow><mml:mrow><mml:mo>(</mml:mo><mml:mrow><mml:mn>10</mml:mn><mml:mo>¯</mml:mo></mml:mrow><mml:mn>12</mml:mn></mml:mrow></mml:mover) Tj twin boundary in titanium. Acta Materialia, 2018, 156, 11-19.	3.8	13
39699	Thermoelectric properties of TcX2(X=S, Se, Te). Journal of Alloys and Compounds, 2018, 764, 505-511.	2.8	6
39700	Formation of Fe-doped In2O3 nanowires and influence evolution of Fe ions on its photoluminescence property. Journal of Alloys and Compounds, 2018, 764, 861-868.	2.8	7
39701	Structural and electronic properties of point defects in Haeckelite GaN monolayer. Physica E: Low-Dimensional Systems and Nanostructures, 2018, 103, 289-293.	1.3	9
39702	Insight into the thermodynamic properties of tungsten disilicides. Vacuum, 2018, 155, 361-363.	1.6	19
39703	Structureâ€“Property Relationship of Low-Dimensional Layered GaSe_xTe_{1â€“x} Alloys. Chemistry of Materials, 2018, 30, 4226-4232.	3.2	16
39704	Hot-Atom-Mediated Dynamical Displacement of CO Adsorbed on Cu(111) by Incident H Atoms: An Ab Initio Molecular Dynamics Study. Journal of Physical Chemistry C, 2018, 122, 15485-15493.	1.5	6
39705	Role of disorder when upscaling magnetocaloric Ni-Co-Mn-Al Heusler alloys from thin films to ribbons. Scientific Reports, 2018, 8, 9147.	1.6	19
39706	Finite-size correction scheme for supercell calculations in Dirac-point two-dimensional materials. Scientific Reports, 2018, 8, 9348.	1.6	4
39707	Origins of possible synergistic effects in the interactions between metal atoms and MoS₂/graphene heterostructures for battery applications. Physical Chemistry Chemical Physics, 2018, 20, 18671-18677.	1.3	7
39708	A first-principles study on Si₂₄ as an anode material for rechargeable batteries. RSC Advances, 2018, 8, 20228-20233.	1.7	8
39709	Effects of H₂ and N₂ treatment for B₂H₆ dosing process on TiN surfaces during atomic layer deposition: an ab initio study. RSC Advances, 2018, 8, 21164-21173.	1.7	4

#	Article	IF	Citations
39710	Silicon-coordinated nitrogen-doped graphene as a promising metal-free catalyst for N₂O reduction by CO: a theoretical study. RSC Advances, 2018, 8, 22322-22330.	1.7	24
39711	The critical role of hydrogen on the stability of oxy-hydroxyl defect clusters in uranium oxide. Journal of Materials Chemistry A, 2018, 6, 11362-11369.	5.2	17
39712	Structural and electronic properties of Ga2O3-Al2O3 alloys. Applied Physics Letters, 2018, 112, .	1.5	198
39713	Topological Dirac semimetal phase in GexSny alloys. Applied Physics Letters, 2018, 112, .	1.5	10
39714	Flexible modulation of electronic and magnetic properties of zigzag H-MoS₂ nanoribbons by crack defects. Journal of Physics Condensed Matter, 2018, 30, 285302.	0.7	3
39715	Î²-tungsten: a promising metal for spintronics. Journal of Physics Condensed Matter, 2018, 30, 305802.	0.7	7
39716	Bifurcation and orientation-dependence of corrugation of 2D hexagonal boron nitride on palladium. 2D Materials, 2018, 5, 045001.	2.0	5
39717	Pressure and Strain Effects on the Structural, Electronic, and Optical Properties of K4 Phosphorus. Zeitschrift Fur Naturforschung - Section A Journal of Physical Sciences, 2018, 73, 661-668.	0.7	3
39718	Direct Observation at Room Temperature of the Orthorhombic Weyl Semimetal Phase in Thin Epitaxial MoTe₂. Advanced Functional Materials, 2018, 28, 1802084.	7.8	31
39719	Computational investigations of mechanical and dynamical properties of gold-based compounds (X3Au, Xâ€¯=â€¯Ti, Zr and V). Chinese Journal of Physics, 2018, 56, 1508-1514.	2.0	3
39720	Air-Stable Direct Bandgap Perovskite Semiconductors: All-Inorganic Tin-Based Heteroleptic Halides A_xSnCl_yI_z (A = Cs, Rb). Chemistry of Materials, 2018, 30, 4847-4856.	3.2	65
39721	Experimental and Theoretical Evidence of Enhanced Visible Light Photoelectrochemical and Photocatalytic Properties in MoS₂/TiO₂ Nanohole Arrays. Journal of Physical Chemistry C, 2018, 122, 15055-15062.	1.5	40
39722	Two-Dimensional Tetragonal Titanium Carbide: a High-Capacity and High-Rate Battery Material. Journal of Physical Chemistry C, 2018, 122, 15118-15124.	1.5	38
39723	p- and n-type Doping Effects on the Electrical and Ionic Conductivities of Li4Ti5O12 Anode Materials. Journal of Physical Chemistry C, 2018, 122, 15155-15162.	1.5	10
39724	First-Principles Calculations of the Rotational Motion and Hydrogen Bond Capability of Large Organic Cations in Hybrid Perovskites. Journal of Physical Chemistry C, 2018, 122, 15966-15972.	1.5	17
39725	Atomic Observation of Filling Vacancies in Monolayer Transition Metal Sulfides by Chemically Sourced Sulfur Atoms. Nano Letters, 2018, 18, 4523-4530.	4.5	83
39726	Enhanced Oxygen Reduction Activity by Selective Anion Adsorption on Non-Precious-Metal Catalysts. ACS Catalysis, 2018, 8, 7104-7112.	5.5	53
39727	A Monolayer of Hexagonal Boron Nitride on Ir(111) as a Template for Cluster Superlattices. ACS Nano, 2018, 12, 6871-6880.	7.3	31

#	Article	IF	Citations
39728	Double thermoelectric power factor of a 2D electron system. Nature Communications, 2018, 9, 2224.	5.8	48
39729	Heterointerface effects in the electrointercalation of van der Waals heterostructures. Nature, 2018, 558, 425-429.	13.7	184
39730	Ab initio inspired design of ternary boride thin films. Scientific Reports, 2018, 8, 9288.	1.6	54
39731	A new 3D Dirac nodal-line semi-metallic graphene monolith for lithium ion battery anode materials. Journal of Materials Chemistry A, 2018, 6, 13816-13824.	5.2	44
39732	Tuning the electronic and magnetic properties of graphene/h-BN hetero nanoribbon: A first-principles investigation. AIP Advances, 2018, 8, .	0.6	7
39733	Superior mechanical flexibility and strained-engineered direct-indirect band gap transition of green phosphorene. Applied Physics Letters, 2018, 112, .	1.5	25
39734	Titanium-hydrogen interaction at high pressure. Journal of Applied Physics, 2018, 123, 235901.	1.1	4
39735	Weak metal-metal transition in the vanadium oxytelluride <mml:math xmlns:mml="http://www.w3.org/1998/Math/MathML"><mml:mrow><mml:msub><mml:mi>Rb</mml:mi><mml:mrow><mml:mn>1</mml:mn> mathvariant="normal">V</mml:mi><mml:mn>2</mml:mn></mml:msub><mml:msub><mml:mi>Te</mml:mi><mml:mn>2</mml:mn> mathvariant="normal">O</mml:mi></mml:mrow></mml:math>. Physical Review B, 2018, 97, .	1.1	9
39736	Polarization fluctuations in the perovskite-structured ferroelectric <mml:math xmlns:mml="http://www.w3.org/1998/Math/MathML"><mml:mrow><mml:mi>AgNb</mml:mi><mml:msub><mml:mi mathvariant="normal">O</mml:mi><mml:mn>3</mml:mn></mml:msub></mml:mrow></mml:math>. Physical Review B, 2018, 97, .	1.1	20
39737	Strain-induced ferroelectricity and spin-lattice coupling in <mml:math xmlns:mml="http://www.w3.org/1998/Math/MathML"><mml:mrow><mml:mi>SrMn</mml:mi><mml:msub><mml:mi mathvariant="normal">O</mml:mi><mml:mn>3</mml:mn></mml:msub></mml:mrow></mml:math> thin films. Physical Review B, 2018, 97, .	1.1	51
39738	Structural and mechanistic revelations on high capacity cation-disordered Li-rich oxides for rechargeable Li-ion batteries. Energy Storage Materials, 2019, 16, 354-363.	9.5	94
39739	Rational synthesis of CaCo2O4 nanoplate as an earth-abundant electrocatalyst for oxygen evolution reaction. Journal of Energy Chemistry, 2019, 31, 125-131.	7.1	12
39740	Controlled Catalytic Energy Release of the Norbornadiene/Quadricyclane Molecular Solar Thermal Energy Storage System on Ni(111). Journal of Physical Chemistry C, 2019, 123, 7654-7664.	1.5	25
39741	Prediction and Characterization of NaGaS₂, A High Thermal Conductivity Mid-Infrared Nonlinear Optical Material for High-Power Laser Frequency Conversion. Inorganic Chemistry, 2019, 58, 93-98.	1.9	30
39742	Photocatalytic water splitting of (F, Ti) codoped heptazine/triazine based g-C3N4 heterostructure: A hybrid DFT study. Applied Surface Science, 2019, 463, 809-819.	3.1	39
39743	Ab initio phase diagrams of Hfâ€“O, Zrâ€“O and Yâ€“O: a comparative study. Faraday Discussions, 2019, 213, 321-337.	1.6	27
39744	A computational search for the zeta phase in the tantalum carbides. Journal of the American Ceramic Society, 2019, 102, 1454-1462.	1.9	13
39745	Forbidden Bandâ€Edge Excitons of Wurtziteâ€GaP: A Theoretical View. Physica Status Solidi (B): Basic Research, 2019, 256, 1800238.	0.7	15

#	Article	IF	Citations
39746	Atomic-registry-dependent electronic structures of sulfur vacancies in ReS2 studied by scanning tunneling microscopy/spectroscopy. Current Applied Physics, 2019, 19, 224-229.	1.1	6
39747	Effect of ceria and zirconia supports on NO reduction over platinum-group metal catalysts: A DFT study with comparative experiments. Catalysis Today, 2019, 332, 236-244.	2.2	20
39748	CO oxidation over BC₃ nanosheet: a theoretical study. Molecular Physics, 2019, 117, 125-135.	0.8	3
39749	The Surface Structure of Cu2O(100): Nature of Defects. Journal of Physical Chemistry C, 2019, 123, 7696-7704.	1.5	13
39750	Improved oxidation of hydrogen off-gas by hydrophobic surface modification: A multiscale density functional theory study. Particuology, 2019, 44, 28-35.	2.0	4
39751	Highâ€throughput computational screening of layered and twoâ€dimensional materials. Wiley Interdisciplinary Reviews: Computational Molecular Science, 2019, 9, e1385.	6.2	43
39752	Facet-Dependent Kinetics and Energetics of Hematite for Solar Water Oxidation Reactions. ACS Applied Materials & Interfaces, 2019, 11, 5616-5622.	4.0	46
39753	Intermetallics in catalysis: An exciting subset of multimetallic catalysts. Catalysis Today, 2019, 330, 2-15.	2.2	70
39754	Promising Graphene-Like Half-Metallic Nanosheets TM-InSe (TM = Mn, Fe, and Co) Induced by TM Adsorption. Journal of Superconductivity and Novel Magnetism, 2019, 32, 229-235.	0.8	1
39755	BaNb3.6O10 nanowires with superior electrochemical performance towards ultrafast and highly stable lithium storage. Energy Storage Materials, 2019, 16, 400-410.	9.5	43
39756	Rational design of graphitic-inorganic Bi-layer artificial SEI for stable lithium metal anode. Energy Storage Materials, 2019, 16, 426-433.	9.5	85
39757	A new six-dimensional potential energy surface for NO/Au(111). Molecular Physics, 2019, 117, 42-57.	0.8	6
39758	Ferroelectric and magnetoelectric origins of multiferroic SmCrO₃. Journal of the American Ceramic Society, 2019, 102, 267-274.	1.9	9
39759	Ab initio phase stabilities and mechanical properties of multicomponent alloys: A comprehensive review for high entropy alloys and compositionally complex alloys. Materials Characterization, 2019, 147, 464-511.	1.9	231
39760	Resistivity saturation in liquid ironâ€“light-element alloys at conditions of planetary cores from first principles computations. Comptes Rendus - Geoscience, 2019, 351, 154-162.	0.4	17
39761	On the kinetics of solvate formation through mechanochemistry. CrystEngComm, 2019, 21, 2097-2104.	1.3	14
39762	CO₂â€”H₂O Capture and Cyclability on Sodium Cobaltate at Low Temperatures (30â€“80ÂÂ°C): Experimental and Theoretical Analysis. Energy Technology, 2019, 7, 1800527.	1.8	4
39763	Theoretical Approach for Nanocarbon-Based Energy Catalyst Design. Nanostructure Science and Technology, 2019, , 159-174.	0.1	0

#	Article	IF	Citations
39764	Electronic and magnetic properties of 5d transition metal atoms doped blue phosphorene: First-principles study. Journal of Magnetism and Magnetic Materials, 2019, 469, 236-244.	1.0	24
39765	First-order grain boundary transformations in Au-doped Si: Hybrid Monte Carlo and molecular dynamics simulations verified by first-principles calculations. Scripta Materialia, 2019, 158, 11-15.	2.6	17
39766	Conductive CaSi2 transparent in the near infra-red range. Journal of Alloys and Compounds, 2019, 770, 710-720.	2.8	15
39767	Large modulation of interface magnetization and interface magnetoelectric effect in SrRuO3|KNbO3 oxide heterostructures: Prediction from first-principles study. Journal of Magnetism and Magnetic Materials, 2019, 469, 138-145.	1.0	5
39768	Phase transition, magnetic and electronic properties of iron mononitride: First-principles calculations. Journal of Alloys and Compounds, 2019, 771, 322-326.	2.8	10
39769	Magnetization on nitrogen in extended honeycomb carbon layers from first principles: Case studies of CxN (xâ€ =â€ 2, 6, 12). Journal of Magnetism and Magnetic Materials, 2019, 469, 46-51.	1.0	3
39770	Reconfiguring graphene for high-performance metal-ion battery anodes. Energy Storage Materials, 2019, 16, 619-624.	9.5	143
39771	Adverse effects of interlayer-gliding in layered transition-metal oxides on electrochemical sodium-ion storage. Energy and Environmental Science, 2019, 12, 825-840.	15.6	205
39772	Density-functional study of the La2Zr2O7 low-index surfaces. Surface Science, 2019, 689, 121235.	0.8	2
39773	Electronic and mechanical responses of two-dimensional HfS2, HfSe2, ZrS2, and ZrSe2 from first-principles. Frontiers of Structural and Civil Engineering, 2019, 13, 486-494.	1.2	41
39774	Elasticity and Anisotropy of the Pyrite-Type FeO2H-FeO2 System in Earthâ€™s Lowermost Mantle. Journal of Earth Science (Wuhan, China), 2019, 30, 1293-1301.	1.1	7
39775	Direct hydroxylation of benzene to phenol on h-BCN nanosheets in the presence of FeCl3 and H2O2 under visible light. Catalysis Today, 2019, 324, 73-82.	2.2	55
39776	Tautomerization of Phenol at the External Lewis Acid Sites of Scandium-, Iron- and Gallium-Substituted Zeolite MFI. Journal of Physical Chemistry C, 2019, 123, 7604-7614.	1.5	7
39777	Spontaneous Formation of Gold Cluster Anions on ZnO/Cu(111) Bilayer Films. Journal of Physical Chemistry C, 2019, 123, 7644-7653.	1.5	12
39778	Fabrication and photocatalytic performance of C, N, F-tridoped TiO2 nanotubes. Catalysis Today, 2019, 327, 182-189.	2.2	29
39779	Study of Li Adsorption on Graphdiyne Using Hybrid DFT Calculations. ACS Applied Materials & Interfaces, 2019, 11, 2677-2683.	4.0	33
39780	First principles investigation of topological phase in XMR material TmSb under hydrostatic pressure. Journal of Physics Condensed Matter, 2019, 31, 335401.	0.7	6
39781	The electronic properties of hydrogenated Janus MoSSe monolayer: a first principles investigation. Materials Research Express, 2019, 6, 105055.	0.8	10

#	Article	IF	Citations
39782	Optimizing electronic structure and charge transport of sulfur/potassium coâ€doped graphitic carbon nitride with efficient photocatalytic hydrogen evolution performance. Applied Organometallic Chemistry, 2019, 33, e5163.	1.7	16
39783	Insight into the Anchoring and Catalytic Effects of VO₂ and VS₂ Nanosheets as Sulfur Cathode Hosts for Liâ€“S Batteries. ChemSusChem, 2019, 12, 4671-4678.	3.6	50
39784	Formation, geometric properties, and surface activities of nSi clusters (nâ€‰=â€‰1â€‰â^'â€‰4) doped graphene as metal-free catalyst. Applied Physics A: Materials Science and Processing, 2019, 125, 1.	1.1	0
39785	Electronic and geometric factors affecting oxygen vacancy formation on CeO2(111) surfaces: A first-principles study from trivalent metal doping cases. Applied Surface Science, 2019, 497, 143732.	3.1	14
39786	Enhanced Generation of Reactive Oxygen Species under Visible Light Irradiation by Adjusting the Exposed Facet of FeWO₄ Nanosheets To Activate Oxalic Acid for Organic Pollutant Removal and Cr(VI) Reduction. Environmental Science & Technology, 2019, 53, 11023-11030.	4.6	160
39787	Enantiospecific Adsorption and Decomposition of Cysteine Enantiomers on the Chiral Cu{421}^R Surface. Journal of Physical Chemistry C, 2019, 123, 20829-20837.	1.5	8
39788	Two-Dimensional Covalent Crystals by Chemical Conversion of Thin van der Waals Materials. Nano Letters, 2019, 19, 6475-6481.	4.5	32
39789	Strain Engineering of a Defect-Free, Single-Layer MoS₂ Substrate for Highly Efficient Single-Atom Catalysis of CO Oxidation. ACS Applied Materials & Interfaces, 2019, 11, 32887-32894.	4.0	33
39790	A chiral molecular propeller designed for unidirectional rotations on a surface. Nature Communications, 2019, 10, 3742.	5.8	58
39791	Directly transforming copper (I) oxide bulk into isolated single-atom copper sites catalyst through gas-transport approach. Nature Communications, 2019, 10, 3734.	5.8	276
39792	Carboxylic acid induced near-surface restructuring of a magnetite surface. Communications Chemistry, 2019, 2, .	2.0	17
39793	Monitoring the electronic, thermal and optical properties of two-dimensional MoO₂ under strain via vibrational spectroscopies: a first-principles investigation. Physical Chemistry Chemical Physics, 2019, 21, 19904-19914.	1.3	24
39794	Heptazine-based porous graphitic carbon nitride: a visible-light driven photocatalyst for water splitting. Journal of Materials Chemistry A, 2019, 7, 20799-20805.	5.2	25
39795	A charge optimized many-body potential for iron/iron-fluoride systems. Physical Chemistry Chemical Physics, 2019, 21, 20118-20131.	1.3	4
39796	Prediction of strain-induced phonon-mediated superconductivity in monolayer YS. Journal of Materials Chemistry C, 2019, 7, 11184-11190.	2.7	11
39797	Pressure-induced phase transitions and superconductivity in a quasiâ€“1-dimensional topological crystalline insulator Î±-Bi ₄ Br ₄. Proceedings of the National Academy of Sciences of the United States of America, 2019, 116, 17696-17700.	3.3	36
39798	Rotational design of BP/XY₂ (Xâ€‰=â€‰Mo, W; Yâ€‰=â€‰S, Se) composites for overall photocat water-splitting. Journal of Physics Condensed Matter, 2019, 31, 465002.	0.7	10
39799	Ab initio study of optoelectronic and magnetic properties of Mn-doped ZnS with and without vacancy defects. Journal of Physics Condensed Matter, 2019, 31, 485706.	0.7	6

#	Article	IF	Citations
39800	van der Waals-corrected density functional study of electric field noise heating in ion traps caused by electrode surface adsorbates. New Journal of Physics, 2019, 21, 053043.	1.2	8
39801	Structural, Electronic, Stability, and Optical Properties of CsPb1â€“xSnxIBr2 Perovskites: A First-Principles Investigation. Journal of Physical Chemistry C, 2019, 123, 20476-20487.	1.5	23
39802	Charge-Carrier Enrichment at BaZrO₃/SrTiO₃ Interfaces. Journal of Physical Chemistry C, 2019, 123, 20808-20816.	1.5	7
39803	Indium-Doped TiO₂ Photocatalysts with High-Temperature Anatase Stability. Journal of Physical Chemistry C, 2019, 123, 21083-21096.	1.5	69
39804	Putting the Squeeze on Lead Chromate Nanorods. Journal of Physical Chemistry Letters, 2019, 10, 4744-4751.	2.1	6
39805	Tailored CsPbX₃ Nanorods for Electron-Emission Nanodevices. ACS Applied Nano Materials, 2019, 2, 5942-5951.	2.4	24
39806	Revealing the Active Sites of Pd Nanocrystals for Propyne Semihydrogenation: From Theory to Experiment. ACS Catalysis, 2019, 9, 8471-8480.	5.5	22
39807	Switching the Spin on a Ni Trimer within a Metalâ€“Organic Motif by Controlling the On-Top Bromine Atom. ACS Nano, 2019, 13, 9936-9943.	7.3	14
39808	High-throughput computation and evaluation of raman spectra. Scientific Data, 2019, 6, 135.	2.4	13
39809	Determining the structures, acidity and adsorption properties of Al substituted HZSM-5. Physical Chemistry Chemical Physics, 2019, 21, 18758-18768.	1.3	18
39810	A proton transfer mechanism along the PO₄ anion chain in the [Zn(HPO₄)(H₂PO₄)]^{2â^'} coordination polymer. Physical Chemistry Chemical Physics, 2019, 21, 18605-18611.	1.3	3
39811	Ultrafine CoO nanoparticles as an efficient cocatalyst for enhanced photocatalytic hydrogen evolution. Nanoscale, 2019, 11, 15633-15640.	2.8	44
39812	Single-atom molybdenum immobilized on photoactive carbon nitride as efficient photocatalysts for ambient nitrogen fixation in pure water. Journal of Materials Chemistry A, 2019, 7, 19831-19837.	5.2	108
39813	Emergence of superconductivity in a Dirac nodal-line Cu₂Si monolayer: ab initio calculations. Journal of Materials Chemistry C, 2019, 7, 10926-10932.	2.7	26
39814	A novel phosphotungstic acid-supported single metal atom catalyst with high activity and selectivity for the synthesis of NH₃ from electrochemical N₂ reduction: a DFT prediction. Journal of Materials Chemistry A, 2019, 7, 19838-19845.	5.2	69
39815	Stochastic wave packet approach to nonadiabatic scattering of diatomic molecules from metals. Journal of Chemical Physics, 2019, 150, 184105.	1.2	9
39816	Structural evolution in liquid GaIn eutectic alloy under high temperature and pressure. Journal of Applied Physics, 2019, 126, .	1.1	6
39817	Structural and topological phase transitions induced by strain in two-dimensional bismuth. Journal of Physics Condensed Matter, 2019, 31, 475001.	0.7	2

#	Article	IF	Citations
39818	Structural phase transitions in a <mml:math xmlns:mml="http://www.w3.org/1998/Math/MathML"><mml:mrow><mml:msub><mml:mi mathvariant="normal">MoWSe</mml:mi><mml:mn>2</mml:mn></mml:msub></mml:mrow></mml:math> monolayer: Molecular dynamics simulations and variational autoencoder analysis. Physical Review B, 2019, 100, .	1.1	10
39819	Confluence of structural distortion and <mml:math xmlns:mml="http://www.w3.org/1998/Math/MathML"><mml:mi>A</mml:mi></mml:math> -site composition in the band gaps of perovskite niobate and tantalate photocatalysts. Physical Review B, 2019, 100, .	1.1	3
39820	Symmetry-Protected Ideal Type-II Weyl Phonons in CdTe. Physical Review Letters, 2019, 123, 065501.	2.9	86
39821	Magnetic Properties of Hole-Doped Pyrochlore Iridate (Y₁₋_x₋_yCu_xCa_y₎₂_I Materials Science Forum, 2019, 966, 269-276.	0.8	1
39822	Effect of electric field on formation energies of point defects around metal/SiC and metal/GaN interfaces: first-principles study. Japanese Journal of Applied Physics, 2019, 58, 091006.	0.8	2
39823	Energetics and electronic structure of native point defects in Î±-Ga₂O₃. Applied Physics Express, 2019, 12, 091001.	1.1	35
39824	Scanning near-field optical microscopy based phase-change optical memory. Applied Physics Express, 2019, 12, 095002.	1.1	1
39825	Electronic, magnetic, and optical properties of Mn-doped GaSb: A first-principles study. Physica B: Condensed Matter, 2019, 572, 225-229.	1.3	5
39826	Unprecedented Piezoresistance Coefficient in Strained Silicon Carbide. Nano Letters, 2019, 19, 6569-6576.	4.5	62
39827	Towards rational catalyst design: boosting the rapid prediction of transition-metal activity by improved scaling relations. Physical Chemistry Chemical Physics, 2019, 21, 19269-19280.	1.3	29
39828	Structural versatility and electronic structures of copper(<scp>i</scp>) thiocyanate (CuSCN)â€“ligand complexes. Journal of Materials Chemistry C, 2019, 7, 12907-12917.	2.7	10
39829	Identification of turbostratic twisting in germanane. Journal of Materials Chemistry C, 2019, 7, 10092-10097.	2.7	4
39830	Embedded atom method potentials for La-Al-Ni ternary alloy. Journal of Applied Physics, 2019, 125, 245109.	1.1	2
39831	Space charge control of point defect spin states in AlN. Applied Physics Letters, 2019, 115, .	1.5	15
39832	Anisotropic interfacial properties of monolayer GeSeâ€”metal contacts. Semiconductor Science and Technology, 2019, 34, 095021.	1.0	7
39833	Mass Transfer and Reaction Kinetic Enhanced Electrode for Highâ€Performance Aqueous Flow Batteries. Advanced Functional Materials, 2019, 29, 1903192.	7.8	50
39834	Novel Pâ€Type Wide Bandgap Manganese Oxide Quantum Dots Operating at Deep UV Range for Optoelectronic Devices. Advanced Optical Materials, 2019, 7, 1900801.	3.6	35
39835	Flexible NO₂â€Functionalized Nâ€Heterocyclic Carbene Monolayers on Au (111) Surface. Chemistry - A European Journal, 2019, 25, 15067-15072.	1.7	39

#	Article	IF	Citations
39836	Unveiling the structures and electronic properties of CH3NH3PbI3 interfaces with TiO2, ZnO, and SnO2: a first-principles study. Journal of Materials Science, 2019, 54, 13594-13608.	1.7	5
39837	Experimental and theoretical investigation on the possible half-metallic behaviour of equiatomic quaternary Heusler alloys: CoRuMnGe and CoRuVZ (Zâ€¯=â€¯Al, Ga). Journal of Magnetism and Magnetic Materials, 2019, 492, 165662.	1.0	35
39838	Structural evolution of low-temperature liquid GaIn eutectic alloy. Journal of Molecular Liquids, 2019, 293, 111464.	2.3	7
39839	Linear Correlations between Adsorption Energies and HOMO Levels for the Adsorption of Small Molecules on TiO₂ Surfaces. Journal of Physical Chemistry C, 2019, 123, 20988-20997.	1.5	23
39840	Unidirectional Spinâ€“Orbit Interaction Induced by the Line Defect in Monolayer Transition Metal Dichalcogenides for High-Performance Devices. Nano Letters, 2019, 19, 6005-6012.	4.5	21
39841	pH-Dependent Distribution of Functional Groups on Titanium-Based MXenes. ACS Nano, 2019, 13, 9171-9181.	7.3	93
39842	Direct atomic insight into the role of dopants in phase-change materials. Nature Communications, 2019, 10, 3525.	5.8	56
39843	Probing the active sites of newly predicted stable Janus scandium dichalcogenides for photocatalytic water-splitting. Catalysis Science and Technology, 2019, 9, 4981-4989.	2.1	28
39844	Lattice-constant and band-gap tuning in wurtzite and zincblende BInGaN alloys. Journal of Applied Physics, 2019, 126, 055702.	1.1	4
39845	Hydroxylation of ZnO/Cu(1â€‰1â€‰1) inverse catalysts under ambient water vapor and the waterâ€“gas shift reaction. Journal Physics D: Applied Physics, 2019, 52, 454001.	1.3	8
39846	Nonadiabatic Effects in Raman Spectra of <mml:math xmlns:mml="http://www.w3.org/1998/Math/MathML" display="inline" overflow="scroll"><mml:msubsup><mml:mrow><mml:mi>Al</mml:mi><mml:mi>Cl</mml:mi></mml:mrow><mml:mn>4</mml:mn><mn -graphite Based Batteries. Physical Review Applied, 2019, 12, .	1.5	11
39847	Thermodynamically stabilized Î²-CsPbI ₃ â€“based perovskite solar cells with efficiencies >18%. Science, 2019, 365, 591-595.	6.0	963
39848	Electronic and optical properties of CsPb₂Br₅: A first-principles study. Modern Physics Letters B, 2019, 33, 1950266.	1.0	4
39849	Detwinning Mechanism for Nanotwinned Cubic Boron Nitride with Unprecedented Strength: A First-Principles Study. Nanomaterials, 2019, 9, 1117.	1.9	5
39850	Adsorption and Diffusion of Atoms of Groups 1, 2 and 13 Elements on Antimony Telluride Surface. Russian Physics Journal, 2019, 62, 512-518.	0.2	0
39851	Temperature dependent GrÃ¼neisen parameter. Science China Technological Sciences, 2019, 62, 1565-1576.	2.0	15
39852	Predicting the Strength of Metalâ€“Support Interaction with Computational Descriptors for Adhesion Energies. Journal of Physical Chemistry C, 2019, 123, 20443-20450.	1.5	20
39853	Methane Pyrolysis with a Molten Cuâ€“Bi Alloy Catalyst. ACS Catalysis, 2019, 9, 8337-8345.	5.5	112

#	Article	IF	Citations
39854	Structure and Reactivity of the Mo/ZSM-5 Dehydroaromatization Catalyst: An Operando Computational Study. ACS Catalysis, 2019, 9, 8731-8737.	5.5	52
39855	Tunable giant magnetoresistance in a single-molecule junction. Nature Communications, 2019, 10, 3599.	5.8	50
39856	Zigzag spin chains in the spin-5/2 antiferromagnet Ba₂Mn(PO₄)₂. Inorganic Chemistry Frontiers, 2019, 6, 2736-2746.	3.0	7
39857	Interaction of Oâ€“Y and Oâ€“Yâ€“Ti clusters embedded in bcc Fe with He, vacancies and self-interstitial atoms. Journal of Physics Condensed Matter, 2019, 31, 485702.	0.7	1
39858	Determining the Optimal Phase-Change Material via High-Throughput Calculations. MRS Advances, 2019, 4, 2679-2687.	0.5	4
39859	New Perspectives on the Electronic and Geometric Structure of Au70S20(PPh3)12 Cluster: Superatomic-Network Core Protected by Novel Au12(Âµ3-S)10 Staple Motifs. Nanomaterials, 2019, 9, 1132.	1.9	13
39860	Ni 1â€x Co x O y , Ni 1â€x Co x S y and Ni 1â€x Co x P y Catalysts Prepared from Ni 1â€x Co x â€ŽIFâ€67â€‰for Hydrogen Production by Electrolysis in Alkaline Media. ChemCatChem, 2019, 11, 5131-5138.	1.8	8
39861	Assessment of ductile character in superhard Ta-C-N thin films. Acta Materialia, 2019, 179, 17-25.	3.8	32
39862	Experimental and density functional theory investigations of catechol sensing properties of ZnO/RGO nanocomposites. Applied Surface Science, 2019, 495, 143588.	3.1	20
39863	Three-dimensional graphene networks modified with acetylenic linkages for high-performance optoelectronics and Li-ion battery anode material. Carbon, 2019, 154, 478-484.	5.4	10
39864	Rapid screening of ternary rare-earth â€“ Transition metal catalysts for dry reforming of methane and characterization of final structures. Journal of Catalysis, 2019, 377, 332-342.	3.1	16
39865	Elucidating Structureâ€“Spectral Property Relationships of Negative Thermal Expansion Zr₂(WO₄)(PO₄)₂: A First-Principles Study with Experimental Validation. Journal of Physical Chemistry C, 2019, 123, 21607-21616.	1.5	2
39866	Fast Energy Storage in Two-Dimensional MoO₂ Enabled by Uniform Oriented Tunnels. ACS Nano, 2019, 13, 9091-9099.	7.3	59
39867	Effect of surface termination on the lattice thermal conductivity of monolayer Ti3C2Tz MXenes. Journal of Applied Physics, 2019, 126, .	1.1	55
39868	Insight into the role of nitrogen in the phase-change material Sb. Journal Physics D: Applied Physics, 2019, 52, 455107.	1.3	6
39869	Raman spectroscopic evidence of impurityâ€induced structural distortion in SmB₆. Journal of Raman Spectroscopy, 2019, 50, 1661-1671.	1.2	16
39870	Effective cluster interactions and preâ€“precipitate morphology in binary Al-based alloys. Acta Materialia, 2019, 179, 70-84.	3.8	20
39871	Hydrogen storage in Na-decorated H4,4,4-graphyne: A density functional theory and Monte Carlo study. Applied Surface Science, 2019, 495, 143621.	3.1	20

#	Article	IF	Citations
39872	High temperatureâ€“high pressure phase transformation of Cu. Computational Materials Science, 2019, 170, 109154.	1.4	4
39873	Atomic-level insights in tuning defective structures for nitrogen photofixation over amorphous SmOCl nanosheets. Nano Energy, 2019, 65, 104003.	8.2	36
39874	High-performance corrosion-resistant fluorine-doped tin oxide as an alternative to carbon support in electrodes for PEM fuel cells. Nano Energy, 2019, 65, 104008.	8.2	31
39875	Investigating behavior of hydrogen in zirconium by first-principles: From dissolution, diffusion to the interaction with vacancy. Nuclear Instruments & Methods in Physics Research B, 2019, 458, 1-6.	0.6	5
39876	Tuning the electronic and magnetic properties of zigzag silicene nanoribbons by 585 defects. Physics Letters, Section A: General, Atomic and Solid State Physics, 2019, 383, 125869.	0.9	6
39877	Coordination-Engineered Cuâ€“N_x Single-Site Catalyst for Enhancing Oxygen Reduction Reaction. ACS Applied Energy Materials, 2019, 2, 6497-6504.	2.5	58
39878	Study of Higher Discharge Capacity, Phase Transition, and Relative Structural Stability in Li₂FeSiO₄ Cathode upon Lithium Extraction Using an Experimental and Theoretical Approach and Full Cell Prototype Study. ACS Applied Energy Materials, 2019, 2, 6584-6598.	2.5	21
39879	A Prolific Solvate Former, Galunisertib, under the Pressure of Crystal Structure Prediction, Produces Ten Diverse Polymorphs. Journal of the American Chemical Society, 2019, 141, 13887-13897.	6.6	109
39880	Prediction of C₇N₆ and C₉N₄: stable and strong porous carbon-nitride nanosheets with attractive electronic and optical properties. Journal of Materials Chemistry C, 2019, 7, 10908-10917.	2.7	57
39881	High-efficiency spin polarization in electron transport through the graphene nanoribbon coupled to chromium triiodide. Journal Physics D: Applied Physics, 2019, 52, 435304.	1.3	2
39882	3D graphene-cellulose nanofiber hybrid scaffolds for cortical reconstruction in brain injuries. 2D Materials, 2019, 6, 045043.	2.0	14
39883	First-Principle Computed Structural and Thermodynamic Properties of Cu2ZnSn(SxSe1â^'x)4 Pentanary Solid Solution. Journal of Electronic Materials, 2019, 48, 6991-7002.	1.0	5
39884	Enhanced cyclability and safety performance of LiNi0.6Co0.2Mn0.2O2 at elevated temperature by AlPO4 modification. Journal of Alloys and Compounds, 2019, 810, 151834.	2.8	28
39885	First-principles study of metal-semiconductor contact between MX2 (Mâ€¯=â€¯Nb, Pt; Xâ€¯=â€¯S, Se) monolayers. Physics Letters, Section A: General, Atomic and Solid State Physics, 2019, 383, 125867.	0.9	8
39886	De Haasâ€“van Alphen study on three-dimensional topological semimetal pyrite PtBi2. Science Bulletin, 2019, 64, 1496-1501.	4.3	4
39887	Tailored Plasmons in Pentacene/Graphene Heterostructures with Interlayer Electron Transfer. Nano Letters, 2019, 19, 6058-6064.	4.5	19
39888	Micropore-confined amorphous SnO₂ subnanoclusters as robust anode materials for Na-ion capacitors. Journal of Materials Chemistry A, 2019, 7, 21711-21721.	5.2	32
39889	Surface chemistry and reactivity of Î±-MoO3 toward methane: A SCAN-functional based DFT study. Journal of Chemical Physics, 2019, 151, 044708.	1.2	14

#	Article	IF	Citations
39890	Extraordinarily large kinetic isotope effect on alkene hydrogenation over Rh-based intermetallic compounds. Science and Technology of Advanced Materials, 2019, 20, 805-812.	2.8	6
39891	Highly Ordered Nâ€Ðoped Carbon Dots Photosensitizer on Metalâ€“Organic Frameworkâ€Ðecorated ZnO Nanotubes for Improved Photoelectrochemical Water Splitting. Small, 2019, 15, e1902771.	5.2	66
39892	TiN and TiC as stable and promising supports for oxygen reduction reaction: Theoretical and experimental study. Applied Surface Science, 2019, 495, 143620.	3.1	15
39893	Bonding structure and etching characteristics of amorphous carbon for a hardmask deposited by DC sputtering. Carbon, 2019, 154, 277-284.	5.4	12
39894	Theoretical studies on the hydrous lower mantle and Dâ€³ layer minerals. Earth and Planetary Science Letters, 2019, 525, 115753.	1.8	4
39895	Structural, elastic, electronic and vibrational properties of XAl2O4 (XÂ=ÂCa, Sr and Cd) semiconductors with orthorhombic structure. Journal of Alloys and Compounds, 2019, 809, 151773.	2.8	9
39896	Topological-magnetic proximity effect in Sb2Te3/CrI3 heterostructures. Physica B: Condensed Matter, 2019, 573, 77-80.	1.3	7
39897	Hydride Conductivity in an Anion-Ordered Fluorite Structure LnHO with an Enlarged Bottleneck. Chemistry of Materials, 2019, 31, 7360-7366.	3.2	52
39898	Engineering of K₃YSi₂O₇ To Tune Photoluminescence with Selected Activators and Site Occupancy. Chemistry of Materials, 2019, 31, 7770-7778.	3.2	89
39899	Mechanism of Photocatalytic Reduction of CO₂ by Ag₃PO₄(111)/g-C₃N₄ Nanocomposite: A First-Principles Study. Journal of Physical Chemistry C, 2019, 123, 22191-22201.	1.5	38
39900	Dissociative Chemisorption of Methane on Stepped Ir(332) Surface: Density Functional Theory and Ab Initio Molecular Dynamics Studies. Journal of Physical Chemistry C, 2019, 123, 20893-20902.	1.5	12
39901	Oxidation Mechanism on One-Dimensional Pt-Induced Nanowires on Ge(001). Journal of Physical Chemistry C, 2019, 123, 21645-21650.	1.5	2
39902	Spectroscopically Resolved Binding Sites for the Adsorption of Sarin Gas in a Metalâ€“Organic Framework: Insights beyond Lewis Acidity. Journal of Physical Chemistry Letters, 2019, 10, 5142-5147.	2.1	24
39903	Boron Nitride Nanotube Nucleation via Network Fusion during Catalytic Chemical Vapor Deposition. Journal of the American Chemical Society, 2019, 141, 13385-13393.	6.6	23
39904	Novel two-dimensional tetragonal vanadium carbides and nitrides as promising materials for Li-ion batteries. Physical Chemistry Chemical Physics, 2019, 21, 19513-19520.	1.3	26
39905	Ammonium salt conversion towards Mn4+ doped (NH4)2NaScF6 narrow-band red-emitting phosphor. Journal of Alloys and Compounds, 2019, 811, 151945.	2.8	12
39906	Theoretical investigation on electronic and optical properties of the graphene-MoSe2-graphene sandwich heterostructure. Materials and Design, 2019, 183, 108129.	3.3	31
39907	Revealing the structural, electronic and optical properties of lead-free perovskite derivatives of Rb2SnX6(Xâ€¯=â€¯Cl, Br and I): A theory calculation. Solar Energy, 2019, 190, 272-277.	2.9	50

#	Article	IF	Citations
39908	Spinodal Decomposition During Anion Exchange in Colloidal Mn²⁺-Doped CsPbX₃ (X = Cl, Br) Perovskite Nanocrystals. Chemistry of Materials, 2019, 31, 7711-7722.	3.2	36
39909	Photoinduced Carrier Dynamics at the Interface of Pentacene and Molybdenum Disulfide. Journal of Physical Chemistry A, 2019, 123, 7693-7703.	1.1	22
39910	Adsorption of Formic Acid on CH3NH3PbI3 Leadâ€“Halide Organicâ€“Inorganic Perovskites. Journal of Physical Chemistry C, 2019, 123, 22873-22886.	1.5	5
39911	Material Consequences of Hydrogen Dissolution in Palladium Alloys Observed from First Principles. Journal of Physical Chemistry C, 2019, 123, 22158-22171.	1.5	8
39912	Investigation of Stacking Effects of Bilayer MoSSe on Photocatalytic Water Splitting. Journal of Physical Chemistry C, 2019, 123, 22570-22577.	1.5	41
39913	Encapsulating MnSe Nanoparticles Inside 3D Hierarchical Carbon Frameworks with Lithium Storage Boosted by in Situ Electrochemical Phase Transformation. ACS Applied Materials & Interfaces, 2019, 11, 33022-33032.	4.0	40
39914	The Key Role of Support Surface Hydrogenation in the CH₄ to CH₃OH Selective Oxidation by a ZrO₂-Supported Single-Atom Catalyst. ACS Catalysis, 2019, 9, 8903-8909.	5.5	65
39915	Multiscale Buffering Engineering in Siliconâ€“Carbon Anode for Ultrastable Li-Ion Storage. ACS Nano, 2019, 13, 10179-10190.	7.3	73
39916	Controlled Growth of Large-Area Bilayer Tungsten Diselenides with Lateral Pâ€“N Junctions. ACS Nano, 2019, 13, 10490-10498.	7.3	39
39917	Oxygen Evolution Reaction (OER) on Clean and Oxygen Deficient Low-Index SrTiO₃ Surfaces: A Theoretical Systematic Study. ACS Sustainable Chemistry and Engineering, 2019, 7, 15346-15353.	3.2	16
39918	Strain-tunable CO₂ storage by black phosphorene and Î±-PC from combined first principles and molecular dynamics studies. Physical Chemistry Chemical Physics, 2019, 21, 20107-20117.	1.3	11
39919	Electronic and optical properties of GaNâ€“MoS₂ heterostructure from first-principles calculations*. Chinese Physics B, 2019, 28, 086104.	0.7	9
39920	Visualization of point defects in ultrathin layered 1T-PtSe ₂. 2D Materials, 2019, 6, 041005.	2.0	52
39921	Two-dimensional Weyl half-semimetal and tunable quantum anomalous Hall effect. Physical Review B, 2019, 100, .	1.1	101
39922	Interplay between in-plane and flexural phonons in electronic transport of two-dimensional semiconductors. Physical Review B, 2019, 100, .	1.1	11
39923	Ballistic thermoelectric properties of monolayer semiconducting transition metal dichalcogenides and oxides. Physical Review B, 2019, 100, .	1.1	60
39924	Grain-boundary corrosion of nickel-based alloy by synchrotron radiation technology. Surface Innovations, 2019, 7, 278-283.	1.4	3
39925	The Reactivity of Ambident Nucleophiles: Marcus Theory or Hard and Soft Acids and Bases Principle?. Journal of Computational Chemistry, 2019, 40, 2761-2777.	1.5	12

#	Article	IF	Citations
39926	Deactivation reactions on a commercial lean nox-trap - Effect of hydrocarbon nature, concentration and operation temperature. Applied Catalysis A: General, 2019, 585, 117178.	2.2	3
39927	Controllable synthesis of cerium zirconium oxide nanocomposites and their application for photocatalytic degradation of sulfonamides. Applied Catalysis B: Environmental, 2019, 259, 118107.	10.8	57
39928	Intrinsic photoluminescence of amine-functionalized graphene derivatives for bioimaging applications. Applied Materials Today, 2019, 17, 112-122.	2.3	25
39929	Interfacial charge transfers and interactions drive rectifying and negative differential resistance behaviors in InAs/graphene van der Waals heterostructure. Applied Surface Science, 2019, 496, 143629.	3.1	29
39930	Motif-Based Design of an Oxysulfide Class of Lithium Superionic Conductors: Toward Improved Stability and Record-High Li-Ion Conductivity. Chemistry of Materials, 2019, 31, 7265-7276.	3.2	25
39931	Enhanced N₂-Fixation by Engineering the Edges of Two-Dimensional Transition-Metal Disulfides. Journal of Physical Chemistry C, 2019, 123, 22221-22227.	1.5	53
39932	Prediction of the Reactivity of Argon with Xenon under High Pressures. ACS Omega, 2019, 4, 13640-13644.	1.6	4
39933	Unlocking the key to persistent luminescence with X-ray absorption spectroscopy: a local structure investigation of Cr-substituted spinel-type phosphors. Physical Chemistry Chemical Physics, 2019, 21, 19349-19358.	1.3	6
39934	CO2 adsorption on hydroxylated In2O3(110). Physical Chemistry Chemical Physics, 2019, 21, 21698-21708.	1.3	23
39935	Catalytic manganese oxide nanostructures for the reverse water gas shift reaction. Nanoscale, 2019, 11, 16677-16688.	2.8	31
39936	Migration of carbon from Ga sites to N sites in GaN: a combined PAS and hybrid DFT study. Japanese Journal of Applied Physics, 2019, 58, 090901.	0.8	6
39937	Site-Dependent Activity and Selectivity of H₂O₂ Formation from H₂ and O₂ over Au-Based Catalysts. Industrial & Engineering Chemistry Research, 2019, 58, 15119-15126.	1.8	15
39938	Neutron Spectroscopic and Thermochemical Characterization of Lithiumâ€“Aluminum-Layered Double Hydroxide Chloride: Implications for Lithium Recovery. Journal of Physical Chemistry C, 2019, 123, 20723-20729.	1.5	20
39939	Uncovering the Surface and Phase Effect of Molybdenum Carbides on Hydrogen Evolution: A First-Principles Study. Journal of Physical Chemistry C, 2019, 123, 21878-21887.	1.5	23
39940	Giant Band Gap Reduction and Insulatorâ€“Metal Transition in Two-Dimensional InX (X = Cl, Br, I) Layers. Journal of Physical Chemistry C, 2019, 123, 21763-21767.	1.5	5
39941	Ab Initio Study of the Early Stage of Si Epitaxy on the Chlorinated Si(100) Surface. Journal of Physical Chemistry C, 2019, 123, 19806-19811.	1.5	8
39942	Surface-Plasmon-Induced Ammonia Decomposition on Copper: Excited-State Reaction Pathways Revealed by Embedded Correlated Wavefunction Theory. ACS Nano, 2019, 13, 9944-9957.	7.3	38
39943	Intrinsic doping limit and defect-assisted luminescence in Cs₄PbBr₆. Journal of Materials Chemistry A, 2019, 7, 20254-20261.	5.2	48

#	Article	IF	Citations
39944	Nudged elastic band method for solid-solid transition under finite deformation. Journal of Chemical Physics, 2019, 151, .	1.2	14
39945	Strong Electronic Interaction of Amorphous Fe₂O₃ Nanosheets with Singleâ€Atom Pt toward Enhanced Carbon Monoxide Oxidation. Advanced Functional Materials, 2019, 29, 1904278.	7.8	51
39946	Inâ€...Operando Visualization of the Electrochemical Formation of Liquid Polybromide Microdroplets. Angewandte Chemie - International Edition, 2019, 58, 15228-15234.	7.2	27
39947	Electrodeposition of Silver Vanadate Films: A Tale of Two Polymorphs. ChemPhysChem, 2019, 20, 2635-2646.	1.0	10
39948	Synthesis and Characterization of Sodiumâ€“Iron Antimonate Na2FeSbO5: One-Dimensional Antiferromagnetic Chain Compound with a Spin-Glass Ground State. Inorganic Chemistry, 2019, 58, 11333-11350.	1.9	8
39949	On the Origin of the Negative Thermal Expansion Behavior of YCu. Inorganic Chemistry, 2019, 58, 11819-11827.	1.9	0
39950	Carrier Lifetimes and Recombination Pathways in Metalâ€“Organic Frameworks. Journal of Physical Chemistry Letters, 2019, 10, 5041-5046.	2.1	14
39951	Effects of Ni and Cu Antisite Substitution on the Phase Stability of CuGa2 from Liquid Ga/Cuâ€“Ni Interfacial Reaction. ACS Applied Materials & Interfaces, 2019, 11, 32523-32532.	4.0	10
39952	Seismic velocities of CaSiO3 perovskite can explain LLSVPs in Earthâ€™s lower mantle. Nature, 2019, 572, 643-647.	13.7	52
39953	Realizing giant tunneling electroresistance in two-dimensional graphene/BiP ferroelectric tunnel junction. Nanoscale, 2019, 11, 16837-16843.	2.8	35
39954	Improved thermoelectric performance of bilayer Bi₂O₂Se by the band convergence approach. Journal of Materials Chemistry C, 2019, 7, 11029-11039.	2.7	53
39955	Strain tunable spin reorientation of an individual Fe atom on 2D blue phosphorous. Journal of Physics Condensed Matter, 2019, 31, 485802.	0.7	3
39956	Computational characterization of the structural and mechanical properties of Al x CoCrFeNiTi1â^'x high entropy alloys. Materials Research Express, 2019, 6, 096519.	0.8	7
39957	Dental Resin Monomer Enables Unique NbO₂/Carbon Lithiumâ€Ion Battery Negative Electrode with Exceptional Performance. Advanced Functional Materials, 2019, 29, 1904961.	7.8	26
39958	Iterative-Learning Strategy for the Development of Application-Specific Atomistic Force Fields. Journal of Physical Chemistry C, 2019, 123, 20715-20722.	1.5	20
39959	p-Type Conductivity of Hydrated Amorphous V₂O₅ and Its Enhanced Photocatalytic Performance in ZnO/V₂O₅/rGO. ACS Applied Electronic Materials, 2019, 1, 1881-1889.	2.0	13
39960	Rationalizing the interphase stability of Li|doped-Li₇La₃Zr₂O₁₂via automated reaction screening and machine learning. Journal of Materials Chemistry A, 2019, 7, 19961-19969.	5.2	59
39961	Phenethylammonium bismuth halides: from single crystals to bulky-organic cation promoted thin-film deposition for potential optoelectronic applications. Journal of Materials Chemistry A, 2019, 7, 20733-20741.	5.2	38

#	Article	IF	Citations
39962	A three dimensional numerical quantum mechanical model of field electron emission from metallic surfaces covered with carbon adsorbates. Journal of Applied Physics, 2019, 126, .	1.1	7
39963	Highly stable hybrid perovskite light-emitting diodes based on Dion-Jacobson structure. Science Advances, 2019, 5, eaaw8072.	4.7	188
39964	Viscosity and Prandtl Number of Warm Dense Water as in Ice Giant Planets. Astrophysical Journal, 2019, 881, 81.	1.6	11
39965	Highâ€Order Shift Current Induced Terahertz Emission from Inorganic Cesium Bromine Lead Perovskite Engendered by Twoâ€Photon Absorption. Advanced Functional Materials, 2019, 29, 1904694.	7.8	26
39966	Theoretical Evidence on the Confinement Effect of Pt@UiO-66-NH₂ for Cinnamaldehyde Hydrogenation. Journal of Physical Chemistry C, 2019, 123, 22114-22122.	1.5	28
39967	Understanding the origin of disorder in kesterite-type chalcogenides A₂ZnBQ₄ (A = Cu, Ag; B = Sn, Ge; Q = S, Se): the influence of inter-layer interactions. Physical Chemistry Chemical Physics, 2019, 21, 19311-19317.	1.3	16
39968	Design triple points, nexus points, and related topological phases by stacking monolayers. Applied Physics Letters, 2019, 115, 073105.	1.5	3
39969	First-principles study of the band gap tuning and doping control in CdSe_xTe_{1â^'x} alloy for high efficiency solar cell*. Chinese Physics B, 2019, 28, 086106.	0.7	50
39970	Inâ€…Operando Visualization of the Electrochemical Formation of Liquid Polybromide Microdroplets. Angewandte Chemie, 2019, 131, 15372-15378.	1.6	5
39971	Thermoradiative Cells Based on a p-type Cu3SbSe4 Semiconductor: Application of a Detailed Balance Model. Journal of Electronic Materials, 2019, 48, 6777-6785.	1.0	4
39972	Strong metalâ€“metal interaction and bonding nature in metal/oxide interfaces with large mismatches. Acta Materialia, 2019, 179, 237-246.	3.8	13
39973	First-principles design of highly-efficient earth-abundant electrocatalysts for hydrogen evolution reaction: TiF3 and its analogs. Applied Surface Science, 2019, 495, 143623.	3.1	13
39974	The tunable ferroelectricity and piezoelectricity of the KNN piezoceramics by Na concentrations: First-principles calculations. Journal of the European Ceramic Society, 2019, 39, 5252-5259.	2.8	12
39975	DFT + U and Low-Temperature XPS Studies of Fe-Depleted Chalcopyrite (CuFeS₂) Surfaces: A Focus on Polysulfide Species. Journal of Physical Chemistry C, 2019, 123, 21031-21041.	1.5	29
39976	Engineering Surface Structure of Spinel Oxides via High-Valent Vanadium Doping for Remarkably Enhanced Electrocatalytic Oxygen Evolution Reaction. ACS Applied Materials & Interfaces, 2019, 11, 33012-33021.	4.0	70
39977	High temperature shockwave stabilized single atoms. Nature Nanotechnology, 2019, 14, 851-857.	15.6	278
39978	Catalyst deactivation via decomposition into single atoms and the role of metal loading. Nature Catalysis, 2019, 2, 748-755.	16.1	171
39979	Effects of vacancies and p-doping on the optoelectronic properties of Cu- and Ag-based transparent conducting oxides. Journal of Applied Physics, 2019, 126, .	1.1	8

#	Article	IF	Citations
39980	Experimental determination of the electro-acoustic properties of thin film AlScN using surface acoustic wave resonators. Journal of Applied Physics, 2019, 126, .	1.1	65
39981	Electrochromic properties of Li4Ti5O12: From visible to infrared spectrum. Applied Physics Letters, 2019, 115, .	1.5	30
39982	Ab initio-informed phase-field modeling of dislocation core structures in equal-molar CoNiRu multi-principal element alloys. Modelling and Simulation in Materials Science and Engineering, 2019, 27, 084001.	0.8	23
39983	Platinum vs transition metal carbide surfaces as catalysts for olefin and alkyne conversion: binding and hydrogenation of ethylidyne. Journal of Physics: Conference Series, 2019, 1247, 012003.	0.3	5
39984	Magnetic Proximity Effect in a van der Waals MoirÃ© Superlattice. Physical Review Applied, 2019, 12, .	1.5	26
39985	Composition dependence of the charge-driven phase transition in group-VI transition metal dichalcogenides. Physical Review B, 2019, 100, .	1.1	12
39986	Effect of stacking structure on lithium adsorption and diffusion in bilayer black phosphorene. Physical Review B, 2019, 100, .	1.1	11
39987	Single pair of Weyl fermions in the half-metallic semimetal <mml:math xmlns:mml="http://www.w3.org/1998/Math/MathML"><mml:mrow><mml:mi>EuC</mml:mi><mml:msub><mml:mi mathvariant="normal">d</mml:mi><mml:mn>2</mml:mn></mml:msub><mml:mi mathvariant="normal">A</mml:mi><mml:msub><mml:mi mathvariant="normal">s</mml:mi><mml:mn>2</mml:mn></mml:msub></mml:mrow></mml:math>. Physical Review B, 2019, 99, .	1.1	83
39988	Titanium Trisulfide as Sensitive Gas Sensor. , 2019, , .		0
39989	The Eigenvalues Slicing Library (EVSL): Algorithms, Implementation, and Software. SIAM Journal of Scientific Computing, 2019, 41, C393-C415.	1.3	23
39990	Tuning the electronic and magnetic properties of Mn-doped graphene by gas adsorption and effect of external electric field: First-principles study. International Journal of Modern Physics B, 2019, 33, 1950166.	1.0	5
39991	Phase Diagram of FÐµâ€“Al Alloys: A Study from First Principles. Bulletin of the Russian Academy of Sciences: Physics, 2019, 83, 844-846.	0.1	3
39992	Formation Mechanism, Geometric Stability and Catalytic Activity of a Single Iron Atom Supported on Nâ€Ðoped Graphene. ChemPhysChem, 2019, 20, 2506-2517.	1.0	14
39993	Electronic properties of size-dependent MoTe 2 /WTe 2 heterostructure. Chinese Physics B, 2019, 28, 107101.	0.7	10
39994	Domain walls in strontium titanate. Journal of Physics: Conference Series, 2019, 1252, 012006.	0.3	2
39995	First-principles calculations of the atomic structure and electronic states of <mml:math xmlns:mml="http://www.w3.org/1998/Math/MathML"><mml:mrow><mml:msub><mml:mi>Li</mml:mi><mml:mi>x</mml:mi></mml:msub><mml:msub><mml:mi>Ir</mml:mi><mml:mn>3</mml:mn></mml:msub></mml:mrow></mml:math> Physical Review B, 2019, 100, .	1.1	13
39996	Sound velocity, shear modulus, and shock melting of beryllium along the Hugoniot. Physical Review B, 2019, 100, .	1.1	17
39997	Pressure-induced structural dimerization in the hyperhoneycomb iridate <mml:math xmlns:mml="http://www.w3.org/1998/Math/MathML"><mml:mi>Î²</mml:mi><mml:mtext>â€™</mml:mtext><mml:mi>Li</mml:mi><mml:msub><mml:mi>IrO</mml:mi><mml:mn>3</mml:mn></mml:msub></mml:math> at low temperatures. Physical Review B, 2019, 100, .	1.1	14

#	Article	IF	Citations
39998	Stability, efficiency, and mechanism of <mml:math xmlns:mml="http://www.w3.org/1998/Math/MathML"><mml:mi>n</mml:mi></mml:math> -type doping by hydrogen adatoms in two-dimensional transition metal dichalcogenides. Physical Review B, 2019, 100, .	1.1	12
39999	Influences of spin-orbit coupling on Fermi surfaces and Dirac cones in ferroelectriclike polar metals. Physical Review B, 2019, 99, .	1.1	6
40000	Predicting the electron affinity of ZnSiP2 semiconductor from first-principle calculations. , 2019, , .		0
40001	Impact of Dopants (Al, Mg, Mn, Co) on the Reactivity of Li_xNiO₂Âwith the Electrolyte of Li-Ion Batteries. Journal of the Electrochemical Society, 2019, 166, A2826-A2833.	1.3	46
40002	Optomechanical control of stacking patterns of h-BN bilayer. Nano Research, 2019, 12, 2634-2639.	5.8	20
40003	Interfacial Electronic Properties Dictate Li Dendrite Growth in Solid Electrolytes. Chemistry of Materials, 2019, 31, 7351-7359.	3.2	165
40004	Auxetic B₄N Monolayer: A Promising 2D Material with in-Plane Negative Poissonâ€™s Ratio and Large Anisotropic Mechanics. ACS Applied Materials & Interfaces, 2019, 11, 33231-33237.	4.0	67
40005	Protecting the Nanoscale Properties of Ag Nanowires with a Solution-Grown SnO₂ Monolayer as Corrosion Inhibitor. Journal of the American Chemical Society, 2019, 141, 13977-13986.	6.6	45
40006	Improving selectivity of CO reduction via reducing the coordination of critical intermediates. Journal of Materials Chemistry A, 2019, 7, 24000-24004.	5.2	14
40007	Toward obtaining 2D and 3D and 1D PtPN with pentagonal pattern. Journal of Materials Science, 2019, 54, 14029-14037.	1.7	4
40008	Understanding the catalytic mechanisms of CO2 hydrogenation to methanol on unsupported and supported Ga-Ni clusters. Applied Energy, 2019, 253, 113623.	5.1	34
40009	A bismuth rich hollow Bi4O5Br2 photocatalyst enables dramatic CO2 reduction activity. Nano Energy, 2019, 64, 103955.	8.2	156
40010	Adsorption and Decomposition of Ethanol on Cu₂O(111) and (100). Journal of Physical Chemistry C, 2019, 123, 20384-20392.	1.5	11
40011	Electrocatalytic Production of H₂O₂ by Selective Oxygen Reduction Using Earth-Abundant Cobalt Pyrite (CoS₂). ACS Catalysis, 2019, 9, 8433-8442.	5.5	167
40012	Lattice doping regulated interfacial reactions in cathode for enhanced cycling stability. Nature Communications, 2019, 10, 3447.	5.8	116
40013	Coverage dependent structure and energy of water dissociative adsorption on clean and O-pre-covered Ni (100) and Ni(110). Catalysis Science and Technology, 2019, 9, 4725-4743.	2.1	8
40014	One-dimensional nearly free electron states in borophene. Nanoscale, 2019, 11, 15605-15611.	2.8	25
40015	NMR shifts in aluminosilicate glasses via machine learning. Physical Chemistry Chemical Physics, 2019, 21, 21709-21725.	1.3	25

#	Article	IF	Citations
40016	Evidence of a purely electronic two-dimensional lattice at the interface of TMD/Bi₂Se₃ heterostructures. Nanoscale, 2019, 11, 15929-15938.	2.8	21
40017	Electronic and magnetic properties of a black phosphorene/Tl2S heterostructure with transition metal atom intercalation: a first-principles study. RSC Advances, 2019, 9, 19418-19428.	1.7	2
40018	Understanding the phase dependent energy storage performance of MnO2 nanostructures. Journal of Applied Physics, 2019, 126, .	1.1	13
40019	Crystal Structure and Mechanical Properties of ThBC2. Crystals, 2019, 9, 389.	1.0	2
40020	Flexible Smart Noncontact Control Systems with Ultrasensitive Humidity Sensors. Small, 2019, 15, e1902801.	5.2	110
40021	Density functional theory study of NOx adsorption on alkaline earth metal oxide and transition metal surfaces. Korean Journal of Chemical Engineering, 2019, 36, 1258-1266.	1.2	7
40022	Unravelling the effects of layered supports on Ru nanoparticles for enhancing N2 reduction in photocatalytic ammonia synthesis. Applied Catalysis B: Environmental, 2019, 259, 118026.	10.8	36
40023	Intrinsic factors affecting the catalytic activity of doped TiC as potential cathode in Li-O2 batteries. Applied Surface Science, 2019, 494, 983-988.	3.1	10
40024	Tunable magnetic and half-metallic properties of the two-dimensional electron gas in LaAlO3/SrTiO3(111) heterostructures. Physical Chemistry Chemical Physics, 2019, 21, 18170-18178.	1.3	4
40025	Functions of hydroxyapatite in fabricating N-doped carbon for excellent catalysts and supercapacitors. Catalysis Science and Technology, 2019, 9, 4952-4960.	2.1	11
40026	Theoretical insights into nitrogen fixation on Ti₂C and Ti₂CO₂ in a lithiumâ€“nitrogen battery. Journal of Materials Chemistry A, 2019, 7, 19950-19960.	5.2	21
40027	Thickness dependence of anomalous Hall conductivity in L1₀-FePt thin film. Journal Physics D: Applied Physics, 2019, 52, 43LT02.	1.3	5
40028	Enhanced low-temperature Li-ion storage in MXene titanium carbide by surface oxygen termination. 2D Materials, 2019, 6, 045025.	2.0	46
40029	The good performance of bilayer Î²-antimoneneas an anode material for the Li-ion battery study. Applied Surface Science, 2019, 495, 143549.	3.1	17
40030	Defect energetics for diffusion in CrMnFeCoNi high-entropy alloy from first-principles calculations. Computational Materials Science, 2019, 170, 109163.	1.4	39
40031	Role of intrinsic dipole on photocatalytic water splitting for Janus MoSSe/nitrides heterostructure: A first-principles study. Progress in Natural Science: Materials International, 2019, 29, 335-340.	1.8	28
40032	Synthesis of Secondary Aldimines from the Hydrogenative Cross-Coupling of Nitriles and Amines over Al₂O₃-Supported Ni Catalysts. ACS Catalysis, 2019, 9, 8413-8423.	5.5	9
40033	Optoelectronic and solar cell applications of Janus monolayers and their van der Waals heterostructures. Physical Chemistry Chemical Physics, 2019, 21, 18612-18621.	1.3	141

#	Article	IF	Citations
40034	A simple chemical guide for finding novel n-type dopable Zintl pnictide thermoelectric materials. Journal of Materials Chemistry A, 2019, 7, 19385-19395.	5.2	29
40035	Single-phase Ni₅P₄â€“copper foam superhydrophilic and aerophobic coreâ€“shell nanostructures for efficient hydrogen evolution reaction. Journal of Materials Chemistry A, 2019, 7, 23989-23999.	5.2	58
40036	Rationalizing accurate structure prediction in the meta-GGA SCAN functional. Physical Review B, 2019, 100, .	1.1	56
40037	Varying topological properties of two-dimensional honeycomb lattices composed of endohedral fullerenes. Physical Review B, 2019, 100, .	1.1	2
40038	Tunable visible-light excitonic absorption and high photoconversion efficiency in two-dimensional group-VI monolayer materials. Physical Review B, 2019, 100, .	1.1	28
40039	pH dependence of dacarbazine adsorption on activated carbon: DFT study. Europhysics Letters, 2019, 126, 58002.	0.7	3
40040	Ultrafine Defective RuO₂ Electrocatayst Integrated on Carbon Cloth for Robust Water Oxidation in Acidic Media. Advanced Energy Materials, 2019, 9, 1901313.	10.2	182
40041	Sn3O4 exfoliation process investigated by density functional theory and modern scotch-tape experiment. Computational Materials Science, 2019, 170, 109160.	1.4	7
40042	Origin and evolution of ferroelectricity in the layered rare-earth-titanate,<mml:math xmlns:mml="http://www.w3.org/1998/Math/MathML" altimg="si210.svg"><mml:mrow><mml:msub><mml:mrow><mml:mi>R</mml:mi></mml:mrow><mml:mrow><mml:mn>2</mml:mn></r Carpy-Galy phases. Polyhedron, 2019, 171, 181-192.	1.0	11
40043	Data-Driven Discovery of Full-Visible-Spectrum Phosphor. Chemistry of Materials, 2019, 31, 6286-6294.	3.2	92
40044	Dispersion XDM with Hybrid Functionals: Delocalization Error and Halogen Bonding in Molecular Crystals. Journal of Chemical Theory and Computation, 2019, 15, 4933-4944.	2.3	22
40045	GdFe_{0.8}Ni_{0.2}O₃: A Multiferroic Material for Low-Power Spintronic Devices with High Storage Capacity. ACS Applied Materials & Interfaces, 2019, 11, 31562-31572.	4.0	25
40046	Topological Lifshitz transitions and Fermi arc manipulation in Weyl semimetal NbAs. Nature Communications, 2019, 10, 3478.	5.8	41
40047	Manganese oxidation as the origin of the anomalous capacity of Mn-containing Li-excess cathode materials. Nature Energy, 2019, 4, 639-646.	19.8	164
40048	Stable InSe transistors with high-field effect mobility for reliable nerve signal sensing. Npj 2D Materials and Applications, 2019, 3, .	3.9	31
40049	Identifying the rate-determining step of the electrocatalytic hydrodechlorination reaction on palladium nanoparticles. Nanoscale, 2019, 11, 15892-15899.	2.8	34
40050	Tailoring cations in a perovskite cathode for proton-conducting solid oxide fuel cells with high performance. Journal of Materials Chemistry A, 2019, 7, 20624-20632.	5.2	115
40051	Modulation of the electronic property of hydrogenated 2D tetragonal Ge by applying external strain. RSC Advances, 2019, 9, 23142-23147.	1.7	8

#	Article	IF	Citations
40052	Systematic exploration of the mechanical properties of 13â€‰621 inorganic compounds. Chemical Science, 2019, 10, 8589-8599.	3.7	24
40053	Understanding the role of functional groups of thiolate ligands in electrochemical CO₂ reduction over Au(111) from first-principles. Journal of Materials Chemistry A, 2019, 7, 19872-19880.	5.2	28
40054	Black phosphorene exhibiting negative thermal expansion and negative linear compressibility. Journal of Physics Condensed Matter, 2019, 31, 465003.	0.7	9
40055	Antimonene on Pb quantum wells. 2D Materials, 2019, 6, 045028.	2.0	18
40056	Calculating the frequencies and intensities of strongly anharmonic modes of adsorbates on surfaces: A low-cost but accurate computational approach. Physical Review B, 2019, 100, .	1.1	1
40057	Vibration signatures of the structural phase transition of Sn/Ge(111) compared to Sn/Si(111). Physical Review B, 2019, 100, .	1.1	3
40058	Adsorption on transition metal surfaces: Transferability and accuracy of DFT using the ADS41 dataset. Physical Review B, 2019, 100, .	1.1	51
40059	Efficient band gap prediction of semiconductors and insulators from a semilocal exchange-correlation functional. Physical Review B, 2019, 100, .	1.1	35
40060	Property control from polyhedral connectivity in ABO3 oxides. Physical Review B, 2019, 100, .	1.1	7
40061	Deuterium Hugoniot: Pitfalls of thermodynamic sampling beyond density functional theory. Physical Review B, 2019, 100, .	1.1	7
40062	Electronic structure and anomalous Hall effect in the ferromagnetic <mml:math xmlns:mml="http://www.w3.org/1998/Math/MathML"><mml:mrow><mml:mn>3</mml:mn><mml:mi>d</mml:mi><mml:mtext>â^'</mm superlattice <mml:math xmlns:mml="http://www.w3.org/1998/Math/MathML"><mml:mrow><mml:msub><mml:mi>SrMnO</mml:mi><mml:mn>3</mml:mn></r Physical Review B, 2019, 99, .	1.1	19
40063	Defective [Bi₂O₂]²⁺ Layers Exhibiting Ultrabroad Nearâ€Infrared Luminescence. Chemistry - A European Journal, 2019, 25, 12842-12848.	1.7	4
40064	Microscopic Modeling of Correlated Systems Under Pressure: Representative Examples. Physica Status Solidi (B): Basic Research, 2019, 256, 1900229.	0.7	6
40065	When a defect is a pathway to improve stability: a case study of the L12 Co3TM superlattice intrinsic stacking fault. Journal of Materials Science, 2019, 54, 13609-13618.	1.7	16
40066	YAGG:Ce transparent ceramics with high luminous efficiency for solid-state lighting application. Journal of Advanced Ceramics, 2019, 8, 389-398.	8.9	56
40067	A unique amorphous cobalt-phosphide-boride bifunctional electrocatalyst for enhanced alkaline water-splitting. Applied Catalysis B: Environmental, 2019, 259, 118051.	10.8	112
40068	Mechanistic origin of the diverging selectivity patterns in catalyzed ethane and ethene oxychlorination. Journal of Catalysis, 2019, 377, 233-244.	3.1	9
40069	Mechanical deformation: A feasible route for reconfiguration of inner interfaces to modulate the high performance of three-dimensional porous carbon material anodes in stretchable lithium-Ion batteries. Journal of Colloid and Interface Science, 2019, 555, 431-437.	5.0	8

#	Article	IF	Citations
40070	Nitrogen-rich GaN5 and GaN6 as high energy density materials with modest synthesis condition. Physics Letters, Section A: General, Atomic and Solid State Physics, 2019, 383, 125859.	0.9	17
40071	LiB6Si: An indirect band gap semiconductor. Physics Letters, Section A: General, Atomic and Solid State Physics, 2019, 383, 125862.	0.9	3
40072	First-Principles Investigations on Sodium Superionic Conductor Na₁₁Sn₂PS₁₂. Chemistry of Materials, 2019, 31, 6066-6075.	3.2	23
40073	The Effect of Jump Attempt Frequencies on the Ionic Conductivity of Doped Ceria. Journal of Physical Chemistry C, 2019, 123, 19437-19446.	1.5	8
40074	Molybdenum-Doped Porous Cobalt Phosphide Nanosheets for Efficient Alkaline Hydrogen Evolution. ACS Applied Energy Materials, 2019, 2, 6302-6310.	2.5	22
40075	Au-MoS₂ Hybrids as Hydrogen Evolution Electrocatalysts. ACS Applied Energy Materials, 2019, 2, 6043-6050.	2.5	43
40076	Confinement-Enhanced Rapid Interlayer Diffusion within Graphene-Supported Anisotropic ReSe₂ Electrodes. ACS Applied Materials & Interfaces, 2019, 11, 31147-31154.	4.0	13
40077	Preadsorption of O₂ on the Exposed (001) Facets of ZnO Nanostructures for Enhanced Sensing of Gaseous Acetone. ACS Applied Nano Materials, 2019, 2, 6144-6151.	2.4	33
40078	Impact of local composition on the energetics of E-centres in Si1â^'xGex alloys. Scientific Reports, 2019, 9, 10849.	1.6	4
40079	Rational design of selective metal catalysts for alcohol amination with ammonia. Nature Catalysis, 2019, 2, 773-779.	16.1	70
40080	Suppression of platinum sintering on Ptâ€"M/ZSM-22 (M = Ce, La, and Re) catalyst for n-dodecane isomerization. New Journal of Chemistry, 2019, 43, 13967-13978.	1.4	16
40081	Hyperfine interactions and diffusion of Cd in TiO2 (rutile). Journal of Applied Physics, 2019, 126, .	1.1	4
40082	Janus single-layer group-III monochalcogenides: a promising visible-light photocatalyst. Journal Physics D: Applied Physics, 2019, 52, 455303.	1.3	26
40083	Large second-harmonic generation and linear electro-optic effect in trigonal selenium and tellurium. Physical Review B, 2019, 100, .	1.1	26
40084	Unconventional superconductivity in a doped quantum spin Hall insulator. Physical Review B, 2019, 100, .	1.1	24
40085	Computer Modeling of Extended PnX3n + 2 Chains (X = F, Cl). Russian Journal of Inorganic Chemistry, 2019, 64, 780-785.	0.3	0
40086	Enhanced superconductivity by Na doping in SnAs-based layered compound Na_{1+x}Sn_{2â^'x}As₂. Japanese Journal of Applied Physics, 2019, 58, 083001.	0.8	11
40087	Oganesson ist ein Halbleiter: Ãœber die relativitische BandlÃ¼ckenkontraktion in den schwersten Edelgasen. Angewandte Chemie, 2019, 131, 14398-14402.	1.6	8

#	Article	IF	Citations
40088	Influence of Surface Passivation on Indium Arsenide Nanowire Band Gap Energies. Journal of Electronic Materials, 2019, 48, 6654-6660.	1.0	2
40089	Electronic and optical properties of graphane, silicane, MoS2 homo-bilayers and hetero-bilayers. Current Applied Physics, 2019, 19, 1222-1232.	1.1	10
40090	Role of water in cyclopentanone self-condensation reaction catalyzed by MCM-41 functionalized with sulfonic acid groups. Journal of Catalysis, 2019, 377, 245-254.	3.1	38
40091	Mid-temperature thermoelectric performance of zone-melted Sb2(Te,Se)3 alloys near phase transition boundary. Journal of Materiomics, 2019, 5, 590-596.	2.8	9
40092	The electronic structures and properties for carbon doped aluminum phosphide. Physics Letters, Section A: General, Atomic and Solid State Physics, 2019, 383, 3138-3142.	0.9	4
40093	Enhanced triethylamine sensing performance of Î±-Fe2O3 nanoparticle/ZnO nanorod heterostructures. Sensors and Actuators B: Chemical, 2019, 298, 126917.	4.0	74
40094	Understanding the Correlation between Electronic Coupling and Energetic Stability of Molecular Crystal Polymorphs: The Instructive Case of Quinacridone. Chemistry of Materials, 2019, 31, 7054-7069.	3.2	9
40095	In-Depth Theoretical Probe into Novel Mixed-Metal Uranium-Based Endohedral Clusterfullerenes Sc₂UX@I_h(31924)-C₈₀ (X = C, N). Inorganic Chemistry, 2019, 58, 10769-10777.	1.9	12
40096	Magnetic properties of the low-dimensional BaM2Si2O7 system (M=Cu,ÂCo,ÂMn). Physical Review B, 2019, 100, .	1.1	2
40097	Magnetization density distribution in the metallic ferromagnet <mml:math xmlns:mml="http://www.w3.org/1998/Math/MathML"><mml:msub><mml:mi>SrRuO</mml:mi><mml:mn>3</mml:mn></mml:msub></m determined by polarized neutron diffraction. Physical Review B, 2019, 100, .	1.1	3
40098	Mechanism for unconventional nonlinear elasticity. Physical Review B, 2019, 100, .	1.1	4
40099	Ground states of Au2Pb and pressure-enhanced superconductivity. Physical Review B, 2019, 100, .	1.1	9
40100	Origin of the anomalous Hall effect in <mml:math xmlns:mml="http://www.w3.org/1998/Math/MathML"><mml:msub><mml:mi>SrCoO</mml:mi><mml:mn>3</mml:mn></mml:msub></m thin films. Physical Review B, 2019, 100, .	1.1	9
40101	Influence of crystal structure on charge carrier effective masses in <mml:math xmlns:mml="http://www.w3.org/1998/Math/MathML"><mml:msub><mml:mi>BiFeO</mml:mi><mml:mn>3</mml:mn></mml:msub></m Physical Review B, 2019, 100, .	1.1	10
40102	Layer-dependent intrinsic anomalous Hall effect in <mml:math xmlns:mml="http://www.w3.org/1998/Math/MathML"><mml:mrow><mml:msub><mml:mi>Fe</mml:mi><mml:mn>3</mml:mn></mml:msub></m Physical Review B, 2019, 100, .	1.1	10
40103	Pressure-induced phase transitions in Na₂B₁₂H₁₂, structural investigation on a candidate for solid-state electrolyte. Acta Crystallographica Section B: Structural Science, Crystal Engineering and Materials, 2019, 75, 406-413.	0.5	22
40104	Partial Local Atomic Ordering in Ge-Sn Alloy. , 2019, , .		0
40105	Ferroicity-driven nonlinear photocurrent switching in time-reversal invariant ferroic materials. Science Advances, 2019, 5, eaav9743.	4.7	62

#	Article	IF	Citations
40106	Surface states in bulk single crystal of topological semimetal Co ₃ Sn ₂ S ₂ toward water oxidation. Science Advances, 2019, 5, eaaw9867.	4.7	118
40107	Quantification and Statistical Analysis of Errors Related to the Approximate Description of Active Site Models in Metalâ€Exchanged Zeolites. ChemCatChem, 2019, 11, 5055-5067.	1.8	3
40108	Structureâ€“Activity Relationship of Iron Oxides for NO Reduction in the Presence of C 3 H 6 , CO, and O 2. Chemistry - A European Journal, 2019, 25, 13964-13971.	1.7	4
40109	The first-principle study on the performance of biaxial strained graphdiyne as the Li-ion battery anode. Applied Surface Science, 2019, 497, 143723.	3.1	24
40110	The role of isotropic and anisotropic Hubbard corrections for the magnetic ordering and absolute band alignment of hematite Î±-Fe2O3(0001) surfaces. Progress in Natural Science: Materials International, 2019, 29, 349-355.	1.8	5
40111	Metal-Free B@g-CN: Visible/Infrared Light-Driven Single Atom Photocatalyst Enables Spontaneous Dinitrogen Reduction to Ammonia. Nano Letters, 2019, 19, 6391-6399.	4.5	236
40112	Enhanced Cycling Performance of Ni-Rich Positive Electrodes (NMC) in Li-Ion Batteries by Reducing Electrolyte Free-Solvent Activity. ACS Applied Materials & Interfaces, 2019, 11, 34973-34988.	4.0	63
40113	Screening highly active perovskites for hydrogen-evolving reaction via unifying ionic electronegativity descriptor. Nature Communications, 2019, 10, 3755.	5.8	139
40114	Planar graphitic ZnS, buckling ZnS monolayers and rolled-up nanotubes as nonlinear optical materials: first-principles simulation. RSC Advances, 2019, 9, 25336-25344.	1.7	6
40115	Design of metal contacts for monolayer Fe3GeTe2 based devices. Applied Physics Letters, 2019, 115, .	1.5	19
40116	Electronic and elastic properties of the multiferroic crystals with the Kagome type lattices -Mn₃V₂O₈ and Ni₃V₂O₈: First principle calculations. Ferroelectrics, 2019, 544, 11-19.	0.3	2
40117	In-plane and out-of-plane properties of a BaFe₂As₂ single crystal. Journal of Physics Condensed Matter, 2019, 31, 214003.	0.7	6
40118	Hydrogen interactions with low-index surface orientations of tungsten. Journal of Physics Condensed Matter, 2019, 31, 255002.	0.7	12
40119	Graphene-based heterostructures with moirÃ© superlattice that preserve the Dirac cone: a first-principles study. Journal of Physics Condensed Matter, 2019, 31, 255302.	0.7	4
40120	Cation ordering, ferrimagnetism and ferroelectric relaxor behavior in Pb(Fe1â^'xScx)2â^•3W1â^•3O3 solid solutions. European Physical Journal B, 2019, 92, 1.	0.6	6
40121	Epitaxial Growth of Largeâ€Scale Orthorhombic CsPbBr₃ Perovskite Thin Films with Anisotropic Photoresponse Property. Advanced Functional Materials, 2019, 29, 1904913.	7.8	55
40122	Highâ€pressureâ€induced phase transition in 1,3â€diphenylurea: The approaching of Nâ€“Hâ‹¯O hydrogenâ€bonded chains. Journal of Raman Spectroscopy, 2019, 50, 1744-1752.	1.2	6
40123	First-Principles Calculations of the Structural, Magnetic, and Electronic Properties of $$hbox {Fe}_{2}hbox {MgB}$$ Full-Heusler Alloy. Journal of Electronic Materials, 2019, 48, 7258-7262.	1.0	4

#	Article	IF	Citations
40124	Modification of a first-generation solid oxide fuel cell cathode with Co3O4 nanocubes having selectively exposed crystal planes. Materials for Renewable and Sustainable Energy, 2019, 8, 1.	1.5	29
40125	Alkali-Glass Behavior in Honeycomb-Type Layered Li_{3â€“x}Na_xNi₂SbO₆ Solid Solution. Inorganic Chemistry, 2019, 58, 11546-11552.	1.9	15
40126	Quantum Dynamics of Dissociative Chemisorption of H₂ on the Stepped Cu(211) Surface. Journal of Physical Chemistry C, 2019, 123, 23049-23063.	1.5	20
40127	Data-Driven Systematic Search of Promising Photocatalysts for Water Splitting under Visible Light. Journal of Physical Chemistry Letters, 2019, 10, 5211-5218.	2.1	31
40128	Stable, Strongly Emitting Cesium Lead Bromide Perovskite Nanorods with High Optical Gain Enabled by an Intermediate Monomer Reservoir Synthetic Strategy. Nano Letters, 2019, 19, 6315-6322.	4.5	101
40129	Epitaxial Growth of Free-Standing Bismuth Film on Graphene Embedded with Nontrivial Properties. ACS Applied Electronic Materials, 2019, 1, 1817-1824.	2.0	12
40130	Anomalous Temperature-Dependent Charge Recombination in CH₃NH₃PbI₃ Perovskite: Key Roles of Charge Localization and Thermal Effect. ACS Applied Materials & Interfaces, 2019, 11, 32069-32075.	4.0	22
40131	Identifying the Ground-State NP Sheet through a Global Structure Search in Two-Dimensional Space and Its Promising High-Efficiency Photovoltaic Properties. , 2019, 1, 375-382.		26
40132	Phonon Anharmonicity in Few-Layer Black Phosphorus. ACS Nano, 2019, 13, 10456-10468.	7.3	34
40133	Surpassing the single-atom catalytic activity limit through paired Pt-O-Pt ensemble built from isolated Pt1 atoms. Nature Communications, 2019, 10, 3808.	5.8	225
40134	Spinâ€“lattice and electronâ€“phonon coupling in 3d/5d hybrid Sr3NiIrO6. Npj Quantum Materials, 2019, 4, .	1.8	6
40135	Room temperature ferromagnetism and antiferromagnetism in two-dimensional iron arsenides. Nanoscale, 2019, 11, 16508-16514.	2.8	18
40136	Transport properties of electron small polarons in a V₂O₅ cathode of Li-ion batteries: a computational study. RSC Advances, 2019, 9, 19483-19494.	1.7	31
40137	The excellent TE performance of photoelectric material CdSe along with a study of Zn(Cd)Se and Zn(Cd)Te based on first-principles. RSC Advances, 2019, 9, 25471-25479.	1.7	7
40138	Fermi surface complexity, effective mass, and conduction band alignment in n-type thermoelectric Mg3Sb2â€‰â€“â€‰xBix from first principles calculations. Journal of Applied Physics, 2019, 126, .	1.1	41
40139	Strain-tunable electronic structure, optical response, and high electron mobility of Bi2O2Se crystals. APL Materials, 2019, 7, .	2.2	12
40140	Interaction between Li, Ultrathin Adsorbed Ionic Liquid Films, and CoO(111) Thin Films: A Model Study of the Solid|Electrolyte Interphase Formation. Chemistry of Materials, 2019, 31, 5537-5549.	3.2	9
40141	Efficient Base-Metal NiMn/TiO₂ Catalyst for CO₂ Methanation. ACS Catalysis, 2019, 9, 7823-7839.	5.5	124

#	Article	IF	Citations
40142	Tunable Covalent Triazine-Based Frameworks (CTF-0) for Visible-Light-Driven Hydrogen and Oxygen Generation from Water Splitting. ACS Catalysis, 2019, 9, 7697-7707.	5.5	131
40143	Getting Insights into the Temperature-Specific Active Sites on Platinum Nanoparticles for CO Oxidation: A Combined in Situ Spectroscopic and ab Initio Density Functional Theory Study. ACS Catalysis, 2019, 9, 7759-7768.	5.5	33
40144	Magnetic Transition in Monolayer VSe₂ via Interface Hybridization. ACS Nano, 2019, 13, 8997-9004.	7.3	94
40145	Implicit solvent effects in the determination of BrÃ¸nstedâ€“Evansâ€“Polanyi relationships for heterogeneously catalyzed reactions. Physical Chemistry Chemical Physics, 2019, 21, 17687-17695.	1.3	4
40146	The effect of compositional engineering of imidazolium lead iodide on the resistive switching properties. Nanoscale, 2019, 11, 14455-14464.	2.8	16
40147	Phonons and anisotropic thermal expansion behavior of NiX (Xâ€‰=â€‰S, Se, Te). Journal of Applied Physics, 2019, 125, .	1.1	2
40148	First principles study of structural, electronic and optical properties of Cs-doped HC(NH2)2PbI3 for photovoltaic applications. AIP Conference Proceedings, 2019, , .	0.3	1
40149	Pressure-induced ferromagnetism and enhanced perpendicular magnetic anisotropy of bilayer CrI₃. Journal of Physics Condensed Matter, 2019, 31, 355001.	0.7	14
40150	Predictions of the structures and properties of the substituted layered ternary compound series (Zr1â’x Tx)3Al3C5 (Tâ€‰=â€‰Hf, Nb, and V) through first-principles studies. Journal of Physics Condensed Matter, 2019, 31, 385702.	0.7	2
40151	Oxygen reduction reaction mechanism of N-doped graphene nanoribbons. Journal of Vacuum Science and Technology B:Nanotechnology and Microelectronics, 2019, 37, .	0.6	4
40152	Realâ€Time Imaging of Nanoscale Redox Reactions over Bimetallic Nanoparticles. Advanced Functional Materials, 2019, 29, 1903242.	7.8	36
40153	Mixedâ€Valenceâ€Driven Quasiâ€1D Sn^{II}Sn^{IV}S₃ with Highly Polarizationâ€Sensitive UVâ€“visâ€“NIR Photoresponse. Advanced Functional Materials, 2019, 29, 1904416.	7.8	39
40154	Practical Considerations for Continuum Models Applied to Surface Electrochemistry. ChemPhysChem, 2019, 20, 3074-3080.	1.0	40
40155	An effective approach to realize graphene based p-n junctions via adsorption of donor and acceptor molecules. Carbon, 2019, 153, 525-530.	5.4	6
40156	Enhanced electrocatalytic HER performance of non-noble metal nickel by introduction of divanadium trioxide. Electrochimica Acta, 2019, 320, 134535.	2.6	18
40157	The effect of reactants adsorption and products desorption for Au/TiO2 in catalyzing CO oxidation. Journal of Catalysis, 2019, 376, 134-145.	3.1	22
40158	Superior triethylamine detection at room temperature by {-112} faceted WO3 gas sensor. Journal of Hazardous Materials, 2019, 380, 120876.	6.5	95
40159	The adsorption and dissolution properties of iron surfaces in liquid lithium and lead under a fusion environment. Journal of Nuclear Materials, 2019, 524, 200-208.	1.3	8

#	Article	IF	Citations
40160	Na2Bi5AuO11 revisited. Materials Research Bulletin, 2019, 119, 110534.	2.7	0
40161	Strain tuned electronic and magnetic anisotropy in SrTiO3 (110) surface. Physics Letters, Section A: General, Atomic and Solid State Physics, 2019, 383, 2685-2691.	0.9	1
40162	Evaluation of cobalt oxides for calcium battery cathode applications. Solid State Ionics, 2019, 340, 115004.	1.3	15
40163	Nitridation of the metallic Mo2C(001) surface from NH3 dissociative adsorptionâ€"A DFT study. Surface Science, 2019, 689, 121466.	0.8	12
40164	Accelerated Discovery of Efficient Solar Cell Materials Using Quantum and Machine-Learning Methods. Chemistry of Materials, 2019, 31, 5900-5908.	3.2	87
40165	Large-Scale Benchmark of Exchangeâ€"Correlation Functionals for the Determination of Electronic Band Gaps of Solids. Journal of Chemical Theory and Computation, 2019, 15, 5069-5079.	2.3	151
40166	Unravelling the Effects of Pressure-Induced Suppressed Electronâ€"Hole Recombination in CsPbBr₃ Perovskite: Time-Domain ab Initio Analysis. Journal of Physical Chemistry Letters, 2019, 10, 4354-4361.	2.1	19
40167	Mechanistic Insights into the Ceria-Catalyzed Synthesis of Carbamates as Polyurethane Precursors. ACS Catalysis, 2019, 9, 7708-7720.	5.5	14
40168	Dynamic shortening of disorder potentials in anharmonic halide perovskites. Nature Communications, 2019, 10, 3141.	5.8	74
40169	Theoretical investigation of the valence states in Au via the Auâ€"F compounds under high pressure. Physical Chemistry Chemical Physics, 2019, 21, 17621-17627.	1.3	11
40170	Size-dependent selective crystallization using an inorganic mixed-oxoanion system for lanthanide separation. Dalton Transactions, 2019, 48, 12808-12811.	1.6	16
40171	Chemical functionalization of the ZnO monolayer: structural and electronic properties. RSC Advances, 2019, 9, 21831-21843.	1.7	33
40172	CO oxidization catalyzed by B, N, and their co-doped fullerenes: a first-principles investigation. RSC Advances, 2019, 9, 21626-21636.	1.7	12
40173	Si-doped MoS2 sheet as phosgene gas sensor: A first principles study. AIP Conference Proceedings, 2019, , .	0.3	1
40174	Computing the self-consistent field in Kohnâ€"Sham density functional theory. Journal of Physics Condensed Matter, 2019, 31, 453001.	0.7	38
40175	Interplay between magnetic, metal/insulator and topological phases in Hg1âˆ'x Mn x Te alloys: prediction of a ferromagnetic Weyl semimetal at xâ€‰â€‰=â€‰â€‰0.25. Journal of Physics Condensed Matter, 2019, 31, 435502.	0.7	13
40176	Cu Doped Crystalline Carbon-Conjugated g-C₃N₄, a Promising Oxygen Reduction Catalyst by Theoretical Study. Journal of the Electrochemical Society, 2019, 166, F755-F759.	1.3	14
40177	First Principles Study of the Vibrational and Thermal Properties of Sn-Based Type II Clathrates, CsxSn136 (0 â‰¤ x â‰¤ 24) and Rb24Ga24Sn112. Inorganics, 2019, 7, 74.	1.2	1

#	Article	IF	Citations
40178	Ultrahigh Thermoelectric Performance Realized in Black Phosphorus System by Favorable Band Engineering through Group VA Doping. Advanced Functional Materials, 2019, 29, 1904346.	7.8	41
40179	Ultralarge interlayer distance and C,N-codoping enable superior sodium storage capabilities of MoS2 nanoonions. Chemical Engineering Journal, 2019, 378, 122249.	6.6	39
40180	First principles calculation of UO2 polymorphs and phase transitions under compressive and tensile loading. Computational Materials Science, 2019, 169, 109124.	1.4	9
40181	A comparative study of Na3LiTi5O12 and Li4Ti5O12: Geometric and electronic structures obtained by density functional theory calculations. Chemical Physics Letters, 2019, 731, 136598.	1.2	9
40182	Promising photocatalysts with high carrier mobility for water splitting in monolayer Ge2P4S2 and Ge2As4S2. International Journal of Hydrogen Energy, 2019, 44, 21536-21545.	3.8	16
40183	The effect of Cr on He segregation and diffusion at Î£3(1â€¯1â€¯2) grain boundary in Î±-Fe. Nuclear Instruments & Methods in Physics Research B, 2019, 456, 7-11.	0.6	5
40184	Water Contributes to Higher Energy Density and Cycling Stability of Prussian Blue Analogue Cathodes for Aqueous Sodium-Ion Batteries. Chemistry of Materials, 2019, 31, 5933-5942.	3.2	66
40185	A First-Principles Investigation of Gas-Phase Ring-Opening Reaction of Furan over HZSM-5 and Ga-Substituted ZSM-5. Industrial & Engineering Chemistry Research, 2019, 58, 15127-15133.	1.8	6
40186	Pathways for O₂ Electroreduction over Substitutional FeN₄, HOFeN₄, and OFeN₄ in Graphene Bulk Sites: Critical Evaluation of Overpotential Predictions Using LGER and CHE Models. Journal of Physical Chemistry C, 2019, 123, 18398-18409.	1.5	20
40187	Quantum Mechanical Screening of Metal-N₄-Functionalized Graphenes for Electrochemical Anodic Oxidation of Light Alkanes to Oxygenates. Journal of Physical Chemistry C, 2019, 123, 19033-19044.	1.5	20
40188	Hydroxamate Titaniumâ€“Organic Frameworks and the Effect of Siderophore-Type Linkers over Their Photocatalytic Activity. Journal of the American Chemical Society, 2019, 141, 13124-13133.	6.6	73
40189	Direct observation and impact of co-segregated atoms in magnesium having multiple alloying elements. Nature Communications, 2019, 10, 3243.	5.8	78
40190	Unveiling chemical reactivity and oxidation of 1T-phased group VI disulfides. Physical Chemistry Chemical Physics, 2019, 21, 17010-17017.	1.3	7
40191	The local electron attachment energy and the electrostatic potential as descriptors of surfaceâ€“adsorbate interactions. Physical Chemistry Chemical Physics, 2019, 21, 17001-17009.	1.3	10
40192	Pressure-induced reversible framework rearrangement and increased polarization in the polar [NH4][Cd(HCOO)3] hybrid perovskite. Inorganic Chemistry Frontiers, 2019, 6, 2379-2386.	3.0	9
40193	Stabilizing the B-site oxidation state in ABO₃ perovskite nanoparticles. Nanoscale, 2019, 11, 14303-14311.	2.8	16
40194	Band-structure engineering of the magnetically Cr-doped topological insulator Sb₂Te₃ under mechanical strain. Journal of Physics Condensed Matter, 2019, 31, 385501.	0.7	8
40195	Reversible direct-indirect band transition in alloying TMDs heterostructures via band engineering. Journal of Physics Condensed Matter, 2019, 31, 435503.	0.7	7

#	Article	IF	Citations
40196	STM Images of Anionic Defects at CeO2(111)â€"A Theoretical Perspective. Frontiers in Chemistry, 2019, 7, 212.	1.8	8
40197	Understanding the Potential of 2D Ga 2 O 3 in Flexible Optoelectronic Devices: Impact of Uniaxial Strain and Electric Field. Advanced Theory and Simulations, 2019, 2, 1900106.	1.3	22
40198	NiSe₂ as Coâ€Catalyst with CdS: Nanocomposites for Highâ€Performance Photodriven Hydrogen Evolution under Visibleâ€Light Irradiation. ChemPlusChem, 2019, 84, 999-1010.	1.3	12
40199	An Old Dog with New Tricks - Additions to the Cesium Lithium Chloride System: Cs3 Li2 Cl5 and the Hydrated Cs3 LiCl4 Â·4H2 O. European Journal of Inorganic Chemistry, 2019, 2019, 3526-3535.	1.0	2
40200	Intermediate Modulation on Noble Metal Hybridized to 2D Metal-Organic Framework for Accelerated Water Electrocatalysis. CheM, 2019, 5, 2429-2441.	5.8	150
40201	Synergistic effects of reduced graphene oxide with freeze drying tuned interfacial structure on performance of transparent and flexible supercapacitors. Journal of Colloid and Interface Science, 2019, 554, 650-657.	5.0	5
40202	Density functional theory model for carbon dot surfaces and their interaction with silver nanoparticles. Physica E: Low-Dimensional Systems and Nanostructures, 2019, 114, 113640.	1.3	18
40203	Effects of lattice parameter manipulations on electronic and optical properties of BaSi2. Thin Solid Films, 2019, 686, 137436.	0.8	10
40204	P3 Na_{0.9}Ni_{0.5}Mn_{0.5}O₂ Cathode Material for Sodium Ion Batteries. Chemistry of Materials, 2019, 31, 5376-5383.	3.2	72
40205	Well-Ordered Monolayer Growth of Crown-Ether Ring Molecules on Cu(111) in Ultra-High Vacuum: An STM, UPS, and DFT Study. Journal of Physical Chemistry C, 2019, 123, 18939-18950.	1.5	12
40206	Outstanding Energy Exchange between Organic Molecules and Metal Surfaces: Decomposition Kinetics of Excited Vinyl Derivatives Driven by the Interaction with a Cu(111) Surface. Journal of Physical Chemistry C, 2019, 123, 19625-19636.	1.5	6
40207	Experimental Visualization of Interstitialcy Diffusion of Li Ion in Î²-Li₂TiO₃. ACS Applied Energy Materials, 2019, 2, 5481-5489.	2.5	19
40208	Tunability in the Optical and Electronic Properties of ZnSe Microspheres via Ag and Mn Doping. ACS Omega, 2019, 4, 12271-12277.	1.6	51
40209	Intermediate-sized molecular sieving of styrene from larger and smaller analogues. Nature Materials, 2019, 18, 994-998.	13.3	133
40210	Possible realization of the high-temperature and multichannel quantum anomalous Hall effect in graphene/CrBr₃ heterostructures under pressure. Physical Chemistry Chemical Physics, 2019, 21, 17087-17095.	1.3	23
40211	On-the-fly machine learning force field generation: Application to melting points. Physical Review B, 2019, 100, .	1.1	233
40212	Group theoretical approach to computing phonons and their interactions. Physical Review B, 2019, 100, .	1.1	14
40213	Tuning of the intrinsic magnetic damping parameter in epitaxial CoNi(001) films : Role of the band-filling effect. Physical Review B, 2019, 100, .	1.1	5

#	Article	IF	Citations
40214	Analysis of over-magnetization of elemental transition metal solids from the SCAN density functional. Physical Review B, 2019, 100, .	1.1	37
40215	Density functional methods for the magnetism of transition metals: SCAN in relation to other functionals. Physical Review B, 2019, 100, .	1.1	42
40216	All Magic Angles in Twisted Bilayer Graphene are Topological. Physical Review Letters, 2019, 123, 036401.	2.9	327
40217	Phonon Mean Free Path - Thermal Conductivity Relation in AlN. , 2019, , .		2
40218	Superlithiophilic Amorphous SiO₂â€“TiO₂ Distributed into Porous Carbon Skeleton Enabling Uniform Lithium Deposition for Stable Lithium Metal Batteries. Advanced Science, 2019, 6, 1900943.	5.6	96
40219	Methane Chemisorption on Oxideâ€Supported Pt Single Atom. ChemPhysChem, 2019, 20, 2217-2220.	1.0	19
40220	Adsorption characteristics of formaldehyde on nitrogen doped graphene-based single atom adsorbents: A DFT study. Applied Surface Science, 2019, 493, 1260-1267.	3.1	21
40221	Graphene/antimonene/graphene heterostructure: A potential anode for sodium-ion batteries. Carbon, 2019, 153, 767-775.	5.4	45
40222	Direct synthesis of Hâ¯-encaged 12CaOÂ·7Al2O3 crystals by high-pressure processes. Ceramics International, 2019, 45, 16028-16031.	2.3	3
40223	Ab Initio and Experimental Insights on Structural, Electronic, Optical, and Magnetic Properties of Cr-Doped Bi₂Ti₂O₇. Inorganic Chemistry, 2019, 58, 9904-9915.	1.9	18
40224	Strongly Compressed Few-Layered SnSe₂ Films Grown on a SrTiO₃ Substrate: The Coexistence of Charge Ordering and Enhanced Interfacial Superconductivity. Nano Letters, 2019, 19, 5304-5312.	4.5	32
40225	High-throughput computational discovery of In2Mn2O7 as a high Curie temperature ferromagnetic semiconductor for spintronics. Npj Computational Materials, 2019, 5, .	3.5	28
40226	Spontaneous full photocatalytic water splitting on 2D MoSe₂/SnSe₂ and WSe₂/SnSe₂ vdW heterostructures. Nanoscale, 2019, 11, 14836-14843.	2.8	156
40227	Electronic structures of ultra-thin tellurium nanoribbons. Nanoscale, 2019, 11, 14134-14140.	2.8	12
40228	Strain-Induced Room-Temperature Ferromagnetic Semiconductors with Large Anomalous Hall Conductivity in Two-Dimensional <mml:math xmlns:mml="http://www.w3.org/1998/Math/MathML" display="inline" overflow="scroll"><mml:msub><mml:mi>Cr</mml:mi><mml:mn>2</mml:mn></mml:msub><mml:msub><mml:mi>Ge</mml:mi><mml:mi><mml:n Physical Review Applied, 2019, 12, .	1.5	68
40229	Unified Assessment of the Effects of Van der Waals Interactions on the Structural and Electronic Properties of Some Layered Organic Solids Î²-(BEDT-TTF)2X. Crystals, 2019, 9, 348.	1.0	0
40230	Controlled Oxygen Redox for Excellent Power Capability in Layered Sodiumâ€Based Compounds. Advanced Energy Materials, 2019, 9, 1901181.	10.2	49
40231	Using irradiation effect to study the disparate anchoring stabilities of polar-organic molecules adsorbed on bulk and thin-film metal surfaces. Applied Surface Science, 2019, 493, 1090-1097.	3.1	1

#	Article	IF	Citations
40232	Similarities and differences for atomic and diatomic molecule adsorption on the B-5 type sites of the HCP(101ì...6) surfaces of Co, Os, and Ru from DFT calculations. Heliyon, 2019, 5, e01924.	1.4	0
40233	Iron-incorporated chalcopyrite of an intermediate band for improving solar wide-spectrum absorption. Journal of Solid State Chemistry, 2019, 277, 388-394.	1.4	4
40234	High-throughput Computational Study of Halide Double Perovskite Inorganic Compounds. Chemistry of Materials, 2019, 31, 5392-5401.	3.2	102
40235	Dilute Pd/Au Alloy Nanoparticles Embedded in Colloid-Templated Porous SiO₂: Stable Au-Based Oxidation Catalysts. Chemistry of Materials, 2019, 31, 5759-5768.	3.2	50
40236	Ultralow Thermal Conductivity and High-Temperature Thermoelectric Performance in n-Type K_{2.5}Bi_{8.5}Se₁₄. Chemistry of Materials, 2019, 31, 5943-5952.	3.2	25
40237	Simulating Surfactantâ€“Iron Oxide Interfaces: From Density Functional Theory to Molecular Dynamics. Journal of Physical Chemistry B, 2019, 123, 6870-6881.	1.2	28
40238	Mitigating Voltage Decay of Li-Rich Layered Oxide by Incorporation of 5d Metal Rhenium. Journal of Physical Chemistry C, 2019, 123, 18870-18876.	1.5	23
40239	Cobalt-Based Nonprecious Metal Catalysts Derived from Metalâ€“Organic Frameworks for High-Rate Hydrogenation of Carbon Dioxide. ACS Applied Materials & Interfaces, 2019, 11, 27717-27726.	4.0	23
40240	Laser-driven shock compression of â€œsynthetic planetary mixturesâ€•of water, ethanol, and ammonia. Scientific Reports, 2019, 9, 10155.	1.6	19
40241	Achieving giant spin-orbit splitting in conduction band of monolayer WS2 via n-p co-doping. AIP Advances, 2019, 9, 075304.	0.6	6
40242	A p-type thermoelectric material BaCu4S3 with high electronic band degeneracy. Journal of Applied Physics, 2019, 126, .	1.1	7
40243	Structural and electronic properties of heterointerface composed of non-polar oxides: SrTiO3 and ferroelectric BaTiO3. Ferroelectrics, 2019, 542, 7-12.	0.3	1
40244	Spin fluctuation induced Weyl semimetal state in the paramagnetic phase of EuCd ₂ As ₂. Science Advances, 2019, 5, eaaw4718.	4.7	122
40245	Electronic, Optical, Mechanical and Lattice Dynamical Properties of MgBi2O6: A First-Principles Study. Applied Sciences (Switzerland), 2019, 9, 1267.	1.3	10
40246	Hole doped Î±-MgAgSb as potential low temperature thermoelectric materials. Physics Letters, Section A: General, Atomic and Solid State Physics, 2019, 383, 125833.	0.9	3
40247	Transition-Metal Distribution in Brownmillerite Ca₂FeCoO₅. Inorganic Chemistry, 2019, 58, 10209-10216.	1.9	3
40248	Structure and Composition Modification of Ultrasmall Palladium Nanoparticles upon Hydrogenation from First Principles. Journal of Physical Chemistry C, 2019, 123, 18609-18619.	1.5	2
40249	Strong Interplay between Sodium and Oxygen in Kesterite Absorbers: Complex Formation, Incorporation, and Tailoring Depth Distributions. Advanced Energy Materials, 2019, 9, 1900740.	10.2	20

#	Article	IF	Citations
40250	Co-adsorption of O₂ and C₂H₄ on a Free Gold Dimer Probed via Infrared Photodissociation Spectroscopy. Journal of the American Society for Mass Spectrometry, 2019, 30, 1895-1905.	1.2	6
40251	Electronic structure and magnetic properties of 3d transition-metal atom adsorbed SnO monolayers. Applied Surface Science, 2019, 493, 404-410.	3.1	17
40252	Superatomic anion Al6O2â^' and the prospect for cluster assembled crystals. Chemical Physics, 2019, 525, 110413.	0.9	0
40253	Toughening and maintaining strength of diamond with substitutional doping boron and nitrogen. Journal of Alloys and Compounds, 2019, 805, 1090-1095.	2.8	5
40254	Ab initio study on Pb2FeOsO6 and possible half metallicity via Na doping. Journal of Magnetism and Magnetic Materials, 2019, 491, 165553.	1.0	5
40255	Structural, electronic and magnetic properties of NM-doped Ni clusters (NM=Cu, Ag, Au). Journal of Molecular Structure, 2019, 1197, 147-153.	1.8	4
40256	Interstitial Oxide Ion Conductivity in the Langasite Structure: Carrier Trapping by Formation of (Ga,Ge)₂O₈ Units in La₃Ga_{5â€“x}Ge_{1+x}O_{14+x/2} (0 <) Tj ETQq0 0 0 rgBT /Overloc	3.2	9
40257	CO₂ Conversion Performance of Perovskite Oxides Designed with Abundant Metals. Industrial & Engineering Chemistry Research, 2019, 58, 12551-12560.	1.8	16
40258	Non-conventional mechanism of ferroelectric fatigue via cation migration. Nature Communications, 2019, 10, 3064.	5.8	23
40259	High temperature-mediated rocksalt to wurtzite phase transformation in cadmium oxide nanosheets and its theoretical evidence. Nanoscale, 2019, 11, 14802-14819.	2.8	15
40260	Two-dimensional ferroelastic topological insulator with tunable topological edge states in single-layer ZrAsX (X = Br and Cl). Journal of Materials Chemistry C, 2019, 7, 9743-9747.	2.7	15
40261	Single Pt atoms stabilized on Mo2TiC2O2 for hydrogen evolution: A first-principles investigation. Journal of Chemical Physics, 2019, 151, 024702.	1.2	22
40262	Evidence for the formation of metallic In after laser irradiation of InP. Journal of Applied Physics, 2019, 126, .	1.1	4
40263	Electronic, magnetic and optical properties of C, N-doped TiO2 anatase: A hybrid density functional study. AIP Conference Proceedings, 2019, , .	0.3	0
40264	Prediction of Mo2CF2 monolayer as a novel anode material for Li-ion batteries: A first principle study. AIP Conference Proceedings, 2019, , .	0.3	5
40265	Oxygen and potassium vacancies in KTP calculated from first principles. Journal of Physics Condensed Matter, 2019, 31, 385401.	0.7	8
40266	Structural Relaxation in Polyanionic Sodium Fluorophosphate Glasses. Frontiers in Materials, 2019, 6, .	1.2	13
40267	Porous MOFâ€205 with multiple modifications for efficiently storing hydrogen and methane as well as separating carbon dioxide from hydrogen and methane. International Journal of Energy Research, 2019, 43, 7517.	2.2	9

#	Article	IF	Citations
40268	Ab initio study of electronic structure properties of CaAFe4As4 (Aâ€¯=â€¯K, Rb and Cs) superconductors. Computational Materials Science, 2019, 169, 109114.	1.4	2
40269	Structural, elastic, vibrational and electronic properties of amorphous Sm2O3 from Ab Initio calculations. Computational Materials Science, 2019, 169, 109119.	1.4	10
40270	Relativistic DFT-1/2 Calculations Combined with a Statistical Approach for Electronic and Optical Properties of Mixed Metal Hybrid Perovskites. Journal of Physical Chemistry Letters, 2019, 10, 4245-4251.	2.1	20
40271	P-Doped Ironâ€“Nickel Sulfide Nanosheet Arrays for Highly Efficient Overall Water Splitting. ACS Applied Materials & Interfaces, 2019, 11, 27667-27676.	4.0	155
40272	Evaluating the Catalytic Efficiency of Paired, Single-Atom Catalysts for the Oxygen Reduction Reaction. ACS Catalysis, 2019, 9, 7660-7667.	5.5	128
40273	Toward a Design of Active Oxygen Evolution Catalysts: Insights from Automated Density Functional Theory Calculations and Machine Learning. ACS Catalysis, 2019, 9, 7651-7659.	5.5	118
40274	Laser-sculptured ultrathin transition metal carbide layers for energy storage and energy harvesting applications. Nature Communications, 2019, 10, 3112.	5.8	91
40275	Building egg-tray-shaped graphenes that have superior mechanical strength and band gap. Npj Computational Materials, 2019, 5, .	3.5	19
40276	Mechanism and kinetics for both thermal and electrochemical reduction of N₂ catalysed by Ru(0001) based on quantum mechanics. Physical Chemistry Chemical Physics, 2019, 21, 17605-17612.	1.3	13
40277	Interrogation of fractional crystallization behavior of a newly exploited chiral resolution method for racemic 1-(pyridin-2-yl)ethylamine via DFT-D3 calculations of cohesive energy. Inorganic Chemistry Frontiers, 2019, 6, 2325-2338.	3.0	1
40278	Electric field-tailored giant transformation of magnetic anisotropy and interfacial spin coupling in epitaxial Î³â€²-Fe₄N/Pb(Mg_{1/3}Nb_{2/3})_{0.7}Ti_{0.3}O₃(011) multiferroic heterostructures. Journal of Materials Chemistry C, 2019, 7, 8537-8545.	2.7	11
40279	Defect tolerant and dimension dependent ferromagnetism in MnSe₂. Physical Chemistry Chemical Physics, 2019, 21, 16718-16725.	1.3	18
40280	Local structure and vibrational dynamics of proton conducting Ba2In2O5(H2O)x. Journal of Materials Chemistry A, 2019, 7, 17626-17636.	5.2	11
40281	Ab-initio study of strain engineering optical properties of RbPbI3. AIP Conference Proceedings, 2019, , .	0.3	2
40282	Strain induced magnetism and half-metallicity in alkali metal substituted aluminene. AIP Conference Proceedings, 2019, , .	0.3	2
40283	Tuning of Schottky barriers in borophene/MoS2 van der Waals heterostructure by external electric field. AIP Conference Proceedings, 2019, , .	0.3	0
40284	The complex non-collinear magnetic orderings in Ba₂YOsO₆: a new approach to tuning spin-lattice interactions and controlling magnetic orderings in frustrated complex oxides. Journal of Physics Condensed Matter, 2019, 31, 445803.	0.7	5
40285	Confinement of Fe2O3 nanoparticles in the shell of N-doped carbon hollow microsphere for efficient oxygen reduction reaction. Chemical Engineering Science, 2019, 207, 235-246.	1.9	32

#	Article	IF	Citations
40286	First-principles investigation of N-triphenylene-graphdiyne nanosheets as an anode material for Na, K, Mg and Ca storage. Computational Materials Science, 2019, 169, 109093.	1.4	19
40287	Giant anisotropy of thermal expansion and thermomechanical properties of monolayer Î±-antimonene: A first-principles study. Computational Materials Science, 2019, 169, 109132.	1.4	1
40288	The ratio law of the structure evolution and stability for TinOm (nâ€¯=â€¯3â€“18, mâ€¯=â€¯1â€“2n) clusters. Chemical Physics Letters, 2019, 731, 136574.	1.2	5
40289	Structural transformation of the binary network in response to selective guest inclusion at liquid/solid interfaces. Physica E: Low-Dimensional Systems and Nanostructures, 2019, 114, 113587.	1.3	1
40290	Discovery of Superconductivity in Potassium-Doped Tri-p-tolylbismuthine. Journal of Physical Chemistry C, 2019, 123, 19105-19111.	1.5	8
40291	Computational Investigation of Aqueous Phase Effects on the Dehydrogenation and Dehydroxylation of Polyols over Pt(111). Journal of Physical Chemistry C, 2019, 123, 19052-19065.	1.5	21
40292	Elucidation of temperature-programmed desorption of high-coverage hydrogen on Pt(211), Pt(221), Pt(533) and Pt(553) based on density functional theory calculations. Physical Chemistry Chemical Physics, 2019, 21, 17142-17151.	1.3	10
40293	Direct observation of delithiation as the origin of analog memristance in LixNbO2. APL Materials, 2019, 7, .	2.2	13
40294	Predicting CO₂ adsorption and reactivity on transition metal surfaces using popular density functional theory methods. Molecular Simulation, 2019, 45, 1163-1172.	0.9	26
40295	Effect of nonmetallic solutes on the ductility of zirconium from first-principles calculations. IOP Conference Series: Materials Science and Engineering, 2019, 479, 012070.	0.3	1
40296	Biomimetic Nitrogen Fixation Catalyzed by Transition Metal Sulfide Surfaces in an Electrolytic Cell. ChemSusChem, 2019, 12, 4265-4273.	3.6	35
40297	Aluminium segregation profiles in the (110), (100) and (111) surface regions of the Fe0.85Al0.15 random body-centered cubic alloy. Applied Surface Science, 2019, 492, 886-895.	3.1	7
40298	Assessments of molar volumes of Co-, Ni- and Ti- related bcc and fcc phases. Calphad: Computer Coupling of Phase Diagrams and Thermochemistry, 2019, 66, 101629.	0.7	7
40299	PtNi colloidal nanoparticle clusters: Tuning electronic structure and boundary density of nanocrystal subunits for enhanced electrocatalytic properties. Journal of Catalysis, 2019, 376, 87-100.	3.1	18
40300	Oxidation simulation study of silicon carbide nanowires: A carbon-rich interface state. Applied Surface Science, 2019, 493, 882-888.	3.1	24
40301	First-principle investigation of hydrogen solubility and diffusivity in transition metal-doped vanadium membranes and their mechanical properties. Journal of Alloys and Compounds, 2019, 805, 747-756.	2.8	28
40302	Understanding the magneto-structural coupling of Ni50Mn35.4In14.6 alloy from first-principles calculations. Journal of Magnetism and Magnetic Materials, 2019, 488, 165339.	1.0	9
40303	Interfacial engineering of oxygenated chemical bathâ€“deposited CdS window layer for highly efficient Sb2Se3 thin-film solar cells. Materials Today Physics, 2019, 10, 100125.	2.9	22

#	Article	IF	Citations
40304	Highly Conducting p-Type Transparent LnCuOS (Ln = La and Nd) and pâ€“n Junction by Using Ink. ACS Applied Electronic Materials, 2019, 1, 1605-1615.	2.0	9
40305	A two-dimensional robust topological insulator with coexisting ferroelectric and valley polarization. Journal of Materials Chemistry C, 2019, 7, 9406-9412.	2.7	13
40306	Hydrodeoxygenation of phenol over Ni-based bimetallic single-atom surface alloys: mechanism, kinetics and descriptor. Catalysis Science and Technology, 2019, 9, 4314-4326.	2.1	65
40307	Biaxial strain induced band transition and valleyâ€“spin coupling in the ferromagnetic semiconducting WSe₂/1T-FeCl₂ heterostructure. Journal of Materials Chemistry C, 2019, 7, 9398-9405.	2.7	9
40308	A first-principles study of interfacial fluorination at the HfO2/Al2O3 interface in charge trapping memory devices. Journal of Applied Physics, 2019, 125, 215303.	1.1	0
40309	Micki: A python-based object-oriented microkinetic modeling code. Journal of Chemical Physics, 2019, 151, 014112.	1.2	18
40310	Quantum chemical methods in charge density studies from X-ray diffraction data. Russian Chemical Reviews, 2019, 88, 677-716.	2.5	18
40311	Lattice Dynamic and Instability in Pentasilicene: A Light Single-Element Ferroelectric Material With High Curie Temperature. Physical Review Applied, 2019, 11, .	1.5	24
40312	Tunable optoelectronic properties in h-BP/h-BAs bilayers: The effect of an external electrical field. Applied Surface Science, 2019, 493, 308-319.	3.1	23
40313	Gibbsite (100) and Kaolinite (100) Sorption of Cadmium(II): A Density Functional Theory and XANES Study of Structures and Energies. Journal of Physical Chemistry A, 2019, 123, 6319-6333.	1.1	9
40314	Transition Metal-Functionalized Janus MoSSe Monolayer: A Magnetic and Efficient Single-Atom Photocatalyst for Water-Splitting Applications. Journal of Physical Chemistry C, 2019, 123, 18347-18354.	1.5	46
40315	Coexistence of Superconductivity with Enhanced Charge Density Wave Order in the Two-Dimensional Limit of TaSe₂. Journal of Physical Chemistry Letters, 2019, 10, 4076-4081.	2.1	44
40316	Spontaneous Delithiation under Operando Condition Triggers Formation of an Amorphous Active Layer in Spinel Cobalt Oxides Electrocatalyst toward Oxygen Evolution. ACS Catalysis, 2019, 9, 7389-7397.	5.5	52
40317	Investigating the Nature of the Active Sites for the CO₂ Reduction Reaction on Carbon-Based Electrocatalysts. ACS Catalysis, 2019, 9, 7668-7678.	5.5	58
40318	Formation of two-dimensional transition metal oxide nanosheets with nanoparticles as intermediates. Nature Materials, 2019, 18, 970-976.	13.3	169
40319	A two-dimensional assembly of ultrafine cobalt oxide nanocrystallites anchored on single-layer Ti₃C₂T_x nanosheets with enhanced lithium storage for Li-ion batteries. Nanoscale, 2019, 11, 16755-16766.	2.8	35
40320	Theory of photo-ionization defects in nano-porous SiC alloys. Journal of Applied Physics, 2019, 125, 215703.	1.1	1
40321	Unraveling anomalous isotope effect on hydrogen diffusivities in fcc metals from first principles including nuclear quantum effects. Physical Review B, 2019, 100, .	1.1	17

#	Article	IF	Citations
40322	Ferromagnetic nodal-line metal in monolayer <mml:math xmlns:mml="http://www.w3.org/1998/Math/MathML"><mml:mi>h</mml:mi></mml:math> -InC. Physical Review B, 2019, 100, .	1.1	14
40323	Role of Pb2+ Adsorbents on the Opto-Electronic Properties of a CsPbBr3 Nanocrystal: A DFT Study. MRS Advances, 2019, 4, 1981-1988.	0.5	4
40324	Controlling Chiral Spin States of a Triangularâ€Lattice Magnet by Cooling in a Magnetic Field. Advanced Functional Materials, 2019, 29, 1900947.	7.8	4
40325	Highâ€Performance Silicon Anodes Enabled By Nonflammable Localized Highâ€Concentration Electrolytes. Advanced Energy Materials, 2019, 9, 1900784.	10.2	175
40326	Firstâ€Principles Study on the Electronic, Magnetic, and Optical Properties in TM Atom Doped Cadmium Sulfide Nanosheets. Physica Status Solidi (B): Basic Research, 2019, 256, 1900182.	0.7	4
40327	Electrocatalytic hydrodechlorination of 2,4-dichlorophenol over palladium nanoparticles: The critical role of hydroxyl group deprotonation. Applied Catalysis A: General, 2019, 583, 117146.	2.2	29
40328	Catalyzed growth of encapsulated carbyne. Carbon, 2019, 153, 1-5.	5.4	11
40329	Aluminum intercalation and transport in TiO2(B) from first principles. Journal of Energy Storage, 2019, 24, 100800.	3.9	4
40330	First-principles study of Hf/Nb/Zr-doped MAX phases Ti3AlC2 and Ti3SiC2. Physica B: Condensed Matter, 2019, 571, 105-111.	1.3	9
40331	Large-Scale Computational Identification of p-Type Oxide Semiconductors by Hierarchical Screening. Chemistry of Materials, 2019, 31, 5475-5483.	3.2	18
40332	Theoretical Investigation of Propylene Epoxidation on Ag(111) by Molecular Oxygen: Na(K,Cl) Effects. Journal of Physical Chemistry C, 2019, 123, 17273-17282.	1.5	22
40333	First-principles study of phase stability, electronic and mechanical properties of plutonium sub-oxides. Physical Chemistry Chemical Physics, 2019, 21, 16818-16829.	1.3	11
40334	Stabilization of a monolayer tellurene phase at CdTe interfaces. Nanoscale, 2019, 11, 14698-14706.	2.8	10
40335	A new reflowing strategy based on lithiophilic substrates towards smooth and stable lithium metal anodes. Journal of Materials Chemistry A, 2019, 7, 18126-18134.	5.2	32
40336	First-principles prediction of high oxygen-ion conductivity in trilanthanide gallates Ln₃GaO₆. Science and Technology of Advanced Materials, 2019, 20, 144-159.	2.8	9
40337	Understanding intercalation compounds for sodium-ion batteries and beyond. Philosophical Transactions Series A, Mathematical, Physical, and Engineering Sciences, 2019, 377, 20190020.	1.6	33
40338	Optical Properties of Vanadium in 4 H Silicon Carbide for Quantum Technology. Physical Review Applied, 2019, 12, .	1.5	51
40339	High-pressure modulated structures in beryllium chalcogenides. Physical Review B, 2019, 100, .	1.1	3

#	Article	IF	Citations
40340	Anisotropic and plane-selective migration of the carbon vacancy in SiC: Theory and experiment. Physical Review B, 2019, 100, .	1.1	20
40341	Fast anharmonic free energy method with an application to vacancies in ZrC. Physical Review B, 2019, 100, .	1.1	10
40342	Putative hybridization gap in <mml:math xmlns:mml="http://www.w3.org/1998/Math/MathML"><mml:mrow><mml:msub><mml:mi>CaMn</mml:mi><mml:mn>2</mml:mn></m under applied pressure. Physical Review B, 2019, 100, .	1.1	3
40343	Tunable band gap and enhanced ferromagnetism by surface adsorption in monolayer <mml:math xmlns:mml="http://www.w3.org/1998/Math/MathML"><mml:mrow><mml:msub><mml:mi>Cr</mml:mi><mml:mn>2</mml:mn></mml:msub></m Physical Review B, 2019, 99, .	3.7	40
40344	Origin of Fermi-level depinning at TiN/Ge(001) interfaces: first-principles study. Japanese Journal of Applied Physics, 2019, 58, 061007.	0.8	0
40345	New insights into the determination of maximum chemical potentials to account for alkali doping in <mml:math xmlns:mml="http://www.w3.org/1998/Math/MathML" altimg="si12.svg"><mml:mrow><mml:mi>Î²</mml:mi><mml:mtext>-</mml:mtext><mml:msub><mml:mrow><mml:mi mathvariant="normal">In</mml:mi></mml:mrow><mml:mrow><mml:mn>2</mml:mn></mml:mrow></mml:msub><mml:msub><mml:mi mathvariant="normal">S</mml:mi></mml:mrow><mml:mrow><mml:mn>3</mml:mn></mml:mrow></mml:msub></mml:mrow></m by ab initio calculati. Computational Materials Science, 2019, 168, 221-228.	1.4	7
40346	Nitrided FeNi: Chemical versus magnetovolume effects from ab initio. Journal of Magnetism and Magnetic Materials, 2019, 491, 165555.	1.0	1
40347	Strain tunable structural, mechanical and electronic properties of monolayer tin dioxides and dichalcogenides SnX2 (X O, S, Se, Te). Materials Research Bulletin, 2019, 119, 110533.	2.7	20
40348	Copper(I)-Based Highly Emissive All-Inorganic Rare-Earth Halide Clusters. Matter, 2019, 1, 180-191.	5.0	35
40349	Ultrahigh carrier mobilities and high thermoelectric performance at room temperature optimized by strain-engineering to two-dimensional aw-antimonene. Nano Energy, 2019, 63, 103870.	8.2	38
40350	Ignition Threshold of Perovskite-Based Oxides for Solid Fuel Oxidation from First-Principles Calculations. Journal of Physical Chemistry C, 2019, 123, 17644-17649.	1.5	2
40351	Revealing the Conducting Character of the Î²-NiOOH Catalyst through Defect Chemistry. Journal of Physical Chemistry C, 2019, 123, 18895-18904.	1.5	4
40352	Formation of AlF_x Gaseous Phases during High Temperature Etching: A Reactive Force Field Based Molecular Dynamics Study. Journal of Physical Chemistry C, 2019, 123, 16823-16835.	1.5	6
40353	Theoretical Investigation of V₃C₂ MXene as Prospective High-Capacity Anode Material for Metal-Ion (Li, Na, K, and Ca) Batteries. Journal of Physical Chemistry C, 2019, 123, 18207-18214.	1.5	100
40354	Potential Applications of Heterostructures of TMDs with MXenes in Sodium-Ion and Naâ€“O₂ Batteries. Nano Letters, 2019, 19, 5577-5586.	4.5	69
40355	In Situ Hybridizing MoS₂ Microflowers on VS₂ Microflakes in a One-Pot CVD Process for Electrolytic Hydrogen Evolution Reaction. ACS Applied Energy Materials, 2019, 2, 5799-5808.	2.5	53
40356	Transition Metal Chalcogenide Single Layers as an Active Platform for Single-Atom Catalysis. ACS Energy Letters, 2019, 4, 1947-1953.	8.8	43
40357	Superior electrocatalytic hydrogen evolution at engineered non-stoichiometric two-dimensional transition metal dichalcogenide edges. Journal of Materials Chemistry A, 2019, 7, 18357-18364.	5.2	30

#	Article	IF	Citations
40358	First-principles study of Ni adatom migration on graphene with vacancies. RSC Advances, 2019, 9, 18823-18834.	1.7	7
40359	Nonlocal effects on the structural transition of gold clusters from planar to three-dimensional geometries. RSC Advances, 2019, 9, 20989-20999.	1.7	6
40360	Pure and Zr-doped YMnO_{3+Î´}as a YSZ-compatible SOFC cathode: a combined computational and experimental approach. Journal of Materials Chemistry A, 2019, 7, 18589-18602.	5.2	17
40361	Tailoring Storage Capacity and Ion Kinetics in Ti2CO2/ Graphene Heterostructures by Functionalization of Graphene. Physical Review Applied, 2019, 12, .	1.5	17
40362	Coexisting spin resonance and long-range magnetic order of Eu in <mml:math xmlns:mml="http://www.w3.org/1998/Math/MathML"><mml:mrow><mml:msub><mml:mi>EuRbFe</mml:mi><mml:mn>4</mml:mn></ml Physical Review B, 2019, 100, .	1.1	34
40363	Thermodynamic stability of hexagonal and rhombohedral boron nitride under chemical vapor deposition conditions from van der Waals corrected first principles calculations. Journal of Vacuum Science and Technology A: Vacuum, Surfaces and Films, 2019, 37, .	0.9	7
40364	Using DFT Models of Thiophene Adsorption at Transition Metal Interfaces to Interpret Periodic Trends in Thiophene Hydrodesulfurization on Transition Metal Sulfides. Catalysis Letters, 2019, 149, 2953-2960.	1.4	5
40365	Understanding the interfacial interactions of bioinspired chitosan-calcite nanocomposites by first principles molecular dynamics simulations and experimental FT-IR spectroscopy. Carbohydrate Polymers, 2019, 223, 115054.	5.1	9
40366	Ab initio atomistic insights into lead-free formamidinium based hybrid perovskites for photovoltaics and optoelectronics. Computational Materials Science, 2019, 169, 109118.	1.4	50
40367	Investigation of the on-site Coulomb correction and temperature dependence of the stability of Uâ€“Si phases using DFT+U. Journal of Nuclear Materials, 2019, 524, 157-163.	1.3	13
40368	Computational study on catalytic performance of BC3 and NC3 nanosheets as cathode electrocatalysts for nonaqueous Liâ€“O2 batteries. Journal of Power Sources, 2019, 436, 226845.	4.0	24
40369	Trimetallic Ptâ€“Pdâ€“Ni octahedral nanocages with subnanometer thick-wall towards high oxygen reduction reaction. Nano Energy, 2019, 64, 103890.	8.2	34
40370	Vibrational properties of uranium fluorides. Physica B: Condensed Matter, 2019, 570, 194-205.	1.3	5
40371	Manipulating electronic and magnetic properties of black phosphorene with 4d series transition metal adsorption. Physics Letters, Section A: General, Atomic and Solid State Physics, 2019, 383, 2765-2771.	0.9	13
40372	Magnetic ordering contribution on diffusion process forming hollow materials. Solid State Ionics, 2019, 339, 115000.	1.3	2
40373	First-principles study of hydrogen-vacancy complexes in Be12Ti. Journal of Nuclear Materials, 2019, 525, 7-13.	1.3	8
40374	Epitaxial Dimers and Auger-Assisted Detrapping in PbS Quantum Dot Solids. Matter, 2019, 1, 250-265.	5.0	56
40375	Gas molecular adsorption effects on the electronic and optical properties of monolayer SnP3. Vacuum, 2019, 168, 108823.	1.6	20

#	Article	IF	Citations
40376	Reaction Behavior of the NO Molecule on the Surface of an M_n Particle (M = Ru,) Tj ETQq0 0 0 rgBT /Overlock 10 Tf Journal of Physical Chemistry A, 2019, 123, 7021-7033.	1.1	24
40377	Scaling Relation of Oxygen Reduction Reaction Intermediates at Defective TiO₂ Surfaces. Journal of Physical Chemistry C, 2019, 123, 19486-19492.	1.5	20
40378	Understanding the Decomposition Mechanisms of LiNH₂, Mg(NH₂)₂, and NaNH₂: A Joint Experimental and Theoretical Study. Journal of Physical Chemistry C, 2019, 123, 18180-18186.	1.5	9
40379	Reversible Tuning of Ca Nanoparticles Embedded in a Superionic CaF2 Matrix. Journal of Physical Chemistry C, 2019, 123, 19945-19951.	1.5	1
40380	Gallium Thiophosphate: An Emerging Bidirectional Auxetic Two-Dimensional Crystal with Wide Direct Band Gap. Journal of Physical Chemistry Letters, 2019, 10, 4455-4462.	2.1	35
40381	Janus Segregation at the Carbon Nanotubeâ€“Catalyst Interface. ACS Nano, 2019, 13, 8836-8841.	7.3	25
40382	An electrostatic spectral neighbor analysis potential for lithium nitride. Npj Computational Materials, 2019, 5, .	3.5	69
40383	A new perspective on metal particles enhanced MoS2 photocatalysis in hydrogen evolution: Excited electric field by surface plasmon resonance. Journal of Applied Physics, 2019, 126, .	1.1	2
40384	The origin of the conductivity maximum in molten salts. III. Zinc halides. Journal of Chemical Physics, 2019, 151, 034507.	1.2	3
40385	Insights into the interfacial bonding strength of TiB/Ti: A first principles study. Journal of Applied Physics, 2019, 126, .	1.1	8
40386	Diameter effects on the quantum confined Ni nanowire arrays. AIP Conference Proceedings, 2019, , .	0.3	0
40387	Enhanced sensitivity of MoSe₂ monolayer for gas adsorption induced by electric field. Journal of Physics Condensed Matter, 2019, 31, 445301.	0.7	35
40388	Structural stability and band alignment in the c-plane ZnO/GaN heterostructure. Semiconductor Science and Technology, 2019, 34, 095008.	1.0	1
40389	Electronic spin transition in <mml:math xmlns:mml="http://www.w3.org/1998/Math/MathML"><mml:msub><mml:mi>FeO</mml:mi><mml:mn>2</mml:mn></mml:msub></mml: : Evidence for Fe(II) with peroxide <mml:math xmlns:mml="http://www.w3.org/1998/Math/MathML"><mml:msubsup><mml:mi mathvariant="normal">O</mml:mi><mml:mrow><mml:mn>2</mml:mn></mml:mrow><mml:mrow><mml:mn>2</mml:mn><mml:mo> Physical Review B, 2019, 100, .	1.1	17
40390	Free-electron effects on the optical absorption of the hybrid perovskite <mml:math xmlns:mml="http://www.w3.org/1998/Math/MathML"><mml:mrow><mml:msub><mml:mi>CH</mml:mi><mml:mn>3</mml:mn></mml: from first principles. Physical Review B, 2019, 100, .	1.1	7
40391	The Effect of Point Defects on the Electronic Density of States of ScMN2-Type (M = V, Nb, Ta) Phases. Condensed Matter, 2019, 4, 70.	0.8	6
40392	Promoting Highly Reversible Sodium Storage of Iron Sulfide Hollow Polyhedrons via Cobalt Incorporation and Graphene Wrapping. Advanced Energy Materials, 2019, 9, 1901584.	10.2	71
40393	Band Gap Prediction for Large Organic Crystal Structures with Machine Learning. Advanced Quantum Technologies, 2019, 2, 1900023.	1.8	51

#	Article	IF	Citations
40394	Interface intrinsic strengthening mechanism on the tensile properties of Al2O3/Al composites. Computational Materials Science, 2019, 169, 109131.	1.4	18
40395	Electron Attachment Leads to Unidirectional In-Plane Molecular Rotation of Para-Chlorostyrene on Si(100). Journal of Physical Chemistry C, 2019, 123, 18425-18431.	1.5	2
40396	Unraveling the Water Degradation Mechanism of CH₃NH₃PbI₃. Journal of Physical Chemistry C, 2019, 123, 19385-19394.	1.5	63
40397	Continuously Tuning Electronic Properties of Few-Layer Molybdenum Ditelluride with in Situ Aluminum Modification toward Ultrahigh Gain Complementary Inverters. ACS Nano, 2019, 13, 9464-9472.	7.3	36
40398	A semiconducting layered metal-organic framework magnet. Nature Communications, 2019, 10, 3260.	5.8	119
40399	Binding and activation of ethylene on tungsten carbide and platinum surfaces. Physical Chemistry Chemical Physics, 2019, 21, 17332-17342.	1.3	9
40400	Impressive performance of proton-conducting solid oxide fuel cells using a first-generation cathode with tailored cations. Journal of Materials Chemistry A, 2019, 7, 18792-18798.	5.2	84
40401	Anion-mediated electronic effects in reducible oxides: Tuning the valence band of ceria via fluorine doping. Journal of Chemical Physics, 2019, 151, 044701.	1.2	4
40402	Single-atom Fe and N co-doped graphene for lithium-sulfur batteries: a density functional theory study. Materials Research Express, 2019, 6, 095620.	0.8	29
40403	Hydrogenation: An effective strategy to improve the thermoelectric properties of multilayer silicene. Physical Review B, 2019, 99, .	1.1	25
40404	Strain Effect Of Band Gap In Snte Monolayer. , 2019, , .		0
40405	Kinetics of the Atomic Structure of Palladium Nanoparticles during the Desorption of Hydrogen According to X-Ray Diffraction. JETP Letters, 2019, 109, 594-599.	0.4	1
40406	Boron Phosphide Nanoparticles: A Nonmetal Catalyst for Highâ€Selectivity Electrochemical Reduction of CO₂ to CH₃OH. Advanced Materials, 2019, 31, e1903499.	11.1	169
40407	On the Accuracy of Density Functional Theory in Zeolite Catalysis. ChemCatChem, 2019, 11, 4368-4376.	1.8	55
40408	Density, distribution and nature of planar faults in silver antimony telluride for thermoelectric applications. Acta Materialia, 2019, 178, 135-145.	3.8	13
40409	Revealing the active species of Cu-based catalysts for heterogeneous Fenton reaction. Applied Catalysis B: Environmental, 2019, 258, 117985.	10.8	107
40410	Edge effects on Li atom adsorption and migration of MoS2 zigzag nanoribbons. Applied Surface Science, 2019, 494, 223-229.	3.1	7
40411	Two-dimensional nanoporous metal chalcogenophosphates MP2X6 with high electron mobilities. Applied Surface Science, 2019, 493, 1334-1339.	3.1	8

#	Article	IF	Citations
40412	Lithium and calcium decorated triphenylene-graphdiyne as potential high-capacity hydrogen storage medium: A first-principles prediction. Applied Surface Science, 2019, 494, 763-770.	3.1	35
40413	Topological nodal lines in three-dimensional single wall carbon nanotube network. Computational Materials Science, 2019, 169, 109123.	1.4	2
40414	Oxygen adsorption on the doped TiAl(1â€¯0â€¯0) surface. Computational Materials Science, 2019, 170, 109136.	1.4	12
40415	First-principles theoretical and experimental studies of effects of ruthenium on precipitation behavior of Î¼ phase and Î¼/matrix interface stability in Ni-based single crystal superalloys. Intermetallics, 2019, 113, 106556.	1.8	19
40416	Temperature dependence of thermodynamic stability and mechanical property of alloying Co3Ta compounds. Journal of Alloys and Compounds, 2019, 808, 151068.	2.8	3
40417	Thermodynamic description of the sintering aid system in silicon carbide ceramics with the addition of yttrium. Journal of the European Ceramic Society, 2019, 39, 4510-4519.	2.8	15
40418	Structural, magnetic and topological properties in rare-earth-adsorbed silicene system. Journal of Magnetism and Magnetic Materials, 2019, 492, 165606.	1.0	7
40419	Tuning the properties of hydrogenated graphene via interfacial contact of cubic BN (111). Physica B: Condensed Matter, 2019, 571, 257-262.	1.3	2
40420	Improving Electrochemical Pb²⁺ Detection Using a Vertically Aligned 2D MoS₂ Nanofilm. Analytical Chemistry, 2019, 91, 11770-11777.	3.2	73
40421	Simulation of Structural Phase Transitions in Perovskite Methylhydrazinium Metalâ€“Formate Frameworks: Coupled Ising and Potts Models. Journal of Physical Chemistry C, 2019, 123, 19912-19919.	1.5	5
40422	Inquisitive Geometric Sites in h-BN Monolayer for Alkali Earth Metal Ion Batteries. Journal of Physical Chemistry C, 2019, 123, 19340-19346.	1.5	18
40423	Computational Evaluation of Electrocatalytic Nitrogen Reduction on TM Single-, Double-, and Triple-Atom Catalysts (TM = Mn, Fe, Co, Ni) Based on Graphdiyne Monolayers. Journal of Physical Chemistry C, 2019, 123, 19066-19076.	1.5	224
40424	Structureâ€“Optical Behavior Correlation, Optimized Photoluminescence, and DFT Calculation of La₇O₆(BO₃)(PO₄)₂:Sm³⁺ Micropowder for Solid State Lighting. ACS Applied Electronic Materials, 2019, 1, 1688-1697.	2.0	26
40425	P-Substituted Ba_{0.95}La_{0.05}FeO_{3â^'Î´} as a Cathode Material for SOFCs. ACS Applied Energy Materials, 2019, 2, 5472-5480.	2.5	36
40426	Tuning ZnO Sensors Reactivity toward Volatile Organic Compounds via Ag Doping and Nanoparticle Functionalization. ACS Applied Materials & Interfaces, 2019, 11, 31452-31466.	4.0	78
40427	Carbon Monoxide Activation on Cobalt Carbide for Fischerâ€“Tropsch Synthesis from First-Principles Theory. ACS Catalysis, 2019, 9, 8093-8103.	5.5	47
40428	Enhancement of CO₂ Methanation over La-Modified Ni/SBA-15 Catalysts Prepared by Different Doping Methods. ACS Sustainable Chemistry and Engineering, 2019, 7, 14647-14660.	3.2	69
40429	Tunable ferromagnetic Weyl fermions from a hybrid nodal ring. Npj Computational Materials, 2019, 5, .	3.5	15

#	Article	IF	Citations
40430	Atomic scale study of stress-induced misaligned subsurface layers in KDP crystals. Scientific Reports, 2019, 9, 10399.	1.6	5
40431	Theoretical study on the intrinsic properties of In2Se3/MoS2 as a photocatalyst driven by near-infrared, visible and ultraviolet light. Catalysis Science and Technology, 2019, 9, 4659-4667.	2.1	31
40432	Revisiting the charge compensation mechanisms in LiNi_{0.8}Co_{0.2â^'y}Al_yO₂ systems. Materials Horizons, 2019, 6, 2112-2123.	6.4	62
40433	Ionic micro-structure and transport properties of low-temperature aluminium electrolytes containing potassium cryolite and sodium cryolite. Physical Chemistry Chemical Physics, 2019, 21, 16573-16582.	1.3	8
40434	Enhanced photocatalytic and photoelectrochemical performance of g-C3N4/BiVO4 heterojunction: A combined experimental and theoretical study. AIP Advances, 2019, 9, .	0.6	19
40435	Validity of perturbative methods to treat the spinâ€“orbit interaction: application to magnetocrystalline anisotropy. New Journal of Physics, 2019, 21, 073054.	1.2	29
40436	A simple rule for finding Dirac cones in bilayered perovskites*. Chinese Physics B, 2019, 28, 077106.	0.7	4
40437	Electronic and magnetic properties of CrI₃ nanoribbons and nanotubes*. Chinese Physics B, 2019, 28, 077301.	0.7	8
40438	Fabrication of large-scale graphene/2D-germanium heterostructure by intercalation. Chinese Physics B, 2019, 28, 078103.	0.7	6
40439	Modulation of magnetic and electrical properties of bilayer graphene quantum dots using rotational stacking faults*. Chinese Physics B, 2019, 28, 078106.	0.7	4
40440	First-principles insight into Li and Na ion storage in graphene oxide*. Chinese Physics B, 2019, 28, 078201.	0.7	3
40441	Calculation of magnetic moments and lattice parameters Co-based Heusler alloys with determination of their energy favorable structure. Journal of Physics: Conference Series, 2019, 1163, 012051.	0.3	0
40442	Dynamics of cleaning, passivating and doping monolayer MoS ₂ by controlled laser irradiation. 2D Materials, 2019, 6, 045031.	2.0	40
40443	First-principles prediction of switchable metallic ferroelectricity in multiferroic tunnel junctions. Physical Review B, 2019, 99, .	1.1	8
40444	Unveiling Electronic Correlation and the Ferromagnetic Superexchange Mechanism in the van der Waals Crystal <mml:math xmlns:mml="http://www.w3.org/1998/Math/MathML" display="inline"><mml:mrow><mml:msub><mml:mrow><mml:mi>CrSiTe</mml:mi></mml:mrow><mml:mrow><mml:mn>3</mml:mn></ Physical Review Letters, 2019, 123, 047203.	2.9	52
40445	Modulation of Electronic Behaviors of InSe Nanosheet and Nanoribbons: The Firstâ€Principles Study. Advanced Theory and Simulations, 2019, 2, 1900099.	1.3	3
40446	Electronic Properties, Phase Transformation, and Anionic Redox of Monoclinic Na₂MnO₃ Cathode Material for Sodiumâ€Ion Batteries: Firstâ€Principle Calculations. ChemElectroChem, 2019, 6, 3987-3993.	1.7	12
40447	Computational Design of Oneâ€Dimensional Ferromagnetic Semiconductors in Transition Metal Embedded Stannaspherene Nanowires. Chinese Journal of Chemistry, 2019, 37, 1021-1024.	2.6	7

#	Article	IF	Citations
40448	Band structure and thermoelectric properties of Al-doped Mg3â^'xAlxSb2 compounds. Journal of Materials Science: Materials in Electronics, 2019, 30, 15206-15213.	1.1	8
40449	Achieving tolerant CO2 electro-reduction catalyst in real water matrix. Applied Catalysis B: Environmental, 2019, 258, 117961.	10.8	19
40450	Theoretical investigation of surface electronic structure and thermodynamic energies of (1x1) polar and nonpolar K1/2Bi1/2TiO3 (001) surfaces. Journal of Physics and Chemistry of Solids, 2019, 135, 109116.	1.9	2
40451	Dislocation core structures and Peierls stresses of the high-entropy alloy NiCoFeCrMn and its subsystems. Materials and Design, 2019, 180, 107955.	3.3	26
40452	High mobility and photocatalytic properties of NaXO2(X=Co, Rh, Ir). Vacuum, 2019, 168, 108824.	1.6	7
40453	Nonprecious Metal Catalysts for Tuning Discharge Product Distribution at Solidâ€“Solid Interfaces of Aprotic Liâ€“O₂ Batteries. Chemistry of Materials, 2019, 31, 7300-7310.	3.2	25
40454	Theoretical Insights into Li-Ion Transport in LiTa₂PO₈. Journal of Physical Chemistry C, 2019, 123, 19282-19287.	1.5	24
40455	Constant Electrode Potential Quantum Mechanical Study of CO₂ Electrochemical Reduction Catalyzed by N-Doped Graphene. ACS Catalysis, 2019, 9, 8197-8207.	5.5	42
40456	First-principles thermodynamics and experimental study of interface oxidation in Ni/Ni₃Al structures. Physical Chemistry Chemical Physics, 2019, 21, 18316-18327.	1.3	5
40457	Methanol oxidation on the Pt(321) surface: a theoretical approach on the role of surface morphology and surface coverage effects. Physical Chemistry Chemical Physics, 2019, 21, 18227-18239.	1.3	14
40458	An electronic structure governed by the displacement of the indium site in Inâ€“S₆ octahedra: LnOInS₂ (Ln = La, Ce, and Pr). Dalton Transactions, 2019, 48, 12272-12278.	1.6	8
40459	Mo6S8-based single-metal-atom catalysts for direct methane to methanol conversion. Journal of Chemical Physics, 2019, 151, 024304.	1.2	13
40460	Ab initio semi-classical electronic transport in ZnSe: the role of inelastic scattering mechanisms. Journal of Physics Condensed Matter, 2019, 31, 345901.	0.7	4
40461	Picosecond Absorption Spectroscopy of Excited States in BaBrCl with and without Eu Dopant and Au Codopant. Physical Review Applied, 2019, 12, .	1.5	5
40462	Modeling the structural distortion and magnetic ground state of the polar lacunar spinel <mml:math xmlns:mml="http://www.w3.org/1998/Math/MathML"><mml:mrow><mml:msub><mml:mi>GaV</mml:mi><mml:mn>4</mml:mn></mml:msub><mml:mo>,</mml:mo></mml:mrow></mml:math> Physical Review B, 2019, 100, .	1.1	9
40463	Electronic band structure and conduction mechanism of mixed valence <mml:math xmlns:mml="http://www.w3.org/1998/Math/MathML"><mml:mrow><mml:mi mathvariant="normal">T</mml:mi><mml:msup><mml:mrow><mml:mi mathvariant="normal">e</mml:mi></mml:mrow><mml:mrow><mml:mn>4</mml:mn><mml:mo>+</mml:mo></mml:mrow></mml:msup><mml:msub><mml:mrow><mml:mi mathvariant="normal">T</mml:mi></mml:mrow><mml:mrow><mml:mi mathvariant="normal">e</mml:mi></mml:mrow><mml:mrow><mml:mn>6</mml:mn><mml:mo>+</mml:mo></mml:mrow></mml:msub></mml:mrow></mml:math>	1.1	5
40464	Anomalous elastic behavior of phase egg, AlSiO3(OH), at high pressures. American Mineralogist, 2019, 104, 130-139.	0.9	7
40465	Great Enhancement of Carbon Energy Storage through Narrow Pores and Hydrogen-Containing Functional Groups for Aqueous Zn-Ion Hybrid Supercapacitor. Molecules, 2019, 24, 2589.	1.7	38

#	Article	IF	Citations
40466	Oganesson Is a Semiconductor: On the Relativistic Bandâ€Gap Narrowing in the Heaviest Nobleâ€Gas Solids. Angewandte Chemie - International Edition, 2019, 58, 14260-14264.	7.2	22
40467	Firstâ€Principles Study of Structure, Magnetic Properties, and Stability of Î·â€Carbides (M,Fe) 3 W 3 C (Mâ€‰=â€‰Ti,) Tj ETQq1 1 0	0.7	3
40468	The new role of surface adsorbed CH (xâ€¯=â€¯1â€“3) intermediates as a co-adsorbed promoter in self-promoting syngas conversion to form CH intermediates and C2 oxygenates on the Rh-doped Cu catalyst. Journal of Catalysis, 2019, 377, 1-12.	3.1	18
40469	The stability of deformation twins in aluminum enhanced by alloying elements. Journal of Materials Science and Technology, 2019, 35, 2625-2629.	5.6	5
40470	Learn-and-Match Molecular Cations for Perovskites. Journal of Physical Chemistry A, 2019, 123, 7323-7334.	1.1	28
40471	Disparity of the Nature of the Band Gap between Halide and Chalcogenide Single Perovskites for Solar Cell Absorbers. Journal of Physical Chemistry Letters, 2019, 10, 4566-4570.	2.1	16
40472	Breakdown of the Static Picture of Defect Energetics in Halide Perovskites: The Case of the Br Vacancy in CsPbBr₃. Journal of Physical Chemistry Letters, 2019, 10, 4490-4498.	2.1	52
40473	Wide-Bandgap Cu(In,Ga)S₂ Photocathodes Integrated on Transparent Conductive F:SnO₂ Substrates for Chalcopyrite-Based Water Splitting Tandem Devices. ACS Applied Energy Materials, 2019, 2, 5515-5524.	2.5	21
40474	TiCaPCON-Supported Pt- and Fe-Based Nanoparticles and Related Antibacterial Activity. ACS Applied Materials & Interfaces, 2019, 11, 28699-28719.	4.0	16
40475	Physicochemical Properties and Complexity of Amino Acids beyond Our Biosphere: Analysis of the Isoleucine Group from Meteorites. ACS Earth and Space Chemistry, 2019, 3, 1955-1965.	1.2	1
40476	Ultrahigh and anisotropic thermal transport in the hybridized monolayer (BC₂N) of boron nitride and graphene: a first-principles study. Physical Chemistry Chemical Physics, 2019, 21, 17306-17313.	1.3	15
40477	Tuning the Bi³⁺-photoemission color over the entire visible region by manipulating secondary cations modulation in the Sc_xP_{1â^'x}O₄:Bi³⁺ (0 â‰¤ x â‰¤ 1) solid solution. Journal of Materials Chemistry C, 2019, 7, 9865-9877.	2.7	48
40478	Potassium titanyl phosphate (KTP) quasiparticle energies and optical response. JPhys Materials, 2019, 2, 045003.	1.8	8
40479	Optimal transport and colossal ionic mechano-conductance in graphene crown ethers. Science Advances, 2019, 5, eaaw5478.	4.7	37
40480	Thermal unequilibrium of strained black CsPbI ₃ thin films. Science, 2019, 365, 679-684.	6.0	444
40481	Hybrid-Functional and Quasi-Particle Calculations of Band Structures of Mg2Si, Mg2Ge, and Mg2Sn. Journal of the Korean Physical Society, 2019, 75, 144-152.	0.3	20
40482	Influence of Van der Waals Interactions on the Solvation Energies of Adsorbates at Ptâ€Based Electrocatalysts. ChemPhysChem, 2019, 20, 2968-2972.	1.0	16
40483	Theoretical investigation of dissociative and non-dissociative acetic-acid on TiO2-B surfaces. Applied Surface Science, 2019, 494, 850-858.	3.1	8

#	Article	IF	Citations
40484	A first-principles study of Cu and Al doping in ZrO2 for RRAM device applications. Vacuum, 2019, 168, 108842.	1.6	24
40485	Sn₂Ga₂S₅: A Polar Semiconductor with Exceptional Infrared Nonlinear Optical Properties Originating from the Combined Effect of Mixed Asymmetric Building Motifs. Chemistry of Materials, 2019, 31, 6268-6275.	3.2	61
40486	Intrinsic and Extrinsic Defects in Layered Nitride Semiconductor SrTiN₂. Journal of Physical Chemistry C, 2019, 123, 19307-19314.	1.5	9
40487	Interface Structure in Li-Metal/[Pyr₁₄][TFSI]-Ionic Liquid System from ab Initio Molecular Dynamics Simulations. Journal of Physical Chemistry Letters, 2019, 10, 4577-4586.	2.1	31
40488	Highly Dispersed Single-Atom Pt and Pt Clusters in the Fe-Modified KL Zeolite with Enhanced Selectivity for n-Heptane Aromatization. ACS Applied Materials & Interfaces, 2019, 11, 29858-29867.	4.0	49
40489	Overwhelming the Performance of Single Atoms with Atomic Clusters for Platinum-Catalyzed Hydrogen Evolution. ACS Catalysis, 2019, 9, 8213-8223.	5.5	68
40490	Water Enables Efficient CO₂ Capture from Natural Gas Flue Emissions in an Oxidation-Resistant Diamine-Appended Metalâ€“Organic Framework. Journal of the American Chemical Society, 2019, 141, 13171-13186.	6.6	107
40491	Computational and experimental demonstrations of one-pot tandem catalysis for electrochemical carbon dioxide reduction to methane. Nature Communications, 2019, 10, 3340.	5.8	150
40492	Ab initio vibrational free energies including anharmonicity for multicomponent alloys. Npj Computational Materials, 2019, 5, .	3.5	79
40493	Direct cation exchange of CdSe nanocrystals into ZnSe enabled by controlled binding between guest cations and organic ligands. Nanoscale, 2019, 11, 15072-15082.	2.8	12
40494	Metal-free perovskites for non linear optical materials. Chemical Science, 2019, 10, 8187-8194.	3.7	46
40495	First-principles microkinetic study of methane and hydrogen sulfide catalytic conversion to methanethiol/dimethyl sulfide on Mo6S8 clusters: activity/selectivity of different promoters. Catalysis Science and Technology, 2019, 9, 4573-4580.	2.1	5
40496	Intrinsic point defects and the n - and p -type dopability of the narrow gap semiconductors GaSb and InSb. Physical Review B, 2019, 100, .	1.1	16
40497	Graphene Supported Tungsten Carbide as Catalyst for Electrochemical Reduction of CO2. Catalysts, 2019, 9, 604.	1.6	12
40498	Impact of Bonding on the Stacking Defects in Layered Chalcogenides. Advanced Functional Materials, 2019, 29, 1902332.	7.8	21
40499	Local structural coupling of A- and B-site disorder in perovskite bismuth-based piezoelectrics. Acta Materialia, 2019, 177, 222-229.	3.8	3
40500	Towards rigorous multiscale flow models of nanoparticle reactivity in chemical looping applications. Catalysis Today, 2019, 338, 152-163.	2.2	7
40501	First-principles study on the mechanical properties of interstitial solid solution Aluminumâ€“Boron alloy. Computational Materials Science, 2019, 170, 109159.	1.4	3

#	Article	IF	Citations
40502	Opto-electronic properties of stable blue photosensitisers on a TiO2 anatase-101 surface for efficient dye-sensitised solar cells. Chemical Physics Letters, 2019, 731, 136624.	1.2	15
40503	Tunable band-gap of the GeC monolayer by strain and electric field: A first-principles study. Optik, 2019, 195, 163147.	1.4	18
40504	Exploring mechanical, electronic, vibrational, and thermoelectric properties of CaGa2P2, CaGa2As2, and SrGa2As2. Solid State Sciences, 2019, 96, 105942.	1.5	5
40505	Assessment of thermodynamic data for CuCrO2 delafossite from calorimetric measurements. Thermochimica Acta, 2019, 680, 178345.	1.2	4
40506	Analysis of Minerals as Electrode Materials for Ca-based Rechargeable Batteries. Scientific Reports, 2019, 9, 9644.	1.6	28
40507	Iridium-catalyzed growth of single-walled carbon nanotubes with a bicentric diameter distribution. Materials Chemistry Frontiers, 2019, 3, 1882-1887.	3.2	8
40508	Structural engineering of bilayer PtSe₂ thin films: a first-principles study. Journal of Physics Condensed Matter, 2019, 31, 455001.	0.7	16
40509	Effect of substitutional impurities on vibrational properties of zircon: a first-principles study. Journal of Physics Condensed Matter, 2019, 31, 455402.	0.7	5
40510	Manipulating efficient light emission in two-dimensional perovskite crystals by pressure-induced anisotropic deformation. Science Advances, 2019, 5, eaav9445.	4.7	130
40511	New Findings on Multilayer Silicene on Si(111)âˆš3Ã—âˆš3R30Â°â€“Ag Template. Materials, 2019, 12, 2258.	1.3	14
40512	Constructing bimetal-complex based hydrogen-bonded framework for highly efficient electrocatalytic water splitting. Applied Catalysis B: Environmental, 2019, 258, 117973.	10.8	55
40513	Atomistic description of phenol, CO and H2O adsorption over crystalline and amorphous silica surfaces for hydrodeoxygenation applications. Applied Surface Science, 2019, 494, 721-730.	3.1	23
40514	Possible Rashba band splitting and thermoelectric properties in CuI-doped Bi2Te2.7Se0.3 bulk crystals. Journal of Alloys and Compounds, 2019, 806, 636-642.	2.8	18
40515	Salt-controlled dissolution in pigment cathode for high-capacity and long-life magnesium organic batteries. Nano Energy, 2019, 65, 103902.	8.2	49
40516	Weak Ferroelectricity in n = 2 Pseudo Ruddlesdenâ€“Popper-Type Niobate Li₂SrNb₂O₇. Chemistry of Materials, 2019, 31, 6257-6261.	3.2	19
40517	First-Principles Investigation of the Structure and Properties of Au Nanoparticles Supported on ZnO. Journal of Physical Chemistry C, 2019, 123, 21185-21194.	1.5	9
40518	Nonmetal-Atom-Doping-Induced Valley Polarization in Single-Layer Tl₂O. Journal of Physical Chemistry Letters, 2019, 10, 4535-4541.	2.1	54
40519	Phase Transition Pathway Sampling via Swarm Intelligence and Graph Theory. Journal of Physical Chemistry Letters, 2019, 10, 5019-5026.	2.1	10

#	Article	IF	Citations
40520	Reexamination of the Schottky Barrier Heights in Monolayer MoS₂ Field-Effect Transistors. ACS Applied Nano Materials, 2019, 2, 4717-4726.	2.4	27
40521	Hollow Porous Ag Spherical Catalysts for Highly Efficient and Selective Electrocatalytic Reduction of CO₂ to CO. ACS Sustainable Chemistry and Engineering, 2019, 7, 14443-14450.	3.2	40
40522	Analysis of Water Coupling in Inelastic Neutron Spectra of Uranyl Fluoride. Scientific Reports, 2019, 9, 10476.	1.6	5
40523	Ti_{n+1}C_n MXenes with fully saturated and thermally stable Cl terminations. Nanoscale Advances, 2019, 1, 3680-3685.	2.2	81
40524	Photocatalytic Facet Selectivity in BiVO4 Nanoparticles: Polaron Electronic Structure and Thermodynamic Stability Considerations for Photocatalysis. Journal of Physical Chemistry C, 2019, 123, 20142-20151.	1.5	18
40525	Defect Thermodynamics in Nonstoichiometric Alluaudite-Based Polyanionic Materials for Na-Ion Batteries. ACS Applied Materials & Interfaces, 2019, 11, 32856-32868.	4.0	5
40526	Nickel Metal Nanoparticles as Anode Electrocatalysts for Highly Efficient Direct Borohydride Fuel Cells. ACS Catalysis, 2019, 9, 8520-8528.	5.5	46
40527	Effect of External Electric Field on Methane Conversion on IrO₂(110) Surface: A Density Functional Theory Study. ACS Catalysis, 2019, 9, 8230-8242.	5.5	34
40528	Active Oxygen Species Promoted Catalytic Oxidation of 5-Hydroxymethyl-2-furfural on Facet-Specific Pt Nanocrystals. ACS Catalysis, 2019, 9, 8306-8315.	5.5	53
40529	Mechanistic Understanding of Metal Phosphide Host for Sulfur Cathode in High-Energy-Density Lithiumâ€“Sulfur Batteries. ACS Nano, 2019, 13, 8986-8996.	7.3	215
40530	Realizing nearly-free-electron like conduction band in a molecular film through mediating intermolecular van der Waals interactions. Nature Communications, 2019, 10, 3374.	5.8	18
40531	Strain and electric field modulated electronic structure of two-dimensional SiP(SiAs)/GeS van der Waals heterostructures. Journal of Materials Chemistry C, 2019, 7, 10491-10497.	2.7	27
40532	Scratch to sensitize: scratch-induced sensitivity enhancement in semiconductor thin-film sensors. Nanoscale, 2019, 11, 15374-15381.	2.8	1
40533	High intrinsic ZT in InP₃ monolayer at room temperature. Journal of Physics Condensed Matter, 2019, 31, 365501.	0.7	6
40534	Electronic structure and RPA spin susceptibility of anti-PbO type CoSe. Solid State Communications, 2019, 300, 113670.	0.9	0
40535	Correlation Between Reactivity and Oxidation State of Cobalt Oxide Catalysts for CO Preferential Oxidation. ACS Catalysis, 2019, 9, 8325-8336.	5.5	58
40536	Investigation of the electrostatic potential of a grain boundary in Y-substituted BaZrO3 using inline electron holography. Physical Chemistry Chemical Physics, 2019, 21, 17662-17672.	1.3	10
40537	Computational acceleration of prospective dopant discovery in cuprous iodide. Physical Chemistry Chemical Physics, 2019, 21, 18839-18849.	1.3	34

#	Article	IF	Citations
40538	Controlling the secondary pollutant on B-doped g-C₃N₄ during photocatalytic NO removal: a combined DRIFTS and DFT investigation. Catalysis Science and Technology, 2019, 9, 4531-4537.	2.1	20
40539	A computational survey of semiconductors for power electronics. Energy and Environmental Science, 2019, 12, 3338-3347.	15.6	26
40540	Ultrahigh elastically compressible and strain-engineerable intermetallic compounds under uniaxial mechanical loading. APL Materials, 2019, 7, .	2.2	8
40541	Density functional study of structural, electronic and magnetic properties of new half-metallic ferromagnetic double perovskite Sr2MnVO6. Journal of Physics Condensed Matter, 2019, 31, 475501.	0.7	4
40542	Large effect of metal substrate on magnetic anisotropy of Co on hexagonal boron nitride. New Journal of Physics, 2019, 21, 073053.	1.2	10
40543	Atomically precise bottom-up synthesis of Ï€-extended [5]triangulene. Science Advances, 2019, 5, eaav7717.	4.7	159
40544	On the Mechanism of Carbon Dioxide Reduction on Sn-Based Electrodes: Insights into the Role of Oxide Surfaces. Catalysts, 2019, 9, 636.	1.6	21
40545	Ethanol- and Methanol-Coordinated and Solvent-Free Dodecahydro closo-Dodecaborates of 3d Transition Metals and of Magnesium. Crystals, 2019, 9, 372.	1.0	14
40546	Electronic and Optical Properties of Two-Dimensional Tellurene: From First-Principles Calculations. Nanomaterials, 2019, 9, 1075.	1.9	40
40547	Fundamental Properties of Transitionâ€Metalsâ€Adsorbed Graphene. ChemPhysChem, 2019, 20, 2473-2481.	1.0	8
40548	Firstâ€Principles Prediction of the Structural, Electronic, and Magnetic Properties of Nonmetal Atoms Doped Singleâ€Layer CrS 2. Physica Status Solidi (B): Basic Research, 2019, 256, 1900149.	0.7	5
40549	Thermochemical investigation of Zr doping in LiNi_{8/12}Co_{2/12}Mn_{2/12}O₂ based on phase equilibria simulation. International Journal of Quantum Chemistry, 2019, 119, e26028.	1.0	5
40550	DFT calculations in periodic boundary conditions of gas-phase acidities and of transition-metal anionic clusters: case study with carboxylate-stabilized ruthenium clusters. Theoretical Chemistry Accounts, 2019, 138, 1.	0.5	4
40551	Boosting the high-capacity with multi-active centers: A first-principles investigation of NiPS3 monolayer as an anode material. Applied Surface Science, 2019, 495, 143534.	3.1	15
40552	First-principle investigation on multiferroicity and interfacial coupling of nonstoichiometric tetragonal La2/3Sr1/3MnO3/BiCoO3 interface. Current Applied Physics, 2019, 19, 1156-1163.	1.1	0
40553	Theoretical investigations on stable structures of C60-nNn (n=2â€“12): Symmetry, model interaction, and global optimization. Carbon, 2019, 154, 140-149.	5.4	4
40554	Adsorption and mechanistic study for phosphate removal by rice husk-derived biochar functionalized with Mg/Al-calcined layered double hydroxides via co-pyrolysis. Composites Part B: Engineering, 2019, 176, 107209.	5.9	129
40555	Size-dependent bond dissociation enthalpies in single-walled carbon nanotubes. Chemical Physics Letters, 2019, 731, 136628.	1.2	2

#	Article	IF	Citations
40556	Transition-metal-element dependence of ideal shear strength and elastic behaviors of Î³â€²-Ni3Al: ab initio study to guide rational alloy design. Journal of Alloys and Compounds, 2019, 806, 1260-1266.	2.8	17
40557	Electronic and magnetic properties of 3d transition-metal atom adsorbed vacancy-defected arsenene: A first-principles study. Journal of Magnetism and Magnetic Materials, 2019, 491, 165613.	1.0	9
40558	Influence of local surrounding on magnetism in Fe-Ni alloy: A first principles study. Journal of Magnetism and Magnetic Materials, 2019, 492, 165657.	1.0	3
40559	Study on impact of Cr and Mo on diffusion of H in 2.25Cr1Mo steel using first-principle calculations. Journal of Nuclear Materials, 2019, 525, 152-160.	1.3	3
40560	Tuning phase evolution of Î²-MnO2 during microwave hydrothermal synthesis for high-performance aqueous Zn ion battery. Nano Energy, 2019, 64, 103942.	8.2	154
40561	Strain dependent electronic structure and optical properties tuning of InN/PtX2 (X=S, Se) van der waals heterostructures. Vacuum, 2019, 168, 108805.	1.6	13
40562	Controlling the Chemical Bonding of Highly Dispersed Co Atoms Anchored on an Ultrathin g-C₃N₄@Carbon Sphere for Enhanced Electrocatalytic Activity of the Oxygen Evolution Reaction. Inorganic Chemistry, 2019, 58, 10802-10811.	1.9	27
40563	Exploring the Mgâ€“Crâ€“H System at High Pressure and Temperature via in Situ Synchrotron Diffraction. Inorganic Chemistry, 2019, 58, 11043-11050.	1.9	6
40564	Crystal Structures and Energy Storage Properties of Ammine Sodium Decahydro-closo-decaboranes (Na2B10H10Â·nNH3, n = 1, 2). Journal of Physical Chemistry C, 2019, 123, 20160-20166.	1.5	10
40565	Single-Layer PtI2: A Multifunctional Material with Promising Photocatalysis toward the Oxygen Evolution Reaction and Negative Poissonâ€™s Ratio. ACS Applied Materials & Interfaces, 2019, 11, 31793-31798.	4.0	18
40566	Bismuth Vacancy-Tuned Bismuth Oxybromide Ultrathin Nanosheets toward Photocatalytic CO₂ Reduction. ACS Applied Materials & Interfaces, 2019, 11, 30786-30792.	4.0	140
40567	Layer-Dependent Interfacial Transport and Optoelectrical Properties of MoS₂ on Ultraflat Metals. ACS Applied Materials & Interfaces, 2019, 11, 31543-31550.	4.0	33
40568	Highly Polarization-Sensitive, Broadband, Self-Powered Photodetector Based on Graphene/PdSe₂/Germanium Heterojunction. ACS Nano, 2019, 13, 9907-9917.	7.3	420
40569	Strong stress-composition coupling in lithium alloy nanoparticles. Nature Communications, 2019, 10, 3428.	5.8	13
40570	Thermodynamic Stability and Structural Insights for CH3NH3Pb1â^'xSixI3, CH3NH3Pb1â^'xGexI3, and CH3NH3Pb1â^'xSnxI3 Hybrid Perovskite Alloys: A Statistical Approach from First Principles Calculations. Scientific Reports, 2019, 9, 11061.	1.6	14
40571	The influence of dilute aluminum and molybdenum on stacking fault and twin formation in FeNiCoCr-based high entropy alloys based on density functional theory. Scientific Reports, 2019, 9, 10940.	1.6	16
40572	First-principles study of alkali-metal intercalation in disordered carbon anode materials. Journal of Materials Chemistry A, 2019, 7, 19070-19080.	5.2	68
40573	Unoccupied electronic band structure of pentagonal Si nanoribbons on Ag(110). Physical Chemistry Chemical Physics, 2019, 21, 17811-17820.	1.3	9

#	Article	IF	Citations
40574	A comparative study on modeling of the ferromagnetic and paramagnetic states of uranium hydride using a DFT+U method. Physical Chemistry Chemical Physics, 2019, 21, 17628-17639.	1.3	5
40575	Intrinsically low thermal conductivity of bismuth oxychalcogenides originating from interlayer coupling. Physical Chemistry Chemical Physics, 2019, 21, 18259-18264.	1.3	12
40576	Atomistic design favored compositions and atomic-level structure of Mgâ€“Caâ€“Ag ternary metallic glasses. AIP Advances, 2019, 9, .	0.6	3
40577	A comprehensive assessment of the low-temperature thermal properties and thermodynamic functions of CeO2. Journal of Chemical Physics, 2019, 151, 044202.	1.2	5
40578	Stress- and electric-field-induced band gap tuning in hexagonal boron phosphide layers. Journal of Physics Condensed Matter, 2019, 31, 465502.	0.7	10
40579	Characterization of the energetics and configurations of hydrogen in vacancy clusters in tungsten. Nuclear Fusion, 2019, 59, 106032.	1.6	16
40580	Highâ€pressure Raman spectroscopy of CeOCl: Observation of the isostructural phase transition. Journal of Raman Spectroscopy, 2019, 50, 1962-1968.	1.2	5
40581	Group-theoretical high-order rotational invariants for structural representations: Application to linearized machine learning interatomic potential. Physical Review B, 2019, 99, .	1.1	31
40582	Insight into the Role of Water on the Methylation of Hexamethylbenzene in Hâ€SAPOâ€34 from First Principle Molecular Dynamics Simulations. ChemCatChem, 2019, 11, 3993-4010.	1.8	17
40583	Microstructure, magnetic and transport properties of a Mn2CoAl Heusler compound. Acta Materialia, 2019, 176, 33-42.	3.8	35
40584	Atomistic simulation of fracture in UO2 under tensile loading. Journal of Alloys and Compounds, 2019, 803, 42-50.	2.8	3
40585	Adsorption, diffusion, and permeation of hydrogen at PdCu surfaces. Journal of Membrane Science, 2019, 588, 117206.	4.1	24
40586	Noncovalent Close Contacts in Fluorinated Thiopheneâ€“Phenyleneâ€“Thiophene Conjugated Units: Understanding the Nature and Dominance of OÂ·Â·Â·H versus SÂ·Â·Â·F and OÂ·Â·Â·F Interactions with Respect to the Control of Polymer Conformation. Chemistry of Materials, 2019, 31, 7070-7079.	3.2	23
40587	Understanding the Acidic Properties of the Amorphous Hydroxylated Silica Surface. Journal of Physical Chemistry C, 2019, 123, 17343-17352.	1.5	37
40588	Electrochemical Synthesis of Cation Vacancy-Enriched Ultrathin Bimetallic Oxyhydroxide Nanoplatelets for Enhanced Water Oxidation. ACS Applied Materials & Interfaces, 2019, 11, 25958-25966.	4.0	25
40589	Impact of Transition Metal Carbide and Nitride Supports on the Electronic Structure of Thin Platinum Overlayers. ACS Catalysis, 2019, 9, 7090-7098.	5.5	30
40590	Monte-Carlo simulation combined with density functional theory to investigate the equilibrium thermodynamics of electrode materials: lithium titanates as model compounds. Physical Chemistry Chemical Physics, 2019, 21, 15551-15559.	1.3	10
40591	Realization of versatile electronic, magnetic properties and new topological phases in hydrogenated bismuthene. Electronic Structure, 2019, 1, 025003.	1.0	2

#	Article	IF	Citations
40592	Magnon-polaron excitations in the noncollinear antiferromagnet Mn3Ge. Physical Review B, 2019, 99, .	1.1	18
40593	Higher-Order Topology of the Axion Insulator <mml:math xmlns:mml="http://www.w3.org/1998/Math/MathML" display="inline"><mml:mrow><mml:mrow><mml:msub><mml:mrow><mml:mi>EuIn</mml:mi></mml:mrow><mml:mrow><mml:mn> Physical Review Letters, 2019, 122, 256402.	2.9	218
40594	Structure and stability of (Cr, Fe)7C3 ternary carbides in solid and liquid state. Journal of Alloys and Compounds, 2019, 804, 566-572.	2.8	8
40595	Doping strain induced bi-Ti3+ pairs for efficient N2 activation and electrocatalytic fixation. Nature Communications, 2019, 10, 2877.	5.8	279
40596	Magnetism in bimetallic PtxNiNâ^'x clusters via cross-atomic coupling. Journal of Materials Chemistry C, 2019, 7, 9293-9300.	2.7	1
40597	Tunable pH-dependent oxygen evolution activity of strontium cobaltite thin films for electrochemical water splitting. Physical Chemistry Chemical Physics, 2019, 21, 16230-16239.	1.3	13
40598	Single molybdenum center supported on N-doped black phosphorus as an efficient electrocatalyst for nitrogen fixation. Nanoscale, 2019, 11, 13600-13611.	2.8	102
40599	Mechanical deformation induced charge redistribution to promote the high performance of stretchable magnesium-ion batteries based on two-dimensional C₂N anodes. Nanoscale, 2019, 11, 15472-15478.	2.8	14
40600	Superflexible C₆₈-graphyne as a promising anode material for lithium-ion batteries. Journal of Materials Chemistry A, 2019, 7, 17357-17365.	5.2	19
40601	First-principles study of electronic, optical and thermal transport properties of group IIIâ€"VI monolayer MX (Mâ€‰=â€‰Ga, In; Xâ€‰=â€‰S, Se). Journal of Applied Physics, 2019, 125, .	1.1	61
40602	Signatures for half-metallicity and nontrivial surface states in the kagome lattice Weyl semimetal <mml:math xmlns:mml="http://www.w3.org/1998/Math/MathML"><mml:mrow><mml:msub><mml:mi>Co</mml:mi><mml:mn>3</mml:mn></mml:msub><mml:msub><mml:mi mathvariant="normal">S</mml:mi><mml:mn>2</mml:mn></mml:msub></mml:mrow></mml:math>. Physical Review B, 2019, 99, .	1.1	38
40603	Effective thickness and mechanical properties of Î²-phases of two-dimensional pnictogen nanosheets. Journal of Nanoparticle Research, 2019, 21, 1.	0.8	4
40604	Electronic Structure and Theoretical Aspects on Sensing Application of 2D Materials. , 2019, , 145-203.		7
40605	Effects of composition and morphology on the hydrogen storage properties of transition metal hydrides: Insights from PtPd nanoclusters. Nano Energy, 2019, 63, 103858.	8.2	15
40606	Geometric and electronic properties of rutile TiO2 with vanadium implantation: A first-principles calculation. Nuclear Instruments & Methods in Physics Research B, 2019, 455, 35-38.	0.6	5
40607	Coupling the High-Throughput Property Map to Machine Learning for Predicting Lattice Thermal Conductivity. Chemistry of Materials, 2019, 31, 5145-5151.	3.2	63
40608	MoTe₂ Lateral Homojunction Field-Effect Transistors Fabricated using Flux-Controlled Phase Engineering. ACS Nano, 2019, 13, 8035-8046.	7.3	75
40609	Effect of structure and composition on the electronic excitation induced amorphization of La2Ti2â^'xZrxO7 ceramics. Scientific Reports, 2019, 9, 8190.	1.6	11

#	Article	IF	Citations
40610	Design and optimization of cobalt-encapsulating vertical graphene nano-hills for hydrogen evolution reaction. Journal of Materials Chemistry A, 2019, 7, 17046-17052.	5.2	11
40611	Transport and topological properties of ThOCh(Ch: S, Se and Te) in bulk and monolayer: a first principles study. Journal of Physics Condensed Matter, 2019, 31, 435504.	0.7	0
40612	Electrical and magnetic properties of thin films of the spin-filter material CrVTiAl. Physical Review B, 2019, 99, .	1.1	11
40613	Anomalous electron transport in epitaxial NdNiO3 films. Physical Review B, 2019, 99, .	1.1	19
40614	Alloy-Free Band Gap Tuning across the Visible Spectrum. Physical Review Letters, 2019, 122, 256403.	2.9	37
40615	Thermodynamic assessment of the Niâ€“Te system. Journal of Materials Science, 2019, 54, 11304-11319.	1.7	18
40616	Scanning Kelvin Probe Force Microscopy and Density Functional Theory Studies on the Surface Potential of the Intermetallics in AA7075-T6 Alloys. Journal of Materials Engineering and Performance, 2019, 28, 4289-4301.	1.2	8
40617	The electronic and optical properties of monovalent atom-doped ZnO monolayers: the density functional theory. Bulletin of Materials Science, 2019, 42, 1.	0.8	14
40618	Mechanical peeling of van der Waals heterostructures: Theory and simulations. Extreme Mechanics Letters, 2019, 30, 100501.	2.0	28
40619	Electronic structure, magnetic, optical and thermodynamic properties of Ni2Mn1-xRexSn and NiMn1-xRexSn Heusler alloys â€“ ab-initio study. Journal of Alloys and Compounds, 2019, 803, 153-164.	2.8	7
40620	Three dimensional metallic porous SiC4 allotropes: Stability and battery applications. Nano Energy, 2019, 63, 103862.	8.2	15
40621	Influence of the vacancy-defect and transition-metal doping in arsenene: A first-principles study. Superlattices and Microstructures, 2019, 132, 106163.	1.4	13
40622	The structure, mechanical and electronic properties of WSi2 from first-principles investigations. Vacuum, 2019, 167, 374-381.	1.6	63
40623	Interplay of Collective Electrostatic Effects and Level Alignment Dictates the Tunneling Rates across Halogenated Aromatic Monolayer Junctions. Journal of Physical Chemistry Letters, 2019, 10, 4142-4147.	2.1	25
40624	KSCN-induced Interfacial Dipole in Black TiO₂ for Enhanced Photocatalytic CO₂ Reduction. ACS Applied Materials & Interfaces, 2019, 11, 25186-25194.	4.0	54
40625	New insights into Li diffusion in Liâ€“Si alloys for Si anode materials: role of Si microstructures. Nanoscale, 2019, 11, 14042-14049.	2.8	17
40626	Unraveling photoexcitation dynamics at â€œdots-in-a-perovskiteâ€•heterojunctions from first-principles. Journal of Materials Chemistry A, 2019, 7, 18012-18019.	5.2	12
40627	Oxygen migration and proton diffusivity in transition-metal (Mn, Fe, Co, and Cu) doped Ruddlesdenâ€“Popper oxides. Journal of Materials Chemistry A, 2019, 7, 18558-18567.	5.2	56

#	Article	IF	Citations
40628	High pressure theoretical and experimental analysis of the bandgap of BaMoO4, PbMoO4, and CdMoO4. Applied Physics Letters, 2019, 115, .	1.5	24
40629	Adsorption of Common Transition Metal Atoms on Arsenene: A First-Principles Study. Russian Journal of Physical Chemistry A, 2019, 93, 1088-1092.	0.1	3
40630	High Thermoelectric Performance in PbSeâ€“NaSbSe₂ Alloys from Valence Band Convergence and Low Thermal Conductivity. Advanced Energy Materials, 2019, 9, 1901377.	10.2	54
40631	Enhanced catalytic performance of Pdâ€Ga bimetallic catalysts for 2â€ethylanthraquinone hydrogenation. Applied Organometallic Chemistry, 2019, 33, e5076.	1.7	6
40632	Triphenyleneâ€Derived Electron Acceptors and Donors on Ag(111): Formation of Intermolecular Chargeâ€Transfer Complexes with Common Unoccupied Molecular States. Small, 2019, 15, e1901741.	5.2	10
40633	Impurity diffusion coefficients in BCC Nb from first-principles calculations. Journal of Alloys and Compounds, 2019, 803, 684-688.	2.8	12
40634	CsPbBrCl2/g-C3N4 type II heterojunction as efficient visible range photocatalyst. Journal of Hazardous Materials, 2019, 380, 120855.	6.5	124
40635	The nature of Ni-O pairs for ethane activation on NiO(100) and NiO(110) surfaces. Molecular Catalysis, 2019, 474, 110417.	1.0	7
40636	Efficient direct electron transfer via band alignment in hybrid metal-semiconductor nanostructures toward enhanced photocatalysts. Nano Energy, 2019, 63, 103841.	8.2	13
40637	Elastic properties of Î±- and Î²-tantalum thin films. Thin Solid Films, 2019, 688, 137403.	0.8	18
40638	Revealing the Mechanism of Multiwalled Carbon Nanotube Growth on Supported Nickel Nanoparticles by in Situ Synchrotron X-ray Diffraction, Density Functional Theory, and Molecular Dynamics Simulations. ACS Catalysis, 2019, 9, 6999-7011.	5.5	36
40639	Transition Metal Atoms Embedded in Graphene: How Nitrogen Doping Increases CO Oxidation Activity. ACS Catalysis, 2019, 9, 6864-6868.	5.5	72
40640	Exploring Metalâ€“Support Interactions To Immobilize Subnanometer Co Clusters on Î³â€“Mo₂N: A Highly Selective and Stable Catalyst for CO₂ Activation. ACS Catalysis, 2019, 9, 9087-9097.	5.5	50
40641	Interfacing Epitaxial Dinickel Phosphide to 2D Nickel Thiophosphate Nanosheets for Boosting Electrocatalytic Water Splitting. ACS Nano, 2019, 13, 7975-7984.	7.3	171
40642	Interface-mediated Kirkendall effect and nanoscale void migration in bimetallic nanoparticles during interdiffusion. Nature Communications, 2019, 10, 2831.	5.8	42
40643	Tailoring phononic, electronic, and thermoelectric properties of orthorhombic GeSe through hydrostatic pressure. Scientific Reports, 2019, 9, 9490.	1.6	21
40644	Improve the performance of machine-learning potentials by optimizing descriptors. Journal of Chemical Physics, 2019, 150, 244110.	1.2	14
40645	Pdâ€“H and Niâ€“H phase diagrams using cluster variation method and Monte Carlo simulation. Philosophical Magazine, 2019, 99, 2376-2392.	0.7	4

#	Article	IF	Citations
40646	Phonon and electron transport in Janus monolayers based on InSe. Journal of Physics Condensed Matter, 2019, 31, 435501.	0.7	27
40647	Electrically controlled spin-switch and evolution of Hanle spin precession in graphene. 2D Materials, 2019, 6, 035042.	2.0	12
40648	Electromagnetic and Chemical Enhancements of Surfaceâ€Enhanced Raman Scattering Spectra from Cu₂O Hexagonal Nanoplates. Advanced Materials Interfaces, 2019, 6, 1900534.	1.9	16
40649	First principles investigations of the structural, elastic, vibrational, and thermodynamic properties of TiMg2O4 oxide spinels: cubic and tetragonal phases. Journal of Molecular Modeling, 2019, 25, 210.	0.8	1
40650	Surface charge-induced activation of Ni-loaded CdS for efficient and robust photocatalytic dehydrogenation of methanol. Applied Catalysis B: Environmental, 2019, 257, 117869.	10.8	41
40651	Development of Pdn/g-C3N4 adsorbent for Hg0 removal â€“ DFT study of influences of the support and Pd cluster size. Fuel, 2019, 254, 115537.	3.4	32
40652	A first-principles simulation of the metal borohydride ammonia borane complex (LiBH4)2(NH3BH3) and the decomposition reaction pathway for hydrogen storage. International Journal of Hydrogen Energy, 2019, 44, 20121-20132.	3.8	3
40653	On the mechanism of alkyne hydrogenation catalyzed by Ga-doped ceria. Journal of Catalysis, 2019, 375, 410-418.	3.1	43
40654	Structural and electronic properties of monolayer group III-VII compounds: A first-principle study. Physica E: Low-Dimensional Systems and Nanostructures, 2019, 114, 113605.	1.3	2
40655	Atomic Layer Deposition of Pt Thin Films Using Dimethyl (N,N-Dimethyl-3-Butene-1-Amine-N) Platinum and O₂ Reactant. Chemistry of Materials, 2019, 31, 5056-5064.	3.2	21
40656	Solving the Coloring Problem in Half-Heusler Structures: Machine-Learning Predictions and Experimental Validation. Inorganic Chemistry, 2019, 58, 9280-9289.	1.9	17
40657	Short-Range and Long-Range Order in AFMâ€“FM Exchange Coupled Compound LiCu2(VO4)(OH)2. Journal of Physical Chemistry C, 2019, 123, 17933-17942.	1.5	2
40658	Unsupervised word embeddings capture latent knowledge from materials science literature. Nature, 2019, 571, 95-98.	13.7	590
40659	Two-dimensional MoS₂/Fe-phthalocyanine hybrid nanostructures as excellent electrocatalysts for hydrogen evolution and oxygen reduction reactions. Nanoscale, 2019, 11, 14266-14275.	2.8	32
40660	Direct observation of reversible conversion and alloying reactions in a Bi₂(MoO₄)₃-based lithium-ion battery anode. Journal of Materials Chemistry A, 2019, 7, 17906-17913.	5.2	9
40661	H permeation in molybdenum: temperature dependence and compensation effect from first-principles simulation. Journal of Nuclear Science and Technology, 2019, 56, 1014-1028.	0.7	2
40662	Estimating the Stability of the Structure of MAX Phases of Ti3AlC2Ââ€“ÂÑ…BÑ… Composition on the Basis of Quantum-Chemical Calculations. Russian Journal of Physical Chemistry A, 2019, 93, 1277-1280.	0.1	1
40663	Experimental Evidence of Large Bandgap Energy in Atomically Thin AlN. Advanced Functional Materials, 2019, 29, 1902608.	7.8	21

#	Article	IF	Citations
40664	Boosting Oxygen Evolution Kinetics by Mnâ€“Nâ€“C Motifs with Tunable Spin State for Highly Efficient Solarâ€Driven Water Splitting. Advanced Energy Materials, 2019, 9, 1901505.	10.2	121
40665	Comparative study of density functionals for the description of lithiumâ€graphite intercalation compounds. Journal of Computational Chemistry, 2019, 40, 2400-2412.	1.5	21
40666	Atomic insights into regulation of graphene sheets vertically attached to the FeF3Â·0.33H2O (002) surface by cation doping. Current Applied Physics, 2019, 19, 1103-1110.	1.1	0
40667	Pressure-induced novel metallic phase in non-stoichiometric cadmium selenides: A first-principles study. Computational Materials Science, 2019, 167, 191-197.	1.4	2
40668	Theoretical investigation of strain-engineered WSe2 monolayers as anode material for Li-ion batteries. Journal of Alloys and Compounds, 2019, 804, 370-375.	2.8	39
40669	Photocatalytic oxidation of methanol to formaldehyde on bismuth-based semiconductors. Journal of Hazardous Materials, 2019, 380, 120822.	6.5	35
40670	A molecular dynamics study of the behavior of Xe in U3Si2. Journal of Nuclear Materials, 2019, 523, 413-420.	1.3	9
40671	Quantum-Dot-Derived Catalysts for CO2 Reduction Reaction. Joule, 2019, 3, 1703-1718.	11.7	106
40672	Stability, electronic and mechanical properties of superhard materials formed by 4+6+8 membered rings of carbon. Journal of Solid State Chemistry, 2019, 277, 454-465.	1.4	4
40673	Enhancement of Ethane Selectivity in Ethaneâ€“Ethylene Mixtures by Perfluoro Groups in Zr-Based Metal-Organic Frameworks. ACS Applied Materials & Interfaces, 2019, 11, 27410-27421.	4.0	69
40674	Multiple superionic states in heliumâ€“water compounds. Nature Physics, 2019, 15, 1065-1070.	6.5	69
40675	High-throughput screening and classification of layered di-metal chalcogenides. Nanoscale, 2019, 11, 13924-13933.	2.8	11
40676	Direct atomic-scale observation of the Ag⁺ diffusion structure in the quasi-2D â€œliquid-likeâ€•state of superionic thermoelectric AgCrSe₂. Journal of Materials Chemistry C, 2019, 7, 9263-9269.	2.7	16
40677	Designing ultrastrong 5d transition metal diborides with excellent stability for harsh service environments. Physical Chemistry Chemical Physics, 2019, 21, 16095-16107.	1.3	7
40678	Pressure-induced modification of the anomalous Hall effect in layered <mml:math xmlns:mml="http://www.w3.org/1998/Math/MathML"><mml:mrow><mml:msub><mml:mi>Fe</mml:mi><mml:mn>1</mml:mn></mml:msub></mml:r Physical Review B, 2019, 100, .	1.1	32
40679	Metallization and superconductivity in potassium-doped methane. International Journal of Modern Physics C, 2019, 30, 1950061.	0.8	11
40680	An unexpected interaction between a H2O2 molecule and anatase TiO2(101) surface. Applied Surface Science, 2019, 493, 926-932.	3.1	5
40681	The chemical nature of N doping on N doped carbon supported noble metal catalysts. Journal of Catalysis, 2019, 375, 456-465.	3.1	76

#	Article	IF	Citations
40682	Activating MoS2 basal planes for hydrogen evolution through the As doping and strain. Physics Letters, Section A: General, Atomic and Solid State Physics, 2019, 383, 2997-3000.	0.9	11
40683	Spatial Phase Distributions in Solution-Based and Evaporated Csâ€“Pbâ€“Br Thin Films. Journal of Physical Chemistry C, 2019, 123, 17666-17677.	1.5	16
40684	The Impact of Coordination Environment on the Thermodynamic Stability of Uranium Oxides. Journal of Physical Chemistry C, 2019, 123, 15985-15995.	1.5	7
40685	Strain-Tailored Valley Polarization and Magnetic Anisotropy in Two-Dimensional 2H-VS₂/Cr₂C Heterostructures. Journal of Physical Chemistry C, 2019, 123, 17440-17448.	1.5	38
40686	Band Alignments, Band Gap, Core Levels, and Valence Band States in Cu₃BiS₃ for Photovoltaics. ACS Applied Materials & Interfaces, 2019, 11, 27033-27047.	4.0	37
40687	High-pressure synthesis of ultraincompressible hard rhenium nitride pernitride Re2(N2)(N)2 stable at ambient conditions. Nature Communications, 2019, 10, 2994.	5.8	65
40688	Dielectric properties and the role of grain boundaries in polycrystalline tetracene at high pressures. CrystEngComm, 2019, 21, 4507-4512.	1.3	6
40689	Fabrication of surface hydroxyl modified g-C₃N₄with enhanced photocatalytic oxidation activity. Catalysis Science and Technology, 2019, 9, 3979-3993.	2.1	51
40690	Strain to alter the covalency and superconductivity in transition metal diborides. Journal of Materials Chemistry C, 2019, 7, 10700-10707.	2.7	9
40691	SrPt3In2â€“ an orthorhombically distorted coloring variant of SrIn5. Dalton Transactions, 2019, 48, 11411-11420.	1.6	0
40692	Ab initio inversion of structure and the lattice dynamics of a metallic glass: the case of Pd₄₀Ni₄₀P₂₀. Modelling and Simulation in Materials Science and Engineering, 2019, 27, 075002.	0.8	5
40693	Correlation effects in the ground state of Ni-(Co)-Mn-Sn Heusler compounds. MRS Advances, 2019, 4, 441-446.	0.5	3
40694	MXene Electrode Materials for Electrochemical Energy Storage: First-Principles and Grand Canonical Monte Carlo Simulations. MRS Advances, 2019, 4, 1833-1841.	0.5	6
40695	cartesius fort - object fortran Library for Chemistry and Materials Science. Lecture Notes in Computer Science, 2019, , 639-651.	1.0	3
40696	Metallic glasses for biodegradable implants. Acta Materialia, 2019, 176, 297-305.	3.8	25
40697	Structure-dependent catalytic properties of mesoporous cobalt oxides in furfural hydrogenation. Applied Catalysis A: General, 2019, 583, 117125.	2.2	22
40698	Facile synthesized Fe nanosheets as superior active catalyst for hydrogen storage in MgH2. International Journal of Hydrogen Energy, 2019, 44, 21955-21964.	3.8	100
40699	Embedded atom potential for Smâ€“Co compounds obtained by force-matching. Journal of Magnetism and Magnetic Materials, 2019, 490, 165468.	1.0	2

#	Article	IF	Citations
40700	Unusual magnetic and electronic properties of Al-substituted Ga2MnNi: An ab initio study. Journal of Magnetism and Magnetic Materials, 2019, 490, 165521.	1.0	3
40701	TiSe2 cathode for beyond Li-ion batteries. Journal of Power Sources, 2019, 436, 226813.	4.0	36
40702	Ligand-Dependent Energetics for Dehydrogenation: Implications in Li-Ion Battery Electrolyte Stability and Selective Oxidation Catalysis of Hydrogen-Containing Molecules. Chemistry of Materials, 2019, 31, 5464-5474.	3.2	28
40703	Environmental stability of bismuthene: oxidation mechanism and structural stability of 2D pnictogens. Journal of Materials Chemistry C, 2019, 7, 9195-9202.	2.7	40
40704	Prominent out-of-plane diffraction in helium scattering from a methyl-terminated Si(111) surface. Physical Chemistry Chemical Physics, 2019, 21, 15879-15887.	1.3	2
40705	Theoretical Modeling of the Thermoelectric Properties of Fe2Ti1 â€“xVxSn Heusler Alloys. Semiconductors, 2019, 53, 865-868.	0.2	1
40706	Theoretical prediction of piezoelectric property of new LiNbO3-type compound AlTlO3. MRS Advances, 2019, 4, 531-537.	0.5	0
40707	The Electronic Structure and Optical Properties of Twoâ€Dimensional BiOXâ€“YO₃ (Xâ€‰=â€‰Cl, Br) Tj ETQq1 1 0.784	0.7	2
40708	BaAs3: a narrow gap 2D semiconductor with vacancy-induced semiconductorâ€“metal transition from first principles. Journal of Materials Science, 2019, 54, 12676-12687.	1.7	3
40709	Effect of Hydrogen on the Substructure of Lenticular Martensite in Fe-31Ni Alloy. Metallurgical and Materials Transactions A: Physical Metallurgy and Materials Science, 2019, 50, 4027-4036.	1.1	7
40710	Computationally Guided Discovery of the Sulfide Li₃AlS₃ in the Liâ€“Alâ€“S Phase Field: Structure and Lithium Conductivity. Chemistry of Materials, 2019, 31, 9699-9714.	3.2	17
40711	Effect of Nonmagnetic Ion Deficiency on Magnetic Structure: Density Functional Study of Sr₂MnO₂Cu_{2â€“x}Te₂, Sr₂MO₂Cu₂Te₂ (M = Co, Mn), and the Oxide-Hydrides Sr₂VO₃H, Sr₃V₂O₅H₂, and Sr₃V₂O₄H. Inorganic Chemistry, 2019, 58, 14769-14776.	1.9	1
40712	Microhydration of Polymer Electrolyte Membranes: A Comparison of Hydrogen-Bonding Networks and Spectral Properties of Nafion and Bis[(perfluoroalkyl)sulfonyl] Imide. Journal of Physical Chemistry B, 2019, 123, 9899-9911.	1.2	3
40713	Electrochemical Oxygen-Reduction Activity and Carbon Monoxide Tolerance of Iron Phthalocyanine Functionalized with Graphene Quantum Dots: A Density Functional Theory Approach. Journal of Physical Chemistry C, 2019, 123, 27483-27491.	1.5	10
40714	Surface Functionalization of Reconstructed Si(111) with Methionine. Journal of Physical Chemistry C, 2019, 123, 26980-26988.	1.5	2
40715	Iodine Adsorption on Ni(110): 2D-Phase Transitions and NiI₂ Growth. Journal of Physical Chemistry C, 2019, 123, 27659-27665.	1.5	3
40716	Inorganic and Pb-Free CsBi₃I₁₀ Thin Film for Photovoltaic Applications. Journal of Physical Chemistry C, 2019, 123, 27423-27428.	1.5	37
40717	Deep Molecular Orbital Driven High-Temperature Hydrogen Tautomerization Switching. Journal of Physical Chemistry Letters, 2019, 10, 6755-6761.	2.1	12

#	Article	IF	Citations
40718	Mo Concentration Controls the Morphological Transitions from Dendritic to Semicompact, and to Compact Growth of Monolayer Crystalline MoS2 on Various Substrates. ACS Applied Materials & Interfaces, 2019, 11, 42751-42759.	4.0	30
40719	A Robust Au/ZnCr₂O₄ Catalyst with Highly Dispersed Gold Nanoparticles for Gas-Phase Selective Oxidation of Cyclohexanol to Cyclohexanone. ACS Catalysis, 2019, 9, 11104-11115.	5.5	20
40720	Elucidating the Mechanism of Electrochemical N₂ Reduction at the Ru(0001) Electrode. ACS Catalysis, 2019, 9, 11137-11145.	5.5	78
40721	Dopant-tuned stabilization of intermediates promotes electrosynthesis of valuable C3 products. Nature Communications, 2019, 10, 4807.	5.8	26
40722	Extreme nonlinear strong-field photoemission from carbon nanotubes. Nature Communications, 2019, 10, 4891.	5.8	16
40723	Three-dimensional open nano-netcage electrocatalysts for efficient pH-universal overall water splitting. Nature Communications, 2019, 10, 4875.	5.8	253
40724	Dynamic oxygen adsorption on single-atomic Ruthenium catalyst with high performance for acidic oxygen evolution reaction. Nature Communications, 2019, 10, 4849.	5.8	416
40725	Electronic, mechanical and lattice dynamical properties of YXB₄ (X = Cr, Mn, Fe, and Co) compounds. Physica Scripta, 2019, 94, 125710.	1.2	6
40726	Structural model of substitutional sulfur in diamond*. Chinese Physics B, 2019, 28, 088102.	0.7	5
40727	Vacancy defects effect on thermal conductivity of Î±-zirconium crystal. Materials Research Express, 2019, 6, 116531.	0.8	3
40728	Magnetic coupling in L10-MnGa/Ni films. Materials Research Express, 2019, 6, 116414.	0.8	1
40729	Electronic structure and mechanical properties of crystalline precipitate phases M₂₃C₆(M=Cr, W, Mo, Fe) in Ni-based superalloys. Materials Research Express, 2019, 6, 116323.	0.8	6
40730	Effects of defects on the electronic and optical properties of TiO ₂ nanosheet. Electronic Structure, 2019, 1, 044002.	1.0	6
40731	Stable Lithium Ion Conducting Thiophosphate Solid Electrolytes Li_x(PS₄)_yX_z (X = Cl, Br, I). Chemistry of Materials, 2019, 31, 8649-8662.	3.2	24
40732	Intrinsically Low Lattice Thermal Conductivity Derived from Rattler Cations in an AMMâ€²Q3 Family of Chalcogenides. Chemistry of Materials, 2019, 31, 8734-8741.	3.2	26
40733	First-Principles Delimitation of the Boundary between Intralayer and Interlayer in Two-Dimensional Structures. Journal of Physical Chemistry C, 2019, 123, 26912-26920.	1.5	19
40734	Sequestration of Radionuclides in Metalâ€“Organic Frameworks from Density Functional Theory Calculations. Journal of Physical Chemistry C, 2019, 123, 26842-26855.	1.5	12
40735	Electrocatalytic Oxygen Reduction Reaction over the Au₂₂(L⁸)₆ Nanocluster with Promising Activity: A DFT Study. Journal of Physical Chemistry C, 2019, 123, 27116-27123.	1.5	19

#	Article	IF	Citations
40736	Li_{0.35}La_{0.55}TiO₃ Nanofibers Enhanced Poly(vinylidene) Tj ETQq0 0 0 rgBT /Overlock 10 Tf 50 74 & Interfaces, 2019, 11, 42206-42213.	4.0	98
40737	Evolution of the Intrinsic Point Defects in Bismuth Telluride-Based Thermoelectric Materials. ACS Applied Materials & Interfaces, 2019, 11, 41424-41431.	4.0	53
40738	Carrier localization in perovskite nickelates from oxygen vacancies. Proceedings of the National Academy of Sciences of the United States of America, 2019, 116, 21992-21997.	3.3	71
40739	Computationally generated maps of surface structures and catalytic activities for alloy phase diagrams. Proceedings of the National Academy of Sciences of the United States of America, 2019, 116, 22044-22051.	3.3	14
40740	Prospects for detecting individual defect centers using spatially resolved electron energy loss spectroscopy. Physical Review B, 2019, 100, .	1.1	5
40741	Single Fe atoms anchored by short-range ordered nanographene boost oxygen reduction reaction in acidic media. Nano Energy, 2019, 66, 104164.	8.2	68
40742	First principles calculation on the newly superhard materials of W-B-C ternary system. Solid State Communications, 2019, 301, 113705.	0.9	6
40743	Molecular-Level Understanding of Hydroxyl Groups Boosted the Catalytic Activity of the CuZnAl Catalyst in the Conversion of Syngas to Ethanol. Industrial & Engineering Chemistry Research, 2019, 58, 19421-19433.	1.8	1
40744	n-Type TaCoSn-Based Half-Heuslers as Promising Thermoelectric Materials. ACS Applied Materials & Interfaces, 2019, 11, 41321-41329.	4.0	44
40745	Level the Conversion/Alloying Voltage Gap by Grafting the Endogenetic Sb₂Te₃ Building Block into Layered GeTe to Build Ge₂Sb₂Te₅ for Li-Ion Batteries. ACS Applied Materials & Interfaces, 2019, 11, 41374-41382.	4.0	15
40746	Strong Thermopower Enhancement and Tunable Power Factor via Semimetal to Semiconductor Transition in a Transition-Metal Dichalcogenide. ACS Nano, 2019, 13, 13317-13324.	7.3	33
40747	Improved Oxygen Reduction Activity in Heteronuclear FeCo-Codoped Graphene: A Theoretical Study. ACS Sustainable Chemistry and Engineering, 2019, 7, 17273-17281.	3.2	56
40748	B-Doped MnN₄-G Nanosheets as Bifunctional Electrocatalysts for Both Oxygen Reduction and Oxygen Evolution Reactions. ACS Sustainable Chemistry and Engineering, 2019, 7, 18711-18717.	3.2	48
40749	Negative piezoelectric response of van der Waals layered bismuth tellurohalides. Physical Review B, 2019, 100, .	1.1	29
40750	Large resistivity reduction in mixed-valent <mml:math xmlns:mml="http://www.w3.org/1998/Math/MathML"><mml:msub><mml:mi>CsAuBr</mml:mi><mml:mn>3</mml:mn></mml:msub></ under pressure. Physical Review B, 2019, 100, .	1.1	4
40751	Effect of Stacking Faults on the Thermoelectric Figure of Merit of Si Nanowires. , 2019, , .		0
40752	Electronically Coupled Uranium and Iron Oxide Heterojunctions as Efficient Water Oxidation Catalysts. Advanced Functional Materials, 2019, 29, 1905005.	7.8	18
40753	Efficient and Stable Inverted Perovskite Solar Cells Incorporating Secondary Amines. Advanced Materials, 2019, 31, e1903559.	11.1	128

#	Article	IF	Citations
40754	Colloidal Singleâ€Layer Photocatalysts for Methanolâ€Storable Solar H₂ Fuel. Advanced Materials, 2019, 31, e1905540.	11.1	39
40755	Interfacial Superâ€Assembled Porous CeO₂/C Frameworks Featuring Efficient and Sensitive Decomposing Li₂O₂ for Smart Liâ€“O₂ Batteries. Advanced Energy Materials, 2019, 9, 1901751.	10.2	71
40756	Enhanced Stability of Li Metal Anodes by Synergetic Control of Nucleation and the Solid Electrolyte Interphase. Advanced Energy Materials, 2019, 9, 1901764.	10.2	108
40757	Crystal Structural Framework of Lithium Superâ€Ionic Conductors. Advanced Energy Materials, 2019, 9, 1902078.	10.2	93
40758	Catalytic Mechanisms and Design Principles for Singleâ€Atom Catalysts in Highly Efficient CO₂ Conversion. Advanced Energy Materials, 2019, 9, 1902625.	10.2	167
40759	Normalized Lithium Growth from the Nucleation Stage for Dendriteâ€Free Lithium Metal Anodes. Angewandte Chemie - International Edition, 2019, 58, 18246-18251.	7.2	60
40760	Electrochemical CO₂ Reduction to C₁ Products on Single Nickel/Cobalt/Ironâ€Doped Graphitic Carbon Nitride: A DFT Study. ChemSusChem, 2019, 12, 5126-5132.	3.6	81
40761	QCM based enantioselective discrimination of enantiomers by a pair of serine derived homochiral coordination polymers. Biosensors and Bioelectronics, 2019, 144, 111667.	5.3	13
40762	Structural stability, electronic, optical and lattice thermal conductivity properties of bulk and monolayer PtS_2. Materials Today Communications, 2019, 21, 100661.	0.9	6
40763	Solid-Form Transition Temperature Prediction from a Virtual Polymorph Screening: A Reality Check. Crystal Growth and Design, 2019, 19, 7132-7137.	1.4	12
40764	Theoretical Investigation of the Role of the Nitride Ion in the Magnetism of Oxynitride MnTaO₂N. Journal of Physical Chemistry C, 2019, 123, 25379-25384.	1.5	3
40765	Borophosphene: A New Anisotropic Dirac Cone Monolayer with a High Fermi Velocity and a Unique Self-Doping Feature. Journal of Physical Chemistry Letters, 2019, 10, 6656-6663.	2.1	45
40766	Theoretical Study of the Mechanism of Furfural Conversion on the NiCuCu(111) Surface. ACS Omega, 2019, 4, 17447-17456.	1.6	11
40767	Thermal equation of state of ruthenium characterized by resistively heated diamond anvil cell. Scientific Reports, 2019, 9, 14459.	1.6	8
40768	A van der Waals epitaxial growth of ultrathin two-dimensional Sn film on graphene covered Cu(111) substrate. Applied Physics Letters, 2019, 115, .	1.5	7
40769	Ferromagnetic, antiferromagnetic, and Peierls distortion states in IVA-VA nanoribbons. Applied Physics Letters, 2019, 115, .	1.5	1
40770	Machine-learning interatomic potential for radiation damage and defects in tungsten. Physical Review B, 2019, 100, .	1.1	79
40771	Strong and Tunable Electrical Anisotropy in Typeâ€II Weyl Semimetal Candidate WP₂ with Broken Inversion Symmetry. Advanced Materials, 2019, 31, e1903498.	11.1	13

#	Article	IF	Citations
40772	Striated 2D Lattice with Subâ€nm 1D Etch Channels by Controlled Thermally Induced Phase Transformations of PdSe₂. Advanced Materials, 2019, 31, e1904251.	11.1	31
40773	The Stereoselective Formation of trans â€Cumulene through Dehalogenative Homocoupling of Alkenyl gem â€Dibromides on Cu(110). ChemCatChem, 2019, 11, 5417-5420.	1.8	4
40774	Lowâ€Energy GeP Monolayers with Natural Typeâ€II Homojunctions for SunLightâ€Driven Water Splitting. Physica Status Solidi - Rapid Research Letters, 2019, 13, 1900470.	1.2	12
40775	A New Reversible Phase Transformation of Intermetallic Ti3Sn. Materials, 2019, 12, 2484.	1.3	7
40776	Temperature-dependent nucleation kinetics of Guinier-Preston zones in Alâ€“Cu alloys: An atomistic kinetic Monte Carlo and classical nucleation theory approach. Acta Materialia, 2019, 179, 262-272.	3.8	31
40777	Hydrogen pickup during oxidation in aqueous environments: The role of nano-pores and nano-pipes in zirconium oxide films. Acta Materialia, 2019, 180, 105-115.	3.8	37
40778	Insights into the fivefold symmetry of the amorphous Sb-based change materials in the rapid phase change from first principles. Acta Materialia, 2019, 181, 439-446.	3.8	6
40779	Investigation of electronic property modulation driven by strain in monolayer tellurium. Chinese Journal of Physics, 2019, 62, 172-178.	2.0	6
40780	First molecule with carbonâ€“carbon bond in methanol-to-olefins process. Chemical Physics Letters, 2019, 737, 136844.	1.2	11
40781	Thermodynamic and mechanical stability of Ni3X-type intermetallic compounds. Intermetallics, 2019, 114, 106604.	1.8	33
40782	Asymmetric-dimer reconstruction and semiconducting properties of Mg2Si(100) surfaces: Prediction from meta-GGA and hybrid functional study. Solid State Sciences, 2019, 98, 106030.	1.5	1
40783	Interaction Mechanisms of Insensitive Explosive FOX-7 and Graphene Oxides from Ab Initio Calculations. Nanomaterials, 2019, 9, 1290.	1.9	6
40784	Mutualistic decomposition pathway of formaldehyde on O-predosed Î´-MnO2. Applied Surface Science, 2019, 498, 143784.	3.1	12
40785	First-principles study of the diffusion of Li in bcc Fe. Fusion Engineering and Design, 2019, 148, 111285.	1.0	5
40786	Fast room temperature lability of aluminosilicate zeolites. Nature Communications, 2019, 10, 4690.	5.8	75
40787	Ge1â^'xSnx alloys: Consequences of band mixing effects for the evolution of the band gap Î“-character with Sn concentration. Scientific Reports, 2019, 9, 14077.	1.6	35
40788	Dehydrogenation of the liquid organic hydrogen carrier system 2-methylindole/2-methylindoline/2-methyloctahydroindole on Pt(111). Journal of Chemical Physics, 2019, 151, 144711.	1.2	19
40789	Quest for Compounds at the Verge of Charge Transfer Instabilities: The Case of Silver(II) Chloride â€. Crystals, 2019, 9, 423.	1.0	8

#	Article	IF	Citations
40790	Theoretical Modeling of Defects, Dopants, and Diffusion in the Mineral Ilmenite. Minerals (Basel,) Tj ETQq0 0 0 rgBT /Overlock 10 Tf 50 7	0.8	5
40791	Compressional behavior of end-member and aluminous iron-bearing diopside at high pressure from single-crystal X-ray diffraction and first principles calculations. Physics and Chemistry of Minerals, 2019, 46, 977-986.	0.3	0
40792	Modified embedded-atom method potential for cadmium. Hyperfine Interactions, 2019, 240, 1.	0.2	0
40793	A comparative investigation of metal (Li, Ca and Sc)-decorated 6,6,12-graphyne monolayers and 6,6,12-graphyne nanotubes for hydrogen storage. Applied Surface Science, 2019, 498, 143763.	3.1	20
40794	Profound softening and shear-induced melting of diamond under extreme conditions: An ab-initio molecular dynamics study. Carbon, 2019, 155, 361-368.	5.4	9
40795	Electron-nuclear hyperfine coupling in quantum kagome antiferromagnets from first-principles calculation and a reflection of the defect effect. Science Bulletin, 2019, 64, 1584-1591.	4.3	0
40796	Two-dimensional inorganic molecular crystals. Nature Communications, 2019, 10, 4728.	5.8	91
40797	Band structure engineering of chemically tunable LnSbTe (Ln = La, Ce, Pr). APL Materials, 2019, 7, .	2.2	16
40798	Experimental and Theoretical In Situ Spectral Magneto-Ellipsometry Study of Layered Ferromagnetic Structures. JETP Letters, 2019, 110, 166-172.	0.4	5
40799	Spin coherent quantum transport of electrons between defects in diamond. Nanophotonics, 2019, 8, 1975-1984.	2.9	11
40800	First-Principle Calculation of High Absorption-TlGaTe2 for Photovoltaic Application. Materials, 2019, 12, 2667.	1.3	1
40801	Optimizing the Performance of CsPbI3-Based Perovskite Solar Cells via Doping a ZnO Electron Transport Layer Coupled with Interface Engineering. Nano-Micro Letters, 2019, 11, 91.	14.4	54
40802	Inducing molecular isomerization assisted by water. Communications Chemistry, 2019, 2, .	2.0	35
40803	Doping single transition metal atom into PtTe sheet for catalyzing nitrogen reduction and hydrogen evolution reactions. Journal of Chemical Physics, 2019, 151, 144710.	1.2	9
40804	Near-infrared optical properties and proposed phase-change usefulness of transition metal disulfides. Applied Physics Letters, 2019, 115, .	1.5	19
40805	Electronic structure of the Pd2Sn surface alloy on Pd(111)-(âˆš3 Ã— âˆš3)R30Â°. European Physical Journal B, 2019, 92, 1.	0.6	3
40806	Fabrication of Robust Hydrogen Evolution Reaction Electrocatalyst Using Ag2Se by Vacuum Evaporation. Nanomaterials, 2019, 9, 1460.	1.9	12
40807	Tuning the Magnetic Properties of Nonmetal-Adsorbed MoSe2 Monolayer by Normal Strain. Journal of Electronic Materials, 2019, 48, 8224-8232.	1.0	0

#	Article	IF	Citations
40808	Three-dimensional fcc C60 polymer. Materials Letters: X, 2019, 4, 100026.	0.3	1
40809	First-principles studies of graphene antidot lattices on monolayer h-BN substrate. Physics Letters, Section A: General, Atomic and Solid State Physics, 2019, 383, 125944.	0.9	1
40810	Rationalizing and engineering Rashba spin-splitting in ferroelectric oxides. Npj Quantum Materials, 2019, 4, .	1.8	59
40811	Ab initio calculation insights into the structural, elastic and mechanical properties of high-k dielectric gadolinium oxide (Gd2O3). Applied Physics A: Materials Science and Processing, 2019, 125, 1.	1.1	4
40812	Poisoning and competitive adsorption effects during phenol hydrogenation on platinum in water-alcohol mixtures. Applied Catalysis A: General, 2019, 585, 117199.	2.2	12
40813	Density-functional-theory calculations of the optical properties of Al2O3: From solid-state to warm dense matter conditions. High Energy Density Physics, 2019, 33, 100718.	0.4	2
40814	Understanding of fission products transport in SiC layer of TRISO fuels by nanoscale characterization and modeling. Journal of Nuclear Materials, 2019, 527, 151793.	1.3	6
40815	First principles modeling of pure black phosphorus devices under pressure. Beilstein Journal of Nanotechnology, 2019, 10, 1943-1951.	1.5	5
40816	Differential Surface Elemental Distribution Leads to Significantly Enhanced Stability of PtNi-Based ORR Catalysts. Matter, 2019, 1, 1567-1580.	5.0	82
40817	Optimized hybrid functionals for defect calculations in semiconductors. Journal of Applied Physics, 2019, 126, 130901.	1.1	27
40818	Thermoelectric transport trends in group 4 half-Heusler alloys. Journal of Applied Physics, 2019, 126, .	1.1	20
40819	A first-principles study of <mml:math xmlns:mml="http://www.w3.org/1998/Math/MathML" altimg="si1.svg"><mml:msubsup><mml:mrow><mml:mi mathvariant="normal">Î²</mml:mi></mml:mrow><mml:mtext>F</mml:mtext><mml:mo>â€²</mml:mo></mml:msubsup></mml:math> phase in magnesium-rare earth binary systems. Computational Materials Science, 2019, 170, 109126.	1.4	8
40820	Metal distribution in iron-nickel sulfide mineral pentlandite: First-principles study. Chemical Physics Letters, 2019, 736, 136786.	1.2	14
40821	Topological nodal lines and hybrid Weyl nodes in YCoC2. APL Materials, 2019, 7, 101109.	2.2	17
40822	Transition from ductilizing to hardening in tungsten: The dependence on rhenium distribution. Acta Materialia, 2019, 181, 110-123.	3.8	26
40823	Mechanistic insight into high-efficiency sodium storage based on N/O/P-functionalized ultrathin carbon nanosheet. Journal of Power Sources, 2019, 442, 227184.	4.0	18
40824	The influence of A- and B-cation substitution on electronic structure of SrFeO3 and SrCoO3. Materials Today: Proceedings, 2019, 12, 21-24.	0.9	4
40825	First-principles study of ferromagnetic metal Fe5GeTe2. Nano Materials Science, 2019, 1, 299-303.	3.9	26

#	Article	IF	Citations
40826	First-principles design of strong solids: Approaches and applications. Physics Reports, 2019, 826, 1-49.	10.3	31
40827	On the Reactivity of the Cu/ZrO₂ System for the Hydrogenation of CO₂ to Methanol: A Density Functional Theory Study. Journal of Physical Chemistry C, 2019, 123, 26904-26911.	1.5	24
40828	Cobalt and Iron Ions in MgO Nanocrystals: Should They Stay or Should They Go. Journal of Physical Chemistry C, 2019, 123, 25991-26004.	1.5	8
40829	Characterization and Simulation of Natural Pyrite Surfaces: A Combined Experimental and Theoretical Study. Journal of Physical Chemistry C, 2019, 123, 26397-26405.	1.5	13
40830	Carrierâ€“Carrier Interaction in Proton-Conducting Perovskites: Carrier Blocking vs Trap-Site Filling. Journal of Physical Chemistry C, 2019, 123, 26823-26830.	1.5	27
40831	Two-Dimensional Fe-Hexaaminobenzene Metalâ€“Organic Frameworks as Promising CO₂ Catalysts with High Activity and Selectivity. Journal of Physical Chemistry C, 2019, 123, 26460-26466.	1.5	16
40832	Fluorinated Phthalocyanine Molecules on Ferromagnetic Cobalt: A Highly Polarized Spinterface. Journal of Physical Chemistry C, 2019, 123, 26475-26480.	1.5	9
40833	Nonstoichiometric Phases of Two-Dimensional Transition-Metal Dichalcogenides: From Chalcogen Vacancies to Pure Metal Membranes. Journal of Physical Chemistry Letters, 2019, 10, 6492-6498.	2.1	15
40834	Hole Localization Inhibits Charge Recombination in Tinâ€“Lead Mixed Perovskites: Timeâ€“Domain ab Initio Analysis. Journal of Physical Chemistry Letters, 2019, 10, 6604-6612.	2.1	21
40835	Activating the MoS₂ Basal Planes for Electrocatalytic Hydrogen Evolution by 2H/1Tâ€² Structural Interfaces. ACS Applied Materials & Interfaces, 2019, 11, 42014-42020.	4.0	34
40836	Atomic Ru Immobilized on Porous h-BN through Simple Vacuum Filtration for Highly Active and Selective CO₂ Methanation. ACS Catalysis, 2019, 9, 10077-10086.	5.5	93
40837	Understanding the Influence of Cation Doping on the Surface Chemistry of NaTaO₃ from First Principles. ACS Catalysis, 2019, 9, 10528-10535.	5.5	13
40838	Nano-compacted Li₂S/Graphene Composite Cathode for High-Energy Lithiumâ€“Sulfur Batteries. ACS Energy Letters, 2019, 4, 2787-2795.	8.8	37
40839	In situ-grown compressed NiCo2S4 barrier layer for efficient and durable polysulfide entrapment. NPG Asia Materials, 2019, 11, .	3.8	27
40840	Path to Overcome Material and Fundamental Obstacles in Spin Valves Based on MoS2 and Other Transition-Metal Dichalcogenides. Physical Review Applied, 2019, 12, .	1.5	13
40841	Composite Dirac semimetals. Physical Review B, 2019, 100, .	1.1	14
40842	Compressive strain induced enhancement of exchange interaction and short-range magnetic order in <mml:math xmlns:mml="http://www.w3.org/1998/Math/MathML"><mml:mrow><mml:mi mathvariant="normal">S</mml:mi><mml:msub><mml:mi mathvariant="normal">r</mml:mi><mml:mn>2</mml:mn></mml:msub><mml:mi>Ir</mml:mi><mml:msub><mml:mi mathvariant="normal">O</mml:mi><mml:mn>4</mml:mn></mml:msub></mml:mrow></mml:math> Investigated by Raman spectroscopy. Physical Review B, 2019, 100, .	1.1	12
40843	Supercompliant and Soft <mml:math xmlns:mml="http://www.w3.org/1998/Math/MathML" display="inline"><mml:mrow><mml:msub><mml:mrow><mml:mo stretchy="false">(</mml:mo><mml:msub><mml:mrow><mml:mi>CH</mml:mi></mml:mrow><mml:mrow><mml:mn>3</mml:mn></mml:mrow></mml:msub><mml:msub><mml:mrow><mml:mi>NH</mml:mi></mml:mrow><mml:mrow><mml:mn>3</mml:mn></mml:mrow></mml:msub><mml:msub><mml:mrow><mml:mi>PbI</mml:mi></mml:mrow><mml:mrow><mml:mn>3</mml:mn></mml:mrow></mml:msub><mml:mo stretchy="false">)</mml:mo></mml:mrow><mml:mrow><mml:mi>n</mml:mi></mml:mrow></mml:msub></mml:mrow></mml:math> Physical Review Letters, 2019, 123, 155901.	2.9	83

#	Article	IF	Citations
40844	Influence of simple metals on the stability of <mml:math xmlns:mml="http://www.w3.org/1998/Math/MathML" altimg="si1.svg"><mml:mrow><mml:mrow><mml:mo>â€ˆ</mml:mo><mml:mrow><mml:mi>a</mml:mi></mml:mrow><mml:mo>â€‰ basal screw dislocations in hexagonal titanium alloys. Acta Materialia, 2019, 180, 42-50.	3.8	22
40845	Hexagonal tungsten oxide-polyaniline hybrid electrodes for high-performance energy storage. Applied Surface Science, 2019, 498, 143872.	3.1	24
40846	Energetically-favorable distribution of oxygen vacancies and metal atoms in perovskite BaCe Zr0.85â^Y0.15O2.925 solid solutions using a genetic algorithm and lattice statics. Computational Materials Science, 2019, 170, 109184.	1.4	6
40847	Atomic bonding and electronic stability of the binary sigma phase. Journal of Alloys and Compounds, 2019, 811, 152053.	2.8	7
40848	BrÃ¸nstedâ€“Evansâ€“Polanyi relation for CO oxidation on metal oxides following the Marsâ€“van Krevelen mechanism. Journal of Catalysis, 2019, 377, 577-581.	3.1	33
40849	Oxygen-terminated BiXenes and derived single atom catalysts for the hydrogen evolution reaction. Journal of Catalysis, 2019, 378, 97-103.	3.1	37
40850	Modelling the influence of strain fields around precipitates on defect equilibria and kinetics under irradiation in ODS steels: A multi scale approach. Journal of Nuclear Materials, 2019, 527, 151807.	1.3	3
40851	An unreported precipitate orientation relationship in Al-Zn-Mg based alloys. Materials Characterization, 2019, 158, 109958.	1.9	20
40852	Thermoelectric properties of silicides with topologically non-trivial electronic structure: Co1-xMxSi (M=Fe, Ni). Materials Today: Proceedings, 2019, 8, 540-545.	0.9	4
40853	Global Geometry Optimization and magnetic properties of Pt and FePt Clusters. Materials Today: Proceedings, 2019, 14, 47-51.	0.9	0
40854	Tuning electronic and magnetic properties of armchair InSe nanoribbons by hydrogenation. Superlattices and Microstructures, 2019, 135, 106282.	1.4	1
40855	Effect of IrO₂ Spatial Distribution on the Stability and Charge Distribution of Ti_{1â€“x}Ir_xO₂ Alloys. Chemistry of Materials, 2019, 31, 8742-8751.	3.2	2
40856	Electrochemical Properties of Three Li₂Ni₂TeO₆ Structural Polymorphs. Chemistry of Materials, 2019, 31, 9379-9388.	3.2	29
40857	Design of Phosphorene for Hydrogen Evolution Performance Comparable to Platinum. Chemistry of Materials, 2019, 31, 8948-8956.	3.2	66
40858	Revisiting Polytypism in Hexagonal Ternary Sulfide ZnIn₂S₄ for Photocatalytic Hydrogen Production Within the Z-Scheme. Chemistry of Materials, 2019, 31, 9148-9155.	3.2	47
40859	Charge Transport in Alkali-Metal Superoxides: A Systematic First-Principles Study. Chemistry of Materials, 2019, 31, 9156-9167.	3.2	19
40860	Imaginary-Time Time-Dependent Density Functional Theory and Its Application for Robust Convergence of Electronic States. Journal of Chemical Theory and Computation, 2019, 15, 6036-6045.	2.3	12
40861	DFT Insights into Comparative Hydrogen Adsorption and Hydrogen Spillover Mechanisms of Pt₄/Graphene and Pt₄/Anatase (101) Surfaces. Journal of Physical Chemistry C, 2019, 123, 25618-25627.	1.5	39

#	Article	IF	Citations
40862	Surface Carbon Hydrogenation on Precovered Fe(110) with Spectator-Coverage-Dependent Chain Initiation and Propagation. Journal of Physical Chemistry C, 2019, 123, 25657-25667.	1.5	6
40863	Nanosized Layered TOT Magnesium Silicates: Equilibrium Morphologies and Surface Speciation, a Computational and Experimental Study. Journal of Physical Chemistry C, 2019, 123, 26965-26979.	1.5	2
40864	Ultrahigh-Pressure Behavior of AO2 (A = Sn, Pb, Hf) Compounds. Journal of Physical Chemistry C, 2019, 123, 27735-27741.	1.5	6
40865	Electronic Structure of Heavy Halogen Atoms Adsorbed on the Cu(111) Surface: A Combined ARPES and First Principles Calculations Study. Journal of Physical Chemistry C, 2019, 123, 26309-26314.	1.5	3
40866	Single Nanoparticle Activities in Ensemble: A Study on Pd Cluster Nanoportals for Electrochemical Oxygen Evolution Reaction. Journal of Physical Chemistry C, 2019, 123, 26124-26135.	1.5	13
40867	First-Principles Study of Oxidation State and Coordination of Cu-Dimers in Cu-SSZ-13 during Methane-to-Methanol Reaction Conditions. Journal of Physical Chemistry C, 2019, 123, 26145-26150.	1.5	17
40868	Sarin Decomposition on Pristine and Hydroxylated ZnO: Quantum-Chemical Modeling. Journal of Physical Chemistry C, 2019, 123, 26432-26441.	1.5	16
40869	Transition-Metal Softener for High-Durability Hydrogen Separation Silica Membranes. Journal of Physical Chemistry C, 2019, 123, 25761-25768.	1.5	6
40870	Engineering Magnetic Phases in Two-Dimensional Non-van der Waals Transition-Metal Oxides. Nano Letters, 2019, 19, 7793-7800.	4.5	45
40871	Probing the Crystal and Electronic Structures of Molybdenum Oxide in Redox Process: Implications for Energy Applications. ACS Applied Energy Materials, 2019, 2, 7709-7716.	2.5	6
40872	Tuning the Electrocatalytic Activity of Co₃O₄ through Discrete Elemental Doping. ACS Applied Materials & Interfaces, 2019, 11, 39706-39714.	4.0	21
40873	Using a Graphene-Polyelectrolyte Complex Reducing Agent To Promote Cracking in Single-Crystalline Gold Nanoplates. ACS Applied Materials & Interfaces, 2019, 11, 41602-41610.	4.0	9
40874	Toward a Unified Theory Correlating Electronic, Thermodynamic, and Mechanical Properties at Defective Al/SiO₂ Nanodevice Interfaces: An Application to Dielectric Breakdown. ACS Applied Nano Materials, 2019, 2, 6836-6848.	2.4	4
40875	Construction of Active Site in a Sintered Copperâ€“Ceria Nanorod Catalyst. Journal of the American Chemical Society, 2019, 141, 17548-17557.	6.6	94
40876	Real Time Monitoring of the Dynamic Intracluster Diffusion of Single Gold Atoms into Silver Nanoclusters. Journal of the American Chemical Society, 2019, 141, 18977-18983.	6.6	73
40877	Ba-induced phase segregation and band gap reduction in mixed-halide inorganic perovskite solar cells. Nature Communications, 2019, 10, 4686.	5.8	105
40878	Statistical learning goes beyond the d-band model providing the thermochemistry of adsorbates on transition metals. Nature Communications, 2019, 10, 4687.	5.8	76
40879	De novo exploration and self-guided learning of potential-energy surfaces. Npj Computational Materials, 2019, 5, .	3.5	132

#	Article	IF	Citations
40880	The encapsulation selectivity for anionic fission products imparted by an electride. Scientific Reports, 2019, 9, 13612.	1.6	14
40881	Enhanced Absorption in MoS₂/Hg_{0.33}Cd_{0.66}Te Heterostructure for Application in Solar Cell Absorbers. IEEE Nanotechnology Magazine, 2019, 18, 989-994.	1.1	17
40882	Electronic structures and optical properties of CuMgVO₄ and AgMgVO₄: a first-principles study. Journal of the Ceramic Society of Japan, 2019, 127, 50-55.	0.5	1
40883	Mechanism behind the Crack Formation in Hydrogen Doping Cz-Si Crystal Growth. Materials Transactions, 2019, 60, 1936-1942.	0.4	3
40884	Hybrid density functional theory description of non-metal doping in perovskite BaTiO3 for visible-light photocatalysis. Journal of Solid State Chemistry, 2019, 280, 121018.	1.4	21
40885	Induction of an atomically thin ferromagnetic semiconductor in 1Tâ€² phase ReS2 by doping with transition metals. Physics Letters, Section A: General, Atomic and Solid State Physics, 2019, 383, 125883.	0.9	5
40886	Computational Exploration of NO Single-Site Disproportionation on Fe-MOF-5. Chemistry of Materials, 2019, 31, 8875-8885.	3.2	20
40887	Partial Oxidation of Methanol on the Fe3O4(111) Surface Studied by Density Functional Theory. Journal of Physical Chemistry C, 2019, 123, 8429-8438.	1.5	17
40888	Optically Driven Magnetic Phase Transition of Monolayer RuCl₃. Nano Letters, 2019, 19, 7673-7680.	4.5	45
40889	First-Principles Computational Screening of Perovskite Hydrides for Hydrogen Release. ACS Combinatorial Science, 2019, 21, 736-742.	3.8	10
40890	Diisopropylammonium Bromide Based Two-Dimensional Ferroelectric Monolayer Molecular Crystal with Large In-Plane Spontaneous Polarization. Journal of the American Chemical Society, 2019, 141, 1452-1456.	6.6	10
40891	Mass Transport and Structural Properties of Binary Liquid Iron Alloys at High Pressure. Geochemistry, Geophysics, Geosystems, 2019, 20, 3556-3568.	1.0	12
40892	Effect of oxygen plasma modification on Pd/Al/Au Ohmic contacts on undoped AlN. Journal Physics D: Applied Physics, 2019, 52, 505106.	1.3	1
40893	Surface-engineered cobalt nitride composite as efficient bifunctional oxygen electrocatalyst. Nanotechnology, 2019, 30, 495406.	1.3	17
40894	Multi-layer elemental 2D materials: antimonene, germanene and stanene grown directly on molybdenum disulfides. Semiconductor Science and Technology, 2019, 34, 105020.	1.0	19
40895	Interface properties and electronic structures of aromatic molecules with anhydride and thio-functional groups on Ag (111) and Au (111) substrates. Chinese Physics B, 2019, 28, 103101.	0.7	1
40896	Electronic structure of molecular beam epitaxy grown 1 T â€² -MoTe₂ film and strain effect*. Chinese Physics B, 2019, 28, 107307.	0.7	7
40897	Theoretical study on orderâ€“disorder phase transition of CH 3 NH 3 PbCl 3. Chinese Physics B, 2019, 28, 116105.	0.7	0

#	Article	IF	Citations
40898	Pd3Te2: an s-wave superconductor with Pd atom coordinated by five Te atoms. Journal of Physics Communications, 2019, 3, 095008.	0.5	1
40899	Orthorhombic to monoclinic phase transition in NbNiTe2. Physical Review B, 2019, 100, .	1.1	1
40900	Structural analysis of an InP(111)A surface using reflection high-energy electron diffraction rocking curves. Japanese Journal of Applied Physics, 2019, 58, SIIA14.	0.8	2
40901	Perpendicularly magnetized Cu₂Sb type (Mn-Cr)AlGe films onto amorphous SiO₂. Applied Physics Express, 2019, 12, 103002.	1.1	8
40902	Suppressed Deep Traps and Bandgap Fluctuations in Cu₂CdSnS₄ Solar Cells with â‰ˆ8% Efficiency. Advanced Energy Materials, 2019, 9, 1902509.	10.2	65
40903	Identifying Copper Vacancies and Their Role in the CuO Based Photocathode for Water Splitting. Angewandte Chemie - International Edition, 2019, 58, 17604-17609.	7.2	82
40904	Ultrafine Ag Nanoparticles as Active Catalyst for Electrocatalytic Hydrogen Production. ChemCatChem, 2019, 11, 5976-5981.	1.8	21
40905	Exploring Main Group Metal Borosulfates: Similarities and Differences of Two New Borosulfates M [B 2 O(SO 4) 3] (M = Sr, Pb). European Journal of Inorganic Chemistry, 2019, 2019, 3975-3981.	1.0	15
40906	Germanium Incorporation in Cu₂ZnSnS₄ and Formation of a Snâ€“Ge Gradient. Physica Status Solidi (A) Applications and Materials Science, 2019, 216, 1900492.	0.8	17
40907	Interlayer Excitons in Transitionâ€Metal Dichalcogenide Heterobilayers. Physica Status Solidi (B): Basic Research, 2019, 256, 1900308.	0.7	15
40908	Coexistence of Weyl and Typeâ€II Triply Degenerate Fermions in a Ternary Topological Semimetal YPtP. Physica Status Solidi - Rapid Research Letters, 2019, 13, 1900421.	1.2	2
40909	Strainâ€Induced Slater Transition in Polar Metal LiOsO₃. Physica Status Solidi - Rapid Research Letters, 2019, 13, 1900436.	1.2	5
40910	Opening of Band Gap of Graphene with High Electronic Mobility by Codoping BN Pairs. Chemical Research in Chinese Universities, 2019, 35, 1058-1061.	1.3	3
40911	First-principle investigation for the hydrogen storage properties of NaXH3 (X= Mn, Fe, Co) perovskite type hydrides. International Journal of Hydrogen Energy, 2019, 44, 30218-30225.	3.8	46
40912	Large Band Offset in Monolayer MoS2 on Oppositely Polarized BiFeO3(0001) Polar Surfaces. Journal of Physical Chemistry C, 2019, 123, 3039-3047.	1.5	11
40913	Design Superior Alkaline Hydrogen Evolution Electrocatalyst by Engineering Dual Active Sites for Water Dissociation and Hydrogen Desorption. ACS Applied Materials & Interfaces, 2019, 11, 38771-38778.	4.0	13
40914	Enhanced Synergetic Catalytic Effect of Mo₂C/NCNTs@Co Heterostructures in Dye-Sensitized Solar Cells: Fine-Tuned Energy Level Alignment and Efficient Charge Transfer Behavior. ACS Applied Materials & Interfaces, 2019, 11, 42156-42171.	4.0	63
40915	Tunable Schottky barrier in graphene/graphene-like germanium carbide van der Waals heterostructure. Scientific Reports, 2019, 9, 5208.	1.6	48

#	Article	IF	Citations
40916	Double-zigzag boron chain-enhanced Vickers hardness and manganese bilayers-induced high d-electron mobility in Mn₃B₄. Physical Chemistry Chemical Physics, 2019, 21, 2697-2705.	1.3	18
40917	Functionalized MXenes as ideal electrodes for Janus MoSSe. Physical Chemistry Chemical Physics, 2019, 21, 70-76.	1.3	35
40918	Blue phosphorene/graphene heterostructure as a promising anode for lithium-ion batteries: a first-principles study with vibrational analysis techniques. Journal of Materials Chemistry A, 2019, 7, 611-620.	5.2	93
40919	C₃N/phosphorene heterostructure: a promising anode material in lithium-ion batteries. Journal of Materials Chemistry A, 2019, 7, 2106-2113.	5.2	81
40920	Pressure-induced emission enhancement in hexaphenylsilole: a computational study. Journal of Materials Chemistry C, 2019, 7, 1388-1398.	2.7	33
40921	A study of strain-induced indirect-direct bandgap transition for silicon nanowire applications. Journal of Applied Physics, 2019, 125, .	1.1	10
40922	Cluster expansion based configurational averaging approach to bandgaps of semiconductor alloys. Journal of Chemical Physics, 2019, 150, 034102.	1.2	15
40923	Effect of sub-surface hydrogen on intrinsic crack tip plasticity in aluminium. Philosophical Magazine, 2019, 99, 2355-2375.	0.7	1
40924	Rare-Earth Elements Modified 1T Phase Mos2 Synergy with Defects for Enhanced Hydrogen Evolution. IOP Conference Series: Earth and Environmental Science, 2019, 252, 022136.	0.2	1
40925	Effect of strain on the magnetism of Fe-doped MoTe₂ monolayer. Modern Physics Letters B, 2019, 33, 1950304.	1.0	5
40926	First-Principle Prediction on STM Tip Manipulation of Ti Adatom on Two-Dimensional Monolayer YBr3. Scanning, 2019, 2019, 1-7.	0.7	3
40927	First Principles Study of Penta-siligraphene as High-Performance Anode Material for Li-Ion Batteries. Nanoscale Research Letters, 2019, 14, 260.	3.1	25
40928	Strain Effect on Thermoelectric Performance of InSe Monolayer. Nanoscale Research Letters, 2019, 14, 287.	3.1	40
40929	Crystal Structures of Al2Cu Revisited: Understanding Existing Phases and Exploring Other Potential Phases. Metals, 2019, 9, 1037.	1.0	26
40930	First-principles based ballistic transport simulation of monolayer and few-layer InSe FETs. Japanese Journal of Applied Physics, 2019, 58, SBBA02.	0.8	5
40931	Tuning Metallic Co0.85Se Quantum Dots/Carbon Hollow Polyhedrons with Tertiary Hierarchical Structure for High-Performance Potassium Ion Batteries. Nano-Micro Letters, 2019, 11, 96.	14.4	51
40932	Reversing the charge transfer between platinum and sulfur-doped carbon support for electrocatalytic hydrogen evolution. Nature Communications, 2019, 10, 4977.	5.8	243
40933	Suppressing Interfacial Dipoles to Minimize Openâ€Circuit Voltage Loss in Quantum Dot Photovoltaics. Advanced Energy Materials, 2019, 9, 1901938.	10.2	14

#	Article	IF	Citations
40934	Identifying Multinuclear Organometallic Intermediates in Onâ€Surface [2+2] Cycloaddition Reactions. Angewandte Chemie - International Edition, 2019, 58, 16485-16489.	7.2	14
40935	Epitaxial Growth of Topological Insulators on Semiconductors (Bi₂Se₃/Te@Se) toward Highâ€Performance Photodetectors. Small Methods, 2019, 3, 1900349.	4.6	45
40936	First-principles study on the mechanical properties of M2CT2 (Mâ€‰=â€‰Ti, Zr, Hf; Tâ€‰=â€‰O, F, OH) MXenes. Nuclear Science and Techniques/Hewuli, 2019, 30, 1.	1.3	14
40937	Coexistence of Magnetism and Ferroelectricity in 3d Transition-Metal-Doped SnTe Monolayer. Journal of Physical Chemistry C, 2019, 123, 28919-28924.	1.5	12
40938	Psesudocubic Phase Tungsten Oxide as a Photocatalyst for Hydrogen Evolution Reaction. ACS Applied Energy Materials, 2019, 2, 8792-8800.	2.5	19
40939	Single-layer CdPSe3: A promising thermoelectric material persisting in high temperatures. Applied Physics Letters, 2019, 115, 193105.	1.5	10
40940	Reentrant melting of sodium, magnesium, and aluminum: General trend. Physical Review B, 2019, 100, .	1.1	17
40941	<mml:math xmlns:mml="http://www.w3.org/1998/Math/MathML"><mml:mi>NiRh</mml:mi><mml:msub><mml:mrow /><mml:mn>2</mml:mn></mml:msub><mml:mi mathvariant="normal">O</mml:mi><mml:msub><mml:mrow /><mml:mn>4</mml:mn></mml:msub></mml:math> : A spin-orbit entangled diamond-lattice paramagnet. Physical Review B, 2019, 100, .	1.1	11
40942	FeO Content of Earthâ€™s Liquid Core. Physical Review X, 2019, 9, .	2.8	7
40944	Microstructural evolution of helium-irradiated 6Hâ€“SiC subjected to different irradiation conditions and annealing temperatures: A multiple characterization study. Acta Materialia, 2019, 181, 160-172.	3.8	70
40945	Interfacial Engineering Enabled Novel Bi-Based Layered Oxide Supercells with Modulated Microstructures and Tunable Physical Properties. Crystal Growth and Design, 2019, 19, 7088-7095.	1.4	6
40946	Synthesis and Fundamental Studies of Si-Compatible (Si)GeSn and GeSn Mid-IR Systems with Ultrahigh Sn Contents. Chemistry of Materials, 2019, 31, 9831-9842.	3.2	26
40947	Fluid Structure of Molten LiClâ€“Li Solutions. Journal of Physical Chemistry B, 2019, 123, 10036-10043.	1.2	10
40948	Tunable Schottky and Ohmic contacts in graphene and tellurene van der Waals heterostructures. Physical Chemistry Chemical Physics, 2019, 21, 23611-23619.	1.3	24
40949	Interfacial aspect of ZnTe/In₂Te₃ heterostructures as an efficient catalyst for the hydrogen evolution reaction. Journal of Materials Chemistry A, 2019, 7, 27441-27449.	5.2	41
40950	Enhanced stability and stacking dependent magnetic/electronic properties of 2D monolayer FeTiO₃ on a Ti₂CO₂ substrate. Journal of Materials Chemistry C, 2019, 7, 15308-15314.	2.7	5
40951	First principles calculations of intrinsic mobilities in tin-based oxide semiconductors SnO, SnO2, and Ta2SnO6. Journal of Applied Physics, 2019, 126, .	1.1	47
40952	Efficient, stable solar cells by using inherent bandgap of Î±-phase formamidinium lead iodide. Science, 2019, 366, 749-753.	6.0	936

#	Article	IF	Citations
40953	The Effect of Hydrogen on Fluctuation Embrittlement of Aluminum. Technical Physics Letters, 2019, 45, 882-885.	0.2	3
40954	Doping-induced insulator-metal transition in the Lifshitz magnetic insulator NaOsO₃. Journal of Physics Condensed Matter, 2019, 31, 244002.	0.7	3
40955	First-principles DFT insights into the structural, elastic, and optoelectronic properties ofÎ±andÎ²-ZnP₂: implications for photovoltaic applications. Journal of Physics Condensed Matter, 2019, 31, 265501.	0.7	4
40956	Influence of magnetism on Dirac semimetallic behavior in nonstoichiometric <mml:math xmlns:mml="http://www.w3.org/1998/Math/MathML"><mml:mrow><mml:msub><mml:mi>Sr</mml:mi><mml:mrow><mml:mn>1</mml:m		

#	Article	IF	Citations
40971	Cobalt-Modulated Molybdenumâ€“Dinitrogen Interaction in MoS₂ for Catalyzing Ammonia Synthesis. Journal of the American Chemical Society, 2019, 141, 19269-19275.	6.6	189
40972	A New Three-Dimensional Subsulfide Ir₂In₈S with Dirac Semimetal Behavior. Journal of the American Chemical Society, 2019, 141, 19130-19137.	6.6	26
40973	CLEASE: a versatile and user-friendly implementation of cluster expansion method. Journal of Physics Condensed Matter, 2019, 31, 325901.	0.7	41
40974	Probing the dephasing time of crystals via spectral properties of high-order harmonic generation. Physical Review A, 2019, 100, .	1.0	14
40975	Two-dimensional topological materials discovery by symmetry-indicator method. Physical Review B, 2019, 100, .	1.1	29
40976	Smooth Flow in Diamond: Atomistic Ductility and Electronic Conductivity. Physical Review Letters, 2019, 123, 195504.	2.9	50
40977	First-principles study of the formation energies and positron lifetimes of vacancies in the Yttrium-Aluminum Garnet Y3Al5O12. European Physical Journal B, 2019, 92, 1.	0.6	9
40978	Using density functional calculations to elucidate atomic ordering of Pd-Rh nanoparticles at sizes relevant for catalytic applications. Chinese Journal of Catalysis, 2019, 40, 1749-1757.	6.9	7
40979	Hydrogen flux of BCC and FCC PdCuAg membranes. International Journal of Hydrogen Energy, 2019, 44, 31160-31171.	3.8	9
40980	CO Adsorption and Activation of Î·-Fe₂C Fischerâ€“Tropsch Catalyst. Industrial & Engineering Chemistry Research, 2019, 58, 21296-21303.	1.8	9
40981	Evaluating Thermal Corrections for Adsorption Processes at the Metal/Gas Interface. Journal of Physical Chemistry C, 2019, 123, 28828-28835.	1.5	17
40982	Large Thermal Conductivity Drops in the Diamondoid Lattice of CuFeS₂ by Discordant Atom Doping. Journal of the American Chemical Society, 2019, 141, 18900-18909.	6.6	66
40983	Atomic-scale spin sensing with a single molecule at the apex of a scanning tunneling microscope. Science, 2019, 366, 623-627.	6.0	60
40984	Strain effect on the electronic and optical properties of ATaO2N (Aâ€‰=â€‰Ca, Sr, and Ba): insights from the first-principles. Applied Physics A: Materials Science and Processing, 2019, 125, 1.	1.1	4
40985	The structural, magnetic, electronic, and mechanical properties of the full Heusler alloys Ti2CoTl1â^'xPbx (xâ€‰=â€‰0.00, 0.25, 0.50, 0.75, 1.00). Applied Physics A: Materials Science and Processing, 2019, 125, 1.	1.1	3
40986	The effect of SnO2(110) supports on the geometrical and electronic properties of platinum nanoparticles. SN Applied Sciences, 2019, 1, 1.	1.5	13
40987	Theoretical study on wetting behavior of B-SWNT: Effects of doping concentration. Applied Surface Science, 2019, 497, 143798.	3.1	6
40988	Tuning the Apparent Stability of Polymorphic Cocrystals through Mechanochemistry. Crystal Growth and Design, 2019, 19, 7271-7279.	1.4	23

#	Article	IF	Citations
40989	Photoinduced Carrier Dynamics at the Interface of Black Phosphorus and Bismuth Vanadate. Journal of Physical Chemistry A, 2019, 123, 10019-10029.	1.1	5
40990	Spin Selection Rule in Single-Site Catalysis of Molecular Oxygen Adsorption on Transition-Metal Phthalocyanines. Journal of Physical Chemistry C, 2019, 123, 28158-28167.	1.5	4
40991	Improving Interfacial Electron Transfer via Tuning Work Function of Electrodes for Electrocatalysis: From Theory to Experiment. Journal of Physical Chemistry C, 2019, 123, 28319-28326.	1.5	30
40992	Tuning Electronic Structure in Layered Hybrid Perovskites with Organic Spacer Substitution. Nano Letters, 2019, 19, 8732-8740.	4.5	41
40993	Confinement-Induced Giant Spinâ€“Orbit-Coupled Magnetic Moment of Co Nanoclusters in TiO₂ Films. ACS Applied Materials & Interfaces, 2019, 11, 43781-43788.	4.0	8
40994	Hexagonal Cu(111) Monolayers for Selective CO₂ Hydrogenation to CH₃OH: Insights from Density Functional Theory. ACS Applied Nano Materials, 2019, 2, 7686-7695.	2.4	21
40995	High Selective Electrochemical Hydrogenation of Cinnamaldehyde to Cinnamyl Alcohol on RuO₂â€“SnO₂â€“TiO₂/Ti Electrode. ACS Catalysis, 2019, 9, 11307-11316.	5.5	47
40996	Voltage-Controlled Magnetic Anisotropy in Heterostructures with Atomically Thin Heavy Metals. Physical Review Applied, 2019, 12, .	1.5	22
40997	Theoretical investigation of magnetic anisotropy at the <mml:math xmlns:mml="http://www.w3.org/1998/Math/MathML"><mml:mrow><mml:mi mathvariant="normal">L</mml:mi><mml:msub><mml:mi mathvariant="normal">a</mml:mi><mml:mrow><mml:mn>0.5</mml:mn></mml:mrow></mml:msub><mml:mi mathvariant="normal">S</mml:mi><mml:msub><mml:mi mathvariant="normal">O</mml:mi><mml:mrow><mml:mn>2.5</mml:mn></mml:mrow></mml:msub></mml:mrow></mml:math>-type doping of <mml:math xmlns:mml="http://www.w3.org/1998/Math/MathML"><mml:mrow><mml:mi>Mn</mml:mi><mml:msub><mml:mi>ZnGeN</mml:mi><mml:mn>2</mml:mn></mml:msub></mml:mrow></mml:math> and <mml:math xmlns:mml="http://www.w3.org/1998/Math/MathML"><mml:mrow><mml:mn>3</mml:mn><mml:mi>R</mml:mi><mml:mo>â^’</mml:mo><mml:mi mathvariant="normal">W</mml:mi><mml:msub><mml:mi mathvariant="normal">S</mml:mi><mml:mn>2</mml:mn></mml:msub></mml:mrow></mml:math>. Physical Review B, 2019, 100, .	1.1	13
40998	Robust circular polarization of indirect Q-K transitions in bilayer <mml:math xmlns:mml="http://www.w3.org/1998/Math/MathML"><mml:msub><mml:mi>ZnGeN</mml:mi><mml:mn>2</mml:mn></mml:msub></mml:math>	1.1	8
40999	Robust circular polarization of indirect Q-K transitions in bilayer <mml:math xmlns:mml="http://www.w3.org/1998/Math/MathML"><mml:mrow><mml:mn>3</mml:mn><mml:mi>R</mml:mi><mml:mo>â^’</mml:mo><mml:mi mathvariant="normal">W</mml:mi><mml:msub><mml:mi mathvariant="normal">S</mml:mi><mml:mn>2</mml:mn></mml:msub></mml:mrow></mml:math>. Physical Review B, 2019, 100, .	1.1	11
41000	Interfacial effects on the superconducting properties of <mml:math xmlns:mml="http://www.w3.org/1998/Math/MathML"><mml:mrow><mml:mi>LaS</mml:mi><mml:msub><mml:mi mathvariant="normal">i</mml:mi><mml:mn>2</mml:mn></mml:msub><mml:mo>(</mml:mo><mml:mn>112</mml:mn></mml:mrow></mml:math> films on Si(111). Physical Review B, 2019, 100, .	1.1	1
41001	Oxygen deficiency induced strong electron localization in lanthanum doped transparent perovskite oxide BaSnO3. Physical Review B, 2019, 100, .	1.1	14
41002	Trigonal Tellurium Nanostructure Formation Energy and Band gap. , 2019, , .		1
41004	2D Ca₃Sn₂S₇ Chalcogenide Perovskite: A Grapheneâ€Like Semiconductor with Direct Bandgap 0.5 eV and Ultrahigh Carrier Mobility 6.7â€‰Ã—â€‰10⁴ cm² V^{â^'1} s^{â^'1}. Advanced Materials, 2019, 31, e1905643.	11.1	28
41005	Vibration uncoupling of germanium with different valence states lowers thermal conductivity of Cs2Ge3Ga6Se14. Science China Materials, 2019, 62, 1788-1797.	3.5	8
41006	Pressure-Induced Structural Transition to the Polar Phase in GdFe₃(BO₃)₄. Crystal Growth and Design, 2019, 19, 6935-6944.	1.4	2
41007	Phase Stability and Ordering in Rock Salt-Based Thermoelectrics: NaSbX₂, AgSbX₂, and Their Alloys with PbX and SnX (X = S, Se, Te). Chemistry of Materials, 2019, 31, 9445-9452.	3.2	15

#	Article	IF	Citations
41008	Elucidating the Electronic Structure and Magnetic and Conducting Properties of Î¼-Oxo Mn-phthalocyanine [MnPc(CN)]₂O Complex. Journal of Physical Chemistry C, 2019, 123, 28359-28369.	1.5	1
41009	Insight into the Oxidation Mechanism of Furanic Compounds on Pt(111). ACS Catalysis, 2019, 9, 11360-11370.	5.5	10
41010	Mysterious SiB₃: Identifying the Relation between Î±- and Î²-SiB₃. ACS Omega, 2019, 4, 18741-18759.	1.6	9
41011	Topological phases in pyrochlore thallium niobate Tl2Nb2O6+x. Npj Computational Materials, 2019, 5, .	3.5	11
41012	Theoretical prediction of a highly responsive material: Spin fluctuations and superconductivity in FeNiB2 system. Applied Physics Letters, 2019, 115, 182601.	1.5	4
41013	On the calculation of the bandgap of periodic solids with MGGA functionals using the total energy. Journal of Chemical Physics, 2019, 151, 161102.	1.2	10
41014	Spin dynamics study in layered van der Waals single-crystal <mml:math xmlns:mml="http://www.w3.org/1998/Math/MathML"><mml:mrow><mml:msub><mml:mi>Cr</mml:mi><mml:mn>2</mml:mn></mml:msub></mml:r Physical Review B, 2019, 100, .	1.1	25
41015	Identification of ferrimagnetic interaction in <mml:math xmlns:mml="http://www.w3.org/1998/Math/MathML"><mml:mrow><mml:mi>MnS</mml:mi><mml:msub><mml:mi mathvariant="normal">b</mml:mi><mml:mn>2</mml:mn></mml:msub><mml:mi mathvariant="normal">T</mml:mi><mml:msub><mml:mi mathvariant="normal">e</mml:mi><mml:mn>4</mml:mn></mml:msub></mml:mrow></mml:math> layer with antiferromagnetic ordering. Physical Review B, 2019, 100, .	1.1	81
41016	Identification of ferrimagnetic orbitals preventing spinel degradation by charge ordering in <mml:math xmlns:mml="http://www.w3.org/1998/Math/MathML"><mml:mrow><mml:msub><mml:mi>Li</mml:mi><mml:mi>x</mml:mi></mml:msub><mml:msub><mml:mi mathvariant="normal">O</mml:mi><mml:mn>4</mml:mn></mml:msub></mml:mrow></mml:math>. Physical Review B, 2019, 100, .	1.1	13
41017	Giant Electrophononic Response in <mml:math xmlns:mml="http://www.w3.org/1998/Math/MathML" display="inline"><mml:mrow><mml:msub><mml:mrow><mml:mi>PbTiO</mml:mi></mml:mrow><mml:mrow><mml:mn>3</mml:mn></mml:mrow> by Strain Engineering. Physical Review Letters, 2019, 123, 185901.	2.9	12
41018	Size, Composition, and Support-Doping Effects on Oxygen Reduction Activity of Platinum-Alloy and on Non-platinum Metal-Decorated-Graphene Nanocatalysts. Frontiers in Chemistry, 2019, 7, 610.	1.8	3
41020	Potassium ion storage properties of Alpha-graphdiyne investigated by first-principles calculations. Electrochimica Acta, 2019, 326, 134955.	2.6	8
41021	Structure and adhesion of Zr/Mo thin-film interface by PVD: A first-principles prediction. Surface and Coatings Technology, 2019, 378, 125082.	2.2	2
41022	Anion Distribution, Structural Distortion, and Symmetry-Driven Optical Band Gap Bowing in Mixed Halide Cs₂SnX₆ Vacancy Ordered Double Perovskites. Chemistry of Materials, 2019, 31, 9430-9444.	3.2	83
41023	Insights into the Most Suitable TiO₂ Surfaces for Photocatalytic O₂ and H₂ Evolution Reactions from DFT Calculations. Journal of Physical Chemistry C, 2019, 123, 28210-28218.	1.5	48
41024	Boron-Doped g-C₆N₆ Layer as a Metal-Free Photoelectrocatalyst for N₂ Reduction Reaction. Journal of Physical Chemistry C, 2019, 123, 28739-28743.	1.5	35
41025	Molecular-Level Insight into the Hydroxylated Monomeric VO_x/Î¸-Al₂O₃(010) and Its Adsorption of Methanol. Journal of Physical Chemistry C, 2019, 123, 27704-27711.	1.5	6
41026	Tuning the Potential Energy Landscape to Suppress Ostwald Ripening in Surface-Supported Catalyst Systems. Nano Letters, 2019, 19, 8388-8398.	4.5	12

#	Article	IF	Citations
41027	Moderate strain induced indirect bandgap and conduction electrons in MoS2 single layers. Npj 2D Materials and Applications, 2019, 3, .	3.9	45
41028	Spin polaronics: Static and dynamic properties of spin polarons in La-doped <mml:math xmlns:mml="http://www.w3.org/1998/Math/MathML"><mml:msub><mml:mi>CaMnO</mml:mi><mml:mn>3</mml:mn></mml:msub></ Physical Review B, 2019, 100, .	1.1	4
41029	Weyl semimetal phase in the noncentrosymmetric superlattice W2XY(X,Y=S,Se,Te,Xâ‰Y). Physical Review B, 2019, 100, .	1.1	3
41030	Band offset modulation in Si-EuO heterostructures via controlled interface formation. Physical Review B, 2019, 100, .	1.1	7
41031	Development of a deep machine learning interatomic potential for metalloid-containing Pd-Si compounds. Physical Review B, 2019, 100, .	1.1	39
41032	Broad luminescence from donor-complexed <mml:math xmlns:mml="http://www.w3.org/1998/Math/MathML"><mml:msub><mml:mi mathvariant="normal">Li</mml:mi><mml:mtext>Zn</mml:mtext></mml:msub></mml:math> and <mml:math xmlns:mml="http://www.w3.org/1998/Math/MathML"><mml:msub><mml:mi mathvariant="normal">Na</mml:mi><mml:mtext>Zn</mml:mtext></mml:msub></mml:math> acceptors in ZnO. Physical Review B, 2019, 100, .	1.1	8
41033	First-principles study of crystal structures and superconductivity of ternary <mml:math xmlns:mml="http://www.w3.org/1998/Math/MathML"><mml:msub><mml:mi>YSH</mml:mi><mml:mn>6</mml:mn></mml:msub></mm and <mml:math xmlns:mml="http://www.w3.org/1998/Math/MathML"><mml:msub><mml:mi>LaSH</mml:mi><mml:mn>6</mml:mn></mml:msub></mm at high pressures. Physical Review B, 2019, 100, .	1.1	33
41034	Two-dimensional antiferromagnetic Dirac fermions in monolayer <mml:math xmlns:mml="http://www.w3.org/1998/Math/MathML"><mml:msub><mml:mi>TaCoTe</mml:mi><mml:mn>2</mml:mn></mml:msub></ Physical Review B, 2019, 100, .	1.1	22
41035	Massless Dirac fermions in stable two-dimensional carbon-arsenic monolayer. Physical Review B, 2019, 100, .	1.1	10
41036	Titanium Carbide MXene as NH₃ Sensor: Realistic First-Principles Study. Journal of Physical Chemistry C, 2019, 123, 29794-29803.	1.5	78
41037	Facile Electron Transfer to CO₂ during Adsorption at the Metal|Solution Interface. Journal of Physical Chemistry C, 2019, 123, 29278-29283.	1.5	36
41038	Improved Description of a Coordinate Bond in the ReaxFF Reactive Force Field. Journal of Physical Chemistry Letters, 2019, 10, 7293-7299.	2.1	7
41039	Ferroelectric Polarization Suppresses Nonradiative Electronâ€“Hole Recombination in CH₃NH₃PbI₃ Perovskites: A Time-Domain ab Initio Study. Journal of Physical Chemistry Letters, 2019, 10, 7237-7244.	2.1	17
41040	Metalâ€“Metal Synergy in Well-Defined Surface Tantalumâ€“Iridium Heterobimetallic Catalysts for H/D Exchange Reactions. Journal of the American Chemical Society, 2019, 141, 19321-19335.	6.6	33
41041	Frustrated and Allowed Structural Transitions: The Theory-Guided Discovery of the Modulated Structure of IrSi. Journal of the American Chemical Society, 2019, 141, 19424-19435.	6.6	12
41042	Evaluation of Tellurium as a Fuel Additive in Neodymium-Containing U-Zr Metallic Fuel. Scientific Reports, 2019, 9, 16043.	1.6	11
41043	An ab initio study of reversible dihydrogen adsorption in metal decorated Î³-graphyne. Journal of Applied Physics, 2019, 126, .	1.1	19
41044	Structural, electronic, and electromechanical properties of MoSSe/blue phosphorene heterobilayer. AIP Advances, 2019, 9, 115302.	0.6	19

#	Article	IF	Citations
41045	Hierarchically pure and M (Cu, Ni)-impregnated ZSM-5 zeolites for the isomerization catalysis of n-hexane and 1-hexene. Materials Research Express, 2019, 6, 125032.	0.8	4
41046	Relevance of the Pauli kinetic energy density for semilocal functionals. Physical Review B, 2019, 100, .	1.1	38
41047	Rashba-like spin-orbit and strain effects in tetragonal <mml:math xmlns:mml="http://www.w3.org/1998/Math/MathML"><mml:msub><mml:mi>PbTiO</mml:mi><mml:mn>3</mml:mn></mml:msub></m Physical Review B, 2019, 100, .	1.1	29
41048	Interplay between boundary conditions and Wilson's mass in Dirac-like Hamiltonians. Physical Review B, 2019, 100, .	1.1	10
41049	Dual topological insulator and insulator-semimetal transition in mirror-symmetric honeycomb materials. Physical Review B, 2019, 100, .	1.1	7
41050	Large Fermi arc and robust Weyl semimetal phase in Ag2S. Physical Review B, 2019, 100, .	1.1	6
41051	Topological crystalline insulator state with type-II Dirac fermions in transition metal dipnictides. Physical Review B, 2019, 100, .	1.1	13
41052	Ab initioinsight into the formation of small polarons: A study across four metal peroxides. Physical Review B, 2019, 100, .	1.1	8
41053	Curie temperature of emerging two-dimensional magnetic structures. Physical Review B, 2019, 100, .	1.1	47
41054	Anomalous Dirac Plasmons in 1D Topological Electrides. Physical Review Letters, 2019, 123, 206402.	2.9	33
41055	Contrasting Oxygen Reduction Reactions on Zero- and One-Dimensional Defects of MoS₂ for Versatile Applications. ACS Applied Materials & Interfaces, 2019, 11, 46327-46336.	4.0	22
41056	Band splitting with vanishing spin polarizations in noncentrosymmetric crystals. Nature Communications, 2019, 10, 5144.	5.8	17
41057	A comprehensive study on the mechanism of ferroelectric phase formation in hafnia-zirconia nanolaminates and superlattices. Applied Physics Reviews, 2019, 6, .	5.5	73
41058	Strain engineering of magnetic and orbital order in perovskite <mml:math xmlns:mml="http://www.w3.org/1998/Math/MathML"><mml:msub><mml:mi>LuMnO</mml:mi><mml:mn>3</mml:mn></mml:msub><(epitaxial films. Physical Review B, 2019, 100, .	1.1	7
41059	Comment on â€œAtomistic Mechanisms of Mg Insertion Reactions in Group XIV Anodes for Mg-Ion Batteriesâ€• ACS Applied Materials & Interfaces, 2019, 11, 45365-45367.	4.0	4
41060	Spinâ€“orbit coupling driven novel magnetism in d ⁵ 6H-perovskite iridates Ba₃IrTi₂O₉ and Ba₃TiIr₂O₉. Journal of Physics Condensed Matter, 2019, 31, 185802.	0.7	5
41061	Boron Phosphide van der Waals p-n Junction via Molecular Adsorption. Physical Review Applied, 2019, 12, .	1.5	10
41062	Degradation of Ka-Band GaN LNA Under High-Input Power Stress: Experimental and Theoretical Insights. IEEE Transactions on Electron Devices, 2019, 66, 5091-5096.	1.6	15

#	Article	IF	Citations
41063	Advanced Li₂S/Si Full Battery Enabled by TiN Polysulfide Immobilizer. Small, 2019, 15, e1902377.	5.2	29
41064	Joint stereochemical and ab initio overview of SnII electron lone pairs (E) and Fâ˜'(E) triplets effects on the crystal networks, the bonding and the electronic structures in a family of tin fluorides. Progress in Solid State Chemistry, 2019, 56, 100252.	3.9	3
41065	Manganese(II) in Tetrahedral Halide Environment: Factors Governing Bright Green Luminescence. Chemistry of Materials, 2019, 31, 10161-10169.	3.2	200
41066	Single Au Anion Can Catalyze Acetylene Hydrochlorination: Tunable Catalytic Performance from Rational Doping. Journal of Physical Chemistry C, 2019, 123, 29203-29208.	1.5	26
41067	Crystal Engineering of Bi₂WO₆ to Polar Aurivillius-Phase Oxyhalides. Journal of Physical Chemistry C, 2019, 123, 29155-29161.	1.5	12
41068	Silver-Intermediated Perovskite La_{0.9}FeO_{3â˜'Î´} toward High-Performance Cathode Catalysts for Nonaqueous Lithiumâ€“Oxygen Batteries. ACS Catalysis, 2019, 9, 11743-11752.	5.5	46
41069	Superlattice-induced ferroelectricity in charge-ordered La _{1/3} Sr _{2/3} FeO ₃. Proceedings of the National Academy of Sciences of the United States of America, 2019, 116, 23972-23976.	3.3	7
41070	A new single-layer structure of MBene family: Ti₂B. Journal of Physics Condensed Matter, 2019, 31, 505401.	0.7	27
41071	Phase diagram of uranium fromab initiocalculations and machine learning. Physical Review B, 2019, 100, .	1.1	28
41072	Theoretical investigation of iron incorporation in hexagonal barium titanate. Physical Review B, 2019, 100, .	1.1	6
41073	Praseodymium polyhydrides synthesized at high temperatures and pressures. Physical Review B, 2019, 100, .	1.1	21
41074	High-Pressure Phase Diagrams of Na2CO3 and K2CO3. Minerals (Basel, Switzerland), 2019, 9, 599.	0.8	11
41076	Equilibrium hydrogen pressures in the Vâ€“H system from first principles. International Journal of Hydrogen Energy, 2019, 44, 28909-28918.	3.8	6
41077	Disparate Essences of Residual, Ion-Exchanged, and Impregnated Na Ions on Topology Structure for Cu/SSZ-13 NH₃ Selective Catalytic Reduction Catalysts. Industrial & Engineering Chemistry Research, 2019, 58, 20610-20619.	1.8	16
41078	Formation and Stability of Nontoxic Perovskite Precursor. Langmuir, 2019, 35, 16217-16225.	1.6	4
41079	NO_x Adsorption and Optical Detection in Rare Earth Metalâ€“Organic Frameworks. ACS Applied Materials & Interfaces, 2019, 11, 43270-43277.	4.0	61
41080	Activity Descriptors Derived from Comparison of Mo and Fe as Active Metal for Methane Conversion to Aromatics. Journal of the American Chemical Society, 2019, 141, 18814-18824.	6.6	52
41081	Mechanisms for hydrogen evolution on transition metal phosphide catalysts and a comparison to Pt(111). Physical Chemistry Chemical Physics, 2019, 21, 24489-24498.	1.3	31

#	Article	IF	Citations
41082	Probing changes in secondary electron yield from copper electrodes due to surface defects and changes in crystal orientation. Journal of Applied Physics, 2019, 126, .	1.1	11
41083	A review on computational modelling of individual device components and interfaces of perovskite solar cells using DFT. AIP Conference Proceedings, 2019, , .	0.3	5
41084	Magnetic anisotropy of the two-dimensional ferromagnetic insulator <mml:math xmlns:mml="http://www.w3.org/1998/Math/MathML"><mml:msub><mml:mi mathvariant="normal">MnBi</mml:mi><mml:mn>2</mml:mn></mml:msub><mml:msub><mml:mi mathvariant="normal">Te</mml:mi><mml:mn>4</mml:mn></mml:msub></mml:math>. Physical Review B, 2019, 100, .	1.1	48
41085	Pressure-tunable large anomalous Hall effect of the ferromagnetic kagome-lattice Weyl semimetal Co3Sn2S2. Physical Review B, 2019, 100, .	1.1	25
41086	Microscopic nonequilibrium energy transfer dynamics in a photoexcited metal/insulator heterostructure. Physical Review B, 2019, 100, .	1.1	18
41087	Electronic and vibrational properties of Pu3M(M=Al,ÂGa,ÂIn,ÂandÂTl) : A first-principles study. Physical Review B, 2019, 100, .	1.1	1
41088	Transition to metallization in warm dense helium-hydrogen mixtures using stochastic density functional theory within the Kubo-Greenwood formalism. Physical Review B, 2019, 100, .	1.1	10
41089	One-Dimensional Pnictogen Allotropes inside Single-Wall Carbon Nanotubes. Inorganic Chemistry, 2019, 58, 15216-15224.	1.9	18
41090	Effect of Chiral Ligand Concentration and Binding Mode on Chiroptical Activity of CdSe/CdS Quantum Dots. ACS Nano, 2019, 13, 13560-13572.	7.3	65
41091	Synergy of a Metallic NiCo Dimer Anchored on a C₂Nâ€“Graphene Matrix Promotes the Electrochemical CO₂ Reduction Reaction. ACS Sustainable Chemistry and Engineering, 2019, 7, 19113-19121.	3.2	91
41092	Chemical and Structural Diversity of Hybrid Layered Double Perovskite Halides. Journal of the American Chemical Society, 2019, 141, 19099-19109.	6.6	144
41093	Pressure-induced metallization of black arsenic. Journal of Physics Condensed Matter, 2019, 31, 505501.	0.7	1
41094	Predicting charge density distribution of materials using a local-environment-based graph convolutional network. Physical Review B, 2019, 100, .	1.1	31
41095	Electron-phonon coupling and Kohn anomaly due to floating two-dimensional electronic bands on the surface of ZrSiS. Physical Review B, 2019, 100, .	1.1	5
41096	Role of TMâ€“TM Connection Induced by Opposite d-Electron States on the Hardness of Transition-Metal (TM = Cr, W) Mononitrides. Inorganic Chemistry, 2019, 58, 15573-15579.	1.9	10
41097	Insight into the Activity and Stability of Transition-Metal Atoms Embedded in MnO for Triiodide Reduction Reaction. ACS Sustainable Chemistry and Engineering, 2019, 7, 19303-19310.	3.2	10
41098	Transition levels of intrinsic defects in type-II InAs/InAs0.5Sb0.5 strained-layer superlattices. Applied Physics Letters, 2019, 115, .	1.5	3
41099	Theoretical understanding of the catalyst-free growth mechanism of GaAs <111>B nanowires. Applied Surface Science, 2019, 497, 143740.	3.1	7

#	Article	IF	Citations
41100	Pressureâ€Induced Coordination Changes in a Pyrolitic Silicate Melt From Ab Initio Molecular Dynamics Simulations. Journal of Geophysical Research: Solid Earth, 2019, 124, 11232-11250.	1.4	27
41101	The MoSeS dynamic omnigami paradigm for smart shape and composition programmable 2D materials. Nature Communications, 2019, 10, 5210.	5.8	15
41102	Superb water splitting activity of the electrocatalyst Fe3Co(PO4)4 designed with computation aid. Nature Communications, 2019, 10, 5195.	5.8	120
41103	Temperature-Dependent Magnetic Properties of Bi-Doped Fe₁₆N₂: First Principles and Atomistic Study. IEEE Transactions on Magnetics, 2019, 55, 1-5.	1.2	2
41104	Negative Surface Energies of Nickel Ferrite Nanoparticles under Hydrothermal Conditions. Journal of Nanomaterials, 2019, 2019, 1-6.	1.5	4
41105	A first-principles microkinetic study on the hydrogenation of carbon dioxide over Cu(211) in the presence of water. Science China Chemistry, 2019, 62, 1686-1697.	4.2	31
41106	Improved optoelectronic properties in CdSexTe1â^'x through controlled composition and short-range order. Solar Energy, 2019, 194, 742-750.	2.9	19
41107	Polarized Raman Reveals Alignment of Few-Layer MoS₂ Films. Journal of Physical Chemistry C, 2019, 123, 29468-29475.	1.5	14
41108	Tuning CO₂ Electroreduction of Cu Atoms on Triphenylene-Cored Graphdiyne. Journal of Physical Chemistry C, 2019, 123, 29776-29782.	1.5	12
41109	Tip-induced superconductivity coexisting with preserved topological properties in line-nodal semimetal ZrSiS. Journal of Physics Condensed Matter, 2019, 31, 485707.	0.7	13
41110	Electronic Property and Negative Thermal Expansion Behavior of Si136-xGex (x = 8, 32, 40, 104) Clathrate Solid Solution from First Principles. Nanomaterials, 2019, 9, 851.	1.9	1
41111	Stability of Coinage Metals Interacting with C60. Nanomaterials, 2019, 9, 1484.	1.9	4
41112	Metal-atom penetration and diffusion in organic solids: difference between Ïƒ- and Ï€- orbital molecular systems. Japanese Journal of Applied Physics, 2019, 58, SIIB28.	0.8	4
41113	Origin of Fermi-level depinning at metal/Ge interfaces: first-principles study on effect of segregation. Japanese Journal of Applied Physics, 2019, 58, SIIB11.	0.8	1
41114	Prediction of dielectric constants using a combination of first principles calculations and machine learning. Japanese Journal of Applied Physics, 2019, 58, SLLC01.	0.8	18
41115	Chemical vapor deposition condition dependence of reconstructed surfaces on 4H-SiC (0001), (000$ar{{f{1}}}$), and (1$ar{{f{1}}}$00) surfaces. Japanese Journal of Applied Physics, 2019, 58, 115501.	0.8	3
41116	Simulating lattice thermal conductivity in semiconducting materials using high-dimensional neural network potential. Applied Physics Express, 2019, 12, 095001.	1.1	29
41117	Visualization of Dopant Oxygen Atoms in a Bi₂Sr₂CaCu₂O₈₊_{Î´} Superconductor. Advanced Functional Materials, 2019, 29, 1903843.	7.8	34

#	Article	IF	Citations
41118	XBi₄S₇ (X = Mn, Fe): New Costâ€Efficient Layered nâ€Type Thermoelectric Sulfides with Ultralow Thermal Conductivity. Advanced Functional Materials, 2019, 29, 1904112.	7.8	24
41119	Enhanced Incorporation of Guanidinium in Formamidiniumâ€Based Perovskites for Efficient and Stable Photovoltaics: The Role of Cs and Br. Advanced Functional Materials, 2019, 29, 1905739.	7.8	41
41120	Halogenated Antimonene: Oneâ€Step Synthesis, Structural Simulation, Tunable Electronic and Photoresponse Property. Advanced Functional Materials, 2019, 29, 1905857.	7.8	33
41121	Enabling Full Conversion Reaction with High Reversibility to Approach Theoretical Capacity for Sodium Storage. Advanced Functional Materials, 2019, 29, 1906680.	7.8	29
41122	Are Cu₂Teâ€Based Compounds Excellent Thermoelectric Materials?. Advanced Materials, 2019, 31, e1903480.	11.1	72
41123	The Fundamental Mechanism Behind Colossal Permittivity in Oxides. Advanced Materials, 2019, 31, e1904746.	11.1	21
41124	Dopant Segregation Boosting Highâ€Voltage Cyclability of Layered Cathode for Sodium Ion Batteries. Advanced Materials, 2019, 31, e1904816.	11.1	89
41125	Rationalization of Diversity in Spinel MgFe₂O₄ Surfaces. Advanced Materials Interfaces, 2019, 6, 1901218.	1.9	14
41126	Titanium(IV) Inclusion as a Versatile Route to Photoactivity in Metalâ€“Organic Frameworks. Advanced Theory and Simulations, 2019, 2, 1900126.	1.3	14
41127	Pressureâ€Dependent Mechanical and Thermal Properties of Leadâ€Free Halide Double Perovskite Cs₂AgBâ€³X₆ (Bâ€³â•In, Bi; Xâ•Cl, Br, I). Advanced Theory and Simulations, 2019, 2, 1900164.	1.3	15
41128	Ballistic Quantum Transport of Subâ€10 nm 2D Sb 2 Te 2 Se Transistors. Advanced Electronic Materials, 2019, 5, 1900813.	2.6	14
41129	Modified Ceria for â€œLowâ€Temperatureâ€•CO₂ Utilization: A Chemical Looping Route to Exploit Industrial Waste Heat. Advanced Energy Materials, 2019, 9, 1901963.	10.2	43
41130	The Capacitive Behavior of Polyluminol on Carbon Nanotubes Electrodes. ChemElectroChem, 2019, 6, 5454-5461.	1.7	27
41131	Itinerant Semiconducting Antiferromagnetism in Metastable V 3 Ga. Physica Status Solidi - Rapid Research Letters, 2019, 13, 1900483.	1.2	5
41132	Relationship between the Auger parameter and the ground state valence charge of the coreâ€ionized atom: The case of Cu(I) and Cu (II) compounds. Surface and Interface Analysis, 2019, 51, 1359-1370.	0.8	9
41133	Highâ€Performance Inverted Planar Perovskite Solar Cells Enhanced by Thickness Tuning of New Dopantâ€Free Hole Transporting Layer. Small, 2019, 15, e1904715.	5.2	47
41134	Structural stability of uranium carbide (UC) under high pressure: ab-initio study. Computational Condensed Matter, 2019, 21, e00431.	0.9	8
41135	Highly dispersed Ni2â^'Mo P nanoparticles on oxygen-defect-rich NiMoO4â^' nanosheets as an active electrocatalyst for alkaline hydrogen evolution reaction. Journal of Power Sources, 2019, 444, 227311.	4.0	32

#	Article	IF	Citations
41136	Understanding why Alite is responsible of the main mechanical characteristics in Portland cement. Cement and Concrete Research, 2019, 126, 105916.	4.6	21
41137	Cohesion and tensile properties of W-TiC interface under irradiation. Fusion Engineering and Design, 2019, 149, 111353.	1.0	6
41138	First-principles study of oxygen reduction reaction on Pd-doped LaxSr1-xCoyFe1-yO3-Î´ cathodes of solid oxide fuel cells. International Journal of Hydrogen Energy, 2019, 44, 28720-28730.	3.8	7
41139	The active site of syngas conversion into ethanol over Cu/ZnO/Al2O3 ternary catalysts in slurry bed. Journal of Catalysis, 2019, 380, 68-82.	3.1	22
41140	Prediction of a new direct-gap silicon phase: T36 silicon. Physics Letters, Section A: General, Atomic and Solid State Physics, 2019, 383, 125903.	0.9	2
41141	YHO, an Air-Stable Ionic Hydride. Inorganic Chemistry, 2019, 58, 14635-14641.	1.9	20
41142	Pressure-Induced Transitions in the 1-Dimensional Vanadium Oxyhydrides Sr2VO3H and Sr3V2O5H2, and Comparison to 2-Dimensional SrVO2H. Inorganic Chemistry, 2019, 58, 15393-15400.	1.9	12
41143	Electrochemical Lithiation Mechanism of Two-Dimensional Transition-Metal Dichalcogenide Anode Materials: Intercalation versus Conversion Reactions. Journal of Physical Chemistry C, 2019, 123, 2139-2146.	1.5	47
41144	NO Adsorption on 4d and 5d Transition-Metal (Rh, Pd, Ag, Ir, and Pt) Nanoparticles: Density Functional Theory Study and Supervised Learning. Journal of Physical Chemistry C, 2019, 123, 28114-28122.	1.5	22
41145	Charge Transfer during the Dissociation of H₂ and the Charge State of H Atoms in Liquid Gallium. Journal of Physical Chemistry C, 2019, 123, 26769-26776.	1.5	7
41146	Coordination Engineering in Cobaltâ€“Nitrogen-Functionalized Materials for CO₂ Reduction. Journal of Physical Chemistry Letters, 2019, 10, 6551-6557.	2.1	42
41147	Enhanced Iridium Mass Activity of 6H-Phase, Ir-Based Perovskite with Nonprecious Incorporation for Acidic Oxygen Evolution Electrocatalysis. ACS Applied Materials & Interfaces, 2019, 11, 42006-42013.	4.0	48
41148	Suppressing Sponge-Like Li Deposition via AlN-Modified Substrate for Stable Li Metal Anode. ACS Applied Materials & Interfaces, 2019, 11, 42261-42270.	4.0	9
41149	Multifarious Interfaces, Band Alignments, and Formation Asymmetry of WSe₂â€“MoSe₂ Heterojunction Grown by Molecular-Beam Epitaxy. ACS Applied Materials & Interfaces, 2019, 11, 43766-43773.	4.0	8
41150	First-Principles Calculations of TiB MBene Monolayers for Hydrogen Evolution. ACS Applied Nano Materials, 2019, 2, 7220-7229.	2.4	45
41151	Enhanced Interfacial H₂ Activation for Nitrostyrene Catalytic Hydrogenation over Rutile Titania-Supported Gold by Coadsorption: A First-Principles Microkinetic Simulation Study. ACS Catalysis, 2019, 9, 11288-11301.	5.5	14
41152	Activity Origin and Multifunctionality of Pt-Based Intermetallic Nanostructures for Efficient Electrocatalysis. ACS Catalysis, 2019, 9, 11242-11254.	5.5	96
41153	New Mechanism for N₂ Reduction: The Essential Role of Surface Hydrogenation. Journal of the American Chemical Society, 2019, 141, 18264-18270.	6.6	166

#	Article	IF	Citations
41154	Ferroelectric switching in bilayer 3R MoS2 via interlayer shear mode driven by nonlinear phononics. Scientific Reports, 2019, 9, 14919.	1.6	19
41155	First-principles study of interfacial energy between alpha-zirconium and zirconium hydride. Journal of Applied Physics, 2019, 126, .	1.1	9
41156	Raman spectra and dimensional effect on the charge density wave transition in GdTe3. Applied Physics Letters, 2019, 115, .	1.5	15
41157	Shock compression of fused silica: An impedance matching standard. Journal of Applied Physics, 2019, 126, .	1.1	13
41158	High thermoelectric properties in full-Heusler X₂YZ alloys (Xâ€‰â€‰=â€‰â€‰Ca, Sr, and Ba; Yâ€‰â€‰=â€‰â€‰Au	1.3	6
41159	Robust cluster expansion of multicomponent systems using structured sparsity. Physical Review B, 2019, 100, .	1.1	18
41160	Phase diagrams and electronic properties of B-S and H-B-S systems under high pressure. Physical Review B, 2019, 100, .	1.1	14
41161	Noncollinear magnetic structure and anisotropic magnetoelastic coupling in cobalt pyrovanadate <mml:math xmlns:mml="http://www.w3.org/1998/Math/MathML"><mml:mrow><mml:msub><mml:mi>Co</mml:mi><mml:mn>2</mml:mn></mml: mathvariant="normal">V</mml:mi><mml:mn>2</mml:mn></mml:msub><mml:msub><mml:mi mathvariant="normal">O</mml:mi><mml:mn>7</mml:mn></mml:msub></mml:mrow></mml:math>.	1.1	12
41162	Simplification of the electron-ion many-body problem: <mml:math xmlns:mml="http://www.w3.org/1998/Math/MathML"><mml:mi>N</mml:mi></mml:math> -representability of pair densities obtained via a classical map for the electrons. Physical Review B, 2019, 100, .	1.1	6
41163	Electronic and lattice properties of noncentrosymmetric superconductors <mml:math xmlns:mml="http://www.w3.org/1998/Math/MathML"><mml:mrow><mml:mi>Th</mml:mi><mml:mi>T</mml:mi><mml:mi>Si</mml:mi> <mml:math		

#	Article	IF	Citations
41172	Investigating possible kinetic limitations to MgB2 hydrogenation. International Journal of Hydrogen Energy, 2019, 44, 31239-31256.	3.8	10
41173	An exploration of measuring lower-length-scale structures in nuclear materials: Thermal conductivity of U-Mo fuel particle. Journal of Nuclear Materials, 2019, 527, 151797.	1.3	3
41174	Stable structure of hydrogen atoms trapped in tungsten divacancy. Journal of Nuclear Materials, 2019, 527, 151825.	1.3	8
41175	Bi substitution effect on superconductivity of novel Pb2Pd alloy. Physica C: Superconductivity and Its Applications, 2019, 565, 1353518.	0.6	1
41176	Dual-Band Luminescent Lead-Free Antimony Chloride Halides with Near-Unity Photoluminescence Quantum Efficiency. Chemistry of Materials, 2019, 31, 9363-9371.	3.2	206
41177	Intrinsic Controllable Magnetism of Graphene Grown on Fe. Journal of Physical Chemistry C, 2019, 123, 26870-26876.	1.5	10
41178	Boron Nitride Nanotube Nucleation during Ni-Catalyzed Boron Oxide Chemical Vapor Deposition. Journal of Physical Chemistry C, 2019, 123, 27875-27883.	1.5	9
41179	Curious Mechanism of the Dissociative Chemisorption of Ammonia on Ru(0001). Journal of Physical Chemistry C, 2019, 123, 28291-28300.	1.5	10
41180	Intrinsic Electric Field-Induced Properties in Janus MoSSe van der Waals Structures. Journal of Physical Chemistry Letters, 2019, 10, 559-565.	2.1	98
41181	Electronâ€“Phonon Scattering Is Much Weaker in Carbon Nanotubes than in Graphene Nanoribbons. Journal of Physical Chemistry Letters, 2019, 10, 7179-7187.	2.1	21
41182	Computational Design of Novel Hydrogen-Rich YSâ€“H Compounds. ACS Omega, 2019, 4, 14317-14323.	1.6	17
41183	Ti₃C₂ MXene-Based Sensors with High Selectivity for NH₃ Detection at Room Temperature. ACS Sensors, 2019, 4, 2763-2770.	4.0	355
41184	Integrating Density Functional Theory Calculations with Vibrational and Nuclear Magnetic Resonance Spectroscopy. ACS Symposium Series, 2019, , 89-102.	0.5	0
41185	Electronic structure of YbB6 dependent on onsite Coulomb interaction U and internal parameter of B atom. Chinese Physics B, 2019, 28, 116201.	0.7	2
41186	Cooperative Effect in a Graphite Intercalation Compound: Enhanced Mobility of <mml:math xmlns:mml="http://www.w3.org/1998/Math/MathML" display="inline" overflow="scroll"><mml:msub><mml:mrow><mml:mi>Al</mml:mi><mml:mi>Cl</mml:mi></mml:mrow><mml:mn>4</mml:mn></mml:r in the Graphite Cathode of Aluminum-Ion Batteries. Physical Review Applied, 2019, 12, .	1.5	15
41187	Phonon dynamics in the layered negative thermal expansion compounds CuxNi2â^'x(CN)4. Physical Review B, 2019, 100, .	1.1	9
41188	Theoretical study of fluorine doping in layered <mml:math xmlns:mml="http://www.w3.org/1998/Math/MathML"><mml:mrow><mml:mi>LaOBi</mml:mi><mml:msub><mml:mi mathvariant="normal">S</mml:mi><mml:mn>2</mml:mn></mml:msub></mml:mrow></mml:math> -type compounds. Physical Review B, 2019, 100, .	1.1	7
41189	Accessing thermal conductivity of complex compounds by machine learning interatomic potentials. Physical Review B, 2019, 100, .	1.1	73

#	Article	IF	Citations
41190	Ab initio calculation of field emission from metal surfaces with atomic-scale defects. Physical Review B, 2019, 100, .	1.1	12
41191	Configuration entropy effect on temperature coefficient of redox potential of P2-Na_xCoO₂. Japanese Journal of Applied Physics, 2019, 58, 065501.	0.8	7
41192	Planar Silicene: A New Silicon Allotrope Epitaxially Grown by Segregation. Advanced Functional Materials, 2019, 29, 1906053.	7.8	37
41193	Versatile and Highly Efficient Controls of Reversible Topotactic Metalâ€“Insulator Transitions through Proton Intercalation. Advanced Functional Materials, 2019, 29, 1907072.	7.8	28
41194	Estimating vibrational and thermodynamic properties of adsorbates with uncertainty using data driven surrogates. AICHE Journal, 2019, 65, e16838.	1.8	5
41195	Identifying Multinuclear Organometallic Intermediates in Onâ€Surface [2+2] Cycloaddition Reactions. Angewandte Chemie, 2019, 131, 16637-16641.	1.6	4
41196	Normalized Lithium Growth from the Nucleation Stage for Dendriteâ€Free Lithium Metal Anodes. Angewandte Chemie, 2019, 131, 18414-18419.	1.6	10
41197	An Uncommon Hypervalent Fluorooxosilicophosphate. Chemistry - an Asian Journal, 2019, 14, 4174-4178.	1.7	4
41198	Pristineâ€Grapheneâ€Supported Nitrogenâ€Doped Carbon Selfâ€Assembled from Glucaminiumâ€Based Ionic Liquids as Metalâ€Free Catalyst for Oxygen Evolution. ChemSusChem, 2019, 12, 5041-5050.	3.6	25
41199	Effect of the Local Environment on the Magnetic Properties of Mn₃Si: Hybrid Ab Initio and Model Study. Physica Status Solidi (B): Basic Research, 2019, 256, 1900228.	0.7	3
41200	Optimized Substrates and Measurement Approaches for Raman Spectroscopy of Graphene Nanoribbons. Physica Status Solidi (B): Basic Research, 2019, 256, 1900343.	0.7	26
41201	Firstâ€Principles Study of Interaction of Bismuthene with Small Gas Molecules. ChemistrySelect, 2019, 4, 10928-10933.	0.7	12
41202	Anisotropic Growth and Scanning Tunneling Microscopy Identification of Ultrathin Evenâ€Layered PdSe₂ Ribbons. Small, 2019, 15, e1902789.	5.2	50
41203	Van der Waals Integration of Bismuth Quantum Dotsâ€“Decorated Tellurium Nanotubes (Te@Bi) Heterojunctions and Plasmaâ€Enhanced Optoelectronic Applications. Small, 2019, 15, e1903233.	5.2	45
41204	Tuning the Optical and Electrical Properties of Fewâ€Layer Black Phosphorus via Physisorption of Small Solvent Molecules. Small, 2019, 15, e1903432.	5.2	21
41205	Spinel/Lithiumâ€Rich Manganese Oxide Hybrid Nanofibers as Cathode Materials for Rechargeable Lithiumâ€Ion Batteries. Small Methods, 2019, 3, 1900350.	4.6	44
41206	Fluorescence imaging of Cys in keratinocytes upon UVB exposure using phenyl doped graphitic carbon nitride Nanosheets-Au nanoparticles nanocomposite. Analytica Chimica Acta, 2019, 1091, 127-134.	2.6	6
41207	Enhancing superconductivity in bulk Î²â€²Bi2Pd by negative pressure induced by quantum electronic stress. Physical Review B, 2019, 100, .	1.1	4

#	Article	IF	Citations
41208	Phonon-induced electronic relaxation in a strongly correlated system: The Sn/Si(111) <mml:math xmlns:mml="http://www.w3.org/1998/Math/MathML"><mml:mrow><mml:mo>(</mml:mo><mml:msqrt><mml:mn>3</mml:mn></mml:msqrt><mml:mo>×</mml:mo><mml:mn>3</mml:mn></mml: adlayer revisited. Physical Review B, 2019, 100, .	1.1	2
41209	Machine learning the density functional theory potential energy surface for the inorganic halide perovskite <mml:math xmlns:mml="http://www.w3.org/1998/Math/MathML"><mml:msub><mml:mi mathvariant="normal">CsPbBr</mml:mi><mml:mn>3</mml:mn></mml:msub></mml:math>. Physical Review B, 2019, 100, .	1.1	14
41210	Spin-spiral formalism based on the multiple-scattering Green's function technique with applications to ultrathin magnetic films and multilayers. Physical Review B, 2019, 100, .	1.1	3
41211	Ground state and low-temperature magnetism of the quasi-two-dimensional honeycomb compound <mml:math xmlns:mml="http://www.w3.org/1998/Math/MathML"><mml:mrow><mml:msub><mml:mi>InCu</mml:mi><mml:mrow><mml:mn>2</mml:mn> mathvariant="normal">V</mml:mi><mml:mrow><mml:mn>1</mml:mn><mml:mo>/</mml:mo><mml:mn>3</mml:mn></mml:mrow> mathvariant="normal">O</mml:mi><mml:mn>3</mml:mn></mml:msub></mml:mrow></mml:math>. Physical Review B, 2019, 100, .	1.1	5
41212	Impact of phonons and spin-orbit coupling on Auger recombination in InAs. Physical Review B, 2019, 100, .	1.1	2
41213	Valley drift and valley current modulation in strained monolayer <mml:math xmlns:mml="http://www.w3.org/1998/Math/MathML"><mml:mrow><mml:mi>Mo</mml:mi><mml:msub><mml:mi mathvariant="normal">S</mml:mi><mml:mn>2</mml:mn></mml:msub></mml:mrow></mml:math>. Physical Review B, 2019, 100, .	1.1	27
41214	Review of high-throughput approaches to search for piezoelectric nitrides. Journal of Vacuum Science and Technology A: Vacuum, Surfaces and Films, 2019, 37, .	0.9	14
41215	Metastable Conducting Crystalline Hydrogen at High Pressure. JETP Letters, 2019, 110, 206-210.	0.4	8
41216	First-Principles Study of the Impact of Grain Boundary Formation in the Cathode Material LiFePO4. Condensed Matter, 2019, 4, 80.	0.8	8
41217	Correlations of Equilibrium Properties and Electronic Structure of Pure Metals. Materials, 2019, 12, 2932.	1.3	2
41218	Partitioning of Interstitial Segregants during Decohesion: A DFT Case Study of the Î£3 Symmetric Tilt Grain Boundary in Ferritic Steel. Materials, 2019, 12, 2971.	1.3	4
41219	Structural Stability, Electronic Structures, Mechanical Properties and Debye Temperature of Transition Metal Impurities in Tungsten: A First-Principles Study. Metals, 2019, 9, 967.	1.0	23
41220	Potential Application of Graphene/Antimonene Herterostructure as an Anode for Li-Ion Batteries: A First-Principles Study. Nanomaterials, 2019, 9, 1430.	1.9	20
41221	First-principles study of pressure and SiO-incorporation effect on dynamical properties of silicon oxide. Japanese Journal of Applied Physics, 2019, 58, 111004.	0.8	2
41222	Defect Engineering of Grain Boundaries in Leadâ€Free Halide Double Perovskites for Better Optoelectronic Performance. Advanced Functional Materials, 2019, 29, 1805870.	7.8	30
41223	Tunable Graphene Electronics with Local Ultrahigh Pressure. Advanced Functional Materials, 2019, 29, 1806715.	7.8	15
41224	The Contacts of the Monolayer Semiconductor C₂N with 2D Metal Electrodes. Advanced Theory and Simulations, 2019, 2, 1800161.	1.3	19
41225	Effect of Ca doping on structural, magnetic and electronic properties of TbMnO3. Journal of Magnetism and Magnetic Materials, 2019, 477, 77-82.	1.0	4

#	Article	IF	Citations
41226	Tuning the hydrogen activation reactivity on topological insulator heterostructures. Nano Energy, 2019, 58, 40-46.	8.2	49
41227	Unusual synergistic effect in layered Ruddlesdenâ^'Popper oxide enables ultrafast hydrogen evolution. Nature Communications, 2019, 10, 149.	5.8	187
41228	Chromium-ruthenium oxide solid solution electrocatalyst for highly efficient oxygen evolution reaction in acidic media. Nature Communications, 2019, 10, 162.	5.8	396
41229	Deep acceptors and their diffusion in Ga2O3. APL Materials, 2019, 7, .	2.2	143
41230	Atomic and electronic structure of domains walls in a polar metal. Physical Review B, 2019, 99, .	1.1	19
41231	Broadband excitation spectrum of bulk crystals and thin layers of <mml:math xmlns:mml="http://www.w3.org/1998/Math/MathML"><mml:msub><mml:mi>PtTe</mml:mi><mml:mn>2</mml:mn></mml:msub></mml:math> Physical Review B, 2019, 99, .	1.1	18
41232	Vibrational properties of sodosilicate glasses from first-principles calculations. Physical Review B, 2019, 99, .	1.1	23
41233	Intertwined Solitons and Impurities in a Quasi-One-Dimensional Charge-Density-Wave System: <mml:math xmlns:mml="http://www.w3.org/1998/Math/MathML" display="inline"><mml:mrow><mml:mi>In</mml:mi><mml:mo>/</mml:mo><mml:mi>Si</mml:mi><mml:mo stretchy="false">(</mml:mo><mml:mn>111</mml:mn><mml:mo) Tj ETQq1 1 0.784314 rgBT /Overlock 10 Tf 50 447 Td (stretchy="false	2.9	16
41234	The alkali resistance of CuNbTi catalyst for selective reduction of NO by NH3: A comparative investigation with VWTi catalyst. Applied Catalysis B: Environmental, 2019, 246, 166-179.	10.8	96
41235	h-C63: A new hexagonal superhard metallic carbon allotrope. Results in Physics, 2019, 15, 102738.	2.0	3
41236	Designing High-Performance CdSe Nanocrystal Thin-Film Transistors Based on Solution Process of Simultaneous Ligand Exchange, Trap Passivation, and Doping. Chemistry of Materials, 2019, 31, 9389-9399.	3.2	23
41237	Lead-Free Broadband Orange-Emitting Zero-Dimensional Hybrid (PMA)₃InBr₆ with Direct Band Gap. Inorganic Chemistry, 2019, 58, 15602-15609.	1.9	81
41238	Variability of Câ€"F Bonds Governs the Formation of Specific Structural Motifs in Fluorinated Graphenes. Journal of Physical Chemistry C, 2019, 123, 27896-27903.	1.5	22
41239	Translational Manipulation of Magnetic Cobalt Adatoms on the Si(100)-2 Ã— 1 Surface at 9 K. Journal of Physical Chemistry C, 2019, 123, 26415-26423.	1.5	3
41240	First-Principles Calculation of Triplet Exciton Diffusion in Crystalline Poly(p-phenylene) Tj ETQq0 0 0 rgBT /Overlock 10 Tf 50 182	1.5	7
41241	Quantitative Studies of the Coverage Effects on Microkinetic Simulations for NO Oxidation on Pt(111). Journal of Physical Chemistry C, 2019, 123, 27594-27602.	1.5	30
41242	Formation of Reversible Adducts by Adsorption of Oxygen on Ceâ€"ZrO₂: An Unusual Î·² Ionic Superoxide. Journal of Physical Chemistry C, 2019, 123, 27088-27096.	1.5	14
41243	Rational Design of Porous Nodal-Line Semimetallic Carbon for K-Ion Battery Anode Materials. Journal of Physical Chemistry Letters, 2019, 10, 6360-6367.	2.1	31

#	Article	IF	Citations
41244	Upcycling Single-Use Polyethylene into High-Quality Liquid Products. ACS Central Science, 2019, 5, 1795-1803.	5.3	283
41245	Identification of stable adsorption sites and diffusion paths on nanocluster surfaces: an automated scanning algorithm. Npj Computational Materials, 2019, 5, .	3.5	6
41246	Structure and energetics of carbon defects in SiC (0001)/SiO2 systems at realistic temperatures: Defects in SiC, SiO2, and at their interface. Journal of Applied Physics, 2019, 126, .	1.1	44
41247	Interaction between water and carbon nanostructures: How good are current density functional approximations?. Journal of Chemical Physics, 2019, 151, 164702.	1.2	47
41248	Oxygen migration around the filament region in HfOx memristors. AIP Advances, 2019, 9, .	0.6	8
41249	Two-dimensional XSe₂ (X= Mn, V) based magnetic tunneling junctions with high Curie temperature*. Chinese Physics B, 2019, 28, 107504.	0.7	22
41250	Recent progress on the prediction of two-dimensional materials using CALYPSO. Chinese Physics B, 2019, 28, 107306.	0.7	24
41251	Physical properties of ternary thallium chalcogenes Tl 2 MQ 3 (M = Zr, Hf; Q = S, Se, Te) via ab - initio calculations. Chinese Physics B, 2019, 28, 106301.	0.7	1
41252	Anisotropy in elasticity and physical properties of Ti₂B under high pressure. Materials Research Express, 2019, 6, 1065c4.	0.8	5
41253	The mechanical properties and strain effect on the electronic properties of III-nitride monolayers: ab-initio study. Materials Research Express, 2019, 6, 115915.	0.8	7
41254	First principle calculations on electronic, magnetic and optical properties of Mn doped and N co-doped CdS. Materials Research Express, 2019, 6, 116126.	0.8	9
41255	Fully analytic valence force field model for the elastic and inner elastic properties of diamond and zincblende crystals. Physical Review B, 2019, 100, .	1.1	5
41256	Tunneling anisotropic magnetoresistance of Pb and Bi adatoms and dimers on Mn/W(110): A first-principles study. Physical Review B, 2019, 100, .	1.1	3
41257	Crystalline phase transitions and vibrational spectra of silicon up to multiterapascal pressures. Physical Review B, 2019, 100, .	1.1	9
41258	Observation of topological transition in high- <mml:math xmlns:mml="http://www.w3.org/1998/Math/MathML"><mml:msub><mml:mi>T</mml:mi><mml:mi>c</mml:mi></mml:msub></mml:ma superconducting monolayer <mml:math xmlns:mml="http://www.w3.org/1998/Math/MathML"><mml:msub><mml:mi mathvariant="normal">FeTe</mml:mi><mml:mrow><mml:mn>1</mml:mn><mml:mo>â^'</mml:mo><mml:mi>x</mml:mi></mml:mrow mathvariant="normal">Se</mml:mi><mml:mi>x</mml:mi></mml:msub></mml:math> films on <mml:math	1.1	37
41259	Controlled switching of a single CuPc molecule on Cu(111) at low temperature. Physical Review B, 2019, 100, .	1.1	6
41260	Topological semimetallic phase in PbO2 promoted by temperature. Physical Review B, 2019, 100, .	1.1	8
41261	Nonhelical spin texture in the normal states of the centrosymmetric superconductor <mml:math xmlns:mml="http://www.w3.org/1998/Math/MathML"><mml:mrow><mml:mi>Î²</mml:mi><mml:mtext>â^'</mml:mtext><mml:msub Physical Review B, 2019, 100, .	1.1	10

#	Article	IF	Citations
41262	Two-dimensional spin-valley locking spin valve. Physical Review B, 2019, 100, .	1.1	57
41263	Local metallic and structural properties of the strongly correlated metal LaNiO3 using 8Li Î²â€“NMR. Physical Review B, 2019, 100, .	1.1	10
41264	Electronic and hyperbolic dielectric properties of <mml:math xmlns:mml="http://www.w3.org/1998/Math/MathML"><mml:mrow><mml:mi>Zr</mml:mi><mml:msub><mml:mi mathvariant="normal">S</mml:mi><mml:mn>2</mml:mn></mml:msub><mml:mo>/</mml:mo><mml:mi>Hf</mml:mi><mml:msub><mml:mi mathvariant="normal">S</mml:mi><mml:mn>2</mml:mn></mml:msub></mml:mrow></mml:math> heterostructures. Physical Review B, 2019, 100, .	1.1	12
41265	Origins of significant reduction of lattice thermal conductivity in graphene allotropes. Physical Review B, 2019, 100, .	1.1	18
41266	Duality of Ring and Ladder Diagrams and Its Importance for Many-Electron Perturbation Theories. Physical Review Letters, 2019, 123, 156401.	2.9	19
41267	Interstitial defects in the van der Waals gap of Bi₂Se₃. Acta Crystallographica Section B: Structural Science, Crystal Engineering and Materials, 2019, 75, 717-732.	0.5	14
41268	High-surface-area corundum by mechanochemically induced phase transformation of boehmite. Science, 2019, 366, 485-489.	6.0	130
41269	Theoretical Determination of Size Effects in Zeolite-Catalyzed Alcohol Dehydration. Catalysts, 2019, 9, 700.	1.6	11
41270	Two-Dimensional SiP, SiAs, GeP and GeAs as Promising Candidates for Photocatalytic Applications. Coatings, 2019, 9, 522.	1.2	32
41271	In Situ Electrochemical Atomic Force Microscopy and Auger Electro Spectroscopy Study on the Passive Film Structure of 2024â€T3 Aluminum Alloy Combined with a Density Functional Theory Calculation. Advanced Engineering Materials, 2019, 21, 1900386.	1.6	28
41272	Methane functionalization by an Ir(III) catalyst supported on a metalâ€“organic framework: an alternative explanation of steric confinement effects. Theoretical Chemistry Accounts, 2019, 138, 1.	0.5	12
41273	Influence of graphene surface chemistry on Ir-catalyzed hydrogenation of p-chloronitrobenzene and cinnamaldehyde: Weak molecule-support interactions. Journal of Catalysis, 2019, 377, 524-533.	3.1	13
41274	Data-Driven Discovery of Photoactive Quaternary Oxides Using First-Principles Machine Learning. Chemistry of Materials, 2019, 31, 7221-7230.	3.2	45
41275	Phase transition and electronic properties of skutterudite-type IrP₃ under high pressure. Physical Chemistry Chemical Physics, 2019, 21, 21262-21266.	1.3	6
41276	Sulfurization synthesis of a new anode material for Li-ion batteries: understanding the role of sulfurization in lithium ion conversion reactions and promoting lithium storage performance. Journal of Materials Chemistry A, 2019, 7, 21270-21279.	5.2	14
41277	Unique magnetic order in layered van der Waals, layered, and anisotropic <mml:math xmlns:mml="http://www.w3.org/1998/Math/MathML"><mml:mrow><mml:mi mathvariant="normal">B</mml:mi><mml:msub><mml:mi mathvariant="normal">i</mml:mi><mml:mn>2</mml:mn></mml:msub><mml:msub><mml:mi mathvariant="normal">O</mml:mi><mml:mn>2</mml:mn></mml:msub><mml:mi>Se</mml:mi></mml:mrow></mml:math> : Competition between exchange interaction mechanisms. Physical Review B, 2019, 100, .	1.1	8
41278	Oxygen Evolution Reaction on 2D Ferromagnetic Fe₃GeTe₂: Boosting the Reactivity by the Selfâ€Reduction of Surface Hydroxyl. Advanced Functional Materials, 2019, 29, 1904782.	7.8	42
41279	Dynamic Interplay between Defective UiOâ€66 and Protic Solvents in Activated Processes. Chemistry - A European Journal, 2019, 25, 15315-15325.	1.7	13

#	Article	IF	Citations
41280	Improved Moisture Stability of Perovskite Solar Cells Using N719 Dye Molecules. Solar Rrl, 2019, 3, 1900345.	3.1	30
41281	Experimental and Theoretical Investigations on the Influence of A on the Hydrogen Sorption Properties of ANiy Compounds, A = {Y, Sm, Gd}. Journal of Physical Chemistry C, 2019, 123, 23334-23341.	1.5	6
41282	Tuning the Electronic and Magnetic Properties of In-Planar Graphene/Boron Nitride Heterostructure by Doping 3d Transition Metal Atom. Journal of Physical Chemistry C, 2019, 123, 22403-22412.	1.5	5
41283	Electronâ€“Phonon Relaxation at Au/Ti Interfaces Is Robust to Alloying: Ab Initio Nonadiabatic Molecular Dynamics. Journal of Physical Chemistry C, 2019, 123, 22842-22850.	1.5	9
41284	Polarization Control of the Interface Ferromagnetic to Antiferromagnetic Phase Transition in Co/Pb(Zr,Ti)O₃. ACS Applied Materials & Interfaces, 2019, 11, 34399-34407.	4.0	6
41285	Rattling-Induced Ultralow Thermal Conductivity Leading to Exceptional Thermoelectric Performance in AgIn₅S₈. ACS Applied Materials & Interfaces, 2019, 11, 33894-33900.	4.0	25
41286	Largely Enhanced Seebeck Coefficient and Thermoelectric Performance by the Distortion of Electronic Density of States in Ge₂Sb₂Te₅. ACS Applied Materials & Interfaces, 2019, 11, 34046-34052.	4.0	38
41287	High-Performance Flexible Solid-State Asymmetric Supercapacitors Based on Bimetallic Transition Metal Phosphide Nanocrystals. ACS Nano, 2019, 13, 10612-10621.	7.3	214
41288	Structural and Electronic Properties of Iron-Doped Sodium Montmorillonite Clays: A First-Principles DFT Study. ACS Omega, 2019, 4, 14369-14377.	1.6	10
41289	New insights into the origin of unstable sodium graphite intercalation compounds. Physical Chemistry Chemical Physics, 2019, 21, 19378-19390.	1.3	68
41290	Transition metal embedded C₃N monolayers as promising catalysts for the hydrogen evolution reaction. Physical Chemistry Chemical Physics, 2019, 21, 20432-20441.	1.3	32
41291	Theoretical search for novel Au or Ag bimetallic alloys capable of transforming CO2 into hydrocarbons. Journal of Materials Chemistry A, 2019, 7, 20567-20573.	5.2	15
41292	Stability and electronic structure of tricycle-type allotropes of pnictogen monolayers. AIP Conference Proceedings, 2019, , .	0.3	1
41293	Thermoelectric properties of non-stoichiometric Cu2+xSn1â^'xS3 compounds. Journal of Applied Physics, 2019, 126, .	1.1	35
41294	Designing an All-Carbon Membrane for Water Desalination. Physical Review Applied, 2019, 12, .	1.5	16
41295	High-pressure polymorphs of gadolinium orthovanadate: X-ray diffraction, Raman spectroscopy, and ab initio calculations. Physical Review B, 2019, 100, .	1.1	22
41296	Assessment of the exact-exchange-only Kohn-Sham method for the calculation of band structures for transition metal oxide and metal halide perovskites. Physical Review B, 2019, 100, .	1.1	5
41297	Rational Design Principles of the Quantum Anomalous Hall Effect in Superlatticelike Magnetic Topological Insulators. Physical Review Letters, 2019, 123, 096401.	2.9	104

#	Article	IF	Citations
41298	Materials Compatibility in Rechargeable Aluminum Batteries: Chemical and Electrochemical Properties between Vanadium Pentoxide and Chloroaluminate Ionic Liquids. Chemistry of Materials, 2019, 31, 7238-7247.	3.2	35
41299	Temperature Dependence of Self-Diffusion in Cr₂O₃ from First Principles. Journal of Physical Chemistry C, 2019, 123, 22139-22150.	1.5	12
41300	Modulation of Crystal and Electronic Structures in Topological Insulators by Rare-Earth Doping. ACS Applied Electronic Materials, 2019, 1, 1929-1936.	2.0	7
41301	Enhancement of Thermoelectric Properties in Pdâ€“In Co-Doped SnTe and Its Phase Transition Behavior. ACS Applied Materials & Interfaces, 2019, 11, 33792-33802.	4.0	32
41302	Probing Photocatalytic Nitrogen Reduction to Ammonia with Water on the Rutile TiO₂ (110) Surface by First-Principles Calculations. ACS Catalysis, 2019, 9, 9178-9187.	5.5	56
41303	Atomic and electronic modulation of self-supported nickel-vanadium layered double hydroxide to accelerate water splitting kinetics. Nature Communications, 2019, 10, 3899.	5.8	355
41304	An Au₂₂(L⁸)₆ nanocluster with in situ uncoordinated Au as a highly active catalyst for O₂ activation and CO oxidation. Physical Chemistry Chemical Physics, 2019, 21, 20144-20150.	1.3	11
41305	Diracâ€“Weyl semimetal phase in noncentrosymmetric transition metal monochalcogenides MoTe and WTe. Journal of Materials Chemistry C, 2019, 7, 12151-12159.	2.7	11
41306	Correlation of cation deficiency and nanostructure to decreased magnetism in a ferroelectric BiMnO3 film. Journal of Applied Physics, 2019, 126, 085303.	1.1	1
41307	Anomalous Hall effect and the role of Berry curvature in <mml:math xmlns:mml="http://www.w3.org/1998/Math/MathML"><mml:mrow><mml:msub><mml:mi>Co</mml:mi><mml:mn>2</mml:mn></mml:msub></mml:mrow></mml:math> Heusler films. Physical Review B, 2019, 100, .	1.1	32
41308	Deformation induced pseudomagnetic fields in complex carbon architectures. Physical Review B, 2019, 100, .	1.1	1
41309	Investigation of growth mechanism for highly oriented TiO2 nanorods: the role of reaction time and annealing temperature. SN Applied Sciences, 2019, 1, 1.	1.5	19
41310	Density functional theory meta GGA study of water adsorption in MIL-53(Cr). Powder Diffraction, 2019, 34, 227-232.	0.4	6
41311	Covalency-driven Structural Evolution in the Polar Pyrochlore Series Cd₂Nb₂O_{7â€“x}S_x. Chemistry of Materials, 2019, 31, 7626-7637.	3.2	18
41312	Toward Fast and Reliable Potential Energy Surfaces for Metallic Pt Clusters by Hierarchical Delta Neural Networks. Journal of Chemical Theory and Computation, 2019, 15, 5614-5627.	2.3	34
41313	Enhanced Interactions of Amino Acids and Nucleic Acid Bases with Bare Black Phosphorene Monolayer Mediated by Coadsorbed Species. Journal of Physical Chemistry C, 2019, 123, 23691-23704.	1.5	10
41314	Exploring the Catalytic Properties of Unsupported and TiO₂-Supported Cu₅ Clusters: CO₂ Decomposition to CO and CO₂ Photoactivation. Journal of Physical Chemistry C, 2019, 123, 23064-23074.	1.5	39
41315	Nanostructure of Cr₂CO₂ MXene Supported Single Metal Atom as an Efficient Bifunctional Electrocatalyst for Overall Water Splitting. ACS Applied Energy Materials, 2019, 2, 6851-6859.	2.5	81

#	Article	IF	Citations
41316	Subnanomolar FRET-Based DNA Assay Using Thermally Stable Phosphorothioated DNA-Functionalized Quantum Dots. ACS Applied Materials & Interfaces, 2019, 11, 33525-33534.	4.0	18
41317	Dendrite-Free Fluorinated Graphene/Lithium Anodes Enabling in Situ LiF Formation for High-Performance Lithiumâ€“Oxygen Cells. ACS Applied Materials & Interfaces, 2019, 11, 39737-39745.	4.0	23
41318	Surface Functionalization of Layered Molybdenum Disulfide for the Selective Detection of Volatile Organic Compounds at Room Temperature. ACS Applied Materials & Interfaces, 2019, 11, 34135-34143.	4.0	79
41319	A General Atomic Surface Modification Strategy for Improving Anchoring and Electrocatalysis Behavior of Ti₃C₂T₂ MXene in Lithiumâ€“Sulfur Batteries. ACS Nano, 2019, 13, 11078-11086.	7.3	232
41320	Markedly Enhanced Oxygen Reduction Activity of Single-Atom Fe Catalysts via Integration with Fe Nanoclusters. ACS Nano, 2019, 13, 11853-11862.	7.3	340
41321	A Supramolecular View on the Cooperative Role of BrÃ¸nsted and Lewis Acid Sites in Zeolites for Methanol Conversion. Journal of the American Chemical Society, 2019, 141, 14823-14842.	6.6	80
41322	The influence of support materials on the structural and electronic properties of gold nanoparticles â€“ a DFT study. Physical Chemistry Chemical Physics, 2019, 21, 19011-19025.	1.3	39
41323	Graphene-like monolayer monoxides and monochlorides. Proceedings of the National Academy of Sciences of the United States of America, 2019, 116, 17213-17218.	3.3	54
41324	Non-Abelian band topology in noninteracting metals. Science, 2019, 365, 1273-1277.	6.0	141
41325	Morphology and Electronic Structure of Sn-Intercalated TiS2(0001) Layers. Journal of Physical Chemistry C, 2019, 123, 22293-22298.	1.5	6
41326	Ab Initio Investigation of Li and Na Migration in Guest-Free, Type I Clathrates. Journal of Physical Chemistry C, 2019, 123, 22812-22822.	1.5	11
41327	Probing Nanoscale Phase Separation at Atomic Resolution within Î²-Type Tiâ€“Mn Alloy: A Potential Candidate for Biomedical Implants. ACS Biomaterials Science and Engineering, 2019, 5, 5005-5014.	2.6	1
41328	Soft Phonon Modes in Ni2MnGa and Ni2MnAl Heusler Alloys. Bulletin of the Russian Academy of Sciences: Physics, 2019, 83, 909-911.	0.1	0
41329	Hg0 oxidation and SO3, Pb0, PbO, PbCl2 and As2O3 adsorption by graphene-based bimetallic catalyst ((Fe,Co)@N-GN): A DFT study. Applied Surface Science, 2019, 496, 143686.	3.1	38
41330	Neural network-based transductive regression model. Applied Soft Computing Journal, 2019, 84, 105682.	4.1	5
41331	In Situ EC-STM Study and DFT Modeling of the Adsorption of Glycerol on Cu(111) in NaOH Solution. Journal of Physical Chemistry C, 2019, 123, 22228-22238.	1.5	7
41332	Initial Steps in PEO Decomposition on a Li Metal Electrode. Journal of Physical Chemistry C, 2019, 123, 22851-22857.	1.5	70
41333	Innovations in (Uâ€“Th)/He, Fission Track, and Trapped Charge Thermochronometry with Applications to Earthquakes, Weathering, Surfaceâ€Mantle Connections, and the Growth and Decay of Mountains. Tectonics, 2019, 38, 3705-3739.	1.3	76

#	Article	IF	Citations
41334	A first principles investigation on the mechanism of TiC act as heterogeneous nucleation substrate of Mg phase to refine grains in AZ91. AIP Advances, 2019, 9, 085105.	0.6	1
41335	Governing factors of supports of ammonia synthesis in an electric field found using density functional theory. Journal of Chemical Physics, 2019, 151, 064708.	1.2	13
41336	Structural, mechanical, and electronic properties of 25 kinds of IIIâ€“V binary monolayers: A computational study with first-principles calculation*. Chinese Physics B, 2019, 28, 086105.	0.7	29
41337	Near-field infrared spectroscopy of monolayer <mml:math xmlns:mml="http://www.w3.org/1998/Math/MathML"><mml:msub><mml:mi mathvariant="normal">MnPS</mml:mi><mml:mn>3</mml:mn></mml:msub></mml:math>. Physical Review B, 2019, 100, .	1.1	15
41338	Insight into the stability of binuclear Irâ€“La catalysts for efficient heterogeneous methanol carbonylation. Journal of Catalysis, 2019, 377, 400-408.	3.1	17
41339	Predicting Adsorption Energies Using Multifidelity Data. Journal of Chemical Theory and Computation, 2019, 15, 5588-5600.	2.3	17
41340	Interaction of Atomic Hydrogen with the Cu₂O(100) and (111) Surfaces. Journal of Physical Chemistry C, 2019, 123, 22172-22180.	1.5	13
41341	First-Principles Mapping of the Electronic Properties of Two-Dimensional Materials for Strain-Tunable Nanoelectronics. ACS Applied Nano Materials, 2019, 2, 5614-5624.	2.4	17
41342	Spectroscopic studies of atomic defects and bandgap renormalization in semiconducting monolayer transition metal dichalcogenides. Nature Communications, 2019, 10, 3825.	5.8	48
41343	Remarkable active-site dependent H2O promoting effect in CO oxidation. Nature Communications, 2019, 10, 3824.	5.8	96
41344	The Dielectric and Piezoelectric Properties of YCa4O(BO3)3 Crystal Annealed in Critical Condition. , 2019, , .		0
41345	Aluminum adsorption on graphene: Theoretical study of dispersion effects. Journal of Theoretical and Computational Chemistry, 2019, 18, 1950019.	1.8	3
41346	Facile and Versatile Functionalization of Twoâ€Dimensional Carbon Nitrides by Design: Magnetism/Multiferroicity, Valleytronics, and Photovoltaics. Advanced Functional Materials, 2019, 29, 1905752.	7.8	19
41347	Dielectric and optical properties of porous graphenes with uniform pore structures. Journal of Molecular Modeling, 2019, 25, 266.	0.8	3
41348	Molecular Dynamics Study of Molecular and Dissociative Adsorption Using System-Specific Force Fields Based on Ab Initio Calculations: CO/Cu(110) and $$ext {CH}_4/ext {Pt(110)}$$. Topics in Catalysis, 2019, 62, 1044-1052.	1.3	8
41349	Rh nanoroses for isopropanol oxidation reaction. Applied Catalysis B: Environmental, 2019, 259, 118082.	10.8	44
41350	An experimental and computational study of enhanced charge storage capacity of chemical vapor deposited Ni3S2-reduced graphene oxide hybrids. Applied Surface Science, 2019, 497, 143789.	3.1	10
41351	A comprehensive insight into the role of barium in catalytic performance of Co/Al2O3 catalyst for Fischer-Tropsch synthesis. Fuel, 2019, 256, 115911.	3.4	23

#	Article	IF	Citations
41352	Stabilization of Ca7Ge-type magnesium compounds by alloying of non-metal elements: AÂnew family material for reversible hydrogen storage applications. International Journal of Hydrogen Energy, 2019, 44, 23216-23224.	3.8	3
41353	Theoretical evaluation on single-atom Fe doped divacancy graphene for catalytic CO and NO oxidation by O2 molecules. Molecular Catalysis, 2019, 476, 110524.	1.0	14
41354	NaB6Si: A novel wide band gap semiconductor with great hardness. Physics Letters, Section A: General, Atomic and Solid State Physics, 2019, 383, 125901.	0.9	1
41355	Kinetically Controlled Low-Temperature Solid-State Metathesis of Manganese Nitride Mn₃N₂. Chemistry of Materials, 2019, 31, 7248-7254.	3.2	26
41356	Broken-Gap Type-III Band Alignment in WTe₂/HfS₂ van der Waals Heterostructure. Journal of Physical Chemistry C, 2019, 123, 23089-23095.	1.5	69
41357	Vertical Silver@Silver Chloride Coreâ€“Shell Nanowire Array for Carbon Dioxide Electroreduction. ACS Applied Energy Materials, 2019, 2, 6163-6169.	2.5	20
41358	Ultrahigh-current-density niobium disulfide catalysts for hydrogen evolution. Nature Materials, 2019, 18, 1309-1314.	13.3	280
41359	Pressure induced semiconductorâ€“semimetalâ€“superconductor transition of magnesium hexaborides. Dalton Transactions, 2019, 48, 14299-14305.	1.6	6
41360	Defect-induced broadband photodetection of layered Î³-In₂Se₃ nanofilm and its application in near infrared image sensors. Journal of Materials Chemistry C, 2019, 7, 11532-11539.	2.7	36
41361	Mechanisms of ammonia and hydrazine synthesis on Î·-Mn₃N₂-(100) surfaces. Physical Chemistry Chemical Physics, 2019, 21, 19365-19377.	1.3	4
41362	Monolayer Î²-tellurene: a promising p-type thermoelectric material via first-principles calculations. Nanoscale, 2019, 11, 18116-18123.	2.8	36
41363	Vertical ferroelectric switching by in-plane sliding of two-dimensional bilayer WTe₂. Nanoscale, 2019, 11, 18575-18581.	2.8	42
41364	Improved cycling stability in high-capacity Li-rich vanadium containing disordered rock salt oxyfluoride cathodes. Journal of Materials Chemistry A, 2019, 7, 21244-21253.	5.2	37
41365	Towards magnetic alumina: uncovering the roles of transition metal doping and electron hybridization in spin delocalization. Journal of Physics Condensed Matter, 2019, 31, 245801.	0.7	2
41366	Nature of the band gap of Ge:C alloys: insights from hybrid functional density functional theory calculations. Semiconductor Science and Technology, 2019, 34, 075007.	1.0	6
41367	A minimal tight-binding model for the quasi-one-dimensional superconductor K₂Cr₃As₃. New Journal of Physics, 2019, 21, 063027.	1.2	17
41368	Band structure of Ge_{1âˆ’x}Sn_x alloy: a full-zone 30-band k Â· p model. New Journal of Physics, 2019, 21, 073037.	1.2	24
41369	SymTopo: An automatic tool for calculating topological properties of nonmagnetic crystalline materials*. Chinese Physics B, 2019, 28, 087102.	0.7	20

#	Article	IF	Citations
41370	Hydrogen adsorption in Metal-Organic Frameworks Cu-BTC and Fe-BTC:A comparative theoretical study.. Journal of Physics: Conference Series, 2019, 1221, 012016.	0.3	3
41371	Influence of thermal conductivity and of non-constant relaxation time on thermoelectricity in Mg₃Sb₂. Journal of Physics: Conference Series, 2019, 1226, 012010.	0.3	3
41372	Search for ferroelectricity in fluoroperovskites: comparison between LiNiF₃ and NaNiF₃. Journal of Physics: Conference Series, 2019, 1247, 012045.	0.3	1
41373	DFT Study on Metamagnetics Î²-M(OH)₂ (M = Mn, Fe, Co, Ni). Journal of Physics: Conference Series, 2019, 1247, 012046.	0.3	2
41374	Ab initio density-functional studies of 13-atom Cu and Ag clusters. Journal of Physics: Conference Series, 2019, 1252, 012009.	0.3	1
41375	Ab initio simulation of oxygen vacancies in LiMgPO₄. Materials Research Express, 2019, 6, 106304.	0.8	15
41376	Assessment of localized and randomized algorithms for electronic structure. Electronic Structure, 2019, 1, 033001.	1.0	7
41377	Internal and external pressure in cubic perovskites: electronic structure effects and systematic accuracy from first principles. Electronic Structure, 2019, 1, 035001.	1.0	6
41378	Ultrafast electron transfer dynamics in lateral transition-metal dichalcogenide heterostructures. Electronic Structure, 2019, 1, 034001.	1.0	9
41379	Metal-Site Dopants in Two-Dimensional Transition Metal Dichalcogenides. , 2019, , .		2
41380	Erasable and recreatable two-dimensional electron gas at the heterointerface of SrTiO ₃ and a water-dissolvable overlayer. Science Advances, 2019, 5, eaaw7286.	4.7	24
41381	Pivotal Role of Nonmetal Atoms in the Stabilities, Geometries, Electronic Structures, and Isoelectronic Chemistry of Sc 3 X@C 80 (X = C, N, and O). Journal of Computational Chemistry, 2019, 40, 2730-2738.	1.5	10
41382	Strain Affects CO Oxidation on Metallic Nanoparticles Non-linearly. Topics in Catalysis, 2019, 62, 660-668.	1.3	9
41383	Highly efficient cobalt nanoparticles anchored porous N-doped carbon nanosheets electrocatalysts for Li-O2 batteries. Journal of Catalysis, 2019, 377, 534-542.	3.1	95
41384	Morphology effects on surface chemical properties and lattice defects of Cu/CeO2 catalysts applied for low-temperature CO oxidation. Scientific Reports, 2019, 9, 12056.	1.6	61
41385	Electronic structures of MgO/Fe interfaces with perpendicular magnetization revealed by hard X-ray photoemission with an applied magnetic field. Science and Technology of Advanced Materials, 2019, 20, 796-804.	2.8	7
41386	Tuneable magnetic moments in superatomic Cu _X Ni _{8â^' X} clusters. Electronic Structure, 2019, 1, 035003.	1.0	2
41387	Composition Dependence of Structural and Electronic Properties of Quaternary InGaNBi. Nanoscale Research Letters, 2019, 14, 178.	3.1	9

#	Article	IF	Citations
41388	Tuning Electronic Properties of Blue Phosphorene/Graphene-Like GaN van der Waals Heterostructures by Vertical External Electric Field. Nanoscale Research Letters, 2019, 14, 174.	3.1	16
41389	Investigation of energy band at atomic layer deposited AZO/Î²-Ga2O3 ($$ overline{2}01 $$) heterojunctions. Nanoscale Research Letters, 2019, 14, 275.	3.1	6
41390	Dependence of Electronic and Optical Properties of MoS2 Multilayers on the Interlayer Coupling and Van Hove Singularity. Nanoscale Research Letters, 2019, 14, 288.	3.1	27
41391	High-Performance Two-Dimensional InSe Field-Effect Transistors with Novel Sandwiched Ohmic Contact for Sub-10 nm Nodes: a Theoretical Study. Nanoscale Research Letters, 2019, 14, 277.	3.1	6
41392	Interaction of carbon with microstructural defects in a W-Re matrix: An ab initio assessment. Journal of Applied Physics, 2019, 126, 075110.	1.1	20
41393	Relaxation volumes of microscopic and mesoscopic irradiation-induced defects in tungsten. Journal of Applied Physics, 2019, 126, .	1.1	35
41394	Cesium desorption mechanism in Cs0.33WO3 by first-principles molecular dynamics calculations. Journal of Applied Physics, 2019, 126, .	1.1	7
41395	Stacking defects in GaP nanowires: Electronic structure and optical properties. Journal of Applied Physics, 2019, 126, 084306.	1.1	3
41396	Atomic structure and electronic properties of lead and tin based hybrid halide perovskite surface for photovoltaic applications. AIP Advances, 2019, 9, .	0.6	9
41397	Ab-initio study of charged oxygen defects in Zn2P2O7. AIP Conference Proceedings, 2019, , .	0.3	0
41398	Stability and electronic properties of two dimensional pentagonal layers of palladium chalcogenides. AIP Conference Proceedings, 2019, , .	0.3	0
41399	Spin-orbit coupling from a two-component self-consistent approach. I. Generalized Hartree-Fock theory. Journal of Chemical Physics, 2019, 151, 074107.	1.2	20
41400	o-C8 carbon: A new allotrope of superhard carbon. Chinese Journal of Chemical Physics, 2019, 32, 357-364.	0.6	5
41401	Role of Coulomb correlations in the charge density wave of CuTe. Physical Review B, 2019, 100, .	1.1	11
41402	Phase stabilities of <mml:math xmlns:mml="http://www.w3.org/1998/Math/MathML"><mml:mrow><mml:mi>C</mml:mi><mml:mi>m</mml:mi><mml:mi>c</mml:mi> and <mml:math xmlns:mml="http://www.w3.org/1998/Math/MathML"><mml:mrow><mml:mi>P</mml:mi><mml:mi>n</mml:mi><mml:mi>m</mml:mi> SnSe studied by phonon quasiparticle approach. Physical Review B, 2019, 100, .	1.1	14
41403	Origin of two-dimensional electronic states at Si- and Gd-terminated surfaces of GdRh2Si2 (001). Physical Review B, 2019, 100, .	1.1	4
41404	Pressure effect on Kohn anomaly and electronic topological transition in single-crystal tantalum. Physical Review B, 2019, 100, .	1.1	13
41405	Band edge evolution of transparent <mml:math xmlns:mml="http://www.w3.org/1998/Math/MathML"><mml:mrow><mml:mi>Zn</mml:mi><mml:msubsup><mml:mi>M</mml:mi><mml:mi>		

#	Article	IF	Citations
41406	Momentum-resolved lattice dynamics of parent and electron-doped <mml:math xmlns:mml="http://www.w3.org/1998/Math/MathML"><mml:mrow><mml:msub><mml:mi>Sr</mml:mi><mml:mn>2</mml:mn></mml:msub><mml:mi>Ir</mml:mi><mml:msub><mml:mi>O</mml:mi><mml:mn></mml:mn></mml:r Physical Review B, 2019, 100, .	1.1	7
41407	Spin-orbit entangled <mml:math xmlns:mml="http://www.w3.org/1998/Math/MathML"><mml:mrow><mml:mi>j</mml:mi><mml:mo>=</mml:mo><mml:mfrac><mml:mn moments in <mml:math xmlns:mml="http://www.w3.org/1998/Math/MathML"><mml:mrow><mml:msub><mml:mi>Ba</mml:mi><mml:mn>2</mml:mn></mml:msub> : A frustrated fcc quantum magnet. Physical Review B, 2019, 100, .	1.1	40
41408	Route to a Superconducting Phase above Room Temperature in Electron-Doped Hydride Compounds under High Pressure. Physical Review Letters, 2019, 123, 097001.	2.9	255
41409	Comparative analysis of electronic structure evolution in Ge_{1-x}Sn_x and Ge_{1â^'x}Pb_x alloys. , 2019, , .		2
41410	Improved Unconstrained Energy Functional Method for Eigensolvers in Electronic Structure Calculations. , 2019, , .		0
41411	A density functional theory study of the oxygen reduction reaction on the (111) and (100) surfaces of cobalt(II) oxide. Progress in Reaction Kinetics and Mechanism, 2019, 44, 122-131.	1.1	6
41412	THz Emission by Frequency Down-conversion in Topological Insulator Quantum Dots. Physical Review Applied, 2019, 12, .	1.5	8
41413	Higher Energy Barrier for Interfacial Li-Ion Transfer from EC/LiPF6 Electrolyte into (010) LiFePO4 Cathode Surface than Bulk Li-Ion Diffusion within Both Cathode and Electrolyte. Journal of the Electrochemical Society, 2019, 166, A2966-A2972.	1.3	9
41414	Cesium Bismuth Iodide Solar Cells from Systematic Molar Ratio Variation of CsI and BiI₃. Inorganic Chemistry, 2019, 58, 12040-12052.	1.9	45
41415	Role of Hydroxyl Species in Hydrogen Oxidation Reaction: A DFT Study. Journal of Physical Chemistry C, 2019, 123, 23931-23939.	1.5	35
41416	Breaking Linear Scaling Relationships with Secondary Interactions in Confined Space: A Case Study of Methane Oxidation by Fe/ZSM-5 Zeolite. ACS Catalysis, 2019, 9, 9276-9284.	5.5	44
41417	Kinetic Isolation between Turnovers on Au₁₈ Nanoclusters: Formic Acid Decomposition One Molecule at a Time. ACS Catalysis, 2019, 9, 9446-9457.	5.5	20
41418	First-Principles Study of Piezoelectric Properties and Bonding Analysis in (Mg, X, Al)N Solid Solutions (X = Nb, Ti, Zr, Hf). ACS Omega, 2019, 4, 15081-15086.	1.6	31
41419	Room-Temperature Ferroelectricity in Group-IV Metal Chalcogenide Nanowires. Journal of the American Chemical Society, 2019, 141, 15040-15045.	6.6	44
41420	Theoretical analysis of spectral lineshapes from molecular dynamics. Npj Computational Materials, 2019, 5, .	3.5	6
41421	Magnetic field-temperature phase diagram of multiferroic (NH4)2FeCl5Â·H2O. Npj Quantum Materials, 2019, 4, .	1.8	10
41422	Nitrogen-based gas molecule adsorption of monolayer phosphorene under metal functionalization. Scientific Reports, 2019, 9, 12498.	1.6	25
41423	Janus MoSSe/WSeTe heterostructures: a direct Z-scheme photocatalyst for hydrogen evolution. Journal of Materials Chemistry A, 2019, 7, 21835-21842.	5.2	119

#	Article	IF	Citations
41424	An alkali metalâ€“selenium battery with a wide temperature range and low self-discharge. Journal of Materials Chemistry A, 2019, 7, 21774-21782.	5.2	38
41425	Graphene quantum dot/Co(OH)₂ electrode on nanoporous Auâ€“Ag alloy for superior hybrid micro-supercapacitors. Journal of Materials Chemistry C, 2019, 7, 11441-11448.	2.7	22
41426	Theoretical study of the photoconduction and photomagnetism of the BPY[Ni(dmit)2]2 molecular crystal. Dalton Transactions, 2019, 48, 13789-13798.	1.6	1
41427	NaSbSe2 as a promising light-absorber semiconductor in solar cells: First-principles insights. APL Materials, 2019, 7, 081122.	2.2	11
41428	Strain effects and electronic structures of narrow band P-R ferroelectrics: First principles calculation. Ferroelectrics, 2019, 544, 1-10.	0.3	0
41429	Large out-of-plane piezoelectricity of oxygen functionalized MXenes for ultrathin piezoelectric cantilevers and diaphragms. Nano Energy, 2019, 65, 104058.	8.2	49
41430	Experimental and DFT Mechanistic Study of Dehydrohalogenation of 1-Chloro-1,1-difluoroethane over Metal Fluorides. Industrial & Engineering Chemistry Research, 2019, 58, 18149-18159.	1.8	10
41431	Dynamical Study of the Dissociative Chemisorption of CHD₃ on Pd(111). Journal of Physical Chemistry C, 2019, 123, 24013-24023.	1.5	11
41432	Chlorine-Doped Perovskite Oxide: A Platinum-Free Cathode for Dye-Sensitized Solar Cells. ACS Applied Materials & Interfaces, 2019, 11, 35641-35652.	4.0	15
41433	Pt/Pd Single-Atom Alloys as Highly Active Electrochemical Catalysts and the Origin of Enhanced Activity. ACS Catalysis, 2019, 9, 9350-9358.	5.5	106
41434	Imaging and Dynamics of Water Hexamer Confined in Nanopores. ACS Nano, 2019, 13, 10622-10630.	7.3	10
41435	Ionic and Electronic Conduction in TiNb₂O₇. Journal of the American Chemical Society, 2019, 141, 16706-16725.	6.6	134
41436	Highly efficient decomposition of ammonia using high-entropy alloy catalysts. Nature Communications, 2019, 10, 4011.	5.8	376
41437	Prediction of Site Preference of Implanted Transition Metal Dopants in Rock-salt Oxides. Scientific Reports, 2019, 9, 12593.	1.6	13
41438	IRMOF-74(n)â€“Mg: a novel catalyst series for hydrogen activation and hydrogenolysis of Câ€“O bonds. Chemical Science, 2019, 10, 9880-9892.	3.7	23
41439	Efficient perovskite solar cells fabricated by manganese cations incorporated in hybrid perovskites. Journal of Materials Chemistry C, 2019, 7, 11943-11952.	2.7	46
41440	The influence of oxygen vacancy on the electronic and optical properties of ABO₃â^Î´</sub> (A =) Tj ETQq0 0 0 rgBT /Overlock 10	1.3	41
41441	In situ growth of minimal Ir-incorporated CoxNi1-xO nanowire arrays on Ni foam with improved electrocatalytic activity for overall water splitting. Chinese Journal of Catalysis, 2019, 40, 1576-1584.	6.9	25

#	Article	IF	Citations
41442	Quantum capacitance of transition metal and nitrogen co-doped graphenes as supercapacitors electrodes: A DFT study. Applied Surface Science, 2019, 496, 143659.	3.1	58
41443	DFT investigations into surface stability and morphology of Î´-MoC catalyst. Applied Surface Science, 2019, 497, 143790.	3.1	12
41444	Doped graphene and Ag(1â€¯1â€¯1) hybrid material as fuel cell electrode: New insights on interfacial features and oxygen adsorption from dispersion-corrected density functional theory. Computational Materials Science, 2019, 169, 109141.	1.4	2
41445	Electronic and optical properties of the ZrS2/HfSe2 van der Waals heterobilayer with native type-II band alignment. Chemical Physics Letters, 2019, 734, 136703.	1.2	10
41446	Hydrogen generation from formic acid decomposition on Pdâ€“Cu nanoalloys. International Journal of Hydrogen Energy, 2019, 44, 24098-24109.	3.8	17
41447	The n- and p-type thermoelectricity property of GeTe by first-principles study. Journal of Alloys and Compounds, 2019, 810, 151838.	2.8	13
41448	Dehybridization effect in improved dehydrogenation of LiAlH4 by doping with two-dimensional Ti3C2. Materials Today Nano, 2019, 8, 100054.	2.3	26
41449	Stable Ordered Phases of Cuprous Iodide with Complexes of Copper Vacancies. Chemistry of Materials, 2019, 31, 7877-7882.	3.2	17
41450	Indium-Free Amorphous Caâ€“Alâ€“O Thin Film as a Transparent Conducting Oxide. Chemistry of Materials, 2019, 31, 8019-8025.	3.2	9
41451	Ionic Transport in Potential Coating Materials for Mg Batteries. Chemistry of Materials, 2019, 31, 8087-8099.	3.2	82
41452	Combined Experimental and Theoretical Insights into Energy Storage Applications of a VO₂(D)â€“Graphene Hybrid. Journal of Physical Chemistry C, 2019, 123, 24280-24288.	1.5	37
41453	Ultrafast Charge Separation and Recombination across a Molecule/CsPbBr₃ Quantum Dot Interface from First-Principles Nonadiabatic Molecular Dynamics Simulation. Journal of Physical Chemistry C, 2019, 123, 23800-23806.	1.5	8
41454	Nickel Hydrides under High Pressure. Journal of Physical Chemistry C, 2019, 123, 24243-24247.	1.5	3
41455	Computational Insights into the Working Mechanism of the LiPF₆â€“Graphite Dual-Ion Battery. Journal of Physical Chemistry C, 2019, 123, 23863-23871.	1.5	31
41456	Unveiling the Role of Oxygen Vacancy in Li₂MnO₃ upon Delithiation. Journal of Physical Chemistry C, 2019, 123, 23403-23409.	1.5	14
41457	Suppressed Carrier Recombination in Janus MoSSe Bilayer Stacks: A Time-Domain Ab Initio Study. Journal of Physical Chemistry Letters, 2019, 10, 5564-5570.	2.1	23
41458	Two-Dimensional T-NiSe₂ as a Promising Anode Material for Potassium-Ion Batteries with Low Average Voltage, High Ionic Conductivity, and Superior Carrier Mobility. ACS Applied Materials & Interfaces, 2019, 11, 35661-35666.	4.0	49
41459	Understanding Active Sites in Pyrolyzed Feâ€“Nâ€“C Catalysts for Fuel Cell Cathodes by Bridging Density Functional Theory Calculations and ⁵⁷Fe MÃ¶ssbauer Spectroscopy. ACS Catalysis, 2019, 9, 9359-9371.	5.5	167

#	Article	IF	Citations
41460	Sulfated Tin Oxide as Highly Selective Catalyst for the Chlorination of Methane to Methyl Chloride. ACS Catalysis, 2019, 9, 9398-9410.	5.5	22
41461	Tailoring exciton dynamics of monolayer transition metal dichalcogenides by interfacial electron-phonon coupling. Communications Physics, 2019, 2, .	2.0	27
41462	A comprehensive study of the molecular vibrations in solid-state benzylic amide [2]catenane. Physical Chemistry Chemical Physics, 2019, 21, 19538-19547.	1.3	4
41463	Hydrogenated PtP₂ monolayer: theoretical predictions on the structure and charge carrier mobility. Journal of Materials Chemistry C, 2019, 7, 12231-12239.	2.7	21
41464	Ab initio investigation of the elastic properties of bismuth-based alloys. Physical Review B, 2019, 100, .	1.1	15
41465	First-principles study of the electronic structure and the Fermi surface in rare-earth filled skutterudites <mml:math xmlns:mml="http://www.w3.org/1998/Math/MathML"><mml:mrow><mml:mi>R</mml:mi><mml:msub><mml:mi>Pt</mml:mi><mml:mn Physical Review B, 2019, 100, .	1.1	6
41466	Superioniclike Diffusion in an Elemental Crystal: bcc Titanium. Physical Review Letters, 2019, 123, 105501.	2.9	28
41467	Atomically precise, custom-design origami graphene nanostructures. Science, 2019, 365, 1036-1040.	6.0	156
41468	Multiple fermions in MoP. Modern Physics Letters B, 2019, 33, 1950293.	1.0	0
41469	Defects, Diffusion, and Dopants in Li2Ti6O13: Atomistic Simulation Study. Materials, 2019, 12, 2851.	1.3	12
41470	Hydrogen evolution reaction mechanism on 2H-MoS2 electrocatalyst. Applied Surface Science, 2019, 498, 143869.	3.1	65
41471	Site dependent substitution and half-metallic behaviour in Heusler compounds: A case study for Mn2RhSi, Co2RhSi and CoRhMnSi. Computational Condensed Matter, 2019, 21, e00423.	0.9	3
41472	Lithium ion storage in lithium titanium germanate. Nano Energy, 2019, 66, 104094.	8.2	15
41473	Synthesis and structural characterization of 3-[1-[4-(2-methylpropyl)phenyl]ethyl]-6-(4-fluorophenyl)-1,2,4-triazolo[3,4-b]-1,3,4-thiadiazole. Powder Diffraction, 2019, 34, 325-330.	0.4	1
41474	The sp² character of new two-dimensional AsB with tunable electronic properties predicted by theoretical studies. Physical Chemistry Chemical Physics, 2019, 21, 20981-20987.	1.3	5
41475	Core-dependent properties of copper nanoclusters: valence-pure nanoclusters as NIR TADF emitters and mixed-valence ones as semiconductors. Chemical Science, 2019, 10, 10122-10128.	3.7	42
41476	ReaxFF reactive force field for molecular dynamics simulations of liquid Cu and Zr metals. Journal of Chemical Physics, 2019, 151, 094503.	1.2	12
41477	Comparative First-Principles Study of Antiperovskite Oxides and Nitrides as Thermoelectric Material: Multiple Dirac Cones, Low-Dimensional Band Dispersion, and High Valley Degeneracy. Physical Review Applied, 2019, 12, .	1.5	14

#	Article	IF	Citations
41478	Evolution of structural, magnetic, and transport properties in <mml:math xmlns:mml="http://www.w3.org/1998/Math/MathML"><mml:mrow><mml:msub><mml:mi>MnBi</mml:mi><mml:mrow><mml:mn>2</mml:mn></mml:mrow></mml:msub></mml:mrow></mml:math> Physical Review B, 2019, 100, .	1.1	16
41479	Dirac-node-line and Hall effect in the <mml:math xmlns:mml="http://www.w3.org/1998/Math/MathML"><mml:mn>6</mml:mn><mml:mi>H</mml:mi></mml:math> -perovskite iridate <mml:math xmlns:mml="http://www.w3.org/1998/Math/MathML"><mml:mrow><mml:msub><mml:mi>Ba</mml:mi><mml:mn>3</mml:mn></mml:msub><mml:msub><mml:mi mathvariant="normal">O</mml:mi><mml:mn>9</mml:mn></mml:msub></mml:mrow></mml:math>. Physical Review B, 2019, 100, .	1.1	16
41480	Density functional theory study of the effect of Vanadium doping on electronic and optical properties of NiO. International Journal of Computational Materials Science and Engineering, 2019, 08, 1950007.	0.5	1
41481	Monofunctional platinum(II) compounds and nucleolar stress: is phenanthriplatin unique?. Journal of Biological Inorganic Chemistry, 2019, 24, 899-908.	1.1	15
41482	Thermodynamics of graphite intercalation binary alloys of Li-Na, Na-K, and Li-K from van der Waals density functionals. Journal of Solid State Electrochemistry, 2019, 23, 2825-2834.	1.2	2
41483	Effect of surface intrinsic defects on the structural stability and electronic properties of the all-inorganic halide perovskite CsPbI3(0â€¯0â€¯1) film. Chemical Physics Letters, 2019, 734, 136719.	1.2	19
41484	Thermodynamics and kinetics of ordered and disordered Cu/Au alloys from first principles calculations. Journal of Alloys and Compounds, 2019, 809, 151615.	2.8	10
41485	Adsorption geometries and interface electronic structure of C60 on Si(100)2â€Ã—â€1 reconstruction surface. Surface Science, 2019, 690, 121484.	0.8	2
41486	Electrostatic force driven helium insertion into ammonia and water crystals under pressure. Communications Chemistry, 2019, 2, .	2.0	15
41487	Mechanism of photocatalytic toluene oxidation with ZnWO₄: a combined experimental and theoretical investigation. Catalysis Science and Technology, 2019, 9, 5692-5697.	2.1	20
41488	Selective electrochemical reduction of CO₂ to CO on CuO/In₂O₃ nanocomposites: role of oxygen vacancies. Catalysis Science and Technology, 2019, 9, 5339-5349.	2.1	25
41489	Out-of-plane ion transport makes nitrogenated holey graphite a promising high-rate anode for both Li and Na ion batteries. Nanoscale, 2019, 11, 18758-18768.	2.8	22
41490	Tuning graphene transistors through ad hoc electrostatics induced by a nanometer-thick molecular underlayer. Nanoscale, 2019, 11, 19705-19712.	2.8	13
41491	Toward rational catalyst design for partial hydrogenation of dimethyl oxalate to methyl glycolate: a descriptor-based microkinetic analysis. Catalysis Science and Technology, 2019, 9, 5763-5773.	2.1	19
41492	Computer Design of Two-Dimensional Monolayers with Octahedral 1,6-Carborane Units. Russian Journal of Inorganic Chemistry, 2019, 64, 1031-1034.	0.3	3
41493	Hybrid-improper ferroelectric behavior in Ba3SiO/Ba3GeO oxide antiperovskite superlattices. European Physical Journal B, 2019, 92, 1.	0.6	5
41494	Two-Dimensional Room-Temperature Ferromagnetic Semiconductors with Quantum Anomalous Hall Effect. Physical Review Applied, 2019, 12, .	1.5	60
41495	Anomalous ferromagnetism and magneto-optical Kerr effect in semiconducting double perovskite Ba2NiOsO6 and its (111) (Ba2NiOsO6)/(BaTiO3)10 superlattice. Physical Review B, 2019, 100, .	1.1	7

#	Article	IF	Citations
41496	Unusual lattice thermal conductivity in the simple crystalline compounds <mml:math xmlns:mml="http://www.w3.org/1998/Math/MathML"><mml:mrow><mml:mrow><mml:mi>Tl</mml:mi><mml:mi>X</mml:mi></mml:mr mathvariant="normal">Te</mml:mi><mml:mn>2</mml:mn></mml:msub></mml:mrow><mml:mrow><mml:mo>(</mml:mo><mml:mrow Physical Review B, 2019, 100, .	1.1	16
41497	One-step hydrothermal synthesis of Cu-doped MnO2 coated diatomite for degradation of methylene blue in Fenton-like system. Journal of Colloid and Interface Science, 2019, 556, 466-475.	5.0	39
41498	Computer-Generated Kinetics for Coupled Heterogeneous/Homogeneous Systems: A Case Study in Catalytic Combustion of Methane on Platinum. Industrial & Engineering Chemistry Research, 2019, 58, 17682-17691.	1.8	26
41499	Revelation of the Nature of the Ligandâ€“PbS Bond and Its Implication on Chemical Functionalization of PbS. Journal of Physical Chemistry C, 2019, 123, 22981-22988.	1.5	2
41500	Highly Anisotropic Thermal Transport in LiCoO₂. Journal of Physical Chemistry Letters, 2019, 10, 5552-5556.	2.1	17
41501	Surface Pb-Dimer Passivated by Molecule Oxygen Notably Suppresses Charge Recombination in CsPbBr₃ Perovskites: Time-Domain Ab Initio Analysis. Journal of Physical Chemistry Letters, 2019, 10, 5499-5506.	2.1	22
41502	Zeeman-type spin splitting in nonmagnetic three-dimensional compounds. Npj Quantum Materials, 2019, 4, .	1.8	23
41503	Formation of a uranyl hydroxide hydrateviahydration of [(UO₂F₂)(H₂O)]₇Â·4H₂O. Dalton Transactions, 2019, 48, 13685-13698.	1.6	15
41504	First principles study of g-Mg₃N₂ as an anode material for Na-, K-, Mg-, Ca- and Al-ion storage. RSC Advances, 2019, 9, 27378-27385.	1.7	24
41505	Experimental and computational analysis of binary Fe-Sn ferromagnetic compounds. Acta Materialia, 2019, 180, 126-140.	3.8	14
41506	Non-trivial band gaps and charge transfer in Janus-like functionalized bilayer boron arsenide. Computational Materials Science, 2019, 170, 109186.	1.4	4
41507	On-Surface Synthesis of Chiral Ï€-Conjugate Porphyrin Tapes by Substrate-Regulated Dehydrogenative Coupling. Journal of Physical Chemistry C, 2019, 123, 23007-23013.	1.5	14
41508	Strain-tunable electric structure and magnetic anisotropy in monolayer CrSI. Physical Chemistry Chemical Physics, 2019, 21, 20892-20900.	1.3	25
41509	Ab initio molecular dynamics simulation of vibrational energy redistribution of selective excitation of Câ€“H stretching vibrations for solid nitromethane. Physical Chemistry Chemical Physics, 2019, 21, 20822-20828.	1.3	5
41510	Theoretical studies on the energy structures and optical properties of copper cysteamine â€“ a novel sensitizer. Physical Chemistry Chemical Physics, 2019, 21, 21084-21093.	1.3	7
41511	Layer-dependent dielectric and optical properties of centimeter-scale 2D WSe₂: evolution from a single layer to few layers. Nanoscale, 2019, 11, 22762-22771.	2.8	55
41512	Topological metal and noncentrosymmetric superconductor Î±-BiPd as an efficient candidate for the hydrogen evolution reaction. Materials Chemistry Frontiers, 2019, 3, 2184-2189.	3.2	11
41513	Controllable oxygen-incorporated interlayer-expanded ReS₂ nanosheets deposited on hollow mesoporous carbon spheres for improved redox kinetics of Li-ion storage. Journal of Materials Chemistry A, 2019, 7, 22070-22078.	5.2	10

#	Article	IF	Citations
41514	A first principles study of a spin-polarized two-dimensional polar metal at the SrVO3/PbTiO3 heterostructure interface. Journal of Applied Physics, 2019, 126, .	1.1	8
41515	Thickness dependence of the anomalous Hall effect in thin films of the topological semimetal <mml:math xmlns:mml="http://www.w3.org/1998/Math/MathML"><mml:mrow><mml:msub><mml:mi>Co</mml:mi><mml:mn>2</mml:mn></mml Physical Review B, 2019, 100, .	1.1	66
41516	Atomic and Effective Pair Interactions in FeC Alloy with Point Defects: A Cluster Expansion Study. ISIJ International, 2019, 59, 2343-2351.	0.6	0
41517	Observation of the Same New Sheet Topology in Both the Layered Uranyl Oxide-Phosphate Cs11[(UO2)12(PO4)3O13] and the Layered Uranyl Oxyfluoride-Phosphate Rb11[(UO2)12(PO4)3O12F2] Prepared by Flux Crystal Growth. Frontiers in Chemistry, 2019, 7, 583.	1.8	12
41518	The Kinetic Behaviors of H Impurities in the Li/Ta Bilayer: Application for the Accelerator-Based BNCT. Nanomaterials, 2019, 9, 1107.	1.9	3
41519	Engineering anion defect in LaFeO2.85Cl0.15 perovskite for boosting oxygen evolution reaction. International Journal of Hydrogen Energy, 2019, 44, 24077-24085.	3.8	26
41520	Reactivity and selectivity descriptors of dioxygen activation routes on metal oxides. Journal of Catalysis, 2019, 377, 692-710.	3.1	9
41521	Reduced graphene oxide supported Ni-Ce catalysts for CO2 methanation: The support and ceria promotion effects. Journal of CO2 Utilization, 2019, 34, 676-687.	3.3	85
41522	Computational Discovery of Inorganic Electrides from an Automated Screening. Matter, 2019, 1, 1293-1303.	5.0	42
41523	Global discovery of stable and non-toxic hybrid organic-inorganic perovskites for photovoltaic systems by combining machine learning method with first principle calculations. Nano Energy, 2019, 66, 104070.	8.2	48
41524	Spontaneous low-temperature crystallization of Î±-FAPbI3 for highly efficient perovskite solar cells. Science Bulletin, 2019, 64, 1608-1616.	4.3	58
41525	Diffusion in CaCO₃ Calcite Investigated by Atomic-Scale Simulations. Journal of Physical Chemistry C, 2019, 123, 21825-21837.	1.5	3
41526	Controlling Molecular Switching via Chemical Functionality: Ethyl vs Methoxy Rotors. Journal of Physical Chemistry C, 2019, 123, 23738-23746.	1.5	9
41527	Two-Dimensional Effects on the Oxygen Reduction Reaction and Irreversible Surface Oxidation of Metallic Ru Nanosheets and Nanoparticles. ACS Applied Nano Materials, 2019, 2, 5743-5751.	2.4	16
41528	Pressure-Induced Superconductivity and Flattened Se₆ Rings in the Wide Band Gap Semiconductor Cu₂I₂Se₆. Journal of the American Chemical Society, 2019, 141, 15174-15182.	6.6	9
41529	Triggered reversible phase transformation between layered and spinel structure in manganese-based layered compounds. Nature Communications, 2019, 10, 3385.	5.8	42
41530	In situ observation of picosecond polaron self-localisation in Î±-Fe2O3 photoelectrochemical cells. Nature Communications, 2019, 10, 3962.	5.8	93
41531	Zn-Doped Cu(100) facet with efficient catalytic ability for the CO₂ electroreduction to ethylene. Physical Chemistry Chemical Physics, 2019, 21, 21341-21348.	1.3	25

#	Article	IF	Citations
41532	Evaluation of interfacial stability and strength of cermets based on work function. Physical Chemistry Chemical Physics, 2019, 21, 20706-20719.	1.3	2
41533	Ru@UiO-66(Ce) catalyzed acceptorless dehydrogenation of primary amines to nitriles: the roles of Lewis acidâ€“base pairs in the reaction. Green Chemistry, 2019, 21, 5386-5393.	4.6	37
41534	Magnetism and hybrid improper ferroelectricity in LaMO₃/YMO₃ superlattices. Physical Chemistry Chemical Physics, 2019, 21, 20132-20136.	1.3	8
41535	First-principles investigation of the hydrogen evolution reaction on different surfaces of pyrites MnS₂, FeS₂, CoS₂, NiS₂. Physical Chemistry Chemical Physics, 2019, 21, 21561-21567.	1.3	20
41536	Metalâ€“organic-framework-derived porous 3D heterogeneous NiFe_x/NiFe₂O₄@NC nanoflowers as highly stable and efficient electrocatalysts for the oxygen-evolution reaction. Journal of Materials Chemistry A, 2019, 7, 21338-21348.	5.2	71
41537	Stacking induced indirect-to-direct bandgap transition in layered group-IV monochalcogenides for ideal optoelectronics. Journal of Materials Chemistry C, 2019, 7, 11858-11867.	2.7	10
41538	A comparative study of optical properties of site specific doping in GaNbO4. AIP Conference Proceedings, 2019, , .	0.3	2
41539	Geometries, electronic and magnetic properties of Aun and Aun-1Li (n=2-6) clusters using density functional theory. AIP Conference Proceedings, 2019, , .	0.3	0
41540	First-principles study of ultrathin molybdenum sulfides nanowires: Electronic and catalytic hydrogen evolution properties. Chinese Journal of Chemical Physics, 2019, 32, 267-272.	0.6	3
41541	Ab-Initio Study of (111) to (001) Texture Transformation in Ag Thin Films. Materials Transactions, 2019, 60, 437-440.	0.4	1
41542	Analysis of surface adsorption kinetics of SiH4 and Si2H6 for deposition of a hydrogenated silicon thin film using intermediate pressure SiH4 plasmas. Applied Surface Science, 2019, 496, 143728.	3.1	16
41543	Site occupation and 4f â†' 5d transitions of Ce3+ ions at mixed Ca2+/Y3+ sites in CaYAlO4: Insights from first-principles calculations. Journal of Luminescence, 2019, 216, 116726.	1.5	9
41544	Insight into the improved cycling stability of sphere-nanorod-like micro-nanostructured high voltage spinel cathode for lithium-ion batteries. Nano Energy, 2019, 66, 104100.	8.2	38
41545	Electron-Rich Ruthenium on Nitrogen-Doped Carbons Promoting Levulinic Acid Hydrogenation to Î³-Valerolactone: Effect of Metalâ€“Support Interaction. ACS Sustainable Chemistry and Engineering, 2019, 7, 16501-16510.	3.2	64
41546	Highly Exposed Active Sites of Defect-Enriched Derived MOFs for Enhanced Oxygen Reduction Reaction. ACS Sustainable Chemistry and Engineering, 2019, 7, 17855-17862.	3.2	66
41547	A high-performance oxygen evolution catalyst in neutral-pH for sunlight-driven CO2 reduction. Nature Communications, 2019, 10, 4081.	5.8	57
41548	Intermediate band solar cell materials through the doping of group-VA elements (N, P, As and Sb) in Cu₂ZnSiSe₄. RSC Advances, 2019, 9, 28234-28240.	1.7	3
41549	Integrated insights into Na⁺ storage mechanism and electrochemical kinetics of ultrafine V₂O₃/S and N co-doped rGO composites as anodes for sodium ion batteries. Journal of Materials Chemistry A, 2019, 7, 22429-22435.	5.2	29

#	Article	IF	Citations
41550	Effect of doping Ti on the vacancy trapping mechanism for helium in ZrCo from first principles. Physical Chemistry Chemical Physics, 2019, 21, 20909-20918.	1.3	10
41551	Boronated holey graphene: a case of 2D ferromagnetic metal. Physical Chemistry Chemical Physics, 2019, 21, 21128-21135.	1.3	3
41552	Unravelling the effects of oxidation state of interstitial iodine and oxygen passivation on charge trapping and recombination in CH₃NH₃PbI₃ perovskite: a time-domain ab initio study. Chemical Science, 2019, 10, 10079-10088.	3.7	44
41553	Exploring high-performance anodes of Li-ion batteries based on the rules of pore-size dependent band gaps in porous carbon foams. Journal of Materials Chemistry A, 2019, 7, 21976-21984.	5.2	31
41554	First-principles study of bandgap bowing in BGaN alloys. Journal of Applied Physics, 2019, 126, 095706.	1.1	18
41555	Preparation, Performance, and Work Function Model of Impregnated Tungstate Cathodes. IEEE Transactions on Electron Devices, 2019, 66, 3592-3598.	1.6	4
41556	Structural, mechanical, and thermodynamic properties of R-3m ReB4 under high pressure. European Physical Journal B, 2019, 92, 1.	0.6	2
41557	Predication of screened hybrid functional on transition metal monoxides: From Mott insulator to charge transfer insulator. Journal of Alloys and Compounds, 2019, 808, 151707.	2.8	2
41558	Revealing Electronic Signatures of Lattice Oxygen Redox in Lithium Ruthenates and Implications for High-Energy Li-Ion Battery Material Designs. Chemistry of Materials, 2019, 31, 7864-7876.	3.2	47
41559	Structure-Driven Photoluminescence Enhancement in a Zn-Based Metalâ€“Organic Framework. Chemistry of Materials, 2019, 31, 7933-7940.	3.2	21
41560	What Is the Best Size of Subnanometer Copper Clusters for CO₂ Conversion to Methanol at Cu/TiO₂ Interfaces? A Density Functional Theory Study. Journal of Physical Chemistry C, 2019, 123, 24118-24132.	1.5	32
41561	Controlling Selectivity in Unsaturated Aldehyde Hydrogenation Using Single-Site Alloy Catalysts. ACS Catalysis, 2019, 9, 9150-9157.	5.5	55
41562	Amplification of Elementary Surface Reaction Steps on Transition Metal Surfaces Using Liquid Crystals: Dissociative Adsorption and Dehydrogenation. Journal of the American Chemical Society, 2019, 141, 16003-16013.	6.6	18
41563	Arm Growth and Facet Modulation in Perovskite Nanocrystals. Journal of the American Chemical Society, 2019, 141, 16160-16168.	6.6	84
41564	Emergent honeycomb network of topological excitations in correlated charge density wave. Nature Communications, 2019, 10, 4038.	5.8	38
41565	Reaction selectivity of homochiral versus heterochiral intermolecular reactions of prochiral terminal alkynes on surfaces. Nature Communications, 2019, 10, 4122.	5.8	27
41566	Magnetism and in-gap states of 3d transition metal atoms on superconducting Re. Npj Quantum Materials, 2019, 4, .	1.8	29
41567	Selective control of surface spin current in topological pyrite-type OsX2 (Xâ€‰=â€‰Se, Te) crystals. Npj Quantum Materials, 2019, 4, .	1.8	8

#	Article	IF	Citations
41568	Energy of the 229Th nuclear clock transition. Nature, 2019, 573, 243-246.	13.7	151
41569	Stability of non-metal dopants to tune the photo-absorption of TiO2 at realistic temperatures and oxygen partial pressures: A hybrid DFT study. Scientific Reports, 2019, 9, 11427.	1.6	17
41570	Phase-change like process through bond switching in distorted and resonantly bonded crystal. Scientific Reports, 2019, 9, 12816.	1.6	4
41571	Callistemon-like Zn and S codoped CoP nanorod clusters as highly efficient electrocatalysts for neutral-pH overall water splitting. Journal of Materials Chemistry A, 2019, 7, 22453-22462.	5.2	76
41572	A type of robust superlattice type-I Weyl semimetal with four Weyl nodes. Nanoscale, 2019, 11, 18358-18366.	2.8	12
41573	Unconventional inner-TL electric polarization in TL-LaOBiS₂ with ultrahigh carrier mobility. Nanoscale, 2019, 11, 18436-18443.	2.8	9
41574	Surface properties of rare-earth metals and the effects of their substitutional doping on work function of the W(110) surface. EPJ Applied Physics, 2019, 87, 11301.	0.3	0
41575	Electronic structure and optical properties of Cu-doped SnO₂. Ferroelectrics, 2019, 547, 137-147.	0.3	7
41576	Interplay of electronic, magnetic, and structural properties of <mml:math xmlns:mml="http://www.w3.org/1998/Math/MathML"><mml:msub><mml:mi>GdB</mml:mi><mml:mn>6</mml:mn></mml:msub></mm from first principles. Physical Review B, 2019, 100, .	1.1	9
41577	Ultrathin Orthorhombic PbS Nanosheets. Chemistry of Materials, 2019, 31, 8145-8153.	3.2	37
41578	Molecular Encapsulation of Cinnamaldehyde within Cyclodextrin Inclusion Complex Electrospun Nanofibers: Fast-Dissolution, Enhanced Water Solubility, High Temperature Stability, and Antibacterial Activity of Cinnamaldehyde. Journal of Agricultural and Food Chemistry, 2019, 67, 11066-11076.	2.4	65
41579	Elaboration of Aggregated Polysulfide Phases: From Molecules to Large Clusters and Solid Phases. Nano Letters, 2019, 19, 7487-7493.	4.5	12
41580	Improving the Oxygen Reduction Reaction Activity of FeN₄â€“Graphene via Tuning Electronic Characteristics. ACS Applied Energy Materials, 2019, 2, 6634-6641.	2.5	37
41581	Unlocking the Potential of Fluoride-Based Solid Electrolytes for Solid-State Lithium Batteries. ACS Applied Energy Materials, 2019, 2, 7196-7203.	2.5	47
41582	Carrier lifetime enhancement in halide perovskite via remote epitaxy. Nature Communications, 2019, 10, 4145.	5.8	93
41583	Comprehensive understanding of intrinsic mobility in the monolayers of IIIâ€“VI group 2D materials. Physical Chemistry Chemical Physics, 2019, 21, 21898-21907.	1.3	32
41584	Electronic stripes and transport properties in borophene heterostructures. Nanoscale, 2019, 11, 17894-17903.	2.8	21
41585	Single molybdenum atom anchored on 2D Ti₂NO₂ MXene as a promising electrocatalyst for N₂ fixation. Nanoscale, 2019, 11, 18132-18141.	2.8	55

#	Article	IF	Citations
41586	An emerging Janus MoSeTe material for potential applications in optoelectronic devices. Journal of Materials Chemistry C, 2019, 7, 12312-12320.	2.7	85
41587	Temperature-induced molecular reorganization on Au(111) driven by oligomeric defects. Nanoscale, 2019, 11, 19468-19476.	2.8	9
41588	Magnetostriction, Soft Magnetism, and Microwave Properties in <mml:math xmlns:mml="http://www.w3.org/1998/Math/MathML" display="inline" overflow="scroll"><mml:mi>Co</mml:mi><mml:mtext>â^'</mml:mtext><mml:mi>Fe</mml:mi><mml:mtext>â^'</mml:mtext><mml:mi>C</mml:mi></mml:mrow></mml:mrow></mml:math> Alloy Films. Physical Review Applied, 2019, 12, .	4.6	16
41589	A group-theory based method to study structural phase transitions in dynamically unstable crystals, with new insights on the<mml:math xmlns:mml="http://www.w3.org/1998/Math/MathML"><mml:mi>Î²</mml:mi></mml:math>to<mml:math xmlns:mml="http://www.w3.org/1998/Math/MathML"><mml:mi>Ï‰</mml:mi></mml:math>transformation in titanium. Physical Review B, 2019, 100, .	1.1	12
41590	Discovery of Weyl Nodal Lines in a Single-Layer Ferromagnet. Physical Review Letters, 2019, 123, 116401.	2.9	70
41591	Shape regulation of high-index facet nanoparticles by dealloying. Science, 2019, 365, 1159-1163.	6.0	108
41592	Acrylic acid hydrodeoxygenation reaction mechanism over molybdenum carbide studied by DFT calculations. Journal of Molecular Modeling, 2019, 25, 309.	0.8	2
41593	Synthesis of Tunable-Aspect-Ratio Calcite Nanoparticles via Mg2+ Doping. Crystal Growth and Design, 2019, 19, 6784-6791.	1.4	4
41594	Photoactive Ag(I)-Based Coordination Polymer as a Potential Semiconductor for Photocatalytic Water Splitting and Environmental Remediation: Experimental and Theoretical Approach. Journal of Physical Chemistry C, 2019, 123, 23940-23950.	1.5	12
41595	Transition Metal Substitution of Hollandite Î±-MnO₂: Enhanced Potential and Structural Stability on Lithiation from First-Principles Calculation. Journal of Physical Chemistry C, 2019, 123, 25042-25051.	1.5	14
41596	Theoretical Investigation on the Single Transition-Metal Atom-Decorated Defective MoS₂ for Electrocatalytic Ammonia Synthesis. ACS Applied Materials & Interfaces, 2019, 11, 36506-36514.	4.0	88
41597	Creating multiferroic and conductive domain walls in common ferroelastic compounds. Npj Computational Materials, 2019, 5, .	3.5	4
41598	Predicting two-dimensional topological phases in Janus materials by substitutional doping in transition metal dichalcogenide monolayers. Npj 2D Materials and Applications, 2019, 3, .	3.9	53
41599	Assessment of van der Waals inclusive density functional theory methods for adsorption and selective dehydrogenation of formic acid on Pt(111) surface. Physical Chemistry Chemical Physics, 2019, 21, 21049-21056.	1.3	23
41600	A type-II C₂N/Î±-Te van der Waals heterojunction with improved optical properties by external perturbation. Physical Chemistry Chemical Physics, 2019, 21, 21753-21760.	1.3	20
41601	Two-Dimensional Li-Based Ternary Chalcogenides for Photocatalysis. Journal of Physical Chemistry Letters, 2019, 10, 6061-6066.	2.1	31
41602	Machine Learning Protocol for Surface-Enhanced Raman Spectroscopy. Journal of Physical Chemistry Letters, 2019, 10, 6026-6031.	2.1	60
41603	Anatase TiO₂ Nanorods as Cathode Materials for Aluminum-Ion Batteries. ACS Applied Nano Materials, 2019, 2, 6428-6435.	2.4	40

#	Article	IF	Citations
41604	Inhibitor, Co-Catalyst, or Co-Reactant? Probing the Different Roles of H₂S during CO₂ Hydrogenation on the MoS₂ Catalyst. ACS Catalysis, 2019, 9, 10044-10059.	5.5	24
41605	Magnetism and Optical Anisotropy in van der Waals Antiferromagnetic Insulator CrOCl. ACS Nano, 2019, 13, 11353-11362.	7.3	97
41606	Theoretical prediction of strain-induced carrier effective mass modulation in 4H-SiC and GaN. Applied Physics Letters, 2019, 115, .	1.5	13
41607	Discovery of topological Weyl fermion lines and drumhead surface states in a room temperature magnet. Science, 2019, 365, 1278-1281.	6.0	374
41608	Fermi-arc diversity on surface terminations of the magnetic Weyl semimetal Co ₃ Sn ₂ S ₂. Science, 2019, 365, 1286-1291.	6.0	441
41609	Magnetic Weyl semimetal phase in a KagomÃ© crystal. Science, 2019, 365, 1282-1285.	6.0	518
41610	First-principles investigations on the formation of H2O defects in lizardite with influence on the elastic property. Physics and Chemistry of Minerals, 2019, 46, 935-946.	0.3	4
41611	Distribution of boron and phosphorus and roles of co-doping in colloidal silicon nanocrystals. Acta Materialia, 2019, 178, 186-193.	3.8	12
41612	Paving the way for cristobalite TiO2 and GeO2 attainable under moderate tensile stress: A DFT study of transformation paths and activation barriers in cristobalite-rutile transformations of MO2 (Mâ€“â€“Si, Ge,) Tj ETQq1 1 0.784314 rgBT /Overlock	1.0	0
41613	Temperature dependence of vacancy concentration and void growth mechanism in Al with constant hydrogen concentration: A first-principles study. Engineering Fracture Mechanics, 2019, 216, 106508.	2.0	4
41614	Realizing high thermoelectric properties of SnTe via synergistic band engineering and structure engineering. Nano Energy, 2019, 65, 104056.	8.2	116
41615	Orthorhombic C10: A new superdense carbon allotrope. Physics Letters, Section A: General, Atomic and Solid State Physics, 2019, 383, 125861.	0.9	10
41616	Strong Vibrational Relaxation of NO Scattered from Au(111): Importance of the Adiabatic Potential Energy Surface. Journal of Physical Chemistry Letters, 2019, 10, 5969-5974.	2.1	35
41617	Green Emission Induced by Intrinsic Defects in All-Inorganic Perovskite CsPb₂Br₅. Journal of Physical Chemistry Letters, 2019, 10, 6118-6123.	2.1	28
41618	Nanoporous Ni₃P Evolutionarily Structured onto a Ni Foam for Highly Selective Hydrogenation of Dimethyl Oxalate to Methyl Glycolate. ACS Applied Materials & Interfaces, 2019, 11, 37635-37643.	4.0	26
41619	Chemical Trend of Transition-Metal Doping in WSe2. Physical Review Applied, 2019, 12, .	1.5	16
41620	Nanoscale topological defects and improper ferroelectric domains in multiferroic barium hexaferrite nanocrystals. Physical Review B, 2019, 100, .	1.1	14
41621	Thermal transport and phonon focusing in complex molecular crystals: Ab initio study of polythiophene. Physical Review B, 2019, 100, .	1.1	8

#	Article	IF	Citations
41622	Superconductivity with strong electron-phonon coupling in noncentrosymmetric <mml:math xmlns:mml="http://www.w3.org/1998/Math/MathML"><mml:mrow><mml:msub><mml:mi mathvariant="normal">W</mml:mi><mml:mn>3</mml:mn></mml:msub><mml:msub><mml:mi>Al</mml:mi><mml:mn>2</mml:mn></mml:msub><mml:mi mathvariant="normal">C</mml:mi></mml:mrow></mml:math>. Physical Review B, 2019, 100, .	1.1	13
41623	Deformed octagon-hexagon-square structure of group-IV and group-V elements and III-V compounds. Physical Review B, 2019, 100, .	1.1	7
41624	Carrier-Density-Induced Ferromagnetism in <mml:math xmlns:mml="http://www.w3.org/1998/Math/MathML" display="inline"><mml:mrow><mml:msub><mml:mrow><mml:mi>EuTiO</mml:mi></mml:mrow><mml:mrow><mml:mn>3</mml:mn></mml:mrow> Bulk and Heterostructures. Physical Review Letters, 2019, 123, 127201.	2.9	18
41625	Dangling Bonds in Hexagonal Boron Nitride as Single-Photon Emitters. Physical Review Letters, 2019, 123, 127401.	2.9	68
41626	The effect of Ru on Ti50Pd50 high temperature shape memory alloy: a first-principles study. MRS Advances, 2019, 4, 2419-2429.	0.5	8
41627	BaCoxFe0.7-xZr0.3O3-Î´(0.2â‰xâ‰0.5) as cathode materials for proton-based SOFCs. Ceramics International, 2019, 45, 23948-23953.	2.3	17
41628	Insight into the enhancement effect of rhenium-rich precipitation on hydrogen retention in tungsten by investigating the behaviors of hydrogen in tungsten-rhenium sigma phase. International Journal of Hydrogen Energy, 2019, 44, 24880-24894.	3.8	5
41629	Parallel BFS implementing optimized decomposition of space and kMC simulations for diffusion of vacancies for quantum storage. Journal of Computational Science, 2019, 36, 101018.	1.5	7
41630	Enhanced Catalyst Durability for Bio-Based Adipic Acid Production by Atomic Layer Deposition. Joule, 2019, 3, 2219-2240.	11.7	12
41631	The adsorption and activation of oxygen molecule on nickel clusters doped graphene-based support by DFT. Molecular Catalysis, 2019, 477, 110547.	1.0	12
41632	Influence of Excess Volumes Induced by Re and W on Dislocation Motion and Creep in Ni-Base Single Crystal Superalloys: A 3D Discrete Dislocation Dynamics Study. Metals, 2019, 9, 637.	1.0	9
41633	Topological insulator nanoribbons â€“ A new paradigm for high thermoelectric performance. Nano Energy, 2019, 66, 104092.	8.2	6
41634	Synergistically Optimizing Carrier Concentration and Decreasing Sound Velocity in n-type AgInSe₂ Thermoelectrics. Chemistry of Materials, 2019, 31, 8182-8190.	3.2	23
41635	Role of Ligandâ€“Ligand Interactions in the Stabilization of Thin Layers of Tin Bromide Perovskite: An Ab Initio Study of the Atomic and Electronic Structure, and Optical Properties. Journal of Physical Chemistry C, 2019, 123, 25176-25184.	1.5	14
41636	Phase Stability and Electronic Structure of Tin Sulfide Compounds for Li-ion Batteries. Journal of Physical Chemistry C, 2019, 123, 29086-29095.	1.5	2
41637	Two-Dimensional COF with Rather Low Exciton Binding Energies Comparable to 3D Inorganic Semiconductors in the Visible Range for Water Splitting. Journal of Physical Chemistry C, 2019, 123, 24626-24633.	1.5	11
41638	Combined Experimental and Theoretical Molecular Approach of the Catalytically Active Hydrotreating MoS₂ Phases Promoted by 3d Transition Metals. Journal of Physical Chemistry C, 2019, 123, 24659-24669.	1.5	8
41639	Strain Gradient Mediated Magnetism and Polarization in Monolayer VSe₂. Journal of Physical Chemistry C, 2019, 123, 24988-24993.	1.5	9

#	Article	IF	Citations
41640	High-Capacity Interstitial Mn-Incorporated Mn_xFe_{3â€“x}O₄/Graphene Nanocomposite for Sodium-Ion Battery Anodes. ACS Applied Materials & Interfaces, 2019, 11, 37812-37821.	4.0	40
41641	Mechanistic Role of the Protonâ€“Hydride Pair in Heteroarene Catalytic Hydrogenation. ACS Catalysis, 2019, 9, 9418-9437.	5.5	16
41642	Oxygen Vacancy Promoted O₂ Activation over Perovskite Oxide for Low-Temperature CO Oxidation. ACS Catalysis, 2019, 9, 9751-9763.	5.5	296
41643	Identifying the Origins of Vacancies in the Crystal Structures of Rock Salt-type Chalcogenide Superconductors. ACS Omega, 2019, 4, 15721-15728.	1.6	7
41644	Polar and phase domain walls with conducting interfacial states in a Weyl semimetal MoTe2. Nature Communications, 2019, 10, 4211.	5.8	50
41645	Robust magnetoresistance in TaAs2 under pressure up to about 37 GPa. Applied Physics Letters, 2019, 115, 122403.	1.5	5
41646	Dynamical Magnetic Field Accompanying the Motion of Ferroelectric Domain Walls. Physical Review Letters, 2019, 123, 127601.	2.9	28
41647	First-principles thermal compatibility between Ru-based Re-substitute alloys and Ir coatings. Computational Materials Science, 2019, 170, 109199.	1.4	2
41648	Quasi-chemical theory for anion hydration and specific ion effects: <mml:math xmlns:mml="http://www.w3.org/1998/Math/MathML" altimg="si36.svg"><mml:mrow><mml:msup><mml:mrow><mml:mi mathvariant="normal">Cl</mml:mi></mml:mrow><mml:mrow><mml:mo>-</mml:mo></mml:mrow></mml:msup></mml:mrow></mml:math> vs. <mml:math xmlns:mml="http://www.w3.org/1998/Math/MathML" altimg="si37.svg"><mml:mrow><mml:msup><mml:mrow><mml:mi mathvariant="normal">F</mml:mi></	2.1	15
41649	Influence of trigonal deformation on band structure and Seebeck coefficient of tellurium. Journal of Physics and Chemistry of Solids, 2019, 135, 109114.	1.9	17
41650	Oxygen vacancy mediated cubic phase stabilization at room temperature in pure nano-crystalline zirconia films: a combined experimental and first-principles based investigation. Physical Chemistry Chemical Physics, 2019, 21, 22482-22490.	1.3	16
41651	Quantum oscillations and nontrivial topological state in a compensated semimetal <mml:math xmlns:mml="http://www.w3.org/1998/Math/MathML"><mml:msub><mml:mi>TaP</mml:mi><mml:mn>2</mml:mn></mml:msub></m Physical Review B, 2019, 100, .	1.1	15
41652	Surface electronic structure of bismuth oxychalcogenides. Physical Review B, 2019, 100, .	1.1	18
41653	Fully spin-polarized open and closed nodal lines in <mml:math xmlns:mml="http://www.w3.org/1998/Math/MathML"><mml:mi>Î²</mml:mi></mml:math> -borophene by magnetic proximity effect. Physical Review B, 2019, 100, .	1.1	16
41654	Si-Cmma: A silicon thin film with excellent stability and Dirac nodal loop. Physical Review B, 2019, 100, .	1.1	36
41655	Crystal Structure Exploration of Boron Nitride Polymorphs Using Anharmonic Downward Distortion Following Method with Potential Energy Surface Modified by the Inverse of Lattice Volume. Chemistry Letters, 2019, 48, 1288-1291.	0.7	4
41656	Theoretical and FTIR Investigations of the Acetonitrile Hydrogenation Pathways on Platinum. Topics in Catalysis, 2019, 62, 1076-1085.	1.3	11
41657	Deep Dehalogenation of Florfenicol Using Crystalline CoP Nanosheet Arrays on a Ti Plate via Direct Cathodic Reduction and Atomic H. Environmental Science & Technology, 2019, 53, 11932-11940.	4.6	67

#	Article	IF	Citations
41658	Structure-property correlations of bis(nitrofurazano) furazan(BNFF-1): A density functional theory study. AIP Conference Proceedings, 2019, , .	0.3	0
41659	Density functional theory calculations of generalized stacking fault energy surfaces for eight face-centered cubic transition metals. Journal of Applied Physics, 2019, 126, .	1.1	39
41660	Gaussian approximation potential for studying the thermal conductivity of silicene. Journal of Applied Physics, 2019, 126, .	1.1	21
41661	Topological hybrid nodal-loop semimetal in a carbon allotrope constructed by interconnected Riemann surfaces. Physical Review B, 2019, 100, .	1.1	26
41662	Magnetically controllable topological quantum phase transitions in the antiferromagnetic topological insulator <mml:math xmlns:mml="http://www.w3.org/1998/Math/MathML"><mml:mrow><mml:msub><mml:mi>MnBi</mml:mi><mml:mn>2</mml:mn></mml:mr Physical Review B, 2019, 100, .	1.1	93
41663	Structure of an epitaxial <mml:math xmlns:mml="http://www.w3.org/1998/Math/MathML"><mml:mrow><mml:mi mathvariant="normal">N</mml:mi><mml:msub><mml:mi mathvariant="normal">b</mml:mi><mml:mn>2</mml:mn></mml:msub><mml:msub><mml:mi mathvariant="normal">O</mml:mi><mml:mn>3</mml:mn></mml:msub></mml:mrow></mml:math> honeycomb monolayer on Au(111). Physical Review B, 2019, 100, .	1.1	14
41664	Electron pairing by remote-phonon scattering in oxide-supported graphene. Physical Review B, 2019, 100, .	1.1	0
41665	Capture and dissociation of dichloromethane on Fe, Ni, Pd and Pt decorated phosphorene. Applied Surface Science, 2019, 495, 143533.	3.1	12
41666	Effects of Morphology and Surface Properties of Copper Oxide on the Removal of Hydrogen Sulfide from Gaseous Streams. Industrial & Engineering Chemistry Research, 2019, 58, 18836-18847.	1.8	21
41667	Adsorption, Absorption, Diffusion, and Permeation of Hydrogen and Its Isotopes in bcc Bulk Fe and Fe(100) Surface: Plane Wave-Based Density Functional Theoretical Investigations. Journal of Physical Chemistry C, 2019, 123, 23951-23966.	1.5	11
41668	Cu₄Bi₄Se₉: A Thermoelectric Symphony of Rattling, Anharmonic Lone-pair, and Structural Complexity. ACS Applied Materials & Interfaces, 2019, 11, 36616-36625.	4.0	20
41669	Nodeless superconductivity and its evolution with pressure in the layered dirac semimetal 2M-WS2. Npj Quantum Materials, 2019, 4, .	1.8	20
41670	Enhanced catalytic activity of SO_x-incorporated graphene for the hydrogen evolution reaction. Journal of Materials Chemistry A, 2019, 7, 22615-22620.	5.2	4
41671	Ultrahigh conductivity of graphene nanoribbons doped with ordered nitrogen. Nanoscale Advances, 2019, 1, 4359-4364.	2.2	4
41672	Crystal structure of vyacheslavite, U(PO₄)(OH), solved from natural nanocrystal: a precession electron diffraction tomography (PEDT) study and DFT calculations. RSC Advances, 2019, 9, 19657-19661.	1.7	11
41673	Hydrated Sodium Ion Clusters [Na+(H2O)n (n = 1â€“6)]: An ab initio Study on Structures and Non-covalent Interaction. Frontiers in Chemistry, 2019, 7, 624.	1.8	24
41674	Two-dimensional MoS₂â€“melamine hybrid nanostructures for enhanced catalytic hydrogen evolution reaction. Journal of Materials Chemistry A, 2019, 7, 22571-22578.	5.2	14
41675	Long-range order imposed by short-range interactions in methylammonium lead iodide: Comparing point-dipole models to machine-learning force fields. Physical Review B, 2019, 100, .	1.1	14

#	Article	IF	Citations
41676	Effect of thermal lattice and magnetic disorder on phonons in bcc Fe: A first-principles study. Physical Review B, 2019, 100, .	1.1	8
41677	Valleyite: A new magnetic mineral with the sodalite-type structure. American Mineralogist, 2019, 104, 1238-1245.	0.9	11
41678	Structural, electronic and magnetic properties of MxPt1-X, (M= Co, Ni and V) binary alloys. Heliyon, 2019, 5, e02433.	1.4	6
41679	Stabilizing the oxygen lattice and reversible oxygen redox in Na-deficient cathode oxides. Journal of Power Sources, 2019, 439, 227086.	4.0	27
41680	Bimetallic Composition-Promoted Electrocatalytic Hydrodechlorination Reaction on Silverâ€“Palladium Alloy Nanoparticles. ACS Catalysis, 2019, 9, 10803-10811.	5.5	115
41681	Enhancement of interlayer exchange in an ultrathin two-dimensional magnet. Nature Physics, 2019, 15, 1255-1260.	6.5	165
41682	Pronounced <mml:math xmlns:mml="http://www.w3.org/1998/Math/MathML"><mml:mfrac><mml:mn>2</mml:mn><mml:mn>3</mml:mn></mml:mfrac></mml magnetization plateau in a frustrated <mml:math xmlns:mml="http://www.w3.org/1998/Math/MathML"><mml:mrow><mml:mi>S</mml:mi><mml:mo>=</mml:mo><mml:mn>1</mml:mn> isolated spin-triangle compound: Interplay between Heisenberg and biquadratic exchange interactions. Physical Review B, 2019, 100, .	1.1	7
41683	Optical spectroscopy study of the topological property in PrSb. Physical Review B, 2019, 100, .	1.1	3
41684	Observation of a topological nodal-line semimetal in <mml:math xmlns:mml="http://www.w3.org/1998/Math/MathML"><mml:msub><mml:mi>YbMnSb</mml:mi><mml:mn>2</mml:mn></mml:msub><mml through optical spectroscopy. Physical Review B, 2019, 100, .	1.1	26
41685	Predicting the Structure Stability of Layered Heteroanionic Materials Exhibiting Anion Order. Inorganic Chemistry, 2019, 58, 13229-13240.	1.9	9
41686	Gd³⁺-Doped Î±-CsPbI₃ Nanocrystals with Better Phase Stability and Optical Properties. Journal of Physical Chemistry C, 2019, 123, 24865-24872.	1.5	55
41687	Transparent Conductive Films Derived from Single-Walled Aluminosilicate Nanotubes. ACS Applied Nano Materials, 2019, 2, 6677-6689.	2.4	5
41688	Intermetallic PdIn catalyst for CO₂ hydrogenation to methanol: mechanistic studies with a combined DFT and microkinetic modeling method. Catalysis Science and Technology, 2019, 9, 6102-6113.	2.1	45
41689	Green persistent luminescence and the electronic structure of Î²-Sialon:Eu²⁺. Journal of Materials Chemistry C, 2019, 7, 12544-12551.	2.7	38
41690	Density functional theory (DFT) study of BaScO₃H_{0.5} compound and its hydrogen storage properties. Canadian Journal of Physics, 2019, 97, 1191-1199.	0.4	6
41691	Comparison of first principles and semi-empirical models of the structural and electronic properties of $$hbox {Ge}_{1-x}hbox {Sn}_{x}$$ alloys. Optical and Quantum Electronics, 2019, 51, 1.	1.5	19
41692	Superwadeites: Elucidation of a Structural Family Related to the Wadeite Structure and Prediction of Cs2Ge5O11. Crystal Growth and Design, 2019, 19, 5477-5482.	1.4	5
41693	Reactivity of Cu and Co Nanoparticles Supported on Mo-Doped MgO. Industrial & Engineering Chemistry Research, 2019, 58, 18213-18222.	1.8	4

#	Article	IF	Citations
41694	Modeling of Diffusion and Incorporation of Interstitial Oxygen Ions at the TiN/SiO₂ Interface. ACS Applied Materials & Interfaces, 2019, 11, 36232-36243.	4.0	9
41695	Thermodynamic Assessment of Coating Materials for Solid-State Li, Na, and K Batteries. ACS Applied Materials & Interfaces, 2019, 11, 36607-36615.	4.0	21
41696	Flux crystal growth of uranium(<scp>v</scp>) containing oxyfluoride perovskites. Inorganic Chemistry Frontiers, 2019, 6, 3203-3214.	3.0	11
41697	Semilocal exchange-correlation potentials for solid-state calculations: Current status and future directions. Journal of Applied Physics, 2019, 126, .	1.1	41
41698	Evolution of carbides and performance of knives made of aged 8Cr13MoV steel. Materials Science and Technology, 2019, 35, 1988-1996.	0.8	4
41699	Pressure-induced superconductivity in the layered pnictogen diselenide NdO0.8F0.2Sb1â^'xBixSe2(x=0.3and0.7). Physical Review B, 2019, 100, .	1.1	3
41700	Topological semimetal phases manifested in transition metal dichalcogenides intercalated with <mml:math xmlns:mml="http://www.w3.org/1998/Math/MathML"><mml:mn>3</mml:mn><mml:mi>d</mml:mi></mml:math> metals. Physical Review B, 2019, 100, .	1.1	15
41701	Charge qubit in van der Waals heterostructures. Physical Review B, 2019, 100, .	1.1	15
41702	Precipitate evolution and strengthening behavior during aging process in a 2.5 GPa grade maraging steel. Acta Materialia, 2019, 179, 296-307.	3.8	120
41703	Thermodynamic description of the Coâ€“Niâ€“Ta system. Calphad: Computer Coupling of Phase Diagrams and Thermochemistry, 2019, 66, 101649.	0.7	13
41704	Electrochemical performance of pure Al, Alâ€“Sn, Alâ€“Mg and Alâ€“Mgâ€“Sn anodes for Al-air batteries. Journal of Alloys and Compounds, 2019, 808, 151708.	2.8	84
41705	First principles prediction of the ground state crystal structures of antiperovskite compounds A3PN (A= Be, Mg, Ca, Sr, Ba and Zn). Materials Today: Proceedings, 2019, 8, 294-300.	0.9	5
41706	Electronic Properties of a New Family of Layered Materials from Groups 14 and 15: First-Principles Simulations. Journal of Physical Chemistry C, 2019, 123, 25470-25476.	1.5	13
41707	Optical Properties and Chemical Ordering of Agâ€“Pt Nanoalloys: A Computational Study. Journal of Physical Chemistry C, 2019, 123, 25482-25491.	1.5	11
41708	Real-Space Imaging of Orbital Selectivity on SrTiO₃(001) Surface. ACS Applied Materials & Interfaces, 2019, 11, 37279-37284.	4.0	5
41709	Modulation of Phosphorene for Optimal Hydrogen Evolution Reaction. ACS Applied Materials & Interfaces, 2019, 11, 37787-37795.	4.0	38
41710	W Doping and Voltage Driven Metalâ€“Insulator Transition in VO₂ Nano-Films for Smart Switching Devices. ACS Applied Nano Materials, 2019, 2, 6738-6746.	2.4	36
41711	[{(PhSn)₃SnS₆}{(MCp)₃S₄}] (M = W, Mo): Minimal Molecular Models of the Covalent Attachment of Metal Chalcogenide Clusters on Doped Transition Metal Dichalcogenide Layers. Journal of the American Chemical Society, 2019, 141, 16494-16500.	6.6	14

#	Article	IF	Citations
41712	Concentration-Diversified Magnetic and Electronic Properties of Halogen-Adsorbed Silicene. Scientific Reports, 2019, 9, 13746.	1.6	14
41713	Surface-vacancy-induced metallicity and layer-dependent magnetic anisotropy energy in Cr2Ge2Te6. Journal of Applied Physics, 2019, 126, .	1.1	13
41714	Unique Crystal Structure of Ca2RuO4 in the Current Stabilized Semimetallic State. Physical Review Letters, 2019, 123, 137204.	2.9	31
41715	Mechanical and Electronic Stabilization of Solid Electrolyte Interphase with Sulfite Additive for Lithium Metal Batteries. Journal of the Electrochemical Society, 2019, 166, A3201-A3206.	1.3	8
41716	Electrochemical Properties and Challenges of Type II Silicon Clathrate Anode in Sodium Ion Batteries. Journal of the Electrochemical Society, 2019, 166, A3051-A3058.	1.3	6
41717	Electronic and Optical Properties of Cubic Perovskites CsPbCl_{3â^'} _yI_y (y = 0, 1, 2, 3). Zeitschrift Fur Naturforschung - Section A Journal of Physical Sciences, 2019, 74, 905-913.	0.7	19
41718	Carrier mobility and relaxation time in BiCuSeO. Physics Letters, Section A: General, Atomic and Solid State Physics, 2019, 383, 125990.	0.9	10
41719	Surface Induced Phenytoin Polymorph. 1. Full Structure Solution by Combining Grazing Incidence X-ray Diffraction and Crystal Structure Prediction. Crystal Growth and Design, 2019, 19, 6058-6066.	1.4	5
41720	Fluoroethylene Carbonate Breakdown Mechanisms and Energetics on Two Lithium Silicide Surfaces. Journal of Physical Chemistry C, 2019, 123, 26743-26751.	1.5	4
41721	Bifunctional Electrocatalytic Activity of Bis(iminothiolato)nickel Monolayer for Overall Water Splitting. Journal of Physical Chemistry C, 2019, 123, 25651-25656.	1.5	17
41722	The Endocyclic Carbon Substituent of Guanidinate and Amidinate Precursors Controlling Atomic Layer Deposition of InN Films. Journal of Physical Chemistry C, 2019, 123, 25691-25700.	1.5	19
41723	Magnesiophilic Graphitic Carbon Nanosubstrate for Highly Efficient and Fast-Rechargeable Mg Metal Batteries. ACS Applied Materials & Interfaces, 2019, 11, 38754-38761.	4.0	24
41724	Improved CO Oxidation via Surface Stabilization of Ceria Nanoparticles Induced by Rare-Earth Metal Dopants. ACS Applied Nano Materials, 2019, 2, 6473-6481.	2.4	13
41725	Understanding CO₂ Adsorption on a M₁ (M₂)-Promoted (Doped) MgOâ€“CaO(100) Surface (M₁ = Li, Na, K, and Rb, M₂ = Sr): A DFT Theoretical Study. ACS Sustainable Chemistry and Engineering, 2019, 7, 16979-16984.	3.2	18
41726	Anionic redox reaction in layered NaCr2/3Ti1/3S2 through electron holes formation and dimerization of Sâ€“S. Nature Communications, 2019, 10, 4458.	5.8	38
41727	Anchoring Cu1 species over nanodiamond-graphene for semi-hydrogenation of acetylene. Nature Communications, 2019, 10, 4431.	5.8	224
41728	First-principles investigation on electronic properties and band alignment of group III monochalcogenides. Scientific Reports, 2019, 9, 13289.	1.6	23
41729	Chern insulator with a nearly flat band in the metal-organic-framework-based Kagome lattice. Scientific Reports, 2019, 9, 13807.	1.6	17

#	Article	IF	Citations
41730	Defect evolution of oxygen induced Vth-shift for ON-state biased AlGaN/GaN HEMTs. Applied Physics Letters, 2019, 115, .	1.5	6
41731	Effect of SiC nano-size fillers on the aging resistance of XLPE insulation: A first-principles study. Journal of Molecular Graphics and Modelling, 2019, 93, 107438.	1.3	5
41732	Ge3P2: New viable two-dimensional semiconductors with ultrahigh carrier mobility. Applied Surface Science, 2019, 497, 143803.	3.1	17
41733	Mechanism of glass-forming ability enhancement upon micro solute addition for Ce-Ga-Cu-Ni bulk metallic glasses. Intermetallics, 2019, 114, 106603.	1.8	1
41734	Aluminium substituted Î²â€“type NaMn1-Al O2: A stable and enhanced electrochemical kinetic sodium-ion battery cathode. Journal of Power Sources, 2019, 438, 227025.	4.0	20
41735	Giant Magnetoelectric Coupling in Multiferroic PbTi_{1â€“x}V_xO₃ from Density Functional Calculations. ACS Omega, 2019, 4, 16743-16755.	1.6	1
41736	Bottom-up growth of homogeneous MoirÃ© superlattices in bismuth oxychloride spiral nanosheets. Nature Communications, 2019, 10, 4472.	5.8	59
41737	Local electronic descriptors for solute-defect interactions in bcc refractory metals. Nature Communications, 2019, 10, 4484.	5.8	19
41738	Segregation of the major alloying elements to Al3(Sc,Zr) precipitates in an Alâ€“Znâ€“Mgâ€“Cuâ€“Scâ€“Zr alloy. Materials Characterization, 2019, 157, 109898.	1.9	33
41739	Ionothermal Synthesis of Metal Chalcogenides M₂Ag₃Sb₃S₇ (M = Rb, Cs) Displaying Nonlinear Optical Activity in the Infrared Region. Inorganic Chemistry, 2019, 58, 12582-12589.	1.9	16
41740	Interaction of H₂O with the Platinum Pt (001), (011), and (111) Surfaces: A Density Functional Theory Study with Long-Range Dispersion Corrections. Journal of Physical Chemistry C, 2019, 123, 27465-27476.	1.5	33
41741	Nanoscale Ordering and Depolymerization of Calcium Silicate Hydrates in the Presence of Alkalis. Journal of Physical Chemistry C, 2019, 123, 24873-24883.	1.5	30
41742	Compression Behavior of Copper Hydroxyfluoride CuOHF as a Case Study of the High-Pressure Responses of the Hydrogen-Bonded Two-Dimensional Layered Materials. Journal of Physical Chemistry C, 2019, 123, 25492-25500.	1.5	6
41743	Anisotropy of Elastic Properties of Metalâ€“Organic Frameworks and the Breathing Phenomenon. Journal of Physical Chemistry C, 2019, 123, 24651-24658.	1.5	18
41744	Suppression of Electronâ€“Hole Recombination by Intrinsic Defects in 2D Monoelemental Material. Journal of Physical Chemistry Letters, 2019, 10, 6151-6158.	2.1	62
41745	Monolayer HfTeSe₄: A Promising Two-Dimensional Photovoltaic Material for Solar Cells with High Efficiency. ACS Applied Materials & Interfaces, 2019, 11, 37901-37907.	4.0	34
41746	Highly Water-Resistant La-Doped Co₃O₄ Catalyst for CO Oxidation. ACS Catalysis, 2019, 9, 10093-10100.	5.5	126
41747	PdMo bimetallene for oxygen reduction catalysis. Nature, 2019, 574, 81-85.	13.7	935

#	Article	IF	Citations
41748	High nitrogen doped carbon nanofiber aerogels for sodium ion batteries: synergy of vacancy defects to boost sodium ion storage. Applied Surface Science, 2019, 496, 143717.	3.1	30
41749	Rationally Designed High-Performance Spin Filter Based on Two-Dimensional Half-Metal Cr2NO2. Matter, 2019, 1, 1304-1315.	5.0	30
41750	Boosting the photocatalytic hydrogen evolution performance via an atomically thin 2D heterojunction visualized by scanning photoelectrochemical microscopy. Nano Energy, 2019, 65, 104053.	8.2	18
41751	Three-Dimensional Silicon Carbide from Siligraphene as a High Capacity Lithium Ion Battery Anode Material. Journal of Physical Chemistry C, 2019, 123, 27295-27304.	1.5	26
41752	Magnetic Proximity Coupling of Quantum Emitters in WSe₂ to van der Waals Ferromagnets. Nano Letters, 2019, 19, 7301-7308.	4.5	21
41753	Stabilizing Low-Coordinated O Ions To Operate Cationic and Anionic Redox Chemistry of Li-Ion Battery Materials. ACS Applied Materials & Interfaces, 2019, 11, 37768-37778.	4.0	13
41754	High Thermoelectric Performance in Hexagonal 2D PdTe₂ Monolayer at Room Temperature. ACS Applied Materials & Interfaces, 2019, 11, 38819-38827.	4.0	42
41755	Theoretical Analysis, Synthesis, and Characterization of 2D W_{1.33}C (MXene) with Ordered Vacancies. ACS Applied Nano Materials, 2019, 2, 6209-6219.	2.4	37
41756	Atomic Structure and Dynamics of Epitaxial Platinum Bilayers on Graphene. ACS Nano, 2019, 13, 12162-12170.	7.3	15
41757	A model of hardness and fracture toughness of solids. Journal of Applied Physics, 2019, 126, .	1.1	133
41758	Phase transitions and elastic properties of InN1â€“xBix under high pressure. Phase Transitions, 2019, 92, 889-898.	0.6	1
41759	Boosting Sodium Storage of Fe1â^'xS/MoS2 Composite via Heterointerface Engineering. Nano-Micro Letters, 2019, 11, 80.	14.4	77
41760	Theoretical prediction of a novel aluminum nitride nanostructure: Atomistic exposure. Ceramics International, 2019, 45, 23690-23693.	2.3	3
41761	NiCoP nanopeapods embedded in carbon nanotube arrays as bifunctional catalysts for efficient overall water splitting. Materials Today Nano, 2019, 8, 100053.	2.3	17
41762	Growth of carbon nanosheets on carbon nanotube arrays for the fabrication of three-dimensional micro-patterned supercapacitors. Carbon, 2019, 155, 453-461.	5.4	38
41763	Effect of water chemistry on the composition of oxides formed on stainless steel surfaces in light water reactors. Journal of Nuclear Materials, 2019, 526, 151773.	1.3	0
41764	First principles study of H2O adsorption on U2Ti (1â€¯1â€¯0) surface. Nuclear Instruments & Methods in Physics Research B, 2019, 457, 63-71.	0.6	5
41765	K₂Ge₃As₃: Fiberlike Crystals of a Narrow-Band-Gap Zintl Phase with a One-Dimensional Substructure _{â^ž}¹{(Ge₃As₃)^{2â€“}}. Chemistry of Materials, 2019, 31, 8839-8849.	3.2	4

#	Article	IF	Citations
41766	Toward an Understanding of Deformation Mechanisms in Metallic Lithium and Sodium from First-Principles. Chemistry of Materials, 2019, 31, 8222-8229.	3.2	17
41767	Influence of the Iron Proportion on the Efficiency of an Oil-Soluble Niâ€“Fe Catalyst Applied in the Co-liquefaction of Lignite and Heavy Residue. Industrial & Engineering Chemistry Research, 2019, 58, 19072-19081.	1.8	9
41768	Encapsulating Halometallates into 3-D Lanthanide-Viologen Frameworks: Controllable Emissions, Reversible Thermochromism, Photocurrent Responses, and Electrical Bistability Behaviors. Inorganic Chemistry, 2019, 58, 13862-13880.	1.9	45
41769	Active Sites in Single-Layer BiOX (X = Cl, Br, and I) Catalysts for the Hydrogen Evolution Reaction. Inorganic Chemistry, 2019, 58, 13195-13202.	1.9	29
41770	S-Functionalized Mo₂C Monolayer as a Novel Electrode Material in Li-Ion Batteries. Journal of Physical Chemistry C, 2019, 123, 25052-25060.	1.5	33
41771	Large-Gap Quantum Spin Hall States in the Bilayer Hexagonal Structure of Rhenium and Technetium Dinitrides: A First-Principles Study. Journal of Physical Chemistry C, 2019, 123, 25524-25530.	1.5	6
41772	Predictions on High-Power Trivalent Metal Pentazolate Salts. Journal of Physical Chemistry Letters, 2019, 10, 6166-6173.	2.1	62
41773	Scalable Production of Two-Dimensional Metallic Transition Metal Dichalcogenide Nanosheet Powders Using NaCl Templates toward Electrocatalytic Applications. Journal of the American Chemical Society, 2019, 141, 18694-18703.	6.6	56
41774	In Situ Methods for Identifying Reactive Surface Intermediates during Hydrogenolysis Reactions: Câ€“O Bond Cleavage on Nanoparticles of Nickel and Nickel Phosphides. Journal of the American Chemical Society, 2019, 141, 16671-16684.	6.6	30
41775	Characterization of nitrogen doped graphene bilayers synthesized by fast, low temperature microwave plasma-enhanced chemical vapour deposition. Scientific Reports, 2019, 9, 13715.	1.6	33
41776	Spin-driven electrical power generation at room temperature. Communications Physics, 2019, 2, .	2.0	9
41777	First-principles study of the structural, electronic, magnetic, and ferroelectric properties of a charge-ordered iron(ii)-iron(iii) formate framework. Journal of Chemical Physics, 2019, 151, 124704.	1.2	4
41778	Synthesis of Manganese Mononitride with Tetragonal Structure under Pressure. Crystals, 2019, 9, 511.	1.0	3
41779	Stabilization of E-type antiferromagnetic ordering in La and Y substituted orthorhombic LuMnO3: A first-principles study. Physics Letters, Section A: General, Atomic and Solid State Physics, 2019, 383, 125950.	0.9	4
41780	Broadband transparent optical phase change materials for high-performance nonvolatile photonics. Nature Communications, 2019, 10, 4279.	5.8	349
41781	Effects of Zn and Cr additions on precipitation and creep behavior of a dilute Alâ€“Zrâ€“Erâ€“Si alloy. Acta Materialia, 2019, 181, 249-261.	3.8	35
41782	Role of defects on the surface properties of HfC. Applied Surface Science, 2019, 495, 143500.	3.1	7
41783	Understanding of ammonia detection of PbS in inert ambient: Experimental and computational approach. Applied Surface Science, 2019, 495, 143605.	3.1	3

#	Article	IF	Citations
41784	The sustainable cyclic process of water molecule dissociation on the boron-functionalized graphene monovacancy: First-principles study. Applied Surface Science, 2019, 498, 143823.	3.1	13
41785	Modified embedded-atom method interatomic potential for the Mgâ€“Znâ€“Ca ternary system. Calphad: Computer Coupling of Phase Diagrams and Thermochemistry, 2019, 67, 101674.	0.7	5
41786	The structures, stabilities and electronic properties of PdnB (nâ€¯=â€¯1â€“10) clusters. Computational and Theoretical Chemistry, 2019, 1164, 112554.	1.1	4
41787	Net-Y as a high performance electrode material for Na-ion battery. Chemical Physics Letters, 2019, 734, 136733.	1.2	11
41788	The top-down crystallisation of Mercury's core. Earth and Planetary Science Letters, 2019, 528, 115838.	1.8	11
41789	Quantitative evaluation of the surface stability and morphological changes of Cu2O particles. Heliyon, 2019, 5, e02500.	1.4	22
41790	Aluminum-silicon hydride clusters for prospective hydrogen storage. International Journal of Hydrogen Energy, 2019, 44, 26459-26468.	3.8	5
41791	Site occupancy effects of Mg impurities in BaTiO3. Journal of Alloys and Compounds, 2019, 809, 151847.	2.8	8
41792	An advanced high energy-efficiency rechargeable aluminum-selenium battery. Nano Energy, 2019, 66, 104159.	8.2	39
41793	Study of the role of alkaline sodium additive in selective hydrogenation of phenol. Chinese Journal of Catalysis, 2019, 40, 1516-1524.	6.9	28
41794	Ionic Conductivity and Its Dependence on Structural Disorder in Halogenated Argyrodites Li₆PS₅X (X = Br, Cl, I). Chemistry of Materials, 2019, 31, 8673-8678.	3.2	43
41795	Tailoring a Moleculeâ€™s Optical Absorbance Using Surface Plasmonics. Journal of Physical Chemistry C, 2019, 123, 26498-26508.	1.5	4
41796	Monolayer Nitrides Doped with Transition Metals as Efficient Catalysts for Water Oxidation: The Singular Role of Nickel. Journal of Physical Chemistry C, 2019, 123, 26289-26298.	1.5	12
41797	Temperature-Dependent Structural Evolution in Au₄₄Ga₅₆ Liquid Eutectic Alloy. Journal of Physical Chemistry C, 2019, 123, 25209-25219.	1.5	10
41798	Modeling the Size Dependency of the Stability of Metal Nanoparticles. Journal of Physical Chemistry C, 2019, 123, 25464-25469.	1.5	20
41799	Design of a One-Dimensional Stacked Spin Peierls System with Room-Temperature Switching from Quantum Mechanical Predictions. Journal of Physical Chemistry Letters, 2019, 10, 6432-6437.	2.1	1
41800	Predicting Wettability and the Electrochemical Window of Lithium-Metal/Solid Electrolyte Interfaces. ACS Applied Materials & Interfaces, 2019, 11, 39940-39950.	4.0	22
41801	High-Performance M_aZrO_x (M_a = Cd, Ga) Solid-Solution Catalysts for CO₂ Hydrogenation to Methanol. ACS Catalysis, 2019, 9, 10253-10259.	5.5	137

#	Article	IF	Citations
41802	A Universal Length-Dependent Vibrational Mode in Graphene Nanoribbons. ACS Nano, 2019, 13, 13083-13091.	7.3	36
41803	Elemental Substitution of Two-Dimensional Transition Metal Dichalcogenides (MoSe₂ and) Tj ETQq1 1 0.784314 rgBT /Ove	4.0	109
41804	K_x[Bi_{4â€“x}Mn_xS₆], Design of a Highly Selective Ion Exchange Material and Direct Gap 2D Semiconductor. Journal of the American Chemical Society, 2019, 141, 16903-16914.	6.6	22
41805	Atomically ordered non-precious Co3Ta intermetallic nanoparticles as high-performance catalysts for hydrazine electrooxidation. Nature Communications, 2019, 10, 4514.	5.8	80
41806	Waterproof molecular monolayers stabilize 2D materials. Proceedings of the National Academy of Sciences of the United States of America, 2019, 116, 20844-20849.	3.3	32
41807	High thermoelectric performance in low-cost SnS _{0.91} Se _{0.09} crystals. Science, 2019, 365, 1418-1424.	6.0	395
41808	Structural Evolution of AlN Nanoclusters and the Elemental Chemisorption Characteristics: Atomistic Insight. Nanomaterials, 2019, 9, 1420.	1.9	4
41809	Electronic Structure of Sr1â^'yCayFe2(As1â^'xPx)2 (x = 0.25, y = 0.08) Revealed by Angle-Resolved Photoemission Spectroscopy. Journal of the Physical Society of Japan, 2019, 88, 084701.	0.7	1
41810	First-principles and machine learning predictions of elasticity in severely lattice-distorted high-entropy alloys with experimental validation. Acta Materialia, 2019, 181, 124-138.	3.8	113
41811	Synergetic effects of solute and strain in biocompatible Zn-based and Mg-based alloys. Acta Materialia, 2019, 181, 423-438.	3.8	18
41812	Computational insight of monolayer SnS2 as anode material for potassium ion batteries. Applied Surface Science, 2019, 496, 143625.	3.1	63
41813	Controlling magnetism of monolayer Janus MoSSe by embedding transition-metal atoms. Applied Surface Science, 2019, 496, 143692.	3.1	27
41814	Tunable electronic structures in BP/MoSSe van der Waals heterostructures by external electric field and strain. Applied Surface Science, 2019, 497, 143809.	3.1	71
41815	Ti Substitution Facilitating Oxygen Oxidation in Na2/3Mg1/3Ti1/6Mn1/2O2 Cathode. CheM, 2019, 5, 2913-2925.	5.8	75
41816	Molecular insights into the activity and stability of popular methane reforming catalysts using quantum mechanical tools. Current Opinion in Chemical Engineering, 2019, 26, 38-45.	3.8	9
41817	Origin of high hydrogen evolution activity on InSe nanoribbons: A first-principles study. International Journal of Hydrogen Energy, 2019, 44, 24174-24183.	3.8	9
41818	Thermodynamic modeling of YO1.5-TaO2.5 system and the effects of elastic strain energy and diffusion on phase transformation of YTaO4. Journal of the European Ceramic Society, 2019, 39, 5036-5047.	2.8	27
41819	Study of electronic structure and magnetism in d4 double perovskite iridates A2ScIrO6 (Aâ€¯=â€¯Ba, Sr). Journal of Magnetism and Magnetic Materials, 2019, 492, 165708.	1.0	4

#	Article	IF	Citations
41820	A detailed physical analysis on the interaction between transition elements (3d, 4d and 5d) and point defects in molybdenum for nuclear material application. Journal of Nuclear Materials, 2019, 527, 151805.	1.3	6
41821	Precipitate/vanadium interface and its strengthening on the vanadium alloys: A first-principles study. Journal of Nuclear Materials, 2019, 527, 151821.	1.3	13
41822	Promoting effect of H2O over macroporous Ce-Zr catalysts in soot oxidation. Molecular Catalysis, 2019, 474, 110416.	1.0	9
41823	Carbon nanotube-supported bimetallic Cu-Fe catalysts for syngas conversion to higher alcohols. Molecular Catalysis, 2019, 479, 110610.	1.0	15
41824	Few-layer transition metal dichalcogenides (MoS2, WS2, and WSe2) for water splitting and degradation of organic pollutants: Understanding the piezocatalytic effect. Nano Energy, 2019, 66, 104083.	8.2	181
41825	New predicted two-dimensional MXenes and their structural, electronic and lattice dynamical properties. Solid State Communications, 2019, 303-304, 113739.	0.9	31
41826	Preserved Layered Structure Enables Stable Cyclic Performance of MoS₂ upon Potassium Insertion. Chemistry of Materials, 2019, 31, 8801-8809.	3.2	39
41827	Two-Dimensional CuTe₂X (X = Cl, Br, and I): Potential Photocatalysts for Water Splitting under the Visible/Infrared Light. Journal of Physical Chemistry C, 2019, 123, 25543-25548.	1.5	6
41828	Competition of Secondary versus Tertiary Carbenium Routes for the Type B Isomerization of Alkenes over Acid Zeolites Quantified by Ab Initio Molecular Dynamics Simulations. ACS Catalysis, 2019, 9, 9813-9828.	5.5	35
41829	Vicinal metal surfaces as potential catalysts for phosphorene epitaxial growth. Applied Physics Letters, 2019, 115, .	1.5	1
41830	Negative thermal expansion behavior in orthorhombic Sc2(MoO4)3 and Sc2(WO4)3. Journal of Applied Physics, 2019, 126, 125114.	1.1	11
41831	Interfacial charge-transfer Mott state in iridateâ€“nickelate superlattices. Proceedings of the National Academy of Sciences of the United States of America, 2019, 116, 19863-19868.	3.3	31
41832	Structural and electronic properties of boron-induced defects on the Si(001) surface. Physical Review B, 2019, 100, .	1.1	0
41833	Mechanical Deformation and Electronic Structure of a Blue Copper Azurin in a Solid-State Junction. Biomolecules, 2019, 9, 506.	1.8	16
41834	Single Mn atom as a promising electrocatalyst for CO reduction to C2H5OH and C3H6: A computational study. Applied Surface Science, 2019, 498, 143868.	3.1	15
41835	Carbonate doped Bi2MoO6 hierarchical nanostructure with enhanced transformation of active radicals for efficient photocatalytic removal of NO. Journal of Colloid and Interface Science, 2019, 557, 816-824.	5.0	24
41836	From NaZn₄Sb₃ to HT-Na_{1â€“x}Zn_{4â€“y}Sb₃: Panoramic Hydride Synthesis, Structural Diversity, and Thermoelectric Properties. Chemistry of Materials, 2019, 31, 8695-8707.	3.2	19
41837	Highly Selective CO₂ Uptake in Novel Fishnet-like Polybenzoxazine-Based Porous Carbon. Energy & Fuels, 2019, 33, 11454-11464.	2.5	33

#	Article	IF	Citations
41838	First-Principles Study of Divalent 3d Transition-Metal Carbodiimides. Journal of Physical Chemistry A, 2019, 123, 9328-9335.	1.1	16
41839	DFT-Based Global Optimization of Sub-nanometer Niâ€“Pd Clusters. Journal of Physical Chemistry C, 2019, 123, 26583-26596.	1.5	21
41840	Controlled Single-Crystalline Polymerization of C₁₀H₈Â·C₁₀F₈ under Pressure. Macromolecules, 2019, 52, 7557-7563.	2.2	33
41841	Design and Tuning of the Electrochemical Properties of Vanadium-Based Cation-Disordered Rock-Salt Oxide Positive Electrode Material for Lithium-Ion Batteries. ACS Applied Materials & Interfaces, 2019, 11, 39848-39858.	4.0	21
41842	Amorphous Surface PdO_X and Its Activity toward Methane Combustion. ACS Catalysis, 2019, 9, 10317-10323.	5.5	34
41843	Translucency of Graphene to van der Waals Forces Applies to Atoms/Molecules with Different Polar Character. ACS Nano, 2019, 13, 12230-12241.	7.3	11
41844	Vibrational spectroscopy at atomic resolution with electron impact scattering. Nature Physics, 2019, 15, 1237-1241.	6.5	78
41845	Novel Unexpected Reconstructions of (100) and (111) Surfaces of NaCl: Theoretical Prediction. Scientific Reports, 2019, 9, 14267.	1.6	21
41846	Observation of two collapsed phases in <mml:math xmlns:mml="http://www.w3.org/1998/Math/MathML"><mml:mrow><mml:mi>CaRbF</mml:mi><mml:msub><mml:mi mathvariant="normal">e</mml:mi><mml:mn>4</mml:mn></mml:msub><mml:mi mathvariant="normal">A</mml:mi><mml:msub><mml:mi mathvariant="normal">s</mml:mi><mml:mn>4</mml:mn></mml:msub></mml:mrow></mml:math>. Physical Review B, 2019, 100, .	1.1	9
41847	Realization of large band gap opening of graphene and type-I band alignment with BN intercalation layer in graphene/ <mml:math xmlns:mml="http://www.w3.org/1998/Math/MathML"><mml:mrow><mml:mi>M</mml:mi><mml:msub><mml:mi>X</mml:mi></mml:msub></mml:mrow></mml:math> heterojunctions. Physical Review B, 2019, 100, .	1.1	11
41848	Magnetoelectric control of topological phases in graphene. Physical Review B, 2019, 100, .	1.1	17
41849	Equation of state, ionic structure, and phase diagram of warm dense krypton. Physical Review E, 2019, 100, 033214.	0.8	6
41850	Effect of Ag addition on the precipitation evolution and interfacial segregation for Alâ€“Mgâ€“Si alloy. Acta Materialia, 2019, 180, 301-316.	3.8	76
41851	A DFT study of the surface charge transfer doping of diamond by chromium trioxide. Applied Surface Science, 2019, 496, 143604.	3.1	27
41852	Breaking the anisotropy of Î±-CNH and improving the photoelectric performance by constructing Van der Waals heterojunction. Applied Surface Science, 2019, 497, 143787.	3.1	17
41853	Wetting of surfaces and grain boundaries in cemented carbides and the effect from local chemistry. Materialia, 2019, 8, 100470.	1.3	10
41854	B₄C₃ Monolayer with Impressive Electronic, Optical, and Mechanical Properties: A Potential Metal-Free Photocatalyst for CO₂ Reduction under Visible Light. Journal of Physical Chemistry C, 2019, 123, 25091-25101.	1.5	19
41855	Investigation of Methane Adsorption in Strained IRMOF-1. Journal of Physical Chemistry C, 2019, 123, 24592-24597.	1.5	8

#	Article	IF	Citations
41856	Multiferroic Metalâ€“PbNb_{0.12}Ti_{0.88}O_{3â^Î´} Films on Nb-Doped STO. ACS Applied Electronic Materials, 2019, 1, 2109-2115.	2.0	13
41857	New Sb₂Te_{3â€“x}Se_x Monolayers with High Electron Mobilities and Wide Absorption Range. ACS Applied Materials & Interfaces, 2019, 11, 37216-37228.	4.0	12
41858	CO₂ Adsorption and Activation on the (110) Chalcopyrite Surfaces: AÂDispersion-Corrected DFT + U Study. ACS Omega, 2019, 4, 15935-15946.	1.6	6
41859	Phonon limited anisotropic quantum transport in phosphorene field effect transistors. Journal of Applied Physics, 2019, 126, .	1.1	6
41860	Prediction of improved magnetization and stability in Fe16N2 through alloying. Journal of Applied Physics, 2019, 126, .	1.1	18
41861	Dependence of a cooling rate on structural and vibrational properties of amorphous silicon: A neural network potential-based molecular dynamics study. Journal of Chemical Physics, 2019, 151, 114101.	1.2	18
41862	Nanoscale stacking faultâ€“assisted room temperature plasticity in flash-sintered TiO ₂. Science Advances, 2019, 5, eaaw5519.	4.7	82
41863	Covalent Organic Frameworks for the Capture, Fixation, or Reduction of CO2. Frontiers in Energy Research, 2019, 7, .	1.2	91
41864	Charge Density Wave Transition in Monolayer CuTe driven by Coulomb Correlation. Journal of the Korean Physical Society, 2019, 75, 394-397.	0.3	2
41865	First-principles investigation of hydrogen behavior in different oxides in ODS steels. International Journal of Hydrogen Energy, 2019, 44, 17105-17113.	3.8	5
41866	Surface Induced Phenytoin Polymorph. 2. Structure Validation by Comparing Experimental and Density Functional Theory Raman Spectra. Crystal Growth and Design, 2019, 19, 6067-6073.	1.4	1
41867	Rational Design of Mixed Solvent and Porous Graphene-Supported Spinel Oxide Electrodes for High-Rate and Long Cycle-Life Mg Batteries. ACS Applied Materials & Interfaces, 2019, 11, 37595-37601.	4.0	3
41868	Valence Engineering via Dual-Cation and Boron Doping in Pyrite Selenide for Highly Efficient Oxygen Evolution. ACS Nano, 2019, 13, 11469-11476.	7.3	68
41869	Ideal maximum strengths and defect-induced softening in nanocrystalline-nanotwinned metals. Nature Materials, 2019, 18, 1207-1214.	13.3	87
41870	Assessing exchange-correlation functional performance in the chalcogenide lacunar spinels <mml:math xmlns:mml="http://www.w3.org/1998/Math/MathML"><mml:mrow><mml:mi>Ga</mml:mi><mml:msub><mml:mi>M</mml:mi><mml:m <mml:math		

#	Article	IF	Citations
41874	Cooperation of Ni and CaO at Interface for CO₂ Reforming of CH₄: A Combined Theoretical and Experimental Study. ACS Catalysis, 2019, 9, 10060-10069.	5.5	68
41875	Simultaneously Achieving High Activity and Selectivity toward Two-Electron O₂ Electroreduction: The Power of Single-Atom Catalysts. ACS Catalysis, 2019, 9, 11042-11054.	5.5	314
41876	Solvation effect on binding modes of model lignin dimer compounds on MWW 2D-zeolite. Journal of Chemical Physics, 2019, 151, 114708.	1.2	2
41877	Efficient thermal conductivity modulation by manipulating interlayer interactions: A comparative study of bilayer graphene and graphite. Journal of Applied Physics, 2019, 126, .	1.1	21
41878	Concentration-tuned tetragonal strain in alloys: Application to magnetic anisotropy of <mml:math xmlns:mml="http://www.w3.org/1998/Math/MathML"><mml:mrow><mml:msub><mml:mi>FeNi</mml:mi><mml:mrow><mml:mn>1</m Physical Review B, 2019, 100, .	1.1	1
41879	Modeling of Ionic Conductivity in Inorganic Compounds with Multivalent Cations. Russian Journal of Electrochemistry, 2019, 55, 762-777.	0.3	11
41880	Fe(CN)₅@PIL-derived N-doped porous carbon with FeC_xN_y active sites as a robust electrocatalyst for the oxygen reduction reaction. Catalysis Science and Technology, 2019, 9, 97-105.	2.1	10
41881	Elementary kinetics of nitrogen electroreduction to ammonia on late transition metals. Catalysis Science and Technology, 2019, 9, 174-181.	2.1	47
41882	A dimer path for CO dissociation on PtSn. Catalysis Science and Technology, 2019, 9, 695-701.	2.1	9
41883	Molecular or dissociative adsorption of water on clean and oxygen pre-covered Ni(111) surfaces. Catalysis Science and Technology, 2019, 9, 199-212.	2.1	9
41884	Oxygen vacancy-rich MoO_{3â^'x} nanobelts for photocatalytic N₂ reduction to NH₃ in pure water. Catalysis Science and Technology, 2019, 9, 803-810.	2.1	71
41885	The role of H₂S addition on Pt/Al₂O₃ catalyzed propane dehydrogenation: a mechanistic study. Catalysis Science and Technology, 2019, 9, 867-876.	2.1	21
41886	Crystal field modulation-control, bandgap engineering and shallow/deep traps tailoring-guided design of a color-tunable long-persistent phosphor (Ca,) Tj ETQq0 0 0 rgBT /Overlock 10 Tf 50 262 Td (Sr)Ga₄O<sub>7</su 253-265.	1.6	38
41887	Defect engineering of nickel hydroxide nanosheets by Ostwald ripening for enhanced selective electrocatalytic alcohol oxidation. Green Chemistry, 2019, 21, 578-588.	4.6	71
41888	Lanthanide complexes as molecular dopants for realizing air-stable n-type graphene logic inverters with symmetric transconductance. Materials Horizons, 2019, 6, 743-750.	6.4	9
41889	Au quantum dots engineered room temperature crystallization and magnetic anisotropy in CoFe₂O₄ thin films. Nanoscale Horizons, 2019, 4, 434-444.	4.1	77
41890	How the moirÃ© superstructure determines the formation of highly stable graphene quantum dots on Ru(0001) surface. Nanoscale Horizons, 2019, 4, 625-633.	4.1	4
41891	Realizing a stable high thermoelectric zT â¼ 2 over a broad temperature range in Ge_{1â^'xâ^'y}Ga_xSb_yTe via band engineering and hybrid flash-SPS processing. Inorganic Chemistry Frontiers, 2019, 6, 63-73.	3.0	78

#	Article	IF	Citations
41892	Synthesis, crystal and electronic structure, physical properties and121Sb and151Eu MÃ¶ssbauer spectroscopy of the Eu14AlPn11series (Pn = As, Sb). Inorganic Chemistry Frontiers, 2019, 6, 137-147.	3.0	17
41893	A new metallic Ï€-conjugated carbon sheet used for the cathode of Liâ€“S batteries. RSC Advances, 2019, 9, 92-98.	1.7	6
41894	Determination of the structure and geometry of N-heterocyclic carbenes on Au(111) using high-resolution spectroscopy. Chemical Science, 2019, 10, 930-935.	3.7	64
41895	Metallic P₃C monolayer as anode for sodium-ion batteries. Journal of Materials Chemistry A, 2019, 7, 405-411.	5.2	75
41896	High throughput identification of Li ion diffusion pathways in typical solid state electrolytes and electrode materials by BV-Ewald method. Journal of Materials Chemistry A, 2019, 7, 1300-1306.	5.2	12
41897	Charge carrier transport dynamics in W/Mo-doped BiVO₄: first principles-based mesoscale characterization. Journal of Materials Chemistry A, 2019, 7, 3054-3065.	5.2	51
41898	Carrier density control in Cu2HgGeTe4and discovery of Hg2GeTe4viaphase boundary mapping. Journal of Materials Chemistry A, 2019, 7, 621-631.	5.2	27
41899	Unexpectedly high cross-plane thermoelectric performance of layered carbon nitrides. Journal of Materials Chemistry A, 2019, 7, 2114-2121.	5.2	44
41900	Pressure-driven band gap engineering in ion-conducting semiconductor silver orthophosphate. Journal of Materials Chemistry A, 2019, 7, 4451-4458.	5.2	5
41901	Unique SchrÃ¶dinger semimetal state in ternary Be₂P₃N honeycomb lattice. Journal of Materials Chemistry C, 2019, 7, 4118-4123.	2.7	8
41902	Highly efficient photogenerated electron transfer at a black phosphorus/indium selenide heterostructure interface from ultrafast dynamics. Journal of Materials Chemistry C, 2019, 7, 1864-1870.	2.7	53
41903	Overlapped embedded fragment stochastic density functional theory for covalently-bonded materials. Journal of Chemical Physics, 2019, 150, 034106.	1.2	25
41904	Current Enhancement via a TiO2 Window Layer for CSS Sb2Se3 Solar Cells: Performance Limits and High V _{oc}. IEEE Journal of Photovoltaics, 2019, 9, 544-551.	1.5	65
41905	Thermochromic Leadâ€Free Halide Double Perovskites. Advanced Functional Materials, 2019, 29, 1807375.	7.8	120
41906	Robust Aboveâ€Roomâ€Temperature Ferromagnetism in Fewâ€Layer Antimonene Triggered by Nonmagnetic Adatoms. Advanced Functional Materials, 2019, 29, 1808746.	7.8	38
41907	Highly Efficient Solarâ€Driven Carbon Dioxide Reduction on Molybdenum Disulfide Catalyst Using Choline Chlorideâ€Based Electrolyte. Advanced Energy Materials, 2019, 9, 1803536.	10.2	34
41908	Graphene: Properties, Synthesis, and Applications. , 2019, , 219-332.		1
41909	Effect of Cu doping on the anatase-to-rutile phase transition in TiO2 photocatalysts: Theory and experiments. Applied Catalysis B: Environmental, 2019, 246, 266-276.	10.8	119

#	Article	IF	Citations
41910	Oxygenated (113) diamond surface for nitrogen-vacancy quantum sensors with preferential alignment and long coherence time from first principles. Carbon, 2019, 145, 273-280.	5.4	24
41911	Ab initio calculations for crystalline PEO6:LiPF6 polymer electrolytes. Computational Materials Science, 2019, 160, 173-179.	1.4	11
41912	A site-sensitive quasi-in situ strategy to characterize Mo/HZSM-5 during activation. Journal of Catalysis, 2019, 370, 321-331.	3.1	40
41913	Effects of transport direction and carrier concentration on the thermoelectric properties of AgIn5Te8: A first-principles study. Materials Research Bulletin, 2019, 113, 77-83.	2.7	6
41914	Application of quantitative prediction to design new organic dyes in dye sensitized solar cells. Journal of Molecular Liquids, 2019, 278, 484-490.	2.3	9
41915	Electronic structure and magnetic order in Cu Zn(1â^')O: A study GGA and GGAÂ+ÂU. Physica B: Condensed Matter, 2019, 557, 74-81.	1.3	7
41916	Different Dissociation Rates of Singlet and Triplet Excitons of Pentacene at the Interface in Solar Cells. Journal of Physical Chemistry C, 2019, 123, 3541-3551.	1.5	9
41917	Contacting MoS₂ to MXene: Vanishing p-Type Schottky Barrier and Enhanced Hydrogen Evolution Catalysis. Journal of Physical Chemistry C, 2019, 123, 3719-3726.	1.5	47
41918	Identifying Active Sites for Parasitic Reactions at the Cathodeâ€“Electrolyte Interface. Journal of Physical Chemistry Letters, 2019, 10, 589-594.	2.1	31
41919	Direct Observation of Magnetization Reversal by Electric Field at Room Temperature in Co-Substituted Bismuth Ferrite Thin Film. Nano Letters, 2019, 19, 1767-1773.	4.5	23
41920	Electrides with Dinitrogen Ligands. ACS Applied Materials & Interfaces, 2019, 11, 5256-5263.	4.0	15
41921	Excitation to defect-bound band edge states in two-dimensional semiconductors and its effect on carrier transport. Npj Computational Materials, 2019, 5, .	3.5	20
41922	Observation of ballistic avalanche phenomena in nanoscale vertical InSe/BP heterostructures. Nature Nanotechnology, 2019, 14, 217-222.	15.6	153
41923	The first atomic layer deposition process for Fe_xN films. Chemical Communications, 2019, 55, 1943-1946.	2.2	9
41924	2D planar penta-MN₂ (M = Pd, Pt) sheets identified through structure search. Physical Chemistry Chemical Physics, 2019, 21, 246-251.	1.3	32
41925	Theoretical design of a series of 2D TMâ€“C₃N₄ and TMâ€“C₃N₄@graphene (TM = V, Nb and Ta) nanostructures with highly efficient catalytic activity for the hydrogen evolution reaction. Physical Chemistry Chemical Physics, 2019, 21, 1773-1783.	1.3	27
41926	Unusual interfacial magnetic interactions for Ï„-MnAl with Fe(Co) atomic layers. Physical Chemistry Chemical Physics, 2019, 21, 2443-2452.	1.3	4
41927	Molecular mechanism and binding free energy of doxorubicin intercalation in DNA. Physical Chemistry Chemical Physics, 2019, 21, 3877-3893.	1.3	70

#	Article	IF	Citations
41928	Single tungsten atom supported on N-doped graphyne as a high-performance electrocatalyst for nitrogen fixation under ambient conditions. Physical Chemistry Chemical Physics, 2019, 21, 1546-1551.	1.3	126
41929	Effects of the number of layers on the vibrational, electronic and optical properties of alpha lead oxide. Physical Chemistry Chemical Physics, 2019, 21, 3868-3876.	1.3	25
41930	Ferromagnetic ligand holes in cobalt perovskite electrocatalysts as an essential factor for high activity towards oxygen evolution. Physical Chemistry Chemical Physics, 2019, 21, 2977-2983.	1.3	32
41931	Effect of ammonia on cobalt Fischerâ€“Tropsch synthesis catalysts: a surface science approach. Catalysis Science and Technology, 2019, 9, 702-710.	2.1	5
41932	Phase evolution in calcium molybdate nanoparticles as a function of synthesis temperature and its electrochemical effect on energy storage. Nanoscale Advances, 2019, 1, 565-580.	2.2	49
41933	KTlO: a metal shrouded 2D semiconductor with high carrier mobility and tunable magnetism. Nanoscale, 2019, 11, 1131-1139.	2.8	50
41934	First-principles study of the electric, magnetic, and orbital structure in perovskite ScMnO₃. RSC Advances, 2019, 9, 2143-2151.	1.7	3
41935	Insights into the roles of water on the aqueous phase reforming of glycerol. Reaction Chemistry and Engineering, 2019, 4, 383-392.	1.9	25
41936	Origins of ultralow thermal conductivity in 1-2-1-4 quaternary selenides. Journal of Materials Chemistry A, 2019, 7, 2589-2596.	5.2	28
41937	Controllable nitrogen-doping of nanoporous carbons enabled by coordination frameworks. Journal of Materials Chemistry A, 2019, 7, 647-656.	5.2	43
41938	Probing ring-opening pathways for efficient photocatalytic toluene decomposition. Journal of Materials Chemistry A, 2019, 7, 3366-3374.	5.2	166
41939	Prediction of new ZnSâ€“CaS alloys with anomalous electronic properties. Journal of Materials Chemistry C, 2019, 7, 1246-1254.	2.7	5
41940	Observation of a Dirac state in borophene hetero-bilayers by Cr intercalation. Journal of Materials Chemistry C, 2019, 7, 2068-2075.	2.7	7
41941	Microscopic origin of pressure-induced phase-transitions in urea: a detailed investigation through first principles calculations. Physical Chemistry Chemical Physics, 2019, 21, 884-900.	1.3	16
41942	Effect of Ho dopant on the ferromagnetic characteristics of MoS₂ nanocrystals. Physical Chemistry Chemical Physics, 2019, 21, 232-237.	1.3	14
41943	Shell model extension to the valence force field: application to single-layer black phosphorus. Physical Chemistry Chemical Physics, 2019, 21, 322-328.	1.3	5
41944	Exploring new approaches towards the formability of mixed-ion perovskites by DFT and machine learning. Physical Chemistry Chemical Physics, 2019, 21, 1078-1088.	1.3	45
41945	Carbon chain growth by formyl coupling over the Cu/Î³-AlOOH(001) surface in syngas conversion. Physical Chemistry Chemical Physics, 2019, 21, 148-159.	1.3	12

#	Article	IF	Citations
41946	Achieving a direct band gap and high power conversion efficiency in an SbI₃/BiI₃ type-II vdW heterostructure via interlayer compression and electric field application. Physical Chemistry Chemical Physics, 2019, 21, 2619-2627.	1.3	13
41947	Mixed phononic and non-phononic transport in hybrid lead halide perovskites: glass-crystal duality, dynamical disorder, and anharmonicity. Energy and Environmental Science, 2019, 12, 216-229.	15.6	51
41948	Electron-induced molecular dissociation at a surface leads to reactive collisions at selected impact parameters. Faraday Discussions, 2019, 214, 89-103.	1.6	6
41949	Effects of precursor pre-treatment on the vapor deposition of WS₂ monolayers. Nanoscale Advances, 2019, 1, 953-960.	2.2	17
41950	Theoretical study on the influence of electric field direction on the photovoltaic performance of aryl amine organic dyes for dye-sensitized solar cells. New Journal of Chemistry, 2019, 43, 651-661.	1.4	7
41951	A unified model of impact sensitivity of metal azides. New Journal of Chemistry, 2019, 43, 1459-1468.	1.4	18
41952	2D group-VA fluorinated antimonene: synthesis and saturable absorption. Nanoscale, 2019, 11, 1762-1769.	2.8	49
41953	Powder exfoliated MoS₂ nanosheets with highly monolayer-rich structures as high-performance lithium-/sodium-ion-battery electrodes. Nanoscale, 2019, 11, 1887-1900.	2.8	93
41954	Influence of the support on stabilizing local defects in strained monolayer oxide films. Nanoscale, 2019, 11, 2412-2422.	2.8	10
41955	A chemical-bond-driven edge reconstruction of Sb nanoribbons and their thermoelectric properties from first-principles calculations. RSC Advances, 2019, 9, 1047-1054.	1.7	2
41956	Strong interfacial interactions induced a large reduction in lateral thermal conductivity of transition-metal dichalcogenide superlattices. RSC Advances, 2019, 9, 1387-1393.	1.7	7
41957	A hypervalent and cubically coordinated molecular phase of IF₈predicted at high pressure. Chemical Science, 2019, 10, 2543-2550.	3.7	36
41958	Local structure and vibrational dynamics in indium-doped barium zirconate. Journal of Materials Chemistry A, 2019, 7, 7360-7372.	5.2	24
41959	Understanding on the structural and electrochemical performance of orthorhombic sodium manganese oxides. Journal of Materials Chemistry A, 2019, 7, 202-211.	5.2	39
41960	Correlating lattice distortions, ion migration barriers, and stability in solid electrolytes. Journal of Materials Chemistry A, 2019, 7, 3216-3227.	5.2	68
41961	Ultrafast diffusive cross-sheet motion of lithium through antimonene with 2 + 1 dimensional kinetics. Journal of Materials Chemistry A, 2019, 7, 2901-2907.	5.2	19
41962	Photo-oxidative degradation of methylammonium lead iodide perovskite: mechanism and protection. Journal of Materials Chemistry A, 2019, 7, 2275-2282.	5.2	105
41963	2D boron dichalcogenides from the substitution of Mo with ionic B₂ pair in MoX₂ (X = S, Se and Te): high stability, large excitonic effect and high charge carrier mobility. Journal of Materials Chemistry C, 2019, 7, 1651-1658.	2.7	17

#	Article	IF	Citations
41964	An experimental and theoretical study into NaSbS₂ as an emerging solar absorber. Journal of Materials Chemistry C, 2019, 7, 2059-2067.	2.7	25
41965	A three dimensional numerical quantum mechanical model of electronic field emission from metallic surfaces with nanoscale corrugation. Journal of Applied Physics, 2019, 125, .	1.1	13
41966	First-principles study of electron dynamics with explicit treatment of momentum dispersion on Si nanowires along different directions. Molecular Physics, 2019, 117, 2293-2302.	0.8	7
41967	Calculations of defect states in various sizes of InN nanowires. Nanotechnology, 2019, 30, 205705.	1.3	0
41968	Theoretical investigations on structural, elastic, thermodynamic and electronic properties of Al₃Ti and Al₃V compounds in L1₂ structure under high pressure. Materials Research Express, 2019, 6, 056536.	0.8	8
41969	Correlation effects on ground-state properties of ternary Heusler alloys: First-principles study. Physical Review B, 2019, 99, .	1.1	28
41970	Lattice dynamics and negative thermal expansion in the framework compound <mml:math xmlns:mml="http://www.w3.org/1998/Math/MathML"><mml:mrow><mml:mi>ZnNi</mml:mi><mml:msub><mml:mrow><mml:mo>(</m with two-dimensional and three-dimensional local environments. Physical Review B, 2019, 99, .	1.1	26
41971	Stone-Wales graphene: A two-dimensional carbon semimetal with magic stability. Physical Review B, 2019, 99, .	1.1	95
41972	Computer-Aided Design of Nanoceria Structures as Enzyme Mimetic Agents: The Role of Bodily Electrolytes on Maximizing Their Activity. ACS Applied Bio Materials, 2019, 2, 1098-1106.	2.3	25
41973	CO₂ Electrochemical Reduction Catalyzed by Graphene Supported Palladium Cluster: A Computational Guideline. ACS Applied Energy Materials, 2019, 2, 1544-1552.	2.5	17
41974	Platinum-trimer decorated cobalt-palladium core-shell nanocatalyst with promising performance for oxygen reduction reaction. Nature Communications, 2019, 10, 440.	5.8	115
41975	Electronic and optical properties of lead-free hybrid double perovskites for photovoltaic and optoelectronic applications. Scientific Reports, 2019, 9, 718.	1.6	130
41976	New high-pressure phases of Fe7N3 and Fe7C3 stable at Earth's core conditions: evidences for carbonâ€“nitrogen isomorphism in Fe-compounds. RSC Advances, 2019, 9, 3577-3581.	1.7	15
41977	Vibrational and electron-phonon coupling properties of Î²-Ga2O3 from first-principles calculations: Impact on the mobility and breakdown field. AIP Advances, 2019, 9, .	0.6	40
41978	A modified generalized Langevin oscillator model for activated gas-surface reactions. Journal of Chemical Physics, 2019, 150, 024704.	1.2	9
41979	[2+1] Additions of (n,0)(n=6â^'10) single-walled carbon nanotubes with di-vacancies based on defect curvature: A first-principles study. Journal of Theoretical and Computational Chemistry, 2019, 18, 1950004.	1.8	1
41980	Toward Improving Ambient Volta Potential Measurements with SKPFM for Corrosion Studies. Journal of the Electrochemical Society, 2019, 166, C3018-C3027.	1.3	19
41981	Room Temperature Commensurate Charge Density Wave in Epitaxial Strained TiTe₂ Multilayer Films. Advanced Materials Interfaces, 2019, 6, 1801850.	1.9	34

#	Article	IF	Citations
41982	Structural Insight into Layered Silicon Hydrogen Phosphates Containing [SiO 6] Octahedra Prepared by Different Reaction Routes. European Journal of Inorganic Chemistry, 2019, 2019, 828-836.	1.0	3
41983	Multi-Objective Optimization as a Tool for Material Design. , 2019, , 1-15.		3
41984	First-principles molecular dynamics study on ultrafast potassium ion transport in silicon anode. Journal of Power Sources, 2019, 415, 119-125.	4.0	36
41985	Adsorption of NO and NO2 molecules on defected-graphene and ozone-treated graphene: First-principles analysis. Surface Science, 2019, 684, 28-36.	0.8	39
41986	Photoexcited Electron Lifetimes Influenced by Momentum Dispersion in Silicon Nanowires. Journal of Physical Chemistry C, 2019, 123, 7457-7466.	1.5	9
41987	Dynamically Switching the Electronic and Electrostatic Properties of Indiumâ€“Tin Oxide Electrodes with Photochromic Monolayers: Toward Photoswitchable Optoelectronic Devices. ACS Applied Nano Materials, 2019, 2, 1102-1110.	2.4	20
41988	The Mechanism of Steam-Ethanol Reforming on Co₁₃/CeO_{2â€“x}: A DFT Study. ACS Catalysis, 2019, 9, 2355-2367.	5.5	30
41989	Controllable in Situ Surface Restructuring of Cu Catalysts and Remarkable Enhancement of Their Catalytic Activity. ACS Catalysis, 2019, 9, 2213-2221.	5.5	53
41990	van der Waals Stacking Induced Transition from Schottky to Ohmic Contacts: 2D Metals on Multilayer InSe. Journal of the American Chemical Society, 2019, 141, 3110-3115.	6.6	162
41991	Structural selectivity of supported Pd nanoparticles for catalytic NH3 oxidation resolved using combined operando spectroscopy. Nature Catalysis, 2019, 2, 157-163.	16.1	74
41992	Dirac cones in a snub trihexagonal tiling lattice with reflective symmetry breaking. Journal of Physics Condensed Matter, 2019, 31, 155001.	0.7	5
41993	Polaron-enhanced giant strain effect on defect formation: The case of oxygen vacancies in rutile <mml:math xmlns:mml="http://www.w3.org/1998/Math/MathML"><mml:msub><mml:mi>TiO</mml:mi><mml:mn>2</mml:mn></mml:msub></m Physical Review B, 2019, 99, .	1.1	8
41994	Strong decoupling between magnetic subsystems in the low-dimensional spin- <mml:math xmlns:mml="http://www.w3.org/1998/Math/MathML"><mml:mfrac><mml:mn>1</mml:mn><mml:mn>2</mml:mn></mml:mfrac></mml antiferromagnet <mml:math xmlns:mml="http://www.w3.org/1998/Math/MathML"><mml:msub><mml:mi>SeCuO</mml:mi><mml:mn>3</mml:mn></mml:msub></ Physical Review B, 2019, 99, .	1.1	8
41995	Density functional theory study explaining the underperformance of copper oxides as photovoltaic absorbers. Physical Review B, 2019, 99, .	1.1	40
41996	Oxygen Redox Promoted by Na Excess and Covalency in Hexagonal and Monoclinic Na_{2â^'x}RuO₃ Polymorphs. Journal of the Electrochemical Society, 2019, 166, A5343-A5348.	1.3	8
41997	Ultrathin 2D TiS₂ Nanosheets for High Capacity and Longâ€Life Sodium Ion Batteries. Advanced Energy Materials, 2019, 9, 1803210.	10.2	100
41998	Planar penta-transition metal phosphide and arsenide as narrow-gap semiconductors with ultrahigh carrier mobility. Journal of Materials Science, 2019, 54, 7035-7047.	1.7	20
41999	Application of highly stretchable and conductive two-dimensional 1T VS2 and VSe2 as anode materials for Li-, Na- and Ca-ion storage. Computational Materials Science, 2019, 160, 360-367.	1.4	60

#	Article	IF	Citations
42000	Negative Poisson's ratio in monolayer PdSe2. Computational Materials Science, 2019, 160, 309-314.	1.4	29
42001	Geometry optimizations and evaluation of electronic properties of prism carbon tubes by density functional theory using plane waves. Chemical Physics Letters, 2019, 718, 32-37.	1.2	1
42002	Directly catalytic reduction of NO without NH3 by single atom iron catalyst: A DFT calculation. Fuel, 2019, 243, 262-270.	3.4	94
42003	Hydrogen adsorption, dissociation, and diffusion on high-index Mg(10<mml:math) Tj ETQq1 1 0.784314 rgBT /Overlock 10 Tf 50 642 Td and their comparisons with Mg(0001): A systematic first-principles study. International Journal of Hydrogen Energy, 2019, 44, 4897-4906.	3.8	11
42004	Interfacial electronic properties of ferroelectric nanocomposites for energy storage application. Materials Today Energy, 2019, 12, 136-145.	2.5	23
42005	Surface energies, adhesion energies, and exfoliation energies relevant to copper-graphene and copper-graphite systems. Surface Science, 2019, 685, 48-58.	0.8	74
42006	Local electronic structure of doping defects on Tl/Si(111)1x1. Scientific Reports, 2019, 9, 779.	1.6	2
42007	Theoretical investigation of the platinum substrate influence on BaTiO₃ thin film polarisation. Physical Chemistry Chemical Physics, 2019, 21, 4367-4374.	1.3	8
42008	Ultra-small Mo₂C nanodots encapsulated in nitrogen-doped porous carbon for pH-universal hydrogen evolution: insights into the synergistic enhancement of HER activity by nitrogen doping and structural defects. Journal of Materials Chemistry A, 2019, 7, 4734-4743.	5.2	90
42009	High Thermoelectric Power Factor and Efficiency from a Highly Dispersive Band in <mml:math xmlns:mml="http://www.w3.org/1998/Math/MathML" display="inline" overflow="scroll"><mml:msub><mml:mi>Ba</mml:mi><mml:mn>2</mml:mn></mml:msub><mml:mi>Bi</mml:mi><mml:mi>Au</mml:m Physical Review Applied, 2019, 11, .	1.5	49
42010	Gate-tunable magnetism of C adatoms on graphene. Physical Review B, 2019, 99, .	1.1	10
42011	Racemic Amino Acid Piezoelectric Transducer. Physical Review Letters, 2019, 122, 047701.	2.9	59
42012	Superconductivity in SrTiO3: Dielectric Function Method for Non-Parabolic Bands. Journal of Superconductivity and Novel Magnetism, 2019, 32, 2739-2744.	0.8	12
42013	Magnesium based materials for hydrogen based energy storage: Past, present and future. International Journal of Hydrogen Energy, 2019, 44, 7809-7859.	3.8	460
42014	Indirect tail states formation by thermal-induced polar fluctuations in halide perovskites. Nature Communications, 2019, 10, 484.	5.8	88
42015	Microscopic calculation of the optical properties and intrinsic losses in the methylammonium lead iodide perovskite system. APL Materials, 2019, 7, 011107.	2.2	2
42016	Parameter transferability, self-doping, and metallicity in LaNiO3/LaMnO3 superlattices. Physical Review B, 2019, 99, .	1.1	4
42017	Structure and phase regulation in MoxC (Î±-MoC1-x/Î²-Mo2C) to enhance hydrogen evolution. Applied Catalysis B: Environmental, 2019, 247, 78-85.	10.8	123

#	Article	IF	Citations
42018	Defect levels induced by double substitution of B and N in 4H-SiC. Nuclear Instruments & Methods in Physics Research B, 2019, 442, 41-46.	0.6	2
42019	State-of-Matter-Dependent Charge-Transfer Interactions between Planar Molecules for Doping Applications. Chemistry of Materials, 2019, 31, 1237-1249.	3.2	32
42020	Graphene/hBN Heterostructures as High-Capacity Cathodes with High Voltage for Next-Generation Aluminum Batteries. Journal of Physical Chemistry C, 2019, 123, 3959-3967.	1.5	30
42021	Predicting Structure and Electrochemistry of Dilithium Thiophene-2,5-Dicarboxylate Electrodes by Density Functional Theory and Evolutionary Algorithms. Journal of Physical Chemistry C, 2019, 123, 4691-4700.	1.5	10
42022	PCF-Graphene: A 2D sp²-Hybridized Carbon Allotrope with a Direct Band Gap. Journal of Physical Chemistry C, 2019, 123, 4567-4573.	1.5	29
42023	Functionalization: An Effective Approach to Open and Close Channels for Electron Transfer in Nitrogenated Holey Graphene C₂N Anodes in Sodium-Ion Batteries. Journal of Physical Chemistry Letters, 2019, 10, 721-726.	2.1	37
42024	Phonon Scattering by Dislocations in GaN. ACS Applied Materials & Interfaces, 2019, 11, 8175-8181.	4.0	25
42025	Two-Dimensional Hydroxyl-Functionalized and Carbon-Deficient Scandium Carbide, ScC_xOH, a Direct Band Gap Semiconductor. ACS Nano, 2019, 13, 1195-1203.	7.3	30
42026	Learning-in-Templates Enables Accelerated Discovery and Synthesis of New Stable Double Perovskites. Journal of the American Chemical Society, 2019, 141, 3682-3690.	6.6	27
42027	Perovskite-polymer composite cross-linker approach for highly-stable and efficient perovskite solar cells. Nature Communications, 2019, 10, 520.	5.8	405
42028	Synergy of the catalytic activation on Ni and the CeO₂â€“TiO₂/Ce₂Ti₂O₇ stoichiometric redox cycle for dramatically enhanced solar fuel production. Energy and Environmental Science, 2019, 12, 767-779.	15.6	90
42029	Metal-free electrocatalyst for reducing nitrogen to ammonia using a Lewis acid pair. Journal of Materials Chemistry A, 2019, 7, 4865-4871.	5.2	115
42030	Exfoliation of borophenes from silver substrates assisted by Li/Mg atomsâ€”a density functional theory study. Journal of Materials Chemistry C, 2019, 7, 4043-4048.	2.7	15
42031	Structural origin of the high glass-forming ability of Ce70Ga10Cu20 alloys. Physical Chemistry Chemical Physics, 2019, 21, 4209-4214.	1.3	3
42032	3D hierarchical porous indium catalyst for highly efficient electroreduction of CO₂. Journal of Materials Chemistry A, 2019, 7, 4505-4515.	5.2	134
42033	Thermoelectric properties of topological insulator lanthanum phosphide via first-principles study. Journal of Applied Physics, 2019, 125, .	1.1	16
42034	Pressure effect on the electronic, structural, and vibrational properties of layered <mml:math xmlns:mml="http://www.w3.org/1998/Math/MathML"><mml:mrow><mml:mn>2</mml:mn><mml:mi>H</mml:mi><mml:mo>’</mml:m Physical Review B, 2019, 99, .	1.1	26
42035	Interlayer excitons in bilayer <mml:math xmlns:mml="http://www.w3.org/1998/Math/MathML"><mml:msub><mml:mi>MoS</mml:mi><mml:mn>2</mml:mn></mml:msub></m with strong oscillator strength up to room temperature. Physical Review B, 2019, 99, .	1.1	88

#	Article	IF	Citations
42036	Observation of highly dispersive bands in pure thin film <mml:math xmlns:mml="http://www.w3.org/1998/Math/MathML"><mml:msub><mml:mi mathvariant="normal">C</mml:mi><mml:mn>60</mml:mn></mml:msub></mml:math>. Physical Review B, 2019, 99, .	1.1	9
42037	Theoretical studies on the structures, material properties, and IR spectra of polymorphs of 3,4-bis(1H-5-tetrazolyl)furoxan. Journal of Molecular Modeling, 2019, 25, 51.	0.8	3
42038	Interfacial coupling effects in g-C3N4/SrTiO3 nanocomposites with enhanced H2 evolution under visible light irradiation. Applied Catalysis B: Environmental, 2019, 247, 1-9.	10.8	139
42039	Valence and core excitons in solids from velocity-gauge real-time TDDFT with range-separated hybrid functionals: An LCAO approach. Computational Condensed Matter, 2019, 18, e00348.	0.9	18
42040	Transparent Conducting Oxides as Cathodes in Liâ€“O₂ Batteries: A First Principles Computational Investigation. Journal of Physical Chemistry C, 2019, 123, 4623-4631.	1.5	2
42041	Assessment of Constant-Potential Implicit Solvation Calculations of Electrochemical Energy Barriers for H₂ Evolution on Pt. Journal of Physical Chemistry C, 2019, 123, 4116-4124.	1.5	71
42042	Janus Chromium Dichalcogenide Monolayers with Low Carrier Recombination for Photocatalytic Overall Water-Splitting under Infrared Light. Journal of Physical Chemistry C, 2019, 123, 4186-4192.	1.5	54
42043	Sub-Band Gap Absorption Mechanisms Involving Oxygen Vacancies in Hydroxyapatite. Journal of Physical Chemistry C, 2019, 123, 4856-4865.	1.5	26
42044	Thermodynamic Overpotentials and Nucleation Rates for Electrodeposition on Metal Anodes. ACS Applied Materials & Interfaces, 2019, 11, 7954-7964.	4.0	44
42045	Probing the Active Sites of MoS₂ Based Hydrotreating Catalysts Using Modulation Excitation Spectroscopy. ACS Catalysis, 2019, 9, 2568-2579.	5.5	43
42046	Epitaxial Growth of PbSe Few-Layers on SrTiO₃: The Effect of Compressive Strain and Potential Two-Dimensional Topological Crystalline Insulator. ACS Nano, 2019, 13, 2615-2623.	7.3	7
42047	Emergence of Topological insulator and Nodal line semi-metal states in XXâ€²Bi (Xâ€‰=â€‰Na, K, Rb, Cs; Xâ€²â€‰=â€‰Ca, Sr). Scientific Reports, 2019, 9, 527.	1.6	13
42048	Stability and magnetism of FeN high-pressure phases. Physical Chemistry Chemical Physics, 2019, 21, 5262-5273.	1.3	12
42049	An essential descriptor for the oxygen evolution reaction on reducible metal oxide surfaces. Chemical Science, 2019, 10, 3340-3345.	3.7	63
42050	Electronic structure, optical properties, and phonon transport in Janus monolayer PtSSe via first-principles study. Philosophical Magazine, 2019, 99, 1025-1040.	0.7	58
42051	Hybrid Organic-Inorganic Perovskites as Promising Substrates for Pt Single-Atom Catalysts. Physical Review Letters, 2019, 122, 046101.	2.9	25
42052	High-Pressure Third-Order Elastic Constants of MgO Single Crystal: First-Principles Investigation. Zeitschrift Fur Naturforschung - Section A Journal of Physical Sciences, 2019, 74, 447-456.	0.7	3
42053	Size-Dependent Critical Temperature and Anomalous Optical Dispersion in Ferromagnetic CrI3 Nanotubes. Nanomaterials, 2019, 9, 153.	1.9	5

#	Article	IF	Citations
42054	Toward Computational Design of Catalysts for CO₂ Selective Reduction via Reaction Phase Diagram Analysis. Advanced Theory and Simulations, 2019, 2, 1800200.	1.3	10
42055	Revealing the Unusual Rigid Boron Chain Substructure in Hard and Superconductive Tantalum Monoboride. Chemistry - A European Journal, 2019, 25, 5051-5057.	1.7	9
42056	Role of Mineral Surfaces in Prebiotic Chemical Evolution. In Silico Quantum Mechanical Studies. Life, 2019, 9, 10.	1.1	44
42057	New Insights on the Role of Chloride During the Onset of Local Corrosion: TEM, APT, Surface Energy, and Morphological Instability. Corrosion, 2019, 75, 616-627.	0.5	15
42058	Ion Conductivity Enhancement in Antiâ€Spinel Li₃OBr with Intrinsic Vacancies. Advanced Theory and Simulations, 2019, 2, 1800138.	1.3	14
42059	Comments on â€œNi nanoparticle-decorated reduced graphene oxide for non-enzymatic glucose sensing: An experimental and modeling study [Electrochim. Acta 240 (2017) 388â€“398]â€. Electrochimica Acta, 2019, 299, 933-935.	2.6	0
42060	Elastic properties of the TiZrNbTaMo multi-principal element alloy studied from first principles. Intermetallics, 2019, 106, 130-140.	1.8	29
42061	Photoluminescence and phosphorescence of Mn2+ ion activated green phosphor Na2ZnSiO4:Mn2+ synthesized by self-reduction. Materials Research Bulletin, 2019, 113, 90-96.	2.7	31
42062	Effect of surface morphology on initial hydrogen diffusion in vanadium alloys. Materials Letters, 2019, 241, 100-103.	1.3	4
42063	Functionalized Rutile TiO₂(110) as a Sorbent To Capture CO₂ through Noncovalent Interactions: A Computational Investigation. Journal of Physical Chemistry C, 2019, 123, 3491-3504.	1.5	16
42064	Selective Desorption of Ethylene after Dimethyl Sulfide Reaction on Cold Gold Surface. Journal of Physical Chemistry C, 2019, 123, 1874-1879.	1.5	3
42065	Single-Layer Janus-Type Platinum Dichalcogenides and Their Heterostructures. Journal of Physical Chemistry C, 2019, 123, 4549-4557.	1.5	81
42066	Boosting Potassium-Ion Battery Performance by Encapsulating Red Phosphorus in Free-Standing Nitrogen-Doped Porous Hollow Carbon Nanofibers. Nano Letters, 2019, 19, 1351-1358.	4.5	239
42067	Breaking Long-Range Order in Iridium Oxide by Alkali Ion for Efficient Water Oxidation. Journal of the American Chemical Society, 2019, 141, 3014-3023.	6.6	337
42068	Switchable valley splitting by external electric field effect in graphene/CrI3 heterostructures. Npj 2D Materials and Applications, 2019, 3, .	3.9	43
42069	Two-dimensional honeycomb borophene oxide: strong anisotropy and nodal loop transformation. Nanoscale, 2019, 11, 2468-2475.	2.8	84
42070	Reaction mechanism between small-sized Ce clusters and water molecules: an ab initio investigation on Ce_n + H₂O. Physical Chemistry Chemical Physics, 2019, 21, 4006-4014.	1.3	8
42071	First-principle investigation on electronic structures and magnetic properties of EuNbO₃ phases. EPJ Applied Physics, 2019, 85, 10601.	0.3	1

#	Article	IF	Citations
42072	First-principles investigation of the electronic structures and Seebeck coefficients of PbTe/SrTe interfaces. Journal of Applied Physics, 2019, 125, 035107.	1.1	5
42073	Defect-induced magnetism in II-VI quantum dots. Physical Review B, 2019, 99, .	1.1	5
42074	Magnetoresistance from Fermi surface topology. Physical Review B, 2019, 99, .	1.1	60
42075	Hybrid density functional theory study of vanadium doping in stoichiometric and congruent <mml:math xmlns:mml="http://www.w3.org/1998/Math/MathML"><mml:mrow><mml:mi>LiNb</mml:mi><mml:msub><mml:mi mathvariant="normal">O</mml:mi><mml:mn>3</mml:mn></mml:msub></mml:mrow></mml:math>. Physical Review B, 2019, 99, .	1.1	11
42076	Theoretical Aspects of the Study on the Thermoelectric Properties of Pnictogen-Dichalcogenide Layered Compounds. Journal of the Physical Society of Japan, 2019, 88, 041010.	0.7	11
42077	NMR Crystallography: Evaluation of Hydrogen Positions in Hydromagnesite by ¹³C{¹H} REDOR Solidâ€State NMR and Density Functional Theory Calculation of Chemical Shielding Tensors. Angewandte Chemie - International Edition, 2019, 58, 4210-4216.	7.2	18
42078	Assembling Allâ€Solidâ€State Lithiumâ€“Sulfur Batteries with Li₃Nâ€Protected Anodes. ChemPlusChem, 2019, 84, 183-189.	1.3	28
42080	Understanding Competition of Polyalcohol Dehydration Reactions in Hot Water. Journal of Physical Chemistry B, 2019, 123, 1662-1671.	1.2	4
42081	Thickness-Dependent Phase Stability and Electronic Properties of GaN Nanosheets and MoS₂/GaN van der Waals Heterostructures. Journal of Physical Chemistry C, 2019, 123, 3861-3867.	1.5	38
42082	Single-Metal Atom Anchored on Boron Monolayer (Î²₁₂) as an Electrocatalyst for Nitrogen Reduction into Ammonia at Ambient Conditions: A First-Principles Study. Journal of Physical Chemistry C, 2019, 123, 4274-4281.	1.5	86
42083	Surface Activity of Early Transition-Metal Oxycarbides: CO₂ Adsorption Case Study. Journal of Physical Chemistry C, 2019, 123, 3664-3671.	1.5	10
42084	Single Transition Metal Atom-Doped Graphene Supported on a Nickel Substrate: Enhanced Oxygen Reduction Reactions Modulated by Electron Coupling. Journal of Physical Chemistry C, 2019, 123, 3703-3710.	1.5	27
42085	Real-Space Observation of Quantum Tunneling by a Carbon Atom: Flipping Reaction of Formaldehyde on Cu(110). Journal of Physical Chemistry Letters, 2019, 10, 645-649.	2.1	9
42086	Bifacial Raman Enhancement on Monolayer Two-Dimensional Materials. Nano Letters, 2019, 19, 1124-1130.	4.5	10
42087	Understanding the Different Diffusion Mechanisms of Hydrated Protons and Potassium Ions in Titanium Carbide MXene. ACS Applied Materials & Interfaces, 2019, 11, 7087-7095.	4.0	36
42088	Metal Chalcogenides Janus Monolayers for Efficient Hydrogen Generation by Photocatalytic Water Splitting. ACS Applied Nano Materials, 2019, 2, 890-897.	2.4	93
42089	Revisiting the Polyol Synthesis of Silver Nanostructures: Role of Chloride in Nanocube Formation. ACS Nano, 2019, 13, 1849-1860.	7.3	69
42090	WO₃ nanolayer coated 3D-graphene/sulfur composites for high performance lithium/sulfur batteries. Journal of Materials Chemistry A, 2019, 7, 4596-4603.	5.2	47

#	Article	IF	Citations
42091	Prediction of phonon-mediated superconductivity in two-dimensional Mo₂B₂. Journal of Materials Chemistry C, 2019, 7, 2589-2595.	2.7	39
42092	Polymorphism in p-aminobenzoic acid. CrystEngComm, 2019, 21, 2034-2042.	1.3	30
42093	In situ preparation of a Nbâ€“Pb codoped and Pd loaded TiO₂ photocatalyst from waste multi-layer ceramic capacitors by a chlorinationâ€“leaching process. Green Chemistry, 2019, 21, 874-884.	4.6	15
42094	The electronic structure of Îµ-Ga2O3. APL Materials, 2019, 7, .	2.2	49
42095	Single-layer ferromagnetic and piezoelectric CoAsS with pentagonal structure. APL Materials, 2019, 7, .	2.2	14
42096	Polyamorphic transition in a transition metal based metallic glass under high pressure. Physical Review B, 2019, 99, .	1.1	15
42097	Tuning the magnetocrystalline anisotropy ofFe3Snby alloying. Physical Review B, 2019, 99, .	1.1	17
42098	Observation of intercalation-driven zone folding in quasi-free-standing graphene energy bands. Physical Review B, 2019, 99, .	1.1	6
42099	Exciton in phosphorene: Strain, impurity, thickness, and heterostructure. Physical Review B, 2019, 99, .	1.1	17
42100	Design and control of gas diffusion process in a nanoporous soft crystal. Science, 2019, 363, 387-391.	6.0	332
42101	Chemical Control of Correlated Metals as Transparent Conductors. Advanced Functional Materials, 2019, 29, 1808609.	7.8	30
42102	Alkaliâ€Metalâ€Intercalated Percolation Network Regulates Selfâ€Assembled Electronic Aromatic Molecules. Advanced Materials, 2019, 31, e1807178.	11.1	11
42103	Unraveling Highâ€Yield Phaseâ€Transition Dynamics in Transition Metal Dichalcogenides on Metallic Substrates. Advanced Science, 2019, 6, 1802093.	5.6	23
42104	Rational Design of Grapheneâ€Supported Single Atom Catalysts for Hydrogen Evolution Reaction. Advanced Energy Materials, 2019, 9, 1803689.	10.2	279
42105	Carbon Permeation: The Prerequisite Elementary Step in Iron-Catalyzed Fischerâ€“Tropsch Synthesis. Catalysis Letters, 2019, 149, 645-664.	1.4	19
42106	DFT studies of bulk and surfaces of the electrocatalyst cobalt phosphide CoP2. Chemical Physics Letters: X, 2019, 737, 100008.	2.1	10
42107	High-throughput fabrication of 3D N-doped graphenic framework coupled with Fe3C@porous graphite carbon for ultrastable potassium ion storage. Energy Storage Materials, 2019, 22, 185-193.	9.5	91
42108	Insights into the new 3dâ€“5f heterometallic quaternary fluorides: Synthesis, crystal structures, spectroscopic properties, and thermodynamic stability. Inorganica Chimica Acta, 2019, 487, 362-368.	1.2	2

#	Article	IF	Citations
42109	Tunable band gap of N V co-doped Ca:TiO2B (CaTi5O11) for visible-light photocatalysis. International Journal of Hydrogen Energy, 2019, 44, 4716-4723.	3.8	12
42110	Structural, Dynamic, and Thermodynamic Study of KFâ€“AlF₃ Melts by Combining High-Temperature NMR and Molecular Dynamics Simulations. Journal of Physical Chemistry C, 2019, 123, 2147-2156.	1.5	8
42111	Mixed Cs and FA Cations Slow Electronâ€“Hole Recombination in FAPbI₃ Perovskites by Time-Domain Ab Initio Study: Lattice Contraction versus Octahedral Tilting. Journal of Physical Chemistry Letters, 2019, 10, 672-678.	2.1	29
42112	Effect of Defects on the Properties of ZnGa₂O₄ Thin-Film Transistors. ACS Applied Electronic Materials, 2019, 1, 253-259.	2.0	18
42113	One-Dimensional/Two-Dimensional Coreâ€“Shell-Structured Bi₂O₄/BiO_{2â€“x} Heterojunction for Highly Efficient Broad Spectrum Light-Driven Photocatalysis: Faster Interfacial Charge Transfer and Enhanced Molecular Oxygen Activation Mechanism. ACS Applied Materials & Interfaces, 2019, 11, 7112-7122.	4.0	111
42114	Anionic Single-Atom Catalysts for CO Oxidation: Support-Independent Activity at Low Temperatures. ACS Catalysis, 2019, 9, 1595-1604.	5.5	54
42115	Control of Hierarchical Structure and Framework-Al Distribution of ZSM-5 via Adjusting Crystallization Temperature and Their Effects on Methanol Conversion. ACS Catalysis, 2019, 9, 2880-2892.	5.5	90
42116	Robust and synthesizable photocatalysts for CO2 reduction: a data-driven materials discovery. Nature Communications, 2019, 10, 443.	5.8	125
42117	Controlling the Polarity of the Molecular Beam Epitaxy Grown In-Bi Atomic Film on the Si(111) Surface. Scientific Reports, 2019, 9, 756.	1.6	6
42118	Physicalâ€“chemical properties of M@Fe₃O₄core@shell nanowires (M = Cu, Co,) Tj ETQq1 1 0.784314 rgB	1.3	2
42119	Perseverance of direct bandgap in multilayer 2D PbI ₂ under an experimental strain up to 7.69%. 2D Materials, 2019, 6, 025014.	2.0	20
42120	Single-Crystal Permanent Magnets: Extraordinary Magnetic Behavior in theTa-,Cu-, andFe-SubstitutedCeCo5Systems. Physical Review Applied, 2019, 11, .	1.5	15
42121	The existence and impact of persistent ferroelectric domains in MAPbI ₃. Science Advances, 2019, 5, eaas9311.	4.7	77
42122	Electronic Structure and Band Alignments of Various Phases of Titania Using the Self-Consistent Hybrid Density Functional and DFT+U Methods. Frontiers in Chemistry, 2019, 7, 47.	1.8	12
42123	Electronic and Optical Properties of Functionalized GaNâ€(101Â¯0) Surfaces using Hybridâ€Density Functionals. Physica Status Solidi (B): Basic Research, 2019, 256, 1800455.	0.7	2
42124	Effect of Mn and C on Age Hardening of Feâ€“Mnâ€“Alâ€“C Lightweight Steels. Metals and Materials International, 2019, 25, 683-696.	1.8	24
42125	Encapsulation of cadmium telluride nanocrystals within single walled carbon nanotubes. Inorganica Chimica Acta, 2019, 488, 246-254.	1.2	8
42126	Effect of Co doping on mechanism and kinetics of ammonia synthesis on Fe(1â€¯1â€¯1) surface. Journal of Catalysis, 2019, 370, 364-371.	3.1	13

#	Article	IF	Citations
42127	Group-IV analogues of MXene: Promising two-dimensional semiconductors. Solid State Communications, 2019, 291, 51-53.	0.9	4
42128	Understanding the effect of Ce and Zr on chemical expansion in yttrium doped strontium cerate and zirconate by high temperature X-ray analysis and density functional theory. Solid State Ionics, 2019, 333, 1-8.	1.3	13
42129	Theoretical Insights into Propene Epoxidation on Au₇/Anatase TiO_{2â€“x}(001) Catalysts: Effect of the Interface and Reaction Atmosphere. Journal of Physical Chemistry C, 2019, 123, 3568-3578.	1.5	5
42130	Interaction-Dependent Interfacial Charge-Transfer Behavior in Solar Water-Splitting Systems. Nano Letters, 2019, 19, 1234-1241.	4.5	42
42131	A Systematic Theoretical Study of Water Gas Shift Reaction on Cu(111) and Cu(110): Potassium Effect. ACS Catalysis, 2019, 9, 2261-2274.	5.5	77
42132	Indirect to Direct Gap Crossover in Two-Dimensional InSe Revealed by Angle-Resolved Photoemission Spectroscopy. ACS Nano, 2019, 13, 2136-2142.	7.3	63
42133	Multi-loop node line states in ternary MgSrSi-type crystals. Npj Computational Materials, 2019, 5, .	3.5	14
42134	Self-recoverable Pdâ€“Ru/TiO₂ nanocatalysts with ultrastability towards ethanol electrooxidation. Nanoscale, 2019, 11, 3311-3317.	2.8	25
42135	Tunable electronic structure and magnetic anisotropy of two dimensional van der Waals GeS/FeCl₂ multiferroic heterostructures. Journal of Materials Chemistry C, 2019, 7, 2049-2058.	2.7	28
42136	Strain Enhanced Visibleâ€“Ultraviolet Absorption of Blue Phosphorene/MoX 2 (Xâ€‰=â€‰S,Se) Heterolayers. Physica Status Solidi - Rapid Research Letters, 2019, 13, 1800659.	1.2	5
42137	PdIn intermetallic material with isolated single-atom Pd sites â€“ A promising catalyst for direct formic acid fuel cell. Chemical Engineering Science, 2019, 199, 64-78.	1.9	25
42138	The role of chemical disorder and structural freedom in radiation-induced amorphization of silicon carbide deduced from electron spectroscopy and ab initio simulations. Journal of Nuclear Materials, 2019, 514, 299-310.	1.3	9
42139	First-principles calculations and experiments for Ce4+ effects on structure and chemical stabilities of Zr1-Ce SiO4. Journal of Nuclear Materials, 2019, 514, 276-283.	1.3	11
42140	Microstructure, indentation and first principles study of AlCuFeMn alloy. Materialia, 2019, 5, 100206.	1.3	4
42141	The Janus structures of group-III chalcogenide monolayers as promising photocatalysts for water splitting. Applied Surface Science, 2019, 478, 522-531.	3.1	78
42142	Defect-rich activated carbons as active and stable metal-free catalyst for acetylene hydrochlorination. Carbon, 2019, 146, 406-412.	5.4	78
42143	Theoretical Design of Layered AlGaS3 as a New Nonlinear Optical Material with a Strong Second Harmonic Generation Response. Crystal Growth and Design, 2019, 19, 1632-1639.	1.4	1
42144	Visible Light-Driven Photocatalytic H₂ Generation and Mechanism Insights into Bi₂O₂CO₃/G-C₃N₄ Z-Scheme Photocatalyst. Journal of Physical Chemistry C, 2019, 123, 4795-4804.	1.5	71

#	Article	IF	Citations
42145	Role of Long-Range Dispersion Forces in Modeling of MXenes as Battery Electrode Materials. Journal of Physical Chemistry C, 2019, 123, 4064-4071.	1.5	5
42146	Cu-Based Single-Atom Catalysts Boost Electroreduction of CO₂ to CH₃OH: First-Principles Predictions. Journal of Physical Chemistry C, 2019, 123, 4380-4387.	1.5	68
42147	A Water Solvation Shell Can Transform Gold Metastable Nanoparticles in the Fluxional Regime. Journal of Physical Chemistry Letters, 2019, 10, 1092-1098.	2.1	14
42149	Superior Performance of Ag over Pt for Hydrogen Evolution Reaction in Water Electrolysis under High Overpotentials. ACS Applied Energy Materials, 2019, 2, 1221-1228.	2.5	27
42150	Structure- and Temperature-Dependence of Pt-Catalyzed Ammonia Oxidation Rates and Selectivities. ACS Catalysis, 2019, 9, 2407-2414.	5.5	58
42151	Infrared-pump electronic-probe of methylammonium lead iodide reveals electronically decoupled organic and inorganic sublattices. Nature Communications, 2019, 10, 482.	5.8	25
42152	Stabilities and novel electronic structures of three carbon nitride bilayers. Scientific Reports, 2019, 9, 1025.	1.6	13
42153	Tuning polaronic redox behavior in olivine phosphate. Physical Chemistry Chemical Physics, 2019, 21, 4578-4583.	1.3	12
42154	Metal/graphene heterobilayers as hydrogen evolution reaction cathodes: a first-principles study. Physical Chemistry Chemical Physics, 2019, 21, 4594-4599.	1.3	6
42155	A general route to modify diatomite with niobates for versatile applications of heavy metal removal. RSC Advances, 2019, 9, 3816-3827.	1.7	11
42156	Effect of spin contamination error on surface catalytic reaction: NO reduction by core-shell catalysts. Molecular Physics, 2019, 117, 2251-2259.	0.8	22
42157	Low lattice thermal conductivity and high thermoelectric figure of merit in <mml:math xmlns:mml="http://www.w3.org/1998/Math/MathML"><mml:mrow><mml:msub><mml:mi>Na</mml:mi><mml:mn>2</mml:mn></mml:msub></mml:mrow></mml:math> Physical Review B, 2019, 99, .	1.7	18
42158	Heterostructured Nanocubeâ€Shaped Binary Sulfide (SnCo)S₂ Interlaced with Sâ€Doped Graphene as a Highâ€Performance Anode for Advanced Na⁺ Batteries. Advanced Functional Materials, 2019, 29, 1807971.	7.8	154
42159	Liquid bismuth initiated growth of phosphorus microbelts with efficient charge polarization for photocatalysis. Applied Catalysis B: Environmental, 2019, 247, 100-106.	10.8	38
42160	A stable mesoporous super-acid nanocatalyst for eco-friendly synthesis of biodiesel. Chemical Engineering Journal, 2019, 364, 111-122.	6.6	38
42161	Roles of oxygen vacancies and pH induced size changes on photo- and radioluminescence of undoped and Eu3+-doped La2Zr2O7 nanoparticles. Journal of Luminescence, 2019, 209, 302-315.	1.5	36
42162	Reactivity-Guided Interface Design in Na Metal Solid-State Batteries. Joule, 2019, 3, 1037-1050.	11.7	120
42163	Syntheses and first-principles calculations of the pseudobrookite compound AlTi2O5. Journal of Physics and Chemistry of Solids, 2019, 127, 252-257.	1.9	7

#	Article	IF	Citations
42164	Hydrogen Chemisorption Isotherms on Platinum Particles at Catalytic Temperatures: Langmuir and Two-Dimensional Gas Models Revisited. Journal of Physical Chemistry C, 2019, 123, 8447-8462.	1.5	28
42165	Comparing Rate and Mechanism of Ethane Hydrogenolysis on Transition-Metal Catalysts. Journal of Physical Chemistry C, 2019, 123, 5421-5432.	1.5	31
42166	Enhanced flexoelectricity at reduced dimensions revealed by mechanically tunable quantum tunnelling. Nature Communications, 2019, 10, 537.	5.8	64
42167	Insight of the thermal conductivity of Ïµ-iron at Earthâ€™s core conditions from the newly developed direct ab initio methodology. Journal of Applied Physics, 2019, 125, .	1.1	5
42168	Highly Controllable Synthesis and DFT Calculations of Double/Triple-Halide CsPbX3 (X = Cl, Br, I) Perovskite Quantum Dots: Application to Light-Emitting Diodes. Nanomaterials, 2019, 9, 172.	1.9	21
42169	Synergistic optimization of thermoelectric performance in p-type Ag2Te through Cu substitution. Journal of Materiomics, 2019, 5, 489-495.	2.8	33
42170	Deciphering Charge Transfer and Electronic Polarization Effects at Gold Nanocatalysts on Reduced Titania Support. Journal of Physical Chemistry C, 2019, 123, 5495-5506.	1.5	12
42171	Metalâ€“oxygen decoordination stabilizes anion redox in Li-rich oxides. Nature Materials, 2019, 18, 256-265.	13.3	280
42172	Stabilizing amorphous Sb by adding alien seeds for durable memory materials. Physical Chemistry Chemical Physics, 2019, 21, 4494-4500.	1.3	31
42173	Towards topological quasifreestanding stanene via substrate engineering. Physical Review B, 2019, 99, .	1.1	17
42174	Porous Cobaltâ€“Nickel Hydroxide Nanosheets with Active Cobalt Ions for Overall Water Splitting. Small, 2019, 15, e1804832.	5.2	46
42175	Transport properties of liquid metals and semiconductors from molecular dynamics simulation with the Kubo-Greenwood formula. Applied Surface Science, 2019, 478, 818-830.	3.1	10
42176	Screening of active center and reactivity descriptor in acetylene hydrochlorination on metal-free doped carbon catalysts from first principle calculations. Applied Surface Science, 2019, 478, 574-580.	3.1	21
42177	Magnetism in Cu2Si zigzag nanoribbon. Computational Materials Science, 2019, 161, 119-126.	1.4	5
42178	First-principles studies on the doping effect of Niâˆ’1TM (nâ€¯=â€¯13, 19, 55). Computational and Theoretical Chemistry, 2019, 1152, 32-40.	1.1	2
42179	Hydrogenation of acetylenic contaminants over Ni-Based catalyst: Enhanced performance by addition of silver. Journal of Cleaner Production, 2019, 220, 289-297.	4.6	6
42180	Enhanced thermoelectric performance in the n-type NbFeSb half-Heusler compound with heavy element Ir doping. Materials Today Physics, 2019, 8, 62-70.	2.9	44
42181	Investigating the interlayer electron transport and its influence on the whole electric properties of black phosphorus. Science Bulletin, 2019, 64, 254-260.	4.3	16

#	Article	IF	Citations
42182	Insights into the CO Formation Mechanism during Steam Reforming of Dimethyl Ether over NiO/Cu-Based Catalyst. Industrial & Engineering Chemistry Research, 2019, 58, 3440-3449.	1.8	9
42183	Theoretical Investigation of On-Purpose Propane Dehydrogenation over the Two-Dimensional Ruâ€“Pc Framework. Journal of Physical Chemistry C, 2019, 123, 4969-4976.	1.5	28
42184	Fiber-Shaped Electrochemical Capacitors Based on Plasma-Engraved Graphene Fibers with Oxygen Vacancies for Alternating Current Line Filtering Performance. ACS Applied Energy Materials, 2019, 2, 993-999.	2.5	16
42185	Super Large Sn_{1â€“x}Se Single Crystals with Excellent Thermoelectric Performance. ACS Applied Materials & Interfaces, 2019, 11, 8051-8059.	4.0	43
42186	Nanoclay-modulated oxygen vacancies of metal oxide. Communications Chemistry, 2019, 2, .	2.0	84
42187	Highly oriented GeSe thin film: self-assembly growth via the sandwiching post-annealing treatment and its solar cell performance. Nanoscale, 2019, 11, 3968-3978.	2.8	38
42188	Quenching of photoluminescence in a Zn-MOF sensor by nitroaromatic molecules. Journal of Materials Chemistry C, 2019, 7, 2625-2632.	2.7	54
42189	Discovery of a ferroelastic topological insulator in a two-dimensional tetragonal lattice. Physical Chemistry Chemical Physics, 2019, 21, 5165-5169.	1.3	5
42190	The AFLOW Library of Crystallographic Prototypes: Part 2. Computational Materials Science, 2019, 161, S1-S1011.	1.4	70
42191	Strain distribution in (InAs) âˆ•(InSb) multilayer: A first principles calculations. Solid State Communications, 2019, 291, 24-27.	0.9	1
42192	Facile One-Pot Synthesis of Pd@Pt_{1L} Octahedra with Enhanced Activity and Durability toward Oxygen Reduction. Chemistry of Materials, 2019, 31, 1370-1380.	3.2	41
42193	Mechanism of Hg⁰ and O₂ Interaction on the IrO₂ (110) Surface: A Density Functional Theory Study. Energy & Fuels, 2019, 33, 1354-1362.	2.5	16
42194	Energy Dissipation Effects on the Adsorption Dynamics of N2 on W(100). Journal of Physical Chemistry C, 2019, 123, 2900-2910.	1.5	5
42195	Origin of High-Efficiency Photoelectrochemical Water Splitting on Hematite/Functional Nanohybrid Metal Oxide Overlayer Photoanode after a Low Temperature Inert Gas Annealing Treatment. ACS Omega, 2019, 4, 1449-1459.	1.6	20
42196	The role of decomposition reactions in assessing first-principles predictions of solid stability. Npj Computational Materials, 2019, 5, .	3.5	63
42197	Electronic and Magnetic Properties of Lanthanum and Strontium Doped Bismuth Ferrite: A First-Principles Study. Scientific Reports, 2019, 9, 194.	1.6	42
42198	Symmetry-breaking induced large piezoelectricity in Janus tellurene materials. Physical Chemistry Chemical Physics, 2019, 21, 1207-1216.	1.3	134
42199	Silver route to cuprate analogs. Proceedings of the National Academy of Sciences of the United States of America, 2019, 116, 1495-1500.	3.3	47

#	Article	IF	Citations
42200	Discovery of ABO₃ perovskites as thermal barrier coatings through high-throughput first principles calculations. Materials Research Letters, 2019, 7, 145-151.	4.1	60
42201	Engineering the magnetic properties of PtSe₂ monolayer through transition metal doping. Journal of Physics Condensed Matter, 2019, 31, 145502.	0.7	36
42202	Local order in Cr-Fe-Co-Ni: Experiment and electronic structure calculations. Physical Review B, 2019, 99, .	1.1	40
42203	Polymorphism of bulk boron nitride. Science Advances, 2019, 5, eaau5832.	4.7	33
42204	Fast Flux Reaction Approach for the Preparation of Sn₂TiO₄: Tuning Particle Sizes and Photocatalytic Properties. Journal of the Electrochemical Society, 2019, 166, H3084-H3090.	1.3	12
42205	Synthesis, X-ray structure, and DFT modeling of a new polymeric zinc(II) complex of 2-mercaptonicotinic acid (MntH), {[Zn(Mntâ€“Mnt)(en)]·H2O}n. Monatshefte FÃ¼r Chemie, 2019, 150, 219-231.	0.9	3
42206	Regression model for stabilization energies associated with anion ordering in perovskite-type oxynitrides. Journal of Energy Chemistry, 2019, 36, 7-14.	7.1	21
42207	Combined Theoretical Approach for Identifying Battery Materials: Al³⁺ Mobility in Oxides. Chemistry of Materials, 2019, 31, 737-747.	3.2	36
42208	Structure and optical properties of sputter deposited pseudobrookite Fe₂TiO₅ thin films. CrystEngComm, 2019, 21, 34-40.	1.3	30
42209	Tuning oxygen electrocatalysis via strain on LaNiO3(001). Physical Chemistry Chemical Physics, 2019, 21, 4738-4745.	1.3	14
42210	Hydrogen adsorption on transition metal carbides: a DFT study. Physical Chemistry Chemical Physics, 2019, 21, 5335-5343.	1.3	42
42211	Band structure engineering of SnS₂/polyphenylene van der Waals heterostructure via interlayer distance and electric field. Physical Chemistry Chemical Physics, 2019, 21, 1521-1527.	1.3	26
42212	Unraveling the effect of B-site antisite defects on the electronic and magnetic properties of the quadruple perovskite CaCu₃Fe₂Nb₂O₁₂. Physical Chemistry Chemical Physics, 2019, 21, 3059-3065.	1.3	5
42213	Coexistence of piezoelectricity and magnetism in two-dimensional vanadium dichalcogenides. Physical Chemistry Chemical Physics, 2019, 21, 132-136.	1.3	80
42214	Infrared and Raman spectroscopy of non-conventional hydrogen bonding between N,Nâ€²-disubstituted urea and thiourea groups: a combined experimental and theoretical investigation. Physical Chemistry Chemical Physics, 2019, 21, 3310-3317.	1.3	15
42215	Transition-metal single atoms in nitrogen-doped graphenes as efficient active centers for water splitting: a theoretical study. Physical Chemistry Chemical Physics, 2019, 21, 3024-3032.	1.3	122
42216	Theoretical insight into the mechanism of photoreduction of CO₂ to CO by graphitic carbon nitride. Physical Chemistry Chemical Physics, 2019, 21, 1514-1520.	1.3	13
42217	Transition-metal dichalcogenides/Mg(OH)₂ van der Waals heterostructures as promising water-splitting photocatalysts: a first-principles study. Physical Chemistry Chemical Physics, 2019, 21, 1791-1796.	1.3	106

#	Article	IF	Citations
42218	A single boron atom doped boron nitride edge as a metal-free catalyst for N₂ fixation. Physical Chemistry Chemical Physics, 2019, 21, 1110-1116.	1.3	107
42219	Computational discovery and characterization of new B₂O phases. Physical Chemistry Chemical Physics, 2019, 21, 2499-2506.	1.3	7
42220	Valley polarization and ferroelectricity in a two-dimensional GaAsC₆ monolayer. Physical Chemistry Chemical Physics, 2019, 21, 3954-3959.	1.3	7
42221	Sulfation of a PdO(101) methane oxidation catalyst: mechanism revealed by first principles calculations. Catalysis Science and Technology, 2019, 9, 232-240.	2.1	10
42223	Atomically dispersed Ni as the active site towards selective hydrogenation of nitroarenes. Green Chemistry, 2019, 21, 704-711.	4.6	98
42224	Direct probe of the nuclear modes limiting charge mobility in molecular semiconductors. Materials Horizons, 2019, 6, 182-191.	6.4	53
42225	Two-dimensional spinâ€“valley-coupled Dirac semimetals in functionalized SbAs monolayers. Materials Horizons, 2019, 6, 781-787.	6.4	38
42226	Eighteen functional monolayer metal oxides: wide bandgap semiconductors with superior oxidation resistance and ultrahigh carrier mobility. Nanoscale Horizons, 2019, 4, 592-600.	4.1	78
42227	Molecular evidence for feedstock-dependent nucleation mechanisms of CNTs. Nanoscale Horizons, 2019, 4, 674-682.	4.1	11
42228	Germagraphene as a promising anode material for lithium-ion batteries predicted from first-principles calculations. Nanoscale Horizons, 2019, 4, 457-463.	4.1	48
42229	Catalytic performance of graphene quantum dot supported manganese phthalocyanine for efficient oxygen reduction: density functional theory approach. New Journal of Chemistry, 2019, 43, 348-355.	1.4	19
42230	Effects of pore surfaces on the electronic states of metal complexes formed on bipyridine periodic mesoporous organosilica. New Journal of Chemistry, 2019, 43, 2471-2478.	1.4	6
42231	Intrinsic multiferroicity in two-dimensional VOCl₂ monolayers. Nanoscale, 2019, 11, 1103-1110.	2.8	62
42232	Insights into defective TiO₂ in electrocatalytic N₂ reduction: combining theoretical and experimental studies. Nanoscale, 2019, 11, 1555-1562.	2.8	126
42233	Origins of complex solvent effects on chemical reactivity and computational tools to investigate them: a review. Reaction Chemistry and Engineering, 2019, 4, 165-206.	1.9	108
42234	Surface phonons of lithium ion battery active materials. Sustainable Energy and Fuels, 2019, 3, 508-513.	2.5	18
42235	A Janus MoSSe monolayer: a superior and strain-sensitive gas sensing material. Journal of Materials Chemistry A, 2019, 7, 1099-1106.	5.2	187
42236	Carbon-vacancy modified graphitic carbon nitride: enhanced CO₂ photocatalytic reduction performance and mechanism probing. Journal of Materials Chemistry A, 2019, 7, 1556-1563.	5.2	178

#	Article	IF	Citations
42237	Enhancement of photocatalytic H2 production by metal complex electrostatic adsorption on TiO2 (B) nanosheets. Journal of Materials Chemistry A, 2019, 7, 3797-3804.	5.2	11
42238	Achieving high energy density for lithium-ion battery anodes by Si/C nanostructure design. Journal of Materials Chemistry A, 2019, 7, 2165-2171.	5.2	113
42239	Uniform Pd_{0.33}Ir_{0.67} nanoparticles supported on nitrogen-doped carbon with remarkable activity toward the alkaline hydrogen oxidation reaction. Journal of Materials Chemistry A, 2019, 7, 3161-3169.	5.2	50
42240	Intercalated complexes of 1Tâ€²-MoS₂ nanosheets with alkylated phenylenediamines as excellent catalysts for electrochemical hydrogen evolution. Journal of Materials Chemistry A, 2019, 7, 2334-2343.	5.2	41
42241	Extremely high tensile strength and superior thermal conductivity of an sp3-hybridized superhard C24 fullerene crystal. Journal of Materials Chemistry A, 2019, 7, 3426-3431.	5.2	8
42242	New understanding of crystal control and facet selectivity of titanium dioxide ruling photocatalytic performance. Journal of Materials Chemistry A, 2019, 7, 8156-8166.	5.2	63
42243	Proposal of a stable B₃S nanosheet as an efficient hydrogen evolution catalyst. Journal of Materials Chemistry A, 2019, 7, 3752-3756.	5.2	41
42244	TlP₅: an unexplored direct band gap 2D semiconductor with ultra-high carrier mobility. Journal of Materials Chemistry C, 2019, 7, 639-644.	2.7	30
42245	Monitoring the crystal orientation of black-arsenic via vibrational spectra. Journal of Materials Chemistry C, 2019, 7, 1228-1236.	2.7	13
42246	How to predict the location of the defect levels induced by 3d transition metal ions at octahedral sites of aluminate phosphors. Journal of Materials Chemistry C, 2019, 7, 95-103.	2.7	16
42247	A new 2D high-pressure phase of PdSe₂ with high-mobility transport anisotropy for photovoltaic applications. Journal of Materials Chemistry C, 2019, 7, 2096-2105.	2.7	70
42248	Unraveling the highest oxidation states of actinides in solid-state compounds with a particular focus on plutonium. Physical Chemistry Chemical Physics, 2019, 21, 4732-4737.	1.3	16
42249	Theoretical study on the reaction mechanism and selectivity of acetylene semi-hydrogenation on Niâ€“Sn intermetallic catalysts. Physical Chemistry Chemical Physics, 2019, 21, 1384-1392.	1.3	10
42250	Morphology evolution of magnesium facets: DFT and KMC simulations. Physical Chemistry Chemical Physics, 2019, 21, 2434-2442.	1.3	20
42251	Nâ€“H bond activation in ammonia by TM-SSZ-13 (Fe, Co, Ni and Cu) zeolites: a first-principles calculation. Physical Chemistry Chemical Physics, 2019, 21, 1506-1513.	1.3	8
42252	Evenâ€“odd oscillation of bandgaps in GeP₃ nanoribbons and a tunable 1D lateral homogenous heterojunction. Physical Chemistry Chemical Physics, 2019, 21, 275-280.	1.3	6
42253	A novel hydrogenated boronâ€“carbon monolayer with high stability and promising carrier mobility. Physical Chemistry Chemical Physics, 2019, 21, 2572-2577.	1.3	6
42254	Topologically nontrivial phase and tunable Rashba effect in half-oxidized bismuthene. Physical Chemistry Chemical Physics, 2019, 21, 2899-2909.	1.3	10

#	Article	IF	Citations
42255	Effects of tensile strain and finite size on thermal conductivity in monolayer WSe₂. Physical Chemistry Chemical Physics, 2019, 21, 468-477.	1.3	60
42256	Density functional theory calculations and thermodynamic analysis of bridgmanite surface structure. Physical Chemistry Chemical Physics, 2019, 21, 1009-1013.	1.3	3
42257	Electronic structure of Al, Ga, In and Cu doped ZnO/Cu(111) bilayer films. Physical Chemistry Chemical Physics, 2019, 21, 369-377.	1.3	28
42258	Half-metal state of a Ti₂C monolayer by asymmetric surface decoration. Physical Chemistry Chemical Physics, 2019, 21, 3318-3326.	1.3	22
42259	Intrinsic effects of strain on low-index surfaces of platinum: roles of the five 5d orbitals. Physical Chemistry Chemical Physics, 2019, 21, 3242-3249.	1.3	23
42260	First-principles calculations of carrier localization in fluctuated InGaN quantum wells. Japanese Journal of Applied Physics, 2019, 58, SCCB05.	0.8	0
42261	An atomic scale structural investigation of nanometre-sized Î·Âprecipitates in the 7050 aluminium alloy. Acta Materialia, 2019, 174, 351-368.	3.8	110
42262	Electrochemically active novel amorphous carbon (a-C)/Cu3P peapod nanowires by low-temperature chemical vapor phosphorization reaction as high efficient electrocatalysts for hydrogen evolution reaction. Electrochimica Acta, 2019, 318, 374-383.	2.6	13
42263	Prediction of intrinsic ferromagnetism in two-dimension planar metal-organic framework semiconductors. Journal of Magnetism and Magnetic Materials, 2019, 488, 165354.	1.0	17
42264	First principles investigation into the phase stability and enhanced hardness of TiN-ScN and TiN-YN alloys. Thin Solid Films, 2019, 688, 137284.	0.8	16
42265	NH₃-SCR over Vâ€“W/TiO₂ Investigated by Operando X-ray Absorption and Emission Spectroscopy. Journal of Physical Chemistry C, 2019, 123, 14338-14349.	1.5	20
42266	First-Principles Prediction of the ZnO Morphology in the Perovskite Solar Cell. Journal of Physical Chemistry C, 2019, 123, 14164-14172.	1.5	4
42267	Type-II InSe/g-C₃N₄ Heterostructure as a High-Efficiency Oxygen Evolution Reaction Catalyst for Photoelectrochemical Water Splitting. Journal of Physical Chemistry Letters, 2019, 10, 3122-3128.	2.1	142
42268	Distinct Catalytic Reactivity of Sn Substituted in Framework Locations and at Defect Grain Boundaries in Sn-Zeolites. ACS Catalysis, 2019, 9, 6146-6168.	5.5	52
42269	Gate tunable giant anisotropic resistance in ultra-thin GaTe. Nature Communications, 2019, 10, 2302.	5.8	72
42270	Computational screening of M/Cu core/shell nanoparticles and their applications for the electro-chemical reduction of CO₂ and CO. Nanoscale, 2019, 11, 11351-11359.	2.8	14
42271	First-principles investigation on anion order, electronic structure and dielectric properties of BaTaO₂N. Journal of Materials Chemistry A, 2019, 7, 14583-14591.	5.2	15
42272	Long- and short-range structures of Ti_{1â^'x}Hf_xNi_{1.0/1.1}Sn half-Heusler compounds and their electric transport properties. CrystEngComm, 2019, 21, 3330-3342.	1.3	4

#	Article	IF	Citations
42273	Cracked eight-awn star TaS₂ with fractal structures used as an efficient electrocatalyst for the hydrogen evolution reaction. CrystEngComm, 2019, 21, 3517-3524.	1.3	5
42274	The magnetism of 1T-MX₂ (M = Zr, Hf; X = S, Se) monolayers by hole doping. RSC Advances, 2019, 9, 13561-13566.	1.7	16
42275	Tuning the electronic and magnetic properties of metal-doped phenanthrene by codoping method. AIP Advances, 2019, 9, .	0.6	2
42276	Carbon doping of WS ₂ monolayers: Bandgap reduction and p-type doping transport. Science Advances, 2019, 5, eaav5003.	4.7	119
42277	Analyzing the Electronic Coupling in Molecular Crystalsâ€"The Instructive Case of Î±â€Quinacridone. Advanced Theory and Simulations, 2019, 2, 1800204.	1.3	10
42278	Fine-tuning the ductile-brittle transition temperature of Mg2Si intermetallic compound via Al doping. International Journal of Minerals, Metallurgy and Materials, 2019, 26, 507-515.	2.4	10
42279	Hierarchical analysis of alloying element effects on gas nitriding rate of Fe alloys: A DFT, microkinetic and kMC study. Acta Materialia, 2019, 174, 173-180.	3.8	5
42280	Reversible displacive transformation with continuous transition interface in a metastable Î² titanium alloy. Acta Materialia, 2019, 174, 217-226.	3.8	18
42281	Effective hydrogenation of TiO2 photocatalysts with CH3OH for enhanced water splitting: A computational and X-ray study. Applied Surface Science, 2019, 488, 546-554.	3.1	11
42282	Thermal atomic layer deposition of metallic Ru using H2O as a reactant. Applied Surface Science, 2019, 488, 896-902.	3.1	17
42283	Strategy to enhance intrinsic ductility and surface stability of Mg-Zn-R (Râ€¯=â€¯La to Sm) alloys from a first-principles study. Computational Materials Science, 2019, 165, 96-100.	1.4	5
42284	The modulation of the magnetocrystalline anisotropy of the halogen functionalize metal-phthalocyanine networks. Chemical Physics Letters, 2019, 728, 181-185.	1.2	2
42285	Exploration of crystal structure and the origin of unexpected intrinsic ductility of Ï‡Co7Ta2. Journal of Alloys and Compounds, 2019, 797, 1198-1204.	2.8	5
42286	Theoretical study on Frenkel pair formation and recombination in single crystal silicon. Journal of Crystal Growth, 2019, 520, 1-10.	0.7	3
42287	Effects of Zr and V additions on the stability and migration of He in bcc W: A first-principles study. Physics Letters, Section A: General, Atomic and Solid State Physics, 2019, 383, 2777-2783.	0.9	5
42288	Structural and electronic properties of 2H phase Janus transition metal dichalcogenide bilayers. Superlattices and Microstructures, 2019, 131, 8-14.	1.4	23
42289	Defect chemistry in cubic Li6.25Al0.25La3Zr2O12 solid electrolyte: A density functional theory study. Solid State Ionics, 2019, 338, 74-79.	1.3	22
42290	Organic Semiconductors Derived from Dinaphtho-Fused s-Indacenes: How Molecular Structure and Film Morphology Influence Thin-Film Transistor Performance. Chemistry of Materials, 2019, 31, 6962-6970.	3.2	41

#	Article	IF	Citations
42291	Impact of lattice relaxations on phase transitions in a high-entropy alloy studied by machine-learning potentials. Npj Computational Materials, 2019, 5, .	3.5	110
42292	Electric field tuning of the anomalous Hall effect at oxide interfaces. Npj Computational Materials, 2019, 5, .	3.5	18
42293	Spin-dependent scattering induced negative magnetoresistance in topological insulator Bi2Te3 nanowires. Scientific Reports, 2019, 9, 7836.	1.6	16
42294	Effects and distribution of Zr introduced in Ni-based cathode material for Li-ion batteries. Physical Chemistry Chemical Physics, 2019, 21, 12505-12517.	1.3	27
42295	Single Pt atom supported on penta-graphene as an efficient catalyst for CO oxidation. Physical Chemistry Chemical Physics, 2019, 21, 12201-12208.	1.3	27
42296	Electronic structure and high-temperature thermochemistry of BaZrO_{3â^'Î´}perovskite from first-principles calculations. Physical Chemistry Chemical Physics, 2019, 21, 12468-12476.	1.3	7
42297	Physical properties of epitaxial SrMnO_{2.5â^'Î´}F_{Î³} oxyfluoride films. Journal of Physics Condensed Matter, 2019, 31, 365602.	0.7	5
42298	First-principles study of structural, mechanical, and electronic properties of W alloying with Zr. Chinese Physics B, 2019, 28, 046301.	0.7	6
42299	First Principles Calculations on the Stoichiometric and Defective (101) Anatase Surface and Upon Hydrogen and H2Pc Adsorption: The Influence of Electronic Exchange and Correlation and of Basis Set Approximations. Frontiers in Chemistry, 2019, 7, 220.	1.8	6
42300	Quantum Well Energetics of an n = 2 Ruddlesdenâ€“Popper Phase Perovskite. Advanced Energy Materials, 2019, 9, 1901005.	10.2	25
42301	Cd/Cr dopings in CuAg nano-clusters: a transition towards strong alloying. Journal of Nanoparticle Research, 2019, 21, 1.	0.8	2
42302	Interface reaction of high-strength low-alloy steel with Alâ€“43.4Znâ€“1.6Si (wt.%) metallic coating. Journal of Iron and Steel Research International, 2019, 26, 1304-1314.	1.4	2
42303	Electronic interaction between single Pt atom and vacancies on boron nitride nanosheets and its influence on the catalytic performance in the direct dehydrogenation of propane. Chinese Journal of Catalysis, 2019, 40, 819-825.	6.9	25
42304	MoS2 nanoflower supported Pt nanoparticle as an efficient electrocatalyst for ethanol oxidation reaction. International Journal of Hydrogen Energy, 2019, 44, 16411-16423.	3.8	31
42305	Theoretical Screening of Single-Atom-Embedded MoSSe Nanosheets for Electrocatalytic N₂ Fixation. Journal of Physical Chemistry C, 2019, 123, 14501-14507.	1.5	72
42306	Rich Polymorphism of a Metalâ€“Organic Framework in Pressureâ€“Temperature Space. Journal of the American Chemical Society, 2019, 141, 9330-9337.	6.6	68
42307	Energy storage properties of a two-dimensional TiB₄ monolayer. Physical Chemistry Chemical Physics, 2019, 21, 13151-13156.	1.3	11
42308	Large tetragonality and room temperature ferroelectricity in compressively strained CaTiO3 thin films. APL Materials, 2019, 7, .	2.2	10

#	Article	IF	Citations
42309	Predicting three-dimensional icosahedron-based boron <mml:math xmlns:mml="http://www.w3.org/1998/Math/MathML"><mml:msub><mml:mi mathvariant="normal">B</mml:mi><mml:mn>60</mml:mn></mml:msub></mml:math>. Physical Review B, 2019, 99,	1.1	21
42310	Magnetism and the emergence of frustration in the sawtooth lattice chalcogenide olivines <mml:math xmlns:mml="http://www.w3.org/1998/Math/MathML"><mml:mrow><mml:msub><mml:mi>Mn</mml:mi><mml:mn>2</mml:mn></mml:msub></mml:mrow></mml:math>		

#	Article	IF	Citations
42327	External strain-enhanced cysteine enantiomeric separation ability on alloyed stepped surfaces. Journal of Chemical Physics, 2019, 150, 154701.	1.2	4
42328	Strongly Enhanced Gilbert Damping in 3 d Transition-Metal Ferromagnet Monolayers in Contact with the Topological Insulator <mml:math xmlns:mml="http://www.w3.org/1998/Math/MathML" display="inline" overflow="scroll"><mml:msub><mml:mi>Bi</mml:mi><mml:mn>2</mml:mn></mml:msub><mml:msub><mml:mi>Se</mml:mi><mml:mi><mm Physical Review Applied, 2019, 11, .	1.5	15
42329	Two-dimensional silicon phosphide: low effective mass and direct band gap for future devices applications. Journal of Materials Science, 2019, 54, 11878-11888.	1.7	14
42330	Thermoelectric Properties of Two-Dimensional Gallium Telluride. Journal of Electronic Materials, 2019, 48, 5988-5994.	1.0	22
42331	Construction the Ni@Carbon nanostructure with dual-reaction surfaces for the selective hydrogenation reaction. Applied Surface Science, 2019, 489, 786-795.	3.1	20
42332	Sorption mechanism and dynamic behavior of graphene oxide as an effective adsorbent for the removal of chlorophenol based environmental-hormones: A DFT and MD simulation study. Chemical Engineering Journal, 2019, 375, 121964.	6.6	74
42333	Effect of Si doping on the structure and optical properties of Ge2Sb2Te5 studied by ab initio calculations. Computational Materials Science, 2019, 168, 253-259.	1.4	8
42334	(Sr0.6Bi0.305)2Bi2O7 as a new visible-light-responsive photocatalyst: An experimental and theoretical study. Materials Research Bulletin, 2019, 118, 110484.	2.7	16
42335	First principles investigation of the vacancy-mediated impurity diffusion in dilute Zr-X (Xâ€¯=â€¯Sc, Y, Ce) alloys. Nuclear Instruments & Methods in Physics Research B, 2019, 453, 75-78.	0.6	5
42336	Continuous, Ultra-lightweight, and Multipurpose Super-aligned Carbon Nanotube Tapes Viable over a Wide Range of Temperatures. Nano Letters, 2019, 19, 6756-6764.	4.5	17
42337	Amorphous Rhenium Disulfide Nanosheets: A Methanol-Tolerant Transition Metal Dichalcogenide Catalyst for Oxygen Reduction Reaction. ACS Applied Nano Materials, 2019, 2, 4480-4488.	2.4	17
42338	Metal-catalyst-free access to multiwalled carbon nanotubes/silica nanocomposites (MWCNT/SiO₂) from a single-source precursor. Dalton Transactions, 2019, 48, 11018-11033.	1.6	11
42339	Direction-control of anisotropic electronic behaviors via ferroelasticity in two-dimensional Î±-MPI (M = Zr, Hf). Materials Horizons, 2019, 6, 1930-1937.	6.4	39
42340	Experimental and first-principles investigation of Cr-driven color change in cesium lead halide perovskites. Journal of Applied Physics, 2019, 125, 225705.	1.1	3
42341	Negative Thermal Expansion of GaFe(CN)₆ and Effect of Na Insertion by First-Principles Calculations*. Chinese Physics Letters, 2019, 36, 066301.	1.3	6
42342	Ordering of Fe and Zn Ions and the Magnetic Properties of FeZnMo3O8. JETP Letters, 2019, 109, 786-789.	0.4	10
42343	Identifying rhenium substitute candidate multiprincipal-element alloys from electronic structure and thermodynamic criteria. Journal of Materials Research, 2019, 34, 3296-3304.	1.2	8
42344	Greatly Enhanced Electrocatalytic N₂ Reduction on TiO₂ via V Doping. Small Methods, 2019, 3, 1900356.	4.6	164

#	Article	IF	Citations
42345	Tunable first order transition in La(Fe,Cr,Si)13 compounds: Retaining magnetocaloric response despite a magnetic moment reduction. Acta Materialia, 2019, 175, 406-414.	3.8	45
42346	Transition-metal doping/adsorption induced valley polarization in Janus WSSe: First-principles calculations. Applied Surface Science, 2019, 490, 172-177.	3.1	30
42347	Electrodeposition behavior of lithium metal on carbon substrates with surface silvering. Carbon, 2019, 152, 503-510.	5.4	16
42348	First-principles study of dopant stability and related optical properties in CdSiP2 crystal. Journal of Alloys and Compounds, 2019, 802, 310-317.	2.8	2
42349	Equation of state of LiNi0.8Co0.1Mn0.1O2 at high pressure. Solid State Communications, 2019, 299, 113656.	0.9	9
42350	Structural Diversity in Cesium Bismuth Halide Nanocrystals. Chemistry of Materials, 2019, 31, 4685-4697.	3.2	80
42351	Chromate Effect on Iodate Incorporation into Calcite. ACS Earth and Space Chemistry, 2019, 3, 1624-1630.	1.2	16
42352	End-Bonded Metal Contacts on WSe₂ Field-Effect Transistors. ACS Nano, 2019, 13, 8146-8154.	7.3	44
42353	Trace doping of multiple elements enables stable battery cycling of LiCoO2 at 4.6â€‰V. Nature Energy, 2019, 4, 594-603.	19.8	572
42354	A map of the inorganic ternary metal nitrides. Nature Materials, 2019, 18, 732-739.	13.3	274
42355	Defect induced, layer-modulated magnetism in ultrathin metallic PtSe2. Nature Nanotechnology, 2019, 14, 674-678.	15.6	162
42356	Identification of active sites for acidic oxygen reduction on carbon catalysts with and without nitrogen doping. Nature Catalysis, 2019, 2, 688-695.	16.1	423
42357	Anisotropic thermoelectric properties of Weyl semimetal NbX (X = P and As): a potential thermoelectric material. Physical Chemistry Chemical Physics, 2019, 21, 15167-15176.	1.3	31
42358	A high-pressure induced stable phase of Li₂MnSiO₄ as an effective poly-anion cathode material from simulations. Journal of Materials Chemistry A, 2019, 7, 16406-16413.	5.2	6
42359	Mapping the sodium intercalation mechanism, electrochemical properties and structural evolution in non-stoichiometric alluaudite Na_{2+2Î´}Fe_{2â^'Î´}(SO₄)₃ cathode materials. Journal of Materials Chemistry A, 2019, 7, 17446-17455.	5.2	11
42360	Influence of Ca adsorption on the heterogeneous nucleation of Î±-Mg on Al4C3 particles: First-principles calculation and experiment. Applied Surface Science, 2019, 491, 187-194.	3.1	19
42361	Micromachining of ferrous metal with an ion implanted diamond cutting tool. Carbon, 2019, 152, 598-608.	5.4	27
42362	Enhanced overall water electrolysis on a bifunctional perovskite oxide through interfacial engineering. Electrochimica Acta, 2019, 318, 120-129.	2.6	39

#	Article	IF	Citations
42363	Structure engineering of Cu-based nanoparticles for electrochemical reduction of CO2. Journal of Catalysis, 2019, 375, 234-241.	3.1	20
42364	Fe and N Co-Doped Porous Carbon Nanospheres with High Density of Active Sites for Efficient CO₂ Electroreduction. Journal of Physical Chemistry C, 2019, 123, 16651-16659.	1.5	54
42365	Formation of Silicene on Ultrathin Pb(111) Films. Journal of Physical Chemistry C, 2019, 123, 17019-17025.	1.5	40
42366	Enhancement Effects of Co Doping on Interfacial Properties of Sn Electrodeâ^'Collector: A First-Principles Study. ACS Applied Materials & Interfaces, 2019, 11, 24648-24658.	4.0	19
42367	Sn-Doping Enhanced Ultrahigh Mobility In_{1â€“x}Sn_xSe Phototransistor. ACS Applied Materials & Interfaces, 2019, 11, 24269-24278.	4.0	17
42368	Strong charge polarization effect enabled by surface oxidized titanium nitride for lithium-sulfur batteries. Communications Chemistry, 2019, 2, .	2.0	29
42369	Recyclable and superior selective CO₂ adsorption of C₄B₃₂ and Ca@C₄B₃₂: a new category of perfect cubic heteroborospherenes. Physical Chemistry Chemical Physics, 2019, 21, 15541-15550.	1.3	14
42370	Fine tuning of Fermi level by charged impurity-defect cluster formation and thermoelectric properties in n-type PbTe-based compounds. Journal of Materials Chemistry A, 2019, 7, 16488-16500.	5.2	24
42371	Thickness-dependent bandgap and electrical properties of GeP nanosheets. Journal of Materials Chemistry A, 2019, 7, 16526-16532.	5.2	45
42372	Stable, one-dimensional suspended and supported monatomic chains of pnictogens: a metalâ€“insulator framework. Physical Chemistry Chemical Physics, 2019, 21, 14832-14845.	1.3	9
42373	Topology on a new facet of bismuth. Proceedings of the National Academy of Sciences of the United States of America, 2019, 116, 13255-13259.	3.3	61
42374	Ab initio electronic structure calculations using a real-space Chebyshev-filtered subspace iteration method. Journal of Physics Condensed Matter, 2019, 31, 455901.	0.7	11
42375	Route to achieving enhanced quantum capacitance in functionalized graphene based supercapacitor electrodes. Journal of Physics Condensed Matter, 2019, 31, 475502.	0.7	26
42376	Inverse pressure-induced Mott transition in TiPO4. Physical Review B, 2019, 99, .	1.1	2
42377	Concentrated Electrolytes for Enhanced Stability of Al-Alloy Negative Electrodes in Li-Ion Batteries. Journal of the Electrochemical Society, 2019, 166, A1867-A1874.	1.3	28
42378	Origins of promising thermoelectric performance in quaternary selenide BaAg₂SnSe₄. Applied Physics Express, 2019, 12, 071006.	1.1	4
42379	Investigation of Alkaliâ€Ion (Li, Na, and K) Intercalation in K_xVPO₄F (x â^¼ 0) Cathode. Advanced Functional Materials, 2019, 29, 1902392.	7.8	35
42380	Two-dimensional silicon chalcogenides with high carrier mobility for photocatalytic water splitting. Journal of Materials Science, 2019, 54, 11485-11496.	1.7	30

#	Article	IF	Citations
42381	Multiscale Entropy and Its Implications to Critical Phenomena, Emergent Behaviors, and Information. Journal of Phase Equilibria and Diffusion, 2019, 40, 508-521.	0.5	17
42382	Theoretical picture of positive electrodeâ€“solid electrolyte interface in all-solid-state battery from electrochemistry and semiconductor physics viewpoints. Current Opinion in Electrochemistry, 2019, 17, 149-157.	2.5	40
42383	Band structure manipulated by high pressure-assisted Te doping realizing improvement in thermoelectric performance of BiCuSeO system. Journal of Materiomics, 2019, 5, 649-656.	2.8	12
42384	Magnetostructural Coupling Drives Magnetocaloric Behavior: The Case of MnB versus FeB. Chemistry of Materials, 2019, 31, 4873-4881.	3.2	24
42385	First-Principle Study on Heterofullerenes: Effective and Multifunctional in Hg Removal. Industrial & Engineering Chemistry Research, 2019, 58, 11101-11110.	1.8	8
42386	CO₂ Activation and Reduction on Pt-CeO₂-Based Catalysts. Journal of Physical Chemistry C, 2019, 123, 17092-17101.	1.5	31
42387	Quantitative Understanding of the Sluggish Kinetics of Hydrogen Reactions in Alkaline Media Based on a Microscopic Hamiltonian Model for the Volmer Step. Journal of Physical Chemistry C, 2019, 123, 17325-17334.	1.5	38
42388	Role of Superexchange Interactions on the Arrangement of Fe and Mn in LiMn_xFe_{1â€“x}PO₄. Journal of Physical Chemistry C, 2019, 123, 17002-17009.	1.5	6
42389	Two-Dimensional Gold Sulfide Monolayers with Direct Band Gap and Ultrahigh Electron Mobility. Journal of Physical Chemistry Letters, 2019, 10, 3773-3778.	2.1	34
42390	Magnetoresistance in Metallic Ferroelectrics. ACS Applied Electronic Materials, 2019, 1, 1225-1232.	2.0	4
42391	Role of Cation Vacancies in Cu₂SnSe₃ Thermoelectrics. ACS Applied Materials & Interfaces, 2019, 11, 24212-24220.	4.0	30
42392	Three-Dimensional Optical Anisotropy of Low-Symmetry Layered GeS. ACS Applied Materials & Interfaces, 2019, 11, 24247-24253.	4.0	27
42393	Hexagonal CuCl Monolayer for Water Splitting: A DFT Study. ACS Applied Nano Materials, 2019, 2, 4238-4246.	2.4	25
42394	Ultrahigh-Performance Optoelectronics Demonstrated in Ultrathin Perovskite-Based Vertical Semiconductor Heterostructures. ACS Nano, 2019, 13, 7996-8003.	7.3	64
42395	Plasmonic Photocatalysis of Nitrous Oxide into N₂ and O₂ Using Aluminumâ€“Iridium Antennaâ€“Reactor Nanoparticles. ACS Nano, 2019, 13, 8076-8086.	7.3	83
42396	Unraveling Oxygen Evolution in Li-Rich Oxides: A Unified Modeling of the Intermediate Peroxo/Superoxo-like Dimers. Journal of the American Chemical Society, 2019, 141, 10751-10759.	6.6	82
42397	Thermodynamics and Electronic Properties of Heterometallic Multinuclear Actinide-Containing Metalâ€“Organic Frameworks with â€œStructural Memoryâ€• Journal of the American Chemical Society, 2019, 141, 11628-11640.	6.6	71
42398	Computational polymorph screening reveals late-appearing and poorly-soluble form of rotigotine. Communications Chemistry, 2019, 2, .	2.0	39

#	Article	IF	Citations
42399	Thickness dependent thermal stability of 2D gallenene. Chemical Communications, 2019, 55, 8872-8875.	2.2	19
42400	Unravelling the polarity of InN quantum dots using a modified approach of negative-spherical-aberration imaging. Nanoscale, 2019, 11, 13632-13638.	2.8	9
42401	New scaling relations to compute atom-in-material polarizabilities and dispersion coefficients: part 1. Theory and accuracy. RSC Advances, 2019, 9, 19297-19324.	1.7	16
42402	A CoMoO₄â€“Co₂Mo₃O₈ heterostructure with valence-rich molybdenum for a high-performance hydrogen evolution reaction in alkaline solution. Journal of Materials Chemistry A, 2019, 7, 16761-16769.	5.2	50
42403	Direct synthesis of furfuryl alcohol from furfural: catalytic performance of monometallic and bimetallic Mo and Ru phosphides. Catalysis Science and Technology, 2019, 9, 3656-3668.	2.1	35
42404	Template-free synthesis of oxygen-containing ultrathin porous carbon quantum dots/g-C₃N₄ with superior photocatalytic activity for PPCPs remediation. Environmental Science: Nano, 2019, 6, 2565-2576.	2.2	55
42405	Ti-Ti Ïƒ bond at oxygen vacancy inducing the deep defect level in anatase TiO2 (101) surface. Journal of Chemical Physics, 2019, 150, 224702.	1.2	25
42406	Tunable electronic properties of monolayer MnPSe₃/MoTe₂ heterostructure: a first principles study. Journal of Physics Condensed Matter, 2019, 31, 405705.	0.7	13
42407	Real-space observation on standing configurations of phenylacetylene on Cu (111) by scanning probe microscopy*. Chinese Physics B, 2019, 28, 066801.	0.7	2
42408	Role of defects in the metal-insulator transition in <mml:math xmlns:mml="http://www.w3.org/1998/Math/MathML"><mml:msub><mml:mi mathvariant="normal">VO</mml:mi><mml:mn>2</mml:mn></mml:msub></mml:math> and <mml:math xmlns:mml="http://www.w3.org/1998/Math/MathML"><mml:msub><mml:mi mathvariant="normal">V</mml:mi><mml:mn>2</mml:mn></mml:msub><mml:msub><mml:mi	1.1	32
42409	Possible emergence of a skyrmion phase in ferroelectric <mml:math xmlns:mml="http://www.w3.org/1998/Math/MathML"><mml:mrow><mml:mi>GaM</mml:mi><mml:msub><mml:mi mathvariant="normal">o</mml:mi><mml:mn>4</mml:mn></mml:msub><mml:msub><mml:mi mathvariant="normal">S</mml:mi><mml:mn>8</mml:mn></mml:msub></mml:mrow></mml:math>. Physical Review B, 2019, 99, .	1.1	18
42410	Dynamics of the Structural Transformation of Crystalline Hydrogen upon the Transition into the Conductive State under Compression. Doklady Physics, 2019, 64, 145-149.	0.2	5
42411	Selfâ€Supported and Flexible Sulfur Cathode Enabled via Synergistic Confinement for Highâ€Energyâ€Density Lithiumâ€“Sulfur Batteries. Advanced Materials, 2019, 31, e1902228.	11.1	216
42412	A 3D and Stable Lithium Anode for Highâ€Performance Lithiumâ€“Iodine Batteries. Advanced Materials, 2019, 31, e1902399.	11.1	137
42413	Identification of Nonâ€Carbonaceous Cathodes in Al Batteries: Potential Applicability of Black and Blue Phosphorene Monolayers. Chemistry - an Asian Journal, 2019, 14, 2831-2837.	1.7	6
42414	Chemisorption of NO₂ to MoS₂ Nanostructures and its Effects for MoS₂ Sensors. ChemNanoMat, 2019, 5, 1123-1130.	1.5	41
42415	Porous-hollow nanorods constructed from alternate intercalation of carbon and MoS2 monolayers for lithium and sodium storage. Nano Research, 2019, 12, 1912-1920.	5.8	39
42416	A novel highly selective and sensitive NH3 gas sensor based on monolayer Hf2CO2. Applied Surface Science, 2019, 492, 116-124.	3.1	61

#	Article	IF	Citations
42417	Hydrogen-Induced Degradation of NaMnO₂. Chemistry of Materials, 2019, 31, 5224-5228.	3.2	10
42418	Theoretical Prediction of Catalytic Activity of Ti₂C MXene as Cathode for Liâ€“O₂ Batteries. Journal of Physical Chemistry C, 2019, 123, 17466-17471.	1.5	53
42419	Î²-As Monolayer: Vibrational Properties and Raman Spectra. ACS Omega, 2019, 4, 10171-10175.	1.6	13
42420	Site-selectively generated photon emitters in monolayer MoS2 via local helium ion irradiation. Nature Communications, 2019, 10, 2755.	5.8	132
42421	The geometry of hexagonal boron nitride clusters in the initial stages of chemical vapor deposition growth on a Cu(111) surface. Nanoscale, 2019, 11, 13366-13376.	2.8	21
42422	Low-dimensional perovskite nanoplatelet synthesis using in situ photophysical monitoring to establish controlled growth. Nanoscale, 2019, 11, 17262-17269.	2.8	18
42423	BaZrSe3: Ab initio study of anion substitution for bandgap tuning in a chalcogenide material. Journal of Applied Physics, 2019, 125, .	1.1	10
42424	Ultrathin LaNiO $$_{3}$$. Springer Theses, 2019, , 65-77.	0.0	0
42425	Strain-induced band modulation of surface F-functionalized two-dimensional Sc2C. Applied Surface Science, 2019, 491, 276-285.	3.1	23
42426	Effect of sulfur dopant atoms on the electronic band gap and optical properties of tin iodide. Chemical Physics Letters, 2019, 730, 557-561.	1.2	8
42427	Ab initio calculations on three dimensional antiferromagnet Cu3TeO6. Journal of Physics and Chemistry of Solids, 2019, 134, 182-186.	1.9	6
42428	Prediction of two-dimensional monochalcogenides: MoS and WS. Physics Letters, Section A: General, Atomic and Solid State Physics, 2019, 383, 2914-2921.	0.9	10
42429	Highly Active and CO-Tolerant Trimetallic NiPtPd Hollow Nanocrystals as Electrocatalysts for Methanol Electro-oxidation Reaction. ACS Applied Energy Materials, 2019, 2, 4763-4773.	2.5	23
42430	Effects of Mo alloying on stability and diffusion of hydrogen in the Nb16H phase: a first-principles investigation. RSC Advances, 2019, 9, 19495-19500.	1.7	5
42431	Influence of HfO2 interlayers on magnetocrystalline anisotropy in Fe |MgO |Fe magnetic tunnel junction: First-principles investigation. Journal of Applied Physics, 2019, 125, 233905.	1.1	0
42432	Weakened interlayer coupling in two-dimensional MoSe2 flakes with screw dislocations. Nano Research, 2019, 12, 1900-1905.	5.8	23
42433	Theoretical investigating of graphene/antimonene heterostructure as a promising high cycle capability anodes for fast-charging lithium ion batteries. Applied Surface Science, 2019, 491, 451-459.	3.1	33
42434	Investigation on the formation and regulation of yttrium aluminosilicate fiber driven by spontaneous element migration. Ceramics International, 2019, 45, 19182-19188.	2.3	6

#	Article	IF	Citations
42435	Sublattice formation in CoCrFeNi high-entropy alloy. Intermetallics, 2019, 112, 106542.	1.8	20
42436	Insight into the robust multiple Dirac cones in perovskite <mml:math xmlns:mml="http://www.w3.org/1998/Math/MathML" altimg="si1.svg"><mml:mrow><mml:mi>R</mml:mi><mml:mrow><mml:mover accent="true"><mml:mrow><mml:mn>3</mml:mn></mml:mrow><mml:mo stretchy="true">Â¯</mml:mo></mml:mover></mml:mrow><mml:mi>c</mml:mi></mml:mrow></mml:math> phase CaBO3 semimetal from first-principles. Journal of Molecular Graphics and Modelling, 2019, 91, 18.	1.3	1
42437	A superhard orthorhombic carbon with all six-membered-ring in sp3 bonding networks. Physics Letters, Section A: General, Atomic and Solid State Physics, 2019, 383, 2809-2812.	0.9	19
42438	Influence of local lattice distortions on electrical transport of refractory high entropyÂalloys. Scripta Materialia, 2019, 170, 189-194.	2.6	26
42439	Mechanistic insight into CO activation, methanation and C-C bond formation from coverage dependent CO hydrogenation on Fe(110). Surface Science, 2019, 689, 121456.	0.8	10
42440	Highly Efficient Ni-Doped Iron Catalyst for Ammonia Synthesis from Quantum-Mechanics-Based Hierarchical High-Throughput Catalyst Screening. Journal of Physical Chemistry C, 2019, 123, 17375-17383.	1.5	16
42441	Biaxial strain effect on the electronic structure and valleytronic properties of a MoS₂/CoO(111) heterostructure. Physical Chemistry Chemical Physics, 2019, 21, 15151-15156.	1.3	4
42442	Quantifying the activation energies of ROS-induced NOx conversion: Suppressed toxic intermediates generation and clarified reaction mechanism. Chemical Engineering Journal, 2019, 375, 122026.	6.6	19
42443	Database of novel magnetic materials for high-performance permanent magnet development. Computational Materials Science, 2019, 168, 188-202.	1.4	41
42444	Scalable atomistic simulations of quantum electron transport using empirical pseudopotentials. Computer Physics Communications, 2019, 244, 156-169.	3.0	23
42445	First-principles study of structural, electronic, ferroelectric, and vibrational properties of BiInO3 under high pressure. Journal of Physics and Chemistry of Solids, 2019, 134, 225-237.	1.9	8
42446	Which Transition Metal Atoms Can Be Embedded into Two-Dimensional Molybdenum Dichalcogenides and Add Magnetism?. Nano Letters, 2019, 19, 4581-4587.	4.5	61
42447	Highly active enzymeâ€“metal nanohybrids synthesized in proteinâ€“polymer conjugates. Nature Catalysis, 2019, 2, 718-725.	16.1	115
42448	Low-temperature selective oxidation of methane over distant binuclear cationic centers in zeolites. Communications Chemistry, 2019, 2, .	2.0	31
42449	Elastic anisotropy and single-crystal moduli of solid argon up to 64ÂGPa from time-domain Brillouin scattering. Physical Review B, 2019, 99, .	1.1	10
42450	A class of two-dimensional SiAs monolayers with novel electronic and optical properties from ab initio investigations. European Physical Journal Plus, 2019, 134, 1.	1.2	8
42451	Site Occupation of Nb in Î³-TiAl: Beyond the Point Defect Gas Approximation. Acta Metallurgica Sinica (English Letters), 2019, 32, 1511-1520.	1.5	5
42452	Defect induced magnetism in monolayer HfSe2: An ab initio study. Applied Surface Science, 2019, 491, 517-525.	3.1	7

#	Article	IF	Citations
42453	Transition metal-doped janus monolayer SMoSe with excellent thermal spin filter and spin Seebeck effect. Applied Surface Science, 2019, 491, 750-756.	3.1	17
42454	In-situ coalesced vacancies on MoSe2 mimicking noble metal: Unprecedented Tafel reaction in hydrogen evolution. Nano Energy, 2019, 63, 103846.	8.2	41
42455	The N-type Pb-doped single crystal SnSe thermoelectric material synthesized by a Sn-flux method. Physica B: Condensed Matter, 2019, 570, 128-132.	1.3	13
42456	Theoretical Investigation of Metal-Shrouded Tl₂O Monolayers: Pudding-Mold-Type Band Structure and Thermoelectric Performance. ACS Applied Nano Materials, 2019, 2, 4061-4066.	2.4	26
42457	A comparative first-principles study of orthorhombic and full-Heusler phases in Ti₂AlNb intermetallic. Materials Research Express, 2019, 6, 096510.	0.8	6
42458	Itinerant ferromagnetism in <mml:math xmlns:mml="http://www.w3.org/1998/Math/MathML"><mml:mi>p</mml:mi></mml:math> -doped monolayers of <mml:math xmlns:mml="http://www.w3.org/1998/Math/MathML"><mml:msub><mml:mi>MoS</mml:mi><mml:mn>2</mml:mn></mml:msub></mml:math> Physical Review B, 2019, 99, .	1.1	16
42459	Linear Dichroism Conversion in Quasiâ€1D Perovskite Chalcogenide. Advanced Materials, 2019, 31, e1902118.	11.1	41
42460	Theoretical Screening of Single Transition Metal Atoms Embedded in MXene Defects as Superior Electrocatalyst of Nitrogen Reduction Reaction. Small Methods, 2019, 3, 1900337.	4.6	213
42461	Molecular modeling and computational study of the chiral-dependent structures and properties of self-assembling diphenylalanine peptide nanotubes. Journal of Molecular Modeling, 2019, 25, 199.	0.8	27
42462	Geometric and Optical Properties of Cluster Model of Yb-doped Silica Optical Fiber. Journal of Cluster Science, 2019, 30, 1205-1210.	1.7	7
42463	Density functional theory calculation on two-dimensional MoS2/BiOX (Xâ€¯=â€¯Cl, Br, I) van der Waals heterostructures for photocatalytic action. Applied Surface Science, 2019, 492, 157-165.	3.1	65
42464	Corrosion mechanism of annealed equiatomic AlCoCrFeNi tri-phase high-entropy alloy in 0.5 M H2SO4 aerated aqueous solution. Corrosion Science, 2019, 157, 462-471.	3.0	89
42465	Crystal orientation-dependent activity of tungsten-based catalysts for selective catalytic reduction of NO with NH3. Journal of Catalysis, 2019, 375, 294-303.	3.1	16
42466	Experimental and theoretical study on static recrystallization of a low-density ferritic steel containing 4 mass% aluminum. Materials and Design, 2019, 180, 107924.	3.3	18
42467	Strain effects on magnetic states of monolayer MoS2 doped with group IIIA to VA atoms. Physica E: Low-Dimensional Systems and Nanostructures, 2019, 114, 113609.	1.3	8
42468	High Pressure Investigation of the Sâ€“N₂ System up to the Megabar Range: Synthesis and Characterization of the SN₂ Solid. Inorganic Chemistry, 2019, 58, 9195-9204.	1.9	17
42469	Phthalocyanine and Metal Phthalocyanines Adsorbed on Graphene: A Density Functional Study. Journal of Physical Chemistry C, 2019, 123, 16614-16620.	1.5	33
42470	Influence of the N,N,N-Trimethyl-1-adamantyl Ammonium Structure-Directing Agent on Al Substitution in SSZ-13 Zeolite. Journal of Physical Chemistry C, 2019, 123, 17454-17458.	1.5	20

#	Article	IF	Citations
42471	Manganese Doping of MoSe₂ Promotes Active Defect Sites for Hydrogen Evolution. ACS Applied Materials & Interfaces, 2019, 11, 25155-25162.	4.0	70
42472	Turning a Methanation Co Catalyst into an Inâ€“Co Methanol Producer. ACS Catalysis, 2019, 9, 6910-6918.	5.5	88
42473	Effective Promotion of Oxygen Reduction Reaction by in Situ Formation of Nanostructured Catalyst. ACS Catalysis, 2019, 9, 7137-7142.	5.5	42
42474	Activity and Selectivity Trends in Electrocatalytic Nitrate Reduction on Transition Metals. ACS Catalysis, 2019, 9, 7052-7064.	5.5	369
42475	Chemical Vapor Deposition Grown Large-Scale Atomically Thin Platinum Diselenide with Semimetalâ€“Semiconductor Transition. ACS Nano, 2019, 13, 8442-8451.	7.3	87
42476	Conformation-Driven Self-Assembly: From a 1D Metalâ€“Organic Polymer to an Infinite Double Nanotube. ACS Omega, 2019, 4, 10755-10760.	1.6	0
42477	Self-compensation in chlorine-doped CdTe. Scientific Reports, 2019, 9, 9194.	1.6	13
42478	Electronic band dispersion determination in azimuthally disordered transition-metal dichalcogenide monolayers. Communications Physics, 2019, 2, .	2.0	11
42479	Tunable valley splitting and an anomalous valley Hall effect in hole-doped WS₂ by proximity coupling with a ferromagnetic MnO₂ monolayer. Nanoscale, 2019, 11, 13567-13575.	2.8	51
42480	Effect of Stoneâ€“Wales defects and transition-metal dopants on arsenene: a DFT study. RSC Advances, 2019, 9, 19048-19056.	1.7	23
42481	Self-supported multidimensional Niâ€“Fe phosphide networks with holey nanosheets for high-performance all-solid-state supercapacitors. Journal of Materials Chemistry A, 2019, 7, 17386-17399.	5.2	72
42482	Effect of toxic ligands on O2 binding to heme and their toxicity mechanism. Physical Chemistry Chemical Physics, 2019, 21, 14957-14963.	1.3	2
42483	Novel structures of two-dimensional tungsten boride and their superconductivity. Physical Chemistry Chemical Physics, 2019, 21, 15327-15338.	1.3	23
42484	Importance of zero-point energy for crystalline ice phases: A comparison of force fields and density functional theory. Journal of Chemical Physics, 2019, 150, 234504.	1.2	7
42485	Investigation of atomic and electronic properties of 2D-MoS₂/3D-GaN mixed-dimensional heterostructures. Nanotechnology, 2019, 30, 404002.	1.3	12
42486	Electrical and optical properties of Zr doped Î²-Ga₂O₃ single crystals. Applied Physics Express, 2019, 12, 085502.	1.1	38
42487	Stable Dynamics Performance and High Efficiency of ABX₃â€Type Superâ€Alkali Perovskites First Obtained by Introducing H₅O₂ Cation. Advanced Energy Materials, 2019, 9, 1900664.	10.2	113
42488	Unlocking Fewâ€Layered Ternary Chalcogenides for Highâ€Performance Potassiumâ€Ion Storage. Advanced Energy Materials, 2019, 9, 1901560.	10.2	53

#	Article	IF	Citations
42489	Interface Engineering via Sputtered Oxygenated CdS:O Window Layer for Highly Efficient Sb₂Se₃ Thinâ€Film Solar Cells with Efficiency Above 7%. Solar Rrl, 2019, 3, 1900225.	3.1	42
42490	DFT Study of Pyrolysis Gasoline Hydrogenation on Pd(100), Pd(110) and Pd(111) Surfaces. Catalysis Letters, 2019, 149, 2226-2233.	1.4	3
42491	Carboneyane: A nodal line topological carbon with spâ^'sp2Ââ^'sp3 chemical bonds. Carbon, 2019, 152, 909-914.	5.4	13
42492	Structural, elastic, and quasiparticle bandstructure of 4,4â€²-Bis(nitramino)azofurazan from first principles theory. Computational Materials Science, 2019, 169, 109081.	1.4	5
42493	Importance of heteroatom doping site in tuning the electronic structure and magnetic properties of graphdiyne. Physica E: Low-Dimensional Systems and Nanostructures, 2019, 114, 113590.	1.3	17
42494	High-Energy Gain Upconversion in Monolayer Tungsten Disulfide Photodetectors. Nano Letters, 2019, 19, 5595-5603.	4.5	41
42495	Insight into the Intrinsic Active Site for Selective Production of Light Olefins in Cobalt-Catalyzed Fischerâ€“Tropsch Synthesis. ACS Catalysis, 2019, 9, 7073-7089.	5.5	60
42496	Low-Temperature Solid-State Ion-Exchange Method for Preparing Cu-SSZ-13 Selective Catalytic Reduction Catalyst. ACS Catalysis, 2019, 9, 6962-6973.	5.5	37
42497	Interlayer epitaxy of wafer-scale high-quality uniform AB-stacked bilayer graphene films on liquid Pt3Si/solid Pt. Nature Communications, 2019, 10, 2809.	5.8	43
42498	Role of hole confinement in the recombination properties of InGaN quantum structures. Scientific Reports, 2019, 9, 9047.	1.6	6
42499	Predicted superhard phases of Zrâ€“B compounds under pressure. Physical Chemistry Chemical Physics, 2019, 21, 15609-15614.	1.3	10
42500	Simultaneous enzyme mimicking and chemical reduction mechanisms for nanoceria as a bio-antioxidant: a catalytic model bridging computations and experiments for nanozymes. Nanoscale, 2019, 11, 13289-13299.	2.8	100
42501	Shock compression of niobium from first-principles. Journal of Applied Physics, 2019, 125, .	1.1	11
42502	Temperature dependent transport spin-polarization in the low Curie temperature complex itinerant ferromagnet EuTi_{1â^'x}Nb_xO₃. Journal of Physics Condensed Matter, 2019, 31, 415601.	0.7	5
42503	Modulating the Electrical Transport in the Two-Dimensional Electron Gas at <mml:math xmlns:mml="http://www.w3.org/1998/Math/MathML" display="inline"><mml:mrow><mml:msub><mml:mrow><mml:mi>LaAlO</mml:mi></mml:mrow><mml:mrow><mml:mn>3</mml:mn></mml:mrow><mml:mrow><mml:mi>x</mml:mi></mml:mrow></mml:msub></mml:mrow></mml:math>/<mml:math xmlns:mml="http://www.w3.org/1998/Math/MathML" display="inline"><mml:mrow><mml:msub><mml:mrow><mml:mi>SrTiO</mml:mi></mml:mrow><mml:mrow><mml:mn>3</mml:mn></mml:mrow></mml:msub></mml:mrow></mml:math> Heterostructures by Interfacial Flexoelectricity. Physical Review Letters, 2019, 122, 257601.	2.9	72
42504	Theoretical investigation of the structural and electronic properties of Al-decorated TiO2/perovskite interfaces. Applied Surface Science, 2019, 492, 369-373.	3.1	4
42505	Improving the Performance of Taoâ€“Mo Non-empirical Density Functional with Broader Applicability in Quantum Chemistry and Materials Science. Journal of Physical Chemistry A, 2019, 123, 6356-6369.	1.1	29
42506	Toward Heterolytic Bond Dissociation of Dihydrogen: The Study of Hydrogen in Arsenolite under High Pressure. Journal of Physical Chemistry C, 2019, 123, 16868-16872.	1.5	6

#	Article	IF	Citations
42507	Synthesis of Regioisomeric Graphene Nanoribbon Junctions via Heteroprecursors. Journal of Physical Chemistry C, 2019, 123, 17632-17638.	1.5	8
42508	Ab Initio Investigation of Migration Mechanisms in La Apatites. ACS Applied Energy Materials, 2019, 2, 4708-4717.	2.5	5
42509	Novel Ordered Rocksalt-Type Lithium-Rich Li₂Ru_{1â€“x}Ni_xO_{3â^'Î´} (0.3 â‰¤ x â‰¤ 0.5) Cathode Material with Tunable Anionic Redox Potential. ACS Applied Energy Materials, 2019, 2, 5933-5944.	2.5	22
42510	Synergistically Improved Electronic and Thermal Transport Properties in Nb-Doped Nb_yMo_{1â€“y}Se_{2â€“2x}Te_{2x} Solid Solutions Due to Alloy Phonon Scattering and Increased Valley Degeneracy. ACS Applied Materials & Interfaces, 2019, 11, 26069-26081.	4.0	9
42511	Highly Active Pt₃Sn{110}-Excavated Nanocube Cocatalysts for Photocatalytic Hydrogen Production. ACS Applied Materials & Interfaces, 2019, 11, 25844-25853.	4.0	28
42512	Complex electronic structure and compositing effect in high performance thermoelectric BiCuSeO. Nature Communications, 2019, 10, 2814.	5.8	81
42513	Penta- and hexa-coordinated beryllium and phosphorus in high-pressure modifications of CaBe2P2O8. Nature Communications, 2019, 10, 2800.	5.8	20
42514	Topological phase transition induced by p_{x,y} and p_z band inversion in a honeycomb lattice. Nanoscale, 2019, 11, 13807-13814.	2.8	9
42515	Effects of out-of-plane strains and electric fields on the electronic structures of graphene/MTe (M =) Tj ETQq0 0 0 rgBT /Overlock 10 Tf 5	2.8	34
42516	Cu supported on polymeric carbon nitride for selective CO₂ reduction into CH₄: a combined kinetics and thermodynamics investigation. Journal of Materials Chemistry A, 2019, 7, 17014-17021.	5.2	90
42517	Temperature-dependent properties of magnetic CuFeS2 from first-principles calculations: Structure, mechanics, and thermodynamics. AIP Advances, 2019, 9, 065021.	0.6	11
42518	Comprehensive calculations and prominent thermoelectric properties of Li3P and Li3As. Physics Letters, Section A: General, Atomic and Solid State Physics, 2019, 383, 2802-2808.	0.9	3
42519	High-temperature â€œion baseballâ€•for enhancing concentrated solar power efficiency. Solar Energy Materials and Solar Cells, 2019, 200, 109974.	3.0	5
42520	Effects of vacancy defects on the electronic structure and optical properties of GaN:Fe. Superlattices and Microstructures, 2019, 133, 106152.	1.4	7
42521	Water-Mediated Reduction of Aqueous N-Nitrosodimethylamine with Pd. Environmental Science & Technology, 2019, 53, 7551-7563.	4.6	11
42522	General Atomic Neighborhood Fingerprint for Machine Learning-Based Methods. Journal of Physical Chemistry C, 2019, 123, 15859-15866.	1.5	33
42523	Control of the Reaction Mechanism of Alkylaromatics Transalkylation by Means of Molecular Confinement Effects Associated to Zeolite Channel Architecture. ACS Catalysis, 2019, 9, 5935-5946.	5.5	29
42524	Hierarchical Nanoassembly of MoS₂/Co₉S₈/Ni₃S₂/Ni as a Highly Efficient Electrocatalyst for Overall Water Splitting in a Wide pH Range. Journal of the American Chemical Society, 2019, 141, 10417-10430.	6.6	653

#	Article	IF	Citations
42525	Chemical doping of the SnSe monolayer: a first-principle calculation. Physical Chemistry Chemical Physics, 2019, 21, 14629-14637.	1.3	9
42526	Ferroelastic lattice rotation and band-gap engineering in quasi 2D layered-structure PdSe₂under uniaxial stress. Nanoscale, 2019, 11, 12317-12325.	2.8	32
42527	Catalytic properties of Al₁₃TM₄complex intermetallics: influence of the transition metal and the surface orientation on butadiene hydrogenation. Science and Technology of Advanced Materials, 2019, 20, 557-567.	2.8	25
42528	Moisture effect on the diffusion of Cu ions in Cu/Ta₂O₅/Pt and Cu/SiO₂/Pt resistance switches: a first-principles study. Science and Technology of Advanced Materials, 2019, 20, 580-588.	2.8	10
42529	Improving the Activity for Oxygen Evolution Reaction by Tailoring Oxygen Defects in Double Perovskite Oxides. Advanced Functional Materials, 2019, 29, 1901783.	7.8	152
42530	Defectâ€Rich Nitrogen Doped Co₃O₄/C Porous Nanocubes Enable Highâ€Efficiency Bifunctional Oxygen Electrocatalysis. Advanced Functional Materials, 2019, 29, 1902875.	7.8	233
42531	Coupled Biphase (1Tâ€2H)â€MoSe₂ on Mold Spore Carbon for Advanced Hydrogen Evolution Reaction. Small, 2019, 15, e1901796.	5.2	87
42532	First-principles explorations of Li2S@V2CT hybrid structure as cathode material for lithiumâ€'sulfur battery. Applied Surface Science, 2019, 489, 677-683.	3.1	39
42533	Transition metal embedded C2N with efficient polysulfide immobilization and catalytic oxidation for advanced lithium-sulfur batteries: A first principles study. Ceramics International, 2019, 45, 17996-18002.	2.3	58
42534	Theoretical prediction of germanium selenium nanosheet as a potential anode material for high-performance alkali-metal based battery. Journal of Solid State Chemistry, 2019, 277, 17-24.	1.4	7
42535	Structural and Electronic Properties of Frenkel and Schottky Defects at the MgO{100} Surface: Spin Polarization, Mid-Band Gap States, and Charge Trapping at Vacancy Sites. Journal of Physical Chemistry C, 2019, 123, 14408-14420.	1.5	10
42536	Role of Dissolution Intermediates in Promoting Oxygen Evolution Reaction at RuO₂(110) Surface. Journal of Physical Chemistry C, 2019, 123, 22151-22157.	1.5	86
42537	Hydrogen Chemisorption on Pd-Doped Copper Clusters. Journal of Physical Chemistry C, 2019, 123, 15834-15840.	1.5	18
42538	Tuning the Catalytic Property of Phosphorene for Oxygen Evolution and Reduction Reactions by Changing Oxidation Degree. Journal of Physical Chemistry Letters, 2019, 10, 3440-3446.	2.1	43
42539	Synergistic Effect of Bismuth and Indium Codoping for High Thermoelectric Performance of Melt Spinning SnTe Alloys. ACS Applied Materials & Interfaces, 2019, 11, 23337-23345.	4.0	30
42540	Modulation of electronic and optical properties by surface vacancies in low-dimensional Î²-Ga2O3. Physical Chemistry Chemical Physics, 2019, 21, 14745-14752.	1.3	13
42541	Synergistic effect of Zr-MOF on phosphomolybdic acid promotes efficient oxidative desulfurization. Applied Catalysis B: Environmental, 2019, 256, 117804.	10.8	131
42542	Se-modified polymeric carbon nitride nanosheets with improved photocatalytic activities. Journal of Catalysis, 2019, 375, 104-112.	3.1	44

#	Article	IF	Citations
42543	Ultralow thermal conductivity of BaAg2SnSe4 and the effect of doping by Ga and In. Materials Today Physics, 2019, 9, 100098.	2.9	17
42544	First-principles investigations of a new trigonal boron nitride. Physica E: Low-Dimensional Systems and Nanostructures, 2019, 114, 113573.	1.3	3
42545	High-throughput prediction of the ground-state collinear magnetic order of inorganic materials using Density Functional Theory. Npj Computational Materials, 2019, 5, .	3.5	69
42546	Two-dimensional ZnO for the selective photoreduction of CO₂. Journal of Materials Chemistry A, 2019, 7, 16294-16303.	5.2	62
42547	Point defects in group III nitrides: A comparative first-principles study. Journal of Applied Physics, 2019, 125, .	1.1	41
42548	Plasmonic control of solar-driven CO2 conversion at the metal/ZnO interfaces. Applied Catalysis B: Environmental, 2019, 256, 117823.	10.8	95
42549	Thermodynamic stability of nitrogen functionalities and defects in graphene and graphene nanoribbons from first principles. Carbon, 2019, 152, 715-726.	5.4	22
42550	Insights into the role of graphene in hybrid photocatalytic system by in-situ shell-isolated nanoparticle-enhanced Raman spectroscopy. Carbon, 2019, 152, 305-315.	5.4	4
42551	A spatial/temporal dual-mode optical thermometry platform based on synergetic luminescence of Ti4+-Eu3+ embedded flexible 3D micro-rod arrays: High-sensitive temperature sensing and multi-dimensional high-level secure anti-counterfeiting. Chemical Engineering Journal, 2019, 374, 992-1004.	6.6	142
42552	Structural and electronic anisotropy, negative Poissonâ€™s ratio, strain-sensitive Dirac-like cone in monolayer Î±-CSe: Tailoring electronic properties. Computational Materials Science, 2019, 168, 87-95.	1.4	12
42553	DFT investigation of Ca mobility in reduced-perovskite and oxidized-marokite oxides. Energy Storage Materials, 2019, 21, 354-360.	9.5	21
42554	Ab initio aided strain gradient elasticity theory in prediction of nanocomponent fracture. Mechanics of Materials, 2019, 136, 103074.	1.7	9
42555	Preparation of Size- and Composition-Controlled Pt_nSn_x/SiO₂ (n = 4, 7, 24) Bimetallic Model Catalysts with Atomic Layer Deposition. Journal of Physical Chemistry C, 2019, 123, 16194-16209.	1.5	25
42556	Bilayer tellureneâ€“metal interfaces. Journal of Semiconductors, 2019, 40, 062003.	2.0	9
42557	Electronic band structures and optical properties of atomically thin AuSe: first-principle calculations. Journal of Semiconductors, 2019, 40, 062004.	2.0	7
42558	Inorganic and Organic Functionalisation of Silicon Studied by Density Functional Theory. , 2019, , 153-166.		0
42559	Electronic structure and adsorption geometry of Pt and Pd metal complexes with 1,3-dithiole-2-thione-4,5-dithiolate ligand on TiO2(101) surface from first-principles calculations. Theoretical Chemistry Accounts, 2019, 138, 1.	0.5	2
42560	Atomic and electronic structures of graphene-decorated graphitic carbon nitride (g-C3N4) as a metal-free photocatalyst under visible-light. Applied Catalysis B: Environmental, 2019, 256, 117850.	10.8	19

#	Article	IF	Citations
42561	Tailoring the electronic properties of graphyne/blue phosphorene heterostructure via external electric field and vertical strain. Chemical Physics Letters, 2019, 730, 277-282.	1.2	12
42562	Boosting exciton dissociation and molecular oxygen activation by in-plane grafting nitrogen-doped carbon nanosheets to graphitic carbon nitride for enhanced photocatalytic performance. Journal of Colloid and Interface Science, 2019, 553, 59-70.	5.0	26
42563	Specific Reaction Parameter Density Functional Based on the Meta-Generalized Gradient Approximation: Application to H₂ + Cu(111) and H₂ + Ag(111). Journal of Physical Chemistry A, 2019, 123, 5395-5406.	1.1	28
42564	Effects of Defect, Doping, Geometrical Configuration, and Size on Plasmon Excitations for Three Silicon Nanostructures. Journal of Physical Chemistry C, 2019, 123, 15707-15716.	1.5	3
42565	Effect of Hydration on Promoting Oxidative Reactions with Aluminum Oxide and Oxyhydroxide Nanoparticles. Journal of Physical Chemistry C, 2019, 123, 15017-15026.	1.5	8
42566	Achieving a High Thermoelectric Performance of Tetrahedrites by Adjusting the Electronic Density of States and Enhancing Phonon Scattering. ACS Applied Materials & Interfaces, 2019, 11, 23361-23371.	4.0	16
42567	Role of Acetaldehyde in the Roadmap from Initial Carbonâ€“Carbon Bonds to Hydrocarbons during Methanol Conversion. ACS Catalysis, 2019, 9, 6491-6501.	5.5	60
42568	Pt-like hydrogen evolution on a V₂O₅/Ni(OH)₂ electrocatalyst. Journal of Materials Chemistry A, 2019, 7, 15794-15800.	5.2	31
42569	Interface dipoles of Ir(ppy)₃on Cu(111). Nanoscale, 2019, 11, 12695-12703.	2.8	3
42570	Monolayer triphosphates MP₃ (M = Sn, Ge) with excellent basal catalytic activity for hydrogen evolution reaction. Nanoscale, 2019, 11, 12210-12219.	2.8	76
42571	Prediction of low energy phase transition in metal doped MoTe2 from first principle calculations. Journal of Applied Physics, 2019, 125, .	1.1	5
42572	Heavily phosphorus doped germanium: Strong interaction of phosphorus with vacancies and impact of tin alloying on doping activation. Journal of Applied Physics, 2019, 125, .	1.1	6
42573	Magnetism and magneto-optical effects in bulk and few-layer CrI₃: a theoretical GGAÂ+ÂU study. New Journal of Physics, 2019, 21, 053012.	1.2	62
42574	Lateral Spin Valve Based on the Two Dimensional <mml:math xmlns:mml="http://www.w3.org/1998/Math/MathML" display="inline" overflow="scroll"><mml:mrow><mml:mi>Cr</mml:mi><mml:mi mathvariant="normal">N</mml:mi></mml:mrow></mml:math> / <mml:math xmlns:mml="http://www.w3.org/1998/Math/MathML" display="inline"	1.5	37
42575	Structure and one-dimensional metallicity of rare-earth silicide nanowires on Si(001). Physical Review B, 2019, 99, .	1.1	9
42576	Evidence for bulk nodal loops and universality of Dirac-node arc surface states in <mml:math xmlns:mml="http://www.w3.org/1998/Math/MathML"><mml:mrow><mml:mi>ZrGe</mml:mi><mml:msub><mml:mi>X</mml:mi> (<mml:math) Tj ETQq1 1 0.784314 rgBT /Overlock 10 Tf 50 137 Td (xmlns:mml="http://www.w3.org/1998/Math/MathML"><mml:mr	1.1	17
42577	Quasiparticle electronic structure and optical spectra of single-layer and bilayer <mml:math xmlns:mml="http://www.w3.org/1998/Math/MathML"><mml:msub><mml:mi>PdSe</mml:mi><mml:mn>2</mml:mn></mml:msub></mml : Proximity and defect-induced band gap renormalization. Physical Review B, 2019, 99, .	1.1	49
42578	Large Enhancement of Thermoelectric Efficiency Due to a Pressure-Induced Lifshitz Transition in SnSe. Physical Review Letters, 2019, 122, 226601.	2.9	46

#	Article	IF	Citations
42579	Half-Metallic Property Induced by Double Exchange Interaction in the Double Perovskite Bi2BBâ€²O6 (B, Bâ€²) Tj ETQq0 0 0 rgBT /Overl	1.3	17
42580	Mixed Two-Dimensional Organic-Inorganic Halide Perovskites for Highly Efficient and Stable Photovoltaic Application. Molecules, 2019, 24, 2144.	1.7	2
42581	Enhancing Interconnect Reliability and Performance by Converting Tantalum to 2D Layered Tantalum Sulfide at Low Temperature. Advanced Materials, 2019, 31, e1902397.	11.1	35
42582	The Influence of Size and Shape of Pd Nanoparticles on the Performances of Pd/Beta Catalysts for nâ€Heptane Hydroisomerization. ChemCatChem, 2019, 11, 3542-3551.	1.8	13
42583	Origin of electronic structure dependent activity of spinel ZnNixCo2-xO4 oxides for complete methane oxidation. Applied Catalysis B: Environmental, 2019, 256, 117844.	10.8	35
42584	Chromium phosphide CrP as highly active and stable electrocatalysts for oxygen electroreduction in alkaline media. Applied Catalysis B: Environmental, 2019, 256, 117846.	10.8	20
42585	Characteristics of atomic layer depositionâ€“grown zinc oxide thin film with and without aluminum. Applied Surface Science, 2019, 491, 535-543.	3.1	4
42586	High brightness and precise adjustment of multicolor-tunable luminescence of Lu2GeO5:Tb3+, Eu3+ phosphors for white LEDs. Current Applied Physics, 2019, 19, 1052-1061.	1.1	13
42587	Computational study of metal/ceramic interfacial adhesion and barriers to shear displacement. Computational Materials Science, 2019, 168, 104-115.	1.4	12
42588	New stable structures of HeN3 predicted using first-principles calculations. Journal of Alloys and Compounds, 2019, 800, 505-511.	2.8	6
42589	First-principles prediction of magnetically ordered half-metals above room temperature. Journal of Materiomics, 2019, 5, 404-412.	2.8	13
42590	Theoretical studies on the switching mechanism of VMCO memories. Microelectronic Engineering, 2019, 215, 110997.	1.1	1
42591	Prediction of directional magnetic-exchange coupling in Mn doped Î³-InSe monolayer. Results in Physics, 2019, 14, 102416.	2.0	3
42592	KBaTeBiO₆: A Lead-Free, Inorganic Double-Perovskite Semiconductor for Photovoltaic Applications. Chemistry of Materials, 2019, 31, 4769-4778.	3.2	46
42593	Giant Stokes Shifts in AgInS₂ Nanocrystals with Trapped Charge Carriers. Journal of Physical Chemistry C, 2019, 123, 16430-16438.	1.5	29
42594	Quinone-Facilitated Coordinated Bipyrene and Polypyrene on Au(111) by Capture of Gold Adatoms. Journal of Physical Chemistry C, 2019, 123, 16281-16287.	1.5	8
42595	Transition-Metal Diboride: A New Family of Two-Dimensional Materials Designed for Selective CO₂ Electroreduction. Journal of Physical Chemistry C, 2019, 123, 16294-16299.	1.5	43
42596	Effects of Î³-Al2O3 Support on the Morphology and Electronic Structure of Pt Nanoparticles. Journal of Physical Chemistry C, 2019, 123, 16893-16901.	1.5	7

#	Article	IF	Citations
42597	Two-Dimensional Ferroelectric Tunnel Junction: The Case of Monolayer In:SnSe/SnSe/Sb:SnSe Homostructure. ACS Applied Electronic Materials, 2019, 1, 1133-1140.	2.0	69
42598	Reactivity of Bioinspired Magnesiumâ€“Organic Networks under CO₂ and O₂ Exposure. ACS Omega, 2019, 4, 9850-9859.	1.6	6
42599	Cross-dimensional electron-phonon coupling in van der Waals heterostructures. Nature Communications, 2019, 10, 2419.	5.8	60
42600	Stepwise on-surface dissymmetric reaction to construct binodal organometallic network. Nature Communications, 2019, 10, 2545.	5.8	26
42601	Unconventional topological phase transition in non-symmorphic material KHgX (Xâ€‰=â€‰As, Sb, Bi). Npj Computational Materials, 2019, 5, .	3.5	9
42602	First-principles study of the complex magnetism in Fe16N2. Scientific Reports, 2019, 9, 8381.	1.6	7
42603	Highâ€Performance Hydrogen Evolution by Ru Single Atoms and Nitridedâ€Ru Nanoparticles Implanted on Nâ€Doped Graphitic Sheet. Advanced Energy Materials, 2019, 9, 1900931.	10.2	224
42604	Exploring the catalytic activity of MXenes Mn+1CnO2 for hydrogen evolution. Journal of Materials Science, 2019, 54, 11378-11389.	1.7	14
42605	Noble metal dopants modified two-dimensional zinc oxide: Electronic structures and magnetic properties. Journal of Alloys and Compounds, 2019, 798, 149-157.	2.8	15
42606	The role of strong electron correlations in determination of band structure and charge distribution of transition metal dihalide monolayers. Journal of Physics and Chemistry of Solids, 2019, 134, 324-332.	1.9	23
42607	Controlling siloxene oxidization to tailor SiOx anodes for high performance lithium ion batteries. Journal of Power Sources, 2019, 432, 65-72.	4.0	32
42608	Atomic and electron analyzing of irradiation damage in Si/SiO2 interfaces caused by irradiation: First-principle calculation. Nuclear Instruments & Methods in Physics Research B, 2019, 451, 89-92.	0.6	1
42609	Tuning the electronic and magnetic properties of 2D g-GaN by H adsorption: An ab-initio study. Physica B: Condensed Matter, 2019, 569, 57-61.	1.3	17
42610	Crossover from 2D metal to 3D Dirac semimetal in metallic PtTe2 films with local Rashba effect. Science Bulletin, 2019, 64, 1044-1048.	4.3	44
42611	All Precursors Are Not Equal: Morphology Control via Distinct Precursorâ€“Facet Interactions in Eu³⁺-Doped NaLa(WO₄)₂. Crystal Growth and Design, 2019, 19, 3945-3954.	1.4	9
42612	Hybrid-Functional Study of Native Defects and W/Mo-Doped in Monoclinic-Bismuth Vanadate. Journal of Physical Chemistry C, 2019, 123, 14508-14516.	1.5	9
42613	A New Class of Bifunctional Perovskites BaMX₄ (M = Co, Ni, Fe, Mn; X = F, Cl, Br, I): An n-Type Semiconductor with Combined Multiferroic and Photovoltaic Properties. Journal of Physical Chemistry C, 2019, 123, 14303-14311.	1.5	1
42614	Effect of Hydrogen-Induced Metallization on Chemisorption. Journal of Physical Chemistry C, 2019, 123, 15171-15175.	1.5	3

#	Article	IF	Citations
42615	Construction of Oxygen-Deficient La(OH)₃ Nanorods Wrapped by Reduced Graphene Oxide for Polysulfide Trapping toward High-Performance Lithium/Sulfur Batteries. ACS Applied Materials & Interfaces, 2019, 11, 23271-23279.	4.0	71
42616	Infinitesimal sulfur fusion yields quasi-metallic bulk silicon for stable and fast energy storage. Nature Communications, 2019, 10, 2351.	5.8	57
42617	Stable zigzag and tripodal all-nitrogen anion N44â¯ in BeN2. AIP Advances, 2019, 9, 055116.	0.6	8
42618	Hematene: a 2D magnetic material in van der Waals or non-van der Waals heterostructures. 2D Materials, 2019, 6, 045002.	2.0	24
42619	Ab initio playing of pentagonal puzzles. Electronic Structure, 2019, 1, 015004.	1.0	7
42620	Sampling-dependent systematic errors in effective harmonic models. Physical Review B, 2019, 99, .	1.1	6
42621	Electronic structure of La2/3Sr1/3MnO3 : Interplay of oxygen octahedra rotations and epitaxial strain. Physical Review B, 2019, 99, .	1.1	5
42622	Fermi-level Dirac crossings in <mml:math xmlns:mml="http://www.w3.org/1998/Math/MathML"><mml:mrow><mml:mn>4</mml:mn><mml:mi>d</mml:mi></mml:mrow></mml:math> and <mml:math xmlns:mml="http://www.w3.org/1998/Math/MathML"><mml:mrow><mml:mn>5</mml:mn><mml:mi>d</mml:mi></mml:mrow></mml:math> cubic metal oxides: <mml:math xmlns:mml="http://www.w3.org/1998/Math/MathML"><mml:mrow><mml:msub><mml:mi>NaPd</mml:mi><mml:mn>3</mml:mn></mml:mrow></mml:math>	1.1	7
42623	Highly Polarized Photoelectrical Response in vdW ZrS₃ Nanoribbons. Advanced Electronic Materials, 2019, 5, 1900419.	2.6	45
42624	N-doped peanut-shaped carbon nanotubes for efficient CO2 electrocatalytic reduction. Carbon, 2019, 152, 241-246.	5.4	29
42625	First principles study on hydrogen storage in yttrium doped graphyne: Role of acetylene linkage in enhancing hydrogen storage. International Journal of Hydrogen Energy, 2019, 44, 16735-16744.	3.8	72
42626	Sn4+ doping combined with hydrogen treatment for CdS/TiO2 photoelectrodes: An efficient strategy to improve quantum dots loading and charge transport for high photoelectrochemical performance. Journal of Power Sources, 2019, 430, 80-89.	4.0	37
42627	Visualization of facet-dependent pseudo-photocatalytic behavior of TiO2 nanorods for water splitting using In situ liquid cell TEM. Nano Energy, 2019, 62, 507-512.	8.2	44
42628	Benchmarking the accuracy of coverage-dependent models: adsorption and desorption of benzene on Pt (1â€¯1â€¯1) and Pt3Sn (1â€¯1â€¯1) from first principles. Progress in Surface Science, 2019, 94, 100538.	3.8	10
42629	Polarâ€“Nonpolar Phase Transition Accompanied by Negative Thermal Expansion in Perovskite-Type Bi_{1â€“x}Pb_xNiO₃. Chemistry of Materials, 2019, 31, 4748-4758.	3.2	21
42630	Electrochemical Stability Window of Polymeric Electrolytes. Chemistry of Materials, 2019, 31, 4598-4604.	3.2	83
42631	Single Ru Sites-Embedded Rutile TiO2 Catalyst for Non-Oxidative Direct Conversion of Methane: A First-Principles Study. Journal of Physical Chemistry C, 2019, 123, 14391-14397.	1.5	13
42632	Insights into Hydrogen Transport Behavior on Perovskite Surfaces: Transition from the Grotthuss Mechanism to the Vehicle Mechanism. Langmuir, 2019, 35, 9962-9969.	1.6	29

#	Article	IF	Citations
42633	Effect of Zeolite Topology and Reactor Configuration on the Direct Conversion of CO₂ to Light Olefins and Aromatics. ACS Catalysis, 2019, 9, 6320-6334.	5.5	144
42634	Stable and hard hafnium borides: A first-principles study. Journal of Applied Physics, 2019, 125, .	1.1	13
42635	First-principles calculation study of Mg₂XH₆ (X=Fe, Ru) on thermoelectric properties. Materials Research Express, 2019, 6, 085536.	0.8	4
42636	Correlation of Interface Structure with Magnetic Exchange in a Hard/Soft Magnetic Model Nanostructure. Physical Review Applied, 2019, 11, .	1.5	9
42637	Is Hydrogen Diffusion along Grain Boundaries Fast or Slow? Atomistic Origin and Mechanistic Modeling. Physical Review Letters, 2019, 122, 215501.	2.9	31
42638	Adsorption of phosgene on Si-embedded MoS2 sheet and electric field-assisted desorption: insights from DFT calculations. Journal of Materials Science, 2019, 54, 11497-11508.	1.7	14
42639	Structural, Electronic and Optical Characterization of ZnO Thin Film-Seeded Platforms for ZnO Nanostructures: Solâ€“Gel Method Versus Ab Initio Calculations. Journal of Electronic Materials, 2019, 48, 5028-5038.	1.0	48
42640	DFT study of Ni segregation at the B2-NiTi(110)/rutile-TiO2(110) interface. Applied Surface Science, 2019, 489, 287-296.	3.1	6
42641	Effect of Gd3+ doping on structural, optical and magnetic properties of SnO crystals. Ceramics International, 2019, 45, 17529-17535.	2.3	9
42642	Interstitialcy diffusion of fluoride ions in LaOF by DFT-based first-principles calculations. Computational Materials Science, 2019, 167, 92-99.	1.4	9
42643	Intrinsic magnetism in monolayer transition metal trihalides: A comparative study. Journal of Magnetism and Magnetic Materials, 2019, 489, 165384.	1.0	43
42644	Novel 3D flower-like micro/nano-structure FeS/N-doped-C composites as advanced cathodes with high lithium storage performances. Journal of Power Sources, 2019, 431, 226-231.	4.0	25
42645	Oriented Attachment Revisited: Does a Chemical Reaction Occur?. Matter, 2019, 1, 690-704.	5.0	27
42646	Electrical transport and thermoelectric properties of Teâ€“Se solid solutions. Physics Letters, Section A: General, Atomic and Solid State Physics, 2019, 383, 2615-2620.	0.9	12
42647	Band alignments and polarization properties in ZnO (11<mml:math) Tj ETQq0 0 0 rgBT /Overlock 10 Tf 50 192 Td (xmlns:mml="http://w (001) heterostructures. Vacuum, 2019, 166, 264-269.	1.6	4
42648	Atomic Repartition in MXenes by Electron Probes. Chemistry of Materials, 2019, 31, 4385-4391.	3.2	17
42649	Phase Stability Diagrams of Group 6 MagnÃ©li Oxides and Their Implications for Photon-Assisted Applications. Chemistry of Materials, 2019, 31, 4282-4290.	3.2	38
42650	Room-Temperature Quantum Anomalous Hall Effect in Single-Layer CrP₂S₆. Journal of Physical Chemistry C, 2019, 123, 14707-14711.	1.5	7

#	Article	IF	Citations
42651	Two-Dimensional Carbon-Based Auxetic Materials for Broad-Spectrum Metal-Ion Battery Anodes. Journal of Physical Chemistry Letters, 2019, 10, 3269-3275.	2.1	64
42652	Ultrathin Porous NiCo₂O₄ Nanosheets for Lithiumâ€“Oxygen Batteries: An Excellent Performance Deriving from an Enhanced Solution Mechanism. ACS Applied Energy Materials, 2019, 2, 4215-4223.	2.5	18
42653	Understanding the Role of Overpotentials in Lithium Ion Conversion Reactions: Visualizing the Interface. ACS Nano, 2019, 13, 7825-7832.	7.3	16
42654	Control of Functionalities in GO: Effect of Bronsted Acids as Supported by Ab Initio Simulations and Experiments. ACS Omega, 2019, 4, 9407-9418.	1.6	10
42655	Building Up a Picture of the Electrocatalytic Nitrogen Reduction Activity of Transition Metal Single-Atom Catalysts. Journal of the American Chemical Society, 2019, 141, 9664-9672.	6.6	642
42656	Understanding of transition metal (Ru, W) doping into Nb for improved thermodynamic stability and hydrogen permeability: density functional theory calculations. Physical Chemistry Chemical Physics, 2019, 21, 17538-17545.	1.3	5
42657	LiAl5O8 as a potential coating material in lithium-ion batteries: a first principles study. Physical Chemistry Chemical Physics, 2019, 21, 13758-13765.	1.3	17
42658	A new family of cation-disordered Zn(Cu)â€“Siâ€“P compounds as high-performance anodes for next-generation Li-ion batteries. Energy and Environmental Science, 2019, 12, 2286-2297.	15.6	53
42659	Dimension engineering of single-layer PtN 2 with the Cairo tessellation. Journal of Applied Physics, 2019, 125, 204302.	1.1	4
42660	First-Principles Prediction of Possible Rare-Earth Free Permanent Magnet of Tetragonal <mml:math xmlns:mml="http://www.w3.org/1998/Math/MathML" display="inline" overflow="scroll"><mml:mrow><mml:mi>Fe</mml:mi><mml:mi>Co</mml:mi></mml:mrow></mml:math> with Enhanced Magnetic Anisotropy and Energy Product through Interstitial Nitrogen. Physical Review Applied, 2019, 11, .	1.5	21
42661	Data-driven material models for atomistic simulation. Physical Review B, 2019, 99, .	1.1	45
42662	Materials Informatics Approach to the Identification of One-Band Correlated Materials Analogous to the Cuprates. Physical Review X, 2019, 9, .	2.8	4
42663	From 3D to 2D: Structural, Spectroscopic and Theoretical Investigations of the Dimensionality Reduction in the [PtAl₂]^{Î´â^’} Polyanions of the Isotypic MPtAl₂ Series (M=Caâ€“Ba, Eu). Chemistry - A European Journal, 2019, 25, 10735-10747.	1.7	24
42664	Designing Highly Efficient and Longâ€Term Durable Electrocatalyst for Oxygen Evolution by Coupling B and P into Amorphous Porous NiFeâ€Based Material. Small, 2019, 15, e1901020.	5.2	71
42665	Interfacial properties of water/heavy water layer encapsulate in bilayer graphene nanochannel and nanocapacitor. Journal of Materials Science: Materials in Electronics, 2019, 30, 11964-11975.	1.1	2
42666	H2 Dissociation and Oxygen Vacancy Formation on Ce2O3 Surfaces. Topics in Catalysis, 2019, 62, 956-967.	1.3	9
42667	Cooperative transport enabling fast Li-ion diffusion in Thio-LISICON Li10SiP2S12 solid electrolyte. Nano Energy, 2019, 62, 844-852.	8.2	42
42668	Adsorption of Polyaromatic Backbone Impacts the Performance of Anion Exchange Membrane Fuel Cells. Chemistry of Materials, 2019, 31, 4195-4204.	3.2	91

#	Article	IF	Citations
42669	Phase Identification of the Layered Perovskite Ce_xSr_{2â€“x}MnO₄ and Application for Solar Thermochemical Water Splitting. Inorganic Chemistry, 2019, 58, 7705-7714.	1.9	24
42670	Separation of Radiolytic Species at the Boehmiteâ€“Water Interface. Journal of Physical Chemistry C, 2019, 123, 15534-15539.	1.5	8
42671	Etching and Exfoliation Properties of Cr₂AlC into Cr₂CO₂ and the Electrocatalytic Performances of 2D Cr₂CO₂ MXene. Journal of Physical Chemistry C, 2019, 123, 15629-15636.	1.5	29
42672	How is Honeycomb Borophene Stabilized on Al(111)?. Journal of Physical Chemistry C, 2019, 123, 14858-14864.	1.5	35
42673	On-surface synthesis of 2D COFs on Cu(111) via the formation of thermodynamically stable organometallic networks as the template. Physical Chemistry Chemical Physics, 2019, 21, 13222-13229.	1.3	20
42674	Surface thermodynamics of silicate compounds: the case of Zn₂SiO₄(001) surfaces and thin films. Physical Chemistry Chemical Physics, 2019, 21, 13287-13295.	1.3	11
42675	Mixing thermodynamics and electronic structure of the Pt_{1â^'x}Ni_x (0 â‰¤ Tj ETQq0 0 0 rgBT /Overlock 10 Tf 5	1.7	10
42676	Thermodynamic Stabilities of Perfect and Vacancy-Defected <mml:math xmlns:mml="http://www.w3.org/1998/Math/MathML" display="inline" overflow="scroll"><mml:msub><mml:mi>Li</mml:mi><mml:mn>2</mml:mn></mml:msub><mml:msub><mml:mrow><mml:mi>Ti</mml:mi> mathvariant="normal">O</mml:mi></mml:mrow><mml:mn>3</mml:mn></mml:msub></mml:math> (001) Surfaces From First-Principles Analyses. Physical Review Applied, 2019, 11, .	4.5	8
42677	Magnetocaloric effect in <mml:math xmlns:mml="http://www.w3.org/1998/Math/MathML"><mml:mrow><mml:msub><mml:mi>Fe</mml:mi><mml:mn>2</mml:mn></mml:msub><mml:msub><mml:mi mathvariant="normal">P</mml:mi></mml:mrow></mml:math> : Magnetic and phonon degrees of freedom. Physical Review B, 2019, 99, .	1.1	8
42678	Optimization of Mechanical Properties in Aluminum Alloys <i>via</i> Hydrogen Partitioning Control. Tetsu-To-Hagane/Journal of the Iron and Steel Institute of Japan, 2019, 105, 240-253.	0.1	0
42679	Understanding the improved electrochemical performance of nitrogen-doped hard carbons as an anode for sodium ion battery. Electrochimica Acta, 2019, 317, 164-172.	2.6	70
42680	Non-flammable electrolyte for dendrite-free sodium-sulfur battery. Energy Storage Materials, 2019, 23, 8-16.	9.5	92
42681	Tuning defect and hollow size of metallic KxCoF3 for ultrastable potassium storage. Energy Storage Materials, 2019, 21, 196-202.	9.5	16
42682	Prediction of stable high-pressure structures of tantalum nitride TaN2. Journal of Materials Science and Technology, 2019, 35, 2297-2304.	5.6	8
42683	Atomic scandium and nitrogen-codoped graphene for oxygen reduction reaction. Journal of Power Sources, 2019, 431, 265-273.	4.0	39
42684	Rational design of D-Ï€-A organic dyes to prevent â€œtrade offâ€•effect in dye-sensitized solar cells. Spectrochimica Acta - Part A: Molecular and Biomolecular Spectroscopy, 2019, 221, 117167.	2.0	5
42685	Tuning Electrical and Raman Scattering Properties of Cadmium Sulfide Nanoribbons via Surface Charge Transfer Doping. Journal of Physical Chemistry C, 2019, 123, 15794-15801.	1.5	7
42686	CHD₃ Dissociation on the Kinked Pt(210) Surface: A Comparison of Experiment and Theory. Journal of Physical Chemistry C, 2019, 123, 14530-14539.	1.5	14

#	Article	IF	Citations
42687	Balancing Competing Reactions in Hydride Transfer Catalysis via Catalyst Surface Doping: The Ionization Energy Descriptor. Journal of the American Chemical Society, 2019, 141, 9895-9901.	6.6	9
42688	Identification of the mechanism responsible for the boron oxygen light induced degradation in silicon photovoltaic cells. Journal of Applied Physics, 2019, 125, .	1.1	36
42689	Magnetizing topological surface states of Bi ₂ Se ₃ with a CrI ₃ monolayer. Science Advances, 2019, 5, eaaw1874.	4.7	78
42690	Boronâ€•and nitrogenâ€doped pentaâ€graphene as a promising material for hydrogen storage: A computational study. International Journal of Energy Research, 2019, 43, 4867-4878.	2.2	44
42691	Unique electronic structure of Mg/O co-decorated amorphous carbon nitride enhances the photocatalytic tetracycline hydrochloride degradation. Chinese Journal of Catalysis, 2019, 40, 776-785.	6.9	13
42692	Electron-configuration stabilized (W,Al)B2 solid solutions. Acta Materialia, 2019, 174, 398-405.	3.8	15
42693	Theoretical study of the role of the interface of Ag4 nanoclusters deposited on TiO2(110) and TiO2(101). Applied Surface Science, 2019, 490, 343-351.	3.1	17
42694	Combination of experimental and theoretical investigation on Ti-doped g-C3N4 with improved photo-catalytic activity. Applied Surface Science, 2019, 489, 427-434.	3.1	67
42695	phq: A Fortran code to compute phonon quasiparticle properties and dispersions. Computer Physics Communications, 2019, 243, 110-120.	3.0	18
42696	Monometallic nanoporous nickel with high catalytic performance towards hydrazine electro-conversion and its DFT calculations. Electrochimica Acta, 2019, 317, 449-458.	2.6	8
42697	Structural, electronic and adsorption properties of monolayer 2H-MoS2 on graphene substrates: A computational study. Inorganic Chemistry Communication, 2019, 106, 135-138.	1.8	10
42698	Effects of B on the segregation of Mo at the Fe-Cr-NiΣ5(210) grain boundary. Physica B: Condensed Matter, 2019, 568, 25-30.	1.3	16
42699	Dynamics of dissociative chemisorption of O2 on Cu(100) surface: A theoretical study. Surface Science, 2019, 688, 45-50.	0.8	7
42700	Tuning Adsorption and Catalytic Properties of Î±-Cr₂O₃ and ZnO in Propane Dehydrogenation by Creating Oxygen Vacancy and Doping Single Pt Atom: A Comparative First-Principles Study. Industrial & Engineering Chemistry Research, 2019, 58, 10199-10209.	1.8	38
42701	Ground-State Geometry and Vibrations of Polyphenylenevinylene Oligomers. Journal of Physical Chemistry Letters, 2019, 10, 3232-3239.	2.1	14
42702	Enhancement of catalytic activity by UV-light irradiation in CeO2 nanocrystals. Scientific Reports, 2019, 9, 8018.	1.6	14
42703	Computational design of alkali metals decorated 2D GeSe for hydrogen storage: a first principle study. Materials Research Express, 2019, 6, 085538.	0.8	5
42704	Revealing the Nature of Chemical Bonding in an ALn2Ag3Te5-Type Alkaline-Metal (A) Lanthanide (Ln) Silver Telluride. Inorganics, 2019, 7, 70.	1.2	12

#	Article	IF	Citations
42705	Atomicâ€Level Customization of 4 in. Transition Metal Dichalcogenide Multilayer Alloys for Industrial Applications. Advanced Materials, 2019, 31, e1901405.	11.1	52
42706	Thermodynamic Properties of W x (TaTiVCr) 1â^' x Highâ€Entropy(â€Like) Alloy and Influence of Tungsten Content. Physica Status Solidi (B): Basic Research, 2019, 256, 1800741.	0.7	2
42707	Structural, Electronic, and Optical Properties of ZnO_{1â€‰â€“â€‰x}Te_x Alloys. Physica Status Solidi - Rapid Research Letters, 2019, 13, 1900155.	1.2	3
42708	The pivotal effects of oxygen vacancy on Bi2MoO6: Promoted visible light photocatalytic activity and reaction mechanism. Chinese Journal of Catalysis, 2019, 40, 647-655.	6.9	86
42709	Non-oxidative dehydrogenation of ethane to ethylene over ZSM-5 zeolite supported iron catalysts. Applied Catalysis B: Environmental, 2019, 256, 117816.	10.8	84
42710	Computational design of multilayer frameworks to achieve DOE target for on-board methane delivery. Carbon, 2019, 152, 206-217.	5.4	5
42711	First-principles calculations of initial Cr deposition on the Fe surface. Computational Materials Science, 2019, 167, 183-190.	1.4	1
42712	Electronic structures and thermoelectric properties of polytype phases of bismuth. Journal of Physics and Chemistry of Solids, 2019, 134, 52-57.	1.9	13
42713	Dilute Cu2Te-alloying enables extraordinary performance of r-GeTe thermoelectrics. Materials Today Physics, 2019, 9, 100096.	2.9	74
42714	Investigating CO₂ Sorption in SIFSIX-3-M (M = Fe, Co, Ni, Cu, Zn) through Computational Studies. Crystal Growth and Design, 2019, 19, 3732-3743.	1.4	35
42715	First-Principles Study of Structural Transitions in LiNiO₂ and High-Throughput Screening for Long Life Battery. Journal of Physical Chemistry C, 2019, 123, 14126-14131.	1.5	27
42716	Computational Study of the Bulk and Surface Properties of Minor Actinide Dioxides MAnO₂ (MAn = Np, Am, and Cm); Water Adsorption on Stoichiometric and Reduced {111}, {110}, and {100} Surfaces. Journal of Physical Chemistry C, 2019, 123, 15540-15550.	1.5	14
42717	Novel Metallic Clathrates of Group-IV Elements and Their Compounds in a Dense Hexagonal Lattice. Journal of Physical Chemistry C, 2019, 123, 15330-15338.	1.5	5
42718	Band Gap Narrowing of Zinc Orthogermanate by Dimensional and Defect Modification. Journal of Physical Chemistry C, 2019, 123, 14573-14581.	1.5	6
42719	Decomposition and Recombination of Binary Interalkali Na₂K at High Pressures. Journal of Physical Chemistry Letters, 2019, 10, 3006-3012.	2.1	10
42720	Doping-Induced Rapid Decoherence Suppresses Charge Recombination in Mono/Divalent Cation Mixed Perovskites from Nonadiabatic Molecular Dynamics Simulation. Journal of Physical Chemistry Letters, 2019, 10, 3433-3439.	2.1	24
42721	Direct Oxidation of Methane to Methanol Enabled by Electronic Atomic Monolayerâ€“Metal Support Interaction. ACS Catalysis, 2019, 9, 6073-6079.	5.5	36
42722	On-surface synthesis of planar dendrimers via divergent cross-coupling reaction. Nature Communications, 2019, 10, 2414.	5.8	17

#	Article	IF	Citations
42723	Real-Time Observation of Carbon Oxidation by Driven Motion of Catalytic Ceria Nanoparticles within Low Pressure Oxygen. Scientific Reports, 2019, 9, 8082.	1.6	4
42724	Unravelling the synergy effects of defect-rich 1T-MoS₂/carbon nanotubes for the hydrogen evolution reaction by experimental and calculational studies. Sustainable Energy and Fuels, 2019, 3, 2100-2110.	2.5	34
42725	Deep insights into the exfoliation properties of MAX to MXenes and the hydrogen evolution performances of 2D MXenes. Journal of Materials Chemistry A, 2019, 7, 15862-15870.	5.2	58
42726	The n- and p-type thermoelectric response of a semiconducting Co-based quaternary Heusler alloy: a density functional approach. Journal of Materials Chemistry C, 2019, 7, 7664-7671.	2.7	20
42727	Ab-initio calculation of band alignments for opto-electronic simulations. AIP Advances, 2019, 9, 055328.	0.6	1
42728	Single-layer BiOBr: An effective p-type 2D thermoelectric material. Journal of Applied Physics, 2019, 125, .	1.1	22
42729	ICET â€“ A Python Library for Constructing and Sampling Alloy Cluster Expansions. Advanced Theory and Simulations, 2019, 2, 1900015.	1.3	91
42730	Understanding the effects of metal particle size on the NO2 reduction from a DFT study. Applied Surface Science, 2019, 489, 1019-1029.	3.1	10
42731	Design of highly efficient adsorbents for removal of gaseous methyl iodide using tertiary amine-impregnated activated carbon: Integrated experimental and first-principles approach. Chemical Engineering Journal, 2019, 373, 1003-1011.	6.6	27
42732	Mechanistic insight into the selective catalytic oxidation for NO and CO on co-doping graphene sheet: A theoretical study. Fuel, 2019, 253, 1531-1544.	3.4	31
42733	A New sp2â€“sp3-Hybridized Metallic Carbon Network for Lithium-Ion Battery Anode with Enhanced Safety and Lithium-Ion Diffusion Rate. Journal of Physical Chemistry C, 2019, 123, 15412-15418.	1.5	14
42734	Efficient, Full Spectrum-Driven H₂ Evolution Z-Scheme Co₂P/CdS Photocatalysts with Coâ€“S Bonds. ACS Applied Materials & Interfaces, 2019, 11, 22297-22306.	4.0	90
42735	Nucleation and Conversion Transformations of the Transition Metal Polysulfide VS₄ in Lithium-Ion Batteries. ACS Applied Materials & Interfaces, 2019, 11, 22307-22313.	4.0	21
42736	Surface Structure of Co₃O₄ (111) under Reactive Gas-Phase Environments. ACS Catalysis, 2019, 9, 6380-6392.	5.5	27
42737	Strain-tunable van der Waals interactions in few-layer black phosphorus. Nature Communications, 2019, 10, 2447.	5.8	98
42738	Catalysis-Hub.org, an open electronic structure database for surface reactions. Scientific Data, 2019, 6, 75.	2.4	163
42739	First-principles study on the magnetic properties of Î²-Ti68.75Nb25X6.25 (X=Mo, Sn, Ta, Zr, Fe) alloys. AIP Advances, 2019, 9, 065102.	0.6	0
42740	Electric field control of the semiconductor-metal transition in two dimensional CuInP2S6/germanene van der Waals heterostructure. Applied Physics Letters, 2019, 114, .	1.5	22

#	Article	IF	Citations
42741	Magnetotransport properties of the correlated topological nodal-line semimetal YbCdGe. Physical Review B, 2019, 99, .	1.1	32
42742	Ferroelectricity with Asymmetric Hysteresis in Metallic <mml:math xmlns:mml="http://www.w3.org/1998/Math/MathML" display="inline"><mml:mrow><mml:msub><mml:mrow><mml:mi>LiOsO</mml:mi></mml:mrow><mml:mrow><mml:mn>3</mml:mn> Ultrathin Films. Physical Review Letters, 2019, 122, 227601.	2.9	34
42743	First-principles study of two-dimensional bilayer GaN: structure, electronic properties and temperature effect. Japanese Journal of Applied Physics, 2019, 58, SCCB35.	0.8	3
42744	Modulation of Heavy Metal/Ferromagnetic Metal Interface for Highâ€Performance Spintronic Devices. Advanced Electronic Materials, 2019, 5, 1900134.	2.6	64
42745	Î²-PtO2: Phononic, thermodynamic, and elastic properties derived from first-principles calculations. Frontiers of Physics, 2019, 14, 1.	2.4	3
42746	Nuclear magnetic resonance and theoretical simulation study on Cs ion co-adsorbed with other alkali cations on illite. Applied Surface Science, 2019, 489, 766-775.	3.1	9
42747	Reversible hydrogen storage properties of defect-engineered <mml:math xmlns:mml="http://www.w3.org/1998/Math/MathML" altimg="si1.svg"><mml:mrow><mml:msub><mml:mrow><mml:mi mathvariant="bold">C</mml:mi></mml:mrow><mml:mrow><mml:mn mathvariant="bold">4</mml:mn></mml:mrow></mml:msub><mml:mi mathvariant="bold">N</mml:mi></mml:mrow></mml:math> nanosheets under ambient conditions. Car	5.4	69
42748	An efficient palm waste derived hierarchical porous carbon for electrocatalytic hydrogen evolution reaction. Carbon, 2019, 152, 188-197.	5.4	41
42749	Metal-free N2-to-NH3 thermal conversion at the boron-terminated zigzag edges of hexagonal boron nitride: Mechanism and kinetics. Journal of Catalysis, 2019, 375, 68-73.	3.1	11
42750	Influence of strain and substitution on magnetocrystalline anisotropy of R2Fe14B (R=Pr, Dy and Y). Journal of Magnetism and Magnetic Materials, 2019, 488, 165370.	1.0	0
42751	Syntheses and Characterization of Diammineâ€“Nickel/Cobalt(II)â€“Bisdicyanamide M(NH₃)₂[N(CN)₂]₂ with M = Ni and Co. Inorganic Chemistry, 2019, 58, 7803-7811.	1.9	3
42752	Adsorption Features of Formaldehyde on TiO₂(110) Surface Probed by High-Resolution Scanning Tunnelling Microscopy. Journal of Physical Chemistry Letters, 2019, 10, 3352-3358.	2.1	13
42753	Why Do Colloidal Wurtzite Semiconductor Nanoplatelets Have an Atomically Uniform Thickness of Eight Monolayers?. Journal of Physical Chemistry Letters, 2019, 10, 3465-3471.	2.1	17
42754	Connecting Solution-Phase to Single-Molecule Properties of Ni(Salophen). Journal of Physical Chemistry Letters, 2019, 10, 3525-3530.	2.1	8
42755	Approaching the Intrinsic Limit in Transition Metal Diselenides via Point Defect Control. Nano Letters, 2019, 19, 4371-4379.	4.5	161
42756	Defect-Mediated Charge-Carrier Trapping and Nonradiative Recombination in WSe₂ Monolayers. Journal of the American Chemical Society, 2019, 141, 10451-10461.	6.6	81
42757	Strain-induced reversible manipulation of orbital magnetic moments in Ni/Cu multilayers on ferroelectric BaTiO3. Npj Quantum Materials, 2019, 4, .	1.8	21
42758	Freestanding crystalline oxide perovskites down to the monolayer limit. Nature, 2019, 570, 87-90.	13.7	398

#	Article	IF	Citations
42759	Tuning the electronic and magnetic properties of MoS2 nanotubes with vacancy defects. RSC Advances, 2019, 9, 17203-17210.	1.7	12
42760	Adsorption of toxic gases on silicene/Ag(111). Physical Chemistry Chemical Physics, 2019, 21, 17521-17537.	1.3	17
42761	Acetylenic linkage dependent electronic and optical behaviour of morphologically distinct â€˜ynesâ€™. Physical Chemistry Chemical Physics, 2019, 21, 13795-13808.	1.3	37
42762	Inducing magnetism in non-magnetic Î±-FeSi2 by distortions and/or intercalations. Physical Chemistry Chemical Physics, 2019, 21, 13835-13846.	1.3	4
42763	Convertible and conformationally constrained nucleic acids (C₂NAs). Organic and Biomolecular Chemistry, 2019, 17, 6386-6397.	1.5	2
42764	First-principles computational investigation of nitrogen-doped carbon nanotubes as anode materials for lithium-ion and potassium-ion batteries. RSC Advances, 2019, 9, 17299-17307.	1.7	11
42765	A new phase of monolayer group-V binary compounds with direct bandgap and giant piezoelectric properties. Journal of Applied Physics, 2019, 125, .	1.1	13
42766	First-order liquid-liquid phase transition in compressed hydrogen and critical point. Journal of Chemical Physics, 2019, 150, 204114.	1.2	6
42767	Electronic properties of spin excitation in multiferroics with a spinel structure: first principles calculation. Ferroelectrics, 2019, 539, 41-49.	0.3	0
42768	Two-dimensional ferromagnetic-ferroelectric multiferroics in violation of the <mml:math xmlns:mml="http://www.w3.org/1998/Math/MathML"><mml:msup><mml:mi>d</mml:mi><mml:mn>0</mml:mn></mml:msup></mml:m rule. Physical Review B, 2019, 99, .	1.1	6
42769	Trends in Oxygen Electrocatalysis of 3â€‰dâ€Layered (Oxy)(Hydro)Oxides. ChemCatChem, 2019, 11, 3423-3431.	1.8	33
42770	Calculation of the anisotropic coefficients of thermal expansion: A first-principles approach. Computational Materials Science, 2019, 167, 257-263.	1.4	16
42771	A first-principles study of the effect of surface oxygen during the early stage of graphene growth on a Cu(1â€¯1â€¯1) surface. Computational Materials Science, 2019, 168, 17-24.	1.4	8
42772	Electronic band gaps corrections using total energy with DFT/LDA-Â½ quasi-particle approximation. Computational Materials Science, 2019, 167, 228-236.	1.4	6
42773	[Ni(phen)3]Sn3Se7Â·1.5H2O: A new two-dimensional layered selenidostannate templated by [Ni(phen)3]2+ complexes. Inorganic Chemistry Communication, 2019, 106, 76-80.	1.8	10
42774	Propose two-dimensional Sb₂Te₂X (X = S, Se) with isotropic electron mobility and remarkable visible-light response. Physical Chemistry Chemical Physics, 2019, 21, 14904-14910.	1.3	2
42775	Dinitrogen activation by zirconium dimer loaded C60. AIP Advances, 2019, 9, 055331.	0.6	0
42776	An ultralow-density porous ice with the largest internal cavity identified in the water phase diagram. Proceedings of the National Academy of Sciences of the United States of America, 2019, 116, 12684-12691.	3.3	16

#	Article	IF	Citations
42777	Ni/ZnO heterostructured microspheres: electronic structure engineering for enhanced photocatalytic activity. Materials Research Express, 2019, 6, 0850e5.	0.8	0
42778	Lithium diffusion in <mmlmath xmlns:mml="http://www.w3.org/1998/Math/MathML"><mml:mrow><mml:mi mathvariant="normal">L</mml:mi><mml:msub><mml:mi mathvariant="normal">i</mml:mi><mml:mn>2</mml:mn></mml:msub><mml:mi>X</mml:mi></mml:mrow></mml:math>		

#	Article	IF	Citations
42795	Initial Fe₃O₄(100) Formation on Fe(100). Journal of Physical Chemistry C, 2019, 123, 16317-16325.	1.5	8
42796	Bandlike Transport in PbS Quantum Dot Superlattices with Quantum Confinement. Journal of Physical Chemistry Letters, 2019, 10, 3756-3762.	2.1	10
42797	Functionalization and Defect-Driven Water Splitting Mechanism on a Quasi-Two-Dimensional TiO2 Hexagonal Nanosheet. ACS Applied Energy Materials, 2019, 2, 5074-5082.	2.5	8
42798	Absolute energy level positions in tin- and lead-based halide perovskites. Nature Communications, 2019, 10, 2560.	5.8	381
42799	Characteristic fast Hâ˜ ion conduction in oxygen-substituted lanthanum hydride. Nature Communications, 2019, 10, 2578.	5.8	70
42800	Prediction of quantum anomalous Hall effect and giant magnetic anisotropy in graphene with adsorbed Ir-based dimers. Journal of Applied Physics, 2019, 125, 193903.	1.1	6
42801	Electronic structure and superconductivity in hexagonal Li3B2 and Li2B2H phases under pressure. Journal of Applied Physics, 2019, 125, 223902.	1.1	0
42802	Topological phase transition induced by magnetic proximity effect in two dimensions. Journal of Physics Condensed Matter, 2019, 31, 395502.	0.7	4
42803	Topological states in A15 superconductors. Physical Review B, 2019, 99, .	1.1	16
42804	Mechanism and control parameters of the coupled structural and metal-insulator transition in nickelates. Physical Review B, 2019, 99, .	1.1	38
42805	Onâ€Surface Synthesis and Characterization of Aceneâ€Based Nanoribbons Incorporating Fourâ€Membered Rings. Chemistry - A European Journal, 2019, 25, 12074-12082.	1.7	38
42806	Ab initio phase stability and electronic conductivity of the doped-Li4Ti5O12 anode for Li-ion batteries. Acta Materialia, 2019, 175, 196-205.	3.8	35
42807	Short-range ordered structure and phase stability of supersaturated nitrided layer on austenitic stainless steel. Acta Materialia, 2019, 175, 314-323.	3.8	16
42808	Vacancy-enhanced cycle life and electrochemical performance of lithium-rich layered oxide Li2RuO3. Ceramics International, 2019, 45, 18315-18319.	2.3	57
42809	Tuning the electronic properties of monolayer MoS2, MoSe2 and MoSSe by applying z-axial strain. Chemical Physics Letters, 2019, 730, 191-197.	1.2	29
42810	Dimensional Crossover and Topological Nature of the Thin Films of a Three-Dimensional Topological Insulator by Band Gap Engineering. Nano Letters, 2019, 19, 4627-4633.	4.5	16
42811	Perfect planar tetra-coordinated MC₆ monolayer: superior anode material for Li-ion battery. Physical Chemistry Chemical Physics, 2019, 21, 15187-15194.	1.3	14
42812	Optimizing the thermoelectric transport properties of Bi₂O₂Se monolayer via biaxial strain. Physical Chemistry Chemical Physics, 2019, 21, 15097-15105.	1.3	76

#	Article	IF	Citations
42813	Theory and practice of modeling van der Waals interactions in electronic-structure calculations. Chemical Society Reviews, 2019, 48, 4118-4154.	18.7	114
42814	Quantum chemical models for the absorption of endohedral clusters on Si(111)-(7 Ã— 7): a subtle balance between Wâ€“Si and Siâ€“Si bonding. Physical Chemistry Chemical Physics, 2019, 21, 13686-13695.	1.3	0
42815	Absorption edge, urbach tail, and electron-phonon interactions in topological insulator Bi2Se3 and band insulator (Bi0.89In0.11)2Se3. Applied Physics Letters, 2019, 114, .	1.5	10
42816	Crystal structures and sign reversal Hall resistivities in iron-based superconductors Li x (C3H10N2)0.32FeSe $(0.15lt xlt 0.4$). Chinese Physics B, 2019, 28, 067401.	0.7	3
42817	Thickness-driven first-order phase transitions in manganite ultrathin films. Physical Review B, 2019, 99, .	1.1	12
42818	Charge-induced ferromagnetic phase transition and anomalous Hall effect in full <mml:math xmlns:mml="http://www.w3.org/1998/Math/MathML"><mml:mi>d</mml:mi></mml:math> -band nonmagnetic metals. Physical Review B, 2019, 99, .	1.1	9
42819	Monte Carlo Simulation for Formation of Ti and N Atoms Nanoclusters in BCC-Fe. Tetsu-To-Hagane/Journal of the Iron and Steel Institute of Japan, 2019, 105, 334-342.	0.1	3
42820	Inâ€Situ Growth of Gadolinium Phthalocyaninato Sandwich Complexes on the Ag(111) Surface. ChemPhysChem, 2019, 20, 2301-2304.	1.0	4
42821	Theoretical investigation on the structures, electronic and magnetic properties of new 2D/1D composite nanosystems by adsorbing superhalogen MnCl3 on the BN monolayer/nanoribbons. Theoretical Chemistry Accounts, 2019, 138, 1.	0.5	3
42822	First principles study on the oxygen reduction reaction of the Laâ€“Sr MnO coated Baâ€“Sr Coâ€“Fe Oâ€“ cathode for solid oxide fuel cells. International Journal of Hydrogen Energy, 2019, 44, 16359-16367.	3.8	29
42823	Synthesis, structure and characterization of a new triphosphate: CsMg2P3O10. Solid State Sciences, 2019, 94, 133-137.	1.5	0
42824	Numerical methods for Kohnâ€“Sham density functional theory. Acta Numerica, 2019, 28, 405-539.	6.3	23
42825	The Oâ€“O Bonding and Hydrogen Storage in the Pyrite-type PtO₂. Inorganic Chemistry, 2019, 58, 8300-8307.	1.9	6
42826	Enhanced Yellow Persistent Luminescence in Sr₃SiO₅:Eu²⁺ through Ge Incorporation. Inorganic Chemistry, 2019, 58, 8694-8701.	1.9	27
42827	Rational Design of Stable Dianions and the Concept of Super-Chalcogens. Journal of Physical Chemistry A, 2019, 123, 5753-5761.	1.1	10
42828	Two-Dimensional CuO Inside the Supportive Bilayer Graphene Matrix. Journal of Physical Chemistry C, 2019, 123, 17459-17465.	1.5	12
42829	Multi-Step Topochemical Pathway to Metastable Mo₂AlB₂ and Related Two-Dimensional Nanosheet Heterostructures. Journal of the American Chemical Society, 2019, 141, 10852-10861.	6.6	84
42830	Proton-assisted creation of controllable volumetric oxygen vacancies in ultrathin CeO2â^'x for pseudocapacitive energy storage applications. Nature Communications, 2019, 10, 2594.	5.8	75

#	Article	IF	Citations
42831	Active catalyst construction for CO2 recycling via catalytic synthesis of N-doped carbon on supported Cu. Nature Communications, 2019, 10, 2599.	5.8	23
42832	Atomic-resolution imaging of surface and core melting in individual size-selected Au nanoclusters on carbon. Nature Communications, 2019, 10, 2583.	5.8	48
42833	High-throughput Discovery of Topologically Non-trivial Materials using Spin-orbit Spillage. Scientific Reports, 2019, 9, 8534.	1.6	36
42834	Ab initio thermodynamics of carbon segregation on dislocation cores in bcc iron. Modelling and Simulation in Materials Science and Engineering, 2019, 27, 074002.	0.8	13
42835	The effect of grain boundary on the visible light absorption of BaTi_{1â€x}[Ni_{1/2}Nb_{1/2}]_xO_{3â€Î´} ferroelectric ceramics. Journal of the American Ceramic Society, 2019, 102, 7405-7413.	1.9	16
42836	Prediction of Time-to-Solution in Material Science Simulations Using Deep Learning. , 2019, , .		0
42837	A Theoretical Study on the Inclusion of Fe, Cu, and Zn in Illite Clays. Journal of Nanomaterials, 2019, 2019, 1-14.	1.5	1
42838	Understanding Phase Stability of Metallic 1T-MoS2 Anodes for Sodium-Ion Batteries. Condensed Matter, 2019, 4, 53.	0.8	18
42839	Elasticity of Phases in Fe-Al-Ti Superalloys: Impact of Atomic Order and Anti-Phase Boundaries. Crystals, 2019, 9, 299.	1.0	11
42840	Quantum Mechanical Modeling of the Vibrational Spectra of Minerals with a Focus on Clays. Minerals (Basel, Switzerland), 2019, 9, 141.	0.8	18
42841	Recent Progress on 2D Group IIâ€VI Binary Chalcogenides ZnX and CdX (XÂ=ÂS, Se, Te): From a Theoretical Perspective. Advanced Theory and Simulations, 2019, 2, 1900061.	1.3	10
42842	Structural, Electronic, and Magnetic Properties of Hard Magnetic SmNi2Fe Compound: a DFT Study. Journal of Superconductivity and Novel Magnetism, 2019, 32, 3901-3905.	0.8	3
42843	Prediction of electronic structure in atomistic model using artificial neural network. Computational Materials Science, 2019, 168, 164-171.	1.4	10
42844	First-principles comparative study of UN and Zr corrosion. Journal of Nuclear Materials, 2019, 523, 402-412.	1.3	2
42845	Metalated azolo[1,2,4]triazines. II. Generation, C(4)-substituent dependent stability and electrophile trapping of 7-lithiopyrazolo[5,1-c][1,2,4]triazines. Journal of Organometallic Chemistry, 2019, 896, 168-182.	0.8	17
42846	Tunable electronic and optical properties of the MoS2/MoSe2 heterostructure nanotubes. Superlattices and Microstructures, 2019, 132, 106156.	1.4	8
42847	Ab Initio Search of Polymer Crystals with High Thermal Conductivity. Chemistry of Materials, 2019, 31, 4649-4656.	3.2	9
42848	Properties of Negatively Charged Ruthenium Clusters in Molten Sodium Chloride. Journal of Physical Chemistry C, 2019, 123, 16179-16185.	1.5	5

#	Article	IF	Citations
42849	Heat-Induced Polymorphic Transformation Facilitating the Low Impact-Sensitivity of 2,2-Dinitroethylene-1,1-diamine (FOX-7). Journal of Physical Chemistry C, 2019, 123, 16014-16022.	1.5	25
42850	Automated Detection and Characterization of Surface Restructuring Events in Bimetallic Catalysts. Journal of Physical Chemistry C, 2019, 123, 16332-16344.	1.5	10
42851	Exploring the chemical nature of super-heavy main-group elements by means of efficient plane-wave density-functional theory. Physical Chemistry Chemical Physics, 2019, 21, 18048-18058.	1.3	31
42852	Seeking large Seebeck effects in LaX(X = Mn and Co)O₃/SrTiO₃ superlattices by exploiting high spin-polarized effects. Physical Chemistry Chemical Physics, 2019, 21, 14973-14983.	1.3	7
42853	Infrared and Raman spectra of Bi₂O₂X and Bi₂OX₂ (XÂ= S, Se, and Te) studied from first principles calculations. RSC Advances, 2019, 9, 18042-18049.	1.7	26
42854	Intrinsic magnetic topological insulators in van der Waals layered MnBi ₂ Te ₄ -family materials. Science Advances, 2019, 5, eaaw5685.	4.7	675
42855	Stable group-IIB elements â€”Zn, Cd and Hg at terapascal pressures. Europhysics Letters, 2019, 126, 36001.	0.7	2
42856	Degenerate electron-doping in two-dimensional tungsten diselenide with a dimeric organometallic reductant. Materials Today, 2019, 30, 26-33.	8.3	14
42857	Doping and biaxial deformation engineering the thermoelectric transport properties in selenium crystal. Solid State Communications, 2019, 297, 34-38.	0.9	2
42858	Robust two-dimensional ferroelectricity in single-layer Î³-SbP and Î³-SbAs. Nanoscale, 2019, 11, 11864-11871.	2.8	27
42859	Predicting two-dimensional semiconducting boron carbides. Nanoscale, 2019, 11, 11099-11106.	2.8	29
42860	Tunable photoluminescence and an enhanced photoelectric response of Mn²⁺-doped CsPbCl₃ perovskite nanocrystals via pressure-induced structure evolution. Nanoscale, 2019, 11, 11660-11670.	2.8	15
42861	In situ formed ultrafine NbTi nanocrystals from a NbTiC solid-solution MXene for hydrogen storage in MgH₂. Journal of Materials Chemistry A, 2019, 7, 14244-14252.	5.2	114
42862	Interplay of Strain and Magnetism in FeSe Monolayers[*]. Chinese Physics Letters, 2019, 36, 056801.	1.3	4
42863	Intrinsic phonon-mediated superconductivity in graphene-like BSi lattice. Journal of Physics Condensed Matter, 2019, 31, 345401.	0.7	5
42864	Off-centered-symmetry-based band structure modulation of hexagonal WO₃. Journal of Physics Condensed Matter, 2019, 31, 355501.	0.7	5
42865	Crystal structures and decomposing of Bâ€“P compounds under pressure*. Chinese Physics B, 2019, 28, 056101.	0.7	5
42866	Surface stabilized cubic phase of CsPbI₃ and CsPbBr₃ at room temperature*. Chinese Physics B, 2019, 28, 056402.	0.7	16

#	Article	IF	Citations
42867	Anisotropic thermal expansion and thermodynamic properties of monolayer <mml:math xmlns:mml="http://www.w3.org/1998/Math/MathML"><mml:mi>Î²</mml:mi></mml:math> -Te. Physical Review B, 2019, 99, .	1.1	25
42868	Half-metallicity versus symmetry in half-Heusler alloys based on Pt, Ni, and Co: An ab initio study. Physical Review B, 2019, 99, .	1.1	26
42869	Atomicâ€Scale Spectroscopic Imaging of the Extremeâ€UV Optical Response of Bâ€•and Nâ€Doped Graphene. Advanced Functional Materials, 2019, 29, 1901819.	7.8	7
42870	Strain Effect on the Magnetism of Nâ€Doped Molybdenum Disulfide. Physica Status Solidi (B): Basic Research, 2019, 256, 1900110.	0.7	2
42871	Electronic Doping Controlled Migration of Dislocations in Polycrystalline 2D WS₂. Small, 2019, 15, e1805145.	5.2	4
42872	Nickel Promoted Palladium Nanoparticles for Electrocatalysis of Carbohydrazide Oxidation Reaction. Small, 2019, 15, e1900929.	5.2	8
42873	Adsorption and Photodegradation of Acetaldehyde and Ethylene on TiO2 (001) Surface: Experimental and First Principle Studies. Catalysis Letters, 2019, 149, 2728-2738.	1.4	9
42874	Water dissociation on the reduced PuO2(110) surface from first principles. Science China: Physics, Mechanics and Astronomy, 2019, 62, 1.	2.0	7
42875	Red phosphorus decorated and doped TiO2 nanofibers for efficient photocatalytic hydrogen evolution from pure water. Applied Catalysis B: Environmental, 2019, 255, 117764.	10.8	151
42876	Effect of high pressure on magnetic properties of CrMnFeCoNi high entropy alloy. Journal of Magnetism and Magnetic Materials, 2019, 487, 165333.	1.0	12
42877	Self-assembled two-dimensional layered oxide supercells with modulated layer stacking and tunable physical properties. Materials Today Nano, 2019, 6, 100037.	2.3	14
42878	Electronic transport and thermoelectric properties in a superlattice junction based graphene-In2Te2 nanoribbon bilayer. Physica E: Low-Dimensional Systems and Nanostructures, 2019, 114, 113570.	1.3	1
42879	Structural features and electronic properties of Group-IIIB pnictides nanosheets and nanoribbons. Physics Letters, Section A: General, Atomic and Solid State Physics, 2019, 383, 2744-2750.	0.9	1
42880	Experimental and Density Functional Theory Corroborated Optimization of Durable Metal Embedded Carbon Nanofiber for Oxygen Electrocatalysis. Journal of Physical Chemistry Letters, 2019, 10, 3109-3114.	2.1	16
42881	Limiting Heterovalent B-Site Doping in CsPbI₃ Nanocrystals: Phase and Optical Stability. ACS Energy Letters, 2019, 4, 1364-1369.	8.8	86
42882	Ru passivated and Ru doped Îµ-TaN surfaces as a combined barrier and liner material for copper interconnects: a first principles study. Journal of Materials Chemistry C, 2019, 7, 7959-7973.	2.7	11
42883	Interface-tuned selective reductive coupling of nitroarenes to aromatic azo and azoxy: a first-principles-based microkinetics study. Physical Chemistry Chemical Physics, 2019, 21, 12555-12565.	1.3	10
42884	Strain controlling transport properties of heterostructure composed of monolayer CrI3. Applied Physics Letters, 2019, 114, .	1.5	31

#	Article	IF	Citations
42885	Intercalation of transition metals in aluminene bi-layers: An ab initio study. Journal of Chemical Physics, 2019, 150, 194702.	1.2	3
42886	Methane dissociation on stepped Ni surfaces resolved by impact site, collision energy, vibrational state, and lattice distortion. Journal of Chemical Physics, 2019, 150, 204703.	1.2	14
42887	Ab initio simulation studies on the room-temperature ferroelectricity in two-dimensional Î² -phase GeS. Applied Physics Letters, 2019, 114, .	1.5	72
42888	Raman scattering study of magnetic layered MPS₃ crystals (M = Mn , Fe, Ni)*. Chinese Physics B, 2019, 28, 056301.	0.7	8
42889	Magnetic structure of monatomic Fe chains on Re(0001): Emergence of chiral multispin interactions. Physical Review B, 2019, 99, .	1.1	32
42890	In-plane band bending in hexagonal monolayer WS2 by edge polarization. Physical Review B, 2019, 99, .	1.1	2
42891	Selfâ€healing of TiSiN/Ag coatings induced by Ag. Journal of the American Ceramic Society, 2019, 102, 7521-7532.	1.9	6
42892	Theoretical Analysis on Temperature- and Pressure-Dependences of NO-CO-O₂ Reaction on Rh(111) Surface. Journal of Computer Chemistry Japan, 2019, 18, 70-77.	0.0	1
42893	The Influence of Interface Structure on the Electrical Conductivity of Graphene Embedded in Aluminum Matrix. Advanced Materials Interfaces, 2019, 6, 1900468.	1.9	38
42894	Neutron diffraction study of temperature-dependent elasticity of B19â€² NiTi---Elinvar effect and elastic softening. Acta Materialia, 2019, 173, 281-291.	3.8	24
42895	Assessment of M2O(111) (Mâ€¯=â€¯Li and Na) surfaces for CO2 adsorption based on first-principles calculations. Applied Surface Science, 2019, 486, 571-577.	3.1	9
42896	Comparative electrochemical analysis of rGO-FeVO4 nanocomposite and FeVO4 for supercapacitor application. Applied Surface Science, 2019, 488, 221-227.	3.1	45
42897	Discontinuous model combined with an atomic mechanism simulates the precipitated Î·â€² phase effect in intergranular cracking of 7-series aluminum alloys. Computational Materials Science, 2019, 166, 282-292.	1.4	9
42898	Realization of spin-canted magnetism from lattice site specific spin structure in the double perovskite Nd2CoTiO6. Journal of Magnetism and Magnetic Materials, 2019, 488, 165338.	1.0	4
42899	Ammonothermal Crystal Growth of ATaN₂ with A = Na, K, Rb, and Cs and Their Optical and Electronic Properties. Crystal Growth and Design, 2019, 19, 3484-3490.	1.4	4
42900	Effects of Rb Intercalation on NbSe₂: Phase Formation, Structure, and Physical Properties. Inorganic Chemistry, 2019, 58, 7564-7570.	1.9	9
42901	Divalent Path to Enhance p-Type Conductivity in a SnO Transparent Semiconductor. Journal of Physical Chemistry C, 2019, 123, 14909-14913.	1.5	5
42902	L-Type Ligand-Assisted Acid-Free Synthesis of CsPbBr₃ Nanocrystals with Near-Unity Photoluminescence Quantum Yield and High Stability. Nano Letters, 2019, 19, 4151-4157.	4.5	177

#	Article	IF	Citations
42903	Mechanism and Kinetics of Methylating C₆â€“C₁₂ Methylbenzenes with Methanol and Dimethyl Ether in H-MFI Zeolites. ACS Catalysis, 2019, 9, 6444-6460.	5.5	45
42904	Selective 2-Propanol Oxidation over Unsupported Co₃O₄ Spinel Nanoparticles: Mechanistic Insights into Aerobic Oxidation of Alcohols. ACS Catalysis, 2019, 9, 5974-5985.	5.5	61
42905	On the Study of Ca and Mg Deintercalation from Ternary Tantalum Nitrides. ACS Omega, 2019, 4, 8943-8952.	1.6	18
42906	Regulating the Inner Helmholtz Plane for Stable Solid Electrolyte Interphase on Lithium Metal Anodes. Journal of the American Chemical Society, 2019, 141, 9422-9429.	6.6	429
42907	UV-SWIR broad range photodetectors made from few-layer Î±-In₂Se₃ nanosheets. Nanoscale, 2019, 11, 12817-12828.	2.8	47
42908	Grapheneâ€“boron nitride hybrid-supported single Mo atom electrocatalysts for efficient nitrogen reduction reaction. Journal of Materials Chemistry A, 2019, 7, 15173-15180.	5.2	107
42909	Effect of point defects on electronic and magnetic properties of single-layer SiO. Philosophical Magazine, 2019, 99, 2340-2353.	0.7	3
42910	Electric field gradient study on pure and Cd-doped In(111) surfaces: Correlation between experiments at the atomic scale and first-principles calculations. Physical Review B, 2019, 99, .	1.1	2
42911	Defect Engineering in Two Common Types of Dielectric Materials for Electromagnetic Absorption Applications. Advanced Functional Materials, 2019, 29, 1901236.	7.8	469
42912	Modulation of New Excitons in Transition Metal Dichalcogenideâ€Perovskite Oxide System. Advanced Science, 2019, 6, 1900446.	5.6	6
42913	Carbonate-intercalated defective bismuth tungstate for efficiently photocatalytic NO removal and promotion mechanism study. Applied Catalysis B: Environmental, 2019, 254, 206-213.	10.8	58
42914	Highly active metallic nickel sites confined in N-doped carbon nanotubes toward significantly enhanced activity of CO2 electroreduction. Carbon, 2019, 150, 52-59.	5.4	84
42915	Investigating the optical, photosensitivity and photocatalytic properties of double perovskites A2LuTaO6 (A = Ba, Sr): A combined experimental and density functional theory study. Ceramics International, 2019, 45, 15496-15504.	2.3	14
42916	Germanium as key dopant to boost the catalytic performance of small platinum clusters for alkane dehydrogenation. Journal of Catalysis, 2019, 374, 93-100.	3.1	35
42917	Ordered double-M elements MXenes TiMC: Large in-plane stiffness and ferromagnetism. Journal of Magnetism and Magnetic Materials, 2019, 486, 165280.	1.0	14
42918	Tunable magnetism in defective MoS2 monolayer with nonmetal atoms adsorption. Superlattices and Microstructures, 2019, 130, 346-353.	1.4	4
42919	Mass transport properties of quasiharmonic vs. anharmonic transition-metal nitrides. Thin Solid Films, 2019, 688, 137297.	0.8	7
42920	High-Efficiency Violet-Emitting All-Inorganic Perovskite Nanocrystals Enabled by Alkaline-Earth Metal Passivation. Chemistry of Materials, 2019, 31, 3974-3983.	3.2	90

#	Article	IF	Citations
42921	Understanding Hysteresis in Carbon Dioxide Sorption in Porous Metalâ€“Organic Frameworks. Inorganic Chemistry, 2019, 58, 6811-6820.	1.9	19
42922	Correlations of Crystal and Electronic Structure via NMR and X-ray Photoelectron Spectroscopies in the RETMAl₂ (RE = Sc, Y, Laâ€“Nd, Sm, Gdâ€“Tm, Lu; TM = Ni, Pd, Pt) Series. Inorganic Chemistry, 2019, 58, 7010-7025.	1.9	16
42923	Unveiling Oxygen Adsorption States on One-Dimensional Pt-Induced Nanowires on Ge(001). Journal of Physical Chemistry C, 2019, 123, 13263-13268.	1.5	1
42924	Low-Temperature Heterolytic Adsorption of H₂ on ZnO(101Ì…0) Surface. Journal of Physical Chemistry C, 2019, 123, 13283-13287.	1.5	21
42925	van der Waals Correction to the Physisorption of Graphene on Metal Surfaces. Journal of Physical Chemistry C, 2019, 123, 13748-13757.	1.5	18
42926	High-Temperature Ferromagnetism in an Fe₃P Monolayer with a Large Magnetic Anisotropy. Journal of Physical Chemistry Letters, 2019, 10, 2733-2738.	2.1	79
42927	Exotic Hydrogen Bonding in Compressed Ammonia Hydrides. Journal of Physical Chemistry Letters, 2019, 10, 2761-2766.	2.1	25
42928	Quaternary Coreâ€“Shell Oxynitride Nanowire Photoanode Containing a Hole-Extraction Gradient for Photoelectrochemical Water Oxidation. ACS Applied Materials & Interfaces, 2019, 11, 19077-19086.	4.0	35
42929	Dynamic Frustrated Lewis Pairs on Ceria for Direct Nonoxidative Coupling of Methane. ACS Catalysis, 2019, 9, 5523-5536.	5.5	54
42930	Binding Site Diversity Promotes CO₂ Electroreduction to Ethanol. Journal of the American Chemical Society, 2019, 141, 8584-8591.	6.6	338
42931	Strong hopping induced Dzyaloshinskiiâ€“Moriya interaction and skyrmions in elemental cobalt. Npj Computational Materials, 2019, 5, .	3.5	7
42932	Implementation of distortion symmetry for the nudged elastic band method with DiSPy. Npj Computational Materials, 2019, 5, .	3.5	2
42933	On the nature of active sites for formic acid decomposition on gold catalysts. Catalysis Science and Technology, 2019, 9, 2836-2848.	2.1	24
42934	Lead-free double perovskites Cs₂InCuCl₆ and (CH₃NH₃)₂InCuCl₆: electronic, optical, and electrical properties. Nanoscale, 2019, 11, 11173-11182.	2.8	35
42935	Strain-induced Nâ€“N bonding and magnetic changes in monolayer intrinsic ferromagnetic TmN₂ (Tmâ€‰â€‰=â€‰â€‰Tc and Nb). Journal of Physics Condensed Matter, 2019, 31, 335801.	0.7	6
42936	Assessing the Role of Fluorine in the Performance of <mml:math xmlns:mml="http://www.w3.org/1998/Math/MathML" display="inline" overflow="scroll"><mml:msub><mml:mi>Al</mml:mi><mml:mi>x</mml:mi></mml:msub><mml:msub><mml:mi>Ga</mml:mi><mml:mi mathvariant="normal">N</mml:mi></mml:mrow></mml:mrow><mml:mo>/</mml:mo><mml:mrow><mml:mi>Ga</mml:mi><mml:mi mathvariant="normal">N</mml:mi></mml:mrow></mml:msub></mml:math> Heterostructure Field-Effect Transistors. Physical Review Applied, 2019, 11, .	4.6	11
42937	Pressure-enhanced interplay between lattice, spin, and charge in the mixed perovskite La2FeMnO6. Physical Review B, 2019, 99, .	1.1	9
42938	Sâ€Doped Grapheneâ€Regional Nucleation Mechanism for Dendriteâ€Free Lithium Metal Anodes. Advanced Energy Materials, 2019, 9, 1804000.	10.2	74

#	Article	IF	Citations
42939	Improving Polysulfides Adsorption and Redox Kinetics by the Co₄N Nanoparticle/Nâ€Doped Carbon Composites for Lithiumâ€Sulfur Batteries. Small, 2019, 15, e1901454.	5.2	130
42940	Explicating the Sodium Storage Kinetics and Redox Mechanism of Highly Pseudocapacitive Binary Transition Metal Sulfide via Operando Techniques and Ab Initio Evaluation. Small Methods, 2019, 3, 1900112.	4.6	21
42941	Sandwiched SiO2@Ni@ZrO2 as a coke resistant nanocatalyst for dry reforming of methane. Applied Catalysis B: Environmental, 2019, 254, 612-623.	10.8	92
42942	The effect of oxygen coverages on hydrogenation of Mg (0001) surface. Applied Surface Science, 2019, 487, 510-518.	3.1	8
42943	Computational prediction and characterization of two-dimensional pentagonal arsenopyrite FeAsS. Computational Materials Science, 2019, 166, 105-110.	1.4	9
42944	Influence of the exchange-correlation potential and magnetic properties on the Li2FeSiO4 cathode materials. Computational Materials Science, 2019, 168, 260-267.	1.4	7
42945	Catalytic mechanism of silver in the oxidative dissolution process of chalcopyrite: Experiment and DFT calculation. Hydrometallurgy, 2019, 187, 18-29.	1.8	29
42946	Tuning CO2 hydrogenation selectivity via metal-oxide interfacial sites. Journal of Catalysis, 2019, 374, 60-71.	3.1	115
42947	Tunable catalytic activity of cobalt-intercalated layered MnO2 for water oxidation through confinement and local ordering. Journal of Catalysis, 2019, 374, 143-149.	3.1	13
42948	Thermal conductivity and diffusion mechanisms of noble gases in uranium dioxide: A DFT+U study. Journal of Nuclear Materials, 2019, 521, 137-145.	1.3	21
42949	Double Half-Heuslers. Joule, 2019, 3, 1226-1238.	11.7	103
42950	RGO induced one-dimensional bimetallic carbide nanorods: An efficient and pH-universal hydrogen evolution reaction electrocatalyst. Nano Energy, 2019, 62, 85-93.	8.2	53
42951	High-pressure phases and pressure-induced phase transition of MoN6 and ReN6. Physics Letters, Section A: General, Atomic and Solid State Physics, 2019, 383, 2429-2435.	0.9	39
42952	Co-doped Na2FePO4F fluorophosphates as a promising cathode material for rechargeable sodium-ion batteries. Solid State Sciences, 2019, 93, 62-69.	1.5	25
42953	Computational Screening of Electrocatalytic Activity of Transition Metal-Doped CdS Nanotubes for Water Splitting. Journal of Physical Chemistry C, 2019, 123, 13419-13427.	1.5	10
42954	Metal@SiO2 Coreâ€“Shells with Self-Arrested Migrating Core. Nano Letters, 2019, 19, 3627-3633.	4.5	6
42955	Iron-Doping-Induced Phase Transformation in Dual-Carbon-Confined Cobalt Diselenide Enabling Superior Lithium Storage. ACS Nano, 2019, 13, 6113-6124.	7.3	108
42956	Cooperativity and coverage dependent molecular desorption in self-assembled monolayers: computational case study with coronene on Au(111) and HOPG. Physical Chemistry Chemical Physics, 2019, 21, 10505-10513.	1.3	11

#	Article	IF	Citations
42957	Experimental and theoretical study of multinuclear indiumâ€“oxo clusters in CHA zeolite for CH₄ activation at room temperature. Physical Chemistry Chemical Physics, 2019, 21, 13415-13427.	1.3	18
42958	Interface engineering in the BNNS@Ti₃C₂ intercalation structure for enhanced electrocatalytic hydrogen evolution. New Journal of Chemistry, 2019, 43, 8613-8619.	1.4	17
42959	Bi₂Te₃ single crystals with high room-temperature thermoelectric performance enhanced by manipulating point defects based on first-principles calculation. RSC Advances, 2019, 9, 14422-14431.	1.7	28
42960	Dispersive non-noble metal phosphide embedded in alumina arrays derived from layered double hydroxide precursor toward efficient oxygen evolution reaction and biomass upgrading. Journal of Materials Chemistry A, 2019, 7, 13695-13704.	5.2	36
42961	Reduction of Fermi level pinning at Cuâ€“BP interfaces by atomic passivation. Nanoscale, 2019, 11, 11569-11576.	2.8	5
42962	A simple numerical approach for reconstructing the atomic stresses at grain boundaries from quantum-mechanical calculations. Journal of Chemical Physics, 2019, 150, 144702.	1.2	5
42963	First principle study on the predicted phase transition of MN (Mâ€‰â€‰=â€‰â€‰Zr, La and Th). Journal of Physics Condensed Matter, 2019, 31, 335402.	0.7	5
42964	Coupling of Spinons with Defects and Phonons in the Spin Chain Compound <mml:math xmlns:mml="http://www.w3.org/1998/Math/MathML" display="inline"><mml:mrow><mml:msub><mml:mrow><mml:mi>Ca</mml:mi></mml:mrow><mml:mn>2</mml:mn></mml:msub><mml:mn> Physical Review Letters, 2019, 122, 185901.	2.9	9
42965	Formation of defects and impurities in MoSx and their effect on electronic properties. Journal of Vacuum Science and Technology A: Vacuum, Surfaces and Films, 2019, 37, 030905.	0.9	0
42966	First-principles calculations of the site preference, phase stability and brittle versus ductile behaviors of TiAl intermetallic alloyed with ternary elements. International Journal of Modern Physics B, 2019, 33, 1950097.	1.0	4
42967	Polyanions Enhance Conversion Reactions for Lithium/Sodiumâ€ion Batteries: The Case of SbVO₄ Nanoparticles on Reduced Graphene Oxide. Small Methods, 2019, 3, 1900231.	4.6	31
42968	Unexpected capture of Guinier-Preston zone and Î³â€³ phase in as-cast Mg-Gd-Y-Zn-Ni-Mn alloy: Atomic-scale insights. Materials Characterization, 2019, 153, 103-107.	1.9	8
42969	Symmetry-Induced Stability in Alkali-Doped Calcium Silicate Hydrate. Journal of Physical Chemistry C, 2019, 123, 14081-14088.	1.5	13
42970	Ferroelectricity and Large Piezoelectric Response of AlN/ScN Superlattice. ACS Applied Materials & Interfaces, 2019, 11, 20482-20490.	4.0	47
42971	Accumulation of Deep Traps at Grain Boundaries in Halide Perovskites. ACS Energy Letters, 2019, 4, 1321-1327.	8.8	117
42972	Understanding Enantioselective Interactions by Pulling Apart Molecular Rotor Complexes. ACS Nano, 2019, 13, 5939-5946.	7.3	8
42973	Engineering atomic-level complexity in high-entropy and complex concentrated alloys. Nature Communications, 2019, 10, 2090.	5.8	182
42974	Ab initio study of electronic temperature effects on magnetic materials properties. Physical Review B, 2019, 99, .	1.1	4

#	Article	IF	Citations
42975	Engineering single-atom dynamics with electron irradiation. Science Advances, 2019, 5, eaav2252.	4.7	61
42976	Reversible Intercalation of Multivalent Al³⁺ Ions into Potassiumâ€Rich Cryptomelane Nanowires for Aqueous Rechargeable Alâ€Ion Batteries. ChemSusChem, 2019, 12, 3753-3760.	3.6	50
42977	C2 oxygenates formation from syngas over the promoter M(Mâ€¯=â€¯Rh, Co) monolayer-modified Cu(111) surface: Probing into the role of monolayer promoter on the selectivity. Applied Surface Science, 2019, 488, 434-444.	3.1	6
42978	MnO2 polymorph selection for non-enzymatic glucose detection: An integrated experimental and density functional theory investigation. Applied Surface Science, 2019, 487, 1033-1042.	3.1	31
42979	Thermodynamic modeling of the Si-Y system aided by first-principles and phonon calculations. Calphad: Computer Coupling of Phase Diagrams and Thermochemistry, 2019, 65, 282-290.	0.7	7
42980	Vacancy effect on the generalized stacking fault energy of alloyed Î³-Ni system: A first-principles study. Computational Materials Science, 2019, 166, 187-192.	1.4	11
42981	Hydrogen storage properties of Li-decorated B2S monolayers: A DFT study. International Journal of Hydrogen Energy, 2019, 44, 16803-16810.	3.8	53
42982	Transition metal doping activated basal-plane catalytic activity of two-dimensional 1Tâ€™-ReS₂ for hydrogen evolution reaction: a first-principles calculation study. Nanoscale, 2019, 11, 10402-10409.	2.8	56
42983	High Performance Anion Exchange Membrane Fuel Cells Enabled by Fluoropoly(olefin) Membranes. Advanced Functional Materials, 2019, 29, 1902059.	7.8	128
42984	Characterization of two-dimensional Ga1â^'Al N ordered alloys with varying chemical composition. Computational Materials Science, 2019, 167, 13-18.	1.4	3
42985	First-principles study of structures, electronic and elastic properties of LaNi5â^'Fe (x: 0.25â€“1.25). Journal of Molecular Graphics and Modelling, 2019, 90, 258-264.	1.3	2
42986	Atomic structure and enhanced thermostability of a new structure MgYZn4 formed by ordered substitution of Y for Mg in MgZn2 in a Mg-Zn-Y alloy. Journal of Materials Science and Technology, 2019, 35, 2058-2063.	5.6	9
42987	Thermal and diffusional properties of (Th,Np)O2 and (U,Np)O2 mixed oxides. Journal of Nuclear Materials, 2019, 521, 89-98.	1.3	6
42988	Effect of mono-halogen-substitution on the electron transporting properties of perylene diimides: A density functional theory study. Journal of Molecular Liquids, 2019, 287, 110968.	2.3	4
42989	Effects of surface structure and halogen substitution on electronic charge transfer in adlayers of (BETS)2-GaCl4 on silver surfaces. Surface Science, 2019, 687, 34-40.	0.8	3
42990	Relative stability of diamond and graphite as seen through bonds and hybridizations. Physical Chemistry Chemical Physics, 2019, 21, 10961-10969.	1.3	20
42991	Surfactant-assisted synthesis of large Cu-BTC MOF single crystals and their potential utilization as photodetectors. CrystEngComm, 2019, 21, 3948-3953.	1.3	19
42992	Contrasting motif preferences of platinum and gold nanoclusters between 55 and 309 atoms. Nanoscale Advances, 2019, 1, 2416-2425.	2.2	17

#	Article	IF	Citations
42993	Topological semimetal porous carbon as a high-performance anode for Li-ion batteries. Journal of Materials Chemistry A, 2019, 7, 14253-14259.	5.2	36
42994	Thermal stability of aluminum oxide nanoparticles: role of oxygen concentration. Inorganic Chemistry Frontiers, 2019, 6, 1701-1706.	3.0	6
42995	Double perovskites as p-type conducting transparent semiconductors: a high-throughput search. Journal of Materials Chemistry A, 2019, 7, 14705-14711.	5.2	32
42996	Structural, Electronic, and Mechanical Properties of A₃Mn₂O₇ (Aâ€‰=â€‰Sr, Ca): Ab Initio Calculation. Ferroelectrics, 2019, 538, 135-145.	0.3	8
42997	Crystallographic-orientation dependent Li ion migration and reactions in layered MoSe ₂. 2D Materials, 2019, 6, 035027.	2.0	13
42998	Interfacial structure and mechanical properties of a new Nb/Re laminated composite. Materials Research Express, 2019, 6, 1065b1.	0.8	1
42999	Magnetoâ€Structural Properties of the Layered Quasiâ€2D Triangularâ€Lattice Antiferromagnets Cs 2 CuCl 4â^' x Br x for x â€‰=â€‰0, 1, 2, and 4. Physica Status Solidi (B): Basic Research, 2019, 256, 1900044.	0.7	4
43000	Graphene-like carbon-nitrogen materials as anode materials for Li-ion and mg-ion batteries. Applied Surface Science, 2019, 487, 1026-1032.	3.1	85
43001	An investigation of thin Zn films on 4H-SiC(0001) graphene. Applied Surface Science, 2019, 487, 1348-1355.	3.1	8
43002	First principles investigation of magnetic new carbon-rich layered compounds UC (n= 2, 6, 12). Computational Condensed Matter, 2019, 21, e00397.	0.9	0
43003	Towards better efficiency of interatomic linear machine learning potentials. Computational Materials Science, 2019, 166, 200-209.	1.4	37
43004	Pd-catalyzed decarbonylation of furfural: Elucidation of support effect on Pd size and catalytic activity using in-situ XAFS. Journal of Catalysis, 2019, 374, 320-327.	3.1	30
43005	Dirac nodal surfaces and nodal lines in ZrSiS. Science Advances, 2019, 5, eaau6459.	4.7	125
43006	Blue phosphorene monolayers as potential nano sensors for volatile organic compounds under point defects. Applied Surface Science, 2019, 486, 52-57.	3.1	87
43007	Pressure-induced structure, vibrational properties, and initial decomposition mechanisms of Î²-HMX crystal: A periodic DFT study. Journal of Molecular Graphics and Modelling, 2019, 90, 144-152.	1.3	5
43008	Thermal transport properties in monolayer GeS. Physics Letters, Section A: General, Atomic and Solid State Physics, 2019, 383, 2499-2503.	0.9	12
43009	Distinction between Intrinsic and X-ray-Induced Oxidized Oxygen States in Li-Rich 3d Layered Oxides and LiAlO₂. Journal of Physical Chemistry C, 2019, 123, 13201-13207.	1.5	33
43010	Adsorption and Diffusion of H Atoms on Î²-PtO₂ Surface: The Role of Nuclear Quantum Effects. Journal of Physical Chemistry C, 2019, 123, 13804-13811.	1.5	9

#	Article	IF	Citations
43011	Theoretical Resolution of the Exceptional Oxygen Reduction Activity of Au(100) in Alkaline Media. ACS Catalysis, 2019, 9, 5567-5573.	5.5	93
43012	Selective Acetylene Hydrogenation over Single-Atom Alloy Nanoparticles by Kinetic Monte Carlo. Journal of the American Chemical Society, 2019, 141, 8541-8549.	6.6	63
43013	â€œSwitching onâ€•iron in clay minerals. Environmental Science: Nano, 2019, 6, 1704-1715.	2.2	21
43014	Rational design of two-dimensional hybrid Co/N-doped carbon nanosheet arrays for efficient bi-functional electrocatalysis. Sustainable Energy and Fuels, 2019, 3, 1757-1763.	2.5	11
43015	Galvanic replacement of liquid metal galinstan with Pt for the synthesis of electrocatalytically active nanomaterials. Nanoscale, 2019, 11, 9705-9715.	2.8	43
43016	Bilayer MSe₂ (MÂ= Zr, Hf) as promising two-dimensional thermoelectric materials: a first-principles study. RSC Advances, 2019, 9, 12394-12403.	1.7	35
43017	Enhanced bulk photovoltaic response in Sn doped BaTiO3 through composition dependent structural transformation. Applied Physics Letters, 2019, 114, .	1.5	23
43018	Nonlinear elasticity of É› -Fe: The pressure effect. Physical Review B, 2019, 99, .	1.1	2
43019	Dynamics of optical excitations in a Fe/MgO(001) heterostructure from time-dependent density functional theory. Physical Review B, 2019, 99, .	1.1	7
43020	Renaissance of 1,2,5â€Oxadiazolyl Diazonium Salts: Synthesis and Reactivity. European Journal of Organic Chemistry, 2019, 2019, 4248-4259.	1.2	12
43021	Multifunctional electrocatalyst PtM with low Pt loading and high activity towards hydrogen and oxygen electrode reactions: A computational study. Applied Catalysis B: Environmental, 2019, 255, 117743.	10.8	66
43022	Ultrahigh stretching bond force constants of linear chains of carbon and boron nitride. Carbon, 2019, 150, 349-355.	5.4	5
43023	Multiscale modelling from quantum level to reactor scale: An example of ethylene epoxidation on silver catalysts. Catalysis Today, 2019, 338, 128-140.	2.2	27
43024	Magnetism and ferroelectricity in BiFeO3 doped with Ga at Fe sites. Journal of Alloys and Compounds, 2019, 797, 117-121.	2.8	13
43025	Computational Screening of Indirect-Gap Semiconductors for Potential Photovoltaic Absorbers. Chemistry of Materials, 2019, 31, 4072-4080.	3.2	31
43026	Ab Initio Flexible Force Field for Metalâ€“Organic Frameworks Using Dummy Model Coordination Bonds. Journal of Chemical Theory and Computation, 2019, 15, 3666-3677.	2.3	9
43027	Role of Surface Species Interactions in Identifying the Reaction Mechanism of Methanol Synthesis from CO₂Hydrogenation over Intermetallic PdIn(310) Steps. Journal of Physical Chemistry C, 2019, 123, 13615-13623.	1.5	32
43028	Anisotropic Compositional Expansion and Chemical Potential of Lithiated SiO₂ Electrodes: Multiscale Mechanical Analysis. ACS Applied Materials & Interfaces, 2019, 11, 19183-19190.	4.0	18

#	Article	IF	Citations
43029	Ab Initio Modeling of Transition Metal Dissolution from the LiNi_{0.5}Mn_{1.5}O₄ Cathode. ACS Applied Materials & Interfaces, 2019, 11, 20110-20116.	4.0	30
43030	Single atom tungsten doped ultrathin Î±-Ni(OH)2 for enhanced electrocatalytic water oxidation. Nature Communications, 2019, 10, 2149.	5.8	363
43031	Carbon dioxide and water co-adsorption on the low-index surfaces of TiC, VC, ZrC and NbC: a DFT study. Physical Chemistry Chemical Physics, 2019, 21, 10750-10760.	1.3	25
43032	Heterostructures of doped graphene and MoX₂ (X = S and Se) as promising anchoring materials for lithiumâ€“sulfur batteries: a first-principles study. New Journal of Chemistry, 2019, 43, 9396-9402.	1.4	17
43033	The origin of intrinsic charge transport for Dirac carbon sheet materials: roles of acetylenic linkage and electronâ€“phonon couplings. Nanoscale, 2019, 11, 10828-10837.	2.8	12
43034	Prediction on elastic properties of Nb-doped Ni systems. Molecular Simulation, 2019, 45, 935-941.	0.9	10
43035	Chemical and structural stability of 2D layered materials. 2D Materials, 2019, 6, 042001.	2.0	94
43036	Structural instability and magnetism of superconducting <mml:math xmlns:mml="http://www.w3.org/1998/Math/MathML"><mml:mrow><mml:msub><mml:mi>KCr</mml:mi><mml:mn>3</mml:mn></mml:msub></mml:mrow></mml:math> Physical Review B, 2019, 99, .	1.1	11
43037	Electrical and optical properties of iron in GaN, AlN, and InN. Physical Review B, 2019, 99, .	1.1	30
43038	Superstructure-Induced Splitting of Dirac Cones in Silicene. Physical Review Letters, 2019, 122, 196801.	2.9	26
43039	An Ab Initio Study of Vacancies in Disordered Magnetic Systems: A Case Study of Fe-Rich Fe-Al Phases. Materials, 2019, 12, 1430.	1.3	11
43040	High-performance Li-ion capacitor based on black-TiO2-x/graphene aerogel anode and biomass-derived microporous carbon cathode. Nano Research, 2019, 12, 1713-1719.	5.8	64
43041	Sulfur-deficient MoS2-x promoted lithium polysulfides conversion in lithium-sulfur battery: A first-principles study. Applied Surface Science, 2019, 487, 452-463.	3.1	58
43042	Uniform nucleation of sodium in 3D carbon nanotube framework via oxygen doping for long-life and efficient Na metal anodes. Energy Storage Materials, 2019, 23, 137-143.	9.5	72
43043	New insights into CO2 methanation mechanisms on Ni/MgO catalysts by DFT calculations: Elucidating Ni and MgO roles and support effects. Journal of CO2 Utilization, 2019, 33, 55-63.	3.3	71
43044	The electronic, magnetic and optical properties of single-layer CrS2 with vacancy defects. Journal of Magnetism and Magnetic Materials, 2019, 487, 165300.	1.0	16
43045	Uniaxial magnetocrystalline anisotropy of tetragonal Mn Ga100âˆ' (50â€¯â‰¤â€¯xâ€¯â‰¤â€¯75) alloys. Journal of Magnetism and Magnetic Materials, 2019, 489, 165308.	1.0	8
43046	Metal-support interaction boosted electrocatalysis of ultrasmall iridium nanoparticles supported on nitrogen doped graphene for highly efficient water electrolysis in acidic and alkaline media. Nano Energy, 2019, 62, 117-126.	8.2	151

#	Article	IF	Citations
43047	Hierarchical nanosheets constructed by integration of bimetallic sulfides into N-Doped carbon: Enhanced diffusion kinetics and cycling stability for sodium storage. Nano Energy, 2019, 62, 239-249.	8.2	84
43048	Preactive Site in Zieglerâ€“Natta Catalysts. Journal of Physical Chemistry C, 2019, 123, 14490-14500.	1.5	11
43049	Impact of Structural Transformation on Electrochemical Performances of Li-Rich Cathode Materials: The Case of Li₂RuO₃. Journal of Physical Chemistry C, 2019, 123, 13491-13499.	1.5	29
43050	Hot-Electron-Mediated Ion Diffusion in Semiconductors for Ion-Beam Nanostructuring. Nano Letters, 2019, 19, 3939-3947.	4.5	15
43051	Exciton Fine Structure in Perovskite Nanocrystals. Nano Letters, 2019, 19, 4068-4077.	4.5	128
43052	Selenium Edge as a Selective Anchoring Site for Lithiumâ€“Sulfur Batteries with MoSe₂/Graphene-Based Cathodes. ACS Applied Materials & Interfaces, 2019, 11, 19986-19993.	4.0	67
43053	Electronic Metalâ€“Support Interaction To Modulate MoS₂-Supported Pd Nanoparticles for the Degradation of Organic Dyes. ACS Applied Nano Materials, 2019, 2, 3385-3393.	2.4	43
43054	Defect-Mediated Phase Transformation in Anisotropic Two-Dimensional PdSe₂ Crystals for Seamless Electrical Contacts. Journal of the American Chemical Society, 2019, 141, 8928-8936.	6.6	81
43055	Noncollinearity-modulated Electronic Properties of Monolayer CrI3. Physical Review Applied, 2019, 11, .	1.5	3
43056	Long-range magnetic order stabilized by acceptors. Physical Review B, 2019, 99, .	1.1	3
43057	Negative-<mml:math xmlns:mml="http://www.w3.org/1998/Math/MathML"><mml:mi>U</mml:mi></mml:math>and polaronic behavior of the Zn-O divacancy in ZnO. Physical Review B, 2019, 99, .	1.1	13
43058	Triplet superconductivity in the Dirac semimetal germanene on a substrate. Physical Review B, 2019, 99, .	1.1	16
43059	Incommensurate Magnetism Near Quantum Criticality in CeNiAsO. Physical Review Letters, 2019, 122, 197203.	2.9	3
43060	Electrolyte Effects on the Stability of Niâ^'Mo Cathodes for the Hydrogen Evolution Reaction. ChemSusChem, 2019, 12, 3491-3500.	3.6	37
43061	Two dimensional InSe/C2N van der Waals heterojunction as enhanced visible-light-responsible photocatalyst for water splitting. Applied Surface Science, 2019, 485, 375-380.	3.1	61
43062	Novel high/ultrahigh pressure structures of TiO2 with low band gaps. Computational Materials Science, 2019, 166, 303-310.	1.4	4
43063	Predicting the formation of <câ€¯+â€¯a> dislocations in magnesium alloys from multiple stacking fault energies. Materialia, 2019, 7, 100352.	1.3	16
43064	Ion Beam Induced Artifacts in Lead-Based Chalcogenides. Microscopy and Microanalysis, 2019, 25, 831-839.	0.2	6

#	Article	IF	Citations
43065	ZnO composite nanolayer with mobility edge quantization for multi-value logic transistors. Nature Communications, 2019, 10, 1998.	5.8	67
43066	A â€œnon-dynamicalâ€•way of describing room-temperature paramagnetic manganese oxide. Physical Chemistry Chemical Physics, 2019, 21, 15932-15939.	1.3	6
43067	The enhanced ferromagnetism of single-layer CrX₃ (X = Br and I) via van der Waals engineering. Physical Chemistry Chemical Physics, 2019, 21, 11949-11955.	1.3	26
43068	A comparative test of different density functionals for calculations of NH₃-SCR over Cu-Chabazite. Physical Chemistry Chemical Physics, 2019, 21, 10923-10930.	1.3	40
43069	Niobium oxide dihalides NbOX₂: a new family of two-dimensional van der Waals layered materials with intrinsic ferroelectricity and antiferroelectricity. Nanoscale Horizons, 2019, 4, 1113-1123.	4.1	43
43070	Inducing half metallicity with alloying in Heusler Compound CoFeMnSb. Journal of Physics Condensed Matter, 2019, 31, 335702.	0.7	2
43071	Drastic enhancement of the Raman intensity in few-layer InSe by uniaxial strain. Physical Review B, 2019, 99, .	1.1	28
43072	Magnetic borophenes from an evolutionary search. Physical Review B, 2019, 99, .	1.1	25
43073	Promising thermoelectric materials of Cu3VX4 (X=S, Se, Te): A Cu-V-X framework plus void tunnels. International Journal of Modern Physics C, 2019, 30, 1950045.	0.8	10
43074	Thermodynamic Stability, Thermoelectric, Elastic and Electronic Structure Properties of ScMN2-Type (M = V, Nb, Ta) Phases Studied by ab initio Calculations. Condensed Matter, 2019, 4, 36.	0.8	2
43075	Chiral Recognition of Hexahelicene on a Surface via the Forming of Asymmetric Heterochiral Trimers. International Journal of Molecular Sciences, 2019, 20, 2018.	1.8	13
43076	Hierarchical and ultrathin copper nanosheets synthesized via galvanic replacement for selective electrocatalytic carbon dioxide conversion to carbon monoxide. Applied Catalysis B: Environmental, 2019, 255, 117736.	10.8	56
43077	Developing a die casting magnesium alloy with excellent mechanical performance by controlling intermetallic phase. Journal of Alloys and Compounds, 2019, 795, 436-445.	2.8	43
43078	Systematic first-principles study on the Ni and X (Xâ€¯=â€¯C, N, O, F, P, S, Cl, Se, and Te) codoped monolayer WS2 (W15Ni1S26X6). Journal of Magnetism and Magnetic Materials, 2019, 486, 165255.	1.0	5
43079	Transport properties and abnormal breakdown of the Stokes-Einstein relation in computer simulated Al72Ni16Co12 metallic melt. Journal of Non-Crystalline Solids, 2019, 517, 83-95.	1.5	8
43080	The anisotropy of three-component medium entropy alloys in AlCoCrFeNi system: First-principle studies. Journal of Solid State Chemistry, 2019, 276, 232-237.	1.4	21
43081	Control and Theoretical Modeling of the Growth Process of AlN Six-fold and Multifold Armed Dendritic Crystals. Crystal Growth and Design, 2019, 19, 3244-3252.	1.4	3
43082	Computational Discovery of Transparent Conducting In-Plane Ordered MXene (i-MXene) Alloys. Chemistry of Materials, 2019, 31, 4124-4132.	3.2	19

#	Article	IF	Citations
43083	Point Defects and Localized Excitons in 2D WSe₂. ACS Nano, 2019, 13, 6050-6059.	7.3	127
43084	Characteristics of sulfur atoms adsorbed on Ag(100), Ag(110), and Ag(111) as probed with scanning tunneling microscopy: experiment and theory. Physical Chemistry Chemical Physics, 2019, 21, 10540-10551.	1.3	11
43085	Single-crystalline melem (C₆N₁₀H₆) nanorods: a novel stable molecular crystal photocatalyst with modulated charge potentials and dynamics. Journal of Materials Chemistry A, 2019, 7, 13234-13241.	5.2	22
43086	Crystal structure prediction of ReN at high pressure: a new incompressible phase. Phase Transitions, 2019, 92, 595-602.	0.6	1
43087	Interstitial Zn-modulated ferromagnetism in Co-doped ZnSe. Materials Research Express, 2019, 6, 106121.	0.8	2
43088	First-principles study of the melting temperature of MgO. Physical Review B, 2019, 99, .	1.1	21
43089	Large spin gaps in the half-metals <mml:math xmlns:mml="http://www.w3.org/1998/Math/MathML"><mml:mi>M</mml:mi><mml:msub><mml:mrow><mml:mi mathvariant="normal">N</mml:mi></mml:mrow><mml:mn>4</mml:mn></mml:msub></mml:math> () Tj ETQq0 0 0 rgBT /Overlock 10	1.1	10
43090	xmlns:mml="http://www.w3.org/1998/Math/MathML"><mml:msub><mml:mrow><mml:mi mathvariant="n Proximity of Ferromagnetic Nickel to Paramagnetic Instability. JETP Letters, 2019, 109, 276-279.	0.4	1
43091	Gas Sensors Based on Mechanically Exfoliated MoS2 Nanosheets for Room-Temperature NO2 Detection. Sensors, 2019, 19, 2123.	2.1	70
43092	Morphological and structural engineering in amorphous Cu2MoS4 nanocages for remarkable electrocatalytic hydrogen evolution. Science China Materials, 2019, 62, 1275-1284.	3.5	23
43093	Machine learning for hierarchical prediction of elastic properties in Fe-Cr-Al system. Computational Materials Science, 2019, 166, 119-123.	1.4	20
43094	The effect of oxygen vacancy on magnetism of geometrically frustrated triangular lattice CuFeO2: Ab initio study. Journal of Magnetism and Magnetic Materials, 2019, 486, 165295.	1.0	7
43095	High-Temperature Grafting Silylation for Minimizing Leaching of Acid Functionality from Hydrophobic Mesoporous Silicas Used as Catalysts in the Liquid Phase. Langmuir, 2019, 35, 6838-6852.	1.6	19
43096	Self-Combustion Synthesis of Novel Metastable Ternary Molybdenum Nitrides. , 2019, 1, 64-70.		20
43097	Family-dependent magnetism in atomic boron adsorbed armchair graphene nanoribbons. Journal of Materials Chemistry C, 2019, 7, 6241-6245.	2.7	16
43098	DFT and MÃ¶ssbauer Spectroscopy Study of a FeTe0.5Se0.5 Single Crystal. JETP Letters, 2019, 109, 266-269.	0.4	1
43099	DFT Study on the Interaction of Subnanometer Cobalt Clusters with Pristine/Defective Graphene. Bulletin of the Korean Chemical Society, 2019, 40, 446-452.	1.0	6
43100	Effect of Ba addition to Ga-Î±-Al2O3 catalyst on structure and catalytic selectivity for dehydrogenation of ethane. Applied Catalysis A: General, 2019, 581, 23-30.	2.2	21

#	Article	IF	Citations
43101	Local structures of nitrogen-doped graphdiynes determined by computational X-ray spectroscopy. Carbon, 2019, 149, 672-678.	5.4	22
43102	Investigation of the temperature in dense carbon near the solid-liquid phase transition between 100ÂGPa and 200ÂGPa with spectrally resolved X-ray scattering. High Energy Density Physics, 2019, 32, 56-62.	0.4	5
43103	First-principles study of impurity segregation in zirconia, hafnia, and yttria-stabilized-zirconia grain boundaries. Journal of the European Ceramic Society, 2019, 39, 3812-3820.	2.8	10
43104	First principles study of electronic structure, magnetism and ferroelectric properties of rhombohedral AgFeO2. Journal of Magnetism and Magnetic Materials, 2019, 487, 165296.	1.0	5
43105	First-principles study of the surface properties of Î³-LiAlO2: Stability and tritium adsorption. Journal of Nuclear Materials, 2019, 522, 1-10.	1.3	17
43106	Studying the insulating characters of cubic ZrO2 slabs with nine terminations within three lower index Miller planes (001), (110) and (111). Microelectronic Engineering, 2019, 213, 77-85.	1.1	9
43107	Competition between formation of Al2O3 and Cr2O3 in oxidation of Al0.3CoCrCuFeNi high entropy alloy: A first-principles study. Scripta Materialia, 2019, 168, 139-143.	2.6	28
43108	Chirality Transfer in Gold Nanoparticles by <scp>l</scp>-Cysteine Amino Acid: A First-Principles Study. Journal of Physical Chemistry C, 2019, 123, 13758-13764.	1.5	23
43109	Electron Transport through Metal/MoS₂ Interfaces: Edge- or Area-Dependent Process?. Nano Letters, 2019, 19, 3641-3647.	4.5	42
43110	CO₂ Photoreduction via Quantum Tunneling: Thin TiO₂-Coated GaP with Coherent Interface To Achieve Electron Tunneling. ACS Catalysis, 2019, 9, 5668-5678.	5.5	22
43111	Cation and anion immobilization through chemical bonding enhancement with fluorides for stable halide perovskite solar cells. Nature Energy, 2019, 4, 408-415.	19.8	831
43112	Building aqueous K-ion batteries for energy storage. Nature Energy, 2019, 4, 495-503.	19.8	630
43113	Pressure dependence of direct optical transitions in ReS2 and ReSe2. Npj 2D Materials and Applications, 2019, 3, .	3.9	35
43114	Strain sensitivity of band structure and electron mobility in perovskite BaSnO₃: first-principles calculation. RSC Advances, 2019, 9, 14072-14077.	1.7	16
43115	The effect of water on the validity of LÃ¶wenstein's rule. Chemical Science, 2019, 10, 5705-5711.	3.7	37
43116	Evidence of ferromagnetic ground state and strong spin phonon coupling in Zr₂TiAl with bi-axial strain: first principles study. Journal of Physics Communications, 2019, 3, 055010.	0.5	0
43117	High-pressure phases of boron arsenide with potential high thermal conductivity. Physical Review B, 2019, 99, .	1.1	15
43118	Contrasting the magnetism in La2â^'xSrxFeCoO6(x=0,1,2) double perovskites: The role of electronic and cationic disorder. Physical Review B, 2019, 99, .	1.1	13

#	Article	IF	Citations
43119	Crucial role of atomic corrugation on the flat bands and energy gaps of twisted bilayer graphene at the magic angle <mml:math xmlns:mml="http://www.w3.org/1998/Math/MathML"><mml:mrow><mml:mi>Î¸</mml:mi><mml:mo>â‰¼</mml:mo><mml:mn>1</mml:mn></mml: Physical Review B, 2019, 99, .	1.1	119
43120	Weyl points created by a three-dimensional flat band. Physical Review B, 2019, 99, .	1.1	23
43121	Using Doping to Modify the Properties of SrFeO3 and SrCoO3 Oxides: DFT Calculations of the Electronic Structure. Journal of Structural Chemistry, 2019, 60, 171-178.	0.3	4
43122	First-Principles Investigation of the Stability of the Oxygen Framework of Li-Rich Battery Cathodes. MRS Advances, 2019, 4, 813-820.	0.5	4
43123	Low-temperature anharmonicity and the thermal conductivity of cesium iodide. Physical Review B, 2019, 99, .	1.1	11
43124	Atomistic behavior of metal surfaces under high electric fields. Physical Review B, 2019, 99, .	1.1	15
43125	Probing and imaging spin interactions with a magnetic single-molecule sensor. Science, 2019, 364, 670-673.	6.0	83
43126	Molecular Structures Polymorphism the Role of Fâ€¦F Interactions in Crystal Packing of Fluorinated Tosylates. Crystals, 2019, 9, 242.	1.0	13
43127	DFT modelling of the edge dislocation in 4H-SiC. Journal of Materials Science, 2019, 54, 10737-10745.	1.7	13
43128	New physical insight in structural and electronic properties of InSb nano-sheet being rolled up into single-wall nanotubes. Applied Surface Science, 2019, 487, 550-557.	3.1	9
43129	Improving the charge transfer performance of Si nanomaterial through C surface modification: A first-principles study. Current Applied Physics, 2019, 19, 817-821.	1.1	1
43130	Updated comments on projector augmented wave (PAW) implementations within various electronic structure code packages. Computer Physics Communications, 2019, 243, 25-29.	3.0	10
43131	Super-stretchability in two-dimensional RuCl3 and RuBr3 confirmed by first-principles simulations. Physica E: Low-Dimensional Systems and Nanostructures, 2019, 113, 79-85.	1.3	9
43132	Insight into delithiation process on the LiFePO4 (010) surface from a novel viewpoint of the work function. Solid State Ionics, 2019, 338, 25-30.	1.3	10
43133	Structureâ€“Performance Relationships for Propane Dehydrogenation over Aluminum Supported Vanadium Oxide. ACS Catalysis, 2019, 9, 5816-5827.	5.5	76
43134	Graphene Oxide Promoted Cadmium Uptake by Rice in Soil. ACS Sustainable Chemistry and Engineering, 2019, 7, 10283-10292.	3.2	29
43135	NO gas sensor based on ZnGa2O4 epilayer grown by metalorganic chemical vapor deposition. Scientific Reports, 2019, 9, 7459.	1.6	50
43136	Atomically tailoring vacancy defects in FeF_{2.2}(OH)_{0.8} toward ultra-high rate and long-life Li/Na-ion batteries. Journal of Materials Chemistry A, 2019, 7, 14180-14191.	5.2	4

#	Article	IF	Citations
43137	Pyrite-type ruthenium disulfide with tunable disorder and defects enables ultra-efficient overall water splitting. Journal of Materials Chemistry A, 2019, 7, 14222-14232.	5.2	50
43138	The performance of adsorption, dissociation and diffusion mechanism of hydrogen on the Ti-doped ZrCo(110) surface. Physical Chemistry Chemical Physics, 2019, 21, 12597-12605.	1.3	14
43139	Visualization of fast â€œhydrogen pumpâ€•in coreâ€“shell nanostructured Mg@Pt through hydrogen-stabilized Mg₃Pt. Journal of Materials Chemistry A, 2019, 7, 14629-14637.	5.2	62
43140	Ti-fraction-induced electronic and magnetic transformations in titanium oxide films. Journal of Chemical Physics, 2019, 150, 154704.	1.2	2
43141	Stabilizing the metastable superhard material wurtzite boron nitride by three-dimensional networks of planar defects. Proceedings of the National Academy of Sciences of the United States of America, 2019, 116, 11181-11186.	3.3	19
43142	Atomic-scale analyses of Nb₃Sn on Nb prepared by vapor diffusion for superconducting radiofrequency cavity applications: a correlative study. Superconductor Science and Technology, 2019, 32, 024001.	1.8	25
43143	Interaction of two symmetric monovacancy defects in graphene. Chinese Physics B, 2019, 28, 046801.	0.7	2
43144	Alloy structure of rare earth Ce with Pt base metal, and the adsorption of CO. Materials Research Express, 2019, 6, 046538.	0.8	0
43145	Incipient adsorption of water and hydroxyl on hematite (0001) surface. Journal of Physics Communications, 2019, 3, 035023.	0.5	7
43146	First-principles investigation of the effect of substitution and surface adsorption on the magnetostrictive performance of Fe-Ga alloys. Physical Review B, 2019, 99, .	1.1	7
43147	Non-PGM Electrocatalysts for PEM Fuel Cells: Thermodynamic Stability and DFT Evaluation of Fluorinated FeN₄-Based ORR Catalysts. Journal of the Electrochemical Society, 2019, 166, F3277-F3286.	1.3	25
43148	The Enhancement of H2 Evolution over Sr1â^'1.5xTbxWO4 Solid Solution under Ultraviolet Light Irradiation. Materials, 2019, 12, 1487.	1.3	4
43149	Efficient Calculation Methods for the Diffusion Coefficient of Interstitial Solutes in Dilute Alloys. Materials, 2019, 12, 1491.	1.3	3
43150	The Effect of Alloying Elements on the Structural Stability, and Mechanical and Electronic Properties of Al3Sc: A First-Principles Study. Materials, 2019, 12, 1539.	1.3	7
43151	Tuning Electronic Properties of the SiC-GeC Bilayer by External Electric Field: A First-Principles Study. Micromachines, 2019, 10, 309.	1.4	3
43152	First-Principles Analysis of Vibrational Properties of Type II SiGe Alloy Clathrates. Nanomaterials, 2019, 9, 723.	1.9	3
43153	Structural Stability and Electronic and Optical Properties of Coinage-Metal (4, 2) Alloy Nanotubes: A First-Principles Study. Journal of the Korean Physical Society, 2019, 74, 555-562.	0.3	0
43154	Resolving the FCC/HCP interface of the <mml:math xmlns:mml="http://www.w3.org/1998/Math/MathML" altimg="si1.svg"><mml:mrow><mml:mi>Î³</mml:mi><mml:mo>'</mml:mo></mml:mrow></mml:math> (<mml:math xmlns:mml="http://www.w3.org/1998/Math/MathML") Tj ETQq1 1 0.784314 rgBT /Overlock 10 Tf 50 52 Td (altimg="si2.svg precipitate phase in aluminium. Acta Materialia, 2019, 174, 116-130.	3.8	20

#	Article	IF	Citations
43155	Theoretical prediction of tunable electronic and magnetic properties of monolayer antimonene by vacancy and strain. Applied Surface Science, 2019, 488, 98-106.	3.1	20
43156	Impurity influence on the oxygen adsorption on Ti3Al(0001) surface. Applied Surface Science, 2019, 487, 898-906.	3.1	14
43157	Structure and physical properties of Ni-based quasi-one-dimensional selenides Rb0.9Ni3.1Se3 and K0.7Ni3.1Se3. Journal of Alloys and Compounds, 2019, 793, 425-432.	2.8	6
43158	Effect of organic coating on the charge distribution of CoFe2O4 nanoparticles. Journal of Alloys and Compounds, 2019, 796, 9-12.	2.8	8
43159	Structural origin of blue luminescence in Ce-doped Ba2Y5B5O17 and Ba3Y2B6O15 with multiple cation sites and occupational disorder. Journal of Alloys and Compounds, 2019, 797, 890-895.	2.8	5
43161	High pressure structural stability of ThN: ab-initio study. Journal of Nuclear Materials, 2019, 521, 161-166.	1.3	7
43162	Interlayer vibration of twisted bilayer graphene: A first-principles study. Physics Letters, Section A: General, Atomic and Solid State Physics, 2019, 383, 2628-2632.	0.9	16
43163	Elucidation of the Structure and Vibrational Spectroscopy of Synthetic Metaschoepite and Its Dehydration Product. Inorganic Chemistry, 2019, 58, 7310-7323.	1.9	19
43164	Coordination corrected ab initio formation enthalpies. Npj Computational Materials, 2019, 5, .	3.5	38
43165	Structural prediction of stabilized atomically thin tin layers. Npj 2D Materials and Applications, 2019, 3, .	3.9	14
43166	Reaction mechanism and kinetics for ammonia synthesis on the Fe(211) reconstructed surface. Physical Chemistry Chemical Physics, 2019, 21, 11444-11454.	1.3	27
43167	Computational investigation of the Mg-ion conductivity and phase stability of MgZr₄(PO₄)₆. RSC Advances, 2019, 9, 12590-12595.	1.7	24
43168	Unraveling the metastability of the SI and SII carbon monoxide hydrate with a combined DFT-neutron diffraction investigation. Journal of Chemical Physics, 2019, 150, 184705.	1.2	12
43169	Surface chemistry of 2,3-dibromosubstituted norbornadiene/quadricyclane as molecular solar thermal energy storage system on Ni(111). Journal of Chemical Physics, 2019, 150, 184706.	1.2	17
43170	Thin Ti adhesion layer breaks bottleneck to hot hole relaxation in Au films. Journal of Chemical Physics, 2019, 150, 184701.	1.2	14
43171	Tailoring the Functionality of Organic Spacer Cations for Efficient and Stable Quasiâ€2D Perovskite Solar Cells. Advanced Functional Materials, 2019, 29, 1900221.	7.8	144
43172	Computationâ€Guided Design of LiTaSiO₅, a New Lithium Ionic Conductor with Sphene Structure. Advanced Energy Materials, 2019, 9, 1803821.	10.2	35
43173	Interfacial Interactions and Enhanced Optoelectronic Properties in CsSnI 3 â€“Black Phosphorus van der Waals Heterostructures. Physica Status Solidi (B): Basic Research, 2019, 256, 1800540.	0.7	34

#	Article	IF	Citations
43174	Oxygenationâ€Induced Twoâ€Dimensional Topological Insulators in Antimony Arsenide. Physica Status Solidi - Rapid Research Letters, 2019, 13, 1900146.	1.2	1
43175	Enhanced Photodetection Properties of Tellurium@Selenium Rollâ€toâ€Roll Nanotube Heterojunctions. Small, 2019, 15, e1900902.	5.2	120
43176	Investigation on heterogeneous nucleation substrate of Y2O3 as NbC in hypereutectic Feâ€“Crâ€“C hardfacing coating by experiment and first-principles calculation. Journal of Materials Science, 2019, 54, 10102-10118.	1.7	9
43177	Ab initio studies of copper hydrides under high pressure. Frontiers of Physics, 2019, 14, 1.	2.4	9
43178	Effect of stacking fault segregation and local phase transformations on creep strength in Ni-base superalloys. Acta Materialia, 2019, 172, 55-65.	3.8	71
43179	Octahedral-shaped perovskite CaCu3Ti4O12 with dual defects and coexposed {(001), (111)} facets for visible-light photocatalysis. Applied Catalysis B: Environmental, 2019, 254, 86-97.	10.8	48
43180	Foamâ€“like Co9S8/Ni3S2 heterostructure nanowire arrays for efficient bifunctional overall waterâ€“splitting. Applied Catalysis B: Environmental, 2019, 253, 246-252.	10.8	138
43181	Covalent bonding versus total energy: On the attainability of certain predicted low-energy carbon allotropes. Carbon, 2019, 148, 151-158.	5.4	14
43182	BC2N monolayers as promising anchoring materials for lithium-sulfur batteries: First-principles insights. Carbon, 2019, 149, 530-537.	5.4	44
43183	Effect of mass transfer process on hydrogen adsorption on polycrystalline platinum electrode in sulfuric acid solution. Chinese Chemical Letters, 2019, 30, 1168-1172.	4.8	6
43184	Robust band gap topological insulators of SbS and SbSH. Chemical Physics, 2019, 523, 110-113.	0.9	4
43185	Alternatives to conventional ensemble averages for thermodynamic properties. Current Opinion in Chemical Engineering, 2019, 23, 70-76.	3.8	11
43186	General adsorption model for H2S, H2Se, H2Te, NH3, PH3, AsH3 and SbH3 on the V2O5(0 0 1) surface including the van der Waals interaction. Chemical Physics Letters, 2019, 720, 58-63.	1.2	30
43187	Two-dimensional van der Waals heterostructure of indium selenide/antimonene: Efficient carrier separation. Chemical Physics Letters, 2019, 727, 50-54.	1.2	6
43188	Chemical optimization towards superior electrocatalysis of Janus 1T-MoSX (Xâ€¯=â€¯O, Se, Te) for hydrogen evolution: Small composition tuning makes big difference. Electrochimica Acta, 2019, 310, 153-161.	2.6	9
43189	Density functional theory study of furfural electrochemical oxidation on the Pt (1â€¯1â€¯1) surface. Journal of Catalysis, 2019, 373, 322-335.	3.1	37
43190	Prediction of robust multiple Dirac-cones in newly designed perovskite R3Âc phase AgBO3 from first-principles. Results in Physics, 2019, 13, 102301.	2.0	5
43191	Effect of Axial Coordination of Iron Porphyrin on Their Nanostructures and Photocatalytic Performance. Crystal Growth and Design, 2019, 19, 3279-3287.	1.4	13

#	Article	IF	Citations
43192	Probing the Stability and Band Gaps of Cs₂AgInCl₆ and Cs₂AgSbCl₆ Lead-Free Double Perovskite Nanocrystals. Chemistry of Materials, 2019, 31, 3134-3143.	3.2	144
43193	Size-Driven Stability of Lanthanide Thiophosphates Grown from an Iodide Flux. Inorganic Chemistry, 2019, 58, 6565-6573.	1.9	19
43194	Parallel Multistream Training of High-Dimensional Neural Network Potentials. Journal of Chemical Theory and Computation, 2019, 15, 3075-3092.	2.3	124
43195	CO₂ Activation on Ni(111) and Ni(100) Surfaces in the Presence of H₂O: An Ambient-Pressure X-ray Photoelectron Spectroscopy Study. Journal of Physical Chemistry C, 2019, 123, 12176-12182.	1.5	36
43196	Plutonium Oxidation States in Complex Molecular Solids. Journal of Physical Chemistry C, 2019, 123, 12096-12103.	1.5	18
43197	Investigation of the (100) Surface of the Ce3Pd20Si6 Intermetallic Cage Compound. Journal of Physical Chemistry C, 2019, 123, 12355-12366.	1.5	3
43198	Stable AA-Stacked Pt Nanoclusters Supported on Graphene/Ru(0001) and the Selective Catalysis: A Theoretical Study. ACS Applied Nano Materials, 2019, 2, 2921-2925.	2.4	7
43199	First-Principles Kinetic and Spectroscopic Insights into Single-Atom Catalysis. ACS Catalysis, 2019, 9, 5002-5010.	5.5	37
43200	Adsorption Preference Determines Segregation Direction: A Shortcut to More Realistic Surface Models of Alloy Catalysts. ACS Catalysis, 2019, 9, 5011-5018.	5.5	27
43201	Understanding Oxygen Activation on Nanoporous Gold. ACS Catalysis, 2019, 9, 5204-5216.	5.5	26
43202	Photochromic Lanthanide(III) Materials with Ion Sensing Based on Pyridinium Tetrazolate Zwitterion. ACS Omega, 2019, 4, 7492-7497.	1.6	10
43203	Ultrafast charge transfer coupled with lattice phonons in two-dimensional covalent organic frameworks. Nature Communications, 2019, 10, 1873.	5.8	93
43204	Optimizing reaction paths for methanol synthesis from CO2 hydrogenation via metal-ligand cooperativity. Nature Communications, 2019, 10, 1885.	5.8	116
43205	Thermal stability and electronic and magnetic properties of atomically thin 2D transition metal oxides. Npj 2D Materials and Applications, 2019, 3, .	3.9	55
43206	Atomic structure observations and reaction dynamics simulations on triple phase boundaries in solid-oxide fuel cells. Communications Chemistry, 2019, 2, .	2.0	16
43207	Thermodynamics, kinetics and electronic properties of point defects in Î²-FeSi₂. Physical Chemistry Chemical Physics, 2019, 21, 10497-10504.	1.3	15
43208	Self-ordering of chemisorbed PTCDA molecules on Ge(001) driven by repulsive forces. Physical Chemistry Chemical Physics, 2019, 21, 9504-9511.	1.3	4
43209	Tunable valley and spin splitting in 2H-VSe₂/BiFeO₃(111) triferroic heterostructures. Nanoscale, 2019, 11, 10329-10338.	2.8	38

#	Article	IF	Citations
43210	Thermally driven homonuclear-stacking phase of MoS₂ through desulfurization. Nanoscale, 2019, 11, 11138-11144.	2.8	4
43211	Two-dimensional hexagonal boronâ€“carbonâ€“nitrogen atomic layers. Nanoscale, 2019, 11, 10454-10462.	2.8	34
43212	First principles study of graphene on metals with the SCAN and SCAN+rVV10 functionals. Journal of Chemical Physics, 2019, 150, 154702.	1.2	17
43213	A full additive QM/MM scheme for the computation of molecular crystals with extension to many-body expansions. Journal of Chemical Physics, 2019, 150, 154118.	1.2	6
43214	Energetics of native defects in ZnRh2O4 spinel from hybrid density functional calculations. Journal of Applied Physics, 2019, 125, .	1.1	3
43215	Local screened Coulomb correction approach to strongly correlated d-electron systems. Journal of Chemical Physics, 2019, 150, 154116.	1.2	22
43216	Emergence of topological electronic phases in elemental lithium under pressure. Proceedings of the National Academy of Sciences of the United States of America, 2019, 116, 9197-9201.	3.3	10
43217	Thermal conductivity of dissociating waterâ€”an ab initio study. New Journal of Physics, 2019, 21, 023007.	1.2	12
43218	Theoretical investigation of the anchoring and activity of a gold cluster on two-dimensional substrates. Materials Research Express, 2019, 6, 075069.	0.8	2
43219	A facile reduction treatment to derive Mo₆S₈ from exfoliated MoS₂ for efficient microwave absorption applications. Materials Research Express, 2019, 6, 085049.	0.8	11
43220	From an atomic layer to the bulk: Low-temperature atomistic structure and ferroelectric and electronic properties of SnTe films. Physical Review B, 2019, 99, .	1.1	39
43221	Renormalized interactions in truncated cluster expansions. Physical Review B, 2019, 99, .	1.1	9
43222	Quantum oscillations in iron-doped single crystals of the topological insulator<mml:math xmlns:mml="http://www.w3.org/1998/Math/MathML"><mml:mrow><mml:mi mathvariant="normal">S</mml:mi><mml:msub><mml:mi mathvariant="normal">b</mml:mi><mml:mn>2</mml:mn></mml:msub><mml:mi mathvariant="normal">T</mml:mi><mml:msub><mml:mi mathvariant="normal">e</mml:mi><mml:mn>3</mml:mn></mml:msub></mml:mrow></mml:math>. Physi	1.1	26
43223	Band-Resolved Imaging of Photocurrent in a Topological Insulator. Physical Review Letters, 2019, 122, 167401.	2.9	55
43224	First-Principles Prediction of Potentials and Space-Charge Layers in All-Solid-State Batteries. Physical Review Letters, 2019, 122, 167701.	2.9	57
43225	Ion Association in Lanthanide Chloride Solutions. Chemistry - A European Journal, 2019, 25, 8725-8740.	1.7	5
43226	Phosphoreneâ€Supported Transitionâ€Metal Dimer for Effective N₂ Electroreduction. ChemPhysChem, 2019, 20, 3141-3146.	1.0	24
43227	Strong Charge Transfer at 2Hâ€“1T Phase Boundary of MoS₂ for Superb Highâ€Performance Energy Storage. Small, 2019, 15, e1900131.	5.2	53

#	Article	IF	Citations
43228	BiVO4 nanocrystals with controllable oxygen vacancies induced by Zn-doping coupled with graphene quantum dots for enhanced photoelectrochemical water splitting. Chemical Engineering Journal, 2019, 372, 399-407.	6.6	102
43229	Optical properties of oxygen vacancy in gamma-LiAlO2: A computational study. Chemical Physics Letters, 2019, 727, 85-89.	1.2	5
43230	Efficient and Stable CsPbI₃ Solar Cells via Regulating Lattice Distortion with Surface Organic Terminal Groups. Advanced Materials, 2019, 31, e1900605.	11.1	209
43231	Role of Water and Defects in Photoâ€Oxidative Degradation of Methylammonium Lead Iodide Perovskite. Small Methods, 2019, 3, 1900154.	4.6	49
43232	Site Selective Detection of Methane Dissociation on Stepped Pt Surfaces. Topics in Catalysis, 2019, 62, 859-873.	1.3	17
43233	A new insight into catalytic role of copper sulfate on elemental mercury oxidation: DFT and experimental study. Fuel, 2019, 252, 10-18.	3.4	15
43234	Theoretical study of Mâ€“H (M=Ti, V, Zr or Nb) structure phase diagram at high pressures. International Journal of Hydrogen Energy, 2019, 44, 13592-13605.	3.8	4
43235	Coexistence of Different Charge-Transfer Mechanisms in the Hot-Carrier Dynamics of Hybrid Plasmonic Nanomaterials. Nano Letters, 2019, 19, 3187-3193.	4.5	34
43236	Interpreting Electrochemical and Chemical Sodiation Mechanisms and Kinetics in Tin Antimony Battery Anodes Using in Situ Transmission Electron Microscopy and Computational Methods. ACS Applied Energy Materials, 2019, 2, 3578-3586.	2.5	14
43237	Computational Design of Mixed-Valence Tin Sulfides as Solar Absorbers. ACS Applied Materials & Interfaces, 2019, 11, 24867-24875.	4.0	11
43238	Improved Electrocatalytic Water Splitting Reaction on CeO₂(111) by Strain Engineering: A DFT+U Study. ACS Catalysis, 2019, 9, 4853-4861.	5.5	37
43239	Nucleobase Stacking at Clay Edges, a Favorable Interaction for RNA/DNA Oligomerization. ACS Earth and Space Chemistry, 2019, 3, 1023-1033.	1.2	5
43240	Natural arsenic with a unique order structure: potential for new quantum materials. Scientific Reports, 2019, 9, 6275.	1.6	11
43241	Computational study of the mixed B-site perovskite SmB_xCo_{1â^'x}O_{3â^'d} (B = Mn, Fe, Ni, Cu) for next generation solid oxide fuel cell cathodes. Physical Chemistry Chemical Physics, 2019, 21, 9407-9418.	1.3	20
43242	Valence mediated tunable magnetism and electronic properties by ferroelectric polarization switching in 2D FeI₂/In₂Se₃ van der Waals heterostructures. Nanoscale, 2019, 11, 9931-9936.	2.8	75
43243	Transferability of the SRP32-vdW specific reaction parameter functional to CHD3 dissociation on Pt(110)-(2 Ã— 1). Journal of Chemical Physics, 2019, 150, 124702.	1.2	17
43244	Prediction of high-mobility two-dimensional electron gas at KTaO 3 -based heterointerfaces. Chinese Physics B, 2019, 28, 047101.	0.7	7
43245	Tunable type-II <mml:math xmlns:mml="http://www.w3.org/1998/Math/MathML" display="inline" overflow="scroll"><mml:msub><mml:mrow><mml:mi>Bi</mml:mi><mml:mi>VO</mml:mi></mml:mrow><mml:mn>4</mml:mn></mml:msub></mml:math> /g- <mml:math xmlns:mml="http://www.w3.org/1998/Math/MathML" display="inline" overflow="scroll"><mml:msub><mml:mrow><mml:mrow><mml:mi mathvariant="normal">C</mml:mi></mml:mrow></mml:mrow><mml:mn>3</mml:mn></mml:msub></mml:math> Physical Review Applied, 201	1.5	23

#	Article	IF	Citations
43246	Magnetic ground state, field-induced transitions, electronic structure, and optical band gap of the frustrated antiferromagnet GeCo2O4. Physical Review B, 2019, 99, .	1.1	22
43247	Experimental and Theoretical Trends of PGM-Free Electrocatalysts for the Oxygen Reduction Reaction with Different Transition Metals. Journal of the Electrochemical Society, 2019, 166, F3136-F3142.	1.3	42
43248	Large Second Harmonic Generation (SHG) Effect and High Laserâ€Induced Damage Threshold (LIDT) Observed Coexisting in Gallium Selenide. Angewandte Chemie, 2019, 131, 8171-8175.	1.6	37
43249	Large Second Harmonic Generation (SHG) Effect and High Laserâ€Induced Damage Threshold (LIDT) Observed Coexisting in Gallium Selenide. Angewandte Chemie - International Edition, 2019, 58, 8087-8091.	7.2	145
43250	Identifying the general trend of activity of non-stoichiometric metal oxide phases for CO oxidation on Pd(111). Science China Chemistry, 2019, 62, 784-789.	4.2	13
43251	Toughness enhancement in TiN/WN superlattice thin films. Acta Materialia, 2019, 172, 18-29.	3.8	72
43252	Misfit strain induced phase transformation at a basal/prismatic twin boundary in deformation of magnesium. Computational Materials Science, 2019, 164, 186-194.	1.4	16
43253	Influence of changes in electronic structure on magnetocrystalline anisotropy of <mml:math xmlns:mml="http://www.w3.org/1998/Math/MathML" altimg="si5.gif" overflow="scroll"><mml:mrow><mml:mi mathvariant="normal">Y</mml:mi><mml:mi mathvariant="normal">C</mml:mi><mml:msub><mml:mi mathvariant="normal">o</mml:mi><mml:mn>5</mml:mn></mml:msub></mml:mrow></mml:math> and related compounds. Journal of Magnetism and Magnetic Materials, 2019, 485, 61-68.	1.0	9
43254	Shedding Light on the Intrinsic Characteristics of 3D Distorted Fluorite-Type Zirconium Tellurite Single Crystals. Inorganic Chemistry, 2019, 58, 7794-7802.	1.9	10
43255	Mechanistic Investigations on Thermal Hydrogenation of CO₂ to Methanol by Nanostructured CeO₂(100): The Crystal-Plane Effect on Catalytic Reactivity. Journal of Physical Chemistry C, 2019, 123, 11763-11771.	1.5	35
43256	Atomic-Scale Dynamics and Storage Performance of Na/K on FeF₃ Nanosheet. ACS Applied Materials & Interfaces, 2019, 11, 17425-17434.	4.0	8
43257	Ab initio calculation of multilayer magnetic structures by VASP on OpenPOWER high performance system. Journal of Physics: Conference Series, 2019, 1163, 012059.	0.3	0
43258	The Structural stabilities and Band Gap Engineering of Core-Shell Nanowires. IOP Conference Series: Materials Science and Engineering, 2019, 490, 022021.	0.3	1
43259	Negative Te spin polarization responsible for ferromagnetic order in the doped topological insulator <mml:math xmlns:mml="http://www.w3.org/1998/Math/MathML"><mml:mrow><mml:msub><mml:mi mathvariant="normal">V</mml:mi><mml:mrow><mml:mn>0.04</mml:mn></mml:mrow></mml:msub><mml:msub><mml:mrow><mml:m Physical Review B, 2019, 99, .	1.1	12
43260	Fragility of Fermi arcs in Dirac semimetals. Physical Review B, 2019, 99, .	1.1	19
43261	Origin of giant negative piezoelectricity in a layered van der Waals ferroelectric. Science Advances, 2019, 5, eaav3780.	4.7	157
43262	Band alignment tuning in GeS/arsenene staggered heterostructures. Journal of Alloys and Compounds, 2019, 793, 283-288.	2.8	13
43263	Unraveling the Hidden Martensitic Phase Transition in BaClF and PbClF under High Pressure Using an Ab Initio Evolutionary Approach. Inorganic Chemistry, 2019, 58, 5886-5899.	1.9	9

#	Article	IF	Citations
43264	Computational Screening of Defective Group IVA Monochalcogenides as Efficient Catalysts for Hydrogen Evolution Reaction. Journal of Physical Chemistry C, 2019, 123, 11791-11797.	1.5	24
43265	Phase transitions and ferroelasticityâ€“multiferroicity in bulk and two-dimensional silver and copper monohalides. Nanoscale Horizons, 2019, 4, 1106-1112.	4.1	32
43266	Ferroelectricity driven by soft phonon and spin order in multiferroic BiMn 3 Cr 4 O 12. Journal of the American Ceramic Society, 2019, 102, 6048-6059.	1.9	4
43267	Transition Metal Diborides: A New Type of Highâ€performance Electrocatalysts for Nitrogen Reduction. ChemCatChem, 2019, 11, 2624-2633.	1.8	37
43268	Role of the Shortâ€Range Order in Amorphous Oxide on MoS₂/aâ€SiO₂ and MoS₂/aâ€HfO₂ Interfaces. Physica Status Solidi (B): Basic Research, 2019, 256, 1900002.	0.7	3
43269	Ab initio study of phosphorus effect on vacancy-mediated process in nickel alloys â€“ An insight into Ni2Cr ordering. Acta Materialia, 2019, 172, 30-43.	3.8	14
43270	The mixing state of mineral dusts with typical anthropogenic pollutants: A mechanism study. Atmospheric Environment, 2019, 209, 192-200.	1.9	7
43271	Photosensitivity and charge injection dynamics of pentacene based thin-film transistors: influence of substrate temperature. Organic Electronics, 2019, 70, 172-178.	1.4	5
43272	In Situ Imaging Facet-Induced Spatial Heterogeneity of Electrocatalytic Reaction Activity at the Subparticle Level via Electrochemiluminescence Microscopy. Analytical Chemistry, 2019, 91, 6829-6835.	3.2	35
43273	From the Terrace Contraction to the Hexameric Sulfur Phase in the Au(100) Surface: A Combined Density Functional Theory and Scanning Tunneling Microscopy Study. Journal of Physical Chemistry C, 2019, 123, 12183-12194.	1.5	0
43274	Surface Structure Dependence of Mechanochemical Etching: Scanning Probe-Based Nanolithography Study on Si(100), Si(110), and Si(111). ACS Applied Materials & Interfaces, 2019, 11, 20583-20588.	4.0	30
43275	Valence Engineering via Selective Atomic Substitution on Tetrahedral Sites in Spinel Oxide for Highly Enhanced Oxygen Evolution Catalysis. Journal of the American Chemical Society, 2019, 141, 8136-8145.	6.6	220
43276	Energetics of the coupled electronicâ€“structural transition in the rare-earth nickelates. Npj Quantum Materials, 2019, 4, .	1.8	28
43277	Reversible and cooperative photoactivation of single-atom Cu/TiO2 photocatalysts. Nature Materials, 2019, 18, 620-626.	13.3	501
43278	Injection of oxygen vacancies in the bulk lattice of layered cathodes. Nature Nanotechnology, 2019, 14, 602-608.	15.6	321
43279	Single-atom Pt on non-metal modified graphene sheets as efficient catalysts for CO oxidation. New Journal of Chemistry, 2019, 43, 9555-9565.	1.4	16
43280	Effects of nitrogen doping in amorphous carbon layers on the diffusion of fluorine atoms: A first-principles study. Journal of Applied Physics, 2019, 125, 155701.	1.1	10
43281	New interaction potentials for alkali and alkaline-earth aluminosilicate glasses. Journal of Chemical Physics, 2019, 150, 154505.	1.2	41

#	Article	IF	Citations
43282	First-principles calculation of mechanical properties of simulated debris ZrxU1â˜xO2. Journal of Nuclear Science and Technology, 2019, 56, 915-921.	0.7	2
43283	Band engineering of B 2 H 2 nanoribbons. Chinese Physics B, 2019, 28, 046803.	0.7	12
43284	Theoretical Study of Sulphur Atomsâ€™ Adsorption and Migration Behaviors on Diamond (001) Surface. Coatings, 2019, 9, 184.	1.2	1
43285	Thermal Expansion and Other Thermodynamic Properties of Î±2-Ti3Al and Î³-TiAl Intermetallic Phases from First Principles Methods. Materials, 2019, 12, 1292.	1.3	12
43286	A Metastable Fo-III Wedge in Cold Slabs Subducted to the Lower Part of the Mantle Transition Zone: A Hypothesis Based on First-Principles Simulations. Minerals (Basel, Switzerland), 2019, 9, 186.	0.8	2
43287	Defectâ€Driven Structural Distortions at the Surface of Relaxor Ferroelectrics. Advanced Functional Materials, 2019, 29, 1900344.	7.8	35
43288	Hâ€dTâ€MoS₂â€onâ€MXene Heterostructures as Promising 2D Anode Materials for Lithiumâ€Ion Batteries: Insights from First Principles. Advanced Theory and Simulations, 2019, 2, 1900045.	1.3	20
43289	Threshold Voltage Modulation of a Grapheneâ€“ZnO Barristor Using a Polymer Doping Process. Advanced Electronic Materials, 2019, 5, 1800805.	2.6	17
43290	Understanding the Photocatalytic Properties of Pt/CeO_x/TiO₂: Structural Effects on Electronic and Optical Properties. ChemPhysChem, 2019, 20, 1624-1629.	1.0	8
43291	Structural Transformation of 2,7â€Dibromopyrene on Au(111) Mediated by Halogenâ€Bonding Motifs. ChemPhysChem, 2019, 20, 2376-2381.	1.0	10
43292	Ab initio molecular dynamics simulations study on initial decompositions of Î²â€HMX at high temperature coupled with high pressures. Journal of the Chinese Chemical Society, 2019, 66, 1429-1435.	0.8	7
43293	Internal electric field construction on dual oxygen group-doped carbon nitride for enhanced photodegradation of pollutants under visible light irradiation. Applied Catalysis B: Environmental, 2019, 256, 117705.	10.8	74
43294	Surface modification of NiCo2Te4 nanoclusters: a highly efficient electrocatalyst for overall water-splitting in neutral solution. Applied Catalysis B: Environmental, 2019, 254, 424-431.	10.8	59
43295	Prediction of electronic and magnetic properties in 3d-transition-metal X-doped bismuthene (Xâ€¯=â€¯V, Cr,) Tj ETQq1 1 0.784314 rgBT	3.1	21
43296	Effect of oxygen doping on the stability and band structure of borophene nanoribbons. Chemical Physics Letters, 2019, 728, 53-56.	1.2	32
43297	Practical Microkinetic Modeling Approach for Methanol Synthesis from Syngas over a Cu-Based Catalyst. Industrial & Engineering Chemistry Research, 2019, 58, 8663-8673.	1.8	22
43298	Reshuffling of Electronic Environment by Introducing CH₃NH₂F⁺ as an Organic Cation for Enhanced Power Conversion Efficiency and Stability of the Designed Hybrid Organicâ€“Inorganic Perovskite. Journal of Physical Chemistry C, 2019, 123, 13385-13393.	1.5	5
43299	Statistical Analysis of Tri-Cresyl Phosphate Conversion on an Iron Oxide Surface Using Reactive Molecular Dynamics Simulations. Journal of Physical Chemistry C, 2019, 123, 12886-12893.	1.5	18

#	Article	IF	Citations
43300	Solar Energy Harvesting in Type II van der Waals Heterostructures of Semiconducting Group III Monochalcogenide Monolayers. Journal of Physical Chemistry C, 2019, 123, 12666-12675.	1.5	86
43301	Electronically-Coupled Phase Boundaries in Î±-Fe₂O₃/Fe₃O₄ Nanocomposite Photoanodes for Enhanced Water Oxidation. ACS Applied Nano Materials, 2019, 2, 334-342.	2.4	32
43302	Dissolution of Sodium Halides by Confined Water on Au(111) via Langmuirâ€“Hinshelwood Process. ACS Nano, 2019, 13, 6025-6032.	7.3	7
43303	Gas reactions under intrapore condensation regime within tailored metalâ€“organic framework catalysts. Nature Communications, 2019, 10, 2076.	5.8	45
43304	Chiral topological semimetal with multifold band crossings and long Fermi arcs. Nature Physics, 2019, 15, 759-765.	6.5	184
43305	Improved phase stability of the CsPbI₃ perovskite via organic cation doping. Physical Chemistry Chemical Physics, 2019, 21, 11175-11180.	1.3	45
43306	First-principles studies of superhard BC8N structures. Journal of Applied Physics, 2019, 125, .	1.1	14
43307	A computational study of gadolinium-doped ceria: Relationship between atomic arrangement and electrostriction. APL Materials, 2019, 7, .	2.2	5
43308	Thermoelectric transport properties of Ni-, Pd-, and Pt- doped skutterudites with S-filling as charge compensation. AIP Advances, 2019, 9, .	0.6	10
43309	The role of magnetic order in VOCl. Journal of Physics Condensed Matter, 2019, 31, 325502.	0.7	5
43310	Strain-tunable electronic structures and optical properties of semiconducting MXenes. Nanotechnology, 2019, 30, 345205.	1.3	29
43311	Equation of state of LiCoO ₂ under 30 GPa pressure. Chinese Physics B, 2019, 28, 016402.	0.7	6
43312	Raman fingerprint of stacking order in <mml:math xmlns:mml="http://www.w3.org/1998/Math/MathML"><mml:mrow><mml:msub><mml:mi>HfS</mml:mi><mml:mn>2</mml:mn></mml	1.2	26
	heterobilayer. Physical Review B, 2019, 99, .		
43313	Electronic structures and magnetic properties of CrSiTe3 single-layer nanoribbons. Physics Letters, Section A: General, Atomic and Solid State Physics, 2019, 383, 2346-2351.	0.9	9
43314	Charge Delocalization, Oxidation States, and Silver Mobility in the Mixed Silverâ€“Copper Oxide AgCuO₂. Inorganic Chemistry, 2019, 58, 7026-7035.	1.9	5
43315	Growing Ultrathin Cu₂O Films on Highly Crystalline Cu(111): A Closer Inspection from Microscopy and Theory. Journal of Physical Chemistry C, 2019, 123, 12716-12721.	1.5	14
43316	Three-Dimensional Crystalline Modification of Graphene in all-sp² Hexagonal Lattices with or without Topological Nodal Lines. Journal of Physical Chemistry Letters, 2019, 10, 2515-2521.	2.1	16
43317	From Two- to Three-Dimensional van der Waals Layered Structures of Boron Crystals: An Ab Initio Study. ACS Omega, 2019, 4, 8015-8021.	1.6	19

#	Article	IF	Citations
43318	High-surface energy enables efficient and stable photocatalytic toluene degradationviathe suppression of intermediate byproducts. Catalysis Science and Technology, 2019, 9, 2952-2959.	2.1	20
43319	Non-linear enhancement of thermoelectric performance of a TiSe₂ monolayer due to tensile strain, from first-principles calculations. Journal of Materials Chemistry C, 2019, 7, 7308-7317.	2.7	22
43320	First-principles investigations of the magnetic phase diagram of <mml:math xmlns:mml="http://www.w3.org/1998/Math/MathML"><mml:mrow><mml:msub><mml:mi>Gd</mml:mi><mml:mrow><mml:mn>1</mml:mn></mml:mrow></mml:msub><mml:mi>Ni</mml:mi><mml:msub><mml:mi>Sn</mml:mi><mml:mn>2</mml:mn></mml:msub></mml:mrow></mml:math>. Physical Review B, 2019, 99, .	1.1	9
43321	Structural, thermodynamic, and local probe investigations of the honeycomb material <mml:math xmlns:mml="http://www.w3.org/1998/Math/MathML"><mml:mrow><mml:msub><mml:mi>Ag</mml:mi><mml:mn>3</mml:mn></mml:msub><mml:msub><mml:mi>Ni</mml:mi><mml:mn>2</mml:mn></mml:msub><mml:msub><mml:mi mathvariant="normal">O</mml:mi><mml:mn>6</mml:mn></mml:msub></mml:mrow></mml:math>. Physical Review B, 2019, 99, .	1.1	10
43322	Rh Doping in Pd Nanocubes Optimizes the Adsorption of 3â€Nitrostyrene towards Selective Hydrogenation of Vinyl Group. ChemCatChem, 2019, 11, 2793-2798.	1.8	8
43323	Thermodynamic constitution of the Alâ€“Cuâ€“Ni system modeled by CALPHAD and ab initio methodology for designing high entropy alloys. Calphad: Computer Coupling of Phase Diagrams and Thermochemistry, 2019, 65, 346-369.	0.7	32
43324	Investigation of structural, electronic and lattice dynamical properties of XNiH (XÂ=ÂLi, Na and K) perovskite type hydrides and their hydrogen storage applications. International Journal of Hydrogen Energy, 2019, 44, 15173-15182.	3.8	56
43325	Influence of Nb concentration on the structure, stability, and electronic and mechanical properties of D022 Al3Ti by first-principles calculations and experiments. Journal of Physics and Chemistry of Solids, 2019, 131, 243-253.	1.9	11
43326	Electronic structures of twist-stacked 1T-TaS2 bilayers. Physics Letters, Section A: General, Atomic and Solid State Physics, 2019, 383, 2302-2308.	0.9	5
43327	Adsorption of toxic gas molecules on pristine and transition metal doped hexagonal GaN monolayer: A first-principles study. Vacuum, 2019, 165, 35-45.	1.6	74
43328	Oxygen Vacancies Promoted the Selective Photocatalytic Removal of NO with Blue TiO₂ via Simultaneous Molecular Oxygen Activation and Photogenerated Hole Annihilation. Environmental Science & Technology, 2019, 53, 6444-6453.	4.6	215
43329	Computational Screening for Developing Optimal Intermetallic Transition Metal Pt-Based ORR Catalysts at the Predictive Volcano Peak. Journal of Physical Chemistry C, 2019, 123, 13236-13245.	1.5	21
43330	Zn_xMg_{60â€“x}O₆₀ Nanoclusters with Tunable Near-Ultraviolet Energy Gaps. Journal of Physical Chemistry C, 2019, 123, 13083-13093.	1.5	0
43331	Improvement of Visible-Light Photocatalytic Efficiency in a Novel InSe/Zr₂CO₂ Heterostructure for Overall Water Splitting. Journal of Physical Chemistry C, 2019, 123, 12781-12790.	1.5	80
43332	Defect Healing in Layered Materials: A Machine Learning-Assisted Characterization of MoS₂ Crystal Phases. Journal of Physical Chemistry Letters, 2019, 10, 2739-2744.	2.1	19
43333	Predicting Novel 2D MB₂ (M = Ti, Hf, V, Nb, Ta) Monolayers with Ultrafast Dirac Transport Channel and Electron-Orbital Controlled Negative Poissonâ€™s Ratio. Journal of Physical Chemistry Letters, 2019, 10, 2567-2573.	2.1	65
43334	Molecular Rectifiers on Silicon: High Performance by Enhancing Top-Electrode/Molecule Coupling. ACS Applied Materials & Interfaces, 2019, 11, 18564-18570.	4.0	21
43335	Stacking stability of C2N bilayer nanosheet. Scientific Reports, 2019, 9, 6861.	1.6	9

#	Article	IF	Citations
43336	CO₂ electrochemical reduction at thiolate-modified bulk Au electrodes. Catalysis Science and Technology, 2019, 9, 2689-2701.	2.1	22
43337	Encapsulation of heavy metals by a nanoporous complex oxide 12CaOâ€‰Â·â€‰7Al2O3. Journal of Applied Physics, 2019, 125, .	1.1	7
43338	Strong spin-orbit coupling and Dirac nodal lines in the three-dimensional electronic structure of metallic rutile <mml:math xmlns:mml="http://www.w3.org/1998/Math/MathML"><mml:msub><mml:mi>IrO</mml:mi><mml:mn>2</mml:mn></mml:msub></mml Physical Review B, 2019, 99, .	1.1	18
43339	Orbital degrees of freedom in artificial electron lattices on a metal surface. Physical Review B, 2019, 99, .	1.1	7
43340	Observation of Weyl Nodes in Robust Type-II Weyl Semimetal <mml:math xmlns:mml="http://www.w3.org/1998/Math/MathML" display="inline"><mml:mrow><mml:msub><mml:mrow><mml:mi>WP</mml:mi></mml:mrow><mml:mrow><mml:mn>2</mml:mn></m Physical Review Letters, 2019, 122, 176402.	2.9	42
43343	3D Stackable and Scalable Binary Ovonic Threshold Switch Devices with Excellent Thermal Stability and Low Leakage Current for Highâ€Density Crossâ€Point Memory Applications. Advanced Electronic Materials, 2019, 5, 1900196.	2.6	27
43344	WS₂ Nanosheets with Highlyâ€Enhanced Electrochemical Activity by Facile Control of Sulfur Vacancies. ChemCatChem, 2019, 11, 2667-2675.	1.8	57
43345	Theoretical insight into the effect of Si-doped sites on the photocatalytic properties of SrTiO3. Applied Physics A: Materials Science and Processing, 2019, 125, 1.	1.1	4
43346	Electronic properties and defect levels induced by group III substitutionâ€“interstitial complexes in Ge. Journal of Materials Science, 2019, 54, 10798-10808.	1.7	4
43347	Towards an integrated modeling of the plasma-solid interface. Frontiers of Chemical Science and Engineering, 2019, 13, 201-237.	2.3	34
43348	Transition metal substitution on Mg(101Â¯3) and Mg(0001) surfaces for improved hydrogenation and dehydrogenation: A systematic first-principles study. Applied Surface Science, 2019, 479, 626-633.	3.1	6
43349	First-principles search for alloying elements that increase corrosion resistance of Mg with second-phase particles of transition metal impurities. Computational Materials Science, 2019, 165, 154-166.	1.4	29
43350	Enhanced photovoltaic performance of dye-sensitized solar cells by the adsorption of Zn-porphyrin dye molecule on TiO2 surfaces. Journal of Alloys and Compounds, 2019, 794, 35-44.	2.8	4
43351	Na-doped ruthenium perovskite electrocatalysts with improved oxygen evolution activity and durability in acidic media. Nature Communications, 2019, 10, 2041.	5.8	227
43352	Unexpected hydrolytic transformation of new type hybrid bromobismuthates with methylpyrazinium dications. Dalton Transactions, 2019, 48, 7602-7611.	1.6	9
43353	Ultralow lattice thermal conductivity induced high thermoelectric performance in the Î´-Cu₂S monolayer. Nanoscale, 2019, 11, 10306-10313.	2.8	43
43354	Ab initiocomputation for solid-state³¹P NMR of inorganic phosphates: revisiting X-ray structures. Physical Chemistry Chemical Physics, 2019, 21, 10070-10074.	1.3	10
43355	Non-intuitive concomitant enhancement of dielectric permittivity, breakdown strength and energy density in percolative polymer nanocomposites by trace Ag nanodots. Journal of Materials Chemistry A, 2019, 7, 15198-15206.	5.2	61

#	Article	IF	Citations
43356	Perpendicular magnetic anisotropy modulated by interfacial magnetoelectric coupling in Fe₄N/0.75Pb(Mg_{1/3}Nb_{2/3})O₃-0.25PbTiO₃ multiferroic heterostructures. Journal Physics D: Applied Physics, 2019, 52, 335001.	1.3	5
43357	Genetic algorithm prediction of pressure-induced multiferroicity in the perovskite <mml:math xmlns:mml="http://www.w3.org/1998/Math/MathML"><mml:mrow><mml:mi>PbCo</mml:mi><mml:msub><mml:mi mathvariant="normal">O</mml:mi><mml:mn>3</mml:mn></mml:msub></mml:mrow></mml:math>. Physical Review B, 2019, 99, .	1.1	6
43358	Theoretical study of quantum size effects in thin Al(100), Al(110), and Al(111) films. Physical Review B, 2019, 99, .	1.1	8
43359	NMR Crystallography: Evaluation of Hydrogen Positions in Hydromagnesite by 13 C{ 1 H} REDOR Solidâ€State NMR and Density Functional Theory Calculation of Chemical Shielding Tensors. Angewandte Chemie, 2019, 131, 4254-4260.	1.6	2
43360	Kinetically Controlled Synthesis of Fourâ€•and Sixâ€Member Cyclic Products via Sequential Arylâ€Aryl Coupling on a Au(111) Surface. ChemPhysChem, 2019, 20, 2292-2296.	1.0	6
43361	Defining the optimal morphology of Rhn nanoparticles for efficient hydrazine adsorption: a DFT-D3 study. Journal of Materials Science, 2019, 54, 9533-9542.	1.7	5
43362	Boron-phosphide monolayer as a potential anchoring material for lithium-sulfur batteries: A first-principles study. Applied Surface Science, 2019, 486, 281-286.	3.1	53
43363	Strengthening and toughening by partial slip in nanotwinned diamond. Carbon, 2019, 150, 1-7.	5.4	29
43364	Ultra-fast NH4+ Storage: Strong H Bonding between NH4+ and Bi-layered V2O5. CheM, 2019, 5, 1537-1551.	5.8	207
43365	SIMPLE-NN: An efficient package for training and executing neural-network interatomic potentials. Computer Physics Communications, 2019, 242, 95-103.	3.0	81
43366	A DFT study of H2 adsorption on lithium decorated 3D hybrid Boron-Nitride-Carbon frameworks. International Journal of Hydrogen Energy, 2019, 44, 15183-15192.	3.8	14
43367	Development of Water Reactive Potentials for Sodium Silicate Glasses. Journal of Physical Chemistry B, 2019, 123, 4452-4461.	1.2	27
43368	Ultrathin Amorphous Titania on Nanowires: Optimization of Conformal Growth and Elucidation of Atomic-Scale Motifs. Nano Letters, 2019, 19, 3457-3463.	4.5	14
43369	Topological superconducting phase in high-Tc superconductor MgB2 with Diracâ€“nodal-line fermions. Npj Computational Materials, 2019, 5, .	3.5	52
43370	Electronic transport properties of MoS2 nanoribbons embedded in butadiene solvent. Physical Chemistry Chemical Physics, 2019, 21, 11359-11366.	1.3	11
43371	Enhancing electrostatic interactions to activate polar molecules: ammonia borane methanolysis on a Cu/Co(OH)₂ nanohybrid. Catalysis Science and Technology, 2019, 9, 2828-2835.	2.1	14
43372	The charge regulation of electronic structure and optical properties of graphitic carbon nitride under strain. RSC Advances, 2019, 9, 7464-7468.	1.7	19
43373	Site preference and magnetic properties of Zn-Sn-substituted strontium hexaferrite. Journal of Applied Physics, 2019, 125, .	1.1	15

#	Article	IF	Citations
43374	Surface Reconstruction, Oxidation Mechanism, and Stability of Cd₃As₂. Advanced Functional Materials, 2019, 29, 1900965.	7.8	13
43375	A Roomâ€Temperature Ferroelectric Ferromagnet in a 1D Tetrahedral Chain Network. Advanced Materials, 2019, 31, e1808104.	11.1	22
43376	Tandem Conversion of CO₂ to Valuable Hydrocarbons in Highly Concentrated Potassium Iron Catalysts. ChemCatChem, 2019, 11, 2879-2886.	1.8	57
43377	Enhancing High Humidity Stability of Quasiâ€2D Perovskite Thin Films through Mixed Cation Doping and Solvent Engineering. ChemNanoMat, 2019, 5, 1280-1288.	1.5	13
43378	On the origin of the difference between type A and type B skeletal isomerization of alkenes catalyzed by zeolites: The crucial input of ab initio molecular dynamics. Journal of Catalysis, 2019, 373, 361-373.	3.1	38
43379	A first principles study of CO oxidation over gold clusters: The catalytic role of boron nitride support and water. Molecular Catalysis, 2019, 471, 44-53.	1.0	10
43380	Stanene on a SiC(0001) surface: a candidate for realizing quantum anomalous Hall effect. Physical Chemistry Chemical Physics, 2019, 21, 11150-11157.	1.3	18
43381	First-principles study of thermal transport properties in the two- and three-dimensional forms of Bi₂O₂Se. Physical Chemistry Chemical Physics, 2019, 21, 10931-10938.	1.3	43
43382	First-principles study of the layered thermoelectric material TiNBr. RSC Advances, 2019, 9, 12886-12894.	1.7	18
43383	Tunable gap in stable arsenene nanoribbons opens the door to electronic applications. RSC Advances, 2019, 9, 11818-11823.	1.7	3
43384	Full orientation control of epitaxial <mml:math xmlns:mml="http://www.w3.org/1998/Math/MathML"><mml:msub><mml:mi>MoS</mml:mi><mml:mn>2</mml:mn></mml:msub></mm on hBN assisted by substrate defects. Physical Review B, 2019, 99, .	1.1	37
43385	Manipulating the Mixedâ€Perovskite Crystallization Pathway Unveiled by In Situ GIWAXS. Advanced Materials, 2019, 31, e1901284.	11.1	127
43386	Prediction of the terminations and Miller planes of the tetragonal zirconia thin films as a gate dielectric layer in integratedâ€circuit industry. Surface and Interface Analysis, 2019, 51, 774-782.	0.8	2
43387	Flexoelectric Effects in Corrugated Boron Nitride Nanoribbons. Journal of Electronic Materials, 2019, 48, 4515-4523.	1.0	7
43388	Two-Dimensional Silver(I)-Dithiocarboxylate Coordination Polymer Exhibiting Strong Near-Infrared Photothermal Effect. Inorganic Chemistry, 2019, 58, 6601-6608.	1.9	28
43389	Spin Polarization Enhancement of an Fe3O4(100) Surface by Coadsorption of Atomic Hydrogen and Molecular Nitric Oxide. Journal of Physical Chemistry C, 2019, , .	1.5	2
43390	Prediction of the Role of Bismuth Dopants in Organicâ€“Inorganic Lead Halide Perovskites on Photoelectric Properties and Photovoltaic Performance. Journal of Physical Chemistry C, 2019, 123, 12684-12693.	1.5	24
43391	Hydrogen Passivated Silicon Grain Boundaries Greatly Reduce Charge Recombination for Improved Silicon/Perovskite Tandem Solar Cell Performance: Time Domain Ab Initio Analysis. Journal of Physical Chemistry Letters, 2019, 10, 2445-2452.	2.1	14

#	Article	IF	Citations
43392	Computational Screening of Layered Materials for Multivalent Ion Batteries. ACS Omega, 2019, 4, 7822-7828.	1.6	33
43393	Heteroepitaxial passivation of Cs2AgBiBr6 wafers with suppressed ionic migration for X-ray imaging. Nature Communications, 2019, 10, 1989.	5.8	252
43394	Understanding the effects of oxygen defects on the redox reaction pathways in LiVPO₄F by combining ab initio calculations with experiments. Journal of Materials Chemistry A, 2019, 7, 13060-13070.	5.2	7
43395	Dirac fermions in the layered titanium-based oxypnictide superconductor <mml:math xmlns:mml="http://www.w3.org/1998/Math/MathML"><mml:mrow><mml:msub><mml:mi>BaTi</mml:mi><mml:mn>2</mml:mn></mml:msub><mml:msub><mml:mi mathvariant="normal">O</mml:mi></mml:mrow></mml:math>. Physical Review B, 2019, 99, .	1.1	2
43396	Superconductivity and Its Enhancement in Polycyclic Aromatic Hydrocarbons. Frontiers in Physics, 2019, 7, .	1.0	11
43397	A Novel Strategy for the Selection of Polysulfide Adsorbents Toward Highâ€Performance Lithiumâ€Sulfur Batteries. Advanced Materials Interfaces, 2019, 6, 1900393.	1.9	7
43398	Ab Initio Simulation of Ta₂O₅: A High Symmetry Ground State Phase with Application to Interface Calculation. Annalen Der Physik, 2019, 531, 1800524.	0.9	12
43399	Temperature- and pressure-dependent adsorption configuration of NO molecules on Rh(111) surface: A theoretical study. Surface Science, 2019, 686, 58-62.	0.8	6
43400	Metalâ€“Organic Frameworks with Metalâ€“Catecholates for O₂/N₂ Separation. Journal of Physical Chemistry C, 2019, 123, 12935-12946.	1.5	33
43401	Regulating the Catalytic Performance of Single-Atomic-Site Ir Catalyst for Biomass Conversion by Metalâ€“Support Interactions. ACS Catalysis, 2019, 9, 5223-5230.	5.5	87
43402	Degenerately Doped Transition Metal Dichalcogenides as Ohmic Homojunction Contacts to Transition Metal Dichalcogenide Semiconductors. ACS Nano, 2019, 13, 5103-5111.	7.3	39
43403	Black phosphorene as a hole extraction layer boosting solar water splitting of oxygen evolution catalysts. Nature Communications, 2019, 10, 2001.	5.8	222
43404	Constructive coupling effect of topological states and topological phase transitions in plumbene. Physical Review B, 2019, 99, .	1.1	25
43405	Zeroâ€Field Nernst Effect in a Ferromagnetic Kagomeâ€Lattice Weylâ€Semimetal Co₃Sn₂S₂. Advanced Materials, 2019, 31, e1806622.	11.1	180
43406	Birnessite Nanosheet Arrays with High K Content as a Highâ€Capacity and Ultrastable Cathode for Kâ€Ion Batteries. Advanced Materials, 2019, 31, e1900060.	11.1	183
43407	H₂ Adsorption on Wurtzite ZnO and on ZnO/M(111) (M=Cu, Ag and Au) Bilayer Films. ChemNanoMat, 2019, 5, 932-939.	1.5	8
43408	The Structural, Elastic and Electronic Properties of Ni3â^'xCuxSn4 (xâ€‰=â€‰0, 0.5, 1 and 1.5) Intermetallic Compounds via Ab Initio Calculations. Journal of Electronic Materials, 2019, 48, 4533-4543.	1.0	9
43409	Realizing n-type BiCuSeO through halogens doping. Ceramics International, 2019, 45, 14953-14957.	2.3	11

#	Article	IF	Citations
43410	Enhancing CO2 electroreduction on nanoporous silver electrode in the presence of halides. Electrochimica Acta, 2019, 313, 561-569.	2.6	29
43411	Bandgap alignment of Î±-CsPbI3 perovskites with synergistically enhanced stability and optical performance via B-site minor doping. Nano Energy, 2019, 61, 389-396.	8.2	67
43412	Nonvolatile Electrical Control and Heterointerfaceâ€Induced Halfâ€Metallicity of 2D Ferromagnets. Advanced Functional Materials, 2019, 29, 1901420.	7.8	109
43413	Tuning electron density of metal nickel by support defects in Ni/ZrO2 for selective hydrogenation of fatty acids to alkanes and alcohols. Applied Catalysis B: Environmental, 2019, 253, 170-178.	10.8	133
43414	The experimental and theoretical insights towards the CO induced Pd-Graphene and their multifunctional energy conversion applications. Carbon, 2019, 149, 307-317.	5.4	7
43415	Crystallographic and compositional analysis of impurity phase U2MoSi2C in UMo alloys. Journal of Nuclear Materials, 2019, 519, 287-291.	1.3	11
43416	Atomistic modeling of out-of-pile xenon diffusion by vacancy clusters in UO2. Journal of Nuclear Materials, 2019, 520, 96-109.	1.3	27
43417	Thermodynamic of intrinsic defects in Î²-Ga2O3. Journal of Physics and Chemistry of Solids, 2019, 132, 104-109.	1.9	12
43418	Promoting ring-opening efficiency for suppressing toxic intermediates during photocatalytic toluene degradation via surface oxygen vacancies. Science Bulletin, 2019, 64, 669-678.	4.3	159
43419	Conceptual Design of Yttrium Oxyhydrides: Phase Diagram, Structure, and Properties. Crystal Growth and Design, 2019, 19, 2574-2582.	1.4	16
43420	Exploration of Properties from Both the Bulk and Surface of Iron Silicides: A Unified Theoretical Study. Journal of Physical Chemistry C, 2019, 123, 11939-11949.	1.5	4
43421	Energy, Phonon, and Dynamic Stability Criteria of Two-Dimensional Materials. ACS Applied Materials & Interfaces, 2019, 11, 24876-24884.	4.0	76
43422	Band engineering of two-dimensional Ruddlesdenâ€“Popper perovskites for solar utilization: the relationship between chemical components and electronic properties. Journal of Materials Chemistry A, 2019, 7, 11530-11536.	5.2	17
43423	GeSe@SnS: stacked Janus structures for overall water splitting. Journal of Materials Chemistry A, 2019, 7, 12060-12067.	5.2	66
43424	Theoretical discovery of Dirac half metal in experimentally synthesized two dimensional metal semiquinoid frameworks. Journal of Materials Chemistry C, 2019, 7, 5792-5796.	2.7	16
43425	Optical properties of single crystalline copper iodide with native defects: Experimental and density functional theoretical investigation. Journal of Applied Physics, 2019, 125, .	1.1	26
43426	Separated and intermixed phases of borophene as anode material for lithium-Ion batteries. Journal Physics D: Applied Physics, 2019, 52, 245501.	1.3	19
43427	Preparation and structure study of phosphorus-doped porous graphdiyne and its efficient lithium storage application. 2D Materials, 2019, 6, 035020.	2.0	52

#	Article	IF	Citations
43428	Low-Scaling Algorithm for Nudged Elastic Band Calculations Using a Surrogate Machine Learning Model. Physical Review Letters, 2019, 122, 156001.	2.9	116
43429	Thermoelectric Properties of Hexagonal M2C3 (M = As, Sb, and Bi) Monolayers from First-Principles Calculations. Nanomaterials, 2019, 9, 597.	1.9	22
43430	Metastable molecular fluid hydrogen at high pressures. Contributions To Plasma Physics, 2019, 59, e201800173.	0.5	6
43431	Borohydride as Magnetic Superexchange Pathway in Late Lanthanide Borohydrides. European Journal of Inorganic Chemistry, 2019, 2019, 1776-1783.	1.0	18
43432	Effect of Power Density on the Electrochemical Properties of Undoped Amorphous Carbon (aâ€€) Thin Films. Electroanalysis, 2019, 31, 746-755.	1.5	6
43433	Origin of Intrinsic Direct Band Gap of Janus Groupâ€III Chalcogenide Monolayers. Physica Status Solidi (B): Basic Research, 2019, 256, 1900070.	0.7	12
43434	Synthesis and Properties of Au Hydride. ChemistrySelect, 2019, 4, 4287-4292.	0.7	4
43435	Stability and physical properties tuning via interstitials chemical engineering of Zr5Sn3: a first-principles study. Journal of Materials Science, 2019, 54, 10284-10296.	1.7	4
43436	Structural and electronic properties of predicting two-dimensional BC2P and BC3P3 monolayers by the global optimization method. Chemical Physics Letters, 2019, 726, 69-76.	1.2	16
43437	The physical properties of bismuth replacement in lead halogen perovskite solar cells: CH3NH3Pb1â^'Bi I3 compounds by ab-initio calculations. Results in Physics, 2019, 13, 102278.	2.0	14
43438	Band Gap Tuning in Bismuth Oxide Carbodiimide Bi₂O₂NCN. Inorganic Chemistry, 2019, 58, 6467-6473.	1.9	28
43439	DFT Characterization of Metallole-Decorated Silicon (001) Surface. Journal of Physical Chemistry C, 2019, 123, 11639-11648.	1.5	0
43440	Effects of O₂ and H₂O in the Oxidative Steam-Reforming Reaction of Ethanol on Rh Catalysts. Journal of Physical Chemistry C, 2019, 123, 11649-11661.	1.5	10
43441	Multi-ion Conduction in Li₃OCl Glass Electrolytes. Journal of Physical Chemistry Letters, 2019, 10, 2264-2269.	2.1	38
43442	Multifidelity Information Fusion with Machine Learning: A Case Study of Dopant Formation Energies in Hafnia. ACS Applied Materials & Interfaces, 2019, 11, 24906-24918.	4.0	49
43443	Benzo-Fused Periacenes or Double Helicenes? Different Cyclodehydrogenation Pathways on Surface and in Solution. Journal of the American Chemical Society, 2019, 141, 7399-7406.	6.6	49
43444	Anomalous Nernst effect beyond the magnetization scaling relation in the ferromagnetic Heusler compound Co2MnGa. NPG Asia Materials, 2019, 11, .	3.8	190
43445	Selective photoelectrochemical oxidation of glycerol to high value-added dihydroxyacetone. Nature Communications, 2019, 10, 1779.	5.8	185

#	Article	IF	Citations
43446	Topological Dirac states in transition-metal monolayers on graphyne. Physical Chemistry Chemical Physics, 2019, 21, 9310-9316.	1.3	7
43447	Enhancing the photocatalytic activity of ZnSn(OH)₆ achieved by gradual sulfur doping tactics. Nanoscale, 2019, 11, 9444-9456.	2.8	19
43448	Unraveling the high-activity nature of Feâ€“Nâ€“C electrocatalysts for the oxygen reduction reaction: the extraordinary synergy between Feâ€“N₄ and Fe₄N. Journal of Materials Chemistry A, 2019, 7, 11792-11801.	5.2	84
43449	Surface-mediated assembly, polymerization and degradation of thiophene-based monomers. Chemical Science, 2019, 10, 5167-5175.	3.7	28
43450	Adsorption, diffusion, and limited dissociation of a single water molecule on the Î±-Pu₂O₃ (1â€‰1â€‰1) surface. Journal of Physics Condensed Matter, 2019, 31, 265001.	0.7	4
43451	Large-scale spin-polarized DFT calculation of electronic properties of GaAs with defects. Materials Research Express, 2019, 6, 055914.	0.8	7
43452	Photocatalytic performance enhancement of two-dimensional Ruddlesden-Popper type perovskite K₂La₂Ti₃O₁₀ by nitrogen-doping. Materials Research Express, 2019, 6, 075047.	0.8	11
43453	An Ab Initio Molecular Dynamics study of Low Temperature Effects in Crystalline Î±â€HMX. Physica Status Solidi (B): Basic Research, 2019, 256, 1900057.	0.7	2
43454	The epitaxial growth of ZnO films on Cu(111) surface: Thickness dependence. Applied Surface Science, 2019, 483, 133-139.	3.1	11
43455	Ni structural doping induced spin polarization effects on the optical and electric properties of nano-SiC film. Applied Surface Science, 2019, 483, 626-632.	3.1	5
43456	Atomistic simulation of the structural and conductance evolution of Au break junctions. Computational Materials Science, 2019, 164, 147-152.	1.4	1
43457	Optimized photoluminescence and electronic properties of europium doped phosphate red phosphor. Results in Physics, 2019, 13, 102258.	2.0	12
43458	Synthesis, Crystal Structure Analysis, and Electrochemical Properties of Rock-Salt Type Mg_xNi_yCo_zO₂ as a Cathode Material for Mg Rechargeable Batteries. Inorganic Chemistry, 2019, 58, 5664-5670.	1.9	16
43459	High-Pressure Single-Crystal X-ray Diffraction of Lead Chromate: Structural Determination and Reinterpretation of Electronic and Vibrational Properties. Inorganic Chemistry, 2019, 58, 5966-5979.	1.9	13
43460	Approaching the Quantitative Description of Enantioselective Adsorption by the Density Functional Theory Means. Journal of Physical Chemistry C, 2019, 123, 11714-11722.	1.5	5
43461	MoS₂/Ti₂CT₂ (T = F, O) Heterostructures as Promising Flexible Anodes for Lithium/Sodium Ion Batteries. Journal of Physical Chemistry C, 2019, 123, 11493-11499.	1.5	62
43462	Exploring planar and nonplanar siligraphene: a first-principles study. RSC Advances, 2019, 9, 12276-12281.	1.7	6
43463	Electronic structure properties of CuZn2InTe4 and AgZn2InTe4 quaternary chalcogenides. Journal of Applied Physics, 2019, 125, 155101.	1.1	17

#	Article	IF	Citations
43464	Elastic properties and intrinsic strength of two-dimensional InSe flakes. Nanotechnology, 2019, 30, 335703.	1.3	27
43465	Systematic understanding of half-metallicity of ternary compounds in Heusler and Inverse Heusler structures with 3d and 4d elements. Physica Scripta, 2019, 94, 125001.	1.2	17
43466	Thermoelectric optimization of <mml:math xmlns:mml="http://www.w3.org/1998/Math/MathML"><mml:mrow><mml:mi>AgBiS</mml:mi><mml:msub><mml:mi mathvariant="normal">e</mml:mi><mml:mn>2</mml:mn></mml:msub></mml:mrow></mml:math> by defect engineering for room-temperature applications. Physical Review B, 2019, 99, .	1.1	38
43467	Fermions and bosons in nonsymmorphic <mml:math xmlns:mml="http://www.w3.org/1998/Math/MathML"><mml:msub><mml:mi>PdSb</mml:mi><mml:mn>2</mml:mn></mml:msub></mml:math> with sixfold degeneracy. Physical Review B, 2019, 99, .	1.1	24
43468	Large anomalous Hall and Nernst effects from nodal line symmetry breaking in <mml:math xmlns:mml="http://www.w3.org/1998/Math/MathML"><mml:msub><mml:mi mathvariant="normal">Fe</mml:mi><mml:mn>2</mml:mn></mml:msub><mml:mi>Mn</mml:mi><mml:mi>X</mml:mi></mml:math> (<mml:math xmlns:mml="http://www.w3.org/1998/Math/MathML"><mml:mi>X</mml:mi></mml:math> =) Tj ETQq0 0 0 rgBT /Overlock	1.1	38
43469	Versatile electrical behavior of <mml:math xmlns:mml="http://www.w3.org/1998/Math/MathML"><mml:mrow><mml:mn>1</mml:mn><mml:mi>T</mml:mi></mml:mrow></mml:math> elucidated from a theoretical study. Physical Review B, 2019, 99, .	1.1	21
43470	Dissolution, diffusion, and penetration of H in the group VB metals investigated by first-principles method. International Journal of Hydrogen Energy, 2019, 44, 29083-29091.	3.8	18
43471	Rhenium disulfide nanosheets/carbon composite as novel anodes for high-rate and long lifespan sodium-ion batteries. Nano Energy, 2019, 61, 626-636.	8.2	46
43472	High-throughput modeling of atomic diffusion migration energy barrier of fcc metals. Progress in Natural Science: Materials International, 2019, 29, 341-348.	1.8	20
43473	The Pressure Gap for Thiols: Methanethiol Self-Assembly on Au(111) from Vacuum to 1 bar. Journal of Physical Chemistry C, 2019, 123, 12382-12389.	1.5	7
43474	Nitrogen-Doped Cobalt Phosphide for Enhanced Hydrogen Evolution Activity. ACS Applied Materials & Interfaces, 2019, 11, 17359-17367.	4.0	40
43475	Defective Graphene on the Transition-Metal Surface: Formation of Efficient Bifunctional Catalysts for Oxygen Evolution/Reduction Reactions in Alkaline Media. ACS Applied Materials & Interfaces, 2019, 11, 17410-17415.	4.0	34
43476	Synergy of Single-Atom Ni₁ and Ru₁ Sites on CeO₂ for Dry Reforming of CH₄. Journal of the American Chemical Society, 2019, 141, 7283-7293.	6.6	272
43477	A Large Family of Synthetic Two-Dimensional Metal Hydrides. Journal of the American Chemical Society, 2019, 141, 7899-7905.	6.6	25
43478	Elucidation of the Reaction Mechanism for High-Temperature Water Gas Shift over an Industrial-Type Copperâ€“Chromiumâ€“Iron Oxide Catalyst. Journal of the American Chemical Society, 2019, 141, 7990-7999.	6.6	60
43479	Dramatic differences in carbon dioxide adsorption and initial steps of reduction between silver and copper. Nature Communications, 2019, 10, 1875.	5.8	63
43480	Insights into how the aqueous environment influences the kinetics and mechanisms of heterogeneously-catalyzed COH* and CH₃OH* dehydrogenation reactions on Pt(111). Physical Chemistry Chemical Physics, 2019, 21, 9895-9904.	1.3	13
43481	The interaction of ethylammonium tetrafluoroborate [EtNH₃⁺][BF₄^{â^'}] ionic liquid on the Li(001) surface: towards understanding early SEI formation on Li metal. Physical Chemistry Chemical Physics, 2019, 21, 10028-10037.	1.3	20

#	Article	IF	Citations
43482	First-principles calculations of thermal transport properties in MoS₂/MoSe₂ bilayer heterostructure. Physical Chemistry Chemical Physics, 2019, 21, 10442-10448.	1.3	37
43483	Design and synthesis of Ga-doped ZSM-22 zeolites as highly selective and stable catalysts forn-dodecane isomerization. Catalysis Science and Technology, 2019, 9, 2812-2827.	2.1	22
43484	Hydrogen interaction with selectively desulfurized MoS2 surface using Ne+ sputtering. Journal of Applied Physics, 2019, 125, .	1.1	10
43485	Co(CO)n/Cu(001): Towards understanding chemical control of the Kondo effect. Journal of Applied Physics, 2019, 125, 142910.	1.1	4
43486	Imaging covalent bond formation by H atom scattering from graphene. Science, 2019, 364, 379-382.	6.0	76
43487	Complex Band Structures and Lattice Dynamics of Bi₂Te₃â€Based Compounds and Solid Solutions. Advanced Functional Materials, 2019, 29, 1900677.	7.8	135
43488	Unveiling Electrochemical Reaction Pathways of CO₂ Reduction to C_N Species at Sâ€Vacancies of MoS₂. ChemSusChem, 2019, 12, 2671-2678.	3.6	25
43489	Electronic and optical properties of the supercell of 8-Pmmn borophene modified on doping by H, Li, Be, and C: a DFT approach. Applied Physics A: Materials Science and Processing, 2019, 125, 1.	1.1	21
43490	Outstanding strength, optical characteristics and thermal conductivity of graphene-like BC3 and BC6N semiconductors. Carbon, 2019, 149, 733-742.	5.4	126
43491	Coexistence of half-metallicity and martensitic transition in Co2VGa1Sb (xâ€¯=â€¯0, 0.25 and 0.5) Heusler alloys: First-principles calculations combined with structural experiments. Computational Materials Science, 2019, 165, 34-39.	1.4	9
43492	Simulation of hydrogen thermal desorption and stability titanium hydrides TiH. International Journal of Hydrogen Energy, 2019, 44, 29132-29139.	3.8	9
43493	The structure, electrical and magnetic properties of M-doped PbPdO2 (Mâ€¯=â€¯Cu, Co, Fe) thin films: A first-principles and experimental study. Journal of Magnetism and Magnetic Materials, 2019, 485, 271-279.	1.0	6
43494	Subunit volume control mechanism for dehydrogenation performance of AB3-type superlattice intermetallics. Journal of Power Sources, 2019, 427, 145-153.	4.0	28
43495	Strainâ€“Spintronics: Modulating Electronic and Magnetic Properties of Hf₂MnC₂O₂ MXene by Uniaxial Strain. Journal of Physical Chemistry C, 2019, 123, 12451-12459.	1.5	35
43496	Room-Temperature in Vacuo Chemisorption of Xenon Atoms on Ru(0001) under Interface Confinement. Journal of Physical Chemistry C, 2019, 123, 13578-13585.	1.5	5
43497	DFT Analysis of the Adsorption of Phenol on the Nonpolar (101Ì…0) ZnO Surface. Journal of Physical Chemistry C, 2019, 123, 12296-12304.	1.5	26
43498	Boosting the Seebeck Coefficient for Organic Coordination Polymers: Role of Doping-Induced Polaron Band Formation. Journal of Physical Chemistry Letters, 2019, 10, 2493-2499.	2.1	16
43499	High-Throughput Screening for Advanced Thermoelectric Materials: Diamond-Like ABX₂ Compounds. ACS Applied Materials & Interfaces, 2019, 11, 24859-24866.	4.0	72

#	Article	IF	Citations
43500	Greatly Enhanced Photoabsorption and Photothermal Conversion of Antimonene Quantum Dots through Spontaneously Partial Oxidation. ACS Applied Materials & Interfaces, 2019, 11, 17987-17993.	4.0	30
43501	Free Standing Nanoporous Palladium Alloys as CO Poisoning Tolerant Electrocatalysts for the Electrochemical Reduction of CO₂ to Formate. ACS Catalysis, 2019, 9, 5290-5301.	5.5	78
43502	Machine-learned multi-system surrogate models for materials prediction. Npj Computational Materials, 2019, 5, .	3.5	96
43503	Hydrogen interaction with a sulfur-vacancy-induced occupied defect state in the electronic band structure of MoS₂. Physical Chemistry Chemical Physics, 2019, 21, 15302-15309.	1.3	17
43504	Superior spin-polarized electronic structure in MoS₂/MnO₂ heterostructures with an efficient hole injection. Physical Chemistry Chemical Physics, 2019, 21, 10706-10715.	1.3	4
43505	GIGA: a versatile genetic algorithm for free and supported clusters and nanoparticles in the presence of ligands. Nanoscale, 2019, 11, 9042-9052.	2.8	29
43506	Theoretical design of a technetium-like alloy and its catalytic properties. Chemical Science, 2019, 10, 5461-5469.	3.7	5
43507	Transition metal-embedded two-dimensional C₃N as a highly active electrocatalyst for oxygen evolution and reduction reactions. Journal of Materials Chemistry A, 2019, 7, 12050-12059.	5.2	123
43508	A copper single-atom catalyst towards efficient and durable oxygen reduction for fuel cells. Journal of Materials Chemistry A, 2019, 7, 16690-16695.	5.2	140
43509	Engineering difference of band structure between mirror symmetrical adsorption and antisymmetrical adsorption of the identical group on a graphene sheet. EPJ Applied Physics, 2019, 85, 30101.	0.3	0
43510	Influence of defects on the photocatalytic behavior of La3+ ions doped SrBi2Nb2O9 ferroelectric materials. Journal of Applied Physics, 2019, 125, .	1.1	4
43511	First principles investigations of the structural, elastic, electronic, vibrational and thermodynamic properties of hexagonal XAl₂O₄ (X = Cd, Ca and Sr). Materials Research Express, 2019, 6, 085518.	0.8	2
43512	Oneâ€step synthesis of coralâ€like highâ€entropy metal carbide powders. Journal of the American Ceramic Society, 2019, 102, 6372-6378.	1.9	48
43513	Zirconium Monocarbide. , 2019, , 423-675.		2
43514	BTEX adsorption on TiO2 anatase and rutile surfaces: DFT functionals. Journal of Molecular Modeling, 2019, 25, 137.	0.8	8
43515	Spectroscopic signatures of edge states in hexagonal boron nitride. Nano Research, 2019, 12, 1663-1667.	5.8	7
43516	Tandem nanocatalyst design: putting two step-reaction sites into one location towards enhanced hydrogen transfer reactions. Science China Materials, 2019, 62, 1297-1305.	3.5	4
43517	Stabilization of furanics to cyclic ketone building blocks in the vapor phase. Applied Catalysis B: Environmental, 2019, 254, 491-499.	10.8	19

#	Article	IF	Citations
43518	Preservation of the frictional properties of h-BN under chemical modification in the presence of a commensurate Ni(1â€¯1â€¯1) substrate. Computational Materials Science, 2019, 165, 82-87.	1.4	2
43519	The structure stability, diffusion behavior and elastic properties ofÂstoichiometric ZrC bulk with interstitial hydrogen defect: AÂfirst-principles study. Journal of Nuclear Materials, 2019, 521, 146-154.	1.3	11
43520	Theoretical investigations of solid-solution effect on the twinning of Ni. Journal of Physics and Chemistry of Solids, 2019, 133, 1-6.	1.9	5
43521	Earth-abundant photovoltaic semiconductor NaSbS2 in the rocksalt-derived structure: A first-principles study. Progress in Natural Science: Materials International, 2019, 29, 322-328.	1.8	8
43522	Adsorption of 3d transition-metal atom on Stone-Wales defected arsenene: A theoretical study. Superlattices and Microstructures, 2019, 130, 139-146.	1.4	0
43523	Solid Oganesson via a Many-Body Interaction Expansion Based on Relativistic Coupled-Cluster Theory and from Plane-Wave Relativistic Density Functional Theory. Journal of Physical Chemistry A, 2019, 123, 4201-4211.	1.1	23
43524	A-site Excessive (La_{0.8}Sr_{0.2})_{1+x}MnO₃ Perovskite Oxides for Bifunctional Oxygen Catalyst in Alkaline Media. ACS Catalysis, 2019, 9, 5074-5083.	5.5	84
43525	Room temperature electrofreezing of water yields a missing dense ice phase in the phase diagram. Nature Communications, 2019, 10, 1925.	5.8	20
43526	High capacity graphite-like calcium boridecarbides as a novel anode active material for lithium-ion batteries. Sustainable Energy and Fuels, 2019, 3, 1929-1936.	2.5	0
43527	First principles investigation of electronic properties and magnetic response of Fe3Co3Ti2 in non-cubic phase. AIP Conference Proceedings, 2019, , .	0.3	0
43528	First-principles prediction of a new ground state for surface-oxidized phosphorene with remarkable piezoelectricity. Journal Physics D: Applied Physics, 2019, 52, 295301.	1.3	1
43529	Epitaxial strain adaptation in chemically disordered FeRh thin films. Physical Review B, 2019, 99, .	1.1	5
43530	The Ab Initio Calculations on the Areal Specific Resistance of Liâ€Metal/Li₇La₃Zr₂O₁₂ Interphase. Advanced Theory and Simulations, 2019, 2, 1900028.	1.3	25
43531	Tuning the Magnetic and Electronic Properties of Janus MoSSe Nanoribbon by Edge Modification: A Firstâ€Principles Study. Physica Status Solidi (B): Basic Research, 2019, 256, 1900106.	0.7	8
43532	Electronic and optical properties of amorphous carbon with different sp3/sp2 hybridization ratio. Applied Physics A: Materials Science and Processing, 2019, 125, 1.	1.1	13
43533	First-Principles Study of Chemical Driving Force for Face Centered Cubic to Hexagonal Close Packed Martensitic Transformation in Hydrogen-Charged Iron. Metallurgical and Materials Transactions A: Physical Metallurgy and Materials Science, 2019, 50, 3019-3023.	1.1	4
43534	Orientation dependent electronic and optical properties of ZnS nanowires and ZnSâ€”Si core shell nanowires. Applied Surface Science, 2019, 486, 539-545.	3.1	14
43535	Magnetic properties of transition metal doped SnO2: A detailed theoretical study. Computational Condensed Matter, 2019, 21, e00393.	0.9	19

#	Article	IF	Citations
43536	First-principles study on the two-dimensional siligene (2D SiGe) as an anode material of an alkali metal ion battery. Computational Materials Science, 2019, 165, 121-128.	1.4	60
43537	Ab-initio design of novel cathode material LiFeP1-Si O4 for rechargeable Li-ion batteries. Electrochimica Acta, 2019, 313, 70-78.	2.6	2
43538	First principles calculations of behavior of lithium and interaction with helium in molybdenum. Fusion Engineering and Design, 2019, 142, 45-54.	1.0	1
43539	Influence of brÃ¸nsted-acid and cation-exchange sites on ethene adsorption in ZSM-5. Microporous and Mesoporous Materials, 2019, 284, 336-342.	2.2	8
43540	Intrinsic anharmonic localization in thermoelectric PbSe. Nature Communications, 2019, 10, 1928.	5.8	51
43541	B₃S monolayer: prediction of a high-performance anode material for lithium-ion batteries. Journal of Materials Chemistry A, 2019, 7, 12706-12712.	5.2	59
43542	A new and different insight into the promotion mechanisms of Ga for the hydrogenation of carbon dioxide to methanol over a Ga-doped Ni(211) bimetallic catalyst. Nanoscale, 2019, 11, 9969-9979.	2.8	10
43543	Divalent doping-induced thermoelectric power factor increase in p-type Bi2Te3 via electronic structure tuning. Journal of Applied Physics, 2019, 125, .	1.1	11
43544	Computational screening of MX (Mâ€‰â€‰=â€‰â€‰Ga, Ge, Sn, In; Xâ€‰â€‰=â€‰â€‰As, Se) van der Waa heterostructures as suitable candidates for solar cells. Journal Physics D: Applied Physics, 2019, 52, 335303.	1.3	5
43545	Spin-fermion model for skyrmions in MnGe derived from strong correlations. Physical Review B, 2019, 99, .	1.1	10
43546	Predicting Accurate Phonon Spectra: An Improved Description of Lattice Dynamics in Thermoelectric Clathrates Based on the SCAN Meta-GGA Functional. Chemistry of Materials, 2019, 31, 2571-2576.	3.2	9
43547	Syntheses of Colloidal F:In₂O₃ Cubes: Fluorine-Induced Faceting and Infrared Plasmonic Response. Chemistry of Materials, 2019, 31, 2661-2676.	3.2	41
43548	Ligand Effects on the Linear Response Hubbard U: The Case of Transition Metal Phthalocyanines. Journal of Physical Chemistry A, 2019, 123, 3214-3222.	1.1	6
43549	Unexpected Xe Cations and Superconductivity in Yâ€“Xe Intermediate Compounds under Pressure. Journal of Physical Chemistry C, 2019, 123, 9323-9330.	1.5	6
43550	CO, CO2, and H2 Interactions with (0001) and (001) Tungsten Carbide Surfaces: Importance of Carbon and Metal Sites. Journal of Physical Chemistry C, 2019, 123, 8871-8883.	1.5	30
43551	Exploring the Compositional Ternary Diagram of Ge/S/Cu Glasses for Resistance Switching Memories. Journal of Physical Chemistry C, 2019, 123, 9486-9495.	1.5	6
43552	Beyond the Oxygen Redox Strategy in Designing Cathode Material for Batteries: Dynamics of a Prussian Blue-like Cathode Revealed by Operando X-ray Diffraction and X-ray Absorption Fine Structure and by a Theoretical Approach. Journal of Physical Chemistry C, 2019, 123, 8588-8598.	1.5	16
43553	Unsubstituted and Fluorinated Copper Phthalocyanine Overlayers on Si(111)-(âˆš7 Ã— âˆš3)-In Surface: Adsorption Geometry, Charge Polarization, and Effects on Superconductivity. Journal of Physical Chemistry C, 2019, 123, 8951-8958.	1.5	15

#	Article	IF	Citations
43554	Intermetallic Differences at CdSâ€“Metal (Ni, Pd, Pt, and Au) Interfaces: From Single-Atom to Subnanometer Metal Clusters. Journal of Physical Chemistry C, 2019, 123, 9298-9310.	1.5	7
43555	Triferroic Material and Electrical Control of Valley Degree of Freedom. ACS Applied Materials & Interfaces, 2019, 11, 12675-12682.	4.0	52
43556	Syngas to light olefins conversion with high olefin/paraffin ratio using ZnCrOx/AlPO-18 bifunctional catalysts. Nature Communications, 2019, 10, 1297.	5.8	129
43557	Topological chiral crystals with helicoid-arc quantum states. Nature, 2019, 567, 500-505.	13.7	249
43558	Extensive deep neural networks for transferring small scale learning to large scale systems. Chemical Science, 2019, 10, 4129-4140.	3.7	32
43559	Ionic structure and transport properties of KFâ€“NaFâ€“AlF3 fused salt: a molecular dynamics study. Physical Chemistry Chemical Physics, 2019, 21, 7474-7482.	1.3	25
43560	An unexpected organometallic intermediate in surface-confined Ullmann coupling. Nanoscale, 2019, 11, 7682-7689.	2.8	29
43561	Silicene catalysts for CO₂hydrogenation: the number of layers controls selectivity. Nanoscale, 2019, 11, 7734-7743.	2.8	28
43562	DHQ-graphene: a novel two-dimensional defective graphene for corrosion-resistant coating. Journal of Materials Chemistry A, 2019, 7, 8967-8974.	5.2	33
43563	Synergetic effects of strain engineering and substrate defects on generating highly efficient single-atom catalysts for CO oxidation. Journal of Materials Chemistry A, 2019, 7, 9297-9304.	5.2	12
43564	Prediction of superhard B₂N₃ with two-dimensional metallicity. Journal of Materials Chemistry C, 2019, 7, 4527-4532.	2.7	13
43565	Structure dependent optoelectronic properties of monolayer antimonene, bismuthene and their binary compound. Physical Chemistry Chemical Physics, 2019, 21, 7907-7917.	1.3	40
43566	Strong anisotropic nodal lines in the TiBe family. Physical Chemistry Chemical Physics, 2019, 21, 8402-8407.	1.3	10
43567	The shielding effects of a C60 cage on the magnetic moments of transition metal atoms inside the corner holes of Si(111)-(7 Ã— 7). Nanoscale, 2019, 11, 6228-6234.	2.8	2
43568	Identification of divacancy and silicon vacancy qubits in 6H-SiC. Applied Physics Letters, 2019, 114, 112107.	1.5	28
43569	Electronic structure of cobalt/iron carbide from ab-initio calculations. Materials Research Express, 2019, 6, 076302.	0.8	1
43570	Kagome bands disguised in a coloring-triangle lattice. Physical Review B, 2019, 99, .	1.1	42
43571	Low-energy paths for octahedral tilting in inorganic halide perovskites. Physical Review B, 2019, 99, .	1.1	31

#	Article	IF	Citations
43572	Reactivity of Atomically Functionalized C-Doped Boron Nitride Nanoribbons and Their Interaction with Organosulfur Compounds. Nanomaterials, 2019, 9, 452.	1.9	7
43573	Plasma phase transition (by the fiftieth anniversary of the prediction). Contributions To Plasma Physics, 2019, 59, e201800182.	0.5	6
43574	Hybrid Charge-Transfer Semiconductors: (C₇H₇)SbI₄, (C₇H₇)BiI₄, and Their Halide Congeners. Inorganic Chemistry, 2019, 58, 5818-5826.	1.9	37
43575	An effective polysulfide trapping polar interlayer for high rate Liâ€“S batteries. Journal of Materials Chemistry A, 2019, 7, 10067-10076.	5.2	25
43576	Alloy-induced phase transition and enhanced photovoltaic performance: the case of Cs₃Bi₂I_{9â^'x}Br_x perovskite solar cells. Journal of Materials Chemistry A, 2019, 7, 8818-8825.	5.2	87
43577	Morphology evolution of fcc Ru nanoparticles under hydrogen atmosphere. Nanoscale, 2019, 11, 8037-8046.	2.8	18
43578	Orbital Fingerprint of Topological Fermi Arcs in the Weyl Semimetal TaP. Physical Review Letters, 2019, 122, 116402.	2.9	22
43579	Realizing Magnetoelectric Coupling with Hydrogen Intercalation. Physical Review Letters, 2019, 122, 117601.	2.9	13
43580	Factors controlling surface oxygen exchange in oxides. Nature Communications, 2019, 10, 1346.	5.8	69
43581	Phase stability of three-dimensional bulk and two-dimensional monolayer As_{1â^'x}Sb_x solid solutions from first principles. Journal of Physics Condensed Matter, 2019, 31, 245702.	0.7	6
43582	Plasmon damping depends on the chemical nature of the nanoparticle interface. Science Advances, 2019, 5, eaav0704.	4.7	128
43583	Recent Research on Strategies to Improve Ion Conduction in Alkali Metalâ€Ion Batteries. Batteries and Supercaps, 2019, 2, 403-427.	2.4	32
43584	Chemical and Electrochemical Lithiation of van der Waals Tetrelâ€Arsenides. Chemistry - A European Journal, 2019, 25, 6392-6401.	1.7	17
43585	Comprehensive study of the promotional mechanism of F on Ceâ€“Mo/TiO₂ catalysts for wide temperature NH₃-SCR performance: the activation of surface î€‚Tiâ€“F bonds. Catalysis Science and Technology, 2019, 9, 2231-2244.	2.1	18
43586	First Principle Study of New W2N Monolayer: a Promising Candidate for Li+ ion Batteries. International Journal of Electrochemical Science, 2019, 14, 3070-3080.	0.5	18
43587	Searching General Sufficientâ€andâ€Necessary Conditions for Ultrafast Hydrogenâ€Evolving Electrocatalysis. Advanced Functional Materials, 2019, 29, 1900704.	7.8	94
43588	Machine Learning Augmented Discovery of Chalcogenide Double Perovskites for Photovoltaics. Advanced Theory and Simulations, 2019, 2, 1800173.	1.3	54
43589	Electronics of Ba adsorbed on Ge(001). Applied Surface Science, 2019, 481, 1474-1482.	3.1	1

#	Article	IF	Citations
43590	Density functional theory investigation of the adsorption behaviors of SO2 and NO2 on a Pt(111) surface. Colloids and Surfaces A: Physicochemical and Engineering Aspects, 2019, 568, 266-270.	2.3	22
43591	Insight into the effect of surface structure for Pd catalyst on CO oxidative coupling to dimethyl oxalate. Molecular Catalysis, 2019, 470, 19-31.	1.0	8
43592	Theoretical insight into magnetic and thermoelectric properties of Au doped ZnO compounds using density functional theory. Physica B: Condensed Matter, 2019, 562, 67-74.	1.3	25
43593	Modeling Key Pathways Proposed for the Formation and Evolution of â€œCocktailâ€•Type Systems in Pd-Catalyzed Reactions Involving ArX Reagents. ACS Catalysis, 2019, 9, 3991-4005.	5.5	63
43594	Insights into the unusual semiconducting behavior in low-dimensional boron. Nanoscale, 2019, 11, 7866-7874.	2.8	3
43595	3D well-ordered porous phosphorus doped carbon as an anode for sodium storage: structure design, experimental and computational insights. Journal of Materials Chemistry A, 2019, 7, 11400-11407.	5.2	64
43596	Native point defects and carbon clusters in 4H-SiC: A hybrid functional study. Journal of Applied Physics, 2019, 125, .	1.1	55
43597	Electron and phonon interactions and transport in the ultrahigh-temperature ceramic ZrC. Physical Review B, 2019, 99, .	1.1	12
43598	Ab initio modeling of oxygen ion migration in non-stoichiometric bismuth titanate pyrochlore Bi1.5Ti2O6.25. Solid State Ionics, 2019, 335, 135-141.	1.3	12
43599	Dispelling the Myth of Passivated Codoping in TiO₂. Chemistry of Materials, 2019, 31, 2577-2589.	3.2	17
43600	Theoretical Study of the Catalytic Performance of Activated Layered Double Hydroxides in the Cyanoethylation of Alcohols. Journal of Physical Chemistry C, 2019, 123, 8777-8784.	1.5	12
43601	Essential Role of Water in the Autocatalysis Behavior of Methanol Synthesis from CO₂ Hydrogenation on Cu: A Combined DFT and Microkinetic Modeling Study. Journal of Physical Chemistry C, 2019, 123, 8959-8966.	1.5	48
43602	Realization of Strained Stanene by Interface Engineering. Journal of Physical Chemistry Letters, 2019, 10, 1558-1565.	2.1	25
43603	Unique Double-Interstitialcy Mechanism and Interfacial Storage Mechanism in the Graphene/Metal Oxide as the Anode for Sodium-Ion Batteries. Nano Letters, 2019, 19, 3122-3130.	4.5	31
43604	Rapid One-Pot Synthesis and Photoelectrochemical Properties of Copper Vanadates. ACS Applied Energy Materials, 2019, 2, 2837-2847.	2.5	34
43605	Octahedral SnO₂/Graphene Composites with Enhanced Gas-Sensing Performance at Room Temperature. ACS Applied Materials & Interfaces, 2019, 11, 12958-12967.	4.0	54
43606	Symmetry-enforced chiral hinge states and surface quantum anomalous Hall effect in the magnetic axion insulator Bi2â€“xSmxSe3. Nature Physics, 2019, 15, 577-581.	6.5	112
43607	Methane selective oxidation to methanol by metal-exchanged zeolites: a review of active sites and their reactivity. Catalysis Science and Technology, 2019, 9, 1744-1768.	2.1	148

#	Article	IF	Citations
43608	A 2D nonsymmorphic Dirac semimetal in a chemically modified group-VA monolayer with a black phosphorene structure. Nanoscale, 2019, 11, 7256-7262.	2.8	22
43609	Structural prediction and multilayer Li⁺ storage in two-dimensional VC₂ carbide studied by first-principles calculations. Journal of Materials Chemistry A, 2019, 7, 8873-8881.	5.2	34
43610	Robust staggered band alignment in one-dimensional van der Waals heterostructures: binary compound nanoribbons in nanotubes. Journal of Materials Chemistry C, 2019, 7, 3829-3836.	2.7	8
43611	Bifunctional mechanism of N, P co-doped graphene for catalyzing oxygen reduction and evolution reactions. Journal of Chemical Physics, 2019, 150, 104701.	1.2	29
43612	General method for atomistic spin-lattice dynamics with first-principles accuracy. Physical Review B, 2019, 99, .	1.1	37
43613	Gate-controlled VO ₂ phase transition for high-performance smart windows. Science Advances, 2019, 5, eaav6815.	4.7	160
43614	Advances in Sustainable Catalysis: A Computational Perspective. Frontiers in Chemistry, 2019, 7, 182.	1.8	36
43615	Synergistic Regulation of Polysulfides Conversion and Deposition by MOFâ€Derived Hierarchically Ordered Carbonaceous Composite for Highâ€Energy Lithiumâ€“Sulfur Batteries. Advanced Functional Materials, 2019, 29, 1900875.	7.8	104
43616	Achieving band convergence by tuning the bonding ionicity in nâ€type Mg₃Sb₂. Journal of Computational Chemistry, 2019, 40, 1693-1700.	1.5	68
43617	The AFLOW Fleet for Materials Discovery. , 2019, , 1-28.		0
43618	Density functional study of the adsorption of NO on Ni (nâ€¯=â€¯1, 2, 3 and 4) clusters doped functionalized graphene support. Applied Surface Science, 2019, 481, 940-950.	3.1	27
43619	Adsorption and dissociation of H2O molecule on the doped monolayer MoS2 with B/Si. Applied Surface Science, 2019, 481, 994-1000.	3.1	16
43620	pyiron: An integrated development environment for computational materials science. Computational Materials Science, 2019, 163, 24-36.	1.4	64
43621	Visiting CH4 formation and C1â€¯+â€¯C1 couplings to tune CH4 selectivity on Fe surfaces. Journal of Catalysis, 2019, 372, 217-225.	3.1	19
43622	Optimized band gap and fast interlayer charge transfer in two-dimensional perovskite oxynitride Ba2NbO3N and Sr2NbO3/Ba2NbO3N bonded heterostructure visible-light photocatalysts for overall water splitting. Journal of Colloid and Interface Science, 2019, 546, 20-31.	5.0	26
43623	A Dirac semimetal phase diagram of the binary compound CuI(R-3m). Journal of Physics and Chemistry of Solids, 2019, 131, 62-68.	1.9	2
43624	Structural Intergrowth in Î´-Al₂O₃. Journal of Physical Chemistry C, 2019, 123, 9454-9460.	1.5	14
43625	Formation of Active Cu-oxo Clusters for Methane Oxidation in Cu-Exchanged Mordenite. Journal of Physical Chemistry C, 2019, 123, 8759-8769.	1.5	60

#	Article	IF	Citations
43626	Electronic Structure of LiCoO₂ Surfaces and Effect of Al Substitution. Journal of Physical Chemistry C, 2019, 123, 8851-8858.	1.5	24
43627	Tunable Dipole Moment in Janus Single-Layer MoSSe via Transition-Metal Atom Adsorption. Journal of Physical Chemistry C, 2019, 123, 9059-9065.	1.5	42
43628	A New Family of Two-Dimensional Crystals: Open-Framework T₃X (T =) Tj ETQq0 0 0 rgBT /Overlock 10 2694-2699.	4.5	11
43629	Simultaneous Immobilization and Conversion of Polysulfides on Co₃O₄â€“CoN Heterostructured Mediators toward High-Performance Lithiumâ€“Sulfur Batteries. ACS Applied Energy Materials, 2019, 2, 2570-2578.	2.5	18
43630	Machine-Learning-Assisted Development and Theoretical Consideration for the Al₂Fe₃Si₃ Thermoelectric Material. ACS Applied Materials & Interfaces, 2019, 11, 11545-11554.	4.0	69
43631	Superoxide/Peroxide Chemistry Extends Charge Carriersâ€™ Lifetime but Undermines Chemical Stability of CH₃NH₃PbI₃ Exposed to Oxygen: Time-Domain ab Initio Analysis. Journal of the American Chemical Society, 2019, 141, 5798-5807.	6.6	102
43632	Improving the electron transport performance by changing side chains in sulfur-containing azaacenes: a combined theoretical investigation on free molecules and an adsorption system. New Journal of Chemistry, 2019, 43, 5414-5422.	1.4	3
43633	Exploring T-carbon for energy applications. Nanoscale, 2019, 11, 5798-5806.	2.8	38
43634	Origin of the isotropic motion in crystalline molecular rotors with carbazole stators. Chemical Science, 2019, 10, 4422-4429.	3.7	11
43635	Two-dimensional ferroelastic semiconductors in single-layer indium oxygen halide InOY (Y = Cl/Br). Physical Chemistry Chemical Physics, 2019, 21, 7440-7446.	1.3	26
43636	Grain boundaries modified uniformly-conjoint metal/oxides via binder strategy as efficient bifunctional electrocatalysts. Journal of Materials Chemistry A, 2019, 7, 10010-10018.	5.2	27
43637	Large magnetoresistance and spin-polarized photocurrent in La_{2/3}Sr_{1/3}MnO₃(Co)/quaterthiophene/La_{2/3}Sr_{1/3}MnO₃ organic magnetic tunnel junctions. Journal of Materials Chemistry C, 2019, 7, 4079-4088.	2.7	20
43638	The effect of oxidation on the electronic properties of penta-graphene: first-principles calculation. RSC Advances, 2019, 9, 8253-8261.	1.7	14
43639	Dynamic Ag⁺-intercalation with AgSnSe₂ nano-precipitates in Cl-doped polycrystalline SnSe₂ toward ultra-high thermoelectric performance. Journal of Materials Chemistry A, 2019, 7, 9761-9772.	5.2	50
43640	Vibrational properties of CdGa2S4 at high pressure. Journal of Applied Physics, 2019, 125, .	1.1	7
43641	First-principles characterization of reversible martensitic transformations. Physical Review B, 2019, 99, .	1.1	12
43642	Identification of point defects using high-resolution electron energy loss spectroscopy. Physical Review B, 2019, 99, .	1.1	6
43643	Interplay between the Coulomb Interaction and Hybridization in Ca and Anomalous Pressure Dependence of the Resistivity. JETP Letters, 2019, 109, 387-391.	0.4	11

#	Article	IF	Citations
43644	Morphologyâ€Dependent Stability of Complex Metal Hydrides and Their Intermediates Using Firstâ€Principles Calculations. ChemPhysChem, 2019, 20, 1340-1347.	1.0	11
43645	Atomistic insight into ordered defect superstructures at novel grain boundaries in CuO nanosheets: From structures to electronic properties. Nano Research, 2019, 12, 1099-1104.	5.8	6
43646	A synergistic reinforcement of Re and W for ideal shear strengths of Î³â€²-Ni3Al phases. Journal of Physics and Chemistry of Solids, 2019, 131, 34-43.	1.9	18
43647	Properties of M₂O₃/Au(111) Honeycomb Monolayers (M = Sc, Ti, V, Cr, Mn, Fe,) Tj ETQq1 1 0.784314 rgBT /O	1.5	21
43648	Understanding the Diverse Coordination Modes of Thiocyanate Anion on Solid Surfaces. Journal of Physical Chemistry C, 2019, 123, 9282-9291.	1.5	10
43649	Symmetry Breaking at MAPbI₃ Perovskite Grain Boundaries Suppresses Charge Recombination: Time-Domain ab Initio Analysis. Journal of Physical Chemistry Letters, 2019, 10, 1617-1623.	2.1	65
43650	Observation of unconventional chiral fermions with long Fermi arcs in CoSi. Nature, 2019, 567, 496-499.	13.7	260
43651	Hierarchical Ni₂P/Cr₂CT_x(MXene) composites with oxidized surface groups as efficient bifunctional electrocatalysts for overall water splitting. Journal of Materials Chemistry A, 2019, 7, 9324-9334.	5.2	54
43652	Tl on the Si(111)- surface: Density Functional Theory. Philosophical Magazine, 2019, 99, 1656-1668.	0.7	1
43653	1 + 1â€² > 2: Heteronuclear Biatom Catalyst Outperforms Its Homonuclear Counterparts for CO Oxidation. Small Methods, 2019, 3, 1800480.	4.6	92
43654	A Bifunctional Saddleâ€Shaped Small Molecule as a Dopantâ€Free Hole Transporting Material and Interfacial Layer for Efficient and Stable Perovskite Solar Cells. Solar Rrl, 2019, 3, 1900011.	3.1	34
43655	Sintering behavior of high-concentration Li2CO3-doped BaTiO3 ceramics. Applied Physics A: Materials Science and Processing, 2019, 125, 1.	1.1	5
43656	Power generation from graphene-water interactions. FlatChem, 2019, 14, 100090.	2.8	38
43657	First-principles study of the ferroelectric phase of AgNbO3. , 2019, , 137-159.		0
43658	Catalytic de-chlorination of products from PVC degradation by magnetite (Fe3O4). Applied Surface Science, 2019, 480, 792-801.	3.1	15
43659	Phase equilibria of the Zn-Ti system: Experiments, first-principles calculations and Calphad assessment. Calphad: Computer Coupling of Phase Diagrams and Thermochemistry, 2019, 64, 213-224.	0.7	7
43660	Finite temperature thermal expansion and elastic properties of (Hf1-xTax)C ultrahigh temperature ceramics. Ceramics International, 2019, 45, 10805-10809.	2.3	17
43661	Theoretical study of the electronic and optical properties of rare-earth (REâ€¯=â€¯La, Ce, Pr, Nd, Eu, Gd,) Tj ETQq1 1 0.784314 rgBT /O	1.4	21

#	Article	IF	Citations
43662	Realization of tetragonal Heusler alloy Mn3-Cr Ga for spintronic applications. Intermetallics, 2019, 108, 87-93.	1.8	13
43663	Realizing high thermoelectric performance of polycrystalline SnS through optimizing carrier concentration and modifying band structure. Journal of Alloys and Compounds, 2019, 789, 485-492.	2.8	34
43664	Protection of one-dimensional Si chains embedded in Pt(111) and protected by a hexagonal boron-nitride monolayer. Surface Science, 2019, 685, 24-33.	0.8	0
43665	Redox-Driven Spin Transition in a Layered Battery Cathode Material. Chemistry of Materials, 2019, 31, 2358-2365.	3.2	19
43666	First-Principles Study of the Effect of Nonmetallic Si Doping on Tritium Release from Li₂TiO₃(001) Surface. Journal of Physical Chemistry C, 2019, 123, 6477-6486.	1.5	8
43667	Structure and Electronic Properties of [Ca₂₄Al₂₈O₆₄]⁴⁺Â·4e^{â€“} Surfaces: Opportunities for Termination-Controlled Electron Transfer. Journal of Physical Chemistry C, 2019, 123, 6030-6036.	1.5	8
43668	Submolecular Imaging of Parallel Offset Ï€â€“Ï€ Stacking in Nonplanar Phthalocyanine Bilayers. Journal of Physical Chemistry C, 2019, 123, 7178-7184.	1.5	4
43669	Insights into the CO₂ Stability-Performance Trade-Off of Antimony-Doped SrFeO_{3â^Î´} Perovskite Cathode for Solid Oxide Fuel Cells. ACS Applied Materials & Interfaces, 2019, 11, 11498-11506.	4.0	36
43670	New insights on the nature of impurity levels in V-doped In₂S₃: why is it impossible to obtain a metallic intermediate band?. Journal of Materials Chemistry A, 2019, 7, 7745-7751.	5.2	12
43671	Hybrid 2D nanodevices (graphene/h-BN): selecting NO_x gas through the device interface. Journal of Materials Chemistry A, 2019, 7, 8905-8911.	5.2	29
43672	Local adsorption structure and bonding of porphine on Cu(111) before and after self-metalation. Journal of Chemical Physics, 2019, 150, 094702.	1.2	11
43673	Eley Rideal recombination of hydrogen atoms on Cu(111): Quantitative role of electronic excitation in cross sections and product distributions. Journal of Chemical Physics, 2019, 150, 061101.	1.2	15
43674	Geometric and electronic properties of MnC60 Â±1,0 (M = Li, Na, K, n = 1â€“12) clusters. Materials Research Express, 2019, 6, 065605.	0.8	0
43675	Pressure-induced evolution of structural and electronic properties in <mml:math xmlns:mml="http://www.w3.org/1998/Math/MathML"><mml:mrow><mml:mi>TiT</mml:mi><mml:msub><mml:mi mathvariant="normal">e</mml:mi><mml:mn>2</mml:mn></mml:msub></mml:mrow></mml:math>. Physical Review B, 2019, 99, .	1.1	12
43676	An MoS₂-Based Piezoelectric FET: A Computational Study of Material Properties and Device Design. IEEE Transactions on Electron Devices, 2019, 66, 1997-2003.	1.6	8
43677	Electronic Properties of SbTa₁₋_xNb_xO₄: Phase-Related Distortions. Journal of the Electrochemical Society, 2019, 166, H3195-H3201.	1.3	6
43678	Phase Stability and Mechanical Properties of Al8Fe4RE via First-Principle Calculations. Materials, 2019, 12, 701.	1.3	4
43679	Structural Basis of CO2 Adsorption in a Flexible Metal-Organic Framework Material. Nanomaterials, 2019, 9, 354.	1.9	10

#	Article	IF	Citations
43680	Ionizationâ€Facilitated Formation of 2D (Alumino)Silicateâ€“Noble Gas Clathrate Compounds. Advanced Functional Materials, 2019, 29, 1806583.	7.8	20
43681	Leadâ€Free Perovskite Derivative Cs₂SnCl_{6â^'}_xBr_x Single Crystals for Narrowband Photodetectors. Advanced Optical Materials, 2019, 7, 1900139.	3.6	123
43682	Understanding the Oxygen Reduction Reaction Activity and Oxidative Stability of Pt Supported on Nbâ€Doped TiO₂. ChemSusChem, 2019, 12, 3468-3480.	3.6	39
43683	Ab Initio Molecular Dynamics Study on the Dissolution of Interfacial Iron Oxides in Hot Compressive Bonding Combined with Experiments. Minerals, Metals and Materials Series, 2019, , 3-15.	0.3	2
43684	First-principles study of mechanical, electronic properties and anisotropic deformation mechanisms of TiB under uniaxial compressions. Applied Physics A: Materials Science and Processing, 2019, 125, 1.	1.1	5
43685	Unraveling the mechanochemical synthesis and luminescence in MnII-based two-dimensional hybrid perovskite (C4H9NH3)2PbCl4. Science China Materials, 2019, 62, 1013-1022.	3.5	26
43686	Design of high efficient oxygen reduction catalyst from the transition metal dimer phthalocyanine monolayer. Applied Surface Science, 2019, 480, 905-911.	3.1	12
43687	Adsorption characteristics of Co-anchored different graphene substrates toward O2 and NO molecules. Applied Surface Science, 2019, 480, 779-791.	3.1	29
43688	Crystal and Magnetic Structures of Melilite-Type Ba₂MnSi₂O₇. Inorganic Chemistry, 2019, 58, 4164-4172.	1.9	8
43689	Theoretical Studies of Electronic and Optical Behaviors of All-Inorganic CsPbI₃ and Two-Dimensional MS₂ (M = Mo, W) Heterostructures. Journal of Physical Chemistry C, 2019, 123, 7158-7165.	1.5	21
43690	Self-Assembly Evolution of Metal-Free Naphthalocyanine Molecules on Ag(111) at the Submonolayer Coverage. Journal of Physical Chemistry C, 2019, 123, 7202-7208.	1.5	5
43691	Understanding the Impact of Defects on Catalytic CO Oxidation of LaFeO₃-Supported Rh, Pd, and Pt Single-Atom Catalysts. Journal of Physical Chemistry C, 2019, 123, 7290-7298.	1.5	36
43692	Assessing structure and stability of polymer/lithium-metal interfaces from first-principles calculations. Journal of Materials Chemistry A, 2019, 7, 8394-8404.	5.2	77
43693	Self-assembly of 5,6-dihydroxyindole-2-carboxylic acid: polymorphism of a eumelanin building block on Au(111). Nanoscale, 2019, 11, 5422-5428.	2.8	9
43694	Ab initio investigation of structural and electronic properties of selenium and tellurium clusters. European Physical Journal B, 2019, 92, 1.	0.6	8
43695	Interaction of Ethylene with Irn (n = 1â€“10): From Bare Clusters to Î³-Al2O3-Supported Nanoparticles. Nanomaterials, 2019, 9, 331.	1.9	6
43696	VI₃â€”a New Layered Ferromagnetic Semiconductor. Advanced Materials, 2019, 31, e1808074.	11.1	157
43697	A Computational Investigation of OMEâ€synthesis through Homogeneous Acid Catalysis. ChemCatChem, 2019, 11, 1949-1954.	1.8	5

#	Article	IF	Citations
43698	Synthesis, Crystal Structure, and Selected Properties of [Au(S₂CNH₂)₂]SCN: A Precursor for Gold Macroâ€Needles Consisting of Gold Nanoparticles Glued by Graphitic Carbon Nitride. Chemistry - A European Journal, 2019, 25, 6763-6772.	1.7	5
43699	Data-enabled structureâ€“property mappings for lanthanide-activated inorganic scintillators. Journal of Materials Science, 2019, 54, 8361-8380.	1.7	9
43700	Effects of Solute Atoms on 9R Phase Stabilization in High-Performance Al Alloys: A First-Principles Study. Jom, 2019, 71, 2047-2053.	0.9	8
43701	Theoretical insight into the hydrogen adsorption on MoS2 (MoSe2) monolayer as a function of biaxial strain/external electric field. Applied Surface Science, 2019, 478, 857-865.	3.1	38
43702	Monolayer Zr2B2: A promising two-dimensional anode material for Li-ion batteries. Applied Surface Science, 2019, 480, 448-453.	3.1	63
43703	Adsorption and migration of selenium atoms on a hydrogen-terminated diamond (0â€¯0â€¯1) surface: A first-principles study. Computational Materials Science, 2019, 162, 186-198.	1.4	4
43704	SLABCC: Total energy correction code for charged periodic slab models. Computer Physics Communications, 2019, 240, 101-105.	3.0	9
43705	Structural stability, electronic structure, and superconductivity of cubic sodium hexaboride NaB6 from first-principle calculations. Chemical Physics Letters, 2019, 722, 80-84.	1.2	8
43706	A first-principles study of novel cubic AlN phases. Journal of Physics and Chemistry of Solids, 2019, 130, 58-66.	1.9	5
43707	Origin of anisotropy and compositional dependence of phonon and electron transport in ZnO based natural superlattices and role of atomic layer interfaces. Nano Energy, 2019, 59, 651-666.	8.2	5
43708	Structural, electronic, magnetic, and optical properties of monolayer WS2 doped with Co-X6 (Xâ€¯=â€¯S, N,) Tj ETQq0 0 0 rgBT /Overloc	0.8	10
43709	Atomically Layered and Ordered Rare-Earth i-MAX Phases: A New Class of Magnetic Quaternary Compounds. Chemistry of Materials, 2019, 31, 2476-2485.	3.2	89
43710	Impact of Hydrogen on the Intermediate Oxygen Clusters and Diffusion in Fluorite Structured UO2+x. Inorganic Chemistry, 2019, 58, 3774-3779.	1.9	3
43711	Double-Spiral Hexagonal Boron Nitride and Shear Strained Coalescence Boundary. Nano Letters, 2019, 19, 4229-4236.	4.5	15
43712	The Opposite Anisotropic Piezoresistive Effect of ReS₂. ACS Nano, 2019, 13, 3310-3319.	7.3	55
43713	Borophene Synthesis on Au(111). ACS Nano, 2019, 13, 3816-3822.	7.3	261
43714	Neural network force fields for simple metals and semiconductors: construction and application to the calculation of phonons and melting temperatures. Physical Chemistry Chemical Physics, 2019, 21, 6506-6516.	1.3	25
43715	Adsorption and migration of alkali metals (Li, Na, and K) on pristine and defective graphene surfaces. Nanoscale, 2019, 11, 5274-5284.	2.8	149

#	Article	IF	Citations
43716	Exciton states and oscillator strength in few-layer Î±-tellurene. Applied Physics Letters, 2019, 114, .	1.5	14
43717	Tunable 2D-gallium arsenide and graphene bandgaps in a graphene/GaAs heterostructure: anab initiostudy. Journal of Physics Condensed Matter, 2019, 31, 265502.	0.7	6
43718	Topological node line semimetal state in two-dimensional tetragonal allotrope of Ge and Sn. New Journal of Physics, 2019, 21, 033005.	1.2	35
43719	Thermal conductivity and phonon hydrodynamics in transition metal dichalcogenides from first-principles. 2D Materials, 2019, 6, 035002.	2.0	39
43720	Origin of Deep <mml:math xmlns:mml="http://www.w3.org/1998/Math/MathML" display="inline" overflow="scroll"><mml:mi>Be</mml:mi></mml:math> Acceptor Levels in Nitride Semiconductors: The Roles of Chemical and Strain Effects. Physical Review Applied, 2019, 11, .	1.5	17
43721	<mml:math xmlns:mml="http://www.w3.org/1998/Math/MathML"><mml:mrow><mml:mi>La</mml:mi><mml:mi>X</mml:mi><mml:msub><mml:mi mathvariant="normal">O</mml:mi><mml:mn>3</mml:mn></mml:msub></mml:mrow></mml:math> bilayers (<mml:math) Ti ETOq1 1 0.784314 rgBT /Overlock 10 Tf 50.522 Td (xmlns:mml="http://www.w3.org/1998/Math/MathML"><mml:	1.1	8
43722	Bulklike band-offset mystery solved through energy minimization: Lessons from perovskite oxide heterojunctions. Physical Review B, 2019, 99, .	1.1	8
43723	Predicted Pressure-Induced Superconducting Transition in Electride <mml:math xmlns:mml="http://www.w3.org/1998/Math/MathML" display="inline"><mml:mrow><mml:msub><mml:mrow><mml:mi>Li</mml:mi></mml:mrow><mml:mrow><mml:mn>2</mml:mn></mml:mrow></mml:msub><mml:mi mathvariant="normal">P</mml:mi></mml:mrow></mml:math>. Physical Review Letters, 2019, 122, 027002.	2.6	94
43724	Molecular mechanisms of atomic layer etching of cobalt with sequential exposure to molecular chlorine and diketones. Journal of Vacuum Science and Technology A: Vacuum, Surfaces and Films, 2019, 37, 021004.	0.9	41
43725	A First-Principles Study on the Multiferroic Property of Two-Dimensional BaTiO3 (001) Ultrathin Film with Surface Ba Vacancy. Nanomaterials, 2019, 9, 269.	1.9	9
43726	Ordered Mesoporous CeO₂â€supported Ag as an Effective Catalyst for Carboxylative Coupling Reaction Using CO₂. ChemCatChem, 2019, 11, 2089-2098.	1.8	24
43727	Nonadiabatic scattering of NO off Au₃ clusters: A simple and robust diabatic state manifold generation method for multiconfigurational wavefunctions. Journal of Computational Chemistry, 2019, 40, 794-810.	1.5	10
43728	Interfacial Properties for a Monolayer CrS 2 Contact with Metal: A Theoretical Perspective. Physica Status Solidi (B): Basic Research, 2019, 256, 1800597.	0.7	8
43729	Periodic DFT modeling and vibrational analysis of silver(I) cyanide complexes of thioureas. Journal of Molecular Modeling, 2019, 25, 90.	0.8	8
43730	Understanding the role of Ru dopant on selective catalytic reduction of NO with NH3 over Ru-doped CeO2 catalyst. Chemical Engineering Journal, 2019, 369, 124-133.	6.6	33
43731	Chemical and mechanical degradation and mitigation strategies for Si anodes. Journal of Power Sources, 2019, 419, 208-218.	4.0	32
43732	Characterization of Phonon Vibrations of Silica Bilayer Films. Journal of Physical Chemistry C, 2019, 123, 7110-7117.	1.5	8
43733	Atomically Thin Metal Films on Foreign Substrates: From Lattice Mismatch to Electrocatalytic Activity. ACS Catalysis, 2019, 9, 3467-3481.	5.5	25

#	Article	IF	Citations
43734	Structureâ€“Activity Relationships That Identify Metalâ€“Organic Framework Catalysts for Methane Activation. ACS Catalysis, 2019, 9, 3576-3587.	5.5	105
43735	Room Temperature Methane Capture and Activation by Ni Clusters Supported on TiC(001): Effects of Metalâ€“Carbide Interactions on the Cleavage of the Câ€“H Bond. Journal of the American Chemical Society, 2019, 141, 5303-5313.	6.6	57
43736	MoS₂â€“OH Bilayer-Mediated Growth of Inch-Sized Monolayer MoS₂ on Arbitrary Substrates. Journal of the American Chemical Society, 2019, 141, 5392-5401.	6.6	87
43737	Magnetic proximity effect induced spin-dependent electronic structure in two-dimensional SnO by half-metallic monolayer CrN ferromagnet. Physical Chemistry Chemical Physics, 2019, 21, 6984-6990.	1.3	11
43738	Electronic structure basis for enhanced overall water splitting photocatalysis with aluminum doped SrTiO₃ in natural sunlight. Energy and Environmental Science, 2019, 12, 1385-1395.	15.6	134
43739	Organic enantiomeric high- T _c ferroelectrics. Proceedings of the National Academy of Sciences of the United States of America, 2019, 116, 5878-5885.	3.3	137
43740	Oxygen-Vacancy Dynamics and Entanglement with Polaron Hopping at the Reduced <mml:math xmlns:mml="http://www.w3.org/1998/Math/MathML" display="inline"><mml:mrow><mml:msub><mml:mrow><mml:mi>CeO</mml:mi></mml:mrow><mml:mn>2</mml:mn></mml:msub><m stretchy="false">(</mml:mo><mml:mn>111</mml:mn><mml:mo) Tj ETQq0 0 0 rgBT /Overlock 10 Tf 50 492 Td (stretchy="false">)</mm	2.9	43
43741	096101. Ab Initio Study of the Combined Effects of Alloying Elements and H on Grain Boundary Cohesion in Ferritic Steels. Metals, 2019, 9, 291.	1.0	14
43742	Nanoporous graphene: A 2D semiconductor with anisotropic mechanical, optical and thermal conduction properties. Carbon, 2019, 147, 377-384.	5.4	46
43743	Phase diagram and bonding states of Ir-P binary compounds at high pressures. Journal of Alloys and Compounds, 2019, 791, 1257-1262.	2.8	7
43744	Anisotropic magnetic property and exchange bias effect in a homogeneous Sillen-Aurivillius layered oxide. Journal of the European Ceramic Society, 2019, 39, 2685-2691.	2.8	6
43745	Antiferromagnetic coupling of van der Waals ferromagnetic Fe₃GeTe₂. Nanotechnology, 2019, 30, 245701.	1.3	53
43746	Diversity of structural and electronic properties ofPâ€“AuBr of different dimensions. Materials Research Express, 2019, 6, 065010.	0.8	1
43747	Phase evolution in the ferroelectric relaxor <mml:math xmlns:mml="http://www.w3.org/1998/Math/MathML"><mml:mrow><mml:mi>Ba</mml:mi><mml:mrow><mml:mo>(</mml:mo><mml:mn mathvariant="normal">O</mml:mi><mml:mn>3</mml:mn></mml:msub></mml:mrow></mml:math> from atomistic simulations. Physical Review B, 2019, 99, .	1.1	14
43748	Accelerating crystal structure prediction by machine-learning interatomic potentials with active learning. Physical Review B, 2019, 99, .	1.1	229
43749	Strain and screening: Optical properties of a small-diameter carbon nanotube from first principles. Physical Review B, 2019, 99, .	1.1	10
43750	Geometry and electronic structure of monolayer, bilayer, and multilayer Janus WSSe. Physical Review B, 2019, 99, .	1.1	100
43751	Paramagnetic-to-Diamagnetic Transition in Dense Liquid Iron and Its Influence on Electronic Transport Properties. Physical Review Letters, 2019, 122, 086601.	2.9	17

#	Article	IF	Citations
43752	Ultrafast electron calorimetry uncovers a new long-lived metastable state in 1 T -TaSe ₂ mediated by mode-selective electron-phonon coupling. Science Advances, 2019, 5, eaav4449.	4.7	43
43753	Interface and heterostructure design in polyelemental nanoparticles. Science, 2019, 363, 959-964.	6.0	171
43754	Design and Prediction of a Novel Two-Dimensional Carbon Nanostructure with In-Plane Negative Poissonâ€™s Ratio. Journal of Nanomaterials, 2019, 2019, 1-10.	1.5	2
43755	Large figure of merit ZT = 1.88 at 873 K achieved with nanostructured Si_{0.55}Ge_{0.35}(P_{0.10}Fe_{0.01}). Applied Physics Express, 2019, 12, 045507.	1.1	21
43756	Dramatically reduced lattice thermal conductivity of Mg2Si thermoelectric material from nanotwinning. Acta Materialia, 2019, 169, 9-14.	3.8	30
43757	Exploring reaction mechanisms for CO oxidation on boron-doped carbon nanotubes: A computational approach. Applied Surface Science, 2019, 480, 63-69.	3.1	8
43758	Modulating the Schottky barriers in MoS2/MXenes heterostructures via surface functionalization and electric field. Applied Surface Science, 2019, 480, 199-204.	3.1	58
43759	First-principles investigation of structural, mechanical and thermodynamic properties of NiPt2 bimetallic nanomaterial. Chemical Physics Letters, 2019, 719, 34-38.	1.2	19
43760	First-principles study on visible light absorption of defected SrNbO3. Journal of Photochemistry and Photobiology A: Chemistry, 2019, 375, 175-180.	2.0	6
43761	First principles calculations on CeO2 doped with Tb3+ ions. Optical Materials, 2019, 90, 76-83.	1.7	3
43762	Tuning the Electrical Conductivity of Ti₂CO₂ MXene by Varying the Layer Thickness and Applying Strains. Journal of Physical Chemistry C, 2019, 123, 6802-6811.	1.5	49
43763	Martensitic transformation of Ti50(Ni50â^'xCux) and Ni50(Ti50â^'xZrx) shape-memory alloys. Scientific Reports, 2019, 9, 3221.	1.6	13
43764	Evidence of the Oâ€“Pdâ€“O and Pdâ€“O₄ structure units as oxide seeds and their origin on Pd(211): revealing the mechanism of surface oxide formation. Physical Chemistry Chemical Physics, 2019, 21, 6499-6505.	1.3	7
43765	Electronic and optical properties of perovskite compounds MA_{1â^'Î±}FA_{Î±}PbI_{3â^'Î²}X_{Î²} (X = Cl, Br) explored for photovoltaic applications. RSC Advances, 2019, 9, 7015-7024.	1.7	20
43766	Comparison of hydrogen vacancies in KDP and ADP crystals: a combination of density functional theory calculations and experiment. Physical Chemistry Chemical Physics, 2019, 21, 6186-6197.	1.3	29
43767	Magnetism, stability and electronic properties of a novel one-dimensional infinite monatomic copper wire: a density functional study. New Journal of Chemistry, 2019, 43, 5065-5069.	1.4	1
43768	High Curie temperature and intrinsic ferromagnetic half-metallicity in two-dimensional Cr₃X₄ (X = S, Se, Te) nanosheets. Nanoscale Horizons, 2019, 4, 859-866.	4.1	84
43769	Highly-efficient heterojunction solar cells based on two-dimensional tellurene and transition metal dichalcogenides. Journal of Materials Chemistry A, 2019, 7, 7430-7436.	5.2	90

#	Article	IF	Citations
43770	Functionalization of monolayer AsP phases by adatoms: a first-principles study. Materials Research Express, 2019, 6, 065032.	0.8	5
43771	Evolution of Local Structural Ordering and Chemical Distribution upon Delithiation of a Rock Saltâ€“Structured Li_{1.3}Ta_{0.3}Mn_{0.4}O₂ Cathode. Advanced Functional Materials, 2019, 29, 1808294.	7.8	41
43772	Evidence of the Plaquette Structure of Fe 1+ x Te Iron Telluride: MÃ¶ssbauer Spectroscopy Study. Physica Status Solidi (B): Basic Research, 2019, 256, 1800698.	0.7	1
43773	Passivating Crystal Boundaries with Potassiumâ€Rich Phase in Organic Halide Perovskite. Solar Rrl, 2019, 3, 1900053.	3.1	64
43774	Possible indirect to direct bandgap transition in SnS2 via nickel doping. Chemical Physics, 2019, 522, 59-64.	0.9	21
43775	Realizing discrete growth of thin Li2O2 sheets on black phosphorus quantum dots-decorated Î´-MnO2catalyst for long-life lithiumâ€“oxygen cells. Energy Storage Materials, 2019, 23, 684-692.	9.5	24
43776	Flexible quantum spin Hall insulator in O-functionalized GaSe monolayer. Journal of Alloys and Compounds, 2019, 788, 1113-1118.	2.8	7
43777	Correlating structural and mechanical properties of AlN/TiN superlattice films. Scripta Materialia, 2019, 165, 159-163.	2.6	29
43778	Machine-Learned Fragment-Based Energies for Crystal Structure Prediction. Journal of Chemical Theory and Computation, 2019, 15, 2743-2758.	2.3	33
43779	Adsorption of CO, NO, and H₂ on the Pd_nAu_{55â€“n} Nanoclusters: A Density Functional Theory Investigation within the van der Waals D3 Corrections. Journal of Physical Chemistry C, 2019, 123, 7431-7439.	1.5	15
43780	Prediction of Synthesis of 2D Metal Carbides and Nitrides (MXenes) and Their Precursors with Positive and Unlabeled Machine Learning. ACS Nano, 2019, 13, 3031-3041.	7.3	187
43781	Structural principles to steer the selectivity of the electrocatalytic reduction of aliphatic ketones on platinum. Nature Catalysis, 2019, 2, 243-250.	16.1	95
43782	IIIâ€“VI van der Waals heterostructures for sustainable energy related applications. Nanoscale, 2019, 11, 6431-6444.	2.8	88
43783	Strain effects on electronic and magnetic properties of the monolayer Î±-RuCl3: A first-principles and Monte Carlo study. Journal of Applied Physics, 2019, 125, .	1.1	32
43784	Role of intrinsic defects on the persistent luminescence of pristine and Mn doped ZnGa2O4. Journal of Applied Physics, 2019, 125, .	1.1	9
43785	Electrical contacts of coplanar 2H/1Tâ€² MoTe2 monolayer. Journal of Applied Physics, 2019, 125, 075104.	1.1	7
43786	Carbon in GaN: Calculations with an optimized hybrid functional. Physical Review B, 2019, 99, .	1.1	32
43787	Temperature dependence of the <mml:math xmlns:mml="http://www.w3.org/1998/Math/MathML"><mml:mmultiscripts><mml:mi mathvariant="normal">C</mml:mi><mml:mprescripts /><mml:none /><mml:mn>13</mml:mn></mml:mmultiscripts></mml:math> hyperfine structure of the negatively charged nitrogen-vacancy center in diamond. Physical Review B, 2019, 99, .	1.1	9

#	Article	IF	Citations
43788	Fabricating Singleâ€Atom Catalysts from Chelating Metal in Open Frameworks. Advanced Materials, 2019, 31, e1808193.	11.1	153
43789	Efficient Solar Cells Employing Lightâ€Harvesting Sb_{0.67}Bi_{0.33}SI. Advanced Materials, 2019, 31, e1808344.	11.1	40
43790	Engineering Vacancies in Bi₂S₃ yielding Subâ€Bandgap Photoresponse and Highly Sensitive Shortâ€Wave Infrared Photodetectors. Advanced Optical Materials, 2019, 7, 1900258.	3.6	37
43791	The Role of Zr Doping in Stabilizing Li[Ni_{0.6}Co_{0.2}Mn_{0.2}]O₂ as a Cathode Material for Lithiumâ€Ion Batteries. ChemSusChem, 2019, 12, 2439-2446.	3.6	61
43792	Kinetic Simulations of Cu Doping in Chlorinated CdSeTe PV Absorbers. Physica Status Solidi (A) Applications and Materials Science, 2019, 216, 1800887.	0.8	17
43793	Shape-preserving machining produces gradient nanolaminate medium entropy alloys with high strain hardening capability. Acta Materialia, 2019, 170, 176-186.	3.8	41
43794	Chemical state of surrounding iron species affects the activity of Fe-Nx for electrocatalytic oxygen reduction. Applied Catalysis B: Environmental, 2019, 251, 240-246.	10.8	101
43796	On the presence of Ga2O sub-oxide in high-pressure water vapor annealed AlGaN surface by combined XPS and first-principles methods. Applied Surface Science, 2019, 481, 1120-1126.	3.1	11
43797	Fewer-layer BN nanosheets-deposited on Bi2MoO6 microspheres with enhanced visible light-driven photocatalytic activity. Applied Surface Science, 2019, 483, 572-580.	3.1	45
43798	A novel anions and cations co-doped strategy for developing high-performance cobalt-free cathode for intermediate-temperature proton-conducting solid oxide fuel cells. International Journal of Hydrogen Energy, 2019, 44, 11079-11087.	3.8	24
43799	Theoretical study on the mechanical and thermal properties of uranium dioxide doped with lanthanide fission products. Journal of Nuclear Materials, 2019, 519, 128-136.	1.3	11
43800	First-principles calculation study on phonon thermal conductivity of thorium and plutonium dioxides: Intrinsic anharmonic phonon-phonon and extrinsic grain-boundaryâ€“phonon scattering effects. Journal of Nuclear Materials, 2019, 519, 45-51.	1.3	13
43801	Discovering superior basal plane active two-dimensional catalysts for hydrogen evolution. Materials Today, 2019, 25, 28-34.	8.3	58
43802	Mechanistic understanding of enhanced photocatalytic activity of N-doped BiVO4 towards degradation of ibuprofen: An experimental and theoretical approach. Molecular Catalysis, 2019, 470, 8-18.	1.0	27
43803	The BrÃ¸nsted acidity of three- and two-dimensional zeolites. Microporous and Mesoporous Materials, 2019, 282, 121-132.	2.2	21
43804	Photothermal hydrocarbon synthesis using alumina-supported cobalt metal nanoparticle catalysts derived from layered-double-hydroxide nanosheets. Nano Energy, 2019, 60, 467-475.	8.2	67
43805	Structure-magnetic property relations in FeNbO4 polymorphs: A spin glass perspective. Progress in Solid State Chemistry, 2019, 54, 20-30.	3.9	15
43806	Surface multiferroics in silicon enabled by hole-carrier doping. Science Bulletin, 2019, 64, 331-336.	4.3	2

#	Article	IF	Citations
43807	Pb4S3I2â€“A high-pressure phase in the PbS-PbI2 system. Solid State Sciences, 2019, 91, 49-53.	1.5	5
43808	Probing Electrochemically Induced Structural Evolution and Oxygen Redox Reactions in Layered Lithium Iridate. Chemistry of Materials, 2019, 31, 4341-4352.	3.2	26
43809	Computational Investigation and Experimental Realization of Disordered High-Capacity Li-Ion Cathodes Based on Ni Redox. Chemistry of Materials, 2019, 31, 2431-2442.	3.2	50
43810	Doping Effects on the Performance of Paired Metal Catalysts for the Hydrogen Evolution Reaction. Journal of Chemical Information and Modeling, 2019, 59, 2242-2247.	2.5	15
43811	Methane Activation at the Metalâ€“Support Interface of Ni₄â€“CeO₂(111) Catalyst: A Theoretical Study. Journal of Physical Chemistry C, 2019, 123, 9788-9798.	1.5	48
43812	High-Pressure Behavior of C2I2 and Polymerization to a Conductive Polymer. Journal of Physical Chemistry C, 2019, 123, 11369-11377.	1.5	14
43813	Pervasive Cation Vacancies and Antisite Defects in Copper Indium Diselenide (CuInSe₂) Nanocrystals. Journal of Physical Chemistry C, 2019, 123, 9544-9551.	1.5	26
43814	Oligomerization of Proline Catalyzed by Nickel on a Au(111) Surface. Journal of Physical Chemistry C, 2019, 123, 9935-9943.	1.5	1
43815	Initial Decomposition of HMX Energetic Material from Quantum Molecular Dynamics and the Molecular Structure Transition of Î²-HMX to Î´-HMX. Journal of Physical Chemistry C, 2019, 123, 9231-9236.	1.5	28
43816	Carbon Monoxide Mediated Hydrogen Release from PtCu Single-Atom Alloys: The Punctured Molecular Cork Effect. Journal of Physical Chemistry C, 2019, 123, 10419-10428.	1.5	19
43817	Valence Electron and Chemical State Analysis of Be₁₂M (M = Ti, V) Beryllides by Soft X-ray Emission Spectroscopy. ACS Applied Energy Materials, 2019, 2, 2889-2895.	2.5	9
43818	Tin-Assisted Fully Exposed Platinum Clusters Stabilized on Defect-Rich Graphene for Dehydrogenation Reaction. ACS Catalysis, 2019, 9, 5998-6005.	5.5	150
43819	Photodriven Dipole Reordering: Key to Carrier Separation in Metalorganic Halide Perovskites. ACS Nano, 2019, 13, 4402-4409.	7.3	38
43820	Mechanical, Electronic, and Magnetic Properties of NiX₂ (X = Cl, Br, I) Layers. ACS Omega, 2019, 4, 5714-5721.	1.6	40
43821	Enhancement of Thermoelectric Performance for n-Type PbS through Synergy of Gap State and Fermi Level Pinning. Journal of the American Chemical Society, 2019, 141, 6403-6412.	6.6	67
43822	Firstâ€Principles Study of Thermodynamics and Spin Transition in FeSiO 3 Liquid at High Pressure. Geophysical Research Letters, 2019, 46, 3706-3716.	1.5	6
43823	Identifying Pb-free perovskites for solar cells by machine learning. Npj Computational Materials, 2019, 5, .	3.5	129
43824	Intercalation-conversion hybrid cathodes enabling Liâ€“S full-cell architectures with jointly superior gravimetric and volumetric energy densities. Nature Energy, 2019, 4, 374-382.	19.8	449

#	Article	IF	Citations
43825	Colossal barocaloric effects in plastic crystals. Nature, 2019, 567, 506-510.	13.7	253
43826	Effects of iron spin transition on the electronic structure, thermal expansivity and lattice thermal conductivity of ferropericlase: a first principles study. Scientific Reports, 2019, 9, 4172.	1.6	10
43827	Excellent catalysis of TiO₂ nanosheets with high-surface-energy {001} facets on the hydrogen storage properties of MgH₂. Nanoscale, 2019, 11, 7465-7473.	2.8	89
43828	Sodium bismuth dichalcogenides: candidates for ferroelectric high-mobility semiconductors for multifunctional applications. Physical Chemistry Chemical Physics, 2019, 21, 8553-8558.	1.3	21
43829	Electronic structures and transport properties of SnSâ€“SnSe nanoribbon lateral heterostructures. Physical Chemistry Chemical Physics, 2019, 21, 9296-9301.	1.3	8
43830	The influence of hydroxy groups on the adsorption of three-carbon alcohols on Ni(111), Pd(111) and Pt(111) surfaces: a density functional theory study within the D3 dispersion correction. Physical Chemistry Chemical Physics, 2019, 21, 8434-8444.	1.3	20
43831	Exploring the microscopic mechanism of pseudocapacitance with electronic structures in monolayer 1T-MoS₂ electrodes for supercapacitors. Materials Chemistry Frontiers, 2019, 3, 1310-1316.	3.2	4
43832	First-principles studies of a two-dimensional electron gas at the interface of polar/polar LaAlO₃/KNbO₃ superlattices. Physical Chemistry Chemical Physics, 2019, 21, 8046-8053.	1.3	9
43833	Polymorphic expressions of ultrathin oxidic layers of Mo on Au(111). Nanoscale, 2019, 11, 6023-6035.	2.8	8
43834	Direct observation of an electrically degenerate interface layer in a GaN/sapphire heterostructure. Nanoscale, 2019, 11, 8281-8292.	2.8	12
43835	Hybrid-functional calculations of electronic structure and phase stability of MO (M = Zn, Cd, Be, Mg,) Tj ETQq0 0 0 rgBT /Overlock 10 Tf 8507-8514.	1.7	9
43836	First-principles study of the effect of dopants (Pd, Ni) on the formation and desorption of T₂O from a Li₂TiO₃ (001) surface. RSC Advances, 2019, 9, 8490-8497.	1.7	5
43837	First-principles assessment of thermoelectric properties of CuFeS2. Journal of Applied Physics, 2019, 125, .	1.1	22
43838	Vacancies and interstitials in yttrium. Journal of Physics Condensed Matter, 2019, 31, 185401.	0.7	3
43839	Singling out the effect of quenched disorder in the phase diagram of cuprates. Journal of Physics Condensed Matter, 2019, 31, 184002.	0.7	1
43840	Quantum anomalous Hall effects and various topological mechanisms in functionalized Sn monolayers. New Journal of Physics, 2019, 21, 023010.	1.2	2
43841	Transition metal doping engineered octagonal ZnO monolayer magnetic properties. Materials Research Express, 2019, 6, 056106.	0.8	1
43842	Potential high- <mml:math xmlns:mml="http://www.w3.org/1998/Math/MathML"><mml:msub><mml:mi>T</mml:mi><mml:mi>c</mml:mi></mml:msub></mml:ma superconductivity in <mml:math xmlns:mml="http://www.w3.org/1998/Math/MathML"><mml:msub><mml:mi>CaYH</mml:mi><mml:mn>12</mml:mn></mml:msub> under pressure. Physical Review B, 2019, 99, .	1.1	109

#	Article	IF	Citations
43843	Spin-gapless semiconducting nature of Co-rich <mml:math xmlns:mml="http://www.w3.org/1998/Math/MathML"><mml:mrow><mml:msub><mml:mi>Co</mml:mi><mml:mrow><mml:mn>1</mml:mn> mathvariant="italic">x</mml:mi></mml:mrow></mml:msub><mml:msub><mml:mi>Fe</mml:mi><mml:mrow><mml:mn>1</mml:mn> mathvariant="italic">x</mml:mi></mml:mrow></mml:msub><mml:mi>CrGa</mml:mi></mml:mrow></mml:math>. Physical Review B, 2019, 99, .	1.1	32
43844	Thermally driven topology in frustrated systems. Physical Review B, 2019, 99, .	1.1	2
43845	Robust type-II band alignment in Janus-MoSSe bilayer with extremely long carrier lifetime induced by the intrinsic electric field. Physical Review B, 2019, 99, .	1.1	63
43846	Anharmonic and Anomalous Trends in the High-Pressure Phase Diagram of Silicon. Physical Review Letters, 2019, 122, 125701.	2.9	15
43847	Synthesis and Photocatalytic Activity of Fluorine DOPED-g-C₃N₄. Applied Mechanics and Materials, 0, 889, 24-32.	0.2	15
43848	Direct Oneâ€pot Synthesis of Carbon Supported Agâ€Pt Alloy Nanoparticles as High Performance Electrocatalyst for Fuel Cell Application. Fuel Cells, 2019, 19, 169-176.	1.5	7
43849	C H versus O H bond scission in methanol decomposition on Pt(111): Role of the dispersion interaction. Applied Surface Science, 2019, 481, 1327-1334.	3.1	17
43850	Corrosion inhibition of magnesium alloy in NaCl solution by ionic liquid: Synthesis, electrochemical and theoretical studies. Journal of Alloys and Compounds, 2019, 791, 681-689.	2.8	49
43851	Edge-doping modulation of N, P-codoped porous carbon spheres for high-performance rechargeable Zn-air batteries. Nano Energy, 2019, 60, 536-544.	8.2	247
43853	Controlling the surface chemistry towards unsaturated carbon-carbon bonds over non-oxide transition metal ceramics: Trends in adsorption and distortion energies and adsorbate â€œactivationâ€. Surface Science, 2019, 686, 1-9.	0.8	8
43854	Innovating e-waste recycling: From waste multi-layer ceramic capacitors to Nb Pb codoped and ag-Pd-Sn-Ni loaded BaTiO3 nano-photocatalyst through one-step ball milling process. Sustainable Materials and Technologies, 2019, 21, e00101.	1.7	14
43855	Thermochemical analysis of Mo-C-H system for synthesis of molybdenum carbides. Thermochimica Acta, 2019, 676, 27-32.	1.2	4
43856	Assessment of Two Problems of Specific Reaction Parameter Density Functional Theory: Sticking and Diffraction of H₂ on Pt(111). Journal of Physical Chemistry C, 2019, 123, 10406-10418.	1.5	10
43857	Cu/Sb Codoping for Tuning Carrier Concentration and Thermoelectric Performance of GeTe-Based Alloys with Ultralow Lattice Thermal Conductivity. ACS Applied Energy Materials, 2019, 2, 2596-2603.	2.5	45
43858	Thickness-Dependent Ultrafast Photonics of SnS₂ Nanolayers for Optimizing Fiber Lasers. ACS Applied Nano Materials, 2019, 2, 2697-2705.	2.4	48
43859	Nanolayered Ti₃C₂ and SrTiO₃ Composites for Photocatalytic Reduction and Removal of Uranium(VI). ACS Applied Nano Materials, 2019, 2, 2283-2294.	2.4	119
43860	Mesoporous Hollow Cuâ€“Ni Alloy Nanocage from Coreâ€“Shell Cu@Ni Nanocube for Efficient Hydrogen Evolution Reaction. ACS Catalysis, 2019, 9, 5084-5095.	5.5	116
43861	Electronic Band Structure of Ultimately Thin Silicon Oxide on Ru(0001). ACS Nano, 2019, 13, 4720-4730.	7.3	14

#	Article	IF	Citations
43862	Identification of the Reaction Sequence of the MTO Initiation Mechanism Using Ab Initio-Based Kinetics. Journal of the American Chemical Society, 2019, 141, 5908-5915.	6.6	64
43863	Low Lattice Thermal Conductivity of a Two-Dimensional Phosphorene Oxide. Scientific Reports, 2019, 9, 5149.	1.6	16
43864	Theoretical assessment of wettability on silane coatings: from hydrophilic to hydrophobic. Physical Chemistry Chemical Physics, 2019, 21, 8257-8263.	1.3	4
43865	Coreâ€“shell MOF-derived N-doped yolkâ€“shell carbon nanocages homogenously filled with ZnSe and CoSe₂ nanodots as excellent anode materials for lithium- and sodium-ion batteries. Journal of Materials Chemistry A, 2019, 7, 11016-11037.	5.2	173
43866	Effects of alloying on mode-selectivity in H2O dissociation on Cu/Ni bimetallic surfaces. Journal of Chemical Physics, 2019, 150, 114702.	1.2	19
43867	First principles research on the dynamic conductance and transient current of black phosphorus transistor. Journal Physics D: Applied Physics, 2019, 52, 165303.	1.3	5
43868	Grain-boundary segregation of 3d-transition metal solutes in bcc Fe: ab initio local-energy and d-electron behavior analysis. Journal of Physics Condensed Matter, 2019, 31, 115001.	0.7	23
43869	Shubnikovâ€“de Haas and de Haasâ€“van Alphen oscillations in the topological semimetal CaAl4. Physical Review B, 2019, 99, .	1.1	5
43870	Electronic structure of gadolinium-doped ceria system: A DFT study. Modern Physics Letters B, 2019, 33, 1950095.	1.0	2
43871	Adsorption and desorption of hydrogen on/from single-vacancy and double-vacancy graphenes. Nuclear Science and Techniques/Hewuli, 2019, 30, 1.	1.3	14
43872	Atomistic insights into the growth of Bi (110) thin films on Cu (111) substrate. Applied Surface Science, 2019, 481, 1449-1458.	3.1	5
43873	Two-dimensional haeckelite h567: A promising high capacity and fast Li diffusion anode material for lithium-ion batteries. Carbon, 2019, 148, 344-353.	5.4	59
43874	A sodium perchlorate-based hybrid electrolyte with high salt-to-water molar ratio for safe 2.5â€¯V carbon-based supercapacitor. Energy Storage Materials, 2019, 23, 603-609.	9.5	102
43875	First-principles study on the structure and electronic properties of Ge2H2 and Ge2Li2 nanosheets under electric fields. Physica B: Condensed Matter, 2019, 567, 95-99.	1.3	4
43876	Modulating the electronic structures and sensing properties of metal and non-metal atoms modified graphene sheets. Physica E: Low-Dimensional Systems and Nanostructures, 2019, 111, 206-217.	1.3	8
43877	Theoretical Investigation on the Microscopic Mechanism of Lattice Thermal Conductivity of ZnXP₂ (X = Si, Ge, and Sn). Inorganic Chemistry, 2019, 58, 4320-4327.	1.9	12
43878	Incommensurate Quantum Size Oscillations of Oligoacene Wires Adsorbed on Au(111). Journal of Physical Chemistry C, 2019, 123, 8902-8907.	1.5	8
43879	The effect of protons on the Mg²⁺ migration in an Î±-V₂O₅ cathode for magnesium batteries: a first-principles investigation. Physical Chemistry Chemical Physics, 2019, 21, 7406-7411.	1.3	18

#	Article	IF	Citations
43880	MoSSe nanotube: a promising photocatalyst with an extremely long carrier lifetime. Journal of Materials Chemistry A, 2019, 7, 7885-7890.	5.2	52
43881	Prevention of Hydrogen Damage Using MoS2 Coating on Iron Surface. Nanomaterials, 2019, 9, 382.	1.9	4
43882	Hydrogen Isotope Absorption in Unary Oxides and Nitrides with Anion Vacancies and Substitution. ChemPhysChem, 2019, 20, 1369-1375.	1.0	2
43883	Electronic, magnetic properties of 4d series transition metal substituted black phosphorene: A first-principles study. Applied Surface Science, 2019, 480, 802-809.	3.1	29
43884	MoO2 and graphene heterostructure as promising flexible anodes for lithium-ion batteries. Carbon, 2019, 147, 357-363.	5.4	46
43885	Tuning the photoluminescence of large Ti3C2Tx MXene flakes. Ceramics International, 2019, 45, 11468-11474.	2.3	22
43886	Structural, magnetic and electronic properties of CunNi55â^'n (nâ€¯=â€¯0â€“55) nanoparticles: Combination artificial bee colony algorithm with DFT. Computational and Theoretical Chemistry, 2019, 1154, 11-16.	1.1	10
43887	Flexible and Transferable ab Initio Force Field for Zeolitic Imidazolate Frameworks: ZIF-FF. Journal of Physical Chemistry A, 2019, 123, 3000-3012.	1.1	34
43888	Atomic electrostatic maps of 1D channels in 2D semiconductors using 4D scanning transmission electron microscopy. Nature Communications, 2019, 10, 1127.	5.8	62
43889	Unusual properties and potential applications of strain BN-MS2 (Mâ€‰=â€‰Mo, W) heterostructures. Scientific Reports, 2019, 9, 3518.	1.6	14
43890	Ab initio investigations of orthogonal ScC₂ and ScN₂ monolayers as promising anode materials for sodium-ion batteries. Journal of Materials Chemistry A, 2019, 7, 8897-8904.	5.2	49
43891	Ab-initio study of the optical properties of beryllium-sulphur co-doped graphene. AIP Advances, 2019, 9, 025221.	0.6	5
43892	Defect engineering of black phosphorene towards an enhanced polysulfide host and catalyst for lithium-sulfur batteries: A first principles study. Journal of Applied Physics, 2019, 125, .	1.1	39
43893	Benchmarking the performance of approximate van der Waals methods for the structural and energetic properties of SiO2 and AlPO4 frameworks. Journal of Chemical Physics, 2019, 150, 094102.	1.2	24
43894	First-principles calculations of photoluminescence and defect states of <mml:math xmlns:mml="http://www.w3.org/1998/Math/MathML"><mml:mrow><mml:mi mathvariant="normal">C</mml:mi><mml:msup><mml:mrow><mml:mi mathvariant="normal">e</mml:mi></mml:mrow><mml:mrow><mml:mn>3</mml:mn><mml:mo>+</mml:mo></mml:mrow></mml:msup> -doped <mml:math		

#	Article	IF	Citations
43898	Effects of transmutation elements in tungsten. Computational Materials Science, 2019, 162, 133-139.	1.4	11
43899	Ab initio study of the structures and transport properties of warm dense nitrogen. High Energy Density Physics, 2019, 31, 52-58.	0.4	5
43900	Hydrogen activation enabled by the interfacial frustrated Lewis pairs on cobalt borate nanosheets. Journal of Catalysis, 2019, 372, 142-150.	3.1	27
43901	Strain study of epitaxial Al1â^'xGaxN based on first-principles theory. Journal of Crystal Growth, 2019, 514, 60-64.	0.7	1
43902	Vacancy-interface-helium interaction in Zr-Nb multi-layer system: A first-principles study. Journal of Nuclear Materials, 2019, 518, 11-20.	1.3	21
43903	Superstructures of Se adsorbates on Au(111): Scanning tunneling microscopy and spectroscopy study. Surface Science, 2019, 685, 19-23.	0.8	4
43904	From 0D Cs₃Bi₂I₉ to 2D Cs₃Bi₂I₆Cl₃: Dimensional Expansion Induces a Direct Band Gap but Enhances Electronâ€“Phonon Coupling. Chemistry of Materials, 2019, 31, 2644-2650.	3.2	111
43905	Accelerated Discovery of New 8-Electron Half-Heusler Compounds as Promising Energy and Topological Quantum Materials. Journal of Physical Chemistry C, 2019, 123, 7074-7080.	1.5	38
43906	First-Principles Study of Ferroelastic Twins in Halide Perovskites. Journal of Physical Chemistry Letters, 2019, 10, 1416-1421.	2.1	21
43907	Potassium Ordering and Structural Phase Stability in Layered K_xCoO₂. ACS Applied Energy Materials, 2019, 2, 2629-2636.	2.5	29
43908	Low Contact Barrier in 2H/1Tâ€² MoTe₂ In-Plane Heterostructure Synthesized by Chemical Vapor Deposition. ACS Applied Materials & Interfaces, 2019, 11, 12777-12785.	4.0	70
43909	Ferromagnetic van der Waals Crystal VI₃. Journal of the American Chemical Society, 2019, 141, 5326-5333.	6.6	153
43910	Exploring the ternary interactions in Cuâ€“ZnOâ€“ZrO2 catalysts for efficient CO2 hydrogenation to methanol. Nature Communications, 2019, 10, 1166.	5.8	258
43911	Growth and Thermo-driven Crystalline Phase Transition of Metastable Monolayer 1Tâ€²-WSe2 Thin Film. Scientific Reports, 2019, 9, 2685.	1.6	19
43912	Origin of ferromagnetism in Cu-doped ZnO. Scientific Reports, 2019, 9, 2461.	1.6	63
43913	Engineering the electronic structure of single atom Ru sites via compressive strain boosts acidic water oxidation electrocatalysis. Nature Catalysis, 2019, 2, 304-313.	16.1	757
43914	Superconductivity of boron-doped graphane under high pressure. RSC Advances, 2019, 9, 7680-7686.	1.7	4
43915	Structure and binding in halide perovskites: Analysis of static and dynamic effects from dispersion-corrected density functional theory. APL Materials, 2019, 7, .	2.2	31

#	Article	IF	Citations
43916	Energetics of Cu adsorption and intercalation at graphite step edges. Physical Review B, 2019, 99, .	1.1	15
43917	Direct Cation Exchange in Monolayer <mml:math xmlns:mml="http://www.w3.org/1998/Math/MathML" display="inline"><mml:mrow><mml:msub><mml:mrow><mml:mi>MoS</mml:mi></mml:mrow><mml:mn>2</mml:mn></mml:msub></ via Recombination-Enhanced Migration. Physical Review Letters, 2019, 122, 106101.	2.9	21
43918	Direct Detection of Dimer Orbitals in<mml:math xmlns:mml="http://www.w3.org/1998/Math/MathML" display="inline"><mml:mrow><mml:mrow><mml:msub><mml:mrow><mml:mi>Ba</mml:mi></mml:mrow><mml:mrow><mml:mn>5</m mathvariant="normal">O</mml:mi></mml:mrow><mml:mrow><mml:mn>11</mml:mn></mml:mrow></mml:msub></mml:mrow></mm Physical Review Letters, 2019, 122, 106401.	2.9	15
43919	Band Structure Engineering of Interfacial Semiconductors Based on Atomically Thin Lead Iodide Crystals. Advanced Materials, 2019, 31, e1806562.	11.1	79
43920	Edgeâ€Exposed Molybdenum Disulfide with Nâ€Doped Carbon Hybridization: A Hierarchical Hollow Electrocatalyst for Carbon Dioxide Reduction. Advanced Energy Materials, 2019, 9, 1900072.	10.2	62
43921	Doubleâ€holeâ€mediated coupling of anionic dopants in perovskite NaNbO₃ for efficient solar water splitting. International Journal of Quantum Chemistry, 2019, 119, e25930.	1.0	11
43922	Tuning the electronic structures of all-inorganic lead halide perovskite CsPbI3 via heterovalent doping: A first-principles investigation. Chemical Physics Letters, 2019, 722, 90-95.	1.2	22
43923	Defect-assisted surface modification enhances the visible light photocatalytic performance of g-C3N4@C-TiO2 direct Z-scheme heterojunctions. Chinese Journal of Catalysis, 2019, 40, 424-433.	6.9	228
43924	Atomistic Insight into Glide-Driven Phase Transformations in Layered Oxides for Sodium-Ion Batteries: A Case Study on Na_xVO₂. ACS Applied Materials & Interfaces, 2019, 11, 12562-12569.	4.0	13
43925	Materials design of perovskite solid solutions for thermochemical applications. Energy and Environmental Science, 2019, 12, 1369-1384.	15.6	122
43926	Medium-temperature thermoelectric GeTe: vacancy suppression and band structure engineering leading to high performance. Energy and Environmental Science, 2019, 12, 1396-1403.	15.6	233
43927	Intrinsic ferromagnetism and topological properties in two-dimensional rhenium halides. Nanoscale, 2019, 11, 6101-6107.	2.8	31
43928	A low-cost â€œwater-in-saltâ€•electrolyte for a 2.3 V high-rate carbon-based supercapacitor. Journal of Materials Chemistry A, 2019, 7, 7541-7547.	5.2	260
43929	Intricate modulation of interlayer coupling at the graphene oxide/ <mml:math xmlns:mml="http://www.w3.org/1998/Math/MathML"><mml:mrow><mml:mi>MoS</mml:mi><mml:msub><mml:mi mathvariant="normal">e</mml:mi><mml:mn>2</mml:mn></mml:msub></mml:mrow></mml:math> interface: Application in time-dependent optics and device transport. Physical Review B, 2019, 99, .	1.1	15
43930	Origin of <mml:math xmlns:mml="http://www.w3.org/1998/Math/MathML"><mml:mi>n</mml:mi></mml:math> -type conductivity of monolayer <mml:math xmlns:mml="http://www.w3.org/1998/Math/MathML"><mml:msub><mml:mi>MoS</mml:mi><mml:mn>2</mml:mn></mml:msub></mm Physical Review B, 2019, 99, .	1.1	72
43931	Mn3O4 nanoparticles@reduced graphene oxide composite: An efficient electrocatalyst for artificial N2 fixation to NH3 at ambient conditions. Nano Research, 2019, 12, 1093-1098.	5.8	93
43932	Reactivity of Atomic Layer Deposition Precursors with OH/H2O-Containing Metal Organic Framework Materials. Chemistry of Materials, 2019, 31, 2286-2295.	3.2	16
43933	Boosting Rechargeable Batteries R&D by Multiscale Modeling: Myth or Reality?. Chemical Reviews, 2019, 119, 4569-4627.	23.0	204

#	Article	IF	Citations
43934	Nitrogen-Doped Graphene on Copper: Edge-Guided Doping Process and Doping-Induced Variation of Local Work Function. Journal of Physical Chemistry C, 2019, 123, 8802-8812.	1.5	7
43935	Unraveling the Mechanism of Photocatalytic Water Splitting in Î±-Ga₂O₃ Loaded with a Nickel Oxide Cocatalyst: A First-Principles Investigation. Journal of Physical Chemistry C, 2019, 123, 8990-9000.	1.5	10
43936	Screening Diffusion of Small Molecules in Flexible Zeolitic Imidazolate Frameworks Using a DFT-Parameterized Force Field. Journal of Physical Chemistry C, 2019, 123, 9153-9167.	1.5	30
43937	Unlocking the potential of weberite-type metal fluorides in electrochemical energy storage. Npj Computational Materials, 2019, 5, .	3.5	13
43938	Effects of intercalated atoms on electronic structure of graphene nanoribbon/hexagonal boron nitride stacked layer. Scientific Reports, 2019, 9, 3623.	1.6	2
43939	Formation of DY center as n-type limiting defects in octahedral semiconductors: the case of Bi-doped hybrid halide perovskites. Journal of Materials Chemistry C, 2019, 7, 4230-4234.	2.7	41
43940	Enhanced photocatalysis for water splitting in layered tin chalcogenides with high carrier mobility. Physical Chemistry Chemical Physics, 2019, 21, 7559-7566.	1.3	36
43941	A theoretical study of several fully hydrogenated borophenes. Physical Chemistry Chemical Physics, 2019, 21, 7630-7634.	1.3	16
43942	Band engineering and crystal field screening in thermoelectric Mg₃Sb₂. Journal of Materials Chemistry A, 2019, 7, 8922-8928.	5.2	36
43943	Two-dimensional honeycomb-kagome Ta₂S₃: a promising single-spin Dirac fermion and quantum anomalous hall insulator with half-metallic edge states. Nanoscale, 2019, 11, 5666-5673.	2.8	26
43944	Antidoping in Insulators and Semiconductors Having Intermediate Bands with Trapped Carriers. Physical Review Letters, 2019, 122, 106403.	2.9	28
43945	Planar Hall Effect in Antiferromagnetic MnTe Thin Films. Physical Review Letters, 2019, 122, 106602.	2.9	29
43946	Unique Thickness-Dependent Properties of the van der Waals Interlayer Antiferromagnet <mml:math xmlns:mml="http://www.w3.org/1998/Math/MathML" display="inline"><mml:mrow><mml:msub><mml:mrow><mml:mi>MnBi</mml:mi></mml:mrow><mml:mrow><mml:mn>2</mml:mn></mml:mrow></mml:msub></mml:mrow></mml:math> Films. Physical Review Letters, 2019, 122, 107202.	2.9	415
43947	Atomistic modeling of nanoscale plasticity in high-entropy alloys. Journal of Materials Research, 2019, 34, 1509-1532.	1.2	36
43948	Initial Mechanisms for the Unimolecular Thermal Decomposition of 2,6-Diamino-3,5-dinitropyrazine-1-oxide. Molecules, 2019, 24, 125.	1.7	18
43949	Unraveling the Factors Behind the Efficiency of Hydrogen Evolution in Endohedrally Doped C₆₀ Structures via Ab Initio Calculations and Insights from Machine Learning Models. Advanced Theory and Simulations, 2019, 2, 1800202.	1.3	6
43950	Switchable Outâ€ofâ€Plane Polarization in 2D LiAlTe₂. Advanced Electronic Materials, 2019, 5, 1900089.	2.6	20
43951	Synergistic Engineering of Defects and Architecture in Binary Metal Chalcogenide toward Fast and Reliable Lithiumâ€“Sulfur Batteries. Advanced Energy Materials, 2019, 9, 1900228.	10.2	177

#	Article	IF	Citations
43952	Compositionâ€€Controlled Synthesis of Hybrid Perovskite Nanoparticles by Ionic Metathesis: Bandgap Engineering Studies from Experiments and Theoretical Calculations. Chemistry - A European Journal, 2019, 25, 9892-9901.	1.7	18
43953	Phase transitions and magnetic properties of Fe30Co29Ni29Zr7B4Cu1 high-entropy alloys. Journal of Alloys and Compounds, 2019, 789, 762-767.	2.8	12
43954	Control of surface reactivity towards unsaturated C C bonds and H over Ni-based intermetallic compounds in semi-hydrogenation of acetylene. Journal of Catalysis, 2019, 372, 151-162.	3.1	23
43955	Adsorption state of NO on Ir(111) surfaces under excess O2 coexisting condition. Surface Science, 2019, 685, 1-6.	0.8	7
43956	First-Principles Study on Structural, Electronic, and Optical Properties of Inorganic Ge-Based Halide Perovskites. Inorganic Chemistry, 2019, 58, 4134-4140.	1.9	68
43957	Phase Segregation, Transition, or New Phase Formation of Plutonium Dioxide: The Roles of Transition Metals. Inorganic Chemistry, 2019, 58, 4350-4364.	1.9	21
43958	Breaking Ï€â€“Ï€ Interactions in Carboxylic Acid Monolayers on Rutile TiO₂(110) Leads to Unexpected Long-Range Ordering. Journal of Physical Chemistry C, 2019, 123, 8836-8842.	1.5	5
43959	Dimensionality Control of Self-Assembled Azobenzene Derivatives on a Gold Surface. Journal of Physical Chemistry C, 2019, 123, 8859-8864.	1.5	2
43960	Decreasing Nanocrystal Structural Disorder by Ligand Exchange: An Experimental and Theoretical Analysis. Journal of Physical Chemistry Letters, 2019, 10, 1471-1476.	2.1	19
43961	Distinctive Signatures of the Spin- and Momentum-Forbidden Dark Exciton States in the Photoluminescence of Strained WSe₂ Monolayers under Thermalization. Nano Letters, 2019, 19, 2299-2312.	4.5	34
43962	Axion Insulator State in a Ferromagnet/Topological Insulator/Antiferromagnet Heterostructure. Nano Letters, 2019, 19, 2472-2477.	4.5	24
43963	Horizontal-to-Vertical Transition of 2D Layer Orientation in Low-Temperature Chemical Vapor Deposition-Grown PtSe₂ and Its Influences on Electrical Properties and Device Applications. ACS Applied Materials & Interfaces, 2019, 11, 13598-13607.	4.0	77
43964	Two-Dimensional Anisotropic C₁₀ Carbon Allotrope with Mechanically Tunable Band Gap. ACS Omega, 2019, 4, 5002-5011.	1.6	6
43965	IrF₈ Molecular Crystal under High Pressure. Journal of the American Chemical Society, 2019, 141, 5409-5414.	6.6	40
43966	Radiation tolerance of two-dimensional material-based devices for space applications. Nature Communications, 2019, 10, 1202.	5.8	91
43967	Structural and electronic properties of Mo6S3I6 nanowires by newly proposed theoretical compositional ordering. Scientific Reports, 2019, 9, 1222.	1.6	7
43968	Double-well potential energy surface in the interaction between h-BN and Ni(111). Physical Chemistry Chemical Physics, 2019, 21, 10888-10894.	1.3	7
43969	Impacts of 5d electron binding energy and electronâ€“phonon coupling on luminescence of Ce³⁺ in Li₆Y(BO₃)₃. RSC Advances, 2019, 9, 7908-7915.	1.7	17

#	Article	IF	Citations
43970	Electronic properties of heterogenized Ru(<scp>ii</scp>) polypyridyl photoredox complexes on covalent triazine frameworks. Journal of Materials Chemistry A, 2019, 7, 8433-8442.	5.2	6
43971	Thermodynamic evidence of fractionalized excitations in <mml:math xmlns:mml="http://www.w3.org/1998/Math/MathML"><mml:mrow><mml:mi>Î±</mml:mi><mml:mo>â^'</mml:mo><mml:mi>RuC</mml:mi> mathvariant="normal">I</mml:mi><mml:mn>3</mml:mn></mml:msub></mml:mrow></mml:math>. Physical Review B, 2019, 99, .	1.1	52
43972	Quadratic and cubic nodal lines stabilized by crystalline symmetry. Physical Review B, 2019, 99, .	1.1	89
43973	Origin of the Insulating Phase and First-Order Metal-Insulator Transition in <mml:math xmlns:mml="http://www.w3.org/1998/Math/MathML" display="inline"><mml:mrow><mml:mn>1</mml:mn><mml:mi>T</mml:mi><mml:mtext>â^'</mml:mtext><mml:msub><mml:mrow> Physical Review Letters, 2019, 122, 106404.	2.9	126
43974	Dependence of Carbon Concentration and Alloying Elements on the Stability of Iron Carbides. ISIJ International, 2019, 59, 1128-1135.	0.6	16
43975	Enhanced Supercapacitor Performance Based on CoAl Layered Double Hydroxide-Polyaniline Hybrid Electrodes Manufactured Using Hydrothermal-Electrodeposition Technology. Molecules, 2019, 24, 976.	1.7	19
43976	The Modulation Effect of MoS2 Monolayers on the Nucleation and Growth of Pd Clusters: First-Principles Study. Nanomaterials, 2019, 9, 395.	1.9	13
43977	Rational design of multi-functional CoS@rGO composite for performance enhanced Li-S cathode. Journal of Power Sources, 2019, 421, 132-138.	4.0	54
43978	Transport properties of 2D As1-xPx binary compounds as a potential thermoelectric materials. Physica E: Low-Dimensional Systems and Nanostructures, 2019, 111, 79-83.	1.3	10
43979	Tunable Single-Photon Emission by Defective Boron-Nitride Nanotubes for High-Precision Force Detection. Journal of Physical Chemistry C, 2019, 123, 9624-9628.	1.5	5
43980	Spin-charge-lattice coupling in YBaCuFeO5: Optical properties and first-principles calculations. Scientific Reports, 2019, 9, 3223.	1.6	7
43981	Band alignment of Pbâ€“Sn mixed triple cation perovskites for inverted solar cells with negligible hysteresis. Journal of Materials Chemistry A, 2019, 7, 9154-9162.	5.2	54
43982	Extent of Spin Contamination Errors in DFT/Plane-wave Calculation of Surfaces: A Case of Au Atom Aggregation on a MgO Surface. Molecules, 2019, 24, 505.	1.7	26
43983	Solid-State Divalent Ion Conduction in ZnPS₃. Chemistry of Materials, 2019, 31, 3652-3661.	3.2	37
43984	Free Energies of Catalytic Species Adsorbed to Pt(111) Surfaces under Liquid Solvent Calculated Using Classical and Quantum Approaches. Journal of Chemical Information and Modeling, 2019, 59, 2190-2198.	2.5	37
43985	One-Dimensional-Sn₂X₃ (X = S, Se) as Promising Optoelectronic and Thermoelectronic Materials: A Comparison with Three-Dimensional-Sn₂X₃. ACS Applied Materials & Interfaces, 2019, 11, 12733-12744.	4.0	22
43986	Upshift of the d Band Center toward the Fermi Level for Promoting Silver Ion Release, Bacteria Inactivation, and Wound Healing of Alloy Silver Nanoparticles. ACS Applied Materials & Interfaces, 2019, 11, 12224-12231.	4.0	53
43987	Strategy to Induce Multiferroic Property in (RTiO 3) n /(RVO 3) n Superlattices: A Firstâ€Principles Study. ChemPhysChem, 2019, 20, 1145-1152.	1.0	0

#	Article	IF	Citations
43988	Theoretical realization of two-dimensional M3(C6X6)2 (M = Co, Cr, Cu, Fe, Mn, Ni, Pd, Rh and X = O, S,) Tj ETQq0 0 0 rgBT /Overlock 10	2.3	37
43989	Effect of the intra- and inter-triazine N-vacancies on the photocatalytic hydrogen evolution of graphitic carbon nitride. Chemical Engineering Journal, 2019, 369, 263-271.	6.6	55
43990	Lattice Strain Advances Thermoelectrics. Joule, 2019, 3, 1276-1288.	11.7	333
43991	First-principles prediction of three new graphitic C3N4 allotropes with potentials for application in sun-light-driven water splitting. Physica B: Condensed Matter, 2019, 562, 131-134.	1.3	12
43992	Optimizing Proton Conductivity in Zirconates through Defect Engineering. ACS Applied Energy Materials, 2019, 2, 2611-2619.	2.5	25
43993	Liquid Iron Equation of State to the Terapascal Regime From Ab Initio Simulations. Journal of Geophysical Research: Solid Earth, 2019, 124, 3350-3364.	1.4	23
43994	The effect of Fe vacancies and Cu adhesion on the magnetic properties of Fe₃GeTe₂. Physical Chemistry Chemical Physics, 2019, 21, 7588-7593.	1.3	11
43995	Bilayer phosphorene under high pressure: in situ Raman spectroscopy. Physical Chemistry Chemical Physics, 2019, 21, 7298-7304.	1.3	19
43996	Neutral oxygen-vacancy defect in cubic boron nitride: A plausible qubit candidate. Applied Physics Letters, 2019, 114, .	1.5	12
43997	Use of Cernox thermometers in AC specific heat measurements under pressure. Review of Scientific Instruments, 2019, 90, 023911.	0.6	17
43998	Microscopic investigation of low dimensional magnet Sc₂Cu₂O₅: combined experimental and ab initio approach. Journal of Physics Condensed Matter, 2019, 31, 245802.	0.7	9
43999	Surface energies and electronic properties of intermetallic compound B2-AgMg. Modern Physics Letters B, 2019, 33, 1950097.	1.0	1
44000	Covalency a Pathway for Achieving High Magnetisation in TMFe₂O₄Compounds. Journal of the Physical Society of Japan, 2019, 88, 044706.	0.7	15
44001	Materials Design of Solar Cell Absorbers Beyond Perovskites and Conventional Semiconductors via Combining Tetrahedral and Octahedral Coordination. Advanced Materials, 2019, 31, e1806593.	11.1	48
44002	Amino Acid Immobilization of Copper Surface Diffusion on Cu(111). Advanced Materials Interfaces, 2019, 6, 1900021.	1.9	7
44003	Unusual Fermiâ€Level Pinning and Ohmic Contact at Monolayer Bi 2 O 2 Seâ€“Metal Interface. Advanced Theory and Simulations, 2019, 2, 1800178.	1.3	20
44004	Identification of Phase Control of Carbonâ€Confined Nb₂O₅ Nanoparticles toward Highâ€Performance Lithium Storage. Advanced Energy Materials, 2019, 9, 1802695.	10.2	161
44005	The Solâ€“gel method synthesis of Bi4NbO8Cl with (001) facets exposed for high visible-light activity. Journal of Materials Science: Materials in Electronics, 2019, 30, 7907-7915.	1.1	4

#	Article	IF	Citations
44006	Materials Discovery of Stable and Nontoxic Halide Perovskite Materials for Highâ€Efficiency Solar Cells. Advanced Functional Materials, 2019, 29, 1804354.	7.8	61
44007	Giant Enhancements of Perpendicular Magnetic Anisotropy and Spinâ€Orbit Torque by a MoS₂ Layer. Advanced Materials, 2019, 31, e1900776.	11.1	65
44008	2D Diluted Multiferroic Semiconductors upon Intercalation. Advanced Electronic Materials, 2019, 5, 1800960.	2.6	21
44009	Unveiling the Interfacial Effects for Enhanced Hydrogen Evolution Reaction on MoS₂/WTe₂ Hybrid Structures. Small, 2019, 15, e1900078.	5.2	58
44010	Transitory phase transformations during <mml:math xmlns:mml="http://www.w3.org/1998/Math/MathML" altimg="si1.gif" overflow="scroll"><mml:mrow><mml:mo stretchy="true">{</mml:mo><mml:mn>10</mml:mn><mml:mrow><mml:mover accent="true"><mml:mn>1</mml:mn><mml:mo>Â¯</mml:mo></mml:mover></mml:mrow><mml:mn>2</mml:mn><mml:mo stretchy="true">}</mml:mo></mml:mrow></mml:math> twinning in titanium. Acta Materialia, 2019, 171,	3.8	43
44011	Adsorption of Nin (nâ€‰=â€‰1â€’4) clusters on perfect and O-defective CuAl2O4 surfaces: A DFT study. Chinese Chemical Letters, 2019, 30, 1147-1152.	4.8	19
44012	Single-layer Ag6S2: First principles investigation of a new two-dimensional direct bandgap semiconductor. Computational Materials Science, 2019, 163, 278-281.	1.4	13
44013	Improving hydrogen evolution activity of perovskite BaTiO3 with Mo doping: Experiments and first-principles analysis. International Journal of Hydrogen Energy, 2019, 44, 11695-11704.	3.8	34
44014	Two-dimensional copper nanosheets for electrochemical reduction of carbon monoxide to acetate. Nature Catalysis, 2019, 2, 423-430.	16.1	368
44015	Bi vacancy formation in BiFeO₃ epitaxial thin films under compressive (001)-strain from first principles. Journal of Materials Chemistry C, 2019, 7, 4870-4878.	2.7	8
44016	Vacancy diffusion barriers in TaON and Ta₃N₅ water-splitting photocatalysts. Journal of Materials Chemistry A, 2019, 7, 13029-13035.	5.2	25
44017	Pt-embedded in monolayer g-C₃N₄ as a promising single-atom electrocatalyst for ammonia synthesis. Journal of Materials Chemistry A, 2019, 7, 11908-11914.	5.2	78
44018	Spectrally Stable Defect Qubits with no Inversion Symmetry for Robust Spin-To-Photon Interface. Physical Review Applied, 2019, 11, .	1.5	43
44019	Converting a two-dimensional ferromagnetic insulator into a high-temperature quantum anomalous Hall system by means of an appropriate surface modification. Physical Review B, 2019, 99, .	1.1	23
44020	Methanol Câ€“O Bond Activation by Free Gold Clusters Probed via Infrared Photodissociation Spectroscopy. Zeitschrift Fur Physikalische Chemie, 2019, 233, 865-880.	1.4	3
44021	First-principles Calculations of the Effects of Mn, Cr, and Ni on Hydrogen Diffusion in BCC, FCC, and HCP Fe. Tetsu-To-Hagane/Journal of the Iron and Steel Institute of Japan, 2019, 105, 231-239.	0.1	3
44022	A DFT Study of Hydrogen Storage in High-Entropy Alloy TiZrHfScMo. Nanomaterials, 2019, 9, 461.	1.9	60
44023	Molecular dynamics study of a new metastable allotropic crystalline form of galliumâ€”supertetrahedral gallium. Journal of Computational Chemistry, 2019, 40, 1861-1865.	1.5	4

#	Article	IF	Citations
44024	The Effect of Pressure on Elastic Anisotropy, Vibration and Optical Properties of a AgScSi Compound. Journal of Electronic Materials, 2019, 48, 4050-4056.	1.0	9
44025	Insight into the effect of morphology on catalytic performance of porous CeO2 nanocrystals for H2S selective oxidation. Applied Catalysis B: Environmental, 2019, 252, 98-110.	10.8	213
44026	Thermodynamic modelling of Al-B-N system. Calphad: Computer Coupling of Phase Diagrams and Thermochemistry, 2019, 65, 291-298.	0.7	9
44027	Behavior of H2O molecule in carbon nanotube/boron nitride nanotube heterostructure. Current Applied Physics, 2019, 19, 675-678.	1.1	5
44028	Co, Fe, and Mn in La-perovskite oxides for low temperature thermochemical CO2 conversion. Catalysis Today, 2019, 338, 52-59.	2.2	40
44029	Hydrogen chloride adsorption on large defective PAHs modeling soot surfaces and influence on water trapping: A DFT and AIMD study. Chemical Physics, 2019, 523, 18-27.	0.9	9
44030	Electronic properties of h-BN/g-C2N van der Waals heterojunction: A first-principles calculation. Chemical Physics Letters, 2019, 725, 75-79.	1.2	12
44031	Coupling of spin-orbit interaction with phonon anharmonicity leads to significant impact on thermoelectricity in SnSe. Nano Energy, 2019, 60, 673-679.	8.2	17
44032	Tunable band offset in black Phosphorus/ReS2 van der Waals heterostructure with robust direct band and inherent anisotropy. Superlattices and Microstructures, 2019, 129, 274-281.	1.4	6
44033	First-principles predictions of half-metallic, magnetic, and optical properties of the (001) surface of Ge doped half-Heusler alloys Mn2GexAs1-x (xâ€¯=â€¯0.00, 0.25, 0.50, 0.75, and 1.00). Thin Solid Films, 2019, 679, 99-109.	0.8	4
44034	Modeling Câ€“H Bond Activation and Oxidations of Alkanes over Cuâ€“MOR Using First-Principles Methods. Journal of Physical Chemistry C, 2019, 123, 10356-10366.	1.5	9
44035	A Guideline for Tailoring Lattice Oxygen Activity in Lithium-Rich Layered Cathodes by Strain. Journal of Physical Chemistry Letters, 2019, 10, 2202-2207.	2.1	6
44036	Analysis of Defect Recovery in Reduced Graphene Oxide and Its Application as a Heater for Self-Healing Polymers. ACS Applied Materials & Interfaces, 2019, 11, 16804-16814.	4.0	19
44037	Complicated and Unconventional Defect Properties of the Quasi-One-Dimensional Photovoltaic Semiconductor Sb₂Se₃. ACS Applied Materials & Interfaces, 2019, 11, 15564-15572.	4.0	145
44038	Significant THz absorption in CH3NH2 molecular defect-incorporated organic-inorganic hybrid perovskite thin film. Scientific Reports, 2019, 9, 5811.	1.6	26
44039	Nanostructures of solid electrolyte interphases and their consequences for microsized Sn anodes in sodium ion batteries. Energy and Environmental Science, 2019, 12, 1550-1557.	15.6	167
44040	Optical properties for the oxygen vacancies in Î²-Ga₂O₃ based on first-principles calculations. Materials Research Express, 2019, 6, 075913.	0.8	10
44041	Out-of-plane excitons in two-dimensional crystals. Physical Review B, 2019, 99, .	1.1	30

#	Article	IF	Citations
44042	Identification of a monoclinic metallic state in VO2 from a modified first-principles approach. Modern Physics Letters B, 2019, 33, 1950148.	1.0	0
44043	On the Nature of the Cathodic Reaction during Corrosion of Copper in Anoxic Sulfide Solutions. Journal of the Electrochemical Society, 2019, 166, C196-C208.	1.3	6
44044	First-principles study of elastic, dielectric, and vibrational properties of orthoferrites RFeO3 (R = Ho,) Tj ETQq0 0 0 rgBT /Overlock 10 Tf 5	0.8	3
44045	Moderate Adsorption of Oxygen Molecular Induced Better Performance of Oxygen Reduction Reaction. Journal of the Electrochemical Society, 2019, 166, F386-F392.	1.3	8
44046	Experimental Chemistry and Structural Stability of AlNb3 Enabled by Antisite Defects Formation. Materials, 2019, 12, 1104.	1.3	8
44047	Adsorption Energy Shifts for Oxygen and Hydroxyl on 4-atom Metal-Decorated Graphene Catalysts Via Solvation, pH, and Substrate Dopants: Effects on ORR Activity. Metals, 2019, 9, 227.	1.0	4
44048	Ab initio Study on Adsorption of Transition-Metal Phthalocyanine on a Quasi-One-Dimensional Metallic Surface, In/Si(111)-4Ã—1. Journal of the Korean Physical Society, 2019, 74, 251-255.	0.3	2
44049	Oneâ€Pot Synthesis of Framework Porphyrin Materials and Their Applications in Bifunctional Oxygen Electrocatalysis. Advanced Functional Materials, 2019, 29, 1901301.	7.8	63
44050	Lithium Chlorides and Bromides as Promising Solidâ€State Chemistries for Fast Ion Conductors with Good Electrochemical Stability. Angewandte Chemie, 2019, 131, 8123-8127.	1.6	27
44051	Lithium Chlorides and Bromides as Promising Solidâ€State Chemistries for Fast Ion Conductors with Good Electrochemical Stability. Angewandte Chemie - International Edition, 2019, 58, 8039-8043.	7.2	322
44052	Construction of Pd/BiOCl Catalyst for Highlyâ€selective Synthesis of Benzoin Ethyl Ether by Chlorine Promoted Coupling Reaction. ChemCatChem, 2019, 11, 2676-2682.	1.8	4
44053	Halfâ€Metallicity in Quaternary Heusler Alloys with 3d and 4d Elements: Observations and Insights from DFT Calculations. Physica Status Solidi (B): Basic Research, 2019, 256, 1900039.	0.7	9
44054	Intrinsically Optimizing Charge Transfer via Tuning Charge/Discharge Mode for Lithiumâ€“Oxygen Batteries. Small, 2019, 15, 1900154.	5.2	7
44055	Firstâ€Principles Study of Naâ€Ion Battery Performance and Reaction Mechanism of Tin Sulfide as Negative Electrode. Chemical Record, 2019, 19, 811-816.	2.9	11
44056	Two-dimensional black arsenic for Li-ion battery applications: a DFT study. Journal of Materials Science, 2019, 54, 9543-9552.	1.7	31
44057	Role of defects in tuning the adsorption of CO over graphene-supported Co13 cluster. Applied Surface Science, 2019, 481, 1080-1088.	3.1	16
44058	Superconductivity at 23â€¯K in MgLi compound at ultrahigh pressure. Computational Materials Science, 2019, 164, 158-165.	1.4	0
44059	Interfacial Effects on the Band Edges of Ta3N5 Photoanodes in an Aqueous Environment: A Theoretical View. IScience, 2019, 13, 432-439.	1.9	10

#	Article	IF	Citations
44060	Electronic and magnetic properties of MoS2 monolayers with antisite defects. Journal of Physics and Chemistry of Solids, 2019, 131, 119-124.	1.9	15
44061	Electronic structures of two-dimensional hydrogenated bilayer diamond films with Si dopant and Si-V center. Results in Physics, 2019, 13, 102240.	2.0	14
44062	First-principles study on magnetoelectric coupling effect of M/BiFeO3 (M = Co, Fe) multiferroic superlattice. Vacuum, 2019, 165, 105-112.	1.6	43
44063	Effect of trace Ni on the resistance of high-Cr cast iron to slurry erosion. Wear, 2019, 426-427, 605-611.	1.5	11
44064	Inconvenient Truths about Solid Form Landscapes Revealed in the Polymorphs and Hydrates of Gandotinib. Crystal Growth and Design, 2019, 19, 2947-2962.	1.4	32
44065	Effect of Functional and Electron Correlation on the Structure and Spectroscopy of the Al₂O₃(001)â€“H₂O Interface. Journal of Physical Chemistry Letters, 2019, 10, 2031-2036.	2.1	22
44066	Carbonate-Promoted Drift of Alkali Cations in Small Pore Zeolites: Ab Initio Molecular Dynamics Study of CO₂ in NaKA Zeolite. Journal of Physical Chemistry Letters, 2019, 10, 2191-2195.	2.1	9
44067	Light Emission Enhancement by Tuning the Structural Phase of APbBr₃ (A =) Tj ETQq1 1 0.784314 rgBT /Overlock 10 Tf 50 2135-2142.	2.1	12
44068	Spin Filtering in CrI₃ Tunnel Junctions. ACS Applied Materials & Interfaces, 2019, 11, 15781-15787.	4.0	71
44069	RuN₄ Doped Graphene Oxide, a Highly Efficient Bifunctional Catalyst for Oxygen Reduction and CO₂ Reduction from Computational Study. ACS Sustainable Chemistry and Engineering, 2019, 7, 8136-8144.	3.2	29
44070	In-situ local phase-transitioned MoSe2 in La0.5Sr0.5CoO3-Î´ heterostructure and stable overall water electrolysis over 1000 hours. Nature Communications, 2019, 10, 1723.	5.8	143
44071	Integration of a (â€“Cuâ€“Sâ€“)n plane in a metalâ€“organic framework affords high electrical conductivity. Nature Communications, 2019, 10, 1721.	5.8	134
44072	Alkyl substituted 4-pyrrolidinopyridinium salts encapsulated in the cavity of cucurbit[10]uril. New Journal of Chemistry, 2019, 43, 7028-7034.	1.4	7
44073	B-terminated (111) polar surfaces of BP and BAs: promising metal-free electrocatalysts with large reaction regions for nitrogen fixation. Journal of Materials Chemistry A, 2019, 7, 13284-13292.	5.2	87
44074	In situ exsolved FeNi₃ nanoparticles on nickel doped Sr₂Fe_{1.5}Mo_{0.5}O_{6â”Î´} perovskite for efficient electrochemical CO₂ reduction reaction. Journal of Materials Chemistry A, 2019, 7, 11967-11975.	5.2	159
44075	Elucidating the electronic structure of CuWO₄ thin films for enhanced photoelectrochemical water splitting. Journal of Materials Chemistry A, 2019, 7, 11895-11907.	5.2	67
44076	A combined DFT/topological analysis approach for modeling disordered solid electrolytes. EPJ Web of Conferences, 2019, 201, 02005.	0.1	1
44077	Direct Synthesis of Metalâ€Doped Phosphorene with Enhanced Electrocatalytic Hydrogen Evolution. Small Methods, 2019, 3, 1900083.	4.6	56

#	Article	IF	Citations
44078	Chabazite Architecture Dominates the Structure of SAPO-34â€™s Surface Methoxy Species. Catalysis Letters, 2019, 149, 2104-2109.	1.4	4
44079	From predicting to correlating the bonding properties of iron sulfide phases. Computational Materials Science, 2019, 164, 99-107.	1.4	13
44080	Cr2N2Se covalent ferromagnet proposed from first principles with properties close to CrO2. Solid State Sciences, 2019, 92, 53-59.	1.5	1
44081	SnTe monolayer: Tuning its electronic properties with doping. Superlattices and Microstructures, 2019, 130, 12-19.	1.4	8
44082	Cluster Expansion Framework for the Sr(Ti1â€“xFex)O3â€“x/2 (0 < x < 1) Mixed Ionic Electronic Conductor: Properties Based on Realistic Configurations. Chemistry of Materials, 2019, 31, 3144-3153.	3.2	6
44083	Six Quaternary Chalcogenides of the Pavonite Homologous Series with Ultralow Lattice Thermal Conductivity. Chemistry of Materials, 2019, 31, 3430-3439.	3.2	28
44084	Improved DFT Adsorption Energies with Semiempirical Dispersion Corrections. Journal of Chemical Theory and Computation, 2019, 15, 3250-3259.	2.3	43
44085	Correlation between Composition and Mechanical Properties of Calcium Silicate Hydrates Identified by Infrared Spectroscopy and Density Functional Theory. Journal of Physical Chemistry C, 2019, 123, 10868-10873.	1.5	25
44086	Metal- and Nonmetal-Atom-Modified Graphene as Efficient Catalysts for CO Oxidation Reactions. Journal of Physical Chemistry C, 2019, 123, 10926-10939.	1.5	28
44087	Oxygen-Induced In Situ Manipulation of the Interlayer Coupling and Exciton Recombination in Bi₂Se₃/MoS₂ 2D Heterostructures. ACS Applied Materials & Interfaces, 2019, 11, 15913-15921.	4.0	19
44088	Exploration of Long-Life Pt/Heteroatom-Doped Graphene Catalysts in Hydrogen Atmosphere. ACS Omega, 2019, 4, 6573-6584.	1.6	2
44089	Abnormal diffusion behaviors of Cu atoms in van der Waals layered material MoS₂. Journal of Materials Chemistry C, 2019, 7, 6052-6058.	2.7	18
44090	Band structure and thermoelectric performances of antimony under trigonal transformation. Journal of Applied Physics, 2019, 125, .	1.1	20
44091	Scalable and efficient Sb2S3 thin-film solar cells fabricated by close space sublimation. APL Materials, 2019, 7, .	2.2	72
44092	Evidence of a Nodal Line in the Superconducting Gap Symmetry of Noncentrosymmetric <mml:math xmlns:mml="http://www.w3.org/1998/Math/MathML" display="inline"><mml:mrow><mml:msub><mml:mrow><mml:mi>ThCoC</mml:mi></mml:mrow><mml:mrow><mml:mn>2</mml:mn></ Physical Review Letters, 2019, 122, 147001.	2.9	30
44093	Interplay of noncovalent interactions in antiseptic quaternary ammonium surfactant Miramistin. Acta Crystallographica Section C, Structural Chemistry, 2019, 75, 402-411.	0.2	7
44094	Magnification Effects in Scanning Tunneling Microscopy: the Role of Surface Radicals. Journal of Experimental and Theoretical Physics, 2019, 128, 94-97.	0.2	2
44095	Origin of the anomalous trends in band alignment of GaX/ZnGeX₂ (X = N, P, As, Sb) heterojunctions. Journal of Semiconductors, 2019, 40, 042102.	2.0	10

#	Article	IF	Citations
44096	Dynamics of ruthenium mirror under action of soft x-ray ultrashort laser pulse. Journal of Physics: Conference Series, 2019, 1147, 012070.	0.3	0
44097	Electronic structure and magnetic ordering of NiN and Ni ₂ N from first principles. Electronic Structure, 2019, 1, 015002.	1.0	6
44098	Ab initio and nuclear inelastic scattering studies of Fe3Si/GaAs heterostructures. Physical Review B, 2019, 99, .	1.1	5
44099	Role of the crystal electric field on the two magnetic transitions in the orthorhombic <mml:math xmlns:mml="http://www.w3.org/1998/Math/MathML"><mml:msub><mml:mi>YbMnO</mml:mi><mml:mn>3</mml:mn></mml:msub></ perovskite. Physical Review B, 2019, 99, .	1.1	1
44100	Substrate-mediated umklapp scattering at the incommensurate interface of a monatomic alloy layer. Physical Review B, 2019, 99, .	1.1	10
44101	Precipitation, planar defects and dislocations in alloys: Simulations on Ni3Si and Ni3Al precipitates. European Physical Journal: Special Topics, 2019, 227, 1559-1574.	1.2	6
44102	Surface Compositions of Ptâ€“Pd/Pd(111) Alloys in the Presence of O and OH during Oxygen Reduction Reaction: A First-Principles Study. Journal of the Physical Society of Japan, 2019, 88, 044802.	0.7	2
44103	Single crystal growth, structural analysis and electronic band structure of a nitrogen-containing polyacene Benzo[i]benzo[6â€²,7â€²]quinoxalino[2â€²,3â€²:9,10]phenanthro[4,5-abc]phenazine. Japanese Journal of Applied Physics, 2019, 58, SBBG08.	1.5	3
44104	Mono-C,O-chelated bromo- and triflatosilanes with an amino acid moiety: salts or covalently bonded complexes?. Russian Chemical Bulletin, 2019, 68, 137-148.	0.4	10
44105	A Bi/BiOI/(BiO)2CO3 heterostructure for enhanced photocatalytic NO removal under visible light. Chinese Journal of Catalysis, 2019, 40, 362-370.	6.9	63
44106	Electric field tunable electronic properties of P-ZnO and SiC-ZnO van der Waals heterostructures. Computational Materials Science, 2019, 164, 166-170.	1.4	27
44107	The experimental compression behavior of platinum hydride to 128â€¯GPa. Materials Letters, 2019, 249, 84-86.	1.3	5
44108	First-principle study of metal-organic frameworks of the 4d and 5d transition metal series with phthalocyanine and tetracyanobenzene. Superlattices and Microstructures, 2019, 130, 122-126.	1.4	3
44109	Structural, electronic and optical properties of pulsed laser deposited Cu2SnS3 photo absorber thin films: A combined experimental and computational study. Thin Solid Films, 2019, 677, 62-67.	0.8	9
44110	First-Principles Molecular Dynamics of Monomethylhydrazine and Nitrogen Dioxide. Journal of Physical Chemistry Letters, 2019, 10, 2394-2399.	2.1	8
44111	Modification of Electrical and Magnetic Properties of Fe₃O₄ Epitaxial Thin Films by Nitrogen Substitution for Oxygen. ACS Applied Electronic Materials, 2019, 1, 595-599.	2.0	3
44112	Stretchable and dynamically stable promising two-dimensional thermoelectric materials: ScPÂand ScAs. Journal of Materials Chemistry A, 2019, 7, 12604-12615.	5.2	40
44113	Novel two-dimensional molybdenum carbides as high capacity anodes for lithium/sodium-ion batteries. Journal of Materials Chemistry A, 2019, 7, 12145-12153.	5.2	106

#	Article	IF	Citations
44114	A simple local expression for the prefactor in transition state theory. Journal of Chemical Physics, 2019, 150, 144105.	1.2	7
44115	Structural and electronic properties of T graphene nanotubes: a first-principles study. New Journal of Physics, 2019, 21, 053015.	1.2	12
44116	Double dependence of H diffusion in tungsten from first-principles determination: strain and temperature. Materials Research Express, 2019, 6, 075520.	0.8	1
44117	New insights on the GeSe _x Te_{1â^'x} phase diagram from theory and experiment. Acta Crystallographica Section B: Structural Science, Crystal Engineering and Materials, 2019, 75, 246-256.	0.5	6
44118	A Facile Strategy for the Growth of an Anodic Oxidation Film of the Ti13Nb13Zr Alloy Driven by Residual Stress. International Journal of Electrochemical Science, 2019, , 2224-2239.	0.5	2
44119	Mottâ€“Schottky Effect Leads to Alkyne Semihydrogenation over Pd-Nanocube@N-Doped Carbon. ACS Catalysis, 2019, 9, 4632-4641.	5.5	93
44120	Graphene Liquid Cell Electron Microscopy of Initial Lithiation in Co₃O₄ Nanoparticles. ACS Omega, 2019, 4, 6784-6788.	1.6	11
44121	Network topological model of reconstructive solid-state transformations. Scientific Reports, 2019, 9, 6007.	1.6	21
44122	Study of electronic structure in the L-edge spectroscopy of actinide materials: UO₂ as an example. Physical Chemistry Chemical Physics, 2019, 21, 7789-7801.	1.3	8
44123	Chlorine-assisted fabrication of hybrid supramolecular structures via electrostatic interactions. Physical Chemistry Chemical Physics, 2019, 21, 9357-9361.	1.3	9
44124	Carboxylic acid-capped ruthenium nanoparticles: experimental and theoretical case study with ethanoic acid. Nanoscale, 2019, 11, 9392-9409.	2.8	19
44125	Structural, electronic, and dynamical properties of the tetragonal and collapsed tetragonal phases of KFe2As2. Physical Review B, 2019, 99, .	1.1	10
44126	Ethanol chemisorption on coreâ€“shell Pt-nanoparticles: an ab initio study. European Physical Journal B, 2019, 92, 1.	0.6	6
44127	The Effect of Lanthanum Doping and Oxygen Vacancy on Perovskite, Pyrochlore Oxide and Lanthanide Titanates: A First Principle Study. MRS Advances, 2019, 4, 1167-1175.	0.5	0
44128	Ab initio Study of Anchoring Groups for CuGaO2 Delafossite-Based p-Type Dye Sensitized Solar Cells. Frontiers in Chemistry, 2019, 7, 158.	1.8	15
44129	A descriptor of â€œmaterial genesâ€• Effective atomic size in structural unit of ionic crystals. Science China Technological Sciences, 2019, 62, 849-855.	2.0	6
44130	Structure, charge transfer, and superconductivity of M-doped phenanthrene (M = Al, Ga, and In): A comparative study of K-doped cases. Science China: Physics, Mechanics and Astronomy, 2019, 62, 1.	2.0	4
44131	Strain effects on phase transitions in transition metal dichalcogenides. Current Applied Physics, 2019, 19, 690-696.	1.1	7

#	Article	IF	Citations
44132	Two-dimensional graphyne-like carbon nitrides: Moderate band gaps, high carrier mobility, high flexibility and type-II band alignment. Carbon, 2019, 149, 234-241.	5.4	38
44133	Dominant in-plane cleavage direction of CrPS4. Computational Materials Science, 2019, 162, 277-280.	1.4	6
44134	Comparison of interatomic potential models on the molecular dynamics simulation of fast-ion conductors: A case study of a Li garnet oxide Li7La3Zr2O12. Computational Materials Science, 2019, 162, 333-339.	1.4	10
44135	Impact of solutes on the lattice parameters and elastic stiffness coefficients of hcp Fe from first-principles calculations. Computational Materials Science, 2019, 164, 116-126.	1.4	7
44136	Synergistic effect of N-doping and rich oxygen vacancies induced by nitrogen plasma endows TiO2 superior sodium storage performance. Electrochimica Acta, 2019, 309, 242-252.	2.6	44
44137	Strain effects on the mechanical properties of Group-V monolayers with buckled honeycomb structures. Physica E: Low-Dimensional Systems and Nanostructures, 2019, 112, 59-65.	1.3	20
44138	Synthesis of superfine high-entropy metal diboride powders. Scripta Materialia, 2019, 167, 110-114.	2.6	120
44139	Oxygen Evolution on in Situ Selective Formation of AgO: Plane Is the Key Factor. Journal of Physical Chemistry C, 2019, 123, 10967-10973.	1.5	4
44140	Nonlinear Optical Response in Graphene/WX₂ (X = S, Se, and Te) van der Waals Heterostructures. Journal of Physical Chemistry Letters, 2019, 10, 2090-2100.	2.1	28
44141	Spontaneous Formation of 1D Pattern in Monolayer VSe₂ with Dispersive Adsorption of Pt Atoms for HER Catalysis. Nano Letters, 2019, 19, 4897-4903.	4.5	42
44142	Tunable Ohmic, p-Type Quasi-Ohmic, and n-Type Schottky Contacts of Monolayer SnSe with Metals. ACS Applied Nano Materials, 2019, 2, 2767-2775.	2.4	20
44143	Chemical Properties of Metal-Silicates Rendered by Metal Exchange Reaction. ACS Sustainable Chemistry and Engineering, 2019, 7, 8449-8457.	3.2	10
44144	Stabilization of Oâ€“O Bonds by d⁰ Cations in Li_{4+x}Ni_{1â€“x}WO₆ (0 â‰¤ x â‰¤ 0.25) Rock Salt Oxides as the Origin of Large Voltage Hysteresis. Journal of the American Chemical Society, 2019, 141, 7333-7346.	6.6	61
44145	A BN analog of two-dimensional triphenylene-graphdiyne: stability and properties. Nanoscale, 2019, 11, 9000-9007.	2.8	12
44146	Fundamental insights about interlayer cation migration in Li-ion electrodes at high states of charge. Journal of Materials Chemistry A, 2019, 7, 11996-12007.	5.2	12
44147	Theoretical characterization of C doped SiGe monolayer. Journal of Applied Physics, 2019, 125, 145703.	1.1	4
44148	First principles study of hydrogen in lead zirconate titanate. Smart Materials and Structures, 2019, 28, 034002.	1.8	5
44149	Versatile GaInO ₃ -sheet with strain-tunable electronic structure, excellent mechanical flexibility, and an ideal gap for photovoltaics. Chinese Physics B, 2019, 28, 016105.	0.7	6

#	Article	IF	Citations
44150	Metastable states of fluidâ€“fluid phase transition in warm dense hydrogen. Journal of Physics: Conference Series, 2019, 1147, 012003.	0.3	0
44151	Electrical resistivity of liquid expanded metals by Ziman approach. Journal of Physics: Conference Series, 2019, 1147, 012005.	0.3	1
44152	Structureâ€“Property Relationship in an Organic Semiconductor: Insights from Energy Frameworks, Charge Density Analysis, and Diode Devices. Crystal Growth and Design, 2019, 19, 3019-3029.	1.4	6
44153	Lithium Diffusion Mechanism through Solidâ€“Electrolyte Interphase in Rechargeable Lithium Batteries. Journal of Physical Chemistry C, 2019, 123, 10237-10245.	1.5	181
44154	Silicon Nanocages for Selective Carbon Dioxide Conversion under Visible Light. Journal of Physical Chemistry C, 2019, 123, 9973-9980.	1.5	21
44155	Steric Effects in CO Oxidation on Pt(111) by Impinging Oxygen Atoms Lead to an Exclusive Hot Atom Mechanism. Journal of Physical Chemistry C, 2019, 123, 10509-10516.	1.5	8
44156	Diffusion of Alkali Metals in Polycrystalline CuInSe₂ and Their Role in the Passivation of Grain Boundaries. ACS Applied Materials & Interfaces, 2019, 11, 14821-14829.	4.0	23
44157	Novel graphene-like two-dimensional bilayer germanene dioxide: electronic structure and optical properties. RSC Advances, 2019, 9, 9633-9639.	1.7	4
44158	Penta-PdX₂ (X = S, Se, Te) monolayers: promising anisotropic thermoelectric materials. Journal of Materials Chemistry A, 2019, 7, 11134-11142.	5.2	117
44159	Recovery of metastable dense Bi synthesized by shock compression. Applied Physics Letters, 2019, 114, 120601.	1.5	12
44160	Existence of a critical canting angle of magnetic moments to induce multiferroicity in the Haldane spin-chain system <mml:math xmlns:mml="http://www.w3.org/1998/Math/MathML"><mml:mrow><mml:msub><mml:mi>Tb</mml:mi><mml:mn>2</mml:mn></mml:r Physical Review B, 2019, 99, .	1.1	12
44161	Valley splitting in the van der Waals heterostructure <mml:math xmlns:mml="http://www.w3.org/1998/Math/MathML"><mml:mrow><mml:msub><mml:mi>WSe</mml:mi><mml:mn>2</mml:mn></mml:r : The role of atom superposition. Physical Review B, 2019, 99, .	1.1	17
44162	Toward an Understanding of Capping Molecules on Pt Nanoparticles for Hydrogenation: the Key Role of Hydroxyl Groups. ChemistrySelect, 2019, 4, 3505-3514.	0.7	1
44163	Structural, Elastic, Electronic, and Magnetic Properties of a New Full-Heusler Alloy Mn2MgGe: First-Principles Calculations. Journal of Superconductivity and Novel Magnetism, 2019, 32, 3001-3008.	0.8	9
44164	Recent Developments in Using Computational Materials Design for High-Performance Li4Ti5O12 Anode Material for Lithium-Ion Batteries. Multiscale Science and Engineering, 2019, 1, 87-107.	0.9	13
44165	Magnetic and optical properties of two-dimensional SnS2 nanosheets doped with Ho ions. Applied Surface Science, 2019, 481, 1370-1376.	3.1	23
44166	A theoretical study on tuning band gaps of monolayer and bilayer SnS2 and SnSe2 under external stimuli. Current Applied Physics, 2019, 19, 709-714.	1.1	32
44167	Oxidation states of binary oxides from data analytics of the electronic structure. Computational Materials Science, 2019, 161, 403-414.	1.4	21

#	Article	IF	Citations
44168	Graphene/RuO2 nanocrystal composites as sulfur host for lithium-sulfur batteries. Journal of Energy Chemistry, 2019, 35, 204-211.	7.1	32
44169	Mechanism for the Structural Transformation to the Modulated Superconducting Phase of Compressed Hydrogen Sulfide. Scientific Reports, 2019, 9, 5023.	1.6	12
44170	Copperâ€“nitroxide based breathing crystals: a unified mechanism of gradual magnetostructural transition supported by quantum chemistry calculations. Inorganic Chemistry Frontiers, 2019, 6, 1228-1237.	3.0	5
44171	Hexagonal MASnI3 exhibiting strong absorption of ultraviolet photons. Applied Physics Letters, 2019, 114, .	1.5	5
44172	Cu-Zn disorder in stoichiometric and non-stoichiometric Cu2ZnSnS4/Cu2ZnSnSe4. AIP Advances, 2019, 9, .	0.6	11
44173	Pressure-induced phase transitions and structural evolution across the insulatorâ€“metal transition in bulk and nanoscale BiFeO₃. Journal of Physics Condensed Matter, 2019, 31, 265404.	0.7	4
44174	Î±-MnO₂ under pressure: Possible route to Î´-MnO₂. Materials Research Express, 2019, 6, 076108.	0.8	4
44175	Evolution of elastic moduli through a two-dimensional structural transformation. Physical Review B, 2019, 99, .	1.1	12
44176	Ferromagnetism in nitrogen-doped graphene. Physical Review B, 2019, 99, .	1.1	44
44177	Coexistence of Two Types of Spin Splitting Originating from Different Symmetries. Physical Review Letters, 2019, 122, 126403.	2.9	14
44178	Multiscale Modeling of Agglomerated Ceria Nanoparticles: Interface Stability and Oxygen Vacancy Formation. Frontiers in Chemistry, 2019, 7, 203.	1.8	7
44179	Origin of the ductile-to-brittle transition of metastable Î²-titanium alloys: Self-hardening of Ï‰-precipitates. Acta Materialia, 2019, 170, 187-204.	3.8	76
44180	Enhanced photocatalytic performance of ZnO monolayer for water splitting via biaxial strain and external electric field. Applied Surface Science, 2019, 481, 1064-1071.	3.1	37
44181	First-principles study of a vertical spin switch in atomic scale two-dimensional platform. Journal of Magnetism and Magnetic Materials, 2019, 484, 462-471.	1.0	6
44182	Defect structure in Î´-Bi₅PbY₂O_{11.5}. RSC Advances, 2019, 9, 9640-9653.	1.7	6
44183	Molecular discovery of half-metallic one-dimensional metal-organic framework. Journal of Applied Physics, 2019, 125, .	1.1	8
44184	Thermal conductance across Î²-Ga2O3-diamond van der Waals heterogeneous interfaces. APL Materials, 2019, 7, .	2.2	87
44185	Comparison of Effects of Sodium Bicarbonate and Sodium Carbonate on the Hydration and Properties of Portland Cement Paste. Materials, 2019, 12, 1033.	1.3	53

#	Article	IF	Citations
44186	Stress engineering on the electronic and spintronic properties for a GaSe/HfSe₂ van der Waals heterostructure. Applied Physics Express, 2019, 12, 031002.	1.1	12
44187	Understanding the role of Au in the selective hydrogenation of acetylene on trimetallic PdAgAu catalytic surface. Catalysis Communications, 2019, 124, 41-45.	1.6	16
44188	Reaction mechanism and kinetics for Pt/CNTs catalyzed base-free oxidation of glycerol. Chemical Engineering Science, 2019, 203, 228-236.	1.9	32
44189	High pressure behavior of mercury difluoride (HgF2). Chemical Physics Letters, 2019, 724, 35-41.	1.2	7
44190	Integrated modeling of molar volume of the sigma phase aided by first-principles calculations. Journal of Alloys and Compounds, 2019, 791, 994-1004.	2.8	6
44191	Lithiation of the Two-Dimensional Silicon Carbideâ€“Graphene van der Waals Heterostructure: A First Principles Study. Journal of Physical Chemistry C, 2019, 123, 10738-10745.	1.5	19
44192	Pressure-Stabilized High-Energy-Density Alkaline-Earth-Metal Pentazolate Salts. Journal of Physical Chemistry C, 2019, 123, 10205-10211.	1.5	69
44193	Metalâ€“polymer hybrid nanomaterials for plasmonic ultrafast hydrogen detection. Nature Materials, 2019, 18, 489-495.	13.3	227
44194	Solvent-mediated charge separation drives alternative hydrogenation path of furanics in liquid water. Nature Catalysis, 2019, 2, 431-436.	16.1	171
44195	Activation of CO₂ at the electrodeâ€“electrolyte interface by a co-adsorbed cation and an electric field. Physical Chemistry Chemical Physics, 2019, 21, 8797-8807.	1.3	22
44196	Two-dimensional Blue-AsP monolayers with tunable direct band gap and ultrahigh carrier mobility show promising high-performance photovoltaic properties. Nanoscale, 2019, 11, 8260-8269.	2.8	70
44197	Pursuit of a high-capacity and long-life Mg-storage cathode by tailoring sandwich-structured MXene@carbon nanosphere composites. Journal of Materials Chemistry A, 2019, 7, 16712-16719.	5.2	81
44198	Stability and band offsets between GaAs semiconductor and CeO2 gate dielectric. AIP Advances, 2019, 9, 025117.	0.6	4
44199	Beyond the Drude model in transport and optical properties of dense plasma of silver. Journal of Physics: Conference Series, 2019, 1164, 012017.	0.3	1
44200	Preparation and electronic properties of clean superconducting Nb(110) surfaces. Physical Review B, 2019, 99, .	1.1	31
44201	Stacking tunable interlayer magnetism in bilayer <mml:math xmlns:mml="http://www.w3.org/1998/Math/MathML"><mml:msub><mml:mi>CrI</mml:mi><mml:mn>3</mml:mn></mml:msub></m Physical Review B, 2019, 99, .	1.1	287
44202	Semimetal-to-semiconductor transition and charge-density-wave suppression in <mml:math xmlns:mml="http://www.w3.org/1998/Math/MathML"><mml:mrow><mml:mn>1</mml:mn><mml:mi>T</mml:mi><mml:mo>â^'</mml:m mathvariant="normal">S</mml:mi><mml:mi>x</mml:mi></mml:msub></mml:mrow></mml:math> single crystals. Physical Review B, 2019, 99, .	1.1	21
44203	Electronic Properties of WS₂/WSe₂ Heterostructure Containing Te Impurity: The Role of Substituting Position. International Journal of Nanoscience, 2019, 18, 1940007.	0.4	2

#	Article	IF	Citations
44204	Whiteâ€Light Generation Upon Inâ€Situ Amorphization of Single Crystals of [{(Me 3 P) 3 AuSn}(PhSn) 3 S 6] and [{(Et 3 P) 3 AgSn}(PhSn) 3 S 6]. Advanced Optical Materials, 2019, 7, 1801793.	3.6	23
44205	Abundant Ce³⁺ Ions in Auâ€CeO_x Nanosheets to Enhance CO₂ Electroreduction Performance. Small, 2019, 15, e1900289.	5.2	46
44206	Triple oxygen isotope constraints on the origin of ocean island basalts. Acta Geochimica, 2019, 38, 327-334.	0.7	8
44207	High-pressure characterization of the optical and electronic properties of InVO4, InNbO4, and InTaO4. SN Applied Sciences, 2019, 1, 1.	1.5	42
44208	Two-dimensional blue-phosphorene-phase germanium monochalcogenide photocatalysts for water splitting: From ultraviolet to visible absorption. Journal of Catalysis, 2019, 373, 67-74.	3.1	26
44209	Structure and dynamics of a silver-doped chalcogenide glass: An ab initio study. Journal of Non-Crystalline Solids, 2019, 514, 1-9.	1.5	4
44210	First-Principles study on electronic structure and optical properties of monolayer Mo1-xMx(Mâ€¯=â€¯W or) Tj ETQq0 0 0 rgBT /Overlock	0.9	1
44211	Exploring thiophene desulfurization: The adsorption of thiophene on transition metal surfaces. Surface Science, 2019, 686, 30-38.	0.8	6
44212	Oxidation of Liquid Silicon in Air Atmospheres Containing Water Vapor. Industrial & Engineering Chemistry Research, 2019, 58, 6785-6795.	1.8	7
44213	A Control over Hydrogenation Selectivity of Furfural via Tuning Exposed Facet of Ni Catalysts. ACS Catalysis, 2019, 9, 4226-4235.	5.5	149
44214	Growth Kinetics of Individual Co Particles Ex-solved on SrTi_{0.75}Co_{0.25}O_{3-Î´} Polycrystalline Perovskite Thin Films. Journal of the American Chemical Society, 2019, 141, 6690-6697.	6.6	75
44215	Layered Tl₂O: a model thermoelectric material. Journal of Materials Chemistry C, 2019, 7, 5094-5103.	2.7	46
44216	Multitribe evolutionary search for stable Cuâ€“Pdâ€“Ag nanoparticles using neural network models. Physical Chemistry Chemical Physics, 2019, 21, 8729-8742.	1.3	25
44217	Electronic and magnetic properties of the one-dimensional interfaces of two-dimensional lateral GeC/BP heterostructures. Physical Chemistry Chemical Physics, 2019, 21, 8856-8864.	1.3	7
44218	Electronic Structure and Optical Property Calculation of an Oxygen Vacancy in NH 4 H 2 PO 4 Crystals *. Chinese Physics Letters, 2019, 36, 037801.	1.3	1
44219	Singlet <mml:math xmlns:mml="http://www.w3.org/1998/Math/MathML"><mml:mrow><mml:mi>s</mml:mi><mml:msup><mml:mrow /><mml:mo>Â±</mml:mo></mml:msup></mml:mrow></mml:math> -wave pairing in quasi-one-dimensional <mml:math xmlns:mml="http://www.w3.org/1998/Math/MathML"><mml:mrow><mml:mi>A</mml:mi><mml:msub><mml:mi>Cr</mml:mi><mml:mi		

#	Article	IF	Citations
44222	The Structural, Electronic, and Magnetic Properties of Binary Heusler Alloys ZCl3 (Zâ€‰=â€‰Li, Na, K, Rb) with DO3-Type Structure from First Principle Calculations. Journal of Superconductivity and Novel Magnetism, 2019, 32, 3217-3226.	0.8	4
44223	Grain growth and solid-state dewetting of Bi-Crystal Ni-Fe thin films on sapphire. Acta Materialia, 2019, 168, 237-249.	3.8	17
44224	First-principles study, fabrication and characterization of (Zr0.25Nb0.25Ti0.25V0.25)C high-entropy ceramics. Acta Materialia, 2019, 170, 15-23.	3.8	294
44225	Evolution of Pt and Pd species in functionalized UiO-67 metal-organic frameworks. Catalysis Today, 2019, 336, 33-39.	2.2	19
44226	Sorption of Eu(III) on MXene-derived titanate structures: The effect of nano-confined space. Chemical Engineering Journal, 2019, 370, 1200-1209.	6.6	91
44227	Defect energy levels and persistent luminescence in Cu-doped ZnS. Computational Materials Science, 2019, 163, 63-67.	1.4	25
44228	Structural and electronic properties of bulk and ultrathin layers of V2O5 and MoO3. Computational Materials Science, 2019, 163, 230-240.	1.4	47
44229	First-principles explorations of the universal picture of oxide layer structure over metallic plutonium. Corrosion Science, 2019, 153, 236-248.	3.0	29
44230	Thermodynamic and physical properties of Zr3Fe and ZrFe2 intermetallic compounds. Intermetallics, 2019, 109, 189-196.	1.8	14
44231	P doped MoS2 nanoplates embedded in nitrogen doped carbon nanofibers as an efficient catalyst for hydrogen evolution reaction. Journal of Colloid and Interface Science, 2019, 547, 291-298.	5.0	33
44232	Half-metallic behavior and magnetic properties of various (001) surfaces for the Heusler alloy Y2CrSn. Journal of Physics and Chemistry of Solids, 2019, 131, 164-172.	1.9	7
44233	Optoelectronic Structure and Photocatalytic Applications of Na(Bi,La)S2 Solid Solutions with Tunable Band Gaps. Chemistry of Materials, 2019, 31, 3211-3220.	3.2	13
44234	Accurate Probabilities for Highly Activated Reaction of Polyatomic Molecules on Surfaces Using a High-Dimensional Neural Network Potential: CHD₃ + Cu(111). Journal of Physical Chemistry Letters, 2019, 10, 1763-1768.	2.1	56
44235	Chlorine Passivation of Grain Boundary Suppresses Electronâ€“Hole Recombination in CsPbBr₃ Perovskite by Nonadiabatic Molecular Dynamics Simulation. ACS Applied Energy Materials, 2019, 2, 3419-3426.	2.5	32
44236	Iodine-Deficient BiOI Nanosheets with Lowered Valence Band Maximum To Enable Visible Light Photocatalytic Activity. ACS Sustainable Chemistry and Engineering, 2019, 7, 7900-7907.	3.2	74
44237	Synergistic Mn-Co catalyst outperforms Pt on high-rate oxygen reduction for alkaline polymer electrolyte fuel cells. Nature Communications, 2019, 10, 1506.	5.8	212
44238	Reaction mechanism between small-sized Ce clusters and water molecules II: anab initioinvestigation on Ce_n(n= 1â€“3) +mH₂O (m= 2â€“6). Physical Chemistry Chemical Physics, 2019, 21, 8945-8955.	1.3	8
44239	Lattice constant-dependent anchoring effect of MXenes for lithiumâ€“sulfur (Liâ€“S) batteries: a DFT study. Nanoscale, 2019, 11, 8485-8493.	2.8	93

#	Article	IF	Citations
44240	The complex defect chemistry of antimony selenide. Journal of Materials Chemistry A, 2019, 7, 10739-10744.	5.2	99
44241	Two-dimensional eclipsed arrangement hybrid perovskites for tunable energy level alignments and photovoltaics. Journal of Materials Chemistry C, 2019, 7, 5139-5147.	2.7	22
44242	Structural phase transition in Al-substituted Fe2MnGa Heusler alloy. Journal of Applied Physics, 2019, 125, .	1.1	1
44243	Boronâ€“oxygen complex yields n-type surface layer in semiconducting diamond. Proceedings of the National Academy of Sciences of the United States of America, 2019, 116, 7703-7711.	3.3	60
44244	Magnetocaloric effects from an interplay of magnetic sublattices in Nd2NiMnO6. Journal of Physics Condensed Matter, 2019, 31, 305803.	0.7	8
44245	Tight-binding model for electronic structure of hexagonal boron phosphide monolayer and bilayer. Journal of Physics Condensed Matter, 2019, 31, 285501.	0.7	14
44246	Large Bulk Photovoltaic Response by Symmetry-Breaking Structural Transformation in Ferroelectric [Ba(Zr0.2Ti0.8)O3] 0.5 [(Ba0.7Ca0.3)TiO3] 0.5. Physical Review Applied, 2019, 11, .	1.5	22
44247	Spin-charge conversion in InSe bilayers. Physical Review B, 2019, 99, .	1.1	14
44248	Defect-Rich Nickel Nanoparticles Supported on SiC Derived from Silica Fume with Enhanced Catalytic Performance for CO Methanation. Catalysts, 2019, 9, 295.	1.6	7
44249	Moment tensor potentials as a promising tool to study diffusion processes. Computational Materials Science, 2019, 164, 46-56.	1.4	65
44250	Charge distribution on the water/Î³-Fe2O3 interface. Journal of Magnetism and Magnetic Materials, 2019, 484, 74-82.	1.0	5
44251	Structures and Properties of Coreâ€“Shell B@Mn8@Mg10 Cluster and Brief of Efficient Coreâ€“Shell Cluster Algorithm and Global Minima Algorithm Based on a Sequential Microdisplacement Pressâ€“Expand Method. Journal of Physical Chemistry C, 2019, 123, 11162-11170.	1.5	0
44252	A Comparative Study on the Diffusion Behaviors of Metal and Oxygen Ions in Metal-Oxide-Based Resistance Switches via ab Initio Molecular Dynamics Simulations. ACS Applied Electronic Materials, 2019, 1, 585-594.	2.0	14
44253	Formation and Healing of Defects in Atomically Thin GaSe and InSe. ACS Nano, 2019, 13, 5112-5123.	7.3	35
44254	Initial Steps in Forming the Electrodeâ€“Electrolyte Interface: H2O Adsorption and Complex Formation on the Ag(111) Surface from Combining Quantum Mechanics Calculations and Ambient Pressure X-ray Photoelectron Spectroscopy. Journal of the American Chemical Society, 2019, 141, 6946-6954.	6.6	19
44255	Anion-adaptive crystalline cationic material for 99TcO4â^' trapping. Nature Communications, 2019, 10, 1532.	5.8	87
44256	Intrinsic Thermal conductivities of monolayer transition metal dichalcogenides MX2 (Mâ€‰=â€‰Mo, W; Xâ€‰=â€‰S,) Tj ETQq0 0 0	1.6	62
44257	Silicene-supported TiO2 nanostructures: a theoretical study of electronic and optical properties. Physical Chemistry Chemical Physics, 2019, 21, 9335-9341.	1.3	6

#	Article	IF	Citations
44258	Electronic and spin structure of O- and H-adsorbed <mml:math xmlns:mml="http://www.w3.org/1998/Math/MathML"><mml:msub><mml:mi>Fe</mml:mi><mml:mn>3</mml:mn></mml:msub><mml:r mathvariant="normal">O</mml:mi></mml:mrow><mml:mn>4</mml:mn></mml:msub></mml:math> (111) surfaces. Physical Review B, 2019, 99, .	1.1	6
44259	Search for new nitrogen-doped carbon materials by compressing molecular crystals. Japanese Journal of Applied Physics, 2019, 58, SBBG13.	0.8	2
44260	The Thermoelectric Properties of Bismuth Telluride. Advanced Electronic Materials, 2019, 5, 1800904.	2.6	446
44261	Phosphate Doped Ultrathin FeP Nanosheets as Efficient Electrocatalysts for the Hydrogen Evolution Reaction in Acid Media. ChemCatChem, 2019, 11, 2484-2489.	1.8	17
44262	Distinctive electronic and spin structures at the oppositely polarized ferroelectric BiAlO3(0001) surfaces. Applied Surface Science, 2019, 481, 702-711.	3.1	10
44263	Electric field induced modulation to the magnetic anisotropy of Fe/silicene heterostructures: First-principles study. Journal of Magnetism and Magnetic Materials, 2019, 484, 172-178.	1.0	5
44264	Origin of the R(15â€Ã—â€3) surface reconstruction of carburized W(110) - revisited. Surface Science, 2019, 682, 33-37.	0.8	3
44265	Surface Termination Dependent Work Function and Electronic Properties of Ti₃C₂T_x MXene. Chemistry of Materials, 2019, 31, 6590-6597.	3.2	359
44266	Influence of Cobalt Crystal Structures on Activation of Nitrogen Molecule: A First-Principles Study. Journal of Physical Chemistry C, 2019, 123, 10956-10966.	1.5	19
44267	Influence of Crystal Facet and Phase of Titanium Dioxide on Ostwald Ripening of Supported Pt Nanoparticles from First-Principles Kinetics. Journal of Physical Chemistry C, 2019, 123, 11020-11031.	1.5	26
44268	Anomalously Low Barrier for Water Dimer Diffusion on Cu(111). Nano Letters, 2019, 19, 3049-3056.	4.5	20
44269	Noble gas as a functional dopant in ZnO. Npj Computational Materials, 2019, 5, .	3.5	9
44270	General scaling relations and prediction of transition state energies in CHA/AlPO-34-structured zeolite catalysis related to the methanol-to-olefins conversion. Catalysis Science and Technology, 2019, 9, 2245-2252.	2.1	13
44271	Bandgap engineering of PbTe ultra-thin layers by surface passivations. Journal of Physics Condensed Matter, 2019, 31, 295503.	0.7	2
44272	Experimental molecular adsorption: electronic buffer effect of germanene on Al(1â€‰1â€‰1). 2D Materials, 2019, 6, 035016.	2.0	4
44273	Electronic properties of several two dimensional halides from ab initio calculations. Beilstein Journal of Nanotechnology, 2019, 10, 823-832.	1.5	24
44274	Size Fractionation of Graphene Oxide via Solventâ€Mediated Consecutive Charge Manipulation and Investigation of the Size Effect as Hole Transporting Layer in Perovskite Solar Cells. ChemNanoMat, 2019, 5, 776-783.	1.5	7
44275	The effect of surface vacancies on the interactions of Cl with a Î±-Fe2O3 (0001) surface and the role of Cl in depassivation. Corrosion Science, 2019, 154, 61-69.	3.0	30

#	Article	IF	Citations
44276	Oxygen-vacancies-engaged efficient carrier utilization for the photocatalytic coupling reaction. Journal of Catalysis, 2019, 373, 116-125.	3.1	33
44277	Predicting two-dimensional pentagonal transition metal monophosphides for efficient electrocatalytic nitrogen reduction. Journal of Materials Chemistry A, 2019, 7, 11444-11451.	5.2	49
44278	Porous hydrogen substituted graphyne for high capacity and ultra-stable sodium ion storage. Journal of Materials Chemistry A, 2019, 7, 11186-11194.	5.2	36
44279	Superconductivity with high hardness in Mo₃C₂. Inorganic Chemistry Frontiers, 2019, 6, 1282-1288.	3.0	16
44280	Shifting of Fermi level and realization of topological insulating phase in the oxyfluoride BaBiO₂F. Materials Research Express, 2019, 6, 066309.	0.8	6
44281	Ultrafast quasiparticle dynamics in the correlated semimetal Ca3Ru2O7. Physical Review B, 2019, 99, .	1.1	8
44282	Equation of state of boron nitride combining computation, modeling, and experiment. Physical Review B, 2019, 99, .	1.1	28
44283	Stability of graphite-like ZnO film with Cu doping: First principle study. European Physical Journal Plus, 2019, 134, 1.	1.2	3
44284	Electrochemically Driven Coordination Tuning of FeOOH Integrated on Carbon Fiber Paper for Enhanced Oxygen Evolution. Small, 2019, 15, e1901015.	5.2	46
44285	Effects of phase composition and elemental partitioning on soft magnetic properties of AlFeCoCrMn high entropy alloys. Acta Materialia, 2019, 171, 31-39.	3.8	60
44286	Density-functional-theory approach to determine band offsets and dielectric breakdown properties across metal/crystal oxide and metal/amorphous oxide interfaces: A case study of Al/SiO2. Applied Surface Science, 2019, 483, 616-625.	3.1	5
44287	Application of machine learning-based selective sampling to determine BaZrO3 grain boundary structures. Computational Materials Science, 2019, 164, 57-65.	1.4	4
44288	Superior Mg2+ storage properties of VS2 nanosheets by using an APC-PP14Cl/THF electrolyte. Energy Storage Materials, 2019, 23, 749-756.	9.5	60
44289	MgTiO3Hx and CaTiO3Hx perovskite compounds for hydrogen storage applications. International Journal of Hydrogen Energy, 2019, 44, 11930-11938.	3.8	34
44290	Experimental revelation of multiband transport in heavily doped BaCd2Sb2 with promising thermoelectric performance. Materials Today Physics, 2019, 8, 123-127.	2.9	30
44291	First-principles study of the reorientational motion of the [BH4]- groups in CsBH4's fractionally occupied ground-state phase and the thermal properties. Physica B: Condensed Matter, 2019, 564, 69-79.	1.3	1
44292	Feasible transformation of MgCo2O4 from spinel to defect rocksalt structure under electron irradiation. Scripta Materialia, 2019, 167, 26-30.	2.6	26
44293	Modeling the effect of surface CO coverage on the electrocatalytic reduction of CO₂ to CO on Pd surfaces. Physical Chemistry Chemical Physics, 2019, 21, 9876-9882.	1.3	34

#	Article	IF	Citations
44294	Atomistic approaches to cleavage of interfaces. Modelling and Simulation in Materials Science and Engineering, 2019, 27, 035007.	0.8	24
44295	Carrier transport in two-dimensional topological insulator nanoribbons in the presence of vacancy defects. 2D Materials, 2019, 6, 025011.	2.0	18
44296	Purely rotational symmetry-protected topological crystalline insulator Î± -Bi₄Br₄. 2D Materials, 2019, 6, 031004.	2.0	41
44297	Thermodynamic Modeling of the Al-Ba and Ba-Ge Systems Supported by First-Principles Calculations. Journal of Phase Equilibria and Diffusion, 2019, 40, 195-205.	0.5	3
44298	Adlayer-substrate interactions in controlled growth of graphene/h-BN heterostructure on Ni(111) and Cu(111) surfaces. Applied Surface Science, 2019, 480, 154-161.	3.1	7
44299	Sc2CO2 and Mn-doped Sc2CO2 as gas sensor materials to NO and CO: A first-principles study. Physica E: Low-Dimensional Systems and Nanostructures, 2019, 111, 84-90.	1.3	54
44300	Niobium-Doped TiO₂: Effect of an Interstitial Oxygen Atom on the Charge State of Niobium. Inorganic Chemistry, 2019, 58, 3090-3098.	1.9	14
44301	Crystallography-Derived Youngâ€™s Modulus and Tensile Strength of AlN Nanowires as Revealed by in Situ Transmission Electron Microscopy. Nano Letters, 2019, 19, 2084-2091.	4.5	11
44302	Comparative Study of Ethylene Carbonate-Based Electrolyte Decomposition at Li, Ca, and Al Anode Interfaces. ACS Applied Energy Materials, 2019, 2, 1676-1684.	2.5	36
44303	Synergistic Coupling of Anionic Ligands To Optimize the Electronic and Catalytic Properties of Metalâ€“Organic Framework-Converted Oxygen-Evolving Catalysts. ACS Applied Energy Materials, 2019, 2, 2138-2148.	2.5	31
44304	Kinetics, energetics, and size dependence of the transformation from Pt to ordered PtSn intermetallic nanoparticles. Nanoscale, 2019, 11, 5336-5345.	2.8	25
44305	High thermoelectric efficiency in monolayer PbI₂ from 300 K to 900 K. Inorganic Chemistry Frontiers, 2019, 6, 920-928.	3.0	29
44306	Interfacial competition between a borophene-based cathode and electrolyte for the multiple-sulfide immobilization of a lithium sulfur battery. Journal of Materials Chemistry A, 2019, 7, 7092-7098.	5.2	30
44307	Electronic properties of candidate type-II Weyl semimetal WTe ₂ . A review perspective. Electronic Structure, 2019, 1, 014003.	1.0	32
44308	Schottky Contact in Monolayer WS₂ Fieldâ€Effect Transistors. Advanced Theory and Simulations, 2019, 2, 1900001.	1.3	42
44309	Mechanism of hardening and damage initiation in oxygen embrittlement of body-centred-cubic niobium. Acta Materialia, 2019, 168, 331-342.	3.8	60
44310	Low operating temperature and highly selective NH3 chemiresistive gas sensors based on Ag3PO4 semiconductor. Applied Surface Science, 2019, 479, 1141-1147.	3.1	32
44311	Structural and electronic changes in graphite fluorides as a function of fluorination rate: An XRS, PDF and DFT study. Carbon, 2019, 147, 1-8.	5.4	18

#	Article	IF	Citations
44312	Ductility enhancement of tungsten after plastic deformation. Journal of Alloys and Compounds, 2019, 787, 801-814.	2.8	30
44313	Reaction Mechanisms for Long-Life Rechargeable Zn/MnO₂ Batteries. Chemistry of Materials, 2019, 31, 2036-2047.	3.2	195
44314	Ba₂ScHO₃: H^{â€“} Conductive Layered Oxyhydride with H^{â€“} Site Selectivity. Inorganic Chemistry, 2019, 58, 4431-4436.	1.9	41
44315	Chemical Functionalization of ZnS: A Perspective from the Ligandâ€“ZnS Bond Character. Journal of Physical Chemistry C, 2019, 123, 6054-6061.	1.5	4
44316	Direct Reaction between Copper and Nitrogen at High Pressures and Temperatures. Journal of Physical Chemistry Letters, 2019, 10, 1109-1114.	2.1	30
44317	New Theoretical Insights into the Crystal-Field Splitting and Transition Mechanism for Nd³⁺-Doped Y₃Al₅O₁₂. ACS Applied Materials & Interfaces, 2019, 11, 10745-10750.	4.0	22
44318	Ultrafast Monolayer In/Gr-WS₂-Gr Hybrid Photodetectors with High Gain. ACS Nano, 2019, 13, 3269-3279.	7.3	44
44319	Self- regeneration of Au/CeO2 based catalysts with enhanced activity and ultra-stability for acetylene hydrochlorination. Nature Communications, 2019, 10, 914.	5.8	86
44320	Site stability and pipe diffusion of hydrogen under localised shear in aluminium. Philosophical Magazine, 2019, 99, 1184-1205.	0.7	4
44321	2D selenium allotropes from first principles and swarm intelligence. Journal of Physics Condensed Matter, 2019, 31, 235702.	0.7	21
44322	Ab initiothermodynamics study of ambient gases reacting with amorphous carbon. Physical Review B, 2019, 99, .	1.1	3
44323	Ferroelectricity of stress-free and strained pure SrTiO3 revealed by ab initio calculations with hybrid and density functionals. Physical Review B, 2019, 99, .	1.1	8
44324	Fe/GeTe(111) heterostructures as an avenue towards spintronics based on ferroelectric Rashba semiconductors. Physical Review B, 2019, 99, .	1.1	14
44325	Advances in Density-Functional Calculations for Materials Modeling. Annual Review of Materials Research, 2019, 49, 1-30.	4.3	87
44326	First-Principles Study of Thermo-Physical Properties of Pu-Containing Gd2Zr2O7. Nanomaterials, 2019, 9, 196.	1.9	5
44327	Simultaneously Dual Modification of Niâ€Rich Layered Oxide Cathode for Highâ€Energy Lithiumâ€Ion Batteries. Advanced Functional Materials, 2019, 29, 1808825.	7.8	430
44328	Selfâ€Suppression of Lithium Dendrite in Allâ€Solidâ€State Lithium Metal Batteries with Poly(vinylidene) Tj ETQq0 0 0 rgBT /Overlock 10	11.1	293
44329	The Key Role of Nanocasting in Goldâ€based Fe₂O₃ Nanocasted Catalysts for Oxygen Activation at the Metalâ€support Interface. ChemCatChem, 2019, 11, 1915-1927.	1.8	13

#	Article	IF	Citations
44330	Modulating the electronic and magnetic properties of the marcasite FeS2 via transition metal atoms doping. Journal of Materials Science: Materials in Electronics, 2019, 30, 5891-5901.	1.1	3
44331	Exploring the Origin of Contact Destruction in Tetradymite-Like-Based Thermoelectric Elements. Journal of Electronic Materials, 2019, 48, 1932-1938.	1.0	5
44332	Crystallographic orientation dependent maximum layer thickness of cubic AlN in CrN/AlN multilayers. Acta Materialia, 2019, 168, 190-202.	3.8	31
44333	Energy transfer and tunable luminescence properties in Y3Al2Ga3O12: Tb3+, Eu3+ phosphors. Journal of Alloys and Compounds, 2019, 787, 672-682.	2.8	50
44334	First-principles study of square phase MX2 and Janus MXY (M=Mo, W; X, Y=S, Se, Te) transition metal dichalcogenide monolayers under biaxial strain. Physica E: Low-Dimensional Systems and Nanostructures, 2019, 110, 134-139.	1.3	50
44335	High-Coverage CO Adsorption and Dissociation on Ir(111), Ir(100), and Ir(110) from Computations. Journal of Physical Chemistry C, 2019, 123, 6487-6495.	1.5	12
44336	Enhancing hydrogen evolution on the basal plane of transition metal dichacolgenide van der Waals heterostructures. Npj Computational Materials, 2019, 5, .	3.5	39
44337	Observation of Restored Topological Surface States in Magnetically Doped Topological Insulator. Scientific Reports, 2019, 9, 1331.	1.6	17
44338	Oxygen conduction mechanism in Ca3Fe2Ge3O12 garnet-type oxide. Scientific Reports, 2019, 9, 2593.	1.6	8
44339	A first-principles study of doped black phosphorus carbide monolayers as NO2 and NH3 sensors. Journal of Applied Physics, 2019, 125, .	1.1	17
44340	Materials Informatics for Heat Transfer: Recent Progresses and Perspectives. Nanoscale and Microscale Thermophysical Engineering, 2019, 23, 157-172.	1.4	41
44341	Candidate Inorganic Photovoltaic Materials from Electronic Structure-Based Optical Absorption and Charge Transport Proxies. Chemistry of Materials, 2019, 31, 1561-1574.	3.2	40
44342	Highly Correlated Hydride Ion Tracer Diffusion in SrTiO_{3â€“x}H_x Oxyhydrides. Journal of the American Chemical Society, 2019, 141, 4653-4659.	6.6	20
44343	Electron engineering of metallic multiferroic polarons in epitaxial BaTiO3. Npj Computational Materials, 2019, 5, .	3.5	14
44344	Strong selective oxidization on two-dimensional GaN: a first principles study. Physical Chemistry Chemical Physics, 2019, 21, 6224-6228.	1.3	15
44345	Syngas production from electrocatalytic CO₂ reduction with high energetic efficiency and current density. Journal of Materials Chemistry A, 2019, 7, 7675-7682.	5.2	62
44346	Colossal electric field control of magnetic anisotropy at ferromagnetic interfaces induced by iridium overlayer. Physical Review B, 2019, 99, .	1.1	24
44347	Brightly Luminescent Core/Shell Nanoplatelets with Continuously Tunable Optical Properties. Advanced Optical Materials, 2019, 7, 1801478.	3.6	33

#	Article	IF	Citations
44348	Interplay Between Site Activity and Density of BCC Iron for Ammonia Synthesis Based on Firstâ€Principles Theory. ChemCatChem, 2019, 11, 1928-1934.	1.8	20
44349	From Eâ€Waste to Nbâ€Pb Coâ€Doped and Pdâ€Loaded TiO₂/BaTiO₃ Heterostructure: Highly Efficient Photocatalytic Performance. ChemSusChem, 2019, 12, 2819-2828.	3.6	13
44350	Force Matching Approaches to Extend Density Functional Theory to Large Time and Length Scales. Challenges and Advances in Computational Chemistry and Physics, 2019, , 71-93.	0.6	5
44351	Influence of the valence state change of iron oxidation for pyrolysis by using density functional theory. Applied Surface Science, 2019, 478, 313-318.	3.1	5
44352	Effect of carbon on elastic properties and microstructure of maraging steel: First-principles and phase-field study. Computational Materials Science, 2019, 162, 1-11.	1.4	5
44353	Tuning carburization behaviors of metallic iron catalysts with potassium promoter and CO/syngas/C2H4/C2H2 gases. Journal of Catalysis, 2019, 371, 333-345.	3.1	30
44354	Synthesis, crystallographic structure and thermodynamic properties of T2-Al2MgC2. Journal of Solid State Chemistry, 2019, 273, 150-157.	1.4	8
44355	Adsorption of Cun (n = 1â€'4) clusters on CuAl2O4 spinel surface: A DFT study. Molecular Catalysis, 2019, 468, 29-35.	1.0	20
44356	A family of high-temperature ferromagnetic monolayers with locked spin-dichroism-mobility anisotropy: MnNX and CrCX (Xâ€¯=â€¯Cl, Br, I; Câ€¯=â€¯S, Se, Te). Science Bulletin, 2019, 64, 293-300.	4.3	96
44357	VASP hits the memory wall: Processors efficiency comparison. Concurrency Computation Practice and Experience, 2019, 31, e5136.	1.4	17
44358	Vanadium carbide coating as hydrogen permeation barrier: A DFT study. International Journal of Hydrogen Energy, 2019, 44, 6093-6102.	3.8	27
44359	N-Methylation of amines and nitroarenes with methanol using heterogeneous platinum catalysts. Journal of Catalysis, 2019, 371, 47-56.	3.1	48
44360	Silanization of superficially porous silica particles with p-aminophenyltrimethoxysilane. Microchemical Journal, 2019, 147, 263-268.	2.3	8
44361	Shining a light on amorphous U2O7: A computational approach to understanding amorphous uranium materials. Optical Materials, 2019, 89, 295-298.	1.7	8
44362	Active Role of Methanol in Post-Synthetic Linker Exchange in the Metalâ€“Organic Framework UiO-66. Chemistry of Materials, 2019, 31, 1359-1369.	3.2	43
44363	Dense Post-Barite-type Polymorph of PbSO₄ Anglesite at High Pressures. Inorganic Chemistry, 2019, 58, 2708-2716.	1.9	6
44364	Mechanism of Nitric Oxide Reduction by Hydrogen on Ni(110) and Ir/Ni(110): First Principles and Microkinetic Modeling. Journal of Physical Chemistry C, 2019, 123, 4825-4836.	1.5	12
44365	Magnetic Polymer Chains of Transition Metal Atoms and Zwitterionic Quinone. Journal of Physical Chemistry C, 2019, 123, 4582-4589.	1.5	13

#	Article	IF	Citations
44366	Tunable Topological State, High Hole-Carrier Mobility, and Prominent Sunlight Absorbance in Monolayered Calcium Triarsenide. Journal of Physical Chemistry Letters, 2019, 10, 761-767.	2.1	15
44367	Coordination-Controlled Câ€“C Coupling Products via ortho-Site Câ€“H Activation. ACS Nano, 2019, 13, 1385-1393.	7.3	25
44368	Hidden structural and chemical order controls lithium transport in cation-disordered oxides for rechargeable batteries. Nature Communications, 2019, 10, 592.	5.8	162
44369	Unusual oxidation-induced core-level shifts at the HfO2/InP interface. Scientific Reports, 2019, 9, 1462.	1.6	9
44370	Theoretical prediction of HfB₂ monolayer, a two-dimensional Dirac cone material with remarkable Fermi velocity. RSC Advances, 2019, 9, 2740-2745.	1.7	16
44371	N-, B-, P-, Al-, As-, and Ga-graphdiyne/graphyne lattices: first-principles investigation of mechanical, optical and electronic properties. Journal of Materials Chemistry C, 2019, 7, 3025-3036.	2.7	41
44372	Prediction of intrinsic two-dimensional non-Dirac topological insulators in triangular metal-organic frameworks. Applied Physics Letters, 2019, 114, .	1.5	12
44373	Electronic and optical properties of defective MoSe2 repaired by halogen atoms from first-principles study. AIP Advances, 2019, 9, .	0.6	13
44374	Influence of mass and charge disorder on the phonon thermal conductivity of entropy stabilized oxides determined by molecular dynamics simulations. Journal of Applied Physics, 2019, 125, .	1.1	48
44375	Hyperspatial optimization of structures. Physical Review B, 2019, 99, .	1.1	15
44376	Significant reduction in the thermal conductivity of Si-substituted <mml:math xmlns:mml="http://www.w3.org/1998/Math/MathML"><mml:mrow><mml:msub><mml:mi>Fe</mml:mi><mml:mn>2</mml:mn></mml:msub></mml:mrow></mml:math> epilayers. Physical Review B, 2019, 99, .	1.1	11
44377	Effect of anharmonicity on the hcp to bcc transition in beryllium at high-pressure and high-temperature conditions. Physical Review B, 2019, 99, .	1.1	14
44378	First-Principles Investigation on Type-II Aluminum-Substituted Ternary and Quaternary Clathrate Semiconductors R8Al8Si128 (R = Cs, Rb), Cs8Na16Al24Si112. Applied Sciences (Switzerland), 2019, 9, 125.	1.3	1
44379	Advantageous Interfacial Effects of AgPd/gâ€₃N₄ for Photocatalytic Hydrogen Evolution: Electronic Structure and H₂O Dissociation. Chemistry - A European Journal, 2019, 25, 5058-5064.	1.7	22
44380	The band alignments modulation of gâ€“MoTe2/WTe2 van der Waals heterostructures. Applied Physics A: Materials Science and Processing, 2019, 125, 1.	1.1	5
44381	Intrinsic magnetic properties of SmFe12â^'V alloys with reduced V-concentration. Journal of Alloys and Compounds, 2019, 786, 969-974.	2.8	45
44382	Nonhexagonal Na Sublattice Reconstruction in the Super-Ionic Conductor Na2Zn2TeO6: Insights from Ab Initio Molecular Dynamics. Journal of Physical Chemistry C, 2019, 123, 4654-4663.	1.5	9
44383	Strategy for Fabricating Wafer-Scale Platinum Disulfide. ACS Applied Materials & Interfaces, 2019, 11, 8202-8209.	4.0	37

#	Article	IF	Citations
44384	Disorder in Mn+1AXn phases at the atomic scale. Nature Communications, 2019, 10, 622.	5.8	41
44385	Cyclability evaluation on Si based Negative Electrode in Lithium ion Battery by Graphite Phase Evolution: an operando X-ray diffraction study. Scientific Reports, 2019, 9, 1299.	1.6	5
44386	Water mediated oxygen activation in NH₃ SCR reaction over a Cu-SAPO-34 catalyst: a first principles study. Catalysis Science and Technology, 2019, 9, 1309-1316.	2.1	10
44387	Boosting photochemical activity by Ni doping of mesoporous CoO nanoparticle assemblies. Inorganic Chemistry Frontiers, 2019, 6, 765-774.	3.0	10
44388	Computational design of CO-tolerant Pt₃M anode electrocatalysts for proton-exchange membrane fuel cells. Physical Chemistry Chemical Physics, 2019, 21, 4046-4052.	1.3	14
44389	Tetragonal and trigonal Mo₂B₂ monolayers: two new low-dimensional materials for Li-ion and Na-ion batteries. Physical Chemistry Chemical Physics, 2019, 21, 5178-5188.	1.3	72
44390	First-principles study of intrinsic point defects in MgSiAs2. Physical Chemistry Chemical Physics, 2019, 21, 5295-5304.	1.3	2
44391	A first-principles theoretical study on the potential thermoelectric properties of MgH2 and CaH2. Materials Research Express, 2019, 6, 055510.	0.8	1
44392	Charge disproportionate antiferromagnetism at the verge of the insulator-metal transition in doped <mml:math xmlns:mml="http://www.w3.org/1998/Math/MathML"><mml:msub><mml:mi>LaFeO</mml:mi><mml:mn>3</mml:mn></mml:msub></m Physical Review B, 2019, 99, .	1.1	12
44393	Is Cobalt Needed in Ni-Rich Positive Electrode Materials for Lithium Ion Batteries?. Journal of the Electrochemical Society, 2019, 166, A429-A439.	1.3	259
44394	The Quasiâ€Ptâ€Allotrope Catalyst: Hollow PtCo@singleâ€Atom Pt₁ on Nitrogenâ€Doped Carbon toward Superior Oxygen Reduction. Advanced Functional Materials, 2019, 29, 1807340.	7.8	97
44395	sp3 bonded 2-dimensional allotrope of carbon: A first-principles prediction. Carbon, 2019, 146, 430-437.	5.4	24
44396	Pseudogap Control of Physical and Chemical Properties in CeFeSi-Type Intermetallics. Inorganic Chemistry, 2019, 58, 2848-2855.	1.9	4
44397	Theoretical Study of NO Dissociation on an Open Flat Ru(101Ì…1) Surface. Journal of Physical Chemistry C, 2019, 123, 5488-5494.	1.5	0
44398	Mechanism of Water Splitting on Gadolinium-Doped CeO₂(111): A DFT + U Study. Journal of Physical Chemistry C, 2019, 123, 5507-5517.	1.5	31
44399	Lanthanide Ions as Local Probes in Ionic Hydrides: A Pulsed Electron Nuclear Double Resonance and Thermoluminescence Study of Eu²⁺-Doped Hydride Perovskites. Journal of Physical Chemistry C, 2019, 123, 5031-5041.	1.5	6
44400	First-Principles Study of the Adsorption Behavior of Triptycene Molecular Tripods on Au(111): Site Selectivity and Unambiguous Molecular Orientation. Journal of Physical Chemistry C, 2019, 123, 4401-4406.	1.5	12
44401	Affordable Estimation of Solvation Contributions to the Adsorption Energies of Oxygenates on Metal Nanoparticles. Journal of Physical Chemistry C, 2019, 123, 5578-5582.	1.5	54

#	Article	IF	Citations
44402	Trifluoroacetate induced small-grained CsPbBr3 perovskite films result in efficient and stable light-emitting devices. Nature Communications, 2019, 10, 665.	5.8	350
44403	Selective electroreduction of carbon dioxide to methanol on copper selenide nanocatalysts. Nature Communications, 2019, 10, 677.	5.8	258
44404	Two-dimensional semiconducting and single-crystalline antimony trioxide directly-grown on monolayer graphene. Chemical Communications, 2019, 55, 2473-2476.	2.2	8
44405	Robust Twin Pairs of Weyl Fermions in Ferromagnetic Oxides. Physical Review Letters, 2019, 122, 057205.	2.9	14
44406	Revisiting Bond Breaking and Making in EuCo 2 P 2 : Where are the Electrons?. Chemistry - A European Journal, 2019, 25, 5865-5869.	1.7	5
44407	How oxides affect the stretching modes of carbon monoxide adsorbed on Ni catalyst?. Applied Surface Science, 2019, 478, 1074-1080.	3.1	5
44408	New compounds Mg3IV6V8 (IV=Si, Ge, Sn; V=P, As, Sb) and their potential application to photovoltaic materials. Journal of Alloys and Compounds, 2019, 786, 434-439.	2.8	1
44409	Interaction between Bi Dopants and Intrinsic Defects in LiNbO3 from Local and Hybrid Density Functional Theory Calculations. Inorganic Chemistry, 2019, 58, 3661-3669.	1.9	8
44410	Strain Effects on Oxygen Reduction Activity of Pr₂NiO₄ Caused by Gold Bulk Dispersion for Low Temperature Solid Oxide Fuel Cells. ACS Applied Energy Materials, 2019, 2, 1210-1220.	2.5	22
44411	Sub-stoichiometry-facilitated oxidation kinetics in a Î´-TixC-doped Ti-based alloy. Npj Materials Degradation, 2019, 3, .	2.6	4
44412	Robust quantum anomalous Hall effect with electrically tunable band gap in Ta-decorated silicene. Applied Physics Letters, 2019, 114, .	1.5	5
44413	Ambient Electrosynthesis of Ammonia on a Coreâ€“Shellâ€Structured Au@CeO₂ Catalyst: Contribution of Oxygen Vacancies in CeO₂. Chemistry - A European Journal, 2019, 25, 5904-5911.	1.7	69
44414	Semimetallic Si3C as a high capacity anode material for advanced lithium ion batteries. Applied Surface Science, 2019, 479, 519-524.	3.1	33
44415	Effect of non-Schmid stresses on ã€ˆaã€‰-type screw dislocation core structure and mobility in titanium. Computational Materials Science, 2019, 161, 261-264.	1.4	10
44416	Structural patterns in carbon chemisorption on ultrasmall iron clusters: A first-principles study. Computational and Theoretical Chemistry, 2019, 1150, 49-56.	1.1	0
44417	Mesoporous Cu2-xSe nanocrystals as an ultrahigh-rate and long-lifespan anode material for sodium-ion batteries. Energy Storage Materials, 2019, 22, 275-283.	9.5	88
44418	Mechanochemical reactions and hydrogen storage capacities in MBH4â€“SiS2 systems (M Li or Na). International Journal of Hydrogen Energy, 2019, 44, 7381-7391.	3.8	13
44419	Ab initio study of H, B, C, N, O, and self-interstitial atoms in hcp-Zr. Journal of Alloys and Compounds, 2019, 787, 631-637.	2.8	11

#	Article	IF	Citations
44420	A stable Ta3N5@PANI core-shell photocatalyst: Shell thickness effect, high-efficient photocatalytic performance and enhanced mechanism. Journal of Catalysis, 2019, 371, 175-184.	3.1	47
44421	Restructuring of MFI Framework Zeolite Models and Their Associated Artifacts in Density Functional Theory Calculations. Journal of Physical Chemistry C, 2019, 123, 6572-6585.	1.5	21
44422	Stabilizing High Metal Loadings of Thermally Stable Platinum Single Atoms on an Industrial Catalyst Support. ACS Catalysis, 2019, 9, 3978-3990.	5.5	233
44423	Multi Band Gap Electronic Structure in CH3NH3PbI3. Scientific Reports, 2019, 9, 2144.	1.6	26
44424	Stoichiometric evolutions of PH3 under high pressure: implication for high-Tc superconducting hydrides. National Science Review, 2019, 6, 524-531.	4.6	28
44425	Molecular Topology and the Surface Chemical Bond: Alternant Versus Nonalternant Aromatic Systems as Functional Structural Elements. Physical Review X, 2019, 9, .	2.8	14
44426	First-Principles Calculations of Angular and Strain Dependence on Effective Masses of Two-Dimensional Phosphorene Analogues (Monolayer Î±-Phase Group-IV Monochalcogenides MX). Molecules, 2019, 24, 639.	1.7	13
44427	Artificial Neural Network Model for Atomistic Simulations of $${m {Sb/MoS}_{2}}$$ Sb / MoS 2 van der Waals Heterostructures. Multiscale Science and Engineering, 2019, 1, 119-129.	0.9	9
44428	Design of pentagonal NbX monolayers for electronics and electrocatalysis. Applied Surface Science, 2019, 479, 595-600.	3.1	14
44429	Temperature dependent magnetic properties of Dy-doped Fe16N2: Potential rare-earth-lean permanent magnet. Intermetallics, 2019, 108, 25-31.	1.8	4
44430	Phase and structure modulating of bimetallic CuSn nanowires boosts electrocatalytic conversion of CO2. Nano Energy, 2019, 59, 138-145.	8.2	81
44431	Double-shell Li-rich layered oxide hollow microspheres with sandwich-like carbon@spinel@layered@spinel@carbon shells as high-rate lithium ion battery cathode. Nano Energy, 2019, 59, 184-196.	8.2	194
44432	Hydrogenation of o-Cresol at the Water/Pt(111) Interface. Journal of Physical Chemistry C, 2019, 123, 5378-5384.	1.5	5
44433	Operando DRIFTS and DFT Study of Propane Dehydrogenation over Solid- and Liquid-Supported Ga_xPt_y Catalysts. ACS Catalysis, 2019, 9, 2842-2853.	5.5	83
44434	Magneto-Seebeck effect in Co₂FeAl/MgO/Co₂FeAl: first-principles calculations. Physical Chemistry Chemical Physics, 2019, 21, 5803-5812.	1.3	12
44435	Direct imaging of dopant sites in rare-earth element-doped permanent magnet and correlated magnetism origin. Nanoscale, 2019, 11, 4385-4393.	2.8	11
44436	Tailoring the geometric and electronic structure of tungsten oxide with manganese or vanadium doping toward highly efficient electrochemical and photoelectrochemical water splitting. Journal of Materials Chemistry A, 2019, 7, 6161-6172.	5.2	61
44437	Modeling solution hardening in BCC refractory complex concentrated alloys: NbTiZr, Nb1.5TiZr0.5 and Nb0.5TiZr1.5. Acta Materialia, 2019, 168, 222-236.	3.8	103

#	Article	IF	Citations
44438	Effects of finite temperature on the surface energy in Al alloys from first-principles calculations. Applied Surface Science, 2019, 479, 499-505.	3.1	22
44439	Confined electrochemical catalysis under cover: Enhanced CO2 reduction at the interface between graphdiyne and Cu surface. Applied Surface Science, 2019, 479, 685-692.	3.1	16
44440	Layer dependent electrical transport in exfoliated graphene FETs under UV illumination. Applied Surface Science, 2019, 479, 863-873.	3.1	2
44441	Convergence and machine learning predictions of Monkhorst-Pack k-points and plane-wave cut-off in high-throughput DFT calculations. Computational Materials Science, 2019, 161, 300-308.	1.4	68
44442	Photoelectric properties of InxGa1-xAs: A first-principles study. Superlattices and Microstructures, 2019, 128, 312-318.	1.4	4
44443	Insight into the diffusion mechanism of Cu cluster over Cu(111) surface: Effect of syngas and H2S atmosphere on Cu diffusion. Chemical Physics, 2019, 522, 24-31.	0.9	1
44444	On the possibility of severe corrosion of a Ni-W-Cr alloy in fluoride molten salts at high temperature. Corrosion Science, 2019, 149, 218-225.	3.0	42
44445	Synergy effects between Sn and SiO2 on enhancing the anti-poison ability to CO for ethanol electrooxidation. Electrochimica Acta, 2019, 302, 145-152.	2.6	11
44446	Heterofullerene-linked metalâ€“organic framework with lithium decoration for storing hydrogen and methane gases. International Journal of Hydrogen Energy, 2019, 44, 6702-6708.	3.8	10
44447	Modulation of ferromagnetism and transport in BxCyNz thin films via nitrogen doping and defects. Journal of Magnetism and Magnetic Materials, 2019, 479, 67-73.	1.0	3
44448	Effect of structural defects and S-doped on electronic structure and magnetic properties of HfSe2 monolayer. Journal of Magnetism and Magnetic Materials, 2019, 479, 192-198.	1.0	11
44449	T4,4,4-graphyne: A 2D carbon allotrope with an intrinsic direct bandgap. Solid State Communications, 2019, 293, 23-27.	0.9	15
44450	Thermodynamic and Mechanical Stability of Crystalline Phases of Li2S2. Journal of Physical Chemistry C, 2019, 123, 4674-4681.	1.5	16
44451	Two-Dimensional CH₃NH₃PbI₃ with High Efficiency and Superior Carrier Mobility: A Theoretical Study. Journal of Physical Chemistry C, 2019, 123, 5231-5239.	1.5	41
44452	Machine Learning-Aided Design of Materials with Target Elastic Properties. Journal of Physical Chemistry C, 2019, 123, 5042-5047.	1.5	22
44453	Toward Understanding the Kinetics of CO₂ Capture on Sodium Carbonate. ACS Applied Materials & Interfaces, 2019, 11, 9033-9041.	4.0	21
44454	A high-entropy B₄(HfMo₂TaTi)C and SiC ceramic composite. Dalton Transactions, 2019, 48, 5161-5167.	1.6	47
44455	Novel superconducting structures of BH₂ under high pressure. Physical Chemistry Chemical Physics, 2019, 21, 5466-5473.	1.3	16

#	Article	IF	Citations
44456	Finding a junction partner for candidate solar cell absorbers enargite and bournonite from electronic band and lattice matching. Journal of Applied Physics, 2019, 125, .	1.1	19
44457	Intrinsic origin of enhanced piezoelectricity in alkali niobateâ€based leadâ€free ceramics. Journal of the American Ceramic Society, 2019, 102, 5262-5270.	1.9	18
44458	Synthesis and characterization of the ternary metal diboride solidâ€solution nanopowders. Journal of the American Ceramic Society, 2019, 102, 4956-4962.	1.9	24
44459	Configurational Entropy in Multicomponent Alloys: Matrix Formulation from Ab Initio Based Hamiltonian and Application to the FCC Cr-Fe-Mn-Ni System. Entropy, 2019, 21, 68.	1.1	24
44460	Manipulation of Bi³⁺/In³⁺ Transmutation and Mn²⁺â€Doping Effect on the Structure and Optical Properties of Double Perovskite Cs₂NaBi_{1â€“}_xIn_xCl₆. Advanced Optical Materials, 2019, 7, 1801435.	3.6	157
44461	Electric Field Induced Room Temperature Null to High Spin State Switching: A Computational Prediction. Advanced Theory and Simulations, 2019, 2, 1900005.	1.3	3
44462	A Hydride Route to Ternary Alkali Metal Borides: A Case Study of Lithium Nickel Borides. Chemistry - A European Journal, 2019, 25, 4123-4135.	1.7	22
44463	Big to Small: Ultrafine Mo₂C Particles Derived from Giant Polyoxomolybdate Clusters for Hydrogen Evolution Reaction. Small, 2019, 15, e1900358.	5.2	53
44464	Multiâ€electron Reduction Capacity and Multiple Binding Pockets in Metalâ€“Organic Redox Assembly at Surfaces. Chemistry - A European Journal, 2019, 25, 5565-5573.	1.7	7
44465	Revealing the factors influencing grain boundary segregation of P, As in Si: Insights from first-principles. Acta Materialia, 2019, 168, 52-62.	3.8	26
44466	Enhanced Lewis acid-base adducts in doped stanene: Sensing and photocatalysis. Applied Surface Science, 2019, 478, 946-958.	3.1	10
44467	Phase stabilities and vibrational analysis of hydrogenated diamondized bilayer graphenes: A first principles investigation. Carbon, 2019, 146, 468-475.	5.4	43
44468	First principles study of C diffusion in WC/W interfaces observed in WC/Co tools after Ti-alloy machining. Computational Materials Science, 2019, 161, 236-243.	1.4	5
44469	Interstitial atom ordering in fcc-based Ni4X with Xâ€¯=â€¯N and C. Computational Materials Science, 2019, 161, 209-214.	1.4	5
44470	High Rate Li-Ion Batteries with Cation-Disordered Cathodes. Joule, 2019, 3, 1064-1079.	11.7	12
44471	Defining the composition and electronic structure of large-scale and single-crystalline like Cs2AgBiBr6 films fabricated by capillary-assisted dip-coating method. Materials Today Energy, 2019, 12, 186-197.	2.5	27
44472	Vibrational and thermodynamic properties of pure and gold adsorbed graphene. Vacuum, 2019, 166, 405-412.	1.6	9
44473	Tunable electronic and optical properties of arsenene/MoTe2 van der Waals heterostructures. Vacuum, 2019, 163, 128-134.	1.6	13

#	Article	IF	Citations
44474	Rhodium and Nitrogen Codoped Graphene as a Bifunctional Electrocatalyst for the Oxygen Reduction Reaction and CO₂ Reduction Reaction: Mechanism Insights. Journal of Physical Chemistry C, 2019, 123, 5176-5187.	1.5	44
44475	Ideal Nodal Line Semimetal in a Two-Dimensional Boron Bilayer. Journal of Physical Chemistry C, 2019, 123, 4977-4983.	1.5	35
44476	Polarized Tip-Enhanced Raman Spectroscopy in Understanding Metal-to-Insulator and Structural Phase Transition in VO₂. Journal of Physical Chemistry C, 2019, 123, 11189-11196.	1.5	14
44477	Enhanced Performances of PbS Quantum-Dots-Modified MoS₂ Composite for NO₂ Detection at Room Temperature. ACS Applied Materials & Interfaces, 2019, 11, 9438-9447.	4.0	102
44478	Wet Chemical Method for Black Phosphorus Thinning and Passivation. ACS Applied Materials & Interfaces, 2019, 11, 9213-9222.	4.0	23
44479	Catalytic Chemistry Predicted by a Charge Polarization Descriptor: Synergistic O₂ Activation and CO Oxidation by Auâ€“Cu Bimetallic Clusters on TiO₂(101). ACS Applied Materials & Interfaces, 2019, 11, 9629-9640.	4.0	28
44480	Plasmonic Au Nanoparticles on 2D MoS₂/Graphene van der Waals Heterostructures for High-Sensitivity Surface-Enhanced Raman Spectroscopy. ACS Applied Nano Materials, 2019, 2, 1412-1420.	2.4	53
44481	Morphology and Reactivity Evolution of HCP and FCC Ru Nanoparticles under CO Atmosphere. ACS Catalysis, 2019, 9, 2768-2776.	5.5	36
44482	Properties of Hydrous Aluminosilicate Melts at High Pressures. ACS Earth and Space Chemistry, 2019, 3, 390-402.	1.2	18
44483	Water Adsorption on MO₂ (M = Ti, Ru, and Ir) Surfaces. Importance of Octahedral Distortion and Cooperative Effects. ACS Omega, 2019, 4, 2989-2999.	1.6	28
44484	Non-equilibrium crystallization pathways of manganese oxides in aqueous solution. Nature Communications, 2019, 10, 573.	5.8	66
44485	Exceptionally active iridium evolved from a pseudo-cubic perovskite for oxygen evolution in acid. Nature Communications, 2019, 10, 572.	5.8	254
44486	Cation-swapped homogeneous nanoparticles in perovskite oxides for highÂpower density. Nature Communications, 2019, 10, 697.	5.8	119
44487	eg occupancy as an effective descriptor for the catalytic activity of perovskite oxide-based peroxidase mimics. Nature Communications, 2019, 10, 704.	5.8	199
44488	First-principles-based prediction of yield strength in the RhIrPdPtNiCu high-entropy alloy. Npj Computational Materials, 2019, 5, .	3.5	86
44489	Large piezoelectric response in a family of metal-free perovskite ferroelectric compounds from first-principles calculations. Npj Computational Materials, 2019, 5, .	3.5	45
44490	Equilibrium crystal shape of GaAs and InAs considering surface vibration and new (111)B reconstruction: ab-initio thermodynamics. Scientific Reports, 2019, 9, 1127.	1.6	16
44491	Efficient electrocatalytic conversion of carbon monoxide to propanol using fragmented copper. Nature Catalysis, 2019, 2, 251-258.	16.1	188

#	Article	IF	Citations
44492	The regulation of reaction processes and rate-limiting steps for efficient photocatalytic CO₂ reduction into methane over the tailored facets of TiO₂. Catalysis Science and Technology, 2019, 9, 1451-1456.	2.1	7
44493	Tetragonal C₂₄: a topological nodal-surface semimetal with potential as an anode material for sodium ion batteries. Journal of Materials Chemistry A, 2019, 7, 5733-5739.	5.2	72
44494	Unraveling the role of structural water in bilayer V₂O₅ during Zn²⁺-intercalation: insights from DFT calculations. Journal of Materials Chemistry A, 2019, 7, 5612-5620.	5.2	132
44495	Band gap and band alignment prediction of nitride-based semiconductors using machine learning. Journal of Materials Chemistry C, 2019, 7, 3238-3245.	2.7	48
44496	Intrinsic stability enhancement and ionic migration reduction by fluorinated cations incorporated in hybrid lead halide perovskites. Journal of Materials Chemistry C, 2019, 7, 5299-5306.	2.7	17
44497	Insights into the local structure of dopants, doping efficiency, and luminescence properties of lanthanide-doped CsPbCl₃ perovskite nanocrystals. Journal of Materials Chemistry C, 2019, 7, 3037-3048.	2.7	79
44498	Facile synthesis, characterization and DFT studies of a nanostructured nickelâ€“molybdenumâ€“phosphorous planar electrode as an active electrocatalyst for the hydrogen evolution reaction. Nanoscale, 2019, 11, 9353-9361.	2.8	42
44499	Carbon-encapsulated ultrathin MoS₂ nanosheets epitaxially grown on porous metallic TiNb₂O₆ microspheres with unsaturated oxygen atoms for superior potassium storage. Journal of Materials Chemistry A, 2019, 7, 5760-5768.	5.2	54
44500	Tuning the electrocatalytic properties of a Cu electrode with organic additives containing amine group for CO₂ reduction. Journal of Materials Chemistry A, 2019, 7, 5453-5462.	5.2	28
44501	Evolution of phosphorus-vacancy clusters in epitaxial germanium. Journal of Applied Physics, 2019, 125, .	1.1	13
44502	Boron-graphdiyne as an anode material for Li, Na, and K ion batteries with high capacities and low diffusion barriers. Journal of Renewable and Sustainable Energy, 2019, 11, .	0.8	42
44503	Thermal Resistance by Transition Between Collective and Non-Collective Phonon Flows in Graphitic Materials. Nanoscale and Microscale Thermophysical Engineering, 2019, 23, 247-258.	1.4	11
44504	Recovery of the Dirac states of graphene by intercalating two-dimensional traditional semiconductors. Journal of Physics Condensed Matter, 2019, 31, 194001.	0.7	8
44505	Thermodynamics and superconductivity of <mml:math xmlns:mml="http://www.w3.org/1998/Math/MathML"><mml:mrow><mml:msub><mml:mi mathvariant="normal">S</mml:mi><mml:mi>x</mml:mi></mml:msub><mml:msub><mml:mi>Se</mml:mi><mml:mrow><mml:mn>1</mml:mn></mml:mrow></mml:msub><mml:msub><mml:mi mathvariant="normal">H</mml:mi><mml:mn>3</mml:mn></mml:msub></mml:mrow></mml:math>. Physical Review B, 2019, 99, .	1.1	34
44506	Ternary inorganic electrides with mixed bonding. Physical Review B, 2019, 99, .	1.1	26
44507	Engineering Dirac states in graphene: Coexisting type-I and type-II Floquet-Dirac fermions. Physical Review B, 2019, 99, .	1.1	12
44508	Quantitative modeling of secondary electron emission from slow-ion bombardment on semiconductors. Physical Review B, 2019, 99, .	1.1	9
44509	First-Principles Study of the Electronic, Vibrational Properties and Anharmonic Effects of Some Si-Based Type-II Binary Clathrates. Materials, 2019, 12, 536.	1.3	2

#	Article	IF	Citations
44510	Hydrogen Storage, Magnetism and Electrochromism of Silver Doped FAU Zeolite: First-principles Calculations and Molecular Simulations. Polymers, 2019, 11, 279.	2.0	8
44511	Pancakes under Pressure: A Case Study on Isostructural Dithia- and Diselenadiazolyl Radical Dimers. Inorganic Chemistry, 2019, 58, 3550-3557.	1.9	7
44512	CO Self-Promoting Hydrogenation on CO-Saturated Ru(0001): A New Theoretical Insight into How H₂ Participates in CO Activation. Journal of Physical Chemistry C, 2019, 123, 6508-6515.	1.5	9
44513	Bi(Sb)NCa₃: Expansion of Perovskite Photovoltaics into All-Inorganic Anti-Perovskite Materials. Journal of Physical Chemistry C, 2019, 123, 6363-6369.	1.5	10
44514	Theoretical Surface Science Beyond Gradient-Corrected Density Functional Theory: Water at Î±-Al₂O₃(0001) as a Case Study. Journal of Physical Chemistry C, 2019, 123, 6675-6684.	1.5	15
44515	Bridging the Gap between Direct Dynamics and Globally Accurate Reactive Potential Energy Surfaces Using Neural Networks. Journal of Physical Chemistry Letters, 2019, 10, 1185-1191.	2.1	65
44516	Potential Applications of Halide Double Perovskite Cs₂AgInX₆ (X = Cl, Br) in Flexible Optoelectronics: Unusual Effects of Uniaxial Strains. Journal of Physical Chemistry Letters, 2019, 10, 1120-1125.	2.1	44
44517	Isolation of Single-Wired Transition-Metal Monochalcogenides by Carbon Nanotubes. Nano Letters, 2019, 19, 4845-4851.	4.5	61
44518	Effects of Phosphorus Doping and Postgrowth Laser Annealing on the Structural, Electrical, and Chemical Properties of Phosphorus-Doped Silicon Films. ACS Applied Electronic Materials, 2019, 1, 288-301.	2.0	31
44519	Pd Nanocrystals with Continuously Tunable High-Index Facets as a Model Nanocatalyst. ACS Catalysis, 2019, 9, 3144-3152.	5.5	68
44520	Self-Healing Originated van der Waals Homojunctions with Strong Interlayer Coupling for High-Performance Photodiodes. ACS Nano, 2019, 13, 3280-3291.	7.3	69
44521	Surface Recombination in Ultra-Fast Carrier Dynamics of Perovskite Oxide La0.7Sr0.3MnO3 Thin Films. ACS Nano, 2019, 13, 3457-3465.	7.3	15
44522	Modified carbon nitride nanozyme as bifunctional glucose oxidase-peroxidase for metal-free bioinspired cascade photocatalysis. Nature Communications, 2019, 10, 940.	5.8	349
44523	A highly CO-tolerant atomically dispersed Pt catalyst for chemoselective hydrogenation. Nature Nanotechnology, 2019, 14, 354-361.	15.6	292
44524	Evidence for moirÃ© excitons in van der Waals heterostructures. Nature, 2019, 567, 71-75.	13.7	933
44525	Fundamentals of Câ€“O bond activation on metal oxide catalysts. Nature Catalysis, 2019, 2, 269-276.	16.1	82
44526	Oxygen-functionalized TlTe buckled honeycomb from first-principles study. Physical Chemistry Chemical Physics, 2019, 21, 5689-5694.	1.3	2
44527	In situsynthesized low-PtCo@porous carbon catalyst for highly efficient hydrogen evolution. Journal of Materials Chemistry A, 2019, 7, 6543-6551.	5.2	59

#	Article	IF	Citations
44528	Alignment of semiconducting graphene nanoribbons on vicinal Ge(001). Nanoscale, 2019, 11, 4864-4875.	2.8	26
44529	Surface P atom grafting of g-C₃N₄ for improved local spatial charge separation and enhanced photocatalytic H₂ production. Journal of Materials Chemistry A, 2019, 7, 7628-7635.	5.2	50
44530	Substituting copolymeric poly(alkylenetetrasulfide) for elemental sulfur to diminish the shuttling effect of modified intermediate polysulfides for high-performance lithiumâ€“sulfur batteries. Chemical Communications, 2019, 55, 3729-3732.	2.2	12
44531	Size dependence in two-dimensional lateral heterostructures of transition metal dichalcogenides. Journal of Materials Chemistry C, 2019, 7, 3837-3842.	2.7	7
44532	Enhanced interfacial perpendicular magnetic anisotropy in Fe/MgO heterostructure via interfacial engineering. Applied Physics Letters, 2019, 114, 072407.	1.5	23
44533	From DFT to machine learning: recent approaches to materials scienceâ€“a review. JPhys Materials, 2019, 2, 032001.	1.8	385
44534	Anisotropic resistance switching in hexagonal manganites. Physical Review B, 2019, 99, .	1.1	13
44535	One-dimensionally extended oxygen vacancy states in perovskite oxides. Physical Review B, 2019, 99, .	1.1	8
44536	Role of composition, site ordering, and magnetic structure for the structural stability of off-stoichiometric <mml:math xmlns:mml="http://www.w3.org/1998/Math/MathML"><mml:mrow><mml:msub><mml:mi>Ni</mml:mi><mml:mn>2</mml:mn></mml:r alloys with excess Ni and Mn. Physical Review B, 2019, 99, .	1.1	20
44537	Origin of the transition entropy in vanadium dioxide. Physical Review B, 2019, 99, .	1.1	20
44538	Impact of nonparabolic electronic band structure on the optical and transport properties of photovoltaic materials. Physical Review B, 2019, 99, .	1.1	60
44539	Angara interconnect makes GPU-based Desmos supercomputer an efficient tool for molecular dynamics calculations. International Journal of High Performance Computing Applications, 2019, 33, 507-521.	2.4	45
44540	Theoretical Prediction on the Structural, Electronic, Mechanical, and Thermodynamic Properties of TaSi₂ with a C40 Structure Under Pressure. Zeitschrift Fur Naturforschung - Section A Journal of Physical Sciences, 2019, 74, 353-361.	0.7	9
44541	The Basics of Electronic Structure Theory for Periodic Systems. Frontiers in Chemistry, 2019, 7, 106.	1.8	57
44542	Density Functional Theory Study on Defect Behavior Related to the Bulk Lifetime of Silicon Crystals for Power Device Application. Physica Status Solidi (A) Applications and Materials Science, 2019, 216, 1800615.	0.8	6
44543	Ferromagnetism in p-block-element doped ZnO: An ab-initio approach. Computational Condensed Matter, 2019, 19, e00376.	0.9	3
44544	Quantum-mechanical modeling of divalent cation incorporation into uranium dioxide. Journal of Nuclear Materials, 2019, 517, 362-370.	1.3	3
44545	Nitrogen configuration dependent holey active sites toward enhanced K+ storage in graphite foam. Journal of Power Sources, 2019, 419, 82-90.	4.0	36

#	Article	IF	Citations
44546	Local topology and its effects on grain boundary and solute segregation in HCP magnesium. Materialia, 2019, 6, 100258.	1.3	11
44547	Stability of the Eu²⁺ Dopant in CsPbBr₃ Perovskites: A First-Principles Study. Journal of Physical Chemistry C, 2019, 123, 6965-6969.	1.5	39
44548	Roles of N-Vacancies over Porous g-C₃N₄ Microtubes during Photocatalytic NO_x Removal. ACS Applied Materials & Interfaces, 2019, 11, 10651-10662.	4.0	210
44549	Role of Electric Field and Surface Protonics on Low-Temperature Catalytic Dry Reforming of Methane. ACS Sustainable Chemistry and Engineering, 2019, 7, 5690-5697.	3.2	33
44550	Subnanometer cobalt oxide clusters as selective low temperature oxidative dehydrogenation catalysts. Nature Communications, 2019, 10, 954.	5.8	38
44551	Catalogue of topological electronic materials. Nature, 2019, 566, 475-479.	13.7	600
44552	Density functional theory prediction of Mg₃N₂ as a high-performance anode material for Li-ion batteries. Physical Chemistry Chemical Physics, 2019, 21, 7053-7060.	1.3	16
44553	Density functional theory study of the stability of the tetrabutylphosphonium and tetrabutylammonium montmorillonites. Clay Minerals, 2019, 54, 41-48.	0.2	11
44554	Coloring in the ZrBeSi-type structure. Zeitschrift Fur Naturforschung - Section B Journal of Chemical Sciences, 2019, 74, 307-318.	0.3	14
44555	Theoretical Study on Influence of Cobalt Oxides Valence State Change for C6H5COOH Pyrolysis. Catalysts, 2019, 9, 197.	1.6	2
44556	First-Principles Calculation for the Influence of C and O on the Mechanical Properties of Î³-TiAl Alloy at High Temperature. Metals, 2019, 9, 262.	1.0	5
44557	Ultrahigh Electrical Conductivity of Graphene Embedded in Metals. Advanced Functional Materials, 2019, 29, 1806792.	7.8	126
44558	LiFePO₄ Particles Embedded in Fast Bifunctional Conductor rGO&C@Li₃V₂(PO₄)₃ Nanosheets as Cathodes for Highâ€Performance Liâ€Ion Hybrid Capacitors. Advanced Functional Materials, 2019, 29, 1807895.	7.8	42
44559	Polarizationâ€Sensitive Ultraviolet Photodetection of Anisotropic 2D GeS₂. Advanced Functional Materials, 2019, 29, 1900411.	7.8	120
44560	Slow Cooling of Highâ€Energy C Excitons Is Limited by Intervalleyâ€Transfer in Monolayer MoS 2. Laser and Photonics Reviews, 2019, 13, 1800270.	4.4	22
44561	Landauâ€“Devonshire thermodynamic potentials for displacive perovskite ferroelectrics from first principles. Journal of Materials Science, 2019, 54, 8381-8400.	1.7	10
44562	Coverage dependent CO adsorption manners on seven MoP surfaces with DFT based thermodynamics method. Applied Surface Science, 2019, 480, 172-176.	3.1	9
44563	Prediction on morphologies and phase equilibrium diagram of iron oxides nanoparticles. Applied Surface Science, 2019, 480, 478-486.	3.1	16

#	Article	IF	Citations
44564	Investigation of structural, electronic, elastic and phonon properties of cubic spinel ZnM2O4(Mâ€¯=â€¯Co,) Tj ETQq0 0 0 rgBT /Overlock	2.0	3
44565	Determination of second- and third-order elastic constants for energetic materials. Computational Materials Science, 2019, 161, 379-384.	1.4	12
44566	The effect of phase composition and crystallite size on activity and selectivity of ZrO2 in non-oxidative propane dehydrogenation. Journal of Catalysis, 2019, 371, 313-324.	3.1	74
44567	Phase decomposition and bubble evolution in Xe implanted U3Si2 at 450â˚C. Journal of Nuclear Materials, 2019, 518, 108-116.	1.3	11
44568	Synergistically optimized electrical and thermal transport properties of polycrystalline SnSe via alloying SnS. Journal of Solid State Chemistry, 2019, 273, 85-91.	1.4	23
44569	Cu-doped nickel oxide interface layer with nanoscale thickness for efficient and highly stable printable carbon-based perovskite solar cell. Solar Energy, 2019, 182, 225-236.	2.9	58
44570	A first-principles study: Adsorption of small gas molecules on GeP3 monolayer. Surface Science, 2019, 684, 37-43.	0.8	16
44571	Large-Stokes-Shifted Infrared-Emitting InAsâ€“In(Zn)Pâ€“ZnSeâ€“ZnS Giant-Shell Quantum Dots by One-Pot Continuous-Injection Synthesis. Chemistry of Materials, 2019, 31, 2019-2026.	3.2	21
44572	Origin of Ultralow Thermal Conductivity in n-Type Cubic Bulk AgBiS₂: Soft Ag Vibrations and Local Structural Distortion Induced by the Bi 6s² Lone Pair. Chemistry of Materials, 2019, 31, 2106-2113.	3.2	70
44573	Importance of Specific Heat Characterization when Reporting New Superconductors: An Example of Superconductivity in LiGa₂Rh. Chemistry of Materials, 2019, 31, 2164-2173.	3.2	18
44574	Interfacial Engineering Determines Band Alignment and Steers Charge Separation and Recombination at an Inorganic Perovskite Quantum Dot/WS₂ Junction: A Time Domain Ab Initio Study. Journal of Physical Chemistry Letters, 2019, 10, 1234-1241.	2.1	25
44575	Probing Magnetism in Insulating Cr₂Ge₂Te₆ by Induced Anomalous Hall Effect in Pt. Nano Letters, 2019, 19, 2397-2403.	4.5	81
44576	Simultaneous Activation of CH₄ and CO₂ for Concerted Câ€“C Coupling at Oxideâ€“Oxide Interfaces. ACS Catalysis, 2019, 9, 3187-3197.	5.5	56
44577	Carbon sequestration during core formation implied by complex carbon polymerization. Nature Communications, 2019, 10, 789.	5.8	27
44578	Structural dynamics of a metalâ€“organic framework induced by CO2 migration in its non-uniform porous structure. Nature Communications, 2019, 10, 999.	5.8	54
44579	Unique crystal field splitting and multiband RKKY interactions in Ni-doped EuRbFe4As4. Communications Physics, 2019, 2, .	2.0	17
44580	Watching nanostructure growth: kinetically controlled diffusion and condensation of Xe in a surface metal organic network. Nanoscale, 2019, 11, 4895-4903.	2.8	4
44581	Quantum transport properties of single-crystalline Ag₂Se_{0.5}Te_{0.5} nanowires as a new topological material. Nanoscale, 2019, 11, 5171-5179.	2.8	6

#	Article	IF	Citations
44582	Transition from electron accumulation to depletion at Î²-Ga2O3 surfaces: The role of hydrogen and the charge neutrality level. APL Materials, 2019, 7, .	2.2	62
44583	Strain engineering in perovskite solar cells and its impacts on carrier dynamics. Nature Communications, 2019, 10, 815.	5.8	528
44584	Reaction pathways for HCN on transition metal surfaces. Physical Chemistry Chemical Physics, 2019, 21, 5274-5284.	1.3	4
44585	Design of doped cesium lead halide perovskite as a photo-catalytic CO₂ reduction catalyst. Journal of Materials Chemistry A, 2019, 7, 6911-6919.	5.2	68
44586	Immobilisation of sulphur on cathodes of lithiumâ€“sulphur batteries via B-doped atomic-layer carbon materials. Physical Chemistry Chemical Physics, 2019, 21, 10895-10901.	1.3	19
44587	Interface Schottky barrier in Hf₂NT₂/MSSe (T = F, O, OH; M = Mo, W) heterostructures. Physical Chemistry Chemical Physics, 2019, 21, 5394-5401.	1.3	19
44588	Piezoelectric control of resistance switching in VO2/Pb(Zr0.52Ti0.48)O3 heterostructure. Applied Physics Letters, 2019, 114, .	1.5	5
44589	Electronic and phonon structure of nickel hydroxide: first-principles calculation study. European Physical Journal B, 2019, 92, 1.	0.6	2
44590	Investigation of twoâ€dimensional hfâ€based MXenes as the anode materials for li/naâ€ion batteries: A DFT study. Journal of Computational Chemistry, 2019, 40, 1352-1359.	1.5	38
44591	Exceptionally highly stable cycling performance and facile oxygen-redox of manganese-based cathode materials for rechargeable sodium batteries. Nano Energy, 2019, 59, 197-206.	8.2	100
44592	Electric field effects on the electronic structures of MoS2/antimonene van der Waals heterostructure. Solid State Communications, 2019, 293, 28-32.	0.9	8
44593	First-principles study of elastic, thermal and optical properties of a metal-shrouded two-dimensional semiconductor Tl2O. Solid State Communications, 2019, 293, 40-47.	0.9	6
44594	Structure dependent effect of silicon on the oxidation of Al(111) and Al(100). Surface Science, 2019, 684, 1-11.	0.8	2
44595	Quantitative Determination of How Growth Conditions Affect the 3D Composition of InGaAs Nanowires. Microscopy and Microanalysis, 2019, 25, 524-531.	0.2	1
44596	Fe_{0.36(4)}Pd_{0.64(4)}Se₂: Magnetic Spin-Glass Polymorph of FeSe₂ and PdSe₂ Stable at Ambient Pressure. Inorganic Chemistry, 2019, 58, 3107-3114.	1.9	4
44597	In Situ Measure of Intrinsic Bond Strength in Crystalline Structures: Local Vibrational Mode Theory for Periodic Systems. Journal of Chemical Theory and Computation, 2019, 15, 1761-1776.	2.3	32
44598	Development of the ReaxFF Methodology for Electrolyteâ€“Water Systems. Journal of Physical Chemistry A, 2019, 123, 2125-2141.	1.1	48
44599	High performance of PtCu@TiO₂ nanocatalysts toward methanol oxidation reaction: from synthesis to molecular picture insight. RSC Advances, 2019, 9, 2073-2080.	1.7	18

#	Article	IF	Citations
44600	Modulating charge transfer dynamics for g-C₃N₄ through a dimension and interface engineered transition metal phosphide co-catalyst for efficient visible-light photocatalytic hydrogen generation. Journal of Materials Chemistry A, 2019, 7, 6939-6945.	5.2	64
44601	Pressure-induced insulator to metal transition of mixed valence compound Ce(O,F)SbS2. Journal of Applied Physics, 2019, 125, .	1.1	8
44602	Intersublattice magnetocrystalline anisotropy using a realistic tight-binding method based on maximally localized Wannier functions. Physical Review B, 2019, 99, .	1.1	21
44603	Li and Na Interaction with Ti₂C-MXene: A First-Principles Calculation. Journal of Computer Chemistry Japan, 2019, 18, 84-94.	0.0	12
44604	A Novel TiZrHfMoNb High-Entropy Alloy for Solar Thermal Energy Storage. Nanomaterials, 2019, 9, 248.	1.9	66
44605	Interfaceâ€Driven Partial Dislocation Formation in 2D Heterostructures. Advanced Materials, 2019, 31, e1807486.	11.1	11
44606	Edge Segregated Polymorphism in 2D Molybdenum Carbide. Advanced Materials, 2019, 31, e1808343.	11.1	56
44607	Synthesis, crystal structure, absorption properties, photoelectric behavior of organicâ€“inorganic hybrid (CH₃NH₃)₂CoCl₄. Applied Organometallic Chemistry, 2019, 33, e4795.	1.7	15
44608	Oneâ€Step Preparation of Cobaltâ€Nanoparticleâ€Embedded Carbon for Effective Water Oxidation Electrocatalysis. ChemElectroChem, 2019, 6, 1996-1999.	1.7	11
44609	Theoretical studies of photocatalytic behaviors of isoelectronic C/Si/Ge/Sn-doped TiO2: DFTâ€+â€U. Applied Surface Science, 2019, 484, 1304-1309.	3.1	19
44610	A DFT study and microkinetic analysis of CO oxidation to dimethyl oxalate over Pd stripe and Pd single atom-doped Cu(111) surfaces. Applied Surface Science, 2019, 479, 1057-1067.	3.1	10
44611	Thermodynamic properties of tin: Part I Experimental investigation, ab-initio modelling of Î±-, Î²-phase and a thermodynamic description for pure metal in solid and liquid state from 0â€K. Calphad: Computer Coupling of Phase Diagrams and Thermochemistry, 2019, 65, 50-72.	0.7	32
44612	Influence of the Al concentration in Ti-Al-B coatings on microstructure and mechanical properties using combinatorial sputtering from a segmented TiB2/AlB2 target. Surface and Coatings Technology, 2019, 364, 89-98.	2.2	24
44613	GeSe/BP van der Waals Heterostructures as Promising Anode Materials for Potassium-Ion Batteries. Journal of Physical Chemistry C, 2019, 123, 5157-5163.	1.5	70
44614	Mono-Elemental Properties of 2D Black Phosphorus Ensure Extended Charge Carrier Lifetimes under Oxidation: Time-Domain Ab Initio Analysis. Journal of Physical Chemistry Letters, 2019, 10, 1083-1091.	2.1	74
44615	Thickness Tunable Wedding-Cake-like MoS₂ Flakes for High-Performance Optoelectronics. ACS Nano, 2019, 13, 3649-3658.	7.3	75
44616	Fabrication of SnS₂/Mn₂SnS₄/Carbon Heterostructures for Sodium-Ion Batteries with High Initial Coulombic Efficiency and Cycling Stability. ACS Nano, 2019, 13, 3666-3676.	7.3	205
44617	Composition change-driven texturing and doping in solution-processed SnSe thermoelectric thin films. Nature Communications, 2019, 10, 864.	5.8	62

#	Article	IF	Citations
44618	First-principles calculations of mechanical and thermodynamic properties of tetragonal Be₁₂Ti. RSC Advances, 2019, 9, 5302-5312.	1.7	17
44619	Tin(<scp>ii</scp>) thiocyanate Sn(NCS)₂ â€“ a wide band gap coordination polymer semiconductor with a 2D structure. Journal of Materials Chemistry C, 2019, 7, 3452-3462.	2.7	24
44620	Increasing the optical response of TiO₂ and extending it into the visible region through surface activation with highly stable Cu₅ clusters. Journal of Materials Chemistry A, 2019, 7, 7489-7500.	5.2	35
44621	Tetrapyrroles-decorated graphene nanoribbons: Toward to the half-metal and ferromagnetic semiconductor. Applied Physics Letters, 2019, 114, .	1.5	10
44622	Rediscover Î´5 boron sheet: Interaction with Ni substrate and MoS2 monolayer. Journal of Applied Physics, 2019, 125, 075304.	1.1	0
44623	Covalent organic framework with high capacity for the lithium ion battery anode: insight into intercalation of Li from first-principles calculations. Journal of Physics Condensed Matter, 2019, 31, 205502.	0.7	19
44624	Interfacial and electronic properties of heterostructures of MXene and graphene. Physical Review B, 2019, 99, .	1.1	53
44625	Theoretical study on halide and mixed halide Perovskite solar cells: Effects of halide atoms on the stability and electronic properties. Journal of the Chinese Chemical Society, 2019, 66, 575-582.	0.8	10
44626	Structural and Electronic Properties of Cu₂MnSnS₄ from Experiment and Firstâ€Principles Calculations. Physica Status Solidi (B): Basic Research, 2019, 256, 1800743.	0.7	25
44627	A First Principle Study of Graphene/Metal-Oxides as Nano-Composite Electrode Materials for Supercapacitors. Journal of Electronic Materials, 2019, 48, 2343-2349.	1.0	13
44628	The partial reduction of clean and doped Î±-Fe2O3(0001) from first principles. Applied Catalysis A: General, 2019, 582, 116989.	2.2	6
44629	Modified embedded-atom method potential of niobium for studies on mechanical properties. Computational Materials Science, 2019, 161, 351-363.	1.4	20
44630	Structural and magnetic properties of Pr5Si3-xGex compounds. Journal of Alloys and Compounds, 2019, 788, 468-475.	2.8	1
44631	An experimental and theoretical study on the crystal structure and elastic properties of Ta1â^'xOx coatings. Surface and Coatings Technology, 2019, 364, 289-297.	2.2	1
44632	Band-Edge Engineering at the Carbon Dotâ€“TiO₂ Interface by Substitutional Boron Doping. Journal of Physical Chemistry C, 2019, 123, 5980-5988.	1.5	6
44633	First-Principles Molecular Dynamics Simulations of UCl_nâ€“NaCl (n = 3, 4) Molten Salts. ACS Applied Energy Materials, 2019, 2, 2122-2128.	2.5	39
44634	Charge Transfer Dynamics of Phase-Segregated Halide Perovskites: CH₃NH₃PbCl₃ and CH₃NH₃PbI₃ or (C₄H₉NH₃)₂(CH₃NH₃)_{nâ^'1}Pb<s Mixtures. ACS Applied Materials & Interfaces, 2019, 11, 9583-9593.	4.0	14
44635	Few-Layer P₄O₂: A Promising Photocatalyst for Water Splitting. ACS Applied Materials & Interfaces, 2019, 11, 10163-10170.	4.0	31

#	Article	IF	Citations
44636	Water Splitting Reaction at Polar Lithium Niobate Surfaces. ACS Omega, 2019, 4, 3850-3859.	1.6	16
44637	Kondo-like phonon scattering in thermoelectric clathrates. Nature Communications, 2019, 10, 887.	5.8	35
44638	Promoting electrocatalytic CO2 reduction to formate via sulfur-boosting water activation on indium surfaces. Nature Communications, 2019, 10, 892.	5.8	446
44639	Theoretical study of single transition metal atom modified MoP as a nitrogen reduction electrocatalyst. Physical Chemistry Chemical Physics, 2019, 21, 5950-5955.	1.3	43
44640	A new ab initio modeling scheme for the ion self-diffusion coefficient applied to the Îµ-Cu₃Sn phase of the Cuâ€“Sn alloy. Physical Chemistry Chemical Physics, 2019, 21, 5158-5164.	1.3	2
44641	Unusual strain effect of a Pt-based L1₀ face-centered tetragonal core in core/shell nanoparticles for the oxygen reduction reaction. Physical Chemistry Chemical Physics, 2019, 21, 6477-6484.	1.3	22
44642	Nephelauxetic effect of the hydride ligand in Sr₂LiSiO₄H as a host material for rare-earth-activated phosphors. RSC Advances, 2019, 9, 5282-5287.	1.7	15
44643	Ultrahigh thermal conductivity of carbon allotropes with correlations with the scaled Pugh ratio. Journal of Materials Chemistry A, 2019, 7, 6259-6266.	5.2	23
44644	Impact of the stacking sequence on the bandgap and luminescence properties of bulk, bilayer, and monolayer hexagonal boron nitride. APL Materials, 2019, 7, .	2.2	38
44645	First principles predicting enhanced ductility of boride carbide through magnesium microalloying. Journal of the American Ceramic Society, 2019, 102, 5514-5523.	1.9	14
44646	Tunable intrinsic strain in two-dimensional transition metal electrocatalysts. Science, 2019, 363, 870-874.	6.0	384
44647	Scalable and safe synthetic organic electroreduction inspired by Li-ion battery chemistry. Science, 2019, 363, 838-845.	6.0	305
44648	Tunable Electronic Properties of Nitrogen and Sulfur Doped Graphene: Density Functional Theory Approach. Nanomaterials, 2019, 9, 268.	1.9	39
44649	First-principles rational design of M-doped LiBH4(010) surface for hydrogen release: Role of strain and dopants (M=Na, K, Al, F, or Cl). International Journal of Hydrogen Energy, 2019, 44, 6065-6073.	3.8	7
44650	Study of the NaF-ScF3 system as a molten bath for production of Sc alloys: A combination of NMR and molecular dynamics simulations. Journal of Alloys and Compounds, 2019, 786, 953-959.	2.8	8
44651	Modelling high-performing batteries with Mxenes: The case of S-functionalized two-dimensional nitride Mxene electrode. Nano Energy, 2019, 58, 877-885.	8.2	100
44652	Monolayer MoS2 thermoelectric properties engineering via strain effect. Physica E: Low-Dimensional Systems and Nanostructures, 2019, 109, 248-252.	1.3	21
44653	Heterogeneity in Local Chemical Bonding Explains Spectral Broadening in Quantum Dots with Cu Impurities. Journal of Physical Chemistry C, 2019, 123, 5705-5713.	1.5	12

#	Article	IF	Citations
44654	Role of Ionic Charge Accumulation in Perovskite Solar Cell: Carrier Transfer in Bulk and Extraction at Interface. Journal of Physical Chemistry C, 2019, 123, 5312-5320.	1.5	6
44655	Interconversion of hydrated protons at the interface between liquid water and platinum. Physical Chemistry Chemical Physics, 2019, 21, 5932-5940.	1.3	25
44656	Interfacial active fluorine site-induced electron transfer on TiO₂ (001) facets to enhance polysulfide redox reactions for better liquid Li₂S₆-Based lithiumâ€“sulfur batteries. Journal of Materials Chemistry A, 2019, 7, 6431-6438.	5.2	45
44657	Double graphitic-N doping for enhanced catalytic oxidation activity of carbocatalysts. Physical Chemistry Chemical Physics, 2019, 21, 5481-5488.	1.3	23
44658	Ferroelectrically mediated optical absorption in short-period (LaMnO3)2/BaTiO3/(SrMnO3)2 superlattices: A viewpoint from first-principles. Journal of Applied Physics, 2019, 125, 065301.	1.1	1
44659	Solution effect on improved structural compatibility of NiTi-based alloys by systematic first-principles calculations. Journal of Applied Physics, 2019, 125, .	1.1	4
44660	The half-metallicity and the spin filtering, NDR and spin Seebeck effects in 2D Ag-doped SnSe2 monolayer. Journal of Chemical Physics, 2019, 150, 064701.	1.2	16
44661	Simple and accurate model of fracture toughness of solids. Journal of Applied Physics, 2019, 125, .	1.1	136
44662	Carbon monoxide adsorption at forsterite surfaces as models of interstellar dust grains: An unexpected bathochromic (red) shift of the CO stretching frequency. Journal of Chemical Physics, 2019, 150, 064702.	1.2	4
44663	Cadmium trapping by C60 and B-, Si-, and N-doped C60. Journal of Applied Physics, 2019, 125, 054302.	1.1	7
44664	Phonons in deformable microporous crystalline solids. Zeitschrift Fur Kristallographie - Crystalline Materials, 2019, 234, 513-527.	0.4	7
44665	The impact of lattice vibrations on the macroscopic breathing behavior of MIL-53(Al). Zeitschrift Fur Kristallographie - Crystalline Materials, 2019, 234, 529-545.	0.4	22
44666	Strain-Tunable Visible-Light-Responsive Photocatalytic Properties of Two-Dimensional CdS/g-C3N4: A Hybrid Density Functional Study. Nanomaterials, 2019, 9, 244.	1.9	46
44667	Insight into activation of CO and initial C2 oxygenate formation during synthesis of higher alcohols from syngas on the model catalyst K2O/Cu(111) surface. Applied Surface Science, 2019, 479, 55-63.	3.1	7
44668	Role of unsaturated hydrocarbon lubricant on the friction behavior of amorphous carbon films from reactive molecular dynamics study. Computational Materials Science, 2019, 161, 1-9.	1.4	18
44669	Exchange bias and the effect of phase competition in FePt3 single layer and bilayer films. Journal of Alloys and Compounds, 2019, 786, 848-854.	2.8	1
44670	Cooperative activation effect on H2O adsorption in MnOâ€“Co catalyzed steam methane reforming. Physics Letters, Section A: General, Atomic and Solid State Physics, 2019, 383, 1357-1361.	0.9	4
44671	Fabrication and reduction process of dispersive Er2O3 doped Mo super-fine powders comparing with La2O3 doped Mo powders. Powder Technology, 2019, 346, 78-84.	2.1	9

#	Article	IF	Citations
44672	Tuning the Hematite (110) Surface Properties To Enhance Its Efficiency in Photoelectrochemistry. Journal of Physical Chemistry C, 2019, 123, 5401-5410.	1.5	10
44673	Role of Na and Ca as Isovalent Dopants in Cu₂ZnSnS₄ Solar Cells. ACS Sustainable Chemistry and Engineering, 2019, 7, 5792-5800.	3.2	24
44674	The (eg âŠ— eu) âŠ— Eg product Jahnâ€“Teller effect in the neutral group-IV vacancy quantum bits in diamond. Npj Computational Materials, 2019, 5, .	3.5	35
44675	Photocatalytic performance of few-layer graphitic C₃N₄: enhanced by interlayer coupling. Nanoscale, 2019, 11, 4101-4107.	2.8	34
44676	Jahnâ€“Teller type small polaron assisted Na diffusion in NaMnO₂as a cathode material for Na-ion batteries. Journal of Materials Chemistry A, 2019, 7, 6053-6061.	5.2	27
44677	On the prevalence of smooth polymorphs at the nanoscale: implications for pharmaceuticals. CrystEngComm, 2019, 21, 2203-2211.	1.3	20
44678	Phonon transport and thermoelectric properties of semiconducting Bi₂Te₂X (X = S, Se, Te) monolayers. Physical Chemistry Chemical Physics, 2019, 21, 5679-5688.	1.3	63
44679	Sr- and Co-doped LaGaO_{3â˜Î´} with high O₂ and H₂ yields in solar thermochemical water splitting. Journal of Materials Chemistry A, 2019, 7, 6099-6112.	5.2	46
44680	Synergetic promotion by oxygen doping and Ca decoration on graphene for CO₂ selective adsorption. Physical Chemistry Chemical Physics, 2019, 21, 5133-5141.	1.3	22
44681	Electrically controllable magnetic properties of Fe-doped GaSe monolayer. Journal Physics D: Applied Physics, 2019, 52, 175001.	1.3	2
44682	Weyl-loop half-metal in <mml:math xmlns:mml="http://www.w3.org/1998/Math/MathML"><mml:mrow><mml:msub><mml:mrow><mml:mi>Li</mml:mi></mml:mrow><mm Physical Review B, 2019, 99, .	1.1	61
44683	Direct Vapor Growth of 2D Vertical Heterostructures with Tunable Band Alignments and Interfacial Charge Transfer Behaviors. Advanced Science, 2019, 6, 1802204.	5.6	87
44684	Toward a Reversible Calciumâ€Sulfur Battery with a Lithiumâ€Ion Mediation Approach. Advanced Energy Materials, 2019, 9, 1803794.	10.2	43
44685	Manipulating the electronic and magnetic properties of ZnO monolayer by noble metal adsorption: A first-principles calculations. Applied Surface Science, 2019, 479, 440-448.	3.1	36
44686	A low-cost deep eutectic solvent electrolyte for rechargeable aluminum-sulfur battery. Energy Storage Materials, 2019, 22, 418-423.	9.5	102
44687	First principle studies of ZnO1-xSx alloys under high pressure. Journal of Alloys and Compounds, 2019, 788, 905-911.	2.8	6
44688	Electrical properties of yttrium calcium oxyborate crystal annealed at high temperature and low oxygen partial pressure. Journal of Materiomics, 2019, 5, 363-371.	2.8	9
44689	Properties of fusion-relevant liquid Li-Sn alloys: An ab initio molecular-dynamics study. Nuclear Materials and Energy, 2019, 18, 326-330.	0.6	2

#	Article	IF	Citations
44690	Hydrated and anhydrous dodecahydro closo-dodecaborates of 3d transition metals and of magnesium. Solid State Sciences, 2019, 90, 86-94.	1.5	15
44691	Pressure-induced formation of bulk Ge-Sn compounds with high concentration of Sn. Solid State Communications, 2019, 293, 48-52.	0.9	1
44692	Rapid Prediction of Anisotropic Lattice Thermal Conductivity: Application to Layered Materials. Chemistry of Materials, 2019, 31, 2048-2057.	3.2	20
44693	Comparative Study of C₃N- and Graphene-Supported Single-Atom Pt. Journal of Physical Chemistry C, 2019, 123, 5731-5735.	1.5	12
44694	Spectroscopic Evidence and Density Functional Theory (DFT) Analysis of Low-Temperature Oxidation of Cu⁺ to Cu²⁺NO_x in Cu-CHA Catalysts: Implications for the SCR-NO_x Reaction Mechanism. ACS Catalysis, 2019, 9, 2725-2738.	5.5	55
44695	Aldol Condensation of Cyclopentanone on Hydrophobized MgO. Promotional Role of Water and Changes in the Rate-Limiting Step upon Organosilane Functionalization. ACS Catalysis, 2019, 9, 2831-2841.	5.5	38
44696	Ferromagnetism above 1000â€‰K in a highly cation-ordered double-perovskite insulator Sr3OsO6. Nature Communications, 2019, 10, 535.	5.8	47
44697	Atomic palladium on graphitic carbon nitride as a hydrogen evolution catalyst under visible light irradiation. Communications Chemistry, 2019, 2, .	2.0	57
44698	Facile synthesis of highly luminescent lithium silicate nanocrystals with varying crystal structures and morphology. CrystEngComm, 2019, 21, 1974-1983.	1.3	11
44699	MnX (X = P, As) monolayers: a new type of two-dimensional intrinsic room temperature ferromagnetic half-metallic material with large magnetic anisotropy. Nanoscale, 2019, 11, 4204-4209.	2.8	136
44700	Water adsorption on olivine(010) surfaces: Effect of alkali and transition metal cation doping. Journal of Chemical Physics, 2019, 150, 044703.	1.2	4
44701	Impact of interfacial structure on the charge dynamics in nanocomposite dielectrics. Journal of Applied Physics, 2019, 125, 045109.	1.1	6
44702	Lithiophilicity chemistry of heteroatom-doped carbon to guide uniform lithium nucleation in lithium metal anodes. Science Advances, 2019, 5, eaau7728.	4.7	417
44703	Density fluctuations as door-opener for diffusion on crowded surfaces. Science, 2019, 363, 715-718.	6.0	32
44704	Electronic structure and optical properties of CsSnI3â^'yBry (y = 0, 1, 2, 3) perovskites. International Journal of Modern Physics B, 2019, 33, 1950003.	1.0	5
44705	Lithium insertion in Si electrodes studied by first principles method. IOP Conference Series: Materials Science and Engineering, 2019, 688, 033041.	0.3	0
44706	Single-atom protecting group for on-surface synthesis of graphdiyne nanowires. Chinese Journal of Chemical Physics, 2019, 32, 620-624.	0.6	4
44707	First-principles studies on the structural, electronic and mechanical properties of L1o and L12 FexPt1-x alloys. IOP Conference Series: Materials Science and Engineering, 2019, 655, 012044.	0.3	3

#	Article	IF	Citations
44708	Structure and Stability of the Stoichiometric Al3Fe Phase. Metals, 2019, 9, 1322.	1.0	8
44709	Positron annihilation study on the phase transition of thermally aged Fe-Cr binary alloys at 748K. Philosophical Magazine Letters, 2019, 99, 360-371.	0.5	2
44710	Activating inert basal plane of MoS2 for H2O dissociation and HER via formation of vacancy defects: A DFT study*. , 2019, , .		0
44711	First-Principles Analysis of Deformation and Fracture Properties of Semiconductors. Procedia Structural Integrity, 2019, 23, 372-377.	0.3	0
44712	Prediction of Strain Effect on Hydrogen Evolution Reaction on VMO-SLMOS2 *. , 2019, , .		0
44713	Strengthening Mechanisms of Powder Metallurgy Extruded CP Titanium Materials with Zirconium and Oxygen Solid Solution via Decomposition of ZrO₂ Additives in Sintering. Materials Transactions, 2019, 60, 1881-1889.	0.4	6
44714	Tailoring Polymeric Insulation Materials for DC Cable Dielectrics. , 2019, , .		3
44715	Effects of Ga, Ge and As Modification on Structural, Electrochemical and Electronic Properties of Li2MnSiO4. Journal of the Electrochemical Society, 2019, 166, A3874-A3880.	1.3	5
44716	Role of generated free radicals in synthesis of amorphous hydrogenated boron carbide from orthocarborane using argon bombardment: a ReaxFF molecular dynamics study. Materials Research Express, 2019, 6, 126461.	0.8	0
44717	Prediction of colossal magnetocrystalline anisotropy for transition metal triiodides. Journal of Physics Condensed Matter, 2019, 31, 295801.	0.7	7
44718	First-principles study on the optical spectra of ZrO2 crystal with oxygen vacancy. International Journal of Modern Physics B, 2019, 33, 1950372.	1.0	3
44719	An optimized random structures generator governed by chemical short-range order for multi-component solid solutions. Modelling and Simulation in Materials Science and Engineering, 2019, 27, 085007.	0.8	2
44720	A computational study on the effect of minor yttrium on the interfacial adherence of Al oxide film to aluminum substrate. Journal of Physics Condensed Matter, 2019, 31, 295003.	0.7	2
44721	Positron lifetimes of bare and hydrogenated zirconium vacancies in cubic yttria-stabilized zirconia: an ab initio study. Journal of Physics Condensed Matter, 2019, 31, 315503.	0.7	4
44722	Confinement Effect Driven Quantum Spin Hall Effect in Monolayer AuTe2Cl. Spin, 2019, 09, 1940014.	0.6	1
44723	Impact of single atomic defects and vacancies on the magnetic anisotropy energy of CoPt thin films. Journal of Physics Condensed Matter, 2019, 31, 435803.	0.7	0
44724	Modelling Photocathode Performance using Density Functional Theory. , 2019, , .		1
44725	The Predictive Power of Different Projector-Augmented Wave Potentials for Nuclear Quadrupole Resonance. Crystals, 2019, 9, 507.	1.0	3

#	Article	IF	Citations
44727	Superconductivity at 4.6 K in the Cr-based nitride La3Cr10â€“x N11. Europhysics Letters, 2019, 128, 67002.	0.7	2
44728	Gas Sensing of Monolayer GeSe: A First-Principles Study. Nano, 2019, 14, 1950131.	0.5	13
44729	First-principles investigation of elastic, mechanical, electronic and thermodynamic properties of Al₃Li compound under pressure. Materials Research Express, 2019, 6, 1265g6.	0.8	6
44730	Time-resolved Optical Properties of SiNW Oriented in <211> Crystallographic Direction. MRS Advances, 2019, 4, 2009-2014.	0.5	2
44731	Weyl nodes and magnetostructural instability in antiperovskite Mn3ZnC. APL Materials, 2019, 7, 121104.	2.2	3
44732	Multi-cell Monte Carlo method for phase prediction. Npj Computational Materials, 2019, 5, .	3.5	15
44733	Novel elastic evolution of carbide Mo2Ga2C under pressure: Ab initio theoretical investigation. International Journal of Modern Physics B, 2019, 33, 1950358.	1.0	1
44734	Influence of Octahedral Cation Distribution in Montmorillonite on Interlayer Hydrogen Counter-Ion Retention Strength via First-Principles Calculations. Clays and Clay Minerals, 2019, 67, 439-448.	0.6	4
44736	Gap opening in the most stable phases of K₃ Terphenyl compound. Materials Research Express, 2019, 6, 125111.	0.8	1
44737	Strain and electric field effect on arsenene and antimonene heterobilayers. Materials Research Express, 2019, 6, 125925.	0.8	1
44738	Elastic, Electronic, and Optical properties of NaSnX (X=Sb, Bi, As): First principle calculations. IOP Conference Series: Materials Science and Engineering, 2019, 613, 012011.	0.3	1
44739	Strained epitaxial interfaces of metal (Pd, Pt, Au) overlayers on nonpolar CdS (101Â¯0) surfaces from first-principles. Journal of Physics Condensed Matter, 2019, 31, 505001.	0.7	0
44740	Spin-valley coupled caloritronics with strained honeycomb lattices. , 2019, , .		0
44741	Relaxation of electrons in quantum-confined states in Pb/Si(111) thin films from master equation with first-principles-derived rates. New Journal of Physics, 2019, 21, 123023.	1.2	4
44742	First-principles study of the structure and properties of Fe-Rh-Ir alloys. Journal of Physics: Conference Series, 2019, 1389, 012091.	0.3	0
44743	Calculation of the exchange integrals for Co1-x Ni x alloy by Korring-Kohn-Rostoker method. Journal of Physics: Conference Series, 2019, 1389, 012144.	0.3	1
44744	Investigation of the magnetic and adsorption properties of a Fe_xNi_{1-x} monolayer film on nonmagnetic metal substrates. Journal of Physics: Conference Series, 2019, 1389, 012147.	0.3	0
44745	Adsorption and dissociation of carbon monoxide on rhodium surface: AB INITIO study. IOP Conference Series: Earth and Environmental Science, 2019, 332, 032044.	0.2	0

#	Article	IF	Citations
44746	Ab initio mobility of single-layer MoS₂ and WS₂: comparison to experiments and impact on the device characteristics. , 2019, , .		14
44747	A nanostructuring approach for modification of the features of optical materials: lithium fluoride. IOP Conference Series: Materials Science and Engineering, 2019, 693, 012008.	0.3	4
44748	Identification of an AgS2 Complex on Ag(110). Scientific Reports, 2019, 9, 19842.	1.6	2
44749	Pressure-induced phase transitions and superconductivity in magnesium carbides. Scientific Reports, 2019, 9, 20253.	1.6	4
44750	Flat Band and Hole-induced Ferromagnetism in a Novel Carbon Monolayer. Scientific Reports, 2019, 9, 20116.	1.6	19
44753	Chromium Adsorption Reveals a Persistent Hydroxylation of Vacuum-Annealed Î±-Al₂O₃(0001). Journal of Physical Chemistry C, 2019, 123, 29245-29254.	1.5	7
44754	Mechanism of the transition of solid hydrogen to the conducting state at high pressures. Journal of Physics: Conference Series, 2019, 1147, 012002.	0.3	0
44755	Directed Molecular Stacking for Engineered Fluorescent Threeâ€Dimensional Reduced Graphene Oxide and Coronene Frameworks. ChemistryOpen, 2019, 8, 1383-1398.	0.9	5
44756	First principles investigation on energetics, structure, and mechanical properties of amorphous carbon films doped with B, N, and Cl. Scientific Reports, 2019, 9, 18961.	1.6	12
44757	Hardening tungsten carbide by alloying elements with high work function. Acta Crystallographica Section B: Structural Science, Crystal Engineering and Materials, 2019, 75, 994-1002.	0.5	2
44758	Nano-Phase KNa(Si6Al2)O16 in Adularia: A New Member in the Alkali Feldspar Series with Ordered Kâ€“Na Distribution. Minerals (Basel, Switzerland), 2019, 9, 649.	0.8	5
44759	Optical control of the layer degree of freedom through Wannierâ€“Stark states in polar 3R MoS₂. Journal of Physics Condensed Matter, 2019, 31, 315502.	0.7	5
44760	Direct/indirect band gap tunability in van der Waals heterojunctions based on ternary 2D materials Mo_{1â^'x}W_xY₂. Journal of Physics Condensed Matter, 2019, 31, 505302.	0.7	5
44761	Towards Control of Band Gap in Two-Dimensional Hexagonal Boron Nitride by Doping. , 2019, , .		1
44762	Ultimate Mechanical Properties of Forsterite. Minerals (Basel, Switzerland), 2019, 9, 787.	0.8	12
44763	Computational Prediction of Ferroâ€•and Piezoelectricity in Leadâ€Free Oxyhydrides Ln 2 H 4 O (LnÂ=ÂY, La). Advanced Theory and Simulations, 2019, 2, 1900144.	1.3	2
44764	Electrostatic Potential Anomaly in 2D Janus Transition Metal Dichalcogenides. Annalen Der Physik, 2019, 531, 1900369.	0.9	13
44765	Description of terminal substitutional solid solutions using the sublattice model. Calphad: Computer Coupling of Phase Diagrams and Thermochemistry, 2019, 67, 101685.	0.7	4

#	Article	IF	Citations
44766	Mechanistic origins of the high-pressure inhibition of methanol dehydration rates in small-pore acidic zeolites. Journal of Catalysis, 2019, 380, 161-177.	3.1	40
44767	Coordination Geometry Engineering in a Doped Disordered Matrix for Tunable Optical Response. Journal of Physical Chemistry C, 2019, 123, 29343-29352.	1.5	10
44768	High Thermoelectric Performance of SnTe via In Doping and Cu1.75Se Nanostructuring Approach. ACS Applied Energy Materials, 2019, 2, 8966-8973.	2.5	19
44769	First-principles study of antisite defects in perovskite stannates. Journal of Applied Physics, 2019, 126, 195701.	1.1	9
44770	Magnetic Behavior in TiS3 Nanoribbon. Materials, 2019, 12, 3501.	1.3	3
44771	Evolution of the Structural, Mechanical, and Phonon Properties of GeSe Polymorphs in a Pressure-Induced Second-Order Phase Transition. Materials, 2019, 12, 3612.	1.3	7
44772	Passivating Surface States on Water Splitting Cuprous Oxide Photocatalyst with Bismuth Decoration. Molecules, 2019, 24, 4156.	1.7	2
44773	Improvement of the thermoelectric properties of a MoO₃ monolayer through oxygen vacancies. Beilstein Journal of Nanotechnology, 2019, 10, 2031-2038.	1.5	7
44774	Stabilized Li-decoration and enhanced hydrogen storage on reduced graphene oxides. International Journal of Hydrogen Energy, 2019, 44, 31192-31203.	3.8	20
44775	Hydrodeoxygenation of anisole over different Rh surfaces. Chinese Journal of Catalysis, 2019, 40, 1721-1730.	6.9	17
44776	Rapid Crystallization and Kinetic Freezing of Site-Disorder in the Lithium Superionic Argyrodite Li₆PS₅Br. Chemistry of Materials, 2019, 31, 10178-10185.	3.2	72
44777	Iuliacumite: A Novel Chemical Short-Range Order in a Two-Dimensional Wurtzite Single Monolayer InAs_{1â€“x}Sb_x Shell on InAs Nanowires. Nano Letters, 2019, 19, 8801-8805.	4.5	2
44778	Origin of Band Modulation in GeTe-Rich Geâ€“Sbâ€“Te Thin Film. ACS Applied Electronic Materials, 2019, 1, 2619-2625.	2.0	3
44779	Insight into Two-Dimensional Borophene: Five-Center Bond and Phonon-Mediated Superconductivity. ACS Applied Materials & Interfaces, 2019, 11, 47279-47288.	4.0	14
44780	Unsupervised discovery of solid-state lithium ion conductors. Nature Communications, 2019, 10, 5260.	5.8	150
44781	Frustrated Lewis pairs photocatalyst for visible light-driven reduction of CO to multi-carbon chemicals. Nanoscale, 2019, 11, 20777-20784.	2.8	38
44782	How carbon vacancies can affect the properties of group IV color centers in diamond: A study of thermodynamics and kinetics. Journal of Applied Physics, 2019, 126, 195103.	1.1	10
44783	Spectroscopic Evidence for Electron-Boson Coupling in Electron-Doped <mml:math xmlns:mml="http://www.w3.org/1998/Math/MathML" display="inline"><mml:mrow><mml:msub><mml:mrow><mml:mi>Sr</mml:mi></mml:mrow><mml:mrow><mml:mn>2</mml:mn></mml:mrow> Physical Review Letters, 2019, 123, 216402.	2.9	13

#	Article	IF	Citations
44784	P2 Type Layered Solid-State Electrolyte Na₂Zn₂TeO₆: Crystal Structure and Stacking Faults. Journal of the Electrochemical Society, 2019, 166, A3830-A3837.	1.3	10
44785	Firstâ€Principles Prediction of a New Family of Layered Topological Insulators. Advanced Quantum Technologies, 2019, 2, 1900033.	1.8	6
44786	Dual Interphase Layers In Situ Formed on a Manganese-Based Oxide Cathode Enable Stable Potassium Storage. CheM, 2019, 5, 3220-3231.	5.8	79
44787	Effects of Lattice O Atom Coordination and Pore Confinement on Selectivity Limitations for Ethane Oxidative Dehydrogenation Catalyzed by Vanadium-Oxo Species. Journal of Physical Chemistry C, 2019, 123, 28168-28191.	1.5	20
44788	Analysis of Dihydrogen Bonding in Ammonium Borohydride. Journal of Physical Chemistry C, 2019, 123, 28631-28639.	1.5	22
44789	Controlled Fabrication of K₂Ti₈O₁₇ Nanowires for Highly Efficient and Ultrafast Adsorption toward Methylene Blue. ACS Applied Materials & Interfaces, 2019, 11, 45531-45545.	4.0	31
44790	Low-Temperature Catalytic NO Reduction with CO by Subnanometric Pt Clusters. ACS Catalysis, 2019, 9, 11530-11541.	5.5	70
44791	Atomically dispersed nickel as coke-resistant active sites for methane dry reforming. Nature Communications, 2019, 10, 5181.	5.8	398
44792	Non-glide effects and dislocation core fields in BCC metals. Npj Computational Materials, 2019, 5, .	3.5	31
44793	Computational screening of metalâ€“organic frameworks for biogas purification. Molecular Systems Design and Engineering, 2019, 4, 1125-1135.	1.7	15
44794	Revealing carbon mediated luminescence centers with enhanced lifetime in porous alumina. Journal of Applied Physics, 2019, 126, 164904.	1.1	6
44795	The thermoelectric properties of monolayer SiP and GeP from first-principles calculations. Journal of Applied Physics, 2019, 126, .	1.1	14
44796	Ideal Weyl semimetal induced by magnetic exchange. Physical Review B, 2019, 100, .	1.1	130
44797	Reaction mechanism of N atoms interaction with low-k organosilicate glass films: Dynamic density functional theory study. Journal of Vacuum Science and Technology A: Vacuum, Surfaces and Films, 2019, 37, .	0.9	6
44798	Penta-Graphene as a Potential Gas Sensor for NOx Detection. Nanoscale Research Letters, 2019, 14, 306.	3.1	52
44799	The Nucleation and the Intrinsic Microstructure Evolution of Martensite from 332113Î² Twin Boundary in Î² Titanium: First-Principles Calculations. Metals, 2019, 9, 1202.	1.0	6
44800	Magnetic Properties of YBa₂Cu₃O₆ Studied by Density Functional Theory Calculations. Materials Science Forum, 2019, 966, 257-262.	0.3	2
44801	Effects of the Supercell's Size on Muon Positions Calculations of La₂CuO₄. Materials Science Forum, 2019, 966, 465-470.	0.3	3

#	Article	IF	Citations
44802	Hierarchical Composite of Roseâ€Like VS₂@S/Nâ€Doped Carbon with Expanded (001) Planes for Superior Liâ€Ion Storage. Small, 2019, 15, e1903904.	5.2	64
44803	Photoinduced Carrier Generation and Distribution in Solution-Deposited Titanyl Phthalocyanine Monolayers. Chemistry of Materials, 2019, 31, 10109-10116.	3.2	8
44804	Nonrandomly Distributed Tungsten Vacancies and Interstitial Boron Trimers in Tungsten Tetraboride. Journal of Physical Chemistry C, 2019, 123, 29314-29323.	1.5	12
44805	Propagating DFT Uncertainty to Mechanism Determination, Degree of Rate Control, and Coverage Analysis: The Kinetics of Dry Reforming of Methane. Journal of Physical Chemistry C, 2019, 123, 30389-30397.	1.5	39
44806	Super-resolution energy spectra from neutron direct-geometry spectrometers. Review of Scientific Instruments, 2019, 90, 105109.	0.6	9
44807	Ion-induced n-p inversion of conductivity in TiNiSn compound for thermoelectric applications. Journal of Applied Physics, 2019, 126, 155106.	1.1	3
44808	Comparative Study of Substitutional N and Substitutional P in Diamond. Chinese Physics Letters, 2019, 36, 116101.	1.3	4
44809	Hybrid neural network potential for multilayer graphene. Physical Review B, 2019, 100, .	1.1	38
44810	High-pressure melting line of helium from ab initio calculations. Physical Review B, 2019, 100, .	1.1	10
44811	Effective lattice model of graphene moirÃ© superlattices on hexagonal boron nitride. Physical Review B, 2019, 100, .	1.1	17
44812	Natural van der Waals heterostructural single crystals with both magnetic and topological properties. Science Advances, 2019, 5, eaax9989.	4.7	193
44813	Understanding the Impact of a Nonafluorinated Ether-Based Electrolyte on Li-S Battery. Journal of the Electrochemical Society, 2019, 166, A3653-A3659.	1.3	6
44814	First Principles Investigation of Anomalous Pressure-Dependent Thermal Conductivity of Chalcopyrites. Materials, 2019, 12, 3491.	1.3	8
44815	High-Throughput Screening of Rare-Earth-Lean Intermetallic 1-13-X Compounds for Good Hard-Magnetic Properties. Metals, 2019, 9, 1096.	1.0	7
44816	Characterization and Stability of Janus TiXY (X/Y = S, Se, and Te) Monolayers. Journal of Physical Chemistry C, 2019, 123, 29922-29931.	1.5	30
44817	Ionic Transport in Doped Solid Electrolytes by Means of DFT Modeling and ML Approaches: A Case Study of Ti-Doped KFeO₂. Journal of Physical Chemistry C, 2019, 123, 29533-29542.	1.5	14
44818	Nonvolatile Balanced Ternary Memory Based on The Multiferroelectric Material GeSnTe2. Journal of Physical Chemistry Letters, 2019, 10, 7470-7474.	2.1	6
44819	Single-Layer Cu₂WS₄ with Promising Electrocatalytic Activity toward Hydrogen Evolution Reaction. ACS Applied Materials & Interfaces, 2019, 11, 45818-45824.	4.0	34

#	Article	IF	Citations
44820	Weak antilocalization effect and high-pressure transport properties of ScPdBi single crystal. Applied Physics Letters, 2019, 115, .	1.5	17
44821	Carbon dimer defect as a source of the 4.1 eV luminescence in hexagonal boron nitride. Applied Physics Letters, 2019, 115, .	1.5	77
44822	Improved thermoelectric performance of p-doped half-Heusler Ti0.5Zr0.5CoSb0.5P0.5, Ti0.5Hf0.5CoSb0.5P0.5, and Zr0.5Hf0.5CoSb0.5P0.5 compounds. Materials Research Express, 2019, 6, 126305.	0.8	5
44823	Predictive design of intrinsic half-metallicity in zigzag tungsten dichalcogenide nanoribbons. Physical Review B, 2019, 100, .	1.1	9
44824	Single-layer LaBr2: Two-dimensional valleytronic semiconductor with spontaneous spin and valley polarizations. Applied Physics Letters, 2019, 115, .	1.5	100
44825	Charge-transfer plasmons with narrow conductive molecular bridges: A quantum-classical theory. Journal of Chemical Physics, 2019, 151, 244125.	1.2	11
44826	First-Principles study of two dimensional transition metal phthalocyanine-based metal-organic frameworks in kagome lattice. Chinese Journal of Chemical Physics, 2019, 32, 563-571.	0.6	8
44827	Weak ferromagnetism in hexagonal Mn3Z alloys (Z=Sn,Ge,Ga). Physical Review B, 2019, 100, .	1.1	7
44828	Evidence from first-principles calculations for orbital ordering in <mml:math xmlns:mml="http://www.w3.org/1998/Math/MathML"><mml:msub><mml:mrow><mml:mi>Ba</mml:mi></mml:mrow><mml:mn>2</mml:mn> : A Mott insulator with strong spin-orbit coupling. Physical Review B, 2019, 100, .	1.1	7
44829	Bismuth iron garnet: Ab initio study of electronic properties. Physical Review B, 2019, 100, .	1.1	10
44830	Comment on â€œRegularized SCAN functionalâ€•[J. Chem. Phys. 150, 161101 (2019)]. Journal of Chemical Physics, 2019, 151, 207101.	1.2	21
44831	Ethylene adsorption on Ag(111), Rh(111) and Ir(111) by (meta)-GGA based density functional theory calculations. Chinese Journal of Chemical Physics, 2019, 32, 437-443.	0.6	9
44832	First-Principles Study of Alkyl Derivatives of Boehmite. Journal of the Korean Physical Society, 2019, 75, 490-493.	0.3	1
44833	Conversion of Magnetic Freedoms into Atomic Configurational Freedoms within the Cluster Variation Method. Materials Transactions, 2019, 60, 915-920.	0.4	3
44834	First-Principles Study on Photoluminescence Quenching of Divacancy in 4H SiC. Materials Science Forum, 2019, 963, 714-717.	0.3	1
44835	Water interaction and dissociation on stoichiometric and defective Mn- and Fe-doped CeO2 surfaces. Materials Today Communications, 2019, 21, 100703.	0.9	2
44836	A new tool for validating theoretically derived anisotropic displacement parameters with experiment: directionality of prolate displacement ellipsoids. CrystEngComm, 2019, 21, 6396-6404.	1.3	4
44837	Low-dimensional functional networks of cage-like B₄₀ with effective transition-metal intercalations. Physical Chemistry Chemical Physics, 2019, 21, 22611-22617.	1.3	5

#	Article	IF	Citations
44838	Structureâ€“thermodynamics relationship of schoepite from first-principles. Physical Chemistry Chemical Physics, 2019, 21, 25569-25576.	1.3	4
44839	Beyond molecular nitrogen: revelation of two ambient-pressure metastable single- and double-bonded nitrogen allotropes built from three-membered rings. Physical Chemistry Chemical Physics, 2019, 21, 22930-22938.	1.3	8
44840	Adsorbate induced modulation of strain effects on work functions of a tungsten (100) surface. Physical Chemistry Chemical Physics, 2019, 21, 25763-25772.	1.3	6
44841	Chemical origin of differences in steel corrosion behaviors of s-electron and p-electron liquid metals by first-principles calculation. Physical Chemistry Chemical Physics, 2019, 21, 25916-25924.	1.3	1
44842	Two-dimensional Dirac fermions on oxidized black phosphorus. Physical Chemistry Chemical Physics, 2019, 21, 24206-24211.	1.3	5
44843	Revised values for the X23 benchmark set of molecular crystals. Physical Chemistry Chemical Physics, 2019, 21, 24333-24344.	1.3	31
44844	Designing rare earth free permanent magnets: insights from small Co clusters. Physical Chemistry Chemical Physics, 2019, 21, 22577-22583.	1.3	1
44845	A comprehensive study of the red persistent luminescence mechanism of Y₂O₂S:Eu,Ti,Mg. Physical Chemistry Chemical Physics, 2019, 21, 25118-25125.	1.3	25
44846	A computational study of hydrogen doping induced metal-to-insulator transition in CaFeO₃, SrFeO₃, BaFeO₃ and SmMnO₃. Physical Chemistry Chemical Physics, 2019, 21, 25397-25405.	1.3	8
44847	Defect formation and migration in Nasicon Li_{1+x}Al_xTi_{2â^'x}(PO₄)₃. Physical Chemistry Chemical Physics, 2019, 21, 24232-24238.	1.3	14
44848	Size-controlled excitonic effects on electronic and optical properties of Sb₂S₃ nanowires. Physical Chemistry Chemical Physics, 2019, 21, 26515-26524.	1.3	14
44849	Structural evolution of Ag/BN hybrids via a polyol-assisted fabrication process and their catalytic activity in CO oxidation. Catalysis Science and Technology, 2019, 9, 6460-6470.	2.1	7
44850	Silicon-doped graphene edges: an efficient metal-free catalyst for the reduction of CO₂ into methanol and ethanol. Catalysis Science and Technology, 2019, 9, 6800-6807.	2.1	51
44851	Sb-doped polymeric carbon nitride with charge-capture centers for efficient charge separation and photocatalytic performance in H2 evolution and environmental remediation. Catalysis Science and Technology, 2019, 9, 6627-6637.	2.1	7
44852	Effect of anion substitution on the structural and transport properties of argyrodites Cu₇PSe_{6â^'x}S_x. Dalton Transactions, 2019, 48, 15822-15829.	1.6	17
44853	Insights into the solvent-assisted degradation of organophosphorus compounds by a Zr-based metalâ€“organic framework. Dalton Transactions, 2019, 48, 16153-16157.	1.6	8
44854	Hydrothermally stable ZnAl₂O₄ nanocrystals with controlled surface structures for the design of long-lasting and highly active/selective PdZn catalysts. Green Chemistry, 2019, 21, 6574-6578.	4.6	7
44855	Computational discovery of weak-intermolecular-interaction-tuning ferroelectricity/ferroelasticity of pure organic rotatorâ€“stator-type assemblies designed through a symmetry/structure-limited structure search. Molecular Systems Design and Engineering, 2019, 4, 1136-1144.	1.7	1

#	Article	IF	Citations
44856	Control of highly anisotropic electrical conductance of tellurene by strain-engineering. Nanoscale, 2019, 11, 21775-21781.	2.8	11
44857	Boosting the electrocatalytic activity of amorphous molybdenum sulfide nanoflakes via nickel sulfide decoration. Nanoscale, 2019, 11, 22971-22979.	2.8	19
44858	Two-dimensional MgX₂Se₄ (X = Al, Ga) monolayers with tunable electronic properties for optoelectronic and photocatalytic applications. Nanoscale, 2019, 11, 19806-19813.	2.8	21
44859	Superhigh out-of-plane piezoelectricity, low thermal conductivity and photocatalytic abilities in ultrathin 2D van der Waals heterostructures of boron monophosphide and gallium nitride. Nanoscale, 2019, 11, 21880-21890.	2.8	54
44860	Enhanced catalytic activity of edge-exposed 1T phase WS₂ grown directly on a WO₃ nanohelical array for water splitting. Journal of Materials Chemistry A, 2019, 7, 26378-26384.	5.2	23
44861	Clarifying the controversial catalytic active sites of Co₃O₄ for the oxygen evolution reaction. Journal of Materials Chemistry A, 2019, 7, 23191-23198.	5.2	115
44862	Activating MoS₂ basal planes for hydrogen evolution through direct CVD morphology control. Journal of Materials Chemistry A, 2019, 7, 27603-27611.	5.2	24
44863	FeP₃ monolayer as a high-efficiency catalyst for hydrogen evolution reaction. Journal of Materials Chemistry A, 2019, 7, 25665-25671.	5.2	43
44864	Unveiling the mechanism of improved capacity retention in Pmn₁ Li₂FeSiO₄ cathode by cobalt substitution. Journal of Materials Chemistry A, 2019, 7, 25399-25414.	5.2	11
44865	Li-III-VI bilayers for efficient photocatalytic overall water splitting: the role of intrinsic electric field. Journal of Materials Chemistry A, 2019, 7, 26123-26130.	5.2	40
44866	Study of active sites on Se-MnS/NiS heterojunctions as highly efficient bifunctional electrocatalysts for overall water splitting. Journal of Materials Chemistry A, 2019, 7, 26975-26983.	5.2	104
44867	Topological dual double node-line semimetals NaAlSi(Ge) and their potential as cathode material for sodium ion batteries. Journal of Materials Chemistry C, 2019, 7, 15375-15381.	2.7	34
44868	Tuning valley polarization in two-dimensional ferromagnetic heterostructures. Journal of Materials Chemistry C, 2019, 7, 14932-14937.	2.7	6
44869	The mechanical, electronic and optical properties of two-dimensional transition metal chalcogenides MX₂ and M₂X₃ (M = Ni, Pd; X = S, Se, Te) with hexagonal and orthorhombic structures. Journal of Materials Chemistry C, 2019, 7, 13518-13525.	2.7	58
44870	Lifshitz transition and nontrivial H-doping effect in the Cr-based superconductor <mml:math xmlns:mml="http://www.w3.org/1998/Math/MathML"><mml:msub><mml:mi mathvariant="normal">KCr</mml:mi><mml:mn>3</mml:mn></mml:msub><mml:msub><mml:mi mathvariant="normal">As</mml:mi><mml:mn>3</mml:mn></mml:msub><mml:msub><mml:mi mathvariant="normal">H</mml:mi><mml:mi>x</mml:mi></mml:msub></mml:math>. Physical Review B, 2019, 100, .	1.1	17
44871	Electronic structure of Au-Sn compounds grown on Au(111). Physical Review B, 2019, 100, .	1.1	25
44872	Structure determination of hydrogen-terminated 4H -SiC(0001) by LEED. Physical Review B, 2019, 99, .	1.1	2
44873	Effect of S-vacancy on the oxidation state of Ce in monolayer SnS₂. International Journal of Modern Physics B, 2019, 33, 1950308.	1.0	3

#	Article	IF	Citations
44874	Quantum Spin Hall Insulators in Tin Films: Beyond Stanene. Spin, 2019, 09, 1940012.	0.6	5
44875	Ab Initio Molecular Dynamics Study of Alignment-Resolved O₂ Scattering from Highly Oriented Pyrolytic Graphite. Journal of Physical Chemistry C, 2019, 123, 31094-31102.	1.5	15
44876	Raman Activity of Multilayer Phosphorene under Strain. ACS Omega, 2019, 4, 22418-22425.	1.6	8
44877	Computational Simulation of Trapped Charge Carriers in TiO₂ and Their Impacts on Photocatalytic Water Splitting. ACS Symposium Series, 2019, , 67-100.	0.5	1
44878	Time-Domain ab Initio Studies of Excited State Dynamics at Nanoscale Interfaces. ACS Symposium Series, 2019, , 101-136.	0.5	2
44879	Comprehensive Study of Multiple Exciton Generation in Chiral Carbon Nanotubes Using Many-Body Perturbation Theory Based on Density Functional Theory Simulations. ACS Symposium Series, 2019, , 157-179.	0.5	0
44880	Hydroxide promotes carbon dioxide electroreduction to ethanol on copper via tuning of adsorbed hydrogen. Nature Communications, 2019, 10, 5814.	5.8	201
44881	A computational-experimental investigation on high ethylene selectivity in ethanol dehydration reaction found on WOx/ZrO2-activated carbon bi-support systems. Scientific Reports, 2019, 9, 19738.	1.6	8
44882	Materials with the CrVO₄ structure type as candidate superprotonic conductors. RSC Advances, 2019, 9, 31999-32009.	1.7	10
44883	Polarization properties of AlN (101Ì…0) and (112Ì…0) non-polar surfaces: maximally localized Wannier functions study. EPJ Applied Physics, 2019, 88, 10101.	0.3	0
44884	Atomic interactions between Si and Mn during eutectoid transformation in high-carbon pearlitic steel. Journal of Applied Physics, 2019, 126, .	1.1	5
44885	Electronic structure, phonon and superconductivity for WP 5d-transition metal. Journal of Applied Physics, 2019, 126, 175103.	1.1	9
44886	Magnetic exchange interactions and band gap bowing in NixMg1â^'xO (0.0â€‰â‰€â€‰xâ€‰â‰€â€‰1.0): A GGA+U density functional study. Journal of Applied Physics, 2019, 126, 233904.	1.1	4
44887	Coordination changes in liquid tin under shock compression determined using in situ femtosecond x-ray diffraction. Applied Physics Letters, 2019, 115, .	1.5	22
44888	Enhanced ductility of III-V covalent semiconductors from electrons and holes. Journal of Applied Physics, 2019, 126, .	1.1	5
44889	First-principles investigation of electrochemical dissolution of Pt nanoparticles and kinetic simulation. Journal of Chemical Physics, 2019, 151, 234711.	1.2	10
44890	Oxygen activation on the interface between Pt nanoparticles and mesoporous defective TiO2 during CO oxidation. Journal of Chemical Physics, 2019, 151, 234716.	1.2	37
44891	Î³-GeSe: A two-dimensional ferroelectric material with doping-induced ferromagnetism. Applied Physics Letters, 2019, 115, .	1.5	41

#	Article	IF	Citations
44892	Influence of electric fields on metal self-diffusion barriers and its consequences on dendrite growth in batteries. Journal of Chemical Physics, 2019, 151, 234707.	1.2	16
44893	First-principles calculations of magnetic properties of germanene under strain. Ferroelectrics, 2019, 550, 173-182.	0.3	1
44894	First-principles study of the thermodynamic and vibrational properties of <mml:math xmlns:mml="http://www.w3.org/1998/Math/MathML"><mml:msub><mml:mi>ReS</mml:mi><mml:mn>2</mml:mn></mml:msub></mml under pressure. Physical Review B, 2019, 100, .	1.1	7
44895	Tuning optical properties of TiO2 by dimension reduction: from 3D bulk to 2D sheets along {001} and {101} plane. Materials Research Express, 2019, 6, 1250f1.	0.8	8
44896	Microstructures and characteristics of Ti/Al interface with segregated Si element. Chinese Journal of Physics, 2019, 62, 296-303.	2.0	2
44897	Two-Dimensional Second-Order Topological Insulator in Graphdiyne. Physical Review Letters, 2019, 123, 256402.	2.9	193
44898	Electrical Transport Properties of Nb and Ga Double Substituted Fe2VAl Heusler Compounds. Semiconductors, 2019, 53, 1856-1859.	0.2	1
44899	The Flexible Lubrication Performance of Graphene Used in Diamond Interface as a Solid Lubricant: First-Principles Calculations. Nanomaterials, 2019, 9, 1784.	1.9	4
44900	Theoretical Investigation of NiI₂ Based Bilayer Heterostructures. Key Engineering Materials, 0, 806, 10-16.	0.4	0
44901	Indirect-To-Direct Band Gap Transition of One-Dimensional V₂Se₉: Theoretical Study with Dispersion Energy Correction. ACS Omega, 2019, 4, 18392-18397.	1.6	27
44902	Modeling of Photooxidative Degradation of Aromatics in Water Matrix: A Quantitative Structureâ^'Property Relationship Approach. ACS Symposium Series, 2019, , 257-292.	0.5	0
44903	Continuous strengthening in nanotwinned diamond. Npj Computational Materials, 2019, 5, .	3.5	32
44904	Constructive molecular configurations for surface-defect passivation of perovskite photovoltaics. Science, 2019, 366, 1509-1513.	6.0	846
44905	Functionalized Carbon Nanotube Excited States and Optical Properties. ACS Symposium Series, 2019, , 181-207.	0.5	1
44906	Multistaged discharge constructing heterostructure with enhanced solid-solution behavior for long-life lithium-oxygen batteries. Nature Communications, 2019, 10, 5810.	5.8	80
44907	The influence of edge structure on the optoelectronic properties of Si2BN quantum dot. Journal of Applied Physics, 2019, 126, .	1.1	17
44908	Electronic Structure and Excited State Dynamics of TiO₂Nanowires. ACS Symposium Series, 2019, , 23-46.	0.5	0
44909	Optical Properties of the TiO₂(110) Surface with Adsorbed Ag Atoms Relevant to Photocatalysis and Photovoltaics. ACS Symposium Series, 2019, , 47-66.	0.5	1

#	Article	IF	Citations
44910	Physical Properties of Conjugated Nanopore Materials. ACS Symposium Series, 2019, , 293-308.	0.5	0
44911	Photo-induced Charge Separation and Photoredox Catalysis in Cerium-Based Metalâ€“Organic Frameworks. ACS Symposium Series, 2019, , 309-326.	0.5	5
44912	Excited State Electronic Structure of Single-Site Vanadium Oxide Photocatalysts Supported on Mesoporous Silica. ACS Symposium Series, 2019, , 327-341.	0.5	2
44913	Ferromagnetism from non-magnetic ions: Ag-doped ZnO. Scientific Reports, 2019, 9, 20039.	1.6	42
44914	Thermal annealing effects in polycrystalline EuTiO3 and Eu2Ti2O7. AIP Advances, 2019, 9, 125125.	0.6	9
44915	Evidence for vacancy trapping in Au-hyperdoped Si following pulsed laser melting. APL Materials, 2019, 7, .	2.2	18
44916	Strong Valence Electrons Dependent and Logical Relations of Elemental Impurities in 2D Binary Semiconductor: a Case of GeP3 Monolayer from Ab Initio Studies. Nanoscale Research Letters, 2019, 14, 307.	3.1	2
44917	Phonon-Mediated Ultrafast Hole Transfer from Photoexcited CdSe Quantum Dots to Black Dye. ACS Symposium Series, 2019, , 137-156.	0.5	4
44918	Assessing the usefulness of transition metal carbides for hydrogenation reactions. Chemical Communications, 2019, 55, 12797-12800.	2.2	37
44919	Thermodynamic properties and lattice dynamics investigation of LuB2C: experiment and ab initio calculations. Physical Chemistry Chemical Physics, 2019, 21, 24684-24694.	1.3	2
44920	A theoretical insight into furfural conversion catalyzed on the Ni(111) surface. Physical Chemistry Chemical Physics, 2019, 21, 23685-23696.	1.3	25
44921	Structural phase transitions in VSe₂: energetics, electronic structure and magnetism. Physical Chemistry Chemical Physics, 2019, 21, 22647-22653.	1.3	37
44922	Two-dimensional transition metal dichalcogenides as promising anodes for potassium ion batteries from first-principles prediction. Physical Chemistry Chemical Physics, 2019, 21, 23441-23446.	1.3	40
44923	Structure and electronic properties of rare earth DOBDC metalâ€“organic-frameworks. Physical Chemistry Chemical Physics, 2019, 21, 23085-23093.	1.3	24
44924	A generalized solid strengthening rule for biocompatible Zn-based alloys, a comparison with Mg-based alloys. Physical Chemistry Chemical Physics, 2019, 21, 22629-22638.	1.3	3
44925	Synergy of tellurium and defects in control of activity of phosphorene for oxygen evolution and reduction reactions. Physical Chemistry Chemical Physics, 2019, 21, 22939-22946.	1.3	16
44926	Superconductivity in an organometallic compound. Physical Chemistry Chemical Physics, 2019, 21, 25976-25981.	1.3	10
44927	Strategies for computational design and discovery of two-dimensional transition-metal-free materials for electro-catalysis applications. Physical Chemistry Chemical Physics, 2019, 21, 25535-25547.	1.3	12

#	Article	IF	Citations
44928	Thermoelectric power factor of pure and doped ZnSbviaDFT based defect calculations. Physical Chemistry Chemical Physics, 2019, 21, 23056-23064.	1.3	6
44929	Interpenetrating graphene network bct-C₄₀: a promising anode material for Li ion batteries. Physical Chemistry Chemical Physics, 2019, 21, 23485-23491.	1.3	9
44930	Accurate K-edge X-ray photoelectron and absorption spectra of g-C₃N₄ nanosheets by first-principles simulations and reinterpretations. Physical Chemistry Chemical Physics, 2019, 21, 22819-22830.	1.3	70
44931	Infrared photodissociation spectroscopy of di-manganese oxide cluster cations. Physical Chemistry Chemical Physics, 2019, 21, 23922-23930.	1.3	8
44932	Graphene-covered transition metal halide molecules as efficient and durable electrocatalysts for oxygen reduction and evolution reactions. Physical Chemistry Chemical Physics, 2019, 21, 23094-23101.	1.3	8
44933	The dual-defective SnS₂ monolayers: promising 2D photocatalysts for overall water splitting. Physical Chemistry Chemical Physics, 2019, 21, 26292-26300.	1.3	18
44934	Pressure-induced metallicity and piezoreductive transition of metal-centres in conductive 2-dimensional metalâ€“organic frameworks. Physical Chemistry Chemical Physics, 2019, 21, 25773-25778.	1.3	13
44935	Mechanical properties and superconductivity in two-dimensional B2O under extreme strain. Physical Chemistry Chemical Physics, 2019, 21, 25859-25864.	1.3	4
44936	Thickness biased capture of CO₂ on carbide MXenes. Physical Chemistry Chemical Physics, 2019, 21, 23136-23142.	1.3	55
44937	Theoretical study of the optical and thermodynamic properties of La_xSr_{1âˆ’x}Co_{1âˆ’y}Fe_yO_{3âˆ’Î´} (x/y =) ITβETQq1 1 0.784	1.3	1
44938	Fe-Doped Î±-MnO₂ nanorods for the catalytic removal of NO_x and chlorobenzene: the relationship between lattice distortion and catalytic redox properties. Physical Chemistry Chemical Physics, 2019, 21, 25880-25888.	1.3	39
44939	Theoretical investigation of the cation antisite defect in layer-structured cathode materials for Li-ion batteries. Physical Chemistry Chemical Physics, 2019, 21, 24139-24146.	1.3	8
44940	Trends of the macroscopic behaviors of energetic compounds: insights from first-principles calculations. Physical Chemistry Chemical Physics, 2019, 21, 24034-24041.	1.3	3
44941	Ultra-low lattice thermal conductivity of monolayer penta-silicene and penta-germanene. Physical Chemistry Chemical Physics, 2019, 21, 26033-26040.	1.3	48
44942	Prediction of two-dimensional PC₆ as a promising anode material for potassium-ion batteries. Physical Chemistry Chemical Physics, 2019, 21, 26212-26218.	1.3	47
44943	Interactions between alloy elements and oxygen at the steelâ€“liquid LBE interface determined from first-principles molecular dynamics simulations. Physical Chemistry Chemical Physics, 2019, 21, 25735-25742.	1.3	12
44944	Effect of the oxygen coordination environment of Caâ€“Mn oxides on the catalytic performance of Pd supported catalysts for aerobic oxidation of 5-hydroxymethyl-2-furfural. Catalysis Science and Technology, 2019, 9, 6659-6668.	2.1	25
44945	Selective mild oxidation of methane to methanol or formic acid on Feâ€“MOR catalysts. Catalysis Science and Technology, 2019, 9, 6946-6956.	2.1	29

#	Article	IF	Citations
44946	Chemoselective reduction of quinoline over Rhâ€“C₆₀ nanocatalysts. Catalysis Science and Technology, 2019, 9, 6884-6898.	2.1	16
44947	Influence of organic cation planarity on structural templating in hybrid metal-halides. Dalton Transactions, 2019, 48, 16340-16349.	1.6	12
44948	Experimental and theoretical investigation of lithium-ion conductivity in Li₂LaNbTiO₇. Dalton Transactions, 2019, 48, 17281-17290.	1.6	6
44949	The impact of metal cations on the photochemical properties of hybrid heterostructures with infinite alkaline-earth metal oxide clusters. Dalton Transactions, 2019, 48, 17381-17387.	1.6	20
44950	Scalable production of high-quality boron nitride nanosheets via a recyclable salt-templating method. Green Chemistry, 2019, 21, 6746-6753.	4.6	16
44951	Alkaline earth ion exchange study of pure silica LTA zeolites using periodic first-principles calculations. New Journal of Chemistry, 2019, 43, 16835-16840.	1.4	5
44952	Catalytic trends of nitrogen doped carbon nanotubes for oxygen reduction reaction. Nanoscale, 2019, 11, 18683-18690.	2.8	27
44953	Monolayer SnP₃: an excellent p-type thermoelectric material. Nanoscale, 2019, 11, 19923-19932.	2.8	119
44954	Optimizing PtFe intermetallics for oxygen reduction reaction: from DFT screening to in situ XAFS characterization. Nanoscale, 2019, 11, 20301-20306.	2.8	33
44955	Evolution of intrinsic vacancies and prolonged lifetimes of vacancy clusters in black phosphorene. Nanoscale, 2019, 11, 20987-20995.	2.8	10
44956	Tunable energy storage capacity of two-dimensional Ti₃C₂T_x modified by a facile two-step pillaring strategy for high performance supercapacitor electrodes. Nanoscale, 2019, 11, 21981-21989.	2.8	32
44957	Atomic-scale oxidation mechanisms of single-crystal magnesium. Nanoscale, 2019, 11, 23346-23356.	2.8	5
44958	Synthesis of low-symmetry 2D Ge_(1â^'x)Sn_xSe₂ alloy flakes with anisotropic optical response and birefringence. Nanoscale, 2019, 11, 23116-23125.	2.8	9
44959	Electrochemical exfoliation from an industrial ingot: ultrathin metallic bismuth nanosheets for excellent CO₂ capture and electrocatalytic conversion. Nanoscale, 2019, 11, 22125-22133.	2.8	34
44960	Encapsulation and controlled release characteristics of ethylene gas in cucurbit[n]urils. Polymer Chemistry, 2019, 10, 6021-6030.	1.9	4
44961	A rate equation model for the energy transfer mechanism of a novel multi-color-emissive phosphor, Ca_{1.624}Sr_{0.376}Si₅O₃N₆:Eu²⁺. Inorganic Chemistry Frontiers, 2019, 6, 3493-3500.	3.0	9
44962	The preparation and mechanistic study of highly effective PtSnRu ternary nanorod catalysts toward the ethanol oxidation reaction. Sustainable Energy and Fuels, 2019, 3, 3352-3362.	2.5	9
44963	Laser-engineered oxygen vacancies for improving the NO₂ sensing performance of SnO₂ nanowires. Journal of Materials Chemistry A, 2019, 7, 27205-27211.	5.2	33

#	Article	IF	Citations
44964	Direct emission from quartet excited states triggered by upconversion phenomena in solid-phase synthesized fluorescent lead-free organicâ€“inorganic hybrid compounds. Journal of Materials Chemistry A, 2019, 7, 26504-26512.	5.2	35
44965	Cu single atoms on Ti₂CO₂ as a highly efficient oxygen reduction catalyst in a proton exchange membrane fuel cell. Journal of Materials Chemistry A, 2019, 7, 26062-26070.	5.2	95
44966	Theoretical prediction and atomic-scale investigation of a tetra-VN₂monolayer as a high energy alkali ion storage material for rechargeable batteries. Journal of Materials Chemistry A, 2019, 7, 26858-26866.	5.2	18
44967	Itinerant ferromagnetic half metallic cobaltâ€“iron couples: promising bifunctional electrocatalysts for ORR and OER. Journal of Materials Chemistry A, 2019, 7, 27175-27185.	5.2	122
44968	Hydroxyl group modification improves the electrocatalytic ORR and OER activity of graphene supported single and bi-metal atomic catalysts (Ni, Co, and Fe). Journal of Materials Chemistry A, 2019, 7, 24583-24593.	5.2	126
44969	Insights into the electrochemical processes of rechargeable magnesiumâ€“sulfur batteries with a new cathode design. Journal of Materials Chemistry A, 2019, 7, 25490-25502.	5.2	53
44970	Strong (001) facet-induced growth of multi-hierarchical tremella-like Sn-doped V₂O₅ for high-performance potassium-ion batteries. Journal of Materials Chemistry A, 2019, 7, 25993-26001.	5.2	18
44971	Interfacial synergy of ultralong jagged Pt₈₅Mo₁₅â€“S nanowires with abundant active sites on enhanced hydrogen evolution in an alkaline solution. Journal of Materials Chemistry A, 2019, 7, 24328-24336.	5.2	35
44972	Effect of Cd on cation redistribution and order-disorder transition in Cu₂(Zn,Cd)SnS₄. Journal of Materials Chemistry A, 2019, 7, 26927-26933.	5.2	22
44973	A Setaria-inflorescence-structured catalyst based on nickelâ€“cobalt wrapped silver nanowire conductive networks for highly efficient hydrogen evolution. Journal of Materials Chemistry A, 2019, 7, 26566-26573.	5.2	10
44974	Light enhanced moisture degradation of perovskite solar cell material CH₃NH₃PbI₃. Journal of Materials Chemistry A, 2019, 7, 27469-27474.	5.2	37
44975	Highly polarization-sensitive, visible-blind and self-powered ultraviolet photodetection based on two-dimensional wide bandgap semiconductors: a theoretical prediction. Journal of Materials Chemistry A, 2019, 7, 27503-27513.	5.2	42
44976	Photo-sensitizing thin-film ferroelectric oxides using materials databases and high-throughput calculations. Journal of Materials Chemistry A, 2019, 7, 27323-27333.	5.2	12
44977	Unconventional superconductivity in 3d rocksalt transition metal carbides. Journal of Materials Chemistry C, 2019, 7, 12619-12632.	2.7	18
44978	Boosting the intrinsic carrier mobility of two-dimensional pnictogen nanosheets by 1000 times via hydrogenation. Journal of Materials Chemistry C, 2019, 7, 13080-13087.	2.7	2
44979	Self energy and excitonic effect in (un)doped TiO₂ anatase: a comparative study of hybrid DFT, GW and BSE to explore optical properties. Journal of Materials Chemistry C, 2019, 7, 14284-14293.	2.7	24
44980	High efficiency hydrogen purification through P₂C₃ membrane: A theoretical study*. Chinese Physics B, 2019, 28, 128703.	0.7	6
44981	Role of correlations in determining the Van Hove strain in <mml:math xmlns:mml="http://www.w3.org/1998/Math/MathML"><mml:msub><mml:mi mathvariant="normal">Sr</mml:mi><mml:mn>2</mml:mn></mml:msub><mml:msub><mml:mi mathvariant="normal">RuO</mml:mi><mml:mn>4</mml:mn></mml:msub></mml:math>. Physical Review B, 2019, 100, .	1.1	36

#	Article	IF	Citations
44982	Enhancing Oxygen Electroreduction Activity of Single-Site Feâ€“Nâ€“C Catalysts by a Metal Support. Journal of Physical Chemistry C, 2019, 123, 30335-30340.	1.5	6
44983	Pressure-Induced Novel Stable Stoichiometries in Molybdenumâ€“Phosphorus Phase Diagrams under Pressure. Journal of Physical Chemistry C, 2019, 123, 30187-30197.	1.5	8
44984	X-ray Photoelectron Fingerprints of High-Valence Rutheniumâ€“Oxo Complexes along the Oxidation Reaction Pathway in an Aqueous Environment. Journal of Physical Chemistry Letters, 2019, 10, 7636-7643.	2.1	6
44985	Proton-Detected Multidimensional Solid-State NMR Enables Precise Characterization of Vanadium Surface Species at Natural Abundance. Journal of Physical Chemistry Letters, 2019, 10, 7898-7904.	2.1	12
44986	First-Principles Exploration of Two-Dimensional Transition Metal Dichalcogenides Based on Fe, Co, Ni, and Cu Groups and Their van der Waals Heterostructures. ACS Applied Energy Materials, 2019, 2, 8491-8501.	2.5	27
44987	Solar-to-Steam Generation via Porous Black Membranes with Tailored Pore Structures. ACS Applied Materials & Interfaces, 2019, 11, 48300-48308.	4.0	21
44988	Critical Role of Tricyclic Bridges Including Neighboring Rings for Understanding Raman Spectra of Zeolites. Journal of the American Chemical Society, 2019, 141, 20318-20324.	6.6	32
44989	Strong thermal conductivity dependence on arsenic-vacancy complex formation in arsenic-doped silicon. Journal of Applied Physics, 2019, 126, 195104.	1.1	1
44990	Adiabatic and nonadiabatic energy dissipation during scattering of vibrationally excited CO from Au(111). Physical Review B, 2019, 100, .	1.1	23
44991	Formation of a two-dimensional single-component correlated electron system and band engineering in the nickelate superconductor <mml:math xmlns:mml="http://www.w3.org/1998/Math/MathML"><mml:msub><mml:mi>NdNiO</mml:mi><mml:mn>2</mml:mn></mml:msub> Physical Review B, 2019, 100, .	1.1	161
44992	Fast, scalable and accurate finite-element based ab initio calculations using mixed precision computing. , 2019, , .		28
44993	Bilayer MoSe2/HfS2 Nanocomposite as a Potential Visible-Light-Driven Z-Scheme Photocatalyst. Nanomaterials, 2019, 9, 1706.	1.9	20
44994	Effects of Electric Field on the Performance of Graphene-Based Counter Electrodes for Dye-Sensitized Solar Cells: A Theoretical Study. Journal of Physical Chemistry C, 2019, 123, 30373-30381.	1.5	6
44995	On-Surface Intramolecular Dehalogenation of Vicinal Dibromides for the Direct Formation of Câ€“C Double Bonds. Journal of Physical Chemistry C, 2019, 123, 30467-30472.	1.5	1
44996	Non-Fermi-liquid types of behavior associated with a magnetic quantum critical point in <mml:math xmlns:mml="http://www.w3.org/1998/Math/MathML"><mml:mrow><mml:mi>Sr</mml:mi><mml:msub><mml:mrow><mml:mn>(</mml Physical Review B, 2019, 100, .	1.1	19
44997	Geometric and Electronic Effects Contributing to N₂ Dissociation Barriers on a Range of Active Sites on Ru Nanoparticles. Journal of Physical Chemistry C, 2019, 123, 30458-30466.	1.5	13
44998	Reversible magnetoelectric switching in multiferroic three-dimensional nanocup heterostructure films. NPG Asia Materials, 2019, 11, .	3.8	8
44999	A systematic study of the negative thermal expansion in zinc-blende and diamond-like semiconductors. New Journal of Physics, 2019, 21, 123015.	1.2	10

#	Article	IF	Citations
45000	Electronic properties of binary compounds with high fidelity and high throughput. Journal of Physics: Conference Series, 2019, 1290, 012011.	0.3	6
45001	Mechanism of Ferromagnetic Ordering of Mn Chains in CaMnGe2O6 Clinopyroxene. JETP Letters, 2019, 110, 595-598.	0.4	1
45002	Density Functional Study of the Electronic, Elastic and Optical Properties of Bi₂O₂Te. Zeitschrift Fur Naturforschung - Section A Journal of Physical Sciences, 2019, 75, 73-80.	0.7	6
45003	Tunable Electronic Properties of Graphene/g-AlN Heterostructure: The Effect of Vacancy and Strain Engineering. Nanomaterials, 2019, 9, 1674.	1.9	32
45004	Lanthanum Doping Enabling High Drain Current Modulation in a p-Type Tin Monoxide Thin-Film Transistor. ACS Applied Materials & Interfaces, 2019, 11, 47025-47036.	4.0	26
45005	Real-space observation of far- and near-field-induced photolysis of molecular oxygen on an Ag(110) surface by visible light. Journal of Chemical Physics, 2019, 151, 144705.	1.2	14
45006	Study of the compression behavior and high-pressure strength of a-Si3N4 combining experimental and theoretical methods. AIP Advances, 2019, 9, .	0.6	0
45007	Robust generation of half-metallic transport and pure spin current with photogalvanic effect in zigzag silicene nanoribbons. Journal of Physics Condensed Matter, 2019, 31, 495701.	0.7	18
45008	Detrimental Effects and Prevention of Acidic Electrolytes on Oxygen Reduction Reaction Catalytic Performance of Heteroatom-Doped Graphene Catalysts. Frontiers in Materials, 2019, 6, .	1.2	6
45009	Prediction of room-temperature half-metallicity in layered halide double perovskites. Npj Computational Materials, 2019, 5, .	3.5	19
45010	First-Principles Study of Gas Molecule Adsorption on C-doped Zigzag Phosphorene Nanoribbons. Coatings, 2019, 9, 763.	1.2	11
45011	Theoretical design of a novel 2D tetragonal ZnS/SnO hetero-bilayer as a promising photocatalyst for solar water splitting. International Journal of Hydrogen Energy, 2019, 44, 27816-27824.	3.8	11
45012	Symmetric Small-Molecules with Acceptorâ€“Donorâ€“Acceptor Architecture for Efficient Visible-Light Driven Hydrogen Production: Optical and Thermodynamic Aspects. Journal of Physical Chemistry C, 2019, 123, 30799-30808.	1.5	10
45013	Probing Angle-Dependent Interlayer Coupling in Twisted Bilayer WS₂. Journal of Physical Chemistry C, 2019, 123, 30684-30688.	1.5	28
45014	Tuning Magnetism in Layered Magnet VI₃: A Theoretical Study. Journal of Physical Chemistry C, 2019, 123, 30545-30550.	1.5	37
45015	Cu@g-C₃N₄: An Efficient Single-Atom Electrocatalyst for NO Electrochemical Reduction with Suppressed Hydrogen Evolution. Journal of Physical Chemistry C, 2019, 123, 31043-31049.	1.5	61
45016	A New Metallic In₃O₄ Sheet as an Anode Material for Sodium-Ion Batteries. Journal of Physical Chemistry C, 2019, 123, 30213-30220.	1.5	11
45017	Layer-Dependent Properties of Ultrathin GeS Nanosheets and Application in UVâ€“Vis Photodetectors. ACS Applied Materials & Interfaces, 2019, 11, 47197-47206.	4.0	35

#	Article	IF	Citations
45018	Commensurate-incommensurate phase transition of dense potassium simulated by machine-learned interatomic potential. Physical Review B, 2019, 100, .	1.1	8
45019	Phonon Lifetimes throughout the Brillouin Zone at Elevated Temperatures from Experiment andAbÂInitio. Physical Review Letters, 2019, 123, 235501.	2.9	20
45020	Chiral fermion reversal in chiral crystals. Nature Communications, 2019, 10, 5505.	5.8	35
45021	Effect of electric field on optoelectronic properties of indiene monolayer for photoelectric nanodevices. Scientific Reports, 2019, 9, 17300.	1.6	18
45022	Thermodynamic Properties of Stoichiometric Non-Superconducting Phase Y2BaCuO5. Materials, 2019, 12, 3163.	1.3	1
45023	Plasma Surface Polymerized and Biomarker Conjugated Boron Nitride Nanoparticles for Cancer-Specific Therapy: Experimental and Theoretical Study. Nanomaterials, 2019, 9, 1658.	1.9	6
45024	Influence of Bi doping on physical properties of lead halide perovskites: a comparative first-principles study between CsPbI3 and CsPbBr3. Materials Today Advances, 2019, 3, 100019.	2.5	17
45025	Near 100% CO selectivity in nanoscaled iron-based oxygen carriers for chemical looping methane partial oxidation. Nature Communications, 2019, 10, 5503.	5.8	98
45026	Assessing Relativistic Effects and Electron Correlation in the Actinide Metals Th to Pu. Applied Sciences (Switzerland), 2019, 9, 5020.	1.3	20
45027	Vacancy ordered structures in a nonstoichiometric niobium carbide NbC0.83. Mendeleev Communications, 2019, 29, 707-709.	0.6	7
45028	Coadsorption of CO and H₂ on an Iron Surface and Its Implication on the Hydrogen Embrittlement of Iron. Journal of Physical Chemistry C, 2019, 123, 30265-30273.	1.5	19
45029	Oxidized Silicon Sulfide: Stability and Electronic Properties of a Novel Two-Dimensional Material. Journal of Physical Chemistry C, 2019, 123, 29986-29993.	1.5	2
45030	Mechanical and Electrical Monitoring in the Dynamics of Twisted Phosphorene Nanoflakes on 2D Monolayers. Journal of Physical Chemistry C, 2019, 123, 30704-30713.	1.5	2
45031	Raman Tensor of WSe₂ via Angle-Resolved Polarized Raman Spectroscopy. Journal of Physical Chemistry C, 2019, 123, 29337-29342.	1.5	23
45032	Atom-Resolved Chemical States in the Multivalent U-TM-O (TM: Ti, V, Cr, Mn, Fe, Ni, Nb, Mo, W) Ternary Oxides from First-Principles. Journal of Physical Chemistry C, 2019, 123, 29609-29622.	1.5	11
45033	Probing Structural Reconstruction of Metal Nanoparticles under Annealing and Water Vapor Conditions: A Theoretical Study. Journal of Physical Chemistry C, 2019, 123, 29783-29793.	1.5	7
45034	Elucidating the Nature of Interactions in Collagen Triple-Helix Wrapping. Journal of Physical Chemistry Letters, 2019, 10, 7644-7649.	2.1	10
45035	Kinetic Ionic Permeation and Interfacial Doping of Supported Graphene. Nano Letters, 2019, 19, 9029-9036.	4.5	16

#	Article	IF	Citations
45036	Emergence of Si₂BN Monolayer as Efficient HER Catalyst under Co-functionalization Influence. ACS Applied Energy Materials, 2019, 2, 8441-8448.	2.5	18
45037	A High Capacity Bilayer Cathode for Aqueous Zn-Ion Batteries. ACS Nano, 2019, 13, 14447-14458.	7.3	148
45038	Interrelation between the grain boundary energy and the packing density in Î±-Fe. AIP Conference Proceedings, 2019, , .	0.3	1
45039	First-principles analysis of ferromagnetic properties of molybdenum-doped wide-band-gap oxides. Philosophical Magazine Letters, 2019, 99, 326-337.	0.5	19
45040	Impact of biaxial and uniaxial strain on <mml:math xmlns:mml="http://www.w3.org/1998/Math/MathML"><mml:msub><mml:mi mathvariant="normal">V</mml:mi><mml:mn>2</mml:mn></mml:msub><mml:msub><mml:mi mathvariant="normal">O</mml:mi><mml:mn>3</mml:mn></mml:msub></mml:math>. Physical Review B, 2019, 100, .	1.1	8
45041	Self-supported hydrogenolysis of aromatic ethers to arenes. Science Advances, 2019, 5, eaax6839.	4.7	39
45042	Boron Carbide Secrets. Russian Journal of General Chemistry, 2019, 89, 2069-2074.	0.3	2
45043	Computational Insights into the Interaction between Li 2 S/Li 2 S 2 and Heteroatomâ€Doped Graphene Materials. ChemistrySelect, 2019, 4, 12612-12621.	0.7	3
45044	Tunable optical properties and DFT calculations of RE3+ codoped LaBO3 phosphors. Optical Materials, 2019, 98, 109487.	1.7	6
45045	Dissociation, Dissolution, and Diffusion of Nitrogen on V_xFe_y and V_xCr_y Alloy Membranes Studied by First Principles. Journal of Physical Chemistry C, 2019, 123, 30416-30426.	1.5	1
45046	Strain Controls Charge Carrier Lifetimes in Monolayer WSe₂: Ab Initio Time Domain Analysis. Journal of Physical Chemistry Letters, 2019, 10, 7732-7739.	2.1	36
45047	In Situ Compositing CsPbBr₃ with Exfoliated Layered-Perovskite CsCa₂Ta₃O₁₀: Interfacial Interaction and Enhanced Stability. ACS Applied Materials & Interfaces, 2019, 11, 47227-47236.	4.0	9
45048	Oxygen-Vacancy-Enriched Porous Î±-MoO₃ Nanosheets for Trimethylamine Sensing. ACS Applied Nano Materials, 2019, 2, 8016-8026.	2.4	80
45049	Enhanced Photocatalytic Activity of SiC-Based Ternary Graphene Materials: A DFT Study and the Photocatalytic Mechanism. ACS Omega, 2019, 4, 20142-20151.	1.6	20
45050	In situ formation of mononuclear complexes by reaction-induced atomic dispersion of supported noble metal nanoparticles. Nature Communications, 2019, 10, 5281.	5.8	57
45051	Interface-induced magnetic polar metal phase in complex oxides. Nature Communications, 2019, 10, 5248.	5.8	35
45052	Quasiparticle effects on the linear and nonlinear susceptibility of ZnGeP₂. RSC Advances, 2019, 9, 35771-35779.	1.7	3
45053	Six-dimensional potential energy surfaces for the dissociative chemisorption of HCl on rigid Ag(100) and Ag(110) surfaces. Journal of Chemical Physics, 2019, 151, 144707.	1.2	10

#	Article	IF	Citations
45054	Prediction of the structure, magnetic properties, and martensitic transition of Mg-V-Ga Heusler alloys using first-principles calculations. Journal of Applied Physics, 2019, 126, .	1.1	0
45055	Transmorphic epitaxial growth of AlN nucleation layers on SiC substrates for high-breakdown thin GaN transistors. Applied Physics Letters, 2019, 115, .	1.5	25
45056	Melting curve of vanadium up to 470â€‰GPa simulated by ab initio molecular dynamics. Journal of Applied Physics, 2019, 126, .	1.1	10
45057	Optical injection of spin current into a zigzag nanoribbon of monolayer <mml:math xmlns:mml="http://www.w3.org/1998/Math/MathML"><mml:msub><mml:mi>MoS</mml:mi><mml:mn>2</mml:mn></mml:msub></mml with antiferromagnetic Kekule distortion. Physical Review B, 2019, 100, .	1.1	2
45058	Excitons and narrow bands determine the optical properties of cesium bismuth halides. Physical Review B, 2019, 100, .	1.1	21
45059	Surface- and Strain-Mediated Reversible Phase Transformation in Quantum-Confined ZnO Nanowires. Physical Review Letters, 2019, 123, 216101.	2.9	19
45060	Anisotropic Two-Dimensional Screening at the Surface of Black Phosphorus. Physical Review Letters, 2019, 123, 216403.	2.9	21
45061	Quantum Phase Transition of Correlated Iron-Based Superconductivity in <mml:math xmlns:mml="http://www.w3.org/1998/Math/MathML" display="inline"><mml:mrow><mml:msub><mml:mrow><mml:mi>LiFe</mml:mi></mml:mrow><mml:mrow><mml:mn>1</mml:mn><mml:mn> Physical Review Letters, 2019, 123, 217004.	2.9	19
45062	Evolution of Magnetic Anisotropy of an Organometallic Molecule in a Mechanically Controlled Break Junction: The Roles of Connecting Electrodes. Journal of Physical Chemistry C, 2019, 123, 30754-30764.	1.5	8
45063	A₂Cu₃In₃Te₈ (A = Cd, Zn, Mn, Mg): A Type of Thermoelectric Material with Complex Diamond-like Structure and Low Lattice Thermal Conductivities. ACS Applied Energy Materials, 2019, 2, 8956-8965.	2.5	17
45064	Design of a High-Performance Electrocatalyst for N₂ Conversion to NH₃ by Trapping Single Metal Atoms on Stepped CeO₂. ACS Applied Materials & Interfaces, 2019, 11, 47525-47534.	4.0	64
45065	The 2D InSe/WS₂ Heterostructure with Enhanced Optoelectronic Performance in the Visible Region*. Chinese Physics Letters, 2019, 36, 097301.	1.3	11
45066	The CeFe₁₁Ti permanent magnet: a closer look at the microstructure of the compound. Journal of Physics Condensed Matter, 2019, 31, 505505.	0.7	6
45067	Superconducting TaH5 at high pressure. New Journal of Physics, 2019, 21, 123009.	1.2	6
45068	Experimental and theoretical investigations on the composition-dependent structural phase transition in Cu₂Cd_xZn_{1âˆ’x}SnS₄. Materials Research Express, 2019, 6, 125525.	0.8	9
45069	Electronic and magnetic state of <mml:math xmlns:mml="http://www.w3.org/1998/Math/MathML"><mml:msub><mml:mi>LaMnO</mml:mi><mml:mn>3</mml:mn></mml:msub> epitaxially strained on <mml:math	1.1	11
45070	Anomalous thermal expansion in one-dimensional transition metal cyanides: Behavior of the trimetallic cyanide <mml:math xmlns:mml="http://www.w3.org/1998/Math/MathML"><mml:mrow><mml:mi mathvariant="normal">C</mml:mi><mml:msub><mml:mi mathvariant="normal">u</mml:mi><mml:mrow><mml:mn>1</mml:mn><mml:mo>/</mml:mo><mml:mn>3</mml:mn></mml:mrow></	1.1	3
45071	Observation of bulk states and spin-polarized topological surface states in transition metal dichalcogenide Dirac semimetal candidate <mml:math xmlns:mml="http://www.w3.org/1998/Math/MathML"><mml:msub><mml:mi mathvariant="normal">NiTe</mml:mi><mml:mn>2</mml:mn></mml:msub></mml:math>. Physical Review	1.1	56

#	Article	IF	Citations
45072	Quantum anomalous Hall effect by coupling heavy atomic layers with <mml:math xmlns:mml="http://www.w3.org/1998/Math/MathML"><mml:msub><mml:mi>CrI</mml:mi><mml:mn>3</mml:mn></mml:msub></mml: Physical Review B, 2019, 100, .	1.1	9
45073	Large and controllable spin-valley splitting in two-dimensional <mml:math xmlns:mml="http://www.w3.org/1998/Math/MathML"><mml:mrow><mml:mi mathvariant="normal">W</mml:mi><mml:msub><mml:mi mathvariant="normal">S</mml:mi><mml:mn>2</mml:mn></mml:msub><mml:mo>/</mml:mo><mml:mi>h</mml:mi><mml:mo>â^'</	1.1	49
45074	Electronic structure of rare-earth infinite-layer <mml:math xmlns:mml="http://www.w3.org/1998/Math/MathML"><mml:mrow><mml:mi>R</mml:mi><mml:mi>Ni</mml:mi><mml:msub><mml:mi mathvariant="normal">O</mml:mi><mml:mn>2</mml:mn></mml:msub></mml:mrow><mml:mrow><mml:mo>(</mml:mo><mml:mi>R Physical Review B, 2019, 100, .	1.1	98
45075	Fast nonadiabatic dynamics of many-body quantum systems. Science Advances, 2019, 5, eaaw1634.	4.7	26
45076	Sandwiched NiO/Î²â€Mo₂C/RGO as Improved Electrocatalyst for Hydrogen Evolution Reaction: Solvothermalâ€Assisted Selfâ€Assembly and Catalytic Mechanism. ChemElectroChem, 2019, 6, 5958-5966.	1.7	12
45077	cis-Câ•C Bond and Amide Regulated Oriented Supramolecular Assembly on Two-Dimensional Atomic Crystals. Journal of Physical Chemistry C, 2019, 123, 30996-31002.	1.5	1
45078	Self-Assembly Growth of an Upright Molecular Precursor with a Rigid Framework. Journal of Physical Chemistry C, 2019, 123, 31272-31278.	1.5	4
45079	Why Silicon Doping Accelerates Electron Polaron Diffusion in Hematite. Journal of the American Chemical Society, 2019, 141, 20222-20233.	6.6	42
45080	A comparative study using state-of-the-art electronic structure theories on solid hydrogen phases under high pressures. Npj Computational Materials, 2019, 5, .	3.5	16
45081	Fast, accurate, and transferable many-body interatomic potentials by symbolic regression. Npj Computational Materials, 2019, 5, .	3.5	45
45082	Al5+Î±Si5+ÎN12, a new Nitride compound. Scientific Reports, 2019, 9, 15907.	1.6	4
45083	Chern and Z2 topological insulating phases in perovskite-derived 4d and 5d oxide buckled honeycomb lattices. Scientific Reports, 2019, 9, 17306.	1.6	4
45084	First-principles investigation of the ferroelectric, piezoelectric and nonlinear optical properties of LiNbO3-type ZnTiO3. Scientific Reports, 2019, 9, 17632.	1.6	12
45085	Constraining CO coverage on copper promotes high-efficiency ethylene electroproduction. Nature Catalysis, 2019, 2, 1124-1131.	16.1	214
45086	Crystal field splitting, local anisotropy, and low-energy excitations in the quantum magnet <mml:math xmlns:mml="http://www.w3.org/1998/Math/MathML"><mml:msub><mml:mi>YbCl</mml:mi><mml:mn>3</mml:mn></mml:msub></mml Physical Review B, 2019, 100, .	1.1	26
45087	Origin of up-up-down-down magnetic order in <mml:math xmlns:mml="http://www.w3.org/1998/Math/MathML"><mml:mrow><mml:msub><mml:mi>Cu</mml:mi><mml:mn>2</mml:mn></mml:msub></mml:mrow></mml Physical Review B, 2019, 100, .	1.1	9
45088	Saddle-point Van Hove singularity and dual topological state in <mml:math xmlns:mml="http://www.w3.org/1998/Math/MathML"><mml:mrow><mml:msub><mml:mi>Pt</mml:mi><mml:mn>2</mml:mn></mml:msub></mml:mrow></mml Physical Review B, 2019, 100, .	1.1	21
45089	Experimental characterization of hydrogen adsorption sites for H/W(111) using low energy ion scattering. Physical Review B, 2019, 100, .	1.1	8

#	Article	IF	Citations
45090	Design of Heteroanionic MoON Exhibiting a Peierls Metal-Insulator Transition. Physical Review Letters, 2019, 123, 236402.	2.9	12
45091	Spin polarization properties of two-dimensional MoSeTe induced by transition-metal doping: first-principles calculations. European Physical Journal B, 2019, 92, 1.	0.6	7
45092	Defect-Engineered MoS₂ Nanostructures for Reactive Oxygen Species Generation in the Dark: Antipollutant and Antifungal Performances. ACS Applied Materials & Interfaces, 2019, 11, 48179-48191.	4.0	36
45093	Tailoring Coral-Like Fe₇Se₈@C for Superior Low-Temperature Li/Na-Ion Half/Full Batteries: Synthesis, Structure, and DFT Studies. ACS Applied Materials & Interfaces, 2019, 11, 47886-47893.	4.0	35
45094	Lattice dynamics of the hybrid improper ferroelectrics <mml:math xmlns:mml="http://www.w3.org/1998/Math/MathML"><mml:mrow><mml:msub><mml:mrow><mml:mo>(</mml:mo><mml:mi>Ca</mml:mi> mathvariant="normal">O</mml:mi><mml:mn>7</mml:mn></mml:msub></mml:mrow></mml:math>. Physical Review B, 2019, 100, .	1.1	9
45095	NbS ₂ : A Promising p -Type Ohmic Contact for Two-Dimensional Materials. Physical Review Applied, 2019, 12, .	1.5	36
45096	Magnetic states of iron-based two-leg ladder tellurides. Physical Review B, 2019, 100, .	1.1	20
45097	Strain-driven superplasticity of ultrathin tin (II) oxide films and the modulation of their electronic properties: A first-principles study. Physical Review B, 2019, 100, .	1.1	15
45098	Chemical tuning between triangular and honeycomb structures in a <mml:math xmlns:mml="http://www.w3.org/1998/Math/MathML"><mml:mrow><mml:mn>5</mml:mn><mml:mi>d</mml:mi> spin-orbit Mott insulator. Physical Review B, 2019, 100, .	1.1	4
45099	Large easy-axis anisotropy in the one-dimensional magnet <mml:math xmlns:mml="http://www.w3.org/1998/Math/MathML"><mml:mrow><mml:mi>BaMo</mml:mi><mml:msub><mml:mrow> Physical Review B, 2019, 100, .	1.1	12
45100	Pressure-induced superconductivity in GeAs. Physical Review B, 2019, 100, .	1.1	9
45101	Diversity of structural phases and resulting control of properties in brownmillerite oxides: A first-principles study. Physical Review B, 2019, 100, .	1.1	8
45102	Anisotropic magnetoresistance and nontrivial spin Hall magnetoresistance in <mml:math xmlns:mml="http://www.w3.org/1998/Math/MathML"><mml:mrow><mml:mi>Pt</mml:mi><mml:mo>/</mml:mo><mml:mi>Î±</mml:mi> mathvariant="normal">F</mml:mi><mml:msub><mml:mi mathvariant="normal">e</mml:mi><mml:mn>2</mml:mn></mml:msub><mml:msub><mml:mi mathvariant="normal">O</mml:mi><mml:mn>3</mml:mn></mml:msub></mml:mrow></mml:math> bilayers. Physical Review B, 2019, 100, .	1.1	35
45103	Metastable interlayer Frenkel pair defects in black phosphorus. Physical Review B, 2019, 100, .	1.1	10
45104	First-principles study of high-pressure phase stability and superconductivity of <mml:math xmlns:mml="http://www.w3.org/1998/Math/MathML"><mml:mrow><mml:msub><mml:mi>Bi</mml:mi><mml:mn>4</mml:mn></mml:msub> mathvariant="normal">I</mml:mi><mml:mn>4</mml:mn></mml:msub></mml:mrow></mml:math>. Physical Review B, 2019, 100, .	1.1	9
45105	DFT study of itinerant ferromagnetism in <mml:math xmlns:mml="http://www.w3.org/1998/Math/MathML"><mml:mi>p</mml:mi></mml:math> -doped monolayers of <mml:math xmlns:mml="http://www.w3.org/1998/Math/MathML"><mml:msub><mml:mi>MoS</mml:mi><mml:mn>2</mml:mn></mml:msub> Physical Review B, 2019, 100, .	1.1	9
45106	Interfacial coupling induced critical thickness for the ferroelectric bistability of two-dimensional ferromagnet/ferroelectric van der Waals heterostructures. Physical Review B, 2019, 100, .	1.1	30
45107	Quantum oscillations and electronic structure in the largeâ€“Chern number semimetal RhSn. Physical Review B, 2019, 100, .	1.1	12

#	Article	IF	Citations
45108	Role of charge transfer in hybridization-induced spin transition in metal-organic molecules. Physical Review B, 2019, 100, .	1.1	5
45109	Quantization of spin Hall conductivity in two-dimensional topological insulators versus symmetry and spin-orbit interaction. Physical Review B, 2019, 100, .	1.1	25
45110	Vibrational response and motion of carbon monoxide on Cu(100) driven by femtosecond laser pulses: Molecular dynamics with electronic friction. Physical Review B, 2019, 100, .	1.1	16
45111	Ferroelectric surface chemistry: First-principles study of adsorption on the stoichiometric <mml:math xmlns:mml="http://www.w3.org/1998/Math/MathML"><mml:mrow><mml:mi>LiNb</mml:mi><mml:msub><mml:mi mathvariant="normal">O</mml:mi><mml:mn>3</mml:mn></mml:msub></mml:mrow></mml:math> (0001) surface. Physical Review B, 2019, 100, .	1.1	9
45112	Effect of Hydrogen Doping to MgTiH₃ Perovskite Type Hydride to Enhance Hydrogen Storage Properties. , 2019, , .		1
45113	Fabricating Fe nanocrystals via encapsulation at the graphite surface. Journal of Vacuum Science and Technology A: Vacuum, Surfaces and Films, 2019, 37, 061403.	0.9	14
45114	Quasiparticle interference evidence of the topological Fermi arc states in chiral fermionic semimetal CoSi. Science Advances, 2019, 5, eaaw9485.	4.7	46
45115	A Quantumâ€“Mechanical Study of Clean and Crâ€“Segregated Antiphase Boundaries in Fe3Al. Materials, 2019, 12, 3954.	1.3	7
45116	Theoretical Study of Zirconium Isomorphous Substitution into Zeolite Frameworks. Molecules, 2019, 24, 4466.	1.7	3
45117	Vibrational Characteristics of Two-Dimensional Composite Structures of Hexagonal Boron Nitride and Graphene. Journal of the Korean Physical Society, 2019, 75, 569-576.	0.3	0
45118	Electronic Structure and Polarization of Polar BiOIO3. Journal of the Korean Physical Society, 2019, 75, 990-996.	0.3	6
45119	Atomistic Simulations of Plasmon Mediated Photochemistry. ACS Symposium Series, 2019, , 239-256.	0.5	2
45121	Ferroelectric nonlinear anomalous Hall effect in few-layer WTe2. Npj Computational Materials, 2019, 5, .	3.5	61
45122	Alloying Element Segregation and Grain Boundary Reconstruction, Atomistic Modeling. Metals, 2019, 9, 1319.	1.0	7
45123	Crystal structures and the electronic properties of silicon-rich silicon carbide materials by first principle calculations. Heliyon, 2019, 5, e02908.	1.4	6
45124	BC₂N/Graphene Heterostructure as a Promising Anode Material for Rechargeable Li-Ion Batteries by Density Functional Calculations. Journal of Physical Chemistry C, 2019, 123, 30809-30818.	1.5	22
45125	Thermal Conductivity of Rutile and Anatase TiO2 from First-Principles. Journal of Physical Chemistry C, 2019, 123, 30851-30855.	1.5	11
45126	The ultrathin limit of improper ferroelectricity. Nature Communications, 2019, 10, 5591.	5.8	44

#	Article	IF	Citations
45127	Efficient sky-blue perovskite light-emitting diodes via photoluminescence enhancement. Nature Communications, 2019, 10, 5633.	5.8	267
45128	Janus PtSSe and graphene heterostructure with tunable Schottky barrier. Applied Physics Letters, 2019, 115, .	1.5	69
45129	Disorder-induced localisation and suppression of superconductivity in YSr₂Cu₃O_{6+x}. Journal of Physics Condensed Matter, 2019, 31, 284001.	0.7	1
45130	Phase transitions in titanium with an analytic bond-order potential. Modelling and Simulation in Materials Science and Engineering, 2019, 27, 085008.	0.8	3
45131	Ab Initio Molecular Dynamics Simulation of Divalent Metal Cation Incorporation in Calcite: Implications for Interpreting X-ray Absorption Spectroscopy Data. ACS Earth and Space Chemistry, 2019, 3, 2582-2592.	1.2	11
45132	Edge-State-Induced Stacking of Zigzag Graphene Nanoribbons. ACS Omega, 2019, 4, 22035-22040.	1.6	4
45133	Comparative investigation of the mechanical, electrical and thermal transport properties in graphene-like C3B and C3N. Journal of Applied Physics, 2019, 126, .	1.1	32
45134	Anodic decomposition of surface films on high voltage spinel surfacesâ€"Density function theory and experimental study. Journal of Chemical Physics, 2019, 151, 234713.	1.2	9
45135	DFT study for the mechanical and electronic properties of Mg3BHx (x=l,4,7) compounds for hydrogen storage applications. AIP Conference Proceedings, 2019, , .	0.3	0
45136	Strain-engineered electronic and topological properties of bismuthene on SiC(0001) substrate. Nano Futures, 2019, 3, 045002.	1.0	13
45137	Influence of Mixed Valence on the Formation of Oxygen Vacancy in Cerium Oxides. Materials, 2019, 12, 4041.	1.3	14
45138	Formation of a U(VI)â€"Persulfide Complex during Environmentally Relevant Sulfidation of Iron (Oxyhydr)oxides. Environmental Science & Technology, 2020, 54, 129-136.	4.6	17
45139	Understanding the Electrochemical Reduction of Carbon Dioxide at Copper Surfaces. ACS Symposium Series, 2019, , 209-223.	0.5	1
45140	Topological electronic states in HfRuP family superconductors. Npj Computational Materials, 2019, 5, .	3.5	21
45141	Prediction and observation of an antiferromagnetic topological insulator. Nature, 2019, 576, 416-422.	13.7	701
45142	Distinct dependence on size of Pt and Rh nanoclusters on graphene/Pt(111) in the decomposition of methanol-d4. Journal of Chemical Physics, 2019, 151, 224707.	1.2	19
45143	Ab initio study of enhanced thermal conductivity in ordered AlGaO3 alloys. Applied Physics Letters, 2019, 115, .	1.5	24
45144	Two-Dimensional Fluorine Distribution in a Heavily Distorted Perovskite Nickel Oxyfluoride Revealed by First-Principles Calculation. Journal of Physical Chemistry C, 2019, 123, 31190-31195.	1.5	4

#	Article	IF	Citations
45145	A van der Waals Heterostructure Based on Graphene-like Gallium Nitride and Boron Selenide: A High-Efficiency Photocatalyst for Water Splitting. ACS Omega, 2019, 4, 21689-21697.	1.6	78
45146	Weyl-like points from band inversions of spin-polarised surface states in NbGeSb. Nature Communications, 2019, 10, 5485.	5.8	14
45147	Palladium-bearing intermetallic electride as anÂefficient and stable catalyst for Suzuki cross-coupling reactions. Nature Communications, 2019, 10, 5653.	5.8	43
45148	Structural evolution and the role of native defects in subnanometer MoS nanowires. Physical Review B, 2019, 100, .	1.1	7
45149	Ab initio simulations for expanded gold fluid in metal-nonmetal transition regime. Physics of Plasmas, 2019, 26, 122705.	0.7	4
45150	Electronic properties of Pb-I deficient lead halide perovskites. Journal of Chemical Physics, 2019, 151, 234704.	1.2	7
45151	Mechanical properties of 1T-, 1Tâ€²-, and 1H-MX2 monolayers and their 1H/1Tâ€²-MX2 (M = Mo, W and X = S, Se, Te) heterostructures. AIP Advances, 2019, 9, .	0.6	13
45152	Dynamics of Single-Molecule Dissociation by Selective Excitation of Molecular Phonons. Physical Review Letters, 2019, 123, 246804.	2.9	4
45153	The Conundrum of Relaxation Volumes in First-Principles Calculations of Charged Defects in UO2. Applied Sciences (Switzerland), 2019, 9, 5276.	1.3	11
45154	Interface Structure and Band Alignment of CZTS/CdS Heterojunction: An Experimental and First-Principles DFT Investigation. Materials, 2019, 12, 4040.	1.3	10
45155	Spin-Unrestricted and Spinor Nonradiative Relaxation Dynamics in Functionalized Semiconductors. ACS Symposium Series, 2019, , 1-22.	0.5	1
45156	Quasicubic model for metal halide perovskite nanocrystals. Journal of Chemical Physics, 2019, 151, 234106.	1.2	64
45157	Vertical van der Waals Heterostructure of Single Layer InSe and SiGe. Journal of Physical Chemistry C, 2019, 123, 31232-31237.	1.5	14
45158	Transition Metal Doping of Phase Change Materials: Atomic Arrangement of Cr-Doped Ge₂Sb₂Te₅. Journal of Physical Chemistry C, 2019, 123, 30640-30648.	1.5	10
45159	Effects of Off-Stoichiometry in the Epitaxial NdNiO₃ Film on the Suppression of Its Metal-Insulator-Transition Properties. ACS Applied Electronic Materials, 2019, 1, 2678-2683.	2.0	13
45160	Rh single atoms on TiO2 dynamically respond to reaction conditions by adapting their site. Nature Communications, 2019, 10, 4488.	5.8	191
45161	Nonmagnetic single-molecule spin-filter based on quantum interference. Nature Communications, 2019, 10, 5565.	5.8	57
45162	Electrical charge state identification and control for the silicon vacancy in 4H-SiC. Npj Quantum Information, 2019, 5, .	2.8	54

#	Article	IF	Citations
45163	All-temperature batteries enabled by fluorinated electrolytes with non-polar solvents. Nature Energy, 2019, 4, 882-890.	19.8	557
45164	Enhancement of thermoelectric performance across the topological phase transition in dense lead selenide. Nature Materials, 2019, 18, 1321-1326.	13.3	87
45165	Axionic charge-density wave in the Weyl semimetal (TaSe4)2I. Nature, 2019, 575, 315-319.	13.7	143
45166	Real-space charge-density imaging with sub-Ã¥ngstrÃ¶m resolution by four-dimensional electron microscopy. Nature, 2019, 575, 480-484.	13.7	127
45167	Molecular nitrogen promotes catalytic hydrodeoxygenation. Nature Catalysis, 2019, 2, 1078-1087.	16.1	63
45168	A fast neural network approach for direct covariant forces prediction in complex multi-element extended systems. Nature Machine Intelligence, 2019, 1, 471-479.	8.3	32
45169	Ultra-small Cd@NiAg and Cr@NiAg nano-clusters with enhanced mixing. AIP Advances, 2019, 9, 115316.	0.6	10
45170	One-step solution synthesis of white-light-emitting films via dimensionality control of the Csâ€“Cuâ€“I system. APL Materials, 2019, 7, .	2.2	73
45171	BAlGaN alloys nearly lattice-matched to AlN for efficient UV LEDs. Applied Physics Letters, 2019, 115, .	1.5	10
45172	Effect of point defects and functionalization on structural stability and electron properties of borophene as investigated by means of density functional theory. IOP Conference Series: Materials Science and Engineering, 2019, 672, 012032.	0.3	0
45173	Pressure-induced polymorphism in <mml:math xmlns:mml="http://www.w3.org/1998/Math/MathML"><mml:msub><mml:mi>SrB</mml:mi><mml:mn>6</mml:mn></mml:msub></mml and deformation mechanisms of covalent networks. Physical Review B, 2019, 100, .	1.1	31
45174	Magnetic and atomic short range order in Fe1â^'xCrx alloys. Physical Review B, 2019, 100, .	1.1	6
45175	Defect calculations with hybrid functionals in layered compounds and in slab models. Physical Review B, 2019, 100, .	1.1	9
45176	Mott Metal-Insulator Transitions in Pressurized Layered Trichalcogenides. Physical Review Letters, 2019, 123, 236401.	2.9	44
45177	Improved Moisture Stability of Perovskite Solar Cells Using N719 Dye Molecules. Solar Rrl, 2019, 3, 1970115.	3.1	1
45178	Toward ab Initio Ground States of Gold Clusters via Neural Network Modeling. Journal of Physical Chemistry C, 2019, 123, 30088-30098.	1.5	21
45179	Probing Cerium 4f States across the Volume Collapse Transition by X-ray Raman Scattering. Journal of Physical Chemistry Letters, 2019, 10, 7890-7897.	2.1	8
45180	Strain Manipulation of Magnetic Anisotropy in Room-Temperature Ferrimagnetic Quadruple Perovskite CeCu₃Mn₄O₁₂. ACS Applied Electronic Materials, 2019, 1, 2514-2521.	2.0	5

#	Article	IF	Citations
45181	Incommensurate Phase Transition and Electronic Properties of BaMnF4. IOP Conference Series: Materials Science and Engineering, 2019, 613, 012014.	0.3	0
45182	Assessing the film-substrate interaction in germania films on reconstructed Au(111). Physical Review B, 2019, 100, .	1.1	4
45183	Evidence of charge density wave with anisotropic gap in a monolayer <mml:math xmlns:mml="http://www.w3.org/1998/Math/MathML"><mml:msub><mml:mi mathvariant="normal">VTe</mml:mi><mml:mn>2</mml:mn></mml:msub></mml:math> film. Physical Review B, 2019, 100, .	1.1	43
45184	Ab initio prediction of a two-dimensional variant of the iridate <mml:math xmlns:mml="http://www.w3.org/1998/Math/MathML"><mml:msub><mml:mi>IrO</mml:mi><mml:mn>2</mml:mn></mml:msub></mml Physical Review B, 2019, 100, .	1.1	3
45185	Realistic indirect spin interactions between magnetic impurities on a metallic Pb(110) surface. Physical Review B, 2019, 100, .	1.1	1
45186	Corrosion Resistance and Acidic ORR Activity of Pt-based Catalysts Supported on Nanocrystalline Alloys of Molybdenum and Tantalum Carbide. Journal of the Electrochemical Society, 2019, 166, F1292-F1300.	1.3	13
45187	Probing the edge-related properties of atomically thin MoS2 at nanoscale. Nature Communications, 2019, 10, 5544.	5.8	108
45188	Control of the metal-to-insulator transition by substrate orientation in nickelates. AIP Advances, 2019, 9, 105118.	0.6	0
45189	RPA natural orbitals and their application to post-Hartree-Fock electronic structure methods. Journal of Chemical Physics, 2019, 151, 214106.	1.2	18
45190	Current-induced spin polarization in monolayer InSe. Physical Review B, 2019, 100, .	1.1	14
45191	Coexistence of two different atomic structures in the Î£13 pyramidal twin boundary in Î±-Al₂O₃. Philosophical Magazine Letters, 2019, 99, 435-443.	0.5	4
45192	Bulk Rashba effect in multiferroics: A theoretical prediction for <mml:math xmlns:mml="http://www.w3.org/1998/Math/MathML"><mml:msub><mml:mi>BiCoO</mml:mi><mml:mn>3</mml:mn></mml:msub></m Physical Review B, 2019, 100, .	1.1	29
45193	Stronger role of four-phonon scattering than three-phonon scattering in thermal conductivity of III-V semiconductors at room temperature. Physical Review B, 2019, 100, .	1.1	72
45194	Broadband Nonlinear Optical Response of InSe Nanosheets for the Pulse Generation From 1 to 2 Î¼m. ACS Applied Materials & Interfaces, 2019, 11, 48281-48289.	4.0	51
45195	Phononic Helical Nodal Lines with <mml:math xmlns:mml="http://www.w3.org/1998/Math/MathML" display="inline"><mml:mrow><mml:mi mathvariant="script">PT</mml:mi></mml:mrow></mml:math> Protection in <mml:math xmlns:mml="http://www.w3.org/1998/Math/MathML" display="inline"><mml:msub><mml:mi>MoB</mml:mi><mml:mn>2</mml:mn></mml:msub></mml:math>. Physical Review Letters, 2019, 123, 245302.	2.9	68
45196	Effect of Oxygen Interstitial Ordering on Multiple Order Parameters in Rare Earth Ferrite. Physical Review Letters, 2019, 123, 247601.	2.9	13
45197	A High-Pressure Investigation of the Synthetic Analogue of Chalcomenite, CuSeO3â‹™2H2O. Crystals, 2019, 9, 643.	1.0	8
45198	Lateral InSe pâ€“n Junction Formed by Partial Doping for Use in Ultrathin Flexible Solar Cells. Journal of Physical Chemistry Letters, 2019, 10, 7712-7718.	2.1	20

#	Article	IF	Citations
45199	Single-Phase Borophene on Ir(111): Formation, Structure, and Decoupling from the Support. ACS Nano, 2019, 13, 14511-14518.	7.3	99
45200	Common surface structures of graphene and Au(111): The effect of rotational angle on adsorption and electronic properties. Journal of Chemical Physics, 2019, 151, 214701.	1.2	14
45201	Electron transport properties of mirror twin grain boundaries in molybdenum disulfide: Impact of disorder. Physical Review B, 2019, 100, .	1.1	9
45202	Electronic structure analysis of core structures of threading dislocations in GaN. , 2019, , .		1
45203	Expedient synthesis of E -hydrazone esters and 1 H -indazole scaffolds through heterogeneous single-atom platinum catalysis. Science Advances, 2019, 5, eaay1537.	4.7	31
45204	Effect of Competitive Adsorption at the Interface between Aqueous Electrolyte and Solid Electrode. ACS Symposium Series, 2019, , 225-238.	0.5	5
45205	Atomic order, electronic structure and thermodynamic stability of nickel aluminate. Physical Chemistry Chemical Physics, 2019, 21, 25952-25961.	1.3	10
45206	On the active site for electrocatalytic water splitting on late transition metals embedded in graphene. Catalysis Science and Technology, 2019, 9, 6793-6799.	2.1	9
45207	Defect-mediated selective hydrogenation of nitroarenes on nanostructured WS₂. Chemical Science, 2019, 10, 10310-10317.	3.7	30
45208	Optimizing bidentate N-heterocyclic carbene ligands for the modification of late transition metal surfaces â€“ new insights through theory. Physical Chemistry Chemical Physics, 2019, 21, 24926-24934.	1.3	3
45209	Dependency of f states in fluorite-type XO₂ (X = Ce, Th, U) on the stability and electronic state of doped transition metals. Physical Chemistry Chemical Physics, 2019, 21, 25962-25975.	1.3	10
45210	TiO₂-supported Pt single atoms by surface organometallic chemistry for photocatalytic hydrogen evolution. Physical Chemistry Chemical Physics, 2019, 21, 24429-24440.	1.3	32
45211	Molecular mechanisms for thermal degradation of CO₂-loaded aqueous monoethanolamine solution: a first-principles study. Physical Chemistry Chemical Physics, 2019, 21, 22132-22139.	1.3	22
45212	The doping and oxidation of 2D black and blue phosphorene: a new photocatalyst for nitrogen reduction driven by visible light. Physical Chemistry Chemical Physics, 2019, 21, 24449-24457.	1.3	18
45213	Molecular behaviour of phenol in zeolite Beta catalysts as a function of acid site presence: a quasielastic neutron scattering and molecular dynamics simulation study. Catalysis Science and Technology, 2019, 9, 6700-6713.	2.1	12
45214	Continuous synthesis of carbon dots with full spectrum fluorescence and the mechanism of their multiple color emission. Lab on A Chip, 2019, 19, 3974-3978.	3.1	33
45215	Evidence of a strong perpendicular magnetic anisotropy in Au/Co/MgO/GaN heterostructures. Nanoscale Advances, 2019, 1, 4466-4475.	2.2	5
45216	Fluorine-enriched mesoporous carbon as efficient oxygen reduction catalyst: understanding the defects in porous matrix and fuel cell applications. Nanoscale Advances, 2019, 1, 4926-4937.	2.2	30

#	Article	IF	Citations
45217	Insight into the structure and bonding of copper(i) iodide clusters and a cluster-based coordination polymer. New Journal of Chemistry, 2019, 43, 16176-16187.	1.4	4
45218	Ironâ€“magnesium compounds under high pressure. New Journal of Chemistry, 2019, 43, 17403-17407.	1.4	7
45219	A di-boron pair doped MoS₂ (B2@MoS₂) single-layer shows superior catalytic performance for electrochemical nitrogen activation and reduction. Nanoscale, 2019, 11, 18769-18778.	2.8	87
45220	Anomalous phase transition behavior in hydrothermal grown layered tellurene. Nanoscale, 2019, 11, 20245-20251.	2.8	3
45221	Thermally reduced fluorographenes as efficient electrode materials for supercapacitors. Nanoscale, 2019, 11, 21364-21375.	2.8	15
45222	Electronic structure and transport properties of 2D RhTeCl: a NEGF-DFT study. Nanoscale, 2019, 11, 20461-20466.	2.8	8
45223	New scaling relations to compute atom-in-material polarizabilities and dispersion coefficients: part 2. Linear-scaling computational algorithms and parallelization. RSC Advances, 2019, 9, 33310-33336.	1.7	10
45224	Armchair shaped polymeric nitrogen N8 chains confined in h-BN matrix at ambient conditions: stability and vibration analysis. RSC Advances, 2019, 9, 29987-29992.	1.7	3
45225	Development of a robust tool to extract Mulliken and LÃ¶wdin charges from plane waves and its application to solid-state materials. RSC Advances, 2019, 9, 29821-29830.	1.7	77
45226	Bidirectional heterostructures consisting of graphene and lateral MoS₂/WS₂ composites: a first-principles study. RSC Advances, 2019, 9, 34986-34994.	1.7	4
45227	New red-emitting phosphor Rb_xK_{3â^'x}SiF₇:Mn⁴⁺ (x = 0, 1, 2, 3): DFT predictions and synthesis. RSC Advances, 2019, 9, 39589-39594.	1.7	6
45228	Density functional study of Li/Na adsorption properties of single-layer and double-layer antimonenes. RSC Advances, 2019, 9, 32608-32619.	1.7	8
45229	Two-dimensional polar metals in KNbO3/BaTiO3 superlattices: first-principle calculations. RSC Advances, 2019, 9, 35499-35508.	1.7	6
45230	Strain-tunable magnetic anisotropy in two-dimensional Dirac half-metals: nickel trihalides. RSC Advances, 2019, 9, 35614-35623.	1.7	19
45231	Theoretical prediction of some layered Pa₂O₅ phases: structure and properties. RSC Advances, 2019, 9, 31398-31405.	1.7	4
45232	Halogenation of graphene triggered by heteroatom doping. RSC Advances, 2019, 9, 37507-37511.	1.7	10
45233	First-principles investigation of the microscopic mechanism of the physical and chemical mixed adsorption of graphene on metal surfaces. RSC Advances, 2019, 9, 32712-32720.	1.7	9
45234	A collection of forcefield precursors for metalâ€“organic frameworks. RSC Advances, 2019, 9, 36492-36507.	1.7	21

#	Article	IF	Citations
45235	Nearly spherical CoP nanoparticle/carbon nanosheet hybrids: a high-performance trifunctional electrocatalyst for oxygen reduction and water splitting. RSC Advances, 2019, 9, 39951-39957.	1.7	22
45236	Structural, magnetic and electronic properties of two dimensional NdN: an ab initio study. RSC Advances, 2019, 9, 35917-35923.	1.7	0
45237	Formation of toroidal Li₂O₂ in non-aqueous Liâ€“O₂ batteries with Mo₂CT_x MXene/CNT composite. RSC Advances, 2019, 9, 41120-41125.	1.7	16
45238	Ultralow lattice thermal conductivity and high thermoelectric performance of monolayer KCuTe: a first principles study. RSC Advances, 2019, 9, 36301-36307.	1.7	27
45239	Azugraphene: a new graphene-like hexagonal carbon allotrope with Dirac cones. RSC Advances, 2019, 9, 34481-34485.	1.7	17
45240	First principles calculations of the thermodynamic stability of Ba, Zr, and O vacancies in BaZrO3. RSC Advances, 2019, 9, 34158-34165.	1.7	6
45241	Comparative study on the electronic structures and redox reactions in LiCrX₂ and NaCrX₂ (X = O and S). RSC Advances, 2019, 9, 36867-36874.	1.7	2
45242	Effects of low dimensionality on electronic structure and thermoelectric properties of bismuth. RSC Advances, 2019, 9, 40670-40680.	1.7	10
45243	A first-principles study of strain tuned optical properties in monolayer tellurium. RSC Advances, 2019, 9, 41703-41708.	1.7	6
45244	Tunable magnetic ground states of iron monolayer on nonmagnetic metallic substrates by small in-plane strains. RSC Advances, 2019, 9, 41099-41106.	1.7	4
45245	Biaxial strain modulated the electronic structure of hydrogenated 2D tetragonal silicene. RSC Advances, 2019, 9, 42245-42251.	1.7	7
45246	Search for high-capacity oxygen storage materials by materials informatics. RSC Advances, 2019, 9, 41811-41816.	1.7	10
45247	Tuning the bandgap of Cs₂AgBiBr₆ through dilute tin alloying. Chemical Science, 2019, 10, 10620-10628.	3.7	58
45248	Synergistic adsorptions of Na₂CO₃and Na₂SiO₃on calcium minerals revealed by spectroscopic andab initiomolecular dynamics studies. Chemical Science, 2019, 10, 9928-9940.	3.7	33
45249	Two-dimensional magnetic metalâ€“organic frameworks with the Shastry-Sutherland lattice. Chemical Science, 2019, 10, 10381-10387.	3.7	21
45250	Pillared-layered metalâ€“organic frameworks for mechanical energy storage applications. Journal of Materials Chemistry A, 2019, 7, 22663-22674.	5.2	34
45251	Revealing Ni-based layered double hydroxides as high-efficiency electrocatalysts for the oxygen evolution reaction: a DFT study. Journal of Materials Chemistry A, 2019, 7, 23091-23097.	5.2	75
45252	Cr-doped lithium titanate nanocrystals as Mg ion insertion materials for Mg batteries. Journal of Materials Chemistry A, 2019, 7, 25619-25627.	5.2	16

#	Article	IF	Citations
45253	Storage of Na in layered graphdiyne as high capacity anode materials for sodium ion batteries. Journal of Materials Chemistry A, 2019, 7, 25609-25618.	5.2	20
45254	Depth-dependent oxygen redox activity in lithium-rich layered oxide cathodes. Journal of Materials Chemistry A, 2019, 7, 25355-25368.	5.2	62
45255	Zr vacancy interfaces: an effective strategy for collaborative optimization of ZrNiSn-based thermoelectric performance. Journal of Materials Chemistry A, 2019, 7, 26053-26061.	5.2	16
45256	Discrete color centers in two-dimensional hexagonal boron nitride induced by fast neutron irradiation. Journal of Materials Chemistry C, 2019, 7, 12211-12216.	2.7	10
45257	Topological nodal lines and nodal points in the antiferromagnetic material Î²-Fe₂PO₅. Journal of Materials Chemistry C, 2019, 7, 12657-12663.	2.7	50
45258	Designing iridate-based superlattice with large magnetoelectric coupling. Journal of Materials Chemistry C, 2019, 7, 13294-13300.	2.7	9
45259	Effect of normal strain and external electric field on electronic properties of the GeC bilayer: A first-principles study. AIP Advances, 2019, 9, 125324.	0.6	1
45260	Thermoelectric and galvanomagnetic properties of topologically non-trivial (Co-M)Si semimetals (Mâ€‰=â€‰Fe, Ni) at high temperatures. Journal of Applied Physics, 2019, 126, 245103.	1.1	7
45261	Successive orbital ordering transitions in FeV2O4 from first-principles calculation. Journal of Applied Physics, 2019, 126, .	1.1	2
45262	Construction of interatomic potentials of V-W on the basis of CALPHAD data on the formation enthalpy. AIP Conference Proceedings, 2019, , .	0.3	2
45263	Enhanced catalytic hydrogen evolution reaction in phosphorene nanosheet via cobalt intercalation. Chinese Journal of Chemical Physics, 2019, 32, 572-578.	0.6	4
45264	Density functional theory study of TiPd alloying with Os as potential high temperature shape memory alloys. IOP Conference Series: Materials Science and Engineering, 2019, 655, 012042.	0.3	1
45265	First principle calculations of structural, electronic, optical and thermoelectric properties of tin (II) oxide. Materials Research Express, 2019, 6, 125915.	0.8	9
45266	Treating different bonding situations: Revisiting Au-Cu alloys using the random phase approximation. Physical Review B, 2019, 100, .	1.1	10
45267	Tuning from frustrated magnetism to superconductivity in quasi-one-dimensional <mml:math xmlns:mml="http://www.w3.org/1998/Math/MathML"><mml:mrow><mml:msub><mml:mi>KCr</mml:mi><mml:mn>3</mml:mn></mml through hydrogen doping. Physical Review B, 2019, 100, .	1.1	15
45268	Two-dimensional ferromagnetic van der Waals <mml:math xmlns:mml="http://www.w3.org/1998/Math/MathML"><mml:mrow><mml:mi>CrC</mml:mi><mml:msub><mml:mi mathvariant="normal">I</mml:mi><mml:mn>3</mml:mn></mml:msub></mml:mrow></mml:math> monolayer with enhanced anisotropy and Curie temperature. Physical Review B, 2019, 100, .	1.1	80
45269	Electrons and Phonons Cooperate in the Laser-Induced Desorption of CO from Pd(111). Physical Review Letters, 2019, 123, 246802.	2.9	15
45270	Ordering Sequence in Strongly Nonstoichiometric Niobium Carbide with the Formation of Nb6C5-Type Superstructures. Journal of Experimental and Theoretical Physics, 2019, 129, 863-876.	0.2	8

#	Article	IF	Citations
45271	Density Functional Theory Study on Stability of Fe, Cu, and Ni Atoms Near (001) Surface of Si Wafer. ECS Journal of Solid State Science and Technology, 2019, 8, P573-P579.	0.9	3
45272	Giant Rashba-Type Spin Splitting in Bi/Ag(111) from Asymmetric Interatomic-Hopping. Journal of the Physical Society of Japan, 2019, 88, 124705.	0.7	5
45273	Dual manipulation of ferromagnetism in co-doped ZnO thin films by surfactant and n-type carriers. Chinese Journal of Chemical Physics, 2019, 32, 491-496.	0.6	1
45274	Interface-confined triangular FeOx nanoclusters on Pt(111). Journal of Chemical Physics, 2019, 151, 214704.	1.2	3
45275	Crystal and Electronic Structures of Alluaudite-Type Double Molybdates of Scandium and Indium. Journal of Structural Chemistry, 2019, 60, 1868-1876.	0.3	3
45276	The high-speed channel made of metal for interfacial charge transfer in Z-scheme gâ€“C₃N₄/MoS₂ water-splitting photocatalyst. Materials Research Express, 2019, 6, 115545.	0.8	13
45277	A superhard carbon allotrope: sc-C46 carbon. Europhysics Letters, 2019, 128, 36003.	0.7	2
45278	Tuning electronic, magnetic and optical properties of Cr-doped antimonene via biaxial strain engineering. Applied Surface Science, 2019, 463, 492-497.	3.1	10
45279	Combustion synthesis of AlN doped with carbon and oxygen. Journal of the American Ceramic Society, 2019, 102, 524-532.	1.9	7
45280	Revealing the Critical Role of Titanium in Layered Manganeseâ€Based Oxides toward Advanced Sodiumâ€Ion Batteries via a Combined Experimental and Theoretical Study. Small Methods, 2019, 3, 1800183.	4.6	32
45281	Insights of the role of shell closing model and NICS in the stability of NbGen (nâ€‰=â€‰7â€“18) clusters: a first-principles investigation. Journal of Materials Science, 2019, 54, 515-528.	1.7	26
45282	Hydrogen embrittlement controlled by reaction of dislocation with grain boundary in alpha-iron. International Journal of Plasticity, 2019, 112, 206-219.	4.1	88
45283	Theoretical research on structural, electronic, mechanical, lattice dynamical and thermodynamic properties of layered ternary nitrides Ti2AN (Aâ€¯=â€¯Si, Ge and Sn). Journal of Alloys and Compounds, 2019, 771, 664-673.	2.8	34
45284	Adsorption of water on fluorinated graphene. Journal of Physics and Chemistry of Solids, 2019, 124, 54-59.	1.9	16
45285	Modulation of Magnetism and Magnetic Anistropy at the Heavy-Metal/FeRh Interface. IEEE Transactions on Magnetics, 2019, 55, 1-4.	1.2	4
45286	Phase Stability Diagrams of Tiâ€“Mâ€“Oâ€“C (Mâ€‰=â€‰Zr, Hf, Nb, and Ta) Systems at 1800ÂK. Metals and Materials International, 2019, 25, 396-407.	1.8	3
45287	Large-scale GW calculations on pre-exascale HPC systems. Computer Physics Communications, 2019, 235, 187-195.	3.0	35
45288	X-ray structures, solid state periodic DFT modeling and vibrational study of alkylenediammonium hexachlorostannates compounds NH3(CH2)nNH3SnCl6 (nÂ= 3, 4, 5). Journal of Molecular Structure, 2019, 1177, 55-67.	1.8	5

#	Article	IF	Citations
45289	Enhancing the thermoelectric performance of Bi2S3: A promising earth-abundant thermoelectric material. Frontiers of Physics, 2019, 14, 1.	2.4	24
45290	Lattice dynamics of FeMnP0.5Si0.5 compound from first principles calculation. Journal of Materials Science and Technology, 2019, 35, 127-133.	5.6	3
45291	Copper(<scp>i</scp>) sulfide: a two-dimensional semiconductor with superior oxidation resistance and high carrier mobility. Nanoscale Horizons, 2019, 4, 223-230.	4.1	51
45292	Sr substitution effects on atomic and local electronic structure of Ca₂AlMnO_{5+Î´}. Surface and Interface Analysis, 2019, 51, 65-69.	0.8	4
45293	Mechanisms of oxidation of pure and Si-segregated Î±-Ti surfaces. Applied Surface Science, 2019, 463, 686-692.	3.1	8
45294	A DFT study on dimethyl oxalate synthesis over PdML/Ni(1â€¯1â€¯1) and PdML/Co(1â€¯1â€¯1) surfaces. Applied Surface Science, 2019, 465, 498-508.	3.1	9
45295	Increasing solubility of metal silicates by mixed polymeric antiscalants. Geothermics, 2019, 77, 106-114.	1.5	16
45296	Enhancing thermoelectric performance of SnTe via stepwisely optimizing electrical and thermal transport properties. Journal of Alloys and Compounds, 2019, 773, 571-584.	2.8	37
45297	Theoretical insights into interfacial and electronic structures of NiO /SrTiO3 photocatalyst for overall water splitting. Journal of Energy Chemistry, 2019, 33, 138-148.	7.1	12
45298	Induced defect levels of P and Al vacancy-complexes in <mml:math xmlns:mml="http://www.w3.org/1998/Math/MathML" altimg="si0060.gif" overflow="scroll"><mml:mrow><mml:mn>4</mml:mn><mml:mspace width="0.25em" /><mml:mi>H</mml:mi></mml:mrow></mml:math>-SiC: A hybrid functional study. Materials Science in Semiconductor Processing, 2019, 89, 77-84.	1.9	4
45299	Influence of composition and oxygen-vacancy ordering on lattice parameter and elastic moduli of Ce1-Gd O2-/2: A theoretical study. Scripta Materialia, 2019, 158, 126-130.	2.6	7
45300	Interfacial stability of Î¸â€²/Al in Al-Cu alloys. Scripta Materialia, 2019, 159, 99-103.	2.6	40
45301	DFT study of Rh and Ti dimers decorating N-doped pyridinic and pyrrolic graphene for molecular and dissociative hydrogen adsorption. Applied Surface Science, 2019, 464, 243-254.	3.1	23
45302	Optical and photocatalytic properties of rare earth metal-modified ZnO quantum dots. Applied Surface Science, 2019, 464, 651-663.	3.1	64
45303	On the Carbene-Like Reactions of Imidazolium Acetate Ionic Liquids: Can Theory and Experiments Agree?. European Journal of Organic Chemistry, 2019, 2019, 504-511.	1.2	21
45304	A DFT+u study, including the van der waals interaction, on the adsorption of XO2 molecules on the v2o5(001) surface (x= S, N, O, C). Surface Science, 2019, 679, 110-116.	0.8	1
45305	In situ grown Ni phosphide nanowire array on Ni foam as a high-performance catalyst for hydrazine electrooxidation. Applied Catalysis B: Environmental, 2019, 241, 292-298.	10.8	89
45306	Effect of Coulomb Interactions on the Electronic and Magnetic Properties of Two-Dimensional CrSiTe3 and CrGeTe3 Materials. Journal of Electronic Materials, 2019, 48, 1441-1445.	1.0	34

#	Article	IF	Citations
45307	Dynamic nanoscale imaging of enriched CO adlayer on Pt(111) confined under h-BN monolayer in ambient pressure atmospheres. Nano Research, 2019, 12, 85-90.	5.8	13
45308	Effect of Cr Doping on the Surface Characteristics of Ni Metal Studied with First-Principles Calculation. Acta Metallurgica Sinica (English Letters), 2019, 32, 461-470.	1.5	11
45309	Nitrogenated holey graphene C2N monolayer anodes for lithium- and sodium-ion batteries with high performance. Energy Storage Materials, 2019, 16, 574-580.	9.5	100
45310	Thermodynamic properties and phase stability of the Ba-Bi system: A combined computational and experimental study. Journal of Alloys and Compounds, 2019, 771, 281-289.	2.8	4
45311	The Effects of Dopants on the Cuâ€“ZrO₂ Catalyzed Hydrogenation of Levulinic Acid. Journal of Physical Chemistry C, 2019, 123, 7879-7888.	1.5	21
45312	Atomic-level insight into the mechanism of 0D/2D black phosphorus quantum dot/graphitic carbon nitride (BPQD/GCN) metal-free heterojunction for photocatalysis. Applied Surface Science, 2019, 463, 1148-1153.	3.1	64
45313	High-voltage performance of LiCoO2 cathode studied by single particle microelectrodes â€“influence of surface modification with TiO2. Electrochimica Acta, 2019, 295, 1017-1026.	2.6	33
45314	Understanding the transport and contact properties of metal/BN-MoS2 interfaces to realize high performance MoS2 FETs. Journal of Alloys and Compounds, 2019, 771, 1052-1061.	2.8	10
45315	STM and DFT studies of CO2 adsorption on O-Cu(100) surface. Surface Science, 2019, 679, 50-55.	0.8	15
45316	Phase Diagrams for Binary and Multicomponent Aluminum Systems. , 2019, , 1-131.		1
45317	Influence of Heat Treatment Upon Microstructure of Casting Aluminum Alloys. , 2019, , 235-312.		2
45318	Solvation effects on DFT predictions of ORR activity on metal surfaces. Catalysis Today, 2019, 323, 35-43.	2.2	109
45319	Electrochemical CO2 reduction over nitrogen-doped SnO2 crystal surfaces. Journal of Energy Chemistry, 2019, 33, 22-30.	7.1	38
45320	(0001) Interfaces between M2O3 corundum oxides (MÂ=ÂAl, Ti, V, Cr, Fe).. Surface Science, 2019, 679, 17-23.	0.8	12
45321	The structure of alanine anionic-zwitterionic dimers on Pd(111); formation of salt bridges. Surface Science, 2019, 679, 79-85.	0.8	1
45322	The effects of dye aggregation on the performance of organic dyes in dye-sensitized solar cells: From static model to molecular dynamics simulation. Journal of Luminescence, 2019, 205, 7-13.	1.5	7
45323	Single Ni Sites Supported on CeO₂(111) Reveal Cooperative Effects in the Waterâ€“Gas Shift Reaction. Journal of Physical Chemistry C, 2019, 123, 7749-7757.	1.5	23
45324	Two-dimensional Ï€-conjugated metalâ€“organic nanosheets as single-atom catalysts for the hydrogen evolution reaction. Nanoscale, 2019, 11, 454-458.	2.8	65

#	Article	IF	Citations
45325	Aging Degradation Characteristics and Long-Term Performance of Structural Materials for Energy Conversion Systems. Corrosion, 2019, 75, 254-266.	0.5	0
45326	Stress-dependence of generalized stacking fault energies. Journal of the Mechanics and Physics of Solids, 2019, 122, 262-279.	2.3	42
45327	Prediction of a flexible anode material for Li/Na ion batteries: Phosphorous carbide monolayer (Î±-PC). Carbon, 2019, 141, 444-450.	5.4	70
45328	Rational design of C₂N-based type-II heterojunctions for overall photocatalytic water splitting. Nanoscale Advances, 2019, 1, 154-161.	2.2	70
45329	Emergence of strain induced two dimensional metallic state in ReS2. Journal of Solid State Chemistry, 2019, 269, 138-144.	1.4	7
45330	Room temperature ferromagnetism in Cuâ€“Gd co-doped GaN nanowires: A first-principles study. Physics Letters, Section A: General, Atomic and Solid State Physics, 2019, 383, 54-57.	0.9	9
45331	Deciphering the Microstructure and Energy-Level Splitting of Tm³⁺-Doped Yttrium Aluminum Garnet. Inorganic Chemistry, 2019, 58, 1058-1066.	1.9	23
45332	Edge-doping effects on the electronic and magnetic properties of zigzag germanium selenide nanoribbon. Applied Surface Science, 2019, 464, 236-242.	3.1	21
45333	Three-dimensional honeycomb carbon: Junction line distortion and novel emergent fermions. Carbon, 2019, 141, 417-426.	5.4	48
45334	Spectroscopic and ab initio studies of the pressure-induced Fe2+ high-spin-to-low-spin electronic transition in natural triphyliteâ€“lithiophilite. Physics and Chemistry of Minerals, 2019, 46, 245-258.	0.3	0
45335	Electrocatalytic Reduction of Carbon Dioxide to Methane on Single Transition Metal Atoms Supported on a Defective Boron Nitride Monolayer: First Principle Study. Advanced Theory and Simulations, 2019, 2, 1800094.	1.3	33
45336	Ni catalytic effects for the enhanced hydrogenation properties of Mg17Al12(1â€¯1â€¯0) surface. Applied Surface Science, 2019, 464, 644-650.	3.1	24
45337	First-principles study of oxygen-related defects on 4H-SiC surface: The effects of surface amorphous structure. Applied Surface Science, 2019, 464, 451-454.	3.1	4
45338	Co9S8@carbon yolk-shell nanocages as a high performance direct conversion anode material for sodium ion batteries. Energy Storage Materials, 2019, 18, 51-58.	9.5	89
45339	Adhesion of ZrN and Al2O3 coatings on U metal from first-principles. Applied Surface Science, 2019, 473, 121-126.	3.1	11
45340	First-principles study of structural, mechanical, and electronic properties of typical iron-containing phases in Al-Cu alloys under different pressures. Physica B: Condensed Matter, 2019, 555, 112-117.	1.3	4
45341	Synthesis and Size-Dependent Optical Properties of Intermediate Band Gap Cu₃VS₄ Nanocrystals. Chemistry of Materials, 2019, 31, 532-540.	3.2	39
45342	Bismuth Islands for Low-Temperature Sodium-Beta Alumina Batteries. ACS Applied Materials & Interfaces, 2019, 11, 2917-2924.	4.0	31

#	Article	IF	Citations
45343	Tuning the Electronic Properties of Hexagonal Two-Dimensional GaN Monolayers via Doping for Enhanced Optoelectronic Applications. ACS Applied Nano Materials, 2019, 2, 202-213.	2.4	60
45344	Effect of Substitutionally Doped Graphene on the Activity of Metal Nanoparticle Catalysts for the Hydrogen Oxidation Reaction. ACS Catalysis, 2019, 9, 1129-1139.	5.5	34
45345	Highly Reliable Amorphous In-Ga-Zn-O Thin-Film Transistors Through the Addition of Nitrogen Doping. IEEE Transactions on Electron Devices, 2019, 66, 457-463.	1.6	24
45346	The stability and reactivity of transition metal atoms supported mono and di vacancies defected carbon based materials revealed from first principles study. Applied Surface Science, 2019, 473, 777-784.	3.1	30
45347	Effects of silicon doping on strengthening adhesion at the interface of the hydroxyapatiteâ€“titanium biocomposite: A first-principles study. Computational Materials Science, 2019, 159, 228-234.	1.4	14
45348	Crystal facets-predominated oxygen evolution reaction activity of earth abundant CoMoO4 electrocatalyst. Journal of Alloys and Compounds, 2019, 781, 460-466.	2.8	40
45349	Insight into the low-temperature decomposition of Aroclor 1254 over activated carbon-supported bimetallic catalysts obtained with XANES and DFT calculations. Journal of Hazardous Materials, 2019, 366, 538-544.	6.5	5
45350	Exploring the electronic and magnetic properties of new metal halides from bulk to two-dimensional monolayer: RuX3 (Xâ€¯=â€¯Br, I). Journal of Magnetism and Magnetic Materials, 2019, 476, 111-119.	1.0	48
45351	Application of deep eutectic solvent from phenol and choline chloride in electrolyte to improve stability performance in dye-sensitized solar cells. Journal of Molecular Liquids, 2019, 277, 157-162.	2.3	41
45352	Enhanced hardness and age-hardening of TiAlN coatings through Ru-addition. Scripta Materialia, 2019, 162, 382-386.	2.6	21
45353	Understanding the Polymorphism of A₄[(UO₂)₃(PO₄)₂O₂] (A =) Tj ETQq1 1 0 rgBT /Overlock		
45354	Fundamental Mechanisms of Reversible Dehydrogenation of Formate on N-Doped Graphene-Supported Pd Nanoparticles. Journal of Physical Chemistry C, 2019, 123, 1539-1549.	1.5	28
45355	First-Principles Kinetic Study for Ostwald Ripening of Late Transition Metals on TiO₂(110). Journal of Physical Chemistry C, 2019, 123, 1160-1169.	1.5	19
45356	Mechanically-Controllable Strong 2D Ferroelectricity and Optical Properties of Semiconducting BiN Monolayer. ACS Applied Nano Materials, 2019, 2, 58-63.	2.4	14
45357	Key Factor for the Transformation from hcp to 18R-Type Long-Period Stacking Ordered Structure in Mg Alloys. Materials Transactions, 2019, 60, 237-245.	0.4	12
45358	Enhanced 1Tâ€²â€Phase Stabilization and Chemical Reactivity in a MoTe₂ Monolayer through Contact with a 2D Ca₂N Electride. ChemPhysChem, 2019, 20, 595-601.	1.0	14
45359	Impact of surface adsorbed gases on hydrogen diffusion into Pd(1â€²0â€²0) subsurface from first principles. Applied Surface Science, 2019, 473, 476-485.	3.1	8
45360	A MnN4 moiety embedded graphene as a magnetic gas sensor for CO detection: A first principle study. Applied Surface Science, 2019, 473, 820-827.	3.1	67

#	Article	IF	Citations
45361	Effects of niobium and rare earth elements on microstructure and initial marine corrosion behavior of low-alloy steels. Applied Surface Science, 2019, 475, 83-93.	3.1	60
45362	Thermodynamic assessment and glass forming ability prediction of the Zr-Fe-Cu system. Calphad: Computer Coupling of Phase Diagrams and Thermochemistry, 2019, 64, 175-184.	0.7	12
45363	A high-throughput computation framework for generalized stacking fault energies of pure metals. Computational Materials Science, 2019, 159, 357-364.	1.4	17
45364	Structures of quaternary chromium silicides revealed by a combination of resonant X-ray diffraction and ab initio calculations. Intermetallics, 2019, 105, 130-138.	1.8	1
45365	Epitaxial Growth of Two-Dimensional Metalâ€“Semiconductor Transition-Metal Dichalcogenide Vertical Stacks (VSe₂/MX₂) and Their Band Alignments. ACS Nano, 2019, 13, 885-893.	7.3	102
45366	First principles studies of self-diffusion processes on metallic lithium surfaces. Journal of Chemical Physics, 2019, 150, 041723.	1.2	34
45367	Comparative computational study of CO2 dissociation and hydrogenation over Fe-M (M = Pd, Ni, Co) bimetallic catalysts: The effect of surface metal content. Journal of CO2 Utilization, 2019, 29, 179-195.	3.3	17
45368	Tunable Photocatalytic HER Activity of Single-Layered TiO₂ Nanosheets with Transition-Metal Doping and Biaxial Strain. Journal of Physical Chemistry C, 2019, 123, 526-533.	1.5	34
45369	How Silver Grows on the Silicon (001) Surface: A Theoretical and Experimental Investigation. ACS Applied Electronic Materials, 2019, 1, 122-131.	2.0	4
45370	Elucidating the Role of Support Oxygen in the Waterâ€“Gas Shift Reaction over Ceria-Supported Gold Catalysts Using Operando Spectroscopy. ACS Catalysis, 2019, 9, 1159-1171.	5.5	49
45371	First-principles prediction of two atomic-thin phosphorene allotropes with potentials for sun-light-driven water splitting. Journal of Physics Condensed Matter, 2019, 31, 075702.	0.7	7
45372	Electronic and Optical Properties of CsSnI3â^'yCly (yâ€‰=â€‰0, 1, 2, 3) Perovskites: a DFT Study. Journal of Electronic Materials, 2019, 48, 1243-1251.	1.0	24
45373	The adsorption characteristics of As2O3, Pb0, PbO and PbCl2 on single atom iron adsorbent with graphene-based substrates. Chemical Engineering Journal, 2019, 361, 304-313.	6.6	77
45374	Density functional theory calculations of self- and Xe diffusion in U3Si2. Journal of Nuclear Materials, 2019, 515, 312-325.	1.3	43
45375	Electronic Origin of Oxygen Transport Behavior in La-Based Perovskites: A Density Functional Theory Study. Journal of Physical Chemistry C, 2019, 123, 275-290.	1.5	25
45376	Observation of the nesting and defect-driven 1D incommensurate charge density waves phase in the 2D system. Journal of Physics Condensed Matter, 2019, 31, 115402.	0.7	1
45377	Generalized stacking fault energy of carbon-alloyed paramagnetic $ gamma $ -Fe. Journal of Physics Condensed Matter, 2019, 31, 065703.	0.7	5
45378	Tin Intercalated Ultrathin MoO₃ Nanoribbons for Advanced Lithiumâ€“Sulfur Batteries. Advanced Energy Materials, 2019, 9, 1803137.	10.2	126

#	Article	IF	Citations
45379	OpenMP in VASP: Threading and SIMD. International Journal of Quantum Chemistry, 2019, 119, e25851.	1.0	15
45380	Ab initio investigation into the physisorption of noble gases on graphene. Surface Science, 2019, 682, 38-42.	0.8	12
45381	Oxygen Vacancy Creation Energy in Mn-Containing Perovskites: An Effective Indicator for Chemical Looping with Oxygen Uncoupling. Chemistry of Materials, 2019, 31, 689-698.	3.2	41
45382	Reduction of NO with CO on the Co₃O₄(110)-B and CoO(110) Surfaces: A First-Principles Study. Journal of Physical Chemistry C, 2019, 123, 1770-1778.	1.5	15
45383	Pressure-Induced Band Structure Evolution of Halide Perovskites: A First-Principles Atomic and Electronic Structure Study. Journal of Physical Chemistry C, 2019, 123, 739-745.	1.5	53
45384	Resonance Raman Spectroscopy of Silicene and Germanene. Journal of Physical Chemistry C, 2019, 123, 1995-2008.	1.5	8
45385	One-Pot Synthesis of Co-Doped VSe₂ Nanosheets for Enhanced Hydrogen Evolution Reaction. ACS Applied Energy Materials, 2019, 2, 644-653.	2.5	59
45386	Ethylene Epoxidation on Ag(100), Ag(110), and Ag(111): A Joint Ab Initio and Kinetic Monte Carlo Study and Comparison with Experiments. ACS Catalysis, 2019, 9, 1183-1196.	5.5	45
45387	Interfacial Spin Manipulation of Nickel-Quinonoid Complex Adsorbed on Co(001) Substrate. Magnetochemistry, 2019, 5, 2.	1.0	3
45388	Realizing Ultralow Concentration Gelation of Graphene Oxide with Artificial Interfaces. Advanced Materials, 2019, 31, e1805075.	11.1	16
45389	Linear and Nonlinear Optical Properties of Fewâ€Layer Exfoliated SnSe Nanosheets. Advanced Optical Materials, 2019, 7, 1800579.	3.6	43
45390	Comparative study of magnetic and electronic properties of roomâ€temperature polar magnets ScFeO₃ and InFeO₃. International Journal of Quantum Chemistry, 2019, 119, e25846.	1.0	2
45391	Strain-modulated mechanical, electronic, and thermal transport properties of two-dimensional PdS2 from first-principles investigations. Applied Physics A: Materials Science and Processing, 2019, 125, 1.	1.1	13
45392	Thermal neutron scattering kernels for uranium mono-nitride: A potential advanced tolerant fuel candidate for light water reactors. Annals of Nuclear Energy, 2019, 127, 68-78.	0.9	8
45393	Oxygen vacancy mediated La1-xCexFeO3-Î´ perovskite oxides as efficient catalysts for CWAO of acrylic acid by A-site Ce doping. Applied Catalysis B: Environmental, 2019, 245, 20-28.	10.8	66
45394	Electronic structure of molybdenum-involved amorphous silica buffer layer in MoOx/n-Si heterojunction. Applied Surface Science, 2019, 473, 20-24.	3.1	6
45395	Large enhancement of infrared absorption due to trimer comprised of doping-N and S-S divacancies in the imperfect monolayer MoS2: A first-principles study. Applied Surface Science, 2019, 473, 6-10.	3.1	3
45396	Dopamine sensing by boron and nitrogen co-doped single-walled carbon nanotubes: A first-principles study. Applied Surface Science, 2019, 473, 59-64.	3.1	28

#	Article	IF	Citations
45397	Activation of CO2 at chromia-nanocluster-modified rutile and anatase TiO2. Catalysis Today, 2019, 326, 68-74.	2.2	5
45398	Accurate semiempirical analytical formulas for spontaneous polarization by crystallographic parameters of SrTiO3-BaTiO3 system by ab initio calculations. Computational Materials Science, 2019, 158, 315-323.	1.4	4
45399	Stabilities and electronic properties of vacancy-doped Ti2CO2. Computational Materials Science, 2019, 159, 127-135.	1.4	21
45400	Investigation the origin and mechanical properties of unusual rigid diamond-like net analogues in manganese tetraboride. International Journal of Refractory Metals and Hard Materials, 2019, 85, 104845.	1.7	7
45401	Unique ion diffusion properties in lead-free halide double perovskites: A first-principles study. Journal of Power Sources, 2019, 412, 689-694.	4.0	12
45402	Kinetics of interaction of impurity interstitials with dislocations revisited. Progress in Materials Science, 2019, 101, 172-206.	16.0	34
45403	Structural stability and electronic properties of XTO2 (X= Cu, Ag; T=Al, Cr): An ab initio study including X vacancies and Mg doping. Solid State Sciences, 2019, 88, 48-56.	1.5	15
45404	Ba₁₀Zn₇M₆Q₂₆: Two New Mid-infrared Nonlinear Optical Crystals with T2 Supertetrahedron 3D Framework. Crystal Growth and Design, 2019, 19, 1190-1197.	1.4	8
45405	Electrochemical Properties and Theoretical Capacity for Sodium Storage in Hard Carbon: Insights from First Principles Calculations. Chemistry of Materials, 2019, 31, 658-677.	3.2	60
45406	Theoretical Insights into Heterogeneous (Photo)electrochemical CO₂Reduction. Chemical Reviews, 2019, 119, 6631-6669.	23.0	431
45407	Computationally Designed Crystal Structures of the Supertetrahedral Al₄X (X = B, C, Al,) Tj ETQq0 0 0 rgBT /Overlock 10 Tf	1.1	5
45408	Tailoring the Linear and Second-Order Nonlinear Optical Responses of the Titanium-MIL-125 Metalâ€“Organic Framework through Ligand Functionalization: A First Principles Study. Journal of Physical Chemistry C, 2019, 123, 653-664.	1.5	9
45409	Method for Simultaneous Prediction of Atomic Structure and Stability of Nanoclusters in a Wide Area of Compositions. Journal of Physical Chemistry Letters, 2019, 10, 102-106.	2.1	34
45410	Theoretical Investigation: 2D N-Graphdiyne Nanosheets as Promising Anode Materials for Li/Na Rechargeable Storage Devices. ACS Applied Nano Materials, 2019, 2, 127-135.	2.4	56
45411	Molecular Tunability of Magnetic Exchange Bias and Asymmetrical Magnetotransport in Metalloporphyrin/Co Hybrid Bilayers. ACS Nano, 2019, 13, 894-903.	7.3	14
45412	Exploration of high-pressure structural transition and electronic properties of BaFe2S3. Journal of Physics Condensed Matter, 2019, 31, 115401.	0.7	2
45413	Enhanced Electroreduction of Carbon Dioxide to Methanol Using Zinc Dendrites Pulseâ€Deposited on Silver Foam. Angewandte Chemie - International Edition, 2019, 58, 2256-2260.	7.2	98
45414	A Firstâ€Principles Study on the Adsorption of Small Molecules on Arsenene: Comparison of Oxidation Kinetics in Arsenene, Antimonene, Phosphorene, and InSe. ChemPhysChem, 2019, 20, 575-580.	1.0	42

#	Article	IF	Citations
45415	Insight into room-temperature catalytic oxidation of NO by CrO2(110): A DFT study. Chinese Chemical Letters, 2019, 30, 618-623.	4.8	20
45416	Structural phase transitions and superconductivity of YC2 from first-principles calculations. Computational Materials Science, 2019, 159, 120-126.	1.4	4
45417	Density functional theory-based investigations of solute kinetics and precipitate formation in binary magnesium-rare earth alloys: A review. Computational Materials Science, 2019, 159, 235-256.	1.4	18
45418	Atom doping in Î±-Fe2O3 thin films to prevent hydrogen permeation. International Journal of Hydrogen Energy, 2019, 44, 3221-3229.	3.8	12
45419	Magnetic and structural properties of Co2MnSi based Heusler compound. Journal of Alloys and Compounds, 2019, 781, 216-225.	2.8	27
45420	Free-standing graphene oxide membrane with tunable channels for efficient water pollution control. Journal of Hazardous Materials, 2019, 366, 659-668.	6.5	45
45421	Vacancies inducing electronic and optical properties in 2D ZnO:Be/Mg. Physica B: Condensed Matter, 2019, 555, 47-52.	1.3	5
45422	Single-Atom Electroplating on Two Dimensional Materials. Chemistry of Materials, 2019, 31, 429-435.	3.2	55
45423	Energy Band Gap Modulation in Nd-Doped BiFeO₃/SrRuO₃ Heteroepitaxy for Visible Light Photoelectrochemical Activity. ACS Applied Materials & Interfaces, 2019, 11, 1655-1664.	4.0	25
45424	Ferromagnetic, Ferroelectric, and Optical Modulated Multiple Resistance States in Multiferroic Tunnel Junctions. ACS Applied Materials & Interfaces, 2019, 11, 1057-1064.	4.0	16
45425	Enhanced photocatalytic performance of CdO/g-C₆N₆ heterostructure. Materials Research Express, 2019, 6, 035910.	0.8	12
45426	Co-doped 1T-MoS2 nanosheets embedded in N, S-doped carbon nanobowls for high-rate and ultra-stable sodium-ion batteries. Nano Research, 2019, 12, 2218-2223.	5.8	88
45427	Deformation induced twinning and phase transition in an interstitial intermetallic compound niobium boride. Acta Materialia, 2019, 165, 459-470.	3.8	8
45428	Piezoelectric Effects in Surface-Engineered Two-Dimensional Group III Nitrides. ACS Applied Materials & Interfaces, 2019, 11, 1033-1039.	4.0	47
45429	Adsorption and Destruction of the G-Series Nerve Agent Simulant Dimethyl Methylphosphonate on Zinc Oxide. ACS Catalysis, 2019, 9, 902-911.	5.5	54
45430	Strain engineering the structures and electronic properties of Janus monolayer transition-metal dichalcogenides. Journal of Applied Physics, 2019, 125, .	1.1	39
45431	Accelerated optimization of transparent, amorphous zinc-tin-oxide thin films for optoelectronic applications. APL Materials, 2019, 7, .	2.2	23
45432	Phase diagram of magnetostrictive Fe-Ga alloys: insights from theory and experiment. Phase Transitions, 2019, 92, 101-116.	0.6	33

#	Article	IF	Citations
45433	High pressure structural investigations on hexagonal YInO₃. High Pressure Research, 2019, 39, 17-35.	0.4	6
45434	Understanding selectivity changes during hydrodesulfurization of dibenzothiophene on Mo2C/carbon catalysts. Journal of Catalysis, 2019, 369, 427-439.	3.1	37
45435	Magnetostriction of Fe100-xGax alloys from first principles calculations. Journal of Magnetism and Magnetic Materials, 2019, 476, 120-123.	1.0	7
45436	First-principles calculations of methane adsorption at different coverage on the kaolinite (001) surface. Materials Today Communications, 2019, 18, 199-205.	0.9	10
45437	Charge transfer dynamics in RuO2/perovskite nanohybrid for enhanced electrocatalysis in solid oxide electrolyzers. Nano Energy, 2019, 57, 186-194.	8.2	36
45438	Photocatalytic hydrogen production from water splitting with N-doped Î²-Ga2O3 and visible light. Spectrochimica Acta - Part A: Molecular and Biomolecular Spectroscopy, 2019, 211, 71-78.	2.0	23
45439	Connecting Oxide Nucleation and Growth to Oxygen Diffusion Energetics on Stepped Cu(011) Surfaces: An Experimental and Theoretical Study. Journal of Physical Chemistry C, 2019, 123, 452-463.	1.5	19
45440	Dynamic Phase Diagram of Catalytic Surface of Hexagonal Boron Nitride under Conditions of Oxidative Dehydrogenation of Propane. Journal of Physical Chemistry Letters, 2019, 10, 20-25.	2.1	49
45441	PdSe₂: Flexible Two-Dimensional Transition Metal Dichalcogenides Monolayer for Water Splitting Photocatalyst with Extremely Low Recombination Rate. ACS Applied Energy Materials, 2019, 2, 513-520.	2.5	84
45442	Observation of the nonlinear Hall effect under time-reversal-symmetric conditions. Nature, 2019, 565, 337-342.	13.7	372
45443	Realizing both giant magnetic anisotropy and quantum anomalous Hall effect in graphene with adsorbed Te-Co dimer. Journal of Physics Condensed Matter, 2019, 31, 045802.	0.7	3
45444	Firstâ€Principles Predictions on the Effects of Pb Doping on the Structural, Electronic, Magnetic, and Mechanical Properties of the TiZrCoTl_{1â^'x}Pb_x (xâ€‰=â€‰0.00,) Ti ETQq1 1 0.7843 1800566.	0.7	10
45445	A New Family of Twoâ€Dimensional Topological Materials: CdX (Xâ€‰=â€‰F, Cl, Br, and I). Physica Status Solidi - Rapid Research Letters, 2019, 13, 1800466.	1.2	2
45446	Mechanism Behind the Easy Exfoliation of Ga₂O₃ Ultraâ€Thin Film Along (100) Surface. Physica Status Solidi - Rapid Research Letters, 2019, 13, 1800554.	1.2	36
45447	Twoâ€Dimensional GaX/SnS₂ (Xâ€‰=â€‰S, Se) van der Waals Heterostructures for Photovoltaic Application: Heteroatom Doping Strategy to Boost Power Conversion Efficiency. Physica Status Solidi - Rapid Research Letters, 2019, 13, 1800565.	1.2	35
45448	First-Principles Modeling of Interface Effects in Oxides. , 2019, , 1-30.		0
45449	CALYPSO Method for Structure Prediction and Its Applications to Materials Discovery. , 2019, , 1-28.		6
45450	Adaptive Genetic Algorithm for Structure Prediction and Application to Magnetic Materials. , 2019, , 1-20.		1

#	Article	IF	Citations
45451	Magnetic coupling in 3D-hierarchical MnO2 microsphere. Journal of Materials Science: Materials in Electronics, 2019, 30, 2802-2808.	1.1	7
45452	Phase stability and mechanical properties of novel high entropy transition metal carbides. Acta Materialia, 2019, 166, 271-280.	3.8	422
45453	Structure stability and high Li storage capacity of the unzipped graphene oxide monolayer. Applied Surface Science, 2019, 475, 151-157.	3.1	17
45454	Size effects and active sites of Cu nanoparticle catalysts for CO2 electroreduction. Applied Surface Science, 2019, 475, 20-27.	3.1	51
45455	Atomic-scale simulations of ideal strength and deformation mechanism in Î²-SiC under H/He irradiation. Ceramics International, 2019, 45, 6125-6134.	2.3	4
45456	Physical and chemical insights into molecular adsorption of copolymerâ€™s monomers on Rutile surface. Chemical Physics, 2019, 520, 8-20.	0.9	4
45457	New high pressure phase of yttrium metal under ultrahigh pressure. Computational Materials Science, 2019, 159, 428-431.	1.4	15
45458	ADAIS: Automatic Derivation of Anisotropic Ideal Strength via high-throughput first-principles computations. Computer Physics Communications, 2019, 238, 244-253.	3.0	24
45459	Lithium decoration of boron-doped hybrid fullerenes and nanotubes as a novel 3D architecture for enhanced hydrogen storage: A DFT study. International Journal of Hydrogen Energy, 2019, 44, 2934-2942.	3.8	37
45460	Size effect on the electrochemical reaction path and performance of nano size phosphorus rich skutterudite nickle phosphide. Journal of Alloys and Compounds, 2019, 781, 1059-1068.	2.8	11
45461	Effect of oxygen concentration on the tension and shear strength of Zr-O system: A first-principles study. Journal of Alloys and Compounds, 2019, 781, 919-928.	2.8	8
45462	Understanding structure, optical, and electrical properties of In4Sn3O12 and In4.5Sn2M0.5O12 (Mâ€¯=â€¯Nb) Tj ETQq1 1 0.784314	2.8	5
45463	First-principles predictions for stabilizations of multilayer nanotwins in Al alloys at finite temperatures. Journal of Alloys and Compounds, 2019, 783, 765-771.	2.8	20
45464	Dehydrogenation mechanisms of methyl-cyclohexane on Î³-Al2O3 supported Pt13: Impact of cluster ductility. Journal of Catalysis, 2019, 370, 118-129.	3.1	47
45465	Investigation of electronic, magnetic and structural properties of the Fe1â^'xMnxRh. Journal of Magnetism and Magnetic Materials, 2019, 476, 325-328.	1.0	6
45466	Crystal preferred orientation of Li2MnO3Â·LiMO2 (M=Mn, Co, Ni) nano-particals: Relevance to electrochemical behavior for lithium battery cathode materials. Journal of Power Sources, 2019, 413, 425-431.	4.0	18
45467	Ultra-stable sodium metal-iodine batteries enabled by an in-situ solid electrolyte interphase. Nano Energy, 2019, 57, 692-702.	8.2	72
45468	Transition metal doped puckered arsenene: Magnetic properties and potential as a catalyst. Physica E: Low-Dimensional Systems and Nanostructures, 2019, 108, 153-159.	1.3	55

#	Article	IF	Citations
45469	Magnetic and electronic properties of zigzag boron nitride nanoribbons with nonmetallic atom asymmetric passivation. Physica E: Low-Dimensional Systems and Nanostructures, 2019, 108, 174-180.	1.3	7
45470	Crystal structures of silicon-rich lithium silicides at high pressure. Physics Letters, Section A: General, Atomic and Solid State Physics, 2019, 383, 1047-1051.	0.9	4
45471	Multiscale modeling of PEEK using reactive molecular dynamics modeling and micromechanics. Polymer, 2019, 163, 96-105.	1.8	40
45472	First-principles molecular dynamics simulations of single nitrogen bond structures in a N2H2 system under pressure. Solid State Communications, 2019, 290, 27-30.	0.9	1
45473	Interface properties of nonpolar LiAlO2/SrTiO3 heterostructures. Vacuum, 2019, 161, 98-102.	1.6	2
45474	p-Type Conductivity and Room-Temperature Ferrimagnetism in Spinel MoFe₂O₄ Epitaxial Thin Film. Crystal Growth and Design, 2019, 19, 902-906.	1.4	11
45475	Thermoelectric Material SnPb2Bi2S6: The 4,4L Member of Lillianite Homologous Series with Low Lattice Thermal Conductivity. Inorganic Chemistry, 2019, 58, 1339-1348.	1.9	10
45476	Simultaneous Adsorption and Incorporation of Sr²⁺ at the Barite (001)â€“Water Interface. Journal of Physical Chemistry C, 2019, 123, 1194-1207.	1.5	21
45477	Graphamine: Amine-Functionalized Graphane for Intrinsic Anhydrous Proton Conduction. Journal of Physical Chemistry C, 2019, 123, 1566-1571.	1.5	9
45478	Unravelling the Metastable Nature of the Single Site Tungsten Hydride Metathesis Catalyst Supported on Î³-Alumina from First Principles. Journal of Physical Chemistry C, 2019, 123, 1226-1234.	1.5	2
45479	Bimetallic Pd/Co Embedded in Two-Dimensional Carbon-Nitride for Z-Scheme Photocatalytic Water Splitting. Journal of Physical Chemistry C, 2019, 123, 1846-1851.	1.5	10
45480	Electronic Structure and Properties of Lithium-Rich Complex Oxides. ACS Applied Electronic Materials, 2019, 1, 75-81.	2.0	10
45481	Electrochemical Hydrogen Evolution at the Interface of Monolayer VS₂ and Water from First-Principles Calculations. ACS Applied Materials & Interfaces, 2019, 11, 2944-2949.	4.0	20
45482	CO and H₂ Activation over g-ZnO Layers and w-ZnO(0001). ACS Catalysis, 2019, 9, 1373-1382.	5.5	34
45483	Activation of Cellulose via Cooperative Hydroxyl-Catalyzed Transglycosylation of Glycosidic Bonds. ACS Catalysis, 2019, 9, 1943-1955.	5.5	32
45484	Millimeter-Scale Growth of Single-Oriented Graphene on a Palladium Silicide Amorphous Film. ACS Nano, 2019, 13, 1127-1135.	7.3	1
45485	Defect engineered bioactive transition metals dichalcogenides quantum dots. Nature Communications, 2019, 10, 41.	5.8	168
45486	Band-like transport in small-molecule thin films toward high mobility and ultrahigh detectivity phototransistor arrays. Nature Communications, 2019, 10, 12.	5.8	172

#	Article	IF	Citations
45487	Ultrasensitive detection of miRNA with an antimonene-based surface plasmon resonance sensor. Nature Communications, 2019, 10, 28.	5.8	475
45488	Multiferroic quantum criticality. Nature Materials, 2019, 18, 223-228.	13.3	49
45489	An ultrafast symmetry switch in a Weyl semimetal. Nature, 2019, 565, 61-66.	13.7	307
45490	Catalytic CO2 reduction by palladium-decorated siliconâ€“hydride nanosheets. Nature Catalysis, 2019, 2, 46-54.	16.1	116
45491	Identification of single-atom active sites in carbon-based cobalt catalysts during electrocatalytic hydrogen evolution. Nature Catalysis, 2019, 2, 134-141.	16.1	629
45492	Atomistic study of an ideal metal/thermoelectric contact: The full-Heusler/half-Heusler interface. APL Materials, 2019, 7, 013202.	2.2	7
45493	Phonon properties and thermal conductivity from first principles, lattice dynamics, and the Boltzmann transport equation. Journal of Applied Physics, 2019, 125, .	1.1	141
45494	Failure mode in first-principles computational tensile tests of grain boundaries: effects of a bulk-region size, dominant factors, and local-energy and local-stress analysis. Journal of Physics Condensed Matter, 2019, 31, 095001.	0.7	9
45495	Polarization rotation in Bi4Ti3O12 by isovalent doping at the fluorite sublattice. Physical Review B, 2019, 99, .	1.1	16
45496	Atomistic structure and collective dynamics in liquid Pb along the melting line up to 70 GPa: A first-principles molecular dynamics study. Physical Review B, 2019, 99, .	1.1	12
45497	Defect formation of CuI-doped by group-IIB elements. Modern Physics Letters B, 2019, 33, 1850423.	1.0	2
45498	X3N (X=C and Si) monolayers and their van der Waals Heterostructures with graphene and h-BN: Emerging tunable electronic structures by strain engineering. Carbon, 2019, 145, 1-9.	5.4	36
45499	Assessing Correlations of Perovskite Catalytic Performance with Electronic Structure Descriptors. Chemistry of Materials, 2019, 31, 785-797.	3.2	106
45500	Edge-State-Enhanced CO₂ Electroreduction on Topological Nodal-Line Semimetal Cu₂Si Nanoribbons. Journal of Physical Chemistry C, 2019, 123, 2837-2842.	1.5	26
45501	Two-Dimensional PC₆ with Direct Band Gap and Anisotropic Carrier Mobility. Journal of the American Chemical Society, 2019, 141, 1599-1605.	6.6	144
45502	Switchable Schottky Contacts: Simultaneously Enhanced Output Current and Reduced Leakage Current. Journal of the American Chemical Society, 2019, 141, 1628-1635.	6.6	43
45503	Diffusion of indium in single crystal zinc oxide: a comparison between group III donors. Semiconductor Science and Technology, 2019, 34, 025011.	1.0	4
45504	Topologically trivial states induced by strong spin-orbit coupling and Chern insulators in doped X(C21N3H15) â€‰ (X=Ta , Hf) metal-organic frameworks. Physical Review B, 2019, 99, .	1.1	10

#	Article	IF	Citations
45505	Enhanced Electroreduction of Carbon Dioxide to Methanol Using Zinc Dendrites Pulseâ€Deposited on Silver Foam. Angewandte Chemie, 2019, 131, 2278-2282.	1.6	7
45506	Na3(VO)2(PO4)2F Array for Cathode of Na-Ion Battery. Springer Theses, 2019, , 75-91.	0.0	0
45507	The formation and anisotropic/isotropic diffusion behaviors of vacancy in typical twin boundaries of Î±-Ti: An ab initio study. Computational Materials Science, 2019, 159, 257-264.	1.4	1
45508	Study of the crystal structure effect and mechanism during chemical looping gasification of coal. Journal of the Energy Institute, 2019, 92, 1284-1293.	2.7	9
45509	Probing C3N/Graphene heterostructures as anode materials for Li-ion batteries. Journal of Power Sources, 2019, 413, 117-124.	4.0	68
45510	Impact of Anion Vacancies on the Local and Electronic Structures of Iron-Based Oxyfluoride Electrodes. Journal of Physical Chemistry Letters, 2019, 10, 107-112.	2.1	16
45511	Investigation of structural models for Oâ€“Y and Oâ€“Yâ€“Ti clusters in bcc Fe: a density functional theory study. Journal of Physics Condensed Matter, 2019, 31, 095701.	0.7	3
45512	High Thermoelectric Performance in the Wide Bandâ€Gap AgGa_{1â€‹}_xTe₂ Compounds: Directional Negative Thermal Expansion and Intrinsically Low Thermal Conductivity. Advanced Functional Materials, 2019, 29, 1806534.	7.8	65
45513	Oxidation of Ni 13 clusters. International Journal of Quantum Chemistry, 2019, 119, e25874.	1.0	4
45514	Structural, electronic and optical properties of RbSnCl3: A first-principles calculation. Chemical Physics Letters, 2019, 716, 76-82.	1.2	17
45515	Anion intercalated layered-double-hydroxide structure for efficient photocatalytic NO remove. Green Energy and Environment, 2019, 4, 270-277.	4.7	30
45516	Monitoring the characteristic properties of Ga-doped ZnO by Raman spectroscopy and atomic scale calculations. Journal of Molecular Structure, 2019, 1180, 505-511.	1.8	40
45517	Microfocus Laserâ€Angle-Resolved Photoemission on Encapsulated Mono-, Bi-, and Few-Layer 1Tâ€²-WTe₂. Nano Letters, 2019, 19, 554-560.	4.5	52
45518	High-Magnetization Tetragonal Ferrite-Based Films Induced by Carbon and Oxygen Vacancy Pairs. ACS Applied Materials & Interfaces, 2019, 11, 1049-1056.	4.0	5
45519	Catalytic conversions of atmospheric sulfur dioxide and formation of acid rain over mineral dusts: Molecular oxygen as the oxygen source. Chemosphere, 2019, 217, 18-25.	4.2	30
45520	In-depth synthetic, physicochemical and in vitro biological investigation of a new ternary V(IV) antioxidant material based on curcumin. Journal of Inorganic Biochemistry, 2019, 191, 94-111.	1.5	14
45521	First-principles study of surface properties of uranium silicides. Journal of Nuclear Materials, 2019, 513, 192-197.	1.3	9
45522	First-principles study of thermophysical properties of interaction layer products in U-Mo/Al dispersion fuel. Journal of Nuclear Materials, 2019, 513, 94-101.	1.3	1

#	Article	IF	Citations
45523	First-principles study of transition metal monatomic chains intercalated AA-stacked bilayer graphene nanoribbons. Physica E: Low-Dimensional Systems and Nanostructures, 2019, 106, 114-120.	1.3	13
45524	Effect of non-metallic X(X=F, N, S) and Cr co-doping on properties of BiFeO3: A first-principles study. Physics Letters, Section A: General, Atomic and Solid State Physics, 2019, 383, 383-388.	0.9	8
45525	Fifty Shades of Water: Benchmarking DFT Functionals against Experimental Data for Ionic Crystalline Hydrates. Journal of Chemical Theory and Computation, 2019, 15, 584-594.	2.3	12
45526	Unobvious elastic anisotropy of measured singleâ€“crystal cementite. Materials Research Express, 2019, 6, 016531.	0.8	0
45527	Interaction of gold clusters with graphene and graphene layer over <mml:math xmlns:mml="http://www.w3.org/1998/Math/MathML" altimg="si17.gif" overflow="scroll"><mml:mrow><mml:mi mathvariant="italic">Ni</mml:mi><mml:mo stretchy="false">(</mml:mo><mml:mn>1</mml:mn><mml:mspace width="5.0pt") Tj ETQq0 0 0 rgBT /Overlock 10 Tf 50 577 Td (/><mn Su	3.1	1
45528	1T-MoS2 monolayer doped with isolated Ni atoms as highly active hydrogen evolution catalysts: A density functional study. Applied Surface Science, 2019, 469, 292-297.	3.1	41
45529	Single-layer planar penta-X2N4 (Xâ€¯=â€¯Ni, Pd and Pt) as direct-bandgap semiconductors from first principle calculations. Applied Surface Science, 2019, 469, 456-462.	3.1	48
45530	Insights into unidirectional migration of photo-excited electrons at ZnFe2O4/graphene van der Waals interface. Computational Materials Science, 2019, 157, 60-66.	1.4	7
45531	Origin of Pd-Cu bimetallic effect for synergetic promotion of methanol formation from CO2 hydrogenation. Journal of Catalysis, 2019, 369, 21-32.	3.1	80
45532	Coexistence of nanowire-like hex and (1 Ã— 1) phases in the topmost layer of Au(100) surface. Nanotechnology, 2019, 30, 045704.	1.3	6
45533	Design of Singleâ€Molecule Multiferroics for Efficient Ultrahighâ€Density Nonvolatile Memories. Advanced Science, 2019, 6, 1801572.	5.6	41
45534	Efficient and selective sensing of nitrogen-containing gases by Si2BN nanosheets under pristine and pre-oxidized conditions. Applied Surface Science, 2019, 469, 775-780.	3.1	78
45535	Potassium-Promoted Reduction of Cu₂O/Cu(111) by CO. Journal of Physical Chemistry C, 2019, 123, 8057-8066.	1.5	20
45536	Theory of thermoelectricity in Mg₃Sb₂ with an energy- and temperature-dependent relaxation time. Journal of Physics Condensed Matter, 2019, 31, 065702.	0.7	15
45537	Structural transformations and physical properties of (1â€‰â€‰â€™â€‰â€‰x) Na_{0.5}Bi_{0.5}TiO₃â€‰â€‰â€™â€‰â€‰x BaTiO₃ solid solutions near a morphotropic phase boundary. Journal of Physics Condensed Matter, 2019, 31, 075401.	0.7	45
45538	Width-dependent phase crossover in transition metal dichalcogenide nanoribbons. Nanotechnology, 2019, 30, 075701.	1.3	11
45539	Interplay of solute-mixed self-interstitial atoms and substitutional solutes with interstitial and substitutional helium atoms in tungsten-transition metal alloys. Nuclear Fusion, 2019, 59, 026002.	1.6	8
45540	Dehydrated Na₆[AlSiO₄]₆ sodalite as a promising SO₂ sorbent material: A first principles thermodynamics prediction. Journal of the American Ceramic Society, 2019, 102, 3663-3672.	1.9	9

#	Article	IF	Citations
45541	Theoretical insight into the optoelectronic properties of lead-free perovskite derivatives of Cs3Sb2X9 (Xâ€‰=â€‰Cl, Br, I). Journal of Materials Science, 2019, 54, 4732-4741.	1.7	42
45542	Defects guided wrinkling in graphene on copper substrate. Carbon, 2019, 143, 736-742.	5.4	27
45543	Atomistic understanding of helium behaviors at grain boundaries in vanadium. Computational Materials Science, 2019, 158, 296-306.	1.4	12
45544	Molecular dynamics simulations on the effect of nanovoid on shock-induced phase transition in uranium nitride. Physics Letters, Section A: General, Atomic and Solid State Physics, 2019, 383, 458-463.	0.9	8
45545	Local Electronic Structure of Molecular Heterojunctions in a Singleâ€Layer 2D Covalent Organic Framework. Advanced Materials, 2019, 31, e1805941.	11.1	74
45546	Excitonic effects on layer- and strain-dependent optoelectronic properties of PbI2. Applied Surface Science, 2019, 470, 143-149.	3.1	10
45547	Synthesis and understanding of Na11Sn2PSe12 with enhanced ionic conductivity for all-solid-state Na-ion battery. Energy Storage Materials, 2019, 17, 70-77.	9.5	42
45548	Formation of a new intermediate phase and its evolution toward Î¸' during aging of pre-deformed Al-Cu alloys. Journal of Materials Science and Technology, 2019, 35, 885-890.	5.6	25
45549	A monoclinic form of anhydrous Cs2PdCl4. Solid State Sciences, 2019, 87, 118-123.	1.5	8
45550	Challenges in Modeling Electrochemical Reaction Energetics with Polarizable Continuum Models. ACS Catalysis, 2019, 9, 920-931.	5.5	153
45551	Nitrogen Content in the Earth's Outer Core. Geophysical Research Letters, 2019, 46, 89-98.	1.5	10
45552	Role of Dimensionality for Photocatalytic Water Splitting: CdS Nanotube versus Bulk Structure. ChemPhysChem, 2019, 20, 383-391.	1.0	20
45553	Different limits for convergent Pd-Pd lengths in Pd slabs grown over different oxides. Structural Chemistry, 2019, 30, 489-500.	1.0	7
45554	Electric field induced two-dimensional electron gas and magnetism in LaFeO3/SrTiO3 (0â€¯0â€¯1) heterostructures. Applied Surface Science, 2019, 471, 185-195.	3.1	8
45555	Enhanced lithium storage capability of FeF3Â·0.33H2O single crystal with active insertion site exposed. Nano Energy, 2019, 56, 884-892.	8.2	55
45556	Neutral and zwitterionic dopamine species adsorbed on silver surfaces: A DFT investigation of interaction mechanism. International Journal of Quantum Chemistry, 2019, 119, e25817.	1.0	5
45557	First-principles calculations of phase transition, elasticity, phonon spectra, and thermodynamic properties for hafnium. Computational Materials Science, 2019, 157, 121-131.	1.4	16
45558	Phosphorus-Doped Graphene as a Metal-Free Material for Thermochemical Water Reforming at Unusually Mild Conditions. ACS Sustainable Chemistry and Engineering, 2019, 7, 838-846.	3.2	28

#	Article	IF	Citations
45559	Surface-induced magnetism in intermetallics: Ni3Ge compound as a case study. Journal of Magnetism and Magnetic Materials, 2019, 474, 273-281.	1.0	3
45560	Adsorption and diffusion mechanism of hydrogen atom on the Li2O (111) and (110) surfaces from first principles calculations. Journal of Nuclear Materials, 2019, 513, 232-240.	1.3	6
45561	Magnetic structures and optical properties of rare-earth orthoferrites RFeO3 (Râ€¯=â€¯Ho, Er, Tm and Lu). Solid State Communications, 2019, 288, 10-17.	0.9	36
45562	Novel MnS/(InxCu1-x)2S3 composite for robust solar hydrogen sulphide splitting via the synergy of solid solution and heterojunction. Applied Catalysis B: Environmental, 2019, 243, 790-800.	10.8	36
45563	Quantitative structural determination of active sites from in situ and operando XANES spectra: From standard ab initio simulations to chemometric and machine learning approaches. Catalysis Today, 2019, 336, 3-21.	2.2	70
45564	Benchmarking Computational Alchemy for Carbide, Nitride, and Oxide Catalysts. Advanced Theory and Simulations, 2019, 2, 1800142.	1.3	16
45565	The Coulomb interaction in van der Waals heterostructures. Science China: Physics, Mechanics and Astronomy, 2019, 62, 1.	2.0	25
45566	Atomistic modelling of the diffusion of C in Fe Cr alloys. Acta Materialia, 2019, 165, 638-653.	3.8	13
45567	Highly sensitive H2O2 sensor based on porous bimetallic oxide Ce1â^'xTbxOy derived from homeotypic Ln-MOFs. Applied Surface Science, 2019, 470, 91-98.	3.1	12
45568	Electric and optical properties modulations of armchair silicene nanoribbons by transverse electric fields. Current Applied Physics, 2019, 19, 31-36.	1.1	10
45569	Unlocking the nature of the co-doping effect on the ionic conductivity of CeO2-based electrolyte. Ceramics International, 2019, 45, 3977-3985.	2.3	27
45570	First-principles study of structural, elastic, electronic, vibrational and thermodynamic properties of uranium aluminides. Computational Materials Science, 2019, 158, 26-31.	1.4	15
45571	Structural characterization of Co-doped Pd (n=1â€“12) clusters: First-principles calculations. Chemical Physics Letters, 2019, 715, 141-146.	1.2	8
45572	Defective GP-zones and their evolution in an Al-Cu-Mg alloy during high-temperature aging. Journal of Alloys and Compounds, 2019, 774, 988-996.	2.8	37
45573	Multiple-valley effect on modulation of thermoelectric properties of n-type ZrCuSiAs-structure oxyantimonides LnTSbO (Ln= lanthanides and T=Zn, Mn). Journal of Materiomics, 2019, 5, 51-55.	2.8	4
45574	One-for-multiple substitution of large atoms in beryllium. Scripta Materialia, 2019, 162, 172-175.	2.6	1
45575	Nanopyramid boron-doped diamond electrode realizing nanomolar detection limit of 4-nonylphenol. Sensors and Actuators B: Chemical, 2019, 281, 830-836.	4.0	24
45576	Optimizing hydrogen evolution activity of nanoporous electrodes by dual-step surface engineering. Applied Catalysis B: Environmental, 2019, 244, 87-95.	10.8	22

#	Article	IF	Citations
45577	Predicting pressure-stabilized alkali metal iridides: Aâ˜Ir (Aâ€¯=â€¯Rb, Cs). Computational Materials Science, 2019, 158, 124-129.	1.4	6
45578	Accelerated oxygen evolution kinetics on nickelâ€“iron diselenide nanotubes by modulating electronic structure. Materials Today Energy, 2019, 11, 89-96.	2.5	42
45579	Solid-State Preparation, Structural Characterization, Physical Properties, and Theoretical Studies of a Series of Novel Rare-Earth Metal Chalcogenides with Unprecedented Closed-Cavities. Crystal Growth and Design, 2019, 19, 444-452.	1.4	14
45580	Kinetics-Based Computational Catalyst Design Strategy for the Oxygen Evolution Reaction on Transition-Metal Oxide Surfaces. Journal of Physical Chemistry C, 2019, 123, 8287-8303.	1.5	6
45581	Construction of direct Zâ€Scheme photocatalysts for overall water splitting using twoâ€dimensional van der waals heterojunctions of metal dichalcogenides. Journal of Computational Chemistry, 2019, 40, 980-987.	1.5	48
45582	Generalized stacking fault energies of Cr23C6 carbide: A first-principles study. Computational Materials Science, 2019, 158, 20-25.	1.4	12
45583	2D Fe-containing cobalt phosphide/cobalt oxide lateral heterostructure with enhanced activity for oxygen evolution reaction. Nano Energy, 2019, 56, 109-117.	8.2	223
45584	Fe-porphyrin carbon matrix as a bifunctional catalyst for oxygen reduction and CO₂ reduction from theoretical perspective. Molecular Physics, 2019, 117, 1805-1812.	0.8	12
45585	Total Ionizing Dose Effects and Proton-Induced Displacement Damage on MoS₂-Interlayer-MoS₂Tunneling Junctions. IEEE Transactions on Nuclear Science, 2019, 66, 420-427.	1.2	6
45586	Electronic Structure and Band Alignment of LaMnO₃/SrTiO₃ Polar/Nonpolar Heterojunctions. Advanced Materials Interfaces, 2019, 6, 1801428.	1.9	22
45587	Nonâ€Destructive Surface Energy Measurements on (1Â0Â0) Galfenol. Advanced Theory and Simulations, 2019, 2, 1800043.	1.3	4
45588	Crystal and Electronic Structure and Optical Properties of AE₂SiP₄ (AE = Sr, Eu, Ba) and Ba₄Si₃P₈. Zeitschrift Fur Anorganische Und Allgemeine Chemie, 2019, 645, 242-247.	0.6	17
45589	Electronic structure of Î²-Ta films from X-ray photoelectron spectroscopy and first-principles calculations. Applied Surface Science, 2019, 470, 607-612.	3.1	20
45590	Pressure induced structural phase of lithium disulfide with a close to intermediate product character of lithium-sulfur battery. Journal of Alloys and Compounds, 2019, 778, 588-592.	2.8	6
45591	Ab-initio modeling and experimental investigation of properties of ultra-high temperature solid solutions TaxZr1-xC. Journal of Alloys and Compounds, 2019, 778, 480-486.	2.8	22
45592	Advances on strategies for searching for next generation thermal barrier coating materials. Journal of Materials Science and Technology, 2019, 35, 833-851.	5.6	233
45593	Improving accuracy of interatomic potentials: more physics or more data? A case study of silica. Materials Today Communications, 2019, 18, 74-80.	0.9	32
45594	Conductivity of ironâ€doped strontium titanate in the quenched and degraded states. Journal of the American Ceramic Society, 2019, 102, 3567-3577.	1.9	12

#	Article	IF	Citations
45595	Comprehensive theoretical analysis of the influence of surface alloying by zinc on the catalytic performance of Cu(1â€¯1â€¯0) for the production of methanol from CO2 selective hydrogenation: Part 1 â€“ Thermochemical aspects. Applied Surface Science, 2019, 469, 841-853.	3.1	13
45596	Interaction mechanism between different facet TiO2 and U(VI): Experimental and density-functional theory investigation. Chemical Engineering Journal, 2019, 359, 944-954.	6.6	70
45597	The effects of oxidation on the electronic, thermal and mechanical properties of antimonene: First-principles study. Chemical Physics Letters, 2019, 715, 56-63.	1.2	5
45598	A theoretical study on the stability and ionic conductivity of the Na11M2PS12 (M = Sn, Ge) superionic conductors. Journal of Power Sources, 2019, 409, 94-101.	4.0	27
45599	Excitation Energies of Localized Correlated Defects via Quantum Monte Carlo: A Case Study of Mn⁴⁺-Doped Phosphors. Journal of Physical Chemistry Letters, 2019, 10, 67-74.	2.1	15
45600	Press-engineered funnel effect in MoS2 monolayer homojunction. Journal Physics D: Applied Physics, 2019, 52, 055103.	1.3	1
45601	Polarons in reduced cesium tungsten bronzes studied using the DFT + U method. Materials Research Express, 2019, 6, 026548.	0.8	20
45602	High Bipolar Conductivity and Robust Inâ€Plane Spontaneous Electric Polarization in Selenene. Advanced Electronic Materials, 2019, 5, 1800475.	2.6	32
45603	Glycine self-assembled on graphene enhances the solar absorbance performance. Carbon, 2019, 143, 329-334.	5.4	21
45604	Superprismane: A porous carbon allotrope. Chemical Physics Letters, 2019, 715, 29-33.	1.2	12
45605	Endorsement of Manganese Phthalocyanine microstructures as electrocatalyst in ORR: Experimental and computational study. Electrochimica Acta, 2019, 296, 528-534.	2.6	26
45606	Theoretical investigations of TiNbC MXenes as anode materials for Li-ion batteries. Journal of Alloys and Compounds, 2019, 778, 53-60.	2.8	49
45607	Pd-Ga model SCALMS: Characterization and stability of Pd single atom sites. Journal of Catalysis, 2019, 369, 33-46.	3.1	33
45608	Uncovering the magnetic properties of the <mml:math xmlns:mml="http://www.w3.org/1998/Math/MathML" altimg="si1.gif" overflow="scroll"><mml:mrow><mml:msub><mml:mrow><mml:mtext>Ag</mml:mtext></mml:mrow><mml:mrow><mml:mi>x</mml:mi>		

#	Article	IF	Citations
45613	Properties of Î²/Ï‰ phase interfaces in Ti and their implications on mechanical properties and Ï‰ morphology. Computational Materials Science, 2019, 158, 49-57.	1.4	6
45614	Defect evolution in burnable absorber candidate material: Uranium diboride, UB2. Journal of Nuclear Materials, 2019, 513, 45-55.	1.3	18
45615	Silver atom, trimer and tetramer species supported on a ceria nanoparticle: A density functional study. Surface Science, 2019, 681, 38-46.	0.8	8
45616	Electrocatalysts with Increased Activity for Coelectrolysis of Steam and Carbon Dioxide in Solid Oxide Electrolyzer Cells. ACS Catalysis, 2019, 9, 967-976.	5.5	21
45617	CO Oxidation Promoted by a Pt4/TiO2 Catalyst: Role of Lattice Oxygen at the Metal/Oxide Interface. Catalysis Letters, 2019, 149, 390-398.	1.4	19
45618	Intermetallic Electride Catalyst as a Platform for Ammonia Synthesis. Angewandte Chemie - International Edition, 2019, 58, 825-829.	7.2	104
45619	DFT Calculation about Oxygen Vacancy to Promote Adsorption of a CO Molecule on Single Auâ€Supported Titanium Dioxide. Physica Status Solidi (B): Basic Research, 2019, 256, 1800386.	0.7	7
45620	Formation and temporal evolution of modulated structure in high Nb-containing lamellar Î³-TiAl alloy. Acta Materialia, 2019, 165, 215-227.	3.8	35
45621	Theoretical study of correlations between the coordination structures and catalytic activities in polymerâ€stabilized au nanocluster catalysts. Journal of Computational Chemistry, 2019, 40, 222-228.	1.5	9
45622	Enhanced electron separation on in-plane benzene-ring doped g-C3N4 nanosheets for visible light photocatalytic hydrogen evolution. Applied Catalysis B: Environmental, 2019, 244, 459-464.	10.8	99
45623	A facile and effective sulfur loading method: Direct drop of liquid Li2S8 on carbon coated TiO2 nanowire arrays as cathode towards commercializing lithium-sulfur battery. Energy Storage Materials, 2019, 17, 118-125.	9.5	72
45624	The metal-free magnetism and ferromagnetic narrow gap semiconductor properties in graphene-like carbon nitride. Physica B: Condensed Matter, 2019, 555, 91-95.	1.3	16
45625	Spin-orbital coupling and magnetic properties of Ir-based double perovskites with different 5d (n = 3,) Tj ETQq0 0 0 rgBT /Overlock 10 Tf	0.9	6
45626	CO2 reduction by H2 to CHO on Ru(0001): DFT evaluation of three pathways. Surface Science, 2019, 681, 54-58.	0.8	11
45627	Machine Learning-Assisted Discovery of Solid Li-Ion Conducting Materials. Chemistry of Materials, 2019, 31, 342-352.	3.2	196
45628	Zn-doped MoSe2 nanosheets as high-performance electrocatalysts for hydrogen evolution reaction in acid media. Electrochimica Acta, 2019, 296, 701-708.	2.6	70
45629	Frequency dependent linear and nonlinear optical properties of compositionally tuned inorganic CsSnX (XÂ= Br, I) composites. Journal of Alloys and Compounds, 2019, 779, 497-504.	2.8	10
45630	Penta-AlN2 monolayer: A ferromagnetic insulator. Journal of Magnetism and Magnetic Materials, 2019, 475, 83-87.	1.0	7

#	Article	IF	Citations
45631	Energetics and kinetics of metal impurities in the low-temperature ordered phase of V2C from first-principles calculations. Journal of Nuclear Materials, 2019, 513, 185-191.	1.3	1
45632	Basal slip of âŸ¨aâŸ© screw dislocations in hexagonal titanium. Scripta Materialia, 2019, 162, 296-299.	2.6	22
45633	Atomistic origins of Guinier-Preston zone formation and morphology in Al-Cu and Al-Ag alloys from first principles. Scripta Materialia, 2019, 162, 235-240.	2.6	13
45634	Layered lithium niobium (III) oxideâ€"LiNbO₂ as a visible-light-driven photocatalyst for H₂ evolution. JPhys Energy, 2019, 1, 015001.	2.3	3
45635	The Molecular Surface Property Approach: A Guide to Chemical Interactions in Chemistry, Medicine, and Material Science. Advanced Theory and Simulations, 2019, 2, 1800149.	1.3	36
45636	Efficient energy gap tuning for T-carbon via single atomic doping. Chemical Physics, 2019, 518, 69-73.	0.9	13
45637	First principle analysis for magnetic properties of noble metal doped rutile TiO2. Computational Condensed Matter, 2019, 18, e00349.	0.9	9
45638	Corrosion resistance enhancement of WC cermet coating by carbides alloying. Corrosion Science, 2019, 147, 372-383.	3.0	24
45639	Cobalt hydroxide-black phosphorus nanosheets: A superior electrocatalyst for electrochemical oxygen evolution. Electrochimica Acta, 2019, 297, 40-45.	2.6	27
45640	On the partial enthalpy of mixing of Nb in liquid Al. Thermochimica Acta, 2019, 671, 103-109.	1.2	4
45641	Catalytic Hydrogenation of Carbon Dioxide to Methanol: Synergistic Effect of Bifunctional Cu/Perovskite Catalysts. ACS Catalysis, 2019, 9, 105-116.	5.5	44
45642	Influence of a Preâ€organized Nâ€Donor Group on the Coordination of Trivalent Actinides and Lanthanides by an Aminopolycarboxylate Complexant. Chemistry - A European Journal, 2019, 25, 2545-2555.	1.7	8
45643	Thermodynamic, transport, and optical properties of dense silver plasma calculated using the GreeKuP code. Contributions To Plasma Physics, 2019, 59, 345-353.	0.5	7
45644	Probing Magnetic Excitations in Co^{II} Singleâ€Molecule Magnets by Inelastic Neutron Scattering. European Journal of Inorganic Chemistry, 2019, 2019, 1119-1127.	1.0	14
45645	Hydrogen storage in MIL-88 series. Journal of Materials Science, 2019, 54, 3994-4010.	1.7	27
45646	Insights on hydrogen evolution reaction in transition metal doped monolayer TcS2 from density functional theory calculations. Applied Surface Science, 2019, 470, 107-113.	3.1	22
45647	Design of active bifunctional electrocatalysts using single atom doped transition metal dichalcogenides. Applied Surface Science, 2019, 471, 545-552.	3.1	67
45648	Silicide phase formation by Mg deposition on amorphous Si. Ab initio calculations, growth process and thermal stability. Journal of Alloys and Compounds, 2019, 778, 514-521.	2.8	2

#	Article	IF	Citations
45649	Engineering hydrogenated manganese dioxide nanostructures for high-performance supercapacitors. Journal of Colloid and Interface Science, 2019, 537, 661-670.	5.0	11
45650	Ordering Heterogeneity of [MnO6] Octahedra in Tunnel-Structured MnO2 and Its Influence on Ion Storage. Joule, 2019, 3, 471-484.	11.7	123
45651	A kinetic Monte Carlo study of vacancy diffusion in non-dilute Ni-Re alloys. Materials Science & Engineering A: Structural Materials: Properties, Microstructure and Processing, 2019, 743, 265-273.	2.6	15
45652	Elastic constants of graphene: Comparison of empirical potentials and DFT calculations. Physica E: Low-Dimensional Systems and Nanostructures, 2019, 108, 326-338.	1.3	47
45653	Stability, spontaneous and induced polarization in monolayer MoC, WC, WS, and WSe. Journal of Physics Condensed Matter, 2019, 31, 045301.	0.7	6
45654	2 Ã— 2 charge density wave in single-layer TiTe ₂. 2D Materials, 2019, 6, 015027.	2.0	20
45655	Phase stability and weak metallic bonding within ternaryâ€layered borides CrAlB, Cr₂AlB₂, Cr₃AlB₄, and Cr₄AlB₆. Journal of the American Ceramic Society, 2019, 102, 3715-3727.	1.9	55
45656	First principles investigation of the surface stability and equilibrium morphology of MoO3. Applied Surface Science, 2019, 467-468, 753-759.	3.1	20
45657	Thermo-mechanical properties of Ni-Mo solid solutions: A first-principles study. Computational Materials Science, 2019, 158, 140-148.	1.4	6
45658	Vacancy-ordered yttria stabilized zirconia as a low-temperature electronic conductor achieved by laser melting. Journal of the European Ceramic Society, 2019, 39, 1374-1380.	2.8	10
45659	Co-Fe-P nanotubes electrocatalysts derived from metal-organic frameworks for efficient hydrogen evolution reaction under wide pH range. Nano Energy, 2019, 56, 225-233.	8.2	235
45660	Insights on low-friction mechanism of amorphous carbon films from reactive molecular dynamics study. Tribology International, 2019, 131, 567-578.	3.0	41
45661	Energy Decomposition Analysis for Metal Surfaceâ€“Adsorbate Interactions by Block Localized Wave Functions. Journal of Chemical Theory and Computation, 2019, 15, 265-275.	2.3	13
45662	Effect of pressure on the physical properties of the superconductor NiBi₃. Journal of Physics Condensed Matter, 2019, 31, 035701.	0.7	9
45663	Adiabatic and nonadiabatic charge separation dynamics in graphene oxide quantum dots for overall water splitting. Nanotechnology, 2019, 30, 045201.	1.3	3
45664	Ensemble Design in Nickel Phosphide Catalysts for Alkyne Semiâ€Hydrogenation. ChemCatChem, 2019, 11, 457-464.	1.8	25
45665	Methyl-terminated germanane GeCH3 synthesized by solvothermal method with improved photocatalytic properties. Applied Surface Science, 2019, 467-468, 881-888.	3.1	30
45666	Prediction of Li2B novel phases and superconductivity under varying pressures. Computational Materials Science, 2019, 158, 255-259.	1.4	6

#	Article	IF	Citations
45667	Theoretical study of size effects on the direct synthesis of hydrogen peroxide over palladium catalysts. Journal of Catalysis, 2019, 369, 95-104.	3.1	46
45668	Self-organization of ultra-thin uranium film. Physics Letters, Section A: General, Atomic and Solid State Physics, 2019, 383, 477-481.	0.9	0
45669	Origin of Blue Luminescence in <mml:math xmlns:mml="http://www.w3.org/1998/Math/MathML" display="inline" overflow="scroll"><mml:mi>Mg</mml:mi></mml:math> -Doped <mml:math xmlns:mml="http://www.w3.org/1998/Math/MathML" display="inline" overflow="scroll"><mml:mi>Ga</mml:mi><mml:mi mathvariant="normal">N</mml:mi></mml:math>. Physical Review Applied, 2019, 11, .	1.5	19
45670	Magnetism in cation-disordered 3dâ^'4d/5d double perovskites. Physical Review B, 2019, 99, .	1.1	9
45671	Topological nodal-line semimetals in ferromagnetic rare-earth-metal monohalides. Physical Review B, 2019, 99, .	1.1	51
45672	Surface doping of ZnO nanowires with Bi: Density-functional supercell calculations of defect energetics. Physical Review B, 2019, 99, .	1.1	4
45673	Quantum Paraelastic Two-Dimensional Materials. Physical Review Letters, 2019, 122, 015703.	2.9	13
45674	Hybridization-Switching Induced Mott Transition in <mml:math xmlns:mml="http://www.w3.org/1998/Math/MathML" display="inline"><mml:mrow><mml:mi>A</mml:mi><mml:mi>B</mml:mi><mml:mrow><mml:msub><mml:mrow><mml:mi mathvariant="normal">O</mml:mi></mml:mrow><mml:mrow><mml:mn>3</mml:mn></mml:mrow></mml:msub></mml:mrow></mml:mi Perovskites. Physical Review Letters, 2019, 122, 016404.	2.9	23
45675	Photochemical Etching of Carbonyl Groups from a Carbon Matrix: The (001) Diamond Surface. Physical Review Letters, 2019, 122, 016802.	2.9	7
45676	Interplay between Adsorbates and Polarons: CO on Rutile <mml:math xmlns:mml="http://www.w3.org/1998/Math/MathML" display="inline"><mml:mrow><mml:msub><mml:mrow><mml:mi>TiO</mml:mi></mml:mrow><mml:mrow><mml:mn>2</mml:mn></mml:mrow></mml:msub></mml:mrow></mml:math> (110) Tj ETQq1 1 0.784314 rgBT /Overlock 10 Tf 50 367 Td (stretchy="false">(</mml:mo><mml:mn>110</mml:mn><mml:mo) Tj ETQq1 1 0.784314 rgBT /Overlock 10 Tf 50 367 Td (stretchy="false	2.9	76
45677	Size-Dependent Lattice Dynamics of Atomically Precise Cadmium Selenide Quantum Dots. Physical Review Letters, 2019, 122, 026101.	2.9	12
45678	Structural, electronic, and dielectric properties of a large random network model of amorphous zeolitic imidazolate frameworks and its analogues. Journal of the American Ceramic Society, 2019, 102, 4602-4611.	1.9	13
45679	Li substituent tuning of LED phosphors with enhanced efficiency, tunable photoluminescence, and improved thermal stability. Science Advances, 2019, 5, eaav0363.	4.7	153
45680	Structural, electronic and magnetic properties of stoichiometric cobalt oxide clusters (CoO)nq (n=3â^'10,q=0,+1): A modified basin-hopping Monte Carlo algorithm with spin-polarized DFT. Journal of Theoretical and Computational Chemistry, 2019, 18, 1950003.	1.8	2
45681	Effect of Defects on Spontaneous Polarization in Pure and Doped LiNbO3: First-Principles Calculations. Materials, 2019, 12, 100.	1.3	19
45682	Operando Observations and Firstâ€Principles Calculations of Reduced Lithium Insertion in Auâ€Coated LiMn 2 O 4. Advanced Materials Interfaces, 2019, 6, 1801923.	1.9	11
45683	Mixing Thermodynamics and Photocatalytic Properties of GaPâ€“ZnS solid solutions. Advanced Theory and Simulations, 2019, 2, 1800146.	1.3	7
45684	Synthesis of Nickelâ€Doped Ceria Catalysts for Selective Acetylene Hydrogenation. ChemCatChem, 2019, 11, 1526-1533.	1.8	30

#	Article	IF	Citations
45685	Impact of Defects on Electronic Properties of Heterostructures Constructed From Monolayers of Transition Metal Dichalcogenides. Physica Status Solidi (B): Basic Research, 2019, 256, 1800355.	0.7	10
45686	Calculation of Magnetic Exchange Interactions and Construction of a Spin Model for Low-Dimensional Magnetic Compounds. Journal of Electronic Materials, 2019, 48, 1480-1485.	1.0	0
45687	Half-metallic, Magnetic, and Optical Properties for the (001) Surface of Binary Heusler Alloy MgCl3. Journal of Electronic Materials, 2019, 48, 2563-2571.	1.0	4
45688	Interfacial free energies, nucleation, and precipitate morphologies in Ni-Al-Cr alloys: Calculations and atom-probe tomographic experiments. Acta Materialia, 2019, 166, 702-714.	3.8	18
45689	Electronic and magnetic behaviour of 2D metal structures of Y on Li(1â€¯1â€¯0) surface. Applied Surface Science, 2019, 471, 1005-1010.	3.1	4
45690	Pressure induced semiconductor-metallic transition of selenium nanoribbons generated by laser ablation in liquids. Applied Surface Science, 2019, 473, 564-570.	3.1	15
45691	Experimental investigations and thermodynamic modelling of the Crâ€“Nbâ€“Snâ€“Zr system. Calphad: Computer Coupling of Phase Diagrams and Thermochemistry, 2019, 64, 43-54.	0.7	21
45692	Pushing the frontiers of modeling excited electronic states and dynamics to accelerate materials engineering and design. Computational Materials Science, 2019, 160, 207-216.	1.4	18
45693	First-principles investigation of native point defects in two-dimensional Ti3C2. Computational and Theoretical Chemistry, 2019, 1150, 26-39.	1.1	9
45694	Niobium doped amorphous carbon film on metallic bipolar plates for PEMFCs: First principle calculation, microstructure and performance. International Journal of Hydrogen Energy, 2019, 44, 3144-3156.	3.8	41
45695	Highly anisotropic thermoelectric transport properties responsible for enhanced thermoelectric performance in the hot-deformed tetradymite Bi2Te2S. Journal of Alloys and Compounds, 2019, 783, 448-454.	2.8	15
45696	First-principles study on the structural, electronic, and magnetic properties of bulk and (001) surface of RuS2. Journal of Physics and Chemistry of Solids, 2019, 129, 227-233.	1.9	2
45697	Oxygen vacancy modulated Ti2Nb10O29-x embedded onto porous bacterial cellulose carbon for highly efficient lithium ion storage. Nano Energy, 2019, 58, 355-364.	8.2	137
45698	Electronic structure and photoluminescence of Dy3+ single-doped and Dy3+/Tm3+ co-doped NaBi(WO4)2 phosphors. Optical Materials, 2019, 88, 534-539.	1.7	25
45699	Optoelectronic Properties of TiS2: A Never Ended Story Tackled by Density Functional Theory and Many-Body Methods. Inorganic Chemistry, 2019, 58, 1949-1957.	1.9	12
45700	Toward Fundamentals of Confined Electrocatalysis in Nanoscale Reactors. Journal of Physical Chemistry Letters, 2019, 10, 533-539.	2.1	18
45701	Doping of Monolayer Transition-Metal Dichalcogenides via Physisorption of Aromatic Solvent Molecules. Journal of Physical Chemistry Letters, 2019, 10, 540-547.	2.1	52
45702	Single-Layer Ag₂S: A Two-Dimensional Bidirectional Auxetic Semiconductor. Nano Letters, 2019, 19, 1227-1233.	4.5	165

#	Article	IF	Citations
45703	First-Principles Prediction of a Room-Temperature Ferromagnetic Janus VSSe Monolayer with Piezoelectricity, Ferroelasticity, and Large Valley Polarization. Nano Letters, 2019, 19, 1366-1370.	4.5	292
45704	Revealing the Reaction Mechanism of Sodium Selenide Confined within a Single-Walled Carbon Nanotube: Implications for Naâ€“Se Batteries. ACS Applied Materials & Interfaces, 2019, 11, 4995-5002.	4.0	27
45705	Unusual Electronic States and Superconducting Proximity Effect of Bi Films Modulated by a NbSe₂ Substrate. ACS Nano, 2019, 13, 1885-1892.	7.3	23
45706	Surface-Engineered MXenes: Electric Field Control of Magnetism and Enhanced Magnetic Anisotropy. ACS Nano, 2019, 13, 2831-2839.	7.3	126
45707	Carbonized MoS₂: Super-Active Co-Catalyst for Highly Efficient Water Splitting on CdS. ACS Sustainable Chemistry and Engineering, 2019, 7, 4220-4229.	3.2	68
45708	Cooperative Effects between Hydrophilic Pores and Solvents: Catalytic Consequences of Hydrogen Bonding on Alkene Epoxidation in Zeolites. Journal of the American Chemical Society, 2019, 141, 7302-7319.	6.6	142
45709	Morphology and surface chemistry engineering toward pH-universal catalysts for hydrogen evolution at high current density. Nature Communications, 2019, 10, 269.	5.8	431
45710	Non defect-stabilized thermally stable single-atom catalyst. Nature Communications, 2019, 10, 234.	5.8	452
45711	A welding phenomenon of dissimilar nanoparticles in dispersion. Nature Communications, 2019, 10, 219.	5.8	18
45712	Discovery of TaFeSb-based half-Heuslers with high thermoelectric performance. Nature Communications, 2019, 10, 270.	5.8	227
45713	Electric-field control of spin accumulation direction for spin-orbit torques. Nature Communications, 2019, 10, 248.	5.8	61
45714	Electronic structure and the hydrogen evolution reaction in layered ReS2 regulated by alkali-metal atom intercalation. Journal Physics D: Applied Physics, 2019, 52, 165301.	1.3	3
45715	Predicting ultrafast Dirac transport channel at the one-dimensional interface of the two-dimensional coplanar <mml:math xmlns:mml="http://www.w3.org/1998/Math/MathML"><mml:mrow><mml:mi>ZnO</mml:mi><mml:mo>/</mml:mo><mml:mi>Mo</mml:mi><mml:mathvariant="normal">S</mml:mi><mml:mn>2</mml:mn></mml:msub></mml:mrow></mml:math> heterostructure. Physical Review B, 2019, 99, .	1.1	6
45716	Impact of carbon segregant on microstructure and magnetic properties of FePt-C nanogranular films on MgO (001) substrate. Acta Materialia, 2019, 166, 413-423.	3.8	28
45717	Insight into CaO addition on coking resistance of Ni surface for sorption enhanced methane steam reforming: A density functional study. Applied Surface Science, 2019, 475, 887-895.	3.1	16
45718	Genetic algorithm aided density functional theory simulations unravel the kinetic nature of Au(100) in catalytic CO oxidation. Chinese Chemical Letters, 2019, 30, 1346-1350.	4.8	6
45719	Chemically Accurate Adsorption Energies: CO and H2O on the MgO(001) Surface. Journal of Chemical Theory and Computation, 2019, 15, 1329-1344.	2.3	23
45720	Adsorption Behavior of Organic Molecules: A Study of Benzotriazole on Cu(111) with Spectroscopic and Theoretical Methods. Langmuir, 2019, 35, 882-893.	1.6	22

#	Article	IF	Citations
45721	F-Doped NaTi₂(PO₄)₃/C Nanocomposite as a High-Performance Anode for Sodium-Ion Batteries. ACS Applied Materials & Interfaces, 2019, 11, 3116-3124.	4.0	52
45722	Coreâ€“Shell Structured S@Co(OH)₂ with a Carbon-Nanofiber Interlayer: A Conductive Cathode with Suppressed Shuttling Effect for High-Performance Lithiumâ€“Sulfur Batteries. ACS Applied Materials & Interfaces, 2019, 11, 4065-4073.	4.0	35
45723	Firstâ€principles study, fabrication, and characterization of (Hf_{0.2}Zr_{0.2}Ta_{0.2}Nb_{0.2}Ti_{0.2})C highâ€entropy ceramic. Journal of the American Ceramic Society, 2019, 102, 4344-4352.	1.9	217
45724	Highly Stable and Ultrafast Hydrogen Gas Sensor Based on 15 nm Nanogaps Switching in a Palladiumâ€“Gold Nanoribbons Array. Advanced Materials Interfaces, 2019, 6, 1801442.	1.9	18
45725	Selective reduction of CO2 to CO under visible light by controlling coordination structures of CeOx-S/ZnIn2S4 hybrid catalysts. Applied Catalysis B: Environmental, 2019, 245, 262-270.	10.8	53
45726	Thermodynamic assessment of the Co-Ta system. Calphad: Computer Coupling of Phase Diagrams and Thermochemistry, 2019, 64, 205-212.	0.7	17
45727	Surface thermodynamic stability of Li-rich Li2MnO3: Effect of defective graphene. Energy Storage Materials, 2019, 22, 113-119.	9.5	45
45728	Measuring the mean inner potential of Al2O3 sapphire using off-axis electron holography. Ultramicroscopy, 2019, 198, 18-25.	0.8	9
45729	Fabrication of TiO₂(B)/Anatase Heterophase Junctions at High Temperature via Stabilizing the Surface of TiO₂(B) for Enhanced Photocatalytic Activity. Journal of Physical Chemistry C, 2019, 123, 1779-1789.	1.5	43
45730	Reactive and Nonreactive Scattering of HCl from Au(111): An Ab Initio Molecular Dynamics Study. Journal of Physical Chemistry C, 2019, 123, 2287-2299.	1.5	30
45731	Electronic structure and exciton shifts in Sb-doped MoS2 monolayer. Npj 2D Materials and Applications, 2019, 3, .	3.9	82
45732	Atomistics of pre-nucleation layering of liquid metals at the interface with poor nucleants. Communications Chemistry, 2019, 2, .	2.0	115
45733	An Effective Approach to Improve the Photocatalytic Activity of Graphitic Carbon Nitride via Hydroxyl Surface Modification. Catalysts, 2019, 9, 17.	1.6	15
45734	Engineering an Earthâ€Abundant Elementâ€Based Bifunctional Electrocatalyst for Highly Efficient and Durable Overall Water Splitting. Advanced Functional Materials, 2019, 29, 1807031.	7.8	146
45735	Electronic structure, magnetism properties and optical absorption of organometal halide perovskite CH3NH3XI3 (Xâ€‰=â€‰Fe, Mn). Applied Physics A: Materials Science and Processing, 2019, 125, 1.	1.1	11
45736	Geometries, stabilities, and magnetic properties of Co2Bn (nâ€‰=â€‰1â€“10) clusters. Journal of Molecular Modeling, 2019, 25, 27.	0.8	6
45737	On-surface stereoconvergent synthesis, dimerization and hybridization of organocopper complexes. Science China Chemistry, 2019, 62, 126-132.	4.2	0
45738	First-principles study of the surface reparation of ultrathin InSe with Se-atom vacancies by thiol chemistry. Applied Surface Science, 2019, 475, 487-493.	3.1	6

#	Article	IF	Citations
45739	Hybrid porous flower-like NiO@CeO2microspheres with improved pseudocapacitiveproperties. Electrochimica Acta, 2019, 297, 593-605.	2.6	51
45740	Ni anchored C2N monolayers as low-cost and efficient catalysts for hydrogen production from formic acid. Journal of Power Sources, 2019, 413, 399-407.	4.0	40
45741	Correlations between Density-Based Bond Orders and Orbital-Based Bond Energies for Chemical Bonding Analysis. Journal of Physical Chemistry C, 2019, 123, 2843-2854.	1.5	50
45742	Correlated Roles of Temperature and Dimensionality for Multiple Exciton Generation and Electronic Structures in Quantum Dot Superlattices. Journal of Physical Chemistry C, 2019, 123, 2549-2556.	1.5	6
45743	Insights into the Activation Effect of H₂ Pretreatment on Ag/Al₂O₃ Catalyst for the Selective Oxidation of Ammonia. ACS Catalysis, 2019, 9, 1437-1445.	5.5	78
45744	Few-Nanometer-Sized Î±-CsPbI₃ Quantum Dots Enabled by Strontium Substitution and Iodide Passivation for Efficient Red-Light Emitting Diodes. Journal of the American Chemical Society, 2019, 141, 2069-2079.	6.6	218
45745	Electrical Control of Magnetic Behavior and Valley Polarization of Monolayer Antiferromagnetic <mml:math xmlns:mml="http://www.w3.org/1998/Math/MathML" display="inline" overflow="scroll"><mml:msub><mml:mrow><mml:mi>Mn</mml:mi><mml:mi mathvariant="normal">P</mml:mi><mml:mi>Se</mml:mi></mml:mrow><mml:mn>3</mml:mn></mml:msub></mml:math> on an Insulating Ferroelectric Substrate from First Principles. Physical Review Applied, 2019, 11, .	1.5	36
45746	Anisotropic magnetoresistance in the itinerant antiferromagnetic <mml:math xmlns:mml="http://www.w3.org/1998/Math/MathML"><mml:mrow><mml:mi>EuTi</mml:mi><mml:msub><mml:mi mathvariant="normal">O</mml:mi><mml:mn>3</mml:mn></mml:msub></mml:mrow></mml:math>. Physical Review B, 2019, 99, .	1.1	31
45747	On the Influence of Rare Earth Dopants on Thermal Transport in Thermoelectric Bi₂Te₃ Compounds: An Ab Initio Perspective. Advanced Theory and Simulations, 2019, 2, 1800162.	1.3	8
45748	Pressure-induced Lifshitz transition in the type II Dirac semimetal PtTe2. Science China: Physics, Mechanics and Astronomy, 2019, 62, 1.	2.0	13
45749	Uniform MoS2 nanolayer with sulfur vacancy on carbon nanotube networks as binder-free electrodes for asymmetrical supercapacitor. Applied Surface Science, 2019, 475, 793-802.	3.1	69
45750	Discovery of new ground state structures for Li4Mn2O5 and V2O5 from first principles. Computational Materials Science, 2019, 159, 454-459.	1.4	5
45751	Stable single-atom cobalt as a strong coupling bridge to promote electron transfer and separation in photoelectrocatalysis. Journal of Catalysis, 2019, 370, 176-185.	3.1	46
45752	Silver tellurides: Structural, elastic, and optical properties of AgTe and Ag2Te. Journal of Physics and Chemistry of Solids, 2019, 129, 41-45.	1.9	12
45753	Surface-Templated Assembly of Molecular Methanol on the Thin Film â€œ29â€•Cu(111) Surface Oxide. Journal of Physical Chemistry C, 2019, 123, 2911-2921.	1.5	9
45754	Self-Encapsulation of Silicene in Cubic Diamond Si: Topological Semimetal in Covalent Bonding Networks. Journal of Physical Chemistry C, 2019, 123, 1839-1845.	1.5	4
45755	Transferability of the Specific Reaction Parameter Density Functional for H2 + Pt(111) to H2 + Pt(211). Journal of Physical Chemistry C, 2019, 123, 2973-2986.	1.5	18
45756	Designing Nanoplatelet Alloy/Nafion Catalytic Interface for Optimization of PEMFCs: Performance, Durability, and CO Resistance. ACS Catalysis, 2019, 9, 1446-1456.	5.5	29

#	Article	IF	Citations
45757	What Is Measured When Measuring Acidity in Zeolites with Probe Molecules?. ACS Catalysis, 2019, 9, 1539-1548.	5.5	111
45758	Selective on-surface covalent coupling based on metal-organic coordination template. Nature Communications, 2019, 10, 70.	5.8	55
45759	Impact of proton irradiation on conductivity and deep level defects in Î²-Ga2O3. APL Materials, 2019, 7, .	2.2	143
45760	Equation of state and structural characterization of Cu₄I₄{PPh₂(CH₂CHâ€‰=â€‰CH₂)}₄ under pressure. High Pressure Research, 2019, 39, 69-80.	1.5	
45761	Direct coupling of first-principles calculations with replica exchange Monte Carlo sampling of ion disorder in solids. Journal of Physics Condensed Matter, 2019, 31, 085901.	0.7	7
45762	Tailoring Lithium Deposition via an SEIâ€Functionalized Membrane Derived from LiF Decorated Layered Carbon Structure. Advanced Energy Materials, 2019, 9, 1802912.	10.2	98
45763	First-Principles Study of the Structural Stability and Dynamic Properties of Li2MSiO4 (M = Mn, Co, Ni) Polymorphs. Energies, 2019, 12, 224.	1.6	7
45764	Studies of Functional Defects for Fast Naâ€Ion Conduction in Na_{3â^’}_yPS_{4â^’}_xCl_x with a Combined Experimental and Computational Approach. Advanced Functional Materials, 2019, 29, 1807951.	7.8	51
45765	Photoelectrochemical Synthesis of Ammonia on the Aerophilic-Hydrophilic Heterostructure with 37.8% Efficiency. CheM, 2019, 5, 617-633.	5.8	241
45766	C-57 carbon: A two-dimensional metallic carbon allotrope with pentagonal and heptagonal rings. Computational Materials Science, 2019, 160, 115-119.	1.4	49
45767	Solid Electrolyte Interphase on Native Oxide-Terminated Silicon Anodes for Li-Ion Batteries. Joule, 2019, 3, 762-781.	11.7	185
45768	Phase transition in two-dimensional tellurene under mechanical strain modulation. Nano Energy, 2019, 58, 202-210.	8.2	43
45769	Hydrogen passivation tunes edge magnetism in the ZMoS2NR with a sulfur vacancy. Physics Letters, Section A: General, Atomic and Solid State Physics, 2019, 383, 539-549.	0.9	1
45770	A theoretical study of electrocatalytic ammonia synthesis on single metal atom/MXene. Chinese Journal of Catalysis, 2019, 40, 152-159.	6.9	76
45771	Experimental and Theoretical Elucidation of Electrochemical CO₂ Reduction on an Electrodeposited Cu₃Sn Alloy. Journal of Physical Chemistry C, 2019, 123, 3004-3010.	1.5	28
45772	Unraveling Anhydrous Proton Conduction in Hydroxygraphane. Journal of Physical Chemistry Letters, 2019, 10, 518-523.	2.1	13
45773	Distortion-stabilized ordered structures in A2BBâ€™O7 mixed pyrochlores. Npj Computational Materials, 2019, 5, .	3.5	23
45774	Effective n-type doping of Mg3Sb2 with group-3 elements. Journal of Applied Physics, 2019, 125, .	1.1	37

#	Article	IF	Citations
45775	Isoelectronic analogues of graphene: the BCN monolayers with visible-light absorption and high carrier mobility. Journal of Physics Condensed Matter, 2019, 31, 125301.	0.7	22
45776	Tuning electronic and optical properties of TiO₂ with Pt/Ag doping to a prospective photocatalyst: a first principles DFT study. Materials Research Express, 2019, 6, 045913.	0.8	22
45777	Tunability of magnetic anisotropy of Co on two-dimensional materials by tetrahedral bonding. Physical Review B, 2019, 99, .	1.1	9
45778	Electronic and Magnetic Properties of Transition-Metal-Doped WS₂ Monolayer; First-Principles Investigations. IEEE Transactions on Magnetics, 2019, 55, 1-4.	1.2	6
45779	Disentangling the size-dependent geometric and electronic effects of palladium nanocatalysts beyond selectivity. Science Advances, 2019, 5, eaat6413.	4.7	187
45780	Boosting the electrocatalytic glycerol oxidation performance with highly-dispersed Pt nanoclusters loaded on 3D graphene-like microporous carbon. Applied Catalysis B: Environmental, 2019, 245, 555-568.	10.8	45
45781	N-doped graphene confined Pt nanoparticles for efficient semi-hydrogenation of phenylacetylene. Carbon, 2019, 145, 47-52.	5.4	44
45782	Catalytic benzene oxidation by biogenic Pd nanoparticles over 3D-ordered mesoporous CeO2. Chemical Engineering Journal, 2019, 362, 41-52.	6.6	95
45783	Valley and spin splitting in monolayer TX ₂/antiferromagnetic MnO (Tâ€‰â€‰=â€‰â€‰Mo,) Tj ETQq0 0 0	1.3	17
45784	Topological Landscape of Competing Charge Density Waves in <mml:math xmlns:mml="http://www.w3.org/1998/Math/MathML" display="inline"><mml:mrow><mml:mn>2</mml:mn><mml:mi>H</mml:mi><mml:mtext>â”</mml:mtext><mml:msub><mml:mrow> Physical Review Letters, 2019, 122, 016403.	2.9	30
45785	Deploying Elbrus VLIW CPU Ecosystem for Materials Science Calculations: Performance and Problems. Communications in Computer and Information Science, 2019, , 543-553.	0.4	0
45786	Influence of Pendant Group on Mobility of Organic Thin Film Transistor in Correlation with Reorganization Energy of Molecules. Advanced Functional Materials, 2019, 29, 1805878.	7.8	13
45787	Transitionâ€Metal Oxynitride: A Facile Strategy for Improving Electrochemical Capacitor Storage. Advanced Materials, 2019, 31, e1806088.	11.1	91
45788	Discovery of Calciumâ€Metal Alloy Anodes for Reversible Caâ€Ion Batteries. Advanced Energy Materials, 2019, 9, 1802994.	10.2	61
45789	Enhanced Stability and Optical Absorption in the Perovskiteâ€Based Compounds MA 1â” x Cs x PbI 3â” y Br y. ChemPhysChem, 2019, 20, 489-498.	1.0	6
45790	Fe₂VO₄ Hierarchical Porous Microparticles Prepared via a Facile Surface Solvation Treatment for Highâ€Performance Lithium and Sodium Storage. Small, 2019, 15, e1804706.	5.2	30
45791	Transitionâ€Metal Single Atoms Anchored on Graphdiyne as Highâ€Efficiency Electrocatalysts for Water Splitting and Oxygen Reduction. Small Methods, 2019, 3, 1800419.	4.6	192
45792	C/N Vacancy Coâ€Enhanced Visibleâ€Lightâ€Driven Hydrogen Evolution of gâ€C₃N₄ Nanosheets Through Controlled He⁺ Ion Irradiation. Solar Rrl, 2019, 3, 1800298.	3.1	75

#	Article	IF	Citations
45793	Thermodynamics, structure, and transport properties of the MgOâ€“Al2O3 liquid system. Physics and Chemistry of Minerals, 2019, 46, 501-512.	0.3	2
45794	Influence of internal displacement on band structure, phase transition, and thermoelectric properties of bismuth. Journal of Materials Science, 2019, 54, 6347-6360.	1.7	17
45795	Synthesis of SrCoO3 perovskite as W-based double perovskite and its structural properties. Journal of Materials Science: Materials in Electronics, 2019, 30, 4270-4278.	1.1	2
45796	Using First-Principles Calculations in CALPHAD Models to Determine Carrier Concentration of the Binary PbSe Semiconductor. Journal of Electronic Materials, 2019, 48, 1031-1043.	1.0	8
45797	Two-dimensional amorphous heterostructures of Ag/a-WO3- for high-efficiency photocatalytic performance. Applied Catalysis B: Environmental, 2019, 245, 648-655.	10.8	69
45798	Cu-Pd alloy nanoparticles as highly selective catalysts for efficient electrochemical reduction of CO2 to CO. Applied Catalysis B: Environmental, 2019, 246, 82-88.	10.8	167
45799	Effect of atom adsorption on the electronic, magnetic, and optical properties of the GeP monolayer: A first-principle study. Applied Surface Science, 2019, 475, 863-872.	3.1	14
45800	Low temperature, pressureless sp2 to sp3 transformation of ultrathin, crystalline carbon films. Carbon, 2019, 145, 10-22.	5.4	64
45801	NO2 and H2 sensing properties for urchin-like hexagonal WO3 based on experimental and first-principle investigations. Ceramics International, 2019, 45, 6043-6050.	2.3	67
45802	Experimental and computational modelling study of Ni substitution for Fe in Zr3Fe and its hydride. Journal of Alloys and Compounds, 2019, 781, 131-139.	2.8	3
45803	AlÂâ˜ BN interaction in a high-strength lightweight Al/BN metal-matrix composite: Theoretical modelling and experimental verification. Journal of Alloys and Compounds, 2019, 782, 875-880.	2.8	20
45804	Thermal stability of ternary compounds in the Cu-Li-Sn system and phase transition of the Cu6Sn5 electrode: First-principles calculations and experiment. Journal of Alloys and Compounds, 2019, 783, 44-54.	2.8	2
45805	Effect of similar element substitution on Fe-B-Si-Mo bulk metallic glasses studied by experiment and ab initio molecular dynamics simulation. Journal of Alloys and Compounds, 2019, 784, 1139-1144.	2.8	19
45806	Towards thermal barrier coating application for rare earth silicates RE2SiO5 (RE= La, Nd, Sm, Eu, and) Tj ETQq1 1 0.784314 rgBT /Ove	2.8	70
45807	Role of the Interfacial Rh-layer on Robust Ferromagnetism and Large Perpendicular Magnetic Anisotropy of FeRh Films on MgO(0 0 1). Journal of Magnetism and Magnetic Materials, 2019, 476, 487-496.	1.0	6
45808	First-principles study of Ni-Co-Mn-Sn alloys with regular and inverse Heusler structure. Journal of Magnetism and Magnetic Materials, 2019, 476, 546-550.	1.0	7
45809	Theory-guided bottom-up design of the FeCrAl alloys as accident tolerant fuel cladding materials. Journal of Nuclear Materials, 2019, 516, 63-72.	1.3	27
45810	Influence of hydrostatic strain on the behaviors of rhenium and osmium in tungsten. Journal of Nuclear Materials, 2019, 516, 111-117.	1.3	1

#	Article	IF	Citations
45811	First-principles study of the solute segregation in twin boundaries in Mg and possible descriptors for mechanical properties. Materials and Design, 2019, 165, 107574.	3.3	29
45812	Morphology of MoP catalyst under hydrogenation conditions: A DFT based thermodynamics study. Molecular Catalysis, 2019, 464, 57-62.	1.0	10
45813	Unusual pressure-induced electronic structure evolution in organometal halide perovskite predicted from first-principles. Organic Electronics, 2019, 67, 89-94.	1.4	23
45814	Symmetry and thermodynamics of tellurium vacancies in cadmium telluride. Physica B: Condensed Matter, 2019, 568, 81-87.	1.3	1
45815	A green and facile synthesis for rGO/Ag nanocomposites using one-step chemical co-reduction route at ambient temperature and combined first principles theoretical analyze. Ultrasonics Sonochemistry, 2019, 53, 152-163.	3.8	25
45816	Effective and Noneffective Recombination Center Defects in Cu₂ZnSnS₄: Significant Difference in Carrier Capture Cross Sections. Chemistry of Materials, 2019, 31, 826-833.	3.2	72
45817	Origins and Control of Optical Absorption in a Nondilute Oxide Solid Solution: Sr(Ti,Fe)O_{3â€“x} Perovskite Case Study. Chemistry of Materials, 2019, 31, 1030-1041.	3.2	17
45818	Thermodynamic Ground States of Multifunctional Metal Dodecaborides. Chemistry of Materials, 2019, 31, 1075-1083.	3.2	15
45819	CsCu₅S₃: Promising Thermoelectric Material with Enhanced Phase Transition Temperature. Inorganic Chemistry, 2019, 58, 1371-1376.	1.9	14
45820	Scandium Molybdate Microstructures with Tunable Phase and Morphology: Microwave Synthesis, Theoretical Calculations, and Photoluminescence Properties. Inorganic Chemistry, 2019, 58, 2491-2500.	1.9	12
45821	Understanding Carrier Transport in Organic Semiconductors: Computation of Charge Mobility Considering Quantum Nuclear Tunneling and Delocalization Effects. Journal of Chemical Theory and Computation, 2019, 15, 1477-1491.	2.3	33
45822	Contrasting Bonding-Interaction-Induced Distinct Relaxation in La₆₅Ni₃₅ and La₆₅Al₃₅ Glass-Forming Alloys. Journal of Physical Chemistry B, 2019, 123, 1149-1155.	1.2	6
45823	Size-Dependent Adsorption of Styrene on Pd Clusters: A Density Functional Theory Study. Journal of Physical Chemistry C, 2019, 123, 2182-2188.	1.5	12
45824	Insight Into the Dipeptide Self-Assembly Process Using Density Functional Theory. Journal of Physical Chemistry C, 2019, 123, 2526-2532.	1.5	9
45825	Effect of Interstitial Hydrogen on the Mechanical and Thermal Properties of Tungsten: A First-Principles Study. Journal of Physical Chemistry C, 2019, 123, 1913-1921.	1.5	13
45826	Probing Surface Chemistry at an Atomic Level: Decomposition of 1-Propanethiol on GaP(001) (2 Ã— 4) Investigated by STM, XPS, and DFT. Journal of Physical Chemistry C, 2019, 123, 2964-2972.	1.5	0
45827	Polymorphism, Phase Transition, and Lattice Dynamics of Energetic Oxidizer Ammonium Perchlorate under High Pressure. Journal of Physical Chemistry C, 2019, 123, 2114-2126.	1.5	16
45828	Direct Donation of Protons from H₂O to CO₂ in Artificial Photosynthesis on the Anatase TiO₂(101) Surface. Journal of Physical Chemistry C, 2019, 123, 3019-3023.	1.5	10

#	Article	IF	Citations
45829	Physisorption of Water on Graphene: Subchemical Accuracy from Many-Body Electronic Structure Methods. Journal of Physical Chemistry Letters, 2019, 10, 358-368.	2.1	90
45830	Dynamics of Subnanometer Pt Clusters Can Break the Scaling Relationships in Catalysis. Journal of Physical Chemistry Letters, 2019, 10, 460-467.	2.1	72
45831	Elastic Properties and Fracture Behaviors of Biaxially Deformed, Polymorphic MoTe₂. Nano Letters, 2019, 19, 761-769.	4.5	67
45832	Achieving Fast Kinetics and Enhanced Li Storage Capacity for Ti3C2O2 by Intercalation of Quinone Molecules. ACS Applied Energy Materials, 2019, 2, 1251-1258.	2.5	19
45833	Mn-Doped Fe_{1â€“x}Mn_xF₃Â·0.33H₂O/C Cathodes for Li-Ion Batteries: First-Principles Calculations and Experimental Study. ACS Applied Materials & Interfaces, 2019, 11, 3852-3860.	4.0	25
45834	Strain-Induced Metastable Phase Stabilization in Ga₂O₃ Thin Films. ACS Applied Materials & Interfaces, 2019, 11, 5536-5543.	4.0	42
45835	Theoretical Expectation and Experimental Implementation of In Situ Al-Doped CoS₂ Nanowires on Dealloying-Derived Nanoporous Intermetallic Substrate as an Efficient Electrocatalyst for Boosting Hydrogen Production. ACS Catalysis, 2019, 9, 1489-1502.	5.5	112
45836	Interface Engineering of Au(111) for the Growth of 1Tâ€²-MoSe₂. ACS Nano, 2019, 13, 2316-2323.	7.3	31
45837	Base-Controlled Heck, Suzuki, and Sonogashira Reactions Catalyzed by Ligand-Free Platinum or Palladium Single Atom and Sub-Nanometer Clusters. Journal of the American Chemical Society, 2019, 141, 1928-1940.	6.6	107
45838	Room-temperature electrochemical waterâ€“gas shift reaction for high purity hydrogen production. Nature Communications, 2019, 10, 86.	5.8	62
45839	Significance of hydrogen bonding and other noncovalent interactions in determining octahedral tilting in the CH3NH3PbI3 hybrid organic-inorganic halide perovskite solar cell semiconductor. Scientific Reports, 2019, 9, 50.	1.6	95
45840	A comparative study of mechanisms of the adsorption of CO₂ confined within grapheneâ€“MoS₂ nanosheets: a DFT trend study. Nanoscale Advances, 2019, 1, 1442-1451.	2.2	22
45841	Self-assembling of formic acid on the partially oxidizedp(2 Ã— 1) Cu(110) surface reconstruction at low coverages. Journal of Chemical Physics, 2019, 150, 041720.	1.2	3
45842	First principles study of hBN-AlN short-period superlattice heterostructures. Applied Physics Letters, 2019, 114, 011903.	1.5	5
45843	Strain engineering of electronic and magnetic properties of double-transition metal ferromagnetic semiconductor MXenes. Journal of Applied Physics, 2019, 125, .	1.1	22
45844	Strain-engineering the anisotropic electrical properties of low-symmetry bilayer GeSe. Journal of Applied Physics, 2019, 125, .	1.1	5
45845	Unique mechanical responses of layered phosphorus-like group-IV monochalcogenides. Journal of Applied Physics, 2019, 125, 082519.	1.1	8
45846	Subtlety of TiO2 phase stability: Reliability of the density functional theory predictions and persistence of the self-interaction error. Journal of Chemical Physics, 2019, 150, 014105.	1.2	32

#	Article	IF	Citations
45847	An AIMD study of dissociative chemisorption of methanol on Cu(111) with implications for formaldehyde formation. Journal of Chemical Physics, 2019, 150, 024706.	1.2	9
45848	Electronic structure, mechanical and optical properties of ternary semiconductors Si_{1-x}Ge_xC (Xâ€‰=â€‰0, 0.25, 0.50, 0.75, 1). Philosophical Magazine, 2019, 99, 905-920.	0.7	5
45849	Modification of the electronic and spintronic properties of monolayer GaGeTe with a vertical electric field. Journal Physics D: Applied Physics, 2019, 52, 115101.	1.3	13
45850	Using first principles calculations to interpret XANES experiments: extracting the size-dependence of the (pâ€Š, T) phase diagram of sub-nanometer Cu clusters in an O₂ environment. Journal of Physics Condensed Matter, 2019, 31, 144002.	0.7	6
45851	Performance of van der Waals DFT approaches for helium diffraction on metal surfaces. Journal of Physics Condensed Matter, 2019, 31, 135901.	0.7	4
45852	Transferability of interatomic potentials for molybdenum and silicon. Modelling and Simulation in Materials Science and Engineering, 2019, 27, 025007.	0.8	17
45853	Air-stable n-doped black phosphorus transistor by thermal deposition of metal adatoms. Nanotechnology, 2019, 30, 135201.	1.3	16
45854	Can we rely on hybrid-DFT energies of solid-state problems with local-DFT geometries?. Electronic Structure, 2019, 1, 015008.	1.0	18
45855	Role of Nanostructuring on the Properties of Oxide Materials: The Case of Zirconia Nanoparticles. European Journal of Inorganic Chemistry, 2019, 2019, 751-761.	1.0	8
45856	Two dimensional topological insulators in bilayer BiB. Computational Materials Science, 2019, 160, 82-85.	1.4	1
45857	Effect of nonmagnetic dopants (Ag, Cu or Mg) on ferromagnetic half-metallic properties of NiO. Physica B: Condensed Matter, 2019, 557, 6-11.	1.3	1
45858	Zn segregation in interface between Mg17Al12 precipitate and Mg matrix in Mgâ€“Alâ€“Zn alloys. Scripta Materialia, 2019, 163, 91-95.	2.6	33
45859	Enhanced 1H-X D-HMQC performance through improved 1H homonuclear decoupling. Solid State Nuclear Magnetic Resonance, 2019, 98, 12-18.	1.5	11
45860	Effect of Surface Ni on Oxygen Reduction Reaction in Dealloyed Nanoporous Ptâ€“Ni. Industrial & Engineering Chemistry Research, 2019, 58, 7438-7447.	1.8	9
45861	Design of the Hybrid Metalâ€“Organic Frameworks as Potential Supramolecular Piezo-/Ferroelectrics. Journal of Physical Chemistry C, 2019, 123, 3122-3129.	1.5	37
45862	Mechanism of CO₂ Photocatalytic Reduction to Methane and Methanol on Defected Anatase TiO₂ (101): A Density Functional Theory Study. Journal of Physical Chemistry C, 2019, 123, 3505-3511.	1.5	57
45863	Surface Segregation in CuNi Nanoparticle Catalysts During CO₂ Hydrogenation: The Role of CO in the Reactant Mixture. Journal of Physical Chemistry C, 2019, 123, 8421-8428.	1.5	38
45864	Constructing the Electronic Structure of CH₃NH₃PbI₃ and CH₃NH₃PbBr₃ Perovskite Thin Films from Single-Crystal Band Structure Measurements. Journal of Physical Chemistry Letters, 2019, 10, 601-609.	2.1	78

#	Article	IF	Citations
45865	Two-Dimensional Penta-BN₂ with High Specific Capacity for Li-Ion Batteries. ACS Applied Materials & Interfaces, 2019, 11, 6104-6110.	4.0	58
45866	Enhanced and Faster Potassium Storage in Graphene with Respect to Graphite: A Comparative Study with Lithium Storage. ACS Nano, 2019, 13, 2190-2204.	7.3	27
45867	Unraveling the Impact of Halide Mixing on Perovskite Stability. Journal of the American Chemical Society, 2019, 141, 3515-3523.	6.6	116
45868	Thickness dependent electronic properties of Pt dichalcogenides. Npj 2D Materials and Applications, 2019, 3, .	3.9	138
45869	Stable, color-tunable 2D SCN-based perovskites: revealing the critical influence of an asymmetric pseudo-halide on constituent ions. Nanoscale, 2019, 11, 2608-2616.	2.8	22
45870	The role of the disordered H f O 2 network in the high-Îº n-MOSFET shallow electron trapping. Journal of Applied Physics, 2019, 125, 025705.	1.1	2
45871	Ferromagnetism in graphene traced to antisymmetric orbital combination of involved electronic states. Journal of Physics Condensed Matter, 2019, 31, 095801.	0.7	1
45872	Semiconducting B₁₃C₂ system: structure search and DFT-based analysis. Materials Research Express, 2019, 6, 046544.	0.8	2
45873	First-principles study of the impact of the atomic configuration on the electronic properties of <mml:math xmlns:mml="http://www.w3.org/1998/Math/MathML"><mml:mrow><mml:msub><mml:mi>Al</mml:mi><mml:mi>x</mml:mi></mml:ms mathvariant="normal">N</mml:mi></mml:mrow></mml:math> alloys. Physical Review B, 2019, 99, .	1.1	16
45874	Crystalline topological Dirac semimetal phase in rutile structure <mml:math xmlns:mml="http://www.w3.org/1998/Math/MathML"><mml:mrow><mml:msup><mml:mi>Î²</mml:mi><mml:mo>â€²</mml:mo></mml:m Physical Review B, 2019, 99, .	1.1	12
45875	Conformal deposition of GeTe films with tunable Te composition by atomic layer deposition. Journal of Vacuum Science and Technology A: Vacuum, Surfaces and Films, 2019, 37, 020907.	0.9	13
45876	Lattice phonon modes of the spin crossover crystal [Fe(phen)2(NCS)2] studied by THz, IR, Raman spectroscopies and DFT calculations. European Physical Journal B, 2019, 92, 1.	0.6	47
45877	Multiscale approaches to the mechanical behavior of ceramic nanostructure in electrode using phase field model. , 2019, , .		0
45878	Unusual perpendicular anisotropy in Co2TiSi films. Journal Physics D: Applied Physics, 2019, 52, 035001.	1.3	4
45879	Crystallographic orientation effects of hydrogen diffusion in Î±-uranium from DFT: Interpreting variations in experimental data. Journal of Nuclear Materials, 2019, 513, 293-296.	1.3	5
45880	First-principle studies on the mechanical, thermodynamic and electronic properties of Î²â€³-Mg3Gd and Î²â€²-Mg7Gd alloys under pressure. Journal of Physics and Chemistry of Solids, 2019, 125, 115-122.	1.9	14
45881	The Structural, Electronic, and Magnetic Properties of Cobalt Disulfide Doped with Oxygen, Selenium, or Tellurium. Journal of Electronic Materials, 2019, 48, 483-493.	1.0	0
45882	Effects of surface hydroxyl groups induced by the co-precipitation temperature on the catalytic performance of direct synthesis of isobutanol from syngas. Fuel, 2019, 237, 1021-1028.	3.4	16

#	Article	IF	Citations
45883	Theoretical analysis of the adsorption of ammoniaâ€“borane and their dehydrogenation products on the (001) surface of TiC and ZrC. Surface Science, 2019, 680, 95-106.	0.8	9
45884	Combining the Physics of Metal/Oxide Heterostructure, Interface Dipole, Band Bending, Crystallography, and Surface State to Understand Heterogeneity Contrast in Oxidation and Corrosion. Corrosion, 2019, 75, 152-166.	0.5	12
45885	Density functional investigation on hexagonal nanosheets and bulk thallium nitrides for possible thermoelectric applications. Applied Nanoscience (Switzerland), 2019, 9, 33-42.	1.6	8
45886	Unsaturated edge-anchored Ni single atoms on porous microwave exfoliated graphene oxide for electrochemical CO2. Applied Catalysis B: Environmental, 2019, 243, 294-303.	10.8	243
45887	Theoretical investigation on vanadium dinitrides from first-principles calculations. Ceramics International, 2019, 45, 2457-2465.	2.3	6
45888	Unexpectedly high energy density of a Li-Ion battery by oxygen redox in LiNiO2 cathode: First-principles study. Electrochimica Acta, 2019, 294, 166-172.	2.6	27
45889	Energetics of helium-vacancy complexes in Fe-9Cr alloys from first-principles calculations. Journal of Nuclear Materials, 2019, 513, 143-151.	1.3	26
45890	Defect formations and pH-dependent kinetics in krÃ¶hnkite Na2Fe(SO4)2Â·2H2O based cathode for sodium-ion batteries: Resembling synthesis conditions through chemical potential landscape. Nano Energy, 2019, 55, 123-134.	8.2	13
45891	Generating strong room-temperature photoluminescence in black phosphorus using organic molecules. 2D Materials, 2019, 6, 015009.	2.0	15
45892	On the Ferromagnetism and Band Tailoring of CrI₃ Single Layer. Physica Status Solidi - Rapid Research Letters, 2019, 13, 1800410.	1.2	20
45893	First-Principles Study of the Structures and Electronic Properties for NinGe (nâ€‰=â€‰19â€“29) Clusters. Journal of Cluster Science, 2019, 30, 131-139.	1.7	2
45894	Decohesion Energy of $$Sigma 5(012)$$ Grain Boundaries in Ni as Function of Hydrogen Content. Metallurgical and Materials Transactions A: Physical Metallurgy and Materials Science, 2019, 50, 451-456.	1.1	3
45895	Planar net-Ï„: A new high-performance metallic carbon anode material for lithium-ion batteries. Carbon, 2019, 142, 438-444.	5.4	63
45896	Bifunctional electron transporting layer/perovskite interface linker for highly efficient perovskite solar cells. Electrochimica Acta, 2019, 296, 75-81.	2.6	37
45897	On the stacking fault energy related deformation mechanism of nanocrystalline Cu and Cu alloys: A first-principles and TEM study. Journal of Alloys and Compounds, 2019, 776, 807-818.	2.8	36
45898	First-principles calculations and Bader analysis of oxygen-deficient induced magnetism in cubic BaTiO_{3âˆ’x} and SrTiO_{3âˆ’x}. Philosophical Magazine, 2019, 99, 181-197.	0.7	15
45899	Modeling of the Coadsorption of Chloride and Hydrogen Ions on Copper Electrode Surface. Journal of the Electrochemical Society, 2019, 166, D3042-D3048.	1.3	1
45900	A Theoretical study on the charge and discharge states of Naâ€ion battery cathode material, Na_{1+x}FePO₄F. Journal of Computational Chemistry, 2019, 40, 237-246.	1.5	4

#	Article	IF	Citations
45901	Synergistic integration of Bi metal and phosphate defects on hexagonal and monoclinic BiPO4: Enhanced photocatalysis and reaction mechanism. Applied Catalysis B: Environmental, 2019, 243, 313-321.	10.8	166
45902	Error controlling of the combined Cluster-Expansion and Wangâ€“Landau Monte-Carlo method and its application to FeCo. Computer Physics Communications, 2019, 235, 95-101.	3.0	10
45903	Hexagonal SnS nanoplates assembled onto hierarchical Bi2WO6 with enhanced photocatalytic activity in detoxification and disinfection. Journal of Colloid and Interface Science, 2019, 537, 345-357.	5.0	35
45904	Coupling of Acetaldehyde to Crotonaldehyde on CeO_{2â€“x}(111): Bifunctional Mechanism and Role of Oxygen Vacancies. Journal of Physical Chemistry C, 2019, 123, 8273-8286.	1.5	23
45905	Constructing desired interfacial energy band alignment of Z-scheme TiO2-Pd-Cu2O hybrid by controlling the contact facet for improved photocatalytic performance. Applied Catalysis B: Environmental, 2019, 244, 347-355.	10.8	60
45906	Full spectrum light driven photocatalytic in-situ epitaxy of one-unit-cell Bi2O2CO3 layers on Bi2O4 nanocrystals for highly efficient photocatalysis and mechanism unveiling. Applied Catalysis B: Environmental, 2019, 243, 667-677.	10.8	114
45907	Effect of stereochemical conformation into the corrosion inhibitive behaviour of double azomethine based Schiff bases on mild steel surface in 1â€‰mol Lâ¯1 HCl medium: An experimental, density functional theory and molecular dynamics simulation study. Corrosion Science, 2019, 146, 134-151.	3.0	284
45908	Surface characterization of face-centered cubic crystals. Mechanics of Materials, 2019, 129, 15-22.	1.7	13
45909	Novel insight into the formation of Î±â€³-martensite and Ï‰-phase with cluster structure in metastable Ti-Mo alloys. Acta Materialia, 2019, 164, 322-333.	3.8	63
45910	Analysis of dynamic decomposition for barium dimethyl-naphthalene-sulfonate on an Al3Mg (0â€¯0â€¯1) surface from ab-initio molecular dynamics. Applied Surface Science, 2019, 466, 772-779.	3.1	2
45911	Influence of surface charge density on ligand-metal bonding: A DFT study of NH3 and HCOOH on Mg (0â€¯0â€¯0â€¯1) surface. Applied Surface Science, 2019, 470, 893-898.	3.1	23
45912	Charge collection efficiency of Pt vs. Mg contacts on semi-insulating GaAs. Applied Surface Science, 2019, 467-468, 1219-1225.	3.1	3
45913	Lightweight Metallic MgB2 Mediates Polysulfide Redox and Promises High-Energy-Density Lithium-Sulfur Batteries. Joule, 2019, 3, 136-148.	11.7	256
45914	Intrinsic Properties of Pure and Mixed Monolayer Oxides in the Honeycomb Structure: M₂O₃ and MMâ€²O₃ (M, Mâ€² = Ti, V, Cr, Fe). Journal of Physical Chemistry C, 2019, 123, 7898-7910.	1.5	13
45915	First-principles study of phase stability and elastic properties in metastable Ti-Mo alloys with cluster structure. Molecular Simulation, 2019, 45, 26-34.	0.9	8
45916	GPUs as boosters to analyze scalar and vector fields in quantum chemistry. International Journal of Quantum Chemistry, 2019, 119, e25671.	1.0	28
45917	An Asymptotics-Based Adaptive Finite Element Method for Kohnâ€“Sham Equation. Journal of Scientific Computing, 2019, 79, 464-492.	1.1	2
45918	Experimental and theoretical study of the effect of Si on the oxidative behavior of Ti-6Al-4V alloys. Journal of Alloys and Compounds, 2019, 776, 519-528.	2.8	22

#	Article	IF	Citations
45919	Effect of aging time on the microstructure evolution and mechanical property in an Al-Cu-Li alloy sheet. Materials Science & Engineering A: Structural Materials: Properties, Microstructure and Processing, 2019, 740-741, 157-164.	2.6	54
45920	Dynamics of the phase-change material GeTe across the structural phase transition. Frontiers of Physics, 2019, 14, 1.	2.4	8
45921	An experimental and theoretical investigation on relaxor behavior and local correlations in xBi(Zn0.5Ti0.5)O3-(1-x)BaTiO3 ceramics. Ceramics International, 2019, 45, 3465-3472.	2.3	3
45922	Effects of temperature and O partial pressure on the atomic structure of Al2O3 (0â€¯0â€¯0â€¯1) surface. Computational Materials Science, 2019, 157, 37-42.	1.4	6
45923	First-principles study of fracture toughness enhancement in transition metal nitrides. Surface and Coatings Technology, 2019, 357, 903-909.	2.2	26
45924	A new reconstruction core of the 30Â° partial dislocation in silicon. Philosophical Magazine, 2019, 99, 347-375.	0.7	4
45925	Density functional theory calculation on facet-dependent photocatalytic activity of MoS2/CdS heterostructures. Applied Surface Science, 2019, 469, 27-33.	3.1	63
45926	Measured and calculated properties of B-doped Ï„-phase MnAl â€“ A rare earth free permanent magnet. Journal of Magnetism and Magnetic Materials, 2019, 474, 591-598.	1.0	7
45927	Dislocation pile-ups at Î²1 precipitate interfaces in Mg-rare earth (RE) alloys. Materials Science & Engineering A: Structural Materials: Properties, Microstructure and Processing, 2019, 742, 278-286.	2.6	32
45928	Highly stable tungsten disulfide supported on a self-standing nickel phosphide foam as a hybrid electrocatalyst for efficient electrolytic hydrogen evolution. Nano Energy, 2019, 55, 193-202.	8.2	59
45929	Al Organization in the SSZ-13 Zeolite. Al Distribution and Extraframework Sites of Divalent Cations. Journal of Physical Chemistry C, 2019, 123, 7968-7987.	1.5	63
45930	Li-ion battery material under high pressure: amorphization and enhanced conductivity of Li4Ti5O12. National Science Review, 2019, 6, 239-246.	4.6	49
45931	Corrosion of Si, C, and SiC in molten salt. Corrosion Science, 2019, 146, 1-9.	3.0	24
45932	Thermal decomposition of brominated flame retardants (BFRs): Products and mechanisms. Progress in Energy and Combustion Science, 2019, 70, 212-259.	15.8	168
45933	Prediction of Ti3C2O2 MXene as an effective capturer of formaldehyde. Applied Surface Science, 2019, 469, 770-774.	3.1	40
45934	Correlation between the microstructure of carbon materials and their potassium ion storage performance. Carbon, 2019, 143, 138-146.	5.4	90
45935	Highly U(VI) immobilization on polyvinyl pyrrolidine intercalated molybdenum disulfide: Experimental and computational studies. Chemical Engineering Journal, 2019, 359, 1563-1572.	6.6	45
45936	A superhard allotrope of carbon: Ibam-C and its BN phase. Chemical Physics Letters, 2019, 714, 119-124.	1.2	19

#	Article	IF	Citations
45937	Selective C H bond activation of ethane by free gold clusters. International Journal of Mass Spectrometry, 2019, 435, 241-250.	0.7	9
45938	Experimental and DFT characterization of Î·â€² nano-phase and its interfaces in Al Zn Mg Cu alloys. Acta Materialia, 2019, 164, 207-219.	3.8	113
45939	Stable monolayer of the RuO₂ structure by the Peierls distortion. Philosophical Magazine, 2019, 99, 376-385.	0.7	18
45940	Calculation of the stability and mechanical and phonon properties of NbRuB, TaRuB, and NbOsB compounds. Philosophical Magazine, 2019, 99, 328-346.	0.7	11
45941	Niobium Doping in BiVO₄: Interplay Between Effective Mass, Stability, and Pressure. ChemPhysChem, 2019, 20, 773-784.	1.0	14
45942	New Oneâ€Dimensional Material Nb₂Se₉: Theoretical Prediction of Indirect to Direct Band Gap Transition due to Dimensional Reduction. Physica Status Solidi - Rapid Research Letters, 2019, 13, 1800517.	1.2	20
45943	Hexagonal Double Perovskite Cs₂AgCrCl₆. Zeitschrift Fur Anorganische Und Allgemeine Chemie, 2019, 645, 323-328.	0.6	16
45944	First-principles computational design of unknown flat arsenene epitaxially grown on copper substrate. Applied Surface Science, 2019, 467-468, 561-566.	3.1	15
45945	The preferred slip plane of nuclear material of Hafnium: A first-principles study. Computational Materials Science, 2019, 157, 25-30.	1.4	7
45946	Phosphorous-containing oxygen-deficient cobalt molybdate as an advanced electrode material for supercapacitors. Energy Storage Materials, 2019, 19, 186-196.	9.5	145
45947	The effect of pressure on the structural, elastic, electronic, magnetic, and optical properties of Mo-doped ZnSe alloy. Journal of Magnetism and Magnetic Materials, 2019, 474, 14-24.	1.0	5
45948	Intriguing electronic properties of germanene/ indium selenide and antimonene/ indium selenide heterostructures. Journal of Solid State Chemistry, 2019, 269, 513-520.	1.4	11
45949	Kâ€Birnessite Electrode Obtained by Ion Exchange for Potassiumâ€Ion Batteries: Insight into the Concerted Ionic Diffusion and K Storage Mechanism. Advanced Energy Materials, 2019, 9, 1802739.	10.2	80
45950	Improving the corrosion protection properties of PVB coating by using salicylaldehyde@ZIF-8/graphene oxide two-dimensional nanocomposites. Corrosion Science, 2019, 146, 70-79.	3.0	97
45951	Strain-mediated point defects in thermoelectric p-type bismuth telluride polycrystalline. Nano Energy, 2019, 55, 486-493.	8.2	32
45952	Absence of ferromagnetism in ferroelectric Mnâ€doped BaTiO₃ nanofibers. Journal of the American Ceramic Society, 2019, 102, 2800-2809.	1.9	17
45953	Efficient Prediction of Structural and Electronic Properties of Hybrid 2D Materials Using Complementary DFT and Machine Learning Approaches. Advanced Theory and Simulations, 2019, 2, 1800128.	1.3	55
45954	Kinetic Stability of Bulk LiNiO₂ and Surface Degradation by Oxygen Evolution in LiNiO₂â€Based Cathode Materials. Advanced Energy Materials, 2019, 9, 1802586.	10.2	160

#	Article	IF	Citations
45955	Solvent polarity-induced photoluminescence enhancement (SPIPE): A method enables several-fold increase in quantum yield of silicon nanoparticles. Nano Research, 2019, 12, 315-322.	5.8	12
45956	Highly selective semi-hydrogenation of acetylene over porous gold with twin boundary defects. Applied Catalysis A: General, 2019, 569, 101-109.	2.2	11
45957	Effect of graphene oxide loading on TiO2: Morphological, optical, interfacial charge dynamics-A combined experimental and theoretical study. Carbon, 2019, 143, 51-62.	5.4	37
45958	Hydrogen induced changes of optical and magnetic properties of nanocrystalline Zn0.95Gd0.03M0.02O (M=Al,Mg): Experimental and DFT studies. Journal of Alloys and Compounds, 2019, 776, 575-585.	2.8	3
45959	Influences of isotropic strain on the electronic and magnetic properties of Fe-, Co-, and Ni-doped PbS revealed by density functional calculations. Materials Chemistry and Physics, 2019, 223, 133-139.	2.0	1
45960	Cubic-like BaZrO3 nanocrystals with exposed {001}/{011} facets and tuned electronic band structure for enhanced photocatalytic hydrogen production. Journal of Materials Science, 2019, 54, 1967-1976.	1.7	19
45961	Plastic flow resistance of NiTiCu shape memory alloy-theory and experiments. Acta Materialia, 2019, 163, 173-188.	3.8	8
45962	The adsorption, diffusion and capacity of lithium on novel boron-doped graphene nanoribbon: A density functional theory study. Applied Surface Science, 2019, 466, 737-745.	3.1	26
45963	New nanoporous graphyne monolayer as nodal line semimetal: Double Dirac points with an ultrahigh Fermi velocity. Carbon, 2019, 141, 712-718.	5.4	42
45964	Strain effect of high Tc ferromagnetism in Mo-doped SnS2 monolayer. Computational Materials Science, 2019, 156, 321-324.	1.4	11
45965	Exposed facet engineering design of graphene-SnO2 nanorods for ultrastable Li-ion batteries. Energy Storage Materials, 2019, 19, 39-47.	9.5	53
45966	Two-dimensional InSeF heterostructure: A tunable direct/indirect band gap semiconductor with nontrivially topological properties. Physica E: Low-Dimensional Systems and Nanostructures, 2019, 106, 73-77.	1.3	1
45967	Determination of the structure and properties of an edge dislocation in rutile TiO2. Acta Materialia, 2019, 163, 199-207.	3.8	27
45968	Selective hydrogenation of 1,3-butadiene over single Pt1/Cu(1â€¯1â€¯1) model catalysts: A DFT study. Applied Surface Science, 2019, 466, 946-955.	3.1	23
45969	ZrNiAl-type gallides with pronounced metal-metal bonding, and the dimorphism of ScPdGa. Zeitschrift Fur Naturforschung - Section B Journal of Chemical Sciences, 2019, 74, 15-25.	0.3	2
45970	Role of Metal/Oxide Interfaces in Enhancing the Local Oxide Reducibility. Topics in Catalysis, 2019, 62, 1192-1201.	1.3	14
45971	Highly sulfiphilic Ni-Fe bimetallic oxide nanoparticles anchored on carbon nanotubes enable effective immobilization and conversion of polysulfides for stable lithium-sulfur batteries. Carbon, 2019, 142, 32-39.	5.4	78
45972	First principles calculation of redox potential for tetravalent actinides in molten LiClâ€“KCl eutectic based on vertical substitution and relaxation. Electrochimica Acta, 2019, 293, 466-475.	2.6	14

#	Article	IF	Citations
45973	Strongly canted antiferromagnetic ground state in Cu3(OH)2F4. Journal of Alloys and Compounds, 2019, 776, 16-21.	2.8	3
45974	Investigating detailed mechanism of hydrogen molecules adsorbing on singleâ€wall carbon nanotubes using fitted force field parameters containing carbonâ€“carbon interactions. Journal of Computational Chemistry, 2019, 40, 1073-1083.	1.5	0
45975	First-principles study of CN point defects on sidewall surface of [0â€¯0â€¯0â€¯1]-oriented GaN nanowires. Applied Surface Science, 2019, 467-468, 293-297.	3.1	7
45976	Effect of hole doping and strain modulations on electronic structure and magnetic properties in ZnO monolayer. Applied Surface Science, 2019, 467-468, 22-29.	3.1	32
45977	Investigations of the nickel promotional effect on the reduction and sintering of tungsten compounds. International Journal of Refractory Metals and Hard Materials, 2019, 78, 296-302.	1.7	5
45978	Aqueous electrochemistry of the magnesium surface: Thermodynamic and kinetic profiles. Corrosion Science, 2019, 147, 53-68.	3.0	49
45979	Pd Segregation on the Surface of Bimetallic PdAu Nanoparticles Induced by Low Coverage of Adsorbed CO. Journal of Physical Chemistry C, 2019, 123, 8037-8046.	1.5	40
45980	Toward barrier free contact to MoSe2/WSe2 heterojunctions using two-dimensional metal electrodes. Nanotechnology, 2019, 30, 015707.	1.3	5
45981	The influence of spatial limits on the modeling chemical reactivity: The example of CO₂ hydration in MeX zeolites (Me = K, Rb, Cs). International Journal of Quantum Chemistry, 2019, 119, e25820.	1.0	1
45982	First-principles calculation of multiple hydrogen segregation along aluminum grain boundaries. Computational Materials Science, 2019, 156, 368-375.	1.4	45
45983	Manipulation of Edgeâ€Site Feâ€“N₂ Moiety on Holey Fe, N Codoped Graphene to Promote the Cycle Stability and Rate Capacity of Liâ€“S Batteries. Advanced Functional Materials, 2019, 29, 1807485.	7.8	109
45984	Edgeâ€Functionalized Graphene Nanoplatelets as Metalâ€Free Electrocatalysts for Dyeâ€Sensitized Solar Cells. Advanced Materials, 2019, 31, e1804440.	11.1	44
45985	Structure and dynamics of B2O3 melts and glasses: From ab initio to classical molecular dynamics simulations. Computational Materials Science, 2019, 159, 73-85.	1.4	17
45986	Do Chalcogenide Double Perovskites Work as Solar Cell Absorbers: A First-Principles Study. Chemistry of Materials, 2019, 31, 244-250.	3.2	33
45987	First-Principles Insights into the Oxidation States and Electronic Structures of Ceria-Based Binary, Ternary, and Quaternary Oxides. Journal of Physical Chemistry C, 2019, 123, 175-184.	1.5	10
45988	Improved Thermoelectric Performance of Tellurium by Alloying with a Small Concentration of Selenium to Decrease Lattice Thermal Conductivity. ACS Applied Materials & Interfaces, 2019, 11, 511-516.	4.0	8
45989	Ceramic phases with one-dimensional long-range order. Nature Materials, 2019, 18, 19-23.	13.3	18
45990	Effects of alloying on the interface energy of theÎ´- andÎ·-phase in nickelbase superalloys. Modelling and Simulation in Materials Science and Engineering, 2019, 27, 015002.	0.8	4

#	Article	IF	Citations
45991	New Assembly-Free Bulk Layered Inorganic Vertical Heterostructures with Infrared and Optical Bandgaps. Nano Letters, 2019, 19, 142-149.	4.5	3
45992	Atomistic Mechanisms of Mg Insertion Reactions in Group XIV Anodes for Mg-Ion Batteries. ACS Applied Materials & Interfaces, 2019, 11, 774-783.	4.0	18
45993	Prediction of solid solution characteristics of MC (M = Zr, Nb, and Ta) in TiC lattice using phase stability diagrams. Journal of the American Ceramic Society, 2019, 102, 4285-4295.	1.9	3
45994	Temperature induced twinning in aragonite: transmission electron microscopy experiments and ab initio calculations. Zeitschrift Fur Kristallographie - Crystalline Materials, 2019, 234, 79-84.	0.4	4
45995	First-principles investigation of BiVO3 for thermochemical water splitting. International Journal of Hydrogen Energy, 2019, 44, 1425-1430.	3.8	6
45996	Insights into the Li-Metal/Organic Carbonate Interfacial Chemistry by Combined First-Principles Theory and X-ray Photoelectron Spectroscopy. Journal of Physical Chemistry C, 2019, 123, 347-355.	1.5	10
45997	Toward Free-Standing Lonsdaleite and Diamond Few Layers: The Nitrogen Effect. Journal of Physical Chemistry C, 2019, 123, 798-809.	1.5	5
45998	Coherent Topotactic Interface between Corundum and Rutile Structures. Journal of Physical Chemistry C, 2019, 123, 534-540.	1.5	3
45999	Termination Effects of Pt/v-Ti_{n+1}C_nT₂ MXene Surfaces for Oxygen Reduction Reaction Catalysis. ACS Applied Materials & Interfaces, 2019, 11, 1638-1644.	4.0	88
46000	Solid Oxide Fuel Cell Materials and Interfaces. , 2019, , 1-31.		2
46001	Phase diagrams and elastic properties of the Fe-Cr-Al alloys: A first-principles based study. Calphad: Computer Coupling of Phase Diagrams and Thermochemistry, 2019, 64, 55-65.	0.7	11
46002	Superconductivity and phase stability of potassium-doped p-quinquephenyl. Carbon, 2019, 143, 837-843.	5.4	28
46003	Silicon rods as a negative electrode material for lithium-ion cells: Quantum chemical modeling. Chemical Physics, 2019, 519, 45-51.	0.9	2
46004	Valley polarization and biaxial strain dependent conductivity of WS2/SrRuO3(1â€¯1â€¯1) heterostructures. Computational Materials Science, 2019, 158, 376-381.	1.4	3
46005	Adsorption of Na on silicene for potential anode for Na-ion batteries. Electrochimica Acta, 2019, 297, 497-503.	2.6	35
46006	Modulation of the electronic properties of two-dimensional MoTe2/WSe2 heterostructure by electrical field. Physica E: Low-Dimensional Systems and Nanostructures, 2019, 108, 90-95.	1.3	14
46007	Confined Ionic Liquid in an Ionic Porous Aromatic Framework for Gas Separation. ACS Applied Polymer Materials, 2019, 1, 95-102.	2.0	20
46008	Mn-doped SnS2 nanostructure as a potential efficiency CO catalyst: A first-principles study. Applied Surface Science, 2019, 471, 678-685.	3.1	10

#	Article	IF	Citations
46009	First-principles study on the structural, electronic, and magnetic properties in (001) and (110) surfaces of quaternary Heusler alloy TiZrCoAl. Materials Chemistry and Physics, 2019, 224, 93-99.	2.0	6
46010	Ultralow lattice thermal conductivity and electronic properties of monolayer 1T phase semimetal SiTe2 and SnTe2. Physica E: Low-Dimensional Systems and Nanostructures, 2019, 108, 53-59.	1.3	37
46011	Coordination-Dependent Catalytic Activity and Design Principles of Metalâ€“Organic Frameworks as Efficient Electrocatalysts for Clean Energy Conversion. Journal of Physical Chemistry C, 2019, 123, 214-221.	1.5	10
46012	Local insight into the La-induced structural phase transition in multiferroic BiFeO₃ ceramics by x-ray absorption fine structure spectroscopy. Journal of Physics Condensed Matter, 2019, 31, 085402.	0.7	7
46013	Electrocatalytic N₂ Fixation over Hollow VO₂ Microspheres at Ambient Conditions. ChemElectroChem, 2019, 6, 1014-1018.	1.7	59
46014	A General Twoâ€Step Strategyâ€“Based Highâ€Throughput Screening of Single Atom Catalysts for Nitrogen Fixation. Small Methods, 2019, 3, 1800376.	4.6	303
46015	Ternary LaNi4.75M0.25 hydrogen storage alloys: Surface segregation, hydrogen sorption and thermodynamic stability. International Journal of Hydrogen Energy, 2019, 44, 1760-1773.	3.8	25
46016	Band structure tuning and charge separation of MNX monolayers and MNX/GaS van der Waals heterostructures. Physica E: Low-Dimensional Systems and Nanostructures, 2019, 108, 44-52.	1.3	2
46017	A Study on the Weak Ferromagnetism of Nanocrystalline Stannous Oxide Induced by L-Shaped Oâ€“Snâ€“O Vacancies. Journal of Physical Chemistry C, 2019, 123, 719-724.	1.5	4
46018	Boron and Nitrogen Co-Doping of Graphynes without Inducing Empty or Doubly Filled States in Ï€-Conjugated Systems. Journal of Physical Chemistry C, 2019, 123, 625-630.	1.5	2
46019	Facile Production of Mesoporous WO₃-rGO Hybrids for High-Performance Supercapacitor Electrodes: An Experimental and Computational Study. ACS Sustainable Chemistry and Engineering, 2019, 7, 2350-2359.	3.2	75
46020	Unraveling Oxygen Evolution on Iron-Doped Î²-Nickel Oxyhydroxide: The Key Role of Highly Active Molecular-like Sites. Journal of the American Chemical Society, 2019, 141, 693-705.	6.6	176
46021	Total-Ionizing-Dose Response of MoS₂Transistors With ZrO₂and h-BN Gate Dielectrics. IEEE Transactions on Nuclear Science, 2019, 66, 1584-1591.	1.2	6
46022	On the heat of formation of ye'elimite Ca4Al6O12.SO4 using density functional theory. Advances in Cement Research, 2019, 31, 106-112.	0.7	4
46023	Reconciling Experimental and Theoretical Data in the Structural Analysis of Tiâ€“Ta Shape-Memory Alloys. Shape Memory and Superelasticity, 2019, 5, 6-15.	1.1	5
46024	CO Adsorption on Au(332): Combined Infrared Spectroscopy and Density Functional Theory Study. Journal of Physical Chemistry C, 2019, 123, 8187-8197.	1.5	7
46025	All-Silicon Topological Semimetals with Closed Nodal Line. Journal of Physical Chemistry Letters, 2019, 10, 244-250.	2.1	24
46026	Sodium Superionic Conductors Based on Clusters. ACS Applied Materials & Interfaces, 2019, 11, 963-972.	4.0	44

#	Article	IF	Citations
46027	TiS₂ Monolayer as an Emerging Ultrathin Bifunctional Catalyst: Influence of Defects and Functionalization. ChemPhysChem, 2019, 20, 608-617.	1.0	24
46028	Electronic structure and stability of anionic AuGen (nâ€‰=â€‰1â€“20) clusters and assemblies: a density functional modeling. Structural Chemistry, 2019, 30, 955-963.	1.0	27
46029	Theoretical study on photoelectric properties of lead-free mixed inorganic perovskite RbGe1-xSnxI3. Current Applied Physics, 2019, 19, 279-284.	1.1	42
46030	From Ceria Clusters to Nanoparticles: Superoxides and Supercharging. Journal of Physical Chemistry C, 2019, 123, 1742-1750.	1.5	7
46031	Atomic Layer Deposition of Al₂O₃ Using Aluminum Triisopropoxide (ATIP): A Combined Experimental and Theoretical Study. Journal of Physical Chemistry C, 2019, 123, 485-494.	1.5	9
46032	Structure and Interaction of Ionic Liquid Monolayer on Graphite from First-Principles. Journal of Physical Chemistry C, 2019, 123, 618-624.	1.5	8
46033	Machine-Learning Identification of the Sensing Descriptors Relevant in Molecular Interactions with Metal Nanoparticle-Decorated Nanotube Field-Effect Transistors. ACS Applied Materials & Interfaces, 2019, 11, 1219-1227.	4.0	25
46034	Adsorption Structure of Mono- and Diradicals on a Cu(111) Surface: Chemoselective Dehalogenation of 4-Bromo-3â€³-iodo-p-terphenyl. ACS Nano, 2019, 13, 324-336.	7.3	26
46035	Two-dimensional Janus PtSSe for photocatalytic water splitting under the visible or infrared light. Journal of Materials Chemistry A, 2019, 7, 603-610.	5.2	268
46036	Dipole controlled Schottky barrier in the blue-phosphorene-phase of GeSe based van der Waals heterostructures. Nanoscale Horizons, 2019, 4, 480-489.	4.1	32
46037	Superconducting transition temperatures in the electronic and magnetic phase diagrams of Sr₂VFeAsO_{3âˆ’Î´}, a superconductor. Journal of Physics Condensed Matter, 2019, 31, 115801.	0.7	7
46038	Phonon-Limited Mobility in n-Type Few-Layer InSe Devices From First Principles. IEEE Electron Device Letters, 2019, 40, 333-336.	2.2	12
46039	Computational Screening of Efficient Singleâ€Atom Catalysts Based on Graphitic Carbon Nitride (gâ€C₃N₄) for Nitrogen Electroreduction. Small Methods, 2019, 3, 1800368.	4.6	347
46040	Dataâ€Driven Materials Exploration for Liâ€Ion Conductive Ceramics by Exhaustive and Informaticsâ€Aided Computations. Chemical Record, 2019, 19, 771-778.	2.9	37
46041	Correlation between thermal-vibration-induced large displacement of Cu atoms and phase transition in Cu4SnS4: First-principles investigation. Acta Materialia, 2019, 166, 37-46.	3.8	4
46042	Integration of phenylammoniumiodide (PAI) as a surface coating molecule towards ambient stable MAPbI3 perovskite for solar cell application. Solar Energy Materials and Solar Cells, 2019, 191, 316-328.	3.0	17
46043	A DFT study of CO adsorption on pt (111) using van der Waals functionals. Surface Science, 2019, 681, 143-148.	0.8	15
46044	Metastable Li_{1+Î´}Mn₂O₄ (0 â‰¤ Î´ â‰¤ 1) Spinel Phases Revealed by in Operando Neutron Diffraction and First-Principles Calculations. Chemistry of Materials, 2019, 31, 124-134.	3.2	28

#	Article	IF	Citations
46045	Modulating Hardness in Molybdenum Monoborides by Adjusting an Array of Boron Zigzag Chains. Chemistry of Materials, 2019, 31, 200-206.	3.2	22
46046	Density Functional Theory Calculations and Thermodynamic Analysis of the Forsterite Mg₂SiO₄(010) Surface. Journal of Physical Chemistry C, 2019, 123, 464-472.	1.5	13
46047	In Situ Formed Shields Enabling Li₂CO₃-Free Solid Electrolytes: A New Route to Uncover the Intrinsic Lithiophilicity of Garnet Electrolytes for Dendrite-Free Li-Metal Batteries. ACS Applied Materials & Interfaces, 2019, 11, 898-905.	4.0	147
46048	Synergistic Contribution of the Acidic Metal Oxideâ€“Metal Couple and Solvent Environment in the Selective Hydrogenolysis of Glycerol: A Combined Experimental and Computational Study Using ReO_xâ€“Ir as the Catalyst. ACS Catalysis, 2019, 9, 485-503.	5.5	40
46049	Design of Basal Plane Edges in Metal-Doped Nanostripes-Structured MoSe₂ Atomic Layers To Enhance Hydrogen Evolution Reaction Activity. ACS Sustainable Chemistry and Engineering, 2019, 7, 458-469.	3.2	58
46050	Largely Increased Lithium Storage Ability of Mangnese Oxide through a Continuous Electronic Structure Modulation and Elevated Capacitive Contribution. ACS Sustainable Chemistry and Engineering, 2019, 7, 740-747.	3.2	18
46051	Processing of novel pseudomorphic Cuâ€“Mo hierarchies in thin films. Materials Research Letters, 2019, 7, 1-11.	4.1	26
46052	Guiding Principles for Designing Highly Efficient Metalâ€Free Carbon Catalysts. Advanced Materials, 2019, 31, e1805252.	11.1	110
46053	Triboâ€Induced Structural Transformation and Lubricant Dissociation at Amorphous Carbonâ€“Alpha Olefin Interface. Advanced Theory and Simulations, 2019, 2, 1800157.	1.3	18
46054	The Nature of the Oxygen Vacancy in Amorphous Oxide Semiconductors: Shallow Versus Deep. Physica Status Solidi (B): Basic Research, 2019, 256, 1800486.	0.7	16
46055	First principles study of structural, electronic and optical properties of Cs-doped CH3NH3PbI3 for photovoltaic applications. Vacuum, 2019, 160, 440-444.	1.6	18
46056	Atomic Modeling and Electronic Structure of Mixed Ionicâ€“Electronic Conductor SrTi1â€“xFexO3â€“x/2+Î´ Considered as a Mixture of SrTiO3 and Sr2Fe2O5. Chemistry of Materials, 2019, 31, 233-243.	3.2	13
46057	Superstructural Ordering in Hexagonal CuInSe₂ Nanoparticles. Chemistry of Materials, 2019, 31, 260-267.	3.2	20
46058	Computational Screening of Electrocatalytic Materials for Hydrogen Evolution: Platinum Monolayer on Transitional Metals. Journal of Physical Chemistry C, 2019, 123, 495-503.	1.5	15
46059	Tuning the Magnetic Properties of FeCo Thin Films through the Magnetoelastic Effect Induced by the Au Underlayer Thickness. ACS Applied Materials & Interfaces, 2019, 11, 1529-1537.	4.0	18
46060	Hydrogen Production via Efficient Formic Acid Decomposition: Engineering the Surface Structure of Pd-Based Alloy Catalysts by Design. ACS Catalysis, 2019, 9, 781-790.	5.5	62
46061	Aluminum and Nitrogen Codoped Graphene: Highly Active and Durable Electrocatalyst for Oxygen Reduction Reaction. ACS Catalysis, 2019, 9, 610-619.	5.5	56
46062	Quasi-degenerate magnetic states in Î±-RuCl₃. Journal of Physics Condensed Matter, 2019, 31, 025803.	0.7	4

#	Article	IF	Citations
46063	Combined Experimental and Theoretical Insights into the Synergistic Effect of Cerium Doping and Oxygen Vacancies in BaZrO_{3â^Ï´} Hollow Nanospheres for Efficient Photocatalytic Hydrogen Production. Journal of Physical Chemistry C, 2019, 123, 233-249.	1.5	13
46064	Roles of Hydration and Magnetism on the Structure of Ferrihydrite from First Principles. ACS Earth and Space Chemistry, 2019, 3, 70-78.	1.2	23
46065	In situ Raman spectroscopic evidence for oxygen reduction reaction intermediates at platinum single-crystal surfaces. Nature Energy, 2019, 4, 60-67.	19.8	478
46066	Elementary kinetics of nitrogen electroreduction on Fe surfaces. Journal of Chemical Physics, 2019, 150, 041708.	1.2	32
46067	First-principles investigation of the interface magnetic anisotropy of Fe/SrTiO3. Journal of Physics Condensed Matter, 2019, 31, 075803.	0.7	2
46068	Role of tetrahedrally coordinated dopants in palladium hydrides on their superconductivity and inverse isotope effect. Journal of Physics Condensed Matter, 2019, 31, 075703.	0.7	7
46069	Pmma-XO (X = C, Si, Ge) monolayer as promising anchoring materials for lithiumâ€“sulfur battery: a first-principles study. Nanotechnology, 2019, 30, 085405.	1.3	8
46070	Molten salt synthesis, characterization, and formation mechanism of superfine (Hf_xZr_{1â€x})B₂ solidâ€solution powders. Journal of the American Ceramic Society, 2019, 102, 3763-3770.	1.9	23
46071	Experimental and Theoretical Investigation on the Origin of the High Intercalation Voltage of K₂Zn₃[Fe(CN)₆]₂ Cathode. Journal of the Electrochemical Society, 2019, 166, A5139-A5145.	1.3	18
46072	Effect of oxygen vacancy on structural, optical, and photocatalytic properties of ceria films grown by magnetron sputtering deposition. Surface and Coatings Technology, 2019, 358, 36-42.	2.2	10
46073	Pressure-Driven Reversible Switching between n- and p-Type Conduction in Chalcopyrite CuFeS₂. Journal of the American Chemical Society, 2019, 141, 505-510.	6.6	36
46074	Density functional theory study of structural and thermodynamical stabilities of ferromagnetic MnX (X = P, As, Sb, Bi) compounds. Journal of Physics Condensed Matter, 2019, 31, 054001.	0.7	3
46075	Metal-enhanced hydrogenation of graphene with atomic pattern. Carbon, 2019, 143, 700-705.	5.4	14
46076	Stacking effect on electronic, photocatalytic and optical properties: A comparison between bilayer and monolayer SnS. Computational Materials Science, 2019, 158, 272-281.	1.4	28
46077	When supporting electrolyte matters â€“ Tuning capacitive response of graphene oxide via electrochemical reduction in alkali and alkaline earth metal chlorides. Electrochimica Acta, 2019, 297, 112-117.	2.6	7
46078	Study of carbon-doped Mn3Ga thin films with enhanced magnetization. Intermetallics, 2019, 104, 90-96.	1.8	6
46079	Thermodynamic analysis of the topologically close packed Ïƒ phase in the Co Cr system. Intermetallics, 2019, 105, 13-20.	1.8	17
46080	First principles investigations of Fe, Co, Ni in model honeycomb carbon networks. Solid State Sciences, 2019, 87, 155-162.	1.5	2

#	Article	IF	Citations
46081	Mechanistic Insight into the [4 + 2] Dielsâ€“Alder Cycloaddition over First Row d-Block Cation-Exchanged Faujasites. ACS Catalysis, 2019, 9, 376-391.	5.5	23
46082	Can microsolvation effects be estimated from vacuum computations? A case-study of alcohol decomposition at the H₂O/Pt(111) interface. Physical Chemistry Chemical Physics, 2019, 21, 5368-5377.	1.3	25
46083	Development of 3rd generation Medium Mn duplex steels for automotive applications. Materials Science and Technology, 2019, 35, 204-219.	0.8	18
46084	Electronic and optical properties of SnO₂ (110)/MAPbI₃ (100) interface by first-principles calculations. Materials Research Express, 2019, 6, 026312.	0.8	3
46085	The hardness mechanism and bonding properties of CrN2: A first principle study. Computational Materials Science, 2019, 158, 282-288.	1.4	2
46086	A comprehensive computational study of adatom diffusion on the aluminum (1â€¯0â€¯0) surface. Computational Materials Science, 2019, 158, 353-358.	1.4	9
46087	Single-crystalline (FexNi1-x)2P nanosheets with dominant <mml:math xmlns:mml="http://www.w3.org/1998/Math/MathML" altimg="si0003.gif" overflow="scroll"><mml:mrow><mml:mo stretchy="false">{</mml:mo><mml:mi>01</mml:mi><mml:mover accent="true"><mml:mi mathvariant="bold">1</mml:mi><mml:mo>Â¯</mml:mo></mml:mover><mml:mover accent="true"><mml:mi mathvariant="bold">1</mml:mi><mml:mo>Â¯</mml:mo></mml:mover><mml:mo st	8.2	68
46088	First-principles calculations of magnetic edge states in zigzag CrI3 nanoribbons. Physics Letters, Section A: General, Atomic and Solid State Physics, 2019, 383, 754-758.	0.9	10
46089	Application of the ChIMES Force Field to Nonreactive Molecular Systems: Water at Ambient Conditions. Journal of Chemical Theory and Computation, 2019, 15, 436-447.	2.3	23
46090	Oxygen Electrocatalysis at Mn^{III}â€“O_xâ€“C Hybrid Heterojunction: An Electronic Synergy or Cooperative Catalysis?. ACS Applied Materials & Interfaces, 2019, 11, 706-713.	4.0	7
46091	First-principles study of thermal expansion and thermomechanics of group-V monolayers: blue phosphorene, arsenene, and antimonene. Journal of Physics Condensed Matter, 2019, 31, 065302.	0.7	11
46092	Effect of Zr additions on crystal structures and mechanical properties of binary Wâ€“Zr alloys: A first-principles study. Journal of Materials Research, 2019, 34, 290-300.	1.2	19
46093	Atomic Structure and Electrical Activity of Grain Boundaries and Ruddlesdenâ€“Popper Faults in Cesium Lead Bromide Perovskite. Advanced Materials, 2019, 31, e1805047.	11.1	72
46094	Improved activity and significant SO2 tolerance of samarium modified CeO2-TiO2 catalyst for NO selective catalytic reduction with NH3. Applied Catalysis B: Environmental, 2019, 244, 671-683.	10.8	294
46095	Li-decorated Pmmn8 phase of borophene for hydrogen storage. A van der Waals corrected density-functional theory study. International Journal of Hydrogen Energy, 2019, 44, 1021-1033.	3.8	35
46096	First-principles modeling of water permeation through periodically porous graphene derivatives. Journal of Colloid and Interface Science, 2019, 538, 367-376.	5.0	16
46097	Cluster formation and eventual mobility of helium in a tungsten grain boundary. Journal of Nuclear Materials, 2019, 514, 171-180.	1.3	17
46098	Brownian-snowball-mechanism-induced hierarchical cobalt sulfide for supercapacitors. Journal of Power Sources, 2019, 412, 321-330.	4.0	31

#	Article	IF	Citations
46099	Hydrogen adsorption property of Na-decorated boron monolayer: A first principles investigation. Physica E: Low-Dimensional Systems and Nanostructures, 2019, 107, 170-176.	1.3	27
46100	Width dependent structural and electrical properties of zigzag ZnTe nanoribbons. Physics Letters, Section A: General, Atomic and Solid State Physics, 2019, 383, 748-753.	0.9	4
46101	Van der Waals Heteroepitaxial Growth of Monolayer Sb in a Puckered Honeycomb Structure. Advanced Materials, 2019, 31, e1806130.	11.1	75
46102	Layerâ€Dependent Dielectric Function of Waferâ€Scale 2D MoS₂. Advanced Optical Materials, 2019, 7, 1801250.	3.6	58
46103	Inâ€Plane Optical Anisotropy of Lowâ€Symmetry 2D GeSe. Advanced Optical Materials, 2019, 7, 1801311.	3.6	68
46104	Structure Distortion Induced Monoclinic Nickel Hexacyanoferrate as Highâ€Performance Cathode for Naâ€Ion Batteries. Advanced Energy Materials, 2019, 9, 1803158.	10.2	93
46105	Carbonâ€Supported Divacancyâ€Anchored Platinum Singleâ€Atom Electrocatalysts with Superhigh Pt Utilization for the Oxygen Reduction Reaction. Angewandte Chemie, 2019, 131, 1175-1179.	1.6	73
46106	Carbonâ€Supported Divacancyâ€Anchored Platinum Singleâ€Atom Electrocatalysts with Superhigh Pt Utilization for the Oxygen Reduction Reaction. Angewandte Chemie - International Edition, 2019, 58, 1163-1167.	7.2	252
46107	Starâ€Shaped Molecules as Dopantâ€Free Hole Transporting Materials for Efficient Perovskite Solar Cells: Multiscale Simulation. Chemical Record, 2019, 19, 938-946.	2.9	16
46108	Interpretation of NH3-TPD Profiles from Cu-CHA Using First-Principles Calculations. Topics in Catalysis, 2019, 62, 93-99.	1.3	60
46109	Self-diffusion of Ti interstitial based point defects and complexes in TiC. Acta Materialia, 2019, 165, 381-387.	3.8	18
46110	Two-dimensional Dy doped MoS2 ferromagnetic sheets. Applied Surface Science, 2019, 471, 118-123.	3.1	22
46111	Two-dimensional CdS/g-C6N6 heterostructure used for visible light photocatalysis. Applied Surface Science, 2019, 471, 162-167.	3.1	72
46112	Mechanistic studies of the influence of halogen substituents on the corrosion inhibitive efficiency of selected imidazole molecules: A synergistic computational and experimental approach. Applied Surface Science, 2019, 471, 494-505.	3.1	51
46113	A computational study on linear and bent adsorption of CO2 on different surfaces for its photoreduction. Catalysis Today, 2019, 335, 278-285.	2.2	13
46114	Acoustical characteristics of single-walled noncarbon nanotubes: Longitudinal and torsional waves. Computational Condensed Matter, 2019, 18, e00350.	0.9	2
46115	DFT study on CO oxidative coupling to DMO over Pd4/TiO2 and Pd4/TiO2-Ov: A role of oxygen vacancy on support. Computational Materials Science, 2019, 159, 1-11.	1.4	11
46116	YBaCo2O5+Î´-based double-perovskite cathodes for intermediate-temperature solid oxide fuel cells with simultaneously improved structural stability and thermal expansion properties. Electrochimica Acta, 2019, 297, 344-354.	2.6	39

#	Article	IF	Citations
46117	Tailor-made metal-nitrogen-carbon bifunctional electrocatalysts for rechargeable Zn-air batteries via controllable MOF units. Energy Storage Materials, 2019, 17, 46-61.	9.5	70
46118	Cobalt nitride nanoparticles embedded in porous carbon nanosheet arrays propelling polysulfides conversion for highly stable lithiumâ€“sulfur batteries. Energy Storage Materials, 2019, 21, 210-218.	9.5	79
46119	Thermoelectric properties of n-type Cu Bi2S3 materials fabricated by plasma activated sintering. Journal of Alloys and Compounds, 2019, 780, 35-40.	2.8	18
46120	Predicted semiconducting beryllium sulfides in 3D and 2D configurations: Insights from first-principles calculations. Journal of Alloys and Compounds, 2019, 781, 371-377.	2.8	8
46121	Thermoelectric transport properties of Pb doped SnSe alloys (PbxSn1-xSe): DFT-BTE simulations. Journal of Solid State Chemistry, 2019, 270, 413-418.	1.4	11
46122	Interaction between Ruthenium Oxide Surfaces and Water Molecules. Effect of Surface Morphology and Water Coverage. Journal of Physical Chemistry C, 2019, 123, 7786-7798.	1.5	18
46123	CO oxidation by Pd supported on CeO2(100) and CeO2(111) facets. Applied Catalysis B: Environmental, 2019, 243, 36-46.	10.8	231
46124	Structural, electronic and optical properties of prominent M2Si5N8:Eu2+ phosphors (MÂ= Mg, Ca, Sr,) Tj ETQq1 1 0.784314 rgBT /Ov Compounds, 2019, 775, 30-38.	2.8	9
46125	Continuum embeddings in condensedâ€matter simulations. International Journal of Quantum Chemistry, 2019, 119, e25725.	1.0	40
46126	Segregation Effect and Its Influence on the Stability and Electronic Properties of Icosahedral CuxAg13â^'x (xâ€‰=â€‰0â€“13) Clusters. Journal of Cluster Science, 2019, 30, 77-82.	1.7	2
46127	Key microstructural characteristics in flash sintered 3YSZ critical for enhanced sintering process. Ceramics International, 2019, 45, 1251-1257.	2.3	24
46128	Hetero-interface constructs ion reservoir to enhance conversion reaction kinetics for sodium/lithium storage. Energy Storage Materials, 2019, 18, 107-113.	9.5	105
46129	Formation and migration of point defects in tungsten carbide: Unveiling the sluggish bulk self-diffusivity of WC. Journal of the European Ceramic Society, 2019, 39, 165-172.	2.8	19
46130	Lithiation and Delithiation Reactions of Binary Silicide Electrodes in an Ionic Liquid Electrolyte as Novel Anodes for Lithiumâ€ion Batteries. ChemElectroChem, 2019, 6, 581-589.	1.7	24
46131	Ab Initio Modeling of Y and O Solute Atom Interaction in Small Clusters within the bcc Iron Lattice. Physica Status Solidi (B): Basic Research, 2019, 256, 1800346.	0.7	2
46132	Enhanced magnetism in the VLi8 magnetic superatom supported on graphene. Applied Surface Science, 2019, 465, 207-211.	3.1	8
46133	Insight into phosphate doped BiVO4 heterostructure for multifunctional photocatalytic performances: A combined experimental and DFT study. Applied Surface Science, 2019, 466, 787-800.	3.1	36
46134	Functionalized titanium nitride-based MXenes as promising host materials for lithium-sulfur batteries: A first principles study. Ceramics International, 2019, 45, 1588-1594.	2.3	63

#	Article	IF	Citations
46135	From random stacking faults to polytypes: A 12-layer NiSn4 polytype. Journal of Alloys and Compounds, 2019, 774, 265-273.	2.8	4
46136	Theoretical investigation of lattice dynamics, dielectric properties, infrared reflectivity and Raman intensity spectra of Nowotny chimney-ladder semiconducting silicide Ru2Si3. Materials Chemistry and Physics, 2019, 222, 165-172.	2.0	4
46137	Lithiation-induced interfacial failure of electrode-collector: A first-principles study. Materials Chemistry and Physics, 2019, 222, 193-199.	2.0	9
46138	First-principles study the structures and mechanical properties of binary W-V alloys. Physica B: Condensed Matter, 2019, 552, 165-169.	1.3	17
46139	Magnetocrystalline anisotropy of Pt-doped L10-FeNi compound for clean energy applications. Vacuum, 2019, 159, 186-190.	1.6	6
46140	First-principles investigation of the martensitic transition and magnetic properties in Heusler alloys Mg2YZ (Yâ€¯=â€¯Sc, Ti, V, Zâ€¯=â€¯Al, Ga, In). Journal of Magnetism and Magnetic Materials, 2019, 471, 82-88.	1.0	6
46141	Interactions between dislocations and twins in deformed titanium aluminide crystals. Journal of Materials Science and Technology, 2019, 35, 402-408.	5.6	10
46142	Detailed Structures and Formation Mechanisms of Well-Known Al10RE2Mn7 Phase in Die-Cast Mgâ€“4Alâ€“4REâ€“0.3Mn Alloy. Acta Metallurgica Sinica (English Letters), 2019, 32, 178-186.	1.5	11
46143	Synthesis, characterization and simulation of lithium titanate nanotubes for dye sensitized solar cells. Ceramics International, 2019, 45, 708-717.	2.3	13
46144	Structure and Bonding of La₂NiBi. Zeitschrift Fur Anorganische Und Allgemeine Chemie, 2019, 645, 340-346.	0.6	2
46145	Graphene as an electrochemical transfer layer. Carbon, 2019, 141, 266-273.	5.4	17
46146	Rectification effects of C3N nanoribbons-based Schottky junctions. Carbon, 2019, 141, 363-369.	5.4	15
46147	Reverting fluoroform back to chlorodifluoromethane and dichlorofluoromethane: Intermolecular Cl/F exchange with chloroform at moderate temperatures. Chemical Engineering Journal, 2019, 355, 594-601.	6.6	19
46148	Can fluorine and chlorine functionalization stabilize the graphene like borophene?. Computational Materials Science, 2019, 156, 56-66.	1.4	34
46149	Atomistic insights into the enhanced stability and phase change speed of Alâ€“Sb phase change materials. Materials Letters, 2019, 234, 371-374.	1.3	1
46150	Quantum confinement luminescence of trigonal cesium lead bromide quantum dots. Applied Surface Science, 2019, 466, 119-125.	3.1	22
46151	Identifying the stacking style, intrinsic bandgap and magnetism of pristine graphdyine. Carbon, 2019, 143, 8-13.	5.4	22
46152	Identification of a narrow band red light-emitting phosphor using computational screening of ICSD: Its synthesis and optical characterization. Journal of Alloys and Compounds, 2019, 774, 338-346.	2.8	13

#	Article	IF	Citations
46153	Experimental and first principle study of room temperature ferromagnetism in carbon-doped rutile TiO2. Materials Research Bulletin, 2019, 110, 13-17.	2.7	24
46154	Band alignment of nonpolar (10<mml:math xmlns:mml="http://www.w3.org/1998/Math/MathML") Tj ETQq1 1 0.784314 rgBT /Overlo ZnO on (112) LaAlO3. Solid State Communications, 2019, 287, 23-26.	0.9	3
46155	Anisotropy of the proton kinetic energy in ice Ih. Surface Science, 2019, 679, 174-179.	0.8	2
46156	First-Principles Study of Interface Structures and Charge Rearrangement at the Aluminosilicate/Ru(0001) Heterojunction. Journal of Physical Chemistry C, 2019, 123, 7731-7739.	1.5	11
46157	Nuanced superconductivity in endohedral gallide Mo₈Ga₄₁. Materials Research Express, 2019, 6, 016002.	0.8	9
46158	A bulk adjusted linear combination of atomic orbitals (BAâ€ŁCAO) approach for nanoparticles. Journal of Computational Chemistry, 2019, 40, 212-221.	1.5	3
46159	First-principles Study of Strain-Induced Magnetism in Defective Arsenene. Journal of Superconductivity and Novel Magnetism, 2019, 32, 1735-1740.	0.8	1
46160	Black phosphorus-CdS-La2Ti2O7 ternary composite: Effective noble metal-free photocatalyst for full solar spectrum activated H2 production. Applied Catalysis B: Environmental, 2019, 242, 441-448.	10.8	105
46161	Selective breakdown of phonon quasiparticles across superionic transition in CuCrSe2. Nature Physics, 2019, 15, 73-78.	6.5	88
46162	Two-dimensional g-C₃N₄/InSe heterostructure as a novel visible-light photocatalyst for overall water splitting: a first-principles study. Journal Physics D: Applied Physics, 2019, 52, 015304.	1.3	25
46163	Energetics and Electronic Properties of Interstitial Chlorine in CdTe. Physica Status Solidi (B): Basic Research, 2019, 256, 1800219.	0.7	4
46164	Understanding the role of Pd:Cu ratio, surface and electronic structures in Pd-Cu alloy material applied in direct formic acid fuel cells. Applied Surface Science, 2019, 465, 730-739.	3.1	44
46165	A comparative first-principles study of point defect properties in the layered MX2 (Mâ€¯=â€¯Mo, W; Xâ€¯=â€¯S, Te): Substitution by the groups III, V and VII elements. Computational Materials Science, 2019, 156, 280-285.	1.4	3
46166	Magnetic 3d Transition Metal Atomic Chains Modulated by the Intrinsic Valley Structure in MX Monolayer. Advanced Electronic Materials, 2019, 5, 1800450.	2.6	6
46167	Effect of vacancy on adsorption/dissociation and diffusion of H2S on Fe(1â€¯0â€¯0) surfaces: A density functional theory study. Applied Surface Science, 2019, 465, 833-845.	3.1	27
46168	Tuning the photoluminescence of graphene oxide quantum dots by photochemical fluorination. Carbon, 2019, 141, 331-338.	5.4	31
46169	N-, P-, As-triphenylene-graphdiyne: Strong and stable 2D semiconductors with outstanding capacities as anodes for Li-ion batteries. Carbon, 2019, 141, 291-303.	5.4	73
46170	Prediction of HfB₃ from first-principles calculations: crystal structures, stabilities, electronic properties and hardnesses. Molecular Physics, 2019, 117, 547-556.	0.8	6

#	Article	IF	Citations
46171	Electric Field Induced Raman Scattering at the Sbâ€“InP(110) Interface: The Surface Dipole Contribution. Physica Status Solidi (B): Basic Research, 2019, 256, 1800314.	0.7	3
46172	Forming Atomâ€“Vacancy Interface on the MoS 2 Catalyst for Efficient Hydrodeoxygenation Reactions. Small Methods, 2019, 3, 1800315.	4.6	23
46173	Space-confined growth of monolayer ReSe2 under a graphene layer on Au foils. Nano Research, 2019, 12, 149-157.	5.8	22
46174	Directional electron delivery and enhanced reactants activation enable efficient photocatalytic air purification on amorphous carbon nitride co-functionalized with O/La. Applied Catalysis B: Environmental, 2019, 242, 19-30.	10.8	103
46175	Lead-free perovskite based bismuth for solar cells absorbers. Journal of Alloys and Compounds, 2019, 773, 796-801.	2.8	29
46176	Chalcogens doped BaTiO3 for visible light photocatalytic hydrogen production from water splitting. Spectrochimica Acta - Part A: Molecular and Biomolecular Spectroscopy, 2019, 208, 65-72.	2.0	36
46177	First-principles study of the vibrational characteristics of the heavy element substitution on Cu3SbSe3. Computational Materials Science, 2019, 156, 167-174.	1.4	4
46178	Recent progress on graphene-analogous 2D nanomaterials: Properties, modeling and applications. Progress in Materials Science, 2019, 100, 99-169.	16.0	235
46179	Multiple topological states in iron-based superconductors. Nature Physics, 2019, 15, 41-47.	6.5	170
46180	Stabilization of two-dimensional penta-silicene for flexible lithium-ion battery anodes via surface chemistry reconfiguration. Physical Chemistry Chemical Physics, 2019, 21, 1029-1037.	1.3	27
46181	Elemental site occupancy in the L12 A3B ordered intermetallic phase in Co-based superalloys and its influence on the microstructure. Acta Materialia, 2019, 163, 140-153.	3.8	65
46182	Hydrogen adsorption on alkali metal decorated blue phosphorene nanosheets. Applied Surface Science, 2019, 465, 440-449.	3.1	28
46183	The T phase with the V6Si5 type structure in the Mo-Si-Ti system studied by ab initio calculations and X-ray diffraction. Scripta Materialia, 2019, 159, 76-79.	2.6	1
46184	Theoretical investigation of the effect of phosphate doping on the aggregation of Au atoms on an Al2O3 (0001) surface. Applied Surface Science, 2019, 465, 1003-1013.	3.1	5
46185	Looking for new thermoelectric materials among TMX intermetallics using high-throughput calculations. Computational Materials Science, 2019, 156, 96-103.	1.4	19
46186	The anisotropic thermoelectricity property of AgBi3S5 by first-principles study. Journal of Alloys and Compounds, 2019, 773, 812-818.	2.8	11
46187	Construction of surface lattice oxygen in metallic Nâ^'CuCoS1.97 porous nanowire for wearable Znâ^'air battery. Journal of Energy Chemistry, 2019, 34, 1-9.	7.1	15
46188	CO Oxidation over Unsupported Group 11 Metal Catalysts: New Mechanistic Insight from First-Principles. Journal of Physical Chemistry C, 2019, 123, 7818-7830.	1.5	8

#	Article	IF	Citations
46189	Spatially selective reversible charge carrier density tuning in WS ₂ monolayers via photochlorination. 2D Materials, 2019, 6, 015003.	2.0	13
46190	Computation of stability, elasticity and thermodynamics in equiatomic AlCrFeNi medium-entropy alloys. Journal of Materials Science, 2019, 54, 2566-2576.	1.7	28
46191	Density functional theory study on improved reactivity of alkali-doped Fe2O3 oxygen carriers for chemical looping hydrogen production. Fuel, 2019, 236, 1057-1064.	3.4	38
46192	A first-principles reassessment of the Fe-N phase diagram in the low-nitrogen limit. Journal of Alloys and Compounds, 2019, 775, 758-768.	2.8	9
46193	Theoretical Treatment for Properties of Surfaces and Their Interplay with Bulk Properties of Crystals. Advanced Theory and Simulations, 2019, 2, 1800117.	1.3	2
46194	Mutual modulation of F-distribution and N-configuration in F and N dual-functionalized graphene. Applied Surface Science, 2019, 465, 880-887.	3.1	2
46195	Functionalization Ti3C2 MXene by the adsorption or substitution of single metal atom. Applied Surface Science, 2019, 465, 911-918.	3.1	63
46196	Enhancement of electrical performance via carrier modulation in single crystalline PbTe prepared by Pb-flux method. Journal of Alloys and Compounds, 2019, 774, 282-289.	2.8	9
46197	Structure determination of oxamic acid from laboratory powder X-Ray diffraction data and energy minimization by DFT-D. Journal of Molecular Structure, 2019, 1177, 310-316.	1.8	2
46198	Effect of substrate relaxation on adsorption energies: The example of Î±-Fe2O3(0001) and Fe3O4(111). Surface Science, 2019, 679, 225-229.	0.8	10
46199	Interactions of VOx Species with Amorphous TiO2 Domains on ALD-Derived Alumina-Supported Materials. Journal of Physical Chemistry C, 2019, 123, 7988-7999.	1.5	11
46200	Pyrochlore Pr2Zr1.95In0.05O7+Î´ oxygen conductors: Defect-induced electron transport and enhanced NO2 sensing performances. Electrochimica Acta, 2019, 293, 338-347.	2.6	16
46201	Structure and properties of YAlO3/NbC heterogeneous nucleation interface: First principles calculation and experimental research. Journal of Alloys and Compounds, 2019, 773, 264-276.	2.8	36
46202	hcp â†' Ï‰ phase transition mechanisms in shocked zirconium: A machine learning based atomic simulation study. Acta Materialia, 2019, 162, 126-135.	3.8	17
46203	Improved selectivity and coke resistance of core-shell alloy catalysts for propane dehydrogenation from first principles and microkinetic analysis. Chemical Engineering Journal, 2019, 377, 120049.	6.6	42
46204	Mg-X (X = Ni, Pd, Ti, Nb) interface and atomic mixture effect: a first-principles study. Materials Research Express, 2019, 6, 016305.	0.8	1
46205	Unexpected ground-state crystal structures and mechanical properties of transition metal pernitrides MN2 (M= Ti, Zr, and Hf). Journal of Alloys and Compounds, 2019, 774, 918-925.	2.8	37
46206	Microscopic investigation of Bi2-xSbxTe3-ySey systems: On the origin of a robust intrinsic topological insulator. Journal of Physics and Chemistry of Solids, 2019, 128, 251-257.	1.9	15

#	Article	IF	Citations
46207	Ground state and magnetic properties of the Cr-doped Ni-Mn-(Ga, Ge, In, Sn) alloys: Insights from ab initio study. Journal of Magnetism and Magnetic Materials, 2019, 470, 123-126.	1.0	7
46208	Significant photoluminescence quenching and charge transfer in the MoS2/Bi2Te3 heterostructure. Journal of Physics and Chemistry of Solids, 2019, 128, 337-342.	1.9	11
46209	Topological critical materials of ternary compounds. Journal of Physics and Chemistry of Solids, 2019, 128, 218-224.	1.9	4
46210	Surface modification of TiO2 with copper clusters for band gap narrowing. Catalysis Today, 2019, 321-322, 9-17.	2.2	61
46211	Finite size and volume effects in line node semimetals: A first-principles investigation. Journal of Physics and Chemistry of Solids, 2019, 128, 231-236.	1.9	1
46212	MoirÃ© superlattices and 2D electronic properties of graphite/MoS2 heterostructures. Journal of Physics and Chemistry of Solids, 2019, 128, 325-330.	1.9	14
46213	Density Functional Theory Study of M_n₊₁AX_nPhases: A Review. Critical Reviews in Solid State and Materials Sciences, 2019, 44, 56-107.	6.8	46
46214	Modeling of the structural and magnetic properties of Fe-Rh-(Z) (Zâ€¯=â€¯Mn, Pt) alloys by first principles methods. Journal of Magnetism and Magnetic Materials, 2019, 470, 69-72.	1.0	7
46215	Peculiarities of phonons in Ni-Mn-Ga alloys: Ab initio studies. Journal of Magnetism and Magnetic Materials, 2019, 470, 73-76.	1.0	2
46216	Magnetic properties of Fe100â^'Ga : Ab initio and Monte Carlo study. Journal of Magnetism and Magnetic Materials, 2019, 470, 118-122.	1.0	8
46217	Graphdiyne Containing Atomically Precise N Atoms for Efficient Anchoring of Lithium Ion. ACS Applied Materials & Interfaces, 2019, 11, 2608-2617.	4.0	100
46218	Single-atom supported on graphene grain boundary as an efficient electrocatalyst for hydrogen evolution reaction. Chemical Engineering Science, 2019, 194, 58-63.	1.9	71
46219	Understanding the multifunctionality in Cu-doped BiVO4 semiconductor photocatalyst. Journal of Environmental Sciences, 2019, 75, 84-97.	3.2	56
46220	VSe2-reduced graphene oxide as efficient cathode material for field emission. Journal of Physics and Chemistry of Solids, 2019, 128, 384-390.	1.9	31
46221	Combining Theory and Experiment for Multitechnique Characterization of Activated CO₂ on Transition Metal Carbide (001) Surfaces. Journal of Physical Chemistry C, 2019, 123, 7567-7576.	1.5	22
46222	Ab initio STUDY OF POINT DEFECTS IN 2D GRAPHENE LAYER. Surface Review and Letters, 2019, 26, 1850142.	0.5	6
46223	Electrochemical water oxidation on WO3 surfaces: A density functional theory study. Catalysis Today, 2019, 321-322, 94-99.	2.2	55
46224	The surface reactivity and structural properties of anatase TiO2 (001), (100), (101) and (105) surface researched with DFT. Proceedings of the National Academy of Sciences India Section A - Physical Sciences, 2019, 89, 193-197.	0.8	2

#	Article	IF	Citations
46225	First-principles kinetics study of carbon monoxide promoted Ostwald ripening of Au particles on FeO/Pt(111). Journal of Energy Chemistry, 2019, 30, 108-113.	7.1	12
46226	Interaction-driven spin-orbit effects and Chern insulating phases in corundum-based 4d and 5d oxide honeycomb lattices. Journal of Physics and Chemistry of Solids, 2019, 128, 301-309.	1.9	2
46227	Fate of Lu(III) sorbed on 2-line ferrihydrite at pHÂ5.7 and aged for 12Âyears at room temperature. II: insights from STEM-EDXS and DFT calculations. Environmental Science and Pollution Research, 2019, 26, 5282-5293.	2.7	4
46228	Tailoring magnetic characteristics of phosphorene by the doping of Ce and Ti: A DFT study. Physica E: Low-Dimensional Systems and Nanostructures, 2019, 106, 352-356.	1.3	5
46229	Immobilized Ferrous Ion and Glucose Oxidase on Graphdiyne and Its Application on One-Step Glucose Detection. ACS Applied Materials & Interfaces, 2019, 11, 2647-2654.	4.0	86
46230	Theoretical investigation of loading Ni clusters on the Î±-Ga2O3 surfaces for photocatalytic hydrogen evolution. Journal of Energy Chemistry, 2019, 30, 8-18.	7.1	4
46231	Computational analysis of the intermetallic formation during the dissimilar metal aluminum-to-steel friction stir welding process. Proceedings of the Institution of Mechanical Engineers, Part L: Journal of Materials: Design and Applications, 2019, 233, 1080-1100.	0.7	4
46232	Structural stability of Lanthanum-based oxygen-deficient perovskites in redox catalysis: A density functional theory study. Catalysis Today, 2020, 347, 142-149.	2.2	18
46233	Theoretical understandings on the unusual selectivity of 1,3-Butadiene hydrogenation to butenes over gold catalysts. Catalysis Today, 2020, 347, 134-141.	2.2	14
46234	Effect of low frequency phonons on structural properties of ZIFs with SOD topology. Microporous and Mesoporous Materials, 2020, 304, 109132.	2.2	13
46235	Structural, elastic, thermodynamic and electronic properties of covellite, CuS. Physica B: Condensed Matter, 2020, 582, 311142.	1.3	19
46236	Ab initio calculation of ligand field multiplet parameters for transition metal L-edge spectra. Radiation Physics and Chemistry, 2020, 175, 108051.	1.4	3
46237	High Coverage CO Adsorption on Fe6O6 Cluster Using GGAâ€‰+â€‰U. Journal of Cluster Science, 2020, 31, 591-600.	1.7	5
46238	Treatment of disorder effects in X-ray absorption spectra beyond the conventional approach. Radiation Physics and Chemistry, 2020, 175, 108112.	1.4	16
46239	Mo2TiC2 MXene: A Promising Catalyst for Electrocatalytic Ammonia Synthesis. Catalysis Today, 2020, 339, 120-126.	2.2	102
46240	The important role of N2H formation energy for low-temperature ammonia synthesis in an electric field. Catalysis Today, 2020, 351, 119-124.	2.2	29
46241	Cobalt porphyrin supported on graphene/Ni (111) surface: Enhanced oxygen evolution/reduction reaction and the role of electron coupling. Catalysis Today, 2020, 351, 113-118.	2.2	28
46242	Structural, electronic and catalytic performance of single-atom Fe anchored 3Si-doped graphene. Molecular Physics, 2020, 118, e1580783.	0.8	2

#	Article	IF	Citations
46243	A quantum-chemical study of the CO dissociation mechanism on low-index Miller planes of Ï´-Fe3C. Catalysis Today, 2020, 342, 152-160.	2.2	15
46244	Understanding the conversion of ethanol to propene on In2O3 from first principles. Catalysis Today, 2020, 350, 19-24.	2.2	16
46245	Software tools for thermodynamic calculation of mechanically unstable phases from first-principles data. Computer Physics Communications, 2020, 246, 106712.	3.0	9
46246	Polarization dependent X-ray absorption near-edge spectra of boron nitride nanotubes. Radiation Physics and Chemistry, 2020, 175, 108129.	1.4	1
46247	Reshaping of Rh nanoparticles in operando conditions. Catalysis Today, 2020, 350, 184-191.	2.2	3
46248	Hybrid Cu⁰ and Cu^x⁺ as Atomic Interfaces Promote Highâ€Selectivity Conversion of CO₂ to C₂H₅OH at Low Potential. Small, 2020, 16, e1901981.	5.2	92
46249	A C₂₀-based 3D carbon allotrope with high thermal conductivity. Physical Chemistry Chemical Physics, 2020, 22, 306-312.	1.3	9
46250	Cobalt doping modification for enhanced methane conversion at low temperature in chemical looping reforming systems. Catalysis Today, 2020, 350, 156-164.	2.2	34
46251	Auto-encoder-based generative models for data augmentation on regression problems. Soft Computing, 2020, 24, 7999-8009.	2.1	25
46252	Interaction of hydrogen with flat (0001) and corrugated (11â€“20) and (10â€“12) cobalt surfaces: Insights from experiment and theory. Catalysis Today, 2020, 342, 124-130.	2.2	24
46253	First-principles prediction of crystal structure and physical properties of ScB₃. Molecular Physics, 2020, 118, .	0.8	9
46254	CH4 dissociation and C C coupling on Mo-terminated MoC surfaces: A DFT study. Catalysis Today, 2020, 339, 54-61.	2.2	24
46255	Precipitates and alloying elements distribution in near Î± titanium alloy Ti65. Journal of Materials Science and Technology, 2020, 36, 91-96.	5.6	39
46256	Cobalt-nickel bimetallic Fischer-Tropsch catalysts: A combined theoretical and experimental approach. Catalysis Today, 2020, 342, 88-98.	2.2	27
46257	First-principles based microkinetic modeling of transient kinetics of CO hydrogenation on cobalt catalysts. Catalysis Today, 2020, 342, 131-141.	2.2	29
46258	Characterization of amorphous silica based catalysts using DFT computational methods. Catalysis Today, 2020, 354, 3-18.	2.2	63
46259	Shape selectivity in acidic zeolite catalyzed 2-pentene skeletal isomerization from first principles. Catalysis Today, 2020, 347, 115-123.	2.2	7
46260	High-gravity-assisted preparation of aqueous dispersions of monodisperse palladium nanocrystals as pseudohomogeneous catalyst for highly efficient nitrobenzene reduction. Chemical Engineering Journal, 2020, 382, 122883.	6.6	42

#	Article	IF	Citations
46261	Theoretical investigation on two novel high-pressure orthorhombic phases of superhard C3N2. Journal of Alloys and Compounds, 2020, 815, 152324.	2.8	6
46262	Investigation of adsorption, dissociation, and diffusion properties of hydrogen on the V (1â€¯0â€¯0) surface and in the bulk: A first-principles calculation. Journal of Advanced Research, 2020, 21, 25-34.	4.4	14
46263	High-pressure phase transitions of forsterite from first-principles. Journal of Physics and Chemistry of Solids, 2020, 136, 109161.	1.9	4
46264	Black reduced porous SnO2 nanosheets for CO2 electroreduction with high formate selectivity and low overpotential. Applied Catalysis B: Environmental, 2020, 260, 118134.	10.8	107
46265	ZrS3/MS2 and ZrS3/MXY (M Mo, W; X, Y S, Se, Te; Xâ€â‰ â€Y) type-II van der Waals hetero-bilayers: Prospective candidates in 2D excitonic solar cells. Applied Surface Science, 2020, 499, 143894.	3.1	51
46266	Surface-orientation-dependent growth of SrRuO3 epitaxial thin films. Applied Surface Science, 2020, 499, 143924.	3.1	6
46267	Investigation of the thermodynamic properties of Al4C3: A combined DFT and DSC study. Computational Materials Science, 2020, 171, 109100.	1.4	9
46268	Atomic-scale imaging of incipient interval-layered hydrogenation of single crystal magnesium. Scripta Materialia, 2020, 174, 77-79.	2.6	2
46269	Resonant doping for high mobility transparent conductors: the case of Mo-doped In₂O₃. Materials Horizons, 2020, 7, 236-243.	6.4	64
46270	Boosting defective carbon by anchoring well-defined atomically dispersed metal-N4 sites for ORR, OER, and Zn-air batteries. Applied Catalysis B: Environmental, 2020, 260, 118198.	10.8	216
46271	Neural network aided development of a semi-empirical interatomic potential for titanium. Computational Materials Science, 2020, 171, 109157.	1.4	17
46272	Influence of Ï€ spacer of donor-acceptor-Ï€-acceptor sensitizers on photovoltaic properties in dye-sensitized solar cells. Organic Electronics, 2020, 76, 105429.	1.4	6
46273	Tuning optical properties of Graphene/WSe2 heterostructure by introducing vacancy: First principles calculations. Physica E: Low-Dimensional Systems and Nanostructures, 2020, 116, 113729.	1.3	35
46274	Coupling efficient biomass upgrading with H₂ production via bifunctional Cu_xS@NiCo-LDH coreâ€“shell nanoarray electrocatalysts. Journal of Materials Chemistry A, 2020, 8, 1138-1146.	5.2	132
46275	Semiconducting SN₂ monolayer with three-dimensional auxetic properties: a global minimum with tetracoordinated sulfurs. Nanoscale, 2020, 12, 85-92.	2.8	21
46276	Ripening-resistance of Pd on TiO2(110) from first-principles kinetics. Frontiers of Optoelectronics, 2020, 13, 409-417.	1.9	0
46277	The nano gold rush: Graphynes as atomic sieves for coinage and Pt-group transition metals. Applied Surface Science, 2020, 499, 143927.	3.1	5
46278	Intriguing of two-dimensional Janus surface-functionalized MXenes: An ab initio calculation. Computational Materials Science, 2020, 171, 109231.	1.4	56

#	Article	IF	Citations
46279	Post-side chain engineering of difluorinated benzothiadiazole-based conjugated microporous polymer for enhanced photocatalytic H2 evolution. Applied Surface Science, 2020, 499, 143865.	3.1	33
46280	First-principles calculations on interface stability and migration of H and He in W-ZrC interfaces. Applied Surface Science, 2020, 499, 143995.	3.1	34
46281	First-principles investigation of Î²-Ge3N4 loaded with RuO2 cocatalyst for photocatalytic overall water splitting. Journal of Energy Chemistry, 2020, 44, 24-32.	7.1	11
46282	Co single-atom anchored on Co3O4 and nitrogen-doped active carbon toward bifunctional catalyst for zinc-air batteries. Applied Catalysis B: Environmental, 2020, 260, 118188.	10.8	163
46283	Hydrogenated C3N: Variable-bandgap stable structures and induced antiferromagnetic properties. Chemical Physics, 2020, 528, 110471.	0.9	5
46284	Thermoelectric transport properties of magnetic carbon-based organic chains. Chemical Physics, 2020, 528, 110524.	0.9	2
46285	New modulated structures of solid bromine at high pressure. Computational Materials Science, 2020, 171, 109205.	1.4	7
46286	Role of substituted atoms in stacking fault formation in long-period stacking ordered system. Computational Materials Science, 2020, 171, 109210.	1.4	5
46287	Activation volume dominated diffusivity of Ni50Al50 melt under extreme conditions. Computational Materials Science, 2020, 171, 109263.	1.4	5
46288	Crystal alignment of surface stabilized polymorph in thioindigo films. Dyes and Pigments, 2020, 172, 107847.	2.0	9
46289	Half metallic ferromagnetic and optical properties of ruthenium-doped zincblende ZnS: A first principles study. Journal of Physics and Chemistry of Solids, 2020, 136, 109175.	1.9	21
46290	Functionalization of two-dimensional C4N by atoms adsorption: A first-principles investigation. Physica E: Low-Dimensional Systems and Nanostructures, 2020, 115, 113649.	1.3	6
46291	Evidence of excess oxygen accommodation in yttria partially-stabilized zirconia. Scripta Materialia, 2020, 175, 7-10.	2.6	7
46292	The structure and stability of the low-index surfaces of D8m-Mo5Si3 by first-principles calculations. Ceramics International, 2020, 46, 877-887.	2.3	7
46293	Promotion effect with dispersed Fe-Ni-S catalyst to facilitate hydrogenolysis of lignite and heavy residue. Fuel, 2020, 259, 116303.	3.4	11
46294	The peculiar redox mechanism of copper nitroprusside disclosed by a multi-technique approach. Radiation Physics and Chemistry, 2020, 175, 108336.	1.4	3
46295	Steering elementary steps towards efficient alkaline hydrogen evolution via size-dependent Ni/NiO nanoscale heterosurfaces. National Science Review, 2020, 7, 27-36.	4.6	192
46296	Controlling electronic structure of single-layered $${hbox {HfX}}_{3}$$ ($$hbox {X=S}$$, Se) trichalcogenides through systematic Zr doping. Journal of Materials Science, 2020, 55, 660-669.	1.7	12

#	Article	IF	Citations
46297	Hierarchical NiCo2O4 hollow nanocages for photoreduction of diluted CO2: Adsorption and active sites engineering. Applied Catalysis B: Environmental, 2020, 260, 118208.	10.8	101
46298	Antioxidant behaviors of graphene in marine environment: A first-principles simulation. Applied Surface Science, 2020, 499, 143962.	3.1	24
46299	Modulation of the photocatalytic performance of g-C3N4 by two-sites co-doping using variable valence metal. Applied Surface Science, 2020, 500, 144036.	3.1	20
46300	Effects of nitrogen addition and growth condition on the enhanced mechanical properties of transition metal carbides TMC (TM = Zr, Hf). Ceramics International, 2020, 46, 1124-1136.	2.3	16
46301	Enhancing gas adsorption properties of borophene by embedding transition metals. Computational Condensed Matter, 2020, 22, e00436.	0.9	18
46302	Electronic and magnetic properties of 3d transition metal doped MoSe2 monolayer. Physica E: Low-Dimensional Systems and Nanostructures, 2020, 116, 113745.	1.3	29
46303	Surface electronic structure, relaxations and thermodynamic energies of (100), (110) and (111) surfaces of Mg2Si: A first-principles theoretical study. Surface Science, 2020, 691, 121506.	0.8	4
46304	Reaction mechanisms for reduction of CO2 to CO on monolayer MoS2. Applied Surface Science, 2020, 499, 143964.	3.1	35
46305	Intrinsic properties of nitrogen-rich carbon nitride for oxygen reduction reaction. Applied Surface Science, 2020, 500, 144020.	3.1	21
46306	Evaluating the effect of Pr-doping on the performance of strontium-doped lanthanum ferrite cathodes for protonic SOFCs. Ceramics International, 2020, 46, 4000-4005.	2.3	80
46307	Uncovering the underlying science behind dimensionality in the potassium battery regime. Energy Storage Materials, 2020, 25, 416-425.	9.5	30
46308	Theory of atomic scale quantum dots in silicon: Dangling bond quantum dots on silicon surface. Solid State Communications, 2020, 305, 113752.	0.9	4
46309	Superconducting Hydrides Under Pressure. Annual Review of Condensed Matter Physics, 2020, 11, 57-76.	5.2	149
46310	Towards a better understanding of the structure of diamanoÃ¯ds and diamanoÃ¯d/graphene hybrids. Carbon, 2020, 156, 234-241.	5.4	40
46311	Density functional theory study on the dehydrogenation of 1,2-dimethyl cyclohexane and 2-methyl piperidine on Pd and Pt catalysts. Catalysis Today, 2020, 352, 345-353.	2.2	30
46312	Structural, electronic and magnetic properties of manganese substituted CoFe2O4: A first-principles study. Journal of Magnetism and Magnetic Materials, 2020, 495, 165862.	1.0	16
46313	Synergetic donorâ€“donor codoping strategy for enhanced photoelectrochemical activity of hematite. Applied Catalysis B: Environmental, 2020, 260, 118186.	10.8	5
46314	Pseudopotential for plane-wave density functional theory studies of metallic uranium. Computational Materials Science, 2020, 171, 109221.	1.4	11

#	Article	IF	Citations
46315	Charge-neutral epitaxial graphene on 6Hâ€“SiC(0001) via FeSi intercalation. Carbon, 2020, 156, 187-193.	5.4	12
46316	Metric based on the arctangents of the logderivatives for evaluating scattering properties of pseudopotentials. Computer Physics Communications, 2020, 247, 106929.	3.0	1
46317	An ab initio study on liquid silicon carbide. Journal of Physics and Chemistry of Solids, 2020, 137, 109204.	1.9	7
46318	New LaMnO3 surface energy results obtained from density-functional theory. Surface Science, 2020, 695, 121500.	0.8	6
46319	Orientation Relationships of Pure Tin on Single Crystal Germanium Substrates. Journal of Electronic Materials, 2020, 49, 140-151.	1.0	0
46320	Enhanced visible-light photocatalytic H2 production of hierarchical g-C3N4 hexagon by one-step self-assembly strategy. Applied Surface Science, 2020, 499, 143942.	3.1	16
46321	Compressibility and thermal expansion study of Î´-UZr2 at high pressure and high temperature. Journal of Alloys and Compounds, 2020, 813, 152214.	2.8	3
46322	Enhancing hydrogen evolution reaction by strain engineering in free-standing doped FeS monolayer. Materials Chemistry and Physics, 2020, 239, 122046.	2.0	6
46323	Structural, electronic and photocatalytic properties of g-C3N4 with intrinsic defects: A first-principles hybrid functional investigation. Applied Surface Science, 2020, 499, 143994.	3.1	29
46324	Transition metal doped ZnO nanoparticles with enhanced photocatalytic and antibacterial performances: Experimental and DFT studies. Ceramics International, 2020, 46, 1494-1502.	2.3	287
46325	Oxygen vacancy rich Bi2O4-Bi4O7-BiO2-x composites for UVâ€“vis-NIR activated high efficient photocatalytic degradation of bisphenol A. Journal of Hazardous Materials, 2020, 382, 121121.	6.5	137
46326	High-entropy alumino-silicides: a novel class of high-entropy ceramics. Science China Materials, 2020, 63, 300-306.	3.5	45
46327	Synergistic effect of lattice strain and Co doping on enhancing thermal stability in Fe16N2 thin film with high magnetization. Journal of Magnetism and Magnetic Materials, 2020, 495, 165873.	1.0	3
46328	Effect of Ga substitution for In in LiInSe<mml:math xmlns:mml="http://www.w3.org/1998/Math/MathML" display="inline" id="d1e866" altimg="si108.svg"><mml:msub><mml:mrow /><mml:mrow><mml:mn>2</mml:mn></mml:mrow></mml:msub></mml:math> crystals on carrier transport behaviors and alpha particles detection. Nuclear Instruments and Methods in Physics Research, Section A: Accelerators, Spectrometers, Detectors and Associated Equipment, 2020, 949, 162877.	0.7	4
46329	Mechanical flexibility and strain engineered-band structures of monolayer Bi2O2Se. Physica E: Low-Dimensional Systems and Nanostructures, 2020, 116, 113728.	1.3	10
46330	A new trick for an old support: Stabilizing gold single atoms on LaFeO3 perovskite. Applied Catalysis B: Environmental, 2020, 261, 118178.	10.8	31
46331	Two-dimensional chromium boride MBenes with high HER catalytic activity. Applied Surface Science, 2020, 500, 144248.	3.1	50
46332	Thermoelectric properties of strontium sulfide via first-principles calculations. Solid State Communications, 2020, 305, 113755.	0.9	10

#	Article	IF	Citations
46333	MXenes as promising catalysts for water dissociation. Applied Catalysis B: Environmental, 2020, 260, 118191.	10.8	94
46334	Formation of phenoxy-type Environmental Persistent Free Radicals (EPFRs) from dissociative adsorption of phenol on Cu/Fe and their partial oxides. Chemosphere, 2020, 240, 124921.	4.2	17
46335	Preserving the half-metallicity at the quaternary Heusler CoFeCrAl (001)-oriented thin films: A first-principles study. Materials Chemistry and Physics, 2020, 240, 122262.	2.0	12
46336	The effect of oxygen vacancy at CO oxidation on anatase (001)-supported single-Au catalyst. Materials Chemistry and Physics, 2020, 240, 122291.	2.0	5
46337	Electronic property of bilayer graphene on pristine and rhenium-doped MoS2. Physica E: Low-Dimensional Systems and Nanostructures, 2020, 116, 113775.	1.3	0
46338	First-Principles Study of Black Phosphorus as Anode Material for Rechargeable Potassium-Ion Batteries. Electronic Materials Letters, 2020, 16, 89-98.	1.0	30
46339	2D/2D BiOBr/Ti3C2 heterojunction with dual applications in both water detoxification and water splitting. Journal of Photochemistry and Photobiology A: Chemistry, 2020, 386, 112099.	2.0	54
46340	Single ultrathin WO3 nanowire as a superior gas sensor for SO2 and H2S: Selective adsorption and distinct I-V response. Materials Chemistry and Physics, 2020, 240, 122165.	2.0	55
46341	Site preference and brittleâ€“ductile transition mechanism of B2-NiAl with ternary elements additions form first-principles calculations. Physica B: Condensed Matter, 2020, 576, 411703.	1.3	6
46342	Effect of zinc-doping on tensile strength of Î£5 bcc Fe symmetric tilt grain boundary. Computational Materials Science, 2020, 171, 109204.	1.4	25
46343	Effective Coulomb interaction in actinides from linear response approach. Computational Materials Science, 2020, 171, 109270.	1.4	14
46344	Predicting excellent anisotropic thermoelectric performance of the layered oxychalcogenides BiAgOCh (Châ€¯=â€¯S, Se, and Te). Computational Materials Science, 2020, 171, 109273.	1.4	12
46345	The electronic structure and physicochemical property of boron nitridene. Journal of Molecular Graphics and Modelling, 2020, 94, 107475.	1.3	2
46346	First-principles investigations of effects of solute elements on stability and electronic structure of laves phase/matrix interface in Ni-based superalloys. Journal of Physics and Chemistry of Solids, 2020, 136, 109166.	1.9	18
46347	LiGaOS is a fast Li-Ion conductor: A first-principles prediction. Materials and Design, 2020, 185, 108264.	3.3	6
46348	2D O-PTl monolayer: a robust large bandgap topological insulator. Journal Physics D: Applied Physics, 2020, 53, 025302.	1.3	4
46349	The influence of electrode for electroluminescence devices based on all-inorganic halide perovskite CsPbBr₃. Journal of Physics Condensed Matter, 2020, 32, 065002.	0.7	21
46350	NaTaO3 cubic and orthorhombic surfaces: An intrinsic improvement of photocatalytic properties. Applied Surface Science, 2020, 502, 144206.	3.1	32

#	Article	IF	Citations
46351	Strain-tunable magnetic order and electronic structure in 2D CrAsS4. Journal of Magnetism and Magnetic Materials, 2020, 497, 165941.	1.0	8
46352	Interlayer Transition in a vdW Heterostructure toward Ultrahigh Detectivity Shortwave Infrared Photodetectors. Advanced Functional Materials, 2020, 30, 1905687.	7.8	52
46353	Enhancement of hydrogen storage properties of Ca ₃ CH antiperovskite compound with hydrogen doping. International Journal of Energy Research, 2020, 44, 567-573.	2.2	12
46354	B, Nâ€coâ€doped grapheneâ€supported Ir and Pt clusters for methane activation and Câ”€C coupling: A density functional theory study. Journal of Computational Chemistry, 2020, 41, 194-202.	1.5	9
46355	3D Oxygenâ€Defective Potassium Vanadate/Carbon Nanoribbon Networks as Highâ€Performance Cathodes for Aqueous Zincâ€ion Batteries. Small Methods, 2020, 4, 1900670.	4.6	124
46356	New insights into Li2S2/Li2S adsorption on the graphene bearing single vacancy: A DFT study. Applied Surface Science, 2020, 503, 144446.	3.1	34
46357	Lattice dynamics simulation using machine learning interatomic potentials. Computational Materials Science, 2020, 172, 109333.	1.4	45
46358	Predicting magnetization of ferromagnetic binary Fe alloys from chemical short range order. Computational Materials Science, 2020, 172, 109344.	1.4	10
46359	First-principles analysis of the inhibitive effect of interstitial carbon on an active dissolution of martensitic steel. Corrosion Science, 2020, 163, 108251.	3.0	25
46360	DFT-FE â€“ A massively parallel adaptive finite-element code for large-scale density functional theory calculations. Computer Physics Communications, 2020, 246, 106853.	3.0	119
46361	Role of local coordination in bimetallic sites for oxygen reduction: A theoretical analysis. Journal of Energy Chemistry, 2020, 44, 131-137.	7.1	36
46362	Theoretical investigation of phonon contributions to thermal expansion coefficients for rare earth monosilicates RE2SiO5 (RE = Dy, Ho, Er, Tm, Yb and Lu). Journal of the European Ceramic Society, 2020, 40, 2658-2666.	2.8	41
46363	Structural and magnetic investigations on Cu-doped MnV2O6 compound: Experiment and theory. Journal of Magnetism and Magnetic Materials, 2020, 497, 165995.	1.0	3
46364	Diffusion of hydrogen isotopes in 3C-SiC in HTR-PM: A first-principles study. Progress in Nuclear Energy, 2020, 119, 103181.	1.3	2
46365	Sampling Potential Energy Surfaces in the Condensed Phase with Manyâ€Body Electronic Structure Methods. Chemistry - A European Journal, 2020, 26, 362-368.	1.7	7
46366	Oxychalcogenide Perovskite Solar Cells: A Multiscale Design Approach. Energy Technology, 2020, 8, 1900766.	1.8	1
46367	Structure Evolution, Elastic and Electronic Properties of Ptâ€Doped Ti Alloy under Pressure. Physica Status Solidi (B): Basic Research, 2020, 257, 1900360.	0.7	2
46368	Nitrogenâ€Functionalized Graphene Quantum Dots: A Versatile Platform for Integrated Optoelectronic Devices. Chemical Record, 2020, 20, 429-439.	2.9	11

#	Article	IF	Citations
46369	Ab initio modeling and design of vanadia-based electrode materials for post-lithium batteries. Journal Physics D: Applied Physics, 2020, 53, 083001.	1.3	9
46370	A 2D ZnSe/BiOX vertical heterostructure as a promising photocatalyst for water splitting: a first-principles study. Journal Physics D: Applied Physics, 2020, 53, 055108.	1.3	13
46371	Out-of-plane spontaneous polarization and superior photoelectricity in two-dimensional SiSn. Journal of Physics Condensed Matter, 2020, 32, 065003.	0.7	4
46372	Effect of albumin mediated clustering on the magnetic behavior of MnFe2O4 nanoparticles: experimental and theoretical modeling study. Nanotechnology, 2020, 31, 025707.	1.3	7
46373	Study of selective graphene growth on non-catalytic hetero-substrates. 2D Materials, 2020, 7, 011002.	2.0	5
46374	Chemical and structural stability of superconducting In5Bi3 driven by spinâ€“orbit coupling. JPhys Materials, 2020, 3, 015007.	1.8	1
46375	Selfâ€Assembled Room Temperature Multiferroic BiFeO₃â€LiFe₅O₈ Nanocomposites. Advanced Functional Materials, 2020, 30, 1906849.	7.8	14
46376	Largeâ€Spinâ€Gap Nodalâ€Line Halfâ€Metal and Highâ€Temperature Ferromagnetic Semiconductor in Cr₂X₃ (X=O,S,Se) Monolayers. Advanced Electronic Materials, 2020, 6, 1900490.	2.6	27
46377	Spinâ€Dependent Electronic Structure and Magnetic Anisotropy of 2D Ferromagnetic Janus Cr₂I₃X₃ (X = Br, Cl) Monolayers. Advanced Electronic Materials, 2020, 6, 1900778.	2.6	83
46378	Global Optimization of Adsorbate Covered Supported Cluster Catalysts: The Case of Pt₇H₁₀CH₃ on Î±â€Al₂O₃. ChemCatChem, 2020, 12, 762-770.	1.8	11
46379	Electronic and Spinâ€Dependent Optical Properties of Feâ€Adsorbed Armchair Silicene/Silicane Superlattices. Physica Status Solidi - Rapid Research Letters, 2020, 14, 1900494.	1.2	3
46380	The structure and electronic structure of tin oxides. , 2020, , 11-39.		8
46381	Tuning the structural, optical and photoluminescence properties of hybrid perovskite quantum dots by A-site doping. Applied Materials Today, 2020, 18, 100488.	2.3	6
46382	Mn2C monolayer: A superior anode material offering good conductivity, high storage capacity and ultrafast ion diffusion for Li-ion and Na-ion batteries. Applied Surface Science, 2020, 503, 144091.	3.1	51
46383	Insights into the Pt/Rh(1â€¯1â€¯1) interface for direct ethanol fuel cells. Applied Surface Science, 2020, 502, 144093.	3.1	9
46384	Adsorption or deoxidation of H2 interacted with Fe3O4 surface under different H coverage: A DFT study. Applied Surface Science, 2020, 502, 144097.	3.1	14
46385	Stability of C3-C6 carbonium ions inside zeolites: A first principles study. Applied Surface Science, 2020, 503, 144148.	3.1	7
46386	Interfacial two-dimensional oxide enhances photocatalytic activity of graphene/titania via electronic structure modification. Carbon, 2020, 157, 350-357.	5.4	7

#	Article	IF	Citations
46387	Effects of carbon substitution on electronic properties of the ultra-small boron nitride nanotube using density functional theory. Computational Condensed Matter, 2020, 22, e00442.	0.9	1
46388	Nb2SiTe4 and Nb2GeTe4: Unexplored 2D Ternary Layered Tellurides with High Stability, Narrow Band Gap and High Electron Mobility. Journal of Electronic Materials, 2020, 49, 959-968.	1.0	39
46389	Interfacial electronic structure and electrocatalytic performance modulation in Cu0.81Ni0.19 nanoflowers by heteroatom doping engineering using ionic liquid dopant. Applied Surface Science, 2020, 500, 144052.	3.1	11
46390	The effect of thermal annealing on the magnetic properties of graphene oxide quantum dots. Applied Surface Science, 2020, 501, 144234.	3.1	5
46391	Enhancing the magnetism of 2D carbide MXene Ti3C2Tx by H2 annealing. Carbon, 2020, 157, 90-96.	5.4	49
46392	Lead-free, stable mixed halide double perovskites Cs2AgBiBr6 and Cs2AgBiBr6â^'xClx â€“ A detailed theoretical and experimental study. Chemical Physics, 2020, 529, 110547.	0.9	38
46393	Mechanistic Insight of the Catalytic Role of WOX/SiO2 Catalyst in 2,5-Dimethylfuran to Para-xylene Conversion by DFT Calculation. Catalysis Letters, 2020, 150, 794-801.	1.4	7
46394	Influence of the segregation of 3d transition metal solutes on the elastic modulus of a tilt grain boundary in bcc Fe: ab initio local analysis. Journal of Materials Science, 2020, 55, 3056-3063.	1.7	2
46395	First-principles study of structural and optoelectronic properties of CsSnI3â^'yFy (yâ€‰=â€‰0, 1, 2, 3) perovskites. Indian Journal of Physics, 2020, 94, 1351-1359.	0.9	6
46396	Single-atoms supported (Fe, Co, Ni, Cu) on graphitic carbon nitride for CO2 adsorption and hydrogenation to formic acid: First-principles insights. Applied Surface Science, 2020, 499, 143928.	3.1	47
46397	Uncovering the electrochemical mechanisms for hydrogen evolution reaction of heteroatom doped M2C MXene (Mâ€¯=â€¯Ti, Mo). Applied Surface Science, 2020, 500, 143987.	3.1	93
46398	DFT study of ethanol adsorption on CaO(0â€¯0â€¯1) surface. Applied Surface Science, 2020, 500, 144254.	3.1	25
46399	Electric field and strain effects on the electronic and optical properties of g-C3N4/WSe2 van der Waals heterostructure. Applied Surface Science, 2020, 501, 144262.	3.1	44
46400	Two-dimensional BiP3 with high carrier mobility and moderate band gap for hydrogen generation from water splitting. Applied Surface Science, 2020, 501, 144263.	3.1	59
46401	New strategy for production of primary alcohols from aliphatic olefins by tandem cross-metathesis/hydrogenation. Chinese Chemical Letters, 2020, 31, 1525-1529.	4.8	2
46402	Energy-level engineered hollow N-doped NiS1.03 for Znâ€“Air batteries. Energy Storage Materials, 2020, 25, 202-209.	9.5	62
46403	Unravelling atomically resolved structure of a high-k dielectric oxide-semiconductor interface: Exit wave reconstruction and ab-initio calculation insights. Journal of Alloys and Compounds, 2020, 813, 152232.	2.8	1
46404	Bond relaxation and electronic and magnetic properties of Sc atoms adsorbed on the Li (1â€¯1â€¯0) surface. Journal of Magnetism and Magnetic Materials, 2020, 496, 165910.	1.0	4

#	Article	IF	Citations
46405	Dramatically enhanced carrier mobility and Curie temperature in n-p codoped ZnO by proximity effect. Journal of Magnetism and Magnetic Materials, 2020, 496, 165966.	1.0	4
46406	Structural and electronic features of Si/CH3NH3PbI3 interfaces with optoelectronic applicability: Insights from first-principles. Nano Energy, 2020, 67, 104166.	8.2	6
46407	Novel process for decontamination and additional valorization of steel making dust processing using two-step correlative leaching. Journal of Hazardous Materials, 2020, 384, 121442.	6.5	6
46408	Two-dimensional M2SD (Mâ€¯=â€¯Ge, Sn; Dâ€¯=â€¯Se, Te) monolayers with puckered structure: Electronic structure and optical properties. Physica E: Low-Dimensional Systems and Nanostructures, 2020, 117, 113802.	1.3	10
46409	The mechanism of room temperature catalytic Câ€“H dissociation and oxygenation of formaldehyde over nano-zirconia phase-junction. Chemical Engineering Journal, 2020, 380, 122498.	6.6	19
46410	Vacancyâ€•and dopingâ€dependent electronic and magnetic properties of monolayer SnS₂. Journal of the American Ceramic Society, 2020, 103, 391-402.	1.9	16
46411	Catalytic oxidation of Hg0 with O2 induced by synergistic coupling of CeO2 and MoO3. Journal of Hazardous Materials, 2020, 381, 121037.	6.5	16
46412	Firstâ€Principles Studies of Tiâ€Related Defects in Diamond. Physica Status Solidi (B): Basic Research, 2020, 257, 1900292.	0.7	2
46414	Multi-phase ELAStic Aggregates (MELASA) software tool for modeling anisotropic elastic properties of lamellar composites. Computer Physics Communications, 2020, 247, 106863.	3.0	9
46415	Edge promotion and basal plane activation of MoS2 catalyst by isolated Co atoms for hydrodesulfurization and hydrodenitrogenation. Catalysis Today, 2020, 350, 56-63.	2.2	5
46416	Anomalous crystal structure of Î³â€³ phase in the Mg-RE-Zn(Ag) series alloys: Causality clarified by ab initio study. Journal of Materials Science and Technology, 2020, 36, 167-175.	5.6	17
46417	Theoretical study on the catalytic properties of single-atom catalyst stabilised on silicon-doped graphene sheets. Molecular Physics, 2020, 118, e1652368.	0.8	6
46418	Structural, electronic and vibrational properties of ultra-thin octahedrally coordinated structure of EuO2. Journal of Magnetism and Magnetic Materials, 2020, 493, 165668.	1.0	1
46419	Ï€-Complexation for olefin/paraffin separation using aluminosilicates. Chemical Engineering Journal, 2020, 380, 122482.	6.6	28
46420	Octahedral distortion and electronic properties of the antiperovskite oxide Ba3SiO: First principles study. Journal of Physics and Chemistry of Solids, 2020, 136, 109126.	1.9	9
46421	Electron transport properties of silicene: Intrinsic and dirty cases with screening effects. Journal of Molecular Structure, 2020, 1199, 126878.	1.8	3
46422	A highly asymmetric interfacial superstructure in WC: expanding the classic grain boundary segregation and new complexion theories. Materials Horizons, 2020, 7, 173-180.	6.4	26
46423	An insight of Mg doped ZnO thin films: A comparative experimental and first-principle investigations. Physica E: Low-Dimensional Systems and Nanostructures, 2020, 115, 113658.	1.3	20

#	Article	IF	Citations
46424	Stabilized lithium metal anode by an efficient coating for high-performance Liâ€“S batteries. Energy Storage Materials, 2020, 24, 329-335.	9.5	79
46425	Photoexcited charge carrier behaviors in solar energy conversion systems from theoretical simulations. Wiley Interdisciplinary Reviews: Computational Molecular Science, 2020, 10, e1441.	6.2	7
46426	Nitrogen-rich carbon-supported ultrafine MoC nanoparticles for the hydrotreatment of oleic acid into diesel-like hydrocarbons. Chemical Engineering Journal, 2020, 382, 122464.	6.6	46
46427	Phonon thermal transport in Janus single layer M2XY (Mâ€¯=â€¯Ga; X, Yâ€¯=â€¯S, Se, Te): A study based on first-principles. Physica E: Low-Dimensional Systems and Nanostructures, 2020, 115, 113683.	1.3	33
46428	Modulation of the optical properties of zigzag silicene nanoribbons by double carbon chains. Canadian Journal of Physics, 2020, 98, 260-265.	0.4	0
46429	DFT study of graphene oxide reduction by a dopamine species. Molecular Physics, 2020, 118, .	0.8	9
46430	(Cu, Ag)-DOPED ZnS WITH WIDE VISIBLE LIGHT RANGE ABSORPTION FOR WATER SPLITTING: A THEORETICAL AND EXPERIMENTAL STUDY. Surface Review and Letters, 2020, 27, 1950139.	0.5	1
46431	Coordination dependence of carbon deposition resistance in partial oxidation of methane on Rh catalysts. Catalysis Today, 2020, 355, 422-434.	2.2	8
46432	The electric-field and strain inducing electronic and optical properties of the blue phosphorene/ZnO heterostructures. Physica E: Low-Dimensional Systems and Nanostructures, 2020, 115, 113650.	1.3	6
46433	Effect of La₂O₃ on the oxidation resistance of SiC ceramic at 1973ÂK: Experimental and theoretical study. Journal of the American Ceramic Society, 2020, 103, 614-621.	1.9	15
46434	Controlling the strength of Zr (10 <mml:math xmlns:mml="http://www.w3.org/1998/Math/MathML") Tj ETQq0 0 0 rgBT /Overlock 10 Tf boundary by nonmetallic impurities doping: A DFT study. Journal of Materials Science and Technology, 2020, 36, 140-148.	5.6	12
46435	Selective sodium-ion diffusion channels in Na2-xFe3(PO4)3 positive electrode for Na-ion batteries. Energy Storage Materials, 2020, 24, 343-350.	9.5	14
46436	Study on the NO2 production pathways and the role of NO2 in fast selective catalytic reduction DeNOx at low-temperature over MnOx/TiO2 catalyst. Chemical Engineering Journal, 2020, 379, 122288.	6.6	53
46437	Ab-initio study on opto-electronic properties of non-metal doped TiO2. Materials Today: Proceedings, 2020, 26, 94-96.	0.9	0
46438	Machine learning approaches to XANES spectra for quantitative 3D structural determination: The case of CO2 adsorption on CPO-27-Ni MOF. Radiation Physics and Chemistry, 2020, 175, 108430.	1.4	21
46439	Thermoelectric properties of Bi-doped SnS: First-principle study. Journal of Physics and Chemistry of Solids, 2020, 137, 109182.	1.9	17
46440	Highly durable isotypic heterojunction generated by covalent cross-linking with organic linkers for improving visible-light-driven photocatalytic performance. Applied Catalysis B: Environmental, 2020, 260, 118182.	10.8	20
46441	Active sites of Pt/CNTs nanocatalysts for aerobic base-free oxidation of glycerol. Green Energy and Environment, 2020, 5, 76-82.	4.7	22

#	Article	IF	Citations
46442	Inducing p-orbital magnetic semiconductors and carrier induced half-metallicity in surface oxygen-functionalized two-dimensional <mml:math xmlns:mml="http://www.w3.org/1998/Math/MathML" altimg="si27.svg"><mml:mrow><mml:msub><mml:mrow><mml:mi>X</mml:mi></mml:mrow><mml:mrow><mml:mn>2</mml:mn></m		

#	Article	IF	Citations
46460	Exploring the effects of solute segregation on the strength of Zr <mml:math xmlns:mml="http://www.w3.org/1998/Math/MathML" altimg="si1.svg"><mml:mrow><mml:mo>{</mml:mo><mml:mn>10</mml:mn><mml:mrow><mml:mover accent="true"><mml:mn>1</mml:mn><mml:mo>Â¯</mml:mo></mml:mover></mml:mrow><mml:mn>1</mml:mn><mml:mo stretchy="true">}</mml:mo></mml:mrow></mml:math> grain boundary: A first-principles study. Journal of Alloys and Compounds, 2020, 812, 152153.	2.8	14
46461	Conversion Mechanism From Trivalent Bismuth to Bivalent Bismuth Defect Center in Bi-Doped Silica Optical Fiber. IEEE Journal of Selected Topics in Quantum Electronics, 2020, 26, 1-6.	1.9	8
46462	Theoretical investigation of negatively curved 6.82D carbon based on density functional theory. Computational Materials Science, 2020, 171, 109211.	1.4	4
46463	Ab initio study and thermodynamic modeling of the Pd-Si-C system. Computational Materials Science, 2020, 171, 109238.	1.4	3
46464	Suggest a new approach to fabricate AlFe2B2. Computational Materials Science, 2020, 171, 109239.	1.4	9
46465	Exploring the electronic structure and thermal properties of UAl3 using density functional theory calculations. Journal of Physics and Chemistry of Solids, 2020, 136, 109179.	1.9	3
46466	A Universal Seeding Strategy to Synthesize Single Atom Catalysts on 2D Materials for Electrocatalytic Applications. Advanced Functional Materials, 2020, 30, 1906157.	7.8	91
46467	First-Principles Investigation of Thermodynamic Decomposition of Interfacial Oxides in Hot Compression Bonding. Metallurgical and Materials Transactions A: Physical Metallurgy and Materials Science, 2020, 51, 874-886.	1.1	9
46468	Crystal structure prediction of ReN2 under high pressure. Indian Journal of Physics, 2020, 94, 1711-1716.	0.9	1
46469	First-principles modeling of the hydrogen evolution reaction and its application in electrochemical corrosion of Mg. Acta Materialia, 2020, 183, 377-389.	3.8	50
46470	First-principles calculations on the interface of the Al/TiC aluminum matrix composites. Applied Surface Science, 2020, 505, 144502.	3.1	29
46471	Training data augmentation: An empirical study using generative adversarial net-based approach with normalizing flow models for materials informatics. Applied Soft Computing Journal, 2020, 86, 105932.	4.1	14
46472	High graphene permeability for room temperature silicon deposition: The role of defects. Carbon, 2020, 158, 631-641.	5.4	9
46473	Computer modeling of semiconductor nanotubes for water splitting. Current Opinion in Electrochemistry, 2020, 19, 88-95.	2.5	3
46474	Geometric structures, electronic characteristics, stabilities, catalytic activities, and descriptors of graphene-based single-atom catalysts. Nano Materials Science, 2020, 2, 120-131.	3.9	55
46475	Magnetic resonance imaging (MRI) compatible ZrX (Xâ€¯=â€¯Hf, Mo and Ru) alloys with enhanced mechanical properties as alternative biomedical applications. Scripta Materialia, 2020, 178, 82-85.	2.6	2
46476	A theoretical investigation on the potential of copper- and zinc-doped nanotubes as catalysts for the oxidation of SO2 (SO2â€‰+â€‰Â½O2â€‰â†’â€‰SO3) and CO (COâ€‰+â€‰Â½O2â€‰â†’â€‰CO2). Journal of Computationa 19, 55-61.	1.3	1
46477	Ceria-supported ruthenium clusters transforming from isolated single atoms for hydrogen production via decomposition of ammonia. Applied Catalysis B: Environmental, 2020, 268, 118424.	10.8	83

#	Article	IF	Citations
46478	Transition metal doped arsenene: Promising materials for gas sensing, catalysis and spintronics. Applied Surface Science, 2020, 506, 144660.	3.1	28
46479	A step forward towards the structural characterization of Na2Ti2O5Â·H2O nanotubes and their correlation with optical and electric transport properties. Ceramics International, 2020, 46, 2877-2886.	2.3	12
46480	Impact of the voids on the cracking behavior of the duplex oxide scale on the 18%Cr austenite alloy surface. Corrosion Science, 2020, 163, 108298.	3.0	5
46481	New insights into mechanisms on electrochemical N2 reduction reaction driven by efficient zero-valence Cu nanoparticles. Journal of Power Sources, 2020, 448, 227417.	4.0	22
46482	Lowâ€temperature molten salt synthesis of highâ€entropy carbide nanopowders. Journal of the American Ceramic Society, 2020, 103, 2244-2251.	1.9	50
46483	Revealing the Intrinsic Electronic Structure of 3D Halfâ€Heusler Thermoelectric Materials by Angleâ€Resolved Photoemission Spectroscopy. Advanced Science, 2020, 7, 1902409.	5.6	49
46484	Blue Light Emitting Defective Nanocrystals Composed of Earthâ€Abundant Elements. Angewandte Chemie - International Edition, 2020, 59, 860-867.	7.2	20
46485	Highly Efficient Polarized GeS/MoSe₂ van der Waals Heterostructure for Water Splitting from Ultraviolet to Nearâ€Infrared Light. Physica Status Solidi - Rapid Research Letters, 2020, 14, 1900582.	1.2	14
46486	Half-Heusler alloys: Enhancement of ZT after severe plastic deformation (ultra-low thermal) Tj ETQq0 0 0 rgBT /Overlock 10 Tf 50 422 Td	3.8	44
46487	Electrical conduction mechanism of rare-earth calcium oxyborate high temperature piezoelectric crystals. Acta Materialia, 2020, 183, 165-171.	3.8	14
46488	Uranyl(VI) sorption in calcium silicate hydrate phases. A quantum chemical study of tobermorite models. Applied Geochemistry, 2020, 113, 104463.	1.4	11
46489	Anchoring of single-platinum-adatoms on cyanographene: Experiment and theory. Applied Materials Today, 2020, 18, 100462.	2.3	14
46490	Parametrizing nonbonded interactions between silica and water from first principles. Applied Surface Science, 2020, 504, 144359.	3.1	7
46491	Effect of atomic passivation at Ni-MoS2 interfaces on contact behaviors. Current Applied Physics, 2020, 20, 132-136.	1.1	5
46492	First-principles study on the equilibrium shape of nanometer-sized body-centered cubic Cu precipitates in ferritic steels. Computational Materials Science, 2020, 172, 109351.	1.4	8
46493	Ab initio molecular dynamics study of SiO2 lithiation. Chemical Physics Letters, 2020, 739, 136933.	1.2	8
46494	Dopant screening of modified Fe2O3 oxygen carriers in chemical looping hydrogen production. Fuel, 2020, 262, 116489.	3.4	52
46495	Ab-initio study of electronic and magnetic properties of CoIrMnZ (Zâ€=â€Al, Si, Ga, Ge) Heusler alloys. Journal of Magnetism and Magnetic Materials, 2020, 498, 166092.	1.0	8

#	Article	IF	Citations
46496	Anti-perovskite carbides and nitrides A3BX: A new family of damage tolerant ceramics. Journal of Materials Science and Technology, 2020, 40, 64-71.	5.6	15
46497	Unveiling non-equilibrium metallurgical phases in dissimilar Al-Cu joints processed by vaporizing foil actuator welding. Materials and Design, 2020, 186, 108306.	3.3	20
46498	Superconductivity at 161â€¯K in thorium hydride ThH10: Synthesis and properties. Materials Today, 2020, 33, 36-44.	8.3	187
46499	Re-examining the nature of ordering in CaMnO<mml:math xmlns:mml="http://www.w3.org/1998/Math/MathML" display="inline" id="d1e1263" altimg="si21.svg"><mml:msub><mml:mrow /><mml:mrow><mml:mn>2</mml:mn></mml:mrow></mml:msub></mml:math>: The role of Mn-O covalency in the local structure. Physica B: Condensed Matter, 2020, 581, 411837.	1.3	1
46500	Interfacial magnetic coupling and the confinement effect of spin electrons for Ï„-MnAl/Ni multilayers. Physics Letters, Section A: General, Atomic and Solid State Physics, 2020, 384, 126096.	0.9	0
46501	Impact of V, Hf and Si on oxidation processes in Tiâ€“Alâ€“N: Insights from ab initio molecular dynamics. Surface and Coatings Technology, 2020, 381, 125125.	2.2	21
46502	Hydrogen Adsorption on Ir(111), Ir(100) and Ir(110)â€”Surface and Coverage Dependence. Surface Science, 2020, 692, 121514.	0.8	8
46503	Scanning tunneling microscopic investigations for studying conformational change of underlying Cu(111) and Ni(111) during graphene growth. Surface Science, 2020, 693, 121526.	0.8	6
46504	Magnetism and Distortions in Two-Dimensional Transition-Metal Dioxides: On the Quest for Intrinsic Magnetic Semiconductor Layers. Journal of Physical Chemistry C, 2020, 124, 2634-2643.	1.5	11
46505	Defining Multiple Configurations of Rubrene on a Ag(100) Surface with 5 Ã... Spatial Resolution via Ultrahigh Vacuum Tip-Enhanced Raman Spectroscopy. Journal of Physical Chemistry C, 2020, 124, 2420-2426.	1.5	26
46506	Magnetic proximity, magnetoresistance and spin filtering effect in a binuclear ferric phthalocyanine from first principles. Journal Physics D: Applied Physics, 2020, 53, 035305.	1.3	8
46507	Ab initio dielectric response function of diamond and other relevant high pressure phases of carbon. Journal of Physics Condensed Matter, 2020, 32, 095401.	0.7	17
46508	Realization of noble heterobilayers with enhanced optoelectronic properties. Applied Surface Science, 2020, 505, 144530.	3.1	4
46509	Metalâ€“organic framework-derived high conductivity Fe3C with porous carbon on graphene as advanced anode materials for aqueous battery-supercapacitor hybrid devices. Journal of Power Sources, 2020, 448, 227403.	4.0	60
46510	Dielectric, piezoelectric and nonlinear optical properties of polar iodate BiO(IO3) from first-principles studies. Journal of Solid State Chemistry, 2020, 281, 121057.	1.4	8
46511	Construction of layered h-BN/TiO2 hetero-structure and probing of the synergetic photocatalytic effect. Science China Materials, 2020, 63, 276-287.	3.5	39
46512	Hydrogen evolution over N-doped CoS2 nanosheets enhanced by superaerophobicity and electronic modulation. Applied Surface Science, 2020, 504, 144490.	3.1	50
46513	Wannier90 as a community code: new features and applications. Journal of Physics Condensed Matter, 2020, 32, 165902.	0.7	807

#	Article	IF	Citations
46514	2D Hexagonal Boron Nitride/Cadmium Sulfide Heterostructure as a Promising Waterâ€Splitting Photocatalyst. Physica Status Solidi (B): Basic Research, 2020, 257, 1900431.	0.7	22
46515	Structural, electronic and magnetic properties of a ferromagnetic metal: Nb-doped EuTiO3. Journal of Magnetism and Magnetic Materials, 2020, 497, 166077.	1.0	7
46516	Ferroelectric and dipole control of band alignment in the two dimensional InTe/In₂Se₃ heterostructure. Journal of Physics Condensed Matter, 2020, 32, 055703.	0.7	19
46517	Room-temperature multiferroicity and diversified magnetoelectric couplings in 2D materials. National Science Review, 2020, 7, 373-380.	4.6	50
46518	Electrochemically Derived Grapheneâ€Like Carbon Film as a Superb Substrate for Highâ€Performance Aqueous Znâ€Ion Batteries. Advanced Functional Materials, 2020, 30, 1907120.	7.8	78
46519	Blue Light Emitting Defective Nanocrystals Composed of Earthâ€Abundant Elements. Angewandte Chemie, 2020, 132, 870-877.	1.6	12
46520	Comparison of Ethylation at External Surface and Internal Cavity of Hâ€MCMâ€22 Zeolite from Theoretical Calculations. Chinese Journal of Chemistry, 2020, 38, 50-56.	2.6	5
46521	Atomic scale configuration of planar defects in the Nb-rich C14 Laves phase NbFe2. Acta Materialia, 2020, 183, 362-376.	3.8	29
46522	Crystalline isotype heptazine-/triazine-based carbon nitride heterojunctions for an improved hydrogen evolution. Applied Catalysis B: Environmental, 2020, 268, 118381.	10.8	130
46523	Highly accurate prediction of material optical properties based on density functional theory. Computational Materials Science, 2020, 172, 109315.	1.4	33
46524	An investigation concerning generalized stacking fault behavior of AlCoxCrFeNi (0.25 â‰¤ x â‰¤ 2) high entropy alloys: Insights from first-principles study. Journal of Alloys and Compounds, 2020, 818, 152928.	2.8	23
46525	Intrinsic mechanical behavior of MgAgSb thermoelectric material: An ab initio study. Journal of Materiomics, 2020, 6, 24-32.	2.8	5
46526	Strain engineering of magnetic proximity effect and spin-orbit torque in heavy metal/ferromagnet heterostructures. Journal of Magnetism and Magnetic Materials, 2020, 498, 166112.	1.0	2
46527	Electronic structure based design of thin film metallic glasses with superior fracture toughness. Materials and Design, 2020, 186, 108327.	3.3	13
46528	Solution-Processed Sb₂S₃ Planar Thin Film Solar Cells with a Conversion Efficiency of 6.9% at an Open Circuit Voltage of 0.7 V Achieved via Surface Passivation by a SbCl₃ Interface Layer. ACS Applied Materials & Interfaces, 2020, 12, 4970-4979.	4.0	100
46529	Elastic properties of the molecular crystals of hydrocarbons from first principles calculations. Journal of Physics Condensed Matter, 2020, 32, 085704.	0.7	3
46530	Strengthening boron carbide through lithium dopant. Journal of the American Ceramic Society, 2020, 103, 2012-2023.	1.9	14
46531	Heme Cofactorâ€Resembling Feâ€“N Single Site Embedded Graphene as Nanozymes to Selectively Detect H₂O₂ with High Sensitivity. Advanced Functional Materials, 2020, 30, 1905410.	7.8	171

#	Article	IF	Citations
46532	Critical Assessment of the DFTâ€‰+â€‰U Approach for the Prediction of Vanadium Dioxide Properties. Journal of Computational Chemistry, 2020, 41, 258-265.	1.5	34
46533	Deepâ€Level Defects and Impurities in InGaN Alloys. Physica Status Solidi (B): Basic Research, 2020, 257, 1900534.	0.7	13
46534	Surface speciation of Co based Fischer-Tropsch catalyst under reaction conditions: Deactivation by coke or by oxidation?. Applied Catalysis A: General, 2020, 590, 117332.	2.2	9
46535	DFT study on H2 and H adsorption and the electronic properties of single atom Cu modified Fe (1â€¯1â€¯1) surface. Applied Surface Science, 2020, 505, 144526.	3.1	7
46536	Ionic liquid-reinforced carbon nanofiber matrix enabled lean-electrolyte Li-S batteries via electrostatic attraction. Energy Storage Materials, 2020, 26, 378-384.	9.5	25
46537	Pyrolysis behaviors of coal-related model compounds catalyzed by pyrite. Fuel, 2020, 262, 116526.	3.4	10
46538	Metal oxide sub-nanoclusters decorated Ni catalyst for selective hydrogenation of adiponitrile to hexamethylenediamine. Journal of Catalysis, 2020, 381, 14-25.	3.1	22
46539	Segregation and aggregation of rhenium in tungsten grain boundary: Energetics, configurations and strengthening effects. Journal of Nuclear Materials, 2020, 528, 151867.	1.3	16
46540	A dual-carbon-anchoring strategy to fabricate flexible LiMn2O4 cathode for advanced lithium-ion batteries with high areal capacity. Nano Energy, 2020, 67, 104256.	8.2	46
46541	Structural, magnetic and electronic properties of FeRhxPd1-x compounds: Ab initio study. Physica B: Condensed Matter, 2020, 578, 411882.	1.3	2
46542	A coverage dependent study of the adsorption of pyridine on the (111) coinage metal surfaces. Surface Science, 2020, 693, 121525.	0.8	12
46543	A Firstâ€Principles Study of Electronic Properties of Twisted MoTe 2. Physica Status Solidi (B): Basic Research, 2020, 257, 1900412.	0.7	6
46544	Probing the efficiency of platinum nanotubes for the H2 production by water gas shift reaction: A DFT study. Applied Catalysis B: Environmental, 2020, 263, 118301.	10.8	19
46545	High-efficient electrocatalytic overall water splitting over vanadium doped hexagonal Ni0.2Mo0.8N. Applied Catalysis B: Environmental, 2020, 263, 118330.	10.8	111
46546	Understanding oxygen vacancies in disorder-engineered surface and subsurface of CaTiO3 nanosheets on photocatalytic hydrogen evolution. Applied Catalysis B: Environmental, 2020, 267, 118378.	10.8	86
46547	First-principles study of surface properties of crystalline and amorphous uranium aluminides. Applied Surface Science, 2020, 502, 144132.	3.1	5
46548	Multilayer boron nitride nanofilm as an effective barrier for atomic oxygen irradiation. Applied Surface Science, 2020, 504, 144394.	3.1	6
46549	Rational design of a PC3 monolayer: A high-capacity, rapidly charging anode material for sodium-ion batteries. Carbon, 2020, 157, 420-426.	5.4	49

#	Article	IF	Citations
46550	Surface engineering donor and acceptor sites with enhanced charge transport for low-overpotential lithiumâ€“oxygen batteries. Energy Storage Materials, 2020, 25, 52-61.	9.5	28
46551	The structural, electronic, magnetic and mechanical properties of d0 binary Heusler alloys XF3 (X =) Tj ETQq1 1 0.784314 rgBT /Overlock	1.9	13
46552	First-principles molecular dynamics simulations on the local structure and thermo-kinetic properties of molten magnesium chloride. Journal of Molecular Liquids, 2020, 298, 112063.	2.3	40
46553	Exploring Two-Dimensional Materials Thermodynamic Stability via Machine Learning. ACS Applied Materials & Interfaces, 2020, 12, 20149-20157.	4.0	80
46554	Lowâ€Bandgap Seâ€Deficient Antimony Selenide as a Multifunctional Polysulfide Barrier toward Highâ€Performance Lithiumâ€“Sulfur Batteries. Advanced Materials, 2020, 32, e1904876.	11.1	206
46555	Investigation of 4fâ€Related Electronic Transitions of Rareâ€Earth Doped ZnO Luminescent Materials: Insights from Firstâ€Principles Calculations. ChemPhysChem, 2020, 21, 51-58.	1.0	23
46556	Electrochemical CO ₂ reduction in confined space: Enhanced activity of metal catalysts by graphene overlayer. International Journal of Energy Research, 2020, 44, 784-794.	2.2	9
46557	Solute segregation induced sandwich structure in Al-Cu(-Au) alloys. Acta Materialia, 2020, 184, 17-29.	3.8	28
46558	Interaction of Ge with single layer GaAs: From Ge-island nucleation to formation of novel stable monolayers. Applied Surface Science, 2020, 505, 144218.	3.1	1
46559	Two-dimensional H-TiO2/MoS2(WS2) van der Waals heterostructures for visible-light photocatalysis and energy conversion. Applied Surface Science, 2020, 504, 144425.	3.1	48
46560	Strain rate and temperature effects on the mechanical properties of TiN/VN composite: Molecular dynamics study. Journal of Alloys and Compounds, 2020, 814, 152151.	2.8	7
46561	Pressure induced superconductive 10-fold coordinated TaS₂: a first-principles study. Journal of Physics Condensed Matter, 2020, 32, 085402.	0.7	7
46562	Prediction of staggered stacking 2D BeP semiconductor with unique anisotropic electronic properties. Journal of Physics Condensed Matter, 2020, 32, 085301.	0.7	2
46563	Magnetic order and valence fluctuation in a Puï£¿Ga intermetallic compound studied via a first principles calculation. International Journal of Quantum Chemistry, 2020, 120, e26105.	1.0	7
46564	Pressure-driven catalyst synthesis of Co-doped Fe C@Carbon nano-onions for efficient oxygen evolution reaction. Applied Catalysis B: Environmental, 2020, 268, 118385.	10.8	48
46565	First-principles study on the electronic and magnetic properties of P edge-doped armchair germanium selenide nanoribbon. Computational Materials Science, 2020, 172, 109348.	1.4	16
46566	Crystal facets engineering and rGO hybridizing for synergistic enhancement of photocatalytic activity of nickel disulfide. Journal of Hazardous Materials, 2020, 384, 121402.	6.5	11
46567	MXenes induce epitaxial growth of size-controlled noble nanometals: A case study for surface enhanced Raman scattering (SERS). Journal of Materials Science and Technology, 2020, 40, 119-127.	5.6	73

#	Article	IF	Citations
46568	All roads lead to Rome: Sodiation of different-stacked SnS2. Nano Energy, 2020, 67, 104276.	8.2	14
46569	Effect of doping 3d transition metal (Fe, Co, and Ni) on the electronic, magnetic and optical properties of pentagonal ZnO2 monolayer. Physica E: Low-Dimensional Systems and Nanostructures, 2020, 117, 113806.	1.3	12
46570	Methane dehydrogenation on Cu and Ni surfaces with low and moderate oxygen coverage. International Journal of Quantum Chemistry, 2020, 120, e26065.	1.0	6
46571	Electronic Structures and Catalytic Activities of Niobium Oxides as Electrocatalysts in Liquidâ€Junction Photovoltaic Devices. Solar Rrl, 2020, 4, 1900430.	3.1	29
46572	Electronic and Magnetic Tunability of SnSe Monolayer via Doping of Transition-Metal Atoms. Journal of Electronic Materials, 2020, 49, 290-296.	1.0	13
46573	Structural, Electronic and Thermoelectric Properties of Pb1â^'xSnxTe Alloys. Journal of Electronic Materials, 2020, 49, 586-592.	1.0	4
46574	The formations of C2 species and CH4 over the Co2C catalyst in Fischer-Tropsch synthesis: The effect of surface termination on product selectivity. Computational Materials Science, 2020, 172, 109345.	1.4	2
46575	Surface Ni-rich engineering towards highly stable Li1.2Mn0.54Ni0.13Co0.13O2 cathode materials. Energy Storage Materials, 2020, 25, 76-85.	9.5	47
46576	Effective promotion of oxygen reduction activity by rare earth doping in simple perovskite cathodes for intermediate-temperature solid oxide fuel cells. Journal of Power Sources, 2020, 446, 227360.	4.0	67
46577	Effect of tungsten on the vacancy behaviors in Taâ€“W alloys from first-principles calculations. Solid State Communications, 2020, 306, 113767.	0.9	11
46578	MoS₂/MoTe₂ Heterostructure Tunnel FETs Using Gated Schottky Contacts. Advanced Functional Materials, 2020, 30, 1905970.	7.8	50
46579	First-principles Predictions on Half-Metallic, Mechanical, and Acoustic Properties of CuHg2Ti-Type Mn2LiZ (Z=As, Sb) Compounds. Journal of Superconductivity and Novel Magnetism, 2020, 33, 1065-1072.	0.8	3
46580	Effect of defects on the electronic structure of a PbI2/MoS2 van der Waals heterostructure: A first-principles study. Science China: Physics, Mechanics and Astronomy, 2020, 63, 1.	2.0	1
46581	Extended Î±-phase Bi atomic layer on Si(1â€¯1â€¯1) fabricated by thermal desorption. Applied Surface Science, 2020, 504, 144103.	3.1	6
46582	Enhanced valley polarization at valence/conduction band in transition-metal-doped WTe2 under strain force. Applied Surface Science, 2020, 504, 144367.	3.1	27
46583	The gas sensing performance of borophene/MoS2 heterostructure. Applied Surface Science, 2020, 504, 144412.	3.1	59
46584	First-principles study on the stability and work function of low-index surfaces of TiB2. Computational Materials Science, 2020, 172, 109356.	1.4	18
46585	Adsorption energy engineering of nickel oxide hybrid nanosheets for high areal capacity flexible lithium-ion batteries. Energy Storage Materials, 2020, 25, 41-51.	9.5	261

#	Article	IF	Citations
46586	Chemical and structural engineering of transition metal boride towards excellent and sustainable hydrogen evolution reaction. Nano Energy, 2020, 67, 104245.	8.2	79
46587	Effects of vacancy defects on electronic properties of 2D group-IV Tellurides (XTe, X = Si, Ge, Sn and) Tj ETQq1 1 0.784314 rgBT /Over	1.4	3
46588	Non-Janus WSSe/MoSSe Heterobilayer and Its Photocatalytic Band Offset. Journal of Physical Chemistry C, 2020, 124, 3812-3819.	1.5	11
46589	Unveiling multiferroic proximity effect in graphene. 2D Materials, 2020, 7, 015020.	2.0	7
46590	Theoretical study of the microscopic origin of magnetocrystalline anisotropy in Fe₁₆N₂ and its alloys: comparison with the other L1₀ alloys. Journal of Physics Condensed Matter, 2020, 32, 035801.	0.7	12
46591	Silicene, Siloxene, or Silicane? Revealing the Structure and Optical Properties of Silicon Nanosheets Derived from Calcium Disilicide. Chemistry of Materials, 2020, 32, 795-804.	3.2	59
46592	Atomicâ€Scale Mechanism of Unidirectional Oxide Growth. Advanced Functional Materials, 2020, 30, 1906504.	7.8	30
46593	Construction of host-guest supramolecular bilayer networks at liquid/solid interfaces by scanning tunneling microscopy. Chemical Physics, 2020, 530, 110600.	0.9	3
46594	The effect of N-vacancy and In aggregation on the properties of InAlN. Computational Materials Science, 2020, 172, 109384.	1.4	5
46595	Magnesium partitioning between silicate melt and liquid iron using first-principles molecular dynamics: Implications for the early thermal history of the Earth's core. Earth and Planetary Science Letters, 2020, 531, 115934.	1.8	10
46596	In situ electrochemically synthesized Pt-MoO3â^'x nanostructure catalysts for efficient hydrogen evolution reaction. Journal of Catalysis, 2020, 381, 1-13.	3.1	35
46597	First-principles study of the electronic, magnetic and optical properties of Fe3Se4 in its monoclinic phase. Journal of Magnetism and Magnetic Materials, 2020, 498, 166157.	1.0	6
46598	Tuning electronic structure and optical properties of C3N by B doping. Physica B: Condensed Matter, 2020, 577, 411807.	1.3	2
46599	The energy band engineering for the high-performance infrared photodetectors constructed by CdTe/MoS₂ heterojunction. Journal of Physics Condensed Matter, 2020, 32, 065004.	0.7	20
46600	Survey of acceptor dopants in SrTiO₃: Factors limiting room temperature hole concentration. Journal of the American Ceramic Society, 2020, 103, 1156-1173.	1.9	10
46601	Origin of the existence of interâ€granular glassy films in Î²â€Si₃N₄. Journal of the American Ceramic Society, 2020, 103, 737-743.	1.9	4
46602	An abnormal incorporation behavior of Th in Gd 2 Zr 2 O 7 : A firstâ€principles study. Journal of the American Ceramic Society, 2020, 103, 1846-1853.	1.9	2
46603	Firstâ€Principles Study of Metal Atoms Adsorption on 2D Dumbbell C₄N. Physica Status Solidi (B): Basic Research, 2020, 257, 1900205.	0.7	9

#	Article	IF	Citations
46604	The pivotal roles of spatially separated charge localization centers on the molecules activation and photocatalysis mechanism. Applied Catalysis B: Environmental, 2020, 262, 118251.	10.8	89
46605	Carbon vacancy in C3N4 nanotube: Electronic structure, photocatalysis mechanism and highly enhanced activity. Applied Catalysis B: Environmental, 2020, 262, 118281.	10.8	162
46606	Insight to unprecedented catalytic activity of double-nitrogen defective metal-free catalyst: Key role of coal gangue. Applied Catalysis B: Environmental, 2020, 263, 118316.	10.8	51
46607	A theoretical study of the reverse waterâ€gas shift reaction on Ni(111) and Ni(311) surfaces. Canadian Journal of Chemical Engineering, 2020, 98, 740-748.	0.9	25
46608	The Synergy of Dilute Pd and Surface Oxygen Species for Methane Upgrading on Au₃Pd(111). Energy Technology, 2020, 8, 1900732.	1.8	3
46609	Planar Directionâ€Dependent Interfacial Properties in Monolayer In₂Se₃â€“Metal Contacts. Physica Status Solidi (B): Basic Research, 2020, 257, 1900198.	0.7	19
46610	Low Lying Magnetic States of the Mixed Valence Cobalt Ludwigite. Physica Status Solidi (B): Basic Research, 2020, 257, 1900298.	0.7	3
46611	Pressure variations of the 5f magnetism in UH3. Journal of Magnetism and Magnetic Materials, 2020, 497, 165993.	1.0	6
46612	Point-defect engineering of MoN/TaN superlattice films: A first-principles and experimental study. Materials and Design, 2020, 186, 108211.	3.3	11
46613	Highly-efficient overall water splitting in 2D Janus group-III chalcogenide multilayers: the roles of intrinsic electric filed and vacancy defects. Science Bulletin, 2020, 65, 27-34.	4.3	54
46614	Graphite felt incorporated with MoS2/rGO for electrochemical detoxification of high-arsenic fly ash. Chemical Engineering Journal, 2020, 382, 122763.	6.6	20
46615	Coverage-dependent acrylonitrile adsorption and electrochemical reduction kinetics on Pb electrode. Chemical Engineering Journal, 2020, 382, 123006.	6.6	10
46616	Interfacial potassium induced enhanced Raman spectroscopy for single-crystal TiO2 nanowhisker. Chinese Journal of Chemical Engineering, 2020, 28, 889-895.	1.7	10
46617	A multi-method, multi-scale theoretical study of He and Ne diffusion in zircon. Geochimica Et Cosmochimica Acta, 2020, 268, 348-367.	1.6	22
46618	The atomic structure of a bulk metallic glass resolved by scanning tunneling microscopy and ab-initio molecular dynamics simulation. Journal of Alloys and Compounds, 2020, 816, 152680.	2.8	10
46619	Solid-solution hardening of WC by rhenium. Journal of the European Ceramic Society, 2020, 40, 333-340.	2.8	17
46620	Adsorption behaviors of HCN, SO2, H2S and NO molecules on graphitic carbon nitride with Mo atom decoration. Applied Surface Science, 2020, 501, 144199.	3.1	38
46621	Equilibrium morphology evolution of FCC cobalt nanoparticle under CO and hydrogen environments. Applied Surface Science, 2020, 504, 144469.	3.1	9

#	Article	IF	Citations
46622	Ferromagnetic ordering in cobalt doped methylammonium lead bromide: An ab-initio study. Computational Condensed Matter, 2020, 22, e00444.	0.9	3
46623	Structural, mechanical and electronic properties study on group 5 transition metals ternary mononitrides from first-principles calculations. Journal of Alloys and Compounds, 2020, 813, 152246.	2.8	13
46624	The role of A-site ion on proton diffusion in perovskite oxides (ABO3). Journal of Power Sources, 2020, 445, 227327.	4.0	39
46625	The ferromagnetic and half-metal properties of hydrogen adatoms, fluorine adatoms and boron adatoms adsorbed at edges of zigzag silicene nanoribbon. Physica E: Low-Dimensional Systems and Nanostructures, 2020, 116, 113733.	1.3	9
46626	Dopant-induced magnetism in platinum telluride monolayer regulated by strain engineering. Physica E: Low-Dimensional Systems and Nanostructures, 2020, 116, 113741.	1.3	4
46627	Mechanical properties, lattice thermal conductivity, infrared and Raman spectrum of the fullerite C24. Physics Letters, Section A: General, Atomic and Solid State Physics, 2020, 384, 126035.	0.9	7
46628	A novel metallic silicon hexaboride, Cmca-B6Si. Physics Letters, Section A: General, Atomic and Solid State Physics, 2020, 384, 126075.	0.9	7
46629	Effects of LaAlO3 and La2O2S inclusions on the initialization of localized corrosion of pipeline steels in NaCl solution. Scripta Materialia, 2020, 177, 151-156.	2.6	38
46630	Thermodynamics of low-index surfaces and particle shapes of Y(OH)3 under typical hydrothermal conditions. Surface Science, 2020, 691, 121490.	0.8	1
46631	Biaxial strain tunable photocatalytic properties of 2D ZnO/GeC heterostructure. Journal Physics D: Applied Physics, 2020, 53, 015104.	1.3	65
46632	Monolayer SiP2S6: metal-free photocatalyst with spontaneous hydrogen and oxygen evolution half reactions. Journal Physics D: Applied Physics, 2020, 53, 015304.	1.3	5
46633	Surface and interfacial study of atomic layer deposited Al₂O₃ on MoTe₂ and WTe₂. Nanotechnology, 2020, 31, 055704.	1.3	9
46634	Van der Waals SnSe 2(1â^' x) S 2 x Alloys: Compositionâ€Dependent Bowing Coefficient and Electronâ€“Phonon Interaction. Advanced Functional Materials, 2020, 30, 1908092.	7.8	18
46635	Cubic NaSbS₂ as an Ionicâ€“Electronic Coupled Semiconductor for Switchable Photovoltaic and Neuromorphic Device Applications. Advanced Materials, 2020, 32, e1906976.	11.1	34
46636	Ultrathin ZnIn2S4 nanosheets with active (110) facet exposure and efficient charge separation for cocatalyst free photocatalytic hydrogen evolution. Applied Catalysis B: Environmental, 2020, 265, 118616.	10.8	132
46637	Exploration of pressure induced phase transitions and thermo-mechanical properties in LuX (X=As, Sb,) Tj ETQq1 1 0.784314 rgBT /Ov	0.9	0
46638	Reversible High Capacity and Reaction Mechanism of Cr₂(NCN)₃ Negative Electrodes for Liâ€Ion Batteries. Energy Technology, 2020, 8, 1901260.	1.8	9
46639	Charge reduction in ions in the ionic liquid 1-ethy-2,3-dimethylimidazolium bis(trifluoromethanesulfonyl)imide on the Au(111) surface. Theoretical Chemistry Accounts, 2020, 139, 1.	0.5	1

#	Article	IF	Citations
46640	Crystal structure of NaFeO2 and NaAlO2 and their correlation with ionic conductivity. Ionics, 2020, 26, 2917-2926.	1.2	8
46641	Electronic structure and spin texture of Mo/N co-doped polar 2D-SiC. Applied Surface Science, 2020, 509, 145193.	3.1	3
46642	Shape change of submicron nickel particles under hydrogen and nickel chloride vapor. Applied Surface Science, 2020, 509, 145274.	3.1	4
46643	Segregation of S at Mo(001)/MoSi2(001) interface. Ceramics International, 2020, 46, 5050-5057.	2.3	8
46644	Europium (III) doped LiNa2B5P2O14 phosphor: Surface analysis, DFT calculations and luminescent properties. Journal of Alloys and Compounds, 2020, 822, 153606.	2.8	32
46645	d-electron-dependent transparent conducting oxide of V-doped ZnO thin films. Journal of Alloys and Compounds, 2020, 822, 153706.	2.8	12
46647	MnSnTeO6: A Chiral Antiferromagnet Prepared by a Two-Step Topotactic Transformation. Inorganic Chemistry, 2020, 59, 1532-1546.	1.9	0
46648	Predicted Optimal Bifunctional Electrocatalysts for the Hydrogen Evolution Reaction and the Oxygen Evolution Reaction Using Chalcogenide Heterostructures Based on Machine Learning Analysis of in Silico Quantum Mechanics Based High Throughput Screening. Journal of Physical Chemistry Letters, 2020, 11, 869-876.	2.1	58
46649	Understanding the Enhancement of the Catalytic Properties of Goethite by Transition Metal Doping: Critical Role of O* Formation Energy Relative to OH* and OOH*. ACS Applied Energy Materials, 2020, 3, 1634-1643.	2.5	17
46650	Remarkably High Thermoelectric Efficiencies of the Half-Heusler Compounds BXGa (X = Be, Mg, and Ca). ACS Applied Materials & Interfaces, 2020, 12, 5838-5846.	4.0	39
46651	A Mechanistic Analysis of Phase Evolution and Hydrogen Storage Behavior in Nanocrystalline Mg(BH₄)₂ within Reduced Graphene Oxide. ACS Nano, 2020, 14, 1745-1756.	7.3	29
46652	Theoretical Insight into the Role of Defects and Facets in the Selectivity of Products in Water Oxidation over Bismuth Vanadate (BiVO₄). ACS Sustainable Chemistry and Engineering, 2020, 8, 1980-1988.	3.2	15
46653	uMBD: A Materials-Ready Dispersion Correction That Uniformly Treats Metallic, Ionic, and van der Waals Bonding. Journal of the American Chemical Society, 2020, 142, 2346-2354.	6.6	29
46654	The adsorption characteristics and degradation mechanism of tinidazole on an anatase TiO₂ surface: a DFT study. RSC Advances, 2020, 10, 2104-2112.	1.7	10
46655	Buckling of blue phosphorus nanotubes under axial compression: Insights from molecular dynamics simulations. Journal of Applied Physics, 2020, 127, 014301.	1.1	3
46656	Magnetic ground state of face-centered-cubic structure of iron. Journal of Physics Condensed Matter, 2020, 32, 165806.	0.7	12
46657	Single-crystal synthesis and properties of the open-framework allotrope Si₂₄. Journal of Physics Condensed Matter, 2020, 32, 194001.	0.7	7
46658	Promoted CO2 electroreduction over indium-doped SnP3: A computational study. Journal of Energy Chemistry, 2020, 48, 1-6.	7.1	19

#	Article	IF	Citations
46659	The trend of chemisorption of hydrogen and oxygen atoms on pure transition metals: Magnetism justifies unexpected behaviour of Mn and Cr. Materials Today Communications, 2020, 23, 100894.	0.9	9
46660	The application of artificial neural-network potentials for flexoelectricity: Performance for anatase-type TiO2. Physics Letters, Section A: General, Atomic and Solid State Physics, 2020, 384, 126217.	0.9	5
46661	Introduction to Carbon-Based Nanostructures. , 2020, , 1-10.		0
46662	The New Family of Two-Dimensional Materials and van der Waals Heterostructures. , 2020, , 70-91.		0
46663	Quantum Transport: General Concepts. , 2020, , 92-119.		0
46664	Klein Tunneling and Ballistic Transport in Graphene and Related Materials. , 2020, , 120-144.		0
46665	Quantum Transport in Disordered Graphene-Based Materials. , 2020, , 145-209.		0
46666	Ab Initio Investigation of CO2 Adsorption on 13-Atom 4d Clusters. Journal of Chemical Information and Modeling, 2020, 60, 537-545.	2.5	20
46667	Influence of Electrolyte Composition on Ultrafast Interfacial Electron Transfer in Fe-Sensitized TiO₂-Based Solar Cells. Journal of Physical Chemistry C, 2020, 124, 1794-1811.	1.5	19
46668	Numerical Method for Calculating Nanocrystalsâ€™ Edge Energies from Experimentally Observed Shape Evolution. Journal of Physical Chemistry C, 2020, 124, 3835-3842.	1.5	3
46669	Self-Assembly of a Two-Dimensional Sheet with Ta@Si₁₆ Superatoms and Its Magnetic and Photocatalytic Properties. Journal of Physical Chemistry C, 2020, 124, 6861-6870.	1.5	18
46670	Structure and Chemical State of Cesium on Well-Defined Cu(111) and Cu₂O/Cu(111) Surfaces. Journal of Physical Chemistry C, 2020, 124, 3107-3121.	1.5	16
46671	Efficient and stable Ruddlesdenâ€“Popper perovskite solar cell with tailored interlayer molecular interaction. Nature Photonics, 2020, 14, 154-163.	15.6	443
46672	Electronic structures of 24-valence-electron full Heusler compounds investigated by density functional and GW calculations. Journal of Physics Condensed Matter, 2020, 32, 175501.	0.7	4
46673	ISOBAM-stabilized Ni²⁺ colloidal catalysts: high catalytic activities for hydrogen generation from hydrolysis of KBH₄. Nanotechnology, 2020, 31, 134003.	1.3	12
46674	Light Absorption Properties and Electronic Band Structures of Leadâ€Vanadium Oxyhalide Apatites Pb 5 (VO 4) 3 X (X=F, Cl, Br, I). Chemistry - an Asian Journal, 2020, 15, 540-545.	1.7	6
46675	Tabular electrical conductivity for aluminium. Contributions To Plasma Physics, 2020, 60, e201900123.	0.5	5
46676	Variational projector augmented-wave method: theoretical analysis and preliminary numerical results. Numerische Mathematik, 2020, 144, 271-321.	0.9	3

#	Article	IF	Citations
46677	The effect of atomic point charges on adsorption isotherms of CO2 and water in metal organic frameworks. Adsorption, 2020, 26, 663-685.	1.4	36
46678	Optical Properties of the Oxygen Vacancy in KNbO3 Crystal. Journal of Electronic Materials, 2020, 49, 2137-2143.	1.0	2
46679	Evolution and Growth Mechanism of Cu2(In,Sn) Formed Between In-48Sn Solder and Polycrystalline Cu During Long-Time Liquid-State Aging. Journal of Electronic Materials, 2020, 49, 2651-2659.	1.0	4
46680	Designing rare-earth free permanent magnets in heusler alloys via interstitial doping. Acta Materialia, 2020, 186, 355-362.	3.8	20
46681	An integrated experimental and computational study of diffusion and atomic mobility of the aluminumâ€“magnesium system. Acta Materialia, 2020, 189, 214-231.	3.8	29
46682	Accelerated design of novel W-free high-strength Co-base superalloys with extremely wide Î³/Î³Ê¹ region by machine learning and CALPHAD methods. Acta Materialia, 2020, 186, 425-433.	3.8	57
46683	Theoretical prediction of graphene-based single-atom iron as a novel catalyst for catalytic oxidation of Hg0 by O2. Applied Surface Science, 2020, 508, 145035.	3.1	27
46684	Modulating geometric, electronic, gas sensing and catalytic properties of single-atom Pd supported on divacancy and N-doped graphene sheets. Applied Surface Science, 2020, 508, 145245.	3.1	34
46685	Structure, hydration, and chloride ingress in C-S-H: Insight from DFT calculations. Cement and Concrete Research, 2020, 129, 105965.	4.6	30
46686	Ab initio molecular dynamics simulation of Nd3+ incorporation in calcite. Chemical Geology, 2020, 534, 119460.	1.4	2
46687	First-principles investigation on stability and oxygen adsorption behavior of a O/B2 interface in Ti2AlNb alloys. Journal of Alloys and Compounds, 2020, 818, 152926.	2.8	15
46688	Detrimental role of residual surface acid ions on ozone decomposition over Ce-modified Î³-MnO2 under humid conditions. Journal of Environmental Sciences, 2020, 91, 43-53.	3.2	34
46689	In-situ characterization of initial marine corrosion induced by rare-earth elements modified inclusions in Zr-Ti deoxidized low-alloy steels. Journal of Materials Research and Technology, 2020, 9, 1412-1424.	2.6	35
46690	Calcination of ytterbia aerogels leads to ferromagnetic nanoporous ytterbium oxide networks. Materials Letters, 2020, 261, 126866.	1.3	3
46691	Efficient electroreduction of CO2 to CO by Ag-decorated S-doped g-C3N4/CNT nanocomposites at industrial scale current density. Materials Today Physics, 2020, 12, 100176.	2.9	39
46692	Influence of defects on thermoluminescence in pristine and doped LiMgPO4. Nuclear Instruments & Methods in Physics Research B, 2020, 465, 1-5.	0.6	7
46693	Effects of gas adsorption on electronic and optical properties of palladium-doped graphene: First-principles study. Physica E: Low-Dimensional Systems and Nanostructures, 2020, 118, 113879.	1.3	21
46694	A special triple point in non-centrosymmetric materials Zn3In2Se6 and In2Se3. Physics Letters, Section A: General, Atomic and Solid State Physics, 2020, 384, 126216.	0.9	1

#	Article	IF	Citations
46695	Thermoelectric properties of monolayer Î±-Te: Low lattice thermal conductivity and extremely high dimensionless figure of merit. Physics Letters, Section A: General, Atomic and Solid State Physics, 2020, 384, 126222.	0.9	4
46696	Electronic structure and spin properties study on 2D h-BN nanosheet with Ti or Fe doping. Solid State Communications, 2020, 307, 113803.	0.9	18
46697	Regulating electronic and magnetic properties in chromium trihalide monolayer. Surface Science, 2020, 694, 121560.	0.8	3
46698	Bond Electronegativity as Hydrogen Evolution Reaction Catalyst Descriptor for Transition Metal (TM) Tj ETQq1 1 0.784314 rgBT /Ove	3.2	45
46699	Linear-Response Time-Dependent Density Functional Theory with Stochastic Range-Separated Hybrids. Journal of Chemical Theory and Computation, 2020, 16, 1064-1072.	2.3	19
46700	Structure of Blue Phosphorus Grown on Au(111) Surface Revisited. Journal of Physical Chemistry C, 2020, 124, 2024-2029.	1.5	31
46701	Computational Screening of Single Non-Noble Transition-Metal Atoms Confined Inside Boron Nitride Nanotubes for CO Oxidation. Journal of Physical Chemistry C, 2020, 124, 2030-2038.	1.5	10
46702	Two-Dimensional Ferroelastic Semiconductors in Nb₂SiTe₄ and Nb₂GeTe₄ with Promising Electronic Properties. Journal of Physical Chemistry Letters, 2020, 11, 497-503.	2.1	37
46703	Revealing the Local Electronic Structure of a Single-Layer Covalent Organic Framework through Electronic Decoupling. Nano Letters, 2020, 20, 963-970.	4.5	28
46704	Changing the Phosphorus Allotrope from a Square Columnar Structure to a Planar Zigzag Nanoribbon by Increasing the Diameter of Carbon Nanotube Nanoreactors. Nano Letters, 2020, 20, 1280-1285.	4.5	29
46705	Tuning Palladium Nickel Phosphide toward Efficient Oxygen Evolution Performance. ACS Applied Energy Materials, 2020, 3, 879-888.	2.5	21
46706	New Dimorphs of Na₅V(PO₄)₂F₂ as an Ultrastable Cathode Material for Sodium-Ion Batteries. ACS Applied Energy Materials, 2020, 3, 1181-1189.	2.5	16
46707	Stability and Sensing Enhancement by Nanocubic CeO₂ with {100} Polar Facets on Graphene for NO₂ at Room Temperature. ACS Applied Materials & Interfaces, 2020, 12, 4722-4731.	4.0	23
46708	Artificial Multiferroics and Enhanced Magnetoelectric Effect in van der Waals Heterostructures. ACS Applied Materials & Interfaces, 2020, 12, 6243-6249.	4.0	81
46709	One-Dimensional Sb₂Se₃ Enabling a Highly Flexible Photodiode for Light-Source-Free Heart Rate Detection. ACS Photonics, 2020, 7, 352-360.	3.2	53
46710	Combining experiment and computation to elucidate the optical properties of Ce³⁺ in Ba₅Si₈O₂₁. Physical Chemistry Chemical Physics, 2020, 22, 2327-2336.	1.3	10
46711	Insight into the magnetic moment of iron borides: theoretical consideration from the local coordinative and electronic environment. Dalton Transactions, 2020, 49, 2168-2175.	1.6	2
46712	Single-atom transition metals supported on black phosphorene for electrochemical nitrogen reduction. Nanoscale, 2020, 12, 4903-4908.	2.8	107

#	Article	IF	Citations
46713	Unravelling the early oxidation mechanism of zinc phosphide (Zn₃P₂) surfaces by adsorbed oxygen and water: a first-principles DFT-D3 investigation. Physical Chemistry Chemical Physics, 2020, 22, 1444-1456.	1.3	15
46714	Mechano-chemical stability and water effect on gas selectivity in mixed-metal zeolitic imidazolate frameworks: a systematic investigation from van der Waals corrected density functional theory. Physical Chemistry Chemical Physics, 2020, 22, 1598-1610.	1.3	1
46715	Water dissociation and hydrogen evolution on the surface of Fe-based bulk metallic glasses. Physical Chemistry Chemical Physics, 2020, 22, 700-708.	1.3	8
46716	Quantum mechanical molecular dynamics simulations of polaron formation in methylammonium lead iodide perovskite. Physical Chemistry Chemical Physics, 2020, 22, 97-106.	1.3	23
46717	Combined density functional theory and molecular dynamics study of Sm_{0.75}A_{0.25}Co_{1â^'x}Mn_xO_{2.88} (A = Ca, Sr;) Tj ETQq0 0 0 rgBT /Overl Chemical Physics, 2020, 22, 692-699.	1.3	10
46718	First-principles study on the mechanism of photocatalytic reduction of nitrobenzene on the rutile TiO₂(110) surface. Physical Chemistry Chemical Physics, 2020, 22, 1187-1193.	1.3	14
46719	Thermodynamics of the formation of surface PtO2 stripes on Pt(111) in the absence of subsurface oxygen. Physical Chemistry Chemical Physics, 2020, 22, 10634-10640.	1.3	15
46720	Investigation of the Mn dopant-enhanced photoluminescence performance of lead-free Cs₂AgInCl₆ double perovskite crystals. Physical Chemistry Chemical Physics, 2020, 22, 1815-1819.	1.3	25
46721	Coexistence of three types of sodium motion in double molybdate Na₉Sc(MoO₄)₆: ²³Na and ⁴⁵Sc NMR data and ab initio calculations. Physical Chemistry Chemical Physics, 2020, 22, 144-154.	1.3	9
46722	Effects of a graphene substrate on the structure and properties of atomically thin metal sheets. Physical Chemistry Chemical Physics, 2020, 22, 667-673.	1.3	6
46723	From the perspectives of DFT calculations, thermodynamic modeling, and kinetic Monte Carlo simulations: the interaction between hydrogen and Sc₂C monolayers. Physical Chemistry Chemical Physics, 2020, 22, 4387-4401.	1.3	4
46724	How coverage influences thermodynamic and kinetic isotope effects for H₂/D₂ dissociative adsorption on transition metals. Catalysis Science and Technology, 2020, 10, 671-689.	2.1	26
46725	FSI-inspired solvent and â€œfull fluorosulfonylâ€•electrolyte for 4 V class lithium-metal batteries. Energy and Environmental Science, 2020, 13, 212-220.	15.6	198
46726	Controlling wettability, wet strength, and fluid transport selectivity of nanopaper with atomic layer deposited (ALD) sub-nanometer metal oxide coatings. Nanoscale Advances, 2020, 2, 356-367.	2.2	13
46727	High throughput study on magnetic ground states with Hubbard U corrections in transition metal dihalide monolayers. Nanoscale Advances, 2020, 2, 495-501.	2.2	25
46728	Mo₂B, an MBene member with high electrical and thermal conductivities, and satisfactory performances in lithium ion batteries. Nanoscale Advances, 2020, 2, 347-355.	2.2	38
46729	Computational screening of transition metal-doped phthalocyanine monolayers for oxygen evolution and reduction. Nanoscale Advances, 2020, 2, 710-716.	2.2	30
46730	Highly stable two-dimensional gold selenide with large in-plane anisotropy and ultrahigh carrier mobility. Nanoscale Horizons, 2020, 5, 366-371.	4.1	28

#	Article	IF	Citations
46731	Nano-makisu: highly anisotropic two-dimensional carbon allotropes made by weaving together nanotubes. Nanoscale, 2020, 12, 347-355.	2.8	3
46732	An unexpected surfactant role of immiscible nitrogen in the structural development of silver nanoparticles: an experimental and numerical investigation. Nanoscale, 2020, 12, 1749-1758.	2.8	21
46733	Complementary behaviour of EDL and HER activity in functionalized graphene nanoplatelets. Nanoscale, 2020, 12, 1790-1800.	2.8	10
46734	Composition-induced type I and direct bandgap transition metal dichalcogenides alloy vertical heterojunctions. Nanoscale, 2020, 12, 201-209.	2.8	15
46735	Predictive theoretical screening of phase stability for chemical order and disorder in quaternary 312 and 413 MAX phases. Nanoscale, 2020, 12, 785-794.	2.8	56
46736	Trace fluorinated-carbon-nanotube-induced lithium dendrite elimination for high-performance lithiumâ€“oxygen cells. Nanoscale, 2020, 12, 3424-3434.	2.8	14
46737	Hot carrier relaxation in Cs₂TiI_yBr_{6â^'y} (y = 0, 2 and 6) by a time-domain ab initio study. RSC Advances, 2020, 10, 958-964.	1.7	10
46738	Detection of key transient Cu intermediates in SSZ-13 during NH₃-SCR deNO_x by modulation excitation IR spectroscopy. Chemical Science, 2020, 11, 447-455.	3.7	52
46739	Toward a quantitative theoretical method for infrared and Raman spectroscopic studies on single-crystal electrode/liquid interfaces. Chemical Science, 2020, 11, 1425-1430.	3.7	9
46740	Ir₆In₃₂S₂₁, a polar, metal-rich semiconducting subchalcogenide. Chemical Science, 2020, 11, 870-878.	3.7	7
46741	Discordant nature of Cd in GeTe enhances phonon scattering and improves band convergence for high thermoelectric performance. Journal of Materials Chemistry A, 2020, 8, 1193-1204.	5.2	83
46742	Interlayer separation in hydrogen titanates enables electrochemical proton intercalation. Journal of Materials Chemistry A, 2020, 8, 412-421.	5.2	28
46743	Combined treatment of phonon scattering by electrons and point defects explains the thermal conductivity reduction in highly-doped Si. Journal of Materials Chemistry A, 2020, 8, 1273-1278.	5.2	30
46744	Interfacial stability and ionic conductivity enhanced by dopant segregation in eutectic ceramics: the role of Gd segregation in doped CeO₂/CoO and CeO₂/NiO interfaces. Journal of Materials Chemistry A, 2020, 8, 2591-2601.	5.2	5
46745	Band alignment in multilayered semiconductor homojunctions supported on metals. Journal of Materials Chemistry C, 2020, 8, 959-967.	2.7	15
46746	Superconductivity in predicted two dimensional XB₆ (X = Ga, In). Journal of Materials Chemistry C, 2020, 8, 1704-1714.	2.7	30
46747	Sunlight-activated yellow long persistent luminescence from Nb-doped Sr₃SiO₅:Eu²⁺ for warm-color mark applications. Journal of Materials Chemistry C, 2020, 8, 1143-1150.	2.7	46
46748	Role of W-site substitution on mechanical and electronic properties of cubic tungsten carbide. Journal of Physics Condensed Matter, 2020, 32, 145701.	0.7	5

#	Article	IF	Citations
46749	Distinguishing electronic contributions of surface and sub-surface transition metal atoms in Ti-based MXenes. 2D Materials, 2020, 7, 025015.	2.0	31
46750	A novel multiscale approach to brittle fracture of nano/microâ€sized components. Fatigue and Fracture of Engineering Materials and Structures, 2020, 43, 1630-1645.	1.7	9
46751	The Structural Stability of P2-Layered Na-Based Electrodes during Anionic Redox. Joule, 2020, 4, 420-434.	11.7	89
46752	Gallium Composition-Dependent Structural Phase Transitions in HoFe_{3â€“x}Ga_x(BO₃)₄ Solid Solutions: Crystal Growth, Structure, and Raman Spectroscopy Study. Crystal Growth and Design, 2020, 20, 1058-1069.	1.4	6
46753	Isoelectronic Doping and External Electric Field Regulate the Gas-Separation Performance of Graphdiyne. Journal of Physical Chemistry C, 2020, 124, 2712-2720.	1.5	14
46754	Theoretical Investigations of (Oxidative) Dehydrogenation of Propane to Propylene over Palladium Surfaces. Journal of Physical Chemistry C, 2020, 124, 3171-3176.	1.5	8
46755	Origin of Electronic Modification of Platinum in a Pt₃V Alloy and Its Consequences for Propane Dehydrogenation Catalysis. ACS Applied Energy Materials, 2020, 3, 1410-1422.	2.5	41
46756	Role of Transition Metals in Layered Double Hydroxides for Differentiating the Oxygen Evolution and Nonenzymatic Glucose Sensing. ACS Applied Materials & Interfaces, 2020, 12, 6193-6204.	4.0	48
46757	Rational Design and Characterization of Direct Z-Scheme Photocatalyst for Overall Water Splitting from Excited State Dynamics Simulations. ACS Catalysis, 2020, 10, 1976-1983.	5.5	120
46758	Strain engineering and epitaxial stabilization of halide perovskites. Nature, 2020, 577, 209-215.	13.7	417
46759	Proton-assisted growth of ultra-flat graphene films. Nature, 2020, 577, 204-208.	13.7	111
46760	Synthesis and properties of free-standing monolayer amorphous carbon. Nature, 2020, 577, 199-203.	13.7	250
46761	Dual-phase MoS₂ as a high-performance sodium-ion battery anode. Journal of Materials Chemistry A, 2020, 8, 2114-2122.	5.2	160
46762	Tuning ferroelectricity by charge doping in two-dimensional SnSe. Journal of Applied Physics, 2020, 127, 014101.	1.1	12
46763	Assessment of dynamic structural instabilities across 24 cubic inorganic halide perovskites. Journal of Chemical Physics, 2020, 152, 024703.	1.2	67
46764	Transition metal substituted Fe₂P: potential candidate for MRAM application. Journal of Physics Condensed Matter, 2020, 32, 195804.	0.7	2
46765	Controlled-Atmosphere Flame Fusion Growth of Nickel Poly-oriented Spherical Single Crystalsâ€”Unraveling Decades of Impossibility. Electrocatalysis, 2020, 11, 1-13.	1.5	12
46766	Unravelling local environments in mixed TiO2â€“SiO2 thin films by XPS and ab initio calculations. Applied Surface Science, 2020, 510, 145056.	3.1	23

#	Article	IF	Citations
46767	Theoretical study on double-atom catalysts supported with graphene for electroreduction of nitrogen into ammonia. Electrochimica Acta, 2020, 335, 135667.	2.6	62
46768	Ab initio thermodynamic optimization of Ni-rich Niâ€“Coâ€“Mn oxide cathode coatings. Journal of Power Sources, 2020, 450, 227693.	4.0	15
46769	Both cationic and anionic redox chemistry in a P2-type sodium layered oxide. Nano Energy, 2020, 69, 104474.	8.2	91
46770	Experimental and Computational Studies of CO and NO Adsorption Properties on Rh-Based Single Nanosized Catalysts. Journal of Physical Chemistry C, 2020, 124, 2953-2960.	1.5	8
46771	Three-Dimensional Superlithiophilic Interphase for Dendrite-Free Lithium Metal Anodes. ACS Applied Materials & Interfaces, 2020, 12, 5767-5774.	4.0	36
46772	Role of Intermediate Dynamics in Controlling Hydrogenation Selectivity by Heterogeneous Catalysis. ACS Omega, 2020, 5, 1270-1276.	1.6	2
46773	Electronic structure and hydrogen evolution reaction in Janus monolayer MoSSe regulated by strain engineering. Journal Physics D: Applied Physics, 2020, 53, 125502.	1.3	14
46774	Carbon-boron clathrates as a new class of sp ³ -bonded framework materials. Science Advances, 2020, 6, eaay8361.	4.7	61
46775	Polyol Synthesis of Ag/BN Nanohybrids and their Catalytic Stability in CO Oxidation Reaction. ChemCatChem, 2020, 12, 1691-1698.	1.8	11
46776	Theoretical dopant screening and processing optimization for vanadium disulfide as cathode material for Li-air batteries: A density functional theory study. Applied Surface Science, 2020, 508, 145276.	3.1	8
46777	Regulation of the interface binding and mechanical properties of TiB/Ti via doping-induced chemical and structural effects. Computational Materials Science, 2020, 174, 109506.	1.4	7
46778	A-site deficient perovskite with nano-socketed Ni-Fe alloy particles as highly active and durable catalyst for high-temperature CO2 electrolysis. Electrochimica Acta, 2020, 335, 135683.	2.6	38
46781	Electronic Properties of Carbon-Based Nanostructures. , 2020, , 11-69.		0
46782	Quantum Hall Effects in Graphene. , 2020, , 210-236.		0
46783	Spin-Related Phenomena. , 2020, , 237-277.		0
46784	Ab Initio and Multiscale Quantum Transport in Graphene-Based Materials. , 2020, , 293-353.		0
46788	Defect Interaction and Deformation in Graphene. Journal of Physical Chemistry C, 2020, 124, 2370-2378.	1.5	6
46789	First-Principles and Microkinetic Study on the Mechanism for Ammonia Synthesis Using Ru-Loaded Hydride Catalyst. Journal of Physical Chemistry C, 2020, 124, 2070-2078.	1.5	25

#	Article	IF	Citations
46790	Realizing high-efficiency power generation in low-cost PbS-based thermoelectric materials. Energy and Environmental Science, 2020, 13, 579-591.	15.6	101
46791	Parameterization of a COMPASS force field for single layer blue phosphorene. Nanotechnology, 2020, 31, 145702.	1.3	1
46792	TbMgNi_{4-x}Co_xâ€“(H,D)₂ System. I: Synthesis, Hydrogenation Properties, and Crystal and Electronic Structures. Journal of Physical Chemistry C, 2020, 124, 196-204.	1.5	9
46793	From Trigonal to Cubic LiVO₂: A High-Energy Phase Transition toward Disordered Rock Salt Materials. Journal of Physical Chemistry C, 2020, 124, 2229-2237.	1.5	14
46794	Glide Mirror Plane Protected Nodal-Loop in an Anisotropic Half-Metallic MnNF Monolayer. Journal of Physical Chemistry Letters, 2020, 11, 485-491.	2.1	32
46795	Multielemental singleâ€“atom-thick A layers in nanolaminated V ₂ (Sn, A) C () Tj ETQq1 1 0.784314 rgBT /O Sciences of the United States of America, 2020, 117, 820-825.	3.3	84
46796	Carbon at the nanoscale: Ultrastiffness and unambiguous definition of incompressibility. Carbon, 2020, 160, 228-235.	5.4	10
46797	Effect of polaron formation on electronic, charge and magnetic properties of Nb12O29. Journal of Alloys and Compounds, 2020, 821, 153527.	2.8	3
46798	Elastic properties of long-period stacking ordered phases in Mgâ€“Znâ€“Y and Mgâ€“Niâ€“Y alloys: A first-principles study. Scripta Materialia, 2020, 178, 422-427.	2.6	69
46799	Effect of Hydrotalcites Interlayer Water on Pt-Catalyzed Aqueous-Phase Selective Hydrogenation of Cinnamaldehyde. ACS Applied Materials & Interfaces, 2020, 12, 2516-2524.	4.0	28
46800	Isolated Boron Sites for Electroreduction of Dinitrogen to Ammonia. ACS Catalysis, 2020, 10, 1847-1854.	5.5	161
46801	Self-Assembly and Molecular Recognition in Water: Tubular Stacking and Guest-Templated Discrete Assembly of Water-Soluble, Shape-Persistent Macrocycles. Journal of the American Chemical Society, 2020, 142, 2915-2924.	6.6	44
46802	Realization of Lieb lattice in covalent-organic frameworks with tunable topology and magnetism. Nature Communications, 2020, 11, 66.	5.8	49
46803	Energyâ€“entropy competition in cationâ€“hydroxyl interactions at the liquid waterâ€“Pt(111) interface. Chemical Communications, 2020, 56, 427-430.	2.2	25
46804	High-throughput HSE study on the doping effect in anatase TiO₂. Physical Chemistry Chemical Physics, 2020, 22, 39-53.	1.3	30
46805	Fast prediction of oxygen reduction reaction activity on carbon nanotubes with a localized geometric descriptor. Physical Chemistry Chemical Physics, 2020, 22, 890-895.	1.3	24
46806	Structure, elastic characteristic, ideal strengths, and phonon stability of binary uranium intermetallic UGe₃ of AuCu₃-type. Physical Chemistry Chemical Physics, 2020, 22, 1381-1391.	1.3	4
46807	p-Type conductivity mechanism and defect structure of nitrogen-doped LiNbO3 from first-principles calculations. Physical Chemistry Chemical Physics, 2020, 22, 20-27.	1.3	8

#	Article	IF	Citations
46808	Understanding deep dehydrogenation and cracking of n-butane on Ni(111) by a DFT study. Physical Chemistry Chemical Physics, 2020, 22, 724-733.	1.3	23
46809	Strain-engineering the in-plane electrical anisotropy of GeSe monolayers. Physical Chemistry Chemical Physics, 2020, 22, 914-918.	1.3	16
46810	The influence of adjacent Al atoms on the hydrothermal stability of H-SSZ-13: a first-principles study. Physical Chemistry Chemical Physics, 2020, 22, 2930-2937.	1.3	11
46811	Control of the deprotonation of terephthalic acid assemblies on Ag(111) studied by DFT calculations and low temperature scanning tunneling microscopy. Physical Chemistry Chemical Physics, 2020, 22, 3173-3183.	1.3	3
46812	Structure and reactivity of a water-covered anatase TiO₂(001) surface. Physical Chemistry Chemical Physics, 2020, 22, 1371-1380.	1.3	16
46813	A promising blue phosphorene/C₂N van der Waals type-II heterojunction as a solar photocatalyst: a first-principles study. Physical Chemistry Chemical Physics, 2020, 22, 615-623.	1.3	43
46814	Interface-induced perpendicular magnetic anisotropy in Co₂FeAl/NiFe₂O₄ superlattice: first-principles study. Physical Chemistry Chemical Physics, 2020, 22, 716-723.	1.3	13
46815	Magnetic anisotropy of iridium dimers on two-dimensional materials. Physical Chemistry Chemical Physics, 2020, 22, 238-244.	1.3	11
46816	Three metallic BN polymorphs: 1D multi-threaded conduction in a 3D network. Physical Chemistry Chemical Physics, 2020, 22, 489-496.	1.3	4
46817	Electronic and magnetic properties of the Janus MoSSe/WSSe superlattice nanoribbon: a first-principles study. Physical Chemistry Chemical Physics, 2020, 22, 2498-2508.	1.3	12
46818	New aspects of C2 selectivity in electrochemical CO₂reduction over oxide-derived copper. Physical Chemistry Chemical Physics, 2020, 22, 2046-2053.	1.3	35
46819	Effects of different exchanging ions on the band structure and photocatalytic activity of defect pyrochlore oxide: a case study on KNbTeO₆. Catalysis Science and Technology, 2020, 10, 978-992.	2.1	21
46820	The catalytic mechanism of the Au@TiO_{2â”x}/ZnO catalyst towards a low-temperature water-gas shift reaction. Catalysis Science and Technology, 2020, 10, 768-775.	2.1	9
46821	A systematic theoretical study of the water gas shift reaction on the Pt/ZrO₂ interface and Pt(111) face: key role of a potassium additive. Catalysis Science and Technology, 2020, 10, 876-892.	2.1	22
46822	Adjustable uniaxial zero thermal expansion and zero linear compressibility in unique hybrid semiconductors: the role of the organic chain. Dalton Transactions, 2020, 49, 719-728.	1.6	16
46823	Substituent group-tunable hydrogen evolution activity observed in isostructural Cu(<scp>ii</scp>)-based coordination polymer photocatalysts. Dalton Transactions, 2020, 49, 1674-1680.	1.6	4
46824	Self-doped pâ€“n junctions in two-dimensional In₂X₃ van der Waals materials. Materials Horizons, 2020, 7, 504-510.	6.4	42
46825	Experimental evidence of a new class of massless fermions. Nanoscale Horizons, 2020, 5, 679-682.	4.1	5

#	Article	IF	Citations
46826	Ferroelastic domains drive charge separation and suppress electronâ€“hole recombination in all-inorganic halide perovskites: time-domain ab initio analysis. Nanoscale Horizons, 2020, 5, 683-690.	4.1	20
46827	The role of iodine in the enhancement of the supercapacitance properties of HI-treated flexible reduced graphene oxide film: an experimental study with insights from DFT simulations. New Journal of Chemistry, 2020, 44, 1418-1425.	1.4	13
46828	Boron-decorated C₉N₄ monolayers as promising metal-free catalysts for electrocatalytic nitrogen reduction reaction: a first-principles study. New Journal of Chemistry, 2020, 44, 422-427.	1.4	34
46829	Orbital hybridization-induced band offset phenomena in Ni_xCd_{1â^'x}O thin films. Nanoscale, 2020, 12, 669-686.	2.8	11
46830	Temperature, strain and charge mediated multiple and dynamical phase changes of selenium and tellurium. Nanoscale, 2020, 12, 3249-3258.	2.8	8
46831	Ultra stable superatomic structure of doubly magic Ga₁₃ and Ga₁₃Li electrolyte. Nanoscale, 2020, 12, 289-295.	2.8	3
46832	Largely enhanced thermoelectric effect and pure spin current in silicene-based devices under hydrogen modification. Nanoscale, 2020, 12, 277-288.	2.8	5
46833	Metal single-atom coordinated graphitic carbon nitride as an efficient catalyst for CO oxidation. Nanoscale, 2020, 12, 364-371.	2.8	59
46834	Negative capacitance switching in size-modulated Fe₃O₄nanoparticles with spontaneous non-stoichiometry: confronting its generalized origin in non-ferroelectric materials. Nanoscale, 2020, 12, 1528-1540.	2.8	18
46835	Metal-free highly efficient photocatalysts for overall water splitting: C₃N₅ multilayers. Nanoscale, 2020, 12, 306-315.	2.8	57
46836	Ultra-low thermal conductivity and high thermoelectric performance of two-dimensional triphosphides (InP₃, GaP₃, SbP₃ and SnP₃): a comprehensive first-principles study. Nanoscale, 2020, 12, 3330-3342.	2.8	68
46837	Improved polaronic transport under a strong Mottâ€“Hubbard interaction in Cu-substituted NiO. Inorganic Chemistry Frontiers, 2020, 7, 853-858.	3.0	6
46838	Applying surface strain and coupling with pure or N/B-doped graphene to successfully achieve high HER catalytic activity in 2D layered SnP₃-based nanomaterials: a first-principles investigation. Inorganic Chemistry Frontiers, 2020, 7, 647-658.	3.0	22
46839	Li-decorated carbyne for hydrogen storage: charge induced polarization and van't Hoff hydrogen desorption temperature. Sustainable Energy and Fuels, 2020, 4, 691-699.	2.5	24
46840	A phosphorene-like InP₃ monolayer: structure, stability, and catalytic properties toward the hydrogen evolution reaction. Journal of Materials Chemistry A, 2020, 8, 1307-1314.	5.2	31
46841	Revealing cooperative Li-ion migration in Li_{1+x}Al_xTi_{2â^'x}(PO₄)₃ solid state electrolytes with high Al doping. Journal of Materials Chemistry A, 2020, 8, 342-348.	5.2	41
46842	Theoretical insights into nonprecious oxygen-evolution active sites in Tiâ€“Ir-Based perovskite solid solution electrocatalysts. Journal of Materials Chemistry A, 2020, 8, 218-223.	5.2	15
46843	Local mobility in electrochemically inactive sodium in hard carbon anodes after the first cycle. Journal of Materials Chemistry A, 2020, 8, 743-749.	5.2	28

#	Article	IF	Citations
46844	The stability and reaction mechanism of a LiF/electrolyte interface: insight from density functional theory. Journal of Materials Chemistry A, 2020, 8, 2613-2617.	5.2	13
46845	W supported on g-CN manifests high activity and selectivity for N₂electroreduction to NH₃. Journal of Materials Chemistry A, 2020, 8, 1378-1385.	5.2	93
46846	Fabricating highly efficient heterostructured CuBi₂O₄ photocathodes for unbiased water splitting. Journal of Materials Chemistry A, 2020, 8, 2498-2504.	5.2	57
46847	Bottom-top channeling Li nucleation and growth by a gradient lithiophilic 3D conductive host for highly stable Li-metal anodes. Journal of Materials Chemistry A, 2020, 8, 1678-1686.	5.2	31
46848	The importance of the Mgâ€“Mg interaction in Mg₃Sb₂â€“Mg₃Bi₂ shown through cation site alloying. Journal of Materials Chemistry A, 2020, 8, 2033-2038.	5.2	33
46849	Graphitic carbon nitride doped SnO₂ enabling efficient perovskite solar cells with PCEs exceeding 22%. Journal of Materials Chemistry A, 2020, 8, 2644-2653.	5.2	98
46850	Partial sulfuration-induced defect and interface tailoring on bismuth oxide for promoting electrocatalytic CO₂reduction. Journal of Materials Chemistry A, 2020, 8, 2472-2480.	5.2	82
46851	A composite solid polymer electrolyte incorporating MnO₂ nanosheets with reinforced mechanical properties and electrochemical stability for lithium metal batteries. Journal of Materials Chemistry A, 2020, 8, 2021-2032.	5.2	118
46852	Band structure, phonon spectrum, and thermoelectric properties of Î²-BiAs and Î²-BiSb monolayers. Journal of Materials Chemistry C, 2020, 8, 581-590.	2.7	21
46853	Impurity states in Mo_{1â^'x}M_xSe₂ compounds doped with group VB elements and their electronic and thermal transport properties. Journal of Materials Chemistry C, 2020, 8, 619-629.	2.7	11
46854	Insights into the vacancy behaviour at the interface of Asâ€“Sb lateral heterostructures. Journal of Materials Chemistry C, 2020, 8, 650-662.	2.7	4
46855	A family of all sp²-bonded carbon allotropes of topological semimetals with strain-robust nodal-lines. Journal of Materials Chemistry C, 2020, 8, 1548-1555.	2.7	24
46856	Quantifying the composition dependency of the ground-state structure, electronic property and phase-transition dynamics in ternary transition-metal-dichalcogenide monolayers. Journal of Materials Chemistry C, 2020, 8, 721-733.	2.7	7
46857	Broadband near-infrared (NIR) emission realized by the crystal-field engineering of Y_{3â^'x}Ca_xAl_{5â^'x}Si_xO₁₂:Cr³⁺(x=	2.7	36
46858	Fe doping-stabilized Î³-Ga₂O₃thin films with a high room temperature saturation magnetic moment. Journal of Materials Chemistry C, 2020, 8, 536-542.	2.7	28
46859	As₂S₃, As₂Se₃ and As₂Te₃ nanosheets: superstretchable semiconductors with anisotropic carrier mobilities and optical properties. Journal of Materials Chemistry C, 2020, 8, 2400-2410.	2.7	45
46860	Accurate estimation of the photoelectric conversion efficiency of a series of anthracene-based organic dyes for dye-sensitized solar cells. Journal of Materials Chemistry C, 2020, 8, 2388-2399.	2.7	47
46861	Itinerant ferromagnetism and intrinsic anomalous Hall effect in amorphous iron-germanium. Physical Review B, 2020, 101, .	1.1	10

#	Article	IF	Citations
46862	Formation criterion for binary metal diboride solid solutions established through combinatorial methods. Journal of the American Ceramic Society, 2020, 103, 3338-3348.	1.9	16
46863	Unusual Effect of Trace Water on the Structure and Activity of Ni x Co 1â^' x Electrocatalysts for the Methanol Oxidation Reaction. ChemSusChem, 2020, 13, 964-973.	3.6	14
46864	Cu 2 MgO 3 Electronic and Magnetic Properties â€“ a DFT Study. Israel Journal of Chemistry, 2020, 60, 863-869.	1.0	2
46865	Defectâ€Induced Magnetism in Nonmagnetic Oxides: Basic Principles, Experimental Evidence, and Possible Devices with ZnO and TiO₂. Physica Status Solidi (B): Basic Research, 2020, 257, 1900623.	0.7	26
46866	Simulations of the Oxidation and Degradation of Platinum Electrocatalysts. Small, 2020, 16, 1905159.	5.2	25
46867	Strain effect on the orientation-dependent harmonic spectrum of monolayer aluminum nitride. Science China: Physics, Mechanics and Astronomy, 2020, 63, 1.	2.0	40
46868	A Theoretical Study of Pressure-Induced Effects on Phase Transition and Elastic Properties of AsTh Compound. Journal of Electronic Materials, 2020, 49, 2086-2094.	1.0	3
46869	Scanning tunneling spectroscopic study of monolayer 1T-TaS2 and 1T-TaSe2. Nano Research, 2020, 13, 133-137.	5.8	46
46870	Novel CeMnaOx catalyst for highly efficient catalytic decomposition of ozone. Applied Catalysis B: Environmental, 2020, 264, 118498.	10.8	47
46871	Bi metal prevents the deactivation of oxygen vacancies in Bi2O2CO3 for stable and efficient photocatalytic NO abatement. Applied Catalysis B: Environmental, 2020, 264, 118545.	10.8	197
46872	Environmentally benign synthesis of a PGM-free catalyst for low temperature CO oxidation. Applied Catalysis B: Environmental, 2020, 264, 118547.	10.8	20
46873	Electronic modulation of cobalt phosphide nanosheet arrays via copper doping for highly efficient neutral-pH overall water splitting. Applied Catalysis B: Environmental, 2020, 265, 118555.	10.8	172
46874	Pressure-induced band-gap closure and metallization in two-dimensional transition metal halide CdI2. Applied Materials Today, 2020, 18, 100532.	2.3	9
46875	Vanadium dopant- and strain-dependent magnetic properties of single-layer VI3. Applied Surface Science, 2020, 508, 144937.	3.1	30
46876	Thermal stability of zirconia-doped ceria surfaces: A first-principles molecular dynamics study. Applied Surface Science, 2020, 507, 144942.	3.1	6
46877	Atomic layer deposition of tungsten nitride films as protective barriers to hydrogen. Applied Surface Science, 2020, 507, 145019.	3.1	5
46878	High-pressure topological transport study of Bi2Se3 single crystal. Applied Surface Science, 2020, 507, 145052.	3.1	4
46879	High coverage H2O adsorption on CuAl2O4 surface: A DFT study. Applied Surface Science, 2020, 507, 145162.	3.1	52

#	Article	IF	Citations
46880	Local dimerization and dedimerization of C60 molecules under a tip of scanning tunneling microscope: A first-principles study. Carbon, 2020, 159, 638-647.	5.4	4
46881	Band-gap engineering and structure evolution of confined long linear carbon chains@double-walled carbon nanotubes under pressure. Carbon, 2020, 159, 266-272.	5.4	20
46882	Bco-C24: A new 3D Dirac nodal line semi-metallic carbon honeycomb for high performance metal-ion battery anodes. Carbon, 2020, 159, 542-548.	5.4	30
46883	Pressure difference-induced synthesis of P-doped carbon nanobowls for high-performance supercapacitors. Chemical Engineering Journal, 2020, 385, 123858.	6.6	60
46884	Insights into the difference in metal-free activation of peroxymonosulfate and peroxydisulfate. Chemical Engineering Journal, 2020, 394, 123936.	6.6	63
46885	Orientation dependence of elastic properties of Mg binary alloys: A first-principles study. Computational Condensed Matter, 2020, 22, e00447.	0.9	4
46886	Study of Pt monolayer adsorption on the oppositely polarized BiAlO3 (0ÂÔÂÔÂ1) surfaces by ab initio calculations. Computational Materials Science, 2020, 174, 109470.	1.4	3
46887	First-principle study of the solubility and diffusion of oxygen and boron in <mml:math xmlns:mml="http://www.w3.org/1998/Math/MathML" altimg="si88.svg"><mml:mrow><mml:mi>Î³</mml:mi></mml:mrow></mml:math>-TiAl. Computational Materials Science, 2020, 174, 109475.	1.4	21
46888	Machine learning models for the prediction of energy, forces, and stresses for Platinum. Computational Materials Science, 2020, 174, 109483.	1.4	17
46889	Theoretical investigation of optoelectronic and magnetic properties of Co-doped ZnS and (Al, Co) co-doped ZnS. Computational Materials Science, 2020, 174, 109491.	1.4	17
46890	Elastic constants of pure body-centered cubic Mg in nanolaminates. Computational Materials Science, 2020, 174, 109501.	1.4	18
46891	Insight into inhibition behavior of novel ionic liquids for magnesium alloy in NaCl solution: Experimental and theoretical investigation. Corrosion Science, 2020, 165, 108410.	3.0	48
46892	CALANIE: Anisotropic elastic correction to the total energy, to mitigate the effect of periodic boundary conditions. Computer Physics Communications, 2020, 252, 107130.	3.0	13
46893	Density functional theory analysis of electronic and optical properties of orthorhombic perovskite CH3NH3SnX3 (XÂ=ÂBr, I). Chemical Physics Letters, 2020, 740, 137062.	1.2	5
46894	Tunable metallic and topological properties in two-dimensional ligand-functionalized antimonene films. Chemical Physics Letters, 2020, 740, 137064.	1.2	9
46895	The Agâ€“Li system's experimental and ab initio thermodynamic dataset. Data in Brief, 2020, 28, 104939.	0.5	3
46896	Improving the HER activity of Ni3FeN to convert the superior OER electrocatalyst to an efficient bifunctional electrocatalyst for overall water splitting by doping with molybdenum. Electrochimica Acta, 2020, 333, 135488.	2.6	37
46897	Boosting the electrochemical performance of 3D composite lithium metal anodes through synergistic structure and interface engineering. Energy Storage Materials, 2020, 26, 56-64.	9.5	73

#	Article	IF	Citations
46898	Facet-tailoring five-coordinated Ti sites and structure-optimizing electron transfer in a bifunctional cathode with titanium nitride nanowire array to boost the performance of Li2S6-based lithiumâ€“sulfur batteries. Energy Storage Materials, 2020, 26, 40-45.	9.5	43
46899	Band-gap engineering of layered covalent organic frameworks via controllable exfoliation for enhanced visible-light-driven hydrogen evolution. International Journal of Hydrogen Energy, 2020, 45, 2689-2698.	3.8	32
46900	Direct Z-scheme photocatalytic overall water splitting on two dimensional MoSe2/SnS2 heterojunction. International Journal of Hydrogen Energy, 2020, 45, 2785-2793.	3.8	54
46901	A novel binary metal sulfide hybrid Li-ion battery anode: Three-dimensional ZnCo2S4/NiCo2S4 derived from metal-organic foams enables an improved electron transfer and ion diffusion performance. Journal of Alloys and Compounds, 2020, 817, 153293.	2.8	24
46902	Czochralski growth, electronic structure, luminescence and scintillation properties of Cs2Mo3O10: A new scintillation crystal for 0Î½Î²Î² decay search. Journal of Alloys and Compounds, 2020, 821, 153466.	2.8	17
46903	Ab-initio revelation on the origins of Ti substitution for Ga, Mn and Ni on ferromagnetism, phase stability and elastic properties in Ni2MnGa. Journal of Alloys and Compounds, 2020, 821, 153481.	2.8	27
46904	Yellow persistent luminescence and electronic structure of Ca-Î±-Sialon: Eu2+. Journal of Alloys and Compounds, 2020, 821, 153482.	2.8	13
46905	Insights into the active sites and catalytic mechanism of oxidative esterification of 5-hydroxymethylfurfural by metal-organic frameworks-derived N-doped carbon. Journal of Catalysis, 2020, 381, 570-578.	3.1	56
46906	Bismuth chromate (Bi2CrO6): A promising semiconductor in photocatalysis. Journal of Catalysis, 2020, 382, 40-48.	3.1	57
46907	Fabrication of Ni3N nanorods anchored on N-doped carbon for selective semi-hydrogenation of alkynes. Journal of Catalysis, 2020, 382, 22-30.	3.1	27
46908	The position of lysine controls the catechol-mediated surface adhesion and cohesion in underwater mussel adhesion. Journal of Colloid and Interface Science, 2020, 563, 168-176.	5.0	51
46909	Single-atom Pt supported on holey ultrathin g-C3N4 nanosheets as efficient catalyst for Li-O2 batteries. Journal of Colloid and Interface Science, 2020, 564, 28-36.	5.0	72
46910	Ta-based 413 and 211 MAX phase solid solutions with Hf and Nb. Journal of the European Ceramic Society, 2020, 40, 1829-1838.	2.8	31
46911	Revealing adsorption and the photodegradation mechanism of gas phase o-xylene on carbon quantum dots modified TiO2 nanoparticles. Journal of Hazardous Materials, 2020, 386, 121962.	6.5	25
46912	Composition dependent intrinsic defect structures in ASnO3 (Aâ€¯=â€¯Ca, Sr, Ba). Journal of Materials Science and Technology, 2020, 42, 212-219.	5.6	16
46913	Hydrogen isotope role in the crystal orientation change of erbium oxide coatings. Journal of Nuclear Materials, 2020, 528, 151871.	1.3	4
46914	Intra-layer atomic ordering and semi-conductivity in CsAMS2 (A = Li, Ag; M = Co, Fe). Journal of Solid State Chemistry, 2020, 283, 121134.	1.4	0
46915	Ab initio calculation of mechanical and thermodynamic properties of Gd2Zr2O7 pyrochlore. Materials Chemistry and Physics, 2020, 243, 122565.	2.0	6

#	Article	IF	Citations
46916	Giant reduction in thermal conductivity of Co3O4 with ordered mesopore structures. Microporous and Mesoporous Materials, 2020, 296, 109969.	2.2	12
46917	Multiscale simulation of gas transport in mixed-matrix membranes with interfacial polymer rigidification. Microporous and Mesoporous Materials, 2020, 296, 109982.	2.2	21
46918	Investigation of structural, mechanical, dynamic, electronic and optical properties of seleno-germanates A<mml:math xmlns:mml="http://www.w3.org/1998/Math/MathML" altimg="si1.svg"><mml:msub><mml:mrow /><mml:mn>2</mml:mn></mml:msub></mml:math>GeSe<mml:math xmlns:mml="http://www.w3.org/1998/Math/MathML" altimg="si2.svg"><mml:msub><mml:mrow		

#	Article	IF	Citations
46934	Enhanced Electrochemical Storage Properties of Na- and Mg-Intercalated B-Doped-Graphene Based Heterostructures and Bilayers. Journal of Physical Chemistry C, 2020, 124, 1260-1268.	1.5	4
46935	Electrochemical Interface during Corrosion of Copper in Anoxic Sulfide-Containing Groundwaterâ€"A Computational Study. Journal of Physical Chemistry C, 2020, 124, 469-481.	1.5	8
46936	Isomeric Thiolate Monolayer Protected Au₉₂ and Au₁₀₂ Nanomolecules. Journal of Physical Chemistry C, 2020, 124, 1655-1666.	1.5	9
46937	Importance of Many-Body Dispersion in the Stability of Vacancies and Antisites in Free-Standing Monolayer of MoS₂ from First-Principles Approaches. Journal of Physical Chemistry C, 2020, 124, 1390-1397.	1.5	8
46938	Spatial and Magnetic Factors for CH₄ Oxidation on Pd Slabs in the Presence of Transition-Metal Me Cations Exchanged in Î³-Al₂O₃ Support or MeAl₂O₄ Spinels, Me = Ni, Co, Mn. Journal of Physical Chemistry C, 2020, 124, 605-615.	1.5	4
46939	High-Density COH_x Network Glass. Journal of Physical Chemistry C, 2020, 124, 107-114.	1.5	3
46940	High Thermoelectric Performance of New Two-Dimensional IVâ€"VI Compounds: A First-Principles Study. Journal of Physical Chemistry C, 2020, 124, 1812-1819.	1.5	51
46941	First-Principles Screening of Lead-Free Mixed-Anion Perovskites for Photovoltaics. Journal of Physical Chemistry C, 2020, 124, 1303-1308.	1.5	8
46942	BCN-M: A Free Computational Tool for Generating Wulff-like Nanoparticle Models with Controlled Stoichiometry. Journal of Physical Chemistry C, 2020, 124, 1227-1237.	1.5	13
46943	Transition Metal-doped Ru Nanoparticles Loaded on Metal Hydrides for Efficient Ammonia Synthesis from First Principles. Journal of Physical Chemistry C, 2020, 124, 1529-1534.	1.5	3
46944	Defects in Highly Anisotropic Transition-Metal Dichalcogenide PdSe₂. Journal of Physical Chemistry Letters, 2020, 11, 740-746.	2.1	28
46945	Descriptors for Electron and Hole Charge Carriers in Metal Oxides. Journal of Physical Chemistry Letters, 2020, 11, 438-444.	2.1	22
46946	Covalent Functionalized Black Phosphorus Greatly Inhibits Nonradiative Charge Recombination: A Time Domain Ab Initio Study. Journal of Physical Chemistry Letters, 2020, 11, 478-484.	2.1	22
46947	Shaping and Edge Engineering of Few-Layered Freestanding Graphene Sheets in a Transmission Electron Microscope. Nano Letters, 2020, 20, 2279-2287.	4.5	5
46948	Potassium-Presenting Zinc Oxide Surfaces Induce Vertical Phase Separation in Fullerene-Free Organic Photovoltaics. Nano Letters, 2020, 20, 715-721.	4.5	48
46949	Revealing Grain-Boundary-Induced Degradation Mechanisms in Li-Rich Cathode Materials. Nano Letters, 2020, 20, 1208-1217.	4.5	62
46950	Interface-Charge Induced Giant Electrocaloric Effect in Lead Free Ferroelectric Thin-Film Bilayers. Nano Letters, 2020, 20, 1262-1271.	4.5	95
46951	Lateral MoS₂ Heterostructure for Sensing Small Gas Molecules. ACS Applied Electronic Materials, 2020, 2, 74-83.	2.0	13

#	Article	IF	Citations
46952	Two-Dimensional (001) LaAlO₃/SrTiO₃ Heterostructures with Adjustable Band Gap and Magnetic Properties. ACS Applied Materials & Interfaces, 2020, 12, 3134-3139.	4.0	11
46953	Bioinspired Electrocatalyst for Electrochemical Reduction of N₂ to NH₃ in Ambient Conditions. ACS Applied Materials & Interfaces, 2020, 12, 2445-2451.	4.0	39
46954	Photovoltaic Effect Related to Methylammonium Cation Orientation and Carrier Transport Properties in High-Performance Perovskite Solar Cells. ACS Applied Materials & Interfaces, 2020, 12, 3563-3571.	4.0	9
46955	Ultrafine Tungsten Oxide Nanowires: Synthesis and Highly Selective Acetone Sensing and Mechanism Analysis. ACS Applied Materials & Interfaces, 2020, 12, 3755-3763.	4.0	58
46956	Ultrastrong Ï€-Bonded Interface as Ductile Plastic Flow Channel in Nanostructured Diamond. ACS Applied Materials & Interfaces, 2020, 12, 4135-4142.	4.0	7
46957	Highly Efficient Metal-Free Two-Dimensional Luminescent Melem Nanosheets for Bioimaging. ACS Applied Materials & Interfaces, 2020, 12, 2145-2151.	4.0	27
46958	Atomically Resolved Edge States on a Layered Ferroelectric Oxide. ACS Applied Materials & Interfaces, 2020, 12, 4150-4154.	4.0	9
46959	Enhanced Thermoelectric Performance of Zr_{1â€“x}Ta_xNiSn Half-Heusler Alloys by Diagonal-Rule Doping. ACS Applied Materials & Interfaces, 2020, 12, 3773-3783.	4.0	25
46960	Strain and Doping in Two-Dimensional SnTe Nanosheets: Implications for Thermoelectric Conversion. ACS Applied Nano Materials, 2020, 3, 114-119.	2.4	12
46961	Density Functional Theory Study of Epitaxially Strained Monolayer Transition Metal Chalcogenides for Piezoelectricity Generation. ACS Applied Nano Materials, 2020, 3, 384-390.	2.4	13
46962	Variation in the In₂O₃ Crystal Phase Alters Catalytic Performance toward the Reverse Water Gas Shift Reaction. ACS Catalysis, 2020, 10, 3264-3273.	5.5	112
46963	Effect of Manganese on the Selective Catalytic Hydrogenation of COx in the Presence of Light Hydrocarbons Over Ni/Al2O3: An Experimental and Computational Study. ACS Catalysis, 2020, 10, 1535-1547.	5.5	24
46964	Unraveling the Origins of the Synergy Effect between ZrO₂ and CrO_x in Supported CrZrO_x for Propene Formation in Nonoxidative Propane Dehydrogenation. ACS Catalysis, 2020, 10, 1575-1590.	5.5	46
46965	Robust Net Magnetic Moment in Janus V-Based Nitride MXenes: Insight from First-Principles Calculations. ACS Omega, 2020, 5, 864-870.	1.6	18
46966	Nanoscale percolation in doped BaZrO3 for high proton mobility. Nature Materials, 2020, 19, 338-346.	13.3	73
46967	Targeted chemical pressure yields tuneable millimetre-wave dielectric. Nature Materials, 2020, 19, 176-181.	13.3	27
46968	GeI₂ monolayer: a model thermoelectric material from 300 to 600â€…K. Philosophical Magazine, 2020, 100, 782-796.	0.7	18
46969	Tailoring of nitrogen-vacancy colour centers in diamond epilayers by in situ sulfur and nitrogen anion engineering. Journal Physics D: Applied Physics, 2020, 53, 075107.	1.3	5

#	Article	IF	Citations
46970	HfN₂ monolayer: A new direct-gap semiconductor with high and anisotropic carrier mobility*. Chinese Physics B, 2020, 29, 023102.	0.7	15
46971	Extending Carrier Lifetimes in Lead Halide Perovskites with Alkali Metals by Passivating and Eliminating Halide Interstitial Defects. Angewandte Chemie - International Edition, 2020, 59, 4684-4690.	7.2	78
46972	High Compressionâ€Induced Conductivity in a Layered Cuâ€“Br Perovskite. Angewandte Chemie - International Edition, 2020, 59, 4017-4022.	7.2	23
46973	Effects of Mnâ€Doping on the Structural and Electrochemical Properties of Na 3 Ni 2 SbO 6 for Sodiumâ€Ion Battery.. Batteries and Supercaps, 2020, 3, 402-408.	2.4	6
46974	Bandâ€Gap and Charge Transfer Engineering in Red Phosphorusâ€Based Composites for Enhanced Visibleâ€Lightâ€Driven H₂ Evolution. Chemistry - A European Journal, 2020, 26, 2285-2292.	1.7	19
46975	Effects of noble metal doping on hydrogen sensing performances of monolayer MoS₂. Materials Research Express, 2020, 7, 015501.	0.8	11
46976	Comparison of Effective Exchange Integrals of H-H and H-He-H Chains vs. Single Molecules: A Theoretical Study. Chemistry Letters, 2020, 49, 137-140.	0.7	6
46977	Photoelectrochemistry of Ferrites: Theoretical Predictions vs. Experimental Results. Zeitschrift Fur Physikalische Chemie, 2020, 234, 719-776.	1.4	24
46978	Atomic imaging of the edge structure and growth of a two-dimensional hexagonal ice. Nature, 2020, 577, 60-63.	13.7	149
46979	Phosphorus-Amine-Based Synthesis of Nanoscale Red Phosphorus for Application to Sodium-Ion Batteries. ACS Nano, 2020, 14, 974-984.	7.3	57
46980	Tunable Photocatalytic Water Splitting by the Ferroelectric Switch in a 2D AgBiP₂Se₆ Monolayer. Journal of the American Chemical Society, 2020, 142, 1492-1500.	6.6	229
46981	A-site deficient/excessive effects of LaMnO3 perovskite as bifunctional oxygen catalyst for zinc-air batteries. Electrochimica Acta, 2020, 333, 135566.	2.6	71
46982	Electronic Polarizability as the Fundamental Variable in the Dielectric Properties of Two-Dimensional Materials. Nano Letters, 2020, 20, 841-851.	4.5	70
46983	Engineering the band structures of few-layer black phosphorus by adsorbed metal atoms. Chemical Physics Letters, 2020, 740, 137075.	1.2	4
46984	Synthesis, structure and physical properties of layered quaternary sulfides NaLiMS2 (MÂ= Mn, Fe, Co). Journal of Alloys and Compounds, 2020, 822, 153613.	2.8	4
46985	Atomic and electronic properties of few-layer hexagonal boron. Solid State Communications, 2020, 307, 113804.	0.9	2
46986	Structure and Thermodynamic Stability of Zeolitic Imidazolate Framework Surfaces. Journal of Physical Chemistry C, 2020, 124, 1458-1468.	1.5	9
46987	Mechanochemical Synthesis: A Tool to Tune Cation Site Disorder and Ionic Transport Properties of Li₃MCl₆ (M = Y, Er) Superionic Conductors. Advanced Energy Materials, 2020, 10, 1903719.	10.2	173

#	Article	IF	Citations
46988	MoO3 induces p-type surface conductivity by surface transfer doping in diamond. Applied Surface Science, 2020, 509, 144890.	3.1	30
46989	Ground-state structure of oxidized diamond (100) surface: An electronically nearly surface-free reconstruction. Carbon, 2020, 159, 9-15.	5.4	23
46990	Effects of additives on the morphology and stability of PbO2 films electrodeposited on nickel substrate for light weight lead-acid battery application. Journal of Energy Storage, 2020, 27, 101108.	3.9	9
46991	Adsorption of small molecules on a Pmma CO monolayer. Journal of Physics and Chemistry of Solids, 2020, 139, 109300.	1.9	0
46992	The effect of chemical composition on the structure, chemistry and mechanical properties of magnetron sputtered W-B-C coatings: Modeling and experiments. Surface and Coatings Technology, 2020, 383, 125274.	2.2	16
46993	Bis(iminothiolato)-Based One-Dimensional Metalâ€“Organic Framework: Robust Bipolar Magnetic Semiconductor with Reversal of Spin Polarization. Journal of Physical Chemistry C, 2020, 124, 37-43.	1.5	14
46994	Unraveling the Mechanism of Water-Mediated Sulfur Tolerance via Operando Surface-Enhanced Raman Spectroscopy. ACS Applied Materials & Interfaces, 2020, 12, 2370-2379.	4.0	17
46995	Biogenic Pt/CaCO₃ Nanocomposite as a Robust Catalyst toward Benzene Oxidation. ACS Applied Materials & Interfaces, 2020, 12, 2469-2480.	4.0	44
46996	Catalyst synthesis under CO2 electroreduction favours faceting and promotes renewable fuels electrosynthesis. Nature Catalysis, 2020, 3, 98-106.	16.1	325
46997	DFT-investigation on anisotropy degree of electronic, optical, and mechanical properties of olivine ZnRE2S4 (RE = Er, Tm) compounds. Materials Research Express, 2020, 7, 016305.	0.8	3
46998	Theoryâ€Guided Defect Tuning through Topochemical Reactions for Accelerated Discovery of UVC Persistent Phosphors. Advanced Optical Materials, 2020, 8, 1901727.	3.6	20
46999	Facile, Rapid, and Wellâ€Controlled Preparation of Pt Nanoparticles Decorated on Single Surface of Mos₂ Nanosheets and Application in HER. ChemNanoMat, 2020, 6, 435-441.	1.5	5
47000	Formation of multilayer interfaces and the load transfer in graphene nanoplatelets reinforced Al matrix composites. Materials Characterization, 2020, 159, 110018.	1.9	32
47001	Strain-tunable electronic and optical properties in two dimensional GaSe/g-C3N4 van der Waals heterojunction as photocatalyst for water splitting. Physica E: Low-Dimensional Systems and Nanostructures, 2020, 118, 113896.	1.3	22
47002	Crystalline and Electronic Structures of the Al1+xV2Sn2â€“x (x = 0.19) Intermetallic Compound. Inorganic Chemistry, 2020, 59, 360-366.	1.9	0
47003	Understanding Dealumination Mechanisms in Protonic and Cationic Zeolites. Journal of Physical Chemistry C, 2020, 124, 668-676.	1.5	22
47004	Combined Experimental and Theoretical Assessment of WX_y (X = C, N, S, P) for Hydrogen Evolution Reaction. ACS Applied Energy Materials, 2020, 3, 1082-1088.	2.5	32
47005	Interfacial Hydrogen-Bonding Dynamics in Surface-Facilitated Dehydrogenation of Water on TiO₂(110). Journal of the American Chemical Society, 2020, 142, 826-834.	6.6	31

#	Article	IF	Citations
47006	Enhanced interfacial Dzyaloshinskiiâ€"Moriya interactions in annealed Pt/Co/MgO structures. Nanotechnology, 2020, 31, 155705.	1.3	24
47007	Dendriteâ€Free Lithium Plating Induced by In Situ Transferring Protection Layer from Separator. Advanced Functional Materials, 2020, 30, 1907020.	7.8	43
47008	Subâ€3 nm Intermetallic Ordered Pt₃In Clusters for Oxygen Reduction Reaction. Advanced Science, 2020, 7, 1901279.	5.6	57
47009	RE (La, Nd and Yb) doped CeO2 abrasive particles for chemical mechanical polishing of dielectric materials: Experimental and computational analysis. Applied Surface Science, 2020, 506, 144668.	3.1	50
47010	Intriguing electronic structures and carrier mobilities of two-dimensional GaN nanosheets: Thickness and surface effects. Computational Materials Science, 2020, 172, 109337.	1.4	13
47011	Thermodynamic modelling of the Niâ€"Zr system. Intermetallics, 2020, 116, 106640.	1.8	8
47012	Characterization of (In,Pb)/Si(111): Tuning normal and lateral atom distributions in mixed metal systems. Journal of Alloys and Compounds, 2020, 819, 153030.	2.8	1
47013	Crystal plane dependent electrocatalytic performance of NiS2 nanocrystals for hydrogen evolution reaction. Journal of Catalysis, 2020, 381, 63-69.	3.1	25
47014	Ni clusters embedded in multivacancy graphene substrates. Journal of Physics and Chemistry of Solids, 2020, 138, 109258.	1.9	7
47015	Correlating structure and transport properties in pristine and environmentally-aged superionic conductors based on Li1.3Al0.3Ti1.7(PO4)3 ceramics. Journal of Power Sources, 2020, 448, 227367.	4.0	25
47016	The ultralow thermal conductivity and ultrahigh thermoelectric performance of fluorinated Sn2Bi sheet in room temperature. Nano Energy, 2020, 67, 104283.	8.2	16
47017	M-porphyrin (Mâ€‰=â€‰Mn, Co) carbon materials as oxygen reduction catalysts from density functional studies. Molecular Physics, 2020, 118, e1687949.	0.8	4
47018	Zr vacancies and their complexes with hydrogen in monoclinic zirconia: formation energies and positron lifetimes. Physica Scripta, 2020, 95, 035801.	1.2	0
47019	Strain Engineering for 2D Ferroelectricity in Lead Chalcogenides. Advanced Electronic Materials, 2020, 6, 1900932.	2.6	17
47020	Ultrahigh Sensitivity and Selectivity of Pentagonal SiC₂ Monolayer Gas Sensors: The Synergistic Effect of Composition and Structural Topology. Physica Status Solidi (B): Basic Research, 2020, 257, 1900445.	0.7	11
47021	Ab initio study on physical and chemical interactions at borates and iron oxide interface at high temperature. Chemical Physics, 2020, 529, 110548.	0.9	8
47022	Improving the cycling stability and rate capability of LiMn0.5Fe0.5PO4/C nanorod as cathode materials by LiAlO2 modification. Journal of Materiomics, 2020, 6, 33-44.	2.8	20
47023	A DFT-based simulated annealing method for the optimization of global energy in zeolite framework systems: Application to natrolite, chabazite and clinoptilolite. Microporous and Mesoporous Materials, 2020, 294, 109885.	2.2	13

#	Article	IF	Citations
47024	Janus structure derivatives SnPâ€“InS, GeP-GaS and SiPâ€“AlS monolayers with in-plane and out-of-plane piezoelectric performance. Physica E: Low-Dimensional Systems and Nanostructures, 2020, 117, 113817.	1.3	12
47025	Tunable quadruple-well ferroelectric van der Waals crystals. Nature Materials, 2020, 19, 43-48.	13.3	140
47026	Structural and electronic properties of tungsten oxides under high pressures. Journal of Physics Condensed Matter, 2020, 32, 085403.	0.7	2
47027	Quasi-bonding driven abnormal isotropic thermal transport in intrinsically anisotropic nanostructure: a case of study of a phosphorus nanotube array. Nanotechnology, 2020, 31, 095704.	1.3	3
47028	Epitaxial growth and air-stability of monolayer Cu₂Te*. Chinese Physics B, 2020, 29, 018104.	0.7	22
47029	Interfacial Engineering of W₂N/WC Heterostructures Derived from Solidâ€State Synthesis: A Highly Efficient Trifunctional Electrocatalyst for ORR, OER, and HER. Advanced Materials, 2020, 32, e1905679.	11.1	380
47030	The Dopant Local Effect on the Stability of an Oxygen Vacancy and the Reliability of a Conductive Filament in Rutile Titanium Dioxide. Physica Status Solidi (B): Basic Research, 2020, 257, 1900455.	0.7	3
47031	Insights into the mechanism of formic acid dehydrogenation on Pd-Co@Pd core-shell catalysts: A theoretical study. Applied Surface Science, 2020, 505, 144532.	3.1	10
47032	Nitrogen-Doped graphene coated FeS2 microsphere composite as high-performance anode materials for sodium-ion batteries enhanced by the chemical and structural synergistic effect. Applied Surface Science, 2020, 505, 144633.	3.1	18
47033	Discovering the root of the stability of hexagonal WO3 surfaces from a periodic DFT perspective. Applied Surface Science, 2020, 506, 144719.	3.1	13
47034	Anionic redox in a-(Mo3S11)n polymer cathode for all-solid-state Li-ion battery. Electrochimica Acta, 2020, 332, 135218.	2.6	11
47035	Insight into the effect of high pressure on multiferroic properties of TmNiO3. Journal of Alloys and Compounds, 2020, 815, 152351.	2.8	2
47036	Theoretical study on group III elements and F co-doped ZnO. Journal of Alloys and Compounds, 2020, 819, 153012.	2.8	12
47037	Assessing the adsorption and photocatalytic activity of TiO2 nanoparticles for the gas phase acetaldehyde: A computational and experimental study. Journal of Alloys and Compounds, 2020, 819, 153055.	2.8	13
47038	Design of a two-layer structure to significantly improve the performance of zinc oxide resistive memory. Nanotechnology, 2020, 31, 115209.	1.3	6
47039	Insights into the role of Dâ€Aâ€Ïâ€A type proâ€aromatic organic dyes with thieno[3,4â€b]pyrazine as A acceptor group into dyeâ€sensitized solarâ€cells. A TDâ€DFT/periodic DFT study. International Journal of Quantum Chemistry, 2020, 120, e26108.	1.0	6
47040	Multilayer silicene: Structure, electronics, and mechanical property. Computational Materials Science, 2020, 172, 109354.	1.4	15
47041	First-principles calculations of a new half-metallic Heusler alloy FeCrAs. Journal of Alloys and Compounds, 2020, 820, 153118.	2.8	22

#	Article	IF	Citations
47042	Properties of monolayer black phosphorus affected by uniaxial strain. Physica E: Low-Dimensional Systems and Nanostructures, 2020, 117, 113834.	1.3	5
47043	Low-index surface energies, cleavage energies, and surface relaxations for crystalline NiAl from first-principles calculations. Surface Science, 2020, 695, 121532.	0.8	16
47044	Dipole moment effects in dopamine/N-doped-graphene systems. Surface Science, 2020, 693, 121546.	0.8	6
47045	Random Phase Approximation Applied to Many-Body Noncovalent Systems. Journal of Chemical Theory and Computation, 2020, 16, 427-442.	2.3	12
47046	Controlling the Magnetic Anisotropy of the van der Waals Ferromagnet Fe₃GeTe₂ through Hole Doping. Nano Letters, 2020, 20, 95-100.	4.5	118
47047	Revealing electrolyte oxidation via carbonate dehydrogenation on Ni-based oxides in Li-ion batteries by in situ Fourier transform infrared spectroscopy. Energy and Environmental Science, 2020, 13, 183-199.	15.6	202
47048	Elastic anisotropy and physical properties of semi-transition-metal borides: first-principles calculation. Applied Physics Express, 2020, 13, 015501.	1.1	7
47049	Sn-Doped Hematite for Photoelectrochemical Water Splitting: The Effect of Sn Concentration. Zeitschrift Fur Physikalische Chemie, 2020, 234, 683-698.	1.4	10
47050	Defect engineering of MnO2 nanosheets by substitutional doping for printable solid-state micro-supercapacitors. Nano Energy, 2020, 68, 104306.	8.2	90
47051	Extending Carrier Lifetimes in Lead Halide Perovskites with Alkali Metals by Passivating and Eliminating Halide Interstitial Defects. Angewandte Chemie, 2020, 132, 4714-4720.	1.6	18
47052	Nâ€Doped Graphene Supported on Metalâ€Iron Carbide as a Catalyst for the Oxygen Reduction Reaction: Density Functional Theory Study. ChemSusChem, 2020, 13, 996-1005.	3.6	21
47053	Improved photocatalytic HER activity of Î±-Sb monolayer with doping and strain engineering. Applied Surface Science, 2020, 507, 145194.	3.1	17
47054	Structural and magnetic analyses of the FexCo1â^'xTiSb alloy system: Fe0.5Co0.5TiSb as a prototypical half-Heusler compound. Journal of Alloys and Compounds, 2020, 822, 153408.	2.8	3
47055	A method to predict energy barriers in stress modulated solidâ€“solid phase transitions. Journal of the Mechanics and Physics of Solids, 2020, 137, 103857.	2.3	16
47056	A strategy for designing stable nanocrystalline alloys by thermo-kinetic synergy. Journal of Materials Science and Technology, 2020, 43, 21-31.	5.6	20
47057	Theoretical study of the electronic, thermodynamic, and thermo-conductive properties of Î³-LiAlO2 with 6Li isotope substitutions for tritium production. Journal of Nuclear Materials, 2020, 530, 151963.	1.3	11
47058	Interaction and diffusion of atomic oxygen in monovacancy-containing Cr- and Ti-doped nickel structures. Physica B: Condensed Matter, 2020, 582, 411972.	1.3	1
47059	Visible light-assisted instability of kesterite Cu2ZnSnS4: What are the implications?. Solar Energy Materials and Solar Cells, 2020, 208, 110384.	3.0	8

#	Article	IF	Citations
47060	General trends in Horiuti-Polanyi mechanism vs non-Horiuti-Polanyi mechanism for water formation on transition metal surfaces. Chinese Journal of Catalysis, 2020, 41, 294-301.	6.9	4
47061	Sustainable Synthesis of Biomass-Derived Carbon Electrodes with Hybrid Energy-Storage Behaviors for Use in High-Performance Na-Ion Capacitors. ACS Applied Energy Materials, 2020, 3, 2478-2489.	2.5	33
47062	Tuned Hydrogen Bonding in Rare-Earth Metalâ€“Organic Frameworks for Design of Optical and Electronic Properties: An Exemplar Study of Yâ€“2,5-Dihydroxyterephthalic Acid. ACS Applied Materials & Interfaces, 2020, 12, 4531-4539.	4.0	26
47063	First-Principles Study of Tritium Diffusion in the Li₃TaO₄ Crystal. ACS Omega, 2020, 5, 851-858.	1.6	6
47064	Revealing Principles for Design of Lean-Electrolyte Lithium Metal Anode via In Situ Spectroscopy. Journal of the American Chemical Society, 2020, 142, 2012-2022.	6.6	142
47065	Light-driven methane dry reforming with single atomic site antenna-reactor plasmonic photocatalysts. Nature Energy, 2020, 5, 61-70.	19.8	466
47066	Robust axion insulator and Chern insulator phases in a two-dimensional antiferromagnetic topological insulator. Nature Materials, 2020, 19, 522-527.	13.3	536
47067	Breaking scaling relations for efficient CO₂ electrochemical reduction through dual-atom catalysts. Chemical Science, 2020, 11, 1807-1813.	3.7	230
47068	Surface chemistry dictates stability and oxidation state of supported single metal catalyst atoms. Chemical Science, 2020, 11, 1469-1477.	3.7	16
47069	Photochromic inorganicâ€“organic complex derived from low-cost deep eutectic solvents with tunable photocurrent responses and photocatalytic properties. CrystEngComm, 2020, 22, 1078-1085.	1.3	18
47070	A first-principles study on the influences of metal species Al, Zr, Mo and Tc on the mechanical properties of U₃Si₂. Physical Chemistry Chemical Physics, 2020, 22, 1833-1840.	1.3	8
47071	Boron based layered electrode materials for metal-ion batteries. Physical Chemistry Chemical Physics, 2020, 22, 709-715.	1.3	9
47072	Quantifying the rigidity of 2D carbides (MXenes). Physical Chemistry Chemical Physics, 2020, 22, 2115-2121.	1.3	52
47073	Pore size effect of graphyne supports on CO₂ electrocatalytic activity of Cu single atoms. Physical Chemistry Chemical Physics, 2020, 22, 1181-1186.	1.3	37
47074	Pressure-stabilized polymerization of nitrogen in alkaline-earth-metal strontium nitrides. Physical Chemistry Chemical Physics, 2020, 22, 5242-5248.	1.3	25
47075	Metallization and superconductivity in methane doped by beryllium at low pressure. Physical Chemistry Chemical Physics, 2020, 22, 1069-1077.	1.3	19
47076	Theoretically predicted surface morphology of FCC cobalt nanoparticles induced by Ru promoter. Catalysis Science and Technology, 2020, 10, 187-195.	2.1	9
47077	OH/Na co-functionalized carbon nitride: directional charge transfer and enhanced photocatalytic oxidation ability. Catalysis Science and Technology, 2020, 10, 529-535.	2.1	13

#	Article	IF	Citations
47078	A theoretical indicator of transition-metal nanoclusters applied in the carbon nanotube nucleation process: a DFT study. Dalton Transactions, 2020, 49, 492-503.	1.6	10
47079	Stabilizing atomic Pt with trapped interstitial F in alloyed PtCo nanosheets for high-performance zinc-air batteries. Energy and Environmental Science, 2020, 13, 884-895.	15.6	99
47080	Insight into the active site and reaction mechanism for selective oxidation of methane to methanol using H₂O₂ on a Rh₁/ZrO₂ catalyst. New Journal of Chemistry, 2020, 44, 1632-1639.	1.4	20
47081	Strain-induced phase transition and giant piezoelectricity in monolayer tellurene. Nanoscale, 2020, 12, 167-172.	2.8	25
47082	Intrinsic ferromagnetism and valley polarization in hydrogenated group V transition-metal dinitride (MN₂H₂, M = V/Nb/Ta) nanosheets: insights from first-principles. Nanoscale, 2020, 12, 1002-1012.	2.8	17
47083	Highly efficient N₂ fixation catalysts: transition-metal carbides M₂C (MXenes). Nanoscale, 2020, 12, 538-547.	2.8	71
47084	Strain-engineering enables reversible semiconductorâ€“metal transition of skutterudite IrAs3. Inorganic Chemistry Frontiers, 2020, 7, 1108-1114.	3.0	1
47085	Application of organicâ€“graphene hybrids in high performance photodetectors. Materials Chemistry Frontiers, 2020, 4, 354-368.	3.2	16
47086	Direct synthesis of bifunctional nanorods from a Coâ€“adenineâ€“MoO₃ hybrid for overall water splitting. Materials Chemistry Frontiers, 2020, 4, 546-554.	3.2	17
47087	Photodriven CO dimerization on Cu₂O from an electronic-structure perspective. Sustainable Energy and Fuels, 2020, 4, 670-677.	2.5	0
47088	Elucidating the unexpected electrocatalytic activity of nanoscale PdO layers on Pd electrocatalysts towards ethanol oxidation in a basic solution. Sustainable Energy and Fuels, 2020, 4, 1118-1125.	2.5	22
47089	Strain-tunable electronic properties and lithium storage of 2D transition metal carbide (MXene) Ti₂CO₂ as a flexible electrode. Journal of Materials Chemistry A, 2020, 8, 760-769.	5.2	35
47090	Plasma-etched functionalized graphene as a metal-free electrode catalyst in solid acid fuel cells. Journal of Materials Chemistry A, 2020, 8, 2445-2452.	5.2	20
47091	Highly dispersed nickel nitride nanoparticles on nickel nanosheets as an active catalyst for hydrazine electrooxidation. Journal of Materials Chemistry A, 2020, 8, 632-638.	5.2	44
47092	Weak temperature-dependent hole injection and electronâ€“hole recombination at the CH₃NH₃PbI₃/NiO heterojunction: a time-domain ab initio study. Journal of Materials Chemistry A, 2020, 8, 607-615.	5.2	16
47093	MOF-derived conductive carbon nitrides for separator-modified Liâ€“S batteries and flexible supercapacitors. Journal of Materials Chemistry A, 2020, 8, 1757-1766.	5.2	107
47094	Electrostatic interaction assisted synthesis of a CdS/BCN heterostructure with enhanced photocatalytic effects. Journal of Materials Chemistry C, 2020, 8, 1803-1810.	2.7	48
47095	T-C56: a low-density transparent superhard carbon allotrope assembled from C16 cage-like cluster. Journal of Physics Condensed Matter, 2020, 32, 165701.	0.7	6

#	Article	IF	Citations
47096	Lithium intercalation drives mechanical properties deterioration in bulk and single-layered black phosphorus: a first-principles study. 2D Materials, 2020, 7, 025028.	2.0	10
47097	Closest-Packing Water Monolayer Stably Intercalated in Phyllosilicate Minerals under High Pressure. Langmuir, 2020, 36, 618-627.	1.6	7
47098	Discovery of low-temperature GeTe-based thermoelectric alloys with high performance competing with Bi₂Te₃. Journal of Materials Chemistry A, 2020, 8, 1660-1667.	5.2	43
47099	Kagome-like group-VA monolayers with indirectâ€“direct band gap transition and anisotropic mobility. Journal of Materials Chemistry C, 2020, 8, 2732-2740.	2.7	14
47100	Unraveling the atomic structure, ripening behavior, and electronic structure of supported Au ₂₀ clusters. Science Advances, 2020, 6, eaay4289.	4.7	27
47101	Unveiling the pinning behavior of charged domain walls in BiFeO3 thin films via vacancy defects. Acta Materialia, 2020, 186, 68-76.	3.8	22
47102	First-principle study of the microstructure and electronic properties for Cr3+ doped yttrium orthoaluminate. Computational Materials Science, 2020, 174, 109467.	1.4	11
47103	Activated HER performance of defected single layered TiO2 nanosheet via transition metal doping. International Journal of Hydrogen Energy, 2020, 45, 2681-2688.	3.8	27
47104	Improvement of the homogeneity and oxygen storage capability of Ce1-xZrxO2-Î´ by co-doping: A first-principles study. Journal of Alloys and Compounds, 2020, 817, 153238.	2.8	4
47105	Adsorption and diffusion behaviors of Ni-based filler elements on diamond surface. Journal of Alloys and Compounds, 2020, 822, 153652.	2.8	25
47106	Room temperature ferromagnetic half metal in Mn doped cluster-assembled sodalite phase of III-N compounds. Journal of Magnetism and Magnetic Materials, 2020, 499, 166295.	1.0	4
47107	Pulse electrodeposited bismuth-tellurium superlattices with controllable bismuth content. Journal of Power Sources, 2020, 450, 227605.	4.0	7
47108	Phase Transition from Weak Ferroelectricity to Incipient Ferroelectricity in Li₂Sr(Nb_{1â€“x}Ta_x)₂O₇. Chemistry of Materials, 2020, 32, 744-750.	3.2	16
47109	Fe Enhanced Visible-Light-Driven Nitrogen Fixation on BiOBr Nanosheets. Chemistry of Materials, 2020, 32, 1488-1494.	3.2	113
47110	In-Depth Determination of the Microstructure and Energy Transition Mechanism for Nd³⁺-Doped Yttrium Oxide Laser Crystals. Journal of Physical Chemistry C, 2020, 124, 2113-2119.	1.5	16
47111	Ca₂B₅O₉Cl and Sr₂B₅O₉Cl: Nonlinear Optical Crystals with Deep-Ultraviolet Transparency Windows. ACS Applied Materials & Interfaces, 2020, 12, 4632-4637.	4.0	32
47112	Tuning OH binding energy enables selective electrochemical oxidation of ethylene to ethylene glycol. Nature Catalysis, 2020, 3, 14-22.	16.1	120
47113	A sacrificial Zn strategy enables anchoring of metal single atoms on the exposed surface of holey 2D molybdenum carbide nanosheets for efficient electrocatalysis. Journal of Materials Chemistry A, 2020, 8, 3071-3082.	5.2	48

#	Article	IF	Citations
47114	Palgraphyne: A Promising 2D Carbon Dirac Semimetal with Strong Mechanical and Electronic Anisotropy. Physica Status Solidi - Rapid Research Letters, 2020, 14, 1900670.	1.2	14
47115	Complete catalytic cycle of NO decomposition on a silicon-doped nitrogen-coordinated graphene: Mechanistic insight from a DFT study. Applied Surface Science, 2020, 508, 145255.	3.1	12
47116	Understanding hydrogen in perovskites from first principles. Computational Materials Science, 2020, 174, 109461.	1.4	14
47117	Effects of solute segregation on surface properties of dilute Al-X (XÂ=ÂLi, Sn) alloys from first-principles calculations. Computational Materials Science, 2020, 174, 109502.	1.4	12
47118	Modulated band structures of two-dimensional atomically thick (100) diamond nanofilms with surface functionalization. Diamond and Related Materials, 2020, 101, 107641.	1.8	9
47119	Ruthenium under ultrafast laser excitation: Model and dataset for equation of state, conductivity, and electron-ion coupling. Data in Brief, 2020, 28, 104980.	0.5	11
47120	Interfacial properties and Li-ion dynamics between Li3OCl solid electrolyte and Li metal anode for all solid state Li metal batteries from first principles study. Electrochimica Acta, 2020, 334, 135622.	2.6	17
47121	Generation of molybdenum hydride species via addition of molecular hydrogen across metal-oxygen bond at monolayer oxide/metal composite interface. International Journal of Hydrogen Energy, 2020, 45, 2975-2988.	3.8	10
47122	Three-in-One: Opened Charge-transfer channel, positively shifted oxidation potential, and enhanced visible light response of g-C3N4 photocatalyst through K and S Co-doping. International Journal of Hydrogen Energy, 2020, 45, 4534-4544.	3.8	46
47123	Phase equilibria and diffusion coefficients in the Fe-Zn binary system. Materials and Design, 2020, 188, 108437.	3.3	7
47124	SEHC: A high-throughput materials computing framework with automatic self-evaluation filtering. Materials Science and Engineering B: Solid-State Materials for Advanced Technology, 2020, 252, 114474.	1.7	7
47125	An efficient materials genome method to predict heterostructure interfaces. Materials Today Communications, 2020, 23, 100866.	0.9	1
47126	Oxygen transport in Pr nickelates: Elucidation of atomic-scale features. Solid State Ionics, 2020, 344, 115155.	1.3	6
47127	Theoretical Prediction and Experimental Verification of the Chemically Ordered Atomic-Laminate i-MAX Phases (Cr_{2/3}Sc_{1/3})₂GaC and (Mn_{2/3}Sc_{1/3})₂GaC. Crystal Growth and Design, 2020, 20, 55-61.	1.4	16
47128	Theoretical Investigation of Monolayer RhTeCl Semiconductors as Photocatalysts for Water Splitting. Journal of Physical Chemistry C, 2020, 124, 639-646.	1.5	18
47129	Mechanistic Aspects of CO Activation and Câ€“C Bond Formation on the Fe/C- and Fe-Terminated Fe₃C(010) Surfaces. ACS Catalysis, 2020, 10, 877-890.	5.5	21
47130	Crystal Structure Analysis of Top Dross in a Molten Zinc Bath by First Principle Calculation and Synchrotron X-ray Diffraction. Tetsu-To-Hagane/Journal of the Iron and Steel Institute of Japan, 2020, 106, 205-213.	0.1	0
47131	Anisotropic Elastic, Electronic and Vibrational Properties of the Semiconductor AgScX (X = Ge, C) Compounds. Journal of Electronic Materials, 2020, 49, 1849-1856.	1.0	5

#	Article	IF	Citations
47132	The effect of S-functionalized and vacancies on V2C MXenes as anode materials for Na-ion and Li-ion batteries. Current Applied Physics, 2020, 20, 310-319.	1.1	56
47133	Interstitial diffusion of a helium atom in bulk Li4SiO4 crystal from first-principles calculations. Ceramics International, 2020, 46, 8192-8199.	2.3	7
47134	Electronic structure and thermoelectric properties of PbTe1â^'xSex from first-principles calculations. Computational Materials Science, 2020, 173, 109404.	1.4	3
47135	Activity and selectivity of methanol-to-olefin conversion over Zr-modified H-SAPO-34/H-ZSM-5 zeolites - A theoretical study. Fuel Processing Technology, 2020, 199, 106302.	3.7	20
47136	A comparative study on the high and low symmetric structures of (LaMnO3)n/(LaNiO3)n superlattices by first-principles calculations. Journal of Magnetism and Magnetic Materials, 2020, 499, 166251.	1.0	0
47137	Deactivating deformation twinning in medium-entropy CrCoNi with small additions of aluminum and titanium. Scripta Materialia, 2020, 178, 295-300.	2.6	30
47138	Ab Initio Insights into the Formation Mechanisms of 55-Atom Pt-Based Coreâ€“Shell Nanoalloys. Journal of Physical Chemistry C, 2020, 124, 1158-1164.	1.5	22
47139	Plasmon Localization by H-Induced Band Switching. Journal of Physical Chemistry C, 2020, 124, 958-967.	1.5	9
47140	Quantitative Mapping of the Charge Density in a Monolayer of MoS₂ at Atomic Resolution by Off-Axis Electron Holography. ACS Nano, 2020, 14, 524-530.	7.3	10
47141	Atomicâ€Scale Metalâ€“Insulator Transition in SrRuO₃ Ultrathin Films Triggered by Surface Termination Conversion. Advanced Materials, 2020, 32, e1905815.	11.1	25
47142	Passivating Detrimental DX Centers in CH₃NH₃PbI₃ for Reducing Nonradiative Recombination and Elongating Carrier Lifetime. Advanced Materials, 2020, 32, e1906115.	11.1	53
47143	Atomic-level insights into strain effect on p-nitrophenol reduction via Au@Pd coreâ€“shell nanocubes as an ideal platform. Journal of Catalysis, 2020, 381, 427-433.	3.1	30
47144	Mechanisms of Pressure-Induced Structural Transformation in Confined Sodium Borate Glasses. Journal of Physical Chemistry B, 2020, 124, 277-287.	1.2	5
47145	Understanding the Separation Mechanism of C2H6/C2H4 on Zeolitic Imidazolate Framework ZIF-7 by Periodic DFT Investigations. Journal of Physical Chemistry C, 2020, 124, 256-266.	1.5	9
47146	Suppressing Metal Leaching in a Supported Co/SiO₂ Catalyst with Effective Protectants in the Hydroformylation Reaction. ACS Catalysis, 2020, 10, 914-920.	5.5	44
47147	Enhanced N₂ Electroreduction over LaCoO₃ by Introducing Oxygen Vacancies. ACS Catalysis, 2020, 10, 1077-1085.	5.5	98
47148	A transparent, self-healing and high-Îº dielectric for low-field-emission stretchable optoelectronics. Nature Materials, 2020, 19, 182-188.	13.3	183
47149	High Capacity and Highâ€Rate NASICONâ€Na_{3.75}V_{1.25}Mn_{0.75}(PO₄)₃ Cathode for Naâ€Ion Batteries via Modulating Electronic and Crystal Structures. Advanced Energy Materials, 2020, 10, 1902918.	10.2	68

#	Article	IF	Citations
47150	Pseudocapacitive sodium storage of Fe1â^'xS@N-doped carbon for low-temperature operation. Science China Materials, 2020, 63, 505-515.	3.5	35
47151	Organic-association of Ge in the coal-hosted ore deposits: An experimental and theoretical approach. Ore Geology Reviews, 2020, 117, 103291.	1.1	12
47152	Van der Waals Contact to 2D Semiconductors with a Switchable Electric Dipole: Achieving Both nâ€•and pâ€Type Ohmic Contacts to Metals with a Wide Range of Work Functions. Advanced Electronic Materials, 2020, 6, 1900981.	2.6	20
47153	Charge reordering of MgO (1Â0Â0) surface by Sn cluster deposition: Implications for heterogeneous catalysis. Applied Surface Science, 2020, 506, 144963.	3.1	3
47154	Fabrication of Hollow CoP/TiO_x Heterostructures for Enhanced Oxygen Evolution Reaction. Small, 2020, 16, e1905075.	5.2	117
47155	Solar Driven CO2 Hydrogenation on Ti-Doped Silicon Nanocages. Journal of Cluster Science, 2020, 31, 627-635.	1.7	8
47156	Cathodic Wear by Delamination of the Al4C3 Layer During Aluminium Electrolysis. Metallurgical and Materials Transactions B: Process Metallurgy and Materials Processing Science, 2020, 51, 161-172.	1.0	4
47157	First-Principles Modeling of Oxygen Adsorption on Ag-Doped LaMnO3 (001) Surface. Journal of Electronic Materials, 2020, 49, 1421-1434.	1.0	4
47158	The Effect of Local Arrangement of ExcessÂMn on Phase Stability in Niâ€“Mnâ€“Ga Martensite: An Ab Initio Study. Shape Memory and Superelasticity, 2020, 6, 35-44.	1.1	5
47159	Holey graphitic carbon nitride (g-CN) supported bifunctional single atom electrocatalysts for highly efficient overall water splitting. Applied Catalysis B: Environmental, 2020, 264, 118521.	10.8	137
47160	First-principles computational study of Ni/Î±-Al2O3 hybrid interface reactions under extreme thermodynamic conditions. Applied Surface Science, 2020, 509, 144861.	3.1	3
47161	Lattice dynamical and thermo-elastic properties of M2AlB (MÂ= V, Nb, Ta) MAX phase borides. Journal of Alloys and Compounds, 2020, 819, 153256.	2.8	36
47162	Atomistic building blocks of one-dimensional Guinierâ€“Prestonâ€“Bagaryatsky zones in Al-Cu-Mg alloys. Materials and Design, 2020, 187, 108393.	3.3	14
47163	Gravity field-mediated synthesis of carbon-conjugated quantum dots with tunable defective density for enhanced triiodide reduction. Nano Energy, 2020, 69, 104377.	8.2	19
47164	Understanding the Enhanced Stability of Bromide Substitution in Lead Iodide Perovskites. Chemistry of Materials, 2020, 32, 400-409.	3.2	53
47165	Halide-Assisted Synthesis of Cadmium Chalcogenide Nanoplatelets. Chemistry of Materials, 2020, 32, 566-574.	3.2	29
47166	Proton, Hydroxide Ion, and Oxide Ion Affinities of Closed-Shell Oxides: Importance for the Hydration Reaction and Correlation to Electronic Structure. Journal of Physical Chemistry C, 2020, 124, 1277-1284.	1.5	23
47167	Intercalation-Driven Reversible Switching of 2D Magnetism. Journal of Physical Chemistry C, 2020, 124, 1146-1157.	1.5	10

#	Article	IF	Citations
47168	Cyanate and Cyanurate Adsorption at Silver Electrodes in Neutral Solutions: In Situ ATR-SEIRAS and DFT Studies. Journal of Physical Chemistry C, 2020, 124, 709-721.	1.5	4
47169	Extracting an Empirical Intermetallic Hydride Design Principle from Limited Data via Interpretable Machine Learning. Journal of Physical Chemistry Letters, 2020, 11, 40-47.	2.1	28
47170	Strategies To Improve the Activity While Maintaining the Selectivity of Oxidative Coupling of Methane at La₂O₃: A Density Functional Theory Study. ACS Catalysis, 2020, 10, 586-594.	5.5	50
47171	Insights into the Hydrogen Coverage Effect and the Mechanism of Fischerâ€“Tropsch to Olefins Process on Fe₅C₂ (510). ACS Catalysis, 2020, 10, 689-701.	5.5	41
47172	Robust Ruthenium-Saving Catalyst for High-Temperature Carbon Dioxide Reforming of Methane. ACS Catalysis, 2020, 10, 783-791.	5.5	45
47173	Highly Efficient B-Site Exsolution Assisted by Co Doping in Lanthanum Ferrite toward High-Performance Electrocatalysts for Oxygen Evolution and Oxygen Reduction. ACS Sustainable Chemistry and Engineering, 2020, 8, 302-310.	3.2	48
47174	Bright high-colour-purity deep-blue carbon dot light-emitting diodes via efficient edge amination. Nature Photonics, 2020, 14, 171-176.	15.6	303
47175	Vacancy concentration of films and nanoparticles. Computational Materials Science, 2020, 173, 109416.	1.4	8
47176	Role of electronic correlation effect on charge ordering in Î²-V2OPO4. Computational Materials Science, 2020, 173, 109433.	1.4	0
47177	Effect of interface distance on the electronic properties and optical properties of GaAs/BN novel two-dimensional materials: First-principle calculation. Materials Chemistry and Physics, 2020, 242, 122554.	2.0	4
47178	Unraveling the Active Site and Mechanism for Câ€“S Bond Activation in Alumina-Supported Pt Catalysts: Ab Initio Insights into Catalytic Desulfurization. Journal of Physical Chemistry C, 2020, 124, 446-458.	1.5	4
47179	Interfacial Engineering of MOF-Based Mixed Matrix Membrane through Atomistic Simulations. Journal of Physical Chemistry C, 2020, 124, 594-604.	1.5	39
47180	Novel Superstructure-Phase Two-Dimensional Material 1T-VSe2 at High Pressure. Journal of Physical Chemistry Letters, 2020, 11, 380-386.	2.1	17
47181	Cu- and Fe-Codoped Ni Porous Networks as an Active Electrocatalyst for Hydrogen Evolution in Alkaline Medium. ACS Applied Materials & Interfaces, 2020, 12, 2380-2389.	4.0	26
47182	Unsaturated Single Atoms on Monolayer Transition Metal Dichalcogenides for Ultrafast Hydrogen Evolution. ACS Nano, 2020, 14, 767-776.	7.3	106
47183	Boron Nitride Nanotubes for Ammonia Synthesis: Activation by Filling Transition Metals. Journal of the American Chemical Society, 2020, 142, 308-317.	6.6	105
47184	On-Demand, Ultraselective Hydrogenation System Enabled by Precisely Modulated Pdâ€“Cd Nanocubes. Journal of the American Chemical Society, 2020, 142, 962-972.	6.6	53
47185	Revisiting the conformational adsorption of <scp>L</scp>â€•and <scp>D</scp>â€•cysteine on Au nanoparticles by Raman spectroscopy. Journal of Raman Spectroscopy, 2020, 51, 243-255.	1.2	13

#	Article	IF	Citations
47186	First principles study on methane reforming over Ni/TiO2(110) surface in solid oxide fuel cells under dry and wet atmospheres. Science China Materials, 2020, 63, 364-374.	3.5	17
47187	Grain boundary properties of elemental metals. Acta Materialia, 2020, 186, 40-49.	3.8	115
47188	Insights into KMnO4 etched N-rich carbon nanotubes as advanced electrocatalysts for Zn-air batteries. Applied Catalysis B: Environmental, 2020, 264, 118537.	10.8	81
47189	Mechanistic evaluation of Li2O2 adsorption on carbon nanotube electrodes: A theoretical study. Applied Surface Science, 2020, 506, 145050.	3.1	9
47190	Sequential insulating-metal-insulating phase transition of NbO2 by doping photoexcited carrier. Computational Materials Science, 2020, 173, 109434.	1.4	6
47191	Low Nickel-doped copper as the electrocatalyst for oxidation of formaldehyde and evolution of hydrogen. Electrochimica Acta, 2020, 333, 135542.	2.6	7
47192	Mass diffusivity and thermal conductivity estimation of chloride-based salt hydrates for thermo-chemical heat storage: A molecular dynamics study using the reactive force field.. International Journal of Heat and Mass Transfer, 2020, 149, 119090.	2.5	14
47193	Tungsten solubility in L12-ordered Al3Er and Al3Zr nanoprecipitates formed by aging in an aluminum matrix. Journal of Alloys and Compounds, 2020, 820, 153383.	2.8	16
47194	Recycling waste tantalum capacitors to synthesize high value-added Ta2O5 and polyaniline-decorated Ta2O5 photocatalyst by an integrated chlorination-sintering-chemisorption process. Journal of Cleaner Production, 2020, 252, 117206.	4.6	24
47195	Ab initio study of the magnetic, optical and electronic properties of spinel Co3O4 within DFT and GW approaches. Journal of Magnetism and Magnetic Materials, 2020, 499, 166306.	1.0	6
47196	Probing tribo-interface evolution governing high temperature tribology of nitride ceramic contacts. Materials Characterization, 2020, 160, 110062.	1.9	1
47197	Facet-controlled Ptâ€“Ir nanocrystals with substantially enhanced activity and durability towards oxygen reduction. Materials Today, 2020, 35, 69-77.	8.3	45
47198	Electron Confinement and Magnetism of (LaTiO₃)₁/(SrTiO₃)₅ Heterostructure: A Diffusion Quantum Monte Carlo Study. Journal of Chemical Theory and Computation, 2020, 16, 643-650.	2.3	4
47199	Magnetic Polymer Chains of Iron and Zwitterionic Quinoidal Ligands on the Ag(111) Surface. Journal of Physical Chemistry C, 2020, 124, 1346-1351.	1.5	7
47200	Promotion of Nitrogen Reserve and Electronic Regulation in Bamboo-like Carbon Tubules by Cobalt Nanoparticles for Highly Efficient ORR. ACS Applied Energy Materials, 2020, 3, 2323-2330.	2.5	39
47201	Competing stripe and magnetic phases in the cuprates from first principles. Proceedings of the National Academy of Sciences of the United States of America, 2020, 117, 68-72.	3.3	61
47202	Effect of strain and doping on the polar metal phase in LiOsO₃. Journal of Physics Condensed Matter, 2020, 32, 125501.	0.7	10
47203	Largeâ€Scale Synthesis of Strainâ€Tunable Semiconducting Antimonene on Copper Oxide. Advanced Materials, 2020, 32, e1906873.	11.1	46

#	Article	IF	Citations
47204	Quantumâ€Chemical Study of the FeNCN Conversionâ€Reaction Mechanism in Lithiumâ€•and Sodiumâ€Ion Batteries. Angewandte Chemie - International Edition, 2020, 59, 3718-3723.	7.2	24
47205	Tightâ€Binding Parameterizations of Ti and Ba Oxides and Their Application for the Prediction of 2D Phases. Physica Status Solidi (B): Basic Research, 2020, 257, 1900634.	0.7	2
47206	Influence of oxide support on Pd properties: A gain for O diffusion versus minor impact for CH4 dissociation. Catalysis Today, 2020, 357, 368-379.	2.2	4
47207	BOPcat software package for the construction and testing of tight-binding models and bond-order potentials. Computational Materials Science, 2020, 173, 109455.	1.4	6
47208	Raman spectroscopy and lattice dynamical stability study of 2D ferromagnetic semiconductor Cr2Ge2Te6 under high pressure. Journal of Alloys and Compounds, 2020, 819, 153368.	2.8	14
47209	Nanoscale Pd catalysts decorated WO3â€“SnO2 heterojunction nanotubes for highly sensitive and selective acetone sensing. Sensors and Actuators B: Chemical, 2020, 306, 127575.	4.0	63
47210	Insight into the Characteristics of 4f-Related Electronic Transitions for Rare-Earth-Doped KLuS₂ Luminescent Materials through First-Principles Calculation. Journal of Physical Chemistry C, 2020, 124, 932-938.	1.5	8
47211	Radiation-Induced Evolution of Tungsten Carbide in Fusion Reactors: Accommodation of Defect Clusters and Transmutation Elements. ACS Applied Energy Materials, 2020, 3, 868-878.	2.5	16
47212	Q-Carbon: A New Carbon Allotrope with a Low Degree of sâ€“p Orbital Hybridization and Its Nucleation Lithiation Process in Lithium-Ion Batteries. ACS Applied Materials & Interfaces, 2020, 12, 619-626.	4.0	16
47213	Origin of the Flat Band in Heavily Cs-Doped Graphene. ACS Nano, 2020, 14, 1055-1069.	7.3	28
47214	Enhancing Chemical Interaction of Polysulfide and Carbon through Synergetic Nitrogen and Phosphorus Doping. ACS Sustainable Chemistry and Engineering, 2020, 8, 806-813.	3.2	11
47215	Induced magnetism in oxygen-decorated N-doped graphene. Carbon, 2020, 159, 102-109.	5.4	7
47216	Evidence for bandwidth-control metal-insulator transition in Ti3O5. Computational Materials Science, 2020, 173, 109435.	1.4	7
47217	Zintl phase crystal assembled by magic Al6CNa4 cluster. Chemical Physics Letters, 2020, 739, 137026.	1.2	0
47218	Band inversion induced multiple electronic valleys for high thermoelectric performance of SnTe with strong lattice softening. Nano Energy, 2020, 69, 104395.	8.2	80
47219	Modulation of spinâ€“valley splitting in a two-dimensional MnPSe3/CrBr3 van der Waals heterostructure. Journal Physics D: Applied Physics, 2020, 53, 125104.	1.3	13
47220	Structural, mechanical and electronic properties of two-dimensional chlorine-terminated transition metal carbides and nitrides. Journal of Physics Condensed Matter, 2020, 32, 135302.	0.7	18
47221	The feasibility analysis of growing the modified borophene on substrates: First-principles calculation. Applied Surface Science, 2020, 507, 144154.	3.1	2

#	Article	IF	Citations
47222	First-principles study on structural, electronic, and ferroelectric properties of high-temperature RMn2O5 (Râ€‰=â€‰Sm, Gd, Dy). Materials Today Communications, 2020, 22, 100837.	0.9	3
47223	Experimental and ab Initio Studies of Deep-Bulk Traps in Doped Rare-Earth Oxide Thick Films. Journal of Physical Chemistry C, 2020, 124, 997-1007.	1.5	7
47224	Manipulation of Electronic and Magnetic Properties of 3d Transition Metal (Cr, Mn, Fe) Hexamers on Graphene with Vacancy Defects: Insights from First-Principles Theory. Journal of Physical Chemistry C, 2020, 124, 4270-4278.	1.5	8
47225	Modified Generalized Stacking Fault Energy Surface of IIâ€“VI Ionic Crystals from Excess Electrons and Holes. ACS Applied Electronic Materials, 2020, 2, 56-65.	2.0	3
47226	Size-Controlled Pd Nanoparticles Loaded on Co₃O₄ Nanoparticles by Calcination for Enhanced CO Oxidation. ACS Applied Nano Materials, 2020, 3, 486-495.	2.4	26
47227	Effect of IrO₆ Octahedron Distortion on the OER Activity at (100) IrO₂ Thin Film. ACS Catalysis, 2020, 10, 806-817.	5.5	52
47228	Structure and Properties of Albite Melt at High Pressures. ACS Earth and Space Chemistry, 2020, 4, 1-13.	1.2	8
47229	A Stable Zn-Based Metalâ€“Organic Framework as an Efficient Catalyst for Carbon Dioxide Cycloaddition and Alcoholysis at Mild Conditions. Catalysis Letters, 2020, 150, 1408-1417.	1.4	9
47230	On the Equilibrium Intermetallic Phase in Mg-Nd-Ag Alloys. Metallurgical and Materials Transactions A: Physical Metallurgy and Materials Science, 2020, 51, 1402-1415.	1.1	10
47231	Transport gaps in ideal zigzag-edge graphene nanoribbons with chemical edge disorder. Applied Surface Science, 2020, 512, 144714.	3.1	5
47232	The single-Mo-atom-embedded-graphdiyne monolayer with ultra-low onset potential as high efficient electrocatalyst for N2 reduction reaction. Applied Surface Science, 2020, 506, 144941.	3.1	48
47233	TensorAlloy: An automatic atomistic neural network program for alloys. Computer Physics Communications, 2020, 250, 107057.	3.0	8
47234	Embedding a percolated dual-conductive skeleton with high sodiophilicity toward stable sodium metal anodes. Nano Energy, 2020, 69, 104387.	8.2	70
47235	Strain effect on phonon transport in open framework Si24: A first-principles study. Physica E: Low-Dimensional Systems and Nanostructures, 2020, 118, 113870.	1.3	7
47236	Formulation of Multicomponent Lattice Gas Model Cluster Expansions Parameterized on Ab Initio Data: An Introduction to the Ab Initio Mean-Field Augmented Lattice Gas Modeling Code. Journal of Physical Chemistry C, 2020, 124, 2923-2938.	1.5	10
47237	Stepwise On-Surface Synthesis of Porous Carbon Nanoribbons with Notched Zigzag Edges. Journal of Physical Chemistry C, 2020, 124, 756-763.	1.5	7
47238	Defect Engineering of Iron-Rich Orthosilicate Cathode Materials with Enhanced Lithium-Ion Intercalation Capacity and Kinetics. ACS Applied Energy Materials, 2020, 3, 675-686.	2.5	3
47239	A Flexible Potassium-Ion Hybrid Capacitor with Superior Rate Performance and Long Cycling Life. ACS Applied Materials & Interfaces, 2020, 12, 2424-2431.	4.0	59

#	Article	IF	Citations
47240	Proton Redox and Transport in MXene-Confined Water. ACS Applied Materials & Interfaces, 2020, 12, 763-770.	4.0	53
47241	Synthesis of Mo₄VAlC₄ MAX Phase and Two-Dimensional Mo₄VC₄ MXene with Five Atomic Layers of Transition Metals. ACS Nano, 2020, 14, 204-217.	7.3	429
47242	A Validation of Cluster Modeling in the Description of Matrix Isolation Spectroscopy. Journal of Computational Chemistry, 2020, 41, 751-758.	1.5	5
47243	Fe_{5â^'x}Ge₂Te₂â€”a New Exfoliable Itinerant Ferromagnet with High Curie Temperature and Large Perpendicular Magnetic Anisotropy. Physica Status Solidi - Rapid Research Letters, 2020, 14, 1900666.	1.2	9
47244	Effects of chlorine adatoms on small lithium nanoclusters adsorbed on graphene. Chemical Physics Letters, 2020, 738, 136896.	1.2	4
47245	Investigation of Zr, Gd/Zr, and Pr/Zr â€“ doped ceria for the redox splitting of water. International Journal of Hydrogen Energy, 2020, 45, 160-174.	3.8	37
47246	Phase stability of TiAl-X (X=V, Nb, Ta, Cr, Mo, W, and Mn) alloys. Journal of Alloys and Compounds, 2020, 819, 153291.	2.8	33
47247	In-situ growth of ZnS/FeS heterojunctions on biomass-derived porous carbon for efficient oxygen reduction reaction. Journal of Energy Chemistry, 2020, 47, 79-85.	7.1	32
47248	A phase field model for dislocations in hexagonal close packed crystals. Journal of the Mechanics and Physics of Solids, 2020, 137, 103823.	2.3	20
47249	Effect on electronic and magnetic properties of different Re doping sites on hydrogenated armchair MoSe2 nanoribbon. Physica E: Low-Dimensional Systems and Nanostructures, 2020, 118, 113872.	1.3	5
47250	Investigation of the Structure and Luminescence Mechanism of Tm³⁺-Doped LiYF₄: New Theoretical Perspectives. Inorganic Chemistry, 2020, 59, 1211-1217.	1.9	11
47251	Periodic Electronic Structure Calculations with the Density Matrix Embedding Theory. Journal of Chemical Theory and Computation, 2020, 16, 130-140.	2.3	40
47252	Detection of Spin Transfer from Metal to Molecule by Magnetoresistance Measurement. Nano Letters, 2020, 20, 75-80.	4.5	3
47253	Interfacing Boron Monophosphide with Molybdenum Disulfide for an Ultrahigh Performance in Thermoelectrics, Two-Dimensional Excitonic Solar Cells, and Nanopiezotronics. ACS Applied Materials & Interfaces, 2020, 12, 3114-3126.	4.0	84
47254	Electron Tunneling through Boron Nitride Confirms Marcusâ€“Hush Theory Predictions for Ultramicroelectrodes. ACS Nano, 2020, 14, 993-1002.	7.3	16
47255	MoS₂ and Perylene Derivative Based Typeâ€II Heterostructure: Bandgap Engineering and Giant Photoluminescence Enhancement. Advanced Materials Interfaces, 2020, 7, 1901197.	1.9	26
47256	CaXH ₃ (X = Mn, Fe, Co) perovskiteâ€type hydrides for hydrogen storage applications. International Journal of Energy Research, 2020, 44, 2345-2354.	2.2	46
47257	Intrinsic Defect Limit to the Electrical Conductivity and a Twoâ€Step pâ€Type Doping Strategy for Overcoming the Efficiency Bottleneck of Sb₂S₃â€Based Solar Cells. Solar Rrl, 2020, 4, 1900503.	3.1	79

#	Article	IF	Citations
47258	Activating palladium nanoparticles via a Mott-Schottky heterojunction in electrocatalytic hydrodechlorination reaction. Journal of Hazardous Materials, 2020, 389, 121876.	6.5	39
47259	The effects of dilute concentrations of substitutional Re or Os on the thermodynamics and kinetics of oxygen in tungsten. Physica B: Condensed Matter, 2020, 580, 411937.	1.3	1
47260	Li₁₅P₄S₁₆Cl₃, a Lithium Chlorothiophosphate as a Solid-State Ionic Conductor. Inorganic Chemistry, 2020, 59, 226-234.	1.9	9
47261	Lattice-Strain Control of Flexible Janus Indium Chalcogenide Monolayers for Photocatalytic Water Splitting. Journal of Physical Chemistry C, 2020, 124, 167-174.	1.5	30
47262	Promotional Effect of La in the Three-Way Catalysis of La-Loaded Al₂O₃-Supported Pd Catalysts (Pd/La/Al₂O₃). ACS Catalysis, 2020, 10, 1010-1023.	5.5	46
47263	Mechanical, electronic and optical properties of SeZnO₃: a GGA+U study. Philosophical Magazine, 2020, 100, 601-618.	0.7	8
47264	Effect of IT-M doping on charge transfer and ultrafast carrier dynamics of ternary organic solar cell materials. Journal Physics D: Applied Physics, 2020, 53, 095103.	1.3	4
47265	Two-dimensional hydrogenated buckled gallium arsenide: an ab initio study. Journal of Physics Condensed Matter, 2020, 32, 145502.	0.7	2
47266	New Family of Anisotropic Zinc-Based Semiconductors in a Shallow Energy Landscape. Chemistry of Materials, 2020, 32, 326-332.	3.2	7
47267	Synthesis of orthogonally assembled 3D cross-stacked metal oxide semiconducting nanowires. Nature Materials, 2020, 19, 203-211.	13.3	172
47268	Enhancement of photovoltaic efficiency in CdSe x Te1â^'x (where 0 â©½ x â©½ 1): insights from density functional theory. Journal of Physics Condensed Matter, 2020, 32, 125702.	0.7	15
47269	Deuterium addition to liquid Liâ€“Sn alloys: implications for plasma-facing applications. Nuclear Fusion, 2020, 60, 016025.	1.6	2
47270	Single-atom Sn-Zn pairs in CuO catalyst promote dimethyldichlorosilane synthesis. National Science Review, 2020, 7, 600-608.	4.6	42
47271	Facile CO Oxidation on Oxygenâ€functionalized MXenes via the Marsâ€van Krevelen Mechanism. ChemCatChem, 2020, 12, 1007-1012.	1.8	7
47272	Influence of defects and dopants on the sensitivity of arsenene towards HCN. Applied Surface Science, 2020, 506, 144936.	3.1	61
47273	Structural and electrochemical studies of Fe-doped Na3Mn2P3O11 cathode materials for sodium-ion batteries. Journal of Alloys and Compounds, 2020, 821, 153206.	2.8	12
47274	Phase stability, magnetic and elastic properties of Co2NiGa alloy: A first-principles calculation. Materials Today Communications, 2020, 22, 100810.	0.9	7
47275	Ambipolar and Robust WSe 2 Fieldâ€Effect Transistors Utilizing Selfâ€Assembled Edge Oxides. Advanced Materials Interfaces, 2020, 7, 1901628.	1.9	11

#	Article	IF	Citations
47276	Fabrication of Ti/black TiO2-PbO2 micro/nanostructures with tunable hydrophobic/hydrophilic characteristics and their photoelectrocatalytic performance. Journal of Solid State Electrochemistry, 2020, 24, 375-387.	1.2	14
47277	Free-standing and supported phosphorene nanoflakes: Shape- and size-dependent properties. Applied Surface Science, 2020, 506, 144756.	3.1	8
47278	Thermal evolution and migration behavior of ion-implanted nitrogen in ZnO:In-N films. Applied Surface Science, 2020, 509, 144793.	3.1	4
47279	Tunable high workfunction contacts: Doped graphene. Applied Surface Science, 2020, 509, 144893.	3.1	10
47280	Development and application of EAM potentials for Ti, Al and Nb with enhanced planar fault energy of Ti. Computational Materials Science, 2020, 173, 109432.	1.4	7
47281	Giant tunability of interlayer friction in graphite via ion intercalation. Extreme Mechanics Letters, 2020, 35, 100616.	2.0	6
47282	Capacitive effect: An original of the resistive switching memory. Nano Energy, 2020, 68, 104386.	8.2	102
47283	DFT study of Pt sub-monolayer adsorption on the positive BiFeO3 (0001) surface. Surface Science, 2020, 693, 121553.	0.8	0
47284	Stability of iron-containing nanoparticles for selectively growing single-walled carbon nanotubes. Carbon, 2020, 158, 795-801.	5.4	9
47285	Proton irradiation of Niâ€“Cr alloy: Understanding the evolution of the damage microstructure. Journal of Alloys and Compounds, 2020, 815, 152408.	2.8	4
47286	Self healing of radiation-induced damage in Feâ€“Au and Feâ€“Cu alloys: Combining positron annihilation spectroscopy with TEM and ab initio calculations. Journal of Alloys and Compounds, 2020, 817, 152765.	2.8	20
47287	Chemical doping of transition metal dichalcogenides (TMDCs) based field effect transistors: A review. Superlattices and Microstructures, 2020, 137, 106350.	1.4	37
47288	Methanol synthesis from CO2/H2 on Cu (1â€¯0â€¯0): Two-tier ab initio molecular dynamics study. Applied Surface Science, 2020, 505, 144528.	3.1	5
47289	Vacancy induced p-orbital ferromagnetism in MgO nanocrystallite. Journal of Alloys and Compounds, 2020, 819, 153060.	2.8	11
47290	Designing Highâ€Performance LED Phosphors by Controlling the Phase Stability via a Heterovalent Substitution Strategy. Advanced Optical Materials, 2020, 8, 1901608.	3.6	47
47291	C3N/blue phosphorene heterostructure as a high rate-capacity and stable anode material for lithium ion batteries: Insight from first principles calculations. Applied Surface Science, 2020, 505, 144518.	3.1	44
47292	High Curie temperature ferromagnetism in penta-MnN2 monolayer. Applied Surface Science, 2020, 505, 144620.	3.1	25
47293	Interface-doping modulated structural and electronic properties of two-dimensional silica supported on metal substrate. Applied Surface Science, 2020, 506, 144677.	3.1	1

#	Article	IF	Citations
47294	A CHA zeolite supported Ga-oxo cluster for partial oxidation of CH4 at room temperature. Catalysis Today, 2020, 352, 118-126.	2.2	13
47295	Atomic structure and electronic property of two-dimensional ferroelectric CuInP2Se6. Ceramics International, 2020, 46, 7014-7018.	2.3	5
47296	Origin of anomalous laminar cracking, volume expansion and weight increase of Ti2AlC MAX phase powders at 600 Â°C. Corrosion Science, 2020, 164, 108349.	3.0	5
47297	Interface design based on Ti3C2 MXene atomic layers of advanced battery-type material for supercapacitors. Energy Storage Materials, 2020, 26, 472-482.	9.5	117
47298	Experimental and ab initio study of the Agâ€“Li system for energy storage and high-temperature solders. Journal of Alloys and Compounds, 2020, 817, 152811.	2.8	10
47299	A general rule for transition metals doping on magnetic properties of Fe-based metallic glasses. Journal of Alloys and Compounds, 2020, 819, 153062.	2.8	10
47300	Enhanced cycle stability of rechargeable Li-O2 batteries using immobilized redox mediator on air cathode. Journal of Industrial and Engineering Chemistry, 2020, 83, 14-19.	2.9	6
47301	Non-Heisenberg magnetism in a quaternary spin-gapless semiconductor. Journal of Magnetism and Magnetic Materials, 2020, 497, 166058.	1.0	3
47302	Hydrogen induced AFM to FM magnetic transition in Îµ-FeHx. Journal of Magnetism and Magnetic Materials, 2020, 498, 166147.	1.0	1
47303	Characterizing the degradation of [(UO2F2)(H2O)]7 4H2O under humid conditions. Journal of Nuclear Materials, 2020, 529, 151889.	1.3	11
47304	Thermodynamic stability analysis of Bi-containing III-V quaternary alloys and the effect of epitaxial strain. Journal of Physics and Chemistry of Solids, 2020, 138, 109245.	1.9	6
47305	Electronic and magnetic properties of Fe-doped narrow zigzag boron nitride nanoribbons. Materials Today Communications, 2020, 22, 100753.	0.9	5
47306	Structure and tensile properties of Mx(MnFeCoNi)100-x solid solution strengthened high entropy alloys. Materialia, 2020, 9, 100539.	1.3	10
47307	Fabrication and theoretical investigation of cobaltosic sulfide nanosheets for flexible aqueous Zn/Co batteries. Nano Energy, 2020, 68, 104314.	8.2	51
47308	d-orbital-frustration-induced ferromagnetic monolayer Cu3O2. Physica B: Condensed Matter, 2020, 577, 411826.	1.3	3
47309	Cu-doping impact on the electronic and magnetic properties of Co<mml:math xmlns:mml="http://www.w3.org/1998/Math/MathML" display="inline" id="d1e397" altimg="si28.svg"><mml:msub><mml:mrow /><mml:mrow><mml:mn>2</mml:mn></mml:mrow></mml:msub></mml:math>ZrSn. Physica B: Condensed Matter, 2020, 580, 411836.	1.3	6
47310	Strong Jahn-Teller effect at NiO4 tetrahedron in NiCo2O4 spinel. Physics Letters, Section A: General, Atomic and Solid State Physics, 2020, 384, 126114.	0.9	4
47311	Carbazole-substituted NP-based derivative as hole transporting material for highly efficient perovskite solar cells. Spectrochimica Acta - Part A: Molecular and Biomolecular Spectroscopy, 2020, 228, 117808.	2.0	14

#	Article	IF	Citations
47312	Ultrahigh-strain ferroelasticity in two-dimensional honeycomb monolayers: from covalent to metallic bonding. Science Bulletin, 2020, 65, 147-152.	4.3	21
47313	Core effect of local atomic configuration and design principles in AlxCoCrFeNi high-entropy alloys. Scripta Materialia, 2020, 178, 181-186.	2.6	29
47314	Electronic structures of new layered hexaboron Crâ€“B compounds from first principles. Solid State Sciences, 2020, 99, 106069.	1.5	2
47315	Reversible lithium storage capacity on carbon nitride by electric field. Superlattices and Microstructures, 2020, 137, 106340.	1.4	3
47316	Nano-patterned honeycomb structure of monolayer copper selenide on Cu(111). Thin Solid Films, 2020, 693, 137709.	0.8	4
47317	Imaging defect complexes in scanning transmission electron microscopy: Impact of depth, structural relaxation, and temperature investigated by simulations. Ultramicroscopy, 2020, 209, 112884.	0.8	4
47318	Unusual Mechanism Behind Enhanced Photocatalytic Activity and Surface Passivation of SiC(0001) via Forming Heterostructure with a MoS₂ Monolayer. Journal of Physical Chemistry C, 2020, 124, 1362-1368.	1.5	7
47319	Shining Emitter in a Stable Host: Design of Halide Perovskite Scintillators for X-ray Imaging from Commercial Concept. ACS Nano, 2020, 14, 5183-5193.	7.3	205
47320	Nanoscale amorphous interfaces in phase-change memory materials: structure, properties and design. Journal Physics D: Applied Physics, 2020, 53, 114002.	1.3	4
47321	Low thermal conductivity of peanut-shaped carbon nanotube and its insensitive response to uniaxial strain. Nanotechnology, 2020, 31, 115701.	1.3	4
47322	Non-chemical fluorination of hexagonal boron nitride by high-energy ion irradiation. Nanotechnology, 2020, 31, 125705.	1.3	5
47323	Oxygen Evolution on Metalâ€oxyâ€hydroxides: Beneficial Role of Mixing Fe, Co, Ni Explained via Bifunctional Edge/acceptor Route. ChemCatChem, 2020, 12, 1436-1442.	1.8	21
47324	A decohesion pathway for hydrogen embrittlement in nickel: Mechanism and quantitative prediction. Acta Materialia, 2020, 185, 98-109.	3.8	55
47325	Solute effects on the 123 <mml:math xmlns:mml="http://www.w3.org/1998/Math/MathML" altimg="si1.svg"><mml:mrow><mml:mfenced open="(" ij EtQq1 1 0.784314 rgB1 /Overlock 10 Tf 50 237 Td (close=")"><mml:mrow><mml:mover stretchy="false">[</mml:mo><mml:mn>1</mml:mn><mml:mover accent="true"><mml:mrow><mml:mn>1</mml:mn></mml:mrow><mml:mrow><mml:mo>-</mml:mo></mml:mrow></mml:mover><mml:mover stretchy="false">]</mml:mo></mml:mrow></mml:mrow></mml:math> tilt grain boundary in BCC Fe:	1.4	37
47326	A minimal Tersoff potential for diamond silicon with improved descriptions of elastic and phonon transport properties. Journal of Physics Condensed Matter, 2020, 32, 135901.	0.7	9
47327	Rotation Tunable Photocatalytic Properties of ZnO/GaN Heterostructures. Physica Status Solidi (B): Basic Research, 2020, 257, 1900663.	0.7	11
47328	First-Principles Study of Structural, Elastic, and Thermodynamic Properties of PdSn4 with Ni Addition. Journal of Electronic Materials, 2020, 49, 1435-1444.	1.0	6
47329	ALD-assisted synthesis of V2O5 nanoislands on SnO2 nanowires for improving NO2 sensing performance. Applied Surface Science, 2020, 509, 144821.	3.1	18

#	Article	IF	Citations
47330	Atomic diffusion mediated by vacancy defects in L12-Zr3Al: A first-principles study. Journal of Alloys and Compounds, 2020, 821, 153223.	2.8	9
47331	Exploring the effect of dopant (Si, P, S, Ge, Se, and Sb) in arsenene: A DFT study. Physics Letters, Section A: General, Atomic and Solid State Physics, 2020, 384, 126146.	0.9	8
47332	Band alignment engineering: ultrabroadband photodetection with SnX₂ (Xâ€‰â€‰=â€‰â€‰S, Se)/ZnS heterostructures. Journal of Physics Condensed Matter, 2020, 32, 115703.	0.7	15
47333	The Systematic Refinement for the Phase Change and Conversion Reactions Arising from the Lithiation of Magnetite Nanocrystals. Advanced Functional Materials, 2020, 30, 1907337.	7.8	8
47334	PBCFâ€Graphene: A 2D Sp² Hybridized Honeycomb Carbon Allotrope with a Direct Band Gap. ChemNanoMat, 2020, 6, 139-147.	1.5	54
47335	Insights for optimum cation defects in photocatalysis: A case study of hematite nanostructures. Applied Catalysis B: Environmental, 2020, 264, 118506.	10.8	30
47336	Electronic structure and morphology of thin surface alloy layers formed by deposition of Sn on Au(1â€¯1â€¯1). Applied Surface Science, 2020, 506, 144606.	3.1	13
47337	High conductivity Ni12P5 nanowires as high-rate electrode material for battery-supercapacitor hybrid devices. Chemical Engineering Journal, 2020, 392, 123661.	6.6	78
47338	Thermodynamic modelling of the Feâ€“Snâ€“Zr system based on new experiments and first-principles calculations. Journal of Alloys and Compounds, 2020, 821, 153200.	2.8	12
47339	Electrochemical CO₂ Reduction Reaction on M@Cu(211) Bimetallic Single-Atom Surface Alloys: Mechanism, Kinetics, and Catalyst Screening. ACS Sustainable Chemistry and Engineering, 2020, 8, 210-222.	3.2	86
47340	Rational Synthesis for a Noble Metal Carbide. Journal of the American Chemical Society, 2020, 142, 1247-1253.	6.6	15
47341	Ag-modified Fe₂O₃ nanoparticles on a carbon cloth as an anode material for high-performance supercapacitors. Nanotechnology, 2020, 31, 125405.	1.3	4
47342	Recent Progress in Twoâ€Dimensional Ferroelectric Materials. Advanced Electronic Materials, 2020, 6, 1900818.	2.6	236
47343	Atomic Selfâ€reconstruction of Catalyst Dominated Growth Mechanism of Graphite Structures. ChemCatChem, 2020, 12, 1316-1324.	1.8	6
47344	Iron-doping induced multiferroic in two-dimensional In2Se3. Science China Materials, 2020, 63, 421-428.	3.5	30
47345	In situ no-slot joint integration of half-metallic C(CN)3 cocatalyst into g-C3N4 scaffold: An absolute metal-free in-plane heterosystem for efficient and selective photoconversion of CO2 into CO. Applied Catalysis B: Environmental, 2020, 264, 118470.	10.8	41
47346	Thickness effect on the structural, electronic and energetic properties of the cubic KMgF3 (0Â0Â1) surfaces: A first-principles study. Applied Surface Science, 2020, 506, 144678.	3.1	4
47347	Ohmic contact formation mechanisms of TiN film on 4Hâ€“SiC. Ceramics International, 2020, 46, 7142-7148.	2.3	3

#	Article	IF	Citations
47348	Influence of boron isotope ratio on the thermal conductivity of uranium diboride (UB2) and zirconium diboride (ZrB2). Journal of Nuclear Materials, 2020, 528, 151892.	1.3	12
47349	Theoretical study on structural, mechanical and electronic properties of ternary mononitride Ti0.5W0.5N from first-principles calculations. Materials Chemistry and Physics, 2020, 242, 122476.	2.0	9
47350	Photoninduced charge redistribution of graphene determined by edge structures in the infrared region. Spectrochimica Acta - Part A: Molecular and Biomolecular Spectroscopy, 2020, 229, 117858.	2.0	8
47351	Efficient and tunable one-dimensional charge transport in layered lanthanide metalâ€“organic frameworks. Nature Chemistry, 2020, 12, 131-136.	6.6	214
47352	Two-dimensional MoS₂/GaN van der Waals heterostructures: tunable direct band alignments and excitonic optical properties for photovoltaic applications. Journal Physics D: Applied Physics, 2020, 53, 095107.	1.3	6
47353	A Delicate Balance between Antiferromagnetism and Ferromagnetism: Theoretical and Experimental Studies of A₂MRu₅B₂ (A=Zr, Hf; M=Fe, Mn) Metal Borides. Chemistry - A European Journal, 2020, 26, 1979-1988.	1.7	5
47354	Super strong 2D titanium carbide MXene-based materials: a theoretical prediction. Journal of Physics Condensed Matter, 2020, 32, 11LT01.	0.7	22
47355	Erosion and cathodic arc plasma of Nbâ€“Al cathodes: composite versus intermetallic. Plasma Sources Science and Technology, 2020, 29, 025022.	1.3	10
47356	Role of phonons on phase stabilization of RE2Si2O7 over wide temperature range (RE = Yb, Gd). Journal of the European Ceramic Society, 2020, 40, 780-788.	2.8	8
47357	Cu Intercalation and Br Doping to Thermoelectric SnSe₂ Lead to Ultrahigh Electron Mobility and Temperatureâ€Independent Power Factor. Advanced Functional Materials, 2020, 30, 1908405.	7.8	53
47358	Engineering Active Fe Sites on Nickelâ€“Iron Layered Double Hydroxide through Component Segregation for Oxygen Evolution Reaction. ChemSusChem, 2020, 13, 811-818.	3.6	62
47359	Microscopic Properties of Na and Liâ€”A First Principle Study of Metal Battery Anode Materials. ChemSusChem, 2020, 13, 771-783.	3.6	18
47360	Thicknessâ€Dependent Inâ€Plane Polarization and Structural Phase Transition in van der Waals Ferroelectric CuInP₂S₆. Small, 2020, 16, e1904529.	5.2	50
47361	Lithium and sodium decorated graphdiyne as a candidate for hydrogen storage: First-principles and grand canonical Monte Carlo study. Applied Surface Science, 2020, 509, 144855.	3.1	41
47362	Generalized regular <mml:math xmlns:mml="http://www.w3.org/1998/Math/MathML" altimg="si36.svg"><mml:mrow><mml:mi mathvariant="bold">k</mml:mi></mml:mrow></mml:math>-point grid generation on the fly. Computational Materials Science, 2020, 173, 109340.	1.4	8
47363	pH dependence of aqueous oxalic acid observed by X-ray absorption and emission spectroscopy. Chemical Physics Letters, 2020, 738, 136895.	1.2	1
47364	On preconditioning the self-consistent field iteration in real-space Density Functional Theory. Chemical Physics Letters, 2020, 739, 136983.	1.2	14
47365	Tunable magnetic properties of fluorinated two-dimensional Tetra-MoN2. Chemical Physics Letters, 2020, 739, 136991.	1.2	2

#	Article	IF	Citations
47366	Hole mobility enhancement in strained nanocrystalline architecture of group IV semiconductors. Journal of Alloys and Compounds, 2020, 821, 153212.	2.8	3
47367	A new intermediate phase in compressed nitinol. Journal of Alloys and Compounds, 2020, 817, 153234.	2.8	1
47368	A study on Site Preferences of Eu3+ Dopants in La3+, Ca2+ sites of La2CaB8O16 crystal. Journal of Luminescence, 2020, 219, 116923.	1.5	7
47369	A skin-like sensor for intelligent Braille recognition. Nano Energy, 2020, 68, 104346.	8.2	87
47370	In-situ topochemical nitridation derivative MoO2â€“Mo2N binary nanobelts as multifunctional interlayer for fast-kinetic Li-Sulfur batteries. Nano Energy, 2020, 68, 104356.	8.2	116
47371	Large influence of vacancies on the elastic constants of cubic epitaxial tantalum nitride layers grown by reactive magnetron sputtering. Acta Materialia, 2020, 184, 254-266.	3.8	26
47372	Four distinct resistive states in van der Waals full magnetic 1T-VSe2/CrI3/1T-VSe2 tunnel junction. Applied Surface Science, 2020, 505, 144648.	3.1	23
47373	AICON: A program for calculating thermal conductivity quickly and accurately. Computer Physics Communications, 2020, 251, 107074.	3.0	20
47374	Iron-rich carbonates stabilized by magnetic entropy at lower mantle conditions. Earth and Planetary Science Letters, 2020, 531, 115959.	1.8	12
47375	Theoretical models for hydrogen evolution reaction at combined Mo2C and N â€“ doped graphene. Journal of Catalysis, 2020, 381, 234-247.	3.1	27
47376	Polytetrahedral short-range order and crystallization stability in supercooled <mml:math xmlns:mml="http://www.w3.org/1998/Math/MathML" altimg="si13.svg"><mml:mrow><mml:msub><mml:mrow><mml:mi mathvariant="normal">Cu</mml:mi></mml:mrow><mml:mrow><mml:mn>64.5</mml:mn></mml:mrow></mml:msub><mml:msub><mml:mrow><mml:mi mathvariant="normal">Zr</mml:mi></mml:mrow><mml:mrow><mml:mn>35.5</mml:mn></mml:mrow></mml:msub></mml:mrow> metallic liquid. Journal of Crystal Growth, 2020, 531, 125374.	0.7	1
47377	O-doped graphdiyne as metal-free catalysts for nitrogen reduction reaction. Molecular Catalysis, 2020, 483, 110705.	1.0	44
47378	Oxygen/sulfur decorated 2D MXene V2C for promising lithium ion battery anodes. Materials Today Communications, 2020, 22, 100713.	0.9	27
47379	Interfacial parameters of Pt/Î³-Al2O3: A first-principle and MD simulation study. Physica E: Low-Dimensional Systems and Nanostructures, 2020, 117, 113804.	1.3	2
47380	Coverage-Dependent Adsorption of Phenol on Pt(111) from First Principles. Journal of Physical Chemistry C, 2020, 124, 356-362.	1.5	12
47381	Phase transitions in Fe₃Al-based alloys: ab initio study. Phase Transitions, 2020, 93, 43-53.	0.6	1
47382	Modification of TiO₂ with hBN: high temperature anatase phase stabilisation and photocatalytic degradation of 1,4-dioxane. JPhys Materials, 2020, 3, 015009.	1.8	11
47383	Firstâ€Principles Simulation of Carrier Recombination Mechanisms in Halide Perovskites. Advanced Energy Materials, 2020, 10, 1902830.	10.2	52

#	Article	IF	Citations
47384	Thermodynamically Stable Mesoporous C₃N₇ and C₃N₆ with Ordered Structure and Their Excellent Performance for Oxygen Reduction Reaction. Small, 2020, 16, e1903572.	5.2	53
47385	Atomic scale investigation of the crystal structure and interfaces of the Bâ€² precipitate in Al-Mg-Si alloys. Acta Materialia, 2020, 185, 193-203.	3.8	72
47386	Growth-twins in CrN/AlN multilayers induced by hetero-phase interfaces. Acta Materialia, 2020, 185, 157-170.	3.8	8
47387	Single Fe atoms confined in two-dimensional MoS2 for sulfite activation: A biomimetic approach towards efficient radical generation. Applied Catalysis B: Environmental, 2020, 268, 118459.	10.8	86
47388	Solar-driven efficient methane catalytic oxidation over epitaxial ZnO/La0.8Sr0.2CoO3 heterojunctions. Applied Catalysis B: Environmental, 2020, 265, 118469.	10.8	44
47389	Irreversible structural dynamics on the surface of bimetallic PtNi alloy catalyst under alternating oxidizing and reducing environments. Applied Catalysis B: Environmental, 2020, 264, 118476.	10.8	26
47390	Insights into the role of cation vacancy for significantly enhanced electrochemical nitrogen reduction. Applied Catalysis B: Environmental, 2020, 264, 118477.	10.8	74
47391	Direct observation of the water dimer adsorbed on graphite. Applied Surface Science, 2020, 505, 144600.	3.1	2
47392	C568: A new two-dimensional sp2-sp3 hybridized allotrope of carbon. Carbon, 2020, 158, 827-835.	5.4	62
47393	Emergence of Type-I and Type-II Dirac line nodes in penta-octa-graphene. Carbon, 2020, 158, 210-215.	5.4	18
47394	The lithiation process and Li diffusion in amorphous <mml:math xmlns:mml="http://www.w3.org/1998/Math/MathML" altimg="si1.svg"><mml:mrow><mml:msub><mml:mrow><mml:mtext>SiO</mml:mtext></mml:mrow><mml:mrow><mml:mn>2</mml:mn> and Si from first-principles. Electrochimica Acta, 2020, 331, 135344.	2.6	66
47395	Effects of transition elements on the site preference, elastic properties and phase stability of L12 Î³â€²-Co3(Al, W) from first-principles calculations. Journal of Alloys and Compounds, 2020, 820, 153179.	2.8	15
47396	The role of H2 on the stability of the single-metal-site Ir1/AC catalyst for heterogeneous methanol carbonylation. Journal of Catalysis, 2020, 381, 193-203.	3.1	21
47397	Ge2Sb2Se5 Glass as High-capacity Promising Lithium-ion Battery Anode. Nano Energy, 2020, 68, 104326.	8.2	38
47398	Strain tunable Schottky barriers and tunneling characteristics of borophene/MX2 van der Waals heterostructures. Physica E: Low-Dimensional Systems and Nanostructures, 2020, 120, 113842.	1.3	12
47399	Effective adsorption of uranyl ions with different MoS2-exposed surfaces in aqueous solution. Surfaces and Interfaces, 2020, 18, 100409.	1.5	15
47400	Friction and Wear Behavior of CrN Coating on 316L Stainless Steel in Liquid Sodium at Elevated Temperature. Tribology International, 2020, 143, 106079.	3.0	33
47401	Theoretical studies on the structure and properties of DAT/BTNAT cocrystal under high pressure. Canadian Journal of Chemistry, 2020, 98, 128-133.	0.6	1

#	Article	IF	Citations
47402	â€œFlat/steep band modelâ€•for superconductors containing Bi square nets. Zeitschrift Fur Naturforschung - Section B Journal of Chemical Sciences, 2020, 75, 183-190.	0.3	1
47403	Theoretical Investigations on the Nanowires Assembled by the V1@Si12 Clusters. Journal of Cluster Science, 2020, 31, 637-642.	1.7	3
47404	NaV6O15: A promising cathode material for insertion/extraction of Mg2+ with excellent cycling performance. Nano Research, 2020, 13, 335-343.	5.8	28
47405	HCOOH dissociation over the core-shell M@Pd bimetallic catalysts: Probe into the effect of the core metal type on the catalytic performance. Applied Surface Science, 2020, 506, 144938.	3.1	13
47406	Insights into the trapping mechanism of light metals on C2N-h2D: Utilisation as an anode material for metal ion batteries. Carbon, 2020, 160, 125-132.	5.4	29
47407	Ferromagnetic property of copper doped ZnO: A first-principles study. Computational Condensed Matter, 2020, 23, e00455.	0.9	6
47408	The effect of DOPA hydroxyl groups on wet adhesion to polystyrene surface: An experimental and theoretical study. Materials Chemistry and Physics, 2020, 243, 122606.	2.0	8
47409	New group V graphyne: two-dimensional direct semiconductors with remarkable carrier mobilities, thermoelectric performance, and thermal stability. Materials Today Physics, 2020, 12, 100164.	2.9	17
47410	Structureâ€“Charge Transport Relationships in Fluoride-Doped Amorphous Semiconducting Indium Oxide: Combined Experimental and Theoretical Analysis. Chemistry of Materials, 2020, 32, 805-820.	3.2	16
47411	Relative Stability of Near-Surface Oxygen Vacancies at the CeO₂(111) Surface upon Zirconium Doping. Journal of Physical Chemistry C, 2020, 124, 625-638.	1.5	16
47412	Decisive Role of Interlayer Ionic Couplings for the Electronic Properties of Two-Dimensional Layered Electrides. Journal of Physical Chemistry C, 2020, 124, 1398-1404.	1.5	14
47413	Amorphous Mixture of Two Indium-Free BaSnO₃ and ZnSnO₃ for Thin-Film Transistors with Balanced Performance and Stability. ACS Applied Materials & Interfaces, 2020, 12, 3719-3726.	4.0	15
47414	Facile Combined Experimental and Computational Study: g-C₃N₄@PDMS-Assisted Knoevenagel Condensation Reaction under Phase Transfer Conditions. ACS Sustainable Chemistry and Engineering, 2020, 8, 2350-2360.	3.2	12
47415	Ni₃S₂ anchored to N/S co-doped reduced graphene oxide with highly pleated structure as a sulfur host for lithiumâ€“sulfur batteries. Journal of Materials Chemistry A, 2020, 8, 3834-3844.	5.2	56
47416	2D organ-like molybdenum carbide (MXene) coupled with MoS₂ nanoflowers enhances the catalytic activity in the hydrogen evolution reaction. CrystEngComm, 2020, 22, 1395-1403.	1.3	63
47417	Anomalous lattice thermal conductivity in layered MNCl (M = Zr, Hf) materials driven by lanthanide contraction. Journal of Materials Chemistry A, 2020, 8, 3128-3134.	5.2	14
47418	Two-dimensional graphitic carbon nitride (g-C4N3) for superior selectivity of multiple toxic gases (CO, NO2, and NH3). Nanotechnology, 2020, 31, 145501.	1.3	19
47419	Two-dimensional ferromagnetic superlattices. National Science Review, 2020, 7, 745-754.	4.6	39

#	Article	IF	Citations
47420	Is graphite lithiophobic or lithiophilic?. National Science Review, 2020, 7, 1208-1217.	4.6	126
47421	Evidence for a soft phonon mode driven Peierls-type distortion in <mml:math xmlns:mml="http://www.w3.org/1998/Math/MathML"><mml:msub><mml:mi mathvariant="normal">Sc</mml:mi><mml:mn>3</mml:mn></mml:msub><mml:mi mathvariant="normal">Co</mml:mi><mml:msub><mml:mi mathvariant="normal">C</mml:mi><mml:mn>4</mml:mn></mml:msub></mml:math>. Physical Review B,	1.1	3
47422	Strong spin depolarization in the ferromagnetic Weyl semimetal <mml:math xmlns:mml="http://www.w3.org/1998/Math/MathML"><mml:msub><mml:mi>Co</mml:mi><mml:mn>3</mml:mn></mml:msub><mml:m mathvariant="normal">S</mml:mi><mml:mn>2</mml:mn></mml:msub></mml:math> : Role of spin-orbit coupling. Physical Review B, 2020, 102, .	1.1	10
47423	Coherently coupled quantum-well states in bimetallic Pb/Ag thin films. Physical Review B, 2020, 102, .	1.1	1
47424	Localized dimers drive strong anharmonicity and low lattice thermal conductivity in <mml:math xmlns:mml="http://www.w3.org/1998/Math/MathML"><mml:mrow><mml:mi>Zn</mml:mi><mml:msub><mml:mi>Sb</mml:mi> Physical Review B, 2020, 102, .	1.1	11
47426	Ising Superconductivity and Magnetism in <mml:math xmlns:mml="http://www.w3.org/1998/Math/MathML" display="inline"><mml:mrow><mml:msub><mml:mrow><mml:mi>NbSe</mml:mi></mml:mrow><mml:mrow><mml:mn>2</mml:mn> Physical Review X, 2020, 10, .	2.8	36
47427	Highly Conductive P-Type MAPbI3 Films and Crystals via Sodium Doping. Frontiers in Chemistry, 2020, 8, 754.	1.8	18
47428	Structure and Stability of Iron Fluoride at High Pressureâ€“Temperature and Implication for a New Reservoir of Fluorine in the Deep Earth. Minerals (Basel, Switzerland), 2020, 10, 783.	0.8	6
47429	Highâ€Throughput Computational Characterization of 2D Compositionally Complex Transitionâ€Metal Chalcogenide Alloys. Advanced Theory and Simulations, 2020, 3, 2000195.	1.3	11
47430	Photogalvanicâ€Effectâ€Induced Spinâ€Polarized Current in Defective Silicane with H Vacancies. Physica Status Solidi - Rapid Research Letters, 2020, 14, 2000395.	1.2	13
47431	Shallow Iodine Defects Accelerate the Degradation of Î±-Phase Formamidinium Perovskite. Joule, 2020, 4, 2426-2442.	11.7	173
47432	Enumeration as a Tool for Structure Solution: A Materials Genomic Approach to Solving the Cation-Ordered Structure of Na₃V₂(PO₄)₂F₃. Chemistry of Materials, 2020, 32, 8981-8992.	3.2	14
47433	Magnetocaloric Effect in a Frustrated Gd-Garnet with No Long-Range Magnetic Order. Inorganic Chemistry, 2020, 59, 15144-15153.	1.9	19
47434	Intercalation-Induced Conversion Reactions Give High-Capacity Potassium Storage. ACS Nano, 2020, 14, 14026-14035.	7.3	42
47435	Prediction of superconductivity and topological aspects in single-layer Î²â^'Bi2Pd. Physical Review B, 2020, 102, .	1.1	10
47436	Mayenite Electrides and Their Doped Forms for Oxygen Reduction Reaction in Solid Oxide Fuel Cells. Energies, 2020, 13, 4978.	1.6	0
47437	Dualâ€Metal Interbonding as the Chemical Facilitator for Singleâ€Atom Dispersions. Advanced Materials, 2020, 32, e2003484.	11.1	90
47438	Insights of the anionic redox in P2â€“Na0.67Ni0.33Mn0.67O2. Nano Energy, 2020, 78, 105285.	8.2	49

#	Article	IF	Citations
47439	Predicting Inorganic Photovoltaic Materials with Efficiencies >26% via Structure-Relevant Machine Learning and Density Functional Calculations. Cell Reports Physical Science, 2020, 1, 100179.	2.8	20
47440	Application of Nuclear Inelastic Scattering Spectroscopy to the Frequency Scale Calibration of Ab Initio Calculated Phonon Density of States of Quasi-One-Dimensional Ternary Iron Chalcogenide RbFeSe2. Applied Sciences (Switzerland), 2020, 10, 7212.	1.3	2
47441	Revealing the Bonding Nature in an ALnZnTe3-Type Alkaline-Metal (A) Lanthanide (Ln) Zinc Telluride by Means of Experimental and Quantum-Chemical Techniques. Crystals, 2020, 10, 916.	1.0	10
47442	Strontium Ion Bâ€Site Substitution for Spectralâ€Stable Blue Emitting Perovskite Lightâ€Emitting Diodes. Advanced Optical Materials, 2020, 8, 2001073.	3.6	28
47443	The Mobile and Pinned Grain Boundaries in 2D Monoclinic Rhenium Disulfide. Advanced Science, 2020, 7, 2001742.	5.6	15
47444	Adsorption and Reaction of Trimethyl and Triethyl Phosphite on Fe3O4 by Density Functional Theory. Tribology Letters, 2020, 68, 1.	1.2	0
47445	Development of a Microkinetic Model for the CO2 Methanation with an Automated Reaction Mechanism Generator. Computer Aided Chemical Engineering, 2020, 48, 529-534.	0.3	7
47446	Acid properties of Ni-modified ZSM-12: A first-principles Study. Journal of Fuel Chemistry and Technology, 2020, 48, 704-712.	0.9	4
47447	Catalytic activity of Rh /MegO-nanotube for NO adsorption and dissociation: A van der waals density functional study. Applied Surface Science, 2020, 530, 147179.	3.1	2
47448	Structural and spin state transition in the polar NiO(1 1 1) surface. Applied Surface Science, 2020, 532, 147427.	3.1	11
47449	Design of three-dimensional nanotube-fullerene-interconnected framework for hydrogen storage. Applied Surface Science, 2020, 534, 147606.	3.1	20
47450	First-principles study of FeNi1-xCrx (0â‰¤xâ‰¤1) disordered alloys from special quasirandom structures. Calphad: Computer Coupling of Phase Diagrams and Thermochemistry, 2020, 71, 102007.	0.7	7
47451	First-principles-only CALPHAD phase diagram of the solid aluminium-nickel (Al-Ni) system. Calphad: Computer Coupling of Phase Diagrams and Thermochemistry, 2020, 71, 102008.	0.7	10
47452	Evolutionary search for new compounds in the Tiâ€“Si system. Calphad: Computer Coupling of Phase Diagrams and Thermochemistry, 2020, 71, 102201.	0.7	4
47453	Formaldehyde adsorption effects of chlorine adatoms on lithium-decorated graphene: A DFT study. Chemical Physics Letters, 2020, 761, 138085.	1.2	7
47454	Theoretical and experimental study of reversible intercalation of Li ions in the Jarosite NaFe3(SO4)2(OH)6 structure. Electrochimica Acta, 2020, 359, 136950.	2.6	6
47455	Uncovering the electrochemical interface of low-index copper surfaces in deep groundwater environments. Electrochimica Acta, 2020, 362, 137111.	2.6	5
47456	Boosting up printability of biomacromolecule based bio-ink by modulation of hydrogen bonding pairs. European Polymer Journal, 2020, 141, 110070.	2.6	6

#	Article	IF	Citations
47457	Platinum doped iron carbide for the hydrogen evolution reaction: The effects of charge transfer and magnetic moment by first-principles approach. International Journal of Hydrogen Energy, 2020, 45, 31825-31840.	3.8	16
47458	Dissociative adsorption and linear organization of formic acid on ZnO(1Â0Ââ˜1Â0) surface. Journal of Catalysis, 2020, 390, 109-116.	3.1	9
47459	Recycling prospect and sustainable lubrication mechanism of water-based MoS2 nano-lubricant for steel cold rolling process. Journal of Cleaner Production, 2020, 277, 123991.	4.6	19
47460	Multiple-valued electric polarization in multiferroic GdMn2O5 from first principles. Journal of Magnetism and Magnetic Materials, 2020, 516, 167373.	1.0	4
47461	First principles and molecular dynamics study of Li wetting and diffusion on W surfaces. Journal of Nuclear Materials, 2020, 539, 152345.	1.3	8
47462	Lithium superionic conduction in Î±-Li10P4N10: A promising inorganic solid electrolyte candidate. Journal of Power Sources, 2020, 477, 228744.	4.0	3
47463	Mechanism study on CO2 reforming of methane over platinum cluster doped graphene: A DFT calculation. Molecular Catalysis, 2020, 497, 111205.	1.0	8
47464	Chemical trends of structural, mechanical, electronic and optical properties of Bi2O2X (X = S, Se, Te): A first-principles study. Materials Today Communications, 2020, 25, 101619.	0.9	5
47465	Reducing polarization of lithium-sulfur batteries via ZnS/reduced graphene oxide accelerated lithium polysulfide conversion. Materials Today Energy, 2020, 18, 100519.	2.5	39
47466	Cs0.15FA0.85PbI3/CsxFA1-xPbI3 Core/Shell Heterostructure for Highly Stable and Efficient Perovskite Solar Cells. Cell Reports Physical Science, 2020, 1, 100224.	2.8	35
47467	Boosting Electrocatalytic HER Activity of 3D Interconnected CoSP via Metal Doping: Active and Stable Electrocatalysts for pH-Universal Hydrogen Generation. Chemistry of Materials, 2020, 32, 9591-9601.	3.2	39
47468	Ambient and High Pressure CuNiSb2: Metal-Ordered and Metal-Disordered NiAs-Type Derivative Pnictides. Inorganic Chemistry, 2020, 59, 14058-14069.	1.9	0
47469	A Genetic Algorithmic Approach to Determine the Structure of Liâ€“Al Layered Double Hydroxides. Journal of Chemical Information and Modeling, 2020, 60, 4845-4855.	2.5	4
47470	Hole Polaron Transport in Bismuth Vanadate BiVO₄ from Hybrid Density Functional Theory. Journal of Physical Chemistry C, 2020, 124, 23038-23044.	1.5	20
47471	Poly-p-phenylenes as Novel Bulk-type Anode Materials for Potassium-Ion Batteries: A First-Principles Study. Journal of Physical Chemistry C, 2020, 124, 23045-23051.	1.5	6
47472	Thermodynamic Evolution of Cerium Oxide Nanoparticle Morphology Using Carbon Dioxide. Journal of Physical Chemistry C, 2020, 124, 23210-23220.	1.5	13
47473	Interfacial States, Energetics, and Atmospheric Stability of Large-Grain Antifluorite Cs₂TiBr₆. Journal of Physical Chemistry C, 2020, 124, 24289-24297.	1.5	21
47474	Realization of a Buckled Antimonene Monolayer on Ag(111) via Surface Engineering. Journal of Physical Chemistry Letters, 2020, 11, 8976-8982.	2.1	23

#	Article	IF	Citations
47475	Edge Influence on Charge Carrier Localization and Lifetime in CH₃NH₃PbBr₃ Perovskite: Ab Initio Quantum Dynamics Simulation. Journal of Physical Chemistry Letters, 2020, 11, 9100-9109.	2.1	39
47476	Interlayer Polarization Explains Slow Charge Recombination in Two-Dimensional Halide Perovskites by Nonadiabatic Molecular Dynamics Simulation. Journal of Physical Chemistry Letters, 2020, 11, 9032-9037.	2.1	13
47477	Tuning the Electronic Structure of an Î±-Antimonene Monolayer through Interface Engineering. Nano Letters, 2020, 20, 8408-8414.	4.5	33
47478	Photochemical Construction of Nitrogen-Containing Nanocarbons for Carbon Dioxide Photoreduction. ACS Catalysis, 2020, 10, 12706-12715.	5.5	36
47479	Giant shift upon strain on the fluorescence spectrum of VNNB color centers in h-BN. Npj Quantum Information, 2020, 6, .	2.8	25
47480	Long-range ordered and atomic-scale control of graphene hybridization by photocycloaddition. Nature Chemistry, 2020, 12, 1035-1041.	6.6	41
47481	The role of adsorbed hydroxide in hydrogen evolution reaction kinetics on modified platinum. Nature Energy, 2020, 5, 891-899.	19.8	400
47482	Theoretical study on the interaction of iodide electrolyte/organic dye with the TiO₂ surface in dye-sensitized solar cells. Physical Chemistry Chemical Physics, 2020, 22, 26410-26418.	1.3	7
47483	2D van der Waals heterostructures of graphitic BCN as direct Z-scheme photocatalysts for overall water splitting: the role of polar Ï€-conjugated moieties. Physical Chemistry Chemical Physics, 2020, 22, 23735-23742.	1.3	16
47484	Modulation of band alignment with water redox potentials by biaxial strain on orthorhombic NaTaO₃ thin films. Physical Chemistry Chemical Physics, 2020, 22, 23810-23815.	1.3	5
47485	Enhanced robustness of half-metallicity in VBr₃ nanowires by strains and transition metal doping. Physical Chemistry Chemical Physics, 2020, 22, 24455-24461.	1.3	1
47486	Unveiling the mechanism of rare earth doping to optimize the optical performance of the CsPbBr₃ perovskite. Inorganic Chemistry Frontiers, 2020, 7, 4669-4676.	3.0	15
47487	Layered double hydroxide derived NiAl-oxide hollow nanospheres for selective transfer hydrogenation with improved stability. Journal of Materials Chemistry A, 2020, 8, 23376-23384.	5.2	9
47488	Understanding the electrochemical properties of bulk phase and surface structures of Na₃T^MPO₄CO₃(T^M= Fe, Mn, Co, Ni) from first principles calculations. Physical Chemistry Chemical Physics, 2020, 22, 25325-25334.	1.3	7
47489	Waterâ€“gas shift reaction co-catalyzed by polyoxometalate (POM)â€“gold composites: the â€œmagicâ€•role of POMs. Catalysis Science and Technology, 2020, 10, 8219-8229.	2.1	8
47490	Role of defects in carbon materials during metal-free formic acid dehydrogenation. Nanoscale, 2020, 12, 22768-22777.	2.8	19
47491	Charge separation boosts exciton diffusion in fused ring electron acceptors. Journal of Materials Chemistry A, 2020, 8, 23304-23312.	5.2	18
47492	A density-functional theory study of the Al/AlOx/Al tunnel junction. Journal of Applied Physics, 2020, 128, 155102.	1.1	14

#	Article	IF	Citations
47493	Toughening a superstrong carbon crystal: Sequential bond-breaking mechanisms. Physical Review B, 2020, 102, .	1.1	8
47494	Isosymmetric phase transitions, ultrahigh ductility, and topological nodal lines in <mml:math xmlns:mml="http://www.w3.org/1998/Math/MathML"><mml:mrow><mml:mi>Î±</mml:mi><mml:mo>â^'</mml:mo><mml:mi mathvariant="normal">A</mml:mi><mml:msub><mml:mi mathvariant="normal">g</mml:mi><mml:mn>2</mml:mn></mml:msub><mml:mi mathvariant="normal">S</mml:mi></mml:mrow></mml:math>. Physical Review B, 2020, 102, .	1.1	4
47495	Three-dimensional Weyl hourglass networks in the nonsymmorphic half-metal <mml:math xmlns:mml="http://www.w3.org/1998/Math/MathML"><mml:mrow><mml:msub><mml:mi>Mg</mml:mi><mml:mn>2</mml:mn></mml:msub> Physical Review B, 2020, 102, .	1.1	31
47496	Effects of the substrate-surface reconstruction and orientation on the spin valley polarization in <mml:math xmlns:mml="http://www.w3.org/1998/Math/MathML"><mml:mrow><mml:mi>Mo</mml:mi><mml:msub><mml:mi>Te</mml:mi><mml:mi mathvariant="normal">O</mml:mi></mml:mrow></mml:math>. Physical Review B, 2020, 102, .	1.1	10
47497	Ferroelectricity and ferromagnetism in a <mml:math xmlns:mml="http://www.w3.org/1998/Math/MathML"><mml:mrow><mml:mi>VO</mml:mi><mml:msub><mml:mi mathvariant="normal">I</mml:mi><mml:mn>2</mml:mn></mml:msub></mml:mrow></mml:math> monolayer: Role of the Dzyaloshinskii-Moriya interaction. Physical Review B, 2020, 102, .	1.1	37
47498	Large magnetoresistance and nonzero Berry phase in the nodal-line semimetal <mml:math xmlns:mml="http://www.w3.org/1998/Math/MathML"><mml:mrow><mml:mi>Mo</mml:mi><mml:msub><mml:mi mathvariant="normal">O</mml:mi><mml:mn>2</mml:mn></mml:msub></mml:mrow></mml:math>. Physical Review B, 2020, 102, .	1.1	16
47499	Direct Visualization of Trimerized States in <mml:math xmlns:mml="http://www.w3.org/1998/Math/MathML" display="inline"><mml:mrow><mml:mn>1</mml:mn><mml:msup><mml:mrow><mml:mi>T</mml:mi></mml:mrow><mml:mrow><mml: Physical Review Letters, 2020, 125, 165302.	2.9	17
47500	Charge Ordering and Metal-Insulator Transition: The Different Fates of <mml:math xmlns:mml="http://www.w3.org/1998/Math/MathML" display="inline"><mml:mrow><mml:msub><mml:mrow><mml:mi>NaOsO</mml:mi></mml:mrow><mml:mrow><mml:mn>3</mml:mn></mml:mrow> and <mml:math xmlns:mml="http://www.w3.org/1998/Math/MathML" display="inline"><mml:mrow><mml:msub><mml:mrow><mml:mi>LiOsO</mml:mi></mml:mrow><mml:mrow><mml:mn>3</mml:mn></mml:mrow> Physical Review Letters, 2020, 125, 166402.	2.9	10
47501	Localization and steric effect of the lone electron pair of the tellurium Te⁴⁺cation and other cations of thep-block elements. A systematic study. Journal of Applied Crystallography, 2020, 53, 1243-1251.	1.9	9
47502	Computational design of stable and highly ion-conductive materials using multi-objective bayesian optimization: Case studies on diffusion of oxygen and lithium. Computational Materials Science, 2020, 184, 109927.	1.4	11
47503	Airâ€Stable Lowâ€Symmetry Narrowâ€Bandgap 2D Sulfide Niobium for Polarization Photodetection. Advanced Materials, 2020, 32, e2005037.	11.1	68
47504	Tailoring the Cation Lattice for Chloride Lithiumâ€Ion Conductors. Advanced Energy Materials, 2020, 10, 2002356.	10.2	56
47505	Wide Band Gap Organicâ€“Inorganic Hybrid (CH₃NH₃)₂HgCl₄ as Selfâ€Driven Ultraviolet Photodetector and Photoconductor. Applied Organometallic Chemistry, 2020, 34, e5982.	1.7	1
47506	Optimized Kinetics Match and Charge Balance Toward Potassium Ion Hybrid Capacitors with Ultrahigh Energy and Power Densities. Small, 2020, 16, e2003724.	5.2	62
47507	Screw dislocation-carbon interaction in BCC tungsten: an ab initio study. Acta Materialia, 2020, 200, 481-489.	3.8	20
47508	First principles study of the effect of hydrogen in austenitic stainless steels and high entropy alloys. Acta Materialia, 2020, 200, 932-942.	3.8	38
47509	Remarkable intrinsic ZT in the 2D PtX2(XÂ=ÂO, S, Se, Te) monolayers at room temperature. Applied Surface Science, 2020, 532, 147387.	3.1	27
47510	Black titanium oxynitride thin films prepared by nitrogen plasma-assisted pulsed laser deposition for flat-panel displays. Applied Surface Science, 2020, 534, 147616.	3.1	10

#	Article	IF	Citations
47511	Electrolyte-mediated nanograin intermetallic formation enables superionic conduction and electrode stability in rechargeable batteries. Energy Storage Materials, 2020, 33, 164-172.	9.5	17
47512	An organic nickel salt-based electrolyte additive boosts homogeneous catalysis for lithium-sulfur batteries. Energy Storage Materials, 2020, 33, 290-297.	9.5	69
47513	Methane dry reforming on supported cobalt nanoparticles promoted by boron. Journal of Catalysis, 2020, 392, 126-134.	3.1	32
47514	MoSe2 nanosheets embedded in nitrogen/phosphorus co-doped carbon/graphene composite anodes for ultrafast sodium storage. Journal of Power Sources, 2020, 476, 228660.	4.0	28
47515	Novel two-dimensional Ga(In)S1-Se as high-efficiency OER catalysts for photocatalytic water splitting. Journal of Solid State Chemistry, 2020, 292, 121730.	1.4	4
47516	Nanoscale precipitations in deformed dilute alloying Mg-Zn-Gd alloy. Materials and Design, 2020, 196, 109122.	3.3	36
47517	Amino-functionalized MIL-101(Cr) photodegradation enhancement by sulfur-enriched copper sulfide nanoparticles: An experimental and DFT study. Journal of Molecular Liquids, 2020, 319, 114341.	2.3	22
47518	Inorganic narrow bandgap CsPb0.4Sn0.6I2.4Br0.6 perovskite solar cells with exceptional efficiency. Nano Energy, 2020, 77, 105309.	8.2	25
47519	Heterogeneous interface of Se@Sb@C boosting potassium storage. Nano Energy, 2020, 78, 105345.	8.2	51
47520	Bi-Doped Zirconium Alloys with Enhanced Water Oxidation Resistance. Journal of Physical Chemistry C, 2020, 124, 23116-23125.	1.5	2
47521	Effect of Insertion of B₄C at the Interface Mo/Be Depending on the Film Order. Journal of Physical Chemistry C, 2020, 124, 22601-22609.	1.5	8
47522	Regulating the Grain Orientation and Surface Structure of Primary Particles through Tungsten Modification to Comprehensively Enhance the Performance of Nickel-Rich Cathode Materials. ACS Applied Materials & Interfaces, 2020, 12, 47513-47525.	4.0	36
47523	Probing magnetism in atomically thin semiconducting PtSe2. Nature Communications, 2020, 11, 4806.	5.8	63
47524	Disorderâ€“order and orderâ€“order phase transformations in Ta₅C₄phases predicted using the evolutionary algorithm and symmetry analysis. Physical Chemistry Chemical Physics, 2020, 22, 24116-24132.	1.3	5
47525	Confined pyrolysis of a dye pollutant for two-dimensional F,N,S tri-doped nanocarbon as a high performance oxidative coupling reaction catalyst. Green Chemistry, 2020, 22, 7839-7847.	4.6	6
47526	Effect of Oxygen Adsorption on Electrical and Thermoelectrical Properties of Monolayer <mml:math xmlns:mml="http://www.w3.org/1998/Math/MathML" display="inline" overflow="scroll"><mml:msub><mml:mrow><mml:mi>Mo</mml:mi><mml:mi mathvariant="normal">S</mml:mi></mml:mrow><mml:mn>2</mml:mn></mml:msub></mml:math>. Physical Review Applied, 2020, 14, .	1.5	3
47527	Hidden magnetic order in the triangular-lattice magnet <mml:math xmlns:mml="http://www.w3.org/1998/Math/MathML"><mml:mrow><mml:msub><mml:mi>Li</mml:mi><mml:mn>2</mml:mn></mml:msub></mml:mrow></mml:math>PdO₃. Physical Review B, 2020, 102, .	1.1	6
47528	Continuous crossover from two-dimensional to one-dimensional electronic properties for metallic silicide nanowires. Physical Review B, 2020, 102, .	1.1	4

#	Article	IF	Citations
47529	Twofold quadruple Weyl nodes in chiral cubic crystals. Physical Review B, 2020, 102, .	1.1	65
47530	Research Progress on the Anti-Disproportionation of the ZrCo Alloy by Element Substitution. Materials, 2020, 13, 3977.	1.3	9
47531	Development and application of interatomic potentials to study the stability and shear strength of Ti/TiN and Cu/TiN interfaces. Materials and Design, 2020, 196, 109123.	3.3	14
47532	Cation diffusion in polycrystalline thin films of monoclinic HfO2 deposited by atomic layer deposition. APL Materials, 2020, 8, .	2.2	7
47533	Hierarchical MoS₂@CNTs Hybrid as a Longâ€Life and Highâ€Rate Cathode for Aqueous Rechargeable Znâ€Ion Batteries. ChemElectroChem, 2020, 7, 4218-4223.	1.7	33
47534	PyVibMS: a PyMOL plugin for visualizing vibrations in molecules and solids. Journal of Molecular Modeling, 2020, 26, 290.	0.8	14
47535	Atomic-scale investigation of deep hydrogen trapping in NbC/Î±-Fe semi-coherent interfaces. Acta Materialia, 2020, 200, 686-698.	3.8	125
47536	Theory-Guided Machine Learning Finds Geometric Structure-Property Relationships for Chemisorption on Subsurface Alloys. CheM, 2020, 6, 3100-3117.	5.8	65
47537	Neural Network-Assisted Development of High-Entropy Alloy Catalysts: Decoupling Ligand and Coordination Effects. Matter, 2020, 3, 1318-1333.	5.0	83
47538	Ab initio molecular dynamics study of wet H2S adsorption and dissociation on Fe(100) surface. Journal of Molecular Liquids, 2020, 319, 114135.	2.3	11
47539	Tunable Luminescence in Hybrid Cu(I) and Ag(I) Iodides. Inorganic Chemistry, 2020, 59, 15487-15494.	1.9	8
47540	Strain-induced electronic structures, mechanical anisotropy, and piezoelectricity of transition-metal dichalcogenide monolayer CrS2. Journal of Applied Physics, 2020, 128, .	1.1	26
47541	Magnetoelastic and magnetostrictive properties of <mml:math xmlns:mml="http://www.w3.org/1998/Math/MathML"><mml:msub><mml:mi>Co</mml:mi><mml:mn>2</mml:mn></mml:msub><mml:m Heusler compounds. Physical Review B, 2020, 102, .	1.1	11
47542	Elucidating the role of Ni to enhance the methanol oxidation reaction on Pd electrocatalysts. Electrochimica Acta, 2020, 360, 136954.	2.6	34
47543	Energy landscapes of graphene under general deformations: DFT-to-hyperelasticity upscaling. International Journal of Engineering Science, 2020, 154, 103342.	2.7	9
47544	Re-examining the silicon self-interstitial charge states and defect levels: A density functional theory and bounds analysis study. AIP Advances, 2020, 10, .	0.6	3
47545	Molecular dynamics study on magnesium hydride nanoclusters with machine-learning interatomic potential. Physical Review B, 2020, 102, .	1.1	5
47546	A highly efficient photocatalytic methanol fuel cell based on non-noble metal photoelectrodes: Study on its energy band engineering via experimental and density functional theory method. Journal of Power Sources, 2020, 478, 228756.	4.0	19

#	Article	IF	Citations
47547	Experimental and Theoretical Assessments of Aluminum Proximity in MFI Zeolites and Its Alteration by Organic and Inorganic Structure-Directing Agents. Chemistry of Materials, 2020, 32, 9277-9298.	3.2	55
47548	Benchmarking an Embedded Adaptive Sampling Configuration Interaction Method for Surface Reactions: H₂ Desorption from and CH₄ Dissociation on Cu(111). Journal of Chemical Theory and Computation, 2020, 16, 7078-7088.	2.3	23
47549	The Role of Protons and Hydrides in the Catalytic Hydrogenolysis of Guaiacol at the Ruthenium Nanoparticleâ€“Water Interface. ACS Catalysis, 2020, 10, 12310-12332.	5.5	29
47550	Role of Oxidized Mo Species on the Active Surface of Niâ€“Mo Electrocatalysts for Hydrogen Evolution under Alkaline Conditions. ACS Catalysis, 2020, 10, 12858-12866.	5.5	75
47551	Proximity effect in a superconductorâ€“topological insulator heterostructure based on first principles. Physical Review B, 2020, 102, .	1.1	4
47552	Transition from band insulator to excitonic insulator via alloying Se into monolayer <mml:math xmlns:mml="http://www.w3.org/1998/Math/MathML"><mml:mrow><mml:mi>Ti</mml:mi><mml:msub><mml:mi mathvariant="normal">S</mml:mi><mml:mn>3</mml:mn></mml:msub></mml:mrow></mml:math> : A computational study. Physical Review B, 2020, 102, .	1.1	6
47553	Structures and Properties of Î²-Titanium Alloys Doped with Trace Transition Metals: A Density Functional Theory Study. Russian Journal of Physical Chemistry A, 2020, 94, 2055-2063.	0.1	2
47554	Tuning oxygen reduction activity on chromia surface via alloying: a DFT study. Chemistry - an Asian Journal, 2020, 15, 4087-4092.	1.7	7
47555	Scaleâ€Enhanced Magnetism in Exfoliated Atomically Thin Magnetite Sheets. Small, 2020, 16, e2004208.	5.2	15
47556	Computational study of crystalline and glassy lithium thiophosphates: Structure, thermodynamic stability and transport properties. Journal of Power Sources, 2020, 478, 229041.	4.0	9
47557	Atomic-scale studies of garnet-type Mg3Fe2Si3O12: Defect chemistry, diffusion and dopant properties. Journal of Power Sources Advances, 2020, 3, 100016.	2.6	2
47558	Quasiparticle Band Structure and Optical Properties of the Janus Monolayer and Bilayer SnSSe. Journal of Physical Chemistry C, 2020, 124, 23832-23838.	1.5	23
47559	A Combined Operando Synchrotron X-ray Absorption Spectroscopy and First-Principles Density Functional Theory Study to Unravel the Vanadium Redox Paradox in the Na₃V₂(PO₄)₂F₃â€“Na₃V₂(PO₄ Compositions. Journal of Physical Chemistry C, 2020, 124, 23511-23522.	1.5	19
47560	Theoretical Investigations on the Effect of the Functional Group of Pd@UiO-66 for Formic Acid Dehydrogenation. Journal of Physical Chemistry C, 2020, 124, 23738-23744.	1.5	6
47561	Metal-Encapsulated Boron Nitride Nanocages for Solar-Driven Nitrogen Fixation. Journal of Physical Chemistry C, 2020, 124, 23798-23806.	1.5	12
47562	Giant Piezoresistance in B-Doped SiC Nanobelts with a Gauge Factor of â^'1800. ACS Applied Materials & Interfaces, 2020, 12, 47848-47853.	4.0	6
47563	Electric-Field-Assisted Modulation of Surface Thermochemistry. ACS Catalysis, 2020, 10, 12867-12880.	5.5	23
47564	Theoretical Study of the Catalytic Activity and Anti-SO₂ Poisoning of a MoO₃/V₂O₅ Selective Catalytic Reduction Catalyst. ACS Omega, 2020, 5, 26978-26985.	1.6	9

#	Article	IF	Citations
47565	Auxetic two-dimensional transition metal selenides and halides. Npj Computational Materials, 2020, 6, .	3.5	27
47566	Screening of thermoelectric silicides with atomistic transport calculations. Journal of Applied Physics, 2020, 128, 125105.	1.1	3
47567	The electric and magnetic properties of novel two-dimensional MnBr2 and MnI2 from first-principles calculations. Journal of Applied Physics, 2020, 128, .	1.1	13
47568	Prediction of chlorine and fluorine crystal structures at high pressure using symmetry driven structure search with geometric constraints. Journal of Chemical Physics, 2020, 153, 094111.	1.2	4
47569	Effects of strain on defect-graphene superlattices. AIP Advances, 2020, 10, .	0.6	5
47570	Hydrogen desorption from silicane and germanane crystals: Toward creation of free-standing monolayer silicene and germanene. Journal of Applied Physics, 2020, 128, 125301.	1.1	8
47571	Spinâ€“phonon coupling in NiO nanoparticle. Journal of Applied Physics, 2020, 128, .	1.1	19
47572	Correlating structural, electronic, and magnetic properties of epitaxial VSe2 thin films. Physical Review B, 2020, 102, .	1.1	25
47573	Successive spin reorientations and rare earth ordering in <mml:math xmlns:mml="http://www.w3.org/1998/Math/MathML"><mml:mrow><mml:msub><mml:mi>Nd</mml:mi><mml:mrow><mml:mn>0.5</m mathvariant="normal">O</mml:mi><mml:mn>3</mml:mn></mml:msub></mml:mrow></mml:math> : Experimental and ab initio investigations. Physical Review B, 2020, 102, .	1.1	11
47574	Methylphosphonium Tin Bromide: A 3D Perovskite Molecular Ferroelectric Semiconductor. Advanced Materials, 2020, 32, e2005213.	11.1	66
47575	Can CO₂ and Steam React in the Absence of Electrolysis at High Temperatures?. ChemSusChem, 2020, 13, 6660-6667.	3.6	4
47576	Comparison of Sulfur Incorporation into CuInSe₂ and CuGaSe₂ Thinâ€Film Solar Absorbers. Physica Status Solidi (A) Applications and Materials Science, 2020, 217, 2000415.	0.8	5
47577	Micropillar compression deformation of single crystals of the intermetallic compound Î“-Fe4Zn9. Acta Materialia, 2020, 199, 514-522.	3.8	14
47578	The direct synthesis of hydrogen peroxide over Au and Pd nanoparticles: A DFT study. Catalysis Today, 2021, 381, 76-85.	2.2	11
47579	Mixed incorporation of carbon and hydrogen in silicate melts under varying pressure and redox conditions. Earth and Planetary Science Letters, 2020, 549, 116520.	1.8	12
47580	The effect of dopants on electronic and magnetic properties of symmetric washboard phase bismuthene: A DFT study. Journal of Magnetism and Magnetic Materials, 2020, 516, 167325.	1.0	0
47581	The Rashba Scale: Emergence of Band Anti-crossing as a Design Principle for Materials with Large Rashba Coefficient. Matter, 2020, 3, 145-165.	5.0	21
47582	Physical genetics: Cross-breeding density functional theory and X-ray photoelectron spectroscopy to rationalize chemical shifts of binding energies in solid compounds. Solid State Sciences, 2020, 110, 106359.	1.5	4

#	Article	IF	Citations
47583	Improved Adsorption and Migration of Divalent Ions Over C4N Nanosheets: Potential Anode for Divalent Batteries. Surfaces and Interfaces, 2020, 21, 100758.	1.5	5
47584	Surface structure of 1,4-benzenedithiol on Au(111). Surface Science, 2020, 702, 121717.	0.8	7
47585	Prediction of Highly Selective Electrocatalytic Nitrogen Reduction at Low Overpotential on a Mo-Doped g-GaN Monolayer. ACS Catalysis, 2020, 10, 12841-12857.	5.5	92
47586	Role of Hydrogen-Bonding and OHâ‹¯Ï€ Interactions in the Adhesion of Epoxy Resin on Hydrophilic Surfaces. ACS Omega, 2020, 5, 26211-26219.	1.6	36
47587	Electronic structures of WS2 armchair nanoribbons doped with transition metals. Scientific Reports, 2020, 10, 16452.	1.6	0
47588	Study of the heavily p-type doping of cubic GaN with Mg. Scientific Reports, 2020, 10, 16858.	1.6	25
47589	Two-dimensional molybdenum carbides: active electrocatalysts for the nitrogen reduction reaction. Journal of Materials Chemistry A, 2020, 8, 23947-23954.	5.2	36
47590	A two-dimensional conductive Mo-based covalent organic framework as an efficient electrocatalyst for nitrogen fixation. Journal of Materials Chemistry A, 2020, 8, 23599-23606.	5.2	54
47591	Chemical short-range order in derivative Crâ€“Taâ€“Tiâ€“Vâ€“W high entropy alloys from the first-principles thermodynamic study. Physical Chemistry Chemical Physics, 2020, 22, 23929-23951.	1.3	45
47593	Reproducibility of potential energy surfaces of organic/metal interfaces on the example of PTCDA on Ag(111). Journal of Chemical Physics, 2020, 153, 104701.	1.2	12
47594	Oxidation induced restructuring of Rhâ€“Ga SCALMS model catalyst systems. Journal of Chemical Physics, 2020, 153, 104702.	1.2	9
47595	Ag5-induced stabilization of multiple surface polarons on perfect and reduced TiO2 rutile (110). Journal of Chemical Physics, 2020, 153, 164702.	1.2	14
47596	Templated Growth of Metastable Polymorphs on Amorphous Substrates with Seed Layers. Physical Review Applied, 2020, 13, .	1.5	7
47597	First-principles study of a Mn-doped <mml:math xmlns:mml="http://www.w3.org/1998/Math/MathML"><mml:mrow><mml:msub><mml:mi>In</mml:mi><mml:mn>2</mml:mn></mml:mn> monolayer: Coexistence of ferromagnetism and ferroelectricity with robust half-metallicity and enhanced polarization. Physical Review B, 2020, 102, .	1.1	18
47598	Three-dimensional borophene: A light-element topological nodal-line semimetal with direction-dependent type-II Weyl fermions. Physical Review B, 2020, 102, .	1.1	9
47599	Selective Hydrogenation of Naphthalene over Î³-Al2O3-Supported NiCu and NiZn Bimetal Catalysts. Catalysts, 2020, 10, 1215.	1.6	8
47600	Computational Identification of a New Adsorption Site of CO₂ on the Ag (211) Surface. ChemistrySelect, 2020, 5, 11503-11509.	0.7	4
47601	Identifying Trends in the Field Ionization of Diatomic Molecules over Adsorbate Covered Pd(331) Surfaces. Topics in Catalysis, 2020, 63, 1510-1521.	1.3	0

#	Article	IF	Citations
47602	Investigation on the interface characteristic between TiN and diamond by first-principles calculation. Diamond and Related Materials, 2020, 109, 108023.	1.8	4
47603	Formation Energetics, Electronic Structure and Ferromagnetic Properties of C-, Si- and Ge-Doped Zinc Blende Cadmium Chalcogenides. Materials Today Communications, 2020, 25, 101652.	0.9	2
47604	From LiNiO₂ to Li₂NiO₃: Synthesis, Structures and Electrochemical Mechanisms in Li-Rich Nickel Oxides. Chemistry of Materials, 2020, 32, 9211-9227.	3.2	28
47605	Interlayer Binding Energy of Hexagonal MoS2 as Determined by an In Situ Peeling-to-Fracture Method. Journal of Physical Chemistry C, 2020, 124, 23419-23425.	1.5	23
47606	Solvent Effect on Supramolecular Self-Assembly of Chlorophylls a on Chemically Reduced Graphene Oxide. Langmuir, 2020, 36, 13575-13582.	1.6	9
47607	Superior Anchoring of Sodium Polysulfides to the Polar C₂N 2D Material: A Potential Electrode Enhancer in Sodiumâ€“Sulfur Batteries. Langmuir, 2020, 36, 13104-13111.	1.6	27
47608	Long-Range Spin-Selective Transport in Chiral Metalâ€“Organic Crystals with Temperature-Activated Magnetization. ACS Nano, 2020, 14, 16624-16633.	7.3	51
47609	Dopants fixation of Ruthenium for boosting acidic oxygen evolution stability and activity. Nature Communications, 2020, 11, 5368.	5.8	217
47610	Îµ-InSe single crystals grown by a horizontal gradient freeze method. CrystEngComm, 2020, 22, 7864-7869.	1.3	13
47611	Notes on density matrix perturbation theory. Journal of Chemical Physics, 2020, 153, 164105.	1.2	4
47612	Perovskite Termination-Dependent Charge Transport Behaviors of the CsPbI₃/Black Phosphorus van der Waals Heterostructure*. Chinese Physics Letters, 2020, 37, 107301.	1.3	8
47613	First-principles calculation of higher-order elastic constants using exact deformation-gradient tensors. Physical Review B, 2020, 102, .	1.1	7
47614	Asymmetric modification of the magnetic proximity effect in Pt/Co/Pt trilayers by the insertion of a Ta buffer layer. Physical Review B, 2020, 102, .	1.1	17
47615	One-dimensional electronic instabilities at the edges of MoS2. Physical Review B, 2020, 102, .	1.1	12
47616	Tunable charge density wave in a lateral black/blue phosphorene heterostructure: A first-principles calculation. Physical Review B, 2020, 102, .	1.1	5
47617	Anharmonicity and Phase Diagram of Magnesium Oxide in the Megabar Regime. Physical Review Letters, 2020, 125, 175701.	2.9	24
47618	Shedding light on moirÃ© excitons: A first-principles perspective. Science Advances, 2020, 6, .	4.7	50
47619	Doping quantum materials: Defects and impurities in <mml:math xmlns:mml="http://www.w3.org/1998/Math/MathML"><mml:mrow><mml:mi>Fe</mml:mi><mml:msub><mml:mi>Ga</mml:mi><mml:mi><mm Physical Review B, 2020, 102, .	1.1	5

#	Article	IF	Citations
47620	Magnetic anisotropy and exchange paths for octahedrally and tetrahedrally coordinated <mml:math xmlns:mml="http://www.w3.org/1998/Math/MathML"><mml:msup><mml:mi mathvariant="normal">Mn</mml:mi><mml:mrow><mml:mn>2</mml:mn><mml:mo>+</mml:mo></mml:mrow></mml:msup></mml:ma ions in the honeycomb multiferroic <mml:math xmlns:mml="http://www.w3.org/1998/Math/MathML"><mml:mrow><mml:msub><mml:mi>Mn</mml:mi><mml:mn>2</mml:mn></mml: Physical Review B, 2020, 102, .	1.1	9
47621	Spin/charge density waves at the boundaries of transition metal dichalcogenides. Physical Review B, 2020, 102, .	1.1	11
47622	Understanding the Activity of Single-Atom Catalysis from Frontier Orbitals. Physical Review Letters, 2020, 125, 156001.	2.9	53
47623	Mg2Si Silicide under Pressure: First-Principles Evolution Search Results. Physics of the Solid State, 2020, 62, 880-884.	0.2	1
47624	First Principles Study of Bonding Mechanisms at the TiAl/TiO2 Interface. Metals, 2020, 10, 1298.	1.0	11
47625	Contribution of the Multiplicity Fluctuation in the Temperature Dependence of Phonon Spectra of Rare-Earth Cobaltites. Molecules, 2020, 25, 4316.	1.7	1
47626	Correlating facet orientation, defect-level density and dipole layer formation at the surface of polycrystalline CuInSe2 thin films. Acta Materialia, 2020, 200, 463-470.	3.8	8
47627	Structure and tuneable luminescence in polymeric zinc compounds based on 3-(3-pyridyl)-5-(4-pyridyl)-1,2,4-triazole. Polyhedron, 2020, 191, 114768.	1.0	19
47628	Quantum size effect in conductive properties of silver nanofilms. Thin Solid Films, 2020, 710, 138263.	0.8	9
47629	Lead-Free Antimony Halide Perovskite with Heterovalent Mn²⁺ Doping. Inorganic Chemistry, 2020, 59, 15289-15294.	1.9	25
47630	Understanding the Structureâ€“Performance Relationship of Lithium-Rich Cathode Materials from an Oxygen-Vacancy Perspective. ACS Applied Materials & Interfaces, 2020, 12, 47655-47666.	4.0	44
47631	First-principles investigation on the transport properties of quaternary CoFeRGa (R = Ti, V, Cr, Mn, Cu,) Tj ETQq1 1 0.784314 rgBT /Ove	1.3	7
47632	A two-dimensional h-BN/C₂N heterostructure as a promising metal-free photocatalyst for overall water-splitting. Physical Chemistry Chemical Physics, 2020, 22, 24446-24454.	1.3	41
47633	Stable puckered C₂N₂ nanosheet with giant anisotropic hole carrier mobility: insights from first-principles. Journal of Materials Chemistry C, 2020, 8, 15655-15663.	2.7	4
47634	High-throughput screening of metalâ€“organic frameworks for kinetic separation of propane and propene. Physical Chemistry Chemical Physics, 2020, 22, 23073-23082.	1.3	12
47635	Two-dimensional stable Fe-based ferromagnetic semiconductors: FeI₃ and FeI_{1.5}Cl_{1.5} monolayers. Physical Chemistry Chemical Physics, 2020, 22, 24506-24515.	1.3	13
47636	Fundamental interplay between phase-transition kinetics and thermodynamics of manganese-based sodium layered oxides during cationic and anionic redox. Journal of Materials Chemistry A, 2020, 8, 21142-21150.	5.2	15
47637	Partial cation ordering, relaxor ferroelectricity, and ferrimagnetism in Pb(Fe1â€‰â€²â€‰xYbx)2/3W1/3O3 solid solutions. Journal of Applied Physics, 2020, 128, 134102.	1.1	0

#	Article	IF	Citations
47638	Machine learning formation enthalpies of intermetallics. Journal of Applied Physics, 2020, 128, .	1.1	17
47639	Screw dislocation core structure in the paramagnetic state of bcc iron from first-principles calculations. Physical Review B, 2020, 102, .	1.1	7
47640	Topological electronic structure in the antiferromagnet HoSbTe. Physical Review B, 2020, 102, .	1.1	22
47641	Black phosphorus composites with engineered interfaces for high-rate high-capacity lithium storage. Science, 2020, 370, 192-197.	6.0	336
47642	Clean 2D superconductivity in a bulk van der Waals superlattice. Science, 2020, 370, 231-236.	6.0	64
47643	Identifying Carrier Behavior in Ultrathin Indirectâ€Bandgap CsPbX₃ Nanocrystal Films for Use in UV/Visibleâ€Blind Highâ€Energy Detectors. Small, 2020, 16, e2004513.	5.2	45
47644	Interlayer ligand engineering of Î²-Ni(OH)2 for oxygen evolution reaction. Science China Chemistry, 2020, 63, 1684-1693.	4.2	15
47645	Evaluation of Ni doping for promoting favorable electronic structures in CuCrO2 and AgCrO2 from a first-principles perspective. Ceramics International, 2020, 46, 26777-26783.	2.3	4
47646	Interactions and immobilization of lanthanides with dopants in uranium-based metallic fuels. Journal of Nuclear Materials, 2020, 540, 152372.	1.3	9
47647	Ab initio molecular dynamics study of isotope effects in lithium-ion conductors. Solid State Ionics, 2020, 355, 115434.	1.3	3
47648	First-principles study on sodium storage properties of beryllium and boron dual-doped graphyne. Surface Science, 2020, 702, 121721.	0.8	7
47649	Crystal structures and elastic properties of Ti(Cu,Pt)2 and Ti(Cu,Pt)3 phases. Transactions of Nonferrous Metals Society of China, 2020, 30, 1839-1848.	1.7	9
47650	Mechanically Tunable Near-Field Radiative Heat Transfer between Monolayer Black Phosphorus Sheets. Langmuir, 2020, 36, 12038-12044.	1.6	16
47651	In Situ Confined Co5Ge3 Alloy Nanoparticles in Nitrogen-Doped Carbon Nanotubes for Boosting Lithium Storage. ACS Applied Materials & Interfaces, 2020, 12, 46247-46253.	4.0	11
47652	Effects of the van der Waals Interactions on Structural and Electronic Properties of CH₃NH₃(Pb,Sn)(I,Br,Cl)₃ Halide Perovskites. ACS Omega, 2020, 5, 25723-25732.	1.6	21
47653	A first-principles analysis of the charge transfer in magnesium corrosion. Scientific Reports, 2020, 10, 15006.	1.6	37
47654	Topological Phase and Strong Correlation in Rare-Earth Hexaborides XB6 (X = La, Ce, Pr, Nd, Pm, Sm,) Tj ETQq0 0 0 rgBT /Overlock 10 Tf	1.3	5
47655	Vacancyâ€Induced Oxygen Reduction Activity in Janus Transition Metal Dichalcogenides. ChemElectroChem, 2020, 7, 4233-4238.	1.7	6

#	Article	IF	Citations
47656	Second nearest-neighbor modified embedded atom method interatomic potentials for the Na unary and Na-Sn binary systems. Computational Materials Science, 2020, 185, 109953.	1.4	8
47657	Theoretical study on the electrical and mechanical properties of MXene multilayer structures through strain regulation. Chemical Physics Letters, 2020, 760, 137997.	1.2	13
47658	Stability and bonding nature of tin borohydride. International Journal of Hydrogen Energy, 2020, 45, 23103-23111.	3.8	1
47659	Computational insights into the molecular mechanisms for chromium passivation of stainless-steel surfaces. Materials Today Chemistry, 2020, 17, 100298.	1.7	2
47660	Exploring the Degradation Behavior of Ce-Monazite in Water Solution through Adsorption and Penetration Kinetics. Journal of Physical Chemistry C, 2020, 124, 22173-22184.	1.5	10
47661	A coarse-grain force field based on quantum mechanics (CGq FF) for molecular dynamics simulation of poly(ethylene glycol)-block-poly(Îµ-caprolactone) (PEG-b-PCL) micelles. Physical Chemistry Chemical Physics, 2020, 22, 24028-24040.	1.3	4
47662	Layered electrides as fluoride intercalation anodes. Journal of Materials Chemistry A, 2020, 8, 24469-24476.	5.2	16
47663	Three-dimensional porous borocarbonitride BC₂N with negative Poisson's ratio. Journal of Materials Chemistry C, 2020, 8, 15771-15777.	2.7	5
47664	Tunable ferroelectricity and antiferromagnetism via ferroelastic switching in an FeOOH monolayer. Journal of Materials Chemistry C, 2020, 8, 13982-13989.	2.7	18
47665	Achieving tunable chemical reactivity through photo-initiation of energetic materials at metal oxide surfaces. Physical Chemistry Chemical Physics, 2020, 22, 25284-25296.	1.3	6
47666	ABX₃-type lead-free perovskites using superatom ions with tunable photovoltaic performances. Journal of Materials Chemistry A, 2020, 8, 21993-22000.	5.2	8
47667	Structural and optical properties of transparent, tunable bandgap semiconductor: Î±-(AlxCr1âˆ'x)2O3. Journal of Applied Physics, 2020, 128, 135703.	1.1	1
47668	Role of chemical pressure on the electronic and magnetic properties of the spin- <mml:math xmlns:mml="http://www.w3.org/1998/Math/MathML"><mml:mfrac><mml:mn>1</mml:mn><mml:mn>2</mml:mn></mml:mfrac></mml kagome mineral averievite. Physical Review B, 2020, 102, .	1.4	4
47669	Atomistic mechanism of stress modulated phase transition in monolayer MoTe<mml:math xmlns:mml="http://www.w3.org/1998/Math/MathML" display="inline" id="d1e196" altimg="si10.svg"><mml:msub><mml:mrow /><mml:mrow><mml:mn>2</mml:mn></mml:mrow></mml:msub></mml:math>. Extreme Mechanics Letters, 2020, 40, 100946.	2.0	14
47670	Interactions of Y and Cu on Mg2Ni type hydrogen storage alloys: A study based on experiments and density functional theory calculation. International Journal of Hydrogen Energy, 2020, 45, 28974-28984.	3.8	17
47671	A DFT+U study on the thermodynamic properties of defective Gd2Zr2O7 pyrochlore. Journal of Nuclear Materials, 2020, 542, 152425.	1.3	8
47672	Insights into the Bimetallic Effects of a RhCo Catalyst for Ethene Hydroformylation: Experimental and DFT Investigations. Industrial & Engineering Chemistry Research, 2020, 59, 18771-18780.	1.8	26
47673	Surface Defect Engineering of MoS2 for Atomic Layer Deposition of TiO2 Films. ACS Applied Materials & Interfaces, 2020, 12, 48150-48160.	4.0	7

#	Article	IF	Citations
47674	High temperature pure carbon nanoparticle formation: Validation of AIREBO and ReaxFF reactive molecular dynamics. Carbon, 2020, 170, 606-620.	5.4	51
47675	A three-order-parameter bistable magnetoelectric multiferroic metal. Nature Communications, 2020, 11, 4922.	5.8	8
47676	Stabilizing hidden room-temperature ferroelectricity via a metastable atomic distortion pattern. Nature Communications, 2020, 11, 4944.	5.8	25
47677	A Gd@C82 single-molecule electret. Nature Nanotechnology, 2020, 15, 1019-1024.	15.6	70
47678	Staggering transport of edge states and symmetry analysis of electronic and optical properties of stanene. Nanoscale, 2020, 12, 20890-20897.	2.8	2
47679	Sonication-induced electrostatic assembly of an FeCO₃@Ti₃C₂ nanocomposite for robust lithium storage. Journal of Materials Chemistry A, 2020, 8, 23498-23510.	5.2	32
47680	Two-dimensional ferromagnetic semiconductor VBr₃ with tunable anisotropy. Journal of Materials Chemistry C, 2020, 8, 14782-14788.	2.7	16
47681	Orbital response of single-layer antimony to external magnetic field. Physical Review B, 2020, 102, .	1.1	0
47682	A comparative investigation of sp3-hybridized Pm3n-BN and sc-B12N12 based on density functional theory (DFT). Materials Today Communications, 2020, 25, 101582.	0.9	2
47683	Magnetic Heterostructures of Transition Metal Dichalcogenides: Antiparallel Magnetic Moments and Half-Metallic State. Journal of Physical Chemistry C, 2020, 124, 23352-23360.	1.5	3
47684	Li₅VF₄(SO₄)₂: A Prototype High-Voltage Li-Ion Cathode. ACS Applied Materials & Interfaces, 2020, 12, 48662-48668.	4.0	1
47685	Surface coordination layer passivates oxidation of copper. Nature, 2020, 586, 390-394.	13.7	154
47686	Breakdown of chiral recognition of amino acids in reduced dimensions. Scientific Reports, 2020, 10, 16166.	1.6	9
47687	Effects of native defects and cerium impurity on the monoclinic BiVO₄ photocatalyst obtained via PBE+U calculations. Physical Chemistry Chemical Physics, 2020, 22, 25297-25305.	1.3	17
47688	Gate-tunable high magnetoresistance in monolayer Fe₃GeTe₂ spin valves. Physical Chemistry Chemical Physics, 2020, 22, 25730-25739.	1.3	18
47689	Thermodynamic and kinetic properties of layered-CaCo₂O₄ for the Ca-ion batteries: a systematic first-principles study. Journal of Materials Chemistry A, 2020, 8, 21700-21710.	5.2	5
47690	Enhanced electrochemical oxygen evolution reaction activity on natural single-atom catalysts transition metal phthalocyanines: the substrate effect. Catalysis Science and Technology, 2020, 10, 8339-8346.	2.1	22
47691	Accelerating 2D MXene catalyst discovery for the hydrogen evolution reaction by computer-driven workflow and an ensemble learning strategy. Journal of Materials Chemistry A, 2020, 8, 23488-23497.	5.2	71

#	Article	IF	Citations
47692	Tunable valley splitting and anomalous valley Hall effect in VTe₂/Ga₂S₃ heterostructures. Journal of Materials Chemistry C, 2020, 8, 14895-14901.	2.7	16
47693	Strain-modulated electrical and optical bandgaps of tetragonal WO3: An HSE06 hybrid functional calculation. AIP Advances, 2020, 10, 095202.	0.6	4
47694	Origin of off-stoichiometry and electrical benignity at the grain boundaries in CuInSe2: A first-principles study. Journal of Applied Physics, 2020, 128, 145702.	1.1	0
47695	Lattice dynamics in improper ferroelectric YGaO₃. Ferroelectrics, 2020, 567, 28-36.	0.3	0
47696	Effect of Magnetic Field Annealing on Magnetic Properties of Ironâ€“Gallium Alloys. Physics of the Solid State, 2020, 62, 1746-1754.	0.2	5
47697	Computationâ€Guided Synthesis of New Garnetâ€Type Solidâ€State Electrolytes via an Ultrafast Sintering Technique. Advanced Materials, 2020, 32, e2005059.	11.1	15
47698	Thicknessâ€Dependent, Gateâ€Tunable Rectification and Highly Sensitive Photovoltaic Behavior of Heterostructured GeSe/WS₂ pâ€“n Diode. Advanced Materials Interfaces, 2020, 7, 2000893.	1.9	25
47699	Î²â€CsCu₅Se₃: A Promising Thermoelectric Material going beyond Photovoltaic Application. Advanced Theory and Simulations, 2020, 3, 2000169.	1.3	8
47700	Formation of CaCO3 from calcium sources with different anions in single process of CO2 capture-mineralization. Korean Journal of Chemical Engineering, 2020, 37, 1709-1716.	1.2	1
47701	PAI-graphene: A new topological semimetallic two-dimensional carbon allotrope with highly tunable anisotropic Dirac cones. Carbon, 2020, 170, 477-486.	5.4	42
47702	Hydrogen storage on chains-terminated fullerene C20 with density functional theory. Chemical Physics Letters, 2020, 758, 137940.	1.2	16
47703	A new carbon allotrope: T5-carbon. Scripta Materialia, 2020, 189, 72-77.	2.6	12
47704	Studies of non-trivial band topology and electron-hole compensation in YSb. Solid State Communications, 2020, 321, 114022.	0.9	1
47705	Phase Transition in a Memristive Suspended MoS₂ Monolayer Probed by Opto- and Electro-Mechanics. ACS Nano, 2020, 14, 13611-13618.	7.3	13
47706	New Insights into Silicon Purification by Alloyingâ€“Leaching Refining: A Comparative Study of Mgâ€“Si, Caâ€“Si, and Caâ€“Mgâ€“Si Systems. ACS Sustainable Chemistry and Engineering, 2020, 8, 15953-15966.	3.2	10
47707	Under Pressure: Mechanochemical Effects on Structure and Ion Conduction in the Sodium-Ion Solid Electrolyte Na₃PS₄. Journal of the American Chemical Society, 2020, 142, 18422-18436.	6.6	58
47708	Theoretical Prediction and Synthesis of a Family of Atomic Laminate Metal Borides with In-Plane Chemical Ordering. Journal of the American Chemical Society, 2020, 142, 18583-18591.	6.6	55
47709	Quantum transport evidence of Weyl fermions in an epitaxial ferromagnetic oxide. Nature Communications, 2020, 11, 4969.	5.8	71

#	Article	IF	Citations
47710	Dual redox mediators accelerate the electrochemical kinetics of lithium-sulfur batteries. Nature Communications, 2020, 11, 5215.	5.8	113
47711	Thermodynamic insights into interfacial interactions in TiN/amorphous Al₂O₃ heterostructures: ab initio molecular dynamics and first principles investigation. Inorganic Chemistry Frontiers, 2020, 7, 4347-4356.	3.0	3
47712	Mechanism of enhanced ionic conductivity by rotational nitrite group in antiperovskite Na₃ONO₂. Journal of Materials Chemistry A, 2020, 8, 21265-21272.	5.2	29
47713	High thermopower and power factors in EuFeO3 for high temperature thermoelectric applications: A first-principles approach. Journal of Applied Physics, 2020, 128, .	1.1	8
47714	Tunable Electronic Properties of Type-II SiS2/WSe2 Hetero-Bilayers. Nanomaterials, 2020, 10, 2037.	1.9	8
47715	Effect of the N/P/S and transition-metal co-doping on the quantum capacitance of supercapacitor electrodes based on mono- and multilayer graphene. Carbon, 2020, 170, 368-379.	5.4	65
47716	The structural phase transition of ammonia borane under high pressure. International Journal of Hydrogen Energy, 2020, 45, 33047-33058.	3.8	6
47717	Stabilizing Perovskite Solar Cells to IEC61215:2016 Standards with over 9,000-h Operational Tracking. Joule, 2020, 4, 2646-2660.	11.7	218
47718	Origin of highly efficient photocatalyst NiO/SrTiO3 for overall water splitting: Insights from density functional theory calculations. Journal of Solid State Chemistry, 2020, 292, 121683.	1.4	14
47719	DFT+U study of CO2 reduction and CO oxidation on a reconstructed CeO2â˜(110) facet. Materials Today Advances, 2020, 8, 100111.	2.5	8
47720	Carbon Monoxide Gas Induced 4H-to-fcc Phase Transformation of Gold As Revealed by In-Situ Transmission Electron Microscopy. Inorganic Chemistry, 2020, 59, 14415-14423.	1.9	4
47721	Elucidating Stressâ€“Strain Relations of ZrB₁₂ from First-Principles Studies. Journal of Physical Chemistry Letters, 2020, 11, 9165-9170.	2.1	97
47722	Oriented LiMn₂O₄ Particle Fracture from Delithiation-Driven Surface Stress. ACS Applied Materials & Interfaces, 2020, 12, 49182-49191.	4.0	20
47723	Theoretical Investigations of Electronic Structure and Magnetic and Optical Properties of Transition-Metal Dinuclear Molecules. ACS Omega, 2020, 5, 24520-24525.	1.6	2
47724	Dimer rattling mode induced low thermal conductivity in an excellent acoustic conductor. Nature Communications, 2020, 11, 5197.	5.8	27
47725	Metal chalcogenide hollow polar bipyramid prisms as efficient sulfur hosts for Na-S batteries. Nature Communications, 2020, 11, 5242.	5.8	102
47726	Spectroscopic capture of a low-spin Mn(IV)-oxo species in Niâ€“Mn3O4 nanoparticles during water oxidation catalysis. Nature Communications, 2020, 11, 5230.	5.8	21
47727	Roles of acidic sites in alumina catalysts for efficient <scp>d</scp>-xylose conversion to lactic acid. Green Chemistry, 2020, 22, 8572-8583.	4.6	26

#	Article	IF	Citations
47728	Ferroelectricity and phase transitions in In₂Se₃ van der Waals material. Nanoscale, 2020, 12, 22688-22697.	2.8	35
47729	A structure and activity relationship for single-walled carbon nanotube growth confirmed by in situ observations and modeling. Nanoscale, 2020, 12, 21923-21931.	2.8	9
47730	In operando synchrotron X-ray studies of a novel spinel (Ni_{0.2}Co_{0.2}Mn_{0.2}Fe_{0.2}Ti_{0.2})₃O₄ high-entropy oxide for energy storage applications. Journal of Materials Chemistry A, 2020, 8, 21756-21770.	5.2	66
47731	Tailoring binderâ€“cathode interactions for long-life room-temperature sodiumâ€“sulfur batteries. Journal of Materials Chemistry A, 2020, 8, 22983-22997.	5.2	47
47732	First-principles study of phonon thermal transport in IIâ€“VI group graphenelike materials. Journal of Vacuum Science and Technology A: Vacuum, Surfaces and Films, 2020, 38, 062202.	0.9	2
47733	Explainable and trustworthy artificial intelligence for correctable modeling in chemical sciences. Science Advances, 2020, 6, .	4.7	26
47734	Thermodynamics of Plutonium Monocarbide from Anharmonic and Relativistic Theory. Applied Sciences (Switzerland), 2020, 10, 6524.	1.3	4
47735	Dopantâ€Driven Positive Reinforcement in Exâ€Solution Process: New Strategy to Develop Highly Capable and Durable Catalytic Materials. Advanced Materials, 2020, 32, e2003983.	11.1	26
47736	Fabrication Strategy for Efficient 2D/3D Perovskite Solar Cells Enabled by Diffusion Passivation and Strain Compensation. Advanced Energy Materials, 2020, 10, 2002004.	10.2	97
47737	Investigation of oxygen sources and subsequent thorium oxidation in the iridium DOP â€26 cladding material and PuO 2 fuel system. Engineering Reports, 2020, 2, e12285.	0.9	1
47738	Systematic Enumeration of Lowâ€Energy Graphyne Allotropes Based on a Coordinationâ€Constrained Searching Strategy. Physica Status Solidi - Rapid Research Letters, 2020, 14, 2000437.	1.2	17
47739	Electrical and Optical Properties of Beryllium Deep Acceptors in GaN. Journal of Electronic Materials, 2020, 49, 7472-7478.	1.0	1
47740	Computational thermodynamics and its applications. Acta Materialia, 2020, 200, 745-792.	3.8	91
47741	Enhancing <mml:math xmlns:mml="http://www.w3.org/1998/Math/MathML" altimg="si33.svg"><mml:mrow><mml:mi>Î±</mml:mi></mml:mrow></mml:math>-Fe2O3(0Â0Â0Â1) surfaces reactivity through lattice-strain control. Applied Surface Science, 2020, 534, 147605.	3.1	2
47742	First principle calculations of pressure dependent yielding in solute strengthened aluminium alloys. Computational Materials Science, 2020, 184, 109902.	1.4	7
47743	Tunable friction of monolayer MoS2 by control of interfacial chemistry. Extreme Mechanics Letters, 2020, 41, 100996.	2.0	3
47744	Dual redox-active copper hexacyanoferrate nanosheets as cathode materials for advanced sodium-ion batteries. Energy Storage Materials, 2020, 33, 432-441.	9.5	43
47745	Exploring the initial oxidation of Pt, Pt3Ni, Pt3Au (111) surfaces: a genetic algorithm based global optimization with density functional theory. Green Chemical Engineering, 2020, 1, 56-62.	3.3	10

#	Article	IF	Citations
47746	DFT study of the hydrogen adsorption and storage on Ni4 cluster embedded in multivacancy graphene. International Journal of Hydrogen Energy, 2020, 45, 30805-30817.	3.8	21
47747	Interatomic potentials and defect properties of Feâ€“Crâ€“Al alloys. Journal of Nuclear Materials, 2020, 541, 152421.	1.3	18
47748	Potential of porous nodal-line semi-metallic carbon for sodium-ion battery anode. Journal of Power Sources, 2020, 478, 228746.	4.0	14
47749	Smart 3D Network Nanocomposites Collect Irradiation-Induced â€œTrashâ€• Matter, 2020, 3, 1631-1645.	5.0	9
47750	In situ NMR Investigation of the Photoresponse of Perovskite Crystal. Matter, 2020, 3, 2042-2054.	5.0	12
47751	Highly anisotropic and tunable charge carrier of monolayer phosphorus allotropes by bi-axial strain. Physics Letters, Section A: General, Atomic and Solid State Physics, 2020, 384, 126896.	0.9	0
47752	Powerful predictability of FPMD simulations for the phase transition behavior of NaCl-MgCl2 eutectic salt. Solar Energy, 2020, 209, 568-575.	2.9	24
47753	Investigation of the mono vacancy effects on the structural, electronic and magnetic properties of graphene hexagonal-boron nitride in-plane hybrid embracing diamond shaped graphene island. Solid State Sciences, 2020, 108, 106395.	1.5	2
47754	Adsorption induced magnetic anisotropy in the two-dimensional magnet CrCl3. Solid State Communications, 2020, 321, 114048.	0.9	12
47755	DFT coupled with NEGF study of structural, electronic and transport properties of two-dimensional InOBr. Vacuum, 2020, 182, 109745.	1.6	1
47756	High-Pressure Crystal Growth, Superconducting Properties, and Electronic Band Structure of Nb₂P₅. Chemistry of Materials, 2020, 32, 8781-8788.	3.2	17
47757	First-Principles Calculation Study of Na⁺ Superionic Conduction Mechanism in W- and Mo-Doped Na₃SbS₄ Solid Electrolytes. Chemistry of Materials, 2020, 32, 8373-8381.	3.2	33
47758	Substrate Surface Modification for Enlarging Two-Dimensional SnS Grains at Low Temperatures. Chemistry of Materials, 2020, 32, 9026-9033.	3.2	9
47759	Lattice Thermal Transport in Monolayer Group 13 Monochalcogenides MX (M = Ga, In; X = S, Se, Te): Interplay of Atomic Mass, Harmonicity, and Lone-Pair-Induced Anharmonicity. Inorganic Chemistry, 2020, 59, 14899-14909.	1.9	21
47760	Solvation Free Energies and Adsorption Energies at the Metal/Water Interface from Hybrid Quantum-Mechanical/Molecular Mechanics Simulations. Journal of Chemical Theory and Computation, 2020, 16, 6539-6549.	2.3	34
47761	DFT Study on the Hydrogenation of CO₂ to Methanol on Ho-Doped Cu(211) Surface. Journal of Physical Chemistry C, 2020, 124, 22426-22434.	1.5	13
47762	Band Edge Tailoring in Few-Layer Two-Dimensional Molybdenum Sulfide/Selenide Alloys. Journal of Physical Chemistry C, 2020, 124, 22893-22902.	1.5	9
47763	Understanding and Improving the Kinetics of Bulk Carbonation on Sodium Carbonate. Journal of Physical Chemistry C, 2020, 124, 23106-23115.	1.5	5

#	Article	IF	Citations
47764	Dynamics of H₂O Adsorption on Pt(110)-(1 Ã— 2) Based on a Neural Network Potential Energy Surface. Journal of Physical Chemistry C, 2020, 124, 23190-23199.	1.5	16
47765	Exploring the Coexistence Mechanism of CsPb₂Br₅ and CsPbBr₃ Based on the Competitive Phase Diagram. Journal of Physical Chemistry C, 2020, 124, 23052-23058.	1.5	35
47766	Voxelized Atomic Structure Potentials: Predicting Atomic Forces with the Accuracy of Quantum Mechanics Using Convolutional Neural Networks. Journal of Physical Chemistry Letters, 2020, 11, 9093-9099.	2.1	10
47767	Prediction of a New Layered Polymorph of FeS₂ with Fe³⁺S^{2â€“}(S₂^{2â€“})_{1/2} Structure. Journal of Physical Chemistry Letters, 2020, 11, 8861-8866.	2.1	7
47768	Electrochemical N₂ Reduction to Ammonia Using Single Au/Fe Atoms Supported on Nitrogen-Doped Porous Carbon. ACS Applied Energy Materials, 2020, 3, 10061-10069.	2.5	40
47769	Pseudocapacitive Ti-Doped Niobium Pentoxide Nanoflake Structure Design for a Fast Kinetics Anode toward a High-Performance Mg-Ion-Based Dual-Ion Battery. ACS Applied Materials & Interfaces, 2020, 12, 47539-47547.	4.0	35
47770	Acidic Oxygen Evolution Reaction Activityâ€“Stability Relationships in Ru-Based Pyrochlores. ACS Catalysis, 2020, 10, 12182-12196.	5.5	111
47771	Factors Determining Selectivity of Acid- and Base-Catalyzed Self- and Cross-Condensation of Acetone and Cyclopentanone. ACS Catalysis, 2020, 10, 12790-12800.	5.5	10
47772	Condition-Dependent Pd Speciation and NO Adsorption in Pd/Zeolites. ACS Catalysis, 2020, 10, 12801-12818.	5.5	74
47773	First-Principles Study of the Ferromagnetic Properties of Cr₂CO₂ and Cr₂NO₂ MXenes. ACS Omega, 2020, 5, 25848-25853.	1.6	9
47774	How PM2.5 Affects Pt-Catalyzed Oxygen Reduction Reaction. ACS Sustainable Chemistry and Engineering, 2020, 8, 9385-9392.	3.2	5
47775	Organometallic-Based Hybrid Perovskite Piezoelectrics with a Narrow Band Gap. Journal of the American Chemical Society, 2020, 142, 17787-17794.	6.6	83
47776	Inhibition of oxygen dimerization by local symmetry tuning in Li-rich layered oxides for improved stability. Nature Communications, 2020, 11, 4973.	5.8	66
47777	Determining dimensionalities and multiplicities of crystal nets. Npj Computational Materials, 2020, 6, .	3.5	8
47778	First-principles study of structural, elastic and electronic properties of naphyne and naphdiyne. RSC Advances, 2020, 10, 35349-35355.	1.7	4
47779	Elucidation of the high-voltage phase in the layered sodium ion battery cathode material P3â€“Na_{0.5}Ni_{0.25}Mn_{0.75}O₂. Journal of Materials Chemistry A, 2020, 8, 21151-21162.	5.2	20
47780	Suppressing photoexcited electronâ€“hole recombination in MoSe₂/WSe₂ lateral heterostructures via interface-coupled state engineering: a time-domain ab initio study. Journal of Materials Chemistry A, 2020, 8, 20621-20628.	5.2	18
47781	Optimization of photocarrier dynamics and activity in phosphorene with intrinsic defects for nitrogen fixation. Journal of Materials Chemistry A, 2020, 8, 20570-20580.	5.2	26

#	Article	IF	Citations
47782	Tunable valley polarization, magnetic anisotropy and Dzyaloshinskiiâ€“Moriya interaction in two-dimensional intrinsic ferromagnetic Janus 2H-VSeX (X = S, Te) monolayers. Physical Chemistry Chemical Physics, 2020, 22, 23597-23608.	1.3	33
47783	Two-dimensional van der Waals heterostructure CdO/PtSe₂: promising visible light photocatalyst for overall water splitting. Physical Chemistry Chemical Physics, 2020, 22, 24662-24668.	1.3	10
47784	Prediction of two-dimensional ferromagnetic ferroelectric VOF2 monolayer. Physical Chemistry Chemical Physics, 2020, 22, 24109-24115.	1.3	27
47785	Structural dynamics in Niâ€“Fe catalysts during CO₂ methanation â€“ role of iron oxide clusters. Catalysis Science and Technology, 2020, 10, 7542-7554.	2.1	48
47786	Metathetic synthesis of lead cyanamide as a p-type semiconductor. Dalton Transactions, 2020, 49, 14061-14067.	1.6	16
47787	Tailoring nanoscale polarization patterns and transport properties in ferroelectric tunnel junctions by octahedral tilts in electrodes. RSC Advances, 2020, 10, 35367-35373.	1.7	0
47788	The electronic structures and magnetic properties of mixed-valence Fe-based metalâ€“organic VNU-15 frameworks: a theoretical study from linear response DFT+U calculations. RSC Advances, 2020, 10, 34690-34701.	1.7	1
47789	Cmme-SnS: a two-dimensional tin sulfide nanosheet. Journal of Materials Chemistry A, 2020, 8, 21219-21226.	5.2	4
47790	Visible/infrared light-driven high-efficiency CO₂ conversion into ethane based on a Bâ€“Co synergistic catalyst. Journal of Materials Chemistry A, 2020, 8, 22327-22334.	5.2	24
47791	Phase stability and fast ion transport in P2-type layered Na₂X₂TeO₆ (X = Mg, Zn) solid electrolytes for sodium batteries. Journal of Materials Chemistry A, 2020, 8, 22816-22827.	5.2	20
47792	Phase-controlled synthesis of Ni nanocrystals with high catalytic activity in 4-nitrophenol reduction. Journal of Materials Chemistry A, 2020, 8, 22143-22154.	5.2	22
47793	Phase separation in amorphous tantalum oxide from first principles. APL Materials, 2020, 8, .	2.2	12
47794	Optimization of the Reax force field for the lithiumâ€“oxygen system using a high fidelity charge model. Journal of Chemical Physics, 2020, 153, 084107.	1.2	11
47795	Investigation of local structures and electronic states of Sb-doped Mg2Si by fluorescence XAFS and HAXPES. Applied Physics Letters, 2020, 117, .	1.5	4
47796	Monolayer 1T-LaN2: Dirac spin-gapless semiconductor of p-state and Chern insulator with a high Chern number. Applied Physics Letters, 2020, 117, .	1.5	17
47797	Signatures of a liquidâ€“liquid transition in an ab initio deep neural network model for water. Proceedings of the National Academy of Sciences of the United States of America, 2020, 117, 26040-26046.	3.3	112
47798	First-principles study on the electronic structure and optical properties of BiOBr. Ferroelectrics, 2020, 565, 128-136.	0.3	4
47799	Atomic-scale understanding of the Î³/Îµ2 interface in a TiAl alloy. Journal of Alloys and Compounds, 2020, 846, 156381.	2.8	12

#	Article	IF	Citations
47800	An AIMD+U simulation of low-energy displacement events in UO2. Journal of Nuclear Materials, 2020, 540, 152379.	1.3	5
47801	Electronic and electron emission properties of X/ZnO monolayer (X=Li, Na, K, Rb, or Cs): A first-principles study. Journal of Physics and Chemistry of Solids, 2020, 147, 109618.	1.9	9
47802	Phosphorous incorporation in Pd2Sn alloys for electrocatalytic ethanol oxidation. Nano Energy, 2020, 77, 105116.	8.2	48
47803	Correlation between fracture characteristics and valence electron concentration of sputtered Hf-C-N based thin films. Surface and Coatings Technology, 2020, 399, 126212.	2.2	18
47804	Formaldehyde oxidation on Co-doped reduced CeO2(111): First-principles calculations. Surface Science, 2020, 701, 121693.	0.8	11
47805	Electric Field-Tunable Structural Phase Transitions in Monolayer Tellurium. ACS Omega, 2020, 5, 18213-18217.	1.6	11
47806	Eliminating dissolution of platinum-based electrocatalysts at the atomic scale. Nature Materials, 2020, 19, 1207-1214.	13.3	127
47807	Ln(<scp>iii</scp>)â€“Ni(<scp>ii</scp>) heteropolynuclear metal organic frameworks of oxydiacetate with promising proton-conductive properties. CrystEngComm, 2020, 22, 5638-5648.	1.3	4
47808	Adsorption energy scaling relation on bimetallic magnetic surfaces: role of surface magnetic moments. Physical Chemistry Chemical Physics, 2020, 22, 17960-17968.	1.3	8
47809	Thermal transport properties of novel two-dimensional CSe. Physical Chemistry Chemical Physics, 2020, 22, 17833-17841.	1.3	10
47810	Synthesis and mutual transformations of nitronium tetrakis(nitrooxy)- and tetrakis(2,2,2-trifluoroacetoxy)borates. New Journal of Chemistry, 2020, 44, 13944-13951.	1.4	2
47811	A modified â€˜skeleton/skinâ€™ strategy for designing CoNiP nanosheets arrayed on graphene foam for on/off switching of NaBH₄ hydrolysis. RSC Advances, 2020, 10, 26834-26842.	1.7	11
47812	Large spin splittings due to the orbital degree of freedom and spin textures in a ferroelectric nitride perovskite. Physical Review B, 2020, 102, .	1.1	20
47813	Electronic structure beyond the generalized gradient approximation for <mml:math xmlns:mml="http://www.w3.org/1998/Math/MathML"><mml:mrow><mml:msub><mml:mi>Ni</mml:mi><mml:mn>2</mml:mn></mml:msub></mml:mrow></mml:math> Physical Review B, 2020, 102, .	1.1	13
47814	Enhanced Performance of Zirconiumâ€Doped Ceria Catalysts for the Methoxycarbonylation of Anilines. Chemistry - A European Journal, 2020, 26, 16129-16137.	1.7	6
47815	On the coordination of Mg2+ in aragonite: Ab-initio absorption spectroscopy and isotope fractionation study. Geochimica Et Cosmochimica Acta, 2020, 286, 324-335.	1.6	11
47816	In-situ regulation of formic acid oxidation via elastic strains. Journal of Catalysis, 2020, 389, 631-635.	3.1	10
47817	Î²-PdBi2 monolayer: two-dimensional topological metal with superior catalytic activity for carbon dioxide electroreduction to formic acid. Materials Today Advances, 2020, 8, 100091.	2.5	14

#	Article	IF	Citations
47818	Computational Search for New Wâ€“Moâ€“B Compounds. Chemistry of Materials, 2020, 32, 7028-7035.	3.2	22
47819	Partial Electrooxidation of Glycerol on Close-Packed Transition Metal Surfaces: Insights from First-Principles Calculations. Journal of Physical Chemistry C, 2020, 124, 17907-17915.	1.5	13
47820	Stable Multifunctional Single-Atom Catalysts Resulting from the Synergistic Effect of Anchored Transition-Metal Atoms and Host Covalentâ€“Organic Frameworks. Journal of Physical Chemistry C, 2020, 124, 17675-17683.	1.5	46
47821	Dual Functionalization of Electron Transport Layer via Tailoring Molecular Structure for High-Performance Perovskite Light-Emitting Diodes. ACS Applied Materials & Interfaces, 2020, 12, 37346-37353.	4.0	17
47822	Steaming Drived Chemical Interactions of ZnCl_x with Y Zeolite Framework, Its Regulation to Dealumination/Silicon-Healing as well as Enhanced Availability of BrÃ¸nsted Acidity. ACS Catalysis, 2020, 10, 9197-9214.	5.5	20
47823	Highly durable fuel cell catalysts using crosslinkable block copolymer-based carbon supports with ultralow Pt loadings. Energy and Environmental Science, 2020, 13, 4921-4929.	15.6	61
47824	The rational design of single-atom catalysts for electrochemical ammonia synthesis via a descriptor-based approach. Journal of Materials Chemistry A, 2020, 8, 17078-17088.	5.2	60
47825	Oxygen reduction reaction on Pt-skin Pt₃V(111) fuel cell cathode: a density functional theory study. RSC Advances, 2020, 10, 27346-27356.	1.7	21
47826	Structural, elastic, vibrational, thermophysical properties and pressure-induced phase transitions of ThN2, Th2N3, and Th3N4: An ab initio investigation. Journal of Applied Physics, 2020, 128, .	1.1	6
47827	Experimental and theoretical study on device-processing-incorporated fluorine in AlGaN/GaN heterostructures. AIP Advances, 2020, 10, 065122.	0.6	1
47828	Two-dimensional gallium and indium oxides from global structure searching: Ferromagnetism and half metallicity via hole doping. Journal of Applied Physics, 2020, 128, 034304.	1.1	12
47829	Correlation between Nonlinear Optical Properties and Electronic Band Modification in Cobalt-Doped ZnO Nanorods. Physical Review Applied, 2020, 14, .	1.5	5
47830	Engineering Weyl Phases and Nonlinear Hall Effects in <mml:math xmlns:mml="http://www.w3.org/1998/Math/MathML" display="inline"><mml:mrow><mml:msub><mml:mrow><mml:mi mathvariant="normal">T</mml:mi></mml:mrow><mml:mrow><mml:mi>d</mml:mi></mml:mrow></mml:msub></mml:mrow></mml:ma - <mml:math xmlns:mml="http://www.w3.org/1998/Math/MathML" display="inline"><mml:mrow><mml:msub><mml:mrow><mml:mi>MoTe</mml:mi></mml:mrow><mml:mrow><mml:mn>2</mml:mn></	2.9	45
47831	Zinc Tin Oxide Synaptic Device for Neuromorphic Engineering. IEEE Access, 2020, 8, 130678-130686.	2.6	41
47832	Theoretical Simulation of the Binding Energies and Stretching Frequencies of CO Molecules on PtSn Bimetallic Nanoparticles. Journal of Surface Investigation, 2020, 14, 440-446.	0.1	0
47833	Highly improved electrocatalytic activity of NiSx: Effects of Cr-doping and phase transition. Applied Catalysis B: Environmental, 2020, 267, 118721.	10.8	68
47834	Theoretical study on transport-scheme conversion of g-C3N4/TiO2 heterojunctions by oxygen vacancies. Applied Surface Science, 2020, 531, 147318.	3.1	33
47835	The interplay between the suprafacial and intrafacial mechanisms for complete methane oxidation on substituted LaCoO3 perovskite oxides. Journal of Catalysis, 2020, 390, 1-11.	3.1	32

#	Article	IF	Citations
47836	Diiron in extended carbon networks: Magnetic properties of model Fe2C6 and Fe2C12 from first principles. Journal of Magnetism and Magnetic Materials, 2020, 514, 167213.	1.0	2
47837	Theoretical investigations on structural and thermo-mechanical properties of layered ternary carbide Thâ€“Alâ€“C systems. Journal of Nuclear Materials, 2020, 540, 152358.	1.3	7
47838	Computational Prediction of Boron-Based MAX Phases and MXene Derivatives. Chemistry of Materials, 2020, 32, 6947-6957.	3.2	89
47839	Carrier Dynamics and Transfer across the CdS/MoS₂ Interface upon Optical Excitation. Journal of Physical Chemistry Letters, 2020, 11, 6544-6550.	2.1	13
47840	Mixed Halide Lead-free Double Perovskite Alloys for Band Gap Engineering. ACS Applied Energy Materials, 2020, 3, 7364-7371.	2.5	5
47841	Multicomponent Spinel Metal Oxide Nanocomposites as High-Performance Bifunctional Catalysts in Znâ€“Air Batteries. ACS Applied Energy Materials, 2020, 3, 7710-7718.	2.5	22
47842	Intrinsic Ultralow-Threshold Laser Action from Rationally Molecular Design of Metalâ€“Organic Framework Materials. ACS Applied Materials & Interfaces, 2020, 12, 36485-36495.	4.0	20
47843	Selectively Scissoring Hydrogen-Bonded Cytosine Dimer Structures Catalyzed by Water Molecules. ACS Nano, 2020, 14, 10680-10687.	7.3	10
47845	Exploring the sub-stoichiometric behavior of plutonium mononitride. RSC Advances, 2020, 10, 24877-24881.	1.7	3
47846	Î±-Bi₂Sn₂O₇: a potential room temperature n-type oxide thermoelectric. Journal of Materials Chemistry A, 2020, 8, 16405-16420.	5.2	17
47847	Asymmetrically flexoelectric gating effect of Janus transition-metal dichalcogenides and their sensor applications. Journal of Materials Chemistry C, 2020, 8, 11457-11467.	2.7	15
47848	Dual-site occupancy induced broadband cyan emission in Ba₂CaB₂Si₄O₁₄:Ce³⁺. Journal of Materials Chemistry C, 2020, 8, 15626-15633.	2.7	48
47849	Towards understanding physical origin of 2175ÂÃ... extinction bump in interstellar medium. Monthly Notices of the Royal Astronomical Society, 2020, 497, 2190-2200.	1.6	11
47850	Spin-resolved photomodulated electronic properties of ferromagnetic kagome lattices. Physical Review B, 2020, 102, .	1.1	3
47851	Low-temperature insulating phase of the <mml:math xmlns:mml="http://www.w3.org/1998/Math/MathML"><mml:mi>Si</mml:mi><mml:mo>(</mml:mo><mml:mn>111</mml:mn><mml:mo>)</mml:mo></mml:math> surface. Physical Review B, 2020, 102, .	1.1	11
47852	Effects of structural distortions on the electronic structure of <mml:math xmlns:mml="http://www.w3.org/1998/Math/MathML"><mml:mi>T</mml:mi></mml:math> -type transition metal dichalcogenides. Physical Review B, 2020, 102, .	1.1	5
47853	Intrinsic axion insulating behavior in antiferromagnetic <mml:math xmlns:mml="http://www.w3.org/1998/Math/MathML"><mml:mrow><mml:msub><mml:mi>MnBi</mml:mi><mml:mn>2</mml:mn></mml:msub><mml:mo>(</mml:mo><mml:mn>Bi</mml:mn><mml:mn>2</mml:mn><mml:mn>Te</mml:mn><mml:mn>3</mml:mn><mml:mo>)</mml:mo><mml:mn>3</mml:mn></mml:mrow></mml:math> Physical Review B, 2020, 102, .	1.1	63
47854	Gate-Tuned Interlayer Coupling in van der Waals Ferromagnet <mml:math xmlns:mml="http://www.w3.org/1998/Math/MathML" display="inline"><mml:mrow><mml:msub><mml:mrow><mml:mi>Fe</mml:mi></mml:mrow><mml:mrow><mml:mn>3</mml:mn></mml:mrow></mml:msub></mml:mrow></mml:math> Nanoflakes. Physical Review Letters, 2020, 125, 047202.	2.9	87

#	Article	IF	Citations
47855	Edge Defect-Free Anisotropic Two-Dimensional Sheets with Nearly Direct Band Gaps from a True One-Dimensional Van der Waals Nb₂Se₉ Material. ACS Omega, 2020, 5, 10800-10807.	1.6	14
47856	Novel electronic properties of monoclinic MP4 (M = Cr, Mo, W) compounds with or without topological nodal line. Scientific Reports, 2020, 10, 11502.	1.6	10
47857	Impact of strain, pressure, and electron correlation on magnetism and crystal structure of Mn2GaC from first-principles. Scientific Reports, 2020, 10, 11384.	1.6	13
47858	Alkali ions secure hydrides for catalytic hydrogenation. Nature Catalysis, 2020, 3, 703-709.	16.1	123
47859	Magnetic and electronic properties of 2D TiX3 (X = F, Cl, Br and I). Physical Chemistry Chemical Physics, 2020, 22, 17632-17638.	1.3	12
47860	Emergent multiferroicity and strain-driven metalâ€“semiconductor transitions in LaMnO3/RMnO3 superlattices (R = Pr, Pm, Sm and Gd). Physical Chemistry Chemical Physics, 2020, 22, 17503-17512.	1.3	4
47861	PtSe₂/SiH van der Waals type-II heterostructure: a high efficiency photocatalyst for water splitting. Physical Chemistry Chemical Physics, 2020, 22, 17145-17151.	1.3	36
47862	Uncovering the origin of enhanced field emission properties of rGOâ€“MnO₂heterostructures: a synergistic experimental and computational investigation. RSC Advances, 2020, 10, 25988-25998.	1.7	9
47863	Surface structure and energetics of low index facets of bismuth ferrite. Physical Chemistry Chemical Physics, 2020, 22, 16400-16406.	1.3	4
47864	The optimal co-doping of SrFe_{1â^'x}Co_xO_{3â^'Î´} oxygen carriers in redox applications. Physical Chemistry Chemical Physics, 2020, 22, 16721-16726.	1.3	17
47865	Thermoelectric properties of n-type half-Heusler NbCoSn with heavy-element Pt substitution. Journal of Materials Chemistry A, 2020, 8, 14822-14828.	5.2	44
47866	Bulk and monolayer bismuth oxyiodide (BiOI): Excellent high temperature p-type thermoelectric materials. AIP Advances, 2020, 10, .	0.6	40
47867	Optical response of nickel-based superalloy Inconel-718 for applications in additive manufacturing. Journal of Applied Physics, 2020, 127, .	1.1	10
47868	Modeling the dielectric constants of crystals using machine learning. Journal of Chemical Physics, 2020, 153, 024503.	1.2	29
47869	The geometry, electronic and magnetic properties of VLi_n (nâ€‰=â€‰2â€“13) clusters using the first-principles and PSO method. Molecular Physics, 2020, 118, .	0.8	2
47870	Hydrogen Transport in Tungsten for Nuclear Energy Application: Temperature Dependence and Compensation Effect. Fusion Science and Technology, 2020, 76, 616-631.	0.6	3
47871	Dependence of mechanical properties on the site occupancy of ternary alloying elements in Î³â€²-Ni3Al: Ab initio description for shear and tensile deformation. Chinese Physics B, 2020, 29, 078103.	0.7	4
47872	Polarity-induced electronic and atomic reconstruction at <mml:math xmlns:mml="http://www.w3.org/1998/Math/MathML"><mml:msub><mml:mi>NdNiO</mml:mi><mml:mn>2</mml:mn></mml:msub> interfaces. Physical Review B, 2020, 102, .	1.1	15

#	Article	IF	Citations
47873	<mml:math xmlns:mml="http://www.w3.org/1998/Math/MathML"><mml:mrow><mml:msub><mml:mi mathvariant="normal">K</mml:mi><mml:mn>2</mml:mn></mml:msub><mml:msub><mml:mi>CoS</mml:mi><mml:mn>2</mml:mn></mml:msub></mml:mrow></mml:math> : A two-dimensional in-plane antiferromagnetic insulator. Physical Review B, 2020, 102, .	1.1	3
47874	Electronic structure of the corresponding topological Dirac semimetal <mml:math xmlns:mml="http://www.w3.org/1998/Math/MathML"><mml:mrow><mml:mi>CaA</mml:mi><mml:msub><mml:mi mathvariant="normal">I</mml:mi><mml:mn>2</mml:mn></mml:msub><mml:mi mathvariant="normal">S</mml:mi><mml:msub><mml:mi mathvariant="normal">i</mml:mi><mml:mn>2</mml:mn></mml:msub></mml:mrow></mml:math>. Physical Review B, 2020, 102, .	1.1	9
47875	Symmetry-breaking polymorphous descriptions for correlated materials without interelectronic U. Physical Review B, 2020, 102, .	1.1	48
47876	Influence of high-energy local orbitals and electron-phonon interactions on the band gaps and optical absorption spectra of hexagonal boron nitride. Physical Review B, 2020, 102, .	1.1	13
47877	Anomalous Auger Recombination in PbSe. Physical Review Letters, 2020, 125, 037401.	2.9	16
47878	Exploitable Magnetic Anisotropy of Magnetic CrBr3 Monolayer. JETP Letters, 2020, 112, 58-63.	0.4	5
47879	Atomic-scale insights on the plate-shaped Î³â€³ phase in Mgâ€“Gdâ€“Yâ€“Agâ€“Zr alloy. Journal of Materials Research, 2020, 35, 1837-1845.	1.2	2
47880	Halide Pb-Free Doubleâ€“Perovskites: Ternary vs. Quaternary Stoichiometry. Energies, 2020, 13, 3516.	1.6	10
47881	Strain-induced energetic and electronic properties of stanene nanomeshes. Journal of Computational Electronics, 2020, 19, 1357-1364.	1.3	2
47882	Accelerating inverse crystal structure prediction by machine learning: A case study of carbon allotropes. Frontiers of Physics, 2020, 15, 1.	2.4	17
47883	Interstitial Lithium Doping in BiVO₄ Thin Film Photoanode for Enhanced Solar Water Splitting Activity. Chemistry of Materials, 2020, 32, 6401-6409.	3.2	37
47884	High Voltage Mg-Ion Battery Cathode via a Solid Solution Crâ€“Mn Spinel Oxide. Chemistry of Materials, 2020, 32, 6577-6587.	3.2	48
47885	Theoretical and Experimental Insights into the Effects of Zn Doping on the Magnetic and Magnetocaloric Properties of MnCoGe. Chemistry of Materials, 2020, 32, 6721-6729.	3.2	12
47886	Understanding the Ionic Diffusivity in the (Meta)Stable (Un)doped Solid-State Electrolyte from First-Principles: A Case Study of LISICON. Journal of Physical Chemistry C, 2020, 124, 17485-17493.	1.5	6
47887	Tunning Hydrogen Storage Properties of Carbon Eneâ€“Yne Nanosheets through Selected Foreign Metal Functionalization. Journal of Physical Chemistry C, 2020, 124, 16827-16837.	1.5	15
47888	Multilayer Ion Load and Diffusion on TMD/MXene Heterostructure Anodes for Alkali-Ion Batteries. ACS Applied Energy Materials, 2020, 3, 7699-7709.	2.5	22
47889	KAgX (X = S, Se): High-Performance Layered Thermoelectric Materials for Medium-Temperature Applications. ACS Applied Materials & Interfaces, 2020, 12, 36102-36109.	4.0	68
47890	n-Doping of Quantum Dots by Lithium Ion Intercalation. ACS Applied Materials & Interfaces, 2020, 12, 36523-36529.	4.0	3

#	Article	IF	Citations
47891	Interfacial Chemical-Bond-Modulated Charge Transfer of Heterostructures for Improving Photocatalytic Performance. ACS Applied Materials & Interfaces, 2020, 12, 9872-9880.	4.0	38
47892	Predicting a Novel Phase of 2D SiTe₂. ACS Omega, 2020, 5, 16848-16855.	1.6	4
47893	The stability of P2-layered sodium transition metal oxides in ambient atmospheres. Nature Communications, 2020, 11, 3544.	5.8	204
47894	Enhancing power factor of SnSe sheet with grain boundary by doping germanium or silicon. Npj Computational Materials, 2020, 6, .	3.5	9
47895	Vacancy-enabled N2 activation for ammonia synthesis on an Ni-loaded catalyst. Nature, 2020, 583, 391-395.	13.7	309
47896	Molybdenum defect complexes in bismuth vanadate. Physical Chemistry Chemical Physics, 2020, 22, 16277-16285.	1.3	2
47897	Unexpected bowing band evolution in an all-inorganic CsSn_{1â^'x}Pb_xBr₃perovskite. RSC Advances, 2020, 10, 26407-26413.	1.7	4
47898	Thermoelectric transport of semiconductor full-Heusler VFe₂Al. Journal of Materials Chemistry C, 2020, 8, 10174-10184.	2.7	34
47899	Transferability of neural network potentials for varying stoichiometry: Phonons and thermal conductivity of MnxGey compounds. Journal of Applied Physics, 2020, 127, .	1.1	27
47900	Electronic, magnetic and optical properties of transition-metal and hydroxides doped monolayer g-C₃N₄: a first principles investigation. Journal of Physics Condensed Matter, 2020, 32, 445602.	0.7	8
47901	Eightfold fermionic excitation in a charge density wave compound. Physical Review B, 2020, 102, .	1.1	20
47902	Unit cell restricted Bloch functions basis for first-principle transport models: Theory and application. Physical Review B, 2020, 102, .	1.1	19
47903	Dual topological insulator device with disorder robustness. Physical Review B, 2020, 102, .	1.1	11
47904	Interactions of Calcium with Chlorogenic and Rosmarinic Acids: An Experimental and Theoretical Approach. International Journal of Molecular Sciences, 2020, 21, 4948.	1.8	11
47905	High Curie Temperature Ferromagnetism and High Hole Mobility in Tensile Strained Mnâ€Doped SiGe Thin Films. Advanced Functional Materials, 2020, 30, 2002513.	7.8	20
47906	Structural Relaxation and Crystalline Phase Effects on the Exchange Bias Phenomenon in FeF 2 /Fe Core/Shell Nanoparticles. Advanced Materials Interfaces, 2020, 7, 2000862.	1.9	4
47907	Giant Perpendicular Magnetic Anisotropy in Moâ€Based Doubleâ€Interface Free Layer Structure for Advanced Magnetic Tunnel Junctions. Advanced Electronic Materials, 2020, 6, 2000271.	2.6	26
47908	Identification of Active Sites on High-Performance Pt/Al₂O₃ Catalyst for Cryogenic CO Oxidation. ACS Catalysis, 2020, 10, 8815-8824.	5.5	54

#	Article	IF	Citations
47909	Design of a Vâ€“Tiâ€“Ni alloy with superelastic nano-precipitates. Acta Materialia, 2020, 196, 710-722.	3.8	5
47910	Theoretical exploration of intrinsic facet-dependent CH4 and C2 formation on Fe5C2 particle. Applied Catalysis B: Environmental, 2020, 278, 119308.	10.8	30
47911	1T GdN2 monolayer â€" Spin-orbit induced magnetic Dirac semiconductor stable at room temperature. Applied Surface Science, 2020, 529, 147129.	3.1	3
47912	2D XBiSe3(XÂ=ÂAs, Sb) monolayers with high anisotropic mobility and enhanced optical absorption in visible light region. Applied Surface Science, 2020, 530, 147137.	3.1	13
47913	Electronic structure, lattice dynamics, and dielectric properties in cubic perovskite BiMn3Cr4O12 and LaMn3Cr4O12. Chemical Physics, 2020, 538, 110924.	0.9	3
47914	Atomistic simulations of the face-centered-cubic-to-hexagonal-close-packed phase transformation in the equiatomic CoCrFeMnNi high entropy alloy under high compression. Computational Materials Science, 2020, 184, 109864.	1.4	24
47915	Energetics of heterogeneous Mg {101Â¯2} deformation twinning migration using an atomistically informed phase-field model. Computational Materials Science, 2020, 183, 109907.	1.4	5
47916	Bulk and monolayer As2S3 as promising thermoelectric material with high conversion performance. Computational Materials Science, 2020, 183, 109913.	1.4	24
47917	Radionuclide incorporation in negative thermal expansion <mml:math xmlns:mml="http://www.w3.org/1998/Math/MathML" altimg="si9.svg"><mml:mrow><mml:mi>Î±</mml:mi></mml:mrow></mml:math>-Zr(WO4)2: A density functional theory study. Chemical Physics Letters, 2020, 744, 137172.	1.2	1
47918	Machine learning prediction of monatomic adsorption energies with non-first-principles calculated quantities. Chemical Physics Letters, 2020, 755, 137772.	1.2	7
47919	Morphology evolution and dendrite growth in Li- and Mg-metal batteries: A potential dependent thermodynamic and kinetic multiscale ab initio study. Electrochimica Acta, 2020, 353, 136493.	2.6	28
47920	Hierarchical dense Niâ^'Co layered double hydroxide supported carbon nanofibers for the electrochemical determination of metronidazole in biological samples. Electrochimica Acta, 2020, 354, 136723.	2.6	36
47921	Theoretical analysis of doped graphene as cathode catalyst in Li-O2 and Na-O2 batteries â€" the impact of the computational scheme. Electrochimica Acta, 2020, 354, 136735.	2.6	11
47922	Effects of vanadium, vanadium carbide, and vanadium oxide catalysts on hydrogenation of Mg17Al12 (110) surface: A first principles study. International Journal of Hydrogen Energy, 2020, 45, 28078-28086.	3.8	5
47923	Understanding the structural, electronic and optical properties of CuXY2 (X = Si, Ge, Y = P, As): A DFT +U approach. Optik, 2020, 221, 165212.	1.4	2
47924	Improving Efficiency and Stability of Perovskite Solar Cells Enabled by A Near-Infrared-Absorbing Moisture Barrier. Joule, 2020, 4, 1575-1593.	11.7	88
47925	Exploration of novel High-Pressure Structures of Hf2O3. Materials Chemistry and Physics, 2020, 254, 123532.	2.0	0
47926	Insight into dynamic interaction of molten MgCl2-NaCl-KCl with impurity water via FPMD simulations. Journal of Molecular Liquids, 2020, 314, 113596.	2.3	20

#	Article	IF	Citations
47927	The contrasting fracture behaviour of twin boundaries and general boundaries â€“ A first principles study based on experimental observation. Materials Science & Engineering A: Structural Materials: Properties, Microstructure and Processing, 2020, 781, 139225.	2.6	5
47928	Theoretical investigations on the structural stability, structural and physical properties, and bonding feature for RuX (X = Si, Ge, Sn) with B20 and B2 phases. Materials Today Communications, 2020, 24, 101116.	0.9	2
47929	The electronic and magnetic properties of the Mo doped ZnTe alloys with different configurations. Materials Today Communications, 2020, 24, 101258.	0.9	1
47930	Half-metallicity and enhanced Curie temperature of Ti-embedded CrI3 monolayer. Materials Today Communications, 2020, 25, 101438.	0.9	5
47931	New direction's piezoelectricity and new applications of two-dimensional group V-IV-III-VI films: A theoretical study. Physica E: Low-Dimensional Systems and Nanostructures, 2020, 124, 114214.	1.3	9
47932	First-principles exploration of the stabilization mechanism of long-period stacking ordered structures in high performance Al alloys. Progress in Natural Science: Materials International, 2020, 30, 424-431.	1.8	9
47933	Importance of Au nanostructures in CO2 electrochemical reduction reaction. Science Bulletin, 2020, 65, 796-802.	4.3	44
47934	Mitigation of CO poisoning on functionalized palladium monolayer supported on titanium carbide. Surface and Coatings Technology, 2020, 402, 125925.	2.2	1
47935	Quantum-well states for uniform Ag layers on the Ga-induced Si(111)â€“(3Ã—3)R30Â° surface. Surface Science, 2020, 701, 121684.	0.8	0
47936	Theoretical Investigation of the Heterojunction Effect on the Catalytic Activity and Selectivity of an Au@NiO Coreâ€“Shell Catalyst in Aerobic Oxidation. Journal of Physical Chemistry C, 2020, 124, 17039-17047.	1.5	7
47937	DFT-Based Cu(111)||Cu₂O(111) Model for Copper Metal Covered by Ultrathin Copper Oxide: Structure, Electronic Properties, and Reactivity. Journal of Physical Chemistry C, 2020, 124, 17048-17057.	1.5	27
47938	Thermally Induced Diffusion and Restructuring of Iron Triade (Fe, Co, Ni) Nanoparticles Passivated by Several Layers of Gold. Journal of Physical Chemistry C, 2020, 124, 16680-16688.	1.5	14
47939	Borophene with Large Holes. Journal of Physical Chemistry Letters, 2020, 11, 6235-6241.	2.1	26
47940	Atom-Pair Catalysts Supported by N-Doped Graphene for the Nitrogen Reduction Reaction: d-Band Center-Based Descriptor. Journal of Physical Chemistry Letters, 2020, 11, 6320-6329.	2.1	82
47941	Rational Design of 2D h-BAs Monolayer as Advanced Sulfur Host for High Energy Density Liâ€“S Batteries. ACS Applied Energy Materials, 2020, 3, 7306-7317.	2.5	23
47942	Plasma-Made Graphene Nanostructures with Molecularly Dispersed F and Na Sites for Solar Desalination of Oil-Contaminated Seawater with Complete In-Water and In-Air Oil Rejection. ACS Applied Materials & Interfaces, 2020, 12, 38512-38521.	4.0	32
47943	Exploring the Effects of Node Topology, Connectivity, and Metal Identity on the Binding of Nerve Agents and Their Hydrolysis Products in Metalâ€“Organic Frameworks. ACS Applied Materials & Interfaces, 2020, 12, 35657-35675.	4.0	17
47944	Evaluation of Amorphous Oxide Coatings for High-Voltage Li-Ion Battery Applications Using a First-Principles Framework. ACS Applied Materials & Interfaces, 2020, 12, 35748-35756.	4.0	26

#	Article	IF	Citations
47945	Enhancing the Stability of Orthorhombic CsSnI₃ Perovskite via Oriented Ï€-Conjugated Ligand Passivation. ACS Applied Materials & Interfaces, 2020, 12, 34462-34469.	4.0	26
47946	Catalytic Methane Pyrolysis with Liquid and Vapor Phase Tellurium. ACS Catalysis, 2020, 10, 8223-8230.	5.5	42
47947	Kagome-like silicene: A novel exotic form of two-dimensional epitaxial silicon. Applied Surface Science, 2020, 530, 147195.	3.1	18
47948	Unveiling the critical role of p-d hybridization interaction in M13â^'nGan clusters on CO2 adsorption. Fuel, 2020, 280, 118446.	3.4	9
47949	Reversible photochromism for the enhancement of carrier separation in Zn1-Cu S. Journal of Alloys and Compounds, 2020, 844, 155880.	2.8	4
47950	A comprehensive phonon thermal transport study of 2D hexagonal MX2 and orthorhombic M2X3 (M =) Tj ETQq1 1 0.784314 rgBT /Ov	0.9	7
47951	Effect of biaxial strain on thermal transport in WS2 monolayer from first principles calculations. Physica E: Low-Dimensional Systems and Nanostructures, 2020, 124, 114312.	1.3	31
47952	Electronic Structure Modeling of Metalâ€“Organic Frameworks. Chemical Reviews, 2020, 120, 8641-8715.	23.0	149
47953	Mixed-Anion Control of Câ€“H Bond Activation of Methane on the IrO2 Surface. Journal of Physical Chemistry C, 2020, 124, 17058-17072.	1.5	13
47954	Mechanism of Thermal Atomic Layer Etch of W Metal Using Sequential Oxidation and Chlorination: A First-Principles Study. ACS Applied Materials & Interfaces, 2020, 12, 36670-36680.	4.0	4
47955	Stabilizing Hydrogen Adsorption through Theory-Guided Chalcogen Substitution in Chevrel-Phase Mo₆X₈ (X=S, Se, Te) Electrocatalysts. ACS Applied Materials & Interfaces, 2020, 12, 35995-36003.	4.0	26
47956	Single-Crystalline Mo-Nanowire-Mediated Directional Growth of High-Index-Faceted MoNi Electrocatalyst for Ultralong-Term Alkaline Hydrogen Evolution. ACS Applied Materials & Interfaces, 2020, 12, 36259-36267.	4.0	18
47957	Glycosidic Câ€“O Bond Activation in Cellulose Pyrolysis: Alpha Versus Beta and Condensed Phase Hydroxyl-Catalytic Scission. ACS Catalysis, 2020, 10, 8454-8464.	5.5	19
47958	Multiregion Janus-Featured Cobalt Phosphide-Cobalt Composite for Highly Reversible Room-Temperature Sodium-Sulfur Batteries. ACS Nano, 2020, 14, 10284-10293.	7.3	81
47959	Operando time-resolved X-ray absorption spectroscopy reveals the chemical nature enabling highly selective CO2 reduction. Nature Communications, 2020, 11, 3525.	5.8	242
47960	Canonical, deprotonated, or zwitterionic? II. A computational study on amino acid interaction with the TiO₂(110) rutile surface: comparison with the anatase (101) surface. Physical Chemistry Chemical Physics, 2020, 22, 16862-16876.	1.3	8
47961	A polarization propagation mechanism of Fe and Cu atoms co-doped in two-dimensional-Si₃N₄. New Journal of Chemistry, 2020, 44, 14082-14086.	1.4	0
47962	Two-dimensional metal dicyanamide frameworks of BeTriMe[M(dca)3(H2O)] (BeTriMe =) Tj ETQq1 1 0.784314 rgBT /Overlock 10 Tf 5 magnetic orders and nonlinear optical threshold temperature sensing. Journal of Materials Chemistry C, 2020, 8, 11735-11747.	2.7	14

#	Article	IF	Citations
47963	5d transition-metal atom/5dâ€“3d dimer adsorption tailored electronic structure and magnetic anisotropy of two-dimensional WSe₂ monolayers. Journal of Materials Chemistry C, 2020, 8, 11417-11425.	2.7	8
47964	Machine learning substitutional defect formation energies in ABO3 perovskites. Journal of Applied Physics, 2020, 128, .	1.1	21
47965	A finite volume method preserving maximum principle for steady heat conduction equations with modified Anderson acceleration. Numerical Heat Transfer, Part B: Fundamentals, 2020, 78, 412-438.	0.6	0
47966	Defect-Selective Charge-Density-Wave Condensation in <mml:math xmlns:mml="http://www.w3.org/1998/Math/MathML" display="inline"><mml:mrow><mml:mn>2</mml:mn><mml:mi>H</mml:mi><mml:mtext>â^'</mml:mtext><mml:msub><mml:mrow><m Physical Review Letters, 2020, 125, 036804.	2.9	22
47967	Distinct Topological Surface States on the Two Terminations of <mml:math xmlns:mml="http://www.w3.org/1998/Math/MathML" display="inline"><mml:mrow><mml:mrow><mml:msub><mml:mrow><mml:mi>MnBi</mml:mi></mml:mrow><mml:mrow><mml:mn>4 Physical Review X, 2020, 10, .	2.8	52
47968	Effect of chemical disorder on the electronic stopping of solid solution alloys. Acta Materialia, 2020, 196, 576-583.	3.8	11
47969	Rational designed Co@N-doped carbon catalyst for high-efficient H2S selective oxidation by regulating electronic structures. Chemical Engineering Journal, 2020, 401, 126038.	6.6	43
47970	Effects of L-cysteine on the photoluminescence, electronic and cytotoxicity properties of ZnS:O quantum dots. Journal of Alloys and Compounds, 2020, 825, 154052.	2.8	12
47971	Abnormal elasticity and lattice dynamics in the L10-FePd crystalline alloy at high pressure. Journal of Magnetism and Magnetic Materials, 2020, 510, 166904.	1.0	5
47972	Ultra-low thermal conductivity of orthorhombic CH3NH3SnI3: A first principles investigation. Journal of Solid State Chemistry, 2020, 290, 121541.	1.4	9
47973	A comprehensive study of pressure dependent phase transitions in ferroelectric PbTiO3, PbZrO3 and BaTiO3. Materials Chemistry and Physics, 2020, 254, 123545.	2.0	15
47974	The crystal anisotropy effect of MAPbI3 perovskite on optoelectronic devices. Materials Today Energy, 2020, 17, 100481.	2.5	26
47975	Electronic structures and charge carrier mobilities of boron-graphdiyne sheet and nanoribbons. Physica E: Low-Dimensional Systems and Nanostructures, 2020, 124, 114354.	1.3	6
47976	Frustrated and Allowed Structural Transitions at the Limits of the BaAl₄ Type: The (3 +) Tj ETQq1 1 0.784314 rgBT /Over Chemistry, 2020, 59, 10208-10222.	1.9	5
47977	Hydrodesulfurization of Dibenzothiophene on TiO_{2â€“x}-Modified Fe-Based Catalysts: Electron Transfer Behavior between TiO_{2â€“x} and Fe Species. ACS Catalysis, 2020, 10, 9019-9033.	5.5	31
47978	Single-Atom Vacancy Defect to Trigger High-Efficiency Hydrogen Evolution of MoS₂. Journal of the American Chemical Society, 2020, 142, 4298-4308.	6.6	585
47979	Piezoelectric domain walls in van der Waals antiferroelectric CuInP2Se6. Nature Communications, 2020, 11, 3623.	5.8	47
47980	2D BeP₂ monolayer: investigation of electronic and optical properties by driven modulated strain. RSC Advances, 2020, 10, 26804-26812.	1.7	13

#	Article	IF	Citations
47981	Intrinsic ultra-wide completely spin-polarized state realized in a new CrO₂ monolayer. Physical Chemistry Chemical Physics, 2020, 22, 17038-17041.	1.3	9
47982	Second harmonic generation responses of KH₂PO₄: importance of K and breaking down of Kleinman symmetry. RSC Advances, 2020, 10, 26479-26485.	1.7	14
47983	Multilayer graphene coated vanadium(V) oxide as electrodes for intercalation based brackish water desalination. 2D Materials, 2020, 7, 045025.	2.0	2
47984	Electronic structure of MPX₃ trichalcogenide monolayers in density functional theory: a case study with four compounds (M = Mn, Fe; X = S, Se). Electronic Structure, 2020, 2, 025003.	1.0	19
47985	Time-reversal symmetry breaking in the noncentrosymmetric <mml:math xmlns:mml="http://www.w3.org/1998/Math/MathML"><mml:msub><mml:mrow><mml:mi>Zr</mml:mi></mml:mrow><mml:mn>3</mml:mn> superconductor. Physical Review B, 2020, 102, .	1.1	25
47986	High-precision equation of state data for <mml:math xmlns:mml="http://www.w3.org/1998/Math/MathML"><mml:msub><mml:mi>TiO</mml:mi><mml:mn>2</mml:mn></mml:msub></m : A structural analog of <mml:math xmlns:mml="http://www.w3.org/1998/Math/MathML"><mml:msub><mml:mi>SiO</mml:mi><mml:mn>2</mml:mn></mml:msub></m Physical Review B, 2020, 102, .	1.1	12
47987	Importance of interactions for the band structure of the topological Dirac semimetal <mml:math xmlns:mml="http://www.w3.org/1998/Math/MathML"><mml:mrow><mml:msub><mml:mi mathvariant="normal">Na</mml:mi><mml:mn>3</mml:mn></mml:msub><mml:mi>Bi</mml:mi></mml:mrow></mml:math>. Physical Review B, 2020, 102, .	1.1	7
47988	Coexistence and Interaction of Spinons and Magnons in an Antiferromagnet with Alternating Antiferromagnetic and Ferromagnetic Quantum Spin Chains. Physical Review Letters, 2020, 125, 037204.	2.9	12
47989	The Role of Ceria in a Hybrid Catalyst toward Alkaline Water Oxidation. ChemSusChem, 2020, 13, 5273-5279.	3.6	36
47990	Insight into enhanced visible-light photocatalytic activity of SWCNTs/g-C3N4 nanocomposites from first principles. Applied Surface Science, 2020, 530, 147181.	3.1	30
47991	Systematic exploration of magnetic mechanism of La3Co29Si4B10 by first principles calculation. Computational Materials Science, 2020, 184, 109853.	1.4	1
47992	Migration energy barriers and diffusion anisotropy of point defects on tungsten surfaces. Computational Materials Science, 2020, 184, 109893.	1.4	10
47993	Ab initio molecular dynamics studies on the transport mechanisms of oxygen atoms in the adiabatic reaction of Al/CuO nanothermite. Chemical Physics Letters, 2020, 745, 137278.	1.2	9
47994	Tritium species diffusion on and desorption from Î³-LiAlO2 (100) surface: A first-principles investigation. Journal of Nuclear Materials, 2020, 540, 152394.	1.3	4
47995	Correlated morphological and chemical mechanisms for the superior corrosion resistance of alumina-deposited 2D nanofilms on copper. Materialia, 2020, 11, 100697.	1.3	5
47996	Synthesis, Structure, and Anomalous Magnetic Ordering of the Spin-1/2 Coupled Square Tetramer System K(NbO)Cu₄(PO₄)₄. Inorganic Chemistry, 2020, 59, 10986-10995.	1.9	5
47997	Thermodynamic Full Landscape Searching Scheme for Identifying the Mechanism of Electrochemical Reaction: A Case Study of Oxygen Evolution on Fe- and Co-Doped Grapheneâ€“Nitrogen Sites. Journal of Physical Chemistry A, 2020, 124, 5444-5455.	1.1	1
47998	Modeling Spontaneous Charge Transfer at Metal/Organic Hybrid Heterostructures. Journal of Physical Chemistry C, 2020, 124, 4802-4809.	1.5	8

#	Article	IF	Citations
47999	Giant Photonic Response of Mexican-Hat Topological Semiconductors for Mid-infrared to Terahertz Applications. Journal of Physical Chemistry Letters, 2020, 11, 6119-6126.	2.1	18
48000	Hydrocracking of Fused Aromatic Hydrocarbons Catalyzed by Al-Substituted HZSM-5â€"A Case Study of 9,10-Dihydroanthracene. ACS Catalysis, 2020, 10, 9215-9226.	5.5	13
48001	Magneto-Optical Detection of Photoinduced Magnetism via Chirality-Induced Spin Selectivity in 2D Chiral Hybrid Organicâ€"Inorganic Perovskites. ACS Nano, 2020, 14, 10370-10375.	7.3	61
48002	A General Strategy to Atomically Dispersed Precious Metal Catalysts for Unravelling Their Catalytic Trends for Oxygen Reduction Reaction. ACS Nano, 2020, 14, 1990-2001.	7.3	116
48003	On the mechanism of predominant urea formation from thermal degradation of CO₂-loaded aqueous ethylenediamine. Physical Chemistry Chemical Physics, 2020, 22, 17336-17343.	1.3	12
48004	Production of aromatics from biomass by computer-aided selection of the zeolite catalyst. Green Chemistry, 2020, 22, 5123-5131.	4.6	25
48005	Ultrahigh tunneling magnetoresistance in van der Waals and lateral magnetic tunnel junctions formed by intrinsic ferromagnets Li0.5CrI3 and CrI3. Applied Physics Letters, 2020, 117, 022412.	1.5	17
48006	Synthesis of Highly Stable One-Dimensional Black Phosphorus/h-BN Heterostructures: A Novel Flexible Electronic Platform. Chinese Physics Letters, 2020, 37, 076203.	1.3	8
48007	Tuning the electronic and magnetic properties of pentagraphene through the C1 vacancy. 2D Materials, 2020, 7, 045024.	2.0	6
48008	Universal description of potential energy surface of interlayer interaction in two-dimensional materials by first spatial Fourier harmonics. Physical Review B, 2020, 102, .	1.1	9
48009	Dirac materials for sub-MeV dark matter detection: New targets and improved formalism. Physical Review D, 2020, 101, .	1.6	58
48010	Anisotropic Elastic Properties of Battery Anodes. Journal of the Electrochemical Society, 2020, 167, 110550.	1.3	8
48011	Engineering the Phases and Heterostructures of Ultrathin Hybrid Perovskite Nanosheets. Advanced Materials, 2020, 32, e2002392.	11.1	25
48012	Accelerated Modeling of Lithium Diffusion in Solid State Electrolytes using Artificial Neural Networks. Advanced Theory and Simulations, 2020, 3, 2000097.	1.3	11
48013	Molecular modeling of MCPA herbicide adsorption by goethite (110) surface in dependence of pH. Theoretical Chemistry Accounts, 2020, 139, 1.	0.5	3
48014	Theoretical study of the effects of alloying elements on Cu nanotwins. Science China: Physics, Mechanics and Astronomy, 2020, 63, 1.	2.0	15
48015	Effects of Mo on the mechanical behavior of Î³/Î³Ê¹-strengthened Co-Ti-based alloys. Acta Materialia, 2020, 197, 69-80.	3.8	16
48016	First-principles study of chromium diffusion in the ferritic Fe-Cr alloy. Computational Materials Science, 2020, 181, 109733.	1.4	11

#	Article	IF	Citations
48017	First-principles study of the tritium reaction and diffusion on the Î³-LiAlO2 (1Â0Â0) surface with carbon impurity. Computational Materials Science, 2020, 181, 109748.	1.4	3
48018	First-principles calculations on high-temperature desorption loss from iridium. Computational Materials Science, 2020, 184, 109897.	1.4	0
48019	Pyridinic-to-graphitic conformational change of nitrogen in graphitic carbon nitride by lithium coordination during lithium plating. Energy Storage Materials, 2020, 31, 505-514.	9.5	20
48020	Fluorination effect for stabilizing cationic and anionic redox activities in cation-disordered cathode materials. Energy Storage Materials, 2020, 32, 234-243.	9.5	42
48021	Local lattice relaxation around Tl substitutional impurities in a NaI(Tl) scintillator crystal. Radiation Physics and Chemistry, 2020, 177, 108992.	1.4	2
48022	Atomic scattering of H and N on W(100): Effect of lattice vibration and electronic excitations on the dynamics. Surface Science, 2020, 701, 121678.	0.8	5
48023	Reliable Prediction of New Quantum Materials for Topological and Renewable-Energy Applications: A High-Throughput Screening. Journal of Physical Chemistry Letters, 2020, 11, 6364-6372.	2.1	12
48024	Changing the magnetic states of an Fe/BaTiO₃ interface through crystal field effects controlled by strain. Physical Chemistry Chemical Physics, 2020, 22, 18050-18059.	1.3	1
48025	Hydration of Î±-UO₃following storage under controlled conditions of temperature and relative humidity. Dalton Transactions, 2020, 49, 10452-10462.	1.6	16
48026	Interpretation of experiments on shock compression and isentropic expansion of uranium by quantum molecular dynamics simulations. Journal of Physics: Conference Series, 2020, 1556, 012043.	0.3	0
48027	Quantum Dots of [Na₄Cs₆PbBr₄]⁸⁺, Water Stable in Zeolite X, Luminesce Sharply in the Green. Advanced Materials, 2020, 32, e2001868.	11.1	14
48028	Great Enhancement of Selfâ€Powered Photoresponse Performance of C₃H₈NSiâ€TiO₂ NRAs/nâ€Si Heterojunction by Buildâ€In and Buildâ€Out Electric Field Jointly Promoting Carrier Separation. Advanced Electronic Materials, 2020, 6, 2000501.	2.6	10
48029	Dynamics Study of Superionic Conducting Glass Na 3 PS 4 Using Quasiâ€Elastic Gammaâ€Ray Scattering: Analysis Based on Diffraction and Reverse Monte Carloâ€“Density Functional Theory Modeling. Physica Status Solidi (B): Basic Research, 2020, 257, 2000113.	0.7	3
48030	Systematic Study of Alkali Cations Intercalated Titanium Dioxide Effect on Sodium and Lithium Storage. Small, 2020, 16, 2001391.	5.2	5
48031	Determining the crystal and electronic structures of the magnesium secondary battery cathode material MgCo2â^'xMnxO4 using first-principles calculations and a quantum beam during discharge. Journal of Materials Science, 2020, 55, 13852-13870.	1.7	6
48032	Adsorption structure of adenine on cerium oxide. Applied Surface Science, 2020, 530, 147257.	3.1	8
48033	Origin of magnetic phase transition in RMn2Si2 (RÂ=Ârare-earth ion or Y) intermetallics. Computational Materials Science, 2020, 184, 109901.	1.4	5
48034	Phase-field calculations of sink strength in Al, Ni, and Fe: A detailed study of elastic effects. Computational Materials Science, 2020, 183, 109905.	1.4	5

#	Article	IF	Citations
48035	Intrinsic electronic defect states of anatase using density functional theory. Computational Materials Science, 2020, 184, 109925.	1.4	15
48036	Demonstration of X-ray Thomson scattering as diagnostics for miscibility in warm dense matter. Nature Communications, 2020, 11, 2620.	5.8	27
48037	The microscopic origin of DMI in magnetic bilayers and prediction of giant DMI in new bilayers. Npj Computational Materials, 2020, 6, .	3.5	32
48038	Symmetry-enforced Weyl phonons. Npj Computational Materials, 2020, 6, .	3.5	69
48039	Theoretical dissection of superconductivity in two-dimensional honeycomb borophene oxide B2O crystal with a high stability. Npj Computational Materials, 2020, 6, .	3.5	47
48040	Broken mirror symmetry in excitonic response of reconstructed domains in twisted MoSe2/MoSe2 bilayers. Nature Nanotechnology, 2020, 15, 750-754.	15.6	106
48041	Non-Abelian reciprocal braiding of Weyl points and its manifestation in ZrTe. Nature Physics, 2020, 16, 1137-1143.	6.5	87
48042	Single crystal structure, vibrational spectroscopy, gas sorption and antimicrobial properties of a new inorganic acidic diphosphates material (NH4)2Mg(H2P2O7)2â€¢2H2O. Scientific Reports, 2020, 10, 8909.	1.6	9
48043	Interfacial stabilization for epitaxial CuCrO2 delafossites. Scientific Reports, 2020, 10, 11375.	1.6	8
48044	High performance photocatalytic and thermoelectric two-dimensional asymmetrically ordered Janus-like MXene alloys. Materials Advances, 2020, 1, 1176-1185.	2.6	14
48045	Integrating PtNi nanoparticles on NiFe layered double hydroxide nanosheets as a bifunctional catalyst for hybrid sodiumâ€“air batteries. Journal of Materials Chemistry A, 2020, 8, 16355-16365.	5.2	21
48046	Na-Based monolayer photocatalysts with an extremely high intrinsic electric-field for water splitting. Physical Chemistry Chemical Physics, 2020, 22, 16007-16012.	1.3	7
48047	Synergistic effects of heteroatom-decorated MXene catalysts for CO reduction reactions. Nanoscale, 2020, 12, 15880-15887.	2.8	32
48048	Recent developments in the P<scp>y</scp>SCF program package. Journal of Chemical Physics, 2020, 153, 024109.	1.2	388
48049	Rational design of 2D organic magnets with giant magnetic anisotropy based on two-coordinate 5d transition metals. APL Materials, 2020, 8, .	2.2	10
48050	Spin-polarized electron transmission through B-doped graphene nanoribbons with Fe functionalization: a first-principles study. New Journal of Physics, 2020, 22, 063022.	1.2	2
48051	Emergence of a ferromagnetic insulating state in <mml:math xmlns:mml="http://www.w3.org/1998/Math/MathML"><mml:mrow><mml:msub><mml:mi>LaMnO</mml:mi><mml:mn>3</mml:mn></mml:msub></mml:mrow></ heterostructures: Role of strong electronic correlations and strain. Physical Review B, 2020, 101, .	1.1	9
48052	Active Learning A Neural Network Model For Gold Clusters & Bulk From Sparse First Principles Training Data. ChemCatChem, 2020, 12, 4796-4806.	1.8	17

#	Article	IF	Citations
48053	Magnetic Structure of Bulk GdMnO 3 : Influence of Strain. Physica Status Solidi (B): Basic Research, 2020, 257, 1900632.	0.7	3
48054	Effect of transition metal doping on the structural, magnetic, and vibrational properties of Ten clusters: a DFT study. Journal of Nanoparticle Research, 2020, 22, 1.	0.8	0
48055	Toward Concurrent Engineering of the M1-Based Catalytic Systems for Oxidative Dehydrogenation (ODH) of Alkanes. Topics in Catalysis, 2020, 63, 1667-1681.	1.3	6
48056	The Performance of Ni-Doped Spinel-Type LiMn2O4 for Li-Ion Batteries: First-Principles Calculation. Journal of Electronic Materials, 2020, 49, 5523-5527.	1.0	15
48057	A Preliminary Study on Helium and Sulfur Ion-Irradiated BCC Iron: In Situ Tensile Testing Using a Push-To-Pull Device. Jom, 2020, 72, 2398-2407.	0.9	1
48058	Impact of Antiphase Boundaries on Structural, Magnetic and Vibrational Properties of Fe3Al. Materials, 2020, 13, 4884.	1.3	6
48059	Evaluating Potential Catalytic Active Sites on Nitrogen-Doped Graphene for the Oxygen Reduction Reaction: An Approach Based on Constant Electrode Potential Density Functional Theory Calculations. Journal of Physical Chemistry C, 2020, 124, 25675-25685.	1.5	8
48060	Computational Screening of Atomically Thin Two-Dimensional Nanomaterial-Coated Cs₃Sb Heterostructures for High-Performance Photocathodes. Journal of Physical Chemistry C, 2020, 124, 26396-26403.	1.5	3
48061	Hydrogen Evolution on Restructured B-Rich WB: Metastable Surface States and Isolated Active Sites. ACS Catalysis, 2020, 10, 13867-13877.	5.5	20
48062	Spectroscopic Probe Molecule Selection Using Quantum Theory, First-Principles Calculations, and Machine Learning. ACS Nano, 2020, 14, 17295-17307.	7.3	12
48063	A band-gap database for semiconducting inorganic materials calculated with hybrid functional. Scientific Data, 2020, 7, 387.	2.4	39
48064	Topological semimetals from the perspective of first-principles calculations. Journal of Applied Physics, 2020, 128, .	1.1	15
48065	Phononic Thermal Transport in Yttrium Hydrides Allotropes. Frontiers in Materials, 2020, 7, .	1.2	4
48066	A new cubic superhard large-cell carbon allotrope: c-C200. Results in Physics, 2020, 19, 103457.	2.0	8
48067	Strain tunable ferroelectricity of SnSe/SnTe van der Waals heterostructures. Superlattices and Microstructures, 2020, 148, 106728.	1.4	6
48068	Mixed-Valent Copper Chalcogenides: Tuning Structures and Electronic Properties Using Multiple Anions. Chemistry of Materials, 2020, 32, 10146-10154.	3.2	9
48069	Atomistic Origins of Enhanced Band Gap, Miscibility, and Oxidation Resistance in Î±-CsPb1â€“xSnxI3 Mixed Perovskite. Journal of Physical Chemistry C, 2020, 124, 26124-26133.	1.5	12
48070	Direct Tellurization of Pt to Synthesize 2D PtTe₂ for High-Performance Broadband Photodetectors and NIR Image Sensors. ACS Applied Materials & Interfaces, 2020, 12, 53921-53931.	4.0	48

#	Article	IF	Citations
48071	Copper(I)-Based Flexible Organicâ€“Inorganic Coordination Polymer and Analogues: High-Power Factor Thermoelectrics. ACS Applied Materials & Interfaces, 2020, 12, 53841-53851.	4.0	14
48072	Oxophilicity Drives Oxygen Transfer at a Palladiumâ€“Silver Interface for Increased CO Oxidation Activity. ACS Catalysis, 2020, 10, 13878-13889.	5.5	7
48073	Electronic modulation of nickel selenide by copper doping and in situ carbon coating towards high-rate and high-energy density lithium ion half/full batteries. Nanoscale, 2020, 12, 23645-23652.	2.8	21
48074	Anomalous fracture in two-dimensional rhenium disulfide. Science Advances, 2020, 6, .	4.7	18
48075	Exploring alloying effect on phase stability and mechanical properties of Î³â€³-Ni3Nb precipitates with first-principles calculations. Materials and Design, 2020, 196, 109174.	3.3	22
48076	Kinetic Control of Oxygen Interstitial Interaction with TiO₂(110) via the Surface Fermi Energy. Langmuir, 2020, 36, 12632-12648.	1.6	6
48077	Influence of Aromatic Cations on the Structural Arrangement of Hg(II) Halides. ACS Omega, 2020, 5, 29357-29372.	1.6	3
48078	Voltage-driven motion of nitrogen ions: a new paradigm for magneto-ionics. Nature Communications, 2020, 11, 5871.	5.8	42
48079	Achieving high hydrogen evolution reaction activity of a Mo₂C monolayer. Physical Chemistry Chemical Physics, 2020, 22, 26189-26199.	1.3	9
48080	Two-Dimensional Lateral Heterostructures of Triphosphides: AlP₃â€“GaP₃ as a Promising Photocatalyst for Water Splitting. ACS Applied Materials & Interfaces, 2020, 12, 53731-53738.	4.0	22
48081	Spin Polarization-Induced Facile Dioxygen Activation in Boron-Doped Graphitic Carbon Nitride. ACS Applied Materials & Interfaces, 2020, 12, 52741-52748.	4.0	15
48082	Theoretical Screening of Single Atoms Supported on Two-Dimensional Nb₂CN₂ for Nitrogen Fixation. ACS Applied Nano Materials, 2020, 3, 11274-11281.	2.4	34
48083	Intervalley scattering in GaAs(111)-supported silicene. Physical Chemistry Chemical Physics, 2020, 22, 26402-26409.	1.3	5
48084	Phenazine anodes for ultralongcycle-life aqueous rechargeable batteries. Journal of Materials Chemistry A, 2020, 8, 26013-26022.	5.2	21
48085	(De)lithiation of spinel ferrites Fe₃O₄, MgFe₂O₄, and ZnFe₂O₄: a combined spectroscopic, diffraction and theory study. Physical Chemistry Chemical Physics, 2020, 22, 26200-26215.	1.3	13
48086	Emergence of 2D high-temperature nodal-line half-metal in monolayer AgN. Physical Chemistry Chemical Physics, 2020, 22, 27024-27030.	1.3	13
48087	Unraveling atomic-scale lithiation mechanisms in a NiO thin film electrode. Journal of Materials Chemistry A, 2020, 8, 25198-25207.	5.2	7
48088	Simulation of Phaseâ€Changeâ€Memory and Thermoelectric Materials using Machineâ€Learned Interatomic Potentials: Sb₂Te₃. Physica Status Solidi (B): Basic Research, 2021, 258, 2000416.	0.7	16

#	Article	IF	Citations
48089	Computational modeling of nanoparticles in inert environment. Frontiers of Nanoscience, 2020, 17, 5-26.	0.3	0
48090	Prediction for structure stability and ultrahigh hydrogen evolution performance of monolayer 2H-CrS2. Materials Today Communications, 2020, 25, 101707.	0.9	9
48091	Discovery of Dramatically Improved Ammonia Synthesis Catalysts through Hierarchical High-Throughput Catalyst Screening of the Fe(211) Surface. Chemistry of Materials, 2020, 32, 9914-9924.	3.2	6
48092	Integrated Experimental and Theoretical Approach for Efficient Design and Synthesis of Gold-Based Double Halide Perovskites. Journal of Physical Chemistry C, 2020, 124, 26769-26779.	1.5	10
48093	Intrinsic Ferromagnetic Semiconductors in Two-Dimensional Alkali-Based Chromium Chalcogenides. ACS Applied Electronic Materials, 2020, 2, 3853-3858.	2.0	17
48094	Spontaneous skyrmionic lattice from anisotropic symmetric exchange in a Ni-halide monolayer. Nature Communications, 2020, 11, 5784.	5.8	113
48095	High-rate cathode CrSSe based on anion reactions for lithium-ion batteries. Journal of Materials Chemistry A, 2020, 8, 25739-25745.	5.2	17
48096	High-performance Naâ€“CO₂ batteries with ZnCo₂O₄@CNT as the cathode catalyst. Journal of Materials Chemistry A, 2020, 8, 23974-23982.	5.2	25
48097	Thermodynamic origin of dendrite growth in metal anode batteries. Energy and Environmental Science, 2020, 13, 5186-5197.	15.6	101
48098	Strain induced enhancement in thermoelectric power factor of ZrTe2. AIP Conference Proceedings, 2020, , .	0.3	1
48099	Structure and Noncovalent Interactions of Molybdenum Disulfide Monolayers in the Layered Organo-inorganic Compound with Tetramethylguanidine. Russian Journal of Coordination Chemistry/Koordinatsionnaya Khimiya, 2020, 46, 779-785.	0.3	3
48100	Subtle Variations of the Electronic Structure and Mechanical Properties of High Entropy Alloys With 50% Carbon Composites. Frontiers in Materials, 2020, 7, .	1.2	8
48101	Microscopic Hopping Mechanism of an Isolated PTCDA Molecule on a Reactive Ge(001) Surface. Journal of Physical Chemistry C, 2020, 124, 24704-24712.	1.5	2
48102	Isotopic Exchange Extends Charge Carrier Lifetime in Metal Lead Perovskites by Quantum Dynamics Simulations. Journal of Physical Chemistry Letters, 2020, 11, 10298-10305.	2.1	11
48103	Strain-induced creation and switching of anion vacancy layers in perovskite oxynitrides. Nature Communications, 2020, 11, 5923.	5.8	20
48104	Novel zero-dimensional lead-free bismuth based perovskites: from synthesis to structural and optoelectronic characterization. Materials Advances, 2020, 1, 3439-3448.	2.6	19
48105	Phase Switching as the Origin of Large Piezoelectric Response in Organic-Inorganic Perovskites: A First-Principles Study. Physical Review Letters, 2020, 125, 207601.	2.9	20
48106	Fast analytical evaluation of intermolecular electrostatic interaction energies using the pseudoatom representation of the electron density. III. Application to crystal structures via the Ewald and direct summation methods. Acta Crystallographica Section A: Foundations and Advances, 2020, 76, 630-651.	0.0	5

#	Article	IF	Citations
48107	Layered MoS2 Grown on Anatase TiO2 {001} Promoting Interfacial Electron Transfer to Enhance Photocatalytic Evolution of H2 From H2S. Frontiers in Environmental Chemistry, 2020, 1, .	0.7	2
48108	Towards the selectivity distinction of phenol hydrogenation on noble metal catalysts. Nano Materials Science, 2023, 5, 91-100.	3.9	7
48109	O₂activation by coreâ€“shell Ru₁₃@Pt₄₂particles in comparison with Pt₅₅particles: a DFT study. RSC Advances, 2020, 10, 36090-36100.	1.7	3
48110	Prediction of higher thermoelectric performance in BiCuSeO by weakening electronâ€“polar optical phonon scattering. Journal of Materials Chemistry A, 2020, 8, 25245-25254.	5.2	12
48111	2D Octagon-Structure Carbon and Its Polarization Resolved Raman Spectra. Nanomaterials, 2020, 10, 2252.	1.9	6
48112	Controlling bimerons as skyrmion analogues by ferroelectric polarization in 2D van der Waals multiferroic heterostructures. Nature Communications, 2020, 11, 5930.	5.8	90
48113	Modelling Hydrogen Embrittlement using Density Functional Theory: A theoretical approach to understanding environmentally assisted cracking in 7xxx series aluminium alloys. MATEC Web of Conferences, 2020, 326, 04006.	0.1	0
48114	Crystal Structure and Atomic Vacancy Optimized Thermoelectric Properties in Gadolinium Selenides. Chemistry of Materials, 2020, 32, 10130-10139.	3.2	36
48115	Colloidal Nanoparticles of a Metastable Copper Selenide Phase with Near-Infrared Plasmon Resonance. Chemistry of Materials, 2020, 32, 10227-10234.	3.2	19
48116	2Dâ€“2D Heterojunctions of a Covalent Triazine Framework with a Triphenylphosphine-Based Covalent Organic Framework for Efficient Photocatalytic Hydrogen Evolution. ACS Applied Energy Materials, 2020, 3, 11939-11946.	2.5	33
48117	Selective Photocatalytic Reduction of CO₂ to CH₄ Modulated by Chloride Modification on Bi₂WO₆ Nanosheets. ACS Applied Materials & Interfaces, 2020, 12, 54507-54516.	4.0	62
48118	Conversion of Biomasses and Copper into Catalysts for Photocatalytic CO₂ Reduction. ACS Applied Materials & Interfaces, 2020, 12, 51366-51373.	4.0	25
48119	Highly Active Nanosized Anatase TiO_{2â€“x} Oxide Catalysts In Situ Formed through Reduction and Ostwald Ripening Processes for Propane Dehydrogenation. ACS Catalysis, 2020, 10, 14678-14693.	5.5	39
48120	Intermetallic ZrPd₃-Embedded Nanoporous ZrC as an Efficient and Stable Catalyst of the Suzuki Cross-Coupling Reaction. ACS Catalysis, 2020, 10, 14366-14374.	5.5	13
48121	Charge density wave with anomalous temperature dependence in <mml:math xmlns:mml="http://www.w3.org/1998/Math/MathML"><mml:mrow><mml:msub><mml:mi>UPt</mml:mi><mml:mn>2</mml:mn></mml	1.1	18
	Physical Review B, 2020, 102, .		
48122	Ultrafast formation of a transient two-dimensional diamondlike structure in twisted bilayer graphene. Physical Review B, 2020, 102, .	1.1	8
48123	Hydrogenation engineering of bimetallic Agâ€“Cu-modified-titania photocatalysts for production of hydrogen. Catalysis Today, 2022, 388-389, 79-86.	2.2	4
48124	Atomic-Scale Studies of Overlapping Grain Boundaries between Parallel and Quasi-Parallel Grains in Low-Symmetry Monolayer ReS2. Matter, 2020, 3, 2108-2123.	5.0	11

#	Article	IF	Citations
48125	Negative thermal expansion driven by acoustic phonon modes in rhombohedral Zn2GeO4. Results in Physics, 2020, 19, 103531.	2.0	11
48126	Phase transformation in boron under shock compression. Solid State Sciences, 2020, 108, 106376.	1.5	5
48127	Effect of Sn Doping on Surface States of Bi₂Se₃ Thin Films. Journal of Physical Chemistry C, 2020, 124, 27082-27088.	1.5	12
48128	Design and Synthesis of a Single-Layer Ferromagnetic Metalâ€“Organic Framework with Topological Nontrivial Gaps. Journal of Physical Chemistry C, 2020, 124, 27017-27023.	1.5	22
48129	Polarity- and Pressure-Dependent Hydrogen Dynamics on ZnO Polar Surfaces Revealed by Near-Ambient-Pressure X-ray Photoelectron Spectroscopy. Journal of Physical Chemistry C, 2020, 124, 25431-25436.	1.5	4
48130	Nanopyramidal Reconstruction of Cu2O(111): A Long-Standing Surface Puzzle Solved by STM and DFT. Journal of Physical Chemistry C, 2020, 124, 26937-26943.	1.5	17
48131	Precise Tuning of Band Structures and Electron Correlations by van der Waals Stacking of One-dimensional W6Te6 Wires. Nano Letters, 2020, 20, 8866-8873.	4.5	14
48132	RuN₂ Monolayer: A Highly Efficient Electrocatalyst for Oxygen Reduction Reaction. ACS Applied Materials & Interfaces, 2020, 12, 54517-54523.	4.0	22
48133	Stability, Elastic Properties, and the Li Transport Mechanism of the Protonated and Fluorinated Antiperovskite Lithium Conductors. ACS Applied Materials & Interfaces, 2020, 12, 55011-55022.	4.0	28
48134	Acid Stability and Demetalation of PGM-Free ORR Electrocatalyst Structures from Density Functional Theory: A Model for â€œSingle-Atom Catalystâ€•Dissolution. ACS Catalysis, 2020, 10, 14527-14539.	5.5	105
48135	Competing Effects of pH, Cation Identity, H₂O Saturation, and N₂ Concentration on the Activity and Selectivity of Electrochemical Reduction of N₂ to NH₃ on Electrodeposited Cu at Ambient Conditions. ACS Catalysis, 2020, 10, 14592-14603.	5.5	43
48136	Hybrid Density Functional Theory Study of Native Defects and Nonmetal (C, N, S, and P) Doping in a Bi₂WO₆Photocatalyst. ACS Omega, 2020, 5, 29081-29091.	1.6	33
48137	Synthesis and characterization of a strong ferromagnetic and high hardness intermetallic compound Fe₂B. Physical Chemistry Chemical Physics, 2020, 22, 27425-27432.	1.3	15
48138	Synthesis, structure, and luminescence properties of layered oxychloride Ba₃Y₂O₅Cl₂. Journal of Materials Chemistry C, 2020, 8, 17162-17168.	2.7	3
48139	Probing Efficient Nâ€Type Lanthanide Dopants for Mg₃Sb₂ Thermoelectrics. Advanced Science, 2020, 7, 2002867.	5.6	23
48140	Insights into the stability and thermal properties of WSe2-based nanofluids for concentrating solar power prepared by liquid phase exfoliation. Journal of Molecular Liquids, 2020, 319, 114333.	2.3	10
48141	Multi-fidelity Gaussian process based empirical potential development for Si:H nanowires. Theoretical and Applied Mechanics Letters, 2020, 10, 195-201.	1.3	1
48142	Structure and Optical Properties of Layered Perovskite (MA)2PbI2â€“xBrx(SCN)2 (0 â‰¤ x < 1.6). Inorganic Chemistry, 2020, 59, 17379-17384.	1.9	6

#	Article	IF	Citations
48143	Heavy Metal Effects on the Photovoltaic Properties of Metallocorroles in Dye-Sensitized Solar Cells. ACS Applied Energy Materials, 2020, 3, 12460-12467.	2.5	16
48144	Electron and Ion Transfer across Interfaces of the NASICON-Type LATP Solid Electrolyte with Electrodes in All-Solid-State Batteries: A Density Functional Theory Study via an Explicit Interface Model. ACS Applied Materials & Interfaces, 2020, 12, 54752-54762.	4.0	44
48145	Hydrodeoxygenation of Guaiacol to Phenol over Ceria-Supported Iron Catalysts. ACS Catalysis, 2020, 10, 14624-14639.	5.5	55
48146	High frequency atomic tunneling yields ultralow and glass-like thermal conductivity in chalcogenide single crystals. Nature Communications, 2020, 11, 6039.	5.8	36
48147	First-principles calculations of hyperfine interaction, binding energy, and quadrupole coupling for shallow donors in silicon. Npj Computational Materials, 2020, 6, .	3.5	17
48148	Stoneâ€“Wales defects in hexagonal boron nitride as ultraviolet emitters. Npj Computational Materials, 2020, 6, .	3.5	24
48149	Mechanics and physics of a glass/particles photonic sponge. Scientific Reports, 2020, 10, 19495.	1.6	5
48150	Prediction of topological nontrivial semimetals and pressure-induced Lifshitz transition in 1Tâ€²-MoS₂layered bulk polytypes. Nanoscale, 2020, 12, 22710-22717.	2.8	8
48151	Adsorption and sensing of CO and NH₃ on chemically modified graphene surfaces. RSC Advances, 2020, 10, 42318-42326.	1.7	17
48152	The effect of cation size on hydride-ion conduction in LnSrLiH₂O₂ (Ln = La,) Tj ETQq1 1 0.784314 rgBT /Ov	5.2	15
48153	Tuning the mechanical and electronic properties and carrier mobility of phosphorene via family atom doping: a first-principles study. Journal of Materials Chemistry C, 2020, 8, 14902-14909.	2.7	14
48154	Thermoelectric investigation on Mg3N2 monolayer. AIP Conference Proceedings, 2020, , .	0.3	0
48155	Effects of density and composition on the properties of amorphous alumina: A high-dimensional neural network potential study. Journal of Chemical Physics, 2020, 153, 164119.	1.2	6
48156	Structural, mechanical and thermodynamic properties study on Mgâ€“Y alloys from first-principles calculations. International Journal of Modern Physics B, 2020, 34, 2050220.	1.0	3
48157	The effect of the impurities on the magnetic, electronic and optical properties of Mn5Ge3. Chinese Journal of Physics, 2020, 68, 9-18.	2.0	4
48158	Direct Observation of Electron Beam-Induced Phase Transition in MgCrMnO₄. Chemistry of Materials, 2020, 32, 10456-10462.	3.2	18
48159	Adversarial Generation of Mesoscale Surfaces from Small-Scale Chemical Motifs. Journal of Physical Chemistry C, 2020, 124, 23158-23163.	1.5	9
48160	Density Functional Theory Modeling of Photo-electrochemical Reactions on Semiconductors: H₂ Evolution on 3C-SiC. Journal of Physical Chemistry C, 2020, 124, 26625-26639.	1.5	9

#	Article	IF	Citations
48161	Defects Engineering on Ceria and Câ€“C Coupling Reactions Using [Au₁₁(PPh₃)₇I₃] Nanocluster: A Combined Experimental and Theoretical Study. ACS Nano, 2020, 14, 16681-16688.	7.3	15
48162	Conductive Porous Laminated Vanadium Nitride as Carbon-Free Hosts for High-Loading Sulfur Cathodes in Lithiumâ€“Sulfur Batteries. ACS Nano, 2020, 14, 17308-17320.	7.3	86
48163	Cooperative origin of proton pair diffusivity in yttrium substituted barium zirconate. Communications Physics, 2020, 3, .	2.0	10
48164	Infrared response in photocatalytic polymeric carbon nitride for water splitting via an upconversion mechanism. Communications Materials, 2020, 1, .	2.9	23
48165	Superior anchoring effect of a Cu-benzenehexathial MOF as an aluminiumâ€“sulfur battery cathode host. Materials Advances, 2020, 1, 3572-3581.	2.6	19
48166	Unraveling the effect of Al doping on CO adsorption at ZnO(101Ì„0). RSC Advances, 2020, 10, 40663-40672.	1.7	10
48167	Precise Phase Control of Largeâ€Scale Inorganic Perovskites via Vaporâ€Phase Anionâ€Exchange Strategy. Small, 2020, 16, e2005226.	5.2	17
48168	Efficient Water Splitting Actualized through an Electrochemistryâ€Induced Heteroâ€Structured Antiperovskite/(Oxy)Hydroxide Hybrid. Small, 2020, 16, e2006800.	5.2	36
48169	Adsorption and dissociation of water on halogen pre-adsorbed Ni(111) and Niâ€“Cr(111) surfaces: A DFT study. Solid State Communications, 2020, 321, 114040.	0.9	3
48170	Mechanistic Insight into Hydrogen-Assisted Carbon Dioxide Reduction with Ilmenite. Energy & Fuels, 2020, 34, 15370-15378.	2.5	7
48171	Se Doping Regulates the Activity of NiTe₂ for Electrocatalytic Hydrogen Evolution Reaction. Journal of Physical Chemistry C, 2020, 124, 26793-26800.	1.5	12
48172	Elucidating the Influence of Sulfur Vacancies on Nonradiative Recombination Dynamics in Cu₂ZnSnS₄ Solar Absorbers. Journal of Physical Chemistry Letters, 2020, 11, 10354-10361.	2.1	13
48173	Ionic Conduction through Reaction Products at the Electrolyteâ€“Electrode Interface in All-Solid-State Li⁺ Batteries. ACS Applied Materials & Interfaces, 2020, 12, 55510-55519.	4.0	14
48174	Segregation tendencies of transition-metal dopants in wide band gap semiconductor nanowires. Physical Chemistry Chemical Physics, 2020, 22, 27987-27998.	1.3	2
48175	Unraveling the quantum dynamics origin of high photocatalytic activity in nitrogen-doped anatase TiO₂: time-domain ab initio analysis. Journal of Materials Chemistry A, 2020, 8, 25235-25244.	5.2	19
48176	Tailoring the thermoelectric and structural properties of Cuâ€“Sn based thiospinel compounds [CuM_{1+x}Sn_{1â^'x}S₄ (M = Ti, V, Cr, Co)]. Journal of Materials Chemistry C, 2020, 8, 16368-16383.	2.7	21
48177	Atomically dispersed Cu and Fe on N-doped carbon materials for CO₂electroreduction: insight into the curvature effect on activity and selectivity. RSC Advances, 2020, 10, 43075-43084.	1.7	15
48178	Î±-FeSi2 as a Buffer Layer for Î²-FeSi2 Growth: Analysis of Orientation Relationships in Silicide/Silicon, Silicide/Silicide Heterointerfaces. Journal of Surface Investigation, 2020, 14, 851-861.	0.1	1

#	Article	IF	Citations
48179	Machine Learning in Computational Surface Science and Catalysis: Case Studies on Water and Metalâ€“Oxide Interfaces. Frontiers in Chemistry, 2020, 8, 601029.	1.8	11
48180	Impact of stacking on the optoelectronic properties of 2D ZrS2/GaS heterostructure. Materials Today: Proceedings, 2021, 47, 526-528.	0.9	9
48181	Topological Analysis of Hydroxyquinoline Derivatives Interacting with Aluminum Cations or with an Al(111) Surface. Inorganic Chemistry, 2020, 59, 17916-17928.	1.9	2
48182	Effect of Moleculeâ€“Substrate Interactions on the Adsorption of meso-Dibenzoporphycene Tautomers Studied by Scanning Probe Microscopy and First-Principles Calculations. Journal of Physical Chemistry C, 2020, 124, 26759-26768.	1.5	6
48183	Trends in the Activation of Light Alkanes on Transition-Metal Surfaces. Journal of Physical Chemistry C, 2020, 124, 27503-27510.	1.5	10
48184	Crystal Facet-Dependent CO₂ Photoreduction over Porous ZnO Nanocatalysts. ACS Applied Materials & Interfaces, 2020, 12, 56039-56048.	4.0	52
48185	Kinetics-Limited Two-Step Growth of van der Waals Puckered Honeycomb Sb Monolayer. ACS Nano, 2020, 14, 16755-16760.	7.3	20
48186	Computational Study of Janus Transition Metal Dichalcogenide Monolayers for Acetone Gas Sensing. ACS Omega, 2020, 5, 31398-31406.	1.6	29
48187	Key activity descriptors of nickel-iron oxygen evolution electrocatalysts in the presence of alkali metal cations. Nature Communications, 2020, 11, 6181.	5.8	80
48188	Mechanistic investigations of N-doped graphene/2H(1T)-MoS2 for Li/K-ions batteries. Nano Energy, 2020, 78, 105352.	8.2	20
48189	Defect formation peculiarities and redox properties of novel oxygen carrier material LaCu0.5Ti0.5O3Â± at elevated temperatures. Solid State Sciences, 2020, 110, 106480.	1.5	5
48190	Lithium Ion Conduction in a Cation-Deficient Quadruple Perovskite LiCuTa₃O₉ Epitaxial Thin Film: Theoretical and Experimental Investigations. Chemistry of Materials, 2020, 32, 9753-9760.	3.2	1
48191	Flux Growth of Uranyl Titanates: Rare Examples of TiO₄ Tetrahedra and TiO₅ Square Bipyramids. Journal of Physical Chemistry A, 2020, 124, 9487-9495.	1.1	7
48192	Confinement Effects on Furfuryl Alcohol Reactions over Porous Bilayer Silica-Modified Pd(111). Journal of Physical Chemistry C, 2020, 124, 25437-25446.	1.5	4
48193	Liquid water contains the building blocks of diverse ice phases. Nature Communications, 2020, 11, 5757.	5.8	50
48194	Inverse ZrO2/Cu as a highly efficient methanol synthesis catalyst from CO2 hydrogenation. Nature Communications, 2020, 11, 5767.	5.8	197
48195	Polarization consistent basis sets using the projector augmented wave method: a renovation brought by PAW into Gaussian basis sets. Physical Chemistry Chemical Physics, 2020, 22, 27037-27052.	1.3	2
48196	Effects of perturbation order and basis set on alchemical predictions. Journal of Chemical Physics, 2020, 153, 144118.	1.2	14

#	Article	IF	Citations
48197	Tunable Superconductivity in 2H-NbSe₂ via in situ Li Intercalation. Chinese Physics Letters, 2020, 37, 097402.	1.3	8
48198	Structural, electronic and optical properties of S-doped, Sc-doped and Scâ€“S co-doped anatase TiO2: a DFT + U calculation. European Physical Journal B, 2020, 93, 1.	0.6	4
48199	Timeâ€Dependent Density Functional Theory of Narrow Band Gap Semiconductors Using a Screened Rangeâ€Separated Hybrid Functional. Advanced Theory and Simulations, 2020, 3, 2000220.	1.3	6
48200	Discovery Principles and Materials for Symmetry-Protected Persistent Spin Textures with Long Spin Lifetimes. Matter, 2020, 3, 1211-1225.	5.0	17
48201	Structure and stability of vacancyâ€“solute complexes in Alâ€“Mgâ€“Si alloys. Materialia, 2020, 13, 100853.	1.3	3
48202	Coverage-Dependent Water Dissociative Adsorption Properties on Nickel Surfaces. Journal of Physical Chemistry C, 2020, 124, 25835-25845.	1.5	6
48203	Synthesis of Ultrasmall, Homogeneously Distributed Ni₃Fe Alloy Nanoparticles on N-Doped Porous Graphene as a Bifunctional Electrocatalyst for Rechargeable Flexible Solid Zinc-Air Batteries. ACS Applied Energy Materials, 2020, 3, 12148-12161.	2.5	15
48204	Critical Role of Surface Defects in the Controllable Deposition of Li₂S on Graphene: From Molecule to Crystallite. ACS Applied Materials & Interfaces, 2020, 12, 53435-53445.	4.0	8
48205	Colloidal Synthesis and Optical Properties of Perovskite-Inspired Cesium Zirconium Halide Nanocrystals. , 2020, 2, 1644-1652.		69
48206	Curie temperature engineering in a novel 2D analog of iron ore (hematene) via strain. Nanoscale Advances, 2020, 2, 5890-5896.	2.2	13
48207	Synthesis and Properties of Monolayer Graphene (MLG)-Covered Fe(111). Chemistry of Materials, 2020, 32, 10463-10468.	3.2	1
48208	Encapsulation of Highly Volatile Fragrances in Y Zeolites for Sustained Release: Experimental and Theoretical Studies. ACS Omega, 2020, 5, 31925-31935.	1.6	23
48209	Advanced superhard composite materials with extremely improved mechanical strength by interfacial segregation of dilute dopants. Scientific Reports, 2020, 10, 21008.	1.6	4
48210	Structural and Electronic Properties of Heterostructures Composed of Antimonene and Monolayer MoS2. Nanomaterials, 2020, 10, 2358.	1.9	3
48211	Alloy CsCd_xPb_{1â€“x}Br₃ Perovskite Nanocrystals: The Role of Surface Passivation in Preserving Composition and Blue Emission. Chemistry of Materials, 2020, 32, 10641-10652.	3.2	45
48212	Grapheneâ€“Iron(II) Phthalocyanine Hybrid Systems for Scalable Molecular Spintronics. Journal of Physical Chemistry C, 2020, 124, 27645-27655.	1.5	12
48213	Lattice Dynamics Study of Elemental Bismuth under High Pressure. Journal of Physical Chemistry C, 2020, 124, 26659-26669.	1.5	4
48214	Sulfur-Driven Transition from Vertical to Lateral Growth of 2D SnSâ€“SnS₂ Heterostructures and Their Band Alignments. Journal of Physical Chemistry C, 2020, 124, 27820-27828.	1.5	11

#	Article	IF	Citations
48215	Self-Catalyzed Sensitization of CuO Nanowires via a Solvent-free Click Reaction. Langmuir, 2020, 36, 14539-14545.	1.6	6
48216	Origin of the Enhanced Reusability and Electron Transfer of the Carbon-Coated Mn₃O₄ Nanocube for Persulfate Activation. ACS Catalysis, 2020, 10, 14857-14870.	5.5	151
48217	Stabilization of Îµ-iron carbide as high-temperature catalyst under realistic Fischerâ€“Tropsch synthesis conditions. Nature Communications, 2020, 11, 6219.	5.8	83
48218	Interfacial electronic features in methyl-ammonium lead iodide and p-type oxide heterostructures: new insights for inverted perovskite solar cells. Physical Chemistry Chemical Physics, 2020, 22, 28401-28413.	1.3	12
48219	Na ion dynamics in P2-Nax[Ni1/3Ti2/3]O2: a combination of quasi-elastic neutron scattering and first-principles molecular dynamics study. Journal of Materials Chemistry A, 2020, 8, 25290-25297.	5.2	7
48220	General synthesis of single atom electrocatalystsviaa facile condensationâ€“carbonization process. Journal of Materials Chemistry A, 2020, 8, 25959-25969.	5.2	14
48221	Pressure-induced octahedral tilting distortion and structural phase transition in columbite structured NiNb2O6. Journal of Applied Physics, 2020, 128, .	1.1	9
48222	Tunable two dimensional ferromagnetic topological half-metal CrO2 by electronic correction and spin direction. Applied Physics Letters, 2020, 117, .	1.5	21
48223	Low-Frequency Divergence and Quantum Geometry of the Bulk Photovoltaic Effect in Topological Semimetals. Physical Review X, 2020, 10, .	2.8	95
48224	Structureâ€Ðependent Strain Effects. ChemPhysChem, 2020, 21, 2407-2410.	1.0	11
48225	First-Principles Modeling of Sodium Ion and Water Intercalation into Titanium Disulfide Interlayers for Water Desalination. Chemistry of Materials, 2020, 32, 10678-10687.	3.2	7
48226	Na3FeH7 and Na3CoH6: Hydrogen-Rich First-Row Transition Metal Hydrides from High Pressure Synthesis. Inorganic Chemistry, 2020, 59, 16467-16473.	1.9	12
48227	Beyond the Reverse Horiutiâ€“Polanyi Mechanism in Propane Dehydrogenation over Pt Catalysts. ACS Catalysis, 2020, 10, 14887-14902.	5.5	44
48228	Density-functional tight-binding for phosphine-stabilized nanoscale gold clusters. Chemical Science, 2020, 11, 13113-13128.	3.7	19
48229	Effect of passivation on piezoelectricity of ZnO nanowire. Chinese Journal of Chemical Physics, 2020, 33, 434-442.	0.6	1
48230	Impact of Small Adsorbates in the Vibrational Spectra of Mg- and Zn-MOF-74 Revealed by First-Principles Calculations. ACS Applied Materials & Interfaces, 2020, 12, 54980-54990.	4.0	14
48231	Designer spin order in diradical nanographenes. Nature Communications, 2020, 11, 6076.	5.8	47
48232	Active learning for the power factor prediction in diamond-like thermoelectric materials. Npj Computational Materials, 2020, 6, .	3.5	43

#	Article	IF	Citations
48233	First-principles calculations of an asymmetric MoO₂/graphene nanocomposite as the anode material for lithium-ion batteries. RSC Advances, 2020, 10, 43312-43318.	1.7	4
48234	Electronic Structure Sensitivity to Surface Disorder and Nanometer-Scale Impurity of 2D Titanium Carbide MXene Sheets as Revealed by Electron Energy-Loss Spectroscopy. Journal of Physical Chemistry C, 2020, 124, 27071-27081.	1.5	9
48235	Atomistic Mechanisms for Contrasting Stressâ€“Strain Relations of B₁₃CN and B₁₃C₂. Journal of Physical Chemistry Letters, 2020, 11, 10454-10462.	2.1	9
48236	Ultrahigh strength and ductility in newly developed materials with coherent nanolamellar architectures. Nature Communications, 2020, 11, 6240.	5.8	226
48237	Complete equations of state for PETN and its products from atomistic simulations. Physical Chemistry Chemical Physics, 2020, 22, 27572-27580.	1.3	4
48238	Effects of alloying elements on the Ni/Ni3Al interface strength and vacancy diffusion behavior. Journal of Applied Physics, 2020, 128, .	1.1	7
48239	Quasi-One-Dimensional Free-Electron-Like States Selected by Intermolecular Hydrogen Bonds at the Glycine/Cu(100) Interface*. Chinese Physics Letters, 2020, 37, 117301.	1.3	0
48240	Microwave-enhanced photovoltaic quantum oscillations of Weyl fermions. Physical Review B, 2020, 102, .	1.1	0
48241	Effects of W and Si microadditions on microstructure and the strength of dilute precipitation-strengthened Alâ€“Zrâ€“Er alloys. Materials Science & Engineering A: Structural Materials: Properties, Microstructure and Processing, 2020, 798, 140159.	2.6	17
48242	Oxygen-Mediated Superexchange Interactions and Their Impact on the Structural Stability, Magnetic Order, and Magnetocrystalline Anisotropy of One-Dimensional Co-Oxide Chains on Rh(553) Step-Surfaces. Journal of Physical Chemistry C, 2020, 124, 26026-26036.	1.5	4
48243	Coplanar versus Noncoplanar Carboxyl Groups: The Influence of Sterically Enforced Noncoplanarity on the 2D Mixing Behavior of Benzene Tricarboxylic Acids. Journal of Physical Chemistry C, 2020, 124, 24874-24882.	1.5	9
48244	Charge-Transfer Plasmon Polaritons at Graphene/Î±-RuCl₃ Interfaces. Nano Letters, 2020, 20, 8438-8445.	4.5	53
48245	Single Atoms on a Nitrogen-Doped Boron Phosphide Monolayer: A New Promising Bifunctional Electrocatalyst for ORR and OER. ACS Applied Materials & Interfaces, 2020, 12, 52549-52559.	4.0	95
48246	Facile Synthesis of Defect-Modified Thin-Layered and Porous g-C₃N₄ with Synergetic Improvement for Photocatalytic H₂ Production. ACS Applied Materials & Interfaces, 2020, 12, 52603-52614.	4.0	65
48247	Accelerating Discovery of Metalâ€“Organic Frameworks for Methane Adsorption with Hierarchical Screening and Deep Learning. ACS Applied Materials & Interfaces, 2020, 12, 52797-52807.	4.0	31
48248	Computational Study on Strain-Engineered Graphene Nanopores for Selective Gas Separation. ACS Applied Nano Materials, 2020, 3, 11474-11480.	2.4	6
48249	Ultrafast Real-Time Dynamics of CO Oxidation over an Oxide Photocatalyst. ACS Catalysis, 2020, 10, 13650-13658.	5.5	11
48250	Methodological Issues in First-Principle Calculations of CH₃NH₃PbI₃ Perovskite Surfaces: Quantum Confinement and Thermal Motion. ACS Omega, 2020, 5, 29477-29491.	1.6	9

#	Article	IF	Citations
48251	Exploring the Molecular Conformation Space by Soft Moleculeâ€“Surface Collision. Journal of the American Chemical Society, 2020, 142, 21420-21427.	6.6	41
48252	The magnetism of titanium-defected undoped rutile TiO₂: first-principles calculations. Physical Chemistry Chemical Physics, 2020, 22, 25930-25935.	1.3	3
48253	Selective shortening of gold nanorods: when surface functionalization dictates the reactivity of nanostructures. Nanoscale, 2020, 12, 22658-22667.	2.8	13
48254	Mechanism for hydrogen evolution from water splitting based on a MoS₂/WSe₂ heterojunction photocatalyst: a first-principle study. RSC Advances, 2020, 10, 41127-41136.	1.7	18
48255	Observation of room-temperature long-lived trapped exciton in WS2/RGO heterostructure. Applied Physics Letters, 2020, 117, 142104.	1.5	7
48256	Active learning for robust, high-complexity reactive atomistic simulations. Journal of Chemical Physics, 2020, 153, 134117.	1.2	21
48257	Machine-learning predictions of polymer properties with Polymer Genome. Journal of Applied Physics, 2020, 128, .	1.1	111
48258	Negative-charge-storing mechanism of potassium-ion SiO2-based electrets for vibration-powered generators. Applied Physics Letters, 2020, 117, .	1.5	5
48259	Regulating kinetics and thermodynamics of electrochemical nitrogen reduction with metal single-atom catalysts in a pressurized electrolyser. Proceedings of the National Academy of Sciences of the United States of America, 2020, 117, 29462-29468.	3.3	104
48260	High-throughput calculations screening for new direct band gap superhard carbon allotropes. Chinese Journal of Physics, 2020, 68, 778-787.	2.0	3
48261	Direct sunlight-active Na-doped ZnO photocatalyst for the mineralization of organic pollutants at different pH mediums. Journal of the Taiwan Institute of Chemical Engineers, 2020, 115, 187-197.	2.7	27
48262	Sr₆(Li₂Cd)A₄S₁₆ (A = Ge, Sn): How to Go beyond the Band Gap Limitation via Site-Specific Modification. Crystal Growth and Design, 2020, 20, 8084-8089.	1.4	24
48263	Trace-Level Fluorination of Mesoporous TiO₂ Improves Photocatalytic and Pb(II) Adsorbent Performances. Inorganic Chemistry, 2020, 59, 17631-17637.	1.9	9
48264	Importance of Equilibration Method and Sampling for Ab Initio Molecular Dynamics Simulations of Solventâ€“Lithium-Salt Systems in Lithium-Oxygen Batteries. Journal of Chemical Theory and Computation, 2020, 16, 7255-7266.	2.3	9
48265	Computational Identification of Transition-Metal Dichalcogenides for Electrochemical CO₂ Reduction to Highly Reduced Species Beyond CO and HCOOH. Journal of Physical Chemistry C, 2020, 124, 25812-25820.	1.5	9
48266	Dipentamethylene Thiuram Tetrasulfide-Based Cathodes for Rechargeable Magnesium Batteries. ACS Applied Energy Materials, 2020, 3, 10600-10610.	2.5	5
48267	Unveiling Temperature-Induced Structural Domains and Movement of Oxygen Vacancies in SrTiO₃ with Graphene. ACS Applied Materials & Interfaces, 2020, 12, 52915-52921.	4.0	2
48268	Analysis of Acid-Stable and Active Oxides for the Oxygen Evolution Reaction. ACS Energy Letters, 2020, 5, 3778-3787.	8.8	89

#	Article	IF	Citations
48269	Lattice dynamics of the topological Dirac semimetal LaAgSb2 with charge density wave ordering. Physical Review B, 2020, 102, .	1.1	6
48270	Topological phonons in oxide perovskites controlled by light. Science Advances, 2020, 6, .	4.7	47
48271	New insights into the anti-disproportionation mechanism of ZrCo alloying with Ti, Hf, Sc, Cu, and Fe elements. International Journal of Hydrogen Energy, 2020, 45, 28985-28995.	3.8	13
48272	Novel Ti-decorated borophene <mml:math xmlns:mml="http://www.w3.org/1998/Math/MathML" altimg="si2.svg"><mml:mrow><mml:msub><mml:mi mathvariant="bold-italic">Ï‡</mml:mi><mml:mn>3</mml:mn></mml:msub></mml:mrow></mml:math> as potential high-performance for hydrogen storage medium. International Journal of Hydrogen Energy, 2020, 45, 29059-29069.	3.8	19
48273	Tin Oxynitride-Based Ferroelectric Semiconductors for Solar Energy Conversion Applications. Chemistry of Materials, 2020, 32, 9542-9550.	3.2	15
48274	Reversible Control of Spintronic Properties of Ferromagnetic Metal/Organic Interfaces through Selective Molecular Switching. Chemistry of Materials, 2020, 32, 9609-9615.	3.2	5
48275	Low-Order Scaling G₀W₀ by Pair Atomic Density Fitting. Journal of Chemical Theory and Computation, 2020, 16, 7381-7399.	2.3	45
48276	Spin-Crossover from a Well-Behaved, Low-Cost meta-GGA Density Functional. Journal of Physical Chemistry A, 2020, 124, 9889-9894.	1.1	18
48277	Hydroxide-Enhanced Superexchange Magnetic Couplings in Ionic Clathrate Hydrates. Journal of Physical Chemistry C, 2020, 124, 25455-25464.	1.5	0
48278	Nonradiative Relaxation Dynamics of a Cesium Lead Halide Perovskite Photovoltaic Architecture: Effect of External Electric Fields. Journal of Physical Chemistry Letters, 2020, 11, 9983-9989.	2.1	11
48279	D2h-Symmetric Tetratellurium Clusters in Silicate Glass as a Broadband NIR Light Source for Spectroscopy Applications. ACS Applied Materials & Interfaces, 2020, 12, 51628-51636.	4.0	9
48280	Vertically Aligned 2D MoS₂ Layers with Strain-Engineered Serpentine Patterns for High-Performance Stretchable Gas Sensors: Experimental and Theoretical Demonstration. ACS Applied Materials & Interfaces, 2020, 12, 53174-53183.	4.0	35
48281	Enhanced magnetic anisotropy and Curie temperature of the NiI₂ monolayer by applying strain: a first-principles study. Physical Chemistry Chemical Physics, 2020, 22, 26917-26922.	1.3	21
48282	Wavelet scattering networks for atomistic systems with extrapolation of material properties. Journal of Chemical Physics, 2020, 153, 084109.	1.2	8
48283	Structural, magnetic, and electronic properties of equiatomic quaternary Heusler alloy CoRhTiAl. AIP Conference Proceedings, 2020, , .	0.3	1
48284	Crossover in periodic length dependence of thermal conductivity in <mml:math xmlns:mml="http://www.w3.org/1998/Math/MathML"><mml:mrow><mml:mn>5</mml:mn><mml:mi>d</mml:mi></mml:mrow></mml:math> element substituted <mml:math xmlns:mml="http://www.w3.org/1998/Math/MathML"><mml:mrow><mml:mi mathvariant="normal">F</mml:mi><mml:msub><mml:mi	1.1	6
48285	Temperature-dependent electronic structure in a higher-order topological insulator candidate <mml:math xmlns:mml="http://www.w3.org/1998/Math/MathML"><mml:mrow><mml:mi>Eu</mml:mi><mml:msub><mml:mi>In</mml:mi><mml:mi>m</mml:mi></mml:msub></mml:mrow></mml:math> Physical Review B, 2020, 102, .	1.1	30
48286	Diffusion, permeation and solubility of hydrogen, deuterium and tritium in crystalline tungsten: First principles DFT simulations. International Journal of Hydrogen Energy, 2020, 45, 29095-29109.	3.8	27

#	Article	IF	Citations
48287	First-principles study on stability, electronic and optical properties of Janus-functionalized ZnO monolayer and bilayer for optoelectronic device. Vacuum, 2020, 181, 109749.	1.6	6
48288	Morphology Evolution of FCC and HCP Cobalt Induced by a CO Atmosphere from Ab Initio Thermodynamics. Journal of Physical Chemistry C, 2020, 124, 23200-23209.	1.5	10
48289	Pressure-driven switching of magnetism in layered CrCl₃. Nanoscale, 2020, 12, 22935-22944.	2.8	19
48290	Tuning structural, electronic, and magnetic properties of black-AsP monolayer by adatom adsorptions: A first principles study. Chinese Journal of Chemical Physics, 2020, 33, 311-318.	0.6	9
48291	Stable metal anodes enabled by a labile organic molecule bonded to a reduced graphene oxide aerogel. Proceedings of the National Academy of Sciences of the United States of America, 2020, 117, 30135-30141.	3.3	17
48292	Interfacial Thermal Conductance across Graphene/MoS2 van der Waals Heterostructures. Energies, 2020, 13, 5851.	1.6	12
48293	Embedded atom method potential for hydrogen on palladium surfaces. Journal of Molecular Modeling, 2020, 26, 336.	0.8	4
48294	Exploring Caâ€“Ceâ€“Mâ€“O (M = 3d Transition Metal) Oxide Perovskites for Solar Thermochemical Applications. Chemistry of Materials, 2020, 32, 9964-9982.	3.2	49
48295	And Yet It Moves: LiNiO₂, a Dynamic Jahnâ€“Teller System. Chemistry of Materials, 2020, 32, 10096-10103.	3.2	25
48296	Resolving the Mechanism Complexity of Oxidative Dehydrogenation of Hydrocarbons on Nanocarbon by Microkinetic Modeling. ACS Catalysis, 2020, 10, 14006-14014.	5.5	9
48297	The joint automated repository for various integrated simulations (JARVIS) for data-driven materials design. Npj Computational Materials, 2020, 6, .	3.5	181
48298	Ising ferromagnetism and robust half-metallicity in two-dimensional honeycomb-kagome Cr2O3 layer. Npj 2D Materials and Applications, 2020, 4, .	3.9	26
48299	Effect of van der Waals interactions on the adhesion strength at the interface of the hydroxyapatiteâ€“titanium biocomposite: a first-principles study. RSC Advances, 2020, 10, 37800-37805.	1.7	3
48300	Interface and surface stabilization of the polarization in ferroelectric thin films. Proceedings of the National Academy of Sciences of the United States of America, 2020, 117, 28589-28595.	3.3	32
48301	A Highly Efficient and Stable Blueâ€Emitting Cs₅Cu₃Cl₆I₂ with a 1D Chain Structure. Advanced Materials, 2020, 32, e2002945.	11.1	73
48302	Integrated and Binderâ€Free Air Cathodes of Co₃Fe₇ Nanoalloy and Co_{5.47}N Encapsulated in Nitrogenâ€Doped Carbon Foam with Superior Oxygen Reduction Activity in Flexible Aluminumâ€Air Batteries. Advanced Science, 2020, 7, 2000747.	5.6	67
48303	Multidirectional Intrinsic Piezoelectricity of 2D Metal Chalcogenâ€“Diphosphate ABP 2 X 6 Monolayers. Physica Status Solidi - Rapid Research Letters, 2020, 14, 2000321.	1.2	14
48304	Oxygenâ€Induced 1D to 2D Transformation of Onâ€Surface Organometallic Structures. Small, 2020, 16, 2002393.	5.2	6

#	Article	IF	Citations
48305	Oxygen octahedral coupling mediated ferroelectric-antiferroelectric phase transition based on domain wall engineering. Acta Materialia, 2020, 198, 145-152.	3.8	16
48306	An experimental and modelling study of the reactivity of adsorbed NH3 in the low temperature NH3-SCR reduction half-cycle over a Cu-CHA catalyst. Applied Catalysis B: Environmental, 2020, 279, 119397.	10.8	55
48307	Amorphous carbon to graphene: Carbon diffusion via nickel catalyst. Materials Letters, 2020, 278, 128468.	1.3	3
48308	Lead-free violet-emitting K2CuCl3 single crystal with high photoluminescence quantum yield. Organic Electronics, 2020, 86, 105903.	1.4	27
48309	Mechanochemical Metathesis between AgNO₃ and NaX (X = Cl, Br, I) and Ag₂XNO₃ Double-Salt Formation. Inorganic Chemistry, 2020, 59, 12200-12208.	1.9	7
48310	Transient Spectral Fluctuations of Single Molecules Revealed using an Optical Antenna. Journal of Physical Chemistry C, 2020, 124, 18219-18225.	1.5	0
48311	In Situ Synthesis of Cu Nanoparticles on Carbon for Highly Selective Hydrogenation of Furfural to Furfuryl Alcohol by Using Pomelo Peel as the Carbon Source. ACS Sustainable Chemistry and Engineering, 2020, 8, 12944-12955.	3.2	59
48312	Contribution of Nitrogen Vacancies to Ammonia Synthesis over Metal Nitride Catalysts. Journal of the American Chemical Society, 2020, 142, 14374-14383.	6.6	126
48313	Sustainable lead management in halide perovskite solar cells. Nature Sustainability, 2020, 3, 1044-1051.	11.5	87
48314	New insight into the interaction between divacancy and H/He impurity in Ti3AlC2 using first-principles studies. Physical Chemistry Chemical Physics, 2020, 22, 18040-18049.	1.3	5
48315	A revised mechanistic model for sodium insertion in hard carbons. Energy and Environmental Science, 2020, 13, 3469-3479.	15.6	195
48316	Oxygen defect chemistry for the reversible transformation of titanates for sizeable potassium storage. Journal of Materials Chemistry A, 2020, 8, 17550-17557.	5.2	5
48317	Different structural transitions of rapidly supercooled tantalum melt under pressure. Physical Chemistry Chemical Physics, 2020, 22, 18078-18090.	1.3	9
48318	Sub-5-nm Monolayer Silicane Transistor: A First-Principles Quantum Transport Simulation. Physical Review Applied, 2020, 14, .	1.5	38
48319	Self-learning hybrid Monte Carlo: A first-principles approach. Physical Review B, 2020, 102, .	1.1	15
48320	Exchange-correlation functional challenges in modeling quaternary chalcogenides. Physical Review B, 2020, 102, .	1.1	15
48321	Magnetoelastic excitations in multiferroic hexagonal <mml:math xmlns:mml="http://www.w3.org/1998/Math/MathML"><mml:msub><mml:mi mathvariant="normal">YMnO</mml:mi><mml:mn>3</mml:mn></mml:msub></mml:math> studied by inelastic x-ray scattering. Physical Review B, 2020, 102, .	1.1	4
48322	Quantum anomalous Hall insulator state in ferromagnetically ordered <mml:math xmlns:mml="http://www.w3.org/1998/Math/MathML"><mml:mrow><mml:mi>Mn</mml:mi><mml:msub><mml:mi>Bi</mml:mi><mml:mn mathvariant="normal">V</mml:mi><mml:msub><mml:mi>Bi</mml:mi><mml:mn>2</mml:mn></mml:msub><mml:msub><mml:mi>T</mml:mi> heterostructures. Physical Review B, 2020, 102, .	1.1	25

#	Article	IF	Citations
48323	Symmetry crossover in layered <mml:math xmlns:mml="http://www.w3.org/1998/Math/MathML"><mml:mrow><mml:mi>M</mml:mi><mml:msub><mml:mi>PS</mml:mi><mml:m complexes <mml:math xmlns:mml="http://www.w3.org/1998/Math/MathML"><mml:mo>(</mml:mo><mml:mi>M</mml:mi><mml:mo>=</mml:mo><mml:mi>M via near-field infrared spectros. Physical Review B, 2020, 102, .	1.1	16
48324	Chemical vapor deposition of layered two-dimensional MoSi ₂ N ₄ materials. Science, 2020, 369, 670-674.	6.0	556
48325	Exploration of n- and p-type doping for two-dimensional gallium nitride: charged defect calculation with first principles. European Physical Journal B, 2020, 93, 1.	0.6	2
48326	A Ti-MOF Decorated With a Pt Nanoparticle Cocatalyst for Efficient Photocatalytic H2 Evolution: A Theoretical Study. Frontiers in Chemistry, 2020, 8, 660.	1.8	8
48327	Calphad Modeling of LRO and SRO Using ab initio Data. Metals, 2020, 10, 998.	1.0	2
48328	Strain induced variation of PFOS adsorption on pristine and defected phosphorene: A DFT study. Applied Surface Science, 2020, 532, 147452.	3.1	7
48329	Compositional engineering of tungsten-based carbides toward electrocatalytic hydrogen evolution. Journal of Alloys and Compounds, 2020, 848, 156501.	2.8	5
48330	Enhancing Reactivity of SiC-Supported Graphene by Engineering Intercalated Metal Atoms at the Interface. Journal of Physical Chemistry C, 2020, 124, 18126-18131.	1.5	3
48331	Universal growth of ultra-thin IIIâ€“V semiconductor single crystals. Nature Communications, 2020, 11, 3979.	5.8	34
48332	Theoretically designed two-dimensional Î³-C₄O as an effective gas separation membrane for hydrogen purification. Physical Chemistry Chemical Physics, 2020, 22, 19492-19501.	1.3	8
48333	Superhard sp²â€“sp³ hybridized B₂C₃N₂ with 2D metallicity. Physical Chemistry Chemical Physics, 2020, 22, 22918-22922.	1.3	5
48334	Cobalt doped BiVO₄ with rich oxygen vacancies for efficient photoelectrochemical water oxidation. RSC Advances, 2020, 10, 28523-28526.	1.7	22
48335	Water adlayers on noble metal surfaces: Insights from energy decomposition analysis. Journal of Chemical Physics, 2020, 153, 054703.	1.2	10
48336	Topological phase transition in the layered magnetic compound <mml:math xmlns:mml="http://www.w3.org/1998/Math/MathML"><mml:mrow><mml:msub><mml:mi>MnSb</mml:mi><mml:mn>2</mml:mn></mml:msub><mml:mn><m : Spin-orbit coupling and interlayer coupling dependence. Physical Review B, 2020, 102, .	1.1	50
48337	Hybridization of Bimetallic Molybdenumâ€Tungsten Carbide with Nitrogenâ€Doped Carbon: A Rational Design of Super Active Porous Composite Nanowires with Tailored Electronic Structure for Boosting Hydrogen Evolution Catalysis. Advanced Functional Materials, 2020, 30, 2003198.	7.8	57
48338	Voltageâ€Controlled Dielectric Function of Bilayer Graphene. Advanced Optical Materials, 2020, 8, 2000861.	3.6	11
48339	Superconducting and Superhard Ice. ChemPhysChem, 2020, 21, 2012-2018.	1.0	2
48340	Stable Lithium Sulfur Battery Based on In Situ Electrocatalytically Formed Li₂S on Metallic MoS₂â€“Carbon Cloth Support. Small Methods, 2020, 4, 2000353.	4.6	49

#	Article	IF	Citations
48341	Reaction environment self-modification on low-coordination Ni2+ octahedra atomic interface for superior electrocatalytic overall water splitting. Nano Research, 2020, 13, 3068-3074.	5.8	27
48342	Unveiling the unconventional roles of methyl number on the ring-opening barrier in photocatalytic decomposition of benzene, toluene and o-xylene. Applied Catalysis B: Environmental, 2020, 278, 119318.	10.8	57
48343	Interaction between transition metals (Co, Ni, and Cu) systems and amorphous silica surfaces: A DFT investigation. Applied Surface Science, 2020, 533, 147422.	3.1	20
48344	Single transition metal atoms on nitrogen-doped carbon for CO2 electrocatalytic reduction: CO production or further CO reduction?. Applied Surface Science, 2020, 533, 147466.	3.1	47
48345	Metallic VS2/blue phosphorene heterostructures as promising anode materials for high-performance lithium ion batteries: A first principles study. Applied Surface Science, 2020, 533, 147478.	3.1	37
48346	DFT study of the oxidation of Hg0 by O2 on an Mn-doped buckled g-C3N4 catalyst. Current Applied Physics, 2022, 40, 83-89.	1.1	10
48347	Stacking-dependent electronic properties of aluminene based multilayer van der Waals heterostructures. Computational Materials Science, 2020, 185, 109952.	1.4	3
48348	Microalloying effect in ternary Al-Sm-X (XÂ=ÂAg, Au, Cu) metallic glasses studied by ab initio molecular dynamics. Computational Materials Science, 2020, 185, 109958.	1.4	6
48349	Strain or Electronic Effects? â€“ The influence of alkali metals on the bandgap of Cu2O. Chemical Physics Letters, 2020, 755, 137799.	1.2	1
48350	Combining theory and experiment to determine thermoelectrics of tellurium doped CoSb3. Intermetallics, 2020, 125, 106918.	1.8	5
48351	Strain induced structural transformation, mechanical and phonon stability in silicene derived 2D-SiB. Journal of Industrial and Engineering Chemistry, 2020, 90, 399-406.	2.9	5
48352	Structural and mechanical stability, lattice dynamics and electronic structure of the novel CrVZ (Z =) Tj ETQq1 1 0.784314 rgBT /Over	0.9	12
48353	In-situ passivation perovskite targeting efficient light-emitting diodes via spontaneously formed silica network. Nano Energy, 2020, 78, 105134.	8.2	28
48354	Searching for New Ferroelectric Materials Using High-Throughput Databases: An Experimental Perspective on BiAlO₃ and BiInO₃. Chemistry of Materials, 2020, 32, 7274-7283.	3.2	16
48355	Photocatalytic Properties of Bi_{2â€“x}Ti₂O_{7â€“1.5x} (x = 0, 0.5) Pyrochlores: Hybrid DFT Calculations and Experimental Study. Inorganic Chemistry, 2020, 59, 12385-12396.	1.9	18
48356	Quaternary Arsenides REHfCu_{2+Î´}As₃ (RE = Laâ€“Nd; Î´ â‰ˆ 0.17): Superstructures of the Zr₂Ni₃P₃-Type Structure. Inorganic Chemistry, 2020, 59, 11089-11095.	1.9	2
48357	Energetics of Baseâ€“Acid Pairs for the Design of High-Temperature Fuel Cell Polymer Electrolytes. Journal of Physical Chemistry B, 2020, 124, 7725-7734.	1.2	23
48358	Theoretical Insights into the Structure and Activity of Cobalt Modulated by Surface and Subsurface Carbon in Operando Conditions. Journal of Physical Chemistry C, 2020, 124, 18576-18586.	1.5	5

#	Article	IF	Citations
48359	Fast and Anomalous Exciton Diffusion in Two-Dimensional Hybrid Perovskites. Nano Letters, 2020, 20, 6674-6681.	4.5	44
48360	Experimental Observation of Ultrahigh Mobility Anisotropy of Organic Semiconductors in the Two-Dimensional Limit. ACS Applied Electronic Materials, 2020, 2, 2888-2894.	2.0	6
48361	Revealing the Role of Liquid Metals at the Anodeâ€“Electrolyte Interface for All Solid-State Lithium-Ion Batteries. ACS Applied Materials & Interfaces, 2020, 12, 38232-38240.	4.0	13
48362	High-Resolution Three-Dimensional Sculpting of Two-Dimensional Graphene Oxide by E-Beam Direct Write. ACS Applied Materials & Interfaces, 2020, 12, 39595-39601.	4.0	6
48363	Selective-Area Remote Epitaxy of ZnO Microrods Using Multilayerâ€“Monolayer-Patterned Graphene for Transferable and Flexible Device Fabrications. ACS Applied Nano Materials, 2020, 3, 8920-8930.	2.4	25
48364	In Situ Surface-Enhanced Raman Spectroscopic Evidence on the Origin of Selectivity in CO₂ Electrocatalytic Reduction. ACS Nano, 2020, 14, 11363-11372.	7.3	177
48365	Na Doping in PbTe: Solubility, Band Convergence, Phase Boundary Mapping, and Thermoelectric Properties. Journal of the American Chemical Society, 2020, 142, 15464-15475.	6.6	101
48366	Electronic correlations and flattened band in magnetic Weyl semimetal candidate Co3Sn2S2. Nature Communications, 2020, 11, 3985.	5.8	51
48367	Atomic-scale phase separation induced clustering of solute atoms. Nature Communications, 2020, 11, 3934.	5.8	11
48368	Defect-mediated Rashba engineering for optimizing electrical transport in thermoelectric BiTeI. Npj Computational Materials, 2020, 6, .	3.5	24
48369	Length scales of interfacial coupling between metal and insulator phases in oxides. Nature Materials, 2020, 19, 1182-1187.	13.3	42
48370	Chemically directed structure evolution for crystal structure prediction. Physical Chemistry Chemical Physics, 2020, 22, 18205-18218.	1.3	9
48371	Surface functional group modification induced partial Fermi level pinning and ohmic contact at boropheneâ€“MoS₂ interfaces. Physical Chemistry Chemical Physics, 2020, 22, 19202-19212.	1.3	4
48372	Electronic structures, and optical and photocatalytic properties of the BPâ€“BSe van der Waals heterostructures. New Journal of Chemistry, 2020, 44, 14964-14969.	1.4	11
48373	Correlated migration of ions in a 2D heterostructure anode: guaranteeing a low barrier for a high site occupancy. Journal of Materials Chemistry A, 2020, 8, 17463-17470.	5.2	5
48374	Origin of the abnormal reduction of the dielectric response for ReCOB crystals and its mechanism: theoretical and experimental exploration. Journal of Materials Chemistry C, 2020, 8, 10109-10120.	2.7	1
48375	Impact of linker functionalization on the adsorption of nitrogen-containing compounds in HKUST-1. Dalton Transactions, 2020, 49, 12610-12621.	1.6	16
48376	Pristine edge structures of Tâ€²â€²-phase transition metal dichalcogenides (ReSe₂,) Tj ETQq1 1 0.784314 rgBT /Overloc	2.8	15

#	Article	IF	Citations
48377	Superoxide formation in Li₂VO₂F cathode material â€“ a combined computational and experimental investigation of anionic redox activity. Journal of Materials Chemistry A, 2020, 8, 16551-16559.	5.2	18
48378	Negative effect of oxygen vacancies on ferromagnetism in Ru-doped BaSnO3 materials. Applied Physics Letters, 2020, 117, .	1.5	12
48379	Anomalous lattice shrinking of LaTiO3 thin film on SrTiO3 (111) induced by three-dimensional electron transfer. Journal of Applied Physics, 2020, 128, 035301.	1.1	2
48380	Neural network potential from bispectrum components: A case study on crystalline silicon. Journal of Chemical Physics, 2020, 153, 054118.	1.2	12
48381	Intrinsic ferromagnetism in atomically thin two-dimensional organic-inorganic van der Waals crystals. Physical Review B, 2020, 102, .	1.1	4
48382	Theoretical study on the anomalies of the magnetic susceptibility in the honeycomb lattice compound <mml:math xmlns:mml="http://www.w3.org/1998/Math/MathML"><mml:mrow><mml:msub><mml:mi>Na</mml:mi><mml:mn>2</mml:mn></mml:msub><mml:msub><mml:mi mathvariant="normal">O</mml:mi><mml:mn>6</mml:mn></mml:msub></mml:mrow></mml:math>. Physical Review B, 2020, 102, .	1.1	7
48383	Large lattice thermal conductivity, interplay between phonon-phonon, phonon-electron, and phonon-isotope scatterings, and electrical transport in molybdenum from first principles. Physical Review B, 2020, 102, .	1.1	14
48384	Roles of nitrogen substitution and surface reconstruction in stabilizing nonpassivated single-layer diamond. Physical Review B, 2020, 102, .	1.1	12
48385	Adsorption of alkali metals on graphitic carbon nitride: A first-principles study. Modern Physics Letters B, 2020, 34, 2050361.	1.0	4
48386	A novel high-pressure polymorph of TaSi2. Results in Physics, 2020, 18, 103310.	2.0	2
48387	Optical Gaps and Excitonic Properties of 2D Materials by Hybrid Time-Dependent Density Functional Theory: Evidences for Monolayers and Prospects for van der Waals Heterostructures. Journal of Chemical Theory and Computation, 2020, 16, 5876-5883.	2.3	21
48388	Ultraefficient Singlet Oxygen Generation from Manganese-Doped Cesium Lead Chloride Perovskite Quantum Dots. ACS Nano, 2020, 14, 12596-12604.	7.3	20
48389	Alkali-cation-enhanced benzylammonium passivation for efficient and stable perovskite solar cells fabricated through sequential deposition. Journal of Materials Chemistry A, 2020, 8, 19357-19366.	5.2	13
48390	A posteriori error estimation for the non-self-consistent Kohnâ€“Sham equations. Faraday Discussions, 2020, 224, 227-246.	1.6	8
48391	2D ferromagnetism at finite temperatures under quantum scrutiny. Applied Physics Letters, 2020, 117, .	1.5	14
48392	Improving stability of ALD ZrN thin film coatings over U-Mo dispersion fuel. Applied Surface Science, 2020, 533, 147378.	3.1	4
48393	Surface segregation in Cr-Mn-Fe-Co-Ni high entropy alloys. Applied Surface Science, 2020, 533, 147471.	3.1	46
48394	Synergy of vanadia and ceria in the reaction mechanism of low-temperature selective catalytic reduction of NOx by NH3. Journal of Catalysis, 2020, 391, 145-154.	3.1	30

#	Article	IF	Citations
48395	Transition metal atoms encapsulated within microporous Silicalite-1 zeolite: A systematic computational study. Microporous and Mesoporous Materials, 2020, 308, 110462.	2.2	7
48396	The importance of frontier orbital symmetry in the adsorption of diiodobenzene on MoS2(0001). Surface Science, 2020, 702, 121708.	0.8	3
48397	A Synergistic Approach to Unraveling the Thermodynamic Stability of Binary and Ternary Chevrel Phase Sulfides. Chemistry of Materials, 2020, 32, 7044-7051.	3.2	10
48398	Graphene Oxide-BiOCl Nanoparticle Composites as Catalysts for Oxidation of Volatile Organic Compounds in Nonthermal Plasmas. ACS Applied Nano Materials, 2020, 3, 9363-9374.	2.4	13
48399	Single-Atom Ru-Implanted Metalâ€“Organic Framework/MnO₂ for the Highly Selective Oxidation of NO_x by Plasma Activation. ACS Catalysis, 2020, 10, 10185-10196.	5.5	58
48400	Topological flat bands in frustrated kagome lattice CoSn. Nature Communications, 2020, 11, 4004.	5.8	203
48401	Direct visualization of irreducible ferrielectricity in crystals. Npj Quantum Materials, 2020, 5, .	1.8	9
48402	Directly linked metalloporphyrins: a quest for bio-inspired materials. Materials Advances, 2020, 1, 1895-1908.	2.6	4
48403	Role of carrier-transfer in the optical nonlinearity of graphene/Bi₂Te₃ heterojunctions. Nanoscale, 2020, 12, 16956-16966.	2.8	20
48404	A zero-dimensional nickel, ironâ€“metalâ€“organic framework (MOF) for synergistic N₂electrofixation. Journal of Materials Chemistry A, 2020, 8, 18810-18815.	5.2	52
48405	Development of interatomic potential for Alâ€“Tb alloys using a deep neural network learning method. Physical Chemistry Chemical Physics, 2020, 22, 18467-18479.	1.3	28
48406	An ultra-incompressible Mn3N compound predicted by first-principles genetic algorithm. Journal of Applied Physics, 2020, 128, 055112.	1.1	2
48407	First-principles calculations of finite temperature electronic structures and transport properties of Heusler alloy Co2MnSi. Applied Physics Letters, 2020, 117, 042402.	1.5	15
48408	Shortâ€range ordering in the Liâ€rich disordered rock salt cathode material Li 2 VO 2 F revealed by Raman spectroscopy. Journal of Raman Spectroscopy, 2020, 51, 2095-2101.	1.2	13
48409	How inactive d0 transition metal controls anionic redox in disordered Li-rich oxyfluoride cathodes. Energy Storage Materials, 2020, 32, 253-260.	9.5	16
48410	Tuning electronic and optical properties of SnSe by external strain. Optik, 2020, 218, 165260.	1.4	3
48411	Elucidating dual-defect mechanism in rhenium disulfide nanosheets with multi-dimensional ion transport channels for ultrafast sodium storage. Nano Energy, 2020, 77, 105189.	8.2	31
48412	Superhard high-pressure structures of beryllium diborocarbides. Vacuum, 2020, 180, 109617.	1.6	1

#	Article	IF	Citations
48413	Cyclophosphate MBi(P₄O₁₂) (M = Cs, Rb): Structure Change Giving Rise to Property Enhancement. Crystal Growth and Design, 2020, 20, 6205-6210.	1.4	9
48414	In Search of Surface-Induced Crystal Structures: The Case of Tyrian Purple. Journal of Physical Chemistry C, 2020, 124, 17702-17710.	1.5	3
48415	Dispersed Nickel Boosts Catalysis by Copper in CO₂ Hydrogenation. ACS Catalysis, 2020, 10, 9261-9270.	5.5	52
48416	Alcohol-Induced Low-Temperature Blockage of Supported-Metal Catalysts for Enhanced Catalysis. ACS Catalysis, 2020, 10, 8515-8523.	5.5	18
48417	Construction of Highly Active and Selective Polydopamine Modified Hollow ZnO/Co₃O₄ p-n Heterojunction Catalyst for Photocatalytic CO₂ Reduction. ACS Sustainable Chemistry and Engineering, 2020, 8, 11465-11476.	3.2	84
48418	Hydration of a 2D Supramolecular Assembly: Bitartrate on Cu(110). Journal of the American Chemical Society, 2020, 142, 13814-13822.	6.6	8
48419	Autogenous growth of the hierarchical V-doped NiFe layer double metal hydroxide electrodes for an enhanced overall water splitting. Dalton Transactions, 2020, 49, 11217-11225.	1.6	26
48420	Seamlessly conductive Co(OH)₂ tailored atomically dispersed Pt electrocatalyst with a hierarchical nanostructure for an efficient hydrogen evolution reaction. Energy and Environmental Science, 2020, 13, 3082-3092.	15.6	123
48421	Câ€“H activation of light alkanes on MXenes predicted by hydrogen affinity. Physical Chemistry Chemical Physics, 2020, 22, 18622-18630.	1.3	10
48422	Dilute magnetism in Co-doped spinel Mg3Si6As8. Journal of Applied Physics, 2020, 128, .	1.1	1
48423	First-principles study on the effect of Sn doping in Cu2Sâ€”Acanthite phase as a substitute to low chalcocite for modeling complex doping. Journal of Applied Physics, 2020, 128, .	1.1	7
48424	Monte Carlo simulations of hole transport in 4H-SiC using DOS calculations. Journal of Physics: Conference Series, 2020, 1534, 012006.	0.3	0
48425	Shortcomings of meta-GGA functionals when describing magnetism. Physical Review B, 2020, 102, .	1.1	27
48426	Prediction of exotic magnetic states in the alkali-metal quasi-one-dimensional iron selenide compound Na2FeSe2. Physical Review B, 2020, 102, .	1.1	15
48427	Emergence of Van Hove singularity and topological states in Pb3Bi/Ge(111) Rashba systems. Physical Review B, 2020, 102, .	1.1	10
48428	Strain Tunable Semimetalâ€“Topological-Insulator Transition in Monolayer <mml:math xmlns:mml="http://www.w3.org/1998/Math/MathML" display="inline"><mml:mrow><mml:mn>1</mml:mn><mml:msup><mml:mrow><mml:mi mathvariant="normal">T</mml:mi></mml:mrow><mml:mrow><mml:mo>â€²</mml:mo></mml:mrow></mml:msup><mml:mtext>â^’</mml:mtext> Physical Review Letters, 2020, 125, 046801.	2.9	67
48429	Cooperative carbon capture and steam regeneration with tetraamine-appended metalâ€“organic frameworks. Science, 2020, 369, 392-396.	6.0	249
48430	Prediction of a Stable Organic Metal-Free Porous Material as a Catalyst for Water-Splitting. Catalysts, 2020, 10, 836.	1.6	13

#	Article	IF	Citations
48431	Mechanism of CO Oxidation on Pd/CeO 2 (100): The Unique Surfaceâ€Structure of CeO 2 (100) and the Role of Peroxide. ChemCatChem, 2020, 12, 5164-5172.	1.8	3
48432	Unravelling phosphate adsorption on hydrous ferric oxide surfaces at the molecular level. Chemosphere, 2020, 261, 127776.	4.2	17
48433	Lattice dynamical and elastic properties of Co3-xAlxO4 (xÂ= 0, 1, and 2) spinel oxides: Theoretical investigations. Computational Condensed Matter, 2020, 24, e00476.	0.9	1
48434	Effective interaction model for coupled magnetism and phase stability in bcc Fe-Co systems. Computational Materials Science, 2020, 183, 109906.	1.4	8
48435	Hydrodeoxygenation of phenolic compounds and raw lignin-oil over bimetallic RuNi catalyst: An experimental and modeling study focusing on adsorption properties. Fuel, 2020, 281, 118758.	3.4	39
48436	Dislocation nucleation from Zrâ€“Nb bimetal interfaces cooperating with the dynamic evolution of interfacial dislocations. International Journal of Plasticity, 2020, 135, 102830.	4.1	15
48437	Enhancing the thermoelectric performance of single-walled carbon nanotube-conducting polymer nanocomposites. Journal of Alloys and Compounds, 2020, 845, 156354.	2.8	13
48438	Interaction of irradiation-induced point defects with transmutants (H, He, Li, Be, B, Mg, Al and P) in 3C-SiC ceramics. Journal of the European Ceramic Society, 2020, 40, 5196-5204.	2.8	12
48439	Insights into the nature of optically active defects of ZnO. Journal of Luminescence, 2020, 227, 117536.	1.5	15
48440	Thermodynamic modelling of Yâ€“H and Yâ€“Zrâ€“H system aided by first-principles and its application in bulk hydride moderator fabrication. Journal of Nuclear Materials, 2020, 531, 152035.	1.3	11
48441	Composition-dependent microstructure evolution in liquid MgCl2-KCl: A first-principles molecular dynamics study. Journal of Molecular Liquids, 2020, 309, 113131.	2.3	27
48442	Two-dimensional B3P monolayer as a superior anode material for Li and Na ion batteries: a first-principles study. Materials Today Energy, 2020, 17, 100486.	2.5	15
48443	Magnetic and electronic properties of zigzag BN nanoribbons with nonmetallic atom terminations: A first-principles study. Physics Letters, Section A: General, Atomic and Solid State Physics, 2020, 384, 126483.	0.9	3
48444	Unveiling the adsorption properties of 3d, 4d, and 5d metal adatoms on the MoS2 monolayer: A DFT-D3 investigation. Surface Science, 2020, 701, 121700.	0.8	19
48445	Computationally Guided Investigation of the Optical Spectra of Pure Î²-UO3. Inorganic Chemistry, 2020, 59, 11481-11492.	1.9	14
48446	Phase-controllable growth of ultrathin 2D magnetic FeTe crystals. Nature Communications, 2020, 11, 3729.	5.8	120
48447	Strain-enhanced Dzyaloshinskiiâ€“Moriya interaction at Co/Pt interfaces. Scientific Reports, 2020, 10, 12314.	1.6	20
48448	Reaction probability and kinetics of water splitting on the penta-NiAs₂ monolayer from an ab initio molecular dynamics investigation. Physical Chemistry Chemical Physics, 2020, 22, 18149-18154.	1.3	2

#	Article	IF	Citations
48449	High-pressure elastic properties of dolomite melt supporting carbonate-induced melting in deep upper mantle. Proceedings of the National Academy of Sciences of the United States of America, 2020, 117, 18285-18291.	3.3	15
48450	An insight into indium effect on the crystal structure and thermoluminescence of LiMgPO4: Combined experiment and ab initio calculations. Journal of Alloys and Compounds, 2020, 846, 156242.	2.8	12
48451	EQCM analysis of intercalation species into graphite positive electrodes for Al batteries. Journal of Alloys and Compounds, 2020, 846, 156469.	2.8	13
48452	A study of calcium ion intercalation in perovskite calcium manganese oxide. Journal of Electroanalytical Chemistry, 2020, 874, 114453.	1.9	10
48453	Molybdenum carbide nano-sheet as a high capacity anode material for monovalent alkali metal-ion batteriesâ€"Theoretical investigation. Physics Letters, Section A: General, Atomic and Solid State Physics, 2020, 384, 126688.	0.9	8
48454	Phosphate removal by ZIF-8@MWCNT hybrids in presence of effluent organic matter: Adsorbent structure, wastewater quality, and DFT analysis. Science of the Total Environment, 2020, 745, 141054.	3.9	23
48455	Promising Zintl-Phase Thermoelectric Compound SrAgSb. Chemistry of Materials, 2020, 32, 6983-6989.	3.2	36
48456	Atomic-Scale Analysis of Biphasic Boundaries in the Lithium-Ion Battery Cathode Material LiFePO₄. ACS Applied Energy Materials, 2020, 3, 8009-8016.	2.5	5
48457	Combining Superionic Conduction and Favorable Decomposition Products in the Crystalline Lithiumâ€"Boronâ€"Sulfur System: A New Mechanism for Stabilizing Solid Li-Ion Electrolytes. ACS Applied Materials & Interfaces, 2020, 12, 37957-37966.	4.0	24
48458	Rich essential properties of Si-doped graphene. Scientific Reports, 2020, 10, 12051.	1.6	30
48459	Optical and dielectric properties of lead perovskite and iodoplumbate complexes: an ab initio study. Physical Chemistry Chemical Physics, 2020, 22, 18423-18434.	1.3	13
48460	Combined DFT and geometricalâ€"topological analysis of Li-ion conductivity in complex hydrides. Inorganic Chemistry Frontiers, 2020, 7, 3115-3125.	3.0	17
48461	Heterostructures of Îµ-Fe₂O₃ and Î±-Fe₂O₃: insights from density functional theory. RSC Advances, 2020, 10, 27474-27480.	1.7	8
48462	Two-dimensional penta-SiAs₂: a potential metal-free photocatalyst for overall water splitting. Journal of Materials Chemistry C, 2020, 8, 11980-11987.	2.7	24
48463	Synthesis and high-pressure studies of strontium diazenide by synchrotron X-ray diffraction and DFT calculations. RSC Advances, 2020, 10, 26308-26312.	1.7	0
48464	An accurate and transferable machine learning potential for carbon. Journal of Chemical Physics, 2020, 153, 034702.	1.2	137
48465	Unraveling the abnormal dependence of phase stability on valence electron concentration in Niâ€"Mn-based metamagnetic shape memory alloys. Journal of Applied Physics, 2020, 128, .	1.1	4
48466	Conspicuous interatomic bonding in chalcogenide crystals and implications on electronic, optical, and elastic properties. AIP Advances, 2020, 10, .	0.6	11

#	Article	IF	Citations
48467	Electrically controlled magnetism in iron thin film. Journal of Physics: Conference Series, 2020, 1506, 012009.	0.3	1
48468	The wide-range model of shell effects in hot plasma with semiclassical approximation for bound electrons. Journal of Physics: Conference Series, 2020, 1556, 012044.	0.3	0
48469	Hydrogen adsorption on calcium-decorated planar aluminene using density functional theory. IOP Conference Series: Earth and Environmental Science, 2020, 463, 012104.	0.2	3
48470	Effect of Al-V-B grain refiner on refining aluminium alloys: estimation from ab initio calculations. IOP Conference Series: Materials Science and Engineering, 2020, 861, 012047.	0.3	0
48471	Persistent polar distortions from covalent interactions in doped <mml:math xmlns:mml="http://www.w3.org/1998/Math/MathML"><mml:msub><mml:mi>BaTiO</mml:mi><mml:mn>3</mml:mn></mml:msub></m Physical Review B, 2020, 102, .	1.1	18
48472	Competing magnetic orders in quantum critical <mml:math xmlns:mml="http://www.w3.org/1998/Math/MathML"><mml:msub><mml:mrow><mml:mi>Sr</mml:mi></mml:mrow><mml:mn>3</mn mathvariant="normal">O</mml:mi></mml:mrow><mml:mn>7</mml:mn></mml:msub></mml:math>. Physical Review B, 2020, 102, .	1.1	5
48473	Generalized gradient approximations with local parameters. Physical Review B, 2020, 102, .	1.1	9
48474	Anharmonicity and Ultralow Thermal Conductivity in Lead-Free Halide Double Perovskites. Physical Review Letters, 2020, 125, 045701.	2.9	90
48475	Engineering Graphene Oxide/Water Interface from First Principles to Experiments for Electrostatic Protective Composites. Polymers, 2020, 12, 1596.	2.0	5
48476	Magnetocrystalline anisotropy of small CoPt binary alloy metal clusters: interplay between structure, chemical composition, and spin-orbit coupling. Journal of Nanoparticle Research, 2020, 22, 1.	0.8	4
48477	Composition-balanced trimetallic MOFs as ultra-efficient electrocatalysts for oxygen evolution reaction at high current densities. Applied Catalysis B: Environmental, 2020, 279, 119375.	10.8	102
48478	Catalytic fast pyrolysis of enzymatic hydrolysis lignin over Lewis-acid catalyst niobium pentoxide and mechanism study. Bioresource Technology, 2020, 316, 123853.	4.8	23
48479	Enhanced cycling stability of nickel-rich layered oxide by tantalum doping. Journal of Power Sources, 2020, 473, 228597.	4.0	71
48480	No-monotonic strain effect on the thermal conductivity of blue phosphorene: A first-principles study. Physica E: Low-Dimensional Systems and Nanostructures, 2020, 124, 114341.	1.3	3
48481	Design Principles for Aqueous Na-Ion Battery Cathodes. Chemistry of Materials, 2020, 32, 6875-6885.	3.2	28
48482	Lattice Anharmonicity of Stereochemically Active Lone Pairs Controls Thermochromic Band Gap Reduction of PbVO₃Cl. Chemistry of Materials, 2020, 32, 7404-7412.	3.2	15
48483	A Systematic Study of Methylation from Benzene to Hexamethylbenzene in H-SSZ-13 Using Density Functional Theory and Ab Initio Calculations. ACS Catalysis, 2020, 10, 8916-8925.	5.5	21
48484	Layered Zinc Hydroxide Dihydrate, Zn₅(OH)₁₀Â·2H₂O, from Hydrothermal Conversion of Îµ-Zn(OH)₂ at Gigapascal Pressures and its Transformation to Nanocrystalline ZnO. ACS Omega, 2020, 5, 17617-17627.	1.6	26

#	Article	IF	Citations
48485	Exchange-correlation functionals for band gaps of solids: benchmark, reparametrization and machine learning. Npj Computational Materials, 2020, 6, .	3.5	156
48486	Two-dimensional forms of robust CO2 reduction photocatalysts. Npj 2D Materials and Applications, 2020, 4, .	3.9	20
48487	Ab initio study of band gap properties in metastable BC8/ST12 SixGe1â^'x alloys. Applied Physics Letters, 2020, 117, 032105.	1.5	3
48488	Robust topological Hall effect driven by tunable noncoplanar magnetic state in Mn-Pt-In inverse tetragonal Heusler alloys. Physical Review B, 2020, 102, .	1.1	16
48489	Compositional phase stability of correlated electron materials within DFT+DMFT. Physical Review B, 2020, 102, .	1.1	6
48490	C-2p Spin-Polarizations along with Two Mechanisms in Extended Carbon Multilayers: Insight from First Principles. Condensed Matter, 2020, 5, 48.	0.8	0
48491	First-Principles Study on the Cu/Fe Interface Properties of Ternary Cu-Fe-X Alloys. Materials, 2020, 13, 3112.	1.3	7
48492	Role of Mg Impurity in the Water Adsorption over Low-Index Surfaces of Calcium Silicates: A DFT-D Study. Minerals (Basel, Switzerland), 2020, 10, 665.	0.8	7
48493	First-Principles Study on Stacking Fault Energy of Î³-Feâ€“Mn Alloys. Metals and Materials International, 2020, 27, 3205.	1.8	7
48494	A new concept: Volume photocatalysis for efficient H2 generation ___ Using low polymeric carbon nitride as an example. Applied Catalysis B: Environmental, 2020, 279, 119379.	10.8	104
48495	Two-dimensional clathrate graphene in minimum egg-tray-shape: An ab initio study. Physica E: Low-Dimensional Systems and Nanostructures, 2020, 124, 114378.	1.3	0
48496	Ammoniumâ€“Ammonia Complexes, N2H7+, in Ammonium closo-Borate Ammines: Synthesis, Structure, and Properties. Inorganic Chemistry, 2020, 59, 11449-11458.	1.9	6
48497	Theory-Guided Design of Anode Catalysts for Hydrogenous Liquid Fuels. Journal of Physical Chemistry C, 2020, 124, 17494-17502.	1.5	1
48498	Solution-Processed Sb₂Se₃ on TiO₂ Thin Films Toward Oxidation- and Moisture-Resistant, Self-Powered Photodetectors. ACS Applied Materials & Interfaces, 2020, 12, 38341-38349.	4.0	32
48499	Ab initio modeling of the energy landscape for screw dislocations in body-centered cubic high-entropy alloys. Npj Computational Materials, 2020, 6, .	3.5	58
48500	Ab initio investigation of the role of transition-metal dopants in the adsorption properties of ethylene glycol on doped Pt(100) surfaces. Physical Chemistry Chemical Physics, 2020, 22, 17646-17658.	1.3	3
48501	Superconductivity enhancement in phase-engineered molybdenum carbide/disulfide vertical heterostructures. Proceedings of the National Academy of Sciences of the United States of America, 2020, 117, 19685-19693.	3.3	6
48502	Structural distortion and collinear-to-helical magnetism transition in rutile-type <mml:math xmlns:mml="http://www.w3.org/1998/Math/MathML"><mml:mrow><mml:mi>Fe</mml:mi><mml:msub><mml:mi mathvariant="normal">O</mml:mi><mml:mn>2</mml:mn></mml:msub></mml:mrow></mml:math>. Physical Review B, 2020, 102, .	1.1	1

#	Article	IF	Citations
48503	Static and dynamic spin properties in the quantum triangular lattice antiferromagnet <mml:math xmlns:mml="http://www.w3.org/1998/Math/MathML"><mml:mrow><mml:msub><mml:mi>Ag</mml:mi><mml:mn>2</mml:mn></mml:msub></mml:mrow></mml:math> Physical Review B, 2020, 102, .	1.1	5
48504	Symmetry breaking in the double moirÃ© superlattices of relaxed twisted bilayer graphene on hexagonal boron nitride. Physical Review B, 2020, 102, .	1.1	17
48505	Novel Perspective Coatings for the Optoelectronic Elements: Features of the Carbon Nanotubes to Modify the Surface Relief of BaF2 Materials. Coatings, 2020, 10, 661.	1.2	3
48506	Polar-discontinuity-induced stability of spontaneous polarization in ultrathin perovskite films. Ceramics International, 2020, 46, 26698-26704.	2.3	0
48507	Significant effect of base assisted intercalates in synthesis of 2D semiconductor Ti3C2O2. Surfaces and Interfaces, 2020, 20, 100604.	1.5	1
48508	The Effect of Janus Asymmetry on Thermal Transport in SnSSe. Journal of Physical Chemistry C, 2020, 124, 17476-17484.	1.5	30
48509	Strain-Induced Band Modulation, Work Function, and QTAIM Analysis of Surface O-Functionalized Ti₂C MXene. ACS Omega, 2020, 5, 18403-18410.	1.6	9
48510	2D layered SiC/C2N van der Waals type-II heterostructure: a visible-light-driven photocatalyst for water splitting. New Journal of Chemistry, 2020, 44, 15439-15445.	1.4	21
48511	Addressing the sensitivity of signals from solid/liquid ambient pressure XPS (APXPS) measurement. Journal of Chemical Physics, 2020, 153, 044709.	1.2	16
48512	Quantum dynamics origin of high photocatalytic activity of mixed-phase anatase/rutile TiO2. Journal of Chemical Physics, 2020, 153, 044706.	1.2	26
48513	Emerging piezochromism in transparent lead free perovskite Rb3X2I9 (Xâ€‰=â€‰Sb, Bi) under compression: A comparative theoretical insight. Journal of Applied Physics, 2020, 128, 045102.	1.1	5
48514	Phase diagram and superconductivity of calcium borohyrides at extreme pressures. Physical Review B, 2020, 102, .	1.1	41
48515	One-dimensional Rashba states in Pb atomic chains on a semiconductor surface. Physical Review B, 2020, 102, .	1.1	11
48516	First principles study of bulk and two-dimensional structures of the <mml:math xmlns:mml="http://www.w3.org/1998/Math/MathML"><mml:mi>A</mml:mi><mml:mi mathvariant="normal">MnBi</mml:mi></mml:math> family of materials <mml:math		

#	Article	IF	Citations
48521	Extraordinary Response of H-Charged and H-Free Coherent Grain Boundaries in Nickel to Multiaxial Loading. Crystals, 2020, 10, 590.	1.0	4
48522	The coordination of Al on pyridinic-N doped graphene as electrons reservoir for efficiently catalyzing CO oxidization. Applied Surface Science, 2020, 531, 147310.	3.1	16
48523	A novel two-dimensional sp-sp2-sp3 hybridized carbon nanostructure with a negative in-plane Poisson ratio and high electron mobility. Computational Materials Science, 2020, 185, 109904.	1.4	20
48524	Reaction coordinate mapping of hydrogen evolution mechanism on Mg3N2 monolayer. International Journal of Hydrogen Energy, 2020, 45, 22848-22854.	3.8	7
48525	The structural stability and optical properties of NiPt nanomaterial from first-principles investigations. Materials Science in Semiconductor Processing, 2020, 120, 105306.	1.9	26
48526	A superior electronic conducting tellurium electrode enabled high rate capability rechargeable Mg batteries. Materials Today Energy, 2020, 17, 100450.	2.5	15
48527	Semimetallic features in thermoelectric transport properties of 2Hâ€“3R phase niobium diselenide. Nano Energy, 2020, 78, 105197.	8.2	5
48528	Surface engineering of RhOOH nanosheets promotes hydrogen evolution in alkaline. Nano Energy, 2020, 78, 105224.	8.2	27
48529	Theoretical study of enhanced ferromagnetism and tunable magnetic anisotropy of monolayer CrI3 by surface adsorption. Physics Letters, Section A: General, Atomic and Solid State Physics, 2020, 384, 126754.	0.9	16
48530	Persistent surface states with diminishing gap in MnBi2Te4/Bi2Te3 superlattice antiferromagnetic topological insulator. Science Bulletin, 2020, 65, 2086-2093.	4.3	44
48531	Pressure-induced the formation of Mg(CH3)2 and Ca(CH3)2 studied by the first principles. Solid State Communications, 2020, 320, 114027.	0.9	0
48532	Heat Capacity, Thermal Expansion Coefficient, and GrÃ¼neisen Parameter of CH₄, CO₂, and C₂H₆ Hydrates and Ice I_h via Density Functional Theory and Phonon Calculations. Crystal Growth and Design, 2020, 20, 5947-5955.	1.4	14
48533	Oxygen Affinity: The Missing Link Enabling Prediction of Proton Conductivities in Doped Barium Zirconates. Chemistry of Materials, 2020, 32, 7292-7300.	3.2	25
48534	Predicting the Phase Stability of Multicomponent High-Entropy Compounds. Chemistry of Materials, 2020, 32, 7507-7515.	3.2	37
48535	Correlating Cê•€, Cê•Ǒ, and Cê•Ǹ Hydrogenation Activity with Hydrogen Binding Energies on Niâ€“Fe Bimetallic Catalysts. Journal of Physical Chemistry C, 2020, 124, 18595-18603.	1.5	7
48536	Atomic Layer and Interfacial Oxygen Defect Tailored Magnetic Anisotropy and Dzyaloshinskiiâ€“Moriya Interaction in Perovskite SrRuO₃/SrTiO₃ Heterostructures. ACS Applied Electronic Materials, 2020, 2, 2591-2600.	2.0	8
48537	Effect of Element Substitution on Electrochemical Performance of Silicide/Si Composite Electrodes for Lithium-Ion Batteries. ACS Applied Energy Materials, 2020, 3, 7438-7444.	2.5	8
48538	Mitigation of Polysulfide Shuttling by Interlayer/Permselective Separators in Lithiumâ€“Sulfur Batteries. ACS Applied Energy Materials, 2020, 3, 8095-8129.	2.5	60

#	Article	IF	Citations
48539	Nanoporous V-Doped Ni₅P₄ Microsphere: A Highly Efficient Electrocatalyst for Hydrogen Evolution Reaction at All pH. ACS Applied Materials & Interfaces, 2020, 12, 37092-37099.	4.0	40
48540	Insights into the Structureâ€“Activity Relationships in Metalâ€“Organic Framework-Supported Nickel Catalysts for Ethylene Hydrogenation. ACS Catalysis, 2020, 10, 8995-9005.	5.5	40
48541	Nanoscale Spatial Distribution of Supported Nanoparticles Controls Activity and Stability in Powder Catalysts for CO Oxidation and Photocatalytic H₂ Evolution. Journal of the American Chemical Society, 2020, 142, 14481-14494.	6.6	25
48542	Why Oxygen Increases Carrier Lifetimes but Accelerates Degradation of CH₃NH₃PbI₃ under Light Irradiation: Time-Domain Ab Initio Analysis. Journal of the American Chemical Society, 2020, 142, 14664-14673.	6.6	64
48543	A first-principle perspective on electronic nematicity in FeSe. Npj Quantum Materials, 2020, 5, .	1.8	15
48544	Antiferromagnetism in perfectly ordered L10-MnAl with stoichiometric composition and its mechanism. Scientific Reports, 2020, 10, 12489.	1.6	8
48545	Thermomechanical properties of zero thermal expansion materials from theory and experiments. Physical Chemistry Chemical Physics, 2020, 22, 18518-18525.	1.3	3
48546	Insight into the photophysics of strong dual emission (blue & green) producing graphene quantum dot clusters and their application towards selective and sensitive detection of trace level Fe³⁺ and Cr⁶⁺ ions. RSC Advances, 2020, 10, 26613-26630.	1.7	11
48547	Computational design of (100) alloy surfaces for the hydrogen evolution reaction. Journal of Materials Chemistry A, 2020, 8, 17987-17997.	5.2	47
48548	Boosting the anchoring and catalytic capability of MoS₂ for high-loading lithium sulfur batteries. Journal of Materials Chemistry A, 2020, 8, 17646-17656.	5.2	33
48549	A Cu and Fe dual-atom nanozyme mimicking cytochrome c oxidase to boost the oxygen reduction reaction. Journal of Materials Chemistry A, 2020, 8, 16994-17001.	5.2	109
48550	Metallic antiferromagnets. Journal of Applied Physics, 2020, 128, .	1.1	57
48551	Direct and trapping-mediated pathways to dissociative chemisorption: CH4 dissociation on Ir(111) with step defects. Journal of Chemical Physics, 2020, 153, 034704.	1.2	23
48552	The effects of chemical disorder and external loading conditions on the structural transformation between HCP and FCC phases in CrCoFeNi high-entropy alloys: a first-principles study. Philosophical Magazine, 2020, 100, 2857-2875.	0.7	2
48553	Absence of Oxygen-Vacancy-Related Deep Levels in the Amorphous Mixed Oxide <mml:math xmlns:mml="http://www.w3.org/1998/Math/MathML" display="inline" overflow="scroll"><mml:mo stretchy="false">(</mml:mo><mml:msub><mml:mi>Al</mml:mi><mml:mn>2</mml:mn></mml:msub><mml:msub><mml:mi) Tj ETQq0		

#	Article	IF	Citations
48557	Ni3B as a highly efficient and selective catalyst for the electrosynthesis of hydrogen peroxide. Applied Catalysis B: Environmental, 2020, 279, 119371.	10.8	48
48558	Carbon vacancies and hydroxyls in graphitic carbon nitride: Promoted photocatalytic NO removal activity and mechanism. Applied Catalysis B: Environmental, 2020, 279, 119376.	10.8	83
48559	Improved gas adsorption on functionalized aluminene surface: A first-principles study. Applied Surface Science, 2020, 531, 147364.	3.1	20
48560	Thermodynamic description of the constitutive binaries of the NaCl-KCl-UCl3-PuCl3 system. Calphad: Computer Coupling of Phase Diagrams and Thermochemistry, 2020, 70, 101783.	0.7	22
48561	Surface transformation and interactions of iron oxide in glassy lubricant: An ab initio study. Chemical Physics, 2020, 538, 110919.	0.9	4
48562	Analysis and assessment of the structural, electronic properties of (ZrH2)n (nÂ=Â5â€“24) clusters: Density function theory calculations. Computational and Theoretical Chemistry, 2020, 1188, 112940.	1.1	3
48563	First-principles study of hydrogen trapping behavior in face centered cubic metals (M=Ni, Cu and Al) with monovacancy. International Journal of Hydrogen Energy, 2020, 45, 25555-25566.	3.8	8
48564	An effective method to screen carbon (boron, nitrogen) based two-dimensional hydrogen storage materials. International Journal of Hydrogen Energy, 2020, 45, 25054-25064.	3.8	13
48565	Probing into the global structural prediction, physical and electronic properties of A-X (AÂ= Ca, Sr, Ba;) Tj ETQq0 0 0 rgBT /Overlock 10 T	2.8	5
48566	Oxide-catalyzed self- and cross-condensation of cycloketones. Kinetically relevant steps that determine product distribution. Journal of Catalysis, 2020, 391, 163-174.	3.1	9
48567	Electronic structures, magnetic properties and dielectric properties of Fe3Si@SiO2 core-shell structure from first-principles study. Materials Chemistry and Physics, 2020, 254, 123282.	2.0	6
48568	Formation, evolution and characteristics of copper sulfide nanoparticles in the reactions of aqueous cupric and sulfide ions. Materials Chemistry and Physics, 2020, 255, 123600.	2.0	14
48569	Modeling thermodynamic stability of morphologies and surfaces of YF3. Surface Science, 2020, 700, 121674.	0.8	3
48570	Band Gap Engineering in NaBiO₃Â·2H₂O/NaBiO₃Â·xH₂O Heterostructures for High Photoelectronic Response. Journal of Physical Chemistry C, 2020, 124, 16271-16277.	1.5	16
48571	Pseudogap and Weak Multifractality in 2D Disordered Mott Charge-Density-Wave Insulator. Nano Letters, 2020, 20, 6299-6305.	4.5	5
48572	Local Strain and Polarization Mapping in Ferrielectric Materials. ACS Applied Materials & Interfaces, 2020, 12, 38546-38553.	4.0	14
48573	Pseudo-2-Fold Surface of the Al13Co4 Catalyst: Structure, Stability, and Hydrogen Adsorption. ACS Applied Materials & Interfaces, 2020, 12, 39787-39797.	4.0	5
48574	Highly Efficient Deoxydehydration and Hydrodeoxygenation on MoS₂-Supported Transition-Metal Atoms through a Câ€“H Activation Mechanism. ACS Catalysis, 2020, 10, 11346-11355.	5.5	10

#	Article	IF	Citations
48575	Predicted stable Li₅P₂ and Li₄P at ambient pressure: novel high-performance anodes for lithium-ion batteries. Physical Chemistry Chemical Physics, 2020, 22, 19172-19177.	1.3	4
48576	First principles rates for surface chemistry employing exact transition state theory: application to recombinative desorption of hydrogen from Cu(111). Physical Chemistry Chemical Physics, 2020, 22, 17532-17539.	1.3	10
48577	Why do RuO₂ electrodes catalyze electrochemical CO₂ reduction to methanol rather than methane or perhaps neither of those?. Chemical Science, 2020, 11, 9542-9553.	3.7	17
48578	Optical properties enhancement of buckled Bismuthene in mid-infrared region: a theoretical first-principle study. Molecular Simulation, 2020, 46, 1004-1010.	0.9	4
48579	Ab initio methodology for magnetic exchange parameters: Generic four-state energy mapping onto a Heisenberg spin Hamiltonian. Physical Review B, 2020, 102, .	1.1	24
48580	High-temperature conventional superconductivity in the boron-carbon system: Material trends. Physical Review B, 2020, 102, .	1.1	16
48581	Giant, unconventional anomalous Hall effect in the metallic frustrated magnet candidate, KV ₃ Sb ₅. Science Advances, 2020, 6, eabb6003.	4.7	295
48582	SnxPy Monolayers: a New Type of Two-Dimensional Materials with High Stability, Carrier Mobility, and Magnetic Properties. Nanoscale Research Letters, 2020, 15, 155.	3.1	3
48583	Firstâ€principles investigation of the structure, mechanical and hydrogen adsorption behavior of <scp>NiPt</scp> nanoparticle. International Journal of Energy Research, 2020, 44, 10970-10981.	2.2	23
48584	Oxygen Evolution and Reduction on Fe-doped NiOOH: Influence of Solvent, Dopant Position and Reaction Mechanism. Topics in Catalysis, 2020, 63, 833-845.	1.3	19
48585	Understanding the structural evolution of Au/WO2.7 compounds in hydrogen atmosphere by atomic scale in situ environmental TEM. Nano Research, 2020, 13, 3019-3024.	5.8	13
48586	Effects of Sulfur Doping on Generalized Stacking Fault Energy of Indium Phosphide. Electronic Materials Letters, 2020, 16, 506-511.	1.0	3
48587	Improved thermal stability and fast phase change speed of Y-doped Sb7Se3 thin film for phase change memory applications. Applied Surface Science, 2020, 532, 147370.	3.1	13
48588	Critical evaluation and thermodynamic modeling of the Feâ€“P and Feâ€“Câ€“P system. Calphad: Computer Coupling of Phase Diagrams and Thermochemistry, 2020, 70, 101795.	0.7	6
48589	Raman evidence for the successful synthesis of diamane. Carbon, 2020, 169, 129-133.	5.4	49
48590	Synergistic electron doping and ion conductive phase incorporating of SrCoO3- as desirable cathode materials for intermediate-temperature solid oxide fuel cells. Ceramics International, 2020, 46, 28332-28341.	2.3	6
48591	Structural response of alkali metal borates at Fe2O3 sliding interface: The effect of alkali cations. Computational Materials Science, 2020, 184, 109930.	1.4	4
48592	A first principle based study on the mechanical and thermal properties of UO2: Effect of La and Dy fission product concentrations. Computational Materials Science, 2020, 185, 109933.	1.4	8

#	Article	IF	Citations
48593	A first-principles study on the hydrogen trap characteristics of coherent nano-precipitates in Î±-Fe. International Journal of Hydrogen Energy, 2020, 45, 27941-27949.	3.8	39
48594	Effect of strain on the reactivity of graphene films. Journal of Catalysis, 2020, 390, 67-71.	3.1	12
48595	Magnetic behavior of transition metal solutes in<mml:math xmlns:mml="http://www.w3.org/1998/Math/MathML" altimg="si3.svg"><mml:mrow><mml:mi>Î±</mml:mi></mml:mrow></mml:math>-iron: A classification. Journal of Magnetism and Magnetic Materials, 2020, 513, 167223.	1.0	3
48596	A DFT study on the relationship between local microstructure and oxygen reduction reaction activity over Fe-N4 graphene. Materials Today Communications, 2020, 25, 101524.	0.9	4
48597	Multiferroic properties of three-layer Aurivillius compound Bi4TiFeNbO12: A first-principles and experimental study. Solid State Communications, 2020, 320, 114028.	0.9	3
48598	Electronic properties, anisotropic elasticity, theoretical strengths, and lattice vibrational mode of orthorhombic YSi. Solid State Communications, 2020, 321, 114029.	0.9	4
48599	PdSSe: Two-dimensional pentagonal Janus structures with strong visible light absorption for photovoltaic and photocatalytic applications. Vacuum, 2020, 181, 109649.	1.6	13
48600	Chemical Trends in the Lattice Thermal Conductivity of Li(Ni, Mn, Co)O₂ (NMC) Battery Cathodes. Chemistry of Materials, 2020, 32, 7542-7550.	3.2	28
48601	Calculation of the Thermal Neutron Scattering Cross-Section of Solids Using OCLIMAX. Journal of Chemical Theory and Computation, 2020, 16, 5212-5217.	2.3	14
48602	Flexible Cation Distribution for Stabilizing a Spinel Surface. Journal of Physical Chemistry C, 2020, 124, 16431-16438.	1.5	10
48603	Prediction of Optimal Synthesis Conditions for the Formation of Ordered Double-Transition-Metal MXenes (o-MXenes). Journal of Physical Chemistry C, 2020, 124, 18797-18804.	1.5	11
48604	Tackling the Inertness of CO2: Facile Activation and Electroreduction on the Metal-Free SiN4C4 Monolayer Sheet. Journal of Physical Chemistry C, 2020, 124, 18660-18669.	1.5	8
48605	Monolayer Doping of Germanium with Arsenic: A New Chemical Route to Achieve Optimal Dopant Activation. Langmuir, 2020, 36, 9993-10002.	1.6	7
48606	Understanding Disorder in 2D Materials: The Case of Carbon Doping of Silicene. Nano Letters, 2020, 20, 6336-6343.	4.5	8
48607	First-Principles Calculations on the Adsorption Behavior of Amino Acids on a Titanium Carbide MXene. ACS Applied Bio Materials, 2020, 3, 5913-5921.	2.3	39
48608	SnO₂-Modified Two-Dimensional CuO for Enhanced Electrochemical Reduction of CO₂ to C₂H₄. ACS Applied Materials & Interfaces, 2020, 12, 36128-36136.	4.0	50
48609	Intra-Crystalline Mesoporous Zeolite [Al,Zr]-Y for Catalytic Cracking. ACS Applied Nano Materials, 2020, 3, 9293-9302.	2.4	12
48610	First-Principles Analysis of Coverage, Ensemble, and Solvation Effects on Selectivity Trends in NO Electroreduction on Pt₃Sn Alloys. ACS Catalysis, 2020, 10, 9320-9327.	5.5	27

#	Article	IF	Citations
48611	Predicting the Activity and Selectivity of Bimetallic Metal Catalysts for Ethanol Reforming using Machine Learning. ACS Catalysis, 2020, 10, 9438-9444.	5.5	71
48612	Sharp Increase in Catalytic Selectivity in Acetylene Semihydrogenation on Pd Achieved by a Machine Learning Simulation-Guided Experiment. ACS Catalysis, 2020, 10, 9694-9705.	5.5	30
48613	A Full Solar Light Spectrum Responsive B@ZrO₂â€“OV Photocatalyst: A Synergistic Strategy for Visible-to-NIR Photon Harvesting. ACS Sustainable Chemistry and Engineering, 2020, 8, 13039-13047.	3.2	21
48614	Unique phonon modes of a CH3NH3PbBr3 hybrid perovskite film without the influence of defect structures: an attempt toward a novel THz-based application. NPG Asia Materials, 2020, 12, .	3.8	20
48615	An improved symmetry-based approach to reciprocal space path selection in band structure calculations. Npj Computational Materials, 2020, 6, .	3.5	33
48616	A new class of lightweight, stainless steels with ultra-high strength and large ductility. Scientific Reports, 2020, 10, 12140.	1.6	46
48617	Bulk (in)stability as a possible source of surface reconstruction. Physical Chemistry Chemical Physics, 2020, 22, 19249-19253.	1.3	6
48618	Coupling of triporosity and strong Auâ€“Li interaction to enable dendrite-free lithium plating/stripping for long-life lithium metal anodes. Journal of Materials Chemistry A, 2020, 8, 18094-18105.	5.2	56
48619	Substrate mediated electronic and excitonic reconstruction in a MoS₂ monolayer. Journal of Materials Chemistry C, 2020, 8, 11778-11785.	2.7	9
48620	The first-principles study of nHâ€“V_{Sn} complex: impurity effects on p-type SnO monolayer. Physical Chemistry Chemical Physics, 2020, 22, 19275-19281.	1.3	3
48621	Breaking the scaling relationship via dual metal doping in a cobalt spinel for the OER: a computational prediction. Physical Chemistry Chemical Physics, 2020, 22, 18672-18680.	1.3	5
48622	Novel ultra-thin two-dimensional structures of strontium chloride. Journal of Materials Chemistry C, 2020, 8, 12527-12532.	2.7	2
48623	Ab initio quantum dynamics of charge carriers in graphitic carbon nitride nanosheets. Journal of Chemical Physics, 2020, 153, 054701.	1.2	27
48624	Defect, transport, and dopant properties of andradite garnet Ca3Fe2Si3O12. AIP Advances, 2020, 10, .	0.6	6
48625	Defect formation in a graphene overlayer on ruthenium under high pressure. Physical Review B, 2020, 102, .	1.1	0
48626	Temperature-Programmed Growth of Quasi-Free-Standing N-Doped Graphene Single Crystals from Acetonitrile Molecules. JETP Letters, 2020, 111, 591-597.	0.4	0
48627	Strain Dependence of Energetics and Kinetics of Vacancy in Tungsten. Materials, 2020, 13, 3375.	1.3	11
48628	Voltage Induced Molecular Motors Constitute the Smallest Selfâ€Assembled Molecular Electronic Counter. Advanced Materials Interfaces, 2020, 7, 2000383.	1.9	0

#	Article	IF	Citations
48629	qvasp: A flexible toolkit for VASP users in materials simulations. Computer Physics Communications, 2020, 257, 107535.	3.0	88
48630	Anomalous layer thickness dependent thermal conductivity of Td-WTe2 through first-principles calculation. Physics Letters, Section A: General, Atomic and Solid State Physics, 2020, 384, 126751.	0.9	8
48631	The impact of anion elements on the engineering of the electronic and optical characteristics of the two dimensional monolayer janus MoSSe for nanoelectronic device applications. Results in Physics, 2020, 18, 103284.	2.0	7
48632	Highly Efficient Lead-Free (Bi,Ce)-Codoped Cs₂Ag_{0.4}Na_{0.6}InCl₆ Double Perovskites for White Light-Emitting Diodes. Chemistry of Materials, 2020, 32, 7814-7821.	3.2	108
48633	Anisotropic Electron Transport Limits Performance of Bi₂WO₆ Photoanodes. Journal of Physical Chemistry C, 2020, 124, 18859-18867.	1.5	9
48634	Fast Method for Calculating Spatially Resolved Heterogeneous Electron-Transfer Kinetics and Its Application to Graphene with Defects. Journal of Physical Chemistry C, 2020, 124, 18147-18155.	1.5	10
48635	Electronic and Magneto-Optical Properties of the Molybdenum-Vacancy Center in Zirconia and Its Qubit Applications. Journal of Physical Chemistry C, 2020, 124, 18707-18713.	1.5	7
48636	Layered Perovskite (CH₃NH₃)₂Pb(SCN)₂I₂ Single Crystals: Phase Transition and Moisture Stability. ACS Applied Materials & Interfaces, 2020, 12, 37713-37721.	4.0	20
48637	Exceptionally High Average Power Factor and Thermoelectric Figure of Merit in n-type PbSe by the Dual Incorporation of Cu and Te. Journal of the American Chemical Society, 2020, 142, 15172-15186.	6.6	72
48638	High-throughput gas separation by flexible metalâ€“organic frameworks with fast gating and thermal management capabilities. Nature Communications, 2020, 11, 3867.	5.8	99
48639	Large magnetocaloric effect in gadolinium borotungstate Gd₃BWO₉. Journal of Materials Chemistry C, 2020, 8, 11866-11873.	2.7	29
48640	Noncollinear frustrated antiferromagnetic Mn3P monolayer and its tunability via a spin degree of freedom. Journal of Materials Chemistry C, 2020, 8, 11369-11375.	2.7	3
48641	Transition from an indirect type-I to a direct type-II bandgap in Î±-tellurene/Ca(OH)₂ heterostructures with excellent optical properties. Journal of Materials Chemistry C, 2020, 8, 12291-12301.	2.7	10
48642	Mixed Ionicâ€“Electronic Conductor of Perovskite Li_xLa_yMO_{3â^'}_{Î´} toward Carbonâ€Free Cathode for Reversible Lithiumâ€“Air Batteries. Advanced Energy Materials, 2020, 10, 2001767.	10.2	32
48643	First principles study on optoelectronic properties of energetically stable Si/InS van der Waals heterobilayers. Journal of Materials Science, 2020, 55, 15199-15212.	1.7	17
48644	Electrocatalytic N2 reduction to NH3 with high Faradaic efficiency enabled by vanadium phosphide nanoparticle on V foil. Nano Research, 2020, 13, 2967-2972.	5.8	45
48645	Quantum anomalous Hall insulator phases in Fe-doped GaBi honeycomb. Chinese Journal of Physics, 2020, 67, 246-252.	2.0	9
48646	Cu2Zn(Si,Ge)Se4 quaternary semiconductors as potential photovoltaic materials. Chemical Physics Letters, 2020, 756, 137820.	1.2	3

#	Article	IF	Citations
48647	Borophene-like boron subunits-inserted molybdenum framework of MoB2 enables stable and quick-acting Li2S6-based lithium-sulfur batteries. Energy Storage Materials, 2020, 32, 216-224.	9.5	42
48648	2D intrinsically defective RuO2/Graphene heterostructures as All-pH efficient oxygen evolving electrocatalysts with unprecedented activity. Nano Energy, 2020, 78, 105185.	8.2	58
48649	Flat-band splitting induced tunable magnetism in defective CrI3 monolayer. Solid State Communications, 2020, 321, 114037.	0.9	9
48650	Phase-Selective Solution Synthesis of Perovskite-Related Cesium Cadmium Chloride Nanoparticles. Inorganic Chemistry, 2020, 59, 11688-11694.	1.9	30
48651	Ab Initio Calculations of Free Energy of Activation at Multiple Electronic Structure Levels Made Affordable: An Effective Combination of Perturbation Theory and Machine Learning. Journal of Chemical Theory and Computation, 2020, 16, 6049-6060.	2.3	28
48652	Rethinking Electronic and Geometric Structures of Real Hydrodesulfurization Catalysts by In Situ Photon-In/Photon-Out Spectroscopy. Journal of Physical Chemistry C, 2020, 124, 17586-17598.	1.5	7
48653	Identification of the Active Sites in the Dehydrogenation of Methanol on Pt/Al₂O₃ Catalysts. Journal of Physical Chemistry C, 2020, 124, 19015-19023.	1.5	15
48654	Unsymmetrical Squaraine Dyes for Dye-Sensitized Solar Cells: Position of the Anchoring Group Controls the Orientation and Self-Assembly of Sensitizers on the TiO₂ Surface and Modulates Its Flat Band Potential. Journal of Physical Chemistry C, 2020, 124, 18436-18451.	1.5	14
48655	Deciphering the Growth Mechanism of Self-Assembled Nanowires on Pt-Deposited Ge(001) via Scanning Tunneling Microscopy and Density Functional Theory Calculations. Journal of Physical Chemistry C, 2020, 124, 18165-18172.	1.5	2
48656	Intramolecular Band Alignment and Spinâ€“Orbit Coupling in Two-Dimensional Halide Perovskites. Journal of Physical Chemistry Letters, 2020, 11, 6982-6989.	2.1	24
48657	Revealing the Charge Storage Mechanism of Nickel Oxide Electrochromic Supercapacitors. ACS Applied Materials & Interfaces, 2020, 12, 39098-39107.	4.0	82
48658	Magnetotransport Mechanism of Individual Nanostructures via Direct Magnetoresistance Measurement in situ SEM. ACS Applied Materials & Interfaces, 2020, 12, 39798-39806.	4.0	1
48659	Exploring the Reaction Mechanisms of Furfural Hydrodeoxygenation on a CuNiCu(111) Bimetallic Catalyst Surface from Computation. ACS Omega, 2020, 5, 18040-18049.	1.6	7
48660	Unzipping of black phosphorus to form zigzag-phosphorene nanobelts. Nature Communications, 2020, 11, 3917.	5.8	55
48661	Dielectric ordering of water molecules arranged in a dipolar lattice. Nature Communications, 2020, 11, 3927.	5.8	33
48662	Tunable spin textures in polar antiferromagnetic hybrid organicâ€“inorganic perovskites by electric and magnetic fields. Npj Computational Materials, 2020, 6, .	3.5	22
48663	Facet engineering accelerates spillover hydrogenation on highly diluted metal nanocatalysts. Nature Nanotechnology, 2020, 15, 848-853.	15.6	210
48664	Quantum distance and anomalous Landau levels of flat bands. Nature, 2020, 584, 59-63.	13.7	76

#	Article	IF	Citations
48665	Large and tunable negative thermal expansion induced by a synergistic effect in M₂^{II}[M^{IV}(CN)₈] Prussian blue analogues. Physical Chemistry Chemical Physics, 2020, 22, 18655-18662.	1.3	10
48666	Composition-dependent chemical and structural stabilities of mixed tinâ€“lead inorganic halide perovskites. Physical Chemistry Chemical Physics, 2020, 22, 19787-19794.	1.3	4
48667	Molecular functionalization of all-inorganic perovskite CsPbBr₃thin films. Journal of Materials Chemistry C, 2020, 8, 12587-12598.	2.7	3
48668	Controlling spin-polarized carriers at the <mml:math xmlns:mml="http://www.w3.org/1998/Math/MathML"><mml:mrow><mml:msub><mml:mi>SrTiO</mml:mi><mml:mn>3</mml:mn></ interface via the ferroelectric field effect. Physical Review B, 2020, 102, .	3.7	5
48669	Giant isotope effect on phonon dispersion and thermal conductivity in methylammonium lead iodide. Science Advances, 2020, 6, eaaz1842.	4.7	17
48670	Quantum Simulations of Preferable H₂O Dissociation Pathway on the Ru-Alloyed Pt(111) Surface Based on Density Functional Theory. Key Engineering Materials, 0, 840, 495-500.	0.4	3
48671	First Principle Study of Na and P Co-Doped Heptazine Based Monolayer g-C₃N₄. Materials Science Forum, 0, 978, 369-376.	0.3	5
48672	Catalytic decomposition of toxic phosphine gas on the developed nickel ferrite nanocrystals supported by Halloysite nanotubes. Applied Surface Science, 2020, 530, 147264.	3.1	8
48673	A multi-scale simulation of syngas combustion reactions by Ni-based oxygen carriers for chemical looping combustion. Applied Surface Science, 2020, 531, 147277.	3.1	19
48674	Enhancement of the quantum capacitances of group-14 elemental two-dimensional materials by Ti-doping: A first principles study. Applied Surface Science, 2020, 530, 147301.	3.1	8
48675	DFT thermodynamic study of the adsorption of CO2 and H2O on W3Ox/M(1 1 1) (xâ€¯=â€¯6 or 9 and Mâ€¯=â€¯Cu, Ag) Tj ETQq0 0 0 rg	3.1	11
48676	Fluorescence and photocatalytic activity of metal-free nitrogen-doped carbon quantum dots with varying nitrogen contents. Applied Surface Science, 2020, 531, 147344.	3.1	41
48677	Mechanism of CO2 conversion into methanol and methane at the edge of graphitic carbon nitride sheet: A first-principle study. Carbon, 2020, 169, 73-81.	5.4	9
48678	Zn0.1Ca0.1Sr0.4Ba0.4ZrO3: A non-equimolar multicomponent perovskite ceramic with low thermal conductivity. Journal of the European Ceramic Society, 2020, 40, 6272-6277.	2.8	46
48679	Borophene vs. graphene interfaces: Tuning the electric double layer in ionic liquids. Journal of Molecular Liquids, 2020, 303, 112647.	2.3	8
48680	Theoretical study on the interactions between ibrutinib and gold nanoparticles for being used as drug delivery in the chronic lymphocytic leukemia. Journal of Molecular Liquids, 2020, 316, 113878.	2.3	4
48681	Electron-deficient titanium single-atom electrocatalyst for stable and efficient hydrogen production. Nano Energy, 2020, 78, 105151.	8.2	16
48682	Oxygen vacancy engineering with flame heating approach towards enhanced photoelectrochemical water oxidation on WO3 photoanode. Nano Energy, 2020, 77, 105190.	8.2	65

#	Article	IF	Citations
48683	First-principles study of C3N nanoribbons as anode materials for Li-ion batteries. Physics Letters, Section A: General, Atomic and Solid State Physics, 2020, 384, 126741.	0.9	7
48684	Pinning effect of reactive elements on structural stability and adhesive strength of environmental sulfur segregation on Al2O3/NiAl interface. Scripta Materialia, 2020, 188, 174-178.	2.6	6
48685	Multifold enhancement in water dissociation with Ag/Ni bimetallic alloy surfaces. Surface Science, 2020, 701, 121695.	0.8	11
48686	Crystal Structure Prediction Approach to Explore the Iron Carbide Phases: Novel Crystal Structures and Unexpected Magnetic Properties. Journal of Physical Chemistry C, 2020, 124, 17244-17254.	1.5	8
48687	Computable Bulk and Interfacial Electronic Structure Features as Proxies for Dielectric Breakdown of Polymers. ACS Applied Materials & Interfaces, 2020, 12, 37182-37187.	4.0	21
48688	Atomically Dispersed Ru Catalyst for Low-Temperature Nitrogen Activation to Ammonia via an Associative Mechanism. ACS Catalysis, 2020, 10, 9504-9514.	5.5	47
48689	Synergetic role of charge transfer and strain engineering in improving the catalysis of Pd single-atom-thick motifs stabilized on a defect-free MoS₂/Ag(Au)(111) heterostructure. Journal of Materials Chemistry A, 2020, 8, 17238-17247.	5.2	13
48690	Transition metal-tetracyanoquinodimethane monolayers as single-atom catalysts for the electrocatalytic nitrogen reduction reaction. Materials Advances, 2020, 1, 1285-1292.	2.6	20
48691	First-principles calculations of the electronic structure, chemical bonding, and thermodynamic properties of USiO4. AIP Advances, 2020, 10, .	0.6	6
48692	Investigation on properties of FeNi intermetallics under pressure by First-principles. Journal of Physics: Conference Series, 2020, 1507, 082026.	0.3	3
48693	Aliovalent Doping and Surface Grafting Enable Efficient and Stable Leadâ€Free Blueâ€Emitting Perovskite Derivative. Advanced Optical Materials, 2020, 8, 2000779.	3.6	68
48694	Nonsymmorphic nodal-line metals in the two-dimensional rare earth monochalcogenides MX (Mâ€‰=â€‰Sc, Y;) Tj ETQq1 1 0.7843	1.7	7
48695	Selective hydrogenation of acetylene on graphene-supported non-noble metal single-atom catalysts. Science China Materials, 2020, 63, 1741-1749.	3.5	28
48696	Structures and reactivities of the CeO2/Pt(111) reverse catalyst: A DFT+U study. Chinese Journal of Catalysis, 2020, 41, 1360-1368.	6.9	9
48697	Spinel-Type nitride compounds with improved features as solar cell absorbers. Acta Materialia, 2020, 197, 316-329.	3.8	7
48698	Structural, electronic, and optical properties of pristine and bilayers of hexagonal III-V binary compounds and their hydrogenated counterparts. Applied Surface Science, 2020, 531, 147262.	3.1	13
48699	Molybdenum and sulfur incorporation as oxyanion substitutional impurities in calcium carbonate minerals: A computational investigation. Chemical Geology, 2020, 553, 119796.	1.4	8
48700	Partial core vaporization during Giant Impacts inferred from the entropy and the critical point of iron. Earth and Planetary Science Letters, 2020, 547, 116463.	1.8	7

#	Article	IF	Citations
48701	Effect of titanium on the precipitation behaviors of transmutation elements in tungsten-titanium alloys from first-principles calculations. Fusion Engineering and Design, 2020, 158, 111673.	1.0	4
48702	Computationally Driven Discovery of Layered Quinary Oxychalcogenides: Potential p-Type Transparent Conductors?. Matter, 2020, 3, 759-781.	5.0	15
48703	Novel Mechanistic Insights into Methane Activation over Fe and Cu Active Sites in Zeolites: A Comparative DFT Study Using Meta-GGA Functionals. Journal of Physical Chemistry C, 2020, 124, 18112-18125.	1.5	24
48704	Fine Control of the Chemistry of Nitrogen Doping in TiO₂: A Joint Experimental and Theoretical Study. Journal of Physical Chemistry C, 2020, 124, 17401-17412.	1.5	17
48705	Adsorption of Aspartic Acid on Ni{100}: A Combined Experimental and Theoretical Study. Langmuir, 2020, 36, 9399-9411.	1.6	5
48706	Electronic and Optical Modulation of Metal-Doped Hybrid Organicâ€“Inorganic Perovskites Crystals by Post-Treatment Control. ACS Applied Energy Materials, 2020, 3, 7500-7511.	2.5	10
48707	Unique Behavior of Halide Double Perovskites with Mixed Halogens. ACS Applied Materials & Interfaces, 2020, 12, 37100-37107.	4.0	19
48708	The Vital Role of Step-Edge Sites for Both CO Activation and Chain Growth on Cobalt Fischerâ€“Tropsch Catalysts Revealed through First-Principles-Based Microkinetic Modeling Including Lateral Interactions. ACS Catalysis, 2020, 10, 9376-9400.	5.5	37
48709	Direct hybridization gap from intersite and onsite electronic interactions in CeAg₂Ge₂. RSC Advances, 2020, 10, 24343-24351.	1.7	5
48710	Heavy Mn²⁺-doped near-infrared photon upconversion luminescence in fluoride RbZnF₃:Yb³⁺,Mn²⁺ guided by dopant distribution simulation. Journal of Materials Chemistry C, 2020, 8, 12164-12172.	2.7	14
48711	In situ growth of Fe and Nb co-doped Î²-Ni(OH)₂ nanosheet arrays on nickel foam for an efficient oxygen evolution reaction. Inorganic Chemistry Frontiers, 2020, 7, 3465-3474.	3.0	16
48712	Electrical detection of ferroelectriclike metals through the nonlinear Hall effect. Physical Review B, 2020, 102, .	1.1	22
48713	Two-dimensional chromium pnictides <mml:math xmlns:mml="http://www.w3.org/1998/Math/MathML"><mml:mi>Cr</mml:mi><mml:mi>X</mml:mi><mml:mo>Â</mml:mo><mml:mo>(: Half-metallic ferromagnets with high Curie temperature. Physical Review B, 2020, 102, .	1.1	44
48714	Giant photogalvanic effect and second-harmonic generation in magnetic axion insulators. Physical Review B, 2020, 102, .	1.1	39
48715	Interlayer charge transfer in tin disulphide: Orbital anisotropy and temporal aspects. Physical Review B, 2020, 102, .	1.1	6
48716	Adsorption of Iron Phthalocyanine on a Au(111) Surface. Russian Journal of Physical Chemistry A, 2020, 94, 1704-1707.	0.1	2
48717	Data sets of predicted stable and meta-stable crystalline phase structural of NB-N system under pressure. Data in Brief, 2020, 32, 106054.	0.5	0
48718	Phase diagram, shock equation of states, and elasticity of metal ruthenium under high pressure. Physica B: Condensed Matter, 2020, 598, 412434.	1.3	2

#	Article	IF	Citations
48719	Metastable Rhombohedral Phase Transition of Semiconducting Indium Oxide Controlled by Thermal Atomic Layer Deposition. Chemistry of Materials, 2020, 32, 7397-7403.	3.2	33
48720	Electronic Structure Modulation of 2D Colloidal CdSe Nanoplatelets by Au25 Clusters for High-Performance Photodetectors. Journal of Physical Chemistry C, 2020, 124, 19793-19801.	1.5	20
48721	Collective Spin Manipulation in Antiferroelastic Spin-Crossover Metallo-Supramolecular Chains. ACS Nano, 2020, 14, 11283-11293.	7.3	24
48722	Metal-Specific Reactivity in Single-Atom Catalysts: CO Oxidation on 4d and 5d Transition Metals Atomically Dispersed on MgO. Journal of the American Chemical Society, 2020, 142, 14890-14902.	6.6	75
48723	Adsorption and activation of molecular oxygen over atomic copper(I/II) site on ceria. Nature Communications, 2020, 11, 4008.	5.8	95
48724	Graphitic phosphorus coordinated single Fe atoms for hydrogenative transformations. Nature Communications, 2020, 11, 4074.	5.8	122
48725	Lattice oxygen activation enabled by high-valence metal sites for enhanced water oxidation. Nature Communications, 2020, 11, 4066.	5.8	337
48726	Stability of ferroelectric and antiferroelectric hafniumâ€“zirconium oxide thin films. Journal of Applied Physics, 2020, 128, .	1.1	19
48727	Global optimization of copper clusters at the ZnO(101Â¯0) surface using a DFT-based neural network potential and genetic algorithms. Journal of Chemical Physics, 2020, 153, 054704.	1.2	33
48728	Lattice and spin excitations of <mml:math xmlns:mml="http://www.w3.org/1998/Math/MathML"><mml:mrow><mml:mi mathvariant="normal">Y</mml:mi><mml:mi>Fe</mml:mi><mml:msub><mml:mi mathvariant="normal">O</mml:mi><mml:mn>3</mml:mn></mml:msub></mml:mrow></mml:math> : A [illegible] Physical Review B, 2020, 102, .	1.1	6
48729	Stoichiometric and off-stoichiometric full Heusler <mml:math xmlns:mml="http://www.w3.org/1998/Math/MathML"><mml:mrow><mml:msub><mml:mi>Fe</mml:mi><mml:mn>2</mml:mn></mml: mathvariant="normal">V</mml:mi><mml:mrow><mml:mn>1</mml:mn><mml:mo>â^’</mml:mo><mml:mi>x</mml:mi></mml:mrow></ mathvariant="normal">W</mml:mi><mml:mi>x</mml:mi></mml:msub><mml:mi>Al</mml:mi></mml:mrow></mml:math> [illegible] thermoelectric systems. Physical Review B, 2020, 102, .	1.1	17
48730	<mml:math xmlns:mml="http://www.w3.org/1998/Math/MathML" display="inline"><mml:msup><mml:mi>d</mml:mi><mml:mn>9</mml:mn></mml:msup></mml:math> Nickelate Superconductor <mml:math xmlns:mml="http://www.w3.org/1998/Math/MathML" display="inline"><mml:mrow><mml:mo		

#	Article	IF	Citations
48737	Descriptors for Hydrogen Evolution on Single Atom Catalysts in Nitrogen-Doped Graphene. Journal of Physical Chemistry C, 2020, 124, 19571-19578.	1.5	75
48738	Influence of Strain on Acidâ€“Basic Properties of Oxide Surfaces. Journal of Physical Chemistry C, 2020, 124, 19126-19135.	1.5	7
48739	Insights into Water Permeation through hBN Nanocapillaries by Ab Initio Machine Learning Molecular Dynamics Simulations. Journal of Physical Chemistry Letters, 2020, 11, 7363-7370.	2.1	33
48740	Symmetry Breaking Induced Anisotropic Carrier Transport and Remarkable Thermoelectric Performance in Mixed Halide Perovskites CsPb(I_{1â€“x}Br_x)₃. ACS Applied Materials & Interfaces, 2020, 12, 40453-40464.	4.0	40
48741	Ternary Compounds Cu₃RTe₃ (R = Y, Sm, and Dy): A Family of New Thermoelectric Materials with Trigonal Structures. ACS Applied Materials & Interfaces, 2020, 12, 40486-40494.	4.0	3
48742	Superb Hydrogen Evolution by a Pt Nanoparticle-Decorated Ni₃S₂ Microrod Array. ACS Applied Materials & Interfaces, 2020, 12, 39163-39169.	4.0	41
48743	Sulfur-Doped Titanium Carbide MXenes for Room-Temperature Gas Sensing. ACS Sensors, 2020, 5, 2915-2924.	4.0	92
48744	Ultrafast photoinduced band splitting and carrier dynamics in chiral tellurium nanosheets. Nature Communications, 2020, 11, 3991.	5.8	39
48745	Using statistical learning to predict interactions between single metal atoms and modified MgO(100) supports. Npj Computational Materials, 2020, 6, .	3.5	16
48746	Stable and selective electrosynthesis of hydrogen peroxide and the electro-Fenton process on CoSe₂ polymorph catalysts. Energy and Environmental Science, 2020, 13, 4189-4203.	15.6	134
48747	Physical and optoelectronic features of lead-free A₂AgRhBr₆ (A = Cs, Rb, K,) Tj ETQq0 0 0 rgBT /Overlock 10 Tf 12968-12983.	2.7	19
48748	Two-dimensional BP/ Î² -AsP van der Waals heterostructures as promising photocatalyst for water splitting. Applied Physics Letters, 2020, 117, .	1.5	47
48749	Encapsulation of volatile fission products in a two-dimensional dicalcium nitride electride. Journal of Applied Physics, 2020, 128, 045112.	1.1	3
48750	Large-gap topological insulators in functionalized ordered double transition metal carbide MXenes. Physical Review B, 2020, 102, .	1.1	24
48751	Boron kagome-layer induced intrinsic superconductivity in a <mml:math xmlns:mml="http://www.w3.org/1998/Math/MathML"><mml:msub><mml:mi>MnB</mml:mi><mml:mn>3</mml:mn></mml:msub></mml monolayer with a high critical temperature. Physical Review B, 2020, 102, .	1.1	23
48752	Tunable interlayer magnetism and band topology in van der Waals heterostructures of <mml:math xmlns:mml="http://www.w3.org/1998/Math/MathML"><mml:mrow><mml:mi>Mn</mml:mi><mml:msub><mml:mi>Bi</mml:mi><mml:mn -family materials. Physical Review B, 2020, 102, .	1.1	33
48753	Origin of the monoclinic distortion and its impact on the electronic properties in <mml:math xmlns:mml="http://www.w3.org/1998/Math/MathML"><mml:msub><mml:mi>KO</mml:mi><mml:mn>2</mml:mn></mml:msub></mml Physical Review B, 2020, 102, .	1.1	2
48754	Controlling magnetic order, magnetic anisotropy, and band topology in the semimetals <mml:math xmlns:mml="http://www.w3.org/1998/Math/MathML"><mml:mrow><mml:mi>Sr</mml:mi><mml:mrow><mml:mo>(</mml:mo> and <mml:math xmlns:mml="http://www.w3. Physical Review B, 2020, 102, .	1.1	8

#	Article	IF	Citations
48755	An investigation of hydrogen embrittlement of 12Cr2Mo1R(H) steel by slow strain rate tests and first-principles calculation. Anti-Corrosion Methods and Materials, 2020, 67, 545-555.	0.6	0
48756	Atomically dispersed Ni in cadmium-zinc sulfide quantum dots for high-performance visible-light photocatalytic hydrogen production. Science Advances, 2020, 6, eaaz8447.	4.7	83
48757	Native Point Defects in Monolayer Hexagonal Boron Phosphide from First Principles. Journal of Electronic Materials, 2020, 49, 5782-5789.	1.0	9
48758	Surface dangling bonds dependent magnetic properties in Mn-doped GaAs nanowires. Physics Letters, Section A: General, Atomic and Solid State Physics, 2020, 384, 126815.	0.9	1
48759	Unveiling the Active Site of Metal-Free Nitrogen-doped Carbon for Electrocatalytic Carbon Dioxide Reduction. Cell Reports Physical Science, 2020, 1, 100145.	2.8	53
48760	Tunable Optical Transition in 2H-MoS₂ via Direct Electrochemical Engineering of Vacancy Defects and Surface Sâ€“C Bonds. ACS Applied Materials & Interfaces, 2020, 12, 40870-40878.	4.0	19
48761	Understanding the Improved Activity of Dendritic Sn1Pb3 Alloy for the CO2 Electrochemical Reduction: A Computationalâ€“Experimental Investigation. ACS Catalysis, 2020, 10, 10726-10734.	5.5	11
48762	Tunable 3D/2D magnetism in the (MnBi2Te4)(Bi2Te3)m topological insulators family. Npj Quantum Materials, 2020, 5, .	1.8	138
48763	High mechanical strength and broad optical absorption in underexplored group IV nitride chalcogenides. Chemical Communications, 2020, 56, 10962-10965.	2.2	5
48764	Accepted Degradation of threading dislocations in InAlGaN xmlns:mml="http://www.w3.org/1998/Math/MathML" display="inline" overflow="scroll"><mml:mrow><mml:mrow><mml:mo stretchy="false">(</mml:mo><mml:mi>Al</mml:mi><mml:mo>,</mml:mo><mml:mi>Ga</mml:mi><mml:mo) Tj ET Q q 1 1 0.784314 rg BT mathvariant="normal">N</mml:mi><mml:mo>/</mml:mo><mml:mrow><mml:mi>Ga</mml:mi><mml:mi m	2.1	34
48765	Signatures of possible surface states in TaAs. Physical Review B, 2020, 102, .	1.1	9
48766	Atomic structure of <scp>Co_{92â^’x}B_xTa₈</scp> glassy alloys studied by ab initio molecular dynamics simulations. International Journal of Quantum Chemistry, 2020, 120, e26406.	1.0	1
48767	Searching for the rate determining step of the H2S reaction on Fe (110) surface. Applied Surface Science, 2020, 532, 147470.	3.1	13
48768	Metastable Al-Fe intermetallic stabilised by epitaxial relationship. Applied Surface Science, 2020, 533, 147492.	3.1	5
48769	Insights into ethanol electro-oxidation over solvated Pt(1 0 0): Origin of selectivity and kinetics revealed by DFT. Applied Surface Science, 2020, 533, 147505.	3.1	10
48770	Low thermal conductivity and good thermoelectric performance in mercury chalcogenides. Computational Materials Science, 2020, 185, 109960.	1.4	7
48771	Fingerprint of checkerboard antiferromagnetic order in FeSe monolayer due to magnetic-electric correlation. Materials Today, 2020, 41, 44-50.	8.3	3
48772	Finding Reaction Pathways and Transition States: r-ARTn and d-ARTn as an Efficient and Versatile Alternative to String Approaches. Journal of Chemical Theory and Computation, 2020, 16, 6726-6734.	2.3	21

#	Article	IF	Citations
48773	Electronic Structure Panorama of Halide Perovskites: Approximated DFT-1/2 Quasiparticle and Relativistic Corrections. Journal of Physical Chemistry C, 2020, 124, 18390-18400.	1.5	27
48774	Thermal Stability of Single-Crystalline IrO₂(110) Layers: Spectroscopic and Adsorption Studies. Journal of Physical Chemistry C, 2020, 124, 15324-15336.	1.5	22
48775	Site-Specific Product Selectivity of Stepped Pt Surfaces for Methane Dehydrogenation. Journal of Physical Chemistry C, 2020, 124, 19649-19654.	1.5	11
48776	Low-Temperature Removal of Dissociated Bromine by Silicon Atoms for an On-Surface Ullmann Reaction. Journal of Physical Chemistry C, 2020, 124, 19675-19680.	1.5	10
48777	New Pressure Stabilization Structure in Two-Dimensional PtSe₂. Journal of Physical Chemistry Letters, 2020, 11, 7342-7349.	2.1	15
48778	Transition metal-like carbocatalyst. Nature Communications, 2020, 11, 4091.	5.8	27
48779	Configurational thermodynamics of a 1/2ã€ˆ111ã€‰ screw dislocation core in Moâ€“W solid solutions using cluster expansion. Journal of Applied Physics, 2020, 128, .	1.1	3
48780	First-principle study of puckered arsenene MOSFET. Journal of Semiconductors, 2020, 41, 082006.	2.0	4
48781	The Electronic Structural and Elastic Properties of Mg23Al30 Intermediate Phase under High Pressure. Crystals, 2020, 10, 642.	1.0	4
48782	Leadâ€Free Cs₃Sb₂Br₉ Single Crystals for High Performance Narrowband Photodetector. Advanced Optical Materials, 2020, 8, 2001072.	3.6	46
48783	Structural Diversity and Trends in Properties of an Array of Hydrogen-Rich Ammonium Metal Borohydrides. Inorganic Chemistry, 2020, 59, 12733-12747.	1.9	16
48784	Interactions between Transition-Metal Surfaces and MoS₂ Monolayers: Implications for Hydrogen Evolution and CO₂ Reduction Reactions. Journal of Physical Chemistry C, 2020, 124, 20116-20124.	1.5	12
48785	The Role of Space Charge at Metal/Oxide Interfaces in Proton Ceramic Electrochemical Cells. Journal of Physical Chemistry C, 2020, 124, 20827-20833.	1.5	4
48786	Pressure-Dependent Intermediate Magnetic Phase in Thin Fe3GeTe2 Flakes. Journal of Physical Chemistry Letters, 2020, 11, 7313-7319.	2.1	18
48787	Magnetism, half-metallicity, and topological signatures in Fe_{2â€“x}V_xPO₅ (x = 0, 0.5, 1, 1.5, 2) materials: a potential class of advanced spintronic materials. Physical Chemistry Chemical Physics, 2020, 22, 20027-20036.	1.3	0
48788	Two-dimensional polar metal of a PbTe monolayer by electrostatic doping. Nanoscale Horizons, 2020, 5, 1400-1406.	4.1	16
48789	Double Atom Catalysts: Heteronuclear Transition Metal Dimer Anchored on Nitrogenâ€Doped Graphene as Superior Electrocatalyst for Nitrogen Reduction Reaction. Advanced Theory and Simulations, 2020, 3, 2000190.	1.3	26
48790	In Situ Conversion of Metalâ€“Organic Frameworks into VO₂â€“V₃S₄ Heterocatalyst Embedded Layered Porous Carbon as an â€œAllâ€inâ€Oneâ€•Host for Lithiumâ€“Sulfur Batteries. Small, 2020, 16, e2004806.	5.2	35

#	Article	IF	Citations
48791	A new carbon allotrope with C28 cage: T-C64. Chinese Journal of Physics, 2020, 68, 647-653.	2.0	5
48792	High thermoelectric performance of two-dimensional Î±-GeTe bilayer. Energy, 2020, 211, 118693.	4.5	9
48793	Single Crystal Growth and Structural Characterization of Theoretically Predicted Nanolaminates M2Al2C3, Where M = Sc and Er. Crystal Growth and Design, 2020, 20, 7640-7646.	1.4	3
48794	High Rate Transfer Mechanism of Lithium Ions in Lithiumâ€“Tin and Lithiumâ€“Indium Alloys for Lithium Batteries. Journal of Physical Chemistry C, 2020, 124, 24644-24652.	1.5	23
48795	Mesoporous-Carbon-Based Fully-Printable All-Inorganic Monoclinic CsPbBr₃ Perovskite Solar Cells with Ultrastability under High Temperature and High Humidity. Journal of Physical Chemistry Letters, 2020, 11, 9689-9695.	2.1	23
48796	Molecularly Engineered Strong Metal Oxideâ€“Support Interaction Enables Highly Efficient and Stable CO₂ Electroreduction. ACS Catalysis, 2020, 10, 13227-13235.	5.5	94
48797	Solid-phase hetero epitaxial growth of Î±-phase formamidinium perovskite. Nature Communications, 2020, 11, 5514.	5.8	71
48798	Mechanistic insight into H2-mediated Ni surface diffusion and deposition to form branched Ni nanocrystals: a theoretical study. Physical Chemistry Chemical Physics, 2020, 22, 23869-23877.	1.3	1
48799	Controllable magnetism driven by carrier confinement and ferroelectric polarization in a two-dimensional heterostructure. Journal of Materials Chemistry C, 2020, 8, 17342-17348.	2.7	7
48800	Coupled analysis to probe the effect of angular assignments on the secondary electron yield (SEY) from copper electrodes. Physics of Plasmas, 2020, 27, .	0.7	8
48801	Effects of Monovacancy and Divacancies on Hydrogen Solubility, Trapping and Diffusion Behaviors in fcc-Pd by First Principles. Materials, 2020, 13, 4876.	1.3	5
48802	Molecular Dynamics Simulations of Molten Magnesium Chloride Using Machineâ€Learningâ€Based Deep Potential. Advanced Theory and Simulations, 2020, 3, 2000180.	1.3	24
48803	Non-compact oxide-island growth induced by surface phase transition of the intermetallic NiAl during vacuum annealing. Acta Materialia, 2020, 201, 244-253.	3.8	5
48804	A new hydrous iron oxide phase stable at mid-mantle pressures. Earth and Planetary Science Letters, 2020, 550, 116551.	1.8	5
48805	Natural liquid organic hydrogen carrier with low dehydrogenation energy: A first principles study. International Journal of Hydrogen Energy, 2020, 45, 32089-32097.	3.8	11
48806	Effects of composition modulation on the type of band alignments for Pd2Se3/CsSnBr3 van der waals heterostructure: A transition from type I to type II. Journal of Power Sources, 2020, 478, 229078.	4.0	27
48807	Validation of defect association energy on modulating oxygen ionic conductivity in low temperature solid oxide fuel cell. Journal of Power Sources, 2020, 480, 229106.	4.0	10
48808	Herzbergâ€“Teller Effect on the Vibrationally Resolved Absorption Spectra of Single-Crystalline Pentacene at Finite Temperatures. Journal of Physical Chemistry A, 2020, 124, 9156-9165.	1.1	14

#	Article	IF	Citations
48809	Two-Dimensional Gold Halides: Novel Semiconductors with Giant Spinâ€“Orbit Splitting and Tunable Optoelectronic Properties. Journal of Physical Chemistry Letters, 2020, 11, 9759-9765.	2.1	3
48810	Computational Design of Two-Dimensional Boron-Containing Compounds as Efficient Metal-free Electrocatalysts toward Nitrogen Reduction Independent of Heteroatom Doping. ACS Applied Materials & Interfaces, 2020, 12, 50505-50515.	4.0	20
48811	Measurement of Exciton and Trion Energies in Multistacked hBN/WS2 Coupled Quantum Wells for Resonant Tunneling Diodes. ACS Nano, 2020, 14, 16114-16121.	7.3	15
48812	Electric polarization related Dirac half-metallicity in Mn-trihalide Janus monolayers. Physical Chemistry Chemical Physics, 2020, 22, 26468-26477.	1.3	9
48813	Mechanistic insights of selective syngas conversion over Zn grafted on ZSM-5 zeolite. Catalysis Science and Technology, 2020, 10, 8173-8181.	2.1	6
48814	Understanding activity origin for the oxygen reduction reaction on bi-atom catalysts by DFT studies and machine-learning. Journal of Materials Chemistry A, 2020, 8, 24563-24571.	5.2	71
48815	Structural, electronic, and magnetic properties of Ni nanoparticles supported on the TiC(001) surface. Physical Chemistry Chemical Physics, 2020, 22, 26145-26154.	1.3	8
48816	Hydrogen evolution reaction at the interfaces of two-dimensional lateral heterostructures: a first-principles study. RSC Advances, 2020, 10, 38484-38489.	1.7	10
48817	Unraveling crystal symmetry and strain effects on electronic band structures of SiC polytypes. AIP Advances, 2020, 10, 105014.	0.6	3
48818	Fast, accurate enthalpy differences in spin crossover crystals from DFT+U. Journal of Chemical Physics, 2020, 153, 104107.	1.2	14
48819	Supercell-core software: A useful tool to generate an optimal supercell for vertically stacked nanomaterials. AIP Advances, 2020, 10, 105105.	0.6	4
48820	Solar driven CO2 hydrogenation on transition metal doped Zn12O12 cluster. Journal of Chemical Physics, 2020, 153, 164306.	1.2	6
48821	The search for the new superconductors in the Ni-N system. Journal of Physics: Conference Series, 2020, 1590, 012010.	0.3	1
48822	Titanium-doped MoS2 monolayer as highly efficient catalyst for hydrogen evolution reaction. IOP Conference Series: Earth and Environmental Science, 2020, 558, 032048.	0.2	1
48823	First-principles study of topologically protected vortices and ferroelectric domain walls in hexagonal YGaO3. Physical Review B, 2020, 102, .	1.1	10
48824	Graphene quantum dot states near defects. Physical Review B, 2020, 102, .	1.1	4
48825	Machine learning driven simulated deposition of carbon films: From low-density to diamondlike amorphous carbon. Physical Review B, 2020, 102, .	1.1	44
48826	Blue Phosphorene Bilayer is a Two-Dimensional Metal and an Unambiguous Classification Scheme for Buckled Hexagonal Bilayers. Physical Review Letters, 2020, 125, 196401.	2.9	28

#	Article	IF	Citations
48827	Au_xPd_(300â€x) Alloy Nanoparticles for the Oxygen Reduction Reaction in Alkaline Media. ChemElectroChem, 2020, 7, 3824-3831.	1.7	9
48828	Tuning the electronic properties of C12A7 via Sn doping and encapsulation. Journal of Materials Science: Materials in Electronics, 2020, 31, 21203-21213.	1.1	1
48829	Local probe of the interlayer coupling strength of few-layers SnSe by contact-resonance atomic force microscopy. Frontiers of Physics, 2020, 15, 1.	2.4	8
48830	Silicene oxide: a potential Battery500 cathode for sealed non-aqueous lithiumâ€“oxygen batteries. Materials Today Energy, 2020, 18, 100503.	2.5	6
48831	Insights into the electronic origin of enhancing the catalytic activity of Co3O4 for oxygen evolution by single atom ruthenium. Nano Today, 2020, 34, 100955.	6.2	29
48832	Insight into rare earth yttrium and nitrogen co-decorated graphene as a promising material for NO detection. Physics Letters, Section A: General, Atomic and Solid State Physics, 2020, 384, 126910.	0.9	10
48833	First-principles study of biaxial strain effect on NH3 adsorbed Ti2CO2 monolayer. Vacuum, 2020, 179, 109574.	1.6	17
48834	Emergence of magnetic behavior in AB-stacked bilayer graphene via Fe-doping. Vacuum, 2020, 182, 109685.	1.6	7
48835	Size-Dependent Structural, Energetic, and Spectroscopic Properties of MoS₃ Polymorphs. Crystal Growth and Design, 2020, 20, 7750-7760.	1.4	9
48836	Nonempirical Definition of the Mendeleev Numbers: Organizing the Chemical Space. Journal of Physical Chemistry C, 2020, 124, 23867-23878.	1.5	20
48837	Control of Photocarrier Separation and Recombination at Bismuth Oxyhalide Interface for Nitrogen Fixation. Journal of Physical Chemistry Letters, 2020, 11, 9304-9312.	2.1	13
48838	Predicting aqueous stability of solid with computed Pourbaix diagram using SCAN functional. Npj Computational Materials, 2020, 6, .	3.5	69
48839	Structural transformation of highly active metalâ€“organic framework electrocatalysts during the oxygen evolution reaction. Nature Energy, 2020, 5, 881-890.	19.8	647
48840	PN/PAs-WSe2 van der Waals heterostructures for solar cell and photodetector. Scientific Reports, 2020, 10, 17213.	1.6	12
48841	Interfacial hybridization of Janus MoSSe and BX (X = P, As) monolayers for ultrathin excitonic solar cells, nanopiezotronics and low-power memory devices. Nanoscale, 2020, 12, 22645-22657.	2.8	73
48842	Theoretical investigations of electrochemical CO₂ reduction by transition metals anchored on CNTs. Sustainable Energy and Fuels, 2020, 4, 6156-6164.	2.5	13
48843	Effects of Electric Field on Electronic and Optical Properties of SnSe: A First-Principle Study. Integrated Ferroelectrics, 2020, 211, 167-174.	0.3	2
48844	Topological surface states in strained Dirac semimetal thin films. Physical Review B, 2020, 102, .	1.1	10

#	Article	IF	Citations
48845	Remarkable low-energy properties of the pseudogapped semimetal Be5Pt. Physical Review B, 2020, 102, .	1.1	1
48846	Mechanistic basis of oxygen sensitivity in titanium. Science Advances, 2020, 6, .	4.7	59
48847	Determination of Formation Energies and Phase Diagrams of Transition Metal Oxides with DFT+U. Materials, 2020, 13, 4303.	1.3	13
48848	Adsorption and self-assembly of porphyrins on ultrathin CoO films on Ir(100). Beilstein Journal of Nanotechnology, 2020, 11, 1516-1524.	1.5	6
48849	Geometry and energy barrier of martensite in the initial stage martensitic transformation in B19â€™ TiNi shape memory alloy. Acta Materialia, 2020, 201, 94-101.	3.8	10
48850	Electronic properties of fluorine/hydrogen adsorbed two-dimensional tetrahex-carbon: A first-principles study. Applied Surface Science, 2020, 529, 147150.	3.1	2
48851	First-principles evaluation of the potential of using Mg2SiO4, Mg2VO4, and Mg2GeO4 for CO2 capture. Journal of CO2 Utilization, 2020, 42, 101293.	3.3	8
48852	Direct growth of nanostructural MoS2 over the h-BN nanoplatelets: An efficient heterostructure for visible light photoreduction of CO2 to methanol. Journal of CO2 Utilization, 2020, 42, 101345.	3.3	33
48853	Ab initio study of the stability of H-He clusters at lattice defects in tungsten. Nuclear Instruments & Methods in Physics Research B, 2020, 478, 269-273.	0.6	6
48854	Ab initio and experimental oxygen ion conductivities in Sm-Zr and Gd-Zr co-doped ceria. Solid State Ionics, 2020, 355, 115422.	1.3	7
48855	Role of Methane as a Second Guest Component in Thermodynamic Stability and Isomer Selectivity of Butane Clathrate Hydrates. Journal of Physical Chemistry C, 2020, 124, 18474-18481.	1.5	17
48856	Observation of Molecular Hydrogen Produced from Bridging Hydroxyls on Anatase TiO₂(101). Journal of Physical Chemistry Letters, 2020, 11, 9289-9297.	2.1	16
48857	Predicting the Energetics of Hydrogen Intercalation in Metal Oxides Using Acidâ€“Base Properties. ACS Applied Materials & Interfaces, 2020, 12, 44658-44670.	4.0	10
48858	Accurate elemental boiling points from first principles. Physical Chemistry Chemical Physics, 2020, 22, 24041-24050.	1.3	7
48859	Interplay between local structure, vibrational and electronic properties on CuO under pressure. Physical Chemistry Chemical Physics, 2020, 22, 24299-24309.	1.3	3
48860	Exploring the structure evolution of MoS₂ upon Li/Na/K ion insertion and the origin of the unusual stability in potassium ion batteries. Nanoscale Horizons, 2020, 5, 1618-1627.	4.1	13
48861	A first-principles Quantum Monte Carlo study of two-dimensional (2D) GaSe. Journal of Chemical Physics, 2020, 153, 154704.	1.2	23
48862	Fermionic Analogue of High Temperature Hawking Radiation in Black Phosphorus. Chinese Physics Letters, 2020, 37, 067101.	1.3	18

#	Article	IF	Citations
48863	Inverse design of compounds that have simultaneously ferroelectric and Rashba cofunctionality. Physical Review B, 2020, 102, .	1.1	20
48864	CuTe chains on Cu(111) by deposition of one-third of a monolayer of Te: Atomic and electronic structure. Physical Review B, 2020, 102, .	1.1	5
48865	Superconductivity in <mml:math xmlns:mml="http://www.w3.org/1998/Math/MathML"><mml:msub><mml:mrow><mml:mi>La</mml:mi></mml:mrow><mml:mn>2</mml:mn> Physical Review B, 2020, 102, .	1.1	5
48866	Longitudinal and transverse electron paramagnetic resonance in a scanning tunneling microscope. Science Advances, 2020, 6, .	4.7	33
48867	Electronic Structure and Magnetic Properties of OsCrMnSb and IrCrMnSb from Ab Initio Calculations. Spin, 2020, 10, .	0.6	1
48868	Monolayer Bi2C3: A promising sensor for environmentally toxic NCGs with high sensitivity and selectivity. Applied Surface Science, 2020, 534, 147609.	3.1	23
48869	Nature of active Fe species and reaction mechanism over high-efficiency Fe/CHA catalysts in catalytic decomposition of N2O. Journal of Catalysis, 2020, 392, 322-335.	3.1	27
48870	First-principles simulation of h interacting with transition elements in molybdenum for nuclear material application. Journal of Nuclear Materials, 2020, 541, 152437.	1.3	4
48871	The selective hydrogenation of nitroarenes and alkenes catalyzed by Pd@MOFs: The role of electronic interactions between Pd nanoparticles and MOFs on the reaction. Molecular Catalysis, 2020, 495, 111157.	1.0	15
48872	Role of Buffer Layer and Building Unit in the Monolayer CrI₃ Growth: A First-Principles Perspective. Journal of Physical Chemistry Letters, 2020, 11, 9453-9460.	2.1	10
48873	The Bonding Nature and Adhesion of Polyacrylic Acid Coating on Li-Metal for Li Dendrite Prevention. ACS Applied Materials & Interfaces, 2020, 12, 51007-51015.	4.0	21
48874	Room-Temperature Flexible Quasi-Solid-State Rechargeable Naâ€“O₂ Batteries. ACS Central Science, 2020, 6, 1955-1963.	5.3	25
48875	Optimization of Criteria for an Efficient Screening of New Thermoelectric Compounds: The TiNiSi Structure-Type as a Case-Study. ACS Combinatorial Science, 2020, 22, 813-820.	3.8	6
48876	Emerging piezochromism in lead free alkaline earth chalcogenide perovskite AZrS₃ (A =) Tj ETQq1 1 0.784314 rgBT /Ove	2.7	24
48877	Induced spin polarization in graphene via interactions with halogen doped MoS₂ and MoSe₂ monolayers by DFT calculations. Nanoscale, 2020, 12, 23248-23258.	2.8	13
48878	Hexagonal and Monoclinic Phases of La2O2CO3 Nanoparticles and Their Phase-Related CO2 Behavior. Nanomaterials, 2020, 10, 2061.	1.9	8
48879	Multiple Cations Enhanced Defect Passivation of Blue Perovskite Quantum Dots Enabling Efficient Lightâ€Emitting Diodes. Advanced Optical Materials, 2020, 8, 2001494.	3.6	30
48880	Lithium Cluster Segregation in Coherent Contraction Twin Boundaries of Magnesium Alloys. Acta Materialia, 2020, 201, 477-487.	3.8	13

#	Article	IF	Citations
48881	Atomistic-Benchmarking towards a protocol development for rapid quantitative metrology of piezoelectric biomolecular materials. Applied Materials Today, 2020, 21, 100818.	2.3	15
48882	Evaluating the phase stability of binary titanium alloy Ti-X (X = Mo, Nb, Al, and Zr) using first-principles calculations and a Debye model. Calphad: Computer Coupling of Phase Diagrams and Thermochemistry, 2020, 71, 102207.	0.7	10
48883	Hardness and Young's modulus of Al3Yb single crystal studied by nano indentation. Intermetallics, 2020, 127, 106980.	1.8	5
48884	Cu+ based active sites of different oxides supported Pd-Cu catalysts and electrolytic in-situ H2 evolution for high-efficiency nitrate reduction reaction. Journal of Catalysis, 2020, 392, 231-243.	3.1	25
48885	First-principle investigations of martensitic transformation and magnetic properties in Ni24Mn17â^'In7Cu (xÂ=Â0â€“5) alloys. Journal of Magnetism and Magnetic Materials, 2020, 516, 167363.	1.0	4
48886	Water-silanol interactions on the amorphous silica surface: A dispersion-corrected DFT investigation. Journal of Molecular Liquids, 2020, 320, 114496.	2.3	6
48887	Friction and wear properties of CrSi-based coatings for nuclear fuel cladding. Surface and Coatings Technology, 2020, 402, 126311.	2.2	12
48888	Ab initio calculations and a scratch test study of RF-magnetron sputter deposited hydroxyapatite and silicon-containing hydroxyapatite coatings. Surfaces and Interfaces, 2020, 21, 100727.	1.5	7
48889	Solid-State Phase Transition of Agomelatineâ€“Phosphoric Acid Molecular Complexes along the Saltâ€“Cocrystal Continuum: Ab Initio Powder X-ray Diffraction Structure Determination and DFT-D2 Analysis. Crystal Growth and Design, 2020, 20, 7647-7657.	1.4	10
48890	Doping Modulation of the Charge Injection Barrier between a Covalent Organic Framework Monolayer and Graphene. Chemistry of Materials, 2020, 32, 9228-9237.	3.2	18
48891	Formic Acid Dehydration Rates and Elementary Steps on Lewis Acidâ€“Base Site Pairs at Anatase and Rutile TiO₂ Surfaces. Journal of Physical Chemistry C, 2020, 124, 20161-20174.	1.5	13
48892	Gas Evolution in Li-Ion Batteries: Modeling Ethylene Carbonate Decomposition on LiCoO₂ in the Presence of Surface Magnetism. Journal of Physical Chemistry C, 2020, 124, 24097-24104.	1.5	6
48893	Broad Tunability of Carrier Effective Masses in Two-Dimensional Halide Perovskites. ACS Energy Letters, 2020, 5, 3609-3616.	8.8	54
48894	Simultaneous Observation of Carrier-Specific Redistribution and Coherent Lattice Dynamics in 2H-MoTe₂ with Femtosecond Core-Level Spectroscopy. ACS Nano, 2020, 14, 15829-15840.	7.3	38
48895	High-throughput calculations of magnetic topological materials. Nature, 2020, 586, 702-707.	13.7	241
48896	Morphology of Cu clusters supported on reconstructed polar ZnO (0001) and (000Ì„1Ì„) surfaces. Journal of Materials Chemistry A, 2020, 8, 22840-22857.	5.2	9
48897	Investigation on the formation of Mg metal anode/electrolyte interfaces in Mg/S batteries with electrolyte additives. Journal of Materials Chemistry A, 2020, 8, 22998-23010.	5.2	46
48898	Atomic structure and properties of a perovskite/spinel (111) interface. Physical Review B, 2020, 102, .	1.1	6

#	Article	IF	Citations
48899	Realization of Regularâ€Mixed Quasiâ€1D Borophene Chains with Longâ€Range Order. Advanced Materials, 2020, 32, e2005128.	11.1	30
48900	High-Capacity Li⁺ Storage through Multielectron Redox in the Fast-Charging Wadsleyâ€"Roth Phase (W_{0.2}V_{0.8})₃O₇. Chemistry of Materials, 2020, 32, 9415-9424.	3.2	15
48901	Mn²⁺â€"Mn²⁺ Magnetic Coupling Effect on Photoluminescence Revealed by Photomagnetism in CsMnCl₃. Journal of Physical Chemistry Letters, 2020, 11, 9587-9595.	2.1	49
48902	Dual-Constrained Sulfur in FeS₂@C Nanostructured Lithium-Sulfide Batteries. ACS Applied Energy Materials, 2020, 3, 10950-10960.	2.5	21
48903	Hierarchically Nanostructured Nickelâ€"Cobalt Alloy Supported on Nickel Foam as a Highly Efficient Electrocatalyst for Hydrazine Oxidation. ACS Sustainable Chemistry and Engineering, 2020, 8, 16583-16590.	3.2	29
48904	A general-purpose machine-learning force field for bulk and nanostructured phosphorus. Nature Communications, 2020, 11, 5461.	5.8	72
48905	An investigation of the photovoltaic parameters of ZnS grown on ZnO(101Ì„1). New Journal of Chemistry, 2020, 44, 20600-20609.	1.4	7
48906	Manipulation of planar oxygen defect arrangements in multifunctional magnÃ¨li titanium oxide hybrid systems: from energy conversion to water treatment. Energy and Environmental Science, 2020, 13, 5080-5096.	15.6	15
48907	First principles studies of electronic, mechanical and optical properties of Cr-doped cubic ZrO2. Chemical Physics, 2020, 539, 110972.	0.9	9
48908	Exceptional size-dependent activity enhancement in the catalytic electroreduction of N2 over Mo nanoparticles. International Journal of Hydrogen Energy, 2020, 45, 31841-31848.	3.8	9
48909	Electronic structure, cohesive and magnetic properties of iridium oxide clusters adsorbed on graphene. Journal of Molecular Graphics and Modelling, 2020, 101, 107726.	1.3	1
48910	Tunable electronic properties of silicene based heterojunctions with ultrathin high-Đº La2O3 gate dielectric. Superlattices and Microstructures, 2020, 147, 106686.	1.4	4
48911	Magnetic Interactions in ZnMnO₃: Active Role of Zn 3d¹⁰ Orbitals, in Comparison with MgMnO₃. Inorganic Chemistry, 2020, 59, 16205-16214.	1.9	8
48912	Interaction of Single-Atom Platinumâ€"Oxygen Vacancy Defects for the Boosted Photosplitting Water H₂ Evolution and CO₂ Photoreduction: Experimental and Theoretical Study. Journal of Physical Chemistry C, 2020, 124, 24566-24579.	1.5	48
48913	Boosting Hydrogen Evolution Reaction of Nickel Sulfides by Introducing Nonmetallic Dopants. Journal of Physical Chemistry C, 2020, 124, 24223-24231.	1.5	8
48914	Computationally Predicted High-Throughput Free-Energy Phase Diagrams for the Discovery of Solid-State Hydrogen Storage Reactions. ACS Applied Materials & Interfaces, 2020, 12, 48553-48564.	4.0	6
48915	Excellent thermoelectric properties of monolayer RbAgM (M = Se and Te): first-principles calculations. Physical Chemistry Chemical Physics, 2020, 22, 26364-26371.	1.3	13
48916	LaTiO₂N crystallographic orientation control significantly increases visible-light induced charge extraction. Journal of Materials Chemistry A, 2020, 8, 22867-22873.	5.2	5

#	Article	IF	Citations
48917	Pressure effects on magnetism in <mml:math xmlns:mml="http://www.w3.org/1998/Math/MathML"><mml:mrow><mml:msub><mml:mi>Ca</mml:mi><mml:mn>2</mml:mn></mml: mathvariant="normal">O</mml:mi><mml:mn>5</mml:mn></mml:msub></mml:mrow></mml:math> -type ferrites and manganites. Physical Review B, 2020, 102, .	1.1	2
48918	Great enhancement of Curie temperature and magnetic anisotropy in two-dimensional van der Waals magnetic semiconductor heterostructures. Physical Review B, 2020, 102, .	1.1	34
48919	Second group of high-pressure high-temperature lanthanide polyhydride superconductors. Physical Review B, 2020, 102, .	1.1	116
48920	Hund's metal physics: From <mml:math xmlns:mml="http://www.w3.org/1998/Math/MathML"><mml:msub><mml:mi>SrNiO</mml:mi><mml:mn>2</mml:mn></mml:msub>< to <mml:math xmlns:mml="http://www.w3.org/1998/Math/MathML"><mml:msub><mml:mi>LaNiO</mml:mi><mml:mn>2</mml:mn></mml:msub>< Physical Review B, 2020, 102, .	1.1	82
48921	Blue phosphorus nanoscrolls. Physical Review B, 2020, 102, .	1.1	5
48922	CdPS ₃ nanosheets-based membrane with high proton conductivity enabled by Cd vacancies. Science, 2020, 370, 596-600.	6.0	120
48923	CO2 and H2O Coadsorption and Reaction on the Low-Index Surfaces of Tantalum Nitride: A First-Principles DFT-D3 Investigation. Catalysts, 2020, 10, 1217.	1.6	7
48924	Structures and Properties of the Self-Assembling Diphenylalanine Peptide Nanotubes Containing Water Molecules: Modeling and Data Analysis. Nanomaterials, 2020, 10, 1999.	1.9	21
48925	Microwaveâ€heated Î³â€Alumina Applied to the Reduction of Aldehydes to Alcohols. ChemCatChem, 2020, 12, 6344-6355.	1.8	6
48926	First principle study of electronic structural and physical properties of CaO SiO2Al2O3 ternary slag system by using Ab Initio molecular and lattice dynamics. Journal of Non-Crystalline Solids, 2020, 550, 120384.	1.5	5
48927	Experimental and theoretical Raman study on the HTSC PrxY1â^'xBa2Cu3O7 family for different Pr concentrations and synthesis methods. Materials Chemistry and Physics, 2020, 256, 123737.	2.0	5
48928	Emerging various electronic and magnetic properties of silicene by light rare-earth metal substituted doping. Superlattices and Microstructures, 2020, 148, 106712.	1.4	7
48929	Elucidation of the Underlying Mechanism of CO₂ Capture by Ethylenediamine-Functionalized M₂(dobpdc) (M = Mg, Scâ€"Zn). Inorganic Chemistry, 2020, 59, 16665-16671.	1.9	13
48930	Magnetism and Heterogeneous Catalysis: In Depth on the Quantum Spin-Exchange Interactions in Pt₃M (M = V, Cr, Mn, Fe, Co, Ni, and Y)(111) Alloys. ACS Applied Materials & Interfaces, 2020, 12, 50484-50494.	4.0	22
48931	Atomically dispersed Lewis acid sites boost 2-electron oxygen reduction activity of carbon-based catalysts. Nature Communications, 2020, 11, 5478.	5.8	114
48932	Electronic properties of Janus MXY/graphene (M = Mo, W; X â‰ Y = S, Se) van der Waals structures: a first-principles study. Physical Chemistry Chemical Physics, 2020, 22, 25675-25684.	1.3	16
48933	Boron cage effects on Ndâ€"Feâ€"B crystal structureâ€™s stability. Journal of Chemical Physics, 2020, 153, 114111.	1.2	5
48934	Assessment of PBE+U and HSE06 methods and determination of optimal parameter U for the structural and energetic properties of rare earth oxides. Journal of Chemical Physics, 2020, 153, 164710.	1.2	13

#	Article	IF	Citations
48935	Quasiballistic phonon transport from first principles. Physical Review B, 2020, 102, .	1.1	6
48936	First-principles calculations of vibrational and optical properties of half-Heusler NaScSi. Indian Journal of Physics, 2021, 95, 2303-2312.	0.9	16
48937	Quantitative prediction of Suzuki segregation at stacking faults of the Î³â€™ phase in Ni-base superalloys. Acta Materialia, 2020, 200, 223-235.	3.8	24
48938	Towards defect engineering in hexagonal MoS2 nanosheets for tuning hydrogen evolution and nitrogen reduction reactions. Applied Materials Today, 2020, 21, 100812.	2.3	16
48939	Replacing aromatic Ï€-system with cycloalkyl in triphenylamine dyes to impact intramolecular charge transfer in dyes pertaining to dye-sensitized solar cells application. Journal of Photochemistry and Photobiology A: Chemistry, 2020, 403, 112862.	2.0	18
48940	Three-dimensional porous phosphorus-graphdiyne as a universal anode material for both K- and Ca-ion batteries with high performance. Journal of Power Sources, 2020, 480, 228876.	4.0	28
48941	Identification of the Intrinsic Atomic Disorder in ZrNiSn-based Alloys and Their Effects on Thermoelectric Properties. Nano Energy, 2020, 78, 105372.	8.2	24
48942	GaN and InGaN nanowires prepared by metal-assisted electroless etching: Experimental and theoretical studies. Results in Physics, 2020, 19, 103428.	2.0	9
48943	Evidence of an ordered ternary phase in the section Niâ€“Ti5Sn3 of the ternary Tiâ€“Niâ€“Sn: Crystal structure and phase stability. Solid State Sciences, 2020, 109, 106349.	1.5	2
48944	Favorable Redox Thermodynamics of SrTi_{0.5}Mn_{0.5}O_{3â^Î´} in Solar Thermochemical Water Splitting. Chemistry of Materials, 2020, 32, 9335-9346.	3.2	42
48945	Xenon iron oxides predicted as potential Xe hosts in Earthâ€™s lower mantle. Nature Communications, 2020, 11, 5227.	5.8	27
48946	Application of a long short-term memory for deconvoluting conductance contributions at charged ferroelectric domain walls. Npj Computational Materials, 2020, 6, .	3.5	15
48947	Subtle metastability of the layered magnetic topological insulator MnBi2Te4 from weak interactions. Npj Computational Materials, 2020, 6, .	3.5	8
48948	Aberrant electronic and structural alterations in pressure tuned perovskite NaOsO3. Npj Quantum Materials, 2020, 5, .	1.8	4
48949	Density functional theory-based electric field gradient database. Scientific Data, 2020, 7, 362.	2.4	11
48950	Ab initio study for molecular-scale adsorption, decomposition and desorption on AlN surfaces during MOCVD growth. Scientific Reports, 2020, 10, 17840.	1.6	2
48951	Origin of enhanced chemical precompression in cerium hydride $$hbox {CeH}_{{9}}$$. Scientific Reports, 2020, 10, 16878.	1.6	10
48952	Aqueous ionic effect on electrochemical breakdown of Si-dielectricâ€“electrolyte interface. Scientific Reports, 2020, 10, 16795.	1.6	4

#	Article	IF	Citations
48953	Ultra-strong stability of double-sided fluorinated monolayer graphene and its electrical property characterization. Scientific Reports, 2020, 10, 17562.	1.6	7
48954	Bi2WO6â€“BiOCl heterostructure with enhanced photocatalytic activity for efficient degradation of oxytetracycline. Scientific Reports, 2020, 10, 18401.	1.6	48
48955	Room temperature deformation of single crystals of Ti5Si3 with the hexagonal D88 structure investigated by micropillar compression tests. Scientific Reports, 2020, 10, 17983.	1.6	11
48956	Route to high-$$T_{c}$$ superconductivity of $$hbox {BC}_{{7}}$$ via strong bonding of boronâ€“carbon compound at high pressure. Scientific Reports, 2020, 10, 18090.	1.6	11
48957	Metalâ€“insulator transition tuned by oxygen vacancy migration across TiO2/VO2 interface. Scientific Reports, 2020, 10, 18554.	1.6	24
48958	Understanding the interactions between the bis(trifluoromethylsulfonyl)imide anion and absorbed CO2 using X-ray diffraction analysis of a soft crystal surrogate. Communications Chemistry, 2020, 3, .	2.0	7
48959	Predicted 2D ferromagnetic Janus VSeTe monolayer with high Curie temperature, large valley polarization and magnetic crystal anisotropy. Nanoscale, 2020, 12, 22735-22742.	2.8	64
48960	Intriguing electronic structure and photocatalytic performance of bluePâ€“SMSe and bluePâ€“SeMS (M =) Tj ETQq1 1 0.784314 rgBT /C	1.7	6
48961	Interactions of selected organic molecules with a blue phosphorene monolayer: self-assembly, solvent effect, enhanced binding and fixation through coadsorbed gold clusters. Physical Chemistry Chemical Physics, 2020, 22, 26552-26561.	1.3	6
48962	Combined optical reflectivity measurement and ab initio simulation of expanded gold fluid across the metalâ€“nonmetal transition regime. AIP Advances, 2020, 10, 095008.	0.6	1
48963	Density functional theory calculation of helium segregation and decohesion effect in W110/Ni111 interphase boundary. Journal of Applied Physics, 2020, 128, .	1.1	7
48964	Impact of single and double oxygen vacancies on electronic transport in Fe/MgO/Fe magnetic tunnel junctions. Journal of Applied Physics, 2020, 128, .	1.1	3
48965	A half-metallic ferrimagnet of CeCu3Cr4O12 with 4f itinerant electron. Applied Physics Letters, 2020, 117, 132404.	1.5	1
48966	First-principles study of intrinsic point defects and Xe impurities in uranium monocarbide. Journal of Applied Physics, 2020, 128, .	1.1	7
48967	Rotated angular modulated electronic and optical properties of bilayer phosphorene: A first-principles study. Applied Physics Letters, 2020, 117, .	1.5	10
48968	Achieving low elastic moduli of bcc Tiâ€“V alloys in vicinity of mechanical instability. AIP Advances, 2020, 10, 105322.	0.6	3
48969	Calcium-stannous oxide solid solutions for solar devices. Applied Physics Letters, 2020, 117, .	1.5	2
48970	Promising valleytronic materials with strong spin-valley coupling in two-dimensional MN2X2 (M = Mo,) Tj ETQq1 1 0.784314 rgBT /Ov	1.5	16

#	Article	IF	Citations
48971	Enhanced Ferromagnetism of CrI₃ Bilayer by Self-Intercalation*. Chinese Physics Letters, 2020, 37, 107506.	1.3	25
48972	Spontaneous ferromagnetism and finite surface energy gap in the topological insulator Bi2Se3 from surface BiSe antisite defects. Physical Review B, 2020, 102, .	1.1	3
48973	Stability and electronic properties of edges of <mml:math xmlns:mml="http://www.w3.org/1998/Math/MathML"><mml:mrow><mml:msub><mml:mi>SnS</mml:mi><mml:mn>2</mml:mn></mml Physical Review B, 2020, 102, .	1.1	7
48974	Electron Irradiation Effects and Defects Analysis of the Inverted Metamorphic Four-Junction Solar Cells. IEEE Journal of Photovoltaics, 2020, 10, 1712-1720.	1.5	10
48975	Structural, electronic and mechanical properties of AgIn1â^'XGaXS2 (Xâ€‰=â€‰0, 0.25, 0.50, 0.75, 1) chalcogenides. Indian Journal of Physics, 2021, 95, 1751-1756.	0.9	4
48976	Hydrogen diffusion into Pd(1 0 0) subsurface: Role of co-adsorbed bicomponent species on surface. Applied Surface Science, 2020, 533, 147448.	3.1	3
48977	Interaction of H2S with perfect and S-covered Ni(110) surface: A first-principles study. International Journal of Hydrogen Energy, 2020, 45, 30622-30633.	3.8	13
48978	Unveiling the energetic and structural properties of Pu doped zircon through electrochemical equilibrium diagram from DFT+U calculations. Journal of Nuclear Materials, 2020, 539, 152234.	1.3	0
48979	Nd, SbNd and Sb3Nd4 and their interactions with the cladding alloy HT9. Journal of Nuclear Materials, 2020, 541, 152387.	1.3	5
48980	Adsorption of S on Si(111) with M4ÂÃ—Â4 superstructure. Surface Science, 2020, 701, 121694.	0.8	0
48981	At the Limits of Isolobal Bonding: Ï€-Based Covalent Magnetism in Mn2Hg5. Inorganic Chemistry, 2020, 59, 12304-12313.	1.9	7
48982	Ab Initio Molecular Dynamics Reveals New Metal-Binding Sites in Atomically Dispersed Pt₁/TiO₂ Catalysts. Journal of Physical Chemistry C, 2020, 124, 24187-24195.	1.5	17
48983	Energy Storage Behavior in ErBiO₃-Doped (K,Na)NbO₃ Lead-Free Piezoelectric Ceramics. ACS Applied Electronic Materials, 2020, 2, 3717-3727.	2.0	51
48984	Electronic Band Engineering via MI₃ (M = Sb, Bi) Doping Remarkably Enhances the Air Stability of Perovskite CsSnI₃. ACS Applied Energy Materials, 2020, 3, 10477-10484.	2.5	17
48985	Revealing Interplay of Defects in SnO₂ Quantum Dots for Blue Luminescence and Selective Trace Ammonia Detection at Room Temperature. ACS Applied Materials & Interfaces, 2020, 12, 49227-49236.	4.0	24
48986	Enhanced Charge Transport in Ca₂MnO₄-Layered Perovskites by Point Defect Engineering. ACS Applied Materials & Interfaces, 2020, 12, 49768-49776.	4.0	11
48987	In Situ Study of Molecular Doping of Chlorine on MoS₂ Field Effect Transistor Device in Ultrahigh Vacuum Conditions. ACS Omega, 2020, 5, 28108-28115.	1.6	10
48988	Chemical trends of deep levels in van der Waals semiconductors. Nature Communications, 2020, 11, 5373.	5.8	24

#	Article	IF	Citations
48989	Metastable oxysulfide surface formation on LiNi_{0.5}Mn_{1.5}O₄ single crystal particles by carbothermal reaction with sulfur-doped heterocarbon nanoparticles: new insight into their structural and electrochemical characteristics, and their potential applications. Journal of Materials Chemistry A, 2020, 8, 22302-22314.	5.2	17
48990	A thermodynamic and kinetic study of the catalytic performance of Fe, Mo, Rh and Ru for the electrochemical nitrogen reduction reaction. Physical Chemistry Chemical Physics, 2020, 22, 25973-25981.	1.3	8
48991	Exciton manipulation in rippled transition metal dichalcogenides. Nanoscale, 2020, 12, 21124-21130.	2.8	7
48992	Fermi level dependence of gasâ€“solid oxygen defect exchange mechanism on TiO2 (110) by first-principles calculations. Journal of Chemical Physics, 2020, 153, 124710.	1.2	5
48993	Magnetic properties of one defects on borophene tri-layer structure: a Monte Carlo study. Phase Transitions, 2020, 93, 962-972.	0.6	7
48994	Coupling Stacking Orders with Interlayer Magnetism in Bilayer H-VSe₂*. Chinese Physics Letters, 2020, 37, 107101.	1.3	8
48995	Enhancing Methanol Oxidation Reaction with Platinumâ€based Catalysts using a Nâ€Ðoped Threeâ€dimensional Graphitic Carbon Support. ChemCatChem, 2020, 12, 6000-6012.	1.8	11
48996	Dynamics of Hydroxyl Anions Promotes Lithium Ion Conduction in Antiperovskite Li₂OHCl. Chemistry of Materials, 2020, 32, 8481-8491.	3.2	53
48997	Assessment of Sulfur-Functionalized MXenes for Li-Ion Battery Applications. Journal of Physical Chemistry C, 2020, 124, 21293-21304.	1.5	22
48998	Operando pH Measurements Decipher H⁺/Zn²⁺ Intercalation Chemistry in High-Performance Aqueous Zn/Î´-V₂O₅ Batteries. ACS Energy Letters, 2020, 5, 2979-2986.	8.8	126
48999	Mussel Inspired Highly Aligned Ti₃C₂T_x MXene Film with Synergistic Enhancement of Mechanical Strength and Ambient Stability. ACS Nano, 2020, 14, 11722-11732.	7.3	212
49000	New insights into O and OH adsorption on the Ptâ€“Co alloy surface: effects of Pt/Co ratios and structures. Physical Chemistry Chemical Physics, 2020, 22, 21124-21130.	1.3	4
49001	Unraveling the local structure and luminescence evolution in Nd³⁺-doped LiYF₄: a new theoretical approach. Physical Chemistry Chemical Physics, 2020, 22, 21074-21082.	1.3	3
49002	Octahedral morphology of NiO with (111) facet synthesized from the transformation of NiOHCl for the NO_x detection and degradation: experiment and DFT calculation. Inorganic Chemistry Frontiers, 2020, 7, 3431-3442.	3.0	16
49003	Electric field control of molecular magnetic state by two-dimensional ferroelectric heterostructure engineering. Applied Physics Letters, 2020, 117, .	1.5	12
49004	Orbital-selective superconductivity in a two-band model of infinite-layer nickelates. Physical Review B, 2020, 102, .	1.1	70
49005	Electronic structure and magneto-optical properties of silicon-nitrogen-vacancy complexes in diamond. Physical Review B, 2020, 102, .	1.1	10
49006	Electrochemical Fixation of Carbon Dioxide in Molten Salts on Liquid Zinc Cathode to Zinc@Graphitic Carbon Spheres for Enhanced Energy Storage. Advanced Energy Materials, 2020, 10, 2002241.	10.2	58

#	Article	IF	Citations
49007	Lignin Intermediates on Palladium: Insights into Ketoâ€Enol Tautomerization from Theoretical Modelling. ChemSusChem, 2020, 13, 6574-6581.	3.6	6
49008	The catalytic performance of metalâ€free defected carbon catalyst towards acetylene hydrochlorination revealed from firstâ€principles calculation. International Journal of Quantum Chemistry, 2020, 120, e26418.	1.0	7
49009	Sodiophilically Graded Gold Coating on Carbon Skeletons for Highly Stable Sodium Metal Anodes. Small, 2020, 16, e2003815.	5.2	37
49010	Room temperature ferromagnetism in ultra-thin van der Waals crystals of 1T-CrTe2. Nano Research, 2020, 13, 3358-3363.	5.8	175
49011	Facet Engineered Î±-MnO₂ for Efficient Catalytic Ozonation of Odor CH₃SH: Oxygen Vacancy-Induced Active Centers and Catalytic Mechanism. Environmental Science & Technology, 2020, 54, 12771-12783.	4.6	196
49012	Efficient Ambient Electrocatalytic Ammonia Synthesis by Nanogold Triggered via Boron Clusters Combined with Carbon Nanotubes. ACS Applied Materials & Interfaces, 2020, 12, 42821-42831.	4.0	27
49013	Enhanced Catalytic Conversion of Polysulfides Using Bimetallic Co₇Fe₃ for High-Performance Lithiumâ€“Sulfur Batteries. ACS Nano, 2020, 14, 11558-11569.	7.3	158
49014	Porous Ti-MOF-74 Framework as a Strong-Binding Nitric Oxide Scavenger. Journal of the American Chemical Society, 2020, 142, 16562-16568.	6.6	27
49015	The role of carbon nanotubes in enhanced charge storage performance of VSe₂: experimental and theoretical insight from DFT simulations. RSC Advances, 2020, 10, 31712-31719.	1.7	31
49016	High-throughput computational screening of 2D materials for thermoelectrics. Journal of Materials Chemistry A, 2020, 8, 19674-19683.	5.2	38
49017	Critical role of the defect state in the photo-oxidation of methanol on TiO₂(110). Journal of Materials Chemistry A, 2020, 8, 20082-20090.	5.2	14
49018	Origin of the enhanced oxygen evolution reaction activity and stability of a nitrogen and cerium co-doped CoS2 electrocatalyst. Journal of Materials Chemistry A, 2020, 8, 22694-22702.	5.2	23
49019	Optoelectronic properties of type-II SePtTe/InS van der Waals heterojunction. Journal of Applied Physics, 2020, 128, .	1.1	12
49020	Magnetic states of atomic vacancies in graphite probed by scanning tunneling microscopy. AIP Advances, 2020, 10, 085325.	0.6	0
49021	High-throughput production of force-fields for solid-state electrolyte materials. APL Materials, 2020, 8, 081111.	2.2	15
49022	Predicting short-range order and correlated phenomena in disordered crystalline materials. Science Advances, 2020, 6, eabc2758.	4.7	28
49023	Tunable Cationic Vacancies of Cobalt Oxides for Efficient Electrocatalysis in Liâ€“O₂ Batteries. Advanced Energy Materials, 2020, 10, 2001415.	10.2	113
49024	Modulation of Band Alignment and Electronâ€“Phonon Scattering in Mg3Sb2 via Pressure. ACS Applied Electronic Materials, 2020, 2, 2745-2749.	2.0	8

#	Article	IF	Citations
49025	Power of Aerogel Platforms to Explore Mesoscale Transport in Catalysis. ACS Applied Materials & Interfaces, 2020, 12, 41277-41287.	4.0	13
49026	Decoding of Oxygen Network Distortion in a Layered High-Rate Anode by In Situ Investigation of a Single Microelectrode. ACS Nano, 2020, 14, 11753-11764.	7.3	10
49027	Induced Magnetism of the MoS₂ Monolayer during the Transition Metal (Fe/Ni) Bombardment Process: A Nonadiabatic Ab Initio Collision Dynamics Investigation. ACS Omega, 2020, 5, 16139-16148.	1.6	0
49028	Atomically-precise dopant-controlled single cluster catalysis for electrochemical nitrogen reduction. Nature Communications, 2020, 11, 4389.	5.8	110
49029	A disordered rock salt anode for fast-charging lithium-ion batteries. Nature, 2020, 585, 63-67.	13.7	326
49030	The InSe/SiH type-II van der Waals heterostructure as a promising water splitting photocatalyst: a first-principles study. Physical Chemistry Chemical Physics, 2020, 22, 21436-21444.	1.3	30
49031	A₂AgCrCl₆ (A = Li, Na, K, Rb, Cs) halide double perovskites: a transition metal-based semiconducting material series with appreciable optical characteristics. Physical Chemistry Chemical Physics, 2020, 22, 24337-24350.	1.3	18
49032	Enhanced electrocatalytic nitrogen reduction activity by incorporation of a carbon layer on SnS microflowers. Journal of Materials Chemistry A, 2020, 8, 20677-20686.	5.2	18
49033	Superconducting and antiferromagnetic properties of dual-phase V3Ga. Applied Physics Letters, 2020, 117, 062401.	1.5	5
49034	Out-of-plane magnetic anisotropy engineered via band distortion in two-dimensional materials. Physical Review B, 2020, 102, .	1.1	10
49035	Quantitative and qualitative performance of density functional theory rationalized by reduced density gradient distributions. Physical Review B, 2020, 102, .	1.1	8
49036	The Concept of Negative Capacitance in Ionically Conductive Van der Waals Ferroelectrics. Advanced Energy Materials, 2020, 10, 2001726.	10.2	30
49037	Computational Study of a Novel 2D Ferromagnetic Metal: the Ce 2 C Monolayer. Physica Status Solidi - Rapid Research Letters, 2020, 14, 2000324.	1.2	2
49038	Stabilized Charge, Spin, and Orbital Ordering by the 6s2 Lone Pair in Bi0.5Pb0.5MnO3. Inorganic Chemistry, 2020, 59, 13390-13397.	1.9	2
49039	Defect-Accommodating Intermediates Yield Selective Low-Temperature Synthesis of YMnO₃ Polymorphs. Inorganic Chemistry, 2020, 59, 13639-13650.	1.9	22
49040	First-Principles Study on the Stability of Weberite-Type, Pyrochlore, and Defect-Fluorite Structures of A₂³⁺B₂⁴⁺O₇ (A =) Tj ETQq1 1 0.784314 rgBT	1.5	10
49041	Potential Energy Landscape of CO Adsorbates on NaCl(100) and Implications in Isomerization of Vibrationally Excited CO. Journal of Physical Chemistry C, 2020, 124, 19146-19156.	1.5	12
49042	Enhanced Thermal Conductivity in a Diamine-Appended Metalâ€“Organic Framework as a Result of Cooperative CO₂ Adsorption. ACS Applied Materials & Interfaces, 2020, 12, 44617-44621.	4.0	10

#	Article	IF	Citations
49043	Ferroresistive Diode Currents in Nanometer-Thick Cobalt-Doped BiFeO₃ Films for Memory Applications. ACS Applied Nano Materials, 2020, 3, 8888-8896.	2.4	14
49044	Unveiling the Molecular Mechanism of CO₂ Capture in N-Methylethylenediamine-Grafted M₂(dobpdc). ACS Sustainable Chemistry and Engineering, 2020, 8, 14616-14626.	3.2	24
49045	Localization in the SCAN meta-generalized gradient approximation functional leading to broken symmetry ground states for graphene and benzene. Physical Chemistry Chemical Physics, 2020, 22, 19585-19591.	1.3	8
49046	Me-graphene: a graphene allotrope with near zero Poisson's ratio, sizeable band gap, and high carrier mobility. Nanoscale, 2020, 12, 19359-19366.	2.8	48
49047	Bifunctional water-electrolysis-catalysts meeting band-diagram analysis: case study of â€œFePâ€• electrodes. Journal of Materials Chemistry A, 2020, 8, 20021-20029.	5.2	25
49048	Nitrogen-free TMS₄-centers in metalâ€“organic frameworks for ammonia synthesis. Journal of Materials Chemistry A, 2020, 8, 20047-20053.	5.2	45
49049	Opportunities and challenges of 2D materials in back-end-of-line interconnect scaling. Journal of Applied Physics, 2020, 128, .	1.1	36
49050	Structural Design of Amorphous CoMoP_x with Abundant Active Sites and Synergistic Catalysis Effect for Effective Water Splitting. Advanced Functional Materials, 2020, 30, 2003889.	7.8	128
49051	Highly Efficient Blueâ€Emitting CsPbBr₃ Perovskite Nanocrystals through Neodymium Doping. Advanced Science, 2020, 7, 2001698.	5.6	97
49052	Structural Insight of the Frailty of 2D Janus NbSeTe as an Active Photocatalyst. ChemCatChem, 2020, 12, 6013-6023.	1.8	20
49053	Influence of Polymorphism on the Electronic Structure of Ga₂O₃. Chemistry of Materials, 2020, 32, 8460-8470.	3.2	35
49054	Investigation of the Electronic Structure and Optical, EPR, and ODMR Spectroscopic Properties for ¹⁷¹Yb³⁺-Doped Y₂SiO₅ Crystal: A Combined Theoretical Approach. Inorganic Chemistry, 2020, 59, 13144-13152.	1.9	9
49055	Oxygen Redox Activity in Cathodes: A Common Phenomenon Calling for Density-Based Descriptors. Journal of Physical Chemistry C, 2020, 124, 19962-19968.	1.5	2
49056	Atomically Asymmetric Inversion Scales up to Mesoscopic Single-Crystal Monolayer Flakes. ACS Nano, 2020, 14, 13834-13840.	7.3	11
49057	The Missing Link: Au191(SPh-tBu)66 Janus Nanoparticle with Molecular and Bulk-Metal-like Properties. Journal of the American Chemical Society, 2020, 142, 15799-15814.	6.6	48
49058	Spin-orbit quantum impurity in a topological magnet. Nature Communications, 2020, 11, 4415.	5.8	34
49059	A nitrogen fixation strategy to synthesize NO via the thermally assisted photocatalytic conversion of air. Journal of Materials Chemistry A, 2020, 8, 19623-19630.	5.2	24
49060	Isolated flat bands and physics of mixed dimensions in a 2D covalent organic framework. Nanoscale, 2020, 12, 20279-20286.	2.8	7

#	Article	IF	Citations
49061	A high-pressure study of HfC and nano-crystalline TiC by X-ray diffraction and density functional theory calculations. Modern Physics Letters B, 2020, 34, 2050393.	1.0	7
49062	Elucidating energy scaling between atomic and molecular adsorbates in the presence of solvent. AICHE Journal, 2020, 66, e17036.	1.8	8
49063	Fabrication and manipulation of nanosized graphene homojunction with atomically-controlled boundaries. Nano Research, 2020, 13, 3286-3291.	5.8	3
49064	Accurate and Numerically Efficient r²SCAN Meta-Generalized Gradient Approximation. Journal of Physical Chemistry Letters, 2020, 11, 8208-8215.	2.1	335
49065	Density Functional Theory-Based Method to Predict the Activities of Nanomaterials as Peroxidase Mimics. ACS Catalysis, 2020, 10, 12657-12665.	5.5	92
49066	Extended anharmonic collapse of phonon dispersions in SnS and SnSe. Nature Communications, 2020, 11, 4430.	5.8	46
49067	Novel two-dimensional Î²-GeSe and Î²-SnSe semiconductors: anisotropic high carrier mobility and excellent photocatalytic water splitting. Journal of Materials Chemistry A, 2020, 8, 19612-19622.	5.2	54
49068	Strain-engineering of bandgaps in pristine and fully hydrogenated hexagonal boron phosphide. Journal of Applied Physics, 2020, 128, .	1.1	5
49069	Theoretical Study of the Electronic and Optical Properties of a Heterostructure Based on PTCDA Organic Semiconductor and MoSe2. JETP Letters, 2020, 111, 627-632.	0.4	3
49070	Spontaneous Growth of CaBi4Ti4O15 Piezoelectric Crystal Using Mixed Flux Agents. Crystals, 2020, 10, 698.	1.0	2
49071	Integration and Synergy of Organic Single Crystals and Metalâ€“Organic Frameworks in Coreâ€“Shell Heterostructures Enables Outstanding Gas Selectivity for Detection. Advanced Functional Materials, 2020, 30, 2005727.	7.8	17
49072	Prediction of the Abnormal Properties in Monolayer Î±â€Al_xGa_{2â^'}_xO₃. Advanced Theory and Simulations, 2020, 3, 2000102.	1.3	3
49073	Machine learning corrected alchemical perturbation density functional theory for catalysis applications. AICHE Journal, 2020, 66, e17041.	1.8	10
49074	Accuracy in Resolving the First Hydration Layer on a Transition-Metal Oxide Surface: Experiment (AP-XPS) and Theory. Journal of Physical Chemistry C, 2020, 124, 21407-21417.	1.5	7
49075	Machine Learning Potential for Hexagonal Boron Nitride Applied to Thermally and Mechanically Induced Rippling. Journal of Physical Chemistry C, 2020, 124, 22278-22290.	1.5	25
49076	Temperature-Dependent Cationic Doping-Driven Phonon Dynamics Investigation in CdO Thin Films Using Raman Spectroscopy. Journal of Physical Chemistry C, 2020, 124, 21818-21828.	1.5	4
49077	Tracking the formation, fate and consequence for catalytic activity of Pt single sites on CeO2. Nature Catalysis, 2020, 3, 824-833.	16.1	209
49078	Nanometre-scale spectroscopic visualization of catalytic sites during a hydrogenation reaction on a Pd/Au bimetallic catalyst. Nature Catalysis, 2020, 3, 834-842.	16.1	84

#	Article	IF	Citations
49079	Creating a two-dimensional hole gas in a polar/polar LaAlO₃/KTaO₃ perovskite heterostructure. Journal of Materials Chemistry C, 2020, 8, 14230-14237.	2.7	10
49080	Anomalous elastic properties of superionic ice. Physical Review B, 2020, 102, .	1.1	7
49081	Intrinsic topological phases in <mml:math xmlns:mml="http://www.w3.org/1998/Math/MathML"><mml:mrow><mml:msub><mml:mi>Mn</mml:mi><mml:mn>2</mml:mn></mml: tuned by the layer magnetization. Physical Review B, 2020, 102, .	1.1	22
49082	Methane Conversion over C2N-Supported Fe2 Dimers. Catalysts, 2020, 10, 973.	1.6	1
49083	Hydrogen Adsorption on Ru-Encapsulated, -Doped and -Supported Surfaces of C60. Surfaces, 2020, 3, 408-422.	1.0	5
49084	Phosphorus Pentamers: Floating Nanoflowers form a 2D Network. Advanced Functional Materials, 2020, 30, 2004531.	7.8	12
49085	Family of Magicâ€Sized Carbon Clusters on Transition Metal Substrates. Advanced Functional Materials, 2020, 30, 2006671.	7.8	2
49086	Single Copper Atoms Supported on ZnS as an Efficient Catalyst for Electrochemical Reduction of CO to CH₃OH. ChemNanoMat, 2020, 6, 1806-1811.	1.5	9
49087	Structural evolution, electronic and physicochemical properties of tin ozonide nanoclusters: a density functional theory perspective. Journal of Nanoparticle Research, 2020, 22, 1.	0.8	0
49088	Consequences of ¹³¹I Transmutation in Gas Phase Radioiodine Molecules and Adsorbed on Graphite Surface. Journal of Physical Chemistry C, 2020, 124, 21461-21466.	1.5	0
49089	Strong Electronâ€“Phonon Interaction in 2D Vertical Homovalent IIIâ€“V Singularities. ACS Nano, 2020, 14, 13127-13136.	7.3	8
49090	Preferential phosphate sorption and Al substitution on goethite. Environmental Science: Nano, 2020, 7, 3497-3508.	2.2	11
49091	Optoelectronic and photocatalytic applications of hBPâ€“XMY (M = Mo, W; (X â‰ Y) = S, Se, Te) van der Waals heterostructures. Physical Chemistry Chemical Physics, 2020, 22, 23028-23037.	1.3	7
49092	Prediction of two-dimensional CP₃ as a promising electrode material with a record-high capacity for Na ions. Nanoscale Advances, 2020, 2, 5271-5279.	2.2	12
49093	First-principles surface energies for monoclinic Ga2O3 and Al2O3 and consequences for cracking of (AlxGa1â^'x)2O3. APL Materials, 2020, 8, .	2.2	53
49094	Achieving room-temperature brittle-to-ductile transition in ultrafine layered Fe-Al alloys. Science Advances, 2020, 6, .	4.7	26
49095	Large Impact of Approximate Exchange-Correlation Functionals on Modeling the Water Gas Shift Reaction on Copper. Journal of Physical Chemistry C, 2020, 124, 22506-22520.	1.5	5
49096	Oxygen-Doped VS₄ Microspheres with Abundant Sulfur Vacancies as a Superior Electrocatalyst for the Hydrogen Evolution Reaction. ACS Sustainable Chemistry and Engineering, 2020, 8, 15055-15064.	3.2	25

#	Article	IF	Citations
49097	Structure and Density of H₂Oâ€Rich Mg₂SiO₄ Melts at High Pressure From Ab Initio Simulations. Journal of Geophysical Research: Solid Earth, 2020, 125, e2020JB020365.	1.4	10
49098	Fabrication of a novel magnetic topological heterostructure and temperature evolution of its massive Dirac cone. Nature Communications, 2020, 11, 4821.	5.8	47
49099	First-principles study of phase stability, elastic and thermodynamic properties of AlCrFeNi medium-entropy alloys. International Journal of Modern Physics B, 2020, 34, 2050218.	1.0	5
49100	Atomistic Insights into Interfacial Reactions of FeCr2O4 Oxide Films in High-Temperature Water. International Journal of Electrochemical Science, 2020, , 8662-8673.	0.5	1
49101	Vinyleneâ€Linked Covalent Organic Frameworks (COFs) with Symmetryâ€Tuned Polarity and Photocatalytic Activity. Angewandte Chemie, 2020, 132, 24053-24061.	1.6	39
49102	Adsorption and Diffusion of Potassium on 2D SnC Sheets for Potential Highâ€Performance Anodic Applications of Potassiumâ€Ion Batteries. ChemElectroChem, 2020, 7, 3832-3838.	1.7	33
49103	Interphase Boundary Segregation into an Ordered Coreâ€“Shell Structure with a Shell Containing Two Unit Cells. Crystal Growth and Design, 2020, 20, 6629-6635.	1.4	5
49104	Chiral gold nanoparticles enantioselectively rescue memory deficits in a mouse model of Alzheimerâ€™s disease. Nature Communications, 2020, 11, 4790.	5.8	188
49105	Structural dynamics of basaltic melt at mantle conditions with implications for magma oceans and superplumes. Nature Communications, 2020, 11, 4815.	5.8	17
49106	Structural, optical, transport, and solar cell properties of 2D halide perovskite MAZX3 (Zâ€‰=â€‰Pb, Sn, and) Tj ETQq1 1 0.784314 rg	1.1	18
49107	Tuning Atomically Dispersed Fe Sites in Metalâ€“Organic Frameworks Boosts Peroxidase-Like Activity for Sensitive Biosensing. Nano-Micro Letters, 2020, 12, 184.	14.4	77
49108	Physical state of an early magma ocean constrained by the thermodynamics and viscosity of iron silicate liquid. Earth and Planetary Science Letters, 2020, 551, 116556.	1.8	3
49109	Density functional theoretical study of Au4/In2O3 catalyst for CO2 hydrogenation to methanol: The strong metal-support interaction and its effect. Journal of CO2 Utilization, 2020, 42, 101313.	3.3	39
49110	A theoretical approach to the structural, elastic and electronic properties of Ti8â^'xV4â^'yMox+y+zAl4â^'z lightweight shape memory alloys for biomaterial implant applications. Physica B: Condensed Matter, 2020, 598, 412416.	1.3	5
49111	Surface Charge and Electrostatic Spin Crossover Effects in CoN₄ Electrocatalysts. ACS Catalysis, 2020, 10, 12148-12155.	5.5	69
49112	A density functional theory study on the interface stability between CsPbBr3 and CuI. AIP Advances, 2020, 10, .	0.6	4
49113	Enhanced heterogenous hydration of SO 2 through immobilization of pyridinic-N on carbon materials. Royal Society Open Science, 2020, 7, 192248.	1.1	1
49114	Strain-tunable ferromagnetism and chiral spin textures in two-dimensional Janus chromium dichalcogenides. Physical Review B, 2020, 102, .	1.1	86

#	Article	IF	Citations
49115	Magnetotransport properties and topological phase transition in NaCd4As3. Physical Review B, 2020, 102, .	1.1	1
49116	Doping-driven electronic and lattice dynamics in the phase-change material vanadium dioxide. Physical Review B, 2020, 102, .	1.1	8
49117	Alloying with Sn Suppresses Sintering of Size-Selected Subnano Pt Clusters on SiO₂ with and without Adsorbates. Chemistry of Materials, 2020, 32, 8595-8605.	3.2	19
49118	Halogen-Doping Effect on the Delithiation and Charge Transfer of (Li₂S)₁₀ Cluster. Journal of Physical Chemistry A, 2020, 124, 8949-8958.	1.1	3
49119	Intercalation of Lithium into Graphite: Insights from First-Principles Simulations. Journal of Physical Chemistry C, 2020, 124, 21985-21992.	1.5	11
49120	Adsorption of Acetonitrile on Si(111)-(7 Ã— 7). ACS Omega, 2020, 5, 24179-24185.	1.6	3
49121	Enhancement of van der Waals Interlayer Coupling through Polar Janus MoSSe. Journal of the American Chemical Society, 2020, 142, 17499-17507.	6.6	80
49122	Theoretical study of metal/silica interfaces: Ti, Fe, Cr and Ni on Î²-cristobalite. Physical Chemistry Chemical Physics, 2020, 22, 21453-21462.	1.3	5
49123	An experimentally validated neural-network potential energy surface for H-atom on free-standing graphene in full dimensionality. Physical Chemistry Chemical Physics, 2020, 22, 26113-26120.	1.3	14
49124	Carbon phosphide nanosheets and nanoribbons: insights on modulating their electronic properties by first principles calculations. Physical Chemistry Chemical Physics, 2020, 22, 22520-22528.	1.3	4
49125	Effects of molecular adsorption on the spin-wave spectrum and magnon relaxation in two-dimensional Cr₂Ge₂Te₆. Physical Chemistry Chemical Physics, 2020, 22, 22047-22054.	1.3	11
49126	Establishing the accuracy of density functional approaches for the description of noncovalent interactions in biomolecules. Physical Chemistry Chemical Physics, 2020, 22, 21685-21695.	1.3	4
49127	A DFT and microkinetic study of propylene oxide selectivity over copper-based catalysts: effects of copper valence states. Catalysis Science and Technology, 2020, 10, 7640-7651.	2.1	16
49128	New possible candidate structure for phase IV of solid hydrogen. RSC Advances, 2020, 10, 26443-26450.	1.7	1
49129	How does the Li-distribution in the 16d sites determine the stability of A₃(Li,Ti₅)O₁₂ (A = Li and Na)?. RSC Advances, 2020, 10, 33509-33516.	1.7	6
49130	Photocatalytic, structural and optical properties of mixed anion solid solutions Ba3Sc2â^'xInxO5Cu2S2 and Ba3In2O5Cu2S2â^'ySey. Journal of Materials Chemistry A, 2020, 8, 19887-19897.	5.2	8
49131	Exploring the potential of MnX (S, Sb) monolayers for antiferromagnetic spintronics: A theoretical investigation. Journal of Applied Physics, 2020, 128, .	1.1	15
49132	Charge Density Depinning in Defective MoTe₂ Transistor by Oxygen Intercalation. Advanced Functional Materials, 2020, 30, 2004880.	7.8	20

#	Article	IF	Citations
49133	Vinyleneâ€Linked Covalent Organic Frameworks (COFs) with Symmetryâ€Tuned Polarity and Photocatalytic Activity. Angewandte Chemie - International Edition, 2020, 59, 23845-23853.	7.2	197
49134	Enhancing stability of CsPbBr 3 nanocrystals lightâ€emitting diodes through polymethylmethacrylate physical adsorption. Nano Select, 2020, 1, 372-381.	1.9	5
49135	Lowâ€energy Sr 2 MSbO 5.5 (M = Ca and Sr) structures show significant distortions near oxygen vacancies. International Journal of Quantum Chemistry, 2020, 120, e26356.	1.0	2
49136	Key Experiments and Thermodynamic Description of the Co-Nb-Ni System. Metallurgical and Materials Transactions A: Physical Metallurgy and Materials Science, 2020, 51, 5892-5911.	1.1	11
49137	Structural characterization and property modification for two-dimensional (001) SrTiO3 nanosheets. Applied Nanoscience (Switzerland), 2020, 10, 4273-4279.	1.6	8
49138	Search for adsorption geometry of precursor on surface using genetic algorithm: MoO2Cl2 on SiO2 surface. Journal of the Korean Ceramic Society, 2020, 57, 669-675.	1.1	3
49143	Periodic Solids and Electron Bands. , 2020, , 81-108.		0
49144	Uniform Electron Gas and sp-Bonded Metals. , 2020, , 109-128.		0
49145	Density Functional Theory: Foundations. , 2020, , 129-144.		0
49146	The Kohnâ€“Sham Auxiliary System. , 2020, , 145-170.		0
49147	Functionals for Exchange and Correlation I. , 2020, , 171-187.		0
49148	Functionals for Exchange and Correlation II. , 2020, , 188-214.		0
49149	Electronic Structure of Atoms. , 2020, , 215-229.		0
49150	Pseudopotentials. , 2020, , 230-258.		0
49152	Plane Waves and Grids: Basics. , 2020, , 262-282.		0
49153	Plane Waves and Real-Space Methods: Full Calculations. , 2020, , 283-294.		0
49154	Localized Orbitals: Tight-Binding. , 2020, , 295-319.		0
49155	Localized Orbitals: Full Calculations. , 2020, , 320-331.		0

#	Article	IF	Citations
49156	Augmented Functions: APW, KKR, MTO. , 2020, , 332-364.		0
49157	Augmented Functions: Linear Methods. , 2020, , 365-385.		0
49158	Locality and Linear-Scaling O(N) Methods. , 2020, , 386-410.		0
49159	Quantum Molecular Dynamics (QMD). , 2020, , 411-426.		0
49160	Response Functions: Phonons and Magnons. , 2020, , 427-445.		0
49161	Excitation Spectra and Optical Properties. , 2020, , 446-464.		0
49162	Surfaces, Interfaces, and Lower-Dimensional Systems. , 2020, , 465-480.		0
49163	Wannier Functions. , 2020, , 481-498.		0
49164	Polarization, Localization, and Berry Phases. , 2020, , 499-516.		0
49165	Topology of the Electronic Structure of a Crystal: Introduction. , 2020, , 517-530.		0
49166	Two-Band Models: Berry Phase, Winding, and Topology. , 2020, , 531-546.		0
49167	Topological Insulators I: Two Dimensions. , 2020, , 547-568.		0
49168	Topological Insulators II: Three Dimensions. , 2020, , 569-580.		0
49187	Decomposition of Carbon Tetrachloride on Gold Surfaces. Journal of Physical Chemistry C, 2020, 124, 20874-20880.	1.5	4
49188	Controlling Hydrocarbon (De)Hydrogenation Pathways with Bifunctional PtCu Single-Atom Alloys. Journal of Physical Chemistry Letters, 2020, 11, 8751-8757.	2.1	20
49189	High-Entropy Perovskites as Multifunctional Metal Oxide Semiconductors: Synthesis and Characterization of (Gd_{0.2}Nd_{0.2}La_{0.2}Sm_{0.2}Y_{0.2})CoO₃. ACS Applied Electronic Materials, 2020, 2, 3211-3220.	2.0	43
49190	Sodium Storage Mechanism Investigations through Structural Changes in Hard Carbons. ACS Applied Energy Materials, 2020, 3, 9918-9927.	2.5	56
49191	Engineering the Electronic, Thermoelectric, and Excitonic Properties of Two-Dimensional Group-III Nitrides through Alloying for Optoelectronic Devices (B_{1â€“x}Al_xN, Al_{1â€“x}Ga_xN, and ... J. Phys. Chem. C, 2020, 124, 46416-46428.	4.5	20

#	Article	IF	Citations
49192	Electric Field Tuning of Interlayer Coupling in Noncentrosymmetric 3R-MoS₂ with an Electric Double Layer Interface. ACS Applied Materials & Interfaces, 2020, 12, 46900-46907.	4.0	10
49193	Zn Metal Atom Doping on the Surface Plane of One-Dimesional NiMoO₄ Nanorods with Improved Redox Chemistry. ACS Applied Materials & Interfaces, 2020, 12, 44815-44829.	4.0	67
49194	Enhancing the Rapid Na⁺-Storage Performance via Electron/Ion Bridges through GeS₂/Graphene Heterojunction. ACS Nano, 2020, 14, 13952-13963.	7.3	55
49195	Effect of Hydration on the Molecular Dynamics of Hydroxychloroquine Sulfate. ACS Omega, 2020, 5, 21231-21240.	1.6	8
49196	Long-range focusing of magnetic bound states in superconducting lanthanum. Nature Communications, 2020, 11, 4573.	5.8	19
49197	A picture of pseudogap phase related to charge fluxes. Npj Computational Materials, 2020, 6, .	3.5	7
49198	Identifying candidate hosts for quantum defects via data mining. Npj Computational Materials, 2020, 6, .	3.5	28
49199	Efficient construction of linear models in materials modeling and applications to force constant expansions. Npj Computational Materials, 2020, 6, .	3.5	32
49200	AiiDA 1.0, a scalable computational infrastructure for automated reproducible workflows and data provenance. Scientific Data, 2020, 7, 300.	2.4	142
49201	Nature of the Dirac gap modulation and surface magnetic interaction in axion antiferromagnetic topological insulator $${hbox {MnBi}}_2 {hbox {Te}}_4$$. Scientific Reports, 2020, 10, 13226.	1.6	62
49202	Dimension reduction of thermoelectric properties using barycentric polynomial interpolation at Chebyshev nodes. Scientific Reports, 2020, 10, 13456.	1.6	2
49203	Broken symmetries and the related interface-induced effects at Weyl-system TaAs in proximity of noble metals. Scientific Reports, 2020, 10, 14438.	1.6	0
49204	Hidden porous boron nitride as a high-efficiency membrane for hydrogen purification. Physical Chemistry Chemical Physics, 2020, 22, 22778-22784.	1.3	16
49205	Time-resolved observation of Câ€“C coupling intermediates on Cu electrodes for selective electrochemical CO₂ reduction. Energy and Environmental Science, 2020, 13, 4301-4311.	15.6	197
49206	Pd nanoparticle growth monitored by DRIFT spectroscopy of adsorbed CO. Analyst, The, 2020, 145, 7534-7540.	1.7	17
49207	Hydrogen inserted into the Si(100)-2 Ã— 1-H surface: a first-principles study. Physical Chemistry Chemical Physics, 2020, 22, 21851-21857.	1.3	4
49208	On the structure and electronic properties of Fe₂V_{0.8}W_{0.2}Al thin films. Physical Chemistry Chemical Physics, 2020, 22, 22549-22554.	1.3	3
49209	P-doped nickel sulfide nanosheet arrays for alkaline overall water splitting. Catalysis Science and Technology, 2020, 10, 7581-7590.	2.1	18

#	Article	IF	Citations
49210	Strain-induced band modulation and excellent stability, transport and optical properties of penta-MP₂ (M = Ni, Pd, and Pt) monolayers. Nanoscale Advances, 2020, 2, 4566-4580.	2.2	10
49211	Atomic dynamics of stress-induced lattice misalignment structures in a KDP subsurface. RSC Advances, 2020, 10, 23944-23952.	1.7	4
49212	First-principles study of vacancy defects at interfaces between monolayer MoS₂ and Au. RSC Advances, 2020, 10, 28725-28730.	1.7	9
49213	Biâ€“Zn codoping in GeTe synergistically enhances band convergence and phonon scattering for high thermoelectric performance. Journal of Materials Chemistry A, 2020, 8, 21642-21648.	5.2	36
49214	Substitutional doped GeSe: tunable oxidative states with strain engineering. Journal of Materials Chemistry C, 2020, 8, 13655-13667.	2.7	16
49215	Rethinking the magnetic properties of lepidocrocite: A density functional theory and cluster expansion study. Journal of Applied Physics, 2020, 128, .	1.1	1
49216	Many-body reactive force field development for carbon condensation in C/O systems under extreme conditions. Journal of Chemical Physics, 2020, 153, 054103.	1.2	17
49217	Regular Arrangement of Two-Dimensional Clusters of Blue Phosphorene on Ag(111). Chinese Physics Letters, 2020, 37, 096803.	1.3	17
49218	Hut-shaped lead nanowires with one-dimensional electronic properties. Physical Review B, 2020, 102, .	1.1	3
49219	Structural transition from marcasite to pyrite phase in FeSe2 under high pressure: a first-principles study. European Physical Journal B, 2020, 93, 1.	0.6	10
49220	Band engineering of borophene superlattice based on zigzag nanoribbons: A DFT study. Modern Physics Letters B, 2020, 34, 2050359.	1.0	3
49221	Insights into Interface Charge Extraction in a Noble-Metal-Free Doped Z-Scheme NiO@BiOCl Heterojunction. Catalysts, 2020, 10, 958.	1.6	5
49222	Fe3 Cluster Anchored on the C2N Monolayer for Efficient Electrochemical Nitrogen Fixation. Catalysts, 2020, 10, 974.	1.6	15
49223	Mechanistic Insights for Dry Reforming of Methane on Cu/Ni Bimetallic Catalysts: DFT-Assisted Microkinetic Analysis for Coke Resistance. Catalysts, 2020, 10, 1043.	1.6	30
49224	Superhard Boron-Rich Boron Carbide with Controlled Degree of Crystallinity. Materials, 2020, 13, 3622.	1.3	19
49225	DFT-CEF Approach for the Thermodynamic Properties and Volume of Stable and Metastable Alâ€“Ni Compounds. Metals, 2020, 10, 1142.	1.0	4
49226	Isolated Cobalt Ions Embedded in Magnesium Oxide Nanostructures: Spectroscopic Properties and Redox Activity. Chemistry - A European Journal, 2020, 26, 16049-16056.	1.7	5
49227	Band-Edge Engineering To Eliminate Radiation-Induced Defect States in Perovskite Scintillators. ACS Applied Materials & Interfaces, 2020, 12, 46296-46305.	4.0	19

#	Article	IF	Citations
49228	Computational Study of Borophene with Line Defects as Sensors for Nitrogen-Containing Gas Molecules. ACS Applied Nano Materials, 2020, 3, 9961-9968.	2.4	24
49229	Highly Efficient Photo-/Electrocatalytic Reduction of Nitrogen into Ammonia by Dual-Metal Sites. ACS Central Science, 2020, 6, 1762-1771.	5.3	135
49230	Meron-like topological spin defects in monolayer CrCl3. Nature Communications, 2020, 11, 4724.	5.8	65
49231	First-principles screening of novel ferroelectric MXene phases with a large piezoelectric response and unusual auxeticity. Nanoscale, 2020, 12, 21291-21298.	2.8	48
49232	Stability of epitaxial BiXO3 phases by density-functional theory. APL Materials, 2020, 8, .	2.2	4
49233	Lithium intercalation in <mml:math xmlns:mml="http://www.w3.org/1998/Math/MathML"><mml:msub><mml:mi>MoS</mml:mi><mml:mn>2</mml:mn></mml:msub></mml:math> bilayers and implications for moirÃ© flat bands. Physical Review B, 2020, 102, .	1.1	12
49234	Polar Structures of KNdNb₂O₇ and KNdTa₂O₇. Chemistry of Materials, 2020, 32, 7965-7972.	3.2	8
49235	Cation and Anion Co-doped Perovskite Nanofibers for Highly Efficient Electrocatalytic Oxygen Evolution. ACS Applied Materials & Interfaces, 2020, 12, 41259-41268.	4.0	39
49236	Zn₃B₇O₁₃Cl: A New Deep-Ultraviolet Transparency Nonlinear Optical Crystal with Boracite Structure. ACS Applied Materials & Interfaces, 2020, 12, 42942-42948.	4.0	14
49237	Comparative Study of Olefin Production from CO and CO₂ Using Na- and K-Promoted Zinc Ferrite. ACS Catalysis, 2020, 10, 10742-10759.	5.5	42
49238	Te-Vacancy-Induced Surface Collapse and Reconstruction in Antiferromagnetic Topological Insulator MnBi₂Te₄. ACS Nano, 2020, 14, 11262-11272.	7.3	47
49239	Surface chelation of cesium halide perovskite by dithiocarbamate for efficient and stable solar cells. Nature Communications, 2020, 11, 4237.	5.8	106
49240	Design of two-dimensional carbon-nitride structures by tuning the nitrogen concentration. Npj Computational Materials, 2020, 6, .	3.5	31
49241	Phase segregation reversibility in mixed-metal hydroxide water oxidation catalysts. Nature Catalysis, 2020, 3, 743-753.	16.1	199
49242	Structure dependency of the atomic-scale mechanisms of platinum electro-oxidation and dissolution. Nature Catalysis, 2020, 3, 754-761.	16.1	72
49243	How interface properties control the equilibrium shape of coreâ€“shell Feâ€“Au and Feâ€“Ag nanoparticles. Nanoscale, 2020, 12, 18079-18090.	2.8	15
49244	Nonmonotonic interfacial friction with normal force in two-dimensional crystals. Physical Review B, 2020, 102, .	1.1	9
49245	Nanoscale Mapping of Heterogeneous Strain and Defects in Individual Magnetic Nanocrystals. Crystals, 2020, 10, 658.	1.0	5

#	Article	IF	Citations
49246	Formic Acid: A Hydrogen-Bonding Cocatalyst for Formate Decomposition. ACS Catalysis, 2020, 10, 10812-10825.	5.5	36
49247	Optical excitations and thermoelectric properties of two-dimensional holey graphene. Physical Review B, 2020, 102, .	1.1	28
49248	Radiative capture rates at deep defects from electronic structure calculations. Physical Review B, 2020, 102, .	1.1	14
49249	Highly active dry methane reforming catalysts with boosted in situ grown Ni-Fe nanoparticles on perovskite via atomic layer deposition. Science Advances, 2020, 6, eabb1573.	4.7	79
49250	The Effect of Functional Groups on the Electrocatalytic Activity of Carbon Nanotubes with Different Wall Numbers toward Carbohydrazide Oxidation Reaction. Chemistry - an Asian Journal, 2020, 15, 3451-3455.	1.7	2
49251	Noble-metal-free catalyst with enhanced hydrogen evolution reaction activity based on granulated Co-doped Ni-Mo phosphide nanorod arrays. Nano Research, 2020, 13, 3321-3329.	5.8	37
49252	Crystal Structure and Stoichiometric Composition of Potassium-Intercalated Tetracene. Inorganic Chemistry, 2020, 59, 12545-12551.	1.9	1
49253	Stable Surface Terminations of a Perovskite Oxyhydride from First-Principles. Journal of Physical Chemistry C, 2020, 124, 18557-18563.	1.5	5
49254	Antiferromagnetic and Electric Polarized States in Two-Dimensional Janus Semiconductor Fe2Cl3I3. Journal of Physical Chemistry C, 2020, 124, 19219-19227.	1.5	15
49255	Quantum Accurate Prediction of Plutoniumâ€“Plutonium Dihydride Phase Equilibrium Using a Lattice Gas Model. Journal of Physical Chemistry C, 2020, 124, 20881-20888.	1.5	4
49256	Opposite Hydrogen Behaviors in GaAsN and InAsN Alloys: Band Gap Opening Versus Donor Doping. Journal of Physical Chemistry C, 2020, 124, 19240-19251.	1.5	5
49257	Two-Dimensional Valleytronics in Single-Layer t-ZrNY (Y = Cl, Br) Predicted from First Principles. Journal of Physical Chemistry C, 2020, 124, 20598-20604.	1.5	13
49258	Molecular Dynamics Characterization of Sr-Doped Biomimetic Hydroxyapatite Nanoparticles. Journal of Physical Chemistry C, 2020, 124, 19704-19715.	1.5	6
49259	Understanding the Specific Heat Enhancement in Metal-Containing Nanofluids for Thermal Energy Storage: Experimental and Ab Initio Evidence for a Strong Interfacial Layering Effect. ACS Applied Energy Materials, 2020, 3, 9246-9256.	2.5	20
49260	Coordination engineering of iridium nanocluster bifunctional electrocatalyst for highly efficient and pH-universal overall water splitting. Nature Communications, 2020, 11, 4246.	5.8	221
49261	Modulating oxygen coverage of Ti3C2Tx MXenes to boost catalytic activity for HCOOH dehydrogenation. Nature Communications, 2020, 11, 4251.	5.8	81
49262	Yang-Mills structure for electronâ€“phonon interactions in vanadium dioxide. Scientific Reports, 2020, 10, 12547.	1.6	0
49263	Graphenylene-supported single-atom (Ru and Mo) catalysts for CO and NO oxidations. New Journal of Chemistry, 2020, 44, 15733-15741.	1.4	8

#	Article	IF	Citations
49264	Visible region absorption in TMDs/phosphorene heterostructures for use in solar energy conversion applications. RSC Advances, 2020, 10, 31730-31739.	1.7	20
49265	Autonomous intelligent agents for accelerated materials discovery. Chemical Science, 2020, 11, 8517-8532.	3.7	49
49266	Prediction of single-layer TiVI₆ as a promising two-dimensional valleytronic semiconductor with spontaneous valley polarization. Journal of Materials Chemistry C, 2020, 8, 13220-13225.	2.7	39
49267	Bandgap and strain engineering in epitaxial rocksalt structure (Ti_{0.5}Mg_{0.5})_{1â^'x}Al_xN(001) semiconductors. Journal of Materials Chemistry C, 2020, 8, 12677-12688.	2.7	6
49268	Orbital selectivity of layer-resolved tunneling in the iron-based superconductor <mml:math xmlns:mml="http://www.w3.org/1998/Math/MathML"><mml:mrow><mml:msub><mml:mi>Ba</mml:mi><mml:mrow><mml:mn>0.6</m mathvariant="normal">K</mml:mi><mml:mrow><mml:mn>0.4</mml:mn></mml:mrow></mml:msub><mml:msub><mml:mi>Fe</mml:m Physical Review B, 2020, 102, .	1.1	9
49269	Bond strengthening in lateral heterostructures of transition metal dichalcogenides. Physical Review B, 2020, 102, .	1.1	6
49270	A computational examination of the zeta and eta phases in the hafnium nitrides. Journal of the American Ceramic Society, 2020, 103, 7202-7212.	1.9	2
49271	Electrical Conduction Characteristic of a 2D MXene Device with Cu/Cr2C/TiN Structure Based on Density Functional Theory. Materials, 2020, 13, 3671.	1.3	7
49272	Phase Behavior in Rhombohedral NaSiCON Electrolytes and Electrodes. Chemistry of Materials, 2020, 32, 7908-7920.	3.2	58
49273	The Instability of Monolayer-Thick PbSe on VSe₂. Chemistry of Materials, 2020, 32, 7992-8003.	3.2	5
49274	Structure of a Silica Thin Film on Oxidized Cu(111): Conservation of the Honeycomb Lattice and Role of the Interlayer. Journal of Physical Chemistry C, 2020, 124, 20942-20949.	1.5	9
49275	Interplay of Mechanical and Chemical Tunability of Phosphorene for Flexible Nanoelectronic Applications. Journal of Physical Chemistry C, 2020, 124, 24391-24399.	1.5	5
49276	Two-Dimensional SnSe Composited with One-Dimensional Mn Nanowires: A Promising Thermoelectric with Ultrahigh Power Factor. ACS Applied Energy Materials, 2020, 3, 9234-9245.	2.5	9
49277	Tuning proton-coupled electron transfer by crystal orientation for efficient water oxidization on double perovskite oxides. Nature Communications, 2020, 11, 4299.	5.8	93
49278	Understanding colossal barocaloric effects in plastic crystals. Nature Communications, 2020, 11, 4190.	5.8	30
49279	Exceptional mechano-electronic properties in the HfN₂ monolayer: a promising candidate in low-power flexible electronics, memory devices and photocatalysis. Physical Chemistry Chemical Physics, 2020, 22, 21275-21287.	1.3	18
49280	Computational screening of efficient graphene-supported transition metal single atom catalysts toward the oxygen reduction reaction. Journal of Materials Chemistry A, 2020, 8, 19319-19327.	5.2	49
49281	Semiconductor-to-metal reconstructive phase transition and superconductivity of anti-perovskite Ca3PN under hydrostatic pressure. Journal of Materials Chemistry C, 2020, 8, 13072-13078.	2.7	6

#	Article	IF	Citations
49282	Strain-induced magnetic transition in CaMnO3 ultrathin films. Physical Review B, 2020, 102, .	1.1	5
49283	Honeycomb-Lattice Mott Insulator on Tantalum Disulphide. Physical Review Letters, 2020, 125, 096403.	2.9	8
49284	COMPREHENSIVE EXAMINATION OF DEHYDROXYLATION OF KAOLINITE, DISORDERED KAOLINITE, AND DICKITE: EXPERIMENTAL STUDIES AND DENSITY FUNCTIONAL THEORY. Clays and Clay Minerals, 2020, 68, 319-333.	0.6	37
49285	Magnetoelasticity in CrXTe₃ (X = C, Si) van der Waals Heterobilayers. ACS Applied Electronic Materials, 2020, 2, 3171-3177.	2.0	1
49286	Selective C₃-C₄ Keto-Alcohol Production from Cellulose Hydrogenolysis over Ni-WO_x/C Catalysts. ACS Catalysis, 2020, 10, 10646-10660.	5.5	39
49287	A Mn-N3 single-atom catalyst embedded in graphitic carbon nitride for efficient CO2 electroreduction. Nature Communications, 2020, 11, 4341.	5.8	257
49288	Thermodynamic feasibility of the four-stage chloride-induced depassivation mechanism of iron. Npj Materials Degradation, 2020, 4, .	2.6	11
49289	Observation of gapped state in rare-earth monopnictide HoSb. Scientific Reports, 2020, 10, 12961.	1.6	14
49290	Fermi-crossing Type-II Dirac fermions and topological surface states in NiTe2. Scientific Reports, 2020, 10, 12957.	1.6	29
49291	Quantifying the evolution of atomic interaction of a complex surface with a functionalized atomic force microscopy tip. Scientific Reports, 2020, 10, 14104.	1.6	17
49292	Ultra-thin lead oxide piezoelectric layers for reduced environmental contamination using a liquid metal-based process. Journal of Materials Chemistry A, 2020, 8, 19434-19443.	5.2	29
49293	Computational Design of Copper doped Indium for electrocatalytic Reduction of CO₂ to Formic Acid. ChemCatChem, 2020, 12, 5632-5636.	1.8	13
49294	Heteroatom Promoted Ni/Al₂O₃ Catalysts for Highly Efficient Hydrogenation of 1,4â€Butynediol to 1,4â€Butenediol. ChemistrySelect, 2020, 5, 10072-10080.	0.7	4
49295	Three-Fold Enhancement of In-Plane Thermal Conductivity of Borophene through Metallic Atom Intercalation. Nano Letters, 2020, 20, 7619-7626.	4.5	33
49296	Two-Dimensional Electron Gas at the Spinel/Perovskite Interface: Suppression of Polar Catastrophe by an Ultrathin Layer of Interfacial Defects. ACS Applied Materials & Interfaces, 2020, 12, 42982-42991.	4.0	7
49297	Density Functional Theory Studies of Si₂BN Nanosheets as Anode Materials for Magnesium-Ion Batteries. ACS Applied Nano Materials, 2020, 3, 9055-9063.	2.4	40
49298	Activation of Copper Species on Carbon Nitride for Enhanced Activity in the Arylation of Amines. ACS Catalysis, 2020, 10, 11069-11080.	5.5	29
49299	Surface Functionalization of Ti₃C₂T_x MXene with Highly Reliable Superhydrophobic Protection for Volatile Organic Compounds Sensing. ACS Nano, 2020, 14, 11490-11501.	7.3	247

#	Article	IF	Citations
49300	Pressure-Induced Modulation of Electronic and Optical Properties of Surface O-Functionalized Ti₂C MXene. ACS Omega, 2020, 5, 22248-22254.	1.6	10
49301	Impact of various dopant elements on the electronic structure of Cu₂ZnSnS₄(CZTS) thin films: a DFT study. CrystEngComm, 2020, 22, 5786-5791.	1.3	8
49302	8-Hydroxyquinoline complexes (Alq3) on Al(111): atomic scale structure, energetics and charge distribution. New Journal of Chemistry, 2020, 44, 15209-15222.	1.4	5
49303	Strain gradient induced spatially indirect excitons in single crystalline ZnO nanowires. Nanoscale, 2020, 12, 19083-19087.	2.8	6
49304	Electrically tunable high Curie temperature two-dimensional ferromagnetism in van der Waals layered crystals. Applied Physics Letters, 2020, 117, .	1.5	74
49305	Experimental and Theoretical Investigation of the Energy-Storage Behavior of a Polyaniline-Linked Reduced-Graphene-Oxideâ€“ <mml:math xmlns:mml="http://www.w3.org/1998/Math/MathML" display="inline" overflow="scroll"><mml:msub><mml:mrow><mml:mi>Sn</mml:mi><mml:mi mathvariant="normal">O</mml:mi></mml:mrow><mml:mn>2</mml:mn></mml:msub></mml:math> Ternary Nanohybrid Electrode. Physical Review Applied, 2020, 14, .	1.5	18
49306	Mapping the unoccupied state dispersions in Ta2NiSe5 with resonant inelastic x-ray scattering. Physical Review B, 2020, 102, .	1.1	13
49307	Isoelectronically substituted group-III based monolayers: An ab initio study. Physical Review B, 2020, 102, .	1.1	3
49308	Dualâ€Functional Atomic Zinc Decorated Hollow Carbon Nanoreactors for Kinetically Accelerated Polysulfides Conversion and Dendrite Free Lithium Sulfur Batteries. Advanced Energy Materials, 2020, 10, 2002271.	10.2	137
49309	Adsorption Mechanism and Highâ€Performance Metalâ€Ion Batteries Anode Material for Semimetal Carbon Honeycomb. Physica Status Solidi (A) Applications and Materials Science, 2020, 217, 2000433.	0.8	1
49310	The Yield Strength Anomaly in Coâ€“Ni Design Space. Minerals, Metals and Materials Series, 2020, , 948-958.	0.3	3
49311	Endohedrally Doped Cage Clusters. Chemical Reviews, 2020, 120, 9021-9163.	23.0	164
49312	Elucidating the Coupling Mechanisms of Rapid Intramolecular Vibrational Energy Redistribution in Nitromethane: Ab Initio Molecular Dynamics Simulation. Journal of Physical Chemistry A, 2020, 124, 8184-8191.	1.1	9
49313	Different Thermal Responses of Local Structures in Pd43Cu27Ni10P20 Alloy from Glass to Liquid. Journal of Physical Chemistry C, 2020, 124, 19817-19828.	1.5	5
49314	Physical Properties and Characterization of the Binary Clathrate Hydrate with Methane + 1,1,1,3,3-Pentafluoropropane (HFC-245fa) + Water. Journal of Physical Chemistry C, 2020, 124, 20736-20745.	1.5	7
49315	Ultralow Thermal Conductivity and High Thermoelectric Figure of Merit in Two-Dimensional Thallium Selenide. ACS Applied Energy Materials, 2020, 3, 9315-9325.	2.5	24
49316	Combinatorial Large-Area MoS₂/Anataseâ€“TiO₂ Interface: A Pathway to Emergent Optical and Optoelectronic Functionalities. ACS Applied Materials & Interfaces, 2020, 12, 44345-44359.	4.0	10
49317	Pd Nanoparticles Supported on N- and P-Co-doped Carbon as Catalysts for Reversible Formate-Based Chemical Hydrogen Storage. ACS Applied Nano Materials, 2020, 3, 9209-9217.	2.4	19

#	Article	IF	Citations
49318	Thermal Transformation of Molecular Ni²⁺â€“N₄ Sites for Enhanced CO₂ Electroreduction Activity. ACS Catalysis, 2020, 10, 10920-10931.	5.5	81
49319	Turbulent hydrodynamics in strongly correlated Kagome metals. Nature Communications, 2020, 11, 3997.	5.8	25
49320	Site-dependent reactivity of MoS2 nanoparticles in hydrodesulfurization of thiophene. Nature Communications, 2020, 11, 4369.	5.8	44
49321	Towards intermediate-band photovoltaic absorbers: theoretical insights on the incorporation of Ti and Nb in In2S3. Npj Computational Materials, 2020, 6, .	3.5	10
49322	Uncertainty quantification in molecular simulations with dropout neural network potentials. Npj Computational Materials, 2020, 6, .	3.5	42
49323	Piezochromism in the magnetic chalcogenide MnPS3. Npj Quantum Materials, 2020, 5, .	1.8	26
49324	Anisotropic optical properties of GeS investigated by optical absorption and photoreflectance. Materials Advances, 2020, 1, 1886-1894.	2.6	24
49325	Theoretical study on the photocatalytic properties of 2D InX(X = S, Se)/transition metal disulfide (MoS₂and WS₂) van der Waals heterostructures. Nanoscale, 2020, 12, 20025-20032.	2.8	49
49326	Flux Growth of Single-Crystalline Hollandite-Type Potassium Ferrotitanate Microrods From KCl Flux. Frontiers in Chemistry, 2020, 8, 714.	1.8	3
49327	SnCN₂: A Carbodiimide with an Innovative Approach for Energy Storage Systems and Phosphors in Modern LED Technology. ChemElectroChem, 2020, 7, 4550-4561.	1.7	13
49328	Sr₆(BO₃)₃BN₂: An Oxidoâ€“Nitridoâ€“Borate Phosphor Featuring BN₂ Dumbbells. Chemistry of Materials, 2020, 32, 8587-8594.	3.2	7
49329	Experimental and Ab Initio Studies of Intrinsic Defects in â€œAntizeoliteâ€•Borates with a Ba₁₂(BO₃)₆⁶⁺ Framework and Their Influence on Properties. Inorganic Chemistry, 2020, 59, 13598-13606.	1.9	9
49330	Influence of Acidity on the Methanol-to-DME Reaction in Zeotypes: A First Principles-Based Microkinetic Study. Journal of Physical Chemistry C, 2020, 124, 14658-14663.	1.5	21
49331	Scanning Tunneling Microscopy Studies of Potassium-Doped Picene Films on Au(111) Surface. Journal of Physical Chemistry C, 2020, 124, 22025-22034.	1.5	0
49332	Probing the Dielectric Effects on the Colloidal 2D Perovskite Oxides by Eu³⁺ Luminescence. ACS Applied Materials & Interfaces, 2020, 12, 44961-44969.	4.0	13
49333	Surprisingly good thermoelectric performance of a black phosphorus/blue phosphorus van der Waals heterostructure. Physical Chemistry Chemical Physics, 2020, 22, 22390-22398.	1.3	20
49334	Defective h-BN sheet embedded atomic metals as highly active and selective electrocatalysts for NH₃ fabrication via NO reduction. Physical Chemistry Chemical Physics, 2020, 22, 22627-22634.	1.3	32
49335	Elucidating hydrogen storage properties of two-dimensional siligraphene (SiC₈) monolayers upon selected metal decoration. Sustainable Energy and Fuels, 2020, 4, 5578-5587.	2.5	22

#	Article	IF	Citations
49336	On the importance of hexagonal phases in TM (TMâ€‰=â€‰Ti, Zr, and Hf) mono-nitrides. Journal of Applied Physics, 2020, 128, .	1.1	1
49337	de Haasâ€“van Alphen quantum oscillations and electronic structure in the large-Chern-number topological chiral semimetal CoSi. Physical Review B, 2020, 102, .	1.1	15
49338	Inflection points in the conduction-band structure of <mml:math xmlns:mml="http://www.w3.org/1998/Math/MathML"><mml:mrow><mml:mi>BaSn</mml:mi><mml:msub><mml:mi mathvariant="normal">O</mml:mi><mml:mn>3</mml:mn></mml:msub></mml:mrow></mml:math>. Physical Review B, 2020, 102, .	1.1	3
49339	Prediction of an Extended Ferroelectric Clathrate. Physical Review Letters, 2020, 125, 127601.	2.9	12
49340	DFT study the water-gas shift reaction over Cu/Î±-MoC surface. Journal of Molecular Modeling, 2020, 26, 237.	0.8	9
49341	Selective Ammonium Removal from Synthetic Wastewater by Flow-Electrode Capacitive Deionization Using a Novel K₂Ti₂O₅-Activated Carbon Mixture Electrode. Environmental Science & Technology, 2020, 54, 12723-12731.	4.6	38
49342	Revisiting Competing Paths in Electrochemical CO₂ Reduction on Copper via Embedded Correlated Wavefunction Theory. Journal of Chemical Theory and Computation, 2020, 16, 6528-6538.	2.3	21
49343	Efficient Training of Machine Learning Potentials by a Randomized Atomic-System Generator. Journal of Physical Chemistry B, 2020, 124, 8704-8710.	1.2	4
49344	Nanoscale Mgâ€“B via Surfactant Ball Milling of MgB₂: Morphology, Composition, and Improved Hydrogen Storage Properties. Journal of Physical Chemistry C, 2020, 124, 21761-21771.	1.5	17
49345	Radiation-Induced Interfacial Hydroxyl Transformation on Boehmite and Gibbsite Basal Surfaces. Journal of Physical Chemistry C, 2020, 124, 22185-22191.	1.5	8
49346	Self-Chargeable Flexible Solid-State Supercapacitors for Wearable Electronics. ACS Applied Materials & Interfaces, 2020, 12, 44883-44891.	4.0	32
49347	Layered and Cubic Semiconductors AGaMâ€²Q₄ (A⁺ =) Tj ETQq1 1 0.784314 rgB High Third-Harmonic Generation. Journal of the American Chemical Society, 2020, 142, 17730-17742.	6.6	21
49348	Structural, electronic, and optical properties of cubic formamidinium lead iodide perovskite: a first-principles investigation. RSC Advances, 2020, 10, 32364-32369.	1.7	24
49349	The role of water vapor during the synthesis of hydrogen doped In2O3. Applied Physics Letters, 2020, 117, .	1.5	4
49350	Prediction of high-strain polar phases in antiferroelectric <mml:math xmlns:mml="http://www.w3.org/1998/Math/MathML"><mml:msub><mml:mi>PbZrO</mml:mi><mml:mn>3</mml:mn></mml:msub></m from a multiscale approach. Physical Review B, 2020, 102, .	1.1	1
49351	Dirac fermions in the antiferromagnetic spintronics material CuMnAs. Physical Review B, 2020, 102, .	1.1	8
49352	First-Principles Study of Effects of Combined Ti Supervalent Cations and Lithium Ion Vacancies Doping on Crystal and Electronic Structures and Conductivity in LiFePO₄. Key Engineering Materials, 0, 861, 277-283.	0.4	5
49353	Study of Structural and Magnetic Properties of Spinel Zn Doped Cobalt Ferrites. Solid State Phenomena, 2020, 310, 124-133.	0.3	5

#	Article	IF	Citations
49354	Supramolecular Porous Assemblies of Atomically Precise Catalytically Active Cerium-Based Clusters. Chemistry of Materials, 2020, 32, 8522-8529.	3.2	23
49355	Epitaxial Stabilization of SrCu₃O₄ with Infinite Cu_{3/2}O₂ Layers. Inorganic Chemistry, 2020, 59, 10042-10047.	1.9	4
49356	A Machine Learning Model on Simple Features for CO₂ Reduction Electrocatalysts. Journal of Physical Chemistry C, 2020, 124, 22471-22478.	1.5	125
49357	Quantum Phase Engineering of Two-Dimensional Post-Transition Metals by Substrates: Toward a Room-Temperature Quantum Anomalous Hall Insulator. Nano Letters, 2020, 20, 7186-7192.	4.5	9
49358	Modeling the Interface between Lithium Metal and Its Native Oxide. ACS Applied Materials & Interfaces, 2020, 12, 46015-46026.	4.0	25
49359	Emergent Ferroelectricity in Otherwise Nonferroelectric Oxides by Oxygen Vacancy Design at Heterointerfaces. ACS Applied Materials & Interfaces, 2020, 12, 45602-45610.	4.0	15
49360	High Thermoelectric Performance in Two-Dimensional Janus Monolayer Material WS-X (X = Se) Tj ETQq0 0 0 rgBT /Overlock 10 Tf	4.6	130
49361	Bulk vs Intrinsic Activity of NiFeO_x Electrocatalysts in the Oxygen Evolution Reaction: The Influence of Catalyst Loading, Morphology, and Support Material. ACS Catalysis, 2020, 10, 11768-11778.	5.5	23
49362	Atomic-Level Electronic Properties of Carbon Nitride Monolayers. ACS Nano, 2020, 14, 14008-14016.	7.3	22
49363	Toward lateral heterostructures with two-dimensional MoX₂H₂ (X = As, Sb). Physical Chemistry Chemical Physics, 2020, 22, 22584-22590.	1.3	1
49364	Structural evolution of CrN nanocube electrocatalysts during nitrogen reduction reaction. Nanoscale, 2020, 12, 19276-19283.	2.8	24
49365	Effect of fluorination and Li-excess on the Li migration barrier in Mn-based cathode materials. Journal of Materials Chemistry A, 2020, 8, 19965-19974.	5.2	20
49366	Surface decoration accelerates the hydrogen evolution kinetics of a perovskite oxide in alkaline solution. Energy and Environmental Science, 2020, 13, 4249-4257.	15.6	33
49367	Complexes and compensation in degenerately donor doped GaN. Applied Physics Letters, 2020, 117, .	1.5	15
49368	Facilitating Phase Evolution for a High-Energy-Efficiency, Low-Cost O3-Type Na_xCu_{0.18}Fe_{0.3}Mn_{0.52}O₂ Sodium Ion Battery Cathode. Inorganic Chemistry, 2020, 59, 13792-13800.	1.9	15
49369	Single Fe Site on the Surface of Î³-Al₂O₃: Insights from Density Functional Theory Periodic Boundary Approach. Journal of Physical Chemistry C, 2020, 124, 20931-20941.	1.5	7
49370	Bonding Properties of Isolated Metal Atoms on Two-Dimensional Oxides. Journal of Physical Chemistry C, 2020, 124, 20960-20973.	1.5	9
49371	Insulatorâ€“Metal Transition in the Nd₂CoFeO₆ Disordered Double Perovskite. Journal of Physical Chemistry C, 2020, 124, 22733-22742.	1.5	5

#	Article	IF	Citations
49372	Modulation Effect Generated by A Cations in Hybrid A₂BBâ€™X₆ Double Halogen Perovskite Materials. ACS Applied Materials & Interfaces, 2020, 12, 44798-44804.	4.0	15
49373	Epitaxial Growth and Determination of Band Alignment of Bi₂Te₃â€“WSe₂ Vertical van der Waals Heterojunctions. , 2020, 2, 1351-1359.		9
49374	In Situ Identification of Reaction Intermediates and Mechanistic Understandings of Methane Oxidation over Hematite: A Combined Experimental and Theoretical Study. Journal of the American Chemical Society, 2020, 142, 17119-17130.	6.6	59
49375	Pressure-stabilized divalent ozonide CaO3 and its impact on Earthâ€™s oxygen cycles. Nature Communications, 2020, 11, 4702.	5.8	20
49376	Electric field tuned anisotropic to isotropic thermal transport transition in monolayer borophene without altering its atomic structure. Nanoscale, 2020, 12, 19178-19190.	2.8	15
49377	Vacancy-induced anion and cation redox chemistry in cation-deficient F-doped anatase TiO2. Journal of Materials Chemistry A, 2020, 8, 20393-20401.	5.2	8
49378	Hydrogen doping in wide-bandgap amorphous Inâ€“Gaâ€“O semiconductors. Journal of Materials Chemistry C, 2020, 8, 15436-15449.	2.7	6
49379	Thermal effects on the electronic properties of sodium electride under high pressures. Physical Review B, 2020, 102, .	1.1	10
49380	Density Functional Theory Calculations of the Stability and Statistical Disorder in Crystals of the Kappa Phase of Me3Â+ÂxW10Ââ€“ÂxC3Â+Ây (Me = Fe, Co, Ni). Russian Journal of Physical Chemistry A, 2020, 94, 1369-1374.	0.1	0
49381	Nearâ€Infrared Lightâ€Responsive Cuâ€Doped Cs₂AgBiBr₆. Advanced Functional Materials, 2020, 30, 2005521.	7.8	56
49382	Highâ€Throughput Growth of Waferâ€Scale Monolayer Transition Metal Dichalcogenide via Vertical Ostwald Ripening. Advanced Materials, 2020, 32, e2003542.	11.1	69
49383	Precise Control of Perovskite Crystallization Kinetics via Sequential Aâ€Site Doping. Advanced Materials, 2020, 32, e2004630.	11.1	122
49384	Hybrid Pd38 nanocluster/Ni(OH)2-graphene catalyst for enhanced HCOOH dehydrogenation: First principles approach. Korean Journal of Chemical Engineering, 2020, 37, 1411-1418.	1.2	5
49385	Parallel Nanoimprint Forming of One-Dimensional Chiral Semiconductor for Strain-Engineered Optical Properties. Nano-Micro Letters, 2020, 12, 160.	14.4	8
49386	Nanoscale Modeling of Surface Phenomena in Aluminum Using Machine Learning Force Fields. Journal of Physical Chemistry C, 2020, 124, 22127-22136.	1.5	9
49387	Crystalline Structures and Energetic Properties of Lithium Pentazolate under Ambient Conditions. ACS Omega, 2020, 5, 24946-24953.	1.6	7
49388	A flavin-Cu²⁺ supramolecular complex for highly selective sorting of semiconducting single-walled carbon nanotubes with specific chiralities. Chemical Communications, 2020, 56, 12415-12418.	2.2	2
49389	Magnetism arising from Mexican-hat-like band dispersion in the WSe2/SnS2 heterostructure via interlayer strain. Physical Chemistry Chemical Physics, 2020, 22, 21961-21967.	1.3	1

#	Article	IF	Citations
49390	Atomic structures of high Miller index surfaces of NiO. Journal of Materials Chemistry C, 2020, 8, 14164-14171.	2.7	7
49391	Strain-tunable magnetism and nodal loops in monolayer MnB. Applied Physics Letters, 2020, 117, .	1.5	24
49392	Cause of Extremely Long-Lasting Room-Temperature Persistent Photoconductivity in SrTiO3 and Related Materials. Physical Review Letters, 2020, 125, 126404.	2.9	8
49393	Following the microscopic pathway to adsorption through chemisorption and physisorption wells. Science, 2020, 369, 1461-1465.	6.0	42
49394	Density and sound velocity of liquid Fe-S alloys at Earth's outer core P-T conditions. American Mineralogist, 2020, 105, 1349-1354.	0.9	4
49395	The External Electric Field-Induced Tunability of the Schottky Barrier Height in Graphene/AlN Interface: A Study by First-Principles. Nanomaterials, 2020, 10, 1794.	1.9	8
49396	Tuning band alignment and optical properties of 2D van der Waals heterostructure via ferroelectric polarization switching. Frontiers of Physics, 2020, 15, 1.	2.4	20
49397	Topologization of Î²-antimonene on Bi2Se3 via proximity effects. Scientific Reports, 2020, 10, 14619.	1.6	17
49398	Integrating Conductivity, Captivity, and Immobility Ability into N/O Dualâ€Doped Porous Carbon Nanocage Anchored with CNT as an Effective Se Host for Advanced Kâ€Se Battery. Advanced Functional Materials, 2020, 30, 2003871.	7.8	45
49399	Molecular Functionalization of Chemically Active Defects in WSe 2 for Enhanced Optoâ€Electronics. Advanced Functional Materials, 2020, 30, 2005045.	7.8	22
49400	Photocatalytic Hydrogen Evolution under Ambient Conditions on Polymeric Carbon Nitride/Donorâ€Iâ€Acceptor Organic Molecule Heterostructures. Advanced Functional Materials, 2020, 30, 2005106.	7.8	46
49401	Dirac and Weyl Semimetals in Sn_{1â^'x}In_xTe. Physica Status Solidi - Rapid Research Letters, 2020, 14, 2000362.	1.2	2
49402	Possible quantum paraelectric state in Kitaev spin liquid candidate H3LiIr2O6. Science China: Physics, Mechanics and Astronomy, 2020, 63, 1.	2.0	8
49403	Crystal structure and X-ray absorption spectroscopy of trimethylarsine oxide dihydrate, (CH3)3AsOâ‹…2H2O. Powder Diffraction, 2020, 35, 190-196.	0.4	1
49404	On-Surface Synthesis of Nitrogen-Substituted Gold-Phosphorus Porous Network. Chemistry of Materials, 2020, 32, 8561-8566.	3.2	3
49405	Antiperovskite Oxides as Promising Candidates for High-Performance Ferroelectric Photovoltaics: First-Principles Investigation on Ba₄As₂O and Ba₄Sb₂O. ACS Applied Materials & Interfaces, 2020, 12, 43798-43804.	4.0	13
49406	Machine Learning-Enabled Design of Point Defects in 2D Materials for Quantum and Neuromorphic Information Processing. ACS Nano, 2020, 14, 13406-13417.	7.3	75
49407	Ambient-pressure and low-temperature upgrading of lignin bio-oil to hydrocarbons using a hydrogen buffer catalytic system. Nature Energy, 2020, 5, 759-767.	19.8	65

#	Article	IF	Citations
49408	Highly active and stable stepped Cu surface for enhanced electrochemical CO2 reduction to C2H4. Nature Catalysis, 2020, 3, 804-812.	16.1	298
49409	Unusual features of nitrogen substitutions in silicene. RSC Advances, 2020, 10, 32193-32201.	1.7	8
49410	High elastic moduli, controllable bandgap and extraordinary carrier mobility in single-layer diamond. Journal of Materials Chemistry C, 2020, 8, 13819-13826.	2.7	24
49411	Molecularâ€Scale Strategies to Achieve High Efficiency and Low Efficiency Rollâ€off in Simplified Solutionâ€Processed Organic Lightâ€Emitting Diodes. Advanced Functional Materials, 2020, 30, 2005292.	7.8	21
49412	Highâ€Capacity Sodiumâ€“Prussian Blue Rechargeable Battery through Chelationâ€Induced Nanoâ€Porosity. Advanced Materials Interfaces, 2020, 7, 2000853.	1.9	22
49413	Multifidelity Statistical Machine Learning for Molecular Crystal Structure Prediction. Journal of Physical Chemistry A, 2020, 124, 8065-8078.	1.1	38
49414	Microscopic Mechanism Study of 4f Electronsâ€™ Positive Effect on the Enhanced Proton Conduction in a Pr-Doped BaCeO₃ Electrolyte. Journal of Physical Chemistry C, 2020, 124, 21232-21241.	1.5	10
49415	Minimizing Polymorphic Risk through Cooperative Computational and Experimental Exploration. Journal of the American Chemical Society, 2020, 142, 16668-16680.	6.6	34
49416	Fast Lithium Ion Conductivity in Layered (Liâ€“Ag)CrS₂. Journal of the American Chemical Society, 2020, 142, 18645-18651.	6.6	18
49417	Electronic, optical and thermoelectric properties of boron-doped nitrogenated holey graphene. Physical Chemistry Chemical Physics, 2020, 22, 21147-21157.	1.3	15
49418	Ultralow thermal conductivity in diamondoid lattices: high thermoelectric performance in chalcopyrite Cu_{0.8+y}Ag_{0.2}In_{1â^'y}Te₂. Energy and Environmental Science, 2020, 13, 3693-3705.	15.6	52
49419	[illegible] xmlns:mml="http://www.w3.org/1998/Math/MathML"><mml:mrow><mml:mi>Hf</mml:mi><mml:msub><mml:mi mathvariant="normal">N</mml:mi><mml:mn>2</mml:mn></mml:msub></mml:mrow></mml:math> and valley-contrasting physics at the <mml:math xmlns:mml="http://www.w3.org/1998/Math/MathML"><mml:mrow><mml:mi>Hf</mml:mi><mml:msub><mml:mi mathvariant="normal">N</mml:mi><mml:mn>2</mml:mn></mml:msub><mml:mo>â^'</mml:mo><mml:mi>WS</mml:mi><mml:msub>	1.1	35
49420	Interfacial Properties of Water on Hydrogenated and Fluorinated Graphene Surfaces: Parametrization of Nonbonded Interactions. Journal of Physical Chemistry C, 2020, 124, 21467-21475.	1.5	16
49421	Atomic-Scale Model and Electronic Structure of Cu2O/CH3NH3PbI3 Interfaces in Perovskite Solar Cells. ACS Applied Materials & Interfaces, 2020, 12, 44648-44657.	4.0	16
49422	Hybridisation of perovskite nanocrystals with organic molecules for highly efficient liquid scintillators. Light: Science and Applications, 2020, 9, 156.	7.7	85
49423	Capturing the active sites of multimetallic (oxy)hydroxides for the oxygen evolution reaction. Energy and Environmental Science, 2020, 13, 4225-4237.	15.6	186
49424	Ensemble-machine-learning-based correlation analysis of internal and band characteristics of thermoelectric materials. Journal of Materials Chemistry C, 2020, 8, 13079-13089.	2.7	9
49425	Materials perspective on new lithium chlorides and bromides: insights into thermo-physical properties. Physical Chemistry Chemical Physics, 2020, 22, 22758-22767.	1.3	15

#	Article	IF	Citations
49426	Unraveling the mechanisms of S-doped carbon nitride for photocatalytic oxygen reduction to H₂O₂. Physical Chemistry Chemical Physics, 2020, 22, 21099-21107.	1.3	29
49427	Size-dependent electrocatalytic activity of ORR/OER on palladium nanoclusters anchored on defective MoS₂monolayers. New Journal of Chemistry, 2020, 44, 16135-16143.	1.4	15
49428	First-principles study of two dimensional C₃N and its derivatives. RSC Advances, 2020, 10, 33469-33474.	1.7	15
49429	Giant intrinsic circular dichroism of enantiomorphic flat Chern bands and flatband devices. Physical Review B, 2020, 102, .	1.1	21
49430	Two-Dimensional Dirac Semimetals without Inversion Symmetry. Physical Review Letters, 2020, 125, 116402.	2.9	19
49431	Giant Thermal Enhancement of the Electric Polarization in Ferrimagnetic BiFe1â^'xCoxO3 Solid Solutions near Room Temperature. Physical Review Letters, 2020, 125, 117601.	2.9	9
49432	Confinement of CoP Nanoparticles in Nitrogenâ€Doped Yolkâ€Shell Porous Carbon Polyhedron for Ultrafast Catalytic Oxidation. Advanced Functional Materials, 2020, 30, 2003947.	7.8	97
49433	Computational Discovery of Stable Heteroanionic Oxychalcogenides ABXO (A, B = Metals; X = S, Se, and) Tj ETQq1 1 0.784314 rgBT /O	3.2	21
49434	Effect of Heteroaromaticity on Adsorption of Pyrazine on the Ge(100)-2Ã—1 Surface. Journal of Physical Chemistry C, 2020, 124, 22055-22068.	1.5	3
49435	Tunable Electronic Structure of Two-Dimensional MoX₂ (X = S, Se)/SnS₂ van der Waals Heterostructures. Journal of Physical Chemistry C, 2020, 124, 21357-21365.	1.5	16
49436	From Simple to Complex: Design of Inorganic Crystal Structures with a Topologically Extended Zintlâ€“Klemm Concept. Journal of Physical Chemistry Letters, 2020, 11, 8114-8120.	2.1	1
49437	Mechanisms of Interfacial Charge Transfer and Photocatalytic NO Oxidation on BiOBr/SnO₂ pâ€“n Heterojunctions. ACS Applied Materials & Interfaces, 2020, 12, 43741-43749.	4.0	77
49438	Quantum Transport in Two-Dimensional WS₂ with High-Efficiency Carrier Injection through Indium Alloy Contacts. ACS Nano, 2020, 14, 13700-13708.	7.3	26
49439	Antiferromagnetic topological insulator in stable exfoliated two-dimensional materials. Physical Review B, 2020, 102, .	1.1	21
49440	Immobilizing Pertechnetate in Ettringite via Sulfate Substitution. Environmental Science & Technology, 2020, 54, 13610-13618.	4.6	20
49441	Phonon Spectroscopy in Antimony and Tellurium Oxides. Journal of Physical Chemistry A, 2020, 124, 7869-7880.	1.1	6
49442	Composition-Gradient-Mediated Semiconductorâ€“Metal Transition in Ternary Transition-Metal-Dichalcogenide Bilayers. ACS Applied Materials & Interfaces, 2020, 12, 45184-45191.	4.0	12
49443	Insights into the Influence of CeO₂Crystal Facet on CO₂Hydrogenation to Methanol over Pd/CeO₂Catalysts. ACS Catalysis, 2020, 10, 11493-11509.	5.5	391

#	Article	IF	Citations
49444	Framework for analyzing the thermoreflectance spectra of metal thermal transducers with spectrally tunable time-domain thermoreflectance. Journal of Applied Physics, 2020, 128, 055107.	1.1	7
49445	Prediction of monolayered ferromagnetic <mml:math xmlns:mml="http://www.w3.org/1998/Math/MathML"><mml:msub><mml:mi>CrMnI</mml:mi><mml:mn>6</mml:mn></mml:msub><mml:m as an intrinsic high-temperature quantum anomalous Hall system. Physical Review B, 2020, 102, .	1.1	18
49446	Large Magnetic Anisotropy Energy and Robust Halfâ€Metallic Ferromagnetism in 2D MnXSe₄ (X = As, Sb). Annalen Der Physik, 2020, 532, 2000365.	0.9	4
49447	Ultrahigh Out-of-Plane Piezoelectricity Meets Giant Rashba Effect in 2D Janus Monolayers and Bilayers of Group IV Transition-Metal Trichalcogenides. Journal of Physical Chemistry C, 2020, 124, 21250-21260.	1.5	87
49448	Tuning Electronic and Magnetic Properties of Two-Dimensional Ferromagnetic Semiconductor CrI₃ through Adsorption of Benzene. Journal of Physical Chemistry C, 2020, 124, 22143-22149.	1.5	20
49449	Phase Control and In Situ Passivation of Quasi-2D Metal Halide Perovskites for Spectrally Stable Blue Light-Emitting Diodes. ACS Applied Materials & Interfaces, 2020, 12, 45056-45063.	4.0	49
49450	Atomic Insights into Robust Ptâ€“PdO Interfacial Site-Boosted Hydrogen Generation. ACS Catalysis, 2020, 10, 11417-11429.	5.5	19
49451	Liquidâ€Vapor Coexistence and Critical Point of Mg₂SiO₄ From Ab Initio Simulations. Geophysical Research Letters, 2020, 47, e2020GL089599.	1.5	6
49452	Real and virtual polymorphism of titanium selenide with robust interatomic potentials. Journal of Materials Chemistry A, 2020, 8, 14054-14061.	5.2	8
49453	Crystalline Molecular Standards for Low-Frequency Vibrational Spectroscopies. Journal of Infrared, Millimeter, and Terahertz Waves, 2020, 41, 1284-1300.	1.2	9
49454	Conductivity control via minimally invasive anti-Frenkel defects in a functional oxide. Nature Materials, 2020, 19, 1195-1200.	13.3	20
49455	Hydrogen solution in tungsten (W) under different temperatures and strains: a first principles calculation study. Physical Chemistry Chemical Physics, 2020, 22, 19623-19630.	1.3	4
49456	Prediction of stable energetic beryllium pentazolate salt under ambient conditions. CrystEngComm, 2020, 22, 6057-6062.	1.3	6
49457	Tailoring the phase transition temperature to achieve high-performance cubic GeTe-based thermoelectrics. Journal of Materials Chemistry A, 2020, 8, 18880-18890.	5.2	61
49458	Thickness dependence of electronic structure and optical properties of a correlated van der Waals antiferromagnetic <mml:math xmlns:mml="http://www.w3.org/1998/Math/MathML"><mml:msub><mml:mi>NiPS</mml:mi><mml:mn>3</mml:mn></mml:msub><mml:m thin film. Physical Review B, 2020, 102, .	1.1	26
49459	Polaron-Induced Deep Defect Levels in Brookite TiO₂: A Many-Body Greenâ€™s Function Theory Study. Journal of Physical Chemistry C, 2020, 124, 19024-19032.	1.5	9
49460	How TeO Defects in the MoVNbTeO Catalyst Material Affect the V⁴⁺ Distribution: A Computational Study. Journal of Physical Chemistry C, 2020, 124, 18628-18638.	1.5	5
49461	Computational Screening Single-Atom Catalysts Supported on g-CN for N₂ Reduction: High Activity and Selectivity. ACS Sustainable Chemistry and Engineering, 2020, 8, 13749-13758.	3.2	167

#	Article	IF	Citations
49462	A novel SiO monolayer with a negative Poisson's ratio and Dirac semimetal properties. Physical Chemistry Chemical Physics, 2020, 22, 20107-20113.	1.3	6
49463	Giant magnetoresistance and dual spin filtering effect in ferromagnetic 6,6,12/Î³-graphyne zigzag nanoribbon lateral heterojunction. Physical Chemistry Chemical Physics, 2020, 22, 18548-18555.	1.3	6
49464	Low Ca²⁺ concentration doping enhances the mechanical properties and ionic conductivity of Na₃PS₄ superionic conductors based on first-principles. Physical Chemistry Chemical Physics, 2020, 22, 19816-19822.	1.3	14
49465	Unravelling the role of oxophilic metal in promoting the deoxygenation of catechol on Ni-based alloy catalysts. Catalysis Science and Technology, 2020, 10, 6849-6859.	2.1	25
49466	Screening of transition (Y, Zr, Hf, V, Nb, Mo, and Ru) and rare-earth (La and Pr) elements as potential effective dopants for thermoelectric GeTe â€“ an experimental and theoretical appraisal. Journal of Materials Chemistry A, 2020, 8, 19805-19821.	5.2	43
49467	The geometrical structure and electronic properties of trivalent Ho3+ doped Y2O3 crystals: a first-principles study. RSC Advances, 2020, 10, 28674-28679.	1.7	1
49468	Liquidlike Cu atom diffusion in weakly ionic compounds <mml:math xmlns:mml="http://www.w3.org/1998/Math/MathML"><mml:mrow><mml:msub><mml:mi>Cu</mml:mi><mml:mn>2</mml:mn></mml: mathvariant="normal">S</mml:mi></mml:mrow></mml:math> and <mml:math xmlns:mml="http://www.w3.org/1998/Math/MathML"><mml:mrow><mml:msub><mml:mi>Cu</mml:mi><mml:mn>2</mml:mn></mml: Physical Review B, 2020, 102, .	1.1	12
49469	Pure spin current generation via photogalvanic effect with spatial inversion symmetry. Physical Review B, 2020, 102, .	1.1	43
49470	Molecular Design and Operational Stability: Toward Stable 3D/2D Perovskite Interlayers. Advanced Science, 2020, 7, 2001014.	5.6	43
49471	Effect of Intercalants inside Birnessite-Type Manganese Oxide Nanosheets for Sensor Applications. Inorganic Chemistry, 2020, 59, 15595-15605.	1.9	3
49472	Tuning Adsorption Energies and Reaction Pathways by Alloying: PdZn versus Pd for CO₂ Hydrogenation to Methanol. Journal of Physical Chemistry Letters, 2020, 11, 7672-7678.	2.1	24
49473	One-Dimensional Magnetic Order Stabilized in Edge-Reconstructed MoS₂ Nanoribbon via Bias Voltage. Journal of Physical Chemistry Letters, 2020, 11, 7531-7535.	2.1	13
49474	Microscopic Manipulation of Ferroelectric Domains in SnSe Monolayers at Room Temperature. Nano Letters, 2020, 20, 6590-6597.	4.5	136
49475	Single CuO/Cu₂O/Cu Microwire Covered by a Nanowire Network as a Gas Sensor for the Detection of Battery Hazards. ACS Applied Materials & Interfaces, 2020, 12, 42248-42263.	4.0	36
49476	Large cation ethylammonium incorporated perovskite for efficient and spectra stable blue light-emitting diodes. Nature Communications, 2020, 11, 4165.	5.8	217
49477	Unraveling the relationship between exposed surfaces and the photocatalytic activity of Ag₃PO₄: an in-depth theoretical investigation. RSC Advances, 2020, 10, 30640-30649.	1.7	12
49478	Extremely low-frequency phonon material and its temperature- and photo-induced switching effects. Chemical Science, 2020, 11, 8989-8998.	3.7	23
49479	The fate of aluminium in (Na,Bi)TiO₃-based ionic conductors. Journal of Materials Chemistry A, 2020, 8, 18188-18197.	5.2	12

#	Article	IF	Citations
49480	Sb 5s² lone pairs and band alignment of Sb₂Se₃: a photoemission and density functional theory study. Journal of Materials Chemistry C, 2020, 8, 12615-12622.	2.7	19
49481	Charge transfer and strain tuned antiferromagnetism in the two-dimensional CrCl3/[Mo2C(â€“O)]2 heterojunction. Physical Chemistry Chemical Physics, 2020, 22, 20477-20481.	1.3	1
49482	Visible and near-infrared driven Yb³⁺/Tm³⁺ co-doped InVO₄ nanosheets for highly efficient photocatalytic applications. Dalton Transactions, 2020, 49, 14030-14045.	1.6	21
49483	Computational insights into selective CO₂ hydrogenation to CH₃OH catalysed by ZnO based nanocages. Materials Advances, 2020, 1, 2300-2309.	2.6	12
49484	Molecular engineering of pyrene carbazole dyes with a single bond and double bond as the mode of linkage. New Journal of Chemistry, 2020, 44, 16511-16525.	1.4	11
49485	Strain forces tuned the electronic and optical properties in GaTe/MoS₂ van der Waals heterostructures. RSC Advances, 2020, 10, 25136-25142.	1.7	5
49486	Phase transformation, charge transfer, and ionic diffusion of Na₄MnV(PO₄)₃ in sodium-ion batteries: a combined first-principles and experimental study. Journal of Materials Chemistry A, 2020, 8, 17477-17486.	5.2	23
49487	First-principles study of the catalytic properties of Co-doped molybdenum disulfide nanoribbons for the hydrogen evolution reaction. Journal of Applied Physics, 2020, 128, 045307.	1.1	7
49488	Improving the performance of phase-change memory by grain refinement. Journal of Applied Physics, 2020, 128, 075101.	1.1	25
49489	Magnetocrystalline anisotropy of the easy-plane metallic antiferromagnet <mml:math xmlns:mml="http://www.w3.org/1998/Math/MathML"><mml:mrow><mml:mi mathvariant="normal">F</mml:mi><mml:msub><mml:mi mathvariant="normal">e</mml:mi><mml:mn>2</mml:mn></mml:msub><mml:mi>As</mml:mi></mml:mrow></mml:math>.	1.1	7
49490	Exchange splitting and exchange-induced nonreciprocal photonic behavior of graphene in <mml:math xmlns:mml="http://www.w3.org/1998/Math/MathML"><mml:mrow><mml:mi>Cr</mml:mi><mml:msub><mml:mi mathvariant="normal">I</mml:mi><mml:mn>3</mml:mn></mml:msub></mml:mrow></mml:math> -graphene van der Waals heterostructures. Physical Review B, 2020, 102, .	1.1	9
49491	Microscopic Mechanisms of Glasslike Lattice Thermal Transport in Cubic <mml:math xmlns:mml="http://www.w3.org/1998/Math/MathML" display="inline"><mml:mrow><mml:mrow><mml:msub><mml:mrow><mml:mi>Cu</mml:mi></mml:mrow><mml:mrow><mml:mn>12</mml:mn> <mml:mathvariant="normal">S</mml:mi></mml:mrow><mml:mrow><mml:mn>13</mml:mn></mml:mrow></mml:msub></mml:mrow></. Physical Review Letters, 2020, 125, 085901.	2.9	62
49492	High-Temperature Quantum Anomalous Hall Insulators in Lithium-Decorated Iron-Based Superconductor Materials. Physical Review Letters, 2020, 125, 086401.	2.9	46
49493	Local Disorder-Induced Elevation of Intrinsic Anomalous Hall Conductance in an Electron-Doped Magnetic Weyl Semimetal. Physical Review Letters, 2020, 125, 086602.	2.9	45
49494	Dualâ€Ionâ€Diffusion Induced Degradation in Leadâ€Free Cs₂AgBiBr₆ Double Perovskite Solar Cells. Advanced Functional Materials, 2020, 30, 2002342.	7.8	86
49495	Irradiationâ€Induced Extremes Create Hierarchical Faceâ€/Bodyâ€Centeredâ€Cubic Phases in Nanostructured High Entropy Alloys. Advanced Materials, 2020, 32, 2002652.	11.1	14
49496	Superselective Removal of Lead from Water by Two-Dimensional MoS₂ Nanosheets and Layer-Stacked Membranes. Environmental Science & Technology, 2020, 54, 12602-12611.	4.6	87
49497	Catalytic Performance of Two-Dimensional Bismuth Tuned by Defect Engineering for Nitrogen Reduction Reaction. Journal of Physical Chemistry C, 2020, 124, 19563-19570.	1.5	8

#	Article	IF	Citations
49498	Assessing the Potential of Amorphous Silica Surfaces for the Removal of Phenol from Biofuel: A Density Functional Theory Investigation. Journal of Physical Chemistry C, 2020, 124, 20262-20269.	1.5	11
49499	Elucidating the Structure of Ethanol-Producing Active Sites at Oxide-Derived Cu Electrocatalysts. ACS Catalysis, 2020, 10, 10488-10494.	5.5	35
49500	Phase Evolution of Re_{1â€“x}Mo_xSe₂ Alloy Nanosheets and Their Enhanced Catalytic Activity toward Hydrogen Evolution Reaction. ACS Nano, 2020, 14, 11995-12005.	7.3	59
49501	Direct insights into the role of epoxy groups on cobalt sites for acidic H2O2 production. Nature Communications, 2020, 11, 4181.	5.8	204
49502	Band gap crossover and insulatorâ€“metal transition in the compressed layered CrPS4. Npj Quantum Materials, 2020, 5, .	1.8	23
49503	A folded ice monolayer. Physical Chemistry Chemical Physics, 2020, 22, 20388-20393.	1.3	5
49504	Why does there have to be a residual Na ion as a co-cation on Cu/SSZ-13?. Catalysis Science and Technology, 2020, 10, 6319-6329.	2.1	9
49505	First-principles study of Na insertion at TiO₂ anatase surfaces: new hints for Na-ion battery design. Nanoscale Advances, 2020, 2, 2745-2751.	2.2	75
49506	NECI: N-Electron Configuration Interaction with an emphasis on state-of-the-art stochastic methods. Journal of Chemical Physics, 2020, 153, 034107.	1.2	55
49507	Below bandgap photoluminescence of an AlN crystal: Co-existence of two different charging states of a defect center. APL Materials, 2020, 8, .	2.2	24
49508	High Thermoelectric Performance and Defect Energetics of Multipocketed Full Heusler Compounds. Physical Review Applied, 2020, 14, .	1.5	25
49509	Phonon-mediated dimensional crossover in bilayer <mml:math xmlns:mml="http://www.w3.org/1998/Math/MathML"><mml:mi>Cr</mml:mi><mml:msub><mml:mrow><mml:mi mathvariant="normal">I</mml:mi></mml:mrow><mml:mn>3</mml:mn></mml:msub></mml:math>. Physical Review B, 2020, 102, .	1.1	21
49510	Nonmagnetic doping induced quantum anomalous Hall effect in topological insulators. Physical Review B, 2020, 102, .	1.1	6
49511	Anharmonic Origin of the Giant Thermal Expansion of NaBr. Physical Review Letters, 2020, 125, 085504.	2.9	13
49512	Electrochemical Reduction of CO₂ on Metal-Based Cathode Electrocatalysts of Solid Oxide Electrolysis Cells. Industrial & Engineering Chemistry Research, 2020, 59, 15884-15893.	1.8	17
49513	High Thermoelectric Performance of AgSb_{1â€“x}Pb_xSe₂ Prepared by Fast Nonequilibrium Synthesis. ACS Applied Materials & Interfaces, 2020, 12, 41333-41341.	4.0	15
49514	A universal descriptor based on p_z-orbitals for the catalytic activity of multi-doped carbon bifunctional catalysts for oxygen reduction and evolution. Nanoscale, 2020, 12, 19375-19382.	2.8	28
49515	Dynamics Studies of Nitrogen Interstitial in GaN from Ab Initio Calculations. Materials, 2020, 13, 3627.	1.3	6

#	Article	IF	Citations
49516	A First‐Principles‐Based Sub‐Lattice Formalism for Predicting Off‐Stoichiometry in Materials for Solar Thermochemical Applications: The Example of Ceria. Advanced Theory and Simulations, 2020, 3, 2000112.	1.3	10
49517	Magnetic and Intercalation Properties of BaRu2O6 and SrRu2O6. Chemistry of Materials, 2020, 32, 8471-8480.	3.2	6
49518	Solvent-Induced Bond-Bending Isomerism in Hexaphenyl Carbodiphosphorane: Decisive Dispersion Interactions in the Solid State. Inorganic Chemistry, 2020, 59, 12054-12064.	1.9	9
49519	Modified Single Iteration Synchronous-Transit Approach to Bound Diffusion Barriers for Solid-State Reactions. Journal of Chemical Theory and Computation, 2020, 16, 5912-5922.	2.3	3
49520	The Role of the Height Fluctuation Effect in the Tunable Interfacial Electronic Structure of the Vertically Stacked BP/MoS₂ Heterojunction. Journal of Physical Chemistry C, 2020, 124, 20256-20261.	1.5	4
49521	Spatial Confinement as an Effective Strategy for Improving the Catalytic Selectivity in Acetylene Hydrogenation. ACS Applied Materials & Interfaces, 2020, 12, 39352-39361.	4.0	11
49522	Origin of the Unusual Stability of Zeolite-Encapsulated Sub-Nanometer Platinum. ACS Catalysis, 2020, 10, 11057-11068.	5.5	20
49523	van der Waals heterostructures based on MSSe (M = Mo, W) and graphene-like GaN: enhanced optoelectronic and photocatalytic properties for water splitting. Physical Chemistry Chemical Physics, 2020, 22, 20704-20711.	1.3	37
49524	Basal plane activation in monolayer MoTe₂ for the hydrogen evolution reaction via phase boundaries. Journal of Materials Chemistry A, 2020, 8, 19522-19532.	5.2	19
49525	Raman studies of hydrogen trapped in As4O6Â·2H2 at high pressure and low temperature. Journal of Chemical Physics, 2020, 153, 054501.	1.2	3
49526	Electronic band structure of three-dimensional topological insulators with different stoichiometry composition. Physical Review B, 2020, 102, .	1.1	3
49527	Strain modulation using defects in two-dimensional <mml:math xmlns:mml="http://www.w3.org/1998/Math/MathML"><mml:mrow><mml:mi>Mo</mml:mi><mml:msub><mml:mi mathvariant="normal">S</mml:mi><mml:mn>2</mml:mn></mml:msub></mml:mrow></mml:math>. Physical Review B, 2020, 102, .	1.1	8
49528	The Magnetic Proximity Effect Induced Large Valley Splitting in 2D InSe/FeI2 Heterostructures. Nanomaterials, 2020, 10, 1642.	1.9	7
49529	Dehydrogenation of Ethylene on Supported Palladium Nanoparticles: A Double View from Metal and Hydrocarbon Sides. Nanomaterials, 2020, 10, 1643.	1.9	14
49530	The Adsorption of NH₃ on the FeS₂ (100) Surface: A First-Principles Investigation. Materials Science Forum, 2020, 1001, 22-27.	0.3	0
49531	Thermodynamic Modeling of the Al-Li-Zr Ternary System. Journal of Phase Equilibria and Diffusion, 2020, 41, 623-641.	0.5	2
49532	Unconventional dual-vacancies in nickel diselenide-graphene nanocomposite for high-efficiency oxygen evolution catalysis. Nano Research, 2020, 13, 3292-3298.	5.8	16
49533	Robust In-Zn-O Thin-Film Transistors with a Bilayer Heterostructure Design and a Low-Temperature Fabrication Process Using Vacuum and Solution Deposited Layers. ACS Omega, 2020, 5, 21593-21601.	1.6	2

#	Article	IF	Citations
49534	Borophosphene as a promising Dirac anode with large capacity and high-rate capability for sodium-ion batteries. Physical Chemistry Chemical Physics, 2020, 22, 20851-20857.	1.3	18
49535	The structure, and electronic and magnetic properties of MX (M=GA, IN; X=S, SE, TE) nanoribbons. International Journal of Modern Physics B, 2020, 34, 2050168.	1.0	1
49536	Chemical and Laser Ablation Synthesis of Monometallic and Bimetallic Ni-Based Nanoparticles. Catalysts, 2020, 10, 1453.	1.6	17
49537	Two-Dimensional As/BlueP van der Waals Hetero-Structure as a Promising Photocatalyst for Water Splitting: A DFT Study. Coatings, 2020, 10, 1160.	1.2	9
49538	First Principles Study on the Thermoelectric Performance of CaAl₂Si₂-type Zintl Phase Compounds. Journal of the Physical Society of Japan, 2020, 89, 124707.	0.7	7
49539	Structure and Dynamics of Aqueous Electrolytes Confined in 2D-TiO2/Ti3C2T2 MXene Heterostructures. ACS Applied Materials & Interfaces, 2020, 12, 58378-58389.	4.0	25
49540	Crystal and Electronic Structures of A₂NaIO₆ Periodate Double Perovskites (A = Sr, Ca, Ba): Candidate Wasteforms for I-129 Immobilization. Inorganic Chemistry, 2020, 59, 18407-18419.	1.9	13
49541	Insights into Syngas Combustion on a Defective NiO Surface for Chemical Looping Combustion: Oxygen Migration and Vacancy Effects. Journal of Physical Chemistry C, 2020, 124, 28359-28370.	1.5	17
49542	Prediction of the Curie temperature considering the dependence of the phonon free energy on magnetic states. Npj Computational Materials, 2020, 6, .	3.5	20
49543	Strong spinâ€“orbit quenching via the product Jahnâ€“Teller effect in neutral group IV qubits in diamond. Npj Quantum Materials, 2020, 5, .	1.8	16
49544	Orbital-enhanced warping effect in px,py-derived Rashba spin splitting of monatomic bismuth surface alloy. Npj Quantum Materials, 2020, 5, .	1.8	7
49545	Phonon mode potential and its contribution to anharmonism. Scientific Reports, 2020, 10, 19783.	1.6	5
49546	Probing local distortion around structural defects in half-Heusler thermoelectric NiZrSn alloy. Scientific Reports, 2020, 10, 19820.	1.6	13
49547	Improved magnetostriction in Galfenol alloys by aligning crystal growth direction along easy magnetization axis. Scientific Reports, 2020, 10, 20055.	1.6	8
49548	Ab-initio investigation of preferential triangular self-formation of oxide heterostructures of monolayer $$hbox {WSe}_{2}$$. Scientific Reports, 2020, 10, 21737.	1.6	1
49549	Unveiling giant hidden Rashba effects in two-dimensional Si2Bi2. Npj 2D Materials and Applications, 2020, 4, .	3.9	14
49550	Dependency of solvation effects on metal identity in surface reactions. Communications Chemistry, 2020, 3, .	2.0	15
49551	Photoinduced metastable dd-exciton-driven metal-insulator transitions in quasi-one-dimensional transition metal oxides. Communications Physics, 2020, 3, .	2.0	3

#	Article	IF	Citations
49552	Nonlinear propagating modes beyond the phonons in fluorite-structured crystals. Communications Physics, 2020, 3, .	2.0	17
49553	In silicoinvestigation of Cu(In,Ga)Se₂-based solar cells. Physical Chemistry Chemical Physics, 2020, 22, 26682-26701.	1.3	3
49554	Highly effective and selective molecular nanowire catalysts for hydrogen and ammonia synthesis. Journal of Materials Chemistry A, 2020, 8, 26075-26084.	5.2	11
49555	Aliovalent-doped sodium chromium oxide (Na0.9Cr0.9Sn0.1O2 and Na0.8Cr0.9Sb0.1O2) for sodium-ion battery cathodes with high-voltage characteristics. RSC Advances, 2020, 10, 43273-43281.	1.7	9
49556	Structure, phonons, and orbital degrees of freedom in <mml:math xmlns:mml="http://www.w3.org/1998/Math/MathML"><mml:mrow><mml:msub><mml:mi>Fe</mml:mi><mml:mn>2</mml:mn></mml:r mathvariant="normal">O</mml:mi><mml:mn>8</mml:mn></mml:msub></mml:mrow></mml:math>. Physical Review B, 2020, 102, .	1.1	23
49557	Structure, magnetism, and electronic properties in <mml:math xmlns:mml="http://www.w3.org/1998/Math/MathML"><mml:mrow><mml:mn>3</mml:mn><mml:mi>d</mml:mi></mml:mrow><mml:mn		

#	Article	IF	Citations
49570	The adsorption of HEC and PVA as surfactants on SrTiO3 surface: A theoretical, experimental and applied investigation. Colloids and Surfaces A: Physicochemical and Engineering Aspects, 2020, 606, 125521.	2.3	2
49571	The First-Principles Prediction of Two Dimensional Monolayer Puckered WCAZ2 as the Anode Material of Li-ion Batteries. Materials Today Communications, 2020, 25, 101587.	0.9	1
49572	Effect of external electric field on hydrogen-related defect in amorphous silica. Materials Today Communications, 2020, 25, 101631.	0.9	0
49573	Two unexplored two-dimensional MSe2 (M = Cd, Zn) structures as the photocatalysts of water splitting and the enhancement of their performances by strain. Vacuum, 2020, 182, 109728.	1.6	12
49574	DFT Study of Methane Activation and Coupling on the (0001) and (112Ì…0) Surfaces of Î±-WC. Journal of Physical Chemistry C, 2020, 124, 26722-26729.	1.5	10
49575	Disperse Multimetal Atom-Doped Carbon as Efficient Bifunctional Electrocatalysts for Oxygen Reduction and Evolution Reactions: Design Strategies. Journal of Physical Chemistry C, 2020, 124, 27387-27395.	1.5	16
49576	First-Principles Mechanistic Study of the Initial Growth of SrO by Atomic Layer Deposition on TiO2-Terminated SrTiO3 (001). Journal of Physical Chemistry C, 2020, 124, 28116-28122.	1.5	3
49577	Stabilities and Electronic Structures of Transition Metal (Cu, Ag, Au, Ni, Pd, Pt) Cluster-Confined UiO-66. Journal of Physical Chemistry C, 2020, 124, 28123-28131.	1.5	9
49578	Subsurface Nitrogen Dissociation Kinetics in Lithium Metal from Metadynamics. Journal of Physical Chemistry C, 2020, 124, 26368-26378.	1.5	14
49579	Ultrafast In Situ Synthesis of Large-Area Conductive Metalâ€“Organic Frameworks on Substrates for Flexible Chemiresistive Sensing. ACS Applied Materials & Interfaces, 2020, 12, 57235-57244.	4.0	34
49580	Metal-induced n+/n homojunction for ultrahigh electron mobility transistors. NPG Asia Materials, 2020, 12, .	3.8	6
49581	Hyper oxygen incorporation in CeF₃: a new intermediate-band photocatalyst for antibiotic degradation under visible/NIR light. RSC Advances, 2020, 10, 38798-38804.	1.7	8
49582	Calculation of elastic constants at high pressure from first-principles. AIP Conference Proceedings, 2020, , .	0.3	1
49583	Orientation-dependent band offsets between (AlxGa1â€’x)2O3 and Ga2O3. Applied Physics Letters, 2020, 117, .	1.5	24
49584	Muon Interaction with Negative- <mml:math xmlns:mml="http://www.w3.org/1998/Math/MathML" display="inline" overflow="scroll"><mml:mi>U</mml:mi></mml:math> and High-Spin-State Defects: Differentiating Between <mml:math xmlns:mml="http://www.w3.org/1998/Math/MathML" display="inline" overflow="scroll"><mml:mrow><mml:mrow><mml:mi mathvariant="normal">C</mml:mi></mml:mrow></mml:mrow></mml:math> and <mml:math xmlns:mml="http://www.w3.org/1998/Math/MathML" display="inline" overflow="scroll"><mml:mi>Si</	1.5	7
49585	Three-site transition-metal clusters: Going from localized electrons to molecular orbitals. Physical Review B, 2020, 102, .	1.1	6
49586	Na-functionalized <mml:math xmlns:mml="http://www.w3.org/1998/Math/MathML"><mml:mrow><mml:mi>Ir</mml:mi><mml:msub><mml:mi>Te</mml:mi><mml:mn> monolayer: Suppressed charge ordering and electric field tuned topological phase transition. Physical Review B, 2020, 102, .	1.1	11
49587	Electronic structure and magnetism in infinite-layer nickelates <mml:math xmlns:mml="http://www.w3.org/1998/Math/MathML"><mml:mrow><mml:mi>R</mml:mi><mml:msub><mml:mi>NiO</mml:mi><mml:mn> (<mml:math) Tj ETQq1 1 0.784314 rgBT /Overlock 10 Tf 50 57 Td (xmlns:mml="http://www.w3.org/1998/Math/MathML"><mml:mrow>	1.1	18

#	Article	IF	Citations
49588	Schottky barrier formation at the <mml:math xmlns:mml="http://www.w3.org/1998/Math/MathML"><mml:mrow><mml:mi>Fe</mml:mi><mml:mo>/</mml:mo><mml:msub><mml:m (001) interface: Influence of oxygen vacancies and layer oxidation. Physical Review B, 2020, 102, .	1.1	6
49589	Ab initio determination of pseudospin for paramagnetic defects in SiC. Physical Review B, 2020, 102, .	1.1	10
49590	Temperature-dependent band structure evolution determined by surface geometry in organic halide perovskite single crystals. Physical Review B, 2020, 102, .	1.1	9
49591	Calculations of electronic excitation by protons and Î± particles in silicon. Physical Review B, 2020, 102, .	1.1	2
49592	Benchmarking boron carbide equation of state using computation and experiment. Physical Review E, 2020, 102, 053203.	0.8	6
49593	Melting Curve and Isostructural Solid Transition in Superionic Ice. Physical Review Letters, 2020, 125, 195501.	2.9	30
49594	Stabilization of Competing Ferroelectric Phases of<mml:math xmlns:mml="http://www.w3.org/1998/Math/MathML" display="inline"><mml:mrow><mml:msub><mml:mrow><mml:mi>HfO</mml:mi></mml:mrow><mml:mrow><mml:mn>2</mml:mn></mml:m Epitaxial Strain. Physical Review Letters, 2020, 125, 257603.	2.9	46
49595	New Ternary Compounds of the Composition Cu2SnTi3 and Their Crystal Structures. Applied Sciences (Switzerland), 2020, 10, 8776.	1.3	0
49596	Quantification of the Dislocation Density, Size, and Volume Fraction of Precipitates in Deep Cryogenically Treated Martensitic Steels. Metals, 2020, 10, 1561.	1.0	6
49597	Bandgap engineering of the (001) oriented thin-films of the Heusler alloys Co2â€'xFexCrAl (x=0.00, 0.25,) Tj ETQq1 1 0.784314 rgBT	0.8	2
49598	Identification of Synergistic Actions between Cu⁰ and Cu⁺ Sites in Hydrogenation of Dimethyl Oxalate from Microkinetic Analysis. Industrial & Engineering Chemistry Research, 2020, 59, 22451-22459.	1.8	11
49599	Center-Environment Feature Model for Machine Learning Study of Spinel Oxides Based on First-Principles Computations. Journal of Physical Chemistry C, 2020, 124, 28458-28468.	1.5	17
49600	Surface-Trapped Hole Diffusion in CdS and CdSe: The Superexchange Mechanism. Journal of Physical Chemistry C, 2020, 124, 28244-28251.	1.5	2
49601	Nanomanufacturing of Non-Noble Amorphous Alloys for Electrocatalysis. ACS Applied Energy Materials, 2020, 3, 12099-12107.	2.5	14
49602	Two-Dimensional Direct Semiconductor Boron Monochalcogenide Î³-BTe: Room-Temperature Single-Bound Exciton and Novel Donor Material in Excitonic Solar Cells. ACS Applied Materials & Interfaces, 2020, 12, 58349-58359.	4.0	7
49603	Anomalous Facile Carbamate Formation at High Stripping Temperatures from Carbon Dioxide Reaction with 2-Amino-2-methyl-1-propanol in Aqueous Solution. ACS Sustainable Chemistry and Engineering, 2020, 8, 18671-18677.	3.2	10
49604	Impact of oxygen defects on a ferromagnetic CrI₃ monolayer. RSC Advances, 2020, 10, 42493-42501.	1.7	13
49605	Doping by design: finding new n-type dopable ABX₄ Zintl phases for thermoelectrics. Journal of Materials Chemistry A, 2020, 8, 25306-25315.	5.2	14

#	Article	IF	Citations
49606	Machine learning potentials for multicomponent systems: The Ti-Al binary system. Physical Review B, 2020, 102, .	1.1	20
49607	Short-range and long-range magnetic order in <mml:math xmlns:mml="http://www.w3.org/1998/Math/MathML"><mml:mrow><mml:mi>Fe</mml:mi><mml:mrow><mml:mo>(</mml:mo><mml:mi mathvariant="normal">O</mml:mi><mml:mn>5</mml:mn></mml:msub><mml:mi>Cl</mml:mi></mml:mrow></mml:math>. Physical Review B, 2020, 102, .	1.1	2
49608	Optically Detected Magnetic Resonance in Neutral Silicon Vacancy Centers in Diamond via Bound Exciton States. Physical Review Letters, 2020, 125, 237402.	2.9	36
49609	Tuning the Magnetism in Boron-Doped Strontium Titanate. Materials, 2020, 13, 5686.	1.3	11
49610	Hydrogen Embrittlement at Cleavage Planes and Grain Boundaries in Bcc Ironâ€”Revisiting the First-Principles Cohesive Zone Model. Materials, 2020, 13, 5785.	1.3	13
49611	A Density Functional Theory Study on the Mechanism of Complete Ethanol Oxidation on Ir(100): Surface Diffusion-Controlled Câ€“C Bond Cleavage. Journal of Physical Chemistry C, 2020, 124, 26953-26964.	1.5	22
49612	Highly Selective, Defect-Induced Photocatalytic CO₂ Reduction to Acetaldehyde by the Nb-Doped TiO₂ Nanotube Array under Simulated Solar Illumination. ACS Applied Materials & Interfaces, 2020, 12, 55982-55993.	4.0	39
49613	Structural diversity in conducting bilayer salts (CNB-EDT-TTF)₄A. CrystEngComm, 2020, 22, 8313-8321.	1.3	4
49614	Paramagnetic phases of two-dimensional magnetic materials. Physical Review B, 2020, 102, .	1.1	6
49615	Band Engineering of Large-Twist-Angle <mml:math xmlns:mml="http://www.w3.org/1998/Math/MathML" display="inline"><mml:mrow><mml:mtext>Graphene</mml:mtext><mml:mo>/</mml:mo><mml:mrow><mml:mi>h</mml:mi></mml:mrow></mml:mrow></mml:math> MoirÃ© Superlattices with Pressure. Physical Review Letters, 2020, 125, 226403.	2.9	17
49616	Ni-Doped Epitaxial Graphene Monolayer on the Ni(111) Surface. Physics of Wave Phenomena, 2020, 28, 293-298.	0.3	0
49617	Thermodynamic properties of metaschoepite predicted from density functional perturbation theory. Chemical Physics Letters, 2020, 757, 137878.	1.2	3
49618	Reaction Pathways for Î±-Ga2O3 and Î²-Ga2O3 Phase Transition under Pressure up to 40 GPa: A First-Principles Study. Journal of Physical Chemistry C, 2020, 124, 23280-23286.	1.5	6
49619	Surface Orientation and Pressure Dependence of CO₂ Activation on Cu Surfaces. Journal of Physical Chemistry C, 2020, 124, 27511-27518.	1.5	20
49620	Modeling for Structural Engineering and Synthesis of Two-Dimensional WSe₂ Using a Newly Developed ReaxFF Reactive Force Field. Journal of Physical Chemistry C, 2020, 124, 28285-28297.	1.5	20
49621	False metals, real insulators, and degenerate gapped metals. Applied Physics Reviews, 2020, 7, .	5.5	44
49622	First-Principles Study of Structure and Magnetism in Copper(II)-Containing Hybrid Perovskites. Crystals, 2020, 10, 1129.	1.0	1
49623	Adsorption of NO2 and H2S on ZnGa2O4(111) Thin Films: A First-Principles Density Functional Theory Study. Applied Sciences (Switzerland), 2020, 10, 8822.	1.3	9

#	Article	IF	Citations
49624	Electronic Structure and Surface Properties of Copper Thiocyanate: A Promising Hole Transport Material for Organic Photovoltaic Cells. Materials, 2020, 13, 5765.	1.3	8
49625	Highly Sensitive Gas Sensing Material for Environmentally Toxic Gases Based on Janus NbSeTe Monolayer. Nanomaterials, 2020, 10, 2554.	1.9	17
49626	Poisonous Vapor Adsorption on Pure and Modified Aluminum Nitride Nanosheet for Environmental Safety: A DFT Exploration. Sustainability, 2020, 12, 10097.	1.6	3
49627	Stacking fault energies on {112} planes of an AlNbTaTiV BCC high-entropy alloy from first-principles calculations, analyzed with inferential statistics. Materialia, 2020, 14, 100927.	1.3	4
49628	Understanding filamentary growth and rupture by Ag ion migration through single-crystalline 2D layered CrPS4. NPG Asia Materials, 2020, 12, .	3.8	9
49629	The mechanism of Co oxyhydroxide nano-islands deposited on a Pt surface to promote the oxygen reduction reaction at the cathode of fuel cells. RSC Advances, 2020, 10, 44719-44727.	1.7	7
49630	Structures, electronic properties, and superconductivities of alkaline-earth metal-doped phenanthrene and charge transfer characteristics of metal-doped phenanthrene. Physical Chemistry Chemical Physics, 2020, 22, 23847-23855.	1.3	2
49631	First-principles study on the electron and phonon transport properties of layered Bi2OX2 (X = S, Se). AIP Advances, 2020, 10, .	0.6	4
49632	Screening of Charge Carrier Migration in the MgSc2Se4 Spinel Structure. Frontiers in Energy Research, 2020, 8, .	1.2	13
49633	Modulation of the Crystal Structure and Ultralong Life Span of a Na₃V₂(PO₄)₃-Based Cathode for a High-Performance Sodium-Ion Battery by Niobiumâ€“Vanadium Substitution. Industrial & Engineering Chemistry Research, 2020, 59, 21039-21046.	1.8	15
49634	First-Principles Study on the Oxidation of Supported Î²12-Borophene. Journal of Physical Chemistry C, 2020, 124, 28145-28151.	1.5	13
49635	Valence-Dependent Electrical Conductivity in a 3D Tetrahydroxyquinone-Based Metalâ€“Organic Framework. Journal of the American Chemical Society, 2020, 142, 21243-21248.	6.6	39
49636	Covalent organic framework shows high isobutene adsorption selectivity from C4 hydrocarbons: Mechanism of interpenetration isomerism and pedal motion. Green Energy and Environment, 2020, 7, 296-296.	4.7	8
49637	Mechanistic aspects of facet-dependent CH4/C2+ selectivity over a Ï‡-Fe5C2 Fischerâ€“Tropsch catalyst. Green Energy and Environment, 2022, 7, 449-456.	4.7	8
49638	Engineering electronic structures of titanium vacancies in Ti1-xO2 nanosheets enables enhanced Li-ion and Na-ion storage. Green Energy and Environment, 2022, 7, 734-741.	4.7	6
49639	Surface-mediated iron on porous cobalt oxide with high energy state for efficient water oxidation electrocatalysis. Green Energy and Environment, 2022, 7, 662-671.	4.7	12
49640	Warm hydrogen direct adsorptive separation and purification with highly CO/H2S-tolerant rare earth alloys. Applications in Energy and Combustion Science, 2020, 1-4, 100004.	0.9	1
49641	Dynamics of gold clusters on ceria during CO oxidation. Journal of Catalysis, 2020, 392, 39-47.	3.1	20

#	Article	IF	Citations
49642	The compositional dependence of structural stability and resulting properties for Mn+1CnT2 (M = Sc,) Tj ETQq0 0 0 rgBT /Overlock 10 T Technology, 2020, 9, 14979-14989.	2.6	11
49643	Promising high-temperature thermoelectric response of bismuth oxybromide. Results in Physics, 2020, 19, 103584.	2.0	27
49644	Chemical Reactivity of Supported ZnO Clusters: Undercoordinated Zinc and Oxygen Atoms as Active Sites. ChemPhysChem, 2020, 21, 2553-2564.	1.0	5
49645	Ab Initio Study of Stability, Local Order, and Phase Diagram For a Series of bcc-based Transition Metal Alloys. Journal of Phase Equilibria and Diffusion, 2020, 41, 737-755.	0.5	5
49646	Ferrimagnetic semiconductor of CaCu3Fe2V2O12 with direct bandgap. Chemical Physics Letters, 2020, 759, 137910.	1.2	0
49647	Progressive lithiation of FeP2 nanoparticles constrained inside the carbon shell. Materials Today Energy, 2020, 18, 100545.	2.5	7
49648	Influence of the Fe-Si-O framework in crystal structure on the phase stability and electrochemical performance of Li2FeSiO4 cathode. Solid State Ionics, 2020, 356, 115436.	1.3	5
49649	New n-Type Zintl Phases for Thermoelectrics: Discovery, Structural Characterization, and Band Engineering of the Compounds A₂CdP₂ (A = Sr, Ba, Eu). Chemistry of Materials, 2020, 32, 10697-10707.	3.2	21
49650	Fundamental Mechanisms of Mercury Removal by FeCl₃- and CuCl₂-Impregnated Activated Carbons: Experimental and First-Principles Study. Energy & Fuels, 2020, 34, 16401-16410.	2.5	13
49651	How CuI and NaI Interact with Faujasite Zeolite? A Theoretical Investigation. Journal of Physical Chemistry C, 2020, 124, 28026-28037.	1.5	2
49652	Highly Energetic and Stable Gadolinium/Bismuth Molybdate with a Fast Reactive Species, Redox Mechanism of Aqueous Electrolyte. ACS Applied Energy Materials, 2020, 3, 12385-12399.	2.5	21
49653	Deep Mining Stable and Nontoxic Hybrid Organicâ€“Inorganic Perovskites for Photovoltaics via Progressive Machine Learning. ACS Applied Materials & Interfaces, 2020, 12, 57821-57831.	4.0	20
49654	Colossal Magnetization and Giant Coercivity in Ion-Implanted (Nb and Co) MoS₂ Crystals. ACS Applied Materials & Interfaces, 2020, 12, 58140-58148.	4.0	22
49655	Porous NiCo₂S₄ Nanoneedle Arrays with Highly Efficient Electrocatalysis Anchored on Carbon Cloths as Self-Supported Hosts for High-Loading Liâ€“S Batteries. ACS Applied Materials & Interfaces, 2020, 12, 57975-57986.	4.0	25
49656	Nanostructured LiMnO₂ with Li₃PO₄ Integrated at the Atomic Scale for High-Energy Electrode Materials with Reversible Anionic Redox. ACS Central Science, 2020, 6, 2326-2338.	5.3	22
49657	Intrinsic Activity of Metal Centers in Metalâ€“Nitrogenâ€“Carbon Single-Atom Catalysts for Hydrogen Peroxide Synthesis. Journal of the American Chemical Society, 2020, 142, 21861-21871.	6.6	163
49658	Topological superconductivity in a van der Waals heterostructure. Nature, 2020, 588, 424-428.	13.7	211
49659	A computational search for wurtzite-structured ferroelectrics with low coercive voltages. APL Materials, 2020, 8, .	2.2	19

#	Article	IF	Citations
49660	Micropillar compression deformation of single crystals of Î±-Nb₅Si₃ with the tetragonal D8_l structure. Science and Technology of Advanced Materials, 2020, 21, 805-816.	2.8	7
49661	Role of Defect-Induced Interfacial States in Molecular Sensing: Ultrahigh-Sensitivity Region for Molecular Interaction. Physical Review Applied, 2020, 14, .	1.5	2
49662	Role of Si Doping in Reducing Coercive Fields for Ferroelectric Switching in <mml:math xmlns:mml="http://www.w3.org/1998/Math/MathML" display="inline" overflow="scroll"><mml:msub><mml:mrow><mml:mi>Hf</mml:mi><mml:mi mathvariant="normal">O</mml:mi></mml:mrow><mml:mn>2</mml:mn></mml:msub></mml:math>. Physical Review Applied, 2020, 14, .	1.5	15
49663	Linear and quadratic magnetoresistance in the semimetal <mml:math xmlns:mml="http://www.w3.org/1998/Math/MathML"><mml:mrow><mml:mi>Si</mml:mi><mml:msub><mml:mi mathvariant="normal">P</mml:mi><mml:mn>2</mml:mn></mml:msub></mml:mrow></mml:math>. Physical Review B, 2020, 102, .	1.1	14
49664	Generalized small set of ordered structures method for the solid-solution phase of high-entropy alloys. Physical Review B, 2020, 102, .	1.1	10
49665	Unconventional magnetism and electronic state in the frustrated layered system <mml:math xmlns:mml="http://www.w3.org/1998/Math/MathML"><mml:msub><mml:mi>PdCrO</mml:mi><mml:mn>2</mml:mn></mml:msub></mml:math>. Physical Review B, 2020, 102, .	1.1	8
49666	Anisotropic vortices on superconducting Nb(110). Physical Review B, 2020, 102, .	1.1	12
49667	Observation of tunable single-atom Yu-Shiba-Rusinov states. Physical Review B, 2020, 102, .	1.1	28
49668	Measurement of the sound velocity and GrÃ¼neisen parameter of polystyrene at inertial confinement fusion conditions. Physical Review B, 2020, 102, .	1.1	9
49669	<mml:math xmlns:mml="http://www.w3.org/1998/Math/MathML"><mml:mi>F</mml:mi></mml:math>and<mml:math xmlns:mml="http://www.w3.org/1998/Math/MathML"><mml:mi>M</mml:mi></mml:math>centers in alkali halides: A theoretical study applying self-consistent dielectric-dependent hybrid density functional theory. Physical Review B, 2020, 102, .	1.1	6
49670	Shock compression of vanadium at extremes: Theory and experiment. Physical Review B, 2020, 102, .	1.1	13
49671	Manipulation of giant negative Poisson's ratios in three-dimensional graphene networks. Physical Review B, 2020, 102, .	1.1	5
49672	Similarities and differences between nickelate and cuprate films grown on a <mml:math xmlns:mml="http://www.w3.org/1998/Math/MathML"><mml:msub><mml:mi>SrTiO</mml:mi><mml:mn>3</mml:mn></mml:msub></mml:math> substrate. Physical Review B, 2020, 102, .	1.1	30
49673	Kerker mixing scheme for self-consistent muffin-tin based all-electron electronic structure calculations. Physical Review B, 2020, 102, .	1.1	7
49674	Superconductivity and Fermi-surface nesting in the candidate Dirac semimetal NbC. Physical Review B, 2020, 102, .	1.1	29
49675	Identification of strongly interacting organic semimetals. Physical Review B, 2020, 102, .	1.1	7
49676	Phonons, <mml:math xmlns:mml="http://www.w3.org/1998/Math/MathML"><mml:mrow><mml:mi>Q</mml:mi></mml:mrow></mml:math>-dependent Kondo spin fluctuations, and <mml:math xmlns:mml="http://www.w3.org/1998/Math/MathML"><mml:mrow><mml:mn>4</mml:mn><mml:mi>f</mml:mi></mml:mrow></mml:math> phonon resonance in <mml:math xmlns:mml="http://www.w3.org/1998/Math/MathML"><mml:mrow><mml:mi>Yb</mml:mi><mml:msub><mml:mi	1.1	3
49677	Local ferroelectric polarization in antiferroelectric chalcogenide perovskite BaZrS3 thin films. Physical Review B, 2020, 102, .	1.1	13

#	Article	IF	Citations
49678	<mml:math xmlns:mml="http://www.w3.org/1998/Math/MathML"><mml:mtext>Germanium</mml:mtext><mml:mo>/</mml:mo><mml:msub><mm : Competition between the growth of germanene and intercalation. Physical Review B, 2020, 102, .	1.1	9
49679	Tuning the structure of the skyrmion lattice system Cu2OSeO3 under pressure. Physical Review B, 2020, 102, .	1.1	1
49680	Enhanced charge-transfer character in the monoclinic phase of Mott insulator <mml:math xmlns:mml="http://www.w3.org/1998/Math/MathML"><mml:mrow><mml:mi>La</mml:mi><mml:mi mathvariant="normal">V</mml:mi><mml:msub><mml:mi mathvariant="normal">O</mml:mi><mml:mn>3</mml:mn></mml:msub></mml:mrow></mml:math> thin films. Physical Review B, 2020, 102, .	1.1	5
49681	Experimental and theoretical study of the correlated compound YbCdSn: Evidence for large magnetoresistance and mass enhancement. Physical Review B, 2020, 102, .	1.1	11
49682	Oxyfluoride superlattices <mml:math xmlns:mml="http://www.w3.org/1998/Math/MathML"><mml:mi mathvariant="normal">K</mml:mi><mml:mi>Ta</mml:mi><mml:msub><mml:mrow><mml:mi mathvariant="normal">O</mml:mi></mml:mrow><mml:mn>3</mml:mn></mml:msub><mml:mo>/</mml:mo><mml:mi mathvariant="normal">K</mml:mi><mml:mi>M</mml:mi><mml:msub><mml:mrow><mml:mi mathvariant="normal">F</mml:mi></mml:mrow><mml:mn>3</mml:mn></mml:msub></mml:math>		

#	Article	IF	Citations
49696	Spin-Resolved Contribution to Perpendicular Magnetic Anisotropy and Gilbert Damping in Interface-Engineered Fe/MgAl2O4 Heterostructures. Physical Review Applied, 2020, 14, .	1.5	10
49697	Molecular Mott state in the deficient spinel GaV4S8. Physical Review B, 2020, 102, .	1.1	12
49698	Coupled magnetic and structural phase transitions in the antiferromagnetic polar metal <mml:math xmlns:mml="http://www.w3.org/1998/Math/MathML"><mml:mrow><mml:msub><mml:mi>Pb</mml:mi><mml:mn>2</mml:mn></mml:r mathvariant="normal">O</mml:mi><mml:mn>6</mml:mn></mml:msub></mml:mrow></mml:math> under pressure. Physical Review B, 2020, 102, .	1.1	5
49699	Optical properties of <mml:math xmlns:mml="http://www.w3.org/1998/Math/MathML"><mml:mrow><mml:mi>La</mml:mi><mml:mi>Ni</mml:mi><mml:msub><mml:mi mathvariant="normal">O</mml:mi><mml:mn>3</mml:mn></mml:msub></mml:mrow></mml:math> films tuned from compressive to tensile strain. Physical Review B, 2020, 102, .	1.1	4
49700	Equation of motion and the constraining field in ab initio spin dynamics. Physical Review B, 2020, 102, .	1.1	8
49701	Systematic theoretical study of carbon nanotubes rolled from a two-dimensional tetrahex-carbon nanosheet. Physical Review B, 2020, 102, .	1.1	6
49702	First-Principles Study of Anharmonic Lattice Dynamics in Low Thermal Conductivity <mml:math xmlns:mml="http://www.w3.org/1998/Math/MathML" display="inline"><mml:mrow><mml:msub><mml:mrow><mml:mi>AgCrSe</mml:mi></mml:mrow><mml:mrow><mml:mn>2</mml:mn> : Evidence for a Large Resonant Four-Phonon Scattering. Physical Review Letters, 2020, 125, 245901.	2.9	52
49703	InÂSitu Scanning Transmission Electron Microscopy Observations of Fracture at the Atomic Scale. Physical Review Letters, 2020, 125, 246102.	2.9	34
49704	<mml:math xmlns:mml="http://www.w3.org/1998/Math/MathML" display="inline"><mml:mrow><mml:mi>Cs</mml:mi><mml:msub><mml:mrow><mml:mi mathvariant="normal">V</mml:mi></mml:mrow><mml:mrow><mml:mn>3</mml:mn></mml:mrow></mml:msub><mml:mrow><mml:m : A <mml:math xmlns:mml="http://www.w3.org/1998/Math/MathML" display="inline"><mml:msub><mml:mi mathvariant="double-struck">Z</mml:mi><mml:mn>2</mml:mn>. Physical Review Letters, 2020, 125, 247002.	2.9	468
49705	Stacking Domain Wall Magnons in Twisted van der Waals Magnets. Physical Review Letters, 2020, 125, 247201.	2.9	58
49706	Magnetoelectric Coupling in Multiferroic Bilayer <mml:math xmlns:mml="http://www.w3.org/1998/Math/MathML" display="inline"><mml:mrow><mml:msub><mml:mrow><mml:mi>VS</mml:mi></mml:mrow><mml:mn>2</mml:mn></mml:msub></mml:mr Physical Review Letters, 2020, 125, 247601.	2.9	110
49707	High-throughput search for magnetic and topological order in transition metal oxides. Science Advances, 2020, 6, .	4.7	35
49708	Coexistence of Raritaâ€“Schwingerâ€“Weyl fermion and spin-1 excitation in Bi4Ni6S4. Modern Physics Letters B, 2020, 34, 2150003.	1.0	0
49709	Phase Transition and Electronic Structures of All-d-Metal Heusler-Type X2MnTi Compounds (X = Pd, Pt,) Tj ETQq1 1 0.784314 rgBT /O	1.8	14
49710	Orbital Magnetic Moments of the High-Spin Co²⁺ Ions at Axially-Elongated Octahedral Sites: Unquenched as Reported from Experiment or Quenched as Predicted by Theory?. Inorganic Chemistry, 2020, 59, 18319-18324.	1.9	4
49711	Distance Matrix-Based Crystal Structure Prediction Using Evolutionary Algorithms. Journal of Physical Chemistry A, 2020, 124, 10909-10919.	1.1	3
49712	Identifying and Tuning the In Situ Oxygen-Rich Surface of Molybdenum Nitride Electrocatalysts for Oxygen Reduction. ACS Applied Energy Materials, 2020, 3, 12433-12446.	2.5	17
49713	Design of an Ultrastable and Highly Active Ceria Catalyst for CO Oxidation by Rare-Earth- and Transition-Metal Co-Doping. ACS Catalysis, 2020, 10, 14877-14886.	5.5	23

#	Article	IF	Citations
49714	Insulator-to-conductor transition driven by the Rashbaâ€“Zeeman effect. Npj Computational Materials, 2020, 6, .	3.5	15
49715	Tritium diffusion in a Li2TiO3 crystal terminated with the (001) surface from first-principles calculations. Physical Chemistry Chemical Physics, 2020, 22, 27206-27213.	1.3	1
49716	Calculation of the detonation state of HN3 with quantum accuracy. Journal of Chemical Physics, 2020, 153, 224102.	1.2	14
49717	Se intercalation between <mml:math xmlns:mml="http://www.w3.org/1998/Math/MathML"><mml:mrow><mml:mi>Pt</mml:mi><mml:msub><mml:mi>Se</mml:mi><mml and the Pt surface during synthesis of <mml:math xmlns:mml="http://www.w3.org/1998/Math/MathML"><mml:mrow><mml:mi>Pt</mml:mi><mml:msub><mml:mi>Se</mml:mi><mml by direct selenization of Pt(111). Physical Review B, 2020, 102, .	1.1	3
49718	Pressure-induced ferroelectric phase of <mml:math xmlns:mml="http://www.w3.org/1998/Math/MathML"><mml:msub><mml:mi>LaMoN</mml:mi><mml:mn>3</mml:mn></mml:msub></ Physical Review B, 2020, 102, .	1.1	11
49719	Structure and superconductivity in compressed Li-Si-H compounds: Density functional theory calculations. Physical Review B, 2020, 102, .	1.1	20
49720	Lattice dynamics of YbxCo4Sb12 skutterudite by machine-learning interatomic potentials: Effect of filler concentration and disorder. Physical Review B, 2020, 102, .	1.1	15
49721	Photoinduced Floquet mixed-Weyl semimetallic phase in a carbon allotrope. Physical Review B, 2020, 102, .	1.1	12
49722	Purely Cubic Spin Splittings with Persistent Spin Textures. Physical Review Letters, 2020, 125, 216405.	2.9	35
49723	High-Throughput Study of Lattice Thermal Conductivity in Binary Rocksalt and Zinc Blende Compounds Including Higher-Order Anharmonicity. Physical Review X, 2020, 10, .	2.8	55
49724	Generation of Amorphous Silicon Dioxide Structures via Melting-Quenching Density Functional Modeling. Lobachevskii Journal of Mathematics, 2020, 41, 1581-1590.	0.1	7
49725	Point Defect and Their Influence on the Atomic and Electronic Structure of Î²-(Al_xGa_{1-x})₂O₃ Alloys by STEM-EELS. Microscopy and Microanalysis, 2020, 26, 622-623.	0.2	2
49726	Nitrogen Enables the Intensity Modulation of Charge Transfer and Spin Paramagnetism in Graphdiyne. Chemistry of Materials, 2020, 32, 9001-9007.	3.2	18
49727	Large Power Factors in Wide Band Gap Semiconducting RFeO₃ Materials for High-Temperature Thermoelectric Applications. ACS Applied Energy Materials, 2020, 3, 11193-11205.	2.5	10
49728	Beyond Volume Variation: Anisotropic and Protrusive Lithiation in Bismuth Nanowire. ACS Nano, 2020, 14, 15669-15677.	7.3	18
49729	Influence of tungsten doping on nonradiative electronâ€“hole recombination in monolayer MoSe2 with Se vacancies. Journal of Chemical Physics, 2020, 153, 154701.	1.2	8
49730	First-principle study for influence of normal strain on the magnetic properties of nonmetal adsorbed WSe2 monolayer. Ferroelectrics, 2020, 568, 132-142.	0.3	0
49731	Fe2Ga2S5 as a 2D Antiferromagnetic Semiconductor. Chinese Physics Letters, 2020, 37, 107505.	1.3	3

#	Article	IF	Citations
49732	Insights in the A- and B-siteâ€™s Radii Influence in the Polar Character of ABF₄. Journal of Physics: Conference Series, 2020, 1541, 012012.	0.3	1
49733	Structure properties of warm dense hydrogen. Journal of Physics: Conference Series, 2020, 1556, 012047.	0.3	2
49734	Ab Initio Study of the Effect of Mono-Vacancies on the Metastability of Ga-Stabilized Î´-Pu. Applied Sciences (Switzerland), 2020, 10, 7628.	1.3	4
49735	Experimental and Theoretical Investigation of the Elastic Properties of HfV2O7. Crystals, 2020, 10, 172.	1.0	1
49736	Segregation of P and S Impurities to A Î£9 Grain Boundary in Cu. Metals, 2020, 10, 1362.	1.0	7
49737	The Interstitial Carbonâ€“Dioxygen Center in Irradiated Silicon. Crystals, 2020, 10, 1005.	1.0	3
49738	The Advent of Quantum Crystallography: Form and Structure Factors from Quantum Mechanics for Advanced Structure Refinement and Wavefunction Fitting. Structure and Bonding, 2020, , 65-144.	1.0	17
49739	Molecular modeling and computational study of the chiral-dependent structures and properties of the self-assembling diphenylalanine peptide nanotubes, containing water molecules. Journal of Molecular Modeling, 2020, 26, 326.	0.8	7
49740	Superhard and superconductive nondiamond-like BC structure. Diamond and Related Materials, 2020, 110, 108142.	1.8	0
49741	The Impact of Surface Structure Transformations on the Performance of Li-Excess Cation-Disordered Rocksalt Cathodes. Cell Reports Physical Science, 2020, 1, 100187.	2.8	20
49742	Tunable Electronic Properties and Large Rashba Splittings Found in Few-Layer Bi₂Se₃/PtSe₂ Van der Waals Heterostructures. ACS Applied Electronic Materials, 2020, 2, 3585-3592.	2.0	9
49743	Band Alignment of Sc_xAl_{1â€“x}N/GaN Heterojunctions. ACS Applied Materials & Interfaces, 2020, 12, 52192-52200.	4.0	22
49744	Lowering the Schottky barrier height of G/WSSe van der Waals heterostructures by changing the interlayer coupling and applying external biaxial strain. Physical Chemistry Chemical Physics, 2020, 22, 26231-26240.	1.3	43
49745	Estimation of the spatial distribution of Frenkel defects in NiFe2O4 by simulation of HAADF-STEM images. Nanoscale, 2020, 12, 22668-22673.	2.8	1
49746	Mapping temperature-dependent energyâ€“structureâ€“property relationships for solid solutions of inorganic halide perovskites. Journal of Materials Chemistry C, 2020, 8, 16815-16825.	2.7	10
49747	Rashba band splitting in two-dimensional Ruddlesdenâ€“Popper halide perovskites. Journal of Applied Physics, 2020, 128, 175101.	1.1	11
49748	de Haas-van Alphen Quantum Oscillations in BaSn3 Superconductor with Multiple Dirac Fermions. Chinese Physics Letters, 2020, 37, 087101.	1.3	5
49749	First principles study of the charge ordered phase in <mml:math xmlns:mml="http://www.w3.org/1998/Math/MathML"><mml:mi>Î²</mml:mi><mml:mo>â€²</mml:mo><mml:msub><mml:mi mathvariant="normal">D</mml:mi><mml:mn>3</mml:mn></mml:msub><mml:msub><mml:mrow><mml:mo>(</mml:mo><mml:mte : Stability of <mml:math xmlns:mml="http://www.w3.org/1998/Math/MathML"><mml:mi>Ï€</mml:mi></mml:math> -electron deuterium coupled ordering i. Physical Review B, 2020, 101, .	1.1	6

#	Article	IF	Citations
49750	Ferromagnetic phase of the spinel compound <mml:math xmlns:mml="http://www.w3.org/1998/Math/MathML"><mml:mrow><mml:msub><mml:mi>MgV</mml:mi><mml:mn>2</mml:mn></mm mathvariant="normal">O</mml:mi><mml:mn>4</mml:mn></mml:msub></mml:mrow></mml:math> and its spintronics properties. Physical Review B, 2020, 102, .	1.1	6
49751	Carbon-Deficient Titanium Carbide With Highly Enhanced Hardness. Frontiers in Physics, 2020, 8, .	1.0	9
49752	Spin Alignment Studies on the Muon-Site Determination in La₂CuO₄. Key Engineering Materials, 2020, 860, 154-159.	0.4	1
49753	A Linear Relationship between the Charge Transfer Amount and Level Alignment in Molecule/Two-Dimensional Adsorption Systems. ACS Omega, 2020, 5, 26748-26754.	1.6	11
49754	Single-phase perovskite oxide with super-exchange induced atomic-scale synergistic active centers enables ultrafast hydrogen evolution. Nature Communications, 2020, 11, 5657.	5.8	134
49755	Localized spin-orbit polaron in magnetic Weyl semimetal Co3Sn2S2. Nature Communications, 2020, 11, 5613.	5.8	53
49756	Unusual intrinsic thermoluminescence in LiMgPO₄:Er. Physical Chemistry Chemical Physics, 2020, 22, 27632-27644.	1.3	12
49757	High zT and Its Origin in Sbâ€doped GeTe Single Crystals. Advanced Science, 2020, 7, 2002494.	5.6	36
49758	Designing New Metal Chalcogenide Nanoclusters through Atomâ€byâ€Atom Substitution. Small, 2021, 17, e2002927.	5.2	7
49759	Potential and pH Dependence of the Buried Interface of Membrane-Coated Electrocatalysts. ACS Applied Materials & Interfaces, 2020, 12, 52125-52135.	4.0	2
49760	Continuously Selective Photocatalytic CO₂ Fixation via Controllable S/Se Ratio in a TiO₂â€“MoS_xSe_y Dual-Excitation Heterostructured Nanotree. ACS Photonics, 2020, 7, 3394-3400.	3.2	10
49761	The Critical Point and the Supercritical State of Alkali Feldspars: Implications for the Behavior of the Crust During Impacts. Journal of Geophysical Research E: Planets, 2020, 125, e2020JE006412.	1.5	9
49762	Theoretical investigation on graphene-supported single-atom catalysts for electrochemical CO₂ reduction. Catalysis Science and Technology, 2020, 10, 8465-8472.	2.1	35
49763	Enhancing surface oxygen retention through theory-guided doping selection in Li_{1â^'x}NiO₂ for next-generation lithium-ion batteries. Journal of Materials Chemistry A, 2020, 8, 23293-23303.	5.2	44
49764	Atomistic origins of charge traps in CdSe nanoclusters. Physical Chemistry Chemical Physics, 2020, 22, 26299-26305.	1.3	8
49765	First-principles study on crystal structures and superconductivity of molybdenum hydrides under high pressure. Journal of Applied Physics, 2020, 128, .	1.1	8
49766	Real-space formulation of the stress tensor for O(N) density functional theory: Application to high temperature calculations. Journal of Chemical Physics, 2020, 153, 034112.	1.2	10
49767	The Cs2AgRhCl6 Halide Double Perovskite: A Dynamically Stable Lead-Free Transition-Metal Driven Semiconducting Material for Optoelectronics. Frontiers in Chemistry, 2020, 8, 796.	1.8	24

#	Article	IF	Citations
49768	Boron Concentration Induced Co-Ta-B Composite Formation Observed in the Transition from Metallic to Covalent Glasses. Condensed Matter, 2020, 5, 18.	0.8	1
49769	Physical Fundamentals of Biomaterials Surface Electrical Functionalization. Materials, 2020, 13, 4575.	1.3	11
49770	Deposition of Tetracoordinate Co(II) Complex with Chalcone Ligands on Graphene. Molecules, 2020, 25, 5021.	1.7	15
49771	Bonding of Gold Nanoclusters on Graphene with and without Point Defects. Nanomaterials, 2020, 10, 2109.	1.9	4
49772	First-Principles Exploration of Hazardous Gas Molecule Adsorption on Pure and Modified Al60N60 Nanoclusters. Nanomaterials, 2020, 10, 2156.	1.9	2
49773	Electronic Structure and Optical Properties of a Mn-Doped InSe/WSe2 van der Walls Heterostructure: First Principles Calculations. Journal of the Korean Physical Society, 2020, 77, 587-591.	0.3	2
49774	2D Sandwiched Nano Heterostructures Endow MoSe₂/TiO_{2â˜’}_x/Graphene with High Rate and Durability for Sodium Ion Capacitor and Its Solid Electrolyte Interphase Dependent Sodiation/Desodiation Mechanism. Small, 2020, 16, e2004457.	5.2	38
49775	Multiscale modeling of magnetic nanoparticle systems. Frontiers of Nanoscience, 2020, 17, 27-39.	0.3	0
49776	Mixed metal oxide: A new class of catalyst for methanol activation. Applied Surface Science, 2020, 534, 147449.	3.1	5
49777	Crafting carbon sphere-titania coreâ€“shell interfacial structure to achieve enhanced visible light photocatalysis. Applied Surface Science, 2020, 534, 147566.	3.1	16
49778	Prediction of three-dimensional B3N5 with one-dimensional metallicity. Chemical Physics Letters, 2020, 760, 138002.	1.2	0
49779	Metallic and semiconducting carbon allotropes comprising of pentalene skeletons. Diamond and Related Materials, 2020, 109, 108063.	1.8	19
49780	Role of surface defects in CO2 adsorption and activation on CuFeO2 delafossite oxide. Molecular Catalysis, 2020, 496, 111181.	1.0	29
49781	Unveiling the Remarkable Arsenic Resistance Origin of Alumina Promoted Ceriumâ€“Tungsten Catalysts for NH₃â€“SCR. Environmental Science & Technology, 2020, 54, 14740-14749.	4.6	34
49782	Performance controlled via surface oxygen-vacancy in Ti-based oxide catalyst during methyl oleate epoxidation. Scientific Reports, 2020, 10, 18952.	1.6	27
49783	Computational investigation of Zn-doped and undoped SrEu₂Fe₂O₇ as potential mixed electron and proton conductors. RSC Advances, 2020, 10, 39988-39994.	1.7	1
49784	TM₂B₆: a newly designed ferromagnetic 2D metal-boride with a high Curie temperature. Journal of Materials Chemistry C, 2020, 8, 14805-14811.	2.7	9
49785	Tunable magnetic anisotropy in 2D magnets via molecular adsorption. Journal of Materials Chemistry C, 2020, 8, 14948-14953.	2.7	26

#	Article	IF	Citations
49786	Cyano-bridged perovskite [(CH3)3NOH]2[KM(CN)6], [M: Fe(iii), and Co(iii)] for high-temperature multi-axial ferroelectric applications with enhanced thermal and nonlinear optical performance. Journal of Materials Chemistry C, 2020, 8, 17491-17501.	2.7	26
49787	Featureless adaptive optimization accelerates functional electronic materials design. Applied Physics Reviews, 2020, 7, .	5.5	26
49788	Quantum Oscillations and Electronic Structure in the Large-Chern-Number Topological Chiral Semimetal PtGa. Chinese Physics Letters, 2020, 37, 107504.	1.3	12
49789	First-principles calculations of oxygen vacancy in CaO crystal. European Physical Journal D, 2020, 74, 1.	0.6	1
49790	Monocrystalline Antimonene Nanosheets via Physical Vapor Deposition. Advanced Materials Interfaces, 2020, 7, 2001678.	1.9	14
49791	Predicting mesoscale spectral thermal conductivity using advanced deterministic phonon transport techniques. Advances in Heat Transfer, 2020, 52, 335-488.	0.4	4
49792	Large reduction in switching current driven by spin-orbit torque in W/CoFeB heterostructures with Wâ€“N interfacial layers. Acta Materialia, 2020, 200, 551-558.	3.8	9
49793	Electro-oxidation of furfural on gold is limited by furoate self-assembly. Journal of Catalysis, 2020, 391, 327-335.	3.1	30
49794	Site Occupation and Spectral Assignment in Eu²⁺-Activated Î²-Ca₃(PO₄)₂-Type Phosphors: Insights from First-Principles Calculations. Inorganic Chemistry, 2020, 59, 16760-16768.	1.9	15
49795	Surface-controlled reversal of the selectivity of halogen bonds. Nature Communications, 2020, 11, 5630.	5.8	24
49796	Revealing the veil of the stability of monolayer boron sulfide upon air and humidity exposure. AIP Conference Proceedings, 2020, , .	0.3	0
49797	Misfit epitaxial strain manipulated transport properties in cubic In2O3 hetero-epilayers. Applied Physics Letters, 2020, 117, 102104.	1.5	4
49798	A Study on N-Type Bismuth Sulphochloride (BiSCl): Efficient Synthesis and Characterization. Nano, 2020, 15, 2050116.	0.5	2
49799	Equibiaxial Strained Oxygen Adsorption on Pristine Graphene, Nitrogen/Boron Doped Graphene, and Defected Graphene. Materials, 2020, 13, 4945.	1.3	5
49800	Van der Waals Epitaxial Growth of Mosaicâ€Like 2D Platinum Ditelluride Layers for Roomâ€Temperature Midâ€Infrared Photodetection up to 10.6 Âµm. Advanced Materials, 2020, 32, e2004412.	11.1	202
49801	Scalable Substitutional Reâ€Doping and its Impact on the Optical and Electronic Properties of Tungsten Diselenide. Advanced Materials, 2020, 32, e2005159.	11.1	32
49802	Roomâ€Temperature Synthesis of 2D Janus Crystals and their Heterostructures. Advanced Materials, 2020, 32, e2006320.	11.1	138
49803	Discovering Electronâ€Transferâ€Driven Changes in Chemical Bonding in Lead Chalcogenides (PbX, where) Tj ETQq1 1 0.784314 rgBT	11.1	56

#	Article	IF	Citations
49804	Multiscale Modeling of Defect Phenomena in Platinum Using Machine Learning of Force Fields. Jom, 2020, 72, 4346-4358.	0.9	5
49805	The structural, elastic, thermodynamic, and electronic properties of (Cu6-xAux)Sn5 (xâ€‰=â€‰0, 0.5, 1, 1.5, 2) intermetallic compounds. Indian Journal of Physics, 2020, , 1.	0.9	1
49806	First-principle calculations of lithium adsorption and diffusion on titanium-based monolayers. Chemical Physics, 2020, 539, 110956.	0.9	3
49807	Antiferromagnetism-induced second-order nonlinear optical responses of centrosymmetric bilayer CrI3. Chinese Journal of Physics, 2020, 68, 896-907.	2.0	6
49808	First-principles study of heterostructures of MXene and nitrogen-doped graphene as anode materials for Li-ion batteries. Surfaces and Interfaces, 2020, 21, 100788.	1.5	9
49809	Geometric Analysis and Formability of the Cubic A₂BX₆ Vacancy-Ordered Double Perovskite Structure. Chemistry of Materials, 2020, 32, 9573-9583.	3.2	35
49810	An Efficient Deep Learning Scheme To Predict the Electronic Structure of Materials and Molecules: The Example of Graphene-Derived Allotropes. Journal of Physical Chemistry A, 2020, 124, 9496-9502.	1.1	12
49811	Tuning Câ€“F Bonding of Graphite Fluoride by Applying High Pressure: Experimental and Theoretical Study. Journal of Physical Chemistry C, 2020, 124, 24747-24755.	1.5	6
49812	Understanding the Phase Transition Evolution Mechanism of Partially M2 Phased VO₂ Film by Hydrogen Incorporation. Journal of Physical Chemistry Letters, 2020, 11, 9680-9688.	2.1	16
49813	Stability of Solid-Electrolyte Interphase (SEI) on the Lithium Metal Surface in Lithium Metal Batteries (LMBs). ACS Applied Energy Materials, 2020, 3, 10560-10567.	2.5	37
49814	Stabilization of Catalytic Surfaces through Coreâ€“Shell Structures: Agâ€“Ir/Al₂O₃ Case Study. ACS Catalysis, 2020, 10, 13352-13363.	5.5	4
49815	Phase Stability in Nickel Phosphides at High Pressures. ACS Earth and Space Chemistry, 2020, 4, 1978-1984.	1.2	4
49816	Rare-Earth Single-Atom Laâ€“N Charge-Transfer Bridge on Carbon Nitride for Highly Efficient and Selective Photocatalytic CO₂ Reduction. ACS Nano, 2020, 14, 15841-15852.	7.3	283
49817	Stacking-configuration-enriched essential properties of bilayer graphenes and silicenes. Journal of Chemical Physics, 2020, 153, 154707.	1.2	5
49818	Quantifying the stability of the anion ordering in SrVO2H. Physical Review B, 2020, 102, .	1.1	3
49819	Improved solid stability from a screened range-separated hybrid functional by satisfying semiclassical atom theory and local density linear response. Physical Review B, 2020, 102, .	1.1	19
49820	Changes of Fermi surface topology due to the rhombohedral distortion in SnTe. Physical Review B, 2020, 102, .	1.1	7
49821	Complexity of mixed allotropes of <mml:math xmlns:mml="http://www.w3.org/1998/Math/MathML"><mml:msub><mml:mi mathvariant="normal">MoS</mml:mi><mml:mn>2</mml:mn></mml:msub></mml:math> unraveled by first-principles theory. Physical Review B, 2020, 102, .	1.1	5

#	Article	IF	Citations
49822	Effect of the Free Volume on the Electronic Structure of Cu70Zr30 Metallic Glasses. Materials, 2020, 13, 4911.	1.3	2
49823	Spontaneously Splitting Copper Nanowires into Quantum Dots on Graphdiyne for Suppressing Lithium Dendrites. Advanced Materials, 2020, 32, e2004379.	11.1	74
49824	The structural, electronic, magnetic, and optical properties of the Cr-, Mo-, and W-doped ZnTe alloys. Applied Physics A: Materials Science and Processing, 2020, 126, 1.	1.1	2
49825	Orange peel extracts as biodegradable corrosion inhibitor for magnesium alloy in NaCl solution: Experimental and theoretical studies. Journal of the Taiwan Institute of Chemical Engineers, 2020, 115, 35-46.	2.7	40
49826	Equation of state of LiNi0Â·5Mn1Â·5O4 at high pressure. Solid State Communications, 2020, 321, 114045.	0.9	2
49827	Design of Reversible Low-Field Magnetocaloric Effect at Room Temperature in Hexagonal MnMX Ferromagnets. Physical Review Applied, 2020, 13, .	1.5	13
49828	A general method to synthesize and sinter bulk ceramics in seconds. Science, 2020, 368, 521-526.	6.0	357
49829	2D-layered Ti3C2 MXenes for promoted synthesis of NH3 on P25 photocatalysts. Applied Catalysis B: Environmental, 2020, 273, 119054.	10.8	111
49830	Investigation of alkali-ion (Li, Na and K) intercalation in manganese hexacyanoferrate KxMnFe(CN)6 as cathode material. Chemical Engineering Journal, 2020, 396, 125269.	6.6	44
49831	Bimetallic MOF-derived CNTs-grafted carbon nanocages as sulfur host for high-performance lithiumâ€“sulfur batteries. Electrochimica Acta, 2020, 349, 136378.	2.6	33
49832	The Potential of Overlayers on Tin-based Perovskites for Water Splitting. Journal of Physical Chemistry Letters, 2020, 11, 4124-4130.	2.1	4
49833	In Situ Formation of Free-Standing Single-Atom-Thick Antiferromagnetic Chromium Membranes. Nano Letters, 2020, 20, 4354-4361.	4.5	22
49834	Interface hybridization and spin filter effect in metal-free phthalocyanine spin valves. Physical Chemistry Chemical Physics, 2020, 22, 11663-11670.	1.3	7
49835	Structural evolution and magnetic properties of ScLi_n (n = 2â€“13) clusters: A PSO and DFT investigation*. Chinese Physics B, 2020, 29, 077101.	0.7	5
49836	Source/Drain Materials for Ge nMOS Devices: Phosphorus Activation in Epitaxial Si, Ge, Ge_{1â^'x}Sn_x and Si_yGe_{1â^'xâ^'y}Sn_x. ECS Journal of Solid State Science and Technology, 2020, 9, 044010.	0.9	5
49837	Enhanced Electrochemical CO₂ Reduction of Cu@Cu_xO Nanoparticles Decorated on 3D Vertical Graphene with Intrinsic sp³â€type Defect. Advanced Functional Materials, 2020, 30, 1910118.	7.8	54
49838	Unveiling the Structural Descriptor of A₃B₂X₉ Perovskite Derivatives toward Xâ€Ray Detectors with Low Detection Limit and High Stability. Advanced Functional Materials, 2020, 30, 1910648.	7.8	144
49839	Work Function Evolution in Li Anode Processing. Advanced Energy Materials, 2020, 10, 2000520.	10.2	40

#	Article	IF	Citations
49840	Dendritic Ag/Pd Alloy Nanostructure Arrays for Electrochemical CO 2 Reduction. ChemElectroChem, 2020, 7, 2608-2613.	1.7	12
49841	Bimetallic Pairs Supported on Graphene as Efficient Electrocatalysts for Nitrogen Fixation: Search for the Optimal Coordination Atoms. ChemSusChem, 2020, 13, 3636-3644.	3.6	45
49842	Extendable Machine Learning Model for the Stability of Single Atom Alloys. Topics in Catalysis, 2020, 63, 728-741.	1.3	25
49843	Selectivity switch in transformation of CO2 from ethanol to methanol on Cu embedded in the defect carbon. Science China Chemistry, 2020, 63, 722-730.	4.2	10
49844	An ab initio molecular dynamics exploration of associates in Ba-Bi liquid with strong ordering trends. Acta Materialia, 2020, 190, 81-92.	3.8	13
49845	Short-range chemical order and local lattice distortion in a compositionally complex alloy. Acta Materialia, 2020, 193, 329-337.	3.8	49
49846	PLD-fabricated perovskite oxide nanofilm as efficient electrocatalyst with highly enhanced water oxidation performance. Applied Catalysis B: Environmental, 2020, 272, 119046.	10.8	29
49847	Structural stability and electronic property evaluations for different Bi2Te3 (0Â0Â1) termination surfaces. Applied Surface Science, 2020, 525, 146454.	3.1	4
49848	Unraveling the effects of the coordination number of Mn over Î±-MnO2 catalysts for toluene oxidation. Chemical Engineering Journal, 2020, 396, 125192.	6.6	110
49849	Data on the comprehensive first-principles diffusion study of the aluminum-magnesium system. Data in Brief, 2020, 30, 105381.	0.5	7
49850	First principles investigation on interface properties and formation mechanism of Î³-Fe/CeO2 heterogeneous nucleation interface. Journal of Alloys and Compounds, 2020, 831, 154867.	2.8	16
49851	Interplay of covalency, non-cubic crystal field, and spin-orbit coupling: A comparative study of d5,d4, and d3 double perovskite iridates Sr2MIrO6 (Mâ€¯=â€¯Ce, Sc, Ca). Journal of Magnetism and Magnetic Materials, 2020, 507, 166827.	1.0	3
49852	A new mixed-anion phosphate Cs2Bi2Sr(P2O7)(PO4)2: Synthesis, characterization, structure and its Eu3+-activated luminescence. Journal of Solid State Chemistry, 2020, 288, 121411.	1.4	9
49853	First-principles study on the interfacial segregation at coherent Cu precipitate/Fe matrix interface. Scripta Materialia, 2020, 185, 42-46.	2.6	23
49854	Electronic and optical properties of PdSe2 from monolayer to trilayer. Superlattices and Microstructures, 2020, 142, 106514.	1.4	17
49855	Density Functional Theory Study of Decarboxylation and Decarbonylation of Acetic Acid on Pd(111). Journal of Physical Chemistry C, 2020, 124, 13082-13093.	1.5	13
49856	Fluorine Substitution in Magnesium Hydride as a Tool for Thermodynamic Control. Journal of Physical Chemistry C, 2020, 124, 9109-9117.	1.5	8
49857	Photogenerated-Carrier Separation and Transfer in Two-Dimensional Janus Transition Metal Dichalcogenides and Graphene van der Waals Sandwich Heterojunction Photovoltaic Cells. Journal of Physical Chemistry Letters, 2020, 11, 4070-4079.	2.1	44

#	Article	IF	Citations
49858	Topological Hall Effect in Traditional Ferromagnet Embedded with Black-Phosphorus-Like Bismuth Nanosheets. ACS Applied Materials & Interfaces, 2020, 12, 25135-25142.	4.0	21
49859	Critical Hydrogen Coverage Effect on the Hydrogenation of Ethylene Catalyzed by Î´-MoC(001): An Ab Initio Thermodynamic and Kinetic Study. ACS Catalysis, 2020, 10, 6213-6222.	5.5	21
49860	Superconductivity on Edge: Evidence of a One-Dimensional Superconducting Channel at the Edges of Single-Layer FeTeSe Antiferromagnetic Nanoribbons. ACS Nano, 2020, 14, 6539-6547.	7.3	7
49861	Tuning lithium-peroxide formation and decomposition routes with single-atom catalysts for lithiumâ€“oxygen batteries. Nature Communications, 2020, 11, 2191.	5.8	181
49862	Mechanism of collective interstitial ordering in Feâ€“C alloys. Nature Materials, 2020, 19, 849-854.	13.3	32
49863	Mg₃(Bi,Sb)₂ single crystals towards high thermoelectric performance. Energy and Environmental Science, 2020, 13, 1717-1724.	15.6	91
49864	Origin of high carrier concentration in amorphous wide-bandgap oxides: Role of disorder in defect formation and electron localization in In2O3â^'x. Journal of Applied Physics, 2020, 127, .	1.1	26
49865	Stable single-layers of calcium halides (CaX₂, X = F, Cl, Br, I). Journal of Chemical Physics, 2020, 152, 164116.	1.2	13
49866	Stability of H3O at extreme conditions and implications for the magnetic fields of Uranus and Neptune. Proceedings of the National Academy of Sciences of the United States of America, 2020, 117, 5638-5643.	3.3	23
49867	Modelling of short-range ordering kinetics in dilute multicomponent substitutional solid solutions. Philosophical Magazine, 2020, 100, 1942-1961.	0.7	0
49868	Pnma metal hydride system LiBH: a superior topological semimetal with the coexistence of twofold and quadruple degenerate topological nodal lines. Journal of Physics Condensed Matter, 2020, 32, 365502.	0.7	11
49869	The important role of strain on phonon hydrodynamics in diamond-like bi-layer graphene. Nanotechnology, 2020, 31, 335711.	1.3	30
49870	Computational discovery of a dynamically stable cubic <mml:math xmlns:mml="http://www.w3.org/1998/Math/MathML"><mml:msub><mml:mi>SH</mml:mi><mml:mn>3</mml:mn></mml:msub></mml: -like high-temperature superconductor at 100ÂGPa via <mml:math xmlns:mml="http://www.w3.org/1998/Math/MathML"><mml:msub><mml:mi>CH</mml:mi><mml:mn>4</mml:mn></mml:msub></mml intercalation. Physical Review B, 2020, 101, .	1.1	73
49871	Epitaxial metals for interconnects beyond Cu. Journal of Vacuum Science and Technology A: Vacuum, Surfaces and Films, 2020, 38, .	0.9	29
49872	Composition Tuning of Nanostructured Binary Copper Selenides through Rapid Chemical Synthesis and Their Thermoelectric Property Evaluation. Nanomaterials, 2020, 10, 854.	1.9	17
49873	Titaniumâ€Substituted Tavorite LiFeSO 4 F as Cathode Material for Lithium Ion Batteries: Firstâ€Principles Calculations and Experimental Study. ChemPlusChem, 2020, 85, 900-905.	1.3	1
49874	Simultaneous Enhancements of Ultraviolet-Shielding Properties and Thermal Stability/Photostability of Poly(vinyl chloride) via Incorporation of Defect-Rich CeO₂ Nanoparticles. Industrial & Engineering Chemistry Research, 2020, 59, 9959-9968.	1.8	16
49875	Electrochemical Li Intercalation in Black Phosphorus: In Situ and Ex Situ Studies. Journal of Physical Chemistry C, 2020, 124, 10710-10718.	1.5	18

#	Article	IF	Citations
49876	Highly Enhanced Photoelectrocatalytic Oxidation via Cooperative Effect of Neighboring Two Different Metal Oxides for Water Purification. Journal of Physical Chemistry C, 2020, 124, 11525-11535.	1.5	21
49877	Origin of Confined Catalysis in Nanoscale Reactors between Two-Dimensional Covers and Metal Substrates: Mechanical or Electronic?. Journal of Physical Chemistry C, 2020, 124, 11564-11573.	1.5	14
49878	Oxidation Notably Accelerates Nonradiative Electronâ€“Hole Recombination in MoS2 by Different Mechanisms: Time-Domain Ab Initio Analysis. Journal of Physical Chemistry Letters, 2020, 11, 4086-4092.	2.1	17
49879	Using Site Heterogeneity in Metalâ€“Organic Frameworks with Bimetallic Open Metal Sites for Olefin/Paraffin Separations. ACS Applied Nano Materials, 2020, 3, 5291-5300.	2.4	10
49880	The Role of Fe Species on NiOOH in Oxygen Evolution Reactions. ACS Catalysis, 2020, 10, 6254-6261.	5.5	93
49881	Identification of Active Area as Active Center for CO Oxidation over Single Au Atom Catalyst. ACS Catalysis, 2020, 10, 6094-6101.	5.5	106
49882	Electronegativity and doping in Si1-xGex alloys. Scientific Reports, 2020, 10, 7459.	1.6	13
49883	Semiconducting two-dimensional group VAâ€“VA haeckelite compounds with superior carrier mobility. Physical Chemistry Chemical Physics, 2020, 22, 12260-12266.	1.3	7
49884	Predicted CsSi compound: a promising material for photovoltaic applications. Physical Chemistry Chemical Physics, 2020, 22, 11578-11582.	1.3	7
49885	Substituted SrFeO₃ as robust oxygen sorbents for thermochemical air separation: correlating redox performance with compositional and structural properties. Physical Chemistry Chemical Physics, 2020, 22, 8924-8932.	1.3	43
49886	Topological phase transition and tunable electronic properties of hydrogenated bismuthene: from single-layer to double-layer. Journal of Physics Condensed Matter, 2020, 32, 035501.	0.7	1
49887	First principles calculations of the electric field gradient tensors of Ba₂NaOsO₆, a Mott insulator with strong spin orbit coupling. Journal of Physics Condensed Matter, 2020, 32, 405802.	0.7	3
49888	Influence of edge functionalization on electronic and optical properties of armchair phosphorene nanoribbons: a first-principles study. Electronic Structure, 2020, 2, 025001.	1.0	4
49889	Temperature dependence of surface and grain boundary energies from first principles. Physical Review B, 2020, 101, .	1.1	26
49890	Spin orbitronics at a topological insulator-semiconductor interface. Physical Review B, 2020, 101, .	1.1	11
49891	Topological semimetal in an <mml:math xmlns:mml="http://www.w3.org/1998/Math/MathML"><mml:mrow><mml:mi>s</mml:mi><mml:msup><mml:mi>p</mml:mi><mml:mi>n</mml:mi></mml:msup></mml:mrow></mml:math> hybridized carbon network with nodal rings. Physical Review B, 2020, 101, .	1.1	18
49892	Abundant valley-polarized states in two-dimensional ferromagnetic van der Waals heterostructures. Physical Review B, 2020, 101, .	1.1	42
49893	Metallic Phases on a Pristine Si(111) Surface. Journal of the Korean Physical Society, 2020, 76, 710-714.	0.3	0

#	Article	IF	Citations
49894	Copper phosphosulfides as a highly active and stable photocatalyst for hydrogen evolution reaction. Applied Catalysis B: Environmental, 2020, 273, 118927.	10.8	28
49895	Mechanistic insight into the catalytically active phase of CO2 hydrogenation on Cu/ZnO catalyst. Applied Surface Science, 2020, 525, 146481.	3.1	20
49896	Thermoplastic polyurethane â€“ Ti3C2(Tx) MXene nanocomposite: The influence of functional groups upon the matrixâ€“reinforcement interaction. Applied Surface Science, 2020, 528, 146526.	3.1	24
49897	Role of active sites in N-coordinated Fe-Co dual-metal doped graphene for oxygen reduction and evolution reactions: A theoretical insight. Applied Surface Science, 2020, 525, 146588.	3.1	75
49898	Effect of coordination interaction between water and zinc on photochemistry property of Zn3(PO4)2Â·2H2O. Chemical Physics, 2020, 536, 110811.	0.9	6
49899	Enhancing adhesion of Al2O3 scale on Ti-Al intermetallics by alloying: A first principles study. Computational Materials Science, 2020, 181, 109756.	1.4	9
49900	Design of novel pentagonal 2D transitional-metal sulphide monolayers for hydrogen evolution reaction. International Journal of Hydrogen Energy, 2020, 45, 16201-16209.	3.8	32
49901	Electronic and optical properties of lithium-decorated Î´-graphyne from first principles. Optik, 2020, 216, 164898.	1.4	6
49902	Crystal Site Feature Embedding Enables Exploration of Large Chemical Spaces. Matter, 2020, 3, 433-448.	5.0	33
49903	Engineering of a highly stable metal-organic Co-film for efficient electrocatalytic water oxidation in acidic media. Materials Today Energy, 2020, 17, 100437.	2.5	9
49904	Accurate simulations of atomic diffractive scattering from KCl(0 0 1) under fast grazing incidence conditions. Nuclear Instruments & Methods in Physics Research B, 2020, 476, 1-9.	0.6	5
49905	Ten Facets, One Force Field: The GAL19 Force Field for Waterâ€“Noble Metal Interfaces. Journal of Chemical Theory and Computation, 2020, 16, 4565-4578.	2.3	26
49906	Molecular Dynamics Study of sp-Defect Migration in Odd Fullerene: Possible Role in Synthesis of Abundant Isomers of Fullerenes. Journal of Physical Chemistry C, 2020, 124, 11652-11661.	1.5	9
49907	Identification of Active Sites of Pure and Nitrogen-Doped Carbon Materials for Oxygen Reduction Reaction Using Constant-Potential Calculations. Journal of Physical Chemistry C, 2020, 124, 12016-12023.	1.5	73
49908	Structural Deformation Controls Charge Losses in MAPbI₃: Unsupervised Machine Learning of Nonadiabatic Molecular Dynamics. ACS Energy Letters, 2020, 5, 1930-1938.	8.8	55
49909	Electronic and magnetic structure of infinite-layer NdNiO2: trace of antiferromagnetic metal. Npj Quantum Materials, 2020, 5, .	1.8	66
49910	Tuneable quantum spin Hall states in confined 1T' transition metal dichalcogenides. Scientific Reports, 2020, 10, 6670.	1.6	12
49911	Precursor chemistry of h-BN: adsorption, desorption, and decomposition of borazine on Pt(110). Physical Chemistry Chemical Physics, 2020, 22, 11704-11712.	1.3	6

#	Article	IF	Citations
49912	The effect of DMPO on the formation of hydroxyl radicals on the rutile TiO₂(110) surface. Physical Chemistry Chemical Physics, 2020, 22, 13129-13135.	1.3	12
49913	Atomic and electronic structures of charge-doping VO₂: first-principles calculations. RSC Advances, 2020, 10, 18543-18552.	1.7	17
49914	Mutual dependence of oxygen and vacancy diffusion in bcc Fe and dilute iron alloys. Physical Review B, 2020, 101, .	1.1	3
49915	Two-dimensional <mml:math xmlns:mml="http://www.w3.org/1998/Math/MathML"><mml:msub><mml:mi mathvariant="normal">CP</mml:mi><mml:mn>3</mml:mn></mml:msub></mml:math> monolayer and its fluorinated derivative with promising electronic and optical properties: A theoretical study. Physical Review B, 2020, 101, .	1.1	27
49916	Experimental and DFT insights into elastic, magnetic, electrical, and thermodynamic properties of MABâ€phase Fe₂AlB₂. Journal of the American Ceramic Society, 2020, 103, 5837-5851.	1.9	22
49917	Introducing Highly Redoxâ€Active Atomic Centers into Insertionâ€Type Electrodes for Lithiumâ€Ion Batteries. Advanced Energy Materials, 2020, 10, 2000783.	10.2	30
49918	Synthesis, Structural Characterization and Chemical Bonding of Sr₇Li₆Sn₁₂ and its Quaternary Derivatives with Eu and Alkaline Earth Metal (Mg, Ca, Ba) Substitutions. A Tale of Seven Liâ€Containing Stannides and Two Complex Crystal Structures. European Journal of Inorganic Chemistry, 2020, 2020, 1979-1988.	1.0	0
49919	<mml:math xmlns:mml="http://www.w3.org/1998/Math/MathML" altimg="si43.svg"><mml:mrow><mml:msub><mml:mrow><mml:mtext>Sn</mml:mtext></mml:mrow><mml:mrow><mml:mn>1</mml:mn> <mml:math xmlns:mml="http://www.w3.org/1998/Math/MathML" altimg="si44.svg"><mml:mrow><mml:msub><mml:mrow><mml:mtext>In</mml:mtext></mml:mrow><mml:mrow><mml:mi>x</mml:mi> Computational Materials Science, 2020, 182, 109777.	1.4	5
49920	Comparison of oxygen vacancy and interstitial oxygen in KDP and ADP crystals from density functional theory calculations. Computational Materials Science, 2020, 182, 109783.	1.4	16
49921	Spin Seebeck effect in bipolar magnetic semiconductor: A case of magnetic MoS2 nanotube. Journal of Advanced Research, 2020, 24, 391-396.	4.4	10
49922	Synthesis of mesoscale ordered two-dimensional Ï€-conjugated polymers with semiconducting properties. Nature Materials, 2020, 19, 874-880.	13.3	158
49923	Density functionals combined with van der Waals corrections for graphene adsorbed on layered materials. Physical Review B, 2020, 101, .	1.1	8
49924	A Physical Model for Understanding the Activation of MoS₂ Basalâ€Plane Sulfur Atoms for the Hydrogen Evolution Reaction. Angewandte Chemie - International Edition, 2020, 59, 14835-14841.	7.2	36
49925	Layer construction of topological crystalline insulator LaSbTe. Science China: Physics, Mechanics and Astronomy, 2020, 63, 1.	2.0	12
49926	Microscopic Link between Electron Localization and Chemical Expansion in AMnO3 and ATiO3 Perovskites (A = Ca, Sr, Ba). Journal of Physical Chemistry C, 2020, 124, 12922-12932.	1.5	12
49927	Surface-Enhanced Raman Scattering due to a Synergistic Effect on ZnS and Graphene Oxide. Journal of Physical Chemistry C, 2020, 124, 12742-12751.	1.5	14
49928	Controlling the Oxidation State of Fe-Based Catalysts through Nitrogen Doping toward the Hydrodeoxygenation of m-Cresol. ACS Catalysis, 2020, 10, 7884-7893.	5.5	32
49929	Selective Formation of the Li₄Mn₅O₁₂ Surface Spinel Phase in Sulfur-Doped Li-Excess-Layered Cathode Materials for Improved Cycle Life. ACS Sustainable Chemistry and Engineering, 2020, 8, 8037-8048.	3.2	17

#	Article	IF	Citations
49930	Metal-Free Magnetism in Chemically Doped Covalent Organic Frameworks. Journal of the American Chemical Society, 2020, 142, 11013-11021.	6.6	28
49931	Ab initio study of structure and electrical conductivity of warm dense oxygen. Physics of Plasmas, 2020, 27, 052701.	0.7	1
49932	Structural evolution in gold nanoparticles using artificial neural network based interatomic potentials. Journal of Chemical Physics, 2020, 152, 154302.	1.2	8
49933	Structural, electronic, and magnetic properties of point defects in polyaniline (C3N) and graphene monolayers: A comparative study. Journal of Applied Physics, 2020, 127, 195102.	1.1	8
49934	Bader net charge analysis on doping effects of Sb in SnSe2 and related charge transport properties. Journal of Applied Physics, 2020, 127, .	1.1	7
49935	Electron density modulation of GaN nanowires by manganese incorporation for highly high-rate Lithium-ion storage. Electrochimica Acta, 2020, 350, 136380.	2.6	28
49936	Molecular Layer Deposition of â€œMagnesiconeâ€, a Magnesium-based Hybrid Material. Chemistry of Materials, 2020, 32, 4451-4466.	3.2	17
49937	Cooperative Catalysis by Multiple Active Centers in Nonoxidative Conversion of Methane. Journal of Physical Chemistry C, 2020, 124, 13656-13663.	1.5	18
49938	Ester-Based Electrolytes for Fast Charging of Energy Dense Lithium-Ion Batteries. Journal of Physical Chemistry C, 2020, 124, 12269-12280.	1.5	50
49939	Two-Dimensional van der Waals Supramolecular Frameworks from Co-Hosted Molecular Assembly and C₆₀ Dimerization. Journal of Physical Chemistry C, 2020, 124, 12589-12595.	1.5	7
49940	Thermal Conductivity of High-Temperature Phases of Cu2S from Ab Initio Molecular Dynamics: Advent of Lattice-Site Hopping. Journal of Physical Chemistry C, 2020, 124, 12318-12323.	1.5	0
49941	MAI Termination Favors Efficient Hole Extraction and Slow Charge Recombination at the MAPbI₃/CuSCN Heterojunction. Journal of Physical Chemistry Letters, 2020, 11, 4481-4489.	2.1	22
49942	Harnessing Hot Phonon Bottleneck in Metal Halide Perovskite Nanocrystals via Interfacial Electronâ€“Phonon Coupling. Nano Letters, 2020, 20, 4610-4617.	4.5	60
49943	Optical Properties and First-Principles Study of CH₃NH₃PbBr₃ Perovskite Structures. ACS Omega, 2020, 5, 12313-12319.	1.6	12
49944	Synthesis of Co-based Prussian Blue Analogues/Dual-Doped Hollow Carbon Microsphere Hybrids as High-Performance Bifunctional Electrocatalysts for Oxygen Evolution and Overall Water Splitting. ACS Sustainable Chemistry and Engineering, 2020, 8, 8318-8326.	3.2	45
49945	Promoting effect of tungsten carbide on the catalytic activity of Cu for CO₂ reduction. Physical Chemistry Chemical Physics, 2020, 22, 13666-13679.	1.3	16
49946	Facet engineering of LaNbON₂ transformed from LaKNaNbO₅ for enhanced photocatalytic O₂ evolution. Journal of Materials Chemistry A, 2020, 8, 11743-11751.	5.2	21
49947	First-principles study of the surface reactions of aminosilane precursors over WO₃(001) during atomic layer deposition of SiO₂. RSC Advances, 2020, 10, 16584-16592.	1.7	3

#	Article	IF	Citations
49948	Phonon dispersion, Raman spectra, and evidence for spin-phonon coupling in MnV2O4 from first principles. Physical Review B, 2020, 101, .	1.1	4
49949	Higher-order Dirac fermions in three dimensions. Physical Review B, 2020, 101, .	1.1	56
49950	Probing Nonequilibrium Dynamics of Photoexcited Polarons on a Metal-Oxide Surface with Atomic Precision. Physical Review Letters, 2020, 124, 206801.	2.9	37
49951	Structural stabilities of iron silicides at high pressures and temperatures. International Journal of Modern Physics B, 2020, 34, 2050119.	1.0	1
49952	Thermal Characterization and Modelling of AlGaN-GaN Multilayer Structures for HEMT Applications. Energies, 2020, 13, 2363.	1.6	21
49953	Oxygen Vacancy Modulation of Bimetallic Oxynitride Anodes toward Advanced Liâ€ion Capacitors. Advanced Functional Materials, 2020, 30, 2000350.	7.8	48
49954	Metastability at Defective Metal Oxide Interfaces and Nanoconfined Structures. Advanced Materials Interfaces, 2020, 7, 1902090.	1.9	20
49955	Exploring the Correlation between Stability, Fluxionality, and Absorption Spectra of Ultrasmall CdSe Clusters: A Computational Study. Journal of Physical Chemistry C, 2020, 124, 12672-12681.	1.5	2
49956	Anisotropic High Carrier Mobilities of One-Third-Hydrogenated Group-V Elemental Monolayers. Journal of Physical Chemistry C, 2020, 124, 12628-12635.	1.5	1
49957	Methane Nonoxidative Direct Conversion to C₂ Hydrogenations over CeO₂-Supported Pt Catalysts: A Density Functional Theory Study. Journal of Physical Chemistry C, 2020, 124, 13249-13262.	1.5	16
49958	Excitonic Effect Drives Ultrafast Dynamics in van der Waals Heterostructures. Nano Letters, 2020, 20, 4631-4637.	4.5	46
49959	Artificial Trees for Artificial Photosynthesis: Construction of Dendrite-Structured Î±-Fe₂O₃/g-C₃N₄ Z-Scheme System for Efficient CO₂ Reduction into Solar Fuels. ACS Applied Energy Materials, 2020, 3, 6561-6572.	2.5	67
49960	Porous-Carbon Aerogels with Tailored Sub-Nanopores for High Cycling Stability and Rate Capability Potassium-Ion Battery Anodes. ACS Applied Materials & Interfaces, 2020, 12, 27045-27054.	4.0	16
49961	1D/2D C₃N₄/Graphene Composite as a Preferred Anode Material for Lithium Ion Batteries: Importance of Heterostructure Design via DFT Computation. ACS Applied Materials & Interfaces, 2020, 12, 25875-25883.	4.0	40
49962	Insights into Spectator-Directed Catalysis: CO Adsorption on Amine-Capped Platinum Nanoparticles on Oxide Supports. ACS Applied Materials & Interfaces, 2020, 12, 27765-27776.	4.0	14
49963	Naâ€“Niâ€“H Phase Formation at High Pressures and High Temperatures: Hydrido Complexes [NiH5]3â€“ Versus the Perovskite NaNiH3. ACS Omega, 2020, 5, 8730-8743.	1.6	7
49964	Yield strength and misfit volumes of NiCoCr and implications for short-range-order. Nature Communications, 2020, 11, 2507.	5.8	162
49965	Electronic structure of epitaxial perovskite films in the two-dimensional limit: Role of the surface termination. Applied Physics Letters, 2020, 116, 201601.	1.5	2

#	Article	IF	Citations
49966	Adsorption of small molecules on transition metal doped rhodium clusters Rh3X (Xâ€‰=â€‰3d, 4d atom): a first-principles investigation. Molecular Physics, 2020, 118, e1746424.	0.8	0
49967	Electrical scattering mechanism evolution in un-doped and halogen-doped Bi2O2Se single crystals. Journal of Physics Condensed Matter, 2020, 32, 365705.	0.7	0
49968	High-pressure characterization of multifunctional CrVO₄. Journal of Physics Condensed Matter, 2020, 32, 385403.	0.7	12
49969	Towards simulation of the dynamics of materials on quantum computers. Physical Review B, 2020, 101, .	1.1	23
49970	Stacking Domains and Dislocation Networks in Marginally Twisted Bilayers of Transition Metal Dichalcogenides. Physical Review Letters, 2020, 124, 206101.	2.9	100
49971	Ab Initio Studies of Phase Transformations in Fe100Ââ€“ÂxSix. Physics of the Solid State, 2020, 62, 739-743.	0.2	2
49972	Effects of B on the Segregation Behavior of Mo at the Feâ€“Cr(111)/Cr2O3(0001) Interface: A First-Principles Study. Metals, 2020, 10, 577.	1.0	6
49973	The Role of the Interactions at the Tungsten Disulphide Surface in the Stability and Enhanced Thermal Properties of Nanofluids with Application in Solar Thermal Energy. Nanomaterials, 2020, 10, 970.	1.9	11
49974	Cu Anchored Ti₂NO₂ as High Performance Electrocatalyst for Oxygen Evolution Reaction: A Density Functional Theory Study. ChemCatChem, 2020, 12, 4059-4066.	1.8	27
49975	Introduction of an Al Seed Layer for Facile Adsorption of MoCl₅ during Atomic Layer Deposition of MoS₂. Physica Status Solidi (A) Applications and Materials Science, 2020, 217, 1901042.	0.8	6
49976	Thermal dynamic study of the gradual desolvation in submicropores for carbon-based supercapacitor at low temperature. Ionics, 2020, 26, 4695-4704.	1.2	3
49977	Covalent Encapsulation of Sulfur in a MOFâ€Derived S, Nâ€Doped Porous Carbon Host Realized via the Vaporâ€Infiltration Method Results in Enhanced Sodiumâ€“Sulfur Battery Performance. Advanced Energy Materials, 2020, 10, 2000931.	10.2	118
49978	Substitution of Titanium for Magnesium Ions at the Surface of Mg-Doped Rutile. Journal of Physical Chemistry C, 2020, 124, 11490-11498.	1.5	6
49979	Nanocrystals of Lead Chalcohalides: A Series of Kinetically Trapped Metastable Nanostructures. Journal of the American Chemical Society, 2020, 142, 10198-10211.	6.6	34
49980	Tunable electronic structures and half-metallicity in two-dimensional InSe functionalized with magnetic superatom. Journal of Physics Condensed Matter, 2020, 32, 365501.	0.7	2
49981	Two-Dimensional Multifunctional Metalâ€“Organic Frameworks with Simultaneous Ferro-/Ferrimagnetism and Vertical Ferroelectricity. Journal of Physical Chemistry Letters, 2020, 11, 4193-4197.	2.1	30
49982	Adsorption of Polarized Molecules for Interfacial Band Engineering of Doped TiO₂ Thin Films. Langmuir, 2020, 36, 5839-5846.	1.6	3
49983	Atomically Dispersed Ru on Manganese Oxide Catalyst Boosts Oxidative Cyanation. ACS Catalysis, 2020, 10, 6299-6308.	5.5	51

#	Article	IF	Citations
49984	Single Vanadium Atoms Anchored on Graphitic Carbon Nitride as a High-Performance Catalyst for Non-oxidative Propane Dehydrogenation. ACS Nano, 2020, 14, 5772-5779.	7.3	73
49985	Co-immobilization of a Rh Catalyst and a Keggin Polyoxometalate in the UiO-67 Zr-Based Metalâ€“Organic Framework: In Depth Structural Characterization and Photocatalytic Properties for CO₂ Reduction. Journal of the American Chemical Society, 2020, 142, 9428-9438.	6.6	138
49986	Perovskite neural trees. Nature Communications, 2020, 11, 2245.	5.8	38
49987	New carbon allotropes derived from nanotubes via a three-fold distortion mechanism. Physical Chemistry Chemical Physics, 2020, 22, 12489-12495.	1.3	2
49988	Alâ€“Sc dual-doped LiGe₂(PO₄)₃ â€“ a NASICON-type solid electrolyte with improved ionic conductivity. Journal of Materials Chemistry A, 2020, 8, 11302-11313.	5.2	36
49989	Diffused morphotropic phase boundary in relaxor-PbTiO₃ crystals: High piezoelectricity with improved thermal stability. Applied Physics Reviews, 2020, 7, 021405.	5.5	43
49990	High-temperature ion-thermal behavior from average-atom calculations. Physical Review E, 2020, 101, 053201.	0.8	6
49991	Semimetal States of Crystalline Molecular Hydrogen at High Pressures. JETP Letters, 2020, 111, 162-166.	0.4	5
49992	Ab Initio Study of the Relation between the Structural, Magnetic, and Optical Properties of Normal and Inverse MnGa2O4 Spinels. Journal of Experimental and Theoretical Physics, 2020, 130, 418-422.	0.2	1
49993	Highâ€Voltage Oxygenâ€Redoxâ€Based Cathode for Rechargeable Sodiumâ€Ion Batteries. Advanced Energy Materials, 2020, 10, 2001111.	10.2	72
49994	Fast, Low-Cost Synthesis of ZnO:Eu Nanosponges and the Nature of Ln Doping in ZnO. Inorganic Chemistry, 2020, 59, 7584-7602.	1.9	15
49995	Magneto-Optical Kerr Switching Properties of (CrI₃)₂ and (CrBr₃/CrI₃) Bilayers. ACS Applied Electronic Materials, 2020, 2, 1373-1380.	2.0	32
49996	Reaction mechanism and kinetics for CO2 reduction on nickel single atom catalysts from quantum mechanics. Nature Communications, 2020, 11, 2256.	5.8	140
49997	Orbital ordering and magnetism in layered Perovskite Ruthenate Sr2RuO4. Scientific Reports, 2020, 10, 7089.	1.6	4
49998	An ultrathin two-dimensional vertical ferroelectric tunneling junction based on CuInP₂S₆ monolayer. Nanoscale, 2020, 12, 12522-12530.	2.8	40
49999	Epitaxial fabrication of monolayer copper arsenide on Cu(111)*. Chinese Physics B, 2020, 29, 077301.	0.7	5
50000	Signature of Dirac semimetal states in gray arsenic studied by de Haasâ€“van Alphen and Shubnikovâ€“de Haas quantum oscillations. Physical Review B, 2020, 101, .	1.1	3
50001	Galliumâ€“Boronâ€“Phosphide ($$hbox {GaBP}_{2}$$): a new IIIâ€“V semiconductor for photovoltaics. Journal of Materials Science, 2020, 55, 9448-9460.	1.7	5

#	Article	IF	Citations
50002	Colossal Permittivity Ti_{1â€“x}(Eu_{0.5}Ta_{0.5})_xO₂ Ceramics with Excellent Thermal Stability. ACS Applied Electronic Materials, 2020, 2, 1700-1708.	2.0	23
50003	Structureâ€“Activityâ€“Selectivity Relationships in Propane Dehydrogenation over Rh/ZrO₂ Catalysts. ACS Catalysis, 2020, 10, 6377-6388.	5.5	47
50004	Ultrafast nucleation and growth of high-quality monolayer MoSe₂ crystals via vapor-liquid-solid mechanism. Nanotechnology, 2020, 31, 335601.	1.3	20
50005	Sensitivity of Monte Carlo Simulations to Linear Scaling Relations. Journal of Physical Chemistry C, 2020, 124, 11952-11959.	1.5	5
50006	Sputtered p-Type Cu_xZn_{1â€“x}S Back Contact to CdTe Solar Cells. ACS Applied Energy Materials, 2020, 3, 5427-5438.	2.5	11
50007	Synergy between a Silverâ€“Copper Surface Alloy Composition and Carbon Dioxide Adsorption and Activation. ACS Applied Materials & Interfaces, 2020, 12, 25374-25382.	4.0	19
50008	Anomalous in-plane lattice thermal conductivity in an atomically thin two-dimensional Î±-GeTe layer. Physical Chemistry Chemical Physics, 2020, 22, 12273-12280.	1.3	4
50009	Discovery of multiferroics with tunable magnetism in two-dimensional lead oxide. Applied Physics Letters, 2020, 116, .	1.5	24
50010	Improved transition metal surface energies from a generalized gradient approximation developed for quasi two-dimensional systems. Journal of Chemical Physics, 2020, 152, 151101.	1.2	14
50011	Pseudorotating hydride complexes with high hydrogen coordination: A class of rotatable polyanions in solid matter. Applied Physics Letters, 2020, 116, .	1.5	15
50012	Strain robust spin gapless semiconductors/half-metals in transition metal embedded MoSe₂ monolayer. Journal of Physics Condensed Matter, 2020, 32, 365305.	0.7	9
50013	Band Structure of Strained $mathrm{Ge}_{1-x}~mathrm{Sn}_{x}$ Alloy: A Full-Zone 30-Band ${k}cdot{p}$ Model. IEEE Journal of Quantum Electronics, 2020, 56, 1-8.	1.0	4
50014	Artificial neural network modeling of anisotropic hyperelastic materials based on computational crystal structure data. , 2020, , .		3
50015	Metalâ€“Organic Frameworks Derived Interconnected Bimetallic Metaphosphate Nanoarrays for Efficient Electrocatalytic Oxygen Evolution. Advanced Functional Materials, 2020, 30, 1910498.	7.8	104
50016	Highâ€Performance Overall CO₂ Splitting on Hierarchical Structured Cobalt Disulfide with Partially Removed Sulfur Edges. Advanced Functional Materials, 2020, 30, 2000154.	7.8	26
50017	Theoretical Study of Interfacial and Electronic Properties of Transition Metal Dichalcogenides and Organic Molecules Based van der Waals Heterostructures. Advanced Theory and Simulations, 2020, 3, 2000045.	1.3	25
50018	Discovery of New Polymorphs of Gallium Oxides with Particle Swarm Optimizationâ€Based Structure Searches. Advanced Electronic Materials, 2020, 6, 2000119.	2.6	17
50019	Understanding the Band Engineering in Mg₂Siâ€Based Systems from Wannierâ€Orbital Analysis. Annalen Der Physik, 2020, 532, 1900543.	0.9	5

#	Article	IF	Citations
50020	Ultrafast Relaxation Dynamics and Nonlinear Response of Fewâ€Layer Niobium Carbide MXene. Small Methods, 2020, 4, 2000250.	4.6	84
50021	Thermal Stability of Ag₁₃^{â€“} Clusters Studied by Ab Initio Molecular Dynamics Simulations. Journal of Physical Chemistry A, 2020, 124, 4325-4332.	1.1	4
50022	Trends in the Adsorption of Oxygen and Li₂O₂ on Transition-Metal Carbide Surfaces: A Theoretical Study. Journal of Physical Chemistry C, 2020, 124, 7716-7724.	1.5	9
50023	Highly Selective Cross-Etherification of 5-Hydroxymethylfurfural with Ethanol. ACS Catalysis, 2020, 10, 6771-6785.	5.5	40
50024	Impacts of Oxygen Vacancies on Zinc Ion Intercalation in VO₂. ACS Nano, 2020, 14, 5581-5589.	7.3	267
50025	Tuning the activities of cuprous oxide nanostructures via the oxide-metal interaction. Nature Communications, 2020, 11, 2312.	5.8	31
50026	Enhanced performance of in-plane transition metal dichalcogenides monolayers by configuring local atomic structures. Nature Communications, 2020, 11, 2253.	5.8	112
50027	Efficient electrically powered CO2-to-ethanol via suppression of deoxygenation. Nature Energy, 2020, 5, 478-486.	19.8	363
50028	Strain modulation of TaO4 planarity in tantalates ultrathin films: surface states engineering. Scientific Reports, 2020, 10, 7828.	1.6	5
50029	A quantum chemical study of substituent effects on CN bonds in aryl isocyanide molecules adsorbed on the Pt surface. Physical Chemistry Chemical Physics, 2020, 22, 12200-12208.	1.3	4
50030	Structural trends in the dehydrogenation selectivity of palladium alloys. Chemical Science, 2020, 11, 5066-5081.	3.7	23
50031	Synthetic investigation of competing magnetic interactions in 2D metalâ€“chloranilate radical frameworks. Chemical Science, 2020, 11, 5922-5928.	3.7	13
50032	Density functional theory study of superoxide ions as impurities in alkali halides. Physical Chemistry Chemical Physics, 2020, 22, 13378-13389.	1.3	1
50033	The mechanism and ligand effects of single atom rhodium supported on ZSM-5 for the selective oxidation of methane to methanol. Physical Chemistry Chemical Physics, 2020, 22, 11686-11694.	1.3	22
50034	Surface functionalization of ZnO:Ag columnar thin films with AgAu and AgPt bimetallic alloy nanoparticles as an efficient pathway for highly sensitive gas discrimination and early hazard detection in batteries. Journal of Materials Chemistry A, 2020, 8, 16246-16264.	5.2	38
50035	A physics-based machine learning study of the behavior of interstitial helium in single crystal Wâ€“Mo binary alloys. Journal of Applied Physics, 2020, 127, .	1.1	10
50036	Exchange interactions and long-range magnetic order in the (Mg,Co,Cu,Ni,Zn)O entropy-stabilized oxide: A theoretical investigation. Journal of Applied Physics, 2020, 127, .	1.1	16
50037	Scalable synthesis of water-dispersible 2D manganese dioxide monosheets. Journal of Physics Condensed Matter, 2020, 32, 015301.	0.7	11

#	Article	IF	Citations
50038	Superconducting boron allotropes. Physical Review B, 2020, 101, .	1.1	18
50039	Experimental and Theoretical Study of the Atomic Structure Evolution of High-Entropy Alloys Based on Fe, Cr, Ni, Mn, and Co upon Thermal and Radiation Aging. Physics of the Solid State, 2020, 62, 389-400.	0.2	6
50040	Aluminum electrodeposition from a non-aqueous electrolyteâ€"a combined computational and experimental study. Journal of Solid State Electrochemistry, 2020, 24, 2833-2846.	1.2	7
50041	First-principles insight into the entanglements between superionic diffusion and Li/Al antisite in Al-doped Li1+xAlxGe2â^'x(PO4)3 (LAGP). Science China Technological Sciences, 2020, 63, 1787-1794.	2.0	7
50042	High yield production of ultrathin fibroid semiconducting nanowire of Ta2Pd3Se8. Nano Research, 2020, 13, 1627-1635.	5.8	16
50043	Boosting the bifunctional oxygen electrocatalytic performance of atomically dispersed Fe site via atomic Ni neighboring. Applied Catalysis B: Environmental, 2020, 274, 119091.	10.8	130
50044	Substitutional Mechanisms and Structural Relaxations for Manganese in SrTiO3: Bridging the Concentration Gap for Point-Defect Metrology. Chemistry of Materials, 2020, 32, 4651-4662.	3.2	16
50045	Facile and Controllable Synthesis of Co₂V₂O₇ Microplatelets Anchored on Graphene Layers toward Superior Li-Ion Battery Anodes. Energy & Fuels, 2020, 34, 7616-7621.	2.5	22
50046	Selective Adsorption of Pb(II) on an Annealed Hematite (1<ovl>1</ovl>02) Surface: Evidence from Crystal Truncation Rod X-ray Diffraction and Density Functional Theory. Environmental Science & Technology, 2020, 54, 6651-6660.	4.6	9
50047	Theoretical Studies on the Stability and Reactivity of the Metal-Doped CeO₂(100) Surface: Toward H₂ Dissociation and Oxygen Vacancy Formation. Langmuir, 2020, 36, 5891-5901.	1.6	42
50048	OER Performances of Cationic Substituted (100)-Oriented IrO₂ Thin Films: A Joint Experimental and Theoretical Study. ACS Applied Energy Materials, 2020, 3, 5229-5237.	2.5	14
50049	Highly Stable Two-Dimensional Iron Monocarbide with Planar Hypercoordinate Moiety and Superior Li-Ion Storage Performance. ACS Applied Materials & Interfaces, 2020, 12, 30297-30303.	4.0	21
50050	Trifunctional Electrocatalysts with High Efficiency for the Oxygen Reduction Reaction, Oxygen Evolution Reaction, and Naâ€"O₂ Battery in Heteroatom-Doped Janus Monolayer MoSSe. ACS Applied Materials & Interfaces, 2020, 12, 24066-24073.	4.0	37
50051	Insights into the Oxygen Vacancy Filling Mechanism in CuO/CeO₂ Catalysts: A Key Step Toward High Selectivity in Preferential CO Oxidation. ACS Catalysis, 2020, 10, 6532-6545.	5.5	128
50052	Structural Phase Transitions of Molecular Self-Assembly Driven by Nonbonded Metal Adatoms. ACS Nano, 2020, 14, 6331-6338.	7.3	9
50053	Interlayer quantum transport in Dirac semimetal BaGa2. Nature Communications, 2020, 11, 2370.	5.8	8
50054	Negative Poissonâ€™s ratio in two-dimensional honeycomb structures. Npj Computational Materials, 2020, 6, .	3.5	56
50055	WSe2/SnSe2 vdW heterojunction Tunnel FET with subthermionic characteristic and MOSFET co-integrated on same WSe2 flake. Npj 2D Materials and Applications, 2020, 4, .	3.9	50

#	Article	IF	Citations
50056	Phosphine vapor-assisted construction of heterostructured Ni₂P/NiTe₂ catalysts for efficient hydrogen evolution. Energy and Environmental Science, 2020, 13, 1799-1807.	15.6	105
50057	Experimental and theoretical investigations of the effect of heteroatom-doped carbon microsphere supports on the stability and storage capacity of nano-Co₃O₄ conversion anodes for application in lithium-ion batteries. Nanoscale Advances, 2020, 2, 2914-2924.	2.2	7
50058	Fullerene-based 0D ferroelectrics/multiferroics for ultrahigh-density and ultrafast nonvolatile memories. Physical Chemistry Chemical Physics, 2020, 22, 12039-12043.	1.3	7
50059	Two-dimensional Dirac spin-gapless semiconductors with tunable perpendicular magnetic anisotropy and a robust quantum anomalous Hall effect. Materials Horizons, 2020, 7, 2071-2077.	6.4	45
50060	Ultrathin Î´-MnO₂ nanoflakes with Na⁺ intercalation as a high-capacity cathode for aqueous zinc-ion batteries. RSC Advances, 2020, 10, 17702-17712.	1.7	43
50061	In situconfinement of Pt within three-dimensional MoO₂@porous carbon for efficient hydrogen evolution. Journal of Materials Chemistry A, 2020, 8, 10409-10418.	5.2	35
50062	High-temperature quantum anomalous Hall insulator in two-dimensional Bi2ON. Applied Physics Letters, 2020, 116, .	1.5	4
50063	Exchange-correlation corrections for electronic properties of half-metallic Co2FeSi and nonmagnetic semiconductor CoFeTiAl. Journal of Applied Physics, 2020, 127, .	1.1	10
50064	First-principles studies of Tin+1SiNn (nâ€‰=â€‰1, 2, 3) MAX phase. Philosophical Magazine, 2020, 100, 2183-2204.	0.7	4
50065	Realization of valley polarization in monolayer WS₂ via 3d transition metal atom adsorption. Journal Physics D: Applied Physics, 2020, 53, 384001.	1.3	5
50066	Structure gauges and laser gauges for the semiconductor Bloch equations in high-order harmonic generation in solids. Physical Review A, 2020, 101, .	1.0	60
50067	Vibronic States and Their Effect on the Temperature and Strain Dependence of Silicon-Vacancy Qubits in<mml:math xmlns:mml="http://www.w3.org/1998/Math/MathML" display="inline" overflow="scroll"><mml:mn>4</mml:mn><mml:mi>H</mml:mi></mml:math>-<mml:math xmlns:mml="http://www.w3.org/1998/Math/MathML" display="inline"	1.5	47
50068	Quartic anharmonicity and anomalous thermal conductivity in cubic antiperovskites <mml:math xmlns:mml="http://www.w3.org/1998/Math/MathML"><mml:mrow><mml:msub><mml:mi>A</mml:mi><mml:mn>3</mml:mn></mml:m mathvariant="normal">O</mml:mi></mml:mrow></mml:math> <mml:math		

#	Article	IF	Citations
50074	Fast and stable Mg2+ intercalation in a high voltage NaV2O2(PO4)2F/rGO cathode material for magnesium-ion batteries. Science China Materials, 2020, 63, 1651-1662.	3.5	36
50075	Multielectron Redox and Insulator-to-Metal Transition upon Lithium Insertion in the Fast-Charging, Wadsley-Roth Phase PNb₉O₂₅. Chemistry of Materials, 2020, 32, 4553-4563.	3.2	50
50076	Ammine Lanthanum and Cerium Borohydrides, M(BH₄)₃Â·nNH₃; Trends in Synthesis, Structures, and Thermal Properties. Inorganic Chemistry, 2020, 59, 7768-7778.	1.9	19
50077	Large-Scale Electric-Field Confined Silicon with Optimized Charge-Transfer Kinetics and Structural Stability for High-Rate Lithium-Ion Batteries. ACS Nano, 2020, 14, 7066-7076.	7.3	114
50078	Controlling interlayer excitons in MoS2 layers grown by chemical vapor deposition. Nature Communications, 2020, 11, 2391.	5.8	73
50079	Computational search for magnetic and non-magnetic 2D topological materials using unified spinâ€“orbit spillage screening. Npj Computational Materials, 2020, 6, .	3.5	32
50080	Engineering covalently bonded 2D layered materials by self-intercalation. Nature, 2020, 581, 171-177.	13.7	185
50081	The interaction of two-dimensional Î±- and Î²-phosphorus carbide with environmental molecules: a DFT study. Physical Chemistry Chemical Physics, 2020, 22, 11307-11313.	1.3	6
50082	Pressure-induced isostructural phase transition in Ti₃AlC₂: experimental and theoretical investigation. Physical Chemistry Chemical Physics, 2020, 22, 13136-13142.	1.3	5
50083	Unconventional stable stoichiometry of vanadium peroxide. Physical Chemistry Chemical Physics, 2020, 22, 11460-11466.	1.3	4
50084	Koopmansâ€™ tuning of HSE hybrid density functional for calculations of defects in semiconductors: A case study of carbon acceptor in GaN. Journal of Applied Physics, 2020, 127, 155701.	1.1	8
50085	Investigations of optical and thermoelectric response of GaBi monolayer. AIP Conference Proceedings, 2020, , .	0.3	5
50086	Ab initio investigation of pressure-induced structural transitions and electronic evolution of Th3N4. High Pressure Research, 2020, 40, 267-282.	0.4	3
50087	Superhigh flexibility and out-of-plane piezoelectricity together with strong anharmonic phonon scattering induced extremely low lattice thermal conductivity in hexagonal buckled CdX (X =) Tj ETQq1 1 0.784314 rgBT /Ov	0.7	
50088	Stable edge structures and electronic states in zigzag 1Tâ€²-dichalcogenide nanoribbons. Journal of Physics Condensed Matter, 2020, 32, 365303.	0.7	1
50089	High-Chern-number and high-temperature quantum Hall effect without Landau levels. National Science Review, 2020, 7, 1280-1287.	4.6	251
50090	First-principles study of the low-temperature charge density wave phase in the quasi-one-dimensional Weyl chiral compound <mml:math xmlns:mml="http://www.w3.org/1998/Math/MathML"><mml:mo>(</mml:mo><mml:mrow><mml:msub><mml:mi>TaSe</mml:mi><mml mathvariant="normal">I</mml:mi></mml:mrow></mml:math>. Physical Review B, 2020, 101, .	1.1	36
50091	Phase stability and magnetic properties in fcc Fe-Cr-Mn-Ni alloys from first-principles modeling. Physical Review B, 2020, 101, .	1.1	30

#	Article	IF	Citations
50092	Observation of sixfold degenerate fermions in <mml:math xmlns:mml="http://www.w3.org/1998/Math/MathML"><mml:mrow><mml:mi>PdS</mml:mi><mml:msub><mml:mi mathvariant="normal">b</mml:mi><mml:mn>2</mml:mn></mml:msub></mml:mrow></mml:math>. Physical Review B, 2020, 101, .	1.1	20
50093	Dioxygen dissociation over man-made system at room temperature to form the active Î±-oxygen for methane oxidation. Science Advances, 2020, 6, eaaz9776.	4.7	35
50094	Superior mechanical and thermal properties than diamond: Diamond/lonsdaleite biphasic structure. Journal of Materials Science and Technology, 2020, 48, 114-122.	5.6	8
50095	Characterization of molecular-atomic transformation in fluid hydrogen under pressure via long-wavelength asymptote of charge density fluctuations. Journal of Molecular Liquids, 2020, 312, 113274.	2.3	6
50096	Alkali metals inside bi-layer graphene and MoS2: Insights from first-principles calculations. Nano Energy, 2020, 75, 104927.	8.2	30
50097	Heteroepitaxial oxygen-buffering interface enables a highly stable cobalt-free Li-rich layered oxide cathode. Nano Energy, 2020, 75, 104995.	8.2	74
50098	First-Principles Analyses of Nanoionic Effects at Oxideâ€“Oxide Heterointerfaces for Electrochemical Applications. Journal of Physical Chemistry C, 2020, 124, 14072-14081.	1.5	1
50099	Amorphization of Indirect Band Gap Semiconductors To Tune Their Optoelectronic Properties. Journal of Physical Chemistry C, 2020, 124, 14432-14438.	1.5	7
50100	Tuning the Carrier Lifetime in Black Phosphorene through Family Atom Doping. Journal of Physical Chemistry Letters, 2020, 11, 4662-4667.	2.1	48
50101	Mode-resolved reciprocal space mapping of electron-phonon interaction in the Weyl semimetal candidate Td-WTe2. Nature Communications, 2020, 11, 2613.	5.8	51
50102	Understanding the interface interaction between U3Si2 fuel and SiC cladding. Nature Communications, 2020, 11, 2621.	5.8	11
50103	Enabling materials informatics for 29Si solid-state NMR of crystalline materials. Npj Computational Materials, 2020, 6, .	3.5	11
50104	Thermally induced intra-molecular transformation and metalation of free-base porphyrin on Au(111) surface steered by surface confinement and ad-atoms. Nanoscale Advances, 2020, 2, 2986-2991.	2.2	8
50105	Transport properties of RuV-based half-Heusler semiconductors for thermoelectric applications: a computational study. Journal of Physics Condensed Matter, 2020, 32, 405501.	0.7	7
50106	Anisotropic Optical Properties of 2D Silicon Telluride. MRS Advances, 2020, 5, 1881-1889.	0.5	5
50107	The Effect of Surface Defects on Chloride-Induced Depassivation of Ironâ€”A Density Functional Theory Study. Corrosion, 2020, 76, 690-697.	0.5	14
50108	Effect of manganese dioxide crystal structure on adsorption of SO2 by DFT and experimental study. Applied Surface Science, 2020, 521, 146477.	3.1	36
50109	Adhesion, bonding and mechanical properties of Mo doped diamond/Al (Cu) interfaces: A first principles study. Applied Surface Science, 2020, 527, 146817.	3.1	41

#	Article	IF	Citations
50110	Interplay between Gd and oxygen vacancy on the electronic properties and defect chemistry of Gd-doped CeO2: A DFTÂ+ÂU study. Chemical Physics, 2020, 534, 110741.	0.9	14
50111	Electronic, optical, and thermoelectric properties of sodium pnictogen chalcogenides: A first principles study. Computational Materials Science, 2020, 183, 109818.	1.4	21
50112	Induced valley and spin splitting in monolayer MoS2 by interfacial magnetic proximity of half-Heusler LiBeN substrate. Journal of Magnetism and Magnetic Materials, 2020, 512, 167061.	1.0	2
50113	Superhard monoclinic BN allotrope in M-carbon structure. Physics Letters, Section A: General, Atomic and Solid State Physics, 2020, 384, 126518.	0.9	5
50114	First principles study of the electronic properties and Schottky barrier in Cu2Si/C2N van der Waals heterostructures. Physics Letters, Section A: General, Atomic and Solid State Physics, 2020, 384, 126532.	0.9	0
50115	Detection of Ppb-level NO2 using mesoporous ZnSe/SnO2 core-shell microspheres based chemical sensors. Sensors and Actuators B: Chemical, 2020, 320, 128365.	4.0	44
50116	Unusual Atmospheric Water Trapping and Water Induced Reversible Restacking of 2D Gallium Sulfide Layers in NaGaS₂ Formed by Supertetrahedral Building Unit. Chemistry of Materials, 2020, 32, 5589-5603.	3.2	21
50117	Implanting Ni-O-VOx sites into Cu-doped Ni for low-overpotential alkaline hydrogen evolution. Nature Communications, 2020, 11, 2720.	5.8	113
50118	Dynamic active-site generation of atomic iridium stabilized on nanoporous metal phosphides for water oxidation. Nature Communications, 2020, 11, 2701.	5.8	204
50119	Effect of Sn-self diffusion via H2 treatment on low temperature activation of hematite photoanodes. Catalysis Science and Technology, 2020, 10, 4245-4255.	2.1	3
50120	First-principles study of superionic Na_{9+x}Sn_xM_{3â^'x}S₁₂ (M = P, Sb). Materials Advances, 2020, 1, 184-196.	2.6	15
50121	Schottky barrier height and modulation due to interface structure and defects in Pt|MgO|Pt heterojunctions with implications for resistive switching. Journal of Applied Physics, 2020, 127, 205306.	1.1	1
50122	Degradation in AlGaN-based UV-C LEDs under constant current stress: A study on defect behaviors. Applied Physics Letters, 2020, 116, .	1.5	23
50123	Rational design principles for giant spin Hall effect in 5d -transition metal oxides. Proceedings of the National Academy of Sciences of the United States of America, 2020, 117, 11878-11886.	3.3	20
50124	Computational prediction of aâ€‰â€‰+4 oxidation state in Au via compressed AuO2 compound. Journal of Physics Condensed Matter, 2020, 32, 015402.	0.7	2
50125	Ferrotoroidic polarons in antiferrodistortive <mml:math xmlns:mml="http://www.w3.org/1998/Math/MathML"><mml:mrow><mml:mi>SrTi</mml:mi><mml:msub><mml:mi mathvariant="normal">O</mml:mi><mml:mn>3</mml:mn></mml:msub></mml:mrow></mml:math>. Physical Review B, 2020, 101, .	1.1	6
50126	Real spin and pseudospin topologies in the noncentrosymmetric topological nodal-line semimetal CaAgAs. Physical Review B, 2020, 101, .	1.1	11
50127	pâ€Type Transparent Quadruple Perovskite Halide Conductors: Fact or Fiction?. Advanced Functional Materials, 2020, 30, 1909906.	7.8	17

#	Article	IF	Citations
50128	Regulating the Hidden Solvationâ€Ionâ€Exchange in Concentrated Electrolytes for Stable and Safe Lithium Metal Batteries. Advanced Energy Materials, 2020, 10, 2000901.	10.2	65
50129	Hydrogen/deuterium adsorption and absorption properties on and in palladium using a combined plane wave and localized basis set method. International Journal of Quantum Chemistry, 2020, 120, e26275.	1.0	4
50130	Molecular oxides of high-valent actinides. Structural Chemistry, 2020, 31, 1247-1271.	1.0	8
50131	Role of surface frustrated Lewis pairs on reduced CeO2(110) in direct conversion of syngas. Chinese Journal of Catalysis, 2020, 41, 1906-1915.	6.9	23
50132	Highly efficient mixed-metal spinel cobaltite electrocatalysts for the oxygen evolution reaction. Chinese Journal of Catalysis, 2020, 41, 1855-1863.	6.9	39
50133	A cobalt silicate modified BiVO4 photoanode for efficient solar water oxidation. Applied Catalysis B: Environmental, 2020, 277, 119189.	10.8	67
50134	Visible-light-driven deep oxidation of NO over Fe doped TiO2 catalyst: Synergic effect of Fe and oxygen vacancies. Applied Catalysis B: Environmental, 2020, 277, 119196.	10.8	148
50135	Critical evidence for direct interspecies electron transfer with tungsten-based accelerants: An experimental and theoretical investigation. Bioresource Technology, 2020, 311, 123519.	4.8	42
50136	Competitive adsorption between phosphate and arsenic in soil containing iron sulfide: XAS experiment and DFT calculation approaches. Chemical Engineering Journal, 2020, 397, 125426.	6.6	31
50137	Rh nanoclusters encaged in hollow mesoporous silica nanoreactors with enhanced catalytic performance for phenol selective hydrogenation. Chemical Engineering Journal, 2020, 397, 125484.	6.6	46
50138	Compressive behavior and elastic properties of Ni-based Î³/Î³â€™ ternary model superalloys: First-principles calculations and rule of mixtures predications. Journal of Alloys and Compounds, 2020, 839, 155661.	2.8	7
50139	Structural, magnetic, and electronic properties of small M-Pt (MÂ=ÂFe, Co, and Ni) clusters: Insight from density-functional calculations. Journal of Magnetism and Magnetic Materials, 2020, 512, 167047.	1.0	4
50140	Direct observations of Pdâ€“Te compound formation within noble metal inclusions in spent nuclear fuel. Journal of Nuclear Materials, 2020, 538, 152249.	1.3	2
50141	Enhanced stability and ferromagnetic property in transition metals co-doped rutile TiO2. Journal of Physics and Chemistry of Solids, 2020, 146, 109582.	1.9	3
50142	Enhanced near-ultraviolet and visible light absorption of organic-inorganic halide perovskites by co-doping with cesium and barium: Insight from first-principles calculations. Journal of Solid State Chemistry, 2020, 289, 121477.	1.4	4
50143	Simulation of nickel surfaces using ab-initio and empirical methods. Materialia, 2020, 12, 100675.	1.3	1
50144	Mechanisms of Degradation of Toxic Nerve Agents: Quantum-chemical Insight into Interactions of Sarin and Soman with Molybdenum Dioxide. Surface Science, 2020, 700, 121639.	0.8	7
50145	Se2TiO6E2 Ternary Oxide Characteristic of Isolated TiO6 Octahedra with the Shear Effect of SeIVE Electron Lone Pair (E): Combined Crystal Chemistry and ab Initio Study. Journal of Physical Chemistry C, 2020, 124, 12281-12285.	1.5	0

#	Article	IF	Citations
50146	Selective Dissolution Resistance Control of EUV Photoresist Using Multiscale Simulation: Rational Design of Hybrid System. Macromolecules, 2020, 53, 4748-4763.	2.2	8
50147	Rational Design of Hierarchical SnS₂ Microspheres with S Vacancy for Enhanced Sodium Storage Performance. ACS Sustainable Chemistry and Engineering, 2020, 8, 9519-9525.	3.2	52
50148	Intrinsic ferromagnetic semiconductivity realized in a new MoS₂ monolayer. Physical Chemistry Chemical Physics, 2020, 22, 13363-13367.	1.3	2
50149	Control of transition metalâ€“oxygen bond strength boosts the redox ex-solution in a perovskite oxide surface. Energy and Environmental Science, 2020, 13, 3404-3411.	15.6	36
50150	Understanding the ML black box with simple descriptors to predict clusterâ€“adsorbate interaction energy. New Journal of Chemistry, 2020, 44, 8545-8553.	1.4	7
50151	First principles calculations on the thermoelectric properties of bulk Au₂S with ultra-low lattice thermal conductivity*. Chinese Physics B, 2020, 29, 087202.	0.7	9
50152	Hybrid density functional theory benchmark study on lithium manganese oxides. Physical Review B, 2020, 101, .	1.1	12
50153	Spontaneous antisymmetric spin splitting in noncollinear antiferromagnets without spin-orbit coupling. Physical Review B, 2020, 101, .	1.1	44
50154	Spinon excitations in the quasi-one-dimensional <mml:math xmlns:mml="http://www.w3.org/1998/Math/MathML"><mml:mrow><mml:mi>S</mml:mi><mml:mo>=</mml:mo><mml:mfrac><mml:m chain compound <mml:math xmlns:mml="http://www.w3.org/1998/Math/MathML"><mml:mrow><mml:mi mathvariant="normal">C</mml:mi><mml:msub><mml:mi mathvariant="normal">s</mml:mi><mml:mn>4</mml:mn></mml:msub><mml:mi>CuS</mml:mi><mml:msub><mml:mi mathvariant="normal">b</mml:mi><mml:mn>. Physical Review B, 2020, 101, .	1.1	14
50155	Origin of magnetic inhomogeneity in Cr- and V-doped topological insulators. Physical Review B, 2020, 101, .	1.1	6
50156	Computational Search for Ultrasmall and Fast Skyrmions in the Inverse Heusler Family. IEEE Transactions on Magnetics, 2020, 56, 1-8.	1.2	4
50157	Design of an Accurate Machine Learning Algorithm to Predict the Binding Energies of Several Adsorbates on Multiple Sites of Metal Surfaces. ChemCatChem, 2020, 12, 4611-4617.	1.8	24
50158	Zn-doping enhances the photoluminescence and stability of PbS quantum dots for in vivo high-resolution imaging in the NIR-II window. Nano Research, 2020, 13, 2239-2245.	5.8	33
50159	Oxygen defects boost polysulfides immobilization and catalytic conversion: First-principles computational characterization and experimental design. Nano Research, 2020, 13, 2299-2307.	5.8	36
50160	Ultrafast processes in photochromic material YHxOy studied by excited-state density functional theory simulation. Science China Materials, 2020, 63, 1579-1587.	3.5	14
50161	Structural characterization and electronic properties of Ru-doped Cun (nÂ=Â1â€“12) clusters. Chemical Physics Letters, 2020, 754, 137677.	1.2	7
50162	High selective and efficient Fe2â€“N6 sites for CO2 electroreduction: A theoretical investigation. International Journal of Hydrogen Energy, 2020, 45, 14311-14319.	3.8	26
50163	Ab initio study on exchange integrals and magnetic anisotropy change of BaFe12â^'xScxO19 (xÂ=Â0, 0.5, 1,) Tj ETQq1 1 0.784314 rg	1.0	4

#	Article	IF	Citations
50164	Frank-Read source operation in six body-centered cubic refractory metals. Journal of the Mechanics and Physics of Solids, 2020, 141, 104017.	2.3	43
50165	Theoretical study of half-metallicity in the bulk and (001) oriented thin-films of the CoMn1-xFexCrAl and CoMn1-xCoxCrAl (x=0.00, 0.25, 0.50, 0.75 or 1.00) Heusler alloys. Materials Chemistry and Physics, 2020, 253, 123297.	2.0	1
50166	Enhanced Transformation of Cr(VI) by Heterocyclic-N within Nitrogen-Doped Biochar: Impact of Surface Modulatory Persistent Free Radicals (PFRs). Environmental Science & Technology, 2020, 54, 8123-8132.	4.6	107
50167	Moderate Pressure Stabilized Pentazolate Cyclo-N₅^{â€“} Anion in Zn(N₅)₂ Salt. Inorganic Chemistry, 2020, 59, 8002-8012.	1.9	31
50168	Structural Evolution of Ferroelectric and Ferroelastic Barium Sodium Niobate Tungsten Bronze. Inorganic Chemistry, 2020, 59, 8514-8521.	1.9	12
50169	Insights into Crystal Structure and Diffusion of Biphasic Na₂Zn₂TeO₆. ACS Applied Materials & Interfaces, 2020, 12, 28188-28198.	4.0	14
50170	Sulfur-Doped CoSe₂ Porous Nanosheets as Efficient Electrocatalysts for the Hydrogen Evolution Reaction. ACS Applied Materials & Interfaces, 2020, 12, 28288-28297.	4.0	86
50171	Plasma-Treated Ultrathin Ternary FePSe₃ Nanosheets as a Bifunctional Electrocatalyst for Efficient Zincâ€“Air Batteries. ACS Applied Materials & Interfaces, 2020, 12, 29393-29403.	4.0	10
50172	Relative Humidity Facilitated Urea Particle Reaction with Salicylic Acid: A Combined In Situ Spectroscopy and DFT Study. ACS Earth and Space Chemistry, 2020, 4, 1018-1028.	1.2	12
50173	Electrode interface optimization advances conversion efficiency and stability of thermoelectric devices. Nature Communications, 2020, 11, 2723.	5.8	101
50174	Stabilizing the crystal structures of NaFePO₄ with Li substitutions. Physical Chemistry Chemical Physics, 2020, 22, 13975-13980.	1.3	8
50175	Lead-free perovskite solar cells enabled by hetero-valent substitutes. Energy and Environmental Science, 2020, 13, 2363-2385.	15.6	109
50176	Dopant arrangements in Y-doped BaZrO3 under processing conditions and their impact on proton conduction: a large-scale first-principles thermodynamics study. Journal of Materials Chemistry A, 2020, 8, 12674-12686.	5.2	25
50177	Bimetallenes for selective electrocatalytic conversion of CO₂: a first-principles study. Journal of Materials Chemistry A, 2020, 8, 12457-12462.	5.2	14
50178	Ultra-high selectivity biogas upgrading through porous MXenes. Journal of Materials Chemistry A, 2020, 8, 12296-12300.	5.2	20
50179	First-principles calculations of phonon transport in two-dimensional penta-X2C family. Journal of Applied Physics, 2020, 127, 205106.	1.1	13
50180	Superior and tunable gas sensing properties of Janus PtSSe monolayer. Nano Express, 2020, 1, 010042.	1.2	18
50181	Janus <mml:math xmlns:mml="http://www.w3.org/1998/Math/MathML" display="inline" overflow="scroll"><mml:mi>Pt</mml:mi></mml:math> <mml:math xmlns:mml="http://www.w3.org/1998/Math/MathML" display="inline" overflow="scroll"><mml:msub><mml:mi>X</mml:mi><mml:mi>n</mml:mi></mml:msub><mml:msub><mml:mi>Y</mml:mi><mml:mi><mml:mr		

#	Article	IF	Citations
50182	Exciton <mml:math xmlns:mml="http://www.w3.org/1998/Math/MathML"><mml:mi>g</mml:mi></mml:math> factors of van der Waals heterostructures from first-principles calculations. Physical Review B, 2020, 101, .	1.1	82
50183	Three Jahn-Teller States of Matter in Spin-Crossover System Mn(taa). Physical Review Letters, 2020, 124, 227201.	2.9	11
50184	Probing the Validity of the Zintlâ^'Klemm Concept for Alkaline-Metal Copper Tellurides by Means of Quantum-Chemical Techniques. Materials, 2020, 13, 2178.	1.3	11
50185	Influence of Molecular Orbitals on Magnetic Properties of FeO2Hx. Molecules, 2020, 25, 2211.	1.7	4
50186	Building Artificial Solidâ€Electrolyte Interphase with Uniform Intermolecular Ionic Bonds toward Dendriteâ€Free Lithium Metal Anodes. Advanced Functional Materials, 2020, 30, 2002414.	7.8	104
50187	High Cycling Stability for Solidâ€State Li Metal Batteries via Regulating Solvation Effect in Poly(Vinylidene Fluoride)â€Based Electrolytes. Batteries and Supercaps, 2020, 3, 876-883.	2.4	84
50188	Revealing the Li 2 O 2 Nucleation Mechanisms on CeO 2 Catalysts for Lithiumâ€Oxygen Batteries. ChemCatChem, 2020, 12, 4132-4137.	1.8	1
50189	Bismuth Doping of CdTe: The Effect of Spinâ€"Orbit Coupling. Physica Status Solidi (B): Basic Research, 2020, 257, 1900693.	0.7	0
50190	Hydrogen Terminated Germanene for a Robust Selfâ€Powered Flexible Photoelectrochemical Photodetector. Small, 2020, 16, e2000283.	5.2	58
50191	Effect of potassium on carbon adsorption on the Co(0001) surface. Journal of Molecular Modeling, 2020, 26, 134.	0.8	2
50192	Experimental and Theoretical Contribution to the Phase Equilibria in the Ternary CaO-Al2O3-B2O3 System. Journal of Phase Equilibria and Diffusion, 2020, 41, 443-456.	0.5	3
50193	On the slip and twinning mechanisms on first order pyramidal plane of magnesium: Molecular dynamics simulations and first principal studies. Materials and Design, 2020, 191, 108648.	3.3	18
50194	Perovskite-Type CuNbO₃ Exhibiting Unusual Noncollinear Ferrielectric to Collinear Ferroelectric Dipole Order Transition. Chemistry of Materials, 2020, 32, 5016-5027.	3.2	11
50195	Predictive Model of Charge Mobilities in Organic Semiconductor Small Molecules with Force-Matched Potentials. Journal of Chemical Theory and Computation, 2020, 16, 3494-3503.	2.3	12
50196	Understanding the Linear and Second-Order Nonlinear Optical Properties of UiO-66-Derived Metalâ€"Organic Frameworks: A Comprehensive DFT Study. Journal of Physical Chemistry C, 2020, 124, 11595-11608.	1.5	22
50197	Raman Tensor of van der Waals MoSe₂. Journal of Physical Chemistry Letters, 2020, 11, 4311-4316.	2.1	28
50198	Potassium-Doped g-C₃N₄ Achieving Efficient Visible-Light-Driven CO₂ Reduction. ACS Sustainable Chemistry and Engineering, 2020, 8, 8214-8222.	3.2	126
50199	Mechanism of CO₂conversion to methanol over Cu(110) and Cu(100) surfaces. Dalton Transactions, 2020, 49, 8478-8497.	1.6	28

#	Article	IF	Citations
50200	Deoxydehydration of 1,4-anhydroerythritol over anatase TiO₂(101)-supported ReO_x and MoO_x. Catalysis Science and Technology, 2020, 10, 3731-3738.	2.1	13
50201	Cesium polytungstates with blue-tint-tunable near-infrared absorption. RSC Advances, 2020, 10, 10491-10501.	1.7	9
50202	NWChem: Past, present, and future. Journal of Chemical Physics, 2020, 152, 184102.	1.2	425
50203	Band offsets of Al_xGa_{1â^'x}N alloys using first-principles calculations. Journal of Physics Condensed Matter, 2020, 32, 365504.	0.7	5
50204	Electrical Contact between an Ultrathin Topological Dirac Semimetal and a Two-Dimensional Material. Physical Review Applied, 2020, 13, .	1.5	23
50205	Semirealistic tight-binding model for spin-orbit torques. Physical Review B, 2020, 101, .	1.1	10
50206	Prediction of <mml:math xmlns:mml="http://www.w3.org/1998/Math/MathML"><mml:msub><mml:mi>MnSiTe</mml:mi><mml:mn>3</mml:mn></mml:msub></ as an intrinsic layered half-metal. Physical Review B, 2020, 101, .	1.1	11
50207	Robust Ferromagnetism in Highly Strained <mml:math xmlns:mml="http://www.w3.org/1998/Math/MathML" display="inline"><mml:mrow><mml:msub><mml:mrow><mml:mi>SrCoO</mml:mi></mml:mrow><mml:mrow><mml:mn>3</mml:mn> Thin Films. Physical Review X, 2020, 10, .	2.8	15
50208	Essential Role of Spinel MgFe₂O₄ Surfaces during Discharge. Journal of the Electrochemical Society, 2020, 167, 090506.	1.3	11
50209	Many-Body Effects in FeN4 Center Embedded in Graphene. Applied Sciences (Switzerland), 2020, 10, 2542.	1.3	9
50210	Iodine-doping-assisted tunable introduction of oxygen vacancies on bismuth tungstate photocatalysts for highly efficient molecular oxygen activation and pentachlorophenol mineralization. Chinese Journal of Catalysis, 2020, 41, 1544-1553.	6.9	17
50211	Developing new alkaline ceramics as possible CO2 chemisorbents at high temperatures: The lithium and sodium yttriates (LiYO2 and NaYO2) cases. Chemical Engineering Journal, 2020, 396, 125277.	6.6	8
50212	Structural, elastic, electronic, and magnetic properties of Si-doped Co2MnGe full-Heusler type compounds. Journal of Alloys and Compounds, 2020, 845, 155499.	2.8	17
50213	Crystal chemistry, second-order nonlinear optical, and magnetic properties of Eu8Sn4Se20. Journal of Solid State Chemistry, 2020, 288, 121432.	1.4	8
50214	Influence of Kubas-type interaction of Bâ€“Ni codoped graphdiyne with hydrogen molecules on desorption temperature and storage efficiency. Materials Today Energy, 2020, 16, 100421.	2.5	8
50215	First-principles determination of pressure-induced structure, anisotropic elasticity and ideal strengths of CuInS2 and CuInSe2. Solid State Communications, 2020, 316-317, 113952.	0.9	2
50216	Adsorption of U(VI) on Stoichiometric and Oxidised Mackinawite: a DFT Study. Environmental Science & Technology, 2020, 54, 6792-6799.	4.6	14
50217	Molecules versus Nanoparticles: Identifying a Reactive Molecular Intermediate in the Synthesis of Ternary Coinage Metal Chalcogenides. Inorganic Chemistry, 2020, 59, 7727-7738.	1.9	10

#	Article	IF	Citations
50218	Validation of Pseudopotential Calculations for the Electronic Band Gap of Solids. Journal of Chemical Theory and Computation, 2020, 16, 3620-3627.	2.3	25
50219	Promoting Active Sites for Hydrogen Evolution in MoSe₂ via Transition-Metal Doping. Journal of Physical Chemistry C, 2020, 124, 12324-12336.	1.5	38
50220	Elucidation of the Active Sites for Monodisperse FePt and Pt Nanocrystal Catalysts for p-WSe₂ Photocathodes. Journal of Physical Chemistry C, 2020, 124, 11877-11885.	1.5	10
50221	Enhanced Ferromagnetism and Tunable Magnetism in Fe₃GeTe₂ Monolayer by Strain Engineering. ACS Applied Materials & Interfaces, 2020, 12, 26367-26373.	4.0	83
50222	First-Principles Investigation of the 1T-HfTe₂ Nanosheet for Selective Gas Sensing. ACS Applied Nano Materials, 2020, 3, 5160-5171.	2.4	27
50223	Catalytic Conversion Furfuryl Alcohol to Tetrahydrofurfuryl Alcohol and 2-Methylfuran at Terrace, Step, and Corner Sites on Ni. ACS Catalysis, 2020, 10, 7240-7249.	5.5	31
50224	Transfer Hydrogenation of Cinnamaldehyde Catalyzed by Al₂O₃ Using Ethanol as a Solvent and Hydrogen Donor. ACS Sustainable Chemistry and Engineering, 2020, 8, 8195-8205.	3.2	25
50225	Universal mechanical exfoliation of large-area 2D crystals. Nature Communications, 2020, 11, 2453.	5.8	394
50226	Purely in-plane ferroelectricity in monolayer SnS at room temperature. Nature Communications, 2020, 11, 2428.	5.8	214
50227	Coevolutionary search for optimal materials in the space of all possible compounds. Npj Computational Materials, 2020, 6, .	3.5	18
50228	Optical Absorption Exhibits Pseudo-Direct Band Gap of Wurtzite Gallium Phosphide. Scientific Reports, 2020, 10, 7904.	1.6	18
50229	MBenes: emerging 2D materials as efficient electrocatalysts for the nitrogen reduction reaction. Nanoscale Horizons, 2020, 5, 1106-1115.	4.1	114
50230	High stability and visible-light photocatalysis in novel two-dimensional monolayer silicon and germanium mononitride semiconductors: first-principles study. RSC Advances, 2020, 10, 14225-14234.	1.7	9
50231	Insight into anomalous hydrogen adsorption on rare earth metal decorated on 2-dimensional hexagonal boron nitride: a density functional theory study. RSC Advances, 2020, 10, 12929-12940.	1.7	6
50232	Metal-functionalized 2D boron sulfide monolayer material enhancing hydrogen storage capacities. Journal of Applied Physics, 2020, 127, .	1.1	19
50233	Possible role of grain-boundary and dislocation structure for the magnetic-flux trapping behavior of niobium: A first-principles study. Physical Review B, 2020, 101, .	1.1	7
50234	<mml:math xmlns:mml="http://www.w3.org/1998/Math/MathML"><mml:mrow><mml:mi>DFT</mml:mi><mml:mo>+</mml:mo><mml:mi>DMFT</m study of spin-charge-lattice coupling in covalent <mml:math xmlns:mml="http://www.w3.org/1998/Math/MathML"><mml:msub><mml:mi>LaCoO</mml:mi><mml:mn>3</mml:mn></mml:msub></r Physical Review B, 2020, 101, .	1.1	11
50235	The Microstructure and Electronic Properties of Yttrium Oxide Doped With Cerium: A Theoretical Insight. Frontiers in Chemistry, 2020, 8, 338.	1.8	5

#	Article	IF	Citations
50236	Study of structural, elastic, electronic, and vibrational properties of MRh2O4 (M = Cd and Zn) spinels: DFT-based calculations. Journal of Molecular Modeling, 2020, 26, 140.	0.8	2
50237	Structural and electronic properties of BaSi2(100) thin film on Si(111) substrate. Journal of Materials Science, 2020, 55, 9483-9492.	1.7	2
50238	Direct bandgap engineering with local biaxial strain in few-layer MoS2 bubbles. Nano Research, 2020, 13, 2072-2078.	5.8	25
50239	Exploring phononic properties of two-dimensional materials using machine learning interatomic potentials. Applied Materials Today, 2020, 20, 100685.	2.3	96
50240	Syngas conversion catalyzed by copper-embedded graphene. Applied Surface Science, 2020, 525, 146500.	3.1	8
50241	2D g-C3N4 monolayer for amino acids sequencing. Applied Surface Science, 2020, 528, 146609.	3.1	11
50242	Double-layered yolk-shell microspheres with NiCo2S4-Ni9S8-C hetero-interfaces as advanced battery-type electrode for hybrid supercapacitors. Chemical Engineering Journal, 2020, 396, 125316.	6.6	80
50243	Ultra-thin tubular graphitic carbon Nitride-Carbon Dot lateral heterostructures: One-Step synthesis and highly efficient catalytic hydrogen generation. Chemical Engineering Journal, 2020, 397, 125470.	6.6	72
50244	Topological effects on separation of alkane isomers in metalâ^'organic frameworks. Fluid Phase Equilibria, 2020, 519, 112642.	1.4	8
50245	Facet-dependent electrocatalytic water splitting reaction on CeO2: A DFTÂ+ÂU study. Journal of Catalysis, 2020, 388, 1-10.	3.1	32
50246	Understanding the effect of Mo2C support on the activity of Cu for the hydrodeoxygenation of glycerol. Journal of Catalysis, 2020, 388, 141-153.	3.1	12
50247	Atomically embedded asymmetrical dual-metal dimers on N-doped graphene for ultra-efficient nitrogen reduction reaction. Journal of Catalysis, 2020, 388, 77-83.	3.1	123
50248	Investigation of the thermophysical properties of (Y1-xYbx)TaO4 ceramics. Journal of the European Ceramic Society, 2020, 40, 3111-3121.	2.8	18
50249	Facet- and defect-engineered Pt/Fe2O3 nanocomposite catalyst for catalytic oxidation of airborne formaldehyde under ambient conditions. Journal of Hazardous Materials, 2020, 395, 122628.	6.5	48
50250	Diamond(001)â€“Si(001) and Si(001)â€“Ti(0001) interfaces: A density functional theory study. Journal of Physics and Chemistry of Solids, 2020, 145, 109563.	1.9	5
50251	Enhanced hardness in tungstenâ€“substituted molybdenum diboride solid solutions by local symmetry reduction. Materials Chemistry and Physics, 2020, 251, 123188.	2.0	6
50252	Ab initio investigation and thermodynamic modeling of the Moâ€“Tiâ€“Zr system. Materialia, 2020, 10, 100701.	1.3	7
50253	Human motion interactive mechanical energy harvester based on all inorganic perovskite-PVDF. Nano Energy, 2020, 74, 104870.	8.2	85

#	Article	IF	Citations
50254	Super-hygroscopic film for wearables with dual functions of expediting sweat evaporation and energy harvesting. Nano Energy, 2020, 75, 104873.	8.2	52
50255	Strain-induced work function in h-BN and BCN monolayers. Physica E: Low-Dimensional Systems and Nanostructures, 2020, 123, 114180.	1.3	42
50256	Structural stability and electronic properties of Sr induced (5Ã—4) reconstruction on Si(111) surface. Physics Letters, Section A: General, Atomic and Solid State Physics, 2020, 384, 126540.	0.9	1
50257	Thermoelectric transport properties of PbS and its contrasting electronic band structures. Scripta Materialia, 2020, 185, 76-81.	2.6	7
50258	A first-principles study of hydrogen adsorption on Ni-decorated defective GaN monolayer. Solid State Communications, 2020, 316-317, 113951.	0.9	0
50259	Interdependence of Oxygenation and Hydration in Mixed-Conducting (Ba,Sr)FeO_{3â˜Î´} Perovskites Studied by Density Functional Theory. Journal of Physical Chemistry C, 2020, 124, 11780-11789.	1.5	24
50260	First-Principles Prediction of Na Diffusivity in Doped NaCrO₂ Layered Cathode Materials with van der Waals Interactions. Journal of Physical Chemistry C, 2020, 124, 12239-12248.	1.5	5
50261	Electronic Structure, Optical Properties, and Photoelectrochemical Activity of Sn-Doped Fe₂O₃ Thin Films. Journal of Physical Chemistry C, 2020, 124, 12548-12558.	1.5	56
50262	Interlayer Bonding in Two-Dimensional Materials: The Special Case of SnP₃ and GeP₃. Journal of Physical Chemistry Letters, 2020, 11, 4503-4510.	2.1	24
50263	How Accurately Do Approximate Density Functionals Predict Trends in Acidic Zeolite Catalysis?. Journal of Physical Chemistry Letters, 2020, 11, 4305-4310.	2.1	27
50264	Selective Cl-Decoration on Nanocrystal Facets of Hematite for High-Efficiency Catalytic Oxidation of Cyclohexane: Identification of the Newly Formed Clâ€“O as Active Sites. ACS Applied Materials & Interfaces, 2020, 12, 26733-26745.	4.0	34
50265	Mechanism of the Accelerated Water Formation Reaction under Interfacial Confinement. ACS Catalysis, 2020, 10, 6119-6128.	5.5	20
50266	First principles calculations on order and disorder in La₂Ce₂O₇ and Nd₂Ce₂O₇. Physical Chemistry Chemical Physics, 2020, 22, 13930-13941.	1.3	4
50267	Computational discovery of promising new n-type dopable ABX Zintl thermoelectric materials. Materials Horizons, 2020, 7, 1809-1818.	6.4	30
50268	The magnetic, electronic, and light-induced topological properties in two-dimensional hexagonal FeX2 (Xâ€‰=â€‰Cl, Br, I) monolayers. Applied Physics Letters, 2020, 116, .	1.5	18
50269	Impact of Co-Solvent and LiTFSI Concentration on Ionic Liquid-Based Electrolytes for Li-S Battery. Journal of the Electrochemical Society, 2020, 167, 070528.	1.3	12
50270	A molecular dynamics study of Fe50-XMXAl50 ternary alloy (M=Ag, Pt, Pd). MRS Advances, 2020, 5, 1185-1193.	0.5	1
50271	Interlayer Engineering of Molybdenum Trioxide toward Highâ€Capacity and Stable Sodium Ion Half/Full Batteries. Advanced Functional Materials, 2020, 30, 2001708.	7.8	58

#	Article	IF	Citations
50272	CNTâ€Assembled Octahedron Carbonâ€Encapsulated Cu₃P/Cu Heterostructure by In Situ MOFâ€Derived Engineering for Superior Lithium Storage: Investigations by Experimental Implementation and Firstâ€Principles Calculation. Advanced Science, 2020, 7, 2000736.	5.6	66
50273	Synthesis of Chiral MOFâ€74 Frameworks by Postâ€Synthetic Modification by Using an Amino Acid. Chemistry - A European Journal, 2020, 26, 13957-13965.	1.7	35
50274	Raman scattering of true 1D van der Waals Nb₂Se₉ nanowires. Journal of Raman Spectroscopy, 2020, 51, 1100-1107.	1.2	5
50275	Enhancing Interfacial Properties of Mg₂Siâ€Based Thermoelectric Joint with Mg₂SiNi₃ Compound as Electrodes. Physica Status Solidi (A) Applications and Materials Science, 2020, 217, 1901035.	0.8	7
50276	Vacancy-mediated complex phase selection in high entropy alloys. Acta Materialia, 2020, 194, 540-546.	3.8	31
50277	<mml:math xmlns:mml="http://www.w3.org/1998/Math/MathML" altimg="si105.svg"><mml:mrow><mml:mi mathvariant="italic">DFT</mml:mi><mml:mo linebreak="badbreak">+</mml:mo><mml:mi>U</mml:mi></mml:mrow></mml:math> approach on the electronic and thermal properties of hypostoichiometric <mml:math xmlns:mml="http://www.w3.org/1998/Math/MathML" altimg="si106.svg"><mml:mrow><mml:msub><mml:mrow></mml:mrow><mml:mi mathvariant="normal">UO</mml:mi>	0.9	8
50278	Revealing the role of oxygen vacancies in bimetallic PbBiO2Br atomic layers for boosting photocatalytic CO2 conversion. Applied Catalysis B: Environmental, 2020, 277, 119170.	10.8	77
50279	The importance of atomic charge distributions of solid boron material in N2 electrochemical reduction. Applied Surface Science, 2020, 526, 146606.	3.1	13
50280	Achieving superior high-capacity K-ion batteries with the C57 carbon monolayer anode by first-principles calculations. Applied Surface Science, 2020, 526, 146638.	3.1	12
50281	Giant tunability in electrical contacts and doping via inconsiderable normal electric field strength or gating for a high-performance in ultrathin field effect transistors based on 2D BX/graphene (XÂ=ÂP,) Tj ETQq1 1 0.784314 rgBT /Ov	3.1	51
50282	Ground state structure and physical properties of silicon monoxide sheet. Applied Surface Science, 2020, 527, 146759.	3.1	1
50283	rGO-CNT aerogel embedding iron phosphide nanocubes for high-performance Li-polysulfide batteries. Carbon, 2020, 167, 446-454.	5.4	21
50284	Vacancy effect of antimony on shear deformation mechanisms of CoSb3 thermoelectric material. Computational Materials Science, 2020, 182, 109761.	1.4	6
50285	A general method for large-scale fabrication of metal nanoparticles embedded N-doped carbon fiber cloth with highly efficient hydrogen production in all pH range. Electrochimica Acta, 2020, 353, 136475.	2.6	9
50286	The roles of native defects and transition metal additives in the dehydrogenation mechanism of Mg(AlH4)2. International Journal of Hydrogen Energy, 2020, 45, 17625-17636.	3.8	1
50287	Evolution of high specific surface area lanthanum aerogels to magnetic lanthanum hydroxide nanostructures. Inorganic Chemistry Communication, 2020, 114, 107818.	1.8	2
50288	Atomic cooperation in enhancing magnetism: (Fe, Cu)-doped CeCo5. Journal of Alloys and Compounds, 2020, 839, 155549.	2.8	6
50289	Effect of groundwater ions (Ca2+, Na+, and HCO3â˜) on removal of hexavalent chromium by Fe(II)-phosphate mineral. Journal of Hazardous Materials, 2020, 398, 122948.	6.5	15

#	Article	IF	Citations
50290	A MnOx@Eu-CeOx nanorod catalyst with multiple protective effects: Strong SO2-tolerance for low temperature DeNOx processes. Journal of Hazardous Materials, 2020, 399, 123011.	6.5	26
50291	Structure stability and magnetic properties of Fe-doped Co2VGa Heusler alloys: Insights from first-principles calculations. Journal of Magnetism and Magnetic Materials, 2020, 513, 167059.	1.0	4
50292	Stability, electronic and defect levels induced by substitution of Al and P pair in 4Hâ€“SiC. Journal of Physics and Chemistry of Solids, 2020, 142, 109448.	1.9	1
50293	Minimum Co content limit in layer-structured cathode materials for Li-ion batteries. Journal of Power Sources, 2020, 467, 228351.	4.0	2
50294	Electronic and optical properties of mono and co-doped anatase TiO2: First principles calculations. Materials Chemistry and Physics, 2020, 252, 123285.	2.0	19
50295	Electronic properties and Hirshfeld surface analysis of dihydroxylammonium 5,5â€²-bistetrazole-1,1â€²-diolate under pressure. Materials Today: Proceedings, 2020, 24, 683-689.	0.9	3
50296	Multiscale structure and band configuration tuning to achieve high thermoelectric properties in n-type PbS bulks. Nano Energy, 2020, 74, 104826.	8.2	38
50297	Interfacial kinetics induced phase separation enhancing low-temperature performance of lithium-ion batteries. Nano Energy, 2020, 75, 104977.	8.2	11
50298	Mechanism for structure conversion of FeSi under pressures. Physics Letters, Section A: General, Atomic and Solid State Physics, 2020, 384, 126598.	0.9	3
50299	Thermal expansion and vibrational properties of Îµ-Se and Îµ-TeSe2 based on first-principles calculations. Solid State Communications, 2020, 314-315, 113912.	0.9	1
50300	Local Redox Reaction of High Valence Manganese in Li2MnO3-Based Lithium Battery Cathodes. Cell Reports Physical Science, 2020, 1, 100061.	2.8	25
50301	Toward Establishing Electronic and Phononic Signatures of Reversible Lattice Oxygen Oxidation in Lithium Transition Metal Oxides For Li-Ion Batteries. Chemistry of Materials, 2020, 32, 5502-5514.	3.2	17
50302	Crystal Structure, Lattice Dynamics, and Thermodynamic Properties of a Thermoelectric Orthorhombic BaCu₂Se₂ Compound. Journal of Physical Chemistry C, 2020, 124, 13627-13638.	1.5	6
50303	Mechanism and Effects of Coverage and Particle Morphology on Rh-Catalyzed NOâ€“H₂ Reactions. Journal of Physical Chemistry C, 2020, 124, 13291-13303.	1.5	10
50304	Intrinsic Point Defects and Dopants Ce3+ in SrLiAl3N4: Thermodynamic and Spectral Properties from First Principles. Journal of Physical Chemistry C, 2020, 124, 13400-13408.	1.5	4
50305	Efficient Raman Enhancement in Molybdenum Disulfide by Tuning the Interlayer Spacing. ACS Applied Materials & Interfaces, 2020, 12, 28474-28483.	4.0	23
50306	CoP/RGO-Pd Hybrids with Heterointerfaces as Highly Active Catalysts for Ethanol Electrooxidation. ACS Applied Materials & Interfaces, 2020, 12, 28903-28914.	4.0	16
50307	Colossal flexoresistance in dielectrics. Nature Communications, 2020, 11, 2586.	5.8	21

#	Article	IF	Citations
50308	Graphene-nanoplatelets-supported NiFe-MOF: high-efficiency and ultra-stable oxygen electrodes for sustained alkaline anion exchange membrane water electrolysis. Energy and Environmental Science, 2020, 13, 3447-3458.	15.6	197
50309	On the understanding of the optoelectronic properties of S-doped MoO₃ and O-doped MoS₂ bulk systems: a DFT perspective. Journal of Materials Chemistry C, 2020, 8, 9064-9074.	2.7	44
50310	Structural Transition from Ordered to Disordered of BeZnO2 Alloy. Chinese Physics Letters, 2020, 37, 057101.	1.3	1
50311	Crystal structure and properties of iodine monofluoride compounds at high pressure. Journal of Physics Condensed Matter, 2020, 32, 385404.	0.7	3
50312	Signatures of non-trivial band topology in LaAs/LaBi heterostructure. Journal of Physics Condensed Matter, 2020, 32, 395703.	0.7	1
50313	Adjustable electronic and optical properties of BlueP/MoS2 van der Waals heterostructure by external strain: a first-principles study. Nanotechnology, 2020, 31, 375706.	1.3	11
50314	Constructing realistic effective spin Hamiltonians with machine learning approaches. New Journal of Physics, 2020, 22, 053036.	1.2	16
50315	Structural, electronic, and magnetic properties of quaternary Heusler CrZrCoZ compounds: A first-principles study. Chinese Physics B, 2020, 29, 077105.	0.7	5
50316	Unveiling a facile approach for large-scale synthesis of N-doped graphene with tuned electrical properties. 2D Materials, 2020, 7, 045001.	2.0	31
50317	Phase stability and mechanical response of tantalum nitrides to electronic excitation effect. Materials Research Express, 2020, 7, 066508.	0.8	2
50318	Topological properties of <mml:math xmlns:mml="http://www.w3.org/1998/Math/MathML"><mml:mrow><mml:msub><mml:mi>Mo</mml:mi><mml:mn>2</mml:mn></mml:msub><mml:mi mathvariant="normal">C</mml:mi></mml:mrow></mml:math> and <mml:math xmlns:mml="http://www.w3.org/1998/Math/MathML"><mml:mrow><mml:msub><mml:mi mathvariant="normal">W</mml:mi><mml:mn>2</mml:mn></mml:msub><mml:mi mathvariant="normal">C</mml:mi></mml:mrow></mml:math> superconductors. Physical Review B, 202	1.1	12
50319	Minimax isometry method: A compressive sensing approach for Matsubara summation in many-body perturbation theory. Physical Review B, 2020, 101, .	1.1	24
50320	Effect of dopant on the morphology and electrochemical performance of Ni1-xCaxCo2O4 (0 = x = 0.8) oxide hierarchical structures. MRS Advances, 2020, 5, 2487-2494.	0.5	10
50321	Two-dimensional hexaphosphate BiMP6 (MÂ=ÂAl, Ga, In) with desirable band gaps and ultrahigh carrier mobility for photocatalytic hydrogen evolution. Applied Surface Science, 2020, 517, 146166.	3.1	34
50322	Theoretical study of Li intercalation in TiO2(B) surfaces. Applied Surface Science, 2020, 526, 146460.	3.1	17
50323	Contact barriers modulation of graphene/Î²-Ga2O3 interface for high-performance Ga2O3 devices. Applied Surface Science, 2020, 527, 146740.	3.1	24
50324	Two-dimensional 1T-PS2 as a promising anode material for sodium-ion batteries with ultra-high capacity, low average voltage and appropriate mobility. Chinese Chemical Letters, 2020, 31, 2325-2329.	4.8	42
50325	Exploiting the Ï€-bonding for the separation of benzene and cyclohexane in zeolites. Chemical Engineering Journal, 2020, 398, 125678.	6.6	23

#	Article	IF	Citations
50326	Linear scaling relations for N2H4 decomposition over transition metal catalysts. International Journal of Hydrogen Energy, 2020, 45, 16114-16121.	3.8	4
50327	Sulfur Vacancy Clustering and Its Impact on Electronic Properties in Pyrite FeS₂. Chemistry of Materials, 2020, 32, 4820-4831.	3.2	21
50328	Atom Classification Model for Total Energy Evaluation of Two-Dimensional Multicomponent Materials. Journal of Physical Chemistry A, 2020, 124, 4506-4511.	1.1	13
50329	Explicit Multielement Extension of the Spectral Neighbor Analysis Potential for Chemically Complex Systems. Journal of Physical Chemistry A, 2020, 124, 5456-5464.	1.1	36
50330	Conversion Reaction in the Binder-Free Anode for Fast-Charging Li-Ion Batteries Based on WO₃ Nanorods. ACS Applied Energy Materials, 2020, 3, 6700-6708.	2.5	20
50331	Assessing common approximations in space charge modelling to estimate the proton resistance across grain boundaries in Y-doped BaZrO₃. Physical Chemistry Chemical Physics, 2020, 22, 11891-11902.	1.3	7
50332	Elastic and electronic origins of strain stabilized photovoltaic Î³-CsPbI₃. Physical Chemistry Chemical Physics, 2020, 22, 12706-12712.	1.3	21
50333	Development of Ni-based alloy catalysts to improve the sulfur poisoning resistance of Ni/YSZ anodes in SOFCs. Catalysis Science and Technology, 2020, 10, 4544-4552.	2.1	10
50334	Insights into the regularity of the formation of 2D 3d transition metal monocarbides. Nanoscale, 2020, 12, 13407-13413.	2.8	9
50335	Exploring high-energy and mechanically robust anode materials based on doped graphene for lithium-ion batteries: a first-principles study. RSC Advances, 2020, 10, 13662-13668.	1.7	10
50336	A new large-cell superhard carbon allotrope: orthorhombic oC240. Molecular Physics, 2020, 118, e1767815.	0.8	2
50337	Giant spin Seebeck effect in two-dimensional ferromagnetic CrI₃ monolayer. Nanotechnology, 2020, 31, 455404.	1.3	11
50338	Selective linear etching of monolayer black phosphorus using electron beams*. Chinese Physics B, 2020, 29, 086801.	0.7	2
50339	Optical enhancement of dielectric permittivity in reduced lanthanum aluminate. Physical Review B, 2020, 101, .	1.1	1
50340	Study of Energetic and Magnetic Properties of FexNi1Ââ€“Âx Monolayer Film on Nonmagnetic Metallic Substrates. Physics of the Solid State, 2020, 62, 777-784.	0.2	1
50341	Tailoring the Band Gap in Codoped GaN Nanosheet From First Principle Calculations. Frontiers in Materials, 2020, 7, .	1.2	8
50342	A DFT Insight into the Tuning Effect of Potassium Promoter on the Formation of Carbon Atoms via Carburization Gases Dissociation on Iron-Based Catalysts. Catalysts, 2020, 10, 527.	1.6	5
50343	Theoretical Study of the Direct Conversion of Methane to Methanol Using H₂O₂ as an Oxidant on Pd and Au/Pd Surfaces. Journal of Physical Chemistry C, 2020, 124, 13231-13239.	1.5	17

#	Article	IF	Citations
50344	Ultralow Voltage Manipulation of Ferromagnetism. Advanced Materials, 2020, 32, e2001943.	11.1	44
50345	Tuning Interfacial Thermal and Electrical Conductance across a Metal/MoS₂ Monolayer through Nâ€Methylâ€2â€pyrrolidone Wet Cleaning. Advanced Materials Interfaces, 2020, 7, 2000364.	1.9	7
50346	Exploring Phase Stability and Properties of Iâ€II 2 â€IIIâ€VI 4 Quaternary Chalcogenides. Advanced Theory and Simulations, 2020, 3, 2000041.	1.3	8
50347	Embedded, graphâ€ttheoretically defined manyâ€body approximations for <scp>wavefunctionâ€inâ€DFT</scp> and <scp>DFTâ€inâ€DFT</scp>: Applications to gasâ€•and condensedâ€phase ab initio molecular dynamics, and potential surfaces for quantum nuclear effects. International Journal of Quantum Chemistry, 2020, 120, e26244.	1.0	12
50348	The ï£¿NH x Group Induced Formation of 3D Î±â€Co(OH) 2 Curly Nanosheet Aggregates as Efficient Oxygen Evolution Electrocatalysts. Small, 2020, 16, 2001973.	5.2	22
50349	Methoxy radical adsorption on gold nanoparticles: a comparison with methanethiol and methylamine radicals. Adsorption, 2020, 26, 579-586.	1.4	1
50350	Effects of doping and biaxial strain on the electronic properties of GaN/graphene/WS2 trilayer vdW heterostructure. Journal of Materials Science, 2020, 55, 11999-12007.	1.7	12
50351	Structural transformation of energetic cyclo-pentazolate salt under the pressure. Structural Chemistry, 2020, 31, 1887-1896.	1.0	1
50352	Chevron-type graphene nanoribbons with a reduced energy band gap: Solution synthesis, scanning tunneling microscopy and electrical characterization. Nano Research, 2020, 13, 1713-1722.	5.8	12
50353	Machine-learning-accelerated screening of hydrogen evolution catalysts in MBenes materials. Applied Surface Science, 2020, 526, 146522.	3.1	50
50354	Experimental and DFT insights into an eco-friendly photocatalytic system toward environmental remediation and hydrogen generation based on AgInS2 quantum dots embedded on Bi2WO6. Applied Surface Science, 2020, 525, 146596.	3.1	32
50355	Experimental observation of large tunneling anisotropic magnetoresistance in a magnetic tunnel junction without heavy metals. Applied Surface Science, 2020, 526, 146716.	3.1	0
50356	Monolayer Be2P3N as a high capacity and high energy density anode material for ultrafast charging Na- and K-ion batteries. Applied Surface Science, 2020, 527, 146783.	3.1	16
50357	Enhanced electrocatalytic oxygen evolution by manipulation of electron transfer through cobalt-phosphorous bridging. Chemical Engineering Journal, 2020, 398, 125660.	6.6	20
50358	Magnetic properties of 3C-SiC nanowires doped by transition metal and vacancy. Chemical Physics Letters, 2020, 754, 137643.	1.2	3
50359	Optimize the electrocatalytic performances of NiCoP for water splitting by the synergic effect of S dopant and P vacancy. International Journal of Hydrogen Energy, 2020, 45, 16161-16168.	3.8	34
50360	Correction of band-gap energy and dielectric function of BiOX bulk with GW and BSE. Optik, 2020, 216, 164631.	1.4	10
50361	Investigations on Gilbert damping, electronic, magnetic and Curie temperature for equiatomic quaternary Heusler alloys CrScCoZ. Journal of Magnetism and Magnetic Materials, 2020, 512, 166986.	1.0	10

#	Article	IF	Citations
50362	Ultrahigh electrical conductivities and low lattice thermal conductivities of La, Dy, and Nb Co-doped SrTiO3 thermoelectric materials with complex structures. Journal of Materials Science and Technology, 2020, 52, 172-179.	5.6	25
50363	sp3-Defect and pore engineered carbon framework for high energy density supercapacitors. Journal of Power Sources, 2020, 464, 228203.	4.0	27
50364	The comprehensive first-principle study of the thermoelectric performance of p- and n-type SnS. Materials Today Communications, 2020, 24, 101167.	0.9	8
50365	Realizing high thermoelectricity in polycrystalline tin sulfide via manipulating fermi surface anisotropy and phonon dispersion. Materials Today Physics, 2020, 14, 100221.	2.9	21
50366	Thermo-selenizing to rationally tune surface composition and evolve structure of stainless steel to electrocatalytically boost oxygen evolution reaction. Nano Energy, 2020, 75, 104949.	8.2	44
50367	Effects of local shear strain on the zigzag graphene nanoribbon with a topological line defect. Physica E: Low-Dimensional Systems and Nanostructures, 2020, 123, 114195.	1.3	3
50368	Chemical bonding analysis in Ti1â€“â€“Al Ta N solid solutions. Surface and Coatings Technology, 2020, 395, 125802.	2.2	15
50369	A novel morphology-controlled synthesis of Na+-doped Li- and Mn-rich cathodes by the self-assembly of amphiphilic spherical micelles. Sustainable Materials and Technologies, 2020, 25, e00171.	1.7	10
50370	Semiconducting High-Entropy Chalcogenide Alloys with Ambi-ionic Entropy Stabilization and Ambipolar Doping. Chemistry of Materials, 2020, 32, 6070-6077.	3.2	35
50371	Chemomechanical Failure Mechanism Study in NASICON-Type Li_{1.3}Al_{0.3}Ti_{1.7}(PO₄)₃ Solid-State Lithium Batteries. Chemistry of Materials, 2020, 32, 4998-5008.	3.2	104
50372	XO-PBC: An Accurate and Efficient Method for Molecular Crystals. Journal of Chemical Theory and Computation, 2020, 16, 4271-4285.	2.3	10
50373	Facile Decomposition of Organophosphonates by Dual Lewis Sites on a Fe₃O₄(111) Film. Journal of Physical Chemistry C, 2020, 124, 12432-12441.	1.5	13
50374	Tuning Single-Atom Catalysts of Nitrogen-Coordinated Transition Metals for Optimizing Oxygen Evolution and Reduction Reactions. Journal of Physical Chemistry C, 2020, 124, 13168-13176.	1.5	43
50375	Graph Theory Model of Dry Reforming of Methane Using Rh(111). Journal of Physical Chemistry Letters, 2020, 11, 4917-4922.	2.1	14
50376	Fabrication of a Postfunctionalizable, Biorepellent, Electroactive Polyurethane Interface on a Gold Surface by Surface-Assisted Polymerization. Langmuir, 2020, 36, 6828-6836.	1.6	7
50377	Tuning the Properties of Zero-Field Room Temperature Ferromagnetic Skyrmions by Interlayer Exchange Coupling. Nano Letters, 2020, 20, 4739-4747.	4.5	11
50378	Boron-Induced Nitrogen Fixation in 3D Carbon Materials for Supercapacitors. ACS Applied Materials & Interfaces, 2020, 12, 28075-28082.	4.0	34
50379	A Semiempirical Method to Detect and Correct DFT-Based Gas-Phase Errors and Its Application in Electrocatalysis. ACS Catalysis, 2020, 10, 6900-6907.	5.5	71

#	Article	IF	Citations
50380	Force-Activated Isomerization of a Single Molecule. Journal of the American Chemical Society, 2020, 142, 10673-10680.	6.6	16
50381	High-throughput screening platform for solid electrolytes combining hierarchical ion-transport prediction algorithms. Scientific Data, 2020, 7, 151.	2.4	90
50382	Strain-enhanced power conversion efficiency of a BP/SnSe van der Waals heterostructure. Physical Chemistry Chemical Physics, 2020, 22, 14787-14795.	1.3	21
50383	A topological semimetal Li₂CrN₂ sheet as a promising hydrogen storage material. Nanoscale, 2020, 12, 12106-12113.	2.8	9
50384	Tiny amounts of fluorinated carbon nanotubes remove sodium dendrites for high-performance sodiumâ€“oxygen batteries. Sustainable Energy and Fuels, 2020, 4, 4108-4116.	2.5	3
50385	Strain effect on the catalytic activities of B- and B/N-doped black phosphorene for electrochemical conversion of CO to valuable chemicals. Journal of Materials Chemistry A, 2020, 8, 11986-11995.	5.2	31
50386	A viable method to enhance the electrical conductivity of CNT bundles: direct in situ TEM evaluation. Nanoscale, 2020, 12, 13095-13102.	2.8	10
50387	Just add water to split water: ultrahigh-performance bifunctional electrocatalysts fabricated using eco-friendly heterointerfacing of NiCo diselenides. Journal of Materials Chemistry A, 2020, 8, 12035-12044.	5.2	38
50388	Accelerating hydrogen evolution at neutral pH by destabilization of water with a conducting oxophilic metal oxide. Journal of Materials Chemistry A, 2020, 8, 12169-12176.	5.2	21
50389	First-principles study of the adsorption of 3d transition metals on BaO- and TiO2-terminated cubic-phase BaTiO3(001) surfaces. Journal of Chemical Physics, 2020, 152, 204701.	1.2	10
50390	Effect of cation-vacancy superstructure on the phonon dynamics in <mml:math xmlns:mml="http://www.w3.org/1998/Math/MathML"><mml:mrow><mml:msub><mml:mi>KNi</mml:mi><mml:mn>2</mml:mn></mml Physical Review B, 2020, 101, .	1.1	3
50391	Evidence for pseudoâ€“Jahn-Teller distortions in the charge density wave phase of <mml:math xmlns:mml="http://www.w3.org/1998/Math/MathML"><mml:mrow><mml:mn>1</mml:mn><mml:mi>T</mml:mi><mml:mtext>-</mml Physical Review B, 2020, 101, .	1.1	25
50392	Structural transition, metallization, and superconductivity in quasi-two-dimensional layered <mml:math xmlns:mml="http://www.w3.org/1998/Math/MathML"><mml:mrow><mml:mi>Pd</mml:mi><mml:msub><mml:mi mathvariant="normal">S</mml:mi><mml:mn>2</mml:mn></mml:msub></mml:mrow></mml:math> under compression. Physical Review B, 2020, 101, .	1.1	22
50393	Atomic Diffusion in <mml:math xmlns:mml="http://www.w3.org/1998/Math/MathML" display="inline"><mml:mi>Î±</mml:mi></mml:math> -iron across the Curie Point: An Efficient and Transferable AbÂInitio â€“Based Modeling Approach. Physical Review Letters, 2020, 124, 215901.	2.9	23
50394	Perpendicular Magnetic Anisotropy and Dzyaloshinskii-Moriya Interaction at an Oxide/Ferromagnetic Metal Interface. Physical Review Letters, 2020, 124, 217202.	2.9	27
50395	Control of zeolite pore interior for chemoselective alkyne/olefin separations. Science, 2020, 368, 1002-1006.	6.0	179
50396	Ferric iron in bridgmanite and implications for ULVZs. Physics of the Earth and Planetary Interiors, 2020, 306, 106505.	0.7	3
50397	First-principles analysis of oxide-ion conduction mechanism in neodymium silicate. Solid State Ionics, 2020, 355, 115367.	1.3	2

#	Article	IF	Citations
50398	Visible-Light-Induced Photocatalytic Activity of Stacked MXene Sheets of Y₂CF₂. Journal of Physical Chemistry C, 2020, 124, 14640-14645.	1.5	22
50399	Structural Transition in Oxidized Ca2N Electrenes: CaO/CaN 2D Heterostructures. Journal of Physical Chemistry C, 2020, 124, 14706-14712.	1.5	4
50400	Structural-Defect-Mediated Grafting of Alkylamine on Few-Layer MoS₂ and Its Potential for Enhancement of Tribological Properties. ACS Applied Materials & Interfaces, 2020, 12, 30720-30730.	4.0	30
50401	Sulfate-Modified NiAl Mixed Oxides as Effective Câ€“H Bond-Breaking Agents for the Sole Production of Ethylene from Ethane. ACS Catalysis, 2020, 10, 7619-7629.	5.5	26
50402	First-principles study on the selective hydrogenation of the Cî€Ō and Cî€Ć bonds of acrolein on Ptâ€“Mâ€“Pt (M = Pt, Cu, Ni, Co) surfaces. Physical Chemistry Chemical Physics, 2020, 22, 14645-14650.	1.3	4
50403	Two dimensional ruthenium carbide: structural and electronic features. Physical Chemistry Chemical Physics, 2020, 22, 15488-15495.	1.3	2
50404	Significant tunneling magnetoresistance and excellent spin filtering effect in CrI₃-based van der Waals magnetic tunnel junctions. Physical Chemistry Chemical Physics, 2020, 22, 14773-14780.	1.3	42
50405	Structure of chalcogen overlayers on Au(111): Density functional theory and lattice-gas modeling. Journal of Chemical Physics, 2020, 152, 224706.	1.2	5
50406	Flatband in a three-dimensional tungsten nitride compound. Journal of Chemical Physics, 2020, 152, 224503.	1.2	3
50407	Resolving the adsorption of molecular O ₂ on the rutile TiO ₂ (110) surface by noncontact atomic force microscopy. Proceedings of the National Academy of Sciences of the United States of America, 2020, 117, 14827-14837.	3.3	39
50408	Effects of self-interstitial atom on behaviors of hydrogen and helium in tungsten. Physica Scripta, 2020, 95, 075708.	1.2	7
50409	Phonon thermodynamics and elastic behavior of GaAs at high temperatures and pressures. Physical Review B, 2020, 101, .	1.1	3
50410	Sodium-potassium system at high pressure. Physical Review B, 2020, 101, .	1.1	6
50411	Modulation of electronic and transport properties of bilayer heterostructures: <mml:math xmlns:mml="http://www.w3.org/1998/Math/MathML"><mml:mi>InSe</mml:mi><mml:mo>/</mml:mo><mml:msub><mml:mi>MoS</mml:mi> and <mml:math xmlns:mml="http://www.w3.org/1998/Math/MathML"><mml:mi>InSe</mml:mi><mml:mo>/</mml:mo><mml:mi>h</mml:mi></mml:m -BN as the prototype. Physical Review B, 2020, 101, .	1.1	25
50412	Temperature-Induced Lifshitz Transition and Possible Excitonic Instability in ZrSiSe. Physical Review Letters, 2020, 124, 236601.	2.9	34
50413	Phase Transitions in Tungsten Monoborides. JETP Letters, 2020, 111, 343-349.	0.4	3
50414	It's All in the (Cyanamide) Tilt: Synthesis and Structure of NaSc(NCN)₂. European Journal of Inorganic Chemistry, 2020, 2020, 2596-2602.	1.0	9
50415	Enhanced Thermoelectric Performance in Black Phosphorus Nanotubes by Band Modulation through Tailoring Nanotube Chirality. Small, 2020, 16, e2001820.	5.2	13

#	Article	IF	Citations
50416	Substrate-free flexible thin film solar cells by graphene-mediated peel-off technology. Journal of Materials Science: Materials in Electronics, 2020, 31, 10279-10287.	1.1	1
50417	Carrier capture and emission properties of silicon interstitial defects in near SiC/SiO2 interface region. Applied Surface Science, 2020, 514, 145889.	3.1	15
50418	Enhanced diffusion and permeation of hydrogen species on the partially carbon covered iron surfaces. Applied Surface Science, 2020, 515, 145899.	3.1	8
50419	Structural stability, mechanical, electronic and thermal behaviour of Ru2CrZ (Z=Sb, Si, Pb, Ge) Heusler alloys. Chinese Journal of Physics, 2020, 66, 124-134.	2.0	6
50420	Hydrogen oxidation reaction response of noble-metal based bulk metallic glasses. Electrochimica Acta, 2020, 353, 136616.	2.6	9
50421	Calcium orthocarbonate, Ca2CO4-Pnma: A potential host for subducting carbon in the transition zone and lower mantle. Lithos, 2020, 370-371, 105637.	0.6	23
50422	Band gap engineering of monolayer ZrGeTe4 via strain: A first-principles study. Materials Chemistry and Physics, 2020, 253, 123308.	2.0	10
50423	Phase transformations in novel hot-deformed Alâ€“Znâ€“Mgâ€“Cuâ€“Siâ€“Mnâ€“Fe(â€“Scâ€“Zr) alloys. Materials and Design, 2020, 193, 108821.	3.3	21
50424	Electronic properties of two-dimensional G/GaN(SiC) van der Waals heterostructures. Physica E: Low-Dimensional Systems and Nanostructures, 2020, 124, 114277.	1.3	15
50425	Surface hydrogen bond network spatially confined BiOCl oxygen vacancy for photocatalysis. Science Bulletin, 2020, 65, 1916-1923.	4.3	61
50426	Predicting Elastic Properties of Materials from Electronic Charge Density Using 3D Deep Convolutional Neural Networks. Journal of Physical Chemistry C, 2020, 124, 17262-17273.	1.5	23
50427	On-Surface Synthesis of All-cis Standing Phenanthrene Polymers upon Selective Câ€“H Bond Activation. Journal of Physical Chemistry Letters, 2020, 11, 5022-5028.	2.1	2
50428	Enhancing Electrochemical Hydrogen Evolution Performance of CoMoO₄-Based Microrod Arrays in Neutral Media through Alkaline Activation. ACS Applied Materials & Interfaces, 2020, 12, 30905-30914.	4.0	22
50429	Janus WSSe Monolayer: An Excellent Photocatalyst for Overall Water Splitting. ACS Applied Materials & Interfaces, 2020, 12, 29335-29343.	4.0	86
50430	Fundamental Properties of Metal-Adsorbed Silicene: A DFT Study. ACS Omega, 2020, 5, 13760-13769.	1.6	11
50431	Devil's staircase transition of the electronic structures in CeSb. Nature Communications, 2020, 11, 2888.	5.8	21
50432	Modelling the enthalpy change and transition temperature dependence of the metalâ€“insulator transition in pure and doped vanadium dioxide. Physical Chemistry Chemical Physics, 2020, 22, 13474-13478.	1.3	12
50433	Stoichiometry-controllable optical defects in Cu_xIn_{2â”'x}S_y quantum dots for energy harvesting. Journal of Materials Chemistry A, 2020, 8, 12556-12565.	5.2	8

#	Article	IF	Citations
50434	A new family of two-dimensional ferroelastic semiconductors with negative Poisson's ratios. Nanoscale, 2020, 12, 14150-14159.	2.8	21
50435	Pair-distribution-function guided optimization of fingerprints for atom-centered neural network potentials. Journal of Chemical Physics, 2020, 152, 224102.	1.2	8
50436	Vibrational properties of LaNiO3 films in the ultrathin regime. APL Materials, 2020, 8, .	2.2	13
50437	Metal-insulator and magnetic phase diagram of <mml:math xmlns:mml="http://www.w3.org/1998/Math/MathML"><mml:mrow><mml:msub><mml:mi>Ca</mml:mi><mml:mn>2</mml:mn></mml:msub> from auxiliary field quantum Monte Carlo and dynamical mean field theory. Physical Review B, 2020, 101, .	1.1	9
50438	Boosting Transport Kinetics of Cobalt Sulfides Yolkâ€“Shell Spheres by Anion Doping for Advanced Lithium and Sodium Storage. ChemSusChem, 2020, 13, 4078-4085.	3.6	106
50439	Origin of pâ€Type Conduction in Amorphous CuI: A Firstâ€Principles Investigation. Physica Status Solidi (B): Basic Research, 2020, 257, 2000218.	0.7	6
50440	Synchrotron characterization of clusters for catalysis. Frontiers of Nanoscience, 2020, 15, 1-29.	0.3	1
50441	Vacancy and interstitial interactions with crystal/amorphous, metal/covalent interfaces. Journal of Nuclear Materials, 2020, 539, 152329.	1.3	3
50442	Adsorption of single alkali-metal atoms (Li, Na, K) over the edge-passivated zigzag blue phosphorene nanoribbons. Journal of Physics and Chemistry of Solids, 2020, 146, 109623.	1.9	11
50443	Stability and energetics of HenVm complexes in Feâ€“Cr alloys: Ab initio study. Materials Chemistry and Physics, 2020, 253, 123314.	2.0	4
50444	Fracture properties of thin film TiN at elevated temperatures. Materials and Design, 2020, 194, 108885.	3.3	36
50445	First-principles study of oxygen evolution reaction on Ni3Fe-layered double hydroxides surface with different oxygen coverage. Molecular Catalysis, 2020, 490, 110957.	1.0	2
50446	Accelerated Atomic Data Production in Ab Initio Molecular Dynamics with Recurrent Neural Network for Materials Research. Journal of Physical Chemistry C, 2020, 124, 14838-14846.	1.5	18
50447	Long Radiation Lifetime and Quasi-Isotropic Excitons in Antioxidant Vâ€“V Binary Phosphorene Allotropes with Intrinsic Dipole. Journal of Physical Chemistry C, 2020, 124, 14787-14796.	1.5	2
50448	Structural Phase Transitions, Electronic Properties, and Hardness of RuB₄ under High Pressure in Comparison with FeB₄ and OsB₄. Journal of Physical Chemistry C, 2020, 124, 14804-14810.	1.5	20
50449	Hot-Atom Mechanism in Syngas Methanation on Precovered Pd(100) Surfaces. Journal of Physical Chemistry Letters, 2020, 11, 5312-5317.	2.1	9
50450	2-D Materials for Ultrascaled Field-Effect Transistors: One Hundred Candidates under the Ab Initio Microscope. ACS Nano, 2020, 14, 8605-8615.	7.3	56
50451	Insights into the Anchoring of Polysulfides and Catalytic Performance by Metal Phthalocyanine Covalent Organic Frameworks as the Cathode in Lithiumâ€“Sulfur Batteries. ACS Sustainable Chemistry and Engineering, 2020, 8, 10185-10192.	3.2	37

#	Article	IF	Citations
50452	Iridium single-atom catalyst on nitrogen-doped carbon for formic acid oxidation synthesized using a general hostâ€“guest strategy. Nature Chemistry, 2020, 12, 764-772.	6.6	452
50453	Coupling N2 and CO2 in H2O to synthesize urea under ambient conditions. Nature Chemistry, 2020, 12, 717-724.	6.6	485
50454	Ferroelectric domain wall memory with embedded selector realized in LiNbO3 single crystals integrated on Si wafers. Nature Materials, 2020, 19, 1188-1194.	13.3	92
50455	Controlling the magnetic anisotropy in Cr2Ge2Te6 by electrostatic gating. Nature Electronics, 2020, 3, 460-465.	13.1	145
50456	Covalency competition dominates the water oxidation structureâ€“activity relationship on spinel oxides. Nature Catalysis, 2020, 3, 554-563.	16.1	284
50457	Thermal decomposition and diffusion of methane in clathrate hydrates from quantum mechanics simulations. RSC Advances, 2020, 10, 14753-14760.	1.7	3
50458	Potassium ions promote electrochemical nitrogen reduction on nano-Au catalysts triggered by bifunctional boron supramolecular assembly. Journal of Materials Chemistry A, 2020, 8, 13086-13094.	5.2	44
50459	Mechanistic insight into biopolymer induced iron oxide mineralization through quantification of molecular bonding. Nanoscale Advances, 2020, 2, 3323-3333.	2.2	10
50460	Solution enthalpy calculation for impurity in liquid metal by first-principles calculations: A benchmark test for oxygen impurity in liquid sodium. Journal of Chemical Physics, 2020, 152, 154503.	1.2	4
50461	Predicting the dynamic behavior of the mechanical properties of platinum with machine learning. Journal of Chemical Physics, 2020, 152, 224709.	1.2	4
50462	Intrinsic role of â†‘â†‘â†“â†“-type magnetic structure on magnetoelectric coupling in Y2NiMnO6. Applied Physics Letters, 2020, 116, 242901.	1.5	3
50463	Valley degree of freedom in ferromagnetic Janus monolayer H-VSSe and the asymmetry-based tuning of the valleytronic properties. Physical Review B, 2020, 101, .	1.1	45
50464	Simulation of ab Initio Dynamics of the Formation of Metastable Conducting Solid Hydrogen. Journal of Experimental and Theoretical Physics, 2020, 130, 423-430.	0.2	2
50465	Enhanced Optical Emission from 2D InSe Bent onto Siâ€Pillars. Advanced Optical Materials, 2020, 8, 2000828.	3.6	17
50466	Structural and electronic properties of defective 2D transition metal dichalcogenide heterostructures. Journal of Computational Chemistry, 2020, 41, 1946-1955.	1.5	8
50467	Local structure in amorphous Sm$$_x$$Co$$_{1-x}$$: a combined experimental and theoretical study. Journal of Materials Science, 2020, 55, 12488-12498.	1.7	7
50468	Molecular recognition and homochirality preservation of guanine tetrads in the presence of melamine. Nano Research, 2020, 13, 2427-2430.	5.8	5
50469	Manipulating electronic delocalization of Mn3O4 by manganese defects for oxygen reduction reaction. Applied Catalysis B: Environmental, 2020, 277, 119247.	10.8	65

#	Article	IF	Citations
50470	BiVO4@MoS2 core-shell heterojunction with improved photocatalytic activity for discoloration of Rhodamine B. Applied Surface Science, 2020, 528, 146949.	3.1	89
50471	Synthesis of the porous spinel Co-Al2O4 powder produced by ball milling and annealing. Advanced Powder Technology, 2020, 31, 2742-2748.	2.0	0
50472	Low-temperature growth of carbon shells on gold and copper nanoparticles in transmission electron microscope. Carbon, 2020, 167, 541-547.	5.4	2
50473	Facile synthesis of Mn-doped BiOCl for metronidazole photodegradation: Optimization, degradation pathway, and mechanism. Chemical Engineering Journal, 2020, 400, 125813.	6.6	140
50474	Density functional study of magnetic, structural and electronic properties of quasi-one-dimensional compounds <mml:math xmlns:mml="http://www.w3.org/1998/Math/MathML" altimg="si1.svg"><mml:mrow><mml:msub><mml:mtext>CrSbX</mml:mtext><mml:mn>3</mml:mn></mml:msub></mml:mrow></mml <mml:math xmlns:mml="http://www.w3.org/1998/Math/MathML" altimg="si2.svg"><mml:mrow><mml:mo		

#	Article	IF	Citations
50488	Achieving high thermoelectric quality factor toward high figure of merit in GeTe. Materials Today Physics, 2020, 14, 100239.	2.9	61
50489	Geometric and optical properties of Bi/Er co-doped silica optical fiber. Optical Materials, 2020, 107, 110030.	1.7	5
50490	Ultra-low thermal conductivity and super-slow hot-carrier thermalization induced by a huge phononic gap in multifunctional nanoscale boron pnictides. Physica E: Low-Dimensional Systems and Nanostructures, 2020, 124, 114222.	1.3	21
50491	Influence of Nanoarchitecture on Charge Donation and the Electrical-Transport Properties in [(SnSe)_{1+Î´}][TiSe₂]_q Heterostructures. Chemistry of Materials, 2020, 32, 5802-5813.	3.2	6
50492	Oxygen Ion Migration and Conductivity in LaSrGa₃O₇ Melilites from First Principles. Chemistry of Materials, 2020, 32, 4442-4450.	3.2	18
50493	Design of Nonideal Eutectic Mixtures Based on Correlations with Molecular Properties. Journal of Physical Chemistry B, 2020, 124, 5209-5219.	1.2	16
50494	Two-Dimensional Perovskite Capping Layer Simultaneously Improves the Charge Carriersâ€™ Lifetime and Stability of MAPbI₃ Perovskite: A Time-Domain Ab Initio Study. Journal of Physical Chemistry Letters, 2020, 11, 5100-5107.	2.1	9
50495	Harnessing strong metalâ€“support interactions via a reverse route. Nature Communications, 2020, 11, 3042.	5.8	84
50496	Engineering unsymmetrically coordinated Cu-S1N3 single atom sites with enhanced oxygen reduction activity. Nature Communications, 2020, 11, 3049.	5.8	537
50497	Sub-picosecond photo-induced displacive phase transition in two-dimensional MoTe2. Npj 2D Materials and Applications, 2020, 4, .	3.9	43
50498	A substantial hybridization between correlated Ni-d orbital and itinerant electrons in infinite-layer nickelates. Communications Physics, 2020, 3, .	2.0	97
50499	First-principles investigation of ScX₂ (X = Cl, Br, or I) monolayers for flexible spintronic and electronic applications. Physical Chemistry Chemical Physics, 2020, 22, 14781-14786.	1.3	7
50500	An ab initio approach on the asymmetric stacking of GaAs ã€ˆ111ã€‰ nanowires grown by a vaporâ€“solid method. Nanoscale, 2020, 12, 17703-17714.	2.8	6
50501	Thermally stable indium based metalâ€“organic frameworks with high dielectric permittivity. Journal of Materials Chemistry C, 2020, 8, 9724-9733.	2.7	10
50502	Plane wave basis set correction methods for RPA correlation energies. Journal of Chemical Physics, 2020, 152, 134103.	1.2	7
50503	Nitrogen Doping Improves the Immobilization and Catalytic Effects of Co₉S₈ in Liâ€S Batteries. Advanced Functional Materials, 2020, 30, 2002462.	7.8	86
50504	Potassium Doping to Enhance Green Photoemission of Lightâ€Emitting Diodes Based on CsPbBr₃ Perovskite Nanocrystals. Advanced Optical Materials, 2020, 8, 2000742.	3.6	32
50505	Colloidal Quantum Dot Bulk Heterojunction Solids with Nearâ€Unity Charge Extraction Efficiency. Advanced Science, 2020, 7, 2000894.	5.6	22

#	Article	IF	Citations
50506	Controllable inversion symmetry breaking in single layer graphene induced by sub-lattice contrasted charge polarization. Carbon, 2020, 163, 63-69.	5.4	2
50507	Thin film solar cells based on Ag-substituted CuSbS2 absorber. Chemical Engineering Journal, 2020, 400, 125906.	6.6	22
50508	Unusual crystallographic ordering of two neighbouring elements - Cd and In in Cd2Cu3In, the first example in ternary Laves phase. Journal of Alloys and Compounds, 2020, 844, 156054.	2.8	6
50509	Spin orbit coupling effects on the non-collinear magnetism of structurally relaxed Fe/Cu (001) thin films: First principles calculations. Journal of Magnetism and Magnetic Materials, 2020, 514, 167108.	1.0	5
50510	Activation energy barriers for Na migration in Na12A zeolite: The main contribution to ionic current via doubly occupied NaII site?. Microporous and Mesoporous Materials, 2020, 305, 110288.	2.2	3
50511	Ultrasensitive and robust two-dimensional indium selenide flexible electronics and sensors for human motion detection. Nano Energy, 2020, 76, 105020.	8.2	28
50512	Strong lattice anharmonicity securing intrinsically low lattice thermal conductivity and high performance thermoelectric SnSb2Te4 via Se alloying. Nano Energy, 2020, 76, 105084.	8.2	39
50513	Structural, electronic, and optical properties of ZnO:ZnSnN2 compounds for optoelectronics and photocatalyst applications. Physics Letters, Section A: General, Atomic and Solid State Physics, 2020, 384, 126670.	0.9	4
50514	Strain engineering induced indirect-direct band gap transition of difluorphosphorane. Solid State Communications, 2020, 311, 113873.	0.9	0
50515	Adsorption of O and Cl on Tl/Si(111)â€“â€“Suppressed spin polarization via bilayer formation. Surface Science, 2020, 696, 121598.	0.8	0
50516	One-Dimensional All-Inorganic K₂CuBr₃ with Violet Emission as Efficient X-ray Scintillators. ACS Applied Electronic Materials, 2020, 2, 2242-2249.	2.0	77
50517	Enhanced Oxygen Evolution Reaction Activity by Encapsulating NiFe Alloy Nanoparticles in Nitrogen-Doped Carbon Nanofibers. ACS Applied Materials & Interfaces, 2020, 12, 31503-31513.	4.0	78
50518	PdAg Alloy Nanocatalysts: Toward Economically Viable Nitrite Reduction in Drinking Water. ACS Catalysis, 2020, 10, 7979-7989.	5.5	64
50519	Layer-Dependent Electronic Structure Changes in Transition Metal Dichalcogenides: The Microscopic Origin. ACS Omega, 2020, 5, 15169-15176.	1.6	44
50520	Bi₈Se₇: Delocalized Interlayer Ï€-Bond Interactions Enhancing Carrier Mobility and Thermoelectric Performance near Room Temperature. Journal of the American Chemical Society, 2020, 142, 12536-12543.	6.6	27
50521	Low-temperature and high-rate-charging lithium metal batteries enabled by an electrochemically active monolayer-regulated interface. Nature Energy, 2020, 5, 534-542.	19.8	280
50522	Visualization of moirÃ© superlattices. Nature Nanotechnology, 2020, 15, 580-584.	15.6	187
50523	Strain-engineered high-responsivity MoTe2 photodetector for silicon photonic integrated circuits. Nature Photonics, 2020, 14, 578-584.	15.6	172

#	Article	IF	Citations
50524	Coexistence of valley polarization and Chern insulating states in MoS2 monolayers with n-p codoping. Scientific Reports, 2020, 10, 9851.	1.6	5
50525	Exploring direct and hydrogen-assisted CO activation on iridium surfaces â€“ surface dependent activity. Catalysis Science and Technology, 2020, 10, 4424-4435.	2.1	2
50526	An asymmetric Ti₂CO/WS₂ heterostructure as a promising anchoring material for lithiumâ€“sulfur batteries. Journal of Materials Chemistry A, 2020, 8, 13770-13775.	5.2	32
50527	Thermoelectric properties of monolayer GeAsSe and SnSbTe. Journal of Materials Chemistry C, 2020, 8, 9763-9774.	2.7	22
50528	Two-dimensional type-II g-C₃N₄/SiPâ€“GaS heterojunctions as water splitting photocatalysts: first-principles predictions. Physical Chemistry Chemical Physics, 2020, 22, 15649-15657.	1.3	12
50529	Investigation on the role of amines in the liquefaction and recrystallization process of MAPbI₃ perovskite. Journal of Materials Chemistry A, 2020, 8, 13585-13593.	5.2	11
50530	Descriptors representing two- and three-body atomic distributions and their effects on the accuracy of machine-learned inter-atomic potentials. Journal of Chemical Physics, 2020, 152, 234102.	1.2	71
50531	Bond-breaking induced Lifshitz transition in robust Dirac semimetal VAI ₃. Proceedings of the National Academy of Sciences of the United States of America, 2020, 117, 15517-15523.	3.3	8
50532	Precious metal recovery from electronic waste by a porous porphyrin polymer. Proceedings of the National Academy of Sciences of the United States of America, 2020, 117, 16174-16180.	3.3	133
50533	Temperature effect on the phase stability of hydrogen C2/c phase from first-principles molecular dynamics calculations. Journal of Physics Condensed Matter, 2020, 32, 405404.	0.7	3
50534	Energy Level Engineering in Organic Thin Films by Tailored Halogenation. Advanced Functional Materials, 2020, 30, 2002987.	7.8	9
50535	FCC-to-HCP Phase Transformation in CoCrNix Medium-Entropy Alloys. Acta Metallurgica Sinica (English Letters), 2020, 33, 1151-1158.	1.5	12
50536	Segregation of Ni at early stages of radiation damage in NiCoFeCr solid solution alloys. Acta Materialia, 2020, 196, 44-51.	3.8	39
50537	The deactivation mechanism of toluene on MnOx-CeO2 SCR catalyst. Applied Catalysis B: Environmental, 2020, 277, 119257.	10.8	86
50538	First-principles study on strain-modulated negative differential resistance effect of in-plane device based on heterostructure tellurene. Applied Surface Science, 2020, 528, 146957.	3.1	6
50539	Magnetic and topological properties in hydrogenated transition metal dichalcogenide monolayers. Chinese Journal of Physics, 2020, 66, 15-23.	2.0	25
50540	A combined machine learning and density functional theory study of binary Ti-Nb and Ti-Zr alloys: Stability and Youngâ€™s modulus. Computational Materials Science, 2020, 184, 109830.	1.4	10
50541	Electronic structure and phase stability of Pt3M (MÂ=ÂCo, Ni, and Cu) bimetallic nanoparticles. Computational Materials Science, 2020, 184, 109874.	1.4	9

#	Article	IF	Citations
50542	Room temperature ferromagnetism and visible light absorption of Fe-doped pentra-ZnO2 monolayer: First-principles calculations. Chemical Physics Letters, 2020, 754, 137729.	1.2	5
50543	First principle study of intrinsic point defects in Zintl-phase thermoelectric Eu2ZnSb2. Journal of Alloys and Compounds, 2020, 843, 155981.	2.8	5
50544	Relationship between hydrogen binding energy and activity for hydrogen evolution reaction by palladium supported on sulfur-doped ordered mesoporous carbon. Journal of Industrial and Engineering Chemistry, 2020, 89, 361-367.	2.9	11
50545	Computational and experimental investigation of refractory high entropy alloy Mo15Nb20Re15Ta30W20. Journal of Materials Research and Technology, 2020, 9, 8929-8936.	2.6	39
50546	Density functional theory studies of structural distortion in lone pair substituted LuMnO3. Materials Today Communications, 2020, 24, 101079.	0.9	3
50547	Optical identification of point defects in monolayer beryllium oxide by ab initio calculations. Materials Today Communications, 2020, 24, 101344.	0.9	4
50548	In-built durable Liâ€“S counterparts from Liâ€“TiS2 batteries. Materials Today Energy, 2020, 17, 100439.	2.5	8
50549	Efficient computational search for lanthanide-binding additive dopants for advanced U-Zr based fuels. Materialia, 2020, 10, 100653.	1.3	3
50550	Theoretical investigation of V2xFe2(1-x)Zr and ScxY1-xFe2 (0<x<1) quasi-binary alloy: Stable structures, mechanical and electronical properties. Physics Letters, Section A: General, Atomic and Solid State Physics, 2020, 384, 126658.	0.9	3
50551	Tunable magnetism through edge functionalization in zigzag green phosphorene nanoribbons. Physics Letters, Section A: General, Atomic and Solid State Physics, 2020, 384, 126672.	0.9	0
50552	A comprehensive study of phonon thermal transport in 2D IV-VI semiconductors MX (M = Ge, Sn; X = S,) Tj ETQq0 0 0 rgBT /Overlock 10	0.9	6
50553	Enhancement of the tensile strength by introducing alloy element Fe for Ti based alloy. Solid State Communications, 2020, 318, 113982.	0.9	16
50554	Experimental and theoretical studies on the room-temperature ferromagnetism in new (1-x)Bi1/2Na1/2TiO3+xCoTiO3 solid solution materials. Vacuum, 2020, 179, 109551.	1.6	15
50555	BCN-Encapsulated Nano-nickel Synergistically Promotes Ambient Electrochemical Dinitrogen Reduction. ACS Applied Materials & Interfaces, 2020, 12, 31419-31430.	4.0	33
50556	Reactivity descriptors in acid catalysis: acid strength, proton affinity and hostâ€“guest interactions. Chemical Communications, 2020, 56, 7371-7398.	2.2	27
50557	Cluster expansion Monte Carlo study of indiumâ€“aluminum segregation and homogenization in CuInSe2â€“CuAlSe2 pseudobinary alloys. Physical Chemistry Chemical Physics, 2020, 22, 14694-14703.	1.3	0
50558	DFT and hybrid-DFT calculations on the electronic properties of vanadate materials: theory meets experiments. New Journal of Chemistry, 2020, 44, 11602-11607.	1.4	21
50559	Search for stable cocrystals of energetic materials using the evolutionary algorithm USPEX. Physical Chemistry Chemical Physics, 2020, 22, 16822-16830.	1.3	21

#	Article	IF	Citations
50560	Pressure-Induced Topological and Structural Phase Transitions in an Antiferromagnetic Topological Insulator*. Chinese Physics Letters, 2020, 37, 066401.	1.3	50
50561	Thickness-dependent magnetic order and phase transition in V₅S₈*. Chinese Physics B, 2020, 29, 077504.	0.7	5
50562	An electron-counting rule to determine the interlayer magnetic coupling of the van der Waals materials. 2D Materials, 2020, 7, 045010.	2.0	27
50563	Enhanced voltage-controlled magnetic anisotropy via magnetoelasticity in FePt/MgO(001). Physical Review B, 2020, 101, .	1.1	9
50564	Analysis of Electronic and Optical Properties of Pristine LiNbO3 Using First-Principle Calculations. , 2020, , .		1
50565	Relationships Between Na⁺ Distribution, Concerted Migration, and Diffusion Properties in Rhombohedral NASICON. Advanced Energy Materials, 2020, 10, 2001486.	10.2	64
50566	Enhancement of ferromagnetism for VI3 monolayer. Applied Surface Science, 2020, 524, 146490.	3.1	14
50567	Role of anions on electrochemical exfoliation of graphite into graphene in aqueous acids. Carbon, 2020, 167, 816-825.	5.4	54
50568	Enhanced adsorption properties of bimetallic RuCo catalyst for the hydrodeoxygenation of phenolic compounds and raw lignin-oil. Chemical Engineering Science, 2020, 227, 115920.	1.9	42
50569	AMP2: A fully automated program for ab initio calculations of crystalline materials. Computer Physics Communications, 2020, 256, 107450.	3.0	8
50570	SiI2 monolayer as a promising photocatalyst for water splitting hydrogen production under the irradiation of solar light. International Journal of Hydrogen Energy, 2020, 45, 17517-17524.	3.8	21
50571	First-principles study on a new type of quaternary carbonitride VWCN with outstanding mechanical properties. International Journal of Refractory Metals and Hard Materials, 2020, 92, 105319.	1.7	8
50572	Structural, elastic, electronic and hardness properties of osmium diboride predicted from first principles calculations. Journal of Alloys and Compounds, 2020, 844, 156098.	2.8	12
50573	Modeling competitive precipitations among iron carbides during low-temperature tempering of martensitic carbon steel. Materialia, 2020, 12, 100800.	1.3	10
50574	Self-integrated effects of 2D ZnIn2S4 and amorphous Mo2C nanoparticles composite for promoting solar hydrogen generation. Nano Energy, 2020, 76, 105031.	8.2	106
50575	Identifying the existence and molecular structure of the dissolved HCO3-Ca-As(V) complex in water. Science of the Total Environment, 2020, 724, 138216.	3.9	3
50576	Long-Range Ferromagnetic Exchange Interactions Mediated by Mnâ€“Ce^{IV}â€“Mn Superexchange Involving Empty 4f Orbitals. Inorganic Chemistry, 2020, 59, 8716-8726.	1.9	12
50577	Density of States Effective Mass for p-Type Mg₂Siâ€“Mg₂Sn Solid Solutions: Comparison between Experiments and First-Principles Calculations. Journal of Physical Chemistry C, 2020, 124, 14987-14996.	1.5	10

#	Article	IF	Citations
50578	Na₃Zr₂Si₂PO₁₂: A Stable Na⁺-Ion Solid Electrolyte for Solid-State Batteries. ACS Applied Energy Materials, 2020, 3, 7427-7437.	2.5	77
50579	Metastable Chloride Solid Electrolyte with High Formability for Rechargeable All-Solid-State Lithium Metal Batteries. , 2020, 2, 880-886.		40
50580	Direct Observation of One-Dimensional Peierls-type Charge Density Wave in Twin Boundaries of Monolayer MoTe₂. ACS Nano, 2020, 14, 8299-8306.	7.3	23
50581	Hidden role of Bi incorporation in nonradiative recombination in methylammonium lead iodide. Journal of Materials Chemistry A, 2020, 8, 12964-12967.	5.2	18
50582	Structural, elastic, vibrational and optical properties of energetic material octanitrocubane studied from first-principles theory. Journal of Physics Condensed Matter, 2020, 32, 425502.	0.7	4
50583	The effect of moirÃ© superstructures on topological edge states in twisted bismuthene homojunctions. Science Advances, 2020, 6, eaba2773.	4.7	39
50584	Thermoelasticity of tremolite amphibole: Geophysical implications. American Mineralogist, 2020, 105, 904-916.	0.9	11
50585	Understanding the role of boron and stoichiometric ratio in the catalytic performance of amorphous Co-B catalyst. Applied Surface Science, 2020, 518, 146199.	3.1	7
50586	A record-high ion storage capacity of T-graphene as two-dimensional anode material for Li-ion and Na-ion batteries. Applied Surface Science, 2020, 527, 146849.	3.1	59
50587	PANNA: Properties from Artificial Neural Network Architectures. Computer Physics Communications, 2020, 256, 107402.	3.0	36
50588	Two single-phase ZnWO4: RE3+, Li+ (RE = Sm, Eu) white phosphors with high luminous intensity synthesized by solid-state reaction. Journal of Luminescence, 2020, 226, 117377.	1.5	10
50589	Novel cage-like nanoporous ZnO polymorphs with cubic lattice frameworks. Materials Today Communications, 2020, 24, 101152.	0.9	4
50590	Partial Isovalent Anion Substitution to Access Remarkable Second-Harmonic Generation Response: A Generic and Effective Strategy for Design of Infrared Nonlinear Optical Materials. Chemistry of Materials, 2020, 32, 5890-5896.	3.2	84
50591	Flat Bands and Mechanical Deformation Effects in the MoirÃ© Superlattice of MoS₂-WSe₂ Heterobilayers. ACS Nano, 2020, 14, 7564-7573.	7.3	38
50592	Very sharp diffraction peak in nonglass-forming liquid with the formation of distorted tetraclusters. NPG Asia Materials, 2020, 12, .	3.8	28
50593	A tunable and unidirectional one-dimensional electronic system Nb2n+1SinTe4n+2. Npj Quantum Materials, 2020, 5, .	1.8	15
50594	A super stable assembled P nanowire with variant structural and magnetic/electronic properties via transition metal adsorption. Nanoscale, 2020, 12, 12454-12461.	2.8	8
50595	Uncovering the mechanism of dislocation interaction with nanoscale (<4â€‰nm) interphase precipitates in microalloyed ferritic steels. Materials Research Letters, 2020, 8, 341-347.	4.1	25

#	Article	IF	Citations
50596	Path integral Monte Carlo and density functional molecular dynamics simulations of warm dense <mml:math xmlns:mml="http://www.w3.org/1998/Math/MathML"><mml:msub><mml:mi>MgSiO</mml:mi><mml:mn>3</mml:mn></mml:msub></r Physical Review B, 2020, 101, .	1.1	11
50597	Remote heteroepitaxy of GaN microrod heterostructures for deformable light-emitting diodes and wafer recycle. Science Advances, 2020, 6, eaaz5180.	4.7	80
50598	Highâ€Throughput Analysis of Materials for Chemical Looping Processes. Advanced Energy Materials, 2020, 10, 2000685.	10.2	18
50599	3D uniform nitrogen-doped carbon skeleton for ultra-stable sodium metal anode. Nano Research, 2020, 13, 2136-2142.	5.8	75
50600	Effect of Na, Cs and Ca on propylene epoxidation selectivity over CuOx/SiO2 catalysts studied by catalytic tests, in-situ XAS and DFT. Applied Surface Science, 2020, 528, 146854.	3.1	15
50601	Adsorption of metal ions at kaolinite surfaces: Ion-specific effects, and impacts of charge source and hydroxide formation. Applied Clay Science, 2020, 194, 105706.	2.6	13
50602	Surface electronic structure, thermodynamic stability of Na1/2Bi1/2TiO3 (001) surfaces and their relevance to A-site cation ordering in bulk phases: A first-principles study. Solid State Sciences, 2020, 102, 106161.	1.5	1
50603	Adsorption of Azobenzene on Hexagonal Boron Nitride Nanomesh Supported by Rh(111). Journal of Physical Chemistry C, 2020, 124, 14182-14194.	1.5	6
50604	Strain and Low-Coordination Effects on Monolayer Nanoislands of Pd and Pt on Au(111): A Comparative Analysis Based on Density Functional Results. Journal of Physical Chemistry C, 2020, 124, 13225-13230.	1.5	9
50605	DFT Study of Oxygen Reduction Reaction on Chromia and Hematite: Insights into Corrosion Inhibition. Journal of Physical Chemistry C, 2020, 124, 13799-13808.	1.5	21
50606	Revealing the Formation Energyâ€“Exfoliation Energyâ€“Structure Correlation of MAB Phases Using Machine Learning and DFT. ACS Applied Materials & Interfaces, 2020, 12, 29424-29431.	4.0	15
50607	Instant Postsynthesis Aqueous Dispersion of Sb-Doped SnO₂ Nanocrystals: The Synergy between Small-Molecule Amine and Sb Dopant Ratio. ACS Applied Materials & Interfaces, 2020, 12, 29937-29945.	4.0	3
50608	Dipole-Field Interactions Determine the CO₂ Reduction Activity of 2D Feâ€“Nâ€“C Single-Atom Catalysts. ACS Catalysis, 2020, 10, 7826-7835.	5.5	94
50609	Facet-Specific Photocatalytic Activity Enhancement of Cu₂O Polyhedra Functionalized with 4-Ethynylanaline Resulting from Band Structure Tuning. ACS Central Science, 2020, 6, 984-994.	5.3	42
50610	Hexagonal Stacking Faults Act as Hole-Blocking Layers in Lead Halide Perovskites. ACS Energy Letters, 2020, 5, 2231-2233.	8.8	12
50611	Stability and gas sensing properties of Ta₂X₃M₈ (X = Pd, Pt; M = S,) Tj ETQq1 1 0.784314 rgB 14651-14659.	1.3	6
50612	Dissociation of (Li2O2)0,+ on graphene and boron-doped graphene: insights from first-principles calculations. Physical Chemistry Chemical Physics, 2020, 22, 14216-14224.	1.3	11
50613	The first-principles study of the adsorption of NH3, NO, and NO2 gas molecules on InSe-like phosphorus carbide. New Journal of Chemistry, 2020, 44, 9377-9381.	1.4	9

#	Article	IF	Citations
50614	Stability and metallization of solid oxygen at high pressure. Physical Chemistry Chemical Physics, 2020, 22, 12577-12583.	1.3	5
50615	Dynamic strain aging in Fe-Mn-Al-C lightweight steel. Philosophical Magazine Letters, 2020, 100, 355-364.	0.5	4
50616	Tight-binding modeling of interstitial ordering processes in metals: Application to zirconium hydrides. Physical Review B, 2020, 101, .	1.1	2
50617	Chlorine insertion and manipulation on the Si(100)- <mml:math xmlns:mml="http://www.w3.org/1998/Math/MathML"><mml:mrow><mml:mn>2</mml:mn><mml:mo>Ã—</mml:mo><mml:mn>1</mml:mn> -Cl surface in the regime of local supersaturation. Physical Review B, 2020, 101, .	1.1	9
50618	Water- and acid-stable self-passivated dihafnium sulfide electride and its persistent electrocatalytic reaction. Science Advances, 2020, 6, eaba7416.	4.7	30
50619	Reversible Release and Fixation of Bromine in Vacancyâ€Ordered Bromide Perovskites. Energy and Environmental Materials, 2020, 3, 535-540.	7.3	23
50620	Ohmic contacts of monolayer Tl2O field-effect transistors. Journal of Materials Science, 2020, 55, 11439-11450.	1.7	9
50621	Mechanical-electro-magnetic coupling in strained bilayer CrI3. Science China Technological Sciences, 2020, 63, 1265-1271.	2.0	3
50622	First-principles study of the oxygen reduction reaction on the boron-doped C9N4 metal-free catalyst. Applied Surface Science, 2020, 527, 146828.	3.1	16
50623	Nanoporous C3N4, C3N5 and C3N6 nanosheets; novel strong semiconductors with low thermal conductivities and appealing optical/electronic properties. Carbon, 2020, 167, 40-50.	5.4	72
50624	High thermal conductivity in semiconducting Janus and non-Janus diamanes. Carbon, 2020, 167, 51-61.	5.4	39
50625	Insight into the intrinsic mechanism of improving electrochemical performance via constructing the preferred crystal orientation in lithium cobalt dioxide. Chemical Engineering Journal, 2020, 399, 125708.	6.6	13
50626	Prediction of mechanical properties of grafted kaolinite â€“ A DFT study. Applied Clay Science, 2020, 193, 105692.	2.6	19
50627	The influence of transition metal solutes on the dissolution and diffusion of oxygen in tungsten. Journal of Nuclear Materials, 2020, 537, 152250.	1.3	5
50628	Targeting Productive Composition Space through Machine-Learning-Directed Inorganic Synthesis. Matter, 2020, 3, 261-272.	5.0	11
50629	Elucidating the methanol conversion in H-SAPO-5 from first principles: Nature of hydrocarbon pool and scission style. Molecular Catalysis, 2020, 490, 110948.	1.0	4
50630	Mechanism of pitting corrosion induced by inclusions in Al-Ti-Mg deoxidized high strength pipeline steel. Micron, 2020, 138, 102898.	1.1	19
50631	Structural stabilities and optical properties of Si Ge H nanocrystals. Physics Letters, Section A: General, Atomic and Solid State Physics, 2020, 384, 126597.	0.9	3

#	Article	IF	Citations
50632	First-principles study on electronic, magnetic properties and optical absorption of vanadium doped rutile TiO2. Physics Letters, Section A: General, Atomic and Solid State Physics, 2020, 384, 126637.	0.9	7
50633	Does GaAs bulk lattice really expand due to defects in the low concentration regime?. Solid State Communications, 2020, 316-317, 113918.	0.9	1
50634	Nodal Flexible-surface Semimetals: Case of Carbon Nanotube Networks. Nano Letters, 2020, 20, 5400-5407.	4.5	36
50635	Computational framework for a systematic investigation of anionic redox process in Li-rich compounds. Npj Computational Materials, 2020, 6, .	3.5	17
50636	High-throughput density functional perturbation theory and machine learning predictions of infrared, piezoelectric, and dielectric responses. Npj Computational Materials, 2020, 6, .	3.5	60
50637	Benefits of Ga, Ge and As substitution in Li₂FeSiO₄: a first-principles exploration of the structural, electrochemical and capacity properties. Physical Chemistry Chemical Physics, 2020, 22, 14712-14719.	1.3	6
50638	Synthesis of two new copper-sandwiched polyoxotungstates and the influence of nuclear number on catalytic hydrogen evolution activity. New Journal of Chemistry, 2020, 44, 11035-11041.	1.4	6
50639	Mottness collapse in monolayer 1T-TaSe2 with persisting charge density wave order. Journal of Materials Chemistry C, 2020, 8, 9742-9747.	2.7	18
50640	The transformation of cuboctahedral to icosahedral nanoparticles: atomic structure and dynamics. Physical Chemistry Chemical Physics, 2020, 22, 12939-12945.	1.3	9
50641	Strain tuning of closed topological nodal lines and opposite pockets in quasi-two-dimensional Î±-phase FeSi2. Physical Chemistry Chemical Physics, 2020, 22, 13650-13658.	1.3	16
50642	On the origin of non-monotonic variation of the lattice parameters of LiNi_{1/3}Co_{1/3}Mn_{1/3}O₂ with lithiation/delithiation: a first-principles study. Journal of Materials Chemistry A, 2020, 8, 13832-13841.	5.2	10
50643	Concepts from the linear magnetoelectric effect that might be useful for antiferromagnetic spintronics. Journal of Applied Physics, 2020, 127, .	1.1	29
50644	Local structure of [(GeTe)₂/(Sb₂Te₃)_m]_n super-lattices by x-ray absorption spectroscopy. Journal Physics D: Applied Physics, 2020, 53, 404002.	1.3	9
50645	Understanding the curious magnetic state of <mml:math xmlns:mml="http://www.w3.org/1998/Math/MathML"><mml:mrow><mml:msub><mml:mi>Sr</mml:mi><mml:mn>3</mml:mn> Physical Review B, 2020, 101, .	1.1	4
50646	Examining the surface phase diagram of <mml:math xmlns:mml="http://www.w3.org/1998/Math/MathML"><mml:msub><mml:mi>IrTe</mml:mi><mml:mn>2</mml:mn> with photoemission. Physical Review B, 2020, 101, .	1.1	8
50647	Spin-orbit splitting of quantum well states in <mml:math xmlns:mml="http://www.w3.org/1998/Math/MathML"><mml:mi>n</mml:mi></mml:math> -monolayer Ir/Au(111) heterostructures. Physical Review B, 2020, 101, .	1.1	0
50648	Crystal time-reversal symmetry breaking and spontaneous Hall effect in collinear antiferromagnets. Science Advances, 2020, 6, eaaz8809.	4.7	177
50649	Calculations of selective Si epitaxial growth. Applied Surface Science, 2020, 514, 145888.	3.1	2

#	Article	IF	Citations
50650	Revealing the effect of N-content in Fe doped graphene on its catalytic performance for direct oxidation of methane to methanol. Applied Surface Science, 2020, 527, 146833.	3.1	20
50651	Dielectrophoretic borophene tweezer: Sub-10â€¯mV nano-particle trapping. Applied Surface Science, 2020, 527, 146859.	3.1	4
50652	Realization of ultrathin red 2D carbon nitride sheets to significantly boost the photoelectrochemical water splitting performance of TiO2 photoanodes. Chemical Engineering Journal, 2020, 396, 125267.	6.6	16
50653	Structural, strong magnetic exchange, and room temperature multiferroic properties of single-phase 0.75BiFeO3â€“BaFe1/2Nb1/2O3 bulk ceramics. Ceramics International, 2020, 46, 18707-18715.	2.3	2
50654	The mechanism of V-modification in Li2CoSiO4 cathode material for Li-ion batteries: A combined first-principles and experimental study. Electrochimica Acta, 2020, 353, 136564.	2.6	9
50655	Origin of Ï‰-phase formation in metastable Î²-type Ti-Mo alloys: cluster structure and stacking fault. Scientific Reports, 2020, 10, 8664.	1.6	21
50656	Synergetic defects boost charge separation in CN for enhanced photocatalytic water splitting. Journal of Materials Chemistry C, 2020, 8, 9366-9372.	2.7	15
50657	Mn absorbed on the surface of the monolayer of GeSe Sheet. , 2020, , .		0
50658	Theoretical studies on alloying of germanene supported on Al (111) substrate*. Chinese Physics B, 2020, 29, 108103.	0.7	3
50659	Switching at Less Than 60 mV/Decade with a â€œColdâ€•Metal as the Injection Source. Physical Review Applied, 2020, 13, .	1.5	28
50660	A Study of the Structure and Magnetic Properties of FeRh1Ââ€“ÂxIrx (x = 0.5â€“1) Alloys by First-Principles Methods. Physics of the Solid State, 2020, 62, 963-967.	0.2	2
50661	Exploring the Possibility of Î²â€Phase Arsenicâ€Phosphorus Polymorph Monolayer as Anode Materials for Sodiumâ€ion Batteries. Advanced Theory and Simulations, 2020, 3, 2000023.	1.3	14
50662	Photocatalytic properties of grapheneâ€supported titania clusters from densityâ€functional theory. Journal of Computational Chemistry, 2020, 41, 1921-1930.	1.5	10
50663	Probing Pd_n (n=1â€5) Clusters on Rutile TiO₂ Surfaces by Using Firstâ€Principle Calculations. ChemistrySelect, 2020, 5, 6939-6945.	0.7	5
50664	Nitrogen reduction reaction on small iron clusters supported by N-doped graphene: A theoretical study of the atomically precise active-site mechanism. Nano Research, 2020, 13, 2280-2288.	5.8	59
50665	Interfacial engineering of Ni/V2O3 for hydrogen evolution reaction. Nano Research, 2020, 13, 2407-2412.	5.8	41
50666	Solid-acid-mediated electronic structure regulation of electrocatalysts and scaling relation breaking of oxygen evolution reaction. Applied Catalysis B: Environmental, 2020, 277, 119237.	10.8	42
50667	Phase equilibria and thermodynamic investigation of the Inâ€“Li system. Calphad: Computer Coupling of Phase Diagrams and Thermochemistry, 2020, 70, 101779.	0.7	4

#	Article	IF	Citations
50668	Effect of S vacancy or non-metallic atom (C, N and F) doping on the adsorption behaviors of molecules (H2S, BF4) on monolayer MoS2. Physica E: Low-Dimensional Systems and Nanostructures, 2020, 124, 114292.	1.3	1
50669	Disagreements between space charge models and grain boundary impedance data in yttrium-substituted barium zirconate. Solid State Ionics, 2020, 353, 115369.	1.3	13
50670	Indium-Doped Rutile Titanium Oxide with Reduced Particle Length and Its Sodium Storage Properties. ACS Omega, 2020, 5, 15495-15501.	1.6	12
50671	Hierarchically structured diamond composite with exceptional toughness. Nature, 2020, 582, 370-374.	13.7	141
50672	Remarkably improved oxygen evolution reaction activity of cobalt oxides by an Fe ion solution immersion process. Inorganic Chemistry Frontiers, 2020, 7, 3327-3339.	3.0	29
50673	Functionalized MXenes as effective polyselenide immobilizers for lithiumâ€“selenium batteries: a density functional theory (DFT) study. Nanoscale, 2020, 12, 14087-14095.	2.8	41
50674	High-temperature and multichannel quantum anomalous Hall effect in pristine and alkaliâ€“metal-doped CrBr₃ monolayers. Nanoscale, 2020, 12, 13964-13972.	2.8	16
50675	Coexistence of plastic and partially diffusive phases in a helium-methane compound. National Science Review, 2020, 7, 1540-1547.	4.6	33
50676	CVD synthesis and characterization of thin Mo₂C crystals. Journal of the American Ceramic Society, 2020, 103, 5586-5593.	1.9	37
50677	Silica surface states and their wetting characteristics. Surface Innovations, 2020, 8, 145-157.	1.4	18
50678	The Relationships of Microscopic Evolution to Resistivity Variation of a FIB-Deposited Platinum Interconnector. Micromachines, 2020, 11, 588.	1.4	3
50679	Segregation of alloying elements and their effects on the thermodynamic stability and fracture strength of Î³-Ni/Î³â€²-Ni3Al interface. Journal of Materials Science, 2020, 55, 12513-12524.	1.7	15
50680	Heterojunction architecture of pTTh nanoflowers with CuOx nanoparticles hybridized for efficient photoelectrocatalytic degradation of organic pollutants. Applied Catalysis B: Environmental, 2020, 277, 119249.	10.8	24
50681	Adsorption behavior of CO, CO2, H2, H2O, NO, and O2 on pristine and defective 2D monolayer ferromagnetic Fe3GeTe2. Applied Surface Science, 2020, 527, 146894.	3.1	20
50682	A Directional Synthesis for Topological Defect in Carbon. CheM, 2020, 6, 2009-2023.	5.8	120
50683	Evolutionary multi-objective optimization and Pareto-frontal uncertainty quantification of interatomic forcefields for thermal conductivity simulations. Computer Physics Communications, 2020, 254, 107337.	3.0	9
50684	2D MoSe2/CoP intercalated nanosheets for efficient electrocatalytic hydrogen production. International Journal of Hydrogen Energy, 2020, 45, 19246-19256.	3.8	32
50685	Oxidization of fluid-like Li metal with inherent Li Li2O interface from simulation insights. Journal of Materiomics, 2020, 6, 692-701.	2.8	4

#	Article	IF	Citations
50686	Study of group 5B transition metal monoborides under high pressure. Journal of Physics and Chemistry of Solids, 2020, 146, 109603.	1.9	3
50687	Realizing long-term cycling stability and superior rate performance of 4.5ÂVâ€“LiCoO2 by aluminum doped zinc oxide coating achieved by a simple wet-mixing method. Journal of Power Sources, 2020, 470, 228423.	4.0	57
50688	Synergistic enhancement effect of MoO3@Ag hybrid nanostructures for boosting selective detection sensitivity. Spectrochimica Acta - Part A: Molecular and Biomolecular Spectroscopy, 2020, 241, 118611.	2.0	13
50689	Modulating the electronic, magnetic and optical properties of 1T-SnSe2 monolayer by defects: An ab initio study. Superlattices and Microstructures, 2020, 145, 106621.	1.4	17
50690	Does Spinel Serve as a Rigid Framework for Oxygen Redox?. Chemistry of Materials, 2020, 32, 7181-7187.	3.2	5
50691	Experimental and Computational Investigation of the Role of P in Moderating Ethane Dehydrogenation Performance over Ni-Based Catalysts. Industrial & Engineering Chemistry Research, 2020, 59, 12666-12676.	1.8	14
50692	Multiscale Study of the Mechanism of Catalytic CO₂ Hydrogenation: Role of the Ni(111) Facets. ACS Catalysis, 2020, 10, 8077-8089.	5.5	43
50693	Synergy of Binary Substitutions for Improving the Cycle Performance in LiNiO₂ Revealed by Ab Initio Materials Informatics. ACS Omega, 2020, 5, 13403-13408.	1.6	8
50694	First principles study of reactions in alucone growth: the role of the organic precursor. Dalton Transactions, 2020, 49, 8710-8721.	1.6	8
50695	B5N5 monolayer: a room-temperature light element antiferromagnetic insulator. Nanoscale Advances, 2020, 2, 4421-4426.	2.2	3
50696	In situ modification of BiVO₄ nanosheets on graphene for boosting photocatalytic water oxidation. Nanoscale, 2020, 12, 14853-14862.	2.8	20
50697	Highly spin-polarized electronic structure and magnetic properties of Mn_{2.25}Co_{0.75}Al_{1â^'x}Ge_x Heusler alloys: first-principles calculations. RSC Advances, 2020, 10, 22556-22569.	1.7	2
50698	Superconductivity and topological aspects of the rocksalt carbides NbC and TaC. Physical Review B, 2020, 101, .	1.1	30
50699	Halogen modified two-dimensional covalent triazine frameworks as visible-light driven photocatalysts for overall water splitting. Science China Chemistry, 2020, 63, 1134-1141.	4.2	31
50700	LixNa2â^'xW4O13 nanosheet for scalable electrochromic device. Frontiers of Optoelectronics, 2021, 14, 298-310.	1.9	3
50701	Tuning the high-Î° oxide (HfO2, ZrO2)/4H-SiC interface properties with a SiO2 interlayer for power device applications. Applied Surface Science, 2020, 527, 146843.	3.1	13
50702	Theoretical insights into the origin of highly efficient photocatalyst NiO/NaTaO3 for overall water splitting. International Journal of Hydrogen Energy, 2020, 45, 19357-19369.	3.8	13
50703	Vacancy ordering during selective oxidation of Î²-NiAl. Materialia, 2020, 12, 100783.	1.3	6

#	Article	IF	Citations
50704	Two-Dimensional Layered SnO₂ Nanosheets for Ambient Ammonia Synthesis. ACS Applied Energy Materials, 2020, 3, 6735-6742.	2.5	16
50705	Type-II Interface Band Alignment in the vdW PbI₂â€“MoSe₂ Heterostructure. ACS Applied Materials & Interfaces, 2020, 12, 32099-32105.	4.0	20
50706	Understanding the Enhanced Electrocatalytic Hydrogen Evolution <i>via</i> Integrating Electrochemically Inactive g-C₃N₄: The Effect of Interfacial Engineering. ACS Sustainable Chemistry and Engineering, 2020, 8, 10313-10320.	3.2	28
50707	Reversing abnormal hole localization in high-Al-content AlGaN quantum well to enhance deep ultraviolet emission by regulating the orbital state coupling. Light: Science and Applications, 2020, 9, 104.	7.7	25
50708	Establishing the carrier scattering phase diagram for ZrNiSn-based half-Heusler thermoelectric materials. Nature Communications, 2020, 11, 3142.	5.8	87
50709	Microscopic origin of the extremely low thermal conductivity and outstanding thermoelectric performance of BiSbX₃ (X = S, Se) revealed by first-principles study. Physical Chemistry Chemical Physics, 2020, 22, 15559-15566.	1.3	12
50710	Catalysis to discriminate single atoms from subnanometric ruthenium particles in ultra-high loading catalysts. Catalysis Science and Technology, 2020, 10, 4673-4683.	2.1	18
50711	Synergistic effects of dopant (Ti or Sn) and oxygen vacancy on the electronic properties of hematite: a DFT investigation. RSC Advances, 2020, 10, 23263-23269.	1.7	14
50712	Atomic hydrogen passivation for photoresponsivity enhancement of boron-doped p-BaSi2 films and performance improvement of boron-doped p-BaSi2/n-Si heterojunction solar cells. Journal of Applied Physics, 2020, 127, .	1.1	13
50713	Probing the intermolecular coupled vibrations in a water cluster with inelastic electron tunneling spectroscopy. Journal of Chemical Physics, 2020, 152, 234301.	1.2	2
50714	Combining steady-state photo-capacitance spectra with first-principles calculations: the case of Fe and Ti in Î²-Ga2O3. New Journal of Physics, 2020, 22, 063033.	1.2	10
50715	<mml:math xmlns:mml="http://www.w3.org/1998/Math/MathML"><mml:mrow><mml:msub><mml:mi>SrCu</mml:mi><mml:mn>2</mml:mn></m under pressure: A first-principles study. Physical Review B, 2020, 101, .	1.1	6
50716	Valley polarization investigation of GeS under high pressure. Physical Review B, 2020, 101, .	1.1	10
50717	Mesoscopic electronic transport in twisted bilayer graphene. Physical Review B, 2020, 101, .	1.1	5
50718	First-principle study of electronic structure of montmorillonite at high pressure. Modern Physics Letters B, 2020, 34, 2050263.	1.0	2
50719	Chemical substitution of Zn in the structure of ordered Cu6Zn2Sb2: A structural and theoretical study. Solid State Sciences, 2020, 107, 106333.	1.5	5
50720	Understanding the role of ionic flux on the polarity of the exposed surfaces of ZnO. Physical Chemistry Chemical Physics, 2020, 22, 15427-15436.	1.3	4
50721	Two-dimensional hexagonal chromium chalco-halides with large vertical piezoelectricity, high-temperature ferromagnetism, and high magnetic anisotropy. Physical Chemistry Chemical Physics, 2020, 22, 14503-14513.	1.3	32

#	Article	IF	Citations
50722	Inert basal plane activation of two-dimensional ZnIn₂S₄via Ni atom doping for enhanced co-catalyst free photocatalytic hydrogen evolution. Journal of Materials Chemistry A, 2020, 8, 13376-13384.	5.2	79
50723	Stable halogen 2D materials: the case of iodine and astatine. Journal of Physics Condensed Matter, 2020, 32, 335301.	0.7	1
50724	Synthesis of heteroepitaxial BP and related Al-B-Sb-As-P films via CVD of Al(BH4)3 and MH3 (M=P, As, Sb) at temperatures below 600 Â°C. Semiconductor Science and Technology, 2020, 35, 085034.	1.0	2
50725	Prospects for high carrier mobility in the cubic germanates. Semiconductor Science and Technology, 2020, 35, 085030.	1.0	5
50726	Phase stability and impact of water on CsSnI₃ perovskite. Applied Physics Express, 2020, 13, 071003.	1.1	10
50727	A Physical Model for Understanding the Activation of MoS₂ Basalâ€Plane Sulfur Atoms for the Hydrogen Evolution Reaction. Angewandte Chemie, 2020, 132, 14945-14951.	1.6	9
50728	Topological Phase Transition in 2D 1Tâ€²â€WSTe. Physica Status Solidi (B): Basic Research, 2020, 257, 2000010.	0.7	2
50729	Phosphorus-doped TiO2 for visible light-driven oxidative coupling of benzyl amines and photodegradation of phenol. Applied Surface Science, 2020, 527, 146693.	3.1	37
50730	Amorphous Ag2-xCuxS quantum dots: â€œall-in-oneâ€•theranostic nanomedicines for near-infrared fluorescence/photoacoustics dual-modal-imaging-guided photothermal therapy. Chemical Engineering Journal, 2020, 399, 125777.	6.6	19
50731	FLAME: A library of atomistic modeling environments. Computer Physics Communications, 2020, 256, 107415.	3.0	23
50732	Long structures of H2O molecules adsorbed on the V2O5(0 0 1) surface. A DFTÂ+ÂU study including van der Waals interactions. Chemical Physics Letters, 2020, 749, 137408.	1.2	0
50733	Graphene pillared with hybrid fullerene and nanotube as a novel 3D framework for hydrogen storage: A DFT and GCMC study. International Journal of Hydrogen Energy, 2020, 45, 17637-17648.	3.8	31
50734	Pore opening and breathing transitions in metal-organic frameworks: Coupling adsorption and deformation. Journal of Colloid and Interface Science, 2020, 578, 77-88.	5.0	20
50735	Charge transfer in Pr-Doped cerium oxide: Experimental and theoretical investigations. Materials Chemistry and Physics, 2020, 249, 122967.	2.0	9
50736	Density functional theory study of hydrogen sulfide adsorption onto transition metal-doped bilayer graphene using external electric fields. Physica E: Low-Dimensional Systems and Nanostructures, 2020, 124, 114252.	1.3	14
50737	Organic-inorganic hybrid coordination polymer C3H9CdCl3N co-exhibiting superior Dirac point and nodal surface states. Results in Physics, 2020, 17, 103159.	2.0	4
50738	Enabling Efficient and Accurate Computational Studies of MOF Reactivity via QM/MM and QM/QM Methods. Journal of Physical Chemistry C, 2020, 124, 10550-10560.	1.5	18
50739	Understanding Solidâ€“Gas Reaction Mechanisms by Operando Soft X-Ray Absorption Spectroscopy at Ambient Pressure. Journal of Physical Chemistry C, 2020, 124, 14202-14212.	1.5	19

#	Article	IF	Citations
50740	A Multitechnique Study of Fluorinated Nanodiamonds for Low-Energy Neutron Physics Applications. Journal of Physical Chemistry C, 2020, 124, 14229-14236.	1.5	6
50741	High-Performance Thermoelectric Oxides Based on Spinel Structure. ACS Applied Energy Materials, 2020, 3, 5666-5674.	2.5	18
50742	Molybdenum Nitride Electrocatalysts for Hydrogen Evolution More Efficient than Platinum/Carbon: Mo₂N/CeO₂@Nickel Foam. ACS Applied Materials & Interfaces, 2020, 12, 29153-29161.	4.0	18
50743	Electronic Structure and Magnetic Anisotropy of Single-Layer Rare-Earth Oxybromide. ACS Omega, 2020, 5, 14194-14201.	1.6	10
50744	Fundamental electronic structure and multiatomic bonding in 13 biocompatible high-entropy alloys. Npj Computational Materials, 2020, 6, .	3.5	79
50745	Plasmon-driven carbonâ€“fluorine (C(sp3)â€“F) bond activation with mechanistic insights into hot-carrier-mediated pathways. Nature Catalysis, 2020, 3, 564-573.	16.1	81
50746	Characterization of three phases of liquid carbon by tight-binding molecular dynamics simulations. Physical Chemistry Chemical Physics, 2020, 22, 14630-14636.	1.3	4
50747	Damage mechanism and electro-elastic stability of LiNbO₃ crystals irradiated with 6 MeV Xe²³⁺. RSC Advances, 2020, 10, 21754-21759.	1.7	1
50748	Grafting of iron on amorphous silica surfaces from ab initio calculations. Journal of Chemical Physics, 2020, 152, 214706.	1.2	13
50749	Comparing GGA, GGA+U, and meta-GGA functionals for redox-dependent binding at open metal sites in metalâ€“organic frameworks. Journal of Chemical Physics, 2020, 152, 224101.	1.2	16
50750	Excellent properties of type-II van der Waals Janus-XM2Xâ€™/MX heterojunctions toward solar cell utilization. Journal Physics D: Applied Physics, 2020, 53, 405101.	1.3	5
50751	Theoretical prediction of stable cluster-assembled CdSe bilayer and its functionalization with Co and Cr adatoms. Journal of Physics Condensed Matter, 2020, 32, 015501.	0.7	2
50752	First principles investigation on the nitrogen-doped planar aluminene for hydrogen storage application. IOP Conference Series: Earth and Environmental Science, 2020, 463, 012103.	0.2	2
50753	Modeling mechanical relaxation in incommensurate trilayer van der Waals heterostructures. Physical Review B, 2020, 101, .	1.1	31
50754	Hole antidoping of oxides. Physical Review B, 2020, 101, .	1.1	10
50755	Ion beam irradiation of ABO₄ compounds with the fergusonite, monazite, scheelite, and zircon structures. Journal of the American Ceramic Society, 2020, 103, 5502-5514.	1.9	9
50756	Thermodynamic Analysis of the Fe-Mo-B Ternary System. Tetsu-To-Hagane/Journal of the Iron and Steel Institute of Japan, 2020, 106, 310-320.	0.1	7
50757	Hydrogen states in hydrogen-passivated semiconducting barium disilicide measured via muon spin rotation. Japanese Journal of Applied Physics, 2020, 59, 071004.	0.8	9

#	Article	IF	Citations
50758	Compositional Phase Change of Early Transition Metal Diselenide (VSe₂ and) Tj ETQq0 0 0 rgBT /Overlock 10 Tf 50 747 Td 2000497.	1.9	17
50759	First-principles predication of facet-dependent electronic and optical properties in InSe/GaAs heterostructure with potential in solar energy utilization. Journal of Alloys and Compounds, 2020, 842, 155901.	2.8	15
50760	First-Principles Study on the Oxygenâ€“Light-Induced Iodide Vacancy Formation in FASnI₃ Perovskite. Journal of Physical Chemistry C, 2020, 124, 14147-14157.	1.5	17
50761	Reduction of Carbon Impurities in Aluminum Nitride from Time-Resolved Chemical Vapor Deposition Using Trimethylaluminum. Journal of Physical Chemistry C, 2020, 124, 14176-14181.	1.5	9
50762	Diffusion on a Crowded Surface: kMC Simulations. Journal of Physical Chemistry C, 2020, 124, 15216-15224.	1.5	9
50763	Nature of Terminating Hydroxyl Groups and Intercalating Water in Ti₃C₂T_x MXenes: A Study by ¹H Solid-State NMR and DFT Calculations. Journal of Physical Chemistry C, 2020, 124, 13649-13655.	1.5	35
50764	LaCrO3-Coated La0.6Sr0.4Co0.2Fe0.8O3â^'Î´ Coreâ€“Shell Structured Cathode with Enhanced Cr Tolerance for Intermediate-Temperature Solid Oxide Fuel Cells. ACS Applied Materials & Interfaces, 2020, 12, 29133-29142.	4.0	4
50765	Synergistic Photocatalytic Decomposition of a Volatile Organic Compound Mixture: High Efficiency, Reaction Mechanism, and Long-Term Stability. ACS Catalysis, 2020, 10, 7230-7239.	5.5	98
50766	Discovery of new boron-rich chalcogenides: orthorhombic B6X (X=S, Se). Scientific Reports, 2020, 10, 9277.	1.6	15
50767	An experimental and first-principle investigation of the Ca-substitution effect on P3-type layered Na_xCoO₂. Chemical Communications, 2020, 56, 8107-8110.	2.2	4
50768	Machine-learning interatomic potentials enable first-principles multiscale modeling of lattice thermal conductivity in graphene/borophene heterostructures. Materials Horizons, 2020, 7, 2359-2367.	6.4	124
50769	Weak Coulomb correlations stabilize the electride high-pressure phase of elemental calcium. Journal of Physics Condensed Matter, 2020, 32, 445501.	0.7	10
50770	Raman spectra of MXenes Zr₂X(X=C and N). Nanotechnology, 2020, 31, 405708.	1.3	7
50771	Phonon-mediated superconductivity in aluminum-deposited graphene <mml:math xmlns:mml="http://www.w3.org/1998/Math/MathML"><mml:msub><mml:mi>AlC</mml:mi><mml:mn>8</mml:mn></mml:msub></m Physical Review B, 2020, 101, .	1.1	30
50772	<mml:math xmlns:mml="http://www.w3.org/1998/Math/MathML"><mml:mrow><mml:msub><mml:mi>SrRuO</mml:mi><mml:mn>3</mml:mn></ heterostructure as a possible platform for studying unconventional superconductivity in <mml:math xmlns:mml="http://www.w3.org/1998/Math/MathML"><mml:mrow><mml:msub><mml:mi>Sr</mml:mi><mml:mn>2</mml:mn></mml:r Physical Review B, 2020, 101, .	1.1	6
50773	Symmetry-guaranteed ideal Weyl semimetallic phase in face-centered orthogonal C6. Physical Review B, 2020, 101, .	1.1	7
50774	Non-Fermi-liquid behavior and saddlelike flat band in the layered ferromagnet <mml:math xmlns:mml="http://www.w3.org/1998/Math/MathML"><mml:mrow><mml:msub><mml:mi>AlFe</mml:mi><mml:mn>2</mml:mn></mm mathvariant="normal">B</mml:mi><mml:mn>2</mml:mn></mml:msub></mml:mrow></mml:math>. Physical Review B, 2020, 101, .	1.1	7
50775	Mechanical Properties of the Interface of Al/SiC Heteroparticles and Their Composites: a Theoretical and Experimental Study. Technical Physics Letters, 2020, 46, 342-345.	0.2	1

#	Article	IF	Citations
50776	New Polymorphs of 2D Indium Selenide with Enhanced Electronic Properties. Advanced Functional Materials, 2020, 30, 2001920.	7.8	33
50777	Strainâ€Engineered Anisotropic Optical and Electrical Properties in 2D Chiralâ€Chain Tellurium. Advanced Materials, 2020, 32, e2002342.	11.1	40
50778	Clarification of the Relationship between the Magnetic and Conductive Properties of Infinite Chains in Trioxotriangulene Radical Crystals by Spinâ€Projected DFT/Planeâ€Wave Calculations. Advanced Theory and Simulations, 2020, 3, 2000050.	1.3	10
50779	Enabling reversible phase transition on K5/9Mn7/9Ti2/9O2 for high-performance potassium-ion batteries cathodes. Energy Storage Materials, 2020, 31, 20-26.	9.5	35
50780	Enhanced strength and ductility of superhard boron carbide through injecting electrons. Journal of the European Ceramic Society, 2020, 40, 4428-4435.	2.8	7
50781	Hybridization versus sublattice symmetry breaking in the band gap opening in graphene on Ni(111): A first-principles study. Surface Science, 2020, 700, 121651.	0.8	3
50782	ONETEP + TOSCAM: Uniting Dynamical Mean Field Theory and Linear-Scaling Density Functional Theory. Journal of Chemical Theory and Computation, 2020, 16, 4899-4911.	2.3	5
50783	Tunable Properties of Novel Ga₂O₃ Monolayer for Electronic and Optoelectronic Applications. ACS Applied Materials & Interfaces, 2020, 12, 30659-30669.	4.0	87
50784	Spontaneously separated intermetallic Co3Mo from nanoporous copper as versatile electrocatalysts for highly efficient water splitting. Nature Communications, 2020, 11, 2940.	5.8	146
50785	Te₃O₃(PO₄)₂: a phosphate crystal with large birefringence activated by the highly distorted [TeO₅] group and antiparallel [PO₄] pseudo-layer. Journal of Materials Chemistry C, 2020, 8, 9585-9592.	2.7	23
50786	Molecular and dissociative adsorption of CO and SO on the surface of Ir(111). AIP Advances, 2020, 10, 035021.	0.6	2
50787	Direct observation and catalytic role of mediator atom in 2D materials. Science Advances, 2020, 6, eaba4942.	4.7	7
50788	Interaction of SO2 with the Platinum (001), (011), and (111) Surfaces: A DFT Study. Catalysts, 2020, 10, 558.	1.6	9
50789	Boosting Activity on Co₄N Porous Nanosheet by Coupling CeO₂ for Efficient Electrochemical Overall Water Splitting at High Current Densities. Advanced Functional Materials, 2020, 30, 1910596.	7.8	218
50790	Domain Engineering in ReS₂ by Coupling Strain during Electrochemical Exfoliation. Advanced Functional Materials, 2020, 30, 2003057.	7.8	22
50791	Boosting Catalysis of Pd Nanoparticles in MOFs by Pore Wall Engineering: The Roles of Electron Transfer and Adsorption Energy. Advanced Materials, 2020, 32, e2000041.	11.1	151
50792	Machineâ€Learning Clustering Technique Applied to Powder Xâ€Ray Diffraction Patterns to Distinguish Compositions of ThMn₁₂â€Type Alloys. Advanced Theory and Simulations, 2020, 3, 2000039.	1.3	13
50793	<scp>LOBSTER</scp>: Local orbital projections, atomic charges, and chemicalâ€bonding analysis from <scp>projectorâ€augmentedâ€waveâ€based</scp> densityâ€functional theory. Journal of Computational Chemistry, 2020, 41, 1931-1940.	1.5	523

#	Article	IF	Citations
50794	Shockâ€driven electron redistribution studies of triamino trinitrobenzene using timeâ€resolved Raman spectroscopy and firstâ€principle calculation. Journal of Raman Spectroscopy, 2020, 51, 2007-2015.	1.2	6
50795	Research trend of large-scale supercomputers and applications from the TOP500 and Gordon Bell Prize. Science China Information Sciences, 2020, 63, 1.	2.7	9
50796	All-inorganic perovskite CsPbI2Br as a promising photovoltaic absorber: a first-principles study. Journal of Chemical Sciences, 2020, 132, 1.	0.7	8
50797	The correlation between chemical effect and segregation behavior in metallic Al liquid. Computational Materials Science, 2020, 175, 109611.	1.4	1
50798	A novel antiferromagnetic semiconductor hidden in pyrite. Computational Materials Science, 2020, 183, 109852.	1.4	7
50799	To the synthesis and characterization of layered metal phosphorus triselenides proposed for electrochemical sensing and energy applications. Chemical Physics Letters, 2020, 754, 137627.	1.2	12
50800	Revealing the effect of phosphorus doping on Co@carbon in boosting oxygen evolution catalytic activity. Journal of Alloys and Compounds, 2020, 843, 156001.	2.8	8
50801	First-principles investigation of Mg substitution for Ga on martensitic transformation, magnetism and electronic structures in Ni2MnGa. Journal of Alloys and Compounds, 2020, 843, 156049.	2.8	10
50802	Investigation of martensitic transformation behavior in Ni-Mn-In Heusler alloy from a first-principles study. Journal of Materials Science and Technology, 2020, 58, 100-106.	5.6	5
50803	Polaron transport mechanism in maricite NaFePO4: A combined experimental and simulation study. Journal of Power Sources, 2020, 469, 228348.	4.0	4
50804	External-strain induced transition from Schottky to ohmic contact in Graphene/InS and Graphene/Janus In2SSe heterostructures. Journal of Solid State Chemistry, 2020, 289, 121511.	1.4	24
50805	Stability of B1-type oxides in BCC iron studied using density functional theory calculations. Materials Today Communications, 2020, 25, 101266.	0.9	0
50806	Bilayer B 54 , B 60 , and B 62 Clusters in a Universal Structural Pattern. European Journal of Inorganic Chemistry, 2020, 2020, 3296-3301.	1.0	15
50807	Tuning adsorption strength of CO2 and its intermediates on tin oxide-based electrocatalyst for efficient CO2 reduction towards carbonaceous products. Applied Catalysis B: Environmental, 2020, 277, 119252.	10.8	50
50808	Heterobilayer CaS/CaSe: A promising sensor for environmental toxic NO2 gas with high selectivity and sensitivity. Applied Surface Science, 2020, 528, 146996.	3.1	30
50809	Bi2O2Se as a novel co-catalyst for photocatalytic hydrogen evolution reaction. Chemical Engineering Journal, 2020, 400, 125931.	6.6	45
50810	Interfacial microstructure and thermal resistance of UO2/Mo composites fabricated by spark plasma sintering. Ceramics International, 2020, 46, 23797-23801.	2.3	5
50811	Primary solidification of ternary compounds in Al-rich Alâ€“Ceâ€“Mn alloys. Journal of Alloys and Compounds, 2020, 844, 156048.	2.8	21

#	Article	IF	Citations
50812	Combined Neural Network Potential and Density Functional Theory Study of TiAl₂O₅ Surface Morphology and Oxygen Reduction Reaction Overpotentials. Journal of Physical Chemistry C, 2020, 124, 15171-15179.	1.5	9
50813	Unique 2Dâ€“3D Structure Transformations in Trichalcogenide CrSiTe₃ under High Pressure. Journal of Physical Chemistry C, 2020, 124, 15600-15606.	1.5	15
50814	Protonic solid-state electrochemical synapse for physical neural networks. Nature Communications, 2020, 11, 3134.	5.8	82
50815	Pressure-induced superconductivity and topological phase transitions in the topological nodal-line semimetal SrAs3. Npj Quantum Materials, 2020, 5, .	1.8	27
50816	Structural, mechanical and electronic properties and hardness of ionic vanadium dihydrides under pressure from first-principles computations. Scientific Reports, 2020, 10, 8868.	1.6	12
50817	First-principles study on the anisotropic transport of electrons and phonons in monolayer and bulk GaTe: a comparative study. Physical Chemistry Chemical Physics, 2020, 22, 15270-15280.	1.3	11
50818	1D topological phases in transition-metal monochalcogenide nanowires. Nanoscale, 2020, 12, 14661-14667.	2.8	15
50819	Unconventional Pyridyl Ligand Inclusion within a Flexible Metalâ€Organic Framework Bearing an N , N â€²â€Diethylformamide (DEF)â€Solvated Cd 5 Cluster Secondary Building Unit. ChemPlusChem, 2020, 85, 503-509.	1.3	6
50820	First principles studies of oxygen adsorption on the Î³-U (1â€¯1â€¯0) surface and influences of Mo doping. Computational Materials Science, 2020, 179, 109633.	1.4	16
50821	Theoretical and experimental investigations of mesoporous C3N5/MoS2 hybrid for lithium and sodium ion batteries. Nano Energy, 2020, 72, 104702.	8.2	65
50822	Enhancement of Second-Order Optical Nonlinearity in a Lutetium Selenite by Monodentate Anion Partial Substitution. Chemistry of Materials, 2020, 32, 3043-3053.	3.2	40
50823	Computational Screening of Transition Metalâ€“Phthalocyanines for the Electrochemical Reduction of Carbon Dioxide. Journal of Physical Chemistry C, 2020, 124, 7708-7715.	1.5	27
50824	Phase Diagram and Bonding States of Puâ€“H Binary Compounds at High Pressures. Journal of Physical Chemistry C, 2020, 124, 7361-7369.	1.5	8
50825	Enhancing CO₂ Electroreduction to Ethanol on Copperâ€“Silver Composites by Opening an Alternative Catalytic Pathway. ACS Catalysis, 2020, 10, 4059-4069.	5.5	145
50826	Existence and Properties of Isolated Catalytic Sites on the Surface of Î²-Cristobalite-Supported, Doped Tungsten Oxide Catalysts (WO_x/Î²-SiO₂,) Tj ETQq0 0 0 rgBT /Overlock 10 Tf 50 187 Td (Na-WO<sub> Oxidative Coupling of Methane (OCM): A Combined Periodic DFT and Experimental Study. ACS Catalysis, 2020, 10, 4580-4592.	5.5	33
50827	Electronic transport properties of a lithium-decorated ZrTe5 thin film. Scientific Reports, 2020, 10, 3537.	1.6	1
50828	Spin filtering with Mn-doped Ge-core/Si-shell nanowires. Nanoscale Advances, 2020, 2, 1843-1849.	2.2	4
50829	Incorporating rare-earth cations with moderate electropositivity into iodates for the optimized second-order nonlinear optical performance. Inorganic Chemistry Frontiers, 2020, 7, 2736-2746.	3.0	12

#	Article	IF	Citations
50830	Reversible photoluminescence switching in photochromic material Sr₆Ca₄(PO₄)₆F₂:Eu²⁺ and the modified performance by trap engineering via Ln³⁺ (Ln = La, Y, Gd, Lu) co-doping for erasable optical data storage. Journal of Materials Chemistry C, 2020, 8, 6403-6412.	2.7	19
50831	Effects of a Ni cocatalyst on the photocatalytic hydrogen evolution reaction of anatase TiO₂ by first-principles calculations. New Journal of Chemistry, 2020, 44, 5428-5437.	1.4	8
50832	Study of the GaAs/SiH van der Waals type-II heterostructure: a high efficiency photocatalyst promoted by a built-in electric field. Physical Chemistry Chemical Physics, 2020, 22, 8565-8571.	1.3	27
50833	Ion migration in Br-doped MAPbI3 and its inhibition mechanisms investigated via quantum dynamics simulations. Physical Chemistry Chemical Physics, 2020, 22, 7778-7786.	1.3	10
50834	Mechanism of selective and complete oxidation in La₂O₃-catalyzed oxidative coupling of methane. Catalysis Science and Technology, 2020, 10, 2602-2614.	2.1	28
50835	Vibrational properties of CO2 adsorbed on the Fe3O4 (111) surface: Insights gained from DFT. Journal of Chemical Physics, 2020, 152, 104702.	1.2	13
50836	Phase relations in the Fe-P system at high pressures and temperatures from ab initio computations. High Pressure Research, 2020, 40, 235-244.	0.4	9
50837	The coexistence of ferroelectricity and topological phase transition in monolayer Î±-In₂Se₃ under strain engineering. Journal of Physics Condensed Matter, 2020, 32, 105501.	0.7	24
50838	Modulating the electronic and optical properties for SrTiO₃/LaAlO₃ bilayers treated as the 2D materials by biaxial strains. Journal of Physics Condensed Matter, 2020, 32, 215701.	0.7	4
50839	Disorder-robust bands from anisotropic orbitals in a coordination polymer semiconductor. Journal of Physics Condensed Matter, 2020, 32, 275701.	0.7	5
50840	Computationally aided, entropy-driven synthesis of highly efficient and durable multi-elemental alloy catalysts. Science Advances, 2020, 6, eaaz0510.	4.7	158
50841	Evidence for Interfacial Octahedral Coupling as a Route to Enhance Magnetoresistance in Perovskite Oxide Superlattices. Advanced Materials Interfaces, 2020, 7, 1901576.	1.9	8
50842	Firstâ€Principles Investigation of Î²â€FeOOH for Hydrogen Evolution: Identifying Reactive Sites and Boosting Surface Reactions. Chemistry - A European Journal, 2020, 26, 7118-7123.	1.7	6
50843	Adsorption and migration growth of the Ce, O, and F adatoms on the CeO2(111) surface: A density functional theory study. Surface and Interface Analysis, 2020, 52, 493-498.	0.8	0
50844	Insight into Crystal Phase Dependent CO Dissociation on Rh Catalyst from DFT and Microkinetic Modeling. Journal of Physical Chemistry C, 2020, 124, 6756-6769.	1.5	7
50845	Theoretical Insights into Solid Electrolyte Interphase Formation in an Al Anode Dual-Ion Battery. Journal of Physical Chemistry C, 2020, 124, 7634-7643.	1.5	13
50846	Molecular Recognition at Mineral Interfaces: Implications for the Beneficiation of Rare Earth Ores. ACS Applied Materials & Interfaces, 2020, 12, 16327-16341.	4.0	20
50847	Metal-Free 2D/2D Black Phosphorus and Covalent Triazine Framework Heterostructure for CO₂ Photoreduction. ACS Sustainable Chemistry and Engineering, 2020, 8, 5175-5183.	3.2	74

#	Article	IF	Citations
50848	Two-dimensional Siâ€“Ge monolayers: Stabilities, structures, and electronic properties. Journal of Applied Physics, 2020, 127, .	1.1	6
50849	Ultra-low lattice thermal conductivity and giant phononâ€“electric field coupling in hafnium dichalcogenide monolayers. Journal of Physics Condensed Matter, 2020, 32, 315301.	0.7	22
50850	Temperature dependence of the Kohn anomaly in bcc Nb from first-principles self-consistent phonon calculations. Physical Review B, 2020, 101, .	1.1	11
50851	Discovery of an Unexpected Metal Dissolution of Thinâ€Coated Cathode Particles and Its Theoretical Explanation. Advanced Theory and Simulations, 2020, 3, 2000002.	1.3	8
50852	Selective Electroreduction of Carbon Dioxide over SnO₂â€Nanodot Catalysts. ChemSusChem, 2020, 13, 6353-6359.	3.6	16
50853	Stability, electronic, and optical properties of twoâ€dimensional phosphoborane. Journal of Computational Chemistry, 2020, 41, 1456-1463.	1.5	19
50854	Material Study of Co2CrAl Heusler Alloy Magnetic Thin Film and Co2CrAl/n-Si Schottky Junction Device. Journal of Electronic Materials, 2020, 49, 3652-3658.	1.0	5
50855	Computational Study of the Evolution of Ni-Based Catalysts during the Dry Reforming of Methane. Energy & Fuels, 2020, 34, 4855-4864.	2.5	22
50856	Strain-Engineered Metal-Free h-B₂O Monolayer as a Mechanocatalyst for Photocatalysis and Improved Hydrogen Evolution Reaction. Journal of Physical Chemistry C, 2020, 124, 7884-7892.	1.5	27
50857	Phonons and Anomalous Lattice Behavior in KMnAg₃(CN)₆ and KNiAu₃(CN)₆: Inelastic Neutron Scattering and First-Principles Calculations. Journal of Physical Chemistry C, 2020, 124, 7216-7228.	1.5	2
50858	Experimental Realization of Two-Dimensional Buckled Lieb Lattice. Nano Letters, 2020, 20, 2537-2543.	4.5	12
50859	Stabilization of the High-Energy-Density CuN₅ Salts under Ambient Conditions by a Ligand Effect. ACS Omega, 2020, 5, 6221-6227.	1.6	15
50860	Dynamic stability of active sites in hydr(oxy)oxides for the oxygen evolution reaction. Nature Energy, 2020, 5, 222-230.	19.8	540
50861	Decoupling electrolytes towards stable and high-energy rechargeable aqueous zincâ€“manganese dioxide batteries. Nature Energy, 2020, 5, 440-449.	19.8	430
50862	Effects of stacking periodicity on the electronic and optical properties of GaAs/AlAs superlattice: a first-principles study. Scientific Reports, 2020, 10, 4862.	1.6	6
50863	Structural and electronic properties of NaTaO₃cubic nanowires. Physical Chemistry Chemical Physics, 2020, 22, 7250-7258.	1.3	7
50864	High throughput screening of M₃C₂ MXenes for efficient CO₂ reduction conversion into hydrocarbon fuels. Nanoscale, 2020, 12, 7660-7673.	2.8	64
50865	Nickel iron phosphide ultrathin nanosheets anchored on nitrogen-doped carbon nanoflake arrays as a bifunctional catalyst for efficient overall water splitting. Nanoscale, 2020, 12, 8443-8452.	2.8	55

#	Article	IF	Citations
50866	One-dimensional transition metal dihalide nanowires as robust bipolar magnetic semiconductors. Nanoscale, 2020, 12, 8942-8948.	2.8	10
50867	Mechanism and activity of the oxygen reduction reaction on WTe₂ transition metal dichalcogenide with Te vacancy. RSC Advances, 2020, 10, 8460-8469.	1.7	11
50868	Boosting the activity of transition metal carbides towards methane activation by nanostructuring. Physical Chemistry Chemical Physics, 2020, 22, 7110-7118.	1.3	18
50869	A fast species redistribution approach to accelerate the kinetic Monte Carlo simulation for heterogeneous catalysis. Physical Chemistry Chemical Physics, 2020, 22, 7348-7364.	1.3	9
50870	Composition conserving defects and their influence on the electronic properties of thermoelectric TiNiSn. Physical Chemistry Chemical Physics, 2020, 22, 8035-8047.	1.3	7
50871	The influence of oxygen vacancy and Ce3+ ion positions on the properties of small gold clusters supported on CeO2â˜'x(111). Journal of Materials Chemistry A, 2020, 8, 15695-15705.	5.2	17
50872	Catalytic C2H2 synthesis via low temperature CO hydrogenation on defect-rich 2D-MoS2 and 2D-MoS2 decorated with Mo clusters. Journal of Chemical Physics, 2020, 152, 074706.	1.2	3
50873	Assessing model-dielectric-dependent hybrid functionals on the antiferromagnetic transition-metal monoxides MnO, FeO, CoO, and NiO. Journal of Physics Condensed Matter, 2020, 32, 015502.	0.7	30
50874	On the stability of Cu_xTe polytypes: phase transitions, vibrational and electronic properties. Journal of Physics Condensed Matter, 2020, 32, 045403.	0.7	11
50875	Chemically modified phosphorene as efficient catalyst for hydrogen evolution reaction. Journal of Physics Condensed Matter, 2020, 32, 025202.	0.7	13
50876	First-principles study on photovoltaic properties of 2D Cs₂PbI₄-black phosphorus heterojunctions. Journal of Physics Condensed Matter, 2020, 32, 195501.	0.7	10
50877	Theoretical study on the effect of the optical properties and electronic structure for the Bi-doped CsPbBr₃. Journal of Physics Condensed Matter, 2020, 32, 205504.	0.7	27
50878	Magnetic anisotropy and Curie temperature of two-dimensional VI₃ monolayer. Journal of Physics Condensed Matter, 2020, 32, 245803.	0.7	23
50879	Layer-dependent band engineering of Pd dichalcogenides: a first-principles study. New Journal of Physics, 2020, 22, 053010.	1.2	25
50880	Thermal conductivity measurements in nanosheets via bolometric effect. 2D Materials, 2020, 7, 035003.	2.0	9
50881	Intrinsic skyrmions in monolayer Janus magnets. Physical Review B, 2020, 101, .	1.1	94
50882	Ideal type-III nodal-ring phonons. Physical Review B, 2020, 101, .	1.1	53
50883	Graphene-based Symmetric and Non-Symmetric Magnetoresistive Junctions. Journal of the Physical Society of Japan, 2020, 89, 034708.	0.7	2

#	Article	IF	Citations
50884	Computational Study on the Charge Transport and Optical Spectra of Anthracene Derivatives in Aggregates. ChemPhysChem, 2020, 21, 952-957.	1.0	19
50885	Large Valley Splitting and Enhancement of Curie Temperature in a Two-Dimensional VI₃/CrI₃ Heterostructure. Journal of Physical Chemistry C, 2020, 124, 7156-7162.	1.5	18
50886	Single-Photon Emission from Point Defects in Aluminum Nitride Films. Journal of Physical Chemistry Letters, 2020, 11, 2689-2694.	2.1	35
50887	MoirÃ© Potential, Lattice Corrugation, and Band Gap Spatial Variation in a Twist-Free MoTe₂/MoS₂ Heterobilayer. Journal of Physical Chemistry Letters, 2020, 11, 2637-2646.	2.1	19
50888	Giant renormalization of dopant impurity levels in 2D semiconductor MoS2. Scientific Reports, 2020, 10, 4938.	1.6	8
50889	A possible unaccounted source of atmospheric sulfate formation: amine-promoted hydrolysis and non-radical oxidation of sulfur dioxide. Chemical Science, 2020, 11, 2093-2102.	3.7	11
50890	Hydrolytic dehydrogenation of NH₃BH₃ catalyzed by ruthenium nanoparticles supported on magnesiumâ€“aluminum layered double-hydroxides. RSC Advances, 2020, 10, 9996-10005.	1.7	16
50891	First-Principles Mechanistic Insights into the Hydrogen Evolution Reaction on Ni2P Electrocatalyst in Alkaline Medium. Catalysts, 2020, 10, 307.	1.6	8
50892	Oxygen redox activity with small voltage hysteresis in Na0.67Cu0.28Mn0.72O2 for sodium-ion batteries. Energy Storage Materials, 2020, 28, 300-306.	9.5	105
50893	One-dimensional hexagonal boron nitride conducting channel. Science Advances, 2020, 6, eaay4958.	4.7	37
50894	Synthesis and Electrochemical Properties of Bi2MoO6/Carbon Anode for Lithium-Ion Battery Application. Materials, 2020, 13, 1132.	1.3	16
50895	Scalable Synthesis of a MoS₂/Black Phosphorus Heterostructure for pHâ€Universal Hydrogen Evolution Catalysis. ChemCatChem, 2020, 12, 2840-2848.	1.8	42
50896	Enhancing hydrogen storage by metal substitution in MIL-88A metal-organic framework. Adsorption, 2020, 26, 509-519.	1.4	15
50897	High-loading and thermally stable Pt1/MgAl1.2Fe0.8O4 single-atom catalysts for high-temperature applications. Science China Materials, 2020, 63, 949-958.	3.5	31
50898	Elastic and thermodynamic properties of high entropy carbide (HfTaZrTi)C and (HfTaZrNb)C from ab initio investigation. Ceramics International, 2020, 46, 15104-15112.	2.3	58
50899	Structure and activity of mixed VOx-CeO2 domains supported on alumina in cyclohexane oxidative dehydrogenation. Journal of Catalysis, 2020, 384, 147-158.	3.1	17
50900	Cellulose derived nitrogen and phosphorus co-doped carbon-based catalysts for catalytic reduction of p-nitrophenol. Journal of Colloid and Interface Science, 2020, 571, 100-108.	5.0	46
50901	Strain-regulated electronic structure for hydrogen evolution reaction in Fe3S4 monolayer. Physics Letters, Section A: General, Atomic and Solid State Physics, 2020, 384, 126368.	0.9	3

#	Article	IF	Citations
50902	The effect of strain on the Li-storage performance of V2C and Nb2C: From first-principles study. Solid State Communications, 2020, 311, 113857.	0.9	7
50903	Impact of Active Site Density on Oxygen Reduction Reactions Using Monodispersed Feâ€“Nâ€“C Single-Atom Catalysts. ACS Applied Materials & Interfaces, 2020, 12, 15271-15278.	4.0	55
50904	Evolution of Ni/Li antisites under the phase transition of a layered LiNi_{1/3}Co_{1/3}Mn_{1/3}O₂ cathode. Journal of Materials Chemistry A, 2020, 8, 6337-6348.	5.2	36
50905	Plane-wave many-body corrections to the conductance in bulk tunnel junctions. Physical Review B, 2020, 101, .	1.1	1
50906	High-throughput and data-mining approach to predict new rare-earth free permanent magnets. Physical Review B, 2020, 101, .	1.1	34
50907	Symmetry-Protected Topological Triangular Weyl Complex. Physical Review Letters, 2020, 124, 105303.	2.9	78
50908	Optical insights of indium-doped Î²â€“Ga2O3 nanoparticles and its luminescence mechanism. Journal of Materials Science: Materials in Electronics, 2020, 31, 6185-6191.	1.1	3
50909	Enhanced photoluminescence quantum yield of MAPbBr3 nanocrystals by passivation using graphene. Nano Research, 2020, 13, 932-938.	5.8	11
50910	Structural, electronic and magnetic properties of the ordered binary FePt, MnPt, and CrPt3 alloys. Heliyon, 2020, 6, e03545.	1.4	14
50911	Spherical sodium metal deposition and growth mechanism study in three-electrode sodium-ion full-cell system. Journal of Power Sources, 2020, 455, 227919.	4.0	9
50912	Intermetallic Reactivity: Ca3Cu7.8Al26.2 and the Role of Electronegativity in the Stabilization of Modular Structures. Inorganic Chemistry, 2020, 59, 5018-5029.	1.9	10
50913	Mechanistic Insight into the Oxygen Reduction Reaction on the Mnâ€“N₄/C Single-Atom Catalyst: The Role of the Solvent Environment. Journal of Physical Chemistry C, 2020, 124, 7287-7294.	1.5	51
50914	Orderâ€“Disorder Transition in Kesterite Cu₂ZnSnS₄: Thermopower Enhancement via Electronic Band Structure Modification. Journal of Physical Chemistry C, 2020, 124, 7091-7096.	1.5	30
50915	Inducing Magnetic Phase Transitions in Monolayer CrI₃ via Lattice Deformations. Journal of Physical Chemistry C, 2020, 124, 7585-7590.	1.5	28
50916	[n]Phenacenes: Promising Organic Anodes for Potassium-Ion Batteries. Journal of Physical Chemistry C, 2020, 124, 6964-6970.	1.5	13
50917	Computational Study of Plutoniumâ€“Americium Mixed Oxides (Pu0.92Am0.08O2â€“x); Water Adsorption on {111}, {110}, and {100} Surfaces. Journal of Physical Chemistry C, 2020, 124, 6646-6658.	1.5	10
50918	Sizable Band Gap in Epitaxial Bilayer Graphene Induced by Silicene Intercalation. Nano Letters, 2020, 20, 2674-2680.	4.5	23
50919	Flexoelectricity and Charge Separation in Carbon Nanotubes. Nano Letters, 2020, 20, 3240-3246.	4.5	32

#	Article	IF	Citations
50920	Identifying the Origins of High Thermoelectric Performance in Group IIIA Element Doped PbS. ACS Applied Materials & Interfaces, 2020, 12, 14203-14212.	4.0	12
50921	Contrasting Arene, Alkene, Diene, and Formaldehyde Hydrogenation in H-ZSM-5, H-SSZ-13, and H-SAPO-34 Frameworks during MTO. ACS Catalysis, 2020, 10, 4593-4607.	5.5	38
50922	Accelerated Cu₂O Reduction by Single Pt Atoms at the Metal-Oxide Interface. ACS Catalysis, 2020, 10, 4215-4226.	5.5	34
50923	Prospects of Heterogeneous Hydroformylation with Supported Single Atom Catalysts. Journal of the American Chemical Society, 2020, 142, 5087-5096.	6.6	98
50924	Atomically thin half-van der Waals metals enabled by confinement heteroepitaxy. Nature Materials, 2020, 19, 637-643.	13.3	114
50925	Limits on gas impermeability of graphene. Nature, 2020, 579, 229-232.	13.7	220
50926	Li-ion transport at the interface between a graphite anode and Li₂CO₃ solid electrolyte interphase: ab initio molecular dynamics study. Physical Chemistry Chemical Physics, 2020, 22, 10764-10774.	1.3	14
50927	Electronic properties of bare and functionalized two-dimensional (2D) tellurene structures. Physical Chemistry Chemical Physics, 2020, 22, 6727-6737.	1.3	28
50928	n -hourglass Weyl fermions in nonsymmorphic materials. Physical Review B, 2020, 101, .	1.1	6
50929	Monolayer diboron dinitride: Direct band-gap semiconductor with high absorption in the visible range. Physical Review B, 2020, 101, .	1.1	20
50930	Surface Energy of Au Nanoparticles Depending on Their Size and Shape. Nanomaterials, 2020, 10, 484.	1.9	44
50931	Phosphorusâ€Functionalized Fe 2 VO 4 /Nitrogenâ€Doped Carbon Mesoporous Nanowires with Exceptional Lithium Storage Performance. ChemElectroChem, 2020, 7, 2395-2403.	1.7	9
50932	Relationship between the Auger parameter and the ground state valence charge at the coreâ€ionized site. Surface and Interface Analysis, 2020, 52, 864-868.	0.8	6
50933	Double drumheadlike surface states in elemental group V nodal line semimetals. Nano Research, 2020, 13, 927-931.	5.8	1
50934	First-Principles Study of the Structure and Properties of Fe3Pd and Feâ€“Pdâ€“Rh Alloys. Shape Memory and Superelasticity, 2020, 6, 61-66.	1.1	2
50935	Localized corrosion at nm-scale hardening precipitates in Al-Cu-Li alloys. Acta Materialia, 2020, 189, 204-213.	3.8	43
50936	Synergetic ternary metal oxide nanodots-graphene cathode for high performance zinc energy storage. Chinese Chemical Letters, 2020, 31, 2358-2364.	4.8	21
50937	Electrochemical performance of Bi2Te3 heterostructure thin film and Cu7Te4 nanocrystals on undoped and In3+-doped WO3 films for energy storage applications. Electrochimica Acta, 2020, 341, 136049.	2.6	13

#	Article	IF	Citations
50938	Cu(In,Ga)Se2 for selective and efficient photoelectrochemical conversion of CO2 into CO. Journal of Catalysis, 2020, 384, 88-95.	3.1	36
50939	Phase stability and temperature effect in ScX (X=S, Se and Te) compounds. Physics Letters, Section A: General, Atomic and Solid State Physics, 2020, 384, 126373.	0.9	1
50940	Evaluating Computational Shortcuts in Supercell-Based Phonon Calculations of Molecular Crystals: The Instructive Case of Naphthalene. Journal of Chemical Theory and Computation, 2020, 16, 2716-2735.	2.3	21
50941	Mechanical and Bonding Behaviors Behind the Bending Mechanism of Kaolinite Clay Layers. Journal of Physical Chemistry C, 2020, 124, 7432-7440.	1.5	21
50942	A Scalable Method for Thickness and Lateral Engineering of 2D Materials. ACS Nano, 2020, 14, 4861-4870.	7.3	14
50943	Low Energy Implantation into Transition-Metal Dichalcogenide Monolayers to Form Janus Structures. ACS Nano, 2020, 14, 3896-3906.	7.3	136
50944	Coherent electrical control of a single high-spin nucleus in silicon. Nature, 2020, 579, 205-209.	13.7	79
50945	First-Principles Predictions and Synthesis of B50C2 by Chemical Vapor Deposition. Scientific Reports, 2020, 10, 4454.	1.6	8
50946	Two-dimensional hydrogen hydrates: structure and stability. Physical Chemistry Chemical Physics, 2020, 22, 5774-5784.	1.3	8
50947	Intrinsic insight on localized surface plasmon resonance enhanced methanol electro-oxidation over a Au@AgPt hollow urchin-like nanostructure. Journal of Materials Chemistry A, 2020, 8, 6638-6646.	5.2	19
50948	First-principles simulation of monolayer hydrogen passivated Bi₂O₂S₂â€“metal interfaces. Physical Chemistry Chemical Physics, 2020, 22, 7853-7863.	1.3	9
50949	Scattering Mechanisms and Compositional Optimization of Highâ€Performance Elemental Te as a Thermoelectric Material. Advanced Electronic Materials, 2020, 6, 2000038.	2.6	13
50950	On the adsorption of elemental mercury on single-atom TM (TMÂ=ÂV, Cr, Mn, Co) decorated graphene substrates. Applied Surface Science, 2020, 516, 146037.	3.1	17
50951	Study on the enhanced electron-hole separation capability of IrxZn1-xO/Ti electrodes with high photoelectrocatalysis efficiency. Journal of Hazardous Materials, 2020, 393, 122488.	6.5	19
50952	Effect of group-3 elements doping on promotion of in-plane Seebeck coefficient of n-type Mg3Sb2. Journal of Materiomics, 2020, 6, 274-279.	2.8	13
50953	Energy density-enhancement mechanism and design principles for heteroatom-doped carbon supercapacitors. Nano Energy, 2020, 72, 104666.	8.2	65
50954	Decorating a WSe2 monolayer with Au nanoparticles: A study combined first-principles calculation with material genome approach. Surface and Coatings Technology, 2020, 388, 125563.	2.2	3
50955	GeSe: Optical Spectroscopy and Theoretical Study of a van der Waals Solar Absorber. Chemistry of Materials, 2020, 32, 3245-3253.	3.2	48

#	Article	IF	Citations
50956	Computing the Fukui Function in Solid-State Chemistry: Application to Alkaline Earth Oxides Bulk and Surfaces. Journal of Physical Chemistry A, 2020, 124, 2826-2833.	1.1	20
50957	Specific Response of the Atomic and Electronic Structure of Ta₂Pd₃Se₈ and Ta₂Pt₃Se₈ Nanoribbons to the Uniaxial Strain. Journal of Physical Chemistry C, 2020, 124, 7539-7543.	1.5	17
50958	Pseudo Jahnâ€“Teller Origin of Buckling Deformation of Two-dimensional Group-IV-Based Triphosphides as an Anode of Sodium-Ion Batteries. Journal of Physical Chemistry C, 2020, 124, 7699-7707.	1.5	0
50959	Electronic and Vibrational Contributions to the Bulk Stabilities of Trivalent 3d Transition Metal Oxyhydroxides from Electronic Structure Calculations. Journal of Physical Chemistry C, 2020, 124, 7500-7510.	1.5	0
50960	Investigation on Cu₂O Surface Reconstruction and Catalytic Performance of NH₃-SCO by Experimental and DFT Studies. ACS Applied Energy Materials, 2020, 3, 3465-3476.	2.5	25
50961	Twist Angle-Dependent Atomic Reconstruction and MoirÃ© Patterns in Transition Metal Dichalcogenide Heterostructures. ACS Nano, 2020, 14, 4550-4558.	7.3	172
50962	Î±-Ag₂S: A Ductile Thermoelectric Material with High ZT. ACS Omega, 2020, 5, 5796-5804.	1.6	64
50963	Transforming solid-state precipitates via excess vacancies. Nature Communications, 2020, 11, 1248.	5.8	65
50964	Nickel induced electronic structural regulation of cobalt hydroxide for enhanced water oxidation. Journal of Materials Chemistry A, 2020, 8, 6699-6708.	5.2	29
50965	In situ construction of a MOF-derived carbon-encapsulated LiCoO₂ heterostructure as a superior cathode for elevated-voltage lithium storage: from experimental to theoretical study. Journal of Materials Chemistry A, 2020, 8, 6607-6618.	5.2	46
50966	Multiorbital bond formation for stable oxygen-redox reaction in battery electrodes. Energy and Environmental Science, 2020, 13, 1492-1500.	15.6	60
50967	A unique pentagonal network structure of the NiS₂ monolayer with high stability and a tunable bandgap. Physical Chemistry Chemical Physics, 2020, 22, 7483-7488.	1.3	21
50968	Fast diffusion mechanism in Li₄P₂S₆ via a concerted process of interstitial Li ions. RSC Advances, 2020, 10, 10715-10722.	1.7	11
50969	New interaction potentials for borate glasses with mixed network formers. Journal of Chemical Physics, 2020, 152, 104501.	1.2	28
50970	Catalytic effect of water on the HO3â€‰+â€‰NO formations from the HNOâ€‰+â€‰O3reaction in tropospheric conditions. Molecular Simulation, 2020, 46, 497-505.	0.9	1
50971	Embedded carbon nanowire in black phosphorene and C-doping: the rule to control electronic properties. Nanotechnology, 2020, 31, 275201.	1.3	7
50972	Tunable large spin Hall and spin Nernst effects in the Dirac semimetals <mml:math xmlns:mml="http://www.w3.org/1998/Math/MathML"><mml:mrow><mml:mi>Zr</mml:mi><mml:mi>X</mml:mi><mml:mi>Y</mml:mi> Physical Review B, 2020, 101, .	1.1	28
50973	Temperature dependence of electron-phonon interactions in vanadium. Physical Review B, 2020, 101, .	1.1	12

#	Article	IF	Citations
50974	Tracking the ultrafast nonequilibrium energy flow between electronic and lattice degrees of freedom in crystalline nickel. Physical Review B, 2020, 101, .	1.1	41
50975	XFe4Ge2(X=Y,Lu) and Mn3Pt : Filling-enforced magnetic topological metals. Physical Review B, 2020, 101, .	1.1	5
50976	Room-temperature ferromagnetism in boron-doped oxides: a combined first-principle and experimental study. Philosophical Magazine Letters, 2020, 100, 141-153.	0.5	12
50977	High-efficiency photocatalyst for water splitting: a Janus MoSSe/XN (Xâ€‰â€‰=â€‰â€‰Ga, Al) van der Waals heterostructure. Journal Physics D: Applied Physics, 2020, 53, 185504.	1.3	110
50978	Phonons in magnetically disordered materials: Magnetic versus phononic time scales. Physical Review B, 2020, 101, .	1.1	8
50979	Exchange bias and quantum anomalous Hall effect in the MnBi ₂ Te ₄ /CrI ₃ heterostructure. Science Advances, 2020, 6, eaaz0948.	4.7	89
50980	Crystal facet dependence of carbon chain growth mechanism over the Hcp and Fcc Co catalysts in the Fischer-Tropsch synthesis. Applied Catalysis B: Environmental, 2020, 269, 118847.	10.8	29
50981	Quantifying exchange forces of a spin spiral on the atomic scale. Nature Communications, 2020, 11, 1197.	5.8	7
50982	Uniaxial negative thermal expansion and band renormalization in monolayer <mml:math xmlns:mml="http://www.w3.org/1998/Math/MathML"><mml:msub><mml:mi>T</mml:mi><mml:mi>d</mml:mi></mml:msub><mml:mo mathvariant="normal">MoTe</mml:mi><mml:mn>2</mml:mn></mml:msub></mml:math> at low temperature. Physical Review B, 2020, 101, .	1.1	12
50983	Surface science of shape-selective metal nanocrystal synthesis from first-principles: Growth of Cu nanowires and nanocubes. Journal of Vacuum Science and Technology A: Vacuum, Surfaces and Films, 2020, 38, .	0.9	13
50984	Stabilizing Perovskite Lightâ€Emitting Diodes by Incorporation of Binary Alkali Cations. Advanced Materials, 2020, 32, e1907786.	11.1	64
50985	Highly Efficient Oxygen Evolution by a Thermocatalytic Process Cascaded Electrocatalysis Over Sulfurâ€Treated Feâ€Based Metalâ€“Organicâ€Frameworks. Advanced Energy Materials, 2020, 10, 2000184.	10.2	75
50986	Theoretical Study of Using Kinetics Strategy to Enhance the Stability of Tin Perovskite. Energy and Environmental Materials, 2020, 3, 541-547.	7.3	13
50987	Ruthenium Nanoparticles on Cobaltâ€Doped 1Tâ€² Phase MoS₂ Nanosheets for Overall Water Splitting. Small, 2020, 16, e2000081.	5.2	82
50988	First-principles study of medium-scale X-atoms-doped nickel clusters Ninâ^'1X (Xâ€‰=â€‰C, Si, Ge, Sn, Pb;) Tj ETQq0 0 0 rgBT /Overlo	0.5	1
50989	Structural and physical properties of the new layered transition metal material Na4Cu3TaAs4. Science China Materials, 2020, 63, 816-822.	3.5	0
50990	DFT and thermodynamics calculations of surface cation release in LiCoO2. Applied Surface Science, 2020, 515, 145865.	3.1	34
50991	Contact properties of 2D/3D GaSe/Si(1Â1Â1) heterostructure. Applied Surface Science, 2020, 516, 145969.	3.1	3

#	Article	IF	Citations
50992	Sensing of volatile organic compounds on two-dimensional nitrogenated holey graphene, graphdiyne, and their heterostructure. Carbon, 2020, 163, 213-223.	5.4	77
50993	Comparative study on the activities of different MgO surfaces in CO2 activation and hydrogenation. Catalysis Today, 2020, 356, 535-543.	2.2	18
50994	An effective combination reaction involved with sputtered and selenized Sb precursors for efficient Sb2Se3 thin film solar cells. Chemical Engineering Journal, 2020, 393, 124599.	6.6	95
50995	Study of intermetallics for corrosion and creep resistant microstructure in Mg-RE and Mg-Al-RE alloys through a data-centric high-throughput DFT framework. Computational Materials Science, 2020, 175, 109541.	1.4	15
50996	C-doped TiO2 nanoparticles to detect alcohols with different carbon chains and their sensing mechanism analysis. Sensors and Actuators B: Chemical, 2020, 312, 127942.	4.0	45
50997	Bimetallic Ruâ€“Mo Phosphide Catalysts for the Hydrogenation of CO₂ to Methanol. Industrial & Engineering Chemistry Research, 2020, 59, 6931-6943.	1.8	24
50998	Experimental and DFT Studies of Hybrid Silver/Cdots Nanoparticles. Journal of Physical Chemistry B, 2020, 124, 2425-2435.	1.2	10
50999	Bulk and Monolayer ZrS₃ as Promising Anisotropic Thermoelectric Materials: A Comparative Study. Journal of Physical Chemistry C, 2020, 124, 6536-6543.	1.5	50
51000	Nanocrystal facet modulation to enhance transferrin binding and cellular delivery. Nature Communications, 2020, 11, 1262.	5.8	33
51001	Strong metal-support interaction promoted scalable production of thermally stable single-atom catalysts. Nature Communications, 2020, 11, 1263.	5.8	198
51002	Ruthenium anchored on carbon nanotube electrocatalyst for hydrogen production with enhanced Faradaic efficiency. Nature Communications, 2020, 11, 1278.	5.8	340
51003	Discovery of the soft electronic modes of the trimeron order in magnetite. Nature Physics, 2020, 16, 541-545.	6.5	26
51004	Electronic structure, ion diffusion and cation doping in the Na₄VO(PO₄)₂ compound as a cathode material for Na-ion batteries. Physical Chemistry Chemical Physics, 2020, 22, 6653-6659.	1.3	15
51005	Polymorphism of low dimensional boron nanomaterials driven by electrostatic gating: a computational discovery. Nanoscale, 2020, 12, 10543-10549.	2.8	5
51006	O2 activation by AuAg clusters on a defective (100)MgO surface. Journal of Chemical Physics, 2020, 152, 024303.	1.2	7
51007	The effects of interstitial iodine in hybrid perovskite hot carrier cooling: A non-adiabatic molecular dynamics study. Journal of Chemical Physics, 2020, 152, 091102.	1.2	15
51008	Trace bismuth and iodine co-doping enhanced thermoelectric performance of PbTe alloys. Journal Physics D: Applied Physics, 2020, 53, 245501.	1.3	29
51009	Reducing lead toxicity in the methylammonium lead halide <mml:math xmlns:mml="http://www.w3.org/1998/Math/MathML"><mml:msub><mml:mi mathvariant="normal">MAPbI</mml:mi><mml:mn>3</mml:mn></mml:msub></mml:math> : Why Sn substitution should be preferred to Pb vacancy for optimum solar cell efficiency. Physical Review B, 2020, 101, .	1.1	25

#	Article	IF	Citations
51010	Prediction of quasi-one-dimensional superconductivity in metastable two-dimensional boron. Physical Review B, 2020, 101, .	1.1	12
51011	Induced magnetic two-dimensionality by hole doping in the superconducting infinite-layer nickelate <mml:math xmlns:mml="http://www.w3.org/1998/Math/MathML"><mml:mrow><mml:msub><mml:mi>Nd</mml:mi><mml:mrow><mml:mn>1</mml:mn> Physical Review B, 2020, 101, .	1.1	87
51012	Ultrafast band-gap renormalization and build-up of optical gain in monolayer <mml:math xmlns:mml="http://www.w3.org/1998/Math/MathML"><mml:msub><mml:mi>MoTe</mml:mi><mml:mn>2</mml:mn></mml:msub></m Physical Review B, 2020, 101, .	1.1	22
51013	First-principles modeling of binary layered topological insulators: Structural optimization and exchange-correlation functionals. Physical Review B, 2020, 101, .	1.1	11
51014	Emerging chiral edge states from the confinement of a magnetic Weyl semimetal in <mml:math xmlns:mml="http://www.w3.org/1998/Math/MathML"><mml:mrow><mml:msub><mml:mi>Co</mml:mi><mml:mn>3</mml:mn></mml: mathvariant="normal">S</mml:mi><mml:mn>2</mml:mn></mml:msub></mml:mrow></mml:math>. Physical Review B, 2020, 101, .	1.1	48
51015	Small polarons and the Janus nature of <mml:math xmlns:mml="http://www.w3.org/1998/Math/MathML"><mml:msub><mml:mi>TiO</mml:mi><mml:mn>2</mml:mn></mml:msub></m (110). Physical Review B, 2020, 101, .	1.1	55
51016	Strain Effect on the Hydrogen Evolution Reaction of V_{Mo}-SLMoS₂. IEEE Nanotechnology Magazine, 2020, 19, 192-196.	1.1	3
51017	Two-dimensional ligand-functionalized plumbene: A promising candidate for ferroelectric and topological order with a large bulk band gap. Physica E: Low-Dimensional Systems and Nanostructures, 2020, 120, 114095.	1.3	6
51018	Synergistic trifunctional electrocatalysis of pyridinic nitrogen and single transition-metal atoms anchored on pyrazine-modified graphdiyne. Science Bulletin, 2020, 65, 995-1002.	4.3	34
51019	M-SPARC: Matlab-Simulation Package for Ab-initio Real-space Calculations. SoftwareX, 2020, 11, 100423.	1.2	13
51020	Chemical Properties of Lithium Cluster (Li_x, x = 2â€“8) on Stoneâ€“Wales Defect Graphene Sheet: A DFT Study. Journal of Physical Chemistry C, 2020, 124, 7229-7237.	1.5	8
51021	Monolithic Interface Contact Engineering to Boost Optoelectronic Performances of 2D Semiconductor Photovoltaic Heterojunctions. Nano Letters, 2020, 20, 2443-2451.	4.5	31
51022	Few-Layer Borophene Prepared by Mechanical Resonance and Its Application in Terahertz Shielding. ACS Applied Materials & Interfaces, 2020, 12, 19746-19754.	4.0	22
51023	Coking-Resistant Sub-Nano Dehydrogenation Catalysts: Pt_nSn_x/SiO₂ (n = 4, 7). ACS Catalysis, 2020, 10, 4543-4558.	5.5	40
51024	Rapid Upcycling of Waste Polyethylene Terephthalate to Energy Storing Disodium Terephthalate Flowers with DFT Calculations. ACS Sustainable Chemistry and Engineering, 2020, 8, 6252-6262.	3.2	43
51025	Electronic structure, thermodynamic stability and high-temperature sensing properties of Er-Î±-SiAlON ceramics. Scientific Reports, 2020, 10, 4952.	1.6	17
51026	Defective crystal plane-oriented induced lattice polarization for the photocatalytic enhancement of ZnO. CrystEngComm, 2020, 22, 2709-2717.	1.3	16
51027	The energetics of carbonated PuO₂ surfaces affects nanoparticle morphology: a DFT+U study. Physical Chemistry Chemical Physics, 2020, 22, 7728-7737.	1.3	8

#	Article	IF	Citations
51028	Crystal structure and luminescence properties of lead-free metal halides (C₆H₅CH₂NH₃)₃MBr₆ (M = Bi) Tj ET Q q 0 0 0 rg BT /Overl	2.0	69
51029	First-principles investigations of orthorhombic-cubic phase transition and its effect on thermoelectric properties in cobalt-based ternary alloys. Journal of Physics Condensed Matter, 2020, 32, 055505.	0.7	7
51030	2D honeycomb borophene oxide: a promising anode material offering super high capacity for Li/Na-ion batteries. Journal of Physics Condensed Matter, 2020, 32, 065001.	0.7	16
51031	Theoretical analysis of pressure induced spin crossover phenomenon in a di-nuclear Fe(II) molecular complex. Journal of Physics Condensed Matter, 2020, 32, 165802.	0.7	4
51032	First-principles exploration of defect-pairs in GaN. Journal of Semiconductors, 2020, 41, 032104.	2.0	14
51033	Magnetic-field-induced nontrivial electronic state in the Kondo-lattice semimetal CeSb. Physical Review B, 2020, 101, .	1.1	18
51034	Robustness of topological insulating phase against vacancy, vacancy cluster, and grain boundary bulk defects. Physical Review B, 2020, 101, .	1.1	23
51035	Local structure investigations of accumulated damage in irradiated MgAl₂O₄. Journal of the American Ceramic Society, 2020, 103, 4654-4663.	1.9	6
51036	Photocatalysis with octahedral sulfides. , 2020, , 385-402.		0
51037	Dry reforming of methane over the cobalt catalyst: Theoretical insights into the reaction kinetics and mechanism for catalyst deactivation. Applied Catalysis B: Environmental, 2020, 270, 118859.	10.8	98
51038	Polaron modulation mechanism of H2O and CO2 adsorption on PuO2(111) surface. Applied Surface Science, 2020, 516, 146164.	3.1	10
51039	Insight into electronic structure and optical properties of Nb and F co-doped SnO2 with hybrid functional theoretical method. Ceramics International, 2020, 46, 10341-10347.	2.3	11
51040	First-principles study of hydrogen behavior in Î±-Pu2O3. Computational Materials Science, 2020, 179, 109688.	1.4	7
51041	Revealing the role of tellurium in palladium-tellurium catalysts for the direct synthesis of hydrogen peroxide. Journal of Catalysis, 2020, 385, 21-29.	3.1	31
51042	Modeling of explosives: 1,4,2,3,5,6-dioxatetrazinane as a new green energetic material with enhanced performance. Journal of Physics and Chemistry of Solids, 2020, 142, 109458.	1.9	15
51043	A new proximate structure for the APB (111) in L12 compounds. Scripta Materialia, 2020, 182, 38-42.	2.6	14
51044	First-Principles Study on Self-Activated Luminescence and 4f â†' 5d Transitions of Ce³⁺ in M₅(PO₄)₃X (M = Sr, Ba; X = Cl, Br). Inorganic Chemistry, 2020, 59, 5170-5181.	1.9	17
51045	Inter-Kramers Transitions and Spinâ€"Phonon Couplings in a Lanthanide-Based Single-Molecule Magnet. Inorganic Chemistry, 2020, 59, 5218-5230.	1.9	25

#	Article	IF	Citations
51046	Graphene-Supported Single Nickel Atom Catalyst for Highly Selective and Efficient Hydrogen Peroxide Production. ACS Applied Materials & Interfaces, 2020, 12, 17519-17527.	4.0	99
51047	Doping of MoTe2 via Surface Charge Transfer in Air. ACS Applied Materials & Interfaces, 2020, 12, 18182-18193.	4.0	15
51048	Hierarchical Co₃O₄@N-Doped Carbon Composite as an Advanced Anode Material for Ultrastable Potassium Storage. ACS Nano, 2020, 14, 5027-5035.	7.3	121
51049	Low-temperature paddlewheel effect in glassy solid electrolytes. Nature Communications, 2020, 11, 1483.	5.8	102
51050	The surface hydroxyl and oxygen vacancy dependent Cr(<scp>vi</scp>) adsorption performance of BiOCl. Environmental Science: Nano, 2020, 7, 1454-1463.	2.2	30
51051	Effects of magnetic and structural phase transitions on the normal and anomalous Hall effects in Ni-Mn-In-B Heusler alloys. Physical Review B, 2020, 101, .	1.1	24
51052	Intrinsic orbital moment and prediction of a large orbital Hall effect in two-dimensional transition metal dichalcogenides. Physical Review B, 2020, 101, .	1.1	44
51053	Unexpected softness of bilayer graphene and softening of A-A stacked graphene layers. Physical Review B, 2020, 101, .	1.1	7
51054	First-principles study on composition-dependent properties of quaternary InP1â^'xâ^'yNxBiy alloys. Modern Physics Letters B, 2020, 34, 2050111.	1.0	1
51055	Heavily Hydride-ion-doped 1111-type Iron-based Superconductors: Synthesis, Physical Properties and Electronic Structure. Journal of the Physical Society of Japan, 2020, 89, 051006.	0.7	13
51056	InP/TiO2 heterojunction for photoelectrochemical water splitting under visible-light. International Journal of Hydrogen Energy, 2020, 45, 11615-11624.	3.8	18
51057	Double-centers of V,Ceâ€“Codoped LiNbO₃ from Hybrid Density Functional Theory Calculations: Electron Trapping and Excitation between the Defect Levels. Crystal Growth and Design, 2020, 20, 2774-2780.	1.4	2
51058	Methanol Synthesis from CO₂Hydrogenation over a Potassium-Promoted Cu_xO/Cu(111) (xâ‰ˆ 2) Model Surface: Rationalizing the Potential of Potassium in Catalysis. ACS Catalysis, 2020, 10, 5723-5733.	5.5	36
51059	Metallic FeSe monolayer as an anode material for Li and non-Li ion batteries: a DFT study. Physical Chemistry Chemical Physics, 2020, 22, 8902-8912.	1.3	79
51060	Observation of short-range Yu-Shiba-Rusinov states with threefold symmetry in layered superconductor 2H-NbSe2. Nanoscale, 2020, 12, 8174-8179.	2.8	11
51061	Electron-beam irradiation alters bond strength in zinc oxide single crystal. Applied Physics Letters, 2020, 116, .	1.5	10
51062	Quantum paraelectricity of <mml:math xmlns:mml="http://www.w3.org/1998/Math/MathML"><mml:mrow><mml:msub><mml:mi>BaFe</mml:mi><mml:mn>12</mml:mn></m mathvariant="normal">O</mml:mi><mml:mn>19</mml:mn></mml:msub></mml:mrow></mml:math>. Physical Review B, 2020, 101, .	1.1	8
51063	A Microporous MOF with Inorganic Nitrate Ions Immobilized on a Porous Surface Displaying Efficient C₂H₂ Separation and Purification. European Journal of Inorganic Chemistry, 2020, 2020, 1683-1689.	1.0	17

#	Article	IF	Citations
51064	Design of defected TaN supercells dataset for structural and elastic properties from ab initio simulations and comparison to experimental data. Data in Brief, 2020, 30, 105411.	0.5	1
51065	High-Throughput Approach Exploitation: Two-Dimensional Double-Metal Sulfide (M₂S₂) of Efficient Electrocatalysts for Oxygen Reduction Reaction in Fuel Cells. Energy & Fuels, 2020, 34, 5006-5015.	2.5	27
51066	Ferromagnetic quasi-atomic electrons in two-dimensional electride. Nature Communications, 2020, 11, 1526.	5.8	57
51067	Regulating strain in perovskite thin films through charge-transport layers. Nature Communications, 2020, 11, 1514.	5.8	346
51068	Infrared spectroscopy data- and physics-driven machine learning for characterizing surface microstructure of complex materials. Nature Communications, 2020, 11, 1513.	5.8	77
51069	High-performance phosphorene electromechanical actuators. Npj Computational Materials, 2020, 6, .	3.5	13
51070	Câ€“O bond activation using ultralow loading of noble metal catalysts on moderately reducible oxides. Nature Catalysis, 2020, 3, 446-453.	16.1	131
51071	Comment on â€œLocal, solvation pressures and conformational changes in ethylenediamine aqueous solutions probed using Raman spectroscopyâ€•by M. CÃ¡ceres, A. Lobato, N. J. Mendoza, L. J. Bonales and V. G. Baonza, Phys. Chem. Chem. Phys., 2016, 18, 26192. Physical Chemistry Chemical Physics, 2020, 22, 7119-7125.	1.3	1
51072	Structure of two-dimensional Fe3O4. Journal of Chemical Physics, 2020, 152, 114705.	1.2	10
51073	First-principles calculations of structural and electronic properties of layered AxRhO2 (A = Li, Na, K,) Tj ETQq1 1 0.784314 rgBT /Overlo	0.6	4
51074	Structural, elastic, magnetic and electronic properties of Ti-based Heusler alloys. International Journal of Modern Physics B, 2020, 34, 2050055.	1.0	12
51075	Enhancing Capacitance Performance of Ti3C2Tx MXene as Electrode Materials of Supercapacitor: From Controlled Preparation to Composite Structure Construction. Nano-Micro Letters, 2020, 12, 77.	14.4	136
51076	Electronic Anisotropy and Superconductivity in One-Dimensional Electride Ca₃Si. Journal of Physical Chemistry C, 2020, 124, 7683-7690.	1.5	18
51077	Effect of Structural Phases on Mechanical Properties of Molybdenum Disulfide. ACS Omega, 2020, 5, 5994-6002.	1.6	44
51078	Polycyclic aromatic chains on metals and insulating layers by repetitive [3+2]Âcycloadditions. Nature Communications, 2020, 11, 1490.	5.8	23
51079	Ultrasensitive detection of nucleic acids using deformed graphene channel field effect biosensors. Nature Communications, 2020, 11, 1543.	5.8	251
51080	Trends in Câ€“O and Nâ€“O bond scission on rutile oxides described using oxygen vacancy formation energies. Chemical Science, 2020, 11, 4119-4124.	3.7	16
51081	The role of oxygen vacancies on the vibrational motions of hydride ions in the oxyhydride of barium titanate. Journal of Materials Chemistry A, 2020, 8, 6360-6371.	5.2	9

#	Article	IF	Citations
51082	Boron-terminated diamond (100) surfaces with promising structural and electronic properties. Physical Chemistry Chemical Physics, 2020, 22, 8060-8066.	1.3	20
51083	Elasticity, piezoelectricity, and mobility in two-dimensional BiTeI from a first-principles study. Journal Physics D: Applied Physics, 2020, 53, 245301.	1.3	13
51084	Two dimensional ferromagnetic semiconductor: monolayer CrGeS₃. Journal of Physics Condensed Matter, 2020, 32, 015701.	0.7	20
51085	Tuning electronic structure and magnetic properties of Mn- and Fe-doped arsenene with biaxial strain. Journal of Physics Condensed Matter, 2020, 32, 085802.	0.7	3
51086	Corrosion resistance of itaconic acid doped polyaniline /nanographene oxide composite coating. Nanotechnology, 2020, 31, 285704.	1.3	7
51087	Phonon stability and phonon transport of graphene-like borophene. Nanotechnology, 2020, 31, 315709.	1.3	33
51088	Strain-induced phase transition in CrI₃ bilayers. 2D Materials, 2020, 7, 035008.	2.0	45
51089	Nonadiabatic effects and excitonlike states during the insulator-to-metal transition in warm dense hydrogen. Physical Review B, 2020, 101, .	1.1	7
51090	Carbon Nanotubes as Means to Optimizing the Operation of Liquid Crystal Cells. , 2020, , .		0
51091	Evaluation of alternatives to paraffin for antirelaxation coatings. Journal of Vacuum Science and Technology A: Vacuum, Surfaces and Films, 2020, 38, .	0.9	2
51092	Measurement and ab initio Investigation of Structural, Electronic, Optical, and Mechanical Properties of Sputtered Aluminum Nitride Thin Films. Frontiers in Physics, 2020, 8, .	1.0	28
51093	Heteroleptic Pt(II)-dithiolene-based Colorimetric Chemosensors: Selectivity Control for Hg(II) Ion Sensing. Materials, 2020, 13, 1385.	1.3	6
51094	Unravelling the water oxidation mechanism on NaTaO₃-based photocatalysts. Journal of Materials Chemistry A, 2020, 8, 6812-6821.	5.2	23
51095	A DFT screening of single transition atoms supported on MoS₂ as highly efficient electrocatalysts for the nitrogen reduction reaction. Nanoscale, 2020, 12, 10035-10043.	2.8	94
51096	Honeycombâ€like carbon materials derived from coffee extract via a â€œsaltyâ€•thermal treatment for highâ€performance Liâ€₂ batteries. , 2020, 2, 265-275.		24
51097	Effect of Sr substitution on the property and stability of CH₃NH₃SnI₃perovskite: A firstâ€principles investigation. International Journal of Energy Research, 2020, 44, 5765-5778.	2.2	19
51098	Theoretical study of active Ca element on grain refining of carbon-inoculated Mg-Al alloy. Materials and Design, 2020, 192, 108664.	3.3	5
51099	Adsorption of Water Molecule on Calcium Fluoride and Magnesium Fluoride Surfaces: A Combined Theoretical and Experimental Study. Journal of Physical Chemistry C, 2020, 124, 7853-7859.	1.5	8

#	Article	IF	Citations
51100	Antithermal Quenching of Luminescence in Zero-Dimensional Hybrid Metal Halide Solids. Journal of Physical Chemistry Letters, 2020, 11, 2902-2909.	2.1	49
51101	Covalently Connected Nb₄N_{5â€“x}O_xâ€“MoS₂ Heterocatalysts with Desired Electron Density to Boost Hydrogen Evolution. ACS Nano, 2020, 14, 4925-4937.	7.3	50
51102	Density-Functional Tight-Binding Study of Carbonaceous Species Diffusion on the (100)-i³-Al₂O₃ Surface. ACS Omega, 2020, 5, 6862-6871.	1.6	8
51103	Site-Occupation-Tuned Superionic Li_xScCl_{3+x}Halide Solid Electrolytes for All-Solid-State Batteries. Journal of the American Chemical Society, 2020, 142, 7012-7022.	6.6	260
51104	Inorganic photovoltaic cells based on BiFeO₃: spontaneous polarization, lattice matching, light polarization and their relationship with photovoltaic performance. Physical Chemistry Chemical Physics, 2020, 22, 8658-8666.	1.3	6
51105	Nitrogen fixation on metal-free SiC(111) polar surfaces. Journal of Materials Chemistry A, 2020, 8, 7412-7421.	5.2	26
51106	On stability and kinetics of Li-rich transition metal oxides and oxyfluorides. Journal of Materials Chemistry A, 2020, 8, 7956-7967.	5.2	13
51107	Tuning the electronic properties of bilayer black phosphorene with the twist angle. Journal of Materials Chemistry C, 2020, 8, 6264-6272.	2.7	28
51108	Electronic structure, magnetic anisotropy and Dzyaloshinskiiâ€“Moriya interaction in Janus Cr₂I₃X₃ (X = Br, Cl) bilayers. Physical Chemistry Chemical Physics, 2020, 22, 8647-8657.	1.3	24
51109	Ferrimagnetic semiconductor with a direct bandgap. Applied Physics Letters, 2020, 116, .	1.5	7
51110	Alloying effects on the plasticity of magnesium: comprehensive analysis of influences of all five slip systems. Journal of Physics Condensed Matter, 2020, 32, 015401.	0.7	7
51111	Structures, stabilities and piezoelectric properties of Janus gallium oxides and chalcogenides monolayers. Journal of Physics Condensed Matter, 2020, 32, 08LT01.	0.7	16
51112	2D CrCl₂(pyrazine)₂ monolayer: high-temperature ferromagnetism and half-metallicity. Journal of Physics Condensed Matter, 2020, 32, 135801.	0.7	6
51113	Auxetic Tetrahex Carbon with Ultrahigh Strength and a Direct Band Gap. Physical Review Applied, 2020, 13, .	1.5	23
51114	Strain-induced enhancement of the Seebeck effect in magnetic tunneling junctions via interface resonant tunneling: Ab initio study. Physical Review B, 2020, 101, .	1.1	4
51115	Dynamical properties of organo lead-halide perovskites and their interfaces to titania: insights from Density Functional Theory. Heliyon, 2020, 6, e03427.	1.4	4
51116	Carbon Nitride-Based Single-Atom Cu Catalysts for Highly Efficient Carboxylation of Alkynes with Atmospheric CO₂. Industrial & Engineering Chemistry Research, 2020, 59, 7327-7335.	1.8	53
51117	Entropy-Driven Incommensurability: Chemical Pressure-Guided Polymorphism in PdBi and the Origins of Lock-In Phenomena in Modulated Systems. Inorganic Chemistry, 2020, 59, 4936-4949.	1.9	8

#	Article	IF	Citations
51118	Hydrothermal Synthesis and Crystal Structure of a Mixed-Valence Bismuthate, Na₃Bi₃O₈. Inorganic Chemistry, 2020, 59, 4950-4960.	1.9	13
51119	A Density Functional Theory Study of the Two-Dimensional Bis(iminothiolato)metal Monolayers as Efficient Electrocatalysts for Oxygen Reduction Reaction. Journal of Physical Chemistry C, 2020, 124, 7803-7811.	1.5	10
51120	Optimization of Ptâ€“Oxygen-Containing Species Anodes for Ethanol Oxidation Reaction: High Performance of Pt-AuSnO_x Electrocatalyst. Journal of Physical Chemistry Letters, 2020, 11, 2846-2853.	2.1	11
51121	Pressure-Stabilized Zinc Trifluoride. Journal of Physical Chemistry Letters, 2020, 11, 2854-2858.	2.1	7
51122	Atomically Dispersed Cuâ€“Nâ€“C as a Promising Support for Low-Pt Loading Cathode Catalysts of Fuel Cells. ACS Applied Energy Materials, 2020, 3, 3807-3814.	2.5	22
51123	Selective Growth of Stacking Fault Free âŸ¨100âŸ© Nanowires on a Polycrystalline Substrate for Energy Conversion Application. ACS Applied Materials & Interfaces, 2020, 12, 17676-17685.	4.0	8
51124	Nanoengineering Microstructure of Hybrid Câ€“Sâ€“H/Silicene Gel. ACS Applied Materials & Interfaces, 2020, 12, 17806-17814.	4.0	11
51125	Noble-Metal-Free Niâ€“Wâ€“O-Derived Catalysts for High-Capacity Hydrogen Production from Hydrazine Monohydrate. ACS Sustainable Chemistry and Engineering, 2020, 8, 5595-5603.	3.2	20
51126	Unraveling Reaction Mechanisms of Mo₂C as Cathode Catalyst in a Li-CO₂ Battery. Journal of the American Chemical Society, 2020, 142, 6983-6990.	6.6	133
51127	A yolkâ€“shell structured metalâ€“organic framework with encapsulated iron-porphyrin and its derived bimetallic nitrogen-doped porous carbon for an efficient oxygen reduction reaction. Journal of Materials Chemistry A, 2020, 8, 9536-9544.	5.2	95
51128	Multiferroic hydrogenated graphene bilayer. Physical Chemistry Chemical Physics, 2020, 22, 7962-7968.	1.3	0
51129	MoB₂: a new multifunctional transition metal diboride monolayer. Journal of Physics Condensed Matter, 2020, 32, 055503.	0.7	21
51130	Effects of cage occupancy in hydrate by first-principles calculation and modification of the van der Waalsâ€“Platteeuw hypothesis. Journal of Physics Condensed Matter, 2020, 32, 095402.	0.7	1
51131	Phonon scattering limited mobility in the representative cubic perovskite semiconductors <mml:math xmlns:mml="http://www.w3.org/1998/Math/MathML"><mml:msub><mml:mi>SrGeO</mml:mi><mml:mn>3</mml:mn></mml:msub>, <mml:math xmlns:mml="http://www.w3.org/1998/Math/MathML"><mml:msub><mml:mi>BaSnO</mml:mi><mml:mn>3</mml:mn></mml:msub>, and <mml:math xmlns:mml="http://www.w3.org/1998/Math/MathML"><mml:msub><mml:mi>SrTiO</mml:mi><mml:mn>3</mml:mn></mml:msub>	1.1	11
51132	Electronic and Magnetic Properties of BaFeO3on the Pt(111) Surface in a Quasicrystalline Approximant Structure. Physica Status Solidi (B): Basic Research, 2020, 257, 1900649.	0.7	4
51133	Cation-Size Mismatch as a Design Principle for Enhancing the Efficiency of Garnet Phosphors. Chemistry of Materials, 2020, 32, 3097-3108.	3.2	40
51134	Thermochemistry of FeO_mH_n^z Species: Assessment of Some DFT Functionals. Journal of Chemical Theory and Computation, 2020, 16, 2430-2435.	2.3	7
51135	Room-Temperature Propylene Dehydrogenation and Linear Atomic Chain Formation on Ni(111). Journal of Physical Chemistry C, 2020, 124, 8218-8224.	1.5	4

#	Article	IF	Citations
51136	Room Temperature Bound Excitons and Strain-Tunable Carrier Mobilities in Janus Monolayer Transition-Metal Dichalcogenides. Journal of Physical Chemistry Letters, 2020, 11, 3116-3128.	2.1	38
51137	Ultraheavy and Ultrarelativistic Dirac Quasiparticles in Sandwiched Graphenes. Nano Letters, 2020, 20, 3030-3038.	4.5	80
51138	Synthesis of a Smart Hybrid MXene with Switchable Conductivity for Temperature Sensing. ACS Applied Nano Materials, 2020, 3, 4069-4076.	2.4	26
51139	Splitting Mono- and Dibranched Alkane Isomers by a Robust Aluminum-Based Metalâ€“Organic Framework Material with Optimal Pore Dimensions. Journal of the American Chemical Society, 2020, 142, 6925-6929.	6.6	60
51140	Electric field modulation in the auxetic effect of BP-analog monolayer As and Sb by first-principles calculations. Physical Chemistry Chemical Physics, 2020, 22, 8739-8744.	1.3	5
51141	Highly active hydrogen evolution catalysis on oxygen-deficient double-perovskite oxide PrBaCo₂O_{6â˜Î´}. Materials Chemistry Frontiers, 2020, 4, 1519-1529.	3.2	18
51142	Intersecting nodal rings in orthorhombic-type BaLi₂Sn compound. Journal of Materials Chemistry C, 2020, 8, 5461-5466.	2.7	16
51143	Monolayer Ti₂C MXene: manipulating magnetic properties and electronic structures by an electric field. Physical Chemistry Chemical Physics, 2020, 22, 11266-11272.	1.3	38
51144	Monolayer of PtSe2 on Pt(1â€‰1â€‰1): is it metallic or insulating?. Journal of Physics Condensed Matter, 2020, 32, 235002.	0.7	2
51145	Interaction between Mo and intrinsic or extrinsic defects of Mo doped LiNbO3 from first-principles calculations. Journal of Physics Condensed Matter, 2020, 32, 255701.	0.7	3
51146	Cooper minimum of high-order harmonic spectra from an MgO crystal in an ultrashort laser pulse. Physical Review A, 2020, 101, .	1.0	53
51147	Anomalous dispersion of longitudinal optical phonons in oxygen-doped <mml:math xmlns:mml="http://www.w3.org/1998/Math/MathML"><mml:msub><mml:mrow><mml:mi>La</mml:mi></mml:mrow><mml:mrow><mml:mn>1</mml:mn></mml:mrow></mml:msub></mml:math> Physical Review B, 2020, 101, .	1.1	4
51148	Stacking-dependent topological phase in bilayer <mml:math xmlns:mml="http://www.w3.org/1998/Math/MathML"><mml:mrow><mml:mi>M</mml:mi><mml:mi mathvariant="normal">B</mml:mi><mml:msub><mml:mi mathvariant="normal">i</mml:mi><mml:mn>2</mml:mn></mml:msub><mml:mi mathvariant="normal">T</mml:mi><mml:msub><mml:mi		

#	Article	IF	Citations
51154	Gaussian Basis Sets for Crystalline Solids: All-Purpose Basis Set Libraries vs System-Specific Optimizations. Journal of Chemical Theory and Computation, 2020, 16, 2192-2201.	2.3	18
51155	Inartificial Two-Dimensional Ge₄Se₉ Janus Structures with Appropriate Direct Band Gaps and Intrinsic Polarization Boosted Charge Separation for Photocatalytic Water Splitting. Journal of Physical Chemistry Letters, 2020, 11, 3095-3102.	2.1	26
51156	Tweaking the Physics of Interfaces between Monolayers of Buckled Cadmium Sulfide for a Superhigh Piezoelectricity, Excitonic Solar Cell Efficiency, and Thermoelectricity. ACS Applied Materials & Interfaces, 2020, 12, 18123-18137.	4.0	44
51157	Ternary NiFeTiOOH Catalyst for the Oxygen Evolution Reaction: Study of the Effect of the Addition of Ti at Different Loadings. ACS Catalysis, 2020, 10, 4879-4887.	5.5	21
51158	Multielectron, Cation and Anion Redox in Lithium-Rich Iron Sulfide Cathodes. Journal of the American Chemical Society, 2020, 142, 6737-6749.	6.6	46
51159	Single-atom Rh/N-doped carbon electrocatalyst for formic acid oxidation. Nature Nanotechnology, 2020, 15, 390-397.	15.6	420
51160	Magnetic properties of Fe_{16â^'x}(Ta/W)_xN₂ ternary alloy: first principles and atomistic simulations. Journal of Physics Condensed Matter, 2020, 32, 025801.	0.7	2
51161	Spin-Canting-Induced Band Reconstruction in the Dirac Material Ca1â^'xNaxMnBi2. Physical Review Letters, 2020, 124, 137201.	2.9	11
51162	Theoretical screening of single atoms anchored on defective graphene for electrocatalytic N₂ reduction reactions: a DFT study. Physical Chemistry Chemical Physics, 2020, 22, 9322-9329.	1.3	29
51163	The fox and the hound: in-depth and in-grain Na doping and Ga grading in Cu(In,Ga)Se₂ solar cells. Journal of Materials Chemistry A, 2020, 8, 6471-6479.	5.2	27
51164	Octopus, a computational framework for exploring light-driven phenomena and quantum dynamics in extended and finite systems. Journal of Chemical Physics, 2020, 152, 124119.	1.2	210
51165	Magnetotransport properties of noncentrosymmetric CaAgBi single crystal. Journal of Physics Condensed Matter, 2020, 32, 335701.	0.7	11
51166	In Situ Assessment of Intrinsic Strength of X-Iâ‹¯OA-Type Halogen Bonds in Molecular Crystals with Periodic Local Vibrational Mode Theory. Molecules, 2020, 25, 1589.	1.7	26
51167	Remarkable Rashba spin splitting induced by an asymmetrical internal electric field in polar IIIâ€“VI chalcogenides. Physical Chemistry Chemical Physics, 2020, 22, 9148-9156.	1.3	22
51168	Mixed anion/cation redox in K_{0.78}Fe_{1.60}S₂ for a high-performance cathode in potassium ion batteries. Inorganic Chemistry Frontiers, 2020, 7, 2023-2030.	3.0	8
51169	Substitutional transition metal doping in MoS₂: a first-principles study. Nano Express, 2020, 1, 010008.	1.2	20
51170	Novel Allâ€Nitrogen Molecular Crystals of Aromatic N₁₀. Advanced Science, 2020, 7, 1902320.	5.6	32
51171	Ultrafine Co₃Se₄ Nanoparticles in Nitrogenâ€Doped 3D Carbon Matrix for Highâ€Stable and Longâ€Cycleâ€Life Lithium Sulfur Batteries. Advanced Energy Materials, 2020, 10, 1904273.	10.2	141

#	Article	IF	Citations
51172	2D-Coordination Polymers Based on Rare-Earth Propionates of Layered Topology Demonstrate Polytypism and Controllable Single-Crystal-to-Single-Crystal Phase Transitions. Crystal Growth and Design, 2020, 20, 3316-3324.	1.4	11
51173	Unraveling the Ground-State Structure of BaZrO₃ by Neutron Scattering Experiments and First-Principles Calculations. Chemistry of Materials, 2020, 32, 2824-2835.	3.2	41
51174	Understanding the Origin of Higher Capacity for Ni-Based Disordered Rock-Salt Cathodes. Chemistry of Materials, 2020, 32, 3447-3461.	3.2	16
51175	Prediction of Novel 2D Intrinsic Ferromagnetic Materials with High Curie Temperature and Large Perpendicular Magnetic Anisotropy. Journal of Physical Chemistry C, 2020, 124, 7956-7964.	1.5	42
51176	Accuracy of Localized Resolution of the Identity in Periodic Hybrid Functional Calculations with Numerical Atomic Orbitals. Journal of Physical Chemistry Letters, 2020, 11, 3082-3088.	2.1	17
51177	Reagent-Triggered Isomerization of Fluxional Cluster Catalyst via Dynamic Coupling. Journal of Physical Chemistry Letters, 2020, 11, 3089-3094.	2.1	19
51178	Two-Dimensional Square-A₂B (A = Cu, Ag, Au, and B = S, Se): Auxetic Semiconductors with High Carrier Mobilities and Unusually Low Lattice Thermal Conductivities. Journal of Physical Chemistry Letters, 2020, 11, 2925-2933.	2.1	40
51179	Synthesis and Surface Chemistry of 2D TiVC Solid-Solution MXenes. ACS Applied Materials & Interfaces, 2020, 12, 20129-20137.	4.0	93
51180	Surface Adsorption and Vacancy in Tuning the Properties of Tellurene. ACS Applied Materials & Interfaces, 2020, 12, 19110-19115.	4.0	20
51181	Selective Hydrogenation of Acetylene on Pt_n/TiO₂ (n = 1, 2, 4, 8) Surfaces: Structure Sensitivity Analysis. ACS Catalysis, 2020, 10, 4922-4928.	5.5	45
51182	Ni Nanoparticles on CeO₂(111): Energetics, Electron Transfer, and Structure by Ni Adsorption Calorimetry, Spectroscopies, and Density Functional Theory. ACS Catalysis, 2020, 10, 5101-5114.	5.5	42
51183	Engineering Local and Global Structures of Single Co Atoms for a Superior Oxygen Reduction Reaction. ACS Catalysis, 2020, 10, 5862-5870.	5.5	126
51184	Vibron-assisted spin excitation in a magnetically anisotropic molecule. Nature Communications, 2020, 11, 1619.	5.8	9
51185	High doping efficiency in p-type Al-rich AlGaN by modifying the Mg doping planes. Materials Advances, 2020, 1, 77-85.	2.6	11
51186	A new perspective of lanthanide metalâ€“organic frameworks: tailoring Dy-BTC nanospheres for rechargeable Liâ€“O₂ batteries. Nanoscale, 2020, 12, 9524-9532.	2.8	29
51187	The quest of chirality in the interstellar medium. Astronomy and Astrophysics, 2020, 633, A49.	2.1	13
51188	Theoretical search for possible Liâ€“Niâ€“B crystal structures using an adaptive genetic algorithm. Journal of Applied Physics, 2020, 127, .	1.1	8
51189	Realization of a Heusler alloy Mn2FeAl with B2 ordering. Applied Physics Letters, 2020, 116, .	1.5	8

#	Article	IF	Citations
51190	Pressure-induced amorphization and existence of molecular and polymeric amorphous forms in dense SO ₂. Proceedings of the National Academy of Sciences of the United States of America, 2020, 117, 8736-8742.	3.3	13
51191	Large spin Hall effect in Si at room temperature. Physical Review B, 2020, 101, .	1.1	15
51192	Strain-tunable out-of-plane polarization in two-dimensional materials. Physical Review B, 2020, 101, .	1.1	16
51193	Pressure-induced gap modulation and topological transitions in twisted bilayer and twisted double bilayer graphene. Physical Review B, 2020, 101, .	1.1	19
51194	High Thermoelectric Performance in Sulfideâ€Type Argyrodites Compound Ag₈Sn(S_{1â^'}_xSe_x)₆ Enabled by Ultralow Lattice Thermal Conductivity and Extended Cubic Phase Regime. Advanced Functional Materials, 2020, 30, 2000526.	7.8	38
51195	A Scalable Interfacial Engineering Strategy for a Finely Tunable, Homogeneous MoS 2 /rGOâ€Based HER Catalytic Structure. Advanced Materials Interfaces, 2020, 7, 1902022.	1.9	18
51196	The Long and Winding Road: Predicting Materials Properties Through Theory and Computation. , 2020, , 37-48.		3
51197	Synthesis of Highly-Oriented Black CsPbI₃ Microstructures for High-Performance Solar Cells. Chemistry of Materials, 2020, 32, 3235-3244.	3.2	23
51198	Mechanistic Understanding of NO₂ Dissociation on a Rutile TiO₂ (110) Surface: An Electronic Structure Study. Journal of Physical Chemistry C, 2020, 124, 8786-8794.	1.5	9
51199	Adsorption Preference of HF over Ethylene Carbonate Leads to Dominant Presence of Fluoride Products in LiFePO₄ Cathodeâ€"Electrolyte Interface in Li-Ion Batteries. Journal of Physical Chemistry C, 2020, 124, 9170-9177.	1.5	10
51200	Chemisorption and Physisorption at the Metal/Organic Interface: Bond Energies of Naphthalene and Azulene on Coinage Metal Surfaces. Journal of Physical Chemistry C, 2020, 124, 8257-8268.	1.5	26
51201	Water Oxidation on TiO₂: A Comparative DFT Study of 1e^{â€"}, 2e^{â€"}, and 4e^{â€"} Processes on Rutile, Anatase, and Brookite. Journal of Physical Chemistry C, 2020, 124, 8094-8100.	1.5	30
51202	g-C₃N₄/WTe₂ Hybrid Electrocatalyst for Efficient Hydrogen Evolution Reaction. Journal of Physical Chemistry C, 2020, 124, 8726-8735.	1.5	14
51203	Organic Cations Protect Methylammonium Lead Iodide Perovskites against Small Exciton-Polaron Formation. Journal of Physical Chemistry Letters, 2020, 11, 2983-2991.	2.1	12
51204	Mn Ion Dissolution Mechanism for Lithium-Ion Battery with LiMn₂O₄ Cathode: In Situ Ultravioletâ€"Visible Spectroscopy and Ab Initio Molecular Dynamics Simulations. Journal of Physical Chemistry Letters, 2020, 11, 3051-3057.	2.1	60
51205	Surface Modification Strategy for Promoting the Performance of Non-noble Metal Single-Atom Catalysts in Low-Temperature CO Oxidation. ACS Applied Materials & Interfaces, 2020, 12, 19457-19466.	4.0	12
51206	Towards the understanding of the gold interaction with AIII-BV semiconductors at the atomic level. Nanoscale, 2020, 12, 9067-9081.	2.8	6
51207	A Ti₃C₂O₂ supported single atom, trifunctional catalyst for electrochemical reactions. Journal of Materials Chemistry A, 2020, 8, 7801-7807.	5.2	69

#	Article	IF	Citations
51208	Epitaxially grown Cu2Sb-type MnGaGe films with large perpendicular magnetic anisotropy. Applied Physics Letters, 2020, 116, .	1.5	3
51209	Interlayer coupling in intrinsically magnetic bilayer ScO2 and NbN2. Applied Physics Letters, 2020, 116, .	1.5	2
51210	Photophysics in Cs₃Cu₂X₅ (X = Cl, Br, or I): Highly Luminescent Self-Trapped Excitons from Local Structure Symmetrization. Chemistry of Materials, 2020, 32, 3462-3468.	3.2	177
51211	Theoretical Studies of MoS₂ and Phosphorene Drug Delivery for Antituberculosis Drugs. Journal of Physical Chemistry C, 2020, 124, 8279-8287.	1.5	17
51212	Accurate Ab Initio Calculations on Various PV-Based Materials: Which Functional to Be Used?. Journal of Physical Chemistry C, 2020, 124, 8467-8478.	1.5	15
51213	Synergistic ultraviolet and visible light photo-activation enables intensified low-temperature methanol synthesis over copper/zinc oxide/alumina. Nature Communications, 2020, 11, 1615.	5.8	84
51214	Critical topological nodal points and nodal lines/rings in Kagome graphene. Physical Chemistry Chemical Physics, 2020, 22, 8713-8718.	1.3	2
51215	Synthesis of a flower-like MoS₂/carbon nanocomposite with enhanced adsorption performance toward Eu(<scp>iii</scp>): the cooperative effects between S atoms and carboxyl groups. Environmental Science: Water Research and Technology, 2020, 6, 1482-1494.	1.2	12
51216	Prediction of a two-dimensional high-T_C f-electron ferromagnetic semiconductor. Materials Horizons, 2020, 7, 1623-1630.	6.4	141
51217	Atomic scale insight into the fundamental mechanism of Mn doped LiFePO₄. Sustainable Energy and Fuels, 2020, 4, 2741-2751.	2.5	17
51218	Degradation of the transition metal@Pt coreâ€“shell nanoparticle catalyst: a DFT study. Physical Chemistry Chemical Physics, 2020, 22, 9467-9476.	1.3	7
51219	Unraveling the role of bonding chemistry in connecting electronic and thermal transport by machine learning. Journal of Materials Chemistry A, 2020, 8, 8716-8721.	5.2	21
51220	Engineering Sulfide-Phosphide Based Double Catalysts on 3D Nickel Phosphides Framework for Electrolytic Hydrogen Evolution: Activating Short-range Crystalline MoS₂ with Ni₅P₄-Ni₂P Template. Journal of the Electrochemical Society, 2020, 167, 026511.	1.3	8
51221	Macroscopic and Microscopic Structures of Cesium Lead Iodide Perovskite from Atomistic Simulations. Advanced Functional Materials, 2020, 30, 1909496.	7.8	11
51222	Phase Transition across Anisotropic NbS 3 and Direct Gap Semiconductor TiS 3 at Nominal Titanium Alloying Limit. Advanced Materials, 2020, 32, 2000018.	11.1	16
51223	The discontinuous effect of pressure on twin boundary strength in MgO. Physics and Chemistry of Minerals, 2020, 47, 1.	0.3	1
51224	Microstructural Instability and Precipitation Behaviors of Intermetallic Phases in a Nb-Containing CoNi-Based Superalloy. Metallurgical and Materials Transactions A: Physical Metallurgy and Materials Science, 2020, 51, 2495-2508.	1.1	3
51225	Geometric effect promoted hydrotalcites catalysts towards aldol condensation reaction. Chinese Journal of Catalysis, 2020, 41, 1279-1287.	6.9	20

#	Article	IF	Citations
51226	The adsorption and migration behavior of divalent metals (Mg, Ca, and Zn) on pristine and defective graphene. Carbon, 2020, 163, 276-287.	5.4	36
51227	Adsorption of mercury species on selected CuS surfaces and the effects of HCl. Chemical Engineering Journal, 2020, 393, 124773.	6.6	38
51228	Unexpected band gap increase in the Fe2VAl Heusler compound. Materials Today Physics, 2020, 13, 100203.	2.9	20
51229	Double-layer hybrid chainmail catalyst for high-performance hydrogen evolution. Nano Energy, 2020, 72, 104700.	8.2	35
51230	Spinodal decomposition of reactively sputtered (V0.64Al0.36)0.49N0.51 thin films. Surface and Coatings Technology, 2020, 389, 125641.	2.2	11
51231	Origin of Disorder Tolerance in Piezoelectric Materials and Design of Polar Systems. Chemistry of Materials, 2020, 32, 2836-2842.	3.2	4
51232	Two-Dimensional Honeycomb B₂Se with Orthogonal Lattice: High Stability and Strong Anisotropic Dirac Cone. Journal of Physical Chemistry C, 2020, 124, 7558-7565.	1.5	16
51233	Quantitative Resolution of Complex Stoichiometric Changes during Electrochemical Cycling by Density Functional Theory-Assisted Electrochemical Quartz Crystal Microbalance. ACS Applied Energy Materials, 2020, 3, 3347-3357.	2.5	14
51234	Extrapolated Defect Transition Level in Two-Dimensional Materials: The Case of Charged Native Point Defects in Monolayer Hexagonal Boron Nitride. ACS Applied Materials & Interfaces, 2020, 12, 17055-17061.	4.0	24
51235	Active and Stable Ptâ€“Ni Alloy Octahedra Catalyst for Oxygen Reduction via Near-Surface Atomical Engineering. ACS Catalysis, 2020, 10, 4205-4214.	5.5	98
51236	Achieving a superlubricating ohmic sliding electrical contact via a 2D heterointerface: a computational investigation. Nanoscale, 2020, 12, 7857-7863.	2.8	11
51237	2D PC₃ as a promising thermoelectric material. Physical Chemistry Chemical Physics, 2020, 22, 8625-8632.	1.3	18
51238	Multi-wavelength light emission from InGaN nanowires on pyramid-textured Si(100) substrate grown by stationary plasma-assisted molecular beam epitaxy. Nanoscale, 2020, 12, 8836-8846.	2.8	6
51239	Reversible gas capture using a ferroelectric switch and 2D molecule multiferroics on the In₂Se₃ monolayer. Journal of Materials Chemistry A, 2020, 8, 7331-7338.	5.2	59
51240	Desorption products during linear heating of copper zeolites with pre-adsorbed methanol. Physical Chemistry Chemical Physics, 2020, 22, 6809-6817.	1.3	1
51241	Propene oxidation catalysis and electronic structure of M₅₅particles (M = Pd or Rh): differences and similarities between Pd₅₅and Rh₅₅. Physical Chemistry Chemical Physics, 2020, 22, 11783-11796.	1.3	5
51242	Ti- and Fe-related charge transition levels in Î²â^'Ga2O3. Applied Physics Letters, 2020, 116, .	1.5	37
51243	The water/ceria(111) interface: Computational overview and new structures. Journal of Chemical Physics, 2020, 152, 104709.	1.2	11

#	Article	IF	Citations
51244	The interplay between Peierls distortions and metavalent bonding in IVâ€“VI compounds: comparing GeTe with related monochalcogenides. Journal Physics D: Applied Physics, 2020, 53, 234002.	1.3	43
51245	Improved phase change properties in layered ScxIn2â^'xSe3 for multilevel information storage. Journal Physics D: Applied Physics, 2020, 53, 285101.	1.3	1
51246	Band offsets engineering in asymmetric Janus bilayer transition-metal dichalcogenides. Journal of Physics Condensed Matter, 2020, 32, 035502.	0.7	6
51247	2D AlP₃ with high carrier mobility and tunable band structure. Journal of Physics Condensed Matter, 2020, 32, 055001.	0.7	19
51248	Vanadium doped polyoxometalate: induced active sites and increased hydrogen adsorption. Journal of Physics Condensed Matter, 2020, 32, 195001.	0.7	4
51249	Titanium nitride halides monolayers: promising 2D anisotropic thermoelectric materials. Journal of Physics Condensed Matter, 2020, 32, 205503.	0.7	19
51250	Strain induced optoelectronic properties of two dimensional MnPSe₃/WS₂ heterostructure. Journal of Physics Condensed Matter, 2020, 32, 315501.	0.7	4
51251	Crystal structure reconstruction in the surface monolayer of the quantum spin liquid candidate Î±-RuCl3. 2D Materials, 2020, 7, 035004.	2.0	11
51252	Strain-driven disproportionation at a correlated oxide metal-insulator transition. Physical Review B, 2020, 101, .	1.1	26
51253	Defects and Dopants in CaFeSi2O6: Classical and DFT Simulations. Energies, 2020, 13, 1285.	1.6	11
51254	Excitons and Electronâ€“Hole Liquid State in 2D Î³â€Phase Groupâ€IV Monochalcogenides. Advanced Functional Materials, 2020, 30, 2000533.	7.8	39
51255	Electro-Optical Properties of Monolayer and Bilayer Pentagonal BN: First Principles Study. Nanomaterials, 2020, 10, 440.	1.9	19
51256	Tuning the Catalytic Activity of a Quantum Nutcracker for Hydrogen Dissociation. Surfaces, 2020, 3, 40-47.	1.0	2
51257	First-principles studies of chalcopyrite-type (Cu, Li)GaS2 and (Cu, Li)InS2 systems. Japanese Journal of Applied Physics, 2020, 59, SCCB18.	0.8	0
51258	Impact of hydrogen on lithium storage on graphene edges. Applied Surface Science, 2020, 515, 145886.	3.1	5
51259	Interfacial activation of reactants and intermediates on CaSO4 insulator-based heterostructure for efficient photocatalytic NO removal. Chemical Engineering Journal, 2020, 390, 124609.	6.6	39
51260	DFT and microkinetic comparison of Pt, Pd and Rh-catalyzed ammonia oxidation. Journal of Catalysis, 2020, 383, 322-330.	3.1	33
51261	New Rubidium-Containing Mixed-Metal Titanium Hollandites. Crystal Growth and Design, 2020, 20, 2398-2405.	1.4	6

#	Article	IF	Citations
51262	Structure, Stability, and Mechanical Properties of Boron-Rich Moâ€“B Phases: A Computational Study. Journal of Physical Chemistry Letters, 2020, 11, 2393-2401.	2.1	30
51263	Thickness-Independent Semiconducting-to-Metallic Conversion in Wafer-Scale Two-Dimensional PtSe₂ Layers by Plasma-Driven Chalcogen Defect Engineering. ACS Applied Materials & Interfaces, 2020, 12, 14341-14351.	4.0	51
51264	Thermoelectric Penta-Silicene with a High Room-Temperature Figure of Merit. ACS Applied Materials & Interfaces, 2020, 12, 14298-14307.	4.0	71
51265	Pt₅Se₄ Monolayer: A Highly Efficient Electrocatalyst toward Hydrogen and Oxygen Electrode Reactions. ACS Applied Materials & Interfaces, 2020, 12, 13896-13903.	4.0	26
51266	Synthesis of Monolayer Blue Phosphorus Enabled by Silicon Intercalation. ACS Nano, 2020, 14, 3687-3695.	7.3	52
51267	Anionic Redox Processes in Maricite- and Triphylite-NaFePO₄ of Sodium-Ion Batteries. ACS Omega, 2020, 5, 5192-5201.	1.6	16
51268	Manganese Doping in Cobalt Oxide Nanorods Promotes Catalytic Dehydrogenation. ACS Sustainable Chemistry and Engineering, 2020, 8, 5734-5741.	3.2	19
51269	2D tetragonal transition-metal phosphides: an ideal platform to screen metal shrouded crystals for multifunctional applications. Nanoscale, 2020, 12, 6776-6784.	2.8	21
51270	Exploring the properties of Ag₅â€“TiO₂ interfaces: stable surface polaron formation, UV-Vis optical response, and CO₂ photoactivation. Journal of Materials Chemistry A, 2020, 8, 6842-6853.	5.2	26
51271	Sensing surface lattice strain with Kondo resonance of single Co adatom. Applied Physics Letters, 2020, 116, 051604.	1.5	3
51272	Dynamical and structural properties of adsorbed water molecules at the TiO2 rutile-(110) surface: interfacial hydrogen bonding probed by ab-initio molecular dynamics. Molecular Physics, 2020, 118, e1725166.	0.8	4
51273	Influence of the Facets of Bi24O31Br10 Nanobelts and Nanosheets on Their Photocatalytic Properties. Catalysts, 2020, 10, 257.	1.6	12
51274	Catalytic ethylene oxidation by Cuâ€“Au coreâ€“shell nanoclusters: a computational study. Theoretical Chemistry Accounts, 2020, 139, 1.	0.5	4
51275	Bandgap opening in MoTe2 thin flakes induced by surface oxidation. Frontiers of Physics, 2020, 15, 1.	2.4	12
51276	Effects of the Heterointerface on the Growth Characteristics of a Brownmillerite SrFeO2.5 Thin Film Grown on SrRuO3 and SrTiO3 Perovskites. Scientific Reports, 2020, 10, 3807.	1.6	13
51277	Implications of the fractional charge of hydroxide at the electrochemical interface. Physical Chemistry Chemical Physics, 2020, 22, 6964-6969.	1.3	6
51278	Atomic origin of spin-valve magnetoresistance at the SrRuO3 grain boundary. National Science Review, 2020, 7, 755-762.	4.6	12
51279	Secondary-Phase-Assisted Grain Boundary Migration in CuInSe2. Physical Review Letters, 2020, 124, 095702.	2.9	5

#	Article	IF	Citations
51280	Flux Crystal Growth, Crystal Structure, and Optical Properties of New Germanate Garnet Ce2CaMg2Ge3O12. Frontiers in Chemistry, 2020, 8, 91.	1.8	1
51281	Metalâ€free Catalyst B 2 S Sheet for Effective CO 2 Electrochemical Reduction to CH 3 OH. ChemPhysChem, 2020, 21, 779-784.	1.0	6
51282	Syntheses, Crystal Structures, and Vibrational Properties of Two Lead Azide Halides PbN 3 X (X = Cl,) Tj ETQq0 0 0 rgBT /Overlock 10 Tf	0.6	3
51283	Atomic-scale simulations for lithium dendrite growth driven by strain gradient. Applied Mathematics and Mechanics (English Edition), 2020, 41, 533-542.	1.9	5
51284	Post-redox engineering electron configurations of atomic thick C3N4 nanosheets for enhanced photocatalytic hydrogen evolution. Applied Catalysis B: Environmental, 2020, 270, 118855.	10.8	40
51285	Achieving high conductivity p-type Ga2O3 through Al-N and In-N co-doping. Chemical Physics Letters, 2020, 746, 137308.	1.2	18
51286	A complete computational route to predict reduction of thermal conductivities of complex oxide ceramics by doping: A case study of La2Zr2O7. Journal of Alloys and Compounds, 2020, 826, 154224.	2.8	9
51287	Strain and electric field tuned electronic properties of BAs/MoSe2 van der Waals heterostructures for alternative electrodes and photovoltaic cell in photocatalysis. Physica E: Low-Dimensional Systems and Nanostructures, 2020, 120, 114055.	1.3	12
51288	Adsorption of gas molecules on group III atoms adsorbed g-C3N4: A first-principles study. Vacuum, 2020, 175, 109293.	1.6	43
51289	Facile-Processed Nanocarbon-Promoted Sulfur Cathode for Highly Stable Sodium-Sulfur Batteries. Cell Reports Physical Science, 2020, 1, 100015.	2.8	18
51290	Thickness-Controlled Synthesis of CoX₂ (X = S, Se, and Te) Single Crystalline 2D Layers with Linear Magnetoresistance and High Conductivity. Chemistry of Materials, 2020, 32, 2321-2329.	3.2	35
51291	Anion Ordered and Ferroelectric Ruddlesdenâ€“Popper Oxynitride Ca₃Nb₂N₂O₅ for Visible-Light-Active Photocatalysis. Chemistry of Materials, 2020, 32, 2815-2823.	3.2	18
51292	Rational Synthesis Concept for Cerium Oxide Nanoparticles: On the Impact of Particle Size on the Oxygen Storage Capacity. Journal of Physical Chemistry C, 2020, 124, 8736-8748.	1.5	28
51293	DFT Study on the Mechanism of the Water Gas Shift Reaction Over Ni_xP_y Catalysts: The Role of P. Journal of Physical Chemistry C, 2020, 124, 6598-6610.	1.5	18
51294	Mechanism of Extreme Optical Nonlinearities in Spiral WS₂ above the Bandgap. Nano Letters, 2020, 20, 2667-2673.	4.5	25
51295	(Photo)Electrocatalytic CO₂ Reduction at the Defective Anatase TiO₂ (101) Surface. ACS Catalysis, 2020, 10, 4048-4058.	5.5	42
51296	Reaction Mechanism of Vapor-Phase Formic Acid Decomposition over Platinum Catalysts: DFT, Reaction Kinetics Experiments, and Microkinetic Modeling. ACS Catalysis, 2020, 10, 4112-4126.	5.5	51
51297	Highly Efficient Porous Fe_xCe_{1â€“x}O_{2â^Î´} with Three-Dimensional Hierarchical Nanoflower Morphology for H₂S-Selective Oxidation. ACS Catalysis, 2020, 10, 3968-3983.	5.5	78

#	Article	IF	Citations
51298	Hybrid Functional Study on Small Polaron Formation and Ion Diffusion in the Cathode Material Na₂Mn₃(SO₄)₄. ACS Omega, 2020, 5, 5429-5435.	1.6	6
51299	Synthesis of the Elusive S = ¹/₂ Star Structure: A Possible Quantum Spin Liquid Candidate. Journal of the American Chemical Society, 2020, 142, 5013-5016.	6.6	8
51300	Ultra-high open-circuit voltage of tin perovskite solar cells via an electron transporting layer design. Nature Communications, 2020, 11, 1245.	5.8	408
51301	An automatically curated first-principles database of ferroelectrics. Scientific Data, 2020, 7, 72.	2.4	39
51302	Nanostructuring unlocks high performance of platinum single-atom catalysts for stable vinyl chloride production. Nature Catalysis, 2020, 3, 376-385.	16.1	122
51303	Structural stress and extra optical absorption induced by the intrinsic cation defects in KDP and ADP crystals: a theoretical study. CrystEngComm, 2020, 22, 1962-1969.	1.3	17
51304	Nanoscale lightâ€“matter interactions in metalâ€“organic frameworks cladding optical fibers. Nanoscale, 2020, 12, 9991-10000.	2.8	25
51305	The closed-edge structure of graphite and the effect of electrostatic charging. RSC Advances, 2020, 10, 7994-8001.	1.7	12
51306	A systematic investigation of the catalytic performances of monolayer carbon nitride nanosheets C_{1â^'x}N_x. Physical Chemistry Chemical Physics, 2020, 22, 6772-6782.	1.3	9
51307	Prediction of optimal catalysts for a given chemical reaction. Catalysis Science and Technology, 2020, 10, 2069-2081.	2.1	13
51308	Understanding the structural diversity of freestanding Al₂O₃ ultrathin films through a DFTB-aided genetic algorithm. Nanoscale, 2020, 12, 6153-6163.	2.8	10
51309	Structural, thermodynamic, electronic and elastic properties of Th1â^'xUxO2 and Th1â^'xPuxO2 mixed oxides. Physical Chemistry Chemical Physics, 2020, 22, 6406-6417.	1.3	9
51310	Tunable photoelectronic properties of hydrogenated-silicene/halogenated-silicene superlattices for water splitting. Journal of Applied Physics, 2020, 127, .	1.1	18
51311	Heteroatom doping effects on interaction of H2O and CeO2 (111) surfaces studied using density functional theory: Key roles of ionic radius and dispersion. Journal of Chemical Physics, 2020, 152, 014707.	1.2	13
51312	Leadâ€Free Perovskite Variant Solid Solutions Cs₂Sn_{1â€“}_xTe_xCl₆: Bright Luminescence and High Antiâ€Water Stability. Advanced Materials, 2020, 32, e2002443.	11.1	169
51313	Plasmaâ€Assisted Catalytic Effects of TiO₂/Macroporous SiO₂ on the Synthesis of Light Hydrocarbons from Methane. ChemCatChem, 2020, 12, 5067-5075.	1.8	5
51314	First-principles analysis on the role of rare-earth doping in affecting nitrogen adsorption and diffusion at Fe surface towards clarified catalytic diffusion mechanism in nitriding. Acta Materialia, 2020, 196, 347-354.	3.8	37
51315	The combined DFT and microkinetics methods to investigate the favorite sulfur vacancies of Co(Ni)MoS2 catalysts for maximizing HDS/HYDO selectivity. Applied Catalysis B: Environmental, 2020, 277, 119242.	10.8	25

#	Article	IF	Citations
51316	Superior performance of anion exchange membrane water electrolyzer: Ensemble of producing oxygen vacancies and controlling mass transfer resistance. Applied Catalysis B: Environmental, 2020, 278, 119276.	10.8	80
51317	A first principle study of black phosphorene/N-doped graphene heterostructure: Electronic, mechanical and interface properties. Applied Surface Science, 2020, 528, 146962.	3.1	12
51318	CO2 thermoreduction to methanol on the MoS2 supported single Co atom catalyst: A DFT study. Applied Surface Science, 2020, 528, 147047.	3.1	46
51319	Defective titanium dioxide nanobamboo arrays architecture for photocatalytic nitrogen fixation up to 780Ânm. Chemical Engineering Journal, 2020, 401, 126033.	6.6	47
51320	Platinum doped alkali earth metal oxides as a qubit candidate. Computational Materials Science, 2020, 181, 109754.	1.4	1
51321	Alloying-element dependence of structural, elastic and electronic properties of nickel-based superalloys: Influence of Î³â€™ volume fraction. Journal of Alloys and Compounds, 2020, 838, 155141.	2.8	14
51322	Ab initio investigation of Î±- and Î¶-V2O5 for beyond lithium ion battery cathodes. Journal of Power Sources, 2020, 472, 228096.	4.0	17
51323	Effect of intrinsic vacancy defects on the electronic properties of monoclinic Ag2S. Materials Chemistry and Physics, 2020, 249, 122961.	2.0	14
51324	Ni/SiO2/Graphene-modified separator as a multifunctional polysulfide barrier for advanced lithium-sulfur batteries. Nano Energy, 2020, 76, 105033.	8.2	90
51325	Immobilized trimeric metal clusters: A family of the smallest catalysts for selective CO2 reduction toward multi-carbon products. Nano Energy, 2020, 76, 105049.	8.2	56
51326	Defects levels and VUV/UV luminescence of Ce3+ and Eu3+ doped chloroapatite phosphors M5(PO4)3Cl (M = Ca, Sr, Ba). Optical Materials, 2020, 107, 110014.	1.7	1
51327	The Role of Cation Coordination in the Electrical and Optical Properties of Amorphous Transparent Conducting Oxides. Chemistry of Materials, 2020, 32, 6444-6455.	3.2	9
51328	Mechanisms and Potential-Dependent Energy Barriers for Hydrogen Evolution on Supported MoS₂ Catalysts. Journal of Physical Chemistry C, 2020, 124, 17015-17026.	1.5	9
51329	Importance of the Spinâ€“Orbit Interaction for a Consistent Theoretical Description of Small Polarons in Pr-Doped CeO₂. Journal of Physical Chemistry C, 2020, 124, 15831-15838.	1.5	9
51330	Dynamic structural changes of supported Pd, PdSn, and PdIn nanoparticles during continuous flow high pressure direct H₂O₂ synthesis. Catalysis Science and Technology, 2020, 10, 4726-4742.	2.1	17
51331	Anion order in perovskite oxynitrides AMO₂N (A = Ba, Sr, Ca; M = Ta, Nb): a first-principles based investigation. RSC Advances, 2020, 10, 24410-24418.	1.7	10
51332	Defect compensation in the p-type transparent oxide Ba₂BiTaO₆. Journal of Materials Chemistry C, 2020, 8, 9352-9357.	2.7	16
51333	Semiconductor-to-conductor transition in 2D copper(<scp>ii</scp>) oxide nanosheets through surface sulfur-functionalization. Nanoscale, 2020, 12, 14549-14559.	2.8	6

#	Article	IF	Citations
51334	Mechanism of charge redistribution at the metalâ€“semiconductor and semiconductorâ€“semiconductor interfaces of metalâ€“bilayer MoS2 junctions. Journal of Chemical Physics, 2020, 152, 244701.	1.2	23
51335	Alignment of Polarization against an Electric Field in van der Waals Ferroelectrics. Physical Review Applied, 2020, 13, .	1.5	34
51336	Multiband <mml:math xmlns:mml="http://www.w3.org/1998/Math/MathML"><mml:mrow><mml:mi mathvariant="normal">k</mml:mi><mml:mo>Â·</mml:mo><mml:mi mathvariant="normal">p</mml:mi></mml:mrow></mml:math> model and fitting scheme for ab initio based electronic structure parameters for wurtzite GaAs. Physical Review B, 2020, 101, .	1.1	9
51337	Structure and stability of alkali gallates structurally reminiscent of hollandite. Journal of the American Ceramic Society, 2020, 103, 6531-6542.	1.9	1
51338	Experimental inspection of a computationally-designed NiCrMnSi Heusler alloy with high Curie temperature. Japanese Journal of Applied Physics, 2020, 59, 073003.	0.8	3
51339	Electroplating sludge-derived spinel catalysts for NO removal via NH3 selective catalysis reduction. Applied Surface Science, 2020, 528, 146969.	3.1	11
51340	Studies of surface states in Bi2Se3 induced by the BiSe substitution in the crystal subsurface structure. Applied Surface Science, 2020, 528, 146978.	3.1	13
51341	Importance of structural deformation features in the prediction of hybrid perovskite bandgaps. Computational Materials Science, 2020, 184, 109858.	1.4	22
51342	DFT studies of 2-mercaptobenzothiazole and 2-mercaptobenzimidazole as corrosion inhibitors for copper. Corrosion Science, 2020, 174, 108840.	3.0	58
51343	ELSI â€" An open infrastructure for electronic structure solvers. Computer Physics Communications, 2020, 256, 107459.	3.0	27
51344	Catalytic mechanisms of TiH2 thin layer on dehydrogenation behavior of fluorite-type MgH2: A first principles study. International Journal of Hydrogen Energy, 2020, 45, 21600-21610.	3.8	7
51345	First-principles molecular dynamics studying the solidification of Ti-6Al-4V alloy. Journal of Molecular Liquids, 2020, 315, 113606.	2.3	4
51346	Enhanced photocurrent generation from indiumâ€“tin-oxide/Fe2TiO5 hybrid nanocone arrays. Nano Energy, 2020, 76, 104965.	8.2	9
51347	First principle study on interfacial interaction of black phosphorus and CsBr vdW heterostructure. Physics Letters, Section A: General, Atomic and Solid State Physics, 2020, 384, 126614.	0.9	10
51348	Computational study of the adsorption of bimetallic clusters on alumina substrate. Surface Science, 2020, 700, 121682.	0.8	2
51349	Closing the Gap Between Experiment and Theory: Reactive Scattering of HCl from Au(111). Journal of Physical Chemistry C, 2020, 124, 15944-15960.	1.5	18
51350	â€œStickierâ€•Surface Sb₂Te₃ Templates Enable Fast Memory Switching of Phase Change Material GeSb₂Te₄ with Growth-Dominated Crystallization. ACS Applied Materials & Interfaces, 2020, 12, 33397-33407.	4.0	53
51351	High oscillator strength interlayer excitons in two-dimensional heterostructures for mid-infrared photodetection. Nature Nanotechnology, 2020, 15, 675-682.	15.6	129

#	Article	IF	Citations
51352	Berry curvature memory through electrically driven stacking transitions. Nature Physics, 2020, 16, 1028-1034.	6.5	100
51353	Selective electrocatalysis imparted by metalâ€“insulator transition for durability enhancement of automotive fuel cells. Nature Catalysis, 2020, 3, 639-648.	16.1	79
51354	Molecular-level insights on the reactive facet of carbon nitride single crystals photocatalysing overall water splitting. Nature Catalysis, 2020, 3, 649-655.	16.1	427
51355	Crystal structure and migration paths of alkaline ions in NaVPO₄F. Physical Chemistry Chemical Physics, 2020, 22, 15876-15884.	1.3	7
51356	First-principles studies of electronic properties in lithium metasilicate (Li₂SiO₃). RSC Advances, 2020, 10, 24721-24729.	1.7	13
51357	Two-dimensional IVâ€“VI materials with in-plane negative Poisson's ratio and anisotropic carrier mobility. Journal of Materials Chemistry C, 2020, 8, 10382-10389.	2.7	28
51358	A first-principles study of electronic structure and photocatalytic performance of GaNâ€“MX₂ (M = Mo, W; X= S, Se) van der Waals heterostructures. RSC Advances, 2020, 10, 24683-24690.	1.7	19
51359	A first-principles prediction of an sp3 carbon allotrope comprising four-, five-, six-, and eight-member rings. Journal of Applied Physics, 2020, 127, 245112.	1.1	2
51360	Blocking of the martensitic transition at the nanoscale in a <mml:math xmlns:mml="http://www.w3.org/1998/Math/MathML"><mml:msub><mml:mrow><mml:mi>Ti</mml:mi></mml:mrow> wedge. Physical Review B, 2020, 101, .	1.1	9
51361	Induced spin textures at <mml:math xmlns:mml="http://www.w3.org/1998/Math/MathML"><mml:mrow><mml:mn>3</mml:mn><mml:mi>d</mml:mi> transition metalâ€“topological insulator interfaces. Physical Review B, 2020, 101, .	1.1	6
51362	<mml:math xmlns:mml="http://www.w3.org/1998/Math/MathML"><mml:msub><mml:mi>BaZrO</mml:mi><mml:mn>3</mml:mn> stability under pressure: The role of nonlocal exchange and correlation. Physical Review B, 2020, 101, .	1.1	12
51363	Prediction of orientation relationships and interface structures between Î±-, Î²-, Î³-FeSi₂ and Si phases. Acta Crystallographica Section B: Structural Science, Crystal Engineering and Materials, 2020, 76, 469-482.	0.5	7
51364	Properties and Structural Arrangements of the Electrode Material CuDEPP during Energy Storage. Energy Technology, 2020, 8, 2000388.	1.8	1
51365	The influence of alloying on Zn liquid metal embrittlement in steels. Acta Materialia, 2020, 195, 750-760.	3.8	45
51366	High-efficient hydrogen purification through two-dimensional CrI3 membrane via a first-principles calculation. Applied Surface Science, 2020, 529, 147024.	3.1	8
51367	Optimized interatomic potential for study of structure and phase transitions in Si-Au and Si-Al systems. Computational Materials Science, 2020, 184, 109891.	1.4	26
51368	Segregation of interstitial light elements at grain boundaries in molybdenum. Materials Today Communications, 2020, 25, 101388.	0.9	3
51369	Surfactant-Free Approach for Engineering an Ultrathin Ti-Doped Ni(OH)₂ Nanosheet on Carbon Cloth: Experimental and Theoretical Insight into Boosted Alkaline Water Oxidation Activity. Inorganic Chemistry, 2020, 59, 10253-10261.	1.9	5

#	Article	IF	Citations
51370	The Operando Optical Spectrum of Hematite during Water Splitting through a GWâ€“BSE Calculation. Journal of Chemical Theory and Computation, 2020, 16, 4857-4864.	2.3	13
51371	Predicting the Effect of Dopants on CO₂ Adsorption in Transition Metal Carbides: Case Study on TiC (001). Journal of Physical Chemistry C, 2020, 124, 15969-15976.	1.5	10
51372	Monolayer Cubic Boron Nitride Terminated Diamond (111) Surfaces for Quantum Sensing and Electron Emission Applications. ACS Applied Materials & Interfaces, 2020, 12, 33336-33345.	4.0	14
51373	Highly Efficient Hydrogenation of Nitroarenes by N-Doped Carbon-Supported Cobalt Single-Atom Catalyst in Ethanol/Water Mixed Solvent. ACS Applied Materials & Interfaces, 2020, 12, 34021-34031.	4.0	56
51374	Probing Active-Site Relocation in Cu/SSZ-13 SCR Catalysts during Hydrothermal Aging by In Situ EPR Spectroscopy, Kinetics Studies, and DFT Calculations. ACS Catalysis, 2020, 10, 9410-9419.	5.5	64
51375	A Novel Hyperbolic Two-Dimensional Carbon Material with an In-Plane Negative Poissonâ€™s Ratio Behavior and Low-Gap Semiconductor Characteristics. ACS Omega, 2020, 5, 15783-15790.	1.6	11
51376	Hydrogen adsorption on In₂O₃(111) and In₂O₃(110). Physical Chemistry Chemical Physics, 2020, 22, 16193-16202.	1.3	21
51377	A first-principles study on the magnetoelectric coupling induced by Fe in a two-dimensional BaTiO₃(001) ultrathin film. Physical Chemistry Chemical Physics, 2020, 22, 18284-18293.	1.3	3
51378	Two new Cu-based borate catalysts with cubic supramolecular cages for efficient catalytic hydrogen evolution. Dalton Transactions, 2020, 49, 10156-10161.	1.6	16
51379	Alkali metal insertion into hard carbon â€“ the full picture. Journal of Materials Chemistry A, 2020, 8, 14205-14213.	5.2	27
51380	Enhanced carrier separation in ferroelectric In₂Se₃/MoS₂ van der Waals heterostructure. Journal of Materials Chemistry C, 2020, 8, 11160-11167.	2.7	44
51381	Hydrogen desorption from the surface and subsurface of cobalt. Physical Chemistry Chemical Physics, 2020, 22, 15281-15287.	1.3	7
51382	Understanding the effect of interfacial interaction on metal/metal oxide electrocatalysts for hydrogen evolution and hydrogen oxidation reactions on the basis of first-principles calculations. Catalysis Science and Technology, 2020, 10, 4743-4751.	2.1	29
51383	Examining the order-of-limits problem and lattice constant performance of the Taoâ€“Mo functional. Journal of Chemical Physics, 2020, 152, 244112.	1.2	11
51384	Development of nuclear basis sets for multicomponent quantum chemistry methods. Journal of Chemical Physics, 2020, 152, 244123.	1.2	47
51385	Using principal component analysis for neural network high-dimensional potential energy surface. Journal of Chemical Physics, 2020, 152, 234103.	1.2	11
51386	Orthorhombic alloys of Ga2O3 and Al2O3. Applied Physics Letters, 2020, 116, .	1.5	10
51387	Improper ferroelectricity in 134-type <mml:math xmlns:mml="http://www.w3.org/1998/Math/MathML"><mml:mrow><mml:mi>A</mml:mi><mml:msubsup><mml:mi>A</mml:mi><mml:mi mathvariant="normal">O</mml:mi></mml:mrow><mml:mn>12</mml:mn></mml:msub></mml:math> perovskites. Physical Review B, 2020, 101, .	1.1	3

#	Article	IF	Citations
51388	Accurate electronic band gaps of two-dimensional materials from the local modified Becke-Johnson potential. Physical Review B, 2020, 101, .	1.1	21
51389	Design of Two-Dimensional Multiferroics with Direct Polarization-Magnetization Coupling. Physical Review Letters, 2020, 125, 017601.	2.9	48
51390	First-principles study of magnetism and electric field effects in 2D systems. AVS Quantum Science, 2020, 2, .	1.8	7
51391	Tunable Dualâ€Emission in Monodispersed Sb³⁺/Mn²⁺ Codoped Cs₂NaInCl₆ Perovskite Nanocrystals through an Energy Transfer Process. Small, 2020, 16, e2002547.	5.2	90
51392	Effect of Tin in the Bulk of Platinumâ€“Tin Alloys for Ethane Dehydrogenation. Topics in Catalysis, 2020, 63, 700-713.	1.3	13
51393	Bonding VSe2 ultrafine nanocrystals on graphene toward advanced lithium-sulfur batteries. Nano Research, 2020, 13, 2673-2682.	5.8	62
51394	High-pressure synthesis, crystal structure and physical properties of a new Cr-based arsenide La3CrAs5. Science China Materials, 2020, 63, 1750-1758.	3.5	7
51395	Selective Hydrogenation of 5-Hydroxymethylfurfural via Zeolite Encapsulation to Avoid Further Hydrodehydroxylation. Industrial & Engineering Chemistry Research, 2020, 59, 12004-12012.	1.8	26
51396	Triazine- and Keto-Functionalized Porous Covalent Organic Framework as a Promising Anode Material for Na-Ion Batteries: A First-Principles Study. Journal of Physical Chemistry C, 2020, 124, 15870-15878.	1.5	22
51397	Theoretical Investigation of the Structureâ€“Property Correlation of MXenes as Anode Materials for Alkali Metal Ion Batteries. Journal of Physical Chemistry C, 2020, 124, 14978-14986.	1.5	26
51398	Optical, Electronic, and Contact Properties of Janus-MoSO/MoS₂ Heterojunction. Journal of Physical Chemistry C, 2020, 124, 15988-15994.	1.5	8
51399	Local Distortions and Dynamics in Hydrated Y-Doped BaZrO₃. Journal of Physical Chemistry C, 2020, 124, 16689-16701.	1.5	12
51400	Metal-Free Hybrid Organicâ€“Inorganic Perovskites for Photovoltaics. Journal of Physical Chemistry Letters, 2020, 11, 5938-5947.	2.1	12
51401	Atomically Dispersed Iridium on Indium Tin Oxide Efficiently Catalyzes Water Oxidation. ACS Central Science, 2020, 6, 1189-1198.	5.3	47
51402	Large Zeeman splitting induced anomalous Hall effect in ZrTe5. Npj Quantum Materials, 2020, 5, .	1.8	29
51403	Prediction of two-dimensional antiferromagnetic ferroelasticity in an AgF₂ monolayer. Nanoscale Horizons, 2020, 5, 1386-1393.	4.1	45
51404	Strong influence of strain gradient on lithium diffusion: flexo-diffusion effect. Nanoscale, 2020, 12, 15175-15184.	2.8	9
51405	Reducing the charge overpotential of Liâ€“O₂ batteries through band-alignment cathode design. Energy and Environmental Science, 2020, 13, 2540-2548.	15.6	30

#	Article	IF	Citations
51406	Emergent superconductivity in single-crystalline <mml:math xmlns:mml="http://www.w3.org/1998/Math/MathML"><mml:mrow><mml:msub><mml:mi>MgTi</mml:mi><mml:mn>2</mml:mn></mml:msub><mml:msub><mml:mi mathvariant="normal">O</mml:mi><mml:mn>4</mml:mn></mml:msub></mml:mrow></mml:math> films via structural engineering. Physical Review B, 2020, 101, .	1.1	13
51407	Unconventional spin-orbit torque in transition metal dichalcogenideâ€“ferromagnet bilayers from first-principles calculations. Physical Review B, 2020, 102, .	1.1	29
51408	Generalized dipole correction for charged surfaces in the repeated-slab approach. Physical Review B, 2020, 102, .	1.1	20
51409	Topological Dirac Semimetal Phase in Bismuth Based Anode Materials for Sodium-Ion Batteries. Condensed Matter, 2020, 5, 39.	0.8	4
51410	Molecular Adsorption of NH3 and NO2 on Zr and Hf Dichalcogenides (S, Se, Te) Monolayers: A Density Functional Theory Study. Nanomaterials, 2020, 10, 1215.	1.9	16
51411	Aryl Diammonium Iodide Passivation for Efficient and Stable Hybrid Organâ€inorganic Perovskite Solar Cells. Advanced Functional Materials, 2020, 30, 2002366.	7.8	52
51412	Wideâ€Rangeâ€Tunable pâ€Type Conductivity of Transparent CuI_{1â^'}_xBr_x Alloy. Advanced Functional Materials, 2020, 30, 2003096.	7.8	20
51413	WB 5â^' x : Synthesis, Properties, and Crystal Structureâ€”New Insights into the Longâ€Debated Compound. Advanced Science, 2020, 7, 2000775.	5.6	17
51414	Enhanced electrocatalytic oxygen evolution activity in geometrically designed SrRuO3 thin films. Applied Surface Science, 2020, 529, 147065.	3.1	6
51415	Thermal transport across nanometre gaps: Phonon transmission vs. air conduction. International Journal of Heat and Mass Transfer, 2020, 158, 119963.	2.5	17
51416	Prediction of the Relative Free Energies of Drug Polymorphs above Zero Kelvin. Crystal Growth and Design, 2020, 20, 5211-5224.	1.4	26
51417	Polymorphism and Molten Nitrate Salt-Assisted Single Crystal to Single Crystal Ion Exchange in the Cesium Ferrogermanate Zeotype: CsFeGeO₄. Inorganic Chemistry, 2020, 59, 9699-9709.	1.9	10
51418	Sr₅Ga₈O₃S₁₄: A Nonlinear Optical Oxysulfide with Melilite-Derived Structure and Wide Band Gap. Inorganic Chemistry, 2020, 59, 9944-9950.	1.9	36
51419	A Deep-Learning Potential for Crystalline and Amorphous Liâ€“Si Alloys. Journal of Physical Chemistry C, 2020, 124, 16278-16288.	1.5	43
51420	Synaptic Characteristics of Amorphous Boron Nitride-Based Memristors on a Highly Doped Silicon Substrate for Neuromorphic Engineering. ACS Applied Materials & Interfaces, 2020, 12, 33908-33916.	4.0	52
51421	Mechanistic Insights into Photocatalyzed H₂ Dissociation on Au Clusters. Journal of the American Chemical Society, 2020, 142, 13090-13101.	6.6	48
51422	Isothermal Titration Calorimetry to Explore the Parameter Space of Organophosphorus Agrochemical Adsorption in MOFs. Journal of the American Chemical Society, 2020, 142, 12357-12366.	6.6	53
51423	Sub-5 nm monolayer germanium selenide (GeSe) MOSFETs: towards a high performance and stable device. Nanoscale, 2020, 12, 15443-15452.	2.8	27

#	Article	IF	Citations
51424	Energetics and dynamics of CH₄ and H₂O dissociation on metal surfaces. International Reviews in Physical Chemistry, 2020, 39, 267-318.	0.9	15
51425	Generalizable density functional theory based photoemission model for the accelerated development of photocathodes and other photoemissive devices. Physical Review B, 2020, 101, .	1.1	11
51426	Thermal hybrid exchange-correlation density functional for improving the description of warm dense matter. Physical Review B, 2020, 101, .	1.1	16
51427	Multitype Dirac fermions protected by orthogonal glide symmetries in a noncentrosymmetric system. Physical Review B, 2020, 102, .	1.1	5
51428	Scale-free ferroelectricity induced by flat phonon bands in HfO ₂. Science, 2020, 369, 1343-1347.	6.0	231
51429	Rich essential properties of boron, carbon, and nitrogen substituted germanenes. Applied Physics Express, 2020, 13, 085502.	1.1	6
51430	A 3D porous honeycomb carbon as Na-ion battery anode material with high capacity, excellent rate performance, and robust stability. Carbon, 2020, 168, 163-168.	5.4	25
51431	Solvothermal synthesis of copper-doped BiOBr microflowers with enhanced adsorption and visible-light driven photocatalytic degradation of norfloxacin. Chemical Engineering Journal, 2020, 401, 126012.	6.6	144
51432	Engineering Mo-O-C interface in MoS2@rGO via charge transfer boosts hydrogen evolution. Chemical Engineering Journal, 2020, 399, 126018.	6.6	49
51433	Studies on magnetic and electronic properties of <mml:math xmlns:mml="http://www.w3.org/1998/Math/MathML" altimg="si1.svg"><mml:mi>Î´</mml:mi></mml:math>-Pu<mml:math xmlns:mml="http://www.w3.org/1998/Math/MathML" altimg="si2.svg"><mml:msub><mml:mi>X</mml:mi><mml:mn>3</mml:mn></mml:msub></mml:math>		

#	Article	IF	Citations
51442	Electric filed dependent valley polarization in 2D WSe₂/CrGeTe₃ heterostructure. Nanotechnology, 2020, 31, 425702.	1.3	18
51443	Strain-induced vibrational properties of few layer black phosphorus and MoTe₂ via Raman spectroscopy. Nanotechnology, 2020, 31, 425707.	1.3	26
51444	Ab initio investigation of electronic and magnetic properties of antiferromagnetic/ferroelectric LaMnO3/BaTiO3 interface. Materials Research Express, 2020, 7, 055020.	0.8	15
51445	An experimental and first principles DFT investigation on the effect of Cu addition to Ni/Al2O3 catalyst for the dry reforming of methane. Applied Catalysis A: General, 2020, 602, 117699.	2.2	60
51446	Open Ni site coupled with SO42- functionality to prompt the radical interconversion of OHÂâ†"ÂSO4â•' exploited to decompose refractory pollutants. Chemical Engineering Journal, 2020, 400, 125971.	6.6	20
51447	The impact of crystal structures on the magnetic and electronic properties in double perovskite Sr2NiTeO6. Chemical Physics Letters, 2020, 754, 137776.	1.2	5
51448	Systematical study on the roles of transition alloying substitutions on anti-disproportionation reaction of ZrCo during charging and releasing hydrogen. International Journal of Hydrogen Energy, 2020, 45, 14028-14037.	3.8	11
51449	A computational investigation of the influence of acceptor moieties on photovoltaic performances and adsorption onto the TiO2 surface in triphenylamine-based dyes for DSSC application. Journal of Photochemistry and Photobiology A: Chemistry, 2020, 401, 112745.	2.0	18
51450	Understanding the immobilization mechanisms of hazardous heavy metal ions in the cage of sodalite at molecular level: A DFT study. Microporous and Mesoporous Materials, 2020, 306, 110409.	2.2	13
51451	Hybrid bromobismuthates: Synthesis, thermal stability and crystal structure of multicharged 3-ammoniopyridinium derivatives. Journal of Molecular Structure, 2020, 1221, 128807.	1.8	1
51452	Probing the interactions between interstitial hydrogen atoms in niobium through density functional theory calculations. Materials Today Communications, 2020, 25, 101415.	0.9	3
51453	â€œWater in salt/ionic liquidâ€•electrolyte for 2.8ÂV aqueous lithium-ion capacitor. Science Bulletin, 2020, 65, 1812-1822.	4.3	56
51454	Predicting Thermal Quenching in Inorganic Phosphors. Chemistry of Materials, 2020, 32, 6256-6265.	3.2	64
51455	Thermally Induced Chiral Aggregation of Dihydrobenzopyrenone on Au(111). ACS Applied Materials & Interfaces, 2020, 12, 35547-35554.	4.0	7
51456	Suppressing the Shuttle Effect and Dendrite Growth in Lithiumâ€“Sulfur Batteries. ACS Nano, 2020, 14, 9819-9831.	7.3	209
51457	Out-of-plane carrier spin in transition-metal dichalcogenides under electric current. Proceedings of the National Academy of Sciences of the United States of America, 2020, 117, 16749-16755.	3.3	8
51458	Phenomenon of ultra-fast tracer diffusion of Co in HCP high entropy alloys. Acta Materialia, 2020, 196, 220-230.	3.8	27
51459	Insight into the structure dependence on physical properties of the high temperature ceramics TaB2 boride. Vacuum, 2020, 177, 109427.	1.6	26

#	Article	IF	Citations
51460	Localized High Concentration Electrolytes for High Voltage Lithiumâ€“Metal Batteries: Correlation between the Electrolyte Composition and Its Reductive/Oxidative Stability. Chemistry of Materials, 2020, 32, 5973-5984.	3.2	97
51461	Doping Evolution of the Local Electronic and Structural Properties of the Double Perovskite Ba₂Na_{1â€“x}Ca_xOsO₆. Journal of Physical Chemistry C, 2020, 124, 16577-16585.	1.5	9
51462	Pressure Effect on Electronic and Excitonic Properties of Purely J-Aggregated Monolayer Organic Semiconductor. Journal of Physical Chemistry Letters, 2020, 11, 5896-5901.	2.1	1
51463	Platinumâ€“Nickel Nanowires with Improved Hydrogen Evolution Performance in Anion Exchange Membrane-Based Electrolysis. ACS Catalysis, 2020, 10, 9953-9966.	5.5	19
51464	Proton-transfer-induced 3D/2D hybrid perovskites suppress ion migration and reduce luminance overshoot. Nature Communications, 2020, 11, 3378.	5.8	108
51465	Unveiling hydrocerussite as an electrochemically stable active phase for efficient carbon dioxide electroreduction to formate. Nature Communications, 2020, 11, 3415.	5.8	121
51466	Correlations and incipient antiferromagnetic order within the linear Mn chains of metallic Ti4MnBi2. Physical Review B, 2020, 102, .	1.1	6
51467	Interplay of Magnetism and Topological Superconductivity in Bilayer Kagome Metals. Physical Review Letters, 2020, 125, 026401.	2.9	12
51468	Unravelling the Enigma of Nonoxidative Conversion of Methane on Iron Singleâ€Atom Catalysts. Angewandte Chemie, 2020, 132, 18745-18749.	1.6	12
51469	Unravelling the Enigma of Nonoxidative Conversion of Methane on Iron Singleâ€Atom Catalysts. Angewandte Chemie - International Edition, 2020, 59, 18586-18590.	7.2	44
51470	Mechanisms for As(OH)3 and H3AsO4 adsorption at anhydrous and hydrated surfaces of gibbsite and possibility for anionic As(III) and As(V) formation. Applied Surface Science, 2020, 525, 146494.	3.1	11
51471	Electronic structures and magnetism of Zr-, Th-, and U-based metal-organic frameworks (MOFs) by density functional theory. Computational Materials Science, 2020, 184, 109903.	1.4	25
51472	Paulingâ€™s rules guided Monte Carlo search (PAMCARS): A shortcut of predicting inorganic crystal structures. Computer Physics Communications, 2020, 256, 107486.	3.0	4
51473	The effect of local chemical environment on the energetics of stacking faults and vacancy platelets in<mml:math xmlns:mml="http://www.w3.org/1998/Math/MathML" altimg="si1.svg"><mml:mrow><mml:mi mathvariant="bold-italic">Î±</mml:mi></mml:mrow></mml:math>-zirconium. Journal of Nuclear Materials, 2020, 540, 152339.	1.3	9
51474	Crystal structural, thermal, and mechanical properties of Yb2+Ti2â^'O7â^'/2 solid solutions. Journal of Solid State Chemistry, 2020, 287, 121328.	1.4	4
51475	MCo1.5Sn (MÂ= Ti, Zr, and Hf) ternary compounds: a class of three-quarter Heusler compounds. Materials Today Physics, 2020, 15, 100251.	2.9	17
51476	Ordering and Structural Transformations in Layered K_xCrO₂ for K-Ion Batteries. Chemistry of Materials, 2020, 32, 6392-6400.	3.2	13
51477	Uranium-Incorporated Pyrochlore La₂(U_xMg_xZr_{1â€“2x})₂O₇ for Nuclear Waste Form: Structure and Phase Stability. Inorganic Chemistry, 2020, 59, 9919-9926.	4.7	27

#	Article	IF	Citations
51478	Theoretical Design of Lithium Chloride Superionic Conductors for All-Solid-State High-Voltage Lithium-Ion Batteries. ACS Applied Materials & Interfaces, 2020, 12, 34806-34814.	4.0	68
51479	Cobalt Ferrite Nanoparticles to Form a Catalytic Coâ€“Fe Alloy Carbide Phase for Selective CO₂ Hydrogenation to Light Olefins. ACS Catalysis, 2020, 10, 8660-8671.	5.5	95
51480	Strong Sequestration of Hydrogen Into the Earth's Core During Planetary Differentiation. Geophysical Research Letters, 2020, 47, e2020GL088303.	1.5	31
51481	Gapless spin liquid in a square-kagome lattice antiferromagnet. Nature Communications, 2020, 11, 3429.	5.8	41
51482	Single-atom metal-modified graphenylene as a high-activity catalyst for CO and NO oxidation. Physical Chemistry Chemical Physics, 2020, 22, 16224-16235.	1.3	18
51483	Identifying suitable ionic liquid electrolytes for Al dual-ion batteries: role of electrochemical window, conductivity and voltage. Materials Advances, 2020, 1, 1354-1363.	2.6	23
51484	Screw dislocation that converts p-type GaN to n-type: Microscopic study on Mg condensation and leakage current in pâ€“n diodes. Applied Physics Letters, 2020, 117, 012105.	1.5	22
51485	Magnetic phase transitions and spin density distribution in the molecular multiferroic system GaV4S8. Physical Review B, 2020, 102, .	1.1	10
51486	Quantum spin Hall effect in monolayer and bilayer <mml:math xmlns:mml="http://www.w3.org/1998/Math/MathML"><mml:msub><mml:mi mathvariant="normal">TaIrTe</mml:mi><mml:mn>4</mml:mn></mml:msub></mml:math>. Physical Review B, 2020, 102, .	1.1	16
51487	Observation and control of maximal Chern numbers in a chiral topological semimetal. Science, 2020, 369, 179-183.	6.0	103
51488	Experimental and theoretical studies of chitosan modified titanium dioxide composites for uranium and europium removal. Cellulose, 2020, 27, 7765-7777.	2.4	11
51489	Superconductivity of KFe2As2 Under Pressure: Ab Initio Study of Tetragonal and Collapsed Tetragonal Phases. Journal of Superconductivity and Novel Magnetism, 2020, 33, 2347-2354.	0.8	3
51490	Solute-vacancy clustering in aluminum. Acta Materialia, 2020, 196, 747-758.	3.8	96
51491	First-principles investigations on the mechanism of highly sensitive and selective trimethylamine sensing in MoO3. Applied Surface Science, 2020, 524, 146520.	3.1	12
51492	Formation, electronic, gas sensing and catalytic characteristics of graphene-like materials: A first-principles study. Applied Surface Science, 2020, 530, 147178.	3.1	21
51493	Surface energetics of <mml:math xmlns:mml="http://www.w3.org/1998/Math/MathML" altimg="si35.svg"><mml:mrow><mml:msub><mml:mrow><mml:mi mathvariant="normal">Al</mml:mi></mml:mrow><mml:mrow><mml:mi>x</mml:mi></mml:mrow></mml:msub><mml:msub><mml:mi mathvariant="normal">Ti</mml:mi></mml:mrow><mml:mrow><mml:mn>1</mml:mn><mml:mo>-</mml:mo><mml:mi>x</mml:mi></mml:mrow></mml:msub><mml:mi mathvariant="normal">N</mml:mi></mml:mrow></mml:math> alloys. Computational Materials Science, 2020, 183, 109813.	3.1	11
51494	How to produce isotope anomalies in mantle by using extremely small isotope fractionations: A process-driven amplification effect?. Geochimica Et Cosmochimica Acta, 2020, 291, 19-49.	1.6	4
51495	Microscopic Degradation in Formamidinium-Cesium Lead Iodide Perovskite Solar Cells under Operational Stressors. Joule, 2020, 4, 1743-1758.	11.7	156

#	Article	IF	Citations
51496	Improving the magnetic, electronic and optical properties of the monolayer WSe2 via Mn-X (XÂ=ÂO, S, Se) Tj ETQq0 0 0 rgBT /Overlock	0.8	5
51497	On Hydrogenated Bilayer GaN: New Stable Structures along the c-Plane, m-Plane, or a-Plane. Journal of Physical Chemistry C, 2020, 124, 16888-16894.	1.5	4
51498	An Ab Initio Perspective on the Key Defects of CsCu₅Se₃, a Possible Material for Optoelectronic Applications. Journal of Physical Chemistry C, 2020, 124, 4363-4368.	1.5	7
51499	Giant enhancement of perpendicular magnetic anisotropy and induced quantum anomalous Hall effect in graphene/ <mml:math xmlns:mml="http://www.w3.org/1998/Math/MathML"><mml:msub><mml:mi>NiI</mml:mi><mml:mn>2</mml:mn></mml:msub></mml heterostructures via tuning the van der Waals interlayer distance. Physical Review B, 2020, 101, .	1.1	37
51500	Solutionâ€Based, Anionâ€Doping of Li₄Ti₅O₁₂ Nanoflowers for Lithiumâ€Ion Battery Applications. Chemistry - A European Journal, 2020, 26, 9389-9402.	1.7	19
51501	Electronic and optical properties of gold-doped endohedral fullerenes. Journal of Materials Science, 2020, 55, 12980-12994.	1.7	2
51502	First-principles investigation of mechanical, electronic and optical properties of H-, F- and Cl-diamane. Applied Surface Science, 2020, 528, 147035.	3.1	47
51503	Facile renewable synthesis of nitrogen/oxygen co-doped graphene-like carbon nanocages as general lithium-ion and potassium-ion batteries anode. Carbon, 2020, 167, 685-695.	5.4	69
51504	Hemoglobin-derived Fe-Nx-S species supported by bamboo-shaped carbon nanotubes as efficient electrocatalysts for the oxygen evolution reaction. Carbon, 2020, 168, 588-596.	5.4	12
51505	Molecular dynamics simulations of zinc sulfide deposition on silver sulfide from aqueous solution. Computational Materials Science, 2020, 184, 109821.	1.4	6
51506	Fabrication of reactive flat-sheet ceramic membranes for oxidative degradation of ofloxacin by peroxymonosulfate. Journal of Membrane Science, 2020, 611, 118302.	4.1	55
51507	Frontier Molecular Orbital Based Analysis of Solidâ€“Adsorbate Interactions over Group 13 Metal Oxide Surfaces. Journal of Physical Chemistry C, 2020, 124, 15355-15365.	1.5	22
51508	Understanding Reaction Pathways in High Dielectric Electrolytes Using Î²-Mo₂C as a Catalyst for Liâ€“CO₂ Batteries. ACS Applied Materials & Interfaces, 2020, 12, 32633-32641.	4.0	22
51509	Discovery of superionic conductors by ensemble-scope descriptor. NPG Asia Materials, 2020, 12, .	3.8	16
51510	Tuning reactivity of Fischerâ€“Tropsch synthesis by regulating TiOx overlayer over Ru/TiO2 nanocatalysts. Nature Communications, 2020, 11, 3185.	5.8	114
51511	Unlocking the passivation nature of the cathodeâ€“air interfacial reactions in lithium ion batteries. Nature Communications, 2020, 11, 3204.	5.8	55
51512	Graph theory approach to determine configurations of multidentate and high coverage adsorbates for heterogeneous catalysis. Npj Computational Materials, 2020, 6, .	3.5	37
51513	(Fe,Ni)2P allabogdanite can be an ambient pressure phase in iron meteorites. Scientific Reports, 2020, 10, 8956.	1.6	10

#	Article	IF	Citations
51514	Kinetics mechanism insights into the oxygen evolution reaction on the (110) and (022) crystal facets of Î²-Cu₂V₂O₇. Catalysis Science and Technology, 2020, 10, 5129-5135.	2.1	4
51515	Structure and solvation of confined water and waterâ€“ethanol clusters within microporous BrÃ¸nsted acids and their effects on ethanol dehydration catalysis. Chemical Science, 2020, 11, 7102-7122.	3.7	68
51516	Atomic-layer-deposited SnO₂ on Pt/C prevents sintering of Pt nanoparticles and affects the reaction chemistry for the electrocatalytic glycerol oxidation reaction. Journal of Materials Chemistry A, 2020, 8, 15992-16005.	5.2	18
51517	2D monolayer boron sulfide as an efficient material for optical nanodevices. AIP Conference Proceedings, 2020, , .	0.3	2
51518	Ab initio molecular dynamics simulation of threshold displacement energies and defect formation energies in Y4Zr3O12. Journal of Applied Physics, 2020, 127, .	1.1	10
51519	TiSr antisite: An abundant point defect in SrTiO3. Journal of Applied Physics, 2020, 127, .	1.1	8
51520	Large thermoelectric figure of merit in hexagonal phase of <scp>2D</scp> selenium and tellurium. International Journal of Quantum Chemistry, 2020, 120, e26267.	1.0	19
51521	Metalâ€Halide Perovskite Design for Nextâ€Generation Memories: Firstâ€Principles Screening and Experimental Verification. Advanced Science, 2020, 7, 2001367.	5.6	17
51522	The potentially crucial role of quasi-particle interferences for the growth of silicene on graphite. Nano Research, 2020, 13, 2378-2383.	5.8	6
51523	A Novel Strategy of In Situ Trimerization of Cyano Groups Between the Ti3C2Tx (MXene) Interlayers for High-Energy and High-Power Sodium-Ion Capacitors. Nano-Micro Letters, 2020, 12, 135.	14.4	49
51524	Pressure-Induced Superconductivity in the Wide-Band-Gap Semiconductor Cu2Br2Se6 with a Robust Framework. Chemistry of Materials, 2020, 32, 6237-6246.	3.2	6
51525	Phase-Pure Copper Vanadate (Î±-CuV₂O₆): Solution Combustion Synthesis and Characterization. Chemistry of Materials, 2020, 32, 6247-6255.	3.2	27
51526	Influence of Different Molecular Design Strategies on Photovoltaic Properties of a Series of Triphenylamine-Based Organic Dyes for Dye-Sensitized Solar Cells: Insights from Theoretical Investigations. Journal of Physical Chemistry C, 2020, 124, 15036-15044.	1.5	17
51527	AA-Stacked Borophene-Graphene Bilayer with Covalent Bonding: Ab Initio Investigation of Structural, Electronic and Elastic properties. Journal of Physical Chemistry Letters, 2020, 11, 5668-5673.	2.1	34
51528	Air-Stable Calcium Cyanamide-Supported Ruthenium Catalyst for Ammonia Synthesis and Decomposition. ACS Applied Energy Materials, 2020, 3, 6573-6582.	2.5	27
51529	Zeolitic Imidazolate Framework Cores Decorated with Pd Nanoparticles and Coated Further with Metalâ€“Organic Framework Shells (ZIF-8@Pd@MOF-74) as Nanocatalysts for Chemoselective Hydrogenation Reactions. ACS Applied Nano Materials, 2020, 3, 7242-7251.	2.4	31
51530	Molecular Beam Epitaxy of Transition Metal (Ti-, V-, and Cr-) Tellurides: From Monolayer Ditellurides to Multilayer Self-Intercalation Compounds. ACS Nano, 2020, 14, 8473-8484.	7.3	76
51531	Pairing of Transition Metal Dichalcogenides and Doped Graphene for Catalytically Dual Active Interfaces for the Hydrogen Evolution Reaction. ACS Sustainable Chemistry and Engineering, 2020, , .	3.2	0

#	Article	IF	Citations
51532	Number mismatch between cations and anions as an indicator for low lattice thermal conductivity in chalcogenides. Npj Computational Materials, 2020, 6, .	3.5	13
51533	Complex strengthening mechanisms in the NbMoTaW multi-principal element alloy. Npj Computational Materials, 2020, 6, .	3.5	111
51534	Electronic structure, optoelectronic properties and enhanced photocatalytic response of GaNâ€“GeC van der Waals heterostructures: a first principles study. RSC Advances, 2020, 10, 24127-24133.	1.7	28
51535	Investigation on the thermoelectric properties of single & bilayers of SrS. AIP Conference Proceedings, 2020, , .	0.3	0
51536	Electronic and optical properties of a structural defect in 2D MgF2 monolayer. AIP Conference Proceedings, 2020, , .	0.3	4
51537	Experimental Synthesis of Strained Monolayer Silver Arsenide on Ag(111) Substrates. Chinese Physics Letters, 2020, 37, 068103.	1.3	10
51538	On the effect of supercell size and strain localization in computational tensile tests. Modelling and Simulation in Materials Science and Engineering, 2020, 28, 065011.	0.8	4
51539	Role of Lithium Codoping in Enhancing the Scintillation Yield of Aluminate Garnets. Physical Review Applied, 2020, 13, .	1.5	8
51540	Performance Evaluation and Device Physics Investigation of Negative-Capacitance MOSFETs Based on Ultrathin Body Silicon and Monolayer MoS₂. IEEE Transactions on Electron Devices, 2020, 67, 3049-3055.	1.6	5
51541	Structural, defect, transport and dopant properties of AgNbO 3. ChemNanoMat, 2020, 6, 1337-1345.	1.5	7
51542	Cu Atomic Chain Supported on Graphene Nanoribbon for Effective Conversion of CO 2 to Ethanol. ChemPhysChem, 2020, 21, 1768-1774.	1.0	9
51543	Effect of metal composition on the structure of layer-structured cathode materials for Li-ion batteries. Applied Physics A: Materials Science and Processing, 2020, 126, 1.	1.1	8
51544	Quasiparticle interference and impurity resonances on WTe2. Nano Research, 2020, 13, 2534-2540.	5.8	7
51545	NiBi intermetallic compounds catalyst toward selective hydrogenation of unsaturated aldehydes. Applied Catalysis B: Environmental, 2020, 277, 119273.	10.8	57
51546	Two-level ablation and damage morphology of Ru films under femtosecond extreme UV irradiation. Applied Surface Science, 2020, 528, 146952.	3.1	15
51547	Insights on boosting oxygen evolution reaction performance via boron incorporation into nitrogen-doped carbon electrocatalysts. Applied Surface Science, 2020, 528, 146979.	3.1	18
51548	Boron-, nitrogen-, aluminum-, and phosphorus-doped graphite electrodes for non-lithium ion batteries. Current Applied Physics, 2020, 20, 988-993.	1.1	8
51549	First-principles calculations on two superhard BCN allotropes: P3Â¯m1-BCN and I41md-BCN. Computational Materials Science, 2020, 184, 109869.	1.4	6

#	Article	IF	Citations
51550	A Revisited Mechanism of the Graphite-to-Diamond Transition at High Temperature. Matter, 2020, 3, 864-878.	5.0	30
51551	Ultrasonically controlled growth of monodispersed octahedral BiVO4 microcrystals for improved photoelectrochemical water oxidation. Ultrasonics Sonochemistry, 2020, 68, 105233.	3.8	18
51552	A Density Functional Theory Study of the Hydrogen Absorption in High Entropy Alloy TiZrHfMoNb. Inorganic Chemistry, 2020, 59, 9774-9782.	1.9	31
51553	Predicting Crystal Morphology Using a Geometric Descriptor: A Comparative Study of Elemental Crystals with High-Throughput DFT Calculations. Journal of Physical Chemistry C, 2020, 124, 15920-15927.	1.5	6
51554	Band Gap Engineering in an Efficient Solar-Driven Interfacial Evaporation System. ACS Applied Materials & Interfaces, 2020, 12, 32880-32887.	4.0	73
51555	Monolayered Platinum Nanoparticles as Efficient Electrocatalysts for the Mass Production of Electrolyzed Hydrogen Water. Scientific Reports, 2020, 10, 10126.	1.6	11
51556	New layered perovskite family built from [CeTa₂O₇]^{â˜'} layers: coloring mechanism from unique multi-transitions. Chemical Communications, 2020, 56, 8591-8594.	2.2	6
51557	Heterometallic multinuclear nodes directing MOF electronic behavior. Chemical Science, 2020, 11, 7379-7389.	3.7	14
51558	Electronic and optoelectronic properties of van der Waals heterostructure based on graphene-like GaN, blue phosphorene, SiC, and ZnO: A first principles study. Journal of Applied Physics, 2020, 127, .	1.1	19
51559	Discovery of an unconventional charge modulation on the surface of charge-density-wave material TaTe₄. New Journal of Physics, 2020, 22, 083025.	1.2	7
51560	Band-Structure Engineering of <mml:math xmlns:mml="http://www.w3.org/1998/Math/MathML" display="inline" overflow="scroll"><mml:msub><mml:mi>Zn</mml:mi><mml:mi>x</mml:mi></mml:msub><mml:msub><mml:mi>Cd</mml:mi><mml:mi><mml:m mathvariant="normal">S</mml:mi></mml:mrow></mml:mrow><mml:mi>y</mml:mi></mml:msub><mml:msub><mml:mi>Se</mml:mi> Physical Review Applied, 2020, 13, .	1.5	8
51561	Ab initio description of the <mml:math xmlns:mml="http://www.w3.org/1998/Math/MathML"><mml:mrow><mml:msub><mml:mi>Bi</mml:mi><mml:mn>2</mml:mn></mml:msub><mml:msub><mml:mi mathvariant="normal">O</mml:mi><mml:mrow><mml:mn>8</mml:mn><mml:mo>+</mml:mo><mml:mi>Î´</mml:mi></mml:mrow> electronic structure. Physical Review B, 2020, 101, .	1.1	11
51562	Thermophysical and mechanical properties of novel highâ€entropy metal nitrideâ€carbides. Journal of the American Ceramic Society, 2020, 103, 6475-6489.	1.9	66
51563	Discovery of a Quaternary Sulfide, Ba_{2â€“x}LiAlS₄:Eu²⁺, and Its Potential as a Fast-Decaying LED Phosphor. Chemistry of Materials, 2020, 32, 6697-6705.	3.2	27
51564	First-Principles-Based Microkinetic Simulations of CO₂ Hydrogenation to Methanol over Intermetallic GaPd₂: Method Development to Include Complex Interactions between Surface Adsorbates. Journal of Physical Chemistry C, 2020, 124, 15977-15987.	1.5	16
51565	How Noninnocent Spectator Species Improve the Oxygen Reduction Activity of Single-Atom Catalysts: Microkinetic Models from First-Principles Calculations. ACS Catalysis, 2020, 10, 9129-9135.	5.5	42
51566	Tuning Electrical Conductance in Bilayer MoS₂ through Defect-Mediated Interlayer Chemical Bonding. ACS Nano, 2020, 14, 10265-10275.	7.3	40
51567	New refractory MAB phases and their 2D derivatives: insight into the effects of valence electron concentration and chemical composition. RSC Advances, 2020, 10, 25836-25847.	1.7	9

#	Article	IF	Citations
51568	Motif based high-throughput structure prediction of superconducting monolayer titanium boride. Physical Chemistry Chemical Physics, 2020, 22, 16236-16243.	1.3	8
51569	Van der Waals heterostructures of SiC and Janus MSSe (M = Mo, W) monolayers: a first principles study. RSC Advances, 2020, 10, 25801-25807.	1.7	22
51570	Quasi-one-dimensional Sb2(S,Se)3 alloys as bandgap-tunable and defect-tolerant photocatalytic semiconductors. Journal of Chemical Physics, 2020, 153, 014703.	1.2	32
51571	Image potential states of germanene. 2D Materials, 2020, 7, 035021.	2.0	25
51572	Toggling Valley-Spin Locking and Nonlinear Optical Properties of Single-Element Multiferroic Monolayers via Light. Physical Review Applied, 2020, 14, .	1.5	17
51573	Role of Ga and In adatoms in the epitaxial growth of <mml:math xmlns:mml="http://www.w3.org/1998/Math/MathML"><mml:mrow><mml:mi>Î²</mml:mi><mml:mtext>â^'</mml:mtext><mml:msub><mml:mi mathvariant="normal">O</mml:mi><mml:mn>3</mml:mn></mml:msub></mml:mrow></mml:math>. Physical Review B, 2020, 102, .	1.1	11
51574	Intrinsic anomalous valley Hall effect in single-layer <mml:math xmlns:mml="http://www.w3.org/1998/Math/MathML"><mml:mrow><mml:mi mathvariant="normal">N</mml:mi><mml:msub><mml:mi mathvariant="normal">b</mml:mi><mml:mn>3</mml:mn></mml:msub><mml:msub><mml:mi mathvariant="normal">I</mml:mi><mml:mn>8</mml:mn></mml:msub></mml:mrow></mml:math>. Physical Review B, 2020, 102, .	1.1	108
51575	Nonreciprocal second-harmonic generation in few-layer chromium triiodide. Physical Review B, 2020, 102, .	1.1	13
51576	Structure, stress, and mechanical properties of Mo-Al-N thin films deposited by dc reactive magnetron cosputtering: Role of point defects. Journal of Vacuum Science and Technology A: Vacuum, Surfaces and Films, 2020, 38, .	0.9	12
51577	Collective Dipoleâ€Dominated Doping of Monolayer MoS₂: Orientation and Magnitude Control via the Supramolecular Approach. Advanced Functional Materials, 2020, 30, 2002846.	7.8	27
51578	Novel superhard boron-rich nitrides under pressure. Science China Materials, 2020, 63, 2358-2364.	3.5	17
51579	Defect behavior and radiation tolerance of MAB phases (MoAlB and Fe2AlB2) with comparison to MAX phases. Acta Materialia, 2020, 196, 505-515.	3.8	40
51580	Unveiling the crystallographic facet dependence of the photoelectrochemical glycerol oxidation on bismuth vanadate. Applied Catalysis B: Environmental, 2020, 278, 119303.	10.8	53
51581	Robust tuning metal/carbon heterointerfaces via ketonic oxygen enables hydrogen evolution reaction outperforming Pt/C. Applied Surface Science, 2020, 529, 147080.	3.1	3
51582	Exploring the hydrogen evolution capabilities of earth-abundant ternary metal borides for neutral and alkaline water-splitting. Electrochimica Acta, 2020, 354, 136738.	2.6	30
51583	Towards continuous ammonia electro-oxidation reaction on Pt catalysts with weakened adsorption of atomic nitrogen. International Journal of Hydrogen Energy, 2020, 45, 21816-21824.	3.8	7
51584	Core-shell structured CuCo2S4@CoMoO4 nanorods for advanced electrode materials. Journal of Alloys and Compounds, 2020, 844, 156133.	2.8	81
51585	First-principles study of the surface properties of uranium carbides. Journal of Nuclear Materials, 2020, 542, 152257.	1.3	8

#	Article	IF	Citations
51586	Site preference and atomic ordering in the structure of In3Pd5: AÂtheoretical study. Journal of Solid State Chemistry, 2020, 290, 121567.	1.4	2
51587	Energetic, electronic and structural DFT analysis of point defects in refractory BCC metals. Materials Today Communications, 2020, 24, 101323.	0.9	2
51588	Janus XM-GaS (M=Si, Ge, Sn; X=N, P) monolayers: Multifunctional properties for photocatalysis, piezoelectricity and second harmonic generation. Physica B: Condensed Matter, 2020, 594, 412366.	1.3	12
51589	Two-dimensional Bi2Se3 monolayer with high mobility and enhanced optical absorption in the UVâ€“visible light region. Physica E: Low-Dimensional Systems and Nanostructures, 2020, 124, 114272.	1.3	20
51590	Monolayer NbF4: a 4d1-analogue of cuprates. Science Bulletin, 2020, 65, 1901-1906.	4.3	3
51591	Local Structure Distortion Induced Broad Band Emission in the All-Inorganic BaScO₂F:Eu²⁺ Perovskite. Chemistry of Materials, 2020, 32, 6640-6649.	3.2	39
51592	Theoretical study of the structures and electronic properties for NiX (Xâ€‰=â€‰Naâ€“Cl) clusters. Applied Physics A: Materials Science and Processing, 2020, 126, 1.	1.1	0
51593	Effects of oxygen impurity concentration on the interfacial properties of Ta3N5/Ta5N6 composite photoelectrode: A DFT calculation. Applied Catalysis B: Environmental, 2020, 278, 119296.	10.8	6
51594	Optimizing the electronic structure of cobalt via synergized oxygen vacancy and Co-N-C to boost reversible oxygen electrocatalysis for rechargeable Zn-air batteries. Applied Catalysis B: Environmental, 2020, 278, 119300.	10.8	111
51595	Stabilizing platinum atoms on CeO2 oxygen vacancies by metal-support interaction induced interface distortion: Mechanism and application. Applied Catalysis B: Environmental, 2020, 278, 119304.	10.8	120
51596	Theoretical study on novel orthorhombic ternary monocarbides M0.5Re0.5C (M=V, Nb, Ta) from first-principles calculations. Ceramics International, 2020, 46, 24624-24634.	2.3	10
51597	First-principles study on strain-controllable magnetoelectric coupling behaviour of two-dimensional BaTiO3 (001) ultrathin film with surface Ba vacancy. Ceramics International, 2020, 46, 24682-24688.	2.3	2
51598	Adsorption and decomposition properties of HMX on MgH2(1Â1Â0) surface: A first Principles study. Chemical Physics, 2020, 538, 110875.	0.9	5
51599	Structural, electronic and catalytic properties of bimetallic Pt Ag (n=1â€“7) clusters. Journal of Alloys and Compounds, 2020, 845, 155897.	2.8	15
51600	Investigation on the preference of the martensitic structure in off-stoichiometric Ni-Mn-In alloys by first-principle calculations. Journal of Magnetism and Magnetic Materials, 2020, 514, 167194.	1.0	2
51601	Ab-initio calculations of hydrogen diffusion coefficient in monoclinic zirconia. Journal of Nuclear Materials, 2020, 539, 152333.	1.3	4
51602	Hollow Mn3O4 nanospheres on graphene matrix for oxygen reduction reaction and supercapacitance applications: Experimental and theoretical insight. Journal of Power Sources, 2020, 471, 228465.	4.0	37
51603	Mechanochemical synthesis and ion transport properties of Na3OX (X = Cl, Br, I and BH4) antiperovskite solid electrolytes. Journal of Power Sources, 2020, 471, 228489.	4.0	47

#	Article	IF	Citations
51604	Theoretical investigation of molybdenum/tungsten-vanadium solid solution alloy membranes: Thermodynamic stability and hydrogen permeation. Journal of Membrane Science, 2020, 608, 118200.	4.1	26
51605	Dipotassium terephthalate as promising potassium storing anode with DFT calculations. Materials Today Energy, 2020, 17, 100454.	2.5	12
51606	Positional-Fe-doping-induced spin polarization effects on magnetoelectric properties and spin texture of 2D-SiC. Physica E: Low-Dimensional Systems and Nanostructures, 2020, 122, 114181.	1.3	1
51607	Electronic properties of XPtY-Graphene (X/Y = S, Se and Te) contacts. Physica E: Low-Dimensional Systems and Nanostructures, 2020, 124, 114311.	1.3	8
51608	Properties of RhP predicted by first-principles. Physics Letters, Section A: General, Atomic and Solid State Physics, 2020, 384, 126426.	0.9	0
51609	Orthorhombic carbon oC48: A new superhard carbon allotrope. Solid State Communications, 2020, 319, 113994.	0.9	10
51610	First-principles study of CO and NO adsorption on pristine and transition metal doped blue phosphorene. Vacuum, 2020, 179, 109503.	1.6	28
51611	Tailoring Electronic and Magnetic Properties of Graphene by Phosphorus Doping. ACS Applied Materials & Interfaces, 2020, 12, 34074-34085.	4.0	20
51612	Mechanistic Insight into Bis(amino) Copper Formate Thermochemistry for Conductive Molecular Ink Design. ACS Applied Materials & Interfaces, 2020, 12, 33039-33049.	4.0	14
51613	Boosting hydrogen evolution on MoS2 via co-confining selenium in surface and cobalt in inner layer. Nature Communications, 2020, 11, 3315.	5.8	229
51614	Oxygen-vacancy induced magnetic phase transitions in multiferroic thin films. Npj Computational Materials, 2020, 6, .	3.5	25
51615	Monolayer PC₅/PC₆: promising anode materials for lithium-ion batteries. Physical Chemistry Chemical Physics, 2020, 22, 16665-16671.	1.3	24
51616	Oxidative dehydrogenation of propane on the oxygen adsorbed edges of boron nitride nanoribbons. Catalysis Science and Technology, 2020, 10, 5181-5195.	2.1	10
51617	A first-principles study of damage induced by gaseous species He, Kr, and Xe on the structure of nuclear fuel, U3Si. Journal of Applied Physics, 2020, 127, .	1.1	5
51618	First-principles study of helium behavior in nickel with noble gas incorporation. Journal of Applied Physics, 2020, 127, 175903.	1.1	4
51619	On the elastic anisotropy of the entropy-stabilized oxide (Mg, Co, Ni, Cu, Zn)O compound. Journal of Applied Physics, 2020, 128, .	1.1	14
51620	Probing the continuum scattering and magnetic collapse in single-crystalline <mml:math xmlns:mml="http://www.w3.org/1998/Math/MathML"><mml:mrow><mml:mi>Î±</mml:mi><mml:mtext>â€™</mml:mtext><mml:mi mathvariant="normal">L</mml:mi><mml:msub><mml:mi mathvariant="normal">i</mml:mi><mml:mn>2</mml:mn></mml:msub><mml:mi>Ir</mml:mi><mml:msub><mml:mi mathvariant="normal">O</mml:mi><mml:mn>3</mml:mn></mml:msub></mml:mrow></mml:math> by Raman spectroscopy. Physical Review B, 2020, 101, .	1.1	11
51621	High-pressure silica phase transitions: Implications for deep mantle dynamics and silica crystallization in the protocore. American Mineralogist, 2020, 105, 1014-1020.	0.9	7

#	Article	IF	Citations
51622	Hydrogenation of cinnamaldehyde to cinnamyl alcohol with metal phosphides: Catalytic consequences of product and pyridine doping. Applied Catalysis B: Environmental, 2020, 277, 119272.	10.8	33
51623	The â€œelectric-dipoleâ€•effect of Ptâ€“Ni for enhanced catalytic dehydrogenation of ammonia borane. Journal of Alloys and Compounds, 2020, 844, 156253.	2.8	14
51624	Thermodynamic assessment of the Alâ€“Scâ€“N ternary system and phase-separated region of the strained wurtzite phase. Journal of the European Ceramic Society, 2020, 40, 5410-5422.	2.8	5
51625	First-principle investigation on the interfacial structure evolution of the Î´′/Î¸′/Î′ composite precipitates in Al-Cu-Li alloys. Journal of Materials Science and Technology, 2020, 58, 205-214.	5.6	36
51626	Effect of Al doping on the structural and optical properties of CuO nanoparticles prepared by solution combustion method: Experiment and DFT investigation. Journal of Physics and Chemistry of Solids, 2020, 147, 109646.	1.9	39
51627	Effects of lanthanides doping on the optical properties of graphene/WSe2 heterostructure based on ab-initio calculations. Physics Letters, Section A: General, Atomic and Solid State Physics, 2020, 384, 126663.	0.9	6
51628	Inherent Resistance of Seed-Mediated Grown MoSe₂ Monolayers to Defect Formation. ACS Applied Materials & Interfaces, 2020, 12, 34297-34305.	4.0	7
51629	2D-Covalent Organic Frameworks with Interlayer Hydrogen Bonding Oriented through Designed Nonplanarity. Journal of the American Chemical Society, 2020, 142, 12987-12994.	6.6	51
51630	Ferromagnetic dual topological insulator in a two-dimensional honeycomb lattice. Materials Horizons, 2020, 7, 2431-2438.	6.4	16
51631	Tuning energy barriers by doping 2D group-IV monochalcogenides. Journal of Applied Physics, 2020, 127, .	1.1	4
51632	Mechanisms of hydrogen atom interactions with MoS₂ monolayer. Journal of Physics Condensed Matter, 2020, 32, 445003.	0.7	2
51633	Direct time-domain determination of electron-phonon coupling strengths in chromium. Physical Review B, 2020, 102, .	1.1	4
51634	Adsorption and dissociation of H2O monomer on ceria(111): Density functional theory calculations. Modern Physics Letters B, 2020, 34, 2050254.	1.0	1
51635	Antisite Defectâ€Enhanced Thermoelectric Performance of Topological Crystalline Insulators. Advanced Functional Materials, 2020, 30, 2003162.	7.8	8
51636	Anisotropic Phonon Response of Fewâ€Layer PdSe₂ under Uniaxial Strain. Advanced Functional Materials, 2020, 30, 2003215.	7.8	26
51637	Anomalous Behavior of 2D Janus Excitonic Layers under Extreme Pressures. Advanced Materials, 2020, 32, e2002401.	11.1	36
51638	Preparation and characterization of colorful graphene oxide papers and flexible Nâ€doping graphene papers for supercapacitor and capacitive deionization. , 2020, 2, 656-674.		32
51639	Effect of alkali metal auxiliary in HCHO oxidation on the model catalyst Na2O/Pd(1Â1Â1): A DFT study. Applied Surface Science, 2020, 523, 146488.	3.1	3

#	Article	IF	Citations
51640	High exothermic dissociation in van der Waals like hexagonal two dimensional nitrogene from firstâ€“principles molecular dynamics. Applied Surface Science, 2020, 529, 146552.	3.1	11
51641	2D anisotropic type-I SiS vdW heterostructures toward infrared polarized optoelectronics applications. Applied Surface Science, 2020, 529, 147026.	3.1	6
51642	Vacancy-driven variations in the phonon density of states of fast neutron irradiated nuclear graphite. Carbon, 2020, 168, 42-54.	5.4	13
51643	Lithium vacancy migration in Li2O2: From first principles studies. Computational Materials Science, 2020, 184, 109873.	1.4	6
51644	Bismuthene: Epitaxially grown on MoTe2 and its grain boundary. Journal of Crystal Growth, 2020, 546, 125787.	0.7	3
51645	High-temperature polaronic transport in PrBaCoTa(Nb)O6 perovskite-like phases. Journal of Physics and Chemistry of Solids, 2020, 147, 109645.	1.9	4
51646	Correlation between experimental and theoretical study of scheelite and wolframite-type tungstates. Materials Today Communications, 2020, 25, 101417.	0.9	4
51647	Interfacial chemical binding and improved kinetics assisting stable aqueous Znâ€“MnO2 batteries. Materials Today Energy, 2020, 17, 100475.	2.5	53
51648	First-principles investigations of intrinsic point defects and helium impurities in vanadium monocarbide. Nuclear Instruments & Methods in Physics Research B, 2020, 479, 163-170.	0.6	3
51649	Electronic and optical characteristics of GaS/g-C3N4 van der Waals heterostructures: Effects of biaxial strain and vertical electric field. Vacuum, 2020, 180, 109562.	1.6	35
51650	Boosted Activity for Toluene Selective Photooxidation over Fe-Doped Bi₂WO₆. Industrial & Engineering Chemistry Research, 2020, 59, 13528-13538.	1.8	37
51651	Efficient Method for Modeling Polarons Using Electronic Structure Methods. Journal of Chemical Theory and Computation, 2020, 16, 5264-5278.	2.3	38
51652	Atomic Structure and Work Function Modulations in Two-Dimensional Ultrathin CuI Films on Cu(111) from First-Principles Calculations. Journal of Physical Chemistry C, 2020, 124, 16362-16370.	1.5	8
51653	Polymer Structure Prediction from First Principles. Journal of Physical Chemistry Letters, 2020, 11, 5823-5829.	2.1	20
51654	Symmetry Dictated Grain Boundary State in a Two-Dimensional Topological Insulator. Nano Letters, 2020, 20, 5837-5843.	4.5	16
51655	Contrasting SnTeâ€“NaSbTe₂ and SnTeâ€“NaBiTe₂ Thermoelectric Alloys: High Performance Facilitated by Increased Cation Vacancies and Lattice Softening. Journal of the American Chemical Society, 2020, 142, 12524-12535.	6.6	51
51656	Three-terminal Weyl complex with double surface arcs in a cubic lattice. Npj Computational Materials, 2020, 6, .	3.5	29
51657	Single transition metal atoms anchored on a C₂N monolayer as efficient catalysts for hydrazine electrooxidation. Physical Chemistry Chemical Physics, 2020, 22, 16691-16700.	1.3	12

#	Article	IF	Citations
51658	Sulfur doped Li_{1.3}Al_{0.3}Ti_{1.7}(PO₄)₃ solid electrolytes with enhanced ionic conductivity and a reduced activation energy barrier. Physical Chemistry Chemical Physics, 2020, 22, 17221-17228.	1.3	33
51659	New Liâ€“Mg phosphates with a 3D framework: experimental and ab initio calculations. Dalton Transactions, 2020, 49, 10069-10083.	1.6	0
51660	Optical spectra of 2D monolayers from time-dependent density functional theory. Faraday Discussions, 2020, 224, 467-482.	1.6	8
51661	Theoretical study of two-dimensional bis(iminothiolato)metal monolayers as promising electrocatalysts for carbon dioxide reduction. New Journal of Chemistry, 2020, 44, 12299-12306.	1.4	11
51662	Unleashing ultra-fast sodium ion storage mechanisms in interface-engineered monolayer MoS₂/C interoverlapped superstructure with robust charge transfer networks. Journal of Materials Chemistry A, 2020, 8, 15002-15011.	5.2	26
51663	Comparative investigation of the thermal transport properties of Janus SnSSe and SnS₂ monolayers. Physical Chemistry Chemical Physics, 2020, 22, 16796-16803.	1.3	19
51664	A novel self-assembly approach for synthesizing nanofiber aerogel supported platinum single atoms. Journal of Materials Chemistry A, 2020, 8, 15094-15102.	5.2	5
51665	Sharp-tip enhanced catalytic CO oxidation by atomically dispersed Pt₁/Pt₂on a raised graphene oxide platform. Journal of Materials Chemistry A, 2020, 8, 12485-12494.	5.2	9
51666	Discriminating High-Pressure Water Phases Using Rare-Event Determined Ionic Dynamical Properties. Chinese Physics Letters, 2020, 37, 043101.	1.3	5
51667	Data-driven discovery of 3D and 2D thermoelectric materials. Journal of Physics Condensed Matter, 2020, 32, 475501.	0.7	42
51668	CuAu, a hexagonal two-dimensional metal. 2D Materials, 2020, 7, 045017.	2.0	11
51669	Liquid Phase, Aerobic Oxidation of Benzyl Alcohol over the Catalyst System (Pt/TiO₂+H₂O). ChemCatChem, 2020, 12, 4760-4764.	1.8	10
51670	Modified Failure Mechanism of Silicon through Excess Electrons and Holes. Jom, 2020, 72, 3160-3169.	0.9	0
51671	Anisotropic PC₆N Monolayer with Wide Band Gap and Ultrahigh Carrier Mobility. Journal of Physical Chemistry C, 2020, 124, 4330-4337.	1.5	14
51672	Large Second Harmonic Generation in Elemental Î±-Sb and Î±-Bi Monolayers. Journal of Physical Chemistry C, 2020, 124, 5506-5513.	1.5	14
51673	Strongly Bound Surface Water Affects the Shape Evolution of Cerium Oxide Nanoparticles. Journal of Physical Chemistry C, 2020, 124, 3577-3588.	1.5	26
51674	Rapid Decoherence Induced by Light Expansion Suppresses Charge Recombination in Mixed Cation Perovskites: Time-Domain ab Initio Analysis. Journal of Physical Chemistry Letters, 2020, 11, 1601-1608.	2.1	19
51675	Epitaxial Growth of Flat, Metallic Monolayer Phosphorene on Metal Oxide. ACS Nano, 2020, 14, 2385-2394.	7.3	27

#	Article	IF	Citations
51676	Tuning the Redox Activity of Metalâ€“Organic Frameworks for Enhanced, Selective O₂ Binding: Design Rules and Ambient Temperature O₂ Chemisorption in a Cobaltâ€“Triazolate Framework. Journal of the American Chemical Society, 2020, 142, 4317-4328.	6.6	67
51677	Strain-driven growth of ultra-long two-dimensional nano-channels. Nature Communications, 2020, 11, 772.	5.8	31
51678	Thermochemical stability, and electronic and dielectric properties of Janus bismuth oxyhalide BiOX (X) Tj ETQq0 0 0 rgBT /Overlock 10 Tf	2.2	15
51679	Intrinsic ferromagnetism with high temperature, strong anisotropy and controllable magnetization in the CrX (X = P, As) monolayer. Nanoscale, 2020, 12, 5464-5470.	2.8	48
51680	Potential molecular semiconductor devices: cyclo-C_n (n = 10 and 14) with higher stabilities and aromaticities than acknowledged cyclo-C₁₈. Physical Chemistry Chemical Physics, 2020, 22, 4823-4831.	1.3	31
51681	Ultra-high mechanical flexibility of 2D silicon telluride. Applied Physics Letters, 2020, 116, .	1.5	13
51682	Orbital localization induced magnetization in nonmetal-doped phosphorene. Journal Physics D: Applied Physics, 2020, 53, 155001.	1.3	4
51683	Bright magnetic dipole radiation from two-dimensional lead-halide perovskites. Science Advances, 2020, 6, eaay4900.	4.7	24
51684	Ultrahigh Capacity of Monolayer Dumbbell C₄N as a Promising Anode Material for Lithium-Ion Battery. Journal of the Electrochemical Society, 2020, 167, 020538.	1.3	11
51685	Stability-Ranking of Crystalline Ice Polymorphs Using Density-Functional Theory. Crystals, 2020, 10, 40.	1.0	2
51686	Examination of high-throughput hybrid calculations using coarser reciprocal space meshes. Current Applied Physics, 2020, 20, 379-383.	1.1	10
51687	Strain engineering for Janus palladium-gold bimetallic nanoparticles: Enhanced electrocatalytic performance for oxygen reduction reaction and zinc-air battery. Chemical Engineering Journal, 2020, 389, 124240.	6.6	40
51688	Bimetallic Pd-Based surface alloys promote electrochemical oxidation of formic acid: Mechanism, kinetics and descriptor. Journal of Power Sources, 2020, 451, 227830.	4.0	27
51689	Influence of phase and interface properties on the stress state dependent fracture initiation behavior in DP steels through computational modeling. Materials Science & Engineering A: Structural Materials: Properties, Microstructure and Processing, 2020, 776, 138981.	2.6	9
51690	The effects of vanadium substitution on one-dimensional tunnel structures of cryptomelane: Combined TEM and DFT study. Nano Energy, 2020, 71, 104571.	8.2	11
51691	Electronic and optical properties tuned by strain and external electric field of g-ZnO/2H-TiS2 van der Waals heterostructures. Vacuum, 2020, 174, 109232.	1.6	12
51692	Acidic Properties of Alkaline-Earth Phosphates Determined by an Experimental-Theoretical Approach. Journal of Physical Chemistry C, 2020, 124, 2013-2023.	1.5	3
51693	Role of Rare Earth Ions in the Prevention of Dealumination of Zeolite Y for Fluid Cracking Catalysts. Journal of Physical Chemistry C, 2020, 124, 4626-4636.	1.5	29

#	Article	IF	Citations
51694	Low Pt-Content Ternary PtNiCu Nanoparticles with Hollow Interiors and Accessible Surfaces as Enhanced Multifunctional Electrocatalysts. ACS Applied Materials & Interfaces, 2020, 12, 9600-9608.	4.0	54
51695	Computational discovery of two-dimensional HfO₂ zoo based on evolutionary structure search. Physical Chemistry Chemical Physics, 2020, 22, 4481-4489.	1.3	5
51696	Black arsenene as a promising anisotropic sensor with high sensitivity and selectivity: insights from a first-principles investigation. Journal of Materials Chemistry C, 2020, 8, 4073-4080.	2.7	18
51697	Valley polarization in monolayer CrX₂ (XÂ=ÂS, Se) with magnetically doping and proximity coupling. New Journal of Physics, 2020, 22, 033002.	1.2	31
51698	Ferroelectric polarization switching induced from water adsorption in <mml:math xmlns:mml="http://www.w3.org/1998/Math/MathML"><mml:msub><mml:mi>BaTiO</mml:mi><mml:mn>3</mml:mn></mml:msub></m ultrathin films. Physical Review B, 2020, 101, .	1.1	5
51699	Signatures of Sixfold Degenerate Exotic Fermions in a Superconducting Metal PdSb₂. Advanced Materials, 2020, 32, e1906046.	11.1	36
51700	The Role of the Cu on OSL Emission in Gamma-LiAlO2:Cu Crystal. Journal of Electronic Materials, 2020, 49, 2521-2528.	1.0	1
51701	First-Principles Calculations for Stable Î²-Tiâ€“Mo Alloys Using Cluster-Plus-Glue-Atom Model. Acta Metallurgica Sinica (English Letters), 2020, 33, 968-974.	1.5	5
51702	Analytical modelling of single-walled carbon nanotube energies: the impact of curvature, length and temperature. SN Applied Sciences, 2020, 2, 1.	1.5	3
51703	Thermally stable superhard diborides: An ab initio guided case study for V-W-diboride thin films. Acta Materialia, 2020, 186, 487-493.	3.8	20
51704	Vanadium is an optimal element for strengthening in both fcc and bcc high-entropy alloys. Acta Materialia, 2020, 188, 486-491.	3.8	159
51705	Solute/twin boundary interaction as a new atomic-scale mechanism for dynamic strain aging. Acta Materialia, 2020, 188, 711-719.	3.8	15
51706	Co-N-C in porous carbon with enhanced lithium ion storage properties. Chemical Engineering Journal, 2020, 389, 124377.	6.6	34
51707	N-doped carbon/ultrathin 2D metallic cobalt selenide core/sheath flexible framework bridged by chemical bonds for high-performance potassium storage. Chemical Engineering Journal, 2020, 388, 124396.	6.6	94
51708	Effects of intrinsic defects on the photocatalytic water-splitting activities of PtSe2. International Journal of Hydrogen Energy, 2020, 45, 8549-8557.	3.8	19
51709	Prediction on temperature dependent elastic constants of â€œsoftâ€•metal Al by AIMD and QHA. Journal of Materials Science and Technology, 2020, 45, 92-97.	5.6	7
51710	Electronic and Phonon Instabilities in Bilayer Graphene under Applied External Bias. Materials Today: Proceedings, 2020, 20, 373-382.	0.9	4
51711	First-principles phonon-based model and theory of martensitic phase transformation in NiTi shape memory alloy. Materialia, 2020, 9, 100602.	1.3	10

#	Article	IF	Citations
51712	Luminescence of divalent lanthanide doped BaBrI single crystal under synchrotron radiation excitations. Nuclear Instruments & Methods in Physics Research B, 2020, 467, 17-20.	0.6	14
51713	Thermal dissociation of CO molecules and carbon incorporation on the Si(111)-(7â€ˆâ€Ã—â€ˆâ€7) surface. Surface Science, 2020, 696, 121589.	0.8	1
51714	Density Functional Theory Study of the Gas Phase and Surface Reaction Kinetics for the MOVPE Growth of GaAs_{1â€“y}Bi_y. Journal of Physical Chemistry A, 2020, 124, 1682-1697.	1.1	0
51715	Elucidation of the Nature of Structural Relaxation in Glassy <scp>d</scp>-Sorbitol. Journal of Physical Chemistry B, 2020, 124, 1833-1838.	1.2	1
51716	Real-Space Evidence of Trimeric, Tetrameric, and Pentameric Uracil Clusters Induced by Alkali Metals. Journal of Physical Chemistry C, 2020, 124, 5257-5262.	1.5	5
51717	Charge Density and Redox Potential of LiNiO₂ Using Ab Initio Diffusion Quantum Monte Carlo. Journal of Physical Chemistry C, 2020, 124, 5893-5901.	1.5	16
51718	First-Principles Study of Zinc Phthalocyanine Molecules Adsorbed on Methylammonium Lead Iodide Surfaces. Journal of Physical Chemistry C, 2020, 124, 5167-5173.	1.5	8
51719	Tailoring the Mechanical Properties of Earth-Abundant Transition Metal Borides via Bonding Optimization. Journal of Physical Chemistry C, 2020, 124, 4430-4437.	1.5	5
51720	Experimental Investigation and First-Principles Calculations of a Ni₃Se₄ Cathode Material for Mg-Ion Batteries. ACS Applied Materials & Interfaces, 2020, 12, 9316-9321.	4.0	26
51721	The Coalescence Behavior of Two-Dimensional Materials Revealed by Multiscale In Situ Imaging during Chemical Vapor Deposition Growth. ACS Nano, 2020, 14, 1902-1918.	7.3	35
51722	Electrolyte Reactivity in the Double Layer in Mg Batteries: An Interface Potential-Dependent DFT Study. Journal of the American Chemical Society, 2020, 142, 5146-5153.	6.6	71
51723	Design of a multifunctional polar metal via first-principles high-throughput structure screening. Communications Materials, 2020, 1, .	2.9	65
51724	Metalâ€“organic framework templated Pd/CeO₂@N-doped carbon for low-temperature CO oxidation. Nanoscale Advances, 2020, 2, 755-762.	2.2	3
51725	Rational integration of spatial confinement and polysulfide conversion catalysts for high sulfur loading lithiumâ€“sulfur batteries. Nanoscale Horizons, 2020, 5, 720-729.	4.1	30
51726	Switching of the magnetic anisotropy via strain in two dimensional multiferroic materials: CrSX (Xâ€‰=â€‰Cl, Br, I). Applied Physics Letters, 2020, 116, .	1.5	40
51727	Pursuing the high-temperature quantum anomalous Hall effect in <mml:math xmlns:mml="http://www.w3.org/1998/Math/MathML"><mml:mrow><mml:msub><mml:mi>MnBi</mml:mi><mml:mn>2</mml:mn></mml:msub></mml:mrow></mml:math> heterostructures. Physical Review B, 2020, 101, .	1.1	21
51728	Doping-induced topological phase transition in Bi: The role of quantum electronic stress. Physical Review B, 2020, 101, .	1.1	11
51729	Measurement of diamond nucleation rates from hydrocarbons at conditions comparable to the interiors of icy giant planets. Physical Review B, 2020, 101, .	1.1	10

#	Article	IF	Citations
51730	Coexistence of multiple phases in the half-Heusler materials Co(Ti,Zr)(Sn,Sb). Physical Review B, 2020, 101, .	1.1	4
51731	Effects of lithium intercalation in twisted bilayer graphene. Physical Review B, 2020, 101, .	1.1	21
51732	First-Principles Calculations of Oxygen-Dislocation Interaction in Magnesium. Materials, 2020, 13, 116.	1.3	1
51733	Magnetic and Magneto-Optical Properties of Fe75â^'xMn25Gax Heusler-like Compounds. Materials, 2020, 13, 703.	1.3	5
51734	Study of Structure and Electronic Properties of Heterointerfaces for Photovoltaic Applications. Journal of Physical Chemistry C, 2020, 124, 4141-4151.	1.5	3
51735	N-Coordinated Dual-Metal Single-Site Catalyst for Low-Temperature CO Oxidation. ACS Catalysis, 2020, 10, 2754-2761.	5.5	112
51736	Atomic structure and defect dynamics of monolayer lead iodide nanodisks with epitaxial alignment on graphene. Nature Communications, 2020, 11, 823.	5.8	31
51737	Controllable chemoselective hydrogenation of furfural by PdAg/C bimetallic catalysts under ambient operating conditions: an interesting Ag switch. Green Chemistry, 2020, 22, 1432-1442.	4.6	38
51738	Improving the cycling and air-storage stability of LiNi_{0.8}Co_{0.1}Mn_{0.1}O₂ through integrated surface/interface/doping engineering. Journal of Materials Chemistry A, 2020, 8, 5234-5245.	5.2	56
51739	Assessing the roles of Cu- and Ag-deficient layers in chalcopyrite-based solar cells through first principles calculations. Journal of Applied Physics, 2020, 127, .	1.1	23
51740	On Prediction of a Novel Chiral Material Y2H3O(OH): A Hydroxyhydride Holding Hydridic and Protonic Hydrogens. Materials, 2020, 13, 994.	1.3	1
51741	Searching the crystal structure of silicon using the generalized scaled hypersphere search method with the rapid nuclear motion approximation. Japanese Journal of Applied Physics, 2020, 59, 035503.	0.8	3
51742	Suppression of magnetism and Seebeck effect in Na0.875CoO2 induced by SbCo dopants. Materials for Renewable and Sustainable Energy, 2020, 9, 1.	1.5	4
51743	Strong electronic couple engineering of transition metal phosphides-oxides heterostructures as multifunctional electrocatalyst for hydrogen production. Applied Catalysis B: Environmental, 2020, 269, 118803.	10.8	94
51744	Computational discovery of the novel half-metallic full-Heusler alloys Mn2LiAs and Mn2LiSb. Journal of Magnetism and Magnetic Materials, 2020, 503, 166642.	1.0	8
51745	Enhanced thermoelectric performance of In and Se co-doped GeTe compounds. Journal of Materials Research and Technology, 2020, 9, 4106-4113.	2.6	12
51746	A better nanochannel tungsten film in releasing helium atoms. Journal of Nuclear Materials, 2020, 532, 152044.	1.3	9
51747	Surface functionalization modulates the structural and optoelectronic properties of two-dimensional Ga2O3. Materials Today Physics, 2020, 12, 100192.	2.9	24

#	Article	IF	Citations
51748	One Step Further in the Elucidation of the Crystallographic Structure of Whitlockite. Crystal Growth and Design, 2020, 20, 2553-2561.	1.4	18
51749	Understanding the Key Step of Co₂C-Catalyzed Fischerâ€“Tropsch Synthesis. Journal of Physical Chemistry C, 2020, 124, 5749-5758.	1.5	13
51750	Coverage-Dependent Adsorption of Hydrogen on Fe(100): Determining Catalytically Relevant Surface Structures via Lattice Gas Models. Journal of Physical Chemistry C, 2020, 124, 7254-7266.	1.5	15
51751	MoirÃ© Flat Bands in Twisted Double Bilayer Graphene. Nano Letters, 2020, 20, 2410-2415.	4.5	107
51752	Discovery of n-Type Zintl Phases RbAlSb₄, RbGaSb₄, CsAlSb₄, and CsGaSb₄. ACS Applied Energy Materials, 2020, 3, 2182-2191.	2.5	11
51753	Reducing Anomalous Hysteresis in Perovskite Solar Cells by Suppressing the Interfacial Ferroelectric Order. ACS Applied Materials & Interfaces, 2020, 12, 12275-12284.	4.0	13
51754	Adsorption Behavior of the Hydroxyl Radical and Its Effects on Monolayer MoS₂. ACS Omega, 2020, 5, 1982-1986.	1.6	9
51755	A silicate dynamo in the early Earth. Nature Communications, 2020, 11, 935.	5.8	32
51756	Uncovering near-free platinum single-atom dynamics during electrochemical hydrogen evolution reaction. Nature Communications, 2020, 11, 1029.	5.8	379
51757	A computational study on boron dipyromethene ancillary acceptor-based dyes for dye-sensitized solar cells. New Journal of Chemistry, 2020, 44, 4877-4886.	1.4	17
51758	Copper halide diselenium: predicted two-dimensional materials with ultrahigh anisotropic carrier mobilities. RSC Advances, 2020, 10, 8016-8026.	1.7	10
51759	Hollow-shell structured porous CoSe₂ microspheres encapsulated by MXene nanosheets for advanced lithium storage. Sustainable Energy and Fuels, 2020, 4, 2352-2362.	2.5	39
51760	Two-dimensional Ca4N2 as a one-dimensional electride [Ca4N2]2+Â·2eâ¯ with ultrahigh conductance. Nanoscale, 2020, 12, 5578-5586.	2.8	3
51761	Pressure-induced metallization and reentrant insulativity in elemental crystal of phosphorus: a prediction by ab initio calculations. New Journal of Physics, 2020, 22, 033011.	1.2	5
51762	Robust <mml:math xmlns:mml="http://www.w3.org/1998/Math/MathML"><mml:msub><mml:mi>d</mml:mi><mml:mrow><mml:msup><mml:mi></mml:mi> -wave superconductivity of infinite-layer nickelates. Physical Review B, 2020, 101, .	1.1	151
51763	Optical Properties of a Two-Dimensional GeTe Layer. Journal of the Korean Physical Society, 2020, 76, 221-225.	0.3	2
51764	Synergistically Tuning Electronic Structure of Porous Î²â€Mo₂C Spheres by Co Doping and Moâ€Vacancies Defect Engineering for Optimizing Hydrogen Evolution Reaction Activity. Advanced Functional Materials, 2020, 30, 2000561.	7.8	141
51765	The structural evolution of light-ion implanted 6H-SiC single crystal: Comparison of the effect of helium and hydrogen. Acta Materialia, 2020, 188, 609-622.	3.8	66

#	Article	IF	Citations
51766	Origin of the structural diversity of the alkaline metal borohydride MBH4 (MÂ=ÂLi, Na, K, Rb and Cs): Insights from first-principles calculations. International Journal of Hydrogen Energy, 2020, 45, 9946-9958.	3.8	1
51767	Tuning of interactions between cathode and lithium polysulfide in Li-S battery by rational halogenation. Journal of Energy Chemistry, 2020, 49, 147-152.	7.1	19
51768	Rapidly solidified Sm-Co-Hf-B magnetic Nano-composites: Experimental and DFT studies. Journal of Magnetism and Magnetic Materials, 2020, 504, 166645.	1.0	11
51769	Structural and magnetic properties of Co-Pt clusters: A spin-polarized density functional study. Journal of Magnetism and Magnetic Materials, 2020, 503, 166651.	1.0	3
51770	Band Alignment of the CuGaS2 Chalcopyrite Interfaces Studied by First-Principles Calculations. ACS Omega, 2020, 5, 3294-3301.	1.6	5
51771	Tunable Synthesis of Nitrogen Doped Graphene from Fluorographene under Mild Conditions. ACS Sustainable Chemistry and Engineering, 2020, 8, 4764-4772.	3.2	26
51772	Superconductivity of <mml:math xmlns:mml="http://www.w3.org/1998/Math/MathML"><mml:msub><mml:mi>LaH</mml:mi><mml:mn>10</mml:mn></mml:msub></mml and <mml:math xmlns:mml="http://www.w3.org/1998/Math/MathML"><mml:msub><mml:mi>LaH</mml:mi><mml:mn>16</mml:mn></mml:msub></mml polyhydrides. Physical Review B, 2020, 101, .	1.1	62
51773	two-dimensional square-lattice antimonate <mml:math xmlns:mml="http://www.w3.org/1998/Math/MathML"><mml:mrow><mml:mi>NaMnSb</mml:mi><mml:msub><mml:mi mathvariant="normal">O</mml:mi><mml:mn>4</mml:mn></mml:msub></mml:mrow></mml:math>. Physical Review B, 2020, 101, .	1.1	4
51774	Unusual electronic state of Sn in <mml:math xmlns:mml="http://www.w3.org/1998/Math/MathML"><mml:msub><mml:mi>AgSnSe</mml:mi><mml:mn>2</mml:mn></mml:msub></ Physical Review B, 2020, 101, .	1.1	3
51775	Formation of Bloch Flat Bands in Polar Twisted Bilayers without Magic Angles. Physical Review Letters, 2020, 124, 086401.	2.9	52
51776	Constructing Naâ€ion Cathodes via Alkaliâ€Site Substitution. Advanced Functional Materials, 2020, 30, 1910840.	7.8	28
51777	Phase Modulation and Chemical Activation of MoSe₂ by Phosphorus for Electrocatalytic Hydrogen Evolution Reaction. Energy Technology, 2020, 8, 1901503.	1.8	16
51778	Computational screening of transition metal/pâ€block hybrid electrocatalysts for CO₂ reduction. Journal of Computational Chemistry, 2020, 41, 1384-1394.	1.5	2
51779	Tunable Valley Polarization in a Multiferroic CuCrP₂Te₆ Monolayer. Physica Status Solidi - Rapid Research Letters, 2020, 14, 2000008.	1.2	13
51780	Manipulating the Ge Vacancies and Ge Precipitates through Cr Doping for Realizing the Highâ€Performance GeTe Thermoelectric Material. Small, 2020, 16, e1906921.	5.2	129
51781	Efficient CO₂ Reduction to HCOOH with High Selectivity and Energy Efficiency over Bi/rGO Catalyst. Small Methods, 2020, 4, 1900846.	4.6	70
51782	The importance of residual water for the reactivity of MPTMS with silica on the example of SBA-15. Applied Surface Science, 2020, 513, 145802.	3.1	7
51783	Hollow nanosheet array of phosphorus-anion-decorated cobalt disulfide as an efficient electrocatalyst for overall water splitting. Chemical Engineering Journal, 2020, 390, 124556.	6.6	84

#	Article	IF	Citations
51784	A metal organic foam-derived zinc cobalt sulfide with improved binding energies towards polysulfides for lithiumâ€“sulfur batteries. Ceramics International, 2020, 46, 14056-14063.	2.3	22
51785	TiO2 electrocatalysis via three-electron oxygen reduction for highly efficient generation of hydroxyl radicals. Electrochemistry Communications, 2020, 113, 106687.	2.3	28
51786	Facet effect of Co3O4 nanocatalysts on the catalytic decomposition of ammonium perchlorate. Journal of Hazardous Materials, 2020, 392, 122358.	6.5	96
51787	Mechanism study of TADF and phosphorescence in dinuclear copper (I) molecular crystal using QM/MM combined with an optimally tuned range-separated hybrid functional. Organic Electronics, 2020, 81, 105667.	1.4	13
51788	Design of Lead-Free and Stable Two-Dimensional Dionâ€“Jacobson-Type Chalcogenide Perovskite Aâ€²La2B3S10 (Aâ€² = Ba/Sr/Ca; B = Hf/Zr) with Optimal Band Gap, Strong Optical Absorption, and High Efficiency for Photovoltaics. Chemistry of Materials, 2020, 32, 2450-2460.	3.2	19
51789	Beyond Idealized Models of Nanoscale Metal Hydrides for Hydrogen Storage. Industrial & Engineering Chemistry Research, 2020, 59, 5786-5796.	1.8	15
51790	Oxidation State of GaP Photoelectrode Surfaces under Electrochemical Conditions for Photocatalytic CO₂ Reduction. Journal of Physical Chemistry B, 2020, 124, 2255-2261.	1.2	3
51791	Comparative Catalytic Activity of Graphene Imperfections in Oxygen Reduction Reaction. Journal of Physical Chemistry C, 2020, 124, 6038-6053.	1.5	12
51792	Enhanced Photoresponse of WS₂ Photodetectors through Interfacial Defect Engineering Using a TiO₂ Interlayer. ACS Applied Electronic Materials, 2020, 2, 838-845.	2.0	17
51793	Intermediate Adsorption States Switch to Selectively Catalyze Electrochemical CO₂ Reduction. ACS Catalysis, 2020, 10, 3871-3880.	5.5	89
51794	Kinetic Study of the Hydrogenation of Unsaturated Aldehydes Promoted by CuPt_x/SBA-15 Single-Atom Alloy (SAA) Catalysts. ACS Catalysis, 2020, 10, 3431-3443.	5.5	53
51795	Activating low-temperature diesel oxidation by single-atom Pt on TiO2 nanowire array. Nature Communications, 2020, 11, 1062.	5.8	90
51796	Bismuthene for highly efficient carbon dioxide electroreduction reaction. Nature Communications, 2020, 11, 1088.	5.8	278
51797	A theoretical study on the binding and electrolytic splitting of hydrogen fluoride on Ni(111) and Ni(211). Physical Chemistry Chemical Physics, 2020, 22, 4407-4415.	1.3	3
51798	Enhanced photocurrent in heterostructures formed between CH₃NH₃PbI₃perovskite films and graphdiyne. Physical Chemistry Chemical Physics, 2020, 22, 6239-6246.	1.3	10
51799	Understanding the molecular mechanism of lithium deposition for practical high-energy lithium-metal batteries. Journal of Materials Chemistry A, 2020, 8, 6229-6237.	5.2	29
51800	Theoretical investigation of nonvolatile electrical control behavior by ferroelectric polarization switching in two-dimensional MnCl₃/CuInP₂S₆ van der Waals heterostructures. Journal of Materials Chemistry C, 2020, 8, 4534-4541.	2.7	31
51801	Vibrational dynamics in lead halide hybrid perovskites investigated by Raman spectroscopy. Physical Chemistry Chemical Physics, 2020, 22, 5604-5614.	1.3	61

#	Article	IF	Citations
51802	Magnetic exchange induced Weyl state in a semimetal EuCd2Sb2. APL Materials, 2020, 8, .	2.2	37
51803	First-principles study of electronic and diffusion properties of intrinsic defects in 4H-SiC. Journal of Applied Physics, 2020, 127, .	1.1	32
51804	Novel Mg-ion conductive oxide of Î¼-cordierite Mg_{0.6}Al_{1.2}Si_{1.8}O₆. Science and Technology of Advanced Materials, 2020, 21, 131-138.	2.8	12
51805	Elucidating the Effect of Planar Graphitic Layers and Cylindrical Pores on the Storage and Diffusion of Li, Na, and K in Carbon Materials. Advanced Functional Materials, 2020, 30, 1908209.	7.8	49
51806	Enhancement of chlorobenzene sensing by doping aluminum on nanotubes: A DFT study. Applied Surface Science, 2020, 514, 145897.	3.1	11
51807	Effects of alloy compositions on hydrogen behaviors at a nickel grain boundary and a coherent twin boundary. International Journal of Hydrogen Energy, 2020, 45, 10951-10961.	3.8	14
51808	Quatermetallic Pt-based ultrathin nanowires intensified by Rh enable highly active and robust electrocatalysts for methanol oxidation. Nano Energy, 2020, 71, 104623.	8.2	64
51809	Acepentalene Membrane Sheet: A Metallic Two-Dimensional Carbon Allotrope with High Carrier Mobility for Lithium Ion Battery Anodes. Journal of Physical Chemistry C, 2020, 124, 5999-6011.	1.5	14
51810	Stacking-Independent Ferromagnetism in Bilayer VI₃ with Half-Metallic Characteristic. Journal of Physical Chemistry Letters, 2020, 11, 2158-2164.	2.1	28
51811	Noble-Metal-Free CdS Nanoparticle-Coated Graphene Oxide Nanosheets Favoring Electron Transfer for Efficient Photoreduction of CO₂. ACS Applied Materials & Interfaces, 2020, 12, 12892-12900.	4.0	29
51812	Impact of Surface Modification on the Lithium, Sodium, and Potassium Intercalation Efficiency and Capacity of Few-Layer Graphene Electrodes. ACS Applied Materials & Interfaces, 2020, 12, 19393-19401.	4.0	16
51813	Mechanistic Analysis-Guided Pd-Based Catalysts for Efficient Hydrogen Production from Formic Acid Dehydrogenation. ACS Catalysis, 2020, 10, 3921-3932.	5.5	82
51814	Double-network hydrogel templated FeS/graphene with enhanced PMS activation performance: considering the effect of the template and iron species. Environmental Science: Nano, 2020, 7, 817-828.	2.2	19
51815	Effect of Zr concentration on the mechanical and thermodynamic properties of NbIr3 intermetallic compounds from theoretical estimations. Philosophical Magazine, 2020, 100, 1550-1568.	0.7	0
51816	Three-dimensional graphene nanoribbons as a framework for molecular assembly and local probe chemistry. Science Advances, 2020, 6, eaay8913.	4.7	58
51817	Quantumâ€Chemical Study of the FeNCN Conversionâ€Reaction Mechanism in Lithiumâ€•and Sodiumâ€Ion Batteries. Angewandte Chemie, 2020, 132, 3747-3752.	1.6	2
51818	Controlling Single Molecule Conductance by a Locally Induced Chemical Reaction on Individual Thiophene Units. Angewandte Chemie, 2020, 132, 6266-6271.	1.6	2
51819	Solutionâ€Grown Hypervalent CsI₃ Crystal for Highâ€Sensitive Xâ€Ray Detection. Physica Status Solidi (B): Basic Research, 2020, 257, 2070012.	0.7	1

#	Article	IF	Citations
51820	First-principles study on adsorption behavior of as on the kaolinite (001) and (00$$ar {1}$$) surfaces. Adsorption, 2020, 26, 443-452.	1.4	7
51821	A density functional theory study on the shape of the primary cellulose microfibril in plants: effects of C6 exocyclic group conformation and H-bonding. Cellulose, 2020, 27, 2389-2402.	2.4	29
51822	Energy band gap tuning in Te-doped WS2/WSe2 heterostructures. Journal of Materials Science, 2020, 55, 9695-9702.	1.7	10
51823	Tunability of martensitic transformation in Mg-Sc shape memory alloys: A DFT study. Acta Materialia, 2020, 189, 1-9.	3.8	14
51824	Improving LiNi0.9Co0.08Mn0.02O2â€™s cyclic stability via abating mechanical damages. Energy Storage Materials, 2020, 28, 1-9.	9.5	44
51825	Î±-CsCu₅Se₃: Discovery of a Low-Cost Bulk Selenide with High Thermoelectric Performance. Journal of the American Chemical Society, 2020, 142, 5293-5303.	6.6	46
51826	Ethylene carbonate adsorption on the major surfaces of lithium manganese oxide Li_{1â^'x}Mn₂O₄spinel (0.000 <<i>x</i>< 0.375): a DFT+<i>U</i>-D3 study. Physical Chemistry Chemical Physics, 2020, 22, 6763-6771.	1.3	18
51827	Efficient base-free oxidation of monosaccharide into sugar acid under mild conditions using hierarchical porous carbon supported gold catalysts. Green Chemistry, 2020, 22, 2588-2597.	4.6	23
51828	Elementary reaction pathway study and a deduced macrokinetic model for the unified understanding of Ni-catalyzed steam methane reforming. Reaction Chemistry and Engineering, 2020, 5, 873-885.	1.9	8
51829	CO₂ reduction on p-block metal oxide overlayers on metal substratesâ€”2D MgO as a prototype. Journal of Materials Chemistry A, 2020, 8, 5688-5698.	5.2	20
51830	Modulation of nearly free electron states in hydroxyl-functionalized MXenes: a first-principles study. Journal of Materials Chemistry C, 2020, 8, 5211-5221.	2.7	21
51831	A molecular device providing a remarkable spin filtering effect due to the central molecular stretch caused by lateral zigzag graphene nanoribbon electrodes. Physical Chemistry Chemical Physics, 2020, 22, 6755-6762.	1.3	5
51832	Mirror symmetry origin of Dirac cone formation in rectangular two-dimensional materials. Physical Chemistry Chemical Physics, 2020, 22, 6619-6625.	1.3	14
51833	Enhanced carrier mobility and tunable electronic properties in Î±-tellurene monolayer via an Î±-tellurene and h-BN heterostructure. Physical Chemistry Chemical Physics, 2020, 22, 6434-6440.	1.3	13
51834	NiAg_{0.4} 3D porous nanoclusters with epitaxial interfaces exhibiting Pt like activity towards hydrogen evolution in alkaline medium. Nanoscale, 2020, 12, 8432-8442.	2.8	14
51835	Comparative electrochemical energy storage performance of cobalt sulfide and cobalt oxide nanosheets: experimental and theoretical insights from density functional theory simulations. Physical Chemistry Chemical Physics, 2020, 22, 7903-7911.	1.3	26
51836	Two-sites are better than one: revisiting the OER mechanism on CoOOH by DFT with electrode polarization. Physical Chemistry Chemical Physics, 2020, 22, 7031-7038.	1.3	45
51837	Tunable Rashba spin splitting in Janus transition-metal dichalcogenide monolayers via charge doping. RSC Advances, 2020, 10, 6388-6394.	1.7	55

#	Article	IF	Citations
51838	Two-dimensional boron monochalcogenide monolayer for thermoelectric material. Sustainable Energy and Fuels, 2020, 4, 2363-2369.	2.5	62
51839	Stability diagrams, defect tolerance, and absorption coefficients of hybrid halide semiconductors: High-throughput first-principles characterization. Journal of Chemical Physics, 2020, 152, 084106.	1.2	22
51840	Sn-modification of Pt7/alumina model catalysts: Suppression of carbon deposition and enhanced thermal stability. Journal of Chemical Physics, 2020, 152, 024702.	1.2	25
51841	Phase-dependent electronic and magnetic properties of Ti2C monolayers. Journal of Applied Physics, 2020, 127, .	1.1	30
51842	Influence of hydrogen implantation on emission from the silicon vacancy in 4H-SiC. Journal of Applied Physics, 2020, 127, .	1.1	14
51843	Hall voltage reversal and structural phase transition in VO2thin films. Applied Physics Letters, 2020, 116, 082106.	1.5	1
51844	In situ healing of dendrites in a potassium metal battery. Proceedings of the National Academy of Sciences of the United States of America, 2020, 117, 5588-5594.	3.3	79
51845	First-principles calculations of elastic constants for epsilon-carbide and the consequences. Materials Science and Technology, 2020, 36, 615-622.	0.8	3
51846	Descriptors for dielectric constants of perovskite-type oxides by materials informatics with first-principles density functional theory. Science and Technology of Advanced Materials, 2020, 21, 92-99.	2.8	10
51847	Solute-second phase interaction for Mg, Ag and Zn in Alâ€“Li alloys. Philosophical Magazine, 2020, 100, 1539-1549.	0.7	3
51848	Highly dispersed Co deposited on Al₂O₃ particles via CoCp₂ + H₂ ALD. Nanotechnology, 2020, 31, 175703.	1.3	4
51849	Linear piezoresistive strain sensor based on graphene/g-C₃N₄/PDMS heterostructure. Nanotechnology, 2020, 31, 295501.	1.3	35
51850	Nearly golden-ratio order in Ta metallic glass*. Chinese Physics B, 2020, 29, 046105.	0.7	4
51851	Orbitally-resolved ferromagnetism of monolayer CrI₃. 2D Materials, 2020, 7, 025036.	2.0	68
51852	M-graphene: a metastable two-dimensional carbon allotrope. 2D Materials, 2020, 7, 025047.	2.0	30
51853	Electronic and optical properties of zinc based hybrid organic-inorganic compounds. Materials Research Express, 2020, 7, 035701.	0.8	10
51854	Kagome metal-organic frameworks as a platform for strongly correlated electrons. JPhys Materials, 2020, 3, 025001.	1.8	11
51855	Mo doped TiO₂: impact on oxygen vacancies, anatase phase stability and photocatalytic activity. JPhys Materials, 2020, 3, 025008.	1.8	42

#	Article	IF	Citations
51856	Guided patchwork kriging to develop highly transferable thermal conductivity prediction models. JPhys Materials, 2020, 3, 024006.	1.8	13
51857	On efficiency of earth-abundant chalcogenide photovoltaic materials buffered with CdS: the limiting effect of band alignment. JPhys Energy, 2020, 2, 025002.	2.3	11
51858	Computational screening of Fe-Ta hard magnetic phases. Physical Review B, 2020, 101, .	1.1	11
51859	<mml:math xmlns:mml="http://www.w3.org/1998/Math/MathML"><mml:mi>Ï€</mml:mi></mml:math> -anisotropy: A nanocarbon route to hard magnetism. Physical Review B, 2020, 101, .	1.1	15
51860	Axion insulator state in ferromagnetically ordered <mml:math xmlns:mml="http://www.w3.org/1998/Math/MathML"><mml:mrow><mml:mi>Cr</mml:mi><mml:msub><mml:mi mathvariant="normal">I</mml:mi><mml:mn>3</mml:mn></mml:msub><mml:mo>/</mml:mo><mml:mi mathvariant="normal">B</mml:mi><mml:msub><mml:mi mathvariant="normal">i</mml:mi><mml:mn>2</mml:mn></mml:msub><mml:mi mathvariant="normal">S</mml:mi><mml:msub><mml:mi	1.1	22
51861	Manipulation of valley pseudospin in <mml:math xmlns:mml="http://www.w3.org/1998/Math/MathML"><mml:msub><mml:mi>WSe</mml:mi><mml:mn>2</mml:mn></mml:msub><mml: heterostructures by the magnetic proximity effect. Physical Review B, 2020, 101, .	1.1	58
51862	Ideal two-dimensional molecular sieves for gas separation: Metal trihalides MX3 with precise atomic pores. Journal of Membrane Science, 2020, 602, 117786.	4.1	12
51863	Mechanism of Precursor Blocking by Acetylacetone Inhibitor Molecules during Area-Selective Atomic Layer Deposition of SiO₂. Chemistry of Materials, 2020, 32, 3335-3345.	3.2	39
51864	Structure and Dynamics of the Electronic Heterointerfaces in MoS₂ by First-Principles Simulations. Journal of Physical Chemistry Letters, 2020, 11, 1644-1649.	2.1	9
51865	Study on Ca Segregation toward an Epitaxial Interface between Bismuth Ferrite and Strontium Titanate. ACS Applied Materials & Interfaces, 2020, 12, 12264-12274.	4.0	5
51866	Enhanced Field Emission Properties of Au/SnSe Nano-heterostructure: A Combined Experimental and Theoretical Investigation. Scientific Reports, 2020, 10, 2358.	1.6	10
51867	Computational screening of MN₄ (M = Tiâ€“Cu) based metal organic frameworks for CO₂ reduction using the d-band centre as a descriptor. Nanoscale, 2020, 12, 6188-6194.	2.8	52
51868	Toward a comparative description between transition metal and zeolite catalysts for methanol conversion. Physical Chemistry Chemical Physics, 2020, 22, 5293-5300.	1.3	6
51869	Enhanced room temperature ferromagnetism in MoS2 by N plasma treatment. AIP Advances, 2020, 10, .	0.6	6
51870	Bond relaxation and electronic properties of two-dimensional Sb/MoSe2 and Sb/MoTe2 van der Waals heterostructures. AIP Advances, 2020, 10, .	0.6	8
51871	Encapsulation and substitution of Fe in C12A7 (12CaOâ‹…7Al2O3). AIP Advances, 2020, 10, 015242.	0.6	3
51872	Hydrothermal synthesis and site symmetry tuning of polycrystalline YVO4:Eu nanoparticles via a continuous-flow microreactor. Nanotechnology, 2020, 31, 235603.	1.3	2
51873	Bulk quantum Hall effect of spin-valley coupled Dirac fermions in the polar antiferromagnet BaMnSb2. Physical Review B, 2020, 101, .	1.1	26

#	Article	IF	Citations
51874	An Anionâ€Tuned Solid Electrolyte Interphase with Fast Ion Transfer Kinetics for Stable Lithium Anodes. Advanced Energy Materials, 2020, 10, 1903843.	10.2	186
51875	On the Temperature Limits of Ni-Based Superalloys. Minerals, Metals and Materials Series, 2020, , 785-792.	0.3	2
51876	Analysis of Chemical Activity of Bismuthene in the Presence of Environment Gas Molecules by Means of Ab Initio Calculations. Minerals, Metals and Materials Series, 2020, , 983-991.	0.3	0
51877	Vibrational, thermodynamic, and dielectric properties of Îµ-CL-20: first-principles calculations. Journal of Molecular Modeling, 2020, 26, 47.	0.8	0
51878	Effect of Au Doping on Elastic, Thermodynamic, and Electronic Properties of Î·-Cu6Sn5 Intermetallic. Journal of Electronic Materials, 2020, 49, 3031-3038.	1.0	2
51879	Study of grain boundary self-diffusion in iron with different atomistic models. Acta Materialia, 2020, 188, 560-569.	3.8	28
51880	N-doping activated defective Co3O4 as an efficient catalyst for low-temperature methane oxidation. Applied Catalysis B: Environmental, 2020, 269, 118757.	10.8	85
51881	In-situ hydroxyl modification of monolayer black phosphorus for stable photocatalytic carbon dioxide conversion. Applied Catalysis B: Environmental, 2020, 269, 118760.	10.8	147
51882	True bulk As-antisite defect in GaAs(1Â1Â0) identified by DFT calculations and probed by STM/STS measurements. Applied Surface Science, 2020, 511, 145590.	3.1	8
51883	Electronic and optical properties of halogen (H= F, Cl, Br)-doped Cu2O by hybrid density functional simulations. Optik, 2020, 207, 164440.	1.4	6
51884	Ultra-thin deaminated tri-s-triazine-based crystalline nanosheets with high photocatalytic hydrogen evolution performance. Journal of Alloys and Compounds, 2020, 827, 154307.	2.8	22
51885	A combined experimental and DFT study of H2O effect on In2O3/ZrO2 catalyst for CO2 hydrogenation to methanol. Journal of Catalysis, 2020, 383, 283-296.	3.1	73
51886	Effect of Ba2+ doping on the photoluminescence of YVO4: Eu3+ phosphor and first principles calculations. Journal of Luminescence, 2020, 222, 117117.	1.5	9
51887	Half-metallic ferromagnetism and Ru-induced localization in quaternary Heusler alloy CoRuMnSi. Journal of Magnetism and Magnetic Materials, 2020, 502, 166536.	1.0	15
51888	Design materials based on simulation results of silicon induced segregation at AlSi10Mg interface fabricated by selective laser melting. Journal of Materials Science and Technology, 2020, 46, 145-155.	5.6	33
51889	Temperature dependence of Raman scattering in single crystal SnSe. Vibrational Spectroscopy, 2020, 107, 103034.	1.2	22
51890	Synergic Effect in a New Electrocatalyst Ni₂SbTe₂ for Oxygen Reduction Reaction. Journal of Physical Chemistry C, 2020, 124, 3671-3680.	1.5	11
51891	Molecular Structure and Electronic Properties of para-Hexaphenyl Monolayer on Atomically Flat Rutile TiO₂(110). Journal of Physical Chemistry C, 2020, 124, 5681-5689.	1.5	3

#	Article	IF	Citations
51892	Copper Cobalt Selenide as a High-Efficiency Bifunctional Electrocatalyst for Overall Water Splitting: Combined Experimental and Theoretical Study. ACS Applied Energy Materials, 2020, 3, 3092-3103.	2.5	60
51893	Influence of Hostâ€“Guest Interaction between Chiral Selectors and Probes on the Enantioseparation Properties of Graphene Oxide Membranes. ACS Applied Materials & Interfaces, 2020, 12, 10893-10901.	4.0	27
51894	Blending Ionic and Coordinate Bonds in Hybrid Semiconductor Materials: A General Approach toward Robust and Solution-Processable Covalent/Coordinate Network Structures. Journal of the American Chemical Society, 2020, 142, 4242-4253.	6.6	72
51895	Controlled edge dependent stacking of WS2-WS2 Homo- and WS2-WSe2 Hetero-structures: A Computational Study. Scientific Reports, 2020, 10, 1648.	1.6	19
51896	Epitaxial synthesis of ultrathin Î²-In₂Se₃/MoS₂ heterostructures with high visible/near-infrared photoresponse. Nanoscale, 2020, 12, 6480-6488.	2.8	42
51897	Magnetic properties of 3d transition metal (Scâ€“Ni) doped plumbene. RSC Advances, 2020, 10, 6884-6892.	1.7	9
51898	DFT modelling of explicit solidâ€“solid interfaces in batteries: methods and challenges. Physical Chemistry Chemical Physics, 2020, 22, 10412-10425.	1.3	44
51899	Yolkâ€“shell or yolk-in-shell nanocatalysts? A proof-of-concept study. Journal of Materials Chemistry A, 2020, 8, 10217-10225.	5.2	14
51900	Suppressing the dynamic precipitation and lowering the thermal conductivity for stable and high thermoelectric performance in BaCu2Te2 based materials. Journal of Materials Chemistry A, 2020, 8, 5323-5331.	5.2	16
51901	Effects of short-range order and interfacial interactions on the electronic structure of two-dimensional antimony-arsenic alloys. Journal of Applied Physics, 2020, 127, 025305.	1.1	1
51902	Anomalous solution softening by unique energy balance mediated by kink mechanism in tungsten-rhenium alloys. Journal of Applied Physics, 2020, 127, .	1.1	9
51903	High-throughput first-principles screening of layered magnetic double perovskites Cs₄MSb₂X₁₂ for spintronic applications. Journal of Physics Condensed Matter, 2020, 32, 225705.	0.7	12
51904	Fundamental band gap and alignment of two-dimensional semiconductors explored by machine learning*. Chinese Physics B, 2020, 29, 046101.	0.7	17
51905	Ab initio calculations on oxygen vacancy defects in strained amorphous silica*. Chinese Physics B, 2020, 29, 047103.	0.7	4
51906	Chemisorption characteristics of pyridine on Rh, Pd, Pt and Ni(1â€‰1â€‰1). Electronic Structure, 2020, 2, 015001.	1.0	2
51907	Lattice dynamics and structural transition of the hyperhoneycomb iridate <mml:math xmlns:mml="http://www.w3.org/1998/Math/MathML"><mml:mrow><mml:mi>Î²</mml:mi><mml:mo>â€²</mml:mo></mml:mrow></mml:msub><mml:m investigated by high-pressure Raman scattering. Physical Review B, 2020, 101, .	1.1	9
51908	Materials design of dynamically stable <mml:math xmlns:mml="http://www.w3.org/1998/Math/MathML"><mml:msup><mml:mi>d</mml:mi><mml:mn>9</mml:mn></mml:msup></mml:m layered nickelates. Physical Review B, 2020, 101, .	1.1	62
51909	Structural, Electronic and Optical Properties of Cubic CaCu3Ti_{4â€“x}Ag_xO₁₂ Perovskite Ceramics: A First-Principles Study. IEEE Access, 2020, 8, 19230-19235.	2.6	4

#	Article	IF	Citations
51910	Room-Temperature Activation of Methane and Direct Formations of Acetic Acid and Methanol on Zn-ZSM-5 Zeolite: A Mechanistic DFT Study. Bulletin of the Chemical Society of Japan, 2020, 93, 345-354.	2.0	21
51911	Cation Disorder and Local Structural Distortions in AgxBi1â€“xS2 Nanoparticles. Nanomaterials, 2020, 10, 316.	1.9	2
51912	UV-Initiated Crosslinking Reaction Mechanism and Electrical Breakdown Performance of Crosslinked Polyethylene. Polymers, 2020, 12, 420.	2.0	12
51913	Electrochemistry Induced Giant and Reversible Deformation in Oxides. Advanced Functional Materials, 2020, 30, 1908826.	7.8	2
51914	Zwitterionic Conjugated Surfactant Functionalization of Graphene with pHâ€Independent Dispersibility: An Efficient Electron Mediator for the Oxygen Evolution Reaction in Acidic Media. Small, 2020, 16, 1906635.	5.2	8
51915	A Heterostructure Coupling of Bioinspired, Adhesive Polydopamine, and Porous Prussian Blue Nanocubics as Cathode for Highâ€Performance Sodiumâ€Ion Battery. Small, 2020, 16, e1906946.	5.2	57
51916	Invited Review: Modern Methods for Accurately Simulating the Terahertz Spectra of Solids. Journal of Infrared, Millimeter, and Terahertz Waves, 2020, 41, 491-528.	1.2	35
51917	Phase-field study of IMC growth in Snâ€“Cu/Cu solder joints including elastoplastic effects. Acta Materialia, 2020, 188, 241-258.	3.8	27
51918	The mechanism of dynamic strain aging for type A serrations in tensile flow curves of Fe-18Mn-0.55C (wt.%) twinning-induced plasticity steel. Acta Materialia, 2020, 188, 366-375.	3.8	40
51919	Realizing synergistic effect of electronic modulation and nanostructure engineering over graphitic carbon nitride for highly efficient visible-light H2 production coupled with benzyl alcohol oxidation. Applied Catalysis B: Environmental, 2020, 269, 118772.	10.8	66
51920	Stabilizing CsPbBr3 quantum dots with conjugated aromatic ligands and their regulated optical behaviors. Chemical Engineering Journal, 2020, 389, 124453.	6.6	39
51921	First-principles study of the ideal shear strengths and stacking fault energies of face-centered cubic Al3Ti. Computational Materials Science, 2020, 177, 109596.	1.4	13
51922	DP-GEN: A concurrent learning platform for the generation of reliable deep learning based potential energy models. Computer Physics Communications, 2020, 253, 107206.	3.0	271
51923	Fused pentagon carbon network: A new anode material for Li ion batteries. Chemical Physics Letters, 2020, 745, 137225.	1.2	6
51924	Synthesis of NdSc3(BO3)4 single crystals and study of its structure properties. Journal of Alloys and Compounds, 2020, 828, 154355.	2.8	6
51925	Hydrogen in zirconium: Atomistic simulations of diffusion and interaction with defects using a new embedded atom method potential. Journal of Nuclear Materials, 2020, 532, 152055.	1.3	30
51926	Formation and thermodynamic stability of oxygen vacancies in typical cathode materials for Li-ion batteries: Density functional theory study. Solid State Ionics, 2020, 347, 115257.	1.3	41
51927	Atomic structures of Vâ€“Tiâ€“O intermixed oxide monolayer on rutile TiO2(011) substrate predicted by extensive structural search. Surface Science, 2020, 694, 121559.	0.8	2

#	Article	IF	Citations
51928	Resonant Ta Doping for Enhanced Mobility in Transparent Conducting SnO₂. Chemistry of Materials, 2020, 32, 1964-1973.	3.2	50
51929	Energetics and Structure of Agâ€“Water Clusters Formed in Mordenite. Journal of Physical Chemistry C, 2020, 124, 4517-4524.	1.5	9
51930	Screening Promising Thermoelectric Materials in Binary Chalcogenides through High-Throughput Computations. ACS Applied Materials & Interfaces, 2020, 12, 11852-11864.	4.0	51
51931	First-Principles Calculations of x-Dependent Ground Structures and Optical Properties of Ca_xLa_{1â€“x}B₆. ACS Omega, 2020, 5, 2214-2220.	1.6	1
51932	Light control of surfaceâ€“bulk coupling by terahertz vibrational coherence in a topological insulator. Npj Quantum Materials, 2020, 5, .	1.8	45
51933	Negative and near-zero Poisson's ratios in 2D graphene/MoS₂ and graphene/h-BN heterostructures. Journal of Materials Chemistry C, 2020, 8, 4021-4029.	2.7	24
51934	UI3: a high Curie temperature f-electron two-dimensional magnet. Journal Physics D: Applied Physics, 2020, 53, 185301.	1.3	6
51935	Degenerate doping in Î²-Ga₂O₃ single crystals through Hf-doping. Semiconductor Science and Technology, 2020, 35, 04LT01.	1.0	43
51936	Nonvolatile Ferroelectric Field Control of the Anomalous Hall Effect in <mml:math xmlns:mml="http://www.w3.org/1998/Math/MathML" display="inline" overflow="scroll"><mml:msub><mml:mrow><mml:mi>Bi</mml:mi><mml:mi>Fe</mml:mi><mml:mi mathvariant="normal">O</mml:mi></mml:mrow><mml:mn>3</mml:mn></mml:msub><mml:mo>/</mml:mo><mml:msub><mml:mrow mathvariant="normal">O</mml:mi></mml:mrow><mml:mn>3</mml:mn></mml:msub></mml:math> Bilayer. Physical Review Applied, 2020, 13, .	1.5	15
51937	Semiempirical van der Waals method for two-dimensional materials with incorporated dielectric functions. Physical Review B, 2020, 101, .	1.1	9
51938	Regulating Lithium Nucleation and Deposition via MOFâ€Derived Co@Câ€Modified Carbon Cloth for Stable Li Metal Anode. Advanced Functional Materials, 2020, 30, 1909159.	7.8	170
51939	Asymmetric Lattice Disorder Induced at Oxide Interfaces. Advanced Materials Interfaces, 2020, 7, 1901944.	1.9	13
51940	Tunable Massive Dirac Fermions in Ferromagnetic Fe 3 Sn 2 Kagome Lattice. Physica Status Solidi - Rapid Research Letters, 2020, 14, 1900705.	1.2	12
51941	Liâ€Ion Cooperative Migration and Oxyâ€Sulfide Synergistic Effect in Li₁₄P₂Ge₂S_{16â”6}_xO_x Solidâ€Stateâ€Electrolyte Enables Extraordinary Conductivity and High Stability. Small, 2020, 16, e1906374.	5.2	27
51942	Prediction of corrosion inhibition efficiency of pyridines and quinolines on an iron surface using machine learning-powered quantitative structure-property relationships. Applied Surface Science, 2020, 512, 145612.	3.1	70
51943	Thermodynamic description of the Dyâ€“Siâ€“C system in silicon carbide ceramics. Calphad: Computer Coupling of Phase Diagrams and Thermochemistry, 2020, 68, 101738.	0.7	9
51944	Interphase boundary segregation induced phase transformation in a high-pressure die casting Mg-Al-La-Ca-Mn alloy. Materials and Design, 2020, 190, 108566.	3.3	20
51945	Controlled design of metal oxide-based (Mn2+/Nb5+) anodes for superior sodium-ion hybrid supercapacitors: Synergistic mechanisms of hybrid ion storage. Nano Energy, 2020, 71, 104594.	8.2	67

#	Article	IF	Citations
51946	V₂O₅ Nanobelts Mimick Tandem Enzymes To Achieve Nonenzymatic Online Monitoring of Glucose in Living Rat Brain. Analytical Chemistry, 2020, 92, 4583-4591.	3.2	55
51947	3D Ruthenium Nanoparticle Covalent Assemblies from Polymantane Ligands for Confined Catalysis. Chemistry of Materials, 2020, 32, 2365-2378.	3.2	11
51948	Surface Atomic Configurations of MnO₂ Regulating the Immobilization of Sulfides in Lithium Sulfur Battery. Journal of Physical Chemistry C, 2020, 124, 5565-5573.	1.5	9
51949	Wafer-Scale Growth of 2D PtTe₂ with Layer Orientation Tunable High Electrical Conductivity and Superior Hydrophobicity. ACS Applied Materials & Interfaces, 2020, 12, 10839-10851.	4.0	48
51950	Rotation of Ethoxy and Ethyl Moieties on a Molecular Platform on Au(111). ACS Nano, 2020, 14, 3907-3916.	7.3	15
51951	Room-temperature conversion of Cu_{2âˆ’x}Se to CuAgSe nanoparticles to enhance the photocatalytic performance of their composites with TiO₂. Dalton Transactions, 2020, 49, 3580-3591.	1.6	13
51952	Effect of crystallization on the electronic and optical properties of archetypical porphyrins. Physical Chemistry Chemical Physics, 2020, 22, 3825-3830.	1.3	6
51953	The influence of hydrogen concentration in amorphous carbon films on mechanical properties and fluorine penetration: a density functional theory and ab initio molecular dynamics study. RSC Advances, 2020, 10, 6822-6830.	1.7	8
51954	Metal adsorbate interactions and the convergence of density functional calculations. Journal of Chemical Physics, 2020, 152, 061102.	1.2	0
51955	Ab initio study of the miscibility for solid hydrogenâ€“helium mixtures at high pressure. Journal of Chemical Physics, 2020, 152, 074701.	1.2	3
51956	Tl2O/WTe2 van der Waals heterostructure with tunable multiple band alignments. Journal of Chemical Physics, 2020, 152, 074703.	1.2	6
51957	Making free-energy calculations routine: Combining first principles with machine learning. Physical Review B, 2020, 101, .	1.1	35
51958	Influence of hydrogenation on the vibrational density of states of magnetocaloric <mml:math xmlns:mml="http://www.w3.org/1998/Math/MathML"><mml:mi>LaFe</mml:mi><mml:msub><mml:mrow /><mml:mrow><mml:mn>11.4</mml:mn></mml:mrow></mml:msub><mml:mi>Si</mml:mi><mml:msub><mml:mrow /><mml:mrow><mml:mn>1.6</mml:mn></mml:mrow></mml:msub><mml:mi mathvariant="normal">H</mml:mi><mml:msub><mml:mrow /><mml:mrow><mml:mn>1.6</mml:mn></mml:mrow></mml:msub></mml:math>. Physical Review B, 2020,	1.1	15
51959	Magnetic properties and magnetocaloric effect of two-dimensional ternary <mml:math xmlns:mml="http://www.w3.org/1998/Math/MathML"><mml:mrow><mml:msub><mml:mi>Ga</mml:mi><mml:mn>2</mml:mn></</mml:		

#	Article	IF	Citations
51964	Positive Effect of Ge Vacancies on Facilitating Band Convergence and Suppressing Bipolar Transport in GeTeâ€Based Alloys for High Thermoelectric Performance. Advanced Functional Materials, 2020, 30, 1910059.	7.8	48
51965	Accommodation of Silicon in an Interconnected Copper Network for Robust Liâ€ion Storage. Advanced Functional Materials, 2020, 30, 1910249.	7.8	46
51966	Uncovering the Potential of M1â€Siteâ€Activated NASICON Cathodes for Znâ€ion Batteries. Advanced Materials, 2020, 32, e1907526.	11.1	103
51967	Widely Tunable Optical and Thermal Properties of Dirac Semimetal Cd₃As₂. Advanced Optical Materials, 2020, 8, 1901192.	3.6	27
51968	Controlling the non-linear optical properties of MgO by tailoring the electronic structure. Applied Physics B: Lasers and Optics, 2020, 126, 1.	1.1	13
51969	Salt-assisted growth and ultrafast photocarrier dynamics of large-sized monolayer ReSe2. Nano Research, 2020, 13, 667-675.	5.8	19
51970	Design of assembled composite of Mn3O4@Graphitic carbon porous nano-dandelions: A catalyst for Lowâ€“temperature selective catalytic reduction of NOx with remarkable SO2 resistance. Applied Catalysis B: Environmental, 2020, 269, 118731.	10.8	41
51971	Preparation of electron-rich Fe-based catalyst via electronic structure regulation and its promotion to hydrodesulfurization of dibenzothiophene. Applied Catalysis B: Environmental, 2020, 269, 118779.	10.8	13
51972	Local removal of silicon layers on Si(1Â0Â0)-2ÂÃ—Â1 with chlorine-resist STM lithography. Applied Surface Science, 2020, 509, 145235.	3.1	12
51973	Catalytic decomposition of N2O on Pd Cu alloy catalysts: A density functional theory study. Applied Surface Science, 2020, 510, 145349.	3.1	20
51974	Ullmann coupling of 2,7-dibromopyrene on Au(1Â1Â1) assisted by surface adatoms. Applied Surface Science, 2020, 513, 145797.	3.1	19
51975	Bandstructure engineering in 2D materials using Ferroelectric materials. Applied Surface Science, 2020, 513, 145817.	3.1	9
51976	Two-dimensional tetragonal Ti2BN: A novel potential anode material for Li-ion batteries. Applied Surface Science, 2020, 513, 145821.	3.1	25
51977	Mass difference and polarization lead to low thermal conductivity of graphene-like carbon nitride (C3N). Carbon, 2020, 162, 202-208.	5.4	35
51978	Decorating CoNi layered double hydroxides nanosheet arrays with fullerene quantum dot anchored on Ni foam for efficient electrocatalytic water splitting and urea electrolysis. Chemical Engineering Journal, 2020, 390, 124525.	6.6	118
51979	Symmetry transformation in Pd quasicrystals upon heating and hydrogenation. Computational Materials Science, 2020, 177, 109582.	1.4	0
51980	First-principles study of Ni/Ni3Al interface doped with Re, Ta and W. Computational Materials Science, 2020, 175, 109586.	1.4	22
51981	Effects of Fe doping on enhancing electrochemical properties of NiCo2S4 supercapacitor electrode. Electrochimica Acta, 2020, 340, 135939.	2.6	36

#	Article	IF	Citations
51982	Operando Revealing Dynamic Reconstruction of NiCo Carbonate Hydroxide for High-Rate Energy Storage. Joule, 2020, 4, 673-687.	11.7	88
51983	ZnN and ZnP as novel graphene-like materials with high Li-ion storage capacities. Materials Today Energy, 2020, 16, 100392.	2.5	20
51984	Effect of lattice and dopantâ€“induced strain on the conductivity of solid electrolytes: application of the elastic dipole method. Materialia, 2020, 9, 100607.	1.3	11
51985	Revealing the origin of the beneficial effect of cesium in highly efficient Cu(In,Ga)Se2 solar cells. Nano Energy, 2020, 71, 104622.	8.2	25
51986	Effect of electric field on radiation defects in NPN transistors. Nuclear Instruments & Methods in Physics Research B, 2020, 467, 114-117.	0.6	1
51987	The formation of â€¢OH with Fe-bearing smectite clays and low-molecular-weight thiols: Implication of As(III) removal. Water Research, 2020, 174, 115631.	5.3	24
51988	Ca Cobaltites as Potential Cathode Materials for Rechargeable Ca-Ion Batteries: Theory and Experiment. Journal of Physical Chemistry C, 2020, 124, 5902-5909.	1.5	21
51989	Two-Dimensional Binary Honeycomb Layer Formed by Ag and Te on Ag(111). Journal of Physical Chemistry Letters, 2020, 11, 1609-1613.	2.1	8
51990	Au Nanoparticle/WS₂ Nanodome/Graphene van der Waals Heterostructure Substrates for Surface-Enhanced Raman Spectroscopy. ACS Applied Nano Materials, 2020, 3, 2354-2363.	2.4	27
51991	Role of Defects in the Interplay between Adsorbate Evolving and Lattice Oxygen Mechanisms of the Oxygen Evolution Reaction in RuO₂ and IrO₂. ACS Catalysis, 2020, 10, 3650-3657.	5.5	339
51992	Modulating Electronic Structures of Armchair GaN Nanoribbons by Chemical Functionalization under an Electric Field Effect. ACS Omega, 2020, 5, 1261-1269.	1.6	6
51993	Fe₂CS₂ MXene: a promising electrode for Al-ion batteries. Nanoscale, 2020, 12, 5324-5331.	2.8	35
51994	Gas adsorption and light interaction mechanism in phosphorene-based field-effect transistors. Physical Chemistry Chemical Physics, 2020, 22, 5949-5958.	1.3	14
51995	Magnetic ground state in <mml:math xmlns:mml="http://www.w3.org/1998/Math/MathML"><mml:msub><mml:mi>FeTe</mml:mi><mml:mn>2</mml:mn></mml:msub><m , and <mml:math xmlns:mml="http://www.w3.org/1998/Math/MathML"><mml:msub><mml:mi>NiTe</mml:mi><mml:mn>2</mml:mn></mml:msub></ monolayers: Antiparallel magnetic moments at chalcogen atoms. Physical Review B, 2020, 101, .	1.1	31
51996	Lattice dynamics and thermal properties of thorium metal and thorium monocarbide. Physical Review B, 2020, 101, .	1.1	11
51997	Magnetization-Induced Band Shift in Ferromagnetic Weyl Semimetal <mml:math xmlns:mml="http://www.w3.org/1998/Math/MathML" display="inline"><mml:mrow><mml:mrow><mml:msub><mml:mrow><mml:mi>Co</mml:mi></mml:mrow><mml:mrow><mml:mn>3 mathvariant="normal">S</mml:mi></mml:mrow><mml:mrow><mml:mn>2</mml:mn></mml:mrow></mml:msub></mml:mrow></mml: Physical Review Letters, 2020, 124, 077403.	2.9	48
51998	Exploring the Adsorption Mechanism of Tetracene on Ag(110) by STM and Dispersion-Corrected DFT. Crystals, 2020, 10, 13.	1.0	2
51999	Molecular Modeling of Ammonia Gas Adsorption onto the Kaolinite Surface with DFT Study. Minerals (Basel, Switzerland), 2020, 10, 46.	0.8	10

#	Article	IF	Citations
52000	Hierarchical Self-assembly of Well-Defined Louver-Like P-Doped Carbon Nitride Nanowire Arrays with Highly Efficient Hydrogen Evolution. Nano-Micro Letters, 2020, 12, 52.	14.4	45
52001	Thermodynamic Control in the Synthesis of Quantum-Confined Blue-Emitting CsPbBr₃ Perovskite Nanostrips. Journal of Physical Chemistry Letters, 2020, 11, 2036-2043.	2.1	39
52002	Kinetic Monte Carlo Modeling for the NOâ€“CO Reaction Mechanism on Rh(100) and Rh(111). Langmuir, 2020, 36, 3127-3140.	1.6	7
52003	Inorganic Halide Double Perovskites with Optoelectronic Properties Modulated by Sublattice Mixing. Journal of the American Chemical Society, 2020, 142, 5135-5145.	6.6	62
52004	Electronic effects of transition metal dopants on Fe(100) and Fe5C2(100) surfaces for CO activation. Catalysis Science and Technology, 2020, 10, 2047-2056.	2.1	7
52005	Evolutional carrier mobility and power factor of two-dimensional tin telluride due to quantum size effects. Journal of Materials Chemistry C, 2020, 8, 4181-4191.	2.7	11
52006	Insight into structural stability and helium diffusion behavior of Feâ€“Cr alloys from first-principles. RSC Advances, 2020, 10, 3277-3292.	1.7	12
52007	Spin-polarized quantum transport in Si dangling bond wires. Nanoscale, 2020, 12, 6079-6088.	2.8	4
52008	Probing surface defects of ZnO using formaldehyde. Journal of Chemical Physics, 2020, 152, 074714.	1.2	10
52009	Self-trapped hole and impurity-related broad luminescence in Î²-Ga2O3. Journal of Applied Physics, 2020, 127, .	1.1	87
52010	Quantifying Large Lattice Relaxations in Photovoltaic Devices. Physical Review Applied, 2020, 13, .	1.5	7
52011	Emergence of Nontrivial Lowâ€Energy Dirac Fermions in Antiferromagnetic EuCd₂As₂. Advanced Materials, 2020, 32, e1907565.	11.1	51
52012	A DFT Investigation of the Dehydrogenation of Tetrahydropyrrole on Pt(111). Topics in Catalysis, 2020, 63, 688-699.	1.3	2
52013	A first principles investigation of W1-xMox (x=0â€“68.75Âat.%) alloys: Structural, electronic, mechanical and thermal properties. Journal of Alloys and Compounds, 2020, 829, 154480.	2.8	9
52014	A theoretical study on CO2 electrolysis through synergistic manipulation of Ni/Mn doping and oxygen vacancies in La(Sr)FeO3. Journal of Catalysis, 2020, 383, 273-282.	3.1	25
52015	Origin of Luminescence in La₂MoO₆ and La₂Mo₂O₉ and Their Bi-Doped Variants. Inorganic Chemistry, 2020, 59, 3215-3220.	1.9	22
52016	Band Engineering and Thermoelectric Performance Optimization of p-Type GeTe-Based Alloys through Ti/Sb Co-Doping. Journal of Physical Chemistry C, 2020, 124, 5583-5590.	1.5	16
52017	MoS₂-Supported Fe₂ Clusters Catalyzing Nitrogen Reduction Reaction to Produce Ammonia. Journal of Physical Chemistry C, 2020, 124, 6260-6266.	1.5	69

#	Article	IF	Citations
52018	Effects of the Dopant Site on the Absorption Properties of CsPb1â€“xMxI2Br (M = Ge, Sn, Sr, and Cu): A First-Principles Investigation. Journal of Physical Chemistry C, 2020, 124, 6028-6037.	1.5	10
52019	Dynamics of RS-(Au-SR)_x Staple Motifs on Metal Surfaces: From Nanoclusters to 2D Surfaces. Journal of Physical Chemistry C, 2020, 124, 5452-5459.	1.5	6
52020	Effect of the Nuclearity and Coordination of Cu and Fe Sites in Î² Zeolites on the Oxidation of Hydrocarbons. ACS Catalysis, 2020, 10, 3984-4002.	5.5	38
52021	First-Principles Density Functional Theory Calculations for Formic Acid Adsorption onto Hydro-Garnet Compounds. ACS Omega, 2020, 5, 4083-4089.	1.6	8
52022	Stable single platinum atoms trapped in sub-nanometer cavities in 12CaOÂ·7Al2O3 for chemoselective hydrogenation of nitroarenes. Nature Communications, 2020, 11, 1020.	5.8	94
52023	The exotically stoichiometric compounds in Alâ€“S system under high pressure. Npj Computational Materials, 2020, 6, .	3.5	21
52024	One-dimensional intergrowths in two-dimensional zeolite nanosheets and their effect on ultra-selective transport. Nature Materials, 2020, 19, 443-449.	13.3	91
52025	Bi-directional tuning of thermal transport in SrCoOx with electrochemically induced phase transitions. Nature Materials, 2020, 19, 655-662.	13.3	88
52026	Bandgap tuning of two-dimensional materials by sphere diameter engineering. Nature Materials, 2020, 19, 528-533.	13.3	80
52027	Energy-resolved distribution of electron traps for O/S-doped carbon nitrides by reversed double-beam photoacoustic spectroscopy and the photocatalytic reduction of Cr(<scp>vi</scp>). Chemical Communications, 2020, 56, 3793-3796.	2.2	28
52028	Câ€“C coupling reactions promoted by CNT-supported bimetallic center in Fischerâ€“Tropsch synthesis. Sustainable Energy and Fuels, 2020, 4, 2638-2644.	2.5	2
52029	Effect of thiolate-ligand passivation on the electronic structure and optical absorption properties of ultrathin one and two-dimensional gold nanocrystals. Nanoscale, 2020, 12, 5554-5566.	2.8	6
52030	Magnetic properties of Mn-doped <mml:math xmlns:mml="http://www.w3.org/1998/Math/MathML"><mml:mrow><mml:msub><mml:mi>Bi</mml:mi><mml:mn>2</mml:mn></mml:msub><mml:msub><mml:mi>Te</mml:mi><mml:mn>3</mml:mn></mml:msub></mml:mrow></mml:math> topological insulators: Ab initio calculations. Physical Review B, 2020, 101, .	1.1	9
52031	Indications for Lifshitz transitions in the nodal-line semimetal ZrSiTe induced by interlayer interaction. Physical Review B, 2020, 101, .	1.1	17
52032	Bovine serum albumin templated porous CeO2 to support Au catalyst for benzene oxidation. Molecular Catalysis, 2020, 486, 110849.	1.0	13
52033	First-principles perspective on structural evolution, sequential lithiation and physicochemical properties of tin oxide nanoclusters: Sn3Oz and LixSn3Oz (xâ€¯=â€¯1-10 and zâ€¯=â€¯0, 3-7). Materials Today Communications, 2020, 24, 101026.	0.9	0
52034	Metastable oxygen vacancy ordering state and improved memristive behavior in TiO2 crystals. Science Bulletin, 2020, 65, 631-639.	4.3	15
52035	Correlating the Composition-Dependent Structural and Electronic Dynamics of Inorganic Mixed Halide Perovskites. Chemistry of Materials, 2020, 32, 2470-2481.	3.2	20

#	Article	IF	Citations
52036	Correctly Assessing Defect Tolerance in Halide Perovskites. Journal of Physical Chemistry C, 2020, 124, 6022-6027.	1.5	70
52037	Screening for Planar Carbon Allotropes Using Structure Space Sampling. Journal of Physical Chemistry C, 2020, 124, 6379-6384.	1.5	7
52038	Effects of Sb Deviation from Its Stoichiometric Ratio on the Micro- and Electronic Structures and Thermoelectric Properties of Cu₁₂Sb₄S₁₃. ACS Applied Materials & Interfaces, 2020, 12, 14145-14153.	4.0	9
52039	Doubled Thermoelectric Figure of Merit in p-Type Î²-FeSi₂ via Synergistically Optimizing Electrical and Thermal Transports. ACS Applied Materials & Interfaces, 2020, 12, 12901-12909.	4.0	21
52040	Enhanced Photocatalytic and Antibacterial Ability of Cu-Doped Anatase TiO₂ Thin Films: Theory and Experiment. ACS Applied Materials & Interfaces, 2020, 12, 15348-15361.	4.0	102
52041	Kosterlitz-Thouless melting of magnetic order in the triangular quantum Ising material TmMgGaO4. Nature Communications, 2020, 11, 1111.	5.8	46
52042	Carbon Monoxide Oxidation Promoted by Surface Polarization Charges in a CuO/Ag Hybrid Catalyst. Scientific Reports, 2020, 10, 2552.	1.6	3
52043	Dual Lewis site creation for activation of methanol on Fe₃O₄(111) thin films. Chemical Science, 2020, 11, 2448-2454.	3.7	10
52044	Ultrafast fiber laser based on HfSe₂ saturable absorber. Nanotechnology, 2020, 31, 245204.	1.3	13
52045	Superconducting praseodymium superhydrides. Science Advances, 2020, 6, eaax6849.	4.7	99
52046	DFT calculations of the structure and stability of copper clusters on MoS₂. Beilstein Journal of Nanotechnology, 2020, 11, 391-406.	1.5	8
52047	Facile Selfâ€Forming Superionic Conductors Based on Complex Borohydride Surface Oxidation. Advanced Sustainable Systems, 2020, 4, 1900113.	2.7	14
52048	Onâ€Surface Assembly of Hydrogenâ€•and Halogenâ€Bonded Supramolecular Graphyneâ€Like Networks. Angewandte Chemie, 2020, 132, 9636-9642.	1.6	3
52049	Onâ€Surface Assembly of Hydrogenâ€•and Halogenâ€Bonded Supramolecular Graphyneâ€Like Networks. Angewandte Chemie - International Edition, 2020, 59, 9549-9555.	7.2	21
52050	Explaining Cu@Pt Bimetallic Nanoparticles Activity Based on NO Adsorption. Chemistry - A European Journal, 2020, 26, 11478-11491.	1.7	5
52051	Aminomethylâ€Functionalized Carbon Nanotubes as a Host of Small Sulfur Clusters for Highâ€Performance Lithiumâ€“Sulfur Batteries. ChemSusChem, 2020, 13, 2761-2768.	3.6	9
52052	First Principles Investigation of Cold Curves of Metals. Israel Journal of Chemistry, 2020, 60, 897-904.	1.0	1
52053	K + Intercalation of NH 4 HF 2 â€Exfoliated Ti 3 C 2 MXene as Binderâ€Free Electrodes with High Electrochemical Capacitance. Physica Status Solidi (A) Applications and Materials Science, 2020, 217, 1900806.	0.8	6

#	Article	IF	Citations
52054	An Effective Strategy for Photoelectric Performance Enhancement of 2D Perovskite via Halogenating Organic Cation: A Theoretical Prediction. Physica Status Solidi (B): Basic Research, 2020, 257, 1900599.	0.7	1
52055	Electronic structure and thermoelectric properties of CoAsSb with post-DFT approaches. Applied Physics A: Materials Science and Processing, 2020, 126, 1.	1.1	2
52056	Effects of interlayer coupling and electric field on the electronic properties of PtSe2/ZrSe2 van der Waals heterojunctions. Applied Surface Science, 2020, 510, 145316.	3.1	24
52057	Effects of alloy elements on adsorption of fibrinogen on biodegradable magnesium alloys surfaces: The MD simulations and experimental studies. Applied Surface Science, 2020, 512, 145725.	3.1	6
52058	Deconvoluting the XPS spectra for nitrogen-doped chars: An analysis from first principles. Carbon, 2020, 162, 528-544.	5.4	323
52059	Superior hardness and stiffness of diamond nanoparticles. Carbon, 2020, 162, 497-501.	5.4	7
52060	Spectroscopic identification and catalytic relevance of NH4+ intermediates in selective NOx reduction over Cu-SSZ-13 zeolites. Chemosphere, 2020, 250, 126272.	4.2	21
52061	Influence of defects in graphene on electron transfer kinetics: The role of the surface electronic structure. Electrochimica Acta, 2020, 341, 136011.	2.6	42
52062	Coupling of bowl-like VS2 nanosheet arrays and carbon nanofiber enables ultrafast Na+-Storage and robust flexibility for sodium-ion hybrid capacitors. Energy Storage Materials, 2020, 28, 91-100.	9.5	82
52063	Interactions between hydrogen and the <mml:math xmlns:mml="http://www.w3.org/1998/Math/MathML" altimg="si1.svg"><mml:mrow><mml:mrow><mml:mo		

#	Article	IF	Citations
52072	A new defective 19-electron TiPtSb half-Heusler thermoelectric compound with heavy band and low lattice thermal conductivity. Materials Today Physics, 2020, 13, 100200.	2.9	21
52073	Native point defects in Bi2Se3: A first-principles study. Physics Letters, Section A: General, Atomic and Solid State Physics, 2020, 384, 126281.	0.9	17
52074	A subtle balance between interchain interactions and surface reconstruction at the origin of the alkylthiol/Au(111) self-assembled monolayer geometry. Surface Science, 2020, 696, 121597.	0.8	4
52075	Isotype Heterojunction Solar Cells Using n-Type Sb₂Se₃ Thin Films. Chemistry of Materials, 2020, 32, 2621-2630.	3.2	83
52076	Structural Investigations of MA_{1â€“x}DMA_xPbI₃ Mixed-Cation Perovskites. Inorganic Chemistry, 2020, 59, 3730-3739.	1.9	21
52077	NaMoO₂: a Layered Oxide with Molybdenum Clusters. Inorganic Chemistry, 2020, 59, 4015-4023.	1.9	8
52078	Local Modified Becke-Johnson Exchange-Correlation Potential for Interfaces, Surfaces, and Two-Dimensional Materials. Journal of Chemical Theory and Computation, 2020, 16, 2654-2660.	2.3	42
52079	Large Enantiospecificity of Stepâ€“kink Metal Surfaces: Contributions from the Backbone and Side Chain of Î±-Amino Acids. Journal of Physical Chemistry C, 2020, 124, 742-748.	1.5	5
52080	Theory of Epitaxial Growth of Borophene on Layered Electride: Thermodynamic Stability and Kinetic Pathway. Journal of Physical Chemistry C, 2020, 124, 6063-6069.	1.5	7
52081	Organic Dye Molecules Sensitization-Enhanced Photocatalytic Water-Splitting Activity of MoS₂ from First-Principles Calculations. Journal of Physical Chemistry C, 2020, 124, 6580-6587.	1.5	12
52082	A DFT Study and Microkinetic Simulation in Propylene Oxidation on the â€œ29â€• Cu_xO/Cu(111) Surface. Journal of Physical Chemistry C, 2020, 124, 6611-6623.	1.5	18
52083	Na/K Diffusion in FeP as an Anode Material for Ion Batteries. Journal of Physical Chemistry C, 2020, 124, 6495-6501.	1.5	7
52084	Stoneâ€“Wales Defect Induced Performance Improvement of BC₃ Monolayer for High Capacity Lithium-Ion Rechargeable Battery Anode Applications. Journal of Physical Chemistry C, 2020, 124, 5910-5919.	1.5	52
52085	Understanding How Atomic Sulfur Controls the Selectivity of the Electroreduction of CO₂ to Formic Acid on Metallic Cu Surfaces. Journal of Physical Chemistry C, 2020, 124, 6145-6153.	1.5	25
52086	Formation of Linear Water Chains on Ni(110). Journal of Physical Chemistry Letters, 2020, 11, 2121-2126.	2.1	7
52087	Immobilization of Oxygen Atoms in the Pores of Microporous Metalâ€“Organic Frameworks for C₂H₂ Separation and Purification. ACS Applied Nano Materials, 2020, 3, 2911-2919.	2.4	88
52088	Probing Hydrogen-Bonding Properties of a Negatively Charged MoS₂ Monolayer by Powder X-ray Diffraction and Density Functional Theory Calculations. ACS Omega, 2020, 5, 4603-4610.	1.6	8
52089	Universal Phase Transitions of AlB₂-Type Transition-Metal Diborides. ACS Omega, 2020, 5, 4620-4625.	1.6	9

#	Article	IF	Citations
52090	A First-Principles Study of the Adsorption of H2O on Ru- and Mo-Alloyed Pt(111) Surfaces. Journal of Electronic Materials, 2020, 49, 2642-2650.	1.0	6
52091	SrTiO3/BiOI heterostructure: Interfacial charge separation, enhanced photocatalytic activity, and reaction mechanism. Chinese Journal of Catalysis, 2020, 41, 710-718.	6.9	32
52092	Dual-atom Ag2/graphene catalyst for efficient electroreduction of CO2 to CO. Applied Catalysis B: Environmental, 2020, 268, 118747.	10.8	140
52093	Exploring two-dimensional M2NS2 (Mâ€¯=â€¯Ti, V) MXenes based gas sensors for air pollutants. Applied Materials Today, 2020, 19, 100574.	2.3	44
52094	First-principles study of mechanical and thermodynamic properties of intermetallic Pt3M (MÂ= Al, Hf,) Tj ETQq0 0 0 rgBT /Overlock 10 Tf	0.9	13
52095	First principles study of the elastic and thermodynamic properties of Mg-Al alloys. Computational Materials Science, 2020, 177, 109587.	1.4	4
52096	Computational Investigation of Halogen-Substituted Na Argyrodites as Solid-State Superionic Conductors. Chemistry of Materials, 2020, 32, 1896-1903.	3.2	9
52097	The Intriguing Nature of Fluorine Doping on Li2CuO2 and the Reasons Behind the Inhibition of Oxygen Evolution. ACS Applied Energy Materials, 2020, 3, 2771-2780.	2.5	7
52098	Reversible Electrochemical Phase Change in Monolayer to Bulk-like MoTe₂ by Ionic Liquid Gating. ACS Nano, 2020, 14, 2894-2903.	7.3	37
52099	Artificial relativistic molecules. Nature Communications, 2020, 11, 815.	5.8	5
52100	Effective methane conversion to methanol on bi-functional graphene-oxide-supported platinum nanoclusters (Pt5) â€“ a DFT study. Physical Chemistry Chemical Physics, 2020, 22, 4967-4973.	1.3	15
52101	Giant effect of spinâ€“lattice coupling on the thermal transport in two-dimensional ferromagnetic CrI₃. Journal of Materials Chemistry C, 2020, 8, 3520-3526.	2.7	31
52102	Carrier-mediated ferromagnetism in two-dimensional PtS₂. RSC Advances, 2020, 10, 952-957.	1.7	7
52103	Improving the thermoelectric performance of p-type PbSe via synergistically enhancing the Seebeck coefficient and reducing electronic thermal conductivity. Journal of Materials Chemistry A, 2020, 8, 4931-4937.	5.2	34
52104	High performance supercapacitor electrodes based on spinel NiCo2O4@MWCNT composite with insights from density functional theory simulations. Journal of Chemical Physics, 2020, 152, 064706.	1.2	48
52105	Electronic and magnetic properties of van der Waals ferromagnetic semiconductor <mml:math xmlns:mml="http://www.w3.org/1998/Math/MathML"><mml:msub><mml:mi>VI</mml:mi><mml:mn>3</mml:mn></mml:msub></mml:math> Physical Review B, 2020, 101, .	1.1	28
52106	Electronic properties and topological phases of a two-dimensional allotrope of nitrogenated carbon. Physical Review B, 2020, 101, .	1.1	4
52107	Antiferromagnetic Topological Insulator with Nonsymmorphic Protection in Two Dimensions. Physical Review Letters, 2020, 124, 066401.	2.9	57

#	Article	IF	Citations
52108	Preparation of Surface Modified Ceria Nanoparticles as Abrasives for the Application of Chemical Mechanical Polishing (CMP). ECS Journal of Solid State Science and Technology, 2020, 9, 024015.	0.9	18
52109	Defect-mediated intercalation of dysprosium on buffer layer graphene supported by SiC(0001) substrate. Chemical Physics Letters, 2020, 742, 137162.	1.2	3
52110	Tailoring microstructure and electrical transportation through tensile stress in Bi2Te3 thermoelectric fibers. Journal of Materiomics, 2020, 6, 467-475.	2.8	13
52111	Immobilization of zinc oxide nanoparticles on graphene sheets for lithium ion storage and electromagnetic microwave absorption. Materials Chemistry and Physics, 2020, 245, 122766.	2.0	14
52112	Tailoring Acetylenic Bonds in Graphdiyne for Advanced Lithium Storage. ACS Sustainable Chemistry and Engineering, 2020, 8, 2614-2621.	3.2	30
52113	Enhanced moisture stability of cesium lead iodide perovskite solar cells â€“ a first-principles molecular dynamics study. Physical Chemistry Chemical Physics, 2020, 22, 5693-5701.	1.3	29
52114	Suppressed phase transition of a Rb/K incorporated inorganic perovskite with a water-repelling surface. Nanoscale, 2020, 12, 6571-6581.	2.8	8
52115	Field-enhanced selectivity in nanoconfined ionic transport. Nanoscale, 2020, 12, 6512-6521.	2.8	10
52116	On the divalent character of the Eu atoms in the ternary Zintl phases Eu5In2Pn6and Eu3MAs3(Pn =) Tj ETQq0 0 0 rgBT /Overlock 10 Tf 5	3.2	22
52117	Multi-factor study of the effects of a trace amount of water vapor on low concentration CO₂ capture by 5A zeolite particles. RSC Advances, 2020, 10, 6503-6511.	1.7	12
52118	Abnormally low thermal conductivity of 2D selenene: An ab initio study. Journal of Applied Physics, 2020, 127, .	1.1	26
52119	First principles calculations of optoelectronic and magnetic properties of Co-doped and (Co, Al) co-doped ZnO. Journal of Applied Physics, 2020, 127, 065707.	1.1	10
52120	Plastic flow between nanometer-spaced planar defects in nanostructured diamond and boron nitride. Physical Review B, 2020, 101, .	1.1	6
52121	Diversity of hole-trap centers due to small polarons and bipolarons in Ca-doped <mml:math xmlns:mml="http://www.w3.org/1998/Math/MathML"><mml:mrow><mml:mi>BiFe</mml:mi><mml:msub><mml:mi mathvariant="normal">O</mml:mi><mml:mn>3</mml:mn></mml:msub></mml:mrow></mml:math> : Unveiling dislocation characteristics in <mml:math	1.1	2
52122	xmlns:mml="http://www.w3.org/1998/Math/MathML"><mml:mrow><mml:mi mathvariant="normal">N</mml:mi><mml:msub><mml:mi mathvariant="normal">i</mml:mi><mml:mn>3</mml:mn></mml:msub><mml:mi>Al</mml:mi></mml:mrow></mml:math> from stacking fault energy and ideal strength: A first-principles study via pure alias shear deformation. Physical Review B, 2020, 101, .	1.1	18
52123	Strain stiffening, high load-invariant hardness, and electronic anomalies of boron phosphide under pressure. Physical Review B, 2020, 101, .	1.1	24
52124	Tunable phonon nanocapacitor built by carbon schwarzite based host-guest system. Physical Review B, 2020, 101, .	1.1	20
52125	Benchmarking the effective one-component plasma model for warm dense neon and krypton within quantum molecular dynamics simulation. Physical Review E, 2020, 101, 023302.	0.8	8

#	Article	IF	Citations
52126	HfS2 and TiS2 Monolayers with Adsorbed C, N, P Atoms: A First Principles Study. Catalysts, 2020, 10, 94.	1.6	10
52127	Transition Metal-Hyperdoped InP Semiconductors as Efficient Solar Absorber Materials. Nanomaterials, 2020, 10, 283.	1.9	8
52128	Metalâ€free graphene/boron nitride heterointerface for CO₂ reduction: Surface curvature controls catalytic activity and selectivity. EcoMat, 2020, 2, e12013.	6.8	17
52129	Interlayer coupling prolonged the photogenerated carrier lifetime of few layered Bi₂OS₂ semiconductors. Nanoscale, 2020, 12, 6057-6063.	2.8	18
52130	A density functional theory study on reduction-induced structural transformation of copper-oxide-based oxygen carrier. Journal of Chemical Physics, 2020, 152, 054709.	1.2	8
52131	A Fluorescence Probe for Metal Ions Based on Black Phosphorus Quantum Dots. Advanced Materials Interfaces, 2020, 7, 1902075.	1.9	17
52132	Tuning the Electrochemical Properties of Organic Battery Cathode Materials: Insights from Evolutionary Algorithm DFT Calculations. ChemSusChem, 2020, 13, 2402-2409.	3.6	15
52133	Strain Effects on the 2D van der Waals Heterostructure C₃B/C₃N: A Density Functional Theory and a Tightâ€Binding Study. Physica Status Solidi - Rapid Research Letters, 2020, 14, 2000012.	1.2	10
52134	Unusual mechanical and electronic behaviors of bulk layered hydrogen substituted graphdiyne under biaxial strain. Applied Surface Science, 2020, 513, 145694.	3.1	13
52135	C3N4 with engineered three coordinated (N3C) nitrogen vacancy boosts the production of 1O2 for Efficient and stable NO photo-oxidation. Chemical Engineering Journal, 2020, 389, 124421.	6.6	60
52136	An effective interface-regulating mechanism enabled by non-sacrificial additives for high-voltage nickel-rich cathode. Journal of Power Sources, 2020, 453, 227852.	4.0	26
52137	First-principles study of structural and electronic properties of substitutionally doped arsenene. Physica E: Low-Dimensional Systems and Nanostructures, 2020, 119, 114018.	1.3	11
52138	Understanding the Enhancement Mechanism of A-Site-Deficient La_xNiO₃ as an Oxygen Redox Catalyst. Chemistry of Materials, 2020, 32, 1864-1875.	3.2	54
52139	Defective TiO₂ for Propane Dehydrogenation. Industrial & Engineering Chemistry Research, 2020, 59, 4377-4387.	1.8	49
52140	Critical Role of Interfacial Sites between Nickel and CeO₂ Support in Dry Reforming of Methane: Revisit of Reaction Mechanism and Origin of Stability. Journal of Physical Chemistry C, 2020, 124, 5118-5124.	1.5	36
52141	On the Enhanced Reducibility and Charge Transport Properties of Phosphorus-Doped BiVO4 as Photocatalysts: A Computational Study. Journal of Physical Chemistry C, 2020, 124, 4352-4362.	1.5	10
52142	Centimeter-Scale and Highly Crystalline Two-Dimensional Alcohol: Evidence for Graphenol (C₆OH). Nano Letters, 2020, 20, 2107-2112.	4.5	5
52143	Room Temperature Commensurate Charge Density Wave on Epitaxially Grown Bilayer 2H-Tantalum Sulfide on Hexagonal Boron Nitride. ACS Nano, 2020, 14, 3917-3926.	7.3	27

#	Article	IF	Citations
52144	Realization of Epitaxial NbP and TaP Weyl Semimetal Thin Films. ACS Nano, 2020, 14, 4405-4413.	7.3	31
52145	Band Modulation and Interfacial Engineering to Generate Efficient Visible-Light-Induced Bifunctional Photocatalysts. ACS Sustainable Chemistry and Engineering, 2020, 8, 2919-2930.	3.2	35
52146	Gd(NO₃)(Se₂O₅)Â·3H₂O: a nitrateâ€“selenite nonlinear optical material with a short ultraviolet cutoff edge. Dalton Transactions, 2020, 49, 3253-3259.	1.6	18
52147	Pb dimerization greatly accelerates charge losses in MAPbI3: Time-domain ab initio analysis. Journal of Chemical Physics, 2020, 152, 064707.	1.2	12
52148	Large Valley Splitting in van der Waals Heterostructures with Type-III Band Alignment. Physical Review Applied, 2020, 13, .	1.5	38
52149	Layered <mml:math xmlns:mml="http://www.w3.org/1998/Math/MathML" display="inline" overflow="scroll"><mml:mrow><mml:mi>La</mml:mi><mml:mi>Cu</mml:mi><mml:mi mathvariant="normal">O</mml:mi><mml:mi>Se</mml:mi></mml:mrow></mml:math> : A Promising Anisotropic Thermoelectric Material. Physical Review Applied, 2020, 13, .	1.5	80
52150	Modulating superexchange strength to achieve robust ferromagnetic couplings in two-dimensional semiconductors. Physical Review B, 2020, 101, .	1.1	17
52151	Coulomb correlation in noncollinear antiferromagnetic <mml:math xmlns:mml="http://www.w3.org/1998/Math/MathML"><mml:mi>Î±</mml:mi></mml:math> -Mn. Physical Review B, 2020, 101, .	1.1	27
52152	Decompression-Induced Diamond Formation from Graphite Sheared under Pressure. Physical Review Letters, 2020, 124, 065701.	2.9	41
52153	Particlelike Phonon Propagation Dominates Ultralow Lattice Thermal Conductivity in Crystalline <mml:math xmlns:mml="http://www.w3.org/1998/Math/MathML" display="inline"><mml:mrow><mml:msub><mml:mrow><mml:mi>Tl</mml:mi></mml:mrow><mml:mrow><mml:mn>3</mml:mn></mml:mrow></mml: Physical Review Letters, 2020, 124, 065901.	2.9	122
52154	Observation of a Charge-Neutral Muon-Polaron Complex in Antiferromagnetic <mml:math xmlns:mml="http://www.w3.org/1998/Math/MathML" display="inline"><mml:mrow><mml:msub><mml:mrow><mml:mi>Cr</mml:mi></mml:mrow><mml:mrow><mml:mn>2</mml:mn></mml:mrow></mml: mathvariant="normal">O</mml:mi></mml:mrow><mml:mrow><mml:mn>3</mml:mn></mml:mrow></mml:msub></mml:mrow></mml: Physical Review X, 2020, 10, .	2.8	12
52155	Density-functional-theory-predicted symmetry lowering from cubic to tetragonal in nickel hexacyanoferrate. Journal of Applied Crystallography, 2020, 53, 117-126.	1.9	2
52156	Dilute concentrations of Sb (Bi) dopants in Sn-site enhance the thermoelectric properties of TiNiSn half-Heusler alloys: a first-principles study. Japanese Journal of Applied Physics, 2020, 59, 035003.	0.8	2
52157	Massive Dirac Fermion Behavior in a Low Bandgap Graphene Nanoribbon Near a Topological Phase Boundary. Advanced Materials, 2020, 32, e1906054.	11.1	44
52158	Superior high-temperature properties and deformation-induced planar faults in a novel L12-strengthened high-entropy alloy. Acta Materialia, 2020, 188, 517-527.	3.8	144
52159	Effect of Rh in Ni-based catalysts on sulfur impurities during methane reforming. Applied Catalysis B: Environmental, 2020, 267, 118691.	10.8	42
52160	Boosting aqueous zinc-ion storage in MoS2 via controllable phase. Chemical Engineering Journal, 2020, 389, 124405.	6.6	122
52161	CoSe2 modified Se-decorated CdS nanowire Schottky heterojunctions for highly efficient photocatalytic hydrogen evolution. Chemical Engineering Journal, 2020, 389, 124431.	6.6	57

#	Article	IF	Citations
52162	An orthorhombic D022-like precursor to Al8Mo3 in the Alâ€“Moâ€“Ti system. Journal of Alloys and Compounds, 2020, 823, 153807.	2.8	7
52163	Morphology of Fe2Al5 particles and the interface to WC coating in the context of hot-dip galvanizing: An ab initio study. Journal of Alloys and Compounds, 2020, 824, 153854.	2.8	16
52164	Self-supported MoSx/V2O3 heterostructures as efficient hybrid catalysts for hydrogen evolution reaction. Journal of Alloys and Compounds, 2020, 827, 154262.	2.8	7
52165	Band engineering in intrinsically magnetic CrBr3 monolayer. Journal of Magnetism and Magnetic Materials, 2020, 502, 166608.	1.0	8
52166	The effect of water vapor on surface oxygen exchange kinetics of thin film (La,Sr)(Co,Fe)O3-Î´. Journal of Power Sources, 2020, 451, 227478.	4.0	0
52167	C72: A novel low energy and direct band gap carbon phase. Physics Letters, Section A: General, Atomic and Solid State Physics, 2020, 384, 126325.	0.9	8
52168	Bipolar Doping by Intrinsic Defects and Magnetic Phase Instability in Monolayer CrI₃. Chemistry of Materials, 2020, 32, 1545-1552.	3.2	41
52169	New Perspectives on CO₂â€“Pt(111) Interaction with a High-Dimensional Neural Network Potential Energy Surface. Journal of Physical Chemistry C, 2020, 124, 5174-5181.	1.5	37
52170	Theoretical Investigation of 6-Mercaptopurine Isomersâ€™ Adsorption on the Au(001) Surface: Revealing the Fate of Different Isomers. ACS Omega, 2020, 5, 610-618.	1.6	3
52171	Nitro-Group-Doped Fully Conjugated 2D Covalent Organic Polymers for Enhanced Oxygen Reduction Reaction. ACS Sustainable Chemistry and Engineering, 2020, 8, 3728-3733.	3.2	11
52172	First-Principles Design of Highly Functional Sulfide Electrolyte of Li_{10â^'x}SnP₂S_{12â^'x}Cl_x for All Solid-State Li-Ion Battery Applications. ACS Sustainable Chemistry and Engineering, 2020, 8, 3321-3327.	3.2	26
52173	Energy landscape of Au₁₃: a global view of structure transformation. Physical Chemistry Chemical Physics, 2020, 22, 4402-4406.	1.3	4
52174	Ferroelectric Rashba semiconductors, AgBiP₂X₆ (X = S, Se and Te), with valley polarization: an avenue towards electric and nonvolatile control of spintronic devices. Nanoscale, 2020, 12, 5533-5542.	2.8	13
52175	The influence of dopants on aW-phase antimonene: theoretical investigations. RSC Advances, 2020, 10, 6973-6978.	1.7	34
52176	Steady semiconducting properties of monolayer PtSe2 with non-metal atom and transition metal atom doping. Physical Chemistry Chemical Physics, 2020, 22, 5765-5773.	1.3	15
52177	Effect of interstitial carbon on the evolution of early-stage irradiation damage in equi-atomic FeMnNiCoCr high-entropy alloys. Journal of Applied Physics, 2020, 127, .	1.1	24
52178	Zeeman-splitting-induced topological nodal structure and anomalous Hall conductivity in <mml:math xmlns:mml="http://www.w3.org/1998/Math/MathML"><mml:msub><mml:mi>ZrTe</mml:mi><mml:mn>5</mml:mn></mml:msub></mml:math> Physical Review B, 2020, 101, .	1.1	14
52179	Toward the origin of life over feldspar surfaces: Adsorption of amino acids and catalysis of conformational interconversions. International Journal of Quantum Chemistry, 2020, 120, e26175.	1.0	3

#	Article	IF	Citations
52180	Chloroform Hydrodechlorination on Palladium Surfaces: A Comparative DFT Study on Pd(111), Pd(100), and Pd(211). Topics in Catalysis, 2020, 63, 762-776.	1.3	17
52181	Mechanistic insight into the role of N-doped carbon matrix in electrospun binder-free Si@C composite anode for lithium-ion batteries. Ionics, 2020, 26, 3297-3305.	1.2	14
52182	Towards understanding the role of carbon atoms on transition metal surfaces: Implications for catalysis. Applied Surface Science, 2020, 513, 145765.	3.1	8
52183	High selective catalyst for ethylene epoxidation to ethylene oxide: A DFT investigation. Applied Surface Science, 2020, 513, 145799.	3.1	9
52184	Modelling rutile TiO2nanorod growth preferences: A density functional theory study. Catalysis Today, 2020, 356, 49-55.	2.2	5
52185	Tuning the crystal and electronic structure of Li4Ti5O12 via Mg/La Co-doping for fast and stable lithium storage. Ceramics International, 2020, 46, 12965-12974.	2.3	20
52186	Synthesis of SiC whiskers via catalytic reaction method in self-bonded SiC composites. Ceramics International, 2020, 46, 12975-12985.	2.3	9
52187	Mechanistic insights into heavy metals affinity in magnetic MnO2@Fe3O4/poly(m-phenylenediamine) coreâ"shell adsorbent. Ecotoxicology and Environmental Safety, 2020, 192, 110326.	2.9	29
52188	Stable zigzag edges of transition-metal dichalcogenides with high catalytic activity for oxygen reduction. Electrochimica Acta, 2020, 338, 135865.	2.6	14
52189	First-principles study of phase stability and temperature-dependent mechanical properties of (Cr,) Tj ETQq1 1 0.784314 rgBT /Overloc	2.8	17
52190	The correlation between N deficiency and the mechanical properties of the Ti2AlNy MAX phase. Journal of the European Ceramic Society, 2020, 40, 2279-2286.	2.8	7
52191	Exceptional levofloxacin removal using biochar-derived porous carbon sheets: Mechanisms and density-functional-theory calculation. Chemical Engineering Journal, 2020, 387, 124103.	6.6	63
52192	Synthesis of porous ZnxCo3-xO4 hollow nanoboxes derived from metal-organic frameworks for lithium and sodium storage. Electrochimica Acta, 2020, 335, 135694.	2.6	23
52193	Encapsulated cobalt nanoparticles as a recoverable catalyst for the hydrolysis of sodium borohydride. Energy Storage Materials, 2020, 27, 187-197.	9.5	72
52194	Anomalous short-to-medium-range structural characteristics of P in Pd43Ni43P14 and Pd40Ni40P20 glass-forming liquids. Journal of Alloys and Compounds, 2020, 823, 153101.	2.8	11
52195	Cation impurity-defect complex induced ferromagnetism and hopping conduction in Sb-doped ZnO synthesized under high pressure. Journal of Alloys and Compounds, 2020, 823, 153713.	2.8	4
52196	Thermal radiation and cycling properties of (Ca, Fe) or (Sr, Mn) co-doped La2Ce2O7 coatings. Journal of the European Ceramic Society, 2020, 40, 2020-2029.	2.8	46
52197	Compositional dependence of hydrogenation performance of Ti-Zr-Hf-Mo-Nb high-entropy alloys for hydrogen/tritium storage. Journal of Materials Science and Technology, 2020, 55, 116-125.	5.6	66

#	Article	IF	Citations
52198	Size and phase dependent thermal conductivity of TiO2-water nanofluid with theoretical insight. Journal of Molecular Liquids, 2020, 302, 112499.	2.3	14
52199	Enthalpies and elastic properties of Ni-Co binary system by ab initio calculations and an energy comparison with the CALPHAD approach. Materials Today Communications, 2020, 23, 100905.	0.9	5
52200	New Quasicrystal Approximant in the Scâ€“Pd System: From Topological Data Mining to the Bench. Chemistry of Materials, 2020, 32, 1064-1079.	3.2	10
52201	Performance and Cost Assessment of Machine Learning Interatomic Potentials. Journal of Physical Chemistry A, 2020, 124, 731-745.	1.1	428
52202	Double-Layer Honeycomb AlP: A Promising Anode Material for Li-, Na-, and K-Ion Batteries. Journal of Physical Chemistry C, 2020, 124, 2978-2986.	1.5	11
52203	Predicting the Most Suitable Surface Candidates of Ta₃N₅ Photocatalysts for Water-Splitting Reactions Using Screened Coulomb Hybrid DFT Computations. Journal of Physical Chemistry C, 2020, 124, 2472-2480.	1.5	21
52204	Dual Elements Coupling Effect Induced Modification from the Surface into the Bulk Lattice for Ni-Rich Cathodes with Suppressed Capacity and Voltage Decay. ACS Applied Materials & Interfaces, 2020, 12, 8146-8156.	4.0	56
52205	Atomic-level tuning of Coâ€“Nâ€“C catalyst for high-performance electrochemical H2O2 production. Nature Materials, 2020, 19, 436-442.	13.3	725
52206	A DFT and KMC based study on the mechanism of the water gas shift reaction on the Pd(100) surface. Physical Chemistry Chemical Physics, 2020, 22, 3620-3632.	1.3	22
52207	High-pressure formation of antimony nitrides: a first-principles study. RSC Advances, 2020, 10, 2448-2452.	1.7	3
52208	Octahedrally coordinated single layered CaF₂: robust insulating behaviour. Physical Chemistry Chemical Physics, 2020, 22, 2949-2954.	1.3	11
52209	Undulated silicene and germanene freestanding layers: why not?. Journal of Physics Condensed Matter, 2020, 32, 195503.	0.7	7
52210	Re effects in model Ni-based superalloys investigated with first-principles calculations and atom probe tomography*. Chinese Physics B, 2020, 29, 043103.	0.7	4
52211	Two-dimensional Janus-In2STe/InSe heterostructure with direct gap and staggered band alignment. Applied Surface Science, 2020, 509, 145317.	3.1	23
52212	The role of exfoliating solvents for control synthesis of few-layer graphene-like nanosheets in energy storage applications: Theoretical and experimental investigation. Applied Surface Science, 2020, 509, 145375.	3.1	15
52213	Dual-site activation enhanced photocatalytic removal of no with Au/CeO2. Chemical Engineering Journal, 2020, 386, 124047.	6.6	69
52214	Structural and thermoelectric properties of Zr-doped TiPdSn half-Heusler compound by first-principles calculations. Chemical Physics Letters, 2020, 741, 137055.	1.2	13
52215	Vibrational Raman spectroscopy on adsorbate-induced low-dimensional surface structures. Surface Science Reports, 2020, 75, 100480.	3.8	4

#	Article	IF	Citations
52216	Insight into Size- and Metal-Dependent Activity and the Mechanism for Steam Methane Re-forming in Nanocatalysis. Journal of Physical Chemistry C, 2020, 124, 2501-2512.	1.5	19
52217	Tunable Redox Temperature of a Co_{3â€“x}Mn_xO₄ (0 â‰¤ Tj ETQq1 1 0.784314 gf & Interfaces, 2020, 12, 7010-7020.	4.0	20
52218	Spherical Metal Oxides with High Tap Density as Sulfur Host to Enhance Cathode Volumetric Capacity for Lithiumâ€“Sulfur Battery. ACS Applied Materials & Interfaces, 2020, 12, 5909-5919.	4.0	76
52219	Achieving Both High Ionic Conductivity and High Interfacial Stability with the Li2+xC1â€“xBxO3 Solid-State Electrolyte: Design from Theoretical Calculations. ACS Applied Materials & Interfaces, 2020, 12, 6007-6014.	4.0	17
52220	Cooperative Effect of Multiple Active Sites and Hierarchical Chemical Bonds in Metalâ€“Organic Compounds for Improving Cathode Performance. ACS Energy Letters, 2020, 5, 477-485.	8.8	10
52221	van der Waals Heterojunction between a Bottom-Up Grown Doped Graphene Quantum Dot and Graphene for Photoelectrochemical Water Splitting. ACS Nano, 2020, 14, 1185-1195.	7.3	100
52222	Dehydration Melting Below the Undersaturated Transition Zone. Geochemistry, Geophysics, Geosystems, 2020, 21, e2019GC008712.	1.0	11
52223	Normal-to-topological insulator martensitic phase transition in group-IV monochalcogenides driven by light. NPG Asia Materials, 2020, 12, .	3.8	18
52224	Computational investigation of chalcogenide spinel conductors for all-solid-state Mg batteries. Chemical Communications, 2020, 56, 1952-1955.	2.2	31
52225	Assembly of cerium-based coordination polymer into variant polycrystalline 2Dâ€“3D CeO2â^'x nanostructures. Journal of Materials Chemistry A, 2020, 8, 4753-4763.	5.2	20
52226	Improved description of hematite surfaces by the SCAN functional. Journal of Chemical Physics, 2020, 152, 024706.	1.2	13
52227	Shapes of Fe nanocrystals encapsulated at the graphite surface. New Journal of Physics, 2020, 22, 023016.	1.2	14
52228	Giant tunneling electroresistance in two-dimensional ferroelectric tunnel junctions with out-of-plane ferroelectric polarization. Physical Review B, 2020, 101, .	1.1	52
52229	Reversible control of Dzyaloshinskii-Moriya interaction at the graphene/Co interface via hydrogen absorption. Physical Review B, 2020, 101, .	1.1	19
52230	Titanium 3d ferromagnetism with perpendicular anisotropy in defective anatase. Physical Review B, 2020, 101, .	1.1	10
52231	Probing the Solid Phase of Noble Metal Copper at Terapascal Conditions. Physical Review Letters, 2020, 124, 015701.	2.9	43
52232	B,N Codoped Graphitic Nanotubes Loaded with Co Nanoparticles as Superior Sulfur Host for Advanced Liâ€“S Batteries. Small, 2020, 16, e1906634.	5.2	50
52233	Pdâ€“Cu alloy catalyst synthesized by citric acid-assisted galvanic displacement reaction for N2O reduction. Journal of Applied Electrochemistry, 2020, 50, 395-405.	1.5	6

#	Article	IF	Citations
52234	Hydrogenation of benzoic acid to benzyl alcohol over Pt/SnO2. Applied Catalysis A: General, 2020, 593, 117420.	2.2	15
52235	Effects of carbide forming elements Me on residual stress and mechanical properties of DLC films by molecular dynamics simulation. Materials Today Communications, 2020, 23, 100946.	0.9	7
52236	PC6 monolayer: A potential candidate as NOx sensor with high sensitivity and selectivity. Physica E: Low-Dimensional Systems and Nanostructures, 2020, 118, 113958.	1.3	11
52237	Durability screening of Pt ternary alloy (111) surfaces for oxygen reduction reaction using Density Functional Theory. Surfaces and Interfaces, 2020, 18, 100440.	1.5	2
52238	From the Surface Structure to Catalytic Properties of Al₅Co₂(21Ì...0): A Study Combining Experimental and Theoretical Approaches. Journal of Physical Chemistry C, 2020, 124, 4552-4562.	1.5	11
52239	Reduced Silicon Fragmentation in Lithium Ion Battery Anodes Using Electronic Doping Strategies. ACS Applied Energy Materials, 2020, 3, 1730-1741.	2.5	19
52240	Catalysis Meets Spintronics; Spin Potentials Associated with Open-Shell Orbital Configurations Enhance the Activity of Pt₃Co Nanostructures for Oxygen Reduction: A Density Functional Theory Study. ACS Applied Nano Materials, 2020, 3, 506-515.	2.4	37
52241	Nanoarchitecture through Strained Molecules: Cubane-Derived Scaffolds and the Smallest Carbon Nanothreads. Journal of the American Chemical Society, 2020, 142, 17944-17955.	6.6	32
52242	Synergy between Ion Migration and Charge Carrier Recombination in Metal-Halide Perovskites. Journal of the American Chemical Society, 2020, 142, 3060-3068.	6.6	91
52243	Recreating Giants Impacts in the Laboratory: Shock Compression of Bridgmanite to 14 Mbar. Geophysical Research Letters, 2020, 47, e2019GL085476.	1.5	19
52244	Unfolding the complexity of phonon quasi-particle physics in disordered materials. Npj Computational Materials, 2020, 6, .	3.5	22
52245	Tailoring the physical and chemical properties of Sn_{1â^'x}Co_xO₂ nanoparticles: an experimental and theoretical approach. Physical Chemistry Chemical Physics, 2020, 22, 3702-3714.	1.3	19
52246	Robustness of the electronic structure and charge transfer in topological insulator Bi₂Te₂Se and Bi₂Se₂Te thin films under an external electric field. Physical Chemistry Chemical Physics, 2020, 22, 3867-3874.	1.3	8
52247	Tuning the electronic structure of RhX₃ (X = Cl, Br, I) nonmagnetic monolayers: effects of charge-injection and external strain. Physical Chemistry Chemical Physics, 2020, 22, 4561-4573.	1.3	5
52248	Self-assembled CoTiO₃ nanorods with controllable oxygen vacancies for the efficient photochemical reduction of CO₂ to CO. Catalysis Science and Technology, 2020, 10, 2040-2046.	2.1	22
52249	Temperature-dependent mechanical properties of Ti_{n+1}C_nO₂ (n = 1, 2) MXene monolayers: a first-principles study. Physical Chemistry Chemical Physics, 2020, 22, 3414-3424.	1.3	35
52250	Principle understanding towards synthesizing Fe/N decorated carbon catalysts with pyridinic-N enriched and agglomeration-free features for lithiumâ€“oxygen batteries. RSC Advances, 2020, 10, 3853-3860.	1.7	2
52251	Achieving high-performance p-type SmMg₂Bi₂ thermoelectric materials through band engineering and alloying effects. Journal of Materials Chemistry A, 2020, 8, 15760-15766.	5.2	21

#	Article	IF	Citations
52252	Theoretical study of strain induced magnetic transition of single-layer CrTe3. Journal of Applied Physics, 2020, 127, .	1.1	11
52253	Parameter-free coordination numbers for solutions and interfaces. Journal of Chemical Physics, 2020, 152, 024124.	1.2	11
52254	Theoretical investigation of the crystallographic structure, anisotropic elastic response, and electronic properties of the major borides in Ni-based superalloys. Philosophical Magazine, 2020, 100, 998-1014.	0.7	3
52255	Quantum confinement and edge effects on electronic properties of zigzag green phosphorene nanoribbons. Journal of Physics Condensed Matter, 2020, 32, 175301.	0.7	3
52256	Origin of Rashba-Dresselhaus effect in the ferroelectric nitride perovskite <mml:math xmlns:mml="http://www.w3.org/1998/Math/MathML"><mml:msub><mml:mi>LaWN</mml:mi><mml:mn>3</mml:mn></mml:msub></m Physical Review B, 2020, 101, .	1.1	17
52257	Structural, magnetic, and spin dynamical properties of the polar antiferromagnets <mml:math xmlns:mml="http://www.w3.org/1998/Math/MathML"><mml:mrow><mml:mi mathvariant="normal">N</mml:mi><mml:msub><mml:mi mathvariant="normal">i</mml:mi><mml:mrow><mml:mn>3</mml:mn><mml:mo>â^'</mml:mo><mml:mi>x</mml:mi></mml:mrow></n mathvariant="normal">C</mml:mi><mml:msub><mml:mi	1.1	9
52258	Understanding the origin of the magnetocaloric effects in substitutional <mml:math xmlns:mml="http://www.w3.org/1998/Math/MathML"><mml:mtext>Ni-Mn-Sb-</mml:mtext><mml:mi>Z</mml:mi><mml:mo /><mml:mo>(</mml:mo><mml:mi>Z</mml:mi><mml:mo>=</mml:mo><mml:mi>Fe</mml:mi><mml:mo>,</mml:mo><mml:mi>Co</mm compounds: Insights from first-principles calculations. Physical Review B, 2020, 101, .	1.1	14
52259	Crystal size effects on giant thermopower in <mml:math xmlns:mml="http://www.w3.org/1998/Math/MathML"><mml:msub><mml:mi>CrSb</mml:mi><mml:mn>2</mml:mn></mml:msub></m Physical Review B, 2020, 101, .	1.1	7
52260	Valley-Layer Coupling: A New Design Principle for Valleytronics. Physical Review Letters, 2020, 124, 037701.	2.9	69
52261	Structural and spectral dynamics of single-crystalline Ruddlesden-Popper phase halide perovskite blue light-emitting diodes. Science Advances, 2020, 6, eaay4045.	4.7	88
52262	Visualizing H ₂ O molecules reacting at TiO ₂ active sites with transmission electron microscopy. Science, 2020, 367, 428-430.	6.0	149
52263	First-principles Study of LaOPbBiS₃ and Its Analogous Compounds as Thermoelectric Materials. Journal of the Physical Society of Japan, 2020, 89, 024702.	0.7	8
52264	Extraordinary Strong Bandâ€Edge Absorption in Distorted Chalcogenide Perovskites. Solar Rrl, 2020, 4, 1900555.	3.1	82
52265	Functional group-directed self-installing doors in porous graphene: a theoretical study. Journal of Materials Science, 2020, 55, 5111-5122.	1.7	3
52266	Constructing MoS2/g-C3N4 heterojunction with enhanced oxygen evolution reaction activity: A theoretical insight. Applied Surface Science, 2020, 510, 145489.	3.1	76
52267	Enabling Direct H2O2 Production in Acidic Media through Rational Design of Transition Metal Single Atom Catalyst. CheM, 2020, 6, 658-674.	5.8	418
52268	Responses to comments on the paper â€œTwo-dimensional Sc2C: A reversible and high capacity hydrogen storage material predicted by first-principles calculationsâ€. International Journal of Hydrogen Energy, 2020, 45, 7257-7262.	3.8	3
52269	Noninnocent Influence of Host Î²-NiOOH Redox Activity on Transition-Metal Dopantsâ€™ Efficacy as Active Sites in Electrocatalytic Water Oxidation. ACS Catalysis, 2020, 10, 2720-2734.	5.5	32

#	Article	IF	Citations
52270	Two-dimensional higher-order topology in monolayer graphdiyne. Npj Quantum Materials, 2020, 5, .	1.8	120
52271	Can polarity-inverted membranes self-assemble on Titan?. Science Advances, 2020, 6, eaax0272.	4.7	13
52272	Emergence of Multispinterface and Antiferromagnetic Molecular Exchange Bias via Molecular Stacking on a Ferromagnetic Film. Advanced Functional Materials, 2020, 30, 1908499.	7.8	6
52273	Evaluation of Polaron Transport in Solids from Firstâ€principles. Israel Journal of Chemistry, 2020, 60, 768-786.	1.0	41
52274	Synthesis, Crystal and Electronic Structure of Layered AM Sb Compounds (A = Rb, Cs; M = Zn, Cd). Zeitschrift Fur Anorganische Und Allgemeine Chemie, 2020, 646, 1079-1085.	0.6	4
52275	Selective transformation of ethanol to acetaldehyde catalyzed by Au/h-BN interface prepared on Rh(111) surface. Applied Catalysis A: General, 2020, 592, 117440.	2.2	10
52276	Facet-dependent catalytic activities of Pd/rGO: Exploring dehydrogenation mechanism of dodecahydro-N-ethylcarbazole. Applied Catalysis B: Environmental, 2020, 266, 118658.	10.8	56
52277	Strategy for improving Ag wetting on oxides: Coalescence dynamics versus nucleation density. Applied Surface Science, 2020, 510, 145515.	3.1	32
52278	Mechanical stability and optoelectronic behavior of BeXP2 (X=Si and Ge) chalcopyrite. Chinese Journal of Physics, 2020, 64, 174-182.	2.0	19
52279	Structural and electronic descriptors for atmospheric instability of Li-thiophosphate using density functional theory. Solid State Ionics, 2020, 346, 115225.	1.3	13
52280	Enhanced Bonding of Pentagonâ€“Heptagon Defects in Graphene to Metal Surfaces: Insights from the Adsorption of Azulene and Naphthalene to Pt(111). Chemistry of Materials, 2020, 32, 1041-1053.	3.2	20
52281	Understanding Superionic Conductivity in Lithium and Sodium Salts of Weakly Coordinating Closo-Hexahalocarbaborate Anions. Chemistry of Materials, 2020, 32, 1475-1487.	3.2	35
52282	From Waste-Heat Recovery to Refrigeration: Compositional Tuning of Magnetocaloric Mn_{1+x}Sb. Chemistry of Materials, 2020, 32, 1243-1249.	3.2	18
52283	Nearly Identical but Not Isotypic: Influence of Lanthanide Contraction on Cs₂NaLn(PS₄)₂ (Ln = Laâ€“Nd, Sm, and Gdâ€“Ho). Inorganic Chemistry, 2020, 59, 1905-1916.	1.9	15
52284	High-Pressure Phase Transitions of Zinc Difluoride up to 55 GPa. Inorganic Chemistry, 2020, 59, 2584-2593.	1.9	10
52285	Direct Imaging of Precursor Adcomplex States during Cryogenic-Temperature On-Surface Metalation: Scanning Tunneling Microscopy Study on Porphyrin Array with Fe Adsorption at 78.5 K. Journal of Physical Chemistry C, 2020, 124, 3621-3631.	1.5	6
52286	Surface Functionalization Tailored Electronic Structure and Magnetic Properties of Two-Dimensional CrC₂ Monolayers. Journal of Physical Chemistry C, 2020, 124, 3095-3106.	1.5	13
52287	Chemically Tuning Stability and Superconductivity of Pâ€“H Compounds. Journal of Physical Chemistry Letters, 2020, 11, 935-939.	2.1	40

#	Article	IF	Citations
52288	Key Factors Controlling the Large Second Harmonic Generation in Nonlinear Optical Materials. ACS Applied Materials & Interfaces, 2020, 12, 9434-9439.	4.0	19
52289	Oxygen Evolution Activity on NiOOH Catalysts: Four-Coordinated Ni Cation as the Active Site and the Hydroperoxide Mechanism. ACS Catalysis, 2020, 10, 2581-2590.	5.5	71
52290	Engineering a Highly Defective Stable UiO-66 with Tunable Lewis- BrÃ¸nsted Acidity: The Role of the Hemilabile Linker. Journal of the American Chemical Society, 2020, 142, 3174-3183.	6.6	156
52291	Hematite at its thinnest limit. 2D Materials, 2020, 7, 025029.	2.0	13
52292	Adsorption of CH4 and SO2 on Unsupported Pd1â˜xMxO(101) Surface. Catalysis Letters, 2020, 150, 1870-1877.	1.4	3
52293	Simultaneous electrochemical ozone production and hydrogen evolution by using tantalum-based nanorods electrocatalysts. Applied Catalysis B: Environmental, 2020, 266, 118632.	10.8	42
52294	First-principles study on the structural, electronic, and Li-ion mobility properties of anti-perovskite superionic conductor Li3OCl (1Â0Â0) surface. Applied Surface Science, 2020, 510, 145394.	3.1	12
52295	Orthorhombic CsPbI3 perovskites: Thickness-dependent structural, optical and vibrational properties. Computational Condensed Matter, 2020, 23, e00453.	0.9	8
52296	Accelerating the development of multi-component Cu-Al-based shape memory alloys with high elastocaloric property by machine learning. Computational Materials Science, 2020, 176, 109521.	1.4	19
52297	Triphenylene and tetracene based porous sheet: Stability and electronic properties. Computational Materials Science, 2020, 176, 109529.	1.4	4
52298	First principles modelling of the N-doped Co0.5-terminated (0Â0Â1) Co3O4 surface. Nuclear Instruments & Methods in Physics Research B, 2020, 465, 11-14.	0.6	1
52299	ZnCdO2 monolayer â€" A complex 2D structure of ZnO and CdO monolayers for photocatalytic water splitting driven by visible-light. Spectrochimica Acta - Part A: Molecular and Biomolecular Spectroscopy, 2020, 230, 118068.	2.0	6
52300	The role of P 3s2 lone pair (E) in structure, properties and phase transitions of black phosphorus. Stereochemistry and ab initio topology analyses. Solid State Sciences, 2020, 100, 106068.	1.5	6
52301	Crystal Growth and First-Principles Calculations of the Mid-IR Laser Crystal Dy³⁺:PbGa₂S₄. Crystal Growth and Design, 2020, 20, 845-850.	1.4	10
52302	Defective Phosphorene as a Promising Anchoring Material for Lithiumâ€"Sulfur Batteries. Journal of Physical Chemistry C, 2020, 124, 2739-2746.	1.5	39
52303	Semiconducting Phase and Anisotropic Properties in Borophene via Chemical Surface Functionalization. Journal of Physical Chemistry C, 2020, 124, 5807-5816.	1.5	5
52304	Borophene Concentric Superlattices via Self-Assembly of Twin Boundaries. Nano Letters, 2020, 20, 1315-1321.	4.5	36
52305	Electronic Band Structure of In-Plane Ferroelectric van der Waals Î²â€²-In₂Se₃. ACS Applied Electronic Materials, 2020, 2, 213-219.	2.0	26

#	Article	IF	Citations
52306	Interfacial Control of Ferromagnetism in Ultrathin SrRuO₃ Films Sandwiched between Ferroelectric BaTiO₃ Layers. ACS Applied Materials & Interfaces, 2020, 12, 6707-6715.	4.0	16
52307	Lavender-Like Ga-Doped Pt₃Co Nanowires for Highly Stable and Active Electrocatalysis. ACS Catalysis, 2020, 10, 3018-3026.	5.5	75
52308	Engineering Substrate Interaction To Improve Hydrogen Evolution Catalysis of Monolayer MoS₂ Films beyond Pt. ACS Nano, 2020, 14, 1707-1714.	7.3	97
52309	Complex cobalt silicates and germanates crystallizing in a porous three-dimensional framework structure. CrystEngComm, 2020, 22, 1112-1119.	1.3	8
52310	Water structures on a Pt(111) electrode from ab initio molecular dynamic simulations for a variety of electrochemical conditions. Physical Chemistry Chemical Physics, 2020, 22, 10431-10437.	1.3	65
52311	Electronic properties of dilute-As InGaNAs alloys: A first-principles study. Journal of Applied Physics, 2020, 127, .	1.1	2
52312	Thermal transport properties of GaN with biaxial strain and electron-phonon coupling. Journal of Applied Physics, 2020, 127, .	1.1	59
52313	Intrinsic piezoelectricity of monolayer group IVâ€“V MX2: SiP2, SiAs2, GeP2, and GeAs2. Applied Physics Letters, 2020, 116, .	1.5	30
52314	Quantum critical point and ferromagnetic semiconducting behavior in p -type FeAs2. Physical Review B, 2020, 101, .	1.1	5
52315	Ab initio calculations of the rate of carrier trapping and release at dopant sites in NaI: Tl beyond the harmonic approximation. Physical Review B, 2020, 101, .	1.1	2
52316	Exploring High Transition Temperature Superconductivity in a Freestanding or <mml:math xmlns:mml="http://www.w3.org/1998/Math/MathML" display="inline"><mml:mrow><mml:msub><mml:mrow><mml:mi>SrTiO</mml:mi></mml:mrow><mml:mrow><mml:mn>3</mml:mn></ -Supported CoSb Monolayer. Physical Review Letters, 2020, 124, 027002.	2.9	14
52317	Autonomous Discovery of Materials for Intercalation Electrodes. Batteries and Supercaps, 2020, 3, 488-498.	2.4	25
52318	Multifunctional electrocatalytic activity of coronene-based two-dimensional metal-organic frameworks: TM-PTC. Applied Surface Science, 2020, 511, 145393.	3.1	18
52319	Diameter, strength and resistance tuning of double-walled carbon nanotubes in a transmission electron microscope. Carbon, 2020, 160, 98-106.	5.4	5
52320	Vacancy mediated alloying strengthening effects on Al/Al3Zr interface and stabilization of L12-Al3Zr: A first-principles study. Journal of Alloys and Compounds, 2020, 825, 153825.	2.8	7
52321	Persulfate activation by two-dimensional MoS2 confining single Fe atoms: Performance, mechanism and DFT calculations. Journal of Hazardous Materials, 2020, 389, 122137.	6.5	72
52322	Ab initio molecular dynamic study of structure and atomic motions in SrCoO3-x and SrCo0.875Mo0.125O3-x. Materials Today: Proceedings, 2020, 25, 435-438.	0.9	1
52323	Electronic Structures and Lattice Dynamics of Layered BiOCl Single Crystals. Journal of Physical Chemistry Letters, 2020, 11, 1038-1044.	2.1	39

#	Article	IF	Citations
52324	Real-Space Mapping of Surface-Oxygen Defect States in Photovoltaic Materials Using Low-Voltage Scanning Ultrafast Electron Microscopy. ACS Applied Materials & Interfaces, 2020, 12, 7760-7767.	4.0	12
52325	Aluminum-Induced Interfacial Strengthening in Calcium Silicate Hydrates: Structure, Bonding, and Mechanical Properties. ACS Sustainable Chemistry and Engineering, 2020, 8, 2622-2631.	3.2	28
52326	A type of novel Weyl semimetal candidate: layered transition metal monochalcogenides Mo2XY (X, Y =) Tj ETQq0 0 0 rgBT /Overlock 10	2.8	13
52327	Perovskite-supported Pt single atoms for methane activation. Journal of Materials Chemistry A, 2020, 8, 4362-4368.	5.2	31
52328	Highly conductive n-type CH₃NH₃PbI₃ single crystals doped with bismuth donors. Journal of Materials Chemistry C, 2020, 8, 3694-3704.	2.7	27
52329	Tailoring electronic properties of two-dimensional antimonene with isoelectronic counterparts*. Chinese Physics B, 2020, 29, 037305.	0.7	6
52331	Growth, charge and thermal transport of flowered graphene. Carbon, 2020, 161, 259-268.	5.4	7
52332	Synthesis of novel cubic Ni2Mo3N and its electronic structure regulation by vanadium doping towards high-efficient HER electrocatalyst. Electrochimica Acta, 2020, 337, 135689.	2.6	11
52333	First-principles study on the effects of doping and adsorption on the electronic and magnetic properties of diamond nanothreads. Physica E: Low-Dimensional Systems and Nanostructures, 2020, 118, 113949.	1.3	9
52334	Superconducting thorium hydrides under high pressure. Solid State Communications, 2020, 309, 113820.	0.9	5
52335	The effect of coordination environment on the kinetic and thermodynamic stability of single-atom iron catalysts. Physical Chemistry Chemical Physics, 2020, 22, 3983-3989.	1.3	45
52336	Realizing graphene-like Dirac cones in triangular boron sheets by chemical functionalization. Journal of Materials Chemistry C, 2020, 8, 2798-2805.	2.7	16
52337	Understanding size dependence of phase stability and band gap in CsPbI3 perovskite nanocrystals. Journal of Chemical Physics, 2020, 152, 034702.	1.2	56
52338	Lead-free hybrid organic-inorganic perovskites for solar cell applications. Journal of Chemical Physics, 2020, 152, 014104.	1.2	6
52339	General principles to high-throughput constructing two-dimensional carbon allotropes*. Chinese Physics B, 2020, 29, 037306.	0.7	8
52340	Magnetic and Electronic Properties of Complex Oxides from Firstâ€Principles. Physica Status Solidi (B): Basic Research, 2020, 257, 1900671.	0.7	31
52341	Ternary chalcogenides XGaS₂ (X = Ag or Cu) for photocatalytic hydrogen generation from water splitting under irradiation of visible light. International Journal of Quantum Chemistry, 2020, 120, e26166.	1.0	6
52342	Theoretical study of the modification of the oxide-reducing capacity of titania from selected dopant elements. Journal of Computational Electronics, 2020, 19, 493-506.	1.3	3

#	Article	IF	Citations
52343	Strain-controlled magnetic ordering in 2D carbon metamaterials. Carbon, 2020, 161, 219-223.	5.4	5
52344	Effect of pyridinic- and pyrrolic-nitrogen on electrochemical performance of Pd for formic acid electrooxidation. Electrochimica Acta, 2020, 337, 135758.	2.6	41
52345	Achieving high stability of MgO/carbon nanotube interface via the co-deposition technique. Journal of Alloys and Compounds, 2020, 824, 153889.	2.8	13
52346	Identification of the dehydration active sites in glycerol hydrogenolysis to 1,2-propanediol over Cu/SiO2 catalysts. Journal of Catalysis, 2020, 383, 13-23.	3.1	41
52347	Elementary steps and site requirements in formic acid dehydration reactions on anatase and rutile TiO2 surfaces. Journal of Catalysis, 2020, 383, 60-76.	3.1	26
52348	Comparison of Pd and Pd4S based catalysts for partial hydrogenation of external and internal butynes. Journal of Catalysis, 2020, 383, 51-59.	3.1	17
52349	Enhanced energy storage density and discharge efficiency in potassium sodium niobite-based ceramics prepared using a new scheme. Journal of the European Ceramic Society, 2020, 40, 2357-2365.	2.8	41
52350	Integrating the (311) facet of MnO2 and the fuctional groups of poly(m-phenylenediamine) in coreâ€“shell MnO2@poly(m-phenylenediamine) adsorbent to remove Pb ions from water. Journal of Hazardous Materials, 2020, 389, 122154.	6.5	31
52351	How to get noWear? â€“ A new take on the design of in-situ formed high performing low-friction tribofilms. Materials and Design, 2020, 190, 108519.	3.3	25
52352	A first-principle study on the atomic-level mechanism of surface effect in nanoparticles. Materials Today Communications, 2020, 24, 100948.	0.9	4
52353	Synergy effects on Sn-Cu alloy catalyst for efficient CO2 electroreduction to formate with high mass activity. Science Bulletin, 2020, 65, 711-719.	4.3	142
52354	Application of moisture-induced discoloration material Nickel(II) iodide in humidity detection. Sensors and Actuators B: Chemical, 2020, 309, 127769.	4.0	20
52355	Structural stability, defects and competitive oxygen migration in Pr1â^'xYxBaCo2O6â^'Î´. Solid State Ionics, 2020, 347, 115230.	1.3	12
52356	Effect of Titanium Induced Chemical Inhomogeneity on Crystal Structure, Electronic Structure, and Optical Properties of Wide Band Gap Ga₂O₃. Crystal Growth and Design, 2020, 20, 1422-1433.	1.4	21
52357	Unraveling the Role of Lattice Substitutions on the Stabilization of the Intrinsically Unstable Pb₂Sb₂O₇ Pyrochlore: Explaining the Lightfastness of Lead Pyroantimonate Artistsâ€™ Pigments. Chemistry of Materials, 2020, 32, 2863-2873.	3.2	11
52358	Mechanisms of Oxygen Passivation on Surface Defects in MAPbI₃ Revealed by First-Principles Study. Journal of Physical Chemistry C, 2020, 124, 3731-3737.	1.5	10
52359	Isolated Molybdenum(VI) and Tungsten(VI) Oxide Species on Partly Dehydroxylated Silica: A Computational Perspective. Journal of Physical Chemistry C, 2020, 124, 3002-3013.	1.5	15
52360	Stability of Partially Fluorinated Phthalocyanine Monolayers: Influence of Hydrogen Bonding Revisited. Journal of Physical Chemistry C, 2020, 124, 1973-1979.	1.5	5

#	Article	IF	Citations
52361	Tuning Phase Transitions in Metal Oxides by Hydrogen Doping: A First-Principles Study. Journal of Physical Chemistry Letters, 2020, 11, 1075-1080.	2.1	12
52362	The effect of non-analytical corrections on the phononic thermal transport in InX (Xâ€‰=â€‰S, Se, Te) monolayers. Scientific Reports, 2020, 10, 1093.	1.6	23
52363	Valley phenomena in the candidate phase change material WSe2(1-x)Te2x. Communications Physics, 2020, 3, .	2.0	10
52364	Embedding tetrahedral 3d transition metal TM₄ clusters into the cavity of two-dimensional graphdiyne to construct highly efficient and nonprecious electrocatalysts for hydrogen evolution reaction. Physical Chemistry Chemical Physics, 2020, 22, 3254-3263.	1.3	20
52365	Electronic and optical properties of monolayer MoS₂under the influence of polyethyleneimine adsorption and pressure. RSC Advances, 2020, 10, 4201-4210.	1.7	17
52366	A multifunctional MXene additive for enhancing the mechanical and electrochemical performances of the LiNi_{0.8}Co_{0.1}Mn_{0.1}O₂ cathode in lithium-ion batteries. Journal of Materials Chemistry A, 2020, 8, 4494-4504.	5.2	34
52367	Two-dimensional perovskites as sensitive strain sensors. Journal of Materials Chemistry C, 2020, 8, 3814-3820.	2.7	19
52368	Interaction of oxygen with polystyrene and polyethylene polymer films: A mechanistic study. Journal of Applied Physics, 2020, 127, .	1.1	20
52369	First-principles investigation of the structural, dynamical, electronic, and elastic properties of WGe₂ and W₅Ge₃. Philosophical Magazine, 2020, 100, 1129-1149.	0.7	7
52370	Ab initio calculations of the crystal field and phonon dispersions in CePd2Al2 and LaPd2Al2. Journal of Physics Condensed Matter, 2020, 32, 235402.	0.7	1
52371	Atomic and electronic structures of Sn covered W(110) surface. European Physical Journal B, 2020, 93, 1.	0.6	3
52372	Understanding the Role of Graphene in Hydrated Layered V-Oxide Based Cathodes for Rechargeable Aqueous Zn-Ion Batteries. Journal of the Electrochemical Society, 2020, 167, 070515.	1.3	5
52373	Wurtzite materials in alloys of rock salt compounds. Journal of Materials Research, 2020, 35, 972-980.	1.2	2
52374	Unusual Pressureâ€Đriven Phase Transformation and Band Renormalization in 2D vdW Hybrid Lead Halide Perovskites. Advanced Materials, 2020, 32, e1907364.	11.1	23
52375	Ultrathin Scattering Spin Filter and Magnetic Tunnel Junction Implemented by Ferromagnetic 2D van der Waals Material. Advanced Electronic Materials, 2020, 6, 1900968.	2.6	31
52376	Heavy Alkali Treatment of Cu(In,Ga)Se₂Solar Cells: Surface versus Bulk Effects. Advanced Energy Materials, 2020, 10, 1903752.	10.2	107
52377	Amorphous polymerization of nitrogen in compressed cupric azide. Journal of Computational Chemistry, 2020, 41, 1026-1033.	1.5	2
52378	Wideâ€gap (Ag,Cu)(In,Ga)Se₂ solar cells with different buffer materialsâ€”A path to a better heterojunction. Progress in Photovoltaics: Research and Applications, 2020, 28, 237-250.	4.4	47

#	Article	IF	Citations
52379	A high growth rate process of ALD CeOx with amidinato-cerium [(N-iPr-AMD)3Ce] and O3 as precursors. Journal of Materials Science, 2020, 55, 5378-5389.	1.7	7
52380	In situ study of vacancy disordering in crystalline phase-change materials under electron beam irradiation. Acta Materialia, 2020, 187, 103-111.	3.8	27
52381	Theoretical investigation on H2 oxidation mechanisms over pristine and Sm-doped CeO2(1â€¯1â€¯1) surfaces. Applied Surface Science, 2020, 511, 145388.	3.1	12
52382	Structural, elastic, electronic and optical properties of lithium halides (LiF, LiCl, LiBr, and LiI): First-principle calculations. Materials Chemistry and Physics, 2020, 244, 122733.	2.0	22
52383	Theoretical design of SnTe/GeS lateral heterostructures: A first-principles study. Physica B: Condensed Matter, 2020, 583, 412047.	1.3	8
52384	Single-Atom Ptâ€“N₃ Sites on the Stable Covalent Triazine Framework Nanosheets for Photocatalytic N₂ Fixation. ACS Catalysis, 2020, 10, 2431-2442.	5.5	171
52385	Constructing High-Loading Single-Atom/Cluster Catalysts via an Electrochemical Potential Window Strategy. Journal of the American Chemical Society, 2020, 142, 3375-3383.	6.6	147
52386	Resolving the puzzle of single-atom silver dispersion on nanosized Î³-Al2O3 surface for high catalytic performance. Nature Communications, 2020, 11, 529.	5.8	111
52387	Electrotunable liquid sulfurÂmicrodroplets. Nature Communications, 2020, 11, 606.	5.8	22
52388	Intrinsic electronic and transport properties of graphene nanoribbons with different widths. Physical Chemistry Chemical Physics, 2020, 22, 3584-3591.	1.3	14
52389	Hybrid iodoplumbates with metal complexes: syntheses, crystal structures, band gaps and photoelectric properties. Dalton Transactions, 2020, 49, 1803-1810.	1.6	24
52390	First principles study of ferroelectric hexagonal compounds RInO3 (R = Dy, Er, and Ho): electronic structure, optical and dielectric properties. RSC Advances, 2020, 10, 4080-4086.	1.7	4
52391	Superior performance and stability of anion exchange membrane water electrolysis: pH-controlled copper cobalt oxide nanoparticles for the oxygen evolution reaction. Journal of Materials Chemistry A, 2020, 8, 4290-4299.	5.2	73
52392	High-efficiency electrochemical hydrodeoxygenation of bio-phenols to hydrocarbon fuels by a superacid-noble metal particle dual-catalyst system. Energy and Environmental Science, 2020, 13, 917-927.	15.6	68
52393	Direct writing of lateral fluorographene nanopatterns with tunable bandgaps and its application in new generation of moirÃ© superlattice. Applied Physics Reviews, 2020, 7, .	5.5	18
52394	Theoretical model of spintronic device based on tunable anomalous Hall conductivity of monolayer CrI 3. Applied Physics Letters, 2020, 116, 022404.	1.5	9
52395	Tantalum disulfide quantum dots: preparation, structure, and properties. Nanoscale Research Letters, 2020, 15, 20.	3.1	15
52396	First-Principles Study of the Electrochemical Sodiation of Rutile-Type Vanadium Dioxide. MRS Advances, 2020, 5, 1467-1474.	0.5	1

#	Article	IF	Citations
52398	Cu3ErTe3: a new promising thermoelectric material predicated by high-throughput screening. Materials Today Physics, 2020, 12, 100180.	2.9	20
52399	Modified Density Functional Dispersion Correction for Inorganic Layered MFX Compounds (M = Ca, Sr,) Tj ETQq1 1 0.784314 rgBT /O	1.1	5
52400	Understanding the Inhibition of the Shuttle Effect of Sulfides (S â‰¥ 3) in Lithiumâ€“Sulfur Batteries by Heteroatom-Doped Graphene: First-Principles Study. Journal of Physical Chemistry C, 2020, 124, 3644-3649.	1.5	19
52401	Quantum Dynamics Simulation of Doublet Excitation and Magnetic Field Effect in Neutral Radical Materials. Journal of Physical Chemistry Letters, 2020, 11, 1194-1198.	2.1	1
52402	Efficient Methane Electrosynthesis Enabled by Tuning Local CO₂ Availability. Journal of the American Chemical Society, 2020, 142, 3525-3531.	6.6	154
52403	Manipulating spin polarization of titanium dioxide for efficient photocatalysis. Nature Communications, 2020, 11, 418.	5.8	252
52404	Revisiting the anchoring behavior in lithium-sulfur batteries: many-body effect on the suppression of shuttle effect. Npj Computational Materials, 2020, 6, .	3.5	29
52405	First-principles studies on Î±-Fe₂O₃ surface slabs and mechanistic elucidation of a g-C₃N₄/Î±-Fe₂O₃ heterojunction. Catalysis Science and Technology, 2020, 10, 1376-1384.	2.1	20
52406	Defect chemistry of disordered solid-state electrolyte Li₁₀GeP₂S₁₂. Journal of Materials Chemistry A, 2020, 8, 3851-3858.	5.2	27
52407	One-dimensional van der Waals heterostructures. Science, 2020, 367, 537-542.	6.0	238
52408	Atomicâ€Scale Spacing between Copper Facets for the Electrochemical Reduction of Carbon Dioxide. Advanced Energy Materials, 2020, 10, 1903423.	10.2	32
52409	Spin-polarized exciton formation in Co-doped GaN nanowires. Materials Chemistry and Physics, 2020, 245, 122756.	2.0	10
52410	Bi and Sn Co-doping Enhanced Thermoelectric Properties of Cu₃SbS₄ Materials with Excellent Thermal Stability. ACS Applied Materials & Interfaces, 2020, 12, 8271-8279.	4.0	28
52411	Effects of Oxygen Mobility in Laâ€“Fe-Based Perovskites on the Catalytic Activity and Selectivity of Methane Oxidation. ACS Catalysis, 2020, 10, 3707-3719.	5.5	132
52412	Robust Hot Electron and Multiple Topological Insulator States in PtBi₂. ACS Nano, 2020, 14, 2366-2372.	7.3	13
52413	One-step synthesis of dandelion-like lanthanum titanate nanostructures for enhanced photocatalytic performance. NPG Asia Materials, 2020, 12, .	3.8	33
52414	Synergistic effect between atomically dispersed Fe and Co metal sites for enhanced oxygen reduction reaction. Journal of Materials Chemistry A, 2020, 8, 4369-4375.	5.2	100
52415	Is Cs₂TiBr₆ a promising Pb-free perovskite for solar energy applications?. Journal of Materials Chemistry A, 2020, 8, 4049-4054.	5.2	62

#	Article	IF	Citations
52416	A self-adjusting platinum surface for acetone hydrogenation. Proceedings of the National Academy of Sciences of the United States of America, 2020, 117, 3446-3450.	3.3	17
52417	C3N monolayer with substitutional doping and strain modulation serving as anode material of lithium-ion batteries. Applied Surface Science, 2020, 510, 145324.	3.1	24
52418	First-principles study of thermoelectric properties of mixed iodide perovskite Cs(B,Bâ€²)I3 (B, Bâ€² = Ge, Sn,) Tj ETQq0 0 0 rgBT /Overlo	1.9	8
52419	Electrolyte-assisted dissolution-recrystallization mechanism towards high energy density and power density CF cathodes in potassium cell. Nano Energy, 2020, 70, 104552.	8.2	41
52420	Are transition-metal borides promising for Na ion batteries? A first-principles study on transition-metal boride monolayer. Physics Letters, Section A: General, Atomic and Solid State Physics, 2020, 384, 126282.	0.9	30
52421	van der Waals PtO2/MoS2 heterostructure verified from first principles. Physics Letters, Section A: General, Atomic and Solid State Physics, 2020, 384, 126286.	0.9	9
52422	Strong Chemical Bond Hierarchy Leading to Exceptionally High Thermoelectric Figure of Merit in Oxychalcogenide AgBiTeO. ACS Applied Materials & Interfaces, 2020, 12, 8280-8287.	4.0	26
52423	Tuning the photocatalytic water-splitting capability of two-dimensional Î±-In₂Se₃ by strain-driven band gap engineering. Physical Chemistry Chemical Physics, 2020, 22, 3520-3526.	1.3	21
52424	Anomalous phonon-mode dependence in polarized Raman spectroscopy of the topological Weyl semimetal TaP. Physical Review B, 2020, 101, .	1.1	8
52425	The H₂O Dissociation and Hydrogen Evolution Performance of Monolayer MoS₂ Containing Single Mo Vacancy: A Theoretical Study. IEEE Nanotechnology Magazine, 2020, 19, 163-167.	1.1	6
52426	Lateral 2D WSe₂ pâ€“n Homojunction Formed by Efficient Chargeâ€Carrierâ€Type Modulation for Highâ€Performance Optoelectronics. Advanced Materials, 2020, 32, e1906499.	11.1	103
52427	Triple VTe2/graphene/VTe2 heterostructures as perspective magnetic tunnel junctions. Applied Surface Science, 2020, 510, 145315.	3.1	19
52428	Structural stability of Coâ€“V intermetallic phases and thermodynamic description of the Coâ€“V system. Calphad: Computer Coupling of Phase Diagrams and Thermochemistry, 2020, 68, 101729.	0.7	6
52429	Metallic VS2 monolayer as an anchoring material for lithium-sulfur batteries. Chemical Physics Letters, 2020, 741, 137121.	1.2	21
52430	The phase equilibria of the Tiâ€“Vâ€“M (M = Si, Nb, Ta) ternary systems. Intermetallics, 2020, 118, 106701.	1.8	14
52431	Two-Dimensional BAs/InTe: A Promising Tandem Solar Cell with High Power Conversion Efficiency. ACS Applied Materials & Interfaces, 2020, 12, 6074-6081.	4.0	32
52432	Scalable photonic sources using two-dimensional lead halide perovskite superlattices. Nature Communications, 2020, 11, 387.	5.8	29
52433	Magnetism modulation of Co₃S₄ towards the efficient hydrogen evolution reaction. Molecular Systems Design and Engineering, 2020, 5, 565-572.	1.7	8

#	Article	IF	Citations
52434	Nickel nanograins anchored on a carbon framework for an efficient hydrogen evolution electrocatalyst and a flexible electrode. Journal of Materials Chemistry A, 2020, 8, 3499-3508.	5.2	18
52435	Theoretical prediction of T-graphene as a promising alkali-ion battery anode offering ultrahigh capacity. Physical Chemistry Chemical Physics, 2020, 22, 3281-3289.	1.3	51
52436	Phosphorene Degradation: Visualization and Quantification of Nanoscale Phase Evolution by Scanning Transmission X-ray Microscopy. Chemistry of Materials, 2020, 32, 1272-1280.	3.2	17
52437	Insights into the Interaction of Redox Active Organic Molecules and Solvents with the Pristine and Defective Graphene Surfaces from Density Functional Theory. Journal of Physical Chemistry C, 2020, 124, 2799-2805.	1.5	5
52438	A two-dimensional quinazoline based covalent organic framework with a suitable direct gap and superior optical absorption for photovoltaic applications. Journal of Materials Chemistry A, 2020, 8, 3865-3871.	5.2	21
52439	Li-diffusion at the interface between Li-metal and [Pyr14][TFSI]-ionic liquid: Ab initio molecular dynamics simulations. Journal of Chemical Physics, 2020, 152, 031101.	1.2	9
52440	Controlling Single Molecule Conductance by a Locally Induced Chemical Reaction on Individual Thiophene Units. Angewandte Chemie - International Edition, 2020, 59, 6207-6212.	7.2	9
52441	Embedding Sulfur Atoms in Decahedron Bismuth Vanadate Crystals with a Soft Chemical Approach for Expanding the Light Absorption Range. ChemCatChem, 2020, 12, 1585-1590.	1.8	4
52442	Impact of magnetism on the phase stability of rare-earth based hard magnetic materials. Calphad: Computer Coupling of Phase Diagrams and Thermochemistry, 2020, 68, 101731.	0.7	6
52443	Abnormal lattice occupation of Mo and related polarons in LiNbO3: Hybrid density functional theory investigation. Journal of Materiomics, 2020, 6, 183-191.	2.8	2
52444	Mie scattering of phonons by point defects in IV-VI semiconductors PbTe and GeTe. Materials Today Physics, 2020, 12, 100177.	2.9	15
52445	Assessment of the electronic structure, morphology, and photoluminescence properties of Ca9-xAl6O18:xEu3+ phosphor using the hydrothermal assisted solid state method. Powder Technology, 2020, 363, 657-664.	2.1	5
52446	Fluorine edge decoration on zigzag silicene nanoribbons. Superlattices and Microstructures, 2020, 139, 106394.	1.4	9
52447	Novel WS₂-Based Nanofluids for Concentrating Solar Power: Performance Characterization and Molecular-Level Insights. ACS Applied Materials & Interfaces, 2020, 12, 5793-5804.	4.0	22
52448	First-Principles Insights into the Interface Chemistry between 4-Aminothiophenol and Zinc Phosphide (Zn₃P₂) Nanoparticles. ACS Omega, 2020, 5, 1025-1032.	1.6	10
52449	Elucidating Surface Structure with Action Spectroscopy. Journal of the American Chemical Society, 2020, 142, 2665-2671.	6.6	16
52450	Managing grains and interfaces via ligand anchoring enables 22.3%-efficiency inverted perovskite solar cells. Nature Energy, 2020, 5, 131-140.	19.8	894
52451	Voltage decay and redox asymmetry mitigation by reversible cation migration in lithium-rich layered oxide electrodes. Nature Materials, 2020, 19, 419-427.	13.3	328

#	Article	IF	Citations
52452	First principles investigation of dissociative adsorption of H₂ during CO₂ hydrogenation over cubic and hexagonal In₂O₃ catalysts. Physical Chemistry Chemical Physics, 2020, 22, 3390-3399.	1.3	40
52453	Computer modeling investigation of MgV2O4 for Mg-ion batteries. Journal of Applied Physics, 2020, 127, 035106.	1.1	10
52454	Thermodynamic descriptions of the light rareâ€earth elements in silicon carbide ceramics. Journal of the American Ceramic Society, 2020, 103, 3812-3825.	1.9	16
52455	Morphology Evolution of Hcp Cobalt Nanoparticles Induced by Ru Promoter. ChemCatChem, 2020, 12, 2083-2090.	1.8	7
52456	Optimized design of high-temperature microwave absorption properties of CNTs/Sc2Si2O7 ceramics. Journal of Alloys and Compounds, 2020, 823, 153864.	2.8	40
52457	Simple Ethanol Refluxing Method for Production of Blue-Colored Titanium Dioxide with Oxygen Vacancies and Visible Light-Driven Photocatalytic Properties. Journal of Physical Chemistry C, 2020, 124, 3564-3576.	1.5	21
52458	Strain manipulation of the polarized optical response in two-dimensional GaSe layers. Nanoscale, 2020, 12, 4069-4076.	2.8	11
52459	Thermoelectric properties of Janus MXY (Mâ€‰=â€‰Pd, Pt; X, Yâ€‰=â€‰S, Se, Te) transition-metal dichalcogenide monolayers from first principles. Journal of Applied Physics, 2020, 127, .	1.1	90
52460	Highly efficient binary copperâ"iron catalyst for photoelectrochemical carbon dioxide reduction toward methane. Proceedings of the National Academy of Sciences of the United States of America, 2020, 117, 1330-1338.	3.3	93
52461	Phonon transport properties of NbCoSb compound. Materials Research Express, 2020, , .	0.8	4
52462	Controlling neutral and charged excitons in MoS₂ with defects. Journal of Materials Research, 2020, 35, 949-957.	1.2	12
52463	A Study of Cu Doping Effects in P2â€Na_{0.75}Mn_{0.6}Fe_{0.2}(Cu_xNi_{0.2â€x})O₂ Layered Cathodes for Sodiumâ€ion Batteries. Batteries and Supercaps, 2020, 3, 376-387.	2.4	22
52464	Facile NO-CO elimination over zirconia-coated Cu(1Â1Â0) surfaces: Further evidence from DFTÂ+ÂU calculations. Applied Surface Science, 2020, 508, 145252.	3.1	8
52465	Hydrogen-rich syngas production with tar elimination via biomass chemical looping gasification (BCLG) using BaFe2O4/Al2O3 as oxygen carrier. Chemical Engineering Journal, 2020, 387, 124107.	6.6	74
52466	Superconducting atmospheric structure and pressure-induced novel phases of cobalt mononitride. Computational Materials Science, 2020, 174, 109464.	1.4	2
52467	Mechanics of carbon-coated silicon nanowire via second strain gradient theory. European Journal of Mechanics, A/Solids, 2020, 81, 103943.	2.1	5
52468	Spin liquids and spin glasses in Mn-based alloys with the cubic A13 (Î²Mn) structure. Journal of Magnetism and Magnetic Materials, 2020, 501, 166429.	1.0	3
52469	Magnetic semiconductor properties of RbLnSe2 (LnÂ=ÂCe, Pr, Nd, Gd): A density functional study. Journal of Magnetism and Magnetic Materials, 2020, 501, 166448.	1.0	11

#	Article	IF	Citations
52470	Ab-initio study of Cu-based oxychalcogenides: A new class of materials for optoelectronic applications. Journal of Solid State Chemistry, 2020, 284, 121191.	1.4	5
52471	Quantum Transport beyond DC. , 2020, , 278-292.		0
52473	Mechanically Tunable Spontaneous Vertical Charge Redistribution in Few-Layer WTe₂. Journal of Physical Chemistry C, 2020, 124, 2008-2012.	1.5	8
52474	Guiding Lead Optimization for Solubility Improvement with Physics-Based Modeling. Molecular Pharmaceutics, 2020, 17, 666-673.	2.3	17
52475	Electrochemical Polarization Dependence of the Elastic and Electrostatic Driving Forces to Aliovalent Dopant Segregation on LaMnO₃. Journal of the American Chemical Society, 2020, 142, 3548-3563.	6.6	50
52476	Conversion of a conventional superconductor into a topological superconductor by topological proximity effect. Nature Communications, 2020, 11, 159.	5.8	40
52477	Composition effect on elastic properties of model NiCo-based superalloys*. Chinese Physics B, 2020, 29, 026102.	0.7	5
52478	Single crystal growth, structural and transport properties of bad metal RhSb₂*. Chinese Physics B, 2020, 29, 037101.	0.7	2
52479	Defect engineering on the electronic and transport properties of one-dimensional armchair phosphorene nanoribbons*. Chinese Physics B, 2020, 29, 037302.	0.7	7
52480	First-principles study of Zn-doping effects on phase stability and magnetic anisotropy of Ni-Mn-Ga alloys. Materials Research Express, 2020, 7, 026101.	0.8	6
52481	WasserunterstÃ¼tzte homolytische Dissoziation von Propin auf reduzierter CeroxidoberflÃche. Angewandte Chemie, 2020, 132, 6206-6211.	1.6	1
52482	Waterâ€Assisted Homolytic Dissociation of Propyne on a Reduced Ceria Surface. Angewandte Chemie - International Edition, 2020, 59, 6150-6154.	7.2	14
52483	Design, Synthesis and High HER Performances of 3D Ni/Mo Sulfide on Ni Foam. ChemCatChem, 2020, 12, 1647-1652.	1.8	18
52484	In Situ Nâ€Doped Graphene and Mo Nanoribbon Formation from Mo₂Ti₂C₃ MXene Monolayers. Small, 2020, 16, e1907115.	5.2	14
52485	Comparative adsorption capabilities of rubbish tissue paperâ€“derived carbon-doped MgO and CaCO3 for EBT and U(VI), studied by batch, spectroscopy and DFT calculations. Environmental Science and Pollution Research, 2020, 27, 13114-13130.	2.7	10
52486	Effect of coexistence of defect and dopant on the quantum capacitance of graphene-based supercapacitors electrodes. Applied Surface Science, 2020, 510, 145448.	3.1	27
52487	Characteristics of Sr1â^'xYxTi1â^'yRuyO3+/â^'Î´ and Ru-impregnated Sr1â^'xYxTiO3+/â^'Î´ perovskite catalysts as SOFC anode for methane dry reforming. Applied Surface Science, 2020, 510, 145450.	3.1	17
52488	First-principles study on the C-excess C3B for its potential application in sensing NO2 and NO. Applied Surface Science, 2020, 512, 145611.	3.1	10

#	Article	IF	Citations
52489	Engineering oxygen vacancy on iron oxides/hollow carbon cloth electrode toward stable lithium-ion batteries. Chemical Engineering Journal, 2020, 388, 124229.	6.6	26
52490	Scalable structural refining via altering working pressure and in-situ electrochemically-driven Cu-Sb alloying of magnetron sputtered Sb anode in sodium ion batteries. Chemical Engineering Journal, 2020, 388, 124299.	6.6	21
52491	Comparing study of picene thin films on SnSe and Au(1Â1Â1) surfaces. Chemical Physics, 2020, 532, 110689.	0.9	2
52492	Room temperature ferromagnetism in carbon doped MoO3 for spintronic applications: A DFT study. Journal of Magnetism and Magnetic Materials, 2020, 502, 166503.	1.0	19
52493	Design Rules for High Oxygen-Ion Conductivity in Garnet-Type Oxides. Chemistry of Materials, 2020, 32, 1358-1370.	3.2	10
52494	New High Pressure Phases of the Znâ€“N System. Journal of Physical Chemistry C, 2020, 124, 4044-4049.	1.5	36
52495	Particle-Size-Dependent Methane Selectivity Evolution in Cobalt-Based Fischerâ€“Tropsch Synthesis. ACS Catalysis, 2020, 10, 2799-2816.	5.5	46
52496	2D Hybrid Superlattice-Based On-Chip Electrocatalytic Microdevice for in Situ Revealing Enhanced Catalytic Activity. ACS Nano, 2020, 14, 1635-1644.	7.3	36
52497	Metalâ€“Semiconductorâ€“Metal Îµ-Ga₂O₃ Solar-Blind Photodetectors with a Record-High Responsivity Rejection Ratio and Their Gain Mechanism. ACS Photonics, 2020, 7, 812-820.	3.2	152
52498	Ab initio molecular dynamics and high-dimensional neural network potential study of VZrNbHfTa melt. Journal of Physics Condensed Matter, 2020, 32, 214006.	0.7	7
52499	Inhibiting degradation of LiCoO₂ cathode material by anisotropic strain during delithiation. Materials Research Express, 2020, , .	0.8	4
52500	f-Orbital based Dirac states in a two-dimensional uranium compound. JPhys Materials, 2020, 3, 024002.	1.8	9
52501	Prediction of superconductivity in pressure-induced new silicon boride phases. Physical Review B, 2020, 101, .	1.1	12
52502	Finite-size corrections for defect-involving vertical transitions in supercell calculations. Physical Review B, 2020, 101, .	1.1	32
52503	Anisotropic magnetoresistance and de Haas-van Alphen effect in hafnium ditelluride. Physical Review B, 2020, 101, .	1.1	7
52504	Spin and valley splittings in Janus monolayer WSSe on a MnO(111) surface: Large effective Zeeman field and opening of a helical gap. Physical Review B, 2020, 101, .	1.1	30
52505	Coordinatively Unsaturated Metalâ€“Nitrogen Active Sites at Twisted Surfaces in Metallic Porous Nitride Single Crystals Delivering Enhanced Electrocatalysis Activity. Chemistry - A European Journal, 2020, 26, 2327-2332.	1.7	5
52506	Quantum-mechanical oxidation states of metal ions in the solid-state binary sulfides. Acta Materialia, 2020, 186, 597-608.	3.8	5

#	Article	IF	Citations
52507	Critical effect of carbon vacancies on the reverse water gas shift reaction over vanadium carbide catalysts. Applied Catalysis B: Environmental, 2020, 267, 118719.	10.8	69
52508	Role of the surface density of states in understanding size-dependent surface band bending in GaN nanowires. Applied Surface Science, 2020, 510, 145502.	3.1	4
52509	Enhanced selective catalytic reduction of NO with CO over Cu/C nanoparticles synthetized from a Cu-benzene-1,3,5-tricarboxylate metal organic framework by a continuous spray drying process. Chemical Engineering Journal, 2020, 388, 124270.	6.6	25
52510	Density functional investigation of fluorite-based Pa2O5 phases: Structure and properties. Chinese Journal of Physics, 2020, 64, 115-122.	2.0	2
52511	Elastic moduli of high-density, sintered monoliths of yttrium dihydride. Journal of Alloys and Compounds, 2020, 826, 153955.	2.8	22
52512	Role of electronic and magnetic interactions in defect formation and anomalous diffusion in Î´-Pu. Journal of Nuclear Materials, 2020, 532, 152027.	1.3	7
52513	Theoretical study of a few 2D polymer networks and MOFs formed by chiral mTBPB molecules. Materials Chemistry and Physics, 2020, 244, 122705.	2.0	3
52514	C60 structures: Structural, electronic and elastic properties. Materials Today Communications, 2020, 23, 100906.	0.9	4
52515	Abnormally Low Activation Energy in Cubic Na₃SbS₄ Superionic Conductors. Chemistry of Materials, 2020, 32, 2264-2271.	3.2	35
52516	Mechanism of Electrocatalytically Active Precious Metal (Ni, Pd, Pt, and Ru) Complexes in the Graphene Basal Plane for ORR Applications in Novel Fuel Cells. Energy & Fuels, 2020, 34, 2425-2434.	2.5	72
52517	Observation of the Direct Energy Band Gaps of Defect-Tolerant Cu3N by Ultrafast Pump-Probe Spectroscopy. Journal of Physical Chemistry C, 2020, 124, 3459-3469.	1.5	13
52518	Defect Passivation and Photoluminescence Enhancement of Monolayer MoS₂ Crystals through Sodium Halide-Assisted Chemical Vapor Deposition Growth. ACS Applied Materials & Interfaces, 2020, 12, 9563-9571.	4.0	52
52519	Gas-assisted transformation of gold from fcc to the metastable 4H phase. Nature Communications, 2020, 11, 552.	5.8	17
52520	Coexistence of large conventional and planar spin Hall effect with long spin diffusion length in a low-symmetry semimetal at room temperature. Nature Materials, 2020, 19, 292-298.	13.3	77
52521	Exploring the origin of electrochemical performance of Cr-doped LiNi0.5Mn1.5O4. Physical Chemistry Chemical Physics, 2020, 22, 3831-3838.	1.3	13
52522	The effect of phenylalanine ligands on the chiral-selective oxidation of glucose on Au(111). Nanoscale, 2020, 12, 3050-3057.	2.8	16
52523	A novel simplified model for measuring the twinnability of face-centred-cubic metals. Philosophical Magazine Letters, 2020, 100, 63-73.	0.5	1
52524	High Curie temperature and strain-induced semiconductor-metal transition with spin reorientation transition in 2D CrPbTe₃ monolayer. Nanotechnology, 2020, 31, 195704.	1.3	14

#	Article	IF	Citations
52525	Few-Layer <mml:math xmlns:mml="http://www.w3.org/1998/Math/MathML" display="inline" overflow="scroll"><mml:mi>Î²</mml:mi></mml:math> - <mml:math xmlns:mml="http://www.w3.org/1998/Math/MathML" display="inline" overflow="scroll"><mml:mrow><mml:mi>Sn</mml:mi><mml:mi>Se</mml:mi></mml:mrow></mml:math> with Strong Visible Light Absorbance and Ultrahigh Carrier Mobility. Physical Review Applied, 2020, 13, .	1.5	8
52526	A Short Review of Current Computational Concepts for High-Pressure Phase Transition Studies in Molecular Crystals. Crystals, 2020, 10, 81.	1.0	19
52527	Highâ€throughput firstâ€principle calculations of the structural, mechanical, and electronic properties of cubic XTiO₃ (X = Ca, Sr, Ba, Pb) ceramics under high pressure. International Journal of Quantum Chemistry, 2020, 120, e26168.	1.0	4
52528	Mixing enthalpies of alloys with dynamical instability: bcc Ti-V system. Acta Materialia, 2020, 188, 145-154.	3.8	10
52529	Be3BN3 monolayer with ultrawide band gap and promising stability for deep ultraviolet applications. Computational Materials Science, 2020, 177, 109552.	1.4	1
52530	First-principles study of the structural, electronic, magnetic properties of orthorhombic PrCuO3 perovskites. Chemical Physics Letters, 2020, 743, 137166.	1.2	2
52531	Origin of magnetocrystalline anisotropy in Ni-Mn-Ga-Co-Cu tetragonal martensite. Journal of Magnetism and Magnetic Materials, 2020, 503, 166522.	1.0	13
52532	AGaSnS4 (A = Rb, Cs): Three sulfides and their structure diversity. Journal of Solid State Chemistry, 2020, 285, 121233.	1.4	6
52533	Tunable Perovskite-Derived Bismuth Halides: Cs₃Bi₂(Cl_{1â€“x}I_x)₉. Inorganic Chemistry, 2020, 59, 3387-3393.	1.9	23
52534	Surface Hydration and Hydroxyl Configurations of Gibbsite and Boehmite Nanoplates. Journal of Physical Chemistry C, 2020, 124, 5275-5285.	1.5	21
52535	Antiferromagnetic Semimetal in Ti-Intercalated Borophene Heterobilayer. Journal of Physical Chemistry C, 2020, 124, 4709-4716.	1.5	5
52536	Ultrasensitive Plasmon-Free Surface-Enhanced Raman Spectroscopy with Femtomolar Detection Limit from 2D van der Waals Heterostructure. Nano Letters, 2020, 20, 1620-1630.	4.5	60
52537	Descriptor Design in the Computational Screening of Ni-Based Catalysts with Balanced Activity and Stability for Dry Reforming of Methane Reaction. ACS Catalysis, 2020, 10, 3074-3083.	5.5	82
52538	Strong and fragile topological Dirac semimetals with higher-order Fermi arcs. Nature Communications, 2020, 11, 627.	5.8	152
52539	Enhancing the stability of perovskites by constructing heterojunctions of graphene/MASnI₃. Physical Chemistry Chemical Physics, 2020, 22, 3724-3733.	1.3	6
52540	The identification of optimal active boron sites for N₂reduction. Journal of Materials Chemistry A, 2020, 8, 3910-3917.	5.2	44
52541	Metalâ€“2D multilayered semiconductor junctions: layer-number dependent Fermi-level pinning. Journal of Materials Chemistry C, 2020, 8, 3113-3119.	2.7	33
52542	Atomically Dispersed Single Ni Site Catalysts for Nitrogen Reduction toward Electrochemical Ammonia Synthesis Using N₂ and H₂O. Small Methods, 2020, 4, 1900821.	4.6	148

#	Article	IF	Citations
52543	Microwave-assisted synthesis of nano Hf- and Zr-based metal-organic frameworks for enhancement of curcumin adsorption. Microporous and Mesoporous Materials, 2020, 298, 110064.	2.2	74
52544	DFT-Assisted Spectroscopic Studies on the Coordination of Small Ligands to Palladium: From Isolated Ions to Nanoparticles. Journal of Physical Chemistry C, 2020, 124, 4781-4790.	1.5	4
52545	Silicon and Phosphorus Co-doped Bipyridine-Linked Covalent Triazine Framework as a Promising Metal-Free Catalyst for Hydrogen Evolution Reaction: A Theoretical Investigation. Journal of Physical Chemistry Letters, 2020, 11, 1542-1549.	2.1	37
52546	Deciphering the Role of Key Defects in Sb₂Se₃, a Promising Candidate for Chalcogenide-Based Solar Cells. ACS Applied Energy Materials, 2020, 3, 2496-2509.	2.5	49
52547	Electronic structure of AlFeN films exhibiting crystallographic orientation change from c- to a-axis with Fe concentrations and annealing effect. Scientific Reports, 2020, 10, 1819.	1.6	3
52548	Photocatalytic properties and energy band offset of a tungsten disulfide/graphitic carbon nitride van der Waals heterojunction. RSC Advances, 2020, 10, 5260-5267.	1.7	13
52549	Shallow impurity band in ZrNiSn. Journal of Applied Physics, 2020, 127, .	1.1	10
52550	Interactions between interstitial oxygen and substitutional niobium atoms in Tiâ€“Nbâ€“O BCC alloys: First-principles calculations. AIP Advances, 2020, 10, 025309.	0.6	4
52551	Transition from intrinsic to extrinsic anomalous Hall effect in the ferromagnetic Weyl semimetal PrAlGe1â^’xSix. APL Materials, 2020, 8, .	2.2	41
52552	Relationship between the Behavior of Hydrogen and Hydrogen Bubble Nucleation in Vanadium. Materials, 2020, 13, 322.	1.3	4
52553	An Ab Initio Study of Magnetism in Disordered Fe-Al Alloys with Thermal Antiphase Boundaries. Nanomaterials, 2020, 10, 44.	1.9	6
52554	Synthesis of Coâ€Đoped MoS₂ Monolayers with Enhanced Valley Splitting. Advanced Materials, 2020, 32, e1906536.	11.1	84
52555	Effects of halogen substitutions on the properties of CH3NH3Sn0.5Pb0.5I3 perovskites. Computational Materials Science, 2020, 177, 109576.	1.4	5
52556	Biodegradation, hemocompatibility and covalent bonding mechanism of electrografting polyethylacrylate coating on Mg alloy for cardiovascular stent. Journal of Materials Science and Technology, 2020, 46, 114-126.	5.6	28
52557	Descriptor-Based Analysis of Atomic Layer Deposition Mechanisms on Spinel LiMn₂O₄ Lithium-Ion Battery Cathodes. Chemistry of Materials, 2020, 32, 1794-1806.	3.2	29
52558	Mn-Doped Sr/Si(111)-(3 Ã— 2) HCC Surfaces: Antiferromagnetic Semiconductors for Spintronic Applications. ACS Applied Materials & Interfaces, 2020, 12, 9918-9924.	4.0	5
52559	Effects of a Pd/Pt bimetal supported by a Î³-Al₂O₃ surface on methane activation. Physical Chemistry Chemical Physics, 2020, 22, 4692-4698.	1.3	10
52560	Strategy for achieving multiferroic E-type magnetic order in orthorhombic manganites RMnO₃ (R = Laâ€“Lu). Physical Chemistry Chemical Physics, 2020, 22, 4905-4915.	1.3	5

#	Article	IF	Citations
52561	Inelastic neutron scattering evidence for anomalous Hâ€“H distances in metal hydrides. Proceedings of the National Academy of Sciences of the United States of America, 2020, 117, 4021-4026.	3.3	24
52562	Anharmonic lattice dynamics and superionic transition in AgCrSe ₂. Proceedings of the National Academy of Sciences of the United States of America, 2020, 117, 3930-3937.	3.3	73
52563	Copper-doped induced ferromagnetic half-metal zirconium diselenide single crystals. Nanotechnology, 2020, 31, 235704.	1.3	5
52564	Chiral Magnetism and High-Temperature Skyrmions in B20-Ordered Co-Si. Physical Review Letters, 2020, 124, 057201.	2.9	31
52565	Na ⁺ -gated water-conducting nanochannels for boosting CO ₂ conversion to liquid fuels. Science, 2020, 367, 667-671.	6.0	136
52566	First principle studies of oxygen reduction reaction on N doped graphene: Impact of N concentration, position and co-adsorbate effect. Applied Surface Science, 2020, 510, 145470.	3.1	16
52567	Bournonite CuPbSbS3: An electronically-3D, defect-tolerant, and solution-processable semiconductor for efficient solar cells. Nano Energy, 2020, 71, 104574.	8.2	24
52568	Effect of Mn doping defect on 180Â° domain wall in ferroelectric PbTiO3. Physics Letters, Section A: General, Atomic and Solid State Physics, 2020, 384, 126279.	0.9	6
52569	Chemomechanical Design Factors for High Performance in Manganese-Based Spinel Cathode Materials for Advanced Sodium-Ion Batteries. ACS Applied Materials & Interfaces, 2020, 12, 22789-22797.	4.0	15
52570	Oxygen-Plasma-Assisted Enhanced Acetone-Sensing Properties of ZnO Nanofibers by Electrospinning. ACS Applied Materials & Interfaces, 2020, 12, 23084-23093.	4.0	66
52571	Graphene-Based Etch Resist for Semiconductor Device Fabrication. ACS Applied Nano Materials, 2020, 3, 4635-4641.	2.4	4
52572	Prediction of new thermodynamically stable ZnN2O3 at high pressure. Physical Chemistry Chemical Physics, 2020, 22, 10941-10948.	1.3	1
52573	Characterisation of the temperature-dependent M1 to R phase transition in W-doped VO2 nanorod aggregates by Rietveld refinement and theoretical modelling. Physical Chemistry Chemical Physics, 2020, 22, 7984-7994.	1.3	9
52574	Mechanistic insights into the oxidation of copper(<scp>i</scp>) species during NH₃-SCR over Cu-CHA zeolites: a DFT study. Catalysis Science and Technology, 2020, 10, 3586-3593.	2.1	25
52575	Prospects for n-type doping of (AlxGa1â^'x)2O3 alloys. Applied Physics Letters, 2020, 116, .	1.5	44
52576	Interoperability architecture for bridging computational tools: application to steel corrosion in concrete. Modelling and Simulation in Materials Science and Engineering, 2020, 28, 025003.	0.8	3
52577	Polymorphous nature of cubic halide perovskites. Physical Review B, 2020, 101, .	1.1	104
52578	Weyl semimetals with <mml:math xmlns:mml="http://www.w3.org/1998/Math/MathML"><mml:msub><mml:mi>S</mml:mi><mml:mn>4</mml:mn></mml:msub></mml:math> symmetry. Physical Review B, 2020, 101, .	1.1	104

#	Article	IF	Citations
52579	SrPd, a candidate material with extremely large magnetoresistance. Physical Review B, 2020, 101, .	1.1	4
52580	Metaâ€Stable Molecular Configuration Enables Thermally Stable and Solution Processable Organic Charge Transporting Materials. Advanced Functional Materials, 2020, 30, 2000729.	7.8	3
52581	Defectâ€Enhanced Polarization Switching in the Improper Ferroelectric LuFeO₃. Advanced Materials, 2020, 32, e2000508.	11.1	25
52582	Efficient dual-function catalysts for triiodide reduction reaction and hydrogen evolution reaction using unique 3D network aloe waste-derived carbon-supported molybdenum-based bimetallic oxide nanohybrids. Applied Catalysis B: Environmental, 2020, 273, 119004.	10.8	59
52583	Probing the surface structure via the adsorbed hydrogen atoms â€“ The case of Cu(4â€¯1â€¯0). Applied Surface Science, 2020, 528, 146433.	3.1	2
52584	Effect of BN seeds on locating and promoting the initial nucleation of graphene on Cu substrate and its mechanism: A theoretical study. Applied Surface Science, 2020, 523, 146469.	3.1	4
52585	Adsorption of nucleotides on clay surfaces: Effects of mineral composition, pH and solution salts. Applied Clay Science, 2020, 190, 105544.	2.6	10
52586	Low-pressure chemical vapor deposition of Cu on Ru substrate using CuI:<mml:math xmlns:mml="http://www.w3.org/1998/Math/MathML" altimg="si12.svg"><mml:mrow><mml:mi mathvariant="italic">Ab</mml:mi><mml:mspace width="0.35em" /><mml:mi mathvariant="italic">initio</mml:mi></mml:mrow></mml:math>calculations. Chemical Physics Letters, 2020, 741, 137109.	1.2	5
52587	Constructing light-weight polar boron-doped carbon nitride nanosheets with increased active sites and conductivity for high performance lithium-sulfur batteries. International Journal of Hydrogen Energy, 2020, 45, 14940-14952.	3.8	25
52588	Magnetism and magnetocrystalline anisotropy of tetragonally distorted L10-FeNi: N alloy. Journal of Alloys and Compounds, 2020, 835, 155325.	2.8	20
52589	Li+ co-doping induced phase transition as an efficient strategy to enhance upconversion of La2Zr2O7:Er,Yb nanoparticles. Journal of Luminescence, 2020, 224, 117312.	1.5	24
52590	Vacancy induced robust magnetism in graphene hexagonal-boron nitride in-plane hybrids with hexagonal shaped islands. Journal of Magnetism and Magnetic Materials, 2020, 502, 166530.	1.0	4
52591	Comparative quantum chemistry study of the F-center in lanthanum trifluoride. Nuclear Instruments & Methods in Physics Research B, 2020, 474, 57-62.	0.6	9
52592	Phase Transition and Liquid-like Superionic Conduction in Ag₂S. Journal of Physical Chemistry C, 2020, 124, 10150-10158.	1.5	9
52593	Revealing the Interplay Between Covalent and Non-Covalent Interactions Driving the Adsorption of Monosubstituted Thiourea Derivatives on the Au(111) Surface. Journal of Physical Chemistry C, 2020, 124, 9924-9939.	1.5	2
52594	Interaction of C₃â€“C₅Alkenes with Zeolitic BrÃ¸nsted Sites: Ï€-Complexes, Alkoxides, and Carbenium Ions in H-FER. Journal of Physical Chemistry C, 2020, 124, 10067-10078.	1.5	41
52595	Microscopic Mechanism of Carbon-Dopant Manipulating Device Performance in CGeSbTe-Based Phase Change Random Access Memory. ACS Applied Materials & Interfaces, 2020, 12, 23051-23059.	4.0	24
52596	Design of P-Doped Mesoporous Carbon Nitrides as High-Performance Anode Materials for Li-Ion Battery. ACS Applied Materials & Interfaces, 2020, 12, 24007-24018.	4.0	44

#	Article	IF	Citations
52597	Electron Density Modulation of Metallic MoO₂ by Ni Doping to Produce Excellent Hydrogen Evolution and Oxidation Activities in Acid. ACS Energy Letters, 2020, 5, 1908-1915.	8.8	110
52598	High Curie temperature and carrier mobility of novel Fe, Co and Ni carbide MXenes. Nanoscale, 2020, 12, 11627-11637.	2.8	26
52599	Synergy effect of co-doping Sc and Y in Sb₂Te₃ for phase-change memory. Journal of Materials Chemistry C, 2020, 8, 6672-6679.	2.7	24
52600	Strain-tunable III-nitride/ZnO heterostructures for photocatalytic water-splitting: A hybrid functional calculation. APL Materials, 2020, 8, .	2.2	48
52601	Surface Rashba-Edelstein Spin-Orbit Torque Revealed by Molecular Self-Assembly. Physical Review Applied, 2020, 13, .	1.5	9
52602	Charge density wave like behavior with magnetic ordering in orthorhombic <mml:math xmlns:mml="http://www.w3.org/1998/Math/MathML"><mml:mrow><mml:mi mathvariant="normal">S</mml:mi><mml:msub><mml:mi mathvariant="normal">m</mml:mi><mml:mn>2</mml:mn></mml:msub><mml:mi mathvariant="normal">R</mml:mi><mml:msub><mml:mi mathvariant="normal">u</mml:mi><mml:mn>2</mml:mn></mml:msub><mml:mi mathvariant="normal">	1.1	11
52603	Orbital-Driven Rashba Effect in a Binary Honeycomb Monolayer AgTe. Physical Review Letters, 2020, 124, 176401.	2.9	33
52604	Strain-Modulated Slater-Mott Crossover of Pseudospin-Half Square-Lattice in (SrIrO3)1/(SrTiO3)1 Superlattices. Physical Review Letters, 2020, 124, 177601.	2.9	10
52605	Deciphering atomistic mechanisms of the gas-solid interfacial reaction during alloy oxidation. Science Advances, 2020, 6, eaay8491.	4.7	20
52606	Heavy Water Additive in Formamidinium: A Novel Approach to Enhance Perovskite Solar Cell Efficiency. Advanced Materials, 2020, 32, e1907864.	11.1	51
52607	Multiscale and Multimodal Characterization of 2D Titanium Carbonitride MXene. Advanced Materials Interfaces, 2020, 7, 1902207.	1.9	35
52608	Tuning the Topological Bandgap of Bilayerâ€Bi(111) Supported on Graphene. Physica Status Solidi - Rapid Research Letters, 2020, 14, 2000131.	1.2	2
52609	Step-confined thin film growth via near-surface atom migration. Nano Research, 2020, 13, 1552-1557.	5.8	2
52610	Antioxidative and stable PdZn/ZnO/Al2O3 catalyst coatings concerning methanol steam reforming for fuel cell-powered vehicles. Applied Energy, 2020, 268, 115043.	5.1	28
52611	<mml:math xmlns:mml="http://www.w3.org/1998/Math/MathML" altimg="si22.svg"><mml:mrow><mml:mi mathvariant="italic">Ab</mml:mi><mml:mspace width="0.35em" /><mml:mi mathvariant="italic">initio</mml:mi></mml:mrow></mml:math> calculations of the optical and electronic properties of Bi2WO6 doped with Mo, Cr, Fe, and Zn on the Wâ€“lattice site. Applied Surface Science, 2020, 515, 146036.	3.1	13
52612	Compatibility of Zr2AlC MAX phase-based ceramics with oxygen-poor, static liquid leadâ€“bismuth eutectic. Corrosion Science, 2020, 171, 108704.	3.0	24
52613	Wood cellulose as a hydrogen storage material. International Journal of Hydrogen Energy, 2020, 45, 14907-14914.	3.8	9
52614	Sensitivity of positrons at hydrogen storage sites in FeCr alloy containing vacancy and helium atom. International Journal of Hydrogen Energy, 2020, 45, 15571-15577.	3.8	15

#	Article	IF	Citations
52615	One-pot solvothermal method to fabricate 1D-VS4 nanowires as anode materials for lithium ion batteries. Inorganic Chemistry Communication, 2020, 115, 107883.	1.8	25
52616	Rational electronic control of carbon dioxide reduction over cobalt oxide. Journal of Catalysis, 2020, 387, 119-128.	3.1	20
52617	Highly conductive and nonflammable composite polymer electrolytes for rechargeable quasi-solid-state Li-metal batteries. Journal of Power Sources, 2020, 464, 228182.	4.0	27
52618	In-situ synthesis of nanocomposite from metal-organic frameworks template for high-performance rechargeable batteries. Journal of Power Sources, 2020, 464, 228247.	4.0	23
52619	The role of anions on the Helmholtz Plane for the solid-liquid interface in aqueous rechargeable lithium batteries. Nano Energy, 2020, 74, 104864.	8.2	27
52620	Possible origin of ferromagnetism in pristine magnesium oxide film. Physica B: Condensed Matter, 2020, 590, 412214.	1.3	9
52621	The effect of thickness on the Li-ion adsorption behaviors of 2D Ti1C multi-layers from first-principles calculations. Thin Solid Films, 2020, 704, 138019.	0.8	1
52622	Rediscovering Tuning Product Selectivity by an Energy Descriptor: CH₄ Formation and C₁â€“C₁ Coupling on the FCC Co Surface. Journal of Physical Chemistry C, 2020, 124, 11040-11049.	1.5	9
52623	A Helical Monolayer Ice. Journal of Physical Chemistry Letters, 2020, 11, 3860-3865.	2.1	9
52624	Utilizing Site Disorder in the Development of New Energy-Relevant Semiconductors. ACS Energy Letters, 2020, 5, 2027-2041.	8.8	46
52625	Intrinsic Defect-Rich Hierarchically Porous Carbon Architectures Enabling Enhanced Capture and Catalytic Conversion of Polysulfides. ACS Nano, 2020, 14, 6222-6231.	7.3	89
52626	Effect of Mn²⁺ substitution on the structure, properties and HER activity of cadmium phosphochlorides. RSC Advances, 2020, 10, 5134-5145.	1.7	4
52627	Facile synthesis of oxygen-deficient nano-TiO₂coordinated by acetate ligands for enhanced visible-light photocatalytic performance. Catalysis Science and Technology, 2020, 10, 3875-3889.	2.1	11
52628	On the formation of the Gd3Ru4Al12versusthe Y2Co3Ga9type structure â€“ M3Rh4Al12(M = Ca,) Tj ETQq1 1 0.784314 rgBT /Overlo	1.6	7
52629	Ba₆In₆Zn₄Se₁₉: a high performance infrared nonlinear optical crystal with [InSe₃]^{3â^’} trigonal planar functional motifs. Journal of Materials Chemistry C, 2020, 8, 7947-7955.	2.7	15
52630	Photocatalytic hydrogen evolution over nickel cobalt bimetallic phosphate anchored graphitic carbon nitrides by regulation of the d-band electronic structure. Catalysis Science and Technology, 2020, 10, 3654-3663.	2.1	9
52631	A high-pressure study of Cr3C2 by XRD and DFT. Chinese Physics B, 2020, 29, 086401.	0.7	3
52632	Thermodynamics of the insulator-metal transition in dense liquid deuterium. Physical Review B, 2020, 101, .	1.1	6

#	Article	IF	Citations
52633	First-principles study of magnon-phonon interactions in gadolinium iron garnet. Physical Review B, 2020, 101, .	1.1	21
52634	Zigzag Dissociation Mode of ã€ˆâ€‰+â€‰aã€‰ Dislocations on the 101Â¯1â€‰ Plane in Magnesium Alloys. Advances in Materials Science and Engineering, 2020, 2020, 1-5.	1.0	0
52635	Strain-Induced Modulation of Spin Configuration in LaCoO3. Frontiers in Materials, 2020, 7, .	1.2	4
52636	Physi-Sorption of H2 on Pure and Boronâ€“Doped Graphene Monolayers: A Dispersionâ€“Corrected DFT Study. Journal of Carbon Research, 2020, 6, 15.	1.4	13
52637	Manipulatable Interface Electric Field and Charge Transfer in a 2D/2D Heterojunction Photocatalyst via Oxygen Intercalation. Catalysts, 2020, 10, 469.	1.6	5
52638	Lithium Storage in Nanoporous Complex Oxide 12CaOâ€¢7Al2O3 (C12A7). Energies, 2020, 13, 1547.	1.6	4
52639	Influences of Multicenter Bonding and Interstitial Elements on Twinned Î³-TiAl Crystal. Materials, 2020, 13, 2016.	1.3	4
52640	Effect of Mg(II) and Na(I) Doping on the Electronic Structure and Mechanical Properties of Kaolinite. Minerals (Basel, Switzerland), 2020, 10, 368.	0.8	19
52641	High-Throughput Computational Search for Half-Metallic Oxides. Molecules, 2020, 25, 2010.	1.7	1
52642	Integrating Density Functional Theory Modeling with Experimental Data to Understand and Predict Sorption Reactions: Exchange of Salicylate for Phosphate on Goethite. Soil Systems, 2020, 4, 27.	1.0	9
52643	Benchmarking lattice energy of a model 1D molecular HF crystal. Theoretical Chemistry Accounts, 2020, 139, 1.	0.5	3
52644	Multi sites vs single site for catalytic combustion of methane over Co3O4(110): A first-principles kinetic Monte Carlo study. Chinese Journal of Catalysis, 2020, 41, 1369-1377.	6.9	16
52645	Graphene/Îł-tellurene van der Waals heterobilayers: Interlayer coupling and gate-tunable carrier type and Schottky barriers. Applied Surface Science, 2020, 525, 146476.	3.1	8
52646	Trends in transition metal solute diffusion in metals: The case of tungsten. Computational Materials Science, 2020, 179, 109638.	1.4	5
52647	The influence of Ca doping in Bi2O2Se: A first-principles investigation. Computational Materials Science, 2020, 179, 109684.	1.4	1
52648	Visible-light-driven room-temperature gas sensor based on carbyne nanocrystals. Sensors and Actuators B: Chemical, 2020, 316, 128200.	4.0	11
52649	Polyaromatic Nanotweezers on Semiconducting Carbon Nanotubes for the Growth and Interfacing of Lead Halide Perovskite Crystal Grains in Solar Cells. Chemistry of Materials, 2020, 32, 5125-5133.	3.2	45
52650	Targeted Synthesis of Trimeric Organicâ€“Bromoplumbate Hybrids That Display Intrinsic, Highly Stokes-Shifted, Broadband Emission. Chemistry of Materials, 2020, 32, 4431-4441.	3.2	25

#	Article	IF	Citations
52651	Adsorption of Methyl-Substituted Benzylazide on Si(001): Reaction Channels and Final Configurations. Journal of Physical Chemistry C, 2020, 124, 9940-9946.	1.5	7
52652	Theoretical Insights into the Charge and Discharge Processes in Aluminumâ€“Sulfur Batteries. Journal of Physical Chemistry C, 2020, 124, 11317-11324.	1.5	19
52653	Cooperative Nitrogen Activation and Ammonia Synthesis on Densely Monodispersed Moâ€“Nâ€“C Sites. Journal of Physical Chemistry Letters, 2020, 11, 3962-3968.	2.1	23
52654	Helping Thy Neighbor: How Cobalt Doping Alters the Electrocatalytic Properties of Hematite. Journal of Physical Chemistry Letters, 2020, 11, 4402-4407.	2.1	6
52655	Automated Generation and Analysis of the Complex Catalytic Reaction Network of Ethanol Synthesis from Syngas on Rh(111). ACS Catalysis, 2020, 10, 6346-6355.	5.5	40
52656	Se-Rich MoSe₂ Nanosheets and Their Superior Electrocatalytic Performance for Hydrogen Evolution Reaction. ACS Nano, 2020, 14, 6295-6304.	7.3	125
52657	ZnO/CuSCN Nano-Heterostructure as a Highly Efficient Field Emitter: a Combined Experimental and Theoretical Investigation. ACS Omega, 2020, 5, 6715-6724.	1.6	12
52658	In-situ resonant band engineering of solution-processed semiconductors generates high performance n-type thermoelectric nano-inks. Nature Communications, 2020, 11, 2069.	5.8	23
52659	Lattice distortion induced internal electric field in TiO2 photoelectrode for efficient charge separation and transfer. Nature Communications, 2020, 11, 2129.	5.8	108
52660	Tunable relativistic quasiparticle electronic and excitonic behavior of the FAPb(I_{1â^'x}Br_x)₃ alloy. Physical Chemistry Chemical Physics, 2020, 22, 11943-11955.	1.3	18
52661	First-principles mechanism study on distinct optoelectronic properties of Cl-doped 2D hybrid tin iodide perovskite. Journal of Materials Chemistry C, 2020, 8, 9540-9548.	2.7	21
52662	Color-tunable upconversion luminescence and prolonged Eu3+ fluorescence lifetime in fluoride KCdF3:Yb3+,Mn2+,Eu3+via controllable and efficient energy transfer. Journal of Materials Chemistry C, 2020, 8, 9836-9844.	2.7	15
52663	Prediction of a novel high-pressure phase of hydrogen peroxide. Physical Review B, 2020, 101, .	1.1	3
52664	Performance of the standard exchange-correlation functionals in predicting melting properties fully from first principles: Application to Al and magnetic Ni. Physical Review B, 2020, 101, .	1.1	15
52665	Interface-driven giant tunnel magnetoresistance in (111)-oriented junctions. Physical Review B, 2020, 101, .	1.1	13
52666	Origin of the large voltage-controlled magnetic anisotropy in a Cr/Fe/MgO junction with an ultrathin Fe layer: First-principles investigation. Physical Review B, 2020, 101, .	1.1	15
52667	Doping a bad metal: Origin of suppression of the metal-insulator transition in nonstoichiometric <mml:math xmlns:mml="http://www.w3.org/1998/Math/MathML"><mml:msub><mml:mi>VO</mml:mi><mml:mn>2</mml:mn></mml:msub></mml Physical Review B, 2020, 101, .	1.1	21
52668	Chemical trend of a Cu impurity in Zn chalcogenides. Physical Review B, 2020, 101, .	1.1	2

#	Article	IF	Citations
52669	Electron-phonon interactions using the projector augmented-wave method and Wannier functions. Physical Review B, 2020, 101, .	1.1	10
52670	Very large Dzyaloshinskii-Moriya interaction in two-dimensional Janus manganese dichalcogenides and its application to realize skyrmion states. Physical Review B, 2020, 101, .	1.1	156
52671	Suppression of hysteresis in absorption of hydrogen by a Pd-Au alloy. Physical Review E, 2020, 101, 042130.	0.8	5
52672	Controlled Introduction of Defects to Delafossite Metals by Electron Irradiation. Physical Review X, 2020, 10, .	2.8	16
52673	Analogous Diamondene Nanotube Structure Prediction Based on Molecular Dynamics and First-Principle Calculations. Nanomaterials, 2020, 10, 846.	1.9	4
52674	Adsorption of carbonyl sulfide on Pt-doped vacancy-defected SWCNT: A DFT study. Applied Surface Science, 2020, 525, 146331.	3.1	7
52675	The stability, electronic, mechanical and thermal properties of three novel superhard carbon crystals. Computational Materials Science, 2020, 182, 109758.	1.4	10
52676	Interfacial confinement of Ni-V2O3 in molten salts for enhanced electrocatalytic hydrogen evolution. Journal of Energy Chemistry, 2020, 50, 280-285.	7.1	51
52677	First-principles studies of intrinsic stacking fault energies and elastic properties of Al-based alloys. Materials Today Communications, 2020, 24, 101085.	0.9	7
52678	Fluoride ion batteries: Designing flexible M2CH2 (M=Ti or V) MXenes as high-capacity cathode materials. Nano Energy, 2020, 74, 104911.	8.2	27
52679	First-principles investigation on the structural, electronic, vibrational and magnetic properties of the Co-substituted orthorhombic SrSnO3. Physica B: Condensed Matter, 2020, 590, 412216.	1.3	6
52680	Co-segregation of Mg and Zn atoms at the planar Î·1-precipitate/Al matrix interface in an aged Alâ€“Znâ€“Mg alloy. Scripta Materialia, 2020, 185, 51-55.	2.6	21
52681	Identifying Key Structural Subunits and Their Synergism in Low-Iridium Triple Perovskites for Oxygen Evolution in Acidic Media. Chemistry of Materials, 2020, 32, 3904-3910.	3.2	29
52682	Formation of Hexagonal PdSe₂ for Electronics and Catalysis. Journal of Physical Chemistry C, 2020, 124, 10935-10940.	1.5	16
52683	Designing Efficient Dual-Metal Single-Atom Electrocatalyst TMZnN₆ (TM = Mn, Fe, Co, Ni,) Tj ETQq0 0 0 rgBT /Overlock 10	1.5	47
52684	Compensation between Surface Energy and hcp/fcc Phase Energy of Late Transition Metals from First-Principles Calculations. Journal of Physical Chemistry C, 2020, 124, 11005-11014.	1.5	37
52685	1Tâ€´ Transition-Metal Dichalcogenides: Strong Bulk Photovoltaic Effect for Enhanced Solar-Power Harvesting. Journal of Physical Chemistry C, 2020, 124, 11221-11228.	1.5	11
52686	Improved Performance of Thermally Evaporated Sb₂Se₃ Thin-Film Solar Cells via Substrate-Cooling-Speed Control and Hydrogen-Sulfide Treatment. ACS Applied Materials & Interfaces, 2020, 12, 24112-24124.	4.0	34

#	Article	IF	Citations
52687	Effect of Structural Disorders on the Li Storage Capacity of Graphene Nanomaterials: A First-Principles Study. ACS Applied Materials & Interfaces, 2020, 12, 22917-22929.	4.0	8
52688	Confinement Effect of Mesopores: In Situ Synthesis of Cationic Tungsten-Vacancies for a Highly Ordered Mesoporous Tungsten Phosphide Electrocatalyst. ACS Applied Materials & Interfaces, 2020, 12, 22741-22750.	4.0	34
52689	Exploring the configuration spaces of surface materials using time-dependent diffraction patterns and unsupervised learning. Scientific Reports, 2020, 10, 5868.	1.6	4
52690	Synthesis, structure, and electronic properties of the Li11RbGd4Te6O30 single crystal. RSC Advances, 2020, 10, 11450-11454.	1.7	0
52691	Electric-controlled half-metallicity in magnetic van der Waals heterobilayer. Journal of Materials Chemistry C, 2020, 8, 7034-7040.	2.7	29
52692	The role of Ru passivation and doping on the barrier and seed layer properties of Ru-modified TaN for copper interconnects. Journal of Chemical Physics, 2020, 152, 144701.	1.2	6
52693	Optimization and validation of a deep learning CuZr atomistic potential: Robust applications for crystalline and amorphous phases with near-DFT accuracy. Journal of Chemical Physics, 2020, 152, 154701.	1.2	35
52694	Density Functional Theory Based Micro- and Macro-Kinetic Studies of Ni-Catalyzed Methanol Steam Reforming. Catalysts, 2020, 10, 349.	1.6	5
52695	Revisiting the Zintlâ€'Klemm Concept for ALn2Ag3Te5-Type Alkaline-Metal (A) Lanthanide (Ln) Silver Tellurides. Crystals, 2020, 10, 184.	1.0	12
52696	Two-dimensional halogen-substituted graphdiyne: first-principles investigation of mechanical, electronic, optical, and photocatalytic properties. Journal of Materials Science, 2020, 55, 8220-8230.	1.7	17
52697	Monolayered Ru1/TiO2 nanosheet enables efficient visible-light-driven hydrogen evolution. Applied Catalysis B: Environmental, 2020, 271, 118925.	10.8	30
52698	Cd12O12 cage cluster-assembled nanowires and band gap regulation: A first-principles investigation. Physics Letters, Section A: General, Atomic and Solid State Physics, 2020, 384, 126463.	0.9	4
52699	Structural, bonding, and elastic properties of Si:X (X = B, Al, and Ga): a theoretical study. Semiconductor Science and Technology, 2020, 35, 065004.	1.0	1
52700	Microscopic origin of spin-orbit torque in ferromagnetic heterostructures: A first-principles approach. Physical Review B, 2020, 101, .	1.1	19
52701	Anisotropic Thermal Conductivity in Few-Layer and Bulk Titanium Trisulphide from First Principles. Nanomaterials, 2020, 10, 704.	1.9	8
52702	Direct Observation of Bandgap Oscillations Induced by Optical Phonons in Hybrid Lead Iodide Perovskites. Advanced Functional Materials, 2020, 30, 1907982.	7.8	15
52703	Enargite Cu₃PS₄: A Cuâ€"Sâ€Based Thermoelectric Material with a Wurtziteâ€Derivative Structure. Advanced Functional Materials, 2020, 30, 2000973.	7.8	25
52704	High ZT 2D Thermoelectrics by Design: Strong Interlayer Vibration and Complete Bandâ€Extrema Alignment. Advanced Functional Materials, 2020, 30, 2001200.	7.8	32

#	Article	IF	Citations
52705	Large Outâ€ofâ€Plane Second Harmonic Generation Susceptibility in Pentaâ€ZnS 2 Sheet. Advanced Theory and Simulations, 2020, 3, 2000027.	1.3	10
52706	Conductive Li_{3.08}Cr_{0.02}Si_{0.09}V_{0.9}O₄ Anode Material: Novel â€œZeroâ€Strainâ€•Characteristic and Superior Electrochemical Li⁺ Storage. Advanced Energy Materials, 2020, 10, 1904267.	10.2	53
52707	H₂â€Directing Strategy on In Situ Synthesis of Coâ€MoS₂ with Highly Expanded Interlayer for Elegant HER Activity and its Mechanism. Advanced Energy Materials, 2020, 10, 2000291.	10.2	82
52708	Correlating Macro and Atomic Structure with Elastic Properties and Ionic Transport of Glassy Li₂Sâ€P₂S₅ (LPS) Solid Electrolyte for Solidâ€State Li Metal Batteries. Advanced Energy Materials, 2020, 10, 2000335.	10.2	56
52709	Bimetalâ€organic Frameworkâ€derived Co₉S₈/ZnS@NC Heterostructures for Superior Lithiumâ€ion Storage. Chemistry - an Asian Journal, 2020, 15, 1613-1620.	1.7	24
52710	Nanoheterostructures of Partially Oxidized RuNi Alloy as Bifunctional Electrocatalysts for Overall Water Splitting. ChemSusChem, 2020, 13, 2739-2744.	3.6	23
52711	Strain Dependence of Metal Anode Surface Properties. ChemSusChem, 2020, 13, 3147-3153.	3.6	12
52712	Structural, mechanical, electronic, and thermodynamic properties of pure tungsten metal under different pressures: A firstâ€principles study. International Journal of Quantum Chemistry, 2020, 120, e26231.	1.0	14
52713	Composition and Architecture Design of Doubleâ€Shelled Co_{0.85}Se_{1â^'}_xS_x@Carbon/Graphene Hollow Polyhedron with Superior Alkali (Li, Na, K)â€ion Storage. Small, 2020, 16, e1905853.	5.2	44
52714	Phaseâ€Regulated Sensing Mechanism of MoS 2 Based Nanohybrids toward Pointâ€ofâ€Care Prostate Cancer Diagnosis. Small, 2020, 16, 2000307.	5.2	13
52715	Electron nuclear dynamics with plane wave basis sets: complete theory and formalism. Theoretical Chemistry Accounts, 2020, 139, 1.	0.5	2
52716	First-principles study on the structural, electronic and optical properties in bulk and surfaces of full-Heusler alloy X2CoGa (Xâ€‰=â€‰Ti, Hf). Applied Physics A: Materials Science and Processing, 2020, 126, 1.	1.1	3
52717	First-principles microkinetic analysis of dehydrogenation of cyclohexene on the Pt/Cu/Pt (111) surface. Journal of Molecular Modeling, 2020, 26, 89.	0.8	3
52718	Adsorption of hydrogen and carbon dioxide in zeolitic imidazolate framework structure with SOD topology: experimental and modelling studies. Adsorption, 2020, 26, 1027-1038.	1.4	21
52719	Hydrogen sorption capacity of crystal lattice defects and low Miller index surfaces of copper. Journal of Materials Science, 2020, 55, 6623-6636.	1.7	13
52720	The reliability assessment of Auâ€“Al bonds using parallel gap resistance microwelding. Journal of Materials Science: Materials in Electronics, 2020, 31, 6313-6320.	1.1	7
52721	The Structural, Electronic, Magnetic, Thermodynamic, and Mechanical Properties of Quaternary Heusler Alloys TiHfIrZ (Z = Al, Ga, In). Journal of Superconductivity and Novel Magnetism, 2020, 33, 2235-2243.	0.8	8
52722	Catalysis at Metal/Oxide Interfaces: Density Functional Theory and Microkinetic Modeling of Water Gas Shift at Pt/MgO Boundaries. Topics in Catalysis, 2020, 63, 673-687.	1.3	17

#	Article	IF	Citations
52723	Uncertainty quantification of solute transport coefficients. , 2020, , 93-118.		1
52724	Dissociated dislocation-mediated carbon transport and diffusion in austenitic iron. Acta Materialia, 2020, 191, 43-50.	3.8	36
52725	Highly efficient methane decomposition to H2 and CO2 reduction to CO via redox looping of Ca2FexAl2-xO5 supported NiyFe3-yO4 nanoparticles. Applied Catalysis B: Environmental, 2020, 271, 118938.	10.8	24
52726	The high selectivity for benzoic acid formation on Ca2Sb2O7 enables efficient and stable toluene mineralization. Applied Catalysis B: Environmental, 2020, 271, 118948.	10.8	48
52727	Urchin-like TiO2 structures decorated with lanthanide-doped Bi2S3 quantum dots to boost hydrogen photogeneration performance. Applied Catalysis B: Environmental, 2020, 272, 118962.	10.8	68
52728	How a trapeziform flake of monolayer WS2 formed on SiO2(1Â0Â0)? A first-principle study. Applied Surface Science, 2020, 517, 145864.	3.1	2
52729	The influence of iodide in corrosion inhibition by organic compounds on carbon steel: Theoretical and experimental studies. Applied Surface Science, 2020, 514, 145928.	3.1	47
52730	Catalytic nature of iron-nitrogen-graphene heterogeneous catalysts for oxygen evolution reaction and oxygen reduction reaction. Applied Surface Science, 2020, 514, 146073.	3.1	15
52731	Transition from Schottky-to-Ohmic contacts in 1T VSe2-based van der Waals heterojunctions: Stacking and strain effects. Applied Surface Science, 2020, 517, 146168.	3.1	18
52732	Oxygen defect boosted photocatalytic hydrogen evolution from hydrogen sulfide over active {0Â0Â1} facet in anatase TiO2. Applied Surface Science, 2020, 517, 146198.	3.1	28
52733	CO2 hydrogenation to formic acid over platinum cluster doped defective graphene: A DFT study. Applied Surface Science, 2020, 517, 146200.	3.1	27
52734	Bioinspired Mo tape-porphyrin as an efficient and selective electrocatalyst for ammonia synthesis. Applied Surface Science, 2020, 520, 146202.	3.1	11
52735	Metallic two-dimensional C3N allotropes with electron and ion channels for high-performance Li-ion battery anode materials. Applied Surface Science, 2020, 518, 146254.	3.1	26
52736	Enhancing thermoelectric properties of monolayer GeSe via strain-engineering: A first principles study. Applied Surface Science, 2020, 521, 146256.	3.1	27
52737	Thermodynamic reassessment of the Moâ€“Hf and Moâ€“Zr systems supported by first-principles calculations. Calphad: Computer Coupling of Phase Diagrams and Thermochemistry, 2020, 69, 101766.	0.7	11
52738	Interface and valence modulation on scalable phosphorene/phosphide lamellae for efficient water electrolysis. Chemical Engineering Journal, 2020, 395, 124976.	6.6	65
52739	Exploration of stable stoichiometries, ground-state structures, and mechanical properties of the Wâ€“Si system. Ceramics International, 2020, 46, 17034-17043.	2.3	43
52740	Permeability and mechanical properties of arsenene and arsenene/graphene heterostructure: First-principles calculation. Computational Condensed Matter, 2020, 23, e00473.	0.9	4

#	Article	IF	Citations
52741	Electronegativity regulation on opt-electronic properties of non van der Waals two-dimensional material: Ga2O3. Computational Materials Science, 2020, 179, 109692.	1.4	4
52742	Ab initio thermodynamic properties of certain compounds in Nd-Fe-B system. Computational Materials Science, 2020, 180, 109696.	1.4	7
52743	Predicted crystal structures of titanium nitrides at high pressures. Computational Materials Science, 2020, 180, 109720.	1.4	9
52744	Two-dimensional FeC compound with square and triangle lattice structure â€“ Molecular dynamics and DFT study. Computational Materials Science, 2020, 181, 109730.	1.4	4
52745	Quantum chemical exploration of polymerized forms of polycyclic aromatic hydrocarbons: D6h tetramer and polymer of coronene. Chemical Physics Letters, 2020, 747, 137366.	1.2	3
52746	A core-shell structured CoMoO4â‹…nH2O@Co1-xFexOOH nanocatalyst for electrochemical evolution of oxygen. Electrochimica Acta, 2020, 345, 136125.	2.6	9
52747	ATR-FTIR in Kretschmann configuration integrated with electrochemical cell as in situ interfacial sensitive tool to study corrosion inhibitors for magnesium substrates. Electrochimica Acta, 2020, 345, 136166.	2.6	37
52748	An artificial metal-alloy interphase for high-rate and long-life sodiumâ€“sulfur batteries. Energy Storage Materials, 2020, 29, 1-8.	9.5	91
52749	Synergistic H+/Zn2+ dual ion insertion mechanism in high-capacity and ultra-stable hydrated VO2 cathode for aqueous Zn-ion batteries. Energy Storage Materials, 2020, 29, 60-70.	9.5	157
52750	Multi-scale stabilization of high-voltage LiCoO2 enabled by nanoscale solid electrolyte coating. Energy Storage Materials, 2020, 29, 71-77.	9.5	49
52751	Enhanced quantum efficiency and thermal stability in tunable yellow-emitting Sr Ca1-AlSiN3:Ce3+ phosphor. Journal of Alloys and Compounds, 2020, 831, 154791.	2.8	12
52752	A novel double-perovskite LiLaMgTeO6: Mn4+ far-red phosphor for indoor plant cultivation white LEDs: Crystal and electronic structure, and photoluminescence properties. Journal of Alloys and Compounds, 2020, 832, 154905.	2.8	42
52753	Atomic-scale investigation on the structural evolution and deformation behaviors of Cuâ€“Cr nanocrystalline alloys processed by high-pressure torsion. Journal of Alloys and Compounds, 2020, 832, 154994.	2.8	4
52754	Selective activation of methane C H bond in the presence of methanol. Journal of Catalysis, 2020, 386, 12-18.	3.1	6
52755	Kinetics of non-oxidative propane dehydrogenation on Cr2O3 and the nature of catalyst deactivation from first-principles simulations. Journal of Catalysis, 2020, 386, 126-138.	3.1	51
52756	Free-standing phosphorous-doped molybdenum nitride in 3D carbon nanosheet towards hydrogen evolution at all pH values. Journal of Energy Chemistry, 2020, 50, 44-51.	7.1	38
52757	An efficient defect engineering strategy to enhance catalytic performances of Co3O4 nanorods for CO oxidation. Journal of Hazardous Materials, 2020, 394, 122540.	6.5	43
52758	First-principles search for half-metallic ferromagnetism in CsCrZ2 (Z = O, S, Se or Te) Heusler alloys. Journal of Molecular Graphics and Modelling, 2020, 98, 107620.	1.3	5

#	Article	IF	Citations
52759	First-principles study of structural and optical properties contrast for liquid (GeTe)x(xÂ=Â1,2,3)-Sb2Te3 compounds. Journal of Non-Crystalline Solids, 2020, 539, 120051.	1.5	1
52760	Thermal and mechanical properties of U3Si2: A combined ab-initio and molecular dynamics study. Journal of Nuclear Materials, 2020, 533, 152090.	1.3	15
52761	Hydrothermal syntheses and crystal structures of molybdenum tellurites. Journal of Solid State Chemistry, 2020, 287, 121317.	1.4	4
52762	Ab initio calculations on the electronic structures and electrochemical properties of LiVO2 and NaVO2. Journal of Solid State Chemistry, 2020, 288, 121383.	1.4	3
52763	Novel Al-X alloys with improved hardness. Materials and Design, 2020, 192, 108699.	3.3	28
52764	Electrolytic-anion-redox adsorption pseudocapacitance in nanosized lithium-free transition metal oxides as cathode materials for Li-ion batteries. Nano Energy, 2020, 72, 104727.	8.2	49
52765	Strain engineering of oxide thin films for photocatalytic applications. Nano Energy, 2020, 72, 104732.	8.2	26
52766	Charge redistribution within platinumâ€“nitrogen coordination structure to boost hydrogen evolution. Nano Energy, 2020, 73, 104739.	8.2	55
52767	Structures, mobilities, electronic and optical properties of two-dimensional Î±-phase group-VI binary compounds: Î±-Se2Te and Î±-SeTe2. Physics Letters, Section A: General, Atomic and Solid State Physics, 2020, 384, 126431.	0.9	10
52768	Strongly anisotropic thermal conductivity in planar hexagonal borophene oxide sheet. Physics Letters, Section A: General, Atomic and Solid State Physics, 2020, 384, 126457.	0.9	4
52769	Effects of carbon related defects on opto-electronic properties of Î²-Ga2O3: The first principle calculation. Results in Physics, 2020, 17, 103060.	2.0	7
52770	Single-layer CrI3 grown by molecular beam epitaxy. Science Bulletin, 2020, 65, 1064-1071.	4.3	51
52771	Ferroelectric control of single-molecule magnetism in 2D limit. Science Bulletin, 2020, 65, 1252-1259.	4.3	33
52772	Structural, mechanical, electronic and thermodynamic properties of cubic TiC compounds under different pressures: A first-principles study. Solid State Communications, 2020, 311, 113856.	0.9	16
52773	An ab-initio study of H2O adsorption on the calcite (104) surface with different coverages. Solid State Communications, 2020, 313, 113892.	0.9	16
52774	Mechanical properties and thermal stability of reactively sputtered multi-principal-metal Hf-Ta-Ti-V-Zr nitrides. Surface and Coatings Technology, 2020, 389, 125674.	2.2	60
52775	Self-Limiting Temperature Window for Thermal Atomic Layer Etching of HfO₂ and ZrO₂ Based on the Atomic-Scale Mechanism. Chemistry of Materials, 2020, 32, 3414-3426.	3.2	20
52776	Fast Ion Conduction and Its Origin in Li_{6â€“x}PS_{5â€“x}Br_{1+x}. Chemistry of Materials, 2020, 32, 3833-3840.	3.2	75

#	Article	IF	Citations
52777	Unraveling the Origin of Ceria Activity in Waterâ€“Gas Shift by First-Principles Microkinetic Modeling. Journal of Physical Chemistry C, 2020, 124, 7823-7834.	1.5	21
52778	Modulating the Electronic Structure and In-Plane Activity of Two-Dimensional Transition Metal Dichalcogenide (MoS₂, TaS₂, NbS₂) Monolayers by Interfacial Engineering. Journal of Physical Chemistry C, 2020, 124, 8822-8833.	1.5	20
52779	Construction of a Molecular Switch Based on Two Metastable States of Fullerene on Cu(111). Journal of Physical Chemistry C, 2020, 124, 11158-11164.	1.5	6
52780	Mechanism of Proton Conduction in Doped Barium Cerates: A First-Principles Study. Journal of Physical Chemistry C, 2020, 124, 8024-8033.	1.5	22
52781	First-Order Isostructural Phase Transition Induced by High Pressure in Fe(IO₃)₃. Journal of Physical Chemistry C, 2020, 124, 8669-8679.	1.5	24
52782	Electrochemical Properties and Crystal Structure of Li⁺/H⁺ Cation-Exchanged LiNiO₂. ACS Applied Energy Materials, 2020, 3, 4078-4087.	2.5	32
52783	MoSe₂-Amorphous CNT Hierarchical Hybrid Coreâ€“Shell Structure for Efficient Hydrogen Evolution Reaction. ACS Applied Energy Materials, 2020, 3, 5067-5076.	2.5	24
52784	Effects of Surface Terminations of 2D Bi₂WO₆ on Photocatalytic Hydrogen Evolution from Water Splitting. ACS Applied Materials & Interfaces, 2020, 12, 20067-20074.	4.0	78
52785	Emerging One-/Two-Dimensional Heteronanostructure Integrating SiC Nanowires with MoS₂ Nanosheets for Efficient Electrocatalytic Hydrogen Evolution. ACS Applied Materials & Interfaces, 2020, 12, 19519-19529.	4.0	40
52786	Separation Properties of Porous MoS₂ Membranes Decorated with Small Molecules. ACS Applied Materials & Interfaces, 2020, 12, 20096-20102.	4.0	18
52787	MXene (Ti₃C₂T_x) and Carbon Nanotube Hybrid-Supported Platinum Catalysts for the High-Performance Oxygen Reduction Reaction in PEMFC. ACS Applied Materials & Interfaces, 2020, 12, 19539-19546.	4.0	67
52788	Interfacial Roughness Facilitated by Dislocation and a Metal-Fuse Resistor Fabricated Using a Nanomanipulator. ACS Applied Materials & Interfaces, 2020, 12, 24442-24449.	4.0	1
52789	Nucleation Control-Triggering Cocrystal Polymorphism of Charge-Transfer Complexes Differing in Physical and Electronic Properties. ACS Applied Materials & Interfaces, 2020, 12, 19718-19726.	4.0	21
52790	TiO₂/ZrO₂ Nanoparticle Composites for Electrochemical Hydrogen Evolution. ACS Applied Nano Materials, 2020, 3, 3634-3645.	2.4	35
52791	Dual-Site-Mediated Hydrogenation Catalysis on Pd/NiO: Selective Biomass Transformation and Maintenance of Catalytic Activity at Low Pd Loading. ACS Catalysis, 2020, 10, 5483-5492.	5.5	52
52792	Preferential Oxidation of CO in Hydrogen at Nonmetal Active Sites with High Activity and Selectivity. ACS Catalysis, 2020, 10, 5362-5370.	5.5	8
52793	Facile Heterogeneously Catalyzed Nitrogen Fixation by MXenes. ACS Catalysis, 2020, 10, 5049-5056.	5.5	67
52794	Insight into the Effects of Water on the Ethene to Aromatics Reaction with HZSM-5. ACS Catalysis, 2020, 10, 5288-5298.	5.5	39

#	Article	IF	Citations
52795	Gate-Tunable Reversible Rashbaâ€“Edelstein Effect in a Few-Layer Graphene/2H-TaS₂ Heterostructure at Room Temperature. ACS Nano, 2020, 14, 5251-5259.	7.3	50
52796	Epitaxial Growth of Centimeter-Scale Single-Crystal MoS₂ Monolayer on Au(111). ACS Nano, 2020, 14, 5036-5045.	7.3	211
52797	Sub-Angstrom Characterization of the Structural Origin for High In-Plane Anisotropy in 2D GeS₂. ACS Nano, 2020, 14, 4456-4462.	7.3	25
52798	CO Oxidation Mechanisms on CoO_x-Pt Thin Films. Journal of the American Chemical Society, 2020, 142, 8312-8322.	6.6	39
52799	Nature of Reactive Hydrogen for Ammonia Synthesis over a Ru/C12A7 Electride Catalyst. Journal of the American Chemical Society, 2020, 142, 7655-7667.	6.6	59
52800	Microphotoelectrochemical Surface-Enhanced Raman Spectroscopy: Toward Bridging Hot-Electron Transfer with a Molecular Reaction. Journal of the American Chemical Society, 2020, 142, 8483-8489.	6.6	31
52801	Si-Doped Fe Catalyst for Ammonia Synthesis at Dramatically Decreased Pressures and Temperatures. Journal of the American Chemical Society, 2020, 142, 8223-8232.	6.6	28
52802	Time-dependent density-functional theory molecular-dynamics study on amorphization of Sc-Sb-Te alloy under optical excitation. Npj Computational Materials, 2020, 6, .	3.5	32
52803	Intra- and intermolecular self-assembly of a 20-nm-wide supramolecular hexagonal grid. Nature Chemistry, 2020, 12, 468-474.	6.6	88
52804	Magnetically driven phonon instability enables the metalâ€“insulator transition in h-FeS. Nature Physics, 2020, 16, 669-675.	6.5	26
52805	Direct-bandgap emission from hexagonal Ge and SiGe alloys. Nature, 2020, 580, 205-209.	13.7	231
52806	Dynamical Quantum Filtering via Enhanced Scattering of para-H2 on the Orientationally Anisotropic Potential of SrTiO3(001). Scientific Reports, 2020, 10, 5939.	1.6	0
52807	Intrinsic and tunable ferromagnetism in Bi0.5Na0.5TiO3 through CaFeO3-Î´ modification. Scientific Reports, 2020, 10, 6189.	1.6	32
52808	Enhanced magnetic spinâ€“spin interactions observed between porphyrazine derivatives on Au(111). Communications Chemistry, 2020, 3, .	2.0	5
52809	Catalytic properties of Î±-MnO₂ for Liâ€“air battery cathodes: a density functional investigation. Physical Chemistry Chemical Physics, 2020, 22, 9233-9239.	1.3	2
52810	Theoretical understanding of the electrochemical reaction barrier: a kinetic study of CO2 reduction reaction on copper electrodes. Physical Chemistry Chemical Physics, 2020, 22, 9607-9615.	1.3	19
52811	The effects of microstructure, Nb content and secondary Ruddlesdenâ€“Popper phase on thermoelectric properties in perovskite CaMn_{1â^'x}Nb_xO₃ (x) Tj ETQq1 0 0 rgBT /Overlock		
52812	Peculiarities of Brâ‹¯Br bonding in crystal structures of polybromides and bromine solvates. CrystEngComm, 2020, 22, 7361-7370.	1.3	7

#	Article	IF	Citations
52813	Discovery of new polymorphs of the tuberculosis drug isoniazid. CrystEngComm, 2020, 22, 2705-2708.	1.3	26
52814	A two-dimensional CdO/CdS heterostructure used for visible light photocatalysis. Physical Chemistry Chemical Physics, 2020, 22, 9587-9592.	1.3	63
52815	Ab initioinvestigation of quantum size effects on the adsorption of CO₂, CO, H₂O, and H₂on transition-metal particles. Physical Chemistry Chemical Physics, 2020, 22, 8998-9008.	1.3	19
52816	Structural stability of single-layer PdSe₂ with pentagonal puckered morphology and its nanotubes. Physical Chemistry Chemical Physics, 2020, 22, 8289-8295.	1.3	26
52817	Work function and band alignment of few-layer violet phosphorene. Journal of Materials Chemistry A, 2020, 8, 8586-8592.	5.2	43
52818	Nature of terrace edge states (TES) in lower-dimensional halide perovskite. Journal of Materials Chemistry A, 2020, 8, 7659-7670.	5.2	14
52819	High electron mobility, controllable magnetism and anomalous light absorption in a monolayered tin mononitride semiconductor. Journal of Materials Chemistry C, 2020, 8, 6396-6402.	2.7	6
52820	Novel two-dimensional siliconâ€“carbon binaries by crystal structure prediction. Physical Chemistry Chemical Physics, 2020, 22, 8442-8449.	1.3	8
52821	High-efficiency helium separation through an inorganic graphenylene membrane: a theoretical study. Physical Chemistry Chemical Physics, 2020, 22, 9789-9795.	1.3	32
52822	A multiporous carbon family with superior stability, tunable electronic structures and amazing hydrogen storage capability. Physical Chemistry Chemical Physics, 2020, 22, 9734-9739.	1.3	4
52823	Hydrodeoxygenation of anisole to benzene over an Fe₂P catalyst by a direct deoxygenation pathway. Catalysis Science and Technology, 2020, 10, 3015-3023.	2.1	23
52824	Understanding the thermally activated charge transport in NaPb_mSbQ_{m+2} (Q) Tj ETQq1 1 0.784314 rgBT /O carrier scattering. Energy and Environmental Science, 2020, 13, 1509-1518.	15.6	63
52825	Effects of substrate and tip characteristics on the surface friction of fluorinated graphene. RSC Advances, 2020, 10, 10888-10896.	1.7	2
52826	The controllable synthesis of substitutional and interstitial nitrogen-doped manganese dioxide: the effects of doping sites on enhancing the catalytic activity. Journal of Materials Chemistry A, 2020, 8, 8383-8396.	5.2	65
52827	Polyamorphism in K₂Sb₈Se₁₃ for multi-level phase-change memory. Journal of Materials Chemistry C, 2020, 8, 6364-6369.	2.7	14
52828	Electron quantum interference in epitaxial antiferromagnetic NiO thin films. AIP Advances, 2020, 10, 045204.	0.6	1
52829	Impact of transverse and vertical gate electric field on vibrational and electronic properties of MoS2. Journal of Applied Physics, 2020, 127, .	1.1	3
52830	Morphology and reactivity of size-selected titanium oxide nanoclusters on Au(111). Journal of Chemical Physics, 2020, 152, 054714.	1.2	12

#	Article	IF	Citations
52831	Atomic-level calculations and experimental study of dislocations in InSb. Journal of Applied Physics, 2020, 127, 135104.	1.1	8
52832	Structure and properties of CoCrFeNiX multi-principal element alloys from ab initio calculations. Journal of Applied Physics, 2020, 127, .	1.1	19
52833	Influence of 3d, 4d, and 5d dopants on the oxygen evolution reaction at Î±-Fe2O3(0001) under dark and illumination conditions. Journal of Chemical Physics, 2020, 152, 124709.	1.2	9
52834	Solvation at metal/water interfaces: An ab initio molecular dynamics benchmark of common computational approaches. Journal of Chemical Physics, 2020, 152, 144703.	1.2	103
52835	Electronegativity, phase transition, and ferroelectricity of TeSe2 few-layers. Journal of Physics Condensed Matter, 2020, 32, 045301.	0.7	2
52836	Electric field control of Rashba spin splitting in 2D N^{III}X^{VI} (Nâ€‰â€‰=â€‰â€‰Ga, In; Xâ€‰â€‰=â€‰â€‰	0.7	17
52837	A combined laser-based angle-resolved photoemission spectroscopy and two-photon photoemission spectroscopy study of Tdâ€“WTe₂. Journal of Physics Condensed Matter, 2020, 32, 345503.	0.7	3
52838	First-principles calculations of soluteâ€“vacancy interactions in aluminum*. Chinese Physics B, 2020, 29, 066103.	0.7	1
52839	Electronic Structure and Polarization of NaMgF3/NaCaF3 Superlattices: Insight from First-Principles. IOP Conference Series: Materials Science and Engineering, 2020, 774, 012016.	0.3	0
52840	NMR study of defect-induced magnetism in methylammonium lead iodide perovskite. Physical Review B, 2020, 101, .	1.1	15
52841	Prediction of perovskite-related structures in<mml:math xmlns:mml="http://www.w3.org/1998/Math/MathML"><mml:mrow><mml:mi>A</mml:mi><mml:msub><mml:mi>CuO</mml:mi><mml:m	1.1	16
52842	Single-layer Janus black arsenic-phosphorus (b-AsP): Optical dichroism, anisotropic vibrational, thermal, and elastic properties. Physical Review B, 2020, 101, .	1.1	31
52843	Role of spin-orbit coupling in the alloying behavior of multilayer Bi1âˆ’xSbx solid solutions revealed by a first-principles cluster expansion. Physical Review B, 2020, 101, .	1.1	10
52844	Origin of the large interfacial perpendicular magnetic anisotropy in <mml:math xmlns:mml="http://www.w3.org/1998/Math/MathML"><mml:mrow><mml:mi>MgO</mml:mi><mml:mo>/</mml:mo><mml:msub><mml:m Physical Review B, 2020, 101, .	1.1	25
52845	Electronic and magnetic properties of 3d transition-metal adatoms on Mn/W(110). Physical Review B, 2020, 101, .	1.1	1
52846	Two superconducting phases induced at point contacts on the Weyl semimetal TaAs. Physical Review B, 2020, 101, .	1.1	11
52847	Route to high- <mml:math xmlns:mml="http://www.w3.org/1998/Math/MathML"><mml:msub><mml:mi>T</mml:mi><mml:mi>c</mml:mi></mml:msub></mml:ma superconductivity via <mml:math xmlns:mml="http://www.w3.org/1998/Math/MathML"><mml:msub><mml:mi>CH</mml:mi><mml:mn>4</mml:mn></mml:msub></mml -intercalated <mml:math xmlns:mml="http://www.w3.org/1998/Math/MathML"><mml:mrow><mml:msub><mml:mi	1.1	98
52848	Manipulating magnetism in the topological semimetal <mml:math xmlns:mml="http://www.w3.org/1998/Math/MathML"><mml:mrow><mml:msub><mml:mi>EuCd</mml:mi><mml:mn>2</mml:mn></mml:msub><mml:mn></ Physical Review B, 2020, 101, .	1.1	58

#	Article	IF	Citations
52849	Emergence of <mml:math xmlns:mml="http://www.w3.org/1998/Math/MathML"><mml:mi>d</mml:mi></mml:math> -orbital magnetic Dirac fermions in a <mml:math xmlns:mml="http://www.w3.org/1998/Math/MathML"><mml:mrow><mml:mi>Mo</mml:mi><mml:msub><mml:mi mathvariant="normal">S</mml:mi><mml:mn>2</mml:mn></mml:msub></mml:mrow></mml:math>	1.1	7
52850	First-principles calculation of spin and orbital contributions to magnetically ordered moments in <mml:math xmlns:mml="http://www.w3.org/1998/Math/MathML"><mml:mrow><mml:msub><mml:mi>Sr</mml:mi><mml:mn>2</mml:mn></mml:msub></mml:mrow></mml:math> Physical Review B, 2020, 101, .	1.1	23
52851	Exceptionally large anomalous Hall effect due to anticrossing of spin-split bands in the antiferromagnetic half-Heusler compound TbPtBi. Physical Review B, 2020, 101, .	1.1	24
52852	Intrinsic quantum anomalous Hall phase induced by proximity in the van der Waals heterostructure germanene/ <mml:math xmlns:mml="http://www.w3.org/1998/Math/MathML"><mml:mrow><mml:msub><mml:mi>Cr</mml:mi><mml:mn>2</mml:mn></mml:msub></mml:mrow></mml:math> Physical Review B, 2020, 101, .	1.1	23
52853	Competition of defect ordering and site disproportionation in strained <mml:math xmlns:mml="http://www.w3.org/1998/Math/MathML"><mml:msub><mml:mi>LaCoO</mml:mi><mml:mn>3</mml:mn></mml:msub></mml:math> on <mml:math xmlns:mml="http://www.w3.org/1998/Math/MathML"><mml:msub><mml:mi>SrTiO</mml:mi><mml:mn>3</mml:mn></mml:msub></mml:math> (001). Physical Review B, 2020, 101, .	1.1	12
52854	Lattice dynamics and polarization-dependent phonon damping in Î± -phase FeSi2 nanostructures. Physical Review B, 2020, 101, .	1.1	4
52855	Structural Ordering in Liquid Gallium under Extreme Conditions. Physical Review Letters, 2020, 124, 145501.	2.9	15
52856	Anharmonic Eigenvectors and Acoustic Phonon Disappearance in Quantum Paraelectric <mml:math xmlns:mml="http://www.w3.org/1998/Math/MathML" display="inline"><mml:mrow><mml:msub><mml:mrow><mml:mi>SrTiO</mml:mi></mml:mrow><mml:mrow><mml:mn>3</mml:mn></mml:mrow></mml:msub></mml:mrow></mml:math> Physical Review Letters, 2020, 124, 145901.	2.9	33
52857	Vibration-Driven Self-Doping of Dangling-Bond Wires on Si(553)-Au Surfaces. Physical Review Letters, 2020, 124, 146802.	2.9	15
52858	Superconductivity in Compression-Shear Deformed Diamond. Physical Review Letters, 2020, 124, 147001.	2.9	64
52859	Observation of yttrium oxide segregation in a ZrO₂â€“SiO₂ glassâ€ceramic at nanometer dimensions. Journal of the American Ceramic Society, 2020, 103, 7147-7158.	1.9	9
52860	Polymeric Electrolyte Comprising a NAFION Membrane Plasticized by Dimethyl Sulfoxide and the Transport Specifics of Alkali Metal Ions in It: Quantum-Chemical Simulation. Russian Journal of Inorganic Chemistry, 2020, 65, 378-389.	0.3	1
52861	Uniaxial Tensile Strain Induced the Enhancement of Thermoelectric Properties in n-Type BiCuOCh (Ch =) Tj ETQq0 0 0 rgBT /Overlock 10	1.3	7
52862	Ferromagnetic Half-Metal Cyanamides Cr(NCN)2 Predicted from First Principles Investigation. Materials, 2020, 13, 1805.	1.3	2
52863	Catalytic Effect of Hydrogen Bond on Oxhydryl Dehydrogenation in Methanol Steam Reforming on Ni(111). Molecules, 2020, 25, 1531.	1.7	3
52864	Ab Initio Study of Ferroelectric Critical Size of SnTe Low-Dimensional Nanostructures. Nanomaterials, 2020, 10, 732.	1.9	7
52865	Quantum-Mechanical Assessment of the Energetics of Silver Decahedron Nanoparticles. Nanomaterials, 2020, 10, 767.	1.9	3
52866	Effects of Components Modulation on the Type of Band Alignments for PbI 2 /WS 2 van der Waals Heterostructure. Physica Status Solidi - Rapid Research Letters, 2020, 14, 2000016.	1.2	23

#	Article	IF	Citations
52867	HgCuPS₄: An Exceptional Infrared Nonlinear Optical Material with Defect Diamond-like Structure. Chemistry of Materials, 2020, 32, 4331-4339.	3.2	93
52868	Complex Investigation of Water Impact on Li-Ion Conductivity of Li_{1.3}Al_{0.3}Ti_{1.7}(PO₄)₃â€"Electrochemical, Chemical, Structural, and Morphological Aspects. Chemistry of Materials, 2020, 32, 3723-3732.	3.2	24
52869	Surface Oxygen Vacancy Formation Energy Calculations in 34 Orientations of Î²-Ga₂O₃ and Î¸-Al₂O₃. Journal of Physical Chemistry C, 2020, 124, 10509-10522.	1.5	19
52870	Exploring the Magnetic Properties of the Largest Single-Molecule Magnets. Journal of Physical Chemistry Letters, 2020, 11, 3789-3795.	2.1	9
52871	Exotic Two-Dimensional Structure: The First Case of Hexagonal NaCl. Journal of Physical Chemistry Letters, 2020, 11, 3821-3827.	2.1	38
52872	Adsorption Properties and Microscopic Mechanism of CO₂ Capture in 1,1-Dimethyl-1,2-ethylenediamine-Grafted Metalâ€"Organic Frameworks. ACS Applied Materials & Interfaces, 2020, 12, 18533-18540.	4.0	36
52873	Engineering of Charged Defects at Perovskite Oxide Surfaces for Exceptionally Stable Solid Oxide Fuel Cell Electrodes. ACS Applied Materials & Interfaces, 2020, 12, 21494-21504.	4.0	43
52874	Controlling Ionomer Film Morphology through Altering Pt Catalyst Surface Properties for Polymer Electrolyte Membrane Fuel Cells. ACS Applied Polymer Materials, 2020, 2, 1807-1818.	2.0	23
52875	First-Principles Study of the Hydrogen Resistance Mechanism of PuO₂. ACS Omega, 2020, 5, 7211-7218.	1.6	9
52876	Solid-state 1D â† 3D transformation of polynitrile-based coordination polymers by dehydration reaction. Dalton Transactions, 2020, 49, 7084-7092.	1.6	12
52877	Re-examination of complexation behaviors of V(<scp>v</scp>) and V(<scp>iv</scp>): experimental investigation and theoretical simulation. Journal of Analytical Atomic Spectrometry, 2020, 35, 878-885.	1.6	5
52878	Elastic and optical properties of sillenites: First principle calculations. Ferroelectrics, 2020, 557, 98-104.	0.3	8
52879	Lattice dynamics in the spin- 12 frustrated kagome compound herbertsmithite. Physical Review B, 2020, 101, .	1.1	13
52880	Unconventional Photocurrents from Surface Fermi Arcs in Topological Chiral Semimetals. Physical Review Letters, 2020, 124, 166404.	2.9	40
52881	Phase Diagrams of Iron Hydrides at Pressures of 100â€"400 GPa and Temperatures of 0â€"5000 K. JETP Letters, 2020, 111, 145-150.	0.4	10
52882	Selfâ€Supported 3â€‰D Ultrathin Cobaltâ€"Nickelâ€"Boron Nanoflakes as an Efficient Electrocatalyst for the Oxygen Evolution Reaction. ChemSusChem, 2020, 13, 3662-3670.	3.6	25
52883	The Role of Metal Species on Aldehyde Hydrogenation over Co 13 and Ni 13 Supported on Î³â€Al 2 O 3 (110) Surfaces: A Theoretical Study. ChemistrySelect, 2020, 5, 4058-4068.	0.7	6
52884	The (010) Surface of the Al 45 Cr 7 Complex Intermetallic Compound: Insights from Density Functional Theory. Zeitschrift Fur Anorganische Und Allgemeine Chemie, 2020, 646, 1176-1182.	0.6	4

#	Article	IF	Citations
52885	Multimorphism and gap opening of charge-density-wave phases in monolayer VTe2. Nano Research, 2020, 13, 1733-1738.	5.8	29
52886	Magnetic properties of SnSe monolayer doped by transition-metal atoms: A first-principle calculation. Results in Physics, 2020, 17, 103126.	2.0	11
52887	Flux Crystal Growth, Structure, and Optical Properties of the New Germanium Oxysulfide La₄(GeS₂O₂)₃. Crystal Growth and Design, 2020, 20, 4054-4061.	1.4	4
52888	Catalytic Dehydrogenation of Ethane over Doped Perovskite via the Marsâ€“van Krevelen Mechanism. Journal of Physical Chemistry C, 2020, 124, 10462-10469.	1.5	12
52889	Dynamics Studies of O₂ Collision on Pt(111) Using a Global Potential Energy Surface. Journal of Physical Chemistry C, 2020, 124, 10573-10583.	1.5	7
52890	Neural Network Interatomic Potential for Predicting the Formation of Planar Defect in Nanocrystal. Journal of Physical Chemistry C, 2020, 124, 9424-9433.	1.5	5
52891	Topology-Based Machine Learning Strategy for Cluster Structure Prediction. Journal of Physical Chemistry Letters, 2020, 11, 4392-4401.	2.1	25
52892	First-Principles Study of Strain Modulation in S₃P₂/Black Phosphorene vdW Heterostructured Nanosheets for Flexible Electronics. ACS Applied Nano Materials, 2020, 3, 4407-4417.	2.4	20
52893	Voltage- and time-dependent valence state transition in cobalt oxide catalysts during the oxygen evolution reaction. Nature Communications, 2020, 11, 1984.	5.8	120
52894	Molybdenum carbide supported metal catalysts (M_n/Mo_xC; M = Co, Ni, Cu, Pd,) Tj ETQq1 1 0.784314 rgBT 3029-3046.	2.1	15
52895	A Cu₂B₂ monolayer with planar hypercoordinate motifs: an efficient catalyst for CO electroreduction to ethanol. Journal of Materials Chemistry A, 2020, 8, 9607-9615.	5.2	32
52896	Half-occupation approach for the ab initio calculation of strained Ga(AsSb)/GaAs valence band offsets. AIP Advances, 2020, 10, 045207.	0.6	1
52897	A first-principles study on hydrogen distributions in the Î±-U/UO2 interface. Journal of Physics Condensed Matter, 2020, 32, 195002.	0.7	0
52898	Silicene/boron nitride heterostructure for the design of highly efficient anode materials in lithium-ion battery. Journal of Physics Condensed Matter, 2020, 32, 355502.	0.7	11
52899	Realizing small-flake graphene oxide membranes for ultrafast size-dependent organic solvent nanofiltration. Science Advances, 2020, 6, eaaz9184.	4.7	177
52900	Mechanical and Thermal Properties of Low-Density Al20+xCr20-xMo20-yTi20V20+y Alloys. Crystals, 2020, 10, 278.	1.0	20
52901	Penta-C20: A Superhard Direct Band Gap Carbon Allotrope Composed of Carbon Pentagon. Materials, 2020, 13, 1926.	1.3	31
52902	Catalytic Polysulfide Conversion and Physiochemical Confinement for Lithiumâ€“Sulfur Batteries. Advanced Energy Materials, 2020, 10, 1904010.	10.2	165

#	Article	IF	Citations
52903	Achieving indirectâ€toâ€direct band gap transition and enhanced photocatalytic performance in blue phosphorene through doping and strain. International Journal of Quantum Chemistry, 2020, 120, e26230.	1.0	14
52904	Electronic and Optical Properties of Zigzag BN/AlN Nanoribbons with Misfit Dislocations: First-Principles Calculations. Journal of Electronic Materials, 2020, 49, 4100-4110.	1.0	2
52905	Lithium Diffusion in Niobium Tungsten Oxide Shear Structures. Chemistry of Materials, 2020, 32, 3980-3989.	3.2	54
52906	Computational Chemistry-Based Evaluation of Metal Salts and Metal Oxides for Application in Mercury-Capture Technologies. Industrial & Engineering Chemistry Research, 2020, 59, 9015-9022.	1.8	4
52907	Advancement of Actinide Metalâ€“Organic Framework Chemistry via Synthesis of Pu-UiO-66. Journal of the American Chemical Society, 2020, 142, 9363-9371.	6.6	38
52908	Ternary selenides A₂Sb₄Se₈ (A = K, Rb and Cs) as an n-type thermoelectric material with high power factor and low lattice thermal conductivity: importance of the conformationally flexible Sbâ€“Seâ€“Seâ€“Sb bridges. RSC Advances, 2020, 10, 14415-14421.	1.7	5
52909	Interface and polarization effects induced Schottky-barrier-free contacts in two-dimensional MXene/GaN heterojunctions. Journal of Materials Chemistry C, 2020, 8, 7350-7357.	2.7	34
52910	Neutron diffraction study of crystal structure and temperature driven molecular reorientation in solid Î±-CO. AIP Advances, 2020, 10, 045301.	0.6	4
52911	Origin of high strength in the CoCrFeNiPd high-entropy alloy. Materials Research Letters, 2020, 8, 209-215.	4.1	59
52912	Novel mechanism for weak magnetization with high Curie temperature observed in H-adsorption on graphene. Journal of Physics Condensed Matter, 2020, 32, 195802.	0.7	0
52913	Structural and electronic properties of c-BN (111) surface with hydrogen/fluorine functionalization and nitrogen-based small-molecule adsorption. Journal of Physics Condensed Matter, 2020, 32, 265002.	0.7	4
52914	Novel phosphorus-based 2D allotropes with ultra-high mobility. Nanotechnology, 2020, 31, 325702.	1.3	3
52915	Thermodynamic analysis and kinetic optimization of high-energy batteries based on multi-electron reactions. National Science Review, 2020, 7, 1367-1386.	4.6	31
52916	Large anomalous Hall effect in a hexagonal ferromagnetic <mml:math xmlns:mml="http://www.w3.org/1998/Math/MathML"><mml:mrow><mml:mi mathvariant="normal">F</mml:mi><mml:msub><mml:mi mathvariant="normal">e</mml:mi><mml:mn>5</mml:mn></mml:msub><mml:mi mathvariant="normal">S</mml:mi><mml:msub><mml:mi mathvariant="normal">n</mml:mi><mml:mn>3</mml:mn></mml:msub></mml:mrow></mml:math> single	1.1	18
52917	Graphdiyneâ€Based Flexible Photodetectors with High Responsivity and Detectivity. Advanced Materials, 2020, 32, e2001082.	11.1	171
52918	Photochromic Free MOFâ€Based Nearâ€Infrared Optical Switch. Angewandte Chemie, 2020, 132, 15652-15656.	1.6	7
52919	Photochromic Free MOFâ€Based Nearâ€Infrared Optical Switch. Angewandte Chemie - International Edition, 2020, 59, 15522-15526.	7.2	38
52920	Highâ€Performance Nitrogen Fixation over Mo Atom Modified Defective Î±â€MnO₂ (001). ChemCatChem, 2020, 12, 3937-3945.	1.8	5

#	Article	IF	Citations
52921	Highly correlation of CO2 reduction selectivity and surface electron Accumulation: A case study of Au-MoS2 and Ag-MoS2 catalyst. Applied Catalysis B: Environmental, 2020, 271, 118931.	10.8	53
52922	Enhanced catalytic performance and changed reaction chemistry for electrochemical glycerol oxidation by atomic-layer-deposited Pt-nanoparticle catalysts. Applied Catalysis B: Environmental, 2020, 273, 119037.	10.8	28
52923	Using strain to alter the energy bands of the monolayer MoSe2: A systematic study covering both tensile and compressive states. Applied Surface Science, 2020, 521, 146398.	3.1	20
52924	Thermoelectricity of n-type MnBi4S7-7xSe7x solid solution. Chemical Engineering Journal, 2020, 396, 125219.	6.6	8
52925	Second-nearest-neighbor modified embedded-atom method interatomic potential for Cu-M (MÂ=ÂCo, Mo) binary systems. Computational Materials Science, 2020, 178, 109627.	1.4	8
52926	Strain-induced structural phase transition and the rotation of polarization in BaTiO3 films. Computational Materials Science, 2020, 181, 109713.	1.4	3
52927	Exploring the real ground-state structures of W3Si silicides from first-principles calculations. Computational Materials Science, 2020, 180, 109719.	1.4	16
52928	Helium behaviors at Mn6Ni16Si7 precipitate in Î±-Fe: Insights from ab initio modeling. Computational Materials Science, 2020, 181, 109735.	1.4	2
52929	Uranium adsorption on two-dimensional irradiation resistant MXenes from first-principles calculations. Chemical Physics Letters, 2020, 750, 137444.	1.2	22
52930	Effects of valence and spin of Fe in MgSiO3 melts: Structural insights from first-principles molecular dynamics simulations. Geochimica Et Cosmochimica Acta, 2020, 279, 107-118.	1.6	8
52931	Simulated temperature programmed desorption experiments for nanoceria powders. Journal of Catalysis, 2020, 384, 252-259.	3.1	2
52932	Polymer decoration of carbon support to boost Pt-catalyzed hydrogen generation activity and durability. Journal of Catalysis, 2020, 385, 289-299.	3.1	7
52933	The critical role of hydride (Hâ^') ligands in electrocatalytic CO2reduction to HCOOH by [Cu25H22(PH3)12]Cl nanocluster. Journal of Catalysis, 2020, 387, 95-101.	3.1	20
52934	Facile and controllable synthesis of Zn-Al layered double hydroxide/silver hybrid by exfoliation process and its plasmonic photocatalytic activity of phenol degradation. Materials Chemistry and Physics, 2020, 250, 122988.	2.0	18
52935	Quantitative nanoscale tracking of oxygen vacancy diffusion inside single ceria grains by in situ transmission electron microscopy. Materials Today, 2020, 38, 24-34.	8.3	23
52936	Theoretical investigation on defect engineering for tuning photocatalytic activities in isostructural ScxmCuynOzâ^'1 (mÂ=ÂCa, nÂ=ÂNi). Materials Science and Engineering B: Solid-State Materials for Advanced Technology, 2020, 256, 114546.	1.7	0
52937	Strain-tunable photogalvanic effect in phosphorene. Materials Today Communications, 2020, 24, 101154.	0.9	4
52938	Water Promotes the Oxidation of SO₂ by O₂ over Carbonaceous Aerosols. Environmental Science & Technology, 2020, 54, 7070-7077.	4.6	28

#	Article	IF	Citations
52939	Force Field Parameter Development for the Thiolate/Defective Au(111) Interface. Langmuir, 2020, 36, 4098-4107.	1.6	2
52940	Tunable Room-Temperature Ferromagnetism in Two-Dimensional Cr₂Te₃. Nano Letters, 2020, 20, 3130-3139.	4.5	175
52941	Surfactant-Mediated Growth and Patterning of Atomically Thin Transition Metal Dichalcogenides. ACS Nano, 2020, 14, 6570-6581.	7.3	30
52942	Revisiting the Atomistic Structures at the Interface of Au(111) Electrodeâ€“Sulfuric Acid Solution. Journal of the American Chemical Society, 2020, 142, 9439-9446.	6.6	35
52943	Electrolyte design for LiF-rich solidâ€“electrolyte interfaces to enable high-performance microsized alloy anodes for batteries. Nature Energy, 2020, 5, 386-397.	19.8	621
52944	A density functional theory study of high-performance pre-lithiated MS2 (Mâ€‰=â€‰Mo, W, V) Monolayers as the Anode Material of Lithium Ion Batteries. Scientific Reports, 2020, 10, 6897.	1.6	16
52945	The In₂SeS/g-C₃N₄heterostructure: a new two-dimensional material for photocatalytic water splitting. Journal of Materials Chemistry C, 2020, 8, 6923-6930.	2.7	56
52946	Boosting the acidic electrocatalytic nitrogen reduction performance of MoS₂ by strain engineering. Journal of Materials Chemistry A, 2020, 8, 10426-10432.	5.2	59
52947	Correlation of interfacial perpendicular magnetic anisotropy and interlayer exchange coupling in CoFe/W/CoFe structures. Journal Physics D: Applied Physics, 2020, 53, 334001.	1.3	3
52948	Structural and electronic properties of two-dimensional freestanding <mml:math xmlns:mml="http://www.w3.org/1998/Math/MathML"><mml:mrow><mml:mi>BaTi</mml:mi><mml:msub><mml:mi mathvariant="normal">O</mml:mi><mml:mn>3</mml:mn></mml:msub><mml:mo>/</mml:mo><mml:mi>SrTi</mml:mi><mml:msub><mml:mi mathvariant="normal">O</mml:mi><mml:mn>3</mml:mn></mml:msub></mml:mrow></mml:math> heterostructures. Physical Review B, 2020, 101, .	1.1	18
52949	Landscape of coexisting excitonic states in the insulating single-layer cuprates and nickelates. Physical Review B, 2020, 101, .	1.1	7
52950	Evidence for ferromagnetic order in the CoSb layer ofLaCoSb2. Physical Review B, 2020, 101, .	1.1	3
52951	Electric Field Effects on the Adsorption of Dopamine Species on Ag(111): DFT Investigation of Interaction Mechanism. ChemistrySelect, 2020, 5, 4728-4739.	0.7	4
52952	Platinum and Palladium Monolayer Electrocatalysts for Formic Acid Oxidation. Topics in Catalysis, 2020, 63, 742-749.	1.3	17
52953	MoirÃ© patterns arising from bilayer graphone/graphene superlattice. Nano Research, 2020, 13, 1060-1064.	5.8	11
52954	Adaptive hard and tough mechanical response in single-crystal B1 VNx ceramics via control of anion vacancies. Acta Materialia, 2020, 192, 78-88.	3.8	46
52955	The effects of Fe, Co and Ni doping in CuAl2O4 spinel surface and bulk: A DFT study. Applied Surface Science, 2020, 521, 146478.	3.1	35
52956	Ab initio thermodynamics studies on the phase stability of PtO2 under ambient and high-pressure conditions. Computational Materials Science, 2020, 180, 109708.	1.4	5

#	Article	IF	Citations
52957	3d transitional-metal single atom catalysis toward hydrogen evolution reaction on MXenes supports. International Journal of Hydrogen Energy, 2020, 45, 14396-14406.	3.8	59
52958	Ab initio enhanced sampling kinetic study on MTO ethene methylation reaction. Journal of Catalysis, 2020, 388, 38-51.	3.1	24
52959	First-principles study of bcc Fe-Cr-Si binary and ternary random alloys from special quasi-random structure. Physica B: Condensed Matter, 2020, 586, 412085.	1.3	8
52960	Assembling Homometallic Sb₆ and Heterometallic Ti₄Sb₂ Oxo Clusters. Inorganic Chemistry, 2020, 59, 6689-6696.	1.9	5
52961	Azo-Dimerization Mechanisms of p-Aminothiophenol and p-Nitrothiophenol Molecules on Plasmonic Metal Surfaces Revealed by Tip-/Surface-Enhanced Raman Spectroscopy. Journal of Physical Chemistry C, 2020, 124, 11586-11594.	1.5	16
52962	Structure-Sensitivity Factors Based on Highly Active CO₂ Methanation Catalysts Prepared via the Polygonal Barrel-Sputtering Method. Journal of Physical Chemistry C, 2020, 124, 10016-10025.	1.5	12
52963	Theoretical prediction of double perovskite Cs₂Ag_xCu_{1-x}In_yTb_{1-y}Cl₆ for infrared detection. Journal Physics D: Applied Physics, 2020, 53, 265302.	1.3	29
52964	Methods for comparing uncertainty quantifications for material property predictions. Machine Learning: Science and Technology, 2020, 1, 025006.	2.4	78
52965	Interfacial <mml:math xmlns:mml="http://www.w3.org/1998/Math/MathML" display="inline" overflow="scroll"><mml:mrow><mml:mrow><mml:mi mathvariant="normal">N</mml:mi></mml:mrow></mml:mrow></mml:math> Vacancies in <mml:math xmlns:mml="http://www.w3.org/1998/Math/MathML" display="inline" overflow="scroll"><mml:mrow><mml:mi>Ga</mml:mi><mml:mi		

#	Article	IF	Citations
52975	Search for Ferroelectric Binary Oxides: Chemical and Structural Space Exploration Guided by Group Theory and Computations. Chemistry of Materials, 2020, 32, 3823-3832.	3.2	9
52976	Synthesis and Crystal Structure of Three Ga-rich Lithium Gallides, LiGa₆, Li₁₁Ga₂₄, and LiGa₂. Inorganic Chemistry, 2020, 59, 6566-6580.	1.9	2
52977	An Unexpected Role of H During SiC Corrosion in Water. Journal of Physical Chemistry C, 2020, 124, 9394-9400.	1.5	10
52978	Adsorption-Induced Kondo Effect in Metal-Free Phthalocyanine on Ag(111). Journal of Physical Chemistry C, 2020, 124, 10441-10452.	1.5	10
52979	Understanding the Balance of Entropy and Enthalpy in Hydrogenâ€“Halide Noncovalent Bonding. Journal of Physical Chemistry Letters, 2020, 11, 3495-3500.	2.1	3
52980	Stability of Boronium Cation-Based Ionic Liquid Electrolytes on the Li Metal Anode Surface. ACS Applied Energy Materials, 2020, 3, 5497-5509.	2.5	24
52981	Fundamental Limit of the Emission Linewidths of Quantum Dots: An Ab Initio Study of CdSe Nanocrystals. ACS Applied Materials & Interfaces, 2020, 12, 22012-22018.	4.0	12
52982	Chemical Trends in the Thermodynamic Stability and Band Gaps of 980 Halide Double Perovskites: A High-Throughput First-Principles Study. ACS Applied Materials & Interfaces, 2020, 12, 20680-20690.	4.0	68
52983	Evidence for Self-healing Benign Grain Boundaries and a Highly Defective Sb₂Se₃â€“CdS Interfacial Layer in Sb₂Se₃ Thin-Film Photovoltaics. ACS Applied Materials & Interfaces, 2020, 12, 21730-21738.	4.0	57
52984	Revealing Sintering Kinetics of MoS₂-Supported Metal Nanocatalysts in Atmospheric Gas Environments via Operando Transmission Electron Microscopy. ACS Nano, 2020, 14, 4074-4086.	7.3	15
52985	Enhanced Electrocatalytic Hydrogen Evolution Activity in Single-Atom Pt-Decorated VS₂ Nanosheets. ACS Nano, 2020, 14, 5600-5608.	7.3	135
52986	Computational insights into the strain effect on the electrocatalytic reduction of CO₂ to CO on Pd surfaces. Physical Chemistry Chemical Physics, 2020, 22, 9600-9606.	1.3	19
52987	Discovery of stable and intrinsic antiferromagnetic iron oxyhalide monolayers. Physical Chemistry Chemical Physics, 2020, 22, 11731-11739.	1.3	32
52988	DFT coupled with NEGF study of the electronic properties and ballistic transport performances of 2D SbSiTe₃. Nanoscale, 2020, 12, 9958-9963.	2.8	11
52989	Hydration structure and water exchange kinetics at xenotimeâ€“water interfaces: implications for rare earth minerals separation. Physical Chemistry Chemical Physics, 2020, 22, 7719-7727.	1.3	10
52990	Stacking order driving bandgap and conductance of graphene/C3B (C3N) van der Waals heterostructures. Applied Physics Letters, 2020, 116, .	1.5	12
52991	Thermoelectric properties of two-dimensional magnet CrI₃. Nanotechnology, 2020, 31, 315713.	1.3	12
52992	Electronic structure and phase transition engineering in NbS2: Crucial role of van der Waals interactions. Chinese Physics B, 2020, 29, 056201.	0.7	16

#	Article	IF	Citations
52993	Evidence of new 2D material: Cu₂Te. 2D Materials, 2020, 7, 035010.	2.0	16
52994	Electric field modulation of magnetism in ferrimagnetic Heusler heterostructures. Physical Review B, 2020, 101, .	1.1	24
52995	Iodine interstitials as a cause of nonradiative recombination in hybrid perovskites. Physical Review B, 2020, 101, .	1.1	76
52996	Effect of Dopant Ordering on the Stability of Ferroelectric Hafnia. Physica Status Solidi - Rapid Research Letters, 2020, 14, 2000047.	1.2	15
52997	Metal-free carbocatalysis for persulfate activation toward nonradical oxidation: Enhanced singlet oxygen generation based on active sites and electronic property. Chemical Engineering Journal, 2020, 396, 125107.	6.6	74
52998	A first-principle study on hydrogen storage of metal atoms (MÂ=ÂLi, Ca, Sc, and Ti) coated B40 fullerene composites. Computational and Theoretical Chemistry, 2020, 1181, 112823.	1.1	19
52999	Infinite dilution in doped ceria and high activation energies. Solid State Communications, 2020, 314-315, 113939.	0.9	2
53000	Thickness dependence of hydrogen-induced phase transition in <mml:math xmlns:mml="http://www.w3.org/1998/Math/MathML"><mml:msub><mml:mi>MoTe</mml:mi><mml:mn>2</mml:mn></mml:msub><m Physical Review B, 2020, 101, .	1.1	13
53001	Spin-Triplet Excitonic Insulator: The Case of Semihydrogenated Graphene. Physical Review Letters, 2020, 124, 166401.	2.9	35
53002	Novel 2D Transitionâ€Metal Carbides: Ultrahigh Performance Electrocatalysts for Overall Water Splitting and Oxygen Reduction. Advanced Functional Materials, 2020, 30, 2000570.	7.8	186
53003	Ultrastable Sodiumâ€“Sulfur Batteries without Polysulfides Formation Using Slit Ultramicropore Carbon Carrier. Advanced Science, 2020, 7, 1903246.	5.6	109
53004	Palgraphyne: A Promising 2D Carbon Dirac Semimetal with Strong Mechanical and Electronic Anisotropy. Physica Status Solidi - Rapid Research Letters, 2020, 14, 2070020.	1.2	4
53005	Highâ€Performance Threeâ€Dimensional Li Anode Scaffold Enabled by Homogeneous Zn Nanoclusters. Small, 2020, 16, e2001257.	5.2	25
53006	Quantum anomalous Hall effect in two-dimensional Cu-dicyanobenzene coloring-triangle lattice. Nano Research, 2020, 13, 1571-1575.	5.8	14
53007	Enhanced carrier mobility in anisotropic two-dimensional tetrahex-carbon through strain engineering. Carbon, 2020, 165, 37-44.	5.4	15
53008	Surface adsorption configurations of H3PO4 modified TiO2 and its influence on the photodegradation intermediates of gaseous o-xylene. Chemical Engineering Journal, 2020, 393, 124723.	6.6	28
53009	Controllable synthesis and evolution mechanism of monodispersed Sub-10â€¯nm ZrO2 nanocrystals. Chemical Engineering Journal, 2020, 394, 124843.	6.6	8
53010	Designing ZIF-8/hydroxylated MWCNT nanocomposites for phosphate adsorption from water: Capability and mechanism. Chemical Engineering Journal, 2020, 394, 124992.	6.6	85

#	Article	IF	Citations
53011	Diffusion behavior of hydrogen in oxygen saturated and unsaturated plutonium dioxide: An ab initio molecular dynamics study. Journal of Alloys and Compounds, 2020, 834, 155113.	2.8	8
53012	Mechanochemically synthesized gypsum and gypsum drywall waste cocrystals with urea for enhanced environmental sustainability fertilizers. Journal of Environmental Chemical Engineering, 2020, 8, 103965.	3.3	13
53013	Surface charging activated mechanism change: A computational study of O, CO, and CO2 interactions on Ag electrodes. Journal of Energy Chemistry, 2020, 50, 307-313.	7.1	8
53014	Ab initio study of He, Ne, Ar, Kr incorporation in zirconium carbide. Journal of Nuclear Materials, 2020, 534, 152154.	1.3	2
53015	A computational study of phase stability, electronic structure, vibrational and semiconducting properties of ScAu-based half-Heusler alloys. Physica B: Condensed Matter, 2020, 588, 412172.	1.3	4
53016	Growth of Millimeter Size B₆O Single Crystals in a B-H₃BO₃ System at High Pressure and High Temperature. Crystal Growth and Design, 2020, 20, 3732-3736.	1.4	2
53017	Interpreting the Operando XANES of Surface-Supported Subnanometer Clusters: When Fluxionality, Oxidation State, and Size Effect Fight. Journal of Physical Chemistry C, 2020, 124, 10057-10066.	1.5	24
53018	Substituent Effects on the Thermal Decomposition of Phosphate Esters on Ferrous Surfaces. Journal of Physical Chemistry C, 2020, 124, 9852-9865.	1.5	24
53019	CeTi2O6â€"A Promising Oxide for Solar Thermochemical Hydrogen Production. ACS Applied Materials & Interfaces, 2020, 12, 21521-21527.	4.0	14
53020	Magnetic Tunability in RE-DOBDC MOFs via NO_x Acid Gas Adsorption. ACS Applied Materials & Interfaces, 2020, 12, 19504-19510.	4.0	39
53021	Experimental and Theoretical Investigation on Phase Formation and Mechanical Properties in Crâ€"Coâ€"Ni Alloys Processed Using a Novel Thin-Film Quenching Technique. ACS Combinatorial Science, 2020, 22, 232-247.	3.8	3
53022	Two-Dimensional Metal Hexahydroxybenzene Frameworks as Promising Electrocatalysts for an Oxygen Reduction Reaction. ACS Sustainable Chemistry and Engineering, 2020, 8, 7472-7479.	3.2	57
53023	Electric Dipole Descriptor for Machine Learning Prediction of Catalyst Surfaceâ€"Molecular Adsorbate Interactions. Journal of the American Chemical Society, 2020, 142, 7737-7743.	6.6	65
53024	Sulfate modified g-C₃N₄ with enhanced photocatalytic activity towards hydrogen evolution: the role of sulfate in photocatalysis. Physical Chemistry Chemical Physics, 2020, 22, 10116-10122.	1.3	13
53025	Organocatalytic vs. Ru-based electrochemical hydrogenation of nitrobenzene in competition with the hydrogen evolution reaction. Dalton Transactions, 2020, 49, 6446-6456.	1.6	17
53026	Tunable electronic and magnetic properties of monolayer and bilayer Janus Cr₂Cl₃I₃: a first-principles study. Materials Advances, 2020, 1, 244-253.	2.6	22
53027	Electronic properties and enhanced photocatalytic performance of van der Waals heterostructures of ZnO and Janus transition metal dichalcogenides. Physical Chemistry Chemical Physics, 2020, 22, 10351-10359.	1.3	53
53028	Energetic N-azidomethyl derivatives of polynitro hexaazaisowurtzitanes series: CL-20 analogues having the highest enthalpy. New Journal of Chemistry, 2020, 44, 8357-8365.	1.4	19

#	Article	IF	Citations
53029	Strain tunable pudding-mold-type band structure and thermoelectric properties of SnP3 monolayer. Journal of Applied Physics, 2020, 127, .	1.1	16
53030	Atomic-scale defects in the two-dimensional ferromagnet CrI₃ from first principles. Journal Physics D: Applied Physics, 2020, 53, 244003.	1.3	26
53031	Six novel carbon and silicon allotropes with their potential application in photovoltaic field. Journal of Physics Condensed Matter, 2020, 32, 355701.	0.7	20
53032	Eradicating negative-Set behavior of TiO₂-based devices by inserting an oxygen vacancy rich zirconium oxide layer for data storage applications. Nanotechnology, 2020, 31, 325201.	1.3	21
53033	Bulk Fermi surface of the layered superconductor <mml:math xmlns:mml="http://www.w3.org/1998/Math/MathML"><mml:mrow><mml:mi>TaS</mml:mi><mml:msub><mml:mi mathvariant="normal">e</mml:mi><mml:mn>3</mml:mn></mml:msub></mml:mrow></mml:math> with three-dimensional strong topological state. Physical Review B, 2020, 101, .	1.1	16
53034	Interactions between a H2 Molecule and Carbon Nanostructures: A DFT Study. Journal of Carbon Research, 2020, 6, 16.	1.4	8
53035	Molecularâ€Level Design of Pyrrhotite Electrocatalyst Decorated Hierarchical Porous Carbon Spheres as Nanoreactors for Lithiumâ€“Sulfur Batteries. Advanced Energy Materials, 2020, 10, 2000651.	10.2	101
53036	Precursor Engineering for Ambientâ€Compatible Antisolventâ€Free Fabrication of Highâ€Efficiency CsPbI₂Br Perovskite Solar Cells. Advanced Energy Materials, 2020, 10, 2000691.	10.2	106
53037	Dualâ€function catalysis in propane dehydrogenation over <scp>Pt₁â€“Ga₂O₃</scp> catalyst: Insights from a microkinetic analysis. AIChE Journal, 2020, 66, e16232.	1.8	27
53038	Fluorideâ€Based Anion Doping: A New Strategy for Improving the Performance of Protonic Ceramic Conductors of the Form BaZrO₃. ChemElectroChem, 2020, 7, 2242-2247.	1.7	11
53039	Twoâ€Dimensional Layered Metallic VSe₂/SWCNTs/rGO Based Ternary Hybrid Materials for High Performance Energy Storage Applications. Chemistry - A European Journal, 2020, 26, 6662-6669.	1.7	43
53040	Changing the Electronic and Magnetic Properties of Monolayer HfS 2 by Doping and Vacancy Defects: Insight from Firstâ€Principles Calculations. Physica Status Solidi (B): Basic Research, 2020, 257, 1900768.	0.7	7
53041	Unconventional high temperature superconductivity in cubic zinc-blende transition metal compounds. Science China: Physics, Mechanics and Astronomy, 2020, 63, 1.	2.0	7
53042	Highly sensitive tuning of lattice thermal conductivity of graphene-like borophene by fluorination and chlorination. Nano Research, 2020, 13, 1171-1177.	5.8	10
53043	Data-driven acceleration of first-principles saddle point and local minimum search based on scalable Gaussian processes. , 2020, , 119-168.		0
53044	Understanding the interactions between interstitial and substitutional solutes in refractory alloys: The case of Ti-Al-O. Acta Materialia, 2020, 191, 149-157.	3.8	16
53045	Metallic Ni3Mo3N Porous Microrods with Abundant Catalytic Sites as Efficient Electrocatalyst for Large Current Density and Superstability of Hydrogen Evolution Reaction and Water Splitting. Applied Catalysis B: Environmental, 2020, 272, 118956.	10.8	138
53046	Synergistic coupling of NiTe nanoarrays with RuO2 and NiFe-LDH layers for high-efficiency electrochemical-/photovoltage-driven overall water splitting. Applied Catalysis B: Environmental, 2020, 272, 118988.	10.8	101

#	Article	IF	Citations
53047	Intrinsic-strain-induced curling of free-standing two-dimensional Janus MoSSe quantum dots. Applied Surface Science, 2020, 519, 146251.	3.1	10
53048	DFT-D study of single water adsorption on low-index surfaces of calcium silicate phases in cement. Applied Surface Science, 2020, 518, 146255.	3.1	34
53049	Structural transformation induced enhanced multiferroicity in Al3+ and Ti4+ co-doped LaFeO3. Advanced Powder Technology, 2020, 31, 2469-2479.	2.0	11
53050	Theoretical prediction of eliminating the buffer layer and achieving charge neutrality for epitaxial graphene on 6Hâ€“SiC(0001) via boron compound intercalations. Carbon, 2020, 161, 323-330.	5.4	3
53051	First-principles study on the adsorption and diffusion properties of non-noble (Fe, Co, Ni and Cu) and noble (Ru, Rh, Pt and Pd) metal single atom on graphyne. Chemical Physics, 2020, 536, 110783.	0.9	12
53052	Phase transition, elasticity, phonon spectra, and superconductive properties of equiatomic TiZr, TiHf, and ZrHf alloys at high pressure: Ab initio calculations. Computational Materials Science, 2020, 178, 109637.	1.4	3
53053	Ab initio phase diagram of WSe based on crystal structure prediction. Computational Materials Science, 2020, 181, 109732.	1.4	3
53054	The H2S dimer revisited â€“ Insights from wave-function and density functional theory methods. Ab initio molecular dynamics simulations of liquid H2S. Computational and Theoretical Chemistry, 2020, 1180, 112821.	1.1	3
53055	On Distribution of Superconductivity in Metal Hydrides. Current Opinion in Solid State and Materials Science, 2020, 24, 100808.	5.6	104
53056	Two-dimensional van der Waals heterostructure of indium selenide/hexagonal boron nitride with strong interlayer coupling. Chemical Physics Letters, 2020, 749, 137430.	1.2	8
53057	Theoretical study on the effect of Mn promoter for CO2 reforming of CH4 on the Ni(1Â1Â1) surface. Fuel, 2020, 274, 117849.	3.4	8
53058	Understanding the cyan-emitting phosphor RbNa(Li3SiO4)2: Eu2+ by providing Rb ion vacancies. Journal of Alloys and Compounds, 2020, 837, 155084.	2.8	17
53059	Replacement of Pd nanoparticles: Hydrogenation promoted by frustrated Lewis acid-base pairs in carbon quantum dots. Journal of Catalysis, 2020, 383, 304-310.	3.1	20
53060	In situ spectroscopic and theoretical investigation of methane activation on IrO2 nanoparticles: Role of Ir oxidation state on C-H activation. Journal of Catalysis, 2020, 385, 265-273.	3.1	27
53061	Imprinting isolated single iron atoms onto mesoporous silica by templating with metallosurfactants. Journal of Colloid and Interface Science, 2020, 573, 193-203.	5.0	17
53062	Fluorination over Cr doped layered perovskite Sr2TiO4 for efficient photocatalytic hydrogen production under visible light illumination. Journal of Energy Chemistry, 2020, 51, 30-38.	7.1	14
53063	Porous LaFeO3 nanofiber with oxygen vacancies as an efficient electrocatalyst for N2 conversion to NH3 under ambient conditions. Journal of Energy Chemistry, 2020, 50, 402-408.	7.1	87
53064	High infrared emissivity of SiC-AlN ceramics at room temperature. Journal of the European Ceramic Society, 2020, 40, 3528-3534.	2.8	13

#	Article	IF	Citations
53065	Electronic and optical properties of layered Ruddlesden Popper hybrid X2(MA)n-1SnnI3n+1 perovskite insight by first principles. Journal of Physics and Chemistry of Solids, 2020, 144, 109510.	1.9	3
53066	Feasibility of band gap engineering of iron pyrite (FeS2) by codoping Os, Ru or Zn together with O. Materials Chemistry and Physics, 2020, 244, 122742.	2.0	9
53067	First-principles study of two-dimensional zirconium nitrogen compounds: Anode materials for Na-ion batteries. Materials Chemistry and Physics, 2020, 250, 123028.	2.0	13
53068	Direct antimony recovery from wastewater as anode materials for sodium-ion batteries. Materials Today Energy, 2020, 16, 100403.	2.5	7
53069	Promoting electrocatalytic methanol oxidation of platinum nanoparticles by cerium modification. Nano Energy, 2020, 73, 104784.	8.2	54
53070	Ultralow thermal conductivity and negative thermal expansion of CuSCN. Nano Energy, 2020, 73, 104822.	8.2	25
53071	Realizing high thermoelectric performance in eco-friendly SnTe via synergistic resonance levels, band convergence and endotaxial nanostructuring with Cu2Te. Nano Energy, 2020, 73, 104832.	8.2	81
53072	Thermoelastic properties of MgSiO3-majorite at high temperatures and pressures: A first principles study. Physics of the Earth and Planetary Interiors, 2020, 303, 106491.	0.7	1
53073	The magnetism driven by vacancies in Fe-doped 6H-SiC: A first-principles calculation. Physica B: Condensed Matter, 2020, 587, 412109.	1.3	0
53074	First-principles comprehensive study of electronic and mechanical properties of novel uranium hydrides at different pressures. Progress in Natural Science: Materials International, 2020, 30, 251-259.	1.8	8
53075	Unveiling in situ evolved In/In2O3â˜' heterostructure as the active phase of In2O3 toward efficient electroreduction of CO2 to formate. Science Bulletin, 2020, 65, 1547-1554.	4.3	105
53076	Is the alumino-boron carbide Al3BC a promising thermoelectric material? A computational exploration. Solid State Sciences, 2020, 104, 106205.	1.5	2
53077	The electronic structure and the oxygen adsorption at BaO terminated surface of GdBaCo2O5.5: A first principles study. Solid State Communications, 2020, 311, 113871.	0.9	2
53078	Theoretical investigation of structural and mechanical stability of Mo2N. Solid State Communications, 2020, 314-315, 113919.	0.9	4
53079	Mechanical and electronic properties of graphitic carbon nitride (g-C3N4) under biaxial strain. Vacuum, 2020, 176, 109358.	1.6	15
53080	A Biphasic Interphase Design Enabling High Performance in Room Temperature Sodium-Sulfur Batteries. Cell Reports Physical Science, 2020, 1, 100044.	2.8	47
53081	Theoretical Study on the Intrinsic Source of the Large Thermal Conductivity of Li-Based Chalcogenide Nonlinear Optical Crystals: From AgGaS₂ to LiGaS₂. Crystal Growth and Design, 2020, 20, 4150-4156.	1.4	9
53082	Enhanced Catalytic Activity and Stability of the Oxygen Evolution Reaction on Tetravalent Mixed Metal Oxide. Chemistry of Materials, 2020, 32, 3893-3903.	3.2	36

#	Article	IF	Citations
53083	Stabilizing Na₃Zr₂Si₂PO₁₂/Na Interfacial Performance by Introducing a Clean and Na-Deficient Surface. Chemistry of Materials, 2020, 32, 3970-3979.	3.2	72
53084	Discovery of Sodium-Doped Triphenylene Superconductors by Searching the Organic Material Database. Chemistry of Materials, 2020, 32, 3358-3364.	3.2	7
53085	Copper(I) Promotes Silver Sulfide Dissolution and Increases Silver Phytoavailability. Environmental Science & Technology, 2020, 54, 5589-5597.	4.6	9
53086	Precise Characterization of the Rich Structural Landscape Induced by Pressure in Multifunctional FeVO₄. Inorganic Chemistry, 2020, 59, 6623-6630.	1.9	19
53087	Magnetism-Vanishing Stabilizes the Pyrite-Type 3d Transition Metal Peroxides at High Pressures. Journal of Physical Chemistry C, 2020, 124, 10085-10093.	1.5	1
53088	FeRh and Nitrogen Codoped Graphene, a Highly Efficient Bifunctional Catalyst toward Oxygen Reduction and Oxygen Evolution Reactions. Journal of Physical Chemistry C, 2020, 124, 9142-9150.	1.5	8
53089	Built-In Electric Field Hindering Photogenerated Carrier Recombination in Polar Bilayer SnO/BiOX (X =) Tj ETQq0 0 0 rgBT /Overlock 10 Tf	1.5	22
53090	Substituent Effects on Electronic Structures and Peroxidase-Mimicking Activities of Graphyne and Palladium-Doped Graphyne: A Computational Study. Journal of Physical Chemistry C, 2020, 124, 9917-9923.	1.5	10
53091	Properties of Î±-Brass Nanoparticles. 1. Neural Network Potential Energy Surface. Journal of Physical Chemistry C, 2020, 124, 12682-12695.	1.5	27
53092	Optimization of Anticorrosive Zinc Coatings: Tuning the Adhesion of Zinc/Silica Contact by Interfacial Ternary Oxide Formation. Journal of Physical Chemistry C, 2020, 124, 9337-9344.	1.5	2
53093	Modulating the MoS₂ Edge Structures by Doping Transition Metals for Electrocatalytic CO₂ Reduction. Journal of Physical Chemistry C, 2020, 124, 10523-10529.	1.5	38
53094	Optimization of Work Function via Bayesian Machine Learning Combined with First-Principles Calculation. Journal of Physical Chemistry C, 2020, 124, 9958-9970.	1.5	27
53095	Bifunctional HER/OER or OER/ORR Catalytic Activity of Two-Dimensional TM₃(HITP)₂ with TM = Feâ€“Zn. Journal of Physical Chemistry C, 2020, 124, 9350-9359.	1.5	67
53096	Pathway-Switching Mechanism for Water-Catalyzed Ethanol Decomposition on Cu(111). Journal of Physical Chemistry C, 2020, 124, 9385-9393.	1.5	6
53097	Experimental and DFT Investigation into Chloride Poisoning Effects on Nitrogen-Coordinated Ironâ€“Carbon (FeNC) Catalysts for Oxygen Reduction Reaction. Journal of Physical Chemistry C, 2020, 124, 10324-10335.	1.5	23
53098	Computational Screening of 2D Ordered Double Transition-Metal Carbides (MXenes) as Electrocatalysts for Hydrogen Evolution Reaction. Journal of Physical Chemistry C, 2020, 124, 10584-10592.	1.5	62
53099	Local Coordination Environments and Vibrational Dynamics of Protons in Hexagonal and Cubic Sc-Doped BaTiO₃ Proton-Conducting Oxides. Journal of Physical Chemistry C, 2020, 124, 8643-8651.	1.5	6
53100	Two-Dimensional Black Phosphorus Carbide: Rippling and Formation of Nanotubes. Journal of Physical Chemistry C, 2020, 124, 10235-10243.	1.5	32

#	Article	IF	Citations
53101	Magnetic Dioxygen Clathrate Hydrates: A Type of Promising Building Blocks for Icy Crystalline Materials. Journal of Physical Chemistry C, 2020, 124, 10669-10678.	1.5	4
53102	Nanoscale Interfaces of Janus Monolayers of Transition Metal Dichalcogenides for 2D Photovoltaic and Piezoelectric Applications. Journal of Physical Chemistry C, 2020, 124, 10385-10397.	1.5	94
53103	Pressure-Induced Enhancement of Optical Properties in Indium Oxide Nanowires. Journal of Physical Chemistry C, 2020, 124, 10244-10251.	1.5	1
53104	Occupied Electronic States of Li in Li, Li₂O₂, and Li₂O Analyzed by Soft X-ray Emission Spectroscopy. Journal of Physical Chemistry C, 2020, 124, 9256-9260.	1.5	4
53105	Combined Impact of Denticity and Orientation on Molecular-Scale Charge Transport. Journal of Physical Chemistry C, 2020, 124, 9460-9469.	1.5	4
53106	Size and Stoichiometry Effect of FePt Bimetal Nanoparticle Catalyst for CO Oxidation: A DFT Study. Journal of Physical Chemistry C, 2020, 124, 8706-8715.	1.5	18
53107	Tailoring the Dimension of Halide Perovskites Enables Quantum Wires with Enhanced Visible Light Absorption. Journal of Physical Chemistry C, 2020, 124, 11124-11131.	1.5	1
53108	Local Carbon Concentration Determines the Graphene Edge Structure. Journal of Physical Chemistry Letters, 2020, 11, 3451-3457.	2.1	16
53109	Descriptor-Based Design Principle for Two-Dimensional Single-Atom Catalysts: Carbon Dioxide Electroreduction. Journal of Physical Chemistry Letters, 2020, 11, 3481-3487.	2.1	65
53110	Penta-BCN: A New Ternary Pentagonal Monolayer with Intrinsic Piezoelectricity. Journal of Physical Chemistry Letters, 2020, 11, 3501-3506.	2.1	80
53111	Electronic States and Magnetic Response of MnBi₂Te₄ by Scanning Tunneling Microscopy and Spectroscopy. Nano Letters, 2020, 20, 3271-3277.	4.5	71
53112	Strong Interface Enhanced Hydrogen Evolution over Molybdenum-Based Catalysts. ACS Applied Energy Materials, 2020, 3, 5219-5228.	2.5	16
53113	Predicting Device Parameters for Dye-Sensitized Solar Cells from Electronic Structure Calculations to Reproduce Experiment. ACS Applied Energy Materials, 2020, 3, 4367-4376.	2.5	6
53114	Interfacial Reactions between Ga and Cu-10Ni Substrate at Low Temperature. ACS Applied Materials & Interfaces, 2020, 12, 21045-21056.	4.0	19
53115	Synthesis and Mechanical Characterization of a CuMoTaWV High-Entropy Film by Magnetron Sputtering. ACS Applied Materials & Interfaces, 2020, 12, 21070-21079.	4.0	62
53116	Improved Figure of Merit of Cu₂SnSe₃ via Band Structure Modification and Energy-Dependent Carrier Scattering. ACS Applied Materials & Interfaces, 2020, 12, 19693-19700.	4.0	27
53117	A Study of Eu Doping in Nanolayers of CsPbBr₃ using Ab Initio Calculations to Understand fâ€“f Transitions in Eu³⁺-Doped Nanocrystals for Light-Emitting Diodes. ACS Applied Nano Materials, 2020, 3, 4437-4444.	2.4	9
53118	Involvement of the Unoccupied Site Changes the Kinetic Trend Significantly: A Case Study on Formic Acid Decomposition. ACS Catalysis, 2020, 10, 5153-5162.	5.5	14

#	Article	IF	Citations
53119	A Complete Multisite Reaction Mechanism for Low-Temperature NH₃-SCR over Cu-CHA. ACS Catalysis, 2020, 10, 5646-5656.	5.5	118
53120	Impact of Metal and Heteroatom Identities in the Hydrogenolysis of Câ€“X Bonds (X = C, N, O, S, and Cl). ACS Catalysis, 2020, 10, 5086-5100.	5.5	21
53121	Performance of Metal-Catalyzed Hydrodebromination of Dibromomethane Analyzed by Descriptors Derived from Statistical Learning. ACS Catalysis, 2020, 10, 6129-6143.	5.5	23
53122	Au/Pb Interface Allows the Methane Formation Pathway in Carbon Dioxide Electroreduction. ACS Catalysis, 2020, 10, 5681-5690.	5.5	37
53123	Adsorption Energies of Oxygenated Aromatics and Organics on Rhodium and Platinum in Aqueous Phase. ACS Catalysis, 2020, 10, 4929-4941.	5.5	37
53124	Structural Rearrangements of Subnanometer Cu Oxide Clusters Govern Catalytic Oxidation. ACS Catalysis, 2020, 10, 5309-5317.	5.5	36
53125	Gas-Phase Carbonylation of Dimethyl Ether on the Stable Seed-Derived Ferrierite. ACS Catalysis, 2020, 10, 5135-5146.	5.5	35
53126	DNA-Guided Room-Temperature Synthesis of Single-Crystalline Gold Nanostructures on Graphdiyne Substrates. ACS Central Science, 2020, 6, 779-786.	5.3	15
53127	Stacking Effects on Electronâ€“Phonon Coupling in Layered Hybrid Perovskites via Microstrain Manipulation. ACS Nano, 2020, 14, 5806-5817.	7.3	50
53128	Scanning MoirÃ© Fringe Method: A Superior Approach to Perceive Defects, Interfaces, and Distortion in 2D Materials. ACS Nano, 2020, 14, 6034-6042.	7.3	13
53129	Molecular Approach for Engineering Interfacial Interactions in Magnetic/Topological Insulator Heterostructures. ACS Nano, 2020, 14, 6285-6294.	7.3	9
53130	Agglomeration Suppression of a Fe-Supported Catalyst and its Utilization for Low-Temperature Ammonia Synthesis in an Electric Field. ACS Omega, 2020, 5, 6846-6851.	1.6	21
53131	Selective Oxidation of Propylene on Cu₂O(111) and Cu₂O(110) Surfaces: A Systematically DFT Study. ACS Omega, 2020, 5, 6260-6269.	1.6	18
53132	Metal-Free Thiophene-Sulfur Covalent Organic Frameworks: Precise and Controllable Synthesis of Catalytic Active Sites for Oxygen Reduction. Journal of the American Chemical Society, 2020, 142, 8104-8108.	6.6	226
53133	Manipulating dehydrogenation kinetics through dual-doping Co3N electrode enables highly efficient hydrazine oxidation assisting self-powered H2 production. Nature Communications, 2020, 11, 1853.	5.8	229
53134	Self-sustainable protonic ceramic electrochemical cells using a triple conducting electrode for hydrogen and power production. Nature Communications, 2020, 11, 1907.	5.8	227
53135	Doping-free complementary WSe2 circuit via van der Waals metal integration. Nature Communications, 2020, 11, 1866.	5.8	153
53136	CO oxidation activity of non-reducible oxide-supported mass-selected few-atom Pt single-clusters. Nature Communications, 2020, 11, 1888.	5.8	76

#	Article	IF	Citations
53137	Dynamic electrocatalyst with current-driven oxyhydroxide shell for rechargeable zinc-air battery. Nature Communications, 2020, 11, 1952.	5.8	185
53138	Hydrogen-accelerated spontaneous microcracking in high-strength aluminium alloys. Scientific Reports, 2020, 10, 1998.	1.6	38
53139	Chemical manipulation of hydrogen induced high p-type and n-type conductivity in Ga2O3. Scientific Reports, 2020, 10, 6134.	1.6	65
53140	Anisotropic hydrogen bond structures and orientation dependence of shock sensitivity in crystalline 1,3,5-tri-amino-2,4,6-tri-nitrobenzene (TATB). Physical Chemistry Chemical Physics, 2020, 22, 11956-11966.	1.3	15
53141	Thermodynamical stability of substoichiometric plutonium monocarbide from first-principles calculations. Physical Chemistry Chemical Physics, 2020, 22, 9009-9013.	1.3	6
53142	Ni₁₂P₅ nanoparticles bound on graphene sheets for advanced lithiumâ€“sulfur batteries. Nanoscale, 2020, 12, 10760-10770.	2.8	40
53143	Unraveling the effects of linker substitution on structural, electronic and optical properties of amorphous zeolitic imidazolate frameworks-62 (a-ZIF-62) glasses: a DFT study. RSC Advances, 2020, 10, 14013-14024.	1.7	10
53144	Ultrafine carbon encapsulated NiRu alloys as bifunctional electrocatalysts for boosting overall water splitting: morphological and electronic modulation through minor Ru alloying. Journal of Materials Chemistry A, 2020, 8, 9049-9057.	5.2	48
53145	Origin of short- and medium-range order in supercooled liquid Ge₃Sb₂Te₆ using ab initio molecular dynamics simulations. Physical Chemistry Chemical Physics, 2020, 22, 9759-9766.	1.3	4
53146	A tetragonal phase Mn₂B₂ sheet: a stable room temperature ferromagnet with sizable magnetic anisotropy. Physical Chemistry Chemical Physics, 2020, 22, 10893-10899.	1.3	28
53147	N-Promoted Ru₁/TiO₂ single-atom catalysts for photocatalytic water splitting for hydrogen production: a density functional theory study. Physical Chemistry Chemical Physics, 2020, 22, 11392-11399.	1.3	28
53148	Spin-dependent Schottky barriers and vacancy-induced spin-selective ohmic contacts in magnetic vdW heterostructures. Physical Chemistry Chemical Physics, 2020, 22, 9460-9466.	1.3	14
53149	Functionalization of two-dimensional 1Tâ€²-ReS₂ with surface ligands for use as a photocatalyst in the hydrogen evolution reaction: a first-principles calculation study. Physical Chemistry Chemical Physics, 2020, 22, 9415-9423.	1.3	8
53150	Designing an active Ta₃N₅ photocatalyst for H₂ and O₂ evolution reactions by specific exposed facet engineering: a first-principles study. Physical Chemistry Chemical Physics, 2020, 22, 10295-10304.	1.3	10
53151	A 2D Rashba electron gas with large spin splitting in Janus structures of SnPbO₂. Physical Chemistry Chemical Physics, 2020, 22, 11409-11416.	1.3	7
53152	Impact of edge structures on interfacial interactions and efficient visible-light photocatalytic activity of metalâ€“semiconductor hybrid 2D materials. Catalysis Science and Technology, 2020, 10, 3279-3289.	2.1	37
53153	CO activation and methanation mechanism on hexagonal close-packed Co catalysts: effect of functionals, carbon deposition and surface structure. Catalysis Science and Technology, 2020, 10, 3387-3398.	2.1	5
53154	CO, NO, and SO adsorption on Ni nanoclusters: a DFT investigation. Dalton Transactions, 2020, 49, 6407-6417.	1.6	27

#	Article	IF	Citations
53155	Structure, stability and electronic properties of one-dimensional tetrathia- and tetraselena[8]circulene-based materials: a comparative DFT study. New Journal of Chemistry, 2020, 44, 6872-6882.	1.4	5
53156	Tuning the electronic structure of transition metals embedded in nitrogen-doped graphene for electrocatalytic nitrogen reduction: a first-principles study. Nanoscale, 2020, 12, 9696-9707.	2.8	50
53157	Thermodynamic stability, phase separation and Ag grading in (Ag,Cu)(In,Ga)Se₂ solar absorbers. Journal of Materials Chemistry A, 2020, 8, 8740-8751.	5.2	29
53158	Identifying Raman modes of Sb₂Se₃ and their symmetries using angle-resolved polarised Raman spectra. Journal of Materials Chemistry A, 2020, 8, 8337-8344.	5.2	62
53159	Long-lifespan lithiumâ€“metal batteries obtained using a perovskite intercalation layer to stabilize the lithium electrode. Journal of Materials Chemistry A, 2020, 8, 9137-9145.	5.2	4
53160	Monolayer Bi₂Se_{3âˆ'x}Te_x: novel two-dimensional semiconductors with excellent stability and high electron mobility. Physical Chemistry Chemical Physics, 2020, 22, 9685-9692.	1.3	11
53161	Origin of CO₂ as the main carbon source in syngas-to-methanol process over Cu: theoretical evidence from a combined DFT and microkinetic modeling study. Catalysis Science and Technology, 2020, 10, 3346-3352.	2.1	16
53162	Bondingâ€“antibonding state transition induces multiple electron modulations toward oxygen reduction reaction electrocatalysis. New Journal of Chemistry, 2020, 44, 8191-8197.	1.4	6
53163	Confinement of single polyoxometalate clusters in molecular-scale cages for improved flexible solid-state supercapacitors. Nanoscale, 2020, 12, 11887-11898.	2.8	31
53164	Theoretical and experimental investigations on the bulk photovoltaic effect in lead-free perovskites MASnI₃ and FASnI₃. RSC Advances, 2020, 10, 14679-14688.	1.7	60
53165	Plasma-induced on-surface sulfur vacancies in NiCo₂S₄ enhance the energy storage performance of supercapatteries. Journal of Materials Chemistry A, 2020, 8, 9278-9291.	5.2	73
53166	Exploring the landscape of Buckingham potentials for silica by machine learning: Soft vs hard interatomic forcefields. Journal of Chemical Physics, 2020, 152, 051101.	1.2	14
53167	Shape-controlling effects of hydrohalic and carboxylic acids in TiO2 nanoparticle synthesis. Journal of Chemical Physics, 2020, 152, 064702.	1.2	8
53168	Possible monoclinic distortion of Mo2GaC under high pressure. Journal of Applied Physics, 2020, 127, 145103.	1.1	2
53169	Structural coupling and magnetic tuning in Mn2âˆ'xCoxP magnetocalorics for thermomagnetic power generation. APL Materials, 2020, 8, .	2.2	8
53170	Corrosion inhibition and adsorption properties of cerium-amino acid complexes on mild steel in acidic media: Experimental and DFT studies. Journal of Adhesion Science and Technology, 2020, 34, 2047-2074.	1.4	18
53171	Strain-tunable electronic, elastic, and optical properties of CaI₂monolayer: first-principles study. Philosophical Magazine, 2020, 100, 1982-2000.	0.7	8
53172	Kohn anomaly and van Hove singularity in IV^B and V^B group transition metals nitrides and carbides. Journal of Physics Condensed Matter, 2020, 32, 075401.	0.7	0

#	Article	IF	Citations
53173	Investigation of superconducting gap structure in HfIrSi using muon spin relaxation/rotation. Journal of Physics Condensed Matter, 2020, 32, 085601.	0.7	12
53174	Semi-classical electronic transport properties of ternary compound AlGaAs2: role of different scattering mechanisms. Journal of Physics Condensed Matter, 2020, 32, 135704.	0.7	2
53175	Effects of oxygen variation on the improved structural stability, electronic and optical properties of ZnTeO compounds. Journal of Physics Condensed Matter, 2020, 32, 225701.	0.7	3
53176	Thermally stimulated relaxation and behaviors of oxygen vacancies in SrTiO₃ single crystals with (100), (110) and (111) orientations. Materials Research Express, 2020, 7, 046305.	0.8	3
53177	Strain engineering of the electronic and thermoelectric properties of titanium trisulphide monolayers. Nano Express, 2020, 1, 010026.	1.2	6
53178	In-Plane Dual-Gated Spin-Valve Device Based on the Zigzag Graphene Nanoribbon. Physical Review Applied, 2020, 13, .	1.5	22
53179	High-temperature superconductivity in the Ti-H system at high pressures. Physical Review B, 2020, 101, .	1.1	15
53180	Prediction of <mml:math xmlns:mml="http://www.w3.org/1998/Math/MathML"><mml:mrow><mml:mi mathvariant="normal">F</mml:mi><mml:msub><mml:mi mathvariant="normal">e</mml:mi><mml:mn>2</mml:mn></mml:msub><mml:mi mathvariant="normal">P</mml:mi></mml:mrow></mml:math> -type <mml:math xmlns:mml="http://www.w3.org/1998/Math/MathML"><mml:mrow><mml:mi>TiT</mml:mi><mml:msub><mml:mi mathvariant="normal">e</mml:mi><mml:mn>2</mml:mn></mml:msub></mml:mrow></mml:math> under	1.1	9
53181	High-temperature ferromagnetic semiconductors: Janus monolayer vanadium trihalides. Physical Review B, 2020, 101, .	1.1	45
53182	Multiple magnetic transitions and electrical transport transformation of a <mml:math xmlns:mml="http://www.w3.org/1998/Math/MathML"><mml:mrow><mml:mi>BaFe</mml:mi><mml:msub><mml:mi mathvariant="normal">O</mml:mi><mml:mn>3</mml:mn></mml:msub></mml:mrow></mml:math> cubic perovskite single crystal. Physical Review B, 2020, 101, .	1.1	7
53183	Longitudinal spin relaxation model applied to point-defect qubit systems. Physical Review B, 2020, 101, .	1.1	17
53184	Stability, magnetic order, and electronic properties of ultrathin <mml:math xmlns:mml="http://www.w3.org/1998/Math/MathML"><mml:mrow><mml:msub><mml:mi>Fe</mml:mi><mml:mn>3</mml:mn></mml:msub><mml:msub><mml:mi mathvariant="normal">O</mml:mi><mml:mn>4</mml:mn></mml:msub></mml:mrow></mml:math> nanosheets. Physical Review B, 2020, 101, .	1.1	3
53185	Theoretical prediction of low-energy Stone-Wales graphene with an intrinsic type-III Dirac cone. Physical Review B, 2020, 101, .	1.1	53
53186	Gapless Dirac surface states in the antiferromagnetic topological insulator <mml:math xmlns:mml="http://www.w3.org/1998/Math/MathML"><mml:mrow><mml:msub><mml:mi>MnBi</mml:mi><mml:mn>2</mml:mn></mml:msub></mml:mrow></mml:math> Physical Review B, 2020, 101, .	1.1	134
53187	Metal-chalcogen bond-length induced electronic phase transition from semiconductor to topological semimetal in <mml:math xmlns:mml="http://www.w3.org/1998/Math/MathML"><mml:mi>Zr</mml:mi><mml:msub><mml:mi>X</mml:mi><mml:mn>2</mml:mn></mml:msub></mml:mrow></mml:math> (<mml:math) Tj ETQq0 0 0 rgBT /Overlock 10 Tf 50 172 Td (xmlns:mml="http://www.w3.org/1998/Math/MathML"><mml:mi>X</mml:mi>	1.1	31
53188	Realistic dimension-independent approach for charged-defect calculations in semiconductors. Physical Review B, 2020, 101, .	1.1	30
53189	Spin-lattice Coupling and the Emergence of the Trimerized Phase in the <mml:math xmlns:mml="http://www.w3.org/1998/Math/MathML" display="inline"><mml:mi>S</mml:mi><mml:mo>=</mml:mo><mml:mn>1</mml:mn></mml:math> Kagome Antiferromagnet <mml:math xmlns:mml="http://www.w3.org/1998/Math/MathML" display="inline"><mml:mrow><mml:msub><mml:mrow><mml:mi>Na</mml:mi></mml:mrow><mml:mrow><mml:mn>2</mml:mn></mml:mrow> Physical Review Letters, 2020, 124, 167203.	2.9	13
53190	Plastic and Superionic Helium Ammonia Compounds under High Pressure and High Temperature. Physical Review X, 2020, 10, .	2.8	28

#	Article	IF	Citations
53191	Reversible spin storage in metal oxideâ€"fullerene heterojunctions. Science Advances, 2020, 6, eaax1085.	4.7	10
53192	Phase Transformations in Ni(Co)â€"Mn(Cr,C)â€"(In,Sn) Alloys: An Ab Initio Study. Physics of Metals and Metallography, 2020, 121, 202-209.	0.3	4
53193	Structural and electronic transitions of crystalline 2,2â€²-iminobis (acetamide oxime) induced by different pressure. International Journal of Modern Physics C, 2020, 31, 2050025.	0.8	6
53194	Monolayer Honeycomb Borophene: A Promising Anode Material with a Record Capacity for Lithium-Ion and Sodium-Ion Batteries. Journal of the Electrochemical Society, 2020, 167, 090527.	1.3	28
53195	Functionalization of single-layer TaS₂ and formation of ultrathin Janus structures. Journal of Materials Research, 2020, 35, 1397-1406.	1.2	4
53196	Experimental and Computational Studies on Superhard Material Rhenium Diboride under Ultrahigh Pressures. Materials, 2020, 13, 1657.	1.3	15
53197	Stability and Solid Solutions of Hydrous Alumino-Silicates in the Earthâ€™s Mantle. Minerals (Basel,) Tj ETQq0 0 0 rgBT /Overlock 10 Tf 5	0.8	4
53198	The Effect of Vacancies on Grain Boundary Segregation in Ferromagnetic fcc Ni. Nanomaterials, 2020, 10, 691.	1.9	6
53199	Firstâ€Principles Study on the Molecular Mechanism of Solarâ€Driven CO₂ Reduction on Hâ€Terminated Si. ChemSusChem, 2020, 13, 3524-3529.	3.6	3
53200	Converse flexoelectricity around ferroelectric domain walls. Acta Materialia, 2020, 191, 158-165.	3.8	16
53201	Assembled 3D MOF on 2D Nanosheets for Self-boosting Catalytic Synthesis of N-doped Carbon Nanotube Encapsulated Metallic Co Electrocatalysts for Overall Water Splitting. Applied Catalysis B: Environmental, 2020, 271, 118939.	10.8	136
53202	Growth and optical properties of a stoichiometric laser crystal Pr(BO2)3. Journal of Luminescence, 2020, 225, 117288.	1.5	5
53203	Optimizing Band Gap of Inorganic Halide Perovskites by Donorâ€"Acceptor Pair Codoping. Inorganic Chemistry, 2020, 59, 6053-6059.	1.9	8
53204	Quantitative Analysis of Cation Selectivity of the Electrodes in Multi-ion Electrolytes Based on 2H-Phase MoS2. Journal of Physical Chemistry C, 2020, 124, 9665-9672.	1.5	3
53205	Molecular Recognition and Band Alignment in 3D Covalent Organic Frameworks for Cocrystalline Organic Photovoltaics. Journal of Physical Chemistry C, 2020, 124, 9126-9133.	1.5	14
53206	Rational Design of Phenothiazine-Based Organic Dyes for Dye-Sensitized Solar Cells: The Influence of Ï€-Spacers and Intermolecular Aggregation on Their Photovoltaic Performances. Journal of Physical Chemistry C, 2020, 124, 9233-9242.	1.5	50
53207	Yttriumâ€"Sodium Halides as Promising Solid-State Electrolytes with High Ionic Conductivity and Stability for Na-Ion Batteries. Journal of Physical Chemistry Letters, 2020, 11, 3376-3383.	2.1	43
53208	Electric Field-Modulated Magnetic Phase Transition in van der Waals CrI₃ Bilayers. Journal of Physical Chemistry Letters, 2020, 11, 3152-3158.	2.1	41

#	Article	IF	Citations
53209	Positive Effects of H₂O on the Hydrogen Oxidation Reaction on Sr₂Fe_{1.5}Mo_{0.5}O_{6â^'Î´}-Based Perovskite Anodes for Solid Oxide Fuel Cells. ACS Catalysis, 2020, 10, 5567-5578.	5.5	20
53210	Enhancing catalytic performance of dilute metal alloy nanomaterials. Communications Chemistry, 2020, 3, .	2.0	41
53211	Atomic and electronic structure of solids of Ge₂Br₂PN, Ge₂I₂PN, Sn₂Cl₂PN, Sn₂Br₂PN and Sn₂I₂PN inorganic double helices: a first principles study. RSC Advances, 2020, 10, 14714-14719.	1.7	4
53212	Rational design of an efficient descriptor for single-atom catalysts in the hydrogen evolution reaction. Journal of Materials Chemistry A, 2020, 8, 9202-9208.	5.2	41
53213	Charge localization control of electronâ€“hole recombination in multilayer two-dimensional Dionâ€“Jacobson hybrid perovskites. Journal of Materials Chemistry A, 2020, 8, 9168-9176.	5.2	38
53214	Sensing the polar molecules MH3 (M = N, P, or As) with a Janus NbTeSe monolayer. New Journal of Chemistry, 2020, 44, 7932-7940.	1.4	20
53215	On glyphosateâ€“kaolinite surface interactions. A molecular dynamic study. European Journal of Soil Science, 2021, 72, 1231-1242.	1.8	11
53216	Probing the Geometric and Electronic Effects of Aluminumâ€“Magnesium Clusters on Reactivity Toward Oxygen. Journal of Cluster Science, 2021, 32, 445-460.	1.7	2
53217	Chlorine-anion doping induced multi-factor optimization in perovskties for boosting intrinsic oxygen evolution. Journal of Energy Chemistry, 2021, 52, 115-120.	7.1	69
53218	Loading Fe3O4 nanoparticles on paper-derived carbon scaffold toward advanced lithiumâ€“sulfur batteries. Journal of Energy Chemistry, 2021, 52, 1-11.	7.1	42
53219	Study on the optical spectra of MgAl2O4 with oxygen vacancies. Materials Technology, 2021, 36, 279-285.	1.5	7
53220	Electronic, magnetic and optical properties of Fe-doped nano-BN sheet: DFT study. Indian Journal of Physics, 2021, 95, 823-831.	0.9	7
53221	Single Cu atom supported on modified h-BN monolayer as n-p codoped catalyst for CO oxidation: A computational study. Catalysis Today, 2021, 368, 148-160.	2.2	9
53222	CO₂ reduction to acetic acid on the greigite Fe₃S₄{111} surface. Faraday Discussions, 2021, 229, 35-49.	1.6	12
53223	Reaction Mechanism Optimization of Solidâ€State Liâ€“S Batteries with a PEOâ€Based Electrolyte. Advanced Functional Materials, 2021, 31, 2001812.	7.8	116
53224	Rational Design of Mixed Electronicâ€Ionic Conducting Tiâ€Doping Li₇La₃Zr₂O₁₂ for Lithium Dendrites Suppression. Advanced Functional Materials, 2021, 31, 2001918.	7.8	57
53225	Metallurgical pyrolysis toward Co@Nitrogen-doped carbon composite for lithium storage. Green Energy and Environment, 2021, 6, 91-101.	4.7	20
53226	Cu-Al spinel-oxide catalysts for selective hydrogenation of furfural to furfuryl alcohol. Catalysis Today, 2021, 367, 177-188.	2.2	25

#	Article	IF	Citations
53227	Two-dimensional multimetallic sulfide nanosheets with multi-active sites to enhance polysulfide redox reactions in liquid Li2S6-based lithium-polysulfide batteries. Journal of Energy Chemistry, 2021, 52, 163-169.	7.1	28
53228	density functional theory and kinetic Monte Carlo simulation study the strong metalâ€“support interaction of dry reforming of methane reaction over Ni based catalysts. Chinese Journal of Chemical Engineering, 2021, 29, 176-182.	1.7	10
53229	Search for potential K ion battery cathodes by first principles. Journal of Energy Chemistry, 2021, 54, 377-385.	7.1	8
53230	The role of oxygenated species in the catalytic self-coupling of MeOH on O pre-covered Au(111). Faraday Discussions, 2021, 229, 251-266.	1.6	7
53231	Recyclable aqueous metal adsorbent: Synthesis and Cu(II) sorption characteristics of ternary nanocomposites of Fe3O4 nanoparticles@grapheneâ€“poly-N-phenylglycine nanofibers. Journal of Hazardous Materials, 2021, 401, 123283.	6.5	28
53232	Electrocatalytic and photocatalytic performance of noble metal doped monolayer MoS2 in the hydrogen evolution reaction: A first principles study. Nano Materials Science, 2021, 3, 89-94.	3.9	58
53233	Density Functional Theory Studies of Zn12O12 Clusters Doped with Mg/Eu and Defect Complexes. Journal of Cluster Science, 2021, 32, 55-62.	1.7	4
53234	First-principles study on predicting the crystal structures, mechanical properties and electronic structures of HfCxN1-x. Journal of the European Ceramic Society, 2021, 41, 3037-3044.	2.8	7
53235	Heterogeneous single-cluster catalysts (Mn3, Fe3, Co3, and Mo3) supported on nitrogen-doped graphene for robust electrochemical nitrogen reduction. Journal of Energy Chemistry, 2021, 54, 612-619.	7.1	57
53236	First-Principles Prediction of Enhanced Magnetic Anisotropy of Î±â€³-Phase Feâ‚‚Nâ„ With B and C Impurities. IEEE Transactions on Magnetics, 2021, 57, 1-3.	1.2	3
53237	Selective adsorption-involved formation of NMC532/PANI microparticles with high ageing resistance and improved electrochemical performance. Journal of Energy Chemistry, 2021, 54, 668-679.	7.1	11
53238	Boosting thermoelectric performance of n-type PbS through synergistically integrating In resonant level and Cu dynamic doping. Journal of Physics and Chemistry of Solids, 2021, 148, 109640.	1.9	26
53239	Synergy of copper doping and oxygen vacancies in porous CoOOH nanoplates for efficient water oxidation. Chemical Engineering Journal, 2021, 405, 126198.	6.6	38
53240	Acceleration of catalyst discovery with easy, fast, and reproducible computational alchemy. International Journal of Quantum Chemistry, 2021, 121, e26380.	1.0	15
53241	Highâ€throughput computational materials screening and discovery of optoelectronic semiconductors. Wiley Interdisciplinary Reviews: Computational Molecular Science, 2021, 11, .	6.2	52
53242	Limitations of abÂinitio methods to predict the electronic-transport properties of two-dimensional semiconductors: the computational example of 2H-phase transition metal dichalcogenides. Journal of Computational Electronics, 2021, 20, 49-59.	1.3	25
53243	Surface modification of macroporous La0.8Sr0.2CoO3 perovskite oxides integrated monolithic catalysts for improved propane oxidation. Catalysis Today, 2021, 376, 168-176.	2.2	13
53244	High-Pressure Structural and Electronic Properties of Potassium-Based Green Primary Explosives. Journal of Electronic Materials, 2021, 50, 1581-1590.	1.0	3

#	Article	IF	Citations
53245	Inorganic Mediator toward Organosulfide Active Material: Anchoring and Electrocatalysis. Advanced Functional Materials, 2021, 31, 2001493.	7.8	21
53246	Promoting effect of acid sites on NH3-SCO activity with water vapor participation for Pt-Fe/ZSM-5 catalyst. Catalysis Today, 2021, 376, 311-317.	2.2	23
53247	First Principles Study of Structure, Alloying and Electronic Properties of Mg-doped CuAg Nanoalloys. Journal of Cluster Science, 2021, 32, 719-725.	1.7	1
53248	High-precision regulation synthesis of Fe-doped Co2P nanorod bundles as efficient electrocatalysts for hydrogen evolution in all-pH range and seawater. Journal of Energy Chemistry, 2021, 55, 92-101.	7.1	89
53249	Microstructure and mechanical properties of CoCrNi-Mo medium entropy alloys: Experiments and first-principle calculations. Journal of Materials Science and Technology, 2021, 62, 25-33.	5.6	64
53250	Adsorption and diffusion of oxygen on metal surfaces studied by first-principle study: A review. Journal of Materials Science and Technology, 2021, 62, 180-194.	5.6	78
53251	Tailoring catalytic properties of V2O3 to propane dehydrogenation through single-atom doping: A DFT study. Catalysis Today, 2021, 368, 46-57.	2.2	29
53252	Direct conversion of carboxylic acid to olefins over Pt-loaded, oxygen-deficient alkali hexatitanate catalysts with ketonization-hydrogenation-dehydration activity. Catalysis Today, 2021, 375, 418-428.	2.2	4
53253	A DFT study of methane conversion on Mo-terminated Mo2C carbides: Carburization vs Câ€“C coupling. Catalysis Today, 2021, 368, 140-147.	2.2	14
53254	Effects of surface functionalization of mxene-based nanocatalysts on hydrogen evolution reaction performance. Catalysis Today, 2021, 368, 187-195.	2.2	51
53255	Addressing the uncertainty of DFT-determined hydrogenation mechanisms over coinage metal surfaces. Faraday Discussions, 2021, 229, 50-61.	1.6	9
53256	Combination of theoretical and in situ experimental investigations of the role of lithium dopant in manganese nitride: a two-stage reagent for ammonia synthesis. Faraday Discussions, 2021, 229, 281-296.	1.6	9
53257	Cdâ€Based Metalâ€“Organic Framework for Selective Turnâ€On Fluorescent DMSO Residual Sensing. Chemistry - A European Journal, 2021, 27, 3753-3760.	1.7	12
53258	Synthesis and electronic properties of InSe bi-layer on Si(111). Applied Surface Science, 2021, 539, 148144.	3.1	5
53259	Assembly of stacked In2O3 nanosheets for detecting trace NO2 with ultrahigh selectivity and promoted recovery. Applied Surface Science, 2021, 539, 148217.	3.1	28
53260	Tellurium-assisted and space-confined growth of graphene single crystals. Carbon, 2021, 173, 54-60.	5.4	5
53261	Vertically rooting carbon nanotubes on cobalt-loaded hollow Titanium Dioxide spheres as conductive multifunctional sulfur hosts for superior lithium-sulfur performance. Journal of Alloys and Compounds, 2021, 854, 157267.	2.8	9
53262	Structure, thermal stability, optoelectronic and electrophysical properties of Mg- and Na-codoped bismuth niobate pyrochlores: Experimental and theoretical study. Journal of Alloys and Compounds, 2021, 858, 157742.	2.8	12

#	Article	IF	Citations
53263	Development of an angular-dependent potential for radiation damage study in Fe-Si solutions. Journal of Nuclear Materials, 2021, 545, 152643.	1.3	3
53264	Enhanced quantum capacitance in chemically modified graphene electrodes: Insights from first principles electronic structures calculations. Physica B: Condensed Matter, 2021, 604, 412676.	1.3	5
53265	First-principles study on the electric field manipulation of the magnetic property and the electronic structures for monolayer Fe2C MXene. Physics Letters, Section A: General, Atomic and Solid State Physics, 2021, 386, 126960.	0.9	5
53266	A first-principles study of the temperature-dependent diffusion coefficients of silver in the thermoelectric compound PbTe. Acta Materialia, 2021, 202, 243-254.	3.8	12
53267	Antiâ€“corrosive FeO decorated CuCo2S4 as an efficient and durable electrocatalyst for hydrogen evolution reaction. Applied Surface Science, 2021, 539, 148229.	3.1	37
53268	Magnetic, electronic and mechanical properties of SeXO3 (XÂ= Mn, Ni) with the LSDAÂ+ U framework. Journal of Alloys and Compounds, 2021, 850, 156674.	2.8	1
53269	NaTePO5, SrTeP2O8 and Ba2TeP2O9: Three tellurite-phosphates with large birefringence. Journal of Alloys and Compounds, 2021, 854, 157243.	2.8	12
53270	Multifunctional Enhancement for Highly Stable and Efficient Perovskite Solar Cells. Advanced Functional Materials, 2021, 31, 2005776.	7.8	273
53271	The active site of ethanol formation from syngas over Cu4 cluster modified MoS2 catalyst: A theoretical investigation. Applied Surface Science, 2021, 540, 148301.	3.1	4
53272	Revealing the distinct electrochemical properties of TiSe2 monolayer and bulk counterpart in Li-ion batteries by first-principles calculations. Applied Surface Science, 2021, 540, 148314.	3.1	19
53273	Crystal face-dependent methylmercury adsorption onto mackinawite (FeS) nanocrystals: A DFT-D3 study. Chemical Engineering Journal, 2021, 420, 127594.	6.6	16
53274	Catalytic consequences of hydrogen addition events and solvent-adsorbate interactions during guaiacol-H2 reactions at the H2O-Ru(0Â0Â0Â1) interface. Journal of Catalysis, 2021, 395, 467-482.	3.1	15
53275	18 and 12 â€“ Member carbon rings (cyclo[n]carbons) â€“ A density functional study. Materials Science and Engineering B: Solid-State Materials for Advanced Technology, 2021, 263, 114895.	1.7	6
53276	Tailoring the chemical bonding of GeTe-based alloys by MgB2 alloying to simultaneously enhance their mechanical and thermoelectric performance. Materials Today Physics, 2021, 16, 100308.	2.9	29
53277	A first-principles investigation of Janus MoSSe as a catalyst for photocatalytic water-splitting. Applied Surface Science, 2021, 537, 147919.	3.1	36
53278	CO2 reduction by single copper atom supported on g-C3N4 with asymmetrical active sites. Applied Surface Science, 2021, 540, 148293.	3.1	33
53279	Designing piezoresistive materials from first-principles: Dopant effects on 3C-SiC. Computational Materials Science, 2021, 186, 110040.	1.4	8
53280	CCS: A software framework to generate two-body potentials using Curvature Constrained Splines. Computer Physics Communications, 2021, 258, 107602.	3.0	5

#	Article	IF	Citations
53281	Microstructure evolution during AlSi10Mg molten alloy/BN microflake interactions in metal matrix composites obtained through 3D printing. Journal of Alloys and Compounds, 2021, 859, 157765.	2.8	28
53282	Insights into electrochemical nitrogen reduction reaction mechanisms: Combined effect of single transition-metal and boron atom. Journal of Energy Chemistry, 2021, 58, 577-585.	7.1	66
53283	Interplay between transition-metal dopants and sulfur vacancies in MoS2 electrocatalyst. Surface Science, 2021, 704, 121759.	0.8	20
53284	Establishing a Theoretical Landscape for Identifying Basal Plane Active 2D Metal Borides (MBenes) toward Nitrogen Electroreduction. Advanced Functional Materials, 2021, 31, 2008056.	7.8	97
53285	Highly Efficient Nb₂C MXene Cathode Catalyst with Uniform Oâ€Terminated Surface for Lithiumâ€“Oxygen Batteries. Advanced Energy Materials, 2021, 11, .	10.2	130
53286	Electric field control of magnetism at the Î³-FeSi2/Si(001) interface. Journal of Materials Science, 2021, 56, 3804-3813.	1.7	2
53287	Ultra-incompressibility and high energy density of ReN8 with infinite nitrogen chains. Journal of Materials Science, 2021, 56, 3814-3826.	1.7	9
53288	Surface excess free energies and equilibrium Wulff shapes in variable chemical environments at finite temperatures. Applied Surface Science, 2021, 540, 148383.	3.1	10
53289	Strain engineering for C2N/Janus monochalcogenides van der Waals heterostructures: Potential applications for photocatalytic water splitting. Applied Surface Science, 2021, 536, 147845.	3.1	17
53290	Potential energy surfaces of adsorption and migration of transition metal atoms on nanoporus materials: The case of nanoporus bigraphene and G-C3N4. Applied Surface Science, 2021, 540, 148223.	3.1	4
53291	First-principles calculation of structural, magnetic and electronic properties of PuO2-H , 0â‰xâ‰2. Journal of Alloys and Compounds, 2021, 857, 157592.	2.8	6
53292	Tribological properties of V2O5 studied via reactive molecular dynamics simulations. Tribology International, 2021, 154, 106750.	3.0	6
53293	Strain engineering the electronic and photocatalytic properties of WS₂/blue phosphene van der Waals heterostructures. Catalysis Science and Technology, 2021, 11, 179-190.	2.1	12
53294	Atomic Co/Ni active sites assisted MOF-derived rich nitrogen-doped carbon hollow nanocages for enhanced lithium storage. Chemical Engineering Journal, 2021, 420, 127583.	6.6	36
53295	Computational screening of dopants for mitigating degradation behaviors in sodium-ion layered oxide cathode material. Journal of Alloys and Compounds, 2021, 859, 157785.	2.8	5
53296	First-principles studies on behaviors of He impurities in d-MAX phase Zr3Al3C5. Journal of Nuclear Materials, 2021, 544, 152653.	1.3	1
53297	Doping transition-metal atoms in graphene for atomic-scale tailoring of electronic, magnetic, and quantum topological properties. Carbon, 2021, 173, 205-214.	5.4	35
53298	AMMCR: Ab initio model for mobility and conductivity calculation by using Rode Algorithm. Computer Physics Communications, 2021, 259, 107697.	3.0	8

#	Article	IF	Citations
53299	Visible-light overall water splitting on g-C3N4 decorated by subnanometer oxide clusters. Materials Today Physics, 2021, 16, 100312.	2.9	20
53300	Interactive network of the dehydrogenation of alkanes, alkenes and alkynes â€“ surface carbon hydrogenative coupling on Ru(111). Catalysis Science and Technology, 2021, 11, 191-210.	2.1	4
53301	Exploring Janus MoSSe monolayer as a workable media for SOF6 decompositions sensing based on DFT calculations. Computational Materials Science, 2021, 186, 109976.	1.4	21
53302	Thermophysical properties of high-density, sintered monoliths of yttrium dihydride in the range 373â€“773ÂK. Journal of Alloys and Compounds, 2021, 850, 156303.	2.8	12
53303	Synthesis and photoluminescence properties of a novel red emitting Ba3ZnTa2O9: Eu3+ phosphor. Journal of Molecular Structure, 2021, 1224, 129075.	1.8	14
53304	HCOOH Decomposition on Sub-Nanometer Pd6 Cluster Catalysts: The Effect of Defective Boron Nitride Supports Through First Principles. Applied Catalysis B: Environmental, 2021, 280, 119392.	10.8	19
53305	Nanostructured amorphous Fe29Co27Ni23Si9B12 high-entropy-alloy: an efficient electrocatalyst for oxygen evolution reaction. Journal of Materials Science and Technology, 2021, 68, 191-198.	5.6	54
53306	First steps of blue phosphorene growth on Au(1 1 1). Materials Today: Proceedings, 2021, 39, 1153-1156.	0.9	4
53307	Fe3+-stabilized Ti3C2T MXene enables ultrastable Li-ion storage at low temperature. Journal of Materials Science and Technology, 2021, 67, 156-164.	5.6	41
53308	Nanoscale surface modification of P2-type Na0.65[Mn0.70Ni0.16Co0.14]O2 cathode material for high-performance sodium-ion batteries. Chemical Engineering Journal, 2021, 404, 126446.	6.6	32
53309	Oxygen vacancies engineered self-supported B doped Co3O4 nanowires as an efficient multifunctional catalyst for electrochemical water splitting and hydrolysis of sodium borohydride. Chemical Engineering Journal, 2021, 404, 126474.	6.6	122
53310	Probing the enhanced methanol electrooxidation mechanism on platinum-metal oxide catalyst. Applied Catalysis B: Environmental, 2021, 280, 119393.	10.8	68
53311	Free-standing nanoporous NiMnFeMo alloy: An efficient non-precious metal electrocatalyst for water splitting. Chemical Engineering Journal, 2021, 404, 126530.	6.6	88
53312	Diverse morphologies of zinc oxide nanoparticles and their electrocatalytic performance in hydrogen production. Journal of Energy Chemistry, 2021, 56, 162-170.	7.1	18
53313	Forming electron traps deactivates self-assembled crystalline organic nanosheets toward photocatalytic overall water splitting. Science Bulletin, 2021, 66, 265-274.	4.3	18
53314	HCOOH decomposition over the pure and Ag-modified Pd nanoclusters: Insight into the effects of cluster size and composition on the activity and selectivity. Chemical Engineering Science, 2021, 229, 116016.	1.9	14
53315	Electronic origin of the main-group element dependences of elastic moduli in the Ni2Mn-based magnetic shape memory alloys. Journal of Physics and Chemistry of Solids, 2021, 148, 109671.	1.9	8
53316	Alloy design strategies to increase strength and its trade-offs together. Progress in Materials Science, 2021, 117, 100720.	16.0	77

#	Article	IF	Citations
53317	Experimental and DFT study on cerium inclusions in clean steels. Journal of Rare Earths, 2021, 39, 477-486.	2.5	37
53318	Crystal structure and phase stability of Co2N: A combined first-principles and experimental study. Journal of Alloys and Compounds, 2021, 854, 156341.	2.8	1
53319	First-principles calculations for formation energy and magnetism of defect structures in Heusler alloys Mg-V-Z (ZÂ=ÂAl, Ga, In). Physica B: Condensed Matter, 2021, 600, 412388.	1.3	8
53320	Sodiophilic Zn/SnO2 porous scaffold to stabilize sodium deposition for sodium metal batteries. Chemical Engineering Journal, 2021, 404, 126469.	6.6	35
53321	High-index crystal plane of ZnO nanopyramidal structures: Stabilization, growth, and improved photocatalytic performance. Applied Surface Science, 2021, 536, 147326.	3.1	17
53322	CO adsorption on the calcite(10.4) surface: a combined experimental and theoretical study. Physical Chemistry Chemical Physics, 2021, 23, 7696-7702.	1.3	12
53323	Facilitating active species by decorating CeO2 on Ni3S2 nanosheets for efficient water oxidation electrocatalysis. Chinese Journal of Catalysis, 2021, 42, 482-489.	6.9	61
53324	Thermophysical properties of magnesium arsenide with atomistic simulation methods. Journal of Physics and Chemistry of Solids, 2021, 148, 109614.	1.9	2
53325	Growth of large scale PtTe, PtTe2 and PtSe2 films on a wide range of substrates. Nano Research, 2021, 14, 1663-1667.	5.8	26
53326	First-principles calculations of stability of graphene-like BC3 monolayer and its high-performance potassium storage. Chinese Chemical Letters, 2021, 32, 900-905.	4.8	32
53327	Enhanced photocatalytic water oxidation by hierarchical 2D-Bi2MoO6@2D-MXene Schottky junction nanohybrid. Chemical Engineering Journal, 2021, 403, 126328.	6.6	94
53328	Orbital symmetry matching: Achieving superior nitrogen reduction reaction over single-atom catalysts anchored on Mxene substrates. Chinese Journal of Catalysis, 2021, 42, 288-296.	6.9	41
53329	Turning chemistry into information for heterogeneous catalysis. International Journal of Quantum Chemistry, 2021, 121, e26382.	1.0	9
53330	Identifying the Znâ€“Co binary as a robust bifunctional electrocatalyst in oxygen reduction and evolution reactions via shifting the apexes of the volcano plot. Journal of Energy Chemistry, 2021, 55, 162-168.	7.1	33
53331	TMN4 complex embedded graphene as bifunctional electrocatalysts for high efficiency OER/ORR. Journal of Energy Chemistry, 2021, 55, 437-443.	7.1	117
53332	Catalytic mechanism and pathways of 1, 2-dichloropropane oxidation over LaMnO3 perovskite: An experimental and DFT study. Journal of Hazardous Materials, 2021, 402, 123473.	6.5	42
53333	Phase stability of TiPd1-xRux and Ti1-xPdRux shape memory alloys. Materials Today: Proceedings, 2021, 38, 1071-1076.	0.9	2
53334	Enhanced photocatalytic degradation of organic contaminants over CaFe2O4 under visible LED light irradiation mediated by peroxymonosulfate. Journal of Materials Science and Technology, 2021, 62, 34-43.	5.6	78

#	Article	IF	Citations
53335	Enhanced activity and stability of MoS2 through enriching 1T-phase by covalent functionalization for energy conversion applications. Chemical Engineering Journal, 2021, 403, 126318.	6.6	63
53336	Tuning Fermi Levels in Intrinsic Antiferromagnetic Topological Insulators MnBi₂Te₄ and MnBi₄Te₇ by Defect Engineering and Chemical Doping. Advanced Functional Materials, 2021, 31, 2006516.	7.8	68
53337	Twin Boundary and Fivefold Twins in Nickel Oxide. Physica Status Solidi (B): Basic Research, 2021, 258, 2000377.	0.7	5
53338	In Operando Visualization of Cation Disorder Unravels Voltage Decay in Niâ€Rich Cathodes. Small Methods, 2021, 5, e2000730.	4.6	18
53339	Theoretical study of the phase transitions and electronic structure of (Zr0.5, Mg0.5)N and (Hf0.5,) Tj ETQq0 0 0 rgBT /Overlock 10 Tf 50	1.7	11
53340	Water Adsorption and Dissociation Promoted by Co*-/N-C*-Biactive Sites of Metallic Co/N-Doped Carbon Hybrids for Efficient Hydrogen Evolution. Applied Catalysis B: Environmental, 2021, 282, 119463.	10.8	77
53341	Oxygen vacancies and alkaline metal boost CeO2 catalyst for enhanced soot combustion activity: A first-principles evidence. Applied Catalysis B: Environmental, 2021, 281, 119468.	10.8	28
53342	Boosting the electrocatalytic HER performance of Ni3N-V2O3 via the interface coupling effect. Applied Catalysis B: Environmental, 2021, 283, 119590.	10.8	84
53343	Ab initio study of molybdenum sulfo-selenides alloy as a flexible anode for sodium-ion batteries. Applied Surface Science, 2021, 536, 147973.	3.1	15
53344	A monolayer of Pd on ZrC(0 0 1) speeds up O2 dissociation: An ab initio study. Applied Surface Science, 2021, 537, 148050.	3.1	0
53345	Well-defined sub-nanometer graphene ribbons synthesized inside carbon nanotubes. Carbon, 2021, 171, 221-229.	5.4	23
53346	Two-dimensional blue-phase CX (X = S, Se) monolayers with high carrier mobility and tunable photocatalytic water splitting capability. Chinese Chemical Letters, 2021, 32, 1977-1982.	4.8	31
53347	Metallic B2C monolayer as a promising anode material for Li/Na ion storage. Chemical Engineering Journal, 2021, 406, 126812.	6.6	33
53348	Synthesis of mesoporous nickel-cobalt-manganese sulfides as electroactive materials for hybrid supercapacitors. Chemical Engineering Journal, 2021, 405, 126928.	6.6	99
53349	TransOpt. A code to solve electrical transport properties of semiconductors in constant electronâ€“phonon coupling approximation. Computational Materials Science, 2021, 186, 110074.	1.4	55
53350	An in-depth understanding of the effect of aluminum doping in high-nickel cathodes for lithium-ion batteries. Energy Storage Materials, 2021, 34, 229-240.	9.5	120
53351	Thermal transport of boron pyrochlore lattices. International Journal of Heat and Mass Transfer, 2021, 164, 120483.	2.5	2
53352	Generalized stacking fault energies and critical resolved shear stresses of random Î±-Ti-Al alloys from first-principles calculations. Journal of Alloys and Compounds, 2021, 850, 156314.	2.8	29

#	Article	IF	Citations
53353	Porosity and oxygen vacancy engineering of mesoporous WO3 nanofibers for fast and sensitive low-temperature NO2 sensing. Journal of Alloys and Compounds, 2021, 853, 157339.	2.8	58
53354	The first-principles study on the performance of the graphene/WS2 heterostructure as an anode material of Li-ion battery. Journal of Alloys and Compounds, 2021, 855, 157432.	2.8	30
53355	Boron-doping induced lithophilic transition of graphene for dendrite-free lithium growth. Journal of Energy Chemistry, 2021, 56, 463-469.	7.1	18
53356	Enhanced thermoelectric properties of ZnO: C doping and band gap tuning. Journal of the European Ceramic Society, 2021, 41, 1324-1331.	2.8	30
53357	Influence of Ag substitution on thermoelectric properties of the quaternary diamond-like compound Zn2Cu3In3Te8. Journal of Materiomics, 2021, 7, 236-243.	2.8	7
53358	Maximizing ionic transport of Li1+xAlxTi2-xP3O12 electrolytes for all-solid-state lithium-ion storage: A theoretical study. Journal of Materials Science and Technology, 2021, 73, 45-51.	5.6	12
53359	First-principles study of de-twinning in a FCC alloy. Journal of Solid State Chemistry, 2021, 293, 121765.	1.4	4
53360	A theoretical insight into the microstructure and electronic properties of Ho3+-doped potassium gadolinium tungstate. Materials Chemistry and Physics, 2021, 257, 123824.	2.0	3
53361	Theoretically investigating the physical properties of fcc-C32 and mediating its electronic band structure. Materials Chemistry and Physics, 2021, 258, 123853.	2.0	3
53362	Structural, electronic, optical, thermoelectric and photocatalytic properties of SiS/MXenes van der Waals heterostructures. Materials Today Communications, 2021, 26, 101702.	0.9	12
53363	High quantum efficiency and stability of biohybrid quantum dots nanojunctions in bacteriophage-constructed perovskite. Materials Today Nano, 2021, 13, 100099.	2.3	9
53364	Electron transfer in the contact-electrification between corrugated 2D materials: A first-principles study. Nano Energy, 2021, 79, 105386.	8.2	20
53365	Light-activated polydopamine coatings for efficient metal recovery from electronic waste. Separation and Purification Technology, 2021, 254, 117674.	3.9	10
53366	Stable CO/H2 ratio on MoP surfaces under working condition: A DFT based thermodynamics study. Surface Science, 2021, 703, 121738.	0.8	0
53367	Modulation of the adsorption chemistry of a precursor in atomic layer deposition to enhance the growth per cycle of a TiO₂ thin film. Physical Chemistry Chemical Physics, 2021, 23, 2568-2574.	1.3	9
53368	First-principles calculations of phonon behaviors in graphether: a comparative study with graphene. Physical Chemistry Chemical Physics, 2021, 23, 123-130.	1.3	22
53369	In-situ observations of novel single-atom thick 2D tin membranes embedded in graphene. Nano Research, 2021, 14, 747-753.	5.8	13
53370	Two-dimensional carbon allotropes with tunable direct band gaps and high carrier mobility. Applied Surface Science, 2021, 537, 147885.	3.1	39

#	Article	IF	Citations
53371	Aggregation-induced emission and pressure-dependent fluorescence of aryl cyclooctatetrathiophenes. Dyes and Pigments, 2021, 184, 108803.	2.0	8
53372	Native point defects and low p-doping efficiency in Mg2(Si,Sn) solid solutions: A hybrid-density functional study. Journal of Alloys and Compounds, 2021, 853, 157145.	2.8	16
53373	Catalytic activity for hydrogen evolution reaction in square phase Janus MoSSe monolayer: A first-principles study. Physica E: Low-Dimensional Systems and Nanostructures, 2021, 126, 114485.	1.3	4
53374	Unveiling the pseudocapacitive effects of ultramesopores on nanoporous carbon. Applied Surface Science, 2021, 537, 148037.	3.1	9
53375	Compositional effect on water adsorption on metal halide perovskites. Applied Surface Science, 2021, 538, 148058.	3.1	30
53376	pyHMA: A VASP post-processor for precise measurement of crystalline anharmonic properties using harmonically mapped averaging. Computer Physics Communications, 2021, 258, 107554.	3.0	4
53377	Experimental and theoretical study of dense YBO3 and the influence of non-hydrostaticity. Journal of Alloys and Compounds, 2021, 850, 156562.	2.8	5
53378	Phosphorus-doped Fe7S8@C nanowires for efficient electrochemical hydrogen and oxygen evolutions: Controlled synthesis and electronic modulation on active sites. Journal of Materials Science and Technology, 2021, 74, 168-175.	5.6	18
53379	Mechanistic Investigations of the Pyridinic Nâ€“Co Structures in Co Embedded N-Doped Carbon Nanotubes for Catalytic Ozonation. ACS ES&T Engineering, 2021, 1, 32-45.	3.7	50
53380	Nernstian Li⁺ intercalation into few-layer graphene and its use for the determination of K⁺ co-intercalation processes. Chemical Science, 2021, 12, 559-568.	3.7	10
53381	Tunable oxygen vacancy concentration in vanadium oxide as mass-produced cathode for aqueous zinc-ion batteries. Nano Research, 2021, 14, 754-761.	5.8	96
53382	Improving hydrogen evolution reaction performance by combining ditungsten carbide and nitrogen-doped graphene: A first-principles study. Carbon, 2021, 172, 122-131.	5.4	25
53383	A general thermodynamic model for the long-period stacking ordered phases in magnesium alloys. Journal of Magnesium and Alloys, 2021, 9, 144-155.	5.5	13
53384	Selective patterning of out-of-plane piezoelectricity in MoTe2 via focused ion beam. Nano Energy, 2021, 79, 105451.	8.2	17
53385	First-principles investigation of the structural, elastic, anisotropic and electronic properties of Pmma-carbon. Molecular Physics, 2021, 119, e1809729.	0.8	0
53386	Modulation of Single Atomic Co and Fe Sites on Hollow Carbon Nanospheres as Oxygen Electrodes for Rechargeable Znâ€“Air Batteries. Small Methods, 2021, 5, e2000751.	4.6	178
53387	Li-decorated porous hydrogen substituted graphyne: A new member of promising hydrogen storage medium. Applied Surface Science, 2021, 535, 147683.	3.1	36
53388	Catalytic FeP decorated carbon black as a multifunctional conducting additive for high-performance lithium-sulfur batteries. Carbon, 2021, 172, 96-105.	5.4	60

#	Article	IF	Citations
53389	Selective dehydration of glycerol on copper based catalysts. Catalysis Today, 2021, 367, 58-70.	2.2	14
53390	High-throughput computational screening of oxide double perovskites for optoelectronic and photocatalysis applications. Journal of Energy Chemistry, 2021, 57, 351-358.	7.1	17
53391	Self-assembly of highly-dispersed phosphotungstic acid clusters onto graphitic carbon nitride nanosheets as fascinating molecular-scale Z-scheme heterojunctions for photocatalytic solar-to-fuels conversion. Applied Catalysis B: Environmental, 2021, 281, 119473.	10.8	59
53392	Surface-structure sensitive chemical diffusivity and reactivity of CO adsorbates on noble metal electrocatalysts. Applied Catalysis B: Environmental, 2021, 281, 119522.	10.8	11
53393	Atomically-ordered active sites in NiMo intermetallic compound toward low-pressure hydrodeoxygenation of furfural. Applied Catalysis B: Environmental, 2021, 282, 119569.	10.8	92
53394	Noble-metal and cocatalyst free W2N/C/TiO photocatalysts for efficient photocatalytic overall water splitting in visible and near-infrared light regions. Chemical Engineering Journal, 2021, 405, 126913.	6.6	54
53395	Two-dimensional Janus material MoS2(1-x)Se2x (0Â<ÂxÂ<Â1) for photovoltaic applications: A machine learning and density functional study. Computational Materials Science, 2021, 186, 109998.	1.4	9
53396	Structure prediction of two-dimensional materials based on neural network-driven evolutionary technique. Computational Materials Science, 2021, 186, 110046.	1.4	2
53397	Effect of diffusion barrier and interfacial strengthening on the interface behavior between high entropy alloy and diamond. Journal of Alloys and Compounds, 2021, 852, 157023.	2.8	15
53398	Effects of minor alloying on the mechanical properties of Al based metallic glasses. Journal of Alloys and Compounds, 2021, 854, 157266.	2.8	7
53399	Ground state spin structure of GdFeO3: A computational and experimental study. Journal of Magnetism and Magnetic Materials, 2021, 518, 167407.	1.0	3
53400	Enhancement of thermoelectric properties of p-type BiCuSO through strain-induced electronic structures modification. Solid State Communications, 2021, 324, 114076.	0.9	1
53401	Two-dimensional (Zr0.5Hf0.5)2CO2: A promising visible light water-splitting photocatalyst with efficiently carrier separation. Computational Materials Science, 2021, 186, 110013.	1.4	8
53402	Structural, electronic and optical properties of lead-free antimony-copper based hybrid double perovskites for photovoltaics and optoelectronics by first principles calculations. Computational Materials Science, 2021, 186, 110009.	1.4	30
53403	An automated cluster surface scanning method for exploring reaction paths on metal-cluster surfaces. Computational Materials Science, 2021, 186, 110010.	1.4	10
53404	Predicting Nitrogenâ€Based Families of Compounds: Transitionâ€Metal Guanidinates TCN₃ (T=V, Nb, Ta) and Orthoâ€Nitrido Carbonates Tâ€²₂CN₄ (Tâ€²=Ti, Zr, Hf). Angewandte Chemie - International Edition, 2021, 60, 486-492.	7.2	18
53405	Carbon microspheres with embedded FeP nanoparticles as a cathode electrocatalyst in Li-S batteries. Chemical Engineering Journal, 2021, 406, 126823.	6.6	60
53406	Design of grain boundary enriched bimetallic borides for enhanced hydrogen evolution reaction. Chemical Engineering Journal, 2021, 405, 126977.	6.6	56

#	Article	IF	Citations
53407	Physically inspired atom-centered symmetry functions for the construction of high dimensional neural network potential energy surfaces. Computational Materials Science, 2021, 186, 110071.	1.4	8
53408	Ultra-high piezoelectric coefficients and strain-sensitive Curie temperature in hydrogen-bonded systems. National Science Review, 2021, 8, nwaa203.	4.6	9
53409	Electronic structures and topological properties in nickelatesLnn+1NinO2n+2. National Science Review, 2021, 8, nwaa218.	4.6	33
53410	Prediction of giant and ideal Rashba-type splitting in ordered alloy monolayers grown on a polar surface. National Science Review, 2021, 8, nwaa241.	4.6	9
53411	A direct measurement method of quantum relaxation time. National Science Review, 2021, 8, nwaa242.	4.6	4
53412	Effects of H2 pre-etching on BN seed morphology and induced graphene synthesis on Cu substrate: A theoretical study. Applied Surface Science, 2021, 537, 148093.	3.1	1
53413	Tuning a compatible interface with LLZTO integrated on cathode material for improving NCM811/LLZTO solid-state battery. Chemical Engineering Journal, 2021, 405, 127031.	6.6	36
53414	Amorphous phosphatized ruthenium-iron bimetallic nanoclusters with Pt-like activity for hydrogen evolution reaction. Applied Catalysis B: Environmental, 2021, 283, 119583.	10.8	78
53415	Thermoelectric and lattice dynamics properties of layered MX (MÂ=ÂSn, Pb; X Â=ÂS, Te) compounds. Applied Surface Science, 2021, 538, 147911.	3.1	24
53416	Defect states contributed nanoscale contact electrification at ZnO nanowires packed film surfaces. Nano Energy, 2021, 79, 105406.	8.2	22
53417	Theoretical study of adsorption mechanism of heavy metals As and Pb on the calcite (104) surface. Materials Today Communications, 2021, 26, 101742.	0.9	3
53418	Adsorption of phenanthrene and its monohydroxy derivatives on polyvinyl chloride microplastics in aqueous solution: Model fitting and mechanism analysis. Science of the Total Environment, 2021, 764, 142889.	3.9	53
53419	The Strain and Electric Field Effects on the Electronic and Optical Properties of Armchair MoSSe/WSSe Superlattice Nanoribbon: A Firstâ€Principles Study. Physica Status Solidi (B): Basic Research, 2021, 258, 2000361.	0.7	5
53420	Large valley-polarized state in single-layer NbX2 (X = S, Se): Theoretical prediction. Nano Research, 2021, 14, 834-839.	5.8	49
53421	Twin nucleation from a single <c+a> dislocation in hexagonal close-packed crystals. Acta Materialia, 2021, 202, 35-41.	3.8	13
53422	Effect of post-brazing heat treatment on the corrosion mechanism of sandwich multi-layered aluminium sheets. Vacuum, 2021, 183, 109781.	1.6	9
53423	Neural network constitutive model for crystal structures. Computational Mechanics, 2021, 67, 185-206.	2.2	14
53424	A novel strategy to construct supported silver nanocomposite as an ultra-high efficient catalyst. Applied Catalysis B: Environmental, 2021, 283, 119592.	10.8	27

#	Article	IF	Citations
53425	Theoretical investigation of Ti2B monolayer as powerful anode material for Li/Na batteries with high storage capacity. Applied Surface Science, 2021, 538, 148048.	3.1	14
53426	Theoretical insight into the role of nitrogen in the formic acid decomposition over Pt13/N-GNS. Applied Surface Science, 2021, 539, 148192.	3.1	15
53427	Exploring the thickness dependent photocatalytic oxygen evolution performance for Bi4TaO8Cl two-dimensional semiconductor. Applied Surface Science, 2021, 539, 148193.	3.1	8
53428	A robust calcium-based microporous metal-organic framework for efficient CH4/N2 separation. Chemical Engineering Journal, 2021, 408, 127294.	6.6	72
53429	On the irreversible sodiation of tin disulfide. Nano Energy, 2021, 79, 105458.	8.2	14
53430	Adsorption of lead on the surfaces of pristine and B, Si and N-doped graphene. Physica B: Condensed Matter, 2021, 600, 412639.	1.3	21
53431	Effects of guanidinium cations on structural, optoelectronic and photovoltaic properties of perovskites. Journal of Energy Chemistry, 2021, 58, 48-54.	7.1	21
53432	Origin of profuse {11<mml:math xmlns:mml="http://www.w3.org/1998/Math/MathML" altimg="si2.svg"><mml:mover accent="true"><mml:mn>2</mml:mn><mml:mo>Â¯</mml:mo></mml:mover></mml:math>1} deformation twins in Mg-Gd alloys. Scripta Materialia, 2021, 191, 62-66.	2.6	20
53433	FirstâEPrinciples Study of the Structure and Electronic Properties of TiâEÐoped LiCoO₂. Physica Status Solidi (B): Basic Research, 2021, 258, 2000412.	0.7	6
53434	Mechanical behavior of high entropy carbide (<scp>HfTaZrTi</scp>)C and (<scp>HfTaZrNb</scp>)C under high pressure: Ab initio study. International Journal of Quantum Chemistry, 2021, 121, e26509.	1.0	6
53435	Transition metal doping BiOBr nanosheets with oxygen vacancy and exposed {102} facets for visible light nitrogen fixation. Applied Catalysis B: Environmental, 2021, 281, 119516.	10.8	141
53436	Surface engineering induced hierarchical porous Ni12P5-Ni2P polymorphs catalyst for efficient wide pH hydrogen production. Applied Catalysis B: Environmental, 2021, 282, 119609.	10.8	123
53437	Metal-free boron carbonitride with tunable boron Lewis acid sites for enhanced nitrogen electroreduction to ammonia. Applied Catalysis B: Environmental, 2021, 283, 119622.	10.8	108
53438	Efficient electrocatalytic reduction of CO2 to HCOOH by bimetallic In-Cu nanoparticles with controlled growth facet. Applied Catalysis B: Environmental, 2021, 283, 119646.	10.8	102
53439	Bifunctional WO3 microrods decorated RGO composite as catechol sensor and optical limiter. Applied Surface Science, 2021, 536, 147669.	3.1	15
53440	Hole-matrixed carbonylated graphene: Synthesis, properties, and highly-selective ammonia gas sensing. Carbon, 2021, 172, 236-247.	5.4	34
53441	Phonon dispersions and electronic structures of two-dimensional IV-V compounds. Carbon, 2021, 172, 345-352.	5.4	9
53442	Persulfate activation by ZIF-67-derived cobalt/nitrogen-doped carbon composites: Kinetics and mechanisms dependent on persulfate precursor. Chemical Engineering Journal, 2021, 408, 127305.	6.6	72

#	Article	IF	Citations
53443	High-efficiency photocatalytic decomposition of toluene over defective InOOH: Promotive role of oxygen vacancies in ring opening process. Chemical Engineering Journal, 2021, 413, 127389.	6.6	36
53444	Treatment of ammonia-embodied wastewater by a transition-metal-based photochemical catalysis strategy. Chemosphere, 2021, 270, 128614.	4.2	2
53445	Understanding magnetic behaviors of FeCoNiSi0.2M0.2 (M=Cr, Mn) high entropy alloys via first-principle calculation. Journal of Magnetism and Magnetic Materials, 2021, 519, 167432.	1.0	9
53446	Effect of carbon vacancies and oxygen impurities on the dynamical and thermal properties of uranium monocarbide. Journal of Nuclear Materials, 2021, 545, 152547.	1.3	7
53447	Adsorption behavior of explosive molecules on g-C<mml:math xmlns:mml="http://www.w3.org/1998/Math/MathML" display="inline" id="d1e845" altimg="si56.svg"><mml:msub><mml:mrow /><mml:mrow><mml:mn>3</mml:mn></mml:mrow></mml:msub></mml:math>N<mml:math xmlns:mml="http://www.w3.org/1998/Math/MathML" display="inline" id="d1e853" altimg="si57.svg"><mml:msub><mml:mrow /><mml:mrow><mml:mn>4</mml:mn></mml:mrow></mml:ms	1.9	17
53448	Magnetic oxygen in transition metal oxides: A case study of Ba2CoO4. Journal of Physics and Chemistry of Solids, 2021, 150, 109803.	1.9	2
53449	Influence of alloying elements on hot corrosion resistance of nickel-based single crystal superalloys coated with Na2SO4 salt at 900ÂÂ°C. Materials and Design, 2021, 197, 109197.	3.3	37
53450	Optical property in colorless AlN bulk crystals: investigation of native defect-induced UV absorption. Scripta Materialia, 2021, 190, 91-96.	2.6	5
53451	Aliovalent Sc and Li co-doping boosts the performance of p-type NiO sensor. Sensors and Actuators B: Chemical, 2021, 326, 128834.	4.0	21
53452	Surface chemical trapping of optical cycling centers. Physical Chemistry Chemical Physics, 2021, 23, 211-218.	1.3	5
53453	Hydrogen evolution/spillover effect of single cobalt atom on anatase TiO2 from first-principles calculations. Applied Surface Science, 2021, 536, 147831.	3.1	13
53454	Strong coupled spinel oxide with N-rGO for high-efficiency ORR/OER bifunctional electrocatalyst of Zn-air batteries. Journal of Energy Chemistry, 2021, 57, 428-435.	7.1	45
53455	Ab initio prediction and characterization of Hf2CO2 monolayer as a promising adsorbent to capture toxic AsH3 gas. Applied Surface Science, 2021, 535, 147660.	3.1	12
53456	Effect of tungsten/graphene/tungsten interface on helium diffusion kinetics and mechanical properties and defects of tungsten as first wall material - first principle calculation. Journal of Alloys and Compounds, 2021, 851, 156760.	2.8	17
53457	Effect of impurity elements on the structural stability and electronic state in tin iodide perovskite. Journal of Solid State Chemistry, 2021, 293, 121785.	1.4	2
53458	A two-dimensional MoS2/SnS heterostructure for promising photocatalytic performance: First-principles investigations. Physica E: Low-Dimensional Systems and Nanostructures, 2021, 126, 114453.	1.3	17
53459	Dzyaloshinskiiâ€“Moriya-like interaction in ferroelectrics and antiferroelectrics. Nature Materials, 2021, 20, 341-345.	13.3	37
53460	Graphene oxide aerogel assembled by dimethylaminopropylamine /N-isopropylethylenediamine for the removal of copper ions. Chemosphere, 2021, 263, 128273.	4.2	8

#	Article	IF	Citations
53461	Janus MoSSe/graphene heterostructures: Potential anodes for lithium-ion batteries. Journal of Alloys and Compounds, 2021, 854, 157215.	2.8	41
53462	CdInGaS4: An unexplored two- dimensional materials with desirable band gap for optoelectronic devices. Journal of Alloys and Compounds, 2021, 854, 157220.	2.8	19
53463	Impact of B alloying on ductility and phase transition in the Niâ€“Mn-based magnetic shape memory alloys: Insights from first-principles calculation. Journal of Materials Science and Technology, 2021, 74, 27-34.	5.6	25
53464	New theoretical insights into the actual oxidation states of uranium in the solid-state compounds. Journal of Nuclear Materials, 2021, 543, 152563.	1.3	7
53465	A multiscale framework to predict electrochemical characteristics of yttrium doped Barium Zirconate based solid oxide cells. Journal of Power Sources, 2021, 481, 228969.	4.0	6
53466	Tailoring mechanical and electrical properties of graphene oxide film for structural dielectric capacitors. Journal of Power Sources, 2021, 482, 229020.	4.0	14
53467	How fluorine minimizes density fluctuations of silica glass: Molecular dynamics study with machine-learning assisted force-matching potential. Materials and Design, 2021, 197, 109210.	3.3	18
53468	2D SnC sheet with a small strain is a promising Li host material for Li-ion batteries. Materials Today Communications, 2021, 26, 101768.	0.9	12
53469	Band flattening and phonon-defect scattering in cubic SnSeâ€“AgSbTe2 alloy for thermoelectric enhancement. Materials Today Physics, 2021, 16, 100298.	2.9	20
53470	The sources of hydrogen affect the productivity and selectivity of CO2 photoreduction on SiC. Applied Surface Science, 2021, 538, 148010.	3.1	6
53471	Theoretical insights into the performance of single and double transition metal atoms doped on N-graphenes for N2 electroreduction. Applied Surface Science, 2021, 537, 148012.	3.1	27
53472	Direct trapping and rapid conversing of polysulfides via a multifunctional Nb2O5-CNT catalytic layer for high performance lithium-sulfur batteries. Carbon, 2021, 172, 260-271.	5.4	53
53473	Modulation of 2D GaS/BTe vdW heterostructure as an efficient HER catalyst under external electric field influence. Catalysis Today, 2021, 370, 14-25.	2.2	20
53474	Template-free synthesis of mesh-like graphic carbon nitride with optimized electronic band structure for enhanced photocatalytic hydrogen evolution. Chemical Engineering Journal, 2021, 405, 126685.	6.6	28
53475	Accelerating first-principles estimation of thermal conductivity by machine-learning interatomic potentials: A MTP/ShengBTE solution. Computer Physics Communications, 2021, 258, 107583.	3.0	108
53476	Non-catalytic gas phase NO oxidation in the presence of decane. Fuel, 2021, 286, 119388.	3.4	12
53477	A new perspective of co-doping and Nd segregation effect on proton stability and transportation in Y and Nd co-doped BaCeO3. International Journal of Hydrogen Energy, 2021, 46, 1096-1105.	3.8	18
53478	New Icosahedra-based B4N phases by particle swarm optimization. Journal of Alloys and Compounds, 2021, 854, 157255.	2.8	5

#	Article	IF	Citations
53479	Tailoring the equilibrium hydrogen pressure of TiFe via vanadium substitution. Journal of Alloys and Compounds, 2021, 854, 157263.	2.8	23
53480	Effect of surface interactions on spin contamination errors of homogeneous spin dimers, chains, and films: model calculations of Au/MgO and Au/BaO systems. Molecular Physics, 2021, 119, e1791989.	0.8	10
53481	Monoclinic Scheelite Bismuth Vanadate Derived Bismuthene Nanosheets with Rapid Kinetics for Electrochemically Reducing Carbon Dioxide to Formate. Advanced Functional Materials, 2021, 31, 2006704.	7.8	52
53482	A magnetically controllable metastable LiSeHFeO isomer: an ab-initio investigation from bulk to film. Journal of Materials Science, 2021, 56, 1461-1471.	1.7	5
53483	MagGene: A genetic evolution program for magnetic structure prediction. Computer Physics Communications, 2021, 259, 107659.	3.0	4
53484	Surface structures and equilibrium shapes of layered 2D Ruddlesden-Popper perovskite crystals from density functional theory calculations. Materials Today Communications, 2021, 26, 101745.	0.9	5
53485	Strain-modulated electronic and magnetic properties of Co2TMAl. Materials Today Communications, 2021, 26, 101764.	0.9	1
53486	Bidentate Lewis bases are preferred for passivation of MAPbI3 surfaces: A time-domain ab initio analysis. Nano Energy, 2021, 79, 105491.	8.2	33
53487	Ab-initio investigation for the microscopic thermodynamics and kinetics of martensitic transformation. Progress in Natural Science: Materials International, 2021, 31, 121-128.	1.8	6
53488	The structural stability, lattice dynamics, electronic, thermophysical, and mechanical properties of the inverse perovskites A ₃ OX: A comparative firstâ€principles study. International Journal of Energy Research, 2021, 45, 4793-4810.	2.2	21
53489	Improved thermoelectric properties of doped A0.5B0.5NiSn (A, Bâ€‰=â€‰Ti, Zr, Hf) with a special quasirandom structure. Journal of Materials Science, 2021, 56, 4280-4290.	1.7	3
53490	Improved catalytic wet peroxide oxidation of phenol over Pt-Fe2O3/SBA-15: Influence of platinum species and DFT calculations. Applied Surface Science, 2021, 541, 148409.	3.1	10
53491	Product-Specific Active Site Motifs of Cu for Electrochemical CO2 Reduction. CheM, 2021, 7, 406-420.	5.8	72
53492	ADP potential for the Au-Rh system and its application in element segregation of nanoparticles. Computational Materials Science, 2021, 186, 110002.	1.4	8
53493	Potential thermoelectric candidate monolayer silicon diphosphide (SiP2) from a first-principles calculation. Computational Materials Science, 2021, 188, 110154.	1.4	10
53494	A quasi two dimensional metallic state of CaHCl driven by La doping studied from first principles theory. Materials Today Communications, 2021, 26, 101830.	0.9	0
53495	Comparison of the effects of Sr2+ and Ca2+ substitution on the structural and electronic properties of the perovskites CH3NH3Pb1-Y I3 (Y Sr, Ca) by using the Density Functional Theory. Physica B: Condensed Matter, 2021, 600, 412579.	1.3	3
53496	Polyacrylamideâ€Mediated Silver Nanoparticles for Selectively Enhancing Electroreduction of CO₂ towards CO in Water. ChemSusChem, 2021, 14, 721-729.	3.6	11

#	Article	IF	Citations
53497	Alloying Effects on the Oxygen Diffusion in Nb Alloys: A First-Principles Study. Metallurgical and Materials Transactions A: Physical Metallurgy and Materials Science, 2021, 52, 270-283.	1.1	9
53498	Uniaxial compression of [001]-oriented CaFe2As2 single crystals: the effect of microstructure and temperature on superelasticity Part II: Modeling. Acta Materialia, 2021, 203, 116462.	3.8	1
53499	Highly Selective Production of Syngas from Chemical Looping Reforming of Methane with CO2 Utilization on MgO-supported Calcium Ferrite Redox Materials. Applied Energy, 2021, 282, 116111.	5.1	52
53500	Surface property of the Cu doped Î³-Al2O3: A density functional theory study. Applied Surface Science, 2021, 535, 147651.	3.1	18
53501	2D HfN2/graphene interface based Schottky device: Unmatched controllability in electrical contacts and carrier concentration via electrostatic gating and out-of-plane strain. Applied Surface Science, 2021, 540, 148389.	3.1	25
53502	Anti-sintering non-stoichiometric nickel ferrite for highly efficient and thermal-stable thermochemical CO2 splitting. Chemical Engineering Journal, 2021, 404, 127067.	6.6	13
53503	Ultra-fast and accurate binding energy prediction of shuttle effect-suppressive sulfur hosts for lithium-sulfur batteries using machine learning. Energy Storage Materials, 2021, 35, 88-98.	9.5	42
53504	Highly-efficient all-inorganic lead-free 1D CsCu2I3 single crystal for white-light emitting diodes and UV photodetection. Nano Energy, 2021, 81, 105570.	8.2	100
53505	Highâ€temperature persistent luminescence and visual dualâ€emitting optical temperature sensing in selfâ€activated CaNb₂O₆: Tb³⁺ phosphor. Journal of the American Ceramic Society, 2021, 104, 1750-1759.	1.9	106
53506	First demonstration of phosphate enhanced atomically dispersed bimetallic FeCu catalysts as Pt-free cathodes for high temperature phosphoric acid doped polybenzimidazole fuel cells. Applied Catalysis B: Environmental, 2021, 284, 119717.	10.8	28
53507	Conjugated nickel phthalocyanine polymer selectively catalyzes CO2-to-CO conversion in a wide operating potential window. Applied Catalysis B: Environmental, 2021, 284, 119739.	10.8	45
53508	Reaction induced multifunctional TiO2 rod/particle nanostructured materials for screen printed dye sensitized solar cells. Ceramics International, 2021, 47, 8094-8104.	2.3	4
53509	Selection of interfacial metals for Si3N4 ceramics by the density functional theory. Chemical Physics Letters, 2021, 763, 138189.	1.2	2
53510	Structural stability, electronic structures, mechanical properties and debye temperature of W-Re alloys: A first-principles study. Fusion Engineering and Design, 2021, 162, 112081.	1.0	24
53511	Tailoring p-type conductivity of aluminum nitride via transition metal and fluorine doping. Journal of Alloys and Compounds, 2021, 862, 158017.	2.8	2
53512	1D metal-dithiolene wires as a new class of bi-functional oxygen reduction and evolution single-atom electrocatalysts. Journal of Catalysis, 2021, 393, 140-148.	3.1	18
53513	Ab initio comparative study of the magnetic, electronic and optical properties of AB2O4 (A, B= Mn, Fe) spinels. Materials Chemistry and Physics, 2021, 259, 124065.	2.0	16
53514	Synthesis of metal-free nitrogen-enriched porous carbon and its electrochemical sensing behavior for the highly sensitive detection of dopamine: Both experimental and theoretical investigation. Materials Chemistry and Physics, 2021, 260, 124094.	2.0	14

#	Article	IF	Citations
53515	Artificial Intelligence and QM/MM with a Polarizable Reactive Force Field for Next-Generation Electrocatalysts. Matter, 2021, 4, 195-216.	5.0	29
53516	Single atom Fe in favor of carbon disulfide (CS2) adsorption and thus the removal efficiency. Separation and Purification Technology, 2021, 258, 118086.	3.9	28
53517	Charge Disproportionation and Complex Magnetism in a PbMnO3 Perovskite Synthesized under High Pressure. Chemistry of Materials, 2021, 33, 92-101.	3.2	4
53518	Control of the single atom/nanoparticle ratio in Pd/C catalysts to optimize the cooperative hydrogenation of alkenes. Catalysis Science and Technology, 2021, 11, 984-999.	2.1	30
53519	First principles studies of mononuclear and dinuclear Pacman complexes for electrocatalytic reduction of CO2. Catalysis Science and Technology, 2021, 11, 637-645.	2.1	3
53520	Facilitated Water Adsorption and Dissociation on Ni/Ni 3 S 2 Nanoparticles Embedded in Porous Sâ€doped Carbon Nanosheet Arrays for Enhanced Hydrogen Evolution. Advanced Materials Interfaces, 2021, 8, 2001665.	1.9	10
53521	Roles of Enhancement of Câˆ'H Activation and Diminution of Câˆ'O Formation Within M1â€Phase Pores in Propane Selective Oxidation. ChemCatChem, 2021, 13, 882-899.	1.8	9
53522	Enhancement of 1Tâ€MoS₂ Superambient Temperature Stability and Hydrogen Evolution Performance by Intercalating a Phenanthroline Monolayer. ChemNanoMat, 2021, 7, 447-456.	1.5	11
53523	Contemporaneous inverse manipulation of the valence configuration to preferred Co2+ and Ni3+ for enhanced overall water electrocatalysis. Applied Catalysis B: Environmental, 2021, 284, 119725.	10.8	55
53524	Rh-engineered ultrathin NiFe-LDH nanosheets enable highly-efficient overall water splitting and urea electrolysis. Applied Catalysis B: Environmental, 2021, 284, 119740.	10.8	302
53525	Quantum chemical DFT study of molecular adsorption of H2S on clean and chemically modified Au(1 1) Tj ETQq0 0 0 rgBT /Overlock 10	3.1	8
53526	Electronic and thermodynamic properties of lanthanum tetraboride on low-temperature experimental and ab-initio calculation data. Journal of Alloys and Compounds, 2021, 862, 158020.	2.8	4
53527	Novel three-dimensional Ni2P-MoS2 heteronanosheet arrays for highly efficient electrochemical overall water splitting. Journal of Alloys and Compounds, 2021, 856, 158094.	2.8	15
53528	Distinct transport behaviors and electronic structures in Heusler alloys CoFeCrGa and CoFeCrAl. Journal of Magnetism and Magnetic Materials, 2021, 517, 167383.	1.0	4
53529	The mechanism on retention of hydrogen in three representative tungsten nitride compounds in nuclear fusion reactors. Journal of Nuclear Materials, 2021, 544, 152687.	1.3	5
53530	Uncovering the unusual effect of halogenation on crystal packing in an azzaacee-based electron transporting material. Materials Chemistry and Physics, 2021, 259, 124060.	2.0	2
53531	A chemical map of NaSICON electrode materials for sodium-ion batteries. Journal of Materials Chemistry A, 2021, 9, 281-292.	5.2	91
53532	Double Charge Polarity Switching in Sbâ€Doped SnSe with Switchable Substitution Sites. Advanced Functional Materials, 2021, 31, 2008092.	7.8	7

#	Article	IF	Citations
53533	Nanoindentation of Amorphous Carbon: a combined experimental and simulation approach. Acta Materialia, 2021, 203, 116485.	3.8	23
53534	Cobalt carbide nanosheets as effective catalysts toward photothermal degradation of mustard-gas simulants under solar light. Applied Catalysis B: Environmental, 2021, 284, 119703.	10.8	19
53535	Reaction pathways and the role of the carbonates during CO2 hydrogenation over hexagonal In2O3 catalysts. Applied Surface Science, 2021, 542, 148591.	3.1	9
53536	Theoretical investigation of solvent effects on the selective hydrogenation of furfural over Pt(111). International Journal of Hydrogen Energy, 2021, 46, 1592-1604.	3.8	13
53537	Deep in-gap states induced by double-oxygen-vacancy clusters in hydrogenated TiO2. Physica B: Condensed Matter, 2021, 600, 412631.	1.3	3
53538	Functionalized M₂TiC₂T_x MXenes (M = Cr and Mo; T = F, O, and) Tj ETQq1 1 0.784314 rgBT /Ov Physics, 2021, 23, 1038-1049.	1.3	16
53539	Transformation of a graphene nanoribbon into a hybrid 1D nanoobject with alternating double chains and polycyclic regions. Physical Chemistry Chemical Physics, 2021, 23, 425-441.	1.3	4
53540	Entropy driven preference for alkene adsorption at the pore mouth as the origin of pore-mouth catalysis for alkane hydroisomerization in 1D zeolites. Catalysis Science and Technology, 2021, 11, 563-574.	2.1	5
53541	Voltage hysteresis during lithiation/delithiation of graphite associated with meta-stable carbon stackings. Journal of Materials Chemistry A, 2021, 9, 492-504.	5.2	38
53542	Systematic investigations of the electron, phonon, elastic and thermal properties of monolayer so-MoS2 by first-principles calculations. Applied Surface Science, 2021, 539, 148248.	3.1	11
53543	Insights into the catalytic activity of trimetallic Al/Zn/Cu surfaces for the water gas shift reaction. Applied Surface Science, 2021, 542, 148589.	3.1	12
53544	Ï€-electron weak ferromagnetism in potassium-intercalated 9-phenylanthracene. Carbon, 2021, 173, 587-593.	5.4	10
53545	Bipolar magnetic semiconductor materials based on 2D Fe2O3 lattice. Chemical Physics, 2021, 542, 111058.	0.9	10
53546	Influence of different exchangeâ€“correlation potentials on twisted structures of bilayer XS2 (XÂ=ÂMo,) Tj ETQq1 1 0.784314 rgBT /Ov	1.4	3
53547	Theoretical computation of the electrocatalytic performance of CO2 reduction and hydrogen evolution reactions on graphdiyne monolayer supported precise number of copper atoms. International Journal of Hydrogen Energy, 2021, 46, 5378-5389.	3.8	41
53548	Anchoring Mo on C9N4 monolayers as an efficient single atom catalyst for nitrogen fixation. Journal of Energy Chemistry, 2021, 57, 443-450.	7.1	41
53549	Cofactor-free oxidase-mimetic nanomaterials from self-assembled histidine-rich peptides. Nature Materials, 2021, 20, 395-402.	13.3	78
53550	Electric field modulated ion-sieving effects of graphene oxide membranes. Journal of Materials Chemistry A, 2021, 9, 244-253.	5.2	4

#	Article	IF	Citations
53551	Spin-filter induced large magnetoresistance in 2D van der Waals magnetic tunnel junctions. Nanoscale, 2021, 13, 862-868.	2.8	43
53552	Identifying Ionic and Electronic Charge Transfer at Oxide Heterointerfaces. Advanced Materials, 2021, 33, e2004132.	11.1	22
53553	A Highâ€Efficiency Hematite Photoanode with Enhanced Bonding Energy Around Fe Atoms. Chemistry - A European Journal, 2021, 27, 4089-4097.	1.7	3
53554	Fluorinated (Nano)Carbons: CF_x Electrodes and CF_xâ€Based Batteries. Energy Technology, 2021, 9, 2000605.	1.8	31
53555	First-Principles Investigation of Ti2.25Co0.75Si and Ti2.25Co0.75Si0.5X0.5 (X = As and Sb) Heusler Alloys: Spin-Polarized Electronic, Magnetic, and Mechanical Properties. Journal of Superconductivity and Novel Magnetism, 2021, 34, 285-294.	0.8	0
53556	MIL-53 (Al) derived single-atom Rh catalyst for the selective hydrogenation of m-chloronitrobenzene into m-chloroaniline. Chinese Journal of Catalysis, 2021, 42, 824-834.	6.9	9
53557	Characterization of AE(TM)2Bi2O9 (AE: Ca, Sr, Ba; TM: Nb, Ta) as oxide ion conductors. Journal of the European Ceramic Society, 2021, 41, 1352-1359.	2.8	0
53558	First-principles calculations of electronic properties, surface stability and photocatalytic potentials of seleno-germanates A2GeSe4 (Aâ€¯=â€¯Mg; Î³-Sr) surfaces for a promising visible light photocatalytic application. Materials Today Communications, 2021, 26, 101799.	0.9	2
53559	Boosting interfacial charge transfer for alkaline hydrogen evolution via rational interior Se modification. Nano Energy, 2021, 81, 105641.	8.2	118
53560	Optical properties of organosilicon compounds containing sigma-electron delocalization by quasiparticle self-consistent GW calculations. Spectrochimica Acta - Part A: Molecular and Biomolecular Spectroscopy, 2021, 245, 118939.	2.0	9
53561	Realization of an Antiferromagnetic Superatomic Graphene: Dirac Mott Insulator and Circular Dichroism Hall Effect. Nano Letters, 2021, 21, 230-235.	4.5	16
53562	Prediction of room-temperature ferromagnetism and large perpendicular magnetic anisotropy in a planar hypercoordinate FeB₃monolayer. Nanoscale Horizons, 2021, 6, 43-48.	4.1	50
53563	Strainâ€Mediated High Conductivity in Ultrathin Antiferromagnetic Metallic Nitrides. Advanced Materials, 2021, 33, 2005920.	11.1	25
53564	Designed Iron Single Atom Catalysts for Highly Efficient Oxygen Reduction Reaction in Alkaline and Acid Media. Advanced Materials Interfaces, 2021, 8, 2001788.	1.9	11
53565	Identifying the Bottleneck for Heat Transport in Metalâ€“Organic Frameworks. Advanced Theory and Simulations, 2021, 4, 2000211.	1.3	14
53566	Lithiophilic diffusion barrier layer on stainless steel mesh for dendrite suppression and stable lithium metal anode. Applied Materials Today, 2021, 22, 100896.	2.3	8
53567	Ba3[LiSbS2(S2)2Cl2]: The first zero-dimensional (0D) lithium metal thioantimonate featuring molecular anions of [LiSbS2(S2)2Cl2]6â€“. Journal of Solid State Chemistry, 2021, 294, 121873.	1.4	2
53568	NanoMaterialsCAD: Flexible Software for the Design of Nanostructures. Advanced Theory and Simulations, 2021, 4, 2000232.	1.3	2

#	Article	IF	Citations
53569	Wide-band-gaps two dimentional C3XN (XÂ=ÂN and P) for metal-free photocatalytic water splitting. Applied Surface Science, 2021, 542, 148597.	3.1	17
53570	Al, Fe-codoped CoP nanoparticles anchored on reduced graphene oxide as bifunctional catalysts to enhance overall water splitting. Chemical Engineering Journal, 2021, 421, 127856.	6.6	44
53571	Synthesis strategies and emerging mechanisms of metal-organic frameworks for sulfate radical-based advanced oxidation process: A review. Chemical Engineering Journal, 2021, 421, 127863.	6.6	129
53572	High-throughput calculations based on the small set of ordered structures method for non-equimolar high entropy alloys. Computational Materials Science, 2021, 188, 110213.	1.4	14
53573	The effect of naphthalene-based additives on tin electrodeposition on a gold electrode. Electrochimica Acta, 2021, 368, 137606.	2.6	7
53574	The structure, mechanical, electronic and thermodynamic properties of bcc Zr-Nb alloy: A first principles study. Journal of Alloys and Compounds, 2021, 862, 158029.	2.8	18
53575	Size effect in two-dimensional oxide-on-metal catalysts of CO oxidation and its connection to oxygen bonding: An experimental and theoretical approach. Journal of Catalysis, 2021, 393, 100-106.	3.1	7
53576	Calculation of steady-state dynamical phase diagram in U-Mo binary system under irradiation. Journal of Nuclear Materials, 2021, 544, 152698.	1.3	4
53577	Effect of rare-earth doping on adsorption of carbon atom on ferrum surface and in ferrum subsurface: A first-principles study. Journal of Rare Earths, 2021, 39, 1144-1150.	2.5	6
53578	Spin transition mechanism in a cooperatively assembled Al/Fe-doped 2D SiC based on electric field manipulation. Physica E: Low-Dimensional Systems and Nanostructures, 2021, 127, 114546.	1.3	0
53579	FeOx clusters decorated hcp Ni nanosheets as inverse electrocatalyst to stimulate excellent oxygen evolution performance. Applied Catalysis B: Environmental, 2021, 284, 119687.	10.8	33
53580	Template-free fabrication of MoP nanoparticles encapsulated in N-doped hollow carbon spheres for efficient alkaline hydrogen evolution. Chemical Engineering Journal, 2021, 416, 127677.	6.6	56
53581	Multilayer hollow MnCo2O4 microsphere with oxygen vacancies as efficient electrocatalyst for oxygen evolution reaction. Chemical Engineering Journal, 2021, 421, 127831.	6.6	84
53582	Polarized nucleation and efficient decomposition of Li2O2 for Ti2C MXene cathode catalyst under a mixed surface condition in lithium-oxygen batteries. Energy Storage Materials, 2021, 35, 669-678.	9.5	65
53583	Fast-dissolving antibacterial nanofibers of cyclodextrin/antibiotic inclusion complexes for oral drug delivery. Journal of Colloid and Interface Science, 2021, 585, 184-194.	5.0	46
53584	Hierarchical NiMoP2-Ni2P with amorphous interface as superior bifunctional electrocatalysts for overall water splitting. Journal of Materials Science and Technology, 2021, 77, 108-116.	5.6	48
53585	Unraveling the effects of anions in NixAy@CC (A=O, S, P) on Li-sulfur batteries. Materials Today Nano, 2021, 13, 100106.	2.3	5
53586	Selective SO2 detection at low concentration by Ca substituted LaFeO3 chemiresistive gas sensor: A comparative study of LaFeO3 pellet vs thin film. Sensors and Actuators B: Chemical, 2021, 329, 129211.	4.0	45

#	Article	IF	Citations
53587	The electronic and magnetic properties of h-BN/MoS₂ heterostructures intercalated with 3d transition metal atoms. Physical Chemistry Chemical Physics, 2021, 23, 506-513.	1.3	4
53588	Defect formation and its effect on the thermodynamic properties of Pu₂Zr₂O₇ pyrochlore: a firstâ€principles study. Journal of the American Ceramic Society, 2021, 104, 2301-2312.	1.9	2
53589	Machine learning potentials for tobermorite minerals. Computational Materials Science, 2021, 188, 110173.	1.4	15
53590	Not all platinum surfaces are the same: Effect of the support on fundamental properties of platinum adlayer and its implications for the activity toward hydrogen evolution reaction. Electrochimica Acta, 2021, 368, 137598.	2.6	9
53591	Developing micro-kinetic model for electrocatalytic reduction of carbon dioxide on copper electrode. Journal of Catalysis, 2021, 393, 11-19.	3.1	16
53592	Accelerated discovery of stable spinels in energy systems via machine learning. Nano Energy, 2021, 81, 105665.	8.2	30
53593	Synthesis, characterization and first principle modelling of the MAB phase solid solutions: (Mn1-xCrx)2AlB2 and (Mn1-xCrx)3AlB4. Materials Research Letters, 2021, 9, 112-118.	4.1	17
53594	Structural and Raman study of the thermoelectric solid solution Sr 1.9 La 0.1 Nb 2 O 7. Journal of Raman Spectroscopy, 2021, 52, 737-749.	1.2	1
53595	Vacancies and dopants in two-dimensional tin monoxide: An ab initio study. Applied Surface Science, 2021, 538, 147988.	3.1	11
53596	All-carbon-frameworks enabled thick electrode with exceptional high-areal-capacity for Li-Ion storage. Carbon, 2021, 174, 1-9.	5.4	160
53597	Building up bimetallic active sites for electrocatalyzing hydrogen evolution reaction under acidic and alkaline conditions. Chemical Engineering Journal, 2021, 413, 128027.	6.6	35
53598	Low thermal conductivity and good thermoelectric performance in mercury chalcogenides. Computational Materials Science, 2021, 188, 110192.	1.4	0
53599	Modification of spectrum and laser performance on a Tm3+ doped YAlO3 crystal by a specific electron beam radiation. Optik, 2021, 228, 166124.	1.4	1
53600	Tuning of ferromagnetic behavior of GaN films by N ion implantation: An experimental and first principle-based study. Journal of Magnetism and Magnetic Materials, 2021, 523, 167630.	1.0	12
53601	Mechanistic insight of KBiQ₂ (Q = S, Se) using panoramic synthesis towards synthesis-by-design. Chemical Science, 2021, 12, 1378-1391.	3.7	11
53602	Metal Halide Scintillators with Fast and Selfâ€Absorptionâ€Free Defectâ€Bound Excitonic Radioluminescence for Dynamic Xâ€Ray Imaging. Advanced Functional Materials, 2021, 31, 2007921.	7.8	78
53603	Exotic Structural and Optoelectronic Properties of Layered Halide Double Perovskite Polymorphs. Advanced Functional Materials, 2021, 31, 2008620.	7.8	5
53604	Thermoelectric Properties of Novel Semimetals: A Case Study of YbMnSb₂. Advanced Materials, 2021, 33, e2003168.	11.1	34

#	Article	IF	Citations
53605	Hydrogen Evolution Reaction for Vacancyâ€Ordered iâ€MXenes and the Impact of Proton Absorption into the Vacancies. Advanced Sustainable Systems, 2021, 5, 2000158.	2.7	27
53606	Fluxâ€Assisted Synthesis of Prismâ€like Octahedral Ta₃N₅ Singleâ€Crystals with Controllable Facets for Promoted Photocatalytic H₂ Evolution. Solar Rrl, 2021, 5, 2000574.	3.1	10
53607	Thermodynamics of monoclinic and tetragonal hafnium dioxide (HfO2) at ambient pressure. Calphad: Computer Coupling of Phase Diagrams and Thermochemistry, 2021, 72, 102210.	0.7	14
53608	The impact of B-site antisite defects on the magnetic and electronic properties in double perovskite Pb2FeOsO6. Ceramics International, 2021, 47, 992-1001.	2.3	2
53609	Segregation behavior of alloying elements at Ni Î£5 [001](210) symmetrical tilt grain boundary in nickel-based superalloys and their stabilization and strengthening mechanisms for the grain boundary. Materials Chemistry and Physics, 2021, 258, 123977.	2.0	17
53610	Chargeâ€Transferâ€Induced Multivalent States with Resultant Emergent Magnetism in Transitionâ€Metal Oxide Heterostructures. Advanced Electronic Materials, 2021, 7, .	2.6	5
53611	Non-metallic electronic regulation in CuCo oxy-/thio-spinel as advanced oxygen evolution electrocatalysts. Science China Chemistry, 2021, 64, 101-108.	4.2	21
53612	Atomistic origin of high-concentration Ce3+ in {100}-faceted Cr-substituted CeO2 nanocrystals. Acta Materialia, 2021, 203, 116473.	3.8	18
53613	External uniaxial compressive strain induced built-in electric field in bilayer two-dimensional As2S3 for photocatalytic water splitting: A first-principles study. Applied Surface Science, 2021, 535, 147701.	3.1	7
53614	Zero-thermal-quenching and improved chemical stability of a UCr4C4-type phosphor via crystal site engineering. Chemical Engineering Journal, 2021, 420, 127664.	6.6	21
53615	Corrosion-engineered bimetallic oxide electrode as anode for high-efficiency anion exchange membrane water electrolyzer. Chemical Engineering Journal, 2021, 420, 127670.	6.6	51
53616	IrO2â€“CeO2-graphene/Ti porous electrode with high charge-transfer speed and enhanced capacitance. Ceramics International, 2021, 47, 3728-3740.	2.3	8
53617	High capacity reversible hydrogen storage in titanium doped 2D carbon allotrope Î¨-graphene: Density Functional Theory investigations. International Journal of Hydrogen Energy, 2021, 46, 4154-4167.	3.8	100
53618	Active and stable Fe-based catalyst, mechanism, and key role of alkali promoters in ammonia synthesis. Journal of Catalysis, 2021, 394, 353-365.	3.1	16
53619	CO2 electroreduction by transition metal-embedded two-dimensional C3N: A theoretical study. Journal of CO2 Utilization, 2021, 43, 101367.	3.3	19
53620	Electronic structure, optical and vibrational properties of Ti2FeNiSb2 and Ti2Ni2InSb double half heusler alloys. Materials Science in Semiconductor Processing, 2021, 123, 105531.	1.9	18
53621	Comprehensive first-principles study of bulk, bilayer, and monolayer Î±-PtO2 properties. Physica E: Low-Dimensional Systems and Nanostructures, 2021, 127, 114514.	1.3	7
53622	Crystal structure and ON-OFF polymerization mechanism of poly(1,4-phenyleneazine-N,N-dioxide), a possible wide bandgap semiconductor. Polymer, 2021, 214, 123235.	1.8	8

#	Article	IF	Citations
53623	Two-dimensional vanadium tetrafluoride with antiferromagnetic ferroelasticity and bidirectional negative Poisson's ratio. Journal of Materials Chemistry C, 2021, 9, 95-100.	2.7	18
53624	Coercivity dependence of cation distribution in Co-based spinel: correlating theory and experiments. Inorganic Chemistry Frontiers, 2021, 8, 433-443.	3.0	5
53625	Bain Deformation Mechanism and Lifshitz Transition in Magnesium under High Pressure. Physica Status Solidi (B): Basic Research, 2021, 258, 2000279.	0.7	8
53626	Porous rod-like Ni2P/Ni assemblies for enhanced urea electrooxidation. Nano Research, 2021, 14, 1405-1412.	5.8	65
53627	"Materials Studio" Simulation Study of the Adsorption and Polymerization Mechanism of Sodium Silicate on Active Silica Surface at Different Temperatures. International Journal of Metalcasting, 2021, 15, 1091-1098.	1.5	17
53628	Understanding the dehydrogenation mechanism over iron nanoparticles catalysts based on density functional theory. Chinese Chemical Letters, 2021, 32, 286-290.	4.8	10
53629	Selective adsorption of CO2 by Hex-star phosphorene from natural gas: Combining molecular simulation and real adsorbed solution theory. Chemical Engineering Science, 2021, 231, 116283.	1.9	8
53630	First principles investigation of the structural, elastic, electronic and vibrational properties of vanadium-based V3X (X = Fe, Co, and Ni) compounds. Journal of Physics and Chemistry of Solids, 2021, 150, 109854.	1.9	4
53631	Boron nitride nanoribbons with single vacancy defects and doped with 3d transition metals: A first-principles study. Materials Today Communications, 2021, 26, 101861.	0.9	4
53632	Electronic and magnetic properties of 3d transition metal atom adsorbed Zr2CO2 Mxene: First-principles study. Solid State Communications, 2021, 325, 114140.	0.9	9
53633	Theoretical study of Na⁺ transport in the solid-state electrolyte Na₃OBr based on deep potential molecular dynamics. Inorganic Chemistry Frontiers, 2021, 8, 425-432.	3.0	22
53634	Engineering the interface between LiCoO₂ and Li₁₀GeP₂S₁₂ solid electrolytes with an ultrathin Li₂CoTi₃O₈ interlayer to boost the performance of all-solid-state batteries. Energy and Environmental Science, 2021, 14, 437-450.	15.6	82
53635	Dopingâ€Driven Antiferromagnetic to Ferromagnetic Phase Transition in Tetragonal Cr2B2 Monolayer. Physica Status Solidi (B): Basic Research, 2021, 258, 2000396.	0.7	9
53636	Ammonia electro-oxidation mechanism on the platinum (100) surface. Catalysis Today, 2021, 371, 50-57.	2.2	28
53637	Second-nearest-neighbor modified embedded-atom method interatomic potential for V-M (MÂ=ÂCu, Mo,) Tj ETQq0 0 0 rgBT /Overlock 1	1.4	12
53638	Scaling the existence state of hydrogen in metal binary oxides. Acta Materialia, 2021, 203, 116463.	3.8	3
53639	Epoxy oxidized diamond (111)-(2ÂÃ— 1) surface for nitrogen-vacancy based quantum sensors. Carbon, 2021, 173, 485-492.	5.4	9
53640	Atomistic modeling of anisotropic mechanical properties of lanthanum zirconate nanocystal. Materials Chemistry and Physics, 2021, 259, 124024.	2.0	0

#	Article	IF	Citations
53641	First-principles study of structural, electronic and magnetic properties of A-site-ordered quadruple perovskite LaMn3Rh4O12. Materials Science in Semiconductor Processing, 2021, 123, 105586.	1.9	4
53642	Stability of Zener order in martensite: an atomistic evidence. Scripta Materialia, 2021, 194, 113632.	2.6	9
53643	Controllable synthesis of tunable aspect ratios novel h-BN nanorods with an enhanced wetting performance for water repellent applications. Vacuum, 2021, 184, 109927.	1.6	15
53644	Partialâ€Singleâ€Atom, Partialâ€Nanoparticle Composites Enhance Water Dissociation for Hydrogen Evolution. Advanced Science, 2021, 8, 2001881.	5.6	85
53645	2â€•and 2,7â€Substituted paraâ€•Nâ€Methylpyridinium Pyrenes: Syntheses, Molecular and Electronic Structures, Photophysical, Electrochemical, and Spectroelectrochemical Properties and Binding to Doubleâ€Stranded (ds) DNA. Chemistry - A European Journal, 2021, 27, 2837-2853.	1.7	13
53646	Density functional theory study of solute cluster growth processes in Mg-Y-Zn LPSO alloys. Acta Materialia, 2021, 203, 116491.	3.8	25
53647	Design of solute clustering during thermomechanical processing of AA6016 Alâ€“Mgâ€“Si alloy. Acta Materialia, 2021, 203, 116455.	3.8	71
53648	DFTÂ+ÂU study of U1-An O2- (AnÂ=ÂNp, Pu, Am and Cm) {1 1 1}, {1 1 0} and {1 0 0} surfaces. Applied Surface Science, 2021, 537, 147972.	3.1	4
53649	Effect of thermally excited lattice vibrations on the thermodynamic stability of tungsten ditellurides WTe2 under high pressure: A first-principles investigation. Computational Materials Science, 2021, 186, 110024.	1.4	6
53650	Electromagnetic wave absorption performance of Ti2O3 and vacancy enhancement effective bandwidth. Journal of Materials Science and Technology, 2021, 76, 166-173.	5.6	32
53651	First-principles study of persistent luminescence mechanisms in CaB2O4:Ce3+. Optical Materials, 2021, 111, 110647.	1.7	5
53652	Superhierarchical Inorganic/Organic Nanocomposites Exhibiting Simultaneous Ultrahigh Dielectric Energy Density and High Efficiency. Advanced Functional Materials, 2021, 31, 2007994.	7.8	46
53653	First-principles DFT insights into the adsorption of hydrazine on bimetallic Î²1-NiZn catalyst: Implications for direct hydrazine fuel cells. Applied Surface Science, 2021, 536, 147648.	3.1	15
53654	Giant perpendicular magnetic anisotropy induced by double degeneracy of d-orbitals in W/MgO/Ag heterojunction. Applied Surface Science, 2021, 541, 148421.	3.1	6
53655	Stable performance of Li-S battery: Engineering of Li2S smart cathode by reduction of multilayer graphene-embedded 2D-MoS2. Journal of Alloys and Compounds, 2021, 862, 158031.	2.8	11
53656	Structurally ordered intermetallic Ir3V electrocatalysts for alkaline hydrogen evolution reaction. Nano Energy, 2021, 81, 105636.	8.2	45
53657	Enabling selective, room-temperature gas detection using atomically dispersed Zn. Sensors and Actuators B: Chemical, 2021, 329, 129221.	4.0	10
53658	Exploring the anion chemical space of Ln₂OF_{2â^'x}Cl_xH₂ (Ln = Y, La, Gd): a model of electroelastic material with high mechanical sensitivity and energy harvesting. Materials Horizons, 2021, 8, 577-588.	6.4	2

#	Article	IF	Citations
53659	Ultrasmall SnO₂ nanocrystals sandwiched into polypyrrole and Ti₃C₂T_x MXene for highly effective sodium storage. Materials Chemistry Frontiers, 2021, 5, 825-833.	3.2	25
53660	Design of phosphorus-functionalized MXenes for highly efficient hydrogen evolution reaction. Journal of Materials Chemistry A, 2021, 9, 597-606.	5.2	20
53661	Ab initio study of oxygen segregation in silicon grain boundaries: The role of strain and vacancies. Acta Materialia, 2021, 204, 116477.	3.8	12
53662	Where is the unpaired transition metal in substoichiometric diboride line compounds?. Acta Materialia, 2021, 204, 116510.	3.8	21
53663	Gate controllable optical spin current generation in zigzag graphene nanoribbon. Carbon, 2021, 173, 565-571.	5.4	17
53664	Na10SnSb2S12: A nanosized air-stable solid electrolyte for all-solid-state sodium batteries. Chemical Engineering Journal, 2021, 420, 127692.	6.6	36
53665	Quantum capacitance of supercapacitor electrodes based on germanene influenced by vacancy and co-doping: A first-principles study. Computational Materials Science, 2021, 188, 110131.	1.4	24
53666	Designing new tetragonal Heusler materials using V, Cr, Fe and Ni doped Ti2CoGa: A first-principles study. Computational Materials Science, 2021, 188, 110143.	1.4	2
53667	Manipulation of band alignment in InSe/GaTe and InSe/InS van der Waals heterostructures. Computational Materials Science, 2021, 188, 110153.	1.4	3
53668	Investigation of native defects and impurities in X-N (XÂ=ÂAl, Ga, In). Computational Materials Science, 2021, 188, 110169.	1.4	4
53669	Enhancing bifunctional electrocatalysts of hollow Co3O4 nanorods with oxygen vacancies towards ORR and OER for Liâ€“O2 batteries. Electrochimica Acta, 2021, 367, 137490.	2.6	49
53670	Ag@WS2 quantum dots for Surface Enhanced Raman Spectroscopy: Enhanced charge transfer induced highly sensitive detection of thiram from honey and beverages. Food Chemistry, 2021, 344, 128570.	4.2	25
53671	Thermoelectric transport properties in chalcogenides ZnX (X=S, Se): From the role of electron-phonon couplings. Journal of Materiomics, 2021, 7, 310-319.	2.8	24
53672	Vibron quasi-bound state stability for tetragonal CeCuxAg1-xAl3. Journal of Magnetism and Magnetic Materials, 2021, 530, 167541.	1.0	2
53673	The unique carrier mobility of Janus MoSSe/GaN heterostructures. Frontiers of Physics, 2021, 16, 1.	2.4	18
53674	Strain-improved electronic and magnetic properties of V-, Cr-, Mn- and Fe-doped Î±- and Î²-tellurene. Applied Surface Science, 2021, 541, 148454.	3.1	6
53675	Systematic study on mechanical and electronic properties of ternary VAlN, TiAlN and WAlN systems by first-principles calculations. Ceramics International, 2021, 47, 7511-7520.	2.3	29
53676	Exploration of new phase structure of FePd crystalline alloy with a stoichiometric of 1:1. Computational Materials Science, 2021, 188, 110168.	1.4	3

#	Article	IF	Citations
53677	Mineralogical phase transformation of Fe containing sphalerite at acidic environments in the presence of Cu2+. Journal of Hazardous Materials, 2021, 403, 124058.	6.5	12
53678	On the applicability of the single parabolic band model to advanced thermoelectric materials with complex band structures. Journal of Materiomics, 2021, 7, 603-611.	2.8	11
53679	Atomic-scale roles of Zn element in age-hardened AlMgSiZn alloys. Journal of Materials Science and Technology, 2021, 70, 105-112.	5.6	22
53680	First-principles studies of the electronic and magnetic structures and bonding properties of boron subnitride B13N2. Journal of Solid State Chemistry, 2021, 294, 121840.	1.4	3
53681	Low-Index Stoichiometric Surfaces of CuBiW2O8. Surface Science, 2021, 705, 121762.	0.8	1
53682	Effect of Zn atom in Fe-N-C catalysts for electro-catalytic reactions: theoretical considerations. Nano Research, 2021, 14, 611-619.	5.8	52
53683	Analysis of shape, orientation and interface properties of Mo<mml:math xmlns:mml="http://www.w3.org/1998/Math/MathML" altimg="si15.svg"><mml:msub><mml:mrow /><mml:mn>2</mml:mn></mml:msub></mml:math>C precipitates in Fe using ab-initio and finite element method calculations. Acta Materialia, 2021, 204, 116478.	3.8	8
53684	Stability and catalytic activity to NOx and NH3 of single-atom manganese catalyst with graphene-based substrate: A DFT study. Applied Surface Science, 2021, 541, 148460.	3.1	10
53685	An efficient approximation of the supercell approach to the calculation of the full phonon spectrum. Calphad: Computer Coupling of Phase Diagrams and Thermochemistry, 2021, 72, 102215.	0.7	1
53686	Mn-doped ZnO microspheres as cathode materials for aqueous zinc ion batteries with ultrastability up to 10 000 cycles at a large current density. Chemical Engineering Journal, 2021, 421, 127770.	6.6	23
53687	Manipulation of electronic and magnetic properties of Cr2CX2 (X=F,O,OH) monolayer by applying mechanical strains. Journal of Alloys and Compounds, 2021, 850, 156769.	2.8	5
53688	Insights into the Bond Behavior and Mechanical Properties of Hafnium Carbide under High Pressure and High Temperature. Inorganic Chemistry, 2021, 60, 515-524.	1.9	20
53689	Theory-guided construction of electron-deficient sites via removal of lattice oxygen for the boosted electrocatalytic synthesis of ammonia. Nano Research, 2021, 14, 1457-1464.	5.8	10
53690	Mechanically robust, self-healing graphene like defective SiC: A prospective anode of Li-ion batteries. Applied Surface Science, 2021, 541, 148417.	3.1	25
53691	Coupling highly dispersed Sb2S3 nanodots with nitrogen/sulfur dual-doped porous carbon nanosheets for efficient immobilization and catalysis of polysulfides conversion. Chemical Engineering Journal, 2021, 420, 127688.	6.6	29
53692	Relevance of metal (Ca versus Mn) embedded C2N for energy-storage applications: Atomic-scale study. International Journal of Hydrogen Energy, 2021, 46, 2445-2463.	3.8	12
53693	Study on intrinsic defects and copper doping in LiAlO2 crystal from combined first-principles and thermodynamic calculations. Journal of Alloys and Compounds, 2021, 850, 156761.	2.8	4
53694	Unveiling the role of atomic defects on the electronic, mechanical and elemental diffusion properties in CuS. Scripta Materialia, 2021, 192, 94-99.	2.6	12

#	Article	IF	Citations
53695	First-principles investigation of phosphate ester and carboxylic acid on BaTiO3 surfaces with stoichiometric terminations. Surface Science, 2021, 703, 121737.	0.8	5
53696	Magnetic and vibrational properties of small chromium clusters on the Cu(111) surface. Physical Chemistry Chemical Physics, 2021, 23, 7814-7821.	1.3	1
53697	Construction of atomically dispersed Cu-N4 sites via engineered coordination environment for high-efficient CO2 electroreduction. Chemical Engineering Journal, 2021, 407, 126842.	6.6	91
53698	Carbon-coated ultrathin metallic V5Se8 nanosheet for high-energy-density and robust potassium storage. Energy Storage Materials, 2021, 35, 1-11.	9.5	35
53699	Thermal Transport in Graphene Nanomesh: Unraveling the Role of Brillouin Zone Folding, Phonon Localization and Phonon Confinement. International Journal of Heat and Mass Transfer, 2021, 165, 120685.	2.5	14
53700	Black potassium titanate nanobelts: Ultrafast and durable aqueous redox electrolyte energy storage. Journal of Power Sources, 2021, 483, 229140.	4.0	5
53701	â€œInvertedâ€•CO molecules on NaCl(100): a quantum mechanical study. Physical Chemistry Chemical Physics, 2021, 23, 7860-7874.	1.3	5
53702	New insights on cellular structures strengthening mechanisms and thermal stability of an austenitic stainless steel fabricated by laser powder-bed-fusion. Acta Materialia, 2021, 203, 116476.	3.8	234
53703	Fast sodium intercalation in Na3.41Â£0.59FeV(PO4)3: A novel sodium-deficient NASICON cathode for sodium-ion batteries. Energy Storage Materials, 2021, 35, 192-202.	9.5	66
53704	Electronic and optical properties of bismuth oxyhalides from ab initio calculations. Materials Science and Engineering B: Solid-State Materials for Advanced Technology, 2021, 264, 114921.	1.7	16
53705	Introducing and studying origin of deep electron traps in Ba1-xZrSi3O9:xEu for optical data storage. Optical Materials, 2021, 111, 110617.	1.7	1
53706	Anti-phase boundary energy of Î² series precipitates in Mg-Y-Nd system. Scripta Materialia, 2021, 193, 127-131.	2.6	119
53707	The Limits of the Confinement Effect Associated to Cage Topology on the Control of the MTO Selectivity. ChemCatChem, 2021, 13, 1578-1586.	1.8	18
53708	Combined XPS and DFT investigation of the adsorption modes of methyl enol ether functionalized cyclooctyne on Si(001). ChemPhysChem, 2021, 22, 404-409.	1.0	11
53709	How symmetry factors cause potential- and facet-dependent pathway shifts during CO2 reduction to CH4 on Cu electrodes. Applied Catalysis B: Environmental, 2021, 285, 119776.	10.8	28
53710	Enhanced Fe 3d delocalization and moderate spin polarization in Fe Ni atomic pairs for bifunctional ORR and OER electrocatalysis. Applied Catalysis B: Environmental, 2021, 285, 119778.	10.8	131
53711	Boosting Pd-catalysis for electrochemical CO2 reduction to CO on Bi-Pd single atom alloy nanodendrites. Applied Catalysis B: Environmental, 2021, 289, 119783.	10.8	80
53712	Iron-modulated nickel cobalt phosphide embedded in carbon to boost power density of hybrid sodiumâ€“air battery. Applied Catalysis B: Environmental, 2021, 285, 119786.	10.8	32

#	Article	IF	Citations
53713	Hydrogenation and C S bond activation pathways in thiophene and tetrahydrothiophene reactions on sulfur-passivated surfaces of Ru, Pt, and Re nanoparticles. Applied Catalysis B: Environmental, 2021, 291, 119797.	10.8	9
53714	Interfacial engineering of Cu2Se/Co3Se4 multivalent hetero-nanocrystals for energy-efficient electrocatalytic co-generation of value-added chemicals and hydrogen. Applied Catalysis B: Environmental, 2021, 285, 119800.	10.8	51
53715	A robust H-transfer redox mechanism determines the high-efficiency catalytic performance of layered double hydroxides. Applied Catalysis B: Environmental, 2021, 285, 119806.	10.8	21
53716	Engineering defect-rich Fe-doped NiO coupled Ni cluster nanotube arrays with excellent oxygen evolution activity. Applied Catalysis B: Environmental, 2021, 285, 119809.	10.8	103
53717	Dissociative chemisorption of methyl fluoride and its implications for atomic layer etching of silicon nitride. Applied Surface Science, 2021, 543, 148557.	3.1	10
53718	Highly anisotropic electronic and mechanical properties of monolayer and bilayer As2S3. Applied Surface Science, 2021, 542, 148665.	3.1	10
53719	Rational surface modification of ZnO with siloxane polymers for room-temperature-operated thin-film transistor-based gas sensors. Applied Surface Science, 2021, 542, 148704.	3.1	17
53720	Controlled anisotropic growth of layered perovskite nanocrystals for enhanced optoelectronic properties. Chemical Engineering Journal, 2021, 416, 128045.	6.6	15
53721	Proportional modulation of zinc-based MOF/carbon nanotube hybrids for simultaneous removal of phosphate and emerging organic contaminants with high efficiency. Chemical Engineering Journal, 2021, 417, 128063.	6.6	22
53722	Revert stable p-type ZnO with LimN complex co-doping from the first-principles study. Computational Materials Science, 2021, 186, 109894.	1.4	3
53723	Novel structural phase and superconductivity of W-Te compounds under high pressures. Computational Materials Science, 2021, 188, 110222.	1.4	4
53724	Effects of active elements on adhesion of the Al2O3/Fe interface: A first principles calculation. Computational Materials Science, 2021, 188, 110226.	1.4	24
53725	Crystal field module for the general relativistic atomic structure package. Computer Physics Communications, 2021, 261, 107772.	3.0	1
53726	Elastic3rd: A tool for calculating third-order elastic constants from first-principles calculations. Computer Physics Communications, 2021, 261, 107777.	3.0	22
53727	Theoretical study on thienothiophene core hole-transporting materials in perovskite solar cells: S atom position effect. Chemical Physics Letters, 2021, 764, 138264.	1.2	15
53728	Honeycomb Inspired Lithiophilic Scaffold for Ultra-Stable, High-Areal-Capacity Metallic Deposition. Energy Storage Materials, 2021, 35, 378-387.	9.5	11
53729	Fine tuning of the magnetic properties in Mn3-Co Ga Heusler films near the critical regime. Journal of Alloys and Compounds, 2021, 858, 158288.	2.8	1
53730	Behavior of enrichment and migration path of Cuâ€“Agâ€“Pdâ€“Biâ€“Pb in the recovery of waste multilayer ceramic capacitors by eutectic capture of copper. Journal of Cleaner Production, 2021, 287, 125469.	4.6	5

#	Article	IF	Citations
53731	Exploring UiO-66(Zr) frameworks as nanotraps for highly efficient removal of EDTA-complexed heavy metals from water. Journal of Environmental Chemical Engineering, 2021, 9, 104932.	3.3	21
53732	Triple-phase interfaces of graphene-like carbon clusters on antimony trisulfide nanowires enable high-loading and long-lasting liquid Li2S6-based lithium-sulfur batteries. Journal of Energy Chemistry, 2021, 59, 599-607.	7.1	26
53733	Ab initio molecular dynamics investigation of point defects in <mml:math xmlns:mml="http://www.w3.org/1998/Math/MathML" altimg="si1.svg"><mml:mi>Î³</mml:mi></mml:math>-U. Journal of Nuclear Materials, 2021, 545, 152714.	1.3	10
53734	Screening of perovskite materials for solar cell applications by first-principles calculations. Materials and Design, 2021, 198, 109387.	3.3	24
53735	Microscale bonding mechanism of Mg alloy and steel welded joint with nanoscale Al-based intermetallic compound interface layers. Materials Today Communications, 2021, 26, 101924.	0.9	2
53736	First principles prediction of exceptional mechanical and electronic behaviour of Titanite (CaTiSiO5). Materialia, 2021, 15, 100964.	1.3	3
53737	Interface-modulated uniform outer nanolayer: A category of electrodes of nanolayer-encapsulated core-shell configuration for supercapacitors. Nano Energy, 2021, 81, 105667.	8.2	48
53738	Superconductivity from buckled-honeycomb-vacancy ordering. Science Bulletin, 2021, 66, 327-331.	4.3	1
53739	Electronic and optical properties of Quasi-1D barium zinc chalcogenides <mml:math xmlns:mml="http://www.w3.org/1998/Math/MathML" altimg="si1.svg"><mml:mrow><mml:msub><mml:mtext>Ba</mml:mtext><mml:mn>2</mml:mn></mml:msub><mml:msub><mml:mtex		

#	Article	IF	Citations
53749	Defect-rich ZnS nanoparticles supported on reduced graphene oxide for high-efficiency ambient N2-to-NH3 conversion. Applied Catalysis B: Environmental, 2021, 284, 119746.	10.8	46
53750	The thermal and electrical transport properties of layered LaCuOSe under high pressure. Journal of Alloys and Compounds, 2021, 861, 157984.	2.8	15
53751	Theoretical insight into oxidation catalysis of chromite spinel MCr2O4 (MÂ=ÂMg, Co, Cu, and Zn): Volcano plot for oxygen-vacancy formation and catalytic activity. Journal of Catalysis, 2021, 393, 30-41.	3.1	11
53752	Active oxygen promoted electrochemical conversion of methane on two-dimensional carbide (MXenes): From stability, reactivity and selectivity. Journal of Catalysis, 2021, 393, 20-29.	3.1	19
53753	Pressure-driven structural and spin-state transition in a Hofmann clathrate coordination polymer. Journal of Magnetism and Magnetic Materials, 2021, 524, 167637.	1.0	0
53754	One-step synthesis of oxygen doped g-C3N4 for enhanced visible-light photodegradation of Rhodamine B. Journal of Physics and Chemistry of Solids, 2021, 151, 109900.	1.9	64
53755	Strain engineering the electronic and photocatalytic properties of g-C6N6/graphene heterostructures. Materials Today Communications, 2021, 26, 101969.	0.9	2
53756	Tuning the electronic and magnetic properties of monolayer germanium triphosphide adsorbed by halogen atoms: Insights from first principles study. Physica E: Low-Dimensional Systems and Nanostructures, 2021, 127, 114537.	1.3	8
53757	Metastable structures of CaCO₃ and their role in transformation of calcite to aragonite and postaragonite. Crystal Growth and Design, 2021, 21, 65-74.	1.4	16
53758	Isotropic Iodide Adsorption Causes Anisotropic Growth of Copper Microplates. Chemistry of Materials, 2021, 33, 881-891.	3.2	24
53759	Graphene Layer Morphology as an Indicator of the Metal Alloy Formation at the Interface. Journal of Physical Chemistry Letters, 2021, 12, 19-25.	2.1	4
53760	Oxygen evolution reaction over catalytic single-site Co in a well-defined brookite TiO2 nanorod surface. Nature Catalysis, 2021, 4, 36-45.	16.1	189
53761	Half metallicity and ferromagnetism of vanadium nitride nanoribbons: a first-principles study. Physical Chemistry Chemical Physics, 2021, 23, 1127-1138.	1.3	14
53762	Gate tunable self-powered few-layer black phosphorus broadband photodetector. Physical Chemistry Chemical Physics, 2021, 23, 399-404.	1.3	2
53763	Vertical strain and electric field tunable band alignment in type-II ZnO/MoSSe van der Waals heterostructures. Physical Chemistry Chemical Physics, 2021, 23, 1510-1519.	1.3	10
53764	Identification of key oxidative intermediates and the function of chromium dopants in PKU-8: catalytic dehydrogenation of sec-alcohols with tert-butylhydroperoxide. Catalysis Science and Technology, 2021, 11, 1365-1374.	2.1	2
53765	Photovoltaic modulation of ferromagnetism within a FM metal/Pâ€“N junction Si heterostructure. Nanoscale, 2021, 13, 272-279.	2.8	6
53766	Mo₂B₂ MBene-supported single-atom catalysts as bifunctional HER/OER and OER/ORR electrocatalysts. Journal of Materials Chemistry A, 2021, 9, 433-441.	5.2	175

#	Article	IF	Citations
53767	Tuning the Conduction Band Potential of Biâ€based Semiconductors Using a Combination of Organic Ligands. ChemSusChem, 2021, 14, 892-897.	3.6	7
53768	A density functional theory study on the underwater adhesion of catechol onto a graphite surface. Physical Chemistry Chemical Physics, 2021, 23, 1031-1037.	1.3	8
53769	A shape-memory V₃O₇Â·H₂O electrocatalyst for foldable N₂ fixation. Journal of Materials Chemistry A, 2021, 9, 1603-1609.	5.2	16
53770	Ferroelectricity in 2D metal phosphorus trichalcogenides and van der Waals heterostructures for photocatalytic water splitting. Journal of Materials Chemistry A, 2021, 9, 2734-2741.	5.2	27
53771	Exploring Aluminumâ€Ion Insertion into Magnesiumâ€Doped Manjiroite (MnO₂) Nanorods in Aqueous Solution. ChemElectroChem, 2021, 8, 1048-1054.	1.7	9
53772	Firstâ€principles investigations on the groundâ€state bulk properties and lattice constant dependent halfâ€metallic ferrimagnetism of Mn 2 NbSi fullâ€Heusler compound. International Journal of Quantum Chemistry, 2021, 121, e26566.	1.0	3
53773	Gradient multilayer aluminium sheets used in automotive heat exchangers. Journal of Materials Science, 2021, 56, 5215-5232.	1.7	6
53774	Mechanistic insights into efficient reversible hydrogen storage in ferrotitanium. International Journal of Hydrogen Energy, 2021, 46, 906-921.	3.8	11
53775	Improved H2 detection performance of GaN sensor with Pt/Sulfide treatment of porous active layer prepared by metal electroless etching. International Journal of Hydrogen Energy, 2021, 46, 4614-4625.	3.8	8
53776	Insights on alkylidene formation on Mo2C: A potential overlap between direct deoxygenation and olefin metathesis. Journal of Catalysis, 2021, 393, 381-389.	3.1	3
53777	Elastic anisotropies and thermodynamic properties of metal dodecborides under high pressure. Journal of Chemical Thermodynamics, 2021, 154, 106346.	1.0	4
53778	Two-dimensional uranium halide monolayers UX3 (X Cl, Br) with high Curie temperatures. Physics Letters, Section A: General, Atomic and Solid State Physics, 2021, 394, 127078.	0.9	5
53779	Ultrafast H2 gas nanosensor for ppb-level H2 gas detection based on GaN honeycomb nanonetwork. Sensors and Actuators B: Chemical, 2021, 329, 129079.	4.0	12
53780	Enhanced N₂affinity of 1T-MoS₂with a unique pseudo-six-membered ring consisting of Nâ€“Liâ€“Sâ€“Moâ€“Sâ€“Mo for high ambient ammonia electrosynthesis performance. Journal of Materials Chemistry A, 2021, 9, 1230-1239.	5.2	44
53781	Structural phase evolved Ni²⁺â€doped fluoride nanocrystals in KFâ€'ZnF₂â€'SiO₂ glassâ€ceramics. Journal of the American Ceramic Society, 2021, 104, 824-832.	1.9	4
53782	In Situ Construction of Uniform and Robust Cathodeâ€“Electrolyte Interphase for Liâ€Rich Layered Oxides. Advanced Functional Materials, 2021, 31, 2009192.	7.8	81
53783	Tunnel Intergrowth Li_xMnO₂ Nanosheet Arrays as 3D Cathode for Highâ€Performance Allâ€Solidâ€State Thin Film Lithium Microbatteries. Advanced Materials, 2021, 33, e2003524.	11.1	53
53784	Selective decoration of nitrogenated holey graphene (C2N) with titanium clusters for enhanced hydrogen storage application. International Journal of Hydrogen Energy, 2021, 46, 7371-7380.	3.8	63

#	Article	IF	Citations
53785	B36 nanoflake supported nickel as an efficient single-atom catalyst for oxygen reduction reaction: A first-principles study. Molecular Catalysis, 2021, 499, 111302.	1.0	1
53786	Understanding Excess Li Storage beyond LiC₆ in Reduced Dimensional Scale Graphene. ACS Nano, 2021, 15, 797-808.	7.3	50
53787	Radical pair formation due to compression-induced electron transfer in crystals of energetic salts. Physical Chemistry Chemical Physics, 2021, 23, 1520-1526.	1.3	5
53788	An oxygen-passivated vanadium cluster [V@V10O15]â^' with metalâ€“metal coordination produced by reacting Vnâ^' with O2. Physical Chemistry Chemical Physics, 2021, 23, 921-927.	1.3	9
53789	Unprecedented electrocatalytic oxygen evolution performances by cobalt-incorporated molybdenum carbide microflowers with controlled charge re-distribution. Journal of Materials Chemistry A, 2021, 9, 1770-1783.	5.2	13
53790	Vorhersage stickstoffbasierter Verbindungsklassen: Guanidinate TCN₃ (T=V,) Tj ETQq1 1 0.784314 rgBT /O Ãœbergangsmetallen. Angewandte Chemie, 2021, 133, 490-497.	1.6	2
53791	On the Chemical Bonding of Amorphous Sb₂Te₃. Physica Status Solidi - Rapid Research Letters, 2021, 15, 2000485.	1.2	13
53792	Static and dynamic ionic structure of molten CaCl2 via first-principles molecular dynamics simulations. Ionics, 2021, 27, 771-779.	1.2	14
53793	Impact of Aliovalent Alkaline-Earth metal solutes on Ceria Grain Boundaries: A density functional theory study. Acta Materialia, 2021, 205, 116481.	3.8	5
53794	Direction-control of anisotropic electronic properties via ferroelasticity in two-dimensional multiferroic semiconductor XOBr (XÂ=ÂTc, Ru). Chemical Physics Letters, 2021, 763, 138163.	1.2	4
53795	Spin Seebeck effect in the 2D ferromagnetic CrPbTe3. Physica E: Low-Dimensional Systems and Nanostructures, 2021, 126, 114443.	1.3	6
53796	First-principles study on the electronic structures and magnetic properties of InN monolayer doped with Cr, Fe, and Ni. Physica E: Low-Dimensional Systems and Nanostructures, 2021, 127, 114524.	1.3	9
53797	Modeling Auger Processes with Nonadiabatic Molecular Dynamics. Nano Letters, 2021, 21, 756-761.	4.5	29
53798	Cu₂O/CuS Nanocomposites Show Excellent Selectivity and Stability for Formate Generation via Electrochemical Reduction of Carbon Dioxide. , 2021, 3, 100-109.		65
53799	The first-principles and BTE investigation of phonon transport in 1T-TiSe₂. Physical Chemistry Chemical Physics, 2021, 23, 1627-1638.	1.3	9
53800	Generation of the Thermal Scattering Law of Uranium Dioxide with Ab Initio Lattice Dynamics to Capture Crystal Binding Effects on Neutron Interactions. Nuclear Science and Engineering, 2021, 195, 227-238.	0.5	5
53801	Theoretical Insights into the Mechanism of Selective Nitrateâ€toâ€Ammonia Electroreduction on Singleâ€Atom Catalysts. Advanced Functional Materials, 2021, 31, 2008533.	7.8	240
53802	Anharmonicityâ€Driven Rashba Cohelical Excitons Break Quantum Efficiency Limitation. Advanced Materials, 2021, 33, 2005400.	11.1	1

#	Article	IF	Citations
53803	Ruthenium Catalysts Promoted by Lanthanide Oxyhydrides with High Hydrideâ€ion Mobility for Lowâ€Temperature Ammonia Synthesis. Advanced Energy Materials, 2021, 11, 2003723.	10.2	45
53804	To Every Rule There is an Exception: A Rational Extension of Loewenstein's Rule. Angewandte Chemie - International Edition, 2021, 60, 5132-5135.	7.2	4
53805	Singleâ€Molecule Conductance of 1,4â€Azaborine Derivatives as Models of BNâ€doped PAHs. Angewandte Chemie - International Edition, 2021, 60, 6609-6616.	7.2	20
53806	Developing single-site Pt catalysts for the preferential oxidation of CO: A surface science and first principles-guided approach. Applied Catalysis B: Environmental, 2021, 284, 119716.	10.8	19
53807	Quantum well electronic states in spatially decoupled 2D Pb nanoislands on Nb-doped SrTiO3(0 0 1). Applied Surface Science, 2021, 537, 147967.	3.1	1
53808	Unveiling the interaction profile of cisplatin with gold-supported magnesia film. Applied Surface Science, 2021, 540, 148365.	3.1	8
53809	Biomimetic PVDF/LLTO composite polymer electrolyte enables excellent interface contact and enhanced ionic conductivity. Applied Surface Science, 2021, 541, 148434.	3.1	12
53810	First-principles studies of MoF6 absorption on hydroxylated and non-hydroxylated metal oxide surfaces and implications for atomic layer deposition of MoS2. Applied Surface Science, 2021, 541, 148461.	3.1	5
53811	Strong lithium-polysulfide anchoring effect of amorphous carbon for lithiumâ€“sulfur batteries. Current Applied Physics, 2021, 22, 94-103.	1.1	6
53812	Enhanced pseudocapacitive energy storage of oxides grown on nanoporous alloys by solid solution. Chemical Engineering Journal, 2021, 405, 126632.	6.6	6
53813	Ultra-small Sn-RuO2 nanoparticles supported on Nâ€‘doped carbon polyhedra for highly active and durable oxygen evolution reaction in acidic media. Chemical Engineering Journal, 2021, 409, 128155.	6.6	37
53814	Highly efficient H2 generation over Cu2Se decorated CdS0.95Se0.05 nanowires by photocatalytic water reduction. Chemical Engineering Journal, 2021, 409, 128157.	6.6	22
53815	Boosting the electrocatalytic activity of Pd/C by Cu alloying: Insight on Pd/Cu composition and reaction pathway. Journal of Colloid and Interface Science, 2021, 587, 446-456.	5.0	38
53816	Mechanistic insights into NOâ€'H2 reaction over Pt/boron-doped graphene catalyst. Journal of Hazardous Materials, 2021, 406, 124327.	6.5	8
53817	Adsorbed of toxic gas molecules (CO, H2S, and NO) on alkali-metal-doped g-GaN monolayer. Journal of Physics and Chemistry of Solids, 2021, 152, 109857.	1.9	14
53818	Solid-solution strengthening effects in binary Ni-based alloys evaluated by high-throughput calculations. Materials and Design, 2021, 198, 109359.	3.3	24
53819	Electronic and magnetic properties of carbide MXenesâ€"the role of electron correlations. Materials Today Advances, 2021, 9, 100118.	2.5	35
53820	Thermoelectric properties of strontium oxide under pressure: First-principles study. Physics Letters, Section A: General, Atomic and Solid State Physics, 2021, 390, 127083.	0.9	9

#	Article	IF	Citations
53821	First-principles study of electronic and optical properties of ternary compounds AuBX2 (X = S, Se, Te) and AuMTe2 (M = Al, In, Ga). Solid State Sciences, 2021, 111, 106508.	1.5	27
53822	Novel two-dimensional KAB (A = Cu, Au, B = S, Se) photoelectric materials with Prominent carrier mobility and optical properties. Superlattices and Microstructures, 2021, 149, 106773.	1.4	7
53823	First Principles Design of High Hole Mobility p-Type Snâ€“Oâ€“X Ternary Oxides: Valence Orbital Engineering of Sn²⁺ in Sn²⁺â€“Oâ€“X by Selection of Appropriate Elements X. Chemistry of Materials, 2021, 33, 212-225.	3.2	24
53824	Native Defect Engineering in CuInTe₂. Chemistry of Materials, 2021, 33, 359-369.	3.2	18
53825	Effect of the Niobium Doping Concentration on the Charge Storage Mechanism of Mesoporous Anatase Beads as an Anode for High-Rate Li-Ion Batteries. ACS Applied Energy Materials, 2021, 4, 215-225.	2.5	13
53826	Weak Distance Dependence of Hot-Electron-Transfer Rates at the Interface between Monolayer MoS₂ and Gold. ACS Nano, 2021, 15, 819-828.	7.3	27
53827	Atomic Wires of Transition Metal Chalcogenides: A Family of 1D Materials for Flexible Electronics and Spintronics. Jacs Au, 2021, 1, 147-155.	3.6	16
53828	Two-dimensional Ga₂O₂ monolayer with tunable band gap and high hole mobility. Physical Chemistry Chemical Physics, 2021, 23, 666-673.	1.3	9
53829	Identification of hydrogen species on Pt/Al₂O₃ by in situ inelastic neutron scattering and their reactivity with ethylene. Catalysis Science and Technology, 2021, 11, 116-123.	2.1	6
53830	Mechanistic insights into the phase transition and metal ex-solution phenomena of Pr_{0.5}Ba_{0.5}Mn_{0.85}Co_{0.15}O_{3â˜Î´} from simple to layered perovskite under reducing conditions and enhanced catalytic activity. Energy and Environmental Science, 2021, 14, 873-882.	15.6	37
53831	Efficient charge separation and visible-light response of two-dimensional Janus group-III monochalcogenide multilayers. Catalysis Science and Technology, 2021, 11, 542-555.	2.1	20
53832	An aromatic-rich cage-based MOF with inorganic chloride ions decorating the pore surface displaying the preferential adsorption of C₂H₂and C₂H₆over C₂H₄. Inorganic Chemistry Frontiers, 2021, 8, 1243-1252.	3.0	43
53833	Vanadium oxide integrated on hierarchically nanoporous copper for efficient electroreduction of CO₂ to ethanol. Journal of Materials Chemistry A, 2021, 9, 3044-3051.	5.2	32
53834	Tailoring the oxygen content in lithiated silicon oxide for lithiumâ€ion batteries. International Journal of Energy Research, 2021, 45, 7315-7325.	2.2	8
53835	Catalytic mechanism and selectivity prediction for syngas conversion over pure and K-promoted Mo2C catalysts. Applied Catalysis A: General, 2021, 610, 117945.	2.2	8
53836	Adsorption of C6H6 and C7H8 onto pristine and metal (Pd, Pt)-mediated ZnO monolayers: Electronic and gas sensing properties. Applied Surface Science, 2021, 542, 148767.	3.1	29
53837	Atomic-level understanding layer-by-layer formation process of TiCx on carbon film. Electrochimica Acta, 2021, 367, 137514.	2.6	2
53838	Implication of aliovalent cation substitution on structural and thermodynamic stability of Gd2Ti2O7: Experimental and theoretical investigations. Journal of Alloys and Compounds, 2021, 859, 157781.	2.8	7

#	Article	IF	Citations
53839	Deformation modes and yield strength anomaly in L12 compounds. Journal of Alloys and Compounds, 2021, 860, 158411.	2.8	12
53840	Design of Lead-Free Antiferroelectric (1 â€“ x)NaNbO₃â€“xSrSnO₃ Compositions Guided by First-Principles Calculations. Chemistry of Materials, 2021, 33, 266-274.	3.2	50
53841	Computational Methods in Heterogeneous Catalysis. Chemical Reviews, 2021, 121, 1007-1048.	23.0	198
53842	Exploring the Chemical Space of Linear Alkane Pyrolysis via Deep Potential GENerator. Energy & Fuels, 2021, 35, 762-769.	2.5	22
53843	Mitrofanovite, Layered Platinum Telluride, for Active Hydrogen Evolution. ACS Applied Materials & Interfaces, 2021, 13, 2437-2446.	4.0	10
53844	Probing the Local Site Disorder and Distortion in Pyrochlore High-Entropy Oxides. Journal of the American Chemical Society, 2021, 143, 4193-4204.	6.6	60
53845	Collaboration between a Pt-dimer and neighboring Coâ€“Pd atoms triggers efficient pathways for oxygen reduction reaction. Physical Chemistry Chemical Physics, 2021, 23, 1822-1834.	1.3	16
53846	Ultralow thermal conductivity in the quaternary semiconducting chalcogenide Cs₄[Ho₂₆Cd₇Se₄₈] with an unprecedented closed cavity architecture. Inorganic Chemistry Frontiers, 2021, 8, 1049-1055.	3.0	4
53847	A robust heterometallic ultramicroporous MOF with ultrahigh selectivity for propyne/propylene separation. Journal of Materials Chemistry A, 2021, 9, 2850-2856.	5.2	22
53848	Modifying an ultrathin insulating layer to suppress lithium dendrite formation within garnet solid electrolytes. Journal of Materials Chemistry A, 2021, 9, 3576-3583.	5.2	36
53849	First-principles investigation of the hydrogen evolution reaction of transition metal phosphides CrP, MnP, FeP, CoP, and NiP. Physical Chemistry Chemical Physics, 2021, 23, 2305-2312.	1.3	24
53850	Synthesis of novel chromium carbide using laser heated diamond anvil cell. Journal of Solid State Chemistry, 2021, 295, 121899.	1.4	4
53851	Mechanochemistry for ammonia synthesis under mild conditions. Nature Nanotechnology, 2021, 16, 325-330.	15.6	141
53852	Coordination tunes the activity and selectivity of the nitrogen reduction reaction on single-atom iron catalysts: a computational study. Journal of Materials Chemistry A, 2021, 9, 1240-1251.	5.2	135
53853	Interphase boundary layer-dominated strain mechanisms in Cu+ implanted Zr-Nb nanoscale multilayers. Acta Materialia, 2021, 202, 317-330.	3.8	21
53854	The average and local structure of TiVCrNbD<mml:math xmlns:mml="http://www.w3.org/1998/Math/MathML" altimg="si47.svg"><mml:msub><mml:mrow /><mml:mi>x</mml:mi></mml:msub></mml:math> (<mml:math) Tj ETQq1 1 0.784314 rgBT /Overlock 10 Tf 50 142 Td (xmlns:mml="	3.8	33
53855	Effective Ca2+-doping in Sr1-xCaxFeO3-Î´ oxygen carriers for chemical looping air separation: A theoretical and experimental investigation. Applied Energy, 2021, 281, 116040.	5.1	24
53856	First-principles study of dehydration interfaces between diaspore and corundum, gibbsite and boehmite, and boehmite and Î³-Al2O3: Energetic stability, interface charge effects, and dehydration defects. Applied Surface Science, 2021, 541, 148501.	3.1	19

#	Article	IF	Citations
53857	Improving platinum group metalâ€“free oxygen reduction reaction electrocatalyst activity: suggestions from density functional theory studies. Current Opinion in Electrochemistry, 2021, 25, 100631.	2.5	4
53858	First-principles insights into atomic oxygen diffusion inside polyhedral oligomeric silsesquioxane cages. Computational Materials Science, 2021, 186, 110007.	1.4	1
53859	Fully resolved strain field of the <mml:math xmlns:mml="http://www.w3.org/1998/Math/MathML" altimg="si78.svg"><mml:mrow><mml:msup><mml:mrow><mml:mi>Î²</mml:mi></mml:mrow><mml:mrow><mml:mo>â€³</mml:mo><mml:mo> precipitate calculated by density functional theory. Computational Materials Science, 2021, 187, 110054.	1.4	1
53860	Effect of interatomic potential on the sputtering of Pd surfaces. Computational Materials Science, 2021, 188, 110134.	1.4	0
53861	Cu nanoprecipitate morphologies and interfacial energy densities in bcc Fe from density functional theory (DFT). Computational Materials Science, 2021, 188, 110149.	1.4	7
53862	A first-principles study of helium diffusion in quartz and coesite under high pressure up to 12GPa. Geoscience Frontiers, 2021, 12, 1001-1009.	4.3	5
53863	First-principles investigation of the elastic properties and phase stability of (Ti1-xNix)C1-y ternary metastable carbides. Journal of Alloys and Compounds, 2021, 853, 157349.	2.8	2
53864	Strain-induced control of magnetocrystalline anisotropy energy in FeCo thin films. Journal of Magnetism and Magnetic Materials, 2021, 522, 167542.	1.0	4
53865	Chemisorption, diffusion and permeation of hydrogen isotopes in bcc bulk cr and cr(100) surface: First-principles dft simulations. Journal of Nuclear Materials, 2021, 543, 152538.	1.3	11
53866	Suppressing/enhancing effect of rhenium on helium clusters evolution in tungsten: Dependence on rhenium distribution. Journal of Nuclear Materials, 2021, 543, 152545.	1.3	7
53867	Assessment of multiscale hydrogen desorption models from (0001) Be surfaces. Journal of Nuclear Materials, 2021, 543, 152595.	1.3	7
53868	The role of binding energies for phosphorus and sulphur at grain boundaries in copper. Journal of Nuclear Materials, 2021, 544, 152682.	1.3	7
53869	The monolayer alloying and strain effect in weyl semimetal Td-MoTe2. Journal of Physics and Chemistry of Solids, 2021, 148, 109739.	1.9	3
53870	Revealing sodium-ion diffusion in alluaudite-type Na4â€“2M1+(MoO4)3 (M = Mg, Zn, Cd) from 23Na MAS NMR and ab initio studies. Journal of Solid State Chemistry, 2021, 293, 121800.	1.4	5
53871	Three tetragonal superhard sp3 carbon allotropes. Solid State Communications, 2021, 323, 114095.	0.9	8
53872	Tunable band alignments and optical properties in vertical heterojunctions of SnS2 and MoSe2. Solid State Communications, 2021, 323, 114103.	0.9	4
53873	The Tune Effect of Surface Pt/Mo Ratio on the Stability and Morphology of Î±-MoC surfaces. Surfaces and Interfaces, 2021, 22, 100831.	1.5	3
53874	On the signatures of oxygen vacancies in O1s core level shifts. Surface Science, 2021, 705, 121761.	0.8	27

#	Article	IF	Citations
53875	Insights on the optoelectronic properties in two-dimensional Janus lateral In2SeTe/Ga2STe heterostructure. Thin Solid Films, 2021, 718, 138479.	0.8	8
53876	Lattice resolution of vibrational modes in the electron microscope. Ultramicroscopy, 2021, 220, 113162.	0.8	16
53877	Prediction of enhanced thermoelectric performance in two-dimensional black phosphorus nanosheets. Vacuum, 2021, 183, 109790.	1.6	10
53878	The potential application of VS2 as an electrode material for Mg ion battery: A DFT study. Applied Surface Science, 2021, 544, 148775.	3.1	50
53879	First principles calculations of 3d-4d transition metal based LiMgPdSnâ€“type FeCrRuZ (ZÂ=ÂAl, Ga, In, Si) equiatomic quaternary Heusler alloys. Computational Materials Science, 2021, 188, 110116.	1.4	5
53880	First-Principles Study of the Effect of Doped Metal Atoms Pd, Mg and Ti on Tritium Release from Li2O (111) Surface. Computational Materials Science, 2021, 188, 110151.	1.4	1
53881	Reconstructing the Coordination Environment of Platinum Single-Atom Active Sites for Boosting Oxygen Reduction Reaction. ACS Catalysis, 2021, 11, 466-475.	5.5	62
53882	Quantum spin Hall insulators and topological Rashba-splitting edge states in two-dimensional CX₃ (X = Sb, Bi). Physical Chemistry Chemical Physics, 2021, 23, 2134-2140.	1.3	7
53883	Extrinsic Photoconduction Induced Shortâ€Wavelength Infrared Photodetectors Based on Geâ€Based Chalcogenides. Small, 2021, 17, e2006765.	5.2	25
53884	Electronic structure and magnetic properties of two-dimensional h-BN/Janus 2H-VSeX (XÂ=ÂS, Te) van der Waals heterostructures. Applied Surface Science, 2021, 537, 147898.	3.1	25
53885	Irvsp: To obtain irreducible representations of electronic states in the VASP. Computer Physics Communications, 2021, 261, 107760.	3.0	151
53886	Elastic isotropy originating from heterogeneous interlayer elastic deformation in a Ti3SiC2 MAX phase with a nanolayered crystal structure. Journal of the European Ceramic Society, 2021, 41, 2278-2289.	2.8	7
53887	Study of cage-like diamondoid polymeric nitrogen N10 confined inside single-wall carbon-nanotube. Materials Today Communications, 2021, 26, 101670.	0.9	3
53888	Lattice Thermal Conductivity Prediction Using Symbolic Regression and Machine Learning. Journal of Physical Chemistry A, 2021, 125, 435-450.	1.1	32
53889	On-Surface Fabrication of Complex Hybrid Nanostructures. Journal of Physical Chemistry C, 2021, 125, 354-357.	1.5	2
53890	Displacement parameters from density-functional theory and their validation in the experimental charge density of tartaric acid. CrystEngComm, 2021, 23, 1052-1058.	1.3	1
53891	Bornâ€“Oppenheimer molecular dynamics simulations on structures of high-density and low-density water: a comparison of the SCAN meta-GGA and PBE GGA functionals. Physical Chemistry Chemical Physics, 2021, 23, 2298-2304.	1.3	9
53892	Ionic conduction mechanism in Ca-doped lanthanum oxychloride. Dalton Transactions, 2021, 50, 151-156.	1.6	7

#	Article	IF	Citations
53893	First-principles exploration of the versatile configurations at an alkynyl-protected coinage metal(111) interface. Nanoscale, 2021, 13, 819-831.	2.8	4
53894	Ab initio Gibbs ensemble Monte Carlo simulations of the liquidâ€“vapor equilibrium and the critical point of sodium. Physical Chemistry Chemical Physics, 2021, 23, 311-319.	1.3	0
53895	Thermal neutron scattering properties of Bismuth crystal filter. Journal of Nuclear Science and Technology, 2021, 58, 704-713.	0.7	0
53896	Confinement Aided Simultanous Water Cleaning and Energy Harvesting Using Atomically Thin Wurtzite (Wurtzene). Advanced Sustainable Systems, 2021, 5, 2000189.	2.7	4
53897	To Every Rule There is an Exception: A Rational Extension of Loewenstein's Rule. Angewandte Chemie, 2021, 133, 5192-5195.	1.6	1
53898	Computational Design of Ductile Magnesium Alloy Anodes for Magnesium Batteries. Batteries and Supercaps, 2021, 4, 522-528.	2.4	5
53899	Vacancy assisted diffusion on singleâ€atom surface alloys. ChemPhysChem, 2021, 22, 29-39.	1.0	10
53900	The external electricâ€fieldâ€induced <scp>Schottkyâ€toâ€ohmic</scp> contact transition in graphene/ <scp>As ₂ S ₃ </scp> interface: A study by the first principles. International Journal of Energy Research, 2021, 45, 4727-4734.	2.2	4
53901	Quartic anharmonicity and ultraâ€low lattice thermal conductivity of alkali antimonide compounds M 3 Sb (M = K, Rb and Cs). International Journal of Energy Research, 2021, 45, 6958-6965.	2.2	8
53902	Prediction of Strong Converse Magnetoelectric Effect in Nbâ€Doped BaTiO 3 â€Based Polar Metals. Physica Status Solidi (B): Basic Research, 2021, 258, 2000520.	0.7	0
53903	Ab initio molecular dynamics study of the structure and supramolecular organization in mesogenic lanthanum(III) complexes with Î²â€diketones and Lewis bases. International Journal of Quantum Chemistry, 2021, 121, e26569.	1.0	2
53904	Quantumâ€Matter Bi/TiO₂ Heterostructure Embedded in Nâ€Doped Porous Carbon Nanosheets for Enhanced Sodium Storage. Small Structures, 2021, 2, 2000085.	6.9	77
53905	Lateral epitaxial growth of two-dimensional heterostructure linked by gold adatoms. Nano Research, 2021, 14, 887-892.	5.8	3
53906	Inter-facet composition modulation of III-nitride nanowires over pyramid textured Si substrates by stationary molecular beam epitaxy. Nano Research, 2021, 14, 1502-1511.	5.8	2
53907	Mechanisms for suppressing discontinuous precipitation and improving mechanical properties of NiAl-strengthened steels through nanoscale Cu partitioning. Acta Materialia, 2021, 205, 116561.	3.8	48
53908	Surface and segregation energies of Ag based alloys with Ni, Co and Fe: Direct experimental measurement and DFT study. Acta Materialia, 2021, 205, 116565.	3.8	17
53909	Tuning the structure and morphology of Li2O2 by controlling the crystallinity of catalysts for Li-O2 batteries. Chemical Engineering Journal, 2021, 409, 128145.	6.6	45
53910	Ab initio study of hydrogen diffusion in Be and Be12Ti for fusion applications. Computational Materials Science, 2021, 187, 109921.	1.4	9

#	Article	IF	Citations
53911	Segregation and embrittlement of gold grain boundaries. Computational Materials Science, 2021, 187, 110110.	1.4	13
53912	Influence mechanisms of the surface morphologies on the elementary diffusion kinetics on the Cu (1 1) Tj ETQq1 1 0.784314 rgBT /Overlock 10 Tf 50 507 Td (accent="true"><mml	1.4	0
53913	Difference in the electron energy loss spectra between the spinel-type Na3LiTi5O12 and Li4Ti5O12 clarified by density functional theory calculations. Computational Materials Science, 2021, 188, 110240.	1.4	5
53914	Genesis of magnetism in graphene/MoS2 van der Waals heterostructures via interface engineering using Cr-adsorption. Journal of Alloys and Compounds, 2021, 859, 157776.	2.8	47
53915	Exploring the mechanism of Ta3N5/KTaO3 photocatalyst for overall water splitting by first-principles calculations. Journal of Energy Chemistry, 2021, 56, 353-364.	7.1	4
53916	Mechanisms of tensile strengthening and oxygen solid solution in single Î²-phase Ti-35 at.%Ta+O alloys. Materials Science & Engineering A: Structural Materials: Properties, Microstructure and	2.6	16
53917	Influence of interactions between hydrogen and<ml:math xmlns:mml="http://www.w3.org/1998/Math/MathML" altimg="si1.svg"><mml:mo stretchy="false">(</mml:mo><mml:mn>10</mml:mn><mml:mover) Tj ETQq0 0 0 rgBT /Overlock 10 Tf 50 507 Td (accent="true"><mml	0.9	2
53918	Reducing d-p band coupling to enhance CO2 electrocatalytic activity by Mg-doping in Sr2FeMoO6-Î´ double perovskite for high performance solid oxide electrolysis cells. Nano Energy, 2021, 82, 105707.	8.2	67
53919	Type II GaS/AlN van der Waals heterostructure: Vertical strain, in-plane biaxial strain and electric field effect. Physica E: Low-Dimensional Systems and Nanostructures, 2021, 126, 114481.	1.3	9
53920	Curvature-induced effects in semiconducting alkaline-earth metal silicide nanotubes. Physica E: Low-Dimensional Systems and Nanostructures, 2021, 128, 114582.	1.3	4
53921	Improving surface mechanical properties of the selective laser melted 18Ni300 maraging steel via plasma nitriding. Surface and Coatings Technology, 2021, 406, 126675.	2.2	20
53922	Predicting Charge Transfer Stability between Sulfide Solid Electrolytes and Li Metal Anodes. ACS Energy Letters, 2021, 6, 150-157.	8.8	24
53923	In-Plane Optical and Electrical Anisotropy of 2D Black Arsenic. ACS Nano, 2021, 15, 1701-1709.	7.3	41
53924	Tailoring Binding Abilities by Incorporating Oxophilic Transition Metals on 3D Nanostructured Ni Arrays for Accelerated Alkaline Hydrogen Evolution Reaction. Journal of the American Chemical Society, 2021, 143, 1399-1408.	6.6	161
53925	Entropy-driven stabilization of the cubic phase of MaPbI₃ at room temperature. Journal of Materials Chemistry A, 2021, 9, 1089-1099.	5.2	35
53926	First-principles study of aziridinium tin iodide perovskites for photovoltaics. Journal of Materials Chemistry C, 2021, 9, 982-990.	2.7	7
53927	Highly anisotropic gas sensing of atom-thin borophene: a first-principles study. Journal of Materials Chemistry C, 2021, 9, 1069-1076.	2.7	28
53928	Impact of molecular and packing structure on the charge-transport properties of hetero[8]circulenes. Journal of Materials Chemistry C, 2021, 9, 1451-1466.	2.7	11

#	Article	IF	Citations
53929	Magnetic, transport and thermal properties of Î´-phase UZr₂. Philosophical Magazine Letters, 2021, 101, 1-11.	0.5	5
53930	Simulation of fullerene formation in a carbon-helium plasma. Fullerenes Nanotubes and Carbon Nanostructures, 2021, 29, 337-342.	1.0	6
53931	CVD growth of layered Cr2O3 hexagonal flakes for optoelectronic applications. Applied Surface Science, 2021, 536, 147713.	3.1	10
53932	Determining the hydration energetics on carbon-supported Ru catalysts: An adsorption calorimetry and density functional theory study. Catalysis Today, 2021, 365, 172-180.	2.2	3
53933	Room temperature d ferromagnetism in nitrogen doped WO3 for spintronic applications: A first-principles study. Chemical Physics Letters, 2021, 762, 138075.	1.2	12
53934	Origin of structural heterogeneity in Zr-Co-Al metallic glasses from the point of view of liquid structures. Journal of Non-Crystalline Solids, 2021, 553, 120501.	1.5	8
53935	MXenes: promising donor and acceptor materials for high-efficiency heterostructure solar cells. Sustainable Energy and Fuels, 2021, 5, 135-143.	2.5	32
53936	The adsorption thermodynamics of H2O and CO2 on PuO2(1 1 1) surface: A comparative study based on DFT+U-D3. Applied Surface Science, 2021, 537, 147882.	3.1	10
53937	Prediction of semiconducting SiP2 monolayer with negative Possionâ€™s ratio, ultrahigh carrier mobility and CO2 capture ability. Chinese Chemical Letters, 2021, 32, 1089-1094.	4.8	42
53938	Two-dimensional MgSiP2 with anisotropic electronic properties and good performances for Na-ion batteries. Chinese Chemical Letters, 2021, 32, 1081-1085.	4.8	26
53939	First-principles study of oxygen-terminated periodically porous graphene. Computational Materials Science, 2021, 187, 110102.	1.4	1
53940	Ru to W electron donation for boosted HER from acidic to alkaline on Ru/WNO sponges. Nano Energy, 2021, 80, 105531.	8.2	85
53941	Complexly electronic structure induced largely tunable anisotropic mobility for monolayer GeTe by uniaxial strain. Applied Surface Science, 2021, 538, 148009.	3.1	2
53942	Adsorption mechanism of typical VOCs on pristine and Al-modified MnO2 monolayer. Applied Surface Science, 2021, 539, 148164.	3.1	21
53943	Solution processed Ni2Co layered double hydroxides for high performance electrochemical sensors. Applied Surface Science, 2021, 541, 148270.	3.1	14
53944	Confining ultrasmall CoP nanoparticles into nitrogen-doped porous carbon via synchronous pyrolysis and phosphorization for enhanced potassium-ion storage. Chemical Engineering Journal, 2021, 413, 127508.	6.6	41
53945	Ab initio investigation of Co/TaC interfaces. Journal of Alloys and Compounds, 2021, 853, 156944.	2.8	10
53946	Reducing the acceptor levels of p-type Î²-Ga2O3 by (metal, N) co-doping approach. Journal of Alloys and Compounds, 2021, 854, 157247.	2.8	18

#	Article	IF	Citations
53947	Heterostructural phase diagram of Ga2O3â€“based solid solution with Al2O3. Journal of the European Ceramic Society, 2021, 41, 611-616.	2.8	19
53948	Flux crystal growth of a new BaTa2O6 polymorph, and of the novel tantalum oxyfluoride salt inclusion phase [Ba3F]Ta4O12F: Flux dependent phase formation. Journal of Solid State Chemistry, 2021, 294, 121833.	1.4	2
53949	New monomeric mixed-ligand complex of iron(III)-3-chloropyridine: Synthesis, structure, luminescence, electrochemical and magnetic properties. Journal of Molecular Structure, 2021, 1225, 129160.	1.8	4
53950	Arsenic K4 crystal: A new stable direct-gap semiconductor allotrope. Solid State Communications, 2021, 323, 114128.	0.9	2
53951	First-principles investigation of grain boundary structure effects on hydrogen solubility and segregation in tungsten. Journal of Nuclear Science and Technology, 2021, 58, 207-217.	0.7	6
53952	Tunable magnetism in layered CoPS3 by pressure and carrier doping. Science China Materials, 2021, 64, 673-682.	3.5	22
53953	A computational study of CO oxidation on IrO2 (1 1 0) surface. Applied Surface Science, 2021, 539, 148244.	3.1	10
53954	Highly sensitive NO2 response and abnormal P-N sensing transition with ultrathin Mo-doped SnS2 nanosheets. Chemical Engineering Journal, 2021, 420, 127572.	6.6	46
53955	Density functional theory calculations of diffusion barriers of organic molecules through the 8-ring of H-SSZ-13. Chemical Physics, 2021, 541, 111033.	0.9	9
53956	[Fe(CN)6] vacancy-boosting oxygen evolution activity of Co-based Prussian blue analogues for hybrid sodium-air battery. Materials Today Energy, 2021, 20, 100572.	2.5	17
53957	Layer Edge States Stabilized by Internal Electric Fields in Two-Dimensional Hybrid Perovskites. Nano Letters, 2021, 21, 182-188.	4.5	14
53958	DFT calculations and in situ DRIFTS study of CO oxidation on CeO2/Co3O4 catalyst. Structural Chemistry, 2021, 32, 799-804.	1.0	0
53959	Investigations of the stability and electronic properties of two-dimensional Ga2O3 nanosheet in air from first-principles calculations. Applied Surface Science, 2021, 537, 147883.	3.1	14
53960	Charge transfer driven interaction of CH4, CO2 and NH3 with TiS2 monolayer: Influence of vacancy defect. Catalysis Today, 2021, 370, 189-195.	2.2	5
53961	MAISE: Construction of neural network interatomic models and evolutionary structure optimization. Computer Physics Communications, 2021, 259, 107679.	3.0	22
53962	Quasi three-dimensional lead iodide perovskite using pyridine-2,5-diamine and 4,4â€²-bipyridine with tunable electronic structure, carrier transport, optical absorption properties. Journal of Alloys and Compounds, 2021, 856, 157391.	2.8	1
53963	Half-metallic ferromagnetism in molybdenum doped methylammonium lead halides (MAPbX3, XÂ=ÂCl, Br, I) system: First-principles study. Journal of Magnetism and Magnetic Materials, 2021, 519, 167463.	1.0	11
53964	Tunable electronic, optical, and spintronic properties in InSe/MTe2 (M = Pd, Pt) van der Waals heterostructures. Vacuum, 2021, 183, 109859.	1.6	15

#	Article	IF	Citations
53965	Modulating Electronic Structure of Monolayer Transition Metal Dichalcogenides by Substitutional Nbâ€Doping. Advanced Functional Materials, 2021, 31, 2006941.	7.8	54
53966	Uncertainty Quantification in Atomistic Modeling of Metals and Its Effect on Mesoscale and Continuum Modeling: A Review. Jom, 2021, 73, 149-163.	0.9	7
53967	Band alignment towards high-efficiency NiOx-based Sn-Pb mixed perovskite solar cells. Science China Materials, 2021, 64, 537-546.	3.5	23
53968	A first principles investigation of the hydrogen-strain synergy on the formation and phase transition of hydrides in zirconium. Acta Materialia, 2021, 202, 222-231.	3.8	11
53969	Band engineering of XBi (XÂ=ÂSi, Ge, Sn, and Pb) single layers via strain and surface chemical-modulation. Applied Surface Science, 2021, 540, 148268.	3.1	6
53970	Enhanced direct interspecies electron transfer with transition metal oxide accelerants in anaerobic digestion. Bioresource Technology, 2021, 320, 124294.	4.8	52
53971	Morphogenesis of mesoscopic surface patterns formed in polarized two-photon etching of diamond. Carbon, 2021, 173, 271-285.	5.4	5
53972	A non-iterative method for vertex corrections of the Kubo formula for electric conductivity. Computer Physics Communications, 2021, 258, 107551.	3.0	1
53973	Interface magnetoelectric effect and its sensitivity on interface structures in Fe/AgNbO3 and SrRuO3/AgNbO3 heterostructures: A first-principles investigation. Journal of Magnetism and Magnetic Materials, 2021, 517, 167372.	1.0	2
53974	Influence of Cr-substitution on the structural, magnetic, electron transport, and mechanical properties of Fe3â^'Cr Ge Heusler alloys. Journal of Magnetism and Magnetic Materials, 2021, 521, 167398.	1.0	17
53975	Electronic structure, elastic, optical and thermal properties of chalcopyrite CuBY2 (B = In, Ga, In0.5) Tj ETQq0 0 0 rgBT /Overlock 10 Tf 5	0.9	2
53976	Enhanced power factor and thermoelectric performance for n-type Bi2Te2.7Se0.3 based composites incorporated with 3D topological insulator nanoinclusions. Nano Energy, 2021, 80, 105512.	8.2	44
53977	Ab initio identification of two-dimensional square-octagonal bismuthene doped with 3d transition metals as potential spin gapless semiconductor, bipolar magnetic semiconductor, and quantum anomalous Hall insulator. Physica E: Low-Dimensional Systems and Nanostructures, 2021, 126, 114390.	1.3	4
53978	Configurational kinetics studied by Path Probability Method. Progress in Materials Science, 2021, 120, 100765.	16.0	6
53979	Tailoring M7C3 carbide via electron work function-guided modification. Scripta Materialia, 2021, 190, 168-173.	2.6	19
53980	The growth of anti-friction and wear-resistance TiO2 nanotube arrays driven by residual stress. Tribology International, 2021, 154, 106736.	3.0	11
53981	Stable Janus TaSe2 single-layers via surface functionalization. Applied Surface Science, 2021, 538, 148064.	3.1	7
53982	High-loading lateral Li deposition realized by a Scalable Fluorocarbon Bonded Laminates. Carbon, 2021, 171, 894-906.	5.4	8

#	Article	IF	Citations
53983	Au modified single vacancy graphene as anchoring material for lithiumâ€“sulfur batteries. Chemical Physics Letters, 2021, 762, 138101.	1.2	2
53984	Mn4+ doped narrowband red phosphors with short fluorescence lifetime and high color stability for fast-response backlight display application. Journal of Alloys and Compounds, 2021, 855, 157347.	2.8	21
53985	Atomic-scale identification of invisible cation vacancies at an oxide homointerface. Materials Today Physics, 2021, 16, 100302.	2.9	7
53986	rh.-B12 as host of interstitial atoms: Review of a large family with illustrative study of B12{CN2} from first-principles. Progress in Solid State Chemistry, 2021, 61, 100296.	3.9	5
53987	A new 2D Si3X(X=S, 0) direct band gap semiconductor with anisotropic carrier mobility. Surface Science, 2021, 704, 121736.	0.8	4
53988	Theoretical study on the two-dimensional bis(iminothiolato)rhodium as oxygen reduction reaction catalyst. Molecular Physics, 2021, 119, e1817593.	0.8	0
53989	Selective CO2 conversion tuned by periodicities in Au8n+4(TBBT)4n+8 nanoclusters. Nano Research, 2021, 14, 807-813.	5.8	8
53990	On the relevance of point defects for the selection of contacting electrodes: Ag as an example for Mg2(Si,Sn)-based thermoelectric generators. Materials Today Physics, 2021, 16, 100309.	2.9	19
53991	First-principles study on the Jahn-Teller distortion in trigonal bipyramidal coordinated LiFe1â^'xMxBO3 (Mâ€‰=â€‰Mn, Co, and Ni) compounds. Journal of Solid State Electrochemistry, 2021, 25, 627-635.	1.2	5
53992	Interlayer coupling effect in van der Waals heterostructures of transition metal dichalcogenides. Frontiers of Physics, 2021, 16, 1.	2.4	15
53993	Single-Atom Cobalt-Based Electrochemical Biomimetic Uric Acid Sensor with Wide Linear Range and Ultralow Detection Limit. Nano-Micro Letters, 2021, 13, 7.	14.4	76
53994	Indirect interactions of metal nanoparticles through graphene. Carbon, 2021, 174, 132-137.	5.4	11
53995	Electric field-induced band modulation of predicted ternary 2D MXC3 [M:XÂ= As:Ge, Sb:Sn and Bi:Pb] with strong stability and optical properties. Carbon, 2021, 172, 791-803.	5.4	21
53996	Lanthanum ions decorated 2-dimensional g-C3N4 for ciprofloxacin photodegradation. Chemosphere, 2021, 268, 128780.	4.2	41
53997	Design of half-heusler thermoelectric compound TiFe0.5Ni0.5Sb with special quasi-random structure using 18-electron rule. Journal of Alloys and Compounds, 2021, 858, 157689.	2.8	7
53998	Adsorption mechanisms of fatty acids on fluorite unraveled by infrared spectroscopy and first-principles calculations. Journal of Colloid and Interface Science, 2021, 583, 692-703.	5.0	50
53999	High-throughput identification of high activity and selectivity transition metal single-atom catalysts for nitrogen reduction. Nano Energy, 2021, 80, 105527.	8.2	66
54000	Rectifying Characteristics of the Perovskite Oxide La 1â^' x Sr x MnO 3 /Nbâ€0.7 wt%â€Doped SrTiO 3 Heterojunction. Physica Status Solidi - Rapid Research Letters, 2021, 15, 2000360.	1.2	1

#	Article	IF	Citations
54001	Mechanical properties of lateral transition metal dichalcogenide heterostructures. Frontiers of Physics, 2021, 16, 1.	2.4	19
54002	An unexpected role of atomic oxygen dopants in Au evolution from clusters to a layer. Acta Materialia, 2021, 202, 277-289.	3.8	15
54003	DFT insights into hydrogen activation on the doping Ni2P surfaces under the hydrodesulfurization condition. Applied Surface Science, 2021, 538, 148160.	3.1	11
54004	Revisiting surface chemistry in TiO2: A critical role of ionic passivation for pH-independent and anti-corrosive photoelectrochemical water oxidation. Chemical Engineering Journal, 2021, 407, 126929.	6.6	11
54005	Single- and multi-layer arsenene as an anode material for Li, Na, and K-ion battery applications. Computational Materials Science, 2021, 186, 110000.	1.4	11
54006	An efficient Z-scheme (Cr, B) codoped g-C3N4/BiVO4 photocatalyst for water splitting: A hybrid DFT study. International Journal of Hydrogen Energy, 2021, 46, 247-261.	3.8	59
54007	Theoretical insights into nitrogen oxide activation on halogen defect-rich {001} facets of bismuth oxyhalide. Journal of Materials Science and Technology, 2021, 77, 217-222.	5.6	6
54008	Vacancy defects on optoelectronic properties of double perovskite Cs2AgBiBr6. Materials Science in Semiconductor Processing, 2021, 123, 105541.	1.9	27
54009	Direct observation of highly confined phonon polaritons in suspended monolayer hexagonal boron nitride. Nature Materials, 2021, 20, 43-48.	13.3	84
54010	Hybrid Functional Study of H-Abstraction from Methane by Li-Doped, Pristine and Stepped MgO(100) and MgO(110) Surfaces. Catalysis Letters, 2021, 151, 627-633.	1.4	7
54011	Deposition of the Spin Crossover Fe II â€“Pyrazolylborate Complex on Au(111) Surface at the Molecular Level. Chemistry - A European Journal, 2021, 27, 712-723.	1.7	12
54012	Ultra-small hollow ternary alloy nanoparticles for efficient hydrogen evolution reaction. National Science Review, 2021, 8, nwaa204.	4.6	33
54013	A computational study of water in <scp>UiO</scp>â€66 <scp>Zrâ€MOFs</scp>: Diffusion, hydrogen bonding network, and confinement effect. AICHE Journal, 2021, 67, e17035.	1.8	16
54014	Integrated <scp>SnSSe</scp> bulk and monolayer as industrial waste heat thermoelectric materials. International Journal of Energy Research, 2021, 45, 2085-2099.	2.2	16
54015	High-energy-density pentazolate salts: CaN10 and BaN10. Science China: Physics, Mechanics and Astronomy, 2021, 64, 1.	2.0	19
54016	Hydrodechlorination and deep hydrogenation on single-palladium-atom-based heterogeneous catalysts. Applied Catalysis B: Environmental, 2021, 282, 119518.	10.8	39
54017	Cu2O(100) surface as an active site for catalytic furfural hydrogenation. Applied Catalysis B: Environmental, 2021, 282, 119576.	10.8	43
54018	DFT investigation of 2-mercaptobenzothiazole adsorption on model oxidized copper surfaces and relationship with corrosion inhibition. Applied Surface Science, 2021, 537, 147802.	3.1	47

#	Article	IF	Citations
54019	Detection of SOF2 and SO2F2 through aluminium nitride nanosheets: A DFT study. Applied Surface Science, 2021, 538, 147899.	3.1	19
54020	Discovering a New class of fluoride solid-electrolyte materials via screening the structural property of Li-ion sublattice. Nano Energy, 2021, 79, 105407.	8.2	24
54021	Large family of two-dimensional ferroelectric metals discovered via machine learning. Science Bulletin, 2021, 66, 233-242.	4.3	40
54022	Atomic-resolution electron microscopy of nanoscale local structure in lead-based relaxor ferroelectrics. Nature Materials, 2021, 20, 62-67.	13.3	100
54023	Ab initio calculations of interaction between Ni and Si in Î±-Fe. Journal of Nuclear Science and Technology, 2021, 58, 201-206.	0.7	0
54024	Studies of 2D Bulk and Nanoribbon Band Structures in Mo x W 1â€“ x S 2 Alloy System Using Full sp 3 d 5 Tightâ€Binding Model. Physica Status Solidi (B): Basic Research, 2021, 258, 2000375.	0.7	1
54025	Structural, elastic, and electronic properties of MgB 2 C 2 under pressure from firstâ€principles calculations. International Journal of Quantum Chemistry, 2021, 121, e26442.	1.0	1
54026	Normal and off-normal incidence dissociative dynamics of O₂(v,J) on ultrathin Cu films grown on Ru(0001). Physical Chemistry Chemical Physics, 2021, 23, 7768-7776.	1.3	0
54027	Physical Properties and Electronic Structure of Cr 2 B Under Pressure. Physica Status Solidi (B): Basic Research, 2021, 258, 2000212.	0.7	1
54028	Development of benchmark automation suite and evaluation of various high-performance computing systems. Cluster Computing, 2021, 24, 159-179.	3.5	2
54029	Formation and superconducting properties of predicted ternary hydride <scp>ScYH₆</scp> under pressures. International Journal of Quantum Chemistry, 2021, 121, e26459.	1.0	20
54030	Strong coupling and pressure engineering in WSe2â€“MoSe2 heterobilayers. Nature Physics, 2021, 17, 92-98.	6.5	140
54031	Tracking structural evolution: operando regenerative CeOx/Bi interface structure for high-performance CO2 electroreduction. National Science Review, 2021, 8, nwaa187.	4.6	50
54032	Self-aldol condensation of aldehydes over Lewis acidic rare-earth cations stabilized by zeolites. Chinese Journal of Catalysis, 2021, 42, 595-605.	6.9	24
54033	Phase Stability and Thermo-Physical Properties of Nickel-Aluminum Binary Chemically Disordered Systems via First-Principles Study. Metals and Materials International, 2021, 27, 1469-1477.	1.8	1
54034	Hydrogenation of substituted nitroaromatics on non-noble metal catalysts: mechanistic insights to improve selectivity. Faraday Discussions, 2021, 229, 297-317.	1.6	7
54035	A multiscale modelling approach to elucidate the mechanism of the oxygen evolution reaction at the hematiteâ€“water interface. Faraday Discussions, 2021, 229, 89-107.	1.6	11
54036	Theoretical Investigation of the CO2 Capture Properties of Î³-LiAlO2 and Î±-Li5AlO4. Micro and Nanosystems, 2021, 13, 32-41.	0.3	7

#	Article	IF	Citations
54037	Design of a unique anion framework in halospinels for outstanding performance of all solid-state Li-ion batteries: first-principles approach. Journal of Materials Chemistry A, 2021, 9, 15605-15612.	5.2	12
54038	Defect structures of the Cr₂O₃(112Ì„0) surface: effect of electron beam irradiation. Journal of Materials Chemistry C, 2021, 9, 6324-6331.	2.7	6
54039	Two-dimensional topological insulators exfoliated from Na3Bi-like Dirac semimetals. Physical Chemistry Chemical Physics, 2021, 23, 10545-10550.	1.3	1
54040	Optoelectronic properties and strain regulation of the 2D WS₂/ZnO van der Waals heterostructure. RSC Advances, 2021, 11, 14085-14092.	1.7	18
54041	Unravelling charge-transfer in Pd to pyrrolic-N bond for superior electrocatalytic performance. Journal of Materials Chemistry A, 2021, 9, 10966-10978.	5.2	15
54042	Phase stability of monolayer Si1â^'xGex alloys with a Dirac cone. Nanoscale, 2021, 13, 8607-8613.	2.8	3
54043	Nonequilibrium Greenâ€™s functions (NEGF) in vibrational energy transport: a topical review. Nanoscale and Microscale Thermophysical Engineering, 2021, 25, 1-24.	1.4	11
54044	Probing Kinetics and Mechanism of Formation of Mixed Metallic Nanoparticles in a Polymer Membrane by Galvanic Replacement between Two Immiscible Metals: Case Study of Nickel/Silver Nanoparticle Synthesis. Langmuir, 2021, 37, 1637-1650.	1.6	4
54045	Out-of-Plane Deformations Determined Mechanics of Vanadium Disulfide (VS₂) Sheets. ACS Applied Materials & Interfaces, 2021, 13, 3040-3050.	4.0	21
54046	Identification of Potential Optoelectronic Applications for Metal Thiophosphates. ACS Applied Materials & Interfaces, 2021, 13, 3836-3844.	4.0	9
54047	Implications of in situ chalcogen substitutions in polysulfides for rechargeable batteries. Energy and Environmental Science, 2021, 14, 5423-5432.	15.6	43
54048	Drastic Modification of Lattice Thermal Conductivity in Thermoelectrics Induced by Electronâ€“Hole Pairs. ACS Applied Materials & Interfaces, 2021, 13, 3911-3918.	4.0	2
54049	Pressure-Driven Structural Phase Transitions and Superconductivity of Ternary Hydride MgVH₆. Journal of Physical Chemistry C, 2021, 125, 3150-3156.	1.5	18
54050	Semiconducting Î±â€²-boron sheet with high mobility and low all-boron contact resistance: a first-principles study. Nanoscale, 2021, 13, 8474-8480.	2.8	15
54051	First-principles study of vacancy ordered structures, mechanical properties and electronic properties of ternary Hf-C-N system. Wuli Xuebao/Acta Physica Sinica, 2021, 70, 216101.	0.2	1
54052	Adsorption of water in Na-LTA zeolites: an ab initio molecular dynamics investigation. Physical Chemistry Chemical Physics, 2021, 23, 19032-19042.	1.3	9
54053	Metallic VS₂/graphene heterostructure as an ultra-high rate and high-specific capacity anode material for Li/Na-ion batteries. Physical Chemistry Chemical Physics, 2021, 23, 18784-18793.	1.3	20
54054	A novel route to obtain TiO2 nanoparticles using green synthesis with vanillin and Bougainvillea glabra Choisy extract. Applied Nanoscience (Switzerland), 2021, 11, 887-894.	1.6	2

#	Article	IF	Citations
54055	The bonding variation of Î³-TiAl during deformation. Physical Chemistry Chemical Physics, 2021, 23, 3905-3914.	1.3	5
54056	Interplay of physically different properties leading to challenges in separating lanthanide cations â€“ an ab initio molecular dynamics and experimental study. Physical Chemistry Chemical Physics, 2021, 23, 5750-5759.	1.3	3
54057	Pentagonal B₂C monolayer with extremely high theoretical capacity for Li-/Na-ion batteries. Physical Chemistry Chemical Physics, 2021, 23, 6278-6285.	1.3	30
54058	Combined Ab Initio and Experimental Study of Hydrogen Sorption in Dual-Phase Steels. Minerals, Metals and Materials Series, 2021, , 730-741.	0.3	0
54059	Cation-disorder zinc blende Zn_{0.5}Ge_{0.5}P compound and Zn_{0.5}Ge_{0.5}Pâ€“TiCâ€“C composite as high-performance anodes for Li-ion batteries. Journal of Materials Chemistry A, 2021, 9, 9124-9133.	5.2	8
54060	Operandoanalysis of graphite intercalation compounds with fluoride-containing polyatomic anions in aqueous solutions. Materials Advances, 2021, 2, 2310-2317.	2.6	3
54061	Partial sulfidation for constructing Cu₂Oâ€“CuS heterostructures realizing enhanced electrochemical glucose sensing. New Journal of Chemistry, 2021, 45, 7204-7209.	1.4	11
54062	Surface oxidation for enhancing the hydrogen evolution reaction of metal nitrides: a theoretical study on vanadium nitride. Materials Advances, 0, , .	2.6	4
54063	Defects as catalytic sites for the oxygen evolution reaction in Earth-abundant MOF-74 revealed by DFT. Catalysis Science and Technology, 2021, 11, 1443-1450.	2.1	17
54064	Two-dimensional aluminium, gallium, and indium metallic crystals by first-principles design. Journal of Physics Condensed Matter, 2021, 33, 125901.	0.7	12
54065	Tuning the electronic and magnetic properties of hydrogen saturated zigzag silicene nanoribbon doped with B atoms chain. Ferroelectrics, 2021, 570, 77-87.	0.3	0
54066	Lattice Dynamics of KAgF3 Perovskite, Unique 1D Antiferromagnet. Chemistry, 2021, 3, 94-103.	0.9	6
54067	The mechanism of hydrogen-accelerated melting of polycrystalline copper. Physical Chemistry Chemical Physics, 2021, 23, 3942-3948.	1.3	0
54068	Dynamic stabilization and heat transport characteristics of monolayer SnSe at finite temperature: A study by phonon quasiparticle approach. Physical Review B, 2021, 103, .	1.1	3
54069	Impact of the vertical strain on the Schottky barrier height for graphene/AlN heterojunction: a study by the first-principles method. European Physical Journal B, 2021, 94, 1.	0.6	6
54070	Co-free CuFeMnNi high-entropy alloy with tunable tensile properties by thermomechanical processing. Journal of Materials Science, 2021, 56, 7670-7680.	1.7	10
54071	Polycomponent doping responsible for the improvement of the thermoelectric performance of Cu3SbSe4-based solid solutions. Wuli Xuebao/Acta Physica Sinica, 2021, .	0.2	0
54072	Anomalous plasmons in a two-dimensional Dirac nodal-line Lieb lattice. Nanoscale Advances, 2021, 3, 1127-1135.	2.2	6

#	Article	IF	Citations
54073	Dense as diamond: Pn-C10, a superhard sp3 carbon allotrope. Applied Physics Letters, 2021, 118, .	1.5	6
54074	Equation of state measurements of dense krypton up to the insulator-metal transition regime: Evaluating the exchange-correlation functionals. Physical Review B, 2021, 103, .	1.1	2
54075	A new two-dimensional all-sp³ carbon allotrope with an indirect band gap and superior carrier mobility. Physical Chemistry Chemical Physics, 2021, 23, 2906-2913.	1.3	7
54076	Code for nuclear materials. , 2021, , 483-494.		0
54077	Magnetoelastic coupling and spin contributions to entropy and thermal transport in biferroic yttrium orthochromite [*]. Journal of Physics Condensed Matter, 2021, 33, 125702.	0.7	2
54078	Topological semimetal state with triply degenerate nodal points in a stable Cu2Te structure. Physical Chemistry Chemical Physics, 2021, 23, 3116-3122.	1.3	2
54079	Solute-point defect interactions, coupled diffusion, and radiation-induced segregation in fcc nickel. Physical Review Materials, 2021, 5, .	0.9	9
54080	Adsorption of 4,4â€³-Diamino-p-Terphenyl on Cu(001): A First-Principles Study. Surfaces, 2021, 4, 31-38.	1.0	1
54081	First-principles prediction of rare-earth free permanent magnet: FeNi with enhanced magnetic anisotropy and stability through interstitial boron. AIP Advances, 2021, 11, .	0.6	5
54082	The first principle study of magnetic, electronic, and optical properties of Co- and Mn-doped boron nitride nanosheets. Indian Journal of Physics, 2022, 96, 419-431.	0.9	3
54083	Prediction of scandium tetraboride from first-principles calculations: crystal structures, phase stability, mechanical properties, and hardness. Chinese Physics B, 0, , .	0.7	3
54084	Deep learning of accurate force field of ferroelectric <mml:math xmlns:mml="http://www.w3.org/1998/Math/MathML"><mml:msub><mml:mrow><mml:mi>HfO</mml:mi></mml:mrow><mml:mn>2</mml:mn> Physical Review B, 2021, 103, .	1.1	39
54085	Intrinsic spinâ€“valley-coupled Dirac state in Janus functionalized Î²-BiAs monolayer. Nanoscale Horizons, 2021, 6, 283-289.	4.1	9
54086	Surface Modifications of 2D-Ti3C2O2 by Nonmetal Doping for Obtaining High Hydrogen Evolution Reaction Activity: A Computational Approach. Catalysts, 2021, 11, 161.	1.6	4
54087	Chern insulating phases and thermoelectric properties of EuO/MgO(001) superlattices. Physical Review B, 2021, 103, .	1.1	4
54088	Enabling simulations of helium bubble nucleation and growth: A strategy for interatomic potentials. Physical Review B, 2021, 103, .	1.1	5
54089	Robust transport of charge carriers in in-plane 1Tâ€²-2H MoTe2 homojunctions with ohmic contact. Nano Research, 2021, 14, 1311-1318.	5.8	16
54090	Magnetic <mml:math xmlns:mml="http://www.w3.org/1998/Math/MathML"><mml:mrow><mml:mn>3</mml:mn><mml:mi>d</mml:mi> adatoms on free-standing and Ni(111)-supported graphene. Physical Review Materials, 2021, 5, .	1.0	3

#	Article	IF	Citations
54091	Structure, Magnetism, and First-Principles Modeling of the Na_{0.5}La_{0.5}RuO₃ Perovskite. Chemistry of Materials, 2021, 33, 600-607.	3.2	5
54093	Various half-metallic nodal loops in organic Cr₂N₆C₃ monolayers. Nanoscale, 2021, 13, 3161-3172.	2.8	6
54094	A combined theoretical/experimental study highlighting the formation of carbides on Ru nanoparticles during CO hydrogenation. Nanoscale, 2021, 13, 6902-6915.	2.8	9
54095	Highly tunable electronic structure and linear dichroism in 90Â° twisted Î±-phosphorus carbide bilayer: a first-principles calculation. Physical Chemistry Chemical Physics, 2021, 23, 7080-7087.	1.3	9
54096	Designing chemically selective liquid crystalline materials that respond to oxidizing gases. Journal of Materials Chemistry C, 2021, 9, 6507-6517.	2.7	9
54097	N-doped carbon nanofibers encapsulated Cu2-xSe with the improved lithium storage performance and its structural evolution analysis. Electrochimica Acta, 2021, 367, 137449.	2.6	20
54098	All-boron planar ferromagnetic structures: from clusters to monolayers. Nanoscale, 2021, 13, 9881-9887.	2.8	7
54099	Understanding the unusual stiffness of hydrophobic dipeptide crystals. Physical Chemistry Chemical Physics, 2021, 23, 11931-11936.	1.3	4
54100	First principles calculations of magneto-crystalline anisotropy of rare-earth magnets. Journal of Physics Communications, 2021, 5, 015013.	0.5	0
54101	Electronically Driven 1D Cooperative Diffusion in a Simple Cubic Crystal. Physical Review X, 2021, 11, .	2.8	12
54102	First-principles study on magneto-optical effects in the ferromagnetic semiconductors <mml:math xmlns:mml="http://www.w3.org/1998/Math/MathML"><mml:mrow><mml:msub><mml:mi mathvariant="normal">Y</mml:mi><mml:mn>3</mml:mn></mml:msub><mml:msub><mml:mi>Fe</mml:mi><mml:mn>5</mml:mn></mml:msub><mml:msub><mml:mi mathvariant="normal">O</mml:mi><mml:mn>12</mml:mn></mml:msub></mml:mrow></mml:math> and <mml:math xmlns:mml="http://www.w3.org/1998/Math/MathML"><mml:mrow><mml:msub><mml:mi>Bi</mml:mi><mml:mn>3</mml:mn></mml:msub>.	1.1	14
54103	Magnetocaloric behavior and magnetic ordering in MnPdGa. Physical Review Materials, 2021, 5, .	0.9	4
54104	Tuning the magnetic and electronic properties of strontium titanate by carbon doping. Frontiers of Physics, 2021, 16, 1.	2.4	9
54105	Improvement of alkali metal ion batteries via interlayer engineering of anodes: from graphite to graphene. Nanoscale, 2021, 13, 12521-12533.	2.8	14
54106	Organic cation (DMPI) intercalated graphite anode for high voltage next generation dual-ion batteries. Materials Advances, 2021, 2, 5213-5223.	2.6	6
54107	Selective Construction of Magic Hierarchical Metalâ€“Organic Clusters on Surfaces. Journal of Physical Chemistry C, 2021, 125, 358-365.	1.5	8
54108	Bishop's hat silicene: a planar square silicon bilayer decorated with adatoms. Physical Chemistry Chemical Physics, 2021, 23, 16942-16947.	1.3	0
54109	Adsorption of ethylenediamine on Cu surfaces: attributes of a successful capping molecule using first-principles calculations. Nanoscale, 2021, 13, 13529-13537.	2.8	5

#	Article	IF	Citations
54110	Enhanced degradation of norfloxacin by Ce-mediated Fe-MIL-101: catalytic mechanism, degradation pathways, and potential applications in wastewater treatment. Environmental Science: Nano, 2021, 8, 2347-2359.	2.2	26
54111	Enabling multifunctional electrocatalysts by modifying the basal plane of unifunctional 1Tâ€²-MoS₂ with anchored transition metal single atoms. Nanoscale, 2021, 13, 13390-13400.	2.8	69
54112	Evolution of the structural, magnetic, and electronic properties of the triple perovskite <mml:math xmlns:mml="http://www.w3.org/1998/Math/MathML"><mml:mrow><mml:msub><mml:mi>Ba</mml:mi><mml:mn>3</mml:mn></mml:r mathvariant="normal">O</mml:mi><mml:mn>9</mml:mn></mml:msub></mml:mrow></mml:math>. Physical Review B, 2021, 103, .	1.1	14
54113	Functionalization induced quantum spin Hall to quantum anomalous Hall phase transition in monolayer jacutingaite. Nanoscale, 2021, 13, 2527-2533.	2.8	8
54114	Carrier-specific dynamics in 2H-MoTe2 observed by femtosecond soft x-ray absorption spectroscopy using an x-ray free-electron laser. Structural Dynamics, 2021, 8, 014501.	0.9	14
54115	MC₂ (M = Y, Zr, Nb, and Mo) monolayers containing C₂ dimers: prediction of anode materials for high-performance sodium ion batteries. Nanoscale Advances, 2021, 3, 6617-6627.	2.2	8
54116	Unraveling the structural transition mechanism of room-temperature compressed graphite carbon. Physical Chemistry Chemical Physics, 2021, 23, 20560-20566.	1.3	7
54117	Formation of oxygen vacancies in Li₂FeSiO₄: first-principles calculations. Physical Chemistry Chemical Physics, 2021, 23, 20444-20452.	1.3	3
54118	Designing C₆N₆/C₂N van der Waals heterostructures for photogenerated charge carrier separation. Physical Chemistry Chemical Physics, 2021, 23, 3925-3933.	1.3	25
54119	Mixed Coordination Silica at Megabar Pressure. Physical Review Letters, 2021, 126, 035701.	2.9	20
54120	Improved thermoelectric properties of WS₂â€“WSe₂ phononic crystals: insights from first-principles calculations. Nanoscale, 2021, 13, 7176-7192.	2.8	24
54121	Formic acid dehydrogenation over PdNi alloys supported on N-doped carbon: synergistic effect of Pdâ€“Ni alloying on hydrogen release. Physical Chemistry Chemical Physics, 2021, 23, 11515-11527.	1.3	16
54122	Effect of chemical substitution on polytypes and extended defects in chalcopyrites: A density functional theory study. Journal of Applied Physics, 2021, 129, 025703.	1.1	5
54123	Tri-atomic Pt clusters induce effective pathways in a Co_{core}â€“Pd_{shell} nanocatalyst surface for a high-performance oxygen reduction reaction. Physical Chemistry Chemical Physics, 2021, 23, 18012-18025.	1.3	5
54124	Ab initio design of a new family of 2D materials: transition metal carbon nitrogen compounds (MCNs). Journal of Materials Chemistry C, 2021, 9, 4748-4756.	2.7	8
54125	Lattice-distorted lithiation behavior of a square phase Janus MoSSe monolayer for electrode applications. Nanoscale Advances, 2021, 3, 2902-2910.	2.2	9
54126	Modulating formation rates of active species population by optimizing electron transport channels for boosting the photocatalytic activity of a Bi₂S₃/BiO_{1â^'x}Cl heterojunction. Catalysis Science and Technology, 2021, 11, 4196-4207.	2.1	8
54127	Giant Dzyaloshinskii-Moriya Interaction and Room-Temperature Nanoscale Skyrmions in CoFeB/MgO Heterostructures. SSRN Electronic Journal, 0, , .	0.4	0

#	Article	IF	Citations
54128	Chalcopyrite bioleaching catalyzed by silver. , 2021, , 183-209.		0
54129	Enhancement of the anomalous Nernst effect in Ni/Pt superlattices. Physical Review B, 2021, 103, .	1.1	34
54130	Tuning the structural skeleton of a phenanthroline-based covalent organic framework for better electrochemical performance as a cathode material for Zn-ion batteries: a theoretical exploration. Physical Chemistry Chemical Physics, 2021, 23, 12644-12653.	1.3	19
54131	Mixed formamidiniumâ€“methylammonium lead iodide perovskite from first-principles: hydrogen-bonding impact on the electronic properties. Physical Chemistry Chemical Physics, 2021, 23, 7376-7385.	1.3	25
54132	A key step for preparing highly active Mgâ€“Co composite oxide catalysts for N₂O decomposition. Catalysis Science and Technology, 2021, 11, 3737-3745.	2.1	6
54133	Atomistic understanding of the LiNiO₂â€“NiO₂ phase diagram from experimentally guided lattice models. Journal of Materials Chemistry A, 2021, 9, 14928-14940.	5.2	31
54134	A theoretical study on the role of ammonium ions in the double-layered V₂O₅ electrode. Physical Chemistry Chemical Physics, 2021, 23, 4187-4194.	1.3	3
54135	Prediction of pressure-induced superconductivity in the novel ternary system ScCaH_{2n}(n= 1â€“6). Journal of Materials Chemistry C, 2021, 9, 7284-7291.	2.7	21
54136	Strain-modified ionic conductivity in rare-earth substituted ceria: effects of migration direction, barriers, and defect-interactions. Journal of Materials Chemistry A, 2021, 9, 8630-8643.	5.2	5
54137	Self-limiting lithiation of vanadium diboride nanosheets as ultra-stable mediators towards high-sulfur loading and long-cycle lithium sulfur batteries. Sustainable Energy and Fuels, 2021, 5, 3134-3142.	2.5	10
54138	Research on metallic chalcogen-functionalized monolayer-puckered V₂CX₂ (X) Tj ETQq0 0 0 rgBT /Overlock 1 4672-4681.	3.2	8
54139	Selective visible-light driven highly efficient photocatalytic reduction of CO₂ to C₂H₅OH by two-dimensional Cu₂S monolayers. Nanoscale Horizons, 2021, 6, 661-668.	4.1	15
54140	Crystal structure and electrochemical properties of phosphosulphate NaFe2PO4(SO4)2. MATEC Web of Conferences, 2021, 340, 01012.	0.1	0
54141	Approaching a high-rate and sustainable production of hydrogen peroxide: oxygen reduction on Coâ€“Nâ€“C single-atom electrocatalysts in simulated seawater. Energy and Environmental Science, 2021, 14, 5444-5456.	15.6	126
54142	CuBi₂O₄: Electronic Structure, Optical Properties, and Photoelectrochemical Performance Limitations of the Photocathode. Chemistry of Materials, 2021, 33, 934-945.	3.2	45
54143	Investigating charge carrier scattering processes in anisotropic semiconductors through first-principles calculations: the case of p-type SnSe. Physical Chemistry Chemical Physics, 2021, 23, 900-913.	1.3	13
54144	Pockels effect in low-temperature rhombohedral <mml:math xmlns:mml="http://www.w3.org/1998/Math/MathML"><mml:mrow><mml:mi>BaTi</mml:mi><mml:msub><mml:mi mathvariant="normal">O</mml:mi><mml:mn>3</mml:mn></mml:msub></mml:mrow></mml:math>. Physical Review B, 2021, 103, .	1.1	11
54145	Segregation mechanism of arsenic dopants at grain boundaries in silicon. Science and Technology of Advanced Materials Methods, 2021, 1, 169-180.	0.4	3

#	Article	IF	Citations
54146	Denary oxide nanoparticles as highly stable catalysts for methane combustion. Nature Catalysis, 2021, 4, 62-70.	16.1	153
54147	Ultrasensitive broadband photodetectors based on two-dimensional Bi₂O₂Te films. Journal of Materials Chemistry C, 2021, 9, 13713-13721.	2.7	12
54148	Ab initio study on crystal structure and phase stability of ZrC2 under high pressure. Chinese Physics B, 2021, 30, 016101.	0.7	3
54149	Spin-orbit effects in ferroelectric <mml:math xmlns:mml="http://www.w3.org/1998/Math/MathML"><mml:mrow><mml:mi>Pb</mml:mi><mml:mi>Ti</mml:mi><mml:msub><mml:mi mathvariant="normal">O</mml:mi><mml:mn>3</mml:mn></mml:msub></mml:mrow></mml:math> under tensile strain. Physical Review B, 2021, 103, .	1.1	8
54150	Nitrogen and boron coordinated single-atom catalysts for low-temperature CO/NO oxidations. Journal of Materials Chemistry A, 2021, 9, 15329-15345.	5.2	26
54151	Electronic and thermal transport in novel carbon-based bilayer with tetragonal rings: a combined study using first-principles and machine learning approach. Physical Chemistry Chemical Physics, 2021, 23, 14608-14616.	1.3	19
54152	Coupling the chemical reactivity of bimetallic surfaces to the orientations of liquid crystals. Materials Horizons, 2021, 8, 2050-2056.	6.4	8
54153	Different structural evolutions of inorganic perovskite CsGeI₃. CrystEngComm, 2021, 23, 4917-4922.	1.3	13
54154	First-principles microkinetic simulations revealing the scaling relations and structure sensitivity of CO₂ hydrogenation to C₁ & C₂ oxygenates on Pd surfaces. Catalysis Science and Technology, 2021, 11, 4866-4881.	2.1	5
54155	CrySPY: a crystal structure prediction tool accelerated by machine learning. Science and Technology of Advanced Materials Methods, 2021, 1, 87-97.	0.4	5
54156	Oxygen vacancy mediated room-temperature ferromagnetism and band gap narrowing in DyFe_{0.5}Cr_{0.5}O₃ nanoparticles. Dalton Transactions, 2021, 50, 9519-9528.	1.6	8
54157	Self-passivation leads to semiconducting edges of black phosphorene. Nanoscale Horizons, 2021, 6, 148-155.	4.1	14
54158	Edge reconstructions of black phosphorene: a global search. Nanoscale, 2021, 13, 4085-4091.	2.8	15
54159	Selective filling of n-hexane in a tight nanopore. Nature Communications, 2021, 12, 310.	5.8	21
54160	Optimization of thermoelectric transport performance of nickel-doped CuGaTe₂. Wuli Xuebao/Acta Physica Sinica, 2021, 70, 207101.	0.2	1
54161	Tailoring the catalytic activity of nickel sites in NiFe₂O₄ by cobalt substitution for highly enhanced oxygen evolution reaction. Sustainable Energy and Fuels, 2021, 5, 2668-2677.	2.5	12
54162	Solvent Effects for Methanol Electrooxidation on Gold. Journal of Physical Chemistry C, 2021, 125, 1355-1360.	1.5	13
54163	Exfoliation Energy as a Descriptor of MXenes Synthesizability and Surface Chemical Activity. Nanomaterials, 2021, 11, 127.	1.9	22

#	Article	IF	Citations
54164	Systematic cluster growth: a structure search method for transition metal clusters. Physical Chemistry Chemical Physics, 2021, 23, 4935-4943.	1.3	12
54165	Electron deficiency but semiconductive diamond-like B₂CN originated from three-center bonds. Physical Chemistry Chemical Physics, 2021, 23, 3087-3092.	1.3	4
54166	CuS₂ sheets: a hidden anode material with a high capacity for sodium-ion batteries. Journal of Materials Chemistry C, 2021, 9, 1387-1395.	2.7	12
54167	Discovery of intrinsic two-dimensional antiferromagnets from transition-metal borides. Nanoscale, 2021, 13, 8254-8263.	2.8	31
54168	N-Induced Electron Transfer Effect on Low-Temperature Activation of Nitrogen for Ammonia Synthesis over Co-Based Catalysts. ACS Sustainable Chemistry and Engineering, 2021, 9, 1529-1539.	3.2	11
54169	Titanium and fluorine synergetic modification improves the electrochemical performance of Li(Ni_{0.8}Co_{0.1}Mn_{0.1})O₂. Journal of Materials Chemistry A, 2021, 9, 9354-9363.	5.2	62
54170	Integrating SnS₂ Quantum Dots with Nitrogen-Doped Ti₃C₂T_x MXene Nanosheets for Robust Sodium Storage Performance. ACS Applied Energy Materials, 2021, 4, 846-854.	2.5	40
54171	2D auxetic material with intrinsic ferromagnetism: a copper halide (CuCl₂) monolayer. Physical Chemistry Chemical Physics, 2021, 23, 22078-22085.	1.3	7
54172	Unambiguous determination of crystal orientation in black phosphorus by angle-resolved polarized Raman spectroscopy. Nanoscale Horizons, 2021, 6, 809-818.	4.1	20
54173	Unique surface patterns emerging during solidification of liquid metal alloys. Nature Nanotechnology, 2021, 16, 431-439.	15.6	104
54174	Mechanistic insights into interfaces and nitrogen vacancies in cobalt hydroxide/tungsten nitride catalysts to enhance alkaline hydrogen evolution. Journal of Materials Chemistry A, 2021, 9, 11323-11330.	5.2	12
54175	Unravelling the origin of bifunctional OER/ORR activity for single-atom catalysts supported on C₂N by DFT and machine learning. Journal of Materials Chemistry A, 2021, 9, 16860-16867.	5.2	93
54176	In Situ Strong Metalâ€“Support Interaction (SMSI) Affects Catalytic Alcohol Conversion. ACS Catalysis, 2021, 11, 1938-1945.	5.5	50
54177	Ultralow lattice thermal conductivity and dramatically enhanced thermoelectric properties of monolayer InSe induced by an external electric field. Physical Chemistry Chemical Physics, 2021, 23, 13633-13646.	1.3	10
54178	Me-graphane: tailoring the structural and electronic properties of Me-grapheneviahydrogenation. Physical Chemistry Chemical Physics, 2021, 23, 9483-9491.	1.3	9
54179	Advanced DFTâ€“NEGF Transport Techniques for Novel 2-D Material and Device Exploration Including HfS₂/WSe₂ van der Waals Heterojunction TFET and WTe₂/WS₂ Metal/Semiconductor Contact. IEEE Transactions on Electron Devices, 2021, 68, 5372-5379.	1.6	24
54180	Labile oxygen participant adsorbate evolving mechanism to enhance oxygen reduction in SmMn₂O₅ with double-coordinated crystal fields. Journal of Materials Chemistry A, 2021, 9, 380-389.	5.2	14
54181	Photo-assisted high performance single atom electrocatalysis of the N₂ reduction reaction by a Mo-embedded covalent organic framework. Journal of Materials Chemistry A, 2021, 9, 19949-19957.	5.2	27

#	Article	IF	Citations
54182	Role of additives and solvents in the synthesis of chiral isoreticular MOF-74 topologies. Dalton Transactions, 2021, 50, 12159-12167.	1.6	4
54183	Combined Merits of High Dielectric Breakdown Strength and Low Sintering Temperature Acquired in Mgo-Baseddielectric Ceramics: From Theoretical Prediction to Experimental Validation. SSRN Electronic Journal, 0, , .	0.4	0
54184	Activating the FeS (001) Surface for CO2 Adsorption and Reduction through the Formation of Sulfur Vacancies: A DFT-D3 Study. Catalysts, 2021, 11, 127.	1.6	16
54185	Tunable valley polarization in Janus WSSe by magnetic proximity coupling to a CrI₃ layer. Physical Chemistry Chemical Physics, 2021, 23, 18182-18188.	1.3	7
54186	Ferromagnetic Dirac half-metallicity in transition metal embedded honeycomb borophene. Physical Chemistry Chemical Physics, 2021, 23, 17150-17157.	1.3	12
54187	Efficient electrocatalytic conversion of CO₂ to syngas for the Fischerâ€“Tropsch process using a partially reduced Cu₃P nanowire. Journal of Materials Chemistry A, 2021, 9, 17876-17884.	5.2	11
54188	Atomic-level localization of Ï€-electrons in defect engineered tri-s-triazine units for increased photocatalytic hydrogen generation of polymeric carbon nitride. Catalysis Science and Technology, 2021, 11, 5663-5670.	2.1	9
54189	Syntheses of five new layered quaternary chalcogenides SrScCuSe₃, SrScCuTe₃, BaScCuSe₃, BaScCuTe₃, and BaScAgTe₃: crystal structures, thermoelectric properties, and electronic structures. Inorganic Chemistry Frontiers, 2021, 8, 4086-4101.	3.0	37
54190	Density Functional Theory Studies of Doping and Curvature Effects on the Electrocatalytic Hydrogen Evolution Activity of Carbon Nanotubes. ACS Applied Nano Materials, 2021, 4, 600-611.	2.4	14
54191	Composites of SnSb Nanoparticles Embedded in Porous Carbon Nanofibers Wrapped with Reduced Graphene Oxide for Sodium Storage. ACS Applied Nano Materials, 2021, 4, 826-833.	2.4	4
54192	An ideal two-dimensional nodal-ring semimetal in tetragonal borophene oxide. Physical Chemistry Chemical Physics, 2021, 23, 17348-17353.	1.3	3
54193	Defect Chemistry and Hydrogen Transport in La/Sr-Based Oxyhydrides. Journal of Physical Chemistry C, 2021, 125, 2250-2256.	1.5	3
54194	Spin valve effect in VN/GaN/VN van der Waals heterostructures. Physical Review B, 2021, 103, .	1.1	21
54195	Microscopic mechanism of unusual lattice thermal transport in TlInTe2. Npj Computational Materials, 2021, 7, .	3.5	26
54196	The crystal structure and electrical/thermal transport properties of Li_{1â^'x}Sn_{2+x}P₂and its performance as a Li-ion battery anode material. Journal of Materials Chemistry A, 2021, 9, 7034-7041.	5.2	7
54197	First-principles study of strain effect on the thermoelectric properties of LaP and LaAs. Physical Chemistry Chemical Physics, 2021, 23, 18189-18196.	1.3	7
54198	Chemical ordering in Ptâ€“Au, Ptâ€“Ag and Ptâ€“Cu nanoparticles from density functional calculations using a topological approach. Materials Advances, 2021, 2, 6589-6602.	2.6	12
54199	Electronic and optical properties of two-dimensional heterostructures based on Janus XSSe (X = Mo,) Tj ETQq1 1 0.784314 rgBT /Ove	1.7	24

#	Article	IF	Citations
54200	Nanoscale synthesis of ionic analogues of bilayer silicene with high carrier mobility. Journal of Materials Chemistry C, 2021, 9, 8545-8551.	2.7	4
54201	Exploring the Intrinsic Point Defects in Cesium Copper Halides. Journal of Physical Chemistry C, 2021, 125, 1592-1598.	1.5	15
54202	Implication of Mechanical Properties of Li-S Binary Compounds Obtained from the First-Principles Study. Journal of Physical Chemistry C, 2021, 125, 290-294.	1.5	9
54203	Defect Trapping and Phase Separation in Chemically Doped Bulk AgF₂. Inorganic Chemistry, 2021, 60, 1561-1570.	1.9	4
54204	Temperature-Dependent Band Renormalization in CoSb₃ Skutterudites Due to Sb-Ring-Related Vibrations. Chemistry of Materials, 2021, 33, 1046-1052.	3.2	16
54205	The role of the A-cations in the polymorphic stability and optoelectronic properties of lead-free ASnI3 perovskites. Physical Chemistry Chemical Physics, 2021, 23, 2286-2297.	1.3	11
54206	Revisiting trends in the exchange current for hydrogen evolution. Catalysis Science and Technology, 2021, 11, 6832-6838.	2.1	21
54207	Oxygen vacancy induced MnO₂ catalysts for efficient toluene catalytic oxidation. Catalysis Science and Technology, 2021, 11, 6708-6723.	2.1	52
54208	Tuning the electronic structure of layered vanadium pentoxide by pre-intercalation of potassium ions for superior room/low-temperature aqueous zinc-ion batteries. Nanoscale, 2021, 13, 2399-2407.	2.8	86
54209	Achieving large uniform tensile elasticity in microfabricated diamond. Science, 2021, 371, 76-78.	6.0	95
54210	Materials design of sodium chloride solid electrolytes Na₃MCl₆ for all-solid-state sodium-ion batteries. Journal of Materials Chemistry A, 2021, 9, 23037-23045.	5.2	23
54211	High-throughput screening of TMOCl cathode materials based on the full-cell system for chloride-ion batteries. Journal of Materials Chemistry A, 2021, 9, 23169-23177.	5.2	9
54212	Highly selective oxidation of monosaccharides to sugar acids at room temperature over palladium supported on surface functionalized carbon nanotubes. Green Chemistry, 2021, 23, 7084-7092.	4.6	4
54213	Heterogenisation of polyoxometalates and other metal-based complexes in metalâ€“organic frameworks: from synthesis to characterisation and applications in catalysis. Chemical Society Reviews, 2021, 50, 6152-6220.	18.7	164
54214	Oxygen chemistry of halogen-doped CeO₂(111). Physical Chemistry Chemical Physics, 2021, 23, 19375-19385.	1.3	2
54215	Uncovering the Encapsulation Effect of Reduced Graphene Oxide Sheets on Hydrogen Storage Properties of Palladium Nanocubes. Nanoscale, 2021, 13, 16942-16951.	2.8	8
54216	High-efficient ab initio Bayesian active learning method and applications in prediction of two-dimensional functional materials. Nanoscale, 2021, 13, 14694-14704.	2.8	9
54217	Room temperature spontaneous valley polarization in two-dimensional FeClBr monolayer. Nanoscale, 2021, 13, 14807-14813.	2.8	53

#	Article	IF	Citations
54218	Z-Scheme versus type-II junction in g-C₃N₄/TiO₂ and g-C₃N₄/SrTiO₃/TiO₂ heterostructures. Catalysis Science and Technology, 2021, 11, 3589-3598.	2.1	25
54219	First-principles microkinetic analysis of Lewis acid sites in Zn-ZSM-5 for alkane dehydrogenation and its implication to methanol-to-aromatics conversion. Catalysis Science and Technology, 2021, 11, 2031-2046.	2.1	23
54220	A new strategy for achieving high K⁺ storage capacity with fast kinetics: realizing covalent sulfur-rich carbon by phosphorous doping. Nanoscale, 2021, 13, 4911-4920.	2.8	17
54221	Modulating oxidation state of Ni/CeO₂ catalyst for steam methane reforming: a theoretical prediction with experimental verification. Catalysis Science and Technology, 2021, 11, 1965-1973.	2.1	10
54222	Unravelling the facets-dependent behavior among H₂O₂, O₃ and oxygen vacancies on CeO_x and the promotion of peroxone reaction at under acidic conditions. Environmental Science: Nano, 2021, 8, 3138-3152.	2.2	4
54223	Ab Initio Study of Adsorption of Fission Gas Atoms Xe and Kr on MoS₂ Monolayer Functionalized with 3d Transition Metals. Journal of Physical Chemistry C, 2021, 125, 1493-1508.	1.5	14
54224	Transition-metal single atoms embedded into defective BC₃as efficient electrocatalysts for oxygen evolution and reduction reactions. Nanoscale, 2021, 13, 1331-1339.	2.8	27
54225	The spinâ€“orbit interaction controls photoinduced interfacial electron transfer in fullereneâ€“perovskite heterojunctions: C₆₀versus C₇₀. Physical Chemistry Chemical Physics, 2021, 23, 6536-6543.	1.3	11
54226	A first-principles study on the electronic and optical properties of a type-II C₂N/g-ZnO van der Waals heterostructure. Physical Chemistry Chemical Physics, 2021, 23, 3963-3973.	1.3	24
54227	Generating large out-of-plane piezoelectric properties of atomically thin MoS₂via defect engineering. Physical Chemistry Chemical Physics, 2021, 23, 23945-23952.	1.3	2
54228	Construction of polymeric carbon nitride and dibenzothiophene dioxide-based intramolecular donorâ€“acceptor conjugated copolymers for photocatalytic H₂ evolution. Nanoscale Advances, 2021, 3, 1699-1707.	2.2	22
54229	Global Activity Search Uncovers Reaction Induced Concomitant Catalyst Restructuring for Alkane Dissociation on Model Pt Catalysts. ACS Catalysis, 2021, 11, 1877-1885.	5.5	26
54230	Interface coupling and charge doping in graphene on ferroelectric BiAlO₃(0001) polar surfaces. Physical Chemistry Chemical Physics, 2021, 23, 3407-3416.	1.3	7
54231	Dual effect of the coordination field and sulphuric acid on the properties of a single-atom catalyst in the electrosynthesis of H₂O₂. Physical Chemistry Chemical Physics, 2021, 23, 21338-21349.	1.3	15
54232	Self-reconstruction mediates isolated Pt tailored nanoframes for highly efficient catalysis. Journal of Materials Chemistry A, 2021, 9, 22501-22508.	5.2	5
54233	Tunnel barrier engineering of spin-polarized mild band gap vertical ternary heterostructures. Physical Chemistry Chemical Physics, 2021, 23, 22418-22422.	1.3	1
54234	Electrocatalytic nitrogen reduction on the transition-metal dimer anchored N-doped graphene: performance prediction and synergetic effect. Physical Chemistry Chemical Physics, 2021, 23, 4018-4029.	1.3	90
54235	Mechanistic Framework and Effects of High Coverage in Vinyl Acetate Synthesis. ACS Catalysis, 2021, 11, 1841-1857.	5.5	6

#	Article	IF	Citations
54236	MoirÃ© metrology of energy landscapes in van der Waals heterostructures. Nature Communications, 2021, 12, 242.	5.8	60
54237	Vacancy-induced high activity of MoS₂ monolayers for CO electroreduction: a computational study. Sustainable Energy and Fuels, 2021, 5, 4932-4943.	2.5	4
54238	Lithium ion diffusion mechanism on the inorganic components of the solidâ€“electrolyte interphase. Journal of Materials Chemistry A, 2021, 9, 10251-10259.	5.2	66
54239	Valley pseudospin in monolayer <mml:math xmlns:mml="http://www.w3.org/1998/Math/MathML"><mml:mrow><mml:mi>Mo</mml:mi><mml:msub><mml:mi>Si</mml:mi><mml:mi mathvariant="normal">N</mml:mi><mml:mn>4</mml:mn></mml:msub></mml:mrow></mml:math> and <mml:math xmlns:mml="http://www.w3.org/1998/Math/MathML"><mml:mrow><mml:mi>Mo</mml:mi><mml:msub><mml:mi>Si</mml:mi><mml:mi mathvariant="normal">N</mml:mi><mml:mn>4</mml:mn></mml:msub></mml:mrow></mml:math> Physical Review B, 2021, 103, .	1.1	82
54240	Theoretical study on the adsorption and electronic properties of toxic gas molecules on single-atom Pt-doped B/N-coordinated graphene. New Journal of Chemistry, 0, , .	1.4	1
54241	Semiconducting Metalâ€“Organic Polymer Nanosheets for a Photoinvolved Liâ€“O₂ Battery under Visible Light. Journal of the American Chemical Society, 2021, 143, 1941-1947.	6.6	124
54242	Bifunctional PGM-free metal organic framework-based electrocatalysts for alkaline electrolyzers: trends in the activity with different metal centers. Nanoscale, 2021, 13, 4576-4584.	2.8	8
54243	Synthesis of molecular metallic barium superhydride: pseudocubic BaH12. Nature Communications, 2021, 12, 273.	5.8	66
54244	Selecting a stable solid form of remdesivir using microcrystal electron diffraction and crystal structure prediction. RSC Advances, 2021, 11, 17408-17412.	1.7	9
54245	Selective hydrogenation of 5-(hydroxymethyl)furfural to 5-methylfurfural over single atomic metals anchored on Nb2O5. Nature Communications, 2021, 12, 584.	5.8	92
54246	Coalescence and shape oscillation of Au nanoparticles in CO₂ hydrogenation to methanol. Nanoscale, 2021, 13, 18218-18225.	2.8	6
54247	Efficient nitric oxide reduction to ammonia on a metal-free electrocatalyst. Journal of Materials Chemistry A, 2021, 9, 5434-5441.	5.2	74
54248	Bonding of C₁ fragments on metal nanoclusters: a search for methane conversion catalysts with swarm intelligence. Physical Chemistry Chemical Physics, 2021, 23, 14004-14015.	1.3	12
54249	From Infection Clusters to Metal Clusters: Significance of the Lowest Occupied Molecular Orbital (LOMO). ACS Omega, 2021, 6, 1339-1351.	1.6	6
54250	Dual-site electrocatalytic nitrate reduction to ammonia on oxygen vacancy-enriched and Pd-decorated MnO₂ nanosheets. Nanoscale, 2021, 13, 17504-17511.	2.8	27
54251	Stabilization of Al ₃Zr Allotropes in Dilute Aluminum Alloys Via the Addition of Ternary Elements. SSRN Electronic Journal, 0, , .	0.4	0
54252	Ironâ€“oxygen covalency in perovskites to dominate syngas yield in chemical looping partial oxidation. Journal of Materials Chemistry A, 2021, 9, 13008-13018.	5.2	43
54253	Electron leakage through heterogeneous LiF on lithiumâ€“metal battery anodes. Physical Chemistry Chemical Physics, 2021, 23, 3214-3218.	1.3	22

#	Article	IF	Citations
54254	Efficient electrocatalytic nitrogen reduction to ammonia with aqueous silver nanodots. Communications Chemistry, 2021, 4, .	2.0	36
54255	Effects of Nitrogen/Fluorine Codoping on Photocatalytic Rutile TiO₂ Crystal Studied by First-Principles Calculations. Inorganic Chemistry, 2021, 60, 2381-2389.	1.9	9
54256	ANNMDD: Strength of Artificial Neural Network Types for Medical Diagnosis Domain. International Journal of Advanced Computer Science and Applications, 2021, 12, .	0.5	0
54257	Identification of vanadium dopant sites in the metalâ€“organic framework DUT-5(Al). Physical Chemistry Chemical Physics, 2021, 23, 7088-7100.	1.3	1
54258	Stacking effects in van der Waals heterostructures of blueP and Janus XYO (X = Ti, Zr, Hf: Y = S, Se) monolayers. RSC Advances, 2021, 11, 12189-12199.	1.7	7
54259	Poly(thiourea triethylene glycol) as a multifunctional binder for enhanced performance in lithium-sulfur batteries. Green Energy and Environment, 2022, 7, 1206-1216.	4.7	10
54260	Extended UV detection bandwidth: h-BN/Al powder nanocomposites photodetectors sensitive in a middle UV region due to localized surface plasmon resonance effect. Europhysics Letters, 2021, 133, 28002.	0.7	3
54261	Combined healing and doping of transition metal dichalcogenides through molecular functionalization. Journal of Materials Chemistry C, 2021, 9, 16247-16256.	2.7	7
54262	Pressure-induced stability and polymeric nitrogen in alkaline earth metal N-rich nitrides (XN6, X = Ca,) Tj ETQq0 0 0 rgBT /Overlock 10 Tf	1.7	0
54263	Theoretical insight for supercapacitors based on 2D materials from DFT simulations. , 2021, , 105-128.		3
54264	Electronic and magnetic properties of single-layer FeCl2 with defects. Physical Review B, 2021, 103, .	1.1	9
54265	Sulfur doped ruthenium nanoparticles as a highly efficient electrocatalyst for the hydrogen evolution reaction in alkaline media. Catalysis Science and Technology, 2021, 11, 3865-3872.	2.1	6
54266	Phosgene Gas Sensing of Ti₂CT₂ (T = F^{â^'}, O^{â^'},) Tj ETQq0 0 0 rgBT /Overlock 10 Tf	1.3	30
54267	Atomic insights into the oxygen incorporation in atomic layer deposited conductive nitrides and its mitigation by energetic ions. Nanoscale, 2021, 13, 10092-10099.	2.8	7
54268	Metal-to-insulator transition in Pt-doped TiSe2 driven by emergent network of narrow transport channels. Npj Quantum Materials, 2021, 6, .	1.8	10
54269	A multifunctional colorimetric sensor originating from a cadmium naphthalene diimide-based metalâ€“organic framework: photochromism, hydrochromism, and vapochromism. CrystEngComm, 2021, 23, 4513-4521.	1.3	13
54270	Thickness-dependent anisotropic transport of phonons and charges in few-layered PdSe₂. Physical Chemistry Chemical Physics, 2021, 23, 18869-18884.	1.3	17
54271	A systematic theoretical study of hydrogen activation, spillover and desorption in single-atom alloys. Applied Catalysis A: General, 2021, 610, 117948.	2.2	16

#	Article	IF	Citations
54272	Theoretical study of the H/D isotope effect of CH₄/CD₄ adsorption on a Rh(111) surface using a combined plane wave and localized basis sets method. RSC Advances, 2021, 11, 10253-10257.	1.7	4
54273	Adsorption of toxic gases on borophene: surface deformation links to chemisorptions. RSC Advances, 2021, 11, 18279-18287.	1.7	21
54274	Ultralow Thermal Conductivity and Enhanced Figure of Merit for CuSbSe₂ via Cd-Doping. ACS Applied Energy Materials, 2021, 4, 1637-1643.	2.5	16
54275	The CdTiO₃/BaTiO₃ superlattice interface from first principles. Nanoscale, 2021, 13, 8506-8513.	2.8	3
54276	Electronic Tuning of Monolayer Graphene with Polymeric â€œZwitteristsâ€• ACS Nano, 2021, 15, 2762-2770.	7.3	17
54277	Precise Control of Nanoscale Cu Etching via Gas-Phase Oxidation and Chemical Complexation. Journal of Physical Chemistry C, 2021, 125, 1819-1832.	1.5	7
54278	Density functional theory study of thiophene desulfurization and conversion of desulfurization products on the Ni(111) surface and Ni₅₅ cluster: implication for the mechanism of reactive adsorption desulfurization over Ni/ZnO catalysts. Catalysis Science and Technology, 2021, 11, 1615-1625.	2.1	12
54279	Descriptor-Guided Design and Experimental Synthesis of Metal-Doped TiO₂ for Propane Dehydrogenation. Industrial & Engineering Chemistry Research, 2021, 60, 1200-1209.	1.8	8
54280	Dual-Band Plasmonic Perfect Absorber Based on the Hybrid Halide Perovskite in the Communication Regime. Coatings, 2021, 11, 67.	1.2	14
54281	The unique carrier mobility of monolayer Janus MoSSe nanoribbons: a first-principles study. Dalton Transactions, 2021, 50, 10252-10260.	1.6	8
54282	Metastable piezoelectric group-IV monochalcogenide monolayers with a buckled honeycomb structure. Physical Review B, 2021, 103, .	1.1	23
54284	First-principles study of boron segregation in fcc-Fe grain boundaries and its influence on interface adhesive strength. Wuli Xuebao/Acta Physica Sinica, 2021, 70, 166401.	0.2	3
54286	Porous hydrogen substituted graphyne as a promising anode for lithium-ion batteries. RSC Advances, 2021, 11, 22079-22087.	1.7	1
54287	Doping and strain effect on hydrogen evolution reaction catalysts of NiP₂. Wuli Xuebao/Acta Physica Sinica, 2021, 70, 148802-148802.	0.2	0
54288	All-inorganic tin-doped Cs₂BiAgCl₆ double perovskites with stable blue photoluminescence for WLEDs. Journal of Materials Chemistry C, 2021, 9, 8862-8873.	2.7	11
54289	Relationship between bonding characteristic and thermal property of amorphous carbon structure: Ab initio molecular dynamics study. Diamond and Related Materials, 2021, 111, 108211.	1.8	10
54290	Electronic properties of bilayer g-SiC3 system. Journal of Materials Science: Materials in Electronics, 2021, 32, 1888-1896.	1.1	0
54291	Tuning the magnetic properties of Sn_{1â^'xâ^'y}Ce_{4+x}Ce_{3+y}O₂ nanoparticles: an experimental and theoretical approach. Nanoscale Advances, 2021, 3, 1484-1495.	2.2	5

#	Article	IF	Citations
54293	First-principle study of new phase of layered Bi₂Se₃. Wuli Xuebao/Acta Physica Sinica, 2021, 70, 027102.	0.2	1
54294	Tunable electronic and optical properties in buckling a non-lamellar B₃S monolayer. Physical Chemistry Chemical Physics, 2021, 23, 18669-18677.	1.3	4
54295	Two-dimensional metallic carbon allotrope with multiple rings for ion batteries. Physical Chemistry Chemical Physics, 2021, 23, 18770-18776.	1.3	17
54296	Discovery of high performance thermoelectric chalcogenides through first-principles high-throughput screening. Journal of Materials Chemistry C, 2021, 9, 13226-13235.	2.7	8
54297	Room-temperature ferromagnetism in two-dimensional transition metal borides: a first-principles investigation. Physical Chemistry Chemical Physics, 2021, 23, 10615-10620.	1.3	18
54298	Phase Transformation and Superstructure Formation in (Ti0.5, Mg0.5)N Thin Films through High-Temperature Annealing. Coatings, 2021, 11, 89.	1.2	2
54299	Classical and cubic Rashba effect in the presence of in-plane <mml:math xmlns:mml="http://www.w3.org/1998/Math/MathML"><mml:mn>4</mml:mn><mml:mi>f</mml:mi></mml:math> magnetism at the iridium silicide surface of the antiferromagnet <mml:math xmlns:mml="http://www.w3.org/1998/Math/MathML"><mml:msub><mml:mrow><mml:mi>GdIr</mml:mi></mml:mrow><mml:mn>2</m Physical Review B, 2021, 103, .	1.1	15
54300	Orientation-Dependent Conversion of VLS-Grown Lead Iodide Nanowires into Organic-Inorganic Hybrid Perovskites. Nanomaterials, 2021, 11, 223.	1.9	1
54301	Tunable Magnetic and Electronic Properties of the 2D CoO₂ Layer. Journal of Physical Chemistry C, 2021, 125, 873-877.	1.5	1
54302	Effect of Alloying Elements on the Mechanical Properties of Mo3Si. Metals, 2021, 11, 129.	1.0	2
54303	Orbital competition of Mn³⁺ and V³⁺ ions in Mn_{1+x}V_{2-x}O₄. Journal of Physics Condensed Matter, 2021, 33, 134002.	0.7	1
54304	A High Thermoelectric Performance ZT in p-Type LaSe₂ Crystal. Key Engineering Materials, 0, 871, 203-207.	0.4	1
54305	Topological surface states in epitaxial <mml:math		

#	Article	IF	Citations
54311	Prediction of Superhard BN2 with High Energy Density*. Chinese Physics Letters, 2021, 38, 018101.	1.3	5
54312	Reducing the reverse leakage current of AlGaN/GaN heterostructures via low-fluence neutron irradiation. Journal of Materials Chemistry C, 2021, 9, 3177-3182.	2.7	13
54313	Analysis of defects in In2O3:H synthesized in presence of water vapor and hydrogen gas mixture. Journal of Applied Physics, 2021, 129, .	1.1	5
54314	Phonon spectrum and thermoelectric properties of square/octagon structure of bismuth monolayer. RSC Advances, 2021, 11, 5107-5117.	1.7	2
54315	Computational assessment of the crystallization tendency of 1-ethyl-3-methylimidazolium ionic liquids. Physical Chemistry Chemical Physics, 2021, 23, 4951-4962.	1.3	8
54316	Variation in the interface strength of silicon with surface engineered Ti₃C₂ MXenes. Physical Chemistry Chemical Physics, 2021, 23, 5540-5550.	1.3	7
54317	The high power conversion efficiency of a two-dimensional GeSe/AsP van der Waals heterostructure for solar energy cells. Physical Chemistry Chemical Physics, 2021, 23, 6042-6050.	1.3	22
54318	Study on the Photoluminescence Properties and First-Principles Calculations of L-cysteine Capped ZnS Quantum Dots. Journal of Physics: Conference Series, 2021, 1775, 012008.	0.3	2
54319	Charge carrier dynamics investigation of Cu₂Sâ€“In₂S₃ heterostructures for the conversion of dinitrogen to ammonia via photo-electrocatalytic reduction. Journal of Materials Chemistry A, 2021, 9, 10497-10507.	5.2	19
54320	The dome of gold nanolized for catalysis. Chemical Science, 2021, 12, 5664-5671.	3.7	3
54321	Stoner enhancement from interstitial electrons in Y2C toward a spontaneous ferromagnetic electride. Dalton Transactions, 2021, 50, 5446-5451.	1.6	0
54322	Accelerated Discovery of Thermoelectric Materials Using Machine Learning. Springer Series in Materials Science, 2021, , 133-152.	0.4	1
54323	Revealing the role of defects in graphene oxide in the evolution of magnesium nanocrystals and the resulting effects on hydrogen storage. Journal of Materials Chemistry A, 2021, 9, 9875-9881.	5.2	27
54324	High-energetic and low-sensitive 1,3,5-triamino 2,4,6-trinitrobenzene (TATB) crystal: first principles investigation and Hirshfeld surface analysis. New Journal of Chemistry, 2021, 45, 6136-6143.	1.4	9
54325	Atomic adsorption on monolayer Cu₂Se: a first-principles study. Physical Chemistry Chemical Physics, 2021, 23, 9814-9821.	1.3	5
54326	Effect of axial molecules and linker length on CO₂ adsorption and selectivity of CAU-8: a combined DFT and GCMC simulation study. RSC Advances, 2021, 11, 12460-12469.	1.7	0
54327	Types of Nanoparticles Used in XLPE Systems. Materials Horizons, 2021, , 19-47.	0.3	0
54328	First-Principles Investigations of Electronic Structures, Mechanical Properties, and Thermodynamic Characteristics of Scandium Carbide Compounds. Russian Journal of Physical Chemistry A, 2021, 95, 29-37.	0.1	1

#	Article	IF	Citations
54329	A first-principles study on the properties of Sn-doped LiCoO₂ for Li-ion batteries. Dalton Transactions, 2021, 50, 4680-4685.	1.6	7
54330	Theoretical evidence of water serving as a promoter for lithium superoxide disproportionation in Liâ€“O₂ batteries. Physical Chemistry Chemical Physics, 2021, 23, 10440-10447.	1.3	1
54331	Intrinsic defect formation and the effect of transition metal doping on transport properties in a ductile thermoelectric material Î±-Ag₂S: a first-principles study. Physical Chemistry Chemical Physics, 2021, 23, 9773-9784.	1.3	13
54332	Pressure-induced Naâ€“Au compounds with novel structural units and unique charge transfer. Physical Chemistry Chemical Physics, 2021, 23, 6455-6461.	1.3	8
54333	The interaction between vacancy defects in gallium sulfide monolayer and a new vacancy defect model. Physical Chemistry Chemical Physics, 2021, 23, 13623-13632.	1.3	6
54334	Two-dimensional oxide quasicrystal approximants with tunable electronic and magnetic properties. Nanoscale, 2021, 13, 10771-10779.	2.8	7
54335	Atomic-thin hexagonal CuCo nanocrystals with d-band tuning for CO₂ reduction. Journal of Materials Chemistry A, 2021, 9, 7496-7502.	5.2	24
54336	Selective hydrogenation of acetylene on Cuâ€“Pd intermetallic compounds and Pd atoms substituted Cu(111) surfaces. Physical Chemistry Chemical Physics, 2021, 23, 8653-8660.	1.3	9
54337	State of charge dependent ordered and disordered phases in a Li[Ni1/3Co1/3Mn1/3]O2 cathode material. Materials Advances, 2021, 2, 3965-3970.	2.6	2
54338	Facilitating electrocatalytic hydrogen evolution via multifunctional tungsten@tungsten disulfide coreâ€“shell nanospheres. Journal of Materials Chemistry A, 2021, 9, 9272-9280.	5.2	13
54339	Defect-nucleated phase transition in atomically-thin WS₂. 2D Materials, 2021, 8, 025017.	2.0	5
54340	Electronic and photochemical properties of hybrid binary silicon and germanium derived Janus monolayers. Physical Chemistry Chemical Physics, 2021, 23, 17502-17511.	1.3	8
54341	Revisiting the role of Zr doping in Ni-rich layered cathodes for lithium-ion batteries. Journal of Materials Chemistry A, 2021, 9, 17415-17424.	5.2	56
54342	Performance and limits of 2.0 eV bandgap CuInGaS₂ solar absorber integrated with CdS buffer on F:SnO₂ substrate for multijunction photovoltaic and photoelectrochemical water splitting devices. Materials Advances, 2021, 2, 5752-5763.	2.6	4
54343	Dual electrocatalytic heterostructures for efficient immobilization and conversion of polysulfides in Liâ€“S batteries. Journal of Materials Chemistry A, 2021, 9, 18477-18487.	5.2	15
54344	Dimensionality control of magnetic coupling at interfaces of cuprateâ€“manganite superlattices. Materials Horizons, 2021, 8, 2485-2493.	6.4	5
54345	Plasmonic Au nanoclusters dispersed in nitrogen-doped graphene as a robust photocatalyst for light-to-hydrogen conversion. Journal of Materials Chemistry A, 2021, 9, 22810-22819.	5.2	26
54346	The Effects of photoelectric properties of monolayer MoS2 under Tensile strains. Wuli Xuebao/Acta Physica Sinica, 2021, .	0.2	1

#	Article	IF	Citations
54347	Effect of monovacancy on stability and hydrogen storage property of Sc/Ti/V-decorated graphene. Wuli Xuebao/Acta Physica Sinica, 2021, 70, 218802.	0.2	1
54348	Crystallization of the P₃Sn₄ Phase upon Cooling P₂Sn₅ Liquid by Molecular Dynamics Simulation Using a Machine Learning Interatomic Potential. Journal of Physical Chemistry C, 2021, 125, 3127-3133.	1.5	7
54349	A XANES study of lithium polysulfide solids: a first-principles study. Materials Advances, 2021, 2, 6403-6410.	2.6	6
54350	Structural, Topological, and Superconducting Properties of Twoâ€Ðimensional Tellurium Allotropes from Ab Initio Predictions. Advanced Theory and Simulations, 2021, 4, 2000265.	1.3	4
54351	Consecutive metal oxides with self-supported nanoarchitecture achieves highly stable and enhanced photoelectrocatalytic oxidation for water purification. Journal of Solid State Electrochemistry, 2021, 25, 1083-1092.	1.2	9
54352	The electronic pseudo band gap states and electronic transport of the full-Heusler compound Fe₂VAl. Journal of Materials Chemistry C, 2021, 9, 2073-2085.	2.7	17
54353	Climbing to the Top of Mount Fuji: Uniting Theory and Observations of Oxygen Triple Isotope Systematics. Reviews in Mineralogy and Geochemistry, 2021, 86, 97-135.	2.2	8
54354	Lithium-ion attack on yttrium oxide in the presence of copper powder during Li plating in a super-concentrated electrolyte. RSC Advances, 2021, 11, 6361-6366.	1.7	2
54355	Atomic Resonant Tunneling in the Surface Diffusion of H Atoms on Pt(111). Journal of Physical Chemistry C, 2021, 125, 464-480.	1.5	8
54356	Unveiling the Origin of Alloy-Seeded and Nondendritic Growth of Zn for Rechargeable Aqueous Zn Batteries. ACS Energy Letters, 2021, 6, 404-412.	8.8	148
54357	Composition-dependent effects of oxygen on atomic structure and mechanical properties of metallic glasses. Physical Chemistry Chemical Physics, 2021, 23, 1335-1342.	1.3	10
54358	First-principles study of the electronic structures and optical and photocatalytic performances of van der Waals heterostructures of SiS, P and SiC monolayers. RSC Advances, 2021, 11, 14263-14268.	1.7	14
54359	On the happiness of ferroelectric surfaces and its role in water dissociation: The example of bismuth ferrite. Journal of Chemical Physics, 2021, 154, 024702.	1.2	17
54360	One-step synthesis of single-site vanadium substitution in 1T-WS2 monolayers for enhanced hydrogen evolution catalysis. Nature Communications, 2021, 12, 709.	5.8	137
54361	Broadband Nonlinear Photonics in Fewâ€Layer Borophene. Small, 2021, 17, e2006891.	5.2	42
54362	Density functional theory predictions of the mechanical properties of crystalline materials. CrystEngComm, 2021, 23, 5697-5710.	1.3	41
54363	Tuning the structural, electronic and dynamical properties of Janus M4X3Y3 (M = Pd, Ni and Co; X,Y = S,) Tj ETQq0 0 0 rgBT /Overlock 10	1.3	3
54364	Isolated single iron atoms anchored on a N, S-codoped hierarchically ordered porous carbon framework for highly efficient oxygen reduction. Journal of Materials Chemistry A, 2021, 9, 10110-10119.	5.2	37

#	Article	IF	Citations
54365	An artificial hybrid interphase for an ultrahigh-rate and practical lithium metal anode. Energy and Environmental Science, 2021, 14, 4115-4124.	15.6	376
54366	Topological Phase Transition and Phonon-Space Dirac Topology Surfaces in <mml:math xmlns:mml="http://www.w3.org/1998/Math/MathML" display="inline"><mml:mrow><mml:msub><mml:mrow><mml:mi>ZrTe</mml:mi></mml:mrow><mml:mrow><mml:mn>5</mml:mn></m Physical Review Letters, 2021, 126, 016401.	2.9	16
54367	Significantly improved conductivity of spinel Co₃O₄ porous nanowires partially substituted by Sn in tetrahedral sites for high-performance quasi-solid-state supercapacitors. Journal of Materials Chemistry A, 2021, 9, 7005-7017.	5.2	31
54368	Synthesis, Crystal and Electronic Structure of La 2 SiP 4. Zeitschrift Fur Anorganische Und Allgemeine Chemie, 2021, 647, 91-97.	0.6	8
54369	Micro-electrochemical Properties and Pitting Corrosion Resistance of Microstructures of Carbon Steels. Tetsu-To-Hagane/Journal of the Iron and Steel Institute of Japan, 2021, 107, .	0.1	0
54370	Role of lone-pair electrons in determining the thermal transport behavior of LiAsS₂: first-principles investigation. CrystEngComm, 2021, 23, 4109-4115.	1.3	4
54371	Mn ions' site and valence in PbTiO3 based on the native vacancy defects. Condensed Matter Physics, 2021, 24, 23705.	0.3	0
54372	Can T-carbon serve as a Li storage material and a Li battery anode?. Materials Advances, 0, , .	2.6	1
54373	In situ coating of a lithiophilic interphase on a biporous Cu scaffold with vertical microchannels for dendrite-free Li metal batteries. Journal of Materials Chemistry A, 2021, 9, 13642-13652.	5.2	9
54374	A theoretical investigation of 38-atom CuPd clusters: the effect of potential parameterisation on structure and segregation. Physical Chemistry Chemical Physics, 2021, 23, 15950-15964.	1.3	3
54375	Doping dependence of electronic structure of infinite-layer <mml:math xmlns:mml="http://www.w3.org/1998/Math/MathML"><mml:msub><mml:mrow><mml:mi>NdNiO</mml:mi></mml:mrow><mml:mrow><mml:mn>2 Physical Review B, 2021, 103, .	1.1	24
54376	Interfacial atomic Ni tetragon intercalation in a NiO₂-to-Pd hetero-structure triggers superior HER activity to the Pt catalyst. Journal of Materials Chemistry A, 2021, 9, 12019-12028.	5.2	19
54377	A novel design of SiH/CeO₂(111) van der Waals type-II heterojunction for water splitting. Physical Chemistry Chemical Physics, 2021, 23, 2812-2818.	1.3	49
54378	Growing Nanostructured CuO on Copper Foil via Chemical Etching to Upgrade Metallic Lithium Anode. ACS Applied Materials & Interfaces, 2021, 13, 6367-6374.	4.0	20
54379	Freestanding perovskite oxide monolayers as two-dimensional semiconductors. Nanotechnology, 2021, 32, 145705.	1.3	11
54380	Influence of surface defects on activity and selectivity: a quantitative study of structure sensitivity of Pd catalysts for acetylene hydrogenation. Catalysis Science and Technology, 0, , .	2.1	17
54381	Reconstruction and catalytic activity of hybrid Pd(100)/(111) monolayer on Î³-Al₂O₃(100) in CH₄, H₂O, and O₂ dissociation. Dalton Transactions, 2021, 50, 8863-8876.	1.6	2
54382	Investigating the innate selectivity issues of methane to methanol: consideration of an aqueous environment. Chemical Science, 2021, 12, 4443-4449.	3.7	17

#	Article	IF	Citations
54383	Efficient photogeneration of nonacene on nanostructured graphene. Nanoscale Horizons, 2021, 6, 744-750.	4.1	9
54384	How oxidation state and lattice distortion influence the oxygen evolution activity in acid of iridium double perovskites. Journal of Materials Chemistry A, 2021, 9, 2980-2990.	5.2	36
54385	Ab initio study of alloying of MnBi to enhance the energy product. RSC Advances, 2021, 11, 30955-30960.	1.7	3
54386	Enhanced performance of Se-alloyed CdTe solar cells: The role of Se-segregation on the grain boundaries. Journal of Applied Physics, 2021, 129, .	1.1	8
54387	Directional Monte Carlo Lattice Search Algorithm for the Structure Search of Alumina Clusters (Al2O3)n (n=1~50). Acta Chimica Sinica, 2021, 79, 1154.	0.5	1
54388	Convergence Analysis of Direct Minimization and Self-Consistent Iterations. SIAM Journal on Matrix Analysis and Applications, 2021, 42, 243-274.	0.7	22
54389	Direct and Broadband Plasmonic Charge Transfer to Enhance Water Oxidation on a Gold Electrode. ACS Nano, 2021, 15, 3188-3200.	7.3	23
54390	Computational design of a switchable heterostructure electrocatalyst based on a two-dimensional ferroelectric In₂Se₃ material for the hydrogen evolution reaction. Journal of Materials Chemistry A, 2021, 9, 11553-11562.	5.2	15
54391	The origins of charge separation in anisotropic facet photocatalysts investigated through first-principles calculations. RSC Advances, 2021, 11, 18500-18508.	1.7	5
54392	Blue-AsP monolayer as a promising anode material for lithium- and sodium-ion batteries: a DFT study. Physical Chemistry Chemical Physics, 2021, 23, 5143-5151.	1.3	28
54393	Thermoelectric properties of Î± -In2Se3 monolayer. Applied Physics Letters, 2021, 118, .	1.5	36
54394	Theoretical prediction by DFT and experimental observation of heterocation-doping effects on hydrogen adsorption and migration over the CeO₂(111) surface. Physical Chemistry Chemical Physics, 2021, 23, 4509-4516.	1.3	7
54395	Quenchable amorphous glass-like material from VF₃. Dalton Transactions, 2021, 50, 3005-3010.	1.6	1
54396	Ga2OSe monolayer: A promising hydrogen evolution photocatalyst screened from two-dimensional gallium chalcogenides and the derived janus. Green Energy and Environment, 2022, 7, 1045-1052.	4.7	12
54397	Tunable anomalous Hall transport in bulk and two-dimensional <mml:math xmlns:mml="http://www.w3.org/1998/Math/MathML"><mml:mrow><mml:mn>1</mml:mn><mml:mi>T</mml:mi></mml:mrow><mml:m mathvariant="normal">CrTe</mml:mi><mml:mn>2</mml:mn></mml:msub></mml:math> : A first-principles study. Physical Review B, 2021, 103, .	1.1	24
54398	Evaluation of the role of graphene-based Cu(<scp>i</scp>) catalysts in borylation reactions. Catalysis Science and Technology, 2021, 11, 3501-3513.	2.1	8
54399	In situ coating amorphous boride on ternary pyrite-type boron sulfide for highly efficient oxygen evolution. Journal of Materials Chemistry A, 2021, 9, 12283-12290.	5.2	8
54400	Tuning adlayer-substrate interactions of graphene/h-BN heterostructures on Cu(111)â€“Ni and Ni(111)â€“Cu surface alloys. RSC Advances, 2021, 11, 1916-1927.	1.7	2

#	Article	IF	Citations
54401	Surface activation by electron scavenger metal nanorod adsorption on TiH₂, TiC, TiN, and Ti₂O₃. Physical Chemistry Chemical Physics, 2021, 23, 16577-16593.	1.3	9
54402	Magnetization textures in twisted bilayer <mml:math xmlns:mml="http://www.w3.org/1998/Math/MathML"><mml:mrow><mml:mi>Cr</mml:mi><mml:msub><mml:mi mathvariant="normal">X</mml:mi><mml:mn>3</mml:mn></mml:msub></mml:mrow></mml:math> () Tj ETQq1 1 0.784314 rgBT /Ov	1.3	18
54403	Mechanistic investigation of benzene esterification by K2CO3/TiO2: the catalytic role of the multifunctional interface. Chemical Communications, 2021, 57, 7890-7893.	2.2	2
54404	Copolymers of bipyridinium and metal (Zn & Ni) porphyrin derivatives; theoretical insights and electrochemical activity towards CO₂. RSC Advances, 2021, 11, 19844-19855.	1.7	1
54405	Low-cost and multi-level structured NiFeMn alloy@NiFeMn oxyhydroxide electrocatalysts for highly efficient overall water splitting. Inorganic Chemistry Frontiers, 2021, 8, 2713-2724.	3.0	5
54406	A NiN₃-embedded MoS₂monolayer as a promising electrocatalyst with high activity for the oxygen evolution reaction: a computational study. Sustainable Energy and Fuels, 2021, 5, 3330-3339.	2.5	7
54407	Disorder effects of vacancies on the electronic transport properties of realistic topological insulator nanoribbons: The case of bismuthene. Physical Review Materials, 2021, 5, .	0.9	14
54408	Activation of phosphorene-like two-dimensional GeSe for efficient electrocatalytic nitrogen reductionviastates filtering of Ru. Journal of Materials Chemistry A, 2021, 9, 16056-16064.	5.2	19
54409	Boron position-dependent surface reconstruction and electronic states of boron-doped diamond(111) surfaces: anab initiostudy. Physical Chemistry Chemical Physics, 2021, 23, 15628-15634.	1.3	5
54410	Competitive adsorption of phenol and toluene onto silica-supported transition metal clusters for biofuel purification. Molecular Systems Design and Engineering, 2021, 6, 817-824.	1.7	7
54411	Highly dispersed Pt atoms and clusters on hydroxylated indium tin oxide: a view from first-principles calculations. Journal of Materials Chemistry A, 2021, 9, 15724-15733.	5.2	8
54412	Effect of Adding Third Element on Deformability of Mgâ€“Al Alloy. Minerals, Metals and Materials Series, 2021, , 37-44.	0.3	0
54413	Surface Functionalization Utilizing Mesoporous Silica Nanoparticles for Enhanced Evanescent-Field Mid-Infrared Waveguide Gas Sensing. Coatings, 2021, 11, 118.	1.2	11
54414	Understanding carbon contamination in the proton-conducting zirconates and cerates. Physical Chemistry Chemical Physics, 2021, 23, 14205-14211.	1.3	3
54415	Modification of thermal transport in few-layer MoS₂ by atomic-level defect engineering. Nanoscale, 2021, 13, 11561-11567.	2.8	12
54416	Interactions between water and rhodium clusters: molecular adsorption versus cluster adsorption. Nanoscale, 2021, 13, 11396-11402.	2.8	5
54417	Identification of electronic descriptors for catalytic activity of transition-metal and non-metal doped MoS₂. Physical Chemistry Chemical Physics, 2021, 23, 15101-15106.	1.3	3
54418	Ultraâ€Small 2D PbS Nanoplatelets: Liquidâ€Phase Exfoliation and Emerging Applications for Photoâ€Electrochemical Photodetectors. Small, 2021, 17, e2005913.	5.2	50

#	Article	IF	Citations
54419	Intrinsic carbon-doping induced synthesis of oxygen vacancies-mediated TiO2 nanocrystals: Enhanced photocatalytic NO removal performance and mechanism. Journal of Catalysis, 2021, 393, 179-189.	3.1	25
54420	Interfacial magnetism in a fused superatomic cluster [Co₆Se₈(PEt₃)₅]₂. Nanoscale, 2021, 13, 15763-15769.	2.8	6
54421	Understanding charge storage in Nb₂CT_x MXene as an anode material for lithium ion batteries. Physical Chemistry Chemical Physics, 2021, 23, 23173-23183.	1.3	12
54422	A method to restore the intrinsic dielectric functions of 2D materials in periodic calculations. Nanoscale, 2021, 13, 17057-17067.	2.8	11
54423	Machine learned features from density of states for accurate adsorption energy prediction. Nature Communications, 2021, 12, 88.	5.8	108
54424	Ultra-low thermal conductivity and high thermoelectric performance of monolayer BiP₃: a first principles study. Physical Chemistry Chemical Physics, 2021, 23, 19834-19840.	1.3	2
54425	Theoretical assessment of Raman spectra on MXene Ti₂C: from monolayer to bilayer. Physical Chemistry Chemical Physics, 2021, 23, 19884-19891.	1.3	9
54426	A computational investigation of the adsorption of small copper clusters on the CeO₂(110) surface. Physical Chemistry Chemical Physics, 2021, 23, 19329-19342.	1.3	7
54427	Design Principles for Cationâ€Mixed Sodium Solid Electrolytes. Advanced Energy Materials, 2021, 11, 2003196.	10.2	13
54428	Surface reconstruction inducedin situphosphorus doping in nickel oxides for an enhanced oxygen evolution reaction. Journal of Materials Chemistry A, 2021, 9, 6432-6441.	5.2	38
54429	Confining Aqueous Znâ€“Br Halide Redox Chemistry by Ti₃C₂T_X MXene. ACS Nano, 2021, 15, 1718-1726.	7.3	78
54430	The role of surface oxidation and Feâ€“Ni synergy in Feâ€“Niâ€“S catalysts for CO₂ hydrogenation. Faraday Discussions, 2021, 230, 30-51.	1.6	21
54431	H4,4,4-graphyne with double Dirac points as high-efficiency bifunctional electrocatalysts for water splitting. Journal of Materials Chemistry A, 2021, 9, 4082-4090.	5.2	28
54432	N-Doped carbon encapsulating Bi nanoparticles derived from metalâ€“organic frameworks for high-performance sodium-ion batteries. Journal of Materials Chemistry A, 2021, 9, 22048-22055.	5.2	33
54433	A comparative study of Bi, Sb, and BiSb for electrochemical nitrogen reduction leading to a new catalyst design strategy. Journal of Materials Chemistry A, 2021, 9, 20453-20465.	5.2	15
54434	Switching interlayer magnetic order in bilayer CrI₃ by stacking reversal. Nanoscale, 2021, 13, 16172-16181.	2.8	20
54435	Penta-MS₂ (M = Mn, Ni, Cu/Ag and Zn/Cd) monolayers with negative Poisson's ratios and tunable bandgaps as water-splitting photocatalysts. Journal of Materials Chemistry A, 2021, 9, 6993-7004.	5.2	42
54436	Influence of the particle size on selective 2-propanol gas-phase oxidation over Co₃O₄ nanospheres. Catalysis Science and Technology, 2021, 11, 7552-7562.	2.1	9

#	Article	IF	Citations
54437	Insights into the electronic structure of Fe penta-coordinated complexes. Spectroscopic examination and electrochemical analysis for the oxygen reduction and oxygen evolution reactions. Journal of Materials Chemistry A, 2021, 9, 23802-23816.	5.2	27
54438	Using phase boundary mapping to resolve discrepancies in the Mg₂Siâ€“Mg₂Sn miscibility gap. Journal of Materials Chemistry A, 2021, 9, 7208-7215.	5.2	11
54439	Metallization of Shock-Compressed Liquid Ammonia. Physical Review Letters, 2021, 126, 025003.	2.9	21
54440	Promotion of Inorganic Phosphorus on Rh Catalysts in Styrene Hydroformylation: Geometric and Electronic Effects. ACS Catalysis, 2021, 11, 1787-1796.	5.5	43
54441	Computational study of 4,4â€²-dimethoxy triphenylamine donor linked with low band gap Ï€-spacers by single and double bonds for DSSC applications. New Journal of Chemistry, 2021, 45, 16989-17001.	1.4	5
54442	GeP₃/NbX₂ (X=S, Se) Nano-Heterostructures: Promising Isotropic Flexible Anodes for Lithium-Ion Batteries with High Lithium Storage Capacity. ACS Omega, 2021, 6, 2956-2965.	1.6	6
54443	A new nitrogen fixation strategy: the direct formation of *N₂^{â*} excited state on metal-free photocatalyst. Journal of Materials Chemistry A, 2021, 9, 6214-6222.	5.2	8
54444	Carbon nano-onion encapsulated cobalt nanoparticles for oxygen reduction and lithium-ion batteries. Journal of Materials Chemistry A, 2021, 9, 7227-7237.	5.2	21
54445	Two-Dimensional Carbon Allotropes and Nanoribbons based on 2,6-Polyazulene Chains: Stacking Stabilities and Electronic Properties. Journal of Physical Chemistry Letters, 2021, 12, 732-738.	2.1	41
54446	Ultra-bright green-emitting phosphors with an internal quantum efficiency of over 90% for high-quality WLEDs. Dalton Transactions, 2021, 50, 4159-4166.	1.6	26
54447	PyXtal_FF: a python library for automated force field generation. Machine Learning: Science and Technology, 2021, 2, 027001.	2.4	18
54448	Carburized cobalt catalyst for the Fischerâ€“Tropsch synthesis. Catalysis Science and Technology, 2021, 11, 6564-6572.	2.1	3
54449	Different Oxygen Desorption Durabilities of Lithium Titanium Oxides as Confirmed by Transmission Electron Energy-Loss Spectroscopy Analysis of Li₄Ti₅O₁₂ and Î²-Li₂TiO₃ Biphase Specimens. ACS Applied Energy Materials, 2021, 4, 1377-1386.	2.5	6
54450	Strong Modulation of Electronic Properties in Monolayer MoTe2 Using a Ferroelectric LiNbO3(0001) Substrate. Journal of Materials Chemistry C, 0, , .	2.7	1
54451	Boosting magnesium storage in MoS₂via a 1T phase introduction and interlayer expansion strategy: theoretical prediction and experimental verification. Sustainable Energy and Fuels, 2021, 5, 5471-5480.	2.5	4
54452	Single atom catalysts supported on N-doped graphene toward fast kinetics in Liâ€“S batteries: a theoretical study. Journal of Materials Chemistry A, 2021, 9, 12225-12235.	5.2	62
54453	New theoretical insights into the photoinduced carrier transfer dynamics in WS₂/WSe₂ van der Waals heterostructures. Physical Chemistry Chemical Physics, 2021, 23, 694-701.	1.3	11
54454	Defects of monolayer PbI₂: a computational study. Physical Chemistry Chemical Physics, 2021, 23, 20553-20559.	1.3	4

#	Article	IF	Citations
54455	Unexpected spontaneous dynamic oxygen migration on carbon nanotubes. Nanoscale, 2021, 13, 15231-15237.	2.8	6
54456	First-principles prediction of polar half-metallicity and out-of-plane piezoelectricity in two-dimensional quintuple layered cobalt selenide. Journal of Materials Chemistry C, 2021, 9, 12046-12050.	2.7	11
54457	Electrochemical oxidation of molecular nitrogen to nitric acid â€“ towards a molecular level understanding of the challenges. Chemical Science, 2021, 12, 6442-6448.	3.7	43
54458	Electric-field-driven octahedral rotation in perovskite. Npj Quantum Materials, 2021, 6, .	1.8	7
54459	Hierarchical superhydrophilic/superaerophobic CoMnP/Ni₂P nanosheet-based microplate arrays for enhanced overall water splitting. Journal of Materials Chemistry A, 2021, 9, 22129-22139.	5.2	45
54460	Microstructures and electronic characters of Î²-Ga₂O₃ on different substrates: exploring the role of surface chemistry and structures. Physical Chemistry Chemical Physics, 2021, 23, 21874-21882.	1.3	3
54461	Bond Valence Pathway Analyzerâ€"An Automatic Rapid Screening Tool for Fast Ion Conductors within softBV. Chemistry of Materials, 2021, 33, 625-641.	3.2	112
54462	Combined electrochemical and DFT investigations of iron selenide: a mechanically bendable solid-state symmetric supercapacitor. Sustainable Energy and Fuels, 2021, 5, 5001-5012.	2.5	34
54463	A new 2D auxetic CN₂ nanostructure with high energy density and mechanical strength. Physical Chemistry Chemical Physics, 2021, 23, 4353-4364.	1.3	8
54464	Monitoring the active sites for the hydrogen evolution reaction at model carbon surfaces. Physical Chemistry Chemical Physics, 2021, 23, 10051-10058.	1.3	21
54465	Observation and control of the weak topological insulator state in ZrTe5. Nature Communications, 2021, 12, 406.	5.8	43
54466	Efficient Charge Migration in Chemically-Bonded Prussian Blue Analogue/CdS with Beaded Structure for Photocatalytic H₂ Evolution. Jacs Au, 2021, 1, 212-220.	3.6	47
54467	Enhanced performance of Mo₂P monolayer as lithium-ion battery anode materials by carbon and nitrogen doping: a first principles study. Physical Chemistry Chemical Physics, 2021, 23, 4030-4038.	1.3	26
54468	An antibonding valence band maximum enables defect-tolerant and stable GeSe photovoltaics. Nature Communications, 2021, 12, 670.	5.8	58
54469	Pentagonal two-dimensional noble-metal dichalcogenide PdSSe for photocatalytic water splitting with pronounced optical absorption and ultrahigh anisotropic carrier mobility. Journal of Materials Chemistry C, 2021, 9, 7753-7764.	2.7	30
54470	Origins of structural and electronic transitions in disordered silicon. Nature, 2021, 589, 59-64.	13.7	192
54471	First-principles study on photoelectric and transport properties of CsXBr3 (Xâ€‰=â€‰Ge, Sn) and blue phosphorus van der Waals heterojunctions. Journal of Applied Physics, 2021, 129, .	1.1	9
54472	Theoretical investigations of novel Janus Pb₂SSe monolayer as a potential multifunctional material for piezoelectric, photovoltaic, and thermoelectric applications. Nanoscale, 2021, 13, 15611-15623.	2.8	12

#	Article	IF	Citations
54473	Coreâ€“Shell Double Doping of Zn and Ca on Î²-Ga₂O₃ Photocatalysts for Remarkable Water Splitting. ACS Catalysis, 2021, 11, 1911-1919.	5.5	28
54474	Sliver Doped Sodium Antimonate with Greatly Reduced the Band Gap for Efficiently Enhanced Photocatalytic Activities Under Visible Light (Experiment and DFT Calculation). Materials Research, 2021, 24, .	0.6	9
54475	Predicting lanthanide coordination structures in solution with molecular simulation. Methods in Enzymology, 2021, 651, 193-233.	0.4	3
54476	Alkaline-earth metal substitution stabilizes the anionic redox of Li-rich oxides. Journal of Materials Chemistry A, 2021, 9, 10364-10373.	5.2	10
54477	A defective MoS₂ monolayer as an efficient electrocatalyst for the nitrogen reduction reaction: a combined theoretical and experimental study. Sustainable Energy and Fuels, 2021, 5, 2415-2418.	2.5	5
54478	Two-dimensional palladium diselenide for the oxygen reduction reaction. Materials Chemistry Frontiers, 2021, 5, 4970-4980.	3.2	5
54479	A novel spin-valley-coupled nodal-ring semimetal in single-layer Ta₂C₃. Physical Chemistry Chemical Physics, 2021, 23, 12280-12287.	1.3	4
54480	An Introduction to Discretization Error Analysis for Computational Chemists. Lecture Notes in Quantum Chemistry II, 2021, , 103-128.	0.3	0
54481	Pesticide degradation on solid surfaces: a moisture dependent process governed by the interaction between TiO₂ and H₂O. New Journal of Chemistry, 0, , .	1.4	0
54482	Multiscale exploration of hydrocarbon adsorption and hopping through ZSM-5 channels â€“ from Monte Carlo modelling to experiment. Physical Chemistry Chemical Physics, 2021, 23, 2981-2990.	1.3	4
54483	Ab initio based models for temperature-dependent magnetochemical interplay in bcc Fe-Mn alloys. Physical Review B, 2021, 103, .	1.1	12
54484	An origin of excess vibrational entropies at grain boundaries in Al, Si and MgO: a first-principles analysis with lattice dynamics. Physical Chemistry Chemical Physics, 2021, 23, 10118-10129.	1.3	3
54485	DFT insights into structural effects of Niâ€“Cu/CeO₂ catalysts for CO selective reaction towards waterâ€“gas shift. Physical Chemistry Chemical Physics, 2021, 23, 3826-3836.	1.3	12
54486	Proton transport mechanism and pathways in the superprotonic phase of M3H(AO4)2 solid acids from ab initio molecular dynamics simulations. Physical Chemistry Chemical Physics, 2021, 23, 17026-17032.	1.3	1
54487	Controlled over-growth for nail-like and urchin-like cobalt with enhanced CO hydrogenation activity. Applied Surface Science, 2021, 537, 147931.	3.1	1
54488	Novel ReSe semiconductor designed by structure prediction and phase diagram calculation. Journal of Materials Science, 2021, 56, 6878-6890.	1.7	2
54489	Theoretical study on water adsorption and dissociation on the nickel surfaces. Journal of Molecular Modeling, 2021, 27, 36.	0.8	1
54490	An Integrated Methodology for Screening Hydrogen Evolution Reaction Catalysts: Pt/Mo2C as an Example. Springer Series in Materials Science, 2021, , 719-731.	0.4	0

#	Article	IF	Citations
54491	Intriguing electronic, optical and mechanical properties of the vertical and lateral heterostructures on the boron phosphide and GaN monolayers. Journal of Materials Science, 2021, 56, 7451-7463.	1.7	3
54492	Hydrogenation and oxidation enhances the thermoelectric performance of Si₂BN monolayer. New Journal of Chemistry, 2021, 45, 3892-3900.	1.4	8
54493	Helical magnetic order and Fermi surface nesting in noncentrosymmetric ScFeGe. Physical Review B, 2021, 103, .	1.1	5
54494	Local Electronic Structure and Dynamics of Muon-Polaron Complexes in <mml:math xmlns:mml="http://www.w3.org/1998/Math/MathML" display="inline"><mml:mrow><mml:msub><mml:mrow><mml:mi>Fe</mml:mi></mml:mrow><mml:mrow><mml:mi mathvariant="normal">O</mml:mi></mml:mrow><mml:mrow><mml:mn>3</mml:mn></mml:mrow></mml:msub></mml:mrow></mml: Physical Review Letters, 2021, 126, 037202.	2.9	10
54495	Single-Layer BI: A Multifunctional Semiconductor with Ferroelectricity, Ultrahigh Carrier Mobility, and Negative Poissonâ€™s Ratio. Physical Review Applied, 2021, 15, .	1.5	3
54496	Strain-controlled electronic and magnetic properties of tVS₂/hVS₂ van der Waals heterostructures. Physical Chemistry Chemical Physics, 2021, 23, 4669-4680.	1.3	5
54497	Hydrothermal synthesis of palladium nitrides as robust multifunctional electrocatalysts for fuel cells. Journal of Materials Chemistry A, 2021, 9, 6196-6204.	5.2	33
54498	First principle studies of ammonium chloride under high pressure. RSC Advances, 2021, 11, 5149-5155.	1.7	0
54499	Activated Lone-Pair Electrons Lead to Low Lattice Thermal Conductivity: A Case Study of Boron Arsenide. SSRN Electronic Journal, 0, , .	0.4	0
54500	Curvature-induced bandgap reduction in TiO2 double-walled nanotubes. Journal of Applied Physics, 2021, 129, 024303.	1.1	0
54501	Engineering the ligand states by surface functionalization: a new way to enhance the ferromagnetism of CrI₃. Nanoscale, 2021, 13, 4821-4827.	2.8	3
54502	The electronic and optical properties of SiO2â€“Alâ€“SiO2 withÂdensityÂfunctional theory. Modern Physics Letters B, 2021, 35, 2150136.	1.0	0
54503	Geometric and electronic properties of Au_lPt_m (l + m â‰¤ 10) clusters: a first-principles study. Physical Chemistry Chemical Physics, 2021, 23, 3050-3062.	1.3	0
54504	Evaluation of Yttrium Hydride (Î´-YH_{2-x}) Thermal Neutron Scattering Laws and Thermophysical Properties. Nuclear Science and Engineering, 2021, 195, 563-577.	0.5	4
54505	Structural diversities in centrosymmetric La8S4Cl8La12S8Cl4[SbS3]8 and non-centrosymmetric Ln12S8Cl8[SbS3]4 (Ln = La and Ce): syntheses, crystal and electronic structures, and optical properties. Dalton Transactions, 2021, 50, 2075-2082.	1.6	4
54506	Analysis and Growth Modeling of CuInSe2 Films by Electrodeposition for Photocell Applications. Brazilian Journal of Physics, 2021, 51, 406-419.	0.7	2
54507	Edge-effect enhanced catalytic CO oxidation by atomically dispersed Pt on nitride-graphene. Journal of Materials Chemistry A, 2021, 9, 2093-2098.	5.2	5
54508	Novel (110) Double-Layered Guanidinium-Lead Iodide Perovskite Material: Crystal Structure, Electronic Structure, and Broad Luminescence. Journal of Physical Chemistry C, 2021, 125, 964-972.	1.5	4

#	Article	IF	Citations
54509	Atomistic prediction on the configuration- and temperature-dependent dielectric constant of Be_{0.25}Mg_{0.75}O superlattice as a high-Î¹dielectric layer. Journal of Materials Chemistry C, 2021, 9, 851-859.	2.7	7
54510	Site-dependent photoinduced charge carrier dynamics in nitrogen/fluorine doped TiO2 nanoparticles. Journal of Materials Chemistry C, 2021, 9, 1992-2000.	2.7	0
54511	Pressure tuning of the iron-based superconductor (Ca0.73La0.27)FeAs2. Physical Review B, 2021, 103, .	1.1	3
54512	Adsorption properties of acetylene, ethylene and ethane in UiO-66 with linker defects and NO2 functionalization. Materials Advances, 2021, 2, 426-433.	2.6	3
54513	Anion ordering and vacancy defects in niobium perovskite oxynitrides. Materials Advances, 2021, 2, 2398-2407.	2.6	3
54514	New insights into the 1D carbon chain through the RPA. Physical Chemistry Chemical Physics, 2021, 23, 5254-5260.	1.3	6
54515	Band alignment of monolayer CaP₃, CaAs₃, BaAs₃ and the role of pâ€“d orbital interactions in the formation of conduction band minima. Physical Chemistry Chemical Physics, 2021, 23, 7418-7425.	1.3	0
54516	Mechanistic aspects of ammonia synthesis on Ta₃N₅ surfaces in the presence of intrinsic nitrogen vacancies. Physical Chemistry Chemical Physics, 2021, 23, 6959-6963.	1.3	2
54517	An Ab-initio Study of Structural, Elastic, Electronic, Vibrational and Optical Properties of Semiconductor NaAlSi Compound for Optoelectronic Applications. Advances in Material Research and Technology, 2021, , 125-144.	0.3	0
54518	Single metal atom anchored on a CN monolayer as an excellent electrocatalyst for the nitrogen reduction reaction. Physical Chemistry Chemical Physics, 2021, 23, 2658-2662.	1.3	10
54519	Surface phase structures responsible for the activity and deactivation of the fcc MoC (111)-Mo surface in steam reforming: a systematic kinetic and thermodynamic investigation. Catalysis Science and Technology, 2021, 11, 823-835.	2.1	2
54520	Curvature-induced electronic tuning of molecular catalysts for CO₂ reduction. Catalysis Science and Technology, 2021, 11, 2491-2496.	2.1	11
54521	Computational screening of MBene monolayers with high electrocatalytic activity for the nitrogen reduction reaction. Nanoscale, 2021, 13, 15002-15009.	2.8	22
54522	All solid thick oxide cathodes based on low temperature sintering for high energy solid batteries. Energy and Environmental Science, 2021, 14, 5044-5056.	15.6	41
54523	Digital-intellectual design of microporous organic polymers. Physical Chemistry Chemical Physics, 2021, 23, 22835-22853.	1.3	2
54524	Laboratory Operando XAS Study of Sodium Iron Titanite Cathode in the Li-Ion Half-Cell. Nanomaterials, 2021, 11, 156.	1.9	7
54525	First-Principles Calculations for the Interfaces of Perovskite Solar Cells. , 2021, , 95-158.		0
54526	Solute-adsorption enhanced heterogeneous nucleation: the effect of Cu adsorption on Î±-Al nucleation at the sapphire substrate. Physical Chemistry Chemical Physics, 2021, 23, 5270-5282.	1.3	12

#	Article	IF	Citations
54527	Improving the Mn2+ emission and stability of CsPb(Cl/Br)3 nanocrystals by Ni2+ doping in ambient air. Journal of Materials Science, 2021, 56, 7494-7507.	1.7	10
54528	Rational catalyst design for CO oxidation: a gradient-based optimization strategy. Catalysis Science and Technology, 2021, 11, 2604-2615.	2.1	5
54529	Electric field induced giant valley polarization in two dimensional ferromagnetic WSe2/CrSnSe3 heterostructure. Npj 2D Materials and Applications, 2021, 5, .	3.9	27
54530	Influence of Bismuth Substitution with Nb, Y, and P Elements on the Electronic Structure of Vacancy Filled BiCuSeO-Based System for the Thermoelectric Application. SSRN Electronic Journal, 0, , .	0.4	0
54531	Ti₃C₂T_x with a hydroxyl-rich surface for metal sulfides as high performance electrode materials for sodium/lithium storage. Journal of Materials Chemistry A, 2021, 9, 14013-14024.	5.2	32
54532	Selective hydrogenation of acetylene to ethylene on anatase TiO₂ through first-principles studies. Journal of Materials Chemistry A, 2021, 9, 14064-14073.	5.2	23
54533	Quasi-2D lead-free halide perovskite using superalkali cations for red-light-emitting diodes. Nanoscale, 2021, 13, 13152-13157.	2.8	4
54534	Enhanced strain-induced magnetoelectric coupling in polarization-free Fe/BaTiO3 heterostructures. Physical Chemistry Chemical Physics, 2021, 23, 16053-16059.	1.3	0
54535	Enhanced out-of-plane electromechanical response of Janus ZrSeO. Physical Chemistry Chemical Physics, 2021, 23, 16289-16295.	1.3	9
54536	Pressure-induced novel nitrogen-rich aluminum nitrides: AlN6, Al2N7 and AlN7 with polymeric nitrogen chains and rings. Physical Chemistry Chemical Physics, 2021, 23, 12350-12359.	1.3	8
54537	Dopants and grain boundary effects in monolayer MoS₂: a first-principles study. Physical Chemistry Chemical Physics, 2021, 23, 11937-11943.	1.3	4
54538	The unexpected discovery of the ninth polymorph of tolfenamic acid. CrystEngComm, 2021, 23, 3636-3647.	1.3	25
54539	Theoretical design of asymmetric Aâ€“D₁Aâ€²D₂â€“A type non-fullerene acceptors for organic solar cells. Physical Chemistry Chemical Physics, 2021, 23, 12321-12328.	1.3	20
54540	Electrochemical epitaxial (200) PbSe submicron-plates on single-layer graphene for an ultrafast infrared response. Journal of Materials Chemistry C, 2021, 9, 6536-6543.	2.7	8
54541	First-principle investigation of hybrid improper ferroelectricity of n = 2 Ruddlesden-Popper Sr₃B₂Se₇ (B = Zr, Hf). Wuli Xuebao/Acta Physica Sinica, 2021, 70, 116302-116302.	0.2	0
54542	First principles study of electrical and magnetic properties of two-dimensional ferromagnetic semiconductors CrI₃ adsorbed by atoms. Wuli Xuebao/Acta Physica Sinica, 2021, 70, 117101.	0.2	2
54543	Stability of hydrogen-terminated graphene edges. Physical Chemistry Chemical Physics, 2021, 23, 13261-13266.	1.3	11
54544	Scintillation materials based on metal iodates by rare earth doping modifications for use in radioluminescence and X-ray imaging. CrystEngComm, 2021, 23, 4103-4108.	1.3	9

#	Article	IF	Citations
54545	3D self-supported porous vanadium-doped nickel nitride nanosheet arrays as efficient bifunctional electrocatalysts for urea electrolysis. Journal of Materials Chemistry A, 2021, 9, 4159-4166.	5.2	89
54546	Zero-dimensional plate-shaped copper halide crystals with green-yellow emissions. Materials Advances, 2021, 2, 3744-3751.	2.6	12
54547	Effects of support and oxygen vacancies on the energetics of NiO reduction with H₂ for the chemical looping combustion (CLC) reaction; a DFT study. Physical Chemistry Chemical Physics, 2021, 23, 12795-12806.	1.3	7
54548	Dendrite-free Lithium Based on Lessons Learned from Lithium and Magnesium Electrodeposition Morphology Simulations. Cell Reports Physical Science, 2021, 2, 100294.	2.8	19
54549	Phase-selective active sites on ordered/disordered titanium dioxide enable exceptional photocatalytic ammonia synthesis. Chemical Science, 2021, 12, 9619-9629.	3.7	25
54550	Hydrothermal synthesis of hexagonal YMnO₃ and YbMnO₃ below 250 Â°C. Dalton Transactions, 2021, 50, 9904-9913.	1.6	2
54551	Electronic and magnetic states of Fe ions in Co2FeBO5. Dalton Transactions, 2021, 50, 9735-9745.	1.6	4
54552	A first-principles study of the stability, electronic structure, and optical properties of halide double perovskite Rb₂Sn_{1â^'x}Te_xI₆ for solar cell applications. Physical Chemistry Chemical Physics, 2021, 23, 4646-4657.	1.3	19
54553	Density functional theory design of double donor dyes and electron transfer on dye/TiO₂(101) composite systems for dye-sensitized solar cells. RSC Advances, 2021, 11, 3071-3078.	1.7	10
54554	The defect chemistry of non-stoichiometric PuO_{2Â±x}. Physical Chemistry Chemical Physics, 2021, 23, 4544-4554.	1.3	11
54555	A high-throughput study of oxynitride, oxyfluoride and nitrofluoride perovskites. Journal of Materials Chemistry A, 2021, 9, 8501-8513.	5.2	18
54556	Nitrogen and oxygen tailoring of a solid carbon active site for two-electron selectivity electrocatalysis. Inorganic Chemistry Frontiers, 2021, 8, 173-181.	3.0	11
54557	Exploring the synergistic effect of Bâ€“N doped defective graphdiyne for N₂ fixation. New Journal of Chemistry, 2021, 45, 6327-6335.	1.4	13
54558	MÃ¶ssbauer studies of spin and charge modulations in BaFe2(As1â^'xPx)2. Physical Review B, 2021, 103, .	1.1	2
54559	Progress on Diamane and Diamanoid Thin Film Pressureless Synthesis. Journal of Carbon Research, 2021, 7, 9.	1.4	11
54560	Electronic structure and transport properties of coupled CdS/ZnSe quantum dots. Journal of Physics Condensed Matter, 2021, 33, 125002.	0.7	3
54561	Theoretical investigation of the side-chain mechanism of the MTO process over H-SSZ-13 using DFT and ab initio calculations. Catalysis Science and Technology, 2021, 11, 3826-3833.	2.1	12
54562	Understanding Superatomic Ag Nanohydrides. Small, 2021, 17, e2004808.	5.2	4

#	Article	IF	Citations
54563	Green CsSnX₃ (X = Cl, Br, I)-Derived Quantum Dots for Photovoltaic Applications: First-Principles Investigations. Journal of Physical Chemistry C, 2021, 125, 2592-2606.	1.5	19
54564	CrSbS₃ monolayer: a potential phase transition ferromagnetic semiconductor. Nanoscale, 2021, 13, 14067-14072.	2.8	5
54565	Novel structures and mechanical properties of Zr₂N: Ab initio description under high pressures*. Chinese Physics B, 2021, 30, 016403.	0.7	3
54566	Properties and Detailed Adsorption of CO₂ by M₂(dobpdc) with N,N-Dimethylethylenediamine Functionalization. Inorganic Chemistry, 2021, 60, 2656-2662.	1.9	11
54567	Enormous passivation effects of a surrounding zeolitic framework on Pt clusters for the catalytic dehydrogenation of propane. Catalysis Science and Technology, 0, , .	2.1	10
54568	In situ construction of active interfaces towards improved high-rate performance of CoSe₂. Journal of Materials Chemistry A, 2021, 9, 14582-14592.	5.2	44
54569	A two-dimensional MoSe₂/MoSi₂N₄ van der Waals heterostructure with high carrier mobility and diversified regulation of its electronic properties. Journal of Materials Chemistry C, 2021, 9, 10073-10083.	2.7	32
54570	A defect-induced broadband photodetector based on WS₂/pyramid Si 2D/3D mixed-dimensional heterojunction with a light confinement effect. Nanoscale, 2021, 13, 13550-13557.	2.8	48
54571	Semiconducting and superconducting Moâ€“Ga frameworks: total energy and chemical bonding. Inorganic Chemistry Frontiers, 2021, 8, 1702-1709.	3.0	5
54572	Intrinsic Valley Polarization and High-Temperature Ferroelectricity in Two-Dimensional Orthorhombic Lead Oxide. ACS Applied Materials & Interfaces, 2021, 13, 6480-6488.	4.0	10
54573	Dual Role of Adsorbent and Non-monotonic Transfer p-Doping of Diamond. ACS Applied Materials & Interfaces, 2021, 13, 4676-4681.	4.0	2
54574	Interplay of Anionic Quasi-Atoms and Interstitial Point Defects in Electrides: Abnormal Interstice Occupation and Colossal Charge State of Point Defects in Dense fcc-Lithium. ACS Applied Materials & Interfaces, 2021, 13, 6130-6139.	4.0	8
54575	Epitaxial Growth of Two-Dimensional Insulator Monolayer Honeycomb BeO. ACS Nano, 2021, 15, 2497-2505.	7.3	42
54576	Euâ€“Mn Charge Transfer and the Strong Chargeâ€“Spinâ€“Electronic Coupling Behavior in EuMnO₃. Inorganic Chemistry, 2021, 60, 1367-1379.	1.9	2
54577	Noncentrosymmetric Weyl phase and topological phase transition in bulk MoTe. Physical Chemistry Chemical Physics, 2021, 23, 23196-23202.	1.3	2
54578	Phase formation and ionic conduction in Na-doped Sr₂MgSi₂O₇ melilite-type silicate. Journal of Materials Chemistry A, 2021, 9, 22064-22071.	5.2	12
54579	TiO₂ protection layer and well-matched interfaces enhance the stability of Cu₂ZnSnS₄/CdS/TiO₂ for visible light driven water splitting. Catalysis Science and Technology, 2021, 11, 5505-5517.	2.1	14
54580	Piezoelectricity of Graphene-like Monolayer ZnO and GaN. Wuji Cailiao Xuebao/Journal of Inorganic Materials, 2021, 36, 492.	0.6	2

#	Article	IF	Citations
54581	An Element-Based Generalized Coordination Number for Predicting the Oxygen Binding Energy on Pt₃M (M = Co, Ni, or Cu) Alloy Nanoparticles. ACS Omega, 2021, 6, 3218-3226.	1.6	17
54582	Screening of effective NRR electrocatalysts among the Si-based MSi₂N₄ (M =) Tj ETQq1 1 0.784314 rgBT /O	5.2	34
54583	Two-dimensional materials as a stabilized interphase for the solid-state electrolyte Li₁₀GeP₂S₁₂ in lithium metal batteries. Journal of Materials Chemistry A, 2021, 9, 4810-4821.	5.2	12
54584	Computational determination of coordination structure impact on adsorption and acidity of pristine and sulfated MOF-808. Materials Advances, 2021, 2, 4246-4254.	2.6	9
54585	Orbital-dependent spin textures in ferroelectric Rashba systems. Physical Review B, 2021, 103, .	1.1	5
54586	First-Principles Calculation and Experimental Investigation of a Three-Atoms-Type MXene V₂C and Its Effects on Memristive Devices. IEEE Nanotechnology Magazine, 2021, 20, 512-516.	1.1	6
54587	Tribological properties of a series of carbon dots modified by ionic liquids with various anion species: experimental findings and density functional theory calculations. Dalton Transactions, 2021, 50, 9185-9197.	1.6	22
54588	A general strategy for designing two-dimensional high-efficiency layered thermoelectric materials. Energy and Environmental Science, 2021, 14, 4059-4066.	15.6	24
54589	Atomic-scale insight into the enhanced surface stability of methylammonium lead iodide perovskite by controlled deposition of lead chloride. Energy and Environmental Science, 2021, 14, 4541-4554.	15.6	31
54590	Influence of the Pdâ€‰:â€‰Bi ratio on Pdâ€“Bi/Al₂O₃ catalysts: structure, surface and activity in glucose oxidation. Physical Chemistry Chemical Physics, 2021, 23, 14889-14897.	1.3	4
54591	Ru single atoms for efficient chemoselective hydrogenation of nitrobenzene to azoxybenzene. Green Chemistry, 2021, 23, 4753-4761.	4.6	35
54592	Multi-core yolkâ€“shell-structured Bi₂Se₃@C nanocomposite as an anode for high-performance lithium-ion batteries. Dalton Transactions, 2021, 50, 10758-10764.	1.6	13
54593	Mechanism of Li nucleation at graphite anodes and mitigation strategies. Journal of Materials Chemistry A, 2021, 9, 16798-16804.	5.2	13
54594	Hafniumâ€“zirconium oxide interface models with a semiconductor and metal for ferroelectric devices. Nanoscale Advances, 2021, 3, 4750-4755.	2.2	3
54595	Predicting stable crystalline compounds using chemical similarity. Npj Computational Materials, 2021, 7, .	3.5	41
54596	A systematic computational investigation of the water splitting and N₂ reduction reaction performances of monolayer MBenes. Physical Chemistry Chemical Physics, 2021, 23, 6613-6622.	1.3	9
54597	Reactive force fields for modeling oxidative degradation of organic matter in geological formations. RSC Advances, 2021, 11, 29298-29307.	1.7	6
54598	Pillar-beam structures prevent layered cathode materials from destructive phase transitions. Nature Communications, 2021, 12, 13.	5.8	85

#	Article	IF	Citations
54599	Structure and electronic bandgap tunability of m-plane GaN multilayers. Physical Chemistry Chemical Physics, 2021, 23, 5431-5437.	1.3	10
54600	Enrichment of the field emission properties of NiCo₂O₄ nanostructures by UV/ozone treatment. Materials Advances, 2021, 2, 2658-2666.	2.6	8
54601	Two-dimensional Janus semiconductor BiTeCl and BiTeBr monolayers: a first-principles study on their tunable electronic properties via an electric field and mechanical strain. Physical Chemistry Chemical Physics, 2021, 23, 15216-15223.	1.3	32
54602	Computational study of the staircase molecular conductivity of polyoxovanadates adsorbed on Au(111). Dalton Transactions, 2021, 50, 5540-5551.	1.6	7
54603	Unlocking the potential of ruthenium catalysts for nitrogen fixation with subsurface oxygen. Journal of Materials Chemistry A, 2021, 9, 6575-6582.	5.2	14
54604	High-quality borophene quantum dot realization and their application in a photovoltaic device. Journal of Materials Chemistry A, 2021, 9, 24036-24043.	5.2	14
54605	Boosting the photon absorption, exciton dissociation, and photocatalytic hydrogen- and oxygen-evolution reactions by built-in electric fields in Janus platinum dichalcogenides. Journal of Materials Chemistry C, 2021, 9, 15026-15033.	2.7	28
54606	Research on the quantum confinement effect and enhanced luminescence of red-emitting P⁵⁺-doped CaAl₁₂O₁₉:Mn⁴⁺,Mg²⁺ phosphors. Dalton Transactions, 2021, 50, 13112-13123.	1.6	13
54607	Search of stable structures in cation deficient (V,Nb)CoSb half-Heusler alloys by an atomic cluster expansion. Journal of Materials Chemistry A, 2021, 9, 21111-21122.	5.2	5
54608	Optical properties of orthorhombic germanium selenide: an anisotropic layered semiconductor promising for optoelectronic applications. Journal of Materials Chemistry C, 2021, 9, 14838-14847.	2.7	9
54609	Delicate control of crystallographic Cu₂O derived Niâ€“Co amorphous double hydroxide nanocages for high-performance hybrid supercapacitors: an experimental and computational investigation. Nanoscale, 2021, 13, 8562-8574.	2.8	41
54611	Effects of paramagnetic fluctuations on the thermochemistry of MnO(100) surfaces in the oxygen evolution reaction. Physical Chemistry Chemical Physics, 2021, 23, 859-865.	1.3	4
54613	The First Principle Study of <i>β</i>-CuAgSe Subcells. Journal of Applied Mathematics and Physics, 2021, 09, 1549-1559.	0.2	0
54614	Single-atom catalysts based on TiN for the electrocatalytic hydrogen evolution reaction: a theoretical study. Physical Chemistry Chemical Physics, 2021, 23, 15685-15692.	1.3	6
54615	Atomistic Simulation of Permanent Magnets With Reduced Rare-Earth Content. , 2021, , 169-178.		0
54616	Pd Single-Atom Sites on the Surface of PdAu Nanoparticles: A DFT-Based Topological Search for Suitable Compositions. Nanomaterials, 2021, 11, 122.	1.9	8
54617	B₄₈^{â^'}: a bilayer boron cluster. Nanoscale, 2021, 13, 3868-3876.	2.8	43
54618	Local structure and NO adsorption/desorption property of Pd²⁺ cations at different paired Al sites in CHA zeolite. Physical Chemistry Chemical Physics, 2021, 23, 22273-22282.	1.3	15

#	Article	IF	Citations
54619	Parameter space exploration reveals interesting Mn-doped SrTiO3 structures. Physical Chemistry Chemical Physics, 2021, 23, 23486-23500.	1.3	3
54620	A hierarchical Co₃O₄/CoS microbox heterostructure as a highly efficient bifunctional electrocatalyst for rechargeable Znâ€“air batteries. Journal of Materials Chemistry A, 2021, 9, 17344-17352.	5.2	40
54621	Bifunctional Role of Zn in Î±-Fe ₂O ₃ Boosts the Photoelectrochemical Water Oxidation: Zn ²⁺ Doping and Catalytic Effect. SSRN Electronic Journal, 0, , .	0.4	0
54622	Influence of diluent concentration in localized high concentration electrolytes: elucidation of hidden diluent-Li⁺ interactions and Li⁺ transport mechanism. Journal of Materials Chemistry A, 2021, 9, 17459-17473.	5.2	28
54623	Lithium nickel borides: evolution of [NiB] layers driven by Li pressure. Inorganic Chemistry Frontiers, 2021, 8, 1675-1685.	3.0	7
54624	The complementary graphene growth and etching revealed by large-scale kinetic Monte Carlo simulation. Npj Computational Materials, 2021, 7, .	3.5	20
54625	Two-dimensional ScN with high carrier mobility and unexpected mechanical properties. Nanotechnology, 2021, 32, 155201.	1.3	3
54626	Unraveling the activity of iron carbide clusters embedded in silica for thermocatalytic conversion of methane. Catalysis Science and Technology, 0, , .	2.1	4
54627	Hydrogen-doped viscoplastic liquid metal microparticles for stretchable printed metal lines. Nature Materials, 2021, 20, 533-540.	13.3	111
54628	Novel copper fluoride analogs of cuprates. Physical Chemistry Chemical Physics, 2021, 23, 15989-15993.	1.3	5
54629	Atomistic Insights into Lithium Storage Mechanisms in Anatase, Rutile, and Amorphous TiO₂ Electrodes. ACS Applied Materials & Interfaces, 2021, 13, 1791-1806.	4.0	32
54630	Oxygen reduction reaction on a 68-atom-gold cluster supported on carbon nanotubes: theoretical and experimental analysis. Materials Chemistry Frontiers, 2021, 5, 7529-7539.	3.2	6
54631	Magnetoresistance and Kondo Effect in Nodal-Line Semimetal VAs2 *. Chinese Physics Letters, 2021, 38, 017202.	1.3	9
54632	Stacking fault, dislocation dissociation, and twinning in Pt3Hf compounds: a DFT study. Rare Metals, 2021, 40, 1020-1030.	3.6	15
54633	Design of an efficient photocatalyst: a type II heterojunction for enhanced hydrogen production driven by visible light. Physical Chemistry Chemical Physics, 2021, 23, 11893-11899.	1.3	5
54634	Defect chemistry and doping of BiCuSeO. Journal of Materials Chemistry A, 2021, 9, 20685-20694.	5.2	23
54635	Ru/Mo₂C@NC Schottky junction-loaded hollow nanospheres as an efficient hydrogen evolution electrocatalyst. Journal of Materials Chemistry A, 2021, 9, 20518-20529.	5.2	30
54636	Self-trapped exciton emission in an Sn(<scp>ii</scp>)-doped all-inorganic zero-dimensional zinc halide perovskite variant. Nanoscale, 2021, 13, 15285-15291.	2.8	23

#	Article	IF	Citations
54637	Enhanced reversible solid-state photoswitching of a cationic dithienylethene assembled with a polyoxometalate unit. Journal of Materials Chemistry C, 2021, 9, 13072-13076.	2.7	5
54638	Core level shifts as indicators of Cr chemistry on hydroxylated Î±-Al2O3(0001): a combined photoemission and first-principles study. Physical Chemistry Chemical Physics, 2021, 23, 21852-21862.	1.3	1
54639	Ethanol steam reforming on Rh: microkinetic analyses on the complex reaction network. Catalysis Science and Technology, 2021, 11, 7009-7017.	2.1	5
54640	A new deep hole-trapping site for water splitting on the rutile TiO₂(110) surface. Journal of Materials Chemistry A, 2021, 9, 7650-7655.	5.2	10
54641	Real-space density functional theory adapted to cyclic and helical symmetry: Application to torsional deformation of carbon nanotubes. Physical Review B, 2021, 103, .	1.1	22
54642	The charge transfer effect on SERS in a gold-decorated surface defect anatase nanosheet/methylene blue (MB) system. New Journal of Chemistry, 2021, 45, 19775-19786.	1.4	8
54643	Origin of the magnetic and orbital ordering in Î±â˜Sr2CrO4. Physical Review B, 2021, 103, .	1.1	13
54644	Substitution of copper atoms into defect-rich molybdenum sulfides and their electrocatalytic activity. Nanoscale Advances, 2021, 3, 1747-1757.	2.2	3
54645	A Queueâ€Ordered Layered Mnâ€Based Oxides with Al Substitution as Highâ€Rate and Highâ€Stabilized Cathode for Sodiumâ€Ion Batteries. Small, 2021, 17, e2006259.	5.2	22
54646	A flexible electron-blocking interfacial shield for dendrite-free solid lithium metal batteries. Nature Communications, 2021, 12, 176.	5.8	136
54647	Pressure-induced superconducting CS₂H₁₀ with an H₃S framework. Physical Chemistry Chemical Physics, 2021, 23, 22779-22784.	1.3	16
54648	High-temperature proton conductors based on the (110) layered perovskite BaNdScO₄. Journal of Materials Chemistry A, 2021, 9, 8607-8619.	5.2	31
54649	Modulating the kinetics of CoSe₂ yolkâ€“shell spheres via nitrogen doping with high pseudocapacitance toward ultra-high-rate capability and high-energy density sodium-ion half/full batteries. Materials Chemistry Frontiers, 2021, 5, 6873-6882.	3.2	10
54650	Machine Learning and Monte Carlo Methods for Surface-Assisted Molecular Self-Assembly. Fundamental Biomedical Technologies, 2021, , 45-64.	0.2	0
54651	Challenges for density functional theory: calculation of CO adsorption on electrocatalytically relevant metals. Physical Chemistry Chemical Physics, 2021, 23, 9394-9406.	1.3	15
54652	Boosting the thermoelectric performance of GeTe by manipulating the phase transition temperature via Sb doping. Journal of Materials Chemistry C, 2021, 9, 6484-6490.	2.7	19
54653	Indium Gallium Oxide Alloys: Electronic Structure, Optical Gap, Surface Space Charge, and Chemical Trends within Common-Cation Semiconductors. ACS Applied Materials & Interfaces, 2021, 13, 2807-2819.	4.0	50
54654	Imidazole-graphyne: a new 2D carbon nitride with a direct bandgap and strong IR refraction. Physical Chemistry Chemical Physics, 2021, 23, 10274-10280.	1.3	4

#	Article	IF	Citations
54655	Boosting the photocatalytic hydrogen evolution performance of monolayer C₂N coupled with MoSi₂N₄: density-functional theory calculations. Physical Chemistry Chemical Physics, 2021, 23, 8318-8325.	1.3	49
54656	Strain engineering of polar optical phonon scattering mechanism â€“ an effective way to optimize the power-factor and lattice thermal conductivity of ScN. Physical Chemistry Chemical Physics, 2021, 23, 23288-23302.	1.3	4
54657	Manipulation of Cl/Br transmutation in zero-dimensional Mn²⁺-based metal halides toward tunable photoluminescence and thermal quenching behaviors. Journal of Materials Chemistry C, 2021, 9, 2047-2053.	2.7	44
54658	Effect of Sodium on Ni-Promoted MoS2 Catalyst for Hydrodesulfurization Reaction: Combined Experimental and Simulation Study. Energy & Fuels, 2021, 35, 2368-2378.	2.5	8
54659	Evidence for a higher-order topological insulator in a three-dimensional material built from van der Waals stacking of bismuth-halide chains. Nature Materials, 2021, 20, 473-479.	13.3	98
54660	Linking in situ charge accumulation to electronic structure in doped SrTiO3 reveals design principles for hydrogen-evolving photocatalysts. Nature Materials, 2021, 20, 511-517.	13.3	82
54661	YttriumâĐoped Barium ZirconateâCerate Solid Solution as Proton Conducting Electrolyte: Why Higher Cerium Concentration Leads to Better Performance for Fuel Cells and Electrolysis Cells. Advanced Energy Materials, 2021, 11, 2003149.	10.2	75
54662	Design of non-transition-metal-doped nanoribbon catalysis to achieve efficient nitrogen fixation. Materials Advances, 2021, 2, 7423-7430.	2.6	2
54663	Stepped M@Pt(211) (M = Co, Fe, Mo) single-atom alloys promote the deoxygenation of lignin-derived phenolics: mechanism, kinetics, and descriptors. Catalysis Science and Technology, 2021, 11, 7047-7059.	2.1	13
54664	Factors determining surface oxygen vacancy formation energy in ternary spinel structure oxides with zinc. Physical Chemistry Chemical Physics, 2021, 23, 23768-23777.	1.3	12
54665	First-Principles Study of Câ“C Coupling Pathways for CO₂ Electrochemical Reduction Catalyzed by Cu(110). Journal of Physical Chemistry C, 2021, 125, 2464-2476.	1.5	21
54666	Rashba Effect and Raman Spectra of Tl₂O/PtS₂ Heterostructure. ACS Omega, 2021, 6, 4044-4050.	1.6	6
54667	Microscopic (Dis)order and Dynamics of Cations in Mixed FA/MA Lead Halide Perovskites. Journal of Physical Chemistry C, 2021, 125, 1742-1753.	1.5	28
54668	Unraveling the nature of sulfur poisoning on Cu/SSZ-13 as a selective reduction catalyst. Journal of the Taiwan Institute of Chemical Engineers, 2021, 118, 38-47.	2.7	14
54669	Tuning electrochemically driven surface transformation in atomically flat LaNiO3 thin films for enhanced water electrolysis. Nature Materials, 2021, 20, 674-682.	13.3	105
54670	Multilevel oxygen-vacancy conductive filaments in Î²-Ga₂O₃ based resistive random access memory. Physical Chemistry Chemical Physics, 2021, 23, 5975-5983.	1.3	21
54671	Electronic and optical properties of silicene on GaAs(111) with hydrogen intercalation: a first-principles study. RSC Advances, 2021, 11, 16040-16050.	1.7	1
54672	Density functional theory study of transition metal single-atoms anchored on graphyne as efficient electrocatalysts for the nitrogen reduction reaction. Physical Chemistry Chemical Physics, 2021, 23, 10418-10428.	1.3	68

#	Article	IF	Citations
54673	Fast operando spectroscopy tracking in situ generation of rich defects in silver nanocrystals for highly selective electrochemical CO2 reduction. Nature Communications, 2021, 12, 660.	5.8	68
54674	Local Kondo scattering in 4d-electron RuO_x nanoclusters on atomically-resolved ultrathin SrRuO₃ films. Physical Chemistry Chemical Physics, 2021, 23, 22526-22531.	1.3	0
54675	Revealing practical specific capacity and carbonyl utilization of multi-carbonyl compounds for organic cathode materials. Physical Chemistry Chemical Physics, 2021, 23, 13159-13169.	1.3	7
54676	Designing Zn-doped nickel sulfide catalysts with an optimized electronic structure for enhanced hydrogen evolution reaction. Nanoscale, 2021, 13, 10127-10132.	2.8	26
54677	Topological quantum phase transition in the magnetic semimetal HoSb. Journal of Materials Chemistry C, 2021, 9, 6996-7004.	2.7	4
54678	Preparing high purity Î»-Ti₃O₅ and Li/Î»-Ti₃O₅ as high-performance electromagnetic wave absorbers. Journal of Materials Chemistry C, 0, , .	2.7	6
54679	Stable nitrogen-rich scandium nitrides and their bonding features under ambient conditions. Physical Chemistry Chemical Physics, 2021, 23, 6863-6870.	1.3	20
54680	Theoretical evidence of the spinâ€“valley coupling and valley polarization in two-dimensional MoSi₂X₄ (X = N, P, and As). Physical Chemistry Chemical Physics, 2021, 23, 3144-3151.	1.3	53
54681	Spatial-confinement induced electroreduction of CO and CO₂ to diols on densely-arrayed Cu nanopyramids. Chemical Science, 2021, 12, 8079-8087.	3.7	22
54682	First-principles study of bilayer hexagonal structure of SN₂ nanosheet: a highly stable non-metal platform for the quantum anomalous Hall effect. Journal of Materials Chemistry C, 2021, 9, 5961-5969.	2.7	4
54683	Ultrafast Dynamics of Electronic Resonances in Molecules Adsorbed on Metal Surfaces: A Wave Packet Propagation Approach. Journal of Chemical Theory and Computation, 2021, 17, 639-654.	2.3	2
54684	Enhanced polarization in epitaxially strained monoclinic potassium niobate for lead-free electromechanical applications. Journal of Materials Chemistry C, 2021, 9, 13420-13431.	2.7	5
54685	Hard and superconducting cubic boron phase via swarm-intelligence structural prediction driven by a machine-learning potential. Physical Review B, 2021, 103, .	1.1	16
54686	Valley splitting in the antiferromagnetic heterostructure MnPSe₃/WSe₂. Journal of Materials Chemistry C, 2021, 9, 3562-3568.	2.7	16
54687	The exceptionally high thermal conductivity after â€˜alloyingâ€™ two-dimensional gallium nitride (GaN) and aluminum nitride (AlN). Nanotechnology, 2021, 32, 135401.	1.3	22
54688	Anomalous Hall effect in the weak-itinerant ferrimagnet <mml:math xmlns:mml="http://www.w3.org/1998/Math/MathML"><mml:mrow><mml:msub><mml:mi>FeCr</mml:mi><mml:mn>2</mml:mn></mml:msub></mml:mrow></mml:math> Physical Review B, 2021, 103, .	1.1	10
54689	Towards controlling the reversibility of anionic redox in transition metal oxides for high-energy Li-ion positive electrodes. Energy and Environmental Science, 2021, 14, 2322-2334.	15.6	41
54690	A synergetic effect between a single Cu site and S vacancy on an MoS₂ basal plane for methanol synthesis from syngas. Catalysis Science and Technology, 2021, 11, 3261-3269.	2.1	7

#	Article	IF	Citations
54691	Relating X-ray photoelectron spectroscopy data to chemical bonding in MXenes. Nanoscale Advances, 2021, 3, 2793-2801.	2.2	11
54692	A membrane-less desalination battery with ultrahigh energy efficiency. Journal of Materials Chemistry A, 2021, 9, 7216-7226.	5.2	10
54693	In-depth first-principle study on novel MoS₂ polymorphs. RSC Advances, 2021, 11, 3759-3769.	1.7	13
54694	Î±-MoC_{1â”'x} nanorods as an efficient hydrogen evolution reaction electrocatalyst. New Journal of Chemistry, 2021, 45, 10396-10401.	1.4	12
54695	Thermoelectric transport properties of two-dimensional materials <i>X</i>Te₂ (<i>X</i> = Pd, Pt) via first-principles calculations. Wuli Xuebao/Acta Physica Sinica, 2021, 70, 116301.	0.2	2
54696	Tuning the Lewis acidity of ZrO₂ for efficient conversion of CH₄ and CO₂ into acetic acid. New Journal of Chemistry, 2021, 45, 8978-8985.	1.4	9
54697	Microscopic origin of graphene nanosheets derived from coal-tar pitch by treating Al4C3 as the intermediate. Physical Chemistry Chemical Physics, 2021, 23, 12449-12455.	1.3	2
54698	Understanding trends in the activity and selectivity of bi-atom catalysts for the electrochemical reduction of carbon dioxide. Journal of Materials Chemistry A, 2021, 9, 8761-8771.	5.2	35
54699	Characterizations of electronic and optical properties of Sb-based phase-change material stabilized by alloying Cr. Applied Physics Letters, 2021, 118, .	1.5	7
54700	Prediction of two-dimensional ferroelectric metal Mxenes. Journal of Materials Chemistry C, 2021, 9, 11343-11348.	2.7	15
54701	Thickness dependence of spin torque effect in Fe/MgO/Fe magnetic tunnel junction: Implementation of divide-and-conquer with first-principles calculation. AIP Advances, 2021, 11, 015036.	0.6	4
54702	Correlated Energy-Level Alignment Effects Determine Substituent-Tuned Single-Molecule Conductance. ACS Applied Materials & Interfaces, 2021, 13, 4267-4277.	4.0	11
54703	Bimetallic RuNi nanoparticles as catalysts for upgrading biomass: metal dilution and solvent effects on selectivity shifts. Green Chemistry, 2021, 23, 8480-8500.	4.6	9
54704	Elastic, mechanical, anisotropic, optical and magnetic properties of V₂NiSb Heusler alloy. Physica Scripta, 2021, 96, 035807.	1.2	9
54705	Band-Gap Tuning in All-Inorganic CsPb_xSn_{1â€“x}Br₃ Perovskites. ACS Applied Materials & Interfaces, 2021, 13, 4203-4210.	4.0	24
54706	Simple Luminescent Phenanthroimidazole Emitters for Solution-processed Non-doped Organic Light-emitting Electrochemical Cells. New Journal of Chemistry, 0, , .	1.4	3
54707	Solar-driven electrochemical synthesis of ammonia using nitrate with 11% solar-to-fuel efficiency at ambient conditions. Energy and Environmental Science, 2021, 14, 6349-6359.	15.6	70
54708	Ba₂Ln_{1â”'x}Mn₂Te₅ (Ln = Pr, Gd, and Yb; x = Ln) Tj ETQq1 1 0.784314 rgB Transactions, 2021, 50, 6688-6701.	1.6	8

#	Article	IF	Citations
54709	LaO as a candidate substrate for realizing superconductivity in an FeSe epitaxial film. Physical Review B, 2021, 103, .	1.1	2
54710	Synthesis of sub-nanometric Cu₂O catalysts for Pd-free Câ€“C coupling reactions. Reaction Chemistry and Engineering, 2021, 6, 929-936.	1.9	3
54711	Thermal Nanostructure Design by Materials Informatics. Springer Series in Materials Science, 2021, , 153-195.	0.4	0
54712	Effects of spinâ€“phonon coupling on two-dimensional ferromagnetic semiconductors: a case study of iron and ruthenium trihalides. Nanoscale, 2021, 13, 7714-7722.	2.8	13
54713	Tunable electron property induced by B-doping in g-C₃N₄. RSC Advances, 2021, 11, 15695-15700.	1.7	8
54714	Abundant topological phases in hydrogenated group-IV binary alloy compounds. RSC Advances, 2021, 11, 14434-14440.	1.7	0
54715	Vibrational energy redistribution in crystalline nitromethane simulated by ab initio molecular dynamics. RSC Advances, 2021, 11, 9557-9567.	1.7	1
54716	Effects of A-site composition of perovskite (Sr1â^'xBaxZrO3) oxides on H atom adsorption, migration, and reaction. RSC Advances, 2021, 11, 7621-7626.	1.7	2
54717	Crystal-plane-controlled selectivity and activity of copper catalysts in propylene oxidation with O₂. Catalysis Science and Technology, 2021, 11, 2896-2907.	2.1	6
54718	Comparative density functional studies of pristine and doped bismuth ferrite polymorphs by GGA+U and meta-GGA SCAN+U. Physical Chemistry Chemical Physics, 2021, 23, 8571-8584.	1.3	14
54719	Theoretical insight into single Rh atoms anchored on N-doped Î³-graphyne as an excellent bifunctional electrocatalyst for the OER and ORR: electronic regulation of graphitic nitrogen. Nanoscale, 2021, 13, 5800-5808.	2.8	23
54720	Highly efficient catalytic properties of Sc and Fe single atoms stabilized on a honeycomb borophene/Al(111) heterostructure via a dual charge transfer effect. Nanoscale, 2021, 13, 5875-5882.	2.8	12
54721	On the structure and reactivity of Pt_nCu_n (n = 1â€“7) alloy clusters. Physical Chemistry Chemical Physics, 2021, 23, 7233-7239.	1.3	10
54722	Significant second-harmonic generation and bulk photovoltaic effect in trigonal selenium and tellurium chains. Physical Chemistry Chemical Physics, 2021, 23, 6823-6831.	1.3	3
54723	Frenkel defects promote polaronic exciton dissociation in methylammonium lead iodide perovskites. Physical Chemistry Chemical Physics, 2021, 23, 6583-6590.	1.3	2
54724	An electrically switchable anti-ferroelectric bilayer In₂Se₃ based opto-spintronic device. Nanoscale, 2021, 13, 8555-8561.	2.8	12
54725	Boosting oxygen evolution reaction activity by tailoring MOF-derived hierarchical Coâ€“Ni alloy nanoparticles encapsulated in nitrogen-doped carbon frameworks. RSC Advances, 2021, 11, 10874-10880.	1.7	9
54726	Mapping surface morphology and phase evolution of iron sulfide nanoparticles. CrystEngComm, 2021, 23, 5645-5654.	1.3	4

#	Article	IF	Citations
54727	A reverse-design-strategy for C@Li₃VO₄ nanoflakes toward superb high-rate Li-ion storage. Journal of Materials Chemistry A, 2021, 9, 17270-17280.	5.2	25
54728	An enhanced oxygen evolution reaction on 2D CoOOH via strain engineering: an insightful view from spin state transition. Journal of Materials Chemistry A, 2021, 9, 17749-17759.	5.2	44
54729	Unoccupied 3d orbitals make Li-unalloyable transition metals usable as anode materials for lithium ion batteries. Journal of Materials Chemistry A, 2021, 9, 17353-17365.	5.2	4
54730	Interfacial electron modulation of MoS₂/black phosphorus heterostructure toward high-rate and high-energy density half/full sodium-ion batteries. Materials Chemistry Frontiers, 2021, 5, 6639-6647.	3.2	9
54731	Induced half-metallic characteristics and enhanced magnetic anisotropy in the two-dimensional Janus V₂I₃Br₃ monolayer by graphyne adsorption. Physical Chemistry Chemical Physics, 2021, 23, 17338-17347.	1.3	7
54732	Surface characterization and methane activation on SnO_x/Cu₂O/Cu(111) inverse oxide/metal catalysts. Physical Chemistry Chemical Physics, 2021, 23, 17186-17196.	1.3	10
54733	Pressure-induced reconstructive phase transitions, polarization with metallicity, and enhanced hardness in antiperovskite MgCNi3. Physical Chemistry Chemical Physics, 2021, 23, 18221-18226.	1.3	1
54734	Theoretical inspection of the spin-crossover [Fe(tzpy)2(NCS)2] complex on Au(100) surface. Journal of Chemical Physics, 2021, 154, 034701.	1.2	6
54735	Tomography for Bridging Nano and Macro: Semi-spontaneous Iinterfacial Debonding. Materia Japan, 2021, 60, 13-18.	0.1	0
54736	Lead-free hybrid perovskite N(CH3)4SnI3 with robust ferroelectricity induced by large and non-polar N(CH3)4+ molecular cation. Nature Communications, 2021, 12, 637.	5.8	19
54737	Tuning spinâ€“orbit coupling in (6,5) single-walled carbon nanotube doped with sp3 defects. Journal of Applied Physics, 2021, 129, .	1.1	6
54738	An embedded atom model for Gaâ€“Pd systems: From intermetallic crystals to liquid alloys. Journal of Chemical Physics, 2021, 154, 014109.	1.2	0
54739	Unravelling the K-promotion effect in highly active and stable Fe5C2 nanoparticles for catalytic linear Î±-olefin production. Materials Advances, 2021, 2, 1050-1058.	2.6	3
54740	Anomalous electronic properties in layered, disordered ZnVSb. Physical Review Materials, 2021, 5, .	0.9	2
54741	First-principles investigation of oxygen interaction with hydrogen/helium/vacancy irradiation defects in Ti3AlC2. Physical Chemistry Chemical Physics, 2021, 23, 5340-5351.	1.3	4
54742	The Parallel and Progress of VASP in OpenMPI Environment. Computer Science and Application, 2021, 11, 84-94.	0.0	0
54743	Discovery and Facile Synthesis of a New Silicon Based Family as Efficient Hydrogen Evolution Reaction Catalysts: A Computational and Experimental Investigation of Metal Monosilicides. Small, 2021, 17, e2006153.	5.2	31
54744	Mechanical and Electronic Properties of CeO ₂ Under Uniaxial Tensile Loading: A DFT Study. SSRN Electronic Journal, 0, , .	0.4	0

#	Article	IF	Citations
54745	Theoretical evaluation of multivalent cation diffusion in the 1T-Î´-MnO2 electrode via potential energy surface. Journal Physics D: Applied Physics, 2021, 54, 115303.	1.3	1
54746	First-principles discovery of stable two-dimensional materials with high-level piezoelectric response. Journal of Physics Condensed Matter, 2021, 33, 115705.	0.7	5
54747	Theoretical estimation of size effects on the electronic transport in tailored graphene nanoribbons. Physical Chemistry Chemical Physics, 2021, 23, 1727-1737.	1.3	1
54748	Metallic and anti-metallic properties of hydrogen adsorbed AnO₂ (An = Th, U, and Pu) surfaces. Physical Chemistry Chemical Physics, 2021, 23, 878-885.	1.3	2
54749	Radiation hardness and abnormal photoresponse dynamics of the CH₃NH₃PbI₃ perovskite photodetector. Journal of Materials Chemistry C, 2021, 9, 2095-2105.	2.7	11
54750	Structural phase transition and Goldstone-like mode in hexagonal BaMnO3. Physical Review B, 2021, 103, .	1.1	1
54751	Mo single atoms in the Cu(111) surface as improved catalytic active centers for deoxygenation reactions. Catalysis Science and Technology, 2021, 11, 4969-4978.	2.1	2
54752	New atomic-scale insights into the I/Ni(100) system: phase transitions and growth of an atomically thin NiI₂ film. Physical Chemistry Chemical Physics, 2021, 23, 1896-1913.	1.3	2
54753	Micromechanism of ferroelectric fatigue and enhancement of fatigue resistance of lead zirconate titanate thin films. Wuli Xuebao/Acta Physica Sinica, 2021, 70, 146302-146302.	0.2	0
54754	Computational modelling of effects of surface coverage on adsorption of benzene on Pt(111) surface. AIP Conference Proceedings, 2021, , .	0.3	0
54755	Quantitative explanation of the Schottky barrier height. Physical Review B, 2021, 103, .	1.1	10
54756	Understanding liquefaction in halide perovskites upon methylamine gas exposure. RSC Advances, 2021, 11, 20423-20428.	1.7	1
54757	Excited state dynamics in a sodium and iodine co-doped lead telluride nanowire. Molecular Physics, 2021, 119, e1874557.	0.8	0
54758	Unravelling high volumetric capacity of Co₃O₄ nanograin-interconnected secondary particles for lithium-ion battery anodes. Journal of Materials Chemistry A, 2021, 9, 6242-6251.	5.2	18
54759	Helium-induced damage in U3Si5 by first-principles studies. RSC Advances, 2021, 11, 26920-26927.	1.7	0
54760	Thermodynamic criterions of the thermoelectric performance enhancement in Mg2Sn through the self-compensation vacancy. Materials Today Physics, 2021, 16, 100327.	2.9	22
54761	Electrochemical Performance Enhancement of Nitrogen-Doped TiO₂ for Lithium-Ion Batteries Investigated by a Film Electrode Model. Energy & Fuels, 2021, 35, 2717-2726.	2.5	21
54762	Graphene-Based Dual-Metal Sites for Oxygen Reduction Reaction: A Theoretical Study. Journal of Physical Chemistry C, 2021, 125, 2334-2344.	1.5	32

#	Article	IF	Citations
54763	Nonvolatile Controlling Valleytronics by Ferroelectricity in 2H-VSe₂/Sc₂CO₂ van der Waals Heterostructure. Journal of Physical Chemistry C, 2021, 125, 2802-2809.	1.5	20
54764	A solid electrolyte interphase to protect the sulfurized polyacrylonitrile (SPAN) composite for Liâ€“S batteries: computational approach addressing the electrolyte/SPAN interfacial reactivity. Journal of Materials Chemistry A, 2021, 9, 7888-7902.	5.2	9
54765	Interaction of First Row Transition Metals with M₂C (M = Ti, Zr, Hf, V, Nb, Ta, Cr, Mo, and) Tj ETQq0 0 0 rgBT /Overlock 10 T	1.5	38
54766	Polycrystalline Few-Layer Graphene as a Durable Anticorrosion Film for Copper. Nano Letters, 2021, 21, 1161-1168.	4.5	39
54767	Electronic structures and defect properties of lithium-rich manganese-based ternary material Li1.21Ni0.33Co0.04Mn0.42O2. Wuli Xuebao/Acta Physica Sinica, 2021, .	0.2	0
54768	Structure, phase transition and properties of the one-dimensional antiferromagnet Cu(2,6-dimethylpyrazine)Br2. RSC Advances, 2021, 11, 22565-22570.	1.7	0
54769	A GGA + U investigation into the effects of cations on the electromagnetic properties of transition metal spinels. RSC Advances, 2021, 11, 21851-21856.	1.7	8
54770	Low-Sintering-Temperature Garnet Oxides by Conformal Sintering-Aid Coating. SSRN Electronic Journal, 0, , .	0.4	1
54771	Properties of lithium phosphorus oxynitride (LiPON) solid electrolyte - Li anode interfaces. Wuli Xuebao/Acta Physica Sinica, 2021, 70, 136801-136801.	0.2	1
54772	Effect of Si, Be, Al, N and S dual doping on arsenene: first-principles insights. RSC Advances, 2021, 11, 25217-25227.	1.7	3
54773	Atomistic Simulation of Nickel Surface and Interface Properties. , 2021, , 179-189.		0
54774	Significant Enhancement of Piezoelectric Response in AlN by Yb Addition. Materials, 2021, 14, 309.	1.3	13
54776	Tailoring the cationic and anionic sites of LaFeO₃-based perovskite generates multiple vacancies for efficient water oxidation. Journal of Materials Chemistry A, 2021, 9, 16906-16916.	5.2	29
54777	First-principles-based kinetic Monte Carlo simulations of CO oxidation on catalytic Au(110) and Ag(110) surfaces. Physical Chemistry Chemical Physics, 2021, 23, 14037-14050.	1.3	7
54778	Lead-free perovskite compounds CsSn_{1â^'x}Ge_xI_{3â^'y}Br_y explored for superior visible-light absorption. Physical Chemistry Chemical Physics, 2021, 23, 14449-14456.	1.3	10
54779	Properties of diamane anchored with different groups. Physical Chemistry Chemical Physics, 2021, 23, 14195-14204.	1.3	8
54780	Magnetism of elemental two-dimensional metals. Journal of Materials Chemistry C, 2021, 9, 4554-4561.	2.7	15
54781	Hypercoordinate two-dimensional transition-metal borides for spintronics and catalyst applications. Journal of Materials Chemistry C, 0, , .	2.7	18

#	Article	IF	Citations
54782	Tuning the electrochemical performance of Ti₃C₂ and Hf₃C₂ monolayer by functional groups for metal-ion battery applications. Nanoscale, 2021, 13, 11534-11543.	2.8	25
54783	First-principles study of a topological phase transition induced by image potential states in MXenes. Physical Review B, 2021, 103, .	1.1	6
54784	Controllable synthesis of CoFe₂Se₄/NiCo₂Se₄ hybrid nanotubes with heterointerfaces and improved oxygen evolution reaction performance. Nanoscale, 2021, 13, 6241-6247.	2.8	9
54785	Unlocking veiled oxygen redox in Na-based earth-abundant binary layered oxide. Journal of Materials Chemistry A, 2021, 9, 15179-15187.	5.2	10
54786	Evidence for a spin acoustic surface plasmon from inelastic atom scattering. Scientific Reports, 2021, 11, 1506.	1.6	7
54787	Investigation of the half-metallicity, magnetism and spin transport properties of double half-Heusler alloys Mn₂CoCrZ₂ (Z = P, As). Physical Chemistry Chemical Physics, 2021, 23, 17984-17991.	1.3	20
54788	Bromideâ€“acetate co-mediated high-power density rechargeable aqueous zincâ€“manganese dioxide batteries. Journal of Materials Chemistry A, 2021, 9, 21888-21896.	5.2	9
54789	Ultralow magnetic damping of a common metallic ferromagnetic film. Science Advances, 2021, 7, .	4.7	3
54790	Lithium and sodium intercalation in a 2D NbSe₂bilayer-stacked homostructure: comparative study of ionic adsorption and diffusion behavior. Physical Chemistry Chemical Physics, 2021, 23, 19811-19818.	1.3	8
54791	On the limit of proton-coupled electronic doping in a Ti(<scp>iv</scp>)-containing MOF. Chemical Science, 2021, 12, 11779-11785.	3.7	6
54792	Hydrogen induced interface engineering in Fe₂O₃â€“TiO₂ heterostructures for efficient charge separation for solar-driven water oxidation in photoelectrochemical cells. RSC Advances, 2021, 11, 4297-4307.	1.7	16
54793	Direct formation of interlayer exciton in two-dimensional van der Waals heterostructures. Materials Horizons, 2021, 8, 2208-2215.	6.4	1
54794	An evaluation of solvent effects and ethanol oxidation. Physical Chemistry Chemical Physics, 2021, 23, 16180-16192.	1.3	7
54795	Mechanism of creation and destruction of oxygen interstitial atoms by nonpolar zinc oxide(101Ì„0) surfaces. Physical Chemistry Chemical Physics, 2021, 23, 16423-16435.	1.3	4
54796	Improved thermoelectric transport properties of Ge₄Se₃Te through dimensionality reduction. Journal of Materials Chemistry C, 2021, 9, 1804-1813.	2.7	17
54797	Direct measurement and modeling of spontaneous charge migration across anataseâ€“brookite nanoheterojunctions. Journal of Materials Chemistry A, 2021, 9, 7782-7790.	5.2	14
54798	Thermoelectric performance of 2D materials: the band-convergence strategy and strong intervalley scatterings. Materials Horizons, 2021, 8, 1253-1263.	6.4	25
54799	Tilting and Distortion in Rutile-Related Mixed Metal Ternary Uranium Oxides: A Structural, Spectroscopic, and Theoretical Investigation. Inorganic Chemistry, 2021, 60, 2246-2260.	1.9	13

#	Article	IF	Citations
54800	Graphdiyne as a novel nonactive anode for wastewater treatment: A theoretical study. Chinese Chemical Letters, 2021, 32, 2819-2822.	4.8	7
54801	Atomic Bonding and Electronic Binding Energy of Two-Dimensional Bi/Li(110) Heterojunctions via BOLS-BB Model. ACS Omega, 2021, 6, 3252-3258.	1.6	0
54802	The impact of hydrogen valence on its bonding and transport in molten fluoride salts. Journal of Materials Chemistry A, 2021, 9, 1784-1794.	5.2	18
54803	Investigation on the interlayer coupling and bonding in layered nitride-halides ThNF and ThNCl. RSC Advances, 2021, 11, 28698-28703.	1.7	0
54804	Understanding ultrafast charge transfer processes in SnS and SnS₂: using the core hole clock method to measure attosecond orbital-dependent electron delocalisation in semiconducting layered materials. Journal of Materials Chemistry C, 2021, 9, 11859-11872.	2.7	5
54805	A two-dimensional ferroelectric ferromagnetic half semiconductor in a VOF monolayer. Journal of Materials Chemistry C, 2021, 9, 9130-9136.	2.7	20
54806	MGa₂B₂O₇:Bi³⁺,Al³⁺ (M = Sr, Ba) blue phosphors with a quantum yield of 99% and negative thermal quenching. Inorganic Chemistry Frontiers, 2021, 8, 4257-4266.	3.0	7
54807	Suppressing void formation in all-solid-state batteries: the role of interfacial adhesion on alkali metal vacancy transport. Journal of Materials Chemistry A, 2021, 9, 19901-19913.	5.2	12
54808	Hydrogen Induced Dislocation Core Reconstruction in Bcc Metals. SSRN Electronic Journal, 0, , .	0.4	0
54809	Electrochemically Driven Phase Transition in LiCoO2 Cathode. Materials, 2021, 14, 242.	1.3	20
54810	Hydrogen Clathrate Structures in Uranium Hydrides at High Pressures. ACS Omega, 2021, 6, 3946-3950.	1.6	3
54811	Mechanical Properties of Atomically Thin Tungsten Dichalcogenides: WS₂, WSe₂, and WTe₂. ACS Nano, 2021, 15, 2600-2610.	7.3	65
54812	Promises of Main-Group Metal Chalcogenide-Based Broken-Gap van der Waals Heterojunctions for Tunneling Field Effect Transistors. ACS Applied Electronic Materials, 2021, 3, 898-904.	2.0	9
54813	Doping-Induced Charge Localization Suppresses Electronâ€“Hole Recombination in Copper Zinc Tin Sulfide: Quantum Dynamics Combined with Deep Neural Networks Analysis. Journal of Physical Chemistry Letters, 2021, 12, 835-842.	2.1	15
54814	Synthesis of CaSnN₂ via a High-Pressure Metathesis Reaction and the Properties of II-Sn-N₂ (II = Ca, Mg, Zn) Semiconductors. Inorganic Chemistry, 2021, 60, 1773-1779.	1.9	18
54815	Hydrostatic Pressure Tuning of Thermal Conductivity for PbTe and PbSe Considering Pressure-Induced Phase Transitions. ACS Omega, 2021, 6, 3980-3990.	1.6	6
54816	Accurately predicting optical properties of rare-earth, aluminate scintillators: influence of electronâ€“hole correlation. Journal of Materials Chemistry C, 2021, 9, 7292-7301.	2.7	8
54817	Computational design of a polymorph for 2D IIIâ€“V orthorhombic monolayers by first principles calculations: excellent anisotropic, electronic and optical properties. Physical Chemistry Chemical Physics, 2021, 23, 3771-3778.	1.3	20

#	Article	IF	Citations
54818	Improving phase transition temperature of VO2 via Ge doping: a combined experimental and theoretical study. Rare Metals, 2021, 40, 1337-1346.	3.6	14
54819	Crystal structures and superconductivity of lithium and fluorine implanted gold hydrides under high pressures. Physical Chemistry Chemical Physics, 2021, 23, 21544-21553.	1.3	3
54820	Synthesis and first-principles study of structural, electronic and optical properties of tetragonal hybrid halobismuthathes [Py₂(XK)]₂[Bi₂Br_{10â^'x}I_x]. New Journal of Chemistry, 2021, 45, 18349-18357.	1.4	4
54821	Balancing Stability and Li-ion Conductivity of Li10SiP2O12 for Solid-State Electrolytes with Assistance of body-centered cubic oxygen framework. Journal of Materials Chemistry A, 0, , .	5.2	2
54822	The hidden impact of structural water â€“ how interlayer water largely controls the Raman spectroscopic response of birnessite-type manganese oxide. Journal of Materials Chemistry A, 2021, 9, 18466-18476.	5.2	9
54823	Structural Origins of Elastic and 2D Plastic Flexibility of Molecular Crystals Investigated with Two Polymorphs of Conformationally Rigid Coumarin. Chemistry of Materials, 2021, 33, 1053-1060.	3.2	50
54824	Noble metal (Ag, Au, Pd and Pt) doped TaS₂ monolayer for gas sensing: a first-principles investigation. Physical Chemistry Chemical Physics, 2021, 23, 18359-18368.	1.3	28
54825	Highly efficient and stable broadband near-infrared-emitting lead-free metal halide double perovskites. Journal of Materials Chemistry C, 2021, 9, 13474-13483.	2.7	13
54826	Lattice oxygen of PbO₂ induces crystal facet dependent electrochemical ozone production. Journal of Materials Chemistry A, 2021, 9, 9010-9017.	5.2	25
54827	Engineering SnO₂ nanorods/ethylenediamine-modified graphene heterojunctions with selective adsorption and electronic structure modulation for ultrasensitive room-temperature NO₂ detection. Nanotechnology, 2021, 32, 155505.	1.3	14
54828	Epitaxial growth of CsPbBr3-PbS vertical and lateral heterostructures for visible to infrared broadband photodetection. Nano Research, 2021, 14, 3879-3885.	5.8	25
54829	Absence of phonon gap driven ultralow lattice thermal conductivity in half-Heusler LuNiBi. Journal of Materials Chemistry C, 2021, 9, 12420-12425.	2.7	8
54830	Ca₄Sb₂O and Ca₄Bi₂O: two promising mixed-anion thermoelectrics. Journal of Materials Chemistry A, 2021, 9, 20417-20435.	5.2	22
54831	Towards superior X-ray detection performance of two-dimensional halide perovskite crystals by adjusting the anisotropic transport behavior. Journal of Materials Chemistry A, 2021, 9, 13209-13219.	5.2	34
54832	Prominent nonequilibrium effects beyond the standard first-principles approach in nanoscale electronic devices. Nanoscale Horizons, 2021, 6, 801-808.	4.1	3
54833	The influence of co-doping on the luminescence and thermoluminescence properties of Cu-containing fluoride borate crystals. CrystEngComm, 2021, 23, 6599-6609.	1.3	7
54834	Hierarchical computational screening of layered lead-free metal halide perovskites for optoelectronic applications. Journal of Materials Chemistry A, 2021, 9, 6476-6486.	5.2	15
54835	Strain-tunable electronic structure and anisotropic transport properties in Janus MoSSe and g-SiC van der Waals heterostructure. Physical Chemistry Chemical Physics, 2021, 23, 9440-9447.	1.3	9

#	Article	IF	Citations
54836	Solid-state synthesis of single-phase nickel monophosphosulfide for the oxygen evolution reaction. Dalton Transactions, 2021, 50, 12870-12878.	1.6	4
54837	Direct Identification of Ferromagnetic Ordering in Two-Dimensional Materials by Magnetic Force Microscopy. ACS Applied Materials & Interfaces, 2021, 13, 39602-39609.	1.1	36
54838	Giant negative Poisson's ratio in two-dimensional V-shaped materials. Nanoscale Advances, 2021, 3, 4554-4560.	2.2	15
54839	Heterojunction TiO₂@TiOF₂ nanosheets as superior anode materials for sodium-ion batteries. Journal of Materials Chemistry A, 2021, 9, 5720-5729.	5.2	51
54840	First-principles investigation of two-dimensional covalentâ€“organic framework electrocatalysts for oxygen evolution/reduction and hydrogen evolution reactions. Sustainable Energy and Fuels, 2021, 5, 5615-5626.	2.5	13
54841	A novel and efficient method of MOF-derived electrocatalyst for HER performance through doping organic ligands. Materials Chemistry Frontiers, 2021, 5, 7833-7842.	3.2	8
54842	Facet-dependent CO₂ reduction reactions on kesterite Cu₂ZnSnS₄ photo-electro-integrated electrodes. Physical Chemistry Chemical Physics, 2021, 24, 48-55.	1.3	4
54843	Design of a noble-metal-free direct Z-scheme photocatalyst for overall water splitting based on a SnC/SnSSe van der Waals heterostructure. Physical Chemistry Chemical Physics, 2021, 23, 21641-21651.	1.3	30
54844	Two-dimensional heterostructures of AuSe/SnS for the photocatalytic hydrogen evolution reaction with a Z-scheme. Journal of Materials Chemistry C, 2021, 9, 12231-12238.	2.7	61
54845	Cooperation and competition between magnetism and chemisorption. Physical Chemistry Chemical Physics, 2021, 23, 3802-3809.	1.3	3
54846	First-principles prediction of ferroelasticity tuned anisotropic auxeticity and carrier mobility in two-dimensional AgO. Journal of Materials Chemistry C, 2021, 9, 3155-3160.	2.7	11
54847	Phenylalkylammonium passivation enables perovskite light emitting diodes with record high-radiance operational lifetime: the chain length matters. Nature Communications, 2021, 12, 644.	5.8	109
54848	The impact of framework flexibility and defects on the water adsorption in CAU-10-H. Physical Chemistry Chemical Physics, 2021, 23, 21329-21337.	1.3	17
54849	Interfacial Oxide Formation Limits the Photovoltage of Î±â€SnWO₄/NiO_x Photoanodes Prepared by Pulsed Laser Deposition. Advanced Energy Materials, 2021, 11, 2003183.	10.2	23
54850	Two-dimensional ferroelectric metal for electrocatalysis. Materials Horizons, 2021, 8, 3387-3393.	6.4	17
54851	Improving the power factor and figure of merit of p-type CuSbSe₂via introducing Sb vacancies. Journal of Materials Chemistry C, 2021, 9, 14858-14865.	2.7	19
54852	Mechano-Ferroelectric Coupling: Stabilization Enhancement and Polarization Switching in Bent AgBiP2Se6 Monolayer. Nanoscale Horizons, 2021, 6, 971-978.	4.1	2
54853	MoS₂and Janus (MoSSe) based 2D van der Waals heterostructures: emerging direct Z-scheme photocatalysts. Nanoscale Advances, 2021, 3, 2837-2845.	2.2	27

#	Article	IF	Citations
54854	Tuning the Interfacial Dipole Moment of Spacer Cations for Charge Extraction in Efficient and Ultrastable Perovskite Solar Cells. Journal of Physical Chemistry C, 2021, 125, 1256-1268.	1.5	56
54855	Two-dimensional van der Waals electrical contact to monolayer MoSi2N4. Applied Physics Letters, 2021, 118, .	1.5	134
54856	A rechargeable zinc-air battery based on zinc peroxide chemistry. Science, 2021, 371, 46-51.	6.0	551
54857	Carbide-Supported PtRu Catalysts for Hydrogen Oxidation Reaction in Alkaline Electrolyte. ACS Catalysis, 2021, 11, 932-947.	5.5	56
54858	Ab initio predictions of graphite-like phase with anomalous grain boundaries and flexoelectricity from collapsed carbon nanotubes. Journal of Chemical Physics, 2021, 154, 044701.	1.2	5
54859	Propane Dehydrogenation on Ga₂O₃-Based Catalysts: Contrasting Performance with Coordination Environment and Acidity of Surface Sites. ACS Catalysis, 2021, 11, 907-924.	5.5	55
54860	Promoting the Reversible Oxygen Redox Reaction of Liâ€Excess Layered Cathode Materials with Surface Vanadium Cation Doping. Advanced Science, 2021, 8, 2003013.	5.6	21
54861	Graphdiyne Visibleâ€Light Photodetector with Ultrafast Detectivity. Advanced Optical Materials, 2021, 9, 2001916.	3.6	25
54862	A universal screening strategy for the accelerated design of superior oxygen evolution/reduction electrocatalysts. Journal of Materials Chemistry A, 2021, 9, 3511-3519.	5.2	21
54863	Hydrogenation of TiO₂ nanosheets and nanoparticles: typical reduction stages and orientation-related anisotropic disorder. Journal of Materials Chemistry A, 2021, 9, 22603-22614.	5.2	5
54864	Modulating the Multiple Intrinsic Properties of Platinum-Iron Alloy Nanowires towards Enhancing Collaborative Electrocatalysis. Materials Chemistry Frontiers, 0, , .	3.2	6
54865	Transformation of Bulk Pd to Pd Cations in Small-Pore CHA Zeolites Facilitated by NO. Jacs Au, 2021, 1, 201-211.	3.6	34
54866	Ag (111) surface for ambient electrolysis of nitrogen to ammonia. Journal of Molecular Modeling, 2021, 27, 38.	0.8	15
54867	Ultra-thin structures of manganese fluorides: conversion from manganese dichalcogenides by fluorination. Physical Chemistry Chemical Physics, 2021, 23, 10218-10224.	1.3	1
54868	Subtle Details in Crystal Structure of SHS Products by DFT Calculations. International Journal of Self-Propagating High-Temperature Synthesis, 2021, 30, 15-21.	0.2	0
54869	Ab initio two-sites occupancy and broadband near-infrared emission of Cr³⁺ in Li₂MgZrO₄. Materials Chemistry Frontiers, 2021, 5, 4334-4342.	3.2	44
54870	Switchable electronic and enhanced magnetic properties of CrI₃ edges. Physical Chemistry Chemical Physics, 2021, 23, 10518-10523.	1.3	6
54871	Crystals springing into action: metalâ€“organic framework CUK-1 as a pressure-driven molecular spring. Chemical Science, 2021, 12, 5682-5687.	3.7	21

#	Article	IF	Citations
54872	Amorphous Si_{1â^'y}C_y composite anode materials: ab initio molecular dynamics for behaviors of Li and Na in the framework. Physical Chemistry Chemical Physics, 2021, 23, 5571-5577.	1.3	0
54873	PdRuIr ternary alloy as an effective NO reduction catalyst: insights from first-principles calculation. Physical Chemistry Chemical Physics, 2021, 23, 7153-7163.	1.3	2
54874	Strain-driven phase transition and spin polarization of Re-doped transition-metal dichalcogenides. Physical Chemistry Chemical Physics, 2021, 23, 9962-9970.	1.3	1
54875	Designing of magnetic MAB phases for energy applications. Journal of Materials Chemistry A, 2021, 9, 8805-8813.	5.2	26
54876	High-pressure phase transition of AB3-type compounds: case of tellurium trioxide. RSC Advances, 2021, 11, 14316-14322.	1.7	0
54877	Bridging experiment and theory: enhancing the electrical conductivities of soft-templated niobium-doped mesoporous titania films. Physical Chemistry Chemical Physics, 2021, 23, 3219-3224.	1.3	6
54878	Dynamical correlation enhanced orbital magnetization in <mml:math xmlns:mml="http://www.w3.org/1998/Math/MathML"><mml:msub><mml:mi>VI</mml:mi><mml:mn>3</mml:mn></mml:msub></mml:m Physical Review B, 2021, 103, .	1.1	9
54879	A revised mechanism of band gap evolution of TMDC nanotubes and its application to Janus TMDC nanotubes: negative electron and hole compressibility. Journal of Materials Chemistry C, 0, , .	2.7	7
54880	A nitrogenous pre-intercalation strategy for the synthesis of nitrogen-doped Ti₃C₂T_x MXene with enhanced electrochemical capacitance. Journal of Materials Chemistry A, 2021, 9, 6393-6401.	5.2	45
54881	An Ab Initio Study of Pressure-Induced Changes of Magnetism in Austenitic Stoichiometric Ni2MnSn. Materials, 2021, 14, 523.	1.3	13
54882	Crystal and Electronic Structures of MoSi₂-Type CrGe₂ Synthesized under High Pressure. Inorganic Chemistry, 2021, 60, 1767-1772.	1.9	3
54883	P- or S-Doped graphdiyne as a superior metal-free electrocatalyst for the hydrogen evolution reaction: a computational study. New Journal of Chemistry, 2021, 45, 8101-8108.	1.4	14
54884	First-principles calculations of hybrid inorganicâ€“organic interfaces: from state-of-the-art to best practice. Physical Chemistry Chemical Physics, 2021, 23, 8132-8180.	1.3	36
54885	Janus 2D titanium nitride halide TiNX_{0.5}Y_{0.5} (X, Y = F, Cl, or Br, and X â‰ Y) monolayers with giant out-of-plane piezoelectricity and high carrier mobility. Physical Chemistry Chemical Physics, 2021, 23, 3637-3645.	1.3	15
54886	First-principles explorations on P₈ and N₂ assembled nanowire and nanosheet. Nano Express, 2021, 2, 010004.	1.2	3
54887	Robust charge spatial separation and linearly tunable band gap of low-energy tube-edge phosphorene nanoribbon. Nanoscale Advances, 2021, 3, 4416-4423.	2.2	3
54888	Correlation between surface chemistry and magnetism in iron nanoparticles. Nanoscale Advances, 2021, 3, 4471-4481.	2.2	3
54889	First-Principles Calculations of Phase Stability, Electronic Structure, and Defect Properties of Perovskites for SOFC/SOEC Electrodes. , 2021, , 143-154.		0

#	Article	IF	Citations
54890	Formation of Extra Vacancies in Nucleating Î³ Phase during Î´-Î³ Massive-like Phase Transformation in Carbon Steel. Journal of Smart Processing, 2021, 10, 202-207.	0.0	0
54891	Effect of Impurities on the Initiation of the Methanol-to-Olefins Process: Kinetic Modeling Based on Ab Initio Rate Constants. Catalysis Letters, 2021, 151, 2595-2602.	1.4	4
54892	Optimizing kesterite solar cells from Cu₂ZnSnS₄ to Cu₂CdGe(S,Se)₄. Journal of Materials Chemistry A, 2021, 9, 9882-9897.	5.2	18
54893	Single-atom catalysts of TMâ€“porphyrin for alkali oxygen batteries: reaction mechanism and universal design principle. Journal of Materials Chemistry A, 2021, 9, 16998-17005.	5.2	6
54894	Correlating Li-Ion Solvation Structures and Electrode Potential Temperature Coefficients. Journal of the American Chemical Society, 2021, 143, 2264-2271.	6.6	44
54895	Lattice-Matched Metalâ€“Semiconductor Heterointerface in Monolayer Cu₂Te. ACS Nano, 2021, 15, 3415-3422.	7.3	19
54896	Robust Magnetoelectric Effect in the Decorated Graphene/In₂Se₃ Heterostructure. ACS Applied Materials & Interfaces, 2021, 13, 3033-3039.	4.0	15
54897	Theoretical Combined Experimental Study of Unique He Behaviors in High-Entropy Alloys. Inorganic Chemistry, 2021, 60, 1388-1397.	1.9	12
54898	Pressure-Driven Metallization in Hafnium Diselenide. Inorganic Chemistry, 2021, 60, 1746-1754.	1.9	8
54899	C₉N₄ and C₂N₆S₃ monolayers as promising anchoring materials for lithiumâ€“sulfur batteries: weakening the shuttle effect via optimizing lithium bonds. Physical Chemistry Chemical Physics, 2021, 23, 12958-12967.	1.3	9
54900	Magnon relaxation time in ferromagnetic Cr2Ge2Te6 monolayer governed by magnon-phonon interaction. Applied Physics Letters, 2021, 118, .	1.5	11
54901	Crown ethers in hydrogenated graphene. Physical Chemistry Chemical Physics, 2021, 23, 18983-18989.	1.3	11
54902	Cerium hydride generated during ball milling and enhanced by graphene for tailoring hydrogen sorption properties of sodium alanate. International Journal of Hydrogen Energy, 2021, 46, 4168-4180.	3.8	8
54903	Impact of temperature and mode polarization on the acoustic phonon range in complex crystalline phases: A case study on intermetallic clathrates. Physical Review Research, 2021, 3, .	1.3	3
54904	Cobalt-based magnetic Weyl semimetals with high-thermodynamic stabilities. Npj Computational Materials, 2021, 7, .	3.5	13
54905	Catalytic activity of PtCu intermetallic compound for CO oxidation: A theoretical insight. Catalysis Today, 2022, 383, 339-344.	2.2	2
54906	Exfoliation of boron carbide into ultrathin nanosheets. Nanoscale, 2021, 13, 1652-1662.	2.8	16
54907	Effect of surface steps on chemical ordering in the subsurface of Cu(Au) solid solutions. Physical Review B, 2021, 103, .	1.1	5

#	Article	IF	Citations
54908	Stable deep blue emission with unity quantum yield in organicâ€“inorganic halide perovskite 2D nanosheets doped with cerium and terbium at high concentrations. Journal of Materials Chemistry C, 2021, 9, 2437-2454.	2.7	15
54909	First-Principles Study of the Electronic Properties and Thermal Expansivity of a Hybrid 2D Carbon and Boron Nitride Material. Journal of Carbon Research, 2021, 7, 5.	1.4	1
54910	Novel structural phases and the properties of LaX (X = P, As) under high pressure: first-principles study. RSC Advances, 2021, 11, 3058-3070.	1.7	4
54911	Out-of-plane ferroelectricity and multiferroicity in elemental bilayer phosphorene, arsenene, and antimonene. Applied Physics Letters, 2021, 118, .	1.5	15
54912	Theoretical investigation of tetrahedral distortion of four-coordinate iron(<scp>ii</scp>) centres in FePd(CN)₄. Dalton Transactions, 2021, 50, 1990-1994.	1.6	2
54913	Defects and dopants in zinc-blende aluminum arsenide: a first-principles study. New Journal of Physics, 2021, 23, 013018.	1.2	1
54914	Ferroic dislocations in paraelectric <mml:math xmlns:mml="http://www.w3.org/1998/Math/MathML"><mml:mi>Sr</mml:mi><mml:mi>Ti</mml:mi><mml:msub><mml:mrow><mml:mi mathvariant="normal">O</mml:mi></mml:mrow><mml:mn>3</mml:mn></mml:msub></mml:math>. Physical Review B, 2021, 103, .	1.1	4
54915	Decoupled strain response of ferroic properties in a multiferroic <mml:math xmlns:mml="http://www.w3.org/1998/Math/MathML"><mml:msub><mml:mi mathvariant="normal">VOCl</mml:mi><mml:mn>2</mml:mn></mml:msub></mml:math> monolayer. Physical Review B, 2021, 103, .	1.1	9
54916	On the Reaction Mechanism of Direct H₂O₂ Formation over Pd Catalysts. ACS Catalysis, 2021, 11, 2735-2745.	5.5	50
54917	Mechanical properties of M-Zr (M=Cr, Al, Mn) co-doped ceria: A first-principles study. IOP Conference Series: Earth and Environmental Science, 0, 657, 012032.	0.2	0
54918	Incorporation of Si atoms into CrCoNiFe high-entropy alloy: a DFT study. Journal of Physics Condensed Matter, 2021, 33, 135703.	0.7	5
54919	The influence of alloying on the stacking fault energy of gold from density functional theory calculations. Computational Materials Science, 2021, 188, 110236.	1.4	11
54920	Oxygen vacancy induced site-selective Mott transition in <mml:math xmlns:mml="http://www.w3.org/1998/Math/MathML"><mml:msub><mml:mi>LaNiO</mml:mi><mml:mn>3</mml:mn></mml:msub></mml:math>. Physical Review B, 2021, 103, .	1.1	12
54921	First-principles study of <mml:math xmlns:mml="http://www.w3.org/1998/Math/MathML"><mml:msup><mml:mrow><mml:mi>Bi</mml:mi></mml:mrow><mml:mrow><mml:mn -related luminescence and traps in the perovskites <mml:math xmlns:mml="http://www.w3.org/1998/Math/MathML"><mml:mrow><mml:mi>Ca</mml:mi><mml:mi>M</mml:mi><mml:msub><mml:mn		

#	Article	IF	Citations
54927	Elucidating the Influence of Electric Fields toward CO2 Activation on YSZ (111). Catalysts, 2021, 11, 271.	1.6	5
54928	Computationally Guided Searches for Efficient Catalysts through Chemical/Materials Space: Progress and Outlook. Journal of Physical Chemistry C, 2021, 125, 6495-6507.	1.5	4
54929	Role of strain and composition on the piezoelectric and dielectric response of AlxGa1â^'xN: Implications for power electronics device reliability. Journal of Applied Physics, 2021, 129, 075701.	1.1	1
54930	Automated fragmentation quantum mechanical calculation of 13C and 1H chemical shifts in molecular crystals. Journal of Chemical Physics, 2021, 154, 064502.	1.2	6
54931	Transition-metal adatoms on 2D-GaAs: a route to chiral magnetic 2D materials by design. Journal of Physics Condensed Matter, 2021, 33, 145803.	0.7	0
54932	Density functional theory study of ultra-thin InSe electrodes for Na and Mg ion storage and transport. Materials Letters, 2021, 285, 129091.	1.3	3
54933	The electronic properties and structural stability of LaFeO3 oxide by niobium doping: A density functional theory study. International Journal of Hydrogen Energy, 2021, 46, 9193-9198.	3.8	10
54934	Hydrogenolysis and Î²â€“elimination mechanisms for C S bond scission of dibenzothiophene on CoMoS edge sites. Journal of Catalysis, 2021, 403, 32-42.	3.1	1
54935	Interfacial Electronic Properties and Adjustable Schottky Barrier at Graphene/CsPbI₃ van der Waals Heterostructures. Physica Status Solidi - Rapid Research Letters, 2021, 15, 2000555.	1.2	2
54936	Calculation and interpretation of classical turning surfaces in solids. Npj Computational Materials, 2021, 7, .	3.5	6
54937	Thermodynamic stability and electronic structure of pristine wurtzite <mml:math xmlns:mml="http://www.w3.org/1998/Math/MathML"><mml:mrow><mml:mi>ZnO</mml:mi><mml:mo>{</mml:mo><mml:mn>0001</mml:mn></mml:mrow> inversion domain boundaries. Physical Review Materials, 2021, 5, .	3.1	2
54938	Structural and electronic properties of solid molecular hydrogen from many-electron theories. Physical Review B, 2021, 103, .	1.1	3
54939	High-Throughput Screening of Synergistic Transition Metal Dual-Atom Catalysts for Efficient Nitrogen Fixation. Nano Letters, 2021, 21, 1871-1878.	4.5	223
54940	Electrical conductivity of warm dense silica from double-shock experiments. Nature Communications, 2021, 12, 840.	5.8	9
54941	Improving the stability of perovskite by covering graphene on <scp> FAPbI ₃ </scp> surface. International Journal of Energy Research, 2021, 45, 10808-10820.	2.2	7
54942	Pore Tuning of Metalâ€Organic Framework Membrane Anchored on Grapheneâ€Oxide Nanoribbon. Advanced Functional Materials, 2021, 31, 2011146.	7.8	29
54943	First-principles calculations of the electronic and optical properties of $$ext {WSe}_2/ext {Cd}_{0.9}ext {Zn}_{0.1}ext {Te}$$ van der Waals heterostructure. Journal of Computational Electronics, 2021, 20, 13-20.	1.3	2
54944	Binary and Ternary Colloidal Cuâ€Snâ€Te Nanocrystals for Thermoelectric Thin Films. Small, 2021, 17, e2006729.	5.2	8

#	Article	IF	Citations
54945	Two-dimensional oxygen functionalized honeycomb and zigzag dumbbell silicene with robust Dirac cones. New Journal of Physics, 2021, 23, 023007.	1.2	2
54946	Direct insight into the structure-property relation of interfaces from constrained crystal structure prediction. Nature Communications, 2021, 12, 811.	5.8	10
54947	Experimental study, first-principles calculation and thermodynamic modelling of the Crâ€“Feâ€“Nbâ€“Snâ€“Zr quinary system for application as cladding materials in nuclear reactors.. Journal of Nuclear Materials, 2021, 544, 152692.	1.3	7
54948	Strain Engineering for Tuning the Photocatalytic Activity of Metal-Organic Frameworks-Theoretical Study of the UiO-66 Case. Catalysts, 2021, 11, 264.	1.6	3
54949	Structural and electronic properties of realistic two-dimensional amorphous topological insulators. 2D Materials, 2021, 8, 025032.	2.0	16
54950	Tailoring the electronic structure and magnetic properties of pyrochlore Co₂Ti_{1â^'x}Ge_xO₄: a GGA + U ab initio study. Journal of Physics Condensed Matter, 2021, 33, 145504.	0.7	4
54951	Oxidation and Storage Mechanisms for Nitrogen Oxides on Variously Terminated (001) Surfaces of SrFeO_{3â^'Î´} and Sr₃Fe₂O_{7â^'Î´} Perovskites. ACS Applied Materials & Interfaces, 2021, 13, 7216-7226.	4.0	14
54952	Assessing Atomic-Phase Transitions and Ion Transport in Layered NaxNiO2 (x â‰ 0.67) Cathode Materials. Journal of Physical Chemistry C, 2021, 125, 4930-4937.	1.5	1
54953	Boosted Catalytic Hydrogenation Performance Using Isolated Co Sites Anchored on Nitrogen-Incorporated Hollow Porous Carbon. Journal of Physical Chemistry C, 2021, 125, 5088-5098.	1.5	18
54954	2DEG and 2DHG in NaTaO₃ polar thin films: thickness and strain dependency. Nano Express, 2021, 2, 010016.	1.2	6
54955	Design of a Series of Metallic BxNx+1 with Tunable Mechanical Properties. Journal of Physical Chemistry Letters, 2021, 12, 1979-1984.	2.1	3
54956	Alkali Dispersion in (Ag,Cu)(In,Ga)Se₂ Thin Film Solar Cellsâ€”Insight from Theory and Experiment. ACS Applied Materials & Interfaces, 2021, 13, 7188-7199.	4.0	22
54957	Anisotropic Thermoelectric Materials: Pentagonal PtM₂ (M = S, Se, Te). ACS Applied Materials & Interfaces, 2021, 13, 8700-8709.	4.0	52
54958	Tunable Threshold Voltage of ZnTe-Based Ovonic Switching Devices via Isovalent Cation Exchange. ACS Applied Electronic Materials, 2021, 3, 1107-1114.	2.0	3
54959	A Nanometer-Sized Graphite/Boron-Doped Diamond Electrochemical Sensor for Sensitive Detection of Acetaminophen. ACS Omega, 2021, 6, 6326-6334.	1.6	30
54960	Stabilization Factor of Anion-Excess Fluorite Phase for Fast Anion Conduction. Chemistry of Materials, 2021, 33, 1867-1874.	3.2	10
54961	A First-Principles Study of Impurity-Enhanced Adhesion and Lubricity of Graphene on Iron Oxide Surface. Journal of Physical Chemistry C, 2021, 125, 4310-4321.	1.5	6
54962	Effect of Oxygen Vacancies on Adsorption of Small Molecules on Anatase and Rutile TiO₂ Surfaces: A Frontier Orbital Approach. Journal of Physical Chemistry C, 2021, 125, 3827-3844.	1.5	18

#	Article	IF	Citations
54963	Probing the Interaction of Water Molecules with Oxidized Graphene by First Principles. Journal of Physical Chemistry C, 2021, 125, 4580-4587.	1.5	14
54964	Chemical Way to Tune Spin Excitation of Magnetic Atoms in SierpiÅ„ski Triangles. Journal of Physical Chemistry C, 2021, 125, 5581-5586.	1.5	5
54965	Operation Mechanism in Hybrid Mgâ€“Li Batteries with TiNb₂O₇ Allowing Stable High-Rate Cycling. ACS Applied Materials & Interfaces, 2021, 13, 6309-6321.	4.0	13
54966	Complex Dirac-like Electronic Structure in Atomic Site-Ordered Rh₃In_{3.4}Ge_{3.6}. Chemistry of Materials, 2021, 33, 1218-1227.	3.2	1
54967	Modeling Charge Redistribution at Magnetite Interfaces in Empirical Force Fields. Journal of Physical Chemistry C, 2021, 125, 4794-4805.	1.5	13
54968	Calculation for High Pressure Behaviour of Potential Solar Cell Materials Cu2FeSnS4 and Cu2MnSnS4. Crystals, 2021, 11, 151.	1.0	1
54969	Enhanced optical absorption and photocatalytic water splitting of g-C3N4/TiO2 heterostructure through C&B codoping: A hybrid DFT study. International Journal of Hydrogen Energy, 2021, 46, 9417-9432.	3.8	26
54970	Confinement effect enhanced Stoner ferromagnetic instability in monolayer 1T-VSe₂. New Journal of Physics, 2021, 23, 023027.	1.2	13
54971	Impact of the degree of dehydrogenation in ethanol Câ€“C bond cleavage on Ir(100). Journal of Chemical Physics, 2021, 154, 054705.	1.2	9
54972	Chemically Controllable Magnetic Transition Temperature and Magnetoâ€Elastic Coupling in MnZnSb Compounds. Advanced Functional Materials, 2021, 31, 2100108.	7.8	9
54973	Tunable electronic structure and magnetic anisotropy in bilayer ferromagnetic semiconductor Cr2Ge2Te6. Scientific Reports, 2021, 11, 2744.	1.6	15
54974	Electronic structure of <mml:math xmlns:mml="http://www.w3.org/1998/Math/MathML"><mml:msub><mml:mi mathvariant="normal">TiSe</mml:mi><mml:mn>2</mml:mn></mml:msub></mml:math> from a quasi-self-consistent <mml:math xmlns:mml="http://www.w3.org/1998/Math/MathML"><mml:mrow><mml:msub><mml:mi>G</mml:mi><mml:mn>0</mml:mn></mml:msub></mml:mr approach. Physical Review B, 2021, 103	1.1	8
54975	Engineering Cationic Sulfur-Doped Co₃O₄ Architectures with Exposing High-Reactive (112) Facets for Photoelectrocatalytic Water Purification. ACS Applied Materials & Interfaces, 2021, 13, 8405-8416.	4.0	37
54976	Determining structural and chemical heterogeneities of surface species at the single-bond limit. Science, 2021, 371, 818-822.	6.0	77
54977	Selective-etching of MOF toward hierarchical porous Mo-doped CoP/N-doped carbon nanosheet arrays for efficient hydrogen evolution at all pH values. Chemical Engineering Journal, 2021, 405, 126981.	6.6	55
54978	Effect of Fluoroethylene Carbonate Additives on the Initial Formation of the Solid Electrolyte Interphase on an Oxygen-Functionalized Graphitic Anode in Lithium-Ion Batteries. ACS Applied Materials & Interfaces, 2021, 13, 8169-8180.	4.0	23
54979	Tailoring Electrodeâ€“Electrolyte Interfaces in Lithium-Ion Batteries Using Molecularly Engineered Functional Polymers. ACS Applied Materials & Interfaces, 2021, 13, 9919-9931.	4.0	27
54980	Catalytic hydrocracking of synthetic polymers into grid-compatible gas streams. Cell Reports Physical Science, 2021, 2, 100332.	2.8	28

#	Article	IF	Citations
54981	Fast Molecular Compression by a Hyperthermal Collision Gives Bond-Selective Mechanochemistry. Physical Review Letters, 2021, 126, 056001.	2.9	22
54982	Gold Stability and Diffusion in the Au/TS-1 Catalyst. Journal of Physical Chemistry C, 2021, 125, 4519-4531.	1.5	12
54983	Monoclinic and Orthorhombic NaMnO2 for Secondary Batteries: A Comparative Study. Energies, 2021, 14, 1230.	1.6	19
54984	Near-Broken-Gap Alignment between FeWO₄ and Fe₂WO₆ for Ohmic Direct pâ€“n Junction Thermoelectrics. ACS Applied Materials & Interfaces, 2021, 13, 7416-7422.	4.0	11
54985	Establishment of the Potential of Zero Charge of Metals in Aqueous Solutions: Different Faces of Water Revealed by Ab Initio Molecular Dynamics Simulations. Journal of Physical Chemistry C, 2021, 125, 3972-3979.	1.5	33
54986	Impact of Oxygen on the Properties of Cu₃N and Cu_{3â€“x}N_{1â€“x}O_x. Journal of Physical Chemistry C, 2021, 125, 3680-3688.	1.5	11
54987	Properties of Methane and Carbon Adsorbed at the Interface between Molten NaBr and Ni(111). Journal of Physical Chemistry C, 2021, 125, 3980-3987.	1.5	3
54988	Energy Barrier of Proton Transfer in 3d Transition Metal-Doped Boehmite. Journal of Physical Chemistry C, 2021, 125, 3804-3810.	1.5	3
54989	Stability of Pt Skin Intermetallic Core Catalysts and Adsorption Properties for the Oxygen Reduction Reaction. Journal of Physical Chemistry C, 2021, 125, 3527-3534.	1.5	7
54990	Structural Engineering of Ultrathin ReS₂ on Hierarchically Architectured Graphene for Enhanced Oxygen Reduction. ACS Nano, 2021, 15, 5560-5566.	7.3	24
54991	Novel Two-Dimensional Layered MoSi2Z4 (Z = P, As): New Promising Optoelectronic Materials. Nanomaterials, 2021, 11, 559.	1.9	52
54992	An Analysis of the Hydrogen Embrittlement Resistance of Aluminum Alloys. Technical Physics Letters, 2021, 47, 170-173.	0.2	0
54993	Graphene for next generation magnetic devices: A first-principles study. , 2021, , .		1
54994	Modified Graphene Sheets as Promising Cathode Catalysts for Liâ€“O₂ Batteries: A First-Principles Study. Journal of Physical Chemistry C, 2021, 125, 4363-4370.	1.5	12
54995	A first-principles study of Li and Na co-decorated T4,4,4-graphyne for hydrogen storage. International Journal of Hydrogen Energy, 2021, 46, 8104-8112.	3.8	10
54996	Realizing Efficient Overall Water Splitting by Tuning the Cobalt Content in Selfâ€Supported Ni x â^'Co y â^'P Microarrays. ChemElectroChem, 2021, 8, 1307-1315.	1.7	5
54997	FeCoP₂ Nanoparticles Embedded in N and P Co-doped Hierarchically Porous Carbon for Efficient Electrocatalytic Water Splitting. ACS Applied Materials & Interfaces, 2021, 13, 8832-8843.	4.0	67
54998	A stable cathode-solid electrolyte composite for high-voltage, long-cycle-life solid-state sodium-ion batteries. Nature Communications, 2021, 12, 1256.	5.8	110

#	Article	IF	Citations
54999	Unveiling Temperature-Mediated Dual-Band Edge in TiO2 Nanotubes with Enhanced Photocatalytic Effect. Journal of Physical Chemistry C, 2021, 125, 4846-4859.	1.5	10
55000	Microkinetic Modeling of the CO₂ Desorption from Supported Multifaceted Ni Catalysts. Journal of Physical Chemistry C, 2021, 125, 2984-3000.	1.5	20
55001	Nonlinear Band Gap Dependence of Mixed Pbâ€“Sn 2D Ruddlesdenâ€“Popper PEA₂Pb_{1â€“x}Sn_xI₄ Perovskites. Journal of Physical Chemistry Letters, 2021, 12, 1501-1506.	2.1	9
55002	Vanadium Cluster Neutrals Reacting with Water: Superatomic Features and Hydrogen Evolution in a Fishing Mode. Journal of Physical Chemistry Letters, 2021, 12, 1593-1600.	2.1	21
55003	The inhibition behavior of novel ionic liquids for magnesium alloy in NaCl solution: Experimental and theoretical investigation. Journal of Molecular Liquids, 2021, 324, 114732.	2.3	12
55004	Electronic, structural and optical properties of cerium and zinc co-doped organic-inorganic halide perovskites for photovoltaic application. Physica B: Condensed Matter, 2021, 603, 412703.	1.3	4
55005	Singleâ€Molecule Conductance of 1,4â€Azaborine Derivatives as Models of BNâ€doped PAHs. Angewandte Chemie, 2021, 133, 6683-6690.	1.6	2
55006	One- and two-dimensional electrical contacts and transport properties in monolayer black phosphoreneâ€“Ni interface. Journal of Physics Condensed Matter, 2021, 33, 145001.	0.7	3
55007	Ab initio study of electronic and magnetic properties of Mn2RuZ/MgO (001) heterojunctions (Z = Al,) Tj ETQq0 0 0 rgBT /Overlock 10 Tf	0.7	2
55008	Pushing the limits in photosensitizer-catalyst interaction via a short cyanide bridge for water oxidation. Cell Reports Physical Science, 2021, 2, 100319.	2.8	7
55009	Investigation of the Electrocatalytic Activity of CuRu Alloy and Its Mechanism for Hydrogen Evolution Reaction. ChemElectroChem, 2021, 8, 705-711.	1.7	7
55010	Experimental and theoretical study of magnetization and magnetocaloric effect in Nd1âˆ’xSmxFeO3. Journal of Applied Physics, 2021, 129, 063902.	1.1	0
55011	Electronic and magnetic properties of yttria-stabilized zirconia (6.7Âmol% in Y2O3) doped with Er3+ ions from first-principle computations. Journal of Materials Science, 2021, 56, 8014-8023.	1.7	0
55012	New strontium titanate polymorphs under high pressure. Journal of Computational Chemistry, 2021, 42, 699-705.	1.5	8
55013	Firstâ€principles studies on structure stability, segregation, and work function of <scp>Mg</scp> doped with metal elements. International Journal of Quantum Chemistry, 2021, 121, e26626.	1.0	4
55014	Defect-assisted nonradiative recombination in <mml:math xmlns:mml="http://www.w3.org/1998/Math/MathML"><mml:mrow><mml:msub><mml:mi>Cu</mml:mi><mml:mn>2</mml:mn></ : A comparative study with <mml:math xmlns:mml="http://www.w3.org/1998/Math/MathML"><mml:mrow><mml:msub><mml:mi>Cu</mml:mi><mml:mn>2</mml:mn></ mathvariant="normal">S</mml:mi><mml:mn>4</mml:mn></mml. Physical Review Materials, 2021, 5, .	0.9	8
55015	Role of symmetry mismatch, charge transfer and low dimensionality in the magnetic order of CaMnO3/SrTiO3 ultrathin heterostructures. AIP Advances, 2021, 11, 025319.	0.6	0
55016	Theoretical investigation of quantum capacitance in the functionalized MoS₂-monolayer. Electronic Structure, 2021, 3, 025003.	1.0	4

#	Article	IF	Citations
55017	The carbon state in dilute germanium carbides. Journal of Applied Physics, 2021, 129, 055701.	1.1	6
55018	Hybrid nodal chain in an orthorhombic graphene network. Physical Review B, 2021, 103, .	1.1	12
55019	Effect of alloying on the dynamics of coherent acoustic phonons in bismuth double perovskite single crystals. Optics Express, 2021, 29, 7948.	1.7	4
55020	Atomistic Site Control of Pd in Crystalline MnO₂ Nanofiber for Enhanced Electrocatalysis. Advanced Materials Interfaces, 2021, 8, 2002060.	1.9	1
55021	Adsorption and Surface Diffusion of Metals on Î±-Al2O3 for Advanced Manufacturing Applications. Jom, 2021, 73, 1062-1070.	0.9	1
55023	Influence of lattice deformations on the electronic structure of the molybdenum disulfide monolayer. , 2021, 65, 40-45.	0.0	0
55024	Quaternary Chalcohalides CdSnSX₂ (X = Cl or Br) with Neutral Layers: Syntheses, Structures, and Photocatalytic Properties. Inorganic Chemistry, 2021, 60, 3431-3438.	1.9	10
55025	Cr-Doped Ge-Core/Si-Shell Nanowire: An Antiferromagnetic Semiconductor. Nano Letters, 2021, 21, 1856-1862.	4.5	4
55026	Formation of Highly Doped Nanostripes in 2D Transition Metal Dichalcogenides via a Dislocation Climb Mechanism. Advanced Materials, 2021, 33, e2007819.	11.1	13
55027	Enhancing performance of NiCo2S4/Ni3S2 supercapacitor electrode by Mn doping. Electrochimica Acta, 2021, 368, 137634.	2.6	38
55028	Electroless Formation of a Fluorinated Li/Na Hybrid Interphase for Robust Lithium Anodes. Journal of the American Chemical Society, 2021, 143, 2829-2837.	6.6	119
55029	Adsorption and diffusion of Li/Na atom on blue phosphorene with defects by first-principles calculations. Canadian Journal of Physics, 0, , 1-8.	0.4	1
55030	Type-III Dirac fermions in HfxZr1â^'xTe2 topological semimetal candidate. Journal of Applied Physics, 2021, 129, .	1.1	9
55031	Atomic Zn Sites on N and S Codoped Biomass-Derived Graphene for a High-Efficiency Oxygen Reduction Reaction in both Acidic and Alkaline Electrolytes. ACS Applied Energy Materials, 2021, 4, 2481-2488.	2.5	21
55032	Concomitant Photoresponsive Chiroptics and Magnetism in Metal-Organic Frameworks at Room Temperature. Research, 2021, 2021, 5490482.	2.8	18
55033	Cooperative Activation of Cellulose with Natural Calcium. Jacs Au, 2021, 1, 272-281.	3.6	9
55034	Structural twinning-induced insulating phase in CrN (111) films. Physical Review Materials, 2021, 5, .	0.9	12
55035	Semihard Iron-Based Permanent-Magnet Materials. Physical Review Applied, 2021, 15, .	1.5	11

#	Article	IF	Citations
55036	Structure, phase stability, half-metallicity, and fully spin-polarized Weyl states in compound NaV2O4 : An example for topological spintronic material. Physical Review Materials, 2021, 5, .	0.9	7
55037	Interfacial Atomistic Mechanisms of Lithium Metal Stripping and Plating in Solidâ€State Batteries. Advanced Materials, 2021, 33, e2008081.	11.1	53
55038	Mechanism and Enhancement of the Low-Temperature Selective Catalytic Reduction of NOx with NH₃ by Bifunctional Catalytic Mixtures. Industrial & Engineering Chemistry Research, 2021, 60, 6446-6454.	1.8	11
55039	Anisotropic correlation between the piezoelectricity and anion-polarizability difference in 2D phosphorene-type ternary GaXY (Xâ€‰=â€‰Se, Te; Yâ€‰=â€‰F, Cl, Br, I) monolayers. Journal of Materials Science, 2021, 56, 8024-8036.	1.7	9
55040	8-16-4 graphyne: Square-lattice two-dimensional nodal line semimetal with a nontrivial topological Zak index. Physical Review B, 2021, 103, .	1.1	26
55041	Simple physical mixing of zeolite prevents sulfur deactivation of vanadia catalysts for NOx removal. Nature Communications, 2021, 12, 901.	5.8	49
55042	Machine learning metadynamics simulation of reconstructive phase transition. Physical Review B, 2021, 103, .	1.1	15
55043	Metathesis and Redetermination of the Crystal Structure of Cadmium Carbodiimide, CdNCN. Zeitschrift Fur Anorganische Und Allgemeine Chemie, 2021, 647, 496-499.	0.6	3
55044	Selective Etching Quaternary MAX Phase toward Single Atom Copper Immobilized MXene (Ti₃C₂Cl_x) for Efficient CO₂ Electroreduction to Methanol. ACS Nano, 2021, 15, 4927-4936.	7.3	139
55045	Vacancy ordering induced topological electronic transition in bulk Eu ₂ ZnSb ₂. Science Advances, 2021, 7, .	4.7	21
55046	Strong self-trapping by deformation potential limits photovoltaic performance in bismuth double perovskite. Science Advances, 2021, 7, .	4.7	98
55047	Chemically Switchable n-Type and p-Type Conduction in Bismuth Selenide Nanoribbons for Thermoelectric Energy Harvesting. ACS Nano, 2021, 15, 2791-2799.	7.3	14
55048	Atomistic Insights into the Hydrogen Oxidation Reaction of Palladium-Ceria Bifunctional Catalysts for Anion-Exchange Membrane Fuel Cells. ACS Catalysis, 2021, 11, 2561-2571.	5.5	30
55049	Strain-tunable giant anisotropic conductivity in the polar metal of KNbO3/BaTiO3 ferroelectric superlattice. Computational Materials Science, 2021, 188, 110235.	1.4	0
55050	Prediction of a Heusler alloy with switchable metal-to-half-metal behavior. Physical Review B, 2021, 103, .	1.1	8
55051	First-principles study of an <mml:math xmlns:mml="http://www.w3.org/1998/Math/MathML"><mml:mrow><mml:mi>S</mml:mi><mml:mo>=</mml:mo><mml:mn>1</mml:mn></mml:mr quasi one-dimensional quantum molecular magnetic material. Physical Review B, 2021, 103, .	1.1	1
55052	Effect of zinc doping on electrical properties of LaAlO₃ perovskite. Chimica Techno Acta, 2021, 8, .	0.3	7
55053	Electronic, magnetic and optical properties of blue phosphorene doped with Y, Zr, Nb and Mo: A first-principles study. Thin Solid Films, 2021, 720, 138523.	0.8	12

#	Article	IF	Citations
55054	Monte Carlo simulations of electron transport in 4H-SiC using the DFT-calculated density of states. Journal of Computational Electronics, 2021, 20, 791-797.	1.3	4
55055	Magnetic and electron transport properties of <mml:math xmlns:mml="http://www.w3.org/1998/Math/MathML"><mml:mrow><mml:msub><mml:mi>Co</mml:mi><mml:mn>2</mml:mn></mml:msub> nanomagnets. Physical Review Materials, 2021, 5, .	2.4	6
55056	Hydrogen Oxidation Pathway Over Niâ€“Ceria Electrode: Combined Study of DFT and Experiment. Frontiers in Chemistry, 2020, 8, 591322.	1.8	6
55058	Half-auxetic effect and ferroelasticity in a two-dimensional monolayer TiSe. Journal of Physics Condensed Matter, 2021, 33, 144002.	0.7	1
55059	Pressure-controlled anomalous Hall conductivity in the half-Heusler antiferromagnet GdPtBi. Physical Review B, 2021, 103, .	1.1	7
55060	Two-dimensional iodine-monofluoride epitaxy on WSe2. Npj 2D Materials and Applications, 2021, 5, .	3.9	5
55061	Solution of two-electron SchrÃ¶dinger equations using a residual minimization method and one-dimensional basis functions. AIP Advances, 2021, 11, .	0.6	6
55062	Precipitation of dopants on acceptor-doped LaMnO3Â±Î´ revealed by defect chemistry from first principles. Journal of Chemical Physics, 2021, 154, 064702.	1.2	4
55063	Electron Density-based Estimation of Diradical Character: An Easy Scheme for DFT/Plane-wave Calculations. Chemistry Letters, 2021, 50, 392-396.	0.7	6
55064	Interfacial giant tunnel magnetoresistance and bulk-induced large perpendicular magnetic anisotropy in (111)-oriented junctions with fcc ferromagnetic alloys: A first-principles study. Physical Review B, 2021, 103, .	1.1	14
55065	Optical and physical properties of hydrocarbons with metal impurities in the warm dense matter regime. Physics of Plasmas, 2021, 28, 022705.	0.7	0
55066	Metal-insulator transition in <mml:math xmlns:mml="http://www.w3.org/1998/Math/MathML"><mml:mrow><mml:msub><mml:mi mathvariant="normal">V</mml:mi><mml:mn>2</mml:mn></mml:msub><mml:msub><mml:mi mathvariant="normal">O</mml:mi><mml:mn>3</mml:mn></mml:msub></mml:mrow></mml:math> with intrinsic defects. Physical Review B, 2021, 103, .	1.1	5
55067	Design of memristor materials from ordered-vacancy zincblende semiconductors. Physical Review Materials, 2021, 5, .	0.9	4
55068	Photoemission spectrum in paramagnetic FeO under pressure: Towards an ab initio description. Physical Review Research, 2021, 3, .	1.3	7
55069	First-principles study of the anomalous Hall effect based on exact muffin-tin orbitals. Physical Review B, 2021, 103, .	1.1	5
55070	Morphology evolution of SmCox permanent magnetic nanoparticles. Science China: Physics, Mechanics and Astronomy, 2021, 64, 1.	2.0	2
55071	First-principles insights into the electronic structure, optical and band alignment properties of earth-abundant Cu2SrSnS4 solar absorber. Scientific Reports, 2021, 11, 4755.	1.6	18
55072	Metal-Element-Incorporation Induced Superconducting Hydrogen Clathrate Structure at High Pressure. Chinese Physics Letters, 2021, 38, 027401.	1.3	8

#	Article	IF	Citations
55073	Anisotropic superconductivity in the spin-vortex antiferromagnetic superconductor <mml:math xmlns:mml="http://www.w3.org/1998/Math/MathML"><mml:mrow><mml:mi>CaK</mml:mi><mml:msub><mml:mrow><mml:mo>(</mml:mo> Physical Review B, 2021, 103, .	1.1	12
55075	Unlocking the origin of compositional fluctuations in InGaN light emitting diodes. Physical Review Materials, 2021, 5, .	0.9	7
55076	Stretchable and Ultrasensitive Intelligent Sensors for Wireless Humanâ€“Machine Manipulation. Advanced Functional Materials, 2021, 31, 2009466.	7.8	41
55077	Pentadiamond: A Highly Efficient Electron Transport Layer for Perovskite Solar Cells. Journal of Physical Chemistry C, 2021, 125, 5372-5379.	1.5	18
55078	New Insight into Microstructure Engineering of Niâ€Rich Layered Oxide Cathode for High Performance Lithium Ion Batteries. Advanced Functional Materials, 2021, 31, 2010095.	7.8	113
55079	Comparison of coherent phonon generation by electronic and ionic Raman scattering in <mml:math xmlns:mml="http://www.w3.org/1998/Math/MathML"><mml:msub><mml:mi>LaAlO</mml:mi><mml:mn>3</mml:mn></mml:msub><mml:m Physical Review Research, 2021, 3, .	1.3	9
55080	Stabilization and electronic topological transition of hydrogen-rich metal Li5MoH11 under high pressures from first-principles predictions. Scientific Reports, 2021, 11, 4079.	1.6	12
55081	Density functional theory study of single-molecule ferroelectricity in Preyssler-type polyoxometalates. APL Materials, 2021, 9, .	2.2	5
55082	Tunable electronic properties of SnS2/WSe2 hetero-structure: A frist principle study. Superlattices and Microstructures, 2021, 150, 106806.	1.4	10
55083	Self-Consistent Potential Correction for Charged Periodic Systems. Physical Review Letters, 2021, 126, 076401.	2.9	44
55084	In situ electron microscopy study of structural transformations in 2D CoSe2. Npj 2D Materials and Applications, 2021, 5, .	3.9	13
55085	Dirac Nodal Line Semimetal of Three-Dimensional Cross-Linked Graphene Network as Anode Materials for Li-Ion Battery beyond Graphite. ACS Applied Energy Materials, 2021, 4, 2091-2097.	2.5	6
55086	¹⁷O-ESR Evidence for Zeolite Matrix Isolation of a Square Planar ZnO₃ Ring Radical with C_{2v} Symmetry. Journal of Physical Chemistry C, 2021, 125, 5136-5145.	1.5	2
55087	Insights into adsorption, diffusion, and reactions of atomic nitrogen on a highly oriented pyrolytic graphite surface. Journal of Chemical Physics, 2021, 154, 074708.	1.2	5
55088	Self-Assembled Pyrene Stacks and Peptide Monolayers Tune the Electronic Properties of Functionalized Electrolyte-Gated Graphene Field-Effect Transistors. ACS Applied Materials & Interfaces, 2021, 13, 9134-9142.	4.0	13
55089	Atomistic Imaging of Competition between Surface Diffusion and Phase Transition during the Intermetallic Formation of Faceted Particles. ACS Nano, 2021, 15, 5284-5293.	7.3	17
55090	Mechanism Insights into the Aerobic Oxidation of 5-Hydroxymethylfurfural to 2,5-Furandicarboxylic Acid over MnO₂ Catalysts. Journal of Physical Chemistry C, 2021, 125, 3818-3826.	1.5	12
55091	Tungsten Hexanitride with Single-Bonded Armchairlike Hexazine Structure at High Pressure. Physical Review Letters, 2021, 126, 065702.	2.9	52

#	Article	IF	Citations
55092	Reemergence of superconductivity in pressurized quasi-one-dimensional superconductor K2Mo3As3. Physical Review Materials, 2021, 5, .	0.9	5
55093	Understanding the Strength of the Seleniumâ€“Graphene Interfaces for Energy Storage Systems. Langmuir, 2021, 37, 2029-2039.	1.6	11
55094	Exploring Heat-Shielding Nanoparticle-Based Materials via First-Principles Calculations and Transfer Learning. ACS Applied Nano Materials, 2021, 4, 1932-1939.	2.4	2
55095	Pronounced Enhancement of Superconductivity in ZrN via Strain Engineering. Journal of Physical Chemistry Letters, 2021, 12, 1985-1990.	2.1	15
55096	Atomic-level-designed copper atoms on hierarchically porous gold architectures for high-efficiency electrochemical CO2 reduction. Science China Materials, 2021, 64, 1900-1909.	3.5	26
55097	Berry Phase Engineering in SrRuO₃/SrIrO₃/SrTiO₃ Superlattices Induced by Band Structure Reconstruction. ACS Nano, 2021, 15, 5086-5095.	7.3	19
55098	One-Dimensional Silver-Thiolate Cluster-Assembly: Effect of Argentophilic Interactions on Excited-State Dynamics. Journal of Physical Chemistry Letters, 2021, 12, 2154-2159.	2.1	10
55099	Detailed Characterization of MoO_x-Modified Rh Metal Particles by Ambient-Pressure XPS and DFT Calculations. Journal of Physical Chemistry C, 2021, 125, 4540-4549.	1.5	21
55100	Role of Surface Paramagnetic Oxygen Species in the Desulfurization Reactions on Zinc Oxide. Journal of Physical Chemistry C, 2021, 125, 4559-4566.	1.5	1
55101	A Battery-Like Self-Selecting Biomemristor from Earth-Abundant Natural Biomaterials. ACS Applied Bio Materials, 2021, 4, 1976-1985.	2.3	30
55102	Nonâ€Rareâ€Earth UVC Persistent Phosphors Enabled by Bismuth Doping. Advanced Optical Materials, 2021, 9, 2002065.	3.6	27
55103	Helium-nitrogen mixtures at high pressure. Physical Review B, 2021, 103, .	1.1	16
55104	Direct imaging and electronic structure modulation of moirÃ© superlattices at the 2D/3D interface. Nature Communications, 2021, 12, 1290.	5.8	48
55105	High Efficiency Cu₂ZnSn(S,Se)₄ Solar Cells with Shallow Li_{Zn} Acceptor Defects Enabled by Solutionâ€Based Li Postâ€Deposition Treatment. Advanced Energy Materials, 2021, 11, 2003783.	10.2	57
55106	Comparison of electrochemical response and electric field emission characteristics of pristine La2NiO4 and La2NiO4/CNT composites: Origin of multi-functionality with theoretical penetration by density functional theory. Electrochimica Acta, 2021, 369, 137676.	2.6	15
55107	Bias dependence and defect analysis of Bi on Si(111) <mml:math xmlns:mml="http://www.w3.org/1998/Math/MathML"><mml:mrow><mml:msqrt><mml:mn>3</mml:mn></mml:msqrt><mml:mo>Ã— width="4pt" /><mml:mi>Î²</mml:mi></mml:mrow></mml:math> -phase. Physical Review B, 2021, 103, .	1.1	8
55108	Cage Structure and Near Room-Temperature Superconductivity in TbH_n (n =) Tj ETQq0 0 0 rgBT /Overlock 10	1.5	23
55109	Electro-mechanical coupling in FCC metal rhodium from first-principles simulations. Journal of Materials Research, 2021, 36, 2662-2673.	1.2	0

#	Article	IF	Citations
55110	Directional Design of Materials Based on Multi-Objective Optimization: A Case Study of Two-Dimensional Thermoelectric SnSe. Chinese Physics Letters, 2021, 38, 027301.	1.3	14
55111	Efficient hierarchical models for reactivity of organic layers on semiconductor surfaces. Journal of Computational Chemistry, 2021, 42, 827-839.	1.5	2
55112	Chemical transformation and dissociation of amino acids on metal sulfide surface: Insights from DFT into the effect of surface vacancies on alanine-sphalerite system. Applied Surface Science, 2021, 540, 148304.	3.1	15
55113	Robust S-doped TiO2@N,S-codoped carbon nanotube arrays as free-binder anodes for efficient sodium storage. Journal of Energy Chemistry, 2021, 53, 175-184.	7.1	37
55114	Li interaction-induced phase transition from black to blue phosphorene. Physical Review Materials, 2021, 5, .	0.9	11
55115	Higher-Order Band Topology in Twisted MoirÃ© Superlattice. Physical Review Letters, 2021, 126, 066401.	2.9	56
55116	High-temperature topological superconductivity in twisted double-layer copper oxides. Nature Physics, 2021, 17, 519-524.	6.5	90
55117	Building Ab Initio Interface Pourbaix diagrams to Investigate Electrolyte Stability in the Electrochemical Double Layer: Application to Magnesium Batteries. ACS Applied Materials & Interfaces, 2021, 13, 8263-8273.	4.0	25
55118	Mechanically robust amino acid crystals as fiber-optic transducers and wide bandpass filters for optical communication in the near-infrared. Nature Communications, 2021, 12, 1326.	5.8	67
55119	Scaling of Transition State Vibrational Frequencies and Application of d-Band Theory to the BrÃ¸nstedâ€“Evansâ€“Polanyi Relationship on Surfaces. Journal of Physical Chemistry C, 2021, 125, 7119-7129.	1.5	3
55120	Kinetically Controlled, Scalable Synthesis of Î³â€²-FeOOH Nanosheet Arrays on Nickel Foam toward Efficient Oxygen Evolution: The Key Role of Inâ€Situâ€Generated Î³â€²-NiOOH. Advanced Materials, 2021, 33, e2005587.	11.1	115
55121	Co₂N/Co₂Mo₃O₈ Heterostructure as a Highly Active Electrocatalyst for an Alkaline Hydrogen Evolution Reaction. ACS Applied Materials & Interfaces, 2021, 13, 8337-8343.	4.0	50
55122	Elucidating the origin of selective dehydrogenation of propane on Î³-alumina under H2S treatment and co-feed. Journal of Catalysis, 2021, 394, 142-156.	3.1	21
55123	Tunable Rashba Spin Splitting in Two-Dimensional Polar Perovskites. Journal of Physical Chemistry Letters, 2021, 12, 1932-1939.	2.1	22
55124	Nitriding synthesis and structural change of phosphorus nitrides at high pressures. Journal of Raman Spectroscopy, 2021, 52, 1064-1072.	1.2	8
55125	Water enables mild oxidation of methane to methanol on gold single-atom catalysts. Nature Communications, 2021, 12, 1218.	5.8	138
55126	Photocatalytic Nitrogen Reduction by Ti₃C₂ MXene Derived Oxygen Vacancyâ€Rich C/TiO₂. Advanced Sustainable Systems, 2021, 5, 2000282.	2.7	37
55127	Efficient Oxygen Evolution Electrocatalysis on CaFe₂O₄ and Its Reaction Mechanism. ACS Applied Energy Materials, 2021, 4, 3057-3066.	2.5	22

#	Article	IF	Citations
55128	Theoretical Investigation on the Adsorption and Interface Bonding between N-Heterocyclic Carbenes and Metal Surfaces. Journal of Physical Chemistry C, 2021, 125, 4489-4497.	1.5	11
55129	Strain tunable electronic states of MoSe2 monolayer. Chemical Physics Letters, 2021, 765, 138286.	1.2	13
55130	Estimation of spin contamination errors in DFT/plane-wave calculations of solid materials using approximate spin projection scheme. Chemical Physics Letters, 2021, 765, 138291.	1.2	14
55131	Bipolar ferromagnetic semiconductors and doping-tuned room-temperature half-metallicity in monolayer <mml:math xmlns:mml="http://www.w3.org/1998/Math/MathML"><mml:mrow><mml:mi>Mo</mml:mi><mml:msub><mml:mi>X</mml:mi><mml:mi><mml:math		

#	Article	IF	Citations
55146	Graphitic SiC : A potential anode material for Naâ€ion battery with extremely high storage capacity. International Journal of Quantum Chemistry, 2021, 121, e26608.	1.0	2
55147	Initiating Ullmann-like coupling of Br2Py by a semimetal surface. Scientific Reports, 2021, 11, 3414.	1.6	9
55148	Effect of vanadium substitution in LixFeF3 by first-principles calculations. AIP Advances, 2021, 11, 025218.	0.6	0
55149	Statistical data set for first-principles calculations of stacking fault energies in an AlNbTaTiV high entropy alloy. Data in Brief, 2021, 34, 106670.	0.5	4
55150	Splitting dioxygen over distant binuclear transition metal cationic sites in zeolites. Effect of the transition metal cation. International Journal of Quantum Chemistry, 2021, 121, e26611.	1.0	5
55151	Comparison study of exchange-correlation functionals on prediction of ground states and structural properties. Current Applied Physics, 2021, 22, 61-64.	1.1	7
55152	The effects of local strain on the cubic Li7La3Zr2O12(001)/Li(001) interface: A first-principles study. Solid State Ionics, 2021, 360, 115546.	1.3	5
55153	Atomic mechanism of ionic confinement in the thermoelectric Cu2Se based on a low-cost electric-current method. Cell Reports Physical Science, 2021, 2, 100345.	2.8	12
55154	Improved Thermoelectric Properties of N-Type Mg₃Sb₂ through Cation-Site Doping with Gd or Ho. ACS Applied Materials & Interfaces, 2021, 13, 10964-10971.	4.0	21
55155	Highly Stable and Recyclable Sequestration of CO₂ Using Supported Melamine on Layered-Chain Clay Mineral. ACS Applied Materials & Interfaces, 2021, 13, 10933-10941.	4.0	15
55156	Magnesium polysulfide catholyte (MgSx): Synthesis, electrochemical and computational study for magnesium-sulfur battery application. Journal of Power Sources, 2021, 486, 229326.	4.0	21
55157	Inducing High-Energy-Barrier Tribochemical Reaction Pathways; Acetic Acid Decomposition on Copper. Tribology Letters, 2021, 69, 1.	1.2	17
55158	Ab initio and force field molecular dynamics study of bulk organophosphorus and organochlorine liquid structures. Journal of Chemical Physics, 2021, 154, 084503.	1.2	8
55159	Behavior of Atomic Vacancy in Puckered Arsenene. Journal of Physical Chemistry C, 2021, 125, 4175-4182.	1.5	0
55160	Influence of Structural Distortion and Lattice Dynamics on Li-Ion Diffusion in Li₃OCl_{1â€“x}Br_x Superionic Conductors. ACS Applied Energy Materials, 2021, 4, 2107-2114.	2.5	16
55161	Curvature Constrained Splines for DFTB Repulsive Potential Parametrization. Journal of Chemical Theory and Computation, 2021, 17, 1771-1781.	2.3	12
55162	Understanding the Noncollinear Antiferromagnetic IrMn3 Surfaces and Their Exchange-Biased Heterostructures from First-Principles. ACS Applied Electronic Materials, 2021, 3, 1086-1096.	2.0	3
55163	Tunable Lithium-Ion Transport in Mixed-Halide Argyrodites Li_{6â€“x}PS_{5â€“x}ClBr_x: An Unusual Compositional Space. Chemistry of Materials, 2021, 33, 1435-1443.	3.2	78

#	Article	IF	Citations
55164	Codoping Mg-Mn Based Oxygen Carrier with Lithium and Tungsten for Enhanced C₂ Yield in a Chemical Looping Oxidative Coupling of Methane System. ACS Sustainable Chemistry and Engineering, 2021, 9, 2651-2660.	3.2	22
55165	4.7 V Operation of the Cr⁴⁺/Cr³⁺ Redox Couple in Na₃Cr₂(PO₄)₂F₃. Chemistry of Materials, 2021, 33, 1373-1379.	3.2	9
55166	Mitigating the Effect of Nanoscale Porosity on Thermoelectric Power Factor of Si. ACS Applied Energy Materials, 2021, 4, 1915-1923.	2.5	10
55167	Computational Insights into As(V) Removal from Water by the UiO-66 Metalâ€“Organic Framework. Journal of Physical Chemistry C, 2021, 125, 3157-3168.	1.5	17
55168	Discovering Effective Descriptors for CO₂ Electroreduction to Predict the Catalysts with Different Selectivity. Journal of Physical Chemistry C, 2021, 125, 4550-4558.	1.5	2
55169	The Combined Role of Faceting and Heteroatom Doping for Hydrogen Evolution on a WC Electrocatalyst in Aqueous Solution: A Density Functional Theory Study. Journal of Physical Chemistry C, 2021, 125, 4602-4613.	1.5	13
55170	Data-Driven Discovery and Understanding of Ultrahigh-Modulus Crystals. Chemistry of Materials, 2021, 33, 1276-1284.	3.2	16
55171	Single-Atom Catalysts for Improved Cathode Performance in Naâ€“S Batteries: A Density Functional Theory (DFT) Study. Journal of Physical Chemistry C, 2021, 125, 4458-4467.	1.5	45
55172	Tunable and sizeable band gaps in strained SiC3/hBN vdW heterostructures: A potential replacement for graphene in future nanoelectronics. Computational Materials Science, 2021, 188, 110233.	1.4	8
55173	r2SCAN-3c: A â€œSwiss army knifeâ€•composite electronic-structure method. Journal of Chemical Physics, 2021, 154, 064103.	1.2	290
55174	Tuning the Conductivity of Hexa-Zirconium(IV) Metalâ€“Organic Frameworks by Encapsulating Heterofullerenes. Chemistry of Materials, 2021, 33, 1182-1189.	3.2	17
55175	B-Site Stoichiometry Control of the Magnetotransport Properties of Epitaxial Sr2FeMoO6 Thin Film. ACS Applied Electronic Materials, 2021, 3, 597-604.	2.0	5
55176	Unusual solute segregation phenomenon in coherent twin boundaries. Nature Communications, 2021, 12, 722.	5.8	60
55177	Pressure-induced structural transition and huge enhancement of superconducting properties of single-crystal Fe0.99Ni0.01Se0.5Te0.5 unconventional superconductor. Journal of Materials Research, 2021, 36, 1624-1636.	1.2	1
55178	Theoretical Study of NO Dissociative Adsorption onto 3d Metal Particles M₅₅ (M = Fe, Co,) Tj ETQq0 0 0 rgBT /Overlock 10 ACS Omega, 2021, 6, 4888-4898.	1.6	5
55179	Transition of Cationic Local Structures in Mg1-xNixAl2O4. Journal of Physical Chemistry C, 2021, 125, 5269-5277.	1.5	3
55180	Multistability of isolated and hydrogenated Gaâ€“O divacancies in <mml:math xmlns:mml="http://www.w3.org/1998/Math/MathML"><mml:mi>Î²</mml:mi><mml:mo>â^'</mml:mo><mml:msub><mml:mrow><mml:mathvariant="normal">O</mml:mi></mml:mrow><mml:mn>3</mml:mn></mml:msub></mml:math>. Physical Review Materials, 2021, 5, .	0.9	28
55181	Mimicking efferent nerves using a graphdiyne-based artificial synapse with multiple ion diffusion dynamics. Nature Communications, 2021, 12, 1068.	5.8	115

#	Article	IF	Citations
55182	Metalâ€“Organic Framework-Derived Hierarchical MnO/Co with Oxygen Vacancies toward Elevated-Temperature Li-Ion Battery. ACS Nano, 2021, 15, 4594-4607.	7.3	121
55183	Aâ€Site Management Prompts the Dynamic Reconstructed Active Phase of Perovskite Oxide OER Catalysts. Advanced Energy Materials, 2021, 11, 2003755.	10.2	171
55184	Theory of the Thermal Stability of Silicon Vacancies and Interstitials in 4Hâ€“SiC. Crystals, 2021, 11, 167.	1.0	17
55185	Layer-by-layer anionic diffusion in two-dimensional halide perovskite vertical heterostructures. Nature Nanotechnology, 2021, 16, 584-591.	15.6	88
55186	First-Principles Identification of Single Photon Emitters Based on Carbon Clusters in Hexagonal Boron Nitride. Journal of Physical Chemistry A, 2021, 125, 1325-1335.	1.1	51
55187	Redox Photochemistry on Van Der Waals Surfaces for Reversible Doping in 2D Materials. Advanced Functional Materials, 2021, 31, 2009166.	7.8	9
55188	Constructing Surface Plasmon Resonance on Bi₂WO₆ to Boost High-Selective CO₂ Reduction for Methane. ACS Nano, 2021, 15, 3529-3539.	7.3	113
55189	Electronic Origin of Catalytic Activity of TiH₂for Ammonia Synthesis. Journal of Physical Chemistry C, 2021, 125, 3948-3960.	1.5	13
55190	First-principles study of the co-effect of carbon doping and oxygen vacancies in ZnO photocatalyst*. Chinese Physics B, 2021, 30, 026301.	0.7	7
55191	Multiple Reaction Pathways for the Oxygen Evolution Reaction May Contribute to IrO₂ (110)â€™s High Activity. Journal of the Electrochemical Society, 2021, 168, 024506.	1.3	12
55192	Structural and Electrical Properties of Be_xZn_{1â€“x}O Alloys under High Pressure. Chinese Physics Letters, 2021, 38, 026101.	1.3	7
55193	First-Principles Calculations on Thermoelectric Properties of Layered Transition Metal Phosphides MP2 (M = Ni, Pd, Pt). Journal of Electronic Materials, 2021, 50, 2510-2520.	1.0	6
55194	Possibility of interstitial Na as electron donor in Yb14MgSb11. MRS Communications, 2021, 11, 226-232.	0.8	4
55195	Jahn-Teller distortion assisted interstitial nitrogen engineering: enhanced oxygen dehydrogenation activity of N-doped MnxCo3â^'xO4 hierarchical micro-nano particles. Nano Research, 2021, 14, 2637-2643.	5.8	13
55196	Theoretical Study of Two-Dimensional Î±-Tellurene with Pseudo-Heterospecies as a Promising Elemental Anchoring Material for Lithiumâ€“Sulfur Batteries. Journal of Physical Chemistry C, 2021, 125, 4623-4631.	1.5	12
55197	Density Functional Theory Investigation of Structureâ€“Activity Relationship for Efficient Electrochemical CO₂ Reduction on Defective SnSe₂ Nanosheets. ACS Applied Nano Materials, 2021, 4, 2760-2767.	2.4	6
55198	Studies on the Sodium Storage Performances of Na₃Al_xV_{2â€“x}(PO₄)₃@C Composites from Calculations and Experimental Analysis. ACS Applied Energy Materials, 2021, 4, 1120-1129.	2.5	15
55199	Operando Electrochemical Spectroscopy for CO on Cu(100) at pH 1 to 13: Validation of Grand Canonical Potential Predictions. ACS Catalysis, 2021, 11, 3173-3181.	5.5	6

#	Article	IF	Citations
55200	Shape-Selective Synthesis of Intermetallic Pd₃Pb Nanocrystals and Enhanced Catalytic Properties in the Direct Synthesis of Hydrogen Peroxide. ACS Catalysis, 2021, 11, 2288-2301.	5.5	27
55201	Two-Dimensional Antiferroelectric Tunnel Junction. Physical Review Letters, 2021, 126, 057601.	2.9	52
55202	Comparative computational study of antiferromagnetic and mixed-valent diamagnetic phase of AgF2: Crystal, electronic and phonon structure and p-T phase diagram. Computational Materials Science, 2021, 188, 110250.	1.4	7
55203	Identifying Metallic Transition-Metal Dichalcogenides for Hydrogen Evolution through Multilevel High-Throughput Calculations and Machine Learning. Journal of Physical Chemistry Letters, 2021, 12, 2102-2111.	2.1	43
55204	Direct band gap and strong Rashba effect in van der Waals heterostructures of InSe and Sb single layers. Journal of Physics Condensed Matter, 2021, 33, 155001.	0.7	4
55205	First-principles calculation on Î³-Fe/La2O3 interface properties and austenite refinement mechanism by La2O3. Materials Chemistry and Physics, 2021, 259, 124194.	2.0	12
55206	Enormous Valley Splitting in Monolayer WS₂ by Coupling with an Nâ€Terminated GaN Substrate. Physica Status Solidi - Rapid Research Letters, 2021, 15, 2000493.	1.2	3
55207	Nitrogen-doped char as a catalyst for wet oxidation of phenol-contaminated water. Biomass Conversion and Biorefinery, 2024, 14, 5861-5875.	2.9	4
55208	Atomicâ€Scale Visualization and Quantification of Configurational Entropy in Relation to Thermal Conductivity: A Proofâ€ofâ€Principle Study in tâ€GeSb₂Te₄. Advanced Science, 2021, 8, 2002051.	5.6	16
55209	Coexistence of fully spin-polarized Weyl nodal loop, nodal surface, and Dirac point in a family of quasi-one-dimensional half-metals. Physical Review B, 2021, 103, .	1.1	16
55210	First-principles characterization of the magnetic properties of <mml:math xmlns:mml="http://www.w3.org/1998/Math/MathML"><mml:mrow><mml:msub><mml:mi>Cu</mml:mi><mml:mn>2</mml:mn></mml: Physical Review Materials, 2021, 5, .	2.4	4
55211	Quantum Confinement Effects on Excitonic Properties in the 2D vdW quantum system: The ZnO/WSe₂ Case. Advanced Photonics Research, 2021, 2, 2000114.	1.7	5
55212	First-principles study of two-dimensional puckered and buckled honeycomb-like carbon sulfur systems. Journal of Computational Electronics, 2021, 20, 759-774.	1.3	3
55213	Electronic and Thermophysical Properties of Gas Hydrates: Ab Initio Simulation Results. Physics of the Solid State, 2021, 63, 372-376.	0.2	4
55214	High thermoelectric performance at room temperature of n-type Mg3Bi2-based materials by Se doping. Journal of Magnesium and Alloys, 2022, 10, 1024-1032.	5.5	18
55215	Electric-polarization-driven magnetic phase transition in a ferroelectricâ€“ferromagnetic heterostructure. Applied Physics Letters, 2021, 118, .	1.5	4
55216	Tripleâ€Site Dopantâ€“Defect Complexes in Mgâ€“Hâ€Codoped GaN: Firstâ€Principles Identification. Physica Status Solidi (A) Applications and Materials Science, 2021, 218, 2000723.	0.8	0
55217	Influence of extended defects on the formation energy, hyperfine structure, and zero-field splitting of NV centers in diamond. Physical Review B, 2021, 103, .	1.1	4

#	Article	IF	Citations
55218	Quantum spin Hall effect in antiferromagnetic topological heterobilayers. Physical Review B, 2021, 103, .	1.1	15
55219	Mercury exchange in zeolites Na-A and Na-Y studied by classical molecular dynamics simulations and ion exchange experiments. Microporous and Mesoporous Materials, 2021, 315, 110903.	2.2	15
55220	Deep learning-based initial guess for minimum energy path calculations. Korean Journal of Chemical Engineering, 2021, 38, 406-410.	1.2	1
55221	Nanodomain structure of single crystalline nickel oxide. Scientific Reports, 2021, 11, 3496.	1.6	12
55222	Half-metallic ferromagnetism in layered CdOHCl induced by hole doping. 2D Materials, 2021, 8, 025027.	2.0	10
55223	Colossal switchable photocurrents in topological Janus transition metal dichalcogenides. Npj Computational Materials, 2021, 7, .	3.5	27
55224	Model Studies on the Formation of the Solid Electrolyte Interphase: Reaction of Li with Ultrathin Adsorbed Ionicâ€Liquid Films and Co 3 O 4 (111) Thin Films. ChemPhysChem, 2021, 22, 441-454.	1.0	9
55225	First-Principles Study of Electronic Properties of SnO2/CsPbI2Br Interface. Journal of Electronic Materials, 2021, 50, 2129-2136.	1.0	4
55226	Type-III Weyl semimetals: <mml:math xmlns:mml="http://www.w3.org/1998/Math/MathML"><mml:mrow><mml:msub><mml:mrow><mml:mo>(</mml:mo><mml:mi mathvariant="normal">I</mml:mi></mml:mrow></mml:math>. Physical Review B, 2021, 103, .	1.1	52
55227	Topology Selectivity in On-Surface Dehydrogenative Coupling Reaction: Dendritic Structure versus Porous Graphene Nanoribbon. ACS Nano, 2021, 15, 4617-4626.	7.3	15
55228	Exotic Long-Range Surface Reconstruction on La_{0.7}Sr_{0.3}MnO₃ Thin Films. ACS Applied Materials & Interfaces, 2021, 13, 9166-9173.	4.0	6
55229	Computational scanning tunneling microscope image database. Scientific Data, 2021, 8, 57.	2.4	15
55230	IrN4 and IrN7 as potential high-energy-density materials. Journal of Chemical Physics, 2021, 154, 054706.	1.2	11
55231	Accelerating water dissociation kinetic in Co9S8 electrocatalyst by mn/N Co-doping toward efficient alkaline hydrogen evolution. International Journal of Hydrogen Energy, 2021, 46, 7989-8001.	3.8	23
55232	Unveiling oxidation mechanism of bulk ZrS2. MRS Advances, 2021, 6, 303-306.	0.5	3
55233	Effects of Hydration on the Adsorption of Benzohydroxamic Acid on the Lead-Ion-Activated Cassiterite Surface: A DFT Study. Langmuir, 2021, 37, 2205-2212.	1.6	25
55234	Direct Observation and Quantitative Analysis of Lithium Dendrite Growth by In Situ Transmission Electron Microscopy. Journal of the Electrochemical Society, 2021, 168, 020535.	1.3	11
55235	Direct observation of knock-on reaction with umbrella inversion arising from zero-impact-parameter collision at a surface. Communications Chemistry, 2021, 4, .	2.0	5

#	Article	IF	Citations
55236	Low-frequency Raman signature of Ag-intercalated few-layer MoS₂. 2D Materials, 2021, 8, 025031.	2.0	9
55237	Itinerant ferromagnetism mediated by giant spin polarization of the metallic ligand band in the van der Waals magnet <mml:math xmlns:mml="http://www.w3.org/1998/Math/MathML"><mml:mrow><mml:msub><mml:mi>Fe</mml:mi><mml:mn>5</mml:mn></mml:msub></mml:mrow></mml:math> Physical Review B, 2021, 103, .	1.1	22
55238	Modeling the high-temperature phase coexistence region of mixed transition metal oxides fromab initiocalculations. Physical Review Research, 2021, 3, .	1.3	4
55239	Layered oxygen-deficient double perovskite GdBaFe2O5+Î´ as electrode material for symmetrical solid-oxide fuel cells. Electrochimica Acta, 2021, 370, 137807.	2.6	28
55240	Correct Structural Phase Stability of FeS₂, TiO₂, and MnO₂ from a Semilocal Density Functional. Journal of Physical Chemistry C, 2021, 125, 4284-4291.	1.5	14
55241	PbSe Nanocrystals Produced by Facile Liquid Phase Exfoliation for Efficient UVâ€“Vis Photodetectors. Advanced Functional Materials, 2021, 31, 2010401.	7.8	35
55242	Structural and vibrational study of<mml:math xmlns:mml="http://www.w3.org/1998/Math/MathML"><mml:mrow><mml:mi>Zn</mml:mi><mml:msub><mml:mrow><mml:mo>(</mml:mo> high-pressure experiments and density-functional theory. Physical Review B, 2021, 103, .	1.1	19
55243	Reactions of the Li₂MnO₃ Cathode in an All-Solid-State Thin-Film Battery during Cycling. ACS Applied Materials & Interfaces, 2021, 13, 7650-7663.	4.0	13
55244	Partially Crystallized Ultrathin Interfaces between GaN and SiN_x Grown by Low-Pressure Chemical Vapor Deposition and Interface Editing. ACS Applied Materials & Interfaces, 2021, 13, 7725-7734.	4.0	3
55245	Rewritable High-Mobility Electrons in Oxide Heterostructure of Layered Perovskite/Perovskite. ACS Applied Materials & Interfaces, 2021, 13, 7812-7821.	4.0	6
55246	Preventing Superoxide Generation on Molecule-Protected CH₃NH₃PbI₃ Perovskite: A Time-Domain Ab Initio Study. Journal of Physical Chemistry Letters, 2021, 12, 1664-1670.	2.1	13
55247	Local Structural Disorder in Metavanadates MV₂O₆ (M = Zn and Cu) Synthesized by the Deep Eutectic Solvent Route: Photoactive Oxides with Oxygen Vacancies. Chemistry of Materials, 2021, 33, 1667-1682.	3.2	21
55248	Thermal Reductive Perforation of Graphene Cathode for Highâ€Performance Aluminumâ€Ion Batteries. Advanced Functional Materials, 2021, 31, 2010569.	7.8	41
55249	Uncovering the influence of Cu on the thickening and strength of the Î´â€²/Î¸â€²/Îˆâ€² nano-composite precipitate in Alâ€“Cuâ€“Li alloys. Journal of Materials Science, 2021, 56, 10092-10107.	1.7	11
55250	Thermodynamic and Kinetic Competition between Câ€“H and Oâ€“H Bond Formation Pathways during Electrochemical Reduction of CO on Copper Electrodes. ACS Catalysis, 2021, 11, 2422-2434.	5.5	20
55251	First-principles study of co-adsorption behavior of O₂ and CO₂ molecules on Î´-Pu(100) surface. Chinese Physics B, 2021, 30, 026601.	0.7	5
55252	Discovery of an Environmentally Friendly Water-Soluble Luminous Material with Interstitial Site Occupancy. ACS Sustainable Chemistry and Engineering, 2021, 9, 2717-2726.	3.2	8
55253	A comparison between Sc and Cu segregation to Al (1 0 0)/Al3Li (1 0 0) interface. Indian Journal of Physics, 2021, 95, 2009-2013.	0.9	0

#	Article	IF	Citations
55254	Effects of Solidification Cooling Rates on Microstructures and Physical Properties of Fe-6.5%Si Alloys. Acta Materialia, 2021, 205, 116575.	3.8	30
55255	Electrochemical Synthesis and Crystal Structure of the Organic Ion Intercalated Superconductor (TMA)_{0.5}Fe₂Se₂ with T_c = 43 K. Journal of the American Chemical Society, 2021, 143, 3043-3048.	6.6	21
55256	Chirality-driven topological electronic structure of DNA-like materials. Nature Materials, 2021, 20, 638-644.	13.3	83
55257	Prediction of stable BC3N2 monolayer from first-principles calculations: Stoichiometry, crystal structure, electronic and adsorption properties. Chinese Chemical Letters, 2021, 32, 3149-3154.	4.8	57
55258	Robust Surface Reconstruction Induced by Subsurface Ni/Li Antisites in Niâ€Rich Cathodes. Advanced Functional Materials, 2021, 31, 2010291.	7.8	36
55259	Expansive open Fermi arcs and connectivity changes induced by infrared phonons in <mml:math xmlns:mml="http://www.w3.org/1998/Math/MathML"><mml:mrow><mml:mi>Zr</mml:mi><mml:msub><mml:mi>Te</mml:mi> Physical Review B, 2021, 103, .	3.7	9
55260	Regulating Zn Deposition via an Artificial Solidâ€“Electrolyte Interface with Aligned Dipoles for Long Life Zn Anode. Nano-Micro Letters, 2021, 13, 79.	14.4	117
55261	Iron-Content-Dependent, Quasi-Static Dielectric Resonances and Oxidative Transitions in Bornite and Chalcopyrite Copper Iron Sulfide Nanocrystals. Chemistry of Materials, 2021, 33, 1821-1831.	3.2	17
55262	Pd single-atom monolithic catalyst: Functional 3D structure and unique chemical selectivity in hydrogenation reaction. Science China Materials, 2021, 64, 1919-1929.	3.5	75
55263	The Role of H⁺- and Cu⁺-Sites for N₂O Formation during NH₃-SCR over Cu-CHA. Journal of Physical Chemistry C, 2021, 125, 4595-4601.	1.5	28
55264	Deep moirÃ© potentials in twisted transition metal dichalcogenide bilayers. Nature Physics, 2021, 17, 720-725.	6.5	124
55265	First-principles study on Fe2B2 as efficient catalyst for nitrogen reduction reaction. Chinese Chemical Letters, 2021, 32, 3137-3142.	4.8	38
55266	Giant linear magnetoelectric effect at the morphotropic phase boundary of epitaxial <mml:math xmlns:mml="http://www.w3.org/1998/Math/MathML"><mml:mrow><mml:msub><mml:mi>Sr</mml:mi><mml:mrow> films. Physical Review B, 2021, 103, .	3.7	6
55267	Firstâ€principles exploration of MgTi 2 O 5 and MgV 2 O 5 for CO 2 capture and conversion. International Journal of Quantum Chemistry, 2021, 121, e26637.	1.0	3
55268	Fieldâ€Free Manipulation of Skyrmion Creation and Annihilation by Tunable Strain Engineering. Advanced Functional Materials, 2021, 31, 2008715.	7.8	31
55269	Electronic charge transfer during metal/SiO2 contact: Insight from density functional theory. Journal of Applied Physics, 2021, 129, .	1.1	12
55270	Comparative Study of NO and CO Oxidation Reactions on Singleâ€Atom Catalysts Anchored Grapheneâ€like Monolayer. ChemPhysChem, 2021, 22, 606-618.	1.0	6
55271	Boosting the thermoelectric performance of <mml:math xmlns:mml="http://www.w3.org/1998/Math/MathML"><mml:mrow><mml:msub><mml:mi>Fe</mml:mi><mml:mn>2</mml:mn></mml:msub> Heusler compounds by band engineering. Physical Review B, 2021, 103, .	3.7	41

#	Article	IF	Citations
55273	Electronic structures and impurity segregation around extended defects in pentacene films: first-principles study. Japanese Journal of Applied Physics, 2021, 60, SBBG05.	0.8	1
55274	Defect-mediated ab initio thermodynamics of metastable Î³-MoN(001). Journal of Chemical Physics, 2021, 154, 064703.	1.2	0
55275	Boron dangling bonds in a monolayer of hexagonal boron nitride. Journal of Applied Physics, 2021, 129, .	1.1	7
55276	Two-dimensional centrosymmetrical antiferromagnets for spin photogalvanic devices. Npj Quantum Information, 2021, 7, .	2.8	18
55277	Manipulation of electronic property of epitaxial graphene on SiC substrate by Pb intercalation. Physical Review B, 2021, 103, .	1.1	11
55278	Effect of electron transfer on metal-atom penetration into SiO₂ in electric field: first-principles study. Japanese Journal of Applied Physics, 2021, 60, 031005.	0.8	3
55279	Odd-Parity Spin-Triplet Superconductivity in Centrosymmetric Antiferromagnetic Metals. Physical Review Letters, 2021, 126, 067001.	2.9	1
55280	Superconductivity in Mo₅GeB₂ with a tetragonal structure. Superconductor Science and Technology, 2021, 34, 035030.	1.8	0
55281	Singleâ€Atom Alloys for the Electrochemical Oxygen Reduction Reaction. ChemPhysChem, 2021, 22, 499-508.	1.0	20
55282	The hydrogen-termination effect on the electronic, magnetic, and optical properties of the (001) surface of Heusler alloy ZCl3 (ZÂ=ÂLi, Na, and K). Thin Solid Films, 2021, 719, 138504.	0.8	0
55283	A Biaxial Strain Sensor Using a Single MoS2 Grating. Nanoscale Research Letters, 2021, 16, 31.	3.1	2
55284	Physical Origin of the Mechanochemical Coupling at Interfaces. Physical Review Letters, 2021, 126, 076001.	2.9	17
55285	Multishock to Quasi-Isentropic Compression of Dense Gaseous Deuterium-Helium Mixtures up to 120ÂGPa: Probing the Sound Velocities Relevant to Planetary Interiors. Physical Review Letters, 2021, 126, 075701.	2.9	6
55286	Doping and temperature-dependent UV-Vis optical constants of cubic SrTiO₃: a combined spectroscopic ellipsometry and first-principles study. Optical Materials Express, 2021, 11, 895.	1.6	7
55287	Mitigation of the internal p-n junction in <mml:math xmlns:mml="http://www.w3.org/1998/Math/MathML"><mml:mrow><mml:msub><mml:mi>CoS</mml:mi><mml:mn>2</mml:mn></mml:msub></mml:mrow></mml:math>-contacted <mml:math xmlns:mml="http://www.w3.org/1998/Math/MathML"><mml:mrow><mml:msub><mml:mi>FeS</mml:mi><mml:mn>2</mml:mn></mml:msub></mml:mrow></mml:math> single crystals: Accessing bulk semiconducting transport. Physical Review Materials, 2021, 5, .	0.9	4
55288	All-carbon-based semimetal for sodium-ion batteries anode material: A first principle study. Physics Letters, Section A: General, Atomic and Solid State Physics, 2021, 390, 127113.	0.9	8
55289	Enantioselective Effects in the Electrical Excitation of Amine Single-Molecule Rotors. Journal of Physical Chemistry C, 2021, 125, 3584-3589.	1.5	3
55290	Large-Scale Screening of Interface Parameters in the WC/W System Using Classical Force Field and First-Principles Calculations. Journal of Physical Chemistry C, 2021, 125, 3631-3639.	1.5	3

#	Article	IF	Citations
55291	Pressure-Induced Emergence of Visible Luminescence in Lead Free Halide Perovskite Cs₃Bi₂Br₉: Effect of Structural Distortion. Journal of Physical Chemistry C, 2021, 125, 3432-3440.	1.5	12
55292	Influences on Subsurface Plutonium and Americium Migration. ACS Earth and Space Chemistry, 2021, 5, 279-294.	1.2	4
55293	Hetero-Metallic Active Sites in Omega (MAZ) Zeolite-Catalyzed Methane Partial Oxidation: A DFT Study. Industrial & Engineering Chemistry Research, 2021, 60, 2400-2409.	1.8	12
55294	First-principles study on band gaps and transport properties of van der Waals WSe₂/WTe₂ heterostructure. Zeitschrift Fur Naturforschung - Section A Journal of Physical Sciences, 2021, 76, 361-370.	0.7	5
55295	Connecting experimental synthetic variables with the microstructure and electronic properties of doped ferroelectric perovskites for solar cell applications using high-throughput frameworks. Acta Materialia, 2021, 204, 116466.	3.8	4
55296	Theoretical investigation on stability and electronic properties of Janus MoSSe nanotubes for optoelectronic applications. Optik, 2021, 227, 166105.	1.4	11
55297	Efficient strain-induced light emission in lonsdaleite germanium. Physical Review Materials, 2021, 5, .	0.9	16
55298	Solvation Structure and Dynamics of Mg(TFSI)₂ Aqueous Electrolyte. Energy and Environmental Materials, 2022, 5, 295-304.	7.3	19
55299	Topological transitions to Weyl states in bulk Bi2Se3: Effect of hydrostatic pressure and doping. Journal of Applied Physics, 2021, 129, .	1.1	2
55300	Effect of doping on the GR/MoS2/GR selector: first-principle calculations. Nanotechnology, 2021, 32, 195204.	1.3	2
55301	Tuning Rashba effect, band inversion, and spin-charge conversion of Janus <mml:math xmlns:mml="http://www.w3.org/1998/Math/MathML"><mml:mrow><mml:mi>X</mml:mi><mml:msub><mml:mi>Sn</mml:mi> monolayers via an external field. Physical Review B, 2021, 103, .	1.1	48
55302	Elucidating the Structure of Bimetallic NiW/SiO₂ Catalysts and Its Consequences on Selective Deoxygenation of m-Cresol to Toluene. ACS Catalysis, 2021, 11, 2935-2948.	5.5	32
55303	Structural and magnetic properties of two-dimensional layered <mml:math xmlns:mml="http://www.w3.org/1998/Math/MathML"><mml:mrow><mml:mi>BiFe</mml:mi><mml:msub><mml:mi mathvariant="normal">O</mml:mi><mml:mn>3</mml:mn></mml:msub></mml:mrow></mml:math> from first principles. Physical Review B, 2021, 103, .	1.1	12
55304	Half-Magnetic Topological Insulator with Magnetization-Induced Dirac Gap at a Selected Surface. Physical Review X, 2021, 11, .	2.8	39
55305	Investigation into Cation-Ordered Magnetic Polar Double Perovskite Oxides. Chemistry of Materials, 2021, 33, 1594-1606.	3.2	22
55306	Structural Phase Transitions of NbO₂: Bulk versus Surface. Chemistry of Materials, 2021, 33, 1416-1425.	3.2	14
55307	A First-Principles Microkinetics for Homogeneousâ€“Heterogeneous Reactions: Application to Oxidative Coupling of Methane Catalyzed by Magnesium Oxide. ACS Catalysis, 2021, 11, 2691-2700.	5.5	20
55308	Magnetic Exchange Field Modulation of Quantum Hall Ferromagnetism in 2D van der Waals CrCl₃/Graphene Heterostructures. ACS Applied Materials & Interfaces, 2021, 13, 10656-10663.	4.0	17

#	Article	IF	Citations
55309	Splitting Dioxygen over Distant Binuclear Fe Sites in Zeolites. Effect of the Local Arrangement and Framework Topology. ACS Catalysis, 2021, 11, 2340-2355.	5.5	14
55310	B₄ Cluster-Based 3D Porous Topological Metal as an Anode Material for Both Li- and Na-Ion Batteries with a Superhigh Capacity. Journal of Physical Chemistry Letters, 2021, 12, 1548-1553.	2.1	16
55311	Two-Dimensional Carbonitride MXenes as an Efficient Electrocatalyst for Hydrogen Evolution. Journal of Physical Chemistry C, 2021, 125, 4477-4488.	1.5	13
55312	Glucose-Induced Monodisperse Iron Oxide/Graphene Oxide Catalysts for Efficient Fischerâ€“Tropsch Synthesis. Energy & Fuels, 2021, 35, 4428-4436.	2.5	3
55313	Coexisting Mechanisms for the Ferroelectric Phase Transition in Li₂SrNb₂O₇. Chemistry of Materials, 2021, 33, 1257-1264.	3.2	12
55314	Physicochemical Design Principles Enabling High-Energy and -Power Low-Cost Na Storage Materials. Journal of Physical Chemistry C, 2021, 125, 3305-3313.	1.5	6
55315	Hollow Molybdate Microspheres as Catalytic Hosts for Enhancing the Electrochemical Performance of Sulfur Cathode under High Sulfur Loading and Lean Electrolyte. Advanced Functional Materials, 2021, 31, 2010693.	7.8	57
55316	Fluorides of Silver Under Large Compression**. Chemistry - A European Journal, 2021, 27, 5536-5545.	1.7	14
55318	Oxygen Evolution and Reduction Reaction Activity Investigations on Fe, Co or Ni embedded Tetragonal Graphene by A Thermodynamical Fullâ€Łandscape Searching Scheme. ChemistryOpen, 2021, 10, 672-680.	0.9	0
55319	Edge-Propagation Discharge Mechanism in CF_x Batteriesâ€”A First-Principles and Experimental Study. Chemistry of Materials, 2021, 33, 1760-1770.	3.2	34
55320	Irradiation and Size Effects on Redox Reaction Mechanisms in Iron Oxides. Chemistry of Materials, 2021, 33, 1860-1866.	3.2	7
55321	High-entropy-stabilized chalcogenides with high thermoelectric performance. Science, 2021, 371, 830-834.	6.0	546
55322	Coherent Electronic Band Structure of TiTe₂/TiSe₂ MoirÃ© Bilayer. ACS Nano, 2021, 15, 3359-3364.	7.3	7
55323	Piezoelectric networks and ferroelectric domains in twistronic superlattices in WS₂/MoS₂ and WSe₂/MoSe₂ bilayers. 2D Materials, 2021, 8, 025030.	2.0	36
55324	Metavalent bonding induced abnormal phonon transport in diamondlike structures: Beyond conventional theory. Physical Review B, 2021, 103, .	1.1	22
55325	Strain-induced semiconductor to metal transition in <mml:math xmlns:mml="http://www.w3.org/1998/Math/MathML"><mml:mrow><mml:mi>M</mml:mi><mml:msub><mml:mi>A</mml:mi><mml:mi>		

#	Article	IF	Citations
55328	Evidence for a large Rashba splitting in PtPb4 from angle-resolved photoemission spectroscopy. Physical Review B, 2021, 103, .	1.1	3
55329	Adsorption and Diffusion of Aluminum on Î²-Ga₂O₃(010) Surfaces. ACS Applied Materials & Interfaces, 2021, 13, 10650-10655.	4.0	7
55330	Physical properties and structure characteristics of titanium-modified antimony-selenium phase change thin film. Applied Physics Letters, 2021, 118, .	1.5	12
55331	Structural phase transition in monolayer gold(I) telluride: From a room-temperature topological insulator to an auxetic semiconductor. Physical Review B, 2021, 103, .	1.1	10
55332	Magnetic crystalline-symmetry-protected axion electrodynamics and field-tunable unpinned Dirac cones in Euln2As2. Nature Communications, 2021, 12, 999.	5.8	44
55333	Atomistic Understanding of the Ferroelectric Properties of a Wurtziteâ€Structure (AlN)_n/(ScN)_m Superlattice. Physica Status Solidi - Rapid Research Letters, 2021, 15, 2100009.	1.2	14
55334	Strain-Induced Anion-Site Occupancy in Perovskite Oxyfluoride Films. Chemistry of Materials, 2021, 33, 1811-1820.	3.2	10
55335	Topological effects of phonons in GaN and AlGaN: A potential perspective for tuning phonon transport. Journal of Applied Physics, 2021, 129, .	1.1	17
55336	Nacre-like Mechanically Robust Heterojunction for Lithium-Ion Extraction. Matter, 2021, 4, 737-754.	5.0	69
55337	MoSi₂N₄ single-layer: a novel two-dimensional material with outstanding mechanical, thermal, electronic and optical properties. Journal Physics D: Applied Physics, 2021, 54, 155303.	1.3	160
55338	Spin-valley coupling in a two-dimensional <mml:math xmlns:mml="http://www.w3.org/1998/Math/MathML"><mml:mrow><mml:mi mathvariant="normal">V</mml:mi><mml:msub><mml:mi>Si</mml:mi><mml:mn>2</mml:mn></mml:msub><mml:msub><mml:mi mathvariant="normal">N</mml:mi><mml:mn>4</mml:mn></mml:msub></mml:mrow></mml:math> monolayer. Physical Review B, 2021, 103, .	1.1	114
55339	Nondegenerate Pâ€Type Inâ€Doped SnS₂ Monolayer Transistor. Advanced Electronic Materials, 2021, 7, 2001168.	2.6	13
55340	Prediction of intrinsic topological superconductivity in Mn-doped GeTe monolayer from first-principles. Npj Computational Materials, 2021, 7, .	3.5	15
55341	Theoretical study of the strain influence on lead-free bismuth-based halide perovskites. Journal of Materials Science, 2021, 56, 11377-11385.	1.7	4
55342	Charging Effects on the Adsorption and Diffusion of Au Adatoms on MgO(100). Journal of the Physical Society of Japan, 2021, 90, 034602.	0.7	4
55343	High Thermoelectric Performance in the Cubic Inorganic Cesium Iodide Perovskites CsBI₃ (B = Pb, Sn, and Ge) from First-Principles. Journal of Physical Chemistry C, 2021, 125, 6013-6019.	1.5	18
55344	Assessment of Mo2N Monolayer as Li-ion battery anodes with high cycling stability. Materials Today Communications, 2021, 26, 102100.	0.9	3
55345	First-principles analysis of phonon thermal transport properties of two-dimensional WS₂/WSe₂ heterostructures*. Chinese Physics B, 2021, 30, 034401.	0.7	13

#	Article	IF	Citations
55347	Quantum engineering of non-equilibrium efficient p-doping in ultra-wide band-gap nitrides. Light: Science and Applications, 2021, 10, 69.	7.7	42
55348	Modeling the electrical double layer at solid-state electrochemical interfaces. Nature Computational Science, 2021, 1, 212-220.	3.8	35
55349	Temperature-Induced Structural Changes in the Liquid GaInSn Eutectic Alloy. Journal of Physical Chemistry C, 2021, 125, 7413-7420.	1.5	8
55350	Interfacial molecular layering enhances specific heat of nanofluids: Evidence from molecular dynamics. Journal of Molecular Liquids, 2021, 325, 115217.	2.3	30
55351	Significantly Enhanced Overall Water Splitting Performance by Partial Oxidation of Ir through Au Modification in Coreâ€“Shell Alloy Structure. Journal of the American Chemical Society, 2021, 143, 4639-4645.	6.6	160
55352	Tunable Electrocatalytic Behavior of Sodiated MoS₂ Active Sites toward Efficient Sulfur Redox Reactions in Roomâ€Temperature Naâ€“S Batteries. Advanced Materials, 2021, 33, e2100229.	11.1	66
55353	Spectroscopic evidence for the realization of a genuine topological nodal-line semimetal in LaSbTe. Physical Review B, 2021, 103, .	1.1	28
55354	The promising thermoelectric performance of newly synthesized bulk SrCu2GeSe4 and BaCu2SnSe4 associated with superior band degeneracy. Applied Physics Express, 2021, 14, 045502.	1.1	1
55355	Accelerating the development of new solar absorbers by photoemission characterization coupled with density functional theory. JPhys Energy, 2021, 3, 032001.	2.3	2
55356	Quantification of Coulomb interactions in layered lithium and sodium battery cathode materials. Physical Review Materials, 2021, 5, .	0.9	8
55357	Observation of inverse magnetocaloric effect in magnetic-field-induced austenite phase of Heusler alloys <mml:math xmlns:mml="http://www.w3.org/1998/Math/MathML"><mml:mrow><mml:msub><mml:mi>Ni</mml:mi><mml:mrow><mml:mn>50</mml:mn></mr Physical Review Materials, 2021, 5, .	0.9	4
55358	Band structure engineering of van der Waals heterostructures using ferroelectric clamped sandwich structures. Physical Review B, 2021, 103, .	1.1	11
55359	Surface localized magnetism in transition metal doped alumina. Scientific Reports, 2021, 11, 6410.	1.6	5
55360	Structural and electronic properties of XP4(X = Ru, Os) compounds. Solid State Communications, 2021, 326, 114173.	0.9	0
55361	Dehydrogenation mechanisms of liquid organic hydrogen carriers over Pt, Pd, Rh, and Ni surfaces: Cyclohexane as a model compound. Applied Surface Science, 2021, 543, 148769.	3.1	20
55362	Crystal Structure Analysis of Top Dross in Molten Zinc Bath by First Principles Calculation and Synchrotron X-ray Diffraction. ISIJ International, 2021, 61, 929-936.	0.6	3
55363	Predicted open-framework crystal structures of sodium-silicon at high pressures. Physics Letters, Section A: General, Atomic and Solid State Physics, 2021, 392, 127146.	0.9	2
55364	The structural, electronic, elastic, dielectric, dynamical, thermal and optical properties of Janus ZrOS monolayer: A first-principles investigation. Solid State Communications, 2021, 327, 114207.	0.9	5

#	Article	IF	Citations
55365	Structural, electronic and magnetic properties of Mott insulating Y1-xLaxTiO3 from hybrid density functional calculations. Solid State Communications, 2021, 327, 114208.	0.9	0
55366	Atomic arrangement matters: band-gap variation in composition-tunable (Ga1â€“xZnx)(N1â€“xOx) nanowires. Matter, 2021, 4, 1054-1071.	5.0	14
55367	Population analysis with Wannier orbitals. Journal of Chemical Physics, 2021, 154, 104111.	1.2	3
55368	Tunable electronic properties and large optical anisotropy in the CsPbXnY3-n (X, YÂ=ÂCl, Br, I) perovskite. Solar Energy, 2021, 217, 165-172.	2.9	2
55369	Pressure-induced ferroelectric-like transition creates a polar metal in defect antiperovskites Hg3Te2X2 (Xâ€‰=â€‰Cl, Br). Nature Communications, 2021, 12, 1509.	5.8	14
55370	Quasi-One-Dimensional Fermi Surface Nesting and Hidden Nesting Enable Multiple Kohn Anomalies in <mml:math xmlns:mml="http://www.w3.org/1998/Math/MathML" display="inline"><mml:mi>Î±</mml:mi></mml:math> -Uranium. Physical Review Letters, 2021, 126, 096401.	2.9	12
55371	Superionic iron oxideâ€“hydroxide in Earthâ€™s deep mantle. Nature Geoscience, 2021, 14, 174-178.	5.4	36
55372	A molecular-level strategy to boost the mass transport of perovskite electrocatalyst for enhanced oxygen evolution. Applied Physics Reviews, 2021, 8, .	5.5	20
55373	Current-Driven Domain Wall Dynamics in Ferrimagnetic Nickel-Doped Mn₄N Films: Very Large Domain Wall Velocities and Reversal of Motion Direction across the Magnetic Compensation Point. Nano Letters, 2021, 21, 2580-2587.	4.5	48
55374	Diamond(001)â€“Si(001) and Si(001)â€“Ti(0001) interfaces: A density functional theory study. Journal of Physics and Chemistry of Solids, 2021, 150, 109865.	1.9	4
55375	Microstructure â€“ electron work function relationship: A crucial step towards â€œelectronic metallurgyâ€• Materials Today Communications, 2021, 26, 101977.	0.9	2
55376	Calcium decoration of boron nitride nanotubes with vacancy defects as potential hydrogen storage materials: A first-principles investigation. Materials Today Communications, 2021, 26, 101985.	0.9	9
55377	Itinerant magnetism in the half-metallic Heusler compound <mml:math xmlns:mml="http://www.w3.org/1998/Math/MathML"><mml:msub><mml:mi mathvariant="normal">Co</mml:mi><mml:mn>2</mml:mn></mml:msub><mml:mi mathvariant="normal">HfSn</mml:mi></mml:math> : Evidence from critical behavior combined with first-principles calculations. Physical Review B, 2021, 103, .	1.1	11
55378	Electronic and Topological Properties of Ultraflat Stanene Functionalized by Hydrogen and Halogen Atoms. Journal of Electronic Materials, 2021, 50, 3334-3340.	1.0	9
55379	Hole Dopants Disentangling Peierlsâ€“Mott Relevance States of VO₂ by First-Principles Calculation. Journal of Physical Chemistry C, 2021, 125, 5816-5823.	1.5	13
55380	Identification of structural phases in ferroelectric hafnium zirconium oxide by density-functional-theory-assisted EXAFS analysis. Applied Physics Letters, 2021, 118, .	1.5	6
55381	Ab initio molecular dynamics simulation of the structural and electronic properties of aluminoborosilicate glass. Journal of the American Ceramic Society, 2021, 104, 3198-3211.	1.9	8
55382	Realization of a tunable surface Dirac gap in Sb-doped <mml:math xmlns:mml="http://www.w3.org/1998/Math/MathML"><mml:mrow><mml:msub><mml:mi>MnBi</mml:mi><mml:mn>2</mml:mn></mml:msub><mml:mn> Physical Review B, 2021, 103, .	1.1	27

#	Article	IF	Citations
55383	Discovery of a weak topological insulating state and van Hove singularity in triclinic RhBi2. Nature Communications, 2021, 12, 1855.	5.8	15
55384	Topology conversion of 1T MoS2 to S-doped 2H-MoTe2 nanosheets with Te vacancies for enhanced electrocatalytic hydrogen evolution. Science China Materials, 2021, 64, 2202-2211.	3.5	19
55385	First principles study of small hole polaron formation in doped olivine LiFe1â^'Co PO4: Effects of Li deficiency. Materials Today Communications, 2021, 26, 102043.	0.9	1
55386	Ab initio investigations of the interfacial bond of Fe(001)/Al(001). Materials Today Communications, 2021, 26, 102107.	0.9	3
55387	Paramagnetism of carbyne nanocrystals. Materials Today Communications, 2021, 26, 102152.	0.9	1
55388	Prediction of massless Dirac fermions in a carbon nitride covalent network. Applied Physics Letters, 2021, 118, .	1.5	6
55389	Solvent engineered synthesis of layered SnO for high-performance anodes. Npj 2D Materials and Applications, 2021, 5, .	3.9	11
55390	Effect of alloying on stability of grain boundary in Î³ phase of the Uâ€“Mo and Uâ€“Nb systems. Calphad: Computer Coupling of Phase Diagrams and Thermochemistry, 2021, 72, 102241.	0.7	7
55391	Ultralong-Lifespan Magnesium Batteries Enabled by the Synergetic Manipulation of Oxygen Vacancies and Electronic Conduction. ACS Applied Materials & Interfaces, 2021, 13, 12049-12058.	4.0	11
55392	Extrinsic Photoluminescence and Resonant Raman Spectra of CsPb₂Br₅ Microspheres. Journal of Physical Chemistry C, 2021, 125, 6767-6772.	1.5	9
55393	Atomic-Step Enriched Rutheniumâ€“Iridium Nanocrystals Anchored Homogeneously on MOF-Derived Support for Efficient and Stable Oxygen Evolution in Acidic and Neutral Media. ACS Catalysis, 2021, 11, 3402-3413.	5.5	87
55394	Efficient Photoexcited Charge Separation at the Interface of a Novel 0D/2D Heterojunction: A Time-Dependent Ultrafast Dynamic Study. Journal of Physical Chemistry Letters, 2021, 12, 2312-2319.	2.1	23
55395	Pressure effect on band inversion in AECd2As2 (AE=Ca,ÂSr,ÂBa). Physical Review B, 2021, 103, .	1.1	6
55396	Theoretical investigation of the intercalation mechanism of VS2/MXene heterostructures as anode materials for metal-ion batteries. Applied Surface Science, 2021, 543, 148772.	3.1	43
55397	Switchable Enhanced Spin Photocurrent in Rashba and Cubic Dresselhaus Ferroelectric Semiconductors. Nano Letters, 2021, 21, 2265-2271.	4.5	15
55398	Structural Evolution and Underlying Mechanism of Single-Atom Centers on Mo2C(100) Support during Oxygen Reduction Reaction. ACS Applied Materials & Interfaces, 2021, 13, 17075-17084.	4.0	4
55399	High-Throughput Screening of Nitrogen-Coordinated Bimetal Catalysts for Multielectron Reduction of CO₂ to CH₄ with High Selectivity and Low Limiting Potential. Journal of Physical Chemistry C, 2021, 125, 7155-7165.	1.5	36
55400	A comparison of the mixing thermodynamics of the antifluorite-structured Mg2Si1â^'xGex, Mg2Sn1â^'xGex and Mg2Si1â^'xSnx alloys from first principles. Vacuum, 2021, 185, 110018.	1.6	2

#	Article	IF	Citations
55401	CO₂ Adsorption Properties of a N,N-Diethylethylenediamine-Appended M₂(dobpdc) Series of Materials and Their Detailed Microprocess. Crystal Growth and Design, 2021, 21, 2474-2480.	1.4	9
55402	Ab Initio Molecular Dynamics Simulations of Amorphous Calcium Carbonate: Interpretation of Pair Distribution Function and X-ray Absorption Spectroscopy Data. Crystal Growth and Design, 2021, 21, 2212-2221.	1.4	10
55403	Balancing Cost and Accuracy in Quantum Mechanical Simulations on Collagen Protein Models. Journal of Chemical Theory and Computation, 2021, 17, 2566-2574.	2.3	9
55404	Size and Stoichiometry Effects on the Reactivity of MoC_y Nanoparticles toward Ethylene. Journal of Physical Chemistry C, 2021, 125, 6287-6297.	1.5	5
55405	Crystal and Electronic Structures of Palladium Sesquichalcogenides. Chemistry of Materials, 2021, 33, 2298-2306.	3.2	5
55406	Lithium Thiostannate Spinels: Air-Stable Cubic Semiconductors. Chemistry of Materials, 2021, 33, 2080-2089.	3.2	6
55407	Complex Structure of Molten NaClâ€“CrCl₃ Salt: Crâ€“Cl Octahedral Network and Intermediate-Range Order. ACS Applied Energy Materials, 2021, 4, 3044-3056.	2.5	14
55408	Electronic structures of trivalent cations doped bulk and cubic La2Mo2O9 oxide ion conductors. Journal of Solid State Chemistry, 2021, 295, 121918.	1.4	2
55409	Comparative study of half-metallic ferromagnetic behaviour in ZnO monolayer doped with boron and carbon atoms. International Nano Letters, 2021, 11, 113.	2.3	3
55410	First-Principles Prediction of Two-Dimensional B₃C₂P₃ and B₂C₄P₂: Structural Stability, Fundamental Properties, and Renewable Energy Applications. Journal of Physical Chemistry Letters, 2021, 12, 3436-3442.	2.1	34
55411	Single WTe₂ Sheet-Based Electrocatalytic Microdevice for Directly Detecting Enhanced Activity of Doped Electronegative Anions. ACS Applied Materials & Interfaces, 2021, 13, 14302-14311.	4.0	15
55412	Mechanical and electronic properties of CeO2 under uniaxial tensile loading: A DFT study. Materialia, 2021, 15, 101050.	1.3	14
55413	High-throughput screening of transition metal single-atom catalyst anchored on Janus MoSSe basal plane for hydrogen evolution reaction. International Journal of Hydrogen Energy, 2021, 46, 10337-10345.	3.8	30
55414	Improvement of the catalytic properties of porous lanthanum manganite for the oxygen reduction reaction by partial substitution of strontium for lanthanum. Electrochemistry Communications, 2021, 124, 106964.	2.3	41
55415	Tuning topological phases and electronic properties of monolayer ternary transition metal chalcogenides (ABX4, A/B = Zr, Hf, or Ti; X = S, Se, or Te). Applied Physics Letters, 2021, 118, .	1.5	16
55416	A Highly Efficient and Stable Photocatalyst; N-Doped ZnO/CNT Composite Thin Film Synthesized via Simple Sol-Gel Drop Coating Method. Molecules, 2021, 26, 1470.	1.7	23
55417	Structural Modulation from Cu₃PS₄ to Cu₅Zn_{0.5}P₂S₈: Single-Site Aliovalent-Substitution-Driven Second-Harmonic-Generation Enhancement. Inorganic Chemistry, 2021, 60, 4357-4361.	1.9	11
55418	p-type transparent conducting oxide: Doping of bismuth-alloyed<mml:math xmlns:mml="http://www.w3.org/1998/Math/MathML"><mml:mrow><mml:msub><mml:mi>Ga</mml:mi><mml:mn>2</mml:mn></mml:msub><mml:mathvariant="normal">O</mml:mi><mml:mn>3</mml:mn></mml:msub></mml:mrow></mml:math>with a strongly correlated band edge state. Physical Review B, 2021, 103, .	1.1	24

#	Article	IF	Citations
55419	Tin Alloying Enhances Catalytic Selectivity of Copper Surface: A Mechanistic Study Based on First-Principles Calculations. Journal of Physical Chemistry Letters, 2021, 12, 3031-3037.	2.1	4
55420	Magnetically driven short-range order can explain anomalous measurements in CrCoNi. Proceedings of the National Academy of Sciences of the United States of America, 2021, 118, .	3.3	56
55421	Discovery of NLO Semiorganic (C₅H₆ON)⁺(H₂PO₄)^{â^'}: Dipole Moment Modulation and Superior Synergy in Solar-Blind UV Region. Journal of the American Chemical Society, 2021, 143, 3647-3654.	6.6	99
55422	Coherent electric field manipulation of Fe ³⁺ spins in PbTiO ₃. Science Advances, 2021, 7, .	4.7	17
55423	Interfacial superstructures and chemical bonding transitions at metal-ceramic interfaces. Science Advances, 2021, 7, .	4.7	24
55424	Multiâ€Phase Heterostructure of CoNiP/Co_xP for Enhanced Hydrogen Evolution Under Alkaline and Seawater Conditions by Promoting H₂O Dissociation. Small, 2021, 17, e2007557.	5.2	83
55425	Synthesis of borophane polymorphs through hydrogenation of borophene. Science, 2021, 371, 1143-1148.	6.0	129
55426	Controllable Approach to Carbonâ€Deficient and Oxygenâ€Doped Graphitic Carbon Nitride: Robust Photocatalyst Against Recalcitrant Organic Pollutants and the Mechanism Insight. Advanced Functional Materials, 2021, 31, 2010763.	7.8	135
55427	Density Functional Theory Studies on Sulfurâ€“Polyacrylonitrile as a Cathode Host Material for Lithiumâ€“Sulfur Batteries. ACS Omega, 2021, 6, 9700-9708.	1.6	11
55428	Accelerated Discovery of Zeolite Structures with Superior Mechanical Properties via Active Learning. Journal of Physical Chemistry Letters, 2021, 12, 2334-2339.	2.1	16
55429	Thermoelectric and mechanical properties of XHfSn (X=Ni, Pd and Pt) semiconducting Half-heusler alloys: A first-principles study. Computational Condensed Matter, 2021, 26, e00539.	0.9	13
55430	Spin-lattice model for cubic crystals. Physical Review B, 2021, 103, .	1.1	15
55431	Three-Dimensionally Interconnected Nanoporous IrRe Thin Films Prepared by Selective Etching of Re for Oxygen Evolution Reaction. ACS Applied Energy Materials, 2021, 4, 4173-4180.	2.5	8
55432	Direct Optoelectronic Imaging of 2D Semiconductorâ€“3D Metal Buried Interfaces. ACS Nano, 2021, 15, 5618-5630.	7.3	35
55433	Coffee ground derived biochar embedded Ov-NiCoO2 nanoparticles for efficiently catalyzing a boronâ€“hydrogen bond break. Science of the Total Environment, 2021, 761, 144192.	3.9	8
55434	Tunable double Weyl phonons driven by chiral point group symmetry. Physical Review B, 2021, 103, .	1.1	22
55435	Highly Active Ir/In₂O₃ Catalysts for Selective Hydrogenation of CO₂ to Methanol: Experimental and Theoretical Studies. ACS Catalysis, 2021, 11, 4036-4046.	5.5	108
55436	D-<mml:math xmlns:mml="http://www.w3.org/1998/Math/MathML" altimg="si16.svg"><mml:mrow><mml:mi>Ï€</mml:mi></mml:mrow></mml:math>-A dye attached on TiO2(101) and TiO2(001) surfaces: Electron transfer properties from ab initio calculations. Solar Energy, 2021, 216, 266-273.	2.9	13

#	Article	IF	Citations
55437	Leaf-inspired design of mesoporous Sb2S3/N-doped Ti3C2Tx composite towards fast sodium storage. Science China Chemistry, 2021, 64, 964-973.	4.2	50
55438	Reaction pathways in the solid state and the Hubbard U correction. Journal of Chemical Physics, 2021, 154, 124121.	1.2	6
55439	Uracil-Doped Graphitic Carbon Nitride for Enhanced Photocatalytic Performance. ACS Applied Materials & Interfaces, 2021, 13, 12118-12130.	4.0	27
55440	Rolling the WSSe Bilayer into Double-Walled Nanotube for the Enhanced Photocatalytic Water-Splitting Performance. Nanomaterials, 2021, 11, 705.	1.9	15
55441	Controlling the Formation of Sodium/Black Phosphorus IntercalationCompounds Towards High Sodium Content. Batteries and Supercaps, 2021, 4, 1304-1309.	2.4	3
55442	First-principles investigation on the photovoltaic properties of lead free earth abundant (CH3NH3)2SnI6 perovskite. Journal of Applied Physics, 2021, 129, 125701.	1.1	1
55443	Zn content mediated fibrinogen adsorption on biodegradable Mg-Zn alloys surfaces. Journal of Magnesium and Alloys, 2021, 9, 2145-2154.	5.5	8
55444	Atomistic insights into lithium adsorption and migration on phosphorusâ€doped graphene. International Journal of Quantum Chemistry, 2021, 121, e26659.	1.0	6
55445	Enhanced catalytic conversion of polysulfides using high-percentage 1T-phase metallic WS2 nanosheets for Liâ€“S batteries. Green Energy and Environment, 2022, 7, 1340-1348.	4.7	14
55446	Elucidating the electro-catalytic oxidation of hydrazine over carbon nanotube-based transition metal single atom catalysts. Nano Research, 2021, 14, 4650-4657.	5.8	23
55447	Effect of Monovalent Metal Iodide Additives on the Optoelectric Properties of Two-Dimensional Sn-Based Perovskite Films. Chemistry of Materials, 2021, 33, 2498-2505.	3.2	28
55448	Coexistence of Ferroelectricity and Ferromagnetism in One-Dimensional SbN and BiN Nanowires. ACS Applied Materials & Interfaces, 2021, 13, 13517-13523.	4.0	18
55449	Stacking Order Effects on the Electronic and Optical Properties of Graphene/Transition Metal Dichalcogenide Van der Waals Heterostructures. ACS Applied Electronic Materials, 2021, 3, 1671-1680.	2.0	12
55450	Nanoporous Silver Telluride for Active Hydrogen Evolution. ACS Nano, 2021, 15, 6540-6550.	7.3	10
55451	Orientation-dependent mechanical response of graphene/BN hybrid nanostructures. Nanotechnology, 2021, 32, 235703.	1.3	8
55452	AZn(PO₃)₃ (A = K, Rb): Deep-Ultraviolet Nonlinear Optical Phosphates Derived from Synergy of a Unique [ZnO₆] Octahedron and a [PO₃]_{â^ž} Chain. Crystal Growth and Design, 2021, 21, 2445-2452.	1.4	15
55453	Nitrogen Hydrate Cage Occupancy and Bulk Modulus Inferred from Density Functional Theory-Derived Cell Parameters. Journal of Physical Chemistry C, 2021, 125, 6433-6441.	1.5	3
55454	Hot Hole Cooling and Transfer Dynamics from Lead Halide Perovskite Nanocrystals Using Porphyrin Molecules. Journal of Physical Chemistry C, 2021, 125, 5859-5869.	1.5	37

#	Article	IF	Citations
55455	Organic Functionalization at the Si(001) Dimer Vacancy Defectâ€"Structure, Bonding, and Reactivity. Journal of Physical Chemistry C, 2021, 125, 5635-5646.	1.5	4
55456	Experimental and Theoretical Study of the Electronic Structures of Lanthanide Indium Perovskites LnInO₃. Journal of Physical Chemistry C, 2021, 125, 6387-6400.	1.5	11
55457	Two Lead Halides with Strong SHG Response Obtained by the Isovalent Substitutions of Alkali Metal Cation and Halogen Anion. Inorganic Chemistry, 2021, 60, 5290-5296.	1.9	14
55458	Unveiling The Effect of Dopants on the Hydration Reaction and Proton Conduction of Nd and Y Co-Doped BaZrO3 in Solid Oxide Fuel Cells. Journal of the Electrochemical Society, 2021, 168, 034517.	1.3	7
55459	Semiconductor-to-metal transition in bilayer MoSi2N4 and WSi2N4 with strain and electric field. Applied Physics Letters, 2021, 118, .	1.5	65
55460	Detailed structural, mechanical, and electronic study of five structures for CaF2 under high pressure*. Chinese Physics B, 2021, 30, 030502.	0.7	2
55461	Polarization-resolved Raman spectra of Î±-PtO2 *. Chinese Physics B, 2021, 30, 047102.	0.7	2
55462	First-principles study on growth mechanism of TiN on MgO (1 0 0) and (1 1 0) surfaces. Computational Materials Science, 2021, 189, 110257.	1.4	5
55463	Isothermal conversion of methane to methanol over CuxOy@UiO-bpy. Materials Today Sustainability, 2021, 11-12, 100061.	1.9	9
55464	The effect of vacancy defect on quantum capacitance, electronic and magnetic properties of <scp>Sc₂CF₂</scp> monolayer. International Journal of Quantum Chemistry, 2021, 121, e26666.	1.0	4
55465	Trimeron-phonon coupling in magnetite. Physical Review B, 2021, 103, .	1.1	8
55466	Impact of point defects on the electrical properties of selenium: A density functional theory investigation with discussion of the entropic term. Physical Review B, 2021, 103, .	1.1	7
55467	Design principles and physical properties of two-dimensional heterostructured borides. Physical Review Materials, 2021, 5, .	0.9	2
55468	Effect of atom substitutions on the magnetic properties in Ce2Fe17: Toward permanent magnet applications. Journal of Applied Physics, 2021, 129, 103902.	1.1	4
55469	Hund's physics and the magnetic ground state of<mml:math xmlns:mml="http://www.w3.org/1998/Math/MathML"><mml:mrow><mml:mi>CrO</mml:mi><mml:mi>X</mml:mi></mml:mrow></mml xmlns:mml="http://www.w3.org/1998/Math/MathML"><mml:mo>(</mml:mo><mml:mrow><mml:mi>X</mml:mi><mml:mo>) Physical Review Materials, 2021, 5, .	0.9	9
55470	Large transport gap modulation in graphene via electric-field-controlled reversible hydrogenation. Nature Electronics, 2021, 4, 254-260.	13.1	19
55471	Thermomechanical Manipulation of Electric Transport in MoTe 2. Advanced Electronic Materials, 2021, 7, 2000823.	2.6	5
55472	The Jahn-Teller Effect for Amorphization of Molybdenum Trioxide towards High-Performance Fiber Supercapacitor. Research, 2021, 2021, 6742715.	2.8	14

#	Article	IF	Citations
55473	<scp>BSSEâ€corrected</scp> consistent Gaussian basis sets of <scp>tripleâ€zeta</scp> valence with polarization quality of the sixth period for <scp>solidâ€state</scp> calculations. Journal of Computational Chemistry, 2021, 42, 1064-1072.	1.5	24
55474	Magnetic, Electronic, and Optical Properties of the Tetraborates NiB4O7 and CoB4O7 in Three Structural Modifications. Physics of the Solid State, 2021, 63, 468-476.	0.2	2
55475	Novel Facile Oneâ€Pot Synthesis of Bi₂S₃â^'BiOCl Ultrathin Heteroâ€nanosheets for Selective Alcohol Oxidation. ChemCatChem, 2021, 13, 2293-2302.	1.8	11
55476	High Charge-Storage Performance of Morphologically Modified Anatase TiO 2 : Experimental and Theoretical Insight. Physical Review Applied, 2021, 15, .	1.5	6
55477	Ni Doping: A Viable Route to Make Body-Centered-Cubic Fe Stable at Earthâ€™s Inner Core. Minerals (Basel,) Tj ETQq0 0 0 rgBT /Overloc	0.8	7
55478	Computational Study of Solute Effects in Tungsten under Irradiation. Materials Science Forum, 0, 1024, 87-94.	0.3	1
55479	Interplay between multipolar spin interactions, Jahn-Teller effect, and electronic correlation in a <mml:math xmlns:mml="http://www.w3.org/1998/Math/MathML"><mml:mrow><mml:msub><mml:mi>J</mml:mi><mml:mtext>eff</mml:mtext></ insulator. Physical Review B, 2021, 103, .	1.1	14
55480	Ab initio study of the behavior of helium in different Erbium hydrides. Materials Today Communications, 2021, 26, 102039.	0.9	0
55481	Electronic, optical properties and stress-driven modulation of monolayer MNb3O8 (Mâ€¯=â€¯H,Li,Na,K): An ab-initio investigation. Materials Today Communications, 2021, 26, 101867.	0.9	2
55482	Thermoelectric performance of BaBiNa and SrBiNa: A first-principle study. Materials Today Communications, 2021, 26, 101971.	0.9	3
55483	Monolayer Fe₃GeX₂ (X = S, Se, and Te) as Highly Efficient Electrocatalysts for Lithiumâ€“Sulfur Batteries. ACS Applied Materials & Interfaces, 2021, 13, 11845-11851.	4.0	45
55484	The electronic structures, elastic constants, dielectric permittivity, phonon spectra, thermal properties and optical response of monolayer zirconium dioxide: A first-principles study. Thin Solid Films, 2021, 721, 138549.	0.8	7
55485	Solute segregation induced stabilizing and strengthening effects on Ni Î£3 [110](111) symmetrical tilt grain boundary in nickel-based superalloys. Journal of Materials Research and Technology, 2021, 11, 1281-1289.	2.6	18
55486	Nodeless kagome superconductivity in <mml:math xmlns:mml="http://www.w3.org/1998/Math/MathML"><mml:mrow><mml:msub><mml:mi>LaRu</mml:mi><mml:mn>3</mml:mn></ Physical Review Materials, 2021, 5, .	0.9	37
55487	Ultralow Lattice Thermal Conductivity and Superhigh Thermoelectric Figureâ€ofâ€Merit in (Mg, Bi) Coâ€Doped GeTe. Advanced Materials, 2021, 33, e2008773.	11.1	112
55488	High intrinsic lattice thermal conductivity in monolayer MoSi₂N₄. New Journal of Physics, 2021, 23, 033005.	1.2	74
55489	Enlisting Potential Cathode Materials for Rechargeable Ca Batteries. Chemistry of Materials, 2021, 33, 2488-2497.	3.2	20
55490	Revealing the Underlying Mechanisms of the Stacking Order and Interlayer Magnetism of Bilayer CrBr₃. Journal of Physical Chemistry C, 2021, 125, 7314-7320.	1.5	16

#	Article	IF	Citations
55491	Band Gap as a Novel Descriptor for the Reactivity of 2D Titanium Dioxide and its Supported Pt Single Atom for Methane Activation. Journal of Physical Chemistry Letters, 2021, 12, 2484-2488.	2.1	8
55492	Pressure effect of the mechanical, electronics and thermodynamic properties of Mgâ€“B compounds A first-principles investigations. Scientific Reports, 2021, 11, 6096.	1.6	5
55493	Narrowing Bandgap of HfS₂ by Te Substitution for Shortâ€Wavelength Infrared Photodetection. Advanced Optical Materials, 2021, 9, 2002248.	3.6	17
55494	Fluoridation of HfO2. Inorganic Chemistry, 2021, 60, 4463-4474.	1.9	7
55495	Direct identification of Mott Hubbard band pattern beyond charge density wave superlattice in monolayer 1T-NbSe2. Nature Communications, 2021, 12, 1978.	5.8	45
55496	Defect states and passivation mechanism at grain boundaries of zinc-blende semiconductors. Semiconductor Science and Technology, 2021, 36, 045028.	1.0	2
55497	Thermodynamics of boron incorporation in BGaN. Physical Review Materials, 2021, 5, .	0.9	10
55498	Computer simulations for the adsorption and separation of CH4/H2/CO2/N2 gases by hybrid ultramicroporous materials. Materials Today Communications, 2021, 26, 101987.	0.9	4
55499	Structural modelling and mechanical behaviors of graphene/carbon nanotubes reinforced metal matrix composites via atomic-scale simulations: A review. Composites Part C: Open Access, 2021, 4, 100120.	1.5	11
55500	Polarization Dependent Bulk-sensitive Valence Band Photoemission Spectroscopy and Density Functional Theory Calculations: Part II. 4d Transition Metals. Journal of the Physical Society of Japan, 2021, 90, 034706.	0.7	2
55501	Spin transport properties in Dirac spin gapless semiconductors Cr2X3 with high Curie temperature and large magnetic anisotropic energy. Applied Physics Letters, 2021, 118, .	1.5	23
55502	Interactions between cadmium and Al3Li precipitates: A new mechanism of accelerating dissolution and transformation of phases in Alâ€“Liâ€“Cu alloy. Materials Science & Engineering A: Structural Materials: Properties, Microstructure and Processing, 2021, 806, 140607.	2.6	5
55503	Molecular dynamics study on the coâ€doping effect of Al₂O₃ and fluorine to reduce Rayleigh scattering of silica glass. Journal of the American Ceramic Society, 2021, 104, 5001-5015.	1.9	13
55504	From triple-point materials to multiband nodal links. Physical Review B, 2021, 103, .	1.1	28
55505	Concentric Approximation for Fast and Accurate Numerical Evaluation of Nonadiabatic Coupling with Projector Augmented-Wave Pseudopotentials. Journal of Physical Chemistry Letters, 2021, 12, 3082-3089.	2.1	41
55506	Implications of doping on microstructure, processing, and thermoelectric performance: The case of PbSe. Journal of Materials Research, 2021, 36, 1272-1284.	1.2	8
55507	Potential-Dependent Mechanistic Study of Ethanol Electro-oxidation on Palladium. ACS Applied Materials & Interfaces, 2021, 13, 16602-16610.	4.0	20
55508	High-Throughput Ab Initio Investigation of the Elastic Properties of Inorganic Electrolytes for All-Solid-State Na-Ion Batteries. Journal of the Electrochemical Society, 2021, 168, 030541.	1.3	8

#	Article	IF	Citations
55509	Anisotropic Janus SiP₂ Monolayer as a Photocatalyst for Water Splitting. Journal of Physical Chemistry Letters, 2021, 12, 2464-2470.	2.1	49
55510	Perovskite Lightâ€Emitting Diodes with Near Unit Internal Quantum Efficiency at Low Temperatures. Advanced Materials, 2021, 33, e2006302.	11.1	16
55511	Deep potential generation scheme and simulation protocol for the Li10GeP2S12-type superionic conductors. Journal of Chemical Physics, 2021, 154, 094703.	1.2	49
55512	Acidity and Local Confinement Effect in Mordenite Probed by Solid-State NMR Spectroscopy. Journal of Physical Chemistry Letters, 2021, 12, 2413-2422.	2.1	17
55513	Switchable two-dimensional electrides: A first-principles study. Physical Review B, 2021, 103, .	1.1	9
55514	Tunable electronic properties of two-dimensional type-I 1T-SN2/hBN and type-II 1T-XN2/hBN (XÂ=ÂSe, Te) van der Waals heterostructures from first-principle study. Applied Surface Science, 2021, 542, 148659.	3.1	6
55515	Adsorption and Activation of CO₂ on Small-Sized Cuâ€“Zr Bimetallic Clusters. Journal of Physical Chemistry A, 2021, 125, 2558-2572.	1.1	25
55516	Rapid Charge Separation Boosts Solar Hydrogen Generation at the Grapheneâ€“MoS₂ Junction: Time-Domain Ab Initio Analysis. Journal of Physical Chemistry Letters, 2021, 12, 2763-2769.	2.1	16
55517	Stabilization of 3-D trigonal phase in guanidinium (C(NH2)3) lead triiodide (GAPbI3) films. Applied Surface Science, 2021, 542, 148575.	3.1	12
55518	Structural and electronic properties of C60 fullerene network self-assembled on metal-covered semiconductor surfaces. Journal of Chemical Physics, 2021, 154, 104703.	1.2	4
55519	Increasing electrocatalytic nitrate reduction activity by controlling adsorption through PtRu alloying. Journal of Catalysis, 2021, 395, 143-154.	3.1	94
55520	Thermal conductivity and enhanced thermoelectric performance of SnTe bilayer. Journal of Materials Science, 2021, 56, 10424-10437.	1.7	11
55521	Ni nanoparticles on active (001) facet-exposed rutile TiO2 nanopyramid arrays for efficient hydrogen evolution. Applied Catalysis B: Environmental, 2021, 282, 119548.	10.8	40
55522	First-principles modeling of plasmons in aluminum under ambient and extreme conditions. Physical Review B, 2021, 103, .	1.1	28
55523	Disclosure of charge storage mechanisms in molybdenum oxide nanobelts with enhanced supercapacitive performance induced by oxygen deficiency. Rare Metals, 2021, 40, 2447-2454.	3.6	36
55524	Structures of bulk hexagonal post transition metal chalcogenides from dispersion-corrected density functional theory. Physical Review B, 2021, 103, .	1.1	6
55525	Fast and Accurate Machine Learning Strategy for Calculating Partial Atomic Charges in Metalâ€“Organic Frameworks. Journal of Chemical Theory and Computation, 2021, 17, 3052-3064.	2.3	53
55526	Ultrahigh Thermal Conductivity of <mml:math xmlns:mml="http://www.w3.org/1998/Math/MathML" display="inline"><mml:mi>Î¸</mml:mi></mml:math> -Phase Tantalum Nitride. Physical Review Letters, 2021, 126, 115901.	2.9	46

#	Article	IF	Citations
55527	Transient birefringence and dichroism in ZnO studied with fs-time-resolved spectroscopic ellipsometry. Physical Review Research, 2021, 3, .	1.3	8
55528	Decisive role of interstitial defects in half-Heusler semiconductors: An ab initio study. Physical Review Materials, 2021, 5, .	0.9	6
55529	Band engineering of honeycomb monolayer CuSe via atomic modification*. Chinese Physics B, 2021, 30, 106807.	0.7	1
55530	Optical emission enhancement of bent InSe thin films. Science China Information Sciences, 2021, 64, 1.	2.7	6
55531	Effects of water on the kinetics of acetone hydrogenation over Pt and Ru catalysts. Journal of Catalysis, 2021, 403, 215-227.	3.1	10
55532	Impact of Orientation Misalignments on Black Phosphorus Ultrascaled Field-Effect Transistors. IEEE Electron Device Letters, 2021, 42, 434-437.	2.2	4
55533	Current State-of-the-art In-house and Cloud-Based Applications of Virtual Polymorph Screening of Pharmaceutical Compounds: A Challenging Case ofAZD1305. Crystal Growth and Design, 2021, 21, 1972-1983.	1.4	17
55534	Realization of AlSb in the Double-Layer Honeycomb Structure: A Robust Class of Two-Dimensional Material. ACS Nano, 2021, 15, 8184-8191.	7.3	20
55535	Relating Gain Degradation to Defects Production in Neutron-Irradiated 4H-SiC Transistors. IEEE Transactions on Nuclear Science, 2021, 68, 312-317.	1.2	6
55536	Lowâ€Temperature Growth of Highâ€Quality Ag₂HgS₂ Crystals for Setup of Weakâ€Light UVâ€“Visibleâ€“NIR Photodetectors. Advanced Optical Materials, 2021, 9, 2002080.	3.6	3
55537	Microscopic Kinetics Pathway of Salt Crystallization in Graphene Nanocapillaries. Physical Review Letters, 2021, 126, 136001.	2.9	22
55538	Ab initio molecular dynamics studies on the ignition and combustion mechanisms, twice exothermic characteristics, and mass transport properties of Al/NiO nanothermite. Journal of Materials Science, 2021, 56, 11364-11376.	1.7	4
55539	High temperature stability, metallic character and bonding of the Si2BN planar structure. Journal of Physics Condensed Matter, 2021, 33, 165001.	0.7	2
55540	Transition metal doped C3N monolayer as efficient electrocatalyst for carbon dioxide electroreduction: A computational study. Applied Surface Science, 2021, 542, 148568.	3.1	14
55541	Structural, mechanical, electronic properties, and Debye temperature of quaternary carbide Ti₃NiAl₂C ceramics under high pressure: A first-principles study*. Chinese Physics B, 2021, 30, 036202.	0.7	1
55542	Hierarchical thermal transport mechanisms in Yb2Si2O7 multifunctional thermal and environmental barrier coating (TEBC) material. Scripta Materialia, 2021, 194, 113704.	2.6	5
55543	The interactions between nitrogen oxides and Î±-uranium surface. Nuclear Materials and Energy, 2021, 26, 100945.	0.6	0
55544	Strong valley splitting in d 0 two-dimensional SnO induced by magnetic proximity effect. Nanotechnology, 2021, 32, 225201.	1.3	1

#	Article	IF	Citations
55545	Dipole-assisted carrier transport in bis(trifluoromethane) sulfonamide-treated O-ReS2 field-effect transistor. Nano Research, 2021, 14, 2207-2214.	5.8	2
55546	First-principles study of cubic alkaline-earth metal zirconate perovskites. Journal of Physics Communications, 2021, 5, 035006.	0.5	9
55547	Lattice and electronic properties of VO$$_2$$ with the SCAN(+U) approach. Journal of the Korean Physical Society, 2021, 78, 613-617.	0.3	5
55549	Intensity and wavelength dependence of anisotropic nonlinear absorption inside MgO. Optical and Quantum Electronics, 2021, 53, 1.	1.5	3
55550	NO adsorption on the (111) surface of Al-based intermetallic L1$$_{{2}}$$-Al$$_3$$Sc. European Physical Journal D, 2021, 75, 1.	0.6	0
55551	Evoking ordered vacancies in metallic nanostructures toward a vacated Barlow packing for high-performance hydrogen evolution. Science Advances, 2021, 7, .	4.7	64
55552	Uniaxial strain-induced phase transition in the 2D topological semimetal IrTe2. Communications Materials, 2021, 2, .	2.9	25
55553	Eu₂CuSe₃ Revisited by Means of Experimental and Quantumâ€Chemical Techniques. European Journal of Inorganic Chemistry, 2021, 2021, 1510-1517.	1.0	9
55554	Enhanced Ion Sieving of Graphene Oxide Membranes via Surface Amine Functionalization. Journal of the American Chemical Society, 2021, 143, 5080-5090.	6.6	99
55555	Effects of La and Ce doping on electronic structure and optical properties of janus MoSSe monolayer. Superlattices and Microstructures, 2021, 151, 106841.	1.4	6
55556	Tuning the valence and concentration of europium and luminescence centers in GaN through co-doping and defect association. Physical Review Materials, 2021, 5, .	0.9	11
55557	First Principles, Explicit Interface Studies of Oxygen Vacancy and Chloride in Alumina Films for Corrosion Applications. Journal of the Electrochemical Society, 2021, 168, 031511.	1.3	16
55558	Chemical Composition Engineering Leading to the Significant Improvement in the Thermoelectric Performance of AgBiSe₂-Based n-Type Solid Solutions. ACS Applied Energy Materials, 2021, 4, 2899-2907.	2.5	5
55560	Role of zirconium in neodymium-dopants interactions within uranium-based metallic fuels. Nuclear Materials and Energy, 2021, 26, 100912.	0.6	2
55561	Designing a Family of Aluminum-Containing Fluoroborate Crystals with Enhanced Birefringence and Second-Harmonic Generation Coefficients Based on the First-Principles Methods. Journal of Physical Chemistry C, 2021, 125, 7431-7438.	1.5	3
55562	Rare-Earth-Free Magnets: Enhancing Magnetic Anisotropy and Spin Exchange Toward High-T_C Hf₂MIr₅B₂ (M = Mn, Fe). Journal of the American Chemical Society, 2021, 143, 4205-4212.	6.6	11
55563	Tunable topological states in layered magnetic materials of <mml:math xmlns:mml="http://www.w3.org/1998/Math/MathML"><mml:mrow><mml:mi>Mn</mml:mi><mml:msub><mml:mi>Sb</mml:mi><mml:mi><mml:r , and <mml:math xmlns:mml="http:/. Physical Review B, 2021, 103, .	1.5	30
55564	Cu-Si bond and Cl defect synergistical catalysis for SiCl4 dissociation on CuCl2(1 0 0): A DFT study. Applied Surface Science, 2021, 543, 148777.	3.1	2

#	Article	IF	Citations
55565	Evaluating Materials Design Parameters of Hole-Selective Contacts for Silicon Heterojunction Solar Cells. IEEE Journal of Photovoltaics, 2021, 11, 247-258.	1.5	7
55566	Evidences for pressure-induced two-phase superconductivity and mixed structures of NiTe2 and NiTe in type-II Dirac semimetal NiTe2-x (xÂ= 0.38 Â± 0.09) single crystals. Materials Today Physics, 2021, 17, 100339.	2.9	13
55567	Single-metal-atom site with high-spin state embedded in defective BN nanosheet promotes electrocatalytic nitrogen reduction. Nano Research, 2021, 14, 4211-4219.	5.8	55
55568	oI20-carbon: A new superhard carbon allotrope. Diamond and Related Materials, 2021, 113, 108284.	1.8	9
55569	Nonoxidative Conversion of Methane, Ethane, and Ethylene on Flat Ir(111) and Stepped Ir(211) Surfaces. Journal of Physical Chemistry C, 2021, 125, 5602-5615.	1.5	1
55570	Origin of Magnetism in Î³-FeSi2/Si(111) Nanostructures. Nanomaterials, 2021, 11, 849.	1.9	6
55571	Ab Initio Thermodynamics and Kinetics of the Lattice Oxygen Evolution Reaction in Iridium Oxides. ACS Energy Letters, 2021, 6, 1124-1133.	8.8	56
55572	Indentation Strengths of Zirconium Diboride: Intrinsic versus Extrinsic Mechanisms. Journal of Physical Chemistry Letters, 2021, 12, 2848-2853.	2.1	54
55573	Noncollinear ferromagnetic Weyl semimetal with anisotropic anomalous Hall effect. Physical Review B, 2021, 103, .	1.1	42
55574	Fibrous Phase Red Phosphorene as a New Photocatalyst for Carbon Dioxide Reduction and Hydrogen Evolution. Small, 2021, 17, e2008004.	5.2	31
55575	Anisotropic magnetoresistance and planar Hall effect in (001) and (111) LaVO3/SrTiO3 heterostructures. Physical Review B, 2021, 103, .	1.1	14
55576	Structural and chemical mechanisms governing stability of inorganic Janus nanotubes. Npj Computational Materials, 2021, 7, .	3.5	22
55577	Titanium Iodates with a Second-Harmonic-Generation Response. Inorganic Chemistry, 2021, 60, 5821-5828.	1.9	6
55578	Intrinsic mechanism of active metal dependent primary amine selectivity in the reductive amination of carbonyl compounds. Journal of Catalysis, 2021, 395, 293-301.	3.1	22
55579	Radiation damage behavior of amorphous SiOC polymer-derived ceramics: the role of in situ formed free carbon. Journal of Nuclear Materials, 2021, 545, 152652.	1.3	1
55581	Time-Domain Ab Initio Insights into the Reduced Nonradiative Electronâ€“Hole Recombination in ReSe₂/MoS₂ van der Waals Heterostructure. Journal of Physical Chemistry Letters, 2021, 12, 2682-2690.	2.1	20
55582	Quantum and Classical Proton Diffusion in Superconducting Clathrate Hydrides. Physical Review Letters, 2021, 126, 117002.	2.9	17
55583	Plasmon-Induced CO₂ Conversion on Al@Cu₂O: A DFT Study. Journal of Physical Chemistry C, 2021, 125, 6108-6115.	1.5	14

#	Article	IF	Citations
55584	Monte Carlo study of Cu precipitation in bcc-Fe: temperature-dependent cluster expansion versus local chemical environment potentials. Modelling and Simulation in Materials Science and Engineering, 2021, 29, 035014.	0.8	3
55585	Development of robust neural-network interatomic potential for molten salt. Cell Reports Physical Science, 2021, 2, 100359.	2.8	40
55586	Vacancy-defects turn off conjugated Ï€ bond shield activated catalytic molecular adsorption process. Applied Surface Science, 2021, 543, 148790.	3.1	4
55587	Iron Coordination Polymer, Fe(oxalate)(H₂O)₂ Nanorods Grown on Nickel Foam via One-Step Electrodeposition as an Efficient Electrocatalyst for Oxygen Evolution Reaction. Inorganic Chemistry, 2021, 60, 5140-5152.	1.9	9
55588	Towards cubic symmetry for <mml:math xmlns:mml="http://www.w3.org/1998/Math/MathML"><mml:msup><mml:mi mathvariant="normal">Ir</mml:mi><mml:mrow><mml:mn>4</mml:mn><mml:mo>+</mml:mo></mml:mrow></mml:msup></mml:math : Structure and magnetism of the antifluorite <mml:math xmlns:mml="http://www.w3.org/1998/Math/MathML"><mml:mrow><mml:msub><mml:mi mathvariant="normal">K</mml:mi><mml:mn>2</mml:mn></mml:msub><mml:msub><mml:mi>IrBr</mml:mi><mml:mn>6</mml:mn></	1.1	13
55589	Boosting electrocatalytic activity for CO2 reduction on nitrogen-doped carbon catalysts by co-doping with phosphorus. Journal of Energy Chemistry, 2021, 54, 143-150.	7.1	43
55590	Superior Oxidative Dehydrogenation Performance toward NH₃ Determines the Excellent Low-Temperature NH₃-SCR Activity of Mn-Based Catalysts. Environmental Science & Technology, 2021, 55, 6995-7003.	4.6	83
55591	Reactivity of Single Transition Metal Atoms on a Hydroxylated Amorphous Silica Surface: A Periodic Conceptual DFT Investigation. Chemistry - A European Journal, 2021, 27, 6050-6063.	1.7	11
55592	Theoretical Prediction of P-Triphenylene-Graphdiyne as an Excellent Anode Material for Li, Na, K, Mg, and Ca Batteries. Applied Sciences (Switzerland), 2021, 11, 2308.	1.3	7
55593	Theoretical Insights into Morphologies of Alkali-Promoted Cobalt Carbide Catalysts for Fischerâ€“Tropsch Synthesis. Journal of Physical Chemistry C, 2021, 125, 6061-6072.	1.5	12
55594	Modeling of vibrational and configurational degrees of freedom in hexagonal and cubic tungsten carbide at high temperatures. Physical Review Materials, 2021, 5, .	0.9	10
55595	High-throughput first-principles search for ceramic superlattices with improved ductility and fracture resistance. Acta Materialia, 2021, 206, 116615.	3.8	19
55596	Adsorption and cracking of propane by zeolites of different pore size. Journal of Catalysis, 2021, 395, 117-128.	3.1	29
55597	Fastâ€Charging and Ultrahighâ€Capacity Zinc Metal Anode for Highâ€Performance Aqueous Zincâ€Ion Batteries. Advanced Functional Materials, 2021, 31, 2100398.	7.8	203
55598	Fabrication of Black In₂O₃ with Dense Oxygen Vacancy through Dual Functional Carbon Doping for Enhancing Photothermal CO₂ Hydrogenation. Advanced Functional Materials, 2021, 31, 2100908.	7.8	66
55599	Sodium-storage behavior of electron-rich element-doped amorphous carbon. Applied Physics Reviews, 2021, 8, .	5.5	22
55600	CO₂ Activation and Capture on a Si-Doped h-BN Sheet: Insight into the Local Bonding Effect of Single Si Sites. Journal of Physical Chemistry C, 2021, 125, 5048-5055.	1.5	9
55601	Interfacing spinel NiCo2O4 and NiCo alloy derived N-doped carbon nanotubes for enhanced oxygen electrocatalysis. Chemical Engineering Journal, 2021, 408, 127814.	6.6	106

#	Article	IF	Citations
55602	Enhanced tunable second harmonic generation from twistable interfaces and vertical superlattices in boron nitride homostructures. Science Advances, 2021, 7, .	4.7	73
55603	Anchoring Polysulfides and Accelerating Redox Reaction Enabled by Feâ€Based Compounds in Lithiumâ€“Sulfur Batteries. Advanced Functional Materials, 2021, 31, 2100970.	7.8	94
55604	Mechanistic Origin of Superionic Lithium Diffusion in Anion-Disordered Li₆PS₅X Argyrodites. Chemistry of Materials, 2021, 33, 2004-2018.	3.2	63
55605	Van der Waals epitaxial growth of air-stable CrSe2 nanosheets with thickness-tunable magnetic order. Nature Materials, 2021, 20, 818-825.	13.3	206
55606	Localized Electron Density Engineering for Stabilized B-Î³ CsSnI₃-Based Perovskite Solar Cells with Efficiencies >10%. ACS Energy Letters, 0, , 1480-1489.	8.8	125
55607	Photoelectrochemical Behavior and Computational Insights for Pristine and Doped NdFeO₃ Thin-Film Photocathodes. ACS Applied Materials & Interfaces, 2021, 13, 14150-14159.	4.0	18
55608	Zeolitic imidazole framework-derived FeN5-doped carbon as superior CO2 electrocatalysts. Journal of Catalysis, 2021, 395, 63-69.	3.1	27
55609	Enabling a Stable Room-Temperature Sodiumâ€“Sulfur Battery Cathode by Building Heterostructures in Multichannel Carbon Fibers. ACS Nano, 2021, 15, 5639-5648.	7.3	70
55610	Two-Dimensional Tetrahex-GeC₂: A Material with Tunable Electronic and Optical Properties Combined with Ultrahigh Carrier Mobility. ACS Applied Materials & Interfaces, 2021, 13, 14489-14496.	4.0	15
55611	Intrinsic room-temperature ferromagnetic semiconductor InCrTe3 monolayers with large magnetic anisotropy and large piezoelectricity. Applied Physics Letters, 2021, 118, .	1.5	32
55612	Novel Coâ€Doped Y₂GeO₅:Pr³⁺,Tb³⁺: Deep Trap Level Formation and Analog Binary Optical Storage with Submicron Information Points. Advanced Optical Materials, 2021, 9, 2002090.	3.6	16
55613	Quantum spin Hall effect in <mml:math xmlns:mml="http://www.w3.org/1998/Math/MathML"><mml:mrow><mml:msub><mml:mi>Ta</mml:mi><mml:mn>2</mml:mn></mml: <mml:math xmlns:mml="http://www.w3.org/1998/Math/MathML"><mml:mrow><mml:mo>(</mml:mo><mml:mi>M</mml:mi><mml:mo>=</mml:	1.1	22
55614	Constructed Interfacial Oxygenâ€Bridge Chemical Bonding in Coreâ€Shell Transition Metal Phosphides/Carbon Hybrid Boosting Oxygen Evolution Reaction. ChemSusChem, 2021, 14, 2188-2197.	3.6	26
55615	A First-Principles Study of Hydrogen Desorption from High Entropy Alloy TiZrVMoNb Hydride Surface. Metals, 2021, 11, 553.	1.0	4
55616	A strategy of optimizing magnetism and hysteresis simultaneously in Niâ€“Mn-based metamagnetic shape memory alloys. Intermetallics, 2021, 130, 107063.	1.8	8
55617	One-Dimensional Metal Embedded in Two-Dimensional Semiconductor in Nb₂Si_{xâ€“1}Te₄. ACS Nano, 2021, 15, 7149-7154.	7.3	14
55618	Quantitative Studies of the Key Aspects in Selective Acetylene Hydrogenation on Pd(111) by Microkinetic Modeling with Coverage Effects and Molecular Dynamics. ACS Catalysis, 2021, 11, 4094-4106.	5.5	37
55619	The Mechanism of Graphene Vaporâ€“Solid Growth on Insulating Substrates. ACS Nano, 2021, 15, 7399-7408.	7.3	23

#	Article	IF	Citations
55620	Construction of Spatial Effect from Atomically Dispersed Co Anchoring on Subnanometer Ru Cluster for Enhanced N₂-to-NH₃ Conversion. ACS Catalysis, 2021, 11, 4430-4440.	5.5	28
55621	Ab Initio Analysis of Periodic Self-Assembly Phases of Borophene as Anode Material for Na-Ion Batteries. Journal of Physical Chemistry C, 2021, 125, 5436-5446.	1.5	13
55622	Unveiling Atomic-Scale MoirÃ© Features and Atomic Reconstructions in High-Angle Commensurately Twisted Transition Metal Dichalcogenide Homobilayers. Nano Letters, 2021, 21, 3262-3270.	4.5	15
55623	Frustrated Packing in Simple Structures: Chemical Pressure Hindrance to Isolobal Bonds in the TiAl₃ type and ZrAl_{2.6}Sn_{0.4}. Inorganic Chemistry, 2021, 60, 4779-4791.	1.9	7
55624	Ternary Cu₂SnS₃: Synthesis, Structure, Photoelectrochemical Activity, and Heterojunction Band Offset and Alignment. Chemistry of Materials, 2021, 33, 1983-1993.	3.2	30
55625	Graphitic Carbon Nitride Sheet Supported Single-Atom Metal-Free Photocatalyst for Oxygen Reduction Reaction: A First-Principles Analysis. Journal of Physical Chemistry Letters, 2021, 12, 2788-2795.	2.1	38
55626	Phosphor-Free Electrically Driven White Light Emission from Nanometer-Thick Bariumâ€“Organic Framework Films. ACS Applied Nano Materials, 2021, 4, 2395-2403.	2.4	6
55627	Nanostructure of nickel-promoted indium oxide catalysts drives selectivity in CO2 hydrogenation. Nature Communications, 2021, 12, 1960.	5.8	90
55628	Influence of Confinement on Barriers for Alkoxide Formation in Acidic Zeolites. ChemCatChem, 2021, 13, 2451-2458.	1.8	6
55629	Spin state crossover in <mml:math xmlns:mml="http://www.w3.org/1998/Math/MathML"><mml:mrow><mml:msub><mml:mi>Co</mml:mi><mml:mn>3</mml:mn></mml:msub></mml:mrow></mml:math> Physical Review B, 2021, 103, .	1.1	13
55630	Nanoburl Graphites. Advanced Materials, 2021, 33, e2007513.	11.1	19
55631	Quantum Transport across Amorphous-Crystalline Interfaces in Tunnel Oxide Passivated Contact Solar Cells: Direct versus Defect-Assisted Tunneling. Chinese Physics Letters, 2021, 38, 036301.	1.3	3
55632	Origin of magnetovolume effect in a cobaltite. Physical Review B, 2021, 103, .	1.1	3
55633	PASP: Property analysis and simulation package for materials. Journal of Chemical Physics, 2021, 154, 114103.	1.2	32
55634	Measurement of electronic structure and surface reconstruction in the superionic Cu2â^'xTe. Physical Review B, 2021, 103, .	1.1	2
55635	A generic Slaterâ€“Koster description of the electronic structure of centrosymmetric halide perovskites. Journal of Chemical Physics, 2021, 154, 104706.	1.2	6
55636	Theoretical insight into the effect of Br, Na co-doping on electronic structure, photocatalytic and optical characteristics of g-C3N4 using first-principles and optical simulations. Journal of Materials Science, 2021, 56, 10382-10392.	1.7	9
55637	Buckled hexagonal carbon selenium nanosheet for thermoelectric performance. Applied Physics A: Materials Science and Processing, 2021, 127, 1.	1.1	1

#	Article	IF	Citations
55638	Effect of Cu-doping on the magnetic and electrical transport properties of three-quarter Heusler alloy ZrCo1.5Sn. Journal of Applied Physics, 2021, 129, 125106.	1.1	3
55639	Ab initio anharmonic thermodynamic properties of cubic <mml:math xmlns:mml="http://www.w3.org/1998/Math/MathML"><mml:mrow><mml:mi>Ca</mml:mi><mml:mi>Si</mml:mi><mml:msub><mml:mi mathvariant="normal">O</mml:mi><mml:mn>3</mml:mn></mml:msub></mml:mrow></mml:math> perovskite. Physical Review B, 2021, 103, .	1.1	7
55640	Observation of novel charge ordering and spin reorientation in perovskite oxide PbFeO3. Nature Communications, 2021, 12, 1917.	5.8	17
55641	Surface band characters of the Weyl semimetal candidate material <mml:math xmlns:mml="http://www.w3.org/1998/Math/MathML"><mml:msub><mml:mrow><mml:mi>MoTe</mml:mi></mml:mrow><mml:mn> revealed by one-step angle-resolved photoemission theory. Physical Review B, 2021, 103, .	1.1	5
55642	Change in the Positron Annihilation Lifetime of Vacancy Clusters Containing Hydrogen Atoms in Electron-Irradiated F82H. Materials Science Forum, 0, 1024, 71-78.	0.3	0
55643	Simulations of hydrogen outgassing and sticking coefficients at a copper electrode surface: Dependencies on temperature, incident angle and energy. Physical Review Research, 2021, 3, .	1.3	4
55644	Computational approaches to point defect simulations for semiconductor solid solution alloys. Journal of Chemical Physics, 2021, 154, 094705.	1.2	1
55645	Different segregation effects for Sc and Ce in an Al/Î´Â´ interface. Journal of the Korean Physical Society, 2021, 78, 706-711.	0.3	0
55646	Thermal conductivity of the nâ€‰=â€‰1â€“5 and 10 members of the (SrTiO3)nSrO Ruddlesdenâ€“Popper superlattices. Applied Physics Letters, 2021, 118, .	1.5	9
55647	Design Principles for the Enhanced Transparency Range ofÂCorrelated Transparent Conductors. Laser and Photonics Reviews, 2021, 15, 2000444.	4.4	9
55648	Organic Modifiers Promote Furfuryl Alcohol Ring Hydrogenation via Surface Hydrogen-Bonding Interactions. ACS Catalysis, 2021, 11, 3730-3739.	5.5	14
55649	Theoretical Study of Oxygen-Vacancy Distribution in In₂O₃. Journal of Physical Chemistry C, 2021, 125, 7077-7085.	1.5	19
55650	Multiferroicity of Non-Janus MXY (X = Se/S, Y = Te/Se) Monolayers with Giant In-Plane Ferroelectricity. Journal of Physical Chemistry C, 2021, 125, 7458-7465.	1.5	4
55651	Tailored Electronic Band Gap and Valance Band Edge of Nickel Oxide via p-Type Incorporation. Journal of Physical Chemistry C, 2021, 125, 7495-7501.	1.5	12
55652	Determination of mechanical and vibrational properties of the Sr(Zn1âˆ’xAl)13 intermetallic compound. Intermetallics, 2021, 130, 107056.	1.8	4
55653	Investigation of the (1Â0Â0) and (0Â0Â1) surfaces of the Al5Fe2 intermetallic compound. Applied Surface Science, 2021, 542, 148540.	3.1	4
55654	On the atomic structure of Pt(1 1 1)/Î³-Al2O3(1 1 1) interfaces and the changes in their interfacial energy with temperature and oxygen pressure. Applied Surface Science, 2021, 542, 148594.	3.1	5
55655	Free energy of (CoxMn1âˆ’x)3O4 mixed phases from machine-learning-enhanced ab initio calculations. Physical Review Materials, 2021, 5, .	0.9	5

#	Article	IF	Citations
55656	Large magnetic anisotropy in an OsIr dimer anchored in defective graphene. Nanotechnology, 2021, 32, 230001.	1.3	10
55657	Low-frequency and MoirÃ©â€“Floquet engineering: A review. Annals of Physics, 2021, 435, 168434.	1.0	42
55658	Enhanced Hardness in Transition-Metal Monocarbides via Optimal Occupancy of Bonding Orbitals. ACS Applied Materials & Interfaces, 2021, 13, 14365-14376.	4.0	11
55659	Fast Correction of Errors in the DFTâ€Calculated Energies of Gaseous Nitrogenâ€Containing Species. ChemCatChem, 2021, 13, 2508-2516.	1.8	21
55660	Li₆SiO₄Cl₂: A Hexagonal Argyrodite Based on Antiperovskite Layer Stacking. Chemistry of Materials, 2021, 33, 2206-2217.	3.2	6
55661	Oxygen-promoted synthesis of armchair graphene nanoribbons on Cu(111). Science China Chemistry, 2021, 64, 636-641.	4.2	8
55662	Efficacy of the radial pair potential approximation for molecular dynamics simulations of dense plasmas. Physics of Plasmas, 2021, 28, .	0.7	13
55663	Origin of low thermal conductivity in monolayer PbI2. Solid State Communications, 2021, 327, 114223.	0.9	7
55664	Application of Optimization Algorithms in Clusters. Frontiers in Chemistry, 2021, 9, 637286.	1.8	6
55665	Electrostatic doping of graphene from a LiNbO₃ (0001) substrate. Journal Physics D: Applied Physics, 2021, 54, 235303.	1.3	3
55666	Post-lithium-ion batteries: characterization of phosphorous and tin for potassium-ion anodes. Journal of Materials Science, 2021, 56, 10926-10937.	1.7	3
55667	Chemical short-range ordering and its strengthening effect in refractory high-entropy alloys. Physical Review B, 2021, 103, .	1.1	27
55668	Composition-dependent micro-structure and photocatalytic performance of g-C3N4 quantum dots@SnS2 heterojunction. Nano Research, 2021, 14, 4188-4196.	5.8	26
55669	Sulfur vacancy-rich MoS2 as a catalyst for the hydrogenation of CO2 to methanol. Nature Catalysis, 2021, 4, 242-250.	16.1	308
55670	Sustainable scale-up synthesis of MIL-68(Al) using IPA as solvent for acetic acid capture. Microporous and Mesoporous Materials, 2021, 316, 110943.	2.2	6
55671	Prediction of the two-dimensional cobalt carbonitride compounds <mml:math xmlns:mml="http://www.w3.org/1998/Math/MathML"><mml:mrow><mml:msub><mml:mi>CoN</mml:mi><mml:mn>4</mml:mn></mml:msub><mml:msub><mml:mi mathvariant="normal">C</mml:mi><mml:mn>10</mml:mn></mml:msub></mml:mrow></mml:math> , <mml:math xmlns:mml="http://www.w3.org/1998/Math/MathML"><mml:mrow><mml:msub><mml:mi>Co</mml:mi><mml:mn>2</mml:mn></mml:msub><mml:msub><mml:mi mathvariant="normal">N</mml:mi><mml:mn>8</mml:mn></mml:msub></mml:mrow></mml:math> : Physical Review	1.1	12
55672	Strainâ€Engineered Formation, Migration, and Electronic Properties of Polaronic Defects in CeO₂. Physica Status Solidi (B): Basic Research, 2021, 258, 2100020.	0.7	4
55673	From Monolayers to Nanotubes: Toward Catalytic Transition-Metal Dichalcogenides for Hydrogen Evolution Reaction. Energy & Fuels, 2021, 35, 6282-6288.	2.5	10

#	Article	IF	Citations
55674	High-throughput screening to modulate electronic and optical properties of alloyed Cs₂AgBiCl₆ for enhanced solar cell efficiency. JPhys Materials, 2021, 4, 025005.	1.8	14
55675	Fluorescent Detection of Carbon Disulfide by a Highly Emissive and Robust Isoreticular Series of Zr-Based Luminescent Metal Organic Frameworks (LMOFs). Chemistry, 2021, 3, 327-337.	0.9	11
55676	Dimensional transformation of chemical bonding during crystallization in a layered chalcogenide material. Scientific Reports, 2021, 11, 4782.	1.6	16
55677	Activate Fe₃S₄ Nanorods by Ni Doping for Efficient Dye-Sensitized Photocatalytic Hydrogen Production. ACS Applied Materials & Interfaces, 2021, 13, 14198-14206.	4.0	34
55678	First-principles study on the structural, elastic, piezoelectric and electronic properties of (BaTiO3,) Tj ETQq0 0 0 rgBT /Overlock 10 Tf 50	0.9	4
55679	Structural, electronic, elastic, magnetic, phonon and thermodynamic properties of inverse-Heusler-Ti2FeX (X=Si, Ge, and Sn): Insights from DFT-based computer simulation. Materials Today Communications, 2021, 26, 102036.	0.9	2
55680	Adsorption of cyanogen halides (X-CN; Xâ€¯=â€¯F, Cl and Br) on pristine and Fe, Mn doped C60: A highly potential gas sensor. Materials Today Communications, 2021, 26, 101901.	0.9	12
55681	Unusual magnetic transitions and phonon instabilities in tetragonal SrIrO3 under epitaxial strain. Journal of Magnetism and Magnetic Materials, 2021, 522, 167547.	1.0	0
55682	Structure-sensitive scaling relations among carbon-containing species and their possible impact on CO2 electroreduction. Journal of Catalysis, 2021, 395, 136-142.	3.1	6
55683	Tunable Covalent Organic Frameworks with Different Heterocyclic Nitrogen Locations for Efficient Cr(VI) Reduction, Escherichia coli Disinfection, and Paracetamol Degradation under Visible-Light Irradiation. Environmental Science & Technology, 2021, 55, 5371-5381.	4.6	79
55684	Interface Interaction of Benzohydroxamic Acid with Lead Ions on Oxide Mineral Surfaces: A Coordination Mechanism Study. Langmuir, 2021, 37, 3490-3499.	1.6	16
55685	Selectivity of the First Two Glycerol Dehydrogenation Steps Determined Using Scaling Relationships. ACS Catalysis, 2021, 11, 3487-3497.	5.5	19
55686	Unraveling the intrinsic atomic physics behind x-ray absorption line shifts in warm dense silicon plasmas. Physical Review E, 2021, 103, 033202.	0.8	10
55687	Redirecting dynamic surface restructuring of a layered transition metal oxide catalyst for superior water oxidation. Nature Catalysis, 2021, 4, 212-222.	16.1	266
55688	Optical anisotropy in bare and janus tellurene allotropes from ultraviolet to visible region: A first principle study. Materials Science and Engineering B: Solid-State Materials for Advanced Technology, 2021, 265, 115014.	1.7	8
55689	Highly Stable and Active Solidâ€Solutionâ€Alloy Threeâ€Way Catalyst by Utilizing Configurationalâ€Entropy Effect. Advanced Materials, 2021, 33, e2005206.	11.1	22
55690	Tuning the electronic and optical properties of two-dimensional gallium nitride by chemical functionalization. Vacuum, 2021, 185, 110008.	1.6	17
55691	Polymorphic transformations of CaSi2 and CaGe2. Journal of Solid State Chemistry, 2021, 295, 121919.	1.4	12

#	Article	IF	Citations
55692	Novel 2D B₂S₃ as a metal-free photocatalyst for water splitting. Nanotechnology, 2021, 32, 225401.	1.3	11
55693	Giant tunnel electroresistance in ferroelectric tunnel junctions with metal contacts to two-dimensional ferroelectric materials. Physical Review B, 2021, 103, .	1.1	26
55694	Ca Doping Effect on the Competition of NH₃â€“SCR and NH₃ Oxidation Reactions over Vanadium-Based Catalysts. Journal of Physical Chemistry C, 2021, 125, 6128-6136.	1.5	32
55695	Defective BC₂N as an Anode Material with Improved Performance for Lithium-Ion Batteries. Journal of Physical Chemistry C, 2021, 125, 4946-4954.	1.5	15
55696	Vibrational signatures for the identification of single-photon emitters in hexagonal boron nitride. Physical Review B, 2021, 103, .	1.1	20
55697	Investigation of Sr_{0.7}Ca_{0.3}FeO₃ Oxygen Carriers with Variable Cobalt Bâ€Site Substitution. ChemSusChem, 2021, 14, 1893-1901.	3.6	7
55698	Real-time GW -BSE investigations on spin-valley exciton dynamics in monolayer transition metal dichalcogenide. Science Advances, 2021, 7, .	4.7	70
55699	Engineering the surface of cuprous oxide via surface coordination for efficient catalysis on aerobic oxidation of benzylic alcohols under ambient conditions. Applied Surface Science, 2021, 543, 148840.	3.1	13
55700	Robustness of the Half-Metallicity at the Interfaces in <mml:math xmlns:mml="http://www.w3.org/1998/Math/MathML" display="inline" overflow="scroll"><mml:msub><mml:mi>Co</mml:mi><mml:mn>2</mml:mn></mml:msub><mml:mrow><mml:mi>Mn</mml:mi><mml -Based All-Full-Heusler-Alloy Spintronic Devices. Physical Review Applied, 2021, 15, .	1.5	19
55701	Revisit the Role of Metal Dopants in Enhancing the Selectivity of Ag-Catalyzed Ethylene Epoxidation: Optimizing Oxophilicity of Reaction Site via Cocatalytic Mechanism. ACS Catalysis, 2021, 11, 3371-3383.	5.5	25
55702	Comprehensive Study on Ni- or Ir-Based Alloy Catalysts in the Hydrogenation of Olefins and Mechanistic Insight. ACS Catalysis, 2021, 11, 3293-3309.	5.5	20
55703	Epitaxial Singleâ€Crystal Growth of Transition Metal Dichalcogenide Monolayers via the Atomic Sawtooth Au Surface. Advanced Materials, 2021, 33, e2006601.	11.1	55
55704	Stability of the peroxide group in<mml:math xmlns:mml="http://www.w3.org/1998/Math/MathML"><mml:mrow><mml:mi>Ba</mml:mi><mml:msub><mml:mi mathvariant="normal">O</mml:mi><mml:mn>2</mml:mn></mml:msub></mml:mrow></mml:math>under high pressure. Physical Review B, 2021, 103, .	1.1	1
55705	Prediction of two-dimensional <mml:math xmlns:mml="http://www.w3.org/1998/Math/MathML"><mml:mrow><mml:msub><mml:mi>Cu</mml:mi><mml:mn>2</mml:mn></mml mathvariant="normal">C</mml:mi></mml:mrow></mml:math> with polyacetylene-like motifs and Dirac nodal line. Physical Review Materials, 2021, 5, .	0.9	8
55706	Combining wavefunction frozen-density embedding with one-dimensional periodicity. Journal of Chemical Physics, 2021, 154, 104114.	1.2	4
55707	First-Principles Study of Mechanical and Thermodynamic Properties of Binary and Ternary CoX (X = W) Tj ETQq1 1 0.784314 rgBT /Ov	1.3	2
55708	Measurement of the sound velocity of shock compressed water. Scientific Reports, 2021, 11, 6116.	1.6	3
55709	Low-energy electron transport in gold: mesoscopic potential calculation and its impact on electron emission yields. European Physical Journal Plus, 2021, 136, 1.	1.2	0

#	Article	IF	Citations
55710	Distinctive magnetic properties of <mml:math xmlns:mml="http://www.w3.org/1998/Math/MathML"><mml:mrow><mml:mi>Cr</mml:mi><mml:msub><mml:mi mathvariant="normal">I</mml:mi><mml:mn>3</mml:mn></mml:msub></mml:mrow></mml:math> and <mml:math xmlns:mml="http://www.w3.org/1998/Math/MathML"><mml:mrow><mml:mi>Cr</mml:mi><mml:msub><mml:mi>Br</mml:mi><mml:m monolayers caused by spin-orbit coupling. Physical Review B, 2021, 103, .	1.1	26
55711	Beyond templating: Electronic structure impacts of aromatic cations in organicâ€“inorganic antimony chlorides. Zeitschrift Fur Anorganische Und Allgemeine Chemie, 2021, 647, 857-866.	0.6	1
55712	Propane dehydrogenation catalyzed by single Lewis acid site in Sn-Beta zeolite. Journal of Catalysis, 2021, 395, 155-167.	3.1	54
55713	Chemical-Affinity Disparity and Exclusivity Drive Atomic Segregation, Short-Range Ordering, and Cluster Formation in High-Entropy Alloys. Acta Materialia, 2021, 206, 116638.	3.8	45
55714	Insights into the CO₂ Reduction Pathway through the Electrolysis of Aldehydes on Copper. ACS Catalysis, 2021, 11, 3867-3876.	5.5	8
55715	The Critical Role of Stereochemically Active Lone Pair in Introducing High Temperature Ferroelectricity. Inorganic Chemistry, 2021, 60, 4068-4075.	1.9	10
55716	Regioselective Construction of Chemically Transformed Phosphideâ€“Metal Nanoheterostructures for Enhanced Hydrogen Evolution Catalysis. Inorganic Chemistry, 2021, 60, 7269-7275.	1.9	4
55717	Tunable Magnetism and Insulatorâ€“Metal Transition in Bilayer Perovskites. Journal of Physical Chemistry C, 2021, 125, 6157-6162.	1.5	6
55718	A Global-Optimization Study of the Phase Diagram of Free-Standing Hydrogenated Two-Dimensional Silicon. Journal of Physical Chemistry C, 2021, 125, 6298-6305.	1.5	4
55719	Pushing Optical Switch into Deep Mid-Infrared Region: Band Theory, Characterization, and Performance of Topological Semimetal Antimonene. ACS Nano, 2021, 15, 7430-7438.	7.3	13
55720	Dynamic and Intermediate-Specific Local Coverage Controls the Syngas Conversion on Rh(111) Surfaces: An Operando Theoretical Analysis. ACS Catalysis, 2021, 11, 3830-3841.	5.5	9
55721	Ferromagnetism in two-dimensional <mml:math xmlns:mml="http://www.w3.org/1998/Math/MathML"><mml:mrow><mml:msub><mml:mi>Fe</mml:mi><mml:mn>3</mml:mn></mml:msub></mml:mrow></mml:math> ; Tunability by hydrostatic pressure. Physical Review B, 2021, 103, .	3.1	18
55722	Spinterface Formation at Î±-Sexithiophene/Ferromagnetic Conducting Oxide. Journal of Physical Chemistry C, 2021, 125, 6073-6081.	1.5	6
55723	Catalytic activity of Ru supported on SmCeOx for ammonia decomposition: The effect of Sm doping. Journal of Solid State Chemistry, 2021, 295, 121946.	1.4	13
55724	Accuracy of Cluster Model Calculations for Quasicrystal Surface. Materials Transactions, 2021, 62, 350-355.	0.4	2
55725	Unlocking the Intrinsic Origin of the Reversible Oxygen Redox Reaction in Sodiumâ€Based Layered Oxides. ChemElectroChem, 2021, 8, 1464-1472.	1.7	14
55726	Pt/Au surface adsorption on the ZnO surface: A first-principles study. Solid State Communications, 2021, 327, 114204.	0.9	1
55727	A first-principles and machine learning combined method to investigate the interfacial friction between corrugated graphene. Modelling and Simulation in Materials Science and Engineering, 2021, 29, 035011.	0.8	2

#	Article	IF	Citations
55728	Solventâ€Assisted Kinetic Trapping in Quaternary Perovskites. Advanced Materials, 2021, 33, e2008690.	11.1	6
55729	Disorder effect of 3d transition elements in DO3 Heusler alloy Mn2FeAl. Applied Physics Letters, 2021, 118, 132408.	1.5	3
55730	Sapphire <mml:math xmlns:mml="http://www.w3.org/1998/Math/MathML"><mml:mi>Î±</mml:mi><mml:mo>â^'</mml:mo><mml:mrow><mml:msub><mml:r mathvariant="normal">O</mml:mi><mml:mn>3</mml:mn></mml:msub></mml:mrow></mml:math> puzzle: Joint <mml:math xmlns:mml="http://www.w3.org/1998/Math/MathML"><mml:mrow><mml:mi>Î¼</mml:mi><mml:mi>SR</mml:mi></mml:mrow></mml and density functional theory study. Physical Review B, 2021, 103, .	1.1	3
55731	Theory of nonvolatile resistive switching in monolayer molybdenum disulfide with passive electrodes. Npj 2D Materials and Applications, 2021, 5, .	3.9	15
55732	Robust quantum anomalous Hall effect in a pentagonal MoS2 monolayer grown on CuI(001) substrates. Physical Review B, 2021, 103, .	1.1	2
55733	Surface localized phonon modes at the Si(553)-Au nanowire system. Physical Review B, 2021, 103, .	1.1	6
55734	Shock-compressed silicon: Hugoniot and sound speed up to 2100 GPa. Physical Review B, 2021, 103, .	1.1	13
55735	First-principles calculation of the Dzyaloshinskii-Moriya interaction: A Green's function approach. Physical Review B, 2021, 103, .	1.1	14
55736	Synthesis of superconducting SbS and SbS2 antimony chalcogenide compounds at high pressures. Physical Review B, 2021, 103, .	1.1	2
55737	Evaluation of similarities and differences of LiTaO₃ and LiNbO₃ based on high-T-conductivity, nonlinear optical fs-spectroscopy and ab initio modeling of polaronic structures. New Journal of Physics, 2021, 23, 033016.	1.2	19
55738	A Convenient Method for Synthesis of Fe₃O₄/FeS₂ as High-Performance Electrocatalysts for Oxygen Evolution Reaction and Zinc-Air Batteries. Journal of the Electrochemical Society, 2021, 168, 030517.	1.3	4
55739	Ion beam engineered hydrogen titanate nanotubes for superior energy storage application. Electrochimica Acta, 2021, 371, 137774.	2.6	19
55740	Enhancement of Catalytic Activity and Durability of Pt Nanoparticle through Strong Chemical Interaction with Electrically Conductive Support of MagnÃ©li Phase Titanium Oxide. Nanomaterials, 2021, 11, 829.	1.9	14
55741	Ultrahigh hydrogen storage capacity of holey graphyne. Nanotechnology, 2021, 32, 215402.	1.3	28
55742	Superalkali NLi4 anchored on BN sheets for reversible hydrogen storage. Applied Physics Letters, 2021, 118, .	1.5	10
55743	Structural phase transitions of LaScO3 from first principles. Materials Today Communications, 2021, 26, 102048.	0.9	8
55744	DFT study on the mechanism of methanol to methyl formate on the M@C16B8 surface. Materials Today Communications, 2021, 26, 102090.	0.9	3
55745	An Ingenious Strategy to Integrate Multiple Electrocatalytically Active Components within a Well-Aligned Nitrogen-Doped Carbon Nanotube Array Electrode for Electrocatalysis. ACS Catalysis, 2021, 11, 3958-3974.	5.5	32

#	Article	IF	Citations
55746	Enhanced interfacial electronic transfer of BiVO₄ coupled with 2D gâ€C₃N₄ for visibleâ€light photocatalytic performance. Journal of the American Ceramic Society, 2021, 104, 3004-3018.	1.9	13
55747	Electric field induced topological phase transition and large enhancements of spin-orbit coupling and Curie temperature in two-dimensional ferromagnetic semiconductors. Physical Review B, 2021, 103, .	1.1	33
55748	Confined interfacial alloying of multilayered Pd-Ni nanocatalyst for widening hydrogen detection capacity. Sensors and Actuators B: Chemical, 2021, 330, 129378.	4.0	6
55749	Pressure-Induced Phase Transition of Î²-RDX Single Crystals. Journal of Physical Chemistry C, 2021, 125, 6418-6426.	1.5	9
55750	Synchronized Câ€“H Activations at Proximate Dinuclear Pd²⁺ Sites on Silicotungstate for Oxidative Câ€“C Coupling. ACS Catalysis, 2021, 11, 3455-3465.	5.5	3
55751	Mechanistic Insight into the Hydrodeoxygenation of Hydroquinone over Au/a-TiO₂ Catalyst. Journal of Physical Chemistry C, 2021, 125, 6660-6672.	1.5	7
55752	High-Dimensional Atomistic Neural Network Potential to Study the Alignment-Resolved O2 Scattering from Highly Oriented Pyrolytic Graphite. Journal of Physical Chemistry A, 2021, 125, 2588-2600.	1.1	8
55753	Electrical Switch of Poissonâ€™s Ratio in IVâ€“VI Monolayers via Pseudophase Transitions. Journal of Physical Chemistry Letters, 2021, 12, 3217-3223.	2.1	1
55754	Photothermal synergic catalytic degradation of the gaseous organic pollutant isopropanol in oxygen vacancies utilizing ZnFe₂O₄. Journal of Chemical Research, 2021, 45, 773-780.	0.6	2
55755	Multivalent Ion Transport in Anti-Perovskite Solid Electrolytes. Chemistry of Materials, 2021, 33, 2187-2197.	3.2	9
55756	Hydrogen Adsorption on Au-Supported Pt and Pd Nanoislands: A Computational Study of Hydrogen Coverage Effects. Journal of Physical Chemistry C, 2021, 125, 5110-5115.	1.5	6
55757	Wholeâ€Voltageâ€Range Oxygen Redox in P2â€Layered Cathode Materials for Sodiumâ€Ion Batteries. Advanced Materials, 2021, 33, e2008194.	11.1	108
55758	Glass crystallization making red phosphor for high-power warm white lighting. Light: Science and Applications, 2021, 10, 56.	7.7	104
55759	Insights into the Microstructures and Energy Levels of Pr³⁺-Doped YAlO₃ Scintillating Crystals. Inorganic Chemistry, 2021, 60, 5107-5113.	1.9	6
55760	High-capacity and small-polarization aluminum organic batteries based on sustainable quinone-based cathodes with Al3+ insertion. Cell Reports Physical Science, 2021, 2, 100354.	2.8	32
55761	Surface Functionalization of 2D MXenes: Trends in Distribution, Composition, and Electronic Properties. Journal of Physical Chemistry Letters, 2021, 12, 2377-2384.	2.1	90
55762	Nominal Effect of Mg Intercalation on the Superconducting Properties of 2Hâ€“NbSe₂. Inorganic Chemistry, 2021, 60, 4588-4598.	1.9	9
55763	Construction of an Anion-Pillared MOF Database and the Screening of MOFs Suitable for Xe/Kr Separation. ACS Applied Materials & Interfaces, 2021, 13, 11039-11049.	4.0	60

#	Article	IF	Citations
55764	Enhancement of basal plane electrocatalytic hydrogen evolution activity via joint utilization of trivial and non-trivial surface states. Applied Materials Today, 2021, 22, 100921.	2.3	12
55765	Interface Engineering of Cu(In,Ga)Se₂ Solar Cells by Optimizing Cd- and Zn-Chalcogenide Alloys as the Buffer Layer. ACS Applied Materials & Interfaces, 2021, 13, 15237-15245.	4.0	13
55766	High thermal conductivity in covalently bonded bi-layer honeycomb boron arsenide. Materials Today Physics, 2021, 17, 100346.	2.9	15
55767	N-doping enabled defect-engineering of MoS2 for enhanced and selective adsorption of CO2: A DFT approach. Applied Surface Science, 2021, 542, 148556.	3.1	37
55768	Polyelemental Nanoparticles as Catalysts for a Liâ€“O₂ Battery. ACS Nano, 2021, 15, 4235-4244.	7.3	38
55769	TiO2 as a Photocatalyst for Water Splittingâ€”An Experimental and Theoretical Review. Molecules, 2021, 26, 1687.	1.7	114
55770	Diversified Phenomena in Metal- and Transition-Metal-Adsorbed Graphene Nanoribbons. Nanomaterials, 2021, 11, 630.	1.9	5
55771	Highly Efficient Oxygen Reduction Reaction Activity of Nâ€Doped Carbonâ€“Cobalt Boride Heterointerfaces. Advanced Energy Materials, 2021, 11, 2100157.	10.2	190
55772	Superconductivity in the <mml:math xmlns:mml="http://www.w3.org/1998/Math/MathML"><mml:msub><mml:mi mathvariant="double-struck">Z</mml:mi><mml:mn>2</mml:mn></mml:msub></mml:math> kagome metal <mml:math xmlns:mml="http://www.w3.org/1998/Math/MathML"><mml:mrow><mml:msub><mml:mi>KV</mml:mi><mml:mn>3</mml:mn></mml:msub></mml:mrow></mml:math>. Physical Review Materials, 2021, 5, .	0.9	280
55773	Bifunctional Fluorinated Separator Enabling Polysulfide Trapping and Li Deposition for Lithiumâ€“Sulfur Batteries. ACS Applied Materials & Interfaces, 2021, 13, 11920-11929.	4.0	20
55774	Noncovalently functionalization of Janus MoSSe monolayer with organic molecules. Physica E: Low-Dimensional Systems and Nanostructures, 2021, 127, 114503.	1.3	56
55775	Tipâ€Induced Nanoâ€Engineering of Strain, Bandgap, and Exciton Funneling in 2D Semiconductors. Advanced Materials, 2021, 33, e2008234.	11.1	44
55776	First-Principles Study of Bi³⁺-Related Luminescence and Electron and Hole Traps in (Y/Lu/La)PO₄. Inorganic Chemistry, 2021, 60, 4434-4446.	1.9	34
55777	Efficient and bright warm-white electroluminescence from lead-free metal halides. Nature Communications, 2021, 12, 1421.	5.8	99
55778	Spontaneous phase segregation of Sr ₂ NiO ₃ and SrNi ₂ O ₃ during SrNiO ₃ heteroepitaxy. Science Advances, 2021, 7, .	4.7	12
55779	Sodium-Mediated Bimetallic Feâ€“Ni Catalyst Boosts Stable and Selective Production of Light Aromatics over HZSM-5 Zeolite. ACS Catalysis, 2021, 11, 3553-3574.	5.5	50
55780	Mechanism and Active Species in NH₃ Dehydrogenation under an Electrochemical Environment: An Ab Initio Molecular Dynamics Study. ACS Catalysis, 2021, 11, 4310-4318.	5.5	37
55781	Crystal structure of 3,3â€²-(E)-diazene-1,2-diylbis{4-[(3,4-dinitro-1H-pyrazol-1-yl)-NNO-azoxy]-1,2,5-oxadiazole}. Powder Diffraction, 2021, 36, 134-139.	0.4	2

#	Article	IF	Citations
55782	A Comparative Study of Electron Radiation Responses of Pu2Zr2O7 and La2Zr2O7: An abinitio Molecular Dynamics Study. Materials, 2021, 14, 1516.	1.3	1
55783	Theoretical prediction of structural stability, elastic and magnetic properties for Mn₂NiGa alloy. Modern Physics Letters B, 2021, 35, 2150231.	1.0	2
55784	Iron(III) and cobalt(III) complexes with pentadentate pyridoxal Schiff base ligand â€“ structure, spectral, electrochemical, magnetic properties and DFT calculations. Polyhedron, 2021, 197, 115019.	1.0	7
55785	Synergistic catalysis of cluster and atomic copper induced by copper-silica interface in transfer-hydrogenation. Nano Research, 2021, 14, 4601-4609.	5.8	12
55786	Polymerization of silanes through dehydrogenative Siâ€“Si bond formation on metal surfaces. Nature Chemistry, 2021, 13, 350-357.	6.6	11
55787	Investigating phase transitions from local crystallographic analysis based on statistical learning of atomic environments in 2D MoS2-ReS2. Applied Physics Reviews, 2021, 8, 011409.	5.5	7
55788	Double band inversion in the topological phase transition of Ge1-x Snx alloys. Europhysics Letters, 2021, 133, 57001.	0.7	1
55789	Element-specific investigations of ultrafast dynamics in photoexcited Cu2ZnSnS4 nanoparticles in solution. Structural Dynamics, 2021, 8, 024501.	0.9	1
55790	Extended HÃ¼ckel Semi-Empirical Approach as an Efficient Method for Structural Defects Analysis in 4H-SiC. Materials, 2021, 14, 1247.	1.3	2
55791	Embedment of Multiple Transition Metal Impurities into WS₂ Monolayer for Bandstructure Modulation. Small, 2021, 17, e2007171.	5.2	6
55792	Crystalline symmetry-protected non-trivial topology in prototype compound BaAl4. Npj Quantum Materials, 2021, 6, .	1.8	7
55794	Correlation driven topological nodal ring ferromagnetic spin gapless semimetal: CsMnF4. Journal of Physics Condensed Matter, 2021, 33, .	0.7	1
55795	Manipulating Weyl quasiparticles by orbital-selective photoexcitation in WTe2. Nature Communications, 2021, 12, 1885.	5.8	25
55796	Stability of Zr-Al-C and Ti-Al-C MAX phases: A theoretical study. Physical Review Materials, 2021, 5, .	0.9	5
55797	In silico design of a thermal atomic layer etch process of cobalt. Journal of Vacuum Science and Technology A: Vacuum, Surfaces and Films, 2021, 39, .	0.9	5
55798	Accurate calculation of excitonic signatures in the absorption spectrum of BiSBr using semiconductor Bloch equations. Physical Review B, 2021, 103, .	1.1	3
55799	Phase stability of Au-Li binary systems studied using neural network potential. Physical Review B, 2021, 103, .	1.1	12
55800	Theoretical prediction on the redox potentials of rare-earth ions by deep potentials. Ionics, 2021, 27, 2079-2088.	1.2	8

#	Article	IF	Citations
55801	Identification of materials with strong magnetostructural coupling using computational high-throughput screening. Physical Review Materials, 2021, 5, .	0.9	3
55802	Modified embedded-atom method potentials for the plasticity and fracture behaviors of unary fcc metals. Physical Review B, 2021, 103, .	1.1	5
55803	Advanced First-Principle Modeling of Relativistic Ruddlesdenâ€"Popper Strontium Iridates. Applied Sciences (Switzerland), 2021, 11, 2527.	1.3	5
55804	Engineering the electronic and optical properties of 2D porphyrin-paddlewheel metal-organic frameworks. JPhys Energy, 2021, 3, 034005.	2.3	7
55805	Adsorption of crotonaldehyde on metal surfaces: Cu vs Pt. Journal of Chemical Physics, 2021, 154, 104701.	1.2	10
55806	Distorted planar defects stabilize tetragonal boron. Scripta Materialia, 2021, 194, 113685.	2.6	1
55807	Stability and residual stresses of sputtered wurtzite AlScN thin films. Physical Review Materials, 2021, 5, .	0.9	19
55808	Construction of poly-naphthalocyanine linked by [4]-radialene-like structures on silver surfaces. Nano Research, 2021, 14, 4563.	5.8	2
55809	First-principles hydration free energies of oxygenated species at waterâ€"platinum interfaces. Journal of Chemical Physics, 2021, 154, 094107.	1.2	11
55810	Strain-dependent optical properties of the novel monolayer group-IV dichalcogenides SiS₂ semiconductor: a first-principles study. Nanotechnology, 2021, 32, 235201.	1.3	6
55811	An atomistic model for predicting charge distribution in hexagonal boron nitride. Physica E: Low-Dimensional Systems and Nanostructures, 2021, 127, 114567.	1.3	3
55812	ab initio study of oxygen vacancy effects on structural, electronic and thermoelectric behavior of AZr1-xMxO3 (AÂ= Ba, Ca, Sr; M= Al, Cu, xÂ= 0.25) for application of memory devices. Journal of Molecular Graphics and Modelling, 2021, 103, 107825.	1.3	14
55813	Enhanced thermoelectric properties in two-dimensional monolayer Si₂BN by adsorbing halogen atoms*. Chinese Physics B, 2021, 30, 037304.	0.7	6
55814	Mixed-cation driven magnetic interaction of interstitial electrons for ferrimagnetic two-dimensional electride. Npj Quantum Materials, 2021, 6, .	1.8	4
55815	Topological surface states on the nonpolar (110) and (111) surfaces of <mml:math xmlns:mml="http://www.w3.org/1998/Math/MathML"><mml:msub><mml:mi>SmB</mml:mi><mml:mn>6</mml:mn></mml:msub></mml:math> Physical Review B, 2021, 103, .	1.1	8
55816	Assessing the accuracy of screened range-separated hybrids for bulk properties of semiconductors. Physical Review Materials, 2021, 5, .	0.9	4
55817	Unique Coordination Structure of Cobalt Single-Atom Catalyst Supported on Dopant-Free Carbon. Journal of Physical Chemistry C, 2021, 125, 6735-6742.	1.5	1
55818	Exfoliation of Quasi-Two-Dimensional Nanosheets of Metal Diborides. Journal of Physical Chemistry C, 2021, 125, 6787-6799.	1.5	32

#	Article	IF	Citations
55819	Thiazoleâ€Linked Covalent Organic Framework Promoting Fast Twoâ€Electron Transfer for Lithiumâ€Organic Batteries. Advanced Energy Materials, 2021, 11, 2003735.	10.2	78
55820	Effects of BrÃ¸nsted acid site proximity in chabazite zeolites on OH infrared spectra and protolytic propane cracking kinetics. Journal of Catalysis, 2021, 395, 210-226.	3.1	27
55821	Molecular Mechanism of Thermal Dry Etching of Iron in a Two-Step Atomic Layer Etching Process: Chlorination Followed by Exposure to Acetylacetone. Journal of Physical Chemistry C, 2021, 125, 7142-7154.	1.5	10
55822	Band Engineering and Van Hove Singularity on HfX₂ Thin Films (X = S, Se, or Te). ACS Applied Electronic Materials, 2021, 3, 1071-1079.	2.0	17
55823	Reasonably Introduced ZnIn₂S₄@C to Mediate Polysulfide Redox for Long-Life Lithiumâ€“Sulfur Batteries. ACS Applied Materials & Interfaces, 2021, 13, 14169-14180.	4.0	13
55824	On-surface preparation of coordinated lanthanide-transition-metal clusters. Nature Communications, 2021, 12, 1619.	5.8	20
55825	Peierls transition, ferroelectricity, and spin-singlet formation in monolayer <mml:math xmlns:mml="http://www.w3.org/1998/Math/MathML"><mml:msub><mml:mi>VOI</mml:mi><mml:mn>2</mml:mn></mml:msub></mml:mm Physical Review B, 2021, 103, .	1.1	21
55826	Theory prediction of PC3 monolayer as a promising anode material in potassium-ion batteries. Ionics, 2021, 27, 2465-2471.	1.2	7
55827	The study of self-assembly behavior of phthalocyanine-before (PCB) molecules on Au(111) substrate. Materials Research Express, 2021, 8, 035005.	0.8	0
55828	Enforced Long-Range Order in 1D Wires by Coupling to Higher Dimensions. Physical Review Letters, 2021, 126, 106101.	2.9	14
55829	First-principles prediction of ideal type-II Weyl phonons in wurtzite ZnSe. Physical Review B, 2021, 103, .	1.1	21
55830	Research on Bulk-metallic Glasses and High-entropy Alloys in Peter K. Liawâ€™s Group and with His Colleagues. Metallurgical and Materials Transactions A: Physical Metallurgy and Materials Science, 2021, 52, 2033-2093.	1.1	7
55831	Activating Edge-Mo of 2H-MoS₂ via Coordination with Pyridinic Nâ€“C for pH-Universal Hydrogen Evolution Electrocatalysis. ACS Catalysis, 2021, 11, 4486-4497.	5.5	74
55832	2D Nb₂SiTe₄ and Nb₂GeTe₄: promising thermoelectric figure of merit and gate-tunable thermoelectric performance. Nanotechnology, 2021, 32, 245203.	1.3	10
55833	Coverage-dependent structure and reactivity of vanadia clusters supported on anatase TiO2(1 0 1) surface. Applied Surface Science, 2021, 543, 148774.	3.1	4
55834	Importance of Crystallographic Sites on Sodium-Ion Extraction from NASICON-Structured Cathodes for Sodium-Ion Batteries. ACS Applied Materials & Interfaces, 2021, 13, 14312-14320.	4.0	35
55835	Solidâ€“liquid phase transition induced electrocatalytic switching from hydrogen evolution to highly selective CO2 reduction. Nature Catalysis, 2021, 4, 202-211.	16.1	89
55836	Anomalous Highâ€Temperature Superconductivity in YH₆. Advanced Materials, 2021, 33, e2006832.	11.1	196

#	Article	IF	Citations
55837	MXene Phase with C₃ Structure Unit: A Family of 2D Electrides. Advanced Functional Materials, 2021, 31, 2100009.	7.8	13
55838	Theoretical analysis of the adsorption of phosphoric acid and model phosphate monoesters on CeO2(111). Surface Science, 2021, 705, 121776.	0.8	6
55839	Oxygenation of conducting polymers facilitated by structureâ€breaking anions. Journal of Polymer Science, 2021, 59, 745-753.	2.0	4
55840	Ionic Liquids Achieve the Exfoliation of Ultrathin Two-Dimensional VOPO₄Â·2H₂O Crystalline Nanosheets: Implications on Energy Storage and Catalysis. ACS Applied Nano Materials, 2021, 4, 2503-2514.	2.4	5
55841	Phase Relations in the Niâ€“S System at High Pressures from ab Initio Computations. ACS Earth and Space Chemistry, 2021, 5, 596-603.	1.2	2
55842	Atomic-Scale Superlubricity in Ti₂CO₂@MoS₂ Layered Heterojunctions Interface: A First Principles Calculation Study. ACS Omega, 2021, 6, 9013-9019.	1.6	16
55843	Band-Gap Landscape Engineering in Large-Scale 2D Semiconductor van der Waals Heterostructures. ACS Nano, 2021, 15, 7279-7289.	7.3	28
55844	Epitaxial Stabilization and Oxygen Evolution Reaction Activity of Metastable Columbite Iridium Oxide. ACS Applied Energy Materials, 2021, 4, 3074-3082.	2.5	7
55845	Insights into the Mechanical and Electrical Properties of a Metalâ€“Phosphorene Interface: An Ab Initio Study with a Wide Range of Metals. ACS Omega, 2021, 6, 7795-7803.	1.6	1
55846	PSIQUE: Protein Secondary Structure Identification on the Basis of Quaternions and Electronic Structure Calculations. Journal of Chemical Information and Modeling, 2021, 61, 1789-1800.	2.5	5
55847	Density-Functional Tight-Binding Parameters for Bulk Zirconium: A Case Study for Repulsive Potentials. Journal of Physical Chemistry A, 2021, 125, 2184-2196.	1.1	2
55848	N-Doped Graphene-Supported Diatomic Niâ€“Fe Catalyst for Synergistic Oxidation of CO. Journal of Physical Chemistry C, 2021, 125, 5616-5622.	1.5	23
55849	HoHO: A Paramagnetic Air-Resistant Ionic Hydride with Ordered Anions. Inorganic Chemistry, 2021, 60, 3972-3979.	1.9	11
55850	Graphene on Rh(111): A template for growing ordered arrays of metal nanoparticles with different periodicities. Carbon, 2021, 173, 1073-1081.	5.4	10
55851	A comparative study on the twinning boundaries of five-fold twinned copper and gold nanorods. Applied Surface Science, 2021, 543, 148764.	3.1	6
55852	Strong metalâ€“support interaction between palladium and gallium oxide within monodisperse nanoparticles: self-supported catalysts for propyne semi-hydrogenation. Journal of Catalysis, 2021, 395, 36-45.	3.1	21
55853	Experimental and Theoretical Investigation of the Structural and Optoâ€electronic Properties of Feâ€Doped Leadâ€Free Cs₂AgBiCl₆ Double Perovskite. Chemistry - A European Journal, 2021, 27, 7408-7417.	1.7	28
55854	Interaction of Aromatic Molecules with Forsterite: Accuracy of the Periodic DFT-D4 Method. Journal of Physical Chemistry A, 2021, 125, 2770-2781.	1.1	2

#	Article	IF	Citations
55855	On the origin of precipitation of transition metals implanted in MgO. European Physical Journal B, 2021, 94, 1.	0.6	5
55856	Highâ€Throughput Oneâ€Photon Excitation Pathway in 0D/3D Heterojunctions for Visibleâ€Light Driven Hydrogen Evolution. Advanced Functional Materials, 2021, 31, 2100816.	7.8	92
55857	Adsorption of redox-active Schiff bases and corrosion inhibiting property for mild steel in 1 molLâ^'1 H2SO4: Experimental analysis supported by ab initio DFT, DFTB and molecular dynamics simulation approach. Journal of Molecular Liquids, 2021, 326, 115215.	2.3	38
55858	Hydroxyl-Boosted Nitrogen Reduction Reaction: The Essential Role of Surface Hydrogen in Functionalized MXenes. ACS Applied Materials & Interfaces, 2021, 13, 14283-14290.	4.0	34
55859	Revealing the Complex Nature of Bonding in the Binary High-Pressure Compound <mml:math xmlns:mml="http://www.w3.org/1998/Math/MathML" display="inline"><mml:mrow><mml:msub><mml:mrow><mml:mi>FeO</mml:mi></mml:mrow><mml:mrow><mml:mn>2</mml:mn></m Physical Review Letters, 2021, 126, 106001.	2.9	21
55860	Novel Physics-Based Ensemble Modeling Approach That Utilizes 3D Molecular Conformation and Packing to Access Aqueous Thermodynamic Solubility: A Case Study of Orally Available Bromodomain and Extraterminal Domain Inhibitor Lead Optimization Series. Journal of Chemical Information and Modeling, 2021, 61, 1412-1426.	2.5	12
55861	Highâ€Throughput Screening for Phaseâ€Change Memory Materials. Advanced Functional Materials, 2021, 31, 2009803.	7.8	43
55862	Surface-tuning nanoporous AuCu3 engineering syngas proportion by electrochemical conversion of CO2. Nano Research, 2021, 14, 3907-3912.	5.8	15
55863	Dirac Semimetals in Homogeneous Holey Carbon Nitride Monolayers. Journal of Physical Chemistry C, 2021, 125, 6082-6089.	1.5	17
55864	Origins of Minimized Lattice Thermal Conductivity and Enhanced Thermoelectric Performance in WS₂/WSe₂ Lateral Superlattice. ACS Omega, 2021, 6, 7879-7886.	1.6	15
55865	Neodymiumâ€Doped IrO₂ Electrocatalysts Supported on Titanium Plates for Enhanced Chlorine Evolution Reaction Performance. ChemElectroChem, 2021, 8, 1204-1210.	1.7	15
55866	Efficient Electrical Spin Splitter Based on Nonrelativistic Collinear Antiferromagnetism. Physical Review Letters, 2021, 126, 127701.	2.9	83
55867	Switching polymorph stabilities with impurities provides a thermodynamic route to benzamide form III. Communications Chemistry, 2021, 4, .	2.0	25
55868	Entropy matters in grain boundary segregation. Acta Materialia, 2021, 206, 116597.	3.8	21
55869	Ultrahigh tribocorrosion resistance of metals enabled by nano-layering. Acta Materialia, 2021, 206, 116609.	3.8	15
55870	Properties of (001) <mml:math xmlns:mml="http://www.w3.org/1998/Math/MathML"><mml:msub><mml:mi mathvariant="normal">NaNbO</mml:mi><mml:mn>3</mml:mn></mml:msub></mml:math> films under epitaxial strain: A first-principles study. Physical Review B, 2021, 103, .	1.1	14
55871	Breaking atomic-level ordering via biaxial strain in functional oxides: A DFT study. Journal of Applied Physics, 2021, 129, 095301.	1.1	8
55872	Thickness and Spin Dependence of Raman Modes in Magnetic Layered Fe₃GeTe₂. Advanced Electronic Materials, 2021, 7, 2001159.	2.6	16

#	Article	IF	Citations
55873	From NWChem to NWChemEx: Evolving with the Computational Chemistry Landscape. Chemical Reviews, 2021, 121, 4962-4998.	23.0	39
55874	Deposition of Atomically Thin Pt Shells on Amorphous Palladium Phosphide Cores for Enhancing the Electrocatalytic Durability. ACS Nano, 2021, 15, 7348-7356.	7.3	53
55875	NÃ©el-type skyrmions and their current-induced motion in van der Waals ferromagnet-based heterostructures. Physical Review B, 2021, 103, .	1.1	110
55876	Zoology of domain walls in quasi-2D correlated charge density wave of 1T-TaS2. Npj Quantum Materials, 2021, 6, .	1.8	15
55877	Direct Z-scheme photocatalytic CO2 conversion to solar fuels in a two-dimensional C2N/aza-CMP heterostructure. Applied Surface Science, 2021, 541, 148630.	3.1	19
55878	Short-Range Ordered Iridium Single Atoms Integrated into Cobalt Oxide Spinel Structure for Highly Efficient Electrocatalytic Water Oxidation. Journal of the American Chemical Society, 2021, 143, 5201-5211.	6.6	287
55879	Interplay between London Dispersion, Hubbard U, and Metastable States for Uranium Compounds. Journal of Physical Chemistry A, 2021, 125, 2791-2799.	1.1	4
55880	Regulating the Interfacial Synergy of Ni/Ga₂O₃ for CO₂ Hydrogenation toward the Reverse Waterâ€“Gas Shift Reaction. Industrial & Engineering Chemistry Research, 2021, 60, 9448-9455.	1.8	21
55881	Role of Hydrogen-bonded Bimolecular Formic Acidâ€“Formate Complexes for Formic Acid Decomposition on Copper: A Combined First-Principles and Microkinetic Modeling Study. ACS Catalysis, 2021, 11, 4349-4361.	5.5	19
55882	Two-dimensional intrinsic ferrovalley <mml:math xmlns:mml="http://www.w3.org/1998/Math/MathML"><mml:mrow><mml:mi>Gd</mml:mi><mml:msub><mml:mi mathvariant="normal">I</mml:mi><mml:mn>2</mml:mn></mml:msub></mml:mrow></mml:math> with large valley polarization. Physical Review B, 2021, 103, .	1.1	85
55883	First-Principles Investigation of Electronic Structure and Energy Level Scheme of Phosphors: The Lanthanide-Doped Sr2P2O7. ECS Journal of Solid State Science and Technology, 0, , .	0.9	1
55884	Strain engineering on electrocaloric effect in PbTiO3 and BaTiO3. Advanced Composites and Hybrid Materials, 2021, 4, 1239-1247.	9.9	6
55885	Manipulation of CO adsorption over Me1/CeO2 by heterocation doping: Key roles of single-atom adsorption energy. Journal of Chemical Physics, 2021, 154, 164705.	1.2	5
55886	Local electronic structure of dilute hydrogen in <mml:math xmlns:mml="http://www.w3.org/1998/Math/MathML"><mml:mrow><mml:mi>Î²</mml:mi><mml:mtext>â^'</mml:mtext><mml:msub> Physical Review B, 2021, 103, .	1.1	1
55887	Effect of local geometry on magnetic property of nitric oxide on <mml:math xmlns:mml="http://www.w3.org/1998/Math/MathML"><mml:mi>Au</mml:mi><mml:mo>(</mml:mo><mml:mn>11 Physical Review B, 2021, 103, .	1.1	1
55888	Local decomposition of hybridization functions: Chemical insight into correlated molecular adsorbates. Journal of Chemical Physics, 2021, 154, 144108.	1.2	2
55889	Superior thermoelectric performance of Î±-Se₂Te monolayer. Materials Research Express, 2021, 8, 045507.	0.8	4
55890	Columnar antiferromagnetic order of a MBene monolayer. Physical Review B, 2021, 103, .	1.1	10

#	Article	IF	Citations
55891	The indispensable role of orbital states in studying the magnetism of Mo-doped BaSnO3. Applied Physics Letters, 2021, 118, .	1.5	1
55892	Minority-spin conduction in ferromagnetic <mml:math xmlns:mml="http://www.w3.org/1998/Math/MathML"><mml:mrow><mml:msub><mml:mi>Mn</mml:mi><mml:mn>5</mml:mn></mml:msub><mml:mathvariant="normal">C</mml:mi><mml:mi>x</mml:mi></mml:msub></mml:mrow></mml:math> and <mml:math xmlns:mml="http://www.w3.org/1998/Math/MathML"><mml:mrow><mml:msub><mml:mi>Mn</mml:mi><mml:mn>5</mml:mn></mml:msub></mml:mrow></mml:math>. Physical Review B, 2021, 103, .	1.1	5
55893	Rules of formation of Hâ€“Câ€“Nâ€“O compounds at high pressure and the fates of planetary ices. Proceedings of the National Academy of Sciences of the United States of America, 2021, 118, .	3.3	11
55894	Quantum transport observed in films of the magnetic topological semimetal EuSb2. Physical Review B, 2021, 103, .	1.1	1
55895	On the mechanism underlying the elimination of nitrogen-oxygen shallow thermal donors in nitrogen-doped Czochralski silicon at elevated temperatures. Journal of Applied Physics, 2021, 129, .	1.1	3
55896	Investigation of optoelectronic properties of AgIn1â^'xGaxY2 (Yâ€‰=â€‰Se, Te) semiconductors. Indian Journal of Physics, 0, , 1.	0.9	0
55897	Development of Ni44Ti35Zr15Cu6 Quaternary Shape Memory Alloy: Experimental and Density Functional Theory Studies. Journal of Materials Engineering and Performance, 2021, 30, 3624-3631.	1.2	0
55898	Derivation of a hydrodynamic heat equation from the phonon Boltzmann equation for general semiconductors. Physical Review B, 2021, 103, .	1.1	25
55899	Mechanisms of the Planar Growth of Lithium Metal Enabled by the 2D Lattice Confinement from a Ti₃C₂T_x MXene Intermediate Layer. Advanced Functional Materials, 2021, 31, 2010987.	7.8	33
55900	Synchronized ion and electron transfer in a blue T-Nb2O5-x with solid-solution-like process for fast and high volumetric charge storage. Energy Storage Materials, 2021, 36, 213-221.	9.5	27
55901	MOF-Derived CoS₂/N-Doped Carbon Composite to Induce Short-Chain Sulfur Molecule Generation for Enhanced Sodiumâ€“Sulfur Battery Performance. ACS Applied Materials & Interfaces, 2021, 13, 18010-18020.	4.0	48
55902	Half-metallicity and enhanced magnetism in monolayer T-CrTe2 by lithium adsorption. Physics Letters, Section A: General, Atomic and Solid State Physics, 2021, 394, 127195.	0.9	5
55903	Electronic structure evolution of the transition metals substituted tetragonal graphene: a first-principles investigations. Journal of Physics Condensed Matter, 2021, 33, 205502.	0.7	2
55904	Toward accurate electronic, optical, and vibrational properties of hexagonal Si, Ge, and Si1â^'xGex alloys from first-principle simulations. Journal of Applied Physics, 2021, 129, .	1.1	10
55905	Structural properties, magnetism and reactivity of <mml:math xmlns:mml="http://www.w3.org/1998/Math/MathML" altimg="si21.svg"><mml:mrow><mml:msub><mml:mrow><mml:mi mathvariant="italic">Ni</mml:mi></mml:mrow><mml:mrow><mml:mn>13</mml:mn></mml:mrow></mml:msub><mml:msub><mml:mrow><mml:mi mathvariant="italic">Fe</mml:mi></mml:mrow><mml:mrow><mml:mi>x</mml:mi></mml:mrow></mml:msub></mml:mrow></mml:math> nanoalloys. Journal of Magnetism and Magnetic Materials, 2021, 524, 167636.	1.0	5
55906	Mg adsorption on MgAl2O4 surfaces and the effect of additive Ca: A combined experimental and theoretical study. Journal of Alloys and Compounds, 2021, 861, 158564.	2.8	4
55907	Effect of strain on electrochemical performance of Janus MoSSe monolayer anode material for Li-ion batteries: First-principles study*. Chinese Physics B, 2021, 30, 046301.	0.7	4
55908	High-contrast, reversible change of thermal conductivity in hexagonal nickel-iron sulfides. Acta Materialia, 2021, 208, 116709.	3.8	13

#	Article	IF	Citations
55909	Ultra-low Youngâ€™s modulus and high super-exchange interactions in monolayer CrN: A promising candidate for flexible spintronic applications*. Chinese Physics B, 2021, 30, 047105.	0.7	3
55910	Quantization of the band at the surface of charge density wave material 2H-TaSe₂ *. Chinese Physics B, 2021, 30, 047305.	0.7	1
55911	Remarkably improving dielectric response of polymer/hybrid ceramic composites based on 0D/2D-stacked CuO/V2C MXene heterojunction. Applied Surface Science, 2021, 545, 149008.	3.1	17
55912	Boron vacancy color center in diamond: Ab initio study. Diamond and Related Materials, 2021, 114, 108341.	1.8	3
55913	Theoretical investigation of the reactivity of flat Ni (111) and stepped Ni (211) surfaces for acetic acid hydrogenation to ethanol. International Journal of Hydrogen Energy, 2021, 46, 15454-15470.	3.8	7
55914	Theoretical perspective on the electronic structure and optoelectronic properties of type-II SiC/CrS₂ van der Waals heterostructure with high carrier mobilities. Journal of Physics Condensed Matter, 2021, 33, 215302.	0.7	7
55915	VS₂ nanosheet as a promising candidate of recycle and reuse NO₂ gas sensor and capturer: a DFT study. Journal of Physics Condensed Matter, 2021, 33, 165501.	0.7	10
55916	Cooperative evolution of polar distortion and nonpolar rotation of oxygen octahedra in oxide heterostructures. Science Advances, 2021, 7, .	4.7	20
55917	Initial Stages of Oxidation Reactions of Ethylene Carbonate and Fluoroethylene Carbonate on Li_xCoO₂ Surfaces: A DFT Study. Journal of the Electrochemical Society, 2021, 168, 050505.	1.3	11
55918	A Metalâ€“Organic Framework Nanorodâ€Assembled Superstructure and Its Derivative: Unraveling the Fast Potassium Storage Mechanism in Nitrogenâ€Modified Micropores. Small, 2021, 17, e2100135.	5.2	19
55919	Structural and optical properties of ionic liquid-based hybrid perovskitoid: A combined experimental and theoretical investigation. Functional Materials Letters, 2021, 14, 2150008.	0.7	1
55920	Exploring few and single layer CrPS₄ with near-field infrared spectroscopy. 2D Materials, 2021, 8, 035020.	2.0	10
55921	Electron transfer in LiMn1.5Ni0.5O4 during charging studied with soft X-ray spectrometry. Microscopy (Oxford, England), 2021, 70, 450-460.	0.7	0
55922	The (Inâ€)Stability of the Ionic Liquids [(TMEDA)BH₂][TFSI] and â^'[FSI] on the Li(001) Surface. Batteries and Supercaps, 2021, 4, 1126-1134.	2.4	5
55923	Mixed Solvothermal Synthesis of Tn Cluster-Based Indium and Gallium Sulfides Using Versatile Ammonia or Amine Structure-Directing Agents. Inorganic Chemistry, 2021, 60, 7115-7127.	1.9	11
55925	When Fluxionality Beats Size Selection: Acceleration of Ostwald Ripening of Subâ€Nano Clusters. Angewandte Chemie, 2021, 133, 12080-12089.	1.6	3
55926	Gas sensing properties of palladium-modified zinc oxide nanofilms: A DFT study. Applied Surface Science, 2021, 544, 148868.	3.1	20
55927	MoirÃ© superlattice on the surface of a topological insulator. Physical Review B, 2021, 103, .	1.1	28

#	Article	IF	Citations
55928	Strong Roomâ€Temperature Ferroelectricity in Strained SrTiO₃ Homoepitaxial Film. Advanced Materials, 2021, 33, e2008316.	11.1	28
55929	Electronic and optical properties of Janus monolayers MoXB2 (X=S, Se): first-principles prediction. EPJ Applied Physics, 2021, 94, 10301.	0.3	0
55930	Magnetic Improvement and Relaxation Mechanism of the Tb-Phthalocyanine Single-Molecule Magnet by Absorbing CH₂Cl₂ Molecules. Journal of Physical Chemistry C, 2021, 125, 10165-10172.	1.5	5
55931	Metal-Free Supramolecular Catalytic Hydrolysis of Ammonia Borane through Cucurbituril Nanocavitands. ACS Applied Materials & Interfaces, 2021, 13, 16218-16226.	4.0	19
55932	Performance of Made Simple Meta-GGA Functionals with rVV10 Nonlocal Correlation for H₂ + Cu(111), D₂ + Ag(111), H₂ + Au(111), and D₂ + Pt(111) Journal of Physical Chemistry C, 2021, 125, 8993-9010.	1.5	11
55933	Phonons and Adsorption-Induced Deformations in ZIFs: Is It Really a Gate Opening?. Journal of Physical Chemistry C, 2021, 125, 7999-8005.	1.5	10
55934	FTIR Measurement of the Hydrogenated Si(100) Surface: The Structure-Vibrational Interpretation by Means of Periodic DFT Calculation. Journal of Physical Chemistry C, 2021, 125, 9219-9228.	1.5	2
55935	Heavy-Atom Antiferromagnet GdBiTe: An Interplay of Magnetism and Topology in a Symmetry-Protected Topological Semimetal. Chemistry of Materials, 2021, 33, 2420-2435.	3.2	5
55936	Predicted Electrocatalyst Properties on Metal Insulator MoTe₂ for Hydrogen Evolution Reaction and Oxygen Reduction Reaction Application in Fuel Cells. Energy & Fuels, 2021, 35, 8275-8285.	2.5	11
55937	Achieving Highly Efficient Carbon Dioxide Electrolysis by In Situ Construction of the Heterostructure. ACS Applied Materials & Interfaces, 2021, 13, 20060-20069.	4.0	32
55938	Bonding behavior and passivation mechanism of organic ligands (-SH, -NH2, -COOH) on ZnS (<mml:math) Tj ETQq0 0 0 rgBT /Overlock 1	3.1	9
55939	surface from first-principles calculations. Applied Surface Science, 2021, 545, 148970. Phase and defect evolution in uranium-nitrogen-oxygen system under irradiation. Acta Materialia, 2021, 208, 116778.	3.8	21
55940	Highly Sensitive and Selective Gas Sensor Using Heteroatom Doping Graphdiyne: A DFT Study. Advanced Electronic Materials, 2021, 7, 2001244.	2.6	37
55941	Phase Boundary Mapping of Tinâ€Doped ZnSb Reveals Thermodynamic Route to High Thermoelectric Efficiency. Advanced Energy Materials, 2021, 11, 2100181.	10.2	17
55942	Density functional theory study of the mechanical behavior of silicene and development of a Tersoff interatomic potential model tailored for elastic behavior. Nanotechnology, 2021, 32, 295702.	1.3	10
55943	Excitonic Effects on Two-Dimensional Transition-Metal Dichalcogenide Monolayers: Impact on Solar Cell Efficiency. ACS Applied Energy Materials, 2021, 4, 3265-3278.	2.5	26
55944	First-principles study of hydrogen storage on Ca-decorated defective boron nitride nanosheets. Physica E: Low-Dimensional Systems and Nanostructures, 2021, 128, 114588.	1.3	29
55945	Mechanism of MoS₂ Growth on a Au(111) Surface: An Ab Initio Molecular Dynamics Study. Chemistry of Materials, 2021, 33, 3241-3248.	3.2	11

#	Article	IF	Citations
55946	Adhesion property and bonding characteristic between TiN and 2D-MoS2: A first-principles study. Journal of Materials Research, 2021, 36, 1990-2000.	1.2	3
55947	How dopants limit the ultrahigh thermal conductivity of boron arsenide: a first principles study. Npj Computational Materials, 2021, 7, .	3.5	21
55948	Crystal Orbital Bond Index: Covalent Bond Orders in Solids. Journal of Physical Chemistry C, 2021, 125, 7959-7970.	1.5	96
55949	Prediction of theoretical strength of diamond under complex loadings. Extreme Mechanics Letters, 2021, 44, 101233.	2.0	11
55950	Revealing the Effect of Sodium on Iron-Based Catalysts for CO₂ Hydrogenation: Insights from Calculation and Experiment. Journal of Physical Chemistry C, 2021, 125, 7637-7646.	1.5	20
55951	The atlas of ferroicity in two-dimensional MGeX3 family: Room-temperature ferromagnetic half metals and unexpected ferroelectricity and ferroelasticity. Nano Research, 2021, 14, 4732-4739.	5.8	17
55952	Efficient and selective oxidation of cyclohexane to cyclohexanone over flake hexagonal boron nitride/titanium dioxide hybrid photocatalysts. Molecular Catalysis, 2021, 505, 111530.	1.0	4
55953	Treecode-accelerated Green iteration for Kohn-Sham density functional theory. Journal of Computational Physics, 2021, 430, 110101.	1.9	3
55954	Complete mapping of magnetic anisotropy for prototype Ising van der Waals FePS₃. 2D Materials, 2021, 8, 035011.	2.0	14
55955	The Ti2CO2 MXene as a nucleobase 2D sensor: A first-principles study. Applied Surface Science, 2021, 544, 148946.	3.1	27
55956	Terahertz Driven Reversible Topological Phase Transition of Monolayer Transition Metal Dichalcogenides. Advanced Science, 2021, 8, e2003832.	5.6	25
55957	Discovery of electrochemically induced grain boundary transitions. Nature Communications, 2021, 12, 2374.	5.8	25
55958	Electrochemically induced in-situ surface self-reconstruction on Ni, Fe, Zn ternary-metal hydroxides towards the oxygen-evolution performance. Chemical Engineering Journal, 2021, 410, 128331.	6.6	22
55959	Design of a Multilayered Oxygenâ€Evolution Electrode with High Catalytic Activity and Corrosion Resistance for Saline Water Splitting. Advanced Functional Materials, 2021, 31, 2101820.	7.8	103
55960	Intrinsically low lattice thermal conductivity of monolayer hexagonal aluminum nitride (h-AlN) from first-principles: A comparative study with graphene. International Journal of Thermal Sciences, 2021, 162, 106772.	2.6	23
55961	Highly efficient photosynthesis of hydrogen peroxide in ambient conditions. Proceedings of the National Academy of Sciences of the United States of America, 2021, 118, .	3.3	80
55962	Highly efficient conversion of methane to formic acid under mild conditions at ZSM-5-confined Fe-sites. Nano Energy, 2021, 82, 105718.	8.2	47
55963	Theory-Guided Synthesis of Highly Luminescent Colloidal Cesium Tin Halide Perovskite Nanocrystals. Journal of the American Chemical Society, 2021, 143, 5470-5480.	6.6	49

#	Article	IF	Citations
55964	Highly Lithiophilic Copper-Reinforced Scaffold Enables Stable Li Metal Anode. ACS Applied Materials & Interfaces, 2021, 13, 20240-20250.	4.0	24
55965	Biâ€“Sn Oxides for Highly Selective CO₂Electroreduction to Formate in a Wide Potential Window. ChemSusChem, 2021, 14, 2247-2254.	3.6	34
55966	Enhanced Thermoelectric Performance in High Entropy Alloys Sn_{0.25}Pb_{0.25}Mn_{0.25}Ge_{0.25}Te. ACS Applied Materials & Interfaces, 2021, 13, 18638-18647.	4.0	43
55967	Plasma-Assisted Catalysis of Ammonia Using Tungsten at Low Pressures: A Parametric Study. ACS Applied Energy Materials, 2021, 4, 4385-4394.	2.5	10
55968	Realistic flat-band model based on degenerate p-orbitals in two-dimensional ionic materials. Science Bulletin, 2021, 66, 765-770.	4.3	7
55969	Predicted Superconductivity in the Electride Li₅C. Journal of Physical Chemistry C, 2021, 125, 8899-8906.	1.5	24
55970	Observation of Electric-Field-Induced Structural Dislocations in a Ferroelectric Oxide. Nano Letters, 2021, 21, 3386-3392.	4.5	9
55971	Effect of the Co-cation on Cu Speciation in Cu-Exchanged Mordenite and ZSM-5 Catalysts for the Oxidation of Methane to Methanol. ACS Catalysis, 2021, 11, 4973-4987.	5.5	31
55972	Formic Acid Electrooxidation on Pt or Pd Monolayer on Transition-Metal Single Crystals: A First-Principles Structure Sensitivity Analysis. ACS Catalysis, 2021, 11, 5294-5309.	5.5	15
55973	CrI₃/Y₂CH₂ Heterointerface-Induced Stable Half-Metallicity of Two-Dimensional CrI₃ Monolayer Ferromagnets. ACS Applied Materials & Interfaces, 2021, 13, 16694-16703.	4.0	8
55974	Photovoltaic properties of metal-free semiconductor DMEDAÂ·I6: A first-principles investigation. Materials Research Express, 2021, 8, 045901.	0.8	1
55975	Observation of local vibrational modes in N-doped 6H-SiC. Indian Journal of Physics, 0, , 1.	0.9	0
55976	1D metallic states at 2D transition metal dichalcogenide semiconductor heterojunctions. Npj 2D Materials and Applications, 2021, 5, .	3.9	2
55977	High-throughput screening for Weyl semimetals with <mml:math xmlns:mml="http://www.w3.org/1998/Math/MathML" altimg="si89.svg"><mml:mrow><mml:msub><mml:mrow><mml:mi mathvariant="normal">S</mml:mi></mml:mrow><mml:mrow><mml:mn>4</mml:mn></mml:mrow></mml:msub></mml:mrow></mml symmetry. Science Bulletin, 2021, 66, 667-675.	4.3	16
55978	Available Active Sites on Îµâ€Fe₃N Nanoparticles Synthesized by a Facile Route for Hydrogen Evolution Reaction. Advanced Materials Interfaces, 2021, 8, 2100070.	1.9	12
55979	High-performance flexible self-powered strain sensor based on carbon nanotube/ZnSe/CoSe2 nanocomposite film electrodes. Nano Research, 2022, 15, 170-178.	5.8	33
55980	PyXtal: A Python library for crystal structure generation and symmetry analysis. Computer Physics Communications, 2021, 261, 107810.	3.0	40
55981	Spatially Confined Formation of Single Atoms in Highly Porous Carbon Nitride Nanoreactors. ACS Nano, 2021, 15, 7790-7798.	7.3	33

#	Article	IF	Citations
55982	Interfacial Carrier-Transfer Channel Optimization Based on Hydrogen Bonds for High-Performance Organic Solar Cells. ACS Applied Energy Materials, 2021, 4, 3881-3890.	2.5	5
55983	Metallic-State MoS₂ Nanosheets with Atomic Modification for Sodium Ion Batteries with a High Rate Capability and Long Lifespan. ACS Applied Materials & Interfaces, 2021, 13, 19894-19903.	4.0	20
55984	Disordered but Efficient: Understanding the Role of Structure and Composition of the Coâ€“Pt Alloy on the Electrocatalytic Methanol Oxidation Reaction. Journal of Physical Chemistry C, 2021, 125, 7611-7624.	1.5	7
55985	Mn Dimer Can Be Described Accurately with Density Functional Calculations When Self-Interaction Correction Is Applied. Journal of Physical Chemistry Letters, 2021, 12, 4240-4246.	2.1	7
55986	What is the Role of Nb on Preferential Hydriding of Double-Phased Uranium, Stabilizing Î³-U, or Avoiding Hydrogen Aggregation?. Journal of Physical Chemistry C, 2021, 125, 9364-9370.	1.5	0
55987	Activating electrocatalytic hydrogen evolution performance of two-dimensional <mml:math xmlns:mml="http://www.w3.org/1998/Math/MathML"><mml:mrow><mml:mi>M</mml:mi><mml:msub><mml:mi>Si</mml:mi><mml:mn mathvariant="normal">N</mml:mi><mml:mn>4</mml:mn></mml:msub><mml:mrow><mml:mo>(</mml:mo><mml:mi>M</mml:mi> theoretical pred. Physical Review Materials, 2021, 5, .	3.1	30
55988	Water Splitting with a Single-Atom Cu/TiO₂ Photocatalyst: Atomistic Origin of High Efficiency and Proposed Enhancement by Spin Selection. Jacs Au, 2021, 1, 550-559.	3.6	58
55989	Passivation of PEA+ to MAPbI3 (110) surface states by first-principles calculations*. Chinese Physics B, 2021, 30, 047101.	0.7	1
55990	Data-Driven Discovery and Synthesis of High Entropy Alloy Hydrides with Targeted Thermodynamic Stability. Chemistry of Materials, 2021, 33, 4067-4076.	3.2	33
55991	Anharmonic effects on the dynamics of solid aluminium from ab initio simulations. Journal of Physics Condensed Matter, 2021, 33, 175501.	0.7	3
55992	Reductant-free synthesis of oxygen vacancies-mediated TiO2 nanocrystals with enhanced photocatalytic NO removal performance: An experimental and DFT study. Applied Surface Science, 2021, 544, 148923.	3.1	15
55993	Accommodation and diffusion of Nd in uranium silicide - U3Si2. Journal of Nuclear Materials, 2021, 547, 152794.	1.3	0
55994	Molecular alignment descriptor to search for the most stable adsorption sites of saturated cyclic compounds on metal surfaces. Applied Surface Science, 2021, 544, 148904.	3.1	4
55995	A V₃C₂ MXene/graphene heterostructure as a sustainable electrode material for metal ion batteries. Journal of Physics Condensed Matter, 2021, 33, 175001.	0.7	14
55996	Semiconducting MnB₅ monolayer as a potential photovoltaic material. Journal of Physics Condensed Matter, 2021, 33, 175702.	0.7	1
55997	Tuning the magnetic properties of Fe3GeTe2 by doping with 3d transition-metals. Physics Letters, Section A: General, Atomic and Solid State Physics, 2021, 396, 127219.	0.9	7
55998	The Band-Gap Studies of Short-Period CdO/MgO Superlattices. Nanoscale Research Letters, 2021, 16, 59.	3.1	12
55999	Materials Studio simulation for the adsorption properties of CO2 molecules at the surface of sodium silicate and potassium silicate solution under different pressure conditions. International Journal of Metalcasting, 2022, 16, 242-251.	1.5	8

#	Article	IF	Citations
56000	Growth of h-BN/graphene heterostructure using proximity catalysis. Nanotechnology, 2021, 32, 275602.	1.3	4
56001	Efficient electronic passivation scheme for computing low-symmetry compound semiconductor surfaces in density-functional theory slab calculations. Physical Review Materials, 2021, 5, .	0.9	0
56002	Preferential hole defect formation in monolayer WSe2 by electron-beam irradiation. Physical Review Materials, 2021, 5, .	0.9	4
56003	Simultaneous tuning of the magnetic anisotropy and thermal stability of $$alpha ^{''}$$-phase Fe$$_{16}$$N$$_{2}$$. Scientific Reports, 2021, 11, 7823.	1.6	6
56004	Finite-size correction for slab supercell calculations of materials with spontaneous polarization. Npj Computational Materials, 2021, 7, .	3.5	14
56005	Kinetics and Thermodynamics of Fe-X (X= Al, Cr, Mn, Ti, B, and C) Melts under High Pressure. , 0, 29, 143-160.		0
56006	A tightly bonded reduced graphene oxide coating on magnesium alloy with photothermal effect for tumor therapy. Journal of Magnesium and Alloys, 2022, 10, 3031-3040.	5.5	7
56007	Enhancing gas sensing properties of novel palladium-decorated zinc oxide surface: a first-principles study. Materials Research Express, 2021, 8, 045004.	0.8	10
56009	High-throughput search for magnetic topological materials using spin-orbit spillage, machine learning, and experiments. Physical Review B, 2021, 103, .	1.1	22
56010	Tunable Negative Poissonâ€™s Ratio in Van der Waals Superlattice. Research, 2021, 2021, 1904839.	2.8	5
56011	Nanometer-size Na cluster formation in micropore of hard carbon as origin of higher-capacity Na-ion battery. Npj Computational Materials, 2021, 7, .	3.5	39
56012	Unconventional line defects engineering in two-dimensional boron monolayers. Physical Review Materials, 2021, 5, .	0.9	7
56013	Pressure-induced superconductivity in the quasi-one-dimensional charge density wave material CuTe. Physical Review B, 2021, 103, .	1.1	10
56014	Assessment, improvement, and comparison of different computational tools used for the simulation of heat transport in nanostructures. Simulation, 0, , 003754972110096.	1.1	1
56015	Conversation from antiferromagnetic MnBr2 to ferromagnetic Mn3Br8 monolayer with large MAE. Nanoscale Research Letters, 2021, 16, 72.	3.1	1
56016	Calculation of Phase Diagrams and First-Principles Study of Germanium Impacts on Phosphorus Distribution in Czochralski Silicon. Journal of Electronic Materials, 2021, 50, 4272-4288.	1.0	0
56017	Formaldehyde Oxidation over Co@N-Doped Carbon at Room Temperature: Tunable Co Size and Intensified Surface Electron Density. ACS ES&T Engineering, 2021, 1, 917-927.	3.7	14
56018	On the Spatial Design of Co-Fed Amines for Selective Dehydration of Methyl Lactate to Acrylates. ACS Catalysis, 2021, 11, 5718-5735.	5.5	6

#	Article	IF	Citations
56019	Diffusional-displacive transformation mechanism for the Î²1 precipitate in a model Mg-rare-earth alloy. Materials Characterization, 2021, 174, 111018.	1.9	8
56020	Perfect Spherical Tetrahedral Metallo-Borospherene Ta₄B₁₈ as a Superatom Following the 18-Electron Rule. ACS Omega, 2021, 6, 10991-10996.	1.6	13
56021	Vibrational properties and thermal transport in quaternary chalcogenides: The case of Te-based compositions. Physical Review Materials, 2021, 5, .	0.9	7
56022	Inactivating SARS-CoV-2 by electrochemical oxidation. Science Bulletin, 2021, 66, 720-726.	4.3	18
56023	New structure candidates for the experimentally synthesized heptazine-based and triazine-based two dimensional graphitic carbon nitride. Physica E: Low-Dimensional Systems and Nanostructures, 2021, 128, 114535.	1.3	2
56024	Dispersing and semi-flat bands in the wide band gap two-dimensional semiconductor bilayer silicon oxide. 2D Materials, 2021, 8, 035021.	2.0	3
56025	Effect of Pd Coordination and Isolation on the Catalytic Reduction of O₂ to H₂O₂ over PdAu Bimetallic Nanoparticles. Journal of the American Chemical Society, 2021, 143, 5445-5464.	6.6	101
56026	A Transferable Force Field for Predicting Adsorption and Diffusion of Hydrocarbons and Small Molecules in Silica Zeolites with Coupled-Cluster Accuracy. Journal of Physical Chemistry C, 2021, 125, 8418-8429.	1.5	11
56027	Cobalt-doped oxygen-deficient titanium dioxide coated by carbon layer as high-performance sulfur host for Li/S batteries. Journal of Alloys and Compounds, 2021, 861, 157969.	2.8	18
56028	Manipulating Zn anode reactions through salt anion involving hydrogen bonding network in aqueous electrolytes with PEO additive. Nano Energy, 2021, 82, 105739.	8.2	115
56029	Synthesis, characterization, and photocatalytic activity of stannum-doped MgIn2S4 microspheres. Journal of Alloys and Compounds, 2021, 860, 158446.	2.8	14
56030	Correlating Surface Crystal Orientation and Gas Kinetics in Perovskite Oxide Electrodes. Advanced Materials, 2021, 33, e2100977.	11.1	17
56031	Lithiophilic N-doped carbon bowls induced Li deposition in layered graphene film for advanced lithium metal batteries. Nano Research, 2022, 15, 352-360.	5.8	93
56032	First-principles study of multiple-site substitutions of alloying elements in Ni-based single crystal superalloys. Science China Technological Sciences, 2021, 64, 1276-1284.	2.0	6
56033	Monoclinic <mml:math xmlns:mml="http://www.w3.org/1998/Math/MathML" display="inline"><mml:mrow><mml:msub><mml:mrow><mml:mi>EuSn</mml:mi></mml:mrow><mml:mrow><mml:mn>2</mml:mn></mml:mrow></mml:msub></mml:mrow></mml:math> : A Novel High-Pressure Network Structure. Physical Review Letters, 2021, 126, 155701.	2.9	24
56034	UiO-66 Metalâ€“Organic Framework as an Anode for a Potassium-Ion Battery: Quantum Mechanical Analysis. Journal of Physical Chemistry C, 2021, 125, 9679-9687.	1.5	21
56035	Nanoporous carbon oxynitride and its enhanced lithium-ion storage performance. Nano Energy, 2021, 82, 105733.	8.2	13
56036	Theoretical Calculations Meet Experiment to Explain the Luminescence Properties and the Presence of Defects in m-ZrO₂. Chemistry of Materials, 2021, 33, 2984-2992.	3.2	9

#	Article	IF	Citations
56037	New Cadmiumâ€“Nitrogen Compounds at High Pressures. Inorganic Chemistry, 2021, 60, 6772-6781.	1.9	31
56038	Two-dimensional MnN utilized as high-capacity anode for Li-ion batteries*. Chinese Physics B, 2021, 30, 046302.	0.7	4
56039	Enhancing the Hydrogen Evolution Properties of Kesterite Absorber by Siâ€Doping in the Surface of CZTS Thin Film. Advanced Materials Interfaces, 2021, 8, 2002124.	1.9	8
56040	Surface plasmon mediates the visible lightâ€“responsive lithiumâ€“oxygen battery with Au nanoparticles on defective carbon nitride. Proceedings of the National Academy of Sciences of the United States of America, 2021, 118, .	3.3	74
56041	The mechanism of alkali doping in CsPbBr3: A first-principles perspective. Journal of Applied Physics, 2021, 129, .	1.1	7
56042	Composition Stability and Cr-Rich Phase Formation in W-Cr-Y and W-Cr-Ti Smart Alloys. Metals, 2021, 11, 743.	1.0	4
56043	Impact of training and validation data on the performance of neural network potentials: A case study on carbon using the CA-9 dataset. Carbon Trends, 2021, 3, 100027.	1.4	3
56044	Structural, Electronic, Magnetic, and Elastic Properties of CoXâ€²CrZ (Xâ€²â€‰=â€‰Sc, Ti; Zâ€‰=â€‰Al, Ga) Quaternary Heusler Alloys: Firstâ€Principles Study. Physica Status Solidi (B): Basic Research, 2021, 258, 2100004.	0.7	4
56045	<mml:math xmlns:mml="http://www.w3.org/1998/Math/MathML"><mml:mrow><mml:msub><mml:mi>CoN</mml:mi><mml:mn>4</mml:mn></mml mathvariant="normal">C</mml:mi><mml:mn>2</mml:mn></mml:msub></mml:mrow></mml:math> : Two-dimensional cobalt carbonitride with a flat-band feature. Physical Review B, 2021, 103, .	1.1	13
56046	The superconductivity of Nâ€“Siâ€“H compounds at high pressure. Solid State Communications, 2021, 329, 114260.	0.9	6
56047	Molecular engineering of near-infrared active boron dipyrromethene moiety with various donors and acceptors for tuning the absorption behavior and electron injection of the resultant dyes. Journal of Photochemistry and Photobiology A: Chemistry, 2021, 410, 113161.	2.0	12
56048	An improved electrochemical model for strain dependent electrochemical polarization and corrosion kinetics. Materials and Design, 2021, 202, 109555.	3.3	5
56049	Computational high-throughput screening of alloy nanoclusters for electrocatalytic hydrogen evolution. Npj Computational Materials, 2021, 7, .	3.5	46
56050	Superior Conversion Efficiency Achieved in GeP₃/h-BN Heterostructures as Novel Flexible and Ultralight Thermoelectrics. ACS Applied Materials & Interfaces, 2021, 13, 18800-18808.	4.0	14
56051	Flexible borophosphene monolayer: A potential Dirac anode for high-performance non-lithium ion batteries. Applied Surface Science, 2021, 544, 148895.	3.1	44
56052	Thermochemical electronegativities of the elements. Nature Communications, 2021, 12, 2087.	5.8	141
56053	Crystal and electronic structure engineering of tin monoxide by external pressure. Journal of Advanced Ceramics, 2021, 10, 565-577.	8.9	11
56054	Influence of Fe and Ni Doping on the OER Performance at the Co₃O₄(001) Surface: Insights from DFT+UCalculations. ACS Catalysis, 2021, 11, 5601-5613.	5.5	86

#	Article	IF	Citations
56055	Seeded 2D epitaxy of large-area single-crystal films of the van der Waals semiconductor 2H MoTe ₂. Science, 2021, 372, 195-200.	6.0	143
56056	Prediction of high thermoelectric performance in the low-dimensional metal halide Cs3Cu2I5. Npj Computational Materials, 2021, 7, .	3.5	26
56057	Toward an In-Depth Material Model for Cermet Nuclear Thermal Rocket Fuel Elements. Nuclear Technology, 2021, 207, 825-835.	0.7	2
56058	Surface Reactivity and Surface Characterization of the Layered Î²(III)-CoOOH Material: an Experimental and Computational Study. Journal of Physical Chemistry C, 2021, 125, 8570-8581.	1.5	11
56059	Peierls transition driven ferroelasticity in the two-dimensional <mml:math xmlns:mml="http://www.w3.org/1998/Math/MathML"><mml:mrow><mml:mi>d</mml:mi><mml:mtext>â^'</mml:mtext><mml:mi>f</mml:mi> hybrid magnets. Physical Review B, 2021, 103, .	1.1	24
56060	Microbial methylation potential of mercury sulfide particles dictated by surface structure. Nature Geoscience, 2021, 14, 409-416.	5.4	36
56061	Hydrogenation of benzoic acid derivatives over Pt/TiO2 under mild conditions. Communications Chemistry, 2021, 4, .	2.0	19
56062	Ca₂C MXene monolayer as a superior anode for metal-ion batteries. 2D Materials, 2021, 8, 035015.	2.0	44
56063	Valenceâ€State Effect of Iridium Dopant in NiFe(OH)₂ Catalyst for Hydrogen Evolution Reaction. Small, 2021, 17, e2100203.	5.2	31
56064	Tuning local chemistry of P2 layered-oxide cathode for high energy and long cycles of sodium-ion battery. Nature Communications, 2021, 12, 2256.	5.8	183
56065	Effect of Surface Charge Distribution of Phosphorus-Doped MoS₂ on Hydrogen Evolution Reaction. ACS Applied Energy Materials, 2021, 4, 4887-4896.	2.5	25
56066	Intercalated architecture of MA2Z4 family layered van der Waals materials with emerging topological, magnetic and superconducting properties. Nature Communications, 2021, 12, 2361.	5.8	199
56067	Sn²⁺-Regulated Synthesis of a Bone-like Fe₃O₄@N-Doped Carbon Composite as the Anode for High-Performance Lithium Storage. ACS Applied Energy Materials, 2021, 4, 3785-3793.	2.5	8
56068	Carbonâ€Coordinated Single Cr Site for Efficient Electrocatalytic N₂ Fixation. Advanced Theory and Simulations, 2021, 4, 2100044.	1.3	24
56069	High-Throughput Screening of a Single-Atom Alloy for Electroreduction of Dinitrogen to Ammonia. ACS Applied Materials & Interfaces, 2021, 13, 16336-16344.	4.0	58
56070	Generation of the TSL for Zirconium Hydrides from Ab Initio Methods. Journal of Nuclear Engineering, 2021, 2, 105-113.	0.7	7
56071	Electronic and vibrational properties of the high T _c superconductor Bi₂Sr₂CaCu₂O₈: an ab initio study. Journal of Physics Condensed Matter, 2021, 33, 185705.	0.7	7
56072	Theoretical insights into strong intrinsic piezoelectricity of blue-phosphorus-like group-IV monochalcogenides. Nano Research, 2022, 15, 209-216.	5.8	17

#	Article	IF	Citations
56073	Strong trilinear coupling of phonon instabilities drives the avalanche-like hybrid improper ferroelectric transition in <mml:math xmlns:mml="http://www.w3.org/1998/Math/MathML"><mml:mrow><mml:msub><mml:mi>SrBi</mml:mi><mml:mn>2</mml:mn></mml:msub><mml:msub><mml:mi mathvariant="normal">O</mml:mi><mml:mn>9</mml:mn></mml:msub></mml:mrow></mml:math>. Physical Review B, 2021, 103, .	1.1	0
56074	The cageâ€like structure enhanced magnetic moment in ScK n (n = 2â€“12) clusters: A firstâ€principles jointed particle swarm optimization investigation. International Journal of Quantum Chemistry, 2021, 121, e26654.	1.0	2
56075	Ab initio study of lithium decoration of popgraphene and hydrogen storage capacity of the hybrid nanostructure. International Journal of Hydrogen Energy, 2021, 46, 15724-15737.	3.8	16
56076	Structure-Dependent Doppler Broadening Using a Generalized Thermal Scattering Law. Journal of Nuclear Engineering, 2021, 2, 124-131.	0.7	0
56077	Sizeable bandgap modulation in Y2Hf2O7 pyrochlore oxide thin films through B-site substitution. Applied Physics Letters, 2021, 118, 141902.	1.5	2
56078	Electric control of nearly free electron states and ferromagnetism in the transition-metal dichalcogenides monolayers. Journal of Physics Condensed Matter, 2021, 33, 205702.	0.7	3
56079	Manipulating Berry curvature of SrRuO₃thin films via epitaxial strain. Proceedings of the National Academy of Sciences of the United States of America, 2021, 118, .	3.3	41
56080	First-principles study of the role of surface in the heavy-fermion compound <mml:math xmlns:mml="http://www.w3.org/1998/Math/MathML"><mml:mrow><mml:msub><mml:mi>CeRh</mml:mi><mml:mn>2</mml:mn></mml:msub></mml:mrow></mml:math>. Physical Review B, 2021, 103, .	1.1	8
56081	Ionothermal Synthesis of Two New Thioantimonates with Transition Metal Regulation. Journal of Cluster Science, 2022, 33, 1457-1465.	1.7	1
56082	Defect-engineered three-dimensional vanadium diselenide microflowers/nanosheets on carbon cloth by chemical vapor deposition for high-performance hydrogen evolution reaction. Nanotechnology, 2021, 32, 265402.	1.3	10
56083	Large anomalous Hall effect in the kagome ferromagnet LiMn6Sn6. Physical Review B, 2021, 103, .	1.1	35
56084	Borophene-Based Three-Dimensional Porous Structures as Anode Materials for Alkali Metal-Ion Batteries with Ultrahigh Capacity. Chemistry of Materials, 2021, 33, 2976-2983.	3.2	20
56085	Structural and electronic properties of AlY (Y B, N, O) dual-doped twin graphene: A density functional theory study. Physica E: Low-Dimensional Systems and Nanostructures, 2021, 128, 114619.	1.3	7
56086	Modulation on the Iron Centers by Selective Synthesis of Organic Ligands with Stereoâ€Specific Conformations. Small, 2021, 17, e2008036.	5.2	2
56087	Edgeâ€Confined Pt₁/MoS₂ Singleâ€Atom Catalyst Promoting the Selective Activation of Carbonâ€Oxygen Bond. ChemCatChem, 2021, 13, 2783-2793.	1.8	18
56088	Possibility of Doping <mml:math xmlns:mml="http://www.w3.org/1998/Math/MathML" display="inline" overflow="scroll"><mml:msub><mml:mrow><mml:mi>Cu</mml:mi><mml:mi>Ga</mml:mi><mml:mi>Se</mml:mi></mml:mrow><mml:mn>2</mml:mn></mml:msub></mml:math> n -Type by Hydrogen. Physical Review Applied, 2021, 15, .	1.5	2
56089	Spin-polarized gate-tuned transport property of a four-terminal MoS2 device: a theoretical study. Journal of Materials Science, 2021, 56, 11847-11865.	1.7	1
56090	Ab initio lattice thermal conductivity of <mml:math xmlns:mml="http://www.w3.org/1998/Math/MathML"><mml:mrow><mml:mi>Mg</mml:mi><mml:mi>Si</mml:mi><mml:msub><mml:mi mathvariant="normal">O</mml:mi><mml:mn>3</mml:mn></mml:msub></mml:mrow></mml:math> across the perovskite-postperovskite phase transition. Physical Review B, 2021, 103, .	1.1	8

#	Article	IF	Citations
56091	Atomic properties of sodium silicate glasses obtained from the building-block method. Physical Review B, 2021, 103, .	1.1	3
56092	Influence of anisotropic strain and temperature on hydrogen dissolution in tungsten. Modelling and Simulation in Materials Science and Engineering, 2021, 29, 055011.	0.8	0
56093	Investigating 3,4-bis(3-nitrofurazan-4-yl)furoxan detonation with a rapidly tuned density functional tight binding model. Journal of Chemical Physics, 2021, 154, 164115.	1.2	12
56094	First-order liquid-liquid phase transition in nitrogen-oxygen mixtures. Physical Review B, 2021, 103, .	1.1	4
56095	A DFT study of NO2 and SO2 gas-sensing properties of InX (Xâ€‰=â€‰Cl, Br and I) monolayers. Journal of Materials Science, 2021, 56, 11828-11837.	1.7	12
56096	Theoretical study of GaN (0001) surface reconstructions and La and Ga adatoms under N- and Ga-rich conditions. Physical Review Materials, 2021, 5, .	0.9	0
56097	Inversion domain boundaries in wurtzite GaN. Physical Review B, 2021, 103, .	1.1	1
56099	The stability analysis of the monolayer triangular borophene adsorbed on substrates: First-principles simulation. Computational Materials Science, 2021, 190, 110271.	1.4	0
56100	Carbon phase adjustment by multi-configuration ligand in endohedral metallofullerene derivatives Gd@C82(morpholine)7 under high pressure. Nano Today, 2021, 37, 101079.	6.2	0
56101	Intermediates for catalytic reduction of CO2 on p-block element surfaces. Journal of Industrial and Engineering Chemistry, 2021, 96, 236-242.	2.9	20
56102	Temperature-dependent electronic structure of bixbyite Î±-Mn₂O₃ and the importance of a subtle structural change on oxygen electrocatalysis. Science and Technology of Advanced Materials, 2021, 22, 141-149.	2.8	5
56103	Oxidation behavior of different La2O3-content modified SiC ceramic at 1700ÂÂ°C. Ceramics International, 2021, 47, 11560-11567.	2.3	8
56104	Mechanism insights into direct conversion of syngas into C2 oxygenates via key intermediate C2O2 over Ni-Supported graphene. Carbon, 2021, 175, 322-333.	5.4	5
56105	Ab-initio characterization of B4C3 monolayer as a toxic gases sensing material. Applied Surface Science, 2021, 544, 148877.	3.1	14
56106	Structural and Electronic Properties of (HfH2)n (n = 5â€“30) Clusters: Theoretical Investigation. Physica E: Low-Dimensional Systems and Nanostructures, 2021, 128, 114634.	1.3	3
56107	First principles study of behavior of helium at Fe(110)â€“graphene interface*. Chinese Physics B, 2021, 30, 046802.	0.7	2
56108	Ab-initio study of the effects of charging on the adsorption and diffusion of Au2 on MgO(100). Current Applied Physics, 2021, 24, 39-45.	1.1	4
56109	Synthesis of Au sponges based on agarose template. Scripta Materialia, 2021, 196, 113769.	2.6	3

#	Article	IF	Citations
56110	Mechanical Vibrational Relaxation of NO Scattering from Metal and Insulator Surfaces: When and Why They Are Different. Physical Review Letters, 2021, 126, 156101.	2.9	16
56111	Origin of shuttle-free sulfurized polyacrylonitrile in lithium-sulfur batteries. Journal of Power Sources, 2021, 492, 229508.	4.0	33
56112	First-principles investigation of electronic, optical, mechanical and heat transport properties of pentadiamond: A comparison with diamond. Carbon Trends, 2021, 3, 100036.	1.4	16
56113	Olefin oligomerization by main group Ga3+ and Zn2+ single site catalysts on SiO2. Nature Communications, 2021, 12, 2322.	5.8	26
56114	Theoretical studies of methane adsorption on Silica-Kaolinite interface for shale reservoir application. Applied Surface Science, 2021, 546, 149164.	3.1	23
56115	Origin of itinerant ferromagnetism in two-dimensional Fe₃GeTe₂ *. Chinese Physics B, 2021, 30, 047502.	0.7	6
56116	Changes in CO2 Adsorption Affinity Related to Ni Doping in FeS Surfaces: A DFT-D3 Study. Catalysts, 2021, 11, 486.	1.6	6
56117	A Theoretical Study on the Thermal Conductivity and Thermoelectric Properties of CoNbSi and CoNbSn. Journal of Physical Chemistry C, 2021, 125, 10068-10076.	1.5	3
56118	Effect of Water Vapor on Alumina Scale Growth Based on First-Principles Calculations. Journal of Physical Chemistry C, 2021, 125, 9736-9746.	1.5	6
56119	Ultralow Thermal Conductivity in Diamondoid Structures and High Thermoelectric Performance in (Cu_{1â€“x}Ag_x)(In_{1â€“y}Ga_y)Te₂. Journal of the American Chemical Society, 2021, 143, 5978-5989.	6.4	49
56120	First-Principles Simulations for the Surface Evolution and Mn Dissolution in the Fully Delithiated Spinel LiMn₂O₄. Langmuir, 2021, 37, 5252-5259.	1.6	17
56121	Optimized effective potentials from the random-phase approximation: Accuracy of the quasiparticle approximation. Journal of Chemical Physics, 2021, 154, 154103.	1.2	8
56122	Semi-grand canonical Monte Carlo simulation of the acrolein induced surface segregation and aggregation of AgPd with machine learning surrogate models. Journal of Chemical Physics, 2021, 154, 134701.	1.2	11
56123	First-principles calculations of interface engineering for 2D Î±-In2Se3-based van der Waals multiferroic heterojunctions. Applied Surface Science, 2021, 545, 149024.	3.1	28
56124	Layered oxides as cathode materials for beyond-Li batteries: A computational study of Ca and Al intercalation in bulk V2O5 and MoO3. Computational Materials Science, 2021, 191, 110324.	1.4	15
56125	Enhancing Ferromagnetism and Tuning Electronic Properties of CrI₃ Monolayers by Adsorption of Transition-Metal Atoms. ACS Applied Materials & Interfaces, 2021, 13, 21593-21601.	4.0	30
56126	First-Principles Hydrothermal Synthesis Design to Optimize Conditions and Increase the Yield of Quaternary Heteroanionic Oxychalcogenides. Chemistry of Materials, 2021, 33, 2726-2741.	3.2	15
56127	Atomic-Scale Local Work Function Characterizations of Br Islands on Cu(111). Journal of Physical Chemistry C, 2021, 125, 7944-7949.	1.5	6

#	Article	IF	Citations
56128	Highly Anisotropic Thermoelectric Properties of Two-Dimensional As₂Te₃. ACS Applied Electronic Materials, 2021, 3, 1610-1620.	2.0	24
56129	Understanding the Role of Oxygen Vacancies in the Stability of ZnO(0001)-(1 Ã— 3) Surface Reconstructions. Journal of Physical Chemistry C, 2021, 125, 7980-7989.	1.5	8
56130	Broad-Spectrum Solvent-free Layered Black Phosphorus as a Rapid Action Antimicrobial. ACS Applied Materials & Interfaces, 2021, 13, 17340-17352.	4.0	24
56131	Coordination and activation of nitrous oxide by iron zeolites. Nature Catalysis, 2021, 4, 332-340.	16.1	49
56132	Design of Cobalt Fischerâ€“Tropsch Catalysts for the Combined Production of Liquid Fuels and Olefin Chemicals from Hydrogen-Rich Syngas. ACS Catalysis, 2021, 11, 4784-4798.	5.5	46
56133	Optical Cycling Functionalization of Arenes. Journal of Physical Chemistry Letters, 2021, 12, 3989-3995.	2.1	20
56134	Enhanced Stability and Epitaxial Growth Mechanism of the Honeycomb Borophene Monolayer on a Two-Dimensional Ti₂C Substrate. Journal of Physical Chemistry C, 2021, 125, 8589-8596.	1.5	6
56135	NaNbO₃/NaTaO₃ Superlattices: Cation-Ordering Improved Band-Edge Alignment for Water Splitting and CO₂ Photocatalysis. Langmuir, 2021, 37, 4493-4503.	1.6	10
56136	Thermoelectric Properties of the As/P-Based Zintl Compounds EuIn₂As_{2â€“x}P_x (x = 0â€“2) and SrSn₂As₂. ACS Applied Energy Materials, 2021, 4, 5155-5164.	2.5	16
56137	Unraveling the Causes of the Instability of Au_n(SR)_x Nanoclusters on Au(111). Chemistry of Materials, 2021, 33, 3428-3435.	3.2	3
56138	Spin-induced linear polarization of photoluminescence in antiferromagnetic van der Waals crystals. Nature Materials, 2021, 20, 964-970.	13.3	59
56139	Accurate prediction and applying the <mml:math xmlns:mml="http://www.w3.org/1998/Math/MathML" display="inline"><mml:mi>Si</mml:mi><mml:mo stretchy="false">(</mml:mo><mml:mn>111</mml:mn><mml:mo) Tj ETQq1 1 0.784314 rgBT /Overlock 10 Tf 50 307 Td (stretchy="false">(</mml:mo><mml:mn>7</mml:mn><mml:mo>Ã—</mml:mo><mml:mn>7</mml:mn><mml:mo) Tj ETQq1 1 0.784314 Neural Netwo	2.9	12
56140	Importance of the oxyl character on the IrO2 surface dependent catalytic activity for the oxygen evolution reaction. Journal of Catalysis, 2021, 396, 192-201.	3.1	18
56141	Few-layer tin sulfide (SnS): Controlled synthesis, thickness dependent vibrational properties, and ferroelectricity. Nano Today, 2021, 37, 101082.	6.2	34
56142	Liquid-phase exfoliation of F-diamane-like nanosheets. Carbon, 2021, 175, 124-130.	5.4	26
56143	Formaldehyde gas sensing properties of transition metal-doped graphene: a first-principles study. Journal of Materials Science, 2021, 56, 12256-12269.	1.7	21
56144	Pentagonal B2N3-based 3D metallic boron nitride with high energy density. Journal of Physics Condensed Matter, 2021, 33, 165702.	0.7	1
56145	First-principles calculations of diffusion activation energies for designing anti-self-aging biodegradable zinc alloys. Journal of Materials Research, 2021, 36, 1475-1486.	1.2	6

#	Article	IF	Citations
56146	Reduction of dopant ions and enhancement of magnetic properties by UV irradiation in Ce-doped TiO2. Scientific Reports, 2021, 11, 7668.	1.6	4
56147	Ferroelectricity and multiferroicity in antiâ€“Ruddlesdenâ€“Popper structures. Proceedings of the National Academy of Sciences of the United States of America, 2021, 118, .	3.3	9
56148	SnS₂ Nanosheets Anchored on Nitrogen and Sulfur Co-Doped MXene Sheets for High-Performance Potassium-Ion Batteries. ACS Applied Materials & Interfaces, 2021, 13, 17668-17676.	4.0	49
56149	Memristors Based on (Zr, Hf, Nb, Ta, Mo, W) Highâ€Entropy Oxides. Advanced Electronic Materials, 2021, 7, 2001258.	2.6	22
56150	High Performance Generation of H₂O₂ under Piezophototronic Effect with Multiâ€Layer In₂S₃ Nanosheets Modified by Spherical ZnS and BaTiO₃ Nanopiezoelectrics. Small Methods, 2021, 5, e2100269.	4.6	34
56151	Potassium-activated anionic copper and covalent Cuâ€“Cu bonding in compressed Kâ€“Cu compounds. Journal of Chemical Physics, 2021, 154, 134708.	1.2	5
56152	Anchoring single Pt atoms and black phosphorene dual co-catalysts on CdS nanospheres to boost visible-light photocatalytic H2 evolution. Nano Today, 2021, 37, 101080.	6.2	105
56153	Experimentally Driven Automated Machine-Learned Interatomic Potential for a Refractory Oxide. Physical Review Letters, 2021, 126, 156002.	2.9	28
56154	Blackbody-sensitive room-temperature infrared photodetectors based on low-dimensional tellurium grown by chemical vapor deposition. Science Advances, 2021, 7, .	4.7	121
56155	First-principle study of Ti2XS2 (XÂ=ÂC/N) MXenes as high capacity anodes for rechargeable potassium-ion batteries. Applied Surface Science, 2021, 546, 149096.	3.1	12
56156	Strong Modulation of Band Gap, Carrier Mobility and Lifetime in Two-Dimensional Black Phosphorene through Acoustic Phonon Excitation. Journal of Physical Chemistry Letters, 2021, 12, 3960-3967.	2.1	30
56157	In Situ Construction of Mo₂C Quantum Dotsâ€Đecorated CNT Networks as a Multifunctional Electrocatalyst for Advanced Lithiumâ€“Sulfur Batteries. Small, 2021, 17, e2100460.	5.2	81
56158	Quantifying the interplay between fine structure and geometry of an individual molecule on a surface. Physical Review B, 2021, 103, .	1.1	25
56159	Heterophase Interface Dominated Deformation and Mechanical Properties in Alâ€Cuâ€Li Alloys. Advanced Theory and Simulations, 2021, 4, 2100059.	1.3	5
56160	Crystal structure of 3-[(3,4-dinitro-1H-pyrazol-1-yl)-NNO-azoxy]-4-nitro-1,2,5-oxadiazole. Powder Diffraction, 2021, 36, 176-180.	0.4	2
56161	Effect of Chemical Potential and Atomic-Scale Vibration of Nucleant Surface on Liquid Layering and Heterogeneous Nucleation. Metallurgical and Materials Transactions A: Physical Metallurgy and Materials Science, 2021, 52, 2136-2143.	1.1	4
56162	Metastable 1Tâ€²-phase group VIB transition metal dichalcogenide crystals. Nature Materials, 2021, 20, 1113-1120.	13.3	119
56163	Ultralow Thermal Conductivity and High Thermopower in a New Family of Zintl Antimonides Ca₁₀MSb₉ (M = Ga, In, Mn, Zn) with Complex Structures and Heavy Disorder. Chemistry of Materials, 2021, 33, 3172-3186.	3.2	26

#		IF	Citations
56164	Electronic structure and topological phases of the magnetic layered materials <mml:math xmlns:mml="http://www.w3.org/1998/Math/MathML"><mml:msub><mml:mi mathvariant="normal">MnBi</mml:mi><mml:mn>2</mml:mn></mml:msub><mml:msub><mml:mi mathvariant="normal">Te</mml:mi><mml:mn>4</mml:mn></mml:msub><mml:mo>,</mml:mo><mml:mo>Â</mml:mo><mml:msub><mml:mi mathvariant="normal">MnBi</mml:mi><mml:mn>2</mml:mn></mml:msub><mml:msub><mml:mi mathvariant="normal">Se</mml:mi><mml:mn>4</mml:mn></mml:msub></mml:math> , and <. Physical Ke	1.1	21
56165	Vertex function compliant with the Ward identity for quasiparticle self-consistent calculations beyond <mml:math xmlns:mml="http://www.w3.org/1998/Math/MathML"><mml:mrow><mml:mi>G</mml:mi><mml:mi>W</mml:mi></mml:mrow></mml:m Physical Review B, 2021, 103, .	1.1	15
56166	Syntheses, crystal structures, optical, and theoretical study of two ternary chalcogenides CsSc5Te8 and Cs0.6(1)Ti6Se8 with tunnel structures. Solid State Sciences, 2021, 114, 106577.	1.5	4
56167	Investigating the CO activation mechanism on hcp-Fe7C3 (211) via density functional theory. Molecular Catalysis, 2021, 505, 111506.	1.0	2
56168	Electronic structure, dynamic stability, elastic, and optical properties of MgTMN2 (TMâ€‰=â€‰Ti, Zr, Hf) ternary nitrides from first-principles calculations. Journal of Applied Physics, 2021, 129, 135103.	1.1	3
56169	Observation of topological Dirac fermions and surface states in superconducting <mml:math xmlns:mml="http://www.w3.org/1998/Math/MathML"><mml:mrow><mml:mi>Ba</mml:mi><mml:msub><mml:mi>Sn Physical Review B, 2021, 103, .	1.1	8
56170	Polymorphism of praseodymium orthovanadate under high pressure. Physical Review B, 2021, 103, .	1.1	7
56171	First-principles investigations on the electronic structures, polycrystalline elastic properties, ideal strengths and elastic anisotropy of U3Si2. European Physical Journal Plus, 2021, 136, 1.	1.2	5
56172	Multiple Weyl fermions in the noncentrosymmetric semimetal LaAlSi. Physical Review B, 2021, 103, .	1.1	20
56173	Pressure-induced yttrium oxides with unconventional stoichiometries and novel properties. Physical Review Materials, 2021, 5, .	0.9	8
56174	Anisotropies in Elasticity, Sound Velocity, and Minimum Thermal Conductivity of Low Borides VxBy Compounds. Metals, 2021, 11, 577.	1.0	3
56175	Inherited weak topological insulator signatures in the topological hourglass semimetal <mml:math xmlns:mml="http://www.w3.org/1998/Math/MathML"><mml:mrow><mml:msub><mml:mi>Nb</mml:mi><mml:mn>3</mml:mn></mml:m <mml:math		

#	Article	IF	Citations
56182	Doping-Mediated Metalâ€“Support Interaction Promotion toward Light-Assisted Methanol Production over Cu/ZnO/Al₂O₃. ACS Catalysis, 2021, 11, 5818-5828.	5.5	16
56183	Strain-induced bandgap engineering in C3N nanotubes. Chemical Physics Letters, 2021, 768, 138390.	1.2	4
56184	Tunable electro-optical properties of doped chiral graphene nanoribbons. Chemical Physics, 2021, 544, 111116.	0.9	11
56185	Fermi surfaces of the topological semimetal CaSn₃ probed through de Haas van Alphen oscillations. Journal of Physics Condensed Matter, 2021, 33, 17LT01.	0.7	4
56186	A first-principles study on the electronic property and magnetic anisotropy of ferromagnetic CrOF and CrOCl monolayers. Journal of Physics Condensed Matter, 2021, 33, 195804.	0.7	19
56187	Ground-state structure and physical properties of YB3 predicted from first-principles calculations*. Chinese Physics B, 2021, 30, 046101.	0.7	3
56188	Electrochemiluminescence sensor based on cyclic peptides-recognition and Au nanoparticles assisted graphitic carbon nitride for glucose determination. Mikrochimica Acta, 2021, 188, 151.	2.5	8
56189	Hydrothermal Synthesis and Structural Investigation of a Crystalline Uranyl Borosilicate. Inorganics, 2021, 9, 25.	1.2	3
56190	Design of Graphene/Ionic Liquid Composites for Carbon Capture. ACS Applied Materials & Interfaces, 2021, 13, 17511-17516.	4.0	17
56191	Electronic Challenges of Retrofitting 2D Electrically Conductive MOFs to Form 3D Conductive Lattices. ACS Applied Electronic Materials, 2021, 3, 2017-2023.	2.0	11
56192	Role of High-Index Facet Cu(711) Surface in Controlling the C2 Selectivity for CO₂ Reduction Reactionâ€”A DFT Study. Journal of Physical Chemistry C, 2021, 125, 10919-10925.	1.5	17
56193	Maintaining a Flat Li Surface during the Li Stripping Process via Interface Design. Chemistry of Materials, 2021, 33, 2814-2823.	3.2	25
56194	Atomic Pt Embedded in BNC Nanotubes for Enhanced Electrochemical Ozone Production via an Oxygen Intermediate-Rich Local Environment. ACS Catalysis, 2021, 11, 5438-5451.	5.5	36
56195	Formation of Mg-Orthocarbonate through the Reaction MgCO₃ + MgO = Mg₂CO₄ at Earthâ€™s Lower Mantle Pâ€“T Conditions. Crystal Growth and Design, 2021, 21, 2986-2992.	1.4	19
56196	Gallium nitride catalyzed the direct hydrogenation of carbon dioxide to dimethyl ether as primary product. Nature Communications, 2021, 12, 2305.	5.8	45
56197	Manipulation of the Electronic State of Mott Iridate Superlattice through Protonation Induced Electronâ€Filling. Advanced Functional Materials, 2021, 31, 2100261.	7.8	7
56198	Tuning the electronic structure of nanoporous Ag via alloying effect from Cu to boost the ORR and Zn-air battery performance. Applied Surface Science, 2021, 545, 149042.	3.1	18
56199	Searching Configurations in Uncertainty Space: Active Learning of High-Dimensional Neural Network Reactive Potentials. Journal of Chemical Theory and Computation, 2021, 17, 2691-2701.	2.3	39

#	Article	IF	Citations
56200	Identification of Active Sites for CO₂ Reduction on Grapheneâ€Supported Singleâ€Atom Catalysts. ChemSusChem, 2021, 14, 2475-2480.	3.6	5
56201	Need for Rationally Designed SnWO₄ Photo(electro)catalysts to Overcome the Performance Limitations for O₂ and H₂ Evolution Reactions. Journal of Physical Chemistry C, 2021, 125, 8488-8496.	1.5	7
56202	Ferroelectricity in boron-substituted aluminum nitride thin films. Physical Review Materials, 2021, 5, .	0.9	53
56203	Activating PtSe2 monolayer for hydrogen evolution reaction by defect engineering and Pd doping. Applied Surface Science, 2021, 545, 149013.	3.1	23
56204	Modeling and physical properties of diphenylalanine peptide nanotubes containing water molecules. Ferroelectrics, 2021, 574, 78-91.	0.3	11
56205	High-Efficiency Water Gas Shift Reaction Catalysis on Î±-MoC Promoted by Single-Atom Ir Species. ACS Catalysis, 2021, 11, 5942-5950.	5.5	65
56206	Theoretical Study of an almost Barrier-Free Water Dissociation on a Platinum (111) Surface Alloyed with Ruthenium and Molybdenum. ACS Omega, 2021, 6, 10770-10775.	1.6	2
56207	Tunable Synthesis of Ethanol or Methyl Acetate via Dimethyl Oxalate Hydrogenation on Confined Iron Catalysts. ACS Catalysis, 2021, 11, 4908-4919.	5.5	15
56208	Disassembly of TEMPO-Oxidized Cellulose Fibers: Intersheet and Interchain Interactions in the Isolation of Nanofibers and Unitary Chains. Journal of Physical Chemistry B, 2021, 125, 3717-3724.	1.2	6
56209	Enhancement of Pseudocapacitive Behavior, Cyclic Performance, and Field Emission Characteristics of Reduced Graphene Oxide Reinforced NiGa₂O₄ Nanostructured Electrode: A First Principles Calculation to Correlate with Experimental Observation. Journal of Physical Chemistry C, 2021, 125, 7898-7912.	1.5	15
56210	Controlling Charge Carrier Trapping and Recombination in BiVO₄ with the Oxygen Vacancy Oxidation State. Journal of Physical Chemistry Letters, 2021, 12, 3514-3521.	2.1	33
56211	Transition of the Type of Band Alignments for All-Inorganic Perovskite van der Waals Heterostructures CsSnBr₃/WS_{2(1â€“x)}Se_{2x}. Journal of Physical Chemistry Letters, 2021, 12, 3809-3818.	2.1	20
56212	Mobility of F Centers in Alkali Halides. Journal of Physical Chemistry C, 2021, 125, 9085-9095.	1.5	8
56213	A Combined Experimental and First-Principles Based Assessment of Finite-Temperature Thermodynamic Properties of Intermetallic Al3Sc. Materials, 2021, 14, 1837.	1.3	5
56214	Spin-orbit coupling induced splitting of Yu-Shiba-Rusinov states in antiferromagnetic dimers. Nature Communications, 2021, 12, 2040.	5.8	48
56215	Understanding the Hardness of Doped WB4.2. Journal of Physical Chemistry C, 2021, 125, 9486-9496.	1.5	5
56216	Degradation behavior of mixed and isolated aromatic ring containing VOCs: Langmuir-Hinshelwood kinetics, photodegradation, in-situ FTIR and DFT studies. Journal of Environmental Chemical Engineering, 2021, 9, 105069.	3.3	60
56217	Data-driven enhancement of cubic phase stability in mixed-cation perovskites. Machine Learning: Science and Technology, 2021, 2, 025030.	2.4	17

#	Article	IF	Citations
56218	Exploring the Possible Anionic Redox Mechanism in Li-Rich Transition-Metal Carbodiimides. Journal of Physical Chemistry C, 2021, 125, 8479-8487.	1.5	2
56219	Layer-Dependent Magnetism in Two-Dimensional Transition-Metal Chalcogenides M_nT_{nÂ+Â1} (M = V, Cr, and Mn; T = S, Se, and Te; and n = 2, 3,) Tj ETQq1 1 0.784314 r	1.5	34
56220	Two-dimensional MoSSe/g-GeC van der waals heterostructure as promising multifunctional system for solar energy conversion. Applied Surface Science, 2021, 545, 148952.	3.1	45
56221	Theoretical Insight on Anion Ordering, Strain, and Doping Engineering of the Oxygen Evolution Reaction in BaTaO2N. Chemistry of Materials, 2021, 33, 3297-3303.	3.2	15
56222	Strain-Engineered Rippling and Manipulation of Single-Layer WS₂ by Atomic Force Microscopy. Journal of Physical Chemistry C, 2021, 125, 8696-8703.	1.5	9
56223	Atomistic insight into hydrogen trapping at MC/BCC-Fe phase boundaries: The role of local atomic environment. Acta Materialia, 2021, 208, 116744.	3.8	36
56224	Material exploration via designing spatial arrangement of octahedral units: a case study of lead halide perovskites. Frontiers of Optoelectronics, 2021, 14, 252-259.	1.9	66
56225	Characterizing armchaired and zigzagged phases: Antimony on oxide layer of Cu(110). Vacuum, 2021, 186, 110036.	1.6	3
56226	Photocatalytic and Photoelectrochemical Hydrogen Evolution from Water over Cu₂Sn_xGe_{1â€“x}S₃ Particles. Journal of the American Chemical Society, 2021, 143, 5698-5708.	6.6	33
56227	Tribological behavior of WC-Co-CaF2 self-lubricating cemented carbides. International Journal of Refractory Metals and Hard Materials, 2021, 96, 105492.	1.7	4
56228	Few-Layer Siloxene as an Electrode for Superior High-Rate Zinc Ion Hybrid Capacitors. ACS Energy Letters, 2021, 6, 1786-1794.	8.8	50
56229	Band-potential fluctuation in C3N4/BiOCl hetero-junction for boosting photo-catalytic activity. Separation and Purification Technology, 2021, 261, 118258.	3.9	25
56230	Synthesis of Y6-xCa1.5xSi11N20O:Ce3+ (x = 0 ~ 2.5) Oxynitride Phosphor with Broad Emission Wavelength for 1pc-LED. Korean Journal of Materials Research, 2021, 31, 188-194.	0.1	1
56231	Automated coordination corrected enthalpies with AFLOW-CCE. Physical Review Materials, 2021, 5, .	0.9	9
56232	Structural, electronic, and charge transfer features for two kinds of MoS2/Cs2PbI4 interfaces with optoelectronic applicability: Insights from first-principles. Applied Physics Letters, 2021, 118, .	1.5	4
56233	Tuning charge and orbital ordering in DyNiO3 by biaxial strain. Chinese Physics B, 0, , .	0.7	0
56235	Asymmetric equilibrium core structures of pyramidal-II <mml:math xmlns:mml="http://www.w3.org/1998/Math/MathML"><mml:mrow><mml:mo>âŒ©</mml:mo><mml:mi>c</mml:mi><mml:mo>+</mm dislocations in ten hexagonal-close-packed metals. Physical Review Materials, 2021, 5, .	0.9	3
56237	Metal substrates-induced phase transformation of monolayer transition metal dichalcogenides for hydrogen evolution catalysis*. Chinese Physics B, 2021, 30, 116401.	0.7	3

#	Article	IF	Citations
56238	SierpiÅ„ski Structure and Electronic Topology in Bi Thin Films on InSb(111)B Surfaces. Physical Review Letters, 2021, 126, 176102.	2.9	20
56239	Machine learning classification of binary semiconductor heterostructures. Physical Review Materials, 2021, 5, .	0.9	6
56240	Ultrafast hole transfer from monolayer ReS2 to thin-film F8ZnPc. Applied Physics Letters, 2021, 118, .	1.5	6
56241	Theoretical Study on the Lewis Acidity of the Pristine AlF3 and Cl-Doped Î±-AlF3 Surfaces. Catalysts, 2021, 11, 565.	1.6	5
56242	Magnetic and electronic properties of Mn doped SrISi(111)-(3 Ã— 2) HCC surface. , 2021, , .		0
56243	Ferroelastic-ferroelectric multiferroics in a bilayer lattice. Physical Review B, 2021, 103, .	1.1	31
56244	Strain driven emergence of topological non-triviality in YPdBi thin films. Scientific Reports, 2021, 11, 7535.	1.6	6
56245	Concepts, models, and methods in computational heterogeneous catalysis illustrated through <scp>CO₂</scp> conversion. Wiley Interdisciplinary Reviews: Computational Molecular Science, 2021, 11, e1530.	6.2	24
56246	Interplay between Valence Band Tuning and Redox Stability in SnTiO₃: Implications for Directed Design of Photocatalysts. Chemistry of Materials, 2021, 33, 2824-2836.	3.2	16
56247	SrZn₂N₂ as a Solar Absorber: Theoretical Defect Chemistry and Synthesis by Metal Alloy Nitridation. Chemistry of Materials, 2021, 33, 2864-2870.	3.2	12
56248	Formation Mechanism of Î²-Li₃PS₄ through Decomposition of Complexes. Inorganic Chemistry, 2021, 60, 6964-6970.	1.9	19
56249	Ferromagnetism in Mn-Doped ZnO: A Joint Theoretical and Experimental Study. Journal of Physical Chemistry C, 2021, 125, 7734-7745.	1.5	24
56250	Structural, Electronic, and Optical Properties of the Vacancy-Ordered Bismuthâ€“Antimony Perovskites (CH3NH3)3(Bi1â€“xSbx)2I9. Journal of Physical Chemistry C, 2021, 125, 8938-8946.	1.5	5
56251	Formation of Corrugated n = 1 2D Tin Iodide Perovskites and Their Use as Lead-Free Solar Absorbers. ACS Nano, 2021, 15, 6395-6409.	7.3	18
56252	Surface Defect-Induced Site-Specific Dispersion of Pd Nanoclusters on TiO₂ Nanoparticles for Semihydrogenation of Phenyl Acetylene. ACS Applied Nano Materials, 2021, 4, 4688-4698.	2.4	21
56253	Carbon Nitride Monolayers as Efficient Immobilizers toward Lithium Selenides: Potential Applications in Lithiumâ€“Selenium Batteries. ACS Applied Energy Materials, 2021, 4, 3891-3904.	2.5	10
56254	AuPt Bimetal-Functionalized SnSe₂ Microflower-Based Sensors for Detecting Sub-ppm NO₂ at Low Temperatures. ACS Applied Materials & Interfaces, 2021, 13, 20336-20348.	4.0	60
56255	Support Effect of Metalâ€“Organic Frameworks on Ethanol Production through Acetic Acid Hydrogenation. ACS Applied Materials & Interfaces, 2021, 13, 19992-20001.	4.0	12

#	Article	IF	Citations
56256	Two-Dimensional Nanomaterials as Anticorrosion Surface Coatings for Uranium Metal: Physical Insights from First-Principles Theory. ACS Applied Nano Materials, 2021, 4, 5038-5046.	2.4	4
56257	Pyridine Grafted on SnO₂â€Loaded Carbon Nanotubes Acting as Cocatalyst for Highly Efficient Electroreduction of CO₂. ChemSusChem, 2021, 14, 2769-2779.	3.6	10
56258	Activated edge of single layered TiO2 nanoribbons through transition metal doping and strain approaches for hydrogen production. Applied Surface Science, 2021, 545, 148947.	3.1	10
56259	sp3-Hybridized superhard trigonal carbon allotropes: A first principle study. Computational Materials Science, 2021, 190, 110269.	1.4	3
56260	Real-time atomic-resolution observation of coherent twin boundary migration in CrN. Acta Materialia, 2021, 208, 116732.	3.8	10
56261	Toward two-dimensional ionic crystals with intrinsic ferromagnetism. Physics Letters, Section A: General, Atomic and Solid State Physics, 2021, 395, 127229.	0.9	1
56262	MultiShifter: Software to generate structural models of extended two-dimensional defects in 3D and 2D crystals. Computational Materials Science, 2021, 191, 110310.	1.4	7
56263	Metastable Ce-terminated (1 1 1) surface of ceria. Applied Surface Science, 2021, 546, 148972.	3.1	7
56264	Microscopic evidence of strong interactions between chemical vapor deposited 2D MoS2 film and SiO2 growth template. Nano Convergence, 2021, 8, 11.	6.3	20
56265	A simple method to calculate solution-phase free energies of charged species in computational electrocatalysis. Journal of Physics Condensed Matter, 2021, 33, 204001.	0.7	7
56266	Towards constant potential modeling of CO-CO coupling at liquid water-Cu(1 0 0) interfaces. Journal of Catalysis, 2021, 396, 251-260.	3.1	16
56267	Large magnetoresistance in a <mml:math xmlns:mml="http://www.w3.org/1998/Math/MathML"><mml:mrow><mml:mi>Co</mml:mi><mml:mo>/</mml:mo><mml:mi>Mo</mml:mi><mml:mathvariant="normal">S</mml:mi><mml:mn>2</mml:mn></mml:msub><mml:mo>/</mml:mo><mml:mi>graphene</mml:mi><mml:mathvariant="normal">S</mml:mi><mml:mn>2</mml:mn></mml:msub><mml:mo>/</mml:mo><mml:mi>Co</mml:mi></mml:mrow> magnetic tunnel junction. Physical Review B, 2021, 103, .	1.1	7
56268	Ab initio investigation of the atomic volume, thermal expansion, and formation energy of WTi solid solutions. Physical Review Materials, 2021, 5, .	0.9	4
56269	Indirect-direct band gap transition driven by strain in semiconducting Cu2Se monolayer. Materials Research Express, 2021, 8, 045003.	0.8	2
56270	Defect-induced <mml:math xmlns:mml="http://www.w3.org/1998/Math/MathML"><mml:mrow><mml:mn>4</mml:mn><mml:mi>p</mml:mi></mml:mrow></mml:math> -magnetism in layered platinum diselenide. Physical Review B, 2021, 103, .	1.1	6
56271	Understanding the Effect of Oxygen on the Glass-Forming Ability of Zr55Cu55Al9Be9 Bulk Metallic Glass by ab initio Molecular Dynamics Simulations. Metallurgical and Materials Transactions A: Physical Metallurgy and Materials Science, 2021, 52, 2501-2511.	1.1	6
56272	Layer and spontaneous polarizations in perovskite oxides and their interplay in multiferroic bismuth ferrite. Journal of Chemical Physics, 2021, 154, 154702.	1.2	14
56273	Modulation of electronic and magnetic properties of monolayer chromium trihalides by alloy and strain engineering. Journal of Applied Physics, 2021, 129, 155104.	1.1	3

#	Article	IF	Citations
56274	Silicon carbide detectors for sub-GeV dark matter. Physical Review D, 2021, 103, .	1.6	59
56275	Topological gimbal phonons in <mml:math xmlns:mml="http://www.w3.org/1998/Math/MathML"><mml:mi>T</mml:mi></mml:math> -carbon. Physical Review B, 2021, 103, .	1.1	31
56276	Double Dirac nodal line semimetal with a torus surface state. Physical Review B, 2021, 103, .	1.1	21
56277	Quantum spin Hall and quantum anomalous Hall states in magnetic Ti₂Te₂O single layer. Journal of Physics Condensed Matter, 2021, 33, 21LT01.	0.7	2
56278	Absolute Volume Deformation Potentials of Inorganic ABX₃ Halide Perovskites: The Chemical Trends. Advanced Theory and Simulations, 2021, 4, 2100060.	1.3	11
56279	Phosphatized GaZnInON nanocrystals with core-shell structures for efficient and stable pure water splitting via four-electron photocatalysis. Chemical Engineering Journal, 2021, 410, 128391.	6.6	15
56280	First-principles study of electronic structures and elasticity of Al2Fe3Si3. Journal of Physics Condensed Matter, 2021, 33, 195501.	0.7	10
56281	High capacity reversible hydrogen storage in zirconium doped 2D-covalent triazine frameworks: Density Functional Theory investigations. International Journal of Hydrogen Energy, 2021, 46, 14520-14531.	3.8	41
56282	The MoNâ€“TaN system: Role of vacancies in phase stability and mechanical properties. Materials and Design, 2021, 202, 109568.	3.3	8
56283	Giant tunneling magnetoresistance in van der Waals magnetic tunnel junctions formed by interlayer antiferromagnetic bilayer <mml:math xmlns:mml="http://www.w3.org/1998/Math/MathML"><mml:msub><mml:mi mathvariant="normal">CoBr</mml:mi><mml:mn>2</mml:mn></mml:msub></mml:math>. Physical Review B, 2021, 103, .	1.1	17
56284	Mechanisms of carrier lifetime enhancement and conductivity-type switching on hydrogen-incorporated arsenic-doped BaSi2. Thin Solid Films, 2021, 724, 138629.	0.8	8
56285	In Situ Surface Structures of PdAg Catalyst and Their Influence on Acetylene Semihydrogenation Revealed by Machine Learning and Experiment. Journal of the American Chemical Society, 2021, 143, 6281-6292.	6.6	58
56286	Graphene Antiadhesion Layer for the Effective Peel-and-Pick Transfer of Metallic Electrodes toward Flexible Electronics. ACS Applied Materials & Interfaces, 2021, 13, 22000-22008.	4.0	2
56287	Single-Molecule Vibrational Spectroscopy: Cobalt Tetraphenylporphyrin Deposited on a Cu2N Ultrathin Insulating Layer. Journal of Physical Chemistry C, 2021, 125, 9695-9702.	1.5	0
56288	Fast Ion-Conducting Thioboracite with a Perovskite Topology and Argyrodite-like Lithium Substructure. Journal of the American Chemical Society, 2021, 143, 6952-6961.	6.6	16
56289	Polarization-Controlled Surface Defect Formation in a Hybrid Perovskite. Journal of Physical Chemistry Letters, 2021, 12, 3898-3906.	2.1	6
56290	Energetic segregation of B, C, N, O at the Î³-TiAl/Î±2-Ti3Al interface via DFT approach. Vacuum, 2021, 186, 110045.	1.6	11
56291	High-Pressure Synthesis of Dirac Materials: Layered van der Waals Bonded <mml:math xmlns:mml="http://www.w3.org/1998/Math/MathML" display="inline"><mml:msub><mml:mrow><mml:mi>BeN</mml:mi></mml:mrow><mml:mrow><mml:mn>4</mml:mn></mml:mrow></mml:msub></mml:math> Polymorph. Physical Review Letters, 2021, 126, 175501.	2.9	90

#	Article	IF	Citations
56292	Impact of Water Coadsorption on the Electrode Potential of H-Pt(1 1 1)-Liquid Water Interfaces. Physical Review Letters, 2021, 126, 166802.	2.9	21
56293	pâ€Type Plastic Inorganic Thermoelectric Materials. Advanced Energy Materials, 2021, 11, 2100883.	10.2	40
56294	Ampere-hour-scale zincâ€“air pouch cells. Nature Energy, 2021, 6, 592-604.	19.8	149
56295	Single transition metal atom catalysts on Ti2CN2 for efficient CO2 reduction reaction. International Journal of Hydrogen Energy, 2021, 46, 12886-12896.	3.8	38
56296	Pyridinic-Type N-Doped Graphene on Cobalt Substrate as Efficient Electrocatalyst for Oxygen Reduction Reaction in Acidic Solution in Fuel Cell. Journal of Physical Chemistry Letters, 2021, 12, 3552-3559.	2.1	20
56297	Simultaneously enhancing piezoelectric performance and thermal depolarization in lead-free (Bi,Na)TiO3-BaTiO3 via introducing oxygen-defect perovskites. Acta Materialia, 2021, 208, 116711.	3.8	32
56298	Transfer learning for materials informatics using crystal graph convolutional neural network. Computational Materials Science, 2021, 190, 110314.	1.4	34
56299	Enhancement of heterogeneous photo-Fenton performance of core-shell structured boron-doped reduced graphene oxide wrapped magnetical Fe3O4 nanoparticles: Fe(II)/Fe(III) redox and mechanism. Applied Surface Science, 2021, 544, 148886.	3.1	43
56300	Boosting Electron Transfer with Heterointerface Effect for High-Performance Lithium-Ion Storage. Energy Storage Materials, 2021, 36, 365-375.	9.5	61
56301	Synergized Multimetal Oxides with Amorphous/Crystalline Heterostructure as Efficient Electrocatalysts for Lithiumâ€“Oxygen Batteries. Advanced Energy Materials, 2021, 11, 2100110.	10.2	72
56302	Ultrathin Layered Double Hydroxide Nanosheets Enabling Composite Polymer Electrolyte for Allâ€Solidâ€State Lithium Batteries at Room Temperature. Advanced Functional Materials, 2021, 31, 2101168.	7.8	75
56303	Interfacial Electron Engineering of Palladium and Molybdenum Carbide for Highly Efficient Oxygen Reduction. Journal of the American Chemical Society, 2021, 143, 6933-6941.	6.6	62
56304	Electronic structure and optical properties of SnO2/HC(NH2)2PbI3 interfaces from first-principles calculations. Surfaces and Interfaces, 2021, 23, 100913.	1.5	3
56305	When Fluxionality Beats Size Selection: Acceleration of Ostwald Ripening of Subâ€Nano Clusters. Angewandte Chemie - International Edition, 2021, 60, 11973-11982.	7.2	13
56306	Electronic, magnetism and optical properties of transition metals adsorbed puckered arsenene. Superlattices and Microstructures, 2021, 152, 106852.	1.4	62
56307	Enhanced fast response to Hg0 by adsorption-induced electronic structure evolution of Ti2C nanosheet. Applied Surface Science, 2021, 544, 148925.	3.1	22
56308	Bilayer MoTe2/XS2 (XÂ=ÂHf,Sn,Zr) heterostructures with efficient carrier separation and light absorption for photocatalytic water splitting into hydrogen. Applied Surface Science, 2021, 544, 148842.	3.1	24
56310	Comprehensive anisotropic linear optical properties of the Weyl semimetals TaAs and NbAs. Physical Review B, 2021, 103, .	1.1	11

#	Article	IF	Citations
56311	Combined Effects of Mn, C, and H on the Stacking Fault Energy in Austenitic Mn Steels. Steel Research International, 2021, 92, 2000550.	1.0	1
56312	First-principles design of halide-reduced electrides: Magnetism and topological phases. Physical Review Materials, 2021, 5, .	0.9	5
56313	Computing inelastic neutron scattering spectra from molecular dynamics trajectories. Scientific Reports, 2021, 11, 7938.	1.6	7
56314	First-principles identification of topological crystalline insulators with C2 rotation anomaly. Physical Review B, 2021, 103, .	1.1	0
56315	Prediction and observation of intermodulation sidebands from anharmonic phonons in NaBr. Physical Review B, 2021, 103, .	1.1	1
56316	Effects of Zn and Mg Segregations on the Grain Boundary Sliding and Cohesion in Al: Ab Initio Modeling. Metals, 2021, 11, 631.	1.0	8
56317	Interfacial magnetic coupling and orbital hybridization for D022-Mn3Ga/Fe films. Physica Scripta, 2021, 96, 075804.	1.2	1
56318	Atomic configurations for materials research: A case study of some simple binary compounds. AIP Advances, 2021, 11, .	0.6	4
56319	Control of the metal-insulator transition in <mml:math xmlns:mml="http://www.w3.org/1998/Math/MathML"><mml:msub><mml:mi mathvariant="normal">NdNiO</mml:mi><mml:mn>3</mml:mn></mml:msub></mml:math> thin films through the interplay between structural and electronic properties. Physical Review Materials, 2021, 5, .	0.9	6
56320	New boron nitride monolith phases from high-pressure compression of double-walled boron nitride nanotubes. Journal of Chemical Physics, 2021, 154, 134702.	1.2	8
56321	Predicting an ideal 2D carbon nanostructure with negative Poisson's ratio from first principles: implications for nanomechanical devices. Carbon Letters, 2021, 31, 1227-1235.	3.3	3
56322	Ferromagnetism in a Semiconductor with Mobile Carriers via Low-Level Nonmagnetic Doping. Physical Review Applied, 2021, 15, .	1.5	3
56323	Structural, electronic paramagnetic resonance and magnetic properties of praseodymium-doped rare earth CeO2 semiconductors. Ceramics International, 2021, 47, 20768-20780.	2.3	13
56324	Evolution of Topological Surface States Following Sb Layer Adsorption on Bi2Se3. Materials, 2021, 14, 1763.	1.3	7
56325	A systematic first-principles study of volatile iodine adsorption onto zeolitic imidazolate frameworks. Microporous and Mesoporous Materials, 2021, 317, 111017.	2.2	14
56326	Photocatalytic selective H₂ release from formic acid enabled by CO₂ captured carbon nitride. Nanotechnology, 2021, 32, 275404.	1.3	3
56327	A Raman probe of phonons and electronâ€“phonon interactions in the Weyl semimetal NbIrTe4. Scientific Reports, 2021, 11, 8155.	1.6	10
56328	The Principal Hugoniot of Ironâ€Bearing Olivine to 1465ÂGPa. Geophysical Research Letters, 2021, 48, e2021GL092471.	1.5	2

#	Article	IF	Citations
56329	In-situ self-assembled Cu2O/ZnO core-shell catalysts synergistically enhance the durability of methanol steam reforming. Applied Catalysis A: General, 2021, 616, 118072.	2.2	28
56330	Van der Waals direction transformation induced by shear strain in layered PdSe2. Extreme Mechanics Letters, 2021, 44, 101231.	2.0	7
56331	Quarter-filled Kane-Mele Hubbard model: Dirac half metals. Physical Review B, 2021, 103, .	1.1	7
56332	How CO2 poisons La2O3 in an OCM catalytic reaction: A study by in situ XRD-MS and DFT. Journal of Catalysis, 2021, 396, 202-214.	3.1	14
56333	A density functional theory and neutron diffraction study of the ambient condition properties of sub-stoichiometric yttrium hydride. Journal of Nuclear Materials, 2021, 547, 152837.	1.3	11
56334	Discovery of higher-order topological insulators using the spin Hall conductivity as a topology signature. Npj Computational Materials, 2021, 7, .	3.5	15
56335	Optical bioelectronic nose of outstanding sensitivity and selectivity toward volatile organic compounds implemented with genetically engineered bacteriophage: Integrated study of multi-scale computational prediction and experimental validation. Biosensors and Bioelectronics, 2021, 177, 112979.	5.3	20
56336	Effects of irradiation defects on the adsorption of oxygen on 3C-SiC low index surfaces. Computational Materials Science, 2021, 190, 110267.	1.4	3
56337	Mechanical manipulation of electronic properties of SnO2 monolayer. Computational Materials Science, 2021, 190, 110268.	1.4	1
56338	BiSbWO6: Properties of a mixed 5s/6s lone-pair-electron system. Chemical Physics, 2021, 544, 111117.	0.9	4
56339	Strain engineering in novel Î±-SbP binary material with tensile-robust and compress-sensitive band structures. Physica E: Low-Dimensional Systems and Nanostructures, 2021, 128, 114623.	1.3	4
56340	Modelling the primary damage in Fe and W: Influence of the short range interactions on the cascade properties: Part 1 â€“ Energy transfer. Journal of Nuclear Materials, 2021, 547, 152816.	1.3	10
56341	Volumetric Strain Dependence of Quantum Diffusion of Hydrogen in bcc Iron. ISIJ International, 2021, 61, 1294-1299.	0.6	2
56342	Local insight to the structural phase transition sequence of Bi₂Se₃ under quasi-hydrostatic and nonhydrostatic pressure. Journal of Physics Condensed Matter, 2021, 33, 215402.	0.7	3
56343	Theoretical study of tunable magnetism of two-dimensional MnSe₂ through strain, charge, and defect. Journal of Physics Condensed Matter, 2021, 33, 215803.	0.7	12
56344	Ab initio study of structural, elastic and thermodynamic properties of Fe3S at high pressure: Implications for planetary cores. American Mineralogist, 2022, 107, 248-256.	0.9	0
56345	Configuration of transition-metal atoms on iridium-doped graphene. Journal of Physics B: Atomic, Molecular and Optical Physics, 2021, 54, 085101.	0.6	1
56346	Adsorption of polycyclic aromatic hydrocarbons on FeOOH polymorphs: A theoretical study. Surface Science, 2021, 706, 121795.	0.8	7

#	Article	IF	Citations
56347	Ab initio Molecular Dynamics Investigations of the Speciation and Reactivity of Deep Eutectic Electrolytes in Aluminum Batteries. ChemSusChem, 2021, 14, 2034-2041.	3.6	6
56348	Mass enhancement in <mml:math xmlns:mml="http://www.w3.org/1998/Math/MathML"><mml:mrow><mml:mn>3</mml:mn><mml:mi>d</mml:mi></mml:mrow></mml:r and <mml:math xmlns:mml="http://www.w3.org/1998/Math/MathML"><mml:mrow><mml:mi>s</mml:mi><mml:mtext>â^'</mml:mtext><mml:mi>p</mml:m perovskites from symmetry breaking. Physical Review B, 2021, 103, .	1.1	24
56349	Improved Pd/CeO₂ Catalysts for Low-Temperature NO Reduction: Activation of CeO₂ Lattice Oxygen by Fe Doping. ACS Catalysis, 2021, 11, 5614-5627.	5.5	44
56350	Revisiting Understanding of Electrochemical CO₂ Reduction on Cu(111): Competing Proton-Coupled Electron Transfer Reaction Mechanisms Revealed by Embedded Correlated Wavefunction Theory. Journal of the American Chemical Society, 2021, 143, 6152-6164.	6.6	65
56351	Experimental and theoretical studies on induced ferromagnetism of new (1 â^') Tj ETQq0 0 0 rgBT /Overlock 10 Tf 50 582 Td (x)Na0.5Bi0	1.6	21
56352	Birefringence and Dichroism in Quasiâ€1D Transition Metal Trichalcogenides: Direct Experimental Investigation. Small, 2021, 17, e2100457.	5.2	17
56353	The Role of Metal Ions in the Electron Transport through Azurin-Based Junctions. Applied Sciences (Switzerland), 2021, 11, 3732.	1.3	6
56354	Low thermal conductivity of SrTiO 3 â^'LaTiO 3 and SrTiO 3 â^'SrNbO 3 thermoelectric oxide solid solutions. Journal of the American Ceramic Society, 2021, 104, 4075-4085.	1.9	5
56355	(W_{1â€x},M_x)C carbides with desired combinations of compatible density and properties â€“ A firstâ€principles study. Journal of the American Ceramic Society, 2021, 104, 4239-4256.	1.9	7
56356	Intrinsic triferroicity in a two-dimensional lattice. Physical Review B, 2021, 103, .	1.1	22
56357	Photocatalytic activity of co-doped Janus monolayer MoSSe for solar water splitting: A computational investigation. Applied Surface Science, 2021, 544, 148741.	3.1	25
56358	Efficient calculation of carrier scattering rates from first principles. Nature Communications, 2021, 12, 2222.	5.8	205
56359	Exceptional piezoelectricity, high thermal conductivity and stiffness and promising photocatalysis in two-dimensional MoSi2N4 family confirmed by first-principles. Nano Energy, 2021, 82, 105716.	8.2	303
56360	Density Functional Theory Study of Water Activation at Au-Ceria Interfaces. Korean Journal of Materials Research, 2021, 31, 232-236.	0.1	0
56361	Confinement effects on the solvation structure of solvated alkaline metal cations in a single-digit 1T-MoS2 nanochannel: A first-principles study. Journal of Chemical Physics, 2021, 154, 164706.	1.2	9
56362	Valley polarization, magnetic anisotropy and Dzyaloshinskii-Moriya interaction of two-dimensional graphene/Janus 2H-VSeX (XÂ= S, Te) heterostructures. Carbon, 2021, 174, 540-555.	5.4	47
56363	Large-Area Bernal-Stacked Bilayer Graphene Film on a Uniformly Rough Cu Surface via Chemical Vapor Deposition. ACS Applied Electronic Materials, 2021, 3, 2497-2503.	2.0	4
56364	R10-graphene: A predicted two-dimensional metallic carbon. Diamond and Related Materials, 2021, 114, 108315.	1.8	10

#	Article	IF	Citations
56365	Atomically Dispersed Pt on TiO₂ Nanosheets for Catalytic Gaseous Acetaldehyde Abatement. ACS Applied Nano Materials, 2021, 4, 3799-3810.	2.4	13
56366	Atomic Undercoordination in Ag Islands on Ru(0001) Grown via Size-Selected Cluster Deposition: An Experimental and Theoretical High-Resolution Core-Level Photoemission Study. Journal of Physical Chemistry C, 2021, 125, 9556-9563.	1.5	4
56367	Enhancing the Surface Reactivity of Black Phosphorus on Hydrogen Evolution by Covalent Chemistry. Journal of Physical Chemistry C, 2021, 125, 7581-7589.	1.5	14
56368	Insights into the Electrochemical Stability and Lithium Conductivity of Li₄MS₄ (M = Si, Ge, and Sn). ACS Applied Materials & Interfaces, 2021, 13, 22438-22447.	4.0	7
56369	Revealing the Potential Crystal Structures of Earth-Abundant Nontoxic Photovoltaic CuBiI₄. Crystal Growth and Design, 2021, 21, 2850-2855.	1.4	8
56370	Mechanochemical Redox: Calcinationâ€free Synthesis of Ceriaâ€hybrid Catalyst with Ultraâ€High Surface Area. ChemCatChem, 2021, 13, 2434-2443.	1.8	4
56371	Methanol carbonylation over acid mordenite: Insights from ab initio molecular dynamics and machine learning thermodynamic perturbation theory. Journal of Catalysis, 2021, 396, 166-178.	3.1	11
56372	Preparation, characterization and adsorption properties of tetraalkylphosphonium organobeidellites. Applied Clay Science, 2021, 204, 105989.	2.6	7
56373	Structural, Electrical, and Electromechanical Properties of Inverse Hybrid Perovskites from First-Principles: The Case of (CH₃NH₃)₃OI. Journal of Physical Chemistry C, 2021, 125, 8794-8802.	1.5	5
56374	Proton-assisted calcium-ion storage in aromatic organic molecular crystal with coplanar stacked structure. Nature Communications, 2021, 12, 2400.	5.8	107
56375	A single-molecule van der Waals compass. Nature, 2021, 592, 541-544.	13.7	75
56376	CsPbBr₃ Perovskite Nanocrystal: A Robust Photocatalyst for Realizing NO Abatement. ACS ES&T Engineering, 2021, 1, 1021-1027.	3.7	18
56377	Rational Design of Single-Atom-Doped Ga₂O₃ Catalysts for Propane Dehydrogenation: Breaking through Volcano Plot by Lewis Acidâ€“Base Interactions. ACS Catalysis, 2021, 11, 5135-5147.	5.5	41
56378	Boron Doping and LiBO₂ Coating Synergistically Enhance the High-Rate Performance of LiNi_{0.6}Co_{0.1}Mn_{0.3}O₂ Cathode Materials. ACS Sustainable Chemistry and Engineering, 2021, 9, 5322-5333.	3.2	25
56379	Computational Assessment of Novel Predicted Compounds in Ni-Re Alloy System. Journal of Phase Equilibria and Diffusion, 2021, 42, 315-320.	0.5	3
56380	Unlocking Rapid and Robust Sodium Storage Performance of Zinc-Based Sulfide via Indium Incorporation. ACS Nano, 2021, 15, 8507-8516.	7.3	36
56381	Ba with Unusual Oxidation States in Ba Chalcogenides under Pressure. Journal of Physical Chemistry Letters, 2021, 12, 4203-4210.	2.1	11
56382	Suppressing bias stress degradation in high performance solution processed organic transistors operating in air. Nature Communications, 2021, 12, 2352.	5.8	48

#	Article	IF	Citations
56383	A New Porous Metallic Carbon Allotrope with Interlocking Pentagons for Sodiumâ€Ion Battery Anode Material. Advanced Theory and Simulations, 2021, 4, 2100025.	1.3	9
56384	Experimental and computational studies of sonochemical assisted anchoring of carbon quantum dots on reduced graphene oxide sheets towards the photocatalytic activity. Applied Surface Science, 2021, 545, 148962.	3.1	19
56385	High-rate nanofluidic energy absorption in porous zeolitic frameworks. Nature Materials, 2021, 20, 1015-1023.	13.3	52
56386	Minimizing hydrogen vacancies to enable highly efficient hybrid perovskites. Nature Materials, 2021, 20, 971-976.	13.3	92
56387	Oxygen vacancies and interfacial electric field co-induced photocatalytic performance of OVs-BiOI/Î±-Bi2O3 heterojunctions. Colloids and Surfaces A: Physicochemical and Engineering Aspects, 2021, 615, 126262.	2.3	17
56388	Theoretical Study on the Carrier Mobility and Optical Properties of CsPbI₃ by DFT. ACS Omega, 2021, 6, 11545-11555.	1.6	41
56389	Van der Waals contact between 2D magnetic VSe2 and transition metals and demonstration of high-performance spin-field-effect transistors. Science China Materials, 2021, 64, 2786-2794.	3.5	4
56390	Single Transition Metal Atom Bound to the Unconventional Phase of the MoS₂Monolayer for Catalytic Oxygen Reduction Reaction: A First-Principles Study. ACS Applied Materials & Interfaces, 2021, 13, 17412-17419.	4.0	26
56391	Chemical bonding and Born charge in 1T-HfS2. Npj 2D Materials and Applications, 2021, 5, .	3.9	15
56392	NiMoO₄ Nanosheets Anchored on Nï£¿S Doped Carbon Clothes with Hierarchical Structure as a Bidirectional Catalyst toward Accelerating Polysulfides Conversion for Liï£¿S Battery. Advanced Functional Materials, 2021, 31, 2101285.	7.8	119
56393	Unveiling decaying mechanism through quantitative structure-activity relationship in electrolytes for lithium-ion batteries. Nano Energy, 2021, 83, 105843.	8.2	23
56394	CO adsorption on MnO(100): Experimental benchmarks compared to DFT. Surface Science, 2021, 707, 121808.	0.8	8
56395	Role of Al on the electrochemical performances of quaternary nickel-rich cathode LiNi0.8Co0.1Mn0.1â^'Al O2 (0Ââ‰ÂxÂâ‰Â0.06) for lithium-ion batteries. Journal of Electroanalytical Chemistry, 2021, 888, 115200.	1.9	15
56396	Antiphase boundary migration as a diffusion mechanism in a P3 sodium layered oxide. Physical Review Materials, 2021, 5, .	0.9	5
56397	Phase transition pathway of hybrid halide perovskites under compression: Insights from first-principles calculations. Physical Review Materials, 2021, 5, .	0.9	6
56398	Predicted half-metallicity and ferromagnetism in the Fe (III) doped BaZrO3 perovskite: A theoretical insight. AIP Advances, 2021, 11, 055104.	0.6	1
56399	Understanding Correlation Between CO₂ Insertion Mechanism and Chain Length of Diamine in Metalâ€Organic Framework Adsorbents. ChemSusChem, 2021, 14, 2426-2433.	3.6	6
56400	Dual occupations of sulfur induced band flattening and chemical bond softening in p-type S Co4Sb12-2S2 skutterudites. Journal of Materiomics, 2022, 8, 88-95.	2.8	6

#	Article	IF	Citations
56401	Revisiting the thermal conductivity of Si, Ge and diamond from first principles: roles of atomic mass and interatomic potential. Journal of Physics Condensed Matter, 2021, 33, 285702.	0.7	6
56402	Grain Boundaries and Their Impact on Li Kinetics in Layered-Oxide Cathodes for Li-Ion Batteries. Journal of Physical Chemistry C, 2021, 125, 10284-10294.	1.5	26
56403	Metal-to-Semiconductor Transition in Two-Dimensional Metalâ€“Organic Frameworks: An Ab Initio Dynamics Perspective. ACS Applied Materials & Interfaces, 2021, 13, 25270-25279.	4.0	8
56404	IIâ€“VI Organicâ€“Inorganic Hybrid Nanostructures with Greatly Enhanced Optoelectronic Properties, Perfectly Ordered Structures, and Shelf Stability of Over 15 Years. ACS Nano, 2021, 15, 10565-10576.	7.3	9
56405	Effects of Vacancy and Ti Doping in 2D Janus MoSSe on Photocatalysis. Journal of Physical Chemistry C, 2021, 125, 11939-11949.	1.5	14
56406	Ultralarge Photoluminescence Enhancement of Monolayer Molybdenum Disulfide by Spontaneous Superacid Nanolayer Formation. ACS Applied Materials & Interfaces, 2021, 13, 25280-25289.	4.0	8
56407	Calculations of Hydrogen Associative Desorption on Mono- and Bimetallic Catalysts. Journal of Physical Chemistry C, 2021, 125, 12028-12037.	1.5	12
56408	Addressing the High-Voltage Structural and Electrochemical Instability of Ni-Containing Layered Transition Metal (T_M) Oxide Cathodes by â€œBlockingâ€•the â€œT_M-Migrationâ€• Pathway in the Lattice. ACS Applied Materials & Interfaces, 2021, 13, 25836-25849.	4.0	16
56409	Mixed Anion Control of the Partial Oxidation of Methane to Methanol on the Î²-PtO₂Surface. ACS Omega, 2021, 6, 13858-13869.	1.6	9
56410	Stretchable AgX (X = Se, Te) for Efficient Thermoelectrics and Photovoltaics. ACS Applied Materials & Interfaces, 2021, 13, 25121-25136.	4.0	10
56411	First-Principles Study of the Atomic Structures and Catalytic Properties of Monolayer TaS₂ with Intrinsic Defects. Journal of Physical Chemistry C, 2021, 125, 10362-10369.	1.5	22
56412	Effect of Mg Doping on Structural, Alloying, Electronic, Optical, and Bactericidal Properties of CunAg25â€“n Nanoclusters: A Computational Study. Journal of Physical Chemistry C, 2021, 125, 11066-11074.	1.5	1
56413	Multiscale Catalyst Design for Steam Methane Reforming Assisted by Deep Learning. Journal of Physical Chemistry C, 2021, 125, 10860-10867.	1.5	4
56414	Hydrogen evolution reaction on in-plane platinum and palladium dichalcogenides via single-atom doping. International Journal of Hydrogen Energy, 2021, 46, 18294-18304.	3.8	23
56415	Small Polarons in Two-Dimensional Pnictogens: A First-Principles Study. Journal of Physical Chemistry Letters, 2021, 12, 4674-4680.	2.1	7
56416	Plasmon Triggered, Enhanced Lightâ€“Matter Interactions in Auâ€“MoS₂ Coupled System with Superior Photosensitivity. Journal of Physical Chemistry C, 2021, 125, 11023-11034.	1.5	18
56417	Nonplanar core structure of 1/2<111> screw dislocations: An anisotropic Peierls-Nabarro model. Mechanics of Materials, 2021, 156, 103794.	1.7	4
56419	Carbon Defects Induced Delocalization of Ï€ Electrons Enables Efficient Charge Separation in Graphitic Carbon Nitride for Increased Photocatalytic H2 Generation. Catalysis Letters, 2022, 152, 669-678.	1.4	6

#	Article	IF	Citations
56420	Superior Mechanical Properties of GaAs Driven by Lattice Nanotwinning. Chinese Physics Letters, 2021, 38, 046201.	1.3	4
56421	Feature-Rich Geometric and Electronic Properties of Carbon Nanoscrolls. Nanomaterials, 2021, 11, 1372.	1.9	2
56422	Soft anharmonic phonons and ultralow thermal conductivity in Mg ₃ (Sb, Bi) ₂ thermoelectrics. Science Advances, 2021, 7, .	4.7	52
56423	A kinetic model for halogenation of the zinc content in franklinite. Applied Surface Science, 2021, 562, 150105.	3.1	13
56424	Regulating the interfacial behavior of carbon nanotubes for fast lithium storage. Electrochimica Acta, 2021, 388, 138591.	2.6	7
56425	Bulk Crystalline <mml:math xmlns:mml="http://www.w3.org/1998/Math/MathML" display="inline"><mml:mrow><mml:mn>4</mml:mn><mml:mrow><mml:mi>H</mml:mi></mml:mrow></mml:mrow></mml:math> -Silicon through a Metastable Allotropic Transition. Physical Review Letters, 2021, 126, 215701.	2.9	18
56426	28â€3: Degradation of Organic Molecular Complex Dependent on Atmosphere. Digest of Technical Papers SID International Symposium, 2021, 52, 357-360.	0.1	0
56427	Hydrogen Transportation Behaviour of Vâ€“Ni Solid Solution: A First-Principles Investigation. Materials, 2021, 14, 2603.	1.3	5
56428	Behavior of S, SO, and SO3 on Pt (001), (011), and (111) surfaces: A DFT study. Journal of Chemical Physics, 2021, 154, 194701.	1.2	4
56429	Pressure-dependent modifications in the <mml:math xmlns:mml="http://www.w3.org/1998/Math/MathML"><mml:mrow><mml:mi>LaAu</mml:mi><mml:msub><mml:mi>Sb</mml:mi><mml:mi> charge density wave system. Physical Review B, 2021, 103, .	1.1	6
56430	Valley Two-Qubit System in a <mml:math xmlns:mml="http://www.w3.org/1998/Math/MathML" display="inline" overflow="scroll"><mml:msub><mml:mrow><mml:mi>Mo</mml:mi><mml:mi mathvariant="normal">S</mml:mi></mml:mrow><mml:mn>2</mml:mn></mml:msub></mml:math> -Monolayer Gated Double Quantum dot. Physical Review Applied, 2021, 15, .	1.5	11
56431	Tuning the electronic and optical properties of the sphalerite by adsorbing halogen and alkali metals. IET Optoelectronics, 2021, 15, 270-280.	1.8	2
56432	Ag-Doped and Antibiotic-Loaded Hexagonal Boron Nitride Nanoparticles as Promising Carriers to Fight Different Pathogens. ACS Applied Materials & Interfaces, 2021, 13, 23452-23468.	4.0	17
56433	Data driven discovery of conjugated polyelectrolytes for optoelectronic and photocatalytic applications. Npj Computational Materials, 2021, 7, .	3.5	19
56434	Effects of Eu3+/Ta5+ nonstoichiometric ratio on dielectric properties of (EuxTa1-x)0.08Ti0.92O2 ceramics with colossal permittivity: Experiments and first-principle calculations. Ceramics International, 2021, 47, 24868-24876.	2.3	12
56435	First-Principles DFT Study on Inverse Ruddlesdenâ€“Popper Tetragonal Compounds as Solid Electrolytes for All-Solid-State Li⁺-Ion Batteries. Chemistry of Materials, 2021, 33, 5859-5871.	3.2	13
56436	Influence of transition group elements on the stability of the Î³â€³-phase in nickelbase alloys. Modelling and Simulation in Materials Science and Engineering, 2021, 29, 055006.	0.8	6
56437	Band gap opening in tetragonal stanene monolayer by hydrogenation engineering. Solid State Communications, 2021, 331, 114268.	0.9	4

#	Article	IF	Citations
56438	Origin of destruction of multiferroicity in Tb2BaNiO5 by Sr doping and its implications. Journal of Alloys and Compounds, 2021, 862, 158514.	2.8	2
56439	Structural, Electronic, and Optical Properties of Hexagonal XC 6 (X=N, P, As, and Sb) Monolayers. ChemPhysChem, 2021, 22, 1124-1133.	1.0	0
56440	Strain-tuned magnetism and half-metal to metal transition in defective BCN monolayer. Journal of Physics Condensed Matter, 2021, 33, 235502.	0.7	3
56441	Rotation Tunable Typeâ€Ⅰ/Typeâ€Ⅱ Band Alignment and Photocatalytic Performance of gâ€C 3 N 4 /InSe van der Waals Heterostructure. Physica Status Solidi - Rapid Research Letters, 2021, 15, 2100171.	1.2	6
56442	Comparative study of Sr$$_{2}ext {Fe}_{3}ext {Ch}_{2}ext {O}_{3}$$(Ch=S, Se): 2-D AFM spin S = 2 ladder systems. European Physical Journal B, 2021, 94, 1.	0.6	0
56443	The effects of transitional metal element doping on the Cs(I) adsorption of kaolinite (0 0 1): A density functional theory study. Applied Surface Science, 2021, 547, 149210.	3.1	15
56444	Nanoporous <scp>Titaniumâ€Oxo</scp> Molecular Cluster for <scp>CO₂</scp> Selective Adsorption. Bulletin of the Korean Chemical Society, 2021, 42, 1014-1019.	1.0	2
56445	AlCl₃-Dosed Si(100)-2 Ã— 1: Adsorbates, Chlorinated Al Chains, and Incorporated Al. Journal of Physical Chemistry C, 2021, 125, 11336-11347.	1.5	14
56446	Engineering Electronic Structure and Band Alignment of 2D Mg(OH)2 via Anion Doping for Photocatalytic Applications. Materials, 2021, 14, 2640.	1.3	3
56447	Simple pair-potentials and pseudo-potentials for warm-dense matter applications. Physics of Plasmas, 2021, 28, 052108.	0.7	3
56448	Novel Chain and Ribbon ZnO Nanoporous Crystalline Phases in Cubic Lattice. Physica Status Solidi (B): Basic Research, 2021, 258, 2100067.	0.7	0
56449	Identification of the Nitrogen Interstitial as Origin of the 3.1â€‰eV Photoluminescence Band in Hexagonal Boron Nitride. Physica Status Solidi (B): Basic Research, 2021, 258, 2100031.	0.7	3
56450	Fermi surface studies of the topologically nontrivial compound YSi. Physical Review B, 2021, 103, .	1.1	3
56451	Formation of ordered precipitates in Al-Sc-Er-(Si/Zr) alloy from first-principles study. Journal of Rare Earths, 2021, 39, 609-620.	2.5	13
56452	Understanding solid-state processing of pharmaceutical cocrystals via milling: Role of tablet excipients. International Journal of Pharmaceutics, 2021, 601, 120514.	2.6	19
56453	Graphene-based mesoporous frameworks with ultrahigh nitrogen contents for highly efficient and selective sulfur dioxide capture. Chemical Engineering Journal, 2021, 412, 128677.	6.6	13
56454	Free electron to electride transition in dense liquid potassium. Nature Physics, 2021, 17, 955-960.	6.5	15
56455	Computational and experimental evidence of Pd supported P-doped porous graphitic carbon nitride as a highly efficient and exceptionally durable photocatalyst for boosted visible-light-driven benzyl alcohol oxidation. Journal of Physics and Chemistry of Solids, 2021, 152, 109985.	1.9	11

#	Article	IF	Citations
56456	Constrained crystals deep convolutional generative adversarial network for the inverse design of crystal structures. Npj Computational Materials, 2021, 7, .	3.5	50
56457	Unified theory for light-induced halide segregation in mixed halide perovskites. Nature Communications, 2021, 12, 2687.	5.8	70
56458	Chalcogenide Dopant-Induced Lattice Expansion in Cobalt Vanadium Oxide Nanosheets for Enhanced Supercapacitor Performance. ACS Applied Energy Materials, 2021, 4, 4758-4771.	2.5	20
56459	Strain modulation of magnetic properties of monolayer and bilayer FePS3 antiferromagnet. Journal of Magnetism and Magnetic Materials, 2021, 525, 167687.	1.0	23
56460	Ultralow Lattice Thermal Conductivity of A_{0.5}RhO₂ (A = K, Rb, Cs) Induced by Interfacial Scattering and Resonant Scattering. Journal of Physical Chemistry C, 2021, 125, 11648-11655.	1.5	2
56461	Enhanced Reactant Activation and Transformation for Efficient Photocatalytic Acetone Degradation on SnO₂ via Hf Doping. Advanced Sustainable Systems, 2021, 5, 2100115.	2.7	8
56462	Supramolecular Selfâ€Assembled Multiâ€Electronâ€Acceptor Organic Molecule as Highâ€Performance Cathode Material for Liâ€Ion Batteries. Advanced Energy Materials, 2021, 11, 2100330.	10.2	48
56463	Tuning the Conduction Band for Interfacial Electron Transfer: Dye-Sensitized Sn_xTi_{1â€“x}O₂ Photoanodes for Water Splitting. ACS Applied Energy Materials, 2021, 4, 4695-4703.	2.5	4
56464	Structural motifs and bonding in two families of boron structures predicted at megabar pressures. Physical Review Materials, 2021, 5, .	0.9	8
56465	Cation-synergy stabilizing anion redox of Chevrel phase Mo6S8 in aluminum ion battery. Energy Storage Materials, 2021, 37, 87-93.	9.5	31
56466	Deciphering the structures and electronic features of Yb3+-doped Y2O3 crystal: A theoretical perspective study. Computational Materials Science, 2021, 192, 110340.	1.4	6
56467	Structural Effectiveness of AgCl-decorated Ag Nanowires Enhancing Oxygen Reduction. ACS Sustainable Chemistry and Engineering, 2021, 9, 7519-7528.	3.2	14
56468	Determining the Criticality of Liâ€Excess for Disorderedâ€Rocksalt Liâ€Ion Battery Cathodes. Advanced Energy Materials, 2021, 11, 2100204.	10.2	31
56469	Novel high voltage polymer insulators using computational and data-driven techniques. Journal of Chemical Physics, 2021, 154, 174906.	1.2	12
56470	Enhanced photogalvanic effects in the two-dimensional <mml:math xmlns:mml="http://www.w3.org/1998/Math/MathML" altimg="si7.svg"><mml:mrow><mml:msub><mml:mrow><mml:mi mathvariant="normal">WTe</mml:mi></mml:mrow><mml:mrow><mml:mn>2</mml:mn></mml:mrow></mml:msub></mml:mrow></mml monolayer by vacancy- and substitution-doping. Applied Surface Science, 2021, 548, 148751.	3.1	33
56471	Ru-supported lanthania-ceria composite as an efficient catalyst for COx-free H2 production from ammonia decomposition. Applied Catalysis B: Environmental, 2021, 285, 119831.	10.8	54
56472	Dual-atom Pt heterogeneous catalyst with excellent catalytic performances for the selective hydrogenation and epoxidation. Nature Communications, 2021, 12, 3181.	5.8	156
56473	Engineering of cation and anion vacancies in Co3O4 thin nanosheets by laser irradiation for more advancement of oxygen evolution reaction. Nano Energy, 2021, 83, 105800.	8.2	50

#	Article	IF	Citations
56474	Atomically dispersed antimony on carbon nitride for the artificial photosynthesis of hydrogen peroxide. Nature Catalysis, 2021, 4, 374-384.	16.1	474
56475	Density Functional Theory Study of a Graphdiyne-Supported Single Au Atom Catalyst for Highly Efficient Acetylene Hydrochlorination. ACS Applied Nano Materials, 2021, 4, 6152-6159.	2.4	22
56476	Spin-polarized oxygen evolution reaction under magnetic field. Nature Communications, 2021, 12, 2608.	5.8	242
56477	A hierarchical Ti2Nb10O29 composite electrode for high-power lithium-ion batteries and capacitors. Materials Today, 2021, 45, 8-19.	8.3	61
56478	The Versatile Electronic, Magnetic and Photoâ€Electro Catalytic Activity of a New 2D MA₂Z₄ Family**. Chemistry - A European Journal, 2021, 27, 9925-9933.	1.7	44
56479	Regulating coordination number in atomically dispersed Pt species on defect-rich graphene for n-butane dehydrogenation reaction. Nature Communications, 2021, 12, 2664.	5.8	111
56480	Tomographic Study of Mesopore Formation in Ceria Nanorods. Journal of Physical Chemistry C, 2021, 125, 10077-10089.	1.5	7
56481	Amorphization-induced surface electronic states modulation of cobaltous oxide nanosheets for lithium-sulfur batteries. Nature Communications, 2021, 12, 3102.	5.8	103
56482	Folic Acid Self-Assembly Enabling Manganese Single-Atom Electrocatalyst for Selective Nitrogen Reduction to Ammonia. Nano-Micro Letters, 2021, 13, 125.	14.4	39
56483	Engineering new limits to magnetostriction through metastability in iron-gallium alloys. Nature Communications, 2021, 12, 2757.	5.8	14
56484	Uncertainty of exchangeâ€correlation functionals in density functional theory calculations for lithiumâ€based solid electrolytes on the case study of lithium phosphorus oxynitride. Journal of Computational Chemistry, 2021, 42, 1283-1295.	1.5	6
56485	<mml:math xmlns:mml="http://www.w3.org/1998/Math/MathML"><mml:mi>Î±</mml:mi><mml:mtext>â^'</mml:mtext><mml:mi>Î²</mml:mi></mml: phase transition of zirconium predicted by on-the-fly machine-learned force field. Physical Review Materials, 2021, 5, .	0.9	21
56486	Theoretical insights into bimetallic atoms supported on PC6 as highly efficient electrocatalysts for N2 electroreduction to NH3. Applied Surface Science, 2021, 547, 149208.	3.1	25
56487	Influence of Group III and IV Elements on the Hydrogen Evolution Reaction of MoS₂ Disulfide. Journal of Physical Chemistry C, 2021, 125, 11848-11856.	1.5	70
56488	Nonâ€selfâ€sustained electron beam RFâ€generated plasma in application for functional surface pretreatment. Plasma Processes and Polymers, 2021, 18, 2100007.	1.6	6
56489	First-Principles Predicting Improved Ductility of Boron Carbide through Element Doping. Journal of Physical Chemistry C, 2021, 125, 11591-11603.	1.5	7
56490	Pressure-Induced Insulatorâ€“Metal Transition in Silicon Telluride from First-Principles Calculations. Journal of Physical Chemistry C, 2021, 125, 11532-11539.	1.5	2
56491	Fabrication of Ionic Covalent Triazine Framework-Linked Membranes via a Facile Solâ€“Gel Approach. Chemistry of Materials, 2021, 33, 3386-3393.	3.2	20

#	Article	IF	Citations
56492	Structure-activity correlation of Ti₂CT₂ MXenes for Câ€“H activation. Journal of Physics Condensed Matter, 2021, 33, 235201.	0.7	5
56493	Metal cyclopropenylidene sandwich cluster and nanowire: structural, electronic, and magnetic properties. Journal of Physics Condensed Matter, 2021, 33, 235301.	0.7	2
56494	Tuning electronic properties of conductive 2D layered metalâ€“organic frameworks via hostâ€“guest interactions: Dioxygen as an electroactive chemical stimuli. APL Materials, 2021, 9, .	2.2	7
56495	Thermoelectric transports in pristine and functionalized boron phosphide monolayers. Scientific Reports, 2021, 11, 10030.	1.6	10
56496	Evolutionary inverse design of defects at graphene 2D lateral interfaces. Journal of Applied Physics, 2021, 129, 185302.	1.1	1
56497	Improving the Catalytic CO2 Reduction on Cs2AgBiBr6 by Halide Defect Engineering: A DFT Study. Materials, 2021, 14, 2469.	1.3	13
56498	An Ab Initio Study of Allâ€Heusler Heterostructures: The Case of Ultrathin Multilayers. Physica Status Solidi - Rapid Research Letters, 2021, 15, 2100139.	1.2	2
56499	Mechanistic study of efficient producing CO2 electroreduction via 2D metal-organic frameworks M3(2,3,6,7,10,11-hexaiminotriphenylene)2 surface. Electrochimica Acta, 2021, 378, 138028.	2.6	15
56500	Importance of Lattice Constants in QM/MM Calculations on Metalâ€“Organic Frameworks. Journal of Physical Chemistry B, 2021, 125, 5786-5793.	1.2	5
56501	Effect of Electron Doping on the Crystal Structure and Physical Properties of an n = 3 Ruddlesdenâ€“Popper Compound La₄Ni₃O₁₀. ACS Applied Electronic Materials, 2021, 3, 2671-2684.	2.0	1
56502	Gold-Cage Perovskites: A Three-Dimensional Au^{III}â€“X Framework Encasing Isolated MX₆^{3â€“} Octahedra (M^{III} = In, Sb, Bi; X = Cl^{â€“},) Tj ETQq0 0 0 rgBT /Overlock 10 Tf	6.6	11
56503	Modeling LiF and FLiBe Molten Salts with Robust Neural Network Interatomic Potential. ACS Applied Materials & Interfaces, 2021, 13, 24582-24592.	4.0	22
56504	2D Niobium-Doped MoS₂: Tuning the Exciton Transitions and Potential Applications. ACS Applied Electronic Materials, 2021, 3, 2564-2572.	2.0	12
56505	Surface Chemistry of Gold Nanoparticles Produced by Laser Ablation in Pure and Saline Water. Langmuir, 2021, 37, 5783-5794.	1.6	20
56506	O3-Type NaCrO₂ as a Superior Cathode Material for Sodium/Potassium-Ion Batteries Ensured by High Structural Reversibility. ACS Applied Materials & Interfaces, 2021, 13, 22635-22645.	4.0	20
56507	Liquid-Metal-Assisted Growth of Vertical GaSe/MoS₂ pâ€“n Heterojunctions for Sensitive Self-Driven Photodetectors. ACS Nano, 2021, 15, 10039-10047.	7.3	73
56508	Nonmonotonous Distance Dependence of van der Waals Screening by a Dielectric Layer. Journal of Physical Chemistry Letters, 2021, 12, 4993-4999.	2.1	3
56509	Magnetic order and critical temperature of substitutionally doped transition metal dichalcogenide monolayers. Npj 2D Materials and Applications, 2021, 5, .	3.9	48

#	Author	Formation of SO<mml:math xmlns:mml="http://www.w3.org/1998/Math/MathML" altimg="si1.svg"><mml:msub><mml:mrow /><mml:mn>4</mml:mn></mml:msub></mml:math>H<mml:math xmlns:mml="http://www.w3.org/1998/Math/MathML" altimg="si2.svg"><mml:msub><mml:mrow	IF	Citations
56510				

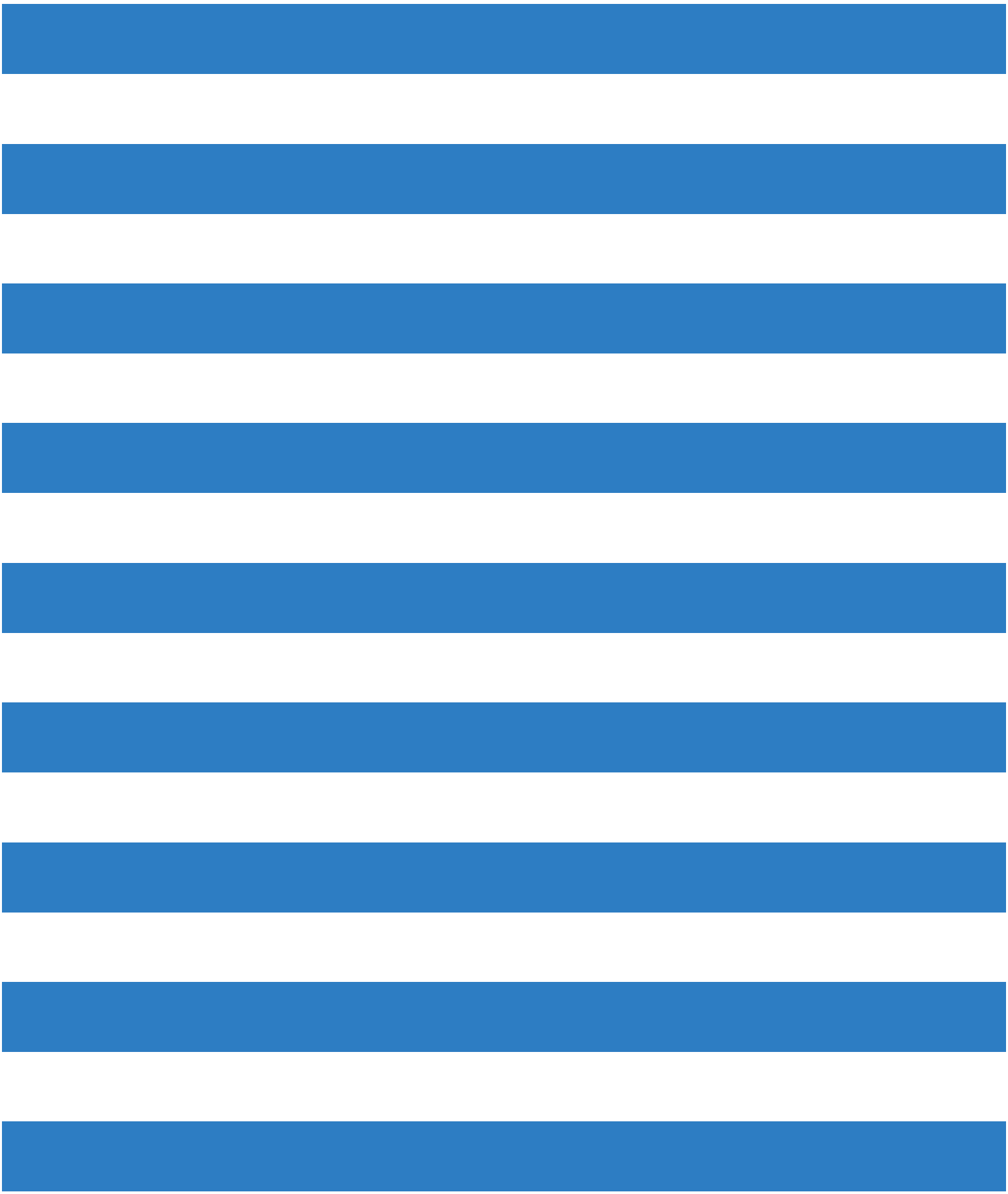

#	Article	IF	Citations
56528	Phonons and lithium diffusion in <mml:math xmlns:mml="http://www.w3.org/1998/Math/MathML"><mml:msub><mml:mi>LiAlO</mml:mi><mml:mn>2</mml:mn></mml:msub></mml:math>. Physical Review B, 2021, 103, .	3.7	11
56529	Magnetic switch and electronic properties in chromium-intercalated two-dimensional <mml:math xmlns:mml="http://www.w3.org/1998/Math/MathML"><mml:msub><mml:mi>GeP</mml:mi><mml:mn>3</mml:mn></mml:msub></mml:math>. Physical Review Materials, 2021, 5, .	3.1	4
56530	Fe4−Nia−N based alloys as rare-earth free high-performance permanent magnet across<mml:math xmlns:mml="http://www.w3.org/1998/Math/MathML" altimg="si46.svg"><mml:mrow><mml:mi>Î±</mml:mi><mml:mtext>'</mml:mtext><mml:mtext>'</mml:mtext></mml:mrow></mml:math> transition: A theoretical insight. Acta Materialia, 2021, 210, 116807.	3.8	6
56531	Surface Structures of CaFe₂O₄ (001), (100), (110) and (111): A Density Functional Theory Study. ISIJ International, 2021, 61, 1370-1378.	0.6	2
56532	Hydration mechanisms of scheelite from adsorption isotherms and ab initio molecular dynamics simulations. Applied Surface Science, 2021, 562, 150137.	3.1	19
56533	First-Principles Observation of Bonded 2D B4C3 Bilayers. ACS Omega, 2021, 6, 13218-13224.	1.6	0
56534	Phaseâ€Changeâ€Memory Process at the Limit: A Proposal for Utilizing Monolayer Sb₂Te₃. Advanced Science, 2021, 8, 2004185.	5.6	25
56535	Structure and Band Alignment of InP Photocatalysts Passivated by TiO₂ Thin Films. Journal of Physical Chemistry C, 2021, 125, 11620-11627.	1.5	7
56536	Photoluminescence enhancement of Gd2Zr2O7:Eu3+ red phosphor sensitized by co-doped Al3+ ions. Ceramics International, 2021, 47, 13071-13077.	2.3	12
56537	Density functional theory of transition metal oxide (FeO, CuO and MnO) adsorbed on TiO2 surface. Journal of Physics and Chemistry of Solids, 2021, 152, 109957.	1.9	7
56538	Ultrafast Growth of Largeâ€Area Uniform, Millimeterâ€Size MoSe 2 Single Crystals on Lowâ€Cost Sodaâ€Lime Glass. Advanced Materials Interfaces, 2021, 8, 2100415.	1.9	11
56539	Decomposition mechanism on different surfaces of copper azide. Journal of Physics Condensed Matter, 2021, 33, 255001.	0.7	1
56540	Theoretical approach to point defects in a single transition metal dichalcogenide monolayer: conductance and force calculations in MoS<mml:math xmlns:mml="http://www.w3.org/1998/Math/MathML"><mml:msub><mml:mrow /> <mml:mn>2</mml:mn></mml:msub></mml:math>. Comptes Rendus Physique, 2021, 22, 23-41.	0.3	1
56541	Solubility and vacancy-mediated inter-diffusion in the Zr-Nb-Cr system. Journal of Nuclear Materials, 2021, 548, 152867.	1.3	5
56542	Coupled deep-mantle carbon-water cycle: Evidence from lower-mantle diamonds. Innovation(China), 2021, 2, 100117.	5.2	6
56543	Localized Wannier function based tight-binding models for two-dimensional allotropes of bismuth. New Journal of Physics, 2021, 23, 063042.	1.2	3
56544	Large Fermiâ€Energy Shift and Suppression of Trivial Surface States in NbP Weyl Semimetal Thin Films. Advanced Materials, 2021, 33, e2008634.	11.1	7
56545	Layered heterostructure of planar and buckled phases of silicene. 2D Materials, 2021, 8, 035038.	2.0	14

#	Article	IF	Citations
56546	Ab initio study of structural and electronic properties of lithium fluoride nanotubes. Journal of Applied Physics, 2021, 129, .	1.1	2
56547	Functional Groupâ€induced pâ€Doping of MoS₂ by Titanium(IV) Bis(ammonium lactato) Dihydroxide Physisorption. Chemistry - an Asian Journal, 2021, 16, 1756-1761.	1.7	4
56548	Tuning network topology and vibrational mode localization to achieve ultralow thermal conductivity in amorphous chalcogenides. Nature Communications, 2021, 12, 2817.	5.8	29
56549	Stability and electronic structure of stacking faults and polytypes in $${hbox {ZnSnN}_2}$$, $${hbox {ZnGeN}_2}$$, and $${hbox {ZnSiN}_2}$$. Journal of the Korean Physical Society, 2021, 79, 309-314.	0.3	1
56550	Selective Adsorption of H₂S, H₂O and SO₂ over CH₄ on Graphene Surface Decorated with Alkali Earth Metals: Insights from DFT Study. Materials Science Forum, 0, 1032, 73-77.	0.3	0
56551	Effects of W⁶⁺ occupying Sc³⁺ on the structure, vibration, and thermal expansion properties of scandium tungstate*. Chinese Physics B, 2021, 30, 066501.	0.7	1
56552	Rhodium Singleâ€Atom Catalysts on Titania for Reverse Water Gas Shift Reaction Explored by First Principles Mechanistic Analysis and Compared to Nanoclusters. ChemCatChem, 2021, 13, 3155-3164.	1.8	10
56553	Efficient Schottky Junction Construction in Metalâ€Organic Frameworks for Boosting H₂ Production Activity. Advanced Science, 2021, 8, 2004456.	5.6	11
56554	Interfacial stabilization for inverted perovskite solar cells with long-term stability. Science Bulletin, 2021, 66, 991-1002.	4.3	45
56555	Carbon Nanotubes/Regenerated Silk Composite as a Three-Dimensional Printable Bio-Adhesive Ink with Self-Powering Properties. ACS Applied Materials & Interfaces, 2021, 13, 21007-21017.	4.0	17
56556	Induced anomalous Hall effect of massive Dirac fermions in <mml:math xmlns:mml="http://www.w3.org/1998/Math/MathML"><mml:mrow><mml:mi>Zr</mml:mi><mml:msub><mml:mi>Te</mml:mi><mml:m and <mml:math xmlns:mml="http://www.w3.org/1998/Math/MathML"><mml:mrow><mml:mi>Hf</mml:mi><mml:msub><mml:mi>Te</mml:mi><mml:m thin flakes. Physical Review B, 2021, 103, .	1.1	15
56557	Accurate and scalable graph neural network force field and molecular dynamics with direct force architecture. Npj Computational Materials, 2021, 7, .	3.5	63
56558	Theoretical Study of Selective Hydrogenation of CO₂ to Methanol over Pt₄/In₂O₃ Model Catalyst. Journal of Physical Chemistry C, 2021, 125, 10926-10936.	1.5	29
56559	Direct Observation and Control of Surface Termination in Perovskite Oxide Heterostructures. Nano Letters, 2021, 21, 4160-4166.	4.5	5
56560	Lowâ€Noise Dualâ€Band Polarimetric Image Sensor Based on 1D Bi₂S₃ Nanowire. Advanced Science, 2021, 8, e2100075.	5.6	48
56561	Two-dimensional superconductivity driven by interfacial electron-phonon coupling in a <mml:math xmlns:mml="http://www.w3.org/1998/Math/MathML"><mml:mrow><mml:msub><mml:mi>BaPbO</mml:mi><mml:mn>3</mml:mn></mml:mn></mml:mi></mml:msub> bilayer. Physical Review B, 2021, 103, .	1.1	5
56562	Real-time imaging of Na ⁺ reversible intercalation in â€œJanusâ€•graphene stacks for battery applications. Science Advances, 2021, 7, .	4.7	61
56563	Tunable electronic and magnetic properties in 1ÂT-VSe2 monolayer on BiFeO3(0001) ferroelectric substrate. Applied Surface Science, 2021, 547, 149206.	3.1	19

#	Article	IF	Citations
56564	The feasibility study of the indium oxide supported silver catalyst for selective hydrogenation of CO2 to methanol. Green Energy and Environment, 2022, 7, 807-817.	4.7	45
56565	Rational Design and Effective Control of Goldâ€Based Bimetallic Electrocatalyst for Boosting CO₂ Reduction Reaction: A Firstâ€Principles Study. ChemSusChem, 2021, 14, 2731-2739.	3.6	9
56566	Insight into bulk charge transfer of lithium metal anodes by synergism of nickel seeding and LiF-Li3N-Li2S co-doped interphase. Energy Storage Materials, 2021, 37, 491-500.	9.5	13
56567	Theoretical design of Salenâ€“metal-based materials for highly selective separation of C2H2/C2H4. Chemical Physics Letters, 2021, 771, 138523.	1.2	0
56568	Structure of the superconducting high-pressure phase of <mml:math xmlns:mml="http://www.w3.org/1998/Math/MathML"><mml:mrow><mml:msub><mml:mi>Sc</mml:mi><mml:mn>3</mml:mn></mml:r mathvariant="normal">C</mml:mi><mml:mn>4</mml:mn></mml:msub></mml:mrow></mml:math>. Physical Review B, 2021, 103, .	1.1	3
56569	Compound-tunable embedding potential method and its application to calcium niobate crystal <mml:math xmlns:mml="http://www.w3.org/1998/Math/MathML"><mml:mrow><mml:msub><mml:mi>CaNb</mml:mi><mml:mn>2</mml:mn></mml:msub><mml:msub><mml:mi mathvariant="normal">O</mml:mi><mml:mn>6</mml:mn></mml:msub></mml:mrow></mml:math> with point defects containing tantalum and uranium. Physical Review B, 2021, 103, .	1.1	7
56570	Prediction of low-energy phases of BiFeO3 with large unit cells and complex tilts beyond Glazer notation. Physical Review Materials, 2021, 5, .	0.9	10
56571	Ab initio determination of Raman spectra of Mg₂SiO₄ and Ca₂MgSi₂O₇ showing mixed modes related to LO/TO splitting. Journal of Raman Spectroscopy, 2021, 52, 1346-1359.	1.2	6
56572	Metal-N4@Graphene as Multifunctional Anchoring Materials for Na-S Batteries: First-Principles Study. Nanomaterials, 2021, 11, 1197.	1.9	12
56573	Electronic structure modulation of CoSe2 nanowire arrays by tin doping toward efficient hydrogen evolution. International Journal of Hydrogen Energy, 2021, 46, 17133-17142.	3.8	22
56574	The Phase Stability of Al3Er Studied by the First-Principles Calculations and Experimental Analysis. Metals, 2021, 11, 759.	1.0	4
56575	Foamer-Derived Bulk Nitrogen Defects and Oxygen-Doped Porous Carbon Nitride with Greatly Extended Visible-Light Response and Efficient Photocatalytic Activity. ACS Applied Materials & Interfaces, 2021, 13, 23866-23876.	4.0	25
56576	Density Functional Theory Study of Edge-Induced Atomic-Scale Structural Phase Transitions of MoS2 Nanocrystals: Implications for a High-Performance Catalyst. ACS Applied Nano Materials, 2021, 4, 5496-5502.	2.4	2
56577	Phonon, Electronic Structure and Mechanical Properties of Superhard Material BC2N from First-Principles Calculations. Brazilian Journal of Physics, 2021, 51, 1199-1206.	0.7	2
56578	Chemical ordering as a precursor to formation of ordered Î´-UZr₂ phase: a theoretical and experimental study. Journal of Physics Condensed Matter, 2021, 33, 254003.	0.7	12
56579	The effect of oxygen vacancies on the coordinatively unsaturated Al-O acid-base pairs for propane dehydrogenation. Journal of Catalysis, 2021, 397, 172-182.	3.1	26
56580	Spontaneous formation of filled-shell CsI-Xenon solid solutions under high temperature and high pressure. Computational Materials Science, 2021, 192, 110355.	1.4	0
56581	Water in the crystal structure of CaSiO3 perovskite. American Mineralogist, 2022, 107, 631-641.	0.9	5

#	Article	IF	Citations
56582	The interfacial charge transfer in triphenylphosphine-based COF/PCN heterojunctions and its promotional effects on photocatalytic hydrogen evolution. International Journal of Hydrogen Energy, 2021, 46, 17666-17676.	3.8	10
56583	Negative thermal expansion in NbF3 and NbOF2: A comparative theoretical study*. Chinese Physics B, 2021, 30, 056501.	0.7	2
56584	CuP: A new type of anisotropic and very stable Dirac cone material. Physica E: Low-Dimensional Systems and Nanostructures, 2021, 129, 114637.	1.3	0
56585	Structural, electronic and optical properties of nano-structural BNC3 alloys. Carbon, 2021, 176, 188-197.	5.4	0
56586	Electronic and magnetic properties of X-doped (X=V, Cr, Mn, and Fe) tellurene for the 2D spintronic device: Insights from the first-principles calculations. Physica E: Low-Dimensional Systems and Nanostructures, 2021, 129, 114667.	1.3	4
56587	First-principles study for comparison of the electronic and optic bandgaps of the CH3NH3Pb1-Y I3 (Y=Bi,) Tj ETQq1 1 0.784314 rgBT /O 2021, 608, 412897.	1.3	1
56588	Adsorption of gas molecules on 2D Na3Bi monolayer: A first-principles study. Physics Letters, Section A: General, Atomic and Solid State Physics, 2021, 399, 127280.	0.9	1
56589	Hydrogen in tungsten trioxide by membrane photoemission and density functional theory modeling. Physical Review B, 2021, 103, .	1.1	6
56590	The fate of compound with AgF2:AgO stoichiometryâ€"A theoretical study. Journal of Chemical Physics, 2021, 154, 204705.	1.2	1
56591	Ferromagnetism in two-dimensional black phosphorus induced by phthalocyanine cobalt. Journal of Materials Science, 2021, 56, 13568-13578.	1.7	5
56592	A first principle study: Effect of tin substitution on magnetic properties of bismuth ferrite nanoparticles prepared by sol-gel synthesis method. Inorganic Chemistry Communication, 2021, 127, 108483.	1.8	16
56593	Prediction of crystal structures and motifs in the Fe-Mg-O system at Earthâ€™s core pressures. New Journal of Physics, 0, , .	1.2	1
56594	Simple linear response model for predicting energy band alignment of two-dimensional vertical heterostructures. Physical Review B, 2021, 103, .	1.1	2
56595	Highly stable two-dimensional metal-carbon monolayer with interpenetrating honeycomb structures. Npj 2D Materials and Applications, 2021, 5, .	3.9	7
56596	Epitaxial stannate pyrochlore thin films: Limitations of cation stoichiometry and electron doping. APL Materials, 2021, 9, .	2.2	3
56597	HR-STEM investigation of atomic lattice defects in different types of Î· precipitates in creep-age forming Alâ€"Znâ€"Mgâ€"Cu aluminium alloy. Materials Science & Engineering A: Structural Materials: Properties, Microstructure and Processing, 2021, 815, 141213.	2.6	22
56598	Uniform Strain-Dependent Thermal Conductivity of Pentagonal and Hexagonal Silicene. Frontiers in Materials, 2021, 8, .	1.2	1
56599	High-Temperature p-Orbital Half-Metallicity and Out-of-Plane Piezoelectricity in a GaN Monolayer Induced by Superhalogens. Journal of Physical Chemistry C, 2021, 125, 10027-10033.	1.5	9

#	Article	IF	Citations
56600	Cadmium(II) Removal by Mackinawite under Anoxic Conditions. ACS Earth and Space Chemistry, 2021, 5, 1306-1315.	1.2	9
56601	Insights into the mechanism and kinetics of propene oxidation and ammoxidation over bismuth molybdate catalysts derived from experiments and theory. Journal of Catalysis, 2022, 408, 436-452.	3.1	18
56602	Reducing Dzyaloshinskii-Moriya interaction and field-free spin-orbit torque switching in synthetic antiferromagnets. Nature Communications, 2021, 12, 3113.	5.8	47
56603	Robust ferromagnetism in single-atom-thick ternary chromium carbonitride CrN4C2. Applied Physics Letters, 2021, 118, .	1.5	12
56604	Symmetry-enforced band crossings in tetragonal materials: Dirac and Weyl degeneracies on points, lines, and planes. Physical Review Materials, 2021, 5, .	0.9	18
56605	Effects of rare-earth elements on the oxidation behavior of Î³-Ni in Ni-based single crystal superalloys: A first-principles study from a perspective of surface adsorption. Applied Surface Science, 2021, 547, 149173.	3.1	10
56606	Effect of Impurity Atoms on the Adsorption/Dissociation of Hydrogen Sulfide and Hydrogen Diffusion on the Fe(100) Surface. ACS Omega, 2021, 6, 14701-14712.	1.6	5
56607	Zintl Phase BaAgSb: Low Thermal Conductivity and High Performance Thermoelectric Material in Ab Initio Calculation. Chinese Physics Letters, 2021, 38, 046301.	1.3	11
56608	Arsenic carbide allotropes prediction: An efficient platform for hole-conductions, optical and photocatalysis applications. Applied Surface Science, 2021, 562, 150109.	3.1	2
56609	Polarization of CO2 for improved CO2 adsorption by MgO and Mg(OH)2. Applied Surface Science, 2021, 562, 150187.	3.1	25
56610	B2 ordering in body-centered-cubic AlNbTiV refractory high-entropy alloys. Physical Review Materials, 2021, 5, .	0.9	14
56611	Tuning the electronic structures and anisotropic transport behaviors of GeSe monolayer by substitutional doping. Semiconductor Science and Technology, 2021, 36, 065020.	1.0	5
56612	Ultrafast dynamics of gallium vacancy charge states in <mml:math xmlns:mml="http://www.w3.org/1998/Math/MathML"><mml:mrow><mml:mi>Î²</mml:mi><mml:mtext>â^'</mml:mtext><mml:msub><mathvariant="normal">O</mml:mi><mml:mn>3</mml:mn></mml:msub></mml:mrow></mml:math>. Physical Review Research, 2021, 3, .	1.3	6
56613	Noncentrosymmetric topological Dirac semimetals in three dimensions. Physical Review B, 2021, 103, .	1.1	11
56614	Theoretical Investigation of the Prospect to Tailor ZnO Electronic Properties with VP Thin Films. Nanomaterials, 2021, 11, 1412.	1.9	1
56615	Nonequilibrium phonon tuning and mapping in few-layer graphene with infrared nanoscopy. Physical Review B, 2021, 103, .	1.1	7
56616	Stability and optoelectronic property of lead-free halide double perovskite Cs₂ Bâ€²Bil₆ (Bâ€² = Li, Na and K)*. Chinese Physics B, 2021, 30, 108102.	0.7	11
56617	Hybrid localized graph kernel for machine learning energyâ€related properties of molecules and solids. Journal of Computational Chemistry, 2021, 42, 1390-1401.	1.5	2

#	Article	IF	Citations
56618	First-principles study on site occupancies and excitation spectra of Na3LuSi2O7:Ce3+. Journal of Luminescence, 2021, 242, 118232.	1.5	0
56619	<scp>PtZn</scp> intermetallic nanoalloy encapsulated in silicaliteâ€1 for propane dehydrogenation. AICHE Journal, 2021, 67, e17295.	1.8	34
56620	Tuning Valleys and Wave Functions of van der Waals Heterostructures by Varying the Number of Layers: A Firstâ€Principles Study. Small, 2021, 17, e2008153.	5.2	4
56621	Computational study of first-row transition metals in monodoped 4H-SiC. Modelling and Simulation in Materials Science and Engineering, 2021, 29, 055008.	0.8	2
56622	Modulation of Negative Differential Resistance in Black Phosphorus Transistors. Advanced Materials, 2021, 33, e2008329.	11.1	18
56623	Morphology Control of Tantalum Carbide Nanoparticles through Dopant Additions. Journal of Physical Chemistry C, 2021, 125, 10665-10675.	1.5	6
56624	SERS Selective Enhancement on Monolayer MoS₂ Enabled by a Pressure-Induced Shift from Resonance to Charge Transfer. ACS Applied Materials & Interfaces, 2021, 13, 26551-26560.	4.0	23
56625	Anomalous Stopping and Charge Transfer in Proton-Irradiated Graphene. Nano Letters, 2021, 21, 4816-4822.	4.5	23
56626	Simulation Meets Experiment: Unraveling the Properties of Water in Metalâ€“Organic Frameworks through Vibrational Spectroscopy. Journal of Physical Chemistry C, 2021, 125, 12451-12460.	1.5	16
56627	Catalytic Conversion of CO and H₂ into Hydrocarbons on the Cobalt Co(111) Surface: Implications for the Fischerâ€“Tropsch Process. Journal of Physical Chemistry C, 2021, 125, 11891-11903.	1.5	11
56628	Electronic-structure methods for materials design. Nature Materials, 2021, 20, 736-749.	13.3	96
56629	Tailoring the surface oxygen engineering of a carbon-quantum-dot-sensitized ZnO@H-ZnO1-x multijunction toward efficient charge dynamics and photoactivity enhancement. Applied Catalysis B: Environmental, 2021, 285, 119846.	10.8	20
56630	Dye Anchoring on CuCrO₂ Surfaces for p-Type Dye-Sensitized Solar Cell Applications: An Ab Initio Study. ACS Applied Energy Materials, 2021, 4, 6180-6190.	2.5	7
56631	3D-to-2D Transition of Anion Vacancy Mobility in CsPbBr₃ under Hydrostatic Pressure. Journal of Physical Chemistry Letters, 2021, 12, 5169-5177.	2.1	7
56632	Impact of A-Site Cations on Fluorescence Quenching in Organicâ€“Inorganic Hybrid Perovskite Materials. Journal of Physical Chemistry C, 2021, 125, 11524-11531.	1.5	3
56633	Doping-Enabled Reconfigurable Strongly Correlated Phase in a Quasi-2D Perovskite. Journal of Physical Chemistry Letters, 2021, 12, 5091-5098.	2.1	1
56634	MnNBr Monolayer: A Highâ€Temperature Ferromagnetic Halfâ€Metal with Typeâ€II Weyl Fermions. Physica Status Solidi - Rapid Research Letters, 2021, 15, 2100115.	1.2	7
56635	Modulation of the Electronic Structure of IrSe₂ by Filling the Bi Atom as a Bifunctional Electrocatalyst for pH Universal Water Splitting. Advanced Energy and Sustainability Research, 2021, 2, 2000074.	2.8	10

#	Article	IF	Citations
56636	An origin of corrosion resistance changes of Zr alloys: effects of Sn and Nb on grain boundary strength of surface oxide. Acta Materialia, 2021, 209, 116804.	3.8	31
56637	Strainâ€Dependent Band Structures and Electronic Properties in Sb/Bi Lateral Heterostructures Calculated by First Principles. Physica Status Solidi - Rapid Research Letters, 2021, 15, 2100148.	1.2	9
56638	Decoupling the effects of defects on efficiency and stability through phosphonates in stable halide perovskite solar cells. Joule, 2021, 5, 1246-1266.	11.7	91
56639	Boosting oxygen reduction activity and enhancing stability through structural transformation of layered lithium manganese oxide. Nature Communications, 2021, 12, 3136.	5.8	25
56640	Solar-driven self-powered alkaline seawater electrolysis via multifunctional earth-abundant heterostructures. Chemical Engineering Journal, 2021, 411, 128538.	6.6	37
56641	Analysis of two-level systems and mechanical loss in amorphous ZrO2-doped Ta2O5 by non-cage-breaking and cage-breaking transitions. Journal of Chemical Physics, 2021, 154, 174502.	1.2	3
56642	Annealingâ€Induced Changes in the Atomic Structure of Amorphous Silica, Germania, and Tantala Using Accelerated Molecular Dynamics. Physica Status Solidi (B): Basic Research, 2021, 258, 2000519.	0.7	5
56643	Room temperature ferromagnetic stability of SrTi1â^' x M xO3 (M = V,) Tj ETQq1 1 0.784314 rgB	0.6	3
56644	The interaction of two-dimensional P2SiS nanosheet with environmental toxic NCG molecules for sensor application: A DFT study. Sensors and Actuators A: Physical, 2021, 322, 112608.	2.0	25
56645	Iridium valence variation and carrier sign tuning in (Ca,Ba)xLa2â^'xCuIrO6 double perovskites. Physical Review Materials, 2021, 5, .	0.9	1
56646	An in-situ solidification strategy to block polysulfides in Lithium-Sulfur batteries. Energy Storage Materials, 2021, 37, 224-232.	9.5	55
56647	Theoretical description of optical and x-ray absorption spectra of MgO including many-body effects. Physical Review B, 2021, 103, .	1.1	8
56649	2D/2D heterostructure of ultrathin BiVO4/Ti3C2 nanosheets for photocatalytic overall Water splitting. Applied Catalysis B: Environmental, 2021, 285, 119855.	10.8	109
56650	Kinetics, reaction pathways, and mechanism investigation for improved environmental remediation by 0D/3D CdTe/Bi2WO6 Z-scheme catalyst. Applied Catalysis B: Environmental, 2021, 285, 119877.	10.8	62
56651	Enhancing the structure stability of Ni-rich LiNi0.6Co0.2Mn0.2O2 cathode via encapsulating in negative thermal expansion nanocrystalline shell. Nano Energy, 2021, 83, 105775.	8.2	59
56652	First-principles study on improvement of two-dimensional hole gas concentration and confinement in AlN/GaN superlattices. Chinese Physics B, 2022, 31, 017104.	0.7	2
56653	Theoretical study of structural and electronic properties of <mml:math xmlns:mml="http://www.w3.org/1998/Math/MathML"><mml:mrow><mml:mn>2</mml:mn><mml:mi>H</mml:mi></mml:mrow></mml:m -phase transition metal dichalcogenides. Physical Review B, 2021, 103, .	1.1	17
56654	Realization of semiconducting Cu₂Se by direct selenization of Cu(111)*. Chinese Physics B, 2021, 30, 116802.	0.7	3

#	Article	IF	Citations
56655	First-principles study of phase transformations in Cuâ€“Cr alloys. Journal of Alloys and Compounds, 2021, 862, 158531.	2.8	23
56656	Effects of deuterium content on the thermal stability and deuterium site occupancy of TiZrHfMoNb deuterides. Journal of Solid State Chemistry, 2021, 297, 121999.	1.4	4
56657	Defects, diffusion, dopants and encapsulation of Na in NaZr2(PO4)3. Materialia, 2021, 16, 101039.	1.3	5
56658	A tetragonal high-pressure phase of PtAs2. Results in Physics, 2021, 24, 104188.	2.0	2
56659	Electronic structure of the layered room-temperature antiferromagnet AlMn2B2. Physical Review B, 2021, 103, .	1.1	1
56660	Cleavage-dissolution assisted stress corrosion cracking under elastic loads. Npj Materials Degradation, 2021, 5, .	2.6	9
56661	Native oxide reconstructions on AlN and GaN (0001) surfaces. Journal of Applied Physics, 2021, 129, .	1.1	4
56662	Efficient N2- and O2-Sensing Properties of PtSe2 With Proper Intrinsic Defects. Frontiers in Chemistry, 2021, 9, 676438.	1.8	2
56663	Significance of Coulomb interaction in interlayer coupling, polarized Raman intensities, and infrared activities in the layered van der Waals semiconductor GaSe. Physical Review B, 2021, 103, .	1.1	6
56664	Ag2S nanoparticles decorated graphene as a selective chemical sensor for acetone working at room temperature. Applied Surface Science, 2021, 562, 150201.	3.1	16
56665	Defects and Strain Engineering of Structural, Elastic, and Electronic Properties of Boron-Phosphide Monolayer: A Hybrid Density Functional Theory Study. Nanomaterials, 2021, 11, 1395.	1.9	8
56666	Lithiophilic NiO Nanoarrays-Modified Ni Skeletons with Vertical Channels for High-Loading Li Metal Batteries. Journal of the Electrochemical Society, 2021, 168, 050536.	1.3	1
56667	Single Co Atoms Implanted into N-Doped Hollow Carbon Nanoshells with Non-Planar Co-N₄-1-O₂ Sites for Efficient Oxygen Electrochemistry. Inorganic Chemistry, 2021, 60, 7498-7509.	1.9	17
56668	Unravelling the Role of Strong Metalâ€“Support Interactions in Boosting the Activity toward Hydrogen Evolution Reaction on Ir Nanoparticle/N-Doped Carbon Nanosheet Catalysts. ACS Applied Materials & Interfaces, 2021, 13, 22448-22456.	4.0	34
56669	Three-Dimensional Dirac Phonons with Inversion Symmetry. Physical Review Letters, 2021, 126, 185301.	2.9	58
56670	Low-Dimensional Organic Metal Halide Hybrids with Excitation-Dependent Optical Waveguides from Visible to Near-Infrared Emission. ACS Applied Materials & Interfaces, 2021, 13, 26451-26460.	4.0	23
56671	Origin of Water-Induced Deactivation of MnO₂-Based Catalyst for Room-Temperature NO Oxidation: A First-Principles Microkinetic Study. ACS Catalysis, 2021, 11, 6835-6845.	5.5	8
56672	Improved Thermoelectric Performance of Cu₁₂Sb₄S₁₃ through Gd-Substitution Induced Enhancement of Electronic Density of States and Phonon Scattering. ACS Applied Materials & Interfaces, 2021, 13, 25092-25101.	4.0	18

#	Article	IF	Citations
56673	On-Surface Fabrication of Bimetallic Metalâ€“Organic Frameworks through the Synergy and Competition among Noncovalent Interactions. Journal of Physical Chemistry Letters, 2021, 12, 5228-5232.	2.1	6
56674	Vacancies-Engineered M₂CO₂ MXene as an Efficient Hydrogen Evolution Reaction Electrocatalyst. Journal of Physical Chemistry Letters, 2021, 12, 4805-4813.	2.1	31
56675	Dissociative Sticking Probability of Methane on Pt(110)-(2Ã—1). Journal of Physical Chemistry C, 2021, 125, 11904-11915.	1.5	5
56676	Role of the Hydration Shell in the pH-Dependent Adsorption of Maleic Acid. Journal of Physical Chemistry C, 2021, 125, 12305-12315.	1.5	2
56677	Emergence of Room Temperature Magnetotransport Anomaly in Epitaxial Pt/Î³â€²-Fe₄N/MgO Heterostructures toward Noncollinear Spintronics. ACS Applied Materials & Interfaces, 2021, 13, 26639-26648.	4.0	3
56678	Partially Anion-Ordered Cerium Niobium Oxynitride Perovskite Phase with a Small Band Gap. Chemistry of Materials, 2021, 33, 4045-4056.	3.2	1
56679	Graphene Oxide/Fe₂O₃ Nanocomposite as an Efficient Catalyst for Thermal Decomposition of Ammonium Perchlorate via the Vacuum-Freeze-Drying Method. Langmuir, 2021, 37, 6132-6138.	1.6	34
56680	Tuning Dzyaloshinskii-Moriya interaction in ferrimagnetic GdCo: A first-principles approach. Physical Review B, 2021, 103, .	1.1	13
56681	Atomic scale investigation of aluminum incorporation, defects, and phase stability in Î²-(AlxGa1â^'x)2O3 films. APL Materials, 2021, 9, .	2.2	35
56682	GPU-acceleration of the ELPA2 distributed eigensolver for dense symmetric and hermitian eigenproblems. Computer Physics Communications, 2021, 262, 107808.	3.0	19
56683	Stability and photoelectric nature of polar surfaces of ZnO: Effects of surface reconstruction. Physics Letters, Section A: General, Atomic and Solid State Physics, 2021, 398, 127274.	0.9	4
56684	Insight into the Structure of TMA-Hectorite: A Theoretical Approach. Minerals (Basel, Switzerland), 2021, 11, 505.	0.8	2
56685	Ferromagnetism and intrinsic half-metallicity of two-dimensional MnN monolayer with squareâ€“octagonal structure. Journal of Physics Condensed Matter, 2021, 33, 225804.	0.7	1
56686	Plastic deformation mechanism of CoCrxNi medium entropy alloys. Materials Science & Engineering A: Structural Materials: Properties, Microstructure and Processing, 2021, 814, 141181.	2.6	12
56687	Electronic and optical properties of ASc₂S₄ (AÂ=ÂCa, Sr) compounds. Physica Scripta, 2021, 96, 075805.	1.2	3
56688	Theoretical investigation on the structural, mechanical, electronic and thermodynamic properties of cubic Ti3NiAl2C compound. Physica B: Condensed Matter, 2021, 609, 412917.	1.3	0
56689	Crystal symmetry based selection rules for anharmonic phonon-phonon scattering from a group theory formalism. Physical Review B, 2021, 103, .	1.1	20
56690	Improving oxygen vacancies by cobalt doping in MoO₂ nanorods for efficient electrocatalytic hydrogen evolution reaction. Nano Select, 2021, 2, 2148-2158.	1.9	9

#	Article	IF	Citations
56691	Electronic, optical, and water solubility properties of two-dimensional layered <mml:math xmlns:mml="http://www.w3.org/1998/Math/MathML"><mml:mrow><mml:msub><mml:mi>SnSi</mml:mi><mml:mn>2</mml:mn></mml:msub><mml:msub><mml:mi mathvariant="normal">N</mml:mi><mml:mn>4</mml:mn></mml:msub></mml:mrow></mml:math> from first principles. Physical Review B, 2021, 103, .	1.1	9
56692	Predicting anomalous quantum confinement effect in van der Waals materials. Physical Review Materials, 2021, 5, .	0.9	10
56693	Negative thermal expansion in the Ruddlesden-Popper calcium titanates. Physical Review Materials, 2021, 5, .	0.9	7
56694	Large anomalous Hall effect induced by gapped nodal lines in GdZn and GdCd. Physical Review B, 2021, 103, .	1.1	3
56695	Electrical contacts to few-layer MoS2 with phase-engineering and metal intercalation for tuning the contact performance. Journal of Chemical Physics, 2021, 154, 184705.	1.2	2
56696	Shape Control of Emissive Properties of Mn-Doped CsPbBr3 Nanocrystals. Journal of Physical Chemistry C, 2021, 125, 11462-11467.	1.5	1
56697	Adsorption of CO, H2, H2O, and CO2 on Fe-, Co-, Ni-, Cu-, Pd-, and Pt-Doped Mo2C(101) Surfaces. Journal of Physical Chemistry C, 2021, 125, 11419-11431.	1.5	3
56698	Formation of Polysulfides from Consolidation of Cu Vacancies on CuS (001) Surfaces. Journal of Physical Chemistry C, 2021, 125, 11325-11335.	1.5	4
56699	Lithium-Aluminum-Phosphate coating enables stable 4.6 V cycling performance of LiCoO2 at room temperature and beyond. Energy Storage Materials, 2021, 37, 67-76.	9.5	64
56700	Atomically precise noble metal clusters (Ag10, Au10, Pd10 and Pt10) on alumina support: A comprehensive DFT study for oxidative catalysis. Applied Surface Science, 2021, 547, 149160.	3.1	7
56701	Investigation on thermal quenching of Eu3+ luminescence in Sr2Ca(Mo/W)O6, Gd3B(Mo/W)O9 and Ca(Mo/W)O4. Ceramics International, 2021, 47, 13729-13737.	2.3	3
56702	Electronic and Structural Transitions of LaAlO₃/SrTiO₃ Heterostructure Driven by Polar Fieldâ€Assisted Oxygen Vacancy Formation at the Surface. Advanced Science, 2021, 8, e2002073.	5.6	23
56703	Dirac Semimetal Protected by Nonsymmorphic Mirror Symmetries in TPHâ€Graphene. Physica Status Solidi - Rapid Research Letters, 2021, 15, 2100039.	1.2	7
56704	Manipulation of Perpendicular Magnetic Anisotropy by Interfacial Strain: Development of Orbital Elastic Effect by Electric-Field Induced XMCD. Vacuum and Surface Science, 2021, 64, 230-235.	0.0	0
56705	Twoâ€“dimensional PC3 as a promising anode material for potassium-ion batteries: Firstâ€“principles calculations*. Chinese Physics B, 2021, 30, 056801.	0.7	5
56706	Tunable spin-valley coupling in layered polar Dirac metals. Communications Materials, 2021, 2, .	2.9	7
56707	Isostructural phase transition by point defect reorganization in the binary type-I clathrate Ba7.5Si45. Acta Materialia, 2021, 210, 116824.	3.8	3
56708	Screening of generalized stacking fault energies, surface energies and intrinsic ductile potency of refractory multicomponent alloys. Acta Materialia, 2021, 210, 116800.	3.8	37

#	Article	IF	Citations
56709	Theoretical prediction of room-temperature two-dimensional ferromagnetism in an yttrium iodide electride. Physical Review B, 2021, 103, .	1.1	7
56710	Critical Role of Orderâ€“Disorder Behavior in Perovskite Ferroelectric KNbO₃. Inorganic Chemistry, 2021, 60, 7961-7973.	1.9	13
56711	Origin of Structural Phase Transitions in Ni-Rich Li_xNi_{0.8}Co_{0.1}Mn_{0.1}O₂ with Lithiation/Delithiation: A First-Principles Study. ACS Sustainable Chemistry and Engineering, 2021, 9, 7437-7446.	3.2	18
56712	B-site La, Ce, and Pr-doped Ba0.5Sr0.5Co0.7Fe0.3O3- perovskite cathodes for intermediate-temperature solid oxide fuel cells: Effectively promoted oxygen reduction activity and operating stability. Journal of Power Sources, 2021, 494, 229778.	4.0	50
56713	Combined Density Functional Theory and Microkinetics Study to Predict Optimum Operating Conditions of Si(100) Surface Carbonization by Acetylene for High Power Devices. Journal of Physical Chemistry Letters, 2021, 12, 4558-4568.	2.1	8
56714	Evolutionary computing and machine learning for discovering of low-energy defect configurations. Npj Computational Materials, 2021, 7, .	3.5	24
56715	Spontaneous Enhanced Visible-Light-Driven Photocatalytic Water Splitting on Novel Type-II GaSe/CN and Ga₂SSe/CN vdW Heterostructures. Journal of Physical Chemistry Letters, 2021, 12, 5064-5075.	2.1	95
56716	Distinguishing a Mott Insulator from a Trivial Insulator with Atomic Adsorbates. Physical Review Letters, 2021, 126, 196405.	2.9	37
56717	Ultrabroadband and High-Detectivity Photodetector Based on WS₂/Ge Heterojunction through Defect Engineering and Interface Passivation. ACS Nano, 2021, 15, 10119-10129.	7.3	252
56718	Unlocking the potential of P3 structure for practical Sodium-ion batteries by fabricating zero strain framework for Na+ intercalation. Energy Storage Materials, 2021, 37, 354-362.	9.5	47
56719	Tuning the Electrocatalytic Properties of Black and Gray Arsenene by Introducing Heteroatoms. ACS Omega, 2021, 6, 13124-13133.	1.6	7
56720	Effect of Mo concentration on structural, mechanical, electronic and magnetic properties of Fe₂B: a first-principles study. Philosophical Magazine, 2021, 101, 1549-1572.	0.7	2
56721	Enhancing Lightâ€“Matter Interactions in MoS₂ by Copper Intercalation. Advanced Materials, 2021, 33, e2008779.	11.1	25
56722	Evolution of hydrogen dissolution and superconductivity in Re-based solid solutions under pressure studied by ab initio calculations. Physical Review B, 2021, 103, .	1.1	5
56723	Strong anharmonicity in tin monosulfide evidenced by local distortion, high-energy optical phonons, and anharmonic potential. Physical Review B, 2021, 103, .	1.1	5
56724	General gauge symmetry in the theory and simulation of heat transport in nonsolid materials. Physical Review B, 2021, 103, .	1.1	2
56725	Density functional theory study of formaldehyde adsorption and decomposition on Co-doped defective CeO₂ (110) surface*. Chinese Physics B, 2021, 30, 103101.	0.7	1
56726	Enhancement of piezoelectric property in MgTMAlN (TM = Cr, Mo, W): First-principles study. Journal of Physics and Chemistry of Solids, 2021, 152, 109913.	1.9	10

#	Article	IF	Citations
56727	Precursor Nuclearity and Ligand Effects in Atomicallyâ€Dispersed Heterogeneous Iron Catalysts for Alkyne Semiâ€Hydrogenation. ChemCatChem, 2021, 13, 3247-3256.	1.8	11
56728	Mechanistic insights into carbonâ€“carbon coupling on NiAu and PdAu single-atom alloys. Journal of Chemical Physics, 2021, 154, 204701.	1.2	10
56729	Magnetoelectric coupling of domains, domain walls and vortices in a multiferroic with independent magnetic and electric order. Nature Communications, 2021, 12, 3093.	5.8	24
56730	Dynamic spin fluctuations in the frustrated spin chain compound Li3Cu2SbO6. Physical Review B, 2021, 103, .	1.1	4
56731	Heisenberg and anisotropic exchange interactions in magnetic materials with correlated electronic structure and significant spin-orbit coupling. Physical Review B, 2021, 103, .	1.1	19
56732	Promoting in situ formation of coreâ€shell structured carbides in highâ€Cr cast irons by boron addition. Journal of the American Ceramic Society, 2021, 104, 4891-4901.	1.9	1
56733	New Insights into the Bulk and Surface Defect Structures of Ceria Nanocrystals from Neutron Scattering Study. Chemistry of Materials, 2021, 33, 3959-3970.	3.2	24
56734	A Universal Method for Enhancing the Structural Stability of Ni-Rich Cathodes Via the Synergistic Effect of Dual-Element Cosubstitution. ACS Applied Materials & Interfaces, 2021, 13, 24925-24936.	4.0	43
56735	A solid-like dual-salt polymer electrolyte for Li-metal batteries capable of stable operation over an extended temperature range. Energy Storage Materials, 2021, 37, 609-618.	9.5	49
56736	Mechanism and Timescales of Reversible pâ€Doping of Methylammonium Lead Triiodide by Oxygen. Advanced Materials, 2021, 33, e2100211.	11.1	17
56737	Interpretable Machine Learning-Based Predictions of Methane Uptake Isotherms in Metalâ€“Organic Frameworks. Chemistry of Materials, 2021, 33, 3543-3552.	3.2	38
56738	Unveiling interactions of non-metallic inclusions within advanced ultra-high-strength steel: A spectro-microscopic determination and first-principles elucidation. Scripta Materialia, 2021, 197, 113791.	2.6	8
56739	Sustained production of superoxide radicals by manganese oxides under ambient dark conditions. Water Research, 2021, 196, 117034.	5.3	43
56740	Efficient Dual-Band White-Light Emission with High Color Rendering from Zero-Dimensional Organic Copper Iodide. ACS Applied Materials & Interfaces, 2021, 13, 22749-22756.	4.0	57
56741	Surfaces of VO₂â€Polymorphs: Structure, Stability and the Effect of Doping. ChemPhysChem, 2021, 22, 1018-1026.	1.0	6
56742	Ab initio prediction of semiconductivity in a novel two-dimensional Sb2X3 (X= S, Se, Te) monolayers with orthorhombic structure. Scientific Reports, 2021, 11, 10366.	1.6	44
56743	Effects of Site and Magnetic Disorder on the Oxygen Vacancy Formation and Electronic and Optical Properties of LaxSr1â€“xCoO3â^'Î´ and SrFeyCo1â€“yO3â^'Î´. Journal of Physical Chemistry C, 2021, 125, 12374-12381.	1.5	3
56744	Single Mn Atom Anchored on Nitrogenâ€Doped Graphene as a Highly Efficient Electrocatalyst for Oxygen Reduction Reaction. Chemistry - A European Journal, 2021, 27, 9686-9693.	1.7	15

#	Article	IF	Citations
56745	Enhanced Hydrogen Evolution Activity of Phosphorusâ€Rich Tungsten Phosphide by Cobalt Doping: A Comprehensive Study of the Active Sites and Electronic Structure. ChemElectroChem, 2021, 8, 1658-1664.	1.7	7
56746	Janus two-dimensional transition metal dichalcogenide oxides: First-principles investigation of <mml:math xmlns:mml="http://www.w3.org/1998/Math/MathML"><mml:mrow><mml:mi mathvariant="normal">W</mml:mi><mml:mi>X</mml:mi><mml:mi mathvariant="normal">O</mml:mi></mml:mrow></mml:math> monolayers with <mml:math xmlns:mml="http://www.w3.org/1998/Math/MathML"><mml:mi>X</mml:mi><mml:mo>=</mml:mo><mml:mi mathvariant="normal">S</mml:mi></mml:math> , Se, and Te. Physical Review B, 2021, 103, .	1.1	73
56747	Benchmarking binding energy calculations for organic structure-directing agents in pure-silica zeolites. Journal of Chemical Physics, 2021, 154, 174109.	1.2	26
56748	Bi-functional electrocatalysis through synergetic coupling strategy of atomically dispersed Fe and Co active sites anchored on 3D nitrogen-doped carbon sheets for Zn-air battery. Journal of Catalysis, 2021, 397, 223-232.	3.1	46
56749	Identification of vibrational mode symmetry and phonon anharmonicity in SbCrSe3 single crystal using Raman spectroscopy. Science China Materials, 2021, 64, 2824-2834.	3.5	4
56750	Defect-driven ferrimagnetism and hidden magnetization in <mml:math xmlns:mml="http://www.w3.org/1998/Math/MathML"><mml:msub><mml:mrow><mml:mi>MnBi</mml:mi></mml:mrow><mml:mn>2</mml:mn></mml:msub></mml:math> Physical Review B, 2021, 103, .	1.1	43
56751	Molecular Sieving of Acetylene from Ethylene in a Rigid Ultraâ€microporous Metal Organic Framework.. Chemistry - A European Journal, 2021, 27, 9446-9453.	1.7	20
56752	Gallium oxynitride@carbon cloth with impressive electrochemical performance for supercapacitors. Chemical Engineering Journal, 2021, 411, 128481.	6.6	18
56753	Theoretical study on water behavior on the copper surfaces. Journal of Molecular Modeling, 2021, 27, 149.	0.8	3
56754	Prominent role of oxygen vacancy for superoxide radical and hydroxyl radical formation to promote electro-Fenton like reaction by W-doped CeO2 composites. Applied Surface Science, 2021, 549, 149262.	3.1	55
56755	Manipulation of the Rashba spin-orbit coupling of a distorted <mml:math xmlns:mml="http://www.w3.org/1998/Math/MathML"><mml:mrow><mml:mn>1</mml:mn><mml:mi>T</mml:mi><mml:mtext>-phase</ Janus WSSe monolayer: Dominant role of charge transfer and orbital components. Physical Review B, 2021, 103, .	1.1	13
56756	The significant role of the chemically bonded interfaces in BiVO4/ZnO heterostructures for photoelectrochemical water splitting. Applied Catalysis B: Environmental, 2021, 285, 119833.	10.8	50
56757	Light-induced static magnetization: Nonlinear Edelstein effect. Physical Review B, 2021, 103, .	1.1	11
56758	Revealing the role of the cathodeâ€“electrolyte interface on solid-state batteries. Nature Materials, 2021, 20, 1392-1400.	13.3	106
56759	Band Gap Engineering toward Wavelength Tunable CsPbBr₃ Nanocrystals for Achieving Rec. 2020 Displays. Chemistry of Materials, 2021, 33, 3575-3584.	3.2	32
56760	Matching the kinetics of natural enzymes with a single-atom iron nanozyme. Nature Catalysis, 2021, 4, 407-417.	16.1	517
56761	Dynamically induced magnetism in <mml:math xmlns:mml="http://www.w3.org/1998/Math/MathML"><mml:msub><mml:mi>KTaO</mml:mi><mml:mn>3</mml:mn></mml:msub></m Physical Review Research, 2021, 3, .	1.3	21
56762	Highly active metal-free hetero-nanotube catalysts for the hydrogen evolution reaction. Nanotechnology, 2021, 32, 315402.	1.3	1

#	Article	IF	Citations
56764	Firstâ€Principles Study on Stacking Fault Energy of Disordered Î³-Fe1â€‰â^'â€‰xMnx with Antiferromagnetic Configuration. Metals and Materials International, 0, , 1.	1.8	2
56765	Uniaxial strain induced symmetry lowering and valleys drift in MoS₂. New Journal of Physics, 2021, 23, 053007.	1.2	3
56766	First-principles study of defects at <mml:math xmlns:mml="http://www.w3.org/1998/Math/MathML" display="inline" id="d1e125" altimg="si6.svg"><mml:mrow><mml:mi>Îž</mml:mi><mml:mn>3</mml:mn></mml:mrow></mml:math> grain boundaries in CuGaSe<mml:math xmlns:mml="http://www.w3.org/1998/Math/MathML" display="inline" id="d1e133" altimg="si24.svg"><mml:msub><mml:mrow /><mml:mrow><mml:mn>2</mml:mn></mml:mrow></mml:msub></mml:math>. Solid State Communicati	0.9	3
56767	First-principles study of the surface of silica and sodium silicate glasses. Physical Review B, 2021, 103, .	1.1	6
56768	Temperature-dependent renormalization of magnetic interactions by thermal, magnetic, and lattice disorder from first principles. Physical Review B, 2021, 103, .	1.1	3
56769	Atomistic Simulations of Defect Production in Monolayer and Bulk Hexagonal Boron Nitride under Low- and High-Fluence Ion Irradiation. Nanomaterials, 2021, 11, 1214.	1.9	7
56770	Deciphering water-solid reactions during hydrothermal corrosion of SiC. Acta Materialia, 2021, 209, 116803.	3.8	10
56771	Dynamic Nature of High-Pressure Ice VII. Physical Review Letters, 2021, 126, 185501.	2.9	9
56772	Density-independent plasmons for terahertz-stable topological metamaterials. Proceedings of the National Academy of Sciences of the United States of America, 2021, 118, .	3.3	14
56773	Strain tuning of the Curie temperature and valley polarization in two dimensional ferromagnetic WSe₂/CrSnSe₃ heterostructure. Nanotechnology, 2021, 32, 375708.	1.3	5
56774	Two-dimensional metallic BP as anode material for lithium-ion and sodium-ion batteries with unprecedented performance. Journal of Materials Science, 2021, 56, 13763-13771.	1.7	12
56775	High Thermopower and Optical Properties of A 2 MoS 4 (Aâ€‰=â€‰K, Rb, Cs) and Cs 2 MoSe 4. Physica Status Solidi (B): Basic Research, 2021, 258, 2000587.	0.7	0
56776	Machine Learning in Magnetic Materials. Physica Status Solidi (B): Basic Research, 2021, 258, 2000600.	0.7	18
56777	Barrier-dependent electronic transport properties in two-dimensional MnBi2Te4-based van der Waals magnetic tunnel junctions. Applied Physics Letters, 2021, 118, .	1.5	11
56778	Chemical bath deposition of SnS:Cu/ZnS for solar hydrogen production and solar cells. Journal of Alloys and Compounds, 2021, 863, 158727.	2.8	17
56779	Multiphase tin equation of state using density functional theory. Physical Review B, 2021, 103, .	1.1	14
56780	Influence of Crystallinity of Lithium Thiophosphate Solid Electrolytes on the Performance of Solidâ€State Batteries. Advanced Energy Materials, 2021, 11, 2100654.	10.2	64
56781	Antimonene Allotropes Î±- and Î²-Phases as Promising Anchoring Materials for Lithiumâ€“Sulfur Batteries. Energy & Fuels, 2021, 35, 9001-9009.	2.5	15

#	Article	IF	Citations
56782	Structural and Electronic Properties of MgO/TiO₂ Interfaces: A First-Principles Molecular-Simulation Study. Journal of Physical Chemistry C, 2021, 125, 10795-10802.	1.5	2
56783	Cooperative Single-Atom Active Centers for Attenuating the Linear Scaling Effect in the Nitrogen Reduction Reaction. Journal of Physical Chemistry Letters, 2021, 12, 5233-5240.	2.1	25
56784	Long-Range Magnetic Exchange Pathways in Complex Clusters from First Principles. Journal of Physical Chemistry C, 2021, 125, 11124-11131.	1.5	4
56785	Designing Active Sites for Structure-Sensitive Reactions via the Generalized Coordination Number: Application to Alcohol Dehydrogenation. Journal of Physical Chemistry C, 2021, 125, 10370-10377.	1.5	6
56786	First-Principles Study of the Surfaces and Equilibrium Shape of Discharge Products in Liâ€“Air Batteries. ACS Applied Materials & Interfaces, 2021, 13, 24984-24994.	4.0	7
56787	Spectrum of Exfoliable 1D van der Waals Molecular Wires and Their Electronic Properties. ACS Nano, 2021, 15, 9851-9859.	7.3	16
56788	Magnetic, Electronic, and Mechanical Properties of Bulk Îµ-Fe₂N Synthesized at High Pressures. ACS Omega, 2021, 6, 12591-12597.	1.6	4
56789	A theoretical investigation of the crystal structure and electronic characters of trivalent Er3+ doped yttrium aluminum garnet. Chemical Physics Letters, 2021, 771, 138537.	1.2	2
56790	G-type antiferromagnetism of Mn ions in A-site-ordered perovskite LaMn3Rh4O12 and La0.8Ca0.2Mn3Rh4O12. Physics Letters, Section A: General, Atomic and Solid State Physics, 2021, 397, 127258.	0.9	1
56791	Straightforward strategy toward a shape-deformable carbon-free cathode for flexible Liâ€“air batteries in ambient air. Nano Energy, 2021, 83, 105821.	8.2	12
56792	Stability and electronic properties of bilayer graphene spirals. Physica E: Low-Dimensional Systems and Nanostructures, 2021, 129, 114638.	1.3	5
56793	Induced magnetization in Cu atoms at the Fe-Co/Cu3Au(001) interface: X-ray magnetic circular dichroism experiments and theoretical results. Applied Surface Science, 2021, 548, 149215.	3.1	1
56794	Vertical ferroelectricity in two-dimensional mixed-valence tin sulfide system: Unprecedented piezoelectricity, efficient nanogenerator and facile control of morphotoropic phase transformations. Nano Energy, 2021, 83, 105786.	8.2	7
56795	Distribution characteristics of phosphoric acid and PTFE binder on Pt/C surfaces in high-temperature polymer electrolyte membrane fuel cells: Molecular dynamics simulation approach. International Journal of Hydrogen Energy, 2021, 46, 17295-17305.	3.8	9
56796	Light-matter interactions in high quality manganese-doped two-dimensional molybdenum diselenide. Science China Materials, 2021, 64, 2507-2518.	3.5	6
56797	Spin Contamination Errors in DFT+U/Plane-wave Calculations for Li_xFeF₃ Systems (x = 0â€“1). Chemistry Letters, 2021, 50, 1057-1061.	0.7	4
56798	Effects of gallium and arsenic substitution on the electronic and magnetic properties of monolayer SnS. Physica Scripta, 2021, 96, 095803.	1.2	2
56799	Quantum oscillations in the field-induced ferromagnetic state of <mml:math xmlns:mml="http://www.w3.org/1998/Math/MathML"><mml:mrow><mml:mi>Mn</mml:mi><mml:msub><mml:mi>Bi</mml:mi> Physical Review B, 2021, 103, .	1.1	11

#	Article	IF	Citations
56800	Koopmans' theorem as the mechanism of nearly gapless surface states in self-doped magnetic topological insulators. Physical Review B, 2021, 103, .	1.1	12
56801	The Role of Grain Boundary Precipitates during Intergranular Fracture in 6xxx Series Aluminium Alloys. Metals, 2021, 11, 894.	1.0	7
56802	Evolutionary search for cobalt-rich compounds in the yttrium-cobalt-boron system. Physical Review Materials, 2021, 5, .	0.9	5
56803	Accurate Deep Potential model for the Alâ€“Cuâ€“Mg alloy in the full concentration space*. Chinese Physics B, 2021, 30, 050706.	0.7	25
56804	Structural evolution, lattice dynamics, electronic and thermal properties of VH2 under high pressure. Solid State Communications, 2021, 330, 114287.	0.9	6
56805	Training sets based on uncertainty estimates in the cluster-expansion method. JPhys Energy, 2021, 3, 034012.	2.3	7
56806	Magnetism-mediated transition between crystalline and higher-order topological phases in NpSb. Physical Review B, 2021, 103, .	1.1	15
56807	Molecular Doping of 2D Indium Selenide for Ultrahigh Performance and Lowâ€Power Consumption Broadband Photodetectors. Advanced Functional Materials, 2021, 31, 2103353.	7.8	17
56808	Analogical discovery of disordered perovskite oxides by crystal structure information hidden in unsupervised material fingerprints. Npj Computational Materials, 2021, 7, .	3.5	9
56809	In-plane ordered quaternary M4/3â€²M2/3â€³AlB2 phases (i-MAB): electronic structure and mechanical properties from first-principles calculations. Journal of Physics Condensed Matter, 2021, 33, 255402.	0.7	4
56810	First-principles calculations of K-shell x-ray absorption spectra for warm dense ammonia*. Chinese Physics B, 2021, 30, 057102.	0.7	1
56811	Giant linear magnetoresistance in half-metallic Sr2CrMoO6 thin films. Npj Quantum Materials, 2021, 6, .	1.8	15
56812	Real time imaging of photocatalytic active site formation during H2 evolution by in-situ TEM. Applied Catalysis B: Environmental, 2021, 284, 119743.	10.8	19
56813	Boosting reversible lithium storage in two-dimensional C3N4 by achieving suitable adsorption energy via Si doping. Carbon, 2021, 176, 480-487.	5.4	21
56814	Catalysis of core-shell nanoparticle M@Pt (M Co and Ni) for oxygen reduction reaction and its electronic structure in comparison to Pt nanoparticle. Journal of Catalysis, 2021, 397, 13-26.	3.1	13
56815	Electrochemical Construction of Low-Crystalline CoOOH Nanosheets with Short-Range Ordered Grains to Improve Oxygen Evolution Activity. ACS Catalysis, 2021, 11, 6104-6112.	5.5	103
56816	Mechanisms for Pressure-Induced Isostructural Phase Transitions in EuO. Physical Review Letters, 2021, 126, 196404.	2.9	7
56817	Exceptional Radiation Absorption in a Pentagon-Based Si Allotrope. Nano Letters, 2021, 21, 4287-4291.	4.5	0

#	Article	IF	Citations
56818	Persistent spin texture in tetragonal BiFeO3. Japanese Journal of Applied Physics, 2021, 60, 050906.	0.8	5
56819	Large-area uniform few-layer PtS2: Synthesis, structure and physical properties. Materials Today Physics, 2021, 18, 100376.	2.9	20
56820	Assessing the Electrochemical Stability Window of NASICON-Type Solid Electrolytes. Frontiers in Energy Research, 2021, 9, .	1.2	29
56821	HClâ€Based Hydrothermal Etching Strategy toward Fluorideâ€Free MXenes. Advanced Materials, 2021, 33, e2101015.	11.1	79
56822	Revealing the Various Electrochemical Behaviors of Sn₄P₃ Binary Alloy Anodes in Alkali Metal Ion Batteries. Advanced Functional Materials, 2021, 31, 2102047.	7.8	25
56823	Binding of Oxygen on Single-Atom Sites on Au/Pd(100) Alloys with High Gold Coverages. Journal of Physical Chemistry C, 2021, 125, 9715-9729.	1.5	3
56824	Off-stoichiometric semiconductors Cu1.33+xZn1.33-xIn1.33Se4 (x = 0, 0.1, 0.2 and 0.3): Synthesis, structure, and thermal and electrical properties. Journal of Solid State Chemistry, 2021, 297, 122058.	1.4	3
56825	Phase Transition and Behaviors of Nâ€“N Bonds in Group-IVB Transition-Metal Pernitrides: First-Principles Calculations under High Pressures. Journal of Physical Chemistry C, 2021, 125, 11555-11566.	1.5	1
56826	Optimal Linear Water Density for Proton Transport in Tunnel Oxides. Journal of Physical Chemistry C, 2021, 125, 11508-11512.	1.5	2
56827	Formation of a Small Electron Polaron in Tantalum Oxynitride: Origin of Low Mobility. Journal of Physical Chemistry C, 2021, 125, 11548-11554.	1.5	16
56828	Mechanisms and Properties of Bismuthene and Graphene/Bismuthene Heterostructures as Anodes of Lithium-/Sodium-Ion Batteries by First-Principles Study. Journal of Physical Chemistry C, 2021, 125, 11391-11401.	1.5	11
56829	An Efficient and Reversible Battery Anode Electrode Derived from a Lead-Based Metalâ€“Organic Framework. Energy & Fuels, 2021, 35, 9669-9682.	2.5	13
56830	Coherence in the Ferroelectric A3ClO (A = Li, Na) Family of Electrolytes. Materials, 2021, 14, 2398.	1.3	10
56831	Low-Temperature and High-Quality Growth of Bi₂O₂Se Layered Semiconductors via Cracking Metalâ€“Organic Chemical Vapor Deposition. ACS Nano, 2021, 15, 8715-8723.	7.3	35
56832	Anomalous layer-dependent electronic and piezoelectric properties of 2D GaInS3 nanosheets. Applied Physics Letters, 2021, 118, .	1.5	29
56833	Strain-tunable electronic and optical properties of Zr2CO2 MXene and MoSe2 van der Waals heterojunction: A first principles calculation. Applied Surface Science, 2021, 548, 149249.	3.1	33
56834	Assessing the Impact of Defects on Leadâ€Free Perovskiteâ€Inspired Photovoltaics via Photoinduced Current Transient Spectroscopy. Advanced Energy Materials, 2021, 11, 2003968.	10.2	26
56835	UO2/BeO interfacial thermal resistance and its effect on fuel thermal conductivity. Annals of Nuclear Energy, 2021, 154, 108102.	0.9	9

#	Article	IF	Citations
56836	Introducing spin polarization into atomically thin 2D carbon nitride sheets for greatly extended visible-light photocatalytic water splitting. Nano Energy, 2021, 83, 105783.	8.2	42
56837	Ternary nickelâ€“tungstenâ€“copper alloy rivals platinum for catalyzing alkaline hydrogen oxidation. Nature Communications, 2021, 12, 2686.	5.8	98
56838	Evidence of a topological edge state in a superconducting nonsymmorphic nodal-line semimetal. Physical Review B, 2021, 103, .	1.1	10
56839	The Stability and Elasticity in Ta-Ti-V Medium-Entropy Alloys Using First-Principles Calculations. Frontiers in Materials, 2021, 8, .	1.2	1
56840	Atomically Thin Pythagorean Tilings in Two Dimensions. Journal of Physical Chemistry Letters, 2021, 12, 4972-4979.	2.1	6
56841	Thermodynamic stability and electronic structure properties of the Bi2WO6 (0 0 1) surface: First principle calculation. Applied Surface Science, 2021, 548, 149053.	3.1	9
56842	Generalizable Trends in Electrochemical Protonation Barriers. Journal of Physical Chemistry Letters, 2021, 12, 5193-5200.	2.1	19
56843	Ab initio molecular dynamics investigation of the elastic properties of superionic <mml:math xmlns:mml="http://www.w3.org/1998/Math/MathML"><mml:mrow><mml:msub><mml:mi>Li</mml:mi><mml:mn>2</mml:mn></mml:msub><mml:mi mathvariant="normal">O</mml:mi></mml:mrow></mml:math> under high temperature and pressure. Physical Review B, 2021, 103, .	1.1	6
56844	Direct oxidation of methane to oxygenates on supported single Cu atom catalyst. Applied Catalysis B: Environmental, 2021, 285, 119827.	10.8	72
56845	Interlayer excitonic states in <mml:math xmlns:mml="http://www.w3.org/1998/Math/MathML"><mml:mrow><mml:mi>Mo</mml:mi><mml:msub><mml:mi>Se</mml:mi><mml:mi mathvariant="normal">S</mml:mi><mml:mn>2</mml:mn></mml:msub></mml:mrow></mml:math> van der Waals heterostructures. Physical Review B, 2021, 103, .	1.1	5
56846	Guiding the design of oxidation-resistant Fe-based single atom alloy catalysts with insights from configurational space. Journal of Chemical Physics, 2021, 154, 174709.	1.2	3
56847	van der Waals corrected density functionals for cylindrical surfaces: Ammonia and nitrogen dioxide adsorbed on a single-walled carbon nanotube. Physical Review B, 2021, 103, .	1.1	2
56848	Hybrid assemblies of octagonal C and BN monolayers and their electronic properties. AIP Advances, 2021, 11, 055114.	0.6	1
56849	Molecular dynamics study of the point defects in bcc uranium. Physical Review Materials, 2021, 5, .	0.9	2
56850	Control of Stepwise Hg²⁺ Reduction on Gold to Selectively Tune its Peroxidase and Catalaseâ€Like Activities and the Mechanism. Advanced Materials Interfaces, 2021, 8, 2100086.	1.9	13
56851	Properties of interfaces between copper and copper sulphide/oxide films. Corrosion Science, 2021, 183, 109313.	3.0	9
56852	Ni/NiO hybrid nanostructure supported on biomass carbon for visible-light photocatalytic hydrogen evolution. Journal of Materials Science, 2021, 56, 12775-12788.	1.7	10
56853	Visualization of the strain-induced topological phase transition in a quasi-one-dimensional superconductor TaSe3. Nature Materials, 2021, 20, 1093-1099.	13.3	57

#	Article	IF	Citations
56854	Spirals and skyrmions in antiferromagnetic triangular lattices. Physical Review Materials, 2021, 5, .	0.9	13
56855	On the Structural Transformation of Ni/BaH2 During a N2-H2 Chemical Looping Process for Ammonia Synthesis: A Joint In Situ Inelastic Neutron Scattering and First-Principles Simulation Study. Topics in Catalysis, 2021, 64, 685-692.	1.3	11
56856	Pseudo-copper Ni-Zn alloy catalysts for carbon dioxide reduction to C2 products. Frontiers of Physics, 2021, 16, 1.	2.4	19
56857	Materials Design and Optimization for Next-Generation Solar Cell and Light-Emitting Technologies. Journal of Physical Chemistry Letters, 2021, 12, 4638-4657.	2.1	12
56858	Oxygen vacancies-rich iron-based perovskite-like electrodes for symmetrical solid oxide fuel cells. Ceramics International, 2021, 47, 12916-12925.	2.3	21
56859	The role of M@Ni6 superstructure units in honeycomb-ordered layered oxides for Li/Na ion batteries. Nano Energy, 2021, 83, 105834.	8.2	15
56860	The influence of Cr on He trapping behavior and the coupling effect of Cr/He on the mechanical behavior of the C14-Laves Fe2W phase: Firstâ€“principle and quasi-harmonic approximation studies. Computational Materials Science, 2021, 192, 110359.	1.4	2
56861	High-buckled 3Ã—3 stanene with a topologically nontrivial energy gap. Journal Physics D: Applied Physics, 2021, 54, 304002.	1.3	5
56862	High-throughput identification of one-dimensional atomic wires and first principles calculations of their electronic states*. Chinese Physics B, 2021, 30, 057304.	0.7	11
56863	Hydrogen-Trapping Energy in Screw and Edge Dislocations in Aluminum: First-Principles Calculations. Materials Transactions, 2021, 62, 582-589.	0.4	18
56864	Bandgap Engineering in the Configurational Space of Solid Solutions via Machine Learning: (Mg,Zn)O Case Study. Journal of Physical Chemistry Letters, 2021, 12, 5163-5168.	2.1	8
56865	Ab initio simulations of the surface free energy of TiN(001). Physical Review B, 2021, 103, .	1.1	9
56866	Noble Metal-Free FeOOH/Li_{0.1}WO₃ Coreâ€“Shell Nanorods for Selective Oxidation of Methane to Methanol with Visibleâ€“NIR Light. Environmental Science & Technology, 2021, 55, 7711-7720.	4.6	32
56867	Thermophysical properties of liquid molybdenum in the near-critical region using quantum molecular dynamics. Physical Review B, 2021, 103, .	1.1	12
56868	Multinary Thioantimonates(III) with d10 Transition Metals: Ionothermal Synthesis, Crystal Structures and Physical Properties. Journal of Cluster Science, 0, , 1.	1.7	0
56869	Room temperature weakly ferromagnetic energy band opened graphene quantum dot coupled solid sheets â€“ A possible carbon based dilute magnetic semiconductor. Applied Surface Science, 2021, 548, 149195.	3.1	4
56870	Electric field controlled type-I and type-II conversion of BP/SnS van der Waals heterostructure. Journal of Physics Condensed Matter, 2021, 33, 265301.	0.7	5
56871	Revealing the catalytic micro-mechanism of MoN, WN and WC on hydrogen evolution reaction. International Journal of Hydrogen Energy, 2021, 46, 23615-23628.	3.8	14

#	Article	IF	Citations
56872	Half metallicity and long-range magnetic order in graphene/hematene van der Waals heterostructure. Indian Journal of Physics, 2022, 96, 1963-1968.	0.9	1
56873	Mechanism of highly sensitive strain response in antiferromagnetic chromium. Journal of Applied Physics, 2021, 129, .	1.1	4
56874	Material Design Strategy for Halide Solid Electrolytes Li₃MX₆ (X = Cl, Br, and) Tj ETQq0 0 0 rgBT /Overlock 10	3.2	62
56875	Thermally Strain-Induced Band Gap Opening on Platinum Diselenide-Layered Films: A Promising Two-Dimensional Material with Excellent Thermoelectric Performance. Chemistry of Materials, 2021, 33, 3490-3498.	3.2	18
56876	First-Principles Study of the Effects of Carbon, Nitrogen, and Oxygen on Helium Behavior in Body-Centered-Cubic Vanadium. Fusion Science and Technology, 0, , 1-10.	0.6	0
56877	Interfacial charge transfer and interaction in the <mml:math xmlns:mml="http://www.w3.org/1998/Math/MathML"><mml:mrow><mml:mrow><mml:mi>MXene</mml:mi><mml:mo>/</mml:mo><mml:mathvariant="normal">O</mml:mi><mml:mn>2</mml:mn></mml:msub></mml:mrow></mml:math> heterostructures. Physical Review Materials, 2021, 5, .	3.1	14
56878	Introducing Ag in Ba0.9La0.1FeO3-: Combining cationic substitution with metal particle decoration. Materials Reports Energy, 2021, 1, 100018.	1.7	6
56879	Application of topological quantum chemistry in electrides. Physical Review B, 2021, 103, .	1.1	23
56880	Lattice dynamics and topological surface phonon states in cuprous oxide <mml:math xmlns:mml="http://www.w3.org/1998/Math/MathML"><mml:mrow><mml:msub><mml:mi>Cu</mml:mi><mml:mn>2</mml:mn></mml:msub><mml:mathvariant="normal">O</mml:mi></mml:mrow></mml:math>. Physical Review B, 2021, 103, .	1.1	12
56881	Two-dimensional vanadium carbide for simultaneously tailoring the hydrogen sorption thermodynamics and kinetics of magnesium hydride. Journal of Magnesium and Alloys, 2022, 10, 2551-2565.	5.5	55
56882	Density functional study of structural, electronic and optical properties of quasi-one-dimensional compounds <mml:math xmlns:mml="http://www.w3.org/1998/Math/MathML" altimg="si1.svg"><mml:mrow><mml:msub><mml:mtext>BaTiX</mml:mtext><mml:mn>3</mml:mn></mml:msub><mml:mrow><mml:mstretchy="true">(</mml:mo><mml:mtext>X</mml:mtext><mml:mo) Tj ETQq0 0 0 rgBT /Overlock 10 Tf 50 337 Td (linebreak 12badbreak	1.1	1
56883	Microstructu Atomically Dispersed Platinum Modulated by Sulfide as an Efficient Electrocatalyst for Hydrogen Evolution Reaction. Advanced Science, 2021, 8, 2100347.	5.6	47
56884	Open Catalyst 2020 (OC20) Dataset and Community Challenges. ACS Catalysis, 2021, 11, 6059-6072.	5.5	201
56885	Click Chemistry in Ultraâ€high Vacuum â€“ Tetrazine Coupling with Methyl Enol Ether Covalently Linked to Si(001). Chemistry - A European Journal, 2021, 27, 8082-8087.	1.7	7
56886	Transitionâ€Metal Borides (MBenes) as New Highâ€Efficiency Catalysts for Nitric Oxide Electroreduction to Ammonia by a Highâ€Throughput Approach. Small, 2021, 17, e2100776.	5.2	67
56887	Enhancing Thermopower and Nernst Signal of Highâ€Mobility Dirac Carriers by Fermi Level Tuning in the Layered Magnet EuMnBi₂. Advanced Functional Materials, 2021, 31, 2102275.	7.8	8
56888	Optimization of Doping <mml:math xmlns:mml="http://www.w3.org/1998/Math/MathML" display="inline" overflow="scroll"><mml:mrow><mml:mi>Cd</mml:mi><mml:mi>Te</mml:mi></mml:mrow></mml:math> with Group-V Elements: A First-Principles Study. Physical Review Applied, 2021, 15, .	1.5	11
56889	Effects of doping substitutions on the thermal conductivity of half-Heusler compounds. Physical Review B, 2021, 103, .	1.1	5

#	Article	IF	Citations
56890	Recyclable and Magnetically Functionalized Metalâ€“Organic Framework Catalyst: IL/Fe₃O₄@HKUST-1 for the Cycloaddition Reaction of CO₂ with Epoxides. ACS Applied Materials & Interfaces, 2021, 13, 22836-22844.	4.0	25
56891	Site Mixing for Engineering Magnetic Topological Insulators. Physical Review X, 2021, 11, .	2.8	50
56892	Assessing the Activity of Ni Clusters Supported on TiC(001) toward CO₂ and H₂ Dissociation. Journal of Physical Chemistry C, 2021, 125, 12019-12027.	1.5	15
56893	Stability Changes in Iridium Nanoclusters via Monoxide Adsorption: A DFT Study within the van der Waals Corrections. Journal of Physical Chemistry A, 2021, 125, 4805-4818.	1.1	7
56894	Exploring the Potentials of Ti₃C_iN_{2â€“i}T_x (i = 0, 1,) Tj ETQq0 0 0 rgBT /Overlock 10 Interfaces, 2021, 13, 22341-22350.	4.0	19
56895	Unusual Role of Point Defects in Perovskite Nickelate Electrocatalysts. ACS Applied Materials & Interfaces, 2021, 13, 24887-24895.	4.0	9
56896	Impact of Solution Chemistry on Growth and Structural Features of Mo-Substituted Spinel Iron Oxides. Inorganic Chemistry, 2021, 60, 7217-7227.	1.9	3
56897	Uncovering design principles for amorphous-like heat conduction using two-channel lattice dynamics. Materials Today Physics, 2021, 18, 100344.	2.9	42
56898	Highly dispersed Co/N-rich carbon nanosheets for the oxidative esterification of biomass-derived alcohols: Insights into the catalytic performance and mechanism. Journal of Catalysis, 2021, 397, 148-155.	3.1	28
56899	Vacancy defects in the vertical heterostructures of graphene and MoS2. Surface Science, 2021, 707, 121809.	0.8	9
56900	Effect of biaxial strain and hydrostatic pressure on the magnetic properties of bilayer CrI3. Frontiers of Physics, 2021, 16, 1.	2.4	7
56901	Hematite facet-mediated microbial dissimilatory iron reduction and production of reactive oxygen species during aerobic oxidation. Water Research, 2021, 195, 116988.	5.3	16
56902	Manipulating anion intercalation enables a high-voltage aqueous dual ion battery. Nature Communications, 2021, 12, 3106.	5.8	104
56903	A Highly Efficient Conjoinedâ€Ётwin Porphyrinâ€Ђbased Complex for the Electrochemical Reduction of CO to Ethanol. ChemNanoMat, 2021, 7, 935-941.	1.5	2
56904	Exploring the Sizeâ€Ðependent Hydrogen Storage Property on Tiâ€Ðoped B_n Clusters by Diatomic Deposition: Temperature Controlled H₂ Release. Advanced Theory and Simulations, 2021, 4, 2100043.	1.3	8
56905	Energy Decomposition to Access the Stability Changes Induced by CO Adsorption on Transition-Metal 13-Atom Clusters. Journal of Chemical Information and Modeling, 2021, 61, 2294-2301.	2.5	6
56906	Catalytic Activity of the Transition-Metal Atom Doped Platinum Surface for NO Reduction by CO. Journal of Physical Chemistry C, 2021, 125, 9703-9714.	1.5	4
56907	Experimental and Ab Initio Investigation of the Formation of Phosphoran Olivine. ACS Earth and Space Chemistry, 2021, 5, 1373-1383.	1.2	0

#	Article	IF	Citations
56908	Atomically Precise Control of Carbon Insertion into hBN Monolayer Point Vacancies using a Focused Electron Beam Guide. Small, 2021, 17, e2100693.	5.2	13
56909	Tuning the Charge Transfer Dynamics of the Nanostructured GaN Photoelectrodes for Efficient Photoelectrochemical Detection in the Ultraviolet Band. Advanced Functional Materials, 2021, 31, 2103007.	7.8	50
56910	Computational Discovery of New 2D Materials Using Deep Learning Generative Models. ACS Applied Materials & Interfaces, 2021, 13, 53303-53313.	4.0	36
56911	Theory of Atomic-Scale Vibrational Mapping and Isotope Identification with Electron Beams. ACS Nano, 2021, 15, 9890-9899.	7.3	9
56912	Ce-introduced effects on modification of acidity and Pt electronic states on Pt-Sn/Î³-Al2O3 catalysts for catalytic reforming. Applied Catalysis A: General, 2021, 617, 118116.	2.2	17
56913	Revealing the Role of Bifunctional Molecules in Crystallizing Methylammonium Lead Iodide through Geometric Isomers. Chemistry of Materials, 2021, 33, 4014-4022.	3.2	10
56914	First-principles investigation on the interfacial interaction and electronic structure of BiVO4/WO3 heterostructure semiconductor material. Applied Surface Science, 2021, 549, 149309.	3.1	28
56915	Engineering Ru atomic structures toward enhanced kinetics of hydrogen generation. Chemical Engineering Science, 2021, 235, 116507.	1.9	6
56916	Avoiding Sabatierâ€™s conflict in bifunctional heterogeneous catalysts for the WGS reaction. CheM, 2021, 7, 1271-1283.	5.8	11
56917	Metal Substitution Steering Electron Correlations in Pyrochlore Ruthenates for Efficient Acidic Water Oxidation. ACS Nano, 2021, 15, 8537-8548.	7.3	54
56918	The role of covalent bonding and anionic redox for the performance of sodium cobaltate electrode materials. Energy Storage Materials, 2021, 37, 190-198.	9.5	4
56919	Tuning interlayer spacing of MoS2 for enhanced hydrogen evolution reaction. Journal of Alloys and Compounds, 2021, 864, 158581.	2.8	18
56920	Electronic charge density as a fast approach for predicting Li-ion migration pathways in superionic conductors with first-principles level precision. Computational Materials Science, 2021, 192, 110380.	1.4	8
56921	In-situ fabrication of Bi/BiVO4 heterojunctions with N-doping for efficient elimination of contaminants. Colloids and Surfaces A: Physicochemical and Engineering Aspects, 2021, 617, 126224.	2.3	22
56922	First-Principles Insights into the Stability Difference between ABX₃ Halide Perovskites and Their A₂BX₆ Variants. Journal of Physical Chemistry C, 2021, 125, 9688-9694.	1.5	36
56923	Electronic and Magnetic Characterization of Epitaxial CrBr₃ Monolayers on a Superconducting Substrate. Advanced Materials, 2021, 33, e2006850.	11.1	38
56924	2D/3D Hybrid of MoS₂/GaN for a High-Performance Broadband Photodetector. ACS Applied Electronic Materials, 2021, 3, 2407-2414.	2.0	70
56925	Charge-carrier-mediated lattice softening contributes to high zT in thermoelectric semiconductors. Joule, 2021, 5, 1168-1182.	11.7	37

#	Article	IF	Citations
56926	Machine learning the quantum-chemical properties of metalâ€“organic frameworks for accelerated materials discovery. Matter, 2021, 4, 1578-1597.	5.0	170
56927	M center in 4 H -SiC is a carbon self-interstitial. Physical Review B, 2021, 103, .	1.1	10
56928	Experimental Evidence of Chiral Symmetry Breaking in KekulÃ©-Ordered Graphene. Physical Review Letters, 2021, 126, 206804.	2.9	72
56929	Interfacial toughening with self-assembled monolayers enhances perovskite solar cell reliability. Science, 2021, 372, 618-622.	6.0	313
56930	Prediction of anomalous LA-TA splitting in electrides. Matter and Radiation at Extremes, 2021, 6, .	1.5	8
56931	Tailored Brownmillerite Oxide Catalyst with Multiple Electronic Functionalities Enables Ultrafast Water Oxidation. Chemistry of Materials, 2021, 33, 5233-5241.	3.2	32
56932	Ru-Doped Single Walled Carbon Nanotubes as Sensors for SO2 and H2S Detection. Chemosensors, 2021, 9, 120.	1.8	12
56933	Accurate GW 0 band gaps and their phonon-induced renormalization in solids. Chinese Physics B, 0, , .	0.7	1
56934	Advanced Data Encryption â€‹using 2D Materials. Advanced Materials, 2021, 33, e2100185.	11.1	67
56935	Nanostructured ZnFe2O4: An Exotic Energy Material. Nanomaterials, 2021, 11, 1286.	1.9	40
56936	Surface oxygen vacancies of Pd/Bi2MoO6-x acts as â€œElectron Bridgeâ€•to promote photocatalytic selective oxidation of alcohol. Applied Catalysis B: Environmental, 2021, 285, 119790.	10.8	90
56937	Toward alcohol synthesis from CO hydrogenation on Cu(111)-supported MoS2 â€“ predictions from DFT+KMC. Journal of Chemical Physics, 2021, 154, 174701.	1.2	3
56938	Pure bulk orbital and spin photocurrent in two-dimensional ferroelectric materials. Npj Computational Materials, 2021, 7, .	3.5	34
56939	Theoretical study of the synthesis, characterization and hydrogen storage properties of a high-density hydrogen storage material: (CH3NH3)BH4. International Journal of Hydrogen Energy, 2021, 46, 19498-19507.	3.8	2
56940	Can N, S Cocoordination Promote Single Atom Catalyst Performance in CO₂RR? Feâ€N₂S₂ Porphyrin versus Feâ€N₄ Porphyrin. Small, 2021, 17, e2100949.	5.2	62
56941	Interface Defect Engineering of a Largeâ€Scale CVDâ€Grown MoS₂ Monolayer via Residual Sodium at the SiO₂/Si Substrate. Advanced Materials Interfaces, 2021, 8, 2100428.	1.9	14
56942	On scaling relations of single atom catalysts for electrochemical ammonia synthesis. Applied Surface Science, 2021, 550, 149283.	3.1	15
56943	Theoretical prediction of intrinsic carrier mobility of monolayer C7N6: First-principles study. Physics Letters, Section A: General, Atomic and Solid State Physics, 2021, 401, 127340.	0.9	5

#	Article	IF	Citations
56944	Realizing n-type doping and high carrier mobility of silicene by decamethylcobaltocene molecular adsorption. Thin Solid Films, 2021, 728, 138691.	0.8	0
56945	First-principles study of high-pressure structural stability and mechanical properties of Ni2B. Computational Materials Science, 2021, 194, 110465.	1.4	7
56946	Electrolyte recommender system for batteries using ensemble Bayesian optimization. IFAC Journal of Systems and Control, 2021, 16, 100158.	1.1	5
56947	First-principles identification of deep energy levels of sulfur impurities in silicon and their carrier capture cross sections. Journal Physics D: Applied Physics, 2021, 54, 335103.	1.3	3
56948	Comparative study of As and Cu doping stability in CdSeTe absorbers. Solar Energy Materials and Solar Cells, 2021, 224, 111012.	3.0	22
56949	Colossal barocaloric effects in the complex hydride Li$$_{2}$$B$$_{12}$$H$$_{12}$$. Scientific Reports, 2021, 11, 11915.	1.6	12
56950	Structural Monoclinicity and Its Coupling to Layered Magnetism in Few-Layer CrI₃. ACS Nano, 2021, 15, 10444-10450.	7.3	14
56951	Revealing the Chemical Bonding in Adatom Arrays via Machine Learning of Hyperspectral Scanning Tunneling Spectroscopy Data. ACS Nano, 2021, 15, 11806-11816.	7.3	13
56952	Two-Dimensional and Three-Dimensional Tetrel-Arsenide Frameworks Templated by Li and Cs Cations. Chemistry of Materials, 2021, 33, 4586-4595.	3.2	2
56953	A Molecular View of the Ionic Liquid Catalyst Interface of SCILLs: Coverage-Dependent Adsorption Motifs of [C₄C₁Pyr][NTf₂] on Pd Single Crystals and Nanoparticles. Journal of Physical Chemistry C, 2021, 125, 13264-13272.	1.5	9
56954	Unexpected Negative-Ion Conversion in Grazing Scattering of Negative Ions on HOPG. Journal of Physical Chemistry C, 2021, 125, 13997-14005.	1.5	2
56955	Nanoparticle Size Effects on Phase Stability for Molybdenum and Tungsten Carbides. Chemistry of Materials, 2021, 33, 4606-4620.	3.2	25
56956	First-Principles-Based Prediction of Electrochemical Oxidation and Corrosion of Copper under Multiple Environmental Factors. Journal of Physical Chemistry C, 2021, 125, 14027-14038.	1.5	7
56957	Orderâ€“Disorder Transition in Inorganic Clathrates Controls Electrical Transport Properties. Chemistry of Materials, 2021, 33, 4500-4509.	3.2	8
56958	Synergistic Effect of Co(III) and Co(II) in a 3D Structured Co₃O₄/Carbon Felt Electrode for Enhanced Electrochemical Nitrate Reduction Reaction. ACS Applied Materials & Interfaces, 2021, 13, 28348-28358.	4.0	66
56959	Elucidating the Mechanism of Ambient-Temperature Aldol Condensation of Acetaldehyde on Ceria. ACS Catalysis, 2021, 11, 8621-8634.	5.5	14
56960	Active Site of Catalytic Ethene Epoxidation: Machine-Learning Global Pathway Sampling Rules Out the Metal Sites. ACS Catalysis, 2021, 11, 8317-8326.	5.5	15
56961	All-Electrical High-Sensitivity, Low-Power Dual-Mode Gas Sensing and Recovery with a WSe₂/MoS₂ pn Heterodiode. ACS Applied Materials & Interfaces, 2021, 13, 30785-30796.	4.0	24

#	Article	IF	Citations
56962	Efficient and Tunable Luminescence in Ga_{2â€“x}In_xO₃:Cr³⁺ for Near-Infrared Imaging. ACS Applied Materials & Interfaces, 2021, 13, 31835-31842.	4.0	98
56963	Nitrogen doping in non-magnetic yttrium oxide: Induction of room temperature ferromagnetism from first principles simulations. Journal of Magnetism and Magnetic Materials, 2021, 528, 167840.	1.0	5
56964	Structural, electronic, and optical properties of two-dimensional hafnium monoxide nanosheets. Physica E: Low-Dimensional Systems and Nanostructures, 2021, 130, 114690.	1.3	3
56965	Unraveling the formation mechanism of hydrogenated vacancy at Î³-Ni/Î³'-Ni3Al phase interface and its roles in interfacial stability and strength. Computational Materials Science, 2021, 194, 110449.	1.4	8
56966	Substitutional carbon-dioxygen center in irradiated silicon. Materials Science in Semiconductor Processing, 2021, 127, 105661.	1.9	1
56967	On the constitution and thermodynamic modeling of the phase diagrams Nb-Mn and Ta-Mn. Journal of Alloys and Compounds, 2021, 865, 158715.	2.8	4
56968	Unraveling the mechanism of hydrogen evolution reaction on cobalt compound electrocatalysts. Applied Surface Science, 2021, 550, 149355.	3.1	12
56969	Improving phase stability, hardness, and oxidation resistance of reactively magnetron sputtered (Al,Cr,Nb,Ta,Ti)N thin films by Si-alloying. Surface and Coatings Technology, 2021, 416, 127162.	2.2	31
56970	Tuning structure, electronic, and catalytic properties of non-metal atom doped Janus transition metal dichalcogenides for hydrogen evolution. Applied Surface Science, 2021, 552, 149146.	3.1	33
56971	Carrier Dynamics and Absorption Properties of Gold-Hyperdoped Germanium: Insight Into Tailoring Defect Energetics. Physical Review Applied, 2021, 15, .	1.5	3
56972	Complex magnetic properties associated with competing local and itinerant magnetism in $${ext {Pr}}_2 {ext {Co}}_{0.86} {ext {Si}}_{2.88}$$. Scientific Reports, 2021, 11, 13245.	1.6	8
56973	Uniaxial NÃ©el vector control in perovskite oxide thin films by anisotropic strain engineering. Physical Review B, 2021, 103, .	1.1	1
56974	Manipulation of hot carrier cooling dynamics in two-dimensional Dionâ€“Jacobson hybrid perovskites via Rashba band splitting. Nature Communications, 2021, 12, 3995.	5.8	41
56975	Ambient effect on the Curie temperatures and magnetic domains in metallic two-dimensional magnets. Npj 2D Materials and Applications, 2021, 5, .	3.9	13
56976	One-dimensional polyhedral chain of ThCl6 encapsulated within single-walled carbon nanotubes. AIP Advances, 2021, 11, 065117.	0.6	1
56977	Gold-in-copper at low *CO coverage enables efficient electromethanation of CO2. Nature Communications, 2021, 12, 3387.	5.8	70
56978	Third-order nonlinear Hall effect induced by the Berry-connection polarizability tensor. Nature Nanotechnology, 2021, 16, 869-873.	15.6	50
56979	Computational insight of ZrS2/graphene heterobilayer as an efficient anode material. Applied Surface Science, 2021, 551, 149304.	3.1	20

#	Article	IF	Citations
56980	Interplay of electrochemical and electrical effects induces structural transformations in electrocatalysts. Nature Catalysis, 2021, 4, 479-487.	16.1	68
56981	Automated Mechanism Generation Using Linear Scaling Relationships and Sensitivity Analyses Applied to Catalytic Partial Oxidation of Methane. ACS Catalysis, 2021, 11, 7114-7125.	5.5	20
56982	Magnetic and f-electron effects in LaNiO2 and NdNiO2 nickelates with cuprate-like $$3{d}_{{x}^{2}-{y}^{2}}$$ band. Communications Physics, 2021, 4, .	2.0	38
56983	Enhancing fatigue life by ductile-transformable multicomponent B2 precipitates in a high-entropy alloy. Nature Communications, 2021, 12, 3588.	5.8	102
56984	Phase transitions of alkaline-earth metal sulfides under pressure. Materials Research Express, 2021, 8, 065902.	0.8	4
56985	Band structures of RE₂O₃:Eu (RE = Lu, Y, Sc) from perspective of spin-polarized quasi-particle approximation. Modelling and Simulation in Materials Science and Engineering, 2021, 29, 065002.	0.8	3
56986	Enzyme-like antibacterial activities of Cu9S5 nanoflowers with vacancy-type dependence. Cell Reports Physical Science, 2021, 2, 100456.	2.8	9
56987	IrW nanochannel support enabling ultrastable electrocatalytic oxygen evolution at 2â€‰Aâ€‰cmâ^'2 in acidic media. Nature Communications, 2021, 12, 3540.	5.8	89
56988	A density functional theory and grand canonical Monte Carlo simulations study the hydrogen storage on the Li-decorated net-I„. International Journal of Hydrogen Energy, 2021, 46, 21965-21972.	3.8	3
56989	Revealing the Pressure-Induced Softening/Weakening Mechanism in Representative Covalent Materials. Chinese Physics Letters, 2021, 38, 056101.	1.3	1
56990	A variety of interface and strain tuning electronic properties of the MoS₂/Cr₂CX ₂ van der Waals heterostructures. Journal Physics D: Applied Physics, 2021, 54, 345105.	1.3	3
56991	Out-of-plane and in-plane ferroelectricity of atom-thick two-dimensional InSe. Nanotechnology, 2021, 32, 385202.	1.3	15
56992	Probing Monomer and Dimer Adsorption Trends in the MFI Framework. Journal of Physical Chemistry B, 2021, 125, 7199-7212.	1.2	2
56993	Magnetostriction of <mml:math xmlns:mml="http://www.w3.org/1998/Math/MathML"><mml:mrow><mml:mi>Al</mml:mi><mml:msub><mml:mi>Fe</mml:mi><mml:mi><mml:mathvariant="normal">B</mml:mi><mml:mn>2</mml:mn></mml:msub></mml:mrow></mml:math> in high magnetic fields. Physical Review Materials, 2021, 5, .	0.9	1
56994	Impurity level properties in transition metal doped Î±-Ga₂O₃ for optoelectronic applications. Semiconductor Science and Technology, 0, , .	1.0	15
56995	Adsorption of gas molecules on graphene, silicene, and germanene: A comparative first-principles study. Surfaces and Interfaces, 2021, 24, 101054.	1.5	20
56996	1D/2D van der Waals Heterojunctions Composed of Carbon Nanotubes and a GeSe Monolayer. Nanomaterials, 2021, 11, 1565.	1.9	5
56997	Formation of a Tiâ€“Cu(111) single atom alloy: Structure and CO binding. Journal of Chemical Physics, 2021, 154, 234703.	1.2	13

#	Article	IF	Citations
56998	Understanding and tuning of spinterface for chemisorbed Ni-dinuclear quinonoid on Co(001) substrate. Journal of Physics Condensed Matter, 2021, 33, .	0.7	0
56999	Strain engineering and thermal conductivity of a penta-BCN monolayer: a computational study. Journal Physics D: Applied Physics, 2021, 54, 355301.	1.3	13
57000	Electron work function: an indicative parameter towards a novel material design methodology. Scientific Reports, 2021, 11, 11565.	1.6	17
57001	Unconventional anomalous Hall effect from magnetization parallel to the electric field. Physical Review B, 2021, 103, .	1.1	10
57002	Hybrid improper ferroelectricity and magnetoelectric coupling in a two-dimensional perovskite oxide. Physical Review B, 2021, 103, .	1.1	8
57003	Tuning fermi level and band gap in Li₄Ti₅O₁₂ by doping and vacancy for ultrafast Li⁺ insertion/extraction. Journal of the American Ceramic Society, 2021, 104, 5934-5945.	1.9	17
57004	Ultrafast Adsorbate Excitation Probed with Subpicosecond-Resolution X-Ray Absorption Spectroscopy. Physical Review Letters, 2021, 127, 016802.	2.9	11
57005	4fâ˜Ï€ Molecular Hybrid Exhibiting Rich Conductive Phases and Slow Relaxation of Magnetization. Journal of the American Chemical Society, 2021, 143, 9543-9550.	6.6	11
57006	Design of refractory compositionally complex alloys with optimal mechanical properties. Physical Review Materials, 2021, 5, .	0.9	7
57007	Two-Dimensional Chromium Bismuthate: A Room-Temperature Ising Ferromagnet with Tunable Magneto-Optical Response. Physical Review Applied, 2021, 15, .	1.5	14
57008	Stable humplike Hall effect and noncoplanar spin textures in <mml:math xmlns:mml="http://www.w3.org/1998/Math/MathML"><mml:msub><mml:mrow><mml:mi>SrRuO</mml:mi></mml:mrow><mml:mrow><mml:mn>3</mml:mn></mml:mrow></mml:msub></mml:math> ultrathin films. Physical Review Research, 2021, 3, .	1.3	16
57009	Two-Dimensional Planar BGe Monolayer as an Anode Material for Sodium-Ion Batteries. ACS Applied Materials & Interfaces, 2021, 13, 29764-29769.	4.0	21
57010	Thermal transport properties of semimetal scandium antimonide: a first-principles study. Applied Physics A: Materials Science and Processing, 2021, 127, 1.	1.1	5
57011	A first-principles study of the structural, electronic, optical, and vibrational properties for paramagnetic half-Heusler compound TiIrBi by GGA and GGAâ€ +â€ mBJ functional. Materials Today Communications, 2021, 27, 102246.	0.9	7
57012	Exposed {0 0 1} facet of anatase TiO2 nanocrystals in Ag/TiO2 catalysts for boosting catalytic soot combustion: The facet-dependent activity. Journal of Catalysis, 2021, 398, 109-122.	3.1	39
57013	Direct correlation of oxygen adsorption on platinum-electrolyte interfaces with the activity in the oxygen reduction reaction. Science Advances, 2021, 7, .	4.7	44
57014	Theoretical prediction of transport coefficients of antimony doped tin dioxide. Ceramics International, 2021, 47, 15277-15281.	2.3	4
57015	Helium incorporation induced direct-gap silicides. Npj Computational Materials, 2021, 7, .	3.5	6

#	Article	IF	Citations
57016	Vitamin C-Assisted Synthesized Mnâ€“Co Oxides with Improved Oxygen Vacancy Concentration: Boosting Lattice Oxygen Activity for the Air-Oxidation of 5-(Hydroxymethyl)furfural. ACS Catalysis, 2021, 11, 7828-7844.	5.5	103
57017	Integration of nickel phosphide nanodot-enriched 3D graphene-like carbon with carbon fibers as self-supported sulfur hosts for advanced lithium sulfur batteries. Electrochimica Acta, 2021, 382, 138267.	2.6	17
57018	Integrated computation of corrosion: Modelling, simulation and applications. Corrosion Communications, 2021, 2, 8-23.	2.7	22
57019	High-Entropy 2D Carbide MXenes: TiVNbMoC₃ and TiVCrMoC₃. ACS Nano, 2021, 15, 12815-12825.	7.3	162
57020	A Deep Learning Approach for Molecular Classification Based on AFM Images. Nanomaterials, 2021, 11, 1658.	1.9	15
57021	Atomistic Insights Into the Degradation of Inorganic Halide Perovskite CsPbI₃: A Reactive Force Field Molecular Dynamics Study. Journal of Physical Chemistry Letters, 2021, 12, 5519-5525.	2.1	31
57022	Sandwiched Cathodes Assembled from CoS₂â€Modified Carbon Clothes for Highâ€Performance Lithiumâ€Sulfur Batteries. Advanced Science, 2021, 8, e2101019.	5.6	64
57023	Substitutional Vanadium Sulfide Nanodispersed in MoS₂ Film for Ptâ€Scalable Catalyst. Advanced Science, 2021, 8, e2003709.	5.6	19
57024	Charge Localization and Magnetic Correlations in the Refined Structure of U₃O₇. Inorganic Chemistry, 2021, 60, 10550-10564.	1.9	6
57025	Opening band gaps of low-dimensional materials at the meta-GGA level of density functional approximations. Physical Review Materials, 2021, 5, .	0.9	18
57026	Improving the applicability of the Pauli kinetic energy density based semilocal functional for solids. New Journal of Physics, 2021, 23, 063007.	1.2	13
57027	DFT calculation of square MoS2 nanotubes. Physica E: Low-Dimensional Systems and Nanostructures, 2021, 130, 114693.	1.3	3
57028	Screening performance of methane activation over atomically dispersed metal catalysts on defective boron nitride monolayers: A density functional theory study. Chinese Chemical Letters, 2021, 32, 1972-1976.	4.8	12
57029	Photocatalytic conversion of CO to fuels with water by B-doped graphene/g-C3N4 heterostructure. Science Bulletin, 2021, 66, 1186-1193.	4.3	19
57030	Stability, and electronic and optical properties of ternary nitride phases of MgSnN2: A first-principles study. Journal of Physics and Chemistry of Solids, 2021, 153, 110011.	1.9	21
57031	Magnesium Ion Storage Properties in a Layered (NH₄)₂V₆O₁₆Â·1.5H₂O Nanobelt Cathode Material Activated by Lattice Water. ACS Applied Materials & Interfaces, 2021, 13, 30625-30632.	4.0	20
57032	Weak ferroelectric charge transfer in layer-asymmetric bilayers of 2D semiconductors. Scientific Reports, 2021, 11, 13422.	1.6	29
57033	Magnetic and electronic ordering phenomena in the <mml:math xmlns:mml="http://www.w3.org/1998/Math/MathML"><mml:mrow><mml:msub><mml:mi>Ru</mml:mi><mml:mn>2</mml:mn></mml:msub><mml:msub><mml:mi mathvariant="normal">O</mml:mi><mml:mn>6</mml:mn></mml:msub></mml:mrow></mml:math> -layer honeycomb lattice compound <mml:math xmlns:mml="http://www.w3.org/1998/Math/MathML"><mml:msub><mml:mi>AgRuO</mml:mi><mml:mn>3</mml:mn></mml:msub></mml:math>. Physical Review B, 2021, 103, .	1.1	10

#	Article	IF	Citations
57034	Electrocatalytic Nitrate Reduction on Oxide-Derived Silver with Tunable Selectivity to Nitrite and Ammonia. ACS Catalysis, 2021, 11, 8431-8442.	5.5	125
57035	Lead halide perovskite for efficient optoacoustic conversion and application toward high-resolution ultrasound imaging. Nature Communications, 2021, 12, 3348.	5.8	85
57036	Loofah activated carbon with hierarchical structures for high-efficiency adsorption of multi-level antibiotic pollutants. Applied Surface Science, 2021, 550, 149313.	3.1	33
57037	High solar-to-hydrogen efficiency in Arsenene/GaX (XÂ=ÂS, Se) van der Waals heterostructure for photocatalytic water splitting. Journal of Alloys and Compounds, 2021, 866, 158774.	2.8	56
57038	Magneto-Ionics in Single-Layer Transition Metal Nitrides. ACS Applied Materials & Interfaces, 2021, 13, 30826-30834.	4.0	13
57039	The Thermodynamic Stability, Electronic and Photocatalytic Properties of the ZnWO₄(100) Surface as Predicted by Screened Hybrid Density Functional Theory. ACS Omega, 2021, 6, 15057-15067.	1.6	10
57040	Using Density Functional Theory to Correlate Charge Transport Properties with Gas Sensing by Organic Nanowires. ACS Applied Nano Materials, 2021, 4, 5972-5980.	2.4	5
57041	Detection of nitrobenzene using transition metal doped C24: A DFT study. Structural Chemistry, 2021, 32, 2259-2270.	1.0	26
57042	Ternary Zinc Antimonides Unlocked Using Hydride Synthesis. Inorganic Chemistry, 2021, 60, 10686-10697.	1.9	6
57043	Optical, electrical and structural properties of Fe doped sodium titanate nanostructures. Applied Surface Science, 2021, 552, 149534.	3.1	4
57044	Electronic and magnetic properties of single-layer and double-layer VX ₂ (X = Cl, Br) under biaxial stress*. Chinese Physics B, 2021, 30, 107305.	0.7	2
57045	Influence of thickness on current-induced magnetization switching in L1₀-FePt single layer*. Chinese Physics B, 2021, 30, 107101.	0.7	1
57046	Modeling the spatial control over point defect spin states via processing variables. Journal of Applied Physics, 2021, 129, 225703.	1.1	2
57047	Methods to accelerate high-throughput screening of atomic qubit candidates in van der Waals materials. Journal of Applied Physics, 2021, 129, 225105.	1.1	3
57048	Accurate frozen core approximation for all-electron density-functional theory. Journal of Chemical Physics, 2021, 154, 224107.	1.2	1
57049	Influences of Work Function Changes in NO2 and H2S Adsorption on Pd-Doped ZnGa2O4(111) Thin Films: First-Principles Studies. Applied Sciences (Switzerland), 2021, 11, 5259.	1.3	6
57050	An effective scheme to determine surface energy and its relation with adsorption energy. Acta Materialia, 2021, 212, 116895.	3.8	16
57051	Stabilization of charged substitutional ions in tetragonal zirconia. Materials Today: Proceedings, 2022, 51, 488-495.	0.9	1

#	Article	IF	Citations
57052	DFT + U Study of Strain-Engineered CO2 Reduction on a CeO2â€“x (111) Facet. Journal of Physical Chemistry C, 2021, 125, 14221-14227.	1.5	14
57053	Spinâ€“Orbit Coupling Is the Key to Promote Asynchronous Photoinduced Charge Transfer of Two-Dimensional Perovskites. Jacs Au, 2021, 1, 1178-1186.	3.6	10
57054	Half-Metallicity and Magnetic Anisotropy in Transition-Metal-Atom-Doped Graphitic Germanium Carbide (g-GeC) Monolayers. Journal of Physical Chemistry C, 2021, 125, 13688-13695.	1.5	18
57055	Realizing High Comprehensive Energy Storage and Ultrahigh Hardness in Lead-Free Ceramics. ACS Applied Materials & Interfaces, 2021, 13, 28472-28483.	4.0	78
57056	Tuning the Activity of Molybdenum Carbide MXenes for CO₂ Electroreduction by Embedding the Single Transition-Metal Atom. Journal of Physical Chemistry C, 2021, 125, 13331-13342.	1.5	14
57057	Charge-Induced Two-Step Structural Phase Transition in the MoTe2â€“WSeTe Hetero-Bilayer. Journal of Physical Chemistry C, 2021, 125, 15000-15011.	1.5	0
57058	Self-Powered Broadband Photodetector and Sensor Based on Novel Few-Layered Pd₃(PS₄)₂ Nanosheets. ACS Applied Materials & Interfaces, 2021, 13, 30806-30817.	4.0	13
57059	Giant Huangâ€“Rhys Factor for Electron Capture by the Iodine Intersitial in Perovskite Solar Cells. Journal of the American Chemical Society, 2021, 143, 9123-9128.	6.6	37
57060	DFT Calculations and Thermodynamic Re-Assessment of the Fe-Y Binary System. Journal of Phase Equilibria and Diffusion, 2021, 42, 348-362.	0.5	7
57061	Enhancing magnetic dipole emission in Eu-doped <mml:math xmlns:mml="http://www.w3.org/1998/Math/MathML"><mml:mrow><mml:mi>Sr</mml:mi><mml:mi>M</mml:mi><mml:msub><mml:mi mathvariant="normal">O</mml:mi><mml:mn>3</mml:mn></mml:msub></mml:mrow></mml:math> () Tj ETQq1 1 0.784314 rgBT /O	1.1	4
57062	Crystal structure engineering in multimetallic high-index facet nanocatalysts. Proceedings of the National Academy of Sciences of the United States of America, 2021, 118, .	3.3	23
57063	Theoretical considerations on activity of the electrochemical CO2 reduction on metal single-atom catalysts with asymmetrical active sites. Catalysis Today, 2022, 397-399, 574-580.	2.2	9
57065	Angular-dependent interatomic potential for large-scale atomistic simulation of iron: Development and comprehensive comparison with existing interatomic models. Physical Review Materials, 2021, 5, .	0.9	18
57066	Cleaving plane-dependent electronic structures of transition metal diarsenides. Physical Review Research, 2021, 3, .	1.3	2
57067	Atomic-scale Evidence for Open-system Thermodynamics in the Early Solar Nebula. Planetary Science Journal, 2021, 2, 115.	1.5	5
57068	Hidden Effects of Negative Stacking Fault Energies in Complex Concentrated Alloys. Physical Review Letters, 2021, 126, 255502.	2.9	18
57069	Predicting carbon diffusion in cementite from first principles. Physical Review Materials, 2021, 5, .	0.9	2
57070	Origin of the Improved Performance of <mml:math xmlns:mml="http://www.w3.org/1998/Math/MathML" display="inline" overflow="scroll"><mml:mi>Cu</mml:mi><mml:mo		

#	Article	IF	Citations
57071	Kinetically Stabilized Cation Arrangement in Li₃YCl₆ Superionic Conductor during Solidâ€State Reaction. Advanced Science, 2021, 8, e2101413.	5.6	24
57072	Electronic and optical properties of Zn-doped Î²-Ga2O3 Czochralski single crystals. Journal of Applied Physics, 2021, 129, .	1.1	23
57073	First-principles study on the electronic structures and magnetic properties of TM-doped (TMÂ=ÂV, Cr,) Tj ETQq0 0 0 rgBT /Overlock 10 T	1.6	5
57074	Achieving junction stability in heavily doped epitaxial Si:P. Materials Science in Semiconductor Processing, 2021, 127, 105672.	1.9	6
57075	Structure distortion related magnetic anisotropy in 5d transition-metal dimer adsorbed g-C3N4 monolayers. Physica E: Low-Dimensional Systems and Nanostructures, 2021, 130, 114697.	1.3	2
57076	Electronic structures and optical properties of nanoporous complex oxide 12CaOÂ·7Al2O3 (C12A7) under high pressure. Computational Materials Science, 2021, 194, 110456.	1.4	3
57077	Synthesis and crystal structures of decahydro-closo-decaborates of the divalent cations of strontium and manganese. Journal of Solid State Chemistry, 2021, 298, 122133.	1.4	5
57078	Computational-experimental study of the onset potentials for CO2 reduction on polycrystalline and oxide-derived copper electrodes. Electrochimica Acta, 2021, 380, 138247.	2.6	4
57079	Metallic two-dimensional P2C3: A promising flexible anode for high-performance potassium-ion batteries. Colloids and Surfaces A: Physicochemical and Engineering Aspects, 2021, 619, 126536.	2.3	17
57080	Synthesis and magnetism of MoCo2O4 spinel thin films. Thin Solid Films, 2021, 728, 138696.	0.8	3
57081	Vacancy-induced structural, electronic and optical properties of Hf2CO2 MXene. Journal of Physics and Chemistry of Solids, 2021, 153, 110021.	1.9	5
57082	Key role of interaction between dislocations and hydrogen-vacancy complexes in hydrogen embrittlement of aluminum: discrete dislocation plasticity analysis. Modelling and Simulation in Materials Science and Engineering, 2021, 29, 065003.	0.8	2
57083	One-dimensional yttrium silicide electride (Y5Si3:eâ^') for encapsulation of volatile fission products. Journal of Applied Physics, 2021, 129, .	1.1	2
57084	Adsorbate-assisted migration of the metal atom in atomically dispersed catalysts: An ab initio molecular dynamics study. Journal of Chemical Physics, 2021, 154, 234709.	1.2	5
57085	Novel Twoâ€Dimensional PC 5 with the Dirac Cone and Edge Size Dependence. Physica Status Solidi - Rapid Research Letters, 0, , 2100203.	1.2	4
57086	Observation of the critical state to multiple-type Dirac semimetal phases in KMgBi. Journal of Applied Physics, 2021, 129, .	1.1	1
57087	IR transmission prediction, processing, and characterization of dense La₂Ce₂O₇. Journal of the American Ceramic Society, 2021, 104, 5659-5670.	1.9	8
57088	Coupling experiments with calculations to understand the thermodynamics evolution for the sorption of zwitterionic ciprofloxacin on oxidizing-aged pyrogenic chars in the aquatic system. Journal of Hazardous Materials, 2021, 411, 125101.	6.5	4

#	Article	IF	Citations
57089	Magnetic effects on ordering and surface segregation in NiPt nanoalloys. Applied Physics A: Materials Science and Processing, 2021, 127, 1.	1.1	0
57090	Correlation analysis of materials properties by machine learning: illustrated with stacking fault energy from first-principles calculations in dilute fcc-based alloys. Journal of Physics Condensed Matter, 2021, 33, 295702.	0.7	13
57091	Revealing the boosting role of NO for soot combustion over CeO2(111): A first-principles microkinetic modeling. Molecular Catalysis, 2021, 509, 111582.	1.0	3
57092	Combination of recommender system and single-particle diagnosis for accelerated discovery of novel nitrides. Journal of Chemical Physics, 2021, 154, 224117.	1.2	3
57093	Tuning thermoelectric efficiency of monolayer indium nitride by mechanical strain. Journal of Applied Physics, 2021, 129, 234302.	1.1	3
57094	First-principles prediction of electronic transport in fabricated semiconductor heterostructures via physics-aware machine learning. Npj Computational Materials, 2021, 7, .	3.5	16
57095	An ab initio study on the dynamical properties of U-Nb alloy melt. Chinese Physics B, 0, , .	0.7	0
57096	Magnetic Ni doping induced high power factor of Cu2GeSe3-based bulk materials. Journal of the European Ceramic Society, 2021, 41, 3473-3479.	2.8	11
57097	Jahn-Teller active fluoroperovskites ACrF3 (A=Na+,K+) : Magnetic and thermo-optical properties. Physical Review Materials, 2021, 5, .	0.9	1
57098	Lessons from a Challenging System: Accurate Adsorption Free Energies at the Amino Acid/ZnO Interface. Journal of Chemical Theory and Computation, 2021, 17, 4420-4434.	2.3	5
57099	High-pressure new phase of AgN₃. Modern Physics Letters B, 2021, 35, 2150386.	1.0	3
57100	A density functional theory study of the mechanism and onset potentials for the major products of NO electroreduction on transition metal catalysts. Applied Surface Science, 2021, 552, 149063.	3.1	28
57101	Strain effect on topological and thermoelectric properties of half Heusler compounds XPtS (X = Sr,) Tj ETQq0 0 0 rgBT /Overlock 10 Tf 5	0.7	3
57102	High pressure lattice dynamics and stress-strain responses of LaIn3 and LaTl3. Solid State Communications, 2021, 332, 114319.	0.9	1
57103	Tailoring the Performance of ZnO for Oxygen Evolution by Effective Transition Metal Doping. ChemSusChem, 2021, 14, 3064-3073.	3.6	9
57104	Insight into interlayer magnetic coupling in <mml:math xmlns:mml="http://www.w3.org/1998/Math/MathML"><mml:mn>1</mml:mn><mml:mi>T</mml:mi></mml:math> -type transition metal dichalcogenides based on the stacking of nonmagnetic atoms. Physical Review B, 2021, 103, .	1.1	7
57105	Large intrinsic anomalous Hall effect in SrIrO3 induced by magnetic proximity effect. Nature Communications, 2021, 12, 3283.	5.8	34
57106	Conversion of Dinitrogen to Ammonia by FeBâ€'Embedded Graphyne. Journal of the Electrochemical Society, 2021, 168, 066503.	1.3	15

#	Article	IF	Citations
57107	Impact of aluminium acetate particles size on the gelation kinetics of polyacrylamideâ€based gels: Rheological and molecular simulation study. Canadian Journal of Chemical Engineering, 2022, 100, 1169-1177.	0.9	4
57108	Hyperdynamics simulations with ab initio forces. Journal of Chemical Physics, 2021, 154, 214112.	1.2	1
57110	Thermodynamic non-ideality and disorder heterogeneity in actinide silicate solid solutions. Npj Materials Degradation, 2021, 5, .	2.6	9
57111	Huge tunneling magnetoresistance in magnetic tunnel junction with Heusler alloy Co2MnSi electrodes. Chinese Journal of Chemical Physics, 2021, 34, 273-280.	0.6	1
57112	New Pentaoctite Phase of Groupâ€V Nanostructures. Physica Status Solidi (B): Basic Research, 2021, 258, 2100112.	0.7	1
57113	In Situ Lattice Tunnel Distortion of Vanadium Trioxide for Enhancing Zinc Ion Storage. Advanced Energy Materials, 2021, 11, 2100973.	10.2	74
57114	On-surface photopolymerization of two-dimensional polymers ordered on the mesoscale. Nature Chemistry, 2021, 13, 730-736.	6.6	68
57115	Role of Oxygen Species toward the Câ€“C Bond Cleavage in Steam Reforming of C₂₊ Alkanes: DFT Studies of Ethane on Ir(100). Journal of Physical Chemistry C, 2021, 125, 14275-14286.	1.5	7
57116	Self-Optimized Metalâ€“Organic Framework Electrocatalysts with Structural Stability and High Current Tolerance for Water Oxidation. ACS Catalysis, 2021, 11, 7132-7143.	5.5	77
57117	A General Ammonium Salt Assisted Synthesis Strategy for Cr³⁺â€Doped Hexafluorides with Highly Efficient Near Infrared Emissions. Advanced Functional Materials, 2021, 31, 2103743.	7.8	107
57118	Stabilization of dissolvable biochar by soil minerals: Release reduction and organo-mineral complexes formation. Journal of Hazardous Materials, 2021, 412, 125213.	6.5	41
57119	Lithium dendrite suppression by facile interfacial barium engineering for stable 5ÂV-class lithium metal batteries with carbonate-based electrolyte. Chemical Engineering Journal, 2021, 414, 128928.	6.6	19
57120	Stability and Catalytic Performance of Single-Atom Catalysts Supported on Doped and Defective Graphene for CO₂Hydrogenation to Formic Acid: A First-Principles Study. ACS Applied Nano Materials, 2021, 4, 6893-6902.	2.4	40
57121	NaOH-Intercalated Iron Chalcogenides (Na1â€“xOH)Fe1â€“yX (X = Se, S): Ion-Exchange Synthesis and Physical Properties. Inorganic Chemistry, 2021, 60, 8742-8753.	1.9	9
57122	Realization of Strong Room-Temperature Ferromagnetism in Atomically Thin 2D Carbon Nitride Sheets by Thermal Annealing. ACS Nano, 2021, 15, 12069-12076.	7.3	27
57123	Unraveling the lithiophilic nature of heteroatom-doped carbons for efficient oxygen reduction in Liâ€“O2 batteries. Carbon, 2021, 178, 436-442.	5.4	14
57124	Metal-organic frameworks functionalized smart textiles for adsorptive removal of hazardous aromatic pollutants from ambient air. Journal of Hazardous Materials, 2021, 411, 125056.	6.5	31
57125	Interfacial <scp>adsorptionâ€“insertion</scp> mechanism induced by phase boundary toward better aqueous <scp>Znâ€ion</scp> battery. InformaÄnÃ-MateriÃ¡ly, 2021, 3, 1028-1036.	8.5	194

#	Article	IF	Citations
57126	Tunable Carbon Dioxide Activation Pathway over Iron Oxide Catalysts: Effects of Potassium. Industrial & Engineering Chemistry Research, 2021, 60, 8705-8713.	1.8	18
57127	Optical quantum technologies with hexagonal boron nitride single photon sources. Scientific Reports, 2021, 11, 12285.	1.6	22
57128	LaHf2Ni5â‾'As4: A filled version of monoclinic LaZr2Ni4â‾'As4. Journal of Solid State Chemistry, 2021, 298, 122118.	1.4	0
57129	Development of modified embedded-atom model and molecular dynamics simulation of cesium. Computational Materials Science, 2021, 194, 110451.	1.4	2
57130	The rise of Nb-, Ta-, and Bi-based oxides/chalcogenides for photocatalytic applications. International Journal of Hydrogen Energy, 2022, 47, 3358-3370.	3.8	6
57131	CNSi/MXene/CNSi: Unique Structure with Specific Electronic Properties for Nanodevices. Small, 2021, 17, 2101482.	5.2	2
57132	Critical Role of Al Pair Sites in Methane Oxidation to Methanol on Cu-Exchanged Mordenite Zeolites. Catalysts, 2021, 11, 751.	1.6	4
57133	Structural disorder-driven topological phase transition in noncentrosymmetric BiTeI. Physical Review B, 2021, 103, .	1.1	7
57134	Defect engineering for high-selection-performance of NO reduction to NH3 over CeO2 (111) surface: A DFT study. Chinese Chemical Letters, 2022, 33, 527-532.	4.8	53
57135	Revealing the vacuum level in an infinite solid by real-space potential unfolding. Physical Review B, 2021, 103, .	1.1	4
57136	Adlayer influence on Dirac-type surface state at W(110). Journal of Physics Condensed Matter, 2021, 33, 285504.	0.7	1
57137	Dynamic Barriers to Crystallization of Calcium Barium Carbonates. Crystal Growth and Design, 2021, 21, 4556-4563.	1.4	5
57138	Atomicâ€Orderingâ€Induced Modulated Properties of Zigzag ZnTe Nanotubes. Physica Status Solidi (B): Basic Research, 2021, 258, 2100115.	0.7	0
57139	Ultrahigh specific strength in a magnesium alloy strengthened by spinodal decomposition. Science Advances, 2021, 7, .	4.7	176
57140	The effect of chromite ore addition on crystallization kinetics of basalt based machinable glass-ceramics. Ceramics International, 2021, 47, 16902-16917.	2.3	6
57141	Strong bulk photovoltaic effect and second-harmonic generation in two-dimensional selenium and tellurium. Physical Review B, 2021, 103, .	1.1	8
57142	Theoretical prediction on the local structure and transport properties of molten alkali chlorides by deep potentials. Journal of Materials Science and Technology, 2021, 75, 78-85.	5.6	31
57143	Nonperturbative phonon scatterings and the two-channel thermal transport in <mml:math xmlns:mml="http://www.w3.org/1998/Math/MathML"><mml:mrow><mml:msub><mml:mi>Tl</mml:mi><mml:mn>3</mml:mn></mml:msub></mml:mrow></mml:math> Physical Review B, 2021, 103, .	1.1	30

#	Article	IF	Citations
57144	A type-II WSe2/HfSe2 van der Waals heterostructure with adjustable electronic and optical properties. Results in Physics, 2021, 25, 104250.	2.0	17
57145	Tunable thermal conductivity of ternary alloy semiconductors from first-principles. Journal Physics D: Applied Physics, 2021, 54, 335302.	1.3	1
57146	Arrangement of polyhedral units for [0001]-symmetrical tilt grain boundaries in zinc oxide. Acta Materialia, 2021, 212, 116864.	3.8	3
57147	Unraveling the selective etching mechanism of silicon nitride over silicon dioxide by phosphoric acid: First-principles study. Applied Surface Science, 2021, 551, 149376.	3.1	10
57148	Novel Two-Dimensional Janus MoSiGeN₄ and WSiGeN₄ as Highly Efficient Photocatalysts for Spontaneous Overall Water Splitting. ACS Applied Materials & Interfaces, 2021, 13, 28090-28097.	4.0	89
57149	Expanded view of electron-hole recollisions in solid-state high-order harmonic generation: Full-Brillouin-zone tunneling and imperfect recollisions. Physical Review A, 2021, 103, .	1.0	23
57150	Kinetics-Driven One-Dimensional Growth of van der Waals Layered SnSe. Journal of Physical Chemistry C, 2021, 125, 12730-12737.	1.5	8
57151	Ohmic-to-Schottky Conversion in Monolayer Tellureneâ€“Metal Interface via Graphene Insertion. Journal of Physical Chemistry C, 2021, 125, 12975-12982.	1.5	2
57152	Engineering Manganese Defects in Mn₃O₄ for Catalytic Oxidation of Carcinogenic Formaldehyde. ACS Applied Materials & Interfaces, 2021, 13, 29664-29675.	4.0	34
57153	Site Occupation and Structural Phase Transformation of the (010) Antiphase Boundary in Boron-Modified L12 Ni3Al. Jom, 2021, 73, 2285-2292.	0.9	2
57154	3C-SiC-induced peak emission intensity in photoluminescence spectrum of SiC/SiO2 coreâ€“shell nanowires using first-principles calculations. AIP Advances, 2021, 11, 065214.	0.6	1
57155	Inclination of self-interstitial dumbbells in molybdenum and tungsten: A first-principles study. AIP Advances, 2021, 11, 065012.	0.6	3
57156	Machine learning based prediction of lattice thermal conductivity for half-Heusler compounds using atomic information. Scientific Reports, 2021, 11, 13410.	1.6	22
57157	Observation of a singular Weyl point surrounded by charged nodal walls in PtGa. Nature Communications, 2021, 12, 3994.	5.8	15
57158	Quasi-four-component method with numeric atom-centered orbitals for relativistic density functional simulations of molecules and solids. Physical Review B, 2021, 103, .	1.1	7
57159	Point defects in hexagonal silicon. Physical Review Materials, 2021, 5, .	0.9	4
57160	Electronic correlations in the normal state of the kagome superconductor <mml:math xmlns:mml="http://www.w3.org/1998/Math/MathML"><mml:mrow><mml:msub><mml:mi>KV</mml:mi><mml:mn>3</mml:mn></mml:msub></mml: Physical Review B, 2021, 103, .	1.1	60
57161	Coexistence of Surface Superconducting and Three-Dimensional Topological Dirac States in Semimetal KZnBi. Physical Review X, 2021, 11, .	2.8	8

#	Article	IF	Citations
57162	Stability and Thermodynamics Properties of CrFeNiCoMn/Pd High Entropy Alloys from First Principles. Journal of Phase Equilibria and Diffusion, 2021, 42, 606-616.	0.5	7
57163	Spin Polarization Properties of Two Dimensional GaP3 Induced by 3d Transition-Metal Doping. Micromachines, 2021, 12, 743.	1.4	2
57164	Commensurate-incommensurate transition and strain relief patterns in monolayer C60 on Cd(0001). Physical Review B, 2021, 103, .	1.1	1
57165	DFT Study of Methylene Blue Adsorption on ZnTiO3 and TiO2 Surfaces (101). Molecules, 2021, 26, 3780.	1.7	21
57166	First principles study of dense and metallic nitric sulfur hydrides. Communications Chemistry, 2021, 4, .	2.0	2
57167	Robust gapless superconductivity in <mml:math xmlns:mml="http://www.w3.org/1998/Math/MathML"><mml:mrow><mml:mn>4</mml:mn><mml:mi>H</mml:mi><mml:mi>b</mml:mi> Physical Review B, 2021, 103, .	1.1	5
57168	Layer-Dependent Photoabsorption and Photovoltaic Effects in Two-Dimensional <mml:math xmlns:mml="http://www.w3.org/1998/Math/MathML" display="inline" overflow="scroll"><mml:msub><mml:mi>Bi</mml:mi><mml:mn>2</mml:mn></mml:msub><mml:msub><mml:mrow><mml:mrow><mm mathvariant="normal">O</mml:mi></mml:mrow></mml:mrow><mml:mn>2</mml:mn></mml:msub><mml:mi>X</mml:mi></mml:math		

#	Article	IF	Citations
57180	Ab initio modelling of interfacial electrochemical properties: beyond implicit solvation limitations. Journal of Physics Condensed Matter, 2021, 33, 304001.	0.7	7
57181	Tuning interchain ferromagnetic instability in A2Cr3As3 ternary arsenides by chemical pressure and uniaxial strain. Physical Review Materials, 2021, 5, .	0.9	7
57182	Computational Chemistry-Guided Syntheses and Crystal Structures of the Heavier Lanthanide Hydride Oxides DyHO, ErHO, and LuHO. Crystals, 2021, 11, 750.	1.0	7
57183	Chemical trends of cation-vacancy-induced d⁰ ferromagnetism in dilute zinc chalcogenides. Journal Physics D: Applied Physics, 2021, 54, 375001.	1.3	2
57184	Strong Metalâ€“Support Interaction in Pd/Ca2AlMnO5+Î´: Catalytic NO Reduction over Mn-Doped CaO Shell. ACS Catalysis, 2021, 11, 7996-8003.	5.5	9
57185	Nb6Mn1â€“xIr6+xB8 (x = 0.25): A Ferrimagnetic Boride Containing Planar B6 Rings Interacting with Ferromagnetic Mn Chains. Journal of Physical Chemistry C, 2021, 125, 13635-13640.	1.5	1
57186	Neural Network Quantum Molecular Dynamics, Intermediate Range Order in GeSe₂, and Neutron Scattering Experiments. Journal of Physical Chemistry Letters, 2021, 12, 6020-6028.	2.1	2
57187	Probing the Limiting Mechanism of Sodium-Ion Extraction in the Na₅V(PO₄)₂F₂ Cathode. Journal of Physical Chemistry C, 2021, 125, 14583-14589.	1.5	3
57188	Polymerization of Nitrogen in Nitrogenâ€“Fluorine Compounds under Pressure. Journal of Physical Chemistry Letters, 2021, 12, 5731-5737.	2.1	11
57189	Stability of Ca₂CO₄-Pnma against the Main Mantle Minerals from Ab Initio Computations. ACS Earth and Space Chemistry, 2021, 5, 1709-1715.	1.2	14
57190	Oxygen Electrocatalysis by [Au₂₅(SR)₁₈]: Charge, Doping, and Ligand Removal Effect. ACS Catalysis, 2021, 11, 7957-7969.	5.5	20
57191	Ab Initio Computational Study on Fe2NiP Schreibersite: Bulk and Surface Characterization. ACS Earth and Space Chemistry, 2021, 5, 1741-1751.	1.2	6
57192	Lattice Dynamics and Structural Phase Transitions in Eu₂O₃. Inorganic Chemistry, 2021, 60, 9571-9579.	1.9	24
57193	On-Site Detection of SARS-CoV-2 Antigen by Deep Learning-Based Surface-Enhanced Raman Spectroscopy and Its Biochemical Foundations. Analytical Chemistry, 2021, 93, 9174-9182.	3.2	58
57194	Strain-Assisted Topochemical Synthesis of La-Doped SrVO2H Films. Crystal Growth and Design, 2021, 21, 3779-3785.	1.4	3
57195	Surface State Passivation Ignited Photoelectrochemical Sensing of Thallium(I) with Ultrathin In₂S₃ Nanosheets. ACS Applied Electronic Materials, 2021, 3, 2490-2496.	2.0	2
57196	Coupled process and device modeling of Cu(In,Ga)Se2 solar cells. , 2021, , .		0
57197	A P3-Type K_{1/2}Mn_{5/6}Mg_{1/12}Ni_{1/12}O₂ Cathode Material for Potassium-Ion Batteries with High Structural Reversibility Secured by the Mgâ€“Ni Pinning Effect. ACS Applied Materials & Interfaces, 2021, 13, 28369-28377.	4.0	29

#	Article	IF	Citations
57198	Strong Electron Localization in Tin Halide Perovskites. Journal of Physical Chemistry Letters, 2021, 12, 5339-5343.	2.1	22
57199	Vacancy-rich 1T-MoS2 monolayer confined to MoO3 matrix: An interface-engineered hybrid for efficiently electrocatalytic conversion of nitrogen to ammonia. Applied Catalysis B: Environmental, 2021, 286, 119870.	10.8	35
57200	Anisotropic strain effect on structural and electronic properties in WSe2/ZnO mixed-dimensional heterostructure. Applied Surface Science, 2021, 551, 149378.	3.1	5
57201	A DFT study of Ti3C2O2 MXenes quantum dots supported on single layer graphene: Electronic structure an hydrogen evolution performance. Frontiers of Physics, 2021, 16, 1.	2.4	12
57202	First-Principles Calculations of Heteroanionic Monochalcogenide Alloy Nanosheets with Direction-dependent Properties for Anisotropic Optoelectronics. ACS Applied Nano Materials, 2021, 4, 5912-5920.	2.4	3
57203	Plastic deformation of single crystals of CrB2, TiB2 and ZrB2 with the hexagonal AlB2 structure. Acta Materialia, 2021, 211, 116857.	3.8	20
57204	Highâ€Efficiency Anionâ€Exchange Membrane Water Electrolyzer Enabled by Ternary Layered Double Hydroxide Anode. Small, 2021, 17, e2100639.	5.2	49
57205	Dual-Ion Substitution-Induced Unique Electronic Modulation to Stabilize an Orthorhombic Lattice towards Reversible Hydrogen Isotope Storage. ACS Sustainable Chemistry and Engineering, 2021, 9, 9139-9148.	3.2	16
57206	Band Engineering of Dirac Semimetals Using Charge Density Waves. Advanced Materials, 2021, 33, e2101591.	11.1	32
57207	Magnetic correlations in single-layer NbSe₂. Journal of Physics Condensed Matter, 2021, 33, 295804.	0.7	10
57208	Highly tunable magneto-optical response from magnesium-vacancy color centers in diamond. Npj Quantum Information, 2021, 7, .	2.8	12
57209	Modulation of electronic structure properties in bilayer phosphorene nanoribbons by transition metal atoms. Physica E: Low-Dimensional Systems and Nanostructures, 2021, 130, 114530.	1.3	5
57210	ZIF-301 MOF/6FDA-DAM polyimide mixed-matrix membranes for CO2/CH4 separation. Separation and Purification Technology, 2021, 264, 118431.	3.9	40
57211	Unravelling the Reaction Mechanisms of N₂ Fixation on Molybdenum Nitride: A Full DFT Study from the Pristine Surface to Heteroatom Anchoring. ChemSusChem, 2021, 14, 3257-3266.	3.6	22
57212	Machine-learning interatomic potential for Wâ€“Mo alloys. Journal of Physics Condensed Matter, 2021, 33, 315403.	0.7	11
57213	Identifying Promising Covalent-Organic Frameworks for Decarburization and Desulfurization from Biogas via Computational Screening. ACS Sustainable Chemistry and Engineering, 2021, 9, 8858-8867.	3.2	10
57214	Structure-activity relationship of VO /TiO2 catalysts for mercury oxidation: A DFT study. Applied Surface Science, 2021, 552, 149462.	3.1	17
57215	Combining Static and Dynamic Analysis to Query Characteristics of HPC Applications. , 2021, , .		0

#	Article	IF	Citations
57216	Hydration and Ionic Conduction Mechanisms of Hexagonal Perovskite Derivatives. Chemistry of Materials, 2021, 33, 4651-4660.	3.2	28
57217	Câ€“doped TiO2(B): A density functional theory characterization. Applied Surface Science, 2021, 551, 149479.	3.1	20
57219	Ternary transition metal chalcogenides Ti2PX2 (XÂ=ÂS, Se, Te) anodes for high performance metal-ion batteries: A DFT study. Applied Surface Science, 2021, 550, 149177.	3.1	30
57220	Promoting the energy density of lithium-ion capacitor by coupling the pore-size and nitrogen content in capacitive carbon cathode. Journal of Power Sources, 2021, 498, 229912.	4.0	36
57221	In Search of the Active Sites for the Selective Catalytic Reduction on Tungsten-Doped Vanadia Monolayer Catalysts Supported by TiO₂. ACS Catalysis, 2021, 11, 7411-7421.	5.5	14
57222	The effects of heteroatoms-doping on the stability, electronic and magnetic properties of CH3NH3PbI3 perovskite. Surfaces and Interfaces, 2021, 24, 101027.	1.5	6
57223	Spin pinning effect to reconstructed oxyhydroxide layer on ferromagnetic oxides for enhanced water oxidation. Nature Communications, 2021, 12, 3634.	5.8	186
57224	Semiconductor-to-metal transition in HfSe2 under high pressure. Journal of Alloys and Compounds, 2021, 867, 158923.	2.8	12
57225	Single Metal Atom Supported on N-Doped 2D Nitride Black Phosphorus: An Efficient Electrocatalyst for the Oxygen Evolution and Oxygen Reduction Reactions. Journal of Physical Chemistry C, 2021, 125, 12541-12550.	1.5	24
57226	Synergistic photocatalytic NO removal of oxygen vacancies and metallic bismuth on Bi12TiO20 nanofibers under visible light irradiation. Chemical Engineering Journal, 2021, 414, 128748.	6.6	30
57227	Molecular switching operation in gate constricted interface of MoS2 and hBN heterostructure. Applied Materials Today, 2021, 23, 100999.	2.3	4
57228	Determination of Thermal Expansion, Defect Formation Energy, and Defect-Induced Strain of Î±-U Via ab Initio Molecular Dynamics. Frontiers in Materials, 2021, 8, .	1.2	10
57229	Machine-learning-accelerated discovery of single-atom catalysts based on bidirectional activation mechanism. Chem Catalysis, 2021, 1, 183-195.	2.9	50
57230	Unusual electronic structure of Dirac material BaMnSb2 revealed by angle-resolved photoemission spectroscopy*. Chinese Physics B, 2021, 30, 067403.	0.7	4
57231	Regulating the Catalytic Performance of a Dual-Atom Iron Species Deposited on Graphitic Carbon Nitride for Electrochemical Nitrogen Reduction. Journal of Physical Chemistry C, 2021, 125, 14253-14262.	1.5	18
57232	A dual strategy for synthesizing carbon/defect comodified polymeric carbon nitride porous nanotubes with boosted photocatalytic hydrogen evolution and synchronous contaminant degradation. Applied Catalysis B: Environmental, 2021, 287, 119995.	10.8	66
57233	The strain-induced excellent thermoelectric performance of PbTe. Physica E: Low-Dimensional Systems and Nanostructures, 2021, 130, 114685.	1.3	18
57234	Effect of intrinsic point-defect complex on elastic properties of Î³â€²-Ni3Al phases. Materials Research Express, 2021, 8, 066517.	0.8	1

#	Article	IF	Citations
57235	Feasibility of mesocarbon mircrobead as an anode for lithium ion batteries work under 115ÂMPa external high pressure. Solid State Ionics, 2021, 364, 115637.	1.3	2
57236	First-principles study of two new boron nitride structures: C12-BN and O16-BN. Chinese Physics B, 2022, 31, 026102.	0.7	0
57237	Bi₂Se₃/Bi₂Se₃ and TlSe/TlSe junctions: enhanced coupling of topological interface states by intercalation. Journal Physics D: Applied Physics, 2021, 54, 345301.	1.3	3
57238	Low-Temperature Mechanical Instabilities Govern High-Temperature Thermodynamics in the Austenite Phase of Shape Memory Alloy Constituents: Ab Initio Simulations of NiTi, NiZr, NiHf, PdTi, and PtTi. Acta Materialia, 2021, 212, 116872.	3.8	18
57239	Quantum Self-Consistent Ab-Initio Lattice Dynamics. Computer Physics Communications, 2021, 263, 107945.	3.0	18
57240	Hydroxyl-terminated carbon dots for efficient conversion of cyclohexane to adipic acid. Journal of Colloid and Interface Science, 2021, 591, 281-289.	5.0	18
57241	Hollow hierarchical zinc cobalt sulfides derived from bimetallic-organic-framework as a non-precious electrocatalyst for oxygen reduction reaction. Molecular Catalysis, 2021, 509, 111614.	1.0	5
57242	Unraveling Reactivity Descriptors and Structure Sensitivity in Low-Temperature NH₃-SCR Reaction over CeTiO_x Catalysts: A Combined Computational and Experimental Study. ACS Catalysis, 2021, 11, 7613-7636.	5.5	75
57243	Computational Characterization of the Intermixing of Iron Triade (Fe, Co, and Ni) Surfaces and Sub-nanometric Clusters with Atomic Gold. ACS Omega, 2021, 6, 16165-16175.	1.6	4
57244	Evidence for Electronically Isolated Atomic Chains: Sbâ€“Pb Structures on the Si(553) Surface. Journal of Physical Chemistry C, 2021, 125, 15061-15068.	1.5	2
57245	Efficient Direct Band-Gap Transition in Germanium by Three-Dimensional Strain. ACS Applied Materials & Interfaces, 2021, 13, 30941-30949.	4.0	14
57246	First-Principles Investigation into Hybrid Improper Ferroelectricity in Ruddlesdenâ€“Popper Perovskite Chalcogenides Sr3B2X7 (B = Ti, Zr, Hf; X = S, Se). Journal of Physical Chemistry C, 2021, 125, 13971-13983.	1.5	3
57247	Linear Relationship between the Dielectric Constant and Band Gap in Low-Dimensional Mixed-Halide Perovskites. Journal of Physical Chemistry C, 2021, 125, 14883-14890.	1.5	21
57248	Properties of Î±-Brass Nanoparticles II: Structure and Composition. Journal of Physical Chemistry C, 2021, 125, 14897-14909.	1.5	9
57249	Crystal Engineering of Binary Organic Eutectics: Significant Improvement in the Physicochemical Properties of Polycyclic Aromatic Hydrocarbons via the Computational and Mechanochemical Discovery of Composite Materials. Crystal Growth and Design, 2021, 21, 4151-4161.	1.4	6
57250	Biaxial Strain Improving the Thermoelectric Performance of a Two-Dimensional MoS₂/WS₂ Heterostructure. ACS Applied Electronic Materials, 2021, 3, 2995-3004.	2.0	26
57251	Boosting Thermoelectric Performance of Cu₂SnSe₃ via Comprehensive Band Structure Regulation and Intensified Phonon Scattering by Multidimensional Defects. ACS Nano, 2021, 15, 10532-10541.	7.3	40
57252	Local Structures of Soft Carbon and Electrochemical Performance of Potassium-Ion Batteries. ACS Applied Materials & Interfaces, 2021, 13, 28261-28269.	4.0	17

#	Article	IF	Citations
57253	A Comparative Study of the Structural and Electronic Properties of Orthorhombic and Cubic CsPbI₃ and Trigonal CsGeI₃ using First-Principles Calculations. , 2021, , .		1
57254	Multidimensional Ti₃C₂T_xMXene ArchitecturesviaInterfacial Electrochemical Self-Assembly. ACS Nano, 2021, 15, 10058-10066.	7.3	46
57255	An interfacial wetting water based hydrogel electrolyte for high-voltage flexible quasi solid-state supercapacitors. Energy Storage Materials, 2021, 38, 489-498.	9.5	28
57256	Phosphorous-doped bimetallic sulfides embedded in heteroatom-doped carbon nanoarrays for flexible all-solid-state supercapacitors. Science China Materials, 2021, 64, 2439-2453.	3.5	19
57257	Tomographic reconstruction of oxygen orbitals in lithium-rich battery materials. Nature, 2021, 594, 213-216.	13.7	56
57258	Anisotropic moirÃ© optical transitions in twisted monolayer/bilayer phosphorene heterostructures. Nature Communications, 2021, 12, 3947.	5.8	33
57259	First-principles study on the electronic structures and ferromagnetism of tetragonal AlN monolayer doped with Be and C. Computational Materials Science, 2021, 193, 110413.	1.4	1
57260	Theoretical study on defect properties of two-dimensional multilayer Ruddlesden-Popper lead iodine perovskite. Computational Materials Science, 2021, 194, 110457.	1.4	7
57261	Thickness- and strain-tunable electronic structures of two-dimensional Bi2O2Se. Computational Materials Science, 2021, 194, 110424.	1.4	10
57262	Alloy thermodynamics via the Multi-cell Monte Carlo (MC)2 method. Computational Materials Science, 2021, 193, 110322.	1.4	4
57263	Electron-Deficient-Type Electride Ca₅Pb₃: Extension of Electride Chemical Space. Journal of the American Chemical Society, 2021, 143, 8821-8828.	6.6	22
57264	Laser-Assisted Synthesis of Pd Aerogel with Compressive Strain for Boosting Formate and Ethanol Electrooxidation. ACS Sustainable Chemistry and Engineering, 2021, 9, 7837-7845.	3.2	14
57265	Thermodynamic stability of defects in hybrid MoS2/InAs heterostructures. Computational Materials Science, 2021, 194, 110426.	1.4	1
57266	Multistep Dissociation of Fluorine Molecules under Extreme Compression. Physical Review Letters, 2021, 126, 225704.	2.9	10
57267	Enhanced electron emission from ternary solid solution-MWCNT hybrid with theoretical validation. Materials Science in Semiconductor Processing, 2021, 127, 105674.	1.9	1
57268	Diffusion behaviour and mechanical properties of binary Mgâ€“Gd system. Intermetallics, 2021, 133, 107171.	1.8	21
57269	Exploring the elastic and electronic properties of chromium molybdenum diboride alloys. Journal of Alloys and Compounds, 2021, 866, 158885.	2.8	8
57270	Tailoring of White Luminescence in a NaLi₃SiO₄:Eu²⁺ Phosphor Containing Broadâ€Band Defectâ€Induced Chargeâ€Transfer Emission. Advanced Materials, 2021, 33, e2101428.	11.1	107

#	Article	IF	Citations
57271	Theoretical new insights into hydrogen interaction with single-atom Zn- and co-doped copper metal catalysts. Applied Surface Science, 2021, 551, 149365.	3.1	2
57272	Activityâ€“Selectivity Enhancement and Catalytic Trend of CO₂ Electroreduction on Metallic Dimers Supported by N-Doped Graphene: A Computational Study. Journal of Physical Chemistry C, 2021, 125, 13176-13184.	1.5	12
57273	Multibounce and Subsurface Scattering of H Atoms Colliding with a van der Waals Solid. Journal of Physical Chemistry A, 2021, 125, 5745-5752.	1.1	8
57274	Highly efficient cataluminescence gas sensor based on nanosized h-BN for trace acetylacetone detection. Measurement Science and Technology, 2021, 32, 095114.	1.4	3
57275	Hydride Conductivity in Nitride Hydrides. ACS Applied Energy Materials, 2021, 4, 6348-6355.	2.5	6
57276	Two-dimensional phosphorus-based binary nanosheets for photocatalyzing water splitting: A first-principles study. Chemical Physics Letters, 2021, 772, 138594.	1.2	6
57277	Ionic liquid-assisted synthesis of porous boron-doped graphitic carbon nitride for photocatalytic hydrogen production. Chemosphere, 2021, 272, 129953.	4.2	49
57278	Surface Lattice Oxygen Activation by Nitrogen-Doped Manganese Dioxide as an Effective and Longevous Catalyst for Indoor HCHO Decomposition. ACS Applied Materials & Interfaces, 2021, 13, 26960-26970.	4.0	32
57279	Activation of Selfâ€Trapped Emission in Stable Bismuthâ€Halide Perovskite by Suppressing Strong Excitonâ€“Phonon Coupling. Advanced Functional Materials, 2021, 31, 2102654.	7.8	67
57281	Electronic structure examination of the topological properties of CaMnSb2 by angle-resolved photoemission spectroscopy. Physical Review B, 2021, 103, .	1.1	6
57282	Enhanced superconductivity in bilayer <mml:math xmlns:mml="http://www.w3.org/1998/Math/MathML"><mml:msub><mml:mrow><mml:mi>PtTe</mml:mi></mml:mrow><mml:mn>2</mml:mn> by alkali-metal intercalations. Physical Review B, 2021, 103, .	1.1	9
57283	Transition of spin gapless semiconductor to semiconductor and half-metal in ferromagnetic Ba2MnTeO6. Results in Physics, 2021, 25, 104315.	2.0	4
57284	CO ₂ reduction on pure Cu produces only H ₂ after subsurface O is depleted: Theory and experiment. Proceedings of the National Academy of Sciences of the United States of America, 2021, 118, .	3.3	41
57285	Lithium-functionalized boron phosphide nanotubes (BPNTs) as an efficient hydrogen storage carrier. International Journal of Hydrogen Energy, 2021, 46, 20586-20593.	3.8	17
57286	Insights into the Coadsorption and Reactivity of O and CO on Ru(0001) and Their Coverage Dependence. Journal of Physical Chemistry C, 2021, 125, 12614-12627.	1.5	9
57287	Metal-to-Ligand Charge-Transfer Spectrum of a Ru-Bipyridine-Sensitized TiO₂ Cluster from Embedded Multiconfigurational Excited-State Theory. Journal of Physical Chemistry A, 2021, 125, 4998-5013.	1.1	5
57288	Truxone-Based Conductive Metalâ€“Organic Frameworks for the Oxygen Reductive Reaction. Journal of Physical Chemistry C, 2021, 125, 12690-12698.	1.5	12
57289	First-Principles Investigation of Ti₂CSO and Ti₂CSSe Janus MXene Structures for Li and Mg Electrodes. Journal of Physical Chemistry C, 2021, 125, 12469-12477.	1.5	15

#	Article	IF	Citations
57290	Proton-Coupled Electron Transfer in Electrochemical Alanine Formation from Pyruvic Acid: Mechanism of Catalytic Reaction at the Interface between TiO₂ (101) and Water. Journal of Physical Chemistry C, 2021, 125, 12603-12613.	1.5	7
57291	Single-Layer MX₂ (M = Zn, Cd and X = Cl, I): Auxetic Semiconductors with Strain-Tunable Optoelectronic Properties. Journal of Physical Chemistry C, 2021, 125, 12983-12990.	1.5	9
57292	Semi-Automated Creation of Density Functional Tight Binding Models through Leveraging Chebyshev Polynomial-Based Force Fields. Journal of Chemical Theory and Computation, 2021, 17, 4435-4448.	2.3	16
57293	In Situ Phase-Transition Crystallization of All-Inorganic Water-Resistant Exciton-Radiative Heteroepitaxial CsPbBr₃â€“CsPb₂Br₅ Coreâ€“Shell Perovskite Nanocrystals. Chemistry of Materials, 2021, 33, 4948-4959.	3.2	47
57294	Projector-Free Capped-Fragment Scheme within Density Functional Embedding Theory for Covalent and Ionic Compounds. Journal of Chemical Theory and Computation, 2021, 17, 4105-4121.	2.3	3
57295	Insights into the thermal decomposition of plutonium(IV) oxalate â€“ a DFT study of the intermediate structures. Journal of Nuclear Materials, 2021, 549, 152864.	1.3	8
57296	Unveiling Oxygen Redox Activity in P2-Type Na_xNi_{0.25}Mn_{0.68}O₂ High-Energy Cathode for Na-Ion Batteries. ACS Energy Letters, 2021, 6, 2470-2480.	8.8	32
57297	Sub-Nanometer Pt Clusters on Defective NiFe LDH Nanosheets as Trifunctional Electrocatalysts for Water Splitting and Rechargeable Hybrid Sodiumâ€“Air Batteries. ACS Applied Materials & Interfaces, 2021, 13, 26891-26903.	4.0	31
57298	Ab initio description of oxygen vacancies in epitaxially strained $$hbox {SrTiO}_{{3}}$$ at finite temperatures. Scientific Reports, 2021, 11, 11499.	1.6	7
57299	Flexoelectricity enhanced water splitting and hydrogen evolution reaction on grain boundaries of monolayer transition metal dichalcogenides. Nano Research, 2022, 15, 978-984.	5.8	15
57300	Dual Dirac points and oddâ€“even oscillated energy gap in zigzag chlorinated stanene nanoribbon. Journal of Physics Condensed Matter, 2021, 33, 325303.	0.7	2
57301	Quasi-graphitic carbon shell-induced Cu confinement promotes electrocatalytic CO2 reduction toward C2+ products. Nature Communications, 2021, 12, 3765.	5.8	99
57302	First-principles study of structural and opto-electronic characteristics of ultra-thin amorphous carbon films. Chinese Physics B, 2022, 31, 016102.	0.7	1
57303	Topological Hall effect in the antiferromagnetic Dirac semimetal EuAgAs. Physical Review B, 2021, 103, .	1.1	19
57304	Origin of hydrogen passivation in <mml:math xmlns:mml="http://www.w3.org/1998/Math/MathML"><mml:mrow><mml:mn>4</mml:mn><mml:mi>H</mml:mi></mml:mrow></mml:math> -SiC. Physical Review Materials, 2021, 5, .	0.9	3
57305	A generally reliable model for composition-dependent lattice constants of substitutional solid solutions. Acta Materialia, 2021, 211, 116865.	3.8	9
57306	Symmetry-enforced topological nodal planes at the Fermi surface of a chiral magnet. Nature, 2021, 594, 374-379.	13.7	29
57307	Optomechanical switching of adsorption configurations of polar organic molecules by UV radiation pressure. Scientific Reports, 2021, 11, 12645.	1.6	0

#	Article	IF	Citations
57308	Machine-Learning-Assisted First-Principles Calculations of Strained InAs1âˆ'xSbx Alloys for Curved Focal-Plane Arrays. Physical Review Applied, 2021, 15, .	1.5	1
57309	Intrinsic two-dimensional multiferroicity in CrNCl₂ monolayer*. Chinese Physics B, 2021, 30, 117503.	0.7	5
57310	Spontaneous interlayer compression in commensurately stacked van der Waals heterostructures. Physical Review B, 2021, 103, .	1.1	7
57311	Unique structure of active platinum-bismuth site for oxidation of carbon monoxide. Nature Communications, 2021, 12, 3342.	5.8	32
57312	Observation of Nonlinear Spin-Charge Conversion in the Thin Film of Nominally Centrosymmetric Dirac Semimetal <mml:math xmlns:mml="http://www.w3.org/1998/Math/MathML" display="inline"><mml:msub><mml:mrow><mml:mi>SrIrO</mml:mi></mml:mrow><mml:mrow><mml:mn>3</mml:mn></mml:mrow></ at Room Temperature. Physical Review Letters, 2021, 126, 236801.	2.9	11
57313	Thermal conductance of nanostructured interfaces from Monte Carlo simulations with ab initio-based phonon properties. Journal of Applied Physics, 2021, 129, .	1.1	4
57314	Efficient dinitrogen fixation on porous covalent organic framework/carbon nanotubes hybrid at low overpotential. Functional Materials Letters, 2021, 14, 2151027.	0.7	2
57315	Design and Process Optimization of a New Reaction Cavity for High-Temperature MOCVD AlGaN Growth. Nano, 2021, 16, 2150084.	0.5	0
57316	Review of the phonon calculations for energetic crystals and their applications. Energetic Materials Frontiers, 2021, 2, 154-164.	1.3	8
57317	Synthesis of ZIF-9(III)/Co LDH layered composite from ZIF-9(I) based on controllable phase transition for enhanced electrocatalytic oxygen evolution reaction. Chemical Engineering Journal, 2021, 414, 128784.	6.6	38
57318	Point Defect Engineering: Coâ€Đoping Synergy Realizing Superior Performance in nâ€Type Bi₂Te₃ Thermoelectric Materials. Small, 2021, 17, e2101328.	5.2	45
57319	CO oxidation activity of Pt/CeO2 catalysts below 0 Â°C: platinum loading effects. Applied Catalysis B: Environmental, 2021, 286, 119931.	10.8	83
57320	Structure-tunable pompon-like RuCo catalysts: Insight into the roles of atomically dispersed Ru-Co sites and crystallographic structures for guaiacol hydrodeoxygenation. Journal of Catalysis, 2021, 398, 76-88.	3.1	34
57321	Elastic dipole tensors and relaxation volumes of point defects in concentrated random magnetic Fe-Cr alloys. Computational Materials Science, 2021, 194, 110435.	1.4	24
57322	Enhanced hydrogen storage of a functional material: Hf2CF2 MXene with Li decoration. Applied Surface Science, 2021, 551, 149484.	3.1	20
57323	Identifying the origin of local flexibility in a carbohydrate polymer. Proceedings of the National Academy of Sciences of the United States of America, 2021, 118, .	3.3	27
57324	Gas-Phase â€œPrehistoryâ€•and Molecular Precursors in Monolayer Metal Dichalcogenides Synthesis: The Case of MoS₂. ACS Nano, 2021, 15, 10525-10531.	7.3	9
57325	Understanding the key role of vanadium in p-type BiVO4 for photoelectrochemical N2 fixation. Chemical Engineering Journal, 2021, 414, 128773.	6.6	50

#	Article	IF	Citations
57326	The thermoelectric performance of new structure SnSe studied by quotient graph and deep learning potential. Materials Today Energy, 2021, 20, 100665.	2.5	11
57327	Phase Diagram of a Deep Potential Water Model. Physical Review Letters, 2021, 126, 236001.	2.9	140
57328	Computational Design and Experimental Validation of the Optimal Bimetal-Doped SrCoO_{3â˜'Î´} Perovskite as Solid Oxide Fuel Cell Cathode. Journal of the American Chemical Society, 2021, 143, 9507-9514.	6.6	48
57329	Pressure-Induced Superconducting Dome and Triple Enhancement of <mml:math xmlns:mml="http://www.w3.org/1998/Math/MathML" display="inline"><mml:msub><mml:mrow><mml:mi>T</mml:mi></mml:mrow><mml:mrow><mml:mi>c</mml:mi></mml:mrow></mml:msub></mml:math> in the Kagome Superconductor <mml:math xmlns:mml="http://www.w3.org/1998/Math/MathML" display="inline"><mml:mrow><mml:msub><mml:mrow><mml:mi>CsV</mml:mi></mml:mrow><mml:mrow><mml:mn>3</mml:mn></mml:mrow></mml:msub></mml:mrow></mml:math>. Physical Review Letters, 2021, 126, 247001.	2.9	240
57330	Temperature-dependent elastic properties of binary and multicomponent high-entropy refractory carbides. Materials and Design, 2021, 204, 109634.	3.3	26
57331	Pressure-induced superconductivity and modification of Fermi surface in type-II Weyl semimetal NbIrTe4. Npj Quantum Materials, 2021, 6, .	1.8	8
57332	Domain wall induced spin-polarized flat bands in antiferromagnetic topological insulators. Physical Review B, 2021, 103, .	1.1	20
57333	Gas sensing materials roadmap. Journal of Physics Condensed Matter, 2021, 33, 303001.	0.7	49
57334	Hydrogen molecules permeate graphene: Permeate way and the breaking and recombination of bonds. Diamond and Related Materials, 2021, 116, 108414.	1.8	0
57335	Antimony allotropes fabricated on oxide layer of Cu(111). Thin Solid Films, 2021, 727, 138669.	0.8	4
57336	Superconductivity in metal intercalated graphite-like boron-carbon-nitrogen. Physics Letters, Section A: General, Atomic and Solid State Physics, 2021, 402, 127348.	0.9	1
57337	Two-dimensional ferromagnetic Chern insulator: WSe2 monolayer. Physics Letters, Section A: General, Atomic and Solid State Physics, 2021, 402, 127344.	0.9	3
57338	First-principles calculations study of the configurations, structural, electronic and magnetic properties of graphene and h-BN monolayers and bilayers adsorbed on Co(0001) surface. Physica B: Condensed Matter, 2021, 611, 412755.	1.3	2
57339	Thermodynamics stability, electronic structures and spectroscopic properties of defects and Ce3+ ions in Y2O3. Current Applied Physics, 2021, 26, 55-63.	1.1	0
57340	Size Effect of Graphene Quantum Dots on Photoluminescence. Molecules, 2021, 26, 3922.	1.7	29
57341	Theoretical Prediction and Experimentally Realizing Cathodic Doping of Sulfur in Li₄Ti₅O₁₂ for Superior Lithium Storage Performance. ACS Applied Energy Materials, 2021, 4, 5995-6004.	2.5	10
57342	First-Principles Study on Structural, Electronic, Elastic, Phonon, and Thermodynamic Properties of Tungsten Oxide-Based Perovskite NaWO3. Journal of Electronic Materials, 2021, 50, 5402-5411.	1.0	3
57343	Boron-Doped MXenes as Electrocatalysts for Nitrogen Reduction Reaction: A Theoretical Study. Frontiers in Chemical Engineering, 2021, 3, .	1.3	4

#	Article	IF	Citations
57344	Impact of interstitial impurities on the trapping of dislocation loops in tungsten. Scientific Reports, 2021, 11, 12333.	1.6	8
57345	High-order harmonic generation from wurtzitic and hexagonal BN. Optical Review, 2021, 28, 342-348.	1.2	0
57346	Effects of Transition Elements on the Structural, Elastic Properties and Relative Phase Stability of L12 Î³â€²-Co3Nb from First-Principles Calculations. Metals, 2021, 11, 933.	1.0	3
57347	Anderson localization of electron states in a quasicrystal. Physical Review B, 2021, 103, .	1.1	9
57348	Type-II Dirac point in <mml:math xmlns:mml="http://www.w3.org/1998/Math/MathML"><mml:mrow><mml:msub><mml:mi>RbAg</mml:mi><mml:mn>5</mml:mn></mml:msub></mml:mrow></mml:math> Physical Review B, 2021, 103, .	1.1	4
57349	Unusual Force Constants Guided Distortion-Triggered Loss of Long-Range Order in Phase Change Materials. Materials, 2021, 14, 3514.	1.3	4
57350	Converting copper sulfide to copper with surface sulfur for electrocatalytic alkyne semi-hydrogenation with water. Nature Communications, 2021, 12, 3881.	5.8	77
57351	Leveraging bipolar effect to enhance transverse thermoelectricity in semimetal Mg2Pb for cryogenic heat pumping. Nature Communications, 2021, 12, 3837.	5.8	24
57352	Synergistic Effect of Metal Doping and Tethered Ligand Promoted Highâ€Selectivity Conversion of CO₂ to C₂ Oxygenates at Ultraâ€Low Potential. Energy and Environmental Materials, 2022, 5, 892-898.	7.3	14
57353	Long-range anisotropic Heisenberg ferromagnets and electrically tunable ordering. Physical Review B, 2021, 103, .	1.1	4
57354	Interplay of high-precision shock wave experiments with first-principles theory to explore molecular systems at extreme conditions: A perspective. Journal of Applied Physics, 2021, 129, .	1.1	3
57355	Interlayer ferromagnetism and high-temperature quantum anomalous Hall effect in <mml:math xmlns:mml="http://www.w3.org/1998/Math/MathML"><mml:mi>p</mml:mi></mml:math> -doped <mml:math xmlns:mml="http://www.w3.org/1998/Math/MathML"><mml:mrow><mml:mi>Mn</mml:mi><mml:msub><mml:mi>Bi</mml:mi><mml:mn> multilayers. Physical Review B, 2021, 103, .	1.1	13
57356	New developments in the <scp>GDIS</scp> simulation package: Integration of <scp>VASP</scp> and <scp>USPEX</scp>. Journal of Computational Chemistry, 2021, 42, 1602-1626.	1.5	3
57357	Thermoelectric performances for both p- and n-type GeSe. Royal Society Open Science, 2021, 8, 201980.	1.1	13
57358	A Ternary Map of Niâ€“Mnâ€“Ga Heusler Alloys from Ab Initio Calculations. Metals, 2021, 11, 973.	1.0	4
57359	Modification of the LiFePO₄ (010) Surface Due to Exposure to Atmospheric Gases. ACS Applied Materials & Interfaces, 2021, 13, 29034-29040.	4.0	10
57360	Tuning the Coordination Environment to Effect the Electrocatalytic Behavior of a Single-Atom Catalyst toward the Nitrogen Reduction Reaction. Journal of Physical Chemistry C, 2021, 125, 11963-11974.	1.5	21
57361	AB₂X₆ Compounds and the Stabilization of Trirutile Oxides. Inorganic Chemistry, 2021, 60, 9224-9232.	1.9	3

#	Article	IF	Citations
57362	Topological Insulating Phase in Single-Layer Pentagonal Covalent Organic Frameworks: A Reticular Design Using Metal Phthalocyanine. Chemistry of Materials, 2021, 33, 4488-4499.	3.2	3
57363	Efficient Waterâ€“Gas Shift Catalysts for H₂O and CO Dissociation Using Cuâ€“Ni Step Alloy Surfaces. Journal of Physical Chemistry C, 2021, 125, 13819-13835.	1.5	18
57364	Electrocatalytic Nitrogen Reduction by Transition Metal Single-Atom Catalysts on Polymeric Carbon Nitride. Journal of Physical Chemistry C, 2021, 125, 13880-13888.	1.5	28
57365	Correlated Octahedral Rotation and Organic Cation Reorientation Assist Halide Ion Migration in Lead Halide Perovskites. Chemistry of Materials, 2021, 33, 4672-4678.	3.2	16
57366	Predictions of Chemical Shifts for Reactive Intermediates in CO2 Reduction under Operando Conditions. ACS Applied Materials & Interfaces, 2021, 13, 31554-31560.	4.0	12
57367	Photocatalytic Water Splitting Reaction Catalyzed by Ion-Exchanged Salts of Potassium Poly(heptazine) Tj ETQq1 1 0.784314 rgBT /Ov	1.5	30
57368	Enhanced Valley Polarization of Bilayer MoSe₂ with Variable Stacking Order and Interlayer Coupling. Journal of Physical Chemistry Letters, 2021, 12, 5879-5888.	2.1	11
57369	Experimental and Theoretical Insights into the Active Sites on WO_x/Pt(111) Surfaces for Dehydrogenation and Dehydration Reactions. ACS Catalysis, 2021, 11, 8023-8032.	5.5	11
57370	Reaction Pathway for Coke-Free Methane Steam Reforming on a Ni/CeO₂ Catalyst: Active Sites and the Role of Metalâ€“Support Interactions. ACS Catalysis, 2021, 11, 8327-8337.	5.5	39
57371	Superconductive Sodium Carbides with Pentagon Carbon at High Pressures. Journal of Physical Chemistry Letters, 2021, 12, 5850-5856.	2.1	16
57372	Pressure-Induced Synthesis and Properties of an H₂Sâ€“H₂Seâ€“H₂ Molecular Alloy. Journal of Physical Chemistry Letters, 2021, 12, 5738-5743.	2.1	1
57373	Unusually High Ion Conductivity in Large-Scale Patternable Two-Dimensional MoS₂ Film. ACS Nano, 2021, 15, 12267-12275.	7.3	11
57374	Factors controlling segregation tendency of solute Ti, Ag and Ta into different symmetrical tilt grain boundaries of tungsten: First-principles and experimental study. Acta Materialia, 2021, 211, 116868.	3.8	22
57375	Reaction mechanisms of chlorine reduction on hydroxylated alumina in titanium nitride growth: First principles study. Applied Surface Science, 2021, 550, 149391.	3.1	5
57376	Blue phosphorene nanosheets with point defects: Electronic structure and hydrogen storage capability. Applied Surface Science, 2021, 551, 149363.	3.1	13
57377	Potential anodic applications of 2D MoS2 for K-ion batteries. Journal of Alloys and Compounds, 2021, 865, 158782.	2.8	38
57378	Cyclic oxidation behavior of Al-Si coating on new Î³â€²-strengthened cobalt-based superalloy: Experimental study and first-principles calculation. Corrosion Science, 2021, 185, 109422.	3.0	10
57379	Investigating the effect of edge and basal plane surface functionalisation of carbonaceous anodes for alkali metal (Li/Na/K) ion batteries. Carbon, 2021, 177, 226-243.	5.4	19

#	Article	IF	Citations
57380	Self-feeding formation of atomically thin molybdenum nanoflakes on MoS₂ monolayer. 2D Materials, 2021, 8, 035054.	2.0	2
57381	Solvato Modulation of the Magnetic Memory in Isotopically Enriched Erbium Polyoxometalate. Chemistry - A European Journal, 2021, 27, 10160-10168.	1.7	10
57382	A first-principles study of hydrogen storage of high entropy alloy TiZrVMoNb. International Journal of Hydrogen Energy, 2021, 46, 21050-21058.	3.8	28
57383	When band convergence is not beneficial for thermoelectrics. Nature Communications, 2021, 12, 3425.	5.8	51
57384	Boron Nanosheet-Supported Rh Catalysts for Hydrogen Evolution: A New Territory for the Strong Metal-Support Interaction Effect. Nano-Micro Letters, 2021, 13, 138.	14.4	37
57385	Effects of strain on the electronic, optical, and ferroelectric transition properties of HfO₂: ab initio simulation study. Journal of Physics Condensed Matter, 2021, 33, 295501.	0.7	6
57386	Neutron thermalization in nuclear graphite: A modern story of a classic moderator. Annals of Nuclear Energy, 2021, 161, 108437.	0.9	4
57387	Data-driven design of a new class of rare-earth free permanent magnets. Acta Materialia, 2021, 212, 116913.	3.8	9
57388	Atomistic insights into the nucleation and growth of platinum on palladium nanocrystals. Nature Communications, 2021, 12, 3215.	5.8	18
57389	Theoretical Predictions of the Structural and Mechanical Properties of Tungstenâ€“Rare Earth Element Alloys. Materials, 2021, 14, 3046.	1.3	5
57390	A15 Nb3Si: a â€˜highâ€™ T c superconductor synthesized at a pressure of one megabar and metastable at ambient conditions. Journal of Physics Condensed Matter, 2021, 33, 285705.	0.7	0
57391	Gate-tunable chiral phonons in low-buckled group-IVA monolayers. Journal of Physics Condensed Matter, 2021, 33, 285704.	0.7	1
57392	Designing zero-dimensional dimer-type all-inorganic perovskites for ultra-fast switching memory. Nature Communications, 2021, 12, 3527.	5.8	38
57393	Band gap engineering in blended organic semiconductor films based on dielectric interactions. Nature Materials, 2021, 20, 1407-1413.	13.3	17
57394	New insights in the electronic structure of doped graphene on adsorption with oxides of nitrogen. Materials Today Communications, 2021, 27, 102417.	0.9	5
57395	Thermoelectric Properties of Arsenic Triphosphide (AsP3) Monolayer: A First-Principles Study. Frontiers in Mechanical Engineering, 2021, 7, .	0.8	2
57396	Chiralities of nodal points along high-symmetry lines with screw rotation symmetry. Physical Review B, 2021, 103, .	1.1	6
57397	Angular dependence of Hall effect and magnetoresistance in <mml:math xmlns:mml="http://www.w3.org/1998/Math/MathML"><mml:msub><mml:mi mathvariant="normal">SrRuO</mml:mi><mml:mn>3</mml:mn></mml:msub><mml:mo>â^•</mml:mo><mml:msub><mml:mi mathvariant="normal">SrIrO</mml:mi><mml:mn>3</mml:mn></mml:msub></mml:math> heterostructures. Physical Review B, 2021, 103, .	1.1	5

#	Article	IF	Citations
57398	Bandgap Engineering and Near-Infrared-II Optical Properties of Monolayer MoS2: A First-Principle Study. Frontiers in Chemistry, 2021, 9, 700250.	1.8	20
57399	Improving Thermodynamic Stability of SmFe12-Type Permanent Magnets from High Entropy Effect. Journal of Phase Equilibria and Diffusion, 2021, 42, 592-605.	0.5	7
57400	Quasiperiodic modulation of electronic states at edges of tellurium nanoribbons on <mml:math xmlns:mml="http://www.w3.org/1998/Math/MathML"><mml:mi>graphene</mml:mi><mml:mo>/</mml:mo><mml:mn>6</mml:mn><mml:mn>3</mml:mn><mml:mr Physical Review B, 2021, 103, .	1.1	3
57401	Magnetoelectric coupling dependent on ferroelectric switching paths in two-dimensional perovskite multiferroics. Physical Review B, 2021, 103, .	1.1	5
57402	Potassium titanyl phosphate Z- and Y-cut surfaces from density-functional theory. Physical Review Materials, 2021, 5, .	0.9	0
57403	Giant GrÃ¼neisen parameter in a superconducting quantum paraelectric. Physical Review B, 2021, 103, .	1.1	6
57404	Geometric, electronic, and optical properties of MoS₂/WSSe van der Waals heterojunctions: a first-principles study. Nanotechnology, 2021, 32, 355705.	1.3	4
57405	Third-order elastic constants and biaxial relaxation coefficient in wurtzite group-III nitrides by hybrid-density functional theory calculations. Journal of Physics Condensed Matter, 2021, 33, .	0.7	3
57406	Momentum-space signatures of Berry flux monopoles in the Weyl semimetal TaAs. Nature Communications, 2021, 12, 3650.	5.8	20
57407	Engineering local coordination environment of atomically dispersed platinum catalyst via lattice distortion of support for efficient hydrogen evolution reaction. Materials Today Energy, 2021, 20, 100653.	2.5	19
57408	Tunable electronic band structure, luminescence properties and thermostability of (Gd1â€“La)2Si2O7:Ce scintillator by adjusting La/Gd ratio. Journal of Rare Earths, 2021, 39, 657-665.	2.5	4
57409	The gate length effect of high-performance monolayer SiAs2 FETs. Semiconductor Science and Technology, 2021, 36, 085006.	1.0	1
57410	Doping effects on mechanical and thermodynamic properties of zirconium carbide systems: a first-principles study. Materials Research Express, 2021, 8, 065012.	0.8	4
57411	Phase-pure two-dimensional FexGeTe2 magnets with near-room-temperature TC. Nano Research, 2022, 15, 457-464.	5.8	21
57412	Enhancing the phase stability of ceramics under radiation via multilayer engineering. Science Advances, 2021, 7, .	4.7	6
57413	Doping Platinum with Germanium: An Effective Way to Mitigate the CO Poisoning. ChemPhysChem, 2021, 22, 1603-1610.	1.0	5
57414	Engineering Co/MnO heterointerface inside porous graphitic carbon for boosting the low-temperature CO2methanation. Applied Catalysis B: Environmental, 2021, 287, 119959.	10.8	36
57415	First-principles calculation identification of ultrahigh hydrogen storage capacity in g-Mg3N2. Journal of Alloys and Compounds, 2021, 867, 158744.	2.8	3

#	Article	IF	Citations
57416	Enhancing energy storage efficiency of lithiated carbon nitride (C7N6) monolayers under co-adsorption of H2 and CH4. International Journal of Hydrogen Energy, 2021, 46, 19988-19997.	3.8	19
57417	Highly efficient catalysts of phytic acid-derivative cobalt phosphide encapsulated in N, P-codoped carbon for activation of peroxymonosulfate in norfloxacin degradation. Separation and Purification Technology, 2021, 264, 118367.	3.9	28
57418	Multifunctional antiperovskites driven by strong magnetostructural coupling. Npj Computational Materials, 2021, 7, .	3.5	22
57419	Quasi-Isentropic Compression of a Nonideal Plasma of Deuterium and its Mixture with Helium at Pressures up to 250 GPa. Journal of Experimental and Theoretical Physics, 2021, 132, 985-998.	0.2	7
57420	Crystallographic and morphological sensitivity of N2 activation over ruthenium. Chinese Journal of Chemical Physics, 2021, 34, 263-272.	0.6	4
57421	Defectâ€Engineered nâ€Doping of WSe₂ via Argon Plasma Treatment and Its Application in Fieldâ€Effect Transistors. Advanced Materials Interfaces, 2021, 8, 2100718.	1.9	18
57422	Structurally Driven Environmental Degradation of Friction in MoS2 Films. Tribology Letters, 2021, 69, 1.	1.2	13
57423	Blister formation in He-H co-implanted InP: A comprehensive atomistic study. Applied Surface Science, 2021, 552, 149426.	3.1	14
57424	Surface Reconstruction for Forming the [IrO₆]â€“[IrO₆] Framework: Key Structure for Stable and Activated OER Performance in Acidic Media. ACS Applied Materials & Interfaces, 2021, 13, 29654-29663.	4.0	26
57425	Stoner Ferromagnetism in Hole-Doped CuM^{IIIA}O₂ with M^{IIIA} = Al, Ga, and In. ACS Applied Materials & Interfaces, 2021, 13, 29770-29779.	4.0	2
57426	Theoretical Study on the NO_x Selective Catalytic Reduction on Single-Cu Sites and BrÃ¸nsted Acid Sites in Cu-SSZ-13. Journal of Physical Chemistry C, 2021, 125, 12594-12602.	1.5	10
57427	High-Pressure Phase Diagram of the Tiâ€“O System. Journal of Physical Chemistry Letters, 2021, 12, 5486-5493.	2.1	5
57428	Polar Ferromagnetic Metal by Intercalation of Metalâ€“Amine Complexes. Chemistry of Materials, 2021, 33, 4936-4947.	3.2	8
57429	Ab initio modelling of helium behavior in Î±-Fe/TaC interface. Nuclear Materials and Energy, 2021, 27, 100956.	0.6	2
57430	Computing with DFT Band Offsets at Semiconductor Interfaces: A Comparison of Two Methods. Nanomaterials, 2021, 11, 1581.	1.9	6
57431	Platinum single-atom catalyst coupled with transition metal/metal oxide heterostructure for accelerating alkaline hydrogen evolution reaction. Nature Communications, 2021, 12, 3783.	5.8	355
57432	First-principles-assisted band gap predictions of methylammonium metal formates. Materials Research Bulletin, 2021, 138, 111239.	2.7	1
57433	Evolution of dielectric loss-dominated electromagnetic patterns in magnetic absorbers for enhanced microwave absorption performances. Nano Research, 2021, 14, 4006-4013.	5.8	56

#	Article	IF	Citations
57434	Hydrodechlorination of 1,2-Dichloroethane on Platinum Catalysts: Insights from Reaction Kinetics Experiments, Density Functional Theory, and Microkinetic Modeling. ACS Catalysis, 2021, 11, 7890-7905.	5.5	12
57435	Dynamically Crosslinked Dry Ionâ€Conducting Elastomers for Soft Iontronics. Advanced Materials, 2021, 33, e2101396.	11.1	128
57436	Gas detection for NO2 and SO2 based on tape-heme monolayer. Molecular Physics, 2021, 119, .	0.8	0
57437	Highly selective metal-organic framework-based electrocatalyst for the electrochemical reduction of CO2 to CO. Materials Research Bulletin, 2021, 138, 111228.	2.7	12
57438	Development of Bimetallic PdNi Electrocatalysts toward Mitigation of Catalyst Poisoning in Direct Borohydride Fuel Cells. ACS Catalysis, 2021, 11, 8417-8430.	5.5	28
57439	Centrosymmetric or Noncentrosymmetric? Transition Metals Talking in K₂TGe₃S₈ (T = Co, Fe). Inorganic Chemistry, 2021, 60, 10603-10613.	1.9	16
57440	The eruption of carbon chains in the oxidation of 2D Tin+1Cn (nÂ=Â1, 2, 3) MXenes. Applied Surface Science, 2021, 550, 149310.	3.1	8
57441	ZnSe/CdSe Z-scheme composites with Se vacancy for efficient photocatalytic CO2 reduction. Applied Catalysis B: Environmental, 2021, 286, 119887.	10.8	74
57442	Membrane-free selective oxidation of thioethers with water over a nickel phosphide nanocube electrode. Cell Reports Physical Science, 2021, 2, 100462.	2.8	18
57443	Nitrogen overgrowth as a catalytic mechanism during diamond chemical vapour deposition. Carbon, 2021, 178, 606-615.	5.4	4
57444	Permeation of chemisorbed hydrogen through graphene: A flipping mechanism elucidated. Carbon, 2021, 178, 718-727.	5.4	10
57445	Computational exploration of magnesium-decorated carbon nitride (g-C3N4) monolayer as advanced energy storage materials. International Journal of Hydrogen Energy, 2021, 46, 21739-21747.	3.8	33
57447	Acoustic Properties of Metal-Organic Frameworks. Research, 2021, 2021, 9850151.	2.8	10
57448	Coexistence of superconductivity and antiferromagentic order in Er2O2Bi with anti-ThCr2Si2 structure. Frontiers of Physics, 2021, 16, 1.	2.4	4
57449	Directional observations of guanine and cytosine pairing structures on HOPG. Chemical Physics, 2021, 546, 111189.	0.9	3
57450	Copperâ^'iron dimer for selective Câ€“C coupling in electrochemical CO2 reduction. Electrochimica Acta, 2021, 380, 138188.	2.6	9
57451	Synergistic effect of substrate and ion-containing water in graphene based hydrovoltaic generators. Nano Energy, 2021, 84, 105939.	8.2	27
57452	Anion ordering enables fast H ^{â^'} conduction at low temperatures. Science Advances, 2021, 7, .	4.7	32

#	Article	IF	Citations
57453	Ab Initio Investigation of the Elastic Properties of CaxSn1â^'x Alloys for Use As Battery Anodes. Journal of Electrochemical Energy Conversion and Storage, 2021, 18, .	1.1	5
57454	Optical and electronic properties of SiTex (xâ€‰=â€‰1, 2) from first-principles. Journal of Applied Physics, 2021, 129, .	1.1	5
57455	Nitrobenzene sensing in pristine and metal doped 2D dichalcogenide MoS2: Insights from density functional theory investigations. Applied Surface Science, 2021, 550, 149395.	3.1	30
57456	Role of V-V dimers on structural, electronic, magnetic, and vibrational properties of <mml:math xmlns:mml="http://www.w3.org/1998/Math/MathML"><mml:msub><mml:mi>VO</mml:mi><mml:mn>2</mml:mn></mml:msub></m by first-principles simulations and Raman spectroscopic analysis. Physical Review B, 2021, 103, .	1.1	11
57457	A single atom change turns insulating saturated wires into molecular conductors. Nature Communications, 2021, 12, 3432.	5.8	16
57458	Ab Initio Investigation of Helium Mobility in La2Zr2O7 Pyrochlore. Crystals, 2021, 11, 667.	1.0	1
57459	Selfâ€Assembled Structure Evolution of Mnï£¿Fe Oxides for High Temperature Thermochemical Energy Storage. Small, 2021, 17, e2101524.	5.2	17
57460	Semiconducting M2X (M = Cu, Ag, Au; X = S, Se, Te) monolayers: A broad range of band gaps and high carrier mobilities. Nano Research, 2021, 14, 2826-2830.	5.8	24
57461	Measuring the structure and equation of state of polyethylene terephthalate at megabar pressures. Scientific Reports, 2021, 11, 12883.	1.6	10
57462	First-principles design of a single-atomâ€“alloy propane dehydrogenation catalyst. Science, 2021, 372, 1444-1447.	6.0	185
57463	Entropic broadening of the spin-crossover pressure in ferropericlase. Physical Review B, 2021, 103, .	1.1	4
57464	Giant ferroelectric modulation of barrier height and width in multiferroic tunnel junctions. Physical Review B, 2021, 103, .	1.1	4
57465	Semiconducting character of LaN: Magnitude of the bandgap and origin of the electrical conductivity. AIP Advances, 2021, 11, .	0.6	2
57466	Fano Resonance Enabled Infrared Nano-Imaging of Local Strain in Bilayer Graphene. Chinese Physics Letters, 2021, 38, 056301.	1.3	7
57467	Influence of Substitutional Defects in ZIF-8 Membranes on Reverse Osmosis Desalination: A Molecular Dynamics Study. Molecules, 2021, 26, 3392.	1.7	8
57468	Searching for cluster Lego blocks for three-dimensional and two-dimensional assemblies. Physical Review Materials, 2021, 5, .	0.9	7
57469	Molecular dynamics simulations of ultrafast radiation induced melting at metalâ€“semiconductor interfaces. Journal of Applied Physics, 2021, 129, .	1.1	4
57470	Linking structures of doubly charged nodal surfaces in centrosymmetric superconductors. Physical Review B, 2021, 103, .	1.1	4

#	Article	IF	Citations
57471	A2(TeO)P2O7 (Aâ€¯=â€¯K, Rb, Cs): Three new tellurite-pyrophosphates with large birefringence. Journal of Alloys and Compounds, 2021, 865, 158785.	2.8	11
57472	sulfides <mml:math xmlns:mml="http://www.w3.org/1998/Math/MathML" altimg="si1.svg"><mml:mrow><mml:msub><mml:mtext>MSnS</mml:mtext><mml:mn>3</mml:mn></mml:msub><mml:mrow><mml:mo stretchy="true">(</mml:mo><mml:mtext>M</mml:mtext><mml:mo) Tj ETQq1 1 0.784314 rgBT /Overlock 10 Tf 50.697 Td (linebreak="	1.6	
57473	First-Principles Studies of the Tunneling Properties through Ferroelectric/Ferromagnetic van der Waals Heterostructures. Journal of Physical Chemistry C, 2021, 125, 14438-14445.	1.5	3
57474	First-principles model for voids decorated by transmutation solutes: Short-range order effects and application to neutron irradiated tungsten. Physical Review Materials, 2021, 5, .	0.9	7
57475	A theoretical study of sulfur poisoning tolerance at the interface of Mo doped Ni/Yttria-Stabilized Zirconia. International Journal of Hydrogen Energy, 2021, 46, 21075-21081.	3.8	3
57476	Combined ab-initio and empirical model for irradiated metal alloys with a focus on uranium alloy fuel thermal conductivity. Journal of Nuclear Materials, 2021, 549, 152891.	1.3	1
57477	Observation of second sound in a rapidly varying temperature field in Ge. Science Advances, 2021, 7, .	4.7	40
57478	Electronic structure and optical properties of InSe/Î±-AsP van der Waals heterostructure from DFT calculations. Physica E: Low-Dimensional Systems and Nanostructures, 2021, 130, 114674.	1.3	12
57479	Electronic structure of reduced CeO2(111) surfaces interacting with hydrogen as revealed through electron energy loss spectroscopy in comparison with theoretical investigations. Journal of Electron Spectroscopy and Related Phenomena, 2021, , 147088.	0.8	6
57480	The newly-assisted catalytic mechanism of surface hydroxyl species performed as the promoter in syngas-to-C2 species on the Cu-based bimetallic catalysts. Green Energy and Environment, 2023, 8, 487-498.	4.7	2
57481	A Hydrothermal Strategy to Fabricate Carbonsâ€Doped Polyaniline Hydrogels with Separationâ€Free for Flexible Allâ€Solidâ€State Supercapacitors. Macromolecular Materials and Engineering, 2021, 306, 2100274.	1.7	3
57482	Two distinct non-Arrhenius behaviors of hydrogen diffusivities in fcc aluminum, silver, and copper determined by ab initio path integral simulations. Physical Review Materials, 2021, 5, .	0.9	8
57483	Structure Sensitivity of Pd Facets for Enhanced Electrochemical Nitrate Reduction to Ammonia. ACS Catalysis, 2021, 11, 7568-7577.	5.5	194
57484	Double-layer honeycomb AlP as a promising catalyst for Li-O2 and Na-O2 batteries. Applied Surface Science, 2021, 550, 149392.	3.1	8
57485	Electronic structure evolution and exciton energy shifting dynamics in WSe₂: from monolayer to bulk. Journal Physics D: Applied Physics, 2021, 54, 354002.	1.3	4
57486	Quasi-one-dimensional uniform spin- 12 Heisenberg antiferromagnet KNaCuP2O7 probed by P31 and Na23 NMR. Physical Review B, 2021, 103, .	1.1	5
57487	CVD Polycrystalline Graphene as Sensing Film of Extended-Gate ISFET for Low-Drift pH Sensor. Journal of the Electrochemical Society, 2021, 168, 067520.	1.3	3
57488	Coexistence of ferroelectricity and metallicity in M-doped BaTiO3 (M = Al, V, Cr, Fe, Ni, and Nb): First-principles study. Materials Today Communications, 2021, 27, 102394.	0.9	3

#	Article	IF	Citations
57489	First-principles investigation of structural and electronic properties of Î± phase In2Se3. Materials Today Communications, 2021, 27, 102452.	0.9	1
57490	First-principles investigation of the elastic, photocatalytic and ferroelectric properties of LiNbO3-type LiSbO3 under high pressure. Materials Today Communications, 2021, 27, 102406.	0.9	1
57491	Ei¬€ect of Thickness and Stacking Order on Raman Spectrum of Layered CrCl3. Journal of Physics Condensed Matter, 2021, 33, .	0.7	5
57492	Origins of anisotropic transport in the electrically switchable antiferromagnet <mml:math xmlns:mml="http://www.w3.org/1998/Math/MathML"><mml:msub><mml:mrow><mml:mi>Fe</mml:mi></mml:mrow><mml:mrow><mml:n Physical Review B, 2021, 103, .	3.7	11
57493	Mass transport induced structural evolution and healing of sulfur vacancy lines and Mo chain in monolayer MoS2. Rare Metals, 2022, 41, 333-341.	3.6	8
57494	Quantifying the Influence of Water on the Mobility of Aluminum Species and Their Effects on Alkane Cracking in Zeolites. ACS Catalysis, 2021, 11, 6982-6994.	5.5	23
57495	Linearly Tailored Work Function of Orthorhombic CsSnI₃ Perovskites. ACS Energy Letters, 2021, 6, 2328-2335.	8.8	11
57496	First-Principles-Based Machine-Learning Molecular Dynamics for Crystalline Polymers with van der Waals Interactions. Journal of Physical Chemistry Letters, 2021, 12, 6000-6006.	2.1	14
57497	DockOnSurf: A Python Code for the High-Throughput Screening of Flexible Molecules Adsorbed on Surfaces. Journal of Chemical Information and Modeling, 2021, 61, 3386-3396.	2.5	13
57498	Single-Dislocation Schottky Diodes. Nano Letters, 2021, 21, 5586-5592.	4.5	5
57499	Surface Electronic Modulation with Hetero-Single Atoms to Enhance Oxygen Evolution Catalysis. ACS Nano, 2021, 15, 11891-11897.	7.3	27
57500	Structural, Vibrational, and Electronic Properties of 1D-TlInTe₂ under High Pressure: A Combined Experimental and Theoretical Study. Inorganic Chemistry, 2021, 60, 9320-9331.	1.9	6
57501	Cu²⁺-Guided Construction of the Amorphous CoMoO₃/Cu Nanocomposite for Highly Efficient Water Electrolysis. ACS Applied Energy Materials, 2021, 4, 6740-6748.	2.5	8
57502	C₂ Vacancy-Mediated N₂ Activation over Ni-Loaded Rare-Earth Dicarbides for Ammonia Synthesis. ACS Catalysis, 2021, 11, 7595-7603.	5.5	5
57503	Efficient electroreduction of CO2 by single-atom catalysts two-dimensional metal hexahydroxybenzene frameworks: A theoretical study. Applied Surface Science, 2021, 550, 149389.	3.1	15
57504	Mn-doped porous interconnected MoP nanosheets for enhanced hydrogen evolution. Applied Surface Science, 2021, 551, 149321.	3.1	31
57505	Improving water desalination via inhomogeneous distribution of [BMIM][BF4] in 2D carbon nanotube networks: Nonequilibrium molecular dynamics simulation. Journal of Molecular Liquids, 2021, 331, 115813.	2.3	8
57506	Strain modulation of the spin-valley polarization in monolayer manganese chalcogenophosphates alloys. Journal of Physics Condensed Matter, 2021, 33, 295503.	0.7	2

#	Article	IF	Citations
57507	CO2 adsorption on graphene supported Ni catalysts. Journal of Physics: Conference Series, 2021, 1949, 012003.	0.3	0
57508	Forging Inspired Processing of Sodiumâ€Fluorinated Graphene Composite as Dendriteâ€Free Anode for Longâ€Life Naâ€“CO₂ Cells. Energy and Environmental Materials, 2022, 5, 572-581.	7.3	8
57509	Modifying Metastable Sr_{1â€“x}BO_{3â^Î´} (B = Nb, Ta, and Mo) Perovskites for Electrode Materials. ACS Applied Materials & Interfaces, 2021, 13, 29788-29797.	4.0	2
57510	A Colossal Enhancement of Thermoelectric Performance of Monolayer SbAs Using Strain Engineering. Physica Status Solidi - Rapid Research Letters, 2021, 15, 2100175.	1.2	1
57511	Laserâ€Ablated Red Phosphorus on Carbon Nanotube Film for Accelerating Polysulfide Conversion toward Highâ€Performance and Flexible Lithiumâ€“Sulfur Batteries. Small Methods, 2021, 5, e2100215.	4.6	19
57512	Coexistence of ferromagnetism, antiferromagnetism, and superconductivity in magnetically anisotropic (Eu,La)FeAs2. Npj Quantum Materials, 2021, 6, .	1.8	4
57513	A theoretical investigation of quantum spin Hall state in ordered Mâ€²2Mâ€³2C3 MXenes (Mâ€² = V, Nb, Ta and Mâ€³) Tj ETQq0 0 0 rg	0.7	3
57514	Predicted Polymeric and Layered Covalent Networks in Transition Metal Pentazolate M(cyclo-N5)x Phases at Ambient and High Pressure: Up to 20 Nitrogen Atoms per Metal. Chemistry of Materials, 2021, 33, 5298-5307.	3.2	10
57515	Sparse Gaussian process potentials: Application to lithium diffusivity in superionic conducting solid electrolytes. Physical Review B, 2021, 103, .	1.1	41
57516	Role of Ferroelectricity, Delocalization, and Occupancy of <mml:math xmlns:mml="http://www.w3.org/1998/Math/MathML" display="inline" overflow="scroll"><mml:mi>d</mml:mi></mml:math> States in the Electrical Control of Interface-Induced Magnetization. Physical Review Applied, 2021, 15, .	1.5	5
57517	Tendency of Gap Opening in Semimetal 1Tâ€²â€MoTe₂ with Proximity to a 3D Topological Insulator. Advanced Functional Materials, 2021, 31, 2103384.	7.8	8
57518	Fluorine-Decorated Graphene Nanoribbons for an Anticorrosive Polymer Electrolyte Membrane Fuel Cell. ACS Applied Materials & Interfaces, 2021, 13, 26936-26947.	4.0	18
57519	Theoretical scanning of bimetallic alloy for designing efficient N2 electroreduction catalyst. Materials Today Energy, 2021, 20, 100684.	2.5	21
57520	Water Reactions on Reconstructed Rutile TiO₂: A Density Functional Theory/Density Functional Tight Binding Approach. Journal of Physical Chemistry C, 2021, 125, 13234-13246.	1.5	9
57521	Strain-tunable triple point Fermions in diamagnetic rare-earth half-Heusler alloys. Scientific Reports, 2021, 11, 12029.	1.6	4
57522	Mechanical Properties and Strain Transfer Behavior of Molybdenum Ditelluride (MoTe2) Thin Films. Journal of Engineering Materials and Technology, Transactions of the ASME, 2022, 144, .	0.8	20
57523	Elimination of Charge Recombination Centers in Metal Halide Perovskites by Strain. Journal of the American Chemical Society, 2021, 143, 9982-9990.	6.6	52
57524	Ferroelectric properties of BaTiO3-BiScO3 weakly coupled relaxor energy-storage ceramics from first-principles calculations. Journal of Alloys and Compounds, 2021, 866, 158933.	2.8	17

#	Article	IF	Citations
57525	Progressive lithiation mechanism of Sn4P3 nanosheets as anodes for Li-ion batteries. Applied Surface Science, 2021, 550, 149247.	3.1	12
57526	Interfacial ferroelectricity by van der Waals sliding. Science, 2021, 372, 1462-1466.	6.0	262
57527	Machine Learning Guided Synthesis of Multinary Chevrel Phase Chalcogenides. Journal of the American Chemical Society, 2021, 143, 9113-9122.	6.6	22
57528	Uniform and robust TiN/HfO2/Pt memristor through interfacial Al-doping engineering. Applied Surface Science, 2021, 550, 149274.	3.1	34
57529	Computational screening study of double transition metal carbonitrides Mâ€²2Mâ€³CNO2-MXene as catalysts for hydrogen evolution reaction. Npj Computational Materials, 2021, 7, .	3.5	63
57530	Hierarchically Assembled Cobalt Oxynitride Nanorods and N-Doped Carbon Nanofibers for Efficient Bifunctional Oxygen Electrocatalysis with Exceptional Regenerative Efficiency. ACS Nano, 2021, 15, 11218-11230.	7.3	45
57531	Low lattice thermal conductivity of pentadiamond. Journal of Applied Physics, 2021, 129, .	1.1	9
57532	Atomic structures of interfacial solute gateways to Î¸â€² precipitates in Al-Cu alloys. Acta Materialia, 2021, 212, 116891.	3.8	18
57533	Bi4O5Br2 nanosheets with vertical aligned facets for efficient visible-light-driven photodegradation of BPA. Applied Catalysis B: Environmental, 2021, 286, 119937.	10.8	69
57534	Design, preparation, characterization, and application of MnxCu1-xOy/Î³-Al2O3 catalysts in ozonation to achieve simultaneous organic carbon and nitrogen removal in pyridine wastewater. Science of the Total Environment, 2021, 774, 145189.	3.9	19
57535	Ferroelectricity in strained <mml:math xmlns:mml="http://www.w3.org/1998/Math/MathML"><mml:mrow><mml:msub><mml:mi>Hf</mml:mi><mml:mn>2</mml:mn></mml:msub></mml:mrow></mml:math> monolayer. Physical Review Materials, 2021, 5, .	2.4	11
57536	Strain-sensitive ferromagnetic two-dimensional Cr2Te3. Nano Research, 2022, 15, 1254-1259.	5.8	26
57537	Evolving Defect Chemistry of (Pu,Am)O_{2Â±x}. Journal of Physical Chemistry C, 2021, 125, 15560-15568.	1.5	4
57538	Tailoring the Optical, Electronic, and Magnetic Properties of MAPbI₃ through Self-Assembled Fe Incorporation. Journal of Physical Chemistry C, 2021, 125, 15636-15646.	1.5	9
57539	Reactivity of the Si(100)-2 Ã— 1-Cl surface with respect to PH₃, PCl₃, and BCl₃: comparison with PH₃ on Si(100)-2 Ã— 1-H. Journal of Physics Condensed Matter, 2021, 33, 384001.	0.7	7
57540	Asymmetric interfaces sandwiched between infinite-layer oxides and perovskite oxides. Physical Review B, 2021, 104, .	1.1	1
57541	High-Throughput Screening of Atomic Defects in MXenes for CO₂ Capture, Activation, and Dissociation. ACS Applied Materials & Interfaces, 2021, 13, 35585-35594.	4.0	30
57542	Point Defects Modeling Explains Multiple Sulfur Species in Sulfur-Doped Na4(Al3Si3O12)Cl Sodalite. Journal of Physical Chemistry C, 2021, 125, 16674-16680.	1.5	6

#	Article	IF	Citations
57543	Computationally Designed Crystal Structures of the Supertetrahedral Ga4C and Ga4Si Solids. Journal of Physical Chemistry A, 2021, 125, 6556-6561.	1.1	1
57544	High carrier mobility and remarkable photovoltaic performance of two-dimensional Ruddlesdenâ€“Popper organicâ€“inorganic metal halides (PA)2(MA)2M3I10 for perovskite solar cell applications. Materials Today, 2021, 47, 45-52.	8.3	12
57545	First principle study on the mechanical response of ZrC and ZrN at high-pressure conditions: anisotropy perspective. Molecular Simulation, 2021, 47, 1135-1148.	0.9	6
57546	Nonlinear Tunable Vibrational Response in Hexagonal Boron Nitride. ACS Nano, 2021, 15, 13415-13426.	7.3	5
57547	Regulating oxygen activity of perovskites to promote NOx oxidation and reduction kinetics. Nature Catalysis, 2021, 4, 663-673.	16.1	54
57548	Strengthening nitrogen affinity on CuAu@Cu coreâ€“shell nanoparticles with ultrathin Cu skin via strain engineering and ligand effect for boosting nitrogen reduction reaction. Applied Catalysis B: Environmental, 2021, 288, 119999.	10.8	35
57549	Construction of a Unique Structure of Ru Sites in the RuP Structure for Propane Dehydrogenation. ACS Applied Materials & Interfaces, 2021, 13, 33045-33055.	4.0	15
57550	Environmental impact of amino acids on the release of selenate immobilized in hydrotalcite: Integrated interpretation of experimental and density-functional theory study. Chemosphere, 2021, 274, 129927.	4.2	5
57551	Exploration of the novel structures and electronic properties for Nd3+ doped CaTiO3. Materials Chemistry and Physics, 2021, 266, 124525.	2.0	2
57552	Alloying non-precious metals into Ni-based electrocatalysts for enhanced hydrogen oxidation reaction in alkaline media: A computational study. Applied Surface Science, 2021, 554, 149627.	3.1	10
57553	New stable two dimensional silicon carbide nanosheets. Journal of Alloys and Compounds, 2021, 868, 159201.	2.8	8
57554	Type-II CeO2(111)/hBN vdW heterojunction for enhanced photocatalytic hydrogen evolution: A first principles study. International Journal of Hydrogen Energy, 2021, 46, 25060-25069.	3.8	19
57555	SPARC: Simulation Package for Ab-initio Real-space Calculations. SoftwareX, 2021, 15, 100709.	1.2	27
57556	Divalent Ion Selectivity in Capacitive Deionization with Vanadium Hexacyanoferrate: Experiments and Quantumâ€Chemical Computations. Advanced Functional Materials, 2021, 31, 2105203.	7.8	38
57557	Gibbs Energy of Hydrogen Adsorption on Pt Surface by Machine Learning Potential and Metadynamics. Chemistry Letters, 2021, 50, 1329-1332.	0.7	1
57558	Insight into the roles of ammonia during direct alcohol amination over supported Ru catalysts. Journal of Catalysis, 2021, 399, 121-131.	3.1	30
57559	Effects of La incorporation in catalytic activity of Ag/La-CeO2 catalysts for soot oxidation. Journal of Hazardous Materials, 2021, 414, 125523.	6.5	31
57560	Assessing the role of mineral particles in the atmospheric photooxidation of typical carbonyl compound. Journal of Environmental Sciences, 2021, 105, 56-63.	3.2	3

#	Article	IF	Citations
57561	Theoretical investigation of lattice dynamics, infrared reflectivity, polarized Raman spectra and nature of interlayer coupling in two-dimensional layered gallium sulfide. Journal of Physics Condensed Matter, 2021, 33, 405001.	0.7	1
57562	Direct probing of phonon mode specific electronâ€“phonon scatterings in two-dimensional semiconductor transition metal dichalcogenides. Nature Communications, 2021, 12, 4520.	5.8	10
57563	Nanostructured Glass Composite for Selfâ€Calibrated Radiation Dose Rate Detection. Advanced Optical Materials, 0, , 2100751.	3.6	6
57564	The trapping of methane on Ir(111): A first-principles quantum study. Journal of Chemical Physics, 2021, 155, 044705.	1.2	5
57565	Flow of polar and nonpolar liquids through nanotubes: A computational study. Physical Review Materials, 2021, 5, .	0.9	2
57566	Inside the electronic structure of the <mml:math xmlns:mml="http://www.w3.org/1998/Math/MathML"><mml:msub><mml:mi mathvariant="normal">Sm</mml:mi><mml:mn>3</mml:mn></mml:msub><mml:msub><mml:mi mathvariant="normal">Fe</mml:mi><mml:mn>5</mml:mn></mml:msub><mml:msub><mml:mi mathvariant="normal">O</mml:mi><mml:mn>12</mml:mn></mml:msub></mml:math> garnet: A mixed	1.1	4
57567	Prediction of monoclinic single-layer Janus <mml:math xmlns:mml="http://www.w3.org/1998/Math/MathML"><mml:mrow><mml:msub><mml:mi>Ga</mml:mi><mml:mn>2</mml:mn></mml: (<mml:math xmlns:mml="http://www.w3.org/1998/Math/MathML"><mml:mi>X</mml:mi></mml:math> = S) Tj ETQq0 0 0 rgBT /Overlo	1.1	12
57568	(111), (001), and (110) surface effects on the stability and electronic-magnetic properties of Mn3P alloy. Physica E: Low-Dimensional Systems and Nanostructures, 2021, 131, 114717.	1.3	3
57569	Adsorbate modification of electronic nonadiabaticity: H atom scattering from p(2 Ã— 2) O on Pt(111). Journal of Chemical Physics, 2021, 155, 034702.	1.2	6
57570	Piezoelectricity in three-dimensional carbon allotropes studied by first-principles calculations. Journal of Materials Science, 2021, 56, 15898-15905.	1.7	0
57571	Understanding the structure-performance relationship of cubic In2O3 catalysts for CO2 hydrogenation. Journal of CO2 Utilization, 2021, 49, 101543.	3.3	10
57572	InSe/Te van der Waals Heterostructure as a High-Efficiency Solar Cell from Computational Screening. Materials, 2021, 14, 3768.	1.3	7
57573	Inversely polarized thermo-electrochemical power generation via the reaction of an organic redox couple on a TiO2/Ti mesh electrode. Scientific Reports, 2021, 11, 13929.	1.6	10
57574	Intrinsic ferroelectricity and large bulk photovoltaic effect in novel two-dimensional buckled honeycomb-like lattice of NbP: first-principles study. Journal of Physics Condensed Matter, 2021, 33, 385302.	0.7	4
57575	Enhanced piezoelectric effect in MoS2 and surface-engineered GaN bilayer. Journal of Applied Physics, 2021, 130, 015113.	1.1	2
57576	High-throughput screening and rational design to drive discovery in molecular water oxidation catalysis. Cell Reports Physical Science, 2021, 2, 100492.	2.8	10
57577	Two-component electronic phase separation in the doped Mott insulator Y1â^'xCaxTiO3. Physical Review B, 2021, 104, .	1.1	3
57578	A multiscale study of the production and recombination of closely correlated defects from irradiation-induced higher order recoils in beryllium. Computational Materials Science, 2021, 195, 110403.	1.4	1

#	Article	IF	Citations
57579	Protonation-Induced B-Site Deficiency in Perovskite-Type Oxides: Fully Hydrated BaSc_{0.67}O(OH)₂ as a Proton Conductor. Chemistry of Materials, 2021, 33, 5935-5942.	3.2	8
57580	Using DFTB to Model Photocatalytic Anataseâ€“Rutile TiO2 Nanocrystalline Interfaces and Their Band Alignment. Journal of Chemical Theory and Computation, 2021, 17, 5239-5247.	2.3	3
57581	Molecular Routes of Dynamic Autocatalysis for Methanol-to-Hydrocarbons Reaction. Journal of the American Chemical Society, 2021, 143, 12038-12052.	6.6	60
57582	Highly CO selective Ca and Zn hybrid metal-organic framework electrocatalyst for the electrochemical reduction of CO2. Current Applied Physics, 2021, 27, 31-37.	1.1	11
57583	MAELAS: MAgneto-ELAStic properties calculation via computational high-throughput approach. Computer Physics Communications, 2021, 264, 107964.	3.0	10
57584	Two dimensional V2O3 and its experimental feasibility as robust room-temperature magnetic Chern insulator. Npj 2D Materials and Applications, 2021, 5, .	3.9	7
57585	Nontrivial topological states in new two-dimensional CdAs. Journal of Physics Condensed Matter, 2021, 33, 365701.	0.7	2
57586	Intravalley $L1_2$-$L1_0$ transition and Stoner ferromagnetism in Janus <mml:math xmlns:mml="http://www.w3.org/1998/Math/MathML"><mml:mrow><mml:mi mathvariant="normal">P</mml:mi><mml:msub><mml:mi>A</mml:mi><mml:mn>2</mml:mn></mml:msub><mml:mi>As</mml:mi></		

#	Article	IF	Citations
57598	Structures and properties of Pd nanoparticles intercalated in layered TiO2: A computational study. Catalysis Today, 2021, , .	2.2	1
57599	Inelastic Neutron Scattering Study of Magnetic Exchange Pathways in MnS. Journal of Physical Chemistry C, 2021, 125, 16183-16190.	1.5	5
57600	In situ formed FeS₂@CoS cathode for long cycling life lithium-ion battery*. Chinese Physics B, 2021, 30, 088201.	0.7	6
57601	Substituted 2D Janus WSSe monolayers as efficient nanosensor toward toxic gases. Journal of Applied Physics, 2021, 130, .	1.1	16
57602	Shear-induced chemical segregation in a Fe-based bulk metallic glass at room temperature. Scientific Reports, 2021, 11, 13650.	1.6	8
57603	An antisite defect mechanism for room temperature ferroelectricity in orthoferrites. Nature Communications, 2021, 12, 4298.	5.8	32
57604	Magnetic proximity effect induced spin splitting in two-dimensional antimonene/Fe₃GeTe₂ van der Waals heterostructures. Chinese Physics B, 2022, 31, 037301.	0.7	6
57605	Surface Chemistry at the Solidâ€Solid Interface; Selectivity and Activity in Mechanochemical Reactions on Surfaces. Chemistry Methods, 2021, 1, 340-349.	1.8	1
57606	Ozonation of Group-IV Elemental Monolayers: A First-Principles Study. ACS Omega, 2021, 6, 19546-19552.	1.6	3
57607	First-Principles Study on the Electronic Properties of PDPP-Based Conjugated Polymer via Density Functional Theory. Journal of Physical Chemistry B, 2021, 125, 8953-8964.	1.2	7
57608	Critical Role of Ti⁴⁺ in Stabilizing Highâ€Voltage Redox Reactions in Liâ€Rich Layered Material. Small, 2021, 17, e2100840.	5.2	13
57609	Trends of higher-order exchange interactions in transition metal trilayers. Physical Review B, 2021, 104, .	1.1	10
57610	Underpotential-deposition synthesis and in-line electrochemical analysis of single-atom copper electrocatalysts. Applied Catalysis B: Environmental, 2021, 289, 120028.	10.8	38
57611	Detecting photoelectrons from spontaneously formed excitons. Nature Physics, 2021, 17, 1024-1030.	6.5	24
57612	Large Anomalous Hall and Nernst Effects in High Curieâ€Temperature Ironâ€Based Heusler Compounds. Advanced Science, 2021, 8, e2100782.	5.6	20
57613	Ab Initio Study of the Defect Chemistry and Substitutional Strategies for Highly Conductive Li₃YX₆ (X = F, Cl, Br, and I) Electrolyte for the Application of Solid-State Batteries. ACS Applied Energy Materials, 2021, 4, 7930-7941.	2.5	19
57614	Stabilizing Oxygen Vacancies in ZrO₂ by Ga₂O₃ Boosts the Direct Dehydrogenation of Light Alkanes. ACS Catalysis, 2021, 11, 10159-10169.	5.5	9
57615	Automated Adsorption Workflow for Semiconductor Surfaces and the Application to Zinc Telluride. Journal of Chemical Information and Modeling, 2021, 61, 3908-3916.	2.5	11

#	Article	IF	Citations
57616	Highâ€Pressureâ€Sinteringâ€Induced Microstructural Engineering for an Ultimate Phonon Scattering of Thermoelectric Halfâ€Heusler Compounds. Small, 2021, 17, e2102045.	5.2	17
57617	Phaseâ€Selective Synthesis of Ultrathin FeTe Nanoplates by Controllable Fe/Te Atom Ratio in the Growth Atmosphere. Small, 2021, 17, 2101616.	5.2	13
57618	Heterostructured Pd/Ti/Pd Thin Films as Highly Efficient Catalysts for Methanol and Formic Acid Oxidation. ACS Applied Materials & Interfaces, 2021, 13, 31725-31732.	4.0	9
57619	Exploring the Evolution Mechanism of Sulfur Vacancies by Investigating the Role of Vacancy Defects in the Interaction between H₂S and the FeS(001) Surface. ACS Omega, 2021, 6, 19212-19221.	1.6	6
57620	High-Throughput Evaluation of Discharge Profiles of Nickel Substitution in LiNiO2 by Ab Initio Calculations. Journal of Physical Chemistry C, 2021, 125, 14517-14524.	1.5	5
57621	First-Principles Calculations of Silicon Interstitial Defects at the Amorphous-SiO₂/Si Interface. Journal of Physical Chemistry C, 2021, 125, 15044-15051.	1.5	4
57622	Efficiently Trained Deep Learning Potential for Graphane. Journal of Physical Chemistry C, 2021, 125, 14874-14882.	1.5	18
57623	A First-Principle Study of Monolayer Transition Metal Carbon Trichalcogenides. Journal of Superconductivity and Novel Magnetism, 2021, 34, 2141-2149.	0.8	3
57624	Experimental and Computational Exploration of the NaFâ€“ThF4 Fuel System: Structure and Thermochemistry. Journal of Physical Chemistry B, 2021, 125, 8558-8571.	1.2	3
57625	Naâ€“CO2 battery with NASICON-structured solid-state electrolyte. Nano Energy, 2021, 85, 105972.	8.2	29
57626	Thermal-Driven Dynamic Shape Change of Bimetallic Nanoparticles Extends Hot Electron Lifetime of Pt/MoS₂ Catalysts. Journal of Physical Chemistry Letters, 2021, 12, 7173-7179.	2.1	8
57627	Pressure-induced 1T to 3R structural phase transition in metallic VSe2 : X-ray diffraction and first-principles theory. Physical Review B, 2021, 104, .	1.1	7
57628	Orthocarbonates of Ca, Sr, and Baâ€”The Appearance of sp³-Hybridized Carbon at a Low Pressure of 5 GPa and Dynamic Stability at Ambient Pressure. ACS Earth and Space Chemistry, 2021, 5, 1948-1957.	1.2	18
57629	Fermi level pinning in Coâ€doped BaTiO₃: Part II. Defect chemistry models. Journal of the American Ceramic Society, 2021, 104, 5859-5872.	1.9	9
57630	Effects of alloying elements on the generalized stacking fault energy of Ti5Si3: A first principle study. Journal of Alloys and Compounds, 2021, 868, 158980.	2.8	7
57631	Predicting core structure variations and spontaneous partial kink formation for Â½<111> screw dislocations in three BCC NbTiZr alloys. Scripta Materialia, 2021, 199, 113834.	2.6	14
57632	Mechanism investigation of iron selenide as polysulfide mediator for long-life lithium-sulfur batteries. Chemical Engineering Journal, 2021, 416, 129166.	6.6	42
57633	Sandwich heterometallic coordination polymers consisting of copper-cluster pillars and layered networks of {Ln6} wheels: synthesis, structures, spectroscopic properties and Juddâ€“Ofelt analysis. Transition Metal Chemistry, 2021, 46, 555-564.	0.7	1

#	Article	IF	Citations
57634	High-temperature phonon transport properties of SnSe from machine-learning interatomic potential. Journal of Physics Condensed Matter, 2021, 33, 405401.	0.7	24
57635	Potential antiferromagnetic Weyl nodal line state in <mml:math xmlns:mml="http://www.w3.org/1998/Math/MathML"><mml:msub><mml:mrow><mml:mi>LiTi</mml:mi></mml:mrow><mml:mn>2</mml:mn></mml:msub><mml:mi mathvariant="normal">O</mml:mi></mml:mrow><mml:mn>4</mml:mn></mml:msub></mml:math> material. Physical Review B, 2021, 104, .	1.1	14
57636	Superconductivity at 253â€¯K in lanthanumâ€“yttrium ternary hydrides. Materials Today, 2021, 48, 18-28.	8.3	119
57637	Electrochemical Oxidative Fluorination of an Oxide Perovskite. Chemistry of Materials, 2021, 33, 5757-5768.	3.2	11
57638	N-doped graphite encapsulated metal nanoparticles catalyst for removal of Bisphenol A via activation of peroxymonosulfate: A singlet oxygen-dominated oxidation process. Chemical Engineering Journal, 2021, 415, 128890.	6.6	108
57639	Epitaxial growth of atomically thick WSe2 nanoribbons. Vacuum, 2021, 189, 110254.	1.6	6
57640	Ensemble learning-iterative training machine learning for uncertainty quantification and automated experiment in atom-resolved microscopy. Npj Computational Materials, 2021, 7, .	3.5	26
57641	Noble gas bubbles in bcc metals: Ab initio-based theory and kinetic Monte Carlo modeling. Acta Materialia, 2021, 213, 116961.	3.8	13
57642	Theoretical and Experimental Studies of KLi6TaO6 as a Li-Ion Solid Electrolyte. Inorganic Chemistry, 2021, 60, 10371-10379.	1.9	4
57643	Effects of anions and alkyl chain length of imidazolium-based ionic liquids at the Au (111) surface on interfacial structure: a first-principles study. Green Chemical Engineering, 2021, 2, 402-402.	3.3	11
57644	Factors that influence hydrogen binding at metal-atop sites. Journal of Chemical Physics, 2021, 155, 024703.	1.2	7
57645	Two-dimensional binary metal-oxide quasicrystal approximants. 2D Materials, 2021, 8, 045002.	2.0	3
57646	Co-regulation of dispersion, exposure and defect sites on CeO2 (111) surface for catalytic oxidation of Hg0. Journal of Hazardous Materials, 2022, 424, 126566.	6.5	15
57647	Tailoring thermal stability of ceria-zirconia mixed oxide by doping of rare earth elements: From theory to experiment. Journal of Rare Earths, 2022, 40, 1272-1280.	2.5	3
57648	How the Copper Dopant Alters the Geometric and Photoelectronic Properties of the Leadâ€Free Cs 2 AgSbCl 6 Double Perovskite. Advanced Theory and Simulations, 2021, 4, 2100142.	1.3	6
57649	2D Vâ€“VI Binary Nanosheets with Square Lattice: A Theoretical Investigation. Physica Status Solidi (B): Basic Research, 2021, 258, 2100178.	0.7	4
57650	Transition Metal-Promoted VC(001) for Overall Water Splitting and Oxygen Reduction. Journal of Physical Chemistry C, 2021, 125, 14607-14615.	1.5	10
57651	Bi₂O₃ Induced Ultralong Cycle Lifespan and High Capacity of MnO₂ Nanotube Cathodes in Aqueous Zinc-Ion Batteries. ACS Applied Energy Materials, 2021, 4, 7355-7364.	2.5	14

#	Article	IF	Citations
57652	Density Functional Theory Studies of Heteroatom-Doped Graphene-like GaN Monolayers as Electrocatalysts for Oxygen Evolution and Reduction. ACS Applied Nano Materials, 2021, 4, 7125-7133.	2.4	9
57653	Atomic structure and electronic properties of the intercalated Pb atoms underneath a graphene layer. Carbon, 2021, 179, 151-158.	5.4	10
57654	Graphitization with Suppressed Carbon Loss for High-Quality Reduced Graphene Oxide. ACS Nano, 2021, 15, 11655-11666.	7.3	17
57655	Promoting Reversible Cathode Reactions in Magnesium Rechargeable Batteries Using Metastable Cubic MgMn₂O₄ Spinel Nanoparticles. ACS Applied Nano Materials, 2021, 4, 8328-8333.	2.4	17
57656	Hydrogen Atom and Molecule Adsorptions on FeCrAl (100) Surface: A First-Principle Study. Frontiers in Energy Research, 2021, 9, .	1.2	0
57657	Strain-Driven Switchable Thermal Conductivity in Ferroelastic PdSe₂. ACS Applied Materials & Interfaces, 2021, 13, 34724-34731.	4.0	14
57658	Controlling the Structural Robustness of Zirconium-Based Metal Organic Frameworks for Efficient Adsorption on Tetracycline Antibiotics. Water (Switzerland), 2021, 13, 1869.	1.2	13
57659	Full energy range primary radiation damage model. Physical Review Materials, 2021, 5, .	0.9	3
57660	Electronic structures and anisotropic carrier mobilities of monolayer ternary metal iodides MLaI₅ (M=Mg, Ca, Sr, Ba). Journal of Physics Condensed Matter, 2021, 33, 355301.	0.7	0
57661	Influence of Magnetic Moment on Single Atom Catalytic Activation Energy Barriers. Catalysis Letters, 2022, 152, 1347-1357.	1.4	6
57662	Screening of II-IV-V2 Materials for Photovoltaic Applications Based on Density Functional Theory Calculations. Crystals, 2021, 11, 883.	1.0	1
57663	<mml:math xmlns:mml="http://www.w3.org/1998/Math/MathML"><mml:mrow><mml:mi>Î²</mml:mi><mml:mtext>â^'</mml:mtext><mml:msub><: Pressure-induced three-dimensional Dirac semimetal with ultralow room-pressure lattice thermal conductivity. Physical Review B, 2021, 104, .	1.1	7
57664	Shear induced deformation twinning evolution in thermoelectric InSb. Npj Computational Materials, 2021, 7, .	3.5	16
57665	On the deactivation mechanisms of MnO2 electrocatalyst during operation in rechargeable zinc-air batteries studied via density functional theory. Journal of Alloys and Compounds, 2021, 869, 159280.	2.8	17
57666	Theoretical studies on the initial oxidation of metallic lithium anodes. Applied Surface Science, 2021, 555, 149447.	3.1	3
57667	Effect of carbon content on the microstructure and bonding properties of hot-rolling pure titanium clad carbon steel plates. Materials Science & Engineering A: Structural Materials: Properties, Microstructure and Processing, 2021, 820, 141572.	2.6	27
57668	A ductility criterion for bcc high entropy alloys. Journal of the Mechanics and Physics of Solids, 2021, 152, 104389.	2.3	44
57669	Two-transition behavior in Bi0.5Sb0.5SeI crystals. Journal of Physics and Chemistry of Solids, 2021, 154, 110031.	1.9	2

#	Article	IF	Citations
57670	Controlled Implantation of Phosphorous Atoms into a Silicon Surface Lattice with a Scanning Tunneling Microscopy Tip. ACS Applied Electronic Materials, 2021, 3, 3338-3345.	2.0	1
57671	Overlooked Binary Compounds Uncovered in the Reinspection of the Laâ€“Au System: Synthesis, Crystal Structures, and Electronic Properties of La₇Au₃, La₃Au₂, and La₃Au₄. Inorganic Chemistry, 2021, 60, 12158-12171.	1.9	1
57672	Bi2S3 and MoS2 Soft Coatings: A Comparative Study of Their Frictional Behavior Under Different Humidity Levels, Normal Loads, and Sliding Speeds. Tribology Letters, 2021, 69, 1.	1.2	8
57673	First-principles calculations to investigate the anisotropic elasticity and thermodynamic properties of FeAl3 under pressure effect. Results in Physics, 2021, 26, 104361.	2.0	12
57674	Theoretical Study of Ethylene Hydroformylation on Atomically Dispersed Rh/Al₂O₃ Catalysts: Reaction Mechanism and Influence of the ReO_x Promoter. ACS Catalysis, 2021, 11, 9506-9518.	5.5	31
57675	Second Floor of Flatland: Epitaxial Growth of Graphene on Hexagonal Boron Nitride. Small, 2021, 17, 2102747.	5.2	1
57676	The theoretical evaluation of new promising solid ion conductors for zinc-ion batteries. Journal of Physics: Conference Series, 2021, 1967, 012059.	0.3	0
57677	Octahedral rotations trigger electronic and magnetic transitions in strontium manganate under volume expansion. Journal of Physics Condensed Matter, 2021, 33, 365501.	0.7	0
57678	NiFeOx decorated Ge-hematite/perovskite for an efficient water splitting system. Nature Communications, 2021, 12, 4309.	5.8	71
57679	First-principles calculations of spontaneous polarization in ScAlN. Journal of Applied Physics, 2021, 130, .	1.1	32
57680	NIRâ€Activated Multimodal Photothermal/Chemodynamic/Magnetic Resonance Imaging Nanoplatform for Anticancer Therapy by Fe(II) Ions Doped MXenes (Feâ€Ti₃C₂). Small, 2021, 17, e2101705.	5.2	49
57681	Harnessing Selective Exsolution of Sn Metal to Enhance Electrical Conductivity in Oxygenâ€Deficient Perovskite Stannates. Advanced Functional Materials, 2021, 31, 2105086.	7.8	11
57682	G-Si C as an anode material for potassium-ion batteries insight from first principles. Materials Chemistry and Physics, 2021, 266, 124541.	2.0	4
57683	Computational screening toward quantum capacitance of transition-metals and vacancy doped/co-doped graphene as electrode of supercapacitors. Electrochimica Acta, 2021, 385, 138432.	2.6	27
57684	Computational Prediction of a Novel Superhard sp ³ Trigonal Carbon Allotrope with Bandgap Larger than Diamond. Chinese Physics Letters, 2021, 38, 076101.	1.3	14
57685	Molecular Beam Epitaxy Growth and Electronic Structures of Monolayer GdTe₃. Chinese Physics Letters, 2021, 38, 077102.	1.3	6
57686	Highly Efficient Activation of HCl Dissociation on Au(111) via Rotational Preexcitation. Journal of Physical Chemistry Letters, 2021, 12, 7252-7260.	2.1	8
57687	Charge Transport in Al₂S₃ and Its Relevance in Secondary Alâ€“S Batteries. Journal of Physical Chemistry C, 2021, 125, 16444-16450.	1.5	2

#	Article	IF	Citations
57688	Low-Cost Pt Alloys for Heterogeneous Catalysis Predicted by Density Functional Theory and Active Learning. Journal of Physical Chemistry Letters, 2021, 12, 7305-7311.	2.1	8
57689	NO2 Interactions with MoO3 and CuO at Atmospherically Relevant Pressures. Journal of Physical Chemistry C, 2021, 125, 16489-16497.	1.5	5
57690	Strain-tunable electronic structure of two-dimensional monolayer SiP. Modern Physics Letters B, 2021, 35, 2150404.	1.0	0
57691	Coordination Polymer-Derived Fe₃N Nanoparticles for Efficient Electrocatalytic Oxygen Evolution. Inorganic Chemistry, 2021, 60, 12136-12150.	1.9	21
57692	Phase Stability of Iron Nitride Fe4N at High Pressureâ€"Pressure-Dependent Evolution of Phase Equilibria in the Feâ€"N System. Materials, 2021, 14, 3963.	1.3	8
57693	Modulating the bonding properties of Li2MoO3 via non-equivalent cationic doping to enhance its stability and electrochemical performance for lithium-ion battery application. Ceramics International, 2021, 47, 18304-18313.	2.3	5
57694	Molecular insertion regulates the donor-acceptor interactions in cocrystals for the design of piezochromic luminescent materials. Nature Communications, 2021, 12, 4084.	5.8	41
57695	Nitrogen and phosphorus dual-doped porous carbons for high-rate potassium ion batteries. Carbon, 2021, 179, 33-41.	5.4	79
57696	Electrochemical Performance of 3D Network CsPbBr₃ Perovskite Anodes for Li-Ion Batteries: Experimental Venture with Theoretical Expedition. Journal of Physical Chemistry C, 2021, 125, 16892-16902.	1.5	18
57697	Coordination and Thermophysical Properties of Transition Metal Chlorocomplexes in LiClâ€"KCl Eutectic. Journal of Physical Chemistry B, 2021, 125, 8876-8887.	1.2	13
57698	Dynamics and Hysteresis of Hydrogen Intercalation and Deintercalation in Palladium Electrodes: A Multimodal In Situ X-ray Diffraction, Coulometry, and Computational Study. Chemistry of Materials, 2021, 33, 5872-5884.	3.2	11
57699	GW100: A Slater-Type Orbital Perspective. Journal of Chemical Theory and Computation, 2021, 17, 5080-5097.	2.3	21
57700	Method for Calculating Excited Electronic States Using Density Functionals and Direct Orbital Optimization with Real Space Grid or Plane-Wave Basis Set. Journal of Chemical Theory and Computation, 2021, 17, 5034-5049.	2.3	12
57701	Development of Density-Functional Tight-Binding Parameters for the Molecular Dynamics Simulation of Zirconia, Yttria, and Yttria-Stabilized Zirconia. ACS Omega, 2021, 6, 20530-20548.	1.6	8
57702	Atomically Dispersed Co to an End-Adsorbing Molecule for Excellent Biomimetically and Prime Sensitively Detecting O₂^{â€¢â€“} Released from Living Cells. Analytical Chemistry, 2021, 93, 10789-10797.	3.2	13
57703	Structure and Energetics of Dye-Sensitized NiO Interfaces in Water from Ab Initio MD and Large-Scale GW Calculations. Journal of Chemical Theory and Computation, 2021, 17, 5225-5238.	2.3	9
57704	Solution-Synthesized SnSe_{1â€“x}S_x: Dual-Functional Materials with Enhanced Electrochemical Storage and Thermoelectric Performance. ACS Applied Materials & Interfaces, 2021, 13, 37201-37211.	4.0	10
57705	Theoretical Approach toward Optimum Anion-Doping on MXene Catalysts for Hydrogen Evolution Reaction: an Ab Initio Thermodynamics Study. ACS Applied Materials & Interfaces, 2021, 13, 37035-37043.	4.0	17

#	Article	IF	Citations
57706	2D-VN2 MXene as a novel anode material for Li, Na and K ion batteries: Insights from the first-principles calculations. Journal of Colloid and Interface Science, 2021, 593, 51-58.	5.0	35
57707	Single-Metallic Thermoresponsive Coordination Network as a Dual-Parametric Luminescent Thermometer. ACS Applied Materials & Interfaces, 2021, 13, 35905-35913.	4.0	5
57708	An ultrasensitive molybdenum-based double-heterojunction phototransistor. Nature Communications, 2021, 12, 4094.	5.8	37
57709	First Principles Study of Oxygen Adsorption on Li-MO₂ (M = Mn, Ti and V) (110) Surface. Journal of the Electrochemical Society, 2021, 168, 070556.	1.3	5
57710	Robust Yellow-Violet Pigments Tuned by Site-Selective Manganese Chromophores. Inorganic Chemistry, 2021, 60, 11579-11590.	1.9	7
57711	Two-Dimensional In₂X₂Xâ€² (X and Xâ€² = S, Se, and Te) Monolayers with an Intrinsic Electric Field for High-Performance Photocatalytic and Piezoelectric Applications. ACS Applied Materials & Interfaces, 2021, 13, 34178-34187.	4.0	38
57712	Metastable V2O3 embedded in 2D N-doped carbon facilitates ion transport for stable and ultrafast sodium-ion storage. Chemical Engineering Journal, 2022, 430, 131156.	6.6	19
57713	First-principles study of the crystal structure, electronic structure, and transport properties of NiTe2 under pressure. Physical Review B, 2021, 104, .	1.1	4
57714	Computational Methods for Determining Martensitic Transformation Characteristics in Binary and Multicomponent Functional Materials. Metallofizika I Noveishie Tekhnologii, 2021, 43, 567-573.	0.2	0
57716	Spectroscopic Analysis of Rare-Earth Silicide Structures on the Si(111) Surface. Materials, 2021, 14, 4104.	1.3	3
57717	Real-space Green's function approach for x-ray spectra at high temperature. Physical Review B, 2021, 104, .	1.1	9
57718	Pt(dithiolene)-Based Colorimetric Chemosensors for Multiple Metal-Ion Sensing. Sustainability, 2021, 13, 8160.	1.6	3
57719	Reconstructed edges of T phase transition metal dichalcogenides. Materials Today Physics, 2021, 19, 100411.	2.9	12
57720	High-throughput design of high-performance lightweight high-entropy alloys. Nature Communications, 2021, 12, 4329.	5.8	112
57721	Superconductivity in an intermetallic oxide Hf3Pt4Ge2O*. Chinese Physics B, 2021, 30, 077403.	0.7	2
57722	Fabrication of sulfur-doped cove-edged graphene nanoribbons on Au(111)*. Chinese Physics B, 2021, 30, 077306.	0.7	6
57723	Quantum computation for predicting electron and phonon properties of solids. Journal of Physics Condensed Matter, 2021, 33, 385501.	0.7	5
57724	Crystal structures and formation mechanisms of boron-rich tungsten borides. Physical Review B, 2021, 104, .	1.1	10

#	Article	IF	Citations
57725	Spatially modulated orbital-selective ferromagnetism in La5Co2Ge3. Physical Review B, 2021, 104, .	1.1	0
57726	Cycloidal Magnetic Order Promoted by Labile Mixed Anionic Paths in M2(SeO3)F2 (M = Mn2+, Ni2+). Inorganic Chemistry, 2021, 60, 12001-12008.	1.9	1
57727	Phase transformation and mechanical stability of niobium aluminide (Nb3Al) induced by high pressures. Journal of Alloys and Compounds, 2021, 869, 159278.	2.8	6
57728	Phaseâ€change memory based on matched <scp>Geâ€Te</scp>, <scp>Sbâ€Te,</scp> and <scp>Inâ€Te</scp> octahedrons: Improved electrical performances and robust thermal stability. InformaÄnÃ-MateriÃ¡ly, 2021, 3, 1008-1015.	8.5	16
57729	Enhanced CO₂ Reduction Performance of BiCuSeOâ€Based Hybrid Catalysts by Synergetic Photoâ€Thermoelectric Effect. Advanced Functional Materials, 2021, 31, 2105001.	7.8	16
57730	Mechanism of transition metal interaction with graphene sheet reflected in its plasmonic excitations: Effect of gas adsorption phenomena studied by a combination of solid state and molecular orbital approaches. Applied Surface Science, 2021, 554, 149585.	3.1	1
57731	Possible half-metallic behavior of <mml:math xmlns:mml="http://www.w3.org/1998/Math/MathML"><mml:mrow><mml:msub><mml:mi>Co</mml:mi><mml:mrow><mml:mn>2</mml:mn> Heusler alloys: Theory and experiment. Physical Review B, 2021, 104, .	1.1	21
57732	First principle investigations of longâ€range magnetic exchange interactions via polyacene couplers. International Journal of Quantum Chemistry, 2021, 121, e26756.	1.0	6
57733	Selective photocatalytic reduction CO2 to CH4 on ultrathin TiO2 nanosheet via coordination activation. Applied Catalysis B: Environmental, 2021, 288, 120000.	10.8	87
57734	Tunable dynamical magnetoelectric effect in antiferromagnetic topological insulator MnBi2Te4 films. Npj Computational Materials, 2021, 7, .	3.5	14
57735	Trends in the Reactivity of Proximate Aluminum Sites in H-SSZ-13. Journal of Physical Chemistry C, 2021, 125, 16508-16515.	1.5	7
57736	An Ab Initio Molecular Dynamics Simulation of Liquid FeOâ€“SiO2 Silicate System with Sulfur Dissolving. Metallurgical and Materials Transactions B: Process Metallurgy and Materials Processing Science, 2021, 52, 3346-3353.	1.0	5
57737	Transformation of nanoscale zero-valent iron with antimony: Effects of the Sb spatial configuration. Chemical Engineering Journal, 2021, 416, 129073.	6.6	24
57738	CO2 capture intensified by solvents with metal hydride. Fuel Processing Technology, 2021, 218, 106859.	3.7	10
57739	Single Au atom supported defect mediated boron nitride monolayer as an efficient catalyst for acetylene hydrochlorination: A first principles study. Molecular Catalysis, 2021, 511, 111753.	1.0	7
57740	1T-MoS2 Coordinated Bimetal Atoms as Active Centers to Facilitate Hydrogen Generation. Materials, 2021, 14, 4073.	1.3	7
57741	Band alignment and interlayer hybridization in monolayer organic/WSe2 heterojunction. Nano Research, 0, , 1.	5.8	10
57742	Precise Layer Control and Electronic State Modulation of a Transition Metal Dichalcogenide via Phaseâ€Transitionâ€Induced Growth. Advanced Materials, 2022, 34, e2103286.	11.1	21

#	Article	IF	Citations
57743	Effect of alloying elements on stacking fault energies and twinnabilities in highâ€entropy transitionâ€metal carbides. Journal of the American Ceramic Society, 2021, 104, 6521-6532.	1.9	2
57744	Deep level study of chlorine-based dry etched Î²â€‰â^'â€‰Ga2O3. Journal of Applied Physics, 2021, 130, .	1.1	8
57745	Unveiling Mn4+ substitution in oxyfluoride phosphor Rb2MoO2F4:Mn4+ applied to wide-gamut fast-response backlight displays. Chemical Engineering Journal, 2021, 415, 128974.	6.6	56
57746	Giant heterogeneous magnetostriction induced by charge accumulation-mediated nanoinclusion formation in dual-phase nanostructured systems. Acta Materialia, 2021, 213, 116975.	3.8	20
57747	New Verbeekite-type polymorphic phase and rich phase diagram in the <mml:math xmlns:mml="http://www.w3.org/1998/Math/MathML"><mml:mrow><mml:msub><mml:mi>PdSe</mml:mi><mml:mrow><mml:mn>2</mml:mn> system. Physical Review B, 2021, 104, .	1.1	16
57748	Surface enrichment and diffusion enabling gradient-doping and coating of Ni-rich cathode toward Li-ion batteries. Nature Communications, 2021, 12, 4564.	5.8	153
57749	An Ice Thickness Measurement Method based on Up-looking Sonar. , 2021, , .		0
57750	Acid Sites of Phosphorus-Modified Zeosils. ACS Catalysis, 2021, 11, 9933-9948.	5.5	9
57751	Indium-doped ZnOas efficient photosensitive material for sunlight driven hydrogen generation and DSSC applications: integrated experimental and computational approach. Journal of Solid State Electrochemistry, 2021, 25, 2279-2292.	1.2	2
57752	Theoretical insight into two-dimensional g-C6N6/InSe van der Waals Heterostructure: A promising visible-light photocatalyst. Applied Surface Science, 2021, 554, 149465.	3.1	13
57753	The early growth process of helium blistering in tungsten and molybdenum: First-principles and statistical model calculations. Journal of Nuclear Materials, 2021, 550, 152938.	1.3	2
57754	Electronic Structure of Molecules, Surfaces, and Molecules on Surfaces with the Local Modified Beckeâ€“Johnson Exchangeâ€“Correlation Potential. Journal of Chemical Theory and Computation, 2021, 17, 4746-4755.	2.3	10
57755	The effect of water on the post-spinel transition and evidence for extreme water contents at the bottom of the transition zone. Earth and Planetary Science Letters, 2021, 565, 116909.	1.8	9
57756	Composition-tuned lithium aluminosilicate as a new humidity-sensing ceramic material with high sensitivity. Sensors and Actuators B: Chemical, 2021, 339, 129928.	4.0	4
57757	Controlled syngas production by electrocatalytic CO2 reduction on formulated Au25(SR)18 and PtAu24(SR)18 nanoclusters. Journal of Chemical Physics, 2021, 155, 014305.	1.2	24
57758	Influence of the second phase on protein adsorption on biodegradable Mg alloysâ€™ surfaces: Comparative experimental and molecular dynamics simulation studies. Acta Biomaterialia, 2021, 129, 323-332.	4.1	16
57759	Strain-tunable electronic and optical properties of h-BN/BC₃ heterostructure with enhanced electron mobility*. Chinese Physics B, 2021, 30, 076801.	0.7	2
57760	Structural and Magnetic Properties of BaFeO_{2.667} Synthesized by Oxidizing BaFeO_{2.5} Obtained via Nebulized Spray Pyrolysis. Inorganic Chemistry, 2021, 60, 10923-10933.	1.9	4

#	Article	IF	Citations
57761	2D MoO_{3â€“x}S_x/MoS₂van der Waals Assembly: A Tunable Heterojunction with Attractive Properties for Photocatalysis. ACS Applied Materials & Interfaces, 2021, 13, 36465-36474.	4.0	29
57762	Unveiling the Origin of Robust Ferroelectricity in Sub-2 nm Hafnium Zirconium Oxide Films. ACS Applied Materials & Interfaces, 2021, 13, 36499-36506.	4.0	24
57763	Survey of Crystallographic Data and Thermodynamic Stabilities of Pharmaceutical Solvates: A Step toward Predicting the Formation of Drug Solvent Adducts. Crystal Growth and Design, 2021, 21, 4362-4371.	1.4	3
57764	Structure and lithium-ion conductivity investigation of the Li_{7-x}La₃Zr_{2-x}Ta_xO₁₂ solid electrolytes. Journal of Physics: Conference Series, 2021, 1967, 012011.	0.3	2
57765	Effects of pyridine-like and pyrrolic-like nitrogen on the photoluminescence blue-shift of nitrogen-doped graphene oxide quantum dots. Journal of Luminescence, 2021, 235, 117983.	1.5	5
57766	Interfacial Dzyaloshinskii-Moriya interaction and perpendicular magnetic anisotropy at cobalt/diamond interfaces. Journal of Magnetism and Magnetic Materials, 2021, 529, 167852.	1.0	4
57767	Modulating Coordination Environment of Single-Atom Catalysts and Their Proximity to Photosensitive Units for Boosting MOF Photocatalysis. Journal of the American Chemical Society, 2021, 143, 12220-12229.	6.6	219
57768	Photoinduced Desorption Dynamics of CO from Pd(111): A Neural Network Approach. Journal of Chemical Theory and Computation, 2021, 17, 4648-4659.	2.3	15
57769	The crystal and electronic structures, dynamical stabilities and thermal properties, elastic constants and mechanical stabilities, Born effective charges and dielectric constants of a novel tetragonal ZrO2 phase: First-principles calculations. Journal of Physics and Chemistry of Solids, 2021, 154, 110046.	1.9	9
57770	Vanadium silicon-oxyfluoride nanowires for lithium storage systems: A perfect synergy for dynamic simple spot synthesis. Materials Science and Engineering B: Solid-State Materials for Advanced Technology, 2021, 269, 115164.	1.7	3
57771	A novel topological crystalline insulator in planar pentacoordinate OsS2 monolayer. Chemical Physics, 2021, 547, 111199.	0.9	1
57772	Transition metal solutes in Ni-based ternary model superalloys: Partitioning and effects on elastic properties from first-principles calculations. Computational Materials Science, 2021, 195, 110447.	1.4	3
57773	Improving the mechanical properties of HfC-based ceramics by exploring composition space of Hf1-Ta C and HfC1-N. Computational Materials Science, 2021, 195, 110464.	1.4	6
57774	Bulk Rashba Effect Splitting and Suppression in Polymorphs of Metal Iodine Perovskites. Journal of Physical Chemistry Letters, 2021, 12, 7245-7251.	2.1	9
57775	Effect of oxygen based functional groups on the nucleation of TiO2 by atomic layer deposition: A theoretical and experimental study. Materials Chemistry and Physics, 2021, 267, 124588.	2.0	5
57776	Unveiling structural, electronic properties and chemical bonding of (VH2)n (n=10â€“30) nanoclusters: DFT investigation. Journal of Molecular Graphics and Modelling, 2021, 106, 107907.	1.3	5
57777	The Vibrational and Thermodynamic Properties of CsPbI₃ Polymorphs: An Improved Description Based on the SCAN meta-GGA Functional. Journal of Physical Chemistry Letters, 2021, 12, 6613-6621.	2.1	24
57778	Reconfiguring graphene to achieve intrinsic negative Poissonâ€™s ratio and strain-tunable bandgap. Nanotechnology, 2021, 32, 415705.	1.3	2

#	Article	IF	Citations
57779	Modulation of Oxygen Vacancy on Midinfrared Lightâ€Induced Ferroelectricity of KTaO 3. Physica Status Solidi (B): Basic Research, 2021, 258, 2100099.	0.7	0
57780	The role of substrate on stabilizing new phases of two-dimensional tin. 2D Materials, 2021, 8, 045003.	2.0	6
57781	Computational Screening of Single Atoms Anchored on Defective Mo₂CO₂ MXene Nanosheet as Efficient Electrocatalysts for the Synthesis of Ammonia. Advanced Engineering Materials, 2021, 23, 2100405.	1.6	13
57782	High Curie temperatures in Gd-dihalide Janus monolayers. Journal of Applied Physics, 2021, 130, .	1.1	10
57783	Mechanical, Structural and Electronic Properties of CO2 Adsorbed Graphitic Carbon Nitride (g-C3N4) under Biaxial Tensile Strain. Materials, 2021, 14, 4110.	1.3	3
57784	Structure prediction of epitaxial inorganic interfaces by lattice and surface matching with Ogre. Journal of Chemical Physics, 2021, 155, 034111.	1.2	7
57785	Density Functional Theory and Machine Learning Description and Prediction of Oxygen Atom Chemisorption on Platinum Surfaces and Nanoparticles. ACS Omega, 2021, 6, 17424-17432.	1.6	9
57786	Orbital coupling of hetero-diatomic nickel-iron site for bifunctional electrocatalysis of CO2 reduction and oxygen evolution. Nature Communications, 2021, 12, 4088.	5.8	259
57787	Activating low-temperature NH3-SCR catalyst by breaking the strong interface between acid and redox sites: A case of model Ce2(SO4)3-CeO2 study. Journal of Catalysis, 2021, 399, 212-223.	3.1	61
57788	Computational Prediction of Superlubric Layered Heterojunctions. ACS Applied Materials & Interfaces, 2021, 13, 33600-33608.	4.0	11
57789	Thermal neutron scattering measurements and modeling of yttrium-hydrides for high temperature moderator applications. Annals of Nuclear Energy, 2021, 157, 108224.	0.9	6
57790	Alkali-Rich Antiperovskite M₃FCh (M = Li, Na; Ch = S, Se, Te): The Role of Anions in Phase Stability and Ionic Transport. Journal of the American Chemical Society, 2021, 143, 10668-10675.	6.6	21
57791	Microstructure and properties of NbVZr refractory complex concentrated alloys. Acta Materialia, 2021, 213, 116919.	3.8	14
57792	Atomically confined calcium in nitrogen-doped graphene as an efficient heterogeneous catalyst for hydrogen evolution. IScience, 2021, 24, 102728.	1.9	19
57793	Oxygen injection during fast vs slow passivation in aqueous solution. Acta Materialia, 2021, 213, 116898.	3.8	11
57794	Defect Properties and Lithium Incorporation in Li2ZrO3. Energies, 2021, 14, 3963.	1.6	6
57795	Thermodynamics and Catalytic Activity of Ruthenium Oxides Grown on Ruthenium Metal from a Machine Learning Atomic Simulation. Journal of Physical Chemistry C, 2021, 125, 17088-17096.	1.5	6
57796	Strain effects on monolayer MoSi2N4: Ideal strength and failure mechanism. Physica E: Low-Dimensional Systems and Nanostructures, 2021, 131, 114753.	1.3	33

#	Article	IF	Citations
57797	High Sodium-Ion Conductivity in Interlocked Quaternary Chalcogenides Built with Supertetrahedral Building Units. ACS Applied Energy Materials, 2021, 4, 7942-7951.	2.5	8
57798	Thermoelectric CoGeTe with an Orthorhombic Crystal Symmetry and Balance of the Electrical and Thermal Properties. Inorganic Chemistry, 2021, 60, 12331-12338.	1.9	1
57799	Dynamic Modification of Palladium Catalysts with Chain Alkylamines for the Selective Hydrogenation of Alkynes. ACS Applied Materials & Interfaces, 2021, 13, 31775-31784.	4.0	30
57800	Effect of One-Coordinated Atoms on the Electronic and Optical Properties of ZnSe Clusters. ACS Omega, 2021, 6, 18711-18718.	1.6	1
57801	Searching Ternary Oxides and Chalcogenides as Positive Electrodes for Calcium Batteries. Chemistry of Materials, 2021, 33, 5809-5821.	3.2	8
57802	Complete Reaction Cycle for Methane-to-Methanol Conversion over Cu-SSZ-13: First-Principles Calculations and Microkinetic Modeling. Journal of Physical Chemistry C, 2021, 125, 14681-14688.	1.5	10
57803	Atomic Layer Deposition of Ru for Replacing Cu-Interconnects. Chemistry of Materials, 2021, 33, 5639-5651.	3.2	27
57804	Large Perpendicular Magnetic Anisotropy in Ta/CoFeB/MgO on Full-Coverage Monolayer MoS₂ and First-Principles Study of Its Electronic Structure. ACS Applied Materials & Interfaces, 2021, 13, 32579-32589.	4.0	11
57805	Photoluminescent Re₆Q₈I₂ (Q = S, Se) Semiconducting Cluster Compounds. Chemistry of Materials, 2021, 33, 5780-5789.	3.2	5
57806	Probing the Effects of Acid Electrolyte Anions on Electrocatalyst Activity and Selectivity for the Oxygen Reduction Reaction. ChemElectroChem, 2021, 8, 2467-2478.	1.7	25
57807	A comparison research on replacements of Ba2+ by Lu3+ and Ba2+-Si4+ by Lu3+-Al3+ in BaSi2O2N2:Eu phosphors. Journal of Rare Earths, 2022, 40, 20-28.	2.5	15
57808	Electrically Controllable Van Der Waals Antiferromagnetic Spin Valve. Physical Review Applied, 2021, 16, .	1.5	9
57809	Superalkali NLi4 decorated graphene: A promising hydrogen storage material with high reversible capacity at ambient temperature. International Journal of Hydrogen Energy, 2021, 46, 23254-23262.	3.8	12
57810	An In Situ Synchrotron Dilatometry and Atomistic Study of Martensite and Carbide Formation during Partitioning and Tempering. Materials, 2021, 14, 3849.	1.3	0
57811	Spin-polarized electronic states and atomic reconstructions at antiperovskite <mml:math xmlns:mml="http://www.w3.org/1998/Math/MathML"><mml:mrow><mml:msub><mml:mi>Sr</mml:mi><mml:mn>3</mml:mn></mml:r mathvariant="normal">O</mml:mi><mml:mrow><mml:mo>(</mml:mo><mml:mn>001</mml:mn><mml:mo>)</mml:mo></mml:mrow> polar surfaces. Physical Review B, 2021, 104, .	1.1	4
57812	Data-processing technique for the Taipan â€œBe-filterâ€•neutron spectrometer at the Australian Nuclear Science and Technology Organisation. Review of Scientific Instruments, 2021, 92, 073304.	0.6	1
57813	In-situ growth of heterophase Ni nanocrystals on graphene for enhanced catalytic reduction of 4-nitrophenol. Nano Research, 2022, 15, 1230-1237.	5.8	21
57814	Enhanced photogalvanic effect in the two-dimensional MgCl2/ZnBr2 vertical heterojunction by inhomogenous tensile stress. Frontiers of Physics, 2022, 17, 1.	2.4	11

#	Article	IF	Citations
57815	Structural Characterization of the Delithiated Noncrystalline Phase in a Li-Rich Li₂VO₂F Cathode Material. Chemistry of Materials, 2021, 33, 5943-5950.	3.2	8
57816	Effect of Alloying Elements on the Stacking Fault Energy and Ductility in Mg₂Si Intermetallic Compounds. ACS Omega, 2021, 6, 20254-20263.	1.6	1
57817	Elaborating the high thermal storage and conductivity of molten NaCl-KCl-NaF eutectic from microstructures by FPMD simulations. Journal of Molecular Liquids, 2022, 346, 117054.	2.3	4
57818	Dimensionality-Inhibited Chemical Doping in Two-Dimensional Semiconductors: The Phosphorene and MoS₂ from Charge-Correction Method. Nano Letters, 2021, 21, 6711-6717.	4.5	14
57819	Theoretical studies of photocatalytic behaviors of isoelectronic Sn/Pb-doped TiO2: DFT+U. Applied Surface Science, 2021, 555, 149714.	3.1	10
57820	Ab initio study of helium in Li4SiO4 crystals: Electronic properties, migration, and vacancy capture mechanism. Ceramics International, 2021, 47, 20239-20247.	2.3	3
57821	Power generation and thermoelectric cooling enabled by momentum and energy multiband alignments. Science, 2021, 373, 556-561.	6.0	270
57822	Nonconventional nucleation and growth of Au nanoparticles with improved adhesion on oxygen-excessive oxide surfaces. Applied Surface Science, 2021, 553, 149385.	3.1	13
57823	Interstitial lithium doping in SrTiO₃. AIP Advances, 2021, 11, 075029.	0.6	2
57824	Ab-Initio Study of Magnetically Intercalated Platinum Diselenide: The Impact of Platinum Vacancies. Materials, 2021, 14, 4167.	1.3	6
57825	Raman Spectrum of layered Ferromagnetic Material VI3 from First-principles. , 2021, , .		0
57826	Engineering single-atomic ruthenium catalytic sites on defective nickel-iron layered double hydroxide for overall water splitting. Nature Communications, 2021, 12, 4587.	5.8	401
57827	Electronic and Magnetic Properties of Building Blocks of Mn and Fe Atomic Chains on Nb(110). Nanomaterials, 2021, 11, 1933.	1.9	7
57828	All-Oxide pâ€“n Junction Thermoelectric Generator Based on SnO_x and ZnO Thin Films. ACS Applied Materials & Interfaces, 2021, 13, 35187-35196.	4.0	21
57829	Epitaxial Molybdenum Disulfide/Gallium Nitride Junctions: Low-Knee-Voltage Schottky-Diode Behavior at Optimized Interfaces. ACS Applied Materials & Interfaces, 2021, 13, 35105-35112.	4.0	3
57830	A Pseudopotential Study of Structural, Mechanical, and Lattice Dynamics Behavior of the Binary Intermetallic Yttrium Tristannide YSn 3. Physica Status Solidi (B): Basic Research, 2021, 258, 2100219.	0.7	1
57831	High-Performance Single-Atom Catalysts for CO Oxidation: the Importance of Hydrogen Bonds and Adsorption Strength of the Reactant. Journal of Physical Chemistry C, 2021, 125, 15987-15993.	1.5	2
57832	Determining the Molecular Orientation on the Metal Nanoparticle Surface through Surface-Enhanced Raman Spectroscopy and Density Functional Theory Simulations. Journal of Physical Chemistry C, 2021, 125, 16289-16295.	1.5	8

#	Article	IF	Citations
57833	Intersecting topological nodal ring and nodal wall states in superhard superconductor <mml:math xmlns:mml="http://www.w3.org/1998/Math/MathML"><mml:msub><mml:mi>FeB</mml:mi><mml:mn>4</mml:mn></mml:msub></mm Physical Review Materials, 2021, 5, .	3.1	14
57834	Lattice dynamics and magnetic exchange interactions in <mml:math xmlns:mml="http://www.w3.org/1998/Math/MathML"><mml:mrow><mml:msub><mml:mi>GeCo</mml:mi><mml:mn>2</mml:mn></mml:msub><mml:mi mathvariant="normal">O</mml:mi><mml:mn>4</mml:mn></mml:mrow></mml:math> : A spinel with <mml:math xmlns:mml="http://www.w3.org/1998/Math/MathML"><mml:mrow><mml:mi>S</mml:mi><mml:mo>=</mml:mo><mml:mfrac> pyrochlore lattice. Physical Review B, 2021, 104,	1.1	7
57835	Electronic and magnetic properties of VOCl/FeOCl antiferromagnetic heterobilayers. 2D Materials, 2021, 8, 045008.	2.0	5
57836	Accurate prediction of bonding properties by a machine learningâ€“based model using isolated states before bonding. Applied Physics Express, 2021, 14, 085503.	1.1	3
57837	Three-dimensional acetylenic modified graphene for high-performance optoelectronics and topological materials. Npj Computational Materials, 2021, 7, .	3.5	4
57838	Investigating the electronic origins of the repulsion between substitutional and interstitial solutes in hcp Ti. Physical Review Materials, 2021, 5, .	0.9	1
57839	Heat transport through propagon-phonon interaction in epitaxial amorphous-crystalline multilayers. Communications Physics, 2021, 4, .	2.0	8
57840	Ligand size effects in two-dimensional hybrid copper halide perovskites crystals. Communications Materials, 2021, 2, .	2.9	12
57841	Machine-learning Interatomic Potential for Predicting Grain Boundary Properties in Semiconductors. Materia Japan, 2021, 60, 416-419.	0.1	0
57842	Melting line of calcium characterized by in situ LH-DAC XRD and first-principles calculations. Scientific Reports, 2021, 11, 15025.	1.6	2
57843	A two-dimensional type I superionic conductor. Nature Materials, 2021, 20, 1683-1688.	13.3	15
57844	Engineering Bimetallic Copperâ€Tin Based Coreâ€Shell Alloy@Oxide Nanowire as Efficient Catalyst for Electrochemical CO₂ Reduction. ChemElectroChem, 2021, 8, 2701-2707.	1.7	9
57845	Ni(OH)₂ Templated Synthesis of Ultrathin Ni₃S₂ Nanosheets as Bifunctional Electrocatalyst for Overall Water Splitting. Small, 2021, 17, e2102097.	5.2	54
57846	High-pressure behavior of disodered kesterite-type Cu2ZnSnS4. Applied Physics A: Materials Science and Processing, 2021, 127, 1.	1.1	3
57847	First-principles molecular dynamics study of the behavior of tritium in molten LiF-BeF2 eutectic. Journal of Molecular Liquids, 2022, 345, 117027.	2.3	5
57848	Effect of Pressure on Mechanical and Thermal Properties of SnSe2. International Journal of Thermophysics, 2021, 42, 1.	1.0	3
57849	Comprehensive Mechanism of CO₂ Electroreduction toward Ethylene and Ethanol: The Solvent Effect from Explicit Waterâ€“Cu(100) Interface Models. ACS Catalysis, 2021, 11, 9688-9701.	5.5	65
57850	Oxidative Dehydrogenation of Ethane with CO₂ as a Soft Oxidant over a PtCe Bimetallic Catalyst. ACS Catalysis, 2021, 11, 9221-9232.	5.5	24

#	Article	IF	Citations
57851	Microscopic understanding about adsorption and transport of different Cr(VI) species at mineral interfaces. Journal of Hazardous Materials, 2021, 414, 125485.	6.5	20
57852	Effects of Charge Transfer on the Critical Distance of the Interlayer Ferromagnetic Order Transition in SCrSeâ€Based van der Waals Bilayers. Physica Status Solidi - Rapid Research Letters, 2021, 15, 2100213.	1.2	0
57853	Robust, Multi-Length-Scale, Machine Learning Potential for Agâ€“Au Bimetallic Alloys from Clusters to Bulk Materials. Journal of Physical Chemistry C, 2021, 125, 17438-17447.	1.5	31
57854	Roomâ€Temperature Negative Differential Resistance in Surfaceâ€Supported Metalâ€Organic Framework Vertical Heterojunctions. Small, 2021, 17, e2101475.	5.2	6
57855	Polarization rotation boosts strong piezoelectric response in the lead-free perovskite ferroelectric <mml:math xmlns:mml="http://www.w3.org/1998/Math/MathML"><mml:mrow><mml:msub><mml:mi mathvariant="normal">K</mml:mi><mml:mrow><mml:mn>0.5</mml:mn></mml:mrow></mml:msub><mml:msub><mml:mi>Na</mml:mi><mml:mr Physical Review B, 2021, 104, .	1.1	9
57856	Synergistic effect of S-bridged Fe-Ni group on hydrogen evolution for pentlandite. Journal of Colloid and Interface Science, 2021, 593, 116-124.	5.0	13
57857	Interaction of Water Molecule with Two-Dimensional Tin Dioxide. Journal of Contemporary Physics, 2021, 56, 265-268.	0.1	0
57858	Anomalous Anisotropy of the Piezoelectric Response in 2D Copperâ€Based Ternary Chalcogenides CuMX₂. Physica Status Solidi - Rapid Research Letters, 2021, 15, 2100304.	1.2	3
57859	Highly Efficient Uniaxial Inâ€Plane Stretching of a 2D Material via Ion Insertion. Advanced Materials, 2021, 33, e2101875.	11.1	16
57860	Simulation of Potential-Dependent Activation Energies in Electrocatalysis: Mechanism of Oâ€“O Bond Formation on RuO₂. Journal of Physical Chemistry C, 2021, 125, 15243-15250.	1.5	28
57861	Microstructural and compositional design principles for Mo-V-Nb-Ti-Zr multi-principal element alloys: a high-throughput first-principles study. Acta Materialia, 2021, 213, 116958.	3.8	14
57862	Tunable Schottky barriers and electronic properties in van der Waals heterostructures of semiconducting monolayer gold sulfides and graphene. Applied Surface Science, 2021, 555, 149654.	3.1	7
57863	Assessing the performances of different continuum solvation models for the calculation of hydration energies of molecules, polymers and surfaces: a comparison between the SMD, VASPsol and FDPB models. Theoretical Chemistry Accounts, 2021, 140, 1.	0.5	13
57864	Intrinsic Defect Limit to the Growth of Orthorhombic HfO₂ and (Hf,Zr)O₂ with Strong Ferroelectricity: Firstâ€Principles Insights. Advanced Functional Materials, 2021, 31, 2104913.	7.8	39
57865	Unraveling the Intermediate Reaction Complexes and Critical Role of Support-Derived Oxygen Atoms in CO Oxidation on Single-Atom Pt/CeO₂. ACS Catalysis, 2021, 11, 8701-8715.	5.5	51
57866	Charge Density Waves and Electronic Properties of Superconducting Kagome Metals. Physical Review Letters, 2021, 127, 046401.	2.9	238
57867	Effects of yttrium on mechanical and cohesion properties of zirconium diboride. Vacuum, 2021, 189, 110246.	1.6	4
57868	Computational evaluation of superalkali-decorated graphene nanoribbon as advanced hydrogen storage materials. International Journal of Hydrogen Energy, 2021, 46, 24510-24516.	3.8	20

#	Article	IF	Citations
57869	Boosting electrocatalytic oxidation of formic acid on SnO2-decorated Pd nanosheets. Journal of Catalysis, 2021, 399, 8-14.	3.1	11
57870	Discovering the role of substrate in aldehyde hydrogenation. Journal of Catalysis, 2021, 399, 162-169.	3.1	9
57871	Constructing Active Sites from Atomicâ€Scale Geometrical Engineering in Spinel Oxide Solid Solutions for Efficient and Robust Oxygen Evolution Reaction Electrocatalysts. Advanced Science, 2021, 8, e2101653.	5.6	31
57872	Tuning 2D magnetism in Fe3+XGeTe2 films by element doping. National Science Review, 2022, 9, .	4.6	7
57873	A First-Principles-Based Microkinetic Study of CO₂ Reduction to CH₃OH over In₂O₃(110). ACS Catalysis, 2021, 11, 9996-10006.	5.5	19
57874	Identification of a Selectivity Descriptor for Propane Dehydrogenation through Density Functional and Microkinetic Analysis on Pure Pd and Pd Alloys. ACS Catalysis, 2021, 11, 9588-9604.	5.5	21
57875	The mechanism of sorbitol dehydration in hot acidic solutions. Journal of Computational Chemistry, 2021, 42, 1783-1791.	1.5	1
57876	Designing super-chalcogens and super-pnictogens with icosahedral metallic clusters: A case application of electron counting rules. Chemical Physics Letters, 2021, 775, 138671.	1.2	0
57877	Nucleation and growth mechanisms of Î³â€™â€™ phase with single-unit-cell height in Mg-RE-Zn(Ag) series alloys: a first-principles study. Journal of Materials Science and Technology, 2021, 79, 133-140.	5.6	6
57878	<mml:math xmlns:mml="http://www.w3.org/1998/Math/MathML"><mml:mrow><mml:mi>La</mml:mi><mml:msub><mml:mi>BH</mml:mi><mml:m : Towards high- <mml:math xmlns:mml="http://www.w3.org/1998/Math/MathML"><mml:msub><mml:mi>T</mml:mi><mml:mi>c</mml:mi></mml:msub></mml:m low-pressure superconductivity in ternary superhydrides. Physical Review B, 2021, 104, .	1.1	95
57879	Vibrational and vibronic structure of isolated point defects: The nitrogen-vacancy center in diamond. Physical Review B, 2021, 104, .	1.1	24
57880	Doping-controllable high temperature magnetic semiconductor. Physica E: Low-Dimensional Systems and Nanostructures, 2021, 131, 114731.	1.3	3
57881	H2O splitting on Run/TiO2(101) surface: Lowered energy barrier due to charge transfer at interface. Physica E: Low-Dimensional Systems and Nanostructures, 2021, 131, 114730.	1.3	2
57882	Prediction quantum anomalous Hall Effect on two-dimensional X3Y2 films. Physica E: Low-Dimensional Systems and Nanostructures, 2021, 131, 114735.	1.3	0
57883	Depression of critical temperature due to residual strain induced by PLD deposition on YBa2Cu3O7-Î´ thin films. Materials Chemistry and Physics, 2021, 266, 124507.	2.0	7
57885	Atomic Structure of the Cu₂O(111) Surface: A Transmission Electron Microscopy and DFTâ€‰+â€‰U Study. Physica Status Solidi (B): Basic Research, 2021, 258, 2100185.	0.7	3
57886	Triple degenerate point in three dimensions: Theory and realization. Physical Review B, 2021, 104, .	1.1	8
57887	Giant Spin Splitting in Chiral Perovskites Based on Local Electrical Field Engineering. Journal of Physical Chemistry Letters, 2021, 12, 6492-6498.	2.1	12

#	Article	IF	Citations
57888	Spin State and Spinâ€šState Transition of Co 3+ Ion in BiCoO 3. Physica Status Solidi (B): Basic Research, 2021, 258, 2100117.	0.7	4
57889	Dynamic structure change of Cu nanoparticles on carbon supports for <scp>CO₂</scp> electroâ€reduction toward multicarbon products. InformaÄnÃ-MateriÃ¡ly, 2021, 3, 1285-1294.	8.5	22
57890	The electronic origins of the â€œrare earthâ€•texture effect in magnesium alloys. Scientific Reports, 2021, 11, 14159.	1.6	17
57891	First principle study of anisotropic thermoelectric material: Sb2Si2Te6. Journal of Applied Physics, 2021, 130, 025102.	1.1	3
57892	Li-ion intercalation enhanced ferromagnetism in van der Waals Fe3GeTe2 bilayer. Applied Physics Letters, 2021, 119, .	1.5	20
57893	Correlation effect on electronic and lattice properties of cerium oxides: Insights from density functional theory to dynamical mean-field theory. Chemical Physics, 2021, 547, 111194.	0.9	1
57894	Embryonic zeolites for highly efficient synthesis of dimethyl ether from syngas. Microporous and Mesoporous Materials, 2021, 322, 111138.	2.2	9
57895	Point defects-induced adsorption and diffusion of lithium on monolayer titanium disulfide: A first-principles study. Applied Surface Science, 2021, 553, 149448.	3.1	11
57896	Understanding the Features of Crystal Structure, Electronic Structure and Electrical Conductivity of RuO2-SiO2 Binary Oxides. International Journal of Electrochemical Science, 2021, 16, 210754.	0.5	1
57897	Defect-induced modulation of magnetic, electronic, and optical properties of the double-perovskite oxide <mml:math xmlns:mml="http://www.w3.org/1998/Math/MathML"><mml:mrow><mml:msub><mml:mi>La</mml:mi><mml:mn>2</mml:mn></mml:mn></mml:r Physical Review B, 2021, 104, .	1.1	6
57898	First-principles and thermodynamic analysis for gas phase reactions and structures of the SiC(0001) surface under conventional CVD and Halide CVD environments. Japanese Journal of Applied Physics, 2021, 60, 085503.	0.8	5
57899	Selective electrocatalytic semihydrogenation of acetylene impurities for the production of polymer-grade ethylene. Nature Catalysis, 2021, 4, 557-564.	16.1	90
57900	Syngas to ethanol on MoCu(2Â1Â1) surface: Effect of promoter Mo on C O bond breaking and C C bond formation. Chinese Journal of Chemical Engineering, 2022, 45, 78-89.	1.7	2
57901	Theoretical Investigation of Proton Diffusion in Dionâ€“Jacobson Layered Perovskite RbBiNb2O7. Nanomaterials, 2021, 11, 1953.	1.9	5
57902	Comparative study of adsorptions, reactions and electronic properties of U atoms on Cu(111), Ag(111), Au(111) and Ru(0001) surfaces. Nanotechnology, 2021, 32, 425704.	1.3	3
57903	Electronic and optical properties of 3N-doped graphdiyne/MoS2 heterostructures tuned by biaxial strain and external electric field. Chinese Physics B, 0, , .	0.7	1
57904	Continuous network structure of two-dimensional silica across a supporting metal step edge: An atomic scale study. Physical Review Materials, 2021, 5, .	0.9	6
57905	Development of Thermokinetic Tools for Phase Transformation Studies of Zr Alloys for Both In-Service and LOCA Conditions. , 2021, , 833-854.		0

#	Article	IF	Citations
57906	Structural, mechanical, electronic properties and Debye temperature of tungsten-technetium alloy: A first-principles study. Fusion Engineering and Design, 2021, 168, 112433.	1.0	10
57907	Arc Synthesis, Crystal Structure, and Photoelectrochemistry of Copper(I) Tungstate. ACS Applied Materials & Interfaces, 2021, 13, 32865-32875.	4.0	11
57908	Cation-Disordered O3-Na_{0.8}Ni_{0.6}Sb_{0.4}O₂ Cathode for High-Voltage Sodium-Ion Batteries. ACS Applied Materials & Interfaces, 2021, 13, 32948-32956.	4.0	21
57909	First-principles investigation of structural, electronic, mechanical, and lattice dynamical properties of Ti-Au intermetallic. Ferroelectrics, 2021, 578, 40-50.	0.3	0
57910	AgPd, AuPd, and AuPt Nanoalloys with Ag- or Au-Rich Compositions: Modeling Chemical Ordering and Optical Properties. Journal of Physical Chemistry C, 2021, 125, 17372-17384.	1.5	15
57911	Symmetry-enforced straight nodal-line phonons. Physical Review B, 2021, 104, .	1.1	37
57912	Structural, Thermal, and Electronic Properties of Twoâ€Dimensional Gallium Oxide (Î²â€Ga₂O₃) from Firstâ€Principles Design. ChemPhysChem, 2021, 22, 2362-2370.	1.0	10
57913	Magnetic and phonon transport properties of two-dimensional room-temperature ferromagnet VSe2. Journal of Materials Science, 2021, 56, 15844-15858.	1.7	11
57914	Structural and Chemical Transformations of Zinc Oxide Ultrathin Films on Pd(111) Surfaces. ACS Applied Materials & Interfaces, 2021, 13, 35113-35123.	4.0	10
57915	Ultra-low lattice thermal conductivity and high thermoelectric efficiency of K3AuO. Journal of Applied Physics, 2021, 130, 045101.	1.1	2
57916	Electronic and optical properties of boron-based hybrid monolayers. Nanotechnology, 2021, 32, 415203.	1.3	2
57917	Defect-free interface between amorphous (Al2O3)1â^'x(SiO2)x and GaN(0001) revealed by first-principles simulated annealing technique. Applied Physics Letters, 2021, 119, .	1.5	2
57918	Ferromagnetism and giant magnetoresistance in zinc-blende FeAs monolayers embedded in semiconductor structures. Nature Communications, 2021, 12, 4201.	5.8	5
57919	Structure and magnetic properties of the S = 3/2 zigzag spin chain antiferromagnet BaCoTe2O7. Science China: Physics, Mechanics and Astronomy, 2021, 64, 1.	2.0	11
57920	Selfconsistent random phase approximation methods. Journal of Chemical Physics, 2021, 155, 040902.	1.2	16
57921	Cu[Ni(2,3-pyrazinedithiolate)₂] Metalâ€“Organic Framework for Electrocatalytic Hydrogen Evolution. ACS Applied Materials & Interfaces, 2021, 13, 34419-34427.	4.0	23
57922	Barriers to carriers: faults and recombination in non-stoichiometric perovskite scintillators. Journal of Materials Science, 2021, 56, 15812-15823.	1.7	0
57923	The Verification of Thermoelectric Performance Obtained by High-Throughput Calculations: The Case of GeS2 Monolayer From First-Principles Calculations. Frontiers in Materials, 2021, 8, .	1.2	5

#	Article	IF	Citations
57924	First-Principles Study on the Elastic Constants and Structural and Mechanical Properties of 30Â° Partial Dislocation in GaAs. Advances in Materials Science and Engineering, 2021, 2021, 1-7.	1.0	0
57925	Modulating reaction pathways of formic acid oxidation for optimized electrocatalytic performance of PtAu/CoNC. Nano Research, 2022, 15, 1221-1229.	5.8	22
57926	Electronic Structure of Ternary Alloys of Group III and Rare Earth Nitrides. Materials, 2021, 14, 4115.	1.3	5
57927	Dy adsorption on and intercalation under graphene on 6 H -SiC(0001) surface from first-principles calculations. Physical Review Materials, 2021, 5, .	0.9	12
57928	Tuning Schottky Barrier and Contact Type of Metalâ€“Semiconductor in Ti₃C₂T₂/MoS₂ (T = F, O, OH) by Strain: A First-Principles Study. Journal of Physical Chemistry C, 2021, 125, 16200-16210.	1.5	29
57929	Impact of Electronic Properties of Grain Boundaries on the Solid Electrolyte Interphases (SEIs) in Li-ion Batteries. Journal of Physical Chemistry C, 2021, 125, 15821-15829.	1.5	18
57930	Computational design of Mg alloys with minimal galvanic corrosion. Journal of Magnesium and Alloys, 2022, 10, 1972-1980.	5.5	15
57931	Ultrafast dynamics of the surface photovoltage in potassium-doped black phosphorus. Physical Review B, 2021, 104, .	1.1	9
57932	Engineering Anisotropic Klein Tunneling in Black Phosphorene through Elemental Substitution. Physica Status Solidi (B): Basic Research, 2021, 258, 2100071.	0.7	2
57933	MXenes@Te as a composite material for high-performance aluminum batteries. Science China Materials, 2022, 65, 85-94.	3.5	10
57934	Electric-field tuning of the magnetic properties of bilayer <mml:math xmlns:mml="http://www.w3.org/1998/Math/MathML"><mml:msub><mml:mi>VI</mml:mi><mml:mn>3</mml:mn></mml:msub></mml:m : A first-principles study. Physical Review B, 2021, 104, .	1.1	
57935	Bulk Diffusion of Cl through O Vacancies in Î±-Cr₂O₃: A Density Functional Theory Study. Journal of the Electrochemical Society, 2021, 168, 071503.	1.3	3
57936	Self-learning hybrid Monte Carlo method for isothermalâ€“isobaric ensemble: Application to liquid silica. Journal of Chemical Physics, 2021, 155, 034106.	1.2	6
57937	Realizing high thermoelectric performance in hot-pressed polycrystalline AlxSn1-xSe through band engineering tuning. Journal of Materiomics, 2022, 8, 475-488.	2.8	9
57938	A new route of synthesizing atomically thin 2D materials embedded in bulk oxides. Journal of Applied Physics, 2021, 130, 035302.	1.1	0
57939	qeirreps: An open-source program for Quantum ESPRESSO to compute irreducible representations of Bloch wavefunctions. Computer Physics Communications, 2021, 264, 107948.	3.0	17
57940	Toward the Development of a High-Voltage Mg Cathode Using a Chromium Sulfide Host. , 2021, 3, 1213-1220.		12
57941	Light-Emitting 0D Hybrid Metal Halide (C₃H₁₂N₂)₂Sb₂Cl₁₀ with Antimony Dimers. Inorganic Chemistry, 2021, 60, 11429-11434.	1.9	13

#	Article	IF	Citations
57942	Formation of porous ice frameworks at room temperature. Proceedings of the National Academy of Sciences of the United States of America, 2021, 118, .	3.3	7
57943	Local and Bulk Probe of Vanadium-Substituted Î±-Manganese Oxide (Î±-K_xV_yMn_{8â€“y}O₁₆) Lithium Electrochemistry. Inorganic Chemistry, 2021, 60, 10398-10414.	1.9	3
57944	Novel Thermoelectric Character of Rhenium Carbonitride, ReCN. ACS Omega, 2021, 6, 18364-18369.	1.6	2
57945	Energy Decomposition Analysis of the Adhesive Interaction between an Epoxy Resin Layer and a Silica Surface. Langmuir, 2021, 37, 8417-8425.	1.6	15
57946	Cobalt Telluride: A Highly Efficient Trifunctional Electrocatalyst for Water Splitting and Oxygen Reduction. ACS Applied Energy Materials, 2021, 4, 8158-8174.	2.5	36
57947	Finite-temperature interplay of structural stability, chemical complexity, and elastic properties of bcc multicomponent alloys from ab initio trained machine-learning potentials. Physical Review Materials, 2021, 5, .	0.9	9
57948	Antiperovskite Gd₃SnC: Unusual Coexistence of Ferromagnetism and Heavy Fermions in Gd Lattice. Advanced Materials, 2021, 33, e2102958.	11.1	2
57949	The Wetâ€Oxidation of a Cu(111) Foil Coated by Single Crystal Graphene. Advanced Materials, 2021, 33, e2102697.	11.1	17
57950	On the Catalytic Activity of Sn Monomers and Dimers at Graphene Edges and the Synchronized Edge Dependence of Diffusing Atoms in Sn Dimers. Advanced Functional Materials, 2021, 31, 2104340.	7.8	4
57951	Unveiling Role of Sulfate Ion in Nickelâ€Iron (oxy)Hydroxide with Enhanced Oxygenâ€Evolving Performance. Advanced Functional Materials, 2021, 31, 2102772.	7.8	158
57952	Pressure-induced high-temperature superconductivity retained without pressure in FeSe single crystals. Proceedings of the National Academy of Sciences of the United States of America, 2021, 118, .	3.3	30
57953	3D-to-2D phase transformation through highly ordered 1D crystals from transition-metal oxides to dichalcogenides. Materials Today, 2021, 47, 38-44.	8.3	3
57954	Î´-SnS: An Emerging Bidirectional Auxetic Direct Semiconductor with Desirable Carrier Mobility and High-Performance Catalytic Behavior toward the Water-Splitting Reaction. ACS Applied Materials & Interfaces, 2021, 13, 31934-31946.	4.0	25
57955	Insights into the Rich Polymorphism of the Na⁺ Ion Conductor Na₃PS₄ from the Perspective of Variable-Temperature Diffraction and Spectroscopy. Chemistry of Materials, 2021, 33, 5652-5667.	3.2	23
57956	The stochastic self-consistent harmonic approximation: calculating vibrational properties of materials with full quantum and anharmonic effects. Journal of Physics Condensed Matter, 2021, 33, 363001.	0.7	70
57957	High tensile strength and thermal conductivity in BeO monolayer: A first-principles study. FlatChem, 2021, 28, 100257.	2.8	24
57958	Optical manipulation of electronic dimensionality in a quantum material. Nature, 2021, 595, 239-244.	13.7	49
57959	Unravelling the chemical heterogeneity of Î±-Pu2O3(111) surface with the site-selective adsorption of H2O and CO2. Journal of Alloys and Compounds, 2021, 870, 159371.	2.8	1

#	Article	IF	Citations
57960	Dominant role of M element on the stability and properties of Prussian blue analogues NaxMFe(CN)6 (MÂ=Â3d transition metal) as cathode material for the sodium-ion batteries. Journal of Alloys and Compounds, 2021, 870, 159533.	2.8	12
57961	FeNi nanoparticles on Mo2TiC2Tx MXene@nickel foam as robust electrocatalysts for overall water splitting. Nano Research, 2021, 14, 3474-3481.	5.8	56
57962	Selective electrocatalytic synthesis of urea with nitrate and carbon dioxide. Nature Sustainability, 2021, 4, 868-876.	11.5	264
57963	Computational identification of B substitutional doped C<mml:math xmlns:mml="http://www.w3.org/1998/Math/MathML" altimg="si2.svg"><mml:msub><mml:mrow /><mml:mn>9</mml:mn></mml:msub></mml:math>N<mml:math xmlns:mml="http://www.w3.org/1998/Math/MathML" altimg="si3.svg"><mml:msub><mml:mrow /><mml:mn>4</mml:mn></mml:msub></mml:math> monolayer for electrocatalytic N<mml:math xmlns:mml="http://www.w3.org/1998/Math/MathML" altimg="si10.svg"><mml:msub><mml:mrow />	1.0	8
57964	Insights on the Catalytic Active Site for CO2 Reduction on Copper-based Catalyst: A DFT study. Molecular Catalysis, 2021, 511, 111725.	1.0	9
57965	Sb³⁺â€Doping in Cesium Zinc Halides Single Crystals Enabling Highâ€Efficiency Nearâ€Infrared Emission. Advanced Functional Materials, 2021, 31, 2105316.	7.8	199
57966	High-Throughput Computation of New Carbon Allotropes with Diverse Hybridization and Ultrahigh Hardness. Crystals, 2021, 11, 783.	1.0	23
57967	Comprehensive Study of Lithium Adsorption and Diffusion on Janus Mo/WXY (X, Y = S, Se, Te) Using First-Principles and Machine Learning Approaches. ACS Applied Materials & Interfaces, 2021, 13, 36388-36406.	4.0	52
57968	Optical absorption spectra of Xene and Xane (X = silic, german, stan). Journal of Physics Condensed Matter, 2021, 33, 355701.	0.7	3
57969	Interfacing or Doping? Role of Ce in Highly Promoted Water Oxidation of NiFeâ€Layered Double Hydroxide. Advanced Energy Materials, 2021, 11, 2101281.	10.2	120
57970	Ultrathin CuNi Nanosheets for CO₂ Reduction and O₂ Reduction Reaction in Fuel Cells. , 2021, 3, 1143-1150.		23
57971	High-Throughput Screening of Alloy Catalysts for Dry Methane Reforming. ACS Catalysis, 2021, 11, 8881-8894.	5.5	47
57972	Towards identification of silicon vacancy-related electron paramagnetic resonance centers in 4H -SiC. Physical Review B, 2021, 104, .	1.1	9
57973	Temperature measurement by extended X-ray absorption fine structure: A new theoretical development. Vacuum, 2021, 189, 110274.	1.6	0
57974	Absence of CO2 electroreduction on copper, gold and silver electrodes without metal cations in solution. Nature Catalysis, 2021, 4, 654-662.	16.1	386
57975	Unveiling the anisotropic behavior of ultrafast electron transfer at the metal/organic interface. Applied Surface Science, 2021, 554, 149311.	3.1	1
57976	The miscibility of calcium silicate perovskite and bridgmanite: A single perovskite solid solution in hot, iron-rich regions. Earth and Planetary Science Letters, 2021, 566, 116973.	1.8	5
57977	Spin-valley locking and bulk quantum Hall effect in a noncentrosymmetric Dirac semimetal BaMnSb2. Nature Communications, 2021, 12, 4062.	5.8	32

#	Article	IF	Citations
57978	Germanene Nanosheets: Achieving Superior Sodiumâ€Ion Storage via Pseudointercalation Reactions. Small Structures, 2021, 2, 2100041.	6.9	20
57979	Extreme Ultraviolet Second Harmonic Generation Spectroscopy in a Polar Metal. Nano Letters, 2021, 21, 6095-6101.	4.5	17
57980	Theoretical Study of Abnormal Thermal Expansion of CuSCN and Effect on Electronic Structure. Frontiers in Materials, 2021, 8, .	1.2	5
57981	Tailored growth of single-crystalline InP tetrapods. Nature Communications, 2021, 12, 4454.	5.8	17
57982	Effect of Calcination Temperature and Chemical Composition of PAN-Derived Carbon Microfibers on N2, CO2, and CH4 Adsorption. Materials, 2021, 14, 3914.	1.3	9
57983	Bimetal single-molecule magnets supported on benzene with large magnetic anisotropy and unquenched orbital moment. Physical Review Research, 2021, 3, .	1.3	3
57984	Insensitivity of the striped charge orders in <mml:math xmlns:mml="http://www.w3.org/1998/Math/MathML"><mml:msub><mml:mrow><mml:mi>IrTe</mml:mi></mml:mrow><mml:mn>2</m to alkali surface doping implies their structural origin. Physical Review Materials, 2021, 5, .	0.9	1
57985	Investigation of the stability of the interface structure between LiC₆ and Î²-Li₃PS₄ by first-principles calculations. Journal of the Ceramic Society of Japan, 2021, 129, 478-480.	0.5	1
57986	Insights into the atomic structure of the interface of ferroelectric <mml:math xmlns:mml="http://www.w3.org/1998/Math/MathML"><mml:mrow><mml:msub><mml:mi>Hf</mml:mi><mml:mrow><mml:mn>0.5</m mathvariant="normal">O</mml:mi><mml:mn>2</mml:mn></mml:msub></mml:mrow></mml:math> grown epitaxially on <mml:math xmlns:mml="http://www.w3.org/1998/Math/MathML"><mml:mrow><mml:msub><mml:mi>La</. Physical Review Materials, 2021, 5, .	0.9	15
57987	Complex pressure-temperature structural phase diagram of the honeycomb iridate Cu2IrO3. Physical Review B, 2021, 104, .	1.1	12
57988	Highly efficient and robust noble-metal free bifunctional water electrolysis catalyst achieved via complementary charge transfer. Nature Communications, 2021, 12, 4606.	5.8	119
57989	Epitaxial growth and transport properties of compressively-strained Ba2IrO4 films*. Chinese Physics B, 2021, 30, 087401.	0.7	2
57990	First-principles study of stability of point defects and their effects on electronic properties of GaAs/AlGaAs superlattice. Chinese Physics B, 2022, 31, 036104.	0.7	3
57991	Magnetic-field-induced robust zero Hall plateau state in MnBi2Te4 Chern insulator. Nature Communications, 2021, 12, 4647.	5.8	43
57992	Temperature-Dependent Properties of Molten Li₂BeF₄ Salt Using Ab Initio Molecular Dynamics. ACS Omega, 2021, 6, 19822-19835.	1.6	17
57993	Enhancing Catalytic Properties of Iron- and Nitrogen-Doped Carbon for Nitrogen Reduction through Structural Distortion: A Density Functional Theory Study. Journal of Physical Chemistry C, 2021, 125, 16004-16012.	1.5	14
57994	Coordination Number-Dependent Complete Oxidation of Methane on NiO Catalysts. ACS Catalysis, 2021, 11, 9837-9849.	5.5	9
57995	Formation of copper boride on Cu(111). Fundamental Research, 2021, 1, 482-487.	1.6	15

#	Article	IF	Citations
57996	Flat Phonon Band-Based Mechanism of Amorphization of MOF-5 at Ultra-low Pressures. Journal of Physical Chemistry C, 2021, 125, 14924-14931.	1.5	4
57997	Cesium-Coated Halide Perovskites as a Photocathode Material: Modeling Insights. Journal of Physical Chemistry Letters, 2021, 12, 6269-6276.	2.1	7
57998	Electric Field Control of the Magnetic Weyl Fermion in an Epitaxial SrRuO₃ (111) Thin Film. Advanced Materials, 2021, 33, e2101316.	11.1	24
57999	Synthesis and ion transport properties of RE3GaO6 (RE = rare earth) oxide ion conductors. Journal of the European Ceramic Society, 2021, 41, 4516-4527.	2.8	5
58000	H2S Dissociation on Defective or Strained Fe (110) and Subsequent Formation of Iron Sulfides: A Density Functional Theory Study. Surface Science, 2021, 709, 121835.	0.8	1
58001	The oxidation of Fe/Ni alloy surface with supercritical water: A ReaxFF molecular dynamics simulation. Applied Surface Science, 2021, 553, 149519.	3.1	18
58002	New honeycomb-like M-based (MÂ=ÂC, Si, Ge and Sn) monochalcogenides polymorphs: An extended family as isoelectronic photocatalysts of Group-VA for water splitting. Applied Surface Science, 2021, 554, 149644.	3.1	10
58003	Origination and evolution of point defects in AlN film annealed at high temperature. Journal of Luminescence, 2021, 235, 118032.	1.5	25
58004	Supported Molybdenum Carbide Nanoparticles as an Excellent Catalyst for CO₂ Hydrogenation. ACS Catalysis, 2021, 11, 9679-9687.	5.5	29
58005	Crystal Structure and Magnetism of Potassium-Intercalated 2,7-Dimethylnaphthalene. Crystals, 2021, 11, 803.	1.0	0
58006	Halogen vacancy migration at surfaces of CsPbBr₃ perovskites: insights from density functional theory. JPhys Energy, 2021, 3, 034017.	2.3	7
58007	Prediction of Co and Ru nanocluster morphology on 2D MoS2 from interaction energies. Beilstein Journal of Nanotechnology, 2021, 12, 704-724.	1.5	0
58008	1,2,4-Azadiphosphole-based piezoelectric penta-CNP sheet with high spontaneous polarization. Applied Surface Science, 2021, 554, 149499.	3.1	21
58009	Machine-Learning-Guided Prediction Models of Critical Temperature of Cuprates. Journal of Physical Chemistry Letters, 2021, 12, 6211-6217.	2.1	19
58010	Atomistic origin of compositional pulling effect in wurtzite (B, Al, In)xGa1â^'xN: A first-principles study. Journal of Applied Physics, 2021, 130, 035704.	1.1	7
58011	Plasma-induced moieties impart super-efficient activity to hydrogen evolution electrocatalysts. Nano Energy, 2021, 85, 106030.	8.2	41
58012	Observation of Surface Ligands-Controlled Etching of Palladium Nanocrystals. Nano Letters, 2021, 21, 6640-6647.	4.5	10
58013	In Situ Mechanistic Studies of Two Divergent Synthesis Routes Forming the Heteroanionic BiOCuSe. Journal of the American Chemical Society, 2021, 143, 12090-12099.	6.6	17

#	Article	IF	Citations
58014	Lattice-Directed Stabilization of Different Spin-State Phases in Metallo-Supramolecular Chains on Au Surfaces. Chemistry of Materials, 2021, 33, 6166-6175.	3.2	4
58015	Marinite Li₂Ni(SO₄)₂ as a New Member of the Bisulfate Family of High-Voltage Lithium Battery Cathodes. Chemistry of Materials, 2021, 33, 6108-6119.	3.2	7
58016	Mechanical and Chemical Interactions in Atomically Defined Contacts. Small, 2021, 17, e2101637.	5.2	6
58017	Carbon clathrates as strong lightweight structures. International Journal of Mechanical Sciences, 2021, 202-203, 106509.	3.6	6
58018	Synthesis of Two New Ni 12 â€Cluster Substituted Sandwiched Phosphotungstates Organicâ€Cluster and their Magnetic Property. European Journal of Inorganic Chemistry, 2021, 2021, 2718-2723.	1.0	2
58019	Ion Substitution Effect on Defect Formation in Two-Dimensional Transition Metal Nitride Semiconductors, AETiN₂ (AE = Ca, Sr, and Ba). Inorganic Chemistry, 2021, 60, 10227-10234.	1.9	3
58020	An integrated experimental and computational investigation of defect and microstructural effects on thermal transport in thorium dioxide. Acta Materialia, 2021, 213, 116934.	3.8	26
58021	The Beginning of HCN Polymerization: Iminoacetonitrile Formation and Its Implications in Astrochemical Environments. ACS Earth and Space Chemistry, 2021, 5, 2152-2159.	1.2	13
58022	Interactions between stearic acid and calcite surfaces: Experimental and computer simulation studies. Biosurface and Biotribology, 2021, 7, 126-132.	0.6	0
58023	Bilateral Interfaces in In₂Se₃-CoIn₂-CoSe₂ Heterostructures for High-Rate Reversible Sodium Storage. ACS Nano, 2021, 15, 13307-13318.	7.3	99
58024	GaAs quantum dot/TiO2 heterojunction for visible-light photocatalytic hydrogen evolution: promotion of oxygen vacancy. Advanced Composites and Hybrid Materials, 2022, 5, 450-460.	9.9	28
58025	Graphite-supported single copper catalyst for electrochemical CO2 reduction: A first-principles approach. Computational and Theoretical Chemistry, 2021, 1201, 113277.	1.1	5
58026	Correlation-induced octahedral rotations in <mml:math xmlns:mml="http://www.w3.org/1998/Math/MathML"><mml:msub><mml:mi>SrMoO</mml:mi><mml:mn>3</mml:mn></mml:msub></ Physical Review B, 2021, 104, .	1.1	10
58027	Structure-sensitivity of direct oxidation methane to methanol over Rhn/ZrO2-x (1 0 1) (nÂ=Â1, 4, 10) surfaces: A DFT study. Applied Surface Science, 2021, 555, 149690.	3.1	11
58028	Reinvestigation of crystal symmetry and fluctuations in <mml:math xmlns:mml="http://www.w3.org/1998/Math/MathML"><mml:mrow><mml:msub><mml:mi>La</mml:mi><mml:mn>12</mml:mn></mml:msub></mml:mrow></mml:m Physical Review B, 2021, 104, .	1.1	10
58029	Specific heat and NMR evidence for the low Fermi-level density of states in semimetallic ScSb. Physical Review B, 2021, 104, .	1.1	1
58030	Low-energy optical properties of the nonmagnetic kagome metal <mml:math xmlns:mml="http://www.w3.org/1998/Math/MathML"><mml:mrow><mml:msub><mml:mi>CsV</mml:mi><mml:mn>3</mml:mn></mml:msub></mml:mrow></mml:m Physical Review B, 2021, 104, .	1.1	12
58031	Structure, Kinetics, and Thermodynamics of Water and Its Ions at the Interface with Monoclinic ZrO2 Resolved via Ab Initio Molecular Dynamics. Journal of Physical Chemistry C, 2021, 125, 15233-15242.	1.5	3

#	Article	IF	Citations
58032	Lateral Interactions and Orderâ€“Disorder Phase Transitions of Metal Phthalocyanines on Ag(111). Journal of Physical Chemistry C, 2021, 125, 15623-15635.	1.5	4
58033	Reduction Mechanism of NO Gas on Ironâ€“Phthalocyanines (Feâ€“PCs): A DFT Investigation. Catalysis Letters, 2022, 152, 1338-1346.	1.4	3
58034	Coupling physics in machine learning to investigate the solution behavior of binary Mg alloys. Journal of Magnesium and Alloys, 2022, 10, 2817-2832.	5.5	23
58035	Halide ion migration in lead-free all-inorganic cesium tin perovskites. Applied Physics Letters, 2021, 119, .	1.5	14
58036	Interplay between Single-Ion and Two-Ion Anisotropies in Frustrated 2D Semiconductors and Tuning of Magnetic Structures Topology. Nanomaterials, 2021, 11, 1873.	1.9	25
58037	Electronic, Vibrational, Elastic, and Piezoelectric Properties of Hâ€, Fâ€Functionalized AlN Sheets. Physica Status Solidi (B): Basic Research, 2021, 258, 2100216.	0.7	3
58038	Crystal structure of copper perchlorophthalocyanine analysed by 3D electron diffraction. Acta Crystallographica Section B: Structural Science, Crystal Engineering and Materials, 2021, 77, 662-675.	0.5	9
58039	First-principles investigation of V-doping effects on Fe₃Cr₄C₃ carbide in hypereutectic Feâ€“Crâ€“C hardfacing coating. Acta Crystallographica Section B: Structural Science, Crystal Engineering and Materials, 2021, 77, 649-661.	0.5	0
58040	Extension of the Linear Response Function of Electron Density to a Plane-wave Basis and the First Application to Periodic Surface Systems. Chemistry Letters, 2021, 50, 1801-1805.	0.7	2
58041	Growth, coalescence, and etching of two-dimensional overlayers on metals modulated by near-surface Ar nanobubbles. Nano Research, 0, , 1.	5.8	1
58042	Water-Soluble Trifunctional Binder for Sulfur Cathodes for Lithiumâ€“Sulfur Battery. ACS Applied Materials & Interfaces, 2021, 13, 33066-33074.	4.0	36
58043	Designing an Electron-Deficient Pd/NiCo₂O₄ Bifunctional Electrocatalyst with an Enhanced Hydrodechlorination Activity to Reduce the Consumption of Pd. Environmental Science & Technology, 2021, 55, 10087-10096.	4.6	64
58044	In Silico Tuning of the Pore Surface Functionality in Al-MOFs for Trace CH₃I Capture. ACS Omega, 2021, 6, 18169-18177.	1.6	10
58045	Impact of residual gas on the optoelectronic properties of Cs-sensitized In0.53Ga0.47As (0 0 1) surface. Journal of Colloid and Interface Science, 2021, 594, 47-53.	5.0	10
58046	Acid-base properties of hydroxyapatite(0001) by the adsorption of probe molecules: An ab initio investigation. Physical Review Materials, 2021, 5, .	0.9	2
58047	Longâ€Range Forces in Rockâ€Saltâ€Type Tellurides and How they Mirror the Underlying Chemical Bonding. Advanced Materials, 2021, 33, e2100163.	11.1	26
58048	Theoretical Inspection of M₁/PMA Single-Atom Electrocatalyst: Ultra-High Performance for Water Splitting (HER/OER) and Oxygen Reduction Reactions (OER). ACS Catalysis, 2021, 11, 8929-8941.	5.5	121
58049	Geometry and Greatly Enhanced Thermoelectric Performance of Monolayer MXY Transitionâ€Metal Dichalcogenide: MoSTe as an Example. Physica Status Solidi - Rapid Research Letters, 2021, 15, 2100166.	1.2	5

#	Article	IF	Citations
58050	Layer Hall effect in a 2D topological axion antiferromagnet. Nature, 2021, 595, 521-525.	13.7	136
58051	The origin of enhanced photocatalytic activity in g-C3N4/TiO2 heterostructure revealed by DFT calculations. Journal of Colloid and Interface Science, 2021, 593, 133-141.	5.0	59
58052	Enhancing electrocatalytic N2-to-NH3 fixation by suppressing hydrogen evolution with alkylthiols modified Fe3P nanoarrays. Nano Research, 2022, 15, 1039-1046.	5.8	74
58053	Theoretical and Experimental Studies of LiBH₄â€“LiBr Phase Diagram. ACS Applied Energy Materials, 2021, 4, 7327-7337.	2.5	12
58054	Block-layer model for intergrowth structures. Nano Research, 2021, 14, 3629-3635.	5.8	8
58055	Electronic and dynamical properties of <mml:math xmlns:mml="http://www.w3.org/1998/Math/MathML"><mml:mrow><mml:msub><mml:mi>CeRh</mml:mi><mml:mn>2</mml:mn></ : Role of <mml:math xmlns:mml="http://www.w3.org/1998/Math/MathML"><mml:mrow><mml:msub><mml:mi>Rh</mml:mi><mml:mn>2</mml:mn></ layers and expected orbital order. Physical Review B, 2021, 104.	1.1	19
58056	Adsorption-Induced Active Vanadium Species Facilitate Excellent Performance in Low-Temperature Catalytic NO_x Abatement. Journal of the American Chemical Society, 2021, 143, 10454-10461.	6.6	64
58057	Dynamics and Site Isolation: Keys to High Propane Dehydrogenation Performance of Silica-Supported PtGa Nanoparticles. Jacs Au, 2021, 1, 1445-1458.	3.6	32
58058	Charge redistribution of Ru nanoclusters on Co3O4 porous nanowire via the oxygen regulation for enhanced hydrogen evolution reaction. Nano Energy, 2021, 85, 105940.	8.2	87
58059	Firstâ€Principles Multiscale Modeling of Mechanical Properties in Graphene/Borophene Heterostructures Empowered by Machineâ€Learning Interatomic Potentials. Advanced Materials, 2021, 33, e2102807.	11.1	171
58060	Biaxial strain tuned magnetic anisotropy of ferromagnetic penta-MnN2 monolayer. Solid State Sciences, 2021, 117, 106634.	1.5	8
58061	Room temperature gas sensing mechanism of SnO2 towards chloroform: Comparing first principles calculations with sensing experiments. Applied Surface Science, 2021, 554, 149603.	3.1	9
58062	How does the defect ZnO@Au surface activate the methane via the precursor-mediated mechanism?. Applied Surface Science, 2021, 555, 149728.	3.1	3
58063	Activity Promotion of Rh_{8â€“x}Co_xP₄ Bimetallic Phosphides in Styrene Hydroformylation: Dual Influence of Adsorption and Surface Reaction. ACS Catalysis, 2021, 11, 9850-9859.	5.5	19
58064	Role of Lithiophilic Metal Sites in Lithium Metal Anodes. Energy & Fuels, 2021, 35, 12746-12752.	2.5	16
58065	Investigation of weak interlayer coupling in 2D layered GeS2 from theory to experiment. Nano Research, 2022, 15, 1013-1019.	5.8	11
58066	Spinney: Post-processing of first-principles calculations of point defects in semiconductors with Python. Computer Physics Communications, 2021, 264, 107946.	3.0	16
58067	Comparative study of electronic structure, optical properties, lattice dynamics and thermal expansion behaviour of energetic ammonium and potassium dinitramide salts. Materials Chemistry and Physics, 2021, 267, 124645.	2.0	4

#	Article	IF	Citations
58068	Atomic and Electronic Edge Structures of Monolayer Ceria on Pt(111). Journal of Physical Chemistry C, 2021, 125, 15599-15605.	1.5	0
58069	Ab initio studies for characterization and identification of nanocrystalline copper pyrophosphate confined in mesoporous silica. Nanotechnology, 2021, 32, 415701.	1.3	6
58070	High-Throughput Screening of Element-Doped Carbon Nanotubes Toward an Optimal One-Dimensional Superconductor. Journal of Physical Chemistry Letters, 2021, 12, 6667-6675.	2.1	4
58071	Flexible Zn-MOF with Rare Underlying scu Topology for Effective Separation of C6 Alkane Isomers. ACS Applied Materials & Interfaces, 2021, 13, 51997-52005.	4.0	22
58072	Tuning the Mn⁴⁺Coordination Environment in Mg₂TiO₄through a Codoping Strategy for Enhancing Luminescence Performance. Journal of Physical Chemistry C, 2021, 125, 15687-15695.	1.5	8
58073	Interacting Electrons in Two-Dimensional Electride Ca2N. Journal of Physical Chemistry C, 2021, 125, 15724-15729.	1.5	8
58074	Transformation of CrSe Monolayers into Room-Temperature Half Metals via Chemical Edge Modification. Journal of Physical Chemistry C, 2021, 125, 15664-15669.	1.5	5
58075	Facet-induced coordination competition for highly ordered CsPbBr3 nanoplatelets with strong polarized emission. Nano Research, 2022, 15, 502-509.	5.8	18
58076	Ionization of carbon at 10â€“100 times the diamond density and in the 106 ÂK temperature range. Physical Review E, 2021, 104, 015201.	0.8	8
58077	Anisotropic superconductivity in the topological crystalline metal <mml:math xmlns:mml="http://www.w3.org/1998/Math/MathML"><mml:msub><mml:mi mathvariant="normal">Pb</mml:mi><mml:mrow><mml:mn>1</mml:mn><mml:mo>/</mml:mo><mml:mn>3</mml:mn></mml:mrow><mml:mi mathvariant="normal">TaS</mml:mi><mml:mn>2</mml:mn></mml:msub></mml:math> with multiple Dirac fermions. Physical Review B, 2021, 104, .	1.1	5
58078	Highly Efficient Photocatalytic CO₂ Reduction in Two-Dimensional Ferroelectric CuInP₂S₆ Bilayers. ACS Applied Materials & Interfaces, 2021, 13, 34486-34494.	4.0	39
58079	Role of anisotropic Coulomb interactions in the superexchange coupling of mixed-valent <mml:math xmlns:mml="http://www.w3.org/1998/Math/MathML"><mml:mrow><mml:msub><mml:mi>Mn</mml:mi><mml:mn>3</mml:mn></mml:msub><mml:msub><mml:mi mathvariant="normal">O</mml:mi><mml:mn>4</mml:mn></mml:msub></mml:mrow></mml:math>. Physical Review B, 2021, 104, .	1.1	4
58080	Effect of Ni Content on Anionic Redox Activity in Ru-Containing Li-Rich Cathode Material. Journal of the Electrochemical Society, 2021, 168, 070552.	1.3	2
58081	Single boron atom anchored on graphitic carbon nitride nanosheet (B/g-C₂N) as a photocatalyst for nitrogen fixation: A first-principles study*. Chinese Physics B, 2021, 30, 083101.	0.7	3
58082	Prediction of the two-dimensional Janus ferrovalley material LaBrI. Physical Review B, 2021, 104, .	1.1	49
58083	Coupling of lattice dynamics and configurational disorder in metal deficient Al1â^'ÎB2 from first-principles. Journal of Applied Physics, 2021, 130, 015110.	1.1	6
58084	Fragile symmetry-protected half metallicity in two-dimensional van der Waals magnets: A case study of monolayer <mml:math xmlns:mml="http://www.w3.org/1998/Math/MathML"><mml:mrow><mml:mi>Fe</mml:mi><mml:msub><mml:mi>Cl</mml:mi> Physical Review B, 2021, 104, .	1.1	11
58085	Quasi-1D XY antiferromagnet Sr2Ni(SeO3)2Cl2 at Sakai-Takahashi phase diagram. Scientific Reports, 2021, 11, 15002.	1.6	1

#	Article	IF	Citations
58086	The Effect of Hydrogen on the Stress-Strain Response in Fe3Al: An ab initio Molecular-Dynamics Study. Materials, 2021, 14, 4155.	1.3	3
58087	Density Functional Theory Study of the Structure of the Pillared Hofmann Compound Ni(3-Methyl-4,4â€²-bipyridine)[Ni(CN)₄] (Ni-BpyMe or PICNIC-21). Journal of Physical Chemistry C, 2021, 125, 15882-15889.	1.5	3
58088	Active-Learning-Based Generative Design for the Discovery of Wide-Band-Gap Materials. Journal of Physical Chemistry C, 2021, 125, 16118-16128.	1.5	12
58089	Heavy carrier doping by hydrogen in the spin-orbit coupled Mott insulator <mml:math xmlns:mml="http://www.w3.org/1998/Math/MathML"><mml:mrow><mml:msub><mml:mi>Sr</mml:mi><mml:mn>2</mml:mn></mml:msub><mml:mi>Ir</mml:mi><mml:mn>1</mml:mn></mml:mrow></mml:math>. Physical Review B, 2021, 104, .	1.1	4
58090	Concurrence of negative in-plane piezoelectricity and photocatalytic properties in 2D ScAgP₂S₆ monolayers. Journal of Physics Condensed Matter, 2021, 33, 375301.	0.7	2
58091	On the temperature and density dependence of dislocation drag from phonon wind. Journal of Applied Physics, 2021, 130, .	1.1	5
58092	Flat bands with fragile topology through superlattice engineering on single-layer graphene. Physical Review Research, 2021, 3, .	1.3	7
58093	Intersection of Organic Molecules and Carbon Materials for Sustainable Society. IEEJ Transactions on Electronics, Information and Systems, 2021, 141, 761-766.	0.1	0
58094	Mechanism for anisotropic diffusion of liquid-like Cu atoms in hexagonal <mml:math xmlns:mml="http://www.w3.org/1998/Math/MathML"><mml:mi>Î²</mml:mi><mml:mo>â^'</mml:mo><mml:msub><mml:mi mathvariant="normal">Cu</mml:mi><mml:mn>2</mml:mn></mml:msub><mml:mi mathvariant="normal">S</mml:mi></mml:math>. Physical Review Materials, 2021, 5, .	0.9	4
58095	Assessment and prediction of band edge locations of nitrides using a self-consistent hybrid functional. Journal of Chemical Physics, 2021, 155, 024120.	1.2	1
58096	Tuning the properties of Ni-based catalyst via La incorporation for efficient hydrogenation of petroleum resin. Chinese Journal of Chemical Engineering, 2022, 45, 41-50.	1.7	8
58097	High-pressure insulating phase of <mml:math xmlns:mml="http://www.w3.org/1998/Math/MathML"><mml:msub><mml:mi mathvariant="normal">Mo</mml:mi><mml:mn>4</mml:mn></mml:msub><mml:msub><mml:mi mathvariant="normal">O</mml:mi><mml:mn>11</mml:mn></mml:msub></mml:math> with collapsed volume. Physical Review B, 2021, 104, .	1.1	1
58098	Metal-insulator alternating behavior in VO2/TiO2 supercells. Journal of Alloys and Compounds, 2021, 870, 159428.	2.8	7
58099	Controllable pâ€Type Doping of 2D WSe₂ via Vanadium Substitution. Advanced Functional Materials, 2021, 31, 2105252.	7.8	40
58100	First-principles insights into the adsorption and interaction mechanism of selenium on selective catalytic reduction catalyst. Chemosphere, 2021, 275, 130057.	4.2	10
58101	Modulating oxygen electronic orbital occupancy of Cr-based MXenes via transition metal adsorbing for optimal HER activity. International Journal of Hydrogen Energy, 2021, 46, 25457-25467.	3.8	7
58102	Structureâ€“composition-property correlations of symmetrical tilt grain boundaries in copper-based binary alloys. Journal of Physics and Chemistry of Solids, 2021, 154, 110082.	1.9	2
58103	Photothermal Catalysis for Selective CO₂ Reduction on the Modified Anatase TiO₂ (101) Surface. ACS Applied Energy Materials, 2021, 4, 7702-7709.	2.5	21

#	Article	IF	Citations
58104	Strain-tunable electronic and optical properties of novel MoSSe/InSe van der Waals heterostructures. Physics Letters, Section A: General, Atomic and Solid State Physics, 2021, 404, 127395.	0.9	10
58105	Mechanical properties and microstructural evolution of pressureless sintered ceramics obtained from high-energy ball-milled TiB2â€“TiC powders. Materials Science & Engineering A: Structural Materials: Properties, Microstructure and Processing, 2021, 819, 141510.	2.6	10
58106	Effective Donor Dopants for Lead Halide Perovskites. Chemistry of Materials, 2021, 33, 6200-6205.	3.2	10
58107	Bismuth-Based Halide Double Perovskite Cs₂LiBiCl₆: Crystal Structure, Luminescence, and Stability. Chemistry of Materials, 2021, 33, 5905-5916.	3.2	39
58108	Strengthening boron carbide by doping Si into grain boundaries. Journal of the American Ceramic Society, 2022, 105, 2978-2989.	1.9	3
58109	Automatic Migration Path Exploration for Multivalent Battery Cathodes using Geometrical Descriptors. Batteries and Supercaps, 2021, 4, 1516-1524.	2.4	11
58110	Properties of orthorhombic Ga2O3 alloyed with In2O3 and Al2O3. Applied Physics Letters, 2021, 119, .	1.5	11
58111	High-throughput screening of carbon-supported single metal atom catalysts for oxygen reduction reaction. Nano Research, 2022, 15, 1054-1060.	5.8	34
58112	Initial micro-galvanic corrosion behavior between Mg2Ca and Î±-Mg via quasi-in situ SEM approach and first-principles calculation. Journal of Magnesium and Alloys, 2023, 11, 958-965.	5.5	15
58113	Ag3PO4/AgSbO3 composite as novel photocatalyst with significantly enhanced activity through a Z-scheme degradation mechanism. Journal of the Iranian Chemical Society, 2022, 19, 821-838.	1.2	11
58115	In Situ Active Site for CO Activation in Fe-Catalyzed Fischerâ€“Tropsch Synthesis from Machine Learning. Journal of the American Chemical Society, 2021, 143, 11109-11120.	6.6	52
58116	Modulation Doping: A Strategy for 2D Materials Electronics. Nano Letters, 2021, 21, 6298-6303.	4.5	48
58117	Light-Tunable Surface State and Hybridization Gap in Magnetic Topological Insulator MnBi₈Te₁₃. Nano Letters, 2021, 21, 6080-6086.	4.5	27
58118	Kondo Holes in the Two-Dimensional Itinerant Ising Ferromagnet Fe₃GeTe₂. Nano Letters, 2021, 21, 6117-6123.	4.5	23
58119	Constructing a novel metal-free g-C3N4/g-CN vdW heterostructure with enhanced visible-light-driven photocatalytic activity for water splitting. Applied Surface Science, 2021, 553, 149550.	3.1	54
58120	Full-Electrical Writing and Reading of Magnetization States in a Magnetic Junction with Symmetrical Structure and Antiparallel Magnetic Configuration. ACS Nano, 2021, 15, 12213-12221.	7.3	7
58121	Orthorhombic Y0.95-xSrxCo0.3Fe0.7O3-Î´ anode for oxygen evolution reaction in solid oxide electrolysis cells. Fundamental Research, 2021, 1, 439-447.	1.6	10
58122	Dealloying-constructed hierarchical nanoporous bismuth-antimony anode for potassium ion batteries. Fundamental Research, 2021, 1, 408-417.	1.6	3

#	Article	IF	Citations
58123	Enhancing crystal structure prediction by decomposition and evolution schemes based on graph theory. Fundamental Research, 2021, 1, 466-471.	1.6	23
58124	Aâ€site Cation Defects (Ba_{0.}<scp>₅Sr₀</scp>_{.5})_{1â€“}<scp>_xCo₀</scp> Perovskites as Active Oxygen Evolution Reaction Catalyst in Alkaline Electrolyte^{â€}. Chinese Journal of Chemistry, 2021, 39, 2692-2698.	2.6	14
58125	Pharmaceutical Salts of Fenbendazole with Organic Counterions: Structural Analysis and Solubility Performance. Crystal Growth and Design, 2021, 21, 4516-4530.	1.4	24
58126	Enhanced Photodetection Performance of Photodetectors Based on Indium-Doped Tin Disulfide Few Layers. ACS Applied Materials & Interfaces, 2021, 13, 35889-35896.	4.0	24
58127	Mechanistic Insights into Interactions of Polysulfides at VS₂ Interfaces in Naâ€“S Batteries: A DFT Study. ACS Applied Materials & Interfaces, 2021, 13, 35848-35855.	4.0	28
58128	First-principles study of the vacancy defects in ZnIn2Te4 and CdIn2Te4. International Journal of Modern Physics C, 0, , 2150166.	0.8	0
58129	Theoretical Design of Effective Multilayer Optical Coatings Using Oxyhydride Thin Films. Physica Status Solidi (B): Basic Research, 2021, 258, 2100179.	0.7	5
58130	Influence of carbon on energetics, electronic structure, and mechanical properties of TiAl alloys. New Journal of Physics, 2021, 23, 073048.	1.2	2
58131	Linear and Nonlinear Optical Properties of Centrosymmetric Sb₄O₅SO₄ and Noncentrosymmetric Sb₄O₄(SO₄)(OH)₂ Induced by Lone Pair Stereoactivity. Inorganic Chemistry, 2021, 60, 11648-11654.	1.9	33
58133	Exploring the Full Potential of Functional Si₂BN Nanoribbons As Highly Reversible Anode Materials for Mg-Ion Battery. Energy & Fuels, 2021, 35, 12688-12699.	2.5	3
58134	Machine learning and evolutionary prediction of superhard B-C-N compounds. Npj Computational Materials, 2021, 7, .	3.5	34
58135	Structures, bonding, and electronic properties of metal thiocyanates. Journal of Physics and Chemistry of Solids, 2021, 154, 110085.	1.9	8
58136	Machine Learning-Based Screening of Highly Stable and Active Ternary Pt Alloys for Oxygen Reduction Reaction. Journal of Physical Chemistry C, 2021, 125, 16963-16974.	1.5	10
58137	Vortexâ€Oriented Ferroelectric Domains in SnTe/PbTe Monolayer Lateral Heterostructures. Advanced Materials, 2021, 33, e2102267.	11.1	11
58138	Hole Trapping at Acceptor Impurities and Alloying Elements in AlN. Physica Status Solidi - Rapid Research Letters, 2021, 15, 2100218.	1.2	3
58139	Understanding the interaction between carboxylates and coinage metals from first principles. Journal of Chemical Physics, 2021, 155, 034301.	1.2	3
58140	Pure spin photocurrent in non-centrosymmetric crystals: bulk spin photovoltaic effect. Nature Communications, 2021, 12, 4330.	5.8	51
58141	A novel two-dimensional SiO sheet with high-stability, strain tunable electronic structure, and excellent mechanical properties*. Chinese Physics B, 2021, 30, 076104.	0.7	2

#	Article	IF	Citations
58142	New insights into Ï‰-embrittlement in high misfit metastable Î²-titanium alloys: Mechanically-driven Ï‰-mediated amorphization. Materials and Design, 2021, 205, 109724.	3.3	6
58143	Revealing the Local Microstates of Feâ€“Mnâ€“Al Medium Entropy Alloy: A Comprehensive First-principles Study. Acta Metallurgica Sinica (English Letters), 2021, 34, 1492-1502.	1.5	2
58144	The lattice thermal conductivity in monolayers group-VA: from elements to binary compounds. Materials Research Express, 2021, 8, 075007.	0.8	2
58145	Multiple Dirac cones and Lifshitz transition in a two-dimensional Cairo lattice as a Hawking evaporation analogue. Journal of Physics Condensed Matter, 2021, 33, 365001.	0.7	5
58146	Intra-unitcell cluster-cluster magnetic compensation and large exchange bias in cubic alloys. Physical Review B, 2021, 104, .	1.1	2
58147	In Situ Coexsolution of Metal Nanoparticle-Decorated Double Perovskites As Anode Materials for Solid Oxide Fuel Cells. ACS Applied Energy Materials, 2021, 4, 7992-8002.	2.5	12
58148	Adjusting the Covalency of Metalâ€“Oxygen Bonds in LaCoO₃ by Sr and Fe Cation Codoping to Achieve Highly Efficient Electrocatalysts for Aprotic Lithiumâ€“Oxygen Batteries. ACS Applied Materials & Interfaces, 2021, 13, 33133-33146.	4.0	25
58149	Taming the Antiferromagnetic Beast: Computational Design of Ultrashort Mnâ‹¯Mn Bonds Stabilized by Nâ€Heterocyclic Carbenes. Chemistry - A European Journal, 2021, 27, 12126-12136.	1.7	6
58150	Experimental and theoretical investigation of the control and balance of active sites on oxygen plasma-functionalized MoSe2 nanosheets for efficient hydrogen evolution reaction. Applied Catalysis B: Environmental, 2021, 288, 119983.	10.8	40
58151	Utilizing the different distribution habit of La and Zr in Li-rich Mn-based cathode to achieve fast lithium-ion diffusion kinetics. Journal of Power Sources, 2021, 499, 229915.	4.0	21
58152	TB2J: A python package for computing magnetic interaction parameters. Computer Physics Communications, 2021, 264, 107938.	3.0	92
58153	Double-Site Doping of a V Promoter on Ni_x-V-MgAl Catalysts for the DRM Reaction: Simultaneous Effect on CH₄ and CO₂ Activation. ACS Catalysis, 2021, 11, 8749-8765.	5.5	40
58154	Voltage control of ferrimagnetic order and voltage-assisted writing of ferrimagnetic spin textures. Nature Nanotechnology, 2021, 16, 981-988.	15.6	45
58155	Fermiology of two-dimensional titanium carbide and nitride MXenes. Physical Review B, 2021, 104, .	1.1	5
58156	A new type of cuprous-cysteamine sensitizers: Synthesis, optical properties and potential applications. Materials Today Physics, 2021, 19, 100435.	2.9	12
58157	Computational Screening of 3â€‰d Transition Metal Atoms Anchored on Defective Graphene for Efficient Electrocatalytic N₂ Fixation. ChemPhysChem, 2021, 22, 1712-1721.	1.0	22
58158	First-principles study of S-doped point defects with different charge states in monolayer g-C3N4. Applied Surface Science, 2021, 554, 149601.	3.1	19
58159	Hydrogenated group IV-V monolayer HAB6: A new type of Dirac material constructed by isoelectronic rule. Applied Surface Science, 2021, 554, 149635.	3.1	7

#	Article	IF	Citations
58160	Understanding the electronic metal-support interactions of the supported Ni cluster for the catalytic hydrogenation of ethylene. Molecular Catalysis, 2021, 511, 111731.	1.0	4
58161	Pushing Cu uphill of the volcano curve: Impact of a WC support on the catalytic activity of copper toward the hydrogen evolution reaction. International Journal of Hydrogen Energy, 2021, 46, 25092-25102.	3.8	7
58162	Lone-pair engineering: Achieving ultralow lattice thermal conductivity and enhanced thermoelectric performance in Al-doped GeTe-based alloys. Materials Today Physics, 2021, 20, 100497.	2.9	15
58163	Defect-Induced Magnetic Skyrmion in a Two-Dimensional Chromium Triiodide Monolayer. Jacs Au, 2021, 1, 1362-1367.	3.6	10
58164	Chemistry of Oxygen Ionosorption on SnO₂ Surfaces. ACS Applied Materials & Interfaces, 2021, 13, 33664-33676.	4.0	35
58165	Computational observation of the strengthening of Cu/TiN metal/ceramic interfaces by sub-nanometer interlayers and dopants. Applied Surface Science, 2021, 554, 149562.	3.1	4
58166	Quantum Mechanical Screening of 2D MBenes for the Electroreduction of CO₂ to C1 Hydrocarbon Fuels. Journal of Physical Chemistry Letters, 2021, 12, 6370-6382.	2.1	23
58167	A facile yet versatile method for adsorption and relayed fluorescent detection of heavy metal ions. Journal of Environmental Chemical Engineering, 2021, 9, 105737.	3.3	7
58168	Bandgap engineering in MnPS3 and ZnPS3 for photocatalytic water splitting: A first-principles study. International Journal of Hydrogen Energy, 2021, 46, 26950-26960.	3.8	11
58169	First-principles study of the electronic, magnetic, and crystal structure of perovskite molybdates. Physical Review Materials, 2021, 5, .	0.9	2
58170	Two-dimensional charge density waves in <mml:math xmlns:mml="http://www.w3.org/1998/Math/MathML"><mml:mrow><mml:mi>Ta</mml:mi><mml:msub><mml:mi>X</mml:mi><mml:mn> (<mml:math) Tj ETQq0 0 0 rgBT /Overlock 10 Tf 50 342 Td (xmlns:mml="http://www.w3.org/1998/Math/MathML"><mml:mrow><mml:mn> Review B, 2021, 104, .	1.1	11
58171	First-principle study of Sr-doping effect in Nd_{1-x} Sr_xNiO₂. Europhysics Letters, 2021, 135, 67001.	0.7	5
58172	Carbon ionization from a quantum average-atom model up to gigabar pressures. Physical Review E, 2021, 104, 025209.	0.8	7
58173	High Thermal Conductivity of Wurtzite Boron Arsenide Predicted by Including Four-Phonon Scattering with Machine Learning Potential. ACS Applied Materials & Interfaces, 2021, 13, 53409-53415.	4.0	26
58174	Origin of anomalous band-gap bowing in two-dimensional tin-lead mixed perovskite alloys. Physical Review B, 2021, 104, .	1.1	9
58175	Chiral phonons in the honeycomb sublattice of layered CoSn-like compounds. Physical Review B, 2021, 104, .	1.1	17
58176	A First-Principles Study on Na and O Adsorption Behaviors on Mo (110) Surface. Metals, 2021, 11, 1322.	1.0	3
58177	Two-band conduction and nesting instabilities in superconducting <mml:math xmlns:mml="http://www.w3.org/1998/Math/MathML"><mml:mrow><mml:msub><mml:mi>Ba</mml:mi><mml:mn>12</mml:mn></mml:m : First-principles study. Physical Review B, 2021, 104, .	1.1	5

#	Article	IF	Citations
58178	Simultaneously enhancing the ultimate strength and ductility of high-entropy alloys via short-range ordering. Nature Communications, 2021, 12, 4953.	5.8	116
58179	Pressure Engineering for Extending Spectral Response Range and Enhancing Photoelectric Properties of Iodine. Advanced Optical Materials, 2021, 9, 2101163.	3.6	16
58180	Allâ€Inorganic Rareâ€Earthâ€Based Double Perovskite Nanocrystals with Nearâ€Infrared Emission. Laser and Photonics Reviews, 2021, 15, 2100218.	4.4	42
58181	Why phenol is selectively hydrogenated to cyclohexanol on Ru (0001): An experimental and theoretical study. Applied Surface Science, 2021, 558, 149880.	3.1	16
58182	Diffusionlessâ€Like Transformation Unlocks Pseudocapacitance with Bulk Utilization: Reinventing Fe₂O₃ in Alkaline Electrolyte. Energy and Environmental Materials, 2023, 6, .	7.3	20
58183	High-pressure study of the low- Z rich superconductor Be22Re. Physical Review B, 2021, 104, .	1.1	2
58184	Dual-cation-doped MoS₂ nanosheets accelerating tandem alkaline hydrogen evolution reaction. Nanotechnology, 2021, 32, 445703.	1.3	10
58185	Density functional theory analysis of symmetry-filtering scandium nitride magnetoresistive junctions. , 2021, , .		0
58186	Defect and Doping Engineered Penta-graphene for Catalysis of Hydrogen Evolution Reaction. Nanoscale Research Letters, 2021, 16, 130.	3.1	19
58187	Critical Evaluation of Various Spontaneous Polarization Models and Induced Electric Fields in III-Nitride Multi-Quantum Wells. Materials, 2021, 14, 4935.	1.3	6
58188	Electronic structures and physical properties of Mg, C, and S doped g-GaN. Superlattices and Microstructures, 2021, 156, 106930.	1.4	5
58189	Giant Bulk Photostriction and Accurate Photomechanical Actuation in Hybrid Perovskites. Advanced Optical Materials, 2021, 9, 2100837.	3.6	12
58190	Interplay between breathing-mode distortions and magnetic order in rare-earth nickelates from ab initio magnetic models. Physical Review B, 2021, 104, .	1.1	4
58191	Coherent thermal transport in nano-phononic crystals: An overview. APL Materials, 2021, 9, .	2.2	26
58192	Atomically dispersed Fe atoms anchored on S and Nâ€“codoped carbon for efficient electrochemical denitrification. Proceedings of the National Academy of Sciences of the United States of America, 2021, 118, .	3.3	49
58193	Can Metal Intermixing Cooperatively Improve Perovskites as Redox Materials for Thermochemical Ammonia Synthesis? A Case Study on (Sr,Y)(Ti,Ru)O₃. Journal of Physical Chemistry C, 2021, 125, 17019-17030.	1.5	2
58194	Deep learning for ultra-fast and high precision screening of energy materials. Energy Storage Materials, 2021, 39, 45-53.	9.5	23
58195	The effect of finite-temperature and anharmonic lattice dynamics on the thermal conductivity of ZrS₂ monolayer: self-consistent phonon calculations. Journal of Physics Condensed Matter, 2021, 33, 425405.	0.7	5

#	Article	IF	Citations
58196	Electronic structure of graphene/Y2C heterostructure and related doping effect. Current Applied Physics, 2021, 28, 13-18.	1.1	5
58197	Slowing Hot-Electron Relaxation in Mix-Phase Nanowires for Hot-Carrier Photovoltaics. Nano Letters, 2021, 21, 7761-7768.	4.5	15
58198	Interplay between Spinâ€Orbit Torques and Dzyaloshinskiiâ€Moriya Interactions in Ferrimagnetic Amorphous Alloys. Advanced Science, 2021, 8, 2100481.	5.6	7
58199	Extraordinary thermoelectric performance in 2D group III monolayer XP₃ (X = Al, Ga, and) Tj ETQq1 1 0.784314 rgBT /Over	1.3	9
58200	Giant anisotropic photonics in the 1D van der Waals semiconductor fibrous red phosphorus. Nature Communications, 2021, 12, 4822.	5.8	32
58201	Ultrahigh stiffness and anisotropic Dirac cones in BeN4 and MgN4 monolayers: a first-principles study. Materials Today Nano, 2021, 15, 100125.	2.3	23
58202	Structural and Electronic Properties of Intertwined Defect in Ruddlesdenâ€“Popper 2D Perovskites Study Using Density Functional Theory Calculations. Multiscale Science and Engineering, 2021, 3, 205.	0.9	0
58203	Effects of Cr doping on structural and electrochemical properties of Li4Ti5O12 nanostructure for sodium-ion battery anode. Journal of Energy Chemistry, 2021, 59, 465-472.	7.1	27
58204	Uncertainty Quantification and Error Propagation in the Enthalpy and Entropy of Surface Reactions Arising from a Single DFT Functional. Journal of Physical Chemistry C, 2021, 125, 18187-18196.	1.5	8
58205	Vacancy-defect modulated pathway of photoreduction of CO2 on single atomically thin AgInP2S6 sheets into olefiant gas. Nature Communications, 2021, 12, 4747.	5.8	128
58206	Two-dimensional valleytronic semiconductor with spontaneous spin and valley polarization in single-layer <mml:math xmlns:mml="http://www.w3.org/1998/Math/MathML"><mml:mrow><mml:msub><mml:mi>Cr</mml:mi><mml:mn>2</mml:mn></mml:m Physical Review B, 2021, 104, .	1.1	32
58207	Carbon complexes in highly C-doped GaN. Physical Review B, 2021, 104, .	1.1	18
58208	A combinatorial study of electrochemical anion intercalation into graphite. Materials Research Express, 2021, 8, 085502.	0.8	5
58209	Support induced phase engineering toward superior electrocatalyst. Nano Research, 2022, 15, 1831-1837.	5.8	13
58210	Theoretical study on Fe2C MXene as electrode material for secondary battery. Chemical Physics, 2021, 548, 111223.	0.9	6
58211	N-type diamond semiconductor induced by co-doping selenium and boron. Computational Materials Science, 2021, 196, 110515.	1.4	9
58212	Density functional theory calculations on acetaldehyde and glycolaldehyde decompositions over stepped Ni surface. Journal of Analytical and Applied Pyrolysis, 2021, 157, 105233.	2.6	0
58213	Machine learning band gaps from the electron density. Physical Review Materials, 2021, 5, .	0.9	7

#	Article	IF	Citations
58214	Charge-induced magnetic instability of atomically thin ferromagnetic semiconductors: The case of <mml:math xmlns:mml="http://www.w3.org/1998/Math/MathML"><mml:mrow><mml:mi>Cr</mml:mi><mml:msub><mml:mi mathvariant="normal">I</mml:mi><mml:mn>3</mml:mn></mml:msub></mml:mrow></mml:math>. Physical Review B, 2021, 104, .	1.1	0
58215	d-Glucose Adsorption on the TiO2 Anatase (100) Surface: A Direct Comparison Between Cluster-Based and Periodic Approaches. Frontiers in Chemistry, 2021, 9, 716329.	1.8	9
58216	Electronic structures of CO adsorbed Pt-skin surface on Pt-Co and Pt-Ni alloys. Current Applied Physics, 2021, 35, 1-1.	1.1	1
58217	Low thermal conductivity in a modular inorganic material with bonding anisotropy and mismatch. Science, 2021, 373, 1017-1022.	6.0	76
58218	Effect of atomic vacancy on the electronic and optical properties, quantum capacitance of Zr2CO2-based electrodes. Vacuum, 2021, 190, 110284.	1.6	15
58219	Effects of alloying elements on the stability and mechanical properties of Î²-Ti0.5X0.5 (X = V, Cr, Mn, Fe;) Tj ETQq1 1 0.784314 rgBT /Ov Communications, 2021, 334-335, 114395.	0.9	1
58220	Interactions between Reduced Graphene Oxide with Monomers of (Calcium) Silicate Hydrates: A First-Principles Study. Nanomaterials, 2021, 11, 2248.	1.9	23
58221	Xenon Trapping in Metalâ€Supported Silica Nanocages. Small, 2021, 17, 2103661.	5.2	2
58222	Manipulation of Magnetic Skyrmion in a 2D van der Waals Heterostructure via Both Electric and Magnetic Fields. Advanced Functional Materials, 2021, 31, 2104452.	7.8	40
58223	Computational identification of efficient 2D Aluminium chalcogenides monolayers for optoelectronics and photocatalysts applications. Applied Surface Science, 2021, 556, 149561.	3.1	31
58224	A theoretical investigation of topological phase modulation in carbide MXenes: Role of image potential states. Carbon, 2021, 181, 370-378.	5.4	6
58225	Anisotropic to Isotropic Transition in Monolayer Group-IV Tellurides. Materials, 2021, 14, 4495.	1.3	4
58226	Design of High-Performance Lead-Free Quaternary Antiperovskites for Photovoltaics via Ion Type Inversion and Anion Ordering. Journal of the American Chemical Society, 2021, 143, 12369-12379.	6.6	24
58227	Enhanced orbital anisotropy through the proximity to a <mml:math xmlns:mml="http://www.w3.org/1998/Math/MathML"><mml:mrow><mml:mi>SrTi</mml:mi><mml:msub><mml:mi mathvariant="normal">O</mml:mi><mml:mn>3</mml:mn></mml:msub></mml:mrow></mml:math> layer in the perovskite iridate superlattices. Physical Review B, 2021, 104, .	1.1	2
58228	Computational Exploration of Stable 4d/5d Transition-Metal MSi₂N₄ (M =) Tj ETQq0 0 0 rgBT /Overlock 10 Tf Physical Chemistry C, 2021, 125, 19580-19591.	1.5	25
58229	Laserâ€Induced Cooperative Transition in Molecular Electronic Crystal. Advanced Materials, 2021, 33, e2103000.	11.1	6
58230	Comparative study on the strain-dependent mechanical and electronic properties of Nb₃Al and Nb₃Sn. Materials Research Express, 2021, 8, 086001.	0.8	4
58231	Substrateâ€Adatom Interface Engineering of Transition Metal Decorated Boronâ€Doped Graphene Sheet for Enhanced Adsorption of Xe and Kr â€“ A Systematic Ab initio Study. Advanced Theory and Simulations, 2021, 4, 2100187.	1.3	2

#	Article	IF	Citations
58232	Designing Allâ€Inorganic EuOâ€Sensitized TiO 2 Solar Cell from 4fâ€3d Composite Bandgap Structure. Advanced Theory and Simulations, 2021, 4, 2100235.	1.3	2
58233	Identifying Order and Disorder in Double Four-Membered Rings via Raman Spectroscopy during Crystallization of LTA Zeolite. Chemistry of Materials, 2021, 33, 6794-6803.	3.2	8
58234	Accelerated Kinetics Revealing Metastable Pathways of Magnesiation-Induced Transformations in MnO₂ Polymorphs. Chemistry of Materials, 2021, 33, 6983-6996.	3.2	32
58235	Boson Subsidiary Solver (BoSS) v1.1. Computer Physics Communications, 2021, 265, 107991.	3.0	5
58236	Pressure- and temperature-dependent physical metallurgy in a face-centered cubic NiCoFeCrMn high entropy alloy and its subsystems. Journal of Alloys and Compounds, 2021, 873, 159843.	2.8	8
58237	Structural, Physical, Theoretical and Spectroscopic Investigations of Mixedâ€Valent Eu 2 Ni 8 Si 3 and Its Structural Anti â€Type Sr 2 Pt 3 Al 8. European Journal of Inorganic Chemistry, 2021, 2021, 3832.	1.0	3
58238	Nonvolatile electric field control of magnetism in bilayer <mml:math xmlns:mml="http://www.w3.org/1998/Math/MathML"><mml:msub><mml:mi>CrI</mml:mi><mml:mn>3</mml:mn></mml:msub></mml: on monolayer <mml:math xmlns:mml="http://www.w3.org/1998/Math/MathML"><mml:mrow><mml:msub><mml:mi>In</mml:mi><mml:mn>2</mml:mn></mml:m Physical Review B, 2021, 104, .	1.1	24
58239	Modifying carbon nanotubes supported palladium nanoparticles via regulating the electronic metalâ€“carbon interaction for phenol hydrogenation. Chemical Engineering Journal, 2022, 436, 131758.	6.6	24
58240	Probing into the In-Situ Exsolution Mechanism of Metal Nanoparticles from Doped Ceria Host. Nanomaterials, 2021, 11, 2114.	1.9	3
58241	Significant enhancement of magnetic anisotropy and conductivity in <mml:math xmlns:mml="http://www.w3.org/1998/Math/MathML"><mml:mi>GaN</mml:mi><mml:mo>/</mml:mo><mml:msub><mml:mi>CrI</mml:mi> van der Waals heterostructures via electrostatic doping. Physical Review B, 2021, 104, .	1.1	18
58242	Screening two-dimensional materials with topological flat bands. Physical Review Materials, 2021, 5, .	0.9	23
58243	Vibrational and Thermodynamic Properties of Hydrous Iron-Bearing Lowermost Mantle Minerals. Minerals (Basel, Switzerland), 2021, 11, 885.	0.8	0
58244	Stress and Strain Prediction of Zirconium Nitride under Oxygen Doping and Vacancy Introduction. Condensed Matter, 2021, 6, 32.	0.8	1
58245	Computational Search for Novel Zn-Ion Conductorsâ€”A Crystallochemical, Bond Valence, and Density Functional Study. Journal of Physical Chemistry C, 2021, 125, 17590-17599.	1.5	12
58246	Achieving Selective and Efficient Electrocatalytic Activity for CO2 Reduction on N-Doped Graphene. Frontiers in Chemistry, 2021, 9, 734460.	1.8	9
58247	Multiple Strategies toward Advanced P2-Type Layered Na_xMnO₂ for Low-Cost Sodium-Ion Batteries. ACS Applied Energy Materials, 2021, 4, 8183-8192.	2.5	11
58248	Surface functionalization with nonalternant aromatic compounds: a computational study of azulene and naphthalene on Si(001). Journal of Physics Condensed Matter, 2021, 33, 444003.	0.7	4
58249	Pressure-induced topological quantum phase transition in the magnetic topological insulator MnBi₂Te₄. New Journal of Physics, 2021, 23, 083030.	1.2	7

#	Article	IF	Citations
58250	Microcrystal-Induced Crystallization Effect for High-Quality Germanium/Silicon Heteroepitaxial Nanofilms. ACS Applied Electronic Materials, 2021, 3, 3391-3399.	2.0	4
58251	Two-Dimensional Janus FeXY (X, Y = Cl, Br, and I, X â‰ Y) Monolayers: Half-Metallic Ferromagnets with Tunable Magnetic Properties under Strain. ACS Applied Materials & Interfaces, 2021, 13, 38897-38905.	4.0	84
58252	Improving the Structure Stability of LiNi_{0.8}Co_{0.15}Al_{0.05}O₂ by Double Modification of Tantalum Surface Coating and Doping. ACS Applied Energy Materials, 2021, 4, 8641-8652.	2.5	52
58253	Unexpectedly low barrier of ferroelectric switching in HfO2 via topological domain walls. Materials Today, 2021, 50, 8-15.	8.3	40
58254	Nickel/Molybdenum Bimetallic Alloy for Dry Reforming of Methane: A Coverage-Dependence Microkinetic Model Simulation Based on the First-Principles Calculation. Journal of Physical Chemistry C, 2021, 125, 18653-18664.	1.5	16
58255	Accurate machine learning models based on small dataset of energetic materials through spatial matrix featurization methods. Journal of Energy Chemistry, 2021, 63, 364-375.	7.1	7
58256	Stacking Sequence, Interlayer Bonding, Termination Group Stability and Li/Na/Mg Diffusion in MXenes. , 2021, 3, 1369-1376.		10
58257	Density Functional Theory Calculations for Insight into the Heterocatalyst Reactivity and Mechanism in Persulfate-Based Advanced Oxidation Reactions. ACS Catalysis, 2021, 11, 11129-11159.	5.5	190
58258	Catalytic Interplay of Ga, Pt, and Ce on the Alumina Surface Enabling High Activity, Selectivity, and Stability in Propane Dehydrogenation. ACS Catalysis, 2021, 11, 10767-10777.	5.5	28
58259	Facet-Dependent Mn Doping on Shaped Co₃O₄ Crystals for Catalytic Oxidation. ACS Catalysis, 2021, 11, 11066-11074.	5.5	69
58260	Effect of Surface Oxidation on Oxidative Propane Dehydrogenation over Chromia: An Ab Initio Multiscale Kinetic Study. ACS Catalysis, 2021, 11, 11233-11247.	5.5	29
58261	Strain-Induced Magnetic Transitions in SrMO_{2.5} (M = Mn, Fe) Thin Films with Ordered Oxygen Vacancies. Inorganic Chemistry, 2021, 60, 13161-13167.	1.9	1
58262	Mechanisms of Double-Bond Isomerization Reactions of n-Butene on Different Lewis Acids. ACS Catalysis, 2021, 11, 11293-11304.	5.5	13
58263	Theoretical screening of 2D materials supported transition-metal single atoms as efficient electrocatalysts for hydrogen evolution reaction. Materialia, 2021, 18, 101168.	1.3	4
58264	Effect of Co doping in tailoring the crystallite size, surface morphology and optical band gap of CuO thin films prepared via thermal spray pyrolysis. Surfaces and Interfaces, 2021, 25, 101269.	1.5	12
58265	Novel Ni/Ni2P@C hollow heterostructure microsphere as efficient sulfur hosts for high-performance lithium-sulfur batteries. Journal of Alloys and Compounds, 2021, 871, 159576.	2.8	20
58266	Unraveling the Ultrafast Self-assembly and Photoluminescence in Zero-Dimensional Mn²⁺-Based Halides with Narrow-Band Green Emissions. ACS Applied Electronic Materials, 2021, 3, 4144-4150.	2.0	16
58267	Spectroscopic Signatures of Interlayer Coupling in Janus MoSSe/MoS₂ Heterostructures. ACS Nano, 2021, 15, 14394-14403.	7.3	36

#	Article	IF	Citations
58268	Thermodynamic Reassessment of the Au-In Binary System Supported with First-Principles Calculations. Journal of Phase Equilibria and Diffusion, 2021, 42, 479-488.	0.5	2
58269	Epitaxial Growth of Quasi-One-Dimensional Bismuth-Halide Chains with Atomically Sharp Topological Non-Trivial Edge States. ACS Nano, 2021, 15, 14850-14857.	7.3	12
58270	Continuous dimethyl carbonate synthesis from CO2 and methanol over BixCe1â^'xOÎ´ monoliths: Effect of bismuth doping on population of oxygen vacancies, activity, and reaction pathway. Nano Research, 2022, 15, 1366-1374.	5.8	51
58271	High Voltageâ€Stabilized Graphdiyne Cathode Interface. Small, 2021, 17, e2102066.	5.2	18
58272	Valley-Contrasting Physics in Single-Layer CrSi₂N₄ and CrSi₂P₄. Journal of Physical Chemistry Letters, 2021, 12, 8341-8346.	2.1	31
58273	Density Functional Theory Study of the Partial Oxidation of Methane to Methanol on Au and Pd Surfaces. Journal of Physical Chemistry C, 2021, 125, 18770-18785.	1.5	2
58274	Insight into the Temperature Evolution of Electronic Structure and Mechanism of Exchange Interaction in EuS. Journal of Physical Chemistry Letters, 2021, 12, 8328-8334.	2.1	7
58275	Defect-Modified Ultrathin BiOX (X = Cl, Br) Nanosheets Via a Topâ€“Down Approach with Effective Visible-Light Photocatalytic Degradation. Journal of Physical Chemistry C, 2021, 125, 18630-18639.	1.5	15
58276	The coupling effect and phase transition behavior of multiple interfaces in GeTe/Sb superlattice-like films. Journal of Alloys and Compounds, 2021, 871, 159467.	2.8	21
58277	Stability and interaction of cation Frenkel pair in wurtzite semiconductor materials. Computational Materials Science, 2021, 196, 110554.	1.4	2
58278	Wafer-scale MoS2 for P-type field effect transistor arrays and defects-related electrical characteristics. Thin Solid Films, 2021, 732, 138798.	0.8	0
58279	Paraffin-Enabled Compressive Folding of Two-Dimensional Materials with Controllable Broadening of the Electronic Band Gap. ACS Applied Materials & Interfaces, 2021, 13, 40922-40931.	4.0	8
58280	Spin-Current Modulation in Hexagonal Buckled ZnTe and CdTe Monolayers for Self-Powered Flexible-Piezo-Spintronic Devices. ACS Applied Materials & Interfaces, 2021, 13, 40872-40879.	4.0	26
58281	Spinâ€“orbit torque engineering in Î²-W/CoFeB heterostructures with Wâ€“Ta or Wâ€“V alloy layers between Î²-W and CoFeB. NPG Asia Materials, 2021, 13, .	3.8	11
58282	Construction of Single-Atom Platinum Catalysts Enabled by CsPbBr₃ Nanocrystals. ACS Nano, 2021, 15, 13129-13139.	7.3	44
58283	Massive Dirac fermions and strong Shubnikovâ€“de Haas oscillations in single crystals of the topological insulator <mml:math xmlns:mml="http://www.w3.org/1998/Math/MathML"><mml:mrow><mml:msub><mml:mi>Bi</mml:mi><mml:mn>2</mml:mn></mml:msub></mml:mrow></mml:math> doped with Sm and Fe. Physical Review B, 2021, 104, .	1.1	6
58284	Role of Coulomb interaction in the phase formation of fcc Ce: Correlation matrix renormalization theory. Physical Review B, 2021, 104, .	1.1	6
58285	Nonvolatile ferromagnetism in bilayer <mml:math xmlns:mml="http://www.w3.org/1998/Math/MathML"><mml:mrow><mml:mi>Cr</mml:mi><mml:msub><mml:mi mathvariant="normal">I</mml:mi><mml:mn>3</mml:mn></mml:msub></mml:mrow></mml:math> induced by a heterointerface. Physical Review B, 2021, 104, .	1.1	7

#	Article	IF	Citations
58286	Neighboring Pd single atoms surpass isolated single atoms for selective hydrodehalogenation catalysis. Nature Communications, 2021, 12, 5179.	5.8	87
58287	Cooperative Effects between Ni-Mo Alloy Sites and Defective Structures over Hierarchical Ni-Mo Bimetallic Catalysts Enable the Enhanced Hydrodeoxygenation Activity. ACS Sustainable Chemistry and Engineering, 2021, 9, 11604-11615.	3.2	39
58288	The Catalysis Effect of Na and Point Defect on NO Heterogeneous Adsorption on Carbon during High-Sodium Zhundong Coal Reburning: Structures, Interactions and Thermodynamic Characteristics. Catalysts, 2021, 11, 1046.	1.6	4
58289	Theoretical Analysis of Si2H6 Adsorption on Hydrogenated Silicon Surfaces for Fast Deposition Using Intermediate Pressure SiH4 Capacitively Coupled Plasma. Coatings, 2021, 11, 1041.	1.2	8
58290	Laser-driven anisotropic and nonlinear Rashba spin splitting in GaAs monolayer. Physical Review B, 2021, 104, .	1.1	1
58291	Atomic-scale defects restricting structural superlubricity: Ab initio study on the example of the twisted graphene bilayer. Physical Review B, 2021, 104, .	1.1	9
58292	Investigation of mechanical and thermodynamic properties of La 2 Zr 2 O 7 pyrochlore. International Journal of Energy Research, 0, , .	2.2	1
58293	Surface microenvironment engineering of black V2O5 nanostructures for visible light photodegradation of methylene blue. Journal of Alloys and Compounds, 2021, 871, 159615.	2.8	26
58294	Promoted H2 splitting on ZnO by pre-adsorbed formic acid. Journal of Catalysis, 2021, 400, 212-217.	3.1	5
58295	Photoinduced Anomalous Electron Transfer Dynamics at a Lateral MoS₂â€“Graphene Covalent Junction. Journal of Physical Chemistry Letters, 2021, 12, 7553-7559.	2.1	12
58296	Low Thermal Conductivity and Magneto-suppressed Thermal Transport in a Highly Oriented FeSb2 Single Crystal. ACS Omega, 2021, 6, 22681-22687.	1.6	2
58297	Cesium manganese chloride: Stable lead-free perovskite from bulk to single layer. Journal of Magnetism and Magnetic Materials, 2021, 531, 167845.	1.0	6
58298	Tuning electronic structure and optical properties of monolayer GeAs and GeAs2 by alloying with nitrogen and phosphorus elements. Physica B: Condensed Matter, 2021, 614, 413033.	1.3	3
58299	Designing efficient single-atomic catalysts for bifunctional oxygen electrocatalysis via a general two-step strategy. Applied Surface Science, 2021, 556, 149779.	3.1	10
58300	Inducing high- Tc ferromagnetism in the van der Waals crystal Mn(ReO4)2 via charge doping: A first-principles study. Physical Review B, 2021, 104, .	1.1	2
58301	Single-Layer Zirconium Dihalides ZrX₂ (X = Cl, Br, and I) with Abnormal Ferroelastic Behavior and Strong Anisotropic Light Absorption Ability. Journal of Physical Chemistry Letters, 2021, 12, 7726-7732.	2.1	11
58302	Spin Hall effect in the monolayer Janus compound MoSSe enhanced by Rashba spin-orbit coupling. Physical Review B, 2021, 104, .	1.1	34
58303	Observation of a molecular muonium polaron and its application to probing magnetic and electronic states. Physical Review B, 2021, 104, .	1.1	0

#	Article	IF	Citations
58304	Bandgap Engineering through Halide Doubleâ€Perovskite Alloys: A Highâ€Throughput Firstâ€Principles Study. Physica Status Solidi - Rapid Research Letters, 2021, 15, 2100343.	1.2	2
58305	Electrochemical release of catalysts in nanoreactors for solid sulfur redox reactions in room-temperature sodium-sulfur batteries. Cell Reports Physical Science, 2021, 2, 100539.	2.8	20
58306	Single-atom doping in carbon black nanomaterials for photothermal antibacterial applications. Cell Reports Physical Science, 2021, 2, 100535.	2.8	8
58307	Incorporating Cobalt Nanoparticles in Nitrogen-Doped Mesoporous Carbon Spheres through Composite Micelle Assembly for High-Performance Lithiumâ€“Sulfur Batteries. ACS Applied Materials & Interfaces, 2021, 13, 38604-38612.	4.0	17
58308	Elucidating active sites and decomposition mechanisms for oxythiomolybdate clusters (Mo₂O₂S_x, xÂ=Â6;8) as catalyzers for hydrogen evolution reactions. Electrochemical Science Advances, 2022, 2, e2100088.	1.2	2
58309	Magnetic phase diagram of rare-earth orthorhombic perovskite oxides. Physical Review B, 2021, 104, .	1.1	11
58310	Slight Zinc Doping by an Ultrafast Electrodeposition Process Boosts the Cycling Performance of Layered Double Hydroxides for Ultralong-Life-Span Supercapacitors. ACS Applied Materials & Interfaces, 2021, 13, 38346-38357.	4.0	36
58311	Collinear magnetism and spin-orbit coupling in Mn₂PtSn. Journal Physics D: Applied Physics, 2021, 54, 455301.	1.3	4
58312	Novel thermoelectric performance of 2D 1T- Se₂Te and SeTe₂ with ultralow lattice thermal conductivity but high carrier mobility. Nanotechnology, 2021, 32, 455401.	1.3	18
58313	On the formation and diffusion of oxygen vacancies in non-stoichiometric mixed Co_{3-x}Mn_xO₄ spinel structures from first-principles calculations. Journal of Physics Condensed Matter, 2021, 33, 444002.	0.7	2
58314	A New Type of Largeâ€Gap Quantum Spin Hall Insulator Material ZrSe₅. Physica Status Solidi (B): Basic Research, 2021, 258, 2100256.	0.7	2
58315	Diverse Structures and Magnetic Properties in Nonlayered Monolayer Chromium Selenide. Journal of Physical Chemistry Letters, 2021, 12, 7752-7760.	2.1	28
58316	Phase Relations in CaSiO3 System up to 100 GPa and 2500 K. Geochemistry International, 2021, 59, 791-800.	0.2	2
58317	Experimental and Theoretical Investigation of Ethylene and 1-MCP Binding Sites in HKUST-1 Metalâ€“Organic Framework. Journal of Physical Chemistry C, 2021, 125, 22295-22300.	1.5	5
58318	Anion-exchange-mediated internal electric field for boosting photogenerated carrier separation and utilization. Nature Communications, 2021, 12, 4952.	5.8	45
58319	Anomalous Hall effect in ferrimagnetic metal RMn6Sn6 (R = Tb, Dy, Ho) with clean Mn kagome lattice. Applied Physics Letters, 2021, 119, .	1.5	29
58320	Facet-dependent catalytic activity of anatase TiO2 for the selective catalytic reduction of NO with NH3: A dispersion-corrected density functional theory study. Applied Catalysis A: General, 2021, 623, 118250.	2.2	9
58321	Molecular-Level Insights on the Facet-Dependent Degradation of Perfluorooctanoic Acid. ACS Applied Materials & Interfaces, 2021, 13, 41584-41592.	4.0	14

#	Article	IF	Citations
58322	Correlations of Ionic Migration and Deep-Level Traps Leads to Surface Defect Formation in Perovskite Solar Cells. Journal of Physical Chemistry C, 2021, 125, 19551-19559.	1.5	10
58323	Distinct Behaviors of Cu- and Ni-ZSM-5 Zeolites toward the Post-activation Reactions of Methane. Journal of Physical Chemistry C, 2021, 125, 19333-19344.	1.5	6
58324	Nucleation and Coalescence of BaTiO₃ Using a Continuous Flow Reactor with Waterâ€“Ethanol Mixed Solvents. Journal of Physical Chemistry C, 2021, 125, 19489-19496.	1.5	2
58325	Computational Investigation of the Catalytic Hydrodeoxygenation of Propanoic Acid over a Cu(111) Surface. Journal of Physical Chemistry C, 2021, 125, 19276-19293.	1.5	3
58326	Roles of Polymerized Anionic Clusters Stimulating for Hydrolysis Deterioration in Li₇P₃S₁₁. Journal of Physical Chemistry C, 2021, 125, 19509-19516.	1.5	10
58327	Two novel semiconducting <scp>B₂CO</scp> monolayers with high carrier mobilities. Journal of Computational Chemistry, 2021, 42, 2024-2030.	1.5	2
58328	Molecular engineering towards efficientwhite-light-emitting perovskite. Nature Communications, 2021, 12, 4890.	5.8	32
58329	Construction of Nickelâ€Based Dual Heterointerfaces towards Accelerated Alkaline Hydrogen Evolution via Boosting Multiâ€Step Elementary Reaction. Advanced Functional Materials, 2021, 31, 2104827.	7.8	42
58330	Atomic Scale Investigation of the CuPcâ€“MAPbX₃ Interface and the Effect of Non-Stoichiometric Perovskite Films on Interfacial Structures. ACS Nano, 2021, 15, 14813-14821.	7.3	8
58331	Effect of alloying elements on the hydrogen diffusion and trapping in high entropy alloys. Scripta Materialia, 2021, 201, 113957.	2.6	30
58332	Liquid metal with solvents for CO 2 capture. , 2021, 11, 988.		1
58333	A Universal Atomic Substitution Conversion Strategy Towards Synthesis of Large-Size Ultrathin Nonlayered Two-Dimensional Materials. Nano-Micro Letters, 2021, 13, 165.	14.4	12
58334	Synthesis of calcium polysulfides at high pressures. Physical Review B, 2021, 104, .	1.1	2
58335	Two types of charge ordering in bismuth nickelate. Physical Review B, 2021, 104, .	1.1	0
58336	Extremely thin interlayer of multi-element intermetallic compound between Sn-based solders and FeCoNiMn high-entropy alloy. Applied Surface Science, 2021, 558, 149945.	3.1	21
58337	Balancing orbital effects and on-site Coulomb repulsion through Na modulations in <mml:math xmlns:mml="http://www.w3.org/1998/Math/MathML"><mml:mrow><mml:msub><mml:mi>Na</mml:mi><mml:mi>x</mml:mi></mml:mi> mathvariant="normal">V</mml:mi><mml:msub><mml:mi mathvariant="normal">O</mml:mi><mml:mn>2</mml:mn></mml:msub></mml:mrow></mml:math>. Physical Review Materials, 2021, 5, .	0.9	4
58338	Layer-Dependent Giant Magnetoresistance in Two-Dimensional <mml:math xmlns:mml="http://www.w3.org/1998/Math/MathML" display="inline" overflow="scroll"><mml:msub><mml:mrow><mml:mi>Cr</mml:mi><mml:mi>PS</mml:mi></mml:mrow><mml:mn>4</mml:mn></mml: Magnetic Tunnel Junctions. Physical Review Applied, 2021, 16, .	1.5	22
58339	Strain Modulation of Black Phosphorene for the Hydrogen Evolution Reaction Activity. Physica Status Solidi (B): Basic Research, 2021, 258, 2100195.	0.7	7

#	Article	IF	Citations
58340	Oxidative Aromatization of 4,7-Dihydro-6-nitroazolo[1,5-a]pyrimidines: Synthetic Possibilities and Limitations, Mechanism of Destruction, and the Theoretical and Experimental Substantiation. Molecules, 2021, 26, 4719.	1.7	5
58341	DFT Investigations on the Boronâ€“Phosphorus Assembled Nanowires. Journal of Cluster Science, 0, , 1.	1.7	1
58342	Electron Lone-Pairs Stereochemistry and Drastic van der Waals and Pressure Effects in AsF3 from First Principles. Condensed Matter, 2021, 6, 31.	0.8	2
58343	Water-Dispersible CsPbBr3 Perovskite Nanocrystals with Ultra-Stability and its Application in Electrochemical CO2 Reduction. Nano-Micro Letters, 2021, 13, 172.	14.4	20
58344	Classification and materials realization of topologically robust nodal ring phonons. Physical Review Materials, 2021, 5, .	0.9	14
58345	Hot Carrier Dynamics at Ligated Silicon(111) Surfaces: A Computational Study. Journal of Physical Chemistry Letters, 2021, 12, 7504-7511.	2.1	3
58346	Defect levels from SCAN and MBJ meta-GGA exchange-correlation potentials. Physical Review B, 2021, 104, .	1.1	5
58347	Combined Spectroscopic and Computational Study of Nitrobenzene Activation on Non-Noble Metals-Based Mono- and Bimetallic Catalysts. Nanomaterials, 2021, 11, 2037.	1.9	5
58348	Bandgap engineering of stacked two-dimensional polyaniline by twist angle. Applied Physics Letters, 2021, 119, 061602.	1.5	7
58349	Ultralow-strain Ti substituted Mn-vacancy layered oxides with enhanced stability for sodium-ion batteries. Journal of Energy Chemistry, 2021, 63, 351-357.	7.1	22
58350	Determination of active sites on Na2SiO3 and Li2SiO3 catalysts for methanol dissociation and methoxide stabilization concerning biodiesel production. Fuel, 2021, 298, 120840.	3.4	9
58351	Electronic properties of intrinsic vacancies in single-layer CaF2 and its heterostructure with monolayer MoS2. Journal of Applied Physics, 2021, 130, .	1.1	3
58352	A stable nanosilver decorated phosphorene nanozyme with phosphorus-doped porous carbon microsphere for intelligent sensing of 8-hydroxy-2â€²-deoxyguanosine. Journal of Electroanalytical Chemistry, 2021, 895, 115522.	1.9	8
58353	Mechanism of Magnesium Transport in Spinel Chalcogenides. Advanced Energy and Sustainability Research, 2021, 2, 2100113.	2.8	12
58354	Self-supported Ni3N nanoarray as an efficient nonnoble-metal catalyst for alkaline hydrogen evolution reaction. International Journal of Hydrogen Energy, 2021, 46, 27037-27043.	3.8	30
58355	Layered Double Hydroxide-Derived Intermetallic Ni₃GaC_{0.25} Catalysts for Dry Reforming of Methane. ACS Catalysis, 2021, 11, 11091-11102.	5.5	26
58356	Lead-Free Cs₂AgBiBr₆ Perovskite with Enriched Surface Defects for Efficient Photocatalytic Hydrogen Evolution. Energy & Fuels, 2021, 35, 15005-15009.	2.5	31
58357	Bulk and surface theoretical investigation of Nb-doped Î´-FeOOH as a promising bifunctional catalyst. Journal of Molecular Modeling, 2021, 27, 249.	0.8	2

#	Article	IF	Citations
58358	Material-Specific Optimization of Gaussian Basis Sets against Plane Wave Data. Journal of Chemical Theory and Computation, 2021, 17, 5611-5622.	2.3	6
58359	Tuning the electronic and optical properties of Ga2SSe janus monolayer by adsorption of metals. Optical and Quantum Electronics, 2021, 53, 1.	1.5	4
58360	Role of Residual Li and Oxygen Vacancies in Ni-rich Cathode Materials. ACS Applied Materials & Interfaces, 2021, 13, 42554-42563.	4.0	56
58361	Induction of planar Li growth with designed interphases for dendrite-free Li metal anodes. Energy Storage Materials, 2021, 39, 250-258.	9.5	44
58362	Boridene: Two-dimensional Mo _{4/3} B _{2-x} with ordered metal vacancies obtained by chemical exfoliation. Science, 2021, 373, 801-805.	6.0	126
58363	Twinning pathways in Fe and Feâ€“Cr alloys from first-principles theory. Acta Materialia, 2021, 215, 117094.	3.8	9
58364	First-principles study of the effect of Al and Hf impurities on Co3W antiphase boundary energies. Acta Materialia, 2021, 215, 117075.	3.8	2
58365	Adsorption of single metallic atoms on self-assembled molecular domain of terephthalic acid. Surfaces and Interfaces, 2021, 25, 101170.	1.5	0
58366	Rational Design of Highly Stable and Active MXeneâ€Based Bifunctional ORR/OER Doubleâ€Atom Catalysts. Advanced Materials, 2021, 33, e2102595.	11.1	137
58367	Cobaltâ€“Nitrogen Compounds at High Pressure. Inorganic Chemistry, 2021, 60, 14022-14030.	1.9	13
58368	High thermoelectric performance enabled by convergence of nested conduction bands in Pb7Bi4Se13 with low thermal conductivity. Nature Communications, 2021, 12, 4793.	5.8	53
58369	Theoretical and Experimental Investigations on Kâ€doped SrCo_{0.9}Nb_{0.1}O_{3â€Î´} as a Promising Cathode for Protonâ€Conducting Solid Oxide Fuel Cells. ChemSusChem, 2021, 14, 3876-3886.	3.6	23
58370	Strong Interlayer Transition in Fewâ€Layer InSe/PdSe₂ van der Waals Heterostructure for Nearâ€Infrared Photodetection. Advanced Functional Materials, 2021, 31, 2104143.	7.8	69
58371	Few-Layer SrRu₂O₆ Nanosheets as Non-Van der Waals Honeycomb Antiferromagnets: Implications for Two-Dimensional Spintronics. ACS Applied Nano Materials, 2021, 4, 9313-9321.	2.4	5
58372	Controlling metalation reaction of phthalocyanine with cobalt at single-molecule level on Au(111) surface. Chinese Journal of Chemical Physics, 2021, 34, 419-428.	0.6	1
58373	An Engineered Pseudoâ€Macrophage for Rapid Treatment of Bacteriaâ€Infected Osteomyelitis via Microwaveâ€Excited Antiâ€Infection and Immunoregulation. Advanced Materials, 2021, 33, e2102926.	11.1	87
58374	Local Structure Regulation in Near-Infrared Persistent Phosphor of ZnGa₂O₄:Cr³⁺ to Fabricate Natural-Light Rechargeable Optical Thermometer. ACS Applied Electronic Materials, 2021, 3, 3789-3803.	2.0	21
58375	Approaching Theoretical Band Gap of ZnSnN₂ Films via Bias Magnetron Cosputtering at Room Temperature. ACS Applied Electronic Materials, 2021, 3, 3855-3866.	2.0	7

#	Article	IF	Citations
58376	Optoelectronic properties of 2D heterojunction ZrO2â€“ MoS2 material using first-principles calculations. Solid State Communications, 2021, 334-335, 114358.	0.9	16
58377	Electronic nature of chiral charge order in the kagome superconductor <mml:math xmlns:mml="http://www.w3.org/1998/Math/MathML"><mml:mrow><mml:mi>Cs</mml:mi><mml:msub><mml:mi mathvariant="normal">V</mml:mi><mml:mn>3</mml:mn></mml:msub><mml:msub><mml:mi>Sb</mml:mi><mml:mn>5</mml:mn></mml:msub></mml:mrow></mml:math>. Physical Review B, 2021, 104, .	1.1	108
58378	Highly Dispersed Ru Nanoparticles on Boronâ€Doped Ti₃C₂T_x (MXene) Nanosheets for Synergistic Enhancement of Electrocatalytic Hydrogen Evolution. Small, 2021, 17, e2102218.	5.2	83
58379	Valley-related multiple Hall effect in monolayer <mml:math xmlns:mml="http://www.w3.org/1998/Math/MathML"><mml:mrow><mml:mi mathvariant="normal">V</mml:mi><mml:msub><mml:mi>Si</mml:mi><mml:mn>2</mml:mn></mml:msub><mml:msub><mml:mi mathvariant="normal">P</mml:mi><mml:mn>4</mml:mn></mml:msub></mml:mrow></mml:math>. Physical Review B, 2021, 104, .	1.1	61
58380	Borophene synthesis beyond the single-atomic-layer limit. Nature Materials, 2022, 21, 35-40.	13.3	137
58381	Tunable mechanical and half-metallic properties of Mn2-XFe1+XSi alloys: A first principles investigation. Physica B: Condensed Matter, 2021, 615, 413044.	1.3	1
58382	Effect of the normal compressive strain and electric filed on the electronic and optical properties of Zr2CO2 MXene and MoSe2 van der Waals Heterojunction: A first principles calculation. Vacuum, 2021, 190, 110290.	1.6	4
58383	Calculating the hyperfine tensors for group-IV impurity-vacancy centers in diamond using hybrid density functional theory. Physical Review B, 2021, 104, .	1.1	9
58384	Band offset in semiconductor heterojunctions. Journal of Physics Condensed Matter, 2021, 33, 415002.	0.7	19
58385	Hourglass phonons jointly protected by symmorphic and nonsymmorphic symmetries. Physical Review B, 2021, 104, .	1.1	35
58386	Kagome-like structure of germanene on Al(111). Physical Review B, 2021, 104, .	1.1	11
58387	Weyl Nodes Close to the Fermi Energy in NbAs. Physica Status Solidi (B): Basic Research, 0, , 2100165.	0.7	2
58389	Low rotational barriers for the most dynamically active methyl groups in the proposed antiviral drugs for treatment of SARS-CoV-2, apilimod and tetrandrine. Chemical Physics Letters, 2021, 777, 138727.	1.2	9
58390	Detection of 1,1 dimethylhydrazine by graphene oxide: first principles study. Journal of Molecular Modeling, 2021, 27, 250.	0.8	2
58391	Machine learning force fields based on local parametrization of dispersion interactions: Application to the phase diagram of <mml:math xmlns:mml="http://www.w3.org/1998/Math/MathML"><mml:msub><mml:mi mathvariant="normal">C</mml:mi><mml:mn>60</mml:mn></mml:msub></mml:math>. Physical Review B, 2021, 104, .	1.1	29
58392	Copper diffusion rates and hopping pathways in superionic Cu2Se. Acta Materialia, 2021, 215, 117026.	3.8	15
58393	Enhancement of vacancy diffusion by C and N interstitials in the equiatomic FeMnNiCoCr high entropy alloy. Acta Materialia, 2021, 215, 117093.	3.8	20
58394	First principles study of the stability and thermal conductivity of novel Li-Be hybrid ceramics. Acta Materialia, 2021, 215, 117052.	3.8	7

#	Article	IF	Citations
58395	Synthesis, Structure and Properties of Layered Phosphide Nitrides Ak Th 2 Mn 4 P 4 N 2 (Ak = Rb, Cs) â€. Chinese Journal of Chemistry, 2021, 39, 2873-2880.	2.6	0
58396	Metavalent Bonding in Crystalline Solids: How Does It Collapse?. Advanced Materials, 2021, 33, e2102356.	11.1	65
58397	A First-Principles Tool to Discover New Pyrometallurgical Refining Options. Jom, 2021, 73, 2900-2910.	0.9	1
58398	sâ€“p Mixing in Stereochemically Active Lone Pairs Drives the Formation of 1D Chains of Lead Bromide Square Pyramids. Inorganic Chemistry, 2021, 60, 12676-12680.	1.9	3
58399	Electronic and optical properties of the SnO2/CsPbI3 interface: Using first principles calculations. Catalysis Today, 2021, 374, 208-213.	2.2	12
58400	Morphology, chemistry, performance trident: Insights from hollow, mesoporous carbon nanofibers for dendrite-free sodium metal batteries. Nano Energy, 2021, 86, 106132.	8.2	34
58401	A study of alkali polyphosphate/borate/carbonate for high temperature lubrication of silicon steel using ball-on-disc tests. Tribology International, 2021, 160, 107015.	3.0	3
58402	Experimental and theoretical realization of an advanced bifunctional 2D Î´-MnO2 electrode for supercapacitor and oxygen evolution reaction via defect engineering. International Journal of Hydrogen Energy, 2021, 46, 28028-28042.	3.8	20
58403	Atomically dispersed low-cost transition metals catalyze efficient hydrogen evolution on two-dimensional SnO nanosheets. International Journal of Hydrogen Energy, 2021, 46, 28602-28612.	3.8	7
58404	Effects of Li adsorption on the physical properties of CrBr3 and CrCl3: From monolayer to multilayer. AIP Advances, 2021, 11, .	0.6	3
58405	Multipole representation for anisotropic Coulomb interactions. Physical Review B, 2021, 104, .	1.1	2
58406	Unravelling the Znâ€Cu Interaction during Activation of a Znâ€promoted Cu/MgO Model Methanol Catalyst. ChemCatChem, 2021, 13, 4120-4132.	1.8	20
58407	Highâ€Throughput Electronic Structures and Ferroelectric Interfaces of HfO 2 by GGA+ U (d,p) Calculations. Physica Status Solidi - Rapid Research Letters, 2021, 15, 2100295.	1.2	5
58408	Inhibition mechanism of capacity degradation in Mg-substituted LaY2-Mg Ni9 hydrogen storage alloys. Journal of Alloys and Compounds, 2021, 873, 159826.	2.8	7
58409	Temperature-Dependent Superplasticity and Strengthening in CoNiCrFeMn High Entropy Alloy Nanowires Using Atomistic Simulations. Nanomaterials, 2021, 11, 2111.	1.9	7
58410	New Insights into the Mechanism of LiDFBOP for Improving the Low-Temperature Performance via the Rational Design of an Interphase on a Graphite Anode. ACS Applied Materials & Interfaces, 2021, 13, 40042-40052.	4.0	35
58411	Effects of Adsorbing Noble Metal Single Atoms on the Electronic Structure and Photocatalytic Activity of Ta₃N₅. Journal of Physical Chemistry C, 2021, 125, 17600-17611.	1.5	9
58412	Role of Dark Excitons in the Excitation Energy Transfer of Carbon Nanotubes. Journal of Physical Chemistry C, 2021, 125, 17861-17869.	1.5	3

#	Article	IF	Citations
58413	Realization of an Ideal Cairo Tessellation in Nickel Diazenide NiN₂: High-Pressure Route to Pentagonal 2D Materials. ACS Nano, 2021, 15, 13539-13546.	7.3	55
58414	Subsurface Carbon as a Selectivity Promotor to Enhance Catalytic Performance in Acetylene Semihydrogenation. ACS Catalysis, 2021, 11, 10257-10266.	5.5	33
58415	Î±-Fe2O3 as a versatile and efficient oxygen atom transfer catalyst in combination with H2O as the oxygen source. Nature Catalysis, 2021, 4, 684-691.	16.1	112
58416	Direct Observation of Knock-on in Surface Reactions at Zero Impact Parameter. Journal of the American Chemical Society, 2021, 143, 12644-12649.	6.6	1
58417	Oxidation of Sn at the Clusterâ€“Support Interface: Sn and Ptâ€“Sn Clusters on TiO₂(110). Journal of Physical Chemistry C, 2021, 125, 17671-17683.	1.5	10
58418	Density Functional Theory Study of Influence of Oxide Thickness and Surface Alloying on Cl Migration within Î±-Al₂O₃. Journal of the Electrochemical Society, 2021, 168, 081508.	1.3	10
58419	Single-atom catalysts with anionic metal centers: Promising electrocatalysts for the oxygen reduction reaction and beyond. Journal of Energy Chemistry, 2021, 63, 285-293.	7.1	15
58420	Bandgap engineering and thermodynamic stability of oxyhalide and chalcohalide antiperovskites. Ceramics International, 2021, 47, 32634-32640.	2.3	9
58421	Self-Assembly and Magnetic Order of Bi-Molecular 2D Spin Lattices of M(II,III) Phthalocyanines on Au(111). Magnetochemistry, 2021, 7, 119.	1.0	4
58422	Ab Initio Energetic Barriers of Gas Permeation across Nanoporous Graphene. ACS Applied Materials & Interfaces, 2021, 13, 39701-39710.	4.0	4
58423	Remote Passivation in Two-Dimensional Materials: The Case of the Monolayerâ€“Bilayer Lateral Junction of MoSe2. Journal of Physical Chemistry Letters, 2021, 12, 8046-8052.	2.1	1
58424	Adsorption of alkali metal atoms on predicted C3N2 sheet. Solid State Communications, 2021, 334-335, 114367.	0.9	2
58425	Exploring the diffusion mechanism of Li ions in different modulated arrangements of La(1-X)/3LixNbO3 with fitted force fields obtained via a metaheuristic algorithm. Solid State Ionics, 2021, 366-367, 115662.	1.3	5
58426	Epitaxial growth of wafer scale antioxidant single-crystal graphene on twinned Pt(111). Carbon, 2021, 181, 225-233.	5.4	12
58427	Conformal coating of lithium-zinc alloy on 3D conducting scaffold for high areal capacity dendrite-free lithium metal batteries. Carbon, 2021, 181, 99-106.	5.4	19
58428	Engineering Na+-layer spacings to stabilize Mn-based layered cathodes for sodium-ion batteries. Nature Communications, 2021, 12, 4903.	5.8	109
58429	Nitrogen-enriched graphene framework from a large-scale magnesiothermic conversion of CO2 with synergistic kinetics for high-power lithium-ion capacitors. NPG Asia Materials, 2021, 13, .	3.8	29
58430	Work Function Trends and New Low-Work-Function Boride and Nitride Materials for Electron Emission Applications. Journal of Physical Chemistry C, 2021, 125, 17400-17410.	1.5	13

#	Article	IF	Citations
58431	Valleytronic and magneto-optical properties of Janus and conventional <mml:math xmlns:mml="http://www.w3.org/1998/Math/MathML"><mml:mrow><mml:mi>TiBrI</mml:mi><mml:mo>/</mml:mo><mml:mi>Cr</mml: mathvariant="normal">I</mml:mi><mml:mn>3</mml:mn></mml:msub></mml:mrow></mml:math> and <mml:math xmlns:mml="http://www.w3.org/1998/Math/MathML"><mml:mrow><mml:mi>Ti</mml:mi><mml:msub><mml:mi>X</mml:mi><mml:mn> mathvarian. Physical Review B, 2021, 104, .	1.1	21
58432	Structural and Optoelectronic Properties of Two-Dimensional Ruddlesdenâ€“Popper Hybrid Perovskite CsSnBr3. Nanomaterials, 2021, 11, 2119.	1.9	7
58433	Impact of NOx and NH3 addition on toluene oxidation over MnOx-CeO2 catalyst. Journal of Hazardous Materials, 2021, 416, 125939.	6.5	37
58434	Evidence of spin reorientation and anharmonicity in kagome ferromagnet Fe3Sn2. Applied Physics Letters, 2021, 119, .	1.5	5
58435	Improved Al-Mg alloy surface segregation predictions with a machine learning atomistic potential. Physical Review Materials, 2021, 5, .	0.9	18
58436	Differentiable sampling of molecular geometries with uncertainty-based adversarial attacks. Nature Communications, 2021, 12, 5104.	5.8	34
58437	Identification of two-dimensional layered dielectrics from first principles. Nature Communications, 2021, 12, 5051.	5.8	44
58438	Identification of active catalysts for the acceptorless dehydrogenation of alcohols to carbonyls. Nature Communications, 2021, 12, 5100.	5.8	21
58439	Nature of the Active Sites on Ni/CeO₂ Catalysts for Methane Conversions. ACS Catalysis, 2021, 11, 10604-10613.	5.5	37
58440	Robust topological state against magnetic impurities observed in the superconductor <mml:math xmlns:mml="http://www.w3.org/1998/Math/MathML"><mml:msub><mml:mi>PbTaSe</mml:mi><mml:mn>2</mml:mn></mml:msub></ Physical Review B, 2021, 104, .	1.1	0
58441	Physicochemical properties of MnTiO3 powders obtained by molten salt method. Ceramics International, 2021, 47, 33315-33321.	2.3	3
58442	Electronic structure of a borophene layer in rare-earth aluminum/chromium boride and its hydrogenated derivative borophane. Physical Review Materials, 2021, 5, .	0.9	13
58443	Evidence for a Magnetic-Field-Induced Ideal Type-II Weyl State in Antiferromagnetic Topological Insulator <mml:math xmlns:mml="http://www.w3.org/1998/Math/MathML" display="inline"><mml:mrow><mml:mi>Mn</mml:mi><mml:msub><mml:mrow><mml:mo stretchy="false">(</mml:mo><mml:msub><mml:mrow><mml:mi>Bi</mml:mi></mml:mrow><mml:mrow><mml:mn>1</mml:mn><mml:	2.8	30
58444	Nonlinear optical property and application of yttrium oxide in erbium-doped fiber lasers. Optics Express, 2021, 29, 29402.	1.7	26
58445	Biaxial Strain-Induced Electronic Structure and Optical Properties of SiP$$_{2}$$S Monolayer. Journal of Electronic Materials, 2021, 50, 6253-6260.	1.0	11
58446	Constructing van der Waals Heterogeneous Photocatalysts Based on Atomically Thin Carbon Nitride Sheets and Graphdiyne for Highly Efficient Photocatalytic Conversion of CO₂ into CO. ACS Applied Materials & Interfaces, 2021, 13, 40629-40637.	4.0	51
58447	High Thermoelectric Performance Achieved in Bulk Selenium with Nanostructural Building Blocks. ACS Applied Electronic Materials, 2021, 3, 3824-3834.	2.0	5
58448	Honeycomb Boron on Al(111): From the Concept of Borophene to the Two-Dimensional Boride. ACS Nano, 2021, 15, 15153-15165.	7.3	20

#	Article	IF	Citations
58449	Atomic-resolution study of charge transfer effects at the <mml:math xmlns:mml="http://www.w3.org/1998/Math/MathML"><mml:mrow><mml:mi>LaTi</mml:mi><mml:msub><mml:mi mathvariant="normal">O</mml:mi><mml:mn>3</mml:mn></mml:msub></mml:mrow><mml:mo>/</mml:mo><mml:mrow><mml:mi>La mathvariant="normal">O</mml:mi><mml:mn>3</mml:mn></mml:msub></mml:mrow></mml:math> interface. Physical Review B, 2021, 104, .	3.7	1
58450	Tuning the kinetics of zinc ion in MoS2 by polyaniline intercalation. Electrochimica Acta, 2021, 388, 138624.	2.6	26
58451	Investigation of Negative Charge Storage Mechanism in the Potassium Ion Electret by First-Principle Calculations. IEEJ Transactions on Sensors and Micromachines, 2021, 141, 292-298.	0.0	0
58452	Theoretical Investigation on Rare Earth Elements of Y, Nd and La Atomsâ€™ Adsorption on the Kaolinite (001) and (001Â¯) Surfaces. Minerals (Basel, Switzerland), 2021, 11, 856.	0.8	6
58453	Nonmetalâ€toâ€metal transition in dense fluid helium. Contributions To Plasma Physics, 0, , e202100105.	0.5	2
58454	Monolayer 1T and 1Tâ€² MoSO as Promising Electrocatalyst for Hydrogen Evolution based on First Principle Calculations. ChemPhysChem, 2021, 22, 2034-2041.	1.0	5
58455	Alloying Process at the Interface of Au-Li Studied Using Neural Network Potential. Vacuum and Surface Science, 2021, 64, 369-374.	0.0	0
58456	One-dimensional ferromagnetic semiconductor <mml:math xmlns:mml="http://www.w3.org/1998/Math/MathML"><mml:mrow><mml:mi>CrSb</mml:mi><mml:msub><mml:mi>Se</mml:mi><mml:mi><m with high Curie temperature and large magnetic anisotropy. Physical Review B, 2021, 104, .	3.7	9
58457	Cyclic Etherâ€“Water Hybrid Electrolyte-Guided Dendrite-Free Lamellar Zinc Deposition by Tuning the Solvation Structure for High-Performance Aqueous Zinc-Ion Batteries. ACS Applied Materials & Interfaces, 2021, 13, 40638-40647.	4.0	40
58458	Au³⁺ Species Boost the Catalytic Performance of Au/ZnO for the Semi-hydrogenation of Acetylene. ACS Applied Materials & Interfaces, 2021, 13, 40429-40440.	4.0	19
58459	Mechanistic studies of oxygen reduction and evolution reactions on Ni3S2 surfaces. Applied Catalysis A: General, 2021, 624, 118324.	2.2	6
58460	Interfacial oxidation of hafnium modified NiAl alloys. Corrosion Science, 2021, 189, 109604.	3.0	8
58461	Ab-initio simulation studies of chromium solvation in molten fluoride salts. Journal of Molecular Liquids, 2021, 335, 116351.	2.3	20
58462	Low Barrier for Exciton Self-Trapping Enables High Photoluminescence Quantum Yield in Cs₃Cu₂I₅. Journal of Physical Chemistry Letters, 2021, 12, 8447-8452.	2.1	16
58463	Initial Steps in CH₄ Pyrolysis on Cu and Ni. Journal of Physical Chemistry C, 2021, 125, 18665-18672.	1.5	4
58464	N-doping in graphdiyne on embedding of metals and its effect in catalysis. Applied Surface Science, 2021, 557, 149815.	3.1	14
58465	B-Site Columnar-Ordered Halide Double Perovskites A₂B(II)â€²_{0.5}B(II)X₅ with B(II)â€²/Vacancy Disordering. Chemistry of Materials, 2021, 33, 7106-7112.	3.2	8
58466	Chemically Accurate Vibrational Free Energies of Adsorption from Density Functional Theory Molecular Dynamics: Alkanes in Zeolites. Journal of Chemical Theory and Computation, 2021, 17, 5849-5862.	2.3	13

#	Article	IF	Citations
58467	A non-polluting method for rapidly purifying uranium-containing wastewater and efficiently recovering uranium through electrochemical mineralization and oxidative roasting. Journal of Hazardous Materials, 2021, 416, 125885.	6.5	30
58468	Tunable Band Gaps in MUV-10(M): A Family of Photoredox-Active MOFs with Earth-Abundant Open Metal Sites. Journal of the American Chemical Society, 2021, 143, 12609-12621.	6.6	26
58469	Theoretical Study of Oxygen Vacancy on Indium Oxide for Promoted Photothermal Catalytic Water Splitting. Journal of Physical Chemistry C, 2021, 125, 19294-19300.	1.5	4
58470	Stability and mechanical, electronic, and optical investigations of a new Heusler alloy: Ag2ScGe. Results in Physics, 2021, 27, 104518.	2.0	3
58471	Accelerating the discovery of novel Î³/Î³' Co-based superalloys by probing temperature and alloying effects on the Î³' precipitates. Materialia, 2021, 18, 101171.	1.3	6
58472	The Role of Roughening to Enhance Selectivity to C₂₊ Products during CO₂ Electroreduction on Copper. ACS Energy Letters, 2021, 6, 3252-3260.	8.8	38
58473	X-ray spectroscopic and first-principles investigation of lead tungstate under pressure. Physical Review B, 2021, 104, .	1.1	3
58474	Mineralization of norfloxacin in a CoFeâ€“LDH/CF cathode-based heterogeneous electro-fenton system: Preparation parameter optimization of the cathode and conversion mechanisms of H2O2 to Â·OH. Chemical Engineering Journal, 2021, 417, 129240.	6.6	66
58475	Titanium Carbide MXene Shows an Electrochemical Anomaly in Water-in-Salt Electrolytes. ACS Nano, 2021, 15, 15274-15284.	7.3	56
58476	Spinâ€Dependent Charge Transport in 1D Chiral Hybrid Leadâ€Bromide Perovskite with High Stability. Advanced Functional Materials, 2021, 31, 2104605.	7.8	44
58477	Controllable CO2 electrocatalytic reduction via ferroelectric switching on single atom anchored In2Se3 monolayer. Nature Communications, 2021, 12, 5128.	5.8	110
58478	Correlation-driven topological and valley states in monolayer <mml:math xmlns:mml="http://www.w3.org/1998/Math/MathML"><mml:mrow><mml:msub><mml:mi>VSi</mml:mi><mml:mn>2</mml:mn></mml:msub><mml:msub><mml:mi mathvariant="normal">P</mml:mi><mml:mn>4</mml:mn></mml:msub></mml:mrow></mml:math>. Physical Review B, 2021, 104, .	1.1	54
58479	High band degeneracy and weak chemical bonds leading to enhanced thermoelectric transport properties in 2Hâ€“MoTe2. Journal of Solid State Chemistry, 2021, 300, 122227.	1.4	2
58480	Electrically controlled valley polarization in 2D buckled honeycomb structures. Modern Physics Letters B, 2021, 35, 2150390.	1.0	1
58481	Spectroscopic and Computational Study of Boronium Ionic Liquids and Electrolytes. Chemistry - A European Journal, 2021, 27, 12826-12834.	1.7	7
58482	Quasi-One-Dimensional Structure and Possible Helical Antiferromagnetism of RbMn₆Bi₅. Inorganic Chemistry, 2021, 60, 12941-12949.	1.9	14
58483	Direct Oxidative Amination of the Methyl Câ€“H Bond in N-Heterocycles over Metal-Free Mesoporous Carbon. ACS Catalysis, 2021, 11, 10902-10912.	5.5	11
58484	Strain induced structural phase transition in TM6X6 (TM = Mo, W; X = S, Se, Te) nanowires. Journal of Solid State Chemistry, 2021, 300, 122194.	1.4	3

#	Article	IF	Citations
58485	On the selectivity of butyric acid photoreforming over Au/TiO2 and Pt/TiO2 by UV and visible radiation: A combined experimental and theoretical study. Applied Catalysis A: General, 2021, 624, 118321.	2.2	8
58486	First-principles study of electron transport in ScN. Physical Review B, 2021, 104, .	1.1	13
58487	Structure, Magnetism, and Thermal Stability of La₂NiO_{2.5}F₃: A Ruddlesdenâ€“Popper Oxyfluoride Crystallizing in Space Group P4₂/nnm. Inorganic Chemistry, 2021, 60, 13646-13657.	1.9	3
58488	Towards ab initio identification of paramagnetic substitutional carbon defects in hexagonal boron nitride acting as quantum bits. Physical Review B, 2021, 104, .	1.1	48
58489	Different Effects of Mg and Si Doping on the Thermal Transport of Gallium Nitride. Frontiers in Materials, 2021, 8, .	1.2	9
58490	Electronic and thermoelectric properties of natural layered structural compounds SrCuChF (Ch=S,) Tj ETQq1 1 0.784314 rgBT /Overlo	1.9	1
58491	Effects of Ce and La elements on interfacial bonding, thermal damage and mechanical performance of brazed diamonds with Ni Cr filler alloy. International Journal of Refractory Metals and Hard Materials, 2021, 98, 105571.	1.7	14
58492	Dynamics of Initial Hydrogen Spillover from a Single Atom Platinum Active Site to the Cu(111) Host Surface: The Impact of Substrate Electronâ€“Hole Pairs. Journal of Physical Chemistry Letters, 2021, 12, 8423-8429.	2.1	19
58493	Flexible Piezoelectricity of Two-Dimensional Materials Governed by Effective Berry Curvature. Journal of Physical Chemistry Letters, 2021, 12, 8220-8228.	2.1	3
58494	The Impact of Vibrational Entropy on the Segregation of Cu to Antiphase Boundaries in Fe3Al. Magnetochemistry, 2021, 7, 108.	1.0	3
58495	Enantioselective Recognition and Separation of C₂ Symmetric Substances via Chiral Metalâ€“Organic Frameworks. ACS Applied Materials & Interfaces, 2021, 13, 37412-37421.	4.0	21
58496	Examining normal modes as fundamental heat carriers in amorphous solids: The case of amorphous silicon. Journal of Applied Physics, 2021, 130, 055101.	1.1	12
58498	Topological Phase and Quantum Anomalous Hall Effect in Ferromagnetic Transition-Metal Dichalcogenides Monolayer 1Tâ€²VSe2. Nanomaterials, 2021, 11, 1998.	1.9	6
58499	Chirality-induced spin texture switching in twisted bilayer graphene. Physical Review B, 2021, 104, .	1.1	5
58500	Atomic-level insights into the activation of nitrogen via hydrogen-bond interaction toward nitrogen photofixation. CheM, 2021, 7, 2118-2136.	5.8	33
58501	Revealing pressure-driven structural transitions in the hybrid improper ferroelectric <mml:math xmlns:mml="http://www.w3.org/1998/Math/MathML"><mml:msub><mml:mi mathvariant="normal">Sr</mml:mi><mml:mn>3</mml:mn></mml:msub><mml:msub><mml:mi mathvariant="normal">Sn</mml:mi><mml:mn>2</mml:mn></mml:msub><mml:msub><mml:mi mathvariant="normal">O</mml:mi><mml:mn>7</mml:mn></mml:msub></mml:math>. Physical Review B, 2021, 104, .	1.1	8
58502	Pressure-tuning structural and electronic transitions in semimetal CoSb. Physical Review B, 2021, 104, .	1.1	4
58503	Phase competition and negative piezoelectricity in interlayer-sliding ferroelectric <mml:math xmlns:mml="http://www.w3.org/1998/Math/MathML"><mml:mrow><mml:mi>Zr</mml:mi><mml:msub><mml:mi mathvariant="normal">I</mml:mi><mml:mn>2</mml:mn></mml:msub></mml:mrow></mml:math>. Physical Review Materials, 2021, 5, .	0.9	18

#	Article	IF	Citations
58504	Common workflows for computing material properties using different quantum engines. Npj Computational Materials, 2021, 7, .	3.5	10
58505	A spontaneously formed plasmonic-MoTe2 hybrid platform for ultrasensitive Raman enhancement. Cell Reports Physical Science, 2021, 2, 100526.	2.8	10
58506	Atomically dispersed S-Fe-N4 for fast kinetics sodium-sulfur batteries via a dual function mechanism. Cell Reports Physical Science, 2021, 2, 100531.	2.8	31
58507	Machine Learning-Aided Materials Design Platform for Predicting the Mechanical Properties of Na-Ion Solid-State Electrolytes. ACS Applied Energy Materials, 2021, 4, 7862-7869.	2.5	14
58508	Restructuring of Lead Electrodes upon Adsorption of NO₃^{â€“} Anions Studied from First-Principles and Its Relevance for the Operation of Lead Quantum Switches. Journal of Physical Chemistry C, 2021, 125, 17962-17970.	1.5	1
58509	Mechanical origin of martensite-like structures in two-dimensional ReS2. Communications Materials, 2021, 2, .	2.9	4
58510	Pressure-Induced Transition from Spin to Superconducting States in Novel MnN₂. ACS Omega, 2021, 6, 21830-21836.	1.6	2
58511	Unusual defect properties in multivalent perovskite <mml:math xmlns:mml="http://www.w3.org/1998/Math/MathML"><mml:mrow><mml:msub><mml:mi>Cs</mml:mi><mml:mn>2</mml:mn></mml:msub><mml:mi mathvariant="normal">I</mml:mi><mml:mn>6</mml:mn></mml:mrow></mml:math> : A first-principles study. Physical Review Materials, 2021, 5, .	0.9	3
58512	Metadynamics sampling in atomic environment space for collecting training data for machine learning potentials. Npj Computational Materials, 2021, 7, .	3.5	7
58513	Unveiling the Local Structure and Luminescence Mechanism of Er³⁺-Doped LiYF₄: A Promising Near-Infrared Laser Crystal. Journal of Physical Chemistry C, 2021, 125, 18015-18021.	1.5	5
58514	Machine-Learning-Enabled Tricks of the Trade for Rapid Host Material Discovery in Liâ€“S Battery. ACS Applied Materials & Interfaces, 2021, 13, 53388-53397.	4.0	21
58515	Universal Machine Learning Interatomic Potentials: Surveying Solid Electrolytes. Journal of Physical Chemistry Letters, 2021, 12, 8115-8120.	2.1	45
58516	Intrinsic Descriptors for Coordination Environment and Synergistic Effects of Metal and Environment in Single-Atom-Catalyzed Carbon Dioxide Electroreduction. Journal of Physical Chemistry C, 2021, 125, 18180-18186.	1.5	6
58517	Partial charge transfer and absence of induced magnetization in EuS(111)/Bi2Se3 heterostructures. Physical Review B, 2021, 104, .	1.1	7
58518	Vast Structural and Polymorphic Varieties of Semiconductors AMMâ€²Q4 (A = K, Rb, Cs, Tl; M = Ga, In; Mâ€² =) Tj ETQq0 0 0 rgBT /Over	3.2	6
58519	Computational Study of the Effect of Doping with Ti on NaAlH4 Nanocluster Dehydrogenation. Russian Journal of Physical Chemistry A, 2021, 95, 1646-1654.	0.1	0
58520	Arene and functionalized arene based two dimensional <scp>organicâ€“inorganic</scp> hybrid perovskites for photovoltaic applications. Journal of Computational Chemistry, 2021, 42, 1982-1990.	1.5	16
58521	Application of germanene monolayers as efficient anchoring material to immobilize lithium polysulfides in Li-S batteries. Applied Surface Science, 2021, 558, 149850.	3.1	8

#	Article	IF	Citations
58522	Observation and manipulation of valley polarization in two-dimensional H-Tl2O/CrI3 heterostructure. Applied Surface Science, 2021, 558, 149604.	3.1	11
58523	Double activation of oxygen intermediates of oxygen reduction reaction by dual inorganic/organic hybrid electrocatalysts. Nano Energy, 2021, 86, 106048.	8.2	5
58524	Transition metal atoms (Fe, Co, Ni, Cu, Zn) doped RuIr surface for the hydrogen evolution reaction: A first-principles study. Applied Surface Science, 2021, 556, 149801.	3.1	27
58525	Selective conversion of nitrate to nitrogen by CuNi alloys embedded mesoporous carbon with breakpoint chlorination. Journal of Water Process Engineering, 2021, 42, 102174.	2.6	6
58526	Sandwiched electrode buffer for efficient and stable perovskite solar cells with dual back surface fields. Joule, 2021, 5, 2148-2163.	11.7	63
58527	Intrinsic Defects in LiMn₂O₄: First-Principles Calculations. ACS Omega, 2021, 6, 21255-21264.	1.6	14
58528	Lattice-matched III-nitride structures comprising BAlN, BGaN, and AlGaN for ultraviolet applications. Materials Research Express, 2021, 8, 086202.	0.8	6
58529	In situ study on the compression deformation of MoNbTaVW high-entropy alloy. Journal of Alloys and Compounds, 2021, 871, 159557.	2.8	7
58530	Band gaps of crystalline solids from Wannier-localizationâ€“based optimal tuning of a screened range-separated hybrid functional. Proceedings of the National Academy of Sciences of the United States of America, 2021, 118, .	3.3	49
58531	Computational investigation of structural, magnetic, electronic and optical properties of the cluster Mn-X6 (X=P, S, Cl, Br or Te) doped monolayer WSe2. Thin Solid Films, 2021, 732, 138793.	0.8	2
58532	Fundamental properties of octalithium plumbate ceramic breeder material. Journal of Nuclear Materials, 2021, 552, 152982.	1.3	3
58533	Solvent-free synthesis of N-doped carbon-based catalyst for high-efficient reduction of 4-nitrophenol. Journal of Environmental Chemical Engineering, 2021, 9, 105649.	3.3	8
58534	Exploration of the Exceptional Capacitive Deionization Performance of CoMn₂O₄ Microspheres Electrode. Energy and Environmental Materials, 2023, 6, .	7.3	8
58535	Strong out-of-plane excitons in 2D hybrid halide double perovskites. Applied Physics Letters, 2021, 119, 051103.	1.5	15
58536	MoirÃ© Skyrmions and Chiral Magnetic Phases in Twisted CrX₃ (X = I, Br, and Cl) Bilayers. Nano Letters, 2021, 21, 6633-6639.	4.5	69
58537	Effect of B-doping on the mechanical properties, thermal stability and oxidation resistance of TiAlN coatings. International Journal of Refractory Metals and Hard Materials, 2021, 98, 105531.	1.7	20
58538	Unveiling the intrinsic band alignment and robust water oxidation features of hierarchical BiVO4 phase junction. Chemical Engineering Journal, 2022, 436, 131516.	6.6	26
58539	Elucidating the Cooperative Roles of Water and Lewis Acidâ€“Base Pairs in Cascade Câ€“C Coupling and Self-Deoxygenation Reactions. Jacs Au, 2021, 1, 1471-1487.	3.6	5

#	Article	IF	Citations
58540	Manipulating crystallization dynamics through chelating molecules for bright perovskite emitters. Nature Communications, 2021, 12, 4831.	5.8	56
58541	In Situ Synthesis of Vacancy-Rich Titanium Sulfide Confined in a Hollow Carbon Nanocage as an Efficient Sulfur Host for Lithiumâ€“Sulfur Batteries. ACS Applied Energy Materials, 2021, 4, 10104-10113.	2.5	15
58542	Remarkable-cycling-performance anode for Li-ion battery: The bilayer Î²-bismuthene. Electrochimica Acta, 2021, 388, 138641.	2.6	7
58543	Elucidating the Impact of Mg Substitution on the Properties of NASICONâ€Na₃₊_yV_{2â€™}_yMg_y(PO₄)₃ Cathodes. Advanced Functional Materials, 2021, 31, 2105463.	18.5	14
58544	Phase Regulation of CsPb₂Br₅/CsPbBr₃ Perovskite Nanocrystals by Doping with Divalent Cations: Implications for Optoelectronic Devices with Enhanced Stability and Reduced Toxicity. ACS Applied Nano Materials, 2021, 4, 9213-9222.	2.4	11
58545	Enhanced microstructural stability of Î³/Î³â€²-strengthened Co-Ti-Mo-based alloys through Al additions. Acta Materialia, 2021, 214, 117011.	3.8	7
58546	Germanene structure enhancement by adjacent insoluble domains of lead. Physical Review Research, 2021, 3, .	1.3	6
58547	Extremely flat band in antiferroelectric bilayer Î±-In₂Se₃ with large twist-angle. New Journal of Physics, 2021, 23, 083019.	1.2	11
58548	MoirÃ© excitons in defective van der Waals heterostructures. Proceedings of the National Academy of Sciences of the United States of America, 2021, 118, .	3.3	16
58549	Low lattice thermal conductivity and high figure of merit in nâ€type doped <scp>fullâ€Heusler</scp> compounds X ₂ <scp>YAu</scp> (XÂ=ÂSr, Ba; YÂ=Âas, Sb). International Journal of Energy Research, 2021, 45, 20949-20958.	2.2	11
58550	Magnetism-driven unconventional effects in Ising superconductors: Role of proximity, tunneling, and nematicity. Physical Review B, 2021, 104, .	1.1	6
58551	CoCrFeNi High-Entropy Alloy as an Enhanced Hydrogen Evolution Catalyst in an Acidic Solution. Journal of Physical Chemistry C, 2021, 125, 17008-17018.	1.5	25
58552	Cr2NX2 MXene (X = O, F, OH): A 2D ferromagnetic half-metal. Applied Physics Letters, 2021, 119, .	1.5	32
58553	Ferroelectric Controlled Gas Adsorption in Doped Graphene/In 2 Se 3 Heterostructure. Advanced Materials Technologies, 0, , 2100463.	3.0	4
58554	Crystal structure, sorption properties, and electronic structure of flexible MOF, (Ni-4,4â€²azopyridine)[Ni(CN)4]. Solid State Sciences, 2021, 118, 106646.	1.5	5
58555	Wetting and interfacial behavior of Alâ€“Ti/4Hâ€“SiC system:A combined study of experiment and DFT simulation. Ceramics International, 2021, 47, 32545-32553.	2.3	6
58556	A First-Principles Study of the Mechanism and Site Requirements for CO₂ Methanation over CeO₂-Supported Ru Catalyst. Journal of Physical Chemistry C, 2021, 125, 18161-18169.	1.5	10
58557	Transient Hydrodynamic Lattice Cooling by Picosecond Laser Irradiation of Graphite. Physical Review Letters, 2021, 127, 085901.	2.9	19

#	Article	IF	Citations
58558	Size-dependent strain-engineered nanostructures in MoS₂monolayer investigated by atomic force microscopy. Nanotechnology, 2021, 32, 465703.	1.3	8
58559	Insights into superconductivity of LaO from experiments and first-principles calculations. Physical Review B, 2021, 104, .	1.1	2
58560	Magnetic Topological Semimetal Phase with Electronic Correlation Enhancement in SmSbTe. Advanced Quantum Technologies, 2021, 4, 2100063.	1.8	11
58561	Ordering of Oxygen Vacancies and Related Ferroelectric Properties in <mml:math xmlns:mml="http://www.w3.org/1998/Math/MathML" display="inline"><mml:mrow><mml:msub><mml:mrow><mml:mi>HfO</mml:mi></mml:mrow><mml:mrow><mml:mn>2</mml:mn><m Physical Review Letters, 2021, 127, 087602.	2.9	31
58562	A Review on Capturing Twin Nucleation in Crystal Plasticity for Hexagonal Metals. Metals, 2021, 11, 1373.	1.0	14
58563	Electronic and Optical Properties of Atomic-Scale Heterostructure Based on MXene and MN (M = Al,) Tj ETQq1 1 0.784314 rgBT /Ove	1.9	33
58564	Preparation and characterization of Ag2ZnSn(S,Se)4 and its application in improvement of power conversion efficiency of Cu2ZnSn(S,Se)4-based solar cells. Ceramics International, 2021, 47, 34473-34480.	2.3	4
58565	Electronic Mechanism of Martensitic Transformation in Nb-doped NiTi Alloys: A First-Principles Investigation. ACS Omega, 2021, 6, 22033-22038.	1.6	2
58566	Surface structure of mass-selected niobium oxide nanoclusters on Au(111). Nanotechnology, 2021, 32, 475601.	1.3	7
58567	Two-Dimensional Boron-Rich Monolayer B_xN as High Capacity for Lithium-Ion Batteries: A First-Principles Study. ACS Applied Materials & Interfaces, 2021, 13, 41169-41181.	4.0	20
58568	Ferroelectricity and Ferromagnetism Achieved via Adjusting Dimensionality in BiFeO₃/BiMnO₃ Superlattices. ACS Applied Materials & Interfaces, 2021, 13, 41315-41322.	4.0	8
58569	Aspects of symmetry and topology in the charge density wave phase of 1Tâ€“TiSe₂. New Journal of Physics, 2021, 23, 083037.	1.2	7
58570	Reversible dual anionic-redox chemistry in NaCrSSe with fast charging capability. Journal of Power Sources, 2021, 502, 230022.	4.0	5
58571	Increasing Accessible Subsurface to Improving Rate Capability and Cycling Stability of Sodiumâ€Ion Batteries. Advanced Materials, 2021, 33, e2100808.	11.1	110
58572	Thermodynamics of Atomic Layer Etching Chemistry on Copper and Nickel Surfaces from First Principles. Chemistry of Materials, 2021, 33, 6774-6786.	3.2	3
58573	Two Coexisting Forms of Simple Molecules for Directing Sesqui-Unit-Cell Zeolite Nanosheets. Chemistry of Materials, 2021, 33, 6934-6941.	3.2	11
58574	Insights into Water Adsorption in Potassium-Exchanged X-type Faujasite Zeolite: Molecular Simulation and Experiment. Journal of Physical Chemistry C, 2021, 125, 19405-19416.	1.5	10
58575	Anchoring an Fe Dimer on Nitrogen-Doped Graphene toward Highly Efficient Electrocatalytic Ammonia Synthesis. ACS Applied Materials & Interfaces, 2021, 13, 43632-43640.	4.0	37

#	Article	IF	Citations
58576	Beyond graphene: Clean, hydrogenated and halogenated silicene, germanene, stanene, and plumbene. Progress in Surface Science, 2021, 96, 100615.	3.8	42
58577	Electronic metal-support interactions and their promotional effect on CO2 methanation on Ru/ZrO2 catalysts. Journal of Catalysis, 2021, 400, 407-420.	3.1	44
58578	Mediating the Local Oxygen-Bridge Interactions of Oxysalt/Perovskite Interface for Defect Passivation of Perovskite Photovoltaics. Nano-Micro Letters, 2021, 13, 177.	14.4	24
58579	First- and second-order phase transitions in RE6Co2Ga (RE = Ho, Dy or Gd) cryogenic magnetocaloric materials. Science China Materials, 2021, 64, 2846-2857.	3.5	62
58580	Electrical performance enhancement by resonant states in PbSe single-crystal growth via Bi-flux method. Journal of Materials Science: Materials in Electronics, 2021, 32, 24198-24208.	1.1	1
58581	Effects of mechanical and electronic properties for B2 FeAl modified by several kinds of point defects: First-principles study. International Journal of Modern Physics B, 2021, 35, .	1.0	0
58582	Vacancy Formation Energy in the Cubic Phase of Magnetite in the Framework of the DFT+U Method. Journal of Experimental and Theoretical Physics, 2021, 133, 206-228.	0.2	6
58583	Evolution of the local structure surrounding nitrogen atoms upon the amorphous to crystalline phase transition in nitrogen-doped Cr2Ge2Te6 phase-change material. Applied Surface Science, 2021, 556, 149760.	3.1	4
58584	Ta₂Ni₃Se₈: 1D van der Waals Material with Ambipolar Behavior. Small, 2021, 17, e2102602.	5.2	15
58585	SpaceGroupIrep: A package for irreducible representations of space group. Computer Physics Communications, 2021, 265, 107993.	3.0	30
58586	Prediction of double-Weyl points in the iron-based superconductor <mml:math xmlns:mml="http://www.w3.org/1998/Math/MathML"><mml:mrow><mml:mi>Ca</mml:mi><mml:mi mathvariant="normal">K</mml:mi><mml:msub><mml:mi>Fe</mml:mi><mml:mn>4</mml:mn></mml:msub><mml:msub><mml:mi>As</mml:mi> Physical Review B, 2021, 104, .	1.1	5
58587	Optical and tuning electronic properties of GeC/MoS2 van der Waals heterostructures by electric field and strain: A first-principles study. Superlattices and Microstructures, 2021, 156, 106935.	1.4	9
58588	First principles study on formation and migration energies of sodium and lithium in graphite. Physical Review Materials, 2021, 5, .	0.9	2
58589	Band Alignment in Monolayer Boron Phosphide with Janus <mml:math xmlns:mml="http://www.w3.org/1998/Math/MathML" display="inline" overflow="scroll"><mml:mrow><mml:mi>Mo</mml:mi><mml:mi mathvariant="normal">S</mml:mi><mml:mi>Se</mml:mi></mml:mrow></mml:math> Heterobilayers under Strain and Electric Field. Physical Review Applied, 2021, 16, .	1.5	31
58590	Demonstration of an x-ray Raman spectroscopy setup to study warm dense carbon at the high energy density instrument of European XFEL. Physics of Plasmas, 2021, 28, 082701.	0.7	11
58591	Atypical behavior of intrinsic defects and promising dopants in two-dimensional <mml:math xmlns:mml="http://www.w3.org/1998/Math/MathML"><mml:msub><mml:mrow><mml:mi>WS</mml:mi></mml:mrow><mml:mn>2</mml:mn> Physical Review Materials, 2021, 5, .	0.9	10
58592	Double Side Interfacial Optimization for Lowâ€Temperature Stable CsPbI₂Br Perovskite Solar Cells with High Efficiency Beyond 16%. Energy and Environmental Materials, 2022, 5, 637-644.	7.3	27
58593	Impact of Cation Substitution in (Ag_xCu_{1â^'x})₂ZnSnSe₄ Absorberâ€Based Solar Cells toward 10% Efficiency: Experimental and Theoretical Analyses. Solar Rrl, 2021, 5, 2100441.	3.1	11

#	Article	IF	Citations
58594	Quantum physical reality of polar-nonpolar oxide heterostructures. Physical Review B, 2021, 104, .	1.1	2
58595	Rashba-Type Dzyaloshinskiiâ€“Moriya Interaction, Perpendicular Magnetic Anisotropy, and Skyrmion States at 2D Materials/Co Interfaces. Nano Letters, 2021, 21, 7138-7144.	4.5	22
58596	Strain-induced electronic, stability and enhancement of thermoelectric performance of 2D Si2C3 monolayer: An emerging material for renewable energy. Physica E: Low-Dimensional Systems and Nanostructures, 2021, 132, 114769.	1.3	3
58597	The dynamic interplay between water and oxygen vacancy at the near-surface of ceria. Journal of Physics Condensed Matter, 2021, 33, 424001.	0.7	2
58598	Coupling between bulk thermal defects and surface segregation dynamics. Physical Review B, 2021, 104, .	1.1	3
58599	Computational study of mechanical stability and phonon properties of MXenes Mo2ScC2T2 (Tâ€‰=â€‰O and) Tj ETQq1 1 0.784314	1.1	2
58600	Advanced Self-Passivating Alloys for an Application under Extreme Conditions. Metals, 2021, 11, 1255.	1.0	12
58601	Reactivity of transition-metal alloys to oxygen and sulfur. Physical Review Materials, 2021, 5, .	0.9	1
58602	First-principles investigations on a two-dimensional S₃N₂/black phosphorene van der Waals heterostructure: mechanical, carrier transport and thermoelectric anisotropy. Journal of Physics Condensed Matter, 2021, 33, 425301.	0.7	7
58603	Polymorph of LiAlP₂O₇: Combined Computational, Synthetic, Crystallographic, and Ionic Conductivity Study. Inorganic Chemistry, 2021, 60, 14083-14095.	1.9	7
58604	Stability, electronic structure, and magnetic moment of vanadium phthalocyanine grafted to the Au(1) Tj ETQq0 0 0 rgBT /Overlock 10 T	1.1	0
58605	Ammonia Decomposition over CaNH-Supported Ni Catalysts via an NH^{2â€“}-Vacancy-Mediated Marsâ€“van Krevelen Mechanism. ACS Catalysis, 2021, 11, 11005-11015.	5.5	45
58606	Understanding creep of a single-crystalline Co-Al-W-Ta superalloy by studying the deformation mechanism, segregation tendency and stacking fault energy. Acta Materialia, 2021, 214, 117019.	3.8	23
58607	Chirality recognition and separation of 4-ethynyltriphenylamine induced by chiral KagomÃ© network on Cu (1 1 1). Chemical Physics, 2021, 548, 111216.	0.9	0
58608	Synergistic effect of solute and strain on the electrochemical degradation in representative Zn-based and Mg-based alloys. Corrosion Science, 2021, 188, 109539.	3.0	4
58609	Insights into vitamin B3, B6 and C as inhibitor of steel reinforcement: A DFTÂ+ÂU study. Construction and Building Materials, 2021, 294, 123571.	3.2	17
58610	Understanding of the crystal structure, mechanical, vibrational properties of Î±-MgSO4 under pressure. Vacuum, 2021, 190, 110280.	1.6	1
58611	The Li ion transport behavior in the defect graphene composite Li3N SEI: a first-principle calculation. Materials Today Chemistry, 2021, 21, 100510.	1.7	6

#	Article	IF	Citations
58612	van der Waals type II carbon nitride homojunctions for visible light photocatalytic hydrogen evolution. Nano Research, 2023, 16, 5864-5872.	5.8	12
58613	Novel B-N-Co surface bonding states constructed on hollow tubular boron doped g-C3N4/CoP for enhanced photocatalytic H2 evolution. Journal of Colloid and Interface Science, 2021, 595, 69-77.	5.0	26
58614	Ab Initio Quantum-Mechanical Predictions of Semiconducting Photocathode Materials. Micromachines, 2021, 12, 1002.	1.4	5
58615	Encapsulation and Adsorption of Halogens into Single-Walled Carbon Nanotubes. Micro, 2021, 1, 140-150.	0.9	2
58616	Topological spin textures in a two-dimensional MnBi2(Se, Te)4 Janus material. Applied Physics Letters, 2021, 119, .	1.5	30
58617	Low-Temperature Fabrication of Phase-Pure Î±-FAPbI3 Films by Cation Exchange from Two-Dimensional Perovskites for Solar Cell Applications. Energy & Fuels, 0, , .	2.5	11
58618	Dissociation of water on atomic oxygen-covered Rh nanoclusters supported on graphene/Ru(0001). Journal of Chemical Physics, 2021, 155, 074701.	1.2	1
58619	Direct Growth of van der Waals Tin Diiodide Monolayers. Advanced Science, 2021, 8, e2100009.	5.6	10
58620	Dissociative and Associative Concerted Mechanism for Ammonia Synthesis over Co-Based Catalyst. Journal of the American Chemical Society, 2021, 143, 12857-12866.	6.6	50
58621	Interfacial Bonding Controls Friction in Diamondâ€“Rock Contacts. Journal of Physical Chemistry C, 2021, 125, 18395-18408.	1.5	9
58622	Purely one-dimensional ferroelectricity and antiferroelectricity from van der Waals niobium oxide trihalides. Npj Computational Materials, 2021, 7, .	3.5	14
58623	Coverage-dependent magnetic and electronic properties of graphene with Co adatoms. International Journal of Modern Physics C, 2021, 32, .	0.8	0
58624	Dielectric screening and electric field control of ferromagnetism at the <mml:math xmlns:mml="http://www.w3.org/1998/Math/MathML"><mml:mrow><mml:msub><mml:mi>CaMnO</mml:mi><mml:mn>3</mml:mn></ interface. Physical Review B, 2021, 104, .	1.1	1
58625	Elucidating the Factors That Cause Cation Diffusion Shutdown in Spinel-Based Electrodes. Chemistry of Materials, 2021, 33, 6421-6432.	3.2	18
58626	Factors Governing Oxygen Vacancy Formation in Oxide Perovskites. Journal of the American Chemical Society, 2021, 143, 13212-13227.	6.6	75
58627	Two-Phase Transition Induced Amorphous Metal Phosphides Enabling Rapid, Reversible Alkali-Metal Ion Storage. ACS Nano, 2021, 15, 13486-13494.	7.3	23
58628	Impact of visible light and humidity on the stability of high-power light emitting diode packaging material. Journal of Applied Physics, 2021, 130, 083101.	1.1	3
58629	Defects Engineering of Lightweight Metalâ€“Organic Frameworks-Based Electrocatalytic Membrane for High-Loading Lithiumâ€“Sulfur Batteries. ACS Nano, 2021, 15, 13803-13813.	7.3	62

#	Article	IF	Citations
58630	Intrinsic anharmonicity and thermal properties of ultralow thermal conductivity <mml:math xmlns:mml="http://www.w3.org/1998/Math/MathML"><mml:mrow><mml:msub><mml:mi>Ba</mml:mi><mml:mn>6</mml:mn></mml:r Physical Review Materials, 2021, 5, .	3.6	8
58631	Tin-pest problem as a test of density functionals using high-throughput calculations. Physical Review Materials, 2021, 5, .	0.9	7
58632	Isomeric Compound Dendrites on a Monolayer WS₂ Substrate: Morphological Engineering and Formation Mechanism. ACS Applied Nano Materials, 2021, 4, 8408-8416.	2.4	7
58633	Stability and reactivity study of bio-molecules brucine and colchicine towards electrophile and nucleophile attacks: Insight from DFT and MD simulations. Journal of Molecular Liquids, 2021, 335, 116192.	2.3	53
58634	Molecular Dynamics Modeling of Mechanical Properties of Polymer Nanocomposites Reinforced by C7N6 Nanosheet. Surfaces, 2021, 4, 240-254.	1.0	3
58635	Carbon Deposition on Heterogeneous Pt Catalysts Promotes the Selective Hydrogenation of Halogenated Nitroaromatics. ACS Applied Materials & Interfaces, 2021, 13, 52193-52201.	4.0	16
58636	Dimensional crossover tuned by pressure in layered magnetic NiPS3. Science China: Physics, Mechanics and Astronomy, 2021, 64, 1.	2.0	16
58637	Theoretical and experimental investigations on mechanical properties of (Fe,Ni)Sn2 intermetallic compounds formed in SnAgCu/Fe-Ni solder joints. Materials Characterization, 2021, 178, 111195.	1.9	5
58638	Surface fluorinated nickel-graphene nanocomposites for high-efficiency methanol electrooxidation. International Journal of Hydrogen Energy, 2021, 46, 27138-27148.	3.8	5
58639	Unsupervised discovery of thin-film photovoltaic materials from unlabeled data. Npj Computational Materials, 2021, 7, .	3.5	13
58640	Multifunctionality in (K,Na)NbO3-based ceramic near polymorphic phase boundary. Journal of Applied Physics, 2021, 130, 064102.	1.1	2
58641	Band Gap Engineering and 14 Electron Superatoms in 2D Superoctahedral Boranes B₄X₂ (B, N, P, As, Sb). Journal of Physical Chemistry C, 2021, 125, 17280-17290.	1.5	6
58642	Pressure-Induced Martensitic Phase Transition and Low Lattice Thermal Conductivity of SrClF. Journal of Physical Chemistry C, 2021, 125, 17261-17270.	1.5	9
58643	Sâ€Scheme Photocatalytic Mechanism of Typeâ€I Band Alignment in Î±â€In₂Se₃/gâ€C₃N₄ Heterostructure. Physica Status Solidi - Rapid Research Letters, 2021, 15, 2100241.	1.2	7
58644	Hydrogen storage on Li-decorated B₄N: a first-principle calculation insight. Journal Physics D: Applied Physics, 2021, 54, 445501.	1.3	15
58645	New interaction potentials for alkaline earth silicate and borate glasses. Journal of Non-Crystalline Solids, 2021, 565, 120853.	1.5	11
58646	Role of Fluorine in Chemomechanics of Cation-Disordered Rocksalt Cathodes. Chemistry of Materials, 2021, 33, 7028-7038.	3.2	8
58647	Influence of Stacking on H⁺ Intercalation in Layered ACoO₂ (A =) Tj ETQq1 1 0.784314 rgBT Investigation. Chemistry of Materials, 2021, 33, 6942-6954.	3.2	15

#	Article	IF	Citations
58648	Giant Rashba-like spinâ€“orbit splitting with distinct spin texture in two-dimensional heterostructures*. Chinese Physics B, 2021, 30, 087307.	0.7	0
58649	A density-functional-theory-based and machine-learning-accelerated hybrid method for intricate system catalysis. Materials Reports Energy, 2021, 1, 100046.	1.7	13
58650	Defect and Impurity-Complex Depassivation During Electron-Beam Irradiation of GaAs. IEEE Transactions on Nuclear Science, 2021, 68, 1548-1555.	1.2	2
58651	Cost-Effective High-Throughput Calculation Based on Hybrid Density Functional Theory: Application to Cubic, Double, and Vacancy-Ordered Halide Perovskites. Journal of Physical Chemistry Letters, 2021, 12, 7885-7891.	2.1	8
58652	Metastable Î²-NdCo2B2: A Triclinic Polymorph with Magnetic Ordering. Chemistry of Materials, 2021, 33, 6374-6382.	3.2	1
58653	DFT-1/2 method applied to 2D topological insulators: fluorinated and hydrogenated group-IV honeycomb systems. Journal of Physics Condensed Matter, 2021, 33, 435501.	0.7	3
58654	Insights into Spontaneous Solid Electrolyte Interphase Formation at Magnesium Metal Anode Surface from Ab Initio Molecular Dynamics Simulations. ACS Applied Materials & Interfaces, 2021, 13, 38816-38825.	4.0	20
58655	Nitrogen-doped graphdiyne for effective metal deposition and heterogeneous Suzuki-Miyaura coupling catalysis. Applied Catalysis A: General, 2021, 623, 118244.	2.2	11
58656	Synthesis, Crystal Structure, Symmetry Relationships, and Electronic Structure of Bismuth Carbodiimide Bi₂(NCN)₃ and Its Ammonia Adduct Bi₂(NCN)₃Â·NH₃. Inorganic Chemistry, 2021, 60, 12664-12670.	1.9	4
58657	Multifunctional Molecule Engineered SnO₂ for Perovskite Solar Cells with High Efficiency and Reduced Lead Leakage. Solar Rrl, 2021, 5, 2100464.	3.1	26
58658	Sr7N2Sn3: a layered antiperovskite-type nitride stannide containing zigzag chains of Sn4 polyanions. Zeitschrift Fur Naturforschung - Section B Journal of Chemical Sciences, 2021, .	0.3	1
58659	Formation and influence of surface hydroxyls on product selectivity during CO2 hydrogenation by Ni/SiO2 catalysts. Journal of Catalysis, 2021, 400, 228-233.	3.1	27
58660	Atomic insights on intermixing of nanoscale nitride multilayer triggered by nanoindentation. Acta Materialia, 2021, 214, 117004.	3.8	19
58661	Pd4O3 Subsurface Oxide on Pd(111) Formed during Oxygen Adsorption-Induced Surface Reconstruction and Its Activity toward Formate Oxidation Reactions. Journal of Physical Chemistry C, 2021, 125, 19497-19508.	1.5	7
58662	Role of Structural Phases and Octahedra Distortions in the Optoelectronic and Excitonic Properties of CsGeX₃ (X = Cl, Br, I) Perovskites. Journal of Physical Chemistry C, 2021, 125, 19142-19155.	1.5	26
58663	Theoretical Evaluation of MBenes as Catalysts for the CO₂ Reduction Reaction. Journal of Physical Chemistry C, 2021, 125, 19183-19189.	1.5	17
58664	Observation of a Half-Metallic Interface State for Pyridine-Adsorbed H/Fe₃O₄(100). Journal of Physical Chemistry Letters, 2021, 12, 8489-8494.	2.1	5
58665	Electronic and Optical Properties of C4N2H14-Based Lead-Less Halide Perovskites Investigated by First Principles. Journal of Physical Chemistry C, 2021, 125, 19445-19454.	1.5	0

#	Article	IF	Citations
58666	Coverage-dependent adsorption of small gas molecules on black phosphorene: a DFT study. Surface Science, 2021, 710, 121860.	0.8	11
58667	Ternary FePSe 3 Atomic Layers with Competitive Temperature Coefficient of Resistance for Uncooled Infrared Bolometers. Advanced Materials Interfaces, 2021, 8, 2100491.	1.9	6
58668	Davis Computational Spectroscopy Workflowâ€"From Structure to Spectra. Journal of Chemical Information and Modeling, 2021, 61, 4486-4496.	2.5	4
58669	Unraveling the decisive role of surface CeO2 nanoparticles in the Pt-CeO2/MnO2 hetero-catalysts for boosting toluene oxidation: Synergistic effect of surface decorated and intrinsic O-vacancies. Chemical Engineering Journal, 2021, 418, 129399.	6.6	132
58670	Introducing tin to develop ternary metal oxides with excellent hydrothermal stability for NH3 selective catalytic reduction of NO. Applied Catalysis B: Environmental, 2021, 291, 120125.	10.8	24
58671	Visible-light-driven photoelectrocatalytic degradation of p-chloronitrobenzene by BiOBr/TiO2 nanotube arrays photoelectrodes: Mechanisms, degradation pathway and DFT calculation. Separation and Purification Technology, 2021, 268, 118699.	3.9	28
58672	Diffusion of silver in titanium nitride: Insights from density functional theory and molecular dynamics. Applied Surface Science, 2021, 556, 149738.	3.1	10
58673	Vibrational Properties of Pristine and Lithiumâ€Intercalated Black Phosphorous under Highâ€Pressure. Annalen Der Physik, 2021, 533, 2100187.	0.9	2
58674	Solventâ€Assisted Anisotropic Cleavage of Transition Metal Carbide into 2D Nanoflakes. Small Structures, 2021, 2, 2100039.	6.9	6
58675	Bayesian Optimization of Hubbard Uâ€™s for Investigating InGaN Superlattices. Electronic Materials, 2021, 2, 370-381.	0.9	1
58676	Effect of <scp>K</scp> on carbon adsorption and deposition on the <scp>Co(111)</scp> surface. International Journal of Quantum Chemistry, 2021, 121, e26812.	1.0	1
58678	The electronic and magnetic properties of KPbM2(PO4)3 (MÂ=ÂCr and Fe) by first-principles calculations. Japanese Journal of Applied Physics, 2021, 60, 083001.	0.8	0
58679	Precipitation during creep in magnesiumâ€"aluminum alloys. Continuum Mechanics and Thermodynamics, 2021, 33, 2363-2374.	1.4	0
58680	Single Atomâ€Modified Hybrid Transition Metal Carbides as Efficient Hydrogen Evolution Reaction Catalysts. Advanced Functional Materials, 2021, 31, 2104285.	7.8	42
58681	Facile Fabrication of Robust Hydrogen Evolution Electrodes under High Current Densities via Pt@Cu Interactions. Advanced Functional Materials, 2021, 31, 2105579.	7.8	45
58682	Selfâ€Reconstruction of Sulfateâ€Containing High Entropy Sulfide for Exceptionally Highâ€Performance Oxygen Evolution Reaction Electrocatalyst. Advanced Functional Materials, 2021, 31, 2106229.	7.8	134
58683	Effects of Zr-Re/W co-segregation behavior on the thermodynamic stability and fracture strength of Î³-Ni/Î³'-Ni3Al interface. Physics Letters, Section A: General, Atomic and Solid State Physics, 2021, 408, 127466.	0.9	3
58684	Effects of the vacancy and doping on the electronic and magnetic characteristics of ZrSe2 monolayer: A first-principles investigation. Thin Solid Films, 2021, 732, 138790.	0.8	10

#	Article	IF	Citations
58685	Orbital-selective Peierls phase in the metallic dimerized chain <mml:math xmlns:mml="http://www.w3.org/1998/Math/MathML"><mml:msub><mml:mrow><mml:mi>MoOCl</mml:mi></mml:mrow><mml:mn>2</mml:mn> Physical Review B, 2021, 104, .	1.1	13
58686	Unraveling the Impact of Graphene Addition to Thermoelectric SrTiO₃ and La-Doped SrTiO₃ Materials: A Density Functional Theory Study. ACS Applied Materials & Interfaces, 2021, 13, 41303-41314.	4.0	14
58687	Two New Hybrid Iodoplumbates with Chain-like Cations. Crystal Growth and Design, 2021, 21, 5317-5324.	1.4	16
58688	Interfacial optimization of PtNi octahedrons@Ti3C2MXene with enhanced alkaline hydrogen evolution activity and stability. Applied Catalysis B: Environmental, 2021, 291, 120100.	10.8	67
58689	Stepwise Evolution of Photocatalytic Spinel-Structured (Co,Cr,Fe,Mn,Ni)3O4 High Entropy Oxides from First-Principles Calculations to Machine Learning. Crystals, 2021, 11, 1035.	1.0	11
58690	Li-decorated carbon nanotubes: charge analysis. Fullerenes Nanotubes and Carbon Nanostructures, 2022, 30, 199-204.	1.0	2
58691	Suppression of axionic charge density wave and onset of superconductivity in the chiral Weyl semimetal <mml:math xmlns:mml="http://www.w3.org/1998/Math/MathML"><mml:mrow><mml:msub><mml:mi>Ta</mml:mi><mml:mn>2</mml:mn></mml:mn></mml:r mathvariant="normal">I</mml:mi></mml:mrow></mml:math>. Physical Review Materials, 2021, 5, .	0.9	12
58692	Signatures of strong interlayer coupling in Î³-InSe revealed by local differential conductivity*. Chinese Physics B, 2021, 30, 087306.	0.7	1
58693	Ultrahigh carrier mobility, Dirac cone and high stretchability in pyrenyl and pyrazinoquinoxaline graphdiyne/graphyne nanosheets confirmed by first-principles. Applied Surface Science, 2021, 557, 149699.	3.1	9
58694	A promising auxetic material of CaAs3 monolayer with anisotropic electro-mechanical and optical properties. Applied Physics Letters, 2021, 119, .	1.5	3
58695	Monolayer puckered pentagonal VTe2: An emergent two-dimensional ferromagnetic semiconductor with multiferroic coupling. Nano Research, 2022, 15, 1486-1491.	5.8	20
58696	Adsorption and dissociation behavior of water on pristine and defected calcite {1 0 4} surfaces: A DFT study. Applied Surface Science, 2021, 556, 149777.	3.1	22
58697	Broadband near-infrared emission of K3ScF6:Cr3+ phosphors for night vision imaging system sources. Chemical Engineering Journal, 2021, 417, 129271.	6.6	95
58698	A new refractory Ni7Nb2 phase identified in Laves eutectic regions by TEM study. Acta Materialia, 2021, 214, 116985.	3.8	9
58699	Onion-like Core-shell Ni@C supported on carbon nanotubes decorated with low Pt as a superior electrocatalyst for hydrogen evolution reaction. Electrochimica Acta, 2021, 386, 138406.	2.6	16
58700	Vertically aligned MoS2 thin film catalysts with Fe-Ni sulfide nanoparticles by one-step sulfurization for efficient solar water reduction. Chemical Engineering Journal, 2021, 418, 129369.	6.6	26
58701	Tuning the electronic and optical properties of molybdenite (MoS2) by adsorption of alkali metals and halogens. Optical Materials, 2021, 118, 111248.	1.7	6
58702	Tunable Alloying Improved Wide Spectrum UV-Vis-NIR and Polarization-Sensitive Photodetector Based on Sbâ€“Sâ€“Se Nanowires. IEEE Transactions on Electron Devices, 2021, 68, 3887-3893.	1.6	15

#	Article	IF	Citations
58703	Comparing alkene-mediated and formaldehyde-mediated diene formation routes in methanol-to-olefins catalysis in MFI and CHA. Journal of Catalysis, 2021, 400, 124-139.	3.1	12
58704	First-principles mechanistic study on nitrate reduction reactions on copper surfaces: Effects of crystal facets and pH. Journal of Catalysis, 2021, 400, 62-70.	3.1	40
58705	Improvement in photocatalytic stability of AgBr under visible light through melt processing. Journal of Catalysis, 2021, 400, 160-165.	3.1	9
58706	Exsolved metal-boosted active perovskite oxide catalyst for stable water gas shift reaction. Journal of Catalysis, 2021, 400, 148-159.	3.1	18
58707	Optimizing Nitrogen Reduction Reaction on Nitrides: A Computational Study on Crystallographic Orientation. Topics in Catalysis, 2022, 65, 252-261.	1.3	14
58708	High-temperature superconductor of sodalite-like clathrate hafnium hexahydride. Scientific Reports, 2021, 11, 16403.	1.6	9
58709	Search for an exotic parity-odd spin- and velocity-dependent interaction using a magnetic force microscope. Physical Review D, 2021, 104, .	1.6	9
58710	Ab initio study of pressure-induced structural and electronic phase transitions in Ca2RuO4. Physical Review B, 2021, 104, .	1.1	3
58711	First-principles study of the quasi-one-dimensional organic-inorganic hybrid perovskites <mml:math xmlns:mml="http://www.w3.org/1998/Math/MathML"><mml:mrow><mml:mrow><mml:mo>(</mml:mo><mml:mi>MV</mml:mi><mml:m mathvariant="normal">I</mml:mi><mml:mn>3</mml:mn></mml:msub><mml:msub><mml:mi>Cl</mml:mi><mml:mn>2</mml:mn></m		

#	Article	IF	Citations
58721	Characteristics of thin InAlAs digital alloy avalanche photodiodes. Optics Letters, 2021, 46, 3841.	1.7	7
58722	Structural features of chalcogenide glass SiTe: An ovonic threshold switching material. APL Materials, 2021, 9, .	2.2	12
58723	First principles study of phase stability in Ba-based tantalate complex double perovskites. Applied Physics Letters, 2021, 119, 052901.	1.5	1
58724	Influence of Amino Acids on the Mobility of Iodide in Hydrocalumite. Minerals (Basel, Switzerland), 2021, 11, 836.	0.8	0
58725	Beyond the Anderson rule: importance of interfacial dipole and hybridization in van der Waals heterostructures. 2D Materials, 2021, 8, 041002.	2.0	11
58726	Pressure-Induced Excitations in the Out-of-Plane Optical Response of the Nodal-Line Semimetal ZrSiS. Physical Review Letters, 2021, 127, 076402.	2.9	6
58727	Comparative Study on the Machine Learning-Based Prediction of Adsorption Energies for Ring and Chain Species on Metal Catalyst Surfaces. Journal of Physical Chemistry C, 2021, 125, 17742-17748.	1.5	10
58728	High-Pressure Yttrium Nitride, Y₅N₁₄, Featuring Three Distinct Types of Nitrogen Dimers. Journal of Physical Chemistry C, 2021, 125, 18077-18084.	1.5	11
58729	Revealing the Unusual Boron-Pinned Layered Substructure in Superconducting Hard Molybdenum Semiboride. ACS Omega, 2021, 6, 21436-21443.	1.6	5
58730	First-Principles Study of Electronic and Optical Properties of Two-Dimensional WSSe/BSe van der Waals Heterostructure with High Solar-to-Hydrogen Efficiency. Catalysts, 2021, 11, 991.	1.6	18
58731	Bimetallic phthalocyanine heterostructure used for highly selective electrocatalytic CO2 reduction. Science China Materials, 2022, 65, 155-162.	3.5	32
58732	Earthâ€™s core could be the largest terrestrial carbon reservoir. Communications Earth & Environment, 2021, 2, .	2.6	6
58733	Weyl-mediated helical magnetism in NdAlSi. Nature Materials, 2021, 20, 1650-1656.	13.3	48
58734	Direct Visualization of Nearly Free Electron States Formed by Superatom Molecular Orbitals in a Li@C₆₀ Monolayer. Journal of Physical Chemistry Letters, 2021, 12, 7812-7817.	2.1	9
58735	Tuning magnetic and optical properties through strain in epitaxial LaCrO3 thin films. Applied Physics Letters, 2021, 119, .	1.5	4
58736	Stable valley-layer coupling and design principle in 2D lattice. Applied Physics Letters, 2021, 119, 073101.	1.5	2
58737	Theoretical investigations on correlations between elastic behavior of Al-based alloys and their electronic structures. International Journal of Materials Research, 2021, 112, 636-641.	0.1	0
58738	Halfâ€Metallic CoO 2 and Semiconducting NiO 2 at High Pressures. Physica Status Solidi (B): Basic Research, 0, , 2100233.	0.7	0

#	Article	IF	Citations
58739	Toward Planar Iodine 2D Crystal Materials. ACS Omega, 2021, 6, 21235-21240.	1.6	0
58740	Revisiting the Electronic Structures and Phonon Properties of Thermoelectric Antimonide-Tellurides: Spinâ€“Orbit Coupling Induced Gap Opening in ZrSbTe and HfSbTe. Crystals, 2021, 11, 917.	1.0	6
58741	Reducing the Energy Band Gap of Cobalt Hydroxide Nanosheets with Silver Atoms and Enhancing Their Electrical Conductivity with Silver Nanoparticles. ACS Omega, 2021, 6, 20804-20811.	1.6	22
58742	Three-Dimensional Fast Na-Ion Transport in Sodium Titanate Nanoarchitectures via Engineering of Oxygen Vacancies and Bismuth Substitution. ACS Nano, 2021, 15, 13604-13615.	7.3	36
58743	Black Phosphorusâ€"Diketopyrrolopyrrole Polymer Semiconductor Hybrid for Enhanced Charge Transfer and Photodetection. Advanced Photonics Research, 2021, 2, 2100150.	1.7	3
58744	Heavy carrier effective masses in van der Waals semiconductor Sn(SeS) revealed by high magnetic fields up to 150 T. Physical Review B, 2021, 104, .	1.1	1
58745	Outstanding Catalytic Effects of 1Tâ€²-MoTe₂ Quantum Dots@3D Graphene in Shuttle-Free Liâ€“S Batteries. ACS Nano, 2021, 15, 13279-13288.	7.3	81
58746	Gaussian Process Regression for Materials and Molecules. Chemical Reviews, 2021, 121, 10073-10141.	23.0	384
58747	Discarded gems: Thermoelectric performance of materials with band gap emerging at the hybrid-functional level. Applied Physics Letters, 2021, 119, .	1.5	3
58748	Modulating composite polymer electrolyte by lithium closo-borohydride achieves highly stable solid-state battery at 25Â°C. Science China Materials, 2022, 65, 95-104.	3.5	12
58749	Modulation on the electrical and optical properties of Na and Rh co-doped Ruddlesden-Popper layered Ca3Ti2O7. Journal of Electroceramics, 2021, 47, 42-50.	0.8	5
58750	P Doping Promotes the Spontaneous Visible-Light-Driven Photocatalytic Water Splitting in Isomorphic Type II GaSe/InS Heterostructure. Journal of Physical Chemistry Letters, 2021, 12, 7892-7900.	2.1	26
58751	In-plane magnetic structure and exchange interactions in the high-temperature antiferromagnet Cr2Al. Physical Review Materials, 2021, 5, .	0.9	1
58752	Approaching Superior Potassium Storage of Carbonaceous Anode Through a Combined Strategy of Carbon Hybridization and Sulfur Doping. Energy and Environmental Materials, 2022, 5, 944-953.	7.3	15
58753	Tuning of electronic structure, magnetic phase, and transition temperature in two-dimensional Cr-based Janus MXenes. Physical Review Materials, 2021, 5, .	0.9	23
58754	Large-scale structure prediction of near-stoichiometric magnesium oxide based on a machine-learned interatomic potential: Crystalline phases and oxygen-vacancy ordering. Physical Review Materials, 2021, 5, .	0.9	5
58755	Empowering hydrogen storage properties of haeckelite monolayers via metal atom functionalization. Applied Surface Science, 2021, 556, 149709.	3.1	20
58756	Water Bridges Substitute for Defects in Amine-Functionalized UiO-66, Boosting CO₂ Adsorption. Langmuir, 2021, 37, 10439-10449.	1.6	12

#	Article	IF	Citations
58757	<scp>MCML</scp>: Combining physical constraints with experimental data for a multiâ€purpose metaâ€generalized gradient approximation. Journal of Computational Chemistry, 2021, 42, 2004-2013.	1.5	10
58758	Investigation of Strain and Transition-Metal Doping Effect on Hydrogen Evolution Reaction Catalysts of Mo₂C, MoP, and Ni₂P. Journal of Physical Chemistry C, 2021, 125, 19119-19130.	1.5	9
58759	Wide Band Gap P₃S Monolayer with Anisotropic and Ultrahigh Carrier Mobility. Journal of Physical Chemistry Letters, 2021, 12, 8481-8488.	2.1	10
58760	Development of the ReaxFF Reactive Force Field for Cu/Si Systems with Application to Copper Cluster Formation during Cu Diffusion Inside Silicon. Journal of Physical Chemistry C, 2021, 125, 19455-19466.	1.5	3
58761	Rational Design of Semiconductor Heterojunctions for Photocatalysis. Chemistry - A European Journal, 2021, 27, 13306-13317.	1.7	44
58762	Stacking fault energy of basal plane for hexagonal closed-packed medium entropy alloy ZrHfTi: Ab initio prediction. Applied Physics A: Materials Science and Processing, 2021, 127, 1.	1.1	1
58763	Quantifying the Impact of Parametric Uncertainty on Automatic Mechanism Generation for CO₂ Hydrogenation on Ni(111). Jacs Au, 2021, 1, 1656-1673.	3.6	30
58764	Quasi-one-dimensional thermal transport in trigonal selenium crystal. Journal of Physics Condensed Matter, 2021, 33, 455402.	0.7	0
58765	Adsorption Mechanisms of Alkali Metal, Alkaline Earth Metal, and Halogen Atoms on Van der Waals Materials. Journal of Physical Chemistry C, 2021, 125, 19259-19267.	1.5	4
58766	On-the-fly assessment of diffusion barriers of disordered transition metal oxyfluorides using local descriptors. Electrochimica Acta, 2021, 388, 138551.	2.6	14
58767	Interfacial Bifunctional Effect Promoted Non-Noble Cu/Fe_yMgO_x Catalysts for Selective Hydrogenation of Acetylene. ACS Catalysis, 2021, 11, 11117-11128.	5.5	24
58768	Direct Oxidation of Cyclohexane to Adipic Acid by a WFeCoO(OH) Catalyst: Role of BrÃ¸nsted Acidity and Oxygen Vacancies. ACS Catalysis, 2021, 11, 10754-10766.	5.5	29
58769	A subtle structure evolution of metal-adsorbed water bilayer and the effect of dispersion correction. Computational Materials Science, 2021, 196, 110533.	1.4	3
58770	Synthesis of 0D SnO2 nanoparticles/2D g-C3N4 nanosheets heterojunction: improved charge transfer and separation for visible-light photocatalytic performance. Journal of Alloys and Compounds, 2021, 871, 159561.	2.8	28
58771	Outâ€Ofâ€Plane Ordered Laminate Borides and Their 2D Tiâ€Based Derivative from Chemical Exfoliation. Advanced Materials, 2021, 33, e2008361.	11.1	14
58772	Proton-Dominated Reversible Aqueous Zinc Batteries with an Ultraflat Long Discharge Plateau. ACS Nano, 2021, 15, 14766-14775.	7.3	38
58773	Manipulating the Electronic Structure of Nickel via Alloying with Iron: Toward High-Kinetics Sulfur Cathode for Naâ€“S Batteries. ACS Nano, 2021, 15, 15218-15228.	7.3	64
58774	Design single nonmetal atom doped 2D Ti2CO2 electrocatalyst for hydrogen evolution reaction by coupling electronic descriptor. Applied Surface Science, 2021, 556, 149778.	3.1	15

#	Article	IF	Citations
58775	Electric-field-driven excitonic instability in an organometallic manganese-cyclopentadienyl wire. Physical Review B, 2021, 104, .	1.1	4
58776	Gateâ€Defined Quantum Confinement in CVD 2D WS₂. Advanced Materials, 2022, 34, e2103907.	11.1	18
58777	Evolving Devil's Staircase Magnetization from Tunable Charge Density Waves in Nonsymmorphic Dirac Semimetals. Advanced Materials, 2021, 33, e2103476.	11.1	14
58778	Electronic structure and enhanced photocatalytic properties in $$hbox {Ca(OH)}_{2}$$/GeC van der Waals heterostructure. European Physical Journal B, 2021, 94, 1.	0.6	2
58779	Fluorine-Doped GeO₂@C Composite with Abundant Oxygen Vacancies for High-Capacity Lithium-Ion Batteries. ACS Applied Energy Materials, 2021, 4, 9848-9857.	2.5	16
58780	Crystal chemistry and ab initio prediction of ultrahard rhombohedral B2N2 and BC2N. Solid State Sciences, 2021, 118, 106667.	1.5	13
58781	Efficient Computation of Structural and Electronic Properties of Halide Perovskites Using Density Functional Tight Binding: GFN1-xTB Method. Journal of Chemical Information and Modeling, 2021, 61, 4415-4424.	2.5	16
58782	Polyethylene Hydrogenolysis at Mild Conditions over Ruthenium on Tungstated Zirconia. Jacs Au, 2021, 1, 1422-1434.	3.6	95
58783	A comparative ab initio study of the mechanical, dynamical and thermophysical characteristics of XC2 (X = La, Ce, Tb, Ho). Vacuum, 2021, 191, 110383.	1.6	5
58784	Ab initio molecular dynamics investigation of Cs adsorption on Mo(0Â0Â1): Beyond a single monolayer coverage. Applied Surface Science, 2021, 559, 149822.	3.1	4
58785	Domain-wall induced giant tunneling electroresistance effect in two-dimensional Graphene/In2Se3 ferroelectric tunnel junctions. Physica E: Low-Dimensional Systems and Nanostructures, 2021, 133, 114783.	1.3	7
58786	Robust silver nanowire membrane with high porosity to construct stable Li metal anodes. Materials Today Energy, 2021, 21, 100751.	2.5	9
58787	Ab-initio study on physical properties of intermetallic LiPb compound. Journal of Computational Science, 2021, 54, 101428.	1.5	3
58788	Understanding the defect levels and photoluminescence in a series of bismuth-doped perovskite oxides: First-principles study. Physical Review B, 2021, 104, .	1.1	25
58789	B₂S₃ monolayer: a two-dimensional direct-gap semiconductor with tunable band-gap and high carrier mobility. Nanotechnology, 2021, 32, 475709.	1.3	10
58790	Enhanced Onâ€Site Hydrogen Peroxide Electrosynthesis by a Selectively Carboxylated Nâ€Doped Graphene Catalyst. ChemCatChem, 2021, 13, 4372-4383.	1.8	15
58791	Adsorbate Free Energies from DFT-Derived Translational Energy Landscapes. Journal of Physical Chemistry C, 2021, 125, 20331-20342.	1.5	10
58792	Effect of Aluminum Siting in H-ZSM-5 on Reaction Barriers. Journal of Physical Chemistry C, 2021, 125, 20373-20379.	1.5	6

#	Article	IF	Citations
58793	Pressure dependent thermoreflectance spectroscopy induced by interband transitions in metallic nano-film. IScience, 2021, 24, 102990.	1.9	5
58794	AICON2: A program for calculating transport properties quickly and accurately. Computer Physics Communications, 2021, 266, 108027.	3.0	22
58795	Ultrahigh thermal conductivity and strength in direct-gap semiconducting graphene-like BC6N: A first-principles and classical investigation. Carbon, 2021, 182, 373-383.	5.4	38
58796	Anisotropic Properties of Quasiâ€1D In₄Se₃: Mechanical Exfoliation, Electronic Transport, and Polarizationâ€Dependent Photoresponse. Advanced Functional Materials, 2021, 31, 2106459.	7.8	11
58797	Twist Effect on the Electronic and Transport Properties of 1D Helical Carbyne Chains. Physica Status Solidi - Rapid Research Letters, 2021, 15, 2100390.	1.2	0
58798	Trimetallic Metalâ€Organic Framework Nanoframe Superstructures: A Stressâ€Buffering Architecture Engineering of Anode Material toward Boosted Lithium Storage Performance. Energy and Environmental Materials, 2023, 6, .	7.3	7
58799	Novel rubidium polyfluorides with F3, F4, and F5 species*. Chinese Physics B, 2021, 30, 066102.	0.7	0
58800	Molybdenum Disorder in Hydrated Sedovite, Ideally U(MoO₄)₂Â·nH₂O, a Microporous Nanocrystalline Mineral Characterized by Three-Dimensional Electron Diffraction, Density Functional Theory Computations, and Complexity Analysis. Inorganic Chemistry, 2021, 60, 15169-15179.	1.9	1
58801	Optimizing the surface distribution of acid sites for cooperative catalysis in condensation reactions promoted by water. Chem Catalysis, 2021, 1, 1065-1087.	2.9	14
58802	Efficient light-free activation of peroxymonosulfate by carbon ring conjugated carbon nitride for elimination of organic pollutants. Chemical Engineering Journal, 2021, 420, 129671.	6.6	24
58803	Projector augmented-wave pseudopotentials for the actinide elements (Acâ€“Bk). Journal of Nuclear Materials, 2021, 553, 153031.	1.3	3
58804	Crystal stabilities and electronic properties of thorium silicide under ambient conditions and high pressures from a first-principles study. Computational Materials Science, 2021, 197, 110561.	1.4	2
58805	Effect of oxygen partial pressure on the stability of Ce0.8Zr0.2O2-Î´ solid solution using genetic algorithm and lattice statics. Computational Materials Science, 2021, 197, 110606.	1.4	0
58806	Theoretical study on the tunable electronic band structure of Cs2PbI2Cl2/CsPbBr3 halide perovskite heterostructure driven by ferroelectric polarization modulation. Journal of Colloid and Interface Science, 2021, 597, 233-241.	5.0	14
58807	Enhanced thermoelectric performance of nominal 19-electron half-Heusler compound NbCoSb with intrinsic Nb and Sb vacancies. Materials Today Physics, 2021, 20, 100450.	2.9	16
58808	Modeling refractory high-entropy alloys with efficient machine-learned interatomic potentials: Defects and segregation. Physical Review B, 2021, 104, .	1.1	46
58809	Transforming 3D CAUâ€10â€H into 2D Materials with High Base Stability for Membrane Separation. Chemistry - an Asian Journal, 2021, 16, 3236-3243.	1.7	6
58810	Electronic properties, contact types and Rashba splitting of two-dimensional graphyne/WSeTe van der Waals heterostructures. Journal of Alloys and Compounds, 2021, 875, 160048.	2.8	16

#	Article	IF	Citations
58811	Static and dynamic oxidation behaviour of silicon carbide at high temperature. Journal of the European Ceramic Society, 2021, 41, 5445-5456.	2.8	14
58812	First-principles investigation on the thickness-dependent optoelectronic properties of two-dimensional perovskite BA2SnI4. Physica B: Condensed Matter, 2021, 616, 413070.	1.3	3
58813	Rapid screening of high-throughput ground state predictions. Calphad: Computer Coupling of Phase Diagrams and Thermochemistry, 2021, 74, 102306.	0.7	2
58814	Synthesizable Double Perovskite Oxide Search via Machine Learning and Highâ€Throughput Computational Screening. Advanced Theory and Simulations, 2021, 4, 2100263.	1.3	14
58815	Electronic structures and optical properties of BiOBr/BiOI heterojunction with an oxygen vacancy. Chemical Physics, 2021, 549, 111264.	0.9	7
58816	Cinnamaldehyde adsorption and thermal decomposition on copper surfaces. Journal of Vacuum Science and Technology A: Vacuum, Surfaces and Films, 2021, 39, 053205.	0.9	3
58817	Unveiling the Ag-Bi miscibility at the atomic level: A theoretical insight. Computational Materials Science, 2021, 197, 110612.	1.4	2
58818	Piezoelectric effect and polarization switching in Al1â^'xScxN. Journal of Applied Physics, 2021, 130, .	1.1	15
58819	Flexible carbon nanofiber film with diatomic Fe-Co sites for efficient oxygen reduction and evolution reactions in wearable zinc-air batteries. Nano Energy, 2021, 87, 106147.	8.2	103
58820	Free energies of iron phases at high pressure and temperature: Molecular dynamics study. Physical Review B, 2021, 104, .	1.1	18
58821	Twoâ€Đimensional Red Phosphorus Nanosheets: Morphology Tuning and Electrochemical Sensing of Aromatic Amines. Small Methods, 2021, 5, e2100720.	4.6	8
58822	Element-resolved local lattice distortion in complex concentrated alloys: An observable signature of electronic effects. Acta Materialia, 2021, 216, 117135.	3.8	22
58823	Stability and stoichiometry of L12 Al3(Sc,Zr) dispersoids in Al-(Si)-Sc-Zr alloys. Acta Materialia, 2021, 216, 117117.	3.8	24
58824	Electronic structures and topological properties of TeSe₂ monolayers*. Chinese Physics B, 2021, 30, 117304.	0.7	0
58825	Epitaxial growth of wafer-scale molybdenum disulfide semiconductor single crystals on sapphire. Nature Nanotechnology, 2021, 16, 1201-1207.	15.6	339
58826	First-principles Calculations of Bulk and Interfacial Thermodynamic Properties of the T1 phase in Al-Cu-Li alloys. Scripta Materialia, 2021, 202, 114009.	2.6	10
58827	Selective Area Growth of Single-Crystalline Alpha-Gallium Oxide on a Sapphire Nanomembrane by Mist Chemical Vapor Deposition. ACS Applied Electronic Materials, 2021, 3, 4328-4336.	2.0	13
58828	The Coordination Chemistry and Stoichiometry of Extracted Diglycolamide Complexes of Lanthanides in Extraction Chromatography Materials. Solvent Extraction and Ion Exchange, 2022, 40, 6-27.	0.8	11

#	Article	IF	Citations
58829	Quantum anomalous Hall effect of Dirac half-metal monolayer TiCl₃ with high Chern number. Europhysics Letters, 2021, 136, 27004.	0.7	3
58830	Indium-contacted van der Waals gap tunneling spectroscopy for van der Waals layered materials. Scientific Reports, 2021, 11, 17790.	1.6	1
58831	New stable 2D and 3D GeC2 crystal structures predicted by first-principles study. Materials Today Communications, 2021, 28, 102567.	0.9	0
58832	Comprehensive mechanism of ferromagnetism enhancement in nitrogen-doped graphene. New Journal of Physics, 2021, 23, 103003.	1.2	3
58833	Anisotropic transport and optical birefringence of triclinic bulk and monolayer NbX₂Y₂ (X = S, Se and Y = Cl, Br, I). Journal of Physics Condensed Matter, 2021, 33, 485501.	0.7	0
58834	Variation of charge dynamics upon antiferromagnetic transitions in the Dirac semimetal <mml:math xmlns:mml="http://www.w3.org/1998/Math/MathML"><mml:msub><mml:mi>EuMnBi</mml:mi><mml:mn>2</mml:mn></mml:msub> Physical Review B, 2021, 104, .	1.1	4
58835	High-energy-density polymeric carbon oxide: Layered <mml:math xmlns:mml="http://www.w3.org/1998/Math/MathML"><mml:mrow><mml:msub><mml:mi mathvariant="normal">C</mml:mi><mml:mi>x</mml:mi></mml:msub><mml:msub><mml:mi mathvariant="normal">O</mml:mi><mml:mi>y</mml:mi></mml:msub></mml:mrow></mml:math> solids under pressure. Physical Review B, 2021, 104, .	1.1	2
58836	xmlns:mml="http://www.w3.org/1998/Math/MathML"><mml:mrow><mml:mi>Mo</mml:mi><mml:msub><mml:mi>Se</mml:mi> and <mml:math xmlns:mml="http://www.w3.org/1998/Math/MathML"><mml:mrow><mml:mi>Mo</mml:mi><mml:msub><mml:mi mathvariant="normal">S</mml:mi><mml:mn>2</mml:mn></mml:msub></mml:mrow></mml:math> : Reexamination of the mechanism. Physical Review B, 2021, 104,	1.1	6
58837	First-principles modeling of complexions at the phase boundaries in Ti-doped WC-Co cemented carbides at finite temperatures. Physical Review Materials, 2021, 5, .	0.9	4
58838	Different shapes of spin textures as a journey through the Brillouin zone. Physical Review B, 2021, 104, .	1.1	23
58839	Li-decorated B2O as potential candidates for hydrogen storage: A DFT simulations study. International Journal of Hydrogen Energy, 2021, 46, 33486-33495.	3.8	35
58840	Strong Electron Coupling of Ru and Vacancyâ€Rich Carbon Dots for Synergistically Enhanced Hydrogen Evolution Reaction. Small, 2021, 17, e2102496.	5.2	31
58841	First-Principles Study on the Stability and Electronic Structure of the Charge-Ordered Phase in Î±-(BEDT-TTF)2I3. Crystals, 2021, 11, 1109.	1.0	3
58842	Pressure- and temperature-dependent diffusion from first-principles: A case study of V and Ti in a TiN matrix. Surface and Coatings Technology, 2021, 422, 127491.	2.2	2
58843	Relevance of Dispersion and the Electronic Spin in the DFT + U Approach for the Description of Pristine and Defective TiO₂ Anatase. ACS Omega, 2021, 6, 23170-23180.	1.6	4
58844	Observation of Spin-Momentum-Layer Locking in a Centrosymmetric Crystal. Physical Review Letters, 2021, 127, 126402.	2.9	12
58845	Computational synthesis of substrates by crystal cleavage. Npj Computational Materials, 2021, 7, .	3.5	2
58846	Identification of a low-energy metastable 1T -type phase for monolayer VSe2. Physical Review B, 2021, 104, .	1.1	2

#	Article	IF	Citations
58847	MEIFUITE, A NEW FERROUS PHYLLOSILICATE MINERAL WITH MODULATED TETRAHEDRAL SHEETS SIMILAR TO MINNESOTAITE. Clays and Clay Minerals, 2021, 69, 672-687.	0.6	0
58848	First low-spin carbodiimide, Fe2(NCN)3, predicted from first-principles investigations. Zeitschrift Fur Naturforschung - Section B Journal of Chemical Sciences, 2021, .	0.3	0
58849	Ab initio investigation of non-metal-doped ZnS monolayer. Applied Physics A: Materials Science and Processing, 2021, 127, 1.	1.1	6
58850	Chemical shielding of H2O and HF encapsulated inside a C60 cage. Communications Chemistry, 2021, 4, .	2.0	7
58851	Abnormal Phase Transition and Band Renormalization of Guanidinium-Based Organicâ€“Inorganic Hybrid Perovskite. ACS Applied Materials & Interfaces, 2021, 13, 44964-44971.	4.0	8
58852	Enhancement of optoelectronic properties of layered MgIn$$_{2}$$Se$$_{4}$$ compound under uniaxial strain, an ab initio study. European Physical Journal B, 2021, 94, 185.	0.6	1
58853	Revealing Mn⁴⁺ Local Symmetry in Narrowband Red-Emitting Phosphor Rb₂NaGaF₆:Mn⁴⁺ for Wide-Color-Gamut Backlighting. ECS Journal of Solid State Science and Technology, 2021, 10, 096011.	0.9	1
58854	Single-atom catalyst for high-performance methanol oxidation. Nature Communications, 2021, 12, 5235.	5.8	113
58855	Development of a solute and defect concentration dependant Ising model for the study of transmutation induced segregation in neutron irradiated Wâ€“(Re, Os) systems. Journal of Physics Condensed Matter, 2021, 33, 475902.	0.7	5
58856	Molecular-Level Insight into the Interfacial Reactivity and Ionic Conductivity of a Li-Argyrodite Li₆PS₅Cl Solid Electrolyte at Bare and Coated Li-Metal Anodes. ACS Applied Materials & Interfaces, 2021, 13, 43734-43745.	4.0	15
58857	Capturing 3D atomic defects and phonon localization at the 2D heterostructure interface. Science Advances, 2021, 7, eabi6699.	4.7	13
58858	A General Principle for DUV NLO Materials: Ï€â€Conjugated Confinement Enlarges Band Gap. Angewandte Chemie, 0, , .	1.6	12
58859	Effect of point defects on electronic and excitonic properties in Janus-MoSSe monolayer. Physical Review B, 2021, 104, .	1.1	14
58860	Actinide Coordination Chemistry on Surfaces: Synthesis, Manipulation, and Properties of Thorium Bis(porphyrinato) Complexes. Journal of the American Chemical Society, 2021, 143, 14581-14591.	6.6	9
58861	Highly selective and efficient electrocatalytic synthesis of glycolic acid in coupling with hydrogen evolution. Chem Catalysis, 2021, 1, 941-955.	2.9	73
58862	Uncovering electronic and geometric descriptors of chemical activity for metal alloys and oxides using unsupervised machine learning. Chem Catalysis, 2021, 1, 923-940.	2.9	22
58863	First-principle-data-integrated machine-learning approach for high-throughput searching of ternary electrocatalyst toward oxygen reduction reaction. Chem Catalysis, 2021, 1, 855-869.	2.9	28
58864	Synergistic Dissociationâ€andâ€Trapping Effect to Promote Liâ€Ion Conduction in Polymer Electrolytes via Oxygen Vacancies. Small, 2021, 17, e2102039.	5.2	38

#	Article	IF	Citations
58865	Regulation of Hole Concentration and Mobility and First-Principle Analysis of Mg-Doping in InGaN Grown by MOCVD. Materials, 2021, 14, 5339.	1.3	2
58866	Unusual spin dynamics in the low-temperature magnetically ordered state of <mml:math xmlns:mml="http://www.w3.org/1998/Math/MathML"><mml:msub><mml:mi mathvariant="normal">Ag</mml:mi><mml:mn>3</mml:mn></mml:msub><mml:msub><mml:mi mathvariant="normal">LiIr</mml:mi><mml:mn>2</mml:mn></mml:msub><mml:msub><mml:mi mathvariant="normal">O</mml:mi><mml:mn>6</mml:mn></mml:msub></mml:math>. Physical Review B, 2021, 104, .	1.1	9
58867	Ostwald ripening microkinetic simulation of Au clusters on MgO(0 0 1). Applied Surface Science, 2022, 572, 151317.	3.1	2
58868	Tuning the magnetic phase diagram of Ni-Mn-Ga by Cr and Co substitution. Journal Physics D: Applied Physics, 0, , .	1.3	1
58869	High thermopower and birefringence in layered mercury-based halides. Materials Today Communications, 2022, 32, 102824.	0.9	0
58870	Elastic and magnetoelastic properties of TbMnO₃ single crystal by nanosecond time resolved acoustics and first-principles calculations. Journal of Physics Condensed Matter, 2021, 33, 495402.	0.7	2
58871	Tunable spin-orbit coupling in two-dimensional InSe. Physical Review B, 2021, 104, .	1.1	9
58872	Theoretical Study on the Contacting Interface-Dependent Band Alignments of CsPbBr₃@MoS₂ van der Waals Heterojunctions: Spinâ€“Orbit Coupling Does Matter. Journal of Physical Chemistry C, 2021, 125, 21678-21688.	1.5	4
58873	Two-Dimensional Graphdiyne-Confined Platinum Catalyst for Hydrogen Evolution and Oxygen Reduction Reactions. ACS Applied Materials & Interfaces, 2021, 13, 47541-47548.	4.0	15
58874	A reversible hydrogen storage material of Li-decorated two-dimensional (2D) C4N monolayer: First principles calculations. International Journal of Hydrogen Energy, 2021, 46, 32936-32948.	3.8	41
58875	Controlling the Shape Anisotropy of Monoclinic Nb₁₂O₂₉ Nanocrystals Enables Tunable Electrochromic Spectral Range. Journal of the American Chemical Society, 2021, 143, 15745-15755.	6.6	23
58876	Defect Passivation in Airâ€Stable Tin(IV)â€Halide Single Crystal for Emissive Selfâ€Trapped Excitons. Advanced Functional Materials, 2021, 31, 2108561.	7.8	41
58877	Design strong anomalous Hall effect via spin canting in antiferromagnetic nodal line materials. Physical Review B, 2021, 104, .	1.1	7
58878	Tunable Band Gap and Rhombohedral Distortion in Lead-Free CsSn1â€“xGexI3 Mixed Perovskites. Journal of Physical Chemistry C, 0, , .	1.5	3
58879	Robust large-gap topological insulator phase in transition-metal chalcogenide ZrTe₄Se. New Journal of Physics, 2021, 23, 093046.	1.2	0
58880	Coronene-Based 2D Metalâ€“Organic Frameworks: A New Family of Promising Single-Atom Catalysts for Nitrogen Reduction Reaction. Journal of Physical Chemistry C, 2021, 125, 20870-20876.	1.5	13
58881	Development of data-driven spd tight-binding models of Fe â€“ parameterisation based on QSGW and DFT calculations including information about higher-order elastic constants.. Modelling and Simulation in Materials Science and Engineering, 0, , .	0.8	1
58882	A Study in Red: The Overlooked Role of Azoâ€Moieties in Polymeric Carbon Nitride Photocatalysts with Strongly Extended Optical Absorption. Chemistry - A European Journal, 2021, 27, 17188-17202.	1.7	4

#	Article	IF	Citations
58883	Mechanistic Similarities and Differences for Hydrogenation of Aromatic Heterocycles and Aliphatic Carbonyls on Sulfided Ru Nanoparticles. ACS Catalysis, 2021, 11, 12585-12608.	5.5	3
58884	Cation Overcrowding Effect on the Oxygen Evolution Reaction. Jacs Au, 2021, 1, 1752-1765.	3.6	48
58885	Prediction of a Kinetic Pathway for Fabricating the Narrowest Zigzag Graphene Nanoribbons on Cu(111). Journal of Physical Chemistry C, 2021, 125, 21933-21942.	1.5	1
58886	Settling the matter of the role of vibrations in the stability of high-entropy carbides. Nature Communications, 2021, 12, 5747.	5.8	28
58887	First-Principles Calculations of the Diffusivity of Interstitial Helium in Alpha-U Considering Anisotropy, Isotope Effects, and Quantum Effects. Journal of Physical Chemistry C, 2021, 125, 21101-21111.	1.5	3
58888	A General Principle for DUV NLO Materials: Ï€â€Conjugated Confinement Enlarges Band Gap**. Angewandte Chemie - International Edition, 2021, 60, 25063-25067.	7.2	79
58889	Dramatic Change in the Step Edges of the Cu(100) Electrocatalyst upon Exposure to CO: Operando Observations by Electrochemical STM and Explanation Using Quantum Mechanical Calculations. ACS Catalysis, 2021, 11, 12068-12074.	5.5	9
58890	2D-layered Mg(OH)2 material adsorbing cellobiose via interfacial chemical coupling and its applications in handling toxic Cd2+ and UO22+ ions. Chemosphere, 2021, 279, 130617.	4.2	8
58891	Structure and energy of the (101) twin boundary in hot-deformed Nd-Fe-B magnets. Materials Characterization, 2021, 179, 111380.	1.9	2
58892	Effects of magnetic excitations and transitions on vacancy formation: Cases of fcc Fe and Ni compared to bcc Fe. Physical Review B, 2021, 104, .	1.1	5
58893	Identification of Topotactic Surfaceâ€Confined Ullmannâ€Polymerization. Small, 2021, 17, e2103044.	5.2	9
58894	Structural and chemical features of Gd:BaTiO3 solid solutions prepared by microwave-assisted heat treatment. Bulletin of Materials Science, 2021, 44, 1.	0.8	1
58895	Ab initio framework for systems with helical symmetry: Theory, numerical implementation and applications to torsional deformations in nanostructures. Journal of the Mechanics and Physics of Solids, 2021, 154, 104515.	2.3	7
58896	Fluorine incorporation into calcite, aragonite and vaterite CaCO3: Computational chemistry insights and geochemistry implications. Geochimica Et Cosmochimica Acta, 2021, 308, 384-392.	1.6	6
58897	Density functional theory study of active sites on nitrogen-doped graphene for oxygen reduction reaction. Royal Society Open Science, 2021, 8, 210272.	1.1	11
58898	Ab initio modelling of intergranular fracture of nickel containing phosphorus: Interfacial excess properties. Nuclear Materials and Energy, 2021, 28, 101055.	0.6	0
58899	Ab-initio studies of electronic and magnetic properties of titanium doped methylammonium lead halides. Computational Condensed Matter, 2021, 28, e00570.	0.9	4
58900	Theoretical investigation of the 70.5<mml:math xmlns:mml="http://www.w3.org/1998/Math/MathML" altimg="si39.svg"><mml:msup><mml:mrow /><mml:mtext>Â°</mml:mtext></mml:msup></mml:math> mixed dislocations in body-centered cubic transition metals. Acta Materialia, 2021, 217, 117154.	3.8	6

#	Article	IF	Citations
58901	Electro-optical and charge transport properties of chalcone derivatives using a dual approach from molecule to material level simulations. Computational and Theoretical Chemistry, 2021, 1203, 113349.	1.1	10
58902	Partial oxidation of propylene with H2 and O2 over Au supported on ZrO2 with different structural and surface properties. Journal of Catalysis, 2021, 401, 188-199.	3.1	9
58903	Optimized interatomic potential for atomistic simulation of Zr-Nb alloy. Computational Materials Science, 2021, 197, 110581.	1.4	19
58904	How to take into account local concentration in Ising-based Monte-Carlo: illustration with zirconium hydrides. Computational Materials Science, 2021, 197, 110547.	1.4	1
58905	An automated approach for developing neural network interatomic potentials with FLAME. Computational Materials Science, 2021, 197, 110567.	1.4	8
58906	Influence of hydrogen isotopes on vacancy formation and antisite defect diffusion in palladium and vanadium metals. Computational Materials Science, 2021, 197, 110641.	1.4	3
58907	Bayesian learning of thermodynamic integration and numerical convergence for accurate phase diagrams. Physical Review B, 2021, 104, .	1.1	6
58908	Importance of the gas-phase error correction for O2 when using DFT to model the oxygen reduction and evolution reactions. Journal of Electroanalytical Chemistry, 2021, 896, 115178.	1.9	37
58909	Third-generation CALPHAD description of pure GeO2 at 1Âatm. Calphad: Computer Coupling of Phase Diagrams and Thermochemistry, 2021, 74, 102299.	0.7	6
58910	Rashba states situated inside the band gap of InTe/PtSe2 heterostructure. Results in Physics, 2021, 28, 104673.	2.0	4
58911	Interlayer ferromagnetic coupling and enhanced magnetism by biaxial strain in MnBi2Te4/VBi2Te4 heterojunction. Journal of Physics: Conference Series, 2021, 2011, 012096.	0.3	0
58912	Ultra-fine Cu clusters decorated hydrangea-like titanium dioxide for photocatalytic hydrogen production. Rare Metals, 2022, 41, 385-395.	3.6	31
58913	Hydrogen states in mixed-cation CuIn(1-x)GaxSe2 chalcopyrite alloys: a combined study by first-principles density-functional calculations and muon-spin spectroscopy. Philosophical Magazine, 0, , 1-23.	0.7	5
58914	Strong electronâ€“phonon coupling influences carrier transport and thermoelectric performances in group-IV/V elemental monolayers. Npj Computational Materials, 2021, 7, .	3.5	19
58915	Pressure-induced atomic packing change in Pd37Ni37S26 metallic glass. Acta Materialia, 2021, 216, 117116.	3.8	3
58916	Defect engineering for high-selection-performance of N2 activation over CeO2(111) surface. Chinese Chemical Letters, 2022, 33, 2188-2194.	4.8	3
58917	Generating Mechanism of Catalytic Effect for Hydrogen Absorption/Desorption Reactions in NaAlH4â€“TiCl3. Applied Sciences (Switzerland), 2021, 11, 8349.	1.3	4
58918	Van der Waals heterostructure of Janus transition metal dichalcogenides monolayers (WSSe-WX2) Tj ETQq1 1 0.784314 rgBT /Overlo	0.9	7

#	Article	IF	Citations
58919	On the design of models for an accurate description of the water â€“ hematite interface. Applied Surface Science, 2021, 560, 149884.	3.1	1
58920	Machine learning for materials discovery: Two-dimensional topological insulators. Applied Physics Reviews, 2021, 8, .	5.5	34
58921	Mitrofanovite Pt₃Te₄: A Topological Metal with Termination-Dependent Surface Band Structure and Strong Spin Polarization. ACS Nano, 2021, 15, 14786-14793.	7.3	13
58922	Mg₃Si₃(MoO₆)₂ as a High-Performance Cathode Active Material for Magnesium-Ion Batteries. ACS Applied Materials & Interfaces, 2021, 13, 47749-47755.	4.0	6
58923	Emergent electronic properties in Co-deposited superatomic clusters. Journal of Chemical Physics, 2021, 155, 124309.	1.2	1
58924	Anomalous Dimensionalityâ€Driven Phase Transition of MoTe₂ in Van der Waals Heterostructure. Advanced Functional Materials, 2021, 31, 2107376.	7.8	14
58925	Giant inverse Rashba-Edelstein effect: Application to monolayer <mml:math xmlns:mml="http://www.w3.org/1998/Math/MathML"><mml:msub><mml:mi>OsBi</mml:mi><mml:mn>2</mml:mn></mml:msub></mml:mr Physical Review B, 2021, 104, .	3.1	8
58926	Dirac nodal line and Rashba spin-split surface states in nonsymmorphic ZrGeTe. New Journal of Physics, 2021, 23, 103019.	1.2	4
58927	3D Tungsten Disulfide/Carbon Nanotube Networks as Separator Coatings and Cathode Additives for Stable and Fast Lithiumâ€“Sulfur Batteries. ACS Applied Materials & Interfaces, 2021, 13, 45547-45557.	4.0	17
58928	Anomalous heavy doping in chemical-vapor-deposited titanium trisulfide nanostructures. Physical Review Materials, 2021, 5, .	0.9	3
58929	In situ loading of MoO3 clusters on ultrathin Bi2MoO6 nanosheets for synergistically enhanced photocatalytic NO abatement. Applied Catalysis B: Environmental, 2021, 292, 120159.	10.8	51
58930	Resolving the intrinsic bandgap and edge effect of BiI3 film epitaxially grown on graphene. Materials Today Physics, 2021, 20, 100454.	2.9	4
58931	Structure and reaction pathways of octanoic acid on copper. Surface Science, 2021, 711, 121875.	0.8	8
58932	Tunable electronic properties and enhanced ferromagnetism in Cr₂Ge₂Te₆ monolayer by strain engineering. Nanotechnology, 2021, 32, 485408.	1.3	7
58933	A saccharide-based binder for efficient polysulfide regulations in Li-S batteries. Nature Communications, 2021, 12, 5375.	5.8	65
58934	Electronic structures of vacancies in Co3Sn2S2 *. Chinese Physics B, 2021, 30, 077102.	0.7	1
58935	Universal Structural Influence on the 2D Electron Gas at SrTiO₃ Surfaces. Advanced Science, 2021, 8, e2100602.	5.6	14
58936	Synergetic effects of Bi5+ and oxygen vacancies in Bismuth(V)-rich Bi4O7 nanosheets for enhanced near-infrared light driven photocatalysis. Journal of Materials Science and Technology, 2021, 85, 1-10.	5.6	41

#	Article	IF	Citations
58937	Investigation of photon emitters in Ce-implanted hexagonal boron nitride. Optical Materials Express, 2021, 11, 3478.	1.6	3
58938	Demonstration of valley anisotropy utilized to enhance the thermoelectric power factor. Nature Communications, 2021, 12, 5408.	5.8	66
58939	Computational design of V-CoCrFeMnNi high-entropy alloys: An atomistic simulation study. Calphad: Computer Coupling of Phase Diagrams and Thermochemistry, 2021, 74, 102317.	0.7	12
58940	Thermodynamic modeling of the Te-X (X = Zr, Ce, Eu) systems. Calphad: Computer Coupling of Phase Diagrams and Thermochemistry, 2021, 74, 102281.	0.7	6
58941	Modification of Lu's (2005) high pressure model for improved high pressure/high temperature extrapolations. Part II: Modeling of osmiumâ€“platinum system at high pressure/high temperature. Calphad: Computer Coupling of Phase Diagrams and Thermochemistry, 2021, 74, 102311.	0.7	2
58942	Insight into the activation energy for the interfacial stability evaluation in all-solid-state Li-ion batteries. Journal of Power Sources, 2021, 506, 230211.	4.0	5
58943	Insight into the structure and tribological and corrosion performance of high entropy (CrNbSiTiZr)C films: First-principles and experimental study. Surface and Coatings Technology, 2021, 421, 127468.	2.2	10
58944	Designing of 0D/2D mixed-dimensional van der waals heterojunction over ultrathin g-C3N4 for high-performance flexible self-powered photodetector. Chemical Engineering Journal, 2021, 420, 129556.	6.6	34
58945	Colloidal synthesis and charge carrier dynamics of Cs4Cd1âˆ’Cu Sb2Cl12 (0Ââ‰ x â‰ 1) layered double perovskite nanocrystals. Matter, 2021, 4, 2936-2952.	5.0	20
58946	2D Pentagonal Pdâ€Based Janus Transition Metal Dichalcogenides for Photocatalytic Water Splitting. Physica Status Solidi - Rapid Research Letters, 2022, 16, 2100344.	1.2	17
58947	Course on the Use of DFT Calculations to Improve Understanding of Phase Diagrams in Solid-State Chemistry. Journal of Chemical Education, 2021, 98, 3207-3217.	1.1	2
58948	Activation of anionic redox in d0 transition metal chalcogenides by anion doping. Nature Communications, 2021, 12, 5485.	5.8	26
58949	First-principles calculations on ferroelectricity and lattice dynamics of Type-II multiferroic SmMn2O5. Current Applied Physics, 2021, 29, 24-32.	1.1	0
58950	Centimeter-Scale Few-Layer PdS₂: Fabrication and Physical Properties. ACS Applied Materials & Interfaces, 2021, 13, 43063-43074.	4.0	28
58951	Adjacent single-atom irons boosting molecular oxygen activation on MnO2. Nature Communications, 2021, 12, 5422.	5.8	114
58952	High-Pressure Synthesis of the Î²-Zn₃N₂ Nitride and the Î±-ZnN₄ and Î²-ZnN₄ Polynitrogen Compounds. Inorganic Chemistry, 2021, 60, 14594-14601.	1.9	15
58953	Spin spiral and topological Hall effect in <mml:math xmlns:mml="http://www.w3.org/1998/Math/MathML"><mml:msub><mml:mi mathvariant="normal">Fe</mml:mi><mml:mn>3</mml:mn></mml:msub><mml:msub><mml:mi mathvariant="normal">Ga</mml:mi><mml:mn>4</mml:mn></mml:msub></mml:math>. Physical Review B, 2021, 104, .	1.1	6
58954	What is the Enthalpy Contribution to the Stabilization of the Coâ€“Crâ€“Feâ€“Mnâ€“Ni Faced-centered Cubic Solid Solution?. Journal of Phase Equilibria and Diffusion, 2021, 42, 561-570.	0.5	4

#	Article	IF	Citations
58955	Effect of metal decoration on sulfur-based gas molecules adsorption on phosphorene. Scientific Reports, 2021, 11, 18179.	1.6	1
58956	Theoretical Insights on Auâ€based Bimetallic Alloy Electrocatalysts for Nitrogen Reduction Reaction with High Selectivity and Activity. ChemSusChem, 2021, 14, 4525-4535.	3.6	11
58957	Cesium polytungstate in sputtered solar control films. II. Electronic structure and water-induced defects. Journal of Applied Physics, 2021, 130, .	1.1	4
58958	Alumina-Mediated Ï€-Activation of Alkynes. Journal of the American Chemical Society, 2021, 143, 15420-15426.	6.6	16
58959	Investigation on the Structureâ€“Performance Correlation of TiC MXenes as Cathode Catalysts for Li-O2 Batteries. Journal of Physical Chemistry C, 0, , .	1.5	10
58960	Theoretical Insight into 20â€Electron Transition Metal Complexes (C₅H₅)₂TM(E₁E₂)₂ (TMâ€‰=â€‰Cr, Bonding Nature. Physica Status Solidi (B): Basic Research, 2021, 258, 2100417.	0.7	6
58961	Assessment of the Accuracy of Density Functionals for Calculating Oxygen Reduction Reaction on Nitrogen-Doped Graphene. Journal of Chemical Theory and Computation, 2021, 17, 6405-6415.	2.3	9
58962	Theoretical and experimental study of (Ga1-xFex)2O3 ternary alloys. Journal of Crystal Growth, 2021, 575, 126353.	0.7	5
58963	Role of Electronic Structure in Li Ordering and Chemical Strain in the Fast Charging Wadsleyâ€“Roth Phase PNb₉O₂₅. Chemistry of Materials, 2021, 33, 7755-7766.	3.2	13
58964	Cyclohexylammoniumâ€Based 2D/3D Perovskite Heterojunction with Funnelâ€Like Energy Band Alignment for Efficient Solar Cells (23.91%). Advanced Energy Materials, 2021, 11, 2102236.	10.2	77
58965	Behavior of intrinsic defects in BaF2 under uniaxial compressions: An ab initio investigation. Materials Today Communications, 2021, 28, 102730.	0.9	5
58966	Neuroevolution machine learning potentials: Combining high accuracy and low cost in atomistic simulations and application to heat transport. Physical Review B, 2021, 104, .	1.1	101
58967	Doping Process of 2D Materials Based on the Selective Migration of Dopants to the Interface of Liquid Metals. Advanced Materials, 2021, 33, e2104793.	11.1	38
58968	Theoretical investigation of metal oxides for SO 2 capture through firstâ€principles calculations. International Journal of Quantum Chemistry, 0, , e26822.	1.0	1
58969	Direct Atomicâ€Scale Structure and Electric Field Imaging of Triazineâ€Based Crystalline Carbon Nitride. Advanced Materials, 2021, 33, e2106359.	11.1	19
58970	Origin of Rashba Spin Splitting and Strain Tunability in Ferroelectric Bulk CsPbF₃. Journal of Physical Chemistry Letters, 2021, 12, 9539-9546.	2.1	10
58971	Nitrogen/oxygen codoped hierarchical porous Carbons/Selenium cathode with excellent lithium and sodium storage behavior. Journal of Colloid and Interface Science, 2022, 608, 265-274.	5.0	20
58972	Coupling Glucoseâ€Assisted Cu(I)/Cu(II) Redox with Electrochemical Hydrogen Production. Advanced Materials, 2021, 33, e2104791.	11.1	126

#	Article	IF	Citations
58973	Tuning reaction pathways of peroxymonosulfate-based advanced oxidation process via defect engineering. Cell Reports Physical Science, 2021, 2, 100550.	2.8	9
58974	Thermoelectric degrees of freedom determining thermoelectric efficiency. IScience, 2021, 24, 102934.	1.9	15
58975	Synthesis modification of hydroxyapatite surface for ethanol conversion: The role of the acidic/basic sites ratio. Journal of Catalysis, 2021, 404, 802-813.	3.1	11
58976	Raman Spectroscopy and Aging of the Low-Loss Ferrimagnet Vanadium Tetracyanoethylene. Journal of Physical Chemistry C, 2021, 125, 20380-20388.	1.5	3
58977	Transport properties of the parent LaNiO$$_2$$. European Physical Journal B, 2021, 94, 1.	0.6	2
58978	Selective Photothermal Reduction of CO₂ to CO over Ni-Nanoparticle/N-Doped CeO₂ Nanocomposite Catalysts. ACS Applied Nano Materials, 2021, 4, 10485-10494.	2.4	21
58979	High thermoelectric power factor of pure and vanadium-alloyed chromium nitride thin films. Materials Today Communications, 2021, 28, 102493.	0.9	9
58980	Correlation between reduced dielectric loss and charge migration kinetics in NdFeO3-modified Ba0.7Sr0.3TiO3 ceramics. Journal of Materials Science: Materials in Electronics, 2021, 32, 24910.	1.1	2
58981	Adsorption and Activation of CO₂ on Nitride MXenes: Composition, Temperature, and Pressure effects. ChemPhysChem, 2021, 22, 2456-2463.	1.0	11
58982	Nobleâ€Metalâ€Assisted Fast Interfacial Oxygen Migration with Topotactic Phase Transition in Perovskite Oxides. Advanced Functional Materials, 2021, 31, 2106765.	7.8	18
58983	Effect of Disorder and Strain on Spin Polarization of a Co₂FeSi Heusler Alloy. ACS Applied Electronic Materials, 2021, 3, 4522-4534.	2.0	8
58984	Acetone sensing mechanism of Ar/O2 plasma modified indium oxide electrospun fibers: A combined DFT and experimental study. Journal of Alloys and Compounds, 2022, 895, 162017.	2.8	15
58985	Termination-dependent electronic structure and atomic-scale screening behavior of the Cu₂O(111) surface. Journal of Physics Condensed Matter, 2021, 33, 484001.	0.7	2
58986	Bandgap engineering of KTaO3 for water-splitting by different doping strategies. International Journal of Hydrogen Energy, 2021, 46, 38663-38677.	3.8	10
58987	Enhancing nitrobenzene reduction to azoxybenzene by regulating the O-vacancy defects over rationally tailored CeO2 nanocrystals. Applied Surface Science, 2022, 572, 151343.	3.1	10
58988	Kitkaite NiTeSe, an Ambientâ€Stable Layered Dirac Semimetal with Lowâ€Energy Typeâ€II Fermions with Application Capabilities in Spintronics and Optoelectronics. Advanced Functional Materials, 0, , 2106101.	7.8	8
58989	Expanded Chemistry and Proton Conductivity in Vanadium-Substituted Variants of Î³-Ba4Nb2O9. Chemistry of Materials, 2021, 33, 7475-7483.	3.2	0
58990	Lateral Modulation of Magnetic Anisotropy in Tricolor 3dâ€“5d Oxide Superlattices. ACS Applied Electronic Materials, 2021, 3, 4210-4217.	2.0	5

#	Article	IF	Citations
58991	Electrostatic Modulation and Mechanism of the Electronic Properties of Monolayer MoS2 via Ferroelectric BiAlO3(0001) Polar Surfaces. ACS Omega, 2021, 6, 26345-26353.	1.6	1
58992	Band Edge Energy Tuning through Electronic Character Hybridization in Ternary Metal Vanadates. Chemistry of Materials, 2021, 33, 7242-7253.	3.2	7
58993	Promoted self-construction of Î²-NiOOH in amorphous high entropy electrocatalysts for the oxygen evolution reaction. Applied Catalysis B: Environmental, 2022, 301, 120764.	10.8	103
58994	Tailoring Layered-Double-Hydroxide Nanostructures toward Long-Lifespan and Fast Kinetics Lithiumâ€“Sulfur Batteries. ACS Applied Energy Materials, 2021, 4, 11752-11760.	2.5	3
58995	The Mystery behind Dynamic Charge Disproportionation in BaBiO₃. Nano Letters, 2021, 21, 8433-8438.	4.5	7
58996	Associative vs. dissociative mechanism: Electrocatalysis of nitric oxide to ammonia. Chinese Chemical Letters, 2022, 33, 1051-1057.	4.8	61
58997	First-principles calculations to investigate stability, electronic and optical properties of fluorinated MoSi2N4 monolayer. Results in Physics, 2021, 30, 104864.	2.0	19
58998	Role of facet in the competitive pathway of ethylene epoxidation. Surface Science, 2022, 716, 121954.	0.8	1
58999	Predicting energy and stability of known and hypothetical crystals using graph neural network. Patterns, 2021, 2, 100361.	3.1	16
59000	Locating Hydrides in Ligand-Protected Copper Nanoclusters by Deep Learning. ACS Applied Materials & Interfaces, 2021, 13, 53468-53474.	4.0	8
59001	Magnetism in Au-Supported Planar Silicene. Nanomaterials, 2021, 11, 2568.	1.9	3
59002	The charge localization deteriorating the thermoelectric properties: The case of kiddcreekite-type Cu6WSnSe8. Journal of Solid State Chemistry, 2021, 304, 122626.	1.4	2
59003	Single germanene phase formed by segregation through Al(111) thin films on Ge(111). 2D Materials, 2021, 8, 045039.	2.0	7
59004	Experimental and computational kinetics study of the liquid-phase hydrogenation of C C and C O bonds. Journal of Catalysis, 2021, 404, 771-785.	3.1	5
59005	Promising Lead-Free Double-Perovskite Photovoltaic Materials Cs₂MMâ€²Br₆ (M) Tj ETQq0 0 0 rgBT /Overlock Journal of Physical Chemistry C, 2021, 125, 21160-21168.	1.5	22
59006	Dioxygen Activation Kinetics over Distinct Cu Site Types in Cu-Chabazite Zeolites. ACS Catalysis, 2021, 11, 11873-11884.	5.5	27
59007	Controlled Asymmetric Charge Distribution of Active Centers in Conjugated Polymers for Oxygen Reduction. Angewandte Chemie, 0, , .	1.6	7
59008	Promotional Role of a Cation Intermediate Complex in C₂ Formation from Electrochemical Reduction of CO₂ over Cu. ACS Catalysis, 2021, 11, 12336-12343.	5.5	60

#	Article	IF	Citations
59009	Vertical growth of nickel sulfide nanosheets on graphene oxide for advanced sodium-ion storage. Carbon, 2021, 182, 194-202.	5.4	24
59010	Structural, electronic and optical properties of M-doped anatase TiO2 (M= Fe or Au): A first principle investigation. Computational Condensed Matter, 2021, 28, e00576.	0.9	10
59011	Silver hollandite (AgxMn8O16 , xâ‰2): A highly anisotropic half-metal for spintronics. Physical Review Materials, 2021, 5, .	0.9	1
59012	Searching for highly efficient multifunctional electrocatalysts based on the single metal doped graphitic carbon nitride. Molecular Physics, 2021, 119, .	0.8	3
59013	Principles Determining the Structure of Transition Metals. Molecules, 2021, 26, 5396.	1.7	1
59014	One-dimensional spin-polarized electron channel in the two-dimensional PbBi compound on silicon. Physical Review B, 2021, 104, .	1.1	9
59015	Rhodium-molybdenum oxide electrocatalyst with dual active sites for electrochemical ammonia synthesis under neutral pH condition. Journal of Electroanalytical Chemistry, 2021, 896, 115157.	1.9	10
59016	Materials informatics platform with three dimensional structures, workflow and thermoelectric applications. Scientific Data, 2021, 8, 236.	2.4	27
59017	Large bulk photovoltaic effect and second-harmonic generation in few-layer pentagonal semiconductors PdS₂ and PdSe₂. New Journal of Physics, 2021, 23, 093028.	1.2	9
59018	Ab initio thermodynamics reveals the nanocomposite structure of ferrihydrite. Communications Chemistry, 2021, 4, .	2.0	17
59019	The Influence of UiOâ€bpy Skeleton for the Direct Methaneâ€toâ€Methanol Conversion on Cu@UiOâ€bpy: Importance of the Encapsulation Effect. ChemCatChem, 2021, 13, 4897-4902.	1.8	5
59020	Boronâ€Mediated Grain Boundary Engineering Enables Simultaneous Improvement of Thermoelectric and Mechanical Properties in Nâ€Type Bi₂Te₃. Small, 2021, 17, e2104067.	5.2	30
59021	Z-scheme systems of ASi2N4 (Aâ€‰=â€‰Mo or W) for photocatalytic water splitting and nanogenerators. Tungsten, 2022, 4, 52-59.	2.0	41
59022	Electronâ€“Hole Plasmaâ€Induced Dephasing in Transition Metal Dichalcogenides. Physica Status Solidi - Rapid Research Letters, 2021, 15, 2100391.	1.2	0
59023	Activation of Transition Metal (Fe, Co and Ni)â€Oxide Nanoclusters by Nitrogen Defects in Carbon Nanotube for Selective CO₂ Reduction Reaction. Energy and Environmental Materials, 2023, 6, .	7.3	16
59024	P removal from Si by Si-Ca-Al alloying-leaching refining: Effect of Al and the CaAl2Si2 phase. Separation and Purification Technology, 2021, 271, 118675.	3.9	7
59025	Liquid structure under extreme conditions: high-pressure x-ray diffraction studies. Journal of Physics Condensed Matter, 2021, 33, 503004.	0.7	8
59026	Influence of Cation Size on the Local Atomic Structure and Electronic Properties of Ta Perovskite Oxynitrides. Inorganic Chemistry, 2021, 60, 14190-14201.	1.9	9

#	Article	IF	Citations
59027	Preparation of CoGe2-type NiSn2 at 10ÂGPa. Zeitschrift Fur Naturforschung - Section B Journal of Chemical Sciences, 2021, .	0.3	0
59028	Entropy stabilized off-stoichiometric cubic Î³-Cu1â^'xIx phase containing high-density Cu vacancies. AIP Advances, 2021, 11, .	0.6	3
59029	Atomic-scale imaging of CH3NH3PbI3 structure and its decomposition pathway. Nature Communications, 2021, 12, 5516.	5.8	36
59030	Evidence of two-dimensional flat band at the surface of antiferromagnetic kagome metal FeSn. Nature Communications, 2021, 12, 5345.	5.8	34
59031	A Combined Experimental and Atomistic Investigation of PTFE Double Transfer Film Formation and Lubrication in Rolling Point Contacts. Tribology Letters, 2021, 69, 1.	1.2	13
59032	Enhancing Effect of Fe²⁺ Doping of Ni/NiO Nanocomposite Films on Catalytic Hydrogen Generation. ACS Applied Materials & Interfaces, 2021, 13, 42909-42916.	4.0	13
59033	Lattice dynamics effects on finite-temperature stability of R1â^'Fe (R = Y, Ce, Nd, Sm, and Dy) alloys from first principles. Journal of Alloys and Compounds, 2021, 874, 159754.	2.8	10
59034	Atomic iridium species anchored on porous carbon network support: An outstanding electrocatalyst for CO2 conversion to CO. Applied Catalysis B: Environmental, 2021, 292, 120173.	10.8	20
59035	Effect of facile nitrogen doping on catalytic performance of NaW/Mn/SiO2 for oxidative coupling of methane. Applied Catalysis B: Environmental, 2021, 292, 120161.	10.8	10
59036	Facile control of surface reconstruction with Co2+ or Co3+-rich (oxy)hydroxide surface on ZnCo phosphate for large-current-density hydrogen evolution in alkali. Materials Today Physics, 2021, 20, 100448.	2.9	14
59037	Ultrahigh hydrogen and nitrogen selectivity achieved by the nanoporous graphene with a precise nanopore. Carbon, 2021, 182, 628-633.	5.4	4
59038	First-principles calculation for displacive phase transition of atomic-scale precipitates in aluminum alloys. Physics Letters, Section A: General, Atomic and Solid State Physics, 2021, 411, 127569.	0.9	4
59039	Quantum Spin-Valley Hall Kink States: From Concept to Materials Design. Physical Review Letters, 2021, 127, 116402.	2.9	25
59040	Complexions and grain growth retardation: First-principles modeling of phase boundaries in WC-Co cemented carbides at elevated temperatures. Acta Materialia, 2021, 216, 117128.	3.8	22
59041	Graphdiyne enables Cu nanoparticles for highly selective electroreduction of CO₂ to formate. 2D Materials, 2021, 8, 044008.	2.0	7
59042	Thickness-dependent Raman active modes of SnS thin films. AIP Advances, 2021, 11, .	0.6	4
59043	Efficient electrochemical reduction of CO to C2 products on the transition metal and boron co-doped black phosphorene. Chinese Chemical Letters, 2022, 33, 2183-2187.	4.8	26
59044	Molecular dynamics simulation of color centers in silicon carbide by helium and dual ion implantation and subsequent annealing. Ceramics International, 2021, 47, 24534-24544.	2.3	11

#	Article	IF	Citations
59045	The formaldehyde adsorption on anatase TiO2 (2Â1Â1) surface. Chemical Physics Letters, 2021, 778, 138771.	1.2	3
59046	Lithium Oxide Superionic Conductors Inspired by Garnet and NASICON Structures. Advanced Energy Materials, 2021, 11, 2101437.	10.2	33
59047	Insights into the HDS/HYDO selectivity with considering stacking effect of Co-MoS2 catalysts by combined DFT and microkinetic method. Fuel, 2021, 300, 120941.	3.4	8
59048	Two-dimensional Al2I2Se2: A promising anisotropic thermoelectric material. Journal of Alloys and Compounds, 2021, 876, 160191.	2.8	37
59049	First principle studies of effects of solute segregation on grain boundary strength in Ni-based alloys. Journal of Alloys and Compounds, 2021, 874, 159795.	2.8	13
59050	Construction of p-n junctions in single-unit-cell ZnIn2S4 nanosheet arrays toward promoted photoelectrochemical performance. Journal of Catalysis, 2021, 401, 262-270.	3.1	18
59051	Phase equilibria in the ZrO₂â€“Ta₂O₅â€“Nb₂O₅ system: Experimental studies and thermodynamic modeling. Journal of the American Ceramic Society, 2022, 105, 668-686.	1.9	24
59052	Dual-Function Reaction Center for Simultaneous Activation of CH₄ and O₂ via Oxygen Vacancies during Direct Selective Oxidation of CH₄ into CH₃OH. ACS Applied Materials & Interfaces, 2021, 13, 46694-46702.	4.0	17
59053	High-Density Ruthenium Single Atoms Anchored on Oxygen-Vacancy-Rich g-C₃N₄-C-TiO₂ Heterostructural Nanosphere for Efficient Electrocatalytic Hydrogen Evolution Reaction. ACS Applied Materials & Interfaces, 2021, 13, 46608-46619.	4.0	20
59054	Surface-Functionalized Boron Arsenide as a Photocathode for CO2 Reduction. Journal of Physical Chemistry C, 0, , .	1.5	0
59055	Investigation of physical properties and superdislocation characters of Ni3Al under uniaxial tension/compression normal to slip plane. Intermetallics, 2021, 136, 107258.	1.8	7
59056	First-principles study of the stability, electronic and mechanical properties of Cr2N and CrN with the variation of Ni doping concentration. Ceramics International, 2021, 47, 24430-24437.	2.3	2
59057	Sizeâ€Đependent Cobalt Catalyst for Lithium Sulfur Batteries: From Single Atoms to Nanoclusters and Nanoparticles. Small Methods, 2021, 5, e2100571.	4.6	39
59058	Atomic-Scale Investigation of Oxidation at the Black Phosphorus Surface. ACS Applied Electronic Materials, 2021, 3, 4066-4072.	2.0	6
59059	Thermophysical properties of hot fluid iron in the protolunar disk. Physics of the Earth and Planetary Interiors, 2021, 321, 106806.	0.7	0
59060	Restructuring highly electron-deficient metal-metal oxides for boosting stability in acidic oxygen evolution reaction. Nature Communications, 2021, 12, 5676.	5.8	92
59061	Devil is in the Defects: Electronic Conductivity in Solid Electrolytes. Chemistry of Materials, 2021, 33, 7484-7498.	3.2	49
59062	Contacts between monolayer black phosphorene and metal electrodes: Ohmic, Schottky, and their regulating strategy. Journal of Applied Physics, 2021, 130, .	1.1	3

#	Article	IF	Citations
59063	Ferromagnetism in 2D Vanadium Diselenide. ACS Nano, 2021, 15, 16236-16241.	7.3	61
59064	Emergent perpendicular magnetic anisotropy at the interface of an oxide heterostructure. Physical Review B, 2021, 104, .	1.1	4
59065	Observation of Unconventional Charge Density Wave without Acoustic Phonon Anomaly in Kagome Superconductors <mml:math xmlns:mml="http://www.w3.org/1998/Math/MathML" display="inline"><mml:mrow><mml:mrow><mml:msub><mml:mrow><mml:mi>A</mml:mi><mml:mi mathvariant="normal">V</mml:mi></mml:mrow><mml:mrow><mml:mn>3</mml:mn></mml:mrow></mml:msub></mml:mrow><mml:mn		

#	Article	IF	Citations
59082	Graphite to AlB2 and MgB2: a comparative study of their tight-binding model and Dirac nodal line. Philosophical Magazine, 0, , 1-15.	0.7	1
59083	Unusual Melting Trend in an Alkali Asymmetric Sulfonamide Salt Series: Single-Crystal Analysis and Modeling. Inorganic Chemistry, 2021, 60, 14679-14686.	1.9	5
59084	Biomimetic assembly to superplastic metalâ€“organic framework aerogels for hydrogen evolution from seawater electrolysis. Exploration, 2021, 1, 217.	5.4	59
59085	Study on the optical spectra of the oxygen vacancy in ZnWO₄crystal. Modern Physics Letters B, 2021, 35, .	1.0	2
59086	Cooperative Oxide-Ion Transport in Pyrochlore Y₂Ti₂O₇: A First-Principles Molecular Dynamics Study. Journal of Physical Chemistry C, 2021, 125, 20460-20467.	1.5	3
59087	Theoretical insight into adsorption and dissociation of water on NiCr binary alloy surfaces: Early-stage oxidation mechanism. Journal of Applied Physics, 2021, 130, .	1.1	1
59088	Study on the optical properties of CdWO4 crystal with oxygen vacancies. Nuclear Instruments & Methods in Physics Research B, 2021, 502, 183-188.	0.6	1
59089	Optical, Electrochemical, and Photoelectrochemical Behavior of Copper Pyrovanadate: A Unified Theoretical and Experimental Study. Journal of Physical Chemistry C, 2021, 125, 19609-19620.	1.5	4
59090	Construction of Indium Oxide/N-Doped Titanium Dioxide Hybrid Photocatalysts for Efficient and Selective Oxidation of Cyclohexane to Cyclohexanone. Journal of Physical Chemistry C, 2021, 125, 19791-19801.	1.5	21
59091	Two-Dimensional Auxetic GeSe₂ Material with Ferroelasticity and Flexoelectricity. Journal of Physical Chemistry C, 2021, 125, 19666-19672.	1.5	9
59092	Immunizing Aqueous Zn Batteries against Dendrite Formation and Side Reactions at Various Temperatures via Electrolyte Additives. Small, 2021, 17, e2103195.	5.2	172
59093	Common Defects Accelerate Charge Carrier Recombination in CsSnI₃ without Creating Mid-Gap States. Journal of Physical Chemistry Letters, 2021, 12, 8699-8705.	2.1	31
59094	New Two-Dimensional Wide Band Gap Hydrocarbon Insulator by Hydrogenation of a Biphenylene Sheet. Journal of Physical Chemistry Letters, 2021, 12, 8889-8896.	2.1	26
59095	Catalyzing Bondâ€Dissociation in Graphene via Alkaliâ€Iodide Molecules. Small, 2021, 17, e2102037.	5.2	1
59096	Intrinsic ferromagnetism with high Curie temperature and strong anisotropy in a ferroelastic <mml:math xmlns:mml="http://www.w3.org/1998/Math/MathML"><mml:mi mathvariant="normal">V</mml:mi><mml:mi>X</mml:mi></mml:math> monolayer <mml:math xmlns:mml="http://www.w3.org/1998/Math/MathML"><mml:mo>(</mml:mo><mml:mi>X</mml:mi><mml:mo>=</mml:mo><mml:mi) Tj	1.1	17
59097	Physical Review B, 2021, 104, . Density-functional theory calculation of magnetic properties of BiFeO3 and BiCrO3 under epitaxial strain. Journal of Applied Physics, 2021, 130, .	1.1	2
59098	Machine-learning-based many-body energy analysis of argon clusters: Fit for size?. Chemical Physics, 2022, 552, 111347.	0.9	3
59099	Electronic, Magnetic, and Mechanical Properties of YXâ€²CrZ (Xâ€² = Fe, Co, Ni; Z = Si, Ge, Sn) Quaternary Heusler Alloys. Journal of Superconductivity and Novel Magnetism, 2021, 34, 3019-3036.	0.8	5

#	Article	IF	Citations
59100	First-principles calculations of structural, electrical, and optical properties of ultra-wide bandgap (Al$$_x$$Ga$$_{1-x}$$)$$_2$$O$$_3$$ alloys. Journal of Materials Research, 2021, 36, 4790-4803.	1.2	25
59101	Microenvironmental Feeding and Stabilization of C₂H₄ Intermediates by Iodide-Doped Copper Nanowire Arrays to Boost C₂H₆ Formation. Energy & Fuels, 2021, 35, 15987-15994.	2.5	12
59102	Large contribution of quasi-acoustic shear phonon modes to thermal conductivity in novel monolayer Ga2O3. Journal of Applied Physics, 2021, 130, .	1.1	5
59103	Can NO x reduction by CO react over carbonâ€based singleâ€atom catalysts at low temperatures? A theoretical study. AICHE Journal, 0, , e17425.	1.8	2
59104	Phonon Anomalies Associated with Spin Reorientation in the Kagome Ferromagnet Fe3Sn2. Physica Status Solidi (B): Basic Research, 2022, 259, 2100169.	0.7	4
59105	Correlating point defects with mechanical properties in nanocrystalline TiN thin films. Materials and Design, 2021, 207, 109844.	3.3	18
59106	A priori control of zeolite phase competition and intergrowth with high-throughput simulations. Science, 2021, 374, 308-315.	6.0	90
59107	Multiple Dirac nodal lines in an in-plane anisotropic semimetal <mml:math xmlns:mml="http://www.w3.org/1998/Math/MathML"><mml:msub><mml:mi mathvariant="normal">TaNiTe</mml:mi><mml:mn>5</mml:mn></mml:msub></mml:math>. Physical Review B, 2021, 104, .	1.1	8
59108	CoS2 quantum dots modified by ZIF-67 and anchored on reduced graphene oxide as an efficient catalyst for hydrogen evolution reaction. Chemical Engineering Journal, 2022, 430, 132634.	6.6	44
59109	Stability and Catalytic Performance of Singleâ€Atom Supported on Ti₂CO₂ for Lowâ€Temperature CO Oxidation: A Firstâ€Principles Study. ChemPhysChem, 2021, 22, 2352-2361.	1.0	11
59110	Understanding of C/Tiâ€Doped SnS₂ Photocatalytic Behaviors from Electronic Structures. Physica Status Solidi - Rapid Research Letters, 2021, 15, 2100340.	1.2	3
59111	Charge Density Wave Orders and Enhanced Superconductivity under Pressure in the Kagome Metal CsV₃Sb₅. Advanced Materials, 2021, 33, e2102813.	11.1	54
59112	Deprotonation and cation adsorption on the NiOOH/water interface: A grand-canonical first-principles investigation. Electrochimica Acta, 2021, 398, 139253.	2.6	3
59113	Growth of Graphene Nanoflakes/hâ€BN Heterostructures. Advanced Materials Interfaces, 2021, 8, 2100766.	1.9	5
59114	Phonon transport anomaly in metavalent bonded materials: contradictory to the conventional theory. Journal of Materials Science, 2021, 56, 18534-18549.	1.7	11
59115	Electron, phonon and thermoelectric properties of Cu7PS6 crystal calculated at DFT level. Scientific Reports, 2021, 11, 19065.	1.6	6
59116	Plasma-engineered organic dyes as efficient polysulfide-mediating layers for high performance lithium-sulfur batteries. Chemical Engineering Journal, 2022, 430, 132679.	6.6	5
59117	High entropy alloy on single sub-lattice in MNiSn compound: Stability and thermoelectric properties. Journal of Alloys and Compounds, 2021, 874, 159940.	2.8	5

#	Article	IF	Citations
59118	Engineering Pt-Bi2O3 Interface to Boost Cyclohexanone Selectivity in Oxidative Dehydrogenation of KA-Oil. Catalysts, 2021, 11, 1187.	1.6	2
59119	Tuning the interaction between Na and Co2C to promote selective CO2 hydrogenation to ethanol. Applied Catalysis B: Environmental, 2021, 293, 120207.	10.8	57
59120	Halogen Edge-Passivated Antimonene Nanoribbons for Photocatalytic Hydrogen Evolution Reaction with High Solar-to-Hydrogen Conversion. Journal of Physical Chemistry C, 2021, 125, 21341-21351.	1.5	12
59121	Roton pair density wave in a strong-coupling kagome superconductor. Nature, 2021, 599, 222-228.	13.7	276
59122	Computational exploration of biomedical HfNbTaTiZr and Hf_{0.5}Nb_{0.5}Ta_{0.5}Ti_{1.5}Zr refractory high-entropy alloys. Materials Research Express, 2021, 8, 096534.	0.8	8
59123	Inherent stochasticity during insulatorâ€“metal transition in VO ₂. Proceedings of the National Academy of Sciences of the United States of America, 2021, 118, .	3.3	15
59124	Nitrogen substituted graphdiyne as electrode for high-performance lithium-ion batteries and capacitors. 2D Materials, 2021, 8, 044013.	2.0	5
59125	High Catalytic Activities of RENi_{5â€“x}Al_x (RE = La, Er) and Low Activity of Mg₂Ni Following Hydrogen Uptake: The Role of Absorbed Hydrogen. Journal of Physical Chemistry C, 2021, 125, 20919-20929.	1.5	4
59126	Cost-Effective Hybrid Density Functional Theory Calculation of Three-Dimensional Band Structure and Search of Band Edge Positions. Journal of Physical Chemistry A, 2021, 125, 8514-8518.	1.1	5
59127	Agent molecule modulated low-temperature activation of solid-state lithium-ion transport for polymer electrolytes. Journal of Power Sources, 2021, 505, 229917.	4.0	4
59128	Chiral Recognition on Bare Gold Surfaces by Quartz Crystal Microbalance. Angewandte Chemie - International Edition, 2021, 60, 25028-25033.	7.2	6
59129	Corrosion inhibition of locally de-passivated surfaces by DFT study of 2-mercaptobenzothiazole on copper. Npj Materials Degradation, 2021, 5, .	2.6	15
59130	Thermal transport and phase transitions of zirconia by on-the-fly machine-learned interatomic potentials. Npj Computational Materials, 2021, 7, .	3.5	57
59131	Single-Atom High-Temperature Catalysis on a Rh₁O₅ Cluster for Production of Syngas from Methane. Journal of the American Chemical Society, 2021, 143, 16566-16579.	6.6	22
59132	Controlling electrical and thermoelectric properties of bilayer SiC by bias voltage. Solid State Sciences, 2021, 121, 106737.	1.5	12
59133	Nano germanium incorporated thin graphite nanoplatelets: A novel germanium based lithium-ion battery anode with enhanced electrochemical performance. Electrochimica Acta, 2021, 391, 139001.	2.6	9
59134	DFT investigation analyzed with data mining technique of rare-earth dihydrides REH2 for hydrogen storage. International Journal of Hydrogen Energy, 2021, 46, 32962-32973.	3.8	11
59135	Type-II AsP/Sc2CO2 van der Waals heterostructure: an excellent photocatalyst for overall water splitting. International Journal of Hydrogen Energy, 2021, 46, 32882-32892.	3.8	23

#	Article	IF	Citations
59136	Pressure-Induced Variation of the Crystal Stacking Order in the Hydrogen-Bonded Quasi-Two-Dimensional Layered Material Cu(OH)Cl. Materials, 2021, 14, 5019.	1.3	0
59137	Direct H-He chemical association in superionic FeO2H2He at Deep-Earth conditions. National Science Review, 0, , .	4.6	18
59138	Controllable Schottky barriers by ferroelectric switching in graphene/In2Te3 heterostructures. Journal Physics D: Applied Physics, 0, , .	1.3	0
59139	Genetic Manipulation of M13 Bacteriophage for Enhancing the Efficiency of Virusâ€Inoculated Perovskite Solar Cells with a Certified Efficiency of 22.3%. Advanced Energy Materials, 2021, 11, 2101221.	10.2	20
59140	How to Look for Compounds: Predictive Screening and inâ€...situ Studies in Naâ^'Znâ^'Bi System. Chemistry - A European Journal, 2021, 27, 15954-15966.	1.7	4
59141	Insights into the borohydride electrooxidation reaction on metallic nickel from operando FTIRS, on-line DEMS and DFT. Electrochimica Acta, 2021, 389, 138721.	2.6	14
59142	DFT study for the absorption spectra evolution of CdS magic-size clusters. Chemical Physics Letters, 2021, 779, 138870.	1.2	6
59143	Basic physical behavior of impurity carbon in molybdenum for nuclear material: A systematical first-principles simulation. Nuclear Materials and Energy, 2021, 28, 101053.	0.6	1
59144	Quantum anomalous Hall effect in Cr₂Ge₂Te₆/Bi₂Se₃/Cr₂Ge₂Te₆ heterostructures. Journal of Physics Condensed Matter, 2021, 33, 465003.	1.7	4
59146	Atomic origin of room-temperature two-dimensional itinerant ferromagnetism in an oxide-monolayer heterostructure. Applied Materials Today, 2021, 24, 101101.	2.3	3
59147	Spin-polarized gap in the magnetic Weyl semimetal <mml:math xmlns:mml="http://www.w3.org/1998/Math/MathML"><mml:mrow><mml:msub><mml:mi>Co</mml:mi><mml:mn>3</mml:mn></mml:msub><mml:mathvariant="normal">S</mml:mi><mml:mn>2</mml:mn></mml:msub></mml:mrow></mml:math>. Physical Review B, 2021, 104, .	1.1	9
59149	Structure, bonding nature and transition dynamics of amorphous Te. Scripta Materialia, 2021, 202, 114011.	2.6	15
59150	Mesoporous WC x Films with NiOâ€Protected Surface: Highly Active Electrocatalysts for the Alkaline Oxygen Evolution Reaction. ChemSusChem, 2021, 14, 4708-4717.	3.6	3
59151	Oxygen-vacancy-assisted construction of FeOOH/CdS heterostructure as an efficient bifunctional photocatalyst for CO2 conversion and water oxidation. Applied Catalysis B: Environmental, 2021, 293, 120203.	10.8	71
59152	Neural network representation of electronic structure from ab initio molecular dynamics. Science Bulletin, 2022, 67, 29-37.	4.3	5
59153	High ICE Hard Carbon Anodes for Lithium-Ion Batteries Enabled by a High Work Function. ACS Applied Materials & Interfaces, 2021, 13, 46813-46820.	4.0	15
59154	Electronic structure, effective masses and g-factors and strain induced crystal field splitting of WZ-InP by kâƒ—Â·Ï€âƒ— method. Physica Scripta, 2021, 96, 125827.	1.2	2
59155	Ab Initio Study of the Influence of Alloying Elements on Stability and Mechanical Properties of Selected TixAly Intermetallic Compounds and Their TixAly/Al, TixAly/Ti Interfaces in Explosively Welded Metalâ€“Metal Composites. Metallurgical and Materials Transactions A: Physical Metallurgy and Materials Science, 2021, 52, 5032-5042.	1.1	2

#	Article	IF	Citations
59156	Theoretical insights for CoNxC4-x-graphene (x = 0â€“4) materials as high performance low-cost electrocatalysts for oxygen reduction reactions. Applied Physics Letters, 2021, 119, .	1.5	2
59157	Electronic structure and signature of Tomonagaâ€“Luttinger liquid state in epitaxial CoSb1â^'x nanoribbons. Npj Quantum Materials, 2021, 6, .	1.8	3
59158	Multiferroic properties of oxygen-functionalized magnetic i-MXene. Physical Review Materials, 2021, 5, .	0.9	13
59159	Interfacial Proton Transfer for Hydrogen Evolution at the Sub-Nanometric Platinum/Electrolyte Interface. ACS Applied Materials & Interfaces, 2021, 13, 47252-47261.	4.0	4
59160	Excellent cryogenic magnetocaloric performances in ferromagnetic Sr2GdNbO6 double perovskite compound. Materials Today Physics, 2021, 20, 100470.	2.9	55
59161	Surface reconstruction of CoO (111) and its effects on the formation of oxygen vacancy and OER activity. Surface Science, 2021, 711, 121862.	0.8	8
59162	Effects of electric field and strain on the Schottky barrier of the bilayer van der Waals heterostructures of graphene and pure/hydrogenated PC3 monolayer. Physica E: Low-Dimensional Systems and Nanostructures, 2021, 133, 114785.	1.3	3
59163	Electronic properties of the one-dimensional interfaces in two dimensional lateral (MoS2)m/(Mo2S3)m heterostructures. Chemical Physics Letters, 2021, 778, 138761.	1.2	3
59164	A permeable electrochemical reactive barrier for underground water remediation using TiO2/graphite composites as heterogeneous electrocatalysts without releasing of chemical substances. Journal of Hazardous Materials, 2021, 418, 126318.	6.5	10
59165	Heat capacity anomalies of the molecular crystal 1-fluoro-adamantane at low temperatures. Scientific Reports, 2021, 11, 18640.	1.6	8
59166	n-Type thermoelectric properties of a hexagonal SiGe polymorph superior to a cubic SiGe. Journal of Alloys and Compounds, 2021, 874, 160007.	2.8	5
59167	Stability and reaction thermodynamics of boron-doped nitrogenated holey graphene (NHG) monolayers and their energy storage properties for Li, Na and K-ion batteries: A first principles investigation. Applied Surface Science, 2021, 559, 149849.	3.1	11
59168	Stable two-dimensional pentagonal tellurene: A high ZT thermoelectric material with a negative Poissonâ€™s ratio. Applied Surface Science, 2021, 559, 149851.	3.1	8
59169	The interplay between twinning and cation inversion in MgAl2O4-spinel: Implications for a nebular thermochronometer. American Mineralogist, 2022, 107, 1470-1476.	0.9	1
59170	Phonon Transport and Thermoelectric Properties of Imidazole-Graphyne. Materials, 2021, 14, 5604.	1.3	3
59171	A Piezoelectric Ionic Cocrystal of Glycine and Sulfamic Acid. Crystal Growth and Design, 2021, 21, 5818-5827.	1.4	17
59172	Efficient Screening of Biâ€“Metallic Electrocatalysts for Glycerol Valorization. Electrochimica Acta, 2021, 398, 139283.	2.6	8
59173	Scalable Fabrication of LiMn₂O₄/Polythiophene with Improved Electrochemical Performance for Lithium-Ion Batteries. Industrial & Engineering Chemistry Research, 2021, 60, 14185-14192.	1.8	4

#	Article	IF	Citations
59174	Computational Exploration of Functional Nanoscale Carbonaceous Materials. Current Nanoscience, 2021, 17, .	0.7	1
59175	Accurate Prediction of Band Structure of FeS2: A Hard Quest of Advanced First-Principles Approaches. Frontiers in Chemistry, 2021, 9, 747972.	1.8	1
59176	Sc, Ge co-doping NASICON boosts solid-state sodium ion batteries' performance. Energy Storage Materials, 2021, 40, 282-291.	9.5	52
59177	Effect of single atom Platinum (Pt) doping and facet dependent on the electronic structure and light absorption of Lanthanum Titanium Oxide (La2Ti2O7): A Density Functional Theory study. Surface Science, 2022, 715, 121949.	0.8	5
59178	Principles for designing CO2 adsorption catalyst: Serving thermal conductivity as the determinant for reactivity. Chinese Chemical Letters, 2022, 33, 990-994.	4.8	36
59179	Investigations of High-Pressure Properties of MnF2 Based on the First-Principles Method. Journal of Physical Chemistry C, 0, , .	1.5	2
59180	Experimental and computational investigations of TiIrB: a new ternary boride with Ti_{1+x}Rh_{2â^'x+y}Ir_{3â^'y}B₃-type structure. Zeitschrift Fur Naturforschung - Section B Journal of Chemical Sciences, 2021, 76, 727-731.	0.3	2
59181	Effects of Interfacial Termination, Oxidation, and Film Thickness on the Magnetic Anisotropy in Mn_{2.25}Co_{0.75}Ga_{0.5}Sn_{0.5}/MgO Heterostructures. ACS Applied Materials & Interfaces, 2021, 13, 47293-47301.	4.0	3
59182	Sulfur Monovacancies in Liquid-Exfoliated MoS₂ Nanosheets for NO₂ Gas Sensing. ACS Applied Nano Materials, 2021, 4, 9459-9470.	2.4	27
59183	Spontaneous symmetry breaking of dislocation core in SrTiO3. Materials Today Physics, 2021, 20, 100453.	2.9	1
59184	Piperazine-based two-dimensional covalent organic framework for high performance anodic lithium storage. Energy Storage Materials, 2021, 40, 124-138.	9.5	34
59185	Unveiling the thermodynamic driving forces for high entropy alloys formation through big data ab initio analysis. Scripta Materialia, 2021, 202, 114000.	2.6	15
59186	Structural and magnetic properties of Sc1-Nb Fe2 intermetallics showing anomalous zero thermal expansion. Intermetallics, 2021, 136, 107252.	1.8	3
59187	Synthesis, characterization, crystal structure prediction, and ab initio study of bandgap of Cu3VSe4. Journal of Solid State Chemistry, 2021, 301, 122336.	1.4	3
59188	Dramatic catalytic activation of kinetically inert disilane hydrolysis in metallic iron particulate via barrierless chemical dissociation: First-principles study. Applied Surface Science, 2021, 560, 149988.	3.1	3
59189	Surface morphology evolution and underlying defects in homoepitaxial growth of GaAs (110). Journal of Alloys and Compounds, 2021, 874, 159848.	2.8	2
59190	Pressure-Enhanced Ferromagnetism in Layered CrSiTe₃ Flakes. Nano Letters, 2021, 21, 7946-7952.	4.5	20
59191	Enhanced Performance of Perovskite Solar Cells via Reactive Postâ€treatment Process Utilizing Guanidine Acetate as Interface Modifier. Solar Rrl, 2021, 5, 2100547.	3.1	16

#	Article	IF	Citations
59192	Glue-assisted grinding exfoliation of large-size 2D materials for insulating thermal conduction and large-current-density hydrogen evolution. Materials Today, 2021, 51, 145-154.	8.3	58
59193	Anisotropic non-split zero-energy vortex bound states in a conventional superconductor. Applied Physics Reviews, 2021, 8, .	5.5	12
59194	First principles calculations on the novel high pressure phase of HfC. International Journal of Modern Physics B, 2021, 35, .	1.0	0
59195	Tuning the Adsorption Properties of Metalâ€“Organic Frameworks through Coadsorbed Ammonia. ACS Applied Materials & Interfaces, 2021, 13, 43661-43667.	4.0	6
59196	Chemical Modifications of Ag Catalyst Surfaces with Imidazolium Ionomers Modulate H₂ Evolution Rates during Electrochemical CO₂ Reduction. Journal of the American Chemical Society, 2021, 143, 14712-14725.	6.6	44
59197	Tuning Metal Elements in Open Frameworks for Efficient Oxygen Evolution and Oxygen Reduction Reaction Catalysts. ACS Applied Materials & Interfaces, 2021, 13, 42715-42723.	4.0	17
59198	Thermoelectric Cu₁₂Sb₄S₁₃â€Based Synthetic Minerals with a Sublimationâ€Derived Porous Network. Advanced Materials, 2021, 33, e2103633.	11.1	46
59199	Thermal conversion of the hydrous aluminosilicate LiAlSiO₃(OH)₂ into Î³-eucryptite. Zeitschrift Fur Naturforschung - Section B Journal of Chemical Sciences, 2021, 76, 599-606.	0.3	1
59200	Novel Narrow Band Cyanâ€Green Phosphor LiK₇[Li₃SiO₄]₈:Eu²⁺ with Enhanced Suppression of Second Broad Band Emission. European Journal of Inorganic Chemistry, 2021, 2021, 4470-4481.	1.0	7
59201	Magnetic structure and exchange interactions in pyrrhotite end member minerals: hexagonal FeS and monoclinic Fe₇S₈. Journal of Physics Condensed Matter, 2021, 33, 465801.	0.7	6
59202	Overcoming Metastable CO₂ Adsorption in a Bulky Diamine-Appended Metalâ€“Organic Framework. Journal of the American Chemical Society, 2021, 143, 15258-15270.	6.6	51
59203	Theoretical Understanding of the Interface Effect in Promoting Electrochemical CO₂ Reduction on Cuâ€“Pd Alloys. Journal of Physical Chemistry C, 2021, 125, 21381-21389.	1.5	17
59204	Epitaxial-Strain-Induced Spontaneous Magnetization in Polar Mn₂Mo₃O₈. Chemistry of Materials, 2021, 33, 7713-7718.	3.2	3
59205	Insight into Fe Activating One-Dimensional Î±-Ni(OH)₂ Nanobelts for Efficient Oxygen Evolution Reaction. Journal of Physical Chemistry C, 2021, 125, 20301-20308.	1.5	17
59206	<mml:math xmlns:mml="http://www.w3.org/1998/Math/MathML"><mml:msup><mml:mrow><mml:mi>Ni</mml:mi></mml:mrow><mml:mrow><mml:mr -induced semiconductor-to-metal transition in spinel nickel cobaltite thin films. Physical Review B, 2021, 104, .	1.1	13
59207	Comparative Studies of the Structural and Transport Properties of Molten Salt FLiNaK Using the Machine-Learned Neural Network and Reparametrized Classical Forcefields. Journal of Physical Chemistry B, 2021, 125, 10562-10570.	1.2	19
59208	Intrinsic Magnetic Topological Insulator State Induced by the Jahnâ€“Teller Effect. Journal of Physical Chemistry Letters, 2021, 12, 9076-9085.	2.1	4
59209	First-Principles Study of NO Reduction by CO on Cu₂O(110) and Pd₁/Cu₂O(110) Surfaces. Journal of Physical Chemistry C, 2021, 125, 20309-20319.	1.5	6

#	Article	IF	Citations
59210	Metalâ€Nitrogenâ€Carbon Clusterâ€Decorated Titanium Carbide is a Durable and Inexpensive Oxygen Reduction Reaction Electrocatalyst. ChemSusChem, 2021, 14, 4680-4689.	3.6	2
59211	Water-Gas-Shift Reaction on Au/TiO_{2â€“x} Catalysts with Various TiO₂ Crystalline Phases: A Theoretical and Experimental Study. Journal of Physical Chemistry C, 2021, 125, 20360-20372.	1.5	11
59212	From Two-, One-, to Zero-Dimensional Vacancies: A Densification Pattern for a Typcial Transition-Metal Dichalcogenide of TiSe₂. Journal of Physical Chemistry Letters, 2021, 12, 9422-9428.	2.1	3
59213	Enhancing thermoelectric performance of SrFBiS2â^’Se via band engineering and structural texturing. Journal of Materiomics, 2021, , .	2.8	2
59214	Polaron formation in Bi-deficient <mml:math xmlns:mml="http://www.w3.org/1998/Math/MathML"><mml:msub><mml:mi mathvariant="normal">BaBiO</mml:mi><mml:mn>3</mml:mn></mml:msub></mml:math>. Physical Review B, 2021, 104, .	1.1	1
59215	Drastic change of magnetic anisotropy in Fe3GeTe2 and Fe4GeTe2 monolayers under electric field studied by density functional theory. Scientific Reports, 2021, 11, 17567.	1.6	20
59216	Bidirectional photocurrent in pâ€“n heterojunction nanowires. Nature Electronics, 2021, 4, 645-652.	13.1	129
59217	In Situ Defect Induction in Closeâ€Packed Lattice Plane for the Efficient Zinc Ion Storage. Small, 2021, 17, e2101944.	5.2	24
59218	Dextran Sulfate Lithium as Versatile Binder to Stabilize Highâ€Voltage LiCoO₂ to 4.6 V. Advanced Energy Materials, 2021, 11, 2101864.	10.2	80
59219	Microstructure evolution and mechanical property of Cu-15Ni-8Sn-0.2Nb alloy during aging treatment. Journal of Materials Science and Technology, 2021, 86, 227-236.	5.6	29
59220	Electronic correlation effects in the kagome magnet <mml:math xmlns:mml="http://www.w3.org/1998/Math/MathML"><mml:msub><mml:mi mathvariant="normal">GdMn</mml:mi><mml:mn>6</mml:mn></mml:msub><mml:msub><mml:mi mathvariant="normal">Sn</mml:mi><mml:mn>6</mml:mn></mml:msub></mml:math>. Physical Review B, 2021, 104, .	1.1	12
59221	Microscopic dynamics of lithium diffusion in single crystal of the solid-state electrolyte <mml:math xmlns:mml="http://www.w3.org/1998/Math/MathML"><mml:msub><mml:mi mathvariant="normal">La</mml:mi><mml:mrow><mml:mn>2</mml:mn><mml:mo>/</mml:mo><mml:mn>3</mml:mn></mml:mrow></mml:msub><mml:msub><mml:mi mathvariant="normal">Li</mml:mi><mml:mrow><mml:mn>3</mml:mn><mml:mi>x</mml:mi></mml:mrow></mml:msub><mml:msub><mml:mi mathvariant="normal">TiO</mml:mi><mml:mn>3</mml:mn></mml:msub></mml:math>. Physical Review B, 2021, 104, .	1.1	6
59222	Dealloying-derived nanoporous deficient titanium oxide as high-performance bifunctional sulfur host-catalysis material in lithium-sulfur battery. Journal of Materials Science and Technology, 2021, 84, 124-132.	5.6	18
59223	Design and fabrication of UN composites: From first principles to pellet production. Journal of Nuclear Materials, 2021, 553, 153047.	1.3	14
59224	Abnormal Hypsochromic Shifts of Surface Plasmon Scattering by Atomic Ordering in Goldâ€“Copper Intermetallic Nanoparticles. Journal of Physical Chemistry C, 2021, 125, 19936-19946.	1.5	7
59225	Identifying a New Pathway for Nitrogen Reduction Reaction on Fe-Doped MoS₂ by the Coadsorption of Hydrogen and N₂. Journal of Physical Chemistry C, 2021, 125, 19980-19990.	1.5	14
59226	Interface-strain-confined synthesis of amorphous TiO2 mesoporous nanosheets with stable pseudocapacitive lithium storage. Chemical Engineering Journal, 2021, 420, 129894.	6.6	28
59227	Tuning the electron structure enables the NiZn alloy for CO2 electroreduction to formate. Journal of Energy Chemistry, 2021, 63, 625-632.	7.1	38

#	Article	IF	Citations
59228	The large perpendicular magnetic anisotropy induced at the Co₂FeAl/MgAl₂O₄ interface and tuned with the strain, voltage and charge doping by first principles study. Nanotechnology, 2021, 32, 495702.	1.3	6
59229	A novel high-pressure phase of ScN₅ with higher stability predicted from first-principles calculations. Journal of Physics Condensed Matter, 2021, 33, 475401.	0.7	5
59230	An atomistic view on Oxygen, antisites and vacancies in the <mml:math xmlns:mml="http://www.w3.org/1998/Math/MathML" altimg="si165.svg"><mml:mrow><mml:mi>Î³</mml:mi></mml:mrow></mml:math>-TiAl phase. Computational Materials Science, 2021, 197, 110655.	1.4	5
59231	First-Principle Study of Co-Adsorption Behavior of H2O and O2 on Î´-Pu (100) Surface. Coatings, 2021, 11, 1098.	1.2	3
59232	Boosting the Electrocatalytic Activity of Feâ^'Co Dualâ€Atom Catalysts for Oxygen Reduction Reaction by Ligandâ€Modification Engineering. ChemCatChem, 2021, 13, 4645-4651.	1.8	11
59233	Janus monolayers of magnetic transition metal dichalcogenides as an all-in-one platform for spin-orbit torque. Physical Review B, 2021, 104, .	1.1	13
59234	Y-doped P2-type Na0.67Ni0.33Mn0.67O2: A sodium-ion battery cathode with fast charging and enhanced cyclic performance. Journal of Alloys and Compounds, 2021, 874, 160027.	2.8	16
59235	Suppressed Phase Segregation in Highâ€Humidityâ€Processed Dionâ€“Jacobson Perovskite Solar Cells Toward High Efficiency and Stability. Solar Rrl, 2021, 5, 2100555.	3.1	6
59236	Novel High-Pressure Yttrium Carbide Î³â^'Y4C5 Containing [C2] and Nonlinear [C3] Units with Unusually Large Formal Charges. Physical Review Letters, 2021, 127, 135501.	2.9	6
59237	Anisotropic Disorder and Thermal Stability of Silicane. ACS Nano, 2021, 15, 14557-14569.	7.3	5
59238	Firstâ€Principles Study of the Electronic and Optical Properties of Bi 2 Se 3 /MoSe 2 Heterojunction. Physica Status Solidi (B): Basic Research, 2021, 258, 2100403.	0.7	5
59239	Impact of Surface Defects on LaNiO₃ Perovskite Electrocatalysts for the Oxygen Evolution Reaction. Chemistry - A European Journal, 2021, 27, 14418-14426.	1.7	19
59240	Cotton pad derived 3D lithiophilic carbon host for robust Li metal anode: In-situ generated ionic conductive Li3N protective decoration. Chemical Engineering Journal, 2022, 430, 132722.	6.6	34
59241	Spin-flip-driven giant magnetotransport in A-type antiferromagnet <mml:math xmlns:mml="http://www.w3.org/1998/Math/MathML"><mml:mrow><mml:mi>NaCr</mml:mi><mml:msub><mml:mi>Te</mml:mi><mml:mi><m Physical Review Materials, 2021, 5, .	0.9	12
59242	Intrinsic nanostructure induced ultralow thermal conductivity yields enhanced thermoelectric performance in Zintl phase Eu2ZnSb2. Nature Communications, 2021, 12, 5718.	5.8	34
59243	Electric field polarized sulfonated carbon dots/NiFe layerd double hydroxide as highly efficient electrocatalyst for oxygen evolution reaction. Chemical Engineering Journal, 2021, 420, 129690.	6.6	16
59244	Cascade of correlated electron states in the kagome superconductor CsV3Sb5. Nature, 2021, 599, 216-221.	13.7	251
59245	System Theoretical Study on the Effect of Variable Nonmetallic Doping on Improving Catalytic Activity of 2D-Ti3C2O2 for Hydrogen Evolution Reaction. Nanomaterials, 2021, 11, 2497.	1.9	6

#	Article	IF	Citations
59246	Unraveling the effects of potassium incorporation routes and positions on toluene oxidation over Î±-MnO2 nanorods: Based on experimental and density functional theory (DFT) studies. Journal of Colloid and Interface Science, 2021, 598, 324-338.	5.0	87
59248	Effects of Axial Functional Groups on Heterogeneous Molecular Catalysts for Electrocatalytic CO₂ Reduction. Small Structures, 2021, 2, 2100093.	6.9	9
59249	Strong magneto-optical effect and anomalous transport in the two-dimensional van der Waals magnets <mml:math xmlns:mml="http://www.w3.org/1998/Math/MathML"><mml:msub><mml:mi mathvariant="normal">Fe</mml:mi><mml:mi>n</mml:mi></mml:msub><mml:msub><mml:mi mathvariant="normal">GeTe</mml:mi><mml:mn>2</mml:mn></mml:msub></mml:math> (<mml:math) Tj ETQq0 0 0 rgBT /Overlock 10	11	26
59250	High-pressure synthesis, crystal structure, and physical properties of NaAlB14 single crystals. Ceramics International, 2022, 48, 1771-1777.	2.3	2
59251	Revealing the stability of CuWO4/g-C3N4 nanocomposite for photocatalytic tetracycline degradation from the aqueous environment and DFT analysis. Environmental Research, 2022, 207, 112112.	3.7	28
59252	A universal electrochemical activation enabling lattice oxygen activation in nickel-based catalyst for efficient water oxidation. Chemical Engineering Journal, 2022, 430, 132736.	6.6	22
59253	Optimizing the Electronic Structure of ZnS via Cobalt Surface Doping for Promoted Photocatalytic Hydrogen Production. Inorganic Chemistry, 2021, 60, 15712-15723.	1.9	14
59254	Computational insights into optoelectronic and magnetic properties of V(III)-doped GaN. Journal of Solid State Chemistry, 2021, 304, 122606.	1.4	4
59255	Highâ€Conductive Protonated Layered Oxides from H₂O Vaporâ€Annealed Brownmillerites. Advanced Materials, 2021, 33, e2104623.	11.1	9
59256	Controlled Asymmetric Charge Distribution of Active Centers in Conjugated Polymers for Oxygen Reduction. Angewandte Chemie - International Edition, 2021, 60, 26483-26488.	7.2	59
59257	Olefin-linked covalent organic frameworks with twisted tertiary amine knots for enhanced ultraviolet detection. Chinese Chemical Letters, 2022, 33, 2621-2624.	4.8	7
59258	The electronic properties and catalytic activity of precious-metals adsorbed silicene for hydrogen evolution reaction and oxygen evolution reaction. Applied Surface Science, 2021, 560, 150041.	3.1	27
59259	Unravelling the metal borides evolution in the transient liquid phase bonding of Ni-based alloys via high-throughput transmission electron microscopy and first-principles thermo-kinetic calculations. Journal of Materials Science and Technology, 2021, 85, 118-128.	5.6	5
59260	Interface and structure engineering of bimetallic selenides toward high-performance sodium-ion half/full batteries. Journal of Power Sources, 2021, 506, 230216.	4.0	55
59261	Theoretical Insights into Na₅M(PO₄)₂F₂ (M = Cr, V): A Fluorophosphate-Based High-Performance Cathode System for Sodium-Ion Batteries. Journal of Physical Chemistry C, 2021, 125, 19593-19599.	1.5	3
59262	Correlating ligand-to-metal charge transfer with voltage hysteresis in a Li-rich rock-salt compound exhibiting anionic redox. Nature Chemistry, 2021, 13, 1070-1080.	6.6	75
59263	Metal-free tellurene cocatalyst with tunable bandgap for enhanced photocatalytic hydrogen production. Materials Today Energy, 2021, 21, 100720.	2.5	18
59264	Improved Dielectric Properties and Grain Boundary Effect of Phenanthrene Under High Pressure. Frontiers in Physics, 2021, 9, .	1.0	2

#	Article	IF	Citations
59265	Mechanism of Nitrogen-Doped Ti₃C₂ Quantum Dots for Free-Radical Scavenging and the Ultrasensitive H₂O₂ Detection Performance. ACS Applied Materials & Interfaces, 2021, 13, 42442-42450.	4.0	30
59266	Structure and Optical Properties of Hybrid-Layered-Double Perovskites (C₈H₂₀N₂)₂AgMBr₈ (M = In, Sb, and Bi). Inorganic Chemistry, 2021, 60, 14629-14635.	1.9	7
59267	Magnetic states of the quasi-one-dimensional iron chalcogenide <mml:math xmlns:mml="http://www.w3.org/1998/Math/MathML"><mml:msub><mml:mrow><mml:mi>Ba</mml:mi></mml:mrow><mml:mn>2</mml:mn> Physical Review B, 2021, 104, .	1.1	10
59268	First principles investigation of the Structural, Mechanical, Electronic Properties and Debye temperature of W-Co alloys. Fusion Engineering and Design, 2021, 170, 112715.	1.0	5
59269	Interdiffusion behaviors and mechanical properties of Znâ€“Cr system. Calphad: Computer Coupling of Phase Diagrams and Thermochemistry, 2021, 74, 102308.	0.7	9
59270	First principles design novel D5 derivative dyes with excellent acceptors for highly efficient dye-sensitized solar cells. Computational and Theoretical Chemistry, 2021, 1203, 113374.	1.1	1
59271	Maximized atomic disordering approach boost the thermoelectric performance of Mg2Sn through the self-compensation effect and steric effect. Acta Materialia, 2021, 217, 117172.	3.8	11
59272	Thermodynamic properties of the Yb-Sb system predicted from first-principles calculations. Acta Materialia, 2021, 217, 117169.	3.8	34
59273	Direct band gap halide-double-perovskite absorbers for solar cells and light emitting diodes: Ab initio study of bulk and layers. Physical Review Materials, 2021, 5, .	0.9	6
59275	Evaluation of electron currents from cesium-coated tungsten emitter arrays with inclusion of space charge effects, workfunction changes, and screening. Journal of Vacuum Science and Technology B:Nanotechnology and Microelectronics, 2021, 39, .	0.6	3
59276	Diverse Spin-Polarized In-Gap States at Grain Boundaries of Rhenium Dichalcogenides Induced by Unsaturated Reâ€“Re Bonding. , 2021, 3, 1513-1520.		4
59277	Visualizing Van der Waals Epitaxial Growth of 2D Heterostructures. Advanced Materials, 2021, 33, e2105079.	11.1	24
59278	EAPOTs: An integrated empirical interatomic potential optimization platform for single elemental solids. Computational Materials Science, 2021, 197, 110626.	1.4	3
59279	First-principles study on the strain-mediated g-C₃N₄/blue phosphorene heterostructures for promising photocatalytic performance. Journal of Physics Condensed Matter, 2021, 33, 485703.	0.7	5
59280	Influence of vacancy defects on the electronic structure and magnetic properties of Cu-doped ZnO monolayers: A first-principles study. Materials Today Communications, 2021, 28, 102722.	0.9	1
59281	Trapping and recombination of tritium in lithium vacancy of the Î³-LiAlO2 (100) surface: A first-principles study. Applied Surface Science Advances, 2021, 5, 100114.	2.9	1
59282	Surface segregation of PdM (M=Cu, Ag, Au) alloys and its implication to acetylene hydrogenation, DFT-based Monte Carlo simulations. Materials Today Communications, 2021, 28, 102475.	0.9	5
59283	Thermal transport of amorphous phase change memory materials using population-coherence theory: a first-principles study. Journal Physics D: Applied Physics, 2021, 54, 505302.	1.3	7

#	Article	IF	Citations
59284	Study on optical properties of the F type color center in the p-CuAlO2 crystal with first principles. Materials Today Communications, 2021, 28, 102482.	0.9	0
59285	The controllable construction of nanochannel in two-dimensional lamellar film for efficient oxygen reduction reaction and lithium-oxygen batteries. Chemical Engineering Journal, 2022, 430, 132489.	6.6	11
59286	Performance improvement of Ï‡3 borophene in nitrogen fixation using singleâ€“atom anchoring: A firstâ€“principles study. Applied Surface Science, 2021, 560, 149667.	3.1	11
59287	First-principles investigation of equilibrium iron isotope fractionation in Fe1â^'S alloys at Earth's core formation conditions. Earth and Planetary Science Letters, 2021, 569, 117059.	1.8	8
59288	The magnetic, electronic, optical, and structural properties of the AB2O4 (AÂ=ÂMn, Fe, co; BÂ=ÂAl, Ga, In) spinels: Ab initio study. Journal of Magnetism and Magnetic Materials, 2021, 533, 168015.	1.0	8
59289	Critical evaluation and thermodynamic modeling of the Ag-X (X=Mn, Y, Sr) binary systems. Intermetallics, 2021, 136, 107260.	1.8	4
59290	Unusual Exchange Couplings and Intermediate Temperature Weyl State in <mml:math xmlns:mml="http://www.w3.org/1998/Math/MathML" display="inline"><mml:mrow><mml:msub><mml:mrow><mml:mi>Co</mml:mi></mml:mrow><mml:mrow><mml:mn>3</mml:mn></mml:mrow></mml:msub><mml:msub><mml:mrow><mml:mi mathvariant="normal">S</mml:mi></mml:mrow><mml:mrow><mml:mn>2</mml:mn></mml:mrow></mml:msub></mml:mrow></mml:math> Physical Review Letters, 2021, 127, 117201.	2.9	26
59291	Regulation of functional groups on graphene quantum dots directs selective CO2 to CH4 conversion. Nature Communications, 2021, 12, 5265.	5.8	89
59292	Chiral separation of Î²-cyclodextrin modified graphene oxide membranes with a complete enantioseparation performance. Journal of Membrane Science, 2021, 634, 119350.	4.1	29
59293	Computational methods for 2D materials modelling. Reports on Progress in Physics, 2021, 84, 106501.	8.1	4
59294	First-principles study of two-dimensional electron gas on a layered <mml:math xmlns:mml="http://www.w3.org/1998/Math/MathML"><mml:mrow><mml:msub><mml:mi>Gd</mml:mi><mml:mn>2</mml:mn></mml:msub><mml:msub><mml:mi mathvariant="normal">C</mml:mi></mml:mrow></mml:math> electride surface. Physical Review B, 2021, 104, .	1.1	7
59295	Theoretical investigation of the chloride effect on aqueous Hg(II) adsorption on the kaolinite(001) surface. Applied Clay Science, 2021, 210, 106120.	2.6	6
59296	Bridge sulfur vacancies in MoS2 catalyst for reverse water gas shift: A first-principles study. Applied Surface Science, 2021, 561, 149925.	3.1	12
59297	H/D isotope effect between adsorbed water (H2O, D2O, and HDO) and H2O- and D2O-ice Ih(0Â0Â0Â1) basal surfaces based on the combined plane wave and localized basis set method. Applied Surface Science, 2021, 561, 150100.	3.1	1
59298	Theoretical and experimental Raman study of molybdenum disulfide. Journal of Physics and Chemistry of Solids, 2021, 156, 110154.	1.9	1
59299	Electrochemical quartz crystal microbalance studies on specific adsorption of nanoparticle stabilizers on platinum surface. Journal of Electroanalytical Chemistry, 2021, 897, 115596.	1.9	1
59300	Facet-dependent stability of near-surface oxygen vacancies and excess charge localization at CeO₂ surfaces. Journal of Physics Condensed Matter, 2021, 33, 504003.	0.7	14
59301	Tunable Electric and Magnetic Properties of Transition Metal@N_xC_yâ€Graphene Materials by Different Metal and Defect Types. Chemistry - an Asian Journal, 2021, 16, 3230-3235.	1.7	3

#	Article	IF	Citations
59302	Enhancing thermoelectric performance of BaMg₂-based compounds by forming solid solutions and biaxial strain. Journal Physics D: Applied Physics, 2021, 54, 485301.	1.3	1
59303	Extremely large magnetoresistance in the â€œordinaryâ€•metal <mml:math xmlns:mml="http://www.w3.org/1998/Math/MathML"><mml:msub><mml:mi>ReO</mml:mi><mml:mn>3</mml:mn></mml:msub></mml:math> Physical Review B, 2021, 104, .	1.1	3
59304	Magnetotransport evidence for the nontrivial topological states in the fully spin-polarized Kondo semimetal CeBi. Journal of Alloys and Compounds, 2021, 875, 159993.	2.8	5
59305	Electrostatic spun hierarchically porous carbon matrix with CoSe2/Co heterostructure as bifunctional electrocatalysts for zinc-air batteries. Journal of Alloys and Compounds, 2021, 875, 160056.	2.8	17
59306	One-step plasma nitriding synthesis of NixN/NF (xÂ=Â3, 4) for efficient hydrogen evolution. Applied Surface Science, 2021, 561, 149972.	3.1	11
59307	A new all-inorganic vacancy-ordered double perovskite Cs2CrI6 for high-performance photovoltaic cells and alpha-particle detection in space environment. Materials Today Physics, 2021, 20, 100446.	2.9	18
59308	Cooperative Sites in Fully Exposed Pd Clusters for Low-Temperature Direct Dehydrogenation Reaction. ACS Catalysis, 2021, 11, 11469-11477.	5.5	51
59309	First-principles prediction of layered MoO₂ and MoOSe as promising cathode materials for magnesium ion batteries. Nanotechnology, 2021, 32, 495405.	1.3	5
59310	Does Explicit Polarizability Improve Simulations of Phase Behavior of Ionic Liquids?. Journal of Chemical Theory and Computation, 2021, 17, 6225-6239.	2.3	7
59311	Electronic Properties and Structure of Boronâ€“Hydrogen Complexes in Crystalline Silicon. Solar Rrl, 2022, 6, 2100459.	3.1	7
59312	Ethylene production by direct conversion of methane over isolated single active centers. Chemical Engineering Journal, 2021, 420, 130493.	6.6	20
59313	Introducing thiophene and benzothiadiazole groups in triphenylamine-based organic dyes with rigidly fused Ï€-bridge to design high-efficiency solar cells: A theoretical investigation. Solar Energy, 2021, 225, 323-332.	2.9	10
59314	Doping engineering: Highly improving hydrogen evolution reaction performance of monolayer SnSe. International Journal of Hydrogen Energy, 2021, 46, 37907-37914.	3.8	7
59315	N-Doped Graphene as an Efficient Metal-Free Electrocatalyst for Indirect Nitrate Reduction Reaction. Nanomaterials, 2021, 11, 2418.	1.9	10
59316	Atomically Dispersed Ruthenium on Nickel Hydroxide Ultrathin Nanoribbons for Highly Efficient Hydrogen Evolution Reaction in Alkaline Media. Advanced Materials, 2021, 33, e2104764.	11.1	70
59317	Electrodeâ€Induced Selfâ€Healed Monolayer MoS₂ for High Performance Transistors and Phototransistors. Advanced Materials, 2021, 33, e2102091.	11.1	26
59318	Magnetic and electronic properties of two-dimensional metal-organic frameworks TM₃(C₂NH)₁₂ *. Chinese Physics B, 2021, 30, 097102.	0.7	5
59319	Van der Waals electride: Toward intrinsic two-dimensional ferromagnetism of spin-polarized anionic electrons. Materials Today Physics, 2021, 20, 100473.	2.9	10

#	Article	IF	Citations
59320	N,Nâ€Dimethylformamideâ€Assisted Shape Evolution of Highly Uniform and Shapeâ€Pure Colloidal Copper Nanocrystals. Small, 2021, 17, e2103302.	5.2	5
59321	First-principles magnetic treatment of the uranium nitride (100) surface and effect on corrosion initiation. Journal of Applied Physics, 2021, 130, 095301.	1.1	2
59322	Theoretical study on single-side fluorinated graphene for lithium storage. Applied Surface Science, 2021, 560, 150033.	3.1	5
59323	Thermal transport property of novel two-dimensional nitride phosphorus: An ab initio study. Applied Surface Science, 2021, 559, 149463.	3.1	16
59324	Impact of three-body interactions in a ReaxFF force field for Ni and Cr transition metals and their alloys on the prediction of thermal and mechanical properties. Computational Materials Science, 2021, 197, 110602.	1.4	9
59325	[illegible] of a reactive force field for <mml:math xmlns:mml="http://www.w3.org/1998/Math/MathML" altimg="si43.svg"><mml:mrow><mml:msub><mml:mrow><mml:mi mathvariant="normal">CaCl</mml:mi></mml:mrow><mml:mrow><mml:mn>2</mml:mn></mml:mrow></mml:msub><mml:mo>Â·</mml:mo> xmlns:mml="http://www.w3.org/1998/Math/MathML" [illegible]	1.4	10
59326	Atomistic study of the structure and deformation behavior of symmetric tilt grain boundaries in <mml:math xmlns:mml="http://www.w3.org/1998/Math/MathML" altimg="si46.svg"><mml:mrow><mml:mi>Î±</mml:mi></mml:mrow></mml:math>-zirconium. Computational Materials Science, 2021, 197, 110600.	1.4	4
59327	Designing and Understanding the Outstanding Triâ€Iodide Reduction of Nâ€Coordinated Magnetic Metal Modified Defectâ€Rich Carbon Dodecahedrons in Photovoltaics. Small, 2021, 17, e2102300.	5.2	46
59328	Tuning of electronic and optical properties of a predicted silicon allotrope: Hexagonal silicon <mml:math xmlns:mml="http://www.w3.org/1998/Math/MathML"><mml:mrow><mml:mi>h</mml:mi><mml:mn>10</mml:mn></mml:mrow></mml -Si. Physical Review B, 2021, 104, .	1.1	7
59329	Amorphous Yolkâ€“Shelled ZIF-67@Co₃(PO₄)₂ as Nonprecious Bifunctional Catalysts for Boosting Overall Water Splitting. Inorganic Chemistry, 2021, 60, 14880-14891.	1.9	18
59330	Dislocation structure and mobility in the layered semiconductor InSe: a first-principles study. 2D Materials, 2021, 8, 045028.	2.0	6
59331	Van der Waals heterostructure <mml:math xmlns:mml="http://www.w3.org/1998/Math/MathML"><mml:msub><mml:mrow><mml:mi>Pt</mml:mi></mml:mrow><mml:mrow><mml:mn>2</mml:mn></mml for topological valleytronics. Physical Review B, 2021, 104, .	1.1	20
59332	Two-dimensional metallic MoS2-amorphous CoNi(OH)2 nanocomposite for enhanced electrochemical water splitting in alkaline solutions. Applied Surface Science, 2021, 561, 150079.	3.1	18
59333	Ti3C2Tx MXene sensor for rapid Hg2+ analysis in high salinity environment. Journal of Hazardous Materials, 2021, 418, 126301.	6.5	27
59334	Rapid preparation of zirconia/zircon composites ceramics by microwave method: Experiment and first-principle investigation. Progress in Nuclear Energy, 2021, 139, 103839.	1.3	2
59335	The evolution and characterizations of Al3(ScxZr1-x) phase in Alâ€“Mg-based alloys proceeded by SLM. Materials Science & Engineering A: Structural Materials: Properties, Microstructure and Processing, 2021, 824, 141863.	2.6	11
59336	Monolayer SnC as anode material for Na ion batteries. Computational Materials Science, 2021, 197, 110617.	1.4	11
59337	How to Identify Lone Pairs, Van der Waals Gaps, and Metavalent Bonding Using Charge and Pair Density Methods: From Elemental Chalcogens to Lead Chalcogenides and Phaseâ€Change Materials. Physica Status Solidi - Rapid Research Letters, 2021, 15, 2000534.	1.2	19

#	Article	IF	Citations
59338	Cs2TiI6: A potential lead-free all-inorganic perovskite material for ultrahigh-performance photovoltaic cells and alpha-particle detection. Nano Research, 2022, 15, 2697-2705.	5.8	22
59339	Vacancy and architecture engineering of porous FeP nanorods for achieving superior Li+ storage. Chemical Engineering Journal, 2022, 429, 132249.	6.6	43
59340	Structural, Electronic, and Mechanical Properties of 2D Oxidized Diamond (100) Nanofilms. Advanced Theory and Simulations, 2021, 4, 2100165.	1.3	2
59341	Surface strain engineered Ni-NiO for boosting hydrogen evolution reaction in alkaline media. Electrochimica Acta, 2021, 391, 138985.	2.6	15
59342	Strainâ€Induced Ideal Topological Semimetal in Ortâ€B₃₂ Holding Parallel Arcâ€Like Nodal Lines and Anisotropic Multiple Weyl Fermions. Physica Status Solidi - Rapid Research Letters, 2021, 15, 2100324.	1.2	0
59343	Stacking effects on the structure and magnetic properties of MoN₂. Europhysics Letters, 2021, 135, 40005.	0.7	1
59344	Chiral Recognition on Bare Gold Surfaces by Quartz Crystal Microbalance. Angewandte Chemie, 2021, 133, 25232-25237.	1.6	1
59345	Unexpected and enhanced electrostatic adsorption capacity of oxygen vacancy-rich cobalt-doped In2O3 for high-sensitive MEMS toluene sensor. Sensors and Actuators B: Chemical, 2021, 342, 129949.	4.0	26
59346	Active oxygen center in oxidative coupling of methane on La2O3 catalyst. Journal of Energy Chemistry, 2021, 60, 649-659.	7.1	28
59347	Mechanism of Mn incorporation into hydroxyapatite: Insights from SR-XRD, Raman, XAS, and DFT calculation. Chemical Geology, 2021, 579, 120354.	1.4	19
59348	Identifying lithium fluorides for promising solid-state electrolyte and coating material of high-voltage cathode. Materials Today Energy, 2021, 21, 100719.	2.5	15
59349	Investigating the Accuracy of Water Models through the Van Hove Correlation Function. Journal of Chemical Theory and Computation, 2021, 17, 5992-6005.	2.3	9
59350	Benign Effects of Twin Boundaries on Charge Carrier Lifetime in Metal Halide Perovskites by a Time-Domain Study. Journal of Physical Chemistry Letters, 2021, 12, 8575-8582.	2.1	13
59351	Fast potassium storage in porous CoV2O6 nanosphere@graphene oxide towards high-performance potassium-ion capacitors. Energy Storage Materials, 2021, 40, 250-258.	9.5	46
59352	Probing metal-molecule contact at the atomic scale via conductance jumps. Physical Review B, 2021, 104, .	1.1	8
59353	A binuclear copper(II) complex based on hydrazone ligand: Characterization, molecular docking, and theoretical and antimicrobial investigation. Applied Organometallic Chemistry, 2022, 36, e6461.	1.7	7
59354	The u<mml:math xmlns:mml="http://www.w3.org/1998/Math/MathML" altimg="si1.svg"><mml:msub><mml:mrow /><mml:mn>3</mml:mn></mml:msub></mml:math>si<mml:math xmlns:mml="http://www.w3.org/1998/Math/MathML" altimg="si2.svg"><mml:msub><mml:mrow /><mml:mn>2</mml:mn></mml:msub></mml:math>-H system. Journal of Nuclear Materials, 2022, 558, 153278.	1.3	9
59355	Study on electronic properties and charge transfer doping of organic molecules adsorbed g-GaN monolayer. Semiconductor Science and Technology, 2021, 36, 125020.	1.0	4

#	Article	IF	Citations
59356	First-Principles Study of Interaction between Molecules and Lewis Acid Zeolites Manipulated by Injection of Energized Charge Carriers. Industrial & Engineering Chemistry Research, 2021, 60, 14124-14133.	1.8	1
59357	Essential Electronic Properties of Silicon Nanotubes. Nanomaterials, 2021, 11, 2475.	1.9	5
59358	Unraveling the Preferable Occupation and Luminescent Properties of Ce³⁺-Doped Ca₉Nd(PO₄)₇. ECS Journal of Solid State Science and Technology, 2021, 10, 096010.	0.9	1
59359	Design of compositionally complex catalysts: Role of surface segregation. Journal of Materials Research and Technology, 2021, 14, 1830-1836.	2.6	3
59360	Structural and optical behaviors of 2D-layered molybdenum disulfide thin film: experimental and ab-initio insights. Journal of Materials Research and Technology, 2021, 14, 780-796.	2.6	4
59361	Strain drived band aligment transition of the ferromagnetic VS₂/C₃N van derWaals heterostructure*. Chinese Physics B, 2021, 30, 097507.	0.7	3
59362	C9N4 as excellent dual electrocatalyst: A first principles study*. Chinese Physics B, 2021, 30, 096802.	0.7	0
59363	Electronic structures and transport properties of low-dimensional GaN nanoderivatives: A first-principles study. Applied Surface Science, 2021, 561, 150038.	3.1	23
59364	Effects of Zn2+/Mg2+ ratio on dielectric properties of BaTiO3-based ceramics with excellent temperature stability: Experiments and the first-principle calculations. Ceramics International, 2022, 48, 847-854.	2.3	10
59365	Observation of a highly conductive warm dense state of water with ultrafast pumpâ€“probe free-electron-laser measurements. Matter and Radiation at Extremes, 2021, 6, .	1.5	6
59366	Tailoring the supercapacitive behaviors of Co/Zn-ZIF derived nanoporous carbon via incorporating transition metal species: A hybrid experimental-computational exploration. Chemical Engineering Journal, 2021, 419, 129636.	6.6	59
59367	Electronic Promotion Effects of Metal Oxides: A Case Study of MnO Impact on Fischerâ€“Tropsch Catalysis. Journal of Physical Chemistry C, 2021, 125, 21390-21401.	1.5	6
59368	Promising Thermoelectric Performance in Two-Dimensional Semiconducting Boron Monolayer. Frontiers in Chemistry, 2021, 9, 739984.	1.8	2
59369	New insights of the interaction of H2S with mackinawite FeS in a wet environment: An ab initio molecular dynamics study. International Journal of Hydrogen Energy, 2021, , .	3.8	2
59370	Alkali-Assisted Hydrothermal Exfoliation and Surfactant-Driven Functionalization of h-BN Nanosheets for Lubrication Enhancement. ACS Applied Nano Materials, 2021, 4, 9143-9154.	2.4	14
59371	Investigations of modulation effect of co-metal ions on the optical properties of the hybrid double perovskites (MA)₂AgBi_{1â^'x}Sb_xBr₆. Journal of Physics Condensed Matter, 2021, 33, 495501.	0.7	2
59372	Identification of the spintronic Ni_{Ga}V_N center in c-GaN and its qubit applications. Journal Physics D: Applied Physics, 2021, 54, 505109.	1.3	5
59373	Solving the Trifunctional Activity Challenge of Catalysts in Unitized Regenerative Fuel Cells via 1T-MoS₂-Coordinated Single Pd Atoms. ACS Omega, 2021, 6, 24731-24738.	1.6	6

#	Article	IF	Citations
59374	Oxygen-vacancy enhanced tunnel electroresistance in LaNiO3/BaTiO3/LaNiO3 ferroelectric tunnel junctions. Applied Physics Letters, 2021, 119, .	1.5	1
59375	Ab initio study of the effect of 2D layer rippling on the electronic properties of 2D/H-terminated diamond (100) heterostructures. Journal of Materials Research, 0, , 1.	1.2	4
59376	Spontaneously formed nanostructures in double perovskite rare-earth tantalates for thermal barrier coatings. Acta Materialia, 2021, 216, 117152.	3.8	13
59378	Switchable Interlayer Magnetic Coupling of Bilayer CrI3. Nanomaterials, 2021, 11, 2509.	1.9	4
59379	BaBi₂O₆: A Promising n-Type Thermoelectric Oxide with the PbSb₂O₆Crystal Structure. Chemistry of Materials, 2021, 33, 7441-7456.	3.2	11
59380	Magnetoelectric Coupling at the Ni/Hf_{0.5}Zr_{0.5}O₂ Interface. ACS Nano, 2021, 15, 14891-14902.	7.3	11
59381	Semiconducting phase of hafnium dioxide under high pressure: a theoretical studied by quasi-particle GW calculations. Materials Research Express, 0, , .	0.8	3
59382	<mml:math xmlns:mml="http://www.w3.org/1998/Math/MathML"><mml:mrow><mml:mi>Mo</mml:mi><mml:msub><mml:mi mathvariant="normal">P</mml:mi><mml:mn>3</mml:mn></mml:msub><mml:mi>Si</mml:mi><mml:msub><mml:mi mathvariant="normal">O</mml:mi><mml:mn>11</mml:mn></mml:msub></mml:mrow></mml:math> : A <mml:math xmlns:mml="http://www.w3.org/1998/Math/MathML"><mml:mrow><mml:mn>4</mml:mn><mml:msup><mml:mi>d</mml:mi><mml:mi>	1.1	3
59383	Ni-based catalysts derived from Ni-Zr-Al ternary hydrotalcites show outstanding catalytic properties for low-temperature CO2 methanation. Applied Catalysis B: Environmental, 2021, 293, 120218.	10.8	62
59384	Electronic and Interface Regulation of Wurtzite Surfaces Promotes Photocatalytic Ammonia Synthesis under Visible Light Irradiation. ACS Sustainable Chemistry and Engineering, 2021, 9, 13630-13639.	3.2	6
59385	DFT calculations on selectivity enhancement by Br addition on Pd catalysts in the direct synthesis of hydrogen peroxide. Catalysis Today, 2022, 397-399, 232-239.	2.2	4
59386	Ultrafast Interlayer Charge Separation, Enhanced Visibleâ€Light Absorption, and Tunable Overpotential in Twisted Graphitic Carbon Nitride Bilayers for Water Splitting. Advanced Materials, 2021, 33, e2104695.	11.1	26
59387	High uptake and fixation ability of BC monolayer for CO and NO toxic gases: a computational analysis. Journal of Materials Science, 2021, 56, 18566-18580.	1.7	0
59388	Understanding the Î²â€“K₂CO₃-Type Na(Na_{0.5}Sc_{0.5})BO₃:Ce₃ + Phosphor. ECS Journal of Solid State Science and Technology, 2021, 10, 096014.	0.9	2
59389	Density Functional Theory Study on Dependence of Stability of Fe, Cu, and Ni Atoms on Surface Orientation of Si Crystal. ECS Journal of Solid State Science and Technology, 2021, 10, 094002.	0.9	0
59390	Highly stable TiOF monolayer as anode material for the applications of Li/Na-ion batteries. Applied Surface Science, 2022, 574, 151296.	3.1	17
59391	Effect of Potassium on Methanol Steam Reforming on the Cu(111) and Cu(110) Surfaces: A DFT Study. Journal of Physical Chemistry C, 2021, 125, 20905-20918.	1.5	12
59392	Unimolecular and bimolecular formic acid decomposition routes on dispersed Cu nanoparticles. Journal of Catalysis, 2021, 404, 814-831.	3.1	5

#	Article	IF	Citations
59393	Vibrational Signature of Metallophilic Interactions in [Pt(terpy)Cl][Au(CN)₂]. Journal of Physical Chemistry C, 2021, 125, 22188-22194.	1.5	7
59394	Developing Proton-Conductive Metal Coordination Polymer as Highly Efficient Electrocatalyst toward Oxygen Reduction. Journal of Physical Chemistry Letters, 2021, 12, 9197-9204.	2.1	15
59395	Efficient Method for Prediction of Metastable or Ground Multipolar Ordered States and Its Application in Monolayer Î±â^'RuX3 (X=Cl , I). Physical Review Letters, 2021, 127, 147202.	2.9	2
59396	Exploring Librational Pathways with on-the-Fly Machine-Learning Force Fields: Methylammonium Molecules in MAPbX₃ (X = I, Br, Cl) Perovskites. Journal of Physical Chemistry C, 2021, 125, 21077-21086.	1.5	14
59397	Thermal Ionization of Hydrogen in Hydrous Olivine With Enhanced and Anisotropic Conductivity. Journal of Geophysical Research: Solid Earth, 2021, 126, e2021JB022939.	1.4	7
59398	Thermodynamic assessment of the As-X (X=Si, Ge, Sn) binary systems. Calphad: Computer Coupling of Phase Diagrams and Thermochemistry, 2021, 74, 102296.	0.7	1
59399	Thermodynamic activity of solute in multicomponent alloy from first-principles: Excess Mg in Mg3(Sb1-Bi)2 as an example. Calphad: Computer Coupling of Phase Diagrams and Thermochemistry, 2021, 74, 102318.	0.7	2
59400	Inductive effects in cobalt-doped nickel hydroxide electronic structure facilitating urea electrooxidation. Chemosphere, 2021, 279, 130550.	4.2	30
59401	An energetic phase of ZnN6 at ambient conditions. Physica B: Condensed Matter, 2021, 617, 413139.	1.3	3
59402	Substrate orientation dependent structural, electronic and magnetic properties of V and Cr linear chains. Physica B: Condensed Matter, 2021, 617, 413132.	1.3	0
59403	Tritium trapping by oxygen and lithium vacancies in Li4TiO4 from first-principles calculations. Ceramics International, 2021, 47, 25567-25573.	2.3	2
59404	Insight into the adsorption of Imidazolium-based ionic liquids on graphene by first principles simulation. Journal of Molecular Liquids, 2021, 338, 116641.	2.3	18
59405	Al/SiC nanocomposites with enhanced thermomechanical properties obtained from microwave plasma-treated nanopowders. Materials Science & Engineering A: Structural Materials: Properties, Microstructure and Processing, 2021, 824, 141817.	2.6	9
59406	Unveiling the Critical Intermediate Stages During Chemical Vapor Deposition of Two-Dimensional Rhenium Diselenide. Chemistry of Materials, 2021, 33, 7039-7046.	3.2	1
59407	Coupling Charge and Topological Reconstructions at Polar Oxide Interfaces. Physical Review Letters, 2021, 127, 127202.	2.9	20
59408	Heterogeneous Two-Atom Single-Cluster Catalysts for the Nitrogen Electroreduction Reaction. Journal of Physical Chemistry C, 2021, 125, 19821-19830.	1.5	27
59409	â€˜Be waterâ€™ strategy of liquid lithium sulfide enables 0.2ÂV potential barrier for high-performance lithiumâ€“sulfur batteries. Materials Today Energy, 2021, 21, 100793.	2.5	8
59410	Three-dimensional perovskite nanowire arrayâ€“based ultrafast resistive RAM with ultralong data retention. Science Advances, 2021, 7, eabg3788.	4.7	29

#	Article	IF	Citations
59411	Tuning the Thermoelectric Properties of Transition Metal Oxide Thin Films and Superlattices on the Quantum Scale. Physica Status Solidi (B): Basic Research, 2022, 259, 2100270.	0.7	6
59412	Macromolecular Ligand Engineering for Programmable Nanoprism Assembly. Journal of the American Chemical Society, 2021, 143, 16163-16172.	6.6	15
59413	Emergence of Ferromagnetism Due to Spontaneous Symmetry Breaking in a Twisted Bilayer Graphene Nanoflex. Nano Letters, 2021, 21, 7548-7554.	4.5	4
59414	Pressure-Induced Enhancement of Thermoelectric Performance in Rubrene. ACS Applied Materials & Interfaces, 2021, 13, 44409-44417.	4.0	8
59415	Highly disordered ionic distribution in Î±â€dicalcium silicate for structure relaxation. Journal of the American Ceramic Society, 2022, 105, 700-711.	1.9	2
59416	Multilevel Theoretical Screening of Novel Two-Dimensional MA₂Z₄ Family for Hydrogen Evolution. Journal of Physical Chemistry Letters, 2021, 12, 9149-9154.	2.1	32
59417	Plumbene: A next generation hydrogen storage medium. International Journal of Hydrogen Energy, 2021, 46, 33197-33205.	3.8	11
59418	Revealing the microscopic mechanism of PuO2 and Î±-Pu2O3 in resisting plutonium hydrogenation via ab initio molecular dynamics simulation. Journal of Alloys and Compounds, 2021, 874, 159904.	2.8	4
59419	Oxidized single nickel atoms embedded in Ru matrix for highly efficient hydrogen evolution reaction. Journal of Alloys and Compounds, 2021, 874, 159909.	2.8	8
59420	Highly selective oxidation of monosaccharides to sugar acids by nickel-embedded carbon nanotubes under mild conditions. Renewable Energy, 2021, 175, 650-659.	4.3	6
59421	Tuning the intermediate reaction barriers by a CuPd catalyst to improve the selectivity of CO2 electroreduction to C2 products. Chinese Journal of Catalysis, 2021, 42, 1500-1508.	6.9	56
59422	Achieving efficient N2 electrochemical reduction by stabilizing the N2H* intermediate with the frustrated Lewis pairs. Journal of Energy Chemistry, 2022, 66, 628-634.	7.1	13
59423	Roles of oxygen-containing functional groups of O-doped g-C3N4 in catalytic ozonation: Quantitative relationship and first-principles investigation. Applied Catalysis B: Environmental, 2021, 292, 120155.	10.8	137
59424	o-C12: A novel orthorhombic metallic superhard carbon phase. Solid State Sciences, 2021, 119, 106607.	1.5	6
59425	First-Principles Predictions of Out-of-Plane Group IV and V Dimers as High-Symmetry, High-Spin Defects in Hexagonal Boron Nitride. ACS Applied Materials & Interfaces, 2021, 13, 45768-45777.	4.0	12
59426	High and Anomalous Thermal Conductivity in Monolayer MSi₂Z₄ Semiconductors. ACS Applied Materials & Interfaces, 2021, 13, 45907-45915.	4.0	27
59427	Zn(O,S) Buffer Layer for in Situ Hydrothermal Sb₂S₃ Planar Solar Cells. ACS Applied Materials & Interfaces, 2021, 13, 45726-45735.	4.0	20
59428	Ca[B₈O₁₁(OH)₄]â€‰:â€‰Eu²⁺ â€“ A Highly Efficient Deep Blueâ€Emitting Phosphor Prepared by Lowâ€Temperature Selfâ€reduction. Chemistry - A European Journal, 2021, 27, 13819-13827.	1.7	6

#	Article	IF	Citations
59429	A universal way to prepare graphyne derivatives with variable band gap and lithium storage properties. Carbon, 2021, 182, 413-421.	5.4	18
59430	An effective approach for bonding of TZM and Nb-Zr system: Microstructure evolution, mechanical properties, and bonding mechanism. Journal of Materials Science and Technology, 2021, 84, 16-26.	5.6	5
59431	Electron beam irradiation induced metastable phase in a Mgâ^'9.8 wt%Sn alloy. Journal of Materials Science and Technology, 2021, 84, 133-138.	5.6	9
59432	Rational design of black phosphorene/g-C3B heterostructures as high-performance electrodes for Li and Na-ion batteries. Applied Surface Science, 2021, 561, 150093.	3.1	13
59433	Axial Ligand-Engineered Single-Atom Catalysts with Boosted Enzyme-Like Activity for Sensitive Immunoassay. Analytical Chemistry, 2021, 93, 12758-12766.	3.2	55
59434	Oxygen vacancy formation and uniformity of conductive filaments in Si-doped Ta2O5 RRAM. Applied Surface Science, 2021, 560, 149960.	3.1	18
59435	Electronic and catalytic engineering in two-dimensional vdW metalâ€“organic frameworks through alloying. Applied Physics Reviews, 2021, 8, 031411.	5.5	3
59436	Structural and electronic properties of the first iridium containing mixed B-site spinel oxide: <mml:math xmlns:mml="http://www.w3.org/1998/Math/MathML"><mml:mrow><mml:mi>Cu</mml:mi><mml:mrow><mml:mo>[</mml:mo><mml:mi mathvariant="normal">O</mml:mi><mml:mn>4</mml:mn></mml:msub></mml:mrow>. Physical Review Materials, 2021, 5, .	3.1	3
59437	Strain-tunable lattice thermal conductivity of the Janus PtSTe monolayer. Journal of Physics Condensed Matter, 2022, 34, 015303.	0.7	6
59438	Nitrogen vacancy enhanced photocatalytic selective oxidation of benzyl alcohol in g-C3N4. International Journal of Hydrogen Energy, 2021, 46, 37782-37791.	3.8	23
59439	Anisotropic Nodalâ€Lineâ€Derived Large Anomalous Hall Conductivity in ZrMnP and HfMnP. Advanced Materials, 2021, 33, 2104126.	11.1	4
59440	Strong intrinsic room-temperature ferromagnetism in freestanding non-van der Waals ultrathin 2D crystals. Nature Communications, 2021, 12, 5688.	5.8	61
59441	One-Dimensional Flat Bands and Anisotropic MoirÃ© Excitons in Twisted Tin Sulfide Bilayers. Chemistry of Materials, 2021, 33, 7432-7440.	3.2	6
59442	Multifaceted moirÃ© superlattice physics in twisted <mml:math xmlns:mml="http://www.w3.org/1998/Math/MathML"><mml:msub><mml:mrow><mml:mi>WSe</mml:mi></mml:mrow><mml:mn>2</mml:mn> bilayers. Physical Review B, 2021, 104, .	3.2	28
59443	Room Temperature Ferromagnetism of Monolayer Chromium Telluride with Perpendicular Magnetic Anisotropy. Advanced Materials, 2021, 33, e2103360.	11.1	84
59444	Role of the Interfacial Effect between the Substrate and Co(OH)₂ Layer in Electrochemical Oxygen Evolution. ACS Applied Energy Materials, 2021, 4, 9487-9497.	2.5	7
59445	Valence State Modulation of Chromium in Selective Hydrogen Peroxide Production Electrocatalysts. ACS Applied Energy Materials, 2021, 4, 10114-10123.	2.5	2
59446	Engineering dâ€p Orbital Hybridization in Singleâ€Atom Metalâ€Embedded Threeâ€Dimensional Electrodes for Liâ€“S Batteries. Advanced Materials, 2021, 33, e2105947.	11.1	209

#	Article	IF	Citations
59447	Anomalous thermophysical properties and electride transition in fcc potassium. Physical Review B, 2021, 104, .	1.1	0
59448	The bonding characteristics of the Cu(111)/WC(0001) interface: An insight from first-principle calculations. Vacuum, 2021, 191, 110218.	1.6	48
59449	Molecular-Scale Insights into Electrochemical Reduction of CO₂ on Hydrophobically Modified Cu Surfaces. ACS Applied Materials & Interfaces, 2021, 13, 47619-47628.	4.0	24
59450	Pathway of in situ polymerization of 1,3-dioxolane in LiPF6 electrolyte on Li metal anode. Materials Today Energy, 2021, 21, 100730.	2.5	22
59451	Enhancing blue light absorption by Sm3+ Co-doing in Ca9Nd(PO4)7: Eu3+ for white light-emitting diodes. Materials Research Express, 2021, 8, 096201.	0.8	1
59452	Photoemission signature of momentum-dependent hybridization in <mml:math xmlns:mml="http://www.w3.org/1998/Math/MathML"><mml:msub><mml:mrow><mml:mi>CeCoIn</mml:mi></mml:mrow><mml:mn Physical Review B, 2021, 104, .	1.1	4
59453	Topological theory of inversion-breaking charge-density-wave monolayer 1T-TiSe₂. New Journal of Physics, 2021, 23, 093025.	1.2	3
59454	Temperature-Induced Structural Phase Transitions in Self-Assembled Hydrogen Bonded Networks at the Liquid/Solid Interface. Russian Journal of Physical Chemistry A, 2021, 95, 1871-1876.	0.1	3
59455	Exploring the frontier between polar intermetallics and Zintl phases for the examples of the prolific ALnTnTe₃-type alkali metal (A) lanthanide (Ln) late transition metal (Tn) tellurides. Zeitschrift Fur Naturforschung - Section B Journal of Chemical Sciences, 2021, 76, 635-642.	0.3	4
59456	Unraveling the Hydrolysis of Z₂Cu²⁺ to ZCu²⁺(OH)^{â^'} and Its Consequences for the Low-Temperature Selective Catalytic Reduction of NO on Cu-CHA Catalysts. ACS Catalysis, 2021, 11, 11616-11625.	5.5	37
59457	On-surface synthesis of 2D COFs via molecular assembly directed photocycloadditions: a first-principles investigation. Journal of Physics Condensed Matter, 2021, 33, 475201.	0.7	0
59459	Mexican-hat potential energy surface in two-dimensional III2-VI3 materials and the importance of entropy barrier in ultrafast reversible ferroelectric phase change. Applied Physics Reviews, 2021, 8, .	5.5	13
59460	Realization of interstitial boron ordering and optimal near-surface electronic structure in Pd-B alloy electrocatalysts. Chemical Engineering Journal, 2021, 419, 129568.	6.6	23
59461	Rise of silicene and its applications in gas sensing. Journal of Molecular Modeling, 2021, 27, 277.	0.8	11
59462	Design and realization of topological Dirac fermions on a triangular lattice. Nature Communications, 2021, 12, 5396.	5.8	19
59463	Site-directed reduction engineering within bimetal-organic frameworks for efficient size-selective catalysis. Matter, 2021, 4, 2919-2935.	5.0	36
59464	Proton distribution visualization in perovskite nickelate devices utilizing nanofocused x rays. Physical Review Materials, 2021, 5, .	0.9	6
59465	Electric Field-Modulated Charge Transfer in Geometrically Tailored MoX₂/WX₂ (X = S, Se) Heterostructures. Journal of Physical Chemistry C, 2021, 125, 22360-22369.	1.5	15

#	Article	IF	Citations
59466	Theoretical and Experimental Characterization of Adsorbed CO and NO on Î³-Al₂O₃-Supported Rh Nanoparticles. Journal of Physical Chemistry C, 2021, 125, 19733-19755.	1.5	9
59467	Prediction of Transition-State Scaling Relationships and Universal Transition-State Vibrational and Entropic Correlations for Dehydrogenations. Journal of Physical Chemistry C, 2021, 125, 19780-19790.	1.5	3
59468	Strain Activation of Surface Chemistry on H-Terminated Si(111). Journal of Physical Chemistry C, 2021, 125, 19811-19820.	1.5	3
59469	Interlayer Interaction Induced Layer-Dependent Catalytic Activity toward a Hydrogen Evolution Reaction on Two-Dimensional PtSe2. Journal of Physical Chemistry C, 2021, 125, 19716-19723.	1.5	1
59470	Density functional study on formic acid decomposition on Pd(111) surface: a revisit and comparison with other density functional methods. Journal of Molecular Modeling, 2021, 27, 285.	0.8	0
59471	Ultrafast crystallization mechanism of amorphous Ge15Sb85 unraveled by pressure-driven simulations. Acta Materialia, 2021, 216, 117123.	3.8	13
59472	Adsorption and Reductive Defluorination of Perfluorooctanoic Acid over Palladium Nanoparticles. Environmental Science & Technology, 2021, 55, 14836-14843.	4.6	26
59473	Synergistic Effects of Co and Fe on the OER activity of LaCoxFe1â^'xO3. Chemistry - A European Journal, 2021, 27, 17145-17158.	1.7	14
59474	Enhanced graphitic domains of unreduced graphene oxide and the interplay of hydration behaviour and catalytic activity. Materials Today, 2021, 50, 44-54.	8.3	27
59475	Long-range migration of H-atoms from electron-induced dissociation of HS on Si(111). Journal of Physics Condensed Matter, 2021, 33, 474001.	0.7	1
59476	Elastic Properties of Photovoltaic Single Crystal Cs2AgBiBr6. Experimental Mechanics, 2022, 62, 117-123.	1.1	4
59477	Structural, electronic, and polarization properties of YN and LaN. Physical Review Materials, 2021, 5, .	0.9	4
59478	A quantitative simulation method for electrochemical infrared and Raman spectroscopies of single-crystal metal electrodes. Journal of Electroanalytical Chemistry, 2021, 896, 115337.	1.9	2
59479	A Green Synthesis of Ru Modified g-C ₃ N ₄ Nanosheets for Enhanced Photocatalytic Ammonia Synthesis. Energy Material Advances, 2021, 2021, .	4.7	36
59480	Optical and Electronic Properties of Organic NIR-II Fluorophores by Time-Dependent Density Functional Theory and Many-Body Perturbation Theory: GW-BSE Approaches. Nanomaterials, 2021, 11, 2293.	1.9	5
59481	Temperatureâ€dependent structural fluctuation and its effect on the electronic structure and charge transport in hybrid perovskite <scp>CH₃NH₃PbI₃</scp>. Journal of Computational Chemistry, 2021, 42, 2213-2220.	1.5	12
59482	Fluorinated Boron-Based Anions for Higher Voltage Li Metal Battery Electrolytes. Nanomaterials, 2021, 11, 2391.	1.9	4
59483	Electrons Meet Alloy Development: A Î³â€TiAlâ€Based Alloy Showcase. Advanced Engineering Materials, 2022, 24, 2100977.	1.6	4

#	Article	IF	Citations
59484	Carrier and magnetism engineering for monolayer SnS₂ by high throughput first-principles calculations*. Chinese Physics B, 2021, 30, 117105.	0.7	2
59485	Novel Ultrabright and Airâ€Stable Photocathodes Discovered from Machine Learning and Density Functional Theory Driven Screening. Advanced Materials, 2021, 33, e2104081.	11.1	7
59486	Surface Properties of Octacalcium Phosphate Nanocrystals Are Crucial for Their Bioactivities. ACS Omega, 2021, 6, 25372-25380.	1.6	4
59487	Beryllium sulfur doped with N, Li and Na: Promising p-type transparent semiconductor. Materials Today Communications, 2021, 28, 102513.	0.9	5
59488	Identifying Migration Channels and Bottlenecks in Monoclinic NASICONâ€Type Solid Electrolytes with Hierarchical Ionâ€Transport Algorithms. Advanced Functional Materials, 2021, 31, 2107747.	7.8	33
59489	Galvanic Deposition of Pt Nanoparticles on Black TiO₂ Nanotubes for Hydrogen Evolving Cathodes. ChemSusChem, 2021, 14, 4993-5003.	3.6	14
59490	Understanding the Role of Oxygen and Hydrogen Defects in Modulating the Optoelectronic Properties of P-Type Metal Oxide Semiconductors. Chemistry of Materials, 2021, 33, 7829-7838.	3.2	12
59491	Origin and Absence of Giant Negative Thermal Expansion in Reduced and Oxidized Ca2RuO4. Chemistry of Materials, 0, , .	3.2	14
59492	Reduced Carbon Monoxide Saturation Coverage on Vicinal Palladium Surfaces: the Importance of the Adsorption Site. Journal of Physical Chemistry Letters, 2021, 12, 9508-9515.	2.1	3
59493	Discrete twinning dynamics and size-dependent dislocation-to twin transition in body-centred cubic tungsten. Journal of Materials Science and Technology, 2022, 106, 33-40.	5.6	19
59494	Atomic layer deposition triggered Fe-In-S cluster and gradient energy band in ZnInS photoanode for improved oxygen evolution reaction. Nature Communications, 2021, 12, 5247.	5.8	36
59495	Steam-created grain boundaries for methane Câ€“H activation in palladium catalysts. Science, 2021, 373, 1518-1523.	6.0	105
59496	Using Neural Network Force Fields to Ascertain the Quality of Ab Initio Simulations of Liquid Water. Journal of Physical Chemistry B, 2021, 125, 10772-10778.	1.2	13
59497	Equilibrium Distribution of Dissolved Carbon in PdCx: Density Functional Theory and Canonical Monte Carlo Simulations. Journal of Physical Chemistry C, 2021, 125, 20930-20939.	1.5	2
59498	First-Principles Characterization of Surface Phonons of Halide Perovskite CsPbI₃ and Their Role in Stabilization. Journal of Physical Chemistry Letters, 2021, 12, 9253-9261.	2.1	4
59499	Atomic-Level Copper Sites for Selective CO₂ Electroreduction to Hydrocarbon. ACS Sustainable Chemistry and Engineering, 2021, 9, 13536-13544.	3.2	14
59500	Coexisting unconventional Rashba- and Zeeman-type spin splitting in Pb-adsorbed monolayer WSe2. Journal of Physics Condensed Matter, 2021, 34, .	0.7	0
59501	High-Performance Binary Moâ€“Ni Catalysts for Efficient Carbon Removal during Carbon Dioxide Reforming of Methane. ACS Catalysis, 2021, 11, 12087-12095.	5.5	61

#	Article	IF	Citations
59502	Metal-organic frameworks derived anatase/rutile heterostructures with enhanced reaction kinetics for lithium and sodium storage. Chemical Engineering Journal, 2022, 430, 132689.	6.6	33
59503	Hierarchically assembling cobalt/nickel carbonate hydroxide on copper nitride nanowires for highly efficient water splitting. Applied Catalysis B: Environmental, 2021, 292, 120148.	10.8	62
59504	Highly exfoliated NiPS3 nanosheets as efficient electrocatalyst for high yield ammonia production. Chemical Engineering Journal, 2022, 430, 132649.	6.6	17
59505	Lattice and electronic structures of BAlN in the deep ultraviolet spectral region. Physica B: Condensed Matter, 2021, 619, 413188.	1.3	3
59506	Theoretical prediction of thermoelectric properties of n-type binary Zintl compounds (KSb and KBi). Physica B: Condensed Matter, 2021, 619, 413206.	1.3	9
59507	Nonrad: Computing nonradiative capture coefficients from first principles. Computer Physics Communications, 2021, 267, 108056.	3.0	50
59508	Temperature-dependent elastic properties of high entropy ceramic (ZrTaNbTi)C from self-consistent quasi-harmonic approximation. Solid State Communications, 2021, 336, 114432.	0.9	3
59509	Modulating electronic, magnetic and mechanical properties of MVN (M = Ti, V, Cr) MXenes by surface functionalization. Solid State Communications, 2021, 336, 114411.	0.9	7
59510	Magnetic properties of Mn-doped monolayer MoS2. Physics Letters, Section A: General, Atomic and Solid State Physics, 2021, 414, 127636.	0.9	6
59511	Hydration structures of barium ions: Ab initio molecular dynamics simulations using the SCAN meta-GGA density functional and EXAFS spectroscopy studies. Chemical Physics Letters, 2021, 780, 138945.	1.2	5
59512	Enhanced activity for electrocatalytic H2 production through cooperative Pr and Bi co-doping of CeO2 in solid oxide electrolysis cells. Journal of Catalysis, 2021, 402, 310-314.	3.1	7
59513	Drastic reduction of thermal conductivity in hexagonal AX (AÂ=ÂGa, In & Tl, XÂ=ÂS, Se & Te) monolayers due to alternative atomic configuration. Nano Energy, 2021, 88, 106248.	8.2	19
59514	Structural, electronic, magnetic and mechanical properties of Fe2SiC. Physica B: Condensed Matter, 2021, 618, 413136.	1.3	2
59515	Vibrational properties of High Entropy Alloy based metal hydrides probed by inelastic neutron scattering. Journal of Alloys and Compounds, 2021, 877, 160320.	2.8	4
59516	Tuning the photocatalytic water-splitting performance with the adjustment of diameter in an armchair WSSe nanotube. Journal of Energy Chemistry, 2021, 61, 228-235.	7.1	16
59517	Mesoporous carbon-supported ultrasmall metal nanoparticles via a mechanochemical-driven redox reaction: A â€œTwo-in-Oneâ€•strategy. Applied Catalysis B: Environmental, 2021, 294, 120232.	10.8	8
59518	Selective N2/H2O adsorption onto 2D amphiphilic amorphous photocatalysts for ambient gas-phase nitrogen fixation. Applied Catalysis B: Environmental, 2021, 294, 120240.	10.8	10
59519	Optimization of hydrogen evolution reaction catalytic activity of Ti2CO2 via surface engineering with an isolated fluorine effect: An ab-initio density functional theory study. Applied Surface Science, 2021, 562, 150149.	3.1	4

#	Article	IF	Citations
59520	Hydrogen storage capacity of Li-decorated borophene and pristine graphene slit pores: A combined ab initio and quantum-thermodynamic study. Applied Surface Science, 2021, 562, 150019.	3.1	15
59521	Superhardness Induced by Grain Boundary Vertical Sliding in (001)-textured ZrB<mml:math xmlns:mml="http://www.w3.org/1998/Math/MathML" altimg="si3.svg"><mml:msub><mml:mrow /><mml:mn>2</mml:mn></mml:msub></mml:math> and TiB<mml:math xmlns:mml="http://www.w3.org/1998/Math/MathML" altimg="si3.svg"><mml:msub><mml:mrow /><mml:mn>2</mml:mn></mml:msub></mml:math> Nano Films. Acta Materialia, 2021, 218, 117212.	3.8	11
59522	First-principle studies on the ferroelectricity and gate-controlled Rashba spin-orbit coupling of d1T-phase transition-metal dichalcogenide monolayers. Physica E: Low-Dimensional Systems and Nanostructures, 2021, 134, 114934.	1.3	5
59523	Monolayer PtTe2: A promising candidate for NO2 sensor with ultrahigh sensitivity and selectivity. Physica E: Low-Dimensional Systems and Nanostructures, 2021, 134, 114925.	1.3	11
59524	Predicting MnB6 monolayer with room temperature ferromagnetism and high magnetic anisotropy. Physica E: Low-Dimensional Systems and Nanostructures, 2021, 134, 114930.	1.3	6
59525	Bi and Al co-doped anatase titania for photosensitized degradation of Rhodamine B under visible-light irradiation. Ceramics International, 2021, 47, 28296-28303.	2.3	14
59526	Electronic and optical properties of ultrathin cerium dioxide: A many-body GW-BSE investigation. Computational Materials Science, 2021, 198, 110696.	1.4	6
59527	Switchable electric polarization of phosphorene in mixed dimensional van der Waals heterostructure. Applied Surface Science, 2021, 563, 150276.	3.1	3
59528	Functionalization of two-dimensional PbTiO3 film by surface modification: A first-principles study. Applied Surface Science, 2021, 563, 150268.	3.1	5
59529	Photo-activated emitting defects in the Ce-doped CaSnF6 fluoride. Materials Research Bulletin, 2021, 142, 111384.	2.7	0
59530	Theoretical investigation of electrochemical reduction mechanism of CO2 on the Cu(1Â1Â1), Sn@Cu(1Â1Â1) and Sn(2Â1Â1) surfaces. Applied Surface Science, 2021, 564, 150418.	3.1	9
59531	Theoretical prediction of topological insulators in two-dimensional ternary transition metal chalcogenides (MM'X4, MÂ=ÂTa, Nb, or V; M'= Ir, Rh, or Co; XÂ=ÂSe or Te). Chinese Journal of Physics, 2021, 73, 95-102.	2.0	11
59532	Revealing the mechanism of grain refinement and anti Si-poisoning induced by (Nb, Ti)B2 with a sandwich-like structure. Acta Materialia, 2021, 219, 117265.	3.8	19
59533	On the role of surface oxygen during nascent single-walled carbon nanotube cap spreading and tube nucleation on iron catalysts. Carbon, 2021, 184, 470-478.	5.4	6
59534	Heterostructure of ultrafine FeOOH nanodots supported on CoAl-layered double hydroxide nanosheets as highly efficient electrocatalyst for water oxidation. Journal of Colloid and Interface Science, 2021, 600, 594-601.	5.0	20
59535	Effect of exchange-correlation functional type and spin-orbit coupling on thermoelectric properties of ZrTe2. Journal of Solid State Chemistry, 2021, 302, 122414.	1.4	6
59536	First principles investigation of elastic and thermodynamic properties of CoSbS thermoelectric material. Journal of Solid State Chemistry, 2021, 302, 122443.	1.4	6
59537	A sensitive chemosensor for nitro-containing compounds based on Au nanoclusters/Ba2+ co-assembly system: The crucial role of ligands to metal charge transfer. Colloids and Surfaces A: Physicochemical and Engineering Aspects, 2021, 627, 127160.	2.3	3

#	Article	IF	Citations
59538	Effects of the V and P doping on the electronic and magnetic properties of the monolayer ZrS2. Thin Solid Films, 2021, 735, 138875.	0.8	3
59539	On the interaction of solute atoms with vacancies in diluted Al-alloys: A paradigmatic experimental and ab-initio study on indium and tin. Acta Materialia, 2021, 219, 117228.	3.8	22
59540	Charge-compensated codoped pseudohexagonal zinc selenide nanosheets towards enhanced visible-light-driven photocatalytic water splitting for hydrogen production. International Journal of Hydrogen Energy, 2021, 46, 34305-34317.	3.8	13
59541	Superior lithium-ion storage of V-doped MoO3 nanosheets via plasma evaporation. Electrochimica Acta, 2021, 394, 139121.	2.6	9
59542	Double bond effects induced by iron selenide as immobilized homogenous catalyst for efficient polysulfides capture. Chemical Engineering Journal, 2021, 421, 129770.	6.6	18
59543	Catechol detection in pure and transition metal decorated 2D MoS2: Acumens from density functional theory approaches. Applied Surface Science, 2021, 562, 150216.	3.1	23
59544	A computational approach on engineering short spacer for carbazole-based dyes for dye-sensitized solar cells. Journal of Photochemistry and Photobiology A: Chemistry, 2021, 419, 113447.	2.0	6
59545	First-Principles Investigation of Structural, Raman and Electronic Characteristics of Single Layer Ge3N4. Applied Surface Science, 2021, 572, 151361.	3.1	1
59546	Exploring Metal Cluster Catalysts Using Swarm Intelligence: Start with Hydrogen Adsorption. Topics in Catalysis, 2022, 65, 215-227.	1.3	2
59547	Completing the picture of initial oxidation on copper. Applied Surface Science, 2021, 562, 150148.	3.1	12
59548	Regulating Water Reduction Kinetics on MoP Electrocatalysts Through Se Doping for Accelerated Alkaline Hydrogen Production. Frontiers in Chemistry, 2021, 9, 737495.	1.8	6
59549	Enhancing Oxygen Evolution Reaction Activity by Using Switchable Polarization in Ferroelectric InSnO₂N. ACS Catalysis, 2021, 11, 12692-12700.	5.5	9
59550	Synthesis, structure, magnetocaloric effect and DFT calculations of a MnII cluster-based inorganic coordination polymer. Journal of Alloys and Compounds, 2021, 878, 160353.	2.8	5
59551	Sulfur vacancies affect the environmental fate, corona formation, and microalgae toxicity of molybdenum disulfide nanoflakes. Journal of Hazardous Materials, 2021, 419, 126499.	6.5	11
59552	Solving the Bethe-Salpeter equation on massively parallel architectures. Computer Physics Communications, 2021, 267, 108081.	3.0	4
59553	MechElastic: A Python library for analysis of mechanical and elastic properties of bulk and 2D materials. Computer Physics Communications, 2021, 267, 108068.	3.0	54
59554	The glass transition and the non-Arrhenian viscosity of carbonate melts. American Mineralogist, 2022, 107, 1053-1064.	0.9	5
59555	Isobutane dehydrogenation over high-performanced sulfide V-K/Î³-Al2O3 catalyst: Modulation of vanadium species and intrinsic effect of potassium. Journal of Colloid and Interface Science, 2021, 600, 440-448.	5.0	3

#	Article	IF	Citations
59556	Enhanced quantum capacitance in 3d-transition metal porphyrin functionalized graphene. Materials Science and Engineering B: Solid-State Materials for Advanced Technology, 2021, 272, 115384.	1.7	4
59557	Elemental partitions and deformation mechanisms of L12-type multicomponent intermetallics. Acta Materialia, 2021, 219, 117238.	3.8	28
59558	Effects of different catalysts on performance of self-bonded SiC refractories. Ceramics International, 2021, 47, 27863-27872.	2.3	6
59559	Design of novel NiSiAlY alloys in marine salt-spray environment: Part I. Al-Si-Y and Ni-Si-Y subsystems. Journal of Materials Science and Technology, 2021, 88, 66-78.	5.6	11
59560	Heterostructure-based devices with enhanced humidity stability for H2 gas sensing applications in breath tests and portable batteries. Sensors and Actuators A: Physical, 2021, 329, 112804.	2.0	17
59561	Metallocene inspired 2D metal intercalated carbon allotropes: Stability and properties via DFT calculations. Carbon, 2021, 184, 714-720.	5.4	3
59562	Inhibition of steel corrosion with imidazolium-based compounds â€“ Experimental and theoretical study. Corrosion Science, 2021, 191, 109716.	3.0	9
59563	Converting cellulose waste into a high-efficiency photocatalyst for Cr(VI) reduction via molecular oxygen activation. Applied Catalysis B: Environmental, 2021, 295, 120253.	10.8	39
59564	Electronic work function, surface energy and electronic properties of binary Mg-Y and Mg- Al alloys: A DFT study. Surface Science, 2021, 712, 121880.	0.8	18
59565	Mechanism investigation of PtPd decorated Zn0.5Cd0.5S nanorods with efficient photocatalytic hydrogen production combining with kinetics and thermodynamics. Chinese Journal of Catalysis, 2021, 42, 1677-1688.	6.9	31
59566	Tuning the electronic and optical properties of two-dimensional AgBiP2Se6 and AgInP2Se6 Janus monolayers. Chemical Physics Letters, 2021, 780, 138933.	1.2	8
59567	CO and H2 adsorption on Au-Ni bimetallic surfaces: a combined experimental and DFT theoretical study. Surface Science, 2021, 712, 121892.	0.8	6
59568	Role of the Cu-ZrO2 interface in the hydrogenation of levulinic acid to Î³-valerolactone. Journal of Energy Chemistry, 2021, 61, 446-458.	7.1	23
59569	La-doped TiO2 nanorods toward boosted electrocatalytic N2-to-NH3 conversion at ambient conditions. Chinese Journal of Catalysis, 2021, 42, 1755-1762.	6.9	35
59570	Borophosphene: A potential anchoring material for lithium-sulfur batteries. Applied Surface Science, 2021, 562, 150157.	3.1	21
59571	Atomic study on phase transformation of the strengthening phase in a die-casting Mgâ€“Alâ€“La alloy via an intermediate phase. Materials and Design, 2021, 208, 109904.	3.3	18
59572	Use of local density approximation within range separated hybrid exchangeâ€“correlation functional to investigate Pb doped SnO<mml:math xmlns:mml="http://www.w3.org/1998/Math/MathML" display="inline" id="d1e1360" altimg="si94.svg"><mml:msub><mml:mrow /><mml:mrow><mml:mn>2</mml:mn></mml:mrow></mml:msub></mml:math>. Physica B: Condensed Matter, 2021, 619, 413226.	1.3	2
59573	Doping and pressure-driven structural transition in BiMnO<mml:math xmlns:mml="http://www.w3.org/1998/Math/MathML" display="inline" id="d1e461" altimg="si72.svg"><mml:msub><mml:mrow /><mml:mrow><mml:mn>3</mml:mn><mml:mo>+</mml:mo><mml:mi>Î´</mml:mi></mml:mrow></mml:msub></mml:math> from first principles. Physica B: Condensed Matter, 2021, 619, 413242.	1.3	1

#	Article	IF	Citations
59574	Interfacing 2D M2X (MÂ=ÂNa, K, Cs; XÂ=ÂO, S, Se, Te) monolayers for 2D excitonic and tandem solar cells. Applied Surface Science, 2021, 563, 150304.	3.1	18
59575	Understanding the surface passivation effects of Lewis base in perovskite solar cells. Applied Surface Science, 2021, 563, 150267.	3.1	25
59576	Improved contact properties of graphene-metal hybrid interfaces by grain boundaries. Applied Surface Science, 2021, 563, 150392.	3.1	0
59577	Au-Ru alloy nanofibers as a highly stable and active bifunctional electrocatalyst for acidic water splitting. Applied Surface Science, 2021, 563, 150293.	3.1	25
59578	Cohesion properties and tensile cracking behavior of CrN coating on Î³-Fe matrix by first principles study. Applied Surface Science, 2021, 563, 150279.	3.1	10
59579	AlAs/SiH van der Waals heterostructures: A promising photocatalyst for water splitting. Physica E: Low-Dimensional Systems and Nanostructures, 2021, 134, 114869.	1.3	20
59580	Ru4+-assisted phase transition in VO2 nanoparticles: Electronic structures and optical properties. Vacuum, 2021, 192, 110495.	1.6	9
59581	JAMIP: an artificial-intelligence aided data-driven infrastructure for computational materials informatics. Science Bulletin, 2021, 66, 1973-1985.	4.3	32
59582	Large gap two-dimensional topological insulators with prominent Rashba effect in ethynyl functionalized â…¢-Bi Buckled-Honeycomb monolayers. Superlattices and Microstructures, 2021, 158, 107026.	1.4	1
59583	Modulation of the selectivity of CO2 to CO electroreduction in palladium rich Palladium-Indium nanoparticles. Journal of Catalysis, 2021, 402, 229-237.	3.1	13
59584	Multi-scale study of Am(III) adsorption on Gaomiaozi bentonite: Combining experiments, modeling and DFT calculations. Chemical Geology, 2021, 581, 120414.	1.4	13
59585	Synthetic accessibility and stability rules of NASICONs. Nature Communications, 2021, 12, 5752.	5.8	47
59586	Grafting nanometer metal/oxide interface towards enhanced low-temperature acetylene semi-hydrogenation. Nature Communications, 2021, 12, 5770.	5.8	43
59587	Prediction of Intrinsic Valley Polarization in Singleâ€Layer GdX₂ (Xâ€‰=â€‰Br, Cl) from a Firstâ€Principles Study. Physica Status Solidi (B): Basic Research, 2021, 258, 2100356.	0.7	8
59588	Promising two-dimensional T-silicene as high capacity anode for rechargeable lithium-ion and sodium-ion batteries. Chemical Physics Letters, 2021, 784, 139097.	1.2	8
59589	Stabilization of Orthorhombic CoSe₂ by 2D-rGO/MWCNT Heterostructures for Efficient Hydrogen Evolution Reaction and Flexible Energy Storage Device Applications. ACS Applied Energy Materials, 2021, 4, 11386-11399.	2.5	30
59590	The Magnetic Proximity Effect at the MoS2/CrI3 Interface. Journal of Physics Condensed Matter, 2021, 34, .	0.7	4
59591	A ternary hybrid of Zn-doped MoS2-RGO for highly effective electrocatalytic hydrogen evolution. Journal of Colloid and Interface Science, 2021, 599, 100-108.	5.0	15

#	Article	IF	Citations
59592	High-performance single-atom Ni catalyst loaded graphyne for H2O2 green synthesis in aqueous media. Journal of Colloid and Interface Science, 2021, 599, 58-67.	5.0	12
59593	Hardness, magnetic, elastic, and electronic properties of manganese semi-boride synthesized by high pressure and high temperature. Journal of Solid State Chemistry, 2021, 302, 122386.	1.4	5
59594	Trimetallic magnetite-Ti-Au nanoparticle formation: A theoretical approach. Materials Chemistry and Physics, 2021, 271, 124847.	2.0	0
59595	A rechargeable 6-electron Alâ€“Se battery with high energy density. Energy Storage Materials, 2021, 41, 667-676.	9.5	44
59596	Effect of ferroelectric polarization field on different carrier migration in photoanode. Materials Science in Semiconductor Processing, 2021, 133, 105958.	1.9	1
59597	Adsorption characteristics of silver atoms and silver ions on silica surface in silver nanoparticle hydrosol system. Applied Surface Science, 2021, 562, 150168.	3.1	6
59598	Transition metal single atom anchored C3N for highly efficient formic acid dehydrogenation: A DFT study. Applied Surface Science, 2021, 562, 150186.	3.1	15
59599	Thermal property and lattice thermal conductivity of three-dimensional pentagonal silicon. Physica B: Condensed Matter, 2021, 618, 413178.	1.3	4
59600	Photoenhanced CO2 methanation over La2O3 promoted Co/TiO2 catalysts. Applied Catalysis B: Environmental, 2021, 294, 120248.	10.8	21
59601	First-Principles investigation on the behavior of Pt single and triple atoms supported on monolayer CuO (1 1 0) in CO oxidation. Applied Surface Science, 2021, 564, 150435.	3.1	3
59602	Quantitative analysis of rhenium in irradiated tungsten. Journal of Nuclear Materials, 2021, 554, 153014.	1.3	0
59603	Mechanical properties of CrN-based superlattices: Impact of magnetism. Acta Materialia, 2021, 218, 117095.	3.8	5
59604	Polyacrylonitrile gel polymer electrolyte as separator in boosting Li-ion storage performance of GeSe2. Ceramics International, 2021, 47, 27916-27924.	2.3	5
59605	The novel positive colossal electroresistance in PbPdO2 thin film with (002) preferred orientation. Ceramics International, 2021, 47, 26768-26778.	2.3	5
59606	Type-II vdW heterojunction SeGa2Te/SeIn2Se as a high-efficiency visible-light-driven water-splitting photocatalyst. Physics Letters, Section A: General, Atomic and Solid State Physics, 2021, 413, 127594.	0.9	9
59607	The design of high performance photoanode of CQDs/TiO2/WO3 based on DFT alignment of lattice parameter and energy band, and charge distribution. Journal of Colloid and Interface Science, 2021, 600, 828-837.	5.0	27
59608	First-principles calculations to investigate electronic structure and transport properties of CrC monolayers: A new horizon for spintronic application. Materials Science and Engineering B: Solid-State Materials for Advanced Technology, 2021, 272, 115379.	1.7	17
59609	Bottom-up approach to quasi-monolayer black phosphorus advancing photocatalytic H2 evolution. Chemical Engineering Journal, 2021, 421, 127841.	6.6	21

#	Article	IF	Citations
59610	Partial Disproportionation Gallium-Oxygen Reaction Boosts Lithium-Oxygen Batteries. Energy Storage Materials, 2021, 41, 475-484.	9.5	12
59611	Structural design enables highly-efficient green emission with preferable blue light excitation from zero-dimensional manganese (II) hybrids. Chemical Engineering Journal, 2021, 421, 129886.	6.6	56
59612	Bi-atom active sites embedded in a two-dimensional covalent organic framework for efficient nitrogen reduction reaction. Applied Surface Science, 2021, 563, 150352.	3.1	25
59613	Theoretical studies of SiC van der Waals heterostructures as anodes of Li-ion batteries. Applied Surface Science, 2021, 563, 150269.	3.1	43
59614	Photodynamic therapy: When van der Waals heterojunction meets tumor. Chemical Engineering Journal, 2021, 421, 129773.	6.6	9
59615	Novel double-perovskite SrLaLiTeO6:Mn4+ far-red phosphor with superior thermal stability for indoor plant growth LED. Journal of Luminescence, 2021, 238, 118286.	1.5	38
59616	Band and optical properties of arsenene and antimonene lateral heterostructure by first-principles calculations. Physica E: Low-Dimensional Systems and Nanostructures, 2021, 134, 114933.	1.3	17
59617	Electrically tunable bandgaps for g-ZnO/ZnX (XÂ= S, Se, Te) 2D semiconductor bilayers. Vacuum, 2021, 192, 110386.	1.6	1
59618	Orthorhombic Fmmm-C80: A new superhard carbon allotrope with direct band gap. Computational Materials Science, 2021, 198, 110689.	1.4	5
59619	A simple method for computing the formation free energies of metal oxides. Computational Materials Science, 2021, 198, 110692.	1.4	0
59620	Prediction of the Rb-Si compounds under high pressure. Computational Materials Science, 2021, 198, 110704.	1.4	1
59621	In situ growth of nano-antioxidants on cellular vesicles for efficient reactive oxygen species elimination in acute inflammatory diseases. Nano Today, 2021, 40, 101282.	6.2	22
59622	FeSe2/Hematite n-n heterojunction with oxygen spillover for highly efficient NO2 gas sensing. Sensors and Actuators B: Chemical, 2021, 345, 130357.	4.0	29
59623	The effect of hydrogen on the mechanical properties of high entropy alloy TiZrHfMoNb: First-principles investigation. Journal of Alloys and Compounds, 2021, 879, 160482.	2.8	15
59624	Tuning reverse water gas shift and methanation reactions during CO2 reduction on Ni catalysts via surface modification by MoOx. Journal of CO2 Utilization, 2021, 52, 101678.	3.3	25
59625	Thermodynamics of the Lu2O3 â€“ SiO2 system and comparison to other rare earth silicates. Journal of Chemical Thermodynamics, 2021, 161, 106483.	1.0	7
59626	A novel perovskite ferroelectric KNbO3-Bi(Ni1/2Ti1/2)O3 nanofibers for photocatalytic hydrogen production. Applied Surface Science, 2022, 572, 151359.	3.1	9
59627	Mixing properties of Al₂O₃(0001)-supported M ₂O₃ and MMâ€²O₃ monolayers (M, Mâ€² = Ti, V, Cr, Fe). Journal of Physics Condensed Matter, 2022, 34, 034002.	0.7	2

#	Article	IF	Citations
59628	Magnetic property of Al-Mg alloys and intermetallic compounds. Journal of Alloys and Compounds, 2021, 877, 160226.	2.8	4
59629	Combined spectroscopic and DFT studies of local defect structures in beta-tricalcium phosphate doped with Nd(III). Journal of Alloys and Compounds, 2021, 877, 160305.	2.8	1
59630	Investigation of p-type doping in Î²- and Î³-Ga2O3. Journal of Alloys and Compounds, 2021, 877, 160227.	2.8	16
59631	Electronic, magnetic, and topological properties of layered ternary chalcogenide CoAsS: A first principles study. Journal of Magnetism and Magnetic Materials, 2021, 536, 168133.	1.0	1
59632	Electric field tunable bandgap and anisotropic high carrier mobility in SiAs2/GeAs2 lateral heterostructure. Computational Materials Science, 2021, 198, 110697.	1.4	6
59633	Can borophenes with Dirac cone be promising electrodes for supercapacitors. Applied Surface Science, 2021, 562, 150154.	3.1	7
59634	Deep Density: Circumventing the Kohn-Sham equations via symmetry preserving neural networks. Journal of Computational Physics, 2021, 443, 110523.	1.9	11
59635	Advanced lithiumâ€“sulfur batteries enabled by a SnS2-Hollow carbon nanofibers Flexible Electrocatalytic Membrane. Carbon, 2021, 184, 1-11.	5.4	27
59636	Effect of defects and defect distribution on Li-diffusion and elastic properties of anti-perovskite Li3OCl solid electrolyte. Energy Storage Materials, 2021, 41, 614-622.	9.5	16
59637	Investigating the formation mechanism of void lattice in tungsten under neutron irradiation: from collision cascades to ordered nanovoids. Acta Materialia, 2021, 219, 117239.	3.8	23
59638	Pressure and temperature dependence of second-order elastic constants from third-order elastic constants in TMC (TM=Nb, Ti, V, Zr). Ceramics International, 2021, 47, 27535-27544.	2.3	11
59639	Carbon dots structural characterization by solution-state NMR and UVâ€“visible spectroscopy and DFT modeling. Applied Surface Science, 2021, 564, 150195.	3.1	26
59640	Towards understanding the trapping, migration and clustering of He atoms in Wâ€“Ta alloy. Journal of Nuclear Materials, 2021, 554, 153095.	1.3	4
59641	Atomistic investigation of uranium oxycarbide (UCO) phase stability at finite temperatures: DFT+<mml:math xmlns:mml="http://www.w3.org/1998/Math/MathML" altimg="si2.svg"><mml:mi>U</mml:mi></mml:math> and AIMD+<mml:math xmlns:mml="http://www.w3.org/1998/Math/MathML" altimg="si2.svg"><mml:mi>U</mml:mi></mml:math> approaches. Journal of Nuclear Materials, 2021, 554, 153046.	1.3	3
59642	Boosting alkaline hydrogen electrooxidation on an unconventional fcc-Ru polycrystal. Journal of Energy Chemistry, 2021, 61, 15-22.	7.1	36
59643	Insight into the wetting and interfacial behavior of Cu-Ti/ZrB2 system: A combined experimental and DFT calculation. Journal of the European Ceramic Society, 2021, 41, 6213-6222.	2.8	4
59644	Hierarchical flower-like TiO2 microspheres for high-selective NH3 detection: A density functional theory study. Sensors and Actuators B: Chemical, 2021, 345, 130303.	4.0	27
59645	Oxidation thermodynamics of Nb-Ti alloys studied via first-principles calculations. Journal of Alloys and Compounds, 2021, 879, 160455.	2.8	13

#	Article	IF	Citations
59646	Two-dimensional Mo-based compounds for the Li-O2 batteries: Catalytic performance and electronic structure studies. Energy Storage Materials, 2021, 41, 650-655.	9.5	35
59647	Exploring sodium storage mechanism of topological insulator Bi2Te3 nanosheets encapsulated in conductive polymer. Energy Storage Materials, 2021, 41, 255-263.	9.5	44
59648	Maximizing the synergistic effect of PdAu catalysts on TiO2(1Â0Â1) for robust CO2 reduction: A DFT study. Applied Surface Science, 2021, 563, 150365.	3.1	6
59649	High electrical transport performance and ultralow thermal conductivity realized in Ga doped single-layer octagon-square nitrogene. Applied Surface Science, 2021, 563, 150244.	3.1	0
59650	First-principle study of electronic properties and quantum capacitance of lithium adsorption on pristine and vacancy-defected O-functionalized Ti2C MXene. Applied Surface Science, 2021, 563, 150264.	3.1	15
59651	Switching the electrical characteristics of TiO2 from n-type to p-type by ion implantation. Applied Surface Science, 2021, 563, 150274.	3.1	6
59652	Simulation of metal-supported metal-Nanoislands: A comparison of DFT methods. Surface Science, 2021, 712, 121889.	0.8	7
59653	Oxygen migration triggering molybdenum exposure in oxygen vacancy-rich ultra-thin Bi2MoO6 nanoflakes: Dual binding sites governing selective CO2 reduction into liquid hydrocarbons. Journal of Energy Chemistry, 2021, 61, 281-289.	7.1	40
59654	Optimized electrocatalytic performance of PtZn intermetallic nanoparticles for methanol oxidation by designing catalyst support and fine-tuning surface composition. Electrochimica Acta, 2021, 394, 139106.	2.6	6
59655	Highly active methanol oxidation electrocatalyst based on 2D NiO porous nanosheets:a combined computational and experimental study. Electrochimica Acta, 2021, 394, 139143.	2.6	13
59656	Reaction of (bromodifluoromethyl)trimethylsilane with HMPA: Structural studies. Journal of Fluorine Chemistry, 2021, 250, 109881.	0.9	1
59657	Synthesis and stability of Sn(II)-containing perovskites: (Ba,SnII)HfIVO3 versus (Ba,SnII)SnIVO3. Journal of Solid State Chemistry, 2021, 302, 122419.	1.4	7
59658	First principles study on planar mechanism and heterostructures of ultraflat stanene. Physica E: Low-Dimensional Systems and Nanostructures, 2021, 134, 114908.	1.3	2
59659	Novel electronic structures and magnetic properties in twisted two-dimensional graphene/Janus 2Hâ€“VSeTe heterostructures. Physica E: Low-Dimensional Systems and Nanostructures, 2021, 134, 114854.	1.3	8
59660	Single transition metal atom modified MoSe2 as a promising electrocatalyst for nitrogen Fixation: A first-principles study. Chemical Physics Letters, 2021, 780, 138939.	1.2	5
59661	First-principles study on the P-induced embrittlement and de-embrittling effect of B and C in ferritic steels. Acta Materialia, 2021, 219, 117260.	3.8	23
59662	Porous N, B co-doped carbon nanotubes as efficient metal-free electrocatalysts for ORR and Zn-air batteries. Chemical Engineering Journal, 2021, 422, 130134.	6.6	98
59663	Two-dimensional IrN2 monolayer: An efficient bifunctional electrocatalyst for oxygen reduction and oxygen evolution reactions. Journal of Colloid and Interface Science, 2021, 600, 711-718.	5.0	27

#	Article	IF	Citations
59664	PbSnSâ„‚-Based Gas Sensor to Detect SFâ‚† Decompositions: DFT and NEGF Calculations. IEEE Transactions on Electron Devices, 2021, 68, 5322-5325.	1.6	13
59665	Chemical transformation approach for high-performance ternary NiFeCo metal compound-based water splitting electrodes. Applied Catalysis B: Environmental, 2021, 294, 120246.	10.8	67
59666	Lithium-mediated electrochemical nitrogen reduction: Mechanistic insights to enhance performance. IScience, 2021, 24, 103105.	1.9	50
59667	Construction of direct Z-scheme Bi5O7I/UiO-66-NH2 heterojunction photocatalysts for enhanced degradation of ciprofloxacin: Mechanism insight, pathway analysis and toxicity evaluation. Journal of Hazardous Materials, 2021, 419, 126466.	6.5	169
59668	Computational prediction and experimental evaluation of nitrate reduction to ammonia on rhodium. Journal of Catalysis, 2021, 402, 1-9.	3.1	14
59669	Single-atom iron as a promising low-temperature catalyst for selective catalytic reduction of NO with NH3: A theoretical prediction. Fuel, 2021, 302, 121041.	3.4	36
59670	A deep learning interatomic potential developed for atomistic simulation of carbon materials. Carbon, 2022, 186, 1-8.	5.4	25
59671	Accelerating materials discovery with Bayesian optimization and graph deep learning. Materials Today, 2021, 51, 126-135.	8.3	44
59672	Persistent radical pairs trigger nano-gold to highly efficiently and highly selectively drive the value-added conversion of nitroaromatics. Chem Catalysis, 2021, 1, 1118-1132.	2.9	10
59673	Computational evaluation of Mg-decorated g-CN as clean energy gas storage media. International Journal of Hydrogen Energy, 2021, 46, 35130-35136.	3.8	22
59674	Tunable Schottky Barrier and Interfacial Electronic Properties in Graphene/ZnSe Heterostructures. Frontiers in Chemistry, 2021, 9, 744977.	1.8	1
59675	Single alloy nanoparticle x-ray imaging during a catalytic reaction. Science Advances, 2021, 7, eabh0757.	4.7	7
59676	Understanding electrochemical and structural properties of copper hexacyanoferrate: Application in hydrogen peroxide analysis. Electrochimica Acta, 2021, 394, 139147.	2.6	5
59677	Cu acting as Fe activity promoter in dual-atom Cu/Fe-NC catalyst in CO2RR to C1 products. Applied Surface Science, 2021, 564, 150423.	3.1	52
59678	Newfound two-dimensional Bi2Se3 monolayers for driving hydrogen evolution reaction with the visible-light. Applied Surface Science, 2021, 564, 150389.	3.1	7
59679	Atomic study of hydrogen behavior in different vanadium carbides. Journal of Nuclear Materials, 2021, 554, 153096.	1.3	3
59680	Half-metallicity in Fe2MnSi and Mn2FeSi heusler compounds: A comparative ab initio study. Materials Chemistry and Physics, 2021, 271, 124897.	2.0	9
59681	Regulating Feâ€“O bond in Ti3C2Tx MXene anode for high-capacity Li-ion batteries. Chemical Engineering Journal, 2021, 422, 130018.	6.6	22

#	Article	IF	Citations
59682	Structural and magnetic transitions of CoFeMnNiAl high-entropy alloys caused by composition and annealing. Intermetallics, 2021, 137, 107298.	1.8	5
59683	Substantial role of charge transfer on the diffusion mechanism of interstitial elements in Î±-titanium: A First-principles study. Scripta Materialia, 2021, 203, 114065.	2.6	12
59684	Modifying Î³-MnO2 to enhance the electrochemical performance of lithium-sulfur batteries. Chemical Engineering Journal, 2021, 421, 129782.	6.6	19
59685	Effect of Al doping on the early-stage oxidation of Ni-Al alloys: A ReaxFF molecular dynamics study. Applied Surface Science, 2021, 563, 150097.	3.1	8
59686	Direct energy minimization based on exponential transformation in density functional calculations of finite and extended systems. Computer Physics Communications, 2021, 267, 108047.	3.0	7
59687	MXenes modified by single transition metal atom for hydrogen evolution reaction catalysts. Applied Surface Science, 2021, 562, 150151.	3.1	25
59688	The tuning on the magnetism and the electronic structures of monolayer Ti2N MXene by electric field. Physica B: Condensed Matter, 2021, 618, 413183.	1.3	8
59689	Catalytic activity of V2CO2 MXene supported transition metal single atoms for oxygen reduction and hydrogen oxidation reactions: A density functional theory calculation study. Chinese Journal of Catalysis, 2021, 42, 1659-1666.	6.9	21
59690	Unraveling the catalytically active phase of carbon dioxide hydrogenation to methanol on Zn/Cu alloy: Single atom versus small cluster. Journal of Energy Chemistry, 2021, 61, 582-593.	7.1	9
59691	Photosensitive antimony triiodide thin films by rapid iodization of chemically deposited antimony sulfide. Materials Research Bulletin, 2021, 142, 111382.	2.7	7
59692	Effective active sites of triangular Mo-S Nano-catalysts from first-principle calculations. Surfaces and Interfaces, 2021, 26, 101373.	1.5	1
59693	Novel two-dimensional <mml:math xmlns:mml="http://www.w3.org/1998/Math/MathML" altimg="si1.svg"><mml:mrow><mml:mtext>C</mml:mtext><mml:mtext>r</mml:mtext><mml:mtext>X</mml:mtext><mml:msub><mml (X=Cr, Ru) metal for high NÃ©el temperature antiferromagnetic spintronics. Journal of Solid State Chemistry, 2021, 302, 122427.	1.4	3
59694	Influence of the Fe-doping on hydrogen behavior on the ZrCo surface. International Journal of Hydrogen Energy, 2021, 46, 33877-33888.	3.8	10
59695	Bi doping stimulation on the visible-light absorption of In2O3 ceramics. Journal of Alloys and Compounds, 2021, 878, 160339.	2.8	5
59696	Local structure elucidation and properties prediction on KClâ€“CaCl2 molten salt: A deep potential molecular dynamics study. Solar Energy Materials and Solar Cells, 2021, 232, 111346.	3.0	26
59697	Enhancing the hydrogen evolution reaction by non-precious transition metal (Non-metal) atom doping in defective MoSi2N4 monolayer. Applied Surface Science, 2021, 563, 150388.	3.1	49
59698	TiO2/Carbon allotrope nanohybrids for supercapacitor application with theoretical insights from density functional theory. Applied Surface Science, 2021, 563, 150259.	3.1	14
59699	Electron reservoir enhances methane conversion on Zn dimer supported by N doped graphene: A DFT study. Applied Surface Science, 2021, 563, 150328.	3.1	4

#	Article	IF	Citations
59700	The new valence state [Ga]â^'5 in Li-Ga-Te system under high pressure. Solid State Communications, 2021, 336, 114402.	0.9	0
59701	Electronic properties of SrFCl and SrFBr monolayers using density functional theory and GW approximation. Solid State Communications, 2021, 336, 114430.	0.9	3
59702	Theoretical investigations for MFe2 (M = Y, La) Laves alloy and hydrides HxMFe2: Structural stability, lattice thermodynamics, and elastic properties. Solid State Communications, 2021, 337, 114452.	0.9	3
59703	ns2-containing vacancy-ordered double perovskites for optoelectronic applications: A first-principles investigation. Solid State Communications, 2021, 337, 114462.	0.9	1
59704	Interaction between hydrogen and solute atoms in bcc iron. Computational Materials Science, 2021, 198, 110652.	1.4	5
59705	Prediction of the diffusion characteristics of the V-Cr system by molecular dynamics based on N-body interatomic potentials. Computational Materials Science, 2021, 198, 110648.	1.4	5
59706	Vacancy effect on the structure and diffusion of a Li adatom on the 2D Janus MoSSe monolayer. Computational Materials Science, 2021, 198, 110687.	1.4	2
59707	Theoretical study on the electronic structure, optical and photocatalytic properties of type-II As/CdO van der Waals heterostructure. Physica E: Low-Dimensional Systems and Nanostructures, 2021, 134, 114888.	1.3	11
59708	Two-dimensional g-C3N4/Ti2CO2 heterostructure as a direct Z-scheme photocatalyst for water splitting: A hybrid density functional theory investigation. Physica E: Low-Dimensional Systems and Nanostructures, 2021, 134, 114872.	1.3	5
59709	Exploring the structural and electronic properties of GeC/BP van der Waals heterostructures. Physica E: Low-Dimensional Systems and Nanostructures, 2021, 134, 114804.	1.3	6
59710	The structure, electronic, magnetic and optical properties of the Co-X (X = B, C, N, O or F) codoped single-layer WS2. Physica E: Low-Dimensional Systems and Nanostructures, 2021, 134, 114917.	1.3	4
59711	Electronic, magnetic and magnetotransport properties of Mn-doped Dirac semimetal Cd<mml:math xmlns:mml="http://www.w3.org/1998/Math/MathML" altimg="si3.svg"><mml:msub><mml:mrow /><mml:mn>3</mml:mn></mml:msub></mml:math>As<mml:math xmlns:mml="http://www.w3.org/1998/Math/MathML" altimg="si4.svg"><mml:msub><mml:mrow /><mml:mn>2</mml:mn></mml:msub></mml:math>. Acta Materialia, 2021, 219, 117249.	3.8	8
59712	Theoretical investigation on thermodynamics and stability of anti-perovskite MgCNi3 superconductor. Chemical Physics Letters, 2021, 780, 138961.	1.2	5
59713	Fatigue resistance of atomically thin graphene oxide. Carbon, 2021, 183, 780-788.	5.4	14
59714	Hex-C558: A new porous metallic carbon allotrope for lithium-ion battery anode. Carbon, 2021, 183, 652-659.	5.4	10
59715	Prediction and optimization of the thermal transport in hybrid carbon-boron nitride honeycombs using machine learning. Carbon, 2021, 184, 492-503.	5.4	4
59716	Very high loading oxidized copper supported on ceria to catalyze the water-gas shift reaction. Journal of Catalysis, 2021, 402, 83-93.	3.1	18
59717	Microstructure and catalytic properties of Fe3O4/BN, Fe3O4(Pt)/BN, and FePt/BN heterogeneous nanomaterials in CO2 hydrogenation reaction: Experimental and theoretical insights. Journal of Catalysis, 2021, 402, 130-142.	3.1	21

#	Article	IF	Citations
59718	Ab initio study on electronic structure and magnetic properties of AlN and BP monolayers with Ti doping. Superlattices and Microstructures, 2021, 158, 107010.	1.4	9
59719	Tailoring the selectivity of ultralow-power heterojunction gas sensors by noble metal nanoparticle functionalization. Nano Energy, 2021, 88, 106241.	8.2	21
59720	Using plant extracts to modify Al electrochemical behavior under corroding and functioning conditions in the air battery with alkaline-ethylene glycol electrolyte. Journal of Industrial and Engineering Chemistry, 2021, 102, 327-342.	2.9	14
59721	Performance enhancement of ZnGa2O4 Schottky type deep-ultraviolet photodetectors by oxygen supercritical fluid treatment. Results in Physics, 2021, 29, 104764.	2.0	12
59722	Ultra-hard rhombohedral carbon by crystal chemistry and ab initio investigations. Journal of Solid State Chemistry, 2021, 302, 122354.	1.4	7
59723	Uncovering the origin of enhanced strengthening in Li-added Alâ€“Cuâ€“Mg alloys. Materials Science & Engineering A: Structural Materials: Properties, Microstructure and Processing, 2021, 827, 142079.	2.6	15
59724	Endogenous NO-releasing Carbon Nanodots for Tumor-specific Gas Therapy. Acta Biomaterialia, 2021, 136, 485-494.	4.1	18
59725	VASPKIT: A user-friendly interface facilitating high-throughput computing and analysis using VASP code. Computer Physics Communications, 2021, 267, 108033.	3.0	2,308
59726	Identifying the Critical Surface Descriptors for the Negative Slopes in the Adsorption Energy Scaling Relationships via Density Functional Theory and Compressed Sensing. Journal of Physical Chemistry Letters, 2021, 12, 9791-9799.	2.1	5
59727	Theoretically Predicted CO Adsorption and Dissociation on Ru-doped Co(100) Surfaces. Applied Surface Science, 2021, 572, 151476.	3.1	1
59728	Singlet-to-Triplet Spin Transitions Facilitate Selective 1-Butene Formation during Ethylene Dimerization in Ni(II)-MFU-4l. Journal of Physical Chemistry C, 2021, 125, 22036-22043.	1.5	5
59729	Origin of ferrimagnetism and the effect of octahedral tilting in double-perovskite compound <mml:math xmlns:mml="http://www.w3.org/1998/Math/MathML" altimg="si9.svg"><mml:mrow><mml:msub><mml:mrow><mml:mi mathvariant="italic">Sr</mml:mi></mml:mrow><mml:mrow><mml:mn>2</mml:mn></mml:mrow></mml:msub><mml:msub><mml:m mathvariant="italic">CoRuO</mml:mi></mml:mrow><mml:mrow><mml:mn>6</mml:mn></mml:mrow></mml:msub></mml:mrow><mml:m Journal of Magnetism and Magnetic Materials, 2021, 535, 168035.	1.0	7
59730	The correlation of NO chemisorption adsorption with its directly catalytic dissociation pathway on Î²-MnO2(1 1 0) and (1 0 1) surfaces. Applied Surface Science, 2021, 562, 150032.	3.1	12
59731	Functionalization of monolayer MoS2 with transition metal oxide nanoclusters. Physica B: Condensed Matter, 2021, 619, 413245.	1.3	2
59732	A DFT+U study about agglomeration of Au atoms on reduced surface of rutile TiO2 (110). Materials Chemistry and Physics, 2021, 271, 124944.	2.0	8
59733	<mml:math xmlns:mml="http://www.w3.org/1998/Math/MathML" altimg="si75.svg"><mml:mrow><mml:mo>{</mml:mo><mml:mrow><mml:mn mathvariant="bold">10</mml:mn><mml:mover accent="true"><mml:mn mathvariant="bold">1</mml:mn><mml:mo>Â¯</mml:mo></mml:mover><mml:mn mathvariant="bold">2</mml:mn></mml:mrow><mml:mo>}</mml:mo></mml:mrow></mml:math> Twin	3.8	12
59734	Engineering of anatase/rutile TiO2 heterophase junction via in-situ phase transformation for enhanced photocatalytic hydrogen evolution. Journal of Colloid and Interface Science, 2021, 599, 795-804.	5.0	34
59735	Large magnetic anisotropy in Tetraoxa[8]circulene-based organometallic nanosheet. Journal of Magnetism and Magnetic Materials, 2021, 535, 168068.	1.0	1

#	Article	IF	Citations
59736	First-principles study of interfacial effects toward oxygen reduction reaction of palladium/La1-xSrxCo1-yFeyO3-Î´ cathodes in solid oxide fuel cells. Applied Surface Science, 2021, 562, 150218.	3.1	6
59737	Variational projector-augmented wave method: A full-potential approach for electronic structure calculations in solid-state physics. Journal of Computational Physics, 2021, 442, 110510.	1.9	2
59738	Ni diffusion in ceria lattice: A combined experimental and theoretical study. Acta Materialia, 2021, 219, 117252.	3.8	9
59739	Theoretical study on the heterostructures of MXenes and B-doped graphene as promising anode materials for lithium-ion batteries. Journal of Solid State Chemistry, 2021, 302, 122418.	1.4	3
59740	Anomalous interfacial dynamics of single proton charges in binary aqueous solutions. Science Advances, 2021, 7, eabg8568.	4.7	8
59741	Synergetic utilization of 3D materials merits and unidirectional electrons transfer of Schottky junction for optimizing optical absorption and charge kinetics. Applied Catalysis B: Environmental, 2021, 295, 120278.	10.8	23
59742	Improved thermoelectric performance of Bi-deficient BiCuSeO material doped with Nb, Y, and P. IScience, 2021, 24, 103145.	1.9	4
59743	Vacancy and solute co-segregated Î·1 interface in over-aged Al-Zn-Mg alloys. Acta Materialia, 2021, 218, 117082.	3.8	14
59744	Insight into the mechanism of nanoparticle induced suppression of interfacial tension. Journal of Molecular Liquids, 2021, 339, 117177.	2.3	3
59745	Sulfur-atom-expanded MoS2 nanosheets with enhanced lithium-ion storage. Applied Surface Science, 2021, 563, 150261.	3.1	4
59746	Tailoring the electronic structure by transition-metal single atom on Ti3C2O2 for improving hydrogen evolution activity. Applied Surface Science, 2021, 563, 150210.	3.1	2
59747	Phosphate functionalised titania for heavy metal removal from acidic sulfate solutions. Journal of Colloid and Interface Science, 2021, 600, 719-728.	5.0	13
59748	S vacancy modulated Zn Cd1âˆ’S/CoP quantum dots for efficient H2 evolution from water splitting under visible light. Journal of Energy Chemistry, 2021, 61, 210-218.	7.1	26
59749	First-principles investigation on electronic structure, magnetic states and optical properties of Mn-doped SnS2 monolayer via strain engineering. Physica E: Low-Dimensional Systems and Nanostructures, 2021, 134, 114842.	1.3	10
59750	A comparison study of the structural, electronic, elastic, dielectric and dynamical properties of Zr-based monolayer dioxides (ZrO2) and dichalcogenides (ZrX2; X = S, Se or Te) as well as their Janus structures (ZrXY; X, Y = O, S, Se or Te, <mml:math xmlns:mml="http://www.w3.org/1998/Math/MathML") Tj ETQq0 0 0 rgBT /Overlock 1	1.3	11
59751	Low-Dimensional Systems and Nanostructures, 2021, 134, 114855. The effects of temperature and pressure on the physical properties and stabilities of point defects and defect complexes in B1-ZrC. Computational Materials Science, 2021, 198, 110694.	1.4	6
59752	Electrical contacts in monolayer Ga2O3 field-effect tansistors. Applied Surface Science, 2021, 564, 150386.	3.1	11
59753	Accurate prediction of high-temperature elastic constants of Ti0.5Al0.5N random alloy. Thin Solid Films, 2021, 735, 138872.	0.8	4

#	Article	IF	Citations
59754	Improvement of thermoelectric properties of SnTe by Mn Bi codoping. Chemical Engineering Journal, 2021, 421, 127795.	6.6	20
59755	Vacancy engineering in VS2 nanosheets for ultrafast pseudocapacitive sodium ion storage. Chemical Engineering Journal, 2021, 421, 129715.	6.6	56
59756	Acetic acid conversion to ketene on Cu2O(1 0 0): Reaction mechanism deduced from experimental observations and theoretical computations. Journal of Catalysis, 2021, 402, 154-165.	3.1	3
59757	Separate-free BiPO4/graphene aerogel with 3D network structure for efficient photocatalytic mineralization by adsorption enrichment and photocatalytic degradation. Chemical Engineering Journal, 2021, 421, 129720.	6.6	39
59758	Controlling Diphenyl Ether Hydrogenolysis Selectivity by Tuning the Pt Support and H-Donors under Mild Conditions. ACS Catalysis, 2021, 11, 12661-12672.	5.5	20
59759	InSe based Janus â...¥-â...¢-â...£-â... monolayers as water-splitting photocatalysts: Role of vacuum level difference. International Journal of Hydrogen Energy, 2021, 46, 35271-35279.	3.8	10
59760	A New Sodium Calcium Cyclotetravanadate Framework: â€œZeroâ€•Strainâ€•during Largeâ€•Capacity Lithium Intercalation. Advanced Functional Materials, 2022, 32, 2105026.	7.8	30
59761	Modulation of optical and electrical properties in hexagonal boron nitride by defects induced via oxygen plasma treatment. 2D Materials, 2021, 8, 045041.	2.0	9
59762	Layer effect on thermal expansion in blue phosphorene monolayer and few-layer. Physics Letters, Section A: General, Atomic and Solid State Physics, 2021, 419, 127726.	0.9	2
59763	A record high average ZT over a wide temperature range in a Single-layer Sb2Si2Te6. Applied Surface Science, 2021, 567, 150873.	3.1	3
59764	Layered quaternary chalcogenides KMgCuSe2 and KMgCuTe2 with paramagnetic semiconducting behavior. Journal of Alloys and Compounds, 2021, 883, 160820.	2.8	4
59765	Role of transport polarization in electrocatalysis: A case study of the Ni-cluster/Graphene interface. Journal of Materials Science and Technology, 2021, 92, 120-128.	5.6	9
59766	Archimedean polyhedron LiCoO2 for ultrafast rechargeable Li-ion batteries. Chemical Engineering Journal, 2021, 423, 130122.	6.6	4
59767	Uncovering the synergy between Mn substitution and O vacancy in ZnAl-LDH photocatalyst for efficient toluene removal. Applied Catalysis B: Environmental, 2021, 296, 120376.	10.8	62
59768	Construction of transition metal-decorated boron doped twin-graphene for hydrogen storage: A theoretical prediction. Fuel, 2021, 304, 121351.	3.4	50
59769	Ultrasensitive formaldehyde gas sensor based on Au-loaded ZnO nanorod arrays at low temperature. Sensors and Actuators B: Chemical, 2021, 346, 130568.	4.0	50
59770	In-situ liquid-phase transformation of SnS2/CNTs composite from SnO2/CNTs for high performance lithium-ion battery anode. Applied Surface Science, 2021, 566, 150645.	3.1	22
59771	Three-dimensional hollow nitrogen-doped carbon shells enclosed monodisperse CoP nanoparticles for long cycle-life sodium storage. Electrochimica Acta, 2021, 395, 139112.	2.6	19

#	Article	IF	Citations
59772	Density functional theory based HSE06 calculations to probe the effects of defect on electronic properties of monolayer TMDCs. Computational and Theoretical Chemistry, 2021, 1205, 113445.	1.1	18
59773	Doping the permanent magnet CeFe11Ti with Co and Ni using ab-initio density functional methods. Physica B: Condensed Matter, 2021, 620, 413241.	1.3	3
59774	Synergistic effects in ordered Co oxides for boosting catalytic activity in advanced oxidation processes. Applied Catalysis B: Environmental, 2021, 297, 120463.	10.8	30
59775	The ionic spin-state, magnetic and electronic structures of double perovskite Pb2CoTeO6:An ab initio study. Solid State Communications, 2021, 338, 114474.	0.9	1
59776	Monoclinic AgSbS2 thin films for photovoltaic applications: Computation, growth and characterization approaches. Materials Science in Semiconductor Processing, 2021, 135, 106074.	1.9	7
59777	Ab initio study of local lattice distortion of hexagonal closed-packed high-entropy (Mo0.25Nb0.25Ta0.25V0.25) (Al0.5Si0.5)2 and the influence on thermodynamic property. Journal of Solid State Chemistry, 2021, 303, 122469.	1.4	3
59778	A mediated fuel cell using alkaline proof alizarin as an anode mediator. Journal of Power Sources, 2021, 511, 230456.	4.0	0
59779	Carbon bearing aluminosilicate melt at high pressure. Geochimica Et Cosmochimica Acta, 2021, 312, 106-123.	1.6	8
59780	Experimental and theoretical investigation of reconstruction and active phases on honeycombed Ni3N-Co3N/C in water splitting. Applied Catalysis B: Environmental, 2021, 297, 120461.	10.8	62
59781	Lead-free Cs2SnX6 (XÂ=ÂCl, Br, I) nanocrystals in mesoporous SiO2 with more stable emission from VIS to NIR light. Chemical Physics Letters, 2021, 782, 139023.	1.2	4
59782	Constructing an efficient conductive network with carbon-based additives in metal hydroxide electrode for high-performance hybrid supercapacitor. Electrochimica Acta, 2021, 397, 139242.	2.6	10
59783	Differential clustering of self-interstitials during Si crystal growth. Journal of Crystal Growth, 2021, 574, 126313.	0.7	1
59784	Experimental and first-principle computational exploration on biomass cellulose/magnesium hydroxide composite: Local structure, interfacial interaction and antibacterial property. International Journal of Biological Macromolecules, 2021, 191, 584-590.	3.6	2
59785	Unraveling surface functionalization of Cr2B2T2 (TÂ=ÂOH, O, Cl, H) MBene by first-principles calculations. Computational Materials Science, 2021, 199, 110810.	1.4	14
59786	Emergence of bulk photovoltaic effect in anion-ordered perovskite sulfur diiodide MASbSI2 with spontaneous out-of-plane ferroelectricity. Materials Today Physics, 2021, 21, 100459.	2.9	4
59787	Strain-induced structural phase transition in GeN monolayer. Applied Surface Science, 2021, 567, 150793.	3.1	9
59788	The role of H2O in the removal of methane mercaptan (CH3SH) on Cu/C-PAN catalyst. Applied Surface Science, 2021, 567, 150851.	3.1	6
59789	Stabilization of unstable and metastable InP native oxide thin films by interface effects. Applied Surface Science, 2021, 567, 150848.	3.1	2

#	Article	IF	Citations
59790	Adsorption and dissociation behavior of H2O on PuH2 (1 1 0) surface: A density functional theory study. Applied Surface Science, 2021, 566, 150733.	3.1	6
59791	Intense sulphurization process can lead to superior heterojunction properties in Cu(In,Ga)(S,Se)2 thin-film solar cells. Nano Energy, 2021, 89, 106375.	8.2	5
59792	First-principles calculations to explore the oxygen effects on WS2 film in marine environments. Applied Surface Science, 2021, 566, 150741.	3.1	5
59793	Initial hydration process of calcium silicates in Portland cement: A comprehensive comparison from molecular dynamics simulations. Cement and Concrete Research, 2021, 149, 106576.	4.6	32
59794	Conversion of CO2 to formic acid by integrated all-solar-driven artificial photosynthetic system. Journal of Power Sources, 2021, 512, 230532.	4.0	21
59795	IZrP: Two-dimensional narrow band gap semiconductor with high Stability, anisotropic electronic properties and high carrier mobility. Computational and Theoretical Chemistry, 2021, 1205, 113458.	1.1	2
59796	Facile synthesis of MoS2/Ni2V3O8 nanosheets for pH-universal efficient hydrogen evolution catalysis. Chemical Engineering Journal, 2021, 423, 130196.	6.6	15
59797	Unlocking fast and reversible sodium intercalation in NASICON Na4MnV(PO4)3 by fluorine substitution. Energy Storage Materials, 2021, 42, 307-316.	9.5	59
59798	Harnessing artificial intelligence to holistic design and identification for solid electrolytes. Nano Energy, 2021, 89, 106337.	8.2	16
59799	Formation of polytypes structures in Mg single crystals. Acta Materialia, 2021, 220, 117266.	3.8	2
59800	Electron-rich NiFe layered double hydroxides via interface engineering for boosting electrocatalytic oxygen evolution. Applied Catalysis B: Environmental, 2021, 297, 120453.	10.8	35
59801	Fine structure of energy levels and electron paramagnetic resonance parameters of Ni2+ doped in CsCdCl3. Journal of Magnetism and Magnetic Materials, 2021, 537, 168216.	1.0	0
59802	A Machine Learning Shortcut for Screening the Spinel Structures of Mg/Zn Ion Battery Cathodes with a High Conductivity and Rapid Ion Kinetics. Energy Storage Materials, 2021, 42, 277-285.	9.5	18
59803	MXene-based mixed-dimensional Schottky heterojunction towards self-powered flexible high-performance photodetector. Materials Today Physics, 2021, 21, 100479.	2.9	13
59804	First-principles study of the surface properties of LiAl5O8: Stability and tritiated water formation. Journal of Nuclear Materials, 2021, 555, 153111.	1.3	5
59805	Engineering of the magnetic anisotropy of CoB6 monolayer by biaxial tensile strain. Physics Letters, Section A: General, Atomic and Solid State Physics, 2021, 416, 127672.	0.9	1
59806	Understanding why dislocation loops are visible in transmission electron microscopy: The tungsten case. Journal of Nuclear Materials, 2021, 555, 153122.	1.3	12
59807	Design and modulation of two-dimensional Dirac materials in beryllium/boron-based binary monolayers. Computational Materials Science, 2021, 199, 110727.	1.4	2

#	Article	IF	Citations
59808	Positron annihilation investigation of thermal cycling induced martensitic transformation in NiTi shape memory alloy. Acta Materialia, 2021, 220, 117298.	3.8	6
59809	Selective synthesis of Ni12P5 and Ni2P nanoparticles: Electronic structures, magnetic and optical properties. Materials Science and Engineering B: Solid-State Materials for Advanced Technology, 2021, 273, 115389.	1.7	7
59810	Advanced analysis of laser-driven pulsed magnetic diffusion based on quantum molecular dynamics simulation. Matter and Radiation at Extremes, 2021, 6, 065901.	1.5	1
59811	Influence of Al location on formation of silver clusters in mordenite. Microporous and Mesoporous Materials, 2021, 327, 111401.	2.2	0
59812	Spinel NiFe2O4 nanoparticles decorated 2D Ti3C2 MXene sheets for efficient water splitting: Experiments and theories. Journal of Colloid and Interface Science, 2021, 602, 232-241.	5.0	63
59813	Ab initio investigation of the adsorption of phenolic compounds, CO, and H<mml:math xmlns:mml="http://www.w3.org/1998/Math/MathML" display="inline" id="d1e943" altimg="si45.svg"><mml:msub><mml:mrow /><mml:mrow><mml:mn>2</mml:mn></mml:mrow></mml:msub></mml:math>O over metallic cluster/silica catalysts for hydrodeoxygenation process. Applied Surface Science, 2021, 567, 150790.	3.1	11
59814	Single tungsten atom steered band-gap engineering for graphitic carbon nitride ultrathin nanosheets boosts visible-light photocatalytic H2 evolution. Chemical Engineering Journal, 2021, 424, 130004.	6.6	39
59815	Microstructural and diffusive properties of Cr solute in MgCl2â€“NaClâ€“KCl eutectic: A First-Principles molecular dynamics study. Journal of Molecular Liquids, 2021, 341, 117321.	2.3	3
59816	The AFLOW Library of Crystallographic Prototypes: Part 3. Computational Materials Science, 2021, 199, 110450.	1.4	16
59817	Electrospun IrP2-carbon nanofibers for hydrogen evolution reaction in alkaline medium. Applied Surface Science, 2021, 565, 150461.	3.1	12
59818	Prediction of half-metallicity and spin-gapless semiconducting behavior in the new series of FeCr-based quaternary Heusler alloys: An Ab initio study. Journal of Alloys and Compounds, 2021, 882, 160500.	2.8	11
59819	The spintronic and optoelectronic applications of substitutional doped CoS2. Materials Chemistry and Physics, 2021, 272, 125052.	2.0	1
59820	Tetragonal distortion induced perpendicular magnetic anisotropy in (Fe0.5Ni0.5) Rh1â^' alloy thin films. Journal of Magnetism and Magnetic Materials, 2021, 538, 168256.	1.0	0
59821	Lithium-metal polysulfide batteries with free-standing MoSxCy thin-film cathodes. Journal of Power Sources, 2021, 511, 230445.	4.0	4
59822	The modulating effect of N coordination on single-atom catalysts researched by Pt-N -C model through both experimental study and DFT simulation. Journal of Materials Science and Technology, 2021, 91, 160-167.	5.6	27
59823	Dual-salt-additive electrolyte enables high-voltage lithium metal full batteries capable of fast-charging ability. Nano Energy, 2021, 89, 106353.	8.2	90
59824	Structural and magnetic properties of SmCo5â^'XNiX intermetallic compounds. Journal of Alloys and Compounds, 2021, 882, 160699.	2.8	6
59825	Mechanisms of bentonite colloid aggregation, retention, and release in saturated porous media: Role of counter ions and humic acid. Science of the Total Environment, 2021, 793, 148545.	3.9	26

#	Article	IF	Citations
59826	Lattice strain and atomic replacement of CoO6 octahedra in layered sodium cobalt oxide for boosted water oxidation electrocatalysis. Applied Catalysis B: Environmental, 2021, 297, 120477.	10.8	30
59827	Tunable electronic structure and magnetic anisotropy of two dimensional Mn2CFCl/MoSSe van der Waals heterostructures by electric field and biaxial strain. Applied Surface Science, 2021, 566, 150683.	3.1	14
59828	First-principles prediction of NO2 and SO2 adsorption on MgO/(Mg0.5Ni0.5)O/MgO(1 0 0). Applied Surface Science, 2021, 566, 150650.	3.1	7
59829	Boosting selective hydrogenation through hydrogen spillover on supported-metal catalysts at room temperature. Applied Catalysis B: Environmental, 2021, 297, 120418.	10.8	50
59830	Achieving exceptional activity and durability toward oxygen reduction based on a cobalt-free perovskite for solid oxide fuel cells. Journal of Energy Chemistry, 2021, 62, 653-659.	7.1	19
59831	Diffusional behaviors and mechanical properties of Ni-Zn system. Journal of Alloys and Compounds, 2021, 881, 160581.	2.8	14
59832	Electron work function as an indicator for tuning the bulk modulus of MC carbide by metal-substitution: A first-principles computational study. Scripta Materialia, 2021, 204, 114148.	2.6	9
59833	B doped Bi2O2CO3 hierarchical microspheres: Enhanced photocatalytic performance and reaction mechanism for NO removal. Catalysis Today, 2021, 380, 230-236.	2.2	14
59834	An efficient and durable trifunctional electrocatalyst for zincâ€“air batteries driven overall water splitting. Applied Catalysis B: Environmental, 2021, 297, 120405.	10.8	127
59835	Interactions of noxious molecules on a single gold atom decorated an ultra-small carbon nanotube: A density functional theory study. Sensors and Actuators A: Physical, 2021, 331, 113024.	2.0	8
59836	Visible-light-driven water splitting by yolk-shelled ZnIn2S4-based heterostructure without noble-metal co-catalyst and sacrificial agent. Applied Catalysis B: Environmental, 2021, 297, 120391.	10.8	58
59837	Flexoelectric-boosted piezoelectricity of BaTiO3@SrTiO3 core-shell nanostructure determined by multiscale simulations for flexible energy harvesters. Nano Energy, 2021, 89, 106469.	8.2	23
59838	Adsorption and spin polarization of pyridine on Fe/W(1 1 0) interface: A DFT study. Computational Materials Science, 2021, 199, 110734.	1.4	3
59839	Cold and hot uranium in DFT calculations: Investigation by the GTH pseudopotential, PAW, and APWÂ+Âlo methods. Computational Materials Science, 2021, 199, 110665.	1.4	3
59840	Electronic, mechanical and optical properties of BC2P/WSe2 van der Waals heterostructures. Solid State Communications, 2021, 339, 114506.	0.9	3
59841	Modulating CoFe2O4 nanocube with oxygen vacancy and carbon wrapper towards enhanced electrocatalytic nitrogen reduction to ammonia. Applied Catalysis B: Environmental, 2021, 297, 120452.	10.8	42
59842	Cobalt tetraphosphate as an efficient bifunctional electrocatalyst for hybrid sodium-air batteries. Nano Energy, 2021, 89, 106485.	8.2	11
59843	The studies of electronic structure, mechanical properties and ideal fracture behavior of U3Si1.75Al0.25: first-principle investigations. Journal of Materials Research and Technology, 2021, 15, 1356-1369.	2.6	4

#	Article	IF	Citations
59844	Unravelling the origin of in-cage vibrations in a La50Al15Ni35 metallic glass. Materials Today Physics, 2021, 21, 100515.	2.9	4
59845	Orientation independent heat transport characteristics of diamond/copper interface with ion beam bombardment. Acta Materialia, 2021, 220, 117283.	3.8	8
59846	Half-metallicity and Curie temperature enhancement of CrI3 through boron atoms adsorption. Superlattices and Microstructures, 2021, 159, 107054.	1.4	7
59847	Electronic, magnetic and optical properties of various surfaces of TiHfIrZ (ZÂ=ÂAl and Ga) quaternary Heusler alloy. Thin Solid Films, 2021, 737, 138952.	0.8	1
59848	Effect of the projector augmented wave potentials on the simulation of thermodynamic properties of vanadium. Matter and Radiation at Extremes, 2021, 6, .	1.5	2
59849	Manipulating selenium molecular configuration in N/O dual-doped porous carbon for high performance potassium-ion storage. Journal of Energy Chemistry, 2021, 62, 581-589.	7.1	19
59850	Electronic, mechanical and thermodynamic properties of ZrC, HfC and their solid solutions studied by first-principles calculation. Solid State Communications, 2021, 338, 114481.	0.9	9
59851	The formation mechanisms of amorphous bands of boron carbide nanopillars under uniaxial compressions and their effects on mechanical properties from molecular dynamics simulation. Computational Materials Science, 2021, 199, 110708.	1.4	4
59852	Vacancy-cluster and off-lattice metal-atom diffusion mechanisms in transition metal carbides. Computational Materials Science, 2021, 199, 110713.	1.4	3
59853	Interactions and electronic properties of adatom/Gra/adatom sandwich complexes. Materials Chemistry and Physics, 2021, 272, 125013.	2.0	0
59854	Magnetism and topological Hall effect in antiferromagnetic Ru2MnSn-based Heusler compounds. Journal of Magnetism and Magnetic Materials, 2021, 537, 168104.	1.0	5
59855	Electronic and magnetic properties of metalâ€“organic polymers with 4d and 5d-transition metal ions. Journal of Magnetism and Magnetic Materials, 2021, 537, 168183.	1.0	6
59856	Dual-doped carbon hollow nanospheres achieve boosted pseudocapacitive energy storage for aqueous zinc ion hybrid capacitors. Energy Storage Materials, 2021, 42, 705-714.	9.5	96
59857	A first-principles study of thiadiazole and dimercapto-thiadiazole adsorption on copper and silver surfaces. Materials Chemistry and Physics, 2021, 273, 125057.	2.0	6
59858	Bridging the gap between simulated and experimental ionic conductivities in lithium superionic conductors. Materials Today Physics, 2021, 21, 100463.	2.9	43
59859	Effect and Mechanism of Hydrogen-Assisted Sulfur Intercalation for Decoupling Graphene from Cu(1 1) Tj ETQq1 1 0.784314 rgBT /O	3.1	2
59860	Dual active site tandem catalysis of metal hydroxyl oxides and single atoms for boosting oxygen evolution reaction. Applied Catalysis B: Environmental, 2021, 297, 120451.	10.8	44
59861	Cadmium copper selenite chloride, CdCu2(SeO3)2Cl2, an insulating spin gap system. Journal of Solid State Chemistry, 2021, 303, 122518.	1.4	0

#	Article	IF	Citations
59862	Thermodynamic functions and vibrational properties of Li intercalation in TiO2(B). Applied Surface Science, 2021, 566, 150679.	3.1	5
59863	Symmetrical dehalogenation of 2, 7-dibromopyrene on Cu(1 1 1) with tunable intermediates and reaction paths. Applied Surface Science, 2021, 566, 150663.	3.1	3
59864	Theoretical insights on the exsolved behavior of ruthenium atom in titanate perovskite. Applied Surface Science, 2021, 566, 150641.	3.1	5
59865	Effects of transition metal doping on surface properties and resistance to Clâ^' adsorption of Î±-Al2O3. Surface Science, 2021, 713, 121909.	0.8	6
59866	DFT investigation of mechanical and vibrational properties of CuTe. Physica B: Condensed Matter, 2021, 620, 413214.	1.3	2
59867	High-throughput approach for estimation of intrinsic barriers in FCC structures for alloy design. Scripta Materialia, 2021, 204, 114126.	2.6	6
59868	Interfacial polymerized copolymers of aniline and phenylenediamine with tunable magnetoresistance and negative permittivity. Materials Today Physics, 2021, 21, 100502.	2.9	34
59869	Trifle Pt coupled with NiFe hydroxide synthesized via corrosion engineering to boost the cleavage of water molecule for alkaline water-splitting. Applied Catalysis B: Environmental, 2021, 297, 120395.	10.8	109
59870	Functional group tuning of two-dimensional carbon nanosheets for boosting oxygen reduction electrocatalysis. Carbon, 2021, 185, 395-403.	5.4	10
59871	A systematic analysis of phase stability in refractory high entropy alloys utilizing linear and non-linear cluster expansion models. Acta Materialia, 2021, 220, 117269.	3.8	10
59872	Point defects in VS2 monolayer towards NH3 synthesis. Materials and Design, 2021, 209, 110006.	3.3	5
59873	Micro-alloying effects of Co on structural and dynamic properties of CeAlCu glass-forming melts by ab initio molecular dynamics simulations. Journal of Non-Crystalline Solids, 2021, 572, 121109.	1.5	2
59874	Bridging the miscibility gap towards higher thermoelectric performance of PbS. Acta Materialia, 2021, 220, 117337.	3.8	17
59875	Combined density functional theory/kinetic Monte Carlo investigation of surface morphology during cycling of Li-Cu electrodes. Electrochimica Acta, 2021, 397, 139272.	2.6	3
59876	Intensified solar thermochemical CO2 splitting over iron-based redox materials via perovskite-mediated dealloying-exsolution cycles. Chinese Journal of Catalysis, 2021, 42, 2049-2058.	6.9	13
59877	The impact of atomic defects on high-temperature stability and electron transport properties in Sr2Mg1â^'xNixMoO6â€“Î´ solid solutions. Journal of Alloys and Compounds, 2021, 883, 160821.	2.8	2
59878	Enhanced singlet oxygen production over a photocatalytic stable metal organic framework composed of porphyrin and Ag. Journal of Colloid and Interface Science, 2021, 602, 300-306.	5.0	15
59879	Adsorption mechanism of CO2 on the single atom doped or promoted Li4SiO4(0 1 0) surface from first principles. Computational and Theoretical Chemistry, 2021, 1205, 113424.	1.1	7

#	Article	IF	Citations
59880	A binder-free lithium-sulfur battery cathode using three-dimensional porous g-C3N4 nanoflakes as sulfur host displaying high binding energies with lithium polysulfides. Journal of Alloys and Compounds, 2021, 881, 160629.	2.8	12
59881	Ultrafast-kinetics, ultralong-cycle-life, bifunctional inorganic open-framework for potassium-ion batteries. Energy Storage Materials, 2021, 42, 806-814.	9.5	7
59882	Formation of noble-metal-free 2D/2D ZnmIn2Sm+3 (mÂ=Â1, 2, 3)/MXene Schottky heterojunction as an efficient photocatalyst for hydrogen evolution. Chemical Engineering Journal, 2021, 424, 130170.	6.6	28
59883	Improved structural stability and adsorption capacity of adsorbent material Li1.6Mn1.6O4 via facile surface fluorination. Colloids and Surfaces A: Physicochemical and Engineering Aspects, 2021, 629, 127465.	2.3	16
59884	Intrinsic point defects and charge carrier trapping in monolayer BiOX (X = I, Br, and Cl). Ceramics International, 2021, 47, 30523-30530.	2.3	5
59885	Insights into the oxidation mechanism of millerite exposed to O2 and H2O using DFT study. Computational and Theoretical Chemistry, 2021, 1205, 113435.	1.1	1
59886	Two-dimensional ferromagnetic semiconductors of rare-earth monolayer GdX2 (XÂ= Cl, Br, I) with large perpendicular magnetic anisotropy and high Curie temperature. Materials Today Physics, 2021, 21, 100514.	2.9	32
59887	In-situ exsolution of Ni nanoparticles to achieve an active and stable solid oxide fuel cell anode catalyst on A-site deficient La0.4Sr0.4Ti0.94Ni0.06O3-Î´. Journal of Industrial and Engineering Chemistry, 2021, 103, 264-274.	2.9	17
59888	Vacancy-mediated electronic localization and phase transition in cubic Sb2Te3. Materials Science in Semiconductor Processing, 2021, 135, 106052.	1.9	8
59889	Density functional theory study on the role of ternary alloying elements in TiFe-based hydrogen storage alloys. Journal of Materials Science and Technology, 2021, 92, 148-158.	5.6	25
59890	Gas (CO and NO) adsorption and sensing based on transition metals functionalized Janus MoSSe. Applied Surface Science, 2021, 565, 150509.	3.1	13
59891	Effects of intrinsic defects and doping on SrFe12O19: A first-principles exploration of the structural, electronic and magnetic properties. Journal of Magnetism and Magnetic Materials, 2021, 538, 168257.	1.0	14
59892	Surface atomic modulation of CoP bifunctional catalyst for high performance Li-O2 battery enabled by high-index (2 1 1) facets. Journal of Colloid and Interface Science, 2021, 601, 114-123.	5.0	12
59893	Confining invasion directions of Li+ to achieve efficient Si anode material for lithium-ion batteries. Energy Storage Materials, 2021, 42, 231-239.	9.5	41
59894	Pressure-induced two magnetic collapses in the ferromagnetic L12-Fe3Pd alloy and related elasticity and lattice dynamics anomalies. Journal of Magnetism and Magnetic Materials, 2021, 538, 168322.	1.0	4
59895	Environmental impact of amino acids on selenate-bearing hydrocalumite: Experimental and DFT studies. Environmental Pollution, 2021, 288, 117687.	3.7	4
59896	Atomic-scale investigation of electronic properties and Na storage performance of Ti3C2Tx-MXene bilayers with various terminations. Applied Surface Science, 2021, 567, 150735.	3.1	6
59897	Stacking induced nonvolatile tuning of band gap in bilayer <mml:math xmlns:mml="http://www.w3.org/1998/Math/MathML" display="inline" id="d1e210" altimg="si8.svg"><mml:mrow><mml:mi>I</mml:mi><mml:msub><mml:mrow><mml:mi>n</mml:mi></mml:mrow><mml:mrow><mm Applied Surface Science, 2021, 567, 150871.	3.1	3

#	Article	IF	Citations
59898	Tellurium vacancy in two-dimensional Si2Te3 for resistive random-access memory. Journal of Solid State Chemistry, 2021, 303, 122448.	1.4	2
59899	First-principles study on electronic structure, optical properties and doping-induced half metallicity in double perovskite Bi2CuCrO6. Journal of Solid State Chemistry, 2021, 303, 122521.	1.4	4
59900	Variation of structural disorder in Zr substituted Y2Sn2O7: Its impact on photocatalysis. Journal of Solid State Chemistry, 2021, 303, 122472.	1.4	4
59901	Experimental and theoretical investigation of the mechanical characteristics of sillenite compound: Bi12GeO20. Journal of Alloys and Compounds, 2021, 882, 160686.	2.8	4
59902	Equiatomic quaternary Heusler compounds TiVFeZ (Z=Al, Si, Ge): Half-metallic ferromagnetic materials. Journal of Alloys and Compounds, 2021, 883, 160869.	2.8	27
59903	A strongly interactive adatom/substrate interface for dendrite-free and high-rate Li metal anodes. Journal of Energy Chemistry, 2021, 62, 179-190.	7.1	22
59904	Two-dimensional SiMI4(MÂ=ÂGe, Sn) monolayers as visible-light-driven photocatalyst of hydrogen production. Spectrochimica Acta - Part A: Molecular and Biomolecular Spectroscopy, 2021, 261, 120013.	2.0	8
59905	Designing artificial carbon clusters using Ge2Sb2Te5/C superlattice-like structure for phase change applications. Journal of Alloys and Compounds, 2021, 882, 160695.	2.8	13
59906	A novel hard superconductor obtained in di-molybdenum carbide (Mo2C) with Moâ€“C octahedral structure. Journal of Alloys and Compounds, 2021, 881, 160631.	2.8	8
59907	First-principles-based high-throughput computation for high entropy alloys with short range order. Journal of Alloys and Compounds, 2021, 882, 160776.	2.8	17
59908	Anomalous temperature and symmetry-dependent electronic excitations in GdB6. Journal of Alloys and Compounds, 2021, 881, 160507.	2.8	0
59909	Magnetocrystalline anisotropy regulations in bulk L10-MnGa alloys by tailoring the tetragonal lattice parameter c: Selectively alloying Al and C atoms. Journal of Alloys and Compounds, 2021, 881, 160646.	2.8	2
59910	C-doped ZnS-ZnO/Rh nanosheets as multijunctioned photocatalysts for effective H2 generation from pure water under solar simulating light. Applied Catalysis B: Environmental, 2021, 297, 120473.	10.8	45
59911	A novel rare-earth luminescent coordination polymer showing potential semiconductor characteristic constructed by anthracene-based dicarboxylic acid ligand (H2L). Journal of Molecular Structure, 2021, 1243, 130788.	1.8	5
59912	Resistive switching characteristics of epitaxial NiO thin films affected by lattice strains and external forces. Applied Surface Science, 2021, 566, 150685.	3.1	5
59913	Coupled Sn/Mo2C nanoparticles wrapped in carbon nanofibers by electrospinning as high-performance electrocatalyst for hydrogen evolution reaction. Applied Surface Science, 2021, 566, 150754.	3.1	22
59914	Addressing electrocatalytic activity and stability of LnBaCo2O5+ perovskites for hydrogen evolution reaction by structural and electronic features. Applied Catalysis B: Environmental, 2021, 297, 120403.	10.8	30
59915	Identifying active sites of boron, nitrogen co-doped carbon materials for the oxygen reduction reaction to hydrogen peroxide. Journal of Colloid and Interface Science, 2021, 602, 799-809.	5.0	32

#	Article	IF	Citations
59916	Short-range ordering governs brittleness and ductility in W-Ta solid solution: Insights from Pugh's shear-to-bulk modulus ratio. Scripta Materialia, 2021, 204, 114136.	2.6	21
59917	Piezotronic-enhanced photocatalytic performance of heterostructured BaTiO3/SrTiO3 nanofibers. Nano Energy, 2021, 89, 106391.	8.2	70
59918	First-principles calculations of precursor adsorption on substrate during atomic layer deposition: The example of SiO2 deposition using tris(dimethylamino)silane. Current Applied Physics, 2021, 31, 228-231.	1.1	1
59919	Multi-objective optimization of alkali/alkaline earth metals doped graphyne for ultrahigh-performance CO2 capture and separation over N2/CH4. Materials Today Physics, 2021, 21, 100539.	2.9	4
59920	Janus WSSe monolayer adsorbed with transition-metal atoms (Fe, Co and Ni): excellent performance for gas sensing and CO catalytic oxidation. Applied Surface Science, 2021, 565, 150558.	3.1	17
59921	First-Principle study of lithium polysulfide adsorption on heteroatom doped graphitic carbon nitride for Lithium-Sulfur batteries. Applied Surface Science, 2021, 565, 150378.	3.1	24
59922	Transition metal single-atom anchored g-CN monolayer for constructing high-activity multifunctional electrocatalyst. Applied Surface Science, 2021, 565, 150547.	3.1	28
59923	Atomic layer deposited boron nitride nanoscale films act as high temperature hydrogen barriers. Applied Surface Science, 2021, 565, 150428.	3.1	9
59924	Effects of atom-to-defect ratio on the thermostability of dispersed Au atoms on reduced TiO2(1 0 1) surface. Applied Surface Science, 2021, 565, 150519.	3.1	2
59925	Insight into the overpotential and thermodynamic mechanism of hydroxyl radical formation on diamond anode. Applied Surface Science, 2021, 565, 150559.	3.1	14
59926	Multi-level phase-change memory with ultralow power consumption and resistance drift. Science Bulletin, 2021, 66, 2217-2224.	4.3	41
59927	Triggering in-plane defect cluster on MoS2 for accelerated dinitrogen electroreduction to ammonia. Journal of Energy Chemistry, 2021, 62, 359-366.	7.1	40
59928	Anomalous Hall and Nernst Conductivities in Co2NbGa: A first principles study. Journal of Magnetism and Magnetic Materials, 2021, 538, 168303.	1.0	6
59929	Structure, magnetism, electronic properties and high magnetic-field-induced stability of alloy carbide M7C3. Journal of Magnetism and Magnetic Materials, 2021, 538, 168263.	1.0	9
59930	Boosting oxygen evolution reaction by enhanced intrinsic activity in Ruddlesdenâ^'Popper iridate oxides. Chemical Engineering Journal, 2021, 423, 130185.	6.6	13
59931	Atomically dispersed Ni on Mo2C embedded in N, P co-doped carbon derived from polyoxometalate supramolecule for high-efficiency hydrogen evolution electrocatalysis. Applied Catalysis B: Environmental, 2021, 296, 120336.	10.8	58
59932	Recording the Pt-beyond hydrogen production electrocatalysis by dirhodium phosphide with an overpotential of only 4.3â€¯mV in alkaline electrolyte. Applied Catalysis B: Environmental, 2021, 297, 120457.	10.8	15
59933	Regulation of Nb3+, Sb3+ and V3+ doping on the photo-induced ferroelectricity of KTaO3. Physica B: Condensed Matter, 2021, 620, 413248.	1.3	1

#	Article	IF	Citations
59934	Various metal (Fe, Mo, V, Co)-doped Ni2P nanowire arrays as overall water splitting electrocatalysts and their applications in unassisted solar hydrogen production with STH 14 %. Applied Catalysis B: Environmental, 2021, 297, 120434.	10.8	82
59935	InterPhon: Ab initio interface phonon calculations within a 3D electronic structure framework. Computer Physics Communications, 2021, 268, 108089.	3.0	0
59936	Internal and external electric field tunable electronic structures for photocatalytic water splitting: Janus transition-metal chalcogenides/C3N4 van der Waals heterojunctions. Applied Surface Science, 2021, 566, 150639.	3.1	12
59937	Reduced interstitial mobility through multicomponent alloying in bcc W. Fusion Engineering and Design, 2021, 172, 112745.	1.0	0
59938	Pt/CeO2 with residual chloride as reusable soft Lewis acid catalysts: Application to highly efficient isomerization of allylic esters. Applied Catalysis B: Environmental, 2021, 296, 120333.	10.8	11
59939	Phonon thermal transport properties of GaN with symmetry-breaking and lattice deformation induced by the electric field. International Journal of Heat and Mass Transfer, 2021, 179, 121659.	2.5	11
59940	Behavior of copper under high pressure: Experimental and theoretical analyses. Current Applied Physics, 2021, 31, 93-98.	1.1	4
59941	Bct-C5: A new body-centered tetragonal carbon allotrope. Diamond and Related Materials, 2021, 119, 108571.	1.8	6
59942	Local structure and luminescent properties of Cs2KGaF6:Mn4+ phosphor for backlight white LEDs. Journal of Alloys and Compounds, 2021, 881, 160624.	2.8	20
59943	Modeling the half-metallicity of the CrN/GaN (1Â1Â1) heterostructure. Applied Surface Science, 2021, 566, 150637.	3.1	4
59944	Unveiling the origins of low lattice thermal conductivity in 122-phase Zintl compounds. Materials Today Physics, 2021, 21, 100480.	2.9	20
59945	Effects of aluminum content on thermoelectric performance of Al CoCrFeNi high-entropy alloys. Journal of Alloys and Compounds, 2021, 883, 160811.	2.8	12
59946	Interfacial charge redistribution in interconnected network of Ni2Pâ€“Co2P boosting electrocatalytic hydrogen evolution in both acidic and alkaline conditions. Chemical Engineering Journal, 2021, 424, 130444.	6.6	76
59947	Fe, N co-doped amorphous carbon as efficient electrode materials for fast and stable Na/K-storage. Electrochimica Acta, 2021, 396, 139265.	2.6	11
59948	Effect of electron localization in theoretical design of Ni-Mn-Ga based magnetic shape memory alloys. Materials and Design, 2021, 209, 109917.	3.3	12
59949	Enhancing plasticity in high-entropy refractory ceramics via tailoring valence electron concentration. Materials and Design, 2021, 209, 109932.	3.3	32
59950	2D ternary nitrides XNY (X=Ti, Zr, Hf; Y F, Cl, Br) with applications as photoelectric and photocatalytic materials featuring mechanical and optical anisotropy: A DFT study. Journal of Solid State Chemistry, 2021, 303, 122517.	1.4	12
59951	V2C MXene synergistically coupling FeNi LDH nanosheets for boosting oxygen evolution reaction. Applied Catalysis B: Environmental, 2021, 297, 120474.	10.8	106

#	Article	IF	Citations
59952	2,5-Bis(hydroxymethyl)furan: A new alternative to HMF for simultaneously electrocatalytic production of FDCA and H2 over CoOOH/Ni electrodes. Applied Catalysis B: Environmental, 2021, 297, 120396.	10.8	56
59953	Organic nanocrystals induced surface passivation towards high-efficiency and stable perovskite solar cells. Nano Energy, 2021, 89, 106445.	8.2	19
59954	Low-temperature growth of crystalline Tin(II) monosulfide thin films by atomic layer deposition using a liquid divalent tin precursor. Applied Surface Science, 2021, 565, 150152.	3.1	11
59955	Density functional theoryâ€"based design of a Pt-skinned PtNi catalyst for the oxygen reduction reaction in fuel cells. Applied Surface Science, 2021, 565, 150518.	3.1	13
59956	Exploring tensile piezoelectricity and bending flexoelectricity of diamane monolayers by machine learning. Carbon, 2021, 185, 558-567.	5.4	13
59957	Remove of triclosan from aqueous solutions by nanoflower MnO2: Insight into the mechanism of oxidation and adsorption. Chemical Engineering Journal, 2021, 426, 131319.	6.6	25
59958	Tuning optical and electrical properties of TixSn1â^'xO2 alloy thin films with dipole-forbidden transition via band gap and defect engineering. Journal of Alloys and Compounds, 2021, 885, 160974.	2.8	5
59959	Large enhancement of magnetic moment in nitridated CeFe12. Journal of Alloys and Compounds, 2021, 886, 161245.	2.8	1
59960	Ab-initio study of the electronic structure and magnetic properties of Ce2Fe17. Journal of Alloys and Compounds, 2021, 888, 161521.	2.8	6
59961	Selective adsorption of glucose towards itaconic acid on amorphous silica surfaces: Insights from density functional theory calculations. Journal of Molecular Liquids, 2021, 343, 117586.	2.3	5
59962	Realization of all-in-one hydrogen-evolving photocatalysts via selective atomic substitution. Applied Catalysis B: Environmental, 2021, 298, 120518.	10.8	49
59963	A tight-binding atomistic approach for point defects and surfaces applied to the o-Al13Co4Âquasicrystalline approximant. Computational Materials Science, 2021, 200, 110826.	1.4	0
59964	Prediction of two-dimensional M2As (MÂ=ÂMn, Fe) with high Curie temperature and large perpendicular magnetic anisotropy. Computational Materials Science, 2021, 200, 110838.	1.4	5
59965	Ab initio thermochemistry study of polymorphism in the Si2N2(NH) analog of Si2N2O. Computational Materials Science, 2021, 200, 110772.	1.4	1
59966	Theoretical study on thermal properties of molybdenum disulfide/silicon heterostructures. Computational Materials Science, 2021, 200, 110835.	1.4	2
59967	Interfacing 2D VS2 with Janus MoSSe: Antiferromagnetic electric polarization and charge transfer driven Half-metallicity. Applied Surface Science, 2021, 570, 151129.	3.1	4
59968	Ultra-deep removal of Pb by functionality tuned UiO-66 framework: A combined experimental, theoretical and HSAB approach. Chemosphere, 2021, 284, 131305.	4.2	29
59969	Hydrogen embrittlement of bulk W-0.5 wt% ZrC alloy induced by annealing in hydrogen atmosphere. Journal of Nuclear Materials, 2021, 556, 153177.	1.3	4

#	Article	IF	Citations
59970	Machine learning enhanced empirical potentials for metals and alloys. Computer Physics Communications, 2021, 269, 108132.	3.0	3
59971	Structural and electronic properties of nitrogen-terminated diamond (100) surfaces. Diamond and Related Materials, 2021, 120, 108601.	1.8	6
59972	Development of a machine learning potential for the study of crack propagation in titanium. International Journal of Pressure Vessels and Piping, 2021, 194, 104514.	1.2	4
59973	The effect of surface carbon on ethylene dimerization. Applied Surface Science, 2021, 570, 151210.	3.1	4
59974	Electronic structure and stability of the (0 0 1) surface of halide double perovskite Cs2AgBiBr6. Applied Surface Science, 2021, 570, 151223.	3.1	1
59975	Rational design of ionic V-MOF with confined Mo species for highly efficient oxidative desulfurization. Applied Catalysis B: Environmental, 2021, 298, 120594.	10.8	40
59976	Tungsten induced defects control on BiVO4 photoanodes for enhanced solar water splitting performance and photocorrosion resistance. Applied Catalysis B: Environmental, 2021, 298, 120610.	10.8	32
59977	Nitrogen-doped graphdiyne for efficient electrocatalytic <mml:math xmlns:mml="http://www.w3.org/1998/Math/MathML" display="inline" id="d1e292" altimg="si39.svg"><mml:msub><mml:mrow><mml:mi mathvariant="normal">N</mml:mi></mml:mrow><mml:mrow><mml:mn>2</mml:mn></mml:mrow></mml:msub></mml:math> reduction: A first-principles study. Applied Surface Science, 2021, 570, 151109.	3.1	14
59978	Laser-induced energetic material ignition with various fluorinated graphenes: Theoretical and experimental studies. Applied Surface Science, 2021, 570, 151187.	3.1	7
59979	Understanding the interaction of organic corrosion inhibitors with copper at the molecular scale: Benzotriazole on Cu(110). Applied Surface Science, 2021, 570, 151206.	3.1	16
59980	Surface termination and thickness dependent magnetic coupling of Cr adlayers on Ni2MnGa(001) surfaces: An ab initio study. Journal of Magnetism and Magnetic Materials, 2021, 540, 168398.	1.0	2
59981	Analysis of electronic structure and properties of Ga2O3/CuAlO2 heterojunction. Applied Surface Science, 2021, 568, 150826.	3.1	16
59982	Atomistic manipulation of interfacial properties in HfN2/MoTe2 van der Waals heterostructure via strain and electric field for next generation multifunctional nanodevice and energy conversion. Applied Surface Science, 2021, 568, 150928.	3.1	15
59983	Electronic modulation of CoP nanoarrays by Cr-doping for efficient overall water splitting. Chemical Engineering Journal, 2021, 425, 130651.	6.6	72
59984	Design of (C3N2H5)(1-)Cs PbI3 as a novel hybrid perovskite with strong stability and excellent photoelectric performance: A theoretical prediction. Solar Energy Materials and Solar Cells, 2021, 233, 111401.	3.0	7
59985	Dual CuCl doped argyrodite superconductor to boost the interfacial compatibility and air stability for all solid-state lithium metal batteries. Nano Energy, 2021, 90, 106542.	8.2	53
59986	Fabrication of cellulose@Mg(OH)2 composite filter via interfacial bonding and its trapping effect for heavy metal ions. Chemical Engineering Journal, 2021, 426, 130812.	6.6	24
59987	Enhanced selective catalytic reduction of NO with NH3 over homoatomic dinuclear sites in defective Î±-Fe2O3. Chemical Engineering Journal, 2021, 426, 131845.	6.6	13

#	Article	IF	Citations
59988	A highly efficient and durable air electrode for intermediate-temperature reversible solid oxide cells. Applied Catalysis B: Environmental, 2021, 299, 120631.	10.8	37
59989	Partial or complete suppression of hysteresis in hydride formation in binary alloys of Pd with other metals. Journal of Alloys and Compounds, 2021, 885, 160956.	2.8	9
59990	Fe-doped CuGaS2 (CuGa1-xFexS2) - Detailed analysis of the intermediate band optical response of chalcopyrite thin films based on first principle calculations and experimental studies. Materials Science in Semiconductor Processing, 2021, 136, 106133.	1.9	11
59991	Nature of electronic topological transition and superconductivity in bismuth under high pressure from ab initio random structure searching. Computational Materials Science, 2021, 200, 110806.	1.4	5
59992	Two-dimensional Al2O3 with ultrawide bandgap and large exciton binding energy for solar-blind ultraviolet photodetectors. Computational Materials Science, 2021, 200, 110775.	1.4	8
59993	Effect of heterostructure engineering on electronic structure and transport properties of two-dimensional halide perovskites. Computational Materials Science, 2021, 200, 110823.	1.4	10
59994	Enhanced overall water splitting under visible light of MoSSeâˆ£WSSe heterojunction by lateral interfacial engineering. Journal of Catalysis, 2021, 404, 18-31.	3.1	13
59995	Suppressing toxic intermediates during photocatalytic degradation of glyphosate by controlling adsorption modes. Applied Catalysis B: Environmental, 2021, 299, 120671.	10.8	18
59996	Ultrafine-grained W-Cr composite prepared by controlled W-Cr solid solution decomposition. Materials Letters, 2021, 304, 130728.	1.3	4
59997	DFT simulation-based screening of single transition metals supported on g-C3N4 for the catalytic oxidation of Hg0. Fuel, 2021, 305, 121456.	3.4	8
59998	Investigation of aluminum concentration on stacking fault energies of hexagonal close-packed high-entropy alloys Hf0.25Ti0.25Zr0.25Sc0.25â^'xAlx (xÂ<Â15%). Journal of Alloys and Compounds, 2021, 887, 161412.	2.8	4
59999	The formation energy and interaction energy of point defects in ZrC. Journal of Nuclear Materials, 2021, 557, 153235.	1.3	12
60000	The fabrication of two-dimensional g-C3N4/NaBiO3Â·2H2O heterojunction for improved photocatalytic CO2 reduction: DFT study and mechanism unveiling. Journal of Colloid and Interface Science, 2021, 604, 122-130.	5.0	30
60001	Fast start-up structured CuFeMg/Al2O3 catalyst applied in microreactor for efficient hydrogen production in methanol steam reforming. Chemical Engineering Journal, 2021, 426, 130644.	6.6	13
60002	Mechanics and strain engineering of bulk and monolayer Bi2O2Se. Journal of the Mechanics and Physics of Solids, 2021, 157, 104626.	2.3	6
60003	Machine learned interatomic potentials for modeling interfacial heat transport in Ge/GaAs. Computational Materials Science, 2021, 200, 110836.	1.4	7
60004	De-hybridization effect of transition metal catalysts on AlH4-based hydrogen storage materials. Physica B: Condensed Matter, 2021, 623, 413343.	1.3	1
60005	Ta cap-induced stabilization of interfacial ferromagnetism and enhanced magnetoelectricity in ultrathin FeRh films. Journal of Magnetism and Magnetic Materials, 2021, 539, 168414.	1.0	1

#	Article	IF	Citations
60006	Adsorption behaviors of NH3 and HCl molecules on Fe-based crystal planes: A DFT study. Chemical Engineering Science, 2021, 246, 116976.	1.9	16
60007	Bulk and surface diffusion of neodymium in alpha-uranium: Ab initio calculations and kinetic Monte Carlo simulations. Journal of Nuclear Materials, 2021, 557, 153307.	1.3	1
60008	Crystallographic facet heterojunction of MIL-125-NH2(Ti) for carbon dioxide photoreduction. Applied Catalysis B: Environmental, 2021, 298, 120524.	10.8	47
60009	Impacts of boron doping on the atomic structure, stability, and photocatalytic activity of Cu3P nanocrystals. Applied Catalysis B: Environmental, 2021, 298, 120515.	10.8	22
60010	Tailoring the redox-active transition metal content to enhance cycling stability in cation-disordered rock-salt oxides. Energy Storage Materials, 2021, 43, 275-283.	9.5	11
60011	Virtual screening of two-dimensional selenides and transition metal doped SnSe for lithium-sulfur batteries: A first-principles study. Applied Surface Science, 2021, 570, 151213.	3.1	36
60012	Field-induced half-metallic phase in epitaxial TcO2 bilayer on rutile TiO2 surface. Journal of Magnetism and Magnetic Materials, 2021, 540, 168478.	1.0	0
60013	Concentration modulate engineering of cobalt-selenium-sulfide electrodes toward water splitting: A first principle study. Applied Surface Science, 2021, 570, 151229.	3.1	5
60014	Construction ZnIn2S4/Ti3C2 of 2D/2D heterostructures with enhanced visible light photocatalytic activity: A combined experimental and first-principles DFT study. Applied Surface Science, 2021, 570, 151183.	3.1	29
60015	Single Ni supported on Ti3C2O2 for uninterrupted CO2 catalytic hydrogenation to formic acid: A DFT study. Separation and Purification Technology, 2021, 279, 119722.	3.9	14
60016	Temperature-dependent elastic and plastic properties of Î±2-Ti3Al. Intermetallics, 2021, 139, 107368.	1.8	4
60017	Micromechanical analysis and theoretical predictions towards thermal shock resistance of HfO2-Si environmental barrier coatings. Composites Part B: Engineering, 2021, 226, 109334.	5.9	20
60018	Controllably synthesized sugar-coated haws-sticklike Au/ZrO2 nanofibers for enhanced cataluminescence in propanal detection. Sensors and Actuators B: Chemical, 2021, 349, 130737.	4.0	6
60019	An improved oxygen reduction reaction activity and CO2-tolerance of La0.6Sr0.4Co0.2Fe0.8O3-Î´ achieved by a surface modification with barium cobaltite coatings. Journal of Power Sources, 2021, 514, 230573.	4.0	24
60020	Li2Ni(WO4)2/C: A potential tungstate anode material for lithium ion batteries. Journal of Alloys and Compounds, 2021, 888, 161535.	2.8	3
60021	Exploring the mechanism of ZrO2 structure features on H2O2 activation in Zrâ€“Fe bimetallic catalyst. Applied Catalysis B: Environmental, 2021, 299, 120685.	10.8	27
60022	Electrochemical catalytic mechanism of N-doped electrode for in-situ generation of OH in metal-free EAOPs to degrade organic pollutants. Separation and Purification Technology, 2021, 277, 119432.	3.9	20
60023	Phase transition of CaTe induced by high-pressure: Structural and elastic DFT study of five structures. Solid State Communications, 2021, 340, 114488.	0.9	2

#	Article	IF	Citations
60024	Charge localization to optimize reactant adsorption on KCu7S4/CuO interfacial structure toward selective CO2 electroreduction. Applied Catalysis B: Environmental, 2021, 298, 120531.	10.8	25
60025	Hybrid heterojunction of molybdenum disulfide/single cobalt atoms anchored nitrogen, sulfur-doped carbon nanotube /cobalt disulfide with multiple active sites for highly efficient hydrogen evolution. Applied Catalysis B: Environmental, 2021, 298, 120630.	10.8	52
60026	High spin polarization ultrafine Rh nanoparticles on CNT for efficient electrochemical N2 fixation to ammonia. Applied Catalysis B: Environmental, 2021, 298, 120592.	10.8	38
60027	Optical properties of arsenene nanoribbons: A first principle study. Materials Science in Semiconductor Processing, 2021, 136, 106139.	1.9	3
60028	Hydrogen diffusion in plutonium hydrides from first principles. Journal of Nuclear Materials, 2021, 557, 153247.	1.3	3
60029	Defect enriched hierarchical iron promoted Bi2MoO6 hollow spheres as efficient electrocatalyst for water oxidation. Chemical Engineering Journal, 2021, 426, 131884.	6.6	16
60030	Engineering the coordination environment in atomic Fe/Ni dual-sites for efficient oxygen electrocatalysis in Zn-air and Mg-air batteries. Chemical Engineering Journal, 2021, 426, 130758.	6.6	30
60031	Observing the spontaneous formation of a sub-critical nucleus in a phase-change amorphous material from ab initio molecular dynamics. Materials Science in Semiconductor Processing, 2021, 136, 106102.	1.9	5
60032	Ab initio investigations on metal ion pre-intercalation strategy of layered V2O5 cathode for magnesium-ion batteries. Applied Surface Science, 2021, 569, 150983.	3.1	11
60033	Structural, mechanical and electronic properties of binary Niâ€“B compounds under pressure. Solid State Communications, 2021, 340, 114524.	0.9	1
60034	Cooling rate dependence of the properties for Ti110Al14V4 alloy investigated by ab initio molecular dynamics. Journal of Molecular Liquids, 2021, 343, 117604.	2.3	4
60035	Electrically-tuned transition of band alignment in arsenene/MoTe2 van der Waals heterostructures. Vacuum, 2021, 194, 110612.	1.6	3
60036	Hydrodeoxygenation of aliphatic acid over NiFe intermetallic compounds: Insights into the mechanism via model compound study. Fuel, 2021, 305, 121545.	3.4	11
60037	Interfacial heteroâ€phase construction in nickel/molybdenum selenide hybrids to promote the water splitting performance. Applied Materials Today, 2021, 25, 101175.	2.3	12
60038	Pressure-induced band anticrossing in two adamantine ordered-vacancy compounds: CdGa2S4 and HgGa2S4. Journal of Alloys and Compounds, 2021, 886, 161226.	2.8	6
60039	Band convergence and thermoelectric performance enhancement of InSb via Bi doping. Intermetallics, 2021, 139, 107347.	1.8	8
60040	Segregation of Ni and Si to coherent bcc Fe-Cu interfaces from density functional theory. Journal of Nuclear Materials, 2021, 556, 153185.	1.3	7
60041	Investigation of the microstructure and electronic features for <mml:math xmlns:mml="http://www.w3.org/1998/Math/MathML" altimg="si2.svg"><mml:mrow><mml:msup><mml:mrow><mml:mi mathvariant="normal">Ce</mml:mi></mml:mrow><mml:mrow><mml:mn>3</mml:mn><mml:mo>+</mml:mo></mml:mrow></mml:ms YAG crystal: A first-principle study. Computational Materials Science, 2021, 200, 110762.	1.4	2

#	Article	IF	Citations
60042	Precisely engineering the electronic structure of active sites boosts the activity of iron-nickel selenide on nickel foam for highly efficient and stable overall water splitting. Applied Catalysis B: Environmental, 2021, 299, 120678.	10.8	61
60043	Investigation of Cu heteroatoms and Cu clusters in Fe-Cu alloy and their special effect mechanisms on the Fenton-like catalytic activity and reusability. Applied Catalysis B: Environmental, 2021, 299, 120662.	10.8	29
60044	Two-dimensional PtSe2/hBN vdW heterojunction as photoelectrocatalyst for the solar-driven oxygen evolution reaction: A first principles study. Applied Surface Science, 2021, 570, 151207.	3.1	24
60045	Spin states modulation of Four-Nitrogen coordinated Transition-Metal (TMN4) embedded graphene. Applied Surface Science, 2021, 570, 151126.	3.1	6
60046	Facile synthesis and first-principles study of nitrogen and sulfur dual-doped porous graphene aerogels/natural graphite as anode materials for Li-ion batteries. Journal of Alloys and Compounds, 2021, 884, 160923.	2.8	18
60047	Rational design of intermetallic compound catalysts for propane dehydrogenation from a descriptor-based microkinetic analysis. Journal of Catalysis, 2021, 404, 32-45.	3.1	15
60048	Photocatalytic production of H2O2 from water and dioxygen only under visible light using organic polymers: Systematic study of the effects of heteroatoms. Applied Catalysis B: Environmental, 2021, 299, 120666.	10.8	22
60049	Density functional theory calculations of the thermodynamic and kinetic properties of point defects in <mml:math xmlns:mml="http://www.w3.org/1998/Math/MathML" altimg="si2.svg"><mml:mi>Î²</mml:mi></mml:math>-U. Journal of Nuclear Materials, 2021, 557, 153238.	1.3	1
60050	Two-dimensional hetero-nanostructured electrocatalyst of Ni/NiFe-layered double oxide for highly efficient hydrogen evolution reaction in alkaline medium. Chemical Engineering Journal, 2021, 426, 131827.	6.6	42
60051	Stone-Wales defect-rich carbon-supported dual-metal single atom sites for Zn-air batteries. Nano Energy, 2021, 90, 106488.	8.2	55
60052	A-site cationic defects induced electronic structure regulation of LaMnO3 perovskite boosts oxygen electrode reactions in aprotic lithiumâ€“oxygen batteries. Energy Storage Materials, 2021, 43, 293-304.	9.5	43
60053	Trimetallic single-cluster catalysts for electrochemical nitrogen reduction reaction: Activity prediction, mechanism, and electronic descriptor. Chemical Engineering Journal, 2021, 426, 130745.	6.6	38
60054	Electronic tuning of SrIrO3 perovskite nanosheets by sulfur incorporation to induce highly efficient and long-lasting oxygen evolution in acidic media. Applied Catalysis B: Environmental, 2021, 298, 120562.	10.8	55
60055	Adjustable electromagnetic response of ultralight 3D Ti3C2T composite via control of crystal defects. Applied Surface Science, 2021, 569, 151053.	3.1	7
60056	Formation of Î²"-related composite precipitates in relation to enhanced thermal stability of Sc-alloyed Al-Mg-Si alloys. Journal of Alloys and Compounds, 2021, 885, 160942.	2.8	15
60057	Revisit of the structure of Î© precipitate in Al-Cu-Mg-Ag alloys. Scripta Materialia, 2021, 205, 114204.	2.6	15
60058	Identification of single-atom-anchored g-CN as pH universal photo- and electro- catalysts for hydrogen evolution. Applied Materials Today, 2021, 25, 101177.	2.3	7
60059	Machine learning aided first-principles studies of structure stability of Co3(Al, X) doped with transition metal elements. Computational Materials Science, 2021, 200, 110787.	1.4	9

#	Article	IF	Citations
60060	Electronic conductivity of two-dimensional VS2 monolayers: A first principles study. Computational Materials Science, 2021, 200, 110767.	1.4	12
60061	Controllable band offset in monolayer MoSe2 driven by surface termination and ferroelectric field of BiFeO3(0001) substrate. Journal of Solid State Chemistry, 2021, 304, 122571.	1.4	1
60062	Bayesian automated weighting of aggregated DFT, MD, and experimental data for candidate thermodynamic models of aluminum with uncertainty quantification. Materialia, 2021, 20, 101216.	1.3	4
60063	Structural, electronic, magnetic, transport and mechanical properties of a new half-metallic quaternary Heusler alloy <mml:math xmlns:mml="http://www.w3.org/1998/Math/MathML" altimg="si125.svg"><mml:mrow><mml:msub><mml:mrow><mml:mi mathvariant="normal">Co</mml:mi></mml:mrow><mml:mrow><mml:mn>2</mml:mn></mml:mrow></mml:msub></mml:mrow></mml:math> xmlns:mml="http://www.w3.org/1998/Math/MathML" altimg="si126.svg"><mml:mrow><mml:msub><mml:mrow><mml:mi mathvariant="normal">Fe</mml:mi>	1.0	10
60064	Stability of the sc16 polymorph of GaAs. Journal of Physics and Chemistry of Solids, 2021, 159, 110233.	1.9	1
60065	CO2 adsorption and dissociation on single and double iron atomic molybdenum disulfide catalysts: A DFT study. Fuel, 2021, 305, 121547.	3.4	16
60066	DFT+U study of the electronic structure changes of WO3 monoclinic and hexagonal surfaces upon Cu, Ag, and Au adsorption. Applications for CO adsorption. Surface Science, 2021, 714, 121907.	0.8	10
60067	Enhancing bifunctional electrodes of oxygen vacancy abundant ZnCo2O4 nanosheets for supercapacitor and oxygen evolution. Chemical Engineering Journal, 2021, 425, 130583.	6.6	70
60068	Study of Adsorption of H<mml:math xmlns:mml="http://www.w3.org/1998/Math/MathML" altimg="si1.svg"><mml:msub><mml:mrow /><mml:mn>2</mml:mn></mml:msub></mml:math>, CO and NO Gas Molecules on Molybdenum Sulfide and Tungsten Sulfide Monolayers from First-Principles Calculations. Surface Science, 2021, 714, 121910.	0.8	6
60069	Screening for lead-free inorganic double perovskites with suitable band gaps and high stability using combined machine learning and DFT calculation. Applied Surface Science, 2021, 568, 150916.	3.1	38
60070	First-principles study of benzene and its homologues upon graphene-metal surfaces: Comparison of London dispersion corrections. Surface Science, 2021, 714, 121919.	0.8	4
60071	Structure, mechanical and phonon stability of the Th-Sn system from ab initio. Journal of Nuclear Materials, 2021, 556, 153187.	1.3	1
60072	High-performance magnetic tunnel junctions based on two-dimensional Bi2O2Se. Journal of Magnetism and Magnetic Materials, 2021, 539, 168346.	1.0	3
60073	Mechanisms for Cr(VI) reduction by alcohols over clay edges: Reactive differences between ethanol and ethanediol, and selective conversions to Cr(IV), Cr(III) and Cr(II) species. Journal of Colloid and Interface Science, 2021, 603, 37-47.	5.0	8
60074	A temperature-dependent phosphorus doping on Ti3C2Tx MXene for enhanced supercapacitance. Journal of Colloid and Interface Science, 2021, 604, 239-247.	5.0	30
60075	Stability and electronic properties of the graphene-supported FeO nanostructures including clusters and monolayer. Applied Surface Science, 2021, 569, 150976.	3.1	4
60076	Theoretical investigation of chemical reaction kinetics of CO2 and vinyl radical under catalytic combustion. Fuel, 2021, 305, 121566.	3.4	3
60077	Strain engineered structural and electronic properties of an organic-crystal through first-principles calculations. Materials Letters, 2021, 304, 130590.	1.3	5

#	Article	IF	Citations
60078	The role of oxygen vacancies on SnO2 in improving formaldehyde competitive adsorption: A DFT study with an experimental verification. Applied Surface Science, 2021, 570, 151110.	3.1	13
60079	ADAQ: Automatic workflows for magneto-optical properties of point defects in semiconductors. Computer Physics Communications, 2021, 269, 108091.	3.0	8
60080	Electronic and magnetic properties of homonuclear and heteronuclear transition metal pairs in graphene. Applied Surface Science, 2021, 569, 150999.	3.1	4
60081	Single-atom platinum or ruthenium on C4N as 2D high-performance electrocatalysts for oxygen reduction reaction. Chemical Engineering Journal, 2021, 426, 131347.	6.6	55
60082	Three Rh-rich ternary germanides in the Ceâ€“Rhâ'Ge system. Journal of Solid State Chemistry, 2021, 304, 122585.	1.4	2
60083	Single atom Ru doping 2H-MoS2 as highly efficient hydrogen evolution reaction electrocatalyst in a wide pH range. Applied Catalysis B: Environmental, 2021, 298, 120490.	10.8	125
60084	Ag nanoparticles modified crumpled borophene supported Co3O4 catalyst showing superior oxygen evolution reaction (OER) performance. Applied Catalysis B: Environmental, 2021, 298, 120529.	10.8	118
60085	Efficient photoreduction strategy for uranium immobilization based on graphite carbon nitride/perovskite oxide heterojunction nanocomposites. Applied Catalysis B: Environmental, 2021, 298, 120625.	10.8	51
60086	Theoretical study of the structural, elastic, vibrational and thermal properties of perovskite halides <mml:math xmlns:mml="http://www.w3.org/1998/Math/MathML" altimg="si96.svg" display="inline" id="d1e2235"><mml:mrow><mml:msub><mml:mrow><mml:mi mathvariant="normal">Cs</mml:mi></mml:mrow><mml:mrow><mml:mn>2</mml:mn></mml:mrow></mml:msub><mml:msub><mml:mi mathvariant="normal">TiBr</mml:mi></mml:mrow><mml:mrow><mml:mn>6</mml:mn><mml:mo>â^'</mml:mo><mml:mi>x</mml:mi> Computational Condensed Matter, 2021, 29, e00587.	0.9	6
60087	Mechanical and optical properties of polymeric nitrogen achieved by compression: DFT study. Materialia, 2021, 20, 101206.	1.3	2
60088	Radial and three-dimensional nonlocal pseudopotential calculations in gradient-corrected Kohnâ€“Sham density functional theory based on higher-order finite element methods. Computer Methods in Applied Mechanics and Engineering, 2021, 386, 114094.	3.4	4
60089	Synthesis, characterization, properties, first principles calculations, and X-ray photoelectron spectroscopy of bulk Mn5SiB2 and Fe5SiB2 ternary borides. Journal of Alloys and Compounds, 2021, 888, 161377.	2.8	8
60090	Structural and thermal stability of B20-type high-pressure phases FeGe and MnGe. Journal of Alloys and Compounds, 2021, 888, 161565.	2.8	4
60091	Oxygen vacancy-enriched Co3O4 as lithiophilic medium for ultra-stable anode of lithium metal batteries. Journal of Alloys and Compounds, 2021, 888, 161553.	2.8	13
60092	LaN structural and topological transitions driven by temperature and pressure. Computational Materials Science, 2021, 200, 110779.	1.4	3
60093	Electrostatic doping determined by band alignment in graphene on ferroelectric LiNbO3(0001) polar surfaces. Computational Materials Science, 2021, 200, 110811.	1.4	1
60094	The unconventionally stoichiometric compounds in the Naâ€“K system at high pressures. Computational Materials Science, 2021, 200, 110818.	1.4	2
60095	Two dimension transition metal boride Y2B2 as a promising anode in Li-ion and Na-ion batteries. Computational Materials Science, 2021, 200, 110776.	1.4	22

#	Article	IF	Citations
60096	Tuning the electronic properties of two dimensional InSe/In2Se3 heterostructure via ferroelectric polarization and strain. Computational Materials Science, 2021, 200, 110819.	1.4	9
60097	Architecture control and electronic structure engineering over Ni-based nitride nanocomposite for boosting ammonia borane dehydrogenation. Applied Catalysis B: Environmental, 2021, 298, 120523.	10.8	42
60098	First-principles study of helium in austenitic Fe 6.3 at% Cr alloys: Structural, stability, energetics, and clustering with vacancies. Materials Today Communications, 2021, 29, 102837.	0.9	4
60099	Investigation of (001), (010), and (100) surface termination and surface energies of the Zintl Ca5Ga2Sb6. Surface Science, 2021, 714, 121918.	0.8	1
60100	Inverse capacity growth and progressive lithiation of SnP-semifilled carbon nanotubes anodes. Applied Surface Science, 2021, 568, 150844.	3.1	3
60101	A Ti-OH bond breaking route for creating oxygen vacancy in titania towards efficient CO2 photoreduction. Chemical Engineering Journal, 2021, 425, 131513.	6.6	23
60102	Finnisâ€“Sinclair-type potential for atomistic simulation of defects behaviour in V-Ti-Ta ternary system. Journal of Nuclear Materials, 2021, 557, 153231.	1.3	11
60103	Vinyl alcohol formation via catalytic Î²-dehydrogenation of ethanol on Ir(100). Chemical Physics Impact, 2021, 3, 100040.	1.7	5
60104	Impact of Ni alloying on Fe-C martensite ageing: an atomistic investigation. Scripta Materialia, 2021, 205, 114182.	2.6	6
60105	First-principles-based microkinetic simulations of syngas to methanol conversion on ZnAl2O4 spinel oxide. Applied Surface Science, 2021, 569, 151064.	3.1	7
60106	Enhanced adsorption of molybdenum(VI) from aquatic solutions by chitosan-coated zirconiumâ€“iron sulfide composite. Separation and Purification Technology, 2021, 279, 119736.	3.9	21
60107	Single, double, and triple transition metal atoms embedded in defective V3C2O2 for nitrogen reduction reaction: A DFT study. Applied Surface Science, 2021, 569, 151020.	3.1	22
60108	Screening MXenes for novel anode material of lithium-ion batteries with high capacity and stability: A DFT calculation. Applied Surface Science, 2021, 569, 151050.	3.1	48
60109	Robust hollow tubular ZnIn2S4 modified with embedded metal-organic-framework-layers: Extraordinarily high photocatalytic hydrogen evolution activity under simulated and real sunlight irradiation. Applied Catalysis B: Environmental, 2021, 298, 120632.	10.8	66
60110	Selective electrocatalytic hydrogenation of nitrobenzene over copper-platinum alloying catalysts: Experimental and theoretical studies. Applied Catalysis B: Environmental, 2021, 298, 120545.	10.8	44
60111	A Yin-Yang hybrid co-catalyst (CoOx-Mo2N) for photocatalytic overall water splitting. Applied Catalysis B: Environmental, 2021, 298, 120491.	10.8	22
60112	Probing the role of surface hydroxyls for Bi, Sn and In catalysts during CO2 Reduction. Applied Catalysis B: Environmental, 2021, 298, 120581.	10.8	54
60113	A supramolecular H12SubPcB-OPhCOPh/TiO2 Z-scheme hybrid assembled via dimeric concave-ligand Ï€-interaction for visible photocatalytic oxidation of tetracycline. Applied Catalysis B: Environmental, 2021, 298, 120550.	10.8	43

#	Article	IF	Citations
60114	Photocatalytic oxidative dehydrogenation of cyclohexane to cyclohexene over oxygen-deficient tungsten trioxide. Applied Catalysis B: Environmental, 2021, 298, 120549.	10.8	16
60115	Structural reconstruction of carbon nitride with tailored electronic structure: A bifunctional photocatalyst for cooperative artificial photosynthesis and selective phenylcarbinol oxidation. Applied Catalysis B: Environmental, 2021, 298, 120517.	10.8	7
60116	Preparation of a novel ion-imprinted membrane using sodium periodate-oxidized polydopamine as the interface adhesion layer for the direction separation of Li+ from spent lithium-ion battery leaching solution. Separation and Purification Technology, 2021, 277, 119519.	3.9	14
60117	Defect stability and intriguing magnetic properties in Janus chromium trihalides monolayer. Applied Surface Science, 2021, 569, 150995.	3.1	5
60118	Electron density modulation of MoP by rare earth metal as highly efficient electrocatalysts for pH-universal hydrogen evolution reaction. Applied Catalysis B: Environmental, 2021, 299, 120657.	10.8	57
60119	Defective C3N4 frameworks coordinated diatomic copper catalyst: Towards mild oxidation of methane to C1 oxygenates. Applied Catalysis B: Environmental, 2021, 299, 120682.	10.8	32
60120	Quantitative assessment of the role of spin fluctuations in 2D Ising superconductor NbSe2. Computational Materials Science, 2021, 200, 110758.	1.4	5
60121	Structural predictions of superconducting phase in tungsten ditellurides WTe2 from first-principles evolutionary techniques under high pressure. Computational Materials Science, 2021, 200, 110795.	1.4	0
60122	First-principles study of vacancy interaction with grain boundaries of tungsten under tensile strains. Computational Materials Science, 2021, 200, 110760.	1.4	3
60123	First-principles study on the electronic properties and enhanced ferromagnetism of alkali metals adsorbed monolayer CrI3. Vacuum, 2021, 194, 110561.	1.6	10
60124	Effect of co-adsorbed water on electrochemical CO2 reduction reaction on transition metal oxide catalysts. Applied Surface Science, 2021, 570, 151031.	3.1	7
60125	A comparative study of the photocatalytic and optical properties of spinel-type titanates: A report for spinel sodium titanate. Journal of Solid State Chemistry, 2021, 304, 122593.	1.4	3
60126	Phase transitions in Fe-(23â^'24)Ga alloys: Experimental results and modeling. Journal of Alloys and Compounds, 2021, 885, 160917.	2.8	3
60127	Tunable broadband emission by bandgap engineering in (Ba,Sr)2(Mg,Zn)WO6 inorganic double-perovskites. Journal of Alloys and Compounds, 2021, 888, 161567.	2.8	10
60128	DFT study of hydrogen sorption on light metal (Li, Be, and Na) decorated novel fullerene-CNTs networks. Applied Surface Science, 2021, 569, 151000.	3.1	12
60129	A robust metal-organic framework with guest molecules induced splint-like pore confinement to construct propane-trap for propylene purification. Separation and Purification Technology, 2021, 279, 119656.	3.9	22
60130	Outstandingly high thermal conductivity, elastic modulus, carrier mobility and piezoelectricity in two-dimensional semiconducting CrC2N4: a first-principles study. Materials Today Energy, 2021, 22, 100839.	2.5	19
60131	The effects of second-alloying-element on the formability of Mg-Sn alloys in respect of the stacking fault energies of slip systems. Materials Today Communications, 2021, 29, 102829.	0.9	9

#	Article	IF	Citations
60132	Crystal chemistry rationale and ab initio investigation of ultra-hard dense rhombohedral carbon and boron nitride. Diamond and Related Materials, 2021, 120, 108607.	1.8	6
60133	Highly surface-active Si-doped TiO2/Ti3C2Tx heterostructure for gas sensing and photodegradation of toxic matters. Chemical Engineering Journal, 2021, 425, 131437.	6.6	33
60134	Van der Waal heterostructure based on BY(Y As, P) and MX<mml:math xmlns:mml="http://www.w3.org/1998/Math/MathML" display="inline" id="d1e981" altimg="si31.svg"><mml:msub><mml:mrow /><mml:mrow><mml:mn>2</mml:mn></mml:mrow></mml:msub></mml:math>(M Mo, W; X S, Se) monolayers. Applied Surface Science, 2021, 568, 150846.	3.1	24
60135	Effects of substantial atomic-oxygen migration across silverÂâ˜Âoxide interfaces during silver growth. Applied Surface Science, 2021, 568, 150927.	3.1	12
60136	The effect of Sr doping on the structural, mechanical, electronic properties and radiation tolerance of MgAl2O4 spinel: A first-principles study. Journal of Alloys and Compounds, 2021, 889, 161614.	2.8	4
60137	Coupling Fe3O4/Fe1-xS@Carbon with carbon-coated MoS2 nanosheets as a superior anode for sodium-ion batteries. Chemical Engineering Journal, 2022, 427, 131652.	6.6	10
60138	Synergistic effect of lithiophilic Zn nanoparticles and N-doping for stable Li metal anodes. Journal of Energy Chemistry, 2022, 65, 439-447.	7.1	16
60139	Supercritically exfoliated Bi2Se3 nanosheets for enhanced photocatalytic hydrogen production by topological surface states over TiO2. Journal of Colloid and Interface Science, 2022, 605, 871-880.	5.0	16
60140	Termination effects of single-atom decorated v-Mo2CTx MXene for the electrochemical nitrogen reduction reaction. Journal of Colloid and Interface Science, 2022, 605, 897-905.	5.0	25
60141	Tuning the reversible chemisorption of hydroxyl ions to promote the electrocatalysis on ultrathin metal-organic framework nanosheets. Journal of Energy Chemistry, 2022, 65, 71-77.	7.1	17
60142	Effect of electronic interactions and coordination spheres on ionic diffusion in LaxSr1-xGayMg1-yO3-Î´. Journal of Physics and Chemistry of Solids, 2022, 161, 110393.	1.9	2
60143	Breaking the linear scaling relations in MXene catalysts for efficient CO2 reduction. Chemical Engineering Journal, 2022, 429, 132171.	6.6	32
60144	Revealing the role of mo doping in promoting oxygen reduction reaction performance of Pt3Co nanowires. Journal of Energy Chemistry, 2022, 66, 16-23.	7.1	36
60145	Tuning of crystal phase of nickel telluride nanosheets to construct superior electrocatalyst for hydrogen evolution. Journal of Alloys and Compounds, 2022, 891, 161955.	2.8	10
60146	Active Co@CoO core/shell nanowire arrays as efficient electrocatalysts for hydrogen evolution reaction. Chemical Engineering Journal, 2022, 429, 132226.	6.6	32
60147	Atomically precise multi-domain GdxFe3â˜xO4 nanoclusters with modulated contrast properties for T2-weighted magnetic resonance imaging of early orthotopic cancer. Chemical Engineering Journal, 2022, 429, 132255.	6.6	6
60148	Experimental Investigations on the Electrical Properties of 4H-SiC Power MOSFETs Under Biaxial and Uniaxial Mechanical Strains. IEEE Transactions on Power Electronics, 2022, 37, 55-58.	5.4	1
60149	3D flower-like perylenetetracarboxylic-Zn(II) superstructures/Bi2WO6 step-scheme heterojunctions with enhanced visible light photocatalytic performance. Chemical Engineering Journal, 2022, 429, 132377.	6.6	25

#	Article	IF	Citations
60150	Enhanced reversibility of the magnetoelastic transition in (Mn,Fe)2(P,Si) alloys via minimizing the transition-induced elastic strain energy. Journal of Materials Science and Technology, 2022, 103, 165-176.	5.6	11
60151	Solution-processed Cd-substituted CZTS nanocrystals for sensitized liquid junction solar cells. Journal of Alloys and Compounds, 2022, 890, 161575.	2.8	9
60152	Enhancement of bacterial inactivation of BiOBr nanoflower through oxygen vacancy engineering. Applied Surface Science, 2022, 571, 151268.	3.1	14
60153	Vertically aligned 1ÂT phase MoS2 nanosheet array for high-performance rechargeable aqueous Zn-ion batteries. Chemical Engineering Journal, 2022, 428, 130981.	6.6	32
60154	Fabrication of surface oxygen vacancies on NiMnAl-LDO catalyst by high-shear mixer-assisted preparation for low-temperature CO2 methanation. Fuel, 2022, 309, 122099.	3.4	14
60155	MagneticTB: A package for tight-binding model of magnetic and non-magnetic materials. Computer Physics Communications, 2022, 270, 108153.	3.0	32
60156	Design the Ï€-stacking type of perovskite-like iodobismuthates to enhance their optoelectronic properties. Journal of Molecular Structure, 2022, 1247, 131332.	1.8	5
60157	2D high temperature ferromagnetic Co2Ti2Sn2 monolayer with tunable magnetic anisotropy and superior mechanical flexibility: A first-principles and Monte Carlo study. Physica E: Low-Dimensional Systems and Nanostructures, 2022, 135, 114939.	1.3	3
60158	Multi-dimensional hybrid flexible films promote uniform lithium deposition and mitigate volume change as lithium metal anodes. Journal of Energy Chemistry, 2022, 65, 583-591.	7.1	6
60159	Facile encapsulating Ag nanoparticles into a Tetrathiafulvalene-based Zr-MOF for enhanced Photocatalysis. Chemical Engineering Journal, 2022, 427, 131970.	6.6	23
60160	Atomically dispersed Fe/Bi dual active sites single-atom nanozymes for cascade catalysis and peroxymonosulfate activation to degrade dyes. Journal of Hazardous Materials, 2022, 422, 126929.	6.5	69
60161	Effect of Li and Li-RE co-doping on structure, stability, optical and electrical properties of bismuth magnesium niobate pyrochlore. Materials Research Bulletin, 2022, 145, 111520.	2.7	6
60162	A comprehensive study of structure and properties of nanocrystalline zinc peroxide. Journal of Physics and Chemistry of Solids, 2022, 160, 110318.	1.9	6
60163	Conductive Fe2N/N-rGO composite boosts electrochemical redox reactions in wide temperature accommodating lithium-sulfur batteries. Chemical Engineering Journal, 2022, 427, 131622.	6.6	12
60164	Niobium carbide (MXene) reduces UHMWPE particle-induced osteolysis. Bioactive Materials, 2022, 8, 435-448.	8.6	38
60165	WloopPHI: A tool for ab initio characterization of Weyl semimetals. Computer Physics Communications, 2022, 270, 108147.	3.0	5
60166	Ga doping enables superior alkaline hydrogen evolution reaction performances of CoP. Chemical Engineering Journal, 2022, 429, 132012.	6.6	25
60167	Two-dimensional MgP3 monolayer with remarkably tunable bandgap and enhanced visible-light and UV optical absorptions. Physica E: Low-Dimensional Systems and Nanostructures, 2022, 135, 114960.	1.3	26

#	Article	IF	Citations
60168	Sulfurized-polyacrylonitrile in lithium-sulfur batteries: Interactions between undercoordinated carbons and polymer structure under low lithiation. Journal of Energy Chemistry, 2022, 66, 587-596.	7.1	13
60169	Enhanced phosphate removal from practical wastewater via in situ assembled dimension-engineered MOF@carbon heterostructures. Chemical Engineering Journal, 2022, 428, 132536.	6.6	40
60170	Topological tuning of Two-Dimensional polytriazine imides by halide anions for selective lead removal from wastewater. Separation and Purification Technology, 2021, 278, 119595.	3.9	5
60171	In-situ conversion growth of carbon-coated MoS2/N-doped carbon nanotubes as anodes with superior capacity retention for sodium-ion batteries. Journal of Materials Science and Technology, 2022, 102, 8-15.	5.6	16
60172	Phase orientation improved the corrosion resistance and conductivity of Cr2AlC coatings for metal bipolar plates. Journal of Materials Science and Technology, 2022, 105, 36-44.	5.6	25
60173	N-doped and oxygen vacancy-rich NiCo2O4 nanograss for supercapacitor electrode. Chemical Engineering Journal, 2022, 429, 132242.	6.6	124
60174	Single Ir atom anchored in pyrrolic-N4 doped graphene as a promising bifunctional electrocatalyst for the ORR/OER: a computational study. Journal of Colloid and Interface Science, 2022, 607, 1005-1013.	5.0	78
60175	Interface modulation mechanism of alloying elements on the interface interaction and mechanical properties of graphene/copper composites. Applied Surface Science, 2022, 571, 151314.	3.1	12
60176	First-principles study of configurations, electronic and photocatalytic properties of carbon-doped anatase TiO2. Physica B: Condensed Matter, 2022, 624, 413443.	1.3	4
60177	Fluorine-doped graphene oxide prepared by direct plasma treatment for supercapacitor application. Chemical Engineering Journal, 2022, 428, 132086.	6.6	41
60178	Carbonized wood membrane decorated with AuPd alloy nanoparticles as an efficient self-supported electrode for electrocatalytic CO2 reduction. Journal of Colloid and Interface Science, 2022, 607, 312-322.	5.0	9
60179	Experimental and first-principles investigation on the structural, electronic and antimicrobial properties of nickel hydroxide nanoparticles. Journal of Physics and Chemistry of Solids, 2022, 160, 110367.	1.9	5
60180	Deposition kinetics and mechanism of pyrocarbon for electromagnetic-coupling chemical vapor infiltration process. Journal of Materials Science and Technology, 2022, 101, 118-127.	5.6	3
60181	A novel Fe-Co double-atom catalyst with high low-temperature activity and strong water-resistant for O3 decomposition: A theoretical exploration. Journal of Hazardous Materials, 2022, 421, 126639.	6.5	16
60182	Ab initio study on magnetism of SnO2 (110) surface with non-metallic elements doping. Materials Science in Semiconductor Processing, 2022, 137, 106194.	1.9	5
60183	Ferromagnetism in Î²-Ag2Se topological semimetal. Journal of Alloys and Compounds, 2022, 891, 162025.	2.8	1
60184	Morphology optimization strategy of flower-like CoNi2S4/Co9S8@MoS2 core@shell nanocomposites to achieve extraordinary microwave absorption performances. Journal of Colloid and Interface Science, 2022, 606, 1128-1139.	5.0	22
60185	Pressure dependent phase transformations of energetic material 2,4â^'dinitroanisole using Raman spectroscopy, X-ray diffraction and first principles calculations. Journal of Molecular Structure, 2022, 1247, 131356.	1.8	3

#	Article	IF	Citations
60186	Spatial carrier separation in cobalt phosphate deposited ZnIn2S4 nanosheets for efficient photocatalytic hydrogen evolution. Journal of Colloid and Interface Science, 2022, 606, 317-327.	5.0	27
60187	Confined Pd clusters with dynamic structure for highly efficient Cascade-type catalysis. Chemical Engineering Journal, 2022, 429, 132128.	6.6	5
60188	A new thermodynamically stable Nb2Ni intermetallic compound phase revealed by peritectoid transition within binary Nb-Ni alloy system. Journal of Materials Science and Technology, 2022, 100, 246-253.	5.6	28
60189	Correlating structure and orbital occupation with the stability and mechanical properties of 3d transition metal carbides. Journal of Alloys and Compounds, 2022, 891, 161866.	2.8	12
60190	1 T-MoSe2 monolayer supported single Pd atom as a highly-efficient bifunctional catalyst for ORR/OER. Journal of Colloid and Interface Science, 2022, 605, 155-162.	5.0	55
60191	Electronic tuning of g-C3N4 via competitive coordination to stimulate high-efficiently photocatalytic for hydrogen evolution. Journal of Alloys and Compounds, 2022, 891, 162027.	2.8	6
60192	Rational design of honeycomb Ni-Co LDH/graphene composite for remarkable supercapacitor via ultrafast microwave synthesis. Applied Surface Science, 2022, 571, 151322.	3.1	62
60193	A simple strategy that may effectively tackle the anode-electrolyte interface issues in solid-state lithium metal batteries. Chemical Engineering Journal, 2022, 427, 131001.	6.6	38
60194	New phases of MBenes M2B (MÂ=ÂSc, Ti, and V) as high-capacity electrode materials for rechargeable magnesium ion batteries. Applied Surface Science, 2022, 571, 151275.	3.1	30
60195	Vacancy ordered phases of nonstoichiometric hafnium carbide from evolutionary crystal structure predictions. Journal of Alloys and Compounds, 2022, 891, 162063.	2.8	5
60196	Small-scale analysis of brittle-to-ductile transition behavior in pure tungsten. Journal of Materials Science and Technology, 2022, 105, 242-258.	5.6	15
60197	ElasTool: An automated toolkit for elastic constants calculation. Computer Physics Communications, 2022, 270, 108180.	3.0	17
60198	Enhanced electronic interaction in hemin@Ni(OH)2 composite for efficient electrocatalytic oxygen evolution. Journal of Alloys and Compounds, 2022, 892, 161780.	2.8	6
60199	Phase transformation of ZrO2 by Si incorporation and catalytic activity for isopropyl alcohol dehydration and dehydrogenation. Chemical Engineering Journal, 2022, 428, 131766.	6.6	16
60200	Palladium-based single atom catalysts for high-performance electrochemical production of hydrogen peroxide. Chemical Engineering Journal, 2022, 428, 131112.	6.6	29
60201	Processing bulk insulating CaTiO3 into a high-performance thermoelectric material. Chemical Engineering Journal, 2022, 428, 131121.	6.6	12
60202	Suppression of Co-Cr antisite defect and robust half metallicity in CoMCrAl (MÂ=ÂMn, Fe) Heusler alloys. Journal of Alloys and Compounds, 2022, 891, 161856.	2.8	4
60203	Influence of alkaline species on the high temperature lubrication of molten carbonate. Tribology International, 2022, 165, 107257.	3.0	1

#	Article	IF	Citations
60204	Directionally maximizing CO selectivity to near-unity over cupric oxide with indium species for electrochemical CO2 reduction. Chemical Engineering Journal, 2022, 427, 131654.	6.6	18
60205	Carbon-coated MoS2 nanosheets@CNTs-Ti3C2 MXene quaternary composite with the superior rate performance for sodium-ion batteries. Journal of Materials Science and Technology, 2022, 100, 101-109.	5.6	29
60206	Monoclinic Cu3(OH)2V2O7Â·2H2O nanobelts/reduced graphene oxide: A novel high-capacity and long-life composite for potassium-ion battery anodes. Journal of Energy Chemistry, 2022, 66, 140-151.	7.1	7
60207	Modulating the stability, electronic and reactivity properties of single-atom catalyst anchored graphene by coordination environments. Physica E: Low-Dimensional Systems and Nanostructures, 2022, 135, 114975.	1.3	5
60208	An integrated strategy based on Schiff base reactions to construct unique two-dimensional nanostructures for intrinsic pseudocapacitive sodium/lithium storage. Chemical Engineering Journal, 2022, 429, 132339.	6.6	12
60209	In-depth understanding of the crystal-facet effect of La2O2CO3 for low-temperature oxidative coupling of methane. Fuel, 2022, 308, 121848.	3.4	10
60210	In-situ vulcanization synthesis of honeycomb-like SnS/C nanocomposites as anode materials for lithium-ion batteries. Journal of Alloys and Compounds, 2022, 891, 162051.	2.8	7
60211	Charge induced reconstruction of glide partial dislocations and electronic properties in GaN. Scripta Materialia, 2022, 207, 114276.	2.6	3
60212	Compression tuned crystalline and amorphous phases of Gd2Si2O7: Raman spectroscopic and first-principles studies. Journal of Alloys and Compounds, 2022, 890, 161864.	2.8	0
60213	Experiment on spin-polarized Dirac concavity Sc<mml:math xmlns:mml="http://www.w3.org/1998/Math/MathML" display="inline" id="d1e736" altimg="si20.svg"><mml:msub><mml:mrow /><mml:mrow><mml:mn>2</mml:mn></mml:mrow></mml:msub></mml:math>CrB<mml:math xmlns:mml="http://www.w3.org/1998/Math/MathML" display="inline" id="d1e744" altimg="si21.svg"><mml:msub><mml:mrow /><mml:mrow><mml:mn>5</mml:mn></mml:mrow></mml:msub></mml:math>	1.3	4
60214	Theoretical insights into the adsorption mechanism of Cd(II) on the basal surfaces of kaolinite. Journal of Hazardous Materials, 2022, 422, 126795.	6.5	15
60215	Phase transformations in Al-Ti-Mg powders consolidated by high-pressure torsion: Experiments and first-principles calculations. Journal of Alloys and Compounds, 2021, 889, 161815.	2.8	8
60216	A theoretical study of the twinned ZnO nanostructures. Applied Surface Science, 2022, 571, 151295.	3.1	0
60217	Intrinsic vacancy suppression and band convergence to enhance thermoelectric performance of (Ge,) Tj ETQq1 1 0.784314 rgBT /Ove	6.6	21
60218	Theoretical insight into surface structures of pentlandite toward hydrogen evolution. Journal of Colloid and Interface Science, 2022, 607, 645-654.	5.0	13
60219	2D XBiSe3(XÂ=ÂGa, In, Tl) monolayers with high carrier mobility and enhanced visible-light absorption. Spectrochimica Acta - Part A: Molecular and Biomolecular Spectroscopy, 2022, 264, 120309.	2.0	7
60220	Phase stability and mechanical properties of carbide solid solutions with 2â€“5 principal metals. Computational Materials Science, 2022, 201, 110869.	1.4	20
60221	Oxygen-containing groups and P doped porous carbon nitride nanosheets towards enhanced photocatalytic activity. Chemosphere, 2022, 287, 132399.	4.2	9

#	Article	IF	Citations
60222	Correlation between precipitates evolution and mechanical properties of Al-Sc-Zr alloy with Er additions. Journal of Materials Science and Technology, 2022, 99, 61-72.	5.6	32
60223	Heat capacity of a MnFe(P,Si,B) compound with first-order magnetic transition. Journal of Magnetism and Magnetic Materials, 2022, 541, 168513.	1.0	2
60224	Effect of dimensional expansion on carrier transport behaviors of the hexagonal Bi-based perovskite crystals. Journal of Energy Chemistry, 2022, 66, 459-465.	7.1	16
60225	Molecule functionalization to facilitate electrocatalytic oxygen reduction on graphdiyne. Journal of Energy Chemistry, 2022, 65, 141-148.	7.1	11
60226	Visible-light deposition of CrO cocatalyst on TiO2: Cr valence regulation for superior photocatalytic CO2 reduction to CH4. Journal of Energy Chemistry, 2022, 64, 103-112.	7.1	25
60227	Role of H-bond along with oxygen and zinc vacancies in the enhancement of ferromagnetic behavior of ZnO films: An experimental and first principle-based study. Journal of Alloys and Compounds, 2021, 889, 161663.	2.8	16
60228	Combined Schottky junction and doping effect in CdxZn1-xS@Au/BiVO4 Z-Scheme photocatalyst with boosted carriers charge separation for CO2 reduction by H2O. Journal of Colloid and Interface Science, 2022, 606, 1469-1476.	5.0	32
60229	Slag design and iron capture mechanism for recovering low-grade Pt, Pd, and Rh from leaching residue of spent auto-exhaust catalysts. Science of the Total Environment, 2022, 802, 149830.	3.9	27
60230	Fabrication of ultra-thin MgAl layered double oxide by cellulose templating and its immobilization effect toward heavy metal ions: cation-exchange and deposition mechanism. Chemical Engineering Journal, 2022, 427, 132017.	6.6	36
60231	Chelating effect between uranyl and pyridine N containing covalent organic frameworks: A combined experimental and DFT approach. Journal of Colloid and Interface Science, 2022, 606, 1617-1626.	5.0	18
60232	Application of hybrid MOF composite in extraction of f-block elements: Experimental and computational investigation. Chemosphere, 2022, 287, 132232.	4.2	12
60233	Effects of electric field on Schottky barrier in graphene and hexagonal boron phosphide heterostructures. Physica E: Low-Dimensional Systems and Nanostructures, 2022, 135, 114973.	1.3	4
60234	The formation of atomic and sub-nano scale pores under tensile strain in oxide films on Zr alloys: A first-principles study. Applied Surface Science, 2022, 571, 151316.	3.1	2
60235	Large-scale defect-rich iron/nitrogen co-doped graphene-based materials as the excellent bifunctional electrocatalyst for liquid and flexible all-solid-state zinc-air batteries. Journal of Colloid and Interface Science, 2022, 607, 1201-1214.	5.0	49
60236	Theoretical study on the formation of diamond germanium vacancy color center. Surface Science, 2022, 715, 121950.	0.8	2
60237	Strain modulation of electronic and optical properties of monolayer MoSi2N4. Physica E: Low-Dimensional Systems and Nanostructures, 2022, 135, 114964.	1.3	20
60238	Taming the challenges of activity and selectivity in catalysts for electrochemical N2 fixation via single metal atom supported on WS2. Applied Surface Science, 2022, 571, 151357.	3.1	16
60239	Structural, electronic, and optic properties of Se nanotubes. Physica B: Condensed Matter, 2022, 624, 413417.	1.3	4

#	Article	IF	Citations
60240	Molecular dynamics and DFT study of 38-atom coinage metal clusters. Computational Materials Science, 2022, 201, 110908.	1.4	9
60241	Graded 2D/3D (CF3-PEA)2FA0.85MA0.15Pb2I7/FA0.85MA0.15PbI3 heterojunction for stable perovskite solar cell with an efficiency over 23.0%. Journal of Energy Chemistry, 2022, 65, 480-489.	7.1	34
60242	Polaron assisted electrical transport and fertile field emission response in polycrystalline LiNi0.33Co0.33Mn0.33O2 with theoretical insight by density functional theory. Journal of Alloys and Compounds, 2022, 891, 162056.	2.8	2
60243	Top-down and facet-selective phase-segregation to construct concave nanocages with strongly coupled hetero-interface for oxygen evolution reaction. Applied Catalysis B: Environmental, 2022, 300, 120727.	10.8	18
60244	Template-controlled in-situ growing of NiCo-MOF nanosheets on Ni foam with mixed linkers for high performance asymmetric supercapacitors. Applied Surface Science, 2022, 572, 151344.	3.1	80
60245	Study on the adsorption of low-concentration VOCs on zeolite composites based on chemisorption of metal-oxides under dry and wet conditions. Separation and Purification Technology, 2022, 280, 119634.	3.9	33
60246	Insertion and diffusion of N and C in <mml:math xmlns:mml="http://www.w3.org/1998/Math/MathML" display="inline" id="d1e1022" altimg="si61.svg"><mml:mi>Î³</mml:mi></mml:math>â€“TiAl: Theoretical study and comparison with O. Physica B: Condensed Matter, 2022, 624, 413370.	1.3	4
60247	A bifunctional MnxCo3-xO4-decorated separator for efficient Li-LiI-O2 batteries: A novel strategy to promote redox coupling and inhibit redox shuttling. Chemical Engineering Journal, 2022, 428, 131105.	6.6	8
60248	A thermally stable isoquinoline based ultra-microporous metal-organic framework for CH4 separation from coal mine methane. Chemical Engineering Journal, 2022, 428, 131136.	6.6	27
60249	Core-shell structured AP/Fe3O4 composite with enhanced catalytic thermal decomposition property: Fabrication and mechanism study. Chemical Engineering Science, 2022, 247, 116899.	1.9	11
60250	Efficient broadband near-infrared luminescence of Cr3+ doped fluoride K2NaInF6 and its NIR-LED application toward veins imaging. Chemical Engineering Journal, 2022, 427, 131740.	6.6	72
60251	High performance of Er-doped Sb2Te material used in phase change memory. Journal of Alloys and Compounds, 2021, 889, 161701.	2.8	14
60252	Intrinsic disorder of dangling OH-bonds in the first water layer on noble metal surfaces. Computational Materials Science, 2022, 201, 110863.	1.4	0
60253	Planar Dual-Layer System for Ultra-Broadband Absorption and Hot-Carrier Photodetection in Longwave Near-Infrared Band. IEEE Journal of Selected Topics in Quantum Electronics, 2022, 28, 1-9.	1.9	0
60254	Carbonaceous-assisted confinement synthesis of refractory high-entropy alloy nanocomposites and their application for seawater electrolysis. Journal of Colloid and Interface Science, 2022, 607, 1580-1588.	5.0	11
60255	MnO2/Mn2O3 with self-triggered oxygen-defects for superior pseudocapacitive energy storage. Applied Surface Science, 2022, 571, 151306.	3.1	13
60256	Hydrogen occupation in Ti4M2O compounds (M = Fe, Co, Ni, Cu, and yÂ=Â0, 1) and their hydrogen storage characteristics. Journal of Alloys and Compounds, 2022, 891, 162050.	2.8	8
60257	First-principles-based microkinetic rate equation theory for oxygen carrier reduction in chemical looping. Chemical Engineering Science, 2022, 247, 117042.	1.9	14

#	Article	IF	Citations
60258	Mechanism study on the high-performance BaFe2O4 during chemical looping gasification. Fuel, 2022, 307, 121847.	3.4	13
60259	Nanostructure Shape-Effects in ZnO heterogeneous photocatalysis. Journal of Colloid and Interface Science, 2022, 606, 588-599.	5.0	32
60260	Monolayer MoSi2N4- as promising electrocatalyst for hydrogen evolution reaction: A DFT prediction. Journal of Materials Science and Technology, 2022, 99, 215-222.	5.6	31
60261	Experimental and density functional theory studies on Cu/Ba-coimpregnated Î³-Al2O3 for low-temperature NO storage and adsorbent regeneration. Chemical Engineering Journal, 2022, 429, 132112.	6.6	7
60262	Dissociative adsorption of H2O and CO2 on the clean and O-pre-covered high index Ru surfaces: Corrugated Ru(11âˆ’21) and stepped Ru(20âˆ’21) surfaces. Surface Science, 2022, 715, 121936.	0.8	3
60263	Structural investigation of metallic Ni nanoparticles with N-doped carbon for efficient oxygen evolution reaction. Chemical Engineering Journal, 2022, 429, 132122.	6.6	35
60264	Boron substitution enhanced activity of BxGa1âˆ’xAs/GaAs photocatalyst for water splitting. Applied Catalysis B: Environmental, 2022, 300, 120690.	10.8	4
60265	Substitutional doping effect of C3N anode material: A first principles calculations study. Applied Surface Science, 2022, 571, 151330.	3.1	11
60266	Tuning the electronic structures of cobalt-molybdenum bimetallic carbides to boost the hydrogen oxidation reaction in alkaline medium. Chemical Engineering Journal, 2022, 428, 131206.	6.6	30
60267	Deep learning for mapping element distribution of high-entropy alloys in scanning transmission electron microscopy images. Computational Materials Science, 2022, 201, 110905.	1.4	8
60268	Experimental investigation and thermodynamic modeling of the ternary Tiâ€“Feâ€“Mn system for hydrogen storage applications. Journal of Alloys and Compounds, 2022, 891, 161957.	2.8	11
60269	Hydroxyapatite and lead-substituted hydroxyapatite near-surface structures: Novel modelling of photoemission lines from X-ray photoelectron spectra. Applied Surface Science, 2022, 571, 151310.	3.1	18
60270	Reactive force fields for aqueous and interfacial magnesium carbonate formation. Physical Chemistry Chemical Physics, 2021, 23, 23106-23123.	1.3	8
60271	A highly sensitive ppb-level H₂S gas sensor based on fluorophenoxy-substituted phthalocyanine cobalt/rGO hybrids at room temperature. RSC Advances, 2021, 11, 5993-6001.	1.7	16
60272	Identifying a Li-rich superionic conductor from chargeâ€“discharge structural evolution study: Li₂MnO₃. Physical Chemistry Chemical Physics, 2021, 23, 4829-4834.	1.3	2
60273	High-temperature superconductivity in transition metallic hydrides MH₁₁(M = Mo, W, Nb,) Tj ETQq1 1 0.784314 rgBT /Ov	1.3	15
60274	Ab initio study of metal carbide hydrides in the 2.25Cr1Mo0.25V steel. Physical Chemistry Chemical Physics, 2021, 23, 5199-5206.	1.3	2
60275	Cesium Lead Bromidesâ€”Structural, Electronic and Optical Properties. Minerals, Metals and Materials Series, 2021, , 3-14.	0.3	0

#	Article	IF	Citations
60276	The thermodynamics and electronic structure analysis of P-doped spinel Co3O4. Physical Chemistry Chemical Physics, 2021, 23, 3588-3594.	1.3	5
60277	Enhanced Interface Phonon Thermal Conductance via Boron Addition in Copper/Diamond Composites. SSRN Electronic Journal, 0, , .	0.4	0
60278	All inorganic lead free solar cell material Cs2PdI6: a first-principles study. Applied Physics Express, 2021, 14, 021005.	1.1	3
60279	Induction of Room Temperature Ferromagnetism in N-Doped Yttrium Oxide: Ab Initio Calculation. JETP Letters, 2021, 113, 120-126.	0.4	0
60280	Deep Insights into the Twinning Mechanism in High-Performance Al Alloys: A Comprehensive First-Principles Study. Metallurgical and Materials Transactions A: Physical Metallurgy and Materials Science, 2021, 52, 955-963.	1.1	6
60281	First-principles study of pristine and metal decorated blue phosphorene for sensing toxic H2S, SO2 and NO2 molecules. Applied Physics A: Materials Science and Processing, 2021, 127, 1.	1.1	5
60282	Nuclearity and Host Effects of Carbonâ€Supported Platinum Catalysts for Dibromomethane Hydrodebromination. Small, 2021, 17, 2005234.	5.2	8
60283	Understanding Cu incorporation in the <mml:math xmlns:mml="http://www.w3.org/1998/Math/MathML"><mml:mrow><mml:msub><mml:mi>Cu</mml:mi><mml:mrow><mml:mn>2</mml:mn> structure using resonant x-ray diffraction. Physical Review Materials, 2021, 5, .	0.9	3
60284	Influence of plastic deformation on the magnetic properties of Heusler MnAu2Al. Physical Review Materials, 2021, 5, .	0.9	3
60285	Tuning the electronic structure of <mml:math xmlns:mml="http://www.w3.org/1998/Math/MathML"><mml:msup><mml:mi>d</mml:mi><mml:mn>0</mml:mn></mml:msup> perovskite oxides by combining distortive modes. Physical Review B, 2021, 103, .	1.1	4
60286	Evidence of Weyl fermions in <mml:math xmlns:mml="http://www.w3.org/1998/Math/MathML"><mml:mrow><mml:mi>Î±</mml:mi><mml:mtext>â€“</mml:mtext><mml:mi>Ru< Physical Review B, 2021, 103, .	1.1	2
60287	First-principles screening of single transition metal atoms anchored on two-dimensional C9N4 for the nitrogen reduction reaction. Physical Chemistry Chemical Physics, 2021, 23, 8784-8791.	1.3	2
60288	Mechanism of monolayer to bilayer silicene transformation in CaSi₂ due to fluorine diffusion. Physical Chemistry Chemical Physics, 2021, 23, 9315-9324.	1.3	0
60289	Stabilized Phase Transition Process of Layered NaxCoO2 via Ca-Substitution. Journal of the Electrochemical Society, 2021, 168, 010509.	1.3	3
60290	Temperature-induced phase transition of two-dimensional semiconductor GaTe*. Chinese Physics B, 2021, 30, 016402.	0.7	2
60291	Alkylation of poly-substituted aromatics to probe effects of mesopores in hierarchical zeolites with differing frameworks and crystal sizes. Molecular Systems Design and Engineering, 2021, 6, 903-917.	1.7	6
60292	Promoting superoxide generation in Bi₂WO₆ by less electronegative substitution for enhanced photocatalytic performance: an example of Te doping. Catalysis Science and Technology, 2021, 11, 6291-6304.	2.1	6
60293	First-principles study of Mn₃ adsorbed on Au(111) and Cu(111) surfaces. RSC Advances, 2021, 11, 31073-31083.	1.7	3

#	Article	IF	Citations
60294	Momentum for Catalysis: How Surface Reactions Shape the RuO2 Flat Surface State. ACS Catalysis, 2021, 11, 1749-1757.	5.5	8
60295	A novel two-dimensional beryllium diphosphide (BeP₂) with superconductivity: the first-principles exploration. Physical Chemistry Chemical Physics, 2021, 23, 12834-12841.	1.3	9
60296	Energy storage performance of 2D MoS₂and carbon nanotube heterojunctions in symmetric and asymmetric configuration. Nanotechnology, 2021, 32, 155403.	1.3	30
60297	Hydrogen-induced tunable electronic and optical properties of a two-dimensional penta-Pt₂N₄ monolayer. Physical Chemistry Chemical Physics, 2021, 23, 10409-10417.	1.3	24
60298	Role of Static Displacements in Stabilizing Body Centered Cubic High Entropy Alloys. Physical Review Letters, 2021, 126, 025501.	2.9	29
60299	Voting Data-Driven Regression Learning for Accelerating Discovery of Advanced Functional Materials and Applications to Two-Dimensional Ferroelectric Materials. Journal of Physical Chemistry Letters, 2021, 12, 973-981.	2.1	11
60300	Hidden spontaneous polarisation in the chalcohalide photovoltaic absorber Sn₂SbS₂I₃. Materials Horizons, 2021, 8, 2709-2716.	6.4	24
60301	Surface self-assembly involving the interaction between S and N atoms. Chemical Communications, 2021, 57, 1328-1331.	2.2	3
60302	Seeking Out Heterogeneous Hydrogen Bonding in a Self-Assembled 2D Cocrystal of Croconic Acid and Benzimidazole on Au(111). Journal of Physical Chemistry C, 2021, 125, 2403-2410.	1.5	8
60303	Chemomechanics in Niâ€“Mn binary cathode for advanced sodium-ion batteries. Journal of Materials Chemistry A, 2021, 9, 24290-24298.	5.2	6
60304	RE-EVALUATION OF THE TSL FOR YTTRIUM HYDRIDE. EPJ Web of Conferences, 2021, 247, 09015.	0.1	4
60305	Predicting activation energies for vacancy-mediated diffusion in alloys using a transition-state cluster expansion. Physical Review Materials, 2021, 5, .	0.9	7
60306	2D hybrid CrCl2(N2C4H4)2 with tunable ferromagnetic half-metallicity. Journal of Materials Chemistry C, 2021, 9, 5985-5991.	2.7	1
60307	Band engineering of Dirac materials in Sb_mBi_n lateral heterostructures. RSC Advances, 2021, 11, 17445-17455.	1.7	2
60308	Structural and proton conductivity studies of fibrous Ï€-Ti₂O(PO₄)₂Â·2H₂O: application in chitosan-based composite membranes. Dalton Transactions, 2021, 50, 7667-7677.	1.6	8
60309	1T-CrO₂monolayer: a high-temperature Dirac half-metal for high-speed spintronics. Nanoscale Advances, 2021, 3, 3093-3099.	2.2	15
60310	Concluding remarks: Reaction mechanisms in catalysis: perspectives and prospects. Faraday Discussions, 2021, 229, 502-513.	1.6	2
60311	On the energy transfer in LiMgPO₄ doped with rare-earth elements. Journal of Materials Chemistry C, 2021, 9, 11272-11283.	2.7	7

#	Article	IF	Citations
60312	Surface morphology controls water dissociation on hydrated IrO₂ nanoparticles. Nanoscale, 2021, 13, 14480-14489.	2.8	8
60313	Nb-Doped nickel nitride-derived catalysts for electrochemical water splitting. Catalysis Science and Technology, 2021, 11, 6455-6461.	2.1	6
60314	Design of 2D materials â€“ MSi₂C_xN_{4â^'x} (M = Cr, Mo, and W;) Tj ETQq0 0 0 rgBT /Overlock 10	2.8	10
60315	Assembling organicâ€“inorganic building blocks for high-capacity electrode design. Materials Horizons, 2021, 8, 1825-1834.	6.4	1
60316	SIn₂Te/TeIn₂Se: a type-II heterojunction as a water-splitting photocatalyst with high solar energy harvesting. Journal of Materials Chemistry C, 2021, 9, 7734-7744.	2.7	10
60317	Stoneâ€“Wales defects preserve hyperuniformity in amorphous two-dimensional networks. Proceedings of the National Academy of Sciences of the United States of America, 2021, 118, .	3.3	28
60318	Mechanism of methanol synthesis on Ni(110). Catalysis Science and Technology, 2021, 11, 3279-3294.	2.1	6
60319	CO₂ electrochemical reduction boosted by the regulated electronic properties of metalloporphyrins through tuning an atomic environment. New Journal of Chemistry, 2021, 45, 10664-10671.	1.4	2
60320	Gate-controlled ambipolar transport in b-AsP crystals and their VIS-NIF photodetection. Nanoscale, 2021, 13, 10579-10586.	2.8	15
60321	BiOCl/group-IV Xene bilayer heterojunctions: stability and electronic and photocatalytic properties. Physical Chemistry Chemical Physics, 2021, 23, 13323-13330.	1.3	3
60322	Isolated and assembled silver aggregates on the Si(001) surface: the initial stage of film formation. Physical Chemistry Chemical Physics, 2021, 23, 4161-4166.	1.3	4
60323	Ternary alkali ion thiogallates, A₅GaS₄ (A = Li and Na), with isolated tetrahedral building units and their ionic conductivities. Dalton Transactions, 2021, 50, 7372-7379.	1.6	9
60324	Structure, intermolecular interactions, and dynamic properties of NTO crystals with impurity defects: a computational study. CrystEngComm, 2021, 23, 2455-2468.	1.3	14
60325	Unveiling the mechanisms behind the ferroelectric response in the Sr(Nb,Ta)O₂N oxynitrides. Physical Chemistry Chemical Physics, 2021, 23, 17142-17149.	1.3	6
60326	Probing the Positions of TeO Moieties in the Channels of the MoVNbTeO M1 Catalyst: A Density Functional Theory Model Study. Catalysis Letters, 2021, 151, 2884-2893.	1.4	4
60327	Double boron atom-doped graphdiynes as efficient metal-free electrocatalysts for nitrogen reduction into ammonia: a first-principles study. Physical Chemistry Chemical Physics, 2021, 23, 17683-17692.	1.3	19
60328	A computational study of the electrochemical cyanide reduction for ambient ammonia production on a nickel cathode. Catalysis Science and Technology, 2021, 11, 5633-5640.	2.1	3
60329	Role of dislocation elastic field on impurity segregation in Fe-based alloys. Scientific Reports, 2021, 11, 1780.	1.6	10

#	Article	IF	Citations
60330	Localized vibration and avoided crossing in SrTi₁₁O₂₀ for oxide thermoelectrics with intrinsically low thermal conductivity. Journal of Materials Chemistry A, 2021, 9, 11674-11682.	5.2	11
60331	Predictive Modeling of Ceramic Materials. , 2021, , 475-480.		0
60332	Stabilization of lithium metal anodes by conductive metalâ€“organic framework architectures. Journal of Materials Chemistry A, 2021, 9, 12099-12108.	5.2	10
60333	Two-dimensional multiferroic FeCl with room temperature ferromagnetism and tunable magnetic anisotropy via ferroelectricity. Journal of Materials Chemistry C, 0, , .	2.7	8
60334	Nonvolatile electrical control of 2D Cr₂Ge₂Te₆ and intrinsic half metallicity in multiferroic hetero-structures. Nanoscale, 2021, 13, 1069-1076.	2.8	13
60335	The induction of half-metallicity and enhanced ferromagnetism in a Cr₂Ge₂Te₆ monolayer via electron doping and alkali metal adsorption. Journal of Materials Chemistry C, 2021, 9, 5952-5960.	2.7	10
60336	Hydroxyl Influence on Adsorption and Lubrication of an Ultrathin Aqueous Triblock Copolymer Lubricant. Langmuir, 2021, 37, 1465-1479.	1.6	4
60337	Effects of doping on photocatalytic water splitting activities of PtS₂/SnS₂ van der Waals heterostructures. Physical Chemistry Chemical Physics, 2021, 23, 18125-18136.	1.3	17
60338	A review on the use of DFT for the prediction of the properties of nanomaterials. RSC Advances, 2021, 11, 27897-27924.	1.7	62
60339	Understanding the Oxidation Degradation Mechanism to Enable Preparation of Ambient Ultra Stable Ti ₃C ₂T _x-MXene. SSRN Electronic Journal, 0, , .	0.4	1
60340	Magnetic order-dependent phonon properties in 2D magnet CrI₃. Nanoscale, 2021, 13, 10882-10890.	2.8	26
60341	Influence of vacancy and adatom defects on the optoelectronic properties of monolayer GeS. AIP Conference Proceedings, 2021, , .	0.3	0
60342	First-Principles Molecular Dynamics Simulation on High Silica Content Na₃AlF₆â€“Al₂O₃â€“SiO₂ Molten Salt. ACS Omega, 2021, 6, 3745-3751.	1.6	8
60343	The formation of TiO₂/VO₂ multilayer structure via directional cationic diffusion. Nanoscale, 2021, 13, 7783-7791.	2.8	10
60344	A Machine Learning Approach for the Prediction of Formability and Thermodynamic Stability of Single and Double Perovskite Oxides. Chemistry of Materials, 2021, 33, 845-858.	3.2	64
60345	Gauging van der Waals interactions in aqueous solutions of 2D MOFs: when water likes organic linkers more than open-metal sites. Physical Chemistry Chemical Physics, 2021, 23, 3135-3143.	1.3	6
60346	First-principles prediction of strain-induced gas-sensing tuning in tin sulfide. Physical Chemistry Chemical Physics, 2021, 23, 18712-18723.	1.3	10
60347	Mechanical properties of nonstoichiometric cubic titanium carbide TiC_y. Physical Chemistry Chemical Physics, 2021, 23, 18558-18567.	1.3	7

#	Article	IF	Citations
60348	High Conversion of Syngas to Ethene and Propene on Bifunctional Catalysts via the Tailoring of SAPO Zeolite Structure. Cell Reports Physical Science, 2021, 2, 100290.	2.8	15
60349	Modulation effects of S vacancy and Mo edge on the adsorption and dissociation behaviors of toxic gas (H₂S, SO₂) molecules on the MoS₂ monolayer. Physical Chemistry Chemical Physics, 2021, 23, 15364-15373.	1.3	7
60351	Materials Screening for Disorderâ€Controlled Chalcogenide Crystals for Phaseâ€Change Memory Applications. Advanced Materials, 2021, 33, e2006221.	11.1	32
60352	Antiferromagnetic spin ordering in two-dimensional honeycomb lattice of SiP₃. Nanoscale Advances, 2021, 3, 2217-2221.	2.2	6
60353	Structural reconstruction and visible-light absorption versus internal electrostatic field in two-dimensional GaNâ€“ZnO alloys. Nanoscale, 2021, 13, 11994-12003.	2.8	9
60354	Diffusion of protons and sodium ions in silicophosphate glasses: insight based on first-principles molecular dynamic simulations. Physical Chemistry Chemical Physics, 2021, 23, 14580-14586.	1.3	4
60355	Oxygen-evolution reactions (OER) on transition-metal-doped Fe₃Co(PO₄)₄ iron-phosphate surfaces: a first-principles study. Catalysis Science and Technology, 2021, 11, 4619-4626.	2.1	4
60356	Oxygen binding energy of doped metal: a shortcut to efficient Ni-based bimetallic catalysts for the hydrodeoxygenation reaction. Catalysis Science and Technology, 2021, 11, 4376-4386.	2.1	10
60357	The effect of Mg₃As₂ alloying on the thermoelectric properties of n-type Mg₃(Sb, Bi)₂. Dalton Transactions, 2021, 50, 9376-9382.	1.6	7
60358	High-throughput screening of single metal atom anchored on N-doped boron phosphide for N₂ reduction. Nanoscale, 2021, 13, 13437-13450.	2.8	18
60359	Distilling nanoscale heterogeneity of amorphous silicon using tip-enhanced Raman spectroscopy (TERS) via multiresolution manifold learning. Nature Communications, 2021, 12, 578.	5.8	25
60360	A highly reversible sodium metal anode by mitigating electrodeposition overpotential. Journal of Materials Chemistry A, 2021, 9, 22892-22900.	5.2	21
60361	Sliding ferroelectricity in two-dimensional MoA₂N₄ (A = Si or Ge) bilayers: high polarizations and MoirÃ© potentials. Journal of Materials Chemistry A, 2021, 9, 19659-19663.	5.2	32
60362	Epitaxial growth of ZrSe₂nanosheets on sapphireviachemical vapor deposition for optoelectronic application. Journal of Materials Chemistry C, 2021, 9, 13954-13962.	2.7	7
60363	Efficient Direct H₂O₂ Synthesis Enabled by PdPb Nanorings via Inhibiting the Oâ€“O Bond Cleavage in O₂ and H₂O₂. ACS Catalysis, 2021, 11, 1106-1118.	5.5	45
60364	Adsorption and reaction pathways of 7-octenoic acid on copper. Physical Chemistry Chemical Physics, 2021, 23, 5834-5844.	1.3	8
60365	Electronic structure and two-band superconductivity in unconventional high- <mml:math xmlns:mml="http://www.w3.org/1998/Math/MathML"><mml:msub><mml:mi>T</mml:mi><mml:mi>c</mml:mi></mml:msub></mml:ma cuprates <mml:math xmlns:mml="http://www.w3.org/1998/Math/MathML"><mml:msub><mml:mi mathvariant="normal">Ba</mml:mi><mml:mn>2</mml:mn></mml:msub><mml:mo>Â</mml:mo><mml:msub><mml:mi mathvariant="normal">CuO</mml:mi><mml:mrow><mml:mn>3</mml:mn><mml:mo>+</mml:mo><mml:mi>Î´</mml:mi></mml:mrow> Physical Review B, 2021, 103.	1.1	9
60366	A linear scaling law for predicting phase transition temperature via averaged effective electronegativity derived from A₂M₃O₁₂-based compounds. Materials Horizons, 2021, 8, 2562-2568.	6.4	14

#	Article	IF	Citations
60367	A sandwich-like Ga₂FeS₄-supported single metal atom as a promising bifunctional electrocatalyst for overall water splitting. Journal of Materials Chemistry A, 2021, 9, 18594-18603.	5.2	4
60368	Suppression of dynamic disorder by electrostatic interactions in structurally close organic semiconductors. Physical Chemistry Chemical Physics, 2021, 23, 15485-15491.	1.3	10
60369	Conflux of tunable Rashba effect and piezoelectricity in flexible magnesium monochalcogenide monolayers for next-generation spintronic devices. Nanoscale, 2021, 13, 8210-8223.	2.8	19
60370	Structureâ€“property relationships in organic battery anode materials: exploring redox reactions in crystalline Na- and Li-benzene diacrylate using combined crystallography and density functional theory calculations. Materials Advances, 2021, 2, 1024-1034.	2.6	7
60371	Morphology dependent interaction between Co(<scp>ii</scp>)-tetraphenylporphyrin and the MgO(100) surface. Physical Chemistry Chemical Physics, 2021, 23, 2105-2116.	1.3	4
60372	Prediction of allotropes of tellurium with molecular, one- and two-dimensional covalent nets for photofunctional applications. RSC Advances, 2021, 11, 29965-29975.	1.7	4
60373	Interfacial antiferromagnetic coupling and high spin polarization in metallic phthalocyanines. Physical Review B, 2021, 103, .	1.1	7
60374	Ruthenium Coreâ€“Shell Engineering with Nickel Single Atoms for Selective Oxygen Evolution via Nondestructive Mechanism. Advanced Energy Materials, 2021, 11, 2003448.	10.2	124
60375	Lattice distortion-enhanced superlubricity of (Mo, X)S₂ (X = Al, Ti, Cr and V) with moirÃ© superlattice. Nanoscale, 2021, 13, 16234-16243.	2.8	6
60376	Understanding the interfacial charge transfer in the CVD grown Bi₂O₂Se/CsPbBr₃ nanocrystal heterostructure and its exploitation in superior photodetection: experiment vs. theory. Nanoscale, 2021, 13, 14945-14959.	2.8	28
60377	Predicting adsorption ability of adsorbents at arbitrary sites for pollutants using deep transfer learning. Npj Computational Materials, 2021, 7, .	3.5	22
60378	Directing the selectivity of CO₂ electroreduction to target C₂ products via non-metal doping on Cu surfaces. Journal of Materials Chemistry A, 2021, 9, 6345-6351.	5.2	25
60379	Reversible multiplexing optical information storage and photoluminescence switching in Eu²⁺-doped fluorophosphate-based tunable photochromic materials. Journal of Materials Chemistry C, 2021, 9, 5930-5944.	2.7	18
60380	Experimental re-evaluation of proton penetration ranges in GaAs and InGaP. Journal Physics D: Applied Physics, 2021, 54, 115302.	1.3	5
60381	Anharmonic Correction to Adsorption Free Energy from DFT-Based MD Using Thermodynamic Integration. Journal of Chemical Theory and Computation, 2021, 17, 1155-1169.	2.3	29
60382	Two-Dimensional IVâ€“V Monolayers with Highly Anisotropic Carrier Mobility and Electric Transport Properties. Journal of Physical Chemistry Letters, 2021, 12, 1058-1065.	2.1	23
60383	Navigating Copper-Atom-Pair Structural Effect inside a Porous Organic Polymer Cavity for Selective Hydrogenation of Biomass-Derived 5-Hydroxymethylfurfural. ACS Sustainable Chemistry and Engineering, 2021, 9, 2136-2151.	3.2	52
60384	Modulating surficial oxygen vacancy of the VO₂ nanostructure to boost its electromagnetic absorption performance. Journal of Materials Chemistry C, 0, , .	2.7	56

#	Article	IF	Citations
60385	Exfoliated Ultrathin ZnIn₂S₄ Nanosheets with Abundant Zinc Vacancies for Enhanced CO₂ Electroreduction to Formate. ChemSusChem, 2021, 14, 852-859.	3.6	45
60386	First-principles calculation of Sb2Te3 topological insulator under pressure. Materials Today: Proceedings, 2021, 47, 1660-1664.	0.9	1
60387	Enhanced Redox Kinetics and Duration of Aqueous I₂/I^{â^'} Conversion Chemistry by MXene Confinement. Advanced Materials, 2021, 33, e2006897.	11.1	121
60388	Vibrational and optical identification of GeO₂ and GeO single layers: a first-principles study. Physical Chemistry Chemical Physics, 2021, 23, 21307-21315.	1.3	3
60389	Quantum well states and sizable Rashba splitting on Pb induced Î±-phase Bi/Si(111) surface reconstruction. Nanoscale, 2021, 13, 16622-16628.	2.8	5
60390	Kust-I: a high-performance two-dimensional graphene-based material for seawater desalination. Journal of Materials Chemistry A, 2021, 9, 21158-21166.	5.2	18
60391	Enhanced methane conversion using Ni-doped calcium ferrite oxygen carriers in chemical looping partial oxidation systems with CO2 utilization. Reaction Chemistry and Engineering, 2021, 6, 1928-1939.	1.9	11
60392	Perovskite Na-ion conductors developed from analogous Li3xLa2/3â^'xTiO3 (LLTO): chemo-mechanical and defect engineering. Journal of Materials Chemistry A, 2021, 9, 21241-21258.	5.2	7
60393	Characterisation of oxygen defects and nitrogen impurities in TiO2 photocatalysts using variable-temperature X-ray powder diffraction. Nature Communications, 2021, 12, 661.	5.8	97
60394	Surface Fluorination Engineering of NiFe Prussian Blue Analogue Derivatives for Highly Efficient Oxygen Evolution Reaction. ACS Applied Materials & Interfaces, 2021, 13, 5142-5152.	4.0	51
60395	Revealing the effect of interfacial electron transfer in heterostructured Co₉S₈@NiFe LDH for enhanced electrocatalytic oxygen evolution. Journal of Materials Chemistry A, 2021, 9, 12244-12254.	5.2	52
60396	Low lattice thermal conductivity of a 5â€“8-peanut-shaped carbon nanotube. Physical Chemistry Chemical Physics, 2021, 23, 5460-5466.	1.3	5
60397	Revealing the role of dopants in mitigating degradation phenomena in sodium-ion layered cathodes. Physical Chemistry Chemical Physics, 2021, 23, 2038-2045.	1.3	5
60398	Endohedral group-14-element clusters TM@E₉ (TM = Co, Ni, Cu; E = Ge, Sn, Pb) and their low-dimensional nanostructures: a first-principles study. Physical Chemistry Chemical Physics, 2021, 23, 20654-20665.	1.3	6
60399	Anionic Oxygen Redox in the High-Lithium Material Li₈SnO₆. Chemistry of Materials, 2021, 33, 834-844.	3.2	10
60400	Enhanced resistive switching performance in yttrium-doped CH₃NH₃PbI₃ perovskite devices. Physical Chemistry Chemical Physics, 2021, 23, 21757-21768.	1.3	12
60401	High-throughput computational search for high carrier lifetime, defect-tolerant solar absorbers. Energy and Environmental Science, 2021, 14, 5057-5073.	15.6	23
60402	Towards bridging the structure gap in heterogeneous catalysis: the impact of defects in dissociative chemisorption of methane on Ir surfaces. Physical Chemistry Chemical Physics, 2021, 23, 4376-4385.	1.3	31

#	Article	IF	Citations
60403	A new 3D metallic carbon allotrope composed of penta-graphene nanoribbons as a high-performance anode material for sodium-ion batteries. Journal of Materials Chemistry A, 2021, 9, 23214-23222.	5.2	17
60404	Self-diffusion in garnet-type Li7La3Zr2O12 solid electrolytes. Scientific Reports, 2021, 11, 451.	1.6	19
60405	Group-IV(A) Janus dichalcogenide monolayers and their interfaces straddle gigantic shear and in-plane piezoelectricity. Nanoscale, 2021, 13, 5460-5478.	2.8	89
60406	DMRG on Top of Plane-Wave Kohnâ€“Sham Orbitals: A Case Study of Defected Boron Nitride. Journal of Chemical Theory and Computation, 2021, 17, 1143-1154.	2.3	16
60407	Intrinsic asymmetric ferroelectricity induced giant electroresistance in ZnO/BaTiO₃ superlattice. RSC Advances, 2021, 11, 2353-2358.	1.7	3
60408	Catalytic separators with Coâ€“Nâ€“C nanoreactors for high-performance lithiumâ€“sulfur batteries. Inorganic Chemistry Frontiers, 2021, 8, 3066-3076.	3.0	29
60409	DART: deep learning enabled topological interaction model for energy prediction of metal clusters and its application in identifying unique low energy isomers. Physical Chemistry Chemical Physics, 2021, 23, 21995-22003.	1.3	7
60410	Phase diagram exploration of Tcâ€“Alâ€“B: from bulk Tc₂AlB₂ to two-dimensional Tc₂B₂. Physical Chemistry Chemical Physics, 2021, 23, 22086-22095.	1.3	3
60411	Tailoring the catalytic performance of single platinum anchored on graphene by vacancy engineering for propane dehydrogenation: a theoretical study. Physical Chemistry Chemical Physics, 2021, 23, 22004-22013.	1.3	4
60412	Defect-driven selective metal oxidation at atomic scale. Nature Communications, 2021, 12, 558.	5.8	47
60413	Boosting thermo-photocatalytic CO2 conversion activity by using photosynthesis-inspired electron-proton-transfer mediators. Nature Communications, 2021, 12, 123.	5.8	75
60414	Thermally induced structural evolution and age-hardening of polycrystalline V1â€“xMoxN (xÂâ‰ˆÂ0.4) thin films. Surface and Coatings Technology, 2021, 405, 126723.	2.2	11
60415	Applications of Few-Layer Nb₂C MXene: Narrow-Band Photodetectors and Femtosecond Mode-Locked Fiber Lasers. ACS Nano, 2021, 15, 954-965.	7.3	176
60416	Neural network reactive force field for C, H, N, and O systems. Npj Computational Materials, 2021, 7, .	3.5	39
60417	A New High Entropy Glycerate for High Performance Oxygen Evolution Reaction. Advanced Science, 2021, 8, 2002446.	5.6	95
60418	A tied Fermi liquid to Luttinger liquid model for nonlinear transport in conducting polymers. Nature Communications, 2021, 12, 58.	5.8	15
60419	Raman and optical characteristics of van der Waals heterostructures of single layers of GaP and GaSe: a first-principles study. Inorganic Chemistry Frontiers, 2021, 8, 2771-2781.	3.0	2
60420	Ionic Phases of Ammonia-Rich Hydrate at High Densities. Physical Review Letters, 2021, 126, 015702.	2.9	5

#	Article	IF	Citations
60421	Transformation of Co₃O₄ nanoparticles to CoO monitored by in situ TEM and predicted ferromagnetism at the Co₃O₄/CoO interface from first principles. Journal of Materials Chemistry C, 2021, 9, 5662-5675.	2.7	31
60422	Biaxial strain, electric field and interlayer distance-tailored electronic structure and magnetic properties of two-dimensional g-C₃N₄/Li-adsorbed Cr₂Ge₂Te₆ van der Waals heterostructures. Physical Chemistry Chemical Physics, 2021, 23, 6171-6181.	1.3	5
60423	Optimized electron occupancy of solid-solution transition metals for suppressing the oxygen evolution of Li₂MnO₃. Journal of Materials Chemistry A, 2021, 9, 9337-9346.	5.2	7
60424	Energetic and electronic properties of CsPbBr₃ surfaces: a first-principles study. Physical Chemistry Chemical Physics, 2021, 23, 7145-7152.	1.3	22
60425	Correlated Li-ion migration in the superionic conductor Li₁₀GeP₂S₁₂. Journal of Materials Chemistry A, 2021, 9, 11278-11284.	5.2	21
60426	Hydrogen solubility and diffusivity at Î£3 grain boundary of PdCu. RSC Advances, 2021, 11, 13644-13652.	1.7	4
60427	The variation of intrinsic defects in XTe (X = Ge, Sn, and Pb) induced by the energy positions of valence band maxima. Journal of Materials Chemistry C, 2021, 9, 5765-5770.	2.7	19
60428	Thermodynamically stable polymorphs of nitrogen-rich carbon nitrides: a C₃N₅ study. Physical Chemistry Chemical Physics, 2021, 23, 6422-6432.	1.3	5
60429	Efficient polysulfide trapping in lithiumâ€“sulfur batteries using ultrathin and flexible BaTiO₃/graphene oxide/carbon nanotube layers. Nanoscale, 2021, 13, 6863-6870.	2.8	3
60430	Controlled synthesis and Raman study of a 2D antiferromagnetic P-type semiconductor: Î±-MnSe. Nanoscale, 2021, 13, 6953-6964.	2.8	20
60431	Reaction mechanism on Ni-C₂-NS single-atom catalysis for the efficient CO₂reduction reaction. Journal of Experimental Nanoscience, 2021, 16, 255-264.	1.3	10
60432	Computational investigation of two-dimensional borides with planar octacoordinated main group elements. Physical Chemistry Chemical Physics, 2021, 23, 15904-15907.	1.3	3
60433	How bulk and surface properties of Ti₄SiC₃, V₄SiC₃, Nb₄SiC₃ and Zr₄SiC₃ tune reactivity: a computational study. Faraday Discussions, 2021, 230, 87-99.	1.6	2
60434	Crystal structure from laboratory X-ray powder diffraction data, DFT-D calculations, Hirshfeld surface analysis, and energy frameworks of a new polymorph of 1-benzothiophene-2-carboxylic acid. Powder Diffraction, 2021, 36, 2-13.	0.4	5
60435	Scintillation in (C₆H₅CH₂NH₃)₂SnBr₄: green-emitting lead-free perovskite halide materials. RSC Advances, 2021, 11, 20635-20640.	1.7	13
60436	First-principles study of properties of rare-earth-doped LiFePO₄. Wuli Xuebao/Acta Physica Sinica, 2021, 70, 158203.	0.2	4
60437	A MoSe₂/N-doped hollow carbon sphere host for rechargeable Naâ€“Se batteries. Dalton Transactions, 2021, 50, 7705-7714.	1.6	17
60438	N-type and p-type molecular doping on monolayer MoS₂. RSC Advances, 2021, 11, 8033-8041.	1.7	15

#	Article	IF	Citations
60439	Potential SiX (X = N, P, As, Sb, Bi) homo-bilayers for visible-light photocatalyst applications. Catalysis Science and Technology, 2021, 11, 4996-5013.	2.1	18
60440	A first-principles study on double-sided decorated boronâ€“nitrogen co-doped graphene by vanadium for enhanced low-temperature reversible hydrogen storage. Sustainable Energy and Fuels, 2021, 5, 2159-2168.	2.5	9
60441	Coexistence of magnetic and electric orderings in a divalent Cr²⁺-based multiaxial molecular ferroelectric. Chemical Science, 2021, 12, 9742-9747.	3.7	33
60442	Environmentally friendly thermoelectric sulphide Cu₂ZnSnS₄ single crystals achieving a 1.6 dimensionless figure of merit ZT. Journal of Materials Chemistry A, 2021, 9, 15595-15604.	5.2	17
60443	Theoretical study of ternary silver fluorides AgMF₄ (M = Cu, Ni, Co) formation at pressures up to 20 GPa. RSC Advances, 2021, 11, 25801-25810.	1.7	6
60444	Gas-phase preparation and the stability of superatomic Nb₁₁O₁₅^{â^'}. Physical Chemistry Chemical Physics, 2021, 23, 15766-15773.	1.3	6
60445	Adsorption-based membranes for air separation using transition metal oxides. Nanoscale Advances, 2021, 3, 4502-4512.	2.2	3
60446	The stability and electronic and photocatalytic properties of the ZnWO4 (010) surface determined from first-principles and thermodynamic calculations. RSC Advances, 2021, 11, 23477-23490.	1.7	3
60447	Tuning the performance of a Mg negative electrode through grain boundaries and alloying toward the realization of Mg batteries. Journal of Materials Chemistry A, 2021, 9, 15207-15216.	5.2	10
60448	The effect of ionic defect interactions on the hydration of yttrium-doped barium zirconate. Physical Chemistry Chemical Physics, 2021, 23, 4882-4891.	1.3	11
60449	Electronic and optical properties of orthorhombic (CH3NH3)BX3 (B = Sn, Pb; X = F, Cl, Br, I) perovskites: a first-principles investigation. RSC Advances, 2021, 11, 22264-22272.	1.7	6
60451	First principles investigations of the optical selectivity of titanium carbide-based materials for concentrating solar power applications. Journal of Materials Chemistry C, 2021, 9, 7591-7598.	2.7	4
60452	Density functional modeling and total scattering analysis of the atomic structure of a quaternary<mml:math xmlns:mml="http://www.w3.org/1998/Math/MathML"><mml:mrow><mml:mi>CaO</mml:mi><mml:mtext>â^'</mml:mtext><mml:mi>M mathvariant="normal">O</mml:mi><mml:mn>3</mml:mn></mml:msub><mml:mtext>â^'</mml:mtext><mml:msub><mml:mi>SiO</mm glass: Uncov. Physical Review Materials, 2021, 5, .	0.9	15
60453	Forced Enhanced Atomic Refinement Modeling of the Metallic Glass Cu 46 Zr 46 Al 8. Physica Status Solidi (B): Basic Research, 2021, 258, 2000415.	0.7	2
60454	Kagome quantum anomalous Hall effect with high Chern number and large band gap. Physical Review B, 2021, 103, .	1.1	17
60455	Raman spectra and elastic light scattering dynamics of V3O5 across insulatorâ€“metal transition. Journal of Applied Physics, 2021, 129, 025111.	1.1	3
60456	What does graphitic carbon nitride really look like?. Physical Chemistry Chemical Physics, 2021, 23, 2853-2859.	1.3	12
60457	Enhancing magnetic anisotropy and stability of Î±â€³-Fe16N2 phase by Co and V co-substitution. AIP Advances, 2021, 11, .	0.6	5

#	Article	IF	Citations
60458	Real-space charge distribution of the cobalt ion and its relation with charge and spin states. Journal of the Korean Physical Society, 2021, 78, 302-306.	0.3	0
60459	Host dependent electrocatalytic hydrogen evolution of Ni/TiO2 composites. Journal of Materials Chemistry A, 2021, 9, 6325-6334.	5.2	10
60460	An efficient and robust lanthanum strontium cobalt ferrite catalyst as a bifunctional oxygen electrode for reversible solid oxide cells. Journal of Materials Chemistry A, 2021, 9, 5507-5521.	5.2	21
60461	In situ TEM study of edge reconstruction and evolution in monolayer black phosphorus. Nanoscale, 2021, 13, 4133-4139.	2.8	9
60462	First-principles calculation for water purification of Pb, Sn and Zn ions adsorption on graplidiyne surface. Journal of Physics: Conference Series, 2021, 1719, 012028.	0.3	3
60463	Alloy engineering in mixed Snâ€“Ge perovskites for photovoltaic application. Journal of Materials Chemistry A, 2021, 9, 6955-6961.	5.2	14
60464	First-Principles Study of Germagraphene as an Anode Material for Lithium-Ion Batteries. Applied Physics, 2021, 11, 44-52.	0.0	0
60465	Layered Transition Metal Electride Hf2Se with Coexisting Two-Dimensional Anionic d-Electrons and Hfâ€“Hf Metallic Bonds*. Chinese Physics Letters, 2021, 38, 017302.	1.3	2
60466	Structure prediction, electronic, and mechanical properties of alkali metal MB₁₂ (M = Be,) Tj ETQq0 0 0 rgBT /Overlock 10 T	0.7	4
60467	Evolution of Water Layer Adsorption on the GaN(0001) Surface and Its Influence on Electronic Properties. Journal of Physical Chemistry C, 2021, 125, 667-674.	1.5	5
60468	Anisotropic Structural Collapse of Mg₃Sb₂ and Mg₃Bi₂ at High Pressure. Chemistry of Materials, 2021, 33, 567-573.	3.2	14
60469	Electric field induced reversal of spin polarization, magnetic anisotropy and tailored Dzyaloshinskiiâ€“Moriya interaction in underoxidized SrRuO3/SrTiO3 heterostructures. Physical Chemistry Chemical Physics, 2021, 23, 3008-3018.	1.3	2
60470	Effect of Halogen Ions on the Low Thermal Conductivity of Cesium Halide Perovskite. Journal of Physical Chemistry C, 2021, 125, 91-97.	1.5	18
60471	Rationalization of promoted reverse water gas shift reaction by Pt3Ni alloy: Essential contribution from ensemble effect. Journal of Chemical Physics, 2021, 154, 014702.	1.2	6
60472	Bain and Nishiyamaâ€“Wassermann transition path separation in the martensitic transitions of Fe. RSC Advances, 2021, 11, 3043-3048.	1.7	6
60473	Experimental and computational study on roles of WOx promoting strong metal support promoter interaction in Pt catalysts during glycerol hydrogenolysis. Scientific Reports, 2021, 11, 530.	1.6	8
60474	Defect-engineering of Pt/Bi₄NbO₈Br heterostructures for synergetic promotional photocatalytic removal of versatile organic contaminants. Journal of Materials Chemistry C, 2021, 9, 2784-2792.	2.7	13
60475	Selfâ€Healing of Broken Bonds and Deep Gap States in Sb₂Se₃ and Sb₂S₃. Advanced Electronic Materials, 2021, 7, 2000908.	2.6	12

#	Article	IF	Citations
60476	Typeâ€II AsP/As van der Waals Heterostructures: Tunable Anisotropic Electronic Structures and Optical Properties. Advanced Materials Interfaces, 2021, 8, 2001555.	1.9	11
60477	Theoretical insight into the CdS/FAPbI₃ heterostructure: a promising visible-light absorber. New Journal of Chemistry, 2021, 45, 4393-4400.	1.4	10
60478	Formation of atomic fluorine anions in 12CaOÂ·7Al2O3. AIP Advances, 2021, 11, 015146.	0.6	0
60479	Computational screening of pristine and functionalized ordered TiVC MXenes as highly efficient anode materials for lithium-ion batteries. Nanoscale, 2021, 13, 2995-3001.	2.8	22
60480	Doping effects on catechol functionalized anatase TiO2(101) surface for dye-sensitized solar cells. Materials Research Express, 2021, 8, 015906.	0.8	3
60481	First-Principles Calculation of Defect Properties on Copper Doped KTaO3 Crystal. ECS Journal of Solid State Science and Technology, 2021, 10, 014009.	0.9	0
60482	Self-inhibition effect of metal incorporation in nanoscaled semiconductors. Proceedings of the National Academy of Sciences of the United States of America, 2021, 118, .	3.3	0
60483	Data-driven analysis of the rotational energy landscapes of an organic cation in a substituted alloy perovskite. Materials Advances, 2021, 2, 2366-2372.	2.6	0
60484	Investigation of the dissolution and diffusion properties of interstitial oxygen at grain boundaries in body-centered-cubic iron by the first-principles study. RSC Advances, 2021, 11, 8643-8653.	1.7	7
60485	Lattice dynamics in the conformational environment of multilayered hexagonal boron nitride (h-BN) results in peculiar infrared optical responses. Physical Chemistry Chemical Physics, 2021, 23, 7247-7260.	1.3	3
60486	Ab initio screening of Pt-based transition-metal nanoalloys using descriptors derived from the adsorption and activation of CO₂. Physical Chemistry Chemical Physics, 2021, 23, 6029-6041.	1.3	14
60487	Effects of S/F doping and Li/Mn site exchange in Li2MnSiO4: A first-principles investigation of the structural, electrochemical and electronic properties. Electrochimica Acta, 2021, 367, 137553.	2.6	3
60488	Half-Dirac semimetals and the quantum anomalous Hall effect in Kagome Cd₂N₃ lattices. Nanoscale Advances, 2021, 3, 847-854.	2.2	6
60489	The impact of cation and anion pairing in ionic salts on surface defect passivation in cesium lead bromide nanocrystals. Journal of Materials Chemistry C, 2021, 9, 991-999.	2.7	0
60490	Polarization-dependence of the Raman response of free-standing strained Ce_{0.8}Gd_{0.2}O₂ membranes. Physical Chemistry Chemical Physics, 2021, 23, 6903-6913.	1.3	1
60491	A photo-induced spin crossover based molecular switch and spin filter operating at room temperature. Dalton Transactions, 2021, 50, 6578-6587.	1.6	4
60492	Rational design of Ti-based oxygen redox layered oxides for advanced sodium-ion batteries. Journal of Materials Chemistry A, 2021, 9, 11762-11770.	5.2	11
60493	La induced Si3 trimer bilayer on the Si(111) surface. Physical Chemistry Chemical Physics, 2021, 23, 11466-11471.	1.3	1

#	Article	IF	Citations
60494	Synergistic modulation of metal-free photocatalysts by the composition ratio change and heteroatom doping for overall water splitting. Journal of Materials Chemistry A, 2021, 9, 11753-11761.	5.2	14
60495	Ideal strength and strain engineering of the Rashba effect in two-dimensional BiTeBr. Physical Chemistry Chemical Physics, 2021, 23, 6552-6560.	1.3	13
60496	Black phosphorene/blue phosphorene van der Waals heterostructure: a potential anode material for lithium-ion batteries. Physical Chemistry Chemical Physics, 2021, 23, 17392-17401.	1.3	6
60497	Giant thermoelectric performance of an n-type 2D GaSe_{0.5}Te_{0.5} alloy. Journal of Materials Chemistry C, 2021, 9, 10497-10504.	2.7	5
60498	Substituted ALPO-5 Zeolites as Promising O2 Sorption Pump Materials: A Density Functional Theory Study. Journal of Physical Chemistry C, 2021, 125, 1269-1281.	1.5	2
60499	Structural Transition with a Sharp Change in the Electrical Resistivity and Spinâ€“Orbit Mott Insulating State in a Rhenium Oxide, Sr₃Re₂O₉. Inorganic Chemistry, 2021, 60, 507-514.	1.9	4
60500	Role of the OH-group in the adsorption properties of methanol, ethanol, and ethylene glycol on 15-atom 3d, 4d, and 5d transition-metal clusters. Physical Chemistry Chemical Physics, 2021, 23, 17553-17566.	1.3	3
60501	Theoretical prediction of solution and order-disorder transition in alloy materials. Wuli Xuebao/Acta Physica Sinica, 2021, .	0.2	1
60502	Tuning metal-insulator transition in Î´-doped La:SrTiO3 superlattice by varying the doping dimensionality and concentration. Wuli Xuebao/Acta Physica Sinica, 2021, .	0.2	0
60503	Prediction of unexpected B_nP_n structures: promising materials for non-linear optical devices and photocatalytic activities. Nanoscale Advances, 2021, 3, 2846-2861.	2.2	9
60504	First principles and machine learning based superior catalytic activities and selectivities for N₂ reduction in MBenes, defective 2D materials and 2D Ï€-conjugated polymer-supported single atom catalysts. Journal of Materials Chemistry A, 2021, 9, 9203-9213.	5.2	67
60505	Modifying Electronic and Elastic Properties of 2-Dimensional [110] Diamond by Nitrogen Substitution. Journal of Carbon Research, 2021, 7, 8.	1.4	8
60506	First-principles investigation of electronic, mechanical and thermoelectric properties of graphene-like XBi (X = Si, Ge, Sn) monolayers. Physical Chemistry Chemical Physics, 2021, 23, 12471-12478.	1.3	16
60507	Ultra-smooth and robust graphene-based hybrid anode for high-performance flexible organic light-emitting diodes. Journal of Materials Chemistry C, 2021, 9, 2106-2114.	2.7	12
60508	Novel Polymorph of Favipiravirâ€”An Antiviral Medication. Pharmaceutics, 2021, 13, 139.	2.0	17
60509	High partial thermal conductivity of luminescence sites: a crucial factor for reducing the heat-induced lowering of the luminescence efficiency. Journal of Materials Chemistry C, 2021, 9, 14439-14443.	2.7	4
60510	Lithiation mechanism of W18O49 anode material for lithium-ion batteries: Experiment and first-principles calculations. Journal of Electroanalytical Chemistry, 2021, 880, 114885.	1.9	10
60511	A theoretical study of de-charging excitations of the NV-center in diamond involving a nitrogen donor [*]. New Journal of Physics, 2020, 22, 123042.	1.2	6

#	Article	IF	Citations
60512	Prediction of Majorana edge states from magnetized topological surface states. Physical Review B, 2021, 103, .	1.1	12
60513	Exploring promising gas sensing and highly active catalysts for CO oxidation: transition-metal (Fe, Co) Tj ETQq1 1 0.784314 rgBT /Ove	1.3	14
60514	Terahertz optics-driven phase transition in two-dimensional multiferroics. Npj 2D Materials and Applications, 2021, 5, .	3.9	16
60515	First-principles study of the morphology and surface structure of LaCoO₃ and La_{0.5}Sr_{0.5}Fe_{0.5}Co_{0.5}O₃ perovskites as air electrodes for solid oxide fuel cells. Science and Technology of Advanced Materials Methods, 2021, 1, 24-33.	0.4	1
60516	Adsorption and diffusion of alkali metals (Li, Na, and K) on heteroatom-doped monolayer titanium disulfide. Dalton Transactions, 2021, 50, 7065-7077.	1.6	7
60517	A size-selective method for increasing the performance of Pt supported on tungstated zirconia catalysts for alkane isomerization: a combined experimental and theoretical DFT study. New Journal of Chemistry, 2021, 45, 10510-10523.	1.4	4
60518	Emerging flat bands in large-angle twisted bi-layer graphene under pressure. Nanoscale, 2021, 13, 9264-9269.	2.8	6
60519	A Dirac nodal surface semi-metallic carbon-based structure as a universal anode material for metal-ion batteries with high performance. Physical Chemistry Chemical Physics, 2021, 23, 18744-18751.	1.3	3
60520	A valence balancing rule for the design of bimetallic phosphides targeting high thermoelectric performance. Physical Chemistry Chemical Physics, 2021, 23, 18916-18924.	1.3	2
60521	Composition and dimension dependent static and dynamic stabilities of inorganic mixed halide antimony perovskites. Journal of Materials Chemistry C, 0, , .	2.7	3
60522	Production of C, N Alternating 2D Materials Using Covalent Modification and Their Electroluminescence Performance. Small Science, 2021, 1, 2000042.	5.8	9
60523	Crystalline red phosphorus for selective photocatalytic reduction of CO₂into CO. Journal of Materials Chemistry A, 2021, 9, 338-348.	5.2	38
60524	<i>Ab Initio</i> Local-Energy and Local-Stress Calculations for Materials Science and Engineering. Materials Transactions, 2021, 62, 1-15.	0.4	12
60525	Ni/NiO heterostructures encapsulated in oxygen-doped graphene as multifunctional electrocatalysts for the HER, UOR and HMF oxidation reaction. Catalysis Science and Technology, 2021, 11, 2480-2490.	2.1	50
60526	Evolutionary exploration of polytypism in lead halide perovskites. Chemical Science, 2021, 12, 12165-12173.	3.7	11
60527	Controlled 2H/1T phase transition in MoS₂ monolayers by a strong interface with M₂C MXenes: a computational study. Physical Chemistry Chemical Physics, 2021, 23, 20107-20116.	1.3	13
60528	Spontaneous flexoelectricity and band engineering in MS₂ (M = Mo, W) nanotubes. Physical Chemistry Chemical Physics, 2021, 23, 20574-20582.	1.3	7
60529	Constructing a 2D/2D interfacial contact in ReS₂/TiO₂via Tiâ€“S bond for efficient charge transfer in photocatalytic hydrogen production. Journal of Materials Chemistry A, 2021, 9, 23687-23696.	5.2	18

#	Article	IF	Citations
60530	Janus PtXO (X = S, Se) monolayers: the visible light driven water splitting photocatalysts with high carrier mobilities. Physical Chemistry Chemical Physics, 2021, 23, 21825-21832.	1.3	18
60531	Pressure-driven electronic phase transition in the high-pressure phase of nitrogen-rich 1H-tetrazoles. RSC Advances, 2021, 11, 21507-21513.	1.7	3
60532	First Principles Calculation of Magnetic Resonance Properties of Cu_{2-<i>δ</i>}X (X = Se, S, Te). Journal of Applied Mathematics and Physics, 2021, 09, 1245-1256.	0.2	1
60533	Type-II lateral SnSe/GeTe heterostructures for solar photovoltaic applications with high efficiency. Nanoscale Advances, 2021, 3, 3643-3649.	2.2	7
60534	Origin of the low conversion efficiency in Cu₂ZnSnS₄ kesterite solar cells: the actual role of cation disorder. Energy and Environmental Science, 2021, 14, 3567-3578.	15.6	43
60535	Sintering Activated Atomic Palladium Catalysts with High-Temperature Tolerance of â^¼1,000Â°C. Cell Reports Physical Science, 2021, 2, 100287.	2.8	7
60536	Enhanced nonradical catalytic oxidation by encapsulating cobalt into nitrogen doped graphene: highlight on interfacial interactions. Journal of Materials Chemistry A, 2021, 9, 7198-7207.	5.2	25
60537	First-Principles Study on Redox Magnetism and Electrochromism of Cyclometalated Triarylamine-Core Triruthenium Complex. Crystals, 2021, 11, 57.	1.0	1
60538	Microcrystal Electron Diffraction for Molecular Design of Functional Non-Fullerene Acceptor Structures. Chemistry of Materials, 2021, 33, 966-977.	3.2	12
60539	Computational mining of Janus Sc₂C-based MXenes for spintronic, photocatalytic, and solar cell applications. Journal of Materials Chemistry A, 2021, 9, 10882-10892.	5.2	52
60540	Atomic-Scale Mechanism of Grain Boundary Effects on the Magnetic and Transport Properties of Fe₃O₄ Bicrystal Films. ACS Applied Materials & Interfaces, 2021, 13, 6889-6896.	4.0	4
60541	Oxygen Adsorption-Induced Morphological Evolution of HÃgg Iron Carbide at High Oxygen Chemical Potentials. Journal of Physical Chemistry C, 2021, 125, 3055-3065.	1.5	3
60542	Nonpolarizing oxygen-redox capacity without O-O dimerization in Na2Mn3O7. Nature Communications, 2021, 12, 631.	5.8	62
60543	Experimental and theoretical evidence of charge transfer in multi-component alloys â€“ how chemical interactions reduce atomic size mismatch. Materials Chemistry Frontiers, 2021, 5, 5746-5759.	3.2	14
60544	Electronic and thermodynamic properties of native point defects in V₂O₅: a first-principles study. Physical Chemistry Chemical Physics, 2021, 23, 11374-11387.	1.3	18
60545	Electrochemical Pourbaix diagrams of Mgâ€“Zn alloys from first-principles calculations and experimental thermodynamic data. Physical Chemistry Chemical Physics, 2021, 23, 19602-19610.	1.3	7
60546	Growth of Monolayer and Multilayer MoS2 Films by Selection of Growth Mode: Two Pathways via Chemisorption and Physisorption of an Inorganic Molecular Precursor. ACS Applied Materials & Interfaces, 2021, 13, 6805-6812.	4.0	16
60547	Kohn-Sham Equations as Regularizer: Building Prior Knowledge into Machine-Learned Physics. Physical Review Letters, 2021, 126, 036401.	2.9	89

#	Article	IF	Citations
60548	Metastable marcasite NiSe₂ nanodendrites on carbon fiber clothes to suppress polysulfide shuttling for high-performance lithiumâ€“sulfur batteries. Nanoscale, 2021, 13, 16487-16498.	2.8	13
60549	Deep levels in cesium lead bromide from native defects and hydrogen. Journal of Materials Chemistry A, 2021, 9, 7491-7495.	5.2	18
60550	Formation of dimethyl carbonateviadirect esterification of CO₂with methanol on reduced or stoichiometric CeO₂(111) and (110) surfaces. Physical Chemistry Chemical Physics, 2021, 23, 16150-16156.	1.3	5
60551	Dimensional reduction upon calcium incorporation in Cs_{0.3}(Ca_{0.3}Ln_{0.7})PS₄ and Cs_{0.5}(Ca_{0.5}Ln_{0.5})PS₄. CrystEngComm, 2021, 23, 831-840.	1.3	5
60552	Surface oxidation-induced restructuring of liquid Pdâ€“Ga SCALMS model catalysts. Physical Chemistry Chemical Physics, 2021, 23, 16324-16333.	1.3	3
60553	Pros and cons of the time-dependent hybrid density functional approach for calculating the optical spectra of solids: a case study of CeO₂. Physical Chemistry Chemical Physics, 2021, 23, 16296-16306.	1.3	5
60554	Strain-induced surface modalities in pnictogen chalcogenide topological insulators. Journal of Applied Physics, 2021, 129, .	1.1	4
60555	Unveiling the critical role of ammonium bromide in blue emissive perovskite films. Nanoscale, 2021, 13, 13497-13505.	2.8	7
60556	MoirÃ© patterns of twisted bilayer antimonene and their structural and electronic transition. Nanoscale, 2021, 13, 13427-13436.	2.8	5
60557	Isosymmetric compression of cubic halide perovskites $$mathrm{ABX}_{3}$$ ($$A=K, Rb, Cs$$;) Tj ETQq1 1 0.784314 rgBT /Overlo Applied Sciences, 2021, 3, 1.	1.5	11
60558	The mechanism of enhanced photocatalytic activity for water-splitting of ReS₂ by strain and electric field engineering. RSC Advances, 2021, 11, 23055-23063.	1.7	5
60559	Modulating the thermal and structural stability of galleneneviavariation of atomistic thickness. Nanoscale Advances, 2021, 3, 499-507.	2.2	10
60560	Infrared spectroscopic measurements of the structure of organic thin films; furfural on Pd(111) and Au(111) surfaces. CrystEngComm, 2021, 23, 4534-4548.	1.3	8
60561	Well-defined Feâ€“Cu diatomic sites for efficient catalysis of CO₂ electroreduction. Journal of Materials Chemistry A, 2021, 9, 23817-23827.	5.2	77
60562	First-principles molecular dynamics study on the surface chemistry and nanotribological properties of MgAl layered double hydroxides. Nanoscale, 2021, 13, 5014-5025.	2.8	12
60563	Vacancy engineering of WO_{3â^’x} nanosheets for electrocatalytic NRR process â€“ a first-principles study. Physical Chemistry Chemical Physics, 2021, 23, 16658-16663.	1.3	9
60564	Selective catalytic reduction of NO over Cu-AFX zeolites: mechanistic insights from in situ/operando spectroscopic and DFT studies. Catalysis Science and Technology, 2021, 11, 4459-4470.	2.1	6
60565	A mechanistic understanding of surface Bi enrichment in dilute GaBi systems. Physical Chemistry Chemical Physics, 2021, 23, 14383-14390.	1.3	2

#	Article	IF	Citations
60566	Incommensurate transition-metal dichalcogenides via mechanochemical reshuffling of binary precursors. Nanoscale Advances, 2021, 3, 4065-4071.	2.2	4
60567	Coreâ€“shell nanoparticles with tensile strain enable highly efficient electrochemical ethanol oxidation. Journal of Materials Chemistry A, 2021, 9, 15373-15380.	5.2	26
60568	Highly efficient photocatalytic water splitting and enhanced piezoelectric properties of 2D Janus group-III chalcogenides. Journal of Materials Chemistry C, 2021, 9, 4989-4999.	2.7	38
60569	Predicting the structural, electronic and magnetic properties of few atomic-layer polar perovskite. Physical Chemistry Chemical Physics, 2021, 23, 5578-5582.	1.3	8
60570	First-Principles Study of Na Intercalation and Diffusion Mechanisms at 2D MoS₂/Graphene Interfaces. Journal of Physical Chemistry C, 2021, 125, 2276-2286.	1.5	23
60571	First-principles-informed energy span and microkinetic analysis of ethanol catalytic conversion to 1,3-butadiene on MgO. Catalysis Science and Technology, 2021, 11, 6682-6694.	2.1	4
60572	First-principles Study on Low Index Surface Structure Optimization and Surface Energy of LiMn2O4 Spinel Oxides. Acta Chimica Sinica, 2021, 79, 1058.	0.5	1
60573	High-throughput systematic topological generation of low-energy carbon allotropes. Npj Computational Materials, 2021, 7, .	3.5	14
60574	CO₂ Photoelectrochemical Reduction Catalyzed by a GaP(001) Photoelectrode. ACS Catalysis, 2021, 11, 1233-1241.	5.5	15
60575	Observation of the correlation between the phonon frequency and long-range magnetic ordering on a MnW octacyanide molecule-based magnet. Journal of Materials Chemistry C, 2021, 9, 10689-10696.	2.7	2
60576	Nonuniversal structure of point defects in face-centered cubic metals. Physical Review Materials, 2021, 5, .	0.9	14
60577	Reply to â€˜Comment on â€œStructural characterization, reactivity, and vibrational properties of silver clusters: A new global minimum for Ag₁₆â€â€™ by P. V. Nhat, N. T. Si, L. V. Duong and M. T. Nguyen, Phys. Chem. Chem. Phys., 2021, 23, DOI: D1CP00646K. Physical Chemistry Chemical Physics, 2021, 23, 12904-12906.	1.3	1
60578	Tunable electronic properties and band alignments of InSâ€“arsenene heterostructures via external strain and electric field. New Journal of Chemistry, 2021, 45, 2508-2519.	1.4	10
60579	Substantial and stable magnetoresistance and spin conductance in phosphorene-based spintronic devices with Co electrodes. Physical Chemistry Chemical Physics, 2021, 23, 10573-10579.	1.3	6
60580	Microstructure and defect characteristics of lithium niobate with different Li concentrations. Inorganic Chemistry Frontiers, 2021, 8, 4006-4013.	3.0	18
60581	Câ€“H Bond Activation of Methane through Electronic Interaction with Pd(110). Journal of Physical Chemistry C, 2021, 125, 1368-1377.	1.5	8
60582	Realizing high thermoelectric performance in SnSe₂<i>via</i> intercalating Cu. Wuli Xuebao/Acta Physica Sinica, 2021, 70, 208401.	0.2	3
60583	Tunable electronic and magnetic properties of transition-metal atoms doped CrBr₃ monolayer. Wuli Xuebao/Acta Physica Sinica, 2021, 70, 247401.	0.2	2

#	Article	IF	Citations
60584	Unveiling the effect of the crystalline phases of iron oxyhydroxide for highly sensitive and selective detection of dopamine. Dalton Transactions, 2021, 50, 13497-13504.	1.6	5
60585	Assessing the stability of Cd₃As₂ Dirac semimetal in humid environments: the influence of defects, steps and surface oxidation. Journal of Materials Chemistry C, 2021, 9, 1235-1244.	2.7	4
60586	Mixed dimensional 0D/3D perovskite heterostructure for efficient green light-emitting diodes. Journal of Materials Chemistry C, 2021, 9, 14318-14326.	2.7	8
60587	Crucial roles of triazinic-Nî€Ò and Cî€Ò groups in photocatalytic water splitting on graphitic carbon nitride. Journal of Materials Chemistry A, 2021, 9, 5522-5532.	5.2	14
60588	Surface Energy-Driven Preferential Grain Growth of Metal Halide Perovskites: Effects of Nanoimprint Lithography Beyond Direct Patterning. ACS Applied Materials & Interfaces, 2021, 13, 5368-5378.	4.0	26
60589	A decomposition mechanism for Mn₂(DSBDC) metalâ€“organic frameworks in the presence of water molecules. Physical Chemistry Chemical Physics, 2021, 23, 22794-22803.	1.3	2
60590	The role of site coordination on the CO₂ electroreduction pathway on stepped and defective copper surfaces. Catalysis Science and Technology, 2021, 11, 2770-2781.	2.1	10
60591	Prediction of tunable spin-orbit gapped materials for dark matter detection. Physical Review Research, 2021, 3, .	1.3	12
60592	Bonding diversity in rock salt-type tellurides: examining the interdependence between chemical bonding and materials properties. RSC Advances, 2021, 11, 20679-20686.	1.7	14
60593	Interface dependence of electrical contact and graphene doping in graphene/XPtY (X, Y = S, Se, and Te) heterostructures. Physical Chemistry Chemical Physics, 2021, 23, 19297-19307.	1.3	9
60594	Subtle structure matters: boosting surface-directed photoelectron transfer via the introduction of specific monovalent oxygen vacancies in TiO₂. Physical Chemistry Chemical Physics, 2021, 23, 19854-19861.	1.3	6
60595	Unveiling the role of the lone electron pair in sesquioxides at high pressure: compressibility of Î²-Sb₂O₃. Dalton Transactions, 2021, 50, 5493-5505.	1.6	7
60596	Machine-Learning-Driven Simulations on Microstructure and Thermophysical Properties of MgCl₂â€“KCl Eutectic. ACS Applied Materials & Interfaces, 2021, 13, 4034-4042.	4.0	44
60597	Two dimensional CrGa₂Se₄: a spin-gapless ferromagnetic semiconductor with inclined uniaxial anisotropy. Nanoscale, 2021, 13, 6024-6029.	2.8	17
60598	Ni nanoparticles/V₄C₃T_x MXene heterostructures for electrocatalytic nitrogen fixation. Materials Chemistry Frontiers, 2021, 5, 2338-2346.	3.2	38
60599	Single site Fe on the (110) surface of Î³-Al₂O₃: insights from a DFT study including the periodic boundary approach. Physical Chemistry Chemical Physics, 2021, 23, 7164-7177.	1.3	9
60600	Strain-controlled single Cr-embedded nitrogen-doped graphene achieves efficient nitrogen reduction. Materials Advances, 2021, 2, 5704-5711.	2.6	9
60601	Theoretically modelling graphene-like carbon matryoshka with strong stability and particular three-center two-electron Ï€ bonds. Physical Chemistry Chemical Physics, 2021, 23, 11907-11916.	1.3	3

#	Article	IF	Citations
60602	A fast and general approach to produce a carbon coated Janus metal/oxide hybrid for catalytic water splitting. Journal of Materials Chemistry A, 2021, 9, 7606-7616.	5.2	17
60603	Effect of Linker Distribution in the Photocatalytic Activity of Multivariate Mesoporous Crystals. Journal of the American Chemical Society, 2021, 143, 1798-1806.	6.6	45
60604	Theoretical investigation of defective MXenes as potential electrocatalysts for CO reduction toward C₂ products. Physical Chemistry Chemical Physics, 2021, 23, 12431-12438.	1.3	11
60605	Stabilized open metal sites in bimetallic metalâ€“organic framework catalysts for hydrogen production from alcohols. Journal of Materials Chemistry A, 2021, 9, 10869-10881.	5.2	20
60606	Ultrafast Charge Transfer Coupled to Quantum Proton Motion at Molecule/Metal Oxide Interface. SSRN Electronic Journal, 0, , .	0.4	0
60607	Reaction Kinetics and Mechanism for the Catalytic Reduction of Propionic Acid over Supported ReO_x Promoted by Pd. ACS Catalysis, 2021, 11, 1435-1455.	5.5	21
60608	Ultra-high thermal conductivities of tetrahedral carbon allotropes with non-simple structures. Physical Chemistry Chemical Physics, 2021, 23, 24550-24556.	1.3	2
60609	NO reduction with CO over CuO_x/CeO₂ nanocomposites: influence of oxygen vacancies and lattice strain. Catalysis Science and Technology, 2021, 11, 6543-6552.	2.1	20
60610	Avoiding dendrite formation by confining lithium deposition underneath Liâ€“Sn coatings. Journal of Materials Research, 2021, 36, 797-811.	1.2	4
60611	Highly efficient degradation of phenol via metal sulphides. AIP Conference Proceedings, 2021, , .	0.3	0
60612	Chemical route to prepare nickel supported on intermetallic Ti₆Si₇Ni₁₆ nanoparticles catalyzing CO methanation. Nanoscale, 2021, 13, 16533-16542.	2.8	4
60613	Enhanced solar-to-hydrogen efficiency for photocatalytic water splitting based on a polarized heterostructure: the role of intrinsic dipoles in heterostructures. Journal of Materials Chemistry A, 2021, 9, 14515-14523.	5.2	32
60614	Impact of S-Vacancies on the Charge Injection Barrier at the Electrical Contact with the MoS₂ Monolayer. ACS Nano, 2021, 15, 2686-2697.	7.3	27
60615	Difference in magnetic anisotropy of the ferromagnetic monolayers <mml:math xmlns:mml="http://www.w3.org/1998/Math/MathML"><mml:mrow><mml:msub><mml:mi mathvariant="normal">VI</mml:mi><mml:mn>3</mml:mn></mml:msub></mml:mrow></mml:math> and <mml:math xmlns:mml="http://www.w3.org/1998/Math/MathML"><mml:mrow><mml:msub><mml:mi>CrI</mml:mi><mml:mn>3</mml:mn></mml:msub></mml:mrow></mml:math>. Physical Review B, 2021, 103, .	1.1	23
60616	Structural, Electronic, Magnetic, and Mechanical Properties of Co_{2-x}V_xFeSi Heusler Alloys. IEEE Transactions on Magnetics, 2022, 58, 1-5.	1.2	4
60617	Can Electron Transport through a Blue-Copper Azurin Be Coherent? An Ab Initio Study. Journal of Physical Chemistry C, 2021, 125, 1693-1702.	1.5	25
60618	Direct arylâ€“aryl coupling of pentacene on Au(110). Physical Chemistry Chemical Physics, 2021, 23, 22155-22159.	1.3	0
60619	Substitutional 4d transition metal doping in atomically thin lead. RSC Advances, 2021, 11, 6182-6187.	1.7	4

#	Article	IF	Citations
60620	In situ manipulation of the active Au-TiO ₂ interface with atomic precision during CO oxidation. Science, 2021, 371, 517-521.	6.0	165
60621	Accurate electronic properties and non-linear optical response of two-dimensional MA2Z4. Nanoscale, 2021, 13, 5479-5488.	2.8	61
60622	Spin-constrained optoelectronic functionality in two-dimensional ferromagnetic semiconductor heterojunctions. Materials Horizons, 2021, 8, 1323-1333.	6.4	11
60623	Band degeneracy enhanced thermoelectric performance in layered oxyselenides by first-principles calculations. Npj Computational Materials, 2021, 7, .	3.5	62
60624	Discovery of Lead-Free Hybrid Organic/Inorganic Perovskites Using Metaheuristic-Driven DFT Calculations. Chemistry of Materials, 2021, 33, 782-798.	3.2	23
60625	Effect of hydrogenation on the thermal conductivity of 2D gallium nitride. Physical Chemistry Chemical Physics, 2021, 23, 22423-22429.	1.3	8
60626	Electrochemically synthesized SnO₂ with tunable oxygen vacancies for efficient electrocatalytic nitrogen fixation. Nanoscale, 2021, 13, 16307-16315.	2.8	13
60627	Scalable Synthesis of Crystalline One-Dimensional Carbon Nanothreads through Modest-Pressure Polymerization of Furan. ACS Nano, 2021, 15, 4134-4143.	7.3	32
60628	Sulfur vacancies in Co₉S_{8â^'x}/N-doped graphene enhancing the electrochemical kinetics for high-performance lithiumâ€“sulfur batteries. Journal of Materials Chemistry A, 2021, 9, 10704-10713.	5.2	53
60629	Prediction of chemically ordered dual transition metal carbides (MXenes) as high-capacity anode materials for Na-ion batteries. Nanoscale, 2021, 13, 7234-7243.	2.8	20
60630	Tracer diffusion coefficients of Li⁺ ions in c-axis oriented Li_xCoO₂ thin films measured by secondary ion mass spectrometry. Physical Chemistry Chemical Physics, 2021, 23, 2438-2448.	1.3	28
60631	The MLIP package: moment tensor potentials with MPI and active learning. Machine Learning: Science and Technology, 2021, 2, 025002.	2.4	181
60632	Ferromagnetic TM₂BC (TM = Cr, Mn) monolayers for spintronic devices with high Curie temperature. Physical Chemistry Chemical Physics, 2021, 23, 6107-6115.	1.3	29
60633	Active Phase on SrCo_{1â€“x}Fe_xO_{3â^'Î´} (0 â‰¤ x â‰¤ 0.5) Perovskite for Water Oxidation: Reconstructed Surface versus Remaining Bulk. Jacs Au, 2021, 1, 108-115.	3.6	47
60634	Thickness-induced band-gap engineering in lead-free double perovskite Cs₂AgBiBr₆ for highly efficient photocatalysis. Physical Chemistry Chemical Physics, 2021, 23, 12439-12448.	1.3	14
60635	Regulation of nitrogen configurations and content in 3D porous carbons for improved lithium storage. Dalton Transactions, 2021, 50, 14390-14399.	1.6	2
60636	Potential thermoelectric materials: first-principles prediction of low lattice thermal conductivity of two-dimensional (2D) orthogonal ScX₂ (X = C and N) compounds. Physical Chemistry Chemical Physics, 2021, 23, 23718-23729.	1.3	2
60637	Exploring the structures and properties of nickel silicides at the pressures of the Earthâ€™s core. Physical Chemistry Chemical Physics, 2021, 23, 14671-14677.	1.3	8

#	Article	IF	Citations
60638	Theoretical exploration of quaternary hexagonal MAB phases and two-dimensional derivatives. Nanoscale, 2021, 13, 13208-13214.	2.8	16
60639	Adsorption energy as a promising single-parameter descriptor for single atom catalysis in the oxygen evolution reaction. Journal of Materials Chemistry A, 2021, 9, 6442-6450.	5.2	18
60640	A DFT-based microkinetic study on methanol synthesis from CO₂ hydrogenation over the In₂O₃ catalyst. Physical Chemistry Chemical Physics, 2021, 23, 1888-1895.	1.3	20
60641	Electrochemical CO2 reduction: water/catalyst interface versus polymer/catalyst interface. Journal of Materials Chemistry A, 2021, 9, 17474-17480.	5.2	5
60642	Hydrogen generation from ammonia borane hydrolysis catalyzed by ruthenium nanoparticles supported on Coâ€“Ni layered double oxides. Sustainable Energy and Fuels, 2021, 5, 2301-2312.	2.5	17
60643	Tunable magneto-optical effect, anomalous Hall effect, and anomalous Nernst effect in the two-dimensional room-temperature ferromagnet <mml:math xmlns:mml="http://www.w3.org/1998/Math/MathML"><mml:mrow><mml:mn>1</mml:mn><mml:mi>T</mml:mi></mml:mrow><mm Physical Review B, 2021, 103, .	1.1	22
60644	Influence of the PO_uN_{4â^’u} structural units on the formation energies and transport properties of lithium phosphorus oxynitride: a DFT study. Physical Chemistry Chemical Physics, 2021, 23, 22567-22588.	1.3	2
60645	Stable, high-performance, dendrite-free, seawater-based aqueous batteries. Nature Communications, 2021, 12, 237.	5.8	174
60646	Tuning the electronic structure of Ag-Pd alloys to enhance performance for alkaline oxygen reduction. Nature Communications, 2021, 12, 620.	5.8	107
60655	Combining Electronic Structure Calculations and Spectroscopy to Unravel the Structure of Grafted Organometallic Complexes. , 0, , 359-374.		1
60656	Selfâ€Compensation in Transparent Conducting Fâ€Doped SnO₂. Advanced Functional Materials, 2018, 28, 1701900.	7.8	85
60657	Alloy Engineering in Fewâ€Layer Manganese Phosphorus Trichalcogenides for Surfaceâ€Enhanced Raman Scattering. Advanced Functional Materials, 2020, 30, 1910171.	7.8	48
60658	Insights of Heteroatoms Dopingâ€Enhanced Bifunctionalities on Carbon Based Energy Storage and Conversion. Advanced Functional Materials, 2021, 31, 2009109.	7.8	58
60659	A Hollowâ€Structured CuS@Cu₂S@Au Nanohybrid: Synergistically Enhanced Photothermal Efficiency and Photoswitchable Targeting Effect for Cancer Theranostics. Advanced Materials, 2017, 29, 1701266.	11.1	252
60660	Homogeneous 2D MoTe₂ pâ€“n Junctions and CMOS Inverters formed by Atomicâ€Layerâ€Depositionâ€Induced Doping. Advanced Materials, 2017, 29, 1701798.	11.1	117
60661	Origin of Fractureâ€Resistance to Large Volume Change in Cuâ€Substituted Co₃O₄ Electrodes. Advanced Materials, 2018, 30, 1704851.	11.1	29
60662	Steric Impediment of Ion Migration Contributes to Improved Operational Stability of Perovskite Solar Cells. Advanced Materials, 2020, 32, e1906995.	11.1	142
60663	Anharmonic Lattice Vibrations in Smallâ€Molecule Organic Semiconductors. Advanced Materials, 2020, 32, 1908028.	11.1	24

#	Article	IF	Citations
60664	Epitaxial Growth of Singleâ€Phase 1T'â€WSe₂ Monolayer with Assistance of Enhanced Interface Interaction. Advanced Materials, 2021, 33, e2004930.	11.1	28
60665	Halogen Substitution in Zeroâ€Dimensional Mixed Metal Halides toward Photoluminescence Modulation and Enhanced Quantum Yield. Advanced Optical Materials, 2020, 8, 2000418.	3.6	29
60666	The Power of Ionic Liquids: Crystal Facet Engineering of SrTiO₃ Nanoparticles for Tailored Photocatalytic Applications. Advanced Sustainable Systems, 2021, 5, 2000180.	2.7	10
60667	Unconventional Ferroelectric Switching via Local Domain Wall Motion in Multiferroic Îµâ€Fe₂O₃ Films. Advanced Electronic Materials, 2020, 6, 1901134.	2.6	11
60668	A Highâ€Energy NASICONâ€Type Cathode Material for Naâ€Ion Batteries. Advanced Energy Materials, 2020, 10, 1903968.	10.2	116
60669	In Situ Polymerized Conjugated Poly(pyreneâ€4,5,9,10â€tetraone)/Carbon Nanotubes Composites for Highâ€Performance Cathode of Sodium Batteries. Advanced Energy Materials, 2021, 11, 2002917.	10.2	69
60670	Fast Proton Insertion in Layered H₂W₂O₇ via Selective Etching of an Aurivillius Phase. Advanced Energy Materials, 2021, 11, .	10.2	16
60671	A₂SnS₅: A Structural Incommensurate Modulation Exhibiting Strong Secondâ€Harmonic Generation and a High Laserâ€Induced Damage Threshold (A=Ba, Sr). Angewandte Chemie, 2020, 132, 11959-11963.	1.6	17
60672	Rechargeable Photoactive Znâ€Air Batteries Using NiCo₂S₄ as an Efficient Bifunctional Photocatalyst towards OER/ORR at the Cathode. Batteries and Supercaps, 2020, 3, 541-547.	2.4	40
60673	On the Limited Role of Electronic Support Effects in Selective Alkyne Hydrogenation: A Kinetic Study of Au/MO_x Catalysts Prepared from Oleylamineâ€Capped Colloidal Nanoparticles. ChemCatChem, 2019, 11, 1650-1664.	1.8	9
60674	GWâ€BSE Calculations of Electronic Band Gap and Optical Spectrum of ZnFe₂O₄: Effect of Cation Distribution and Spin Configuration. ChemPhysChem, 2020, 21, 546-551.	1.0	25
60675	Identifying promising metalâ€“organic frameworks for heterogeneous catalysis via highâ€throughput periodic density functional theory. Journal of Computational Chemistry, 2019, 40, 1305-1318.	1.5	87
60676	Antiâ€Thermalâ€Quenching Bi³⁺ Luminescence in a Cyanâ€Emitting Ba₂ZnGe₂O₇:Bi Phosphor Based on Zinc Vacancy. Laser and Photonics Reviews, 2021, 15, .	4.4	86
60677	Cr³⁺â€Doped Scâ€Based Fluoride Enabling Highly Efficient Near Infrared Luminescence: A Case Study of K₂NaScF₆:Cr³⁺. Laser and Photonics Reviews, 2021, 15, 2000410.	4.4	140
60678	Optical and magnetic properties of some XMnSb and Co ₂ YZ Compounds: ab initio calculations. Physica Status Solidi C: Current Topics in Solid State Physics, 2017, 14, 1600182.	0.8	3
60679	The doping mechanism and electrical performance of polyethylenimineâ€doped MoSÂ-₂ transistor. Physica Status Solidi C: Current Topics in Solid State Physics, 2017, 14, 1600262.	0.8	12
60680	XYO ₃ (X â€‰=â€‰K, Na; Y â€‰=â€‰Nb, Ta) based superlattices for photocatalysis. Physica Status Solidi C: Current Topics in Solid State Physics, 2017, 14, 1700026.	0.8	6
60681	Transport Properties of Grapheneâ€BiTeI Hybrid Structures. Physica Status Solidi C: Current Topics in Solid State Physics, 2017, 14, 1700215.	0.8	3

#	Article	IF	Citations
60682	Defects Engineering Induced Ultrahigh Magnetization in Rare Earth Element Ndâ€doped MoS₂. Advanced Quantum Technologies, 2021, 4, 2000093.	1.8	19
60683	Highly Stable and Ultrahighâ€Rate Li Metal Anode Enabled by Fluorinated Carbon Fibers. Small, 2021, 17, e2006002.	5.2	47
60684	Auâ€Polyoxometalates Aâ€Bâ€Aâ€B Type Copolymerâ€Analogue Subâ€1 nm Nanowires. Small, 2021, 17, e2006260.	5.2	22
60685	Antiblocking Heterostructure to Accelerate Kinetic Process for Naâ€Ion Storage. Small, 2021, 17, e2006374.	5.2	24
60686	Structural Plasticity in the Frankâ€Kasper Realm: Chemical Pressure Roles of the Î¼ â€•and Ï‡â€Phase Units in the Moâ€'Feâ€'Cr System. Zeitschrift Fur Anorganische Und Allgemeine Chemie, 2021, 647, 64-74.	0.6	5
60687	Supercell Methods for Defect Calculations. Topics in Applied Physics, 0, , 29-68.	0.4	10
60688	Applications of Computer Simulations and Statistical Mechanics in Surface Electrochemistry. Modern Aspects of Electrochemistry, 2009, , 131-149.	0.2	2
60689	Density Functional Theory of High-k Dielectric Gate Stacks. Nanostructure Science and Technology, 2008, , 171-190.	0.1	1
60690	Proton Conduction in PEMs: Complexity, Cooperativity and Connectivity. Topics in Applied Physics, 2009, , 385-412.	0.4	11
60691	Ab Initio Study of Ideal Shear Strength. Solid Mechanics and Its Applications, 2004, , 401-410.	0.1	4
60692	Hydrogen Bonds And Solvent Effects In Soil Processes: A Theoretical View. Challenges and Advances in Computational Chemistry and Physics, 2008, , 321-347.	0.6	1
60693	Multiscale Modeling of RPV Embrittlement. NATO Science for Peace and Security Series B: Physics and Biophysics, 2008, , 245-262.	0.2	1
60694	Lithium Ion Batteries, Electrochemical Reactions in. , 2012, , 6067-6097.		2
60695	Density Functional Theory Simulations of High-k Oxides on III-V Semiconductors. , 2010, , 93-130.		3
60696	Challenges in the Design of Active and Durable Alloy Nanocatalysts for Fuel Cells. Modern Aspects of Electrochemistry, 2010, , 351-396.	0.2	3
60697	Can Theory Help in the Search for Better Thermoelectric Materials?. Fundamental Materials Research, 2003, , 259-302.	0.1	3
60698	Syntheses and Properties of Some Bi-Containing Compounds with Noncentrosymmetric Structure. Springer Series in Materials Science, 2013, , 321-341.	0.4	1
60699	Growing SrTiO3 on Si (001) by Molecular Beam Epitaxy. , 2014, , 115-158.		1

#	Article	IF	Citations
60700	Point Defect Energies in L12-Ordered Ni3Al. , 2000, , 187-197.		2
60701	Ab Initio Study of Structure and Compressibility of Garnets. , 2000, , 417-427.		1
60702	Photovoltaic Materials Design by Computational Studies: Metal Sulfides. , 2020, , 123-138.		2
60703	From Molecules to Thin Films: GaP Nucleation on Si Substrates. , 2013, , 185-199.		1
60704	Innovations in Finite-Temperature Density Functionals. Lecture Notes in Computational Science and Engineering, 2014, , 61-85.	0.1	4
60705	Progress in Warm Dense Matter and Planetary Physics. Lecture Notes in Computational Science and Engineering, 2014, , 203-234.	0.1	7
60707	Interfacial Properties and Growth Dynamics of Semiconductor Interfaces. , 2016, , 199-213.		1
60708	Big Data-Driven Materials Science and Its FAIR Data Infrastructure. , 2019, , 1-25.		5
60709	The Long and Winding Road: Predicting Materials Properties Through Theory and Computation. , 2019, , 1-12.		1
60710	Big Data-Driven Materials Science and Its FAIR Data Infrastructure. , 2020, , 49-73.		18
60711	Solid Oxide Fuel Cell Materials and Interfaces. , 2020, , 1275-1305.		2
60712	CALYPSO Method for Structure Prediction and Its Applications to Materials Discovery. , 2020, , 2729-2756.		3
60713	Surface Hydrogenation of the Si(100)-2Ã—1 and Electronic Properties of Silicon Dangling Bonds on the Si(100):H Surfaces. Advances in Atom and Single Molecule Machines, 2017, , 1-24.	0.0	1
60714	Quantum Hamiltonian Computing (QHC) Logic Gates. Advances in Atom and Single Molecule Machines, 2017, , 121-138.	0.0	2
60715	Towards Modelling and Implementation of Reliability and Usability Features for Research-Oriented Cloud Computing Platforms. Communications in Computer and Information Science, 2016, , 158-178.	0.4	3
60716	Porting VASP from MPI to MPI+OpenMP [SIMD]. Lecture Notes in Computer Science, 2017, , 107-122.	1.0	4
60717	Ultrafast dynamics of photoinduced processes at surfaces and interfaces. , 2007, , 387-484.		2
60718	A Theoretical View on the Dielectric Properties of Crystalline and Amorphous High-Îº Materials and Films. , 2007, , 269-292.		1

#	Article	IF	Citations
60719	Structural and Magnetic Properties of Transition Metal Nanoparticles from First Principles. , 2008, , 117-128.		8
60720	Thermodynamic Properties of Materials Using Lattice-Gas Models with Renormalized Potentials. Advances in Materials Research, 2008, , 275-290.	0.2	1
60721	Introduction to Molecular Dynamics. Lecture Notes in Physics, 2008, , 3-40.	0.3	9
60722	Ab initio Simulations of PbTe-CdTe Nanostructures. , 2008, , 107-116.		1
60723	Scanning Tunneling Microscopy of the Si(111)-7Ã—7 Surface and Adsorbed Ge Nanostructures. Nanoscience and Technology, 2009, , 183-220.	1.5	1
60724	Deconstructing the Structural Convergence of the (110) Surface of Rutile TiO2. Springer Proceedings in Physics, 2009, , 26-30.	0.1	1
60725	Metalâ€“Insulator Transition in Dense Hydrogen. Springer Series in Materials Science, 2010, , 63-84.	0.4	3
60726	Adsorption of Cysteine on the Au(110)-surface: A Density Functional Theory Study. , 2010, , 53-60.		1
60727	H2 Carrying Capacity by Considering Charging and Discharging Processes â€“ Case Studies on Small Carbon- and Boron Nitride Nanotubes. , 2010, , 85-109.		1
60728	High-Resolution Electron Microscopy of Semiconductor Heterostructures and Nanostructures. Springer Series in Materials Science, 2012, , 23-62.	0.4	2
60729	Computational Physics on Graphics Processing Units. Lecture Notes in Computer Science, 2013, , 3-26.	1.0	15
60730	Parallel Electronic Structure Calculations Using Multiple Graphics Processing Units (GPUs). Lecture Notes in Computer Science, 2013, , 63-76.	1.0	14
60731	Maximizing Application Performance in a Multi-core, NUMA-Aware Compute Cluster by Multi-level Tuning. Lecture Notes in Computer Science, 2013, , 226-238.	1.0	7
60732	Theoretical Ab Initio Calculations in Ordered-Vacancy Compounds at High Pressures. Springer Series in Materials Science, 2014, , 185-210.	0.4	3
60733	Role of step sites on water dissociation on stoichiometric ceria surfaces. Highlights in Theoretical Chemistry, 2014, , 19-25.	0.0	1
60734	Contrast Mechanisms on Insulating Surfaces. Nanoscience and Technology, 2002, , 305-347.	1.5	2
60735	First-Principles Simulations for CuInGaSe2 (CIGS) Solar Cells. , 2019, , 45-74.		1
60736	Interaction Between Oxygen and Yttrium Impurity Atoms as well as Vacancies in fcc Iron Lattice: Ab Initio Modeling. NATO Science for Peace and Security Series B: Physics and Biophysics, 2012, , 149-159.	0.2	2

#	Article	IF	Citations
60737	First-Principles Study of the Electronic and Magnetic Properties of Defects in Carbon Nanostructures. Carbon Materials, 2013, , 41-76.	0.2	1
60738	Reactivity Theory of Zinc Cation Species in Zeolites. , 2001, , 187-204.		2
60739	Theory of Bayesian Optimization. SpringerBriefs in the Mathematics of Materials, 2017, , 11-28.	0.3	3
60740	Non-regular hexagonal 2D carbon, an allotrope of graphene: a first-principles computational study. Journal of Molecular Modeling, 2020, 26, 150.	0.8	3
60741	Graphitic carbon nitride nanodots: electronic structure and its influence factors. Journal of Materials Science, 2020, 55, 5488-5498.	1.7	3
60742	First-principles investigation of perfect and diffuse antiphase boundaries in HCP-based Ti-Al alloys. Metallurgical and Materials Transactions A: Physical Metallurgy and Materials Science, 2002, 33, 735-741.	1.1	11
60743	Facile synthesis of Au embedded CuOx-CeO2 core/shell nanospheres as highly reactive and sinter-resistant catalysts for catalytic hydrogenation of p-nitrophenol. Nano Research, 2020, 13, 2044-2055.	5.8	39
60744	Carrier mobility tuning of MoS2 by strain engineering in CVD growth process. Nano Research, 2021, 14, 2314.	5.8	27
60745	Elastic Properties and Stacking Fault Energies of Borides, Carbides and Nitrides from First-Principles Calculations. Acta Metallurgica Sinica (English Letters), 2019, 32, 1099-1110.	1.5	18
60746	First-principles study of the anisotropic thermal expansion and thermal transport properties in h-BN. Science China Materials, 2021, 64, 953-963.	3.5	14
60747	Cohesive strength of zirconia/molybdenum interfaces and grain boundaries in molybdenum: A comparative study. Acta Materialia, 2017, 135, 150-157.	3.8	19
60748	Diffusion, defects and understanding the growth of a multicomponent interdiffusion zone between Pt-modified B2 NiAl bond coat and single crystal superalloy. Acta Materialia, 2020, 195, 35-49.	3.8	31
60749	Design of Nickel-Cobalt-Ruthenium multi-principal element alloys. Acta Materialia, 2020, 194, 224-235.	3.8	10
60750	Magnetic properties and excellent cryogenic magnetocaloric performances in B-site ordered RE2ZnMnO6 (REÂ=ÂGd, Dy and Ho) perovskites. Acta Materialia, 2020, 194, 354-365.	3.8	167
60751	Spectroscopic and kinetic responses of Cu-SSZ-13 to SO2 exposure and implications for NOx selective catalytic reduction. Applied Catalysis A: General, 2019, 574, 122-131.	2.2	48
60752	Stability of Mo2C/carbon catalysts during dibenzofuran hydrodeoxygenation. Applied Catalysis A: General, 2020, 600, 117628.	2.2	6
60753	A novel metal-free photocatalyst polyphenylene sulfide: Synthesis, characterization and performance evaluation. Applied Catalysis B: Environmental, 2020, 274, 119073.	10.8	18
60754	Unraveling the selectivity puzzle of H2 evolution over CO2 photoreduction using ZnS nanocatalysts with phase junction. Applied Catalysis B: Environmental, 2020, 274, 119115.	10.8	23

#	Article	IF	Citations
60755	Oxygen vacancy mediated bismuth stannate ultra-small nanoparticle towards photocatalytic CO2-to-CO conversion. Applied Catalysis B: Environmental, 2020, 276, 119156.	10.8	59
60756	A comparative experimental and theoretical investigation on energy storage performance of CoSe2, NiSe2 and MnSe2 nanostructures. Applied Materials Today, 2020, 19, 100568.	2.3	35
60757	Atomic-scale properties of low-index ZnO surfaces. Applied Surface Science, 2004, 237, 336-342.	3.1	49
60758	Modulation of spatial spin polarization at organic spinterface by side groups. Applied Surface Science, 2018, 427, 416-420.	3.1	8
60759	Fabrication of NiSe2 by direct selenylation of a nickel surface. Applied Surface Science, 2018, 428, 623-629.	3.1	33
60760	Insight into the effect of boron doping on electronic structure, photocatalytic and adsorption performance of g-C3N4 by first-principles study. Applied Surface Science, 2020, 511, 145549.	3.1	49
60761	The effect of chlorine vacancy in CuCl2 (0Â0Â1) catalyst on the mechanism of SiCl4 dissociation into SiHCl3: A DFT study. Applied Surface Science, 2020, 515, 146100.	3.1	6
60762	Improving the wettability of Ag/ZrB2 system by Ti, Zr and Hf addition: An insight from first-principle calculations. Applied Surface Science, 2020, 517, 146201.	3.1	29
60763	Nondestructive functionalization of monolayer black phosphorus using Lewis acids: A first-principles study. Applied Surface Science, 2020, 518, 146210.	3.1	6
60764	Surface structure and morphology evolution of iron borides under dynamic conditions: A theoretical study. Applied Surface Science, 2020, 525, 146462.	3.1	6
60765	How does the active site in the MoSe2 surface affect its electrochemical performance as anode material for metal-ion batteries?. Applied Surface Science, 2020, 526, 146637.	3.1	16
60766	Predicting quantum spin hall effect in graphene/GaSb and normal strain-controlled band structures. Applied Surface Science, 2020, 526, 146704.	3.1	1
60767	Synergistic adsorption of lanthanum ions and fatty acids for efficient rare-earth phosphate recovery: Surface analysis and ab initio molecular dynamics studies. Applied Surface Science, 2020, 526, 146725.	3.1	21
60768	Metastable trigonal SnP: A promising anode material for potassium-ion battery. Carbon, 2020, 168, 468-474.	5.4	32
60769	Mechanistic and thermodynamic insights into the deoxygenation of palm oils using Ni2P catalyst: A combined experimental and theoretical study. Chemical Engineering Journal, 2020, 399, 125586.	6.6	15
60770	The photophysical anisotropy and electronic structure of new narrow band gap perovskites Ln2AlMnO6 (Ln = La, Pr, Nd): An experimental and DFT perspective. Ceramics International, 2020, 46, 21021-21032.	2.3	15
60771	Suppressing cation mixing and improving stability by F doping in cathode material LiNiO2 for Li-ion batteries: First-principles study. Colloids and Surfaces A: Physicochemical and Engineering Aspects, 2020, 600, 124940.	2.3	25
60772	First principle study of V-implantation in highly-doped silicon materials. Computational Materials Science, 2017, 136, 207-215.	1.4	6

#	Article	IF	Citations
60773	Potential high-T superconductivity in ZrB2 polymorph under pressure. Computational Materials Science, 2020, 176, 109517.	1.4	5
60774	Migration behavior of tellurium in bcc iron against typical alloying elements: A first-principles study. Computational Materials Science, 2020, 181, 109571.	1.4	7
60775	Effect of transmutation elements Re and Ta on the vacancy formation and dissociation behaviors in W bulk. Computational Materials Science, 2020, 179, 109624.	1.4	9
60776	Tight-Binding Studio: A technical software package to find the parameters of tight-binding Hamiltonian. Computer Physics Communications, 2020, 254, 107379.	3.0	23
60777	The experimental and theoretical insights on the interaction of AuPd bimetallic nanoentities on graphene: A study on electrocatalytic activity towards oxygen reduction reaction. Electrochimica Acta, 2020, 356, 136820.	2.6	10
60778	AlF3-modified anode-electrolyte interface for effective Na dendrites restriction in NASICON-based solid-state electrolyte. Energy Storage Materials, 2020, 30, 170-178.	9.5	86
60779	Towards understanding the strong trapping effects of noble gas elements on hydrogen in tungsten. International Journal of Hydrogen Energy, 2017, 42, 6902-6917.	3.8	31
60780	Atomistic insight into the hydration and proton conducting mechanisms of the cobalt doped Ruddlesden-Popper structure Sr3Fe2O7-Î´. International Journal of Hydrogen Energy, 2020, 45, 14964-14971.	3.8	25
60781	Formation and characterization of gray Ta2O5 and its enhanced photocatalytic hydrogen generation activity. International Journal of Hydrogen Energy, 2020, 45, 16560-16568.	3.8	29
60782	Copper induced phosphide for enhanced electrochemical hydrogen evolution reaction. International Journal of Hydrogen Energy, 2020, 45, 21422-21430.	3.8	15
60783	Atomistic calculations of the generalized stacking fault energies in two refractory multi-principal element alloys. Intermetallics, 2020, 124, 106844.	1.8	40
60784	Electronic and mechanical property of high electron mobility semiconductor Bi2O2Se. Journal of Alloys and Compounds, 2018, 764, 674-678.	2.8	32
60785	Crystal structure and cation ordering in novel perovskite type oxides PrBaCoTa(Nb)O6â€“Î´. Journal of Alloys and Compounds, 2020, 824, 153909.	2.8	6
60786	A DFT study on the austenitic Ni2MnGa (001) surfaces. Journal of Alloys and Compounds, 2020, 836, 155447.	2.8	9
60787	Subtle atomistic processes of S-phase formation in Al-Cu-Mg alloys. Journal of Alloys and Compounds, 2020, 838, 155677.	2.8	14
60788	Prediction of intrinsic electrocatalytic activity for hydrogen evolution reaction in Ti4X3 (Xâ€¯=â€¯C, N). Journal of Catalysis, 2020, 387, 12-16.	3.1	27
60789	Van der Waals heterostructure of graphene and As2S3: Tuning the Schottky barrier height by vertical strain. Journal of Crystal Growth, 2020, 549, 125882.	0.7	1
60790	One-time sintering process to modify xLi2MnO3 (-x)LiMO2 hollow architecture and studying their enhanced electrochemical performances. Journal of Energy Chemistry, 2020, 50, 271-279.	7.1	43

#	Article	IF	Citations
60791	Quantitative insights into the chemical trend of four-coordinated Mn2+ emission in inorganic compounds. Journal of Luminescence, 2020, 225, 117399.	1.5	4
60792	Structural, electronic and optical properties of metalloid element (B, Si, Ge, As, Sb, and Te) doped g-ZnO monolayer: A DFT study. Journal of Molecular Graphics and Modelling, 2020, 101, 107753.	1.3	22
60793	Effect of hydrostatic pressure on electrical resistivity of La0.5Ca0.5Mn1â^'xMoxO3 (xÂ=Â0.03 and 0.05) manganites: Experimental and theoretical approaches. Journal of Magnetism and Magnetic Materials, 2020, 507, 166775.	1.0	3
60794	Effect of Ta capping layer on the magnetic coupling oscillation of L10-MnGa/Co/Ta films. Journal of Magnetism and Magnetic Materials, 2020, 511, 166994.	1.0	2
60795	Molecular reactions and oxidation corrosion on UN (001) surface under exposure to environment gases: A DFT study. Journal of Nuclear Materials, 2020, 533, 152095.	1.3	5
60796	Phonons and thermophysical properties of U1â^'Pu O2 mixed oxide (MOX) fuels. Journal of Nuclear Materials, 2020, 537, 152158.	1.3	6
60797	Insight into interface cohesion and impurity-induced embrittlement in carbide dispersion strengthen tungsten from first principles. Journal of Nuclear Materials, 2020, 538, 152223.	1.3	14
60798	Impact of fission product inclusion on phase development in U3Si2 fuel. Journal of Nuclear Materials, 2020, 537, 152235.	1.3	5
60799	Development of a magnetic nanohybrid for multifunctional application: From immobile photocatalysis to efficient photoelectrochemical water splitting: A combined experimental and computational study. Journal of Photochemistry and Photobiology A: Chemistry, 2020, 397, 112575.	2.0	8
60800	Anisotropic mechanical properties of Tl4Ag18Te11 compound with low thermal conductivity. Journal of Solid State Chemistry, 2020, 289, 121469.	1.4	18
60801	Enhanced age-hardening response of the Mg-Sm alloy via alloying with Cd. Materials Characterization, 2020, 170, 110669.	1.9	9
60802	Structural, mechanical, thermal, magnetic, and electronic properties of the RhMnSb half-Heusler alloy under pressure. Materials Chemistry and Physics, 2020, 251, 123110.	2.0	16
60803	Band gap tuning in aluminum doped two-dimensional hexagonal boron nitride. Materials Chemistry and Physics, 2020, 250, 123176.	2.0	19
60804	Electronic and optical properties of PbFCl and PbFI monolayers using density functional theory and beyond. Materials Chemistry and Physics, 2020, 252, 123233.	2.0	19
60805	Packing high-energy together: Binding the power of pentazolate and high-valence metals with strong bonds. Materials and Design, 2020, 193, 108820.	3.3	14
60806	Surface Defects in Two-Dimensional Photocatalysts for Efficient Organic Synthesis. Matter, 2020, 2, 842-861.	5.0	107
60807	Tunable Second Harmonic Generation in Twisted Bilayer Graphene. Matter, 2020, 3, 1361-1376.	5.0	40
60808	Vanadium carbide with periodic anionic vacancies for effective electrocatalytic nitrogen reduction. Materials Today, 2020, 40, 18-25.	8.3	34

#	Article	IF	Citations
60809	Insight into the formation mechanism of C C chain in ethanol synthesis at the interface of partially hydroxylated Î³-Al2O3 (110D) surface and polyethylene glycol solvent. Molecular Catalysis, 2018, 455, 164-178.	1.0	3
60810	Towards quaternary alloy Auâ€“Pd catalysts for direct synthesis of hydrogen peroxide. Materials Today Energy, 2020, 16, 100399.	2.5	5
60811	Low-temperature synthesis of PdO-CeO2/C toward efficient oxygen reduction reaction. Materials Today Energy, 2020, 18, 100557.	2.5	11
60812	Influence of interatomic interactions on the mechanical properties of face-centered cubic multicomponent Coâ€“Niâ€“Crâ€“Mo alloys. Materialia, 2020, 12, 100742.	1.3	9
60813	Boron-rich environment boosting ruthenium boride on B, N doped carbon outperforms platinum for hydrogen evolution reaction in a universal pH range. Nano Energy, 2020, 75, 104881.	8.2	71
60814	Photochemically deposited Ir-doped NiCo oxyhydroxide nanosheets provide highly efficient and stable electrocatalysts for the oxygen evolution reaction. Nano Energy, 2020, 75, 104885.	8.2	30
60815	Density functional theory calculation of the properties of carbon vacancy defects in silicon carbide. Nami Jishu Yu Jingmi Gongcheng/Nanotechnology and Precision Engineering, 2020, 3, 211-217.	1.7	9
60816	Janus XSSe/SiC (XÂ=ÂMo, W) van der Waals heterostructures as promising water-splitting photocatalysts. Physica E: Low-Dimensional Systems and Nanostructures, 2020, 123, 114207.	1.3	88
60817	Thermal expansion induced reduction of lattice thermal conductivity in light crystals. Physics Letters, Section A: General, Atomic and Solid State Physics, 2017, 381, 3514-3518.	0.9	9
60818	Defect induced room temperature ferromagnetism in methylammonium lead iodide perovskite. Physics Letters, Section A: General, Atomic and Solid State Physics, 2020, 384, 126278.	0.9	18
60819	Evolution of metallization and superconductivity in solid hydrogen. Physics Letters, Section A: General, Atomic and Solid State Physics, 2020, 384, 126571.	0.9	4
60820	Investigating the solution and diffusion properties of hydrogen in Î±-Uranium by first-principles calculations. Progress in Nuclear Energy, 2020, 122, 103268.	1.3	8
60821	Quasi one-dimensional van der Waals gold selenide with strong interchain interaction and giant magnetoresistance. Science Bulletin, 2020, 65, 1451-1459.	4.3	7
60822	Stacking patterns robust to type-I PtSe2/InSe van der Waals heterostructures. Superlattices and Microstructures, 2020, 143, 106552.	1.4	4
60823	Sodium-ion diffusion in alluaudite Na5In(MoO4)4. Solid State Ionics, 2020, 351, 115328.	1.3	9
60824	Structure and ionic conduction study on Li3PO4 and LiPON (Lithium phosphorous oxynitride) with the Density-Functional Tight-Binding (DFTB) method. Solid State Ionics, 2020, 351, 115329.	1.3	8
60825	Improvement in erosion-corrosion resistance of high-chromium cast irons by trace boron. Wear, 2017, 376-377, 578-586.	1.5	17
60826	Lanthanide-regulated oxygen evolution activity of face-sharing IrO6 dimers in 6H-perovskite electrocatalysts. Chinese Journal of Catalysis, 2020, 41, 1692-1697.	6.9	18

#	Article	IF	Citations
60829	Theoretical and Experimental Exploration of a Novel In-Plane Chemically Ordered (Cr_{2/3}M_{1/3})₂AlC i-MAX Phase with M = Sc and Y. Crystal Growth and Design, 2017, 17, 5704-5711.	1.4	79
60830	Boosting Self-Trapped Emissions in Zero-Dimensional Perovskite Heterostructures. Chemistry of Materials, 2020, 32, 5036-5043.	3.2	46
60831	Microscopic Insights into the Reconstructive Phase Transition of KNaNbOF₅ with ¹⁹F NMR Spectroscopy. Chemistry of Materials, 2020, 32, 5715-5722.	3.2	5
60832	Small Electron Polarons in CsPbBr₃: Competition between Electron Localization and Delocalization. Chemistry of Materials, 2020, 32, 8393-8400.	3.2	15
60833	Computation-Motivated Design of Ternary Plasmonic Copper Chalcogenide Nanocrystals. Chemistry of Materials, 2021, 33, 117-125.	3.2	5
60834	Improving Hydride Conductivity in Layered Perovskites via Crystal Engineering. Chemistry of Materials, 2021, 33, 177-185.	3.2	8
60835	Durable Multimetal Oxychloride Intergrowths for Visible Light-Driven Water Splitting. Chemistry of Materials, 2021, 33, 347-358.	3.2	19
60836	Ultrastrong Anion Affinity of Anionic Clay Induced by Its Inherent Nanoconfinement. Environmental Science & Technology, 2021, 55, 930-940.	4.6	18
60837	Sodium Rivals Silver as Single-Atom Active Centers for Catalyzing Abatement of Formaldehyde. Environmental Science & Technology, 2017, 51, 7084-7090.	4.6	70
60838	Understanding CO Heterogeneous Adsorption on the Reduced CaSO₄(010) Surface for Chemical-Looping Combustion: A First-Principles Study. Industrial & Engineering Chemistry Research, 2020, 59, 20022-20032.	1.8	5
60839	Prediction of Stable Ground-State Binary Sodiumâ€“Potassium Interalkalis under High Pressures. Inorganic Chemistry, 2021, 60, 124-129.	1.9	4
60840	Crystal Structures, Superconducting Properties, and the Coloring Problem in ReAlSi and ReGaSi. Inorganic Chemistry, 2020, 59, 17310-17319.	1.9	5
60841	Structural Properties of NdTiO2+xN1â€“x and Its Application as Photoanode. Inorganic Chemistry, 2021, 60, 919-929.	1.9	7
60842	Selective Synthesis of Î±-, Î²-, and Î³-Ag₂WO₄ Polymorphs: Promising Platforms for Photocatalytic and Antibacterial Materials. Inorganic Chemistry, 2021, 60, 1062-1079.	1.9	18
60843	Understanding the Structural and Electronic Properties of Bismuth Trihalides and Related Compounds. Inorganic Chemistry, 2020, 59, 3377-3386.	1.9	9
60844	Energetic Stabilization of Carboxylic Acid Conformers by Manganese Atoms and Clusters. Journal of Physical Chemistry A, 2020, 124, 4990-4997.	1.1	3
60845	Beryllium and Magnesium Metal Clusters: New Globally Stable Structures and G0W0 Calculations. Journal of Physical Chemistry A, 2021, 125, 1424-1435.	1.1	8
60846	Diversity of the Hydrogen Bond Network and Its Impact on NMR Parameters of Amylose B Polymorph: A Study Using Molecular Dynamics and DFT Calculations Within Periodic Boundary Conditions. Journal of Physical Chemistry B, 2021, 125, 158-168.	1.2	2

#	Article	IF	Citations
60847	Synthesis of Two-Dimensional Metalâ€“Organic Frameworks via Dehydrogenation Reactions on a Cu(111) Surface. Journal of Physical Chemistry C, 2020, 124, 12390-12396.	1.5	15
60848	Chemical Synthesis and High-Pressure Reaction of Nb⁵⁺ Monodoped Rutile TiO₂ Nanocrystals. Journal of Physical Chemistry C, 2020, 124, 12808-12815.	1.5	6
60849	Exploring the Electronic Structure of New Doped Salt Hydrates, Mg1â€“xCaxCl2Â·nH2O, for Thermochemical Energy Storage. Journal of Physical Chemistry C, 2020, 124, 24580-24591.	1.5	5
60850	Insights on the Structural and Dynamic Properties of Corundumâ€“Water Interfaces from First-Principle Molecular Dynamics. Journal of Physical Chemistry C, 2021, 125, 295-309.	1.5	4
60851	Structure and Stability of the (001) Surface of Co₃O₄. Journal of Physical Chemistry C, 2020, 124, 25790-25795.	1.5	13
60852	Electronic Band Structure and Ultrafast Carrier Dynamics of Two Dimensional (2D) Semiconductor Nanoplatelets (NPLs) in the Presence of Electron Acceptor for Optoelectronic Applications. Journal of Physical Chemistry C, 2020, 124, 26434-26442.	1.5	9
60853	Pathway Alteration of Water Splitting via Oxygen Vacancy Formation on Anatase Titanium Dioxide in Photothermal Catalysis. Journal of Physical Chemistry C, 2020, 124, 26214-26221.	1.5	19
60854	Oxidation, Stability, and Magnetic Ground States of Two-Dimensional Layered Electrides. Journal of Physical Chemistry C, 2020, 124, 25316-25321.	1.5	6
60855	Insights into the High Activity and Methanol Selectivity of the Zn/ZrO₂ Solid Solution Catalyst for CO₂ Hydrogenation. Journal of Physical Chemistry C, 2020, 124, 27467-27478.	1.5	15
60856	Shedding Light on the Interfacial Structure of Low-Coverage Alkanethiol Lattices. Journal of Physical Chemistry C, 2020, 124, 26748-26758.	1.5	6
60857	Shallow Valence Band of Rutile GeO₂ and P-type Doping. Journal of Physical Chemistry C, 2020, 124, 25721-25728.	1.5	18
60858	Polycyclic Aromatic Hydrocarbons as Prospective Cathodes for Aluminum Organic Batteries. Journal of Physical Chemistry C, 2021, 125, 49-57.	1.5	20
60859	Hydrogenolysis of Asymmetric C_{aryl}â€“Oâ€“C_{alkyl} Bonds in Bio-Oils over Alloyed Catalysts: A Theoretical Insight. Journal of Physical Chemistry C, 2020, 124, 28052-28060.	1.5	14
60860	Theoretical Investigation into the Key Role of Ru in the Epoxidation of Propylene over Cu₂O(111). Journal of Physical Chemistry C, 2020, 124, 28500-28509.	1.5	8
60861	Lead Free Two-Dimensional Mixed Tin and Germanium Halide Perovskites for Photovoltaic Applications. Journal of Physical Chemistry C, 2021, 125, 74-81.	1.5	29
60862	Shape and Surface Morphology of Copper Nanoparticles under CO2 Hydrogenation Conditions from First Principles. Journal of Physical Chemistry C, 2021, 125, 396-409.	1.5	15
60863	Predictive Acid Gas Adsorption in Rare Earth DOBDC Metalâ€“Organic Frameworks via Complementary Cluster and Periodic Structure Models. Journal of Physical Chemistry C, 2020, 124, 26801-26813.	1.5	25
60864	Organic Gas Sensing Performance of the Borophene van der Waals Heterostructure. Journal of Physical Chemistry C, 2021, 125, 427-435.	1.5	30

#	Article	IF	Citations
60865	Lithium Peroxide Growth in Liâ€“O2 Batteries via Chemical Disproportionation and Electrochemical Mechanisms: A Potential-Dependent Ab Initio Study with Implicit Solvation. Journal of Physical Chemistry C, 2021, 125, 436-445.	1.5	8
60866	Electronic Structure of Double-Layer Epitaxial Graphene on SiC(0001) Modified by Gd Intercalation. Journal of Physical Chemistry C, 2020, 124, 28132-28138.	1.5	8
60867	Experimental and Ab Initio Study of Cu₂SnS₃ (CTS) Polymorphs for Thermoelectric Applications. Journal of Physical Chemistry C, 2021, 125, 178-188.	1.5	21
60868	Angle Dependence of Interlayer Coupling in Twisted Transition Metal Dichalcogenide Heterobilayers. Journal of Physical Chemistry C, 2021, 125, 1048-1053.	1.5	12
60869	Doping of IIIâ€“V Arsenide and Phosphide Wurtzite Semiconductors. Journal of Physical Chemistry C, 2020, 124, 27203-27212.	1.5	4
60870	Oxygen Vacancies Altering the Trapping in the Proton Conduction Landscape of Doped Barium Zirconate. Journal of Physical Chemistry C, 2020, 124, 27954-27964.	1.5	14
60871	First-Principles Study of Interhalogen Interactions and Triangular Windmill Structures in Self-Assembly of Fully Halogenated Benzenes on a Silver Surface. Journal of Physical Chemistry C, 2021, 125, 526-535.	1.5	6
60872	Extraordinary Electromechanical Actuation of Ti2C MXene. Journal of Physical Chemistry C, 2021, 125, 1060-1068.	1.5	13
60873	Conductance Switching in Molecular Self-Assembled Monolayers for Application of Data Storage. Journal of Physical Chemistry C, 2021, 125, 1069-1074.	1.5	6
60874	Sublattice Short-Range Order and Modified Electronic Structure in Defective Half-Heusler Nb_{0.8}CoSb. Journal of Physical Chemistry C, 2021, 125, 1125-1133.	1.5	13
60875	Blue Phosphorus Growth on Different Noble Metal Surfaces: From a 2D Alloy Network to an Extended Monolayer. Journal of Physical Chemistry C, 2021, 125, 675-679.	1.5	13
60876	Quasi-Analytical Approach for Modeling of Surface-Enhanced Raman Scattering. Journal of Physical Chemistry C, 2015, 119, 28992-28998.	1.5	13
60877	Intrinsic Structural, Electrical, Thermal, and Mechanical Properties of the Promising Conductor Mo₂C MXene. Journal of Physical Chemistry C, 2016, 120, 15082-15088.	1.5	139
60878	Adsorption Mechanisms of Typical Carbonyl-Containing Volatile Organic Compounds on Anatase TiO₂ (001) Surface: A DFT Investigation. Journal of Physical Chemistry C, 2017, 121, 13717-13722.	1.5	46
60879	A Practical Criterion for Screening Stable Boron Nanostructures. Journal of Physical Chemistry C, 2017, 121, 11950-11955.	1.5	13
60880	Anchoring Bond between Ru and N Atoms of Ru/Ca₂NH Catalyst: Crucial for the High Ammonia Synthesis Activity. Journal of Physical Chemistry C, 2017, 121, 20900-20904.	1.5	33
60881	CO Adsorption on Graphite-like ZnO Bilayers Supported on Cu(111), Ag(111), and Au(111) Surfaces. Journal of Physical Chemistry C, 2017, 121, 27453-27461.	1.5	34
60882	Facilitated Dissociation of Water in the Presence of Lithium Metal at Ambient Temperature as a Requisite for Lithiumâ€“Gas Reactions. Journal of Physical Chemistry C, 2018, 122, 16016-16022.	1.5	10

#	Article	IF	Citations
60883	Properties of Metal-Supported Oxide Honeycomb Monolayers: M₂O₃ and MMâ€²O₃ on Me(111) (M, Mâ€² = Ti, V, Cr, Fe; Me = Ag, Au, Pt). Journal of Physical Chemistry C, 2020, 124, 8186-8197.	1.5	12
60884	Structural Characterization of a Novel Two-Dimensional Material: Cobalt Sulfide Sheets on Au(111). Journal of Physical Chemistry Letters, 2020, 11, 9038-9044.	2.1	8
60885	Group 11 Transition-Metal Halide Monolayers: High Promises for Photocatalysis and Quantum Cutting. Journal of Physical Chemistry Letters, 2021, 12, 525-531.	2.1	25
60886	Point Defects in Two-Dimensional Î³-Phosphorus Carbide. Journal of Physical Chemistry Letters, 2021, 12, 620-626.	2.1	21
60887	An Efficient ab Initio Scheme for Discovering Organicâ€“Inorganic Hybrid Materials by Using Genetic Algorithms. Journal of Physical Chemistry Letters, 2021, 12, 2023-2028.	2.1	7
60888	Formation Mechanism of Ammonium Carbamate for CO₂ Uptake in N,Nâ€²-Dimethylethylenediamine Grafted M₂(dobpdc). Langmuir, 2020, 36, 14104-14112.	1.6	9
60889	Why In₂O₃ Can Make 0.7 nm Atomic Layer Thin Transistors. Nano Letters, 2021, 21, 500-506.	4.5	99
60890	Heterobilayer with Ferroelectric Switching of Topological State. Nano Letters, 2021, 21, 785-790.	4.5	38
60891	ToF-SIMS Investigation of the Initial Stages of MeCpPt(CH₃)₃ Adsorption and Decomposition on Nickel Oxide Surfaces: Exploring the Role and Location of the Ligands. Organometallics, 2020, 39, 1024-1034.	1.1	5
60892	Ultrahigh Power Factors in Ultrawide-Band-Gap GaB₃N₄ and AlB₃N₄ for High-Temperature Thermoelectric Applications. ACS Applied Electronic Materials, 2021, 3, 219-229.	2.0	6
60893	TiO₂ Nanorod Array Conformally Coated with a Monolayer MoS₂ Film: An Efficient Electrocatalyst for Hydrogen Evolution Reaction. ACS Applied Energy Materials, 2020, 3, 10854-10862.	2.5	11
60894	Solar Cells Based on Two-Dimensional WTe₂/PtXY (X, Y = S, Se) Heterostructures with High Photoelectric Conversion Efficiency and Low Power Consumption. ACS Applied Energy Materials, 2021, 4, 357-364.	2.5	25
60895	Surface Electronegativity as an Activity Descriptor to Screen Oxygen Evolution Reaction Catalysts of Liâ€“O₂ Battery. ACS Applied Materials & Interfaces, 2020, 12, 27166-27175.	4.0	12
60896	Silicon as the Anode Material for Multivalent-Ion Batteries: A First-Principles Dynamics Study. ACS Applied Materials & Interfaces, 2020, 12, 55746-55755.	4.0	12
60897	Efficient Heteronuclear Diatom Electrocatalyst for Nitrogen Reduction Reaction: Pdâ€“Nb Diatom Supported on Black Phosphorus. ACS Applied Materials & Interfaces, 2020, 12, 56987-56994.	4.0	49
60898	Mechanical Engineering Effect in Electronic and Optical Properties of Graphene Nanomeshes. ACS Applied Materials & Interfaces, 2020, 12, 55189-55194.	4.0	9
60899	Sulfurized Polyacrylonitrile for High-Performance Lithiumâ€“Sulfur Batteries: In-Depth Computational Approach Revealing Multiple Sulfurâ€™s Reduction Pathways and Hidden Li⁺ Storage Mechanisms for Extra Discharge Capacity. ACS Applied Materials & Interfaces, 2021, 13, 491-502.	4.0	16
60900	Synergistic Effects of Ternary PdOâ€“CeO2â€“OMS-2 Catalyst Afford High Catalytic Performance and Stability in the Reduction of NO with CO. ACS Applied Materials & Interfaces, 2021, 13, 622-630.	4.0	28

#	Article	IF	Citations
60901	Short-Range Order in GeSn Alloy. ACS Applied Materials & Interfaces, 2020, 12, 57245-57253.	4.0	20
60902	Improving the Electrochemical Property of Silicon Anodes through Hydrogen-Bonding Cross-Linked Thiourea-Based Polymeric Binders. ACS Applied Materials & Interfaces, 2021, 13, 639-649.	4.0	36
60903	Degradation of Fatal Toxic Nerve Agents on Dry TiO₂. ACS Applied Materials & Interfaces, 2021, 13, 696-705.	4.0	15
60904	Large Piezoelectric Response and Ferroelectricity in Li and V/Nb/Ta Co-Doped w-AlN. ACS Applied Materials & Interfaces, 2021, 13, 944-954.	4.0	15
60905	Synthesis of Structurally Stable and Highly Active PtCo₃ Ordered Nanoparticles through an Easily Operated Strategy for Enhanced Oxygen Reduction Reaction. ACS Applied Materials & Interfaces, 2021, 13, 827-835.	4.0	13
60906	Morphology and Surface Reactivity Relationship in the Li_{1+x}Mn_{2â€“x}O₄ Spinel with x = 0.05 and 0.10: A Combined First-Principle and Experimental Study. ACS Applied Materials & Interfaces, 2017, 9, 44922-44930.	4.0	21
60907	Interface-Induced Enhancement of Ferromagnetism in Insulating LaMnO₃ Ultrathin Films. ACS Applied Materials & Interfaces, 2017, 9, 44931-44937.	4.0	23
60908	Doping of Cr in Graphene Using Electron Beam Manipulation for Functional Defect Engineering. ACS Applied Nano Materials, 2020, 3, 10855-10863.	2.4	24
60909	Heteroatom Modification of Nanoporous Nickel Surfaces for Electrocatalytic Water Splitting. ACS Applied Nano Materials, 2020, 3, 11298-11306.	2.4	11
60910	Nonmetal-Doped C₂N Nanosheets for Removal of Methoxyphenols: A First-Principles Study. ACS Applied Nano Materials, 2021, 4, 478-486.	2.4	6
60911	Constructing Efficient Single Rh Sites on Activated Carbon via Surface Carbonyl Groups for Methanol Carbonylation. ACS Catalysis, 2021, 11, 682-690.	5.5	19
60912	Understanding the Role of M/Pt(111) (M = Fe, Co, Ni, Cu) Bimetallic Surfaces for Selective Hydrodeoxygenation of Furfural. ACS Catalysis, 2017, 7, 5758-5765.	5.5	76
60913	Pressure-Induced Hydration and Formation of Bilayer Ice in Nacrite, a Kaolin-Group Clay. ACS Earth and Space Chemistry, 2020, 4, 183-188.	1.2	8
60914	Enhanced Photocatalytic VOCs Mineralization via Special Ga-O-H Charge Transfer Channel in Î±-Ga₂O₃/MgAl-LDH Heterojunction. ACS ES&T Engineering, 2021, 1, 501-511.	3.7	32
60915	Synergized Cu/Pb Core/Shell Electrocatalyst for High-Efficiency CO₂ Reduction to C₂₊ Liquids. ACS Nano, 2021, 15, 1039-1047.	7.3	64
60916	Strengthening and Toughening Hierarchical Nanocellulose via Humidity-Mediated Interface. ACS Nano, 2021, 15, 1310-1320.	7.3	85
60917	Spectral Instability of Layered Mixed Halide Perovskites Results from Anion Phase Redistribution and Selective Hole Injection. ACS Nano, 2021, 15, 1486-1496.	7.3	18
60918	Controlling the Shapes of Nanoparticles by Dopant-Induced Enhancement of Chemisorption and Catalytic Activity: Application to Fe-Based Ammonia Synthesis. ACS Nano, 2021, 15, 1675-1684.	7.3	11

#	Article	IF	Citations
60919	Palladium Diselenide Long-Wavelength Infrared Photodetector with High Sensitivity and Stability. ACS Nano, 2019, 13, 2511-2519.	7.3	198
60920	Evaluating the Thermoelectric Properties of BaTiS₃ by Density Functional Theory. ACS Omega, 2020, 5, 12385-12390.	1.6	10
60921	The Anchoring Effect of 2D Graphdiyne Materials for Lithiumâ€“Sulfur Batteries. ACS Omega, 2020, 5, 13424-13429.	1.6	10
60922	Density Functional Tight Binding Theory Approach for the CO2 Reduction Reaction Paths on Anatase TiO2 Surfaces. ACS Omega, 2020, 5, 25819-25823.	1.6	3
60923	A Cyclic Periodic Wave Function Approach for the Study of Infinitely Periodic Solid-State Systems: II. Application to Helical Polysaccharides. ACS Omega, 2020, 5, 27556-27565.	1.6	3
60924	Unraveling Catalytic Mechanisms for CO Oxidation on Boron-Doped Fullerene: A Computational Study. ACS Omega, 2020, 5, 28870-28876.	1.6	4
60925	Superionic Si-Substituted Lithium Argyrodite Sulfide Electrolyte Li_{6+x}Sb_{1â€“x}Si_xS₅I for All-Solid-State Batteries. ACS Sustainable Chemistry and Engineering, 2021, 9, 120-128.	3.2	48
60926	Determining the Effect of Hot Electron Dissipation on Molecular Scattering Experiments at Metal Surfaces. Jacs Au, 2021, 1, 164-173.	3.6	33
60927	Bulk magnetoelectricity in the hexagonal manganites and ferrites. , 0, .		1
60928	An extended defect in graphene as a metallic wire. , 0, .		1
60929	Platinum single-atom and cluster catalysis of the hydrogen evolution reaction. , 0, .		1
60930	Surface reconstruction and chemical evolution of stoichiometric layered cathode materials for lithium-ion batteries. , 0, .		1
60931	Vibrational hierarchy leads to dual-phonon transport in low thermal conductivity crystals. Nature Communications, 2020, 11, 2554.	5.8	79
60932	Tuning the interfacial spin-orbit coupling with ferroelectricity. Nature Communications, 2020, 11, 2627.	5.8	19
60933	Molecular molds for regularizing Kondo states at atom/metal interfaces. Nature Communications, 2020, 11, 2566.	5.8	19
60934	Boron arsenide heterostructures: lattice-matched heterointerfaces and strain effects on band alignments and mobility. Npj Computational Materials, 2020, 6, .	3.5	28
60935	Electrically and magnetically switchable nonlinear photocurrent in ĐĐ¢-symmetric magnetic topological quantum materials. Npj Computational Materials, 2020, 6, .	3.5	43
60936	Spinâ€“valley Hall phenomena driven by Van Hove singularities in blistered graphene. Npj Computational Materials, 2020, 6, .	3.5	4

#	Article	IF	Citations
60937	Efficient training of ANN potentials by including atomic forces via Taylor expansion and application to water and a transition-metal oxide. Npj Computational Materials, 2020, 6, .	3.5	40
60938	Predicting synthesizable multi-functional edge reconstructions in two-dimensional transition metal dichalcogenides. Npj Computational Materials, 2020, 6, .	3.5	23
60939	Aperiodic quantum oscillations in the two-dimensional electron gas at the LaAlO3/SrTiO3 interface. Npj Quantum Materials, 2020, 5, .	1.8	16
60940	Atomic reconstruction in twisted bilayers of transition metal dichalcogenides. Nature Nanotechnology, 2020, 15, 592-597.	15.6	245
60941	Photodoping through local charge carrier accumulation in alloyed hybrid perovskites for highly efficient luminescence. Nature Photonics, 2020, 14, 123-128.	15.6	93
60942	Tweaking the Electronic and Optical Properties of Î±-MoO3 by Sulphur and Selenium Doping â€“ a Density Functional Theory Study. Scientific Reports, 2018, 8, 10144.	1.6	25
60943	Data-driven studies of magnetic two-dimensional materials. Scientific Reports, 2020, 10, 15795.	1.6	39
60944	Quantitative material analysis using secondary electron energy spectromicroscopy. Scientific Reports, 2020, 10, 22144.	1.6	10
60945	Cooperative CO2-to-ethanol conversion via enriched intermediates at moleculeâ€“metal catalyst interfaces. Nature Catalysis, 2020, 3, 75-82.	16.1	390
60946	Raman spectra and phonon structures of BaGa4Se7 crystal. Communications Physics, 2020, 3, .	2.0	9
60947	Design of Advanced Photocatalysis System by Adatom Decoration in 2D Nanosheets of Group-IV and IIIâ€“V Binary Compounds. Scientific Reports, 2016, 6, 23104.	1.6	37
60948	Chemical Bonding Investigations for Materials. , 2018, , 117-175.		2
60949	Variation in surface energy and reduction drive of a metal oxide lithium-ion anode with stoichiometry: a DFT study of lithium titanate spinel surfaces. Journal of Materials Chemistry A, 2016, 4, 17180-17192.	5.2	23
60950	Electronic and optical properties of MoS₂/Î±-Fe₂O₃(0001) heterostructures: a first-principles investigation. CrystEngComm, 2017, 19, 6333-6338.	1.3	10
60951	Water facilitates oxygen migration on gold surfaces. Physical Chemistry Chemical Physics, 2018, 20, 2196-2204.	1.3	17
60952	Exploring perovskites for methane activation from first principles. Catalysis Science and Technology, 2018, 8, 702-709.	2.1	35
60953	Syntheses and characterization of three new sulfides with large band gaps: acentric Ba₄Ga₄SnS₁₂, centric Ba₁₂Sn₄S₂₃ and Ba₇Sn₃S₁₃. Dalton Transactions, 2017, 46, 14771-14778.	1.6	23
60954	Theoretical study of the substitutional solute effect on the interstitial carbon in nickel-based alloy. RSC Advances, 2017, 7, 20567-20573.	1.7	8

#	Article	IF	Citations
60955	Novel magnetic semiconductor Na₂Fe₂Ti₆O₁₆: synthesis, double absorption and strong adsorptive ability. Journal of Materials Chemistry A, 2017, 5, 17589-17600.	5.2	21
60956	Probing the local interface properties at a grapheneâ€“MoSe₂ in-plane lateral heterostructure: an ab initio study. Physical Chemistry Chemical Physics, 2018, 20, 17952-17960.	1.3	16
60957	Intriguing electronic and optical properties of two-dimensional Janus transition metal dichalcogenides. Physical Chemistry Chemical Physics, 2018, 20, 18571-18578.	1.3	141
60958	Na₂C monolayer: a novel 2p Dirac half-metal with multiple symmetry-protected Dirac cones. Nanoscale, 2018, 10, 13645-13651.	2.8	38
60959	Volume expansive pressure (VEP) driven non-trivial topological phase transition in LiMgBi. Physical Chemistry Chemical Physics, 2020, 22, 4602-4609.	1.3	7
60960	Equation of state of water based on the SCAN meta-GGA density functional. Physical Chemistry Chemical Physics, 2020, 22, 4626-4631.	1.3	9
60961	Germanene/GaGeTe heterostructure: a promising electric-field induced data storage device with high carrier mobility. Physical Chemistry Chemical Physics, 2020, 22, 5163-5169.	1.3	12
60962	Catalytic performance of Pd_n (n = 1, 2, 3, 4 and 6) clusters supported on TiO_{2-V} for the formation of dimethyl oxalate via the CO catalytic coupling reaction: a theoretical study. Physical Chemistry Chemical Physics, 2020, 22, 4549-4560.	1.3	11
60963	Interfacial structure-governed SO₂ resistance of Cu/TiO₂ catalysts in the catalytic oxidation of CO. Catalysis Science and Technology, 2020, 10, 1661-1674.	2.1	20
60964	Lone-pair self-containment in pyritohedron-shaped closed cavities: optimized hydrothermal synthesis, structure, magnetism and lattice thermal conductivity of Co₁₅F₂(TeO₃)₁₄. Dalton Transactions, 2020, 49, 2234-2243.	1.6	9
60965	Appraisal of calcium ferrites as cathodes for calcium rechargeable batteries: DFT, synthesis, characterization and electrochemistry of Ca₄Fe₉O₁₇. Dalton Transactions, 2020, 49, 2671-2679.	1.6	17
60966	A new lithium diffusion model in layered oxides based on asymmetric but reversible transition metal migration. Energy and Environmental Science, 2020, 13, 1269-1278.	15.6	39
60967	The adsorption and growth of Agn (n = 1â€“4) clusters on cubic, monoclinic, and tetragonal ZrO2 surfaces: a first-principles study. New Journal of Chemistry, 2020, 44, 2268-2274.	1.4	2
60968	Evolution of local strain in Ag-deposited monolayer MoS₂ modulated by interface interactions. Nanoscale, 2019, 11, 22432-22439.	2.8	12
60969	Magnetic i-MXenes: a new class of multifunctional two-dimensional materials. Nanoscale, 2020, 12, 5995-6001.	2.8	40
60970	Two dimensional ZnO/AlN composites used for photocatalytic water-splitting: a hybrid density functional study. RSC Advances, 2019, 9, 36234-36239.	1.7	12
60971	Investigation of ferrimagnetism and ferroelectricity in Al_xFe_{2â^'x}O₃ thin films. Journal of Materials Chemistry C, 2020, 8, 706-714.	2.7	8
60972	Tunneling magnetoresistance and light modulation in Fe4N(La2/3Sr1/3MnO3)/C60/Fe4N single molecule magnetic tunnel junctions. Journal of Materials Chemistry C, 2020, 8, 3137-3146.	2.7	13

#	Article	IF	Citations
60973	Electron-injection driven phase transition in two-dimensional transition metal dichalcogenides. Journal of Materials Chemistry C, 2020, 8, 4432-4440.	2.7	31
60974	Photon upconversion afterglow materials toward visualized information coding/decoding. Journal of Materials Chemistry C, 2020, 8, 3678-3687.	2.7	14
60975	New germanate and mixed cobalt germanate salt inclusion materials: [(Rb6F)(Rb4F)][Ge14O32] and [(Rb6F)(Rb3.1Co0.9F0.96)][Co3.8Ge10.2O30F2]. CrystEngComm, 2020, 22, 8072-8080.	1.3	9
60976	Two-dimensional tetragonal transition-metal carbide anodes for non-lithium-ion batteries. Physical Chemistry Chemical Physics, 2020, 22, 13680-13688.	1.3	8
60977	Strong dependence of the vertical charge carrier mobility on the Ï€â€“Ï€ stacking distance in molecule/graphene heterojunctions. Physical Chemistry Chemical Physics, 2020, 22, 13802-13807.	1.3	10
60978	Nitrogen fixation on a single Mo atom embedded stanene monolayer: a computational study. Physical Chemistry Chemical Physics, 2020, 22, 13981-13988.	1.3	33
60979	A boron-decorated melon-based carbon nitride as a metal-free photocatalyst for N₂ fixation: a DFT study. Physical Chemistry Chemical Physics, 2020, 22, 21872-21880.	1.3	18
60980	Anharmonic phonon frequency and ultralow lattice thermal conductivity in Î²-Cu₂Se liquid-like thermoelectrics. Physical Chemistry Chemical Physics, 2020, 22, 28086-28092.	1.3	13
60981	Computational prediction of a novel 1D InSeI nanochain with high stability and promising wide-bandgap properties. Physical Chemistry Chemical Physics, 2020, 22, 27441-27449.	1.3	17
60982	Significant enhancement of the thermoelectric properties of CaP₃ through reducing the dimensionality. Materials Advances, 2020, 1, 3322-3332.	2.6	14
60983	Optimisation of the thermoelectric efficiency of zirconium trisulphide monolayers through unixial and biaxial strain. Nanoscale Advances, 2020, 2, 5352-5361.	2.2	8
60984	A high performance N-doped graphene nanoribbon based spintronic device applicable with a wide range of adatoms. Nanoscale Advances, 2020, 2, 5905-5911.	2.2	10
60985	Rational prediction of multifunctional bilayer single atom catalysts for the hydrogen evolution, oxygen evolution and oxygen reduction reactions. Nanoscale, 2020, 12, 20413-20424.	2.8	17
60986	Topology of transition metal dichalcogenides: the case of the coreâ€“shell architecture. Nanoscale, 2020, 12, 23897-23919.	2.8	14
60987	The crystal structures and mechanical properties of the uranyl carbonate minerals roubaultite, fontanite, sharpite, widenmannite, grimselite and Äejkaite. Inorganic Chemistry Frontiers, 2020, 7, 4197-4221.	3.0	9
60988	Perfect cubic La-doped boron clusters La₆&[La@B₂₄]^{+/0}as the embryos of low-dimensional lanthanide boride nanomaterials. RSC Advances, 2020, 10, 12469-12474.	1.7	9
60989	Bandgap engineering of few-layered MoS₂ with low concentrations of S vacancies. RSC Advances, 2020, 10, 15702-15706.	1.7	6
60990	Hydrogen adsorption mechanism of MOF-74 metalâ€“organic frameworks: an insight from first principles calculations. RSC Advances, 2020, 10, 43940-43949.	1.7	13

#	Article	IF	Citations
60991	A self-smoothing Li-metal anode enabled via a hybrid interface film. Journal of Materials Chemistry A, 2020, 8, 12045-12054.	5.2	24
60992	Band convergence and carrier-density fine-tuning as the electronic origin of high-average thermoelectric performance in Pb-doped GeTe-based alloys. Journal of Materials Chemistry A, 2020, 8, 11370-11380.	5.2	41
60993	An ultrathin Al₂O₃ bridging layer between CdS and ZnO boosts photocatalytic hydrogen production. Journal of Materials Chemistry A, 2020, 8, 11031-11042.	5.2	49
60994	Optimizing electron density of nickel sulfide electrocatalysts through sulfur vacancy engineering for alkaline hydrogen evolution. Journal of Materials Chemistry A, 2020, 8, 18207-18214.	5.2	31
60995	Tuning the phase stability and surface HER activity of 1Tâ€²-MoS₂ by covalent chemical functionalization. Journal of Materials Chemistry C, 2020, 8, 15852-15859.	2.7	8
60996	Hydrothermal synthesis of PrVO ₄ nanocubes with enhanced photocatalytic performance through a synergistic effect. Micro and Nano Letters, 2020, 15, 170-175.	0.6	6
60997	Reconstruction of water ice: the neglected process OH + OH â†' H₂O + O. Astronomy and Astrophysics, 2020, 638, A125.	2.1	5
60998	Density functional investigation of the interaction of acetone with small gold clusters. Journal of Chemical Physics, 2007, 126, 014704.	1.2	57
60999	Suppression of phonon transport in multiple Si/PtSi heterostructures. Journal of Applied Physics, 2015, 117, .	1.1	2
61000	Proton dynamics and the phase diagram of dense water ice. Journal of Chemical Physics, 2018, 148, 214501.	1.2	48
61001	Why does NiOOH cocatalyst increase the oxygen evolution activity of Î±-Fe2O3?. Journal of Chemical Physics, 2019, 150, 041729.	1.2	19
61002	Inevitable high density of oxygen vacancies at the surface of polarâ€“nonpolar perovskite heterostructures LaAlO3/SrTiO3. Journal of Applied Physics, 2020, 127, .	1.1	6
61003	Screened range-separated hybrid by balancing the compact and slowly varying density regimes: Satisfaction of local density linear response. Journal of Chemical Physics, 2020, 152, 044111.	1.2	22
61004	A comparative first-principles investigation on the defect chemistry of TiO2 anatase. Journal of Chemical Physics, 2020, 152, 044110.	1.2	12
61005	Extrinsic dopants in quasi-one-dimensional photovoltaic semiconductor Sb2S3: A first-principles study. Journal of Applied Physics, 2020, 127, 183101.	1.1	19
61006	Thermal and pressure ionization in warm, dense MgSiO3 studied with first-principles computer simulations. AIP Conference Proceedings, 2020, , .	0.3	4
61007	Multiphase equation of state and thermoelastic data for polycrystalline beryllium. AIP Conference Proceedings, 2020, , .	0.3	4
61008	First-principles equations of state and structures of liquid metals in multi-megabar conditions. AIP Conference Proceedings, 2020, , .	0.3	2

#	Article	IF	Citations
61009	Half-metallic ferromagnetism in equiatomic quaternary Heusler alloy CoRuMnSb. AIP Conference Proceedings, 2020, , .	0.3	1
61010	First principles study of Mo2N monolayer as potential anode material for na-ion batteries. AIP Conference Proceedings, 2020, , .	0.3	3
61011	A way of resolving the order-of-limit problem of Taoâ€“Mo semilocal functional. Journal of Chemical Physics, 2020, 153, 184112.	1.2	15
61012	Accelerating the convergence of auxiliary-field quantum Monte Carlo in solids with optimized Gaussian basis sets. Journal of Chemical Physics, 2020, 153, 194111.	1.2	12
61013	Prediction of crystalline Ta4O9 phase using first principles-based cluster expansion calculations. APL Materials, 2020, 8, .	2.2	2
61014	The Hubbard-U correction and optical properties of d metal oxide photocatalysts. Journal of Chemical Physics, 2020, 153, 224116.	1.2	10
61015	Anisotropic and trap-limited diffusion of hydrogen/deuterium in monoclinic gallium oxide single crystals. Applied Physics Letters, 2020, 117, .	1.5	16
61016	Defect-related photoluminescence and photoluminescence excitation as a method to study the excitonic bandgap of AlN epitaxial layers: Experimental and ab initio analysis. Applied Physics Letters, 2020, 117, .	1.5	9
61017	Electronic and optical properties of ultrawide bandgap perovskite semiconductors via first principles calculations. Applied Physics Letters, 2020, 117, .	1.5	11
61018	The relationship between the doping concentration and d0 ferromagnetism in n-type 4H-SiC. Journal of Applied Physics, 2020, 128, 193901.	1.1	1
61019	Polarity and charge redistribution induced emergent interfacial ferromagnetism in non-magnetic LaNiO3/SrMnO3 superlattices. Applied Physics Letters, 2020, 117, .	1.5	3
61020	A computational investigation of the interstitial oxidation thermodynamics of a Mo-Nb-Ta-W high entropy alloy beyond the dilute regime. Journal of Applied Physics, 2020, 128, .	1.1	10
61021	Band structure, ferroelectric instability, and spinâ€“orbital coupling effect of bilayer Î±-In2Se3. Journal of Applied Physics, 2020, 128, .	1.1	12
61022	Photovoltaic properties of all-inorganic lead-free perovskite Cs2PdBr6: A first-principles study. AIP Advances, 2020, 10, .	0.6	15
61023	First-principle calculation of electronic and optical properties of VO2 by GGA-1/2 quasiparticle approximation. Journal of Applied Physics, 2020, 128, .	1.1	6
61024	Theoretical investigation of mixing and clustering thermodynamics of Ti1â^'xAlxB2 alloys with potential for age-hardening. Journal of Applied Physics, 2020, 128, 235101.	1.1	7
61025	Simulations of field emission from copper electrodes with inclusion of oxygen surface layer and work function changes based on first-principles calculations. Journal of Applied Physics, 2020, 128, 223302.	1.1	8
61026	Direct and continuous generation of pure acetic acid solutions via electrocatalytic carbon monoxide reduction. Proceedings of the National Academy of Sciences of the United States of America, 2021, 118, .	3.3	93

#	Article	IF	Citations
61027	Influence of Pt and P doping on the performance of g-C3N4 monolayer. Materials and Manufacturing Processes, 2020, 35, 625-634.	2.7	23
61028	Tensorial elastic properties and stability of interface states associated with Î£5(210) grain boundaries in Ni3(Al,Si). Science and Technology of Advanced Materials, 2017, 18, 273-282.	2.8	14
61029	HfX₂ (X = Cl, Br, I) Monolayer and Type II Heterostructures with Promising Photovoltaic Characteristics*. Chinese Physics Letters, 2020, 37, 127101.	1.3	8
61030	Pressure-Stabilized New Phase of CaN₄*. Chinese Physics Letters, 2020, 37, 047101.	1.3	10
61031	Modulation of electron carrier density at the n-type LaAlO3/SrTiO3 interface by water adsorption. Journal of Physics Condensed Matter, 2013, 25, 265004.	0.7	11
61032	Semiconducting phase in borophene: role of defect and strain. Journal Physics D: Applied Physics, 2017, 50, 405103.	1.3	17
61033	A theoretical explanation of RbBH4â€™s fractionally occupied ground-state phase and the reorientational motion of the [BH4]â^' group. Journal Physics D: Applied Physics, 2017, 50, 455501.	1.3	3
61034	Bandgap opening and magnetic anisotropy switching by uniaxial strain in graphene/CrI₃ heterojunction. Journal Physics D: Applied Physics, 2020, 53, 385002.	1.3	9
61035	Electronic structures and electronâ€“phonon superconductivity of Nb2C-based MXenes. Journal Physics D: Applied Physics, 2020, 53, 485301.	1.3	9
61036	Spin-gapless and -gapped band structures of non-compensated bonding BN/Graphene bilayer. Journal Physics D: Applied Physics, 2020, 53, 505101.	1.3	10
61037	Tunable strain effects on the electronic structures and mobility properties of InP/InAs lateral heterostructure. Journal Physics D: Applied Physics, 2020, 53, 505108.	1.3	2
61038	Indium segregation mechanism and V-defect formation at the [0001] InAlN surface: an ab-initio investigation. Journal Physics D: Applied Physics, 2021, 54, 015305.	1.3	4
61039	Energy preference of uniform polarization switching for HfO₂ by first-principle study. Journal Physics D: Applied Physics, 2021, 54, 085304.	1.3	15
61040	Thickness-dependent ultrafast hot carrier and phonon dynamics of PtSe₂ films measured with femtosecond transient optical spectroscopy. Journal Physics D: Applied Physics, 2021, 54, 075102.	1.3	10
61041	Density functional study of carbon vacancies in titanium carbide. Journal of Physics Condensed Matter, 2018, 30, 015702.	0.7	8
61042	Oxygen vacancies and hydrogen doping in LaAlO3/SrTiO3 heterostructures: electronic properties and impact on surface and interface reconstruction. Journal of Physics Condensed Matter, 2019, 31, 295601.	0.7	14
61043	Boron-dopant enhanced stability of diamane with tunable band gap. Journal of Physics Condensed Matter, 2020, 32, 135503.	0.7	5
61044	DFT calculation of ²²⁹thorium-doped magnesium fluoride for nuclear laser spectroscopy. Journal of Physics Condensed Matter, 2020, 32, 255503.	0.7	11

#	Article	IF	Citations
61045	Strong anisotropy and layer-dependent carrier mobility of two-dimensional semiconductor ZrGeTe₄. Journal of Physics Condensed Matter, 2020, 32, 325502.	0.7	9
61046	Thermal transport properties in monolayer group-IV binary compounds. Journal of Physics Condensed Matter, 2020, 32, 305301.	0.7	10
61047	Stable half-metallicity in the (001)-oriented thin films of Co-doped full-Heusler alloys Ti₂Fe_{1â^'x}Co_xSn (x=0.00, 0.25, 0.50, 0.75 or) Tj ETQq0 0 0 rgBT /Overlock	0.7	32
61048	Emergence of weak pyrochlore phase and signature of field induced spin ice ground state in Dy_{2â^' x}La_xZr₂O₇; x = 0, 0.15, 0.3. Journal of Physics Condensed Matter, 2020, 32, 365804.	0.7	5
61049	Theoretical polarization of zero phonon lines in point defects. Journal of Physics Condensed Matter, 2020, 32, 385502.	0.7	9
61050	Robust intrinsic half-metallic ferromagnetism in stable 2D single-layer MnAsS₄. Journal of Physics Condensed Matter, 2020, 32, 385803.	0.7	6
61051	Electronic structure and anisotropic compression of Os₂B₃ to 358 GPa. Journal of Physics Condensed Matter, 2020, 32, 405703.	0.7	9
61052	Anharmonic lattice dynamics and thermal transport of monolayer InSe under equibiaxial tensile strains. Journal of Physics Condensed Matter, 2020, 32, 475702.	0.7	15
61053	Temperature-dependent band gaps in several semiconductors: from the role of electronâ€“phonon renormalization. Journal of Physics Condensed Matter, 2020, 32, 475503.	0.7	23
61054	Electron correlation effect versus spinâ€“orbit coupling for tungsten and impurities. Journal of Physics Condensed Matter, 2020, 32, 445603.	0.7	7
61055	Effect of bond on negative thermal expansion of Prussian blue analogues MCo(CN)₆ (M) Tj ETQq0 0 0 rgBT /Overlock 10 Tf	0.7	14
61056	Ab initio investigation of the temperature-dependent elastic properties of Bi, Te and Cu. Journal of Physics Condensed Matter, 2020, 32, 485902.	0.7	5
61057	Experimental exploration of the amphoteric defect model by cryogenic ion irradiation of a range of wide band gap oxide materials. Journal of Physics Condensed Matter, 2020, 32, 415704.	0.7	7
61058	First-principles investigations of hydrogen trapping in Y₂O₃ and the Y₂O₃|bcc Fe interface. Journal of Physics Condensed Matter, 2020, 32, 495001.	0.7	5
61059	Microscopic Coulomb interaction in transition-metal dichalcogenides. Journal of Physics Condensed Matter, 2021, 33, 035301.	0.7	3
61060	Cation interstitial diffusion in lead telluride and cadmium telluride studied by means of neural network potential based molecular dynamics simulations. Journal of Physics Condensed Matter, 2021, 33, 015901.	0.7	3
61061	Widely tunable direct bandgap of two-dimensional GeSe. Journal of Physics Condensed Matter, 2020, 33, 115301.	0.7	3
61062	Electronic properties of Bi₂Se₃ dopped by 3d transition metal (Mn, Fe, Co, or) Tj ETQq1 1 0.784314 rgBT /O	0.7	16

#	Article	IF	Citations
61063	First principles investigation of electron correlation and Lifshitz transition within iron polynitrides. Journal of Physics Condensed Matter, 2021, 33, 035603.	0.7	9
61064	Dipole control of Rashba spin splitting in a type-II Sb/InSe van der Waals heterostructure. Journal of Physics Condensed Matter, 2021, 33, 045501.	0.7	5
61065	Importance of van der Waals interactions for ab initio studies of topological insulators. Journal of Physics Condensed Matter, 2021, 33, 035702.	0.7	9
61066	Correlation matrix renormalization theory in multi-band lattice systems. Journal of Physics Condensed Matter, 2021, 33, 095902.	0.7	3
61067	Black-box inhomogeneous preconditioning for self-consistent field iterations in density functional theory. Journal of Physics Condensed Matter, 2021, 33, 085503.	0.7	11
61068	Non-hydrostatic pressure-dependent structural and transport properties of BiCuSeO and BiCuSO single crystals. Journal of Physics Condensed Matter, 2021, 33, 105702.	0.7	3
61069	Anab initiobased approach to optical properties of semiconductor heterostructures. Modelling and Simulation in Materials Science and Engineering, 2017, 25, 065001.	0.8	7
61070	Thermal conductance of structured silicon nanocrystals. Modelling and Simulation in Materials Science and Engineering, 2020, 28, 075004.	0.8	1
61071	Electronic origin of grain boundary segregation of Al, Si, P, and S in bcc-Fe: combined analysis of ab initio local energy and crystal orbital Hamilton population. Modelling and Simulation in Materials Science and Engineering, 2021, 29, 015001.	0.8	18
61072	Electronic and effective mass modulation in 2D BCN by strain engineering. Nanotechnology, 2020, 31, 455702.	1.3	7
61073	Two-dimensional ultrathin van der Waals heterostructures of indium selenide and boron monophosphide for superfast nanoelectronics, excitonic solar cells, and digital data storage devices. Nanotechnology, 2020, 31, 495208.	1.3	29
61074	Thermoelectric properties of antimony films: roles of oxidation and topological quantum state. Nanotechnology, 2020, 31, 485704.	1.3	4
61075	Modulation of the transport properties of metal/MoS2 interfaces using BN-graphene lateral tunneling layers. Nanotechnology, 2020, 31, 485204.	1.3	2
61076	High-performance x-ray source based on graphene oxide-coated Cu2S nanowires grown on copper film. Nanotechnology, 2020, 31, 485202.	1.3	3
61077	Two dimensional CdS/ZnO type-II heterostructure used for photocatalytic water-splitting. Nanotechnology, 2020, 31, 485701.	1.3	15
61078	Blue phosphorene reactivity on the Au(111) surface. Nanotechnology, 2020, 31, 495602.	1.3	4
61079	Theoretical design of two-dimensional carbon nitrides. Nanotechnology, 2020, 31, 495707.	1.3	11
61080	Insight the process of hydrazine gas adsorption on layered WS₂: a first principle study. Nanotechnology, 2020, 31, 495703.	1.3	6

#	Article	IF	Citations
61081	A first-principles study of Janus monolayer TiSSe and VSSe as anode materials in alkali metal ion batteries. Nanotechnology, 2021, 32, 025702.	1.3	16
61082	Why thermal conductivity of CaO is lower than that of CaS: a study from the perspective of phonon splitting of optical mode. Nanotechnology, 2021, 32, 025709.	1.3	13
61083	Simulated mechanical properties of finite-size graphene nanoribbons. Nanotechnology, 2021, 32, 045709.	1.3	7
61084	Strain-engineered black arsenene as a promising gas sensor for detecting SO₂ among SF₆ decompositions. Nanotechnology, 2021, 32, 065501.	1.3	9
61085	High thermoelectric performance in two dimensional chalcogenides systems: GaSe and GaTe. Nanotechnology, 2021, 32, 115702.	1.3	22
61086	Switching the soft shearing mode orientation in Niâ€“Mnâ€“Ga non-modulated martensite by Co and Cu doping. Smart Materials and Structures, 2020, 29, 045022.	1.8	12
61087	Topological phase transition from T-carbon to bct-C₁₆. New Journal of Physics, 2020, 22, 073036.	1.2	5
61088	Weyl fermions in ferromagnetic high-temperature phase of K₂Cr₈O₁₆. New Journal of Physics, 2020, 22, 073062.	1.2	2
61089	Ultrafast dynamics of hot charge carriers in an oxide semiconductor probed by femtosecond spectroscopic ellipsometry. New Journal of Physics, 2020, 22, 083066.	1.2	21
61090	Strong lattice anharmonicity exhibited by the high-energy optical phonons in thermoelectric material. New Journal of Physics, 2020, 22, 083083.	1.2	11
61091	Multigap superconductivity in the Mo5PB2 boronâ€“phosphorus compound. New Journal of Physics, 2020, 22, 093016.	1.2	10
61092	Numerical variational solution of hydrogen molecule and ions using one-dimensional hydrogen as basis functions. New Journal of Physics, 2020, 22, 093059.	1.2	8
61093	Topologically nontrivial interband plasmons in type-II Weyl semimetal MoTe2. New Journal of Physics, 2020, 22, 103032.	1.2	10
61094	Pressure-induced superconductivity in a shandite compound Pd3Pb2Se2 with the Kagome lattice. New Journal of Physics, 2020, 22, 123013.	1.2	10
61095	Retention of hydrogen in W-Ti-C, W-Ta-C and W-Zr-C alloys:ab initiostudy. Physica Scripta, 2020, 95, 105707.	1.2	4
61096	First-principles spin-polarized calculations on the adsorption of ethanethiol molecule upon the nonpolar (10$ar{1}$0) ZnO surface. Physica Scripta, 2021, 96, 015803.	1.2	1
61097	Dissociations of O 2 molecules on ultrathin Pb(111) films: first-principles plane wave calculations. Chinese Physics B, 2012, 21, 016801.	0.7	5
61098	Ab initio studies on ammonium iodine under high pressure. Chinese Physics B, 2020, 29, 053104.	0.7	4

#	Article	IF	Citations
61099	Effects of 3d-transition metal doping on the electronic and magnetic properties of one-dimensional diamond nanothread*. Chinese Physics B, 2020, 29, 066101.	0.7	6
61100	Construction of monolayer IrTe2 and the structural transition under low temperatures. Chinese Physics B, 2020, 29, 078102.	0.7	5
61101	Degenerate antiferromagnetic states in spinel oxide LiV2O4. Chinese Physics B, 2020, 29, 077508.	0.7	3
61102	Two ultra-stable novel allotropes of tellurium few-layers*. Chinese Physics B, 2020, 29, 097103.	0.7	5
61103	Epitaxial synthesis and electronic properties of monolayer Pd₂Se₃*. Chinese Physics B, 2020, 29, 098102.	0.7	7
61104	Low lattice thermal conductivity and high figure of merit in p-type doped K₃IO*. Chinese Physics B, 2020, 29, 126501.	0.7	7
61105	Prediction and observation of defect-induced room-temperature ferromagnetism in halide perovskites. Journal of Semiconductors, 2020, 41, 122501.	2.0	5
61106	Comprehensive first-principles studies on phase stability of copper-based halide perovskite derivatives A_lCu_mX_n (A = Rb and Cs; X = Cl, Br, and I). Journal of Semiconductors, 2020, 41, 052201.	2.0	11
61107	Strain tunable band structure of a new 2D carbon allotrope C568. Journal of Semiconductors, 2020, 41, 082005.	2.0	7
61108	Structure dependence of Pt surface activated ammonia oxidation. Journal of Physics: Conference Series, 2008, 117, 012028.	0.3	6
61109	Observation of above-room-temperature ferromagnetism in chemically stable layered semiconductor RhI₃. 2D Materials, 2020, 7, 045034.	2.0	3
61110	In situ transmission electron microscopy study of the formation and migration of vacancy defects in atomically thin black phosphorus. 2D Materials, 2021, 8, 025004.	2.0	11
61111	Interferences of electrostatic moirÃ© potentials and bichromatic superlattices of electrons and excitons in transition metal dichalcogenides. 2D Materials, 2021, 8, 025007.	2.0	17
61112	Magnetic properties and critical behavior of magnetically intercalated WSe₂: a theoretical study. 2D Materials, 2021, 8, 025009.	2.0	16
61113	First-principles investigation on the bonding mechanism between graphyne and the (111) surface of Cu, Ag and Au. Materials Research Express, 2020, 7, 065603.	0.8	4
61114	Superconductivity of superhydride CeH₁₀ under high pressure. Materials Research Express, 2020, 7, 086001.	0.8	26
61115	Lattice thermal conductivity of pure and doped (B, N) Graphene. Materials Research Express, 2020, 7, 095003.	0.8	11
61116	Evaluation of photocatalytic activity of commercial red phosphorus towards the disinfection of E. coli and reduction of Cr (VI) under direct sunlight. Materials Research Express, 2020, 7, 104002.	0.8	13

#	Article	IF	Citations
61117	Fluorination-enhanced photoconductive effect in a wide band gap Ca3Ti2O7-x F x thin films. Materials Research Express, 2020, 7, 126402.	0.8	2
61118	Virtual screening of nitrogen-, phosphorous- and halide-containing materials as p-type transparent conductors. JPhys Materials, 2020, 4, 015004.	1.8	8
61119	On the dependence of ionic transport on crystal orientation in NaSICON-type solid electrolytes. JPhys Energy, 2020, 2, 035003.	2.3	4
61120	Atomic scale structure and its impact on the band gap energy for Cu₂Zn(Sn,Ge)Se₄ kesterite alloys. JPhys Energy, 2020, 2, 035004.	2.3	3
61121	A systematical ab-initio review of promising 2D MXene monolayers towards Li-ion battery applications. JPhys Energy, 2020, 2, 032006.	2.3	34
61122	Robust mixing in self-consistent linearized augmented planewave calculations. Electronic Structure, 2020, 2, 037001.	1.0	5
61123	A charge density prediction model for hydrocarbons using deep neural networks. Machine Learning: Science and Technology, 2020, 1, 025003.	2.4	15
61124	In operando active learning of interatomic interaction during large-scale simulations. Machine Learning: Science and Technology, 2020, 1, 045005.	2.4	11
61125	Low-cost descriptors of electrostatic and electronic contributions to anion redox activity in batteries. IOP SciNotes, 2020, 1, 024805.	0.4	5
61126	Thorium-doped CsI: Implications for the thorium nuclear clock transition. Physical Review A, 2018, 97, .	1.0	2
61127	First-principles Studies of Second-Order Nonlinear Optical Properties of Organic-Inorganic Hybrid Halide Perovskites. Physical Review Applied, 2020, 13, .	1.5	24
61128	Origin of a Simultaneous Suppression of Thermal Conductivity and Increase of Electrical Conductivity and Seebeck Coefficient in Disordered Cubic Cu ₂ ZnSnS ₄. Physical Review Applied, 2020, 14, .	1.5	17
61129	Band Offsets at the Interface between Crystalline and Amorphous Silicon from First Principles. Physical Review Applied, 2017, 8, .	1.5	12
61130	Strain-tuned properties of hybrid improper ferroelectric superlattices through first-principles calculations and machine learning. Physical Review B, 2020, 101, .	1.1	11
61131	Nuclear quantum effect for hydrogen adsorption on Pt(111). Physical Review B, 2020, 101, .	1.1	10
61132	Pressure-induced decomposition of binary lanthanum intermetallic compounds. Physical Review B, 2020, 101, .	1.1	9
61133	Control of magnetic properties of <mml:math xmlns:mml="http://www.w3.org/1998/Math/MathML"><mml:mrow><mml:mi>MnB</mml:mi><mml:msub><mml:mi mathvariant="normal">i</mml:mi><mml:mn>2</mml:mn></mml:msub><mml:mi mathvariant="normal">T</mml:mi><mml:msub><mml:mi mathvariant="normal">e</mml:mi><mml:mn>4</mml:mn></mml:msub></mml:mrow></mml:math> using a van der Waals ferroelectric <mml:math xmlns:mml="http://www.w3.org/1998/Math/MathML"><mml:m	1.1	49
61134	Partially embedded Pb chains on a vicinal Si(113) surface. Physical Review B, 2020, 101, .	1.1	4

#	Article	IF	Citations
61135	Intralayer ferromagnetism between S=52 ions in MnBi2Te4 : Role of empty Bi p states. Physical Review B, 2020, 101, .	1.1	14
61136	Magnetotransport and ab initio calculation studies on the layered semimetal <mml:math xmlns:mml="http://www.w3.org/1998/Math/MathML"><mml:mrow><mml:mi>CaA</mml:mi><mml:msub><mml:mi mathvariant="normal">I</mml:mi><mml:mn>2</mml:mn></mml:msub><mml:mi mathvariant="normal">S</mml:mi><mml:msub><mml:mi mathvariant="normal">i</mml:mi><mml:mn>2</mml:mn></mml:msub></mml:mrow></mml:math> hosting multiple nontrivial topological states. Physical Review B, 2020, 101, .	1.1	7
61137	Magnon valley Hall effect in <mml:math xmlns:mml="http://www.w3.org/1998/Math/MathML"><mml:msub><mml:mrow><mml:mi>CrI</mml:mi></mml:mrow><mml:mn>3</mml:mn> -based van der Waals heterostructures. Physical Review B, 2020, 101, .	1.1	26
61138	Longitudinal spin fluctuations in bcc and liquid Fe at high temperature and pressure calculated with a supercell approach. Physical Review B, 2020, 102, .	1.1	14
61139	Bethe-Slater-curve-like behavior and interlayer spin-exchange coupling mechanisms in two-dimensional magnetic bilayers. Physical Review B, 2020, 102, .	1.1	46
61140	Influence of point defects on the electronic and topological properties of monolayer <mml:math xmlns:mml="http://www.w3.org/1998/Math/MathML"><mml:msub><mml:mi>WTe</mml:mi><mml:mn>2</mml:mn></mml:msub> Physical Review B, 2020, 102, .	1.1	14
61141	Meta-GGA performance in solids at almost GGA cost. Physical Review B, 2020, 102, .	1.1	41
61142	Prediction of Dirac semimetals and hourglass surface states in stacked hydrogenated Xenes (X=Sn) Tj ETQq1 1 0.784314 rgBT /Overlo	1.1	3
61143	Crystal and electronic structure of <mml:math xmlns:mml="http://www.w3.org/1998/Math/MathML"><mml:mrow><mml:mi>Ga</mml:mi><mml:msub><mml:mi>La</mml:mi> from first-principles calculations. Physical Review B, 2020, 102, .	1.1	7
61144	Theory of out-of-equilibrium electron and phonon dynamics in metals after femtosecond laser excitation. Physical Review B, 2020, 102, .	1.1	24
61145	Glassy magnetic state and negative temperature coefficient of resistivity in <mml:math xmlns:mml="http://www.w3.org/1998/Math/MathML"><mml:mrow><mml:msub><mml:mi>Mn</mml:mi> Physical Review B, 2020, 102, .	1.1	9
61146	Electrically switchable Rashba-type Dzyaloshinskii-Moriya interaction and skyrmion in two-dimensional magnetoelectric multiferroics. Physical Review B, 2020, 102, .	1.1	52
61147	Effect of non-Heisenberg magnetic interactions on defects in ferromagnetic iron. Physical Review B, 2020, 102, .	1.1	7
61148	Metallization of dense fluid helium from ab initio simulations. Physical Review B, 2020, 102, .	1.1	10
61149	Multiferroic bismuth ferrite: Perturbed angular correlation studies on its ferroic <mml:math xmlns:mml="http://www.w3.org/1998/Math/MathML"><mml:mi>Î±</mml:mi><mml:mo>â^'</mml:mo><mml:mi>Î² phase transition. Physical Review B, 2020, 102, .	1.1	13
61150	Temporally decoherent and spatially coherent vibrations in metal halide perovskites. Physical Review B, 2020, 102, .	1.1	7
61151	Effects of Sr doping on the electronic and spin-state properties of infinite-layer nickelates: Nature of holes. Physical Review B, 2020, 102, .	1.1	26
61152	Fermiology and type-I superconductivity in the chiral superconductor <mml:math xmlns:mml="http://www.w3.org/1998/Math/MathML"><mml:mi>Nb</mml:mi><mml:msub><mml:mrow><mml:mi>Ge</mml:mi> with Kramers-Weyl fermions. Physical Review B, 2020, 102, .	1.1	9

#	Article	IF	Citations
61153	Koopmans-compliant screened exchange potential with correct asymptotic behavior for semiconductors. Physical Review B, 2020, 102, .	1.1	9
61154	Atomic structure of the (111) surface of the antiferromagnetic 1/1 Au-Al-Tb approximant. Physical Review B, 2020, 102, .	1.1	3
61155	Phonon softening near topological phase transitions. Physical Review B, 2020, 102, .	1.1	10
61156	Valley-dependent properties of monolayer <mml:math xmlns:mml="http://www.w3.org/1998/Math/MathML"><mml:msub><mml:mi mathvariant="normal">MoSi</mml:mi><mml:mn>2</mml:mn></mml:msub><mml:mi mathvariant="normal">N</mml:mi><mml:mn>4</mml:mn></mml:msub><mml:mo>,</mml:mo><mml:mo>Â</mml:mo><mml:msub><mml:mi mathvariant="normal">WSi</mml:mi><mml:mn>2</mml:mn></mml:msub><mml:msub><mml:mi mathvariant="normal">N</mml:mi><mml:mn>4</mml:mn></mml:msub></mml:math> , and <mml:math xmlns	1.1	124
61157	Linear magnetoresistance with a universal energy scale in the strong-coupling superconductor Mo8Ga41 without quantum criticality. Physical Review B, 2020, 102, .	1.1	4
61158	Site substitution in <mml:math xmlns:mml="http://www.w3.org/1998/Math/MathML"><mml:msub><mml:mi>GdMnO</mml:mi><mml:mn>3</mml:mn></mml:msub></mml:math> : Effects on structural, electronic, and magnetic properties. Physical Review B, 2020, 102, .	1.1	16
61159	Hybridization-induced gapped and gapless states on the surface of magnetic topological insulators. Physical Review B, 2020, 102, .	1.1	29
61160	Highly anisotropic two-dimensional metal in monolayer <mml:math xmlns:mml="http://www.w3.org/1998/Math/MathML"><mml:msub><mml:mi>MoOCl</mml:mi><mml:mn>2</mml:mn></mml:msub></mml:math> Physical Review B, 2020, 102, .	1.1	17
61162	Geometric ferroelectricity in rare-earth compounds<mml:math xmlns:mml="http://www.w3.org/1998/Math/MathML" display="inline"><mml:mrow><mml:mi>R</mml:mi><mml:msub><mml:mrow><mml:mtext>GaO</mml:mtext></mml:mrow><mml:mn> xmlns:mml="http://www.w3.org/1998/Math/MathML" display="inline"><mml:mrow><mml:mi>R</mml:mi><mml:msub><mml:mrow><mml:mtext>InO</mml:mtext></mml:mrow><mml:mn>3 Physical Review B, 2009, 79, .	1.1	42
61163	Stabilizing the spin vortex crystal phase in two-dimensional iron-based superconductors. Physical Review B, 2017, 95, .	1.1	20
61164	<mml:math xmlns:mml="http://www.w3.org/1998/Math/MathML"><mml:msub><mml:mi>CoB</mml:mi><mml:mn>6</mml:mn></mml:msub></mml monolayer: A robust two-dimensional ferromagnet. Physical Review B, 2019, 99, .	1.1	58
61165	Vibrational Frequencies of Cerium-Oxide-Bound CO: A Challenge for Conventional DFT Methods. Physical Review Letters, 2020, 125, 256101.	2.9	13
61166	Gapless Quantum Spin Liquid in the Triangular System <mml:math xmlns:mml="http://www.w3.org/1998/Math/MathML" display="inline"><mml:mrow><mml:mrow><mml:msub><mml:mrow><mml:mi>Sr</mml:mi></mml:mrow><mml:mn>3</mml:mn> mathvariant="normal">O</mml:mi></mml:mrow><mml:mrow><mml:mn>9</mml:mn></mml:mrow></mml:msub></mml:mrow></mml: Physical Review Letters, 2020, 125, 267202.	2.9	11
61167	Insight into the Charge Density Wave Gap from Contrast Inversion in Topographic STM Images. Physical Review Letters, 2020, 125, 267603.	2.9	25
61168	Dynamical multiferroicity. Physical Review Materials, 2017, 1, .	0.9	110
61169	Raman studies of the intermediate tin-oxide phase. Physical Review Materials, 2017, 1, .	0.9	54
61170	Amorphous to amorphous insulator-metal transition in GeSe3 :Ag glasses. Physical Review Materials, 2017, 1, .	0.9	8
61171	Synthesis of borophene nanoribbons on Ag(110) surface. Physical Review Materials, 2017, 1, .	0.9	113

#	Article	IF	Citations
61172	Prediction of nontrivial band topology and superconductivity in <mml:math xmlns:mml="http://www.w3.org/1998/Math/MathML"><mml:mrow><mml:mi mathvariant="normal">M</mml:mi><mml:msub><mml:mi mathvariant="normal">g</mml:mi><mml:mn>2</mml:mn></mml:msub><mml:mi>Pb</mml:mi></mml:mrow></mml:math>. Physical Review Materials, 2017, 1, .	0.9	8
61173	High-pressure phase diagram, structural transitions, and persistent nonmetallicity of <mml:math xmlns:mml="http://www.w3.org/1998/Math/MathML"><mml:msub><mml:mi>BaBiO</mml:mi><mml:mn>3</mml:mn></mml:msub></mml:math> : Theory and experiment. Physical Review Materials, 2017, 1, .	0.9	8
61174	Molybdenum-titanium phase diagram evaluated from ab initio calculations. Physical Review Materials, 2017, 1, .	0.9	11
61175	Strain engineering a <mml:math xmlns:mml="http://www.w3.org/1998/Math/MathML"><mml:mrow><mml:mn>4</mml:mn><mml:mi>a</mml:mi><mml:mo>Ã—</mml:mo> charge-density-wave phase in transition-metal dichalcogenide <mml:math xmlns:mml="http://www.w3.org/1998/Math/MathML"><mml:mrow><mml:mn>1</mml:mn><mml:mi mathvariant="normal">T</mml:mi><mml:mtext>â€”</mml:mtext><mml:mi>VS</mml:mi><mml:msub><mml:mi mathvariant="normal">e</mml:mi><mml:mn>2</mml:mn></mml:mm. Physical Review Materials, 2017, 1, .	0.9	42
61176	Heusler compounds with perpendicular magnetic anisotropy and large tunneling magnetoresistance. Physical Review Materials, 2017, 1, .	0.9	46
61177	Polaron formation, native defects, and electronic conduction in metal tungstates. Physical Review Materials, 2017, 1, .	0.9	21
61178	Exploring Cd-Zn-O-S alloys for improved buffer layers in thin-film photovoltaics. Physical Review Materials, 2017, 1, .	0.9	5
61179	Computing elastic anisotropy to discover gum-metal-like structural alloys. Physical Review Materials, 2017, 1, .	0.9	7
61180	Experimental and first-principles calculation study of the pressure-induced transitions to a metastable phase inGaPO4and in the solid solutionAlPO4â€“GaPO4. Physical Review Materials, 2017, 1, .	0.9	3
61181	Thermomechanical response of NiTi shape-memory nanoprecipitates in TiV alloys. Physical Review Materials, 2017, 1, .	0.9	23
61182	Interactions between copper and transition metal dichalcogenides: A density functional theory study. Physical Review Materials, 2017, 1, .	0.9	7
61183	High-throughput screening for antiferromagnetic Heusler compounds using density functional theory. Physical Review Materials, 2017, 1, .	0.9	24
61184	Exchange striction driven magnetodielectric effect and potential photovoltaic effect in polar CaOFeS. Physical Review Materials, 2017, 1, .	0.9	15
61185	Compensation of band-edge positions in titanium-doped <mml:math xmlns:mml="http://www.w3.org/1998/Math/MathML"><mml:mrow><mml:msub><mml:mi>Ta</mml:mi><mml:mn>3</mml:mn></mml:mm mathvariant="normal">N</mml:mi><mml:mn>5</mml:mn></mml:msub></mml:mrow></mml:math> photoanode for enhanced water splitting performance: A first-principles insight. Physical Review Materials, 2017, 1, .	0.9	11
61186	Phase diagram of carbon-nickel-tungsten: A superatom model. Physical Review Materials, 2017, 1, .	0.9	1
61187	Accurate force field for molybdenum by machine learning large materials data. Physical Review Materials, 2017, 1, .	0.9	82
61188	Investigation of vacancy-ordered <mml:math xmlns:mml="http://www.w3.org/1998/Math/MathML"><mml:mrow><mml:mi mathvariant="normal">M</mml:mi><mml:msub><mml:mi mathvariant="normal">o</mml:mi><mml:mrow><mml:mn>1.33</mml:mn></mml:mrow></mml:msub><mml:mi mathvariant="normal">C</mml:mi></mml:mrow></mml:math> MXene from first principles and x-ray photoelectron spectroscopy. Physical Review Materials, 2017, 1, .	0.9	36
61189	Ternary wurtzite CaAgBi materials family: A playground for essential and accidental, type-I and type-II Dirac fermions. Physical Review Materials, 2017, 1, .	0.9	59

#	Article	IF	Citations
61190	Adsorbed or intercalated: Na on graphene/Ir(111). Physical Review Materials, 2017, 1, .	0.9	14
61191	Prediction of a new class of half-metallic ferromagnets from first principles. Physical Review Materials, 2017, 1, .	0.9	13
61192	Controlling the magnetism of oxygen surface vacancies in <mml:math xmlns:mml="http://www.w3.org/1998/Math/MathML"><mml:msub><mml:mi mathvariant="normal">SrTiO</mml:mi><mml:mn>3</mml:mn></mml:msub></mml:math> through charging. Physical Review Materials, 2017, 1, .	0.9	15
61193	Hyperhoneycomb boron nitride with anisotropic mechanical, electronic, and optical properties. Physical Review Materials, 2017, 1, .	0.9	3
61194	Effect of dynamic surface polarization on the oxidative stability of solvents in nonaqueous <mml:math xmlns:mml="http://www.w3.org/1998/Math/MathML"><mml:msub><mml:mrow><mml:mi>Li</mml:mi><mml:mtext>â</mml:mtext> mathvariant="normal">O</mml:mi></mml:mrow><mml:mn>2</mml:mn></mml:msub></mml:math>	0.9	2
61195	<mml:math xmlns:mml="http://www.w3.org/1998/Math/MathML"><mml:mrow><mml:mi mathvariant="normal">C</mml:mi><mml:msub><mml:mi mathvariant="normal">a</mml:mi><mml:mn>3</mml:mn></mml:msub><mml:mi mathvariant="normal">S</mml:mi><mml:msub><mml:mi	0.9	6
61196	Tunable dimensional crossover and magnetocrystalline anisotropy in <mml:math xmlns:mml="http://www.w3.org/1998/Math/MathML"><mml:mrow><mml:msub><mml:mi>Fe</mml:mi><mml:mn>2</mml:mn></mml:msub> mathvariant="normal">P</mml:mi></mml:mrow></mml:math> -based alloys. Physical Review Materials, 2017, 1, .	0.9	7
61197	Polarity-driven oxygen vacancy formation in ultrathin <mml:math xmlns:mml="http://www.w3.org/1998/Math/MathML"><mml:msub><mml:mi>LaNiO</mml:mi><mml:mn>3</mml:mn></mml:msub> films on <mml:math xmlns:mml="http://www.w3.org/1998/Math/MathML"><mml:msub><mml:mi>SrTiO</mml:mi><mml:mn>3</mml:mn></mml:msub>	0.9	25
61198	Anisotropic charge density wave in layered <mml:math xmlns:mml="http://www.w3.org/1998/Math/MathML"><mml:mrow><mml:mn>1</mml:mn><mml:mi>T</mml:mi><mml:mo>â mathvariant="normal">e</mml:mi><mml:mn>2</mml:mn></mml:msub></mml:mrow></mml:math>. Physical Review Materials, 2017, 1, .	0.9	11
61199	Two-dimensional spin-orbit Dirac point in monolayer HfGeTe. Physical Review Materials, 2017, 1, .	0.9	70
61200	Strain-induced band engineering in monolayer stanene on Sb(111). Physical Review Materials, 2017, 1, .	0.9	91
61201	Temperature dependence of the bulk Rashba splitting in the bismuth tellurohalides. Physical Review Materials, 2017, 1, .	0.9	24
61202	New stable ternary alkaline-earth metal Pb(II) oxides: <mml:math xmlns:mml="http://www.w3.org/1998/Math/MathML"><mml:mrow><mml:msub><mml:mrow><mml:mi>Ca</mml:mi><mml:mo>/ mathvariant="normal">O</mml:mi><mml:mn>3</mml:mn></mml:msub></mml:mrow></mml:math> and <mml:math xmlns:mml="http://www.w3.org/1998/Math/MathML"><mml:msub><mml:mi>BaPbO</mml:mi><mml:mn>2</mml:mn></mml:msub> Physical Review Materials, 2017, 1, .	0.9	10
61203	Si(775)-Au atomic chains: Geometry, optical properties, and spin order. Physical Review Materials, 2017, 1, .	0.9	17
61204	Structural and electronic properties of copper-doped chalcogenide glasses. Physical Review Materials, 2017, 1, .	0.9	8
61205	One-dimensional phosphorus chain and two-dimensional blue phosphorene grown on Au(111) by molecular-beam epitaxy. Physical Review Materials, 2017, 1, .	0.9	89
61206	Dynamic interface rearrangement in <mml:math xmlns:mml="http://www.w3.org/1998/Math/MathML"><mml:mrow><mml:msub><mml:mi>LaFeO</mml:mi><mml:mn>3</mml:mn> heterojunctions. Physical Review Materials, 2017, 1, .	0.9	23
61207	Conceptual and practical bases for the high accuracy of machine learning interatomic potentials: Application to elemental titanium. Physical Review Materials, 2017, 1, .	0.9	44

#	Article	IF	Citations
61208	Automated crystal structure solution from powder diffraction data: Validation of the first-principles-assisted structure solution method. Physical Review Materials, 2017, 1, .	0.9	15
61209	Charged iodide in chains behind the highly efficient iodine doping in carbon nanotubes. Physical Review Materials, 2017, 1, .	0.9	25
61210	Theoretical investigation of <mml:math xmlns:mml="http://www.w3.org/1998/Math/MathML"><mml:mrow><mml:mi>CdI</mml:mi><mml:msub><mml:mi mathvariant="normal">n</mml:mi><mml:mn>2</mml:mn></mml:msub><mml:msub><mml:mi mathvariant="normal">S</mml:mi><mml:mn>4</mml:mn></mml:msub></mml:mrow></mml:math> : A possible substitute for CdS in <mml:math xmlns:mml="http://www.w3.org/1998/Math/MathML"><mml:mrow><mml:mi>CuI</mml:mi><mml:msub><mml:mi	0.9	6
61211	Band bowing and the direct-to-indirect crossover in random BAlN alloys. Physical Review Materials, 2017, 1, .	0.9	25
61212	Low lattice thermal conductivity and good thermoelectric performance of cinnabar. Physical Review Materials, 2017, 1, .	0.9	16
61213	Accuracy of ab initio electron correlation and electron densities in vanadium dioxide. Physical Review Materials, 2017, 1, .	0.9	41
61214	Ion-gel-gating-induced oxygen vacancy formation in epitaxial <mml:math xmlns:mml="http://www.w3.org/1998/Math/MathML"><mml:mrow><mml:mi mathvariant="normal">L</mml:mi><mml:msub><mml:mi mathvariant="normal">a</mml:mi><mml:mrow><mml:mn>0.5</mml:mn></mml:mrow></mml:msub><mml:mi mathvariant="normal">S</mml:mi><mml:msub><mml:mi mathvariant="normal">r</mml:mi><mml:mrow><mml:mn>0.5</mml:mn></mml:mrow></mml:msub><mml:mi>Co</mml:mi><mml:msu	0.9	44
61215	Surface buckling of black phosphorus: Determination, origin, and influence on electronic structure. Physical Review Materials, 2017, 1, .	0.9	13
61216	Topological origin of the type-II Dirac fermions in <mml:math xmlns:mml="http://www.w3.org/1998/Math/MathML"><mml:mi>PtSe</mml:mi><mml:msub><mml:mrow /><mml:mn>2</mml:mn></mml:msub></mml:math>. Physical Review Materials, 2017, 1, .	0.9	44
61217	Role of electron filling in the magnetic anisotropy of monolayer <mml:math xmlns:mml="http://www.w3.org/1998/Math/MathML"><mml:msub><mml:mi>WSe</mml:mi><mml:mn>2</mml:mn></mml:msub></mml: doped with <mml:math xmlns:mml="http://www.w3.org/1998/Math/MathML"><mml:mrow><mml:mn>5</mml:mn><mml:mi>d</mml:mi></mml:mrow></mml: transition metals. Physical Review Materials, 2017, 1, .	0.9	18
61218	Achieving giant tunneling electroresistance and magnetoresistance by <mml:math xmlns:mml="http://www.w3.org/1998/Math/MathML"><mml:mrow><mml:msub><mml:mi>BaTiO</mml:mi><mml:mn>3</mml:mn></mml: barrier and Heusler alloy electrode. Physical Review Materials, 2017, 1, .	0.9	8
61219	Prediction of high- <mml:math xmlns:mml="http://www.w3.org/1998/Math/MathML"><mml:msub><mml:mi>T</mml:mi><mml:mi>c</mml:mi></mml:msub></mml: conventional superconductivity in the ternary lithium borohydride system. Physical Review Materials, 2017, 1, .	0.9	38
61220	Tuning the magnetocaloric response in half-Heusler/Heusler <mml:math xmlns:mml="http://www.w3.org/1998/Math/MathML"><mml:mrow><mml:msub><mml:mi>MnNi</mml:mi><mml:mrow><mml:mn>1</mml: solid solutions. Physical Review Materials, 2017, 1, .	0.9	14
61221	First-principles theory of doping in layered oxide electrode materials. Physical Review Materials, 2017, 1, .	0.9	18
61222	Doping Li-rich cathode material <mml:math xmlns:mml="http://www.w3.org/1998/Math/MathML"><mml:mrow><mml:msub><mml:mi>Li</mml:mi><mml:mn>2</mml:mn></mml: : Interplay between lattice site preference, electronic structure, and delithiation mechanism. Physical Review Materials, 2017, 1, .	0.9	21
61223	Twelve inequivalent Dirac cones in two-dimensional <mml:math xmlns:mml="http://www.w3.org/1998/Math/MathML"><mml:msub><mml:mi>ZrB</mml:mi><mml:mn>2</mml:mn></mml: Physical Review Materials, 2018, 2, .	0.9	32
61224	Magnetic proximity effect in <mml:math xmlns:mml="http://www.w3.org/1998/Math/MathML"><mml:mrow><mml:mi>Pt</mml:mi><mml:mo>/</mml:mo><mml:msub><mml:mi mathvariant="normal">O</mml:mi><mml:mn>4</mml:mn></mml:msub></mml:mrow></mml:math> bilayers. Physical Review Materials, 2018, 2, .	0.9	33
61225	Semiconducting cubic titanium nitride in the <mml:math xmlns:mml="http://www.w3.org/1998/Math/MathML"><mml:mrow><mml:msub><mml:mi>Th</mml:mi><mml:mn>3</mml:mn></mml: mathvariant="normal">P</mml:mi><mml:mn>4</mml:mn></mml:msub></mml:mrow></mml:math>structure. Physical Review Materials, 2018, 2, .	0.9	24

#	Article	IF	Citations
61226	Crystal structure prediction accelerated by Bayesian optimization. Physical Review Materials, 2018, 2, .	0.9	94
61227	Matrix- and tensor-based recommender systems for the discovery of currently unknown inorganic compounds. Physical Review Materials, 2018, 2, .	0.9	39
61228	Robust large-gap quantum spin Hall insulators in methyl-functionalized III-Bi buckled honeycombs. Physical Review Materials, 2018, 2, .	0.9	11
61229	Topological Dirac nodal-net fermions in <mml:math xmlns:mml="http://www.w3.org/1998/Math/MathML"><mml:msub><mml:mi>AlB</mml:mi><mml:mn>2</mml:mn></mml:msub></mml -type <mml:math xmlns:mml="http://www.w3.org/1998/Math/MathML"><mml:msub><mml:mi>TiB</mml:mi><mml:mn>2</mml:mn></mml:msub></mml and <mml:math xmlns:mml="http://www.w3.org/1998/Math/MathML"><mml:msub><mml:mi>ZrB</mml:mi><mml:mn>2</mml:mn></mml:msub></mml	0.9	103
61230	Goldstone-like phonon modes in a (111)-strained perovskite. Physical Review Materials, 2018, 2, .	0.9	18
61231	Growth, electrical, structural, and magnetic properties of half-Heusler <mml:math xmlns:mml="http://www.w3.org/1998/Math/MathML"><mml:mrow><mml:mi>CoT</mml:mi><mml:msub><mml:mi mathvariant="normal">i</mml:mi><mml:mrow><mml:mn>1</mml:mn><mml:mo>â^'</mml:mo><mml:mi>x</mml:mi></mml:mrow></ mathvariant="normal">F</mml:mi><mml:msub><mml:mi mathvariant="normal">e</mml:mi><mml:mi>x</mml:mi></mml:msub><mml:mi>Sb</mml:mi></mml:mrow></mml:math>. Physical Review Materials, 2018, 2, .	0.9	8
61232	Opposing effects of stacking faults and antisite domain boundaries on the conduction band edge in kesterite quaternary semiconductors. Physical Review Materials, 2018, 2, .	0.9	15
61234	Band gap and mobility of epitaxial perovskite BaSn1â^'xHfxO3 thin films. Physical Review Materials, 2018, 2, .	0.9	3
61235	Fracture of coherent interfaces between an fcc metal matrix and the <mml:math xmlns:mml="http://www.w3.org/1998/Math/MathML"><mml:mrow><mml:msub><mml:mi>Cr</mml:mi><mml:mn>23</mml:mn></mml mathvariant="normal">C</mml:mi><mml:mn>6</mml:mn></mml:msub></mml:mrow></mml:math> carbide precipitate from first principles. Physical Review Materials, 2018, 2, .	0.9	9
61236	Lattice constant in nonstoichiometric uranium dioxide from first principles. Physical Review Materials, 2018, 2, .	0.9	22
61237	Pressure-stabilized binary compounds of magnesium and silicon. Physical Review Materials, 2018, 2, .	0.9	13
61238	Tetragonal fcc-Fe induced by Îº -carbide precipitates: Atomic scale insights from correlative electron microscopy, atom probe tomography, and density functional theory. Physical Review Materials, 2018, 2, .	0.9	14
61239	Single-layer dual germanene phases on Ag(111). Physical Review Materials, 2018, 2, .	0.9	72
61240	Converged <mml:math xmlns:mml="http://www.w3.org/1998/Math/MathML"><mml:mrow><mml:mi>G</mml:mi><mml:mi>W</mml:mi></mml:mrow></mml quasiparticle energies for transition metal oxide perovskites. Physical Review Materials, 2018, 2, .	0.9	45
61241	Towards novel organic high- <mml:math xmlns:mml="http://www.w3.org/1998/Math/MathML"><mml:msub><mml:mi>T</mml:mi><mml:mi>c</mml:mi></mml:msub></mml:ma superconductors: Data mining using density of states similarity search. Physical Review Materials, 2018, 2, .	0.9	18
61242	High-throughput density functional calculations to optimize properties and interfacial chemistry of piezoelectric materials. Physical Review Materials, 2018, 2, .	0.9	4
61243	Octahedral tilting instabilities in inorganic halide perovskites. Physical Review Materials, 2018, 2, .	0.9	73
61244	High-pressure-assisted design of porous topological semimetal carbon for Li-ion battery anode with high-rate performance. Physical Review Materials, 2018, 2, .	0.9	32

#	Article	IF	Citations
61245	Elastic fields, dipole tensors, and interaction between self-interstitial atom defects in bcc transition metals. Physical Review Materials, 2018, 2, .	0.9	47
61246	Resolving phase stability in the Ti-O binary with first-principles statistical mechanics methods. Physical Review Materials, 2018, 2, .	0.9	17
61247	Evaluation of van der Waals density functionals for layered materials. Physical Review Materials, 2018, 2, .	0.9	71
61248	<mml:math xmlns:mml="http://www.w3.org/1998/Math/MathML"><mml:msub><mml:mi>CsPbBr</mml:mi><mml:mn>3</mml:mn></mml:msub></ perovskites: Theoretical and experimental investigation on water-assisted transition from nanowire	0.9	63
61249	Prediction of new ground-state crystal structure of <mml:math xmlns:mml="http://www.w3.org/1998/Math/MathML"><mml:mrow><mml:mi mathvariant="normal">T</mml:mi><mml:msub><mml:mi mathvariant="normal">a</mml:mi><mml:mn>2</mml:mn></mml:msub><mml:msub><mml:mi mathvariant="normal">O</mml:mi><mml:mn>5</mml:mn></mml:msub></mml:mrow></mml:math>. Physical Review Materials, 2018, 2, .	0.9	19
61250	Study for material analogs of FeSb2 : Material design for thermoelectric materials. Physical Review Materials, 2018, 2, .	0.9	11
61251	Origin of the pressure-dependent <mml:math xmlns:mml="http://www.w3.org/1998/Math/MathML"><mml:msub><mml:mi>T</mml:mi><mml:mi>c</mml:mi></mml:msub></mml:ma valley in superconducting simple cubic phosphorus. Physical Review Materials, 2018, 2, .	0.9	7
61252	Optical and electronic properties of doped p -type CuI: Explanation of transparent conductivity from first principles. Physical Review Materials, 2018, 2, .	0.9	7
61253	Unraveling the oxygen vacancy structures at the reduced <mml:math xmlns:mml="http://www.w3.org/1998/Math/MathML"><mml:mrow><mml:mi>Ce</mml:mi><mml:msub><mml:mi mathvariant="normal">O</mml:mi><mml:mn>2</mml:mn></mml:msub><mml:mrow><mml:mo>(</mml:mo><mml:mn>111</mml:mn> surface. Physical Review Materials, 2018, 2, .	0.9	38
61254	Structure and energetics of carbon, hexagonal boron nitride, and carbon/hexagonal boron nitride single-layer and bilayer nanoscrolls. Physical Review Materials, 2018, 2, .	0.9	23
61255	Predictions of new <mml:math xmlns:mml="http://www.w3.org/1998/Math/MathML"><mml:mrow><mml:mi mathvariant="italic">AB</mml:mi><mml:msub><mml:mi mathvariant="normal">O</mml:mi><mml:mn>3</mml:mn></mml:msub></mml:mrow></mml:math> perovskite compounds by combining machine learning and density functional theory. Physical Review	0.9	127
61256	<mml:math xmlns:mml="http://www.w3.org/1998/Math/MathML"><mml:mrow><mml:mi mathvariant="normal">B</mml:mi><mml:msub><mml:mi mathvariant="normal">i</mml:mi><mml:mn>2</mml:mn></mml:msub><mml:mi mathvariant="normal">S</mml:mi><mml:msub><mml:mi	0.9	4
61257	Antiferromagnetic ground state in the<mml:math xmlns:mml="http://www.w3.org/1998/Math/MathML"><mml:msub><mml:mi>MnGa</mml:mi><mml:mn>4</mml:mn></mml:msub></m compound. Physical Review Materials, 2018, 2, .	0.9	12
61258	Structure and properties of a model conductive filament/host oxide interface in <mml:math xmlns:mml="http://www.w3.org/1998/Math/MathML"><mml:msub><mml:mi>HfO</mml:mi><mml:mn>2</mml:mn></mml:msub></ -based ReRAM. Physical Review Materials, 2018, 2, .	0.9	9
61259	First-principles thermodynamics study of phase stability in inorganic halide perovskite solid solutions. Physical Review Materials, 2018, 2, .	0.9	27
61260	Interfacial strain effects on lithium diffusion pathways in the spinel solid electrolyte Li-doped MgAl2O4. Physical Review Materials, 2018, 2, .	0.9	13
61261	Tin monochalcogenide heterostructures as mechanically rigid infrared band gap semiconductors. Physical Review Materials, 2018, 2, .	0.9	12
61262	Ordered structure of <mml:math xmlns:mml="http://www.w3.org/1998/Math/MathML"><mml:msub><mml:mi>FeGe</mml:mi><mml:mn>2</mml:mn></mml:msub></ formed during solid-phase epitaxy. Physical Review Materials, 2018, 2, .	0.9	4

#	Article	IF	Citations
61263	Structural and electronic properties of the alkali metal incommensurate phases. Physical Review Materials, 2018, 2, .	0.9	20
61264	Optically inactive defects in monolayer and bilayer phosphorene: A first-principles study. Physical Review Materials, 2018, 2, .	0.9	21
61265	Multiple topological electronic phases in superconductor MoC. Physical Review Materials, 2018, 2, .	0.9	10
61266	Tunable inversion symmetry to control indirect-to-direct band gaps transitions. Physical Review Materials, 2018, 2, .	0.9	4
61267	Optical and electronic properties of 2Hâ^'MoS2 under pressure: Revealing the spin-polarized nature of bulk electronic bands. Physical Review Materials, 2018, 2, .	0.9	19
61268	Deep vs shallow nature of oxygen vacancies and consequent<mml:math xmlns:mml="http://www.w3.org/1998/Math/MathML"><mml:mi>n</mml:mi></mml:math>-type carrier concentrations in transparent conducting oxides. Physical Review Materials, 2018, 2, .	0.9	73
61269	Accessible switching of electronic defect type in <mml:math xmlns:mml="http://www.w3.org/1998/Math/MathML"><mml:mrow><mml:mi>SrTi</mml:mi><mml:msub><mml:mi mathvariant="normal">O</mml:mi><mml:mn>3</mml:mn></mml:msub></mml:mrow></mml:math> via biaxial strain. Physical Review Materials, 2018, 2, .	0.9	8
61270	Icosahedral superstrength at the nanoscale. Physical Review Materials, 2018, 2, .	0.9	10
61271	Performance of the strongly constrained and appropriately normed density functional for solid-state materials. Physical Review Materials, 2018, 2, .	0.9	155
61272	Implications of heterostructural alloying for enhanced piezoelectric performance of (Al,Sc)N. Physical Review Materials, 2018, 2, .	0.9	47
61273	Magnetophononics: Ultrafast spin control through the lattice. Physical Review Materials, 2018, 2, .	0.9	53
61274	Atomistic study of the electronic contact resistivity between the half-Heusler alloys (HfCoSb,) Tj ETQq1 1 0.784314 rgBT /Overlock 10	0.9	4
61275	Stability and conductivity of cation- and anion-substituted <mml:math xmlns:mml="http://www.w3.org/1998/Math/MathML"><mml:msub><mml:mi>LiBH</mml:mi><mml:mn>4</mml:mn></mml:msub></mml:math> -based solid-state electrolytes. Physical Review Materials, 2018, 2, .	0.9	15
61276	Thermodynamics of hydrogen release in complexed borohydrides. Physical Review Materials, 2018, 2, .	0.9	2
61277	Plasmon spectroscopy: Robust metallicity of Au wires on Si(557) upon oxidation. Physical Review Materials, 2018, 2, .	0.9	10
61278	Non-Heisenberg covalent magnetism in iron oxide clusters. Physical Review Materials, 2018, 2, .	0.9	6
61279	Effect of fluoropolymer composition on topochemical synthesis of <mml:math xmlns:mml="http://www.w3.org/1998/Math/MathML"><mml:mrow><mml:mi>SrMn</mml:mi><mml:msub><mml:mi mathvariant="normal">O</mml:mi><mml:mrow><mml:mn>3</mml:mn><mml:mtext>â^'</mml:mtext><mml:mi>Î´</mml:mi></mml:mrow></mml:msub><mml:msub><mml:mi mathvariant="normal">F</mml:mi><mml:mi>Î³</mml:mi></mml:msub></mml:mrow></mml:math> oxyfluoride films. Physical Review Materials, 2018, 2, .	0.9	18
61280	Ab initio calculation of thermal expansion with application to understanding Invar behavior in gum metal. Physical Review Materials, 2018, 2, .	0.9	2

#	Article	IF	Citations
61281	Finite-temperature structure of the<mml:math xmlns:mml="http://www.w3.org/1998/Math/MathML"><mml:msub><mml:mi>MAPbI</mml:mi><mml:mn>3</mml:mn></mml:msub></m Comparing density functional approximations and force fields to experiment. Physical Review Materials, 2018, 2, .	0.9	31
61282	Crystallography and substitution patterns in the <mml:math xmlns:mml="http://www.w3.org/1998/Math/MathML"><mml:mrow><mml:mi>Zr</mml:mi><mml:msub><mml:mi mathvariant="normal">O</mml:mi><mml:mn>2</mml:mn></mml:msub><mml:mtext>â^'</mml:mtext><mml:mi>Ta</mml:mi><mml:msub><mml:mi mathvariant="normal">O</mml:mi><mml:mn>4</mml:mn></mml:msub></mml:mrow></mml:math> system. Physical Review Materials, 2018, 2, .	0.9	8
61283	Unusual composition dependence of transformation temperatures in Ti-Ta-X shape memory alloys. Physical Review Materials, 2018, 2, .	0.9	11
61284	Precipitate-induced nonlinearities of diffusion along grain boundaries in Al-based alloys. Physical Review Materials, 2018, 2, .	0.9	13
61285	<mml:math xmlns:mml="http://www.w3.org/1998/Math/MathML"><mml:msub><mml:mi mathvariant="normal">Al</mml:mi><mml:mi>x</mml:mi></mml:msub><mml:msub><mml:mi mathvariant="normal">Ga</mml:mi><mml:mrow><mml:mn>1</mml:mn><mml:mo>â^'</mml:mo><mml:mi>x</mml:mi></mml:mrow><mml: crystals with direct 2 eV band gaps from computational alchemy. Physical Review Materials, 2018, 2, .	0.9	17
61286	Topological band crossings in hexagonal materials. Physical Review Materials, 2018, 2, .	0.9	35
61287	Relativistic <mml:math xmlns:mml="http://www.w3.org/1998/Math/MathML"><mml:mrow><mml:mi>G</mml:mi><mml:mi>W</mml:mi></mml:mrow></mml:m +BSE study of the optical properties of Ruddlesden-Popper iridates. Physical Review Materials, 2018, 2, .	0.9	10
61288	Nontrivial strength of van der Waals epitaxial interaction in soft perovskites. Physical Review Materials, 2018, 2, .	0.9	40
61289	Systematic search for two-dimensional ferromagnetic materials. Physical Review Materials, 2018, 2, .	0.9	81
61290	Combined ab initio and empirical model of the thermal conductivity of uranium, uranium-zirconium, and uranium-molybdenum. Physical Review Materials, 2018, 2, .	0.9	9
61291	First-principles insights on phase stability of titanium interstitial alloys. Physical Review Materials, 2018, 2, .	0.9	10
61292	Influence of vibrational entropy on the concentrations of oxygen interstitial clusters and uranium vacancies in nonstoichiometric <mml:math xmlns:mml="http://www.w3.org/1998/Math/MathML"><mml:mrow><mml:mi mathvariant="normal">U</mml:mi><mml:msub><mml:mi mathvariant="normal">O</mml:mi><mml:mn>2</mml:mn></mml:msub></mml:mrow></mml:math>. Physical Review Materials, 2018, 2, .	0.9	15
61293	Magnetic properties of transition metal dichalcogenides-Fe/Ir(111) interfaces from first principles. Physical Review Materials, 2018, 2, .	0.9	4
61294	Interpenetrating silicene networks: A topological nodal-line semimetal with potential as an anode material for sodium ion batteries. Physical Review Materials, 2018, 2, .	0.9	21
61295	Room-temperature ferrimagnetic multiferroic <mml:math xmlns:mml="http://www.w3.org/1998/Math/MathML"><mml:mrow><mml:mi>BiF</mml:mi><mml:msub><mml:mi mathvariant="normal">e</mml:mi><mml:mrow><mml:mn>0.5</mml:mn></mml:mrow></mml:msub><mml:mi mathvariant="normal">C</mml:mi><mml:msub><mml:mi mathvariant="normal">o</mml:mi><mml:mrow><mml:mn>0.5</mml:mn></mml:mrow></mml:msub><mml:msub><mml:mi mathvariant="normal">O</mml:mi><mml:mn>3</mml:mn></mml:msub></mml:mrow></mml:math> thin f	0.9	12
61296	Structural and magnetic transitions accompanied by large responses in epitaxial Sr0.5Ba0.5MnO3 films. Physical Review Materials, 2018, 2, .	0.9	5
61297	Magnetocrystalline anisotropy in <mml:math xmlns:mml="http://www.w3.org/1998/Math/MathML"><mml:msub><mml:mi>YCo</mml:mi><mml:mn>5</mml:mn></mml:msub></mm and <mml:math xmlns:mml="http://www.w3.org/1998/Math/MathML"><mml:msub><mml:mi>ZrCo</mml:mi><mml:mn>5</mml:mn></mml:msub></m compounds from first-principles real-space pseudopotentials calculations. Physical Review Materials, 2018, 2, .	0.9	4
61298	Real-space pseudopotential method for calculating magnetocrystalline anisotropy. Physical Review Materials, 2018, 2, .	0.9	7

#	Article	IF	Citations
61299	Properties of mixed transition metal oxides:<mml:math xmlns:mml="http://www.w3.org/1998/Math/MathML"><mml:mrow><mml:mi>M</mml:mi><mml:msup><mml:mi>M</mml:mi><mml:mo corundum-type structures<mml:math		

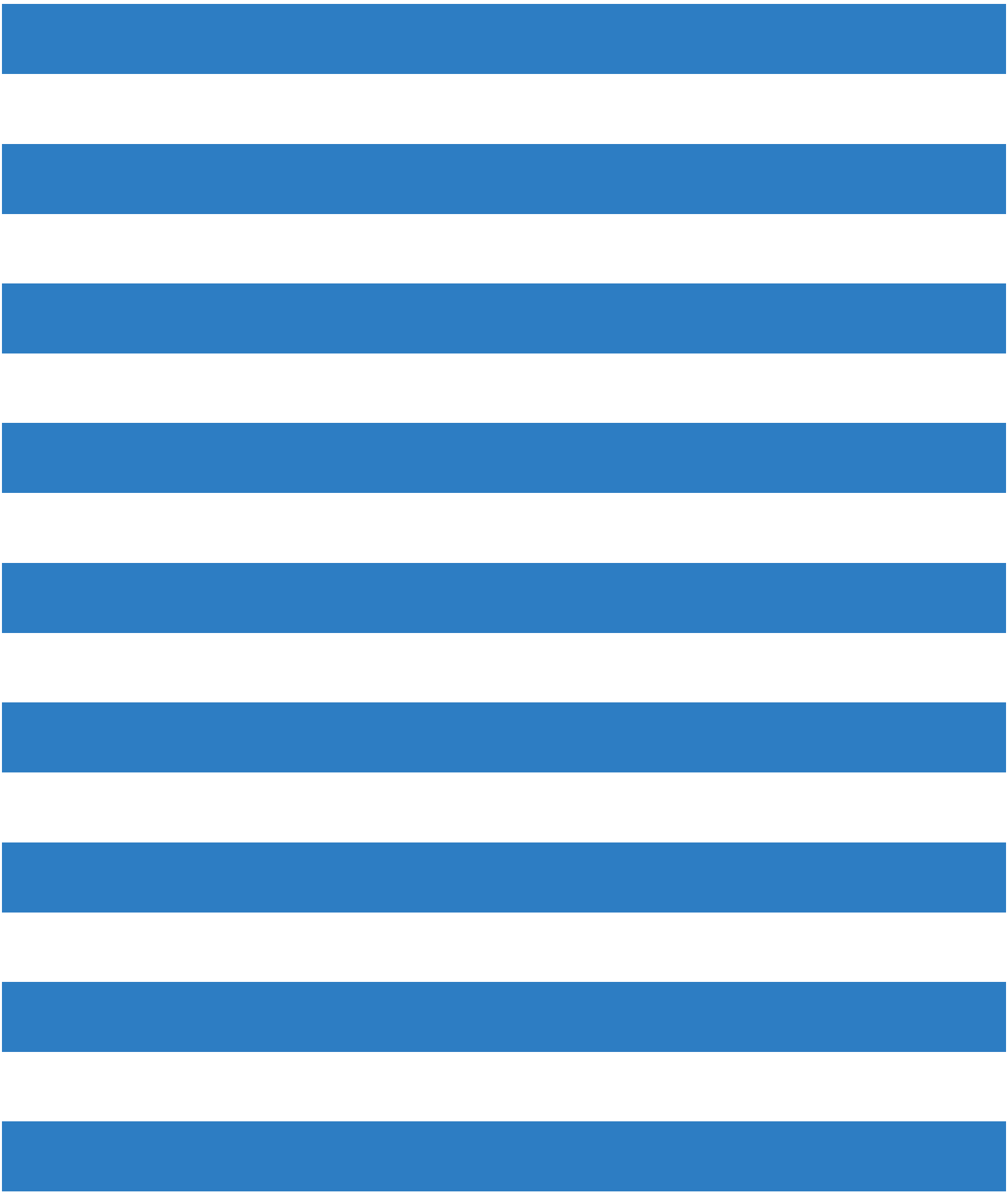

#	Article	IF	Citations
61317	Beyond thermodynamic defect models: A kinetic simulation of arsenic activation in CdTe. Physical Review Materials, 2018, 2, .	0.9	21
61318	Automated construction of symmetrized Wannier-like tight-binding models from ab initio calculations. Physical Review Materials, 2018, 2, .	0.9	32
61319	Highly crystalline synthesis of tellurene sheets on two-dimensional surfaces: Control over helical chain direction of tellurene. Physical Review Materials, 2018, 2, .	0.9	27
61320	Monolayer <mml:math xmlns:mml="http://www.w3.org/1998/Math/MathML"><mml:mrow><mml:msub><mml:mi>Mg</mml:mi><mml:mn>2</mml:mn></mml:msub><mml:mi mathvariant="normal">C</mml:mi></mml:mrow></mml:math> : Negative Poisson's ratio and unconventional two-dimensional emergent fermions. Physical Review Materials, 2018, 2, .	0.9	36
61321	Type-II Dirac line node in strained <mml:math xmlns:mml="http://www.w3.org/1998/Math/MathML"><mml:mrow><mml:msub><mml:mi>Na</mml:mi><mml:mn>3</mml:mn></mml:msub><mml:mi mathvariant="normal">N</mml:mi></mml:mrow></mml:math>. Physical Review Materials, 2018, 2, .	0.9	7
61322	Relationship between crystal structure and multiferroic orders in orthorhombic perovskite manganites. Physical Review Materials, 2018, 2, .	0.9	16
61323	Magnetic structural unit with convex geometry: A building block hosting an exchange-striction-driven magnetoelectric coupling. Physical Review Materials, 2018, 2, .	0.9	13
61324	Polymorphism in Bi-based perovskite oxides: A first-principles study. Physical Review Materials, 2018, 2, .	0.9	10
61325	Surface reconstructions and modified surface states in <mml:math xmlns:mml="http://www.w3.org/1998/Math/MathML"><mml:mrow><mml:mi mathvariant="normal">L</mml:mi><mml:msub><mml:mi mathvariant="normal">a</mml:mi><mml:mrow><mml:mn>1</mml:mn><mml:mo>â^’</mml:mo><mml:mi>x</mml:mi></mml:mrow></mml:msub><mml:mi mathvariant="normal">C</mml:mi><mml:msub><mml:mi mathvariant="normal">a</mml:mi><mml:mi>x</mml:mi></mml:msub><mml:mi>Mn</mml:mi><mml:msub><mml:mi mathvariant="normal">O</mml:mi><mml:mn>3</mml:mn></mml:msub></mml:mrow></mml:math>	0.9	7
61326	Chemical nature of the anion antisite in dilute phosphide <mml:math xmlns:mml="http://www.w3.org/1998/Math/MathML"><mml:mrow><mml:mi>GaA</mml:mi><mml:msub><mml:mi mathvariant="normal">s</mml:mi><mml:mrow><mml:mn>1</mml:mn><mml:mo>â^’</mml:mo><mml:mi>x</mml:mi></mml:mrow></mml:msub><mml:mi mathvariant="normal">P</mml:mi><mml:mi>x</mml:mi></mml:mrow></mml:math> alloy grown at low temperature. Physical Review Materials, 2018, 2, .	0.9	1
61327	Effect of temperature and configurational disorder on the electronic band gap of boron carbide from first principles. Physical Review Materials, 2018, 2, .	0.9	2
61328	Towards bipolar tin monoxide: Revealing unexplored dopants. Physical Review Materials, 2018, 2, .	0.9	9
61329	Influence of <mml:math xmlns:mml="http://www.w3.org/1998/Math/MathML"><mml:mi>Ï€</mml:mi></mml:math> -conjugated cations and halogen substitution on the optoelectronic and excitonic properties of layered hybrid perovskites. Physical Review Materials, 2018, 2, .	0.9	24
61330	Interface-driven thermal rectification in nanoscale systems. Physical Review Materials, 2018, 2, .	0.9	6
61331	Metalorganic vapor phase epitaxy of large size CdTe grains on mica through chemical and van der Waals interactions. Physical Review Materials, 2018, 2, .	0.9	12
61332	First-principles study of phase stability of bcc<mml:math xmlns:mml="http://www.w3.org/1998/Math/MathML"><mml:mrow><mml:mi>X</mml:mi><mml:mi>Zn</mml:mi></mml:mrow></mml:math>	0.9	10
61333	Geometries of edge and mixed dislocations in bcc Fe from first-principles calculations. Physical Review Materials, 2018, 2, .	0.9	18
61334	Autonomous efficient experiment design for materials discovery with Bayesian model averaging. Physical Review Materials, 2018, 2, .	0.9	58

#	Article	IF	Citations
61335	Domain morphology and mechanics of the <mml:math xmlns:mml="http://www.w3.org/1998/Math/MathML"><mml:msup><mml:mrow><mml:mi mathvariant="normal">H</mml:mi><mml:mo>/</mml:mo><mml:mi mathvariant="normal">T</mml:mi></mml:mrow><mml:mo>â€²</mml:mo></mml:msup></mml:math> transition metal dichalcogenide monolayers. Physical Review Materials, 2018, 2, .	0.9	18
61336	<mml:math xmlns:mml="http://www.w3.org/1998/Math/MathML"><mml:msub><mml:mi>PtP</mml:mi><mml:mn>2</mml:mn></mml:msub></mml: : An example of exploring the hidden Cairo tessellation in the pyrite structure for discovering novel two-dimensional materials. Physical Review Materials, 2018, 2, .	0.9	14
61337	Refrigeration in 2D: Electrostaticaloric effect in monolayer materials. Physical Review Materials, 2018, 2, .	0.9	5
61338	Evolution of electronic structure and electron-phonon coupling in ultrathin tetragonal CoSe films. Physical Review Materials, 2018, 2, .	0.9	7
61339	Electronic structure of monolayer antimonene nanoribbons under out-of-plane and transverse bias. Physical Review Materials, 2018, 2, .	0.9	3
61340	Universal superconductivity phase diagram for pressurized tetradymite topological insulators. Physical Review Materials, 2018, 2, .	0.9	8
61341	Topological phonons and thermoelectricity in triple-point metals. Physical Review Materials, 2018, 2, .	0.9	76
61342	Stoichiometry control and electronic and transport properties of pyrochlore <mml:math xmlns:mml="http://www.w3.org/1998/Math/MathML"><mml:mrow><mml:mi mathvariant="normal">B</mml:mi><mml:msub><mml:mi mathvariant="normal">i</mml:mi><mml:mn>2</mml:mn></mml:msub><mml:mi mathvariant="normal">I</mml:mi><mml:msub><mml:mi mathvariant="normal">r</mml:mi><mml:mn>2</mml:mn></mml:msub><mml:msub><mml:mi mathvariant	0.9	7
61343	Charged domain walls in improper ferroelectric hexagonal manganites and gallates. Physical Review Materials, 2018, 2, .	0.9	29
61344	Role of interstitial hydrogen in <mml:math xmlns:mml="http://www.w3.org/1998/Math/MathML"><mml:msub><mml:mi>SrCoO</mml:mi><mml:mrow><mml:mn>2.5</mml:mn antiferromagnetic insulator. Physical Review Materials, 2018, 2, .	0.9	9
61345	Structural dynamics in hybrid halide perovskites: Bulk Rashba splitting, spin texture, and carrier localization. Physical Review Materials, 2018, 2, .	0.9	19
61346	Accurate band alignment at the amorphous <mml:math xmlns:mml="http://www.w3.org/1998/Math/MathML"><mml:mrow><mml:msub><mml:mi>Al</mml:mi><mml:mn>2</mml:mn></mml:msub><mml:mi mathvariant="normal">O</mml:mi><mml:mn>3</mml:mn></mml:mrow></mml:math> Nematicity and superconductivity in orthorhombic superconductor <mml:math xmlns:mml="http://www.w3.org/1998/Math/MathML"><mml:mrow><mml:mi mathvariant="normal">N</mml:mi><mml:msub><mml:mi	0.9	3
61347			

#	Article	IF	Citations
61353	Mechanism of twin-reduced III-V epitaxy on As-modified vicinal Si(111). Physical Review Materials, 2018, 2, .	0.9	2
61354	Effects of composition, crystal structure, and surface orientation on band alignment of divalent metal oxides: A first-principles study. Physical Review Materials, 2018, 2, .	0.9	24
61355	Strain-engineered Peierls instability in layered perovskite <mml:math xmlns:mml="http://www.w3.org/1998/Math/MathML"><mml:mrow><mml:msub><mml:mi>La</mml:mi><mml:mn>3</mml:mn></mml:r mathvariant="normal">O</mml:mi><mml:mn>7</mml:mn></mml:msub></mml:mrow></mml:math> from first principles. Physical Review Materials, 2018, 2, .	0.9	10
61356	Polar metallic behavior of strained antiperovskites ACNi3(A=Mg,Zn,and Cd) from first principles. Physical Review Materials, 2018, 2, .	0.9	14
61357	Presence of water at elevated temperatures, structural transition, and thermal expansion behavior in <mml:math xmlns:mml="http://www.w3.org/1998/Math/MathML"><mml:mrow><mml:mi>LaP</mml:mi><mml:msub><mml:mi 0.9 mathvariant="normal">O</mml:mi><mml:mn>4</mml:mn></mml:msub><mml:mo>:</mml:mo><mml:mi>Eu</mml:mi></mml:mrow></ Physical Review Materials, 2018, 2, .	0.9	4
61358	Protective layer enhanced the stability and superconductivity of tailored antimonene bilayer. Physical Review Materials, 2018, 2, .	0.9	13
61359	New two-dimensional phase of tin chalcogenides: Candidates for high-performance thermoelectric materials. Physical Review Materials, 2019, 3, .	0.9	44
61360	Strain-induced heteronuclear charge disproportionation in <mml:math xmlns:mml="http://www.w3.org/1998/Math/MathML"><mml:msub><mml:mi>EuMnO</mml:mi><mml:mn>3</mml:mn></mml:msub></ Physical Review Materials, 2019, 3, .	0.9	2
61361	Hybrid functional study of nonlinear elasticity and internal strain in zinc-blende III-V materials. Physical Review Materials, 2019, 3, .	0.9	10
61362	Universality of point defect structure in body-centered cubic metals. Physical Review Materials, 2019, 3, .	0.9	53
61363	First-principles study on the grain boundary embrittlement of bcc-Fe by Mn segregation. Physical Review Materials, 2019, 3, .	0.9	23
61364	Deciphering structural and magnetic disorder in the chiral skyrmion host materials <mml:math xmlns:mml="http://www.w3.org/1998/Math/MathML"><mml:mrow><mml:msub><mml:mi>Co</mml:mi><mml:mi>x</mml:mi></mml		

#	Article	IF	Citations
61371	Remarkable thermoelectric performance in <mml:math xmlns:mml="http://www.w3.org/1998/Math/MathML"><mml:msub><mml:mi>BaPdS</mml:mi><mml:mn>2</mml:mn></mml:msub></m via pudding-mold band structure, band convergence, and ultralow lattice thermal conductivity. Physical Review Materials, 2019, 3, .	0.9	11
61372	High thermoelectric figure of merit and thermopower in layered perovskite oxides. Physical Review Materials, 2019, 3, .	0.9	11
61373	Temperature-induced phase transition and Li self-diffusion in <mml:math xmlns:mml="http://www.w3.org/1998/Math/MathML"><mml:mrow><mml:msub><mml:mi>Li</mml:mi><mml:mn>2</mml:mn></mml:m mathvariant="normal">C</mml:mi><mml:mn>2</mml:mn></mml:msub></mml:mrow></mml:math> : A first-principles study. Physical Review Materials, 2019, 3, .	0.9	3
61374	Active learning of uniformly accurate interatomic potentials for materials simulation. Physical Review Materials, 2019, 3, .	0.9	299
61375	Theoretical study of scattering in graphene ribbons in the presence of structural and atomistic edge roughness. Physical Review Materials, 2019, 3, .	0.9	9
61376	Computational design of flexible electrides with nontrivial band topology. Physical Review Materials, 2019, 3, .	0.9	18
61377	High-throughput screening for spin-gapless semiconductors in quaternary Heusler compounds. Physical Review Materials, 2019, 3, .	0.9	79
61378	Effect of N interstitial complexes on the electronic properties of <mml:math xmlns:mml="http://www.w3.org/1998/Math/MathML"><mml:mrow><mml:msub><mml:mi>GaAs</mml:mi><mml:mrow><mml:mn>1 mathvariant="normal">N</mml:mi><mml:mi>x</mml:mi></mml:msub></mml:mrow></mml:math> alloys from first principles. Physical Review Materials, 2019, 3, .	0.9	3
61379	Towards understanding the special stability of <mml:math xmlns:mml="http://www.w3.org/1998/Math/MathML"><mml:msub><mml:mi>SrCoO</mml:mi><mml:mrow><mml:mn>2.5</mml:mn></mml:mrow> and <mml:math xmlns:mml="http://www.w3.org/1998/Math/MathML"><mml:msub><mml:mi>HSrCoO</mml:mi><mml:mrow><mml:mn>2.5</mml:mn></mml:mrow> Physical Review Materials, 2019, 3, .	0.9	8
61380	Insights into the electronic structure of OsO2 using soft and hard x-ray photoelectron spectroscopy in combination with density functional theory. Physical Review Materials, 2019, 3, .	0.9	9
61381	Diffuson-driven ultralow thermal conductivity in amorphous <mml:math xmlns:mml="http://www.w3.org/1998/Math/MathML"><mml:mrow><mml:mi mathvariant="normal">N</mml:mi><mml:msub><mml:mi mathvariant="normal">b</mml:mi><mml:mn>2</mml:mn></mml:msub><mml:msub><mml:mi mathvariant="normal">O</mml:mi><mml:mn>5</mml:mn></mml:msub></mml:mrow></mml:math> thin films. Physical Review Materials, 2019, 3, .	0.9	18
61382	Computational evaluation of new lithium-3 garnets for lithium-ion battery applications as anodes, cathodes, and solid-state electrolytes. Physical Review Materials, 2019, 3, .	0.9	13
61383	Phonons, magnons, and lattice thermal transport in antiferromagnetic semiconductor MnTe. Physical Review Materials, 2019, 3, .	0.9	25
61384	Ferroelectricity in [111]-oriented epitaxially strained <mml:math xmlns:mml="http://www.w3.org/1998/Math/MathML"><mml:msub><mml:mi mathvariant="normal">SrTiO</mml:mi><mml:mn>3</mml:mn></mml:msub></mml:math> from first principles. Physical Review Materials, 2019, 3, .	0.9	11
61385	First-principles calculations of solute transport in zirconium: Vacancy-mediated diffusion with metastable states and interstitial diffusion. Physical Review Materials, 2019, 3, .	0.9	12
61386	First-principles study of phonon anharmonicity and negative thermal expansion in <mml:math xmlns:mml="http://www.w3.org/1998/Math/MathML"><mml:msub><mml:mi>ScF</mml:mi><mml:mn>3</mml:mn></mml:msub></m Physical Review Materials, 2019, 3, .	0.9	66
61387	Density functional study of self-diffusion along an isolated screw dislocation in fcc Ni. Physical Review Materials, 2019, 3, .	0.9	4
61388	Dislocation core structures in Ni-based superalloys computed using a density functional theory based flexible boundary condition approach. Physical Review Materials, 2019, 3, .	0.9	11

#	Article	IF	Citations
61389	Thermal properties of disordered <mml:math xmlns:mml="http://www.w3.org/1998/Math/MathML"><mml:mrow><mml:msub><mml:mi>Li</mml:mi><mml:mi>x</mml:mi></mml:ms /><mml:mn>2</mml:mn></mml:msub></mml:math> : An ab initio study. Physical Review Materials, 2019, 3, .	0.9	4
61390	Influence of strain and chemical substitution on the magnetic anisotropy of antiferromagnetic <mml:math xmlns:mml="http://www.w3.org/1998/Math/MathML"><mml:mrow><mml:msub><mml:mi>Cr</mml:mi><mml:mn>2</mml:mn></mml:msub><mml:msub><mml:mi mathvariant="normal">O</mml:mi><mml:mn>3</mml:mn></mml:msub></mml:mrow></mml:math> : An	0.9	18
61391	Computationally driven high-throughput identification of CaTe and <mml:math xmlns:mml="http://www.w3.org/1998/Math/MathML"><mml:mrow><mml:msub><mml:mi>Li</mml:mi><mml:mn>3</mml:mn></mml:m as promising candidates for high-mobility <mml:math xmlns:mml="http://www.w3.org/1998/Math/MathML"><mml:mi>p</mml:mi></mml:math> -type transparent conducting materials. Physical Review Materials, 2019, 3, .	0.9	16
61392	Accurate electronic and optical properties of hexagonal germanium for optoelectronic applications. Physical Review Materials, 2019, 3, .	0.9	41
61393	Reduced thermal conductivity of epitaxial GaAs on Si due to symmetry-breaking biaxial strain. Physical Review Materials, 2019, 3, .	0.9	20
61394	Enabling visible-light absorption and <mml:math xmlns:mml="http://www.w3.org/1998/Math/MathML"><mml:mi>p</mml:mi></mml:math> -type doping in <mml:math xmlns:mml="http://www.w3.org/1998/Math/MathML"><mml:msub><mml:mrow><mml:msub><mml:mi>In</mml:mi><mml:mn>2</mml:m mathvariant="normal">O</mml:mi></mml:mrow><mml:mn>3</mml:mn></mml:msub></mml:math> by adding Bi. Physical Review Materials, 2019, 3, .	0.9	7
61395	Giant power output in lead-free ferroelectrics by shock-induced phase transition. Physical Review Materials, 2019, 3, .	0.9	29
61396	Ternary mixed-anion semiconductors with tunable band gaps from machine-learning and crystal structure prediction. Physical Review Materials, 2019, 3, .	0.9	16
61397	Influence of lattice dynamics on lithium-ion conductivity: A first-principles study. Physical Review Materials, 2019, 3, .	0.9	45
61398	Bridging molecular dynamics and correlated wave-function methods for accurate finite-temperature properties. Physical Review Materials, 2019, 3, .	0.9	16
61399	Symmetry-broken self-interstitial defects in chromium, molybdenum, and tungsten. Physical Review Materials, 2019, 3, .	0.9	28
61400	Ultralow shear modulus of incommensurate <mml:math xmlns:mml="http://www.w3.org/1998/Math/MathML"><mml:mrow><mml:msub><mml:mrow><mml:mo>[</mml:mo><mml:mi>SnSe</ layers synthesized by the method of modulated elemental reactants. Physical Review Materials, 2019, 3, .	0.9	5
61401	Ab initio investigation of structural stability and exfoliation energies in transition metal dichalcogenides based on Ti-, V-, and Mo-group elements. Physical Review Materials, 2019, 3, .	0.9	44
61402	Electronic structure of a monoatomic <mml:math xmlns:mml="http://www.w3.org/1998/Math/MathML"><mml:msub><mml:mi mathvariant="normal">Cu</mml:mi><mml:mn>2</mml:mn></mml:msub></mml:math> Si layer on a Si(111) substrate. Physical Review Materials, 2019, 3, .	0.9	15
61403	Pressure tuning of the electrical transport properties in the Weyl semimetal TaP. Physical Review Materials, 2019, 3, .	0.9	4
61404	High-pressure lithium as an elemental topological semimetal. Physical Review Materials, 2019, 3, .	0.9	7
61405	Magnetic order effects on the electronic structure of <mml:math xmlns:mml="http://www.w3.org/1998/Math/MathML"><mml:mrow><mml:mi mathvariant="normal">K</mml:mi><mml:mi>M</mml:mi><mml:msub><mml:mi>MnS</mml:mi><mml:mn>2</mml:mn></mml:msub><mml: width="4pt" /><mml:mo>(</mml:mo><mml:mi>M</mml:mi><mml:mo>=</mml:mo><mml:mtext>Cu</mml:mtext><mml:mo>,</mml:mo><mml:mte with the <mml:math xmlns:mml="http://www.w3.org/1998/Math/MathML"><mml:mrow><mml:ms. Physic	0.9	5
61406	First-principles study of self-trapped holes and acceptor impurities in <mml:math xmlns:mml="http://www.w3.org/1998/Math/MathML"><mml:mrow><mml:msub><mml:mi>Ga</mml:mi><mml:mn>2</mml:mn></mml:mn></mml:mrow></mml:math> polymorphs. Physical Review Materials, 2019, 3, .	0.9	80

#	Article	IF	Citations
61407	Rare-earth adatoms on GaN (0001). Physical Review Materials, 2019, 3, .	0.9	3
61408	Electronic structures of quasi-one-dimensional cuprate superconductors <mml:math xmlns:mml="http://www.w3.org/1998/Math/MathML"><mml:mrow><mml:msub><mml:mi>Ba</mml:mi><mml:mn>2</mml:mn></mml:msub></mml:mrow></mml:math>. Physical Review Materials, 2019, 3, .	0.9	15
61409	Hidden kagome-lattice picture and origin of high conductivity in delafossite <mml:math xmlns:mml="http://www.w3.org/1998/Math/MathML"><mml:msub><mml:mi>PtCoO</mml:mi><mml:mn>2</mml:mn></mml:msub></mml:math>. Physical Review Materials, 2019, 3, .	0.9	12
61410	Electronic band structure and optical properties of boron arsenide. Physical Review Materials, 2019, 3, .	0.9	18
61411	Enhanced doping efficiency of ultrawide band gap semiconductors by metal-semiconductor junction assisted epitaxy. Physical Review Materials, 2019, 3, .	0.9	21
61412	First principles high-throughput screening to enhance the ductility of lightweight magnesium alloys. Physical Review Materials, 2019, 3, .	0.9	1
61413	Tunable disorder and localization in the rare-earth nickelates. Physical Review Materials, 2019, 3, .	0.9	8
61414	First-principles study on the effects of twin boundaries on anodic dissolution of Mg. Physical Review Materials, 2019, 3, .	0.9	14
61415	Hourglass Weyl loops in two dimensions: Theory and material realization in monolayer GaTeI family. Physical Review Materials, 2019, 3, .	0.9	44
61416	Phonon mode calculations and Raman spectroscopy of the bulk-insulating topological insulator <mml:math xmlns:mml="http://www.w3.org/1998/Math/MathML"><mml:msub><mml:mi>BiSbTeSe</mml:mi><mml:mn>2</mml:mn></mml:msub></mml:math>. Physical Review Materials, 2019, 3, .	0.9	18
61417	Coexistence of polar displacements and conduction in doped ferroelectrics: An ab initio comparative study. Physical Review Materials, 2019, 3, .	0.9	14
61418	Reversible out-of-plane spin texture in a two-dimensional ferroelectric material for persistent spin helix. Physical Review Materials, 2019, 3, .	0.9	39
61419	Complex dielectric function of <mml:math xmlns:mml="http://www.w3.org/1998/Math/MathML"><mml:mrow><mml:mi>GaA</mml:mi><mml:msub><mml:mi mathvariant="normal">s</mml:mi><mml:mrow><mml:mn>1</mml:mn><mml:mo>â^’</mml:mo><mml:mi>x</mml:mi></mml:mrow></mml:msub><mml:mi mathvariant="normal">B</mml:mi><mml:msub><mml:mi mathvariant="normal">i</mml:mi><mml:mi>x</mml:mi></mml:msub></mml:mrow></mml:math> as a function of Bi content. Physical Review Materials, 2019, 3, .	0.9	6
61420	Oxygen and silicon point defects in <mml:math xmlns:mml="http://www.w3.org/1998/Math/MathML"><mml:mrow><mml:msub><mml:mi>Al</mml:mi><mml:mrow><mml:mn>0.65</mml:mn></mml:mrow></mml:msub><mml:mi mathvariant="normal">N</mml:mi></mml:mrow></mml:math>. Physical Review Materials, 2019, 3, .	0.9	15
61421	Superconductivity in Li-intercalated <mml:math xmlns:mml="http://www.w3.org/1998/Math/MathML"><mml:mrow><mml:mn>1</mml:mn><mml:mi>T</mml:mi><mml:mtext>â^’</mml:mtext></mml:mrow></mml:math> driven by electric field gating. Physical Review Materials, 2019, 3, .	0.9	25
61422	Phase field parameters for battery compounds from first-principles calculations. Physical Review Materials, 2019, 3, .	0.9	8
61423	Structure and basal twinning of topological insulator <mml:math xmlns:mml="http://www.w3.org/1998/Math/MathML"><mml:mrow><mml:mi mathvariant="normal">B</mml:mi><mml:msub><mml:mi mathvariant="normal">i</mml:mi><mml:mn>2</mml:mn></mml:msub><mml:mi mathvariant="normal">S</mml:mi><mml:msub><mml:mi mathvariant="normal">e</mml:mi><mml:mn>3</mml:mn></mml:msub></mml:mrow></mml:math> grow	0.9	12
61424	Formation of two-dimensional electron and hole gases at the interface of half-Heusler semiconductors. Physical Review Materials, 2019, 3, .	0.9	6

#	Article	IF	Citations
61425	Effect of stress on vacancy formation and migration in body-centered-cubic metals. Physical Review Materials, 2019, 3, .	0.9	31
61426	Nonlocal van der Waals functionals for solids: Choosing an appropriate one. Physical Review Materials, 2019, 3, .	0.9	65
61427	van der Waals forces stabilize low-energy polymorphism in <mml:math xmlns:mml="http://www.w3.org/1998/Math/MathML"><mml:mrow><mml:msub><mml:mi mathvariant="normal">B</mml:mi><mml:mn>2</mml:mn></mml:msub><mml:msub><mml:mi mathvariant="normal">O</mml:mi><mml:mn>3</mml:mn></mml:msub></mml:mrow></mml:math> : Implications for the crystallization anomaly. Physical Review Materials, 2019, 3, .	0.9	9
61428	Three-dimensional subnanoscale imaging of unit cell doubling due to octahedral tilting and cation modulation in strained perovskite thin films. Physical Review Materials, 2019, 3, .	0.9	12
61429	Stochastic replica voting machine prediction of stable cubic and double perovskite materials and binary alloys. Physical Review Materials, 2019, 3, .	0.9	10
61430	Atomic-resolution visualization and doping effects of complex structures in intercalated bilayer graphene. Physical Review Materials, 2019, 3, .	0.9	10
61431	Topological semimetal features in the multiferroic hexagonal manganites. Physical Review Materials, 2019, 3, .	0.9	9
61432	Orbital magnetic moments of phonons. Physical Review Materials, 2019, 3, .	0.9	80
61433	High-pressure synthesis of the <mml:math xmlns:mml="http://www.w3.org/1998/Math/MathML"><mml:mrow><mml:mi>BiV</mml:mi><mml:msub><mml:mi mathvariant="normal">O</mml:mi><mml:mn>3</mml:mn></mml:msub></mml:mrow></mml:math> perovskite. Physical Review Materials, 2019, 3, .	0.9	7
61434	Influence of antiphase boundary of the MnAl Ï„ -phase on the energy product. Physical Review Materials, 2019, 3, .	0.9	1
61435	Comparing time-dependent density functional theory with many-body perturbation theory for semiconductors: Screened range-separated hybrids and the <mml:math xmlns:mml="http://www.w3.org/1998/Math/MathML"><mml:mrow><mml:mi>G</mml:mi><mml:mi>W</mml:mi></mml:mrow></mml:n plus Bethe-Salpeter approach. Physical Review Materials, 2019, 3, .	0.9	61
61436	<mml:math xmlns:mml="http://www.w3.org/1998/Math/MathML"><mml:mi>A</mml:mi></mml:math> -site cation size effect on oxygen octahedral rotations in acentric Ruddlesden-Popper alkali rare-earth titanates. Physical Review Materials, 2019, 3, .	0.9	7
61437	Role of the exchange-correlation functional on the structural, electronic, and optical properties of cubic and tetragonal <mml:math xmlns:mml="http://www.w3.org/1998/Math/MathML"><mml:msub><mml:mi>SrTiO</mml:mi><mml:mn>3</mml:mn></mml:msub></m including many-body effects. Physical Review Materials, 2019, 3, .	0.9	13
61438	Hyperbolic dispersion and negative refraction in a metal-organic framework Cu-BHT. Physical Review Materials, 2019, 3, .	0.9	9
61439	Finite temperature optoelectronic properties of BAs from first principles. Physical Review Materials, 2019, 3, .	0.9	13
61440	Marked enhancement of the photoresponsivity and minority-carrier lifetime of <mml:math xmlns:mml="http://www.w3.org/1998/Math/MathML"><mml:mrow><mml:mi>BaS</mml:mi><mml:msub><mml:mi mathvariant="normal">i</mml:mi><mml:mn>2</mml:mn></mml:msub></mml:mrow></mml:math> passivated with atomic hydrogen. Physical Review Materials, 2019, 3, .	0.9	20
61441	Dimensionality reduction and band quantization induced by potassium intercalation in <mml:math xmlns:mml="http://www.w3.org/1998/Math/MathML"><mml:mrow><mml:mn>1</mml:mn><mml:mi>T</mml:mi></mml:mrow><mml:mtext>-</mml:mtext></mml:math>TaS Physical Review Materials, 2019, 3, .	0.9	20
61442	Prediction of threefold fermions in a nearly ideal Dirac semimetal BaAgAs. Physical Review Materials, 2019, 3, .	0.9	24

#	Article	IF	Citations
61443	Topologically protected states and half-metal behaviors: Defect-strain synergy effects in two-dimensional antimonene. Physical Review Materials, 2019, 3, .	0.9	7
61444	Mechanistic insights in phosphorene degradation. Physical Review Materials, 2019, 3, .	0.9	3
61445	Magnetic order in single crystals of <mml:math xmlns:mml="http://www.w3.org/1998/Math/MathML"><mml:mrow><mml:msub><mml:mi>Na</mml:mi><mml:mn>3</mml:mn></mml: with a honeycomb arrangement of <mml:math xmlns:mml="http://www.w3.org/1998/Math/MathML"><mml:mrow><mml:msup><mml:mrow><mml:mn>3</mml:mn><mml:mi mathvariant="normal">d</mml:mi></mml:mrow><mml:mn>7</mml:mn></. Physical Review Materials, 2019, 3, .	0.9	49
61446	Evidence of a second-order Peierls-driven metal-insulator transition in crystalline NbO2. Physical Review Materials, 2019, 3, .	0.9	18
61447	Machine-learning-based interatomic potential for phonon transport in perfect crystalline Si and crystalline Si with vacancies. Physical Review Materials, 2019, 3, .	0.9	40
61448	Role of point defects in the electrical and optical properties of <mml:math xmlns:mml="http://www.w3.org/1998/Math/MathML"><mml:mrow><mml:msub><mml:mi>In</mml:mi><mml:mn>2</mml:mn></ mathvariant="normal">O</mml:mi><mml:mn>3</mml:mn></mml:msub></mml:mrow></mml:math>. Physical Review Materials, 2019, 3, .	0.9	37
61449	Effects of oxygen stoichiometry on the phase stability of sputter-deposited <mml:math xmlns:mml="http://www.w3.org/1998/Math/MathML"><mml:mrow><mml:mi mathvariant="normal">C</mml:mi><mml:msub><mml:mi mathvariant="normal">d</mml:mi><mml:mi>x</mml:mi></mml:msub><mml:mi mathvariant="normal">Z</mml:mi><mml:msub><mml:mi mathvariant="normal">n</mml:mi><mml:mn>1</mml:mn><mml:mo>â^'</mml:mo><mml:mi>x</mml:mi></mml:mrow></	0.9	8
61450	Energy level alignment of <mml:math xmlns:mml="http://www.w3.org/1998/Math/MathML"><mml:mrow><mml:mi>Cu</mml:mi><mml:mrow><mml:mo>(</mml:mo><mml: absorber compounds with <mml:math xmlns:mml="http://www.w3.org/1998/Math/MathML"><mml:mro. Physical Review Materials, 2019, 3, .	0.9	18
61451	Multiple topological Dirac cones in a mixed-valent Kondo semimetal: g -SmS. Physical Review Materials, 2019, 3, .	0.9	11
61452	Parametrization of <mml:math xmlns:mml="http://www.w3.org/1998/Math/MathML"><mml:mrow><mml:mi>LSDA</mml:mi><mml:mo>+</mml:mo><mml:mi>U</mml: for noncollinear magnetic configurations: Multipolar magnetism in <mml:math xmlns:mml="http://www.w3.org/1998/Math/MathML"><mml:msub><mml:mi>UO</mml:mi><mml:mn>2</mml:mn></mml:msub></ Physical Review Materials, 2019, 3, .	0.9	35
61453	Formation of graphene atop a Si adlayer on the C-face of SiC. Physical Review Materials, 2019, 3, .	0.9	3
61454	Transferable screened range-separated hybrids for layered materials: The cases of<mml:math xmlns:mml="http://www.w3.org/1998/Math/MathML"><mml:msub><mml:mi>MoS</mml:mi><mml:mn>2</mml:mn></mml:msub></ h-BN. Physical Review Materials, 2019, 3, .	0.9	26
61455	Two-dimensional nodal-loop half-metal in monolayer MnN. Physical Review Materials, 2019, 3, .	0.9	55
61456	Enhanced ferroelectricity in perovskite oxysulfides. Physical Review Materials, 2019, 3, .	0.9	4
61457	Ab initio phase stabilities of Ce-based hard magnetic materials and comparison with experimental phase diagrams. Physical Review Materials, 2019, 3, .	0.9	18
61458	Segregation tendency of Heusler alloys. Physical Review Materials, 2019, 3, .	0.9	12
61459	Persistent spin helix in Rashba-Dresselhaus ferroelectric <mml:math xmlns:mml="http://www.w3.org/1998/Math/MathML"><mml:msub><mml:mrow><mml:mi>CsBiNb</mml:mi></mml:mrow><mml:mn>2 mathvariant="normal">O</mml:mi></mml:mrow><mml:mn>7</mml:mn></mml:msub></mml:math>. Physical Review Materials, 2019, 3, .	0.9	41
61460	Machine-learning-assisted prediction of magnetic double perovskites. Physical Review Materials, 2019, 3, .	0.9	28

#	Article	IF	Citations
61461	<mml:math xmlns:mml="http://www.w3.org/1998/Math/MathML"><mml:mi>p</mml:mi></mml:math> -type codoping effect in (Ga,Mn)As: Mn lattice location versus magnetic properties. Physical Review Materials, 2019, 3, .	0.9	2
61462	Band alignments at surfaces and heterointerfaces of <mml:math xmlns:mml="http://www.w3.org/1998/Math/MathML"><mml:mrow><mml:msub><mml:mi>Al</mml:mi><mml:mn>2</mml:mn></mml:msub><mml:mi mathvariant="normal">O</mml:mi><mml:mn>3</mml:mn></mml:mrow></mml:math>, <mml:math xmlns:mml="http://www.w3.org/1998/Math/MathML"><mml:mrow><mml:msub><mml:mi>Ga</mml:mi><mml:mn>2</mml:mn></mml:msub><mml:mi mathvariant="normal">O</mml:mi><mml:mn>3</mml:mn></mml:mrow></mml:math>, and <mml:math. Physical Review Materials, 2019, 3, .	0.9	32
61463	Thermal conductivity for III-V and II-VI semiconductor wurtzite and zinc-blende polytypes: The role of anharmonicity and phase space. Physical Review Materials, 2019, 3, .	0.9	14
61464	Strain tuning of plasma frequency in vanadate, niobate, and molybdate perovskite oxides. Physical Review Materials, 2019, 3, .	0.9	18
61465	Role of short- and long-range ordering on diffusion in Ni-Al alloys. Physical Review Materials, 2019, 3, .	0.9	11
61466	Atomic energy mapping of neural network potential. Physical Review Materials, 2019, 3, .	0.9	24
61467	Anharmonic thermodynamics of vacancies using a neural network potential. Physical Review Materials, 2019, 3, .	0.9	14
61468	Ab initio study of magnetic nanopatterning of a hybrid transition metal dichalcogenides/Ir(111) system via magnetic clusters. Physical Review Materials, 2019, 3, .	0.9	4
61469	New kagome prototype materials: discovery of <mml:math xmlns:mml="http://www.w3.org/1998/Math/MathML"><mml:mrow><mml:msub><mml:mi>KV</mml:mi><mml:mn>3</mml:mn></mml:msub></mml:mrow></mml:math>, and <mml:math xmlns:mml="http://www.w3.org/1998/Math/MathML"><mml:mrow><mml:msub><mml:mi>CsV</mml:mi><mml:mn>3</mml:mn></mml:msub></mml:mrow></mml:math>. Physical Review Materials, 2019, 3, .	0.9	398
61470	Effect of local chemistry and structure on thermal transport in doped GaAs. Physical Review Materials, 2019, 3, .	0.9	9
61471	Atomically thin oxide layer on the elemental superconductor Ta(001) surface. Physical Review Materials, 2019, 3, .	0.9	2
61472	Machine-learning model for predicting phase formations of high-entropy alloys. Physical Review Materials, 2019, 3, .	0.9	46
61473	Thermoelectric properties of semimetals. Physical Review Materials, 2019, 3, .	0.9	47
61474	van der Waals heterostructure for photocatalysis: Graphitic carbon nitride and Janus transition-metal dichalcogenides. Physical Review Materials, 2019, 3, .	0.9	14
61475	Discovery of <mml:math xmlns:mml="http://www.w3.org/1998/Math/MathML"><mml:mi>Ï‰</mml:mi></mml:math>-free high-temperature Ti-Ta-<mml:math xmlns:mml="http://www.w3.org/1998/Math/MathML"><mml:mi>X</mml:mi></mml:math>shape memory alloys from first-principles calculations. Physical Review Materials, 2019, 3, .	0.9	7
61476	Cubic and tetragonal perovskites from the random phase approximation. Physical Review Materials, 2019, 3, .	0.9	10
61477	Towards predictive band gaps for halide perovskites: Lessons from one-shot and eigenvalue self-consistent <mml:math xmlns:mml="http://www.w3.org/1998/Math/MathML"><mml:mrow><mml:mi>G</mml:mi><mml:mi>W</mml:mi></mml:mrow></mml:math>. Physical Review Materials, 2019, 3, .	0.9	39
61478	Topological band crossings in epitaxial strained SnTe. Physical Review Materials, 2019, 3, .	0.9	6

#	Article	IF	Citations
61479	Modeling magnetic evolution and exchange hardening in disordered magnets: The example of <mml:math xmlns:mml="http://www.w3.org/1998/Math/MathML"><mml:mrow><mml:msub><mml:mi>Mn</mml:mi><mml:mrow> Heusler alloys. Physical Review Materials, 2019, 3, .	0.9	7
61480	Magnetic frustration control through tunable stereochemically driven disorder in entropy-stabilized oxides. Physical Review Materials, 2019, 3, .	0.9	29
61481	Structural and electronic properties of lithiated Si nanowires: An ab initio study. Physical Review Materials, 2019, 3, .	0.9	3
61482	Computational prediction of nanostructured alloys with enhanced thermoelectric properties. Physical Review Materials, 2019, 3, .	0.9	3
61483	Visualizing the metal- <mml:math xmlns:mml="http://www.w3.org/1998/Math/MathML"><mml:mrow><mml:mi>Mo</mml:mi><mml:msub><mml:mi mathvariant="normal">S</mml:mi><mml:mn>2</mml:mn></mml:msub></mml:mrow></mml:math> contacts in two-dimensional field-effect transistors with atomic resolution. Physical Review Materials, 2019, 3, .	0.9	25
61484	In-plane hexagonal antiferromagnet in the Cu-Mn-As system <mml:math xmlns:mml="http://www.w3.org/1998/Math/MathML"><mml:mrow><mml:msub><mml:mi>Cu</mml:mi><mml:mrow> Physical Review Materials, 2019, 3, .	0.9	4
61485	Finite-temperature simulation of anharmonicity and octahedral tilting transitions in halide perovskites. Physical Review Materials, 2019, 3, .	0.9	28
61486	Materials synthesis, neutron powder diffraction, and first-principles calculations of <mml:math xmlns:mml="http://www.w3.org/1998/Math/MathML"><mml:mrow><mml:mo>(</mml:mo><mml:msub><mml:mi> <mml:math xmlns:mml="http://www.w3.org/1998/. Physical Review Materials, 2019, 3, .	0.9	14
61487	Intrinsic ductility of random substitutional alloys from nonlinear elasticity theory. Physical Review Materials, 2019, 3, .	0.9	9
61488	Dynamics of graphene/Al interfaces using COMB3 potentials. Physical Review Materials, 2019, 3, .	0.9	7
61489	Electronic, magnetic, and thermodynamic properties of the kagome layer compound FeSn. Physical Review Materials, 2019, 3, .	0.9	49
61490	Stabilization of small polarons in <mml:math xmlns:mml="http://www.w3.org/1998/Math/MathML"><mml:msub><mml:mi>BaTiO</mml:mi><mml:mn>3</mml:mn> by local distortions. Physical Review Materials, 2019, 3, .	0.9	16
61491	High-density electron doping of <mml:math xmlns:mml="http://www.w3.org/1998/Math/MathML"><mml:msub><mml:mi>SmNiO</mml:mi><mml:mn>3</mml:mn> from first principles. Physical Review Materials, 2019, 3, .	0.9	24
61492	Boosting ionic conductivity in antiperovskite <mml:math xmlns:mml="http://www.w3.org/1998/Math/MathML"><mml:mrow><mml:msub><mml:mi>Li</mml:mi><mml:mn> via defect engineering: Interstitial versus vacancy. Physical Review Materials, 2019, 3, .	0.9	11
61493	Understanding phonon properties in isoreticular metal-organic frameworks from first principles. Physical Review Materials, 2019, 3, .	0.9	16
61494	Interlayer dielectric function of a type-II van der Waals semiconductor: The <mml:math xmlns:mml="http://www.w3.org/1998/Math/MathML"><mml:mrow><mml:msub><mml:mi>HfS</mml:mi><mml:mrow> heterobilayer. Physical Review Materials, 2019, 3, .	0.9	5
61495	Group-IV monochalcogenide monolayers: Two-dimensional ferroelectrics with weak intralayer bonds and a phosphorenelike monolayer dissociation energy. Physical Review Materials, 2019, 3, .	0.9	19
61496	Unusual valence state in the antiperovskites Sr3SnO and Sr3PbO revealed by x-ray photoelectron spectroscopy. Physical Review Materials, 2019, 3, .	0.9	12

#	Article	IF	Citations
61497	Symmetry-enforced band crossings in trigonal materials: Accordion states and Weyl nodal lines. Physical Review Materials, 2019, 3, .	0.9	20
61498	Magneto-optic response of the metallic antiferromagnet <mml:math xmlns:mml="http://www.w3.org/1998/Math/MathML"><mml:mrow><mml:msub><mml:mi>Fe</mml:mi><mml:mn>2</mml:mn></mml:msub></mml:mrow></mml:math> to ultrafast temperature excursions. Physical Review Materials, 2019, 3, .	0.9	9
61499	Structural, electronic, and magnetic properties of bulk and epitaxial <mml:math xmlns:mml="http://www.w3.org/1998/Math/MathML"><mml:msub><mml:mi mathvariant="normal">LaCoO</mml:mi><mml:mn>3</mml:mn></mml:msub></mml:math> through diffusion Monte Carlo. Physical Review Materials, 2019, 3, .	0.9	13
61500	Dopability of divalent tin containing phosphates for <mml:math xmlns:mml="http://www.w3.org/1998/Math/MathML"><mml:mi>p</mml:mi></mml:math> -type transparent conductors. Physical Review Materials, 2019, 3, .	0.9	5
61501	Impact of organic molecule rotation on the optoelectronic properties of hybrid halide perovskites. Physical Review Materials, 2019, 3, .	0.9	20
61502	Predicting copper gallium diselenide and band structure engineering through order-disordered transition. Physical Review Materials, 2019, 3, .	0.9	5
61503	Influence of crystalline order and defects on the absolute work functions and electron affinities of <mml:math xmlns:mml="http://www.w3.org/1998/Math/MathML"><mml:mrow><mml:mi>Ti</mml:mi><mml:msub><mml:mi mathvariant="normal">O</mml:mi><mml:mn>2</mml:mn></mml:msub></mml:mrow></mml:math> - and SrO-terminated <mml:math xmlns:mml="http://www.w3.org/1998/Math/MathML"><mml:mrow><mml:mi>n</mml:mi><mml:mtext>â^'</mml:mtext><mml:mi>SrTi<	0.9	17
61504	Large-scale interlayer rotations and Te grain boundaries in <mml:math xmlns:mml="http://www.w3.org/1998/Math/MathML"><mml:mrow><mml:msub><mml:mrow><mml:mo>(</mml:mo> <mml:mrow><mm thin films. Physical Review Materials, 2020, 4, .	0.9	10
61505	Insights into the elastic properties of RE- <mml:math xmlns:mml="http://www.w3.org/1998/Math/MathML"><mml:mi>i</mml:mi></mml:math> -MAX phases and their potential exfoliation into two-dimensional RE- <mml:math xmlns:mml="http://www.w3.org/1998/Math/MathML"><mml:mi>i</mml:mi></mml:math> -MXenes. Physical Review Materials, 2020, 4, .	0.9	18
61506	Atomistic description of self-diffusion in molybdenum: A comparative theoretical study of non-Arrhenius behavior. Physical Review Materials, 2020, 4, .	0.9	14
61507	Thickness dependence of transport behaviors in <mml:math xmlns:mml="http://www.w3.org/1998/Math/MathML"><mml:mrow><mml:mi>SrRu</mml:mi><mml:msub><mml:mi mathvariant="normal">O</mml:mi><mml:mn>3</mml:mn></mml:msub><mml:mo>/</mml:mo><mml:mi>SrTi</mml:mi><mml:msub><mml:mi mathvariant="normal">O</mml:mi><mml:mn>3</mml:mn></mml:msub></mml:mrow></mml:math> superlattices. Physical Review Materials, 2020, 4, .	0.9	17
61508	Unveiling the mechanism of abnormal magnetic behavior of FeNiCoMnCu high-entropy alloys through a joint experimental-theoretical study. Physical Review Materials, 2020, 4, .	0.9	18
61509	Investigation of the band gaps and bowing parameter of InAs1â^'xSbx alloys using the modified Becke-Johnson potential. Physical Review Materials, 2020, 4, .	0.9	2
61510	Possible high-potential ilmenite type <mml:math xmlns:mml="http://www.w3.org/1998/Math/MathML"><mml:mrow><mml:mi mathvariant="normal">N</mml:mi><mml:msub><mml:mi mathvariant="normal">a</mml:mi><mml:mn>1</mml:mn></mml:msub><mml:mi>M</mml:mi><mml:msub><mml:mi mathvariant="normal">O</mml:mi><mml:mn>3</mml:mn></mml:msub><mml:mo>Â</mml:mo><mml:mo>(</mml:mo><mml:mi>M<	0.9	2
61511	First-principles study of Li-ion distribution at <mml:math xmlns:mml="http://www.w3.org/1998/Math/MathML"><mml:mrow><mml:mi>Î³</mml:mi><mml:mtext>â^'</mml:mtext><mml:msub> /metal interfaces. Physical Review Materials, 2020, 4, .	0.9	8
61512	Large barocaloric effects in thermoelectric superionic materials. Physical Review Materials, 2020, 4, .	0.9	19
61513	Polar or not polar? The interplay between reconstruction, Sr enrichment, and reduction at the <mml:math xmlns:mml="http://www.w3.org/1998/Math/MathML"><mml:mrow><mml:msub><mml:mi mathvariant="normal">La</mml:mi><mml:mrow><mml:mn>0.75</mml:mn></mml:mrow></mml:msub><mml:msub><mml:mi>Sr</mml:mi> (001) surface. Physical Review Materials, 2020, 4, .	0.9	21
61514	Orbital-adapted electronic structure and anisotropic transport in <mml:math xmlns:mml="http://www.w3.org/1998/Math/MathML"><mml:mrow><mml:mi>Î³</mml:mi><mml:mtext>â^'</mml:mtext><mml:msub><mml:mi mathvariant="normal">O</mml:mi><mml:mn>3</mml:mn></mml:msub><mml:mo>/</mml:mo><mml:msub><mml:mi>SrTiO</mml:mi> heterostructure. Physical Review Materials, 2020, 4, .	0.9	9

#	Article	IF	Citations
61515	Unveiling the influence of interfacial bonding and dynamics on solid/liquid interfacial structures: An ab initio molecular dynamics study of (0001) sapphire-liquid Al interfaces. Physical Review Materials, 2020, 4, .	0.9	12
61516	Hybrid quantum/classical study of hydrogen-decorated screw dislocations in tungsten: Ultrafast pipe diffusion, core reconstruction, and effects on glide mechanism. Physical Review Materials, 2020, 4, .	0.9	11
61517	Ground-state properties and lattice-vibration effects of disordered Fe-Ni systems for phase stability predictions. Physical Review Materials, 2020, 4, .	0.9	7
61518	Theoretical modeling of interstitial carbon impurities in paramagnetic Fe-Mn alloys. Physical Review Materials, 2020, 4, .	0.9	3
61519	Computational screening of magnetocaloric alloys. Physical Review Materials, 2020, 4, .	0.9	13
61520	Synthesis, crystal and magnetic structure of the spin-chain compound Ag2RuO4. Physical Review Materials, 2020, 4, .	0.9	6
61521	Light-induced breathing in photochromic yttrium oxyhydrides. Physical Review Materials, 2020, 4, .	0.9	21
61522	Cosubstitution in Ni-Mn-Sb Heusler compounds: Realization of room-temperature reversible magnetocaloric effect driven by second-order magnetic transition. Physical Review Materials, 2020, 4,	0.9	5
61523	Distinct behavior of localized and delocalized carriers in anatase <mml:math xmlns:mml="http://www.w3.org/1998/Math/MathML"><mml:msub><mml:mi>TiO</mml:mi><mml:mn>2</mml:mn></mml:msub></mml (001) during reaction with <mml:math xmlns:mml="http://www.w3.org/1998/Math/MathML"><mml:msub><mml:mi mathvariant="normal">O</mml:mi><mml:mn>2</mml:mn></mml:msub></mml:math>. Physical Review Materials, 2020, 4, .	0.9	25
61524	Synthesis, structure, and magnetic properties of oxyhydride <mml:math xmlns:mml="http://www.w3.org/1998/Math/MathML"><mml:mrow><mml:mi mathvariant="normal">T</mml:mi><mml:msub><mml:mi mathvariant="normal">i</mml:mi><mml:mrow><mml:mn>1</mml:mn><mml:mo>â^’</mml:mo><mml:mi>x</mml:mi></mml:mrow></mml:msub><mml:msub><mml:mi mathvariant="normal">A</mml:mi><mml:msub><mml:mi mathvariant="normal">l</mml:mi><mml:mi>x</mml:mi></mml:msub></mml:msub></mml:mrow></m	0.9	12
61525	Understanding the lattice thermal conductivity of <mml:math xmlns:mml="http://www.w3.org/1998/Math/MathML"><mml:msub><mml:mi>SrTiO</mml:mi><mml:mn>3</mml:mn></mml:msub></m from an ab initio perspective. Physical Review Materials, 2020, 4, .	0.9	18
61526	Adjusting the descriptor for a crystal structure search using Bayesian optimization. Physical Review Materials, 2020, 4, .	0.9	6
61527	Very high oscillator strength in the band-edge light absorption of zincblende, chalcopyrite, kesterite, and hybrid perovskite solar cell materials. Physical Review Materials, 2020, 4, .	0.9	5
61528	Indentation-strain stiffening in tungsten nitrides: Mechanisms and implications. Physical Review Materials, 2020, 4, .	0.9	41
61529	Order-disorder versus displacive transitions in Jahn-Teller active layered materials. Physical Review Materials, 2020, 4, .	0.9	17
61530	Characterization of the Al-Ga solid-liquid interface using classical and ab initio molecular dynamics simulation. Physical Review Materials, 2020, 4, .	0.9	2
61531	Phonon-assisted diffusion in bcc phase of titanium and zirconium from first principles. Physical Review Materials, 2020, 4, .	0.9	8
61532	Structure-strength relations of distinct MoN phases from first-principles calculations. Physical Review Materials, 2020, 4, .	0.9	41

#	Article	IF	Citations
61533	Pressure effect on the anomalous Hall effect of ferromagnetic Weyl semimetal Co3Sn2S2. Physical Review Materials, 2020, 4, .	0.9	12
61534	Interface-related magnetic and vibrational properties in Fe/MgO heterostructures from nuclear resonant spectroscopy and first-principles calculations. Physical Review Materials, 2020, 4, .	0.9	4
61535	Evolution of noncollinear magnetism in magnetocaloric MnPtGa. Physical Review Materials, 2020, 4, .	0.9	9
61536	First-principles study of site preferences for Fe in <mml:math xmlns:mml="http://www.w3.org/1998/Math/MathML"><mml:mrow><mml:mi>Sm</mml:mi><mml:msub><mml:mrow><mml:mo>(</mml:mo> permanent magnets. Physical Review Materials, 2020, 4, .	0.9	4
61537	Theoretical exploration of mixed-anion antiperovskite semiconductors <mml:math xmlns:mml="http://www.w3.org/1998/Math/MathML"><mml:mrow><mml:msub><mml:mi>M</mml:mi><mml:mn>3</mml:mn></mml:m width="4pt"		

#	Article	IF	Citations
61551	Epitaxial growth and band structure of antiferromagnetic Mott insulator CeOI. Physical Review Materials, 2020, 4, .	0.9	2
61552	Stability of charged sulfur vacancies in 2D and bulk <mml:math xmlns:mml="http://www.w3.org/1998/Math/MathML"><mml:msub><mml:mi>MoS</mml:mi><mml:mn>2</mml:mn></mml:msub></mml from plane-wave density functional theory with electrostatic corrections. Physical Review Materials, 2020, 4, .	0.9	24
61553	Electronic structure of a <mml:math xmlns:mml="http://www.w3.org/1998/Math/MathML"><mml:mrow><mml:mo>(</mml:mo><mml:mn>3</mml:mn><mml:mo>Ã—</mml:mo> silicon layer on Al(111). Physical Review Materials, 2020, 4, .	0.9	5
61554	Structural evolution and skyrmionic phase diagram of the lacunar spinel <mml:math xmlns:mml="http://www.w3.org/1998/Math/MathML"><mml:msub><mml:mi mathvariant="normal">GaMo</mml:mi><mml:mn>4</mml:mn></mml:msub><mml:msub><mml:mi mathvariant="normal">Se</mml:mi><mml:mn>8</mml:mn></mml:msub></mml:math>. Physical Review Materials, 2020, 4, .	0.9	19
61555	Machine learning study of magnetism in uranium-based compounds. Physical Review Materials, 2020, 4, .	0.9	10
61556	Formation and dissociation reactions of complexes involving interstitial carbon and oxygen defects in silicon. Physical Review Materials, 2020, 4, .	0.9	5
61557	Structure and charge transport of amorphous Cu-doped <mml:math xmlns:mml="http://www.w3.org/1998/Math/MathML"><mml:mrow><mml:msub><mml:mi>Ta</mml:mi><mml:mn>2</mml:mn></mml:r mathvariant="normal">O</mml:mi><mml:mn>5</mml:mn></mml:msub></mml:mrow></mml:math> : An ab initio study. Physical Review Materials, 2020, 4, .	0.9	7
61558	Density functional studies of defects and defect-related luminescence in Mg3N2. Physical Review Materials, 2020, 4, .	0.9	2
61559	Boron phosphide as a <mml:math xmlns:mml="http://www.w3.org/1998/Math/MathML"><mml:mi>p</mml:mi></mml:math> -type transparent conductor: Optical absorption and transport through electron-phonon coupling. Physical Review Materials, 2020, 4, .	0.9	11
61560	Prediction of Li intercalation voltages in rechargeable battery cathode materials: Effects of exchange-correlation functional, van der Waals interactions, and Hubbard <mml:math xmlns:mml="http://www.w3.org/1998/Math/MathML"><mml:mi>U</mml:mi></mml:math>. Physical Review Materials, 2020, 4, .	0.9	15
61561	Comprehensive analysis of the influence of dispersion on group-14 rutile-type solids. Physical Review Materials, 2020, 4, .	0.9	1
61562	First-principles calculations of group IIA and group IV impurities in <mml:math xmlns:mml="http://www.w3.org/1998/Math/MathML"><mml:mrow><mml:mi>Î±</mml:mi><mml:mtext>â€”</mml:mtext><mml:mi mathvariant="normal">A</mml:mi><mml:msub><mml:mi mathvariant="normal">I</mml:mi><mml:mn>2</mml:mn></mml:msub><mml:msub><mml:mi mathvariant="normal">O</mml:mi><mml:mn>3</mml:mn></mml:msub></mml:mrow></mml:math>. Physical Review Materials, 2020, 4, .	0.9	11
61563	Equilibrium solute segregation to matrix-Î¸â€² precipitate interfaces in Al-Cu alloys from first principles. Physical Review Materials, 2020, 4, .	0.9	4
61564	Comparative study of Minnesota functionals performance on ferroelectric <mml:math xmlns:mml="http://www.w3.org/1998/Math/MathML"><mml:msub><mml:mi>BaTiO</mml:mi><mml:mn>3</mml:mn></mml:msub> and <mml:math xmlns:mml="http://www.w3.org/1998/Math/MathML"><mml:msub><mml:mi>PbTiO</mml:mi><mml:mn>3</mml:mn></mml:msub> Physical Review Materials, 2020, 4, .	0.9	6
61565	Ferromagnetism and half-metallicity in two-dimensional <mml:math xmlns:mml="http://www.w3.org/1998/Math/MathML"><mml:mrow><mml:mi>M</mml:mi><mml:mi mathvariant="normal">O</mml:mi><mml:mo>Â</mml:mo><mml:mo>(</mml:mo><mml:mi>M</mml:mi><mml:mo>=</mml:mo><mml: monolayers induced by hole doping. Physical Review Materials, 2020, 4, .	0.9	15
61566	Structural, electronic, and magnetic properties of vanadium-based Janus dichalcogenide monolayers: A first-principles study. Physical Review Materials, 2020, 4, .	0.9	23
61567	Tuning hydrogen adsorption and electronic properties from graphene to fluorographone. Physical Review Materials, 2020, 4, .	0.9	5
61568	Simultaneous generation of direct- and indirect-gap photoluminescence in multilayer <mml:math xmlns:mml="http://www.w3.org/1998/Math/MathML"><mml:msub><mml:mi>MoS</mml:mi><mml:mn>2</mml:mn></mml:msub> bubbles. Physical Review Materials, 2020, 4, .	0.9	21

#	Article	IF	Citations
61569	First-principles prediction of two-dimensional copper borides. Physical Review Materials, 2020, 4, .	0.9	8
61570	Oxide at the Al-rich <mml:math xmlns:mml="http://www.w3.org/1998/Math/MathML"><mml:mrow><mml:msub><mml:mi>Fe</mml:mi><mml:mrow><mml:mn>0.85</mml:mn> surface. Physical Review Materials, 2020, 4, .	0.9	4
61571	Primary intrinsic defects and their charge transition levels in <mml:math xmlns:mml="http://www.w3.org/1998/Math/MathML"><mml:mi>Î²</mml:mi><mml:mtext>â€“</mml:mtext><mml:mi>Ga</mml:mi><mml /><mml:mn>2</mml:mn></mml:msub><mml:mi mathvariant="normal">O</mml:mi><mml:msub><mml:mrow /><mml:mn>3</mml:mn></mml:msub></mml:math>. Physical Review Materials, 2020, 4, .	0.9	21
61572	Manifestation of the thermoelectric properties in Ge-based halide perovskites. Physical Review Materials, 2020, 4, .	0.9	14
61573	Efficient thermoelectricity in <mml:math xmlns:mml="http://www.w3.org/1998/Math/MathML"><mml:mrow><mml:msub><mml:mi>Sr</mml:mi><mml:mn>2</mml:mn></mml:m mathvariant="normal">O</mml:mi><mml:mn>7</mml:mn></mml:msub></mml:mrow></mml:math> with energy-dependent relaxation times. Physical Review Materials, 2020, 4, .	0.9	16
61574	xmlns:mml="http://www.w3.org/1998/Math/MathML"><mml:mrow><mml:msub><mml:mi mathvariant="normal">V</mml:mi><mml:mn>2</mml:mn></mml:msub><mml:mi>AlC</mml:mi></mml:mrow></mml:math> and <mml:math xmlns:mml="http://www.w3.org/1998/Math/MathML"><mml:mrow><mml:mi mathvariant="normal">C</mml:mi><mml:msub><mml:mi mathvariant="normal">r</mml:mi><mml:mn>2</mml:mn></mml:msub><mml:mi>AlC</mml:mi></mml:mrow></mml:math>	0.9	4
61575	Role of long-range exact exchange in polaron charge transition levels: The case of MgO. Physical Review Materials, 2020, 4, .	0.9	8
61576	Epitaxial engineering of flat silver fluoride cuprate analogs. Physical Review Materials, 2020, 4, .	0.9	17
61577	Site preference of Y and Mn in nonstoichiometric <mml:math xmlns:mml="http://www.w3.org/1998/Math/MathML"><mml:mi>Ba</mml:mi><mml:mi>Ti</mml:mi><mml:msub><mml:mi mathvariant="normal">O</mml:mi><mml:mn>3</mml:mn></mml:msub></mml:math> from first principles. Physical Review Materials, 2020, 4, .	0.9	6
61578	Trigonal polymorph of <mml:math xmlns:mml="http://www.w3.org/1998/Math/MathML"><mml:msub><mml:mi mathvariant="normal">Li</mml:mi><mml:mn>2</mml:mn></mml:msub><mml:mi>Mn</mml:mi><mml:msub><mml:mi mathvariant="normal">O</mml:mi><mml:mn>3</mml:mn></mml:msub></mml:math>. Physical Review Materials, 2020, 4, .	0.9	2
61579	Tuning the electronic levels of NiO with alkali halides surface modifiers for perovskite solar cells. Physical Review Materials, 2020, 4, .	0.9	9
61580	Effects of band edge positions on defect structure in lead halide perovskites: A case study on the Br vacancy in <mml:math xmlns:mml="http://www.w3.org/1998/Math/MathML"><mml:mrow><mml:mi>Cs</mml:mi><mml:mi>Pb</mml:mi><mml:msub> Physical Review Materials, 2020, 4, .	0.9	20
61581	Mechanical properties of ultrathin gold nanowires from first principles: Interdependencies between size, morphology, and twin boundaries. Physical Review Materials, 2020, 4, .	0.9	5
61582	Discovery of highly polarizable semiconductors BaZrS3 and Ba3Zr2S7. Physical Review Materials, 2020, 4, .	0.9	15
61583	From latent ferroelectricity to hyperferroelectricity in alkali lead halide perovskites. Physical Review Materials, 2020, 4, .	0.9	8
61584	Gaussian approximation potentials for body-centered-cubic transition metals. Physical Review Materials, 2020, 4, .	0.9	24
61585	High-Curie-temperature ferromagnetism in bilayer <mml:math xmlns:mml="http://www.w3.org/1998/Math/MathML"><mml:mrow><mml:mi>Cr</mml:mi><mml:msub><mml:mi mathvariant="normal">I</mml:mi><mml:mn>3</mml:mn></mml:msub></mml:mrow></mml:math> on bulk semiconducting substrates. Physical Review Materials, 2020, 4, .	0.9	24
61586	Interlayer magnetism in <mml:math xmlns:mml="http://www.w3.org/1998/Math/MathML"><mml:mrow><mml:msub><mml:mi>Fe</mml:mi><mml:mrow><mml:mn>3</mml:mn> Physical Review Materials, 2020, 4, .	0.9	11

#	Article	IF	Citations
61587	Impact of impurities on the spin Hall conductivity in <mml:math xmlns:mml="http://www.w3.org/1998/Math/MathML"><mml:mi>Î²</mml:mi></mml:math> -W. Physical Review Materials, 2020, 4, .	0.9	7
61588	Theoretical description of thermodynamic and mechanical properties of multicomponent bcc Fe-Cr-based alloys. Physical Review Materials, 2020, 4, .	0.9	2
61589	Computational assessment of the efficacy of halides as shape-directing agents in nanoparticle growth. Physical Review Materials, 2020, 4, .	0.9	4
61590	Machine learning for metallurgy II. A neural-network potential for magnesium. Physical Review Materials, 2020, 4, .	0.9	32
61591	Ab initio study of chemical disorder as an effective stabilizing mechanism of bcc-based <mml:math xmlns:mml="http://www.w3.org/1998/Math/MathML"><mml:mi>TiAl</mml:mi><mml:mo>(</mml:mo><mml:mo>+</mml:mo><mml:mi> 2020, 4, .	0.9	5
61592	Split-vacancy defect complexes of oxygen in hcp and fcc cobalt. Physical Review Materials, 2020, 4, .	0.9	1
61593	Recoverable high-energy compounds by reacting methane and nitrogen under high pressure. Physical Review Materials, 2020, 4, .	0.9	4
61594	Machine learning models for predicting the dielectric constants of oxides based on high-throughput first-principles calculations. Physical Review Materials, 2020, 4, .	0.9	27
61595	Ab initio investigation of the role of charge transfer in the adsorption properties of H2,ÂN2,ÂO2,CO,NO,CO2,ÂNO2 , and CH4 on the van der Waals layered Sn3O4 semiconductor. Physical Review Materials, 2020, 4, .	0.9	1
61596	Structural signatures of the insulator-to-metal transition in <mml:math xmlns:mml="http://www.w3.org/1998/Math/MathML"><mml:mrow><mml:mi>Ba</mml:mi><mml:msub><mml:mi>Co</mml:mi><mml:mn mathvariant="normal">S</mml:mi><mml:mn>2</mml:mn></mml:msub></mml:mrow></mml:math>. Antiferroelectricity and robust dielectric response owing to competing polar and antipolar instabilities in tetragonal tungsten bronze <mml:math xmlns:mml="http://www.w3.org/1998/Math/MathML"><mml:msub><mml:mi mathvariant="normal">K</mml:mi><mml:mn>2</mml:mn></mml:msub><mml:msub><mml:mrow><mml:mi>R</mml:mi><mml:mi>Nb< mathvariant="normal">O</mml:mi><mml:mn>15</mml:mn></mml:msub></mml:math> (R :) Tj ETQq0 0 0 rgBT /Overlock 10 Tf	0.9	6
61597		0.9	8
61598	Stability, electronic, and optical properties of lead-free halide double perovskites <mml:math xmlns:mml="http://www.w3.org/1998/Math/MathML"><mml:mrow><mml:msub><mml:mrow><mml:mo>(</mml:mo><mml:msub><mml:mi		

#	Article	IF	Citations
61605	Discovering rare-earth-free magnetic materials through the development of a database. Physical Review Materials, 2020, 4, .	0.9	11
61606	Strongly two-dimensional exchange interactions in the in-plane metallic antiferromagnet <mml:math xmlns:mml="http://www.w3.org/1998/Math/MathML"><mml:mrow><mml:msub><mml:mi>Fe</mml:mi><mml:mn>x</mml:mn></mml:msub></mml:mrow></mml:math> probed by inelastic neutron scattering. Physical Review Materials, 2020, 4, .	0.9	5
61607	Electron-phonon coupling superconductivity in two-dimensional orthorhombic <mml:math xmlns:mml="http://www.w3.org/1998/Math/MathML"><mml:mrow><mml:mi>M</mml:mi><mml:msub><mml:mi mathvariant="normal">B</mml:mi><mml:mn>6</mml:mn></mml:msub></mml:mrow></mml:math>		

#	Article	IF	Citations
61623	Spontaneous formation of thermodynamically stable Al-Cu-Fe icosahedral quasicrystal from realistic atomistic simulations. Physical Review Research, 2020, 2, .	1.3	5
61624	Effective Hamiltonian for nickelate oxides <mml:math xmlns:mml="http://www.w3.org/1998/Math/MathML"><mml:mrow><mml:msub><mml:mi>Nd</mml:mi><mml:mrow><mml:mn>1</mml:mn> Physical Review Research, 2020, 2, .	1.3	76
61625	Active learning algorithm for computational physics. Physical Review Research, 2020, 2, .	1.3	14
61626	Interplay between breathing and polar instabilities in transition metal perovskites with active A-sites. Physical Review Research, 2020, 2, .	1.3	2
61627	Superconducting transition temperatures of metallic liquids. Physical Review Research, 2020, 2, .	1.3	4
61628	Noncontacting optostriction driven anisotropic and inhomogeneous strain in two-dimensional materials. Physical Review Research, 2020, 2, .	1.3	9
61629	Diagnosis scheme for topological degeneracies crossing high-symmetry lines. Physical Review Research, 2020, 2, .	1.3	18
61630	Renormalization of the Mott gap by lattice entropy: The case of 1T- TaS2. Physical Review Research, 2020, 2, .	1.3	4
61631	Effect of N, C, and B interstitials on the structural and magnetic properties of alloys with Cu3Au structure. Physical Review Research, 2020, 2, .	1.3	10
61632	Quantum materials interfaces: Graphene/bismuth (111) heterostructures. Physical Review Research, 2020, 2, .	1.3	4
61633	Persistent spin dynamics in the pressurized spin-liquid candidate YbMgGaO4. Physical Review Research, 2020, 2, .	1.3	11
61634	Carbon ionization at gigabar pressures: An ab initio perspective on astrophysical high-density plasmas. Physical Review Research, 2020, 2, .	1.3	34
61635	Mott phase in a van der Waals transition-metal halide at single-layer limit. Physical Review Research, 2020, 2, .	1.3	15
61636	Visualizing the origin of rotational entropy effects in coadsorbed systems. Physical Review Research, 2020, 2, .	1.3	4
61637	Fully consistent density functional theory determination of the insulator-metal transition boundary in warm dense hydrogen. Physical Review Research, 2020, 2, .	1.3	15
61638	Effect of charge self-consistency in DFT+DMFT calculations for complex transition metal oxides. Physical Review Research, 2020, 2, .	1.3	15
61639	Discovery of a low-temperature orthorhombic phase of the <mml:math xmlns:mml="http://www.w3.org/1998/Math/MathML"><mml:mrow><mml:msub><mml:mi>Cd</mml:mi><mml:mn>2</mml:mn></mml: mathvariant="normal">O</mml:mi><mml:mn>7</mml:mn></mml:msub></mml:mrow></mml:math> superconductor. Physical Review Research, 2020, 2, .	1.3	9
61640	Cation order control of correlations in double perovskite <mml:math xmlns:mml="http://www.w3.org/1998/Math/MathML"><mml:mrow><mml:msub><mml:mi>Sr</mml:mi><mml:mn>2</mml:mn> Physical Review Research, 2020, 2, .	1.3	8

#	Article	IF	Citations
61641	Domain wall mobility and roughening in doped ferroelectric hexagonal manganites. Physical Review Research, 2020, 2, .	1.3	11
61642	Search for encapsulation of platinum, silver, and gold at the surface of graphite. Physical Review Research, 2020, 2, .	1.3	13
61643	Superconducting mechanism for the cuprate <mml:math xmlns:mml="http://www.w3.org/1998/Math/MathML"><mml:mrow><mml:msub><mml:mi>Ba</mml:mi><mml:mn>2</mml:mn></mml: mathvariant="normal">O</mml:mi><mml:mrow><mml:mn>3</mml:mn><mml:mo>+</mml:mo><mml:mi>Î´</mml:mi></mml:mrow></ based on a multiorbital Lieb lattice model. Physical Review Research, 2020, 2, .	1.3	17
61644	Ultrabroadband density of states of amorphous In-Ga-Zn-O. Physical Review Research, 2020, 2, .	1.3	11
61645	Kondo screening in Co adatoms with full Coulomb interaction. Physical Review Research, 2020, 2, .	1.3	9
61646	Gate-tunable cross-plane heat dissipation in single-layer transition metal dichalcogenides. Physical Review Research, 2020, 2, .	1.3	4
61647	Interfacial-hybridization-modified Ir ferromagnetism and electronic structure in <mml:math xmlns:mml="http://www.w3.org/1998/Math/MathML"><mml:mrow><mml:msub><mml:mi>LaMnO</mml:mi><mml:mn>3</mml:mn></mml: superlattices. Physical Review Research, 2020, 2, .	1.3	10
61648	Half-magnetization plateau and the origin of threefold symmetry breaking in an electrically switchable triangular antiferromagnet. Physical Review Research, 2020, 2, .	1.3	14
61649	Phono-magnetic analogs to opto-magnetic effects. Physical Review Research, 2020, 2, .	1.3	46
61650	Structural relaxation and low-energy properties of twisted bilayer graphene. Physical Review Research, 2020, 2, .	1.3	39
61651	Higher-order topological crystalline insulating phase and quantized hinge charge in topological electride apatite. Physical Review Research, 2020, 2, .	1.3	17
61652	State-to-state methane-surface scattering as a probe of catalytic activity. Physical Review Research, 2020, 2, .	1.3	11
61653	Pressure controlled trimerization for switching of anomalous Hall effect in triangular antiferromagnet Mn3Sn. Physical Review Research, 2020, 2, .	1.3	11
61654	Lattice dynamics in the double-helix antiferromagnet FeP. Physical Review Research, 2020, 2, .	1.3	4
61655	Thermally induced transformations of Au@Cu₂O coreâ€“shell nanoparticles into Auâ€“Cu nanoparticles from temperature-programmed in situ powder X-ray diffraction. Journal of Applied Crystallography, 2019, 52, 579-586.	1.9	7
61656	X-ray diffraction using focused-ion-beam-prepared single crystals. Journal of Applied Crystallography, 2020, 53, 614-622.	1.9	7
61657	Complex modeling for the quantification of nanoscale disorder using genetic algorithms, density functional theory and line-profile analysis. Journal of Applied Crystallography, 2020, 53, 1087-1100.	1.9	2
61658	A new diffractometer for diffuse scattering studies on the ID28 beamline at the ESRF. Journal of Synchrotron Radiation, 2019, 26, 272-279.	1.0	25

#	Article	IF	Citations
61659	Theoretical development and experimental validation on the measurement of temperature by extended X-ray absorption fine structure. Journal of Synchrotron Radiation, 2020, 27, 436-445.	1.0	5
61660	Hydrogen bonds in crystalline <scp>D</scp>-alanine: diffraction and spectroscopic evidence for differences between enantiomers. IUCrJ, 2018, 5, 6-12.	1.0	7
61661	Conformational aspects of polymorphs and phases of 2-propyl-1H-benzimidazole. IUCrJ, 2018, 5, 706-715.	1.0	7
61662	Self-adapted clustering of solute atoms into a confined two-dimensional prismatic platelet with an ellipse-like quasi-unit cell. IUCrJ, 2018, 5, 823-829.	1.0	10
61663	Robust manipulation of magnetism in LaAO₃/BaTiO₃ (A = Fe, Mn) Tj ETQq0 0 0 rgBT /Overlock	1.0	10
61664	Explainable machine learning for materials discovery: predicting the potentially formable Ndâ€“Feâ€“B crystal structures and extracting the structureâ€“stability relationship. IUCrJ, 2020, 7, 1036-1047.	1.0	7
61665	The crystal structure and phase stability of the zeta phase in the group VB transition metal carbides: a computational investigation. Acta Crystallographica Section B: Structural Science, Crystal Engineering and Materials, 2019, 75, 870-879.	0.5	6
61666	The many flavours of halogen bonds â€“ message from experimental electron density and Raman spectroscopy. Acta Crystallographica Section C, Structural Chemistry, 2019, 75, 1190-1201.	0.2	14
61667	Can we trust the experiment? Anisotropic displacement parameters in 1-(halomethyl)-3-nitrobenzene (halogen = Cl or Br). Acta Crystallographica Section C, Structural Chemistry, 2020, 76, 591-597.	0.2	2
61668	Principles of weakly ordered domains in intermetallics: the cooperative effects of atomic packing and electronics in Fe₂Al₅. Acta Crystallographica Section A: Foundations and Advances, 2019, 75, 297-306.	0.0	12
61669	Bonding network and stability of clusters: the case study of Al13TM4 pseudo-tenfold surfaces. Acta Crystallographica Section A: Foundations and Advances, 2019, 75, 314-324.	0.0	18
61670	Algorithms for target transformations of lattice basis vectors. Acta Crystallographica Section A: Foundations and Advances, 2020, 76, 713-718.	0.0	5
61671	An unusually short intermolecular Nâ€”H...N hydrogen bond in crystals of the hemi-hydrochloride salt of 1-exo-acetamidopyrrolizidine. Acta Crystallographica Section E: Crystallographic Communications, 2020, 76, 77-81.	0.2	2
61672	Multicomponent bulk metal nitride (Nb_{1/3}Ta_{1/3}Ti_{1/3})N_{1â^'}_{Î´} synthesis via reaction flash sintering and characterizations. Journal of the American Ceramic Society, 2020, 103, 4876-4893.	1.9	6
61673	First-Principles Investigation of Intergranular Fracture in Copper by Grain Boundary Segregation of Sulfur. Journal of Engineering Materials and Technology, Transactions of the ASME, 2018, 140, .	0.8	7
61674	Impact of point defects on electrochromism in WO3. , 2018, , .		1
61675	The THz sum-frequency counterparts of stimulated Raman scattering. , 2019, , .		1
61676	Dynamic fracture of tantalum under extreme tensile stress. Science Advances, 2017, 3, e1602705.	4.7	41

#	Article	IF	Citations
61677	Discovery of Lorentz-violating type II Weyl fermions in LaAlGe. Science Advances, 2017, 3, e1603266.	4.7	176
61678	Supercooled liquid sulfur maintained in three-dimensional current collector for high-performance Li-S batteries. Science Advances, 2020, 6, eaay5098.	4.7	95
61679	Competing magnetic phases and fluctuation-driven scalar spin chirality in the kagome metal YMn ₆ Sn ₆. Science Advances, 2020, 6, .	4.7	103
61680	Giant polarization in super-tetragonal thin films through interphase strain. Science, 2018, 361, 494-497.	6.0	173
61681	Can the Highly Symmetric SU(4) Spinâ€"Orbital Model Be Realized in Î±-ZrCl3?. JETP Letters, 2020, 112, 642-646.	0.4	7
61682	Estimation of Enthalpy of Formation of TiCu by Density Functional Method. Physics of Metals and Metallography, 2020, 121, 1188-1192.	0.3	4
61683	Weak Antiferromagnet Iron Borate FeBO3. Classical Object for Magnetism and the State of the Art. Journal of Experimental and Theoretical Physics, 2020, 131, 177-188.	0.2	12
61684	The Optical Properties, Energy Band Structure, and Interfacial Conductance of a 3C-SiC(111)/Si(111) Heterostructure Grown by the Method of Atomic Substitution. Technical Physics Letters, 2020, 46, 1103-1106.	0.2	10
61685	Structural transformation and electronic properties of 2-Methyl-2H-naphtho[1,8-de]triazine under hydrostatic compression. International Journal of Modern Physics C, 2020, 31, 2050133.	0.8	6
61686	Low-pressure superconductivity in lithium-doped methane predicted by first principles. International Journal of Modern Physics C, 2021, 32, 2150032.	0.8	2
61687	Pressure dependence of the electronic structure in kaolinite: A first-principles study. Modern Physics Letters B, 2017, 31, 1750194.	1.0	5
61688	First principles calculation of thermo-mechanical properties of thoria using Quantum ESPRESSO. International Journal of Computational Materials Science and Engineering, 2016, 05, 1650008.	0.5	8
61689	The ESIF-HPC-2 benchmark suite. , 2020, , .		1
61690	Carbon-Decorated Fe₃S₄-Fe₇Se₈ Hetero-Nanowires: Interfacial Engineering for Bifunctional Electrocatalysis Toward Hydrogen and Oxygen Evolution Reactions. Journal of the Electrochemical Society, 2020, 167, 086501.	1.3	14
61691	First-Principles Modeling of the Repassivation of Corrosion Resistant Alloys: Part I. O and Cl Adsorption Energy. Journal of the Electrochemical Society, 2020, 167, 111502.	1.3	10
61692	DFT Analysis of Ethanol Electro-Oxidation on Fe(110) and Fe3C(110) and its Correlation with the Stress Corrosion Cracking of Carbon Steel. Journal of the Electrochemical Society, 2020, 167, 111503.	1.3	2
61693	Density Functional Theory Study of the Initial Stages of Cl-Induced Degradation of Î±-Cr₂O₃ Passive Film. Journal of the Electrochemical Society, 2020, 167, 121508.	1.3	15
61694	Application of the Chloride Susceptibility Index to Study the Effects of Ni, Cr, Mn and Mo on the Repassivation of Stainless Steels. Journal of the Electrochemical Society, 2020, 167, 131510.	1.3	10

#	Article	IF	Citations
61695	Influence of Defects on Activity-Stability of Cu_{1.5}Mn_{1.5}O₄for Acid-Mediated Oxygen Evolution Reaction. Journal of the Electrochemical Society, 2020, 167, 144511.	1.3	7
61696	Adsorption of 2-mercaptobenzimidazole Corrosion Inhibitor on Copper: DFT Study on Model Oxidized Interfaces. Journal of the Electrochemical Society, 2020, 167, 161506.	1.3	21
61697	Direct Demonstration of Unified BrÃ¸nstedâ^'Evansâ^'Polanyi Relationships for Proton-Coupled Electron Transfer Reactions on Transition Metal Surfaces. Journal of the Electrochemical Society, 2020, 167, 166516.	1.3	7
61698	Favorable Lithium Nucleation on Lithiophilic Framework Porphyrin for Dendrite-Free Lithium Metal Anodes. Research, 2019, 2019, 1-11.	2.8	33
61699	Configuration Dependent Electronic and Optical Properties of WZ-CuInS₂. American Journal of Optics and Photonics, 2016, 4, 32.	1.2	2
61700	Quantum-mechanical simulations of the high-pressure behaviour of crystals. , 0, , 193-209.		2
61701	Plastic deformation of minerals at high pressure. , 0, , 389-415.		6
61702	Application of Vibrational Spectroscopy to the Characterization of Phyllosilicates and other Industrial Minerals. , 0, , 171-226.		7
61703	Strain Engineering on the Electronic and Optical Properties of WSSe Bilayer. Nanoscale Research Letters, 2020, 15, 97.	3.1	14
61704	A comprehensive analysis of the history of DFT based on the bibliometric method RPYS. Journal of Cheminformatics, 2019, 11, 72.	2.8	22
61705	Raman tensor of layered black phosphorus. PhotoniX, 2020, 1, .	5.5	29
61706	Theory of InN Bulk Band Structure. , 2009, , 273-313.		2
61707	One-Dimensional Nanosystems. Series in Materials Science and Engineering, 2016, , 47-81.	0.1	1
61709	Thermoelectric properties of half Heusler topological semi-metal LiAuTe. Europhysics Letters, 2020, 132, 67003.	0.7	5
61710	First-Principles Investigation of Electronic Structure and Optical Properties in N-S Codoping ZnO. Applied Physics, 2014, 04, 46-52.	0.0	1
61711	The Magnetism of (Pb_{1-x}Sr_x)TiO₃ and the Effect of Oxygen Vacancy on Its Magnetism by First-Principles Study. Advances in Condensed Matter Physics, 2016, 05, 45-51.	0.1	2
61712	Polarization Properties of Hexagonal AlN(000?1) Surface from Maximally Localized Wannier Functions. Advances in Condensed Matter Physics, 2019, 08, 1-7.	0.1	1
61713	Pressure Dependence of Elastic Constants in Zinc-Blende III-N and Their Influence on the Light Emission in Nitride Heterostructures. Acta Physica Polonica A, 2004, 105, 559-566.	0.2	4

#	Article	IF	Citations
61714	Calculation of Positron Response from Embedded Nanoparticles. Acta Physica Polonica A, 2005, 107, 784-791.	0.2	9
61715	Theoretical Simulations of 0.25 Monolayer Iodine Adsorption on Cu(100). Acta Physica Polonica A, 2008, 114, S-71-S-76.	0.2	3
61716	Impurity Effect on Charge and Spin Density in Î±-Fe - Comparison between Cellular Model, Ab Initio Calculations and Experiment. Acta Physica Polonica A, 2011, 119, 24-27.	0.2	4
61717	Phonon Dispersion Analysis as an Indispensable Tool for Predictions of Solid State Polymorphism and Dynamic Metastability: Case of Compressed Silane. Acta Physica Polonica A, 2011, 119, 895-900.	0.2	8
61718	High-Pressure Phase Transitions and Thermodynamic Behaviors of Cadmium Sulfide. Acta Physica Polonica A, 2011, 120, 501-506.	0.2	36
61719	Electronic Structure of Some Wurtzite Semiconductors: Hybrid Functionals vs. Ab Initio Many Body Calculations. Acta Physica Polonica A, 2012, 121, 1142-1144.	0.2	22
61720	Magnetism in Doped Two-Dimensional Honeycomb Structures of III-V Binary Compounds. Acta Physica Polonica A, 2012, 121, 1240-1241.	0.2	1
61721	Structural and Magnetic Properties of Co Thin Films on Au(111) Substrates. Acta Physica Polonica A, 2012, 121, 653-659.	0.2	7
61722	Effect of Interstitial Iron Defect and Doping on Physical Properties and Stability of Iron Telluride. Acta Physica Polonica A, 2012, 121, 928-931.	0.2	1
61723	Displacive Phase Transformations and Generalized Stacking Faults. Acta Physica Polonica A, 2012, 122, 490-492.	0.2	1
61724	Hardening of (Pb,Cd)Te Crystal Lattice with an Increasing CdTe Content in the Solid Solution. Acta Physica Polonica A, 2016, 130, 1245-1247.	0.2	2
61725	Characterization of Defects in Titanium Created by Hydrogen Charging. Acta Physica Polonica A, 2017, 132, 1606-1611.	0.2	3
61726	Orthorhombic Phase of La_{0.5}Bi_{0.5}NiO₃ Studied by First Principles. Acta Physica Polonica A, 2018, 133, 408-410.	0.2	1
61727	The effect of strain on the electronic properties of MoS₂ monolayers. Multiscale and Multiphysics Mechanics, 2016, 1, 77-86.	0.3	2
61728	Microcantilever biosensor: sensing platform, surface characterization and multiscale modeling. Smart Structures and Systems, 2011, 8, 17-37.	1.9	5
61729	Structural and Spectroscopic Characterization of Montmorillonite Intercalated with N-Butylammonium Cations (N = 1-4) â€" Modeling and Experimental Study. Clays and Clay Minerals, 2016, 64, 401-412.	0.6	19
61730	Filled skutterudites: from single to multiple filling. Scientia Sinica: Physica, Mechanica Et Astronomica, 2011, 41, 706-728.	0.2	7
61731	Two phase transitions in PbZnO₃ at high pressure and the theoretical study of plasmons properties of PbZnO₃ quantum dots. Optics Express, 2019, 27, 16586.	1.7	3

#	Article	IF	Citations
61732	Tunable broadband hyperbolic light dispersion in metal diborides. Optics Express, 2019, 27, 36911.	1.7	12
61733	Twin-ZnSe nanowires as surface enhanced Raman scattering substrate with significant enhancement factor upon defect. Optics Express, 2020, 28, 18843.	1.7	15
61734	Complete optical absorption in hybrid halide perovskites based on critical coupling in the communication band. Optics Express, 2020, 28, 14151.	1.7	12
61735	Localized surface electromagnetic waves in CrI₃-based magnetophotonic structures. Optics Express, 2020, 28, 29155.	1.7	7
61736	Trapped excited electrons in Ni²⁺-doped perovskite KZnF₃ nanocrystals in KFâ€“ZnF₂â€“SiO₂ glass ceramics. Optics Letters, 2020, 45, 4984.	1.7	3
61737	High sensitivity and rapid response ultraviolet photodetector of a tetragonal CsPbCl₃ perovskite single crystal. Optical Materials Express, 2020, 10, 1374.	1.6	34
61738	Mo^6+ substitution induced band structure regulation and efficient near-UV-excited red emission in NaLaMg(W,Mo)O_6:Eu phosphor. Optical Materials Express, 2017, 7, 2660.	1.6	15
61739	Optical properties of MoSe₂ nanosheets: characterization, simulation and application for Q-switching. Optical Materials Express, 2019, 9, 3494.	1.6	12
61740	Temperature dependent optical properties of SnO₂ film study by ellipsometry. Optical Materials Express, 2019, 9, 3691.	1.6	18
61741	Tailoring the local lattice distortion of Nd³⁺ by codoping of Y³⁺ through first principles calculation for tuning the spectroscopic properties. Optical Materials Express, 2019, 9, 4256.	1.6	20
61742	Extreme ultraviolet plasmonics and Cherenkov radiation in silicon. Optica, 2018, 5, 1590.	4.8	24
61743	Third-order nonlinear optical properties of WTe₂ films synthesized by pulsed laser deposition. Photonics Research, 2019, 7, 1493.	3.4	14
61744	â€œConjugate Channelingâ€•Effect in Dislocation Core Diffusion: Carbon Transport in Dislocated BCC Iron. PLoS ONE, 2013, 8, e60586.	1.1	26
61745	A first principles investigation on the interaction of oxomolybdenum porphyrin with O2 - Oxomolybdenum porphyrin as a catalyst for oxygen reduction -. E-Journal of Surface Science and Nanotechnology, 2006, 4, 630-635.	0.1	1
61746	The Use of the “+U” Correction in Describing Defect States at Metal Oxide Surfaces: Oxygen Vacancies on CeO₂ and TiO₂, and Li-doping of MgO. E-Journal of Surface Science and Nanotechnology, 2009, 7, 389-394.	0.1	25
61747	Energetics of Mg, B, Cu, and Ti Atoms Adsorbed on the ZnO Polar Surfaces from First Principles. E-Journal of Surface Science and Nanotechnology, 2011, 9, 199-205.	0.1	2
61748	Density Functional Theory Calculation for Magnetism of Fe-Phthalocyanine Molecules on Au(111). E-Journal of Surface Science and Nanotechnology, 2012, 10, 38-44.	0.1	8
61749	Hydrogen Concentration Estimation Based on Density Functional Theory in Aluminum and Alpha Iron under Gaseous Hydrogen Environments. Transactions of the Materials Research Society of Japan, 2012, 37, 1-6.	0.2	5

#	Article	IF	Citations
61750	Algorithm for Automatic Detection of Surface Atoms. Transactions of the Materials Research Society of Japan, 2020, 45, 115-120.	0.2	6
61751	Extending the knowledge on the quaternary rare earth nickel aluminum germanides of the RENiAl4Ge2 series (RE=Y, Sm, Gdâ€“Tm, Lu) â€“ structural, magnetic and NMR-spectroscopic investigations. Zeitschrift Fur Naturforschung - Section B Journal of Chemical Sciences, 2020, 75, 149-162.	0.3	2
61752	Microstructure and Phase Control in Zr-Fe-Cr-Ni Alloys: Thermodynamic and Kinetic Aspects. Journal of ASTM International, 2005, 2, 12771.	0.2	8
61753	Effect of Hydrogen on Dimensional Changes of Zirconium and the Influence of Alloying Elements: First-Principles and Classical Simulations of Point Defects, Dislocation Loops, and Hydrides. , 2015, , 55-92.		9
61754	Computational Study of Site-Specific Correlations among Oxygen Reduction Intermediates on Pd3Y (111). Journal of Advanced Catalysis Science and Technology, 2014, 1, 1-9.	1.0	1
61755	Quantum Confinement and Piezoresistivity Simulation in 3C-SiC Nanosheet. IEEJ Transactions on Sensors and Micromachines, 2016, 136, 465-472.	0.0	1
61756	Influence of Tantalum on phase stability and mechanical properties of WB2. MRS Communications, 2019, 9, 375-380.	0.8	31
61757	Base-Cataytic Properties of Solid Silicon Imidonitrides. Materials Research Society Symposia Proceedings, 2002, 731, 591.	0.1	2
61758	Atomistic Simulation Study of Controlled Nanostructure Patterning. Materials Research Society Symposia Proceedings, 2003, 775, 9271.	0.1	1
61759	Kinetic Monte Carlo Simulations of Initial Process of Solute Atom Cluster Formations Based on ab initio Data Base. Progress in Nuclear Science and Technology, 2011, 2, 538-542.	0.3	2
61760	Hydrogenâ€“Grain Boundary Interaction in Fe, Feâ€“C, and Feâ€“N Systems. Progress in Nuclear Science and Technology, 2011, 2, 9-15.	0.3	38
61761	Recent Development in Quantum Mechanics/Molecular Mechanics Modeling for Materials. International Journal for Multiscale Computational Engineering, 2011, , .	0.8	1
61762	Investigation on Structural, Elastic, Electronic and Vibrational Properties of LiTiAl Half-Heusler Compound Using First Principles Methods. Cumhuriyet Ãœniversitesi Fen FakÃ¼ltesi Fen Bilimleri Dergisi, 2017, 38, 312-312.	0.1	2
61763	OPTIMIZING THE THERMAL TRANSPORT PROPERTIES OF SINGLE LAYER (2D) TRANSITION METAL DICHALCOGENIDES (TMD). EskiÅŸehir Technical University Journal of Science and Technology A - Applied Sciences and Engineering, 2019, 20, 373-392.	0.4	2
61764	First-Principles Study of Segregation Behavior of Cr/Ti/Y at Grain Boundary in Vanadium. International Journal of Materials Mechanics and Manufacturing, 2018, 6, 31-36.	0.2	2
61765	Estudio DFT de los componentes de una interfaz de tres capas Hf/HfO2/TiN. Avances En Ciencias E IngenierÃas, 2013, 5, .	0.1	1
61767	Structural, elastic, electronic and thermal properties of InAs: A study of functional density. Revista Facultad De IngenierÃa, 2017, 26, 81-91.	0.0	6
61768	A First Principle Study of Electronic Structure and Site Occupancy of Cation doped LiFePO4 Cathode Material. International Journal of Electrochemical Science, 2018, 13, 10427-10439.	0.5	7

#	Article	IF	Citations
61769	GBÂcode: A grain boundary generation code. Journal of Open Source Software, 2018, 3, 900.	2.0	17
61770	pyscal: A python module for structural analysis of atomic environments. Journal of Open Source Software, 2019, 4, 1824.	2.0	25
61771	FHI-vibes: Ab Initio Vibrational Simulations. Journal of Open Source Software, 2020, 5, 2671.	2.0	15
61776	Effects of Moderate Amounts of Sulfur Substitutional Impurities on ZnO Using Density Functional Theory. The Open Nanoscience Journal, 2011, 5, 1-10.	1.8	3
61777	Water Molecular Adsorption on the Low-Index Pt Surface: A Density Functional Study. Indonesian Journal of Chemistry, 2018, 18, 195.	0.3	3
61778	Microstructural impact on electromigration: A TCAD study. Facta Universitatis - Series Electronics and Energetics, 2014, 27, 1-11.	0.6	3
61779	Thermodynamic description of the C-Ge and C-Mg systems. Journal of Mining and Metallurgy, Section B: Metallurgy, 2010, 46, 97-103.	0.3	19
61780	First-principles and CALPHAD-type study of the Ir-Mo and Ir-W systems. Journal of Mining and Metallurgy, Section B: Metallurgy, 2020, 56, 109-118.	0.3	6
61781	Thermodynamic Analysis of the Al-Cu-Mg Ternary System. Nippon Kinzoku Gakkaishi/Journal of the Japan Institute of Metals, 2019, 83, 378-387.	0.2	6
61782	Ab-Initio Multiplet Calculations Using Iterative Algorithms for X-ray Absorption Spectra at Transition Metal L_{2,3}-Edges. Materials Transactions, 2018, 59, 1057-1061.	0.4	4
61783	Prediction of Face-Centered Cubic Single-Phase Formation for Non-Equiatomic Crâ€“Mnâ€“Feâ€“Coâ€“Ni High-Entropy Alloys Using Valence Electron Concentration and Mean-Square Atomic Displacement. Materials Transactions, 2020, 61, 1874-1880.	0.4	13
61784	Hydrogen Trapping in Mg₂Si and Al₇FeCu₂ Intermetallic Compounds in Aluminum Alloy: First-Principles Calculations. Materials Transactions, 2020, 61, 1907-1911.	0.4	20
61785	Thermodynamic Analysis of the Formation Process of Metastable Carbides in Ironâ€“Carbon Martensite. Tetsu-To-Hagane/Journal of the Iron and Steel Institute of Japan, 2020, 106, 342-351.	0.1	4
61786	Parallel Performance Analysis for Electronic Structure Calculation of Metal Nanoparticles. Journal of Computer Chemistry Japan, 2015, 14, 52-53.	0.0	3
61790	Theoretical study of B segregation in Mo(110). Journal of Boron, 0, , .	0.0	1
61791	Stabilization and Metallic to Semiconducting Transition in 2D Boron Sheet. Engineered Science, 2018, , .	1.2	2
61792	Effect of van der Waals Interaction on Ortho-Para Conversion of H2 on Ag(111) Surfaces. Journal of the Vacuum Society of Japan, 2012, 55, 115-117.	0.3	6
61793	A DFT-based Analysis on H2O Molecule Adsorption and Dissociation on the Rutile TiO2 (110) and (100) Surfaces. Journal of the Vacuum Society of Japan, 2012, 55, 341-348.	0.3	1

#	Article	IF	Citations
61794	Theoretical Study of Magnetic Anisotropy in Co/Ni Multi-Layers on W(110). Journal of the Vacuum Society of Japan, 2013, 56, 139-141.	0.3	2
61795	The Naâ€“H system: from first-principles calculations to thermodynamic modeling. International Journal of Materials Research, 2006, 97, 845-853.	0.1	13
61796	Thermochemical stability of Liâ€“Cuâ€“O ternary compounds stable at room temperature analyzed by experimental and theoretical methods. International Journal of Materials Research, 2017, 108, 959-970.	0.1	1
61797	Enhanced Catalysis of Pt3 Clusters Supported on Graphene for Nâ€“H Bond Dissociation. CCS Chemistry, 2019, 1, 215-225.	4.6	21
61798	Synthesis of Iron-Carbide Nanoparticles: Identification of the Active Phase and Mechanism of Fe-Based Fischerâ€“Tropsch Synthesis. CCS Chemistry, 2021, 3, 2712-2724.	4.6	41
61803	Effects of Spin-flip Tunneling on TMR in Tunnel Junctions with Heusler Alloys. Journal of the Magnetics Society of Japan, 2008, 32, 338-342.	0.5	6
61805	Structural and Thermodynamic Properties of the High-Entropy Alloy AlCoCrFeNi Based on First-Principles Calculations. Frontiers in Materials, 2020, 7, .	1.2	6
61806	Oxygen Reduction Reaction Catalyzed by Pt3M (M = 3d Transition Metals) Supported on O-doped Graphene. Catalysts, 2020, 10, 156.	1.6	8
61807	Reaction Mechanism for Methane-to-Methanol in Cu-SSZ-13: First-Principles Study of the Z2[Cu2O] and Z2[Cu2OH] Motifs. Catalysts, 2021, 11, 17.	1.6	2
61808	Inkjet Printing of Sc-Doped TiO2 with Enhanced Photoactivity. Coatings, 2019, 9, 78.	1.2	5
61809	First-Principles Electronic-Structure Study of Graphene Decorated with 4d-Transition Atoms. Crystals, 2021, 11, 29.	1.0	2
61810	Optoelectronic Properties of Ultrathin Indium Tin Oxide Films: A First-Principle Study. Crystals, 2021, 11, 30.	1.0	3
61811	Anomalous Properties of the Dislocation-Free Interface between Si(111) Substrate and 3C-SiC(111) Epitaxial Layer. Materials, 2021, 14, 78.	1.3	9
61812	The symmetry-adapted configurational ensemble approach to the computer simulation of site-disordered solids. , 0, , .		3
61813	Substrate-Controlled Magnetism: Fe Nanowires on Vicinal Cu Surfaces. Nanomaterials, 2020, 10, 159.	1.9	3
61814	A2AgCrBr6 (A = K, Rb, Cs) and Cs2AgCrX6(X = Cl, I) Double Perovskites: A Transition-Metal-Based Semiconducting Material Series with Remarkable Optics. Nanomaterials, 2020, 10, 973.	1.9	27
61815	Facilitating Lithium-Ion Diffusion in Layered Cathode Materials by Introducing Li ⁺ /Ni ²⁺ Antisite Defects for High-Rate Li-Ion Batteries. Research, 2019, 2019, 2198906.	2.8	36
61816	Favorable Lithium Nucleation on Lithiophilic Framework Porphyrin for Dendrite-Free Lithium Metal Anodes. Research, 2019, 2019, 4608940.	2.8	29

#	Article	IF	Citations
61817	Synergistic O ²⁻ /Li ⁺ Dual Ion Transportation at Atomic Scale. Research, 2019, 2019, 9087386.	2.8	3
61818	The Electronic Transport Channel Protection and Tuning in Real Space to Boost the Thermoelectric Performance of Mg _{3+ Î´} Sb _{2- y} Bi _y near Room Temperature. Research, 2020, 2020, 1672051.	2.8	29
61819	Constructing Stable and Potentially High-Performance Hybrid Organic-Inorganic Perovskites with â€œUnstableâ€•Cations. Research, 2020, 2020, 1986576.	2.8	4
61820	Carbon Monoxide Promotes the Catalytic Hydrogenation on Metal Cluster Catalysts. Research, 2020, 2020, 4172794.	2.8	14
61821	The Thermoelectric Properties of n-Type Bismuth Telluride: Bismuth Selenide Alloys Bi2Te3â^'xSex. Research, 2020, 2020, 4361703.	2.8	61
61822	Violation of the T ^{â^'1} Relationship in the Lattice Thermal Conductivity of Mg ₃ Sb ₂ with Locally Asymmetric Vibrations. Research, 2020, 2020, 4589786.	2.8	25
61823	Machine Learning Chemical Guidelines for Engineering Electronic Structures in Half-Heusler Thermoelectric Materials. Research, 2020, 2020, 6375171.	2.8	32
61824	Halide Homogenization for High-Performance Blue Perovskite Electroluminescence. Research, 2020, 2020, 9017871.	2.8	32
61825	Formation of two-dimensional silicide on Ni(100) surface. Japanese Journal of Applied Physics, 2020, 59, 065501.	0.8	4
61826	Charge order of bismuth ions and nature of chemical bonds in double perovskite-type oxide BaBiO₃visualized by synchrotron radiation X-ray diffraction. Japanese Journal of Applied Physics, 2020, 59, 095505.	0.8	2
61827	Carrier mediated ferromagnetism in Ga₂O₃:Cr. Applied Physics Express, 2020, 13, 021002.	1.1	6
61828	Applying Machine Learning Algorithms to Predict Potential Energies and Atomic Forces during C-H Activation. Journal of the Korean Physical Society, 2020, 77, 680-688.	0.3	2
61829	First-Principles Study on Doping of Copper Halides. Journal of the Korean Physical Society, 2020, 77, 764-767.	0.3	3
61830	Informatics-Based Approaches for Accelerated Discovery of Functional Materials. Advances in Chemical and Materials Engineering Book Series, 2016, , 192-223.	0.2	2
61831	Filled Skutterudites: from Single to Multiple Filling. Journal of the Korean Ceramic Society, 2010, 47, 54-60.	1.1	7
61832	Effect of B-Cation Doping on Oxygen Vacancy Formation and Migration in LaBO₃: A Density Functional Theory Study. Journal of the Korean Ceramic Society, 2015, 52, 331-337.	1.1	9
61833	Computational Materials Engineering: Recent Applications of VASP in the MedeAÂ® Software Environment. Journal of the Korean Ceramic Society, 2016, 53, 263-272.	1.1	18
61834	Computational Simulations of Thermoelectric Transport Properties. Journal of the Korean Ceramic Society, 2016, 53, 273-281.	1.1	52

#	Article	IF	Citations
61835	Proton Conduction in Nonstoichiometric â˜3 BaZrO3 (210)[001] Tilt Grain Boundary Using Density Functional Theory. Journal of the Korean Ceramic Society, 2016, 53, 301-305.	1.1	5
61836	Investigation of LiO2 Adsorption on LaB1â˜'xBâ€²xO3(001) for Li-Air Battery Applications: A Density Functional Theory Study. Journal of the Korean Ceramic Society, 2016, 53, 306-311.	1.1	2
61837	The Effect of Domain Wall on Defect Energetics in Ferroelectric LiNbO3 from Density Functional Theory Calculations. Journal of the Korean Ceramic Society, 2016, 53, 312-316.	1.1	4
61838	Initial Reaction of Hexachlorodisilane on Amorphous Silica Surface for Atomic Layer Deposition Using Density Functional Theory. Journal of the Korean Ceramic Society, 2017, 54, 443-447.	1.1	6
61839	Deep Potential: A General Representation of a Many-Body Potential Energy Surface. Communications in Computational Physics, 2018, 23, .	0.7	164
61840	NO Adsorption and Oxidation on Mn Doped CeO2 (111) Surfaces: A DFT+U Study. Aerosol and Air Quality Research, 2018, 18, 1080-1088.	0.9	9
61841	First-Principles Investigation of Energetics and Electronic Structures of Ni and Sc Co-Doped MgH₂. American Journal of Analytical Chemistry, 2016, 07, 34-42.	0.3	10
61842	The Structures and Properties of Y-Substituted Mg₂Ni Alloys and Their Hydrides: A First-Principles Study. American Journal of Analytical Chemistry, 2016, 07, 67-74.	0.3	5
61843	Efficient Theoretical Screening of Solid Sorbents for CO₂ Capture Applications. International Journal of Clean Coal and Energy, 2012, 01, 1-11.	0.2	58
61844	Thermal Properties and Phonon Dispersion of Bi₂Te₃ and CsBi₄Te₆ from First-Principles Calculations. Journal of Applied Mathematics and Physics, 2015, 03, 1563-1570.	0.2	6
61845	A First Principles Investigation of the Mechanical Properties of g-TlN. Modeling and Numerical Simulation of Material Science, 2012, 02, 76-84.	0.5	6
61846	First-Principles Investigation of the Effect of M-Doped (M = Zr, Hf) TiCoSb Half-Heusler Thermoelectric Material. Journal of Materials Science and Chemical Engineering, 2015, 03, 78-86.	0.2	4
61847	First Principles DFT Study of Hydrogen Storage on Graphene with La Decoration. Journal of Materials Science and Chemical Engineering, 2015, 03, 87-94.	0.2	3
61848	Electronic Structures and Magnetic Properties of Co-Adsorbed Monolayer WS₂. Journal of Materials Science and Chemical Engineering, 2016, 04, 32-41.	0.2	2
61849	Characterizing Property of States: Effect of Defects on the Coefficient of Thermal Expansion and the Specific Heat Capacity of ZrB2. New Journal of Glass and Ceramics, 2020, 10, 15-27.	0.6	1
61850	First-Principles Study on Cation-Antisite Defects of Stannate and Titanate Pyrochlores. Open Access Library Journal (oalib), 2014, 01, 1-8.	0.1	3
61851	Electronic and Optical Properties of Rare Earth Oxides: <i>Ab Initio</i> Calculation. World Journal of Condensed Matter Physics, 2015, 05, 78-85.	1.1	8
61852	Structural, Magnetic, and Electronic Properties of Fe: A Screened Hybrid Functional Study. Journal of Magnetics, 2011, 16, 201-205.	0.2	13

#	Article	IF	Citations
61853	Fabrication, Optoelectronic and Photocatalytic Properties of Some Composite Oxide Nanostructures. Transactions on Electrical and Electronic Materials, 2010, 11, 1-10.	1.0	20
61854	First-principles Predictions of Structures and Piezoelectric Properties of PbTiO3Single Crystal. Transactions on Electrical and Electronic Materials, 2016, 17, 29-32.	1.0	5
61855	Fundamental Mechanisms of Platinum Catalyst for Oxygen Reduction Reaction in Fuel Cell: Density Functional Theory Approach. Daehan Hwan'gyeong Gonghag Hoeji, 2016, 38, 242-248.	0.4	3
61856	Reaction of Tri-methylaluminum on Si (001) Surface for Initial Aluminum Oxide Thin-Film Growth. Bulletin of the Korean Chemical Society, 2010, 31, 3579-3582.	1.0	2
61857	Analysis of Spin Exchange Interactions in (C2N2H10)[Fe(HPO3)F3] on the Basis of Electronic Structure Calculations. Bulletin of the Korean Chemical Society, 2011, 32, 467-471.	1.0	2
61858	First-Principles Study of the Three Polymorphs of Crystalline 1,1-Diamino-2,2-dinitrotheylene. Bulletin of the Korean Chemical Society, 2013, 34, 2281-2285.	1.0	4
61859	Synthesis, crystal structure and in vitro anticancer studies of two bis(8-quinolinolato-N,O)-platinum(II) complexes. European Journal of Chemistry, 2019, 10, 37-44.	0.3	2
61860	First principles investigations of HgX (X=S, Se and Te). Archives of Materials Science and Engineering, 2016, 79, 5-11.	0.7	16
61861	Mechanisms of Na adsorption on graphene and graphene oxide: density functional theory approach. Carbon Letters, 2015, 16, 116-120.	3.3	84
61862	Synergy Between First-Principles Computation and Experiment in Study of Earth Science. , 0, , .		1
61863	Electronic States and Piezoresistivity in Silicon Nanowires. , 0, , .		5
61864	Exploring Factors Limiting Three-Na⁺ Extraction from Na₃V₂(PO₄)₃. Electrochemistry, 2020, 88, 457-462.	0.6	14
61866	Elastic Properties of Multi-Component Nickel Solid Solutions. , 2004, , .		2
61867	High pressure phase transition and phonon-dispersion relations of BeO calculated by first-principles method. Wuli Xuebao/Acta Physica Sinica, 2010, 59, 8755.	0.2	8
61868	First-principles calculations of h-BN monolayers by doping with oxygen and sulfur. Wuli Xuebao/Acta Physica Sinica, 2013, 62, 083102.	0.2	11
61869	First-principles study on the electronic structures of Î²-SiC/carbon nanotube core-shell structures. Wuli Xuebao/Acta Physica Sinica, 2013, 62, 107101.	0.2	5
61870	First-principles study on the elastic, electronic and thermodynamic properties of ErNi2B2C under high pressure. Wuli Xuebao/Acta Physica Sinica, 2013, 62, 107402.	0.2	5
61871	The first-principles study on properties of B-doped at interstitial site of Cuâ^'5 grain boundary. Wuli Xuebao/Acta Physica Sinica, 2013, 62, 117102.	0.2	4

#	Article	IF	Citations
61872	Magnetism of V, Cr and Mn doped MoS2 by first-principal study. Wuli Xuebao/Acta Physica Sinica, 2013, 62, 187102.	0.2	9
61873	Study of phase transition of HoVO4 under high pressure by Raman scattering and ab initio calculations. Wuli Xuebao/Acta Physica Sinica, 2013, 62, 246101.	0.2	3
61874	First principles study on molecule doping in MoS2 monolayer. Wuli Xuebao/Acta Physica Sinica, 2014, 63, 117101.	0.2	8
61875	First principles study on influence of oxygen vacancy in HfO2 on charge trapping memory. Wuli Xuebao/Acta Physica Sinica, 2014, 63, 123101.	0.2	3
61876	Properties of Cu1-xWx alloys at high pressure and high temperature from first-principles calculations. Wuli Xuebao/Acta Physica Sinica, 2014, 63, 206501.	0.2	3
61877	First-principles study on the effects of Zn-segregation in CuÎ£5 grain boundary. Wuli Xuebao/Acta Physica Sinica, 2014, 63, 237102.	0.2	4
61878	First-principles study on stability and electronic properties of MC and Mn+1ACn phases. Wuli Xuebao/Acta Physica Sinica, 2014, 63, 237301.	0.2	1
61879	Geometric stability and nitrogen adsorption properties of small BaxOy cluster-modified Ru(0001) surface. Wuli Xuebao/Acta Physica Sinica, 2015, 64, 016802.	0.2	3
61880	First-principles study of electronic properties of MoSi2 thin films. Wuli Xuebao/Acta Physica Sinica, 2015, 64, 047102.	0.2	2
61881	Structural and electronic properties of hydrogenated bilayer silicene. Wuli Xuebao/Acta Physica Sinica, 2015, 64, 076801.	0.2	2
61882	Magnetic coupling properties of Gd-doped ZnO nanowires studied by first-principles calculations. Wuli Xuebao/Acta Physica Sinica, 2015, 64, 178103.	0.2	2
61883	Defect stabilities and magnetic properties of Ni-X-In (X= Mn, Fe and Co) alloys: a first-principle study. Wuli Xuebao/Acta Physica Sinica, 2016, 65, 096103.	0.2	3
61884	First principles investigations of structural, electronic and elastic properties of ammonium perchlorate under high pressures. Wuli Xuebao/Acta Physica Sinica, 2016, 65, 126102.	0.2	8
61885	Research progress of electrochromic performances of WO3. Wuli Xuebao/Acta Physica Sinica, 2016, 65, 168201.	0.2	7
61886	Oxygen vacancy induced band gap narrowing of the low-temperature vanadium dioxide phase. Wuli Xuebao/Acta Physica Sinica, 2017, 66, 163102.	0.2	1
61887	First-principles study on the adsorption of oxygen at NiTi (110) surface. Wuli Xuebao/Acta Physica Sinica, 2017, 66, 216801.	0.2	2
61888	Influence of Zr doping on solubility of Xe in UO2: A first-principle study. Wuli Xuebao/Acta Physica Sinica, 2018, 67, 046101.	0.2	1
61889	First-principle calculation on electronic structures and optical properties of hybrid graphene and BiOI nanosheets. Wuli Xuebao/Acta Physica Sinica, 2018, 67, 116301.	0.2	3

#	Article	IF	Citations
61890	DFT+U calculation of Sm3+ and Sr2+ co-doping effect on performance of CeO2-based electrolyte. Wuli Xuebao/Acta Physica Sinica, 2018, 67, 088202.	0.2	7
61891	Electronic structure calculation of Cr content effect on corrosion resistance of Ti-Nb-Cr alloy. Wuli Xuebao/Acta Physica Sinica, 2018, 67, 197101.	0.2	2
61892	First-principles calculations of magnetic and optical properties of Ga_{1â€“x}Cr_xSb (x = 0.25, 0.50, 0.75). Wuli Xuebao/Acta Physica Sinica, 2019, 68, 176301.	0.2	2
61893	First principle study of formation mechanism of molybdenum-doped amorphous silica in MoO₃/Si interface. Wuli Xuebao/Acta Physica Sinica, 2019, 68, 103101.	0.2	1
61894	Barium as doping element tuning both toxicity and optoelectric properties of lead-based halide perovskites. Wuli Xuebao/Acta Physica Sinica, 2019, 68, 157101.	0.2	8
61895	Sensing performance of two-dimensional WTe₂-based gas sensors. Wuli Xuebao/Acta Physica Sinica, 2019, 68, 197101.	0.2	4
61896	Properties of vacancies and N-doping in monolayer g-ZnO: First-principles calculation and molecular orbital theory analysis. Wuli Xuebao/Acta Physica Sinica, 2019, 68, 246301.	0.2	7
61897	First-Principles Study of Magnetism-Dependent Phonons Governed by Exchange Ligand Field. Journal of the Physical Society of Japan, 2020, 89, 093705.	0.7	9
61898	DFT-based Engineering of Dirac Surface States in Topological-insulator Multilayers. Journal of the Physical Society of Japan, 2020, 89, 094701.	0.7	4
61899	Ferromagnetism Induced by Vacancies in Bulk and the (1010) Surfaces of ZnO: Density Functional Theory Calculations. Japanese Journal of Applied Physics, 2011, 50, 01BE05.	0.8	6
61900	Density Functional Theory Investigation on the Dissociation and Adsorption Processes of N₂on Pd(111) and Pd₃Ag(111) Surfaces. Japanese Journal of Applied Physics, 2011, 50, 045701.	0.8	3
61901	First Principles Calculations of Defect Formation in In-Free Photovoltaic Semiconductors Cu2ZnSnS4and Cu2ZnSnSe4. Japanese Journal of Applied Physics, 2011, 50, 04DP07.	0.8	50
61902	Effect of Lithium Absorption at Tetrahedral Site and Isomorphic Substitution on Montmorillonite Properties: A Density Functional Theory Study. Japanese Journal of Applied Physics, 2011, 50, 055701.	0.8	3
61903	First-Principles Simulation on Piezoresistivity in Alpha and Beta Silicon Carbide Nanosheets. Japanese Journal of Applied Physics, 2011, 50, 06GE05.	0.8	29
61904	Adsorption and Diffusion of Li and Ni on Graphene with Boron Substitution for Hydrogen Storage:Ab-initioMethod. Japanese Journal of Applied Physics, 2011, 50, 06GJ02.	0.8	6
61905	Crystalline Inâ€“Gaâ€“Znâ€“O Density of States and Energy Band Structure Calculation Using Density Function Theory. Japanese Journal of Applied Physics, 2011, 50, 091102.	0.8	24
61906	Effects of Lattice Constant and Sintering Atmosphere on Substitution of Sn2+Ions at Ba Site in (Ba,Ca)TiO3Perovskites: Experimental and Theoretical Studies. Japanese Journal of Applied Physics, 2011, 50, 09NC11.	0.8	4
61907	Theoretical Study on Interactions between Oxygen Vacancy and Doped Rare-Earth Elements in Barium Titanate. Japanese Journal of Applied Physics, 2011, 50, 09NE01.	0.8	23

#	Article	IF	Citations
61908	Anisotropic Permittivity of Tetragonal BaTiO₃: A First-Principles Study. Japanese Journal of Applied Physics, 2011, 50, 09NE02.	0.8	5
61909	Theoretical Calculations for Magnetic Property of FeRh Inter-Metallic Compound with Site-Exchange Defects. Japanese Journal of Applied Physics, 2011, 50, 105803.	0.8	4
61910	Effects of Cluster Size on Platinumâ€“Oxygen Bonds Formation in Small Platinum Clusters. Japanese Journal of Applied Physics, 2012, 51, 035002.	0.8	8
61911	Self-Organized Nanostructures and High Blocking Temperatures in MgO-Based d0Ferromagnets. Japanese Journal of Applied Physics, 2012, 51, 050201.	0.8	7
61912	Theoretical Analysis of Oxygen Vacancy Formation in Zr-Doped BaTiO3. Japanese Journal of Applied Physics, 2012, 51, 09LE01.	0.8	3
61913	A First-Principles Study of the Ferroelectric Phase of AgNbO₃. Japanese Journal of Applied Physics, 2012, 51, 09LE02.	0.8	9
61914	Interaction Effect of Protons on Their Migration in Bulk Undoped Barium Zirconate Using Density Functional Theory. Japanese Journal of Applied Physics, 2012, 51, 09MA01.	0.8	7
61915	First-Principles Study on Cd Doping in Cu₂ZnSnS₄and Cu₂ZnSnSe₄. Japanese Journal of Applied Physics, 2012, 51, 10NC11.	0.8	31
61916	First-Principles Studies of Er2O3(110) Heteroepitaxy on Si(001). International Journal of Applied Physics and Mathematics, 2014, 4, 108-112.	0.3	2
61917	Engineering antiferromagnetic topological insulators in two-dimensional NaMnBi. Journal of Materials Chemistry C, 2021, 9, 16952-16958.	2.7	6
61918	Small radius electron and hole polarons in PbX₂ (X = F, Cl, Br) crystals: a computational study. Journal of Materials Chemistry C, 2021, 9, 16536-16544.	2.7	8
61919	Revealing well-defined cluster-supported bi-atom catalysts for enhanced CO₂ electroreduction: a theoretical investigation. Physical Chemistry Chemical Physics, 2021, 23, 25143-25151.	1.3	4
61920	Effects of external electric field on the sensing property of volatile organic compounds over Janus MoSSe monolayer: a first-principles investigation. RSC Advances, 2021, 11, 33276-33287.	1.7	10
61921	Exploring the electronic band gap of Janus MoSeO and WSeO monolayers and their heterostructures. New Journal of Chemistry, 0, , .	1.4	9
61922	Hybrid density functional theory for the stability and electronic properties of Fe-doped cluster defects in KDP crystal. CrystEngComm, 2021, 23, 7839-7845.	1.3	13
61923	Self-supported efficient hydrogen evolution catalysts with a coreâ€“shell structure designed via phase separation. Nanoscale, 2022, 14, 325-332.	2.8	7
61924	Water dissociation and association on mirror twin boundaries in two-dimensional MoSe₂: insights from density functional theory calculations. Nanoscale Advances, 2021, 3, 6992-7001.	2.2	4
61925	Determining Electronic, Structural, Dielectric, Magnetic, and Transport Properties in Novel Electronic Materials: Using first-principles techniques. IEEE Nanotechnology Magazine, 2021, 15, 68-C3.	0.9	1

#	Article	IF	Citations
61926	Anharmonic lattice dynamics of superionic lithium nitride. Journal of Materials Chemistry A, 2022, 10, 2295-2304.	5.2	9
61927	Antimony doping to greatly enhance the electrocatalytic performance of Sr₂Fe_{1.5}Mo_{0.5}O_{6â^'Î´} perovskite as a ceramic anode for solid oxide fuel cells. Journal of Materials Chemistry A, 2021, 9, 24336-24347.	5.2	23
61928	Low-loading Pt/Î²-Mo2C catalyst for ethanol dissociation. Experimental and theoretical characterization. Physical Chemistry Chemical Physics, 2021, 23, 23567-23575.	1.3	2
61929	One-dimensional van der Waals stacked p-type crystal Ta₂Pt₃Se₈ for nanoscale electronics. Nanoscale, 2021, 13, 17945-17952.	2.8	9
61930	Exemption of lattice collapse in Niâ€“MnO₂ birnessite regulated by the structural water mobility. Journal of Materials Chemistry A, 2021, 9, 23459-23466.	5.2	12
61931	First-principles study on the electronic structures and contact properties of graphene/XC (X = P, As,) Tj ETQq1 1 0.784314 rgBT /Over	1.3	2
61932	Understanding physical chemistry of BaxSr1â^'xTiO3 using ReaxFF molecular dynamics simulations. Physical Chemistry Chemical Physics, 2021, 23, 25056-25062.	1.3	0
61933	Steric effects in the hydrogen evolution reaction based on the TMX₄ active center: Feâ€“BHT as a case study. Physical Chemistry Chemical Physics, 2021, 23, 25239-25245.	1.3	4
61934	Nitride MXenes as sulfur hosts for thermodynamic and kinetic suppression of polysulfide shuttling: a computational study. Journal of Materials Chemistry A, 2021, 9, 25391-25398.	5.2	37
61935	Achieving an Ohmic contact in graphene-based van der Waals heterostructures by intrinsic defects and the inner polarized electric field of Janus AlGaSSe. New Journal of Chemistry, 2021, 45, 21178-21187.	1.4	4
61936	The Z-scheme transfer of photogenerated electrons for CO₂ photocatalytic reduction over g-ZnO/2H-MoS₂ heterostructure. Nanoscale, 2021, 13, 18192-18200.	2.8	11
61937	A comparison of methods for the estimation of the enthalpy of formation of rare earth compounds. Physical Chemistry Chemical Physics, 2021, 23, 24273-24281.	1.3	9
61938	Electronic structure and stability of two-dimensional bimetallic ferromagnetic semiconductor CrMoI₆. Wuli Xuebao/Acta Physica Sinica, 2021, 70, 207301.	0.2	2
61939	Structure prediction of CuBiI ternary compound and first-principles study of photoelectric properties. Wuli Xuebao/Acta Physica Sinica, 2021, 70, 207305.	0.2	0
61940	Origin of the N-coordinated single-atom Ni sites in heterogeneous electrocatalysts for CO₂ reduction reaction. Chemical Science, 2021, 12, 14065-14073.	3.7	35
61941	Controllable fabrication and photocatalytic performance of nanoscale single-layer MoSe₂ islands with substantial edges on an Ag(111) substrate. Nanoscale, 2021, 13, 19165-19171.	2.8	5
61942	Prediction of an Al₄C₄ superatom organic framework (SOF) material based on the superatom network model. Physical Chemistry Chemical Physics, 2021, 23, 24294-24300.	1.3	3
61943	The role of sp-hybridized boron atoms in the highly efficient photocatalytic N₂ reduction activity of boron-doped triphenyleneâ€“graphdiyne. Journal of Materials Chemistry A, 2021, 9, 26077-26085.	5.2	12

#	Article	IF	Citations
61944	Phase relations, and mechanical and electronic properties of nickel borides, carbides, and nitrides from ab initio calculations. RSC Advances, 2021, 11, 33781-33787.	1.7	0
61945	The Dirac cone in two-dimensional tetragonal silicon carbides: a ring coupling mechanism. Nanoscale, 2021, 13, 18267-18272.	2.8	4
61946	Boosting Electrochemical Nitrate-Ammonia Conversion Via Organic Ligands-Tuned Proton Transfer. SSRN Electronic Journal, 0, , .	0.4	0
61947	Using molten salts to probe outer-coordination sphere effects on lanthanide(<scp>iii</scp>)/(<scp>ii</scp>) electron-transfer reactions. Dalton Transactions, 2021, 50, 15696-15710.	1.6	10
61948	Insight into the Fischerâ€“Tropsch mechanism on hcp-Fe7C3 (211) by density functional theory: the roles of surface carbon and vacancies. RSC Advances, 2021, 11, 34533-34543.	1.7	4
61949	The effect of charged defects on the stability of implanted helium and yttrium in cubic ZrO₂: a first-principles study. Physical Chemistry Chemical Physics, 2021, 23, 25727-25735.	1.3	3
61950	Stabilizing orthorhombic CsSnI₃ perovskites with optimized electronic properties by surface ligands with inter-molecular hydrogen bond. Journal of Materials Chemistry A, 2021, 9, 24641-24649.	5.2	9
61951	Two-dimensional ferroelasticity and ferroelastic strain controllable anisotropic transport properties in CuTe monolayer. Nanoscale, 2021, 13, 19012-19022.	2.8	4
61952	Top-down fabrication of Ti doped BiVO₄ nanosheets for efficient water oxidation under visible light. Catalysis Science and Technology, 2021, 11, 7898-7904.	2.1	3
61953	Discovering structureâ€“property relationships for the phonon band structures of hydrocarbon-based organic semiconductor crystals: the instructive case of acenes. Journal of Materials Chemistry C, 2022, 10, 2532-2543.	2.7	6
61954	Theoretical insights into volatile iodine adsorption onto COF-DL229. Physical Chemistry Chemical Physics, 2021, 23, 25365-25373.	1.3	2
61955	Transition of CrI₂ from a two-dimensional network to one-dimensional chain at the monolayer limit. Physical Chemistry Chemical Physics, 2021, 23, 25291-25297.	1.3	3
61956	Construction of frustrated Lewis pairs on carbon nitride nanosheets for catalytic hydrogenation of acetylene. Physical Chemistry Chemical Physics, 2021, 23, 24349-24356.	1.3	14
61957	Stabilizing electrodeâ€“electrolyte interfaces to realize high-voltage Li||LiCoO₂ batteries by a sulfonamide-based electrolyte. Energy and Environmental Science, 2021, 14, 6030-6040.	15.6	84
61958	Calculating the adsorption energy of a charged adsorbent in a periodic metallic system â€“ the case of BH₄^{â^’} hydrolysis on the Ag(111) surface. Physical Chemistry Chemical Physics, 2021, 23, 25667-25678.	1.3	12
61959	Origin of the difference in thermal conductivity and anharmonic phonon scattering between LiNbO₃ and LiTaO₃. CrystEngComm, 2021, 23, 8572-8578.	1.3	2
61960	How to extract adsorption energies, adsorbateâ€“adsorbate interaction parameters and saturation coverages from temperature programmed desorption experiments. Physical Chemistry Chemical Physics, 2021, 23, 24396-24402.	1.3	1
61961	First principles study of electronic and optical properties and photocatalytic performance of GaNâ€“SiS van der Waals heterostructure. RSC Advances, 2021, 11, 32996-33003.	1.7	11

#	Article	IF	Citations
61962	Finding the catalytically active sites on the layered tri-chalcogenide compounds CoPS₃ and NiPS₃ for hydrogen evolution reaction. Physical Chemistry Chemical Physics, 2021, 23, 23967-23977.	1.3	12
61963	Surface passivation induced a significant enhancement of superconductivity in layered two-dimensional MSi₂N₄ (M = Ta and Nb) materials. Nanoscale, 2021, 13, 18947-18954.	2.8	18
61964	An electroactive single-atom copper anchored MXene nanohybrid filter for ultrafast water decontamination. Journal of Materials Chemistry A, 2021, 9, 25964-25973.	5.2	43
61965	The influence of the 6s2 configuration of Bi3+ on the structures of Aâ€²BiNb2O7 (Aâ€² = Rb, Na, Li) layered perovskite oxides. Dalton Transactions, 2021, 50, 15359-15369.	1.6	3
61966	Understanding the role of axial O in CO₂ electroreduction on NiN₄ single-atom catalysts via simulations in realistic electrochemical environment. Journal of Materials Chemistry A, 2021, 9, 23515-23521.	5.2	45
61967	Rational design of boron-containing co-doped graphene as highly efficient electro-catalysts for the nitrogen reduction reaction. Journal of Materials Chemistry A, 2021, 9, 24590-24599.	5.2	14
61968	Stability and structural properties of vacancy-ordered and -disordered ZrC_x. RSC Advances, 2021, 11, 32573-32589.	1.7	6
61969	Ferroelectricity in Novel One-Dimensional P42-InseI Nanowire. SSRN Electronic Journal, 0, , .	0.4	0
61970	Two-dimensional polarized MoTe₂/GeS heterojunction with an intrinsic electric field for photocatalytic water-splitting. RSC Advances, 2021, 11, 34048-34058.	1.7	11
61971	The molecular sieving mechanism of a polysulfide-blocking metalâ€“organic framework separator for lithiumâ€“sulfur batteries. Journal of Materials Chemistry A, 2021, 9, 23929-23940.	5.2	10
61972	Assessing cathode property prediction via exchange-correlation functionals with and without long-range dispersion corrections. Physical Chemistry Chemical Physics, 2021, 23, 24726-24737.	1.3	8
61973	CuZrO₃: If it exists it should be a sandwich. Physical Chemistry Chemical Physics, 2021, 23, 23748-23757.	1.3	2
61974	Enhanced visible light absorption in layered Cs₃Bi₂Br₉ through mixed-valence Sn(<scp>ii</scp>)/Sn(<scp>iv</scp>) doping. Chemical Science, 2021, 12, 14686-14699.	3.7	21
61975	Electrocatalytic nitrate reduction on rhodium sulfide compared to Pt and Rh in the presence of chloride. Catalysis Science and Technology, 2021, 11, 7331-7346.	2.1	13
61976	Facilitating room-temperature oxygen ion migration via Coâ€“O bond activation in cobaltite films. Nanoscale, 2021, 13, 18256-18266.	2.8	8
61977	Structural study and evaluation of thermoelectric properties of single-phase isocubanite (CuFe₂S₃) synthesized via an ultra-fast efficient microwave radiation technique. Sustainable Energy and Fuels, 2021, 5, 5804-5813.	2.5	6
61978	Prediction of 2D ferromagnetism and monovalent europium ions in EuBr/graphene heterojunctions. Physical Chemistry Chemical Physics, 2021, 23, 25500-25506.	1.3	6
61979	Predictions of attainable compositions of layered quaternary i-MAB phases and solid solution MAB phases. Nanoscale, 2021, 13, 18311-18321.	2.8	12

#	Article	IF	Citations
61980	Theoretical Study of Magnetic Phase Transition In La2/3M1/3MnO3 (M=Ca, Sr) Membranes Through Strain and Doping. SSRN Electronic Journal, 0, , .	0.4	0
61981	Adsorption of alkylamines on Cu surfaces: identifying ideal capping molecules using first-principles calculations. Nanoscale, 2021, 13, 18536-18545.	2.8	3
61982	Intrinsic Polarization-Induced Enhanced Ferromagnetism and Self-Doped pâ€“n Junctions in CrBr₃/GaN van der Waals Heterostructures. ACS Applied Materials & Interfaces, 2021, 13, 8764-8773.	4.0	19
61983	Stable and Antisintering Tungsten Carbides with Controllable Active Phase for Selective Cleavage of Aryl Ether Câ€“O Bonds. ACS Applied Materials & Interfaces, 2021, 13, 8274-8284.	4.0	4
61984	Construction of an Iodine Diffusion Barrier Using Network Structure Silicone Resin for Stable Perovskite Solar Cells. ACS Applied Materials & Interfaces, 2021, 13, 8138-8146.	4.0	11
61985	Investigation of Li3P as Electrolyte and Lithium-ion conductor: An Ab- Initio Study. , 2021, , .		0
61986	Selenium Doped Hafnium Disulfide Alloy for Visible Photodetection. , 2021, , .		0
61987	A DFT Investigation on the Electronic Structures and Au Adatom Assisted Hydrogenation of Graphene Nanoflake Array. Chemical Research in Chinese Universities, 2021, 37, 1110-1115.	1.3	2
61988	Application of Computational Chemistry for Contaminant Adsorption on the Components of Soil Surfaces. , 2022, , 171-213.		2
61989	Electrochemical Performance of Aluminum Doped Ni1â^'xAlxCo2O4 Hierarchical Nanostructure: Experimental and Theoretical Study. Processes, 2021, 9, 1750.	1.3	5
61990	Origin of the Ï‰-Strengthening and Embrittlement in Î²-Titanium Alloys: Insight from First Principles. Physical Mesomechanics, 2021, 24, 513-522.	1.0	5
61991	Superconductivity in Shear Strained Semiconductors. Chinese Physics Letters, 2021, 38, 086301.	1.3	17
61992	Symmetry-adapted graph neural networks for constructing molecular dynamics force fields. Science China: Physics, Mechanics and Astronomy, 2021, 64, 1.	2.0	5
61993	Ferroelectric Controlled Spin Texture in Two-Dimensional NbOI2 Monolayer. Chinese Physics Letters, 2021, 38, 087702.	1.3	7
61994	Effective Screening Route for Highly Active and Selective Metalâ^'Nitrogenâ€Doped Carbon Catalysts in CO₂ Electrochemical Reduction. Small, 2021, 17, e2103705.	5.2	12
61995	First-principles study of Ti-doped sapphire. I. Formation and optical transition properties of titanium pairs. Physical Review B, 2021, 104, .	1.1	8
61996	Environmental screening and ligand-field effects to magnetism in CrI3 monolayer. Npj Computational Materials, 2021, 7, .	3.5	19
61997	Evidence for mechanical softening-hardening dual anomaly in transition metals from shock-compressed vanadium. Physical Review B, 2021, 104, .	1.1	5

#	Article	IF	Citations
61998	Magnetic semiconductor in rare-earth-elementâ€“based quaternary Heusler compounds. Europhysics Letters, 2021, 135, 67006.	0.7	2
61999	Spinâ€Dependent Electronic Structure and Magnetic Properties of 2D JANUS Mn₂CFCl/CuBiP₂Se₆ Van Der Waals Multiferroic Heterostructures. Advanced Theory and Simulations, 2021, 4, 2100302.	1.3	5
62000	Structural Dynamics and Thermal Transport in Bismuth Chalcogenide Alloys. Chemistry of Materials, 2021, 33, 8404-8417.	3.2	10
62001	Periodic Trends in Adsorption Energies around Single-Atom Alloy Active Sites. Journal of Physical Chemistry Letters, 2021, 12, 10060-10067.	2.1	16
62002	Combining Experimental and DFT Investigation of the Mechanism Involved in Thermal Etching of Titanium Nitride Using Alternate Exposures of NbF 5 and CCl 4 , or CCl 4 Only. Advanced Materials Interfaces, 2021, 8, 2101085.	1.9	3
62003	First principles study of Janus WSeTe monolayer and its application in photocatalytic water splitting. Nanotechnology, 2022, 33, 025703.	1.3	29
62004	Halide Perovskites: Advanced Photovoltaic Materials Empowered by a Unique Bonding Mechanism. Advanced Functional Materials, 2022, 32, 2110166.	7.8	35
62005	Giant tunneling magnetoresistance induced by bias voltage in spin-filter van der Waals magnetic tunnel junctions with an interlayer antiferromagnetic semiconductor barrier. Physical Review B, 2021, 104, .	1.1	3
62006	Activity Origins of Graphdiyne Based Bifunctional Atom Catalysts for Hydrogen Evolution and Water Oxidation. Chemical Research in Chinese Universities, 2021, 37, 1334-1340.	1.3	4
62007	Selective On-Surface Reactions of the Alkenyl gem-Dibromide Group Directed by Substrate Lattices. Journal of Physical Chemistry C, 2021, 125, 23840-23847.	1.5	3
62008	d- and s-orbital populations in the d block: unbound atoms in physical vacuum versus chemical elements in condensed matter. A Dronskowski-population analysis. Zeitschrift Fur Naturforschung - Section B Journal of Chemical Sciences, 2021, 76, 547-557.	0.3	0
62009	Role of organic cation orientation in formamidine based perovskite materials. Scientific Reports, 2021, 11, 20433.	1.6	11
62010	Theory-Guided Inelastic Neutron Scattering of Crystalline Alkaline Aluminate Salts Bearing Principal Motifs of Solution-State Species. Inorganic Chemistry, 2021, 60, 16223-16232.	1.9	4
62011	Boosting the Redox Kinetics of Highâ€Voltage P2â€Type Cathode by Radially Oriented {010} Exposed Nanoplates for Highâ€Power Sodiumâ€Ion Batteries. Small Structures, 2022, 3, 2100123.	6.9	29
62012	Neural network-based order parameter for phase transitions and its applications in high-entropy alloys. Nature Computational Science, 2021, 1, 686-693.	3.8	14
62013	Asymmetric Sodiophilic Host Based on a Ag-Modified Carbon Fiber Framework for Dendrite-Free Sodium Metal Anodes. ACS Applied Materials & Interfaces, 2021, 13, 48634-48642.	4.0	33
62014	Methane Dry Reforming by Niâ€“Cu Nanoalloys Anchored on Periclase-Phase MgAlO_x Nanosheets for Enhanced Syngas Production. ACS Applied Materials & Interfaces, 2021, 13, 48838-48854.	4.0	25
62015	Quantifying Mechanical Properties of Molecular Crystals: A Critical Overview of Experimental Elastic Tensors. Angewandte Chemie, 2022, 134, .	1.6	7

#	Article	IF	Citations
62016	Surface Chemistry of MoS2 in Remote Oxygen Plasma. Langmuir, 2021, 37, 12112-12117.	1.6	2
62017	Theoretical Prediction and Thin-Film Growth of the Defect-Tolerant Nitride Semiconductor YZn₃N₃. Chemistry of Materials, 2021, 33, 8205-8211.	3.2	7
62018	First-principles study on structural, vibrational, elastic, piezoelectric, and electronic properties of the Janus <mml:math xmlns:mml="http://www.w3.org/1998/Math/MathML"><mml:mrow><mml:mi>Bi</mml:mi><mml:mi>X</mml:mi><mml:mi>Y</mml:mi><mml:mi>		

#	Article	IF	Citations
62034	Strong Rashbaâ€Dresselhaus Effect in Nonchiral 2D Ruddlesdenâ€Popper Perovskites. Advanced Optical Materials, 2022, 10, 2101232.	3.6	14
62035	Enhancing the Intrinsic Activity and Stability of Perovskite Cobaltite at Elevated Temperature Through Surface Stress. Small, 2021, 17, e2104144.	5.2	21
62036	First principles analysis of impurities in silicon carbide grain boundaries. Acta Materialia, 2021, 221, 117421.	3.8	7
62037	TiS₂-graphene heterostructures enabling polysulfide anchoring and fast electrocatalyst for lithium-sulfur batteries: A first-principles calculation. Chinese Physics B, 2022, 31, 047101.	0.7	2
62038	Computationally Accelerated Discovery and Experimental Demonstration of Gd0.5La0.5Co0.5Fe0.5O3 for Solar Thermochemical Hydrogen Production. Frontiers in Energy Research, 2021, 9, .	1.2	12
62039	Substitutionally Doped MoSe₂ for Highâ€Performance Electronics and Optoelectronics. Small, 2021, 17, e2102855.	5.2	24
62040	Impact of Stabilizing Cations on Lithium Intercalation in Tunneled Manganese Oxide Cathodes. ACS Applied Energy Materials, 2021, 4, 12099-12111.	2.5	6
62041	Interplay of topological electrons and magnons in the Kagome magnet CoCu₃(OH)₆Cl₂. New Journal of Physics, 2021, 23, 113007.	1.2	2
62042	First-principles study of pressure-induced phase transitions, mechanical and thermodynamic properties of ThBC. Journal of Physics Condensed Matter, 2022, 34, 044001.	0.7	2
62043	Data-driven simulation and characterisation of gold nanoparticle melting. Nature Communications, 2021, 12, 6056.	5.8	29
62044	Controllable phase transitions between multiple charge density waves in monolayer 1T-VSe2 via charge doping. Applied Physics Letters, 2021, 119, 163101.	1.5	7
62045	A Ta-TaS2 monolith catalyst with robust and metallic interface for superior hydrogen evolution. Nature Communications, 2021, 12, 6051.	5.8	112
62046	First principles study of the 2D Mo(S_{1-X}Te_X)₂ TMD alloy adsorbed on an Al-terminated sapphire (0001)-substrate. Materials Research Express, 2021, 8, 105016.	0.8	0
62048	Design of tough adhesive from commodity thermoplastics through dynamic crosslinking. Science Advances, 2021, 7, eabk2451.	4.7	66
62049	Investigation of Structural, Electronics, Optical, Mechanical and Thermodynamic Properties of YRu2P2 Compound for Superconducting Application. Journal of Superconductivity and Novel Magnetism, 2021, 34, 3089-3097.	0.8	20
62050	Au tailored on g-C3N4/TiO2 heterostructure for enhanced photocatalytic performance. Journal of Alloys and Compounds, 2022, 894, 162338.	2.8	23
62051	Engineering catalyst supports to stabilize PdOx two-dimensional rafts for water-tolerant methane oxidation. Nature Catalysis, 2021, 4, 830-839.	16.1	86
62052	Optimizing the Oxygen Vacancies Concentration of Thin NiO Nanosheets for Efficient Selective CO₂ Photoreduction. Solar Rrl, 2021, 5, 2100703.	3.1	17

#	Article	IF	Citations
62053	Elimination of oxygen sensitivity in Î±-titanium by substitutional alloying with Al. Nature Communications, 2021, 12, 6158.	5.8	41
62054	Tunable properties of ZnSe/graphene heterostructure as a promising candidate for photo/electro-catalyst applications. Applied Surface Science, 2022, 574, 151679.	3.1	20
62055	Breaking the symmetry of spin-sublattices in antiferromagnet by interfacial tailoring in the L10-MnPt/NaCl/Fe junction. Applied Physics Letters, 2021, 119, 172401.	1.5	0
62056	Electronic and lattice strain dual tailoring for boosting Pd electrocatalysis in oxygen reduction reaction. IScience, 2021, 24, 103332.	1.9	10
62057	Rivalry at the Interface: Ion Desolvation and Electrolyte Degradation in Model Ethylene Carbonate Complexes of Li⁺, Na⁺, and Mg²⁺ with PF₆^{â€“} on the Li₄Ti₅O₁₂ (111) Surface. ACS Omega, 2021, 6, 29735-29745.	1.6	4
62058	Light assisted synthesis of poly-para-phenylene on Ag(001). Journal of Physics Condensed Matter, 2022, 34, 055001.	0.7	1
62059	Importance of Surfaces and Many-Body Absorption Spectra for C-Doped TiO2 Photocatalysts. Journal of Physical Chemistry C, 0, , .	1.5	1
62060	Experimental studies and DFT calculations to predict atomic arrangements at twin boundaries and distribution behaviors of different solutes in complex intermetallics. Journal of Physics and Chemistry of Solids, 2022, 161, 110453.	1.9	4
62061	Tuning the selectivity of catalytic nitriles hydrogenation by structure regulation in atomically dispersed Pd catalysts. Nature Communications, 2021, 12, 6194.	5.8	51
62062	Structural, electronic and magnetic properties of weakly correlated metal Sr₂CrTiO₆: a first principles study. Journal of Physics Condensed Matter, 2022, 34, 055501.	0.7	0
62063	Engineering Tetrahedral Co²⁺-Exposed Co₃O₄ Nanosheets toward Highly Efficient Styrene Epoxidation. Industrial & Engineering Chemistry Research, 2021, 60, 15106-15114.	1.8	4
62064	Thermal Transport in Multidimensional Silicon-Graphene Hybrid Nanostructures. ACS Applied Materials & Interfaces, 2021, 13, 50206-50212.	4.0	3
62065	Chemically Activating Tungsten Disulfide via Structural and Electronic Engineering Strategy for Upgrading the Hydrogen Evolution Reaction. ACS Applied Materials & Interfaces, 2021, 13, 49793-49801.	4.0	12
62066	Enhancing Mg²⁺ and Mg²⁺/Li⁺ Storage by Introducing Active Defect Sites and Edge Surfaces in MoSe₂. ChemElectroChem, 2021, 8, 4252-4260.	1.7	3
62067	High-Pressure Behavior and Disorder for Ag₂ZnSnS₄ and Ag₂CdSnS₄. ACS Omega, 2021, 6, 27387-27395.	1.6	3
62068	Facile Synthesis of Palladiumâ€Based Nanocrystals with Different Crystal Phases and a Comparison of Their Catalytic Properties. Advanced Materials, 2021, 33, e2103801.	11.1	18
62069	Deprotonating Melamine to Gain Highly Interconnected Materials: Melaminate Salts of Potassium and Rubidium. Inorganic Chemistry, 2021, 60, 15069-15077.	1.9	3
62070	Zinc cation catalyzed carbonyl hydrazine C N bond cleavage in flash pyrolysis of energetic compound. Journal of Analytical and Applied Pyrolysis, 2021, 160, 105353.	2.6	1

#	Article	IF	Citations
62071	Systematic density functional theory investigations on cubic lithium-rich iron-based Li2FeO3: A multiple electrons cationic and anionic redox cathode material. ETransportation, 2021, 10, 100141.	6.8	8
62072	Adsorption Motifs and Molecular Orientation at the Ionic Liquid/Noble Metal Interface: [C₂C₁Im][NTf₂] on Pt(111). Langmuir, 2021, 37, 12596-12607.	1.6	9
62073	Cr-Doped Fe_{1â€“x}Cr_xF₃Â·0.33H₂O Nanomaterials as Cathode Materials for Sodium-Ion Batteries. ACS Applied Materials & Interfaces, 2021, 13, 48653-48660.	4.0	3
62074	Sign-tunable anomalous Hall effect induced by two-dimensional symmetry-protected nodal structures in ferromagnetic perovskite thin films. Nature Materials, 2021, 20, 1643-1649.	13.3	36
62075	Atomistic simulations of Agâ€“Cuâ€“Sn alloys based on a new modified embedded-atom method interatomic potential. Journal of Materials Research, 2022, 37, 145-161.	1.2	4
62076	Effect of the electronic charge gap on EO bond-stretching phonons in underdoped <mml:math xmlns:mml="http://www.w3.org/1998/Math/MathML"><mml:msub><mml:mi mathvariant="normal">La</mml:mi><mml:mn>2</mml:mn></mml:msub><mml:msub><mml:mi mathvariant="normal">CuO</mml:mi><mml:mn>4</mml:mn></mml:msub></mml:math> calculated using <mml:math xmlns:mml="http://www.w3.org/1998/Math/MathML"><mml:mi mathvariant="normal">LDA</mml:mi><mml:mo>+</mml:mo><mml:mi mathvariant="normal">U</mml:mi></mml:math>	1.1	10
62077	Coherence control of directional nonlinear photocurrent in spatially symmetric systems. Physical Review B, 2021, 104, .	1.1	11
62078	Bond strength between TiN coating and microstructural constituents of a high speed steel determined by first principle calculations. Acta Materialia, 2022, 222, 117439.	3.8	17
62079	Ultrathin 2D NbWO₆ Perovskite Semiconductor Based Gas Sensors with Ultrahigh Selectivity under Low Working Temperature. Advanced Materials, 2022, 34, e2104958.	11.1	46
62080	Hydrogenated Amorphous TiO2â^’x and Its High Visible Light Photoactivity. Nanomaterials, 2021, 11, 2801.	1.9	2
62081	Two-Dimensional TeB Structures with Anisotropic Carrier Mobility and Tunable Bandgap. Molecules, 2021, 26, 6404.	1.7	0
62082	Plasmon-Induced Water Splitting on Ag-Alloyed Pt Single-Atom Catalysts. Frontiers in Chemistry, 2021, 9, 742794.	1.8	6
62083	Effective modulation of ohmic contact and carrier concentration in a graphene- <mml:math xmlns:mml="http://www.w3.org/1998/Math/MathML"><mml:mrow><mml:mi>Mg</mml:mi><mml:mi>X</mml:mi></mml:mrow></mml: (<mml:math) Tj ETQq0 0 0 rgBT /Overlock 10 Tf 50 267 Td (xmlns:mml="http://www.w3.org/1998/Math/MathML"><mml:mrow><mml:r	1.1	30
62084	Re Microscopic theory for the incoherent resonant and coherent off-resonant optical response of tellurium. Physical Review B, 2021, 104, .	1.1	8
62085	Heteroanionic Ruddlesden-Popper ferroelectrics from anion order and octahedral tilts. Physical Review Materials, 2021, 5, .	0.9	0
62086	Uncommon Behavior of Li Doping Suppresses Oxygen Redox in P2â€Type Manganeseâ€Rich Sodium Cathodes. Advanced Materials, 2021, 33, e2107141.	11.1	34
62087	Machine Learning of First-Principles Force-Fields for Alkane and Polyene Hydrocarbons. Journal of Physical Chemistry A, 2021, 125, 9414-9420.	1.1	19
62088	Elemental Topological Dirac Semimetal Î±â€Sn with High Quantum Mobility. Advanced Materials, 2021, 33, e2104645.	11.1	12

#	Article	IF	Citations
62089	Understanding the roles of carbon in carbon/g-C3N4 based photocatalysts for H2 evolution. Nano Research, 0, , 1.	5.8	9
62090	Electron penetration triggering interface activity of Pt-graphene for CO oxidation at room temperature. Nature Communications, 2021, 12, 5814.	5.8	37
62091	Electronic properties and quasiparticle model of monolayer <mml:math xmlns:mml="http://www.w3.org/1998/Math/MathML"><mml:msub><mml:mrow><mml:mi>MoSi</mml:mi></mml:mrow><mml:mn>2</ mathvariant="normal">N</mml:mi></mml:mrow><mml:mn>4</mml:mn></mml:msub></mml:math>. Physical Review B, 2021, 104, .	1.1	17
62092	Rb3Er4Cu5Te10: exploring the frontier between polar intermetallics and Zintlâ€phases via experimental and quantumchemical approaches. European Journal of Inorganic Chemistry, 0, , .	1.0	4
62093	Identification of hidden orbital contributions in the <mml:math xmlns:mml="http://www.w3.org/1998/Math/MathML"><mml:mrow><mml:msub><mml:mi>La</mml:mi><mml:mrow 0.9 <mml:mn>0.65</ valence band. Physical Review Materials, 2021, 5, .	0.9	2
62094	A strategy to identify materials exhibiting a large nonlinear phononics response: tuning the ultrafast structural response of LaAlO₃ with pressure. Journal of Physics Condensed Matter, 2022, 34, 035402.	0.7	3
62095	Competing magnetic interactions and magnetocaloric effect in Ho₅Sn₃. Journal of Physics Condensed Matter, 2022, 34, 025801.	0.7	2
62096	First principles study of photoelectrochemical water splitting in monolayer Sn2S2P4 with high solar-to-hydrogen efficiency. Applied Physics Letters, 2021, 119, .	1.5	17
62097	Modulating charge density wave states in <mml:math xmlns:mml="http://www.w3.org/1998/Math/MathML"><mml:msub><mml:mi>TaSe</mml:mi><mml:mn>2</mml:mn></mml:msub></mml:mrow 1.1 by an electride substrate. Physical Review B, 2021, 104, .	1.1	5
62098	Discovering a Cr-Induced Novel Superstructure on Top of a GaN Pseudo â€œ1 Ã— 1â€•Surface by Scanning Tunneling Microscopy Using a Fe/W Tip. Crystal Growth and Design, 0, , .	1.4	0
62099	Design of a Stable Heusler Alloy with Switchable Metalâ€toâ€Halfâ€Metal Transition at Finite Temperature. Advanced Theory and Simulations, 2021, 4, 2100311.	1.3	6
62100	Single-Step Topochemical Synthesis of NiFe Layered Double Hydroxides for Superior Anion Removal from Aquatic Systems. ACS Applied Materials & Interfaces, 2021, 13, 51186-51197.	4.0	19
62101	Computational examination of the kinetics of electrochemical nitrogen reduction and hydrogen evolution on a tungsten electrode. Journal of Catalysis, 2021, 404, 362-370.	3.1	12
62102	A Computational Comparison of Ether and Ester Electrolyte Stability on a Ca Metal Anode. Energy Material Advances, 2021, 2021, .	4.7	11
62103	Regulation of Te atomic vacancy defects in the intrinsic magnetic topological insulator $$hbox {MnBi}_{{6}}hbox {Te}_{{10}}$$. European Physical Journal B, 2021, 94, 1.	0.6	0
62104	Virial expansion of the electrical conductivity of hydrogen plasmas. Physical Review E, 2021, 104, 045204.	0.8	6
62105	Discovering Catalytic Reaction Networks Using Deep Reinforcement Learning from First-Principles. Journal of the American Chemical Society, 2021, 143, 16804-16812.	6.6	17
62106	Aluminum depletion induced by co-segregation of carbon and boron in a bcc-iron grain boundary. Nature Communications, 2021, 12, 6008.	5.8	24

#	Article	IF	Citations
62107	Bipolar magnetic semiconducting behavior in VNbRuAl. Physical Review B, 2021, 104, .	1.1	13
62108	Bulk Dirac cone and highly anisotropic electronic structure of <mml:math xmlns:mml="http://www.w3.org/1998/Math/MathML"><mml:mrow><mml:mi>Ni</mml:mi><mml:msub><mml:mi>Te</mml:mi> Physical Review B, 2021, 104, .	1.1	4
62109	Kinetics of NH₃ Desorption and Diffusion on Pt: Implications for the Ostwald Process. Journal of the American Chemical Society, 2021, 143, 18305-18316.	6.6	15
62110	Alloying effect on the Câ€“C coupling reactions in acetylene hydrogenation by palladium-coinage metal alloys, a DFT study and microkinetic modeling. Applied Surface Science, 2022, 575, 151513.	3.1	12
62111	Huge Lithium Storage in 2D Bilayer Structures with Point Defects. Journal of Physical Chemistry C, 2021, 125, 23597-23603.	1.5	6
62112	MAELAS 2.0: A new version of a computer program for the calculation of magneto-elastic properties. Computer Physics Communications, 2022, 271, 108197.	3.0	5
62113	Machine Learning Accelerates the Discovery of Light-Absorbing Materials for Double Perovskite Solar Cells. Journal of Physical Chemistry C, 2021, 125, 22483-22492.	1.5	16
62114	Single Metal Atom Catalyst Supported on g-C₃N₄ for Formic Acid Dehydrogenation: A Combining Density Functional Theory and Machine Learning Study. Journal of Physical Chemistry C, 2021, 125, 22513-22521.	1.5	28
62115	Direct methane activation by atomically thin platinum nanolayers on two-dimensional metal carbides. Nature Catalysis, 2021, 4, 882-891.	16.1	63
62116	Multiple spintronic functionalities into single zinc-ferrous ferrite thin films. Journal of Alloys and Compounds, 2022, 895, 162425.	2.8	4
62117	Threshold voltage modulation in monolayer MoS2 field-effect transistors via selective gallium ion beam irradiation. Science China Materials, 2022, 65, 741-747.	3.5	5
62118	Structure Relaxation and Liquidlike Enhanced Cu Diffusion at the Surface of Î²-Cu₂S Chalcocite. Nano Letters, 2021, 21, 8895-8900.	4.5	3
62119	Unraveling the size-dependent effect of Ru-based catalysts on Ammonia synthesis at mild conditions. Journal of Catalysis, 2021, 404, 501-511.	3.1	20
62120	Systematic studies of the effects of group-III dopants (La, Y, Al, and Gd) in Hf0.5Zr0.5O2 ferroelectrics by ab initio simulations. Applied Physics Letters, 2021, 119, .	1.5	13
62121	Theoretical and Experimental Studies on the Ability of Intracrystalline Pores of Î²-La₂(SO₄)₃ To Accommodate Various Gas Species with a Special Focus on Ammonia Insertion Behaviors. ACS Applied Materials & Interfaces, 2021, 13, 52793-52801.	4.0	2
62122	Thermodynamics and Kinetics of Molecular Hydrogen Adsorption and Dissociation on MXenes: Relevance to Heterogeneously Catalyzed Hydrogenation Reactions. ACS Catalysis, 2021, 11, 12850-12857.	5.5	19
62123	Point defects in <mml:math xmlns:mml="http://www.w3.org/1998/Math/MathML"><mml:mrow><mml:mi>p</mml:mi></mml:mrow></mml:math> -type transparent conductive <mml:math xmlns:mml="http://www.w3.org/1998/Math/MathML"><mml:mrow><mml:mi>Cu</mml:mi><mml:mi>M</mml:mi></mml:mrow><mml:m		

#	Article	IF	Citations
62125	Variable precipitation behaviors of Laves phases in an ultralight Mg-Li-Zn alloy. Journal of Magnesium and Alloys, 2023, 11, 2018-2026.	5.5	5
62126	Large Magnetoresistance in Scandium Nitride Magnetic Tunnel Junctions Using First Principles. Advanced Theory and Simulations, 2021, 4, 2100309.	1.3	2
62127	Visualization of Solidâ€State Synthesis for Chalcogenide Na Superionic Conductors by inâ€situ Neutron Diffraction. ChemSusChem, 2021, 14, 5161-5166.	3.6	1
62128	Guaiacol Hydrodeoxygenation over Ironâ€“Ceria Catalysts with Platinum Single-Atom Alloy Clusters as a Promoter. ACS Catalysis, 2021, 11, 12794-12814.	5.5	24
62129	Ti Substitution in Li₅FeO₄: A Li-Rich Cathode Material for Li-Ion Batteries from First Principles Calculations. ECS Journal of Solid State Science and Technology, 2021, 10, 101006.	0.9	2
62130	Tailoring the Pore Size, Basicity, and Binding Energy of Mesoporous C₃N₅ for CO₂ Capture and Conversion. Chemistry - an Asian Journal, 2021, 16, 3999-4005.	1.7	23
62131	Mechanistic insights into proton diffusion in Î£3 BaZrO3 (210)[001] tilt grain boundary. Ceramics International, 2022, 48, 2097-2104.	2.3	4
62132	Confined Monolayer Ice Between CaF2 (111) and Graphene: Structure and Stability. Frontiers in Physics, 2021, 9, .	1.0	0
62133	Predicting Li-Rich Layered Oxide Compounds as High-Conductivity and Stable Solid Electrolytes. ACS Energy Letters, 2021, 6, 3793-3800.	8.8	5
62135	Observation of Defect Luminescence in 2D Dionâ€“Jacobson Perovskites. Advanced Optical Materials, 2021, 9, 2101423.	3.6	19
62136	An Efficient Symmetric Electrolyzer Based On Bifunctional Perovskite Catalyst for Ammonia Electrolysis. Advanced Science, 2021, 8, e2101299.	5.6	34
62137	Solvent Effect on the Structure and Properties of RGD Peptide (1FUV) at Body Temperature (310 K) Using Ab Initio Molecular Dynamics. Polymers, 2021, 13, 3434.	2.0	10
62138	How can the Dualâ€atom Catalyst FeCoâ€“NC Surpass Singleâ€atom Catalysts Feâ€“NC/Coâ€“NC in CO₂RR? â€“ CO Intermediate Assisted Promotion via a Synergistic Effect. Energy and Environmental Materials, 2023, 6, .	7.3	24
62139	Optical activation and detection of charge transport between individual colour centres in diamond. Nature Electronics, 2021, 4, 717-724.	13.1	23
62140	Defect-mediated ferromagnetism in correlated two-dimensional transition metal phosphorus trisulfides. Science Advances, 2021, 7, eabj4086.	4.7	35
62141	Tunable Magnetic Properties in SrRuO₃/BiFeO₃ Heterostructures via Electric Field. Journal of Physical Chemistry C, 2021, 125, 24052-24059.	1.5	4
62142	Six new transformation pathways connecting simple crystal structures and common intermetallic crystal structures. Acta Materialia, 2021, 221, 117429.	3.8	10
62143	DFT study of electronic properties of N-doped ZnO and ZnO/Cu(111) bilayer films. Surface Science, 2022, 716, 121978.	0.8	10

#	Article	IF	Citations
62144	Quasi-layered Crystal Structure Coupled with Point Defects Leading to Ultralow Lattice Thermal Conductivity in n-Type Cu_{2.83}Bi₁₀Se₁₆. ACS Applied Energy Materials, 2021, 4, 11325-11335.	2.5	5
62145	High Anisotropic Optoelectronics in Two Dimensional Layered PbSnX₂ (X = S/Se). Journal of Physical Chemistry Letters, 2021, 12, 10574-10580.	2.1	5
62146	First principles calculation on cohesion properties of PdCu-Mo2C interfaces. Surface Science, 2022, 716, 121962.	0.8	3
62147	First principles study on modulating electronic and optical properties with h-BN intercalation in AlN/MoS₂ heterostructure. Nanotechnology, 2022, 33, 035708.	1.3	5
62148	First-principles study of Suzuki segregation at stacking faults in disordered face-centered cubic Co-Ni alloys. Acta Materialia, 2021, 221, 117358.	3.8	9
62149	First-Principles Investigation on the Heterostructure Photocatalyst Comprising BiVO4 and Few-Layer Black Phosphorus. Journal of Physical Chemistry C, 2021, 125, 21840-21850.	1.5	2
62150	Nonlinear plasmonic response in atomically thin metal films. Nanophotonics, 2021, 10, 4149-4159.	2.9	4
62151	First-Principles Assessment of Anomalous Thermal Degradation of Aqueous 2-Amino-2-methyl-1-propanol for CO₂ Capture. Energy & Fuels, 2021, 35, 16705-16712.	2.5	7
62152	Probing Atomicâ€Scale Fracture of Grain Boundaries in Lowâ€symmetry 2D Materials. Small, 2021, 17, e2102739.	5.2	7
62153	Equilibrium of an arbitrary bunch train with cavity resonators and short range wake: Enhanced iterative solution with Anderson acceleration. Physical Review Accelerators and Beams, 2021, 24, .	0.6	2
62154	Influence of Oxygen Vacancies and Surface Facets on Water Oxidation Selectivity toward Oxygen or Hydrogen Peroxide with BiVO₄. ACS Catalysis, 2021, 11, 13416-13422.	5.5	22
62155	Higher-order quantum magnetic inductions in chiral topological materials. Physical Review B, 2021, 104, .	1.1	0
62156	Novel Dyadic Amorphous-Crystalline Nano-Titania Hybrids for Sacrifiers-Stored Photocatalysis. Journal of Colloid and Interface Science, 2022, 608, 1638-1651.	5.0	5
62157	A First-Principles Microkinetic Rate Equation Theory for Heterogeneous Reactions: Application to Reduction of Fe₂O₃ in Chemical Looping. Industrial & Engineering Chemistry Research, 2021, 60, 15514-15524.	1.8	19
62158	Evolution of water structures in metal-organic frameworks for improved atmospheric water harvesting. Science, 2021, 374, 454-459.	6.0	281
62159	Zero valence iron nanocube decoration of graphitic nanoplatelets. Nanotechnology, 2022, 33, 025704.	1.3	0
62160	Effect of grain boundaries on the work function of hafnium: A first-principles investigation. Journal of Applied Physics, 2021, 130, .	1.1	1
62161	Quantifying Mechanical Properties of Molecular Crystals: A Critical Overview of Experimental Elastic Tensors. Angewandte Chemie - International Edition, 2022, 61, .	7.2	18

#	Article	IF	Citations
62162	Theoretical Insights into Synergistic Effects at Cu/TiC Interfaces for Promoting CO2 Activation. ACS Omega, 2021, 6, 27259-27270.	1.6	4
62163	Mechanistic Probing of Encapsulation and Confined Growth of Lithium Crystals in Carbonaceous Nanotubes. Advanced Materials, 2021, 33, e2105228.	11.1	14
62164	Mechanism and Prediction of Hydrogen Embrittlement in fcc Stainless Steels and High Entropy Alloys. Physical Review Letters, 2021, 127, 175501.	2.9	20
62165	Fast-ion conduction and local environments in BIMEVOX. Philosophical Transactions Series A, Mathematical, Physical, and Engineering Sciences, 2021, 379, 20200430.	1.6	5
62166	Intertwined ferroelectricity and topological state in two-dimensional multilayer. Npj Computational Materials, 2021, 7, .	3.5	12
62167	Influence of Br ^{â˜’} /S ^{2â˜’} site-exchange on Li diffusion mechanism in Li ₆ PS ₅ Br: a computational study. Philosophical Transactions Series A, Mathematical, Physical, and Engineering Sciences, 2021, 379, 20190458.	1.6	2
62168	Transformation of metastable dual-phase (Ti0.25V0.25Zr0.25Hf0.25)B2 to stable high-entropy single-phase boride by thermal annealing. Applied Physics Letters, 2021, 119, .	1.5	9
62169	Epitaxial strain effect on the band gap of a Ga2O3 wide bandgap material. Journal of the Korean Physical Society, 2021, 79, 946-952.	0.3	2
62170	Charge-Density-Wave-Induced Bands Renormalization and Energy Gaps in a Kagome Superconductor <mml:math xmlns:mml="http://www.w3.org/1998/Math/MathML" display="inline"><mml:mrow><mml:msub><mml:mrow><mml:mi>RbV</mml:mi></mml:mrow><mml:mrow><mml:mn>3</mml:mn></m Physical Review X, 2021, 11, .	2.8	60
62171	Fabrication of a NiFe Alloy Oxide Catalyst via Surface Reconstruction for Selective Hydrodeoxygenation of Fatty Acid to Fatty Alcohol. ACS Sustainable Chemistry and Engineering, 2021, 9, 15027-15041.	3.2	12
62172	Excellent Room-Temperature Thermoelectricity of 2D GeP3: Mexican-Hat-Shaped Band Dispersion and Ultralow Lattice Thermal Conductivity. Molecules, 2021, 26, 6376.	1.7	1
62173	Theoretical analysis of reversible phase evolution in Li-ion conductive halides. Applied Surface Science, 2022, 574, 151621.	3.1	2
62174	Artificial intelligence driven in-silico discovery of novel organic lithium-ion battery cathodes. Energy Storage Materials, 2022, 44, 313-325.	9.5	23
62175	2D Silicene Nanosheets for High-Performance Zinc-Ion Hybrid Capacitor Application. ACS Nano, 2021, 15, 16533-16541.	7.3	26
62176	Usability Identification Framework and High-Throughput Screening of Two-Dimensional Materials in Lithium Ion Batteries. ACS Nano, 2021, 15, 16469-16477.	7.3	15
62177	Source of Bright Near-Infrared Luminescence in Gold Nanoclusters. ACS Nano, 2021, 15, 16095-16105.	7.3	41
62178	Quasiparticle energies and optical response of RbTiOPO₄ and KTiOAsO₄. JPhys Materials, 2022, 5, 015002.	1.8	2
62179	Tailoring Interfaces in Solid-State Batteries Using Interfacial Thermochemistry and Band Alignment. Chemistry of Materials, 2021, 33, 8447-8459.	3.2	7

#	Article	IF	Citations
62180	Theoretical investigation of charge transfer between the NVâ˜ center in diamond and substitutional N and P. Journal of Applied Physics, 2021, 130, 155102.	1.1	2
62181	Coordination tailoring of Cu single sites on C3N4 realizes selective CO2 hydrogenation at low temperature. Nature Communications, 2021, 12, 6022.	5.8	132
62182	<scp>Polarizationâ€sensitive</scp> and <scp>wideâ€spectrum</scp> photovoltaic detector based on <scp>quasiâ€1D ZrGeTe₄</scp> nanoribbon. InformaÄnÃ-MateriÃ¡ly, 2022, 4, .	8.5	17
62183	Platinum Deposited Nitrogen-Doped Vertically Aligned Carbon Nanofibers as Methanol Tolerant Catalyst for Oxygen Reduction Reaction with Improved Durability. Applied Nano, 2021, 2, 303-318.	0.9	3
62184	Charge disproportionation and Hund's insulating behavior in a five-orbital Hubbard model applicable to <mml:math xmlns:mml="http://www.w3.org/1998/Math/MathML"><mml:msup><mml:mi>d</mml:mi><mml:mn>4</mml:mn></mml:msup></mml:m perovskites. Physical Review B, 2021, 104, .	1.1	6
62185	Polymorphic Phases of Metal Chlorides in the Confined 2D Space of Bilayer Graphene. Advanced Materials, 2021, 33, e2105898.	11.1	12
62186	Two-dimensional monolayer B2P6 with anisotropic elastic properties and carrier mobility. Vacuum, 2022, 195, 110651.	1.6	9
62187	Increasing Efficiency of Nonadiabatic Molecular Dynamics by Hamiltonian Interpolation with Kernel Ridge Regression. Journal of Physical Chemistry A, 2021, 125, 9191-9200.	1.1	8
62188	Predicting New MXene-like Two-Dimensional Materials Pb₂CO₂ and Sn₂CO₂ as Potential Hydrogen Evolution Reaction Catalysts. Journal of Physical Chemistry C, 2021, 125, 22562-22569.	1.5	5
62189	Assembly of Two-Dimensional Metal Organic Framework Superstructures via Solvent-Mediated Oriented Attachment. Journal of Physical Chemistry C, 2021, 125, 22837-22847.	1.5	7
62190	The Surface and Interface Effects on the CoS2-FeS2 Interfacial Films. Journal of Superconductivity and Novel Magnetism, 2021, 34, 2983-2998.	0.8	0
62191	Single Nickel Atom-Modified Phosphorene Nanosheets for Electrocatalytic CO₂ Reduction. ACS Applied Nano Materials, 2021, 4, 11017-11030.	2.4	24
62192	First-Principles Calculations of Room-Temperature Antiferromagnetism in Crystalline Transition-Metal Borate Nanosheets: Implications for Spintronics Applications. ACS Applied Nano Materials, 2021, 4, 10877-10885.	2.4	6
62193	First-Principles Study of Orderâ€“Disorder Transitions in Pseudobinary Clathrates. Journal of Physical Chemistry C, 2021, 125, 22817-22826.	1.5	0
62194	Microstructure and electronic properties of La2Ti2O7 thin films on SrTiO3 substrates. Applied Surface Science, 2021, , 151599.	3.1	0
62195	Efficient and transferable machine learning potentials for the simulation of crystal defects in bcc Fe and W. Physical Review Materials, 2021, 5, .	0.9	21
62196	Constructing a new 2D Janus black phosphorus/SMoSe heterostructure for spontaneous wide-spectral-responsive photocatalytic overall water splitting. International Journal of Hydrogen Energy, 2021, 46, 39183-39194.	3.8	17
62197	XY magnetism, Kitaev exchange, and long-range frustration in the <mml:math xmlns:mml="http://www.w3.org/1998/Math/MathML"><mml:msub><mml:mi>J</mml:mi><mml:mi>eff</mml:mi></mml:msub><mml:m honeycomb cobaltates. Physical Review B, 2021, 104, .	1.1	30

#	Article	IF	Citations
62198	Simulation and Computer Study of Structures and Physical Properties of Hydroxyapatite with Various Defects. Nanomaterials, 2021, 11, 2752.	1.9	23
62199	Impacts of vacancy-induced polarization and distortion on diffusion in solid electrolyte Li ₃ OCl. Philosophical Transactions Series A, Mathematical, Physical, and Engineering Sciences, 2021, 379, 20190459.	1.6	3
62200	Revisiting Cl-Induced Degradation of MnS Inclusions Using DFT. Journal of Physical Chemistry C, 2021, 125, 24189-24195.	1.5	6
62201	Trends in atomistic simulation software usage [Article v1.0]. Living Journal of Computational Molecular Science, 2021, 3, .	2.2	7
62202	A N â€Heterocyclic Carbeneâ€Palladacycle with Constrained Aliphatic Linker: Synthesis, Characterization and Its Catalytic Application towards Suzukiâ€Miyaura Crossâ€Coupling. Asian Journal of Organic Chemistry, 0, , .	1.3	5
62203	Critical Role of Interfacial Charge Transfer in Reducing Charge Potential of Liâ€“O2 Battery. Journal of Physical Chemistry C, 0, , .	1.5	1
62204	Paradigms of frustration in superionic solid electrolytes. Philosophical Transactions Series A, Mathematical, Physical, and Engineering Sciences, 2021, 379, 20190467.	1.6	16
62205	Promising 2D/2D MoTe₂/Ti₃C₂T_x Hybrid Materials for Boosted Hydrogen Evolution Reaction. ACS Applied Energy Materials, 2021, 4, 11886-11897.	2.5	29
62206	High-throughput crystal structure solution using prototypes. Physical Review Materials, 2021, 5, .	0.9	11
62207	Understanding the Anisotropic Elastic Properties of Metalâ€“Organic Frameworks at the Nanoscale: The Instructive Example of MOF-74. Journal of Physical Chemistry C, 2021, 125, 24728-24745.	1.5	5
62208	Chirality and Magnetocaloricity in GdFeTeO6 as Compared to GdGaTeO6. Materials, 2021, 14, 5954.	1.3	2
62209	Boron adsorption and its effect on stability and CO activation of Ï‡-Fe5C2 catalyst: An ab initio DFT study. Applied Catalysis A: General, 2021, 627, 118382.	2.2	2
62210	Pressure-induced ferromagnetism in the topological semimetal <mml:math xmlns:mml="http://www.w3.org/1998/Math/MathML"><mml:mrow><mml:mi>Eu</mml:mi><mml:msub><mml:mi>Cd</mml:mi><mml:m Physical Review B, 2021, 104, .	1.1	21
62211	A comparative study on pressure-induced structural transformations in a basaltic glass and melt from Ab initio molecular dynamics calculations. Physics and Chemistry of Minerals, 2021, 48, 1.	0.3	3
62212	Multilevel switching in Mg-doped HfOx memristor through the mutual-ion effect. Applied Physics Letters, 2021, 119, .	1.5	20
62213	Topological Anderson Insulator in Cation-Disordered Cu2ZnSnS4. Nanomaterials, 2021, 11, 2595.	1.9	7
62214	Sc2CF2/Janus MoSSe heterostructure: A potential Z-scheme photocatalyst with ultra-high solar-to-hydrogen efficiency. International Journal of Hydrogen Energy, 2021, 46, 39830-39843.	3.8	34
62215	Enhanced Thermoelectric Performance of Polycrystalline Si0.8Ge0.2 Alloys through the Addition of Nanoscale Porosity. Nanomaterials, 2021, 11, 2591.	1.9	7

#	Article	IF	Citations
62216	Î²-CuGaO2: a ferroelectric semiconductor with narrow band gap as degradation catalyst for wastewater environmental remediation. Rare Metals, 2022, 41, 972-981.	3.6	7
62217	Prediction of high- <mml:math xmlns:mml="http://www.w3.org/1998/Math/MathML"><mml:msub><mml:mi>T</mml:mi><mml:mi>c</mml:mi></mml:msub></mml:ma superconductivity in ternary lanthanum borohydrides. Physical Review B, 2021, 104, .	1.1	66
62218	First-principles study of Ti-doped sapphire. II. Formation and reduction of complex defects. Physical Review B, 2021, 104, .	1.1	6
62219	Epitaxial HfTe2 Dirac semimetal in the 2D limit. APL Materials, 2021, 9, .	2.2	7
62220	Contact passivation for defect mitigation in multi-dimensional perovskite interfaces. Applied Physics Letters, 2021, 119, 141602.	1.5	1
62221	Evolution of Structural and Electronic Properties of TiSe₂ under High Pressure. Journal of Physical Chemistry Letters, 2021, 12, 9859-9867.	2.1	21
62222	Electrochemical Production of 2,5-Furandicarboxylic from 5-Hydroxymethylfurfural Using Ultrathin Co(OH)₂ on ZIF-67. ACS Applied Energy Materials, 2021, 4, 12909-12916.	2.5	9
62223	Suppressing Câ€“C Bond Dissociation for Efficient Ethane Dehydrogenation over the Isolated Co(II) Sites in SAPO-34. ACS Catalysis, 2021, 11, 13001-13019.	5.5	29
62224	Competing energetic states in Î³â^'Fe2WO6 with strong spin-charge-lattice coupling. Physical Review B, 2021, 104, .	1.1	0
62225	Pressure-induced structural and magnetic phase transitions in La0.75Ba0.25CoO2.9 studied with scattering methods and first-principle calculations. Physical Review B, 2021, 104, .	1.1	1
62226	Self-Activated and Bismuth-Related Photoluminescence in Rare-Earth Vanadate, Niobate, and Tantalate Seriesâ€"A First-Principles Study. Inorganic Chemistry, 2021, 60, 16614-16625.	1.9	22
62227	Manipulating Uniform Nucleation to Achieve Dendrite-Free Zn Anodes for Aqueous Zn-Ion Batteries. ACS Applied Materials & Interfaces, 2021, 13, 48855-48864.	4.0	31
62228	Reaction Mechanism and Energetics of Decomposition of Tetrakis(1,3-dimethyltetrazol-5-imidoperchloratomanganese(II)) from Quantum-Mechanics-based Reactive Dynamics. Journal of the American Chemical Society, 2021, 143, 16960-16975.	6.6	3
62229	Efficient Alkaline Water Oxidation with a Regenerable Nickel Pseudo-Complex. ACS Applied Materials & Interfaces, 2021, 13, 48661-48668.	4.0	6
62230	Short-range order in SiSn alloy enriched by second-nearest-neighbor repulsion. Physical Review Materials, 2021, 5, .	0.9	3
62231	Ab initio Investigation of Impurity Ferromagnetism in the Pd1â^'xFex Alloys: Concentration and Position Dependences. Crystals, 2021, 11, 1257.	1.0	1
62232	Fabrication of nanohybrids toward improving therapeutic potential of a NIR photo-sensitizer: An optical spectroscopic and computational study. Journal of Photochemistry and Photobiology A: Chemistry, 2022, 424, 113610.	2.0	6
62233	Two-dimensional conducting states in infinite-layer oxide/perovskite oxide hetero-structures. Journal of Physics Condensed Matter, 2022, 34, 035003.	0.7	0

#	Article	IF	Citations
62234	Substitutional synthesis of sub-nanometer InGaN/GaN quantum wells with high indium content. Scientific Reports, 2021, 11, 20606.	1.6	9
62235	Atomistic Insights into Cl^{â€“}-Triggered Highly Selective Ethylene Electrochemical Oxidation to Epoxide on RuO₂: Unexpected Role of the In Situ Generated Intermediate to Achieve Active Site Isolation. ACS Catalysis, 2021, 11, 13660-13669.	5.5	5
62236	Broad Photoluminescence and Second-Harmonic Generation in the Noncentrosymmetric Organicâ€“Inorganic Hybrid Halide (C₆H₅(CH₂)₄NH₃)₄MX₇·H₂O (M = Bi, In, X = Br or I). Chemistry of Materials, 2021, 33, 8106-8111.	3.2	36
62237	Atomic Structure of Dislocations and Grain Boundaries in Two-Dimensional PtSe₂. ACS Nano, 2021, 15, 16748-16759.	7.3	12
62238	Enhanced Thermoelectric Performance Achieved in SnTe via the Synergy of Valence Band Regulation and Fermi Level Modulation. ACS Applied Materials & Interfaces, 2021, 13, 50037-50045.	4.0	18
62239	First-Principles Study on the Stability and Electronic Properties of Dionâ€“Jacobson Halide Aâ€²(MA)_{nâ^'1}B_nX_{3n+1} Perovskites. Journal of Physical Chemistry C, 2021, 125, 24096-24104.	1.5	14
62240	Tailoring the band alignment and magnetic and optical properties of g-C₃N₄/WSe₂ van der Waals heterostructures by vacancies and atomic doping. Modern Physics Letters B, 2021, 35, .	1.0	0
62241	Ga-doped Pd/CeO<mml:math xmlns:mml="http://www.w3.org/1998/Math/MathML" display="inline" id="d1e727" altimg="si34.svg"><mml:msub><mml:mrow /><mml:mrow><mml:mn>2</mml:mn></mml:mrow></mml:msub></mml:math> model catalysts for CO oxidation reactivity: A density functional theory study. Applied Surface Science, 2022, 575, 151655.	3.1	23
62242	Effect of excess Mg to control corrosion in molten MgCl2 and KCl eutectic salt mixture. Corrosion Science, 2022, 194, 109914.	3.0	16
62243	The effect of shape and size in the stability of triangular Janus MoSSe quantum dots. Scientific Reports, 2021, 11, 21061.	1.6	7
62244	Experimental Realization and Phase Engineering of a Two-Dimensional SnSb Binary Honeycomb Lattice. ACS Nano, 2021, 15, 16335-16343.	7.3	5
62245	Dimension-Dependent Bandgap Narrowing and Metallization in Lead-Free Halide Perovskite Cs3Bi2X9 (X) Tj ETQq1 1 0.784314 rgBT /O	1.9	12
62246	High-Pressure and High-Temperature Synthesis of Anion-Disordered Vanadium Perovskite Oxyhydrides. Inorganic Chemistry, 2021, 60, 15751-15758.	1.9	2
62247	Impact of Disorder on Properties of Vacancies: A Case Study of B2 and A2 Polymorphs of Non-Stoichiometric Fe2CoAl. Crystals, 2021, 11, 1207.	1.0	3
62248	Strong interlayer interaction in two-dimensional layered PtTe2. Journal of Solid State Chemistry, 2022, 305, 122657.	1.4	3
62249	Ultrafast Nonlinear Optical Response and Carrier Dynamics in Layered Gallium Sulfide (GaS) Single-Crystalline Thin Films. Frontiers in Materials, 2021, 8, .	1.2	2
62250	Capturing polysulfides by sulfurizedâ€polyacrylonitrile in lithiumâ€sulfur batteries and the sulfurâ€chain effects through Density Functional Theory. Electrochemical Science Advances, 2022, 2, .	1.2	2
62251	3D Porous Metallic Boron Carbide Crystal Structure with Excellent Ductility. Advanced Theory and Simulations, 2021, 4, 2100325.	1.3	3

#	Article	IF	Citations
62252	Ferroelectric and Room-Temperature Ferromagnetic Semiconductors in the 2D M_IM_{II}Ge₂X₆ Family: First-Principles and Machine Learning Investigations. Journal of Physical Chemistry Letters, 2021, 12, 10040-10051.	2.1	15
62253	A review of the multiscale mechanics of silicon electrodes in high-capacity lithium-ion batteries. Journal Physics D: Applied Physics, 2022, 55, 063001.	1.3	9
62254	Lattice dynamics of zircon-type NdVO4 and scheelite-type PrVO4 under high-pressure. Journal of Physics Condensed Matter, 2022, 34, 025404.	0.7	2
62255	Cu9O2(SeO3)4Cl6 revisited: Crystal structure, Raman scattering and first-principles calculations. Journal of Alloys and Compounds, 2022, 894, 162291.	2.8	2
62256	Tunable contacts and device performances in graphene/group-III monochalcogenides MX (Mâ€‰=â€‰In, Ga;) Tj ETQq0 0 0 rgBT /Overl	1.1	8
62257	Equilibrium properties of warm dense deuterium calculated by the wave packet molecular dynamics and density functional theory method. Physical Review E, 2021, 104, 045304.	0.8	2
62258	Exploring Intrinsic Electron-Trapping Centers for Persistent Luminescence in Bi³⁺-Doped LiREGeO₄ (RE = Y, Sc, Lu): Mechanistic Origin from First-Principles Calculations. Inorganic Chemistry, 2021, 60, 16604-16613.	1.9	27
62259	Pressure-induced metalâ€“insulator transition in oxygen-deficient LiNbO3-type ferroelectrics. Journal of Physics Condensed Matter, 2022, 34, 025501.	0.7	2
62260	Understanding the Chemical Composition with Doping Aliovalent Ions, Followed by the Electrochemical Behavior for Surface-Modified Ni-Rich NMC Cathode Materials. Inorganic Chemistry, 2021, 60, 16294-16302.	1.9	3
62261	Fast Generation of Machine Learning-Based Force Fields for Adsorption Energies. Journal of Chemical Theory and Computation, 2021, 17, 7195-7202.	2.3	3
62262	Strainâ€Induced Magnetism in MSi₂N₄ (M = V, Cr): A Firstâ€Principles Study. Annalen Der Physik, 2021, 533, 2100273.	0.9	10
62263	Ab initio molecular dynamics of pipe diffusion in fcc Ni beyond transition state theory. Acta Materialia, 2022, 222, 117357.	3.8	4
62264	Enhancement of monolayer HfSe2 thermoelectric performance by strain engineering: A DFT calculation. Chemical Physics Letters, 2021, 784, 139109.	1.2	10
62265	Self-regulated growth of candidate topological superconducting parkerite by molecular beam epitaxy. APL Materials, 2021, 9, 101110.	2.2	3
62266	Predicted stable high-pressure phases of copper-nitrogen compounds. Journal of Physics Condensed Matter, 2022, 34, 025401.	0.7	2
62267	Tuning Site Energy by XO₆ Units in LiX₂(PO₄)₃ Enables High Li Ion Conductivity and Improved Stability. ACS Applied Materials & Interfaces, 2021, 13, 50948-50956.	4.0	7
62268	Enhancement in magnetic parameters of L10-FeNi on Pd-substitution for permanent magnets. Indian Journal of Physics, 0, , 1.	0.9	0
62269	Joining of titanium diboride-based ultra high-temperature ceramics to refractory metal tantalum using diffusion bonding technology. Journal of the European Ceramic Society, 2022, 42, 344-353.	2.8	13

#	Article	IF	Citations
62270	Molecular Dynamics Simulation of Li-Ion Conduction at Grain Boundaries in NASICON-Type LiZr₂(PO₄)₃ Solid Electrolytes. Journal of Physical Chemistry C, 2021, 125, 23604-23612.	1.5	14
62271	Use of licorice plant extract for controlling corrosion of steel rebar in chloride-polluted concrete pore solution. Journal of Molecular Liquids, 2022, 346, 117856.	2.3	20
62272	Resolving the structure of the striped Ge layer on Ag(111):Ag2Ge surface alloy with alternate fcc and hcp domains. Physical Review B, 2021, 104, .	1.1	7
62273	Rippling Ferroic Phase Transition and Domain Switching In 2D Materials. Advanced Materials, 2021, 33, e2103469.	11.1	14
62274	The role of NaSICON surface chemistry in stabilizing fast-charging Na metal solid-state batteries. JPhys Energy, 2021, 3, 044007.	2.3	18
62275	Unraveling Strain Gradient Induced Electromechanical Coupling in Twisted Double Bilayer Graphene MoirÃ© Superlattices. Advanced Materials, 2021, 33, e2105879.	11.1	25
62276	Intrinsic Linear Dichroism of Organic Single Crystals toward Highâ€Performance Polarizationâ€Sensitive Photodetectors. Advanced Materials, 2022, 34, e2105665.	11.1	23
62277	Construction of an n-Body Potential for Revealing the Atomic Mechanism for Direct Alloying of Immiscible Tungsten and Copper. Materials, 2021, 14, 5988.	1.3	11
62278	Dopant-Tunable Ultrathin Transparent Conductive Oxides for Efficient Energy Conversion Devices. Nano-Micro Letters, 2021, 13, 211.	14.4	13
62279	Bidirectional and reversible tuning of the interlayer spacing of two-dimensional materials. Nature Communications, 2021, 12, 5886.	5.8	42
62280	Encapsulation of selenium in MOF-derived N,O-codoped porous flower-like carbon host for Na-Se batteries. Chemical Engineering Journal, 2022, 430, 132737.	6.6	13
62281	Ultrathin epitaxial Bi film growth on 2D HfTe2 template. Nanotechnology, 2021, 33, .	1.3	1
62282	Screening and Understanding Li Adsorption on Two-Dimensional Metallic Materials by Learning Physics and Physics-Simplified Learning. Jacs Au, 2021, 1, 1904-1914.	3.6	12
62283	Mastering the surface strain of platinum catalysts for efficient electrocatalysis. Nature, 2021, 598, 76-81.	13.7	229
62284	Ethane and methane at high pressures: structure and stability. Journal of Chemical Physics, 2021, 155, 184503.	1.2	2
62285	Revealing the competition between charge density wave and superconductivity in <mml:math xmlns:mml="http://www.w3.org/1998/Math/MathML"><mml:msub><mml:mrow><mml:msub><mml:mi>CsV</mml:mi><mml:mn>3</mml:mn></ through uniaxial strain. Physical Review B, 2021, 104, .	1.1	5
62286	Phaseâ€Controllable Synthesis of Multifunctional 1Tâ€MoSe₂ Nanostructures: Applications in Lithiumâ€Ion Batteries, Electrocatalytic Hydrogen Evolution, and the Hydrogenation Reaction. ChemElectroChem, 2021, 8, 4148-4155.	1.7	4
62287	Quantum Effects in the Dissociative Chemisorption of N₂ on Fe(111): Full-Dimensional Quantum Dynamics and Quasi-Classical Trajectory Study. Journal of Physical Chemistry C, 2021, 125, 23105-23114.	1.5	8

#	Article	IF	Citations
62288	Mechanistic Investigation of Molybdenum Disulfide Defect Photoluminescence Quenching by Adsorbed Metallophthalocyanines. Journal of the American Chemical Society, 2021, 143, 17153-17161.	6.6	12
62289	Novel Two-Dimensional MA₂N₄ Materials for Photovoltaic and Spintronic Applications. Journal of Physical Chemistry Letters, 2021, 12, 10120-10127.	2.1	30
62290	Spin-liquid signatures in geometrically frustrated layered kagome compounds <mml:math xmlns:mml="http://www.w3.org/1998/Math/MathML"><mml:mrow><mml:mi>YBa</mml:mi><mml:msub><mml:mi>Co</mml:mi><mml: mathvariant="normal">O</mml:mi><mml:mrow><mml:mn>7</mml:mn><mml:mo>+</mml:mo><mml:mi>Î´</mml:mi></mml:mrow></m Physical Review B, 2021, 104, .	3.7	2
62291	Genesis of a CO ₂ -rich and H ₂ O-depleted atmosphere from Earthâ€™s early global magma ocean. Science Advances, 2021, 7, eabj0406.	4.7	9
62292	Stimuliâ€Responsive Materials from Ferroceneâ€Based Organic Small Molecule for Wearable Sensors. Small, 2021, 17, e2103125.	5.2	14
62293	An Overcrowded Water-Ion Solvation Structure for a Robust Anode Interphase in Aqueous Lithium-Ion Batteries. ACS Applied Materials & Interfaces, 2021, 13, 51048-51056.	4.0	18
62294	Phase speciation and surface analysis of copper phosphate on high surface area silica support by in situ XAS/XRD and DFT: Assessment for guaiacol hydrodeoxygenation. Applied Surface Science, 2022, 574, 151577.	3.1	9
62295	Bioâ€Derived Surface Layer Suitable for Long Term Cycling Niâ€Rich Cathode for Lithiumâ€Ion Batteries. Small, 2021, 17, e2104532.	5.2	7
62296	Atomically Dispersed Tin-Modified Î³-alumina for Selective Propane Dehydrogenation under H₂S Co-feed. ACS Catalysis, 2021, 11, 13472-13482.	5.5	8
62297	Unveiling the Reversibility and Stability Origin of the Aqueous V₂O₅â€“Zn Batteries with a ZnCl₂ â€œWaterâ€in‐Saltâ€•Electrolyte. Advanced Science, 2021, 8, e2102053.	5.6	60
62298	Antiferromagnetic ferroelastic multiferroics in single-layer VOX (X = Cl, Br) predicted from first-principles. Applied Physics Letters, 2021, 119, 173103.	1.5	14
62299	Synergistic Role of Eg Filling and Anionâ€“Cation Hybridization in Enhancing the Oxygen Evolution Reaction Activity in Nickelates. ACS Applied Energy Materials, 0, , .	2.5	7
62300	Local perturbations of periodic systems. Chemisorption and point defects by GoGreenGo. Journal of Computational Chemistry, 2021, 42, 2352-2368.	1.5	1
62301	Rapid Wafer-Scale Growth of MoS2(1â€“x)Se2x Alloy Monolayers with Tunable Compositions and Optical Properties for High-Performance Photodetectors. ACS Applied Nano Materials, 0, , .	2.4	5
62302	Influence of oxygen vacancies on the ferromagnetism in Co-doped ZnO: An ab-initio study. Solid State Communications, 2022, 341, 114570.	0.9	2
62303	Efficient Iron Phosphide Catalyst as a Counter Electrode in Dye-Sensitized Solar Cells. ACS Applied Energy Materials, 2021, 4, 10618-10626.	2.5	39
62304	Wake-up Free Ferroelectric Rhombohedral Phase in Epitaxially Strained ZrO₂ Thin Films. ACS Applied Materials & Interfaces, 2021, 13, 51383-51392.	4.0	23
62305	Facile synthesis of palladium incorporated NiCo2O4 spinel for low temperature methane combustion: Activate lattice oxygen to promote activity. Journal of Catalysis, 2021, 404, 400-410.	3.1	23

#	Article	IF	Citations
62306	Torsion strained iridium oxide for efficient acidic water oxidation in proton exchange membrane electrolyzers. Nature Nanotechnology, 2021, 16, 1371-1377.	15.6	197
62307	FeCo alloy encased in nitrogen-doped carbon for efficient formaldehyde removal: Preparation, electronic structure, and d-band center tailoring. Journal of Hazardous Materials, 2022, 424, 127593.	6.5	11
62308	Fast-Charging Nonaqueous Potassium-Ion Batteries Enabled by Rational Construction of Oxygen-Rich Porous Nanofiber Anodes. ACS Applied Materials & Interfaces, 2021, 13, 50005-50016.	4.0	15
62309	Superatomic Au25(SC2H5)18 Nanocluster under Pressure. ACS Nanoscience Au, 0, , .	2.0	2
62310	Band gap engineering of amine functionalized Ag(I)-based coordination polymers and their plasmonic Ag0 coupled novel visible light driven photo-redox system for selective oxidation of benzyl alcohol. Applied Catalysis B: Environmental, 2022, 303, 120821.	10.8	6
62311	Airâ€Stable 2D Cr₅Te₈ Nanosheets with Thicknessâ€Tunable Ferromagnetism. Advanced Materials, 2022, 34, e2107512.	11.1	77
62312	The Helium Elemental and Isotopic Compositions of the Earth's Core Based on Ab Initio Simulations. Journal of Geophysical Research: Solid Earth, 2021, 126, e2021JB023106.	1.4	6
62313	Synthesis, Characterisation, and Density Functional Theory Study of Encapsulated Bioactive Components of Ginger. Pertanika Journal of Science and Technology, 2021, 29, .	0.3	0
62314	Boride-derived oxygen-evolution catalysts. Nature Communications, 2021, 12, 6089.	5.8	51
62315	Structure, electronic and magnetic characterization, and calculated electronic structures of two oxyhalide hexagonal perovskites. Physical Review Materials, 2021, 5, .	0.9	0
62316	Engineering Oxidation States of a Platinum Cocatalyst over Chemically Oxidized Graphitic Carbon Nitride Photocatalysts for Photocatalytic Hydrogen Evolution. ACS Sustainable Chemistry and Engineering, 2021, 9, 14537-14549.	3.2	30
62317	Structural Evolution and Electronic Properties of Intermediate Sized Ti_n(n=33–60) Clusters. Advanced Theory and Simulations, 2021, 4, 2100283.	1.3	4
62318	Extraordinary acidic oxygen evolution on new phase 3R-iridium oxide. Joule, 2021, 5, 3221-3234.	11.7	73
62319	Incipient geometric lattice instability of cubic fluoroperovskites. Physical Review B, 2021, 104, .	1.1	11
62320	The distribution effect of sulfur vacancy in 2Hâ€“MoS2 monolayer on its H2 generation mechanism from density functional theory. International Journal of Hydrogen Energy, 2022, 47, 242-249.	3.8	8
62321	Degradation mechanisms of perovskite solar cells under vacuum and one atmosphere of nitrogen. Nature Energy, 2021, 6, 977-986.	19.8	103
62322	Breaking the out-of-plane symmetry of Janus WSSe bilayer with chalcogen substitution for enhanced photocatalytic overall water-splitting. Applied Surface Science, 2022, 574, 151692.	3.1	18
62323	Metal-organic framework-derived LiFePO4 cathode encapsulated in O,F-codoped carbon matrix towards superior lithium storage. Nano Energy, 2022, 91, 106655.	8.2	50

#	Article	IF	Citations
62324	Neutron vibrational spectroscopic evidence for short Hâ^™â^™â^™H contacts in the RNiInH1.4; 1.6 (R = Ce, La) metal hydride. Journal of Alloys and Compounds, 2022, 894, 162381.	2.8	5
62325	High-concentration dual-complex electrolyte enabled a neutral aqueous zinc-manganese electrolytic battery with superior stability. Chemical Engineering Journal, 2022, 430, 133058.	6.6	17
62326	PbTe(core)/PbS(shell) Nanowire: Electronic Structure, Thermodynamic Stability, and Mechanical and Optical Properties. Journal of Physical Chemistry C, 2021, 125, 22660-22667.	1.5	5
62327	Electrocatalytic Glycerol Oxidation with Concurrent Hydrogen Evolution Utilizing an Efficient MoO_x/Pt Catalyst. Small, 2021, 17, e2104288.	5.2	63
62328	Polarimetric Image Sensor and Fermi Level Shifting Induced Multichannel Transition Based on 2D PdPS. Advanced Materials, 2022, 34, e2107206.	11.1	29
62329	Giant Thermal Transport Tuning at a Metal/Ferroelectric Interface. Advanced Materials, 2022, 34, e2105778.	11.1	13
62330	Atomic Heterointerface Boosts the Catalytic Activity toward Oxygen Reduction/Evolution Reaction. Advanced Energy Materials, 2021, 11, 2102235.	10.2	19
62331	Engineering of Ferroic Orders in Thin Films by Anionic Substitution. Advanced Functional Materials, 2022, 32, 2107135.	7.8	9
62332	<scp>Gdâ€Niâ€Sbâ€SnO₂</scp> electrocatalysts for active and selective ozone production. AICHE Journal, 2021, 67, e17486.	1.8	8
62333	Stacking Engineering: A Boosting Strategy for 2D Photocatalysts. Journal of Physical Chemistry Letters, 2021, 12, 10190-10196.	2.1	25
62334	Radiation damage and abnormal photoluminescence enhancement of multilayer MoS₂ under neutron irradiation. Journal of Physics Condensed Matter, 2022, 34, 055701.	0.7	2
62335	A First-Principles Study on Titanium-Decorated Adsorbent for Hydrogen Storage. Energies, 2021, 14, 6845.	1.6	10
62336	Lowâ€Coordinated Coï£¿Nï£¿C on Oxygenated Graphene for Efficient Electrocatalytic H₂O₂ Production. Advanced Functional Materials, 2022, 32, 2106886.	7.8	97
62337	Prospects for n-type conductivity in cubic boron nitride. Applied Physics Letters, 2021, 119, .	1.5	9
62338	Ternary Transition Metal Chalcogenide Nb₂Pd₃Se₈: A New Candidate of 1D Van der Waals Materials for Fieldâ€Effect Transistors. Advanced Functional Materials, 2022, 32, 2108104.	7.8	19
62339	Nitrogen Activation on Defective Potassium Chloride and Sodium Chloride. Journal of Physical Chemistry C, 0, , .	1.5	2
62340	Peculiarities of Phase Formation in Mn-Based Na SuperIonic Conductor (NaSICon) Systems: The Case of Na_{1+2x}Mn_xTi_{2â€“x}(PO₄)₃ (0.0 â‰¤ x â‰¤ 1.5). Chemistry of Materials, 2021, 33, 8394-8403.	3.2	9
62341	Anisotropically large anomalous and topological Hall effect in a kagome magnet. Physical Review B, 2021, 104, .	1.1	23

#	Article	IF	Citations
62342	Topological descendants of a multicritical Dirac semimetal with magnetism and strain. Physical Review B, 2021, 104, .	1.1	2
62343	Tuning band alignment at a semiconductor-crystalline oxide heterojunction via electrostatic modulation of the interfacial dipole. Physical Review Materials, 2021, 5, .	0.9	12
62344	Atomic configurations and energies of Mg symmetric tilt grain boundaries: ab initio local analysis. Modelling and Simulation in Materials Science and Engineering, 2021, 29, 085010.	0.8	3
62345	First-principles studies of the elastic and magnetic properties of monolayer CrN. International Journal of Modern Physics B, 0, , .	1.0	0
62346	Photocatalytic H2 evolution over sulfur vacancy-rich ZnIn2S4 hierarchical microspheres under visible light. Journal of Materials Science, 2021, 56, 19439-19451.	1.7	13
62347	Tuning the Band Alignment and Electronic Properties of <mml:math xmlns:mml="http://www.w3.org/1998/Math/MathML" display="inline" overflow="scroll"><mml:mrow><mml:mi>Ga</mml:mi><mml:mi>Se</mml:mi></mml:mrow><mml:mo>/</mml:mo><mml:mi>Sn</mml:mi><mml:r X <mml:math xmlns:mml="http://www.w3.org/1998/Math/MathML" display="inline"		

#	Article	IF	Citations
62360	Stability, electronic structure, and optical properties of lead-free perovskite monolayer Cs₃ B ₂ X ₉ (B = Sb, Bi; X = Cl, Br, I) and bilayer vertical heterostructure Cs₃ B ₂ X ₉/Cs₃ B2â€² X ₉(B,Bâ€² = Sb, Bi; X = Cl, Br, I). Chinese Physics B, 2022, 31, 027102.	0.7	4
62361	Multiorbital model reveals a second-order topological insulator in <mml:math xmlns:mml="http://www.w3.org/1998/Math/MathML"><mml:mrow><mml:mn>1</mml:mn><mml:mi>H</mml:mi></mml:mrow></mml transition metal dichalcogenides. Physical Review B, 2021, 104, .	3.7	26
62362	Visualizing Spatial Evolution of Electron-Correlated Interface in Two-Dimensional Heterostructures. ACS Nano, 2021, 15, 16589-16596.	7.3	15
62363	Water-Induced Chiral Separation on a Au(111) Surface. ACS Nano, 2021, 15, 16896-16903.	7.3	20
62364	Theoretical Study of Anisotropic Carrier Mobility for Two-Dimensional Nb₂Se₉ Material. ACS Omega, 2021, 6, 26782-26790.	1.6	8
62365	Hydroxyapatite Nanorods Rich in [Caâ€“Oâ€“P] Sites Stabilized Ni Species for Methane Dry Reforming. Industrial & Engineering Chemistry Research, 2021, 60, 15064-15073.	1.8	11
62366	Implications of the Conformationally Flexible, Macrocyclic Structure of the First-Generation, Direct-Acting Anti-Viral Paritaprevir on Its Solid Form Complexity and Chameleonic Behavior. Journal of the American Chemical Society, 2021, 143, 17479-17491.	6.6	27
62367	Emerging Yttrium Phosphides with Tetrahedron Phosphorus and Superconductivity under High Pressures. Chemistry - A European Journal, 2021, 27, 17420-17427.	1.7	5
62368	Valence Band Structure Engineering in Graphene Derivatives. Small, 2021, 17, 2104316.	5.2	8
62369	Cobalt-Based Incorporated Metals in Metalâ€“Organic Framework-Derived Nitrogen-Doped Carbon as a Robust Catalyst for Triiodide Reduction in Photovoltaics. ACS Catalysis, 2021, 11, 13680-13695.	5.5	30
62370	Luminescence Enhancement of Mn⁴⁺-Activated Fluorides via a Heterovalent Co-Doping Strategy for Monochromatic Multiplexing. ACS Applied Materials & Interfaces, 2021, 13, 51255-51265.	4.0	18
62371	Probing active sites on MnPSe3 and FePSe3 tri-chalcogenides as a design strategy for better hydrogen evolution reaction catalysts. International Journal of Hydrogen Energy, 2021, 46, 37928-37938.	3.8	9
62372	Transition metal atom doped Ni3S2 as efficient bifunctional electrocatalysts for overall water splitting: Design strategy from DFT studies. Molecular Catalysis, 2021, 516, 111955.	1.0	7
62373	Cobalt-free LaNi0.4Zn0.1Fe0.5O3-Î´ as a cathode for solid oxide fuel cells using proton-conducting electrolyte. International Journal of Hydrogen Energy, 2021, 46, 38482-38489.	3.8	20
62374	First principles calculation of Li2+2xZn1-xSiO4 (xÂ=Â0.125â€“0.5) as solid electrolyte for lithium-ion battery. Solid State Ionics, 2021, 371, 115767.	1.3	3
62375	Smâ€“Ti binary thermodynamic database and phase diagram. Calphad: Computer Coupling of Phase Diagrams and Thermochemistry, 2021, 75, 102357.	0.7	3
62376	An ab initio study of the oxygen defect formation and oxide ion migration in (Sr1-xPrx)2FeO4Â±Î´. Journal of Power Sources, 2021, 515, 230602.	4.0	5
62377	Electronic coupling induced by structural deformation and magnetic dopants in dual-metal Janus MoReS3 and WReS3 for hydrogen evolution reaction. Chemical Physics Letters, 2021, 785, 139120.	1.2	0

#	Article	IF	Citations
62378	Hybridization of carbon nanotube tissue and MnO2 as a generic advanced air cathode in metalâ€“air batteries. Journal of Power Sources, 2021, 514, 230597.	4.0	5
62379	Ordered clustering of anion vacancies in PtX2 (X=S, Se, Te) monolayer for hydrogen evolution reaction. Surfaces and Interfaces, 2021, 27, 101495.	1.5	2
62380	Control of triboelectricity by mechanoluminescence in ZnS/Mn-containing polymer films. Nano Energy, 2021, 90, 106646.	8.2	28
62381	Tunable electronic structure and magnetic characteristics of two-dimensional graphyne/VI3 van der Waals heterostructures. Superlattices and Microstructures, 2021, 160, 107081.	1.4	6
62382	Supercapacitor properties of V10O14(OH)2 and reduced graphene oxide hybrids: Experimental and theoretical insights. Electrochimica Acta, 2021, 399, 139357.	2.6	12
62383	First principles investigation into the interwoven nature of voltage and mechanical properties of the Li<mml:math xmlns:mml="http://www.w3.org/1998/Math/MathML" display="inline" id="d1e95" altimg="si118.svg"><mml:msub><mml:mrow /><mml:mrow><mml:mi>x</mml:mi></mml:mrow></mml:msub></mml:math>NMC-811 cathode. Journal of Power Sources, 2021, 516, 230620.	4.0	10
62384	CMAS corrosion behavior of Sc doped Gd2Zr2O7 /YSZ thermal barrier coatings and their corrosion resistance mechanisms. Corrosion Science, 2021, 193, 109899.	3.0	26
62385	Ab initio simulations on the pure Cr lattice stability at 0K: Verification with the Fe-Cr and Ni-Cr binary systems. Calphad: Computer Coupling of Phase Diagrams and Thermochemistry, 2021, 75, 102359.	0.7	14
62386	Electronic and magnetic properties in nitrogen-doped 2D titanium carbides (MXenes): Insight from first-principles calculations. Solid State Communications, 2021, 340, 114549.	0.9	7
62387	A novel adsorption-based method for revealing the Si distribution in SAPO molecular sieves: The case of SAPO-11. Microporous and Mesoporous Materials, 2021, 328, 111503.	2.2	5
62388	Transport and interface characteristics of Te-doped NASICON solid electrolyte Li1.3Al0.3Ti1.7(PO4)3. Electrochimica Acta, 2021, 399, 139367.	2.6	33
62389	Hydration of magnesite and dolomite minerals: new insights from ab initio molecular dynamics. Colloids and Surfaces A: Physicochemical and Engineering Aspects, 2021, 631, 127697.	2.3	12
62390	First-principles research on mechanism of sub-band absorption of amorphous silicon induced by ultrafast laser irradiation. Results in Physics, 2021, 31, 104941.	2.0	2
62391	Structure sensitivity of nitrogenâ€“doped carbonâ€“supported metal catalysts in dihalomethane hydrodehalogenation. Journal of Catalysis, 2021, 404, 291-305.	3.1	5
62392	In-situ quantification and density functional theory elucidation of phase transformation in carbon steel during quenching and partitioning. Acta Materialia, 2021, 221, 117361.	3.8	12
62393	Direct thermal annealing synthesis of FeO nanodots anchored on N-doped carbon nanosheet for long-term electrocatalytic oxygen reduction. Electrochimica Acta, 2021, 398, 139361.	2.6	15
62394	Oxygen atom ordering on SiO2/4H-SiC {0001} polar interfaces formed by wet oxidation. Acta Materialia, 2021, 221, 117360.	3.8	5
62395	Strengthening oxygen reduction activity and stability of carbon-supported platinum nanoparticles by fluorination. Electrochimica Acta, 2021, 399, 139409.	2.6	7

#	Article	IF	Citations
62396	Phase stability, mechanical, thermal, electronic properties, anisotropy, lattice dynamics and APB -energies of Ti2AlX intermetallics in Î±2, B2, and O phases: A first principle study. Materials Today Communications, 2021, 29, 102864.	0.9	2
62397	An initio study of influence of substitution of Sc with Al on intrinsic mechanical properties of hexagonal high-entropy alloys Hf0.25Ti0.25Zr0.25Sc0.25â^'xAlx (xÂâ‰Â15%). Materials Today Communications, 2021, 29, 102875.	0.9	2
62398	A subtle functional design of hollow CoP@MoS2 hetero-nanoframes with excellent hydrogen evolution performance. Materials and Design, 2021, 211, 110165.	3.3	10
62399	Impact of the segregation energy spectrum on the enthalpy and entropy of segregation. Acta Materialia, 2021, 221, 117393.	3.8	23
62400	Hybrid Electronic-density-functional/molecular-dynamics Simulation on Parallel Computers: Oxidation of Si Surface. Materials Research Society Symposia Proceedings, 2000, 653, 1.	0.1	0
62401	Ab-Initio Kinetics of Heterogeneous Catalysis: NO+N+O/Rh(111). Lecture Notes in Computer Science, 2001, , 531-540.	1.0	1
62402	Electronic Structure of Oxygen in Delitiated Litmo2 Studied by Electron Energy-Loss Spectrometry. , 2002, , 469-474.		0
62403	Long-Time-Scale Simulations of Al(100) Crystal Growth. , 2002, , 63-74.		0
62405	Large Scale Car-Parrinello Simulation of Fully Hydrated DNA. , 2003, , 207-216.		0
62406	Electronic Structure and Chemisorption Properties of Supported Metal Clusters. , 2003, , .		0
62409	Controlling Role of Electron Concentration in Plasma-Chemical Synthesis. NATO Science Series Series II, Mathematics, Physics and Chemistry, 2004, , 45-51.	0.1	0
62410	Atomic Resolution Electron Energy Loss Spectroscopy. , 2004, , 1-9.		0
62411	Computational Study of the Mechanical Properties of Alumina â€" Copper Interfaces: Ab Initio Calculations and Combination with Mesoscopic Simulations. Solid Mechanics and Its Applications, 2004, , 421-430.	0.1	0
62412	Study on Strength of Microscopic Material by Simulations with Atom and Electron Models. Solid Mechanics and Its Applications, 2004, , 391-399.	0.1	0
62413	Optimum designs of additional elements from first-principles simulations. Keikinzoku/Journal of Japan Institute of Light Metals, 2004, 54, 82-89.	0.1	24
62415	Evaluation of Structural and Mechanical Properties of Amorphous Silicon Surabaces by a Combination Approach of Ab-initio and Classical Molecular Dynamics. Zairyo/Journal of the Society of Materials Science, Japan, 2005, 54, 45-50.	0.1	1
62416	Coherent optical control of electronic excitations in functionalized semiconductor nanostructures. Quantum Information and Computation, 2005, 5, 318-334.	0.1	8
62417	Nonlinear Elasticity in Wurtzite GaN/AlN Planar Superlattices and Quantum Dots. Acta Physica Polonica A, 2005, 108, 749-754.	0.2	1

#	Article	IF	Citations
62418	Current and Force Spectroscopy. Nanoscience and Technology, 2006, , 221-257.	1.5	0
62419	Development of a Bond-Order Potential that can Reproduce the Elastic Constants and Melting Point of Silicon. Zairyo/Journal of the Society of Materials Science, Japan, 2006, 55, 1-7.	0.1	1
62420	A density-functional study of the structural, electronic, and vibrational properties of Ti8C12 metallocarbohedrynes with relevance to ultrafast time-resolved spectroscopy. , 2006, , 80-84.		1
62422	Magnetic Properties of _-CrCl2. , 2006, , 897-900.		0
62423	Global Optimization of 1- and 2-Dimensional Nanoscale Structures. , 2006, , 332-349.		0
62424	Photoexcitation Dynamics on the Nanoscale. Springer Series in Chemical Physics, 2007, , 5-30.	0.2	0
62425	Electronic Properties and Fragmentation Dynamics of Organic Species Deposited on Silicon Surfaces. Challenges and Advances in Computational Chemistry and Physics, 2007, , 505-532.	0.6	0
62426	A Study on the Prediction of the Material Properties of Magnesium Alloys Using Density Functional Theory Method. Korean Journal of Materials Research, 2007, 17, 637-641.	0.1	0
62427	SO2 Reaction on Cu(100): SO3 Structure and Formation â€“Density Functional Theory Investigationâ€“. Journal of the Physical Society of Japan, 2008, 77, 084601.	0.7	0
62428	Structural Evolution on Ag/Si(111) Ag/Si(111)âˆš3Xâˆš3 with Adatom Coverage. Applied Science and Convergence Technology, 2008, 17, 387-393.	0.3	0
62429	Structural Study of Tetragonal-Ni1-xPdxSi/Si (001) Using Density Functional Theory (DFT). Korean Journal of Materials Research, 2008, 18, 482-485.	0.1	1
62430	Defect Formation and Annihilation in Electronic Devices and the Role of Hydrogen. , 2008, , .		0
62431	Selected High-Impact Journal Articles on Defects in Microelectronic Materials and Devices. , 2008, , .		2
62433	Structural Study of Oxygen Vacancy in CaO Stabilized Cubic-HfO2Using Density Functional Theory. Korean Journal of Materials Research, 2008, 18, 673-677.	0.1	0
62434	Structural Study of Interface Layers in Tetragonal-HfO2/Si using Density Functional Theory. Applied Science and Convergence Technology, 2009, 18, 9-14.	0.3	0
62435	The Interior Structure, Composition, and Evolution ofÂGiant Planets. Space Sciences Series of ISSI, 2009, , 423-447.	0.0	0
62436	Effects of molecular adsorption on optical losses of silver surfaces. , 2009, , .		0
62437	Evaluation of Environmental Strength. Yosetsu Gakkai Shi/Journal of the Japan Welding Society, 2009, 78, 461-462.	0.0	0

#	Article	IF	Citations
62438	Indium Nanowire Growth on Si (001) Surface Using Density Functional Theory. Korean Journal of Materials Research, 2009, 19, 137-141.	0.1	2
62439	Magnetism of BN Nanotubes with Transition Metal Substitution. Journal of the Korean Magnetics Society, 2009, 19, 43-46.	0.0	0
62441	Interaction of DEMS with H-terminated Si (001) Surface: A First Principles Study. Journal of the Korean Ceramic Society, 2009, 46, 425-428.	1.1	0
62442	Theory of Native Point Defects and Impurities in InN. , 2009, , 419-444.		0
62443	Applications of Thin Film Oxides in Catalysis. , 2010, , 281-301.		0
62444	Transfer of Oxygen Vacancy and Proton in Y-doped BaZrO₃. Journal of the Korean Ceramic Society, 2009, 46, 695-699.	1.1	2
62445	Electronic Structure Methods Based on Density Functional Theory. , 2009, , 478-488.		0
62446	Structure transition of two-dimensional hexagonal BN under large uniaxial strain. Wuli Xuebao/Acta Physica Sinica, 2010, 59, 8820.	0.2	3
62447	Fist-principle calculation for electronic structure of Mâ€™-GdTaO4. Wuli Xuebao/Acta Physica Sinica, 2010, 59, 2836.	0.2	2
62448	Ab-initio Characterization of Colloidal IV-VI Semiconductor Quantum Dots. , 2010, , 61-73.		0
62449	Theory of HfO2-Based High-k Dielectric Gate Stacks. , 2010, , 51-92.		1
62450	Influence of Zr catalyst on reversible hydrogen storage characteristics of NaAlH4 and Na3AlH6. Wuli Xuebao/Acta Physica Sinica, 2010, 59, 4178.	0.2	3
62451	First-principles investigation on the phase transitions of BiFeO3. Wuli Xuebao/Acta Physica Sinica, 2010, 59, 8789.	0.2	1
62452	Multiple Approaches from Theoretical Simulations and High-Pressure Experiments to Determine Accurate Equation of State for Materials. Review of High Pressure Science and Technology/Koatsuryoku No Kagaku To Gijutsu, 2010, 20, 244-251.	0.1	0
62453	Antiferromagnetic Ordering in the Fe(001) Monolayer Mediated by the Ir Substrate. E-Journal of Surface Science and Nanotechnology, 2010, 8, 152-156.	0.1	0
62454	A first principle study on p-type doped 3C-SiC. Wuli Xuebao/Acta Physica Sinica, 2010, 59, 5652.	0.2	12
62455	First-principles calculation of structural stability and electronic properties of ZnO atomic chains. Wuli Xuebao/Acta Physica Sinica, 2010, 59, 2051.	0.2	3
62456	Antisite defect of LiFePO4: A first-principles study. Wuli Xuebao/Acta Physica Sinica, 2010, 59, 5135.	0.2	3

#	Article	IF	Citations
62457	First-principles study of the multilayer relaxation of Cu stepped surfaces. Wuli Xuebao/Acta Physica Sinica, 2010, 59, 4911.	0.2	1
62458	First-principles study on chemisorption of Cl on Î³-TiAl(111) surface. Wuli Xuebao/Acta Physica Sinica, 2010, 59, 7278.	0.2	9
62459	Evaluation of Proton Transfer in DNA Constituents: Development and Application of Ab Initio Based Reaction Kinetics. Challenges and Advances in Computational Chemistry and Physics, 2010, , 187-211.	0.6	0
62460	Interaction of Di-Methylaluminum Groups with Hydroxyl Groups on a Fully Hydroxyl-Terminated Si (001) Surface. Transactions on Electrical and Electronic Materials, 2010, 11, 11-14.	1.0	1
62461	Mg Atom Substitution for Nonstoichiometric Na⁺Î²-Alumina: A First Principles Study. Korean Journal of Materials Research, 2010, 20, 55-59.	0.1	0
62462	Development of Problem Solving Environment for Large Scale Electronic Structure Calculations Based on Tight Binding Method. Journal of Convergence Information Technology, 2010, 5, 195-203.	0.1	0
62463	Regular Distribution of -OH Fragments on a Si (001)-c(4Ã—2) Surface by Dissociation of Water Molecules. Korean Journal of Materials Research, 2010, 20, 457-462.	0.1	0
62464	Electron Subbands in Thin Silicon Films. Computational Microelectronics, 2011, , 131-167.	1.2	1
62465	Band Structure of Relaxed Silicon. Computational Microelectronics, 2011, , 45-62.	1.2	0
62466	Perturbative Methods for Band Structure Calculations in Silicon. Computational Microelectronics, 2011, , 63-81.	1.2	0
62467	Strain Effects on the Conduction Band of Silicon. Computational Microelectronics, 2011, , 105-121.	1.2	0
62468	Initial Reaction of Zn Precursors with Si (001) Surface for ZnO Thin-Film Growth. Korean Journal of Materials Research, 2010, 20, 463-466.	0.1	0
62470	Strain Effects on the Silicon Crystal Structure. Computational Microelectronics, 2011, , 83-90.	1.2	0
62472	Effect of Volume Variation on Energy Barrier for Proton Conduction in BaZrO3. Journal of the Korean Ceramic Society, 2010, 47, 474-478.	1.1	1
62473	Negative Differential Resistance of Oligo (Phenylene Ethynylene) Self-Assembled Monolayer Systems: The Electric Field Induced Conformational Change Mechanism. Springer Theses, 2011, , 9-26.	0.0	0
62475	Intercalation Voltage and Lithium Ion Conduction in Lithium Cobalt Oxide Cathode for Lithium Ion Battery. Journal of the Korean Electrochemical Society, 2010, 13, 290-294.	0.1	0
62476	First-principles calculations of magnetism of Fe atomic sheet. Wuli Xuebao/Acta Physica Sinica, 2011, 60, 047502.	0.2	3
62477	Pressure induced band-gap changes in (Ba0.5Sr0.5)TiO3 (BST) from first-principles calculations. Wuli Xuebao/Acta Physica Sinica, 2011, 60, 117309.	0.2	2

#	Article	IF	Citations
62478	Ab-initio Characterization of Electronic Properties of PbTe Quantum Dots Embedded in a CdTe Matrix. , 2011, , 135-147.		0
62479	Theoretical mechanical properties of silica glass. Transactions of the Materials Research Society of Japan, 2011, 36, 35-40.	0.2	0
62480	First-principles study on the electronic structures and structural stability of Cd-doped ZnO. Wuli Xuebao/Acta Physica Sinica, 2011, 60, 037101.	0.2	4
62481	Helicity effects on Rh adsorption behavior inside and outside the single-wall carbon nanotubes. Wuli Xuebao/Acta Physica Sinica, 2011, 60, 087102.	0.2	2
62482	Evaluation of the Oxygen Diffusion Coefficient in Nickel-Base Alloys. , 2011, , 1463-1475.		0
62483	Energies, electronic structures and magnetic properties of Ni atomic chain encapsulated in carbon nanotubes: a first-principles calculation. Wuli Xuebao/Acta Physica Sinica, 2011, 60, 078801.	0.2	2
62484	Predicting Mg Strength from First-Principles: Solid-Solution Strengthening, Softening, and Cross-Slip. , 2011, , 13-15.		0
62485	A first principles study of the lattice dynamics property of LiFePO4. Wuli Xuebao/Acta Physica Sinica, 2011, 60, 028201.	0.2	5
62486	The structural stability and electronic properties of monolayer BC2N. Wuli Xuebao/Acta Physica Sinica, 2011, 60, 127305.	0.2	0
62487	Recent Trends and Future Perspectives of Phase Diagram Calculations. Journal of MMIJ, 2011, 127, 473-478.	0.4	2
62488	Thermodynamic Database Integrated by Electron Theory and CALPHAD Modeling. Tetsu-To-Hagane/Journal of the Iron and Steel Institute of Japan, 2011, 97, 166-172.	0.1	1
62489	Electronic structure and magnetic propertiesof post-perovskite CaRhO3. Wuli Xuebao/Acta Physica Sinica, 2011, 60, 047107.	0.2	1
62490	Theorectical study of the oxide-ion conductorLa2Mo2-xMxO9(M=Cr,W). Wuli Xuebao/Acta Physica Sinica, 2011, 60, 046603.	0.2	2
62491	First-principles study of the electronic structure and electric conductivity in W-type hexagonal ferrite BaFe18O27. Wuli Xuebao/Acta Physica Sinica, 2011, 60, 107102.	0.2	2
62492	Organic-Metal Interface: Adsorption of Cysteine on Au(110) from First Principles. , 2011, , 119-134.		0
62493	Effect of Copper Oxide on Migration and Interaction of Protons in Barium Zirconate. Journal of the Korean Ceramic Society, 2011, 48, 195-199.	1.1	0
62495	Molecular and Electronic Tuning of Si/Carbon Nanotube Hybrid System. Japanese Journal of Applied Physics, 2011, 50, 045101.	0.8	0
62497	Multiscale Simulation of Nanostructured Materials and Systems. Japanese Journal of Applied Physics, 2011, 50, 05FE08.	0.8	0

#	Article	IF	Citations
62498	Structural and Elastic Properties of Wurtzite Al-Rich InxAl1 - xN Alloys. Acta Physica Polonica A, 2011, 119, 666-668.	0.2	0
62499	Structural Analysis of Nitride Phosphors. Series in Optics and Optoelectronics, 2011, , 203-261.	0.0	0
62500	First Principles Study of Si/Ge Core-Shell Nanowires ---- Structural and Electronic Properties. , 0, , .		2
62501	Electron Accumulation in LaAlO3/SrTiO3Interfaces by the Broken Symmetry of Crystal Field. Japanese Journal of Applied Physics, 2011, 50, 10PF03.	0.8	0
62503	Effect of Aluminum on Nitrogen Solubility in Zinc Oxide: Density Functional Theory. Korean Journal of Materials Research, 2011, 21, 639-643.	0.1	0
62504	Optical properties of N-doped Cu2O films and relevant analysis with first-principles calculations. Wuli Xuebao/Acta Physica Sinica, 2012, 61, 047104.	0.2	3
62505	First principles investigation of interaction between interstitials H atom and Nb metal. Wuli Xuebao/Acta Physica Sinica, 2012, 61, 047105.	0.2	6
62506	First principles calculations of the electronic structure and optical properties of pure and (Nb, N) co-doped anatase. Wuli Xuebao/Acta Physica Sinica, 2012, 61, 237107.	0.2	1
62507	A first principles study on Mn2NiGa Heusler alloy. Wuli Xuebao/Acta Physica Sinica, 2012, 61, 213102.	0.2	5
62508	The Standard ASW Method. Lecture Notes in Physics, 2012, , 5-44.	0.3	0
62509	Mechanical Properties of Carbon Nanotubes with One-Dimensional Intramolecular Junction. Zairyo/Journal of the Society of Materials Science, Japan, 2012, 61, 149-154.	0.1	0
62510	Conduction modulation of Ï€-stacked ethylbenzene wires on Si(100) with substituent groups. , 2012, , 37-44.		0
62511	First-principles study of nanoscale friction between graphenes. Wuli Xuebao/Acta Physica Sinica, 2012, 61, 106801.	0.2	5
62512	First-principles study of N-doped and N-V co-doped anatase TiO2. Wuli Xuebao/Acta Physica Sinica, 2012, 61, 207103.	0.2	3
62513	Electronic structures and optical properties of AAl2C4 (A=Zn, Cd, Hg; C=S, Se) semiconductors. Wuli Xuebao/Acta Physica Sinica, 2012, 61, 127103.	0.2	1
62514	Cysteine on Gold: An ab-initio Investigation. , 2012, , 105-117.		0
62515	Ab initio calculation of phase transitions, elastic, and thermodynamic properties of MnPd alloys. Wuli Xuebao/Acta Physica Sinica, 2012, 61, 246201.	0.2	1
62516	Geometric structures and nitrogen adsorption properties of BaO adlayer on Ru(0001) surface. Wuli Xuebao/Acta Physica Sinica, 2012, 61, 136802.	0.2	1

#	Article	IF	Citations
62517	Cluster separation phenomena in liquid Ga-In alloys. Wuli Xuebao/Acta Physica Sinica, 2012, 61, 036101.	0.2	3
62518	First-principles study on the sensitization of small molecule adsorbed on ZnO nanowire. Wuli Xuebao/Acta Physica Sinica, 2012, 61, 063103.	0.2	2
62519	First-principles analysis of properties of Cu surfaces. Wuli Xuebao/Acta Physica Sinica, 2012, 61, 016108.	0.2	5
62520	Structural and electronic properties of Al-doped spinel LiMn2O4. Wuli Xuebao/Acta Physica Sinica, 2012, 61, 187306.	0.2	1
62521	Density functional theory study on transparent conductive oxide CuScO2. Wuli Xuebao/Acta Physica Sinica, 2012, 61, 227401.	0.2	2
62522	Effects of oxygen vacancy on impurity distribution and exchange interaction in Co-doped TiO2. Wuli Xuebao/Acta Physica Sinica, 2012, 61, 027503.	0.2	1
62523	Stability of hydrogen in tungsten with carbon impurity: a first-principles study. Wuli Xuebao/Acta Physica Sinica, 2012, 61, 046104.	0.2	0
62524	First-principles study of lattice dynamic of IrTi alloy. Wuli Xuebao/Acta Physica Sinica, 2012, 61, 148105.	0.2	1
62525	Theoretical calculations of high-pressure melting curves of five metals. Wuli Xuebao/Acta Physica Sinica, 2012, 61, 016401.	0.2	0
62526	Strain effect on the intercalation potential of the layered Mn-contained lithium ion batteries cathode materials: a first principles method. Wuli Xuebao/Acta Physica Sinica, 2012, 61, 183101.	0.2	0
62527	First principles caculations of h-BN monolayer with group IA/IIA elements replacing B as impurities. Wuli Xuebao/Acta Physica Sinica, 2012, 61, 236301.	0.2	1
62528	Density functional study on the stability and electronic structure of single layer Si6H4Ph2. Wuli Xuebao/Acta Physica Sinica, 2012, 61, 246801.	0.2	0
62529	First-principles study of (InAs)1/(GaSb)1 superlattice atomic chains. Wuli Xuebao/Acta Physica Sinica, 2012, 61, 117104.	0.2	1
62530	4.3.2 Assessment and modeling of NH3SnO2 interactions using individual nanowire sensors. , 2012, , .		0
62531	Water adsorption on the Be(0001) surface: from monomer to trimer adsorption. Chinese Physics B, 2012, 21, 016802.	0.7	0
62532	Ab Initio Studies on the Hydrogenation at the Edges and Bulk of Graphene. Carbon Nanostructures, 2012, , 203-208.	0.1	0
62533	Nucleation, Structure and Magnetism of Transition Metal Clusters from First Principles. Nanoscience and Technology, 2012, , 77-98.	1.5	0
62534	Electronic structures and dielectric properties of BaCoxZn2-xFe16O27 from first principles. Wuli Xuebao/Acta Physica Sinica, 2012, 61, 207102.	0.2	0

#	Article	IF	Citations
62535	Oxygen adsorption on Nb(110) surface by first-principles calculation. Wuli Xuebao/Acta Physica Sinica, 2012, 61, 047101.	0.2	4
62536	Investigation of the doping failure induced by DB in the SiNWs using first principles method. Wuli Xuebao/Acta Physica Sinica, 2012, 61, 153102.	0.2	1
62537	First principles investigation of dynamic performance in the process of lithium intercalation into black phosphorus. Wuli Xuebao/Acta Physica Sinica, 2012, 61, 247101.	0.2	6
62540	Magnetic Properties of Iron on Strained Graphene: Density Functional Theory Study. Japanese Journal of Applied Physics, 2012, 51, 06FD13.	0.8	0
62542	Density Functional Analysis of the Spin Exchange Interactions in VOSb2O4. Bulletin of the Korean Chemical Society, 2012, 33, 2338-2340.	1.0	0
62543	From Superconductivity Towards Thermoelectricity: Ge-Based Skutterudites. NATO Science for Peace and Security Series B: Physics and Biophysics, 2013, , 115-127.	0.2	2
62544	Results for Various Interfaces: C $$_{60}$$, Benzene, TTF, TCNQ and Pentacene over Au(111). Springer Theses, 2013, , 115-158.	0.0	0
62545	- Gas Adsorption by Fullerenes and Polyhedral Multi-Walled Carbon Nanostructures. , 2012, , 177-202.		0
62546	Lithium Ion Batteries, Electrochemical Reactions in. , 2013, , 239-283.		0
62547	ENHANCEMENT OF GRAPHENE BINDING ENERGY BY Ti 1ML INTERCALATION BETWEEN GRAPHENE AND METAL SURFACES. , 2012, , .		0
62548	Analysis of the origin of lateral interactions in the adsorption of small organic molecules on oxide surfaces. Highlights in Theoretical Chemistry, 2014, , 177-183.	0.0	0
62549	First-principles study of structure and stability in Siâ€“Câ€“O-based materials. Highlights in Theoretical Chemistry, 2014, , 197-201.	0.0	0
62551	Thermodynamic Analysis of the Mg-Y-Zn Ternary System Using the Cluster Variation Method. , 2013, , 1183-1190.		1
62552	Theoretical study of adsorption of propanethiol on Au(111) surface at different coverages. Wuli Xuebao/Acta Physica Sinica, 2013, 62, 223101.	0.2	1
62553	First-principles study on cation-doped Lu2Si2O7. Wuli Xuebao/Acta Physica Sinica, 2013, 62, 147101.	0.2	0
62554	Structural phase transition of Ru at high pressure and temperature. Wuli Xuebao/Acta Physica Sinica, 2013, 62, 176402.	0.2	2
62555	Polarization Dependent Water Adsorption on the Lithium Niobate Z-Cut Surfaces. , 2013, , 155-166.		0
62556	Noncollinear magnetic order and spin-orbit coupling effect in (FeCr)n alloying clusters. Wuli Xuebao/Acta Physica Sinica, 2013, 62, 143601.	0.2	1

#	Article	IF	Citations
62557	Occupancy sites of uranium atom in goethite by first-principles calculation. Wuli Xuebao/Acta Physica Sinica, 2013, 62, 087101.	0.2	0
62558	First-principles study on the electronic and optical properties of the (Eu,N)-codoped anatase TiO2 photocatalyst. Wuli Xuebao/Acta Physica Sinica, 2013, 62, 193103.	0.2	1
62559	Crystal Structure Search based on Evolutionary Algorithm Combined with First-principles Calculation. IEEJ Transactions on Electronics, Information and Systems, 2013, 133, 2291-2296.	0.1	0
62560	Studies on electrical properties of graphene nanoribbons with pore defects. Wuli Xuebao/Acta Physica Sinica, 2013, 62, 057101.	0.2	2
62561	First-principles study of Ag-N dual-doped p-type ZnO. Wuli Xuebao/Acta Physica Sinica, 2013, 62, 167701.	0.2	1
62563	Powder X-Ray Structure Analysis with Density Functional Theory Calculations. Review of High Pressure Science and Technology/Koatsuryoku No Kagaku To Gijutsu, 2013, 23, 133-140.	0.1	0
62564	Stair Magnetism: Distinct Magnetic States of Co₅C₅ Carbide Isomers. Journal of Modern Physics, 2013, 04, 438-441.	0.3	0
62565	First-Principles Study for Phase Diagrams of Cdâ€“Ca and Cdâ€“Y Tsai-Type Approximants Under Pressure. , 2013, , 195-201.		1
62566	Dynamics of H2 Interacting with Substitutional Bimetallic Surface Alloys. Springer Series in Surface Sciences, 2013, , 131-155.	0.3	0
62567	Towards the Interfcae Level Understanding of Internally Oxidized Metal-Oxide Composites: Cu-Al2O3. , 2013, , 265-270.		0
62569	A Theoretical Research on B-N-H for Hydrogen Storage Properties. Advances in Condensed Matter Physics, 2013, 02, 79-87.	0.1	0
62570	Magnetic properties of multiferroic material DyMnO3 in orthorhombic structure. Wuli Xuebao/Acta Physica Sinica, 2013, 62, 227101.	0.2	0
62571	Influences of strain on electronic structure and magnetic properties of CoFe2O4 from first-principles study. Wuli Xuebao/Acta Physica Sinica, 2013, 62, 167502.	0.2	3
62573	Ab initio study of the bcc-to-hcp transition mechanism in Fe under pressure. Wuli Xuebao/Acta Physica Sinica, 2013, 62, 056401.	0.2	0
62576	Computation and Theory. , 2013, , 155-158.		0
62578	Towards the Interface Level Understanding of Internally Oxidized Metal-Oxide Composites: Cu-Al2O3. , 0, , 265-270.		0
62579	First-Principles Investigation of the Surface Properties of LiNiO₂as Cathode Material for Lithium-ion Batteries. Journal of the Korean Electrochemical Society, 2013, 16, 169-176.	0.1	1
62581	Î©-Phase Transformation in Ti3Al2Mo Alloy: A First-Principles Approach. , 0, , 429-433.		0

#	Article	IF	Citations
62582	The Application of Method of Exact MT-orbitals for Modelling of Thermodynamic and Mechanical Properties in Pure Components of Ti- and Zr-Based Alloys. Progress in Physics of Metals, 2013, 14, 319-352.	0.5	0
62583	Stress-diffusion Full Coupled Multiscale Simulation Method for Battery Electrode Design. Journal of the Computational Structural Engineering Institute of Korea, 2013, 26, 409-413.	0.1	0
62584	Electronic Structures and Optical Properties of the Oxygen-Deficient SrTiO₃ from First-Principles Calculation. Modern Physics, 2014, 04, 113-121.	0.1	0
62585	First-principles study of Ag2ZnSnS4 as a photocatalyst. Wuli Xuebao/Acta Physica Sinica, 2014, 63, 247101.	0.2	4
62586	Effect of Pd in NiTi on the martensitic transformation temperatures and hysteresis: a first-principles study. Wuli Xuebao/Acta Physica Sinica, 2014, 63, 233103.	0.2	5
62587	Anylasis and comparison of several methods for calculation of positron bulk lifetime in perfect crystals. Wuli Xuebao/Acta Physica Sinica, 2014, 63, 217804.	0.2	1
62588	Stacking effects in topological insulator Bi2Se3ï¼ša first-principles study. Wuli Xuebao/Acta Physica Sinica, 2014, 63, 187303.	0.2	0
62589	Computational Models of Thermodynamic Properties of Uranium Nitride. , 2014, , .		0
62590	Constrained non-collinear magnetism in disordered Fe and Fe-Cr alloys. , 2014, , .		0
62591	Predictive Engineering of Semiconductor-Oxide Interfaces. , 2014, , 45-61.		0
62592	Integration of Functional Oxides on SrTiO3/Si Pseudo-Substrates. , 2014, , 159-203.		0
62593	Investigation on the electrical properties of anatase and rutile Nb-doped TiO2 by GGA(+U). Wuli Xuebao/Acta Physica Sinica, 2014, 63, 157101.	0.2	0
62594	Investigation of Atomic-Scale Energetics on Liquid Metal Embrittlement of Aluminum due to Gallium. , 2014, , 1069-1076.		0
62595	Density functional study on the different behaviors of Pd and Pt coating on graphene. Wuli Xuebao/Acta Physica Sinica, 2014, 63, 176802.	0.2	1
62596	Research of the synergistic effects in Cu/N co-doped TiO2 surfaceï¼šA DFT calculation. Wuli Xuebao/Acta Physica Sinica, 2014, 63, 157102.	0.2	5
62597	Influence of N Doping on Electronic Properties of ZnO Surface. Advances in Condensed Matter Physics, 2014, 03, 46-52.	0.1	0
62598	A DFT sight of oxygen and carbon monoxide coadsorption on Pt-alloy surfaces. , 0, , .		0
62599	The Scanning Tunneling Microscopy of Adsorbed Molecules on Semiconductors: Some Theoretical Answers to the Experimental Observations. , 2014, , 1-44.		0

#	Article	IF	Citations
62600	Molecular dynamics study on the stability and properties of Î±-Cgeyne. Wuli Xuebao/Acta Physica Sinica, 2014, 63, 207303.	0.2	2
62601	Magnetic and electronic properties of fluorographene sheet with foreign atom substitutions. Wuli Xuebao/Acta Physica Sinica, 2014, 63, 046102.	0.2	5
62602	First-principles study of the lattice dynamics, dielectric and piezoelectric response in BaTiO3/SrTiO3 (1ï¼š1) superlattice. Wuli Xuebao/Acta Physica Sinica, 2014, 63, 126301.	0.2	1
62603	Effects of niobium on helium behaviors in tungsteniï¼ša first-principles investigation. Wuli Xuebao/Acta Physica Sinica, 2014, 63, 046103.	0.2	4
62604	Electronic and magnetic properties of fluorinated graphene sheets with divacancy substitutional doping. Wuli Xuebao/Acta Physica Sinica, 2014, 63, 186101.	0.2	4
62605	Chromium concentration effect on an alloy surface stability and oxidation initiation. , 2014, , .		0
62606	Mechanical properties of transition metals doped Moï¼ša first-principals study. Wuli Xuebao/Acta Physica Sinica, 2014, 63, 087102.	0.2	0
62607	Structural and electronic properties of hydrogenated bilayer boron nitride. Wuli Xuebao/Acta Physica Sinica, 2014, 63, 016801.	0.2	1
62608	Electronic Properties of Si and Ge Pure and Core-Shell Nanowires from First Principle Study. , 2014, , 51-83.		0
62609	Ag Incorporation on ZnO(10 0) Surface: First Principles Study. Applied Physics, 2014, 04, 155-161.	0.0	0
62610	First-principles study on p-type ZnO codoped with F and Na. Wuli Xuebao/Acta Physica Sinica, 2014, 63, 077101.	0.2	5
62613	Magnetism and Magnetocrystalline Anisotropy of CoFe Thin Films: A First-principles Study. Journal of the Korean Magnetics Society, 2014, 24, 35-40.	0.0	2
62614	DFT Study for Adsorption and Decomposition Mechanism of Trimethylene Oxide on Al(111) Surface. Bulletin of the Korean Chemical Society, 2014, 35, 2013-2018.	1.0	0
62615	- Polymer Electrolyte Membranes. , 2014, , 100-195.		0
62617	Electronic Structure and Chemical Bonding of Li1.1Nb0.9O2â^'y as a Negative Electrode Material for Lithium Secondary Batteries. , 2015, , 291-301.		0
62619	Surface Charge of Clean LiNbO3 Z-Cut Surfaces. , 2015, , 163-178.		0
62620	GaP/Si: Studying Semiconductor Growth Characteristics with Realistic Quantum-Chemical Models. , 2015, , 205-218.		0
62622	Study on the electronic structures and the optical absorption mechanism of In2O3 crystals. Wuli Xuebao/Acta Physica Sinica, 2015, 64, 193101.	0.2	0

#	Article	IF	Citations
62623	Tuning the electronic property of monolayer MoS2 adsorbed on metal Au substrate: a first-principles study. Wuli Xuebao/Acta Physica Sinica, 2015, 64, 187101.	0.2	1
62624	Molecular Dynamics Simulation: From â€œAb Initioâ€•to â€œCoarse Grainedâ€• , 2015, , 1-61.		0
62626	Pressure-induced structural transition and thermodynamic properties of NbSi2 from first-principles calculations. Wuli Xuebao/Acta Physica Sinica, 2015, 64, 087103.	0.2	2
62627	Atomic and electronic structures of silicene and germanene on GaAs(111). Wuli Xuebao/Acta Physica Sinica, 2015, 64, 186101.	0.2	5
62628	Multiscale Modelling of In Situ Oil Sands Upgrading with Molybdenum Carbide Nanoparticles. Challenges and Advances in Computational Chemistry and Physics, 2015, , 415-445.	0.6	2
62630	Isotropic and Uniaxial Strain Induced Band Modulation of PbTe. , 0, , .		0
62631	Hydrogen Storage in a Potential Well for Room-Temperature Applications. , 2015, , .		0
62632	First-principles study of effects of quantum confinement and strain on the electronic properties of GaSb nanowires. Wuli Xuebao/Acta Physica Sinica, 2015, 64, 227303.	0.2	3
62633	10.3 Introduction to surface phonons. , 2015, , 586-615.		0
62634	First-principles calculations of the diffusion behaviors of C, N and O atoms in V metal. Wuli Xuebao/Acta Physica Sinica, 2015, 64, 026602.	0.2	2
62635	Charge distribution of Li-doped few-layer MoS2 and comparison to graphene and BN. Wuli Xuebao/Acta Physica Sinica, 2015, 64, 087102.	0.2	0
62636	Phonon stability and magnetism of -Fe4N crystalline state alloys at high pressure. Wuli Xuebao/Acta Physica Sinica, 2015, 64, 156301.	0.2	0
62637	A fully quantum description of the free-energy in high pressure hydrogen. Wuli Xuebao/Acta Physica Sinica, 2015, 64, 183101.	0.2	0
62638	Modeled Catalytic Properties of MOF-Based Compounds. , 2015, , 517-551.		0
62639	Computational Modeling of Catalysis in Metalâ€“Organic Frameworks. , 2015, , 483-516.		0
62640	First-Principles Calculations and Thermodynamic Assessment of the Li-Rh and Tl-Tm Systems. International Journal of Materials Mechanics and Manufacturing, 2015, 4, 135-139.	0.2	0
62641	Domain Decomposition for Heterojunction Problems in Semiconductors. Lecture Notes in Computer Science, 2015, , 92-101.	1.0	2
62642	Density Functional Study of Oxygen Reduction Reaction on Oxygen Doped Graphene. , 0, , .		1

#	Article	IF	Citations
62643	Low energy phonon instabilities and magnetic abnormalities in ordered crystalline state alloys of Fe3Pt at high pressure. Wuli Xuebao/Acta Physica Sinica, 2015, 64, 146301.	0.2	0
62644	First-principles study of stability and electronic structure of N2H4 adsorption on NiFe(111) alloy surface. Wuli Xuebao/Acta Physica Sinica, 2015, 64, 203101.	0.2	1
62645	Material modeling for large scale and complex nanostructures: A semi-empirical Hamiltonian method. Wuli Xuebao/Acta Physica Sinica, 2015, 64, 187302.	0.2	0
62646	Establishment of the Elastic Property Database of Fe-base Alloys. , 0, , .		3
62647	Theoretical study on the influence of rare earth doping on the electronic structure and magnetic properties of cobalt ferrite. Wuli Xuebao/Acta Physica Sinica, 2015, 64, 037501.	0.2	5
62648	First-principles study of the electronic structure, magnetism, and spin-polarization in Heusler alloy Co2MnAl(100) surface. Wuli Xuebao/Acta Physica Sinica, 2015, 64, 147301.	0.2	0
62649	The catalytic effect of transition matel doped Al (111) surfaces for hydrogen splitting. Wuli Xuebao/Acta Physica Sinica, 2015, 64, 038801.	0.2	1
62650	Study of the equation of states for deuterium, helium, and their mixture. Wuli Xuebao/Acta Physica Sinica, 2015, 64, 094702.	0.2	2
62651	Novel properties of 5d transition metal oxides. Wuli Xuebao/Acta Physica Sinica, 2015, 64, 187201.	0.2	3
62652	Computational prediction of lattice defects in multinary compound semiconductors as photovoltaic materials. Wuli Xuebao/Acta Physica Sinica, 2015, 64, 186102.	0.2	3
62653	First Principles Study on Structural Stability of Belite. ACI Materials Journal, 2015, 112, .	0.3	3
62657	Magnetism and Magnetocrystalline Anisotropy of Ni/Fe(001) Surface: A First Principles Study. Journal of the Korean Magnetics Society, 2015, 25, 101-105.	0.0	1
62658	Magnetic Properties of Ni/BN/Co Trilayer Structure: A First Principles Study. Journal of Magnetics, 2015, 20, 201-206.	0.2	0
62660	Effect of H-Atom on Local Structure in Ni-Zr-NbAmorphous Alloy. Acta Physica Polonica A, 2015, 128, 709-713.	0.2	0
62664	Effects of surface regulation on monolayers SbAs and BiSb. Wuli Xuebao/Acta Physica Sinica, 2016, 65, 217101.	0.2	2
62665	Mechanisms on the GeH/ interactions in germanene/germanane bilayer for tuning band structures. Wuli Xuebao/Acta Physica Sinica, 2016, 65, 096801.	0.2	2
62666	Effect of Ga vacancy on the magnetism in GaN:Gd: First-principles calculation. Wuli Xuebao/Acta Physica Sinica, 2016, 65, 127102.	0.2	2
62667	Structural stability and elastic constants of precipitate phases of Mg-5%Al alloy with combined Ca and Sr addition from first-principles calculations. , 2016, , .		0

#	Article	IF	Citations
62668	First-principles calculations of second-order elastic constants and generalized-stacking-fault energy for GaAs. , 2016, , .		0
62669	Submonolayer Rare Earth Silicide Thin Films on the Si(111) Surface. , 2016, , 163-175.		0
62670	Magnesium Technology 2011. , 2016, , .		1
62671	First-principle study of the optical absorption spectra of chalcogen on D-A and D–A copolymers. Wuli Xuebao/Acta Physica Sinica, 2016, 65, 103101.	0.2	1
62672	Effects of point defect concentrations on elastic properties of off-stoichiometric L12-type A13Sc. Wuli Xuebao/Acta Physica Sinica, 2016, 65, 076101.	0.2	4
62673	First-principle studies of the electronic structures and optical properties of diamond crystal co-doped with B and N. Wuli Xuebao/Acta Physica Sinica, 2016, 65, 087101.	0.2	2
62674	Preparation and characterization of orthorhombic Fe2(MoO4)3 and first-principle study of its negative thermal expansion properties. Wuli Xuebao/Acta Physica Sinica, 2016, 65, 056501.	0.2	0
62675	Electronic Structure and XANES Calculations of Silicate Compounds. Journal of Computer Chemistry Japan, 2016, 15, 211-212.	0.0	0
62676	Quantum States of the Hydrogen Isotope in Solid Materialsand on Their Surfaces. Journal of Computer Chemistry Japan, 2016, 15, 124-135.	0.0	1
62677	High Performance Thin-Film Transistors Based on Zinc Oxynitride Semiconductors: Experimental and First-Principles Studies. Korean Journal of Materials Research, 2016, 26, 42-46.	0.1	0
62678	Novel compounds in the hafnium nitride system: first principle study of their crystal structures and mechanical properties. Wuli Xuebao/Acta Physica Sinica, 2016, 65, 118102.	0.2	2
62679	First-principles study on multiphase property and phase transition of monolayer MoS2. Wuli Xuebao/Acta Physica Sinica, 2016, 65, 127101.	0.2	0
62680	First-principle study of the oxygen adsorption on Zr surface with Nb or Ge. Wuli Xuebao/Acta Physica Sinica, 2016, 65, 096802.	0.2	0
62681	First-principles study on the structure stability and doping performance of double layer h-BN/Graphene. Wuli Xuebao/Acta Physica Sinica, 2016, 65, 136101.	0.2	1
62682	Effect of Strain on the Physical Properties of Lanthanum Nickelate. , 2016, , 247-252.		0
62683	Growth, Structural and Electronic Properties of Functional Semiconductors Studied by First Principles. , 2016, , 145-162.		0
62684	Electronic structure and magnetic properties of MnTe from first-principles calculations. Wuli Xuebao/Acta Physica Sinica, 2016, 65, 066101.	0.2	1
62685	First-principles study of the electronic properties and magnetism of LaMnO3/SrTiO3 heterointerface with the different component thickness ratios. Wuli Xuebao/Acta Physica Sinica, 2016, 65, 077301.	0.2	2

#	Article	IF	Citations
62686	Electronic State and Structure of Carbonate in Aqueous Solution by Soft X-ray Spectroscopy. Journal of Computer Chemistry Japan, 2016, 15, 53-54.	0.0	0
62687	Portable SIMD Performance with OpenMP* 4.x Compiler Directives. Lecture Notes in Computer Science, 2016, , 264-277.	1.0	6
62688	Fundamental Structural, Electronic, and Chemical Properties of Carbon Nanostructures: Graphene, Fullerenes, Carbon Nanotubes, and Their Derivatives. , 2016, , 1-84.		0
62689	Theoretical studies of the site preference, electronic and lattice vibration properties of La3Co29-xFexSi4B10. Wuli Xuebao/Acta Physica Sinica, 2016, 65, 057103.	0.2	1
62690	Electronic and Optical Properties of Oxides Nanostructures by First-Principles Approaches. , 2016, , 1071-1084.		0
62691	First-principles Study of Diffusion Coefficients of Alloy Elements in Dilute Mg Alloys. , 2016, , 97-101.		0
62692	Atomic scale piezoelectricity and giant piezoelectric resistance effect in gallium nitride tunnel junctions under compressive strain. Wuli Xuebao/Acta Physica Sinica, 2016, 65, 107701.	0.2	1
62693	The first-principles study on the interaction of Ni with the yttria-stabilized zirconia and the activity of the interface. Wuli Xuebao/Acta Physica Sinica, 2016, 65, 068201.	0.2	0
62694	Theoretical Study of Hydrogen Bonds in Water Nanodroplet on Graphene. Journal of Computer Chemistry Japan, 2016, 15, 85-86.	0.0	0
62695	Comparative Study of the Adsorption of O2 on Al (110) Surface in Different Coverage. International Journal of Material and Mechanical Engineering, 2016, 5, 48.	0.5	0
62696	X-ray Absorption Spectroscopy Studies on Materials Obtained by the Sol-Gel Route. , 2016, , 1-25.		0
62697	Oxygen Reduction Reaction on sulfur doped graphene by density functional study: Oxygen Reduction Reaction on sulfur doped graphene by density functional study. , 2016, , 647-651.		0
62698	Nanocluster-Assembled Materials. , 2016, , 127-162.		0
62699	Na-Ion Anode Based on Na(Li,Ti)O2 System: Effects of Mg Addition. Journal of the Korean Ceramic Society, 2016, 53, 282-287.	1.1	0
62700	First-principles Calculations on Magnetism of 1H/1T Boundary in Monolayer MoS2. Journal of the Korean Magnetics Society, 2016, 26, 71-75.	0.0	0
62701	Optimization problems of nanoscale semiconductor heterostructures. Izvestiya Vysshikh Uchebnykh Zavedenii Materialy Elektronnoi Tekhniki = Materials of Electronics Engineering, 2016, 19, 108-114.	0.1	4
62703	Density Functional Investigation of the Inclusion of Gold Clusters on a CH₃S Self-Assembled Lattice on Au(111). Advances in Chemistry, 2016, 2016, 1-8.	1.1	1
62705	(Ga,Mn)As-Based Magnetic Tunnel Junctions under Electric Field from First Principles. Acta Physica Polonica A, 2016, 130, 1385-1388.	0.2	0

#	Article	IF	Citations
62706	Intrinsic Conductivity in Magnesium-Oxygen Battery Discharge Products: MgO and MgO2. ECS Meeting Abstracts, 2017, , .	0.0	0
62707	First-principle study of effect of asymmetric biaxial tensile strain on band structure of Germanium. Wuli Xuebao/Acta Physica Sinica, 2017, 66, 167101.	0.2	0
62708	Effect of Sr doping on electronic structure of La1-xSrxMnO3/LaAlO3/SrTiO3 heterointerface. Wuli Xuebao/Acta Physica Sinica, 2017, 66, 187301.	0.2	0
62709	Structural and electronic properties of T-graphene and its derivatives. Wuli Xuebao/Acta Physica Sinica, 2017, 66, 166101.	0.2	0
62711	Tunneling Transport Between Transition Metal Dichalcogenides. Springer Theses, 2017, , 49-64.	0.0	0
62712	Theoretical Modelling Methods. Springer Theses, 2017, , 37-66.	0.0	0
62713	Scale Bridging Simulations of Large Elastic Deformations and Bainitic Transformations. Lecture Notes in Computer Science, 2017, , 125-138.	1.0	0
62714	Methodology of Quantum Mechanics/Atomic Simulations. Nanostructure Science and Technology, 2017, , 5-34.	0.1	0
62715	The Nature of Electron Transport and Visible Light Absorption in Strontium Niobateâ€"A Plasmonic Water Splitter. Springer Theses, 2017, , 41-62.	0.0	0
62716	Towards Bridging the Data Exchange Gap Between Atomistic Simulation and Larger Scale Models. Minerals, Metals and Materials Series, 2017, , 45-55.	0.3	0
62717	First-principles investigation of oxygen diffusion mechanism in -titanium crystals. Wuli Xuebao/Acta Physica Sinica, 2017, 66, 116601.	0.2	1
62718	Vertical-Strain Effect on the Band Structures of Sr(Ti_{0.875}Fe_{0.125})O₃ Epitaxial Thin Films. Applied Physics, 2017, 07, 77-83.	0.0	0
62719	Vibration Spectrum Calculation Method for Solid Organic Crystals by Spectral Analysis Method. Journal of Computer Chemistry Japan, 2017, 16, 108-109.	0.0	0
62720	Electronic Properties of a Single Dangling Bond and of Dangling Bond Wires on a Si(001):H Surface. Advances in Atom and Single Molecule Machines, 2017, , 105-120.	0.0	0
62721	Atomic-Scale Modeling of Fe-Al-Mn-C Alloy Using Pair Models and Monte-Carlo Calculations. Minerals, Metals and Materials Series, 2017, , 393-401.	0.3	0
62722	Band Engineering of the Si(001):H Surface by Doping with P and B Atoms. Advances in Atom and Single Molecule Machines, 2017, , 95-104.	0.0	0
62723	Nano Simulation Study of Mechanical Property Parameter for Microstructure-Based Multiscale Simulation. Minerals, Metals and Materials Series, 2017, , 327-332.	0.3	0
62724	Theoretical study of the equation of state for warm dense matter. Wuli Xuebao/Acta Physica Sinica, 2017, 66, 036401.	0.2	2

#	Article	IF	Citations
62725	Surface modification in Cu-Ag codoped TiO2: the first-principle calculation. Wuli Xuebao/Acta Physica Sinica, 2017, 66, 117101.	0.2	0
62726	First-principles Study on the Slip Behavior of Magnesium Alloys. Materia Japan, 2017, 56, 480-483.	0.1	0
62727	Effect of surface passivation on the electronic properties of GaAs nanowire:A first-principle study. Wuli Xuebao/Acta Physica Sinica, 2017, 66, 197302.	0.2	1
62728	Experimental and Theoretical Methods. Springer Theses, 2017, , 31-43.	0.0	0
62729	Informatics-Based Approaches for Accelerated Discovery of Functional Materials. , 2017, , 153-184.		0
62730	Thickness Characterization of Tungsten Diselenide Using Electron Reflectivity Oscillations. Springer Theses, 2017, , 31-47.	0.0	0
62731	The Thermodynamic Approach in Thermoelectric Materials. SpringerBriefs in Materials, 2017, , 17-33.	0.1	0
62732	Transport Properties of Liquid Aluminum at High Pressure from Quantum Molecular Dynamics Simulations. Lecture Notes in Computer Science, 2017, , 787-795.	1.0	1
62733	Principles and Methods. Springer Theses, 2017, , 29-49.	0.0	0
62734	MODELS OF MOLECULAR DYNAMICS: A REVIEW OF EAM POTENTIALS. PART 1: POTENTIALS FOR SINGLE-COMPONENT SYSTEMS. PNRPU Mechanics Bulletin, 2017, , .	0.1	1
62735	First Principles Computational Study of Surface Reactions Toward Design Concepts of High Functional Electrocatalysts for Oxygen Reduction Reaction in a Fuel Cell System. Journal of the Korean Institute of Surface Engineering, 2017, 50, 1-9.	0.1	0
62736	The SrLiAl3N4:Eu2+ Phosphor Synthesized by the Raw Material Model Obtained by DFT Calculations. Journal of the Korean Ceramic Society, 2017, 54, 217-221.	1.1	0
62737	BasÄ±nÃ§ altÄ±nda Î± -PbO2 fazÄ±ndaki SnO2â€™nÄ±n yapÄ±sal ve dinamik Ã¶zelliklerinin araÅŸtÄ±rÄ±lmasÄ±. Sakarya University Journal of Science, 2017, 21, 1-1.	0.3	0
62738	Lattice softening in body-centered-cubic lithium-magnesium alloys. Physical Review Materials, 2017, 1, .	0.9	0
62739	Propiedades piezoelÃ©ctricas del PentÃ³xido de Niobio y PentÃ³xido de Tantalio. Tecno LÃ³gicas, 2017, 20, 43-51.	0.1	0
62740	Influence of Alloying Elements and Effect of Stress on Anisotropic Hydrogen Diffusion in Zr-Based Alloys Predicted by Accelerated Kinetic Monte Carlo Simulations. Minerals, Metals and Materials Series, 2019, , 1815-1826.	0.3	2
62741	High pressure study of structural, electronic, elastic, and vibrational properties of NaNb3O8. Journal of Alloys and Compounds, 2017, 725, 773-782.	2.8	3
62742	Selection of an Appropriate Basis Set for Accurate Description of Binding Energy: A First Principles Study. Journal of Natural and Applied Sciences, 2017, 21, 847.	0.1	0

#	Article	IF	Citations
62743	Ab Initio Study of Magnetism in Nonmetal Adsorption on Arsenene Monolayer. Journal of Superconductivity and Novel Magnetism, 2018, 31, 2221-2225.	0.8	1
62744	A 'Fluid' Nickel-Based Ferrite as an Efficient Redox Material for Thermochemical Two-Step CO ₂ Splitting. SSRN Electronic Journal, 0, , .	0.4	0
62745	First Principles Calculations. Springer Theses, 2018, , 41-73.	0.0	0
62746	First-principles study on Jahn-Teller effect in Cr monolayer film. Wuli Xuebao/Acta Physica Sinica, 2018, 67, 237301.	0.2	2
62747	First principle study on atomic structure of La65X35(X=Ni, Al) metallic glasses. Wuli Xuebao/Acta Physica Sinica, 2018, 67, 178101.	0.2	2
62748	Theoretical study on magnetoelectric effect in multiferroic tetragonal BiMnO3. Wuli Xuebao/Acta Physica Sinica, 2018, 67, 157511.	0.2	1
62749	Intergrading effect of investigation of Carbon monoxide adsorbing on Al-doped SiC(001) Surface. , 2018, , .		0
62750	Hydrohalic acid interaction with copper surfaces: XRD of chloride, bromide, and iodide on Cu(100). , 2018, , 826-831.		0
62751	Future. Springer Series in Surface Sciences, 2018, , 549-562.	0.3	0
62752	Tuning the electronic and magnetic property of semihydrogenated graphene and monolayer boron nitride heterostructure. Wuli Xuebao/Acta Physica Sinica, 2018, 67, 167101.	0.2	2
62753	Effect of electrode position and cross section size on transport properties of molecular devices. Wuli Xuebao/Acta Physica Sinica, 2018, 67, 213101.	0.2	1
62754	First-principles study of H, Cl and F passivation for Cu2ZnSnS4(112) surface states. Wuli Xuebao/Acta Physica Sinica, 2018, 67, 166401.	0.2	0
62755	X-ray Absorption Spectroscopy Studies on Materials Obtained by the Sol-Gel Route. , 2018, , 1231-1255.		0
62756	Theoretical Methods of Surface Dynamics. Springer Series in Surface Sciences, 2018, , 117-142.	0.3	0
62757	The First-Principles Investigation on Adsorption Mechanism of Pb(II) on the Kaolinite (001) Surface. Material Sciences, 2018, 08, 45-52.	0.0	0
62758	Tuning Electronic Transport in WSe2-Graphene. Springer Theses, 2018, , 103-112.	0.0	0
62759	Submolecular-Resolution Imaging of Interfacial Water. Springer Theses, 2018, , 43-71.	0.0	0
62760	Understanding Irradiation Growth through Atomistic Simulations: Defect Diffusion and Clustering in Î±-Zirconium and the Influence of Alloying Elements. , 2018, , 645-675.		0

#	Article	IF	Citations
62761	Development of Hybrid Method Using <i>Ab initio</i> and Classical Molecular Dynamics for Calculating the Thermal Expansion Coefficient of Alloys at High Temperature. Zairyo/Journal of the Society of Materials Science, Japan, 2018, 67, 197-201.	0.1	0
62763	Interlayer Exchange Coupling in Nb/Fe Multilayers. Acta Physica Polonica A, 2018, 133, 605-608.	0.2	0
62765	Modification of Exchange Coupling in Fe/Nb/Fe/Pd Layered Structures using Hydrogen. Acta Physica Polonica A, 2018, 133, 609-612.	0.2	0
62766	Interlayer Exchange Coupling and Proximity Effect in V-Fe Multilayers. Acta Physica Polonica A, 2018, 133, 597-600.	0.2	0
62769	Epitaxial growth of Al9Ir2 intermetallic compound on Al(100): Mechanism and interface structure. Physical Review Materials, 2018, 2, .	0.9	1
62771	Density Functional Theory Study of Separated Adsorption of O₂ and CO on Pt@X(X = Pd,) Tj ETQq1 1 0.784314 rgBT /O	0.1	0
62772	Pair interaction energies and local structures of titanium and nickel atom-pairs in Î²-Sn type silicon. Intermetallics, 2018, 97, 71-76.	1.8	0
62773	First-Principles Calculations of Ionic Conduction in Olivine-Type Li_xFePO₄. Materials Transactions, 2018, 59, 1062-1067.	0.4	2
62774	Electro-chemo-mechanical effects of lithium incorporation in zirconium oxide. Physical Review Materials, 2018, 2, .	0.9	0
62775	First-Principles Modelling of N-Doped Co₃O₄. Latvian Journal of Physics and Technical Sciences, 2018, 55, 36-42.	0.4	1
62776	Nanotechnology approach in macro- and nanostructures. , 2018, , .		0
62777	Reduction in surface state defects in iron pyrite by use of zinc sulfide passivation layers. Optical Materials Express, 2018, 8, 3835.	1.6	4
62778	Electronic Structures and Li Migration in Cubic Nickel Nitrides Intercalation compounds : From First Principles Studies. International Journal of Electrochemical Science, 0, , 12062-12071.	0.5	0
62780	First principles study of structural, electric, and magnetic properties of fluoride perovskite NaFeF₃. Wuli Xuebao/Acta Physica Sinica, 2019, 68, 147101.	0.2	0
62781	First-principles prediction of carbon monoxide nanotube bundles in low pressure phase. Wuli Xuebao/Acta Physica Sinica, 2019, 68, 217101.	0.2	0
62782	NO-CO Reaction Over Metal-supported Ultrathin Oxide Films: Evaluating Novel Catalysts by Density-functional Theory Calculations. Journal of Computer Chemistry Japan, 2019, 18, 1-8.	0.0	0
62783	Theoretical Analysis of NO-CO Reaction Involving Lattice Oxygen. Journal of Computer Chemistry Japan, 2019, 18, 139-141.	0.0	0
62784	First-principles study of rare-earth-doped cathode materials Li₂MnO₃ in Li-ion batteries. Wuli Xuebao/Acta Physica Sinica, 2019, 68, 138201.	0.2	4

#	Article	IF	Citations
62785	Theoretical calculations of stabilities and properties of transition metal borocarbides TM₃B₃C and TM₄B₃C₂ compound. Wuli Xuebao/Acta Physica Sinica, 2019, 68, 096201.	0.2	0
62786	Investigating the Nature of the Active Sites for the CO ₂ Reduction Reaction on Carbon-Based Electrocatalysts. SSRN Electronic Journal, 0, , .	0.4	0
62787	Atomistic Simulations of Hydrogen Effects on Lattice Defects in Alpha Iron. , 2019, , 283-300.		4
62789	The first-principle study on the formation energies of Be, Mg and Mn doped CuInO₂. Wuli Xuebao/Acta Physica Sinica, 2019, 68, 106102.	0.2	2
62790	Thermoelectric Oxide Materials for Energy Conversion. Inorganic Materials Series, 2019, , 188-245.	0.5	0
62791	First-principles study of five isomers of two-dimensional GeSe under in-plane strain. Wuli Xuebao/Acta Physica Sinica, 2019, 68, 113103.	0.2	5
62792	First-principles study of reduction mechanism of oxygen molecule using nitrogen doped graphene as cathode material for lithium air batteries. Wuli Xuebao/Acta Physica Sinica, 2019, 68, 128801.	0.2	3
62793	Importance of Atomic-Like Basis Set Optimization for DFT Modelling of Nanomaterials. Bulletin of the South Ural State University Series Mathematics Mechanics Physics, 2019, 11, 44-50.	0.2	1
62794	Excitonic Character of CDW in TiSe2. Springer Theses, 2019, , 15-29.	0.0	0
62795	FIRST-PRINCIPLES INVESTIGATIONS OF REFERENCE STATES OF Co2CrIn HEUSLER ALLOYS. Bulletin of the South Ural State University Series Mathematics Mechanics Physics, 2019, 11, 59-66.	0.2	0
62796	Synergistic O²⁻/Li⁺ Dual Ion Transportation at Atomic Scale. Research, 2019, 2019, 1-8.	2.8	3
62797	First-principles study of effects of Ga, Ge and As doping on electrochemical properties and electronic structure of Li₂CoSiO₄ serving as cathode material for Li-ion batteries. Wuli Xuebao/Acta Physica Sinica, 2019, 68, 187101.	0.2	1
62798	Theoretical study of density functional of confined CO oxidation reaction between bilayer graphene. Wuli Xuebao/Acta Physica Sinica, 2019, 68, 218101.	0.2	0
62799	First-principles study on the diffusion dynamics of Al atoms on Si surface. Wuli Xuebao/Acta Physica Sinica, 2019, 68, 207302.	0.2	4
62800	High-pressure structure prediction and high-temperature structural stability of periclase. Wuli Xuebao/Acta Physica Sinica, 2019, 68, 126201.	0.2	1
62802	Multiscale Simulation of Precipitation in Copper-Alloyed Pipeline Steels and in Cu-Ni-Si Alloys. , 2019, , 241-281.		1
62803	Possible High- $$T_c$$ T c Superconductivity in â€œHidden Ladderâ€•Materials. Springer Theses, 2019, , 91-111.	0.0	0
62804	Modelling of Rhombohedral Magnetostriction in Fe-Ga Alloys. Bulletin of the South Ural State University, Series: Mathematical Modelling, Programming and Computer Software, 2019, 12, 158-165.	0.1	1

#	Article	IF	Citations
62805	Developments of Interorbitalâ€“band Interaction Analysis and Embedded Cluster Model Incorporating Periodic Electrostatic Potential for Supported Metal Catalysts. Journal of Computer Chemistry Japan, 2019, 18, 49-63.	0.0	0
62806	First-Principles Study on Magnetism and Electronic Structures of Slater Insulators. Advances in Condensed Matter Physics, 2019, 08, 8-15.	0.1	0
62807	The Self-Passivation Mechanism in Degradation of BiVO ₄ Photoanode. SSRN Electronic Journal, 0, , .	0.4	0
62808	Effects of Added Cr and Ni on the Resistance of Î±-Iron Surface to Cl2 Gas Corrosion. Journal of Korean Institute of Metals and Materials, 2019, 57, 108-114.	0.4	1
62809	Characterizing modulated structures with first-principles calculations: a unified superspace scheme of ordering in mullite. Acta Crystallographica Section A: Foundations and Advances, 2019, 75, 260-272.	0.0	1
62810	Effect of mechanical deformations on absorption spectrum of metallic films of nanometer thickness. , 2019, , .		0
62811	BiTel Kristalinde Spin-YÃ¶rÃ¼nge YarÄ±lmasÄ±nÄ±n Gerinim ile DeÄŸiÅŸimi. Bitlis Eren Ãœniversitesi Fen Bilimleri Dergisi, 2019, 8, 19-25.	0.1	0
62812	Tunability of Electronic Properties and Magnetic Behaviour of Nickel Oxide: A Review. Current Nanoscience, 2019, 15, 354-370.	0.7	2
62814	Phase stability of two-dimensional monolayer <mml:math xmlns:mml="http://www.w3.org/1998/Math/MathML"><mml:mrow><mml:msub><mml:mi>As</mml:mi><mml:mrow><mml:mn>1</mml:mn></mml:mrow></mml:msub><mml:mo>+</mml:mo><mml:msub><mml:mi mathvariant="normal">P</mml:mi><mml:mi>x</mml:mi></mml:msub></mml:mrow></mml:math> solid solutions revealed by a first-principles cluster expansion. Physical Review Materials, 2019, 3, .	0.9	2
62815	First-principles study of metal-graphene edge contact for ballistic Josephson junction. Physical Review Materials, 2019, 3, .	0.9	0
62816	Theoretical Study of Metal Atom Adsorption States on Graphene. Vacuum and Surface Science, 2019, 62, 344-349.	0.0	1
62817	Point Defects in Non-metallic Materials from First Principles. Materia Japan, 2019, 58, 320-327.	0.1	0
62819	First-principles screening of ABO3 oxides with two magnetic sublattices. Physical Review Materials, 2019, 3, .	0.9	0
62821	Defect chemistry of Eu dopants in NaI scintillators studied by atomically resolved force microscopy. Physical Review Materials, 2019, 3, .	0.9	0
62822	Thermopower of the electron-doped manganese pnictide LaMnAsO. Physical Review Materials, 2019, 3, .	0.9	1
62823	Origin of dynamical instabilities in some simulated two-dimensional materials: GaSe as a case study. Physical Review Materials, 2019, 3, .	0.9	8
62824	First-principles Study on Formation of LPSO Structures for Ternary Alloys Revisited from Short-range Order. Transactions of the Materials Research Society of Japan, 2019, 44, 149-152.	0.2	0
62825	Ab initio determination of atomic structure of Znâ€“Zr precipitates in a Mgâ€“Ndâ€“Znâ€“Zr alloy. Acta Crystallographica Section B: Structural Science, Crystal Engineering and Materials, 2019, 75, 564-569.	0.5	3

#	Article	IF	Citations
62826	First-principles calculations of phase stability in magnesium based alloy. Keikinzoku/Journal of Japan Institute of Light Metals, 2019, 69, 447-454.	0.1	0
62827	Controlling factors for alignment of solute clusters in magnesium alloys: A first-principles analysis. Keikinzoku/Journal of Japan Institute of Light Metals, 2019, 69, 471-478.	0.1	0
62828	Investigation on origin of Ru-induced deep-level defects in 4H-SiC epilayer based Schottky diodes by DLTS and theoretical calculations. , 2019, , .		1
62829	Strain-gated infrared photodetector based on helical graphene nanoribbon. Physical Review Materials, 2019, 3, .	0.9	0
62830	Synthesis, characterization and crystal structure of a novel tetranuclear Co(II) cubane cluster. European Journal of Chemistry, 2019, 10, 256-262.	0.3	0
62831	Electron accumulation and charge neutrality level at the Eu/EuO interface. Physical Review Materials, 2019, 3, .	0.9	0
62832	First-principles study of the single- and double-walled nanotubes of TiO2. , 2019, , .		0
62833	Dimensionally driven crossover from semimetal to direct semiconductor in layered SbAs. Physical Review Materials, 2019, 3, .	0.9	1
62834	Simulation Studies for Black Phosphorus: From Theory to Experiment. Engineering Materials, 2020, , 101-115.	0.3	0
62835	Asymmetric valley polarization and photoluminescence in MoS₂/MoO₃ heterostructure. Optics Express, 2019, 27, 38451.	1.7	2
62836	Enhanced Reaction of Renewable Hydrogen Energy Production Using Platinum-based Nanoclusters. Daehan Hwan'gyeong Gonghag Hoeji, 2019, 41, 686-694.	0.4	1
62838	Ti interstitial flows giving rutile TiO2 reoxidation process enhancement in (001) surface. Physical Review Materials, 2019, 3, .	0.9	7
62839	Activated layered magnetism from bulk TiN. Physical Review Materials, 2019, 3, .	0.9	0
62840	<mml:math xmlns:mml="http://www.w3.org/1998/Math/MathML"><mml:mrow><mml:mi mathvariant="normal">S</mml:mi><mml:msub><mml:mi mathvariant="normal">b</mml:mi><mml:mn>2</mml:mn></mml:msub><mml:mi mathvariant="normal">S</mml:mi><mml:msub><mml:mi mathvariant="normal">e</mml:mi><mml:mn>3</mml:mn></mml:msub><mml:mo>(</mml:mo><mml:mn>100</mml:mn><mml:mo> : A strongly anisotropic surface. Physical Review Materials, 2019, 3, .	0.9	1
62841	Density Functional Theory Calculations Applied to Nuclear Fuels. , 2020, , 2121-2140.		0
62842	Observing quantum trapping on MoS₂ through the lifetimes of resonant electrons: revealing the Pauli exclusion principle. Nanoscale Advances, 2020, 2, 5848-5856.	2.2	4
62843	Accurate determination of quasi-particle electronic and optical spectra of anatase titanium dioxide. AIP Conference Proceedings, 2020, , .	0.3	0
62844	Origin of the enhanced photocatalytic activity of (Ni, Se, and B) mono- and co-doped anatase TiO2 materials under visible light: a hybrid DFT study. RSC Advances, 2020, 10, 43092-43102.	1.7	7

#	Article	IF	Citations
62845	Natural Topological Insulator Heterostructures. Springer Handbooks, 2020, , 449-470.	0.3	0
62846	Hafnene on Ir(111). Springer Theses, 2020, , 37-46.	0.0	0
62847	Neon diffusion in goethite, Î±-FeO(OH): a theoretical multi-scale study. Physics and Chemistry of Minerals, 2020, 47, 1.	0.3	9
62848	Interplanar stiffness in defect-free monocrystalline graphite. Physical Review Materials, 2020, 4, .	0.9	7
62849	First-Principles Research on Adsorption of NOx on Pt Cluster and BaO Cluster Supported by Î³-Al2O3 (110) Surface. , 0, , .		0
62850	First principles study of liquid uranium at temperatures up to 2050 K. Journal of Physics Condensed Matter, 2020, 32, 304001.	0.7	1
62851	First-Principles Investigations on Magnetic and Optical Properties of Transition-Metal Dopants in Î²-SnSe. Journal of Superconductivity and Novel Magnetism, 2020, 33, 2801-2807.	0.8	3
62852	Intrinsic adsorption behaviour related to the structural and mechanical properties of flexible metal-organic frameworks Co(bdp). Computational Materials Science, 2020, 177, 109543.	1.4	3
62853	Theoretical Investigation of Water Adsorption Chemistry of CeO₂(111) Surfaces by Density Functional Theory. Korean Journal of Materials Research, 2020, 30, 267-271.	0.1	1
62855	Study on the reaction mechanism of acetylene selective hydrogenation catalysts Pd-Ag/Al₂O₃. Inorganic and Nano-Metal Chemistry, 2021, 51, 70-77.	0.9	6
62857	Theoretical design of tetragonal rare-earth-free alloys with high magnetisation and high magnetic anisotropy. Japanese Journal of Applied Physics, 2020, 59, 055506.	0.8	0
62858	Magnetocaloric and Shape Memory Effects in the Mn2NiGa Heusler Alloy. Physics of the Solid State, 2020, 62, 815-820.	0.2	8
62859	Investigation of phase transition in electronic structure and magnetic properties of Fe_{2-x}Co_xTiSn Heusler alloys. Phase Transitions, 2020, 93, 690-708.	0.6	5
62860	Stability of carbon-vacancy complexes in Î±-Fe. IOP Conference Series: Materials Science and Engineering, 0, 835, 012027.	0.3	0
62861	Prediction of ternary alkaline-earth metal Sn(II) and Pb(II) chalcogenide semiconductors. Physical Review Materials, 2020, 4, .	0.9	1
62862	Influence of Na and Cu on the thermodynamic stability and electronic band alignment of the In2S3/ Cu(In,Ga)(Se, S)2 thin-film solar cell interface. , 2020, , .		0
62863	Possible enhancement of superconductivity in ladder-type cuprates by longitudinal compression. Physical Review Research, 2020, 2, .	1.3	6
62864	Projective quasiparticle interference of a single scatterer to analyze the electronic band structure of ZrSiS. Physical Review Research, 2020, 2, .	1.3	1

#	Article	IF	Citations
62865	Electron localisation descriptors in ONETEP: a tool for interpreting localisation and bonding in large-scale DFT calculations. Electronic Structure, 2020, 2, 027001.	1.0	10
62866	Empirical potential optimization for the investigation of lithiation-delithiation cycles of amorphous Si nanowires. Physical Review Materials, 2020, 4, .	0.9	1
62867	Electronic properties and crystal structures of double-perovskites, Ba₂Bi^{III}Bi^VO₆,Ba₂PrBiO₆, and Ba₂PrSbO₆: First-principles study. Materials Research Express, 2020, 7, 065505.	0.8	2
62868	Magnetic and optical properties of Î´-SnSe doped by transition-metal atoms: A first-principle calculation. Optik, 2020, 214, 164810.	1.4	2
62869	RSAVS superconductors: Materials with a superconducting state that is robust against large volume shrinkage. Physical Review Materials, 2020, 4, .	0.9	7
62870	The electronic structure, phase transition, elastic, thermodynamic, and thermoelectric properties of FeRh: high-temperature and high-pressure study. Zeitschrift Fur Naturforschung - Section A Journal of Physical Sciences, 2020, 75, 789-801.	0.7	2
62871	Predicting two-dimensional diphosphorus silicide monolayer by the global optimization method. Chemical Physics Letters, 2020, 752, 137514.	1.2	0
62872	Enhancing perpendicular magnetocrystalline anisotropy in Fe ultrathin films by non-noble transition-metal substrate. International Journal of Modern Physics C, 2020, 31, 2050134.	0.8	0
62873	Oxygen Reduction Reaction Activity of Pt Sub-nano Clusters Supported on Graphene. Vacuum and Surface Science, 2020, 63, 413-418.	0.0	1
62875	Electronic and geometric stability of double titanium-doped silicon clusters. Materials Research Express, 2020, 7, 085006.	0.8	2
62876	Topological transition in monolayer blue phosphorene with transition-metal adatom under strain. Chinese Journal of Chemical Physics, 2020, 33, 443-449.	0.6	1
62877	Theoretical studies on the role of each component in benzotrifuroxan/2,4,6-trinitrotoluene cocrystal. Chemical Physics Letters, 2020, 753, 137608.	1.2	5
62878	First-principles identification of ferroelectric metal-organic frameworks of [CH3NH3][B(HCOO)3] (B =) Tj ETQq0 0 0 rgBT /Overlock 10 T	1.4	1
62880	Modulation of Dirac electrons in epitaxial Bi2Se3 ultrathin films on van der Waals ferromagnet Cr2Si2Te6. Physical Review Materials, 2020, 4, .	0.9	3
62881	Tunable band alignment in boron carbon nitride and blue phosphorene van der Waals heterostructure. Nano Express, 2020, 1, 020021.	1.2	2
62882	Impact of magnetic structure and thermal effects on vibrational excitations and neutron scattering in uranium mononitride. Annals of Nuclear Energy, 2020, 143, 107447.	0.9	2
62883	Influences of hole/electron-lattice coupling on phase transition between Î»-Ti₃O₅ and Î²-Ti₃O₅. Journal of Physics Condensed Matter, 2020, 32, 46LT01.	0.7	1
62884	Insight into the electronic structure of semiconducting <mml:math xmlns:mml="http://www.w3.org/1998/Math/MathML"><mml:mi>Îµ</mml:mi><mml:mtext>â€²</mml:mtext><mml:mi>GaSe</mml:mi><mml:mi></mml:mi> and <mml:math xmlns:mml="http://www.w3.org/1998/Math/MathML"><mml:mi>Îµ</mml:mi><mml:mtext>â€²</mml:mtext><mml:mi>InSe</mml:mi><mml:mi></mml:mi> Physical Review Materials, 2020, 4, .	0.9	4

#	Article	IF	Citations
62885	Absorption of Isopropanol on Surface of Defect Silicene. VNU Journal of Science Mathematics - Physics, 2020, 36, .	0.0	0
62886	Optical Properties and First Principles Study of CH3NH3PbBr3 Perovskite Structures for Solar Cell Application. Lecture Notes in Electrical Engineering, 2021, , 275-282.	0.3	0
62887	First Principles Investigations of Ta4AlX3 (X= B, C, N) MAX Phase Ceramics. Journal of Boron, 0, , .	0.0	1
62888	Enhancement of Curie Temperature under Built-in Electric Field in Multi-Functional Janus Vanadium Dichalcogenides. Chinese Physics Letters, 2020, 37, 087505.	1.3	1
62889	HfSe2 monolayer stability tuning by strain and charge doping. Physics Letters, Section A: General, Atomic and Solid State Physics, 2020, 384, 126534.	0.9	6
62890	First-principles study of the order-disorder transition and its effects on the optoelectronic property of ABiS2 (A=Na , K). Physical Review Materials, 2020, 4, .	0.9	1
62891	Phase diagram of grain boundary facet and line junctions in silicon. Physical Review Materials, 2020, 4, .	0.9	1
62892	Realization of asymmetric spin splitting Dirac cones in antiferromagnetic graphene/CrAs2/graphene heterotrilayer. Journal of Physics Condensed Matter, 2020, 32, 435503.	0.7	4
62893	Mapping the mechanical properties in nitride coatings at the nanometer scale. Acta Materialia, 2020, 194, 343-353.	3.8	6
62894	Manipulation of polarization characteristics in wurtzite Î™Î™Î™-nitride nanowires for linearly polarized emission. Journal Physics D: Applied Physics, 2020, 53, 465108.	1.3	0
62895	Topological superconductivity facilitated by exchange interaction on the surface of FeTe_{0.5}Se_{0.5}. New Journal of Physics, 2020, 22, 083065.	1.2	2
62896	Thermoelectric properties of layered ternary telluride <mml:math xmlns:mml="http://www.w3.org/1998/Math/MathML"><mml:mrow><mml:msub><mml:mi>Nb</mml:mi><mml:mn>3</mml:mn> Physical Review Materials, 2020, 4, .	0.9	4
62897	Defect levels in d-electron containing systems: Comparative study of CdTe using LDA and LDA + U. Journal of Semiconductors, 2020, 41, 102701.	2.0	1
62898	Ab initio modeling of thermal transport through van der Waals materials. Physical Review Materials, 2020, 4, .	0.9	4
62899	Investigation of SiO2-Vo/SiO2 interface induced rectification characteristics at HRS for RRAM devices. Journal of Alloys and Compounds, 2020, 835, 155197.	2.8	1
62900	Dynamical stability and electronic structure of Î²-phosphorus carbide nanowires. Journal of Micromechanics and Molecular Physics, 2020, 05, 2050007.	0.7	2
62901	Molecular dynamics investigation of the configuration and shape of helium clusters in tungsten. Nuclear Fusion, 2020, 60, 126015.	1.6	4
62902	Scalable Production of Freestanding Few-Layer Î²₁₂-Borophene Single Crystalline Sheets as Efficient Electrocatalysts for Lithiumâ€“Sulfur Batteries. ACS Nano, 2021, 15, 17327-17336.	7.3	40

#	Article	IF	Citations
62903	Untangling the structural, magnetic dipole, and charge multipolar orders in <mml:math xmlns:mml="http://www.w3.org/1998/Math/MathML"><mml:msub><mml:mi mathvariant="normal">Ba</mml:mi><mml:mn>2</mml:mn></mml:msub><mml:msub><mml:mi mathvariant="normal">MgReO</mml:mi><mml:mn>6</mml:mn></mml:msub></mml:math>. Physical Review Materials, 2021, 5, .	0.9	6
62904	Construction of N-doped carbon frames anchored with Co single atoms and Co nanoparticles as robust electrocatalyst for hydrogen evolution in the entire pH range. Journal of Energy Chemistry, 2022, 67, 147-156.	7.1	22
62905	Classifying Intermetallic Tetragonal Phase of All-d-Metal Heusler Alloys for Catalysis Applications. Topics in Catalysis, 2022, 65, 208-214.	1.3	5
62906	Computational Auxiliary for the Progress of Sodium-Ion Solid-State Electrolytes. ACS Nano, 2021, 15, 17232-17246.	7.3	42
62907	Potential reversible and high-capacity hydrogen storage medium: Li-decorated B3S monolayers. Materials Today Communications, 2021, 29, 102938.	0.9	12
62908	Phononâ€Related Monochromatic THz Radiation and its Magnetoâ€Modulation in 2D Ferromagnetic Cr₂Ge₂Te₆. Advanced Science, 2022, 9, e2103229.	5.6	4
62909	Large exciton binding energy, superior mechanical flexibility, and ultra-low lattice thermal conductivity in BiI₃ monolayer. Journal of Physics Condensed Matter, 2022, 34, 055302.	0.7	0
62910	Berry curvature generation detected by Nernst responses in ferroelectric Weyl semimetal. Proceedings of the National Academy of Sciences of the United States of America, 2021, 118, .	3.3	7
62911	Magnetism and piezoelectricity in stable transition metal silicate monolayers. Physical Review Materials, 2021, 5, .	0.9	10
62912	Engineering of Fe-pnictide heterointerfaces by electrostatic principles. NPG Asia Materials, 2021, 13, .	3.8	2
62913	Oxygen Coverage Effect on the Magnetic Properties of the Cr₂NO_x (0 â‰) Tj ETQq0 0 0 rgBT /Overloc	2.0	6
62914	Two-Dimensional Defective Boron-Doped Niobic Acid Nanosheets for Robust Nitrogen Photofixation. ACS Nano, 2021, 15, 17820-17830.	7.3	26
62915	Pressure and Spin Effect on the Stability, Electronic and Mechanic Properties of three Equiatomic Quaternary Heusler (FeVHfZ, Z= Al, Si, and Ge) Compounds. Materials Today Communications, 2021, 29, 102941.	0.9	1
62916	Microstructure and Magnetic behaviors of FeCoNi (Al) alloys with Incoherent Nanoprecipitates Prepared by High-pressure Solidification. Journal of Alloys and Compounds, 2021, 894, 162501.	2.8	7
62917	Cooperatively enhanced coking resistance via boron nitride coating over Ni-based catalysts for dry reforming of methane. Applied Catalysis B: Environmental, 2022, 302, 120859.	10.8	61
62918	Structure of Germanene/Al(111): A Two-Layer Surface Alloy. Journal of Physical Chemistry C, 2021, 125, 24702-24709.	1.5	8
62919	Bonding Properties of Manganese Nitrides at High Pressure and the Discovery of MnN₄with Planar N₄Rings. Journal of Physical Chemistry C, 2021, 125, 24605-24612.	1.5	8
62920	Role of Interfacial Oxide in the Preferred Orientation of Ga₂O₃ on Si for Deep Ultraviolet Photodetectors. ACS Omega, 2021, 6, 29149-29156.	1.6	4

#	Article	IF	Citations
62921	Thickness-dependent thermoelectric transporting properties of few-layered SnSe. Journal of Alloys and Compounds, 2022, 894, 162542.	2.8	12
62922	Electronic structure and electrical transport properties of MoS₂single-walled nanotubes based on first principles. International Journal of Modern Physics B, 2021, 35, .	1.0	1
62923	An Feâ€“Niâ€“Crâ€“H interatomic potential and predictions of hydrogen-affected stacking fault energies in austenitic stainless steels. International Journal of Hydrogen Energy, 2022, 47, 651-665.	3.8	19
62924	Toward Zero-Strain Mixed Conductors: Anomalously Low Redox Coefficients of Chemical Expansion in Praseodymium-Oxide Perovskites. Chemistry of Materials, 0, , .	3.2	3
62925	Electrocatalytic oxidation of ammonia on Pt: Mechanistic insights into the formation of N2 in alkaline media. Journal of Catalysis, 2022, 405, 626-633.	3.1	17
62926	Mixed-Valence CsCu₄Se₃: Large Phonon Anharmonicity Driven by the Hierarchy of the Rigid [(Cu⁺)₄(Se^{2â€“})₂](Se^{â€“}) Double Anti-CaF₂ Layer and the Soft Cs⁺ Sublattice. Journal of the American Chemical Society, 2021, 143, 19490-19501.	6.6	25
62927	Unique Arrangement of Atoms Leads to Low Thermal Conductivity: A Comparative Study of Monolayer Mg₂C. Journal of Physical Chemistry Letters, 2021, 12, 10353-10358.	2.1	7
62928	Martensitic transformation in superlattices of two non-transforming metals. Journal of Applied Physics, 2021, 130, 165105.	1.1	1
62929	Anharmonic organic cation vibrations in the hybrid lead halide perovskite <mml:math xmlns:mml="http://www.w3.org/1998/Math/MathML"><mml:msub><mml:mrow><mml:mi>CH</mml:mi></mml:mrow><mml:mn>3</mml:mn> Physical Review Materials, 2021, 5, .	0.9	1
62930	Viable substrates for the honeycomb-borophene growth. Physical Review Materials, 2021, 5, .	0.9	4
62931	Highly effective Ru-based Heusler alloy catalysts for N2 activation: A theoretical study. Applied Surface Science, 2022, 575, 151658.	3.1	9
62932	Electric-Field-Driven Negative Differential Conductance in 2D van der Waals Ferromagnet Fe₃GeTe₂. Nano Letters, 2021, 21, 9233-9239.	4.5	10
62933	Activating Î³-graphyne nanoribbons as bifunctional electrocatalysts toward oxygen reduction and hydrogen evolution reactions by edge termination and nitrogen doping. Chemical Engineering Journal, 2022, 430, 133126.	6.6	17
62934	From Zero- to One-Dimensional, Opportunities and Caveats of Hybrid Iodobismuthates for Optoelectronic Applications. Inorganic Chemistry, 2021, 60, 17123-17131.	1.9	13
62935	Defect Enrichment in Near Inverse Spinel Configuration to Enhance the Persistent Luminescence of Fe³⁺. Advanced Optical Materials, 2022, 10, 2101669.	3.6	26
62936	Rationalizing Surface Electronic Configuration of Niâ€“Fe LDO by Introducing Cationic Nickel Vacancies as Highly Efficient Electrocatalysts for Lithiumâ€“Oxygen Batteries. Small, 2021, 17, e2104349.	5.2	7
62937	Orbital Mapping of Semiconducting Perylenes on Cu(111). Journal of Physical Chemistry C, 2021, 125, 24477-24486.	1.5	2
62938	Optically Induced Ferroelectric Polarization Switching in a Molecular Ferroelectric with Reversible Photoisomerization. Advanced Science, 2021, 8, e2102614.	5.6	31

#	Article	IF	Citations
62939	Strain-induced half-valley metals and topological phase transitions in <mml:math xmlns:mml="http://www.w3.org/1998/Math/MathML"><mml:mrow><mml:mi>M</mml:mi><mml:msub><mml:mi>Br</mml:mi><mml:mn> monolayers <mml:math xmlns:mml="http://www.w3.org/1998/Math/MathML"><mml:mrow><mml:mo>(</mml:mo><mml:mi>M</mml:mi><mml:mo>=</mml:mo> B, 2021, 104, .	1.1	50
62940	Deep vacancy induced low-density fluxional interfacial water. Physical Review Research, 2021, 3, .	1.3	2
62941	Point and complex defects in monolayer <mml:math xmlns:mml="http://www.w3.org/1998/Math/MathML"><mml:mrow><mml:mi>Pd</mml:mi><mml:msub><mml:mi>Se</mml:mi><mml:mn> : Evolution of electronic structure and emergence of magnetism. Physical Review B, 2021, 104, .	1.1	11
62942	Stable Structures and Superconductivity in a Yâ€“Si System under High Pressure. Journal of Physical Chemistry Letters, 2021, 12, 10388-10393.	2.1	10
62943	Density Functional Theory Study of Ethylene Carbonate Adsorption on the (0001) Surface of Aluminum Oxide Î±-Al₂O₃. ACS Omega, 2021, 6, 29577-29587.	1.6	11
62944	Beneficial effect of Au and Pt doping of the Ag-(100) surface for thiophene and pyridine adsorption from density functional theory calculations. Chemical Physics, 2022, 553, 111391.	0.9	3
62945	Mechanism of ammonia oxidation to dinitrogen, nitrite, and nitrate on Î²â€Ni(OH)₂ from firstâ€principles simulations. Electrochemical Science Advances, 2022, 2, 2100142.	1.2	21
62946	High-entropy alloy stabilized active Ir for highly efficient acidic oxygen evolution. Chemical Engineering Journal, 2022, 431, 133251.	6.6	100
62947	Theoretical and experimental studies of compression and shear deformation behavior of Osmium to 280 GPa. Engineering Research Express, 2021, 3, 045017.	0.8	0
62948	Effect of carbon on the phase formation in Fe85-xCr15Cx (x = 10-17) melts at low cooling rates. Journal of Alloys and Compounds, 2021, , 162507.	2.8	0
62949	An integrated surface coating strategy to enhance the electrochemical performance of nickel-rich layered cathodes. Nano Energy, 2022, 91, 106665.	8.2	143
62950	Superâ€Flexible Freestanding BiMnO₃ Membranes with Stable Ferroelectricity and Ferromagnetism. Advanced Science, 2021, 8, e2102178.	5.6	23
62951	Polypeptoid Material as an Anchoring Material for Liâ€“S Batteries. ACS Applied Energy Materials, 2021, 4, 13070-13076.	2.5	8
62952	Floquet-engineered half-valley-metal state in two-dimensional gapped Dirac materials. Physical Review B, 2021, 104, .	1.1	4
62953	Activating COOH* intermediate by Ni/Ni3ZnC0.7 heterostructure in porous N-doped carbon nanofibers for boosting CO2 electroreduction. Applied Catalysis B: Environmental, 2022, 302, 120861.	10.8	32
62954	Steering Metalâ€“Organic Network Structures through Conformations and Configurations on Surfaces. ACS Nano, 2021, , .	7.3	7
62955	Structure, Stability, Properties, and Application of Atomically Thin Coinage Metal Flatland in Graphene Pore: A Density Functional Theory Calculation. Physica Status Solidi (B): Basic Research, 2022, 259, 2100489.	0.7	10
62956	Fe-doped porous Co3O4 nanosheets with highly efficient catalytic performance for soot oxidation. Chemical Engineering Journal, 2022, 431, 133248.	6.6	8

#	Article	IF	Citations
62957	Structural and Elastic Properties of Pd2CrPb Heusler Compound. Issn 2458-9411, 0, , .	0.2	0
62958	Observation of metallic electronic structure in a single-atomic-layer oxide. Nature Communications, 2021, 12, 6171.	5.8	26
62959	Intrinsic Electric Field and Excellent Photocatalytic Solarâ€toâ€Hydrogen Efficiency in 2D Janus Transition Metal Dichalcogenide. Physica Status Solidi - Rapid Research Letters, 2022, 16, 2100417.	1.2	2
62960	Computational Screening of MOFs and Zeolites for Direct Air Capture of Carbon Dioxide under Humid Conditions. Journal of Physical Chemistry C, 2021, 125, 24630-24639.	1.5	30
62961	Revealing the BrÃ¸nsted-Evans-Polanyi relation in halide-activated fast MoS ₂ growth toward millimeter-sized 2D crystals. Science Advances, 2021, 7, eabj3274.	4.7	18
62962	Transferred metal gate to 2D semiconductors for sub-1 V operation and near ideal subthreshold slope. Science Advances, 2021, 7, eabf8744.	4.7	37
62963	Structure and energetics of the elbows in the Au(111) herringbone reconstruction. Physical Review B, 2021, 104, .	1.1	7
62964	Fluorinated Graphite (FG)-Modified Liâ€“S Batteries with Superhigh Primary Specific Capacity and Improved Cycle Stability. ACS Applied Materials & Interfaces, 2021, 13, 52717-52726.	4.0	4
62965	Effects of alloying elements on the atomic structure, elastic and thermodynamic properties of L12-Co3(V, Ti) compound. Materials Today Communications, 2022, 30, 102931.	0.9	2
62966	A Potassium Tungsten Oxyfluoride with Strong Second-Harmonic Generation Response Derived from Anion-Ordered Functional Motif. Inorganic Chemistry, 2021, 60, 17364-17370.	1.9	13
62967	Multiple magnetism-controlled topological states in EuAgAs. Physical Review B, 2021, 104, .	1.1	12
62968	Engineering antiferromagnetic topological insulator by strain in two-dimensional rare-earth pnictide EuCd2Sb2. Applied Physics Letters, 2021, 119, .	1.5	6
62969	Improved photodegradation efficiency in Fe3+-doped Bi3TiNbO9 nanosheets through oxygen vacancies introduction and ferroelectric polarization enhancement simultaneously. Applied Surface Science, 2022, 575, 151749.	3.1	13
62970	Improving robustness of kinetic models for steam reforming based on artificial neural networks and ab initio calculations. Chemical Engineering Journal, 2022, 433, 133201.	6.6	9
62971	A Tandem Electrocatalysis of Sulfur Reduction by Bimetal 2D MOFs. Advanced Energy Materials, 2021, 11, 2102819.	10.2	68
62972	Thermodynamic properties of the Nd-Bi system via emf measurements, DFT calculations, machine learning, and CALPHAD modeling. Acta Materialia, 2022, 223, 117448.	3.8	10
62973	Modified Embedded-Atom Interatomic Potential Parameters of the Tiâ€“Cr Binary and Tiâ€“Crâ€“N Ternary Systems. Frontiers in Chemistry, 2021, 9, 773015.	1.8	2
62974	Comprehensive Mechanism of CO₂ Electroreduction on Nonâ€Noble Metal Singleâ€Atom Catalysts of Mo₂CS₂â€MXene. Chemistry - A European Journal, 2021, 27, 17900-17909.	1.7	16

#	Article	IF	Citations
62975	Water Splitting on Multifaceted SrTiO3 Nanocrystals: Computational Study. Catalysts, 2021, 11, 1326.	1.6	7
62976	On the Origin of Zero Interface Resistance in the Li_{6.25}Al_{0.25}La₃Zr₂O₁₂|Li⁰ System: An Atomistic Investigation. ACS Applied Materials & Interfaces, 2021, 13, 52629-52635.	4.0	4
62977	Atomic-scale characterization of structural and electronic properties of Hf doped Î²-Ga2O3. Applied Physics Letters, 2021, 119, .	1.5	6
62978	Research on the Effects of Sn Dopants of V2O5 Based on the First Principles. Journal of Electronic Materials, 0, , 1.	1.0	4
62979	Increased solar absorption and promoted photocarrier separation in atomically thin 2D carbon nitride sheets for enhanced visible-light photocatalysis. Chemical Engineering Journal, 2022, 431, 133219.	6.6	7
62980	Intrinsic valley polarization and anomalous valley hall effect in single-layer 2H-FeCl2. ChemPhysMater, 2022, 1, 56-61.	1.4	30
62981	Effects of Grain Size on the Thermoelectric Properties of Cu₂SnS₃: An Experimental and First-Principles Study. ACS Applied Energy Materials, 2021, 4, 12604-12612.	2.5	25
62982	Theoretical study of the crystal structure, stability, and properties of phases in the V-N system. Physical Review B, 2021, 104, .	1.1	4
62983	Construction of graphitic-N-rich TiO2-N-C interfaces via dye dissociation and reassembly for efficient oxygen evolution reaction. Chemical Engineering Journal, 2022, 431, 133246.	6.6	11
62984	Solvent Promotion on the Metal-Support Interaction and Activity of Pd@ZrO2 Catalyst: Formation of Metal Hydrides as the New Catalytic Active Phase at the Solid-Liquid Interface. Journal of Catalysis, 2021, , .	3.1	10
62985	Comparative first-principles study of elastic constants of covalent and ionic materials with LDA, GGA, and meta-GGA functionals and the prediction of mechanical hardness. Science China Technological Sciences, 2021, 64, 2755-2761.	2.0	3
62986	In Situ Defect Engineering Route to Optimize the Cationic Redox Activity of Layered Double Hydroxide Nanosheet via Strong Electronic Coupling with Holey Substrate. Advanced Science, 2022, 9, e2103368.	5.6	19
62987	Using a Thin ZnO Film as an Intermediate Layer to Tune the Performance of Mg-Based Nanolaminates: A First-Principles Study. Langmuir, 2021, 37, 12548-12556.	1.6	3
62988	Structure Tuning, Strong Second Harmonic Generation Response, and High Optical Stability of the Polar Semiconductors Na_{1â€“x}K_xAsQ₂. Journal of the American Chemical Society, 2021, 143, 18204-18215.	6.6	24
62989	Passivating buried interface via self-assembled novel sulfonium salt toward stable and efficient perovskite solar cells. Chemical Engineering Journal, 2022, 431, 133209.	6.6	74
62990	Effect of Zr on phase separation, mechanical and corrosion behavior of heterogeneous CoCrFeNiZr high-entropy alloy. Journal of Materials Science and Technology, 2022, 109, 76-85.	5.6	36
62991	Engineering local strain for single-atom nuclear acoustic resonance in silicon. Applied Physics Letters, 2021, 119, .	1.5	6
62992	Breaking the scaling relations of oxygen evolution reaction on amorphous NiFeP nanostructures with enhanced activity for overall seawater splitting. Applied Catalysis B: Environmental, 2022, 302, 120862.	10.8	97

#	Article	IF	Citations
62993	Large Dzyaloshinskii-Moriya interaction and room-temperature nanoscale skyrmions in CoFeB/MgO heterostructures. Cell Reports Physical Science, 2021, 2, 100618.	2.8	14
62994	Adsorption and Decomposition of Sarin on Dry and Wet Cu₂O(111) and CuO(111) Surfaces: Insight from First-Principles Calculations. Journal of Physical Chemistry C, 2021, 125, 24396-24405.	1.5	6
62995	Balancing Anchoring and Diffusion for Screening of Metal Oxide Cathode Materials in Lithiumâ€“Sulfur Batteries. Journal of Physical Chemistry C, 2021, 125, 24318-24327.	1.5	3
62996	Thermoelectric power factor enhancement of calcium-intercalated layered silicene by introducing metastable phase. Applied Physics Express, 2021, 14, 115505.	1.1	9
62997	Role of Intrinsic Points Defects on the Electronic Structure of Metalâ€“Insulator Transition h-FeS. Journal of Physical Chemistry Letters, 2021, 12, 10777-10782.	2.1	5
62998	Large-gap quantum anomalous Hall effect in monolayer halide perovskite. Physical Review B, 2021, 104, .	1.1	3
62999	Efficient Broadband Nearâ€Infrared Emission in the GaTaO₄:Cr³⁺ Phosphor. Advanced Optical Materials, 2022, 10, 2101800.	3.6	93
63000	Defect calculations with quasiparticle correction: A revisited study of iodine defects in CH3NH3PbI3. Chinese Physics B, 0, , .	0.7	0
63001	Mo and Ta addition in NbTiZr medium entropy alloy to overcome tensile yield strength-ductility trade-off. Journal of Materials Science and Technology, 2022, 109, 176-185.	5.6	13
63002	Progressive regulation of Al sites and Cu distribution to increase hydrothermal stability of hierarchical SSZ-13 for the selective catalytic reduction reaction. Applied Catalysis B: Environmental, 2022, 303, 120867.	10.8	10
63003	Molecular dynamics simulation of metallic Alâ€“Ce liquids using a neural network machine learning interatomic potential. Journal of Chemical Physics, 2021, 155, 194503.	1.2	9
63004	Discovery of Domeâ€Shaped Superconducting Phase and Anisotropic Transport in a van der Waals Layered Candidate NbIrTe 4 under Pressure. Advanced Science, 2021, , 2103250.	5.6	5
63005	CO2 activation at atomically dispersed Si sites of N-doped graphenes: Insight into distinct electron mechanisms from first-principles calculations. AIP Advances, 2021, 11, .	0.6	3
63006	Construction of GQDsâ€Đecorated Ultrathin Bi₂WO₆ Nanosheets Hydrogel: a Recyclableâ€Flexible Platform with Excellent Piezoâ€Photocatalytic Activity for Highâ€Performance Water Decontamination and its Theoretical Interpretation. Particle and Particle Systems Characterization, 2021, 38, .	1.2	7
63007	The Adsorption behaviors of pristine MoS2 and N-MoS2 Monolayer: A First-Principles Calculation. Surfaces and Interfaces, 2021, , 101580.	1.5	3
63008	Self-doped Br in Bi5O7Br ultrathin nanotubes: Efficient photocatalytic NO purification and mechanism investigation. Chinese Chemical Letters, 2022, 33, 3161-3166.	4.8	13
63009	Defect induced ferromagnetism in a two-dimensional metal<mml:math xmlns:mml="http://www.w3.org/1998/Math/MathML" display="inline" id="d1e357" altimg="si131.svg"><mml:mo>â^’</mml:mo></mml:math>organic framework. Journal of Magnetism and Magnetic Materials, 2022, 545, 168659.	1.0	2
63010	Thermoelectric performance improvement of p-type Mg3Sb2-based materials by Zn and Ag co-doping. Materials Today Physics, 2021, 21, 100564.	2.9	20

#	Article	IF	Citations
63011	A pathway toward high-throughput quantum Monte Carlo simulations for alloys: A case study of two-dimensional (2D) GaSxSe1â^'x. Journal of Chemical Physics, 2021, 155, 194112.	1.2	7
63012	Tuning the Oxidation State of Cu Electrodes for Selective Electrosynthesis of Ammonia from Nitrate. ACS Applied Materials & Interfaces, 2021, 13, 52469-52478.	4.0	43
63013	Boosting visible light photocatalysis in an Au@TiO2 yolk-in-shell nanohybrid. Applied Catalysis B: Environmental, 2022, 303, 120869.	10.8	39
63014	Enhanced Fluoride Uptake by Layered Double Hydroxides under Alkaline Conditions: Solid-State NMR Evidence of the Role of Surface >MgOH Sites. Environmental Science & Technology, 2021, 55, 15082-15089.	4.6	22
63015	Luminescence and Stability Enhancement of Inorganic Perovskite Nanocrystals via Selective Surface Ligand Binding. ACS Nano, 2021, 15, 17998-18005.	7.3	32
63016	Liquid-Metal-Assisted Deposition and Patterning of Molybdenum Dioxide at Low Temperature. ACS Applied Materials & Interfaces, 2021, 13, 53181-53193.	4.0	19
63017	Effects of hydrogen/halogen â€“edge termination on structural, electronic, and optical properties of planar silicene nanoribbons SiNRs. Physica E: Low-Dimensional Systems and Nanostructures, 2022, 136, 115046.	1.3	5
63018	ZnS/ZnO nanosheets obtained by thermal treatment of ZnS/ethylenediamine as a Z-scheme photocatalyst for H2 generation and Cr(VI) reduction. Applied Surface Science, 2022, 575, 151773.	3.1	41
63019	Excellent multi-color emission and multi-mode optical ratiometric thermometer in (Ca, Tb, Eu,) Tj ETQq0 0 0 rgBT /Overlock 10 Tf 50 422	3.1	25
63020	Ar-plasma activated Au film with under-coordinated facet for enhanced and sustainable CO2 reduction to CO. Journal of CO2 Utilization, 2021, 54, 101776.	3.3	9
63021	Structural stability and mechanical properties of TiAl+Mo alloys: A comprehensive ab initio study. Acta Materialia, 2021, 221, 117427.	3.8	8
63022	Ferroelectricity in novel one-dimensional P42-InSeI nanowires. Results in Physics, 2021, 31, 104960.	2.0	8
63023	BC2P/graphene and BC2P/Black phosphorus van der Waals heterostructures with direct band gap and high carrier mobility, hardness and light absorption. Superlattices and Microstructures, 2021, 160, 107084.	1.4	4
63024	Integration of a Wigner effect-based energy storage system with an advanced nuclear reactor. Nuclear Engineering and Design, 2021, 385, 111521.	0.8	3
63025	Tailoring co-precipitation behavior by molybdenum microalloying in high-strength steels. Materials Characterization, 2021, 182, 111568.	1.9	4
63026	Oxygen ionic transport in LaInO3 and LaIn0.5Zn0.5O2.75 perovskites: Theory and experiment. Solid State Ionics, 2021, 372, 115790.	1.3	9
63027	Zeolite-encapsulated single-atom catalysts for efficient CO2 conversion. Journal of CO2 Utilization, 2021, 54, 101777.	3.3	11
63028	Controlling the Rotational Barrier of Single Porphyrin Rotors on Surfaces. Journal of Physical Chemistry B, 2020, 124, 953-960.	1.2	0

#	Article	IF	Citations
63029	The AFLOW Fleet for Materials Discovery. , 2020, , 1785-1812.		4
63030	First-principles calculations of stabilities and physical properties of ternary niobium borocarbides and tantalum borocarbides. Wuli Xuebao/Acta Physica Sinica, 2020, 69, 116201.	0.2	2
63031	Extending the Scale with Real-Space Methods for the Electronic Structure Problem. , 2020, , 499-522.		0
63032	First-Principles Calculations 1. Springer Series in Materials Science, 2020, , 309-328.	0.4	0
63033	Multi-objective Optimization as a Tool for Material Design. , 2020, , 2777-2790.		1
63034	First-Principles Modeling of Interface Effects in Oxides. , 2020, , 1119-1149.		0
63035	Ferroelectric-driven tunable magnetism in ultrathin platinum films. Physical Review Materials, 2020, 4, .	0.9	4
63036	Theoretical research on novel monoclinic Zr2B5 from first principles calculations. EPJ Applied Physics, 2020, 92, 30401.	0.3	0
63037	First-Principles Investigations of Electronically Excited States in Organic Semiconductors. , 2021, , 155-193.		1
63039	Low energy dissipation readout of single-molecule ferroelectronic states by a spin-Seebeck signal. Physical Review Research, 2020, 2, .	1.3	5
63040	The Features of Phase Stability of GaN and AlN Films at Nanolevel. Nanomaterials, 2021, 11, 8.	1.9	4
63041	Thermal conductivity of h-BN monolayers using machine learning interatomic potential. Journal of Physics Condensed Matter, 2021, 33, 105903.	0.7	9
63043	Vanadium Oxide Clusters Decorated Metallic Cobalt Catalyst for Active Alkaline Hydrogen Evolution. Cell Reports Physical Science, 2020, 1, 100275.	2.8	7
63044	Tunable spin Hall and spin Nernst effects in Dirac line-node semimetals XCuYAs (X=Zr,Hf ; Y=Si,Ge). Physical Review Materials, 2020, 4, .	0.9	7
63045	M-Site Vacancy-Mediated Adsorption and Diffusion of Sodium on Ti₂CO₂ MXene. Journal of Physical Chemistry C, 2021, 125, 82-90.	1.5	10
63046	Cu-Modified SrTiO₃Perovskites Toward Enhanced Waterâ€“Gas Shift Catalysis: A Combined Experimental and Computational Study. ACS Applied Energy Materials, 2021, 4, 452-461.	2.5	15
63047	Deciphering the nature of ion-graphene interaction. Physical Review Research, 2020, 2, .	1.3	9
63048	Changes in the geometric structure and hydrogen-termination modify the electronic and optical properties of porous silicon. Optik, 2020, 224, 165539.	1.4	4

#	Article	IF	Citations
63049	Structure of graphene and a surface carbide grown on the (0001) surface of rhenium. Physical Review Materials, 2020, 4, .	0.9	0
63050	Magnetostructural coupling from competing magnetic and chemical bonding effects. Physical Review Research, 2020, 2, .	1.3	1
63051	Revealing Local Disorder in a Silver-Bismuth Halide Perovskite upon Compression. Journal of Physical Chemistry Letters, 2021, 12, 532-536.	2.1	11
63052	DFT Study of MAX Phase Surfaces for Electrocatalyst Support Materials in Hydrogen Fuel Cells. Materials, 2021, 14, 77.	1.3	7
63053	An antiferromagnetic two-dimensional material: Chromium diiodides monolayer. Journal of Semiconductors, 2020, 41, 122502.	2.0	4
63054	CO Diffusion and Bond Weakening on Cu(410) â€"Probing Surface Structureâ€". E-Journal of Surface Science and Nanotechnology, 2020, 18, 307-311.	0.1	0
63055	First-Principles Investigation of Photoisomeric Switching of Vibrational Heat Current across Molecular Junctions. Physical Review Applied, 2020, 14, .	1.5	1
63056	Highly Selective Electrocatalytic CO₂ Reduction to Methanol on Iridium Dioxide with CO[*] Spectators. ChemElectroChem, 2020, 7, 5036-5043.	1.7	9
63057	New Spiral Form of Carbon Nitride with Ultrasoftness and Tunable Electronic Structures. ACS Omega, 2021, 6, 516-522.	1.6	3
63058	Tuning the electronic properties of highly anisotropic 2D dangling-bond-free sheets from 1D V₂Se₉ chain structures. Nanotechnology, 2021, 32, 095203.	1.3	6
63059	Magnon-magnon interaction and magnon relaxation time in a ferromagnetic <mml:math xmlns:mml="http://www.w3.org/1998/Math/MathML"><mml:mrow><mml:msub><mml:mi>Cr</mml:mi><mml:mn>2</mml:mn></mml:msub></mml:mrow></mml:math> monolayer. Physical Review B, 2020, 102, .	1.1	11
63060	Electronic and Magnetic Structures of New Interstitial Boron Sub-Oxides B12O2:X (X = B, C, N, O). Molecules, 2021, 26, 123.	1.7	3
63061	Two-dimensional CoSe structures: Intrinsic magnetism, strain-tunable anisotropic valleys, magnetic Weyl point, and antiferromagnetic metal state. Physical Review B, 2020, 102, .	1.1	8
63062	The effect of isovalent doping on the electronic band structure of group IV semiconductors. Journal Physics D: Applied Physics, 2021, 54, 085102.	1.3	1
63063	Experimental and theoretical P-V-T equation of state for Os₂B₃. High Pressure Research, 2021, 41, 27-38.	0.4	1
63064	Surface relaxation and rumpling of Sn-doped <mml:math xmlns:mml="http://www.w3.org/1998/Math/MathML"><mml:mrow><mml:mi>Î²</mml:mi><mml:mtext>â^'</mml:mtext><mml:msub><mml:mi mathvariant="normal">O</mml:mi><mml:mn>3</mml:mn></mml:msub><mml:mrow><mml:mo>(</mml:mo><mml:mn>010</mml:mn></mml:mrow></mml:mrow></mml:math> Physical Review B, 2020, 102, .	1.1	4
63065	Anisotropic nonlinear optical response in a graphene oxide-gold nanohybrid. Optics Letters, 2020, 45, 6655.	1.7	2
63066	Contrasting Thermoelectric Transport Behaviors of p -Type PbS Caused by Doping Alkali Metals (Li and Na). Research, 2020, 2020, 4084532.	2.8	2

#	Article	IF	Citations
63067	Rich p -type-doping phenomena in boron-substituted silicene systems. Royal Society Open Science, 2020, 7, 200723.	1.1	5
63068	Defect engineering for nontrivial multiferroic orders inSrTiO3. Physical Review Materials, 2020, 4, .	0.9	8
63069	Designing xenes with two-dimensional triangular lattice. Physical Review Materials, 2020, 4, .	0.9	2
63070	Roomâ€Temperature Ferromagnetism of Singleâ€Layer MoS₂ Induced by Antiferromagnetic Proximity of Yttrium Iron Garnet. Advanced Quantum Technologies, 2021, 4, 2000104.	1.8	9
63071	Study on the optical properties for the F-type color center in BeO crystal with first-principles. Modern Physics Letters B, 2021, 35, 2150148.	1.0	2
63072	Lanthanide-doped metal-organic frameworks with multicolor mechanoluminescence. Science China Materials, 2021, 64, 931-941.	3.5	13
63073	High pressure synthesis of antiferromagnetic semiconductor of ZnMnO3. Physics Letters, Section A: General, Atomic and Solid State Physics, 2020, 384, 126943.	0.9	1
63074	Ab initio modeling framework for Majorana transport in 2D materials: towards topological quantum computing. , 2020, , .		0
63075	Density functional theory study of oxygen vacancy defect diffusion properties in Î»-Ta₂O₅. Japanese Journal of Applied Physics, 2020, 59, 121003.	0.8	4
63076	Strong Boronâ€“Carbon Bonding Interaction Drives CO₂ Reduction to Ethanol over the Boron-Doped Cu(111) Surface: An Insight from the First-Principles Calculations. Journal of Physical Chemistry C, 2021, 125, 572-582.	1.5	12
63077	First principles study of the electronic, elastic, infrared and electrical properties of LiZnPS4. Solid State Communications, 2020, 322, 114057.	0.9	0
63078	Theoretical Assignment of Oxidation State of Uranium in Binary, Ternary, and Quaternary Tellurides. Journal of Physical Chemistry C, 2021, 125, 1029-1040.	1.5	2
63079	First-principles study on structural mechanical and thermodynamic properties of HfMoTaTiZr. Journal of Physics: Conference Series, 2020, 1706, 012148.	0.3	1
63080	Diverse Properties of Carbon-Substituted Silicenes. Frontiers in Physics, 2020, 8, .	1.0	0
63081	Metallic ferroelectric-ferromagnetic multiferroics in strained EuTiO3â^'xHx. Physical Review B, 2020, 102, .	1.1	1
63082	Temperature-induced structural evolution in liquid Ag-Ga alloys. Physical Review B, 2020, 102, .	1.1	1
63083	Statistical approach to obtaining vacancy formation energies in high-entropy crystals from first principles calculations: Application to a high-entropy diboride. Physical Review Materials, 2020, 4, .	0.9	4
63084	Vibrational properties and Raman spectra of 2â€Đ octagonâ€structure nitrogen. Journal of Raman Spectroscopy, 2021, 52, 626-634.	1.2	0

#	Article	IF	Citations
63085	Electron Theory Calculation of Thermodynamic Properties of Steels and Its Application to Theoretical Phase Diagram of the Feâ€“Moâ€“B Ternary System. ISIJ International, 2020, 60, 2963-2972.	0.6	3
63086	First-principles study on the influence of biaxial strain on the electronic and magnetic properties of defective blue phosphorene. Physics Letters, Section A: General, Atomic and Solid State Physics, 2020, 384, 126853.	0.9	1
63087	Various polymorphs of group IIIâ€“VI (GaSe, InSe, GaTe) monolayers with quasi-degenerate energies: facile phase transformations, high-strain plastic deformation, and ferroelastic switching. Materials Today Physics, 2020, 15, 100229.	2.9	4
63088	Unraveling Structural and Optical Properties of Two-Dimensional Mo_xW_{1â€“x}S₂ Alloys. Journal of Physical Chemistry C, 2021, 125, 774-781.	1.5	17
63089	A neural-network based framework of developing cross interaction in alloy embedded-atom method potentials: application to Zrâ€“Nb alloy. Journal of Physics Condensed Matter, 2021, 33, 084004.	0.7	2
63090	Pressure-Induced High-Î° Dielectric Properties and Multiple Phase Transitions between Novel Nonperovskite and Perovskite Phases in LiSbO3: A First-Principles Study. Journal of Physical Chemistry C, 2021, 125, 878-885.	1.5	2
63091	Effect of Nitrogen on the Growth of (100)-, (110)-, and (111)-Oriented Diamond Films. Applied Sciences (Switzerland), 2021, 11, 126.	1.3	1
63092	Firstâ€principles study of Cs 2 Ti 1â^' x M x Br 6 (M = Pb, Sn) and numerical simulation of the solar cells based on Cs 2 Ti 0.25 Sn 0.75 Br 6. International Journal of Energy Research, 2021, 45, 8049-8060.	2.2	5
63093	A computational survey of metal-free polyimide-based photocatalysts within the single-stranded polymer model. Molecular Catalysis, 2020, 497, 111184.	1.0	4
63094	Tunable metalâ€“insulator transition in LaTiO₃/CaVO₃ superlattices: A theoretical study*. Chinese Physics B, 2020, 29, 127303.	0.7	4
63095	Efficient approaches to solutions of partition function for condensed matters. Journal of Physics Condensed Matter, 2021, 33, 115901.	0.7	4
63096	Critical role of parallel momentum in quantum well state couplings in multi-stacked nanofilms: An angle resolved photoemission study. AIP Advances, 2020, 10, 125211.	0.6	1
63097	Antimony oxide nanostructures in the monolayer limit: self-assembly of van der Waals-bonded molecular building blocks. Nanotechnology, 2021, 32, 125701.	1.3	2
63098	Combined experimental and first-principles studies of structural and physical properties of Î²-Ti3SiC2. Journal of Applied Physics, 2020, 128, 225902.	1.1	1
63099	First-principles calculation of the configurational energy density of states for a solid-state ion conductor with a variant of the Wang and Landau algorithm. Physical Review E, 2020, 102, 063304.	0.8	1
63100	Dense and Low Oxygen Permeability Bilayer Ceramic Interconnect for Tubular Anode-Support Solid Oxide Cells. ACS Applied Energy Materials, 2021, 4, 341-349.	2.5	1
63101	Aggregation of retained helium and hydrogen in titanium beryllide Be₁₂Ti: a first-principles study. RSC Advances, 2021, 11, 34860-34869.	1.7	4
63102	Single Non-Noble Metal Atom Doped C2N Catalyst for Chemoselective Hydrogenation of 3-Nitrostyrene. Physical Chemistry Chemical Physics, 2021, 23, 25761-25768.	1.3	1

#	Article	IF	Citations
63103	CO2-Selective Zeolitic Imidazolate Framework Membrane on Graphene Oxide Nanoribbons: Experimental and Theoretical Studies. Journal of Materials Chemistry A, 0, , .	5.2	6
63104	High spin polarized Fe₂ cluster combined with vicinal nonmetallic sites for catalytic ammonia synthesis from a theoretical perspective. Inorganic Chemistry Frontiers, 2021, 8, 5299-5311.	3.0	6
63105	Nodal-loop half metallicity in a two-dimensional Fe₄N₂ pentagon crystal with room-temperature ferromagnetism. Nanoscale, 2021, 13, 19493-19499.	2.8	14
63106	Phase-structure-dependent Na ion transport in yttrium-iodide sodium superionic conductor Na₃YI₆. Journal of Materials Chemistry A, 2021, 9, 26256-26265.	5.2	13
63107	Janus silver/ternary silver halide nanostructures as plasmonic photocatalysts boost the conversion of CO₂ to acetaldehyde. Nanoscale, 2021, 13, 20289-20298.	2.8	5
63108	Prediction of bimetal embedded in two-dimensional materials for CO₂ reduction electrocatalysis with a new integrated descriptor. Physical Chemistry Chemical Physics, 2021, 23, 26241-26249.	1.3	3
63109	Spin-crossover complexes in nanoscale devices: main ingredients of the moleculeâ€“substrate interactions. Nanoscale, 2021, 13, 18702-18713.	2.8	13
63110	First-principles studies of oxygen ion migration behavior for different valence B-site ion doped SrFeO_{3â^’Î´} ceramic membranes. Physical Chemistry Chemical Physics, 2021, 23, 27266-27272.	1.3	4
63111	Methane pyrolysis in low-cost, alkali-halide molten salts at high temperatures. Sustainable Energy and Fuels, 2021, 5, 6107-6123.	2.5	31
63112	Tunable phase stability of negative thermal expansion materials by theory and experiment. Physical Chemistry Chemical Physics, 2021, 23, 25533-25541.	1.3	1
63113	Tunable magnetic coupling and high Curie temperature of twoâ€“dimensional PtBr3 via van der waals heterostructures. Applied Surface Science, 2022, 572, 151478.	3.1	5
63114	Strong hydrophobic affinity and enhanced â€¢OH generation boost energy-efficient electrochemical destruction of perfluorooctanoic acid on robust ceramic/PbO2-PTFE anode. Separation and Purification Technology, 2022, 280, 119919.	3.9	13
63115	Martensitic transformation mechanism of Mg-Sc lightweight shape memory alloys. Scripta Materialia, 2022, 207, 114316.	2.6	10
63116	Pre-doping iodine to restrain formation of low-active graphitic-N in hard carbon for significantly boosting sodium storage performance. Carbon, 2022, 186, 193-204.	5.4	16
63117	Doping with W6+ ions enhances the performance of TiNb2O7 as an anode material for lithium-ion batteries. Applied Surface Science, 2022, 573, 151517.	3.1	25
63118	Coexistence of two gold-induced one-dimensional structures on a single terrace of the Si(11 11 13). Applied Surface Science, 2022, 573, 151501.	3.1	0
63119	Van der Waal heterostructure of hBAs and XMY (MÂ=ÂMo, W; (X<mml:math) Tj ETQq0 0 0 rgBT /Overlock 10 Tf 50 112 Td (xmlns:mml=	0.9	2
63120	A superhard carbon allotrope with cage structure: oS44-carbon. Journal of Solid State Chemistry, 2022, 305, 122653.	1.4	5

#	Article	IF	Citations
63121	Construction of Ti4O7/TiN/carbon microdisk sulfur host with strong polar Nâ€“Tiâ€“O bond for ultralong life lithiumâ€“sulfur battery. Energy Storage Materials, 2022, 44, 180-189.	9.5	74
63122	The thermal and elastic properties of U3Si5 and their variations induced by incorporated aluminum. Journal of Nuclear Materials, 2022, 558, 153331.	1.3	1
63123	Unraveling Electron-deficient Setaria-viridis-like Co3O4@MnO2 heterostructure with superior photoelectrocatalytic efficiency for water remediation. Applied Surface Science, 2022, 573, 151473.	3.1	11
63124	Exploration of the icosahedral clusters in Niâ€“Nb binary metallic glasses via first-principles theory. Journal of Non-Crystalline Solids, 2022, 575, 121232.	1.5	1
63125	Oxidation behaviors of CrNb, CrNbTi, and CrNbTaTi concentrated refractory alloys. Intermetallics, 2022, 140, 107374.	1.8	12
63126	A theoretical study of Cs(I) adsorption on kaolinite basal surfaces. Chemical Physics, 2022, 553, 111380.	0.9	4
63127	Experimental and theoretical study of crystal structure and bandgap of CdBi2S4. Journal of Solid State Chemistry, 2022, 305, 122695.	1.4	1
63128	Influence of vertical strain on the photoelectronic properties of the ReSe2/MoSe2 van der Waals heterostructure. Applied Surface Science, 2022, 572, 151465.	3.1	6
63129	First-principles study of the electronic and magnetic properties of monolayer CrOBr. Solid State Communications, 2022, 341, 114559.	0.9	6
63130	Theoretical insights into mechanisms of electrochemical reduction of CO2 to ethylene catalyzed by Pd3Au. Applied Surface Science, 2022, 572, 151474.	3.1	12
63131	Oxygen promoter on copper-silver coupling for electrochemical carbon dioxide reduction catalysts. Applied Surface Science, 2022, 573, 151532.	3.1	1
63132	Low lattice thermal conductivity and its role in the remarkable thermoelectric performance of newly predicted SiS2 and SiSe2 monolayers. Computational Materials Science, 2022, 201, 110931.	1.4	12
63133	Coverage-dependent adsorption and stability of functionalized Ge(1 0 0) and (1 1 1) surfaces. Applied Surface Science, 2022, 572, 151466.	3.1	0
63134	Scandium decorated C24 fullerene as high capacity reversible hydrogen storage material: Insights from density functional theory simulations. Applied Surface Science, 2022, 573, 151389.	3.1	48
63135	Effect of Al3+ and Mg2+ on the flotation of fluorapatite using fatty- and hydroxamic-acid collectors â€“ A multiscale investigation. Applied Surface Science, 2022, 572, 151499.	3.1	17
63136	Ultrasensitive acetone gas sensor can distinguish the diabetic state of people and its high performance analysis by first-principles calculation. Sensors and Actuators B: Chemical, 2022, 351, 130863.	4.0	39
63137	Prediction of nodal-line semimetals in 2D ScX (XÂ=ÂP, As) with high stability and considerable fermi velocities. Chemical Physics, 2022, 552, 111375.	0.9	0
63138	Exploring thermal expansion of carbon-based nanosheets by machine-learning interatomic potentials. Carbon, 2022, 186, 501-508.	5.4	30

#	Article	IF	Citations
63139	A theoretical study of the controversial surface states of the 2D lead halide perovskites. Applied Surface Science, 2022, 572, 151485.	3.1	4
63140	Fe-Phthalocyanine on Cu(111) and Ag(111): A DFT+vdWs investigation. Surface Science, 2022, 716, 121961.	0.8	6
63141	High-pressure synthesis, crystal structure, and physical properties of NaB13C2 single crystals. Journal of Alloys and Compounds, 2022, 893, 162320.	2.8	1
63142	Boosting polysulfides immobilization and conversion through CoS2 catalytic sites loaded carbon fiber for robust lithium sulfur batteries. Journal of Colloid and Interface Science, 2022, 608, 963-972.	5.0	20
63143	Multisublattice cluster expansion study of short-range ordering in iron-substituted strontium titanate. Computational Materials Science, 2022, 202, 110969.	1.4	0
63144	Construction of machine-learning Zr interatomic potentials for identifying the formation process of c-type dislocation loops. Computational Materials Science, 2022, 202, 110865.	1.4	7
63145	The roles of Rh crystal phase and facet in syngas conversion to ethanol. Chemical Engineering Science, 2022, 248, 117186.	1.9	10
63146	Impact of Sn doping on the hydrogen detection characteristics of ZnO thin films: Insights from experimental and DFT combination. Applied Surface Science, 2022, 574, 151585.	3.1	9
63147	High-performance water gas shift induced by asymmetric oxygen vacancies: Gold clusters supported by ceria-praseodymia mixed oxides. Applied Catalysis B: Environmental, 2022, 301, 120789.	10.8	30
63148	Li-intercalation boosted oxygen vacancies enable efficient electrochemical nitrogen reduction on ultrathin TiO2 nanosheets. Chemical Engineering Journal, 2022, 430, 133085.	6.6	30
63149	Van der Waals heterostructure of graphene Defected&Doped X(X = Au, N) composite ZnO monolayer: AÂFirstÂPrinciple study. Materials Science in Semiconductor Processing, 2022, 138, 106247.	1.9	5
63150	Density functional theory research on the adsorption properties of Ti-doped graphene for acetone and other gases. Materials Science in Semiconductor Processing, 2022, 138, 106252.	1.9	8
63151	Improved photocatalytic CO2 and epoxides cycloaddition via the synergistic effect of Lewis acidity and charge separation over Zn modified UiO-bpydc. Applied Catalysis B: Environmental, 2022, 301, 120793.	10.8	42
63152	Deep learning potential for superionic phase of Ag2S. Computational Materials Science, 2022, 202, 110963.	1.4	12
63153	Segregation behavior of alloying elements and its effects on stacking fault of Î³â€² phase in Ni-based superalloys: First-principles study. Computational Materials Science, 2022, 202, 110990.	1.4	4
63154	2D Ni0.25Mn0.75O2: A high-performance cathode for multivalent ion batteries. Computational Materials Science, 2022, 202, 110948.	1.4	4
63155	Non-peripheral octamethyl-substituted cobalt phthalocyanine nanorods supported on N-doped reduced graphene oxide achieve efficient electrocatalytic CO2 reduction to CO. Chemical Engineering Journal, 2022, 430, 133050.	6.6	29
63156	CO and C3H6 poisoning of hydrogen permeation across Pd77Ag23 alloy membranes: A comparative study with pure palladium. Chemical Engineering Journal, 2022, 430, 133080.	6.6	14

#	Article	IF	Citations
63157	Zinc enhances catalytic performance of pyridine-adsorbed HMOR: Dimethyl ether carbonylation. Fuel, 2022, 310, 122225.	3.4	1
63158	[illegible] interatomic bonding in magnetostrictive Fe<mml:math xmlns:mml="http://www.w3.org/1998/Math/MathML" display="inline" id="d1e222" altimg="si1.svg"><mml:msub><mml:mrow /><mml:mrow><mml:mn>0</mml:mn><mml:mo>.</mml:mo><mml:mn>85</mml:mn></mml:mrow></mml:msub></mml:math>Ga<mml:math xmlns:mml="http://www.w3.org/1998/Math/MathML" display="inline" id="d1e234" altimg="si2.svg"><mml:msub><mml:mrow /><mml:mrow><mml:mn>0</mml:mn><mml:mo>.</mml:mo><mml:m	1.4	3
63159	Porous Carbon/Borocarbonitride hybrid with enhanced tap density as a polar host for ultralong life Lithium-Sulfur batteries. Chemical Engineering Journal, 2022, 430, 132987.	6.6	10
63160	Newtype two-dimensional Cr2O3 monolayer with half-metallicity, high curie temperature, and magnetic anisotropy. Journal of Magnetism and Magnetic Materials, 2022, 543, 168657.	1.0	6
63161	Biochar co-doped with nitrogen and boron switching the free radical based peroxydisulfate activation into the electron-transfer dominated nonradical process. Applied Catalysis B: Environmental, 2022, 301, 120832.	10.8	165
63162	Machine-learning interatomic potential for radiation damage effects in bcc-iron. Computational Materials Science, 2022, 202, 110960.	1.4	9
63163	In situ construction of S-scheme AgBr/BiOBr heterojunction with surface oxygen vacancy for boosting photocatalytic CO2 reduction with H2O. Applied Catalysis B: Environmental, 2022, 301, 120802.	10.8	289
63164	Defect-rich graphene stabilized atomically dispersed Cu3 clusters with enhanced oxidase-like activity for antibacterial applications. Applied Catalysis B: Environmental, 2022, 301, 120826.	10.8	51
63165	Developing machine learning potential for classical molecular dynamics simulation with superior phonon properties. Computational Materials Science, 2022, 202, 111012.	1.4	3
63166	Interface regulation of mixed matrix membranes by ultrathin MOF nanosheet for faster CO2 transfer. Journal of Membrane Science, 2022, 642, 119991.	4.1	17
63167	Effect of the biaxial strain on the electronic structure, quantum capacitance of NH3 adsorption on pristine Hf2CO2 MXene using first-principles calculations. Applied Surface Science, 2022, 575, 151659.	3.1	9
63168	Optimized orbital occupancy of transition metal in spinel Ni-Co oxides with heteroatom doping for Aprotic Li-O2 battery. Chemical Engineering Journal, 2022, 430, 132977.	6.6	37
63169	Density functional theory studies on ortho-position adsorption of SO3 at step sites of a CaO surface with SO2 and CO2. Fuel, 2022, 310, 122174.	3.4	5
63170	Axial chlorine coordinated iron-nitrogen-carbon single-atom catalysts for efficient electrochemical CO2 reduction. Chemical Engineering Journal, 2022, 430, 132882.	6.6	51
63171	Atomic Structures of Single-Layer Nanoislands of Ni, Cu, Rh, Pd, Ag, Ir, Pt, Au Supported on Au(111) from Density Functional Theory Calculations. Surface Science, 2022, 716, 121960.	0.8	1
63172	In situ crystallization of 0D perovskite derivative Cs3Bi2I9 thin films via ultrasonic spray. Journal of Alloys and Compounds, 2022, 893, 162294.	2.8	11
63173	MXene-Bonded hollow MoS2/Carbon sphere strategy for high-performance flexible sodium ion storage. Chemical Engineering Journal, 2022, 430, 132755.	6.6	49
63174	Phonon transport across GaN/AlN interface: Interfacial phonon modes and phonon local non-equilibrium analysis. International Journal of Heat and Mass Transfer, 2022, 183, 122090.	2.5	16

#	Article	IF	Citations
63175	The room-temperature thermoelectric property of PbTe enhanced by mean-free-path filtering. Journal of Alloys and Compounds, 2022, 893, 162296.	2.8	5
63176	CoO anchored on boron nitride nanobelts for efficient removal of water contaminants by peroxymonosulfate activation. Chemical Engineering Journal, 2022, 430, 132915.	6.6	2
63177	Adsorption of benzene on defective Pt surfaces: A DFT study. Surface Science, 2022, 716, 121959.	0.8	3
63178	First-principles and Monte Carlo investigation of magnetic properties of two-dimensional transition metal alloyed boron-carbide<mml:math xmlns:mml="http://www.w3.org/1998/Math/MathML" altimg="si2.svg"><mml:mrow><mml:mi mathvariant="normal">C</mml:mi><mml:mi mathvariant="normal">r</mml:mi><mml:mi mathvariant="normal">F</mml:mi><mml:mi mathvariant="normal">e</mml:mi><mml:mi mathvariant="normal">B</mml:mi><mml:mi mathvariant="normal">C</mml:mi></mml:mrow></mml:math>sheet. Computational Materials Science,	1.4	2
63179	Semiconductor-to-metal transitions in spin-valve-like van der Waals heterostructures based on buckled honeycombs. Journal of Magnetism and Magnetic Materials, 2022, 544, 168706.	1.0	0
63180	First-principles study on the structures and elastic properties of W-Ta-V ternary alloys. Computational Materials Science, 2022, 202, 110940.	1.4	8
63181	Lattice thermal conductivity of half-Heuslers with density functional theory and machine learning: Enhancing predictivity by active sampling with principal component analysis. Computational Materials Science, 2022, 202, 110938.	1.4	17
63182	Cubic to hexagonal tuning in Fe2Mn(Si1â^'Ge) Heusler alloys. Journal of Alloys and Compounds, 2022, 893, 162236.	2.8	3
63183	Synergistic coupling between Fe7S8-MoS2 heterostructure and few layers MoS2-embeded N-/P-doping carbon nanocapsule enables superior Li-S battery performances. Applied Surface Science, 2022, 574, 151586.	3.1	25
63184	Tunable optoelectronic properties of two-dimensional PbSe by strain: First-principles study. Computational Materials Science, 2022, 202, 110957.	1.4	7
63185	The effect of SrFeO25 native point defects on its electrical properties: First principles investigations. Computational Materials Science, 2022, 202, 110922.	1.4	0
63186	Towards predictive simulations of spinodal decomposition in Fe-Cr alloys. Computational Materials Science, 2022, 202, 110955.	1.4	4
63187	Boosting oxygen-reduction catalysis over mononuclear CuN2+2 moiety for rechargeable Zn-air battery. Chemical Engineering Journal, 2022, 430, 133105.	6.6	12
63188	On the ensemble requirement of fully selective chemical looping methane partial oxidation over La-Fe-based perovskites. Applied Catalysis B: Environmental, 2022, 301, 120788.	10.8	34
63189	Thermal transport in planar <mml:math xmlns:mml="http://www.w3.org/1998/Math/MathML" altimg="si16.svg"><mml:msup><mml:mtext>sp</mml:mtext><mml:mn>2</mml:mn></mml:msup></mml:math>-hybridized carbon allotropes: A comparative study of biphenylene network, pentaheptite and graphene. International Journal of Heat and Mass Transfer, 2022, 183, 122060.	2.5	43
63190	A hostâ€“guest self-assembly strategy to enhance Ï€-electron densities in ultrathin porous carbon nitride nanocages toward highly efficient hydrogen evolution. Chemical Engineering Journal, 2022, 430, 132880.	6.6	33
63191	Donor-Acceptor structural polymeric carbon nitride with in-plane electric field accelerating charge separation for efficient photocatalytic hydrogen evolution. Chemical Engineering Journal, 2022, 430, 132725.	6.6	33
63192	Surface strain and co-doping effect on Sm and Y co-doped BaCeO3 in proton conducting solid oxide fuel cells. Computational Materials Science, 2022, 202, 111007.	1.4	9

#	Article	IF	Citations
63193	Tuning selectivity of electrochemical reduction reaction of CO2 by atomically dispersed Pt into SnO2 nanoparticles. Chemical Engineering Journal, 2022, 430, 133035.	6.6	23
63194	Effect of molybdenum on interfacial properties of titanium carbide reinforced Fe composite. Journal of Materials Science and Technology, 2022, 107, 252-258.	5.6	12
63195	Effect of the decrease of Pb concentration on the properties of pentarnary mixed-halide perovskites CsPb8-xSnxIBr2 and CsPb8-xSnxI2Br (1â‰¤xâ‰¤7) for solar-cell applications: A DFT study. Journal of Physics and Chemistry of Solids, 2022, 161, 110429.	1.9	3
63196	Nitrogen containing organics: A promising high capacity anode for potassium ion batteries. Journal of Physics and Chemistry of Solids, 2022, 161, 110415.	1.9	4
63197	The N-body interatomic potential for molecular dynamics simulations of diffusion in tungsten. Computational Materials Science, 2022, 202, 110962.	1.4	4
63198	Role of surface steps in activation of surface oxygen sites on Ir nanocrystals for oxygen evolution reaction in acidic media. Applied Catalysis B: Environmental, 2022, 302, 120834.	10.8	29
63199	On calculations of basic structural parameters in multi-principal element alloys using small atomistic models. Computational Materials Science, 2022, 202, 110942.	1.4	10
63200	Structure dependent and strain tunable magnetic ordering in ultrathin chromium telluride. Journal of Alloys and Compounds, 2022, 893, 162223.	2.8	8
63201	Forming thermodynamics, structure, and electrical conductivity of TiC O compounds fabricated through the carbothermal reduction process. Journal of Alloys and Compounds, 2022, 892, 162201.	2.8	4
63202	Atomic origin of magnetic coupling of antiphase boundaries in magnetite thin films. Journal of Materials Science and Technology, 2022, 107, 92-99.	5.6	8
63203	CO2 reduction mechanism on the Nb2CO2 MXene surface: Effect of nonmetal and metal modification. Computational Materials Science, 2022, 202, 110971.	1.4	16
63204	Theoretical insights into the crystal and fundamental properties of MgAl9Zn compound: First-Principles calculations. Computational Materials Science, 2022, 202, 110951.	1.4	2
63205	Co decoration and charge injection on the electronic structure and magnetic properties of ZnO monolayer: A first-principles study. Journal of Magnetism and Magnetic Materials, 2022, 544, 168707.	1.0	3
63206	Advanced imaging and simulations of precipitate interfaces in aluminium alloys and their role in phase transformations. MATEC Web of Conferences, 2020, 326, 09003.	0.1	0
63207	Ab-initio study of charged oxygen defects in Nd2Zr2O7. AIP Conference Proceedings, 2020, , .	0.3	0
63208	Achieving the robust immobilization of CoP nanoparticles in cellulose nanofiber network-derived carbon via chemical bonding for a stable potassium ion storage. RSC Advances, 2020, 10, 44611-44623.	1.7	6
63209	First-principles investigation of the phase stability and early stages of precipitation in Mg-Sn alloys. Physical Review Materials, 2020, 4, .	0.9	4
63210	Effect of Nb Alloying Addition on Local Phase Transformation at Microtwin Boundaries in Nickel-Based Superalloys. Minerals, Metals and Materials Series, 2020, , 640-650.	0.3	6

#	Article	IF	Citations
63211	Simple mechanisms of CH₄ reforming with CO₂ and H₂O on a supported Ni/ZrO₂ catalyst. Physical Chemistry Chemical Physics, 2021, 23, 26392-26400.	1.3	4
63212	Extended anisotropic phonon dispersion and optical properties of two-dimensional ternary SnSSe. Inorganic Chemistry Frontiers, 2022, 9, 294-301.	3.0	5
63213	Towards Tuning the Modality of Hierarchical Macro-Nanoporous Metals by Controlling the Dealloying Kinetics of Close-to-Eutectic Alloys. Physical Chemistry Chemical Physics, 2021, 23, 25388-25400.	1.3	2
63214	The thermoelectric properties of Î±-XP (X = Sb and Bi) monolayers from first-principles calculations. Physical Chemistry Chemical Physics, 2021, 23, 24598-24606.	1.3	8
63215	Size and crystal symmetry breaking effects on negative thermal expansion in ScF₃ nanostructures. Physical Chemistry Chemical Physics, 2021, 23, 24814-24822.	1.3	1
63216	Factors affecting the electronâ€“phonon coupling in FeSe under pressure. Physical Chemistry Chemical Physics, 2021, 23, 25107-25113.	1.3	3
63217	Spin filtering controller induced by phase transitions in fluorographane. RSC Advances, 2021, 11, 35718-35725.	1.7	1
63218	Controlling thermoelectric transport via native defects in the diamond-like semiconductors Cu2HgGeTe4 and Hg2GeTe4. Journal of Materials Chemistry A, 0, , .	5.2	4
63219	H₂ and CH₄ production from bio-alcohols using condensed poly(heptazine) Tj ETQq0 0 0 rgBT /Overlock 10 Tf	5.2	20
63220	Why are Zn-rich Znâ€“Mg nanoalloys optimal protective coatings against corrosion? A first-principles study of the initial stages of the oxidation process. Physical Chemistry Chemical Physics, 2021, 23, 24685-24698.	1.3	5
63221	Predicting intrinsic antiferromagnetic and ferroelastic MnF₄ monolayer with controllable magnetization. Journal of Materials Chemistry C, 2021, 9, 17152-17157.	2.7	9
63222	Promising thermoelectric candidate based on a CaAs₃ monolayer: A first principles study. Physical Chemistry Chemical Physics, 2021, 23, 24039-24046.	1.3	2
63223	Optical properties and applications of SnS₂ SAs with different thickness. Opto-Electronic Advances, 2021, 4, 200029-200029.	6.4	35
63224	CVD Growth and Characterization of MoS₂ Nanotubes Grown with FeO Nanoparticle Catalysts. Vacuum and Surface Science, 2019, 62, 617-622.	0.0	0
63225	Corrugated graphene exposes the limits of a widely used ab initio van der Waals DFT functional. Physical Review Materials, 2019, 3, .	0.9	2
63226	New accurate molecular dynamics potential function to model the phase transformation of cesium lead triiodide perovskite (CsPbI₃). RSC Advances, 2020, 10, 44503-44511.	1.7	11
63227	Rationalisation of the Micromechanisms Behind the High-Temperature Strength Limit in Single-Crystal Nickel-Based Superalloys. Minerals, Metals and Materials Series, 2020, , 260-272.	0.3	4
63228	Supersolvus Hot Workability and Dynamic Recrystallization in Wrought Coâ€“Alâ€“W-Base Alloys. Minerals, Metals and Materials Series, 2020, , 857-869.	0.3	0

#	Article	IF	Citations
63229	Formamide Dehydration and Condensation on Acidic Montmorillonite: Mechanistic Insights from Ab-Initio Periodic Simulations. Lecture Notes in Computer Science, 2020, , 502-512.	1.0	0
63230	Dependence of Carbon Concentration and Alloying Elements on the Stability of Iron Carbides. Tetsu-To-Hagane/Journal of the Iron and Steel Institute of Japan, 2020, 106, 352-361.	0.1	1
63231	Ferroelectric critical size of SnTe nanoribbon and its mechanical strain engineering. Transactions of the JSME (in Japanese), 2020, 86, 19-00430-19-00430.	0.1	0
63232	Adaptive Genetic Algorithm for Structure Prediction and Application to Magnetic Materials. , 2020, , 2757-2776.		0
63234	Two-dimensional monolayers of arsenides and silicides of Mo and W: A first principles study. AIP Conference Proceedings, 2020, , .	0.3	0
63235	Computational Methodology. Springer Theses, 2020, , 35-49.	0.0	0
63236	Effect of biaxial strain on the gas-sensing of monolayer GeSe. Wuli Xuebao/Acta Physica Sinica, 2020, 69, 196801.	0.2	4
63237	Novel joint catalytic properties of Fe and N co-doped graphene for CO oxidation. Physical Chemistry Chemical Physics, 2020, 22, 28376-28382.	1.3	3
63238	Surface Thermodynamics and Vibrational Entropy. Springer Handbooks, 2020, , 71-93.	0.3	2
63239	A Theoretical Perspective to the Magnetism of Nanoalloys. , 2020, , 225-265.		0
63240	Surface Phonons: Theoretical Methods and Results. Springer Handbooks, 2020, , 737-782.	0.3	2
63241	First-principles on the energy band mechanism for modifying conduction property of graphene nanomeshes. Wuli Xuebao/Acta Physica Sinica, 2020, 69, 047101.	0.2	1
63242	Group III monochalcogenide of single-layered haeckelites structure MX (M = Al, Ga, In;) Tj ETQq0 0 0 rgBT /Overlock 10 Tf	0.2	0
63243	Tuning Schottky barrier in graphene/InSe van der Waals heterostructures by electric field. Wuli Xuebao/Acta Physica Sinica, 2020, 69, 157302.	0.2	3
63244	Oxygen Solid Solution Strengthening of Titanium Materials Fabricated by Selective Laser Melting Process. Journal of Smart Processing, 2020, 9, 158-163.	0.0	0
63245	High Compressionâ€Induced Conductivity in a Layered Cuâ€“Br Perovskite. Angewandte Chemie, 2020, 132, 4046-4051.	1.6	7
63246	Nonadiabatic Effects in Gas-Surface Dynamics. Springer Handbooks, 2020, , 929-965.	0.3	1
63247	Shock compression of niobium oxides from first-principles. AIP Conference Proceedings, 2020, , .	0.3	0

#	Article	IF	Citations
63248	Strain Effect on the Orientation-dependent Harmonic Spectrum of Monolayer Aluminum Nitride. , 2020, , .		0
63249	First-Principles Calculations 2. Springer Series in Materials Science, 2020, , 329-348.	0.4	4
63250	Application of Multiscale Computational Techniques to the Study of Magnetic Nanoparticle Systems. Lecture Notes in Computer Science, 2020, , 301-311.	1.0	0
63251	Recommender Systems for Materials Discovery. Lecture Notes in Physics, 2020, , 427-443.	0.3	0
63252	Structural and Elastic Properties of Fe-Ge Alloys: ab initio studies. Bulletin of the South Ural State University Series Mathematics Mechanics Physics, 2020, 12, 49-56.	0.2	0
63253	Optical properties of mono and bilayer plumbene: A DFT study. AIP Conference Proceedings, 2020, , .	0.3	1
63254	Friedel Oscillations and Helium Bubble Ordering in Molybdenum. SSRN Electronic Journal, 0, , .	0.4	0
63255	Prediction of short range order in high-entropy alloys and its effect on the electronic, magnetic and mechanical properties. Wuli Xuebao/Acta Physica Sinica, 2020, 69, 046102.	0.2	4
63256	Visible Light-Promoted Carbon Dioxide Reforming of Methane Over Pt/TaN Catalysts. Springer Theses, 2020, , 75-91.	0.0	0
63257	First-principles study of Ca₅N₄ at high pressure. Wuli Xuebao/Acta Physica Sinica, 2020, 69, 067101.	0.2	1
63258	Thermodynamic/Electrochemical Description of High-Voltage Spinels for Lithium-Ion Batteries. Journal of the Electrochemical Society, 2020, 167, 130511.	1.3	3
63259	Chemical stability of Ca₃Co_{4â^'x}O_{9+Î´}/CaMnO_{3â^'Î´} pâ€“n junction for oxide-based thermoelectric generators. RSC Advances, 2020, 10, 5026-5031.	1.7	3
63260	High-throughput investigation of the formation of double spinels. Journal of Materials Chemistry A, 2020, 8, 25756-25767.	5.2	36
63261	A Decade of Computational Surface Catalysis. , 2020, , 1309-1319.		3
63262	Methods of estimations of the band gap for kesterite Cu2ZnSnS(Se)4. Materials Today: Proceedings, 2020, 33, 2495-2498.	0.9	1
63263	Atomistic Simulations for Understanding Microscopic Mechanism of Resistive Switches. Advances in Atom and Single Molecule Machines, 2020, , 95-125.	0.0	0
63264	Lattice strain dependent optical properties of BaSnO3: First principle study. AIP Conference Proceedings, 2020, , .	0.3	0
63265	Ab-initio study of thermoelectric properties of Co2XGa (X = Mn, Mo, Pt). AIP Conference Proceedings, 2020, , .	0.3	0

#	Article	IF	Citations
63266	Site occupancy preference, electrical transport property and thermoelectric performance of Ba₈Cu_{6â^'x}Ge_{40+x} single crystals grown by using different metal fluxes. Materials Advances, 2020, 1, 2953-2963.	2.6	1
63267	Machine learning interatomic potential for molten TiZrHfNb. AIP Conference Proceedings, 2020, , .	0.3	0
63268	Mechanical, electronic properties and deformation mechanisms of Ti₃B₄ under uniaxial compressions: a first-principles calculation. Wuli Xuebao/Acta Physica Sinica, 2020, 69, 043102.	0.2	3
63269	First-principles study of atomic bond nature of one-dimensional carbyne chain under different strains. Wuli Xuebao/Acta Physica Sinica, 2020, 69, 246802.	0.2	1
63270	Energetic potential of hexogen constructed by machine learning. Wuli Xuebao/Acta Physica Sinica, 2020, 69, 238702.	0.2	7
63271	Thermodynamic Study on Solubility Products of Ti₄C₂S₂ in Fe Using First-Principles Calculations. Tetsu-To-Hagane/Journal of the Iron and Steel Institute of Japan, 2020, 106, 911-923.	0.1	0
63272	First principles molecular dynamics simulations of high-pressure melting of diamond. AIP Conference Proceedings, 2020, , .	0.3	1
63274	Unconventional crystal-field splitting in noncentrosymmetric <mml:math xmlns:mml="http://www.w3.org/1998/Math/MathML"><mml:msub><mml:mi>BaTiO</mml:mi><mml:mn>3</mml:mn></mml:msub><mml:mi> thin films. Physical Review Materials, 2020, 4, .	0.0	3
63275	Fate of subducted argon in the deep mantle. Scientific Reports, 2020, 10, 1393.	1.6	6
63276	High-pressure crystal structure and properties of BrCl. Journal of Physics Condensed Matter, 2020, 33, 095401.	0.7	2
63277	HOT Graphene and HOT Graphene Nanotubes: New Low Dimensional Semimetals and Semiconductors. Nanoscale Research Letters, 2020, 15, 56.	3.1	4
63278	Tuning CuZn interfaces in metalâ€"organic framework-derived electrocatalysts for enhancement of CO₂ conversion to C₂ products. Catalysis Science and Technology, 2021, 11, 8065-8078.	2.1	17
63279	Establishing the accuracy of density functional approaches for the description of noncovalent interactions in ionic liquids. Physical Chemistry Chemical Physics, 2021, 23, 25558-25564.	1.3	5
63280	Electrocatalytic performance of Mn-adsorbed g-C₃N₄: a first-principles study. Journal of Materials Chemistry A, 2021, 9, 26266-26276.	5.2	12
63281	Electromagnetic interference shielding material for super-broadband: multi-walled carbon nanotube/silver nanowire film with an ultrathin sandwich structure. Journal of Materials Chemistry A, 2021, 9, 25999-26009.	5.2	23
63282	Zn(NH₃)CO₃: a â€œthree-in-oneâ€•UV nonlinear optical crystal built by a polar molecule bonding strategy. Journal of Materials Chemistry C, 2021, 9, 16477-16484.	2.7	8
63283	Nickel-based metalâ€"organic framework-derived Ni/NC/KB as a separator coating for high capacity lithiumâ€"sulfur batteries. Sustainable Energy and Fuels, 2021, 5, 6372-6380.	2.5	6
63284	Coupling between Deformation and Mass Transport in an Immiscible Alloy at High Shear Strains. SSRN Electronic Journal, 0, , .	0.4	0

#	Article	IF	Citations
63285	Intrinsic ferromagnetism in 2D h-CrC semiconductors with strong magnetic anisotropy and high Curie temperatures. Journal of Materials Chemistry C, 2021, 9, 16495-16505.	2.7	15
63286	Revealing the crystal structures and relative dielectric constants of fluorinated silicon oxides. Journal of Materials Chemistry C, 2021, 9, 15983-15989.	2.7	3
63287	Electronic configuration modulation of tin dioxide by phosphorus dopant for pathway change in electrocatalytic water oxidation. Inorganic Chemistry Frontiers, 2021, 9, 83-89.	3.0	5
63288	Mechanical, electronic and optical properties of a novel B₂P₆ monolayer: ultrahigh carrier mobility and strong optical absorption. Physical Chemistry Chemical Physics, 2021, 23, 24915-24921.	1.3	46
63289	Quasi-two-dimensional NaCl crystals encapsulated between graphene sheets and their decomposition under an electron beam. Nanoscale, 2021, 13, 19626-19633.	2.8	6
63290	Study of photogenerated exciton dissociation in transition metal dichalcogenide van der Waals heterojunction A2-MWS₄: a first-principles study. Physical Chemistry Chemical Physics, 2021, 23, 26768-26779.	1.3	2
63291	Capturing excitonic and polaronic effects in lead iodide perovskites using many-body perturbation theory. Journal of Materials Chemistry C, 2021, 9, 17113-17123.	2.7	8
63292	Enhanced valleytronic properties in germanene by direct proximity to heavy metal layer. Journal of Physics Condensed Matter, 2020, 33, 095502.	0.7	0
63294	Electronic and magnetic properties of new binary uranium-boron compounds with 2D and 3D boron networks: A revisit of the U:B system. Solid State Sciences, 2020, 101, 106150.	1.5	2
63295	Wavevector-dependent optical properties from wavevector-independent proper conductivity tensor. European Physical Journal B, 2020, 93, 1.	0.6	1
63296	Topological evolution of correlated band structures and heavy-fermion-like behavior in a molybdenum-based metal organic framework C48S36Mo6. Journal of Physics Condensed Matter, 2020, 32, 295503.	0.7	0
63298	Intrinsic defects of GaSe. Journal of Physics Condensed Matter, 2020, 32, 285503.	0.7	4
63299	Elucidation of the Sulfide Corrosion Mechanism in Piston Pin Bushings. , 0, , .		0
63300	First-principles study on the CO adsorption and electronic properties of Fe (111) modified by Cu single atom. Journal of Fuel Chemistry and Technology, 2020, 48, 440-447.	0.9	3
63301	Thermodynamic Study on Solubility Products of Ti₄C₂S₂ in Fe Using First-Principles Calculations. ISIJ International, 2020, 60, 745-755.	0.6	1
63302	Ab initio modeling of few-layer dilute magnetic semiconductors. , 2021, , .		0
63303	Mechanism Investigation of Temperature Dependent Growth and Etching Process of GeCl4 on SiGe Surface: ab-initio Study. , 2021, , .		0
63304	Advances in atomistic modeling for predictive TCAD applications. , 2021, , .		1

#	Article	IF	Citations
63305	First-principles investigation of amorphous n-type In₂ O₃ for BEOL transistor. , 2021, , .		1
63306	Modeling Contact Resistivity in Monolayer Molybdenum disulfide Edge contacts. , 2021, , .		1
63307	Perovskiteâ€Type SrVO₃ as Highâ€Performance Anode Materials for Lithiumâ€Ion Batteries. Advanced Materials, 2022, 34, e2107262.	11.1	29
63308	Mechanism of Selective Hydrogenation of 4-Nitrophenylacetylene Using Ptâ€“Zn Intermetallic Nanoparticles: The Role of Hydrogen Coverage. Journal of Physical Chemistry C, 2021, 125, 23803-23812.	1.5	2
63309	Understanding the Reversible Reactions of Liâ€N₂ Battery Catalyzed With SnO₂. Energy and Environmental Materials, 2023, 6, .	7.3	7
63310	First-Principles Investigation on Work Function of Martensitic Carbon Steels: Effect of Interstitial Carbon on Anodic Dissolution Resistance. Journal of the Electrochemical Society, 2021, 168, 111503.	1.3	10
63311	Theoretical considerations of superconducting HfBH2 and HfB2H under high pressure. Journal of Applied Physics, 2021, 130, 153904.	1.1	3
63312	Bacterial cellulose-regulated synthesis of metallic Ni catalysts for high-efficiency electrosynthesis of hydrogen peroxide. Science China Materials, 0, , 1.	3.5	6
63313	Impacts of terminal molecules on metal-atom diffusion into alkane SAM films: first-principles study. Japanese Journal of Applied Physics, 0, , .	0.8	0
63314	Electrostatic interaction determines thermal conductivity anisotropy of Bi2O2Se. Cell Reports Physical Science, 2021, 2, 100624.	2.8	8
63315	Surface Properties of LaNi5 and TiFeâ€”Future Opportunities of Theoretical Research in Hydrides. Frontiers in Energy Research, 2021, 9, .	1.2	3
63316	Density Functional Theory Study on the Effect of Isomorphic Substitution of FAU Molecular Sieve on N2 Adsorption Performance. Advances in Condensed Matter Physics, 2021, 2021, 1-9.	0.4	0
63317	Probing into the crystal plane effect on the reduction of Î±-Fe2O3 in CO by Operando Raman spectroscopy. Journal of Fuel Chemistry and Technology, 2021, 49, 1558-1566.	0.9	9
63318	Interplay of magnetism and dimerization in the pressurized Kitaev material <mml:math xmlns:mml="http://www.w3.org/1998/Math/MathML"><mml:mrow><mml:mi>Î²</mml:mi><mml:mtext>â^'</mml:mtext><mml:msub><mml:mi>Physical Review B, 2021, 104, .	1.1	4
63319	Eightfold Degenerate Fermions in Two Dimensions. Physical Review Letters, 2021, 127, 176401.	2.9	11
63320	Prediction of stable Cu structure and phase transition mechanism at ultra-high pressure: A comprehensive properties characterization by DFT calculation. Physica B: Condensed Matter, 2022, 625, 413538.	1.3	1
63321	Identifying the crucial role of water and chloride for efficient mild oxidation of methane to methanol over a [Cu2(Î¼-O)]2+-ZSM-5 catalyst. Journal of Catalysis, 2022, 405, 1-14.	3.1	19
63322	Firstâ€Principles Study of 3d Transition Metal Atoms Doped Ni₁₃ Cluster as Efficient Electrocatalyst for Nitrogen Reduction Reaction. Advanced Theory and Simulations, 2021, 4, 2100353.	1.3	7

#	Article	IF	Citations
63323	Toward Understanding and Simplifying the Reaction Network of Ketene Production on ZnCr₂O₄ Spinel Catalysts. Journal of Physical Chemistry C, 2021, 125, 24902-24914.	1.5	8
63324	H_d-Graphene: A Hexagon-Deficient Carbon-Based Anode for Metal-Ion Batteries with High Charge/Discharge Rates. ACS Applied Electronic Materials, 2021, 3, 5147-5154.	2.0	4
63325	Trends of complete anion substitution on electronic, ferroelectric, and optoelectronic properties of BiFeX3 (X = O, S, Se, and Te). AIP Advances, 2021, 11, 115108.	0.6	0
63326	First-Principles Studies on the Formation of Oxygen Vacancies in Li₂CoSiO₄. Journal of the Electrochemical Society, 2021, 168, 110527.	1.3	2
63327	Molecular Dynamics Study of Heteroepitaxial Growth of HgCdTe on Perfect and Dislocated (211)B CdZnTe Substrates. ACS Applied Electronic Materials, 0, , .	2.0	2
63328	Boron-Nitrogen-Co-Doping Nanocarbons to Create Rich Electroactive Defects toward Simultaneous Sensing Hydroquinone and Catechol. Electrochimica Acta, 2022, 402, 139427.	2.6	10
63329	Borophenes made easy. Science Advances, 2021, 7, eabk1490.	4.7	31
63330	Investigating the Chemical Ordering in Quaternary Clathrate Ba8AlxGa16â€“xGe30. Inorganic Chemistry, 2021, 60, 16977-16985.	1.9	0
63331	Dirac semimetal phase and switching of band inversion in XMg2Bi2 (Xâ€‰=â€‰Ba and Sr). Scientific Reports, 2021, 11, 21937.	1.6	6
63332	Fe doped InVO4 nanosheets with rich surface oxygen vacancies for enhanced electrochemical nitrogen fixation. Chemical Engineering Journal, 2022, 431, 133383.	6.6	15
63333	Realizing Enhanced Thermoelectric Performance and Hardness in Icosahedral Cu₅FeS_{4â^'}_xSe_x with Highâ€Ðensity Twin Boundaries. Small, 2022, 18, e2104592.	5.2	15
63334	Defluorination and adsorption of tetrafluoroethylene (TFE) on TiO2(110) and Cr2O3(0001). Scientific Reports, 2021, 11, 21551.	1.6	0
63335	Layered Transition Metal Oxides as Ca Intercalation Cathodes: A Systematic Firstâ€Principles Evaluation. Advanced Energy Materials, 2021, 11, 2101698.	10.2	8
63336	Dual optimization approach to Mo single atom dispersed g-C3N4 photocatalyst: Morphology and defect evolution. Applied Catalysis B: Environmental, 2022, 303, 120904.	10.8	203
63337	Ultralow lattice thermal conductivity and high thermoelectric performance of penta-Sb2C monolayer: A first principles study. Journal of Applied Physics, 2021, 130, 185104.	1.1	7
63338	Influence of Alloy Atoms on Substitution Properties of Hydrogen by Helium in ZrCoH3. Materials, 2021, 14, 6704.	1.3	1
63339	Lattice thermodynamic behavior in CeO2 from first principles. Physics Letters, Section A: General, Atomic and Solid State Physics, 2021, 423, 127769.	0.9	2
63340	Controllable Polarization and Doping in Ferroelectric In₂Se₃ Monolayers and Heterobilayers via Intrinsic Defect Engineering. Journal of Physical Chemistry C, 2021, 125, 24648-24654.	1.5	12

#	Article	IF	Citations
63341	Atomistic observation of in situ fractured surfaces at a V-doped WC Co interface. Journal of Materials Science and Technology, 2022, 110, 103-108.	5.6	8
63342	Sabatier principle of metal-support interaction for design of ultrastable metal nanocatalysts. Science, 2021, 374, 1360-1365.	6.0	250
63343	Polarization Selectivity of Aloof-Beam Electron Energy-Loss Spectroscopy in One-Dimensional ZnO Nanorods. Physical Review Applied, 2021, 16, .	1.5	1
63344	Discrete quantum geometry and intrinsic spin Hall effect. Physical Review B, 2021, 104, .	1.1	1
63345	Designing high-entropy ceramics via incorporation of the bond-mechanical behavior correlation with the machine-learning methodology. Cell Reports Physical Science, 2021, 2, 100640.	2.8	10
63346	Defectâ€Free Metal Deposition on 2D Materials via Inkjet Printing Technology. Advanced Materials, 2022, 34, e2104138.	11.1	22
63347	Thermal conductivity of <mml:math xmlns:mml="http://www.w3.org/1998/Math/MathML"><mml:msub><mml:mi>CaSiO</mml:mi><mml:mn>3</mml:mn></mml:msub></m perovskite at lower mantle conditions. Physical Review B, 2021, 104, .	1.1	9
63348	Selective Methane Oxidation to Methanol on ZnO/Cu₂O/Cu(111) Catalysts: Multiple Site-Dependent Behaviors. Journal of the American Chemical Society, 2021, 143, 19018-19032.	6.6	41
63349	Aspects of strong electronâ€“phonon coupling in superconductivity of compressed metal hydrides MH6 (Mâ€‰=â€‰Mg, Ca, Sc, Y) with Im-3m structure. Journal of Applied Physics, 2021, 130, 183902.	1.1	5
63350	Thermal conductivity of Î±-U with point defects. Journal of Applied Physics, 2021, 130, .	1.1	6
63351	Electromechanically Actuated MXene Nanotubes for Tunable Mass Transport. Journal of Physical Chemistry C, 2021, 125, 25275-25283.	1.5	1
63352	Comparing the effective enhancement of local and nonlocal spin-orbit couplings on honeycomb lattices due to strong electronic correlations. Physical Review B, 2021, 104, .	1.1	7
63353	Primary radiation damage in silicon from the viewpoint of a machine learning interatomic potential. Physical Review Materials, 2021, 5, .	0.9	3
63354	Photo-Sono Interfacial Engineering Exciting the Intrinsic Property of Herbal Nanomedicine for Rapid Broad-Spectrum Bacteria Killing. ACS Nano, 2021, 15, 18505-18519.	7.3	61
63355	Galliumâ€Based Liquid Metal Reaction Media for Interfacial Precipitation of Bismuth Nanomaterials with Controlled Phases and Morphologies. Advanced Functional Materials, 2022, 32, .	7.8	28
63356	<scp>Inq</scp>, a Modern GPU-Accelerated Computational Framework for (Time-Dependent) Density Functional Theory. Journal of Chemical Theory and Computation, 2021, 17, 7447-7467.	2.3	7
63357	Flexible Alkaliâ€“Halogen Bonding in Two Dimensional Alkali-Metal Organic Frameworks. Journal of Physical Chemistry Letters, 2021, 12, 10808-10814.	2.1	11
63358	Anisotropy in elasticity, sound velocity, thermal conductivity, and thermodynamics properties of dodecaboride Zr 0.5 Y 0.5 B 12. International Journal of Quantum Chemistry, 0, , e26836.	1.0	0

#	Article	IF	Citations
63359	The Restructuring-Induced CoO_x Catalyst for Electrochemical Water Splitting. Jacs Au, 2021, 1, 2216-2223.	3.6	32
63360	Extremely Low Thermal Conductivity and Enhanced Thermoelectric Performance of Porous Gallium-Doped In₂O₃. ACS Applied Energy Materials, 2021, 4, 12943-12953.	2.5	5
63361	NaF-rich solid electrolyte interphase for dendrite-free sodium metal batteries. Energy Storage Materials, 2022, 44, 477-486.	9.5	73
63362	Understanding complex multiple sublattice magnetism in double double perovskites. Scientific Reports, 2021, 11, 21764.	1.6	6
63363	Hexagonal BN- and BNO-supported Au and Pt nanocatalysts in carbon monoxide oxidation and carbon dioxide hydrogenation reactions. Applied Catalysis B: Environmental, 2022, 303, 120891.	10.8	26
63364	Polyphenylene Sulfideâ€Based Solidâ€State Separator for Limited Li Metal Battery. Small, 2021, 17, e2104365.	5.2	12
63365	Spontaneous dynamical disordering of borophenes in MgB2 and related metal borides. Nature Communications, 2021, 12, 6268.	5.8	14
63366	Optimization of Nanostructured Copper Sulfide to Achieve Enhanced Enzyme-Mimic Activities for Improving Anti-Infection Performance. ACS Applied Materials & Interfaces, 2021, 13, 53659-53670.	4.0	11
63367	Structure-related electrochemical behavior of sulfur-rich polymer cathode with solid-solid conversion in lithium-sulfur batteries. Energy Storage Materials, 2022, 45, 1144-1152.	9.5	30
63368	Charged domain boundaries stabilized by translational symmetry breaking in the hybrid improper ferroelectric Ca3â€“xSrxTi2O7. Communications Materials, 2021, 2, .	2.9	8
63369	Strain and electric field tunable electronic and optical properties in antimonene/C3N van der Waals heterostructure. Solid State Sciences, 2021, 122, 106771.	1.5	9
63370	Signatures of bosonic Landau levels in a finite-momentum superconductor. Nature, 2021, 599, 51-56.	13.7	5
63371	Dirac Fermions in Graphene with Stacking Fault Induced Periodic Line Defects. Journal of Physical Chemistry Letters, 2021, 12, 10874-10879.	2.1	12
63372	Computational understanding of Fe-Pt synergy in promoting guaiacol hydrodeoxygenation. Surface Science, 2022, 717, 121985.	0.8	4
63373	Interfacial Covalent Bonding Endowing Ti₃C₂â€Sb₂S₃ Composites High Sodium Storage Performance. Small, 2022, 18, e2104293.	5.2	30
63374	Pressure Dependence of Superconducting Properties, Pinning Mechanism, and Crystal Structure of the Fe_{0.99}Mn_{0.01}Se_{0.5}Te_{0.5}Superconductor. ACS Omega, 2021, 6, 30419-30431.	1.6	2
63375	Modulation of electrical performance of zigzag edged tetra-penta-octagonal graphene nanoribbons based devices via boundary passivations. Results in Physics, 2021, 31, 104945.	2.0	7
63376	Accelerated Discovery of Singleâ€Atom Catalysts for Nitrogen Fixation via Machine Learning. Energy and Environmental Materials, 2023, 6, .	7.3	26

#	Article	IF	Citations
63377	Decoration of Au NPs on hollow structured BiOBr with surface oxygen vacancies for enhanced visible light photocatalytic H2O2 evolution. Journal of Solid State Chemistry, 2022, 306, 122722.	1.4	12
63378	Anionic Redox Regulated via Metalâ€“Ligand Combinations in Layered Sulfides. Advanced Materials, 2022, 34, e2107353.	11.1	11
63379	Understanding the oxygen-vacancy-related catalytic cycle for H2 oxidation on ceria-based SOFC anode and the promotion effect of lanthanide doping from theoretical perspectives. Applied Surface Science, 2022, 576, 151803.	3.1	6
63380	Site occupancy behavior of the binary Î¼ phase. Journal of Solid State Chemistry, 2022, 305, 122704.	1.4	8
63381	Magnetic and structural properties of Co-Ni-<mml:math xmlns:mml="http://www.w3.org/1998/Math/MathML" display="inline" id="d1e1016" altimg="si84.svg"><mml:mi>Z</mml:mi></mml:math>Â(<mml:math) Tj ETQq0 0 0 rgBT /Overlock 10 Tf 50 587 Td (xmlns:mml="http://v	1.0	2
63382	an Effect of Point Defects on Electronic Structure of Monolayer GeS. Nanomaterials, 2021, 11, 2960.	1.9	2
63383	Engineering the low-coordinated single cobalt atom to boost persulfate activation for enhanced organic pollutant oxidation. Applied Catalysis B: Environmental, 2022, 303, 120877.	10.8	54
63384	Influence of Promoters (Fe, Mo, W) on the Structural and Catalytic Properties of Ni/BEA for Guaiacol Hydrodeoxygenation. ACS Sustainable Chemistry and Engineering, 2021, 9, 15673-15682.	3.2	13
63385	Hole-Pinned Defect Clusters for a Large Dielectric Constant up to GHz in Zinc and Niobium Codoped Rutile SnO₂. ACS Applied Materials & Interfaces, 2021, 13, 54124-54132.	4.0	9
63386	Perovskite-like K₃TiOF₅ Exhibits (3 + 1)-Dimensional Commensurate Structure Induced by Octahedrally Coordinated Potassium Ions. Journal of the American Chemical Society, 2021, 143, 18907-18916.	6.6	4
63387	Highly efficient electrochemical carbon dioxide reduction to syngas with tunable ratios over pyridinic- nitrogen rich ultrathin carbon nanosheets. Journal of Colloid and Interface Science, 2022, 608, 2650-2659.	5.0	11
63388	Anomalies in the temperature evolution of Dirac states in the topological crystalline insulator SnTe. Physical Review B, 2021, 104, .	1.1	7
63389	Density Functional Theory Half-Electron Self-Energy Correction for Fast and Accurate Nonadiabatic Molecular Dynamics. Journal of Physical Chemistry Letters, 2021, 12, 10886-10892.	2.1	10
63390	Surface Reconstruction Enabled Efficient Hydrogen Generation on a Cobaltâ€“Iron Phosphate Electrocatalyst in Neutral Water. ACS Applied Materials & Interfaces, 2021, 13, 53798-53809.	4.0	14
63391	Boron Coordination Effect in Niâ^'N_x Doped Graphene Catalysts on the ORR Performance Based on DFT Calculations. ChemPhysChem, 2022, 23, .	1.0	7
63392	Azobenzene-Iron(III)porphyrin Hybrid Composite as a Light-Driven Molecular Spin Regulator: Some Promising Insights from DFT. Chemistry of Materials, 2021, 33, 8786-8799.	3.2	4
63393	Band alignment engineering of a Ruddlesdenâ€“Popper perovskite-based heterostructure constructed using Cs2SnI2Cl2 and Î±-In2Se3: The effects of ferroelectric polarization switching and electric fields. Applied Physics Letters, 2021, 119, 182903.	1.5	10
63394	Two distinct superconducting states controlled by orientations of local wrinkles in LiFeAs. Nature Communications, 2021, 12, 6312.	5.8	16

#	Article	IF	Citations
63395	The barrier free splitting of O-H bond in H2O and CH3OH due to the synergetic effects of single atom (Cu1/Fe1) coordination change and ZnO(1 1 0) surface oxygen activation. Applied Surface Science, 2022, 576, 151750.	3.1	3
63396	Computational Design of Pd Nanoclusters and Pd Single-Atom Catalysts Supported on O-Functionalized Graphene. ACS Applied Nano Materials, 2021, 4, 12235-12249.	2.4	9
63397	<scp>Vacancyâ€“vacancy</scp> pairs induced new phase formation in carbon boride: A design principle to achieve superior performance Li/Naâ€ion battery anodes. EcoMat, 2022, 4, .	6.8	16
63398	Asymmetrical Ï€ back-donation of hetero-dicationic Mo4+-Mo6+ pairs for enhanced electrochemical nitrogen reduction. Nano Research, 2022, 15, 3010-3016.	5.8	22
63399	Controlling Spin Orientation and Metamagnetic Transitions in Anisotropic van der Waals Antiferromagnet CrPS₄ by Hydrostatic Pressure. Advanced Functional Materials, 2022, 32, 2106592.	7.8	6
63400	Switchable valley polarization and quantum anomalous Hall state in the VN2X2Y2 nanosheets (Xâ€‰=â€‰group-III and Yâ€‰=â€‰group-VI elements). Applied Physics Letters, 2021, 119, .	1.5	22
63401	Exceptionally amino-quantitated 3D MOF@CNT-sponge hybrid for efficient and selective recovery of Au(III) and Pd(II). Chemical Engineering Journal, 2022, 431, 133367.	6.6	21
63402	Rules of hierarchical melt and coordinate bond to design crystallization in doped phase change materials. Nature Communications, 2021, 12, 6473.	5.8	17
63403	FeOOH photo-deposited perylene linear polymer with accelerated charge separation for photocatalytic overall water splitting. Science China Chemistry, 2022, 65, 170-181.	4.2	16
63404	Alkyne-Functionalized Cyclooctyne on Si(001): Reactivity Studies and Surface Bonding from an Energy Decomposition Analysis Perspective. Molecules, 2021, 26, 6653.	1.7	1
63405	Unravelling the Mechanism of Intermediateâ€Temperature CO₂ Interaction with Moltenâ€NaNO₃â€Saltâ€Promoted MgO. Advanced Materials, 2022, 34, e2106677.	11.1	21
63406	Growth of Open Honeycomb-like Sn Structures on Ag(111) at Low Temperatures. Journal of Physical Chemistry C, 2021, 125, 25332-25338.	1.5	0
63407	Tuning the carrier type and density of monolayer tin selenide via organic molecular doping. Journal of Physics Condensed Matter, 2022, 34, 085001.	0.7	1
63408	Excellent thermoelectric performances of the SiSe2 monolayer and layered bulk. Applied Surface Science, 2022, 575, 151799.	3.1	16
63409	Adsorption of CH4 on the Pt(111) surface: Random phase approximation compared to density functional theory. Journal of Chemical Physics, 2021, 155, 174702.	1.2	10
63410	Quantifying Spin-Mixed States in Ferromagnets. Physical Review Letters, 2021, 127, 207201.	2.9	10
63411	Quantum anomalous Hall effect in <mml:math xmlns:mml="http://www.w3.org/1998/Math/MathML"><mml:mrow><mml:mi>Mn</mml:mi><mml:msub><mml:mi>Bi</mml:mi><mml:mi><mml:m van der Waals heterostructures. Physical Review Materials, 2021, 5, .	3.1	9
63412	Sol-gel pore-sealing strategy imparts tailored electronic structure to the atomically dispersed Ru sites for efficient oxygen reduction reaction. Energy Storage Materials, 2022, 44, 469-476.	9.5	26

#	Article	IF	Citations
63413	First-principles study of borophene/phosphorene heterojunction as anode material for lithium-ion batteries. Nanotechnology, 2022, 33, 075403.	1.3	2
63414	3-X Structural Model and Common Characteristics of Anomalous Thermal Transport: The Case of Two-Dimensional Boron Carbides. Journal of Physical Chemistry Letters, 2021, 12, 10975-10980.	2.1	10
63415	Quasiparticle band structures and optical properties of twisted bilayer MoS(2). Europhysics Letters, 0, , .	0.7	1
63416	Heterostructures of two-dimensional transition metal dichalcogenides: Formation, ab initio modelling and possible applications. Materials Today: Proceedings, 2021, , .	0.9	0
63417	Intelligent graphene oxide membranes with pH tunable channels for water treatment. Chemical Engineering Journal, 2022, 431, 133462.	6.6	13
63418	Doping limitation due to self-compensation by native defects in In-doped rocksalt Cd_xZn_{1â^'x}O. Journal of Physics Condensed Matter, 2022, 34, 065702.	0.7	1
63419	Determination of the surface states from the ultrafast electronic states in a thermoelectric material. Chinese Physics B, 2022, 31, 027902.	0.7	4
63420	Theoretical Study of Weakly Bound Adsorbates on Au(111): Tests on van der Waals Density Functionals. Journal of Physical Chemistry C, 2021, 125, 24958-24966.	1.5	2
63421	Co-porphyrin/Ru-pincer complex coupled polymer with Z-scheme molecular junctions and dual single-atom sites for visible light-responsive CO2 reduction. Chemical Engineering Journal, 2022, 431, 133357.	6.6	16
63422	Influence of defects on antidoping behavior in <mml:math xmlns:mml="http://www.w3.org/1998/Math/MathML"><mml:mi>Sm</mml:mi><mml:mi>Ni</mml:mi><mml:msub><mml:mi mathvariant="normal">O</mml:mi><mml:mn>3</mml:mn></mml:msub></mml:math>. Physical Review B, 2021, 104, .	1.1	6
63423	Bright luminescence of Sb doping in all-inorganic zinc halide perovskite variant. Journal of Alloys and Compounds, 2022, 895, 162610.	2.8	10
63424	Identification of a Telecom Wavelength Single Photon Emitter in Silicon. Physical Review Letters, 2021, 127, 196402.	2.9	22
63425	A novel Fe-defect induced pure-phase Na4Fe2.91(PO4)2P2O7 cathode material with high capacity and ultra-long lifetime for low-cost sodium-ion batteries. Nano Energy, 2022, 91, 106680.	8.2	67
63426	Rare earth doping effect on the thermal stability of Ce0.35Zr0.60M0.05O2: insights from experiment and simulation. Journal of Physics: Conference Series, 2021, 2079, 012011.	0.3	0
63427	Thermodynamic and electronic properties of ReN2 polymorphs at high pressure. Physical Review B, 2021, 104, .	1.1	1
63428	Photocatalytic Ammonia Synthesis: Mechanistic Insights into N₂ Activation at Oxygen Vacancies under Visible Light Excitation. ACS Catalysis, 2021, 11, 14058-14066.	5.5	35
63429	Solution-Phase Growth of Cu Nanowires with Aspect Ratios Greater Than 1000: Multiscale Theory. ACS Nano, 2021, 15, 18279-18288.	7.3	15
63430	Understanding Dimethyl Methylphosphonate Adsorption and Decomposition on Mesoporous CeO₂. ACS Applied Materials & Interfaces, 2021, 13, 54597-54609.	4.0	16

#	Article	IF	Citations
63431	Molecular Bond Engineering and Feature Learning for the Design of Hybrid Organicâ€“Inorganic Perovskite Solar Cells with Strong Noncovalent Halogenâ€“Cation Interactions. Journal of Physical Chemistry C, 2021, 125, 25316-25326.	1.5	6
63432	xmlns:mml="http://www.w3.org/1998/Math/MathML"><mml:mi>Na</mml:mi><mml:mi>Zn</mml:mi><mml:msub><mml:mi mathvariant="normal">F</mml:mi><mml:mn>3</mml:mn></mml:msub></mml:math> as a low-pressure analog of xmlns:mml="http://www.w3.org/1998/Math/MathML"><mml:mi>Mg</mml:mi><mml:mi>Si</mml:mi><mml:msub><mml:mi mathvariant="normal">O</mml:mi><mml:mn>3</mml:mn></mml:msub></mml:math>. Physical Review Ma	0.9	1
63433	Vacancy-Induced Magnetism in Fluorographene: The Effect of Midgap State. Molecules, 2021, 26, 6666.	1.7	1
63434	Pressure-induced structural and electronic phase transitions of uranium trioxide. Physical Review B, 2021, 104, .	1.1	6
63435	Dual-Silicon-Doped Graphitic Carbon Nitride Sheet: An Efficient Metal-Free Electrocatalyst for Urea Synthesis. Journal of Physical Chemistry Letters, 2021, 12, 10837-10844.	2.1	40
63436	Six-fold symmetry origin of Dirac cone formation in two-dimensional materials. New Journal of Physics, 2021, 23, 113033.	1.2	3
63437	Bornâ€™s valence force-field model for diamond at terapascals: Validity and implications for the primary pressure scale. Matter and Radiation at Extremes, 2021, 6, .	1.5	6
63438	Defect chemistry of Cr-B binary and Cr-Al-B MAB phases: Effects of covalently bonded B networks. Physical Review Materials, 2021, 5, .	0.9	5
63439	Accelerated lithium ions diffusion at the interface between LiFePO4 electrode and electrolyte by surface-nitride treatment. Solid State Ionics, 2021, 373, 115792.	1.3	2
63440	High-pressure monoclinic phase of MoAlB. Results in Physics, 2021, 31, 104980.	2.0	4
63441	Quasiperiodic van der Waals heterostructures of graphene and hexagonal boron nitride. Physica Status Solidi (B): Basic Research, 0, , 2100423.	0.7	0
63442	Catalytic hydrogen evolution reaction on surfaces of metal-nanoparticle-coated zinc-based oxides by first-principles calculations. International Journal of Hydrogen Energy, 2022, 47, 40768-40776.	3.8	3
63443	First-principles study on lattice structures and electronic properties of Li1/2La1/2TiO3/Li2S interface. Solid State Ionics, 2021, 373, 115797.	1.3	1
63444	Hierarchy and delithiation regulations on mesoporous LiCoO2 nanosheets for boosted water oxidation electrocatalysis. Applied Materials Today, 2021, 25, 101241.	2.3	2
63445	Low-loss hyperbolic dispersion and anisotropic plasmonic excitation in nodal-line semimetallic yttrium nitride. Optics Express, 2020, 28, 22076.	1.7	8
63446	Tailoring local coordination structure of the Er³⁺ ions for tuning the up-conversion multicolor luminescence. Optics Express, 2020, 28, 22218.	1.7	6
63447	Site-preferential copper substitution for silicon leads to Cu-chains in the new ternary silicide Ir_{4â^’x}CuSi₂. Zeitschrift Fur Kristallographie - Crystalline Materials, 2020, 235, 391-399.	0.4	0
63448	Denuded zones in zirconium pressure vessels: oxygenâ€™s role examined via multi-scale diffusion model. Modelling and Simulation in Materials Science and Engineering, 2020, 28, 065005.	0.8	0

#	Article	IF	Citations
63449	Ferroelectric atomic displacement in multiferroic tetragonal perovskite <mml:math xmlns:mml="http://www.w3.org/1998/Math/MathML"><mml:mrow><mml:msub><mml:mi>Sr</mml:mi><mml:mrow><mml:mn>1</mml:mn></mml:mrow></mml:msub></mml:mrow></mml:math> Physical Review Research, 2020, 2, .	1.3	2
63452	Born effective charges and electric polarization in bulk Îµ-Fe2O3: An ab-initio approach. Chemical Physics, 2020, 535, 110789.	0.9	3
63453	Thermodynamic analysis of the gas phase reaction of Mg-doped GaN growth by HVPE using MgO. Japanese Journal of Applied Physics, 2020, 59, 088001.	0.8	5
63454	Neutron scattering study of commensurate magnetic ordering in single crystal CeSb2. Journal of Physics Condensed Matter, 2020, 32, 405605.	0.7	3
63455	Control of magnetic interactions between surface adatoms via orbital repopulation. 2D Materials, 2020, 7, 045007.	2.0	4
63456	Theoretical investigation of the structural, elastic, electronic, and dielectric properties of alkali-metal-based bismuth ternary chalcogenides. Physical Review Materials, 2020, 4, .	0.9	7
63457	First-principles investigation of the effect of Co in stabilizing the structures of layer-structured cathodes in delithiated state. Materials Research Express, 2020, 7, 075507.	0.8	0
63458	Gold nanostructures on iron oxide surfaces and their interaction with CO. Journal of Physics Condensed Matter, 2020, 32, 433001.	0.7	1
63459	Structural, Electronic and Mechanical Properties of Few-Layer GaN Nanosheet: A First-Principle Study. Materials Transactions, 2020, 61, 1438-1444.	0.4	3
63460	Effect of site disorder on the electronic, magnetic, and ferroelectric properties of gallium ferrite. Physical Review Materials, 2020, 4, .	0.9	1
63461	Evaluating Solubility and Diffusion Coefficient of Hydrogen in Martensitic Steel Using Computational Mechanics. Materials Transactions, 2020, 61, 1287-1293.	0.4	4
63462	Phononic Engineering for Hot Carrier Solar Cells. Advances in Chemical and Materials Engineering Book Series, 0, , 214-242.	0.2	0
63463	Phononic Engineering for Hot Carrier Solar Cells. , 0, , 1152-1180.		0
63464	Theoretical Methods for Modeling Chemical Processes on Semiconductor Surfaces. , 2004, , 246-265.		0
63465	Neutron Inelastic Scattering and Molecular Modelling. , 2006, , 529-556.		1
63468	Properties of ferroelectric ultrathin films from first principles. , 2006, , 137-145.		3
63469	Large-Scale Ab initio Simulations for Embedded Nanodots. , 2007, , 153-160.		0
63470	Plane Wave Density Functional Model Studies ofÂChemistry at Surfaces. , 2009, , 173-186.		0

#	Article	IF	Citations
63471	Charge Transport through Guanine Crystals. , 2009, , 687-695.		1
63472	The Standard ASW Method. , 2007, , 5-45.		0
63474	A Density-functional Study of Nitrogen and Oxygen Mobility in Fluorite-type Tantalum Oxynitrides. , 2009, , 109-117.		0
63475	Pressure induced nodal line semimetal in YH₃. Zeitschrift Fur Naturforschung - Section A Journal of Physical Sciences, 2020, 75, 971-979.	0.7	1
63476	Mono- to few-layer non-van der Waals 2D lanthanide-doped NaYF₄nanosheets with upconversion luminescence. 2D Materials, 2021, 8, 015005.	2.0	3
63477	Discovery of Ag_xTaS₂ superconductor with stage-3 structure. 2D Materials, 2021, 8, 015007.	2.0	4
63478	Single-layer Mo₅Te₈ â€• A new polymorph of layered transition-metal chalcogenide. 2D Materials, 2021, 8, 015006.	2.0	9
63479	Extension of the LDA-1/2 method to the material class of bismuth containing IIIâ€“V semiconductors. AIP Advances, 2020, 10, 115003.	0.6	1
63480	OH molecule-involved formation of point defects in monolayer graphene. Nanotechnology, 2021, 32, 025704.	1.3	0
63481	Role of tip apices in scanning force spectroscopy on alkali halides at room temperatureâ€”chemical nature of the tip apex and atomic-scale deformations. Nanotechnology, 2021, 32, 035706.	1.3	0
63482	Electrodes with Electrodeposited Water-excluding Polymer Coating Enable High-Voltage Aqueous Supercapacitors. Research, 2020, 2020, 4178179.	2.8	6
63483	Functional Ceramics Materials Study Using First-principle Calculations. Funtai Oyobi Fummatsu Yakin/Journal of the Japan Society of Powder and Powder Metallurgy, 2020, 67, 493-498.	0.1	0
63484	Method of forming time-reversed LEED states from repeated-slab calculations. Journal of Physics Condensed Matter, 2020, 32, 495002.	0.7	0
63485	Density functional study of gallium clusters on graphene: electronic doping and diffusion. Journal of Physics Condensed Matter, 2021, 33, 025002.	0.7	0
63486	Promising room temperature thermoelectric conversion efficiency of zinc-blende AgI from first principles. Journal of Physics Condensed Matter, 2021, 33, 015501.	0.7	2
63487	Trends in elastic properties of Tiâ€“Ta alloys from first-principles calculations. Journal of Physics Condensed Matter, 2021, 33, 035701.	0.7	1
63488	Engineering magnetic anisotropy and exchange couplings in double transition metal MXenes via surface defects. Journal of Physics Condensed Matter, 2021, 33, 035801.	0.7	2
63489	Structural characteristics and elasticities of coesite and coesite-II at high pressure. New Journal of Physics, 2020, 22, 093044.	1.2	1

#	Article	IF	Citations
63490	Tunable Dirac cones in single-layer selenium. New Journal of Physics, 2020, 22, 093055.	1.2	4
63491	Two-dimensional hexagonal manganese carbide monolayer with intrinsic ferromagnetism and half-metallicity. New Journal of Physics, 2020, 22, 103049.	1.2	19
63492	Calculation of Dynamical Phase Diagram in U-Zr Binary System Under Irradiation. Journal of Nuclear Engineering and Radiation Science, 2021, 7, .	0.2	4
63493	Theoretical study on the change of thermoelectric properties by substitution of group 4 elements in Fe₂TiSn. Modern Physics Letters B, 2021, 35, 2150047.	1.0	1
63494	Preferential Energetics of Mg-based Ternary Alloys Revisited by Short-Range Order in Disordered Phases through First Principles. Transactions of the Materials Research Society of Japan, 2020, 45, 167-172.	0.2	0
63495	Ab-initio Study of Magnetically Intercalated Tungsten Diselenide. , 2020, , .		0
63496	TCAD simulation for transition metal dichalcogenide channel Tunnel FETs consistent with ab-initio based NEGF calculation. , 2020, , .		0
63497	First-principles study of dopant trap level and concentration in Si(110)/a-SiO₂ interface. , 2020, , .		0
63498	Ferromagnetism triggered by nitrogen defects in graphitic carbon nitride. Journal Physics D: Applied Physics, 2020, 53, 495002.	1.3	2
63499	Effect of N-type doping and vacancy formation on the thermodynamic, electrical, structural, and bonding properties of Si: X. (X = P, As, and Sb): a theoretical study. Semiconductor Science and Technology, 2020, 35, 125005.	1.0	1
63500	P-doping with beryllium of long-wavelength InAsSb. Semiconductor Science and Technology, 2020, 35, 125001.	1.0	0
63501	Synthesis of black phosphorus structured polymeric nitrogen*. Chinese Physics B, 2020, 29, 106201.	0.7	6
63502	Effects of Re, Ta, andWin [110] (001) dislocation core of Î³/Î³â€² interface to Ni-based superalloys: First-principles study*. Chinese Physics B, 2020, 29, 096101.	0.7	3
63503	Theoretical investigation of twin boundaries in WO3 : Structure, properties, and implications for superconductivity. Physical Review Research, 2020, 2, .	1.3	6
63504	Surface conductivity in antiferromagnetic semiconductor CrSb2. Physical Review Research, 2020, 2, .	1.3	1
63505	Hindered surface diffusion of bonded molecular clusters mediated by surface defects. Physical Review Materials, 2020, 4, .	0.9	1
63506	Anisotropic properties, charge ordering, and ferrimagnetic structures in the strongly correlated <mml:math xmlns:mml="http://www.w3.org/1998/Math/MathML"><mml:mrow><mml:mi>Î²</mml:mi><mml:mtext>â^'</mml:mtext><mml:msub><mathvariant="normal">V</mml:mi><mml:mn>2</mml:mn></mml:msub><mml:msub><mml:mi>PO</mml:mi><mml:mn>5</mml:mn></ single crystal. Physical Review Materials, 2020, 4, .	0.9	0
63507	Carboxyl- and amine-functionalized carboranethiol SAMs on Au(111): A dispersion-corrected density functional theory study. Physical Review Materials, 2020, 4, .	0.9	2

#	Article	IF	Citations
63508	Stacking faults and alternate crystal structures for the shape-memory alloy NiTi. Physical Review Materials, 2020, 4, .	0.9	1
63509	Structural, electronic, and excitonic properties of few-layer <mml:math xmlns:mml="http://www.w3.org/1998/Math/MathML"><mml:mrow><mml:mi>Se</mml:mi><mml:msub><mml:mi mathvariant="normal">S</mml:mi><mml:mn>2</mml:mn></mml:msub></mml:mrow></mml:math> and <mml:math xmlns:mml="http://www.w3.org/1998/Math/MathML"><mml:mrow><mml:mi>Te</mml:mi><mml:msub><mml:mi mathvariant="normal">S</mml:mi><mml:mn>2</mml:mn></mml:msub></mml:mrow></mml:math>. Physical	0.9	3
63510	Breakdown of ion-polarization-correspondence and born effective charges: Algebraic formulas of accurate polarization under field. Physical Review Materials, 2020, 4, .	0.9	1
63511	Statistically averaged molecular dynamics simulations of hydrogen diffusion in magnesium and magnesium hydrides. Physical Review Materials, 2020, 4, .	0.9	2
63512	Experimental verification of a temperature-induced topological phase transition in <mml:math xmlns:mml="http://www.w3.org/1998/Math/MathML"><mml:mrow><mml:msub><mml:mi>TlBiS</mml:mi><mml:mn>2</mml:mn></mml:mn> and <mml:math xmlns:mml="http://www.w3.org/1998/Math/MathML"><mml:mrow><mml:mi>Tl</mml:mi><mml:mi>Bi</mml:mi><mml:msub><mml:mi> Physical Review B, 2020, 102, .	1.1	5
63513	Direct and indirect excitons in two-dimensional covalent organic frameworks. Chinese Journal of Chemical Physics, 2020, 33, 569-577.	0.6	2
63514	Charge localization induced by reorientation of FA cations greatly suppresses nonradiative electron-hole recombination in FAPbI₃ perovskites: A time-domain Ab Initio study. Chinese Journal of Chemical Physics, 2020, 33, 642-648.	0.6	1
63515	First principles investigations of Fe3+ impurity and Fe3+â€‰+â€‰Vâ^'Cd complex in strongly confined CdSe quantum dot. Journal of Applied Physics, 2020, 128, 173901.	1.1	1
63516	The role of anchoring groups in ruthenium(II)-bipyridine sensitized p-type semiconductor solar cellsâ€"a quantum chemical approach. Journal of Physics B: Atomic, Molecular and Optical Physics, 2020, 53, 234001.	0.6	3
63517	Effect of local strain energy to predict accurate phase diagram of IIIâ€"V pseudobinary systems: case of Ga(As,Sb) and (In,Ga)As. Journal Physics D: Applied Physics, 2021, 54, 045104.	1.3	4
63518	Probing the martensite transition and thermoelectric properties of Co_xTaZ (Z = Si, Ge, Sn) Tj ETQq0 0 0 rgBT /Overlock 10 045402.	0.7	5
63519	The recurrence of dense face-centered cubic cesium. Journal of Physics Condensed Matter, 2021, 33, 035404.	0.7	2
63520	Imaginary-time time-dependent density functional theory for periodic systems. Journal of Physics Condensed Matter, 2021, 33, 055903.	0.7	2
63521	Decisive effects of atomic vacancies and structural ordering on stable phases and band structures in copperâ€"galliumâ€"chalcogenide compounds. Journal of Physics Condensed Matter, 2021, 33, 075401.	0.7	0
63522	Interaction between impurity elements (C, N and O) and hydrogen in hcp-Zr: a first-principles study. Modelling and Simulation in Materials Science and Engineering, 2020, 28, 085007.	0.8	3
63523	Superconductivity in scandium borocarbide with orbital hybridization. Materials Research Express, 2020, 7, 116001.	0.8	0
63524	Magnetic structure and phase transition at the surface region of Fe₃O₄(100). Journal of Physics Communications, 2020, 4, 115001.	0.5	2
63525	The transport properties of Cl-decorated arsenene controlled by electric field. Electronic Structure, 2020, 2, 045001.	1.0	0

#	Article	IF	Citations
63526	Magnetic field induced reconstruction of electronic structure in <mml:math xmlns:mml="http://www.w3.org/1998/Math/MathML"><mml:mrow><mml:msub><mml:mi mathvariant="normal">Sr</mml:mi><mml:mn>3</mml:mn></mml:msub><mml:msub><mml:mi mathvariant="normal">Ru</mml:mi><mml:mn>2</mml:mn></mml:msub><mml:msub><mml:mi mathvariant="normal">O</mml:mi><mml:mn>7</mml:mn></mml:msub></mml:mrow></mml:math> nanosheets. Physical Review B, 2020, 102, .	1.1	0
63527	Effect of hydrogen on vacancy diffusion. Physical Review Materials, 2020, 4, .	0.9	6
63528	Combining DFT and CALPHAD for the development of on-lattice interaction models: The case of Fe-Ni system. Physical Review Materials, 2020, 4, .	0.9	3
63529	First-principles investigation of charged dopants and dopant-vacancy defect complexes in monolayer <mml:math xmlns:mml="http://www.w3.org/1998/Math/MathML"><mml:mrow><mml:mi>Mo</mml:mi><mml:msub><mml:mi mathvariant="normal">S</mml:mi><mml:mn>2</mml:mn></mml:msub></mml:mrow></mml:math>. Physical Review Materials, 2020, 4, .	0.9	9
63530	Nature of native atomic defects in <mml:math xmlns:mml="http://www.w3.org/1998/Math/MathML"><mml:msub><mml:mi>ZrTe</mml:mi><mml:mn>5</mml:mn></mml:msub></mml:math> and their impact on the low-energy electronic structure. Physical Review Materials, 2020, 4, .	0.9	7
63531	Designing nickelate superconductors with d8 configuration exploiting mixed-anion strategy. Physical Review Research, 2020, 2, .	1.3	10
63534	Principle study of the europium vacancy color center in a diamond. Optical Materials Express, 2020, 10, 3277.	1.6	2
63535	Asymmetric Schottky Contacts in van der Waals Metal-Semiconductor-Metal Structures Based on Two-Dimensional Janus Materials. Research, 2020, 2020, 6727524.	2.8	11
63536	Fine-Tuning Pyridinic Nitrogen in Nitrogen-Doped Porous Carbon Nanostructures for Boosted Peroxidase-Like Activity and Sensitive Biosensing. Research, 2020, 2020, 8202584.	2.8	19
63537	Iron silicides formation on Si (100) and (111) surfaces through theoretical modeling of sputtering and annealing. Applied Surface Science, 2020, 527, 146736.	3.1	6
63538	PWDFT.jl: A Julia package for electronic structure calculation using density functional theory and plane wave basis. Computer Physics Communications, 2020, 256, 107372.	3.0	6
63539	Prediction of tetragonal monolayer CuN with a quantum spin Hall state. Physica E: Low-Dimensional Systems and Nanostructures, 2020, 124, 114225.	1.3	0
63540	Salt-flux synthesis, crystal structure and theoretical characterization of Rb0.74Ga6.62Ti0Â·38O11. Solid State Sciences, 2020, 109, 106394.	1.5	0
63541	Design of Materials for Nuclear Energy Applications: First-Principles Calculations and Artificial Intelligence Methods. High Temperature, 2020, 58, 907-937.	0.1	3
63542	Strong interlayer coupling in two-dimensional PbSe with high thermoelectric performance. Journal of Physics Condensed Matter, 2021, 33, 325701.	0.7	4
63543	Quantum transport: general concepts. , 0, , 91-117.		1
63544	Atomic-Scale Mechanism of Unidirectional Oxide Growth. Advanced Functional Materials, 2019, 30, .	7.8	2
63545	A Cyclic Periodic Wave Function Approach for the Study of Infinitely Periodic Solid-State Systems. I. Application to the C-HÂ·Â·Â·Ï€(Câ‰¡C) Hydrogen Bonding Systems. ACS Omega, 2020, 5, 27546-27555.	1.6	2

#	Article	IF	Citations
63546	Valley phenomena in the candidate phase change material WSeTe. Communications Physics, 2020, 3, .	2.0	1
63547	Development of a Cyclic Periodic Wave Function Approach for the Study of Infinitely Periodic Solid-State Systems. ACS Omega, 2020, 5, 31060-31068.	1.6	0
63548	Tests on the Accuracy and Scalability of the Full-Potential DFT Method Based on Multiple Scattering Theory. Frontiers in Chemistry, 2020, 8, 590047.	1.8	0
63549	A theoretical study of the electrochemical reduction of CO₂ on cerium dioxide supported palladium single atoms and nanoparticles. Physical Chemistry Chemical Physics, 2021, 23, 26185-26194.	1.3	5
63550	Femtosecond ultrafast pulse generation with high-quality 2H-TaS₂ nanosheets via top-down empirical approach. Nanoscale, 2021, 13, 20471-20480.	2.8	13
63551	Theoretical study on stability and ion transport property with halide doping of Na₃SbS₄ electrolyte for all-solid-state batteries. Journal of Materials Chemistry A, 2022, 10, 2235-2248.	5.2	17
63552	Computer modeling and numerical studies of peptide nanotubes based on diphenylalanine. Keldysh Institute Preprints, 2021, , 1-54.	0.1	1
63553	Rapid large-scale synthesis of ultrathin NiFe-layered double hydroxide nanosheets with tunable structures as robust oxygen evolution electrocatalysts. RSC Advances, 2021, 11, 37624-37630.	1.7	7
63554	Theoretical probing of twenty-coordinate actinide-centered boron molecular drums. Physical Chemistry Chemical Physics, 2021, 23, 26967-26973.	1.3	8
63555	CO₂ reduction to CH₄ on Cu-doped phosphorene: a first-principles study. Nanoscale, 2021, 13, 20541-20549.	2.8	9
63556	Structural characteristics of Al₂O₃ ultra-thin films supported on the NiAl(100) substrate from DFTB-aided global optimization. Nanoscale, 2021, 13, 19500-19510.	2.8	2
63557	Translational dependence of the geometry of metallic mono- and bilayers optimized on semi-ionic supports: the cases of Pd on Î³-Al₂O₃(110), monoclinic ZrO₂(001), and rutile TiO₂(001). CrystEngComm, 2021, 24, 143-155.	1.3	2
63558	Unraveling divalent pillar effects for the prolonged cycling of high-energy-density cathodes. Journal of Materials Chemistry A, 2021, 9, 26820-26828.	5.2	5
63559	Electrical control of topological spin textures in two-dimensional multiferroics. Nanoscale, 2021, 13, 20609-20614.	2.8	11
63560	Theoretical insight into hydroxyl production via H₂O₂ decomposition over the Fe₃O₄(311) surface. RSC Advances, 2021, 11, 36257-36264.	1.7	12
63561	Metallic C₅N monolayer as an efficient catalyst for accelerating redox kinetics of sulfur in lithiumâ€“sulfur batteries. Physical Chemistry Chemical Physics, 2021, 24, 180-190.	1.3	9
63562	CO organization at ambient pressure on stepped Pt surfaces: first principles modeling accelerated by neural networks. Chemical Science, 2021, 12, 15543-15555.	3.7	8
63563	Tantalum based single, double, and triple atom catalysts supported on g-C₂N monolayer for effective nitrogen reduction reaction: a comparative DFT investigation. Catalysis Science and Technology, 2022, 12, 310-319.	2.1	20

#	Article	IF	Citations
63564	A DFT study on magnetic interfaces based on half-metallic Co₂FeGe_{1/2}Ga_{1/2} with h-BN and MoSe₂ monolayers. Physical Chemistry Chemical Physics, 2022, 24, 1023-1028.	1.3	5
63565	First Principles Study of TiO2 as Visible Light Catalyst with Ni Doping. Springer Proceedings in Physics, 2021, , 159-166.	0.1	1
63566	Phase and interface engineering of nickel carbide nanobranches for efficient hydrogen oxidation catalysis. Journal of Materials Chemistry A, 2021, 9, 26323-26329.	5.2	12
63567	Progress in measuring, modeling, and manipulating thermal boundary conductance. Advances in Heat Transfer, 2021, 53, 327-404.	0.4	0
63568	Atomistic Mechanisms Underlying Plasticity and Crack Growth in Ceramics: A Case Study of Aln/Tin Superlattices. SSRN Electronic Journal, 0, , .	0.4	0
63569	High-sensitivity small-molecule detection of microcystin-LR cyano-toxin using a terahertz-aptamer biosensor. Analyst, The, 2021, 146, 7583-7592.	1.7	6
63570	Rapid screening alloying elements for improved corrosion resistance on the Mg(0001) surface using first principles calculations. Physical Chemistry Chemical Physics, 2021, 23, 26887-26901.	1.3	9
63571	Correction methods for first-principles calculations of the solution enthalpy of gases and compounds in liquid metals. Physical Chemistry Chemical Physics, 2022, 24, 757-770.	1.3	3
63572	Ferromagnetic barrier induced large enhancement of tunneling magnetoresistance in van der Waals perpendicular magnetic tunnel junctions. Nanoscale, 2021, 13, 19993-20001.	2.8	5
63573	Enhanced in-plane ferroelectricity, antiferroelectricity, and unconventional 2D emergent fermions in quadruple-layer XSbO₂ (X = Li, Na). Nanoscale, 2021, 13, 19172-19180.	2.8	5
63574	Effects of bipolarons on oxidation states, and the electronic and optical properties of W₁₈O₄₉. Physical Chemistry Chemical Physics, 2021, 23, 25824-25829.	1.3	2
63575	Efficient CO2 reduction with H2O via photothermal chemical reaction based on Au-MgO dual catalytic site on TiO2. Journal of CO2 Utilization, 2022, 55, 101801.	3.3	9
63576	A 3nm-thick, quasi-single crystalline Cu layer with ultralow optoelectrical losses and exceptional durability. Acta Materialia, 2022, 223, 117484.	3.8	5
63577	Revealing the role of Al in the microstructural evolution and creep properties of Mg-2.85Nd-0.92Gd-0.41Zr-0.29Zn alloy. Materials Science & Engineering A: Structural Materials: Properties, Microstructure and Processing, 2022, 832, 142358.	2.6	4
63578	Adsorption behavior and mechanism of multiple Mg atoms on the surface of AlNi compound at Mg alloy/steel interface. Current Applied Physics, 2022, 33, 51-58.	1.1	2
63579	Self-templating synthesis of heteroatom-doped large-scalable carbon anodes for high-performance lithium-ion batteries. Inorganic Chemistry Frontiers, 2022, 9, 1058-1069.	3.0	72
63580	Degradation intermediates of Amitriptyline and fundamental importance of transition metal elements in LDH-based catalysts in Heterogeneous Electro-Fenton system. Separation and Purification Technology, 2022, 283, 120225.	3.9	7
63581	Effects of Zr addition on lattice strains and electronic structures of NbTaTiV high-entropy alloy. Materials Science & Engineering A: Structural Materials: Properties, Microstructure and Processing, 2022, 831, 142293.	2.6	12

#	Article	IF	Citations
63582	Asymmetric janus functionalities induced changes in structural, electronic, optical characteristics of MXenes Ta4C3Tx. Solid State Communications, 2022, 341, 114585.	0.9	3
63583	Optimization of microstructure and properties of as-cast various Si containing Cuâ€“Crâ€“Zr alloy by experiments and first-principles calculation. Materials Science & Engineering A: Structural Materials: Properties, Microstructure and Processing, 2022, 831, 142353.	2.6	9
63584	Mechanistic insight into methanol electro-oxidation catalyzed by PtCu alloy. Chinese Journal of Catalysis, 2022, 43, 167-176.	6.9	19
63585	Ferromagnetic Weyl metal in EuAgP. Materials Today Physics, 2022, 22, 100570.	2.9	3
63586	Computational design of thermoelectric alloys through optimization of transport and dopability. Materials Horizons, 2022, 9, 720-730.	6.4	10
63587	Lithiophilic NiF2 coating inducing LiF-rich solid electrolyte interphase by a novel NF3 plasma treatment for highly stable Li metal anode. Electrochimica Acta, 2022, 402, 139561.	2.6	9
63588	The role of nitrogen and sulfur dual coordination of cobalt in Co-N_{4â^'x}S_x/C single atom catalysts in the oxygen reduction reaction. Sustainable Energy and Fuels, 2021, 6, 179-187.	2.5	10
63589	Oxygen vacancy distributions and electron localization in a CeO₂(100) nanocube. Inorganic Chemistry Frontiers, 2022, 9, 275-283.	3.0	8
63590	Regulating the lattice strain of platinumâ€“copper catalysts for enhancing collaborative electrocatalysis. Inorganic Chemistry Frontiers, 2022, 9, 249-258.	3.0	10
63591	Structural and mechanical properties of predicted vacancy ordered tantalum carbide phases. Acta Materialia, 2022, 223, 117449.	3.8	6
63592	Revealing the influence of Mo addition on interphase precipitation in Ti-bearing low carbon steels. Acta Materialia, 2022, 223, 117475.	3.8	22
63593	NH+-based frameworks as a platform for designing electrodes and solid electrolytes for Na-ion batteries: A screening approach. Solid State Ionics, 2022, 374, 115810.	1.3	7
63594	Toward stable lithium-ion batteries: Accelerating the transfer and alloying reactions of Sn-based anodes via coordination atom regulation and carbon hybridization. Journal of Power Sources, 2022, 519, 230778.	4.0	16
63595	Highly-defective graphene as a metal-free catalyst for chemical vapor deposition growth of graphene glass. Carbon, 2022, 187, 272-279.	5.4	3
63596	Intrinsic doping limitations in inorganic lead halide perovskites. Materials Horizons, 2022, 9, 791-803.	6.4	10
63597	A DFT computational prediction of 2H phase W2C monolayer and the effect of O functional groups. Physics Letters, Section A: General, Atomic and Solid State Physics, 2022, 424, 127842.	0.9	4
63598	Influence of supercell size on Gas-Surface Scattering: A case study of CO scattering from Au(1 1 1). Chemical Physics, 2022, 554, 111423.	0.9	11
63599	Dislocation core structure and motion in pure titanium and titanium alloys: A first-principles study. Computational Materials Science, 2022, 203, 111081.	1.4	13

#	Article	IF	Citations
63600	Defects, dopants and lithium incorporation in LiPON electrolyte. Computational Materials Science, 2022, 202, 111000.	1.4	5
63601	Tuning the hybridization state of Ir-O to improve the OER activity and stability of iridium pyrochlore via Zn doping. Applied Surface Science, 2022, 576, 151840.	3.1	16
63602	Strain-tuneable photocatalytic ability of <mml:math xmlns:mml="http://www.w3.org/1998/Math/MathML" display="inline" id="d1e374" altimg="si4.svg"><mml:mrow><mml:mi>B</mml:mi><mml:msub><mml:mrow><mml:mi>C</mml:mi></mml:mrow><mml:mrow><mml: monolayer: A first principle study. Computational Materials Science, 2022, 202, 111002.	1.4	12
63603	Mechanical and nonlinear optical properties of two-dimensional LiXY2 (X=Al, Ga, In; Y S, Se, Te) monolayers. Physica B: Condensed Matter, 2022, 626, 413531.	1.3	3
63604	First-principle study on catalytic activity of functionalized Ti3C2 MXene as cathode catalyst for Liâ€“O2 batteries. Current Applied Physics, 2022, 34, 24-28.	1.1	8
63605	Effects of size and interstitial element of L12-type clusters on formation of long-period stacking ordered structures in 10H-type Mgâ€“Alâ€“Y alloy. Computational Materials Science, 2022, 203, 111036.	1.4	0
63606	Empathes: A general code for nudged elastic band transition states search. Computer Physics Communications, 2022, 271, 108224.	3.0	4
63607	Atomistic study of the effect of crystallographic orientation on the twinning and detwinning behavior of NiTi shape memory alloys. Computational Materials Science, 2022, 203, 111080.	1.4	6
63608	Effect of coexistence of vacancy and strain on the electronic properties of NH3 adsorption on the Hf2CO2 MXene from first-principles calculations. Vacuum, 2022, 196, 110774.	1.6	15
63609	Extraordinary negative thermal expansion of monolayer biphenylene. Carbon, 2022, 187, 349-353.	5.4	18
63610	Phase transition and electronic properties of barium fluoride at high pressure. Solid State Communications, 2022, 342, 114597.	0.9	4
63611	Covalent organic frameworks promoted single metal atom catalysis: Strategies and applications. Coordination Chemistry Reviews, 2022, 452, 214298.	9.5	132
63612	Strain-stabilized Al-containing high-entropy sublattice nitrides. Acta Materialia, 2022, 224, 117483.	3.8	19
63613	Thermodynamic stability and superconductivity of tantalum carbides from first-principles cluster expansion and isotropic Eliashberg theory. Computational Materials Science, 2022, 202, 111004.	1.4	6
63614	Comparing the hot corrosion of (100), (210) and (110) Ni-based superalloys exposed to the mixed salt of Na2SO4-NaCl at 750ÂÂ°C: Experimental study and first-principles calculation. Corrosion Science, 2022, 195, 109996.	3.0	12
63615	First-principles study on the NiAl/Al2O3 interfacial segregation of Hf during the oxidation of Hf-modified NiAl. Applied Surface Science, 2022, 578, 151917.	3.1	2
63616	Predicting ligand-dependent nanocrystal shapes of InP quantum dots and their electronic structures. Applied Surface Science, 2022, 578, 151972.	3.1	5
63617	Mechanistic insights into the simultaneous removal of As(V) and Cr(VI) oxyanions by a novel hierarchical corolla-like MnO2-decorated porous magnetic biochar composite: A combined experimental and density functional theory study. Applied Surface Science, 2022, 578, 151991.	3.1	16

#	Article	IF	Citations
63618	Cumulative cationic and anionic redox reaction in Mg3V2(SiO4)3 and impact on the battery performance. Journal of Power Sources, 2022, 520, 230828.	4.0	3
63619	Low-cost single-atom transition metals on two-dimensional SnO nanosheets for efficient hydrogen evolution catalysis in all pH-range. Applied Surface Science, 2022, 578, 152021.	3.1	9
63620	Interface structure of (130) twin in the U-14.0Âat.% Nb alloy: an experimental and theoretical study. Scripta Materialia, 2022, 209, 114417.	2.6	3
63621	Sliding energy landscape governs interfacial failure of nanotube-reinforced ceramic nanocomposites. Scripta Materialia, 2022, 210, 114413.	2.6	5
63622	Tribological behaviour of W-S-C coated ceramics in a vacuum environment. Tribology International, 2022, 167, 107375.	3.0	3
63623	Novel 2D boron nitride with optimal direct band gap: A theoretical prediction. Applied Surface Science, 2022, 578, 151929.	3.1	19
63624	Effective modulating the electronic and magnetic properties of VI3 monolayer: A first-principles calculation. Physica E: Low-Dimensional Systems and Nanostructures, 2022, 137, 115079.	1.3	3
63625	A systematic investigation of structural growth patterns and electronic properties of [LuGe]+/0 and [Ge+1]+/0 (nÂ=Â1â€“17) nanoalloy clusters. Materials Today Communications, 2022, 30, 103018.	0.9	3
63626	Nano-phase transformation of composite precipitates in multicomponent Al-Mg-Si(-Sc) alloys. Journal of Materials Science and Technology, 2022, 110, 216-226.	5.6	20
63627	Assembling biphenylene into 3D porous metallic carbon allotrope for promising anode of lithium-ion batteries. Carbon, 2022, 188, 95-103.	5.4	31
63628	Prediction of functionalized graphene as potential catalysts for overall water splitting. Applied Surface Science, 2022, 578, 151989.	3.1	8
63629	NH3-SCR catalysts for heavy-duty diesel vehicles: Preparation of CHA-type zeolites with low-cost templates. Applied Catalysis B: Environmental, 2022, 303, 120928.	10.8	18
63630	In-situ enhanced catalytic reforming behavior of cobalt-based materials with inherent zero-valent aluminum in spent lithium ion batteries. Applied Catalysis B: Environmental, 2022, 303, 120920.	10.8	19
63631	Theoretical estimation of surface magnetic anisotropy on <mml:math xmlns:mml="http://www.w3.org/1998/Math/MathML" altimg="si6.svg"><mml:mrow><mml:mi>L</mml:mi><mml:msub><mml:mn>1</mml:mn><mml:mn>0</mml:mn></mml:msub></mml:m Enhanced Magnetoresistance under Bias Voltage in <mml:math xmlns:mml="http://www.w3.org/1998/Math/MathML" display="inline" thin films: Case of perfect and defect Surfaces. Surface Science, 2022, 717, 121999.	0.8	3
63632	overflow="scroll"><mml:mi>Fe</mml:mi></mml:math> / <mml:math xmlns:mml="http://www.w3.org/1998/Math/MathML" display="inline" overflow="scroll"><mml:mrow><mml:mi>Mg</mml:mi><mml:mi mathvariant="normal">O</mml:mi></mml:mrow></mml:math> / <mml:math xmlns:mml="http://www.w3.	1.5	2
63633	Submonolayer copper telluride phase on Cu(111): Ad-chain and trough formation. Physical Review B, 2021, 104, .	1.1	4
63634	Magneto-optical spectra of the split nickel-vacancy defect in diamond. Physical Review Research, 2021, 3, .	1.3	10
63635	The Mechanical, Electronic and Optical Properties of Sn₂P₂S₆ Compound in Different Phases. Integrated Ferroelectrics, 2021, 220, 56-70.	0.3	1

#	Article	IF	Citations
63636	Slater Insulator Phase of X₂ (Xâ€‰=â€‰Na, Li)IrO₃: First Principles Calculation. Integrated Ferroelectrics, 2021, 220, 80-89.	0.3	0
63637	Recent implementations in LASP 3.0: Global neural network potential with multiple elements and better long-range description. Chinese Journal of Chemical Physics, 2021, 34, 583-590.	0.6	12
63638	Thermodynamic Stabilities of PdRuM (M = Cu, Rh, Ir, Au) Alloy Nanoparticles Assessed by Wangâ€“Landau Sampling Combined with DFT Calculations and Multiple Regression Analysis. Bulletin of the Chemical Society of Japan, 2021, 94, 2484-2492.	2.0	6
63639	Efficient Helium Separation with Two-Dimensional Metalâ€“Organic Framework Fe/Ni-PTC: A Theoretical Study. Membranes, 2021, 11, 927.	1.4	1
63640	Pressure Tuned Structural, Electronic and Elastic Properties of U3Si2C2: A First Principles Study. Crystals, 2021, 11, 1420.	1.0	0
63641	Clusters modification for tunable photoluminescence in Nd3+:SrF2 crystal. Journal of Alloys and Compounds, 2022, 899, 162913.	2.8	15
63642	Regulation of Electrical Properties of ZrOxNy by Oxygen Doping and Zirconium Vacancies. EPJ Applied Physics, 0, , .	0.3	0
63643	Quantum Transport Methodologies forÂSpin Transport. Springer Theses, 2022, , 45-88.	0.0	0
63644	Thioether-Based Polymeric Micelles with Fine-Tuned Oxidation Sensitivities for Chemotherapeutic Drug Delivery. Biomacromolecules, 2022, 23, 77-88.	2.6	10
63645	Ab Initio Calculations for the Electronic, Interfacial and Optical Properties of Two-Dimensional AlN/Zr2CO2 Heterostructure. Frontiers in Chemistry, 2021, 9, 796695.	1.8	14
63646	Incorporation of Kr and Xe in Uranium Mononitride: A Density Functional Theory Study. Journal of Physical Chemistry C, 2021, 125, 26999-27008.	1.5	10
63647	Assessment of the van der Waals, Hubbard U parameter and <scp>spinâ€orbit</scp> coupling corrections on the <scp>2D</scp>/<scp>3D</scp> structures from metal gold congeners clusters. Journal of Computational Chemistry, 2022, 43, 230-243.	1.5	4
63648	Finding the order in complexity: The electronic structure of 14-1-11 zintl compounds. Applied Physics Letters, 2021, 119, .	1.5	6
63649	Significant phonon anharmonicity drives phase transitions in CsPbI3. Applied Physics Letters, 2021, 119, .	1.5	9
63650	Topological nodal line and superconductivity of highly thermally stable two-dimensional <mml:math xmlns:mml="http://www.w3.org/1998/Math/MathML"><mml:msub><mml:mi mathvariant="normal">TiB</mml:mi><mml:mn>4</mml:mn></mml:msub></mml:math>. Physical Review B, 2021, 104, .	1.1	11
63651	Spin-valley coupling and valley splitting in the MoSi2N4/CrCl3 van der Waals heterostructure. Applied Physics Letters, 2021, 119, .	1.5	24
63652	Insights into the effects of single Mo vacancy sites on the adsorption and dissociation of CO2 and H2O over the tertiary N-doped MoS2 monolayers. Applied Surface Science, 2022, 577, 151908.	3.1	4
63653	Effects of thermal annealing on the distribution of boron and phosphorus in p-i-n structured silicon nanocrystals embedded in silicon dioxide. Nanotechnology, 2022, 33, 075709.	1.3	5

#	Article	IF	Citations
63654	First-principles study on the mechanism of water-gas shift reaction on the Fe3O4 (111)-Fetet1. Molecular Catalysis, 2021, 516, 111998.	1.0	2
63655	Theoretical Screening of Transition Metal Doped Defective MoS₂ as Efficient Electrocatalyst for CO Conversion to CH₄. ChemPhysChem, 2022, 23, .	1.0	2
63656	Phonon-assisted electronic states modulation of few-layer PdSe2 at terahertz frequencies. Npj 2D Materials and Applications, 2021, 5, .	3.9	10
63657	Crystalline orientation-related magnetic anisotropy in transition metal dichalcogenides 1Tâ€²-MoTe2/Co heterostructures. Physics Letters, Section A: General, Atomic and Solid State Physics, 2021, , 127866.	0.9	0
63658	Absorption Features of CdTe Nanoclusters: Aspect Ratio Dependency of the Singlet/Doublet from First-Principles Calculations. Journal of Physical Chemistry C, 2021, 125, 25660-25669.	1.5	3
63659	Molecular dynamics simulations of lanthanum chloride by deep learning potential. Computational Materials Science, 2022, 210, 111014.	1.4	13
63660	Computational screening of highly selective and active electrocatalytic nitrogen reduction on single-atom-embedded artificial holey SnN3 monolayers. Journal of Colloid and Interface Science, 2022, 610, 546-556.	5.0	15
63661	Synthesis and Characterization of the Ternary Nitride Semiconductor Zn₂VN₃: Theoretical Prediction, Combinatorial Screening, and Epitaxial Stabilization. Chemistry of Materials, 2021, 33, 9306-9316.	3.2	12
63662	Promoting ethylene production over a wide potential window on Cu crystallites induced and stabilized via current shock and charge delocalization. Nature Communications, 2021, 12, 6823.	5.8	61
63663	P-Type AsP Nanosheet as an Electron Donor for Stable Solar Broad-Spectrum Hydrogen Evolution. ACS Applied Materials & Interfaces, 2021, 13, 55102-55111.	4.0	2
63664	On how the mechanochemical and co-precipitation synthesis method changes the sensitivity and operating range of the Ba2Mg1-xEuxWO6 optical thermometer. Scientific Reports, 2021, 11, 22847.	1.6	13
63665	Phononâ€“phonon interaction assisted electronâ€“hole recombination in WSe2/hBN van der Waals heterostructure. Journal of Applied Physics, 2021, 130, .	1.1	6
63666	Reaching the Excitonic Limit in 2D Janus Monolayers by In Situ Deterministic Growth. Advanced Materials, 2022, 34, e2106222.	11.1	39
63667	Electronic, magnetic and elastic calculations on half-metallic Heusler Ti₂RuTl compound. Philosophical Magazine, 2022, 102, 153-165.	0.7	1
63668	The structure, electronic and optical properties of 4a,5,8,8a-tetrahydro-5,8-ethano-1,4-naphthoquinone under different pressure. Solid State Communications, 2022, 342, 114586.	0.9	1
63669	Computational Study of the Curvature-Promoted Anchoring of Transition Metals for Water Splitting. Nanomaterials, 2021, 11, 3173.	1.9	3
63670	Native Atomic Defects Manipulation for Enhancing the Electronic Transport Properties of Epitaxial SnTe Films. ACS Applied Materials & Interfaces, 2021, 13, 56446-56455.	4.0	2
63671	First-principle predictions of the electric and thermal transport performance on high-temperature thermoelectric semiconductor MnTe2. Journal of Alloys and Compounds, 2022, 898, 162813.	2.8	3

#	Article	IF	Citations
63672	Effect of Dilute Magnetism in a Topological Insulator. Frontiers in Materials, 2021, 8, .	1.2	0
63673	Functionalized nano-MOF for NIR induced bacterial remediation: A combined spectroscopic and computational study. Inorganica Chimica Acta, 2022, 532, 120733.	1.2	6
63674	Scaling and Classification of Ion-Substrate Interaction. Journal of Physical Chemistry C, 2021, 125, 26778-26784.	1.5	1
63675	Exploring DFT+U parameter space with a Bayesian calibration assisted by Markov chain Monte Carlo sampling. Npj Computational Materials, 2021, 7, .	3.5	8
63676	Revealing the Regulation Mechanism of Irâ€“MoO₂ Interfacial Chemical Bonding for Improving Hydrogen Oxidation Reaction. ACS Catalysis, 2021, 11, 14932-14940.	5.5	33
63677	Reversing sintering effect of Ni particles on Î³-Mo2N via strong metal support interaction. Nature Communications, 2021, 12, 6978.	5.8	58
63678	Alkali-metal(Li, Na, and K)-adsorbed MoSi₂N₄ monolayer: an investigation of its outstanding electronic, optical, and photocatalytic properties. Communications in Theoretical Physics, 2022, 74, 015503.	1.1	4
63679	Superconductivity of <mml:math xmlns:mml="http://www.w3.org/1998/Math/MathML"><mml:msub><mml:mrow><mml:mi mathvariant="normal">H</mml:mi></mml:mrow><mml:mn>3</mml:mn></mml:msub><mml:mi mathvariant="normal">S</mml:mi></mml:math> doped with light elements. Physical Review Research, 2021, 3, .	1.3	12
63680	Theoretical Study on V Atom Supported on N and P-Doped Defective Graphene for Electrocatalytic Nitrogen Reduction. Journal of the Electrochemical Society, 2021, 168, 116516.	1.3	5
63681	Quasi-one-dimensional superconductivity in the pressurized charge-density-wave conductor HfTe3. Npj Quantum Materials, 2021, 6, .	1.8	13
63682	Applying design principles to improve hydrogen storage capacity in nanoporous materials. Brazilian Journal of Chemical Engineering, 2022, 39, 919-931.	0.7	3
63683	Unveiling the Selectivity of CO₂ Reduction on Cu₂ZnSnS₄: The Effect of Exposed Termination. Journal of Physical Chemistry C, 2021, 125, 24967-24973.	1.5	6
63684	Non-Equilibrium Sodiation Pathway of CuSbS₂. ACS Nano, 2021, 15, 17472-17479.	7.3	5
63685	From (S = 1) Spin Hexamer to Spin Tetradecamer by CuO Interstitials in A₂Cu₃O(CuO)_x(SO₄)₃ (A = alkali). Inorganic Chemistry, 2021, 60, 18185-18191.	1.9	5
63686	Photocatalytic Properties of a Novel Keratin char-TiO2 Composite Films Made through the Calcination of Wool Keratin Coatings Containing TiO2 Precursors. Catalysts, 2021, 11, 1366.	1.6	2
63687	A theoretical framework for reliable predictions of thermal conductivity of multicomponent molten salt mixtures: KCl-NaCl-MgCl<mml:math xmlns:mml="http://www.w3.org/1998/Math/MathML" display="inline" id="d1e285" altimg="si158.svg"><mml:msub><mml:mrow /><mml:mrow><mml:mn>2</mml:mn></mml:mrow></mml:msub></mml:math> as a case study. Solar Energy Materials and Solar Cells, 2022, 236, 111478.	3.0	9
63688	The influence of A-site deficiency on the electrochemical properties of (Ba0.95La0.05)1-xFeO3-Î´ as an intermediate temperature solid oxide fuel cell cathode. International Journal of Hydrogen Energy, 2022, 47, 1229-1240.	3.8	21
63689	The influence of Fâ˜† ion on the electrochemical behavior and coordination properties of uranium in LiCl-KCl molten salt. Electrochimica Acta, 2022, 404, 139573.	2.6	16

#	Article	IF	Citations
63690	Adsorption and Oxidation of CO on Ceria Nanoparticles Exposing Single-Atom Pd and Ag: A DFT Modelling. Materials, 2021, 14, 6888.	1.3	2
63691	Functionalizing MXenes by Tailoring Surface Terminations in Different Chemical Environments. Chemistry of Materials, 2021, 33, 9108-9118.	3.2	40
63692	Janus Mo₂P₃ Monolayer as an Electrocatalyst for Hydrogen Evolution. ACS Applied Materials & Interfaces, 2021, 13, 57422-57429.	4.0	10
63693	Carrier-Specific Hot Phonon Bottleneck in CH₃NH₃PbI₃ Revealed by Femtosecond XUV Absorption. Journal of the American Chemical Society, 2021, 143, 20176-20182.	6.6	16
63694	Adatoms in the Surface-Confined Ullmann Coupling of Phenyl Groups. Journal of Physical Chemistry Letters, 2021, 12, 11061-11069.	2.1	11
63695	Leadâ€free Double Perovskite Cs₂AgIn_{0.9}Bi_{0.1}Cl₆ Quantum Dots for White Lightâ€Emitting Diodes. Advanced Science, 2022, 9, e2102895.	5.6	46
63696	Stripping away ion hydration shells in electrical double-layer formation: Water networks matter. Proceedings of the National Academy of Sciences of the United States of America, 2021, 118, .	3.3	20
63697	Revisiting properties of CaCoSinO2n+2. Crystal and electronic structure. Journal of Magnetism and Magnetic Materials, 2022, 546, 168858.	1.0	5
63698	Mixed Ionicâ€Electronic Charge Transport in Layered Blackâ€Phosphorus for Lowâ€Power Memory. Advanced Functional Materials, 2022, 32, 2107068.	7.8	16
63699	Effect of ionic disorder on the principal shock Hugoniot. Physical Review E, 2021, 104, 055208.	0.8	2
63700	Engineering Efficient NiIr_x/CNT Hybrid Nanostructures for pH-Universal Oxygen Evolution. Journal of Physical Chemistry C, 2021, 125, 26003-26012.	1.5	6
63701	Pyridinic-N Doped Porous Graphene Supported on Metal Substrates As the Promising Electrocatalyst for Oxygen Reduction Reaction. Energy & Fuels, 2021, 35, 19634-19640.	2.5	1
63702	Weak antilocalization and Shubnikovâ€“de Haas oscillations in single crystal CaCuSb. Physical Review B, 2021, 104, .	1.1	2
63703	Accelerated prediction of Cu-based single-atom alloy catalysts for CO2 reduction by machine learning. Green Energy and Environment, 2023, 8, 820-830.	4.7	16
63704	Aâ€™â€“B Intersite Cooperation-Enhanced Water Splitting in Quadruple Perovskite Oxide CaCu₃Ir₄O₁₂. Chemistry of Materials, 2021, 33, 9295-9305.	3.2	11
63705	Activating MoS₂ Nanoflakes via Sulfur Defect Engineering Wrapped on CNTs for Stable and Efficient Liâ€O₂ Batteries. Advanced Functional Materials, 2022, 32, 2108153.	7.8	74
63706	TaCo₂Te₂: An Airâ€Stable, High Mobility Van der Waals Material with Probable Magnetic Order. Advanced Functional Materials, 2022, 32, .	7.8	10
63707	Nitrogen-incorporation activates NiFeOx catalysts for efficiently boosting oxygen evolution activity and stability of BiVO4 photoanodes. Nature Communications, 2021, 12, 6969.	5.8	109

#	Article	IF	Citations
63708	Pressureâ€Tailored Band Engineering for Significant Enhancements in the Photoelectric Performance of CsI₃ in the Optical Communication Waveband. Advanced Functional Materials, 2022, 32, 2108636.	7.8	18
63709	Interfaceâ€Enhanced Ferromagnetism with Longâ€Distance Effect in van der Waals Semiconductor. Advanced Functional Materials, 2022, 32, 2108953.	7.8	13
63710	Substrate molecule adsorption energy: An activity descriptor for electrochemical oxidation of 5-Hydroxymethylfurfural (HMF). Chemical Engineering Journal, 2022, 433, 133842.	6.6	35
63711	Exploring metastable states in UO₂ using hybrid functionals and dynamical mean field theory. Journal of Physics Condensed Matter, 2022, 34, 094003.	0.7	2
63712	Revealing Size Dependent Structural Transitions in Supported Gold Nanoparticles in Hydrogen at Atmospheric Pressure. Small, 2021, 17, e2104571.	5.2	13
63713	Catalysis stability enhancement of Fe/Co dual-atom site via phosphorus coordination for proton exchange membrane fuel cell. Nano Research, 2022, 15, 3082-3089.	5.8	31
63714	3D graphene-like semiconductor Ba2HfTe4 with electronic structure similar to graphene and bandgap close to silicon. Cell Reports Physical Science, 2021, 2, 100658.	2.8	4
63715	Theoretical limit of how small we can make MoS2 transistor channels. Journal Physics D: Applied Physics, 0, , .	1.3	5
63716	Binderâ€Free Ï‰â€Li₃V₂O₅ Catalytic Network with Multiâ€Polarization Centers Assists Lithiumâ€“Sulfur Batteries for Enhanced Kinetics Behavior. Advanced Functional Materials, 2022, 32, 2110665.	7.8	16
63717	Synthesis and structural characterization of U-phase, [3Ca2Al(OH)6][Na(H2O)6(SO4)2Â·6H2O] layered double hydroxide. Journal of Solid State Chemistry, 2022, 306, 122730.	1.4	3
63718	Tuning the Band Gaps of Oxide and Halide Perovskite Compounds via Biaxial Strain in All Directions. Journal of Physical Chemistry C, 2021, 125, 25951-25958.	1.5	6
63719	Solute drag assessment of grain boundary migration in Au. Acta Materialia, 2022, 224, 117473.	3.8	16
63720	Single-valley state in a two-dimensional antiferromagnetic lattice. Physical Review B, 2021, 104, .	1.1	13
63721	Uncovering the coordination effect on the Ni single-atom catalysts for CO2 reduction including vacancy defect and non-vacancy defect structures. Fuel, 2022, 310, 122472.	3.4	17
63722	First-principles study on the surface oxidation behavior of ternary M6C6 (M6Â=ÂZr5Ti, Zr5Ta, Hf5Ti,) Tj ETQq0 0 0 rgBT /Overlock 10 Tf	1.4	1
63723	Stable polar oxynitrides through epitaxial strain. Physical Review Materials, 2021, 5, .	0.9	2
63724	Externally controlled and switchable two-dimensional electron gas at the Rashba interface between ferroelectrics and heavy d metals. Physical Review Research, 2021, 3, .	1.3	1
63725	Scalable two-step annealing method for preparing ultra-high-density single-atom catalyst libraries. Nature Nanotechnology, 2022, 17, 174-181.	15.6	279

#	Article	IF	Citations
63726	Unified mechanistic understanding of CO2 reduction to CO on transition metal and single atom catalysts. Nature Catalysis, 2021, 4, 1024-1031.	16.1	154
63727	Prediction of structural and phase transitions of Th2CN from ambient pressure to 100 GPa: A first-principles study. Computational Materials Science, 2021, , 110980.	1.4	0
63728	Efficient Helium and Helium Isotopes Separation by Phosphorus Carbide P 2 C 3 Membrane. Advanced Theory and Simulations, 0, , 2100327.	1.3	2
63729	The formation and role of the SiO2 oxidation layer in the 4H-SiC/Î²-Ga2O3 interface. Applied Surface Science, 2022, 581, 151956.	3.1	6
63730	Superexchange-induced valley splitting in two-dimensional transition metal dichalcogenides: A first-principles study for rational design. Physical Review B, 2021, 104, .	1.1	4
63731	Giant Enhancement of Seebeck Coefficient by Deformation of Silicene Buckled Structure in Calciumâ€intercalated Layered Silicene Film. Advanced Materials Interfaces, 2022, 9, 2101752.	1.9	26
63732	Density Functional Theory Calculations on Electrocatalytic CO₂ Hydrogenation to C₂-Based Products over Cu(100) Nanocubes. ACS Applied Nano Materials, 2021, 4, 11907-11919.	2.4	9
63733	Theoretical study of SnS2 encapsulated in Graphene as a promising anode material for Kâ^'ion batteries. Journal of Physics Condensed Matter, 2021, , .	0.7	0
63734	In-situ cation exchange enhances room temperature phosphorescence of a family of metal-organic frameworks. Science China Chemistry, 2022, 65, 128-134.	4.2	16
63735	Structural effect of Nitrogen/Carbon on the stability of anchored Ru catalysts for CO2 hydrogenation to formate. Chemical Engineering Journal, 2022, 433, 133571.	6.6	23
63736	Metal to insulator transition in Ba2Ge2Te5: Synthesis, crystal structure, resistivity, thermal conductivity, and electronic structure. Materials Research Bulletin, 2022, 147, 111641.	2.7	5
63737	First-Principles Study of Pt-Based Bifunctional Oxygen Evolution & Reduction Electrocatalyst: Interplay of Strain and Ligand Effects. Energies, 2021, 14, 7814.	1.6	6
63738	First-Principles Calculations of Magnetic Moment Modulation of 3d Transition Metal Atoms Encapsulated in C60/C70 Cages on Si(100) Surfaces: Implications for Spintronic Devices. ACS Applied Nano Materials, 2021, 4, 12356-12364.	2.4	2
63739	Density functional theory study of adsorption and diffusion of potassium atoms on zigzag graphene nanoribbons with different terminal groups. International Journal of Modern Physics B, 2021, 35, .	1.0	0
63740	Metallization and Superconductivity in the van der Waals Compound CuP₂Se through Pressure-Tuning of the Interlayer Coupling. Journal of the American Chemical Society, 2021, 143, 20343-20355.	6.6	10
63741	Quantitatively regulating defects of 2D tungsten selenide to enhance catalytic ability for polysulfide conversion in a lithium sulfur battery. Energy Storage Materials, 2022, 45, 1229-1237.	9.5	81
63742	Atomistic discharge studies of sulfurized-polyacrylonitrile through ab initio molecular dynamics. Electrochimica Acta, 2022, 403, 139538.	2.6	4
63743	Nonuniformity of Transport Coefficients in Ultrathin Nanoscale Membranes and Nanomaterials. ACS Applied Materials & Interfaces, 2021, 13, 59546-59559.	4.0	6

#	Article	IF	Citations
63744	Atomically dispersed palladium catalyzes H/D exchange and isomerization of alkenes via reversible insertion and elimination. Chem Catalysis, 2021, 1, 1480-1492.	2.9	13
63745	Efficient electrocatalytic acetylene semihydrogenation by electronâ€“rich metal sites in Nâ€“heterocyclic carbene metal complexes. Nature Communications, 2021, 12, 6574.	5.8	30
63746	Sequence control of metals in MOF by coordination number precoding for electrocatalytic oxygen evolution. Chem Catalysis, 2022, 2, 84-101.	2.9	20
63747	Mechanism of Oxygen Reduction Reaction on Monolayer WTe₂ with and without S Dopant at Low Coverage. E-Journal of Surface Science and Nanotechnology, 2021, 19, 119-124.	0.1	0
63748	Engineering Single-Atomic Ni-N₄-O Sites on Semiconductor Photoanodes for High-Performance Photoelectrochemical Water Splitting. Journal of the American Chemical Society, 2021, 143, 20657-20669.	6.6	114
63749	La induced Si3 trimer monolayer on Si(111) surface: An ab initio study. New Journal of Physics, 0, , .	1.2	1
63750	Elucidating the influence of native defects on electrical and optical properties in semiconducting oxides: An experimental and theoretical investigation. Computational Materials Science, 2022, 210, 111037.	1.4	6
63751	<mml:math xmlns:mml="http://www.w3.org/1998/Math/MathML" display="inline"><mml:mrow><mml:mi>P</mml:mi><mml:mi>T</mml:mi></mml:mrow></mml:math> -Symmetry-Enabled Spin Circular Photogalvanic Effect in Antiferromagnetic Insulators. Physical Review Letters, 2021, 127, 207402.	2.9	22
63752	First-principles study of two-dimensional gallium-nitrides on van der Waals epitaxial substrate. Applied Physics Letters, 2021, 119, 203101.	1.5	3
63753	Accurate force field of two-dimensional ferroelectrics from deep learning. Physical Review B, 2021, 104, .	1.1	18
63754	Hydrodenitrogenation of Quinoline with high selectivity to aromatics over Î±-MoC1-x. Molecular Catalysis, 2021, 516, 112002.	1.0	5
63755	First-Principles Modeling of Protein/Surface Interactions. Polyglycine Secondary Structure Adsorption on the TiO₂ (101) Anatase Surface Adopting a Full Periodic Approach. Journal of Chemical Information and Modeling, 2021, 61, 5484-5498.	2.5	2
63756	In-situ release of phosphorus combined with rapid surface reconstruction for Coâ€“Ni bimetallic phosphides boosting efficient overall water splitting. Chemical Engineering Journal, 2022, 433, 133523.	6.6	60
63757	Superconductivity in a quintuple-layer square-planar nickelate. Nature Materials, 2022, 21, 160-164.	13.3	117
63758	Highly Mesoporous Cobalt-Hybridized 2D Cu₃P Nanosheet Arrays as Boosting Janus Electrocatalysts for Water Splitting. Inorganic Chemistry, 2021, 60, 18325-18336.	1.9	8
63759	Al-Modified CuO/Cu₂O for High-Temperature Thermochemical Energy Storage: from Reaction Performance to Modification Mechanism. ACS Applied Materials & Interfaces, 2021, 13, 57274-57284.	4.0	10
63760	High-temperature ideal Weyl semimetal phase and Chern insulator phase in ferromagnetic BaEuNiOsO6 and its (111) (BaEuNiOsO6)/(BaTiO3)10 superlattice. Physical Review B, 2021, 104, .	1.1	0
63761	Ligandâ€Mediated Selfâ€Terminating Growth of Singleâ€Atom Pt on Au Nanocrystals for Improved Formic Acid Oxidation Activity. Advanced Energy Materials, 2022, 12, 2103195.	10.2	17

#	Article	IF	Citations
63762	Gas Permeability and Selectivity of a Porous WS₂ Monolayer. Journal of Physical Chemistry C, 2021, 125, 25055-25066.	1.5	11
63763	Infrared Activities of Adsorbed Species on Metal Surfaces: The Puzzle of Adsorbed Methyl (CH3). Journal of Physical Chemistry Letters, 2021, 12, 11164-11169.	2.1	0
63764	Platinum-silicon doped graphitic carbon nitride: A first principle calculation. Physica B: Condensed Matter, 2022, 627, 413547.	1.3	4
63765	DeepTMC: A deep learning platform to targeted design doped transition metal compounds. Energy Storage Materials, 2022, 45, 1201-1211.	9.5	9
63766	Synergistic electronic and morphological modulation by trace Ir introduction boosting oxygen evolution performance over a wide pH range. Chemical Engineering Journal, 2022, 433, 133577.	6.6	7
63767	Ternary ruthenium complex hydrides for ammonia synthesis via the associative mechanism. Nature Catalysis, 2021, 4, 959-967.	16.1	67
63768	Onset of anharmonicity and thermal conductivity in SnSe. Physical Review B, 2021, 104, .	1.1	5
63769	Finding well-optimized special quasirandom structures with decision diagram. Physical Review Materials, 2021, 5, .	0.9	0
63770	Growth and NO2 gas sensing mechanisms of vertically aligned 2D SnS2 flakes by CVD: Experimental and DFT studies. Sensors and Actuators B: Chemical, 2022, 353, 131078.	4.0	25
63771	The effect of Ti on Ca-pv and Mg-pv phase stability. Physics of the Earth and Planetary Interiors, 2022, 322, 106825.	0.7	1
63772	Electronic Origin of Non-Zone-Center Phonon Condensation: Octahedral Rotation as a Case Study. Physical Review Letters, 2021, 127, 215701.	2.9	7
63773	Hyper-coordinated iodine in HIO3 under pressure. Vibrational Spectroscopy, 2021, 117, 103318.	1.2	1
63774	Vapor-phase self-assembly for generating thermally stable single-atom catalysts. CheM, 2022, 8, 731-748.	5.8	23
63775	Exchange Coupling in Synthetic Anionâ€Engineered Chromia Heterostructures. Advanced Functional Materials, 2022, 32, 2109828.	7.8	3
63776	Characterization of nanostructures in a high pressure die cast Al-Si-Cu alloy. Acta Materialia, 2022, 224, 117500.	3.8	16
63777	Computational Screening and Experimental Synthesis of Doped TiO₂ for Propane Dehydrogenation. Energy & Fuels, 2021, 35, 19624-19633.	2.5	5
63778	Migration Kinetics of Surface Ions in Oxygenâ€Deficient Perovskite During Topotactic Transitions. Small, 2021, 17, e2104356.	5.2	6
63779	A New Hybrid Leadâ€Free Metal Halide Piezoelectric for Energy Harvesting and Human Motion Sensing. Small, 2022, 18, e2103829.	5.2	28

#	Article	IF	Citations
63780	Extended calculation of dark matter-electron scattering in crystal targets. Physical Review D, 2021, 104, .	1.6	28
63781	Electrochemical and transport properties of Te-doped Li4Ti5O12 as anode material for lithium-ion half/full batteries. Journal of Alloys and Compounds, 2022, 897, 162744.	2.8	21
63782	Oxide-ion and proton conductivity of the ordered perovskite BaY1/3Ga2/3O2.5. Journal of Solid State Chemistry, 2022, 306, 122733.	1.4	10
63783	Highly dispersed Ru anchored on nanosheet N-doped carbon for efficient and chemoselective hydrogenation of nitroaromatics to aromatic amines under mild conditions. Chemical Engineering Journal, 2022, 431, 133863.	6.6	19
63784	Defect equilibria and thermophysical properties of CeO 2â€•x based on experimental data and density functional theory calculation result. Journal of the American Ceramic Society, 0, , .	1.9	2
63785	Experimental and theoretical analysis revealing the underlying chemistry accounting for the heterogeneous transesterification reaction in Na2SiO3 and Li2SiO3 catalysts. Renewable Energy, 2022, 184, 845-856.	4.3	6
63786	SnF₂â€Catalyzed Formation of Polymerized Dioxolane as Solid Electrolyte and its Thermal Decomposition Behavior. Angewandte Chemie, 2022, 134, .	1.6	6
63787	Self-Assembled NbOPO₄ Nanosheet/Reduced Graphene Oxide Heterostructure for Capacitive Desalination. ACS Applied Nano Materials, 2021, 4, 12629-12639.	2.4	11
63788	Epitaxial IIIâ€“V/Si Vertical Heterostructures with Hybrid 2Dâ€Semimetal/Semiconductor Ambipolar and Photoactive Properties. Advanced Science, 2022, 9, e2101661.	5.6	13
63789	Remarkable catalysis of spinel ferrite XFe2O4 (XÂ=ÂNi, Co, Mn, Cu, Zn) nanoparticles on the dehydrogenation properties of LiAlH4: An experimental and theoretical study. Journal of Materials Science and Technology, 2022, 111, 189-203.	5.6	18
63790	Significant Effect of Rh on the h-BN-Supported Ni Catalyst for Dry Reformation of CH4: Insights from Density Functional Theory and Microkinetic Analysis. Journal of Physical Chemistry C, 0, , .	1.5	6
63791	Robust evidence for the stabilization of the premartensite phase in Ni-Mn-In magnetic shape memory alloys by chemical pressure. Physical Review Materials, 2021, 5, .	0.9	3
63792	A review of quantum chemical methods for treating energetic molecules. Energetic Materials Frontiers, 2021, 2, 292-305.	1.3	21
63793	Strain and electric field tunable photoelectric properties of multilayer Sb2Se3. Journal of Physics Condensed Matter, 2021, 34, .	0.7	0
63794	Improved electronic structure prediction of chalcopyrite semiconductors from a semilocal density functional based on Pauli kinetic energy enhancement factor. Journal of Physics Condensed Matter, 2022, 34, 075501.	0.7	3
63795	Lattice Dynamics and Optoelectronic Properties of Vacancy-Ordered Double Perovskite Cs₂TeX₆ (X = Cl^{â€“}, Br^{â€“}, I^{â€“}) Single Crystals. Journal of Physical Chemistry C, 2021, 125, 25126-25139.	1.5	17
63796	Unveiling the promotion of accelerated water dissociation kinetics on the hydrogen evolution catalysis of NiMoO4 nanorods. Journal of Energy Chemistry, 2022, 67, 805-813.	7.1	118
63797	High-performance solid-solution potassium-ion intercalation mechanism of multilayered turbostratic graphene nanosheets. Journal of Energy Chemistry, 2022, 67, 814-823.	7.1	13

#	Article	IF	Citations
63798	Photophysical properties of zero-dimensional perovskites studied by PBE0 and GW+BSE methods. Journal of Applied Physics, 2021, 130, 203106.	1.1	4
63799	Ab Initio Molecular Dynamics Study of the Structure and Properties of Nb-Doped Zr-Cu-Al Amorphous Alloys. Metals, 2021, 11, 1821.	1.0	1
63800	In situ formation of ZnOx species for efficient propane dehydrogenation. Nature, 2021, 599, 234-238.	13.7	133
63801	Orally Fast Disintegrating Cyclodextrin/Prednisolone Inclusion-Complex Nanofibrous Webs for Potential Steroid Medications. Molecular Pharmaceutics, 2021, 18, 4486-4500.	2.3	14
63802	Amorphous MoSxOy/h-BNxOy Nanohybrids: Synthesis and Dye Photodegradation. Nanomaterials, 2021, 11, 3232.	1.9	6
63803	Production of methyl levulinate from cellulose over cobalt disulfide: The importance of the crystal facet (111). Bioresource Technology, 2022, 347, 126436.	4.8	3
63804	Incommensurate-commensurate magnetic phase transition in the double tungstate Li2Co(WO4)2. Chinese Physics B, 0, , .	0.7	0
63805	Insight the effect of rigid boron chain substructure on mechanical, magnetic and electrical properties of Î²-FeB. Journal of Alloys and Compounds, 2022, 896, 162767.	2.8	8
63806	Transition metal-doped Ni-rich layered cathode materials for durable Li-ion batteries. Nature Communications, 2021, 12, 6552.	5.8	167
63807	HSH-C10: A new quasi-2D carbon allotrope with a honeycomb-star-honeycomb lattice. Chinese Chemical Letters, 2021, , .	4.8	3
63808	Theoretical and experimental study of effects of Co2+ doping on structural and electronic properties of ZnO. Journal of Physics and Chemistry of Solids, 2021, , 110501.	1.9	5
63809	Synergistic Effect of Neighboring Fe and Cu Cation Sites Boosts FenCum-BEA Activity for the Continuous Direct Oxidation of Methane to Methanol. Catalysts, 2021, 11, 1444.	1.6	7
63810	Tuning the Nanoparticle Interfacial Properties and Stability of the Coreâ€“Shell Structure in Zn-Doped NiMoO₄@AWO₄. ACS Applied Materials & Interfaces, 2021, 13, 56116-56130.	4.0	30
63811	Alkali Metal (Li, Na, and K) Orthocarbonates: Stabilization of sp³-Bonded Carbon at Pressures above 20 GPa. Crystal Growth and Design, 2021, 21, 6744-6751.	1.4	7
63812	Regulating Li nucleation/growth via implanting lithiophilic seeds onto flexible scaffolds enables highly stable Li metal anode. Journal of Colloid and Interface Science, 2022, 609, 606-616.	5.0	12
63813	28.2%-efficient, outdoor-stable perovskite/silicon tandem solar cell. Joule, 2021, 5, 3169-3186.	11.7	99
63814	Discovery of spontaneous de-interpenetration through charged point-point repulsions. CheM, 2022, 8, 225-242.	5.8	11
63815	Tunable Band Alignments in 2D Ferroelectric Î±-In₂Se₃ Based Van der Waals Heterostructures. ACS Applied Electronic Materials, 2021, 3, 5114-5123.	2.0	19

#	Article	IF	Citations
63816	Hydrogen-incorporated vanadium dioxide nanosheets enable efficient uranium confinement and photoreduction. Nano Research, 2022, 15, 2943-2951.	5.8	14
63817	Step-Edge Epitaxy for Borophene Growth on Insulators. ACS Nano, 2021, 15, 18347-18353.	7.3	19
63818	Li_{4.3}AlS_{3.3}Cl_{0.7}: A Sulfideâ€“Chloride Lithium Ion Conductor with Highly Disordered Structure and Increased Conductivity. Chemistry of Materials, 2021, 33, 8733-8744.	3.2	8
63819	Activating Inert MXenes for Hydrogen Evolution Reaction via Anchored Metal Centers. Advanced Theory and Simulations, 2022, 5, .	1.3	2
63820	Promoting propane dehydrogenation via strain engineering on iridium single-atom catalyst. Fuel, 2022, 311, 122580.	3.4	8
63821	Engineering Electronic Band Structure of Binary Thermoelectric Nanocatalysts for Augmented Pyrocatalytic Tumor Nanotherapy. Advanced Materials, 2022, 34, e2106773.	11.1	42
63822	Transition Metal-Modified Co₄ Clusters Supported on Graphdiyne as an Effective Nitrogen Reduction Reaction Electrocatalyst. Inorganic Chemistry, 2021, 60, 18251-18259.	1.9	21
63823	Two-dimensional Pt2P3 monolayer: A promising bifunctional electrocatalyst with different active sites for hydrogen evolution and CO2 reduction. Chinese Chemical Letters, 2022, 33, 3987-3992.	4.8	16
63824	Large magnetoresistance and de Haasâ€“van Alphen oscillations in the topological semimetal candidates BaX4 (X=Ga,Âln). Physical Review B, 2021, 104, .	1.1	0
63825	Structural evolution and phase transition mechanism of $$hbox {MoSe}_2$$ under high pressure. Scientific Reports, 2021, 11, 22090.	1.6	3
63826	The Microstructure in an Alâ€“Ti Alloy Melt: The Wulff Cluster Model from a Partial Structure Factor. Metals, 2021, 11, 1799.	1.0	1
63827	Exotic Spintronic Properties of Transitionâ€Metal Monolayers on Graphyne. Advanced Theory and Simulations, 2022, 5, 2100287.	1.3	1
63828	Defect engineering on V2O3 cathode for long-cycling aqueous zinc metal batteries. Nature Communications, 2021, 12, 6878.	5.8	118
63829	Modulation of magnetoelectric coupling through systematically engineered spin canting in nickelâ€“zinc ferrite. Journal of the American Ceramic Society, 2022, 105, 2655-2662.	1.9	7
63830	A simplified methodology for the modeling of interfaces of elementary metals. AIP Advances, 2021, 11, .	0.6	3
63831	Effect of strain on interactions of Î£ 3{111} silicon grain boundary with oxygen impurities from firstâ€principles. Physica Status Solidi (B): Basic Research, 0, , 2100377.	0.7	3
63832	Interfacial thermal transport in spin caloritronic material systems. Physical Review Materials, 2021, 5, .	0.9	4
63833	Ultrasensitive biochemical sensors based on controllably grown films of high-density edge-rich multilayer WS2 islands. Sensors and Actuators B: Chemical, 2022, 353, 131081.	4.0	5

#	Article	IF	Citations
63834	Distorted <mml:math xmlns:mml="http://www.w3.org/1998/Math/MathML"><mml:mrow><mml:mn>3</mml:mn><mml:mi>Q</mml:mi></mml:mrow></mml: state driven by topological-chiral magnetic interactions. Physical Review B, 2021, 104, .	1.1	5
63835	Quantum Transport Evidence of Topological Band Structures of Kagome Superconductor <mml:math xmlns:mml="http://www.w3.org/1998/Math/MathML" display="inline"><mml:mrow><mml:mrow><mml:msub><mml:mrow><mml:mi>CsV</mml:mi></mml:mrow><mml:mrow><mml:mn> Physical Review Letters, 2021, 127, 207002.	2.9	74
63836	Strain-engineered high-temperature ferromagnetic oxygen-substituted <mml:math xmlns:mml="http://www.w3.org/1998/Math/MathML"><mml:msub><mml:mi>NaMnF</mml:mi><mml:mn>3</mml:mn></mml: from first principles. Physical Review B, 2021, 104, .	1.1	2
63837	Enhanced catalytic performance of atomically dispersed Pd on Pr-doped CeO2 nanorod in CO oxidation. Journal of Hazardous Materials, 2022, 426, 127793.	6.5	26
63838	Hierarchical Stratiform of a Fluorine-Doped NiO Prism as an Enhanced Anode for Lithium-Ion Storage. Journal of Physical Chemistry Letters, 2021, 12, 11460-11469.	2.1	5
63839	A durable and pH-universal self-standing MoCâ€“Mo2C heterojunction electrode for efficient hydrogen evolution reaction. Nature Communications, 2021, 12, 6776.	5.8	169
63840	Robust broadband directional plasmons in a <mml:math xmlns:mml="http://www.w3.org/1998/Math/MathML"><mml:mrow><mml:mi>MoO</mml:mi><mml:msub><mml:mi>Cl</mml:mi> monolayer. Physical Review B, 2021, 104, .	1.1	1
63841	Stronger three-phonon interactions revealed by molecular dynamics in materials with restricted phase space. Journal of Applied Physics, 2021, 130, .	1.1	4
63842	Giant anomalous Nernst signal in the antiferromagnet YbMnBi2. Nature Materials, 2022, 21, 203-209.	13.3	72
63843	Structural Symmetry, Spinâ€“Orbit Coupling, and Valley-Related Properties of Monolayer WSi₂N₄ Family. Journal of Physical Chemistry Letters, 2021, 12, 11622-11628.	2.1	20
63844	Comparing GIPAW with numerically exact chemical shieldings: the role of two-centre contributions to the induced current. Journal of Chemical Physics, 2021, 155, 234101.	1.2	0
63845	Dirac-like band structure and strain-tunable electronic structure of Zr2CCl2 monolayer. Applied Surface Science, 2021, 577, 151931.	3.1	0
63846	Reaction Mechanism and Strategy for Optimizing the Hydrogen Evolution Reaction on Single-Layer 1Tâ€² WSe₂ and WTe₂ Based on Grand Canonical Potential Kinetics. ACS Applied Materials & Interfaces, 2021, 13, 55611-55620.	4.0	14
63847	Mg-stabilized subnanometer Rh particles in zeolite Beta as highly efficient catalysts for selective hydrogenation. Journal of Catalysis, 2022, 405, 489-498.	3.1	8
63848	Theoretical Study of the Propene Combustion Catalysis of Chromite Spinels: Reaction Mechanism and Relation between the Activity and Electronic Structure of Spinels. Journal of Physical Chemistry C, 2021, 125, 25983-26002.	1.5	3
63849	Coreâ€“Shell Co₂VO₄/Carbon Composite Anode for Highly Stable and Fast-Charging Sodium-Ion Batteries. ACS Applied Materials & Interfaces, 2021, 13, 55020-55028.	4.0	65
63850	Electronic reconstruction and charge transfer in strained <mml:math xmlns:mml="http://www.w3.org/1998/Math/MathML"><mml:mrow><mml:msub><mml:mi>Sr</mml:mi><mml:mn>2</mml:mn> double perovskite. Physical Review B, 2021, 104, .	1.1	1
63851	Targeted Regulation of the Electronic States of Nickel Toward the Efficient Electrosynthesis of Benzonitrile and Hydrogen Production. ACS Applied Materials & Interfaces, 2021, 13, 56140-56150.	4.0	21

#	Article	IF	Citations
63852	Machine-learning potentials enable predictive and tractable high-throughput screening of random alloys. Physical Review Materials, 2021, 5, .	0.9	8
63853	A novel free-standing metal organic frameworks-derived cobalt sulfide polyhedron array for shuttle effect suppressive lithiumâ€“sulfur batteries. Nanotechnology, 2022, 33, 105401.	1.3	2
63854	Effect of Fe addition on glass-forming ability, thermal stability of B2 CuZr phase and crystallization kinetics for CuZr-based amorphous alloys. Journal of Materials Research and Technology, 2021, 15, 6464-6475.	2.6	7
63855	Interfacial electronic modulation of Ni3S2 nanosheet arrays decorated with Au nanoparticles boosts overall water splitting. Applied Catalysis B: Environmental, 2022, 304, 120935.	10.8	80
63856	Investigation on hydrogen embrittlement susceptibility in martensitic steels with 1000ÂMPa yield strength. Journal of Materials Research and Technology, 2021, 15, 6883-6900.	2.6	22
63857	Unveiling electronic and magnetic properties of Cu3(SeO3)2Cl2 and Cu3(TeO3)2Br2 oxohalide systems via first-principles calculations. Journal of Physics Condensed Matter, 2021, 34, .	0.7	0
63858	Joining dissimilar metal of Ti and CoCrMo using directed energy deposition. Journal of Materials Science and Technology, 2021, 111, 99-99.	5.6	0
63859	Tuning oxygen-containing groups of pyrene for high hydrogen peroxide production selectivity. Applied Catalysis B: Environmental, 2022, 304, 120908.	10.8	27
63860	Catalytic Hydrogen Evolution of NaBH4 Hydrolysis by Cobalt Nanoparticles Supported on Bagasse-Derived Porous Carbon. Nanomaterials, 2021, 11, 3259.	1.9	21
63861	Phase engineering of Mo-V oxides molecular sieves for zinc-ion batteries. Science China Materials, 2022, 65, 939-946.	3.5	4
63862	Intercalation-deintercalation design in MXenes for high-performance supercapacitors. Nano Research, 2022, 15, 3213-3221.	5.8	17
63863	High-Pressure Synthesis and Lithium-Ion Conduction of Li₄OBr₂ Derivatives with a Layered Inverse-Perovskite Structure. Chemistry of Materials, 2021, 33, 9194-9201.	3.2	8
63864	Grain boundary kinetics in magnesium alloys from first principles. Computational Materials Science, 2022, 210, 111042.	1.4	5
63865	Ferromagnetic Enhancement in LaMnO₃ Films with Release and Flexure. Advanced Materials Interfaces, 2021, 8, .	1.9	8
63866	Gold Carbide: A Predicted Nanotube Candidate from First Principle. Nanomaterials, 2021, 11, 3182.	1.9	0
63867	Magnetic field effect on topological properties of Dirac semimetals PdTe₂/PtTe₂/PtSe₂. Journal of Physics Condensed Matter, 2022, 34, 085802.	0.7	0
63868	Local structural evolution in the anionic solid solution ZnSexS1â^'x. Physical Review B, 2021, 104, .	1.1	2
63869	Coherent phonon spectroscopy and interlayer modulation of charge density wave order in the kagome metal <mml:math xmlns:mml="http://www.w3.org/1998/Math/MathML"><mml:mrow><mml:msub><mml:mi>CsV</mml:mi><mml:mn>3</mml:mn></ Physical Review Materials, 2021, 5, .	0.9	80

#	Article	IF	Citations
63870	Insight into the Interface Engineering of a SnO₂/FAPbI₃ Perovskite Using Lead Halide as an Interlayer: A First-Principles Study. Journal of Physical Chemistry Letters, 2021, 12, 11330-11338.	2.1	8
63871	Structure of mono- and bilayer FeO on Ru(0001): STM and DFT study. Journal of Magnetism and Magnetic Materials, 2022, 546, 168832.	1.0	8
63872	Anisotropic Optical and Vibrational Properties of GeS. Nanomaterials, 2021, 11, 3109.	1.9	7
63873	Enhanced activity of a WOx-incorporated Pt/Al2O3 catalyst for the dehydrogenation of homocyclic LOHCs: Effects of impregnation sequence on Ptâ€“WOx interactions. Fuel, 2022, 313, 122654.	3.4	9
63874	Elucidating the Role of the Metal Catalyst and Oxide Support in the Ru/CeO₂-Catalyzed CO₂Methanation Mechanism. Journal of Physical Chemistry C, 2021, 125, 25533-25544.	1.5	17
63875	Antiferromagnetic topological crystalline insulator and mixed Weyl semimetal in two-dimensional NpAs monolayer. New Journal of Physics, 2021, 23, 123018.	1.2	5
63876	BC6N as a promising sulfur host material for lithium-sulfur batteries. Applied Surface Science, 2022, 577, 151843.	3.1	7
63877	Validation of moment tensor potentials for fcc and bcc metals using EXAFS spectra. Computational Materials Science, 2022, 210, 111028.	1.4	5
63878	Room-temperature non-Dirac quantum anomalous Hall states, half semiconductors, and strain-tuned half metals in monolayer zirconium trihalide. Physical Review B, 2021, 104, .	1.1	3
63879	Tunable spin polarization and electronic structure of bottom-up synthesized <mml:math xmlns:mml="http://www.w3.org/1998/Math/MathML"><mml:msub><mml:mrow><mml:mi>MoSi</mml:mi></mml:mrow><mml:mn>2</ mathvariant="normal">N</mml:mi></mml:mrow><mml:mn>4</mml:mn></mml:msub></mml:math> materials. Physical Review B, 2021, 104, .	1.1	37
63880	Selective Production of 2-Butanol from Hydrogenolysis of Levulinic Acid Catalyzed by the Non-precious NiMn Bimetallic Catalyst. ACS Sustainable Chemistry and Engineering, 2021, 9, 15603-15611.	3.2	14
63881	Screening for Stable Ternary-Metal MXenes as Promising Anode Materials for Sodium/Potassium-Ion Batteries. Journal of Physical Chemistry C, 2021, 125, 26332-26338.	1.5	4
63882	IrRep: Symmetry eigenvalues and irreducible representations of ab initio band structures. Computer Physics Communications, 2022, 272, 108226.	3.0	27
63883	Rationally engineered Co and N co-doped WS2 as bifunctional catalysts for pH-universal hydrogen evolution and oxidative dehydrogenation reactions. Nano Research, 2022, 15, 1993-2002.	5.8	20
63884	Identifying the Atomic Layer Stacking of Mo₂C MXene by Probe Molecule Adsorption. Journal of Physical Chemistry C, 2021, 125, 26808-26813.	1.5	8
63885	Simulation of STM Images of Hematite Î±-Fe₂O₃(0001) Surfaces: Dependence on Distance and Bias. Journal of Physical Chemistry C, 2021, 125, 26711-26717.	1.5	3
63886	Evidence for strong electron correlations in a nonsymmorphic Dirac semimetal. Npj Quantum Materials, 2021, 6, .	1.8	3
63887	Metal Substitution in Rutile TiO2: Segregation Energy and Conductivity. Journal of Electronic Materials, 2022, 51, 609-620.	1.0	6

#	Article	IF	Citations
63888	Photo-fluorination of nanodiamonds catalyzing oxidative dehydrogenation reaction of ethylbenzene. Nature Communications, 2021, 12, 6542.	5.8	14
63889	Heteroatom-doped Clar's goblet: Tunable magnetic order and programmable spin logic gate. Applied Physics Letters, 2021, 119, 192408.	1.5	2
63890	Unveiling the role of cobalt species in the Co/N-C catalysts-induced peroxymonosulfate activation process. Journal of Hazardous Materials, 2022, 426, 127784.	6.5	34
63891	Density functional theory study of the electronic properties and quantum capacitance of pure and doped <scp>Zr₂CO₂</scp> as electrode of supercapacitors. International Journal of Quantum Chemistry, 2022, 122, .	1.0	13
63892	Performance-limiting formation dynamics in mixed-halide perovskites. Science Advances, 2021, 7, eabj1799.	4.7	54
63893	Effect of alloying on the carrier dynamics in high-performance perovskite solar cells. Journal of Energy Chemistry, 2022, 68, 267-274.	7.1	2
63894	Surface energies and relaxation of NiCoCr and NiFeX (X = Cu, Co or Cr) equiatomic multiprincipal element alloys from first principles calculations. Modelling and Simulation in Materials Science and Engineering, 2022, 30, 025001.	0.8	2
63895	Effects of impurity elements on SiC grain boundary stability and corrosion. Nuclear Science and Techniques/Hewuli, 2021, 32, 1.	1.3	7
63896	Lattice Softening in Metastable bcc <mml:math xmlns:mml="http://www.w3.org/1998/Math/MathML" display="inline" overflow="scroll"><mml:msub><mml:mi>Co</mml:mi><mml:mi>x</mml:mi></mml:msub><mml:msub><mml:mi>Mn</mml:mi><mml:m displaystyle="false" scriptlevel="0"><mml:mtext>â^'</mml:mtext></mml:mstyle><mml:mi>x</mml:mi></mml:mrow></mml:msub></mml:math> (001) Ferromagnetic Layers for a Strain-Free Magnetic Tunnel Junction. Physical Review Applied, 2021, 16	1.5	10
63897	Crystal structures and mechanical properties of tungsten monocarbide predicted by first-principles investigations. Journal of Applied Physics, 2021, 130, 195902.	1.1	0
63898	Plasmon-Mediated CO₂ Photoreduction via Indirect Charge Transfer on Small Silver Nanoclusters. Journal of Physical Chemistry C, 2021, 125, 26348-26353.	1.5	10
63899	Sensing properties of NO2 gas sensor based on nonmetal doped Î±-AsP monolayer: A first-principles study. Materials Science in Semiconductor Processing, 2022, 139, 106319.	1.9	15
63900	Synergistically Optimizing Electrical and Thermal Transport Properties of ZrCoSb through Ru Doping. ACS Applied Energy Materials, 2021, 4, 13997-14003.	2.5	9
63901	Intriguing features of Dirac cones in phagraphene with site specific doping. Applied Surface Science, 2021, 577, 151782.	3.1	10
63902	Two-Dimensional Janus Antimony Selenium Telluride with Large Rashba Spin Splitting and High Electron Mobility. ACS Omega, 2021, 6, 31919-31925.	1.6	5
63903	Modulating electronic structure of metal-organic frameworks derived zinc manganates by oxygen vacancies for superior lithium storage. Chemical Engineering Journal, 2022, 433, 133770.	6.6	15
63904	Tuning mobility of intermediate and electron transfer to enhance electrochemical reduction of nitrate to ammonia on Cu2O/Cu interface. Chemical Engineering Journal, 2022, 433, 133680.	6.6	41
63905	Absolute surface energies of wurtzite (10 1Â¯1) surfaces and the instability of the cation-adsorbed surfaces of IIâ€“VI semiconductors. Applied Physics Letters, 2021, 119, 201603.	1.5	0

#	Article	IF	Citations
63906	Understanding the role of lithium bonds in doped graphene nanoribbons as cathode hosts for <scp>Liâ€S</scp> batteries: A firstâ€principles study. International Journal of Energy Research, 2022, 46, 4405-4416.	2.2	8
63907	Interface engineering of tungsten carbide/phosphide heterostructures anchored on N,P-codoped carbon for high-efficiency hydrogen evolution reaction. Science China Materials, 2022, 65, 967-973.	3.5	8
63908	Structural Regulation of ZnMn2O4 cathode material by K, Fe-Double doping to improve its rate and cycling stabilityfor rechargeable aqueous zinc-based batteries. Chemical Engineering Journal, 2022, 431, 133735.	6.6	26
63909	Strain engineering of electronic and optical properties of monolayer diboron dinitride. Physical Review B, 2021, 104, .	1.1	6
63910	Improved hydrothermal durability of Cu-SSZ-13 NH3-SCR catalyst by surface Al modification: Affinity and passivation. Journal of Catalysis, 2022, 405, 199-211.	3.1	28
63911	Highly selective and sensitive detection of mercury (II) and dopamine based on the efficient electrochemiluminescence of Ru(bpy)32+ with acridine orange as a coreactant. Journal of Electroanalytical Chemistry, 2022, 906, 115896.	1.9	8
63912	Artificial Adaptive and Maladaptive Sensory Receptors Based on a Surfaceâ€Dominated Diffusive Memristor. Advanced Science, 2022, 9, e2103484.	5.6	26
63913	Three new orthorhombic superhard metallic carbon allotropes. Diamond and Related Materials, 2022, 121, 108731.	1.8	3
63914	Efficient and Stable Co/Î²-Mo₂C Catalyst for Hydroformylation. ACS Catalysis, 2021, 11, 14319-14327.	5.5	22
63915	Fabrication of a Photocatalyst with Biomass Waste for H₂O₂ Synthesis. ACS Catalysis, 2021, 11, 14480-14488.	5.5	54
63916	Defectâ€Assisted Anchoring of Pt Single Atoms on MoS₂ Nanosheets Produces Highâ€Performance Catalyst for Industrial Hydrogen Evolution Reaction. Small, 2022, 18, e2104824.	5.2	36
63917	Stretchable MoS₂ Artificial Photoreceptors for Eâ€Skin. Advanced Functional Materials, 2022, 32, 2107524.	7.8	24
63918	Highly efficient detection of Cd(II) ions by a stannum and cerium bimetal-modified laser-induced graphene electrode in water. Chemical Engineering Journal, 2022, 433, 133791.	6.6	17
63919	High-Throughput Screening of Two-Dimensional Planar sp² Carbon Space Associated with a Labeled Quotient Graph. Journal of Physical Chemistry Letters, 2021, 12, 11511-11519.	2.1	34
63920	Screening Highly Efficient Hetero-Diatomic Doped PC6 Electrocatalysts for Selective Nitrogen Reduction to Ammonia. Journal of the Electrochemical Society, 2021, 168, 116519.	1.3	3
63921	Dopant binding with vacancies and helium in metal hydrides. Journal of Nuclear Materials, 2022, 559, 153437.	1.3	1
63922	Signatures of the Dichalcogenideâ€“Gold Interaction in the Vibrational Spectra of MoS₂ and MoSe₂ on Au(111). Journal of Physical Chemistry C, 2021, 125, 26645-26651.	1.5	11
63923	Nitric acid-assisted growth of InVO4 nanobelts on protonated ultrathin C3N4 nanosheets as an S-scheme photocatalyst with tunable oxygen vacancies for boosting CO2 conversion. Chemical Engineering Journal, 2022, 434, 133867.	6.6	37

#	Article	IF	Citations
63924	Theoretical study of structure sensitivity on Au doped CeO2 surfaces for formaldehyde oxidation: The effect of crystal planes and Au doping. Chemical Engineering Journal, 2022, 433, 133599.	6.6	7
63925	Unusual terahertz-wave absorptions in Î´/Î±-mixed-phase FAPbI3 single crystals: interfacial phonon vibration modes. NPG Asia Materials, 2021, 13, .	3.8	10
63926	Preferential Growth Mode of Large-Sized Vacancy Clusters in Silicon: A Neural-Network Potential and First-Principles Study. Journal of Physical Chemistry C, 0, , .	1.5	3
63927	Overcoming Asymmetric Contact Resistances in Al-Contacted Mg2(Si,Sn) Thermoelectric Legs. Materials, 2021, 14, 6774.	1.3	14
63928	Electronic and thermal properties of GeTe/Sb2Te3 superlattices by ab initio approach: Impact of Van der Waals gaps on vertical lattice thermal conductivity. Applied Physics Letters, 2021, 119, .	1.5	5
63929	Novel Two-Step Surface Boron Decoration of Graphitic Carbon Nitride Photoelectrodes for Efficient Charge Transport and Separation. Journal of Physical Chemistry C, 2021, 125, 25207-25216.	1.5	9
63930	Two-dimensional quantum-sheet films with sub-1.2â€‰nm channels for ultrahigh-rate electrochemical capacitance. Nature Nanotechnology, 2022, 17, 153-158.	15.6	55
63931	Surface Properties of the Hydrogenâ€“Titanium System. Journal of Physical Chemistry C, 2021, 125, 25339-25349.	1.5	13
63932	Effects of the orientation relationships between TCP phases and matrix on the morphologies of TCP phases in Ni-based single crystal superalloys. Materials Characterization, 2022, 183, 111609.	1.9	10
63933	Nickel Niobate Anodes for High Rate Lithiumâ€Ion Batteries. Advanced Energy Materials, 2022, 12, .	10.2	49
63934	Band structure tuning of g-C₃N₄ via sulfur doping for broadband near-infrared ultrafast photonic applications. Nanophotonics, 2021, 11, 139-151.	2.9	11
63935	Heat-Resistant Black Insulative Thin Films for Flat-Panel Displays in Al-Doped Agâ€“Feâ€“O Systems. ACS Applied Materials & Interfaces, 2021, 13, 57971-57980.	4.0	5
63936	Incorporation of Si and Sn donors in Î²-Ga2O3 through surface reconstructions. Journal of Applied Physics, 2021, 130, 185703.	1.1	7
63937	Interlayer magnetic interactions in Ï€/3-twisted bilayer CrI3. Applied Physics Letters, 2021, 119, .	1.5	9
63938	Pressure-driven electronic and structural phase transition in intrinsic magnetic topological insulator <mml:math xmlns:mml="http://www.w3.org/1998/Math/MathML"><mml:mrow><mml:mi>Mn</mml:mi><mml:msub><mml:mi>Sb</mml:mi><mml:mi><mml:r Physical Review B, 2021, 104, .	1.1	8
63939	Fabrication of Twin-Free Ultrathin NH₂-MIL-125(Ti) Membrane with c-Preferred Orientation Using Transition-Metal Trichalcogenides as Titanium Source. , 2022, 4, 55-60.		10
63940	Unraveling energy and charge transfer in type-II van der Waals heterostructures. Npj Computational Materials, 2021, 7, .	3.5	16
63941	Large valley polarization in a novel two-dimensional semiconductor H-ZrX₂ (X = Cl, Br, I). Journal of Physics Condensed Matter, 2022, 34, 075701.	0.7	6

#	Article	IF	Citations
63942	Temperature dependence of bismuth structures under high pressure. Chinese Physics B, 2022, 31, 056101.	0.7	1
63943	Icosahedral silicon boride: A potential hybrid photovoltaic-thermoelectric for energy harvesting. Physical Review Materials, 2021, 5, .	0.9	4
63944	The color mechanism of iron on quartz by ion implantation. Physica B: Condensed Matter, 2022, 627, 413550.	1.3	4
63945	Quantum Capacitance through Molecular Infiltration of 7,7,8,8-Tetracyanoquinodimethane in Metalâ€“Organic Framework/Covalent Organic Framework Hybrids. ACS Nano, 2021, 15, 18580-18589.	7.3	30
63946	Layered-Template Synthesis of Graphene-like Fe-N-C Nanosheets for Highly Efficient Oxygen Reduction Reaction. Energy & Fuels, 2021, 35, 20349-20357.	2.5	5
63947	Remarkable-cycle-performance Î²-bismuthene/graphene heterostructure anode for Li-ion battery. Chinese Chemical Letters, 2022, 33, 3802-3808.	4.8	8
63948	Insights into the Adsorption of Water and Oxygen on the Cubic CsPbBr3 Surfaces: A First-Principle Study. Chinese Physics B, 0, , .	0.7	1
63949	A Transferable Force Field for Predicting Adsorption and Diffusion of Small Molecules in Alkali Metal Exchanged Zeolites with Coupled Cluster Accuracy. Journal of Physical Chemistry C, 2021, 125, 26832-26846.	1.5	5
63950	Electron beam analysis induces Cl vacancy defects in a NaCl thin film. Nanotechnology, 2021, 33, .	1.3	4
63951	Reorganization of the topological surface mode of topological insulating Î±-Sn. Journal of Physics Condensed Matter, 2021, 34, .	0.7	0
63952	Dipole Engineering of Two-Dimensional van der Waals Heterostructures for Enhanced Power-Conversion Efficiency: The Case of Janus <mml:math xmlns:mml="http://www.w3.org/1998/Math/MathML" display="inline" overflow="scroll"><mml:msub><mml:mi>Ga</mml:mi><mml:mn>2</mml:mn></mml:msub><mml:mrow><mml:mi>Se</mml:mi><mml:mi mathvariant="normal">S</mml:mi></mml:mrow></mml:math>. Physical Review Applied, 2021, 16, .	1.5	39
63953	<mml:math xmlns:mml="http://www.w3.org/1998/Math/MathML"><mml:mrow><mml:mi>A</mml:mi><mml:msub><mml:mi mathvariant="normal">V</mml:mi><mml:mn>3</mml:mn></mml:msub><mml:msub><mml:mi>Sb</mml:mi><mml:mn>5</mml:mn></mml:math>		

#	Article	IF	Citations
63960	First-principles investigations of tricarbon: From the isolated C3 molecule to a novel ultra-hard anisotropic solid. Carbon Trends, 2022, 6, 100132.	1.4	5
63961	Manipulation of crystalline structure, magnetic performance, and topological feature in Mn3Ge films. APL Materials, 2021, 9, .	2.2	4
63962	Activity and stability of alloyed NiCo catalyst for the dry reforming of methane: A combined DFT and microkinetic modeling study. Catalysis Today, 2022, 400-401, 59-65.	2.2	11
63963	Spontaneous valley polarization in two-dimensional organometallic lattices. Physical Review B, 2021, 104, .	1.1	11
63964	In-plane quasi-single-domain BaTiO3 via interfacial symmetry engineering. Nature Communications, 2021, 12, 6784.	5.8	16
63965	Solvothermal synthesis of [Cr7S8(en)8Cl2]Cl3Â·2H2O with magnetically frustrated [Cr7S8]5+ doubleâ€cubes. Chemistry - A European Journal, 2021, , .	1.7	1
63966	First-principles analysis of the grain boundary segregation of transition metal alloying elements in Î³Fe. Computational Materials Science, 2022, 210, 111050.	1.4	20
63967	First-principles investigations on the structural stability, thermophysical and half-metallic properties of the half-Heusler CrMnS alloy. Optical and Quantum Electronics, 2022, 54, 1.	1.5	90
63968	Inorganic gas sensing performance of Ï‡3-borophene and the van der Waals heterostructure. Applied Surface Science, 2022, 581, 151906.	3.1	18
63969	Acidity effect on benzene methylation kinetics over substituted H-MeAlPO-5 catalysts. Journal of Catalysis, 2021, 404, 594-606.	3.1	10
63970	A comprehensive experimental and first-principles study on magnesium-vanadium oxides. Journal of Alloys and Compounds, 2022, 896, 162862.	2.8	10
63971	Kinetically Controlled Linker Binding in Rare Earth-2,5-Dihydroxyterepthalic Acid Metalâ€“Organic Frameworks and Its Predicted Effects on Acid Gas Adsorption. ACS Applied Materials & Interfaces, 2021, 13, 56337-56347.	4.0	15
63972	Quantum dot-like plasmonic modes in twisted bilayer graphene supercells. 2D Materials, 2022, 9, 014004.	2.0	7
63973	Prediction and Validation of the Process Window for Atomic Layer Etching: HF Exposure on TiO₂. Journal of Physical Chemistry C, 2021, 125, 25589-25599.	1.5	8
63974	Molecular-level insights into the electronic effects in platinum-catalyzed carbon monoxide oxidation. Nature Communications, 2021, 12, 6888.	5.8	18
63975	Atomic-scale observation of non-classical nucleation-mediated phase transformation in a titanium alloy. Nature Materials, 2022, 21, 290-296.	13.3	38
63976	A Photoâ€Responsive Chargeâ€Assisted Hydrogenâ€Bonded Organic Network with Ultraâ€Stable Viologen Radicals. Chinese Journal of Chemistry, 2022, 40, 351-356.	2.6	14
63977	Unraveling the Surface Reactivity of Pristine and Ti-Doped Hematite with Water. Journal of Physical Chemistry Letters, 2021, 12, 11520-11527.	2.1	5

#	Article	IF	Citations
63978	Prediction of spin-dependent electronic structures of 3d transition metals doped Hittorf's violet phosphorene towards spintronics. Physica E: Low-Dimensional Systems and Nanostructures, 2022, 138, 115068.	1.3	1
63979	Molybdenum Atom-Mediated Salphen-Based Covalent Organic Framework as a Promising Electrocatalyst for the Nitrogen Reduction Reaction: A First-Principles Study. Journal of Physical Chemistry C, 2021, 125, 26061-26072.	1.5	34
63980	Ab-initio investigation of Er3+ defects in tungsten disulfide. Computational Materials Science, 2021, , 111041.	1.4	2
63981	First-principles estimation of the superconducting transition temperature of a metallic hydrogen liquid. Physical Review B, 2021, 104, .	1.1	3
63982	Evolution of the Nature of Excitons and Electronic Couplings in Hybrid 2D Perovskites as a Function of Organic Cation Ï€â€Conjugation. Advanced Functional Materials, 2022, 32, 2108662.	7.8	15
63983	Sustainable oxidation catalysis supported by light: Fe-poly (heptazine imide) as a heterogeneous single-atom photocatalyst. Applied Catalysis B: Environmental, 2022, 304, 120965.	10.8	46
63984	High-performance proton-conducting solid oxide fuel cells using the first-generation Sr-doped LaMnO3 cathode tailored with Zn ions. Science China Materials, 2022, 65, 675-682.	3.5	65
63985	Electronic states of gallium oxide epitaxial thin films and related atomic arrangement. Applied Surface Science, 2022, 578, 151943.	3.1	4
63986	Descriptor-Based Microkinetic Modeling and Catalyst Screening for CO Hydrogenation. ACS Catalysis, 2021, 11, 14545-14560.	5.5	8
63987	Scalable Synthesis of Nanoâ€Sized Bi for Separator Modifying in 5Vâ€Class Lithium Metal Batteries and Potassium Ion Batteries Anodes. Small, 2022, 18, e2104264.	5.2	19
63988	A DFT study on the crystal stability, mechanical, electronic and thermodynamic properties of Ir3Nb under high pressure and temperature. Journal of Physics and Chemistry of Solids, 2022, 161, 110481.	1.9	9
63989	Pressure-Induced High-Energy-Density BeN4 Materials with Nitrogen Chains: First-Principles Study. Journal of Physical Chemistry C, 2021, 125, 25376-25382.	1.5	7
63990	Understanding the ORR Electrocatalysis on Coâ€“Mn Oxides. Journal of Physical Chemistry C, 2021, 125, 25470-25477.	1.5	11
63991	Photocatalytic HER Performance of TiO2-supported Single Atom Catalyst Based on Electronic Regulation: A DFT Study. Chemical Research in Chinese Universities, 0, , 1.	1.3	8
63992	KP15: Natural van der Waals material with ultra-low thermal conductivity and excellent thermoelectric performance. Journal of Applied Physics, 2021, 130, 195104.	1.1	0
63993	Atomistic studies on waterâ€induced lithium corrosion. ChemSusChem, 2021, , .	3.6	2
63994	Atomic structures and electronic properties of different interface types at Al/c-SiO2 interfaces. Applied Surface Science, 2022, 578, 151932.	3.1	9
63995	Titanium Nitride as a Plasmonic Material from Near-Ultraviolet to Very-Long-Wavelength Infrared Range. Materials, 2021, 14, 7095.	1.3	17

#	Article	IF	Citations
63996	Modeling Potential-Dependent Electrochemical Activation Barriers: Revisiting the Alkaline Hydrogen Evolution Reaction. Journal of the American Chemical Society, 2021, 143, 19341-19355.	6.6	25
63997	SnF₂â€Catalyzed Formation of Polymerized Dioxolane as Solid Electrolyte and its Thermal Decomposition Behavior. Angewandte Chemie - International Edition, 2022, 61, .	7.2	42
63998	Computational and experimental insights into reactive forms of oxygen species on dynamic Ag surfaces under ethylene epoxidation conditions. Journal of Catalysis, 2022, 405, 445-461.	3.1	12
63999	Systemic consequences of disorder in magnetically self-organized topological MnBi₂Te₄/(Bi₂Te₃) _n superlattices. 2D Materials, 2022, 9, 015026.	2.0	11
64000	Phase-modulated mechanical and thermoelectric properties of Ag2S1-xTex ductile semiconductors. Journal of Materiomics, 2022, 8, 656-661.	2.8	31
64001	Nonclassical Crystallization of an Al₂O₃ Film by Positively Charged Secondary Nanoparticles during Aerosol Deposition. Crystal Growth and Design, 2021, 21, 7240-7246.	1.4	4
64002	Structural, hydrogen storage, and electrochemical performance of LaMgNi4 alloy and theoretical investigation of its hydrides. International Journal of Hydrogen Energy, 2022, 47, 1723-1734.	3.8	20
64003	Direct observation of one-dimensional disordered diffusion channel in a chain-like thermoelectric with ultralow thermal conductivity. Nature Communications, 2021, 12, 6709.	5.8	21
64004	Defect Engineering: Electron-Exchange Integral Manipulation to Generate a Large Magnetocaloric Effect in Ni₄₁Mn₄₃Co₆Sn₁₀ Alloys. ACS Applied Materials & Interfaces, 2021, 13, 57372-57379.	4.0	7
64005	Theoretical Prediction of a Bi-Doped Î²-Antimonene Monolayer as a Highly Efficient Photocatalyst for Oxygen Reduction and Overall Water Splitting. ACS Applied Materials & Interfaces, 2021, 13, 56254-56264.	4.0	10
64006	Topological acoustic triple point. Nature Communications, 2021, 12, 6781.	5.8	25
64007	An oxygen vacancy-rich ZnO layer on garnet electrolyte enables dendrite-free solid state lithium metal batteries. Chemical Engineering Journal, 2022, 433, 133665.	6.6	23
64008	Strategic Optimization of the Electronic Transport Properties of Pseudoâ€Ternary Clathrates. Advanced Electronic Materials, 2022, 8, 2100756.	2.6	0
64009	<scp>Twoâ€dimensional</scp> Janus <scp>groupâ€III</scp> ternary chalcogenide monolayer compounds <scp>B₂XY</scp>, <scp>Al₂XY</scp>, and <scp>BAlX₂</scp> (X, Y =) Tj ETQq1 1 0.784314 rgBT	1.1	84
64010	Transition from three- to two-dimensional Ising superconductivity in few-layer <mml:math xmlns:mml="http://www.w3.org/1998/Math/MathML"><mml:msub><mml:mi mathvariant="normal">NbSe</mml:mi><mml:mn>2</mml:mn></mml:msub></mml:math> by proximity effect from van der Waals heterostacking. Physical Review B, 2021, 104, .	1.1	6
64011	Revisiting Î³-alumina surface models through the topotactic transformation of boehmite surfaces. Journal of Catalysis, 2022, 405, 140-151.	3.1	14
64012	Bimetallic nickel-cobalt oxides: A comprehensive insight into Ni/Co ratio, intrinsic structure and electrochemical behaviors. Vacuum, 2022, 196, 110764.	1.6	7
64013	Modification of the Magnetic and Electronic Properties of the Grapheneâ€Ni(111) Interface via Halogens Intercalation. Advanced Theory and Simulations, 0, , 2100319.	1.3	1

#	Article	IF	Citations
64014	Structural speciation in chemical reactivity profiling of binary-ternary systems of Ni(II) with iminodialcohol and aromatic chelators. Polyhedron, 2022, 212, 115577.	1.0	2
64015	Electrically switchable valley polarization, spin/valley filter, and valve effects in transition-metal dichalcogenide monolayers interfaced with two-dimensional ferromagnetic semiconductors. Physical Review B, 2021, 104, .	1.1	14
64016	Stability and Anisotropic Elastic Properties of a Hexagonal Î´-WN Compound. Journal of Electronic Materials, 0, , 1.	1.0	0
64017	Cluster Assembled Silicon-Lithium Nanostructures: A Nanowire Confined Inside a Carbon Nanotube. Frontiers in Chemistry, 2021, 9, 767421.	1.8	1
64018	Efficient approach for optical and morphological characterization of hybrid perovskite films based on reflectance and transmittance measurements. Journal Physics D: Applied Physics, 2022, 55, 115303.	1.3	1
64019	Impact of magnetic transition on Mn diffusion in<mml:math xmlns:mml="http://www.w3.org/1998/Math/MathML"><mml:mi>Î±</mml:mi></mml:math>-iron: Correlative state-of-the-art theoretical and experimental study. Physical Review B, 2021, 104, .	1.1	3
64020	Stability and electronic properties of two-dimensional metalâ€“organic perovskites in Janus phase. APL Materials, 2021, 9, 111105.	2.2	2
64021	Emergent quasi-two-dimensional electron gas between Li1Â±x NbO3 and LaAlO3 and its prospectively switchable magnetism. Physical Review Materials, 2021, 5, .	0.9	2
64022	Stability of Zirconium-Substituted Face-Centered Cubic Yttrium Hydride. Inorganic Chemistry, 2021, 60, 17715-17721.	1.9	0
64023	Synthesis of bilayer borophene. Nature Chemistry, 2022, 14, 25-31.	6.6	105
64024	Structure and Origin of the Second-Harmonic Generation Response of Nonlinear Optical Material Sr₂Be₂B₂O₇. Journal of Physical Chemistry Letters, 2021, 12, 11399-11405.	2.1	5
64025	First-principles calculations of phase transition, elasticity, phonon spectra, and thermodynamic properties for CeO2 polymorphs. Journal of Solid State Chemistry, 2022, 307, 122761.	1.4	6
64026	Role of Dihydride and Dihydrogen Complexes in Hydrogen Evolution Reaction on Single-Atom Catalysts. Journal of the American Chemical Society, 2021, 143, 20431-20441.	6.6	77
64027	IrCrMnZ (Z=Al, Ga, Si, Ge) Heusler alloys as electrode materials for MgO-based magnetic tunneling junctions:A ï¬rst-principles study. Journal Physics D: Applied Physics, 0, , .	1.3	3
64028	Adaptive Learning Framework in Prediction and Validation of Gibbs Free Energy for Inorganic Crystalline Solids. Journal of Physical Chemistry A, 2021, 125, 10103-10110.	1.1	7
64029	Tuning Magnetic Anisotropy in Two-Dimensional Metalâ€“Semiconductor Janus van der Waals Heterostructures. Journal of Physical Chemistry Letters, 2021, 12, 11308-11315.	2.1	2
64030	Novel Braceletlike BiSbX₃ (X = S, Se) Monolayers with an In-Plane Negative Poissonâ€™s Ratio and Anisotropic Photoelectric Properties. Journal of Physical Chemistry Letters, 2021, 12, 11353-11360.	2.1	4
64031	On the doping of the Ga12As12 cluster with groups p and d atomic impurities. Theoretical Chemistry Accounts, 2021, 140, 1.	0.5	13

#	Article	IF	Citations
64032	Evaluation of thermophysical properties of the LiCl-KCl system via ab initio and experimental methods. Journal of Nuclear Materials, 2022, 559, 153414.	1.3	13
64033	Density Functional Theory Study on Anisotropic Arrangement of Interstitial Oxygen Atoms at (001) Interface of Oxide Precipitates in Si Crystal. ECS Journal of Solid State Science and Technology, 2021, 10, 123003.	0.9	1
64034	From pseudo-direct hexagonal germanium to direct silicon-germanium alloys. Physical Review Materials, 2021, 5, .	0.9	7
64035	A First-Principles study of monolayer and heterostructure antimonene as potential anode materials for Magnesium-ion batteries. Applied Surface Science, 2022, 577, 151880.	3.1	11
64036	Impact of stresses and alloying elements on ferrous martensite nanodomains. Materials Letters, 2021, , 131248.	1.3	1
64037	Phase Diagrams and Spectral Characteristics of Hydrofluorocarbon Hydrates: Insights from First-Principles Thermodynamics. ACS Sustainable Chemistry and Engineering, 2021, 9, 16347-16355.	3.2	3
64038	Amorphous transformation of FeP enabling enhanced sulfur catalysis and anchoring in High-performance Li-S batteries. Chemical Engineering Journal, 2022, 431, 133705.	6.6	23
64039	Excellent HER and OER Catalyzing Performance of Seâ€Vacancies in Defectsâ€Engineered PtSe₂: From Simulation to Experiment. Advanced Energy Materials, 2022, 12, 2102359.	10.2	59
64040	First-principles investigation of structural, electronic and optical properties of quasi-one-dimensional barium cadmium chalcogenides Ba2CdX3 (X = S, Se, Te) using HSE06 and GGA-PBE functionals. Journal of Physics and Chemistry of Solids, 2022, 161, 110488.	1.9	19
64041	First-principles study of the double-dome superconductivity in the kagome material <mml:math xmlns:mml="http://www.w3.org/1998/Math/MathML"><mml:mrow><mml:msub><mml:mi>CsV</mml:mi><mml:mn>3</mml:mn></mml:msub></mml:mrow></mml:math> under pressure. Physical Review B, 2021, 104, .	1.1	27
64042	Dual-coupling-guided epitaxial growth of wafer-scale single-crystal WS2 monolayer on vicinal a-plane sapphire. Nature Nanotechnology, 2022, 17, 33-38.	15.6	171
64043	Reversible Manipulation of Photoconductivity Caused by Surface Oxygen Vacancies in Perovskite Stannates with Ultraviolet Light. Advanced Materials, 2022, 34, e2107650.	11.1	17
64044	MEAM interatomic potentials of Ni, Re, and Niâ€“ReÂalloys for atomistic fracture simulations. Modelling and Simulation in Materials Science and Engineering, 2022, 30, 015002.	0.8	2
64045	On-Surface Synthesis of 2D Porphyrin-Based Covalent Organic Frameworks Using Terminal Alkynes. Chemistry of Materials, 2021, 33, 8677-8684.	3.2	2
64046	Intrareticular charge transfer regulated electrochemiluminescence of donorâ€“acceptor covalent organic frameworks. Nature Communications, 2021, 12, 6808.	5.8	81
64047	A general strategy for preparing pyrrolic-N4 type single-atom catalysts via pre-located isolated atoms. Nature Communications, 2021, 12, 6806.	5.8	81
64048	Emergent magnetic states due to stacking and strain in the van der Waals magnetic trilayer CrI3. Physical Review B, 2021, 104, .	1.1	11
64049	Quasinodal lines in rhombohedral magnetic materials. Physical Review B, 2021, 104, .	1.1	3

#	Article	IF	Citations
64050	Rationally designed hierarchical N, P co-doped carbon connected 1T/2H-MoS2 heterostructures with cooperative effect as ultrafast and durable anode materials for efficient sodium storage. Chemical Engineering Journal, 2022, 433, 133778.	6.6	49
64051	Ultrahigh Capacity Retention of a Li₂ZrO₃-Coated Ni-Rich LiNi_{0.8}Co_{0.1}Mn_{0.1}O₂ Cathode Material through Covalent Interfacial Engineering. ACS Applied Energy Materials, 2021, 4, 13785-13795.	2.5	16
64052	Toward Durable Protonic Ceramic Cells: Hydration-Induced Chemical Expansion Correlates with Symmetry in the Y-Doped BaZrO₃â€“BaCeO₃ Solid Solution. Journal of Physical Chemistry C, 2021, 125, 26216-26228.	1.5	12
64053	Investigation of Electronic Structure and Electrochemical Properties of Na2MnSiO4 as a Cathode Material for Na Ion Batteries. Journal of Physical Chemistry C, 2021, 125, 25968-25982.	1.5	6
64054	First-principles study of helium-vacancy complexes in Be12Ti. Physics Letters, Section A: General, Atomic and Solid State Physics, 2021, 424, 127841.	0.9	1
64055	Interplay of Solidâ€“Liquid Interactions and Anisotropic Aggregation in Solution: The Case Study of Î³-AlOOH Crystallites. Journal of Physical Chemistry C, 2021, 125, 26049-26060.	1.5	4
64056	Electrochemical CO₂ Reduction Reaction on 3d Transition Metal Single-Atom Catalysts Supported on Graphdiyne: A DFT Study. Journal of Physical Chemistry C, 2021, 125, 26013-26020.	1.5	38
64057	CH₃^{â€¢}-Generating Capability as a Reactivity Descriptor for Metal Oxides in Oxidative Coupling of Methane. ACS Catalysis, 2021, 11, 14651-14659.	5.5	26
64058	Theoretical Insights into Superior Nitrate Reduction to Ammonia Performance of Copper Catalysts. ACS Catalysis, 2021, 11, 14417-14427.	5.5	150
64059	Atomic-Scale Mechanisms of Electrochemical Pt Dissolution. ACS Catalysis, 2021, 11, 14439-14447.	5.5	19
64060	First-Principles Microkinetic Model for Low-Temperature NH₃-Assisted Selective Catalytic Reduction of NO over Cu-CHA. ACS Catalysis, 2021, 11, 14395-14407.	5.5	25
64061	Hydrogen-passivation modulation on the friction behavior of graphene with vacancy defects under strain engineering. Applied Surface Science, 2022, 579, 152055.	3.1	9
64062	Surface Phase Engineering Modulated Ironâ€Nickel Nitrides/Alloy Nanospheres with Tailored dâ€Band Center for Efficient Oxygen Evolution Reaction. Small, 2022, 18, e2105696.	5.2	41
64063	Intrinsically Honeycombâ€Patterned Hydrogenated Graphene. Small, 2022, 18, e2102687.	5.2	3
64064	First-principles investigation of uranium mononitride (UN): Effect of magnetic ordering, spin-orbit interactions and exchange correlation functional. Journal of Nuclear Materials, 2022, 559, 153401.	1.3	14
64065	Oxygen Reduction Activity of Bâ†Nâ€Containing Organic Molecule Affected by Asymmetric Regulation. Small, 2022, 18, e2105524.	5.2	8
64066	Exploring yttrium doped C24 fullerene as a high-capacity reversible hydrogen storage material: DFT investigations. Journal of Alloys and Compounds, 2022, 897, 162797.	2.8	46
64067	Al2O3 nanofibers prepared from aluminum Di(sec-butoxide)acetoacetic ester chelate exhibits high surface area and acidity. Journal of Catalysis, 2022, 405, 520-533.	3.1	12

#	Article	IF	Citations
64068	Impressive Thermoelectric Figure of Merit in Two-Dimensional Tetragonal Pnictogens: a Combined First-Principles and Machine-Learning Approach. ACS Applied Materials & Interfaces, 2021, 13, 59092-59103.	4.0	24
64069	Interfacial nitrogen engineering of robust silicon/MXene anode toward high energy solid-state lithium-ion batteries. Journal of Energy Chemistry, 2022, 67, 727-735.	7.1	46
64070	Eliminating Edge Electronic and Phonon States of Phosphorene Nanoribbon by Unique Edge Reconstruction. Small, 2022, 18, e2105130.	5.2	9
64071	Stability of Cun (nÂ=Â1â€“4) clusters adsorption on CuAlO2 (11<mml:math) Tj ETQq1 1 0.784314 rgBT /Overlock 10 Tf 50 632 Td (x surfaces using atomic thermodynamics. Applied Surface Science, 2022, 578, 151935.	3.1	1
64072	Thermoelectric properties of Janus AsSBr monolayer from first-principles study. Solid State Communications, 2022, 342, 114612.	0.9	4
64073	Triple-atom catalysts 3TM-GYs (TMÂ=ÂCu, Fe, and Co; GYÂ=Âgraphyne) for high-performance CO2 reduction reaction to C1 products. Applied Materials Today, 2021, 25, 101245.	2.3	10
64074	Competition of Superconductivity and Charge Density Wave in Selective Oxidized <mml:math xmlns:mml="http://www.w3.org/1998/Math/MathML" display="inline"><mml:mrow><mml:mrow><mml:msub><mml:mrow><mml:mi>CsV</mml:mi></mml:mrow><mml:mrow><mml:mn>3<</mml:mn></mml:mrow></mml:msub></mml:mrow></mml:mrow></mml:math> Thin Flakes. Physical Review Letters, 2021, 127, 237001.	2.9	73
64075	Vanadium-phosphorus incorporation induced interfacial modification on cobalt catalyst and its super electrocatalysis for water splitting in alkaline media. Applied Catalysis B: Environmental, 2022, 304, 120985.	10.8	29
64076	Making an artificial px,y -orbital honeycomb electron lattice on a metal surface. Physical Review B, 2021, 104, .	1.1	2
64077	Laser-fabricated channeled Cu6Sn5/Sn as electrocatalyst and gas diffusion electrode for efficient CO2 electroreduction to formate. Applied Catalysis B: Environmental, 2022, 307, 120991.	10.8	26
64078	Role of chemical disorder in tuning the Weyl points in vanadium doped <mml:math xmlns:mml="http://www.w3.org/1998/Math/MathML"><mml:mrow><mml:msub><mml:mi>Co</mml:mi><mml:mn>2</mml:mn></mml:msub><mml:mi>x</mml:mi><mml:mn></mml:mn></mml:mrow></mml:math> Physical Review Materials, 2021, 5, .	3.1	7
64079	A reactive flow model for the 3,3â€²-diamino-4,4â€²-azoxyfurazan based plastic bonded explosive (PBX 9701). Journal of Applied Physics, 2021, 130, .	1.1	3
64080	Bandgap modulation in the two-dimensional core-shell-structured monolayers of WS2. IScience, 2022, 25, 103563.	1.9	4
64081	Effects of trace calcium and strontium on microstructure and properties of Cu-Cr alloys. Journal of Materials Science and Technology, 2022, 112, 11-23.	5.6	29
64082	The influence of doping amount on the catalytic oxidation of formaldehyde by Mn-CeO2 mixed oxide catalyst: A combination of DFT and microkinetic study. Journal of Hazardous Materials, 2022, 425, 127985.	6.5	11
64083	Valence skipping, internal doping, and site-selective Mott transition in <mml:math xmlns:mml="http://www.w3.org/1998/Math/MathML"><mml:msub><mml:mi>PbCoO</mml:mi><mml:mn>3</mml:mn></mml:msub> under pressure. Physical Review B, 2021, 104, .	1.1	4
64084	An understanding of hydrogen embrittlement in nickel grain boundaries from first principles. Materials and Design, 2021, 212, 110283.	3.3	20
64085	Dzyaloshinskii-Moriya anisotropy effect on field-induced magnon condensation in the kagome antiferromagnet <mml:math xmlns:mml="http://www.w3.org/1998/Math/MathML"><mml:mrow><mml:mi>Î±</mml:mi><mml:mtext>â^’</mml:mtext><mml:msub> Physical Review B, 2021, 104, .	1.1	0

#	Article	IF	Citations
64087	Interface coating of iron nitride on carbon cloth for reversible lithium redox in rechargeable battery. Chemical Engineering Journal, 2022, 431, 133961.	6.6	15
64088	Adsorption and migration of a single lithium on TPHâ€graphene nanoribbon: a DFT approach. Physica Status Solidi (B): Basic Research, 0, , 2100369.	0.7	0
64089	Reversible formation of metastable Sn-rich solid solution in SnO2-based anode for high-performance lithium storage. Applied Materials Today, 2021, 25, 101242.	2.3	3
64090	SnS_xSe_{1â€“x}/Ag Nanosheet Thin Films for Solar Energy Water Splitting. ACS Applied Nano Materials, 2021, 4, 13246-13256.	2.4	4
64091	Scalable Molecular GW Calculations: Valence and Core Spectra. Journal of Chemical Theory and Computation, 2021, 17, 7504-7517.	2.3	17
64092	Calculating Entropies of Large Molecules in Aqueous Phase. Journal of Chemical Theory and Computation, 2021, , .	2.3	6
64093	Influence of the Nature and Orientation of the Terminal Group on the Tribochemical Reaction Rates of Carboxylic Acid Monolayers on Copper. Tribology Letters, 2022, 70, 1.	1.2	7
64094	Mechanism of 2D Materialsâ€™ Seamless Coalescence on a Liquid Substrate. ACS Nano, 2021, 15, 19387-19393.	7.3	6
64095	Alkali catalyzes methanethiol synthesis from CO and H2S. Journal of Catalysis, 2022, 405, 116-128.	3.1	8
64096	Porous Co2VO4 Nanodisk as a High-Energy and Fast-Charging Anode for Lithium-Ion Batteries. Nano-Micro Letters, 2022, 14, 5.	14.4	93
64097	Facile hydrothermal synthesis of V2O5 nanofibers as cathode material for aqueous zinc-ion batteries. Journal of Alloys and Compounds, 2022, 896, 163071.	2.8	12
64098	Training data augmentation using generative models with statistical guarantees for materials informatics. Soft Computing, 2022, 26, 1181-1196.	2.1	3
64099	Recruiting Perovskites to Degrade Toxic Trinitrotoluene. Materials, 2021, 14, 7387.	1.3	5
64100	Interface features and electronic structure of Bi2SiO5/Î²-Bi2O3 hetero-junction. , 2021, , .		0
64101	Comparative Study of Oxygen Diffusion in Polyethylene Terephthalate and Polyethylene Furanoate Using Molecular Modeling: Computational Insights into the Mechanism for Gas Transport in Bulk Polymer Systems. Macromolecules, 2022, 55, 498-510.	2.2	14
64102	Exploring the alloying effects on generalized stacking fault energy and ideal strength of Ni and Ni3Al phases in Ni-based superalloys. Mechanics of Materials, 2022, 165, 104183.	1.7	11
64103	First-principles investigation on multiferroic properties of BiFeO3-REMnO3 (RE = Er, Eu, Gd, Ho, La, Tb). Materials Today Communications, 2021, 29, 102976.	0.9	2
64104	Ternary Mo₂NiB₂ as a Superior Bifunctional Electrocatalyst for Overall Water Splitting. Small, 2022, 18, e2104303.	5.2	70

#	Article	IF	Citations
64105	Heterogeneous Atoms Substituted Rock Salt Phase Mn₁_{â€x}Fe_xO Solid Solution with Rich Defects for Advanced Lithiumâ€Ion Batteries. Small, 2022, 18, e2106273.	5.2	2
64106	Adsorption based on weak interaction between phenolic hydroxyl, carboxyl groups and silver nanoparticles in aqueous environment: Experimental and DFT-D3 exploration. Journal of Environmental Chemical Engineering, 2021, 9, 106816.	3.3	8
64107	Dual-Phase Nanocomposite TiB₂/MoS_{1.7}B_{0.3}: An Excellent Ultralow Friction and Ultralow Wear Self-Lubricating Material. ACS Applied Materials & Interfaces, 2021, 13, 59352-59363.	4.0	11
64108	Strain Engineering for Tailored Carrier Transport and Thermoelectric Performance in Mixed Halide Perovskites CsPb(I_{1â€“x}Br_x)₃. ACS Applied Energy Materials, 2021, 4, 14508-14519.	2.5	16
64109	Anisotropic point defects in rhenium diselenide monolayers. IScience, 2021, 24, 103456.	1.9	11
64110	MoirÃ© flat bands in twisted 2D hexagonal vdW materials. 2D Materials, 2022, 9, 014005.	2.0	10
64111	Experimental and theoretical investigation of the formation of two-dimensional Fe silicate on Pd(111). Journal of Vacuum Science and Technology A: Vacuum, Surfaces and Films, 2021, 39, .	0.9	2
64112	O2 on Ag(110): A puzzle for exchange-correlation functionals. Chemical Physics, 2021, 554, 111424.	0.9	0
64113	Modified Embeddedâ€Atom Method Potentials for the Plasticity and Fracture Behaviors of Unary HCP Metals. Advanced Theory and Simulations, 2022, 5, 2100377.	1.3	2
64114	Vapor-Phase Intercalation of Cesium into Black Phosphorous. Journal of Physical Chemistry C, 2021, 125, 27440-27448.	1.5	2
64115	Bi0 and oxygen vacancies co-induced enhanced visible-light photocatalytic detoxication of three typical contaminants over Bi2WO6 treated by NaBH4 solution. Surfaces and Interfaces, 2022, 28, 101648.	1.5	4
64116	Layer-by-layer zinc metal anodes to achieve long-life zinc-ion batteries. Chemical Engineering Journal, 2022, 431, 133902.	6.6	32
64117	Lattice dynamics and thermodynamic properties of Y3Al5O12 (YAG). Journal of Physics and Chemistry of Solids, 2021, 162, 110512.	1.9	6
64118	Size sensitivity of supported Ru catalysts for ammonia synthesis: From nanoparticles to subnanometric clusters and atomic clusters. CheM, 2022, 8, 749-768.	5.8	59
64119	Phase transitions and potential ferroelectricity in noncentrosymmetric KNaNbOF5. Physical Review Materials, 2021, 5, .	0.9	1
64120	Degenerate topological line surface phonons in quasi-1D double helix crystal SnIP. Npj Computational Materials, 2021, 7, .	3.5	19
64121	A non-flammable hydrous organic electrolyte for sustainable zinc batteries. Nature Sustainability, 2022, 5, 205-213.	11.5	277
64122	First-Principles Calculations to Investigate the Third-Order Elastic Constants and Mechanical Properties of Mg, Be, Ti, Zn, Zr, and Cd. Advances in Materials Science and Engineering, 2021, 2021, 1-12.	1.0	2

#	Article	IF	Citations
64123	Highly Efficient Hole Transport Layerâ€Free Low Bandgap Mixed Pbâ€“Sn Perovskite Solar Cells Enabled by a Binary Additive System. Advanced Functional Materials, 2022, 32, 2110069.	7.8	30
64124	Van der Waals Epitaxy of Bi₂Te₂Se/Bi₂O₂Se Vertical Heterojunction for High Performance Photodetector. Small, 2022, 18, e2105211.	5.2	21
64125	Nearly 100% energy transfer at the interface of metal-organic frameworks for X-ray imaging scintillators. Matter, 2022, 5, 253-265.	5.0	53
64126	Copper-Stabilized Pâ€²2-Type Layered Manganese Oxide Cathodes for High-Performance Sodium-Ion Batteries. ACS Applied Materials & Interfaces, 2021, 13, 58665-58673.	4.0	24
64127	Adsorption States of N₂/H₂ Activated on Ru Nanoparticles Uncovered by Modulationâ€“Excitation Infrared Spectroscopy and Density Functional Theory Calculations. ACS Nano, 2021, 15, 20079-20086.	7.3	10
64128	Realizing Near-Unity Quantum Efficiency of Zero-Dimensional Antimony Halides through Metal Halide Structural Modulation. ACS Applied Materials & Interfaces, 2021, 13, 58908-58915.	4.0	36
64129	Oxygen-rich tetrahedral surface phase on high-temperature rutile <mml:math xmlns:mml="http://www.w3.org/1998/Math/MathML"><mml:mrow><mml:mi mathvariant="normal">V</mml:mi><mml:msub><mml:mi mathvariant="normal">O</mml:mi><mml:mn>2</mml:mn></mml:msub><mml:msub><mml:mrow><mml:mo>(</mml:mo><mml:mn>1</mml:mn><mml:mi mathvariant="normal">T</mml:mi></mml:msub></mml:mrow></mml:math> single crystals. Physical Review Materials, 2021, 5, .	0.9	3
64130	Precipitate/matrix incompatibilities related to the {111}Al Î© plates in an Al-Cu-Mg-Ag alloy. Materials Characterization, 2021, 182, 111586.	1.9	11
64131	Two-Dimensional MoS₂ Nanosheet-Functionalized Optical Microfiber for Room-Temperature Volatile Organic Compound Detection. ACS Applied Nano Materials, 2021, 4, 13440-13449.	2.4	10
64132	Augmenting zero-Kelvin quantum mechanics with machine learning for the prediction of chemical reactions at high temperatures. Nature Communications, 2021, 12, 7012.	5.8	10
64133	Alloy Engineering of 2D Van der Waals Chromium Mixed Trihalides as Ferromagnetic Semiconductors. Physica Status Solidi (B): Basic Research, 2022, 259, .	0.7	1
64134	Atomic-scale investigations on dislocation-precipitate interactions influenced by voids in Ni-based superalloys. International Journal of Mechanical Sciences, 2022, 216, 106945.	3.6	5
64135	Unraveling Passivation Mechanism of Imidazolium-Based Ionic Liquids on Inorganic Perovskite to Achieve Near-Record-Efficiency CsPbI2Br Solar Cells. Nano-Micro Letters, 2022, 14, 7.	14.4	58
64136	Observation of electronic structure and electron-boson coupling in the low-dimensional superconductor <mml:math xmlns:mml="http://www.w3.org/1998/Math/MathML"><mml:mrow><mml:msub><mml:mi>Ta</mml:mi><mml:mn>4</mml:mn></mml:msub></mml:mrow></mml:math> Physical Review B, 2021, 104, .	1.1	2
64137	Effect of La vacancies on the oxide-ion conduction in lanthanum silicate apatites. Solid State Ionics, 2021, 373, 115793.	1.3	2
64138	First-principles Study on Piezoelectricity and Spontaneous Polarization in Bi(Fe,Co)O₃. Journal of the Physical Society of Japan, 2021, 90, .	0.7	0
64139	1T-VS₂/MXene Hybrid as a Superior Electrode Material for Asymmetric Supercapacitors: Experimental and Theoretical Investigations. ACS Applied Energy Materials, 2021, 4, 14198-14209.	2.5	34
64140	A study on the stability of gold copper bimetallic clusters on the CeO2(110) surface. Catalysis Communications, 2022, 162, 106376.	1.6	8

#	Article	IF	Citations
64141	The structural, mechanical and electronic properties of novel superhard carbon allotropes: ab initio study. Materials Today Communications, 2021, 29, 102980.	0.9	4
64142	Exploring oxidation mechanism of graphene for insight into its outstanding corrosion resistance in sulfur-containing atmosphere. Materials Today Communications, 2021, 29, 102975.	0.9	0
64143	Physical properties of rare earth perovskites CeMO3 (M = Co, Cu) in the context of density functional theory. Materials Today Communications, 2021, 29, 102973.	0.9	7
64144	Crystal graph attention networks for the prediction of stable materials. Science Advances, 2021, 7, eabi7948.	4.7	37
64145	BC₆P Monolayer: Isostructural and Isoelectronic Analogues of Graphene with Desirable Properties for K-Ion Batteries. Chemistry of Materials, 2021, 33, 9262-9269.	3.2	11
64146	High Curie Temperature and Intrinsic Ferromagnetic Half-Metallicity in Mn₂X₃ (X = S, Se, Te) Nanosheets. Journal of Physical Chemistry Letters, 2021, 12, 11790-11794.	2.1	14
64147	Phase Stability of Nanolaminated Epitaxial (Cr_{1â€“x}Fe_x)₂AlC MAX Phase Thin Films on MgO(111) and Al₂O₃(0001) for Use as Conductive Coatings. ACS Applied Nano Materials, 2021, 4, 13761-13770.	2.4	6
64148	Ultrafast and Selective Nanofiltration Enabled by Graphene Oxide Membranes with Unzipped Carbon Nanotube Networks. ACS Applied Materials & Interfaces, 2022, 14, 1850-1860.	4.0	60
64149	Influence of Ag Clusters on the Electronic Structures of Î²-Ga2O3 Photocatalyst Surfaces. ACS Omega, 2021, 6, 33701-33707.	1.6	0
64150	Spin-Orbit Interaction Effect on Surface Electronic Structure of GdX2Si2 Compound. Russian Physics Journal, 0, , 1.	0.2	0
64151	Carbon dioxide capture over amine functionalized styrene divinylbenzene copolymer: An experimental batch and continuous studies. Journal of Environmental Chemical Engineering, 2022, 10, 106910.	3.3	15
64152	Spin-neutral currents for spintronics. Nature Communications, 2021, 12, 7061.	5.8	63
64153	Ultrafine VN nanodots induced generation of abundant cobalt single-atom active sites on nitrogen-doped carbon nanotube for efficient hydrogen evolution. Journal of Energy Chemistry, 2022, 68, 646-657.	7.1	15
64154	Strain regulated interlayer coupling in WSe₂/WS₂ heterobilayer. Nanotechnology, 2022, 33, 085705.	1.3	5
64155	Role of rare earth sites and vacancies in the anomalous compression of modulated scheelite tungstates <mml:math xmlns:mml="http://www.w3.org/1998/Math/MathML"><mml:msub><mml:mrow><mml:mi>R</mml:mi><mml:mi>E</mml:mi></mml:mrow><mml:mn>3</mml:mn></mml:msub></mml:math> (<mml:math) Tj ETQq0 0 0 rgBT /Overlock 10 Tf 50 172 Td (xmlns:mml="http://www.w3.org/1998/Math/MathML"><mml:mrow><mml:m	0.9	3
64156	Physical Review Materials, 2021, 5, . Modified band alignment method to obtain hybrid functional accuracy from standard DFT: Application to defects in highly mismatched III-V:Bi alloys. Physical Review Materials, 2021, 5, .	0.9	2
64157	Stacking-dependent optical properties in bilayer WSe₂. Nanoscale, 2021, 14, 147-156.	2.8	16
64158	Strain engineering in the oxygen reduction reaction and oxygen evolution reaction catalyzed by Pt-doped Ti₂CF₂. Journal of Materials Chemistry A, 2022, 10, 1390-1401.	5.2	27

#	Article	IF	Citations
64159	High-Pressure Synthesis and Ambient-Pressure Tem Investigation of Mg-Orthocarbonate. SSRN Electronic Journal, 0, , .	0.4	3
64160	All room-temperature synthesis, N2 photofixation and reactivation over 2D cobalt oxides. Applied Catalysis B: Environmental, 2022, 304, 121001.	10.8	11
64161	Evolution of a Snowflake-Like Mn ²⁺ Doped Cs ₂NaBiCl ₆ Nanosheet Phosphor Driven By Cation Exchange. SSRN Electronic Journal, 0, , .	0.4	0
64162	Two-dimensional layered MSi₂N₄ (M = Mo, W) as promising thermal management materials: a comparative study. Physical Chemistry Chemical Physics, 2022, 24, 3086-3093.	1.3	24
64163	Reactive molten-flux assisted syntheses of single crystals of Cs19Ln19Mn10Te48 (Ln = Pr and Gd) crystallizing in a new structure type. CrystEngComm, 2021, 23, 8418-8429.	1.3	2
64164	Tuning the Conductivity of Metallic Nanowires by Hydrogen Adsorption. , 2021, , 133-146.		0
64165	Relativistic quantum theory and algorithms: A toolbox for modeling many-fermion systems in different scenarios. Annual Reports in Computational Chemistry, 2021, 17, 55-111.	0.9	2
64166	Atomistic Mechanisms of Binary Alloy Surface Segregation From Nanoseconds to Seconds Using Accelerated Dynamics. SSRN Electronic Journal, 0, , .	0.4	0
64167	Halide Perovskites for Photonics: Recent History and Perspectives. , 2021, , 1-28.		1
64168	Novel two-dimensional boron oxynitride predicted using the USPEX evolutionary algorithm. Physical Chemistry Chemical Physics, 2021, 23, 26178-26184.	1.3	4
64169	Metal phosphide CuP₂ as a promising thermoelectric material: an insight from a first-principles study. New Journal of Chemistry, 2021, 45, 21569-21576.	1.4	7
64170	Engineering oxygen vacancies in CoO@Co₃O₄/C nanocomposites for enhanced electrochemical performances. Nanoscale, 2021, 13, 19518-19526.	2.8	17
64171	Six- or four-fold band degeneration in CoAs₃, RhAs₃ and RhSb₃ topological semimetals. Physical Chemistry Chemical Physics, 2021, 23, 25944-25950.	1.3	4
64172	Catalytic mechanism of spinel oxides for oxidative electrolyte decomposition in Mg rechargeable batteries. Journal of Materials Chemistry A, 2021, 9, 26401-26409.	5.2	21
64173	High-throughput computation of novel ternary Bâ€“Câ€“N structures and carbon allotropes with electronic-level insights into superhard materials from machine learning. Journal of Materials Chemistry A, 2021, 9, 27596-27614.	5.2	21
64174	Ab initio molecular dynamics study of adsorption of hydroxyl groups on graphene surface. Chinese Journal of Chemical Physics, 2021, 34, 777-784.	0.6	2
64175	High hydrogen production in the InSe/MoSi₂N₄van der Waals heterostructure for overall water splitting. Physical Chemistry Chemical Physics, 2022, 24, 2110-2117.	1.3	16
64176	Selective decomposition of hydrazine over metal free carbonaceous materials. Physical Chemistry Chemical Physics, 2022, 24, 3017-3029.	1.3	3

#	Article	IF	Citations
64177	Elasticity, Mechanical and Thermal Properties of Polycrystalline Hafnium Carbide and Tantalum Carbide at High Pressure. SSRN Electronic Journal, 0, , .	0.4	0
64178	Synthesis of Large Area Graphitic Carbon Nitride Nanosheet by Chemical Vapor Deposition. SSRN Electronic Journal, 0, , .	0.4	0
64179	Feâ^'Nâ^'C Single-Atom Nanozymes Based Sensor Array for Dual Signal Selective Determination of Antioxidants. SSRN Electronic Journal, 0, , .	0.4	0
64180	High Compositional Dependence of Activity of Platinumâ€"Dysprosium Alloys for Oxygen Reduction in Alkaline Media: Experimental and Theoretical Study. SSRN Electronic Journal, 0, , .	0.4	0
64181	Design strategies of two-dimensional metalâ€"organic frameworks toward efficient electrocatalysts for N₂ reduction: cooperativity of transition metals and organic linkers. Nanoscale, 2021, 13, 19247-19254.	2.8	67
64182	Broadband light emitting zero-dimensional antimony and bismuth-based hybrid halides with diverse structures. Journal of Materials Chemistry C, 2021, 9, 15942-15948.	2.7	18
64183	The effect of the composition and pressure on the phase stability and electronic, magnetic, and elastic properties of M₂AX (M = Mn, Fe; A = Al, Ga, Si, Ge; X = C, N) phases. Physical Chemistry Chemical Physics, 2021, 23, 26376-26384.	1.3	5
64184	Electron Theory Calculation of Thermodynamic Properties of Steels and Its Application to Theoretical Phase Diagram of the Fe-Mo-B Ternary System. Tetsu-To-Hagane/Journal of the Iron and Steel Institute of Japan, 2021, 107, 923-933.	0.1	0
64185	Atomic-Scale Probing of Defect-Assisted Ga Intercalation Through Graphene Using ReaxFF Molecular Dynamics Simulations. SSRN Electronic Journal, 0, , .	0.4	0
64186	Modeling Methods for Plasmonic Effects in Halide Perovskite Based Systems for Photonics Applications. , 2021, , 1-52.		0
64187	A flexible Mn_{0.5}Ti₂(PO₄)₃/C nanofiber film with superior cycling stability for potassium-ion batteries. Nanoscale, 2021, 13, 19956-19965.	2.8	9
64188	Time- and momentum-resolved image-potential states of 2H-MoS2 surface. Physical Chemistry Chemical Physics, 2021, 23, 26336-26342.	1.3	1
64189	Enhancing polysulfide confinement and conversion in meso-/microporous coreâ€"shelled MoC/NC microspheres for lithiumâ€"sulfur batteries. Journal of Materials Chemistry A, 2021, 9, 26051-26060.	5.2	16
64190	Two Possible Ways of Forming Ordered Magnetic Chains on a Metal Surface: Monte Carlo Simulations. IEEE Magnetics Letters, 2022, 13, 1-3.	0.6	0
64191	Atomistic Modelling of Electrode Materials for Lithium and Postâ€"lithium Ion Batteries. , 2021, , 161-168.		0
64192	Polyvinylpyrrolidone gel based Pt/Ni(OH)₂ heterostructures with redistributing charges for enhanced alkaline hydrogen evolution reaction. Journal of Materials Chemistry A, 2021, 9, 27061-27071.	5.2	24
64193	Clathrate Structure of Fullerite C ₆₀. SSRN Electronic Journal, 0, , .	0.4	0
64194	Modeling of the Cathodic and Anodic Polarization Curves of Metals and Alloys at an Electronic Level. SSRN Electronic Journal, 0, , .	0.4	0

#	Article	IF	Citations
64195	Using Ion-Beam-Assisted Deposition and Ion Implantation for the Rational Control of Nanomagnetism in Thin Film and Nanostructured Systems. Solid State Physics, 2021, 72, 189-233.	1.3	0
64196	Influence of Doping with Selected Organic Molecules on Magnetic and Electronic Properties of Bare, Surface Terminated and Defect Patterned Ti2C MXene Monolayer. Physical Chemistry Chemical Physics, 2022, , .	1.3	5
64197	Effects of Cr/Ni Ratio on Physical Properties of Crâ€'Mnâ€'Feâ€'Coâ€'Ni High-Entropy Alloys. SSRN Electronic Journal, 0, , .	0.4	0
64198	Cu₄MnGe₂S₇ and Cu₂MnGeS₄: two polar thiogermanates exhibiting second harmonic generation in the infrared and structures derived from hexagonal diamond. Dalton Transactions, 2021, 50, 17524-17537.	1.6	9
64199	PVDF-Stimulated Nanosurface Engineering in Zinc Oxide Targeting Highly Sensitive and Water-Stable Liquid-Phase Hydrazine Sensors. SSRN Electronic Journal, 0, , .	0.4	0
64200	Electronic Properties and Defect Levels Induced by n/p-Type Defect-Complexes in Ge. SSRN Electronic Journal, 0, , .	0.4	0
64201	A Theoretical and Experimental Study of SO ₂ Oxidation on Crystalline MnO ₂ Catalysts. SSRN Electronic Journal, 0, , .	0.4	0
64202	Wrinkle facilitated hydrogen evolution reaction of vacancy-defected transition metal dichalcogenide monolayers. Nanoscale, 2021, 13, 20576-20582.	2.8	7
64203	Rationally designed Ta₃N₅@ReS₂ heterojunctions for promoted photocatalytic hydrogen production. Journal of Materials Chemistry A, 2021, 9, 27084-27094.	5.2	32
64204	Prediction of superconductivity in bilayer borophenes. RSC Advances, 2021, 11, 40220-40227.	1.7	9
64205	Highly Boron-Doped Holey Graphene for Lithium Oxygen Batteries with Enhanced Electrochemical Performance. SSRN Electronic Journal, 0, , .	0.4	0
64206	Diffusion in A15 Nb ₃Sn: An Atomistic Study. SSRN Electronic Journal, 0, , .	0.4	0
64207	Tunable formaldehyde sensing properties of palladium cluster decorated graphene. RSC Advances, 2021, 11, 37120-37130.	1.7	9
64208	Hydrogen Solubility in Zr-Nb Alloys. SSRN Electronic Journal, 0, , .	0.4	0
64209	Computation-Guided Design and Preparation of Durable and Efficient WC-Mo ₂C Heterojunction for Hydrogen Evolution Reaction. SSRN Electronic Journal, 0, , .	0.4	0
64210	Insights from density functional theory calculations into the effects of the adsorption and dissociation of water on the surface properties of zinc diphosphide (ZnP2) nanocrystals. Physical Chemistry Chemical Physics, 2021, 23, 26482-26493.	1.3	1
64211	The Role of Zr in Co-Segregation Behavior of Zr- X Solutes and Their Effects on the Thermodynamic Stability and Fracture Strength of Ni Î£5 [001](210) Grain Boundary. SSRN Electronic Journal, 0, , .	0.4	0
64212	Metal-Free Atom Modified SnS ₂ Sheet for CO ₂ Photoreduction with Significant Activity and Selectivity Improvements: A First-Principles Study. SSRN Electronic Journal, 0, , .	0.4	0

#	Article	IF	Citations
64213	Ultralow lattice thermal conductivity at room temperature in 2D KCuSe from first-principles calculations. Physical Chemistry Chemical Physics, 2022, 24, 3296-3302.	1.3	7
64215	DFT and microkinetic study of acetylene transformation on Pd(111), M(111) and PdM(111) surfaces (M =) Tj ETQq1 1 0.784314 rgBT	1.3	3
64216	Stability of adsorption of Mg and Na on sulfur-functionalized MXenes. Physical Chemistry Chemical Physics, 2021, 23, 25424-25433.	1.3	8
64217	Prediction of Short-Range Order in CrMnFeCoNi High-Entropy Alloy. SSRN Electronic Journal, 0, , .	0.4	0
64218	Adsorption of CO2 on Fe-montmorillonite: A density functional theory study. AIP Conference Proceedings, 2021, , .	0.3	0
64219	The coexistence of superior intrinsic piezoelectricity and thermoelectricity in two-dimensional Janus Î±-TeSSe. Physical Chemistry Chemical Physics, 2021, 23, 26955-26966.	1.3	10
64220	Mixed metalâ€“antimony oxide nanocomposites: low pH water oxidation electrocatalysts with outstanding durability at ambient and elevated temperatures. Journal of Materials Chemistry A, 2021, 9, 27468-27484.	5.2	19
64221	Role of terminal groups in aromatic molecules on the growth of Al₂O₃-based hybrid materials. Dalton Transactions, 2021, 50, 17583-17593.	1.6	5
64222	Two-dimensional XC₆-enes (X = Ge, Sn, Pb) with moderate band gaps, biaxial negative Poisson's ratios, and high carrier mobility. Physical Chemistry Chemical Physics, 2021, 23, 26468-26475.	1.3	2
64223	Insights into Fullerene Polymerization Under the High Pressure: The Role of Endohedral Sc Dimer. SSRN Electronic Journal, 0, , .	0.4	0
64224	Bipolar doping and thermoelectric properties of Zintl arsenide Eu₅In₂As₆. Journal of Materials Chemistry A, 2021, 9, 26362-26370.	5.2	6
64225	Zero-strain Ca_{0.4}Ce_{0.6}VO₄ anode material for high capacity and long-life Na-ion batteries. Journal of Materials Chemistry A, 2021, 9, 25663-25671.	5.2	4
64226	The Influence of Iodide on the Solution-Phase Growth of Cu Microplates: A Multi-Scale Theoretical Analysis from First Principles. Faraday Discussions, 2022, , .	1.6	4
64227	First-principles study of closo-dodecaborates M₂B₁₂H₁₂ (M = Li, Na, K) as solid-state electrolyte materials. Physical Chemistry Chemical Physics, 2021, 23, 27014-27023.	1.3	5
64228	Tunable band gap of layered semiconductor Zn3In2S6 under pressure. Journal of Materials Chemistry C, 0, , .	2.7	6
64229	Formation and properties of iodine- and acetonitrile-functionalized two-dimensional Si materials: a Density Functional Theory study. Physical Chemistry Chemical Physics, 2021, 24, 411-418.	1.3	0
64230	Competing Superior Electronic Structure and Complex Defect Chemistry in Quasi-One-Dimensional Antimony Chalcogenide Photovoltaic Absorbers. ACS Applied Energy Materials, 2022, 5, 492-502.	2.5	14
64231	Fast identification of the stability of atomically dispersed bi-atom catalysts using a structure descriptor-based model. Journal of Materials Chemistry A, 2022, 10, 1451-1462.	5.2	10

#	Article	IF	Citations
64232	Interfacial effects in CuO/Co₃O₄ heterostructures enhance benzene catalytic oxidation performance. Environmental Science: Nano, 2022, 9, 781-796.	2.2	13
64233	Exfoliating silica bilayers via intercalation at the silica/transition metal interface. Nanotechnology, 2022, 33, 135702.	1.3	0
64234	Synthesis of Titanium Molybdenum Nitride-Decorated Electrospun Carbon Nanofiber Membranes as Interlayers to Suppress Polysulfide Shuttling in Lithiumâ€“Sulfur Batteries. ACS Sustainable Chemistry and Engineering, 2022, 10, 776-788.	3.2	21
64235	Ferromagnetism with in-plane magnetization, Dirac spin-gapless semiconducting properties, and tunable topological states in two-dimensional rare-earth metal dinitrides. Physical Review B, 2022, 105, .	1.1	9
64236	Bulk Rashba Spin Splitting and Dirac Surface State in p â€Type (Bi 0.9 Sb 0.1) 2 Se 3 Single Crystal. Physica Status Solidi - Rapid Research Letters, 0, , 2100494.	1.2	1
64237	Superconducting <mml:math xmlns:mml="http://www.w3.org/1998/Math/MathML"><mml:mrow><mml:msub><mml:mi>LaP</mml:mi><mml:mn>2</mml:mn></mml:msub><mml:mrow><mml:math mathvariant="normal">H</mml:mi><mml:mn>2</mml:mn></mml:msub></mml:mrow></mml:math> with graphenelike phosphorus layers. Physical Review B, 2022, 105, .	1.1	8
64238	Molecule in soft-crystal at ground and excited states: Theoretical approach. Journal of Photochemistry and Photobiology C: Photochemistry Reviews, 2022, 51, 100482.	5.6	5
64239	Ab initio study of the phase stability of modulated structures in Co-doped Ni-Mn-In (Sn) Heusler alloys. IOP Conference Series: Materials Science and Engineering, 2022, 1213, 012008.	0.3	1
64240	Improvement of electric insulation in dielectric layered perovskite nickelate films via fluorination. Journal of Materials Chemistry C, 2022, 10, 1711-1717.	2.7	2
64241	Deposition of Electrically Conductive Zirconium Monoxide (ZrO) via Plasma Sprayâ€Physical Vapor Deposition (PSâ€PVD). Journal of the American Ceramic Society, 0, , .	1.9	0
64242	Manipulating the Electronic Properties of Gas-Adsorbed Monolayer GeSe by External Electric Field. Journal of Electronic Materials, 2022, 51, 1232-1240.	1.0	2
64243	Atomistic and electronic structure of metal clusters supported on transition metal carbides: implications for catalysis. Journal of Materials Chemistry A, 2022, 10, 1522-1534.	5.2	13
64244	First-principles calculations to identify key native point defects in Sr₄Al₁₄O₂₅. Physical Chemistry Chemical Physics, 2022, 24, 2482-2490.	1.3	3
64245	Strong Zeeman splitting in orbital-hybridized valleytronic interfaces. Journal of Materials Science, 0, , 1.	1.7	1
64246	Identification of a Stable Ozonide Ion Bound to a Single Cadmium Site within the Zeolite Cavity. Journal of Physical Chemistry C, 0, , .	1.5	1
64247	Strong Edge Stress in Molecularly Thin Organicâ€“Inorganic Hybrid Ruddlesdenâ€“Popper Perovskites and Modulations of Their Edge Electronic Properties. ACS Nano, 2022, 16, 261-270.	7.3	7
64248	BrÃ¸nsted acid properties of hydrodesulfuriaztion catalysts for minimizing the loss of octane number: A DFT and microkinetic study. Microporous and Mesoporous Materials, 2022, 331, 111671.	2.2	4
64250	Room-Temperature Harvesting Oxidase-Mimicking Enzymes with Exogenous ROS Generation in One Step. Inorganic Chemistry, 2022, 61, 1169-1177.	1.9	9

#	Article	IF	Citations
64251	Understanding the mechanism of selective catalytic reduction on spinel TiMn2O4(001) surface. Molecular Catalysis, 2022, 518, 112070.	1.0	1
64252	Reactive phosphine combinatorial co-sputtering of cation disordered ZnGeP₂ films. Journal of Materials Chemistry C, 2022, 10, 870-879.	2.7	8
64253	Atomic-level study of AuSnâ€“Au5Sn eutectic interfaces. Applied Physics Letters, 2022, 120, .	1.5	2
64254	Quantitatively evaluating activity and number of catalytic sites on metal oxide for ammonium perchlorate decomposition. AICHE Journal, 2022, 68, .	1.8	3
64255	Diffusion-enhanced preferential growth of <mml:math xmlns:mml="http://www.w3.org/1998/Math/MathML" display="inline" id="d1e570" altimg="si37.svg"><mml:mi>m</mml:mi></mml:math>-oriented GaN micro-domains on directly grown graphene with a large domain size on Ti/SiO2/Si(001). Materials Today Communications, 2022, 30, 103113.	0.9	3
64256	Electronic properties of TaAs₂ topological semimetal investigated by transport and ARPES. Journal of Physics Condensed Matter, 2022, 34, 125601.	0.7	16
64257	Binary pentagonal auxetic materials for photocatalysis and energy storage with outstanding performances. Nanoscale, 2022, 14, 2041-2051.	2.8	20
64258	Computational Screening of Anode Coatings for Garnetâ€type Solidâ€State Batteries. Batteries and Supercaps, 0, , .	2.4	2
64259	Trace surface fluorination and tungsten-intercalation cooperated dual modification induced photo-activity enhancement of titanium dioxide. Journal of Industrial and Engineering Chemistry, 2022, 108, 195-202.	2.9	0
64260	The Orbital Origins of Chemical Bonding in Geâ^'Sbâ^'Te Phaseâ€Change Materials**. Angewandte Chemie - International Edition, 2022, 61, .	7.2	19
64261	A high-performance and durable direct NH3 tubular protonic ceramic fuel cell integrated with an internal catalyst layer. Applied Catalysis B: Environmental, 2022, 306, 121071.	10.8	33
64262	A new universal force-field for the Li₂Sâ€“P₂S₅system. Physical Chemistry Chemical Physics, 2022, 24, 2567-2581.	1.3	7
64263	Two-dimensional buckling structure induces the ultra-low thermal conductivity: a comparative study of the group GaX (X = N, P, As). Journal of Materials Chemistry C, 2022, 10, 1436-1444.	2.7	13
64264	Quasi-1D electronic transport and isotropic phonon transport in the Zintl Ca5In2Sb6. Materials Today Physics, 2022, 22, 100597.	2.9	3
64265	Dual-role magnesium aluminate ceramic film as an advanced separator and polysulfide trapper in a Liâ€“S battery: experimental and DFT investigations. New Journal of Chemistry, 2022, 46, 3185-3198.	1.4	6
64266	Raised solubility in SnTe by GeMnTe2 alloying enables converged valence bands, low thermal conductivity, and high thermoelectric performance. Nano Energy, 2022, 94, 106940.	8.2	22
64267	Two-dimensional InSb/GaAs- and InSb/InP-based tandem photovoltaic device with matched bandgap. Nanoscale, 2022, 14, 1954-1961.	2.8	9
64268	Phase controlled synthesis of transition metal carbide nanocrystals by ultrafast flash Joule heating. Nature Communications, 2022, 13, 262.	5.8	52

#	Article	IF	Citations
64269	Topological Quantum Cathode Materials for Fast Charging Liâ€Ion Battery Identified by Machine Learning and First Principles Calculation. Advanced Theory and Simulations, 2022, 5, 2100350.	1.3	4
64270	Mechanical, thermal transport, electronic and photocatalytic properties of penta-PdPS, -PdPSe and -PdPTe monolayers explored by first-principles calculations. Journal of Materials Chemistry C, 2021, 10, 329-336.	2.7	14
64271	Theoretical investigations into the hydrogen evolution reaction of the carbon schwarzites: From electronics to structure-catalytic activity relationship. Carbon, 2022, 190, 136-141.	5.4	9
64272	Drastic Reduction of the Solid Electrolyteâ€“Electrode Interface Resistance via Annealing in Battery Form. ACS Applied Materials & Interfaces, 2022, 14, 2703-2710.	4.0	9
64273	Enhanced thermoelectric performance in Sbâ€“Br codoped Bi₂Se₃ with complex electronic structure and chemical bond softening. RSC Advances, 2022, 12, 1653-1662.	1.7	10
64274	Hydrogen trapping and storage in the group IVB-VIB transition metal carbides. Materials and Design, 2022, 214, 110399.	3.3	20
64275	Synergetic effect of Si addition on mechanical properties in face-centered-cubic high entropy alloys: a first-principles study. Modelling and Simulation in Materials Science and Engineering, 2022, 30, 024003.	0.8	8
64276	Au-ZSM-5 catalyses the selective oxidation of CH4 to CH3OH and CH3COOH using O2. Nature Catalysis, 2022, 5, 45-54.	16.1	95
64277	First-Principles Study of Amorphous Al2O3 ALD Coating in Li-S Battery Electrode Design. Energies, 2022, 15, 390.	1.6	3
64278	Topochemical stabilization and single-crystal transformations of a metastable 2D Î³Ê¹-V2O5 intercalation cathode. Cell Reports Physical Science, 2022, 3, 100712.	2.8	5
64279	Routes to High-Carrier-Density Doping in Thermoelectric SnSe. Journal of Physical Chemistry C, 0, , .	1.5	9
64280	Anisotropic Second-Harmonic Generation Induced by Reduction of In-Plane Symmetry in 2D Materials with Strain Engineering. Journal of Physical Chemistry Letters, 2022, 13, 352-361.	2.1	10
64281	Indirect-to-Direct Band Gap Transition and Optical properties of Cs2BiAgX6 with Mechanical Strains: The Density Functional Theory Investigation. Journal of Materials Research and Technology, 2022, 17, 425-425.	2.6	5
64282	Toward benchmarking theoretical computations of elementary rate constants on catalytic surfaces: formate decomposition on Au and Cu. Chemical Science, 2022, 13, 804-815.	3.7	3
64283	One-step conversion of lignin-derived alkylphenols to light arenes by co-breaking of Câ€“O and Câ€“C bonds. New Journal of Chemistry, 2022, 46, 2710-2721.	1.4	5
64284	Accelerated design for elastocaloric performance in NiTi-based alloys through machine learning. Journal of Applied Physics, 2022, 131, .	1.1	7
64285	Carbon allotropes consisting of rings and cubes. Diamond and Related Materials, 2022, 121, 108765.	1.8	7
64286	Ï€-Adsorption promoted electrocatalytic acetylene semihydrogenation on single-atom Ni dispersed N-doped carbon. Journal of Materials Chemistry A, 2022, 10, 6122-6128.	5.2	14

#	Article	IF	Citations
64287	Effect of sp hybridization and bond-length disorder on magnetism in amorphous carbon- A first-principles study. Diamond and Related Materials, 2022, 121, 108725.	1.8	5
64288	Extreme dislocation-mediated plasticity of yttria-stabilized zirconia. Materials Today Physics, 2022, 22, 100588.	2.9	1
64289	Two-dimensional metal structures revealed by evolutionary computations: Pb/Al13Co4(100) as a case study. Journal of Vacuum Science and Technology A: Vacuum, Surfaces and Films, 2022, 40, 012203.	0.9	1
64290	Improving sensing of formaldehyde using ZnO nanostructures with surface-adsorbed oxygen. Nanoscale Advances, 2022, 4, 546-561.	2.2	5
64291	In situ surface reconstruction of a Ni-based perovskite hydroxide catalyst for an efficient oxygen evolution reaction. Journal of Materials Chemistry A, 2022, 10, 1369-1379.	5.2	20
64292	Control of the Cu morphology on Ru-passivated and Ru-doped TaN surfaces â€“ promoting growth of 2D conducting copper for CMOS interconnects. Chemical Science, 2022, 13, 713-725.	3.7	5
64293	Quantum size effects in Ag thin films grown on the fivefold surface of the icosahedral Al-Cu-Fe quasicrystal: Influence of the growth temperature. Journal of Vacuum Science and Technology A: Vacuum, Surfaces and Films, 2022, 40, 013212.	0.9	0
64294	Local orders, lattice distortions, and electronic structure dominated mechanical properties of (ZrHfTaM1M2)C (M = Nb, Ti, V). Journal of the American Ceramic Society, 2022, 105, 4260-4276.	1.9	8
64295	Site occupancy and luminescence of Ce3+-doped NaK2Li[Li3SiO4]4: A first-principles study. Optical Materials, 2022, 123, 111935.	1.7	3
64296	Metastable FeCN₂@nitrogen-doped carbon with high pseudocapacitance as an anode material for sodium ion batteries. Nanoscale, 2022, 14, 780-789.	2.8	7
64297	Dopant precursor adsorption into single-dimer windows: Towards guided self-assembly of dopant arrays on Si(100). Chemical Physics Letters, 2022, 787, 139258.	1.2	2
64298	C₃ production from CO₂ reduction by concerted *CO trimerization on a single-atom alloy catalyst. Journal of Materials Chemistry A, 2022, 10, 5998-6006.	5.2	25
64299	Performance comparison of <mml:math xmlns:mml="http://www.w3.org/1998/Math/MathML"><mml:msup><mml:mrow><mml:mi>r</mml:mi></mml:mrow><mml:mn>2</mml	0.9	31
64300	Spin-crossover Fe(<scp>ii</scp>) complexes on a surface: a mixture of low-spin and high-spin molecules at low temperature from quantum-chemistry calculations. Inorganic Chemistry Frontiers, 2022, 9, 753-760.	3.0	5
64301	Floquet band engineering and topological phase transitions in 1Tâ€™ transition metal dichalcogenides. 2D Materials, 2022, 9, 025005.	2.0	4
64302	Spatial variation of geometry, binding, and electronic properties in the moirÃ© superstructure of MoS₂ on Au(111). 2D Materials, 2022, 9, 025003.	2.0	15
64303	Ultralow-temperature-driven water-based sorption refrigeration enabled by low-cost zeolite-like porous aluminophosphate. Nature Communications, 2022, 13, 193.	5.8	33
64304	Identifying TM-N4 active sites for selective CO2-to-CH4 conversion: A computational study. Applied Surface Science, 2022, 582, 152470.	3.1	16

#	Article	IF	Citations
64305	Electronic state reconfiguration induced by non-metal-dopants in Janus FeReS3 monolayer for hydrogen evolution reaction. Surfaces and Interfaces, 2022, 29, 101718.	1.5	0
64306	Experimental and DFT-D3 study of sensitivity and sensing mechanism of ZnSnO3 nanosheets to C3H6O gas. Journal of Materials Science, 2022, 57, 1-21.	1.7	13
64307	Unconventional materials: the mismatch between electronic charge centers and atomic positions. Science Bulletin, 2022, 67, 598-608.	4.3	32
64308	Structural rule of N-coordinated single-atom catalysts for electrochemical CO₂ reduction. Journal of Materials Chemistry A, 2022, 10, 3585-3594.	5.2	13
64309	Chalcogen dependent metal vacancies and disorder in Ba2Ln1â^'Mn2â^'S5 and Ba2â^'Ln1â^'Mn2â^'Se5 (LnÂ=ÂPr,) Tj ETQq0 0 0 rgBT /Ov	2.8	2
64310	Water Formation Reaction under Interfacial Confinement: Al0.25Si0.75O2 on O-Ru(0001). Nanomaterials, 2022, 12, 183.	1.9	2
64311	Oxygen evolution reaction at the Mo/W-doped bismuth vanadate surface: Assessing the dopant role by DFT calculations. Molecular Catalysis, 2022, 517, 112036.	1.0	11
64312	The effect of ferromagnetism on the CO activation over FCC crystal phase transition metal catalysts: Insights from DFT calculations. Molecular Catalysis, 2022, 518, 112071.	1.0	3
64313	Modulating Thermal Transport in Porous Carbon Honeycomb by Cutting and Deformation Techniques. Physical Chemistry Chemical Physics, 2022, , .	1.3	1
64314	Atomistic origin of lattice softness and its impact on structural and carrier dynamics in three dimensional perovskites. Energy and Environmental Science, 2022, 15, 660-671.	15.6	24
64315	Topological phase transition associated with structural phase transition in ternary half Heusler compound LiAuBi. Journal of Physics Condensed Matter, 2022, 34, 145501.	0.7	0
64316	Interface-Driven Assembly of Pentacene/MoS₂ Lateral Heterostructures. Journal of Physical Chemistry C, 2022, 126, 1132-1139.	1.5	6
64317	Anisotropic nodal loop in NiB₂ monolayer with nonsymmorphic configuration. Nanoscale, 2022, 14, 1264-1270.	2.8	4
64318	First-principles search of hot superconductivity in La-X-H ternary hydrides. Npj Computational Materials, 2022, 8, .	3.5	25
64319	Nitrogenase-Inspired Atomically Dispersed Feâ€“Sâ€“C Linkages for Improved Electrochemical Reduction of Dinitrogen to Ammonia. ACS Catalysis, 2022, 12, 1443-1451.	5.5	58
64320	Invariant expansion of the 30-band <mml:math xmlns:mml="http://www.w3.org/1998/Math/MathML"><mml:mrow><mml:mi>k</mml:mi><mml:mo>Â·</mml:mo><mml:mi>p</mml:mi> model and its parameters for III-V compounds. Physical Review B, 2022, 105, .	1.1	3
64321	Cu/O Frustrated Lewis Pairs on Cu Doped CeO2(111) for Acetylene Hydrogenation: A First-Principles Study. Catalysts, 2022, 12, 74.	1.6	8
64322	First-principles study of the interstitial stability and microscopic diffusion mechanism of hydrogen atom in Zr, Ti elemental and ZrTi2 alloys. Materials Chemistry and Physics, 2022, 277, 125549.	2.0	4

#	Article	IF	Citations
64323	Finite-size scaling effects of chemically induced transformations: From T12â€‘carbon to a composite carbon-cage structure. Diamond and Related Materials, 2022, 122, 108829.	1.8	2
64324	Electronic structure transformation induced by dual-metal orbital hybridization in RexMn1-xS2 monolayer for hydrogen evolution reaction. Surfaces and Interfaces, 2022, 28, 101671.	1.5	1
64325	Roles of hydrogen bond and ion bridge in adsorption of two bisphenols onto montmorillonite: an experimental and DFT study. Applied Clay Science, 2022, 217, 106406.	2.6	17
64326	Carbon adsorption and incorporation on the (110)AlAs surface. Physica B: Condensed Matter, 2022, 627, 413583.	1.3	0
64327	Mg/Si interface reaction: How and why. Towards rational technologies of Mg2Si film growth for energy conversion. Vacuum, 2022, 196, 110798.	1.6	1
64328	Strong phonon coupling induces low thermal conductivity of one-dimensional carbon boron nanotube. Surfaces and Interfaces, 2022, 28, 101690.	1.5	12
64329	First-principles studies of imidazolium chloroaluminate ionic liquids with different substitutions on the Pt(111) surface. Colloids and Surfaces A: Physicochemical and Engineering Aspects, 2022, 635, 128079.	2.3	1
64330	Amorphisation-induced electrochemical stability of solid-electrolytes in Li-metal batteries: The case of Li<mml:math xmlns:mml="http://www.w3.org/1998/Math/MathML" display="inline" id="d1e476" altimg="si18.svg"><mml:msub><mml:mrow /><mml:mrow><mml:mn>3</mml:mn></mml:mrow></mml:msub></mml:math>ClO. Journal of Power Sources, 2022, 521, 230916.	4.0	1
64331	Flower-petal-like Nb2C MXene combined with MoS2 as bifunctional catalysts towards enhanced lithium-sulfur batteries and hydrogen evolution. Electrochimica Acta, 2022, 404, 139781.	2.6	19
64332	Comparative analysis on the structure, electronic and magnetic properties of SrRuO3 and PbRuO3. Solid State Sciences, 2022, 124, 106800.	1.5	2
64333	Influence of WC/C target composition and bias potential on the structure-mechanical properties of non-reactively sputtered WC coatings. Surface and Coatings Technology, 2022, 432, 128036.	2.2	3
64334	High-performance symmetric supercapacitor based on new functionalized graphene oxide composites with pyrimidine nucleotide and nucleoside. Journal of Molecular Liquids, 2022, 348, 118381.	2.3	9
64335	One-dimensional metallic grain boundary in transition metal dichalcogenides. Computational Materials Science, 2022, 203, 111115.	1.4	2
64336	First-principles study on the electronic structures and diffusion behaviors of intrinsic defects in BiOCl. Computational Materials Science, 2022, 203, 111088.	1.4	6
64337	Recommendation of interstitial hydrogen positions in metal oxides. Computational Materials Science, 2022, 203, 111068.	1.4	2
64338	First-principles studies of the concentration-dependent tritium diffusion in the zirconium hydrides with and without Sn impurity. Computational Materials Science, 2022, 203, 111158.	1.4	2
64339	Structural, magnetic, electronic, and phonon properties of NdNiO2 under pressure from first-principles. Journal of Solid State Chemistry, 2022, 306, 122806.	1.4	4
64340	Polarization-dependent Bulk-sensitive Valence Band Photoemission Spectroscopy and Density Functional Theory Calculations: Part III. 5d Transition Metals. Journal of the Physical Society of Japan, 2022, 91, .	0.7	1

#	Article	IF	Citations
64341	Effect of defectiveness of carbon sublattice on elastic properties and microstrains of disordered cubic tantalum carbide TaC. International Journal of Refractory Metals and Hard Materials, 2022, 103, 105760.	1.7	2
64342	Metalloid substitution elevates simultaneously the strength and ductility of face-centered-cubic high-entropy alloys. Acta Materialia, 2022, 225, 117571.	3.8	64
64343	Fe-doping induced electronic structure reconstruction in Ni-based metal-organic framework for improved energy-saving hydrogen production via urea degradation. Journal of Power Sources, 2022, 520, 230882.	4.0	44
64344	Molecular dynamics simulation of molten strontium chloride based on deep potential. Journal of Molecular Liquids, 2022, 348, 118380.	2.3	7
64345	Photoinduced high thermoelectric power factor in strontium titanate. Physica B: Condensed Matter, 2022, 627, 413552.	1.3	2
64346	A type-II PtS2/MoTe2 van der Waals heterostructure with adjustable electronic and optical properties. Results in Physics, 2022, 33, 105172.	2.0	22
64347	Li1+xMn2O4 synthesized by in-situ lithiation for improving sulfur redox kinetics of Li-S batteries. Electrochimica Acta, 2022, 404, 139780.	2.6	5
64348	Ab initio investigation of phase stability, thermo-physical and mechanical properties of (Mo0.2Cr0.2Ta0.2Nb0.2X0.2)Si2 (XÂ=ÂW, V) high-entropy refractory metal silicides. Computational Materials Science, 2022, 203, 111116.	1.4	8
64349	Field-induced semiconductorâ€“metal transition of hybrid ZnO and graphene nanocomposites. Computational Materials Science, 2022, 203, 111138.	1.4	0
64350	In-depth explorations on the microstructural, thermodynamic and kinetic characteristics of MgCl2-KCl eutectic salt. Journal of Molecular Liquids, 2022, 347, 118275.	2.3	6
64351	Hydrothermal synthesis of ammonium vanadate [(NH4)2V7O16â€¢3.6H2O] as a promising zinc-ion cathode: Experimental and theoretical study of its storage. Electrochimica Acta, 2022, 404, 139785.	2.6	9
64352	Atomic structure and evolution of a precursor phase of Î© precipitate in an Al-Cu-Mg-Ag alloy. Acta Materialia, 2022, 225, 117538.	3.8	21
64353	Interactions of hydrogen with zirconium alloying elements and oxygen vacancies in monoclinic zirconia. Acta Materialia, 2022, 225, 117547.	3.8	4
64354	The possible negative state of deuterium in LiAlO2 irradiated by 3keV D2+ at higher temperature. Journal of Nuclear Materials, 2022, 559, 153485.	1.3	1
64355	Microscopic physical origin of polarization induced large tunneling electroresistance in tetragonal-phase BiFeO3. Acta Materialia, 2022, 225, 117564.	3.8	6
64356	The impact of anionic vacancies on the mechanical properties of NbC and NbN: An ab initio study. Computational Materials Science, 2022, 203, 111113.	1.4	2
64357	Phase decomposition and strengthening in HfNbTaTiZr high entropy alloy from first-principles calculations. Acta Materialia, 2022, 225, 117582.	3.8	23
64358	First-principles calculations to investigate electronic structure and optical properties of 2D MgCl2 monolayer. Superlattices and Microstructures, 2022, 162, 107132.	1.4	15

#	Article	IF	Citations
64359	Machine learning assisted design of FeCoNiCrMn high-entropy alloys with ultra-low hydrogen diffusion coefficients. Acta Materialia, 2022, 224, 117535.	3.8	44
64360	Deprivation of unpaired electrons on graphitic carbon nitride-based carbocatalysts by peroxydisulfate driving a nonradical oxidation process. Journal of Cleaner Production, 2022, 334, 130220.	4.6	3
64361	Structure, mechanical stability, lattice dynamics and thermodynamic properties of C15-Laves phase Mg2Ce. Solid State Communications, 2022, 342, 114641.	0.9	1
64362	New high-pressure monoclinic phase of Sn. Solid State Communications, 2022, 342, 114635.	0.9	1
64363	Atomic structure of PbBr2 thin films on Ag (111). Solid State Communications, 2022, 343, 114651.	0.9	1
64364	A comparative study of the structural, vibrational, electronic and thermoelastic properties of Î±â^'SiO2 and Î±â^'Si(NH)2 from first principles. Materials Chemistry and Physics, 2022, 278, 125564.	2.0	0
64365	Structure, stability, and mechanical properties of Nb2B under high pressure. Solid State Communications, 2022, 343, 114650.	0.9	0
64366	Shape stability and electronic structure of Pt3M (MÂ=ÂCo or Ni) alloy nanoparticles. Computational Materials Science, 2022, 203, 111132.	1.4	5
64367	Evaluation of oxygen-vacancy concentration through simulated hydrogen diffusion in amorphous In-Ga-Zn-O. Computational Materials Science, 2022, 203, 111109.	1.4	4
64368	Revealing the key role of bonding states in surface chemisorption. Chemical Engineering Science, 2022, 249, 117345.	1.9	5
64369	Monolayer penta-BCN: A promising candidate for harmful gases detection. Sensors and Actuators A: Physical, 2022, 334, 113326.	2.0	13
64370	Band gap anomaly in cuprous halides. Computational Materials Science, 2022, 203, 111157.	1.4	7
64371	Atomistic study of Al partitioning and its influence on nanoscale precipitation of Cu-rich nanocluster-strengthened steels. Materials Characterization, 2022, 184, 111687.	1.9	0
64372	Blue luminescence origin and Mg acceptor saturation in highly doped zinc-blende GaN with Mg. Journal of Alloys and Compounds, 2022, 897, 163133.	2.8	8
64373	Nickel B-site substitution in bulk Sr1â^'xCaxFeO3 perovskite oxygen carriers: Benefits and limitations. Journal of Alloys and Compounds, 2022, 896, 162783.	2.8	7
64374	Enhanced magnetocaloric effect in aluminum doped Gd3Fe5-Al O12 garnet: Structural, magnetic, and MÃ¶ssbauer study. Materialia, 2022, 21, 101301.	1.3	10
64375	Ab initio predictions of structures and physical properties of the KCuX (X = Se and Te) phases under pressure. Computational Condensed Matter, 2022, 30, e00616.	0.9	2
64376	Surfactant-free synthesis of sub-10Ânm Co3O4 in a rotating packed bed and its high catalytic activity for AP pyrolysis. Chemical Engineering Science, 2022, 250, 117391.	1.9	2

#	Article	IF	Citations
64377	Insight into adsorption mechanism of water on tricalcium silicate from first-principles calculations. Cement and Concrete Research, 2022, 152, 106684.	4.6	11
64378	Formation of metastable aluminum silicide as intermediate stage of Al-Si alloy crystallization. Scripta Materialia, 2022, 210, 114481.	2.6	3
64379	Density functional theory and Monte Carlo study of electronic, magnetic and magnetocaloric properties of Fe3CoN and FeCo3N antiperovskites. Journal of Crystal Growth, 2022, 581, 126497.	0.7	12
64380	Synthesis, crystal structure and luminescence property in Y2ZnGe4O12:Eu3+. Journal of Solid State Chemistry, 2022, 307, 122807.	1.4	1
64381	Ta concentration effect on nucleation of defects in W-Ta alloy from first-principles model. Materials Today Communications, 2022, 30, 103071.	0.9	0
64382	Coexistence of a self-interstitial atom with light impurities in a tungsten grain boundary. Journal of Nuclear Materials, 2022, 560, 153481.	1.3	5
64383	Unlocking the origin of triggering hysteretic oxygen capacity in divalent species incorporated O-type sodium layered-oxide cathodes. Energy Storage Materials, 2022, 45, 432-441.	9.5	7
64384	Deposition of Co islands on Cu(111) and Cuâ€“Al(111): A comparative study from DFT calculations. Vacuum, 2022, 197, 110812.	1.6	1
64385	Compatibility of UN with refractory metals (V, Nb, Ta, Cr, Mo and W): An ab initio approach to interface reactions and diffusion behavior. Journal of Nuclear Materials, 2022, 560, 153482.	1.3	5
64386	Controllable synthesis of Si-based GeSn quantum dots with room-temperature photoluminescence. Applied Surface Science, 2022, 579, 152249.	3.1	3
64387	Computational evaluation of FeMo heteroatom coeffect induced high electroreduction activity of N2-to-NH3. Applied Surface Science, 2022, 579, 152214.	3.1	15
64388	Thermodynamic assessment of the Gaâ€“La and Gaâ€“Pr systems supported by ab-initio calculations. Calphad: Computer Coupling of Phase Diagrams and Thermochemistry, 2022, 76, 102387.	0.7	3
64389	Identification of active sites available for hydrogen evolution of Single-Atom Ni1/TiO2 catalysts. Applied Surface Science, 2022, 579, 152139.	3.1	11
64390	Correlating the dispersion of Li@Mn6 superstructure units with the oxygen activation in Li-rich layered cathode. Energy Storage Materials, 2022, 45, 422-431.	9.5	23
64391	The new stable phases of Fe2Pd crystal alloy and their properties. Computational Materials Science, 2022, 204, 111183.	1.4	1
64392	Flexible Si3C monolayer: A superior anode for high-performance non-lithium ion batteries. Colloids and Surfaces A: Physicochemical and Engineering Aspects, 2022, 637, 128238.	2.3	17
64393	Insights into CrS2 monolayer and <mml:math xmlns:mml="http://www.w3.org/1998/Math/MathML" altimg="si6.svg"><mml:mi>n</mml:mi></mml:math>-CrS2/<mml:math xmlns:mml="http://www.w3.org/1998/Math/MathML" altimg="si7.svg"><mml:mi>p</mml:mi></mml:math>-HfN2 interface for low-power digital and analog nanoelectronics. Applied Surface Science, 2022, 579, 152211.	3.1	14
64394	First-principle investigation on the thermoelectric properties of XCoGe (X = V, Nb, and Ta) half-Heusler compounds. Materials Science in Semiconductor Processing, 2022, 140, 106387.	1.9	9

#	Article	IF	Citations
64395	Exsolved Co3O4 with tunable oxygen vacancies for electrocatalytic H2O2 production. Materials Today Energy, 2022, 24, 100931.	2.5	19
64396	Surface functionalization of Ta4C3 MXene for broadband ultrafast photonics in the near-infrared region. Applied Materials Today, 2022, 26, 101341.	2.3	17
64397	Alkali-metal induced electronic structure evolution in Sn4Sb3 studied by angle-resolved photoemission spectroscopy. Journal of Physics and Chemistry of Solids, 2022, 162, 110526.	1.9	1
64398	Chromium doping: A new approach to regulate electronic structure of cobalt carbonate hydroxide for oxygen evolution improvement. Journal of Colloid and Interface Science, 2022, 609, 414-422.	5.0	14
64399	Surface Termination of BaTiO3(1 1 1) Single Crystal: A Combined DFT and XPS Study. Applied Surface Science, 2022, 578, 152018.	3.1	20
64400	Mechanical and heat transport properties of Ti1â^'xZrxNiSn half-Heuslers: A molecular dynamic simulation study using ab initio-based interaction potentials. Computational Materials Science, 2022, 204, 111147.	1.4	1
64401	Defect modulated electronic structure and magnetism in the 1Tâ€² phase of Janus MoSSe. Chemical Physics, 2022, 555, 111440.	0.9	1
64402	Experimental investigation and thermodynamic re-assessment of the Tiâ€“Zn system and atomic mobility of its bcc phase. Calphad: Computer Coupling of Phase Diagrams and Thermochemistry, 2022, 76, 102392.	0.7	4
64403	Reinforced upconversion and charge separation via mid-gap states in WO3 nanosheet with infrared light driven tetracycline degradation. Chemical Engineering Journal, 2022, 431, 134134.	6.6	12
64404	Metal phthalocyanines as efficient electrocatalysts for acetylene semihydrogenation. Chemical Engineering Journal, 2022, 431, 134129.	6.6	14
64405	Structure, magnetism, and electronic properties of MXene bilayer Fe2NO2H (xÂ=Â1.5, 1)/Ti2CO2 stacked heterojunction. Chemical Physics Letters, 2022, 790, 139319.	1.2	1
64406	Spontaneous etching of B2O3 by HF gas studied using infrared spectroscopy, mass spectrometry, and density functional theory. Journal of Vacuum Science and Technology A: Vacuum, Surfaces and Films, 2022, 40, 022601.	0.9	4
64407	Intrinsic catalytic Sites-Rich Co-doped SnO2 nanoparticles enabling enhanced conversion and capture of polysulfides. Chemical Engineering Journal, 2022, 431, 134033.	6.6	19
64408	3D cubic framework of fluoride perovskite SEI inducing uniform lithium deposition for air-stable and dendrite-free lithium metal anodes. Chemical Engineering Journal, 2022, 431, 134266.	6.6	17
64409	Interfacial electronic modulation on heterostructured NiSe@CoFe LDH nanoarrays for enhancing oxygen evolution reaction and water splitting by facilitating the deprotonation of OH to O. Chemical Engineering Journal, 2022, 431, 134080.	6.6	85
64410	A g-SiC<mml:math xmlns:mml="http://www.w3.org/1998/Math/MathML" display="inline" id="d1e531" altimg="si36.svg"><mml:msub><mml:mrow /><mml:mrow><mml:mn>6</mml:mn></mml:mrow></mml:msub></mml:math> monolayer and its analogs: A new class of tunable Dirac cone materials and novel quantum spin Hall insulators. Applied Surface Science, 2022, 578, 151986.	3.1	4
64411	Thermodynamic assessment of the Feâ€“Niâ€“Rhâ€“Ti system. Calphad: Computer Coupling of Phase Diagrams and Thermochemistry, 2022, 76, 102386.	0.7	0
64412	Excited state charge transfer promoted Raman enhancement of copper phthalocyanine by twisted bilayer graphenes. Carbon, 2022, 188, 305-314.	5.4	1

#	Article	IF	Citations
64413	Designing Pt-based subsurface alloy catalysts for the dehydrogenation of perhydro-dibenzyltoluene: A first-principles study. Applied Surface Science, 2022, 579, 152142.	3.1	13
64414	Temperature-dependent XPS studies on Ga-In alloys through the melting-point. Surface Science, 2022, 717, 122008.	0.8	4
64415	Fe-Sn bimetallic catalysts for an enhanced Fischer-Tropsch synthesis stability via oxygen removal and coking resistance. Fuel, 2022, 311, 122115.	3.4	8
64416	Structural, electronic, elastic, phonon and thermoelectric properties of Heusler-structured intermetallic HfCu2In: Using density functional theory. Physica B: Condensed Matter, 2022, 629, 413633.	1.3	7
64417	Mesoporous IrNiTa metal glass ribbon as a superior self-standing bifunctional catalyst for water electrolysis. Chemical Engineering Journal, 2022, 431, 134210.	6.6	16
64418	Group three nitride clusters as promising components for nanoelectronics. Materials Today Chemistry, 2022, 23, 100751.	1.7	2
64419	Antibacterial nanofibers of pullulan/tetracycline-cyclodextrin inclusion complexes for Fast-Disintegrating oral drug delivery. Journal of Colloid and Interface Science, 2022, 610, 321-333.	5.0	35
64420	Studying GPI zones in Al-Zn-Mg alloys by 4D-STEM. Materials Characterization, 2022, 185, 111675.	1.9	14
64421	Structure of PtRu/Ru(0Â0Â0Â1) and AgPd/Pd(1Â1Â1) surface alloys: A kinetic Monte Carlo study. Chemical Physics, 2022, 555, 111428.	0.9	4
64422	Photocatalytic removal of tetracycline by a Z-scheme heterojunction of bismuth oxyiodide/exfoliated g-C3N4: performance, mechanism, and degradation pathway. Materials Today Chemistry, 2022, 23, 100729.	1.7	32
64423	Temperature-induced orbital polarizations and tunable charge dynamics in layered double perovskite thin films. Materials Today Energy, 2022, 24, 100921.	2.5	5
64424	On intermetallic phases formed during interdiffusion between aluminium alloys and stainless steel. Intermetallics, 2022, 142, 107443.	1.8	13
64425	First-principles study on stability, adhesion and fracture properties of ZrO2/W interface in composite materials. Journal of Nuclear Materials, 2022, 560, 153510.	1.3	3
64426	Investigations on the electronic properties and effect of chitosan capping on the structural and optical properties of zinc aluminate quantum dots. Applied Surface Science, 2022, 579, 152162.	3.1	5
64427	Rationally designed Ta3N5/ZnIn2S4 1D/2D heterojunctions for boosting Visible-Light-driven hydrogen evolution. Chemical Engineering Journal, 2022, 431, 134053.	6.6	42
64428	Adjusting the catalytic activity of C2N/SiH heterojunction for water splitting: A first-principles study. Applied Surface Science, 2022, 579, 152233.	3.1	20
64429	Experimental and DFT studies on the equilibrium properties, kinetics, and mechanism of nitric oxide removal using metal-EDTA and ferrous thiochelates. Chemical Engineering Journal, 2022, 431, 134010.	6.6	2
64430	A machine-learning-based investigation on the mechanical/failure response and thermal conductivity of semiconducting BC2N monolayers. Carbon, 2022, 188, 431-441.	5.4	34

#	Article	IF	Citations
64431	Coralloid-Pt nanodendrites decorated nanoporous gold films with exceptional ORR performance and ab initio DFT studies. Applied Surface Science, 2022, 578, 152117.	3.1	7
64432	A highly efficient narrow-band blue phosphor of Bi3+-activated cubic borate Ba3Lu2B6O15 towards backlight display applications. Chemical Engineering Journal, 2022, 432, 134265.	6.6	28
64433	The effect of W and Mo modification on arsenic adsorption over Cu/Î³-Al2O3 catalyst: Experimental and theoretical analysis. Chemical Engineering Journal, 2022, 432, 134376.	6.6	11
64434	The high piezoelectricity, flexibility and electronic properties of new Janus ZnXY2 (XÂ=ÂGe, Sn, Si and) Tj ETQq1 1 0.784314 rgBT /Ov	3.1	9
64435	Insights into fullerene polymerization under the high pressure: The role of endohedral Sc dimer. Carbon, 2022, 189, 37-45.	5.4	3
64436	Au adsorption on stepped Si(hhk)-Au surfaces. Surface Science, 2022, 718, 122010.	0.8	0
64437	The structural, electronic, magnetic and optical properties of 4d transition metal adatoms (Tc, Ru, Rh) Tj ETQq0 0 0 rgBT /Overlock 10 Tf Nanostructures, 2022, 138, 115116.	1.3	4
64438	Single transition metal atom anchored on VSe2 as electrocatalyst for nitrogen reduction reaction. Applied Surface Science, 2022, 580, 152272.	3.1	15
64439	Atomic insight into iron corrosion exposed to supercritical water environment with an improved Fe-H2O reactive force field. Applied Surface Science, 2022, 580, 152300.	3.1	14
64440	First principles investigations and Hirshfeld surface analysis of high-energetic and low-sensitive 2,6-diamino-3,5-dinitropyrazine-1-oxide (LLM-105) crystal. Journal of Physics and Chemistry of Solids, 2022, 163, 110550.	1.9	1
64441	New insights into the structural, optical, electronic and photocatalytic properties of sulfur doped bulk BiVO4 and surface BiVO4 on {0 1 0} and {1 1 0} via a collective theoretical and experimental investigation. Journal of Photochemistry and Photobiology A: Chemistry, 2022, 426, 113757.	2.0	6
64442	Structure and lattice thermal conductivity of grain boundaries in silicon by using machine learning potential and molecular dynamics. Computational Materials Science, 2022, 204, 111137.	1.4	9
64443	Double charge polarity switching in Sb-doped SnSe for enhanced thermo-electric power generation. Journal of Alloys and Compounds, 2022, 899, 163269.	2.8	4
64444	DFT insights into competitive adsorption and reaction mechanism of benzothiophene and naphthalene on Fe-doped Ni2P catalyst. Fuel, 2022, 314, 123114.	3.4	3
64445	Combined experimental and DFT studies of Co82Zr12V6-xBx melt-spun ribbons to investigate structure and magnetic properties. Journal of Magnetism and Magnetic Materials, 2022, 547, 168940.	1.0	6
64446	First-principles study on luminescent properties of Bi3+-doped ALuGeO4 (A = Li, Na): Insights into effects of host cation on emission wavelength. Journal of Luminescence, 2022, 244, 118700.	1.5	9
64447	Interfacial electronic structure modulation of Pt-MoS2 heterostructure for enhancing electrocatalytic hydrogen evolution reaction. Nano Energy, 2022, 94, 106913.	8.2	119
64448	Graphene/g-carbon nitride (GO/g-C3N4) nanohybrids as a sensor material for the detection of methyl parathion and carbendazim. Chemosphere, 2022, 292, 133450.	4.2	47

#	Article	IF	Citations
64449	Copper-based thiospinel quantum dots as potential candidates for nonlinear optical applications. Optics and Laser Technology, 2022, 148, 107752.	2.2	8
64450	The microstructural, mechanical and thermal properties of TiAlVN, TiAlSiN monolithic and TiAlVN/TiAlSiN multilayered coatings. Journal of Alloys and Compounds, 2022, 899, 163332.	2.8	15
64451	Easy-plane magnetic anisotropy of a single dopant in a single semiconductor nanowire. Journal of Magnetism and Magnetic Materials, 2022, 547, 168915.	1.0	3
64452	Ultrahigh reversible hydrogen capacity and synergetic mechanism of 2LiBH4-MgH2 system catalyzed by dual-metal fluoride. Chemical Engineering Journal, 2022, 433, 134482.	6.6	19
64453	Concunrent manipulation of anion and cation adsorption kinetics in pancake-like carbon achieves ultrastable potassium ion hybrid capacitors. Energy Storage Materials, 2022, 46, 10-19.	9.5	32
64454	Structural phase transition in cobalt oxyfluoride Co3Sb4O6F6 observed by high-resolution synchrotron and neutron diffraction. Journal of Physics and Chemistry of Solids, 2022, 163, 110568.	1.9	2
64455	Revisiting dissolution behavior of interfacial oxides in hot-compression bonding of stainless steel by combination of experiments and first-principles calculations. Applied Surface Science, 2022, 581, 152297.	3.1	3
64456	A DFT study on the adsorption of CO, H<mml:math xmlns:mml="http://www.w3.org/1998/Math/MathML" altimg="si1.svg"><mml:msub><mml:mrow /><mml:mn>2</mml:mn></mml:msub></mml:math>S, PH<mml:math xmlns:mml="http://www.w3.org/1998/Math/MathML" altimg="si3.svg"><mml:msub><mml:mrow /><mml:mn>3</mml:mn></mml:msub></mml:math>, CO<mml:math xmlns:mml="http://www.w3.org/1998/Math/MathML" altimg="si1.svg"><mml:msub><mml:mrow />	0.8	5
64457	Highly boron-doped holey graphene for lithium oxygen batteries with enhanced electrochemical performance. Carbon, 2022, 189, 404-412.	5.4	12
64458	Narrow-Bandgap LaMO3 (MÂ=ÂNi, Co) nanomaterials for efficient interfacial solar steam generation. Journal of Colloid and Interface Science, 2022, 612, 203-212.	5.0	30
64459	Starburst configured imidazole-arylamine organic sensitizers for DSSC applications. Journal of Photochemistry and Photobiology A: Chemistry, 2022, 426, 113735.	2.0	5
64460	Mechanistic insights into chemical reduction of CO2 by reverse water-gas shift reaction on Ru(0001) surface: The water promotion effect. Applied Surface Science, 2022, 581, 152354.	3.1	7
64461	Supercritical CO2 assisted synthesis of highly accessible iron single atoms and clusters on nitrogen-doped carbon as efficient oxygen reduction electrocatalysts. Chemical Engineering Journal, 2022, 433, 134460.	6.6	22
64462	Smart construction of multifunctional Li1.5Al0.5Ge1.5(PO4)3	Li intermediate interfaces for solid-state batteries. Energy Storage Materials, 2022, 46, 68-75.	9.5	34
64463	A simulated-TPD study of H2 desorption on metal surfaces. Surface Science, 2022, 718, 122015.	0.8	7
64464	Heterointerface synergistic Na+ storage fundamental mechanism for CoSeO3 playing as anode for sodium ion batteries/capacitors. Chemical Engineering Journal, 2022, 433, 134567.	6.6	14
64465	Combined experimental and theoretical study of o-xylene elimination on Feâ€“Mn oxides catalysts. Chemosphere, 2022, 292, 133442.	4.2	8
64466	Janus MoCrSSe monolayer: A strong two dimensional polar antiferromagnet. Applied Surface Science, 2022, 581, 152420.	3.1	4

#	Article	IF	Citations
64467	Modulating the blue and green luminescence in the Î²-Ga2O3 films. Journal of Alloys and Compounds, 2022, 900, 163431.	2.8	24
64468	Selective bimetallic sites supported on graphene as a promising catalyst for CO2 Reduction: A first-principles study. Applied Surface Science, 2022, 582, 152472.	3.1	6
64469	Electronic structures and related properties of Ce2Fe17-based magnetocaloric material upon Nd/Si substitution. Journal of Alloys and Compounds, 2022, 900, 163418.	2.8	2
64470	Encapsulated ruthenium nanoparticles activated few-layer carbon frameworks as high robust oxygen evolution electrocatalysts in acidic media. Journal of Colloid and Interface Science, 2022, 612, 488-495.	5.0	10
64471	Synthesis of large area graphitic carbon nitride nanosheet by chemical vapor deposition. Journal of Alloys and Compounds, 2022, 900, 163310.	2.8	4
64472	Remarkable anisotropy in rhombohedral Ge2Sb2Te5 compound: a promising thermoelectric material with multiple conduction bands and acoustic-optical branches coupling. Journal of Alloys and Compounds, 2022, 900, 163471.	2.8	6
64473	High frequency magnetic behavior of FeCoNiMnxAl1âˆ’x high-entropy alloys regulated by ferromagnetic transformation. Journal of Alloys and Compounds, 2022, 900, 163428.	2.8	12
64474	Chlorine-terminated MXene quantum dots for improving crystallinity and moisture stability in high-performance perovskite solar cells. Chemical Engineering Journal, 2022, 432, 134382.	6.6	29
64475	Tuning the magnetic anisotropy of transition-metal atoms on two-dimensional In2Se3 substrate via ferroelectric polarization switching. Applied Surface Science, 2022, 580, 152311.	3.1	4
64476	Adsorption of toxic H2S, CO and NO molecules on pristine and transition metal doped Î±-AsP monolayer by first-principles calculations. Physica E: Low-Dimensional Systems and Nanostructures, 2022, 138, 115109.	1.3	8
64477	Copper and nickel decorated g-C3N4 as superior catalysts for reduction of toxic pollutants: A combined experimental and theoretical approach. Applied Surface Science, 2022, 580, 152137.	3.1	10
64478	Abnormal enhancement of thermal conductivity by planar structure: A comparative study of graphene-like materials. International Journal of Thermal Sciences, 2022, 174, 107438.	2.6	14
64479	Building-block approach to the discovery of Na8Mn2(Ge2Se6)2: A polar chalcogenide exhibiting promising harmonic generation signals with a high laser-induced damage threshold. Journal of Alloys and Compounds, 2022, 900, 163392.	2.8	5
64480	Crystal structure and thermochromic behavior of the quasi-0D lead-free organic-inorganic hybrid compounds (C7H9NF)8M4I16 (M = Bi, Sb). Journal of Alloys and Compounds, 2022, 899, 163278.	2.8	13
64481	Experimental and first-principles investigations on W-Ir mixed matrices cathodes with improved emission performance. Applied Surface Science, 2022, 581, 152379.	3.1	4
64482	Structural and magnetism in metastable bcc Co(Mn)/Mn/Au xmlns:mml="http://www.w3.org/1998/Math/MathML" display="inline" id="d1e604" altimg="si65.svg"><mml:msub><mml:mrow /><mml:mrow><mml:mn>1</mml:mn><mml:mo>â€²</mml:mo><mml:mi>x</mml:mi></mml:mrow></mml:msub></mml:math>Mn<mml xmlns:mml="http://www.w3.org/1998/Math/MathML" display="inline" id="d1e616" altimg="si66.svg"><mml:msub><mml:mrow /><mml:mrow><mml:mi>x</mml:mi></mml:mrow>	3.1	6
64483	The role of Dy doping on cyclic oxidation behavior of Al-Si coating on new cobalt-based Î³/Î³â€² superalloy. Corrosion Science, 2022, 197, 110077.	3.0	1
64484	MoS2/C3N heterostructure: A promising anode material for Lithium-ion batteries. Applied Surface Science, 2022, 580, 152371.	3.1	15

#	Article	IF	Citations
64485	CTAB-functionalized Î´-FeOOH for the simultaneous removal of arsenate and phenylarsonic acid in phenylarsenic chemical warfare. Chemosphere, 2022, 292, 133373.	4.2	11
64486	Alleviating inhibitory effect of H2 on low-temperature water-gas shift reaction activity of Pt/CeO2 catalyst by forming CeO2 nano-patches on Pt nano-particles. Applied Catalysis B: Environmental, 2022, 305, 121038.	10.8	11
64487	Isovalent cation ordering in Bi-based double perovskites: A density functional analysis. Journal of Magnetism and Magnetic Materials, 2022, 548, 168984.	1.0	1
64488	Boosting CO2 hydrogenation performance for light olefin synthesis over GaZrOx combined with SAPO-34. Applied Catalysis B: Environmental, 2022, 305, 121042.	10.8	30
64489	Roles of optical phonons and logarithmic profile of electron-phonon coupling integration in superconducting Sc0.5Y0.5H6 superhydride under pressures. Journal of Alloys and Compounds, 2022, 901, 163524.	2.8	11
64490	Defect-rich Mg-Al MMOs supported TEPA with enhanced charge transfer for highly efficient and stable direct air capture. Journal of Energy Chemistry, 2022, 68, 401-410.	7.1	18
64491	Stabilization of the (1 1 1) surface of NiO and CoO by segregation of point defects. Applied Surface Science, 2022, 582, 152473.	3.1	3
64492	First-principles study of structural, electronic and magnetic properties of transition metal doped Sc2CF2 MXene. Applied Surface Science, 2022, 581, 152360.	3.1	11
64493	Precise identification of active sites of a high bifunctional performance 3D Co/N-C catalyst in Zinc-air batteries. Chemical Engineering Journal, 2022, 433, 134500.	6.6	44
64494	Simultaneous increase of conductivity, active sites and structural strain by nitrogen injection for high-yield CO2 electro-hydrogenation to liquid fuel. Applied Catalysis B: Environmental, 2022, 305, 121080.	10.8	20
64495	Coordination-tuned Fe single-atom catalyst for efficient CO2 electroreduction: The power of B atom. Chemical Engineering Journal, 2022, 433, 134270.	6.6	29
64496	Ultrasonic-assisted soldering of Mg alloy joints using Cu-foam/Sn composite solder foils. Journal of Advanced Joining Processes, 2022, 5, 100092.	1.5	0
64497	Anode-cathode interchangeable strategy for in situ reviving electrocatalystsâ€™ critical active sites for highly stable methanol upgrading and hydrogen evolution reactions. Applied Catalysis B: Environmental, 2022, 305, 121082.	10.8	21
64498	A novel tunable two dimensional ferroelectric material SbAs(CH2OCH3)2 with topological and valley polarized properties. Physica E: Low-Dimensional Systems and Nanostructures, 2022, 138, 115123.	1.3	1
64499	Phase-dependent catalytic performance of MnO2 for solvent-free oxidation of ethybenzene with molecular oxygen. Applied Catalysis B: Environmental, 2022, 305, 121050.	10.8	25
64500	First-principles-based multiscale modelling of heterogeneous CoO oxidation kinetics in high-temperature thermochemical energy storage. Fuel Processing Technology, 2022, 228, 107164.	3.7	7
64501	Visible-light-driven semihydrogenation of alkynes via proton reduction over carbon nitride supported nickel. Applied Catalysis B: Environmental, 2022, 304, 121004.	10.8	17
64502	Atomic Pd-promoted ZnZrO solid solution catalyst for CO2 hydrogenation to methanol. Applied Catalysis B: Environmental, 2022, 304, 120994.	10.8	59

#	Article	IF	Citations
64503	Dry reforming of methane on Ni(1 1 1) surface with different Mo doping ratio: DFT-assisted microkinetic study. Applied Surface Science, 2022, 581, 152310.	3.1	20
64504	Capture and recycling of toxic selenite anions by cobalt-based metal-organic-frameworks for electrocatalytic overall water splitting. Chemical Engineering Journal, 2022, 433, 134553.	6.6	16
64505	Insights into highly efficient photodegradation of poly/perfluoroalkyl substances by In-MOF/BiOF heterojunctions: Built-in electric field and strong surface adsorption. Applied Catalysis B: Environmental, 2022, 304, 121013.	10.8	32
64506	Unraveling the role of cobalt in the direct conversion of CO2 to high-yield liquid fuels and lube base oil. Applied Catalysis B: Environmental, 2022, 305, 121041.	10.8	19
64507	Confinement effect induced conformation change of one-dimensional phosphorus chains filled in carbon nanotubes. Carbon, 2022, 189, 467-473.	5.4	10
64508	Reducing the high hydrogen binding strength of vanadium carbide MXene with atomic Pt confinement for high activity toward HER. Applied Catalysis B: Environmental, 2022, 304, 120989.	10.8	58
64509	Ultrafine Co-MoS2 monolayer catalyst derived from oil-soluble single-molecule polyoxometalates for slurry phase hydrocracking. Fuel, 2022, 315, 123134.	3.4	11
64510	First-principles realistic prediction of gas adsorption on two-dimensional Vanadium Carbide (MXene). Applied Surface Science, 2022, 581, 152105.	3.1	26
64511	Nonmetal doped carbon nitride nanosheet as photocatalyst for degradation of 4, 5-dichloroguaiacol. Environmental Research, 2022, 207, 112623.	3.7	3
64512	Tailoring interphase structure to enable high-rate, durable sodium-ion battery cathode. Journal of Energy Chemistry, 2022, 68, 564-571.	7.1	22
64513	Site-selective doping mechanisms for the enhanced photocatalytic activity of tin oxide nanoparticles. Applied Catalysis B: Environmental, 2022, 305, 121083.	10.8	9
64514	A promising ZnO/Graphene van der Waals heterojunction as solar cell devices: A first-principles study. Energy Reports, 2022, 8, 904-910.	2.5	19
64515	Tuning the structural properties and chemical activities of graphene and hexagonal boron nitride for efficient adsorption of steroidal pollutants. Applied Surface Science, 2022, 580, 152110.	3.1	6
64516	Two-dimensional graphdiyne analogue containing Mo-coordinated porphyrin covalent organic framework as a high-performance electrocatalyst for nitrogen fixation. Applied Surface Science, 2022, 580, 152359.	3.1	12
64517	Different Active Sites of LaCoO3 and LaMnO3 for CH4 Oxidation by Regulation of Precursorâ€™s Ion Concentration. The Global Environmental Engineers, 0, 7, 28-39.	0.3	1
64521	Modeling Photocathode Performance Using MedeA-VASP Simulation Software. IEEE Transactions on Nuclear Science, 2020, 67, 1987-1992.	1.2	0
64524	A Cyclic Periodic Wave Function Approach for the Study of Infinitely Periodic Solid-State Systems. I. Application to the Câ€“HÂ·Â·Â·Ï€(Câ‰¡C) Hydrogen Bonding Systems. ACS Omega, 2020, 5, 27546-27555.	1.6	4
64525	Structural, Electronic and Mechanical Properties of Few-layer Porous Nanosheet from Spheroidal Cage-like ZnO Polymorph. VNU Journal of Science Mathematics - Physics, 2020, 36, .	0.0	0

#	Article	IF	Citations
64527	Development of a Cyclic Periodic Wave Function Approach for the Study of Infinitely Periodic Solid-State Systems. ACS Omega, 2020, 5, 31060-31068.	1.6	2
64528	Density-functional theory of material design: fundamentals and applications-I. Oxford Open Materials Science, 2020, 1, .	0.5	2
64529	Atomistic Insights on Hydrogen Plasma Treatment for Stabilizing High- k/Si Interface. SSRN Electronic Journal, 0, , .	0.4	0
64530	Computational design of materials for metal-ion batteries. , 2023, , 404-429.		4
64531	Chirality Distribution of Single-Walled Carbon Nanotubes Grown from Gold Nanoparticles. SSRN Electronic Journal, 0, , .	0.4	0
64532	Adsorption and Removal of Hazardous Metallic Elements Hg ⁰, Ni ⁰ and Pb ⁰: A DFT Study on g-C ₃N ₄ Monolayer Modified with Pt _n (n=1 - 7) Clusters. SSRN Electronic Journal, 0, , .	0.4	0
64533	Two-Dimensional Sc ₂CCl ₂/SiS ₂ Van Der Waals Heterostructure with High Solar Power Conversion Efficiency. SSRN Electronic Journal, 0, , .	0.4	0
64534	Stability of Low-index Surfaces of Cs₂SnI₆ Studied by First-principles Calculations. Wuji Cailiao Xuebao/Journal of Inorganic Materials, 2022, 37, 691.	0.6	2
64535	89Y chemical shift anisotropy: a sensitive structural probe of layered yttrium hydroxides revealed by solid-state NMR spectroscopy and DFT calculations. Physical Chemistry Chemical Physics, 2021, 23, 27244-27252.	1.3	3
64536	Effect of Hybridization in PdAlY-(Ni/Au/Ir) Metallic Glasses Thin Films on Electrical Resistivity. SSRN Electronic Journal, 0, , .	0.4	0
64537	The Intrinsic Effects of Oxygen Vacancy and Doped Non-Noble Metal in TiO ₂(B) on Photocatalytic Oxidation VOCs by Visible Light Driving. SSRN Electronic Journal, 0, , .	0.4	0
64538	No Adsorption on the Os, IR, and Pt Embedded Tri-S-Triazine Based Graphitic Carbon Nitride: A DFT Study. SSRN Electronic Journal, 0, , .	0.4	0
64539	Mo ₂CS ₂-Mxene Supported Single-Atom Catalysts for Efficient and Selective CO ₂ Electrochemical Reduction. SSRN Electronic Journal, 0, , .	0.4	0
64540	Infinite-layer/perovskite oxide heterostructure-induced high-spin states in SrCuO₂/SrRuO₃ bilayer films. Materials Horizons, 2021, 8, 3468-3476.	6.4	8
64541	Boosting nitrogen reduction on single Mo atom by tuning its coordination environment. Sustainable Energy and Fuels, 2021, 5, 6488-6497.	2.5	7
64542	Atomic structures of twin boundaries in CoO. Physical Chemistry Chemical Physics, 2021, 23, 25590-25596.	1.3	6
64543	Revealing Improved Electrocatalytic Performances of Electrochemically Synthesized S and Ni Doped Fe ₂O ₃ Nanostructure Interfaces. SSRN Electronic Journal, 0, , .	0.4	0
64544	Improvement of Thermoelectric Properties for Silicene by Hydrogenation Effect. SSRN Electronic Journal, 0, , .	0.4	0

#	Article	IF	Citations
64545	Computational Design of BC ₃N ₂ Based Single Atom Catalyst for Dramatic Activation of Inert CO ₂ and CH ₄ Gases into CH ₃COOH with Ultralow CH ₄ Dissociation Barrier. SSRN Electronic Journal, 0, , .	0.4	0
64546	Enhanced Photogenerated Hole Oxidation Capability in Photocatalysis Through Band Structure Modification. SSRN Electronic Journal, 0, , .	0.4	0
64547	Screening of Transition Metal Single-Atom Catalysts Doped on Î“-Graphyne-Like BN Sheet for Efficient Nitrogen Reduction Reaction. SSRN Electronic Journal, 0, , .	0.4	0
64548	High Thermoelectric Properties of Janus WSeS Bilayer Membranes with Different Stacking Modes. SSRN Electronic Journal, 0, , .	0.4	1
64549	A Density Functional Study of the Structural, Electronic and Optical Properties of a Novel Infrared Nonlinear Optical Crystal AgGaS ₂. SSRN Electronic Journal, 0, , .	0.4	0
64550	A Key Role of Soft and Refractory Coke in the Deactivation of Î³-Al ₂O ₃ Catalysts During Low-Temperature Methyl Oleate Epoxidation. SSRN Electronic Journal, 0, , .	0.4	0
64551	High Compositional Dependence of Activity of Platinumâ€“Dysprosium Alloys for Oxygen Reduction in Alkaline Media: Experimental and Theoretical Study. SSRN Electronic Journal, 0, , .	0.4	0
64552	Density Functional Study of Pure/Doped Sodium Borohydride Systems for Hydrogen Storage Applications. SSRN Electronic Journal, 0, , .	0.4	0
64553	The Half-Metallity Induced by Out-of-Plane Electric Field on Phosphorene Nanoribbons. SSRN Electronic Journal, 0, , .	0.4	0
64554	Constrained density functional theory plus the Hubbard U correction approach for the electronic polaron mobility: A case study of TiO₂. Chinese Journal of Chemical Physics, 2021, 34, 541-551.	0.6	1
64555	Interplay of Halogen and Weak Hydrogen Bonds in the Formation of Magic Nanoclusters on Surfaces. Journal of Physical Chemistry C, 2022, 126, 588-596.	1.5	7
64556	Degradation dynamics of quantum dots in white LED applications. Scientific Reports, 2021, 11, 24153.	1.6	4
64557	Understanding copper diffusion in CuInSe2 with first-principles based atomistic and continuum models. Journal of Applied Physics, 2021, 130, .	1.1	1
64558	Bandgap renormalization and indirect optical absorption in MgSiN2 at finite temperature. Journal of Applied Physics, 2021, 130, 225703.	1.1	1
64559	Catalytic and Sulfur-Tolerant Performance of Bimetallic Niâ€“Ru Catalysts on HI Decomposition in the Sulfur-Iodine Cycle for Hydrogen Production. Energies, 2021, 14, 8539.	1.6	0
64560	hcp-phased Ni nanoparticles with generic catalytic hydrogenation activities toward different functional groups. Science China Materials, 2022, 65, 1252-1261.	3.5	5
64561	A First-Principles Study of the Cu-Containing Î²â€³ Precipitates in Al-Mg-Si-Cu Alloy. Materials, 2021, 14, 7879.	1.3	2
64562	Machine-Learning Prediction of Vegard's Law Factor and Volume Size Factor for Binary Substitutional Metallic Solid Solutions. SSRN Electronic Journal, 0, , .	0.4	0

#	Article	IF	Citations
64563	Layer parity dependent Raman-active modes and crystal symmetry in <mml:math xmlns:mml="http://www.w3.org/1998/Math/MathML"><mml:msub><mml:mi mathvariant="normal">ReS</mml:mi><mml:mn>2</mml:mn></mml:msub></mml:math>. Physical Review B, 2022, 105, .	1.1	5
64564	Redox Hyperactive MOF for Li+, Na+ and Mg2+ Storage. Molecules, 2022, 27, 586.	1.7	2
64565	Two-dimensional Dirac semiconductor and its material realization. Physical Review B, 2022, 105, .	1.1	4
64566	Insight into the stacking and the species-ordering dependences of interlayer bonding in SiC/GeC polar heterostructures. Nanotechnology, 2022, 33, 155706.	1.3	5
64567	The Electronic and Optical Properties of Vertically Stacked GaN-WS2 Heterostructure. Journal Wuhan University of Technology, Materials Science Edition, 2022, 37, 28-31.	0.4	1
64568	Real-Time Reconstructed Interphase Enables Reversible Aqueous Zinc Battery Chemistries. SSRN Electronic Journal, 0, , .	0.4	0
64569	Effects of Defect on Work Function and Energy Alignment of PbI₂: Implications for Solar Cell Applications. Chemistry of Materials, 2022, 34, 1020-1029.	3.2	20
64570	Computational screening of single-atom alloys TM@Ru(0001) for enhanced electrochemical nitrogen reduction reaction. Journal of Materials Chemistry A, 2022, 10, 6204-6215.	5.2	33
64571	Growth of high-quality semiconducting tellurium films for high-performance p-channel field-effect transistors with wafer-scale uniformity. Npj 2D Materials and Applications, 2022, 6, .	3.9	25
64572	Enhanced Catalytic Activity of Boron Nitride Nanotubes by Encapsulation of Nickel Wire Toward O2 Activation and CO Oxidation: A Theoretical Study. Frontiers in Chemical Engineering, 2022, 3, .	1.3	1
64573	Ni²⁺-Doped Garnet Solid-Solution Phosphor-Converted Broadband Shortwave Infrared Light-Emitting Diodes toward Spectroscopy Application. ACS Applied Materials & Interfaces, 2022, 14, 4265-4275.	4.0	68
64574	Analysis of Guest Adsorption on Crystal Surfaces Based on the Fragment Molecular Orbital Method. Journal of Physical Chemistry A, 2022, 126, 957-969.	1.1	4
64575	Facet-Selective Dissociation and Radical-Mediated Reaction of Dibenzotetrathiafulvalene Molecules on Low-Index Copper Surfaces. Journal of Physical Chemistry C, 2022, 126, 1281-1288.	1.5	0
64576	Catalytic resonance of ammonia synthesis by simulated dynamic ruthenium crystal strain. Science Advances, 2022, 8, eabl6576.	4.7	24
64577	Understanding the Solid-State Electrodeâ€“Electrolyte Interface of a Model System Using First-Principles Statistical Mechanics and Thin-Film X-ray Characterization. ACS Applied Materials & Interfaces, 2022, 14, 7428-7439.	4.0	1
64578	Exceptional Thermoelectric Properties of Bilayer GeSe: First Principles Calculation. Materials, 2022, 15, 971.	1.3	6
64579	Ultrathin MoS_{1.68}Se_{0.32} Alloy Nanoflakes: An Intercalation-Type Positive Electrode Material for Rechargeable Aluminum-Ion Battery. Journal of Physical Chemistry C, 2022, 126, 2679-2688.	1.5	6
64580	A Microporous Metalâ€“Organic Framework Incorporating Both Primary and Secondary Building Units for Splitting Alkane Isomers. Journal of the American Chemical Society, 2022, 144, 3766-3770.	6.6	36

#	Article	IF	Citations
64581	High activity of step sites on Pd nanocatalysts in electrocatalytic dechlorination. Physical Chemistry Chemical Physics, 2022, 24, 3896-3904.	1.3	10
64582	The synergetic effect of an aqua ligand and metal site on the performance of single-atom catalysts in H2O2 synthesis: a density functional theory study. Physical Chemistry Chemical Physics, 2022, 24, 3905-3917.	1.3	1
64583	New insights into the key bifunctional role of sulfur in Feâ€“Nâ€“C single-atom catalysts for ORR/OER. Nanoscale, 2022, 14, 3212-3223.	2.8	32
64584	The role of Hâ€“H interactions and impurities on the structure and energetics of H/Pd(111). Journal of Chemical Physics, 2022, 156, 044707.	1.2	3
64585	Ba₆(Cu_xZ_y)Sn₄S₁₆ (Z = Mg,) Tj ETQq0 0 0 rgBT /Overlo Inorganic Chemistry, 2022, 61, 2640-2651.	1.9	7
64586	Two-dimensional CdS/SnS₂ heterostructure: a highly efficient direct Z-scheme water splitting photocatalyst. Physical Chemistry Chemical Physics, 2022, 24, 3826-3833.	1.3	18
64587	The Adsorption of Small Molecules on the Copper Paddle-Wheel: Influence of the Multi-Reference Ground State. Molecules, 2022, 27, 912.	1.7	2
64588	A Robust Approach to In Situ Exsolve Highly Dispersed and Stable Electrocatalysts. Small, 2022, 18, e2105741.	5.2	2
64589	Epitaxial Growth of Highâ€Energy Copper Facets for Promoting Hydrogen Evolution Reaction. Small, 2022, 18, e2107481.	5.2	9
64590	Role of Mn-substitution towards the enhanced hydrogen storage performance in FeTi. International Journal of Hydrogen Energy, 2022, 47, 9357-9371.	3.8	4
64591	La@[La5&B30]0/â^'/2â^': endohedral trihedral metallo-borospherenes with spherical aromaticity. Physical Chemistry Chemical Physics, 2022, 24, 3918-3923.	1.3	4
64592	Building a stabilized structure from surface to bulk of Ni-rich cathode for enhanced electrochemical performance. Energy Storage Materials, 2022, 47, 87-97.	9.5	22
64593	Catalytic reduction of 4-nitrophenol using CuO@Na₂Ti(PO₄)₂â‹…H₂O. Journal of Environmental Science and Health - Part A Toxic/Hazardous Substances and Environmental Engineering, 2022, 57, 65-79.	0.9	3
64594	Prediction of new phase 2DC_{2h}group III monochalcogenides with direct bandgaps and highly anisotropic carrier mobilities. Materials Advances, 2022, 3, 2213-2221.	2.6	7
64595	Compression-induced charge disproportionation in the orthorhombic NaTaO$$_{3}$$ (100) monolayer: Structural, electronic, and magnetic transitions. Journal of Materials Research, 2022, 37, 490-499.	1.2	2
64596	Fast Hydride-Ion Conduction in Perovskite Hydrides AELiH₃. ACS Applied Energy Materials, 2022, 5, 2968-2974.	2.5	10
64597	The Thermal and Electronic Properties of the Lateral Janus MoSSe/WSSe Heterostructure. Frontiers in Materials, 2022, 9, .	1.2	9
64598	Negative Piezoelectric Coefficient in Ferromagnetic 1H-LaBr₂ Monolayer. ACS Applied Electronic Materials, 2022, 4, 850-855.	2.0	9

#	Article	IF	Citations
64599	Electron Regulation of Single Indium Atoms at the Active Oxygen Vacancy of In 2 O 3 (110) for Production of Acetic Acid and Acetone through Direct Coupling of CH 4 with CO 2. Chemistry - an Asian Journal, 2022, , e202101383.	1.7	3
64600	Trigonal-to-monoclinic structural transition in <mml:math xmlns:mml="http://www.w3.org/1998/Math/MathML"><mml:msub><mml:mi>TiSe</mml:mi><mml:mn>2</mml:mn></mml:msub></m due to a combined condensation of <mml:math xmlns:mml="http://www.w3.org/1998/Math/MathML"><mml:mrow><mml:mi>q</mml:mi><mml:mo>=</mml:mo><mml:mo>(</mml:m	0.9	6
64601	Hexagonal-to-base-centered-orthorhombic <mml:math xmlns:mml="http://www.w3.org/1998/Math/MathML"><mml:mrow><mml:mn>4</mml:mn><mml:mi>Q</mml:mi></mml:mrow></mml: charge density wave order in kagome metals <mml:math xmlns:mml="http://www.w3.org/1998/Math/MathML"><mml:mrow><mml:msub><mml:mi>KV</mml:mi><mml:mn>3</mml:mn></mml: <mml:math xmlns:mml="http://www.w3.org/1998/Math/MathML"><mml:mrow><mml:ms. Physical Review Materials, 2022, 6, .	0.9	22
64602	The effect of oxygen impurities on the stability and structural properties of vacancy-ordered and -disordered ZrC_x. RSC Advances, 2022, 12, 3198-3215.	1.7	5
64603	Iridium boosts the selectivity and stability of cobalt catalysts for syngas to liquid fuels. CheM, 2022, 8, 1050-1066.	5.8	26
64604	Giant room temperature compression and bending in ferroelectric oxide pillars. Nature Communications, 2022, 13, 335.	5.8	14
64605	Orbital-selective Mott phase and non-Fermi liquid in <mml:math xmlns:mml="http://www.w3.org/1998/Math/MathML"><mml:msub><mml:mrow><mml:mi>FePS</mml:mi></mml:mrow><mml:mn>3</m Physical Review B, 2022, 105, .	1.1	4
64606	Electronic and optical properties of SixGe1â^'xâ^'ySny alloys lattice-matched to Ge. Physical Review Materials, 2022, 6, .	0.9	4
64607	Dispersion interactions in proposed covalent superhydride superconductors. Physical Review B, 2022, 105, .	1.1	2
64608	Copper nanowire with enriched highâ€index facets for highly selective CO₂ reduction. SmartMat, 2022, 3, 142-150.	6.4	19
64609	A study on the evolution of ï‰-phase in Zr-20Nb alloy under the influence of electron irradiation. Journal of Alloys and Compounds, 2022, 904, 163968.	2.8	3
64610	Prediction of semiconducting ferromagnetic CrVI(6) monolayer. Europhysics Letters, 0, , .	0.7	0
64611	Highly stable electronic properties of rippled antimonene under compressive deformation. Physical Review B, 2022, 105, .	1.1	5
64612	Strainâ€induced tunable energy barrier of proton diffusion in Yâ€doped <scp> BaCeO ₃ </scp> and Yâ€doped <scp> BaZrO ₃ </scp>. International Journal of Energy Research, 2022, 46, 7816-7824.	2.2	5
64613	Study on the electronic band structure of ZnOâ€“SnO2 heterostructured nanocomposites with mechanistic investigation on the enhanced photoluminescence and photocatalytic properties. Journal of Materials Science: Materials in Electronics, 2022, 33, 9599-9615.	1.1	2
64614	Synergistic Electronic and Pore Structure Modulation in Open Carbon Nanocages Enabling Efficient Electrocatalytic Production of H₂O₂ in Acidic Medium. Advanced Functional Materials, 2022, 32, .	7.8	33
64615	A comparison study of the structural, electronic and mechanical properties of the pure pyrite FeS2 and oxygen doped pyrite FeO0.25S1.75 under pressure range from 0 to 25â€¯GPa. Physica B: Condensed Matter, 2022, , 413710.	1.3	1
64616	Surface Phosphatization for a Sawdustâ€Derived Carbon Catalyst as Kinetics Promoter and Corrosion Preventer in Lithiumâ€“Oxygen Batteries. Advanced Functional Materials, 2022, 32, .	7.8	21

#	Article	IF	Citations
64617	Electronic properties of graphene oxide: nanoroads towards novel applications. Nanoscale, 2022, 14, 4131-4144.	2.8	3
64618	CO Oxidation with Atomically Dispersed Catalysts: Insights from the Energetic Span Model. ACS Catalysis, 2022, 12, 2064-2076.	5.5	11
64619	Engineering V₂O₃ nanoarrays with abundant localized defects towards high-voltage aqueous supercapacitors. Journal of Materials Chemistry A, 2022, 10, 4825-4832.	5.2	6
64620	Efficient parametrization of the atomic cluster expansion. Physical Review Materials, 2022, 6, .	0.9	23
64621	Orderâ€“Disorder Competitive Cooperation in EquiatomicÂ3dâ€“Transitionâ€“Metal Quaternary Alloys: Phase Stability and Electronic Structure. SSRN Electronic Journal, 0, , .	0.4	1
64622	Lanthanum-doped SrTiO3 theoretical thermoelectric properties. Ionics, 0, , 1.	1.2	3
64623	Understanding Adsorption of Organics on Pt(111) in the Aqueous Phase: Insights from DFT Based Implicit Solvent and Statistical Thermodynamics Models. Journal of Chemical Theory and Computation, 2022, 18, 1849-1861.	2.3	7
64624	p-Type Semiconduction in Oxides with Cation Lone Pairs. Chemistry of Materials, 2022, 34, 643-651.	3.2	12
64625	High-Pressure Synthesis of Polar and Antiferromagnetic Mn₂MnMoO₆. Chemistry of Materials, 2022, 34, 1930-1936.	3.2	3
64626	Ab Initio Investigation of Planar Defects in Immm-Ni ₂(Cr,Mo,W) Strengthened HAYNES 244 Alloy. SSRN Electronic Journal, 0, , .	0.4	0
64627	Thermal behavior and polymorphism of 2,9-didecyldinaphtho[2,3-b:2â€²,3â€²-f]thieno[3,2-b]thiophene thin films. Molecular Systems Design and Engineering, 2022, 7, 507-519.	1.7	6
64628	Unveiling the layer-dependent electronic properties in transition-metal dichalcogenide heterostructures assisted by machine learning. Nanoscale, 2022, 14, 2511-2520.	2.8	6
64629	Experimental and theoretical investigation of the tuning of electronic structure in SnO₂viaCo doping for enhanced styrene epoxidation catalysis. Catalysis Science and Technology, 2022, 12, 1499-1511.	2.1	13
64630	Highly dispersed Ru nanoclusters anchored on B,N co-doped carbon nanotubes for water splitting. Inorganic Chemistry Frontiers, 2022, 9, 968-976.	3.0	15
64631	Preparation of ultrahigh thermally conductive materials of graphene composites by electrophoresis on carbon fiber. Journal of Materials Science, 2022, 57, 4210-4220.	1.7	4
64632	Electronic Structure of Zinc-5,10,15,20-tetraethynylporphyrin: Evolution from the Molecule to a One-Dimensional Chain, a Two-Dimensional Covalent Organic Framework, and a Nanotube. Chemistry of Materials, 2022, 34, 1334-1341.	3.2	10
64633	Wavelength-Specific Product Desorption as a Key to Raising Nitrile Yield of Primary Alcohol Ammoxidation over Illuminated Pd Nanoparticles. ACS Catalysis, 2022, 12, 2280-2289.	5.5	17
64634	Evolution from helical to collinear ferromagnetic order of the Eu2+ spins in RbEu(Fe1â^'xNix)4As4. Physical Review Research, 2022, 4, .	1.3	3

#	Article	IF	Citations
64635	Reshaped Weyl fermionic dispersions driven by Coulomb interactions in<mml:math xmlns:mml="http://www.w3.org/1998/Math/MathML"><mml:msub><mml:mi>MoTe</mml:mi><mml:mn>2</mml:mn></mml:msub></m Physical Review B, 2022, 105, .	1.1	4
64636	Plasma-induced transformation: a new strategy to in situ engineer MOF-derived heterointerface for high-efficiency electrochemical hydrogen evolution. Journal of Materials Chemistry A, 2022, 10, 6596-6606.	5.2	6
64637	From Cc to P6₃mc: Structural Variation in La₃S₂Cl₂[SbS₃] and La₃OSCl₂[SbS₃] Induced by the Isovalent Anion Substitution. Crystal Growth and Design, 2022, 22, 1437-1444.	1.4	8
64638	An ab initio study of size-selected Pd nanocluster catalysts for the hydrogenation of 1-pentyne. Physical Chemistry Chemical Physics, 2022, 24, 3231-3237.	1.3	1
64639	A polyoxometalate cluster-based single-atom catalyst for NH₃ synthesis via an enzymatic mechanism. Journal of Materials Chemistry A, 2022, 10, 6165-6177.	5.2	23
64640	DFT Investigation of Ammonia Formation via a Langmuirâ€“Hinshelwood Mechanism on Mo-Terminated Î´-MoN(0001). ACS Omega, 2022, 7, 4277-4285.	1.6	3
64641	First-Principles Plane-Wave-Based Exploration of Cathode and Anode Materials for Li- and Na-Ion Batteries Involving Complex Nitrogen-Based Anions. Chemistry of Materials, 2022, 34, 652-668.	3.2	9
64642	Phase Evolution, Polymorphism, and Catalytic Activity of Nickel Dichalcogenide Nanocrystals. Chemistry of Materials, 2022, 34, 746-755.	3.2	6
64643	DFT study of NH3 adsorption on 2D monolayer MXenes (M2C, MÂ=ÂCr, Fe) via oxygen functionalization: Suitable materials for gas sensors. FlatChem, 2022, 31, 100329.	2.8	22
64644	Structural phase transition of BiSb and formation of Weyl semimetallic phase under pressure: calculations and experiments. Journal of Materials Chemistry C, 2022, 10, 3531-3537.	2.7	4
64645	Direct observation of hydrogen permeation through grain boundaries in tungsten. Emergent Materials, 2022, 5, 1075-1087.	3.2	6
64646	Theoretical design of transition metal-doped TiO₂ for the selective catalytic reduction of NO with NH₃ by DFT calculations. Catalysis Science and Technology, 2022, 12, 1429-1440.	2.1	5
64647	In situ neutron diffraction unravels deformation mechanisms of a strong and ductile FeCrNi medium entropy alloy. Journal of Materials Science and Technology, 2022, 116, 103-120.	5.6	16
64648	Anisotropic super-hardness of hexagonal WB₂Â±z</sub> thin films. Materials Research Letters, 2022, 10, 70-77.	4.1	21
64649	Short-range magnetic interaction in a monolayer <mml:math xmlns:mml="http://www.w3.org/1998/Math/MathML"><mml:mrow><mml:mn>1</mml:mn><mml:mi>T</mml:mi><mml:mtext>â^'</mm film revealed by element-specific x-ray magnetic circular dichroism. Physical Review Materials, 2022, 6, .	0.9	5
64650	Metalâ€“free C2N doped with sp2â€“hybridized B atom as highâ€“efficiency photocatalyst for nitrobenzene reduction reaction: A density functional theory study. Molecular Catalysis, 2022, 518, 112080.	1.0	3
64651	P-doped melon-carbon nitride for efficient photocatalytic H2O2 production. Journal of Colloid and Interface Science, 2022, 615, 87-94.	5.0	24
64652	Disclosing the response of the surface electronic structure in SrTiO3 (001) to strain. Journal of Vacuum Science and Technology A: Vacuum, Surfaces and Films, 2022, 40, .	0.9	6

#	Article	IF	Citations
64653	Electronic and magnetic properties of quasi-one-dimensional osmium halide OsCl4. Applied Physics Letters, 2022, 120, 023101.	1.5	6
64654	Two-dimensional ferroelasticity and negative Poisson's ratios in monolayer YbX (X = S, Se, Te). Physical Chemistry Chemical Physics, 2022, 24, 2203-2208.	1.3	5
64655	Mechanistic Insight and Local Structure Evolution of NiPS₃ upon Electrochemical Lithiation. ACS Applied Materials & Interfaces, 2022, 14, 3980-3990.	4.0	9
64656	An ab initio study of two-dimensional anisotropic monolayers ScXY (X = S and Se; Y = Cl and Br) for photocatalytic water splitting applications with high carrier mobilities. Physical Chemistry Chemical Physics, 2022, 24, 3770-3779.	1.3	11
64657	Understanding zinc-doped hydroxyapatite structures using first-principles calculations and convolutional neural network algorithm. Journal of Materials Chemistry B, 2022, 10, 1281-1290.	2.9	7
64658	Structural dynamics of Schottky and Frenkel defects in ThO₂: a density-functional theory study. Journal of Materials Chemistry A, 2022, 10, 1861-1875.	5.2	9
64659	Sodiumâ€rich <scp>NASICON</scp>â€structured cathodes for boosting the energy density and lifespan of sodiumâ€freeâ€anode sodium metal batteries. InformaÄnÃ-MateriÃ¡ly, 2022, 4, .	8.5	41
64660	Spin-Orbit Coupling and Spin-Polarized Electronic Structures of Janus Vanadium-Dichalcogenide Monolayers: First-Principles Calculations. Nanomaterials, 2022, 12, 382.	1.9	10
64661	Electronic structure and physical properties of EuAuAs single crystal. Physical Review B, 2022, 105, .	1.1	10
64662	Heat Conduction Theory Including Phonon Coherence. Physical Review Letters, 2022, 128, 015901.	2.9	35
64663	Effects of the incorporation amounts of CdS and Cd(SCN2H4)2Cl2 on the performance of perovskite solar cells. International Journal of Minerals, Metallurgy and Materials, 2022, 29, 283-291.	2.4	16
64664	On the ab initio Calculations within DFT + U Approach of Physical Properties of a Compound with Strong Electron-electron Correlations by the Case of KFeS2. JETP Letters, 2022, 115, 98.	0.4	2
64665	Predicting Lithium Iron Oxysulfides for Battery Cathodes. ACS Applied Energy Materials, 2022, 5, 575-584.	2.5	6
64666	Temperature-Responsive Photoluminescence and Elastic Properties of 1D Lead Halide Perovskites R- and S-(Methylbenzylamine)PbBr3. Molecules, 2022, 27, 728.	1.7	5
64667	A Modeling and Neutron Diffraction Study of the High Temperature Properties of Sub-Stoichiometric Yttrium Hydride for Novel Moderator Applications. Metals, 2022, 12, 199.	1.0	2
64668	Superhard metallic compound <mml:math xmlns:mml="http://www.w3.org/1998/Math/MathML"><mml:msub><mml:mi>TaB</mml:mi><mml:mn>2</mml:mn></mml:msub></m via crystal orientation resolved strain stiffening. Physical Review B, 2022, 105, .	1.1	7
64669	Deep learning-driven molecular dynamics simulations of molten carbonates: 1. Local structure and transport properties of molten Li2CO3-Na2CO3 system. Ionics, 2022, 28, 1231-1248.	1.2	12
64670	Pressure-Induced Increase of the Total Magnetic Moment in Ferrimagnetic Ni_{1.9375}Mn_{1.5625}Sn_{0.5} Martensite: A Quantum-Mechanical Study. Materials Transactions, 2022, 63, 430-435.	0.4	6

#	Article	IF	Citations
64671	Stability of hypothetical AgIICl2 polymorphs under high pressure, revisited: a computational study. Scientific Reports, 2022, 12, 1153.	1.6	1
64672	Identifying the positive role of lithium hydride in stabilizing Li metal anodes. Science Advances, 2022, 8, eabl8245.	4.7	29
64673	All-perovskite tandem solar cells with improved grain surface passivation. Nature, 2022, 603, 73-78.	13.7	544
64674	Investigation of 2D Boridene from First Principles and Experiments. Advanced Functional Materials, 2022, 32, .	7.8	31
64675	Effects of oxygen vacancies on the photoexcited carrier lifetime in rutile TiO₂. Physical Chemistry Chemical Physics, 2022, 24, 4743-4750.	1.3	8
64676	Oxygen Vacancies of Commercial V₂O₅ Induced by Mechanical Force to Enhance the Diffusion of Zinc Ions in Aqueous Zinc Battery. Batteries and Supercaps, 2022, 5, .	2.4	19
64677	The anti-corrosive behavior of benzo-fused N-heterocycles: an in silico study toward developing organic corrosion inhibitors. Physical Chemistry Chemical Physics, 2022, 24, 743-756.	1.3	17
64678	Coexistence of intrinsic room-temperature ferromagnetism and piezoelectricity in monolayer BiCrX₃ (X = S, Se, and Te). Physical Chemistry Chemical Physics, 2022, 24, 1091-1098.	1.3	10
64679	Defect-related luminescence behavior of a Mn⁴⁺ non-equivalently doped fluoroantimonate red phosphor. Dalton Transactions, 2022, 51, 608-617.	1.6	9
64680	Electronic and Vibrational Properties of Feâ„NiAl and Coâ„NiAl Full Heusler Alloys: A First-Principles Comparison. IEEE Transactions on Magnetics, 2022, 58, 1-5.	1.2	0
64681	Dynamic structural transformation induced by defects in nano-rod FeOOH during electrochemical water splitting. Journal of Materials Chemistry A, 2022, 10, 602-610.	5.2	18
64682	Adsorption and dissociation of diatomic molecules on monolayer <mml:math xmlns:mml="http://www.w3.org/1998/Math/MathML"><mml:mrow><mml:mn>1</mml:mn><mml:mi>H</mml:mi></mml:mrow><mml:m Physical Review B, 2022, 105, .	1.1	3
64683	Orbital-selective behavior in cubanite <mml:math xmlns:mml="http://www.w3.org/1998/Math/MathML"><mml:msub><mml:mi mathvariant="normal">CuFe</mml:mi><mml:mn>2</mml:mn></mml:msub><mml:msub><mml:mi mathvariant="normal">S</mml:mi><mml:mn>3</mml:mn></mml:msub></mml:math>. Physical Review B, 2022, 105, .	1.1	1
64684	Engineering of atomic-scale flexoelectricity at grain boundaries. Nature Communications, 2022, 13, 216.	5.8	14
64685	Thermodynamics Modeling for Actinide Monocarbides and Mononitrides from First Principles. Applied Sciences (Switzerland), 2022, 12, 728.	1.3	5
64686	Two-dimensional metalâ€“organic framework Mo₃(C₂O)₁₂ as a promising single-atom catalyst for selective nitrogen-to-ammonia conversion. Journal of Materials Chemistry A, 2022, 10, 4731-4738.	5.2	20
64687	Revealing buckling of an apparently flat monolayer of NaCl on Pt(111). Physical Review B, 2022, 105, .	1.1	1
64688	Effect of lattice strain on magnetism in epitaxial YCrO₃ films. Materials Research Letters, 2022, 10, 29-35.	4.1	5

#	Article	IF	Citations
64689	Disorder-Induced Ordering in Gallium Oxide Polymorphs. Physical Review Letters, 2022, 128, 015704.	2.9	36
64690	First Principles Study of Regulation of Monolayer ZnO and Vacancy Defects Equibiaxial Strain. Journal of Superconductivity and Novel Magnetism, 2022, 35, 925-934.	0.8	2
64691	High-Pressure Structures and Superconductivity of Barium Iodide. Materials, 2022, 15, 522.	1.3	1
64692	Insight into enhanced hydrogen evolution of single-atom Cu1/TiO2 catalysts from first principles. International Journal of Hydrogen Energy, 2022, 47, 4653-4661.	3.8	15
64693	A DFT study of Se_nTe_n clusters. Nanoscale Advances, 2022, 4, 1464-1482.	2.2	3
64694	Effect of Iodine Octahedral Rotations on Dipole Ordering in Organicâ€“Inorganic Hybrid Perovskite CH3NH3PbI3. Journal of Physical Chemistry C, 2022, 126, 779-785.	1.5	2
64695	Study of Ruthenium-Contamination Effect on Oxygen Reduction Activity of Platinum-Based PEMFC and DMFC Cathode Catalyst. Journal of the Electrochemical Society, 2022, 169, 014517.	1.3	3
64696	Finite-temperature force constants are essential for accurately predicting the thermal conductivity of rutile <mml:math xmlns:mml="http://www.w3.org/1998/Math/MathML"><mml:msub><mml:mi mathvariant="normal">TiO</mml:mi><mml:mn>2</mml:mn></mml:msub></mml:math>. Physical Review Materials, 2022, 6, .	0.9	3
64697	Attaining Low Lattice Thermal Conductivity in Half-Heusler Sublattice Solid Solutions: Which Substitution Site Is Most Effective?. Electronic Materials, 2022, 3, 1-14.	0.9	1
64698	Design high-entropy carbide ceramics from machine learning. Npj Computational Materials, 2022, 8, .	3.5	37
64699	Novel trigonal BC11 as model structure of heavily-doped diamond: Crystal chemistry rationale and first principles characterizations. Diamond and Related Materials, 2022, 123, 108842.	1.8	2
64700	Facet-dependent carrier dynamics of cuprous oxide regulating the photocatalytic hydrogen generation. Materials Advances, 2022, 3, 2200-2212.	2.6	15
64701	Enhancing Electron Emission of Hf with an Ultralow Work Function by Bariumâ€“Oxygen Coatings. Journal of Physical Chemistry C, 2022, 126, 2806-2812.	1.5	2
64702	Tunable magnetic order in two-dimensional layered GdGe₂. Journal of Materials Chemistry C, 2022, 10, 1259-1269.	2.7	9
64703	Predicting elastic properties of hard-coating alloys using ab-initio and machine learning methods. Npj Computational Materials, 2022, 8, .	3.5	16
64704	Anti-Ferromagnetic RuO₂: A Stable and Robust OER Catalyst over a Large Range of Surface Terminations. Journal of Physical Chemistry C, 2022, 126, 1337-1345.	1.5	21
64705	Atomistic insight into the formation dynamics of charged point defects: A classical molecular dynamics study of F+ -centers in NaCl. Physical Review Materials, 2022, 6, .	0.9	1
64706	Exploring the Effect of Cation Vacancies in TiO₂: Lithiation Behavior of n-Type and p-Type TiO₂. ACS Applied Materials & Interfaces, 2022, 14, 6560-6569.	4.0	24

#	Article	IF	Citations
64707	Clarification of the relative magnitude of exciton binding energies in ZnO and SnO2. Applied Physics Letters, 2022, 120, .	1.5	8
64708	Two â€˜braking mechanismsâ€™ for tin phthalocyanine molecular rotors on dipolar iron oxide surfaces. Nanoscale Advances, 0, , .	2.2	1
64709	Novel Two-Dimensional ABX₃ Dirac Materials: Achieving a High-Speed Strain Sensor via a Self-Doping Effect. Journal of Physical Chemistry Letters, 2022, 13, 676-685.	2.1	5
64710	Interfacial Chemistry Triggers Ultrafast Radiative Recombination in Metal Halide Perovskites. Angewandte Chemie, 2022, 134, .	1.6	1
64711	Pressure-stabilized hexafluorides of first-row transition metals. Physical Chemistry Chemical Physics, 2022, 24, 1736-1742.	1.3	4
64712	Composition optimization, high-temperature stability, and thermal cycling performance of Sc-doped Gd2Zr2O7 thermal barrier coatings: Theoretical and experimental studies. Journal of Advanced Ceramics, 2022, 11, 454-469.	8.9	42
64713	Sulfur/Nitrogen Coâ€Doped Inâ€Plane Porous Carbon Nanosheets as Superior Anode of Potassiumâ€Ion Batteries. Batteries and Supercaps, 2022, 5, .	2.4	4
64714	Superconductivity in In₂Te₃ under Compression Induced by Electronic and Structural Phase Transitions. Journal of Physical Chemistry Letters, 2022, 13, 1226-1233.	2.1	7
64715	Proton sponge promotion of electrochemical CO2 reduction to multi-carbon products. Joule, 2022, 6, 205-220.	11.7	57
64716	Revisiting catalytic performance of supported metal dimers for oxygen reduction reaction via magnetic coupling from first principles. , 2022, 1, 100031.		31
64717	Ionic Control over Ferroelectricity in 2D Layered van der Waals Capacitors. ACS Applied Materials & Interfaces, 2022, 14, 3018-3026.	4.0	16
64718	Pressure-stabilized high-energy-density material YN₁₀. Journal of Physics Condensed Matter, 2022, 34, 135403.	0.7	5
64719	A metallic Cu₂N monolayer with planar tetracoordinated nitrogen as a promising catalyst for CO₂ electroreduction. Journal of Materials Chemistry A, 2022, 10, 1560-1568.	5.2	13
64720	Room Temperature Cmcm Phase of CaxSn1â€“xSe for Thermoelectric Energy Conversion. ACS Applied Energy Materials, 0, , .	2.5	2
64721	Investigation of anisotropic mechanical, electronic, and charge carrier transport properties of germanium-pnictogen monolayers. Journal Physics D: Applied Physics, 2022, 55, 185302.	1.3	11
64722	The surface phase structure evolution of the fcc MoC (001) surface in a steam reforming atmosphere: systematic kinetic and thermodynamic investigations. Catalysis Science and Technology, 0, , .	2.1	1
64723	Pressure-induced structure, elasticity, intrinsic hardness and ideal strength of tetragonal C₄N. Physical Chemistry Chemical Physics, 2022, 24, 5171-5184.	1.3	5
64724	An Easy, Simple, and Accessible Web-based Machine Learning Platform, SimPL-ML. Integrating Materials and Manufacturing Innovation, 2022, 11, 85.	1.2	0

#	Article	IF	Citations
64725	Designing two-dimensional dodecagonal boron nitride. CrystEngComm, 2022, 24, 471-474.	1.3	7
64726	A Firstâ€Principles Study of CO₂ Hydrogenation on a Niobiumâ€Terminated NbC (111) Surface. ChemPhysChem, 2022, 23, .	1.0	7
64727	<mml:math xmlns:mml="http://www.w3.org/1998/Math/MathML"><mml:mrow><mml:mn>1</mml:mn><mml:mo>/</mml:mo><mml:mi>ï‰</mml:m electric-field noise in surface ion traps from correlated adsorbate dynamics. Physical Review A, 2022, 105, .	1.0	2
64728	Effects of Cr/Ni ratio on physical properties of Cr-Mn-Fe-Co-Ni high-entropy alloys. Acta Materialia, 2022, 227, 117693.	3.8	47
64729	Insight into the Adsorption Structure of TIPS-Pentacene on Noble Metal Surfaces. Journal of Physical Chemistry C, 2022, 126, 2689-2698.	1.5	0
64730	Direct Observation of Orbital Driven Strong Interlayer Coupling in Puckered Twoâ€Dimensional PdSe 2. Small, 2022, , 2106053.	5.2	6
64731	Pressure-induced bandgap engineering and photoresponse enhancement of wurtzite CuInS₂ nanocrystals. Nanoscale, 2022, 14, 2668-2675.	2.8	5
64732	Nickel Quantum Dots Anchored in Biomassâ€Derived Nitrogenâ€Doped Carbon as Bifunctional Electrocatalysts for Overall Water Splitting. Advanced Materials Interfaces, 2022, 9, .	1.9	7
64733	Inverse Materials Design of Doping Strategies with AI, Thermodynamics, and Density Functional Theory. Jom, 2022, 74, 405-413.	0.9	0
64734	Molecular Engineering in Perovskite Solar Cells: A Computational Study on 2â€Mercaptopyridine Derivatives as Surface Passivators against Water. Advanced Materials Interfaces, 2022, 9, .	1.9	11
64735	Modulating the Ferroelectricity of Hafnium Zirconium Oxide Ultrathin Films via Interface Engineering to Control the Oxygen Vacancy Distribution. Advanced Materials Interfaces, 2022, 9, .	1.9	10
64736	Experimental and first-principles studies on superconductivity in noncentrosymmetric <mml:math xmlns:mml="http://www.w3.org/1998/Math/MathML"><mml:msub><mml:mrow><mml:mi>La</mml:mi></mml:mrow><mml:mn>3</mml:mn> Physical Review B, 2022, 105, .	1.1	4
64737	Enormous Berry-Curvature-Based Anomalous Hall Effect in Topological Insulator (Bi,Sb)₂Te₃ on Ferrimagnetic Europium Iron Garnet beyond 400 K. ACS Nano, 2022, 16, 2369-2380.	7.3	6
64738	A facile surface alloy-engineering route to enable robust lithium metal anodes. Physical Chemistry Chemical Physics, 2022, 24, 4751-4758.	1.3	8
64739	Highly Conjugated Graphitic Carbon Nitride Nanofoam for Photocatalytic Hydrogen Evolution. Langmuir, 2022, 38, 1471-1478.	1.6	7
64740	A multiferroic vanadium phosphide monolayer with ferromagnetic half-metallicity and topological Dirac states. Nanoscale Horizons, 2022, 7, 192-197.	4.1	11
64741	First-Principles DFT Insights into the Stabilization of Zinc Diphosphide (ZnP2) Nanocrystals via Surface Functionalization by 4-Aminothiophenol for Photovoltaic Applications. ACS Applied Energy Materials, 0, , .	2.5	0
64742	Wrinkled and flexible N-doped MXene additive for improving the mechanical and electrochemical properties of the nickel-rich LiNi0.8Co0.1Mn0.1O2 cathode. Electrochimica Acta, 2022, 410, 139989.	2.6	6

#	Article	IF	Citations
64743	Development and application of ReaxFF methodology for understanding the chemical dynamics of metal carbonates in aqueous solutions. Physical Chemistry Chemical Physics, 2022, 24, 3322-3337.	1.3	12
64744	Phase stability and sodium-vacancy orderings in a NaSICON electrode. Journal of Materials Chemistry A, 2021, 10, 209-217.	5.2	24
64745	Failure mechanism of solid-state electrolyte Li₁₀GeP₂S₁₂ in a moist atmosphere: a first-principles study. Materials Advances, 2022, 3, 3143-3150.	2.6	7
64746	Computational and experimental characterizations of annealed Cu2ZnSnS4 thin films. Heliyon, 2022, 8, e08683.	1.4	24
64747	Twofold van Hove singularity and origin of charge order in topological kagome superconductor CsV3Sb5. Nature Physics, 2022, 18, 301-308.	6.5	176
64748	Interface engineering of heterogeneous transition metal chalcogenides for electrocatalytic hydrogen evolution. Nanoscale Advances, 2022, 4, 865-870.	2.2	8
64749	Chiral Hybrid Copper(I) Halides for High Efficiency Second Harmonic Generation with a Broadband Transparency Window. Angewandte Chemie, 0, , .	1.6	7
64750	Surprisingly Low Reactivity of Layered Manganese Oxide toward Water Oxidation in Fe/Ni-Free Electrolyte under Alkaline Conditions. Inorganic Chemistry, 2022, 61, 2292-2306.	1.9	21
64751	Î³-BaB₂O₄: High-Pressure High-Temperature Polymorph of Barium Borate with Edge-Sharing BO₄ Tetrahedra. Inorganic Chemistry, 2022, 61, 2340-2350.	1.9	7
64752	A Synergistic Effect of Na⁺ and Al³⁺ Dual Doping on Electrochemical Performance and Structural Stability of LiNi_{0.88}Co_{0.08}Mn_{0.04}O₂ Cathodes for Li-Ion Batteries. ACS Applied Materials & Interfaces, 2022, 14, 5168-5176.	4.0	44
64753	First-principles study of point defects in U₃Si₂: effects on the mechanical and electronic properties. Physical Chemistry Chemical Physics, 2022, 24, 4287-4297.	1.3	7
64754	Novel Two-Dimensional Metal-Based Ï€-d Conjugated Nanosheets as Photocatalyst for Nitrogen Reduction Reaction: The First-Principle Investigation. ACS Applied Materials & Interfaces, 2022, 14, 5384-5394.	4.0	10
64755	Single-atom catalyst of TM@D-siliceneâ€"an effective way to reduce N₂ into ammonia. Physical Chemistry Chemical Physics, 2022, 24, 3486-3497.	1.3	11
64756	Suppression of Rayleigh Scattering in Silica Glass by Codoping Boron and Fluorine: Molecular Dynamics Simulations with Force-Matching and Neural Network Potentials. Journal of Physical Chemistry C, 2022, 126, 2264-2275.	1.5	11
64757	Dual Passivation of Point Defects at Perovskite Grain Boundaries with Ammonium Salts Greatly Inhibits Nonradiative Charge Recombination. Journal of Physical Chemistry Letters, 2022, 13, 954-961.	2.1	10
64758	Forming Platinide Phases under Pressure in the Csâ€"Pt System. Journal of Physical Chemistry C, 2022, 126, 2062-2069.	1.5	0
64759	In Situ Construction of Efficient Interface Layer with Lithiophilic Nanoseeds toward Dendriteâ€Free and Low N/P Ratio Li Metal Batteries. Advanced Science, 2022, 9, e2104391.	5.6	19
64760	Ca₂Ga₄Ge₆ and Ca₃Ga₄Ge₆: Synthesis, Structure, and Electronic Properties. Zeitschrift Fur Anorganische Und Allgemeine Chemie, 2022, 648, .	0.6	0

#	Article	IF	Citations
64761	Mesocrystalline Ordering and Phase Transformation of Iron Oxide Biominerals in the Ultrahard Teeth of Cryptochiton stelleri. Small Structures, 2022, 3, .	6.9	11
64762	Atomically-dispersed NiN₄â€“Cl active sites with axial Niâ€“Cl coordination for accelerating electrocatalytic hydrogen evolution. Journal of Materials Chemistry A, 2022, 10, 6007-6015.	5.2	22
64763	Defect chemistry of LaGaO3 doped with divalent cations. Solid State Ionics, 2022, 374, 115828.	1.3	2
64764	Two-Dimensional MoSi₂N₄: An Excellent 2-D Semiconductor for Field-Effect Transistors. IEEE Transactions on Electron Devices, 2022, 69, 406-413.	1.6	28
64765	Vacancy on Structures, Mechanical and Electronic Properties of Ternary Hf-Ta-C System: a First-principles Study. Wuji Cailiao Xuebao/Journal of Inorganic Materials, 2022, 37, 51.	0.6	4
64766	Crystal-induced transverse current in collinear antiferromagnetic Î³-FeMn. Applied Physics Letters, 2022, 120, .	1.5	3
64767	Bimetallic Goldâ€“Silver Nanostructures Drive Low Overpotentials for Electrochemical Carbon Dioxide Reduction. ACS Applied Materials & Interfaces, 2022, 14, 6604-6614.	4.0	14
64768	Homogenizing the Li-ion flux by multi-element alloying modified for 3D dendrite-free lithium anode. Energy Storage Materials, 2022, 48, 114-122.	9.5	11
64769	Mass Transport in a Highly Immiscible Alloy on Extended Shear Deformation. SSRN Electronic Journal, 0, , .	0.4	0
64770	Highly efficient tree search algorithm for irreducible site-occupancy configurations. Physical Review B, 2022, 105, .	1.1	6
64771	Estimating the lower-limit of fracture toughness from ideal-strength calculations. Materials Horizons, 2022, 9, 825-834.	6.4	4
64772	Phonons as a platform for non-Abelian braiding and its manifestation in layered silicates. Nature Communications, 2022, 13, 423.	5.8	33
64773	Enhanced Photoluminescence in Cd _xZn _(1-x)S Solid Solution Through Defect Activation Strategy to Suppress the Non-Radiative Recombination. SSRN Electronic Journal, 0, , .	0.4	0
64774	Induced activation of the commercial Cu/ZnO/Al2O3 catalyst for the steam reforming of methanol. Nature Catalysis, 2022, 5, 99-108.	16.1	155
64775	Optical absorption by design in a ferroelectric: co-doping in BaTiO₃. Journal of Materials Chemistry C, 2021, 10, 227-234.	2.7	8
64776	Ubiquitous Topological States of Phonons in Solids: Silicon as a Model Material. Nano Letters, 2022, 22, 2120-2126.	4.5	26
64777	Reasonable design of a V2O5-x/TiO2 active interface structure with high polysulfide adsorption energy for advanced lithium-sulfur batteries. Electrochimica Acta, 2022, 403, 139723.	2.6	39
64778	Construction of Pd/Ni2P-Ni foam nanosheet array electrode by in-situ phosphatization-electrodeposition strategy for synergistic electrocatalytic hydrodechlorination. Chemical Engineering Journal, 2022, 435, 134932.	6.6	25

#	Article	IF	Citations
64779	Computational design of double transition metal MXenes with intrinsic magnetic properties. Nanoscale Horizons, 2022, 7, 276-287.	4.1	29
64780	K-Ion intercalated V₆O₁₃ with advanced high-rate long-cycle performance as cathode for Zn-ion batteries. Journal of Materials Chemistry C, 2022, 10, 590-597.	2.7	11
64781	Synthesis of layered vs planar Mo₂C: role of Mo diffusion. 2D Materials, 2022, 9, 015039.	2.0	6
64782	Interaction of hydrogen impurities with intrinsic point defects at the CuInSe$$_2$$/CdS interface of chalcopyrite-based solar cells. European Physical Journal B, 2022, 95, 1.	0.6	0
64783	Synergistic magnetic proximity and ferroelectric field effect on a 2H-VS₂ monolayer by ferromagnetic termination of a BiFeO₃(0001) surface. Journal of Materials Chemistry C, 2022, 10, 1498-1510.	2.7	7
64784	Doping Achieves High Thermoelectric Performance in SnS: A First-Principles Study. ACS Applied Materials & Interfaces, 2022, 14, 6916-6925.	4.0	8
64785	Electronic nature of charge density wave and electron-phonon coupling in kagome superconductor KV3Sb5. Nature Communications, 2022, 13, 273.	5.8	124
64786	Nickel cobaltite/multi-walled carbon nanotube flexible sensor for the electrochemical detection of dopamine released by human neural cells. Journal of Materials Chemistry C, 2022, 10, 3048-3060.	2.7	25
64787	Synergistic Effect of Coordination Fields and Hydrosolvents on the Single-Atom Catalytic Property in H₂O₂ Synthesis: A Density Functional Theory Study. Journal of Physical Chemistry C, 2022, 126, 2349-2364.	1.5	9
64788	Can oxygen vacancies in ceria surfaces be measured by O1s photoemission spectroscopy?. Journal of Physics Condensed Matter, 2022, 34, 174004.	0.7	11
64789	Evidence of a Tetrahedrally Coordinated RuO₄ Surface Complex on RuO₂(100): Density Functional Theory and Beyond. Journal of Physical Chemistry C, 2022, 126, 946-956.	1.5	4
64790	Role of interlayer coupling in second harmonic generation in bilayer transition metal dichalcogenides. Physical Review B, 2022, 105, .	1.1	9
64791	High-temperature ferromagnetism and half-metallicity in hole-doped Janus <mml:math xmlns:mml="http://www.w3.org/1998/Math/MathML"><mml:mrow><mml:mi mathvariant="normal">O</mml:mi><mml:msub><mml:mi>M</mml:mi><mml:mn>2</mml:mn></mml:msub><mml:mi		

#	Article	IF	Citations
64797	Tuning valley degeneracy with band inversion. Journal of Materials Chemistry A, 2022, 10, 1588-1595.	5.2	6
64798	First-principles calculations of stable local structures and electronic structures of magnesium secondary battery cathode materials, MgCo2â˜xMnxO4 (xâ€‰=â€‰0, 0.5), in second charged state after first discharge. Journal of Solid State Electrochemistry, 2022, 26, 663-682.	1.2	3
64799	Large-Gap Quantum Spin Hall State and Temperature-Induced Lifshitz Transition in Bi₄Br₄. ACS Nano, 2022, 16, 3036-3044.	7.3	17
64800	Native point defects and their implications for the Dirac point gap at MnBi2Te4(0001). Npj Quantum Materials, 2022, 7, .	1.8	53
64801	Synergetic stability enhancement with magnesium and calcium ion substitution for Ni/Mn-based P2-type sodium-ion battery cathodes. Chemical Science, 2022, 13, 726-736.	3.7	54
64802	Solutes that reduce yield strength anisotropies in magnesium from first principles. Physical Review Materials, 2022, 6, .	0.9	1
64803	State-of-the-art of computational green chemistry in leading universities in Russia. , 2022, , 55-77.		0
64804	A wafer-scale two-dimensional platinum monosulfide ultrathin film via metal sulfurization for high performance photoelectronics. Materials Advances, 2022, 3, 1497-1505.	2.6	14
64805	Assembling Diverse Skyrmionic Phases in Fe₃GeTe₂ Monolayers. Advanced Materials, 2022, 34, e2107779.	11.1	25
64806	Controlling interlayer magnetic coupling in the two-dimensional magnet <mml:math xmlns:mml="http://www.w3.org/1998/Math/MathML"><mml:mrow><mml:msub><mml:mi>Fe</mml:mi><mml:mn>3</mml:mn></mml:msub><mml:msub><mml:mi>Ge</mml:mi><mml:mn>2</mml:mn></mml:msub><mml:msub><mml:mi>Te</mml:mi><mml:mn>2</mml:mn></mml:msub></mml:mrow></mml:math> Physical Review B, 2022, 105, .	1.1	9
64807	Dynamic Pt Coordination in Dilute AgPt Alloy Nanoparticle Catalysts Under Reactive Environments. Topics in Catalysis, 2022, 65, 1587-1603.	1.3	6
64808	Atomic-Scale Understanding of Li Storage Processes in the Ti₄C₃ and Chemically Ordered Ti₂Ta₂C₃ MXenes: A Theoretical and Experimental Assessment. ACS Applied Energy Materials, 2022, 5, 1801-1809.	2.5	14
64809	Origins of the hydrogen signal in atom probe tomography: case studies of alkali and noble metals. New Journal of Physics, 2022, 24, 013008.	1.2	10
64810	Significant interlayer coupling in bilayer graphene and double-walled carbon nanotubes: A refinement of obtaining strain in low-dimensional materials. Physical Review B, 2022, 105, .	1.1	0
64811	Theoretical Investigation of Half-Metallic Ferrimagnetic Heusler Alloys: the Case of DO3-Type Cr3Z (Zâ€‰=â€‰P, As, Sb, S, Se, and Te). Journal of Superconductivity and Novel Magnetism, 2022, 35, 763.	0.8	1
64812	A transferable machine-learning scheme from pure metals to alloys for predicting adsorption energies. Journal of Materials Chemistry A, 2022, 10, 872-880.	5.2	33
64813	Theoretical insights into TM@PHEs as single-atom catalysts for water splitting based on density functional theory. Physical Chemistry Chemical Physics, 2022, 24, 975-981.	1.3	2
64814	First-principles identification of V_IÂ+ÂCu_i defect cluster in cuprous iodide: origin of red light photoluminescence. Nanotechnology, 2022, 33, 195203.	1.3	7

#	Article	IF	Citations
64815	Simulating intergranular hydrogen enhanced decohesion in aluminium using density functional theory. Modelling and Simulation in Materials Science and Engineering, 2022, 30, 035009.	0.8	3
64816	First principles studies on infrared band structure and absorption of As/Sb lateral heterostructures. Journal of Applied Physics, 2022, 131, 023101.	1.1	4
64817	Thermoelectric performance of MoSi₂As₄monolayer. Europhysics Letters, 2022, 137, 16002.	0.7	6
64818	Doping in the two-dimensional limit: <mml:math xmlns:mml="http://www.w3.org/1998/Math/MathML"><mml:mrow><mml:mi>p</mml:mi><mml:mo>/</mml:mo><mml:mi>n</mml:mi></mml:m -type defects in monolayer ZnO. Physical Review B, 2022, 105, .	1.1	3
64819	Adina Rubellaâ€Like Microsized SiO@Nâ€Doped Carbon Grafted with Nâ€Doped Carbon Nanotubes as Anodes for Highâ€Performance Lithium Storage. Small Science, 2022, 2, .	5.8	33
64820	Analogous Atomic and Electronic Properties between V N and V N. Advances in Condensed Matter Physics, 2022, 2022, 1-6.	0.4	2
64821	Unlocking surface octahedral tilt in two-dimensional Ruddlesden-Popper perovskites. Nature Communications, 2022, 13, 138.	5.8	42
64822	Adsorption Sites on Pd Nanoparticles Unraveled by Machine-Learning Potential with Adaptive Sampling. Molecules, 2022, 27, 357.	1.7	3
64823	Effect of Solute Ta on Grain Refinement of Al-7Si-0.3Mg Based Alloys. Solid State Phenomena, 0, 327, 54-64.	0.3	4
64824	Mechanistic Study of 1,2-Dichloroethane Hydrodechlorination on Cu-Rich Ptâ€“Cu Alloys: Combining Reaction Kinetics Experiments with DFT Calculations and Microkinetic Modeling. ACS Sustainable Chemistry and Engineering, 2022, 10, 1509-1523.	3.2	4
64825	Permeability of boron- and nitrogen-doped graphene nanoflakes for protium/deuterium ions. RSC Advances, 2022, 12, 3883-3891.	1.7	0
64826	Spatially indirect intervalley excitons in bilayer <mml:math xmlns:mml="http://www.w3.org/1998/Math/MathML"><mml:mrow><mml:mi mathvariant="normal">W</mml:mi><mml:msub><mml:mi>Se</mml:mi><mml:mn>2</mml:mn></mml:msub></mml:mrow></mml:m Physical Review B, 2022, 105, .	1.1	11
64827	Machine learned interatomic potentials using random features. Npj Computational Materials, 2022, 8, .	3.5	11
64828	Voltage plateau variation in a bismuth-potassium battery. Journal of Materials Chemistry A, 2022, 10, 2917-2923.	5.2	6
64829	Role of the third dimension in searching for Majorana fermions in <mml:math xmlns:mml="http://www.w3.org/1998/Math/MathML"><mml:mrow><mml:mi>Î±</mml:mi><mml:mtext>â^'</mml:mtext><mml:msub>< via phonons. Physical Review Research, 2022, 4, .	1.3	14
64830	Electrochemical ion-pumping-assisted transfer system featuring a heterogeneous membrane for lithium recovery. Chemical Engineering Journal, 2022, 435, 134955.	6.6	12
64831	In situ tailored strategy to remove capping agents from copper sulfide for building better lithiumâ€“sulfur batteries. Journal of Materials Chemistry A, 2022, 10, 4015-4023.	5.2	7
64832	The Investigation of Adsorption Behavior of Gas Molecules on FeN3-Doped Graphene. Journal of Sensors, 2022, 2022, 1-8.	0.6	2

#	Article	IF	Citations
64833	Exploration of carbon additives to the synthesis of CuMoS structures and their electrocatalytic activity in oxygen reduction reaction. International Journal of Hydrogen Energy, 2022, 47, 5326-5336.	3.8	8
64834	Investigations of Structural, Electronic and Magnetic Properties of MnSe under High Pressure. Materials, 2022, 15, 1109.	1.3	0
64835	Operando generated copperâ€based catalyst enabling efficient electrosynthesis of 2,5â€bis(hydroxymethyl)furan. Fundamental Research, 2023, 3, 763-769.	1.6	7
64836	Dimensionality of the Superconductivity in the Transition Metal Pnictide WP. Materials, 2022, 15, 1027.	1.3	1
64837	Tuning Ferromagnetism in a Single Layer of Fe above Room Temperature. Materials, 2022, 15, 1019.	1.3	1
64838	Photo-assisted Fe2+ modified molybdenum disulfide activated potassium persulfate to degrade sulfadiazine: Insights into the degradation pathway and mechanism from density functional theory. Chemical Engineering Journal, 2022, 435, 134904.	6.6	29
64839	Highly selective production of long-chain aldehydes, ketones or alcohols via syngas at a mild condition. Applied Catalysis B: Environmental, 2022, 307, 121155.	10.8	11
64840	Thermodynamics of carbon point defects in hexagonal boron nitride. Physical Review Materials, 2022, 6, .	0.9	17
64841	Tuning the Interaction between Ruthenium Single Atoms and the Second Coordination Sphere for Efficient Nitrogen Photofixation. Advanced Functional Materials, 2022, 32, .	7.8	22
64842	Promotion effect of Au single-atom support graphene for CO oxidation. Chinese Chemical Letters, 2022, 33, 4822-4827.	4.8	13
64843	Enhancing the Electron Transport, Quantum Yield, and Catalytic Performance of Carbonized Polymer Dots via Mnï£¿O Bridges. Small, 2022, 18, e2106863.	5.2	15
64844	First-Principles Investigation of the Interfacial Stability, Precipitate Formation, and Mechanical Behavior of Al3Li/Al3Zr/Al Interfaces. Metallurgical and Materials Transactions A: Physical Metallurgy and Materials Science, 2022, 53, 1308-1321.	1.1	3
64845	The non-direct band gap in borate glasses; a brief discussion on analysis methodologies and its interpretation. Optical Materials, 2022, 123, 111890.	1.7	1
64846	Wafer-scale single-crystal monolayer graphene grown on sapphire substrate. Nature Materials, 2022, 21, 740-747.	13.3	92
64847	Enhancing Electrocatalytic Methanol Oxidation on PtCuNi Coreâ€“Shell Alloy Structures in Acid Electrolytes. Inorganic Chemistry, 2022, 61, 2612-2618.	1.9	20
64848	Structural Evolution, Redox Mechanism, and Ionic Diffusion in Rhombohedral Na₂FeFe(CN)₆ for Sodium-Ion Batteries: First-Principles Calculations. Journal of the Electrochemical Society, 2022, 169, 010525.	1.3	5
64849	Superionic Silica-Water and Silica-Hydrogen Compounds in the Deep Interiors of Uranus and Neptune. Physical Review Letters, 2022, 128, 035702.	2.9	19
64850	Insights into the binding manners of an Fe doped MOF-808 in high-performance adsorption: a case of antimony adsorption. Environmental Science: Nano, 2022, 9, 254-264.	2.2	10

#	Article	IF	Citations
64851	Electronic and catalytic properties of carbon nitride derivatives tuned by building blocks and linkages. International Journal of Hydrogen Energy, 2022, 47, 8761-8775.	3.8	5
64852	Efficient and selective oxidation of furfural into highâ€value chemicals by cobalt and nitrogen coâ€doped carbon. Canadian Journal of Chemical Engineering, 2023, 101, 354-367.	0.9	4
64853	Redirecting dynamic structural evolution of nickel-contained RuO2 catalyst during electrochemical oxygen evolution reaction. Journal of Energy Chemistry, 2022, 69, 330-337.	7.1	24
64854	Design Rules of a Sulfur Redox Electrocatalyst for Lithiumâ€“Sulfur Batteries. Advanced Materials, 2022, 34, e2110279.	11.1	108
64855	Twist-Stabilized, Coiled Carbon Nanotube Yarns with Enhanced Capacitance. ACS Nano, 2022, 16, 2661-2671.	7.3	31
64856	Length-Gauge Optical Matrix Elements in WIEN2k. Computation, 2022, 10, 22.	1.0	2
64857	Development of the temperature-dependent interatomic potential for molecular dynamics simulation of metal irradiated with an ultrashort pulse laser. Journal of Physics Condensed Matter, 2022, 34, 165901.	0.7	4
64858	Second-Order Real Nodal-Line Semimetal in Three-Dimensional Graphdiyne. Physical Review Letters, 2022, 128, 026405.	2.9	34
64859	Mn⁴⁺ non-equivalent doped fluoride phosphors with a short fluorescence decay time for backlighting. Dalton Transactions, 2022, 51, 2512-2516.	1.6	17
64860	Zero Poisson's ratio in single-layer arsenic. Nanoscale, 2022, 14, 969-975.	2.8	1
64861	A B₂N monolayer: a direct band gap semiconductor with high and highly anisotropic carrier mobility. Nanoscale, 2022, 14, 930-938.	2.8	11
64862	A multiferroic iron arsenide monolayer. Nanoscale Advances, 2022, 4, 1324-1329.	2.2	5
64863	Computational Design of Miniproteins as SARS-CoV-2 Therapeutic Inhibitors. International Journal of Molecular Sciences, 2022, 23, 838.	1.8	15
64864	Manipulation of current rectification in van der Waals ferroionic CuInP2S6. Nature Communications, 2022, 13, 574.	5.8	60
64865	A new MoCN monolayer containing stable cyano structural units as a high-efficiency catalyst for the hydrogen evolution reaction. Nanoscale, 2022, , .	2.8	1
64866	Pressure-induced evolution of crystal and electronic structure of neptunium hydrides. Physical Chemistry Chemical Physics, 2022, 24, 4916-4924.	1.3	0
64867	Clustering feature of metal atoms in pentacene molecular solids: a first-principles study. Japanese Journal of Applied Physics, 2022, 61, 021003.	0.8	2
64868	Theory of Electron Correlation in Disordered Crystals. Materials, 2022, 15, 739.	1.3	2

#	Article	IF	Citations
64869	Ultraâ€deep desulfurization of mercaptan by cyclic selective adsorptionâ€reactive regeneration at room temperature. AICHE Journal, 2022, 68, .	1.8	3
64870	White-light defect emission and enhanced photoluminescence efficiency in a 0D indium-based metal halide. Journal of Materials Chemistry C, 2022, 10, 1999-2007.	2.7	30
64871	The chemical origin of temperature-dependent lithium-ion concerted diffusion in sulfide solid electrolyte Li10GeP2S12. Journal of Energy Chemistry, 2022, 70, 59-66.	7.1	22
64872	A perfect match between borophene and aluminium in the AlB₃ heterostructure with covalent Alâ€“B bonds, multiple Dirac points and a high Fermi velocity. Chemical Science, 2022, 13, 1016-1022.	3.7	5
64873	Thermodynamics and kinetics of H adsorption and intercalation for graphene on 6H-SiC(0001) from first-principles calculations. Journal of Vacuum Science and Technology A: Vacuum, Surfaces and Films, 2022, 40, .	0.9	8
64874	Carrier doping-induced strong magnetoelastic coupling in 2D lattice. Nanoscale, 2022, 14, 3261-3268.	2.8	5
64875	Route to a direct-gap silicon allotrope Si₃₂. Journal of Physics Condensed Matter, 2022, 34, 154006.	0.7	1
64876	Realizing High Thermoelectric Performance in p-Type SnSe Crystals via Convergence of Multiple Electronic Valence Bands. ACS Applied Materials & Interfaces, 2022, 14, 4091-4099.	4.0	8
64877	Electric-field-based control of molecular magnetism in TMPc/Sc₂CO₂ van der Waals systems. Materials Advances, 2022, 3, 1064-1070.	2.6	3
64878	Role of Critical Oxygen Concentration in the Î²-Li₃PS_{4â€“x}O_x Solid Electrolyte. ACS Applied Energy Materials, 2022, 5, 35-41.	2.5	6
64879	Lithium-Ion Storage Mechanism in Metal-N-C Systems: A First-Principles Study. ACS Omega, 2022, 7, 2613-2617.	1.6	0
64880	Thickness-Driven Quantum Anomalous Hall Phase Transition in Magnetic Topological Insulator Thin Films. ACS Nano, 2022, 16, 1134-1141.	7.3	4
64881	Robust Dirac spin gapless semiconductors in a two-dimensional oxalate based organic honeycomb-kagome lattice. Nanoscale, 2022, 14, 2023-2029.	2.8	5
64882	Density Functional Theory Estimate of Halide Perovskite Band Gap: When Spin Orbit Coupling Helps. Journal of Physical Chemistry C, 2022, 126, 2184-2198.	1.5	40
64883	Structural, Electronic, and Physical Properties of a New Layered Cr-Based Oxyarsenide Sr2Cr2AsO3. Materials, 2022, 15, 802.	1.3	1
64884	Understanding the endocrine disruptor and determination of bisphenol A by functional Cu-BTABB-MOF/rGO composite as facile rapid electrochemical sensor: an experimental and DFT investigation. Analytical Methods, 2022, 14, 560-573.	1.3	15
64885	Origin of the different degradation mechanisms of LNCM and LNCA cathodes in Li-ion batteries. Physical Chemistry Chemical Physics, 2022, 24, 3429-3439.	1.3	2
64886	High throughput screening of promising lead-free inorganic halide double perovskites via first-principles calculations. Physical Chemistry Chemical Physics, 2022, 24, 3460-3469.	1.3	26

#	Article	IF	Citations
64887	Mottâ€“Hubbard insulating state for the layered van der Waals $$hbox {FePX}_3$$ (X: S, Se) as revealed by NEXAFS and resonant photoelectron spectroscopy. Scientific Reports, 2022, 12, 735.	1.6	13
64888	MoS₂ nanosheets vertically grown on CoSe₂ hollow nanotube arrays as an efficient catalyst for the hydrogen evolution reaction. Nanoscale, 2022, 14, 2490-2501.	2.8	18
64889	Clustering of metal dopants in defect sites of graphene-based materials. Physical Chemistry Chemical Physics, 2021, 24, 98-111.	1.3	3
64890	Selective, Stable, Biasâ€Free, and Efficient Solar Hydrogen Peroxide Production on Inorganic Layered Materials. Advanced Functional Materials, 2022, 32, .	7.8	19
64891	Lowering the Câ€“H bond activation barrier of methane by means of SAC@Cu(111): periodic DFT investigations. New Journal of Chemistry, 2021, 46, 70-74.	1.4	9
64892	Mapping hidden space-charge distributions across crystalline metal oxide/group IV semiconductor interfaces. Physical Review Materials, 2022, 6, .	0.9	2
64893	Carrier mobility of one-dimensional vanadium selenide (V2Se9) monolayer and nanoribbon systems: DFT study. Nanotechnology, 2022, 33, 135703.	1.3	3
64894	Mechanism Investigations on Water Gas Shift Reaction over Cu(111), Cu(100), and Cu(211) Surfaces. ACS Omega, 2022, 7, 3514-3521.	1.6	12
64895	Giant Optical Oscillator Strengths in Perturbed Hexagonal Germanium. Physica Status Solidi - Rapid Research Letters, 0, , 2100555.	1.2	4
64896	Controllable spin direction in nonmagnetic BX/MX2 (M = Mo or W; X = S, Se and Te) van der Waals heterostructures by switching between the Rashba splitting and valley polarization. Journal of Materials Chemistry C, 2021, 10, 312-320.	2.7	2
64897	Observation of Spinâ€Induced Ferroelectricity in a Layered van der Waals Antiferromagnet CuCrP 2 S 6. Advanced Electronic Materials, 0, , 2101072.	2.6	18
64898	Pentaheptite diamond: a new carbon allotrope. Journal of Physics Condensed Matter, 2022, 34, 184003.	0.7	0
64899	Enhanced superconductivity in C-S-H compounds at high pressure. Physical Review B, 2022, 105, .	1.1	2
64900	Regularized second-order correlation methods for extended systems. Journal of Chemical Physics, 2022, 156, 024106.	1.2	7
64901	p-Type Iodine-Doping of Cu3N and Its Conversion to Î³-CuI for the Fabrication of Î³-CuI/Cu3N p-n Heterojunctions. Electronic Materials, 2022, 3, 15-26.	0.9	8
64902	Influence of strain and external electric field on the performance of PC6/MoSe2 heterostructure. Journal of Materials Science, 2022, 57, 477-488.	1.7	6
64903	Regulation of the luminescence mechanism of two-dimensional tin halide perovskites. Nature Communications, 2022, 13, 60.	5.8	48
64904	Multiband superconductivity in <mml:math xmlns:mml="http://www.w3.org/1998/Math/MathML"><mml:msub><mml:mi mathvariant="normal">V</mml:mi><mml:mn>3</mml:mn></mml:msub><mml:mi>Si</mml:mi></mml:math> determined from studying the response to controlled disorder. Physical Review B, 2022, 105, .	1.1	9

#	Article	IF	Citations
64905	Fulde-Ferrell-Larkin-Ovchinnikov pairing induced by a Weyl nodal line in an Ising superconductor with a high critical field. Physical Review B, 2022, 105, .	1.1	4
64906	Phase-Manipulation-Induced Majorana Mode and Braiding Realization in Iron-Based Superconductor Fe(Te,Se). Physical Review Letters, 2022, 128, 016402.	2.9	13
64907	Computational perspective on recent advances in quantum electronics: from electron quantum optics to nanoelectronic devices and systems. Journal of Physics Condensed Matter, 2022, 34, 163001.	0.7	6
64908	A simple model to engineer single-molecule conductance of acenes by chemical disubstitution. Nanoscale, 2022, 14, 464-472.	2.8	2
64909	Density functional theory of alkali metals at the IL/graphene electrochemical interface. Journal of Chemical Physics, 2022, 156, 014706.	1.2	2
64910	Ceria Nanoparticles as an Unexpected Catalyst to Generate Nitric Oxide from Sâ€Nitrosoglutathione. Small, 2022, 18, e2105762.	5.2	18
64911	Room-Temperature Ferromagnetism at an Oxide-Nitride Interface. Physical Review Letters, 2022, 128, 017202.	2.9	11
64912	Rare-earth defects and defect-related luminescence in ZnS. Journal of Applied Physics, 2022, 131, 015705.	1.1	3
64913	Stabilization of Al3Zr allotropes in dilute aluminum alloys via the addition of ternary elements. Materialia, 2022, 21, 101321.	1.3	6
64914	Dopamine Adsorption on Rutile TiO₂(110): Geometry, Thermodynamics, and Core-Level Shifts from First Principles. ACS Omega, 2022, 7, 4185-4193.	1.6	3
64915	Self-assembled, highly-lithiophilic and well-aligned biomass engineered MXene paper enables dendrite-free lithium metal anode in carbonate-based electrolyte. Journal of Energy Chemistry, 2022, 69, 221-230.	7.1	26
64916	Mechanistic Insights into Electrocatalytic Nitrogen Reduction Reaction on the Pdâ€W Heteronuclear Diatom Supported on C₂N Monolayer: Role of H Preâ€Adsorption. Energy and Environmental Materials, 2023, 6, .	7.3	4
64917	MnBi2Se4-Based Magnetic Modulated Heterostructures. Magnetism, 2022, 2, 1-9.	0.6	1
64918	Determining the Adsorption Energetics of 2,3-Butanediol on RuO2(110): Coupling First-Principles Calculations With Global Optimizers. Frontiers in Energy Research, 2022, 9, .	1.2	0
64919	Band gap, effective masses, and energy level alignment of 2D and 3D halide perovskites and heterostructures using DFT-1/2. Physical Review Materials, 2022, 6, .	0.9	13
64920	Local environment rigidity and the evolution of optical properties in the green-emitting phosphor Ba_{1â^'x}Sr_xScO₂F:Eu²⁺. Journal of Materials Chemistry C, 2022, 10, 2955-2964.	2.7	7
64921	Interlayer exciton emission in a MoS₂/VOPc inorganic/organic van der Waals heterostructure. Materials Horizons, 2022, 9, 1253-1263.	6.4	6
64922	Spin-gapless semiconducting Cl-intercalated phosphorene bilayer: a perfect candidate material to identify its ferroelectric states by spin-Seebeck currents. Journal of Materials Chemistry C, 2022, 10, 3188-3195.	2.7	5

#	Article	IF	Citations
64923	Influence of the hBN Dielectric Layers on the Quantum Transport Properties of MoS2 Transistors. Materials, 2022, 15, 1062.	1.3	3
64924	Screening strain sensitive transition metals using oxygen adsorption. New Journal of Chemistry, 2022, 46, 2178-2188.	1.4	2
64925	Phononic higher-order nodal point in two dimensions. Physical Review B, 2022, 105, .	1.1	20
64926	Photocatalytic reduction of water to hydrogen by CuPbSbS3 nanoflakes. Materials Today Energy, 2022, 25, 100956.	2.5	8
64927	Synergistic effect of Ru-N4 sites and Cu-N3 sites in carbon nitride for highly selective photocatalytic reduction of CO2 to methane. Applied Catalysis B: Environmental, 2022, 307, 121154.	10.8	57
64928	Valley spin polarization in two-dimensional <mml:math xmlns:mml="http://www.w3.org/1998/Math/MathML"><mml:mrow><mml:mi>h</mml:mi><mml:mtext>â^’</mml:mtext><mml:mi>M</mml:mi><mathvariant="normal">N</mml:mi></mml:mrow><mml:mo>Â</mml:mo><mml:mrow><mml:mo>(</mml:mo><mml:mi>M</mml:mi> monolayers: Merger of valleytronics with spintronics. Physical Review B, 2022, 105, .	1.1	20
64929	Simultaneous construction of impermeable dual-shell stabilizing fluoride phosphors for white light-emitting diodes. Chemical Engineering Journal, 2022, 435, 134951.	6.6	10
64930	Transport properties of a quasisymmetric binary nitrogen-oxygen mixture in the warm dense regime. Physical Review E, 2022, 105, 015201.	0.8	1
64931	Oxygen-Vacancy Confined Uranium Single-Atom Over Titanium Dioxide Nanosheets for Efficient Nitrogen Fixation. SSRN Electronic Journal, 0, , .	0.4	0
64932	Unraveling Unique Surface Chemistry of Transition Metal Nitrides in Controlling Selective Câ€“O Bond Scission Pathways of Glycerol. Jacs Au, 2022, 2, 367-379.	3.6	10
64933	Resolving atomic diffusion in <mml:math xmlns:mml="http://www.w3.org/1998/Math/MathML"><mml:mrow><mml:mi>Ru</mml:mi><mml:mrow><mml:mo>(</mml:mo><mml:m<mathvariant="normal">O</mml:mi><mml:mo>(</mml:mo><mml:mn>2</mml:mn><mml:mo>Ã—</mml:mo><mml:mn>2</mml:mn><mml:m with spiral high-speed scanning tunneling microscopy. Physical Review B, 2022, 105, .	1.1	4
64934	Ab initio free energies of liquid metal alloys: Application to the phase diagrams of Li-Na and K-Na. Physical Review Materials, 2022, 6, .	0.9	2
64935	Catalytic production of low-carbon footprint sustainable natural gas. Nature Communications, 2022, 13, 258.	5.8	26
64936	Ultrathick MoS₂ Films with Exceptionally High Volumetric Capacitance. Advanced Energy Materials, 2022, 12, .	10.2	44
64937	Point Defect Generation Probability in Rare-Earth Permanent Magnets in Radiation Environments via First-Principle Calculations. IEEE Transactions on Magnetics, 2022, 58, 1-5.	1.2	1
64938	Photocatalytic Activity and Hole-Scavenging Behaviors on Rutile TiO₂(100) Surfaces: A Theoretical Study. Journal of Physical Chemistry C, 2022, 126, 974-985.	1.5	4
64939	Novel Calcium sp³ Carbonate CaC₂O₅-I4Ì…2d May Be a Carbon Host in Earthâ€™s Lower Mantle. ACS Earth and Space Chemistry, 2022, 6, 73-80.	1.2	13
64940	Revealing the activity of Co₃Mo₃N and Co₃Mo₃N_{0.5} as electrocatalysts for the hydrogen evolution reaction. Journal of Materials Chemistry A, 2022, 10, 855-861.	5.2	11

#	Article	IF	Citations
64941	Controlled CVD growth of ultrathin Mo2C (MXene) flakes. Journal of Applied Physics, 2022, 131, .	1.1	14
64942	Unveiling nonmonotonic chemical trends in the solubility of H in complex Fe-Cr-Mn carbides by means of ab initio based approaches. Physical Review Materials, 2022, 6, .	0.9	1
64943	Data-driven prediction of grain boundary segregation and disordering in high-entropy alloys in a 5D space. Materials Horizons, 2022, 9, 1023-1035.	6.4	14
64944	A new porphyrinic vanadium-based MOF constructed from infinite V(OH)O₄ chains: syntheses, characterization and photoabsorption properties. New Journal of Chemistry, 2022, 46, 632-641.	1.4	12
64945	Fast and recoverable NO₂ detection achieved by assembling ZnO on Ti₃C₂T_x MXene nanosheets under UV illumination at room temperature. Nanoscale, 2022, 14, 3441-3451.	2.8	65
64946	Spinâ€“orbit stable dirac nodal line in monolayer B₆O. Chinese Physics B, 2022, 31, 037305.	0.7	0
64947	Piezoelectricity in two-dimensional aluminum, boron and Janus aluminum-boron monochalcogenide monolayers. Journal Physics D: Applied Physics, 2022, 55, 155301.	1.3	5
64948	Raman Spectroscopy as a Key Method to Distinguish the Ferroelectric Orthorhombic Phase in Thin ZrO₂â€Based Films. Physica Status Solidi - Rapid Research Letters, 2022, 16, .	1.2	15
64949	Twist angle dependent electronic properties in 2D graphene/MoS2 vdW heterostructures. Journal of Applied Physics, 2022, 131, 034301.	1.1	5
64950	Accurate prediction of grain boundary structures and energetics in CdTe: a machine-learning potential approach. Physical Chemistry Chemical Physics, 2022, 24, 1620-1629.	1.3	11
64951	Oxide-ion diffusion in brownmillerite-type Ca₂AlMnO_{5+Î´} from first-principles calculations. Physical Chemistry Chemical Physics, 2022, 24, 1503-1509.	1.3	4
64952	A first-principles study on the phase stability and physical properties of a B-site ordered Nd₂CrFeO₆ double perovskite. Physical Chemistry Chemical Physics, 2022, 24, 1569-1579.	1.3	7
64953	Promotion of the Co₃O₄/TiO₂ Interface on Catalytic Decomposition of Ammonium Perchlorate. ACS Applied Materials & Interfaces, 2022, 14, 3476-3484.	4.0	31
64954	Spin and spinâ€“orbit coupling effects in nickel-based superalloys: A first-principles study on Ni3Al doped with Ta/W/Re. Chinese Physics B, 2022, 31, 016105.	0.7	3
64955	Atomic-scale observation of spontaneous hole doping and concomitant lattice instabilities in strained nickelate films. New Journal of Physics, 2022, 24, 023011.	1.2	0
64956	Exploring the adsorption site coordination as a strategy to tune copper catalysts for CO₂ electro-reduction. Catalysis Science and Technology, 2022, 12, 869-879.	2.1	9
64957	Rational Unraveling of Alkali Metal Concentration-Dependent Photovoltaic Performance of Halide Perovskites: Octahedron Distortion vs Surface Reconstruction. Journal of Physical Chemistry Letters, 2022, 13, 362-370.	2.1	2
64958	Critical assessment of machine-learned repulsive potentials for the density functional based tight-binding method: A case study for pure silicon. Journal of Chemical Physics, 2022, 156, 064101.	1.2	4

#	Article	IF	Citations
64959	Highly efficient two-electron electroreduction of oxygen into hydrogen peroxide over Cu-doped TiO2. Nano Research, 2022, 15, 3880-3885.	5.8	38
64960	Simulations to Cover the Waterfront for Iron Oxide Catalysis. ChemPhysChem, 2022, 23, .	1.0	3
64961	Thermoelectricity and electronic correlation enhancement in FeS by light Se doping. Physical Review B, 2022, 105, .	1.1	3
64962	Electronic properties of zero-line modes in bilayer graphene: An ab initio study. Physical Review B, 2022, 105, .	1.1	2
64963	Generation and Enhancement of Valley Polarization in Monolayer Chromium Dichalcogenides. Journal of Superconductivity and Novel Magnetism, 2022, 35, 787.	0.8	1
64964	Cobalt metal organic framework (Co-MOF) derived CoSe₂/C hybrid nanostructures for the electrochemical hydrogen evolution reaction supported by DFT studies. New Journal of Chemistry, 2022, 46, 2730-2738.	1.4	15
64965	Interfacial engineering of lattice coherency at ZnO-ZnS photocatalytic heterojunctions. Chem Catalysis, 2022, 2, 125-139.	2.9	56
64966	DFT Insights into NO Electrochemical Reduction: A Case Study of Pt(211) and Cu(211) Surfaces. ACS Catalysis, 2022, 12, 1394-1402.	5.5	19
64967	Finding Key Factors for Efficient Water and Methanol Activation at Metals, Oxides, MXenes, and Metal/Oxide Interfaces. ACS Catalysis, 2022, 12, 1237-1246.	5.5	5
64968	Asymmetric donor-acceptor molecule-regulated core-shell-solvation electrolyte for high-voltage aqueous batteries. Joule, 2022, 6, 399-417.	11.7	50
64969	Size Optimization of a N-Doped Graphene Nanocluster for the Oxygen Reduction Reaction. ACS Omega, 2022, 7, 3093-3098.	1.6	3
64970	Breaking the Aristotype: Featurization of Polyhedral Distortions in Perovskite Crystals. Chemistry of Materials, 2022, 34, 562-573.	3.2	8
64971	Structure and Pore Size Distribution in Nanoporous Carbon. Chemistry of Materials, 2022, 34, 617-628.	3.2	29
64972	Theoretical Study of Small Molecules Adsorption on Pristine and Transition Metal Doped GeSe Monolayer for Gas Sensing Application. Langmuir, 2022, 38, 1287-1295.	1.6	15
64973	Ultra-low lattice thermal conductivity and anisotropic thermoelectric transport properties in Zintl compound Î²-K₂Te₂. Physical Chemistry Chemical Physics, 2022, 24, 4666-4673.	1.3	10
64974	Electron-phonon coupling and quantum correction to topological magnetoconductivity in <mml:math xmlns:mml="http://www.w3.org/1998/Math/MathML"><mml:mrow><mml:msub><mml:mi>Bi</mml:mi><mml:mn>2</mml:mn></mml:msub></mml:mrow></mml:math> Physical Review B, 2022, 105, .	1.1	12
64975	Construction of stable Mo_xS_y/CeO₂ heterostructures for the electrocatalytic hydrogen evolution reaction. Physical Chemistry Chemical Physics, 2022, 24, 4891-4898.	1.3	3
64976	Electronic structures of the MoS₂/TiO₂(anatase) heterojunction: influence of physical and chemical modifications at the 2D- or 1D-interfaces. Physical Chemistry Chemical Physics, 2022, 24, 2646-2655.	1.3	6

#	Article	IF	Citations
64977	Topological Luttinger semimetallic phase accompanied with surface states realized in silicon. Physical Review B, 2022, 105, .	1.1	0
64979	Tuning the Carrier Scattering Mechanism by Rare-Earth Element Doping for High Average zT in Mg₃Sb₂-Based Compounds. ACS Applied Materials & Interfaces, 2022, 14, 7022-7029.	4.0	16
64980	Îµ-Ga₂O₃ Grown on c-Plane Sapphire by MOCVD with a Multistep Growth Process. Crystal Growth and Design, 2022, 22, 1837-1845.	1.4	9
64981	Compressed superhydrides: the road to room temperature superconductivity. Journal of Physics Condensed Matter, 2022, 34, 173001.	0.7	12
64982	Giant tunneling magnetoresistance in atomically thin VSi2N4/MoSi2N4/VSi2N4 magnetic tunnel junction. Applied Physics Letters, 2022, 120, .	1.5	17
64983	Two Nonlinear Optical Thiophosphates Cu₅Hg_{0.5}P₂S₈ and AgHg₃PS₆ Activated by Their Tetrahedra-Stacking Architecture. Inorganic Chemistry, 2022, 61, 1620-1626.	1.9	8
64984	Spatially Confined Synthesis of SnSe Spheres Encapsulated in N, Se Dual-Doped Carbon Networks toward Fast and Durable Sodium Storage. ACS Applied Materials & Interfaces, 2022, 14, 4230-4241.	4.0	43
64985	High-Pressure Mgâ€“Scâ€“H Phase Diagram and Its Superconductivity from First-Principles Calculations. Journal of Physical Chemistry C, 2022, 126, 2747-2755.	1.5	17
64986	In silico design of dual-doped nitrogenated graphene (C₂N) employed in electrocatalytic reduction of carbon monoxide to ethylene. Journal of Materials Chemistry A, 2022, 10, 4703-4710.	5.2	12
64987	Ab initio Study of Atomic Structure and Electronic Properties of Different Phases of Polymorphic Ag 2 S. Physica Status Solidi (B): Basic Research, 0, , 2100617.	0.7	0
64988	N-Doped Graphene Supported Cu Single Atoms: Highly Efficient Recyclable Catalyst for Enhanced Câ€“N Coupling Reactions. ACS Nano, 2022, 16, 1142-1149.	7.3	36
64989	Type-II quadratic and cubic Weyl fermions. Physical Review B, 2022, 105, .	1.1	6
64990	Optimizing the Back Contact of Kesterites and Perovskites: Band Edge Design and Defect Engineering in Molybdenum Chalcogenides. Advanced Sustainable Systems, 0, , 2100457.	2.7	4
64991	Deformation and Failure Mechanisms of Thermoelectric Type-I Clathrate Ba₈Au₆Ge₄₀. ACS Applied Materials & Interfaces, 2022, 14, 4326-4334.	4.0	1
64992	Air-grown hybrid copper(<scp>i</scp>) halide single crystals: structural transformations and ultraviolet-pumped photoluminescence applications. Materials Advances, 2022, 3, 2447-2455.	2.6	16
64993	Impact of the dopant-induced ensemble structure of hetero-double atom catalysts in electrochemical NH₃ production. Journal of Materials Chemistry A, 2022, 10, 6216-6230.	5.2	11
64994	Enhancing the photocatalytic activity of defective titania for carbon dioxide photoreduction via surface functionalization. Catalysis Science and Technology, 2022, 12, 509-518.	2.1	15
64995	Cubic halide perovskites as potential low thermal conductivity materials: A combined approach of machine learning and first-principles calculations. Physical Review B, 2022, 105, .	1.1	5

#	Article	IF	Citations
64996	Modulating hardness in Sc₂(Ru_{5â”x}TM_x)B₄ through empirical considerations and computational analysis. Journal of Materials Chemistry C, 2022, 10, 1488-1497.	2.7	1
64997	Controllable and facile preparation of Co₉S₈â€“Ni₃S₂ heterostructures embedded with N,S,O-tri-doped carbon for electrocatalytic oxidation of 5-hydroxymethylfurfural. Green Chemistry, 2022, 24, 1721-1731.	4.6	41
64998	Synergistic Effects of Crystal Phase and Strain for N₂ Dissociation on Ru(0001) Surfaces with Multilayered Hexagonal Close-Packed Structures. ACS Omega, 2022, 7, 4492-4500.	1.6	4
64999	Exploring the Synthesis of Alkali Metal Anti-perovskites. Chemistry of Materials, 2022, 34, 947-958.	3.2	13
65000	Theoretical screening of highly efficient single-atom catalysts for nitrogen reduction based on a defective C3N monolayer. International Journal of Hydrogen Energy, 2022, 47, 5292-5306.	3.8	10
65001	Graphene Lattices with Embedded Transition-Metal Atoms and Tunable Magnetic Anisotropy Energy: Implications for Spintronic Devices. ACS Applied Nano Materials, 2022, 5, 1562-1573.	2.4	13
65002	First-Principles Calculations for the Impact of Hydrogenation on the Electron Behavior and Stability of Borophene Nanosheets: Implications for Boron 2D Electronics. ACS Applied Nano Materials, 2022, 5, 1419-1425.	2.4	2
65003	Intriguing strain-governed magnetic phase transitions in 2D vanadium porphyrin sheets. Physical Chemistry Chemical Physics, 2022, 24, 3834-3843.	1.3	2
65004	Effect of chlorine vacancy on the electronic and optical properties of CsSnCl3 perovskites for optoelectronic applications. Chemical Physics Letters, 2022, 794, 139397.	1.2	5
65005	Machine learning assisted high-throughput screening of transition metal single atom based superb hydrogen evolution electrocatalysts. Journal of Materials Chemistry A, 2022, 10, 6679-6689.	5.2	74
65006	Rational design of Ru species on N-doped graphene promoting water dissociation for boosting hydrogen evolution reaction. Science China Chemistry, 2022, 65, 521-531.	4.2	12
65007	First-principles study of Fe atom adsorbed biphenylene monolayer. Wuli Xuebao/Acta Physica Sinica, 2022, 71, 036801.	0.2	0
65008	Identification of the active site during CF₄ hydrolytic decomposition over Î³-Al₂O₃. Environmental Science: Nano, 2022, 9, 954-963.	2.2	6
65009	N₂O Adsorption and Photochemistry on Ceria Surfaces. Journal of Physical Chemistry C, 2022, 126, 2253-2263.	1.5	1
65010	Unravelling the Impact of Ta Doping on the Electronic and Structural Properties of Titania: A Combined Theoretical and Experimental Approach. Journal of Physical Chemistry C, 2022, 126, 2285-2297.	1.5	2
65011	Promotion of the oxygen evolution reaction via the reconstructed active phase of perovskite oxide. Journal of Materials Chemistry A, 2022, 10, 2271-2279.	5.2	17
65012	Rational Design of Bimetallic Zeolitic Imidazolate Frameworkâ€Derived C, N Dualâ€Doped ZnO/Co for Boosting Lithium Storage. Advanced Sustainable Systems, 2022, 6, .	2.7	1
65013	Valley splitting and magnetic anisotropy in two-dimensional VI₃/MSe₂ (M = W,) Tj ETQq1 1 0.784314 rgBT	1.3	6

#	Article	IF	Citations
65014	Formation of Unconventional Stoichiometric Naâ€“Cl Magicâ€Number Nanoclusters and 2D Assembly on Ir(111). Small Methods, 2022, 6, e2101252.	4.6	1
65015	Insight into the performance of different Pt/KL catalysts for n-alkane (C6â€“C8) aromatization: catalytic role of zeolite channels. Catalysis Science and Technology, 2022, 12, 1610-1618.	2.1	13
65016	Enhanced Electroconversion CO₂â€toâ€Formate by Oxygenâ€Vacancyâ€Rich Ultrasmall Biâ€Based Catalyst Over a Wide Potential Window. ChemCatChem, 2022, 14, .	1.8	7
65017	A self-regulated gradient interphase for dendrite-free solid-state Li batteries. Energy and Environmental Science, 2022, 15, 1325-1333.	15.6	98
65018	Tunable magnetoelectric coupling and electrical features in an ultrathin Cr₂Si₂Te₆/In₂Se₃ heterostructure. Physical Chemistry Chemical Physics, 2022, 24, 3200-3206.	1.3	3
65019	Facile preparation, catalytic performance and reaction mechanism of Mn_xCo_{1â^'x}O_{Î´}/3DOM-m Ti_{0.7}Si_{0.2}W_{0.1}O_ycatalysts for the simultaneous removal of soot and NO_x. Catalysis Science and Technology, 2022, 12, 1959-1967.	2.1	6
65020	Pressure-dependent topological superconductivity on the surface of FeTe0.5Se0.5. New Journal of Physics, 2022, 24, 023001.	1.2	1
65021	Iterative subspace algorithms for finite-temperature solution of Dyson equation. Journal of Chemical Physics, 2022, 156, 094101.	1.2	11
65022	Giant anisotropic in-plane thermal conduction induced by Anomalous phonons in pentagonal PdSe2. Materials Today Physics, 2022, 22, 100599.	2.9	8
65023	On the mechanism of Mn(II)-doping in Scandia stabilized zirconia electrolytes. Acta Materialia, 2022, 227, 117695.	3.8	3
65024	Polaronic Signatures in Doped and Undoped Cesium Lead Halide Perovskite Nanocrystals through a Photoinduced Raman Mode. ACS Applied Materials & Interfaces, 2022, 14, 5567-5577.	4.0	1
65025	Janus Ga₂SeTe/In₂SSe heterostructures: tunable electronic, optical, and photocatalytic properties. Physical Chemistry Chemical Physics, 2022, 24, 4425-4436.	1.3	8
65026	Chiral Hybrid Copper(I) Halides for High Efficiency Second Harmonic Generation with a Broadband Transparency Window. Angewandte Chemie - International Edition, 2022, 61, .	7.2	53
65027	Strain-induced bandgap engineering in CsGeX₃ (X = I, Br or Cl) perovskites: insights from first-principles calculations. Physical Chemistry Chemical Physics, 2022, 24, 5448-5454.	1.3	12
65028	Revealing the Competition between Defectâ€Trapped Exciton and Bandâ€Edge Exciton Photoluminescence in Monolayer Hexagonal WS₂. Advanced Optical Materials, 2022, 10, .	3.6	8
65029	Stressâ€“Strain Relations and Deformation Mechanisms of ZrN and HfN Superconductors. Crystal Growth and Design, 2022, 22, 1104-1109.	1.4	1
65030	A Novel Technique for Controlling Anisotropic Ion Diffusion: Bulk Singleâ€Crystalline Metallic Silicon Clathrate. Advanced Materials, 2021, , 2106754.	11.1	4
65031	Multilayer WSe₂/MoS₂ Heterojunction Phototransistors through Periodically Arrayed Nanopore Structures for Bandgap Engineering. Advanced Materials, 2022, 34, e2108412.	11.1	21

#	Article	IF	Citations
65032	Antisintering Pd₁ Catalyst for Propane Direct Dehydrogenation with In Situ Active Sites Regeneration Ability. ACS Catalysis, 2022, 12, 2244-2252.	5.5	23
65033	Tunable electronic structure and CO2 adsorption of hb-Sb/graphene van der Waals heterostructure. Physica E: Low-Dimensional Systems and Nanostructures, 2022, 139, 115154.	1.3	4
65034	N, O-coupling towards the selectively electrochemical production of H2O2. Chinese Chemical Letters, 2022, 33, 5152-5157.	4.8	19
65035	N2O Hydrogenation on Silver Doped Gold Catalysts, a DFT Study. Nanomaterials, 2022, 12, 394.	1.9	0
65036	Two-dimensional chromium phosphorus monolayer based gas sensors to detect NOx: A first-principles study. Results in Physics, 2022, 32, 105100.	2.0	10
65037	Highly-anisotropic plasmons in two-dimensional hyperbolic copper borides. Optics Express, 2022, 30, 5596.	1.7	6
65038	Exfoliating spent cathode materials with robust interlayer interactions into atomic-thin nanosheets for boosting the oxygen evolution reaction. Journal of Materials Chemistry A, 2022, 10, 3359-3372.	5.2	11
65039	Structural and electronic insight into the effect of indium doping on the photocatalytic performance of TiO₂ for CO₂ conversion. Journal of Materials Chemistry A, 2022, 10, 6054-6064.	5.2	13
65040	Enhanced activity and sulfur resistance of Cu- and Fe-modified activated carbon for the reduction of NO by CO from regeneration gas. Catalysis Science and Technology, 2022, 12, 737-749.	2.1	5
65041	The reaction mechanism of acetylene hydrochlorination on defective carbon supported ruthenium catalysts identified by DFT calculations and experimental approaches. Inorganic Chemistry Frontiers, 2022, 9, 458-467.	3.0	5
65042	Crystal structure, lattice dynamics and superexchange in MAgF₃ 1D antiferromagnets (M =) Tj ETQq0 0 0 rgBT /Overlock 1 CrystEngComm, 2022, 24, 1068-1077.	1.3	2
65043	Double-hybrid density functionals for the condensed phase: Gradients, stress tensor, and auxiliary-density matrix method acceleration. Journal of Chemical Physics, 2022, 156, 074107.	1.2	7
65044	Stabilization of S3O4 at high pressure: implications for the sulfur-excess paradox. Science Bulletin, 2022, 67, 971-976.	4.3	6
65045	A low resistance and stable lithium-garnet electrolyte interface enabled by a multifunctional anode additive for solid-state lithium batteries. Journal of Materials Chemistry A, 2022, 10, 2519-2527.	5.2	22
65046	Computational Evaluation of Li-doped g-C2N Monolayer as Advanced Hydrogen Storage Media. International Journal of Hydrogen Energy, 2022, 47, 3625-3632.	3.8	25
65047	Tuning the Schottky barrier height in a multiferroic In2Se3/Fe3GeTe2 van der Waals heterojunction. Nanoscale, 2021, , .	2.8	11
65048	Spatially Resolved Investigation of the Bandgap Variation across a Î²-(Al_xGa_{1â€“x})₂O₃/Î²-Ga₂O₃ Interface by STEMâ€“VEELS. ACS Applied Electronic Materials, 2022, 4, 585-591.	2.0	2
65049	WO₃ Nanosheet-Supported IrW Alloy for High-Performance Acidic Overall Water Splitting with Low Ir Loading. ACS Applied Energy Materials, 2022, 5, 970-980.	2.5	15

#	Article	IF	Citations
65050	Study on New High-Pressure Phases and Electronic Properties of Iodine Chloride Employing Ab Initio Calculations. Journal of Electronic Materials, 2022, 51, 1632-1638.	1.0	3
65051	Manipulating Interfacial Thermal Conduction of 2D Janus Heterostructure via a Thermoâ€Mechanical Coupling. Advanced Functional Materials, 2022, 32, .	7.8	45
65052	Seeking New Layered Oxyselenides with Promising Thermoelectric Performance. Advanced Functional Materials, 2022, 32, .	7.8	14
65053	Î²-SnS/GaSe heterostructure: a promising solar-driven photocatalyst with low carrier recombination for overall water splitting. Journal of Materials Chemistry A, 2022, 10, 3443-3453.	5.2	28
65054	Janus monolayer HfSO with improved optical properties as a novel material for photovoltaic and photocatalyst applications. New Journal of Chemistry, 2022, 46, 1557-1568.	1.4	4
65055	Coordination modulation of iridium single-atom catalyst maximizing water oxidation activity. Nature Communications, 2022, 13, 24.	5.8	99
65056	Interfacial-confined coordination to single-atom nanotherapeutics. Nature Communications, 2022, 13, 91.	5.8	49
65057	Density-functional-theory predictions of mechanical behaviour and thermal properties as well as experimental hardness of the Ga-bilayer Mo2Ga2C. Journal of Advanced Ceramics, 2022, 11, 273-282.	8.9	26
65058	Strain-Engineered Mn-Doped Transition Metal Dichalcogenides. Journal of Electronic Materials, 2022, 51, 1358-1370.	1.0	1
65059	Two-dimensional B7P2: Dual-purpose functional material for hydrogen evolution reaction/hydrogen storage. International Journal of Hydrogen Energy, 2022, 47, 8338-8347.	3.8	6
65060	Half-Heusler-like compounds with wide continuous compositions and tunable p- to n-type semiconducting thermoelectrics. Nature Communications, 2022, 13, 35.	5.8	20
65061	How palladium inhibits CO poisoning during electrocatalytic formic acid oxidation and carbon dioxide reduction. Nature Communications, 2022, 13, 38.	5.8	44
65062	Phase Stability and Mechanical Properties of the Monoclinic, Monoclinic-Prime and Tetragonal REMO4 (M = Ta, Nb) from First-Principles Calculations. Coatings, 2022, 12, 73.	1.2	8
65063	Substitutional alkaline earth metals delay nonradiative charge recombination in CH3NH3PbI3 perovskite: A time-domain study. Journal of Chemical Physics, 2022, 156, 014702.	1.2	2
65064	Improved Optical and Electronic Properties of Single-Layer MoS₂ by Co Doping for Promising Intermediate - Band Materials. Key Engineering Materials, 0, 905, 96-102.	0.4	0
65065	B2O and B4N monolayers supported single-metal atom as highly efficient bifunctional electrocatalyst for OER and ORR. Journal of Materials Science, 2022, 57, 398-410.	1.7	4
65066	Electronic properties of double-atom catalysts for electrocatalytic oxygen evolution reaction in alkaline solution: a DFT study. Nanoscale, 2021, 14, 187-195.	2.8	17
65067	Facile template-free preparation of silver-coated Cu3SbS4 hollow spheres with enhanced photoelectric properties. Journal of Materials Chemistry C, 2021, 10, 301-311.	2.7	2

#	Article	IF	Citations
65068	Insight into the photoexcitation effect on the catalytic activation of H2 and C-H bonds on TiO2(110) surface. Chinese Chemical Letters, 2022, 33, 4705-4709.	4.8	9
65069	Atomically Thin Indium-Tin-Oxide Transistors Enabled by Atomic Layer Deposition. IEEE Transactions on Electron Devices, 2022, 69, 231-236.	1.6	20
65070	LaFeO₃ meets nitrogen-doped graphene functionalized with ultralow Pt loading in an impactful Z-scheme platform for photocatalytic hydrogen evolution. Journal of Materials Chemistry A, 2022, 10, 3330-3340.	5.2	14
65071	Interpreting the Operando X-ray Absorption Near-Edge Structure of Supported Cu and CuPd Clusters in Conditions of Oxidative Dehydrogenation of Propane: Dynamic Changes in Composition and Size. Journal of Physical Chemistry C, 2022, 126, 1972-1981.	1.5	3
65072	Crystal Structure Prediction Using an Age-Fitness Multiobjective Genetic Algorithm and Coordination Number Constraints. Journal of Physical Chemistry A, 2022, 126, 640-647.	1.1	0
65073	Oxygen deficient Î±-MoO₃ with enhanced adsorption and state-quenching of H₂O for gas sensing: a DFT study. Journal of Materials Chemistry C, 2022, 10, 1839-1849.	2.7	9
65074	The effect of N-doping on the electronic structure property and the li and Na storage capacity of graphene nanomaterials: A first-principles study. Electrochimica Acta, 2022, 403, 139719.	2.6	12
65075	Visualizing the evolution from Mott insulator to Anderson insulator in Ti-doped 1T-TaS2. Npj Quantum Materials, 2022, 7, .	1.8	9
65076	Stabilizing XPbI₃ (X = MA, FA and Cs) cubic perovskites by monolayer Ag₄Se₂ deposition. New Journal of Chemistry, 2022, 46, 1329-1338.	1.4	3
65077	Cationâ€/Anionâ€Based Physicochemical Mechanisms for Anodicallyâ€Coloring Electrochromic Nickel Oxide Thin Films. ChemElectroChem, 0, , .	1.7	1
65078	Understanding the role of spacer cation in 2D layered halide perovskites to achieve stable perovskite solar cells. Materials Advances, 2022, 3, 2464-2474.	2.6	7
65079	Data-Driven Quest for Two-Dimensional Non-van der Waals Materials. Nano Letters, 2022, 22, 989-997.	4.5	35
65080	Ab initio surface free energies of tungsten with full account of thermal excitations. Physical Review B, 2022, 105, .	1.1	10
65081	Giant valley-polarized spin splittings in magnetized Janus Pt dichalcogenides. Physical Review B, 2022, 105, .	1.1	3
65082	Stability and electronic properties of monolayer and multilayer structures of group-IV elements and compounds of complementary groups in biphenylene network. Physical Review B, 2022, 105, .	1.1	22
65083	Edge and Pointâ€Defect Induced Electronic and Magnetic Properties in Monolayer PtSe₂. Advanced Functional Materials, 2022, 32, .	7.8	21
65084	Electronic structure and thermal conductance of the MASnI3/Bi2Te3 interface: a first-principles study. Scientific Reports, 2022, 12, 217.	1.6	5
65085	A superconducting boron allotrope featuring anticlinal pentapyramids. Journal of Materials Chemistry C, 2022, 10, 672-679.	2.7	10

#	Article	IF	Citations
65086	A combined first principles study of the structural, magnetic, and phonon properties of monolayer CrI3. Journal of Chemical Physics, 2022, 156, 014707.	1.2	18
65087	Surface structure of magnetite (111) under oxidizing and reducing conditions. Journal of Physics Condensed Matter, 2022, 34, 164003.	0.7	7
65088	Discovery of Electrides in Electronâ€Rich Nonâ€Electride Materials via Energy Modification of Interstitial Electrons. Advanced Functional Materials, 2022, 32, .	7.8	8
65089	Magnetic field induced valley-polarized quantum anomalous Hall effects in ferromagnetic van der Waals heterostructures. Physical Review B, 2022, 105, .	1.1	11
65090	Ferromagnetic helical nodal line and Kane-Mele spin-orbit coupling in kagome metal <mml:math xmlns:mml="http://www.w3.org/1998/Math/MathML"><mml:msub><mml:mrow><mml:mi>Fe</mml:mi></mml:mrow><mml:mn>3</mml:mn> Physical Review B, 2022, 105, .	1.1	10
65091	Two-step nucleation of the Earthâ€™s inner core. Proceedings of the National Academy of Sciences of the United States of America, 2022, 119, .	3.3	14
65092	Transition metal halide nanowires: A family of one-dimensional multifunctional building blocks. Applied Physics Letters, 2022, 120, .	1.5	10
65093	Aluminium vanadate with unsaturated coordinated V centers and oxygen vacancies: surface migration and partial phase transformation mechanism in high performance zinc-ion batteries. Journal of Materials Chemistry A, 2022, 10, 912-927.	5.2	32
65094	Bulk <mml:math xmlns:mml="http://www.w3.org/1998/Math/MathML"><mml:mrow><mml:mi>NdNi</mml:mi><mml:msub><mml:mi mathvariant="normal">O</mml:mi><mml:mn>2</mml:mn></mml:msub></mml:mrow></mml:math> is thermodynamically unstable with respect to decomposition while hydrogenation reduces the instability and transforms it from metal to insulator. Physical Review B, 2022, 105, .	1.1	33
65095	Atomic Edge-Guided Polyethylene Crystallization on Monolayer Two-Dimensional Materials. Macromolecules, 2022, 55, 559-567.	2.2	6
65096	Two-dimensional AlBiX3(XÂ=ÂS, Se, Te) monolayers for photocatalytic water splitting hydrogen evolution reaction under the irradiation of solar light. FlatChem, 2022, 31, 100331.	2.8	3
65097	H₂O and CO₂ surface contamination of the lithium garnet Li₇La₃Zr₂O₁₂ solid electrolyte. Journal of Materials Chemistry A, 2022, 10, 4960-4973.	5.2	6
65098	<mml:math xmlns:mml="http://www.w3.org/1998/Math/MathML"><mml:msub><mml:mi>C</mml:mi><mml:mi>n</mml:mi></mml:msub></mml:ma -symmetric higher-order topological crystalline insulators in atomically thin transition metal dichalcogenides. Physical Review B, 2022, 105, .	1.1	36
65099	Exploration of trivial and nontrivial electronic phases and of collinear and noncollinear magnetic phases in low-spin d5 perovskites. Physical Review B, 2022, 105, .	1.1	2
65100	Molecular insight into the role of zeolite lattice constraints on methane activation over the Cuâ€“Oâ€“Cu active site. Physical Chemistry Chemical Physics, 2022, 24, 4196-4203.	1.3	7
65101	Bidirectional Phase Transformation of Supramolecular Networks Using Two Molecular Signals. ACS Nano, 2022, 16, 1560-1566.	7.3	1
65102	Ab initio prediction of vacancy energetics in HCP Al-Hf-Sc-Ti-Zr high entropy alloys and the subsystems. Acta Materialia, 2022, 227, 117677.	3.8	22
65103	Highly Dispersed Pt Clusters on F-Doped Tin(IV) Oxide Aerogel Matrix: An Ultra-Robust Hybrid Catalyst for Enhanced Hydrogen Evolution. ACS Nano, 2022, 16, 1625-1638.	7.3	48

#	Article	IF	Citations
65104	High-throughput assessment of two-dimensional electrode materials for energy storage devices. Cell Reports Physical Science, 2022, 3, 100718.	2.8	10
65105	Heterostructural MoS₂/NiS nanoflowers via precise interface modification for enhancing electrocatalytic hydrogen evolution. New Journal of Chemistry, 2022, 46, 5505-5514.	1.4	8
65106	Discerning phase-matrices for individual nitride inclusions within ultra-high-strength steel: experiment driven DFT investigation. Physical Chemistry Chemical Physics, 2022, 24, 1456-1461.	1.3	3
65107	Ammonia synthesis on BaTiO_{2.5}H_{0.5}: computational insights into the role of hydrides. Physical Chemistry Chemical Physics, 2022, 24, 1496-1502.	1.3	4
65108	Atomic-level coupled spinel@perovskite dual-phase oxides toward enhanced performance in Znâ€“air batteries. Journal of Materials Chemistry A, 2022, 10, 1506-1513.	5.2	28
65109	Hole- and electron-injection driven phase transitions in transition metal dichalcogenides and beyond: A unified understanding. Physical Review B, 2022, 105, .	1.1	10
65110	Understanding Alkali Contamination in Colloidal Nanomaterials to Unlock Grain Boundary Impurity Engineering. Journal of the American Chemical Society, 2022, 144, 987-994.	6.6	12
65111	Gapless spin liquid behavior in a kagome Heisenberg antiferromagnet with randomly distributed hexagons of alternate bonds. Physical Review B, 2022, 105, .	1.1	13
65112	Correlation strength, orbital-selective incoherence, and local moments formation in the magnetic MAX-phase<mml:math xmlns:mml="http://www.w3.org/1998/Math/MathML"><mml:mrow><mml:msub><mml:mi>Mn</mml:mi><mml:mn>2</mml:mn></mml: Physical Review B, 2022, 105, .	1.1	3
65113	Co and Ni Incorporated Î³-Al2O3 (110) Surface: A Density Functional Theory Study. Catalysts, 2022, 12, 111.	1.6	3
65114	Intrinsic Valley Polarization in Computationally Discovered Twoâ€Dimensional Ferrovalley Materials: LaI₂ and PrI₂ Monolayers. Advanced Theory and Simulations, 2022, 5, .	1.3	8
65115	Understanding High-Temperature Chemical Reactions on Metal Surfaces: A Case Study on Equilibrium Concentration and Diffusivity of C_xH_y on a Cu(111) Surface. Jacs Au, 2022, 2, 443-452.	3.6	8
65116	Organic molecular dynamics and charge-carrier lifetime in lead iodide perovskite MAPbI ₃. Proceedings of the National Academy of Sciences of the United States of America, 2022, 119, .	3.3	14
65117	Modulation of the Bi³⁺ 6s² Lone Pair State in Perovskites for Highâ€Mobility pâ€Type Oxide Semiconductors. Advanced Science, 2022, 9, e2104141.	5.6	23
65118	Optical detection of the density-wave instability in the kagome metal KV3Sb5. Npj Quantum Materials, 2022, 7, .	1.8	57
65119	Structure and stability of possible new L i-Y-H ternary hydrides. Wuli Xuebao/Acta Physica Sinica, 2022, 71, 017401.	0.2	1
65120	Interface-dependent phononic and optical properties of GeO/MoSO heterostructures. Nanoscale, 2022, 14, 865-874.	2.8	5
65121	Synergizing Surface Hydride Species and Ru Clusters on Sm₂O₃ for Efficient Ammonia Synthesis. ACS Catalysis, 2022, 12, 2178-2190.	5.5	23

#	Article	IF	Citations
65122	Photoinduced Spin Injection and Ferromagnetism in 2D Group III Monochalcogenides. Journal of Physical Chemistry Letters, 2022, 13, 590-597.	2.1	11
65123	Doping and Coating Synergy to Improve the Rate Capability and Cycling Stability of Lithium-Rich Cathode Materials for Lithium-Ion Batteries. Journal of Physical Chemistry C, 2022, 126, 2410-2423.	1.5	7
65124	Monolayer gadolinium halides, GdX₂ (X = F, Cl, Br): intrinsic ferrovalley materials with spontaneous spin and valley polarizations. Physical Chemistry Chemical Physics, 2022, 24, 3865-3874.	1.3	23
65125	High-Throughput Screening of Efficient Biatom Catalysts Based on Monolayer Carbon Nitride for the Nitric Oxide Reduction Reaction. Journal of Physical Chemistry Letters, 2022, 13, 527-535.	2.1	35
65126	Deciphering the Exceptional Performance of NiFe Hydroxide for the Oxygen Evolution Reaction in an Anion Exchange Membrane Electrolyzer. ACS Applied Energy Materials, 2022, 5, 2221-2230.	2.5	22
65127	Oneâ€Step MOFâ€Templated Strategy to Fabrication of Ceâ€Doped ZnIn₂S₄ Tetrakaidecahedron Hollow Nanocages as an Efficient Photocatalyst for Hydrogen Evolution. Advanced Science, 2022, 9, e2104579.	5.6	90
65128	Toward Hydrogenâ€Free and Dendriteâ€Free Aqueous Zinc Batteries: Formation of Zincophilic Protective Layer on Zn Anodes. Advanced Science, 2022, 9, e2104866.	5.6	118
65129	Photocatalytic degradation of methylene blue (MB) with Cu₁â€“ZnO single atom catalysts on graphene-coated flexible substrates. Journal of Materials Chemistry A, 2022, 10, 6231-6241.	5.2	32
65130	Structural, magnetic and ferroelectric properties of VOBr₂monolayer: A first-principles study. Wuli Xuebao/Acta Physica Sinica, 2022, 71, 037101.	0.2	2
65131	Electronic and Magnetic Properties of Eutectoid Growth Mn-rich Ge1-xMnx Dilute Magnetic Semiconductors. Current Chinese Science, 2022, 2, 101-108.	0.2	1
65132	A computational study of the interaction of oxygenates with the surface of rutile TiO2(110). Structural and electronic trends.. Journal of Physics Condensed Matter, 2022, , .	0.7	3
65133	Theoretical Study on Carbon Monoxide Adsorption on Unsupported and Î³-Al₂O₃-Supported Silver Nanoparticles: Size, Shape, and Support Effects. ACS Omega, 2022, 7, 4405-4412.	1.6	8
65134	Large magneto-optical effect and magnetic anisotropy energy in two-dimensional metallic ferromagnet <mml:math xmlns:mml="http://www.w3.org/1998/Math/MathML"><mml:mrow><mml:msub><mml:mi>Fe</mml:mi><mml:mn>3</mml:mn></mml:r Physical Review B, 2022, 105, .	1.1	14
65135	Understanding the Photocatalytic Activity of La₅Ti₂AgS₅O₇ and La₅Ti₂CuS₅O₇ for Green Hydrogen Production: Computational Insights. ACS Applied Energy Materials, 2022, 5, 1992-2001.	2.5	11
65136	Emergent interface vibrational structure of oxide superlattices. Nature, 2022, 601, 556-561.	13.7	40
65137	Highly thermostable white-emitting Ca₉ZnK(PO₄)₇:Ce³⁺,Dy³⁺ single-phase phosphor with tunable photoluminescence and energy transfer. Dalton Transactions, 2022, 51, 2770-2781.	1.6	17
65138	First-principles calculations to study the optical/electronic properties of 2D VS2 with Z doping (Z = N,) Tj ETQq0 0 0 rgBT /Overlock 10 T	1.8	5
65139	Continuous Oxygen Vacancy Gradient in TiO₂ Photoelectrodes by a Photoelectrochemicalâ€Driven â€œSelfâ€Purificationâ€•Process. Advanced Energy Materials, 2022, 12, .	10.2	42

#	Article	IF	Citations
65140	Observation of One-Dimensional Dirac Fermions in Silicon Nanoribbons. Nano Letters, 2022, 22, 695-701.	4.5	12
65141	Green ammonia synthesis using CeO₂/RuO₂ nanolayers on vertical graphene catalyst via electrochemical route in alkaline electrolyte. Nanoscale, 2022, 14, 1395-1408.	2.8	11
65142	CO 2 Hydrogenation to Methanol over Cd 4 /TiO 2 Catalyst: Insight into Multifunctional Interface. ChemCatChem, 0, , .	1.8	1
65143	Bending as a control knob for the electronic and optical properties of phosphorene nanoribbons. Physical Review Materials, 2022, 6, .	0.9	4
65144	<mml:math xmlns:mml="http://www.w3.org/1998/Math/MathML"><mml:msub><mml:mi mathvariant="double-struck">Z</mml:mi><mml:mn>2</mml:mn></mml:msub></mml:math> nontrivial topology of rare-earth binary oxide superconductor LaO. Physical Review B, 2022, 105, .	1.1	2
65145	Synergistic coupling of FeNi3 alloy with graphene carbon dots for advanced oxygen evolution reaction electrocatalysis. Journal of Colloid and Interface Science, 2022, 615, 273-281.	5.0	77
65146	Metalâ€“organic frameworks with mixed-anion secondary building units as efficient photocatalysts for hydrogen generation. Journal of Catalysis, 2022, 407, 10-18.	3.1	5
65147	Analysis of Intermediates and Products from the Dehydrogenation of Mg(BH₄)₂. Journal of Physical Chemistry A, 2022, 126, 444-452.	1.1	6
65148	Low-Temperature Direct Growth of Few-Layer Hexagonal Boron Nitride on Catalyst-Free Sapphire Substrates. ACS Applied Materials & Interfaces, 2022, 14, 7004-7011.	4.0	24
65149	Understanding the Influence of C-Doping on CO₂ Photoreduction at SnS₂ Nanosheets: A First-Principles Study. Journal of Physical Chemistry C, 2022, 126, 1271-1280.	1.5	4
65150	Local Electronic Charge Transfer in the Helical Induction of Cis-Transoid Poly(4-carboxyphenyl)acetylene by Chiral Amines. Journal of Chemical Information and Modeling, 2022, , .	2.5	1
65151	Factors that affect volume change during electrochemical cycling in cathode materials for lithium ion batteries. Physical Chemistry Chemical Physics, 2022, 24, 2167-2175.	1.3	7
65152	Engineering Metallic Heterostructure Based on Ni₃N and 2Mâ€MoS₂ for Alkaline Water Electrolysis with Industryâ€Compatible Current Density and Stability. Advanced Materials, 2022, 34, e2108505.	11.1	104
65153	The Systematic Study on the Stability and Superconductivity of Yâ€Mgâ€H Compounds under High Pressure. Advanced Theory and Simulations, 2022, 5, .	1.3	13
65154	Excited State Dynamics in Dual-Defects Modified Graphitic Carbon Nitride. Journal of Physical Chemistry Letters, 2022, 13, 1033-1041.	2.1	16
65155	A Ï€-extended triphenylamine based dopant-free hole-transporting material for perovskite solar cells via heteroatom substitution. Physical Chemistry Chemical Physics, 2022, 24, 4635-4643.	1.3	9
65156	Effects of potassium on propylene epoxidation by molecular oxygen on Cu₂O (111): a DFT study. Catalysis Science and Technology, 2022, 12, 1487-1498.	2.1	2
65157	Unusual luminescence and its decay behavior of CH3NH3PbBr3 single crystals at orthorhombic phase. Materials Today Physics, 2022, 22, 100621.	2.9	3

#	Article	IF	Citations
65158	Promoted photocarriers separation by straining in 2D/2D van der Waals heterostructures for high-efficiency visible-light photocatalysis. Materials Today Physics, 2022, 22, 100600.	2.9	13
65159	Metalâ€Organic Framework Glass Anode with an Exceptional Cyclingâ€Induced Capacity Enhancement for Lithiumâ€Ion Batteries. Advanced Materials, 2022, 34, e2110048.	11.1	83
65160	Emergence of Magnetic Transition in Cobalt Oxide Nanowires on Vicinal Pt Substrate. IEEE Magnetics Letters, 2022, 13, 1-5.	0.6	1
65161	Effect of the co-adsorption of small molecules from air on the properties of penta-graphene and their proton transfer calculation. Physical Chemistry Chemical Physics, 2022, , .	1.3	0
65162	Hard and soft materials: putting consistent van der Waals density functionals to work. Electronic Structure, 2022, 4, 014001.	1.0	4
65163	Direct band gap and anisotropic transport of ZnSb monolayers tuned by hydrogenation and strain. RSC Advances, 2022, 12, 2693-2700.	1.7	2
65164	Weak-Bonding Elements Lead to High Thermoelectric Performance in BaSnS₃ and SrSnS₃: A First-Principles Study. Chemistry of Materials, 2022, 34, 1289-1301.	3.2	19
65165	Free-standing 2D ironene with magnetic vortex structure at room temperature. Matter, 2022, 5, 291-301.	5.0	13
65166	Formation of twelve-fold iodine coordination at high pressure. Nature Communications, 2022, 13, 412.	5.8	23
65167	Mechanistic differences between methanol and dimethyl ether in zeolite-catalyzed hydrocarbon synthesis. Proceedings of the National Academy of Sciences of the United States of America, 2022, 119, .	3.3	17
65168	Surface dynamics on submonolayer Pb/Cu(001) surfaces. Physical Chemistry Chemical Physics, 2022, 24, 5164-5170.	1.3	0
65169	Relativistic domain-wall dynamics in van der Waals antiferromagnet MnPS3. Npj Computational Materials, 2022, 8, .	3.5	18
65170	From fundamental to CO₂ and COCl₂ gas sensing properties of pristine and defective Si₂BN monolayers. Physical Chemistry Chemical Physics, 2022, 24, 4394-4406.	1.3	10
65171	Enhanced proton irradiation resistance in Cs-doped CH3NH3PbI3 films and solar cells. Journal of Energy Chemistry, 2022, 69, 261-269.	7.1	4
65172	Charged Domain Wall and Polar Vortex Topologies in a Room-Temperature Magnetoelectric Multiferroic Thin Film. ACS Applied Materials & Interfaces, 2022, 14, 5525-5536.	4.0	7
65173	The role of interlayer gases and surface asperities in compression-induced intermetallic formation in Ni/Al nanocomposites. Physical Chemistry Chemical Physics, 2022, 24, 2909-2924.	1.3	3
65174	Water Interaction with Fe2NiP Schreibersite (110) Surface: a Quantum Mechanical Atomistic Perspective. Journal of Physical Chemistry C, 2022, 126, 2243-2252.	1.5	1
65175	Impact of the Polymorphism and Relativistic Effects on the Electronic Properties of Inorganic Metal Halide Perovskites. Journal of Physical Chemistry C, 2022, 126, 2131-2140.	1.5	4

#	Article	IF	Citations
65176	Mechanism of Methanol Synthesis from CO₂ Hydrogenation over Pt₈/In₂O₃ Catalysts: A Combined Study on Density Functional Theory and Microkinetic Modeling. Journal of Physical Chemistry C, 2022, 126, 1761-1769.	1.5	9
65177	Lead-Free Ultra-Wide Direct Bandgap Perovskite EACaI₃. IEEE Nanotechnology Magazine, 2022, 21, 66-70.	1.1	8
65178	Tuning precise numbers of supported nickel clusters on graphdiyne for efficient CO2 electroreduction toward various multi-carbon products. Journal of Energy Chemistry, 2022, 69, 456-465.	7.1	49
65179	Potential outstanding physical properties of novel black arsenic phosphorus As_{0.25}P_{0.75}/As_{0.75}P_{0.25} phases: a first-principles investigation. RSC Advances, 2022, 12, 3745-3754.	1.7	8
65180	Activation of Cellulose with Alkaline Earth Metals. ACS Sustainable Chemistry and Engineering, 2022, 10, 1943-1950.	3.2	4
65181	Adsorption of nitrogen oxides on modified BN nanosheets: improved gas sensing and functionalization. New Journal of Chemistry, 2022, 46, 4373-4384.	1.4	2
65182	Diabolical touching point in the magnetic energy levels of topological nodal-line metals. Physical Review B, 2022, 105, .	1.1	1
65183	Strain-induced topological phase transition and enhanced Curie temperature in <mml:math xmlns:mml="http://www.w3.org/1998/Math/MathML"><mml:mrow><mml:msub><mml:mi>MnBi</mml:mi><mml:mn>2</mml:mn></ heterojunction. Physical Review Materials, 2022, 6, .	0.9	11
65184	CO₂ reduction on single-atom Ir catalysts with chemical functionalization. Physical Chemistry Chemical Physics, 2022, 24, 3733-3740.	1.3	3
65185	Furfural Adsorption and Hydrogenation at the Oxideâ€Metal Interface: Evidence of the Support Influence on the Selectivity of Iridiumâ€Based Catalysts. ChemCatChem, 2022, 14, .	1.8	7
65186	All-optical logic devices based on black arsenicâ€“phosphorus with strong nonlinear optical response and high stability. Opto-Electronic Advances, 2022, 5, 200046-200046.	6.4	25
65187	Magnetic Moment Tensor Potentials for collinear spin-polarized materials reproduce different magnetic states of bcc Fe. Npj Computational Materials, 2022, 8, .	3.5	52
65188	Effect of strain on charge density wave order in Î±-U. Chinese Physics B, 0, , .	0.7	1
65189	ChalcogenÂ·Â·Â·Chalcogen Bonding in Molybdenum Disulfide, Molybdenum Diselenide and Molybdenum Ditelluride Dimers as Prototypes for a Basic Understanding of the Local Interfacial Chemical Bonding Environment in 2D Layered Transition Metal Dichalcogenides. Inorganics, 2022, 10, 11.	1.2	8
65190	Monolayer NbNSe with High Fermi Velocity and Anisotropic Properties. Physica Status Solidi (B): Basic Research, 0, , .	0.7	1
65191	Atomically dispersed Pt sites on porous metalâ€“organic frameworks to enable dual reaction mechanisms for enhanced photocatalytic hydrogen conversion. Journal of Catalysis, 2022, 407, 1-9.	3.1	21
65192	A Nanoscale Design Approach for Enhancing the Li-Ion Conductivity of the Li₁₀GeP₂S₁₂ Solid Electrolyte. , 2022, 4, 424-431.		23
65193	Multi-Bandgap Monolithic Metal Nanowire Percolation Network Sensor Integration by Reversible Selective Laser-Induced Redox. Nano-Micro Letters, 2022, 14, 49.	14.4	26

#	Article	IF	Citations
65194	Experimental verification of semi-metallic band structure in PtSe2 via thermoelectric power measurements. Applied Physics Letters, 2022, 120, 043103.	1.5	2
65195	Hydrothermal synthesis and crystal structure of a novel double-perovskite-type bismuth oxide with 3â€‰:â€‰1 ordering at the B-site. New Journal of Chemistry, 2022, 46, 3595-3601.	1.4	5
65196	Predicting diffusion barriers and diffusivities of C6â€“C12 methylbenzenes in MFI zeolites. Microporous and Mesoporous Materials, 2022, 333, 111705.	2.2	7
65197	High-ammonia selective metalâ€“organic frameworkâ€“derived Co-doped Fe/Fe ₂ O ₃ catalysts for electrochemical nitrate reduction. Proceedings of the National Academy of Sciences of the United States of America, 2022, 119, .	3.3	75
65198	Strain-Tunable Carrier Mobility of Fe-Doped GaN: A First-Principles Study. SSRN Electronic Journal, 0, , .	0.4	0
65199	Electron-Deficient Au Nanoparticles Confined in Organic Molecular Cages for Catalytic Reduction of 4-Nitrophenol. ACS Applied Nano Materials, 2022, 5, 1276-1283.	2.4	21
65200	LaRuSi Electride Disrupts the Scaling Relations for Ammonia Synthesis. Chemistry of Materials, 2022, 34, 1677-1685.	3.2	19
65201	Realizing Efficient Catalytic Performance and High Selectivity for Oxygen Reduction Reaction on a 2D Ni₂SbTe₂ Monolayer. Inorganic Chemistry, 2022, 61, 2284-2291.	1.9	7
65202	Highly stable actinide(III) complexes supported by doubly aromatic ligands. Physical Chemistry Chemical Physics, 2022, , .	1.3	1
65203	Simple structure descriptors quantifying the diffusion of ethene in small-pore zeolites: insights from molecular dynamic simulations. Inorganic Chemistry Frontiers, 2022, 9, 1590-1602.	3.0	4
65204	Stable interphase chemistry of textured Zn anode for rechargeable aqueous batteries. Science Bulletin, 2022, 67, 716-724.	4.3	80
65205	Highly Efficient Pureâ€Blue Perovskite Lightâ€Emitting Diode Leveraging CsPbBr_xCl_{3â^’}_x/Cs₄PbBr_xCl_{6â^’}_x Nanocomposite Emissive Layer with Shallow Valence Band. Advanced Optical Materials, 2022, 10, .		
65206	Insight into the Roles of Metal Loading on CO2 Photocatalytic Reduction Behaviors of TiO2. Nanomaterials, 2022, 12, 474.	1.9	10
65207	SbCl₄: An Exceptional Superhalogen as the Building Block of a Mixed Valence Supercrystal with Unconventional Ferroelectricity. Journal of Physical Chemistry Letters, 2022, 13, 1049-1056.	2.1	6
65208	Density functional theory method for twisted geometries with application to torsional deformations in group-IV nanotubes. Journal of Computational Physics, 2022, 456, 111023.	1.9	6
65209	The role of defects presenting in graphitic SiC sheets and their consequences in the exfoliation of layers â€“ a first principles approach. Physical Chemistry Chemical Physics, 2022, 24, 4262-4269.	1.3	3
65210	Borophane Polymorphs. Journal of Physical Chemistry Letters, 2022, 13, 1107-1113.	2.1	12
65211	Theoretical Understanding of the Effect of Coordination Environment on the Activity of Metal Macrocyclic Complexes as Electrocatalysts for Oxygen Reduction Reactions. SSRN Electronic Journal, 0, , .	0.4	0

#	Article	IF	Citations
65212	Influence of an electrified interface on the entropy and energy of solvation of methanol oxidation intermediates on platinum(111) under explicit solvation. Physical Chemistry Chemical Physics, 2022, 24, 4251-4261.	1.3	5
65213	Interfacial Chemistry Triggers Ultrafast Radiative Recombination in Metal Halide Perovskites. Angewandte Chemie - International Edition, 2022, 61, .	7.2	22
65214	Solute Segregation to Grain Boundaries in Al: A First-Principles Evaluation. Acta Metallurgica Sinica (English Letters), 2022, 35, 1572-1582.	1.5	10
65215	Magnetic properties of new (1â^'x)Bi1/2Na1/2TiO3+xBaNiO3â^ˆÎ´ solid solution materials. Applied Physics A: Materials Science and Processing, 2022, 128, 1.	1.1	3
65216	Host-guest supramolecular interaction behavior at the interface between anode and electrolyte for long life Zn anode. Journal of Energy Chemistry, 2022, 69, 237-243.	7.1	34
65217	First-principles study on the structure, magnetic and electronic properties of cobalt-based double perovskite Sr2CoTeO6. Journal of Solid State Chemistry, 2022, 309, 122958.	1.4	4
65218	Mechanochemically tailoring oxygen vacancies of MnO2 for efficient degradation of tetrabromobisphenol A with peroxymonosulfate. Applied Catalysis B: Environmental, 2022, 307, 121168.	10.8	85
65219	Role of ripples in altering the electronic and chemical properties of graphene. Journal of Chemical Physics, 2022, 156, 054708.	1.2	2
65220	Low Thermal Conductivity in Heteroanionic Materials with Layers of Homoleptic Polyhedra. Journal of the American Chemical Society, 2022, 144, 2569-2579.	6.6	13
65221	Alternate Storage of Opposite Charges in Multisites for Highâ€Energyâ€Density Alâ€“MOF Batteries. Advanced Materials, 2022, 34, e2110109.	11.1	39
65222	Flatten the Liâ€ion Activation in Perfectly Latticeâ€Matched MXene and 1Tâ€MoS 2 Heterostructures via Chemical Functionalization. Advanced Materials Interfaces, 0, , 2101838.	1.9	5
65223	Development and application of a uranium mononitride (UN) potential: Thermomechanical properties and Xe diffusion. Journal of Nuclear Materials, 2022, 562, 153553.	1.3	6
65224	Responses to comments on the paper â€œtwo-dimensional Sc2C: A reversible and high capacity hydrogen storage material predicted by first-principles calculationsâ€• International Journal of Hydrogen Energy, 2022, 47, 9829-9834.	3.8	0
65225	Molecular picture of the adsorption of phenol, toluene, carbon dioxide and water on kaolinite basal surfaces. Applied Surface Science, 2022, 585, 152699.	3.1	13
65226	Boosting the oxygen evolution reaction through migrating active sites from the bulk to surface of perovskite oxides. Journal of Energy Chemistry, 2022, 69, 434-441.	7.1	19
65227	Electron transfer-triggered imaging of EGFR signaling activity. Nature Communications, 2022, 13, 594.	5.8	13
65228	A robust solver for wavefunction-based density functional theory calculations*. Electronic Structure, 2022, 4, 015002.	1.0	0
65229	Two-dimensional graphyne-graphene heterostructure for all-carbon transistors. Journal of Physics Condensed Matter, 2022, , .	0.7	0

#	Article	IF	Citations
65230	Crystallographic engineering to reduce diffusion barrier for enhanced intercalation pseudocapacitance of TiNb2O7 in fast-charging batteries. Energy Storage Materials, 2022, 47, 178-186.	9.5	30
65231	Metallic networks and hydrogen compensation in highly nonstoichiometric amorphous <mml:math xmlns:mml="http://www.w3.org/1998/Math/MathML"><mml:mrow><mml:msub><mml:mi>In</mml:mi><mml:mn>2</mml:mn></mml:msub><mml:msub><mml:mi mathvariant="normal">O</mml:mi><mml:mrow><mml:mn>3</mml:mn><mml:mo>â^'</mml:mo><mml:mi>x</mml:mi></mml:mrow></mml:msub></mml:mrow></mml:math> Physical Review Materials, 2022, 6, .	3.1	6
65232	Decomposition of Organic Perovskite Precursors on MoO₃: Role of Halogen and Surface Defects. ACS Applied Materials & Interfaces, 2022, 14, 34208-34219.	4.0	9
65233	Lattice-Directed Selective Synthesis of Acetylenic and Diacetylenic Organometallic Polyynes. Chemistry of Materials, 2022, 34, 1770-1777.	3.2	11
65234	Two-Dimensional Arsenene/ZrS₂(HfS₂) Heterostructures as Direct Z-Scheme Photocatalysts for Overall Water Splitting. Journal of Physical Chemistry C, 2022, 126, 2587-2595.	1.5	17
65235	Solution-Phase Synthesis of PdH_{0.706} Nanocubes with Enhanced Stability and Activity toward Formic Acid Oxidation. Journal of the American Chemical Society, 2022, 144, 2556-2568.	6.6	42
65236	Crystal Growth, Structure, and Noninteracting Quantum Spins in Cyanochroite, K₂Cu(SO₄)₂Â·6H₂O. ACS Omega, 2022, 7, 5139-5145.	1.6	4
65237	High electrocatalytical performance of FeCoNiCuPd high-entropy alloy for nitrogen reduction reaction. Molecular Catalysis, 2022, 519, 112141.	1.0	13
65238	Electronic properties and controllable Schottky barrier of Janus HfSSe and graphene van der waals heterostructure. Solid State Communications, 2022, 344, 114686.	0.9	3
65239	Effect of pressure on photocatalytic water splitting performance of Z-scheme RP/CH3NH3PbI3 perovskite heterostructure. International Journal of Hydrogen Energy, 2022, 47, 8091-8104.	3.8	8
65240	Orbitale als Ausgangspunkt der Chemischen Bindung in Geâ^'Sbâ^'Teâ€Phasenwechselmaterialien**. Angewandte Chemie, 0, , e202115778.	1.6	0
65241	Janus MoPC Monolayer with Superior Electrocatalytic Performance for the Hydrogen Evolution Reaction. ACS Applied Materials & Interfaces, 2022, 14, 7836-7844.	4.0	13
65242	Ru-Doped NiFe Layered Double Hydroxide as a Highly Active Electrocatalyst for Oxygen Evolution Reaction. Journal of the Electrochemical Society, 2022, 169, 024503.	1.3	15
65243	Molecular Dynamics Study of Reaction Conditions at Active Catalyst-Ionomer Interfaces in Polymer Electrolyte Fuel Cells. Journal of the Electrochemical Society, 2022, 169, 024506.	1.3	1
65244	First-principles study of the oxygen evolution reaction on Ni3Fe-layered double hydroxides surfaces with varying sulfur coverage. Molecular Catalysis, 2022, 519, 112116.	1.0	1
65245	Extrinsic magnetoelectric effect at the BaTiO3/Ni interface. Journal of Applied Physics, 2022, 131, 054101.	1.1	6
65246	Can Substitutions Affect the Oxidative Stability of Lithium Argyrodite Solid Electrolytes?. ACS Applied Energy Materials, 2022, 5, 2045-2053.	2.5	11
65247	Charge Carrier Transport Mechanism in Ta₂O₅, TaON, and Ta₃N₅ Studied by Applying Polaron Hopping and Bandlike Models. ChemPhysChem, 2022, 23, e202100859.	1.0	1

#	Article	IF	Citations
65248	Single-layer honeycomb sheets of zinc selenide and beyond with superior electronic and optical properties. FlatChem, 2022, 32, 100345.	2.8	2
65249	Visualization and control of oxygen dopant ordering in a cuprate superconductor. Materials Today Physics, 2022, 23, 100629.	2.9	2
65250	Magnetically controllable band splittings in <mml:math xmlns:mml="http://www.w3.org/1998/Math/MathML"><mml:mrow><mml:mi>P</mml:mi><mml:mi>n</mml:mi><mml:mi>m</mml:mi><mml:mo</mml:mi> ferromagnetic materials. Physical Review B, 2022, 105, .	3.1	0
65251	Bifunctional Tungsten-Doped Ni(OH)₂/NiOOH Nanosheets for Overall Water Splitting in an Alkaline Medium. ACS Applied Nano Materials, 2022, 5, 2664-2677.	2.4	23
65252	DFT screening of adsorption of biodiesel molecules on aluminum and stainless steel surfaces. Results in Surfaces and Interfaces, 2022, 6, 100050.	1.0	2
65253	Tuning dielectric properties in a rutile TiO2 system via synergistic design of surface structure and microstructure. Applied Surface Science, 2022, 585, 152685.	3.1	6
65254	Density functional modeling of structural and electronic properties of amorphous high temperature oxides. Journal of Non-Crystalline Solids, 2022, 578, 121170.	1.5	6
65255	Structures and energetics of multiple helium atoms in a tungsten monovacancy. Journal of Nuclear Materials, 2022, 561, 153577.	1.3	4
65256	Tetrazine Based Covalent Organic Framework as a Promising Metal-Free Photo and Electro-Catalyst for HER. Catalysis Letters, 0, , 1.	1.4	5
65257	Enhancing the optical absorption of Ga2SeTe Janus monolayer by adsorption of transition metals. European Physical Journal D, 2022, 76, .	0.6	2
65258	Single-atom tailoring of Li2S to Form Li2S2 for building better lithium-sulfur batteries. Energy Storage Materials, 2022, 47, 79-86.	9.5	18
65259	Superior pâ€Type Surface Doping of Cubic Boron Nitride via MoO 3 Adsorption. Advanced Theory and Simulations, 0, , 2100460.	1.3	5
65260	Enhancement of the magnetic anisotropy in single semiconductor nanowires via surface doping and adatom deposition. Nanotechnology, 2022, , .	1.3	1
65261	Thin films made by reactive sputtering of high entropy alloy FeCoNiCuGe: Optical, electrical and structural properties. Thin Solid Films, 2022, 744, 139083.	0.8	3
65262	Density Functional Theory Study of Metallic Silicon (111) Plane Structures. ACS Omega, 2022, 7, 5385-5392.	1.6	8
65263	Electronegativityâ€Induced Charge Balancing to Boost Stability and Activity of Amorphous Electrocatalysts. Advanced Materials, 2022, 34, e2100537.	11.1	39
65264	Two-Dimensional Perovskite/HfS₂ van der Waals Heterostructure as an Absorber Material for Photovoltaic Applications. ACS Applied Energy Materials, 2022, 5, 2300-2307.	2.5	9
65265	Conversion of CO2 to defective porous carbons in one electro-redox cycle for boosting electrocatalytic H2O2 production. Applied Catalysis B: Environmental, 2022, 307, 121161.	10.8	25

#	Article	IF	Citations
65266	Understanding of electrochemical K+/Na+ exchange mechanisms in layered oxides. Energy Storage Materials, 2022, 47, 105-112.	9.5	8
65267	Improved Thermoelectric Performance of P-type SnTe through Synergistic Engineering of Electronic and Phonon Transports. ACS Applied Materials & Interfaces, 2022, , .	4.0	3
65268	Insight into the Enhanced Charge Transport in Quasi-2D Perovskite via Fluorination of Ammonium Cations for Photovoltaic Applications. ACS Applied Materials & Interfaces, 2022, 14, 7917-7925.	4.0	9
65269	Monodisperse Ni-clusters anchored on carbon nitride for efficient photocatalytic hydrogen evolution. Chinese Journal of Catalysis, 2022, 43, 536-545.	6.9	15
65270	The joint effect of spinâ€“orbit coupling and atomistic disorder on bandgap evolution in inorganic CsSn1â^'xPbxI3 mixed perovskite. Journal of Applied Physics, 2022, 131, 055107.	1.1	1
65271	Electronic properties of MoS2/Be2C van der Waals heterostructure: Effect of Bi-axil strain and vertical electric field. Physica E: Low-Dimensional Systems and Nanostructures, 2022, 139, 115172.	1.3	1
65272	Theoretical understanding of electronic and mechanical properties of 1Tâ€² transition metal dichalcogenide crystals. Beilstein Journal of Nanotechnology, 2022, 13, 160-171.	1.5	5
65273	Robust half-metallic spin-gap in Co₂CrAl: doping and strain engineering. Physica Scripta, 2022, 97, 035801.	1.2	1
65274	Identification of Cooperative Reaction Sites in Metalâ^'Organic Framework Catalysts for High Yielding Lactic Acid Production from d â€Xylose. ChemSusChem, 2022, , .	3.6	4
65275	High Performance Space Lubrication of MoS₂ with Tantalum. Advanced Functional Materials, 2022, 32, .	7.8	18
65276	High-capacity reversible hydrogen storage in scandium decorated holey graphyne: Theoretical perspectives. International Journal of Hydrogen Energy, 2022, 47, 7870-7883.	3.8	45
65277	Electronic and Photovoltaic Properties of Superlattices Constructed by Organicâ€“Inorganic Perovskites: a Theoretical Perspective. ACS Applied Energy Materials, 2022, 5, 2430-2441.	2.5	3
65278	Tetragonal distortion in magnetron sputtered bcc-W films with supersaturated carbon. Materials and Design, 2022, 214, 110422.	3.3	1
65279	Water-Stable Nickel Metalâ€“Organic Framework Nanobelts for Cocatalyst-Free Photocatalytic Water Splitting to Produce Hydrogen. Journal of the American Chemical Society, 2022, 144, 2747-2754.	6.6	109
65280	Reactivity of internal vs. external BrÃ¸nsted acid sites in nanosponge MFI: H/D exchange kinetic study. Microporous and Mesoporous Materials, 2022, 332, 111717.	2.2	1
65281	Role of Sb in the superconducting kagome metal CsV$_3$Sb$_5$ revealed by its anisotropic compression. SciPost Physics, 2022, 12, .	1.5	29
65282	Negative linear compressibility in Se at ultra-high pressure above 120 GPa. IUCrJ, 2022, 9, 253-260.	1.0	3
65283	Impact of oxygen content on the thermal stability of Ti-Al-O-N coatings based on computational and experimental studies. Acta Materialia, 2022, 227, 117706.	3.8	8

#	Article	IF	Citations
65284	Band Alignment at Heterointerface with Rapid Charge Transfer Supporting Excellent Photocatalytic Degradation of Methylene Blue under Sunlight. Advanced Materials Interfaces, 2022, 9, .	1.9	9
65285	Magnetic carboxyl-functionalized covalent organic frameworks for adsorption of quinolones with high capacities, fast kinetics and easy regeneration. Journal of Cleaner Production, 2022, 336, 130485.	4.6	27
65286	Insights into the Role of Protonation in Covalent Triazine Framework-Based Photocatalytic Hydrogen Evolution. Chemistry of Materials, 2022, 34, 1481-1490.	3.2	18
65287	First-Principles Study of Transition Metal Ti-Based MXenes (Ti₂MC₂T_x and) Tj ETQq1 1 0.784314 rgBT /Overlock 10 Tf 50 622 Td (M₂Ti ACS Applied Nano Materials, 2022, 5, 2358-2366.	2.4	8
65288	2D CeO₂ and a Partially Phosphated 2D Ni-Based Metalâ€“Organic Framework Formed an S-Scheme Heterojunction for Efficient Photocatalytic Hydrogen Evolution. Langmuir, 2022, 38, 2117-2131.	1.6	119
65289	Fragile topological band in the checkerboard antiferromagnetic monolayer FeSe. Npj Computational Materials, 2022, 8, .	3.5	15
65290	Unveiling the effect of interstitial dopants on CO2 activation over CsPbBr3 catalyst for efficient photothermal CO2 reduction. Chemical Engineering Journal, 2022, 435, 135071.	6.6	35
65291	Surface half metallicity and thermodynamic stability of 001-plane Ti2XSi (X=Mn, Co) Heusler alloys (HAs): A DFT approach. Surfaces and Interfaces, 2022, 28, 101602.	1.5	1
65292	Achieving optical phosphine sensitive h-BN nanosheets through transition metal doping. Applied Surface Science, 2022, 585, 152700.	3.1	5
65293	Facile synthesis of self support Fe doped Ni3S2 nanosheet arrays for high performance alkaline oxygen evolution. Journal of Electroanalytical Chemistry, 2022, 907, 116047.	1.9	6
65294	High entropy alloy CrFeNiCoCu sputter deposited films: Structure, electrical properties, and oxidation. Journal of Vacuum Science and Technology A: Vacuum, Surfaces and Films, 2022, 40, .	0.9	3
65295	Structural, Electronic, Elastic and Dynamical Properties of MCO₃ (M: Mn, Co, Ni) Precursor Materials for Li-Ion Batteries: A First-Principles Study. Journal of the Electrochemical Society, 2022, 169, 020540.	1.3	3
65296	Three-dimensional tetrahexcarbon: Stability and properties. Materials Today Physics, 2022, 23, 100628.	2.9	8
65297	Study on the thermoelectric properties of p-type doped CsCdF3 and CsHgF3 with quartic anharmonicity. Physics Letters, Section A: General, Atomic and Solid State Physics, 2022, 428, 127946.	0.9	8
65298	Non-catalytic, instant iridium (Ir) leaching: A non-negligible aspect in identifying Ir-based perovskite oxygen-evolving electrocatalysts. Chinese Journal of Catalysis, 2022, 43, 885-893.	6.9	17
65299	Size- and shape-dependent phase diagram of Ga-Sb nanoparticles. Calphad: Computer Coupling of Phase Diagrams and Thermochemistry, 2022, 76, 102389.	0.7	1
65300	Adsorption dynamics and intrinsic mechanism of POPs on corrole-based COF: A computational study. Journal of Cleaner Production, 2022, 338, 130566.	4.6	11
65301	Van der Waals epitaxy growth of 2D ferromagnetic Cr(1+Î´)Te2 nanolayers with concentration-tunable magnetic anisotropy. Applied Physics Reviews, 2022, 9, .	5.5	19

#	Article	IF	Citations
65302	Pressure induced structural phase transition and piezochromism in photovoltaic sillen compounds PbBiO2X (XÂ=ÂCl, Br & I). Applied Materials Today, 2022, 26, 101372.	2.3	0
65303	Magnetic properties and giant cryogenic magnetocaloric effect in B-site ordered antiferromagnetic Gd2MgTiO6 double perovskite oxide. Acta Materialia, 2022, 226, 117669.	3.8	131
65304	Improvement of Geant4 Neutron-HP package: From methodology to evaluated nuclear data library. Nuclear Instruments and Methods in Physics Research, Section A: Accelerators, Spectrometers, Detectors and Associated Equipment, 2022, 1027, 166187.	0.7	13
65305	Hybrid density functional theory study on zinc blende GaN and diamond surfaces and interfaces: Effects of size, hydrogen passivation, and dipole corrections. Computational Condensed Matter, 2022, 30, e00653.	0.9	0
65306	Theoretical investigations of selective cation doping as a novel design strategy for high-capacity lithium-rich cathode materials. Computational Materials Science, 2022, 204, 111177.	1.4	0
65307	Intrinsic spin Hall conductivity plateau in topological semimetals with triply degenerate points. Physica B: Condensed Matter, 2022, 629, 413626.	1.3	0
65308	Non-uniform He bubble formation in W/W2C composite: Experimental and ab-initio study. Acta Materialia, 2022, 226, 117608.	3.8	3
65309	Exfoliated Fe3GeTe2 and Ni3GeTe2 materials as water splitting electrocatalysts. FlatChem, 2022, 32, 100334.	2.8	11
65310	Controllable porous perovskite with three-dimensional ordered structure as an efficient oxygen reduction reaction electrocatalyst for flexible aluminum-air battery. Journal of Power Sources, 2022, 523, 231028.	4.0	9
65311	Asymmetric super-exchange interaction induced by inter-site distance effect for hydrogen evolution reaction. Materials Chemistry and Physics, 2022, 279, 125748.	2.0	2
65312	Photoelectric properties of 2D ZnO, graphene, silicene materials and their heterostructures. Composites Part B: Engineering, 2022, 233, 109645.	5.9	33
65313	Low-hysteresis manganese hexacyanoferrate (MnHCF) aqueous battery for low-grade thermal energy harvesting. Journal of Power Sources, 2022, 524, 231080.	4.0	3
65314	Electrochemical, theoretical, and analytical investigation of the phenylurea herbicide fluometuron at a glassy carbon electrode. Electrochimica Acta, 2022, 408, 139945.	2.6	6
65315	First-principles calculations to investigate stability, electronic properties and anisotropy of half-metallic full Heusler alloy Co2NbGa. Results in Physics, 2022, 34, 105237.	2.0	8
65316	Prediction of short-range order in CrMnFeCoNi high-entropy alloy. Results in Physics, 2022, 34, 105285.	2.0	8
65317	Enhance the anchoring and catalytic performance of lithium-sulfur batteries for lithium polysulfide by predicted TiS2 monolayer. Materials Today Communications, 2022, 30, 103196.	0.9	6
65318	Computational screening of spinel structure cathodes for Li-ion battery with low expansion and rapid ion kinetics. Computational Materials Science, 2022, 204, 111187.	1.4	5
65319	Hydrogen induced dislocation core reconstruction in bcc tungsten. Acta Materialia, 2022, 226, 117622.	3.8	16

#	Article	IF	Citations
65320	Intermediate carbon phase. New experimental data and atomic model. Diamond and Related Materials, 2022, 123, 108825.	1.8	2
65321	Defects on Li2S@graphene cathode improves the performance of lithium-sulfur battery, A theoretical study. Acta Materialia, 2022, 226, 117632.	3.8	10
65322	Spin-orbit coupling effect on pressure-induced phase transitions, magnetic, and electronic properties in YFeO3: A first-principles study. Chemical Physics, 2022, 555, 111454.	0.9	1
65323	TD-carbon: A new face-centered cubic carbon allotrope. Chemical Physics, 2022, 555, 111458.	0.9	1
65324	Theoretical investigation on the Ni atom-pair supported by N-doped graphene for the oxygen reduction reaction. Computational and Theoretical Chemistry, 2022, 1209, 113598.	1.1	4
65325	[NH4][Fe(bipy)3]2[Ag6Br11]: Synthesis, structure, characterization and photocurrent response. Inorganic Chemistry Communication, 2022, 137, 109250.	1.8	10
65326	CO2 reduction reaction pathways on single-atom Co sites: Impacts of local coordination environment. Chinese Journal of Catalysis, 2022, 43, 832-838.	6.9	18
65327	On the anomalous diffusion of proton in Y-doped BaZrO3 perovskite oxide. Solid State Ionics, 2022, 376, 115859.	1.3	5
65328	Quantum spin Hall insulating phase and van Hove singularities in Zintl single-quintuple-layer AM2X2 (A = Ca, Sr, or Ba; M = Zn or Cd; X = Sb or Bi) family. Applied Physics Reviews, 2022, 9, .	5.5	17
65329	Origin of the age-hardening and age-softening response in Mg-Li-Zn based alloys. Acta Materialia, 2022, 226, 117673.	3.8	29
65330	Weak dependence of spontaneous polarization on epitaxial strain in ferroelectric BiAlO3: A first-principles study. Current Applied Physics, 2022, 35, 67-71.	1.1	4
65331	Distance between two-dimensional hole gas and the interface of SrTi(Zn, Ti)O<mml:math xmlns:mml="http://www.w3.org/1998/Math/MathML" display="inline" id="d1e303" altimg="si25.svg"><mml:msub><mml:mrow /><mml:mrow><mml:mn>3</mml:mn></mml:mrow></mml:msub></mml:math>/SrTiO<mml:math xmlns:mml="http://www.w3.org/1998/Math/MathML" display="inline" id="d1e311" altimg="si25.svg"><mml:msub><mml:mrow /><mml:mrow><mml:mn>3</mml:mn></mml:mrow></mml:msub></mml:math>	1.4	1
65332	Degradation of chemical warfare agents by nickel doped titanium dioxide powders: Enhanced surface activity. Arabian Journal of Chemistry, 2022, 15, 103678.	2.3	3
65333	Designing superior bifunctional electrocatalyst with high-purity pyrrole-type CoN4 and adjacent metallic cobalt sites for rechargeable Zn-air batteries. Energy Storage Materials, 2022, 46, 553-562.	9.5	70
65334	An efficient gel polymer electrolyte for dendrite-free and long cycle life lithium metal batteries. Energy Storage Materials, 2022, 46, 352-365.	9.5	34
65335	The adsorption characteristics of CO, NO and NO2 on two dimensional metalloporphyrin porous nanosheets: A first-principles study. Applied Surface Science, 2022, 582, 152469.	3.1	9
65336	In-situ synthesized N-doped ZnO for enhanced CO2 sensing: Experiments and DFT calculations. Sensors and Actuators B: Chemical, 2022, 357, 131359.	4.0	15
65337	Precise carbon doping regulation of porous graphitic carbon nitride nanosheets enables elevated photocatalytic oxidation performance towards emerging organic pollutants. Chemical Engineering Journal, 2022, 433, 134551.	6.6	33

#	Article	IF	Citations
65338	Fabrication of 3D CuS@ZnIn2S4 hierarchical nanocages with 2D/2D nanosheet subunits p-n heterojunctions for improved photocatalytic hydrogen evolution. Chemical Engineering Journal, 2022, 433, 134474.	6.6	81
65339	Bridge the activity and durability of Ruthenium for hydrogen evolution reaction with the Ru O C link. Chemical Engineering Journal, 2022, 433, 134421.	6.6	30
65340	Super-hardening and localized plastic deformation behaviors in ZrB2 â€“TaÐ'2 ceramics. Journal of Alloys and Compounds, 2022, 901, 163368.	2.8	9
65341	A first principles study of the adsorption and hydrogenation of formic acid on a Cu3Zn material: Implication for bulk alloying effect on CO2 hydrogenation reactivity of Cu/ZnO-based catalysts. Computational Materials Science, 2022, 205, 111222.	1.4	1
65342	Orbital engineering of C3N monolayer to design efficient synergistic sites electrocatalyst for boosting alkaline hydrogen evolution. Applied Surface Science, 2022, 582, 152474.	3.1	5
65343	First-principles modelling of the new generation of subnanometric metal clusters: Recent case studies. Journal of Colloid and Interface Science, 2022, 612, 737-759.	5.0	13
65344	Adsorption of metal atoms on two-dimensional BC3 and AlC3 nanosheets: Computational studies. Chemical Physics Letters, 2022, 792, 139403.	1.2	5
65345	Semiconducting Sm3GaSe5O with trigonal bipyramidal GaSe5 units. Journal of Solid State Chemistry, 2022, 308, 122901.	1.4	3
65346	ElasT: A toolkit for thermoelastic calculations. Computer Physics Communications, 2022, 273, 108280.	3.0	3
65347	Fabrication of stable substoichiometric WOx films with high SERS sensitivity by thermal treatment. Vacuum, 2022, 198, 110884.	1.6	4
65348	Hybrid density functional theory calculation of orthorhombic CsPbI3â^'3Br3 and CsPbBr3â^'3Cl3. Current Applied Physics, 2022, 36, 93-96.	1.1	2
65349	Modulated carrier concentration and enhanced seebeck coefficient of Ge2Sb2Te5 thin films by Sn doping. Vacuum, 2022, 198, 110881.	1.6	4
65350	Role of Ni on the helium diffusion, stability and energetics of vacancyâ€"type clusters in Feâ€"6.25Crâ€"3.13Ni (at.%) ternary alloys: From first-principles. Computational Materials Science, 2022, 205, 111213.	1.4	1
65351	Improving performance of zinc-manganese battery via efficient deposition/dissolution chemistry. Energy Storage Materials, 2022, 46, 165-174.	9.5	32
65352	Theoretical investigation of the HgTe topological edge states with a Fe impurity. Physica B: Condensed Matter, 2022, 630, 413673.	1.3	0
65353	Orientation-dependent transport properties of Cu3Sn. Acta Materialia, 2022, 227, 117671.	3.8	11
65354	Regulating the electrolyte ion types and exposed crystal facets for pseudocapacitive energy storage of transition metal nitrides. Energy Storage Materials, 2022, 46, 278-288.	9.5	15
65355	Correlation between phase transition characteristics and hydrogen irradiation-induced Frenkel defect formations in FeRh films. Journal of Alloys and Compounds, 2022, 901, 163611.	2.8	2

#	Article	IF	Citations
65356	A new non-stoichiometric quaternary sulfide Ba3.14(4)Sn0.61(1)Bi2.39(1)S8: Synthesis, crystal structure, physical properties, and electronic structure. Journal of Solid State Chemistry, 2022, 308, 122914.	1.4	6
65357	First-principles calculation of chalcogen-doped Sr2M2O7 (M=Nb and Ta) for visible light photocatalysis. Journal of Solid State Chemistry, 2022, 308, 122905.	1.4	2
65358	Highly efficient interface stabilization for ambient-temperature quasi-solid-state sodium metal batteries. Chemical Engineering Journal, 2022, 434, 134679.	6.6	15
65359	Density functional theory analysis of structural and electronic properties of hexagonal hybrid perovskite (CH3NH3)3Bi2I9. Physica B: Condensed Matter, 2022, 630, 413695.	1.3	3
65360	Structural stability, electronic, magnetic and thermoelectric properties for half-metallic quaternary Heusler alloys CrLaCoZ. Journal of Physics and Chemistry of Solids, 2022, 163, 110600.	1.9	15
65361	Element-dependent unique properties of Janus Cr2I3X3 (XÂ=ÂF, Cl, Br) monolayer: Insight from first-principles calculations. Materials Science and Engineering B: Solid-State Materials for Advanced Technology, 2022, 278, 115610.	1.7	7
65362	Electronic and magnetic properties of polar magnets M2Mo3O8 (M = Mn, Fe, Co and Ni) from first principles studies. Journal of Solid State Chemistry, 2022, 308, 122910.	1.4	2
65363	Self-adaptive evolution of nickel silicide nanowires for the enhancement of bifunctional electrocatalytic activities. Chemical Engineering Journal, 2022, 434, 134668.	6.6	5
65364	Charging effects on the vibrational properties of Au and Au2 on MgO(100). Current Applied Physics, 2022, 36, 34-42.	1.1	0
65365	Atomic-scale probing of defect-assisted Ga intercalation through graphene using ReaxFF molecular dynamics simulations. Carbon, 2022, 190, 276-290.	5.4	9
65366	Optimization of persistent luminescence via dopant concentration in LiNbO3. Journal of Luminescence, 2022, 244, 118753.	1.5	2
65367	Highly efficient catalytic debromination of tetrabromodiphenyl ether with hydrazine as reducing agent: The role of the interaction between the catalyst and the reducing agent. Chemical Engineering Journal, 2022, 433, 134364.	6.6	6
65368	Discovery of high thermoelectric performance of WS2-WSe2 nanoribbons with superlattice and Janus structures. Journal of Alloys and Compounds, 2022, 903, 163850.	2.8	7
65369	Designing and optimizing Î²1-borophene organic gas sensor: A theoretical study. Surface Science, 2022, 719, 122030.	0.8	8
65370	First-principles study of the electronic structure and magnetism of the element-doped SnO2 (001) surface. Journal of Physics and Chemistry of Solids, 2022, 163, 110586.	1.9	5
65371	Interface-dependent activity and selectivity for CO2 hydrogenation on Ni/CeO2 and Ni/Ce0.9Sn0.1Ox. Fuel, 2022, 316, 123191.	3.4	12
65372	Synthesis and thermal expansion of chalcogenide MAX phase Hf2SeC. Journal of the European Ceramic Society, 2022, 42, 2084-2088.	2.8	19
65373	Crystal structure of the Ï„11 Al4Fe1.7Si phase from neutron diffraction and ab initio calculations. Journal of Alloys and Compounds, 2022, 902, 163141.	2.8	2

#	Article	IF	Citations
65374	A first principles analysis of oxidation in titanium alloys with aluminum and vanadium. Surface Science, 2022, 719, 122026.	0.8	11
65375	Continuous precipitate modes of the Î'â€²-Al3Li phase in Al-Li alloys. Journal of Alloys and Compounds, 2022, 904, 163800.	2.8	12
65376	Study of Er-Sb and Er-Te parental alloys used in phase change memory. Journal of Alloys and Compounds, 2022, 904, 164057.	2.8	4
65377	Theoretical insight into the interaction between hydrogen and HÃgg carbide (Ï‡-Fe5C2) surfaces. Applied Surface Science, 2022, 583, 152538.	3.1	5
65378	Atomistic and cluster dynamics modeling of fission gas (Xe) diffusivity in TRISO fuel kernels. Journal of Nuclear Materials, 2022, 561, 153539.	1.3	8
65379	Realizing excellent energy storage properties in Na0.5Bi0.5TiO3-based lead-free relaxor ferroelectrics. Journal of the European Ceramic Society, 2022, 42, 2221-2229.	2.8	57
65380	Single-phase formation and mechanical properties of (TiZrNbTaMo)C high-entropy ceramics: First-principles prediction and experimental study. Journal of the European Ceramic Society, 2022, 42, 2021-2027.	2.8	22
65381	Zirconia nanofibers-loaded reduced graphene oxide fabrication for specific electrochemical detection of methyl parathion. Journal of Alloys and Compounds, 2022, 904, 163798.	2.8	20
65382	Identifying the reaction network complexity and structure sensitivity of selective catalytic oxidation of ammonia over Ag surfaces. Applied Surface Science, 2022, 584, 152584.	3.1	3
65383	Direct incorporating small amount of Ce (III) in Cu-SAPO-18 catalysts for enhanced low-temperature NH3-SCR activity: Influence on Cu distribution and Si coordination. Chemical Engineering Journal, 2022, 435, 134890.	6.6	16
65384	High-entropy oxides as advanced anode materials for long-life lithium-ion Batteries. Nano Energy, 2022, 95, 106962.	8.2	86
65385	Coexistence of magnetism in SnX (XÂ=ÂS, Se, Te) monolayers by the adsorption of 3d transition-metal atoms. Journal of Magnetism and Magnetic Materials, 2022, 549, 169021.	1.0	1
65386	DFT insights into the adsorption mechanism of five-membered aromatic heterocycles containing N, O, or S on Fe(1 1 0) surface. Applied Surface Science, 2022, 583, 152524.	3.1	13
65387	A first-principles study of formic acid adsorption on CaO (001). Applied Surface Science, 2022, 583, 152296.	3.1	7
65388	Construction of BiVO4/NiCo2O4 nanosheet Z-scheme heterojunction for highly boost solar water oxidation. Journal of Colloid and Interface Science, 2022, 613, 265-275.	5.0	17
65389	Interfacial electronic modulation by Fe2O3/NiFe-LDHs heterostructures for efficient oxygen evolution at high current density. Applied Catalysis B: Environmental, 2022, 306, 121097.	10.8	138
65390	Pd and octahedra do not get along: Square planar [PdS4] units in non-centrosymmetric La6PdSi2S14. Journal of Alloys and Compounds, 2022, 902, 163756.	2.8	8
65391	N-coordinated bimetallic defect-rich nanocarbons as highly efficient electrocatalysts in advanced energy conversion applications. Chemical Engineering Journal, 2022, 435, 134913.	6.6	23

#	Article	IF	Citations
65392	Synthesis and bader analyzed cobalt-phthalocyanine modified solar UV-blind Î²-Ga2O3 quadrilateral nanorods photocatalysts for wide-visible-light driven H2 evolution. Applied Catalysis B: Environmental, 2022, 307, 121149.	10.8	51
65393	Influence of Cu/W interfacial structure on the resistance against harmful helium atoms: A mechanism analysis. Journal of Alloys and Compounds, 2022, 903, 163817.	2.8	6
65394	Nanotwinning induced decreased lattice thermal conductivity of high temperature thermoelectric boron subphosphide (B12P2) from deep learning potential simulations. Energy and AI, 2022, 8, 100135.	5.8	4
65395	A multifunctional protective layer with biomimetic ionic channel suppressing dendrite and side reactions on zinc metal anodes. Journal of Colloid and Interface Science, 2022, 613, 136-145.	5.0	8
65396	Dynamic dissolution and re-adsorption of molybdate ion in iron incorporated nickel-molybdenum oxyhydroxide for promoting oxygen evolution reaction. Applied Catalysis B: Environmental, 2022, 307, 121150.	10.8	88
65397	Co and Ti effect on hot workability of phosphor bronze. Journal of Alloys and Compounds, 2022, 903, 163778.	2.8	5
65398	One-step synthesis of novel core-shell bimetallic hexacyanoferrate for high performance sodium-storage cathode. Journal of Materials Science and Technology, 2022, 114, 180-190.	5.6	9
65399	Oxygen-mediated selection of Cu crystallographic orientation for growth of single-crystalline graphene. Applied Surface Science, 2022, 584, 152585.	3.1	1
65400	The thermodynamical and optical properties of surface bromine vacancy in two-dimensional CsPbBr3: A first principles study. Applied Surface Science, 2022, 584, 152626.	3.1	3
65401	Thermodynamic and kinetic corrosion behavior of alloys in molten MgCl2â€“NaCl eutectic: FPMD simulations and electrochemical technologies. Solar Energy Materials and Solar Cells, 2022, 238, 111624.	3.0	6
65402	Co-promotion of two-type active sites: PtCu single-atom alloy and copper-ceria interface for preferential oxidation of CO. Applied Catalysis B: Environmental, 2022, 306, 121117.	10.8	29
65403	Nickel polyphthalocyanine with electronic localization at the nickel site for enhanced CO2 reduction reaction. Applied Catalysis B: Environmental, 2022, 306, 121093.	10.8	53
65404	Hydrogen-bond-stabilized high density catechol monolayer on magnetite Fe3O4(111). Surface Science, 2022, 719, 122027.	0.8	1
65405	1T-MoS2 monolayer as a promising anode material for (Li/Na/Mg)-ion batteries. Applied Surface Science, 2022, 584, 152537.	3.1	66
65406	Hydrogen and electricity co-generation from hydrazine-assisted water electrolysis on hierarchical porous heteroatoms-doped CoCu catalysts. Applied Catalysis B: Environmental, 2022, 306, 121132.	10.8	23
65407	Tunable ultraviolet-B full-spectrum delayed luminescence of bismuth-activated phosphors for high-secure data encryption and decryption. Journal of Alloys and Compounds, 2022, 902, 163776.	2.8	12
65408	Low-temperature dielectric relaxation associated with NbO6 octahedron distortion in antimony modified potassium sodium niobate ceramics. Journal of Materials Science and Technology, 2022, 115, 189-198.	5.6	14
65409	First-principles investigations of structural, electronic and thermoelectric properties of Sb/Bi2Se3 van der Waals heterostructure. Materials Science in Semiconductor Processing, 2022, 142, 106472.	1.9	6

#	Article	IF	Citations
65410	In-situ construction of N-doped carbon nanosnakes encapsulated FeCoSe nanoparticles as efficient bifunctional electrocatalyst for overall water splitting. Journal of Energy Chemistry, 2022, 68, 699-708.	7.1	31
65411	Vacancy-defect semiconductor quantum dots induced an S-scheme charge transfer pathway in 0D/2D structures under visible-light irradiation. Applied Catalysis B: Environmental, 2022, 306, 121109.	10.8	60
65412	Non-metal atom modified SnS2 sheet for CO2 photoreduction with significant activity and selectivity improvements: A first-principles study. Applied Surface Science, 2022, 584, 152618.	3.1	8
65413	Simulation of the Physicochemical Properties of Anatase TiO2 with Oxygen Vacancies and Doping of Different Elements for Photocatalysis Processes. Lecture Notes in Networks and Systems, 2022, , 238-249.	0.5	0
65414	Van der Waals 2D Metallic Materials for Low-Resistivity Interconnects. Journal of Materials Chemistry C, 0, , .	2.7	1
65415	A predictive model of surface adsorption in dissolution on transition metals and alloys. Journal of Materials Chemistry A, 2022, 10, 6731-6739.	5.2	7
65416	Circumferential Li metal deposition at high rates enabled by the synergistic effect of a lithiophilic and ionic conductive network. Journal of Materials Chemistry A, 2022, 10, 5391-5401.	5.2	4
65417	The characterisation of commercial 2D carbons: graphene, graphene oxide and reduced graphene oxide. Materials Advances, 2022, 3, 2810-2826.	2.6	16
65418	A novel 2D porous C₃N₂ framework as a promising anode material with ultra-high specific capacity for lithium-ion batteries. Journal of Materials Chemistry A, 2022, 10, 6551-6559.	5.2	22
65419	The dependence of crystal structure and ultraviolet nonlinear optical property of KBe₂BO₃F<sub>2</sub by density functional theory and π-conjugate confinement. Scientia Sinica Chimica, 2022, 52, 947-955.	0.2	2
65420	Performance and reaction mechanisms of tin compounds as high-capacity negative electrodes of lithium and sodium ion batteries. Materials Advances, 2022, 3, 2793-2799.	2.6	4
65421	Giant valley splitting in a MoTe₂/MnSe₂ van der Waals heterostructure with room-temperature ferromagnetism. Materials Advances, 2022, 3, 2927-2933.	2.6	9
65422	Prediction of dielectric constants of ABO₃-type perovskites using machine learning and first-principles calculations. Physical Chemistry Chemical Physics, 2022, 24, 7050-7059.	1.3	12
65423	Tuning the metathesis performance of a molybdenum oxide-based catalyst by silica support acidity modulation and high temperature pretreatment. Catalysis Science and Technology, 2022, 12, 2134-2145.	2.1	2
65424	Ambipolar to Unipolar Irreversible Switching in Nanosheet Transistors: The Role of Ferrocene in Fullerene/Ferrocene Nanosheets. Journal of Materials Chemistry C, 0, , .	2.7	5
65425	Origin of the concentration-dependent effects of N on the stability and electrical resistivity in polycrystalline Ge1Sb2Te4. Journal of Materials Chemistry C, 0, , .	2.7	1
65426	Investigation of factors affecting the stability of compounds formed by isovalent substitution in layered oxychalcogenides, leading to identification of Ba₃Sc₂O₅Cu₂Se₂, Ba₃Y₂O₅Cu₂S₂, Ba₃Sc₂O₅Ag₂Se₂ and Ba₃In₂O₅Ag₂Se₂. Journal of Materials Ch	2.7	1
65427	Chemical order or disorder â€“ a theoretical stability expose for expanding the compositional space of quaternary metal borides. Materials Advances, 2022, 3, 2908-2917.	2.6	9

#	Article	IF	Citations
65428	A biphenylene nanoribbon-based 3D metallic and ductile carbon allotrope. Nanoscale, 2022, 14, 3801-3807.	2.8	9
65429	Optical gaps and excitons in semiconducting transition metal carbides (MXenes). Journal of Materials Chemistry C, 2022, 10, 3919-3928.	2.7	13
65430	NiO nanobelts with exposed {110} crystal planes as an efficient electrocatalyst for the oxygen evolution reaction. Physical Chemistry Chemical Physics, 2022, 24, 6087-6092.	1.3	10
65431	Interpenetrated metalâ€“organic frameworks with enhanced photoluminescence for selective recognition of m-xylene from xylene isomers. Dalton Transactions, 2022, 51, 4790-4797.	1.6	11
65432	Synergistic decarboxylation over Ce-doped Na/SiO₂ facilitating functionalized monomer production from furfural for manufacturing polymers. Green Chemistry, 2022, 24, 2240-2248.	4.6	1
65433	Highly active postspinel-structured catalysts for oxygen evolution reaction. RSC Advances, 2022, 12, 5094-5104.	1.7	3
65435	Synthesis of metal silicides using polyhedral oligomeric silsesquioxane as a silicon source for semi-hydrogenation of phenylacetylene. Inorganic Chemistry Frontiers, 2022, 9, 1386-1394.	3.0	0
65436	Mutual modulationviacharge transfer and unpaired electrons of catalytic sites for the superior intrinsic activity of N₂reduction: from high-throughput computation assisted with a machine learning perspective. Journal of Materials Chemistry A, 2022, 10, 5470-5478.	5.2	26
65437	Pressure-induced phase transition of a series of energetic pentazolate anion salts: a DFT study. New Journal of Chemistry, 2022, 46, 5653-5662.	1.4	3
65438	Superior thermoelectric properties of ternary chalcogenides CsAg₅Q₃ (Q =) Tj ETQq1 1 0.784314 rgBT /Ov 5729-5737.	1.3	4
65439	Layered TiCl₂ Monolayer as an Antiferromagnetic Semiconductor. Spin, 2022, 12, .	0.6	2
65440	Thermally-driven formation method for growing (quantum) dots on sidewalls of self-catalysed thin nanowires. Nanoscale Horizons, 2022, 7, 311-318.	4.1	2
65441	Adsorption behavior of Ti3C2Tx with h-BN nanosheet and their application in waterborne epoxy anti-corrosion coating. Applied Surface Science, 2022, 586, 152778.	3.1	26
65442	Predicting magnetic anisotropy energies using site-specific spin-orbit coupling energies and machine learning: Application to iron-cobalt nitrides. Physical Review Materials, 2022, 6, .	0.9	3
65443	Chemical-Mechanical Effects in Ni-Rich Cathode Materials. Chemistry of Materials, 2022, 34, 1509-1523.	3.2	34
65444	First-Principles Calculations about Elastic and Li⁺ Transport Properties of Lithium Superoxides under High Pressure and High Temperature. Chinese Physics Letters, 2022, 39, 026101.	1.3	2
65445	A novel approach to recovery of lithium element and production of holey graphene based on the lithiated graphite of spent lithium ion batteries. Chemical Engineering Journal, 2022, 436, 135011.	6.6	29
65446	Two-dimensional ZrSe2/ZrS2 heterobilayer tuned by electric field for optoelectronic devices. Journal of the Korean Physical Society, 0, , 1.	0.3	2

#	Article	IF	Citations
65447	Surface Noble Metal Concentration on Ceria as a Key Descriptor for Efficient Catalytic CO Oxidation. ACS Catalysis, 2022, 12, 2473-2486.	5.5	19
65448	Snâ€Doped Black Phosphorene for Enhancing the Selectivity of Nitrogen Electroreduction to Ammonia. Advanced Functional Materials, 2022, 32, .	7.8	41
65449	Basic formulation and first-principles implementation of nonlinear magneto-optical effects. Physical Review B, 2022, 105, .	1.1	12
65450	Tuning valley splitting and magnetic anisotropy of multiferroic <mml:math xmlns:mml="http://www.w3.org/1998/Math/MathML"><mml:mrow><mml:mi>Cu</mml:mi><mml:mi>M</mml:mi><mml:msub><mml:m		

#	Article	IF	Citations
65465	Second-harmonic generation in atomically thin <mml:math xmlns:mml="http://www.w3.org/1998/Math/MathML"><mml:mn>1</mml:mn><mml:mi>T</mml:mi><mml:mtext>â€“</mml:mtext><mml:mm and its possible origin from charge density wave transitions. Physical Review B, 2022, 105, .	3.7	5
65466	Exotic magnetic and electronic properties of layered <mml:math xmlns:mml="http://www.w3.org/1998/Math/MathML"><mml:msub><mml:mi>CrI</mml:mi><mml:mn>3</mml:mn></mml:msub></mml single crystals under high pressure. Physical Review B, 2022, 105, .	3.7	12
65467	Tuning electronic structures and optical properties of graphene/phosphorene heterostructure via electric field. Superlattices and Microstructures, 2022, 164, 107184.	1.4	0
65468	Uncovering electrocatalytic conversion mechanisms from Li2S2 to Li2S: Generalization of computational hydrogen electrode. Energy Storage Materials, 2022, 47, 327-335.	9.5	22
65469	Theoretical investigation of nitrogen-vacancy defects in silicon. AIP Advances, 2022, 12, .	0.6	4
65470	Designing Electrophilic and Nucleophilic Dual Centers in the ReS₂ Plane toward Efficient Bifunctional Catalysts for Li-CO₂ Batteries. Journal of the American Chemical Society, 2022, 144, 3106-3116.	6.6	93
65471	General Descriptors for CO₂-Assisted Selective Câ€“H/Câ€“C Bond Scission in Ethane. Journal of the American Chemical Society, 2022, 144, 4186-4195.	6.6	26
65472	Molecular and Dissociative Hydrogen Adsorption on Bimetallic PdAg/Pd(111) Surface Alloys: A Combined Experimental and Theoretical Study. Journal of Physical Chemistry C, 2022, 126, 3060-3077.	1.5	4
65473	Methylammonium Tin Tribromide Quantum Dots for Heavy Metal Ion Detection and Cellular Imaging. ACS Applied Nano Materials, 2022, 5, 2859-2874.	2.4	45
65474	Enhancement Effect of Chemisorbed Sulfate toward Electrochemical Oxidation of Ethanol on Platinum Electrodes. Journal of Physical Chemistry C, 2022, 126, 3397-3403.	1.5	8
65475	First principle calculations including ab initio molecular dynamics studies for the activation of hydrogen fluoride on Ni(111). Chemical Physics, 2022, 557, 111469.	0.9	1
65476	Efficient Oxygenâ€Vacancy Suppression and Electrical Stabilization of Solutionâ€Processed In₂O₃:Q (Q = S, Se) Thinâ€Film Transistor with Chalcogen Alloying. Advanced Electronic Materials, 2022, 8, .	2.6	7
65477	Shining Mn⁴⁺ in 0D Organometallic Fluoride Hosts towards Highly Efficient Photoluminescence. Advanced Optical Materials, 2022, 10, .	3.6	24
65478	Thermal migration towards constructing W-W dual-sites for boosted alkaline hydrogen evolution reaction. Nature Communications, 2022, 13, 763.	5.8	68
65479	Strain-induced light emission enhancement in CsPbBr3 microwires. Journal of Materials Science, 2022, 57, 5061-5071.	1.7	3
65480	Synthesis and characterization of Taâ€“Bâ€“C coatings prepared by DCMS and HiPIMS co-sputtering. Vacuum, 2022, 199, 110937.	1.6	4
65481	Nanoscale Control of Polar Surface Phases in Layered van der Waals CuInP₂S₆. ACS Nano, 2022, 16, 2452-2460.	7.3	12
65482	Unprecedentedly high activity and selectivity for hydrogenation of nitroarenes with single atomic Co1-N3P1 sites. Nature Communications, 2022, 13, 723.	5.8	91

#	Article	IF	Citations
65483	Effect of interfacial intermixing on spin-orbit torque in Co/Pt bilayers. Physical Review B, 2022, 105, .	1.1	5
65484	Giant interlayer magnetic exchange interaction and charge-spin coupling in a van der Waals magnetic interface driven by <mml:math xmlns:mml="http://www.w3.org/1998/Math/MathML"><mml:mi>p</mml:mi><mml:mo>â^'</mml:mo><mml:mi>d</mml:mi></mml:ma coupling. Physical Review B, 2022, 105, .	1.1	3
65485	Investigation of out-of-plane ordered Ti4MoSiB2 from first principles. Journal of Physics Condensed Matter, 2022, , .	0.7	2
65486	Enhanced Structural Stability and Volumetric Capacity of a 3D Pyknotic Graphene Conductive Network via a Pillar Effect of Sn Nanoparticles for Sodium-Ion Batteries. ACS Applied Materials & Interfaces, 2022, 14, 8086-8094.	4.0	9
65487	Firstâ€principles investigation of elastic and electronic properties of double transition metal carbide MXenes. Journal of the American Ceramic Society, 2022, 105, 4400-4413.	1.9	7
65488	Dynamic structural evolution of iron catalysts involving competitive oxidation and carburization during CO ₂ hydrogenation. Science Advances, 2022, 8, eabm3629.	4.7	92
65489	Fabrication of a Microcavity Prepared by Remote Epitaxy over Monolayer Molybdenum Disulfide. ACS Nano, 2022, 16, 2399-2406.	7.3	13
65490	Size Effect of MgO on the Ionic Conduction Properties of a LiBH₄Â·1/2NH₃â€“MgO Nanocomposite. ACS Applied Materials & Interfaces, 2022, 14, 8947-8954.	4.0	5
65491	First-Principles Study of High-Pressure Phase Stability and Electron Properties of Be-P Compounds. Materials, 2022, 15, 1255.	1.3	0
65492	Sensitivity of the electronic and magnetic structures of cuprate superconductors to density functional approximations. Npj Computational Materials, 2022, 8, .	3.5	12
65493	Semiconducting and Metallic Compounds within the IrIn₃ Structure Type: Stability and Chemical Bonding. Inorganic Chemistry, 2022, 61, 3274-3280.	1.9	4
65494	A distinctive semiconductor-metalloid heterojunction: unique electronic structure and enhanced CO2 photoreduction activity. Journal of Colloid and Interface Science, 2022, 615, 821-830.	5.0	9
65495	Origin of superior pseudocapacitive mechanism of transition metal nitrides. Journal of Energy Chemistry, 2022, 69, 561-568.	7.1	11
65496	xmlns:mml="http://www.w3.org/1998/Math/MathML"><mml:mrow><mml:mi>A</mml:mi></mml:mrow></mml:math> -site <mml:math xmlns:mml="http://www.w3.org/1998/Math/MathML"><mml:msup><mml:mrow><mml:mi>Mn</mml:mi></mml:mrow><mml:mrow> tuned magnetism and electrical transport properties in the transition-metal-only perovskite oxide	10.1	1
65497	Unveiling the Degradation Chemistry of Fibrous Red Phosphorus under Ambient Conditions. ACS Applied Materials & Interfaces, 2022, 14, 9925-9932.	4.0	8
65498	Electrochemical reduction of thin graphene-oxide films in aqueous solutions â€“ Restoration of conductivity. Electrochimica Acta, 2022, 410, 140046.	2.6	10
65499	Direct assessment of confinement effect in zeolite-encapsulated subnanometric metal species. Nature Communications, 2022, 13, 821.	5.8	30
65500	Degradation mechanism and eco-toxicity assessment of bisphenol S based on peroxymonosulfate activated with Co3O4 surfaces. Journal of Cleaner Production, 2022, 341, 130881.	4.6	16

#	Article	IF	Citations
65501	Suppressing effect of tantalum on the radiation-induced clustering of rhenium in tungsten. Journal of Nuclear Materials, 2022, 562, 153588.	1.3	4
65502	Surface ion isolated platinum-thiocyanate catalysts for hydrogen peroxide production via 2-electron oxygen reduction in acidic media. Chemical Engineering Journal, 2022, 435, 135105.	6.6	6
65503	Rational Design of Magnetic Hybrid Transition Metal Double Perovskites in Polyatomic Anionic Systems. Chemistry of Materials, 0, , .	3.2	1
65504	Superionic iron alloys and their seismic velocities in Earthâ€™s inner core. Nature, 2022, 602, 258-262.	13.7	37
65505	Structural, elastic, thermal and mechanical properties of LnTa2O6(Ln Ce-Tb) ceramics from first-principles calculations. Materials Today Communications, 2022, 31, 103251.	0.9	0
65506	Stabilization of Cu₂O through Site-Selective Formation of a Co₁Cu Hybrid Single-Atom Catalyst. Chemistry of Materials, 2022, 34, 2313-2320.	3.2	5
65507	Excellent high-temperature strength and ductility of the ZrC nanoparticles dispersed molybdenum. Acta Materialia, 2022, 227, 117725.	3.8	34
65508	Atomic control of active-site ensembles in ordered alloys to enhance hydrogenation selectivity. Nature Chemistry, 2022, 14, 523-529.	6.6	51
65509	Probing the onset of wurtzite phase formation in (V,Al)N thin films by transmission electron microscopy and atom probe tomography. Surface and Coatings Technology, 2022, 442, 128235.	2.2	7
65510	Manipulating the oxygen reduction reaction pathway on Pt-coordinated motifs. Nature Communications, 2022, 13, 685.	5.8	82
65511	Feâ€•and Coâ€Doped Tungsten Disulfide Monolayers: 2D Ferromagnetic Halfâ€Metals at Room Temperature. Physica Status Solidi - Rapid Research Letters, 2022, 16, .	1.2	4
65512	Cuâ€•doped Ba_{0.5}Sr_{0.5}FeO_{3â€Ž} for electrochemical synthesis of hydrogen peroxide via a 2â€•electron oxygen reduction reaction¹. Electrochemical Science Advances, 2023, 3, .	1.2	0
65513	Computationally Accelerated Discovery of High Entropy Pyrochlore Oxides. Chemistry of Materials, 2022, 34, 1459-1472.	3.2	14
65514	A metal-supported single-atom catalytic site enables carbon dioxide hydrogenation. Nature Communications, 2022, 13, 819.	5.8	83
65515	Efficient electrosynthesis of n-propanol from carbon monoxide using a Agâ€“Ruâ€“Cu catalyst. Nature Energy, 2022, 7, 170-176.	19.8	96
65516	Adaptive sampling methods via machine learning for materials screening. Science and Technology of Advanced Materials Methods, 2022, 2, 55-66.	0.4	2
65517	Herzbergâ€“Teller Effect in Single-Crystalline Hexacene at Finite Temperatures. Journal of Physical Chemistry C, 2022, 126, 3366-3374.	1.5	3
65518	Structural changes of hydrotalcite-based Co-containing mixed oxides with calcination temperature and their effects on NOx adsorption: A combined experimental and DFT study. Chemical Engineering Journal, 2022, 437, 135209.	6.6	6

#	Article	IF	Citations
65519	Presence and absence of intrinsic magnetism in graphitic carbon nitrides designed through Câ€“Nâ€“H building blocks. Scientific Reports, 2022, 12, 2343.	1.6	4
65520	Descriptor and Scaling Relations for Ion Mobility in Crystalline Solids. Jacs Au, 2022, 2, 463-471.	3.6	19
65521	Real-space detection and manipulation of two-dimensional quantum well states in few-layer <mml:math xmlns:mml="http://www.w3.org/1998/Math/MathML"><mml:msub><mml:mi>MoS</mml:mi><mml:mn>2</mml:mn></mml:msub></mm Physical Review B, 2022, 105, .	1.1	4
65522	Growth of Ta₂SnO₆ Films, a Candidate Wide-Band-Gap p-Type Oxide. Journal of Physical Chemistry C, 2022, 126, 3764-3775.	1.5	8
65523	Improving electrochemical performance of (Cu, Sm)CeO2 anode with anchored Cu nanoparticles for direct utilization of natural gas in solid oxide fuel cells. Journal of the European Ceramic Society, 2022, 42, 3254-3263.	2.8	9
65524	Strong laser polarization control of coherent phonon excitation in van der Waals material Fe3GeTe2. Npj 2D Materials and Applications, 2022, 6, .	3.9	5
65525	Photoinduced chiral charge density wave in <mml:math xmlns:mml="http://www.w3.org/1998/Math/MathML"><mml:msub><mml:mi>TiSe</mml:mi><mml:mn>2</mml:mn></mml:msub></mm Physical Review B, 2022, 105, .	1.1	5
65526	Modification of Indium Tin Oxide Surface with HCl for Source/Drain Electrodes in Organic Thin Film Transistors. Advanced Materials Technologies, 2022, 7, .	3.0	6
65527	C₇N₆/Sc₂CCl₂ Weak van der Waals Heterostructure: A Promising Visible-Light-Driven Z-Scheme Water Splitting Photocatalyst with Interface Ultrafast Carrier Recombination. Journal of Physical Chemistry Letters, 2022, 13, 1473-1479.	2.1	16
65528	Thermoelectric performance in the binary semiconductor compound <mml:math xmlns:mml="http://www.w3.org/1998/Math/MathML"><mml:mrow><mml:msub><mml:mi>A</mml:mi><mml:mn>2</mml:mn></mml:mm width="4pt" /><mml:mo>(</mml:mo><mml:mi>A</mml:mi></mml:math> = K, Rb) with host-guest structure. Physical Review B, 2022, 105, .	1.1	25
65529	Exploring Highly Efficient Dual-Metal-Site Electrocatalysts for Oxygen Reduction Reaction by First Principles Screening. Journal of the Electrochemical Society, 2022, 169, 026524.	1.3	9
65530	Unveiling the structural, electronic, and optical effects of carbon-doping on multi-layer anatase TiO2 (1 0 1) and the impact on photocatalysis. Applied Surface Science, 2022, 586, 152641.	3.1	12
65531	The regulation mechanism of cationic substitution in morphology-controlled oxy-spinel for oxygen evolution reaction. Journal of Catalysis, 2022, 407, 221-231.	3.1	14
65532	Effects of Electron Correlation inside Disordered Crystals. Crystals, 2022, 12, 237.	1.0	3
65533	Elucidation of the redox activity of Ca2MnO3.5 and CaV2O4 in calcium batteries using operando XRD: charge compensation mechanism and reversibility. Energy Storage Materials, 2022, 47, 354-364.	9.5	7
65534	Origin of nonlinear magnetoelectric response in rare-earth orthoferrite perovskite oxides. Physical Review B, 2022, 105, .	1.1	6
65535	High-capacity reversible hydrogen storage properties of metal-decorated nitrogenated holey graphenes. International Journal of Hydrogen Energy, 2022, 47, 10654-10664.	3.8	22
65536	Large magnetoresistance and unexpected low thermal conductivity in topological semimetal CrP4 single crystal. Applied Physics A: Materials Science and Processing, 2022, 128, 1.	1.1	3

#	Article	IF	Citations
65537	Non-oxidized bare copper nanoparticles with surface excess electrons in air. Nature Nanotechnology, 2022, 17, 285-291.	15.6	34
65538	Giant and Tunneling Magnetoresistance in Unconventional Collinear Antiferromagnets with Nonrelativistic Spin-Momentum Coupling. Physical Review X, 2022, 12, .	2.8	41
65539	Atomic Layer Deposition of Iridium Using a Tricarbonyl Cyclopropenyl Precursor and Oxygen. Chemistry of Materials, 2022, 34, 1533-1543.	3.2	7
65540	First principle investigation on 2D beryllium chalcogenides for thermoelectric and optical applications. Journal of Physics and Chemistry of Solids, 2022, 164, 110619.	1.9	6
65541	Enhanced interactions of gas molecule with defective graphene induced by strong coupling effect between carbon-Co in Co3O4: A theoretical study. Applied Surface Science, 2022, 587, 152755.	3.1	3
65542	Unraveling the Synergistic Effect of Re and Cs Promoters on Ethylene Epoxidation over Silver Catalysts with Machine Learning-Accelerated First-Principles Simulations. ACS Catalysis, 2022, 12, 2540-2551.	5.5	13
65543	OsPd bimetallic dimer pushes the limit of magnetic anisotropy in atom-sized magnets for data storage. Nanotechnology, 2022, 33, 215001.	1.3	3
65544	The effect of strain and pressure on the electron-phonon coupling and superconductivity in MgB2â€"Benchmark of theoretical methodologies and outlook for nanostructure design. Journal of Applied Physics, 2022, 131, 063902.	1.1	1
65545	Titrating Controlled Defects into Si-LTA Zeolite Crystals Using Multiple Organic Structure-Directing Agents. Chemistry of Materials, 2022, 34, 1789-1799.	3.2	6
65546	A density functional study of the structural, electronic, optical and lattice dynamical properties of AgGaS2. Results in Physics, 2022, 35, 105309.	2.0	9
65547	Thermal-healing of lattice defects for high-energy single-crystalline battery cathodes. Nature Communications, 2022, 13, 704.	5.8	33
65548	Highly Sodiophilic, Defectâ€Rich, Ligninâ€Derived Skeletal Carbon Nanofiber Host for Sodium Metal Batteries. Advanced Energy Materials, 2022, 12, .	10.2	47
65549	W 4f electron binding energies in amorphous W-B-C systems. Applied Surface Science, 2022, 586, 152824.	3.1	4
65550	The intrinsic effects of oxygen vacancy and doped non-noble metal in TiO2(B) on photocatalytic oxidation VOCs by visible light driving. Journal of Environmental Chemical Engineering, 2022, 10, 107390.	3.3	6
65551	Exploring cesiumâ€"tellurium phase space via high-throughput calculations beyond semi-local density-functional theory. Journal of Chemical Physics, 2022, 156, 104108.	1.2	9
65552	Interaction mechanism between lead species and activated carbon in MSW incineration flue gas: Role of different functional groups. Chemical Engineering Journal, 2022, 436, 135252.	6.6	8
65553	CO Oxidation Activity of Au on Spinel Titanate Supports: Improvement of Catalytic Activity via Alkali Cation Substitution from Li4Ti5O12 to Na3LiTi5O12. Chemistry Letters, 2022, 51, 157-161.	0.7	1
65554	Enabling Stable and Nonhysteretic Oxygen Redox Capacity in Liâ€Excess Na Layered Oxides. Advanced Energy Materials, 2022, 12, .	10.2	18

#	Article	IF	Citations
65555	Ab initio comparative study of B2â€“MnX intermetallics with Xâ€‰=â€‰V, Nb, Ta. European Physical Journal B, 2022, 95, 1.	0.6	1
65556	Surface steps dominate the water formation on Pd(111) surfaces. Journal of Chemical Physics, 2022, 156, 064701.	1.2	8
65557	Realizing high thermoelectric performance in p-type RbZn4P3 Zintl compound: a first-principles investigation. Journal of Materials Science, 2022, 57, 10691-10701.	1.7	4
65558	Ultrafast Spinâ€Charge Conversion at SnBi₂Te₄/Co Topological Insulator Interfaces Probed by Terahertz Emission Spectroscopy. Advanced Optical Materials, 2022, 10, .	3.6	13
65559	Multigap topology and non-Abelian braiding of phonons from first principles. Physical Review B, 2022, 105, .	1.1	16
65560	Trigonal multivalent polonium monolayers with intrinsic quantum spin Hall effects. Scientific Reports, 2022, 12, 2129.	1.6	2
65561	Temperature Modulating Fermi Level Pinning in 2D GeSe for Highâ€Performance Transistor. Advanced Electronic Materials, 2022, 8, .	2.6	12
65562	Thiotetrelates Li₂ZnXS₄ (X = Si, Ge, and Sn) As Potential Li-Ion Solid-State Electrolytes. ACS Applied Materials & Interfaces, 2022, 14, 9203-9211.	4.0	2
65563	First-principles study of magnetic states and the anomalous Hall conductivity of <mml:math xmlns:mml="http://www.w3.org/1998/Math/MathML"><mml:mrow><mml:mi>M</mml:mi><mml:msub><mml:mi>Nb</mml:mi><mml:m mathvariant="normal">S</mml:mi><mml:mn>6</mml:mn></mml:msub></mml:mrow></mml:math> <mml:math		

#	Article	IF	Citations
65573	Selective catalytic oxidation of ammonia to nitric oxide via chemical looping. Nature Communications, 2022, 13, 718.	5.8	18
65574	Effect of surface segregation on the oxidation resistance of <mml:math xmlns:mml="http://www.w3.org/1998/Math/MathML"><mml:mrow><mml:msub><mml:mi>Cu</mml:mi><mml:mn>3</mml:mn></mml:msub></mml:mrow></mml:math> Physical Review Materials, 2022, 6, .	0.3	2
65575	Pair structure, diffusion and pressure in liquid CuZr alloys from ab initio simulations: assessing the sensitivity to the energy cutoff. Modelling and Simulation in Materials Science and Engineering, 0, , .	0.8	1
65576	Reversible transition between the polar and antipolar phases and its implications for wake-up and fatigue in HfO2-based ferroelectric thin film. Nature Communications, 2022, 13, 645.	5.8	66
65577	Machine-learning-based exchange correlation functional with physical asymptotic constraints. Physical Review Research, 2022, 4, .	1.3	21
65578	Route to a novel tetragonal carbon allotrope via T-carbon. Diamond and Related Materials, 2022, , 108895.	1.8	0
65579	Highly active and stable BaCo0.8Zr0.1Y0.1O3-Î´ cathode for intermediate temperature solid oxide fuel cells. Journal of the European Ceramic Society, 2022, 42, 2860-2869.	2.8	14
65580	Enhanced absorption in black phosphorene on adsorption of Li and K for use in energy conversion applications. Optical and Quantum Electronics, 2022, 54, 1.	1.5	4
65581	Modification of electronic and thermoelectric properties of InSe/GaSe superlattices by strain engineering. Physical Review Materials, 2022, 6, .	0.9	6
65582	Uniaxially Aligned 1D Sandwich-Molecular Wires: Electronic Structure and Magnetism. Journal of Physical Chemistry C, 2022, 126, 3140-3150.	1.5	4
65583	The Importance of Avoided Crossings in Understanding High Valley Degeneracy in Halfâ€Heusler Thermoelectric Semiconductors. Advanced Electronic Materials, 2022, 8, .	2.6	11
65584	Disorder-mediated quenching of magnetization in NbVTiAl: Theory and experiment. Journal of Magnetism and Magnetic Materials, 2022, 551, 169124.	1.0	4
65585	Metal-Porphyrin Frameworks Supported by Carbon Nanotubes: Efficient Polysulfide Electrocatalysts for Lithium-Sulfur Batteries. Chemical Engineering Journal, 2022, 437, 135150.	6.6	8
65586	Propane Dehydrogenation on Platinum Catalysts: Identifying the Active Sites through Bayesian Analysis. ACS Catalysis, 2022, 12, 2487-2498.	5.5	15
65587	Reversible Dissociation for Effective Storage of Diborane Gas within the UiO-66-NH2 Metalâ€“Organic Framework. ACS Applied Materials & Interfaces, 2022, , .	4.0	4
65588	Low-Cost Biomass-Gel-Induced Conductive Polymer Networks for High-Efficiency Polysulfide Immobilization and Catalytic Conversion in Liâ€“S Batteries. ACS Applied Energy Materials, 2022, 5, 2308-2317.	2.5	11
65589	Correlation Between Viscosity and Local Atomic Structure in Liquid Zr56Co28Al16 Alloy. Microgravity Science and Technology, 2022, 34, 1.	0.7	2
65590	Strainâ€Activated Copper Catalyst for pHâ€Universal Hydrogen Evolution Reaction. Advanced Functional Materials, 2022, 32, .	7.8	46

#	Article	IF	Citations
65591	Dissociating the phononic, magnetic and electronic contributions to thermal conductivity: a computational study in alpha-iron. Journal of Materials Science, 0, , 1.	1.7	6
65592	Electrochemical CO₂ Reduction On Two-Dimensional Metal 1,3,5-triamino-2,4,6-Benzenetriol Frameworks: A Density Functional Study. Journal of the Electrochemical Society, 2022, 169, 024513.	1.3	6
65593	Anharmonic stabilization of ferrielectricity in <mml:math xmlns:mml="http://www.w3.org/1998/Math/MathML"><mml:mrow><mml:msub><mml:mi>CuInP</mml:mi><mml:mn>2</mml:mn></m Physical Review Research, 2022, 4, .	1.3	12
65594	A Library of ROSâ€Catalytic Metalloenzyme Mimics with Atomic Metal Centers. Advanced Materials, 2022, 34, e2200255.	11.1	68
65595	Optical Properties of Epsilon Iron Oxide Nanoparticles in the Millimeter- and Terahertz-Wave Regions. Bulletin of the Chemical Society of Japan, 2022, 95, 538-552.	2.0	24
65596	Epitaxially Constrained Grain Boundary Structures in an Oxide Honeycomb Monolayer. Advanced Materials Interfaces, 2022, 9, .	1.9	2
65597	A Scalable Network Model for Electrically Tunable Ferroelectric Domain Structure in Twistronic Bilayers of Two-Dimensional Semiconductors. Nano Letters, 2022, 22, 1534-1540.	4.5	15
65598	Realistic first-principles calculations of the magnetocaloric effect: applications to hcp Gd. Materials Research Letters, 2022, 10, 156-162.	4.1	4
65599	In situ TEM visualization of LiF nanosheet formation on the cathode-electrolyte interphase (CEI) in liquid-electrolyte lithium-ion batteries. Matter, 2022, 5, 1235-1250.	5.0	56
65600	Ammonia Synthesis on the RRuSi(001) (R = Ca,La) Surfaces: DFT Insights Revealing the Active La Termination of the LaRuSi Electride. Journal of Physical Chemistry C, 2022, 126, 3009-3016.	1.5	3
65601	Few-layer bismuth selenide cathode for low-temperature quasi-solid-state aqueous zinc metal batteries. Nature Communications, 2022, 13, 752.	5.8	49
65602	First-principles determination of magnetic properties of <mml:math xmlns:mml="http://www.w3.org/1998/Math/MathML"><mml:mrow><mml:mi>Co</mml:mi><mml:msub><mml:mi>Cp</mml:mi><mml:mi><mml on the Cr(001) surface. Physical Review B, 2022, 105, .	1.3	0
65603	Adsorption and dissociation mechanism of toluene on Pd (111) and PdO (101) surface: First principle calculation. Surface Science, 2022, 720, 122051.	0.8	12
65604	Impact of local arrangement of Fe and Ni on the phase stability and magnetocrystalline anisotropy in Fe-Ni-Al Heusler alloys. Physical Review Materials, 2022, 6, .	0.9	6
65605	Synthesis of Uranium Single Atom from Radioactive Wastewater for Enhanced Water Dissociation and Hydrogen Evolution. Small, 2022, 18, e2107444.	5.2	17
65606	Ab Initio Study of Energetics, Charge Transfer, and Atomic Structures of FCC Fe/NbC Interfaces with and Without N Doping: From Coherent to Semi-coherent Interfaces. Jom, 2022, 74, 1379-1386.	0.9	3
65607	Tetraphenyl Tetrel Molecules and Molecular Crystals: From Structural Properties to Nonlinear Optics. Journal of Physical Chemistry C, 2022, 126, 3713-3726.	1.5	4
65608	Molecular Packing of Phenoxazine: A Combined Single-Crystal/Crystal Structure Prediction Study. Crystal Growth and Design, 0, , .	1.4	1

#	Article	IF	Citations
65609	Realizing strong visible-light absorption band for 2D crystalline carbon nitride sheets induced by extending Ï€-conjugation and introducing cyano groups. Materials Today Physics, 2022, 23, 100634.	2.9	7
65610	First-Principles Calculations of the Hydrolysis Mechanism of Hexagonal Boron Nitride Nanosheets: Implications for Preventing Hydrolytic Degradation. ACS Applied Nano Materials, 0, , .	2.4	1
65611	Tailoring the coercive field in ferroelectric metal-free perovskites by hydrogen bonding. Nature Communications, 2022, 13, 794.	5.8	24
65612	Super-hydrophobic Cs4PbBr6@PDB composites with water-driven photoluminescence enhancement and dehydration recovery. Chemical Engineering Journal, 2022, 436, 135077.	6.6	10
65613	An MXeneâ€Based Metal Anode with Stepped Sodiophilic Gradient Structure Enables a Large Current Density for Rechargeable Naâ€“O₂ Batteries. Advanced Materials, 2022, 34, e2106565.	11.1	35
65614	Oscillatory bifurcation patterns initiated by seeded surface solidification of liquid metals. , 2022, 1, 158-169.		15
65615	Phase transition and enhanced hardness of LaB4 under pressure. Journal of Physics and Chemistry of Solids, 2022, , 110622.	1.9	0
65616	On the Sensitivity to Densityâ€Functional Approximations for CO Binding Energies of Singleâ€Atom Catalysts in Nitrogenâ€Doped Graphene. ChemPhysChem, 2022, 23, e202100787.	1.0	6
65617	Mechanistic insights into ball milling enhanced montmorillonite modification with tetramethylammonium for adsorption of gaseous toluene. Chemosphere, 2022, 296, 133962.	4.2	16
65618	Atomically dispersed cobalt in core-shell carbon nanofiber membranes as super-flexible freestanding air-electrodes for wearable Zn-air batteries. Energy Storage Materials, 2022, 47, 365-375.	9.5	35
65619	Mechanism and Free-Energy Landscape of Peptide Bond Formation at the Silicaâ€“Water Interface. ACS Catalysis, 2022, 12, 2821-2830.	5.5	7
65620	High-capacity NCNT-encapsulated metal NP catalysts on carbonised loofah with dual-reaction centres over Câ€“M bond bridges for Fenton-like degradation of antibiotics. Applied Catalysis B: Environmental, 2022, 307, 121205.	10.8	37
65621	Facile synthesis of nitrogen- and phosphorus-Co-doped porous carbon nanosheets embedded with FeP clusters for the oxygen reduction reaction using rechargeable zinc-air batteries. Journal of Electroanalytical Chemistry, 2022, 909, 116122.	1.9	2
65622	Electronic Relaxation of Photoexcited Open and Closed Shell Adsorbates on Semiconductors: Ag and Ag2 on TiO2. Journal of Chemical Physics, 2022, 156, 104705.	1.2	3
65623	Experimental and Theoretical Comparison of Potential-dependent Methylation on Chemically Exfoliated WS₂ and MoS₂. ACS Applied Materials & Interfaces, 2022, 14, 9744-9753.	4.0	2
65624	Twoâ€Dimensional Dirac Nodal Line Carbon Nitride to Anchor Singleâ€Atom Catalyst for Oxygen Reduction Reaction. ChemSusChem, 2022, 15, e202102537.	3.6	9
65625	Pressureâ€Driven Magnetoâ€Topological Phase Transition in a Magnetic Weyl Semimetal. Advanced Quantum Technologies, 2022, 5, .	1.8	7
65626	Static and dynamic components of Debyeâ€“Waller coefficients in the novel cubic polymorph of low-temperature disordered Cu₂ZnSnS₄. IUCrJ, 2022, 9, 272-285.	1.0	5

#	Article	IF	Citations
65627	Direct band gap AlPSi3 and GaPSi3 for tandem solar cells. Journal of Power Sources, 2022, 525, 231104.	4.0	0
65628	Hosting AlCl3 on ternary metal oxide composites for catalytic oligomerization of 1-decene: Revealing the role of supports via performance evaluation and DFT calculation. Microporous and Mesoporous Materials, 2022, 333, 111665.	2.2	2
65629	Modulation of the electronic properties of blue phosphorene/stanene heterostructures by electric field and interlayer distance. Results in Physics, 2022, 34, 105252.	2.0	6
65630	Effect of lanthanide fission product concentrations on the mechanical properties of UO2: A first principle based study. Computational and Theoretical Chemistry, 2022, 1209, 113610.	1.1	4
65631	Unsaturated coordination modes of Mn/V in manganese vanadate: Inner capture and surface migration of zinc ions for high performance zinc-ion battery. Journal of Power Sources, 2022, 525, 231134.	4.0	15
65632	Synthesis, structural and spectral characteristics of Cd3O2SO4. Materials Today Communications, 2022, 30, 103215.	0.9	1
65633	First-Principles Study on Cathode Properties of Li2MTiO4 and Na2MTiO4 (M = V, Cr, Mn, Fe, Co, Ni). Journal of the Physical Society of Japan, 2022, 91, .	0.7	0
65634	Ab initio investigation of properties and mobility of helium defects in La2Sn2O7 pyrochlore. Nuclear Materials and Energy, 2022, 30, 101135.	0.6	0
65635	Unraveling roles of lead ions in selective flotation of scheelite and fluorite from atomic force microscopy and first-principles calculations. Minerals Engineering, 2022, 179, 107424.	1.8	14
65636	Effect of neutron irradiation on ductility of tungsten foils developed for tungsten-copper laminates. Nuclear Materials and Energy, 2022, 30, 101133.	0.6	3
65637	Interaction of Mg with the ionic liquid 1-butyl-1-methylpyrrolidinium bis(trifluoromethylsulfonyl)imideâ€"An experimental and computational model study of the electrodeâ€"electrolyte interface in post-lithium batteries. Journal of Vacuum Science and Technology A: Vacuum, Surfaces and Films, 2022, 40, .	0.9	6
65638	Hydrous silicate melts and the deep mantle H2O cycle. Earth and Planetary Science Letters, 2022, 581, 117408.	1.8	9
65639	Enhanced MnO2/peroxymonosulfate activation for phthalic acid esters degradation: Regulation of oxygen vacancy. Chemical Engineering Journal, 2022, 433, 134048.	6.6	17
65640	Pyrolysis-free, facile mechanochemical strategy toward cobalt single-atom/nitrogen-doped carbon for highly efficient water splitting. Chemical Engineering Journal, 2022, 433, 134089.	6.6	13
65641	Doping-induced structural transformation in the spin-1/2 triangular-lattice antiferromagnet Na2Ba1-xSrxCo(PO4)2. Journal of Alloys and Compounds, 2022, 905, 164147.	2.8	2
65642	Electronic reconfiguration in layered Bi2SeO2 surface induced by dual-metal hybridization for hydrogen evolution reaction. Surfaces and Interfaces, 2022, 29, 101779.	1.5	1
65643	New insights on the different corrosion mechanisms of Mg alloys with solute-enriched stacking faults or long period stacking ordered phase. Corrosion Science, 2022, 198, 110163.	3.0	91
65644	Excitation-dependent emissive FeSe nanoparticles induced by chiral interlayer expansion and their multi-color bio-imaging. Nano Today, 2022, 43, 101424.	6.2	9

#	Article	IF	Citations
65645	Comparative study on the radiation resistance of pure and He-doped Gd2Zr2O7 pyrochlore by DFTÂ+ÂU calculation. Nuclear Instruments & Methods in Physics Research B, 2022, 516, 8-14.	0.6	2
65646	Ultralow lattice thermal conductivity and high thermoelectric performance of the WS2/WTe2 van der Waals superlattice. Physics Letters, Section A: General, Atomic and Solid State Physics, 2022, 430, 127986.	0.9	3
65647	Ab initio prediction of a metallic Bi2C monolayer with high light absorption. Solid State Communications, 2022, 345, 114690.	0.9	0
65648	Interfacial boron modification on mesoporous octahedral rhodium shell and its enhanced electrocatalysis for water splitting and oxygen reduction. Chemical Engineering Journal, 2022, 435, 134982.	6.6	13
65649	Barriers to predictive high-throughput screening for spin-crossover. Computational Materials Science, 2022, 206, 111161.	1.4	9
65650	Ultrafast and selective gas transport through highly ordered black phosphorene nanochannels. Separation and Purification Technology, 2022, 288, 120629.	3.9	6
65651	Discharge Induced-Activation of Phosphorus-Doped Nickel Oxyhydroxide for Oxygen Evolution Reaction. Chemical Engineering Journal, 2022, 435, 135049.	6.6	14
65652	Experimental and DFT investigations of the performance of ZrO2 catalysts modified with Ce, La, Y, Mg, and Ba oxides during methyl stearate ketonization. Applied Surface Science, 2022, 585, 152627.	3.1	5
65653	Effect of aluminum substitution on structural, electronic and dielectric properties of cubic CaCu3Ti4O12 ceramics: A first-principles study. Journal of Physics and Chemistry of Solids, 2022, 164, 110617.	1.9	0
65654	Transforming incipient to real ferroelectrics in SrTiO3 upon doping luminescent Eu3+ /Tb3+ ions and the generation of white light for piezo-phototronics application. Journal of Alloys and Compounds, 2022, 904, 164086.	2.8	5
65655	A multi-scale model for syngas combustion on NiO oxygen carrier for chemical looping combustion: The role of nearest neighbors. Fuel Processing Technology, 2022, 229, 107172.	3.7	8
65656	Retarded transport properties of graphene oxide based chiral separation membranes modified with dipeptide. Separation and Purification Technology, 2022, 288, 120642.	3.9	9
65657	A highly stable potassium-ion battery anode enabled by multilayer graphene sheets embedded with SnTe nanoparticles. Chemical Engineering Journal, 2022, 435, 135100.	6.6	29
65658	Combination of Fe(II)-induced oxygen deficiency and metal doping strategy for construction of high efficiency water oxidation electrocatalysts under industrial-scale current density. Chemical Engineering Journal, 2022, 435, 135048.	6.6	6
65659	The atomic structure, magnetic properties and bending ductility of a novel Fe-P-C-B-Si amorphous alloy investigated by experiments and ab initio molecular dynamics. Journal of Alloys and Compounds, 2022, 904, 164101.	2.8	9
65660	Oxygen vacancy inducing phase transition during charge storage in MnOx@rGO supercapacitor electrode. Chemical Engineering Journal, 2022, 435, 135103.	6.6	42
65661	Achieving fast ionic conductivity and high electrochemical stability through polyhedral structure design. Energy Storage Materials, 2022, 47, 70-78.	9.5	2
65662	Construction of Î³-MnS/Î±-MnS hetero-phase junction for high-performance sodium-ion batteries. Chemical Engineering Journal, 2022, 435, 135149.	6.6	16

#	Article	IF	Citations
65663	PVDF-stimulated surface engineering in ZnO for highly sensitive and water-stable hydrazine sensors. Applied Surface Science, 2022, 585, 152747.	3.1	5
65664	A new metallic composite cathode originated from hyperbranched polymer coated MOF for High-performance Lithium-Sulfur batteries. Chemical Engineering Journal, 2022, 435, 135125.	6.6	25
65665	Efficient photocatalytic hydrogen evolution through reverse hydrogen spillover on photoactivated copper-doped mesoporous titania spheres. Applied Materials Today, 2022, 27, 101417.	2.3	2
65666	Defects-/doping-driven modulation of the electronic and magnetic properties of 2H- and Td-phase <mml:math xmlns:mml="http://www.w3.org/1998/Math/MathML" display="inline" id="d1e715" altimg="si41.svg"><mml:mrow><mml:mi>W</mml:mi><mml:mi>T</mml:mi><mml:msub><mml:mrow><mml:mi>e</mml:mi></mml:mrow><mml:mi></mml:mi></mml:msub></mml:mrow></mml:math> monolayers: A first-principle study. Materials Science in Semiconductor Processing, 2022, 143, 106537.	4.9	9
65667	Heterostructured CoPÂ·CoMoP nanocages as advanced electrocatalysts for efficient hydrogen evolution over a wide pH range. Journal of Colloid and Interface Science, 2022, 615, 465-474.	5.0	28
65668	Theoretical investigation of structural, energetic and magnetic properties of B2 type MnM alloys, DFT and data mining approach. Computational Condensed Matter, 2022, 31, e00656.	0.9	0
65669	Two-dimensional hexagonal LaOF with ultrawide bandgap, large exciton energy, and low lattice thermal conductivity. Physica E: Low-Dimensional Systems and Nanostructures, 2022, 140, 115195.	1.3	1
65670	Tuning Ni dopant concentration to enable co-deposited superhydrophilic self-standing Mo2C electrode for high-efficient hydrogen evolution reaction. Applied Catalysis B: Environmental, 2022, 307, 121201.	10.8	36
65671	High thermal conductivity of carbon allotropes and its relationship with mechanical properties: A first-principles study. International Journal of Thermal Sciences, 2022, 176, 107481.	2.6	5
65672	Design and analysis of III-V two-dimensional van der Waals heterostructures for ultra-thin solar cells. Applied Surface Science, 2022, 586, 152799.	3.1	16
65673	Highly efficient electrocatalytic hydrogen evolution coupled with upcycling of microplastics in seawater enabled via Ni3N/W5N4 janus nanostructures. Applied Catalysis B: Environmental, 2022, 307, 121198.	10.8	72
65674	Experimental and Theoretical Insight into the Facet-Dependent Mechanisms of NO Oxidation Catalyzed by Structurally Diverse Mn₂O₃ Nanocrystals. ACS Catalysis, 2022, 12, 397-410.	5.5	38
65675	Hole doping effect of MoS2 via electron capture of He+ ion irradiation. Scientific Reports, 2021, 11, 23590.	1.6	8
65676	Role of Pr-Vacancies and O-Interstitials on the Activity and Stability of (Pr_{1â^'x}Ln_x)₂NiO₄ (Ln = La, Nd, Pm, Sm, Gd, Tb, Dy, and) Tj ETQq1 1 0.784314 rgB 168, 124508.	1.3	3
65677	Coordination environments tune the activity of oxygen catalysis on single atom catalysts: A computational study. Nano Research, 2022, 15, 3073-3081.	5.8	58
65678	Tunable giant nonlinear optical susceptibility in BaSnO3 quantum wells. Physical Review B, 2021, 104, .	1.1	2
65679	Vacancies and interfaces engineering of coreâ€“shell heterostuctured NiCoP/NiO as trifunctional electrocatalysts for overall water splitting and zinc-air batteries. Green Energy and Environment, 2023, 8, 601-611.	4.7	15
65680	Atomic-Scale Visualization of Polar Domain Boundaries in Ferroelectric In₂Se₃ at the Monolayer Limit. Journal of Physical Chemistry Letters, 2021, 12, 11902-11909.	2.1	7

#	Article	IF	Citations
65681	Development of SnO2 Composites as Electron Transport Layer in Unencapsulated CH3NH3PbI3 Solar Cells. Solids, 2021, 2, 407-419.	1.1	4
65682	First-Formed Framework Species and Phosphate Structure Distributions in Phosphorus-Modified MFI Zeolites. Journal of Physical Chemistry C, 2022, 126, 227-238.	1.5	7
65683	First-Principles Investigation on the Significant Anisotropic Thermoelectric Transport Performance of a Hf₂Cl₄ Monolayer. Journal of Physical Chemistry C, 2022, 126, 525-533.	1.5	13
65684	Effect of Aqueous Electrolytes on LiCoO₂ Surfaces: Role of Proton Adsorption on Oxygen Vacancy Formation. Journal of Physical Chemistry C, 2022, 126, 110-119.	1.5	7
65685	The Regulation of O2 Spin State and Direct Oxidation of CO at Room Temperature Using Triboelectric Plasma by Harvesting Mechanical Energy. Nanomaterials, 2021, 11, 3408.	1.9	7
65686	Metastable Antimonyâ€Doped SnO₂ Quantum Wires for Ultrasensitive Gas Sensors. Advanced Electronic Materials, 2022, 8, .	2.6	6
65687	Surfaceâ€Anchored Acetylcholine Regulates Bandâ€Edge States and Suppresses Ion Migration in a 21%â€Efficient Quadrupleâ€Cation Perovskite Solar Cell. Small, 2022, 18, e2105184.	5.2	30
65688	In Situ Grown Coâ€Based Interstitial Compounds: Nonâ€3d Metal and Nonâ€Metal Dual Modulation Boosts Alkaline and Acidic Hydrogen Electrocatalysis. Small, 2022, 18, e2105331.	5.2	122
65689	Selfâ€Optimizing Effect in Lithium Storage of GeO₂ Induced by Heterointerface Regulation. Small, 2022, 18, e2106067.	5.2	5
65690	High Oxideâ€Ion Conductivity in a Hexagonal Perovskiteâ€Related Oxide Ba₇Ta_{3.7}Mo_{1.3}O_{20.15} with Cation Site Preference and Interstitial Oxide Ions. Small, 2022, 18, e2106785.	5.2	21
65691	First-principles investigation on stability and electronic structure of Sc-doped Î¸â€²/Al interface in Alâ€“Cu alloys. Transactions of Nonferrous Metals Society of China, 2021, 31, 3342-3355.	1.7	14
65692	High-Throughput Computational Discovery of Ternary Mixed-Anion Oxypnictides. Chemistry of Materials, 2021, 33, 9486-9500.	3.2	6
65693	High-T_c Superconducting Hydrides Formed by LaH₂₄ and YH₂₄ Cage Structures as Basic Blocks. Chemistry of Materials, 2021, 33, 9501-9507.	3.2	16
65694	Germanium Antimony Bonding in Ba₄Ge₂Sb₂Te₁₀ with Low Thermal Conductivity. Inorganic Chemistry, 2022, 61, 968-981.	1.9	10
65695	Four Discrete Silver Iodobismuthates/Bromobismuthates with Metal Complexes: Syntheses, Structures, Photocurrent Responses, and Theoretical Studies. Inorganic Chemistry, 2022, 61, 406-413.	1.9	14
65696	Capturing Individual Hydrogen Bond Strengths in Ices via Periodic Local Vibrational Mode Theory: Beyond the Lattice Energy Picture. Journal of Chemical Theory and Computation, 2022, 18, 562-579.	2.3	17
65697	Edge Effect Promotes Graphene-Confining Single-Atom Coâ€“N₄ and Rhâ€“N₄ for Bifunctional Oxygen Electrocatalysis. Journal of Physical Chemistry C, 2022, 126, 30-39.	1.5	17
65698	Tuning the Lifetime of Photoexcited Small Polarons on Rutile TiO₂ Surface via Molecular Adsorption. Journal of Physical Chemistry C, 2021, 125, 27275-27282.	1.5	10

#	Article	IF	Citations
65699	Breaking through the Peak Height Limit of the Volcano-Shaped Activity Curve for Metal Catalysts: Role of Distinct Surface Structures on Transition Metal Oxides. Journal of Physical Chemistry C, 2022, 126, 183-191.	1.5	4
65700	Charge State Dependence of Phase Transition Catalysis of Dynamic Cu Clusters in CO₂ Dissociation. Journal of Physical Chemistry C, 2021, 125, 27615-27623.	1.5	2
65701	Uncovering the Self-Organized Nanowires on Au-Modified Ge(001) Surfaces. Journal of Physical Chemistry C, 2021, 125, 27876-27883.	1.5	4
65702	Potential Solid-State Electrolytes with Good Balance between Ionic Conductivity and Electrochemical Stability: Li_{5â€“x}M_{1â€“x}M_xâ€²O₄ (M = Al,	1.5	1
65703	Insights into the Mechanism of Methanol Steam Reforming for Hydrogen Production over Niâ€“Cu-Based Catalysts. ACS Catalysis, 2022, 12, 512-526.	5.5	31
65704	The Role of Cation Acidity on the Competition between Hydrogen Evolution and CO₂ Reduction on Gold Electrodes. Journal of the American Chemical Society, 2022, 144, 1589-1602.	6.6	127
65705	Piezoelectricity in hafnia. Nature Communications, 2021, 12, 7301.	5.8	37
65706	Ti1â€“graphene single-atom material for improved energy level alignment in perovskite solar cells. Nature Energy, 2021, 6, 1154-1163.	19.8	72
65707	Topologically protected oxygen redox in a layered manganese oxide cathode for sustainable batteries. Nature Sustainability, 2022, 5, 214-224.	11.5	44
65708	Surface-substituted Prussian blue analogue cathode for sustainable potassium-ion batteries. Nature Sustainability, 2022, 5, 225-234.	11.5	293
65709	In-situ reconstructed Ru atom array on Î±-MnO2 with enhanced performance for acidic water oxidation. Nature Catalysis, 2021, 4, 1012-1023.	16.1	324
65710	Assessing density functionals for describing methane dissociative chemisorption on Pt(110)-(2Ã—1) surface. Chinese Journal of Chemical Physics, 2021, 34, 883-895.	0.6	2
65711	Recent advances in lattice thermal conductivity calculation using machine-learning interatomic potentials. Journal of Applied Physics, 2021, 130, .	1.1	24
65712	Theory of the charge density wave in <mml:math xmlns:mml="http://www.w3.org/1998/Math/MathML"><mml:mrow><mml:mi>A</mml:mi><mml:msub><mml:mi mathvariant="normal">V</mml:mi><mml:mn>3</mml:mn></mml:msub><mml:msub><mml:mi>Sb</mml:mi><mml:mn>5</mml:mn> kagome metals. Physical Review B, 2021, 104, .	1.1	86
65713	Photoionization of negatively charged NV centers in diamond: Theory and ab initio calculations. Physical Review B, 2021, 104, .	1.1	25
65714	Type-II nodal line fermions in the <mml:math xmlns:mml="http://www.w3.org/1998/Math/MathML"><mml:msub><mml:mi mathvariant="double-struck">Z</mml:mi><mml:mn>2</mml:mn></mml:msub></mml:math> topological semimetals <mml:math xmlns:mml="http://www.w3.org/1998/Math/MathML"><mml:mi>A</mml:mi><mml:msub><mml:mrow><mml:mi mathvariant="normal">V</mml:mi></mml:mrow><mml:mn>6</mml:mn></mml:msub><mml:msub><mml:mrow><mml:mi>Sb</mml:mi>	1.1	8
65715	Second-order topological insulator state in hexagonal lattices and its abundant material candidates. Physical Review B, 2021, 104, .	1.1	27
65716	Quasi-two-dimensional ferromagnetism and anisotropic interlayer couplings in the magnetic topological insulator <mml:math xmlns:mml="http://www.w3.org/1998/Math/MathML"><mml:mrow><mml:msub><mml:mi>MnBi</mml:mi><mml:mn>2</mml:mn></mml:msub></mml:mrow> Physical Review B, 2021, 104, .	1.1	10

#	Article	IF	Citations
65717	Signatures of Weyl Fermion Annihilation in a Correlated Kagome Magnet. Physical Review Letters, 2021, 127, 256403.	2.9	17
65718	Intrinsic Nonlinear Hall Effect in Antiferromagnetic Tetragonal CuMnAs. Physical Review Letters, 2021, 127, 277201.	2.9	59
65719	Intrinsic Second-Order Anomalous Hall Effect and Its Application in Compensated Antiferromagnets. Physical Review Letters, 2021, 127, 277202.	2.9	54
65720	Insights into oxygen vacancies from high-throughput first-principles calculations. Physical Review Materials, 2021, 5, .	0.9	25
65721	First-principles calculations of defects in metal halide perovskites: A performance comparison of density functionals. Physical Review Materials, 2021, 5, .	0.9	12
65722	Exciton landscape in van der Waals heterostructures. Physical Review Research, 2021, 3, .	1.3	19
65723	A scalable metal-organic framework as a durable physisorbent for carbon dioxide capture. Science, 2021, 374, 1464-1469.	6.0	308
65724	The Adsorption Behavior of Gas Molecules on Co/N Coâ€“Doped Graphene. Molecules, 2021, 26, 7700.	1.7	6
65725	Super-Hydrophobic Cs4pbbr6@Pdb Composites with Water-Driven Photoluminescence Enhancement and Dehydration Recovery. SSRN Electronic Journal, 0, , .	0.4	0
65726	Uncovering Electrocatalytic Conversion Mechanisms from Li ₂S ₂ to Li ₂S: Generalization of Computational Hydrogen Electrode. SSRN Electronic Journal, 0, , .	0.4	0
65727	Development of the Electronic Structure Calculation using Imaginary Time Evolution. Journal of Computer Chemistry Japan, 2021, 20, 126-128.	0.0	0
65728	Novel 2D Porous C ₃N ₂ Framework as Promising Anode Materials with Ultra-High Specific Capacity for Lithium-Ion Batteries. SSRN Electronic Journal, 0, , .	0.4	0
65729	Reversible Hydrogen Storage for NLi ₄-Decorated Honeycomb BoropheneOxide. SSRN Electronic Journal, 0, , .	0.4	0
65730	Construction of a Dense and Li-N Rich Solid Electrolyte Interface for Dendrite-Free Lithium Metal Batteries. SSRN Electronic Journal, 0, , .	0.4	0
65731	Microstructure Control and Strengthening Mechanism of Fine-Grained Cast Mg Alloys Based on Grain Boundary Segregation of Al Solute. SSRN Electronic Journal, 0, , .	0.4	0
65732	Experimental and Theoretical Identifications of Durable Feâ€“Nx Configurations Embedded in Graphitic Carbon Nitride for Uranium Photoreduction. SSRN Electronic Journal, 0, , .	0.4	0
65733	Properties of Mo-Based Tmdcs/Ti2ct2(T = O, F, Oh)Vdws Heterostructures for Full Spectrum Electromagnetic Absorption. SSRN Electronic Journal, 0, , .	0.4	0
65734	Single-Atomic Iron-Nitrogen 2d Mof Originated Hierarchically Porous Carbon Catalysts for Enhanced Oxygen Reduction Reaction. SSRN Electronic Journal, 0, , .	0.4	0

#	Article	IF	Citations
65735	Insights into the Alleviation of Dendrite Formation Via F- Induced Dissolution in Rechargeable Aqueous Zn-Ion Batteries. SSRN Electronic Journal, 0, , .	0.4	0
65736	Biobr/Bi2s3 Heterojunction with S-Scheme Structure and Oxygen Defects: In-Situ Construction and Photocatalytic Behavior for Reduction of Co2 with H2o. SSRN Electronic Journal, 0, , .	0.4	0
65737	Enabling Deep Conversion Reactions by Weakening M-O Bonds Through K ⁺ Pre-Intercalation. SSRN Electronic Journal, 0, , .	0.4	0
65738	Construction of Î“-Mns/Î‘-Mns Hetero-Phase Junction for High-Performance Sodium-Ion Batteries. SSRN Electronic Journal, 0, , .	0.4	0
65739	Peroxymonosulfate Activation by Black Tio2 Nanotube Arrays Under Solar Light: Switching the Activation Mechanism and Enhancing Catalytic Activity and Stability. SSRN Electronic Journal, 0, , .	0.4	0
65740	Impact of Ultrathin Coating Layer on Lithium-Ion Intercalation Onto Particles for Lithium-Ion Batteries. SSRN Electronic Journal, 0, , .	0.4	0
65741	Influence of Co and Co-F Co-Doping on Defect-Induced Intrinsic Ferromagnetic Properties of PbPdO ₂ Nanoparticles. SSRN Electronic Journal, 0, , .	0.4	0
65742	Electronic Structure, Magnetism and Disorder Effect in Double Half-Heusler Alloy Mn ₂FeCoSi ₂. SSRN Electronic Journal, 0, , .	0.4	0
65743	Exploration of Potassium Silicide Compounds Under High Pressure. SSRN Electronic Journal, 0, , .	0.4	0
65744	Highly Efficient Interface Stabilization for Ambient-Temperature Solid-State Sodium Metal Batteries. SSRN Electronic Journal, 0, , .	0.4	0
65745	Simultaneous Construction of Impermeable Dual-Shell Stabilizing Fluoride Phosphors for White Light-Emitting Diodes. SSRN Electronic Journal, 0, , .	0.4	0
65746	Stable Nitrogen-Rich Yttrium Nitrides Under High Pressure. SSRN Electronic Journal, 0, , .	0.4	0
65747	One-Pot Synthesis of Novel Porous Carbon Adsorbents Derived from Poly Vinyl Chloride for High Methane Adsorption Uptake. SSRN Electronic Journal, 0, , .	0.4	0
65748	An In-Plane S-Scheme Heterostructure Drives H2 Production with Water and Solar Energy. SSRN Electronic Journal, 0, , .	0.4	0
65749	Li Plating on Alloy with Superior Electro-Mechanical Stability for High Energy Density Anode-Free Batteries. SSRN Electronic Journal, 0, , .	0.4	0
65750	Interfacial Electronic Structure Modulation of Pt-MoS ₂ Heterostructure for Enhancing Electrocatalytic Hydrogen Evolution Reaction. SSRN Electronic Journal, 0, , .	0.4	0
65751	Perpendicular Exchange Bias on Cubic L1 ₂-Mn _{2.6}Ga- Mn ₃Ga Epitaxial Bilayers. SSRN Electronic Journal, 0, , .	0.4	0
65752	Interfacial Boron Modification on Mesoporous Octahedral Rhodium Shell and its Enhanced Electrocatalysis for Water Splitting and Oxygen Reduction. SSRN Electronic Journal, 0, , .	0.4	0

#	Article	IF	Citations
65753	Mg2Sn Stannide under Pressure: First-Principles Evolutionary Search Results. Physics of the Solid State, 2021, 63, 590-594.	0.2	0
65754	Visible-Light Photocatalytic Chlorite Activation Mediated by Oxygen Vacancy for Efficient Chlorine Dioxide Generation and Pollutant Degradation. SSRN Electronic Journal, 0, , .	0.4	0
65755	CH₄ steam reforming on Pt + Pd/Al₂O₃ monolith: impact of Mn_{0.5}Fe_{2.5}O₄ spinel addition. Catalysis Science and Technology, 2022, 12, 2618-2633.	2.1	4
65756	Lone pair driven anisotropy in antimony chalcogenide semiconductors. Physical Chemistry Chemical Physics, 2022, 24, 7195-7202.	1.3	27
65757	Effect of transition metal cations on the local structure and lithium transport in disordered rock-salt oxides. Physical Chemistry Chemical Physics, 2022, 24, 5823-5832.	1.3	8
65758	High Thermoelectric Properties of Janus Wses Bilayer Membranes with Different Stacking Modes. SSRN Electronic Journal, 0, , .	0.4	0
65759	Ultrathin black phosphorus as a pivotal hole extraction layer and oxidation evolution co-catalyst boosting solar water oxidation. Inorganic Chemistry Frontiers, 2022, 9, 2938-2944.	3.0	2
65760	Accommodation of helium in PuO_{2Â±x} and the role of americium. Physical Chemistry Chemical Physics, 2022, 24, 8245-8250.	1.3	3
65761	Exploring mechanistic routes for light alkane oxidation with an ironâ€“triazolate metalâ€“organic framework. Physical Chemistry Chemical Physics, 2022, 24, 8129-8141.	1.3	6
65762	Study on SO₂ and Cl₂ sensor application of 2D PbSe based on first principles calculations. RSC Advances, 2022, 12, 8530-8535.	1.7	4
65763	Predicted structures and superconductivity of LiYH_n (n = 5â€“10) under high pressure. Physical Chemistry Chemical Physics, 2022, 24, 8432-8438.	1.3	0
65764	Abnormal In-Plane Thermal Conductivity Anisotropy in Bilayer Î´-Phase Tellurene. SSRN Electronic Journal, 0, , .	0.4	0
65765	Geometrical Determination of Surface Atom Diffusion Paths. Materials Transactions, 2022, , .	0.4	0
65766	Coordination polymer-derived Al³⁺-doped V₂O₃/C with rich oxygen vacancies for an advanced aqueous zinc-ion battery with ultrahigh rate capability. Sustainable Energy and Fuels, 2022, 6, 2020-2037.	2.5	7
65767	Oxygen-vacancy-rich Fe₃O₄/carbon nanosheets enabling high-attenuation and broadband microwave absorption through the integration of interfacial polarization and charge-separation polarization. Journal of Materials Chemistry A, 2022, 10, 8479-8490.	5.2	26
65768	Post-doping induced morphology evolution boosts Mn²⁺ luminescence in the Cs₂NaBiCl₆:Mn²⁺ phosphor. Physical Chemistry Chemical Physics, 2022, 24, 9866-9874.	1.3	10
65769	Slow excitonic carrier cooling in Sr-doped PbS nanocrystals for hot carrier devices: an integrated experimental and first-principles approach. Journal of Materials Chemistry C, 2022, 10, 6634-6645.	2.7	3
65770	å±,çŠ¶3d²ä½“ç³»VI₃çš„æ™¶ä½“ç»“æž„å'Œ Physica, Mechanica Et Astronomica, 2022, , .	0.2	0

#	Article	IF	Citations
65771	Binder-free S@Ti3C2Tx sandwich structure film as a high-capacity cathode for a stable aluminum-sulfur battery. Science China Materials, 2022, 65, 1463-1475.	3.5	20
65772	Effects of Bi₂Te₃(111) and Al₂O₃(0001) substrates on Electronic and topological properties of Bi(111) bilayer. Wuli Xuebao/Acta Physica Sinica, 2022, .	0.2	0
65773	Tunable Dirac states in doping B₂S₃ monolayer. Physical Chemistry Chemical Physics, 2022, , .	1.3	1
65774	First-Principles Study of the Structural, Electronic, Dynamical, and Mechanical Properties of Pd-Nb Binary Systems. SSRN Electronic Journal, 0, , .	0.4	0
65775	Reactive Species-Dependent Photocatalytic Toluene Mineralization and Deactivation Pathways. SSRN Electronic Journal, 0, , .	0.4	0
65776	Theoretical scheme of nonvolatile strain-switchable high/low resistance based on novel strain-tunable magnetic anisotropy in the Mn_{2.25}Co_{0.75}Ga_{0.5}Sn_{0.5}/MgO superlattice. Physical Chemistry Chemical Physics, 2022, 24, 7826-7835.	1.3	1
65777	Cubic-Spinel Agin5s8-Based Thermoelectric Materials: Synthesis, Phonon Transport and Defect Chemistry. SSRN Electronic Journal, 0, , .	0.4	0
65778	Crystallographic Engineering to Reduce Diffusion Barrier for Enhanced Intercalation Pseudocapacitance of TiNb ₂O ₇ in Fast-Charging Batteries. SSRN Electronic Journal, 0, , .	0.4	0
65779	MoirÃ© bands in twisted trilayer black phosphorene: effects of pressure and electric field. Nanoscale, 2022, 14, 3758-3767.	2.8	4
65780	Understanding Electrochemical Reaction Mechanisms of Precious Metals Au and Ru as Cathode Catalysts in Li-CO ₂ Batteries. SSRN Electronic Journal, 0, , .	0.4	0
65781	Two-dimensional square and hexagonal oxide quasicrystal approximants in SrTiO₃ films grown on Pt(111)/Al₂O₃(0001). Physical Chemistry Chemical Physics, 2022, 24, 7253-7263.	1.3	4
65782	Single-particle and collective excitations of polar water molecules confined in nano-pores within a cordierite crystal lattice. Physical Chemistry Chemical Physics, 2022, 24, 6890-6904.	1.3	8
65783	Na⁺/vacancy disordered manganese-based oxide cathode with ultralow strain enabled by tuning charge distribution. Journal of Materials Chemistry A, 2022, 10, 10391-10399.	5.2	10
65784	Magnetoelectric coupling effects on the band alignments of multiferroic In₂Se₃â€“CrI₃ trilayer heterostructures. Nanoscale, 2022, 14, 5454-5461.	2.8	5
65785	Prediction of atomically thin two-dimensional single monolayer SnGe with high carrier mobility: a DFT study. New Journal of Chemistry, 2022, 46, 5368-5373.	1.4	2
65786	A first-principles study of electronic and optical properties of the tetragonal phase of monolayer ZnS modulated by biaxial strain. RSC Advances, 2022, 12, 6166-6173.	1.7	5
65787	Formation of stable polonium monolayers with tunable semiconducting properties driven by strong quantum size effects. Physical Chemistry Chemical Physics, 2022, 24, 7512-7520.	1.3	0
65788	Giant tunnelling electroresistance through 2D sliding ferroelectric materials. Materials Horizons, 2022, 9, 1422-1430.	6.4	23

#	Article	IF	Citations
65789	Ultralow work function of the electride Sr₃CrN₃. Physical Chemistry Chemical Physics, 2022, 24, 8854-8858.	1.3	3
65790	Mechanistic insights for electrochemical reduction of CO₂ into hydrocarbon fuels over O-terminated MXenes. Catalysis Science and Technology, 2022, 12, 2223-2231.	2.1	22
65791	Computational screening of single-atom catalysts supported by VS₂ monolayers for electrocatalytic oxygen reduction/evolution reactions. Nanoscale, 2022, 14, 6902-6911.	2.8	30
65792	Rational Design of Zr-Mofs Pyrolyzed to Pinpoint Rate-Directing Stage and Catalytic Functions of Surface Acidic Species in Homolytic H2o2 Scission. SSRN Electronic Journal, 0, , .	0.4	0
65793	Structural, magnetic, and electronic properties of EuSi₂ thin films on the Si(111) surface. Physical Chemistry Chemical Physics, 2022, 24, 6782-6787.	1.3	6
65794	Structural, elastic and optoelectronic properties of inorganic cubic FrBX₃ (B = Ge, Sn; X =) Tj ETQq1 1 0.784314 rgBT /O	1.7	35
65795	Ab initio, artificial neural network predictions and experimental synthesis of mischmetal alloying in Smâ€“Co permanent magnets. Nanoscale, 2022, 14, 5824-5839.	2.8	5
65796	Hydride ion intercalation and conduction in the electride Sr₃CrN₃. Journal of Materials Chemistry C, 2022, 10, 6628-6633.	2.7	6
65797	Flexible polyolefin dielectric by strategic design of organic modules for harsh condition electrification. Energy and Environmental Science, 2022, 15, 1307-1314.	15.6	56
65798	Structural and Phase Evolution in U3si2 During Steam Corrosion. SSRN Electronic Journal, 0, , .	0.4	0
65799	Ab Initio Study of the Effects of Cr on Helium Behaviors in Feâ€“Ycr (Y = 9.38, 12.50 At.%) Austenitic Binary Alloys. SSRN Electronic Journal, 0, , .	0.4	0
65800	H2o2 Formation Mechanisms on the (112) and (310) Facets of Sno2 Via Water Oxidation Reaction with the Participation of Bicarbonate: Dft and Experimental Investigations. SSRN Electronic Journal, 0, , .	0.4	0
65801	Dynamic coordination transformation of active sites in single-atom MoS₂ catalysts for boosted oxygen evolution catalysis. Energy and Environmental Science, 2022, 15, 2071-2083.	15.6	33
65802	Designing a descriptor for the computational screening of argyrodite-based solid-state superionic conductors: uniformity of ion-cage size. Journal of Materials Chemistry A, 2022, 10, 7888-7895.	5.2	7
65803	Highly efficient doping of titanium dioxide with sulfur using disulfide-linked macrocycles for hydrogen production under visible light. Green Chemistry, 2022, 24, 2557-2566.	4.6	10
65804	Characterization of Pertechnetates Atco4: A First-Principles Study. SSRN Electronic Journal, 0, , .	0.4	0
65805	Core Structure and Peierls Barrier of Basal Edge Dislocations in Ti3alc2 Max Phase. SSRN Electronic Journal, 0, , .	0.4	0
65806	An analysis of Schottky barrier in silicene/Ga₂SeS heterostructures by employing electric field and strain. Physical Chemistry Chemical Physics, 2022, 24, 10210-10221.	1.3	21

#	Article	IF	Citations
65807	In-Situ Exfoliation and Assembly of 2d/2d G-C3n4/Tio2(B) Hierarchical Microflower: Enhanced Photo-Oxidation of Benzyl Alcohol Under Visible Light. SSRN Electronic Journal, 0, , .	0.4	0
65808	The reaction pathways of 5-hydroxymethylfurfural conversion in a continuous flow reactor using copper catalysts. Catalysis Science and Technology, 2022, 12, 3016-3027.	2.1	9
65809	Oxalate promoted iron dissolution of hematite via proton coupled electron transfer. Environmental Science: Nano, 2022, 9, 1770-1779.	2.2	7
65810	Magnetic single-layer nanoribbons of manganese oxide: edge- and width-dependent electronic properties. Journal of Materials Chemistry C, 2022, 10, 7567-7574.	2.7	1
65811	The consistent behavior of negative Poisson's ratio with interlayer interactions. Materials Advances, 2022, 3, 4334-4341.	2.6	7
65812	Synergistic effects of bithiophene ammonium salt for high-performance perovskite solar cells. Journal of Materials Chemistry A, 2022, 10, 9971-9980.	5.2	14
65813	Adsorption and Dissociation of High-Pressure Hydrogen on Fe (100) and Fe ₂O ₃ (001) Surfaces: Combining DFT Calculation and Statistical Thermodynamics. SSRN Electronic Journal, 0, , .	0.4	0
65814	Modulating the intrinsic properties of platinumâ€“cobalt nanowires for enhanced electrocatalysis of the oxygen reduction reaction. New Journal of Chemistry, 2022, 46, 8122-8130.	1.4	5
65815	A combined experimental and DFT study on the catalysis performance of a Co-doped MoS₂ monolayer for hydrodesulfurization reaction. New Journal of Chemistry, 2022, 46, 5065-5077.	1.4	2
65816	Cu Atoms Induce a New Reconstruction in the Mnga(001) Surface: An Ab-Initio Study. SSRN Electronic Journal, 0, , .	0.4	0
65817	Tailoring defect structure and dopant composition and the generation of various color characteristics in Eu³⁺ and Tb³⁺ doped MgF₂ phosphors. Physical Chemistry Chemical Physics, 2022, 24, 10915-10927.	1.3	5
65818	Lithium Dendrite Suppression with Li3n-Rich Protection LayerÂFormation on 3d Anode Via Ultra-Low Temperature Nitriding. SSRN Electronic Journal, 0, , .	0.4	0
65819	Circumventing the scaling relationship on bimetallic monolayer electrocatalysts for selective CO₂ reduction. Chemical Science, 2022, 13, 3880-3887.	3.7	9
65820	Dft Insights into Hydrodesulfurization Mechanism of 2-Methylthiophene Catalyzed by Ni2p. SSRN Electronic Journal, 0, , .	0.4	0
65821	Synergetic ligand and size effects of boron cage based electrolytes in Li-ion batteries. Physical Chemistry Chemical Physics, 2022, 24, 11345-11352.	1.3	1
65822	Improving the Electrochemical Activity of Pdse2 by Constructing P/T Structural Interfaces. SSRN Electronic Journal, 0, , .	0.4	0
65823	Cation substitution effects on the structural, electronic and sun-light absorption features of all-inorganic halide perovskites. Inorganic Chemistry Frontiers, 2022, 9, 1337-1353.	3.0	2
65824	Spin Polarized Stm Imaging of Nanoscale NÃ©el Skyrmions in an Sriro3/Srruo3 Perovskite Bilayer. SSRN Electronic Journal, 0, , .	0.4	0

#	Article	IF	Citations
65825	Transition Structures, Reaction Paths, and Kinetics: Methods and Applications in Catalysis. , 2024, , 496-518.		0
65826	Low thermal conductivity and high performance anisotropic thermoelectric properties of XSe (X =) Tj ETQq1 1 0.784314 rgBT /Overlo	1.3	19
65827	3d Hierarchical Local Heterojunction as Ultra-High Efficient Fenton-Like Catalyst: Mechanism of Coupling the Proton-Coupled Electron Transfer Under Nanoconfinement Effect. SSRN Electronic Journal, 0, , .	0.4	0
65828	A pre-reaction suppressing strategy for Î±-Ga₂O₃ halide vapor pressure epitaxy using asymmetric precursor gas flow. CrystEngComm, 2022, 24, 3049-3056.	1.3	4
65829	Atomic/molecular layer deposition of cerium(<scp>iii</scp>) hybrid thin films using rigid organic precursors. Dalton Transactions, 2022, 51, 5603-5611.	1.6	3
65830	Effective medium theory for bcc metals: electronically non-adiabatic H atom scattering in full dimensions. Physical Chemistry Chemical Physics, 2022, 24, 8738-8748.	1.3	5
65831	Mechanism of High Magnetic Field Effect on the D03-L12 Phase Transition in Fe-Ga Alloys. SSRN Electronic Journal, 0, , .	0.4	0
65832	Tuning the Activity and Selectivity of Nitrogen Reduction Reaction on Double-Atom Catalysts by B Doping: A Density Functional Theory Study. SSRN Electronic Journal, 0, , .	0.4	0
65833	First principles assessment of the phase stability and transition mechanisms of designated crystal structures of pristine and Janus transition metal dichalcogenides. Physical Chemistry Chemical Physics, 2022, 24, 7430-7441.	1.3	6
65834	Effects of vibrational and rotational excitations on dissociative chemisorption dynamics of N2 on Fe(111). Chinese Journal of Chemical Physics, 2022, 35, 443-450.	0.6	2
65835	Phase Transition and Electronic Properties of Co-As Binary Compounds at High Pressures. SSRN Electronic Journal, 0, , .	0.4	0
65836	Dft Combined with Xanes to Investigate the Sulfur Fixation Mechanisms of H2s on Different Cao Surfaces. SSRN Electronic Journal, 0, , .	0.4	0
65837	Fluorine-free synthesis of ambient-stable delaminated Ti₂CT_x (MXene). Journal of Materials Chemistry A, 2022, 10, 7960-7967.	5.2	17
65838	Ultrahigh-stability SnOX (X = S, Se) nanotubes with a built-in electric field as a highly promising platform for sensing NH₃, NO and NO₂: a theoretical investigation. Journal of Materials Chemistry A, 2022, 10, 7948-7959.	5.2	4
65839	A high-efficiency GeTe-based thermoelectric module for low-grade heat recovery. Journal of Materials Chemistry A, 2022, 10, 7677-7683.	5.2	9
65840	An intrinsic room-temperature half-metallic ferromagnet in a metal-free PN₂ monolayer. Physical Chemistry Chemical Physics, 2022, 24, 7077-7083.	1.3	4
65841	Design of 3D topological nodal-net porous carbon for sodium-ion battery anodes. Journal of Materials Chemistry A, 2022, 10, 7754-7763.	5.2	15
65842	An unprecedented azobenzene-based organic single-component ferroelectric. Chemical Science, 2022, 13, 4936-4943.	3.7	12

#	Article	IF	Citations
65843	Doped Metals IR and Pt on Tio2 in Improving Activity Toward Oxidative Coupling of Methane: Activation Oxygen Species and Reaction Network. SSRN Electronic Journal, 0, , .	0.4	0
65844	Ultra-Fast and Ultra-Efficient Removal of Cr (Vi) by the Aqueous Solutions of Monolayer Mxene (Ti3c2tx). SSRN Electronic Journal, 0, , .	0.4	0
65845	Rashba spin splitting and anomalous spin textures in the bulk ferroelectric oxide perovskite KIO₃. Materials Advances, 2022, 3, 4170-4178.	2.6	10
65846	Realizing Robust and Efficient Acidic Oxygen Evolution by Electronic Modulation of 0d/2d Ceo2 Quantum Dots Decorated Sriro3 Nanosheets. SSRN Electronic Journal, 0, , .	0.4	0
65847	Revisit the Vec Criterion in High Entropy Alloys (Heas) with High-Throughput Ab Initio Calculations: A Case Study with Al-Co-Cr-Fe-Ni System. SSRN Electronic Journal, 0, , .	0.4	0
65848	Lattice Instability and Raman Spectra of Bao Under High Pressure: A First Principles Study. SSRN Electronic Journal, 0, , .	0.4	0
65849	A first-principles and machine-learning investigation on the electronic, photocatalytic, mechanical and heat conduction properties of nanoporous C₅N monolayers. Nanoscale, 2022, 14, 4324-4333.	2.8	26
65850	Lead-free layered Aurivillius-type Sn-based halide perovskite Ba₂X₂[Cs_{nâ^'1}Sn_nX_{3n+1}] (X = I/Br/Cl) with an optimal band gap of â^¼1.26 eV and theoretical efficiency beyond 27% for photovoltaics. Journal of Materials Chemistry A, 2022, 10, 10682-10691.	5.2	1
65851	Phase engineered gallium ferrite: a promising narrow bandgap, room-temperature ferroelectric. Materials Advances, 2022, 3, 3980-3988.	2.6	1
65852	Design of choline chloride modified USY zeolites for palladium-catalyzed acetylene hydrochlorination. RSC Advances, 2022, 12, 9923-9932.	1.7	5
65853	A bimetallic PdCuâ€“Fe₃O₄catalyst with an optimal d-band centre for selectiveN-methylation of aromatic amines with methanol. Catalysis Science and Technology, 2022, 12, 3524-3533.	2.1	6
65854	Development of a Sustainable Nitrogen-Doped Biochar Desulfurizer for Solid Oxide Fuel Cell Systems. SSRN Electronic Journal, 0, , .	0.4	0
65855	Finite-momentum excitons and the role of electronâ€“phonon couplings in the electronic and phonon transport properties of boron arsenide. Physical Chemistry Chemical Physics, 2022, 24, 9384-9393.	1.3	2
65856	PtCu alloy cocatalysts for efficient photocatalytic CO₂ reduction into CH₄ with 100% selectivity. Catalysis Science and Technology, 2022, 12, 3454-3463.	2.1	13
65857	Ultrahigh mechanical flexibility induced superior piezoelectricity of InSeBr-type 2D Janus materials. Physical Chemistry Chemical Physics, 2022, 24, 8371-8377.	1.3	6
65858	Superconductivity in Moâ€“P compounds under pressure and in double-Weyl semimetal Hex-MoP₂. Physical Chemistry Chemical Physics, 2022, 24, 7893-7900.	1.3	3
65859	The quantum size and spinâ€“orbit coupling effects in BiVO₄ with several atomic layers studied by density functional theory. Physical Chemistry Chemical Physics, 2022, 24, 10168-10174.	1.3	3
65860	Mechanism of High- and Low-Valence Doping on Adsorbed Oxygen of SnO ₂-Based Gas Sensors and a Strategy to Combine the Advantages of Both Dopants. SSRN Electronic Journal, 0, , .	0.4	0

#	Article	IF	Citations
65861	Pressure-stabilized graphene-like P layer in superconducting LaP₂. Physical Chemistry Chemical Physics, 2022, 24, 6469-6475.	1.3	5
65862	Bandgap Engineering of TiO₂ as Visible light Photocatalyst with Pd Doping Using First Principles. IOP Conference Series: Materials Science and Engineering, 2022, 1219, 012041.	0.3	2
65863	Higher loadings of Pt single atoms and clusters over reducible metal oxides: application to Câ€“O bond activation. Catalysis Science and Technology, 2022, 12, 2920-2928.	2.1	7
65864	Increasing oxygen vacancies in CeO₂ nanocrystals by Ni doping and reduced graphene oxide decoration towards electrocatalytic hydrogen evolution. CrystEngComm, 2022, 24, 3369-3379.	1.3	9
65865	First-Principles Investigation of Stable Lead-Free Halide Perovskite Materials Cssnclxbryi3-X-Y for Solar Cell Applications. SSRN Electronic Journal, 0, , .	0.4	0
65866	First-row transition metal embedded pyrazine-based graphynes as high-performance single atom catalysts for the CO₂reduction reaction. Journal of Materials Chemistry A, 2022, 10, 9048-9058.	5.2	21
65867	Single-Atom Metal Tuned Sulfur Vacancy for Efficient H2 Activation and Hydrogen Evolution Reaction on Mos2 Basal Plane. SSRN Electronic Journal, 0, , .	0.4	0
65868	Engineering metalâ€“metal oxide surfaces for high-performance oxygen reduction on Agâ€“Mn electrocatalysts. Energy and Environmental Science, 2022, 15, 1611-1629.	15.6	22
65869	Pentagonal PdX2 (X = S, Se) nanosheets with X vacancies as high-performance electrocatalysts for the hydrogen evolution reaction. Physical Chemistry Chemical Physics, 2022, , .	1.3	2
65870	Density Functional Theory Study of N2 Adsorption and DissociationÂOn 3d Transition Metal Atoms DopedÂIr(100)ÂSurface. SSRN Electronic Journal, 0, , .	0.4	0
65871	DNA/RNA sequencing using germanene nanoribbons via two dimensional molecular electronic spectroscopy: an ab initio study. Nanoscale, 2022, 14, 5147-5153.	2.8	2
65872	Unveiling the complex configurational landscape of the intralayer cavities in a crystalline carbon nitride. Chemical Science, 2022, 13, 3187-3193.	3.7	13
65873	Tunable White Light Emission and Energy Transfer in Liymgwo6: Dy3+, Tm3+ Single-Phase Phosphor. SSRN Electronic Journal, 0, , .	0.4	0
65874	Theoretical study of two-dimensional tetragonal transition metal chalcogenides and the potassium derivatives. Sustainable Energy and Fuels, 2022, 6, 1770-1779.	2.5	4
65875	Effects of Phase and Local Structures on the Electronic and Optical Properties of K0.5na0.5nbo3 Solid Solutions. SSRN Electronic Journal, 0, , .	0.4	0
65876	Interface rich CuO/Al₂CuO₄ surface for selective ethylene production from electrochemical CO₂ conversion. Energy and Environmental Science, 2022, 15, 2397-2409.	15.6	54
65877	A Perovskite-Based Sns/Cspbbr3ÂHeterostructure Used for SuperiorÂOptical Absorption. SSRN Electronic Journal, 0, , .	0.4	0
65878	Phosphorus-bridged ternary metal alloy encapsulated in few-layered nitrogen-doped graphene for highly efficient electrocatalytic hydrogen evolution. Journal of Materials Chemistry A, 2022, 10, 7111-7121.	5.2	28

#	Article	IF	Citations
65879	One-pot hydrothermal preparation and defect-enhanced photocatalytic activity of Bi-doped CdWO₄ nanostructures. Physical Chemistry Chemical Physics, 2022, 24, 8775-8786.	1.3	7
65880	A first-principles study of water adsorbed on flat and stepped silver surfaces. Physical Chemistry Chemical Physics, 2022, 24, 6803-6810.	1.3	4
65881	Design of 3d transition metal anchored B₅N₃ catalysts for electrochemical CO₂ reduction to methane. Journal of Materials Chemistry A, 2022, 10, 9737-9745.	5.2	31
65882	Understanding the Unusual-Caged Dynamics from the Microstructure and Interatomic Interaction in Glass-Forming Liquids. SSRN Electronic Journal, 0, , .	0.4	0
65883	Layered post-transition-metal dichalcogenide SnGe₂N₄ as a promising photoelectric material: a DFT study. RSC Advances, 2022, 12, 10249-10257.	1.7	4
65884	Mixed-anion mixed-cation perovskite (FAPbI₃)_{0.875}(MAPbBr₃)_{0.125}: an ab initio molecular dynamics study. Journal of Materials Chemistry A, 2022, 10, 9592-9603.	5.2	4
65885	The Origin of Isotropy to Anisotropy Transformation of Agi-S Bond and Semiconductor-Metal Transition in Monoclinic Ag2s Through Strain Engineering. SSRN Electronic Journal, 0, , .	0.4	0
65886	Revealing the role of HBr in propane dehydrogenation on CeO₂(111) via DFT-based microkinetic simulation. Physical Chemistry Chemical Physics, 2022, 24, 9718-9726.	1.3	3
65887	Low-Temperature Crystallization of Lafeo3 and Inherent Surface Activation for Efficient Oxygen Evolution Reaction Catalysts. SSRN Electronic Journal, 0, , .	0.4	0
65888	Preparation of Ultra-Thin Porous Carbon Nitride and its Photocatalytic H2o2 Production and Photodegradation of Rhb. SSRN Electronic Journal, 0, , .	0.4	0
65889	Microscopic Functionality of Fen4 Sites in Polymeric Carbon Nitride for Efficient H2s Oxidation. SSRN Electronic Journal, 0, , .	0.4	0
65890	In Situ Mitigating Cation Mixing of Ni-Rich Cathode at High Voltage Via Li2mno3 Injection. SSRN Electronic Journal, 0, , .	0.4	0
65891	Gas Sensing Properties of Alkali Metal Decorated Pristine and Defect Î‘-Asp Monolayer Toward Acid So2 and Alkaline Nh3 Molecules. SSRN Electronic Journal, 0, , .	0.4	0
65892	Single atom alloys vs. phase separated alloys in Cu, Ag, and Au atoms with Ni(111) and Ni, Pd, and Pt atoms with Cu(111): a theoretical exploration. Physical Chemistry Chemical Physics, 2022, 24, 10420-10438.	1.3	4
65893	A Hydrophobic and Fluorophilic Coating Layer for Stable and Reversible Aqueous Zinc Metal Anodes. SSRN Electronic Journal, 0, , .	0.4	0
65894	Structural Stability, Mechanical and Optoelectronic Properties of Strain-Tunedmixed-Halide Perovskites Cspbx3-Ayaâƒ°. SSRN Electronic Journal, 0, , .	0.4	0
65895	Effect of oxygen termination on the interaction of first row transition metals with M₂C MXenes and the feasibility of single-atom catalysts. Journal of Materials Chemistry A, 2022, 10, 8846-8855.	5.2	18
65896	Predicting the Optimal Chemical Composition of Functionalized Carbon Catalysts Towards Oxidative Dehydrogenation of Ethanol to Acetaldehyde. SSRN Electronic Journal, 0, , .	0.4	0

#	Article	IF	Citations
65897	Facile Design of Two-Dimensional Heterogeneous Fenton-Like Catalysis for Micropollutants Degradation: Metal Dependence of Reactive Oxygen Species Generation. SSRN Electronic Journal, 0, , .	0.4	0
65898	Dual-metal atom incorporated N-doped graphenes as oxygen evolution reaction electrocatalysts: high activities achieved by site synergies. Journal of Materials Chemistry A, 2022, 10, 8309-8323.	5.2	18
65899	Theoretical design and study of two-dimensional organic ferroelectric monolayer based on cyclobutene-1,2-dicarboxylic acid. Wuli Xuebao/Acta Physica Sinica, 2022, 71, 067302.	0.2	1
65900	Fabrication and Characterisation of Zno@Tio2 Core/Shell Nanowires Using a Versatile Kinetics-Controlled Coating Growth Method. SSRN Electronic Journal, 0, , .	0.4	0
65901	Valley-Dependent Electronic Properties of Metal Monochalcogenides Gax and Janus Ga2xy (X, Y = S, Se,) Tj ETQq0 0 0 rgBT /Overlock 10	0.4	0
65902	Magnetic anisotropy and ferroelectric-driven magnetic phase transition in monolayer Cr₂Ge₂Te₆. Nanoscale, 2022, 14, 3632-3643.	2.8	29
65903	Data-driven design of novel halide perovskite alloys. Energy and Environmental Science, 2022, 15, 1930-1949.	15.6	26
65904	Pressure-induced evolution of structures and promising superconductivity of ScB₆. Physical Chemistry Chemical Physics, 2022, 24, 10079-10084.	1.3	7
65905	High-efficiency red photoluminescence achieved by antimony doping in organicâ€“inorganic halide (C₁₁H₂₄N₂)₂[InBr₆][InBr₄]. Journal of Materials Chemistry C, 2022, 10, 5905-5913.	2.7	17
65906	Nitric oxide reduction reaction for efficient ammonia synthesis on topological nodal-line semimetal Cu₂Si monolayer. Journal of Materials Chemistry A, 2022, 10, 8568-8577.	5.2	21
65907	Tensile Strain of Feni Alloy Coupled with Pyridinic-N Doping Carbon Layers for Activating Water and Urea Oxidation. SSRN Electronic Journal, 0, , .	0.4	0
65908	Theoretical Prediction of High Entropy Intermetallic Compound Phase: A Case of Equimolar Alticuco. SSRN Electronic Journal, 0, , .	0.4	0
65909	The Dynamical Stability, Electronic, Elastic Properties and Ideal Strength of Diamond-Like Cubic B2cn: A First-Principles Study. SSRN Electronic Journal, 0, , .	0.4	0
65910	Pressure-stabilized polymerization of nitrogen in manganese nitrides at ambient and high pressures. Physical Chemistry Chemical Physics, 2022, 24, 5738-5747.	1.3	8
65911	NanostructuredÂZn3v3o8@N-Doped GrapheneÂWith High-Rate and Ultra-Stable Storage as Anode of Lithium-IonÂBatteries. SSRN Electronic Journal, 0, , .	0.4	0
65912	Metal dimers embedded vertically in defect-graphene as gas sensors: a first-principles study. Physical Chemistry Chemical Physics, 2022, 24, 9842-9847.	1.3	5
65913	Unveiling two-dimensional magnesium hydride as a hydrogen storage material via a generative adversarial network. Nanoscale Advances, 2022, 4, 2332-2338.	2.2	2
65914	Influence of different microstructures of cobalt on the catalytic activity for amination of ethylene glycol: comparison of HCP cobalt and FCC cobalt. Catalysis Science and Technology, 2022, 12, 3148-3157.	2.1	3

#	Article	IF	Citations
65915	Supramolecular nanocapsules as two-fold stabilizers of outer-cavity sub-nanometric Ru NPs and inner-cavity ultra-small Ru clusters. Nanoscale Horizons, 2022, 7, 607-615.	4.1	2
65916	Thgraphene: a novel two-dimensional carbon allotrope as a potential multifunctional material for electrochemical water splitting and potassium-ion batteries. Journal of Materials Chemistry A, 2022, 10, 9848-9857.	5.2	20
65918	Phase-Conversion Synthesis of Multi-Type Rare Earth Compounds with Re(Oh)So4 as a New Template: Fast Reaction Kinetic, and Photoluminescence. SSRN Electronic Journal, 0, , .	0.4	0
65919	Interface Engineering Âof GeP/Graphene/BiVO4ÂHeterostructureÂforÂPhotocatalyticÂApplication: A ComputationalÂstudy. SSRN Electronic Journal, 0, , .	0.4	0
65920	Directional Utilization Disorder Charge Via In-Plane Driving Force of Functionalized Graphite Carbon Nitride for the Robust Photocatalytic Degradation of Fluoroquinolone. SSRN Electronic Journal, 0, , .	0.4	0
65921	Integrated Dft and Experimental Study on Co3o4/Ceo2 Catalyst for Direct Synthesis of Dimethyl Carbonate from Co2. SSRN Electronic Journal, 0, , .	0.4	0
65922	Engineering of the Properties of Low Dimensional Materials via Inhomogeneous Strain. Wuli Xuebao/Acta Physica Sinica, 2022, .	0.2	0
65923	Dft Insights into Hydrodesulfurization Mechanism of 2-Methylthiophene Catalyzed by Ni2p. SSRN Electronic Journal, 0, , .	0.4	0
65924	More complex than originally thought: revisiting the origins of the relaxation processes in dimethylammonium zinc formate. Journal of Materials Chemistry C, 2022, 10, 6866-6877.	2.7	5
65925	Single-, double-, and triple-atom catalysts on graphene-like C₂N enable electrocatalytic nitrogen reduction: insight from first principles. Catalysis Science and Technology, 2022, 12, 2604-2617.	2.1	15
65926	Theoretical study of Ni^Iâ€“Ni^{III} cycle mediated by heterogeneous zinc in Câ€“N cross-coupling reaction. Physical Chemistry Chemical Physics, 2022, 24, 7617-7623.	1.3	2
65927	Computational Screening of Single Transition Metal Atom Embedded in Nitrogen Doped Graphene for Ch4 Detection. SSRN Electronic Journal, 0, , .	0.4	0
65928	The twist angle has weak influence on charge separation and strong influence on recombination in the MoS₂/WS₂ bilayer: ab initio quantum dynamics. Journal of Materials Chemistry A, 2022, 10, 8324-8333.	5.2	30
65929	Design and Analysis of Iii-V Two-Dimensional Van Der Waals Heterostructures for Ultra-Thin Solar Cells. SSRN Electronic Journal, 0, , .	0.4	0
65930	Boosting the Fenton-Like Catalytic Degradation Activities on Single Atomic Fe-Catalysts by Acid Etching. SSRN Electronic Journal, 0, , .	0.4	0
65931	Covalent organic framework-based materials as electrocatalysts for fuel cells. , 2022, , 229-250.		1
65932	Tuning Single Metal Atoms Anchored on Graphidyne for Highly Efficient and Selective Nitrate Electroreduction to Ammonia: A Computational Study. SSRN Electronic Journal, 0, , .	0.4	0
65933	Strain Induced Effects on the Electronic and Phononic Properties of 2h and 1t â€² Monolayer Mos 2. SSRN Electronic Journal, 0, , .	0.4	1

#	Article	IF	Citations
65934	Synergetic Optimization of Thermoelectric Properties in Snse Film Via Manipulating Se Vacancies. SSRN Electronic Journal, 0, , .	0.4	0
65935	Photocatalytic activity enhancement of Cu₂O cubes functionalized with 2-ethynyl-6-methoxynaphthalene through band structure modulation. Journal of Materials Chemistry C, 2022, 10, 3980-3989.	2.7	22
65936	Improved H2o2 Photogeneration and Stability on Rational Tailored Polymeric Carbon Nitride Via Enhanced O2 Adsorption. SSRN Electronic Journal, 0, , .	0.4	0
65937	Surface morphology evolution of cobalt nanoparticles induced by hydrogen adsorption: a theoretical study. New Journal of Chemistry, 2022, 46, 9272-9279.	1.4	2
65938	High-throughput oxygen chemical potential engineering of perovskite oxides for chemical looping applications. Energy and Environmental Science, 2022, 15, 1512-1528.	15.6	35
65939	Devices and defects in two-dimensional materials: outlook and perspectives. , 2022, , 339-401.		1
65940	Understanding and controlling the formation of surface anion vacancies for catalytic applications. Catalysis Science and Technology, 2022, 12, 2398-2410.	2.1	2
65941	Near-Infrared-Driven Photoelectrocatalytic Oxidation of Urea on La-Ni-Based Perovskites. SSRN Electronic Journal, 0, , .	0.4	0
65942	Adsorption and exchange reactions of iodine molecules at the alumina surface: modelling alumina-iodine reaction mechanisms. Physical Chemistry Chemical Physics, 2022, , .	1.3	0
65943	Defect Modulated Band Modification in Ni Ion Implanted Mgo Crystal. SSRN Electronic Journal, 0, , .	0.4	0
65944	First-Principles Calculations of Structural, Energetic, Electronic, Optical, and Photocatalytic Properties of Batao2n Low-Index Surfaces. SSRN Electronic Journal, 0, , .	0.4	0
65945	Polymorphism of boron phosphide: theoretical investigation and experimental assessment. Journal of Materials Chemistry C, 2022, 10, 3937-3943.	2.7	8
65946	Tunable topological electronic states in the Honeycomb-kagome lattices of nitrogen/oxygen-doped graphene nanomeshes. Nanoscale Advances, 0, , .	2.2	1
65947	Modulating electronic properties of dinitrosoarene polymers. Journal of Materials Chemistry C, 2022, 10, 5433-5446.	2.7	4
65948	Phonon-mediated superconductivity in two-dimensional hydrogenated phosphorus carbide: HPC₃. Physical Chemistry Chemical Physics, 2022, 24, 9256-9262.	1.3	19
65949	Ab initio molecular dynamics study on disordered Li-Ga-Sn system. Physical Chemistry Chemical Physics, 2022, , .	1.3	1
65950	Mechanistic insights into the photocatalytic reduction of nitric oxide to nitrogen on oxygen-deficient quasi-two-dimensional bismuth-based perovskites. Environmental Science: Nano, 2022, 9, 1453-1465.	2.2	11
65951	Photo-induced lattice distortion in 2H-MoTe₂ probed by time-resolved core level photoemission. Faraday Discussions, 2022, 236, 429-441.	1.6	5

#	Article	IF	Citations
65952	The catalytic activity and adsorption in faujasite and ZSM-5 zeolites: the role of differential stabilization and charge delocalization. Physical Chemistry Chemical Physics, 2022, 24, 7739-7747.	1.3	6
65953	Regulating Anionic Redox Activity of Lithium-Rich Layered Oxides Via Linbo3 Integrated Modification. SSRN Electronic Journal, 0, , .	0.4	0
65954	Investigation of W/Mo Co-Doping with Multiple Concentrations in Photocatalyst Bivo4ÂBy First-Principles Calculations. SSRN Electronic Journal, 0, , .	0.4	0
65955	Experimental and Theoretical Insight into Dsscs Mechanism Influenced by Different Doping Metal Ions. SSRN Electronic Journal, 0, , .	0.4	0
65956	Crystallographic Dependence of Co2 Hydrogenation Pathways Over Hcp-Co and Fcc-Co Catalysts. SSRN Electronic Journal, 0, , .	0.4	0
65957	Hybrid Heterostructure of Transition Metal Dichalcogenides as Potential Photocatalyst for Hydrogen Evolution. SSRN Electronic Journal, 0, , .	0.4	0
65958	Theoretical insights into dual-atom catalysts for the oxygen reduction reaction: the crucial role of orbital polarization. Journal of Materials Chemistry A, 2022, 10, 9150-9160.	5.2	25
65959	Bonding dependent lithium storage behavior of molybdenum oxides for next-generation Li-ion batteries. Journal of Materials Chemistry A, 2022, 10, 7718-7727.	5.2	7
65960	Tuning the Electronic Structure and Inverse Degree of Inverse Spinel Ferrites by Integrating Samarium Orthoferrite for Efficient Water Oxidation. SSRN Electronic Journal, 0, , .	0.4	0
65961	A Study of transition metal dichalcogenides/Chromium Trihalides vdW heterostructure based on band unfolding method. Wuli Xuebao/Acta Physica Sinica, 2022, .	0.2	0
65962	Revealing the role of interfacial heterogeneous nucleation in the metastable thin film growth of rare-earth nickelate electronic transition materials. Physical Chemistry Chemical Physics, 2022, 24, 9333-9344.	1.3	6
65963	Exploring a silicene monolayer as a promising sensor platform to detect and capture NO and CO gas. RSC Advances, 2022, 12, 9828-9835.	1.7	12
65964	Pressure tuned incommensurability and guest structure transition in compressed scandium from machine learning atomic simulation. Physical Chemistry Chemical Physics, 2022, 24, 7007-7013.	1.3	3
65965	X-Ray Induced Coloration Behavior of Lu2o3:Eu Transparent Ceramics and the Impact of Zro2 and Hfo2 Sintering Additives. SSRN Electronic Journal, 0, , .	0.4	0
65966	Nanostructuring determines poisoning: tailoring CO adsorption on PtCu bimetallic nanoparticles. Materials Advances, 2022, 3, 4159-4169.	2.6	7
65967	Chalcogenide MAX Phases Zr ₂Se(B _{1-x}Se) Tj ETQq1 1 0.784314 rgBT /Overlock 10 Tf	0.4	0
65968	XMCD and ab initio study of interface-engineered ultrathin Ru/Co/W/Ru films with perpendicular magnetic anisotropy and strong Dzyaloshinskiiâ€“Moriya interaction. Physical Chemistry Chemical Physics, 2022, 24, 8225-8232.	1.3	3
65969	A heteroepitaxially grown two-dimensional metalâ€“organic framework and its derivative for the electrocatalytic oxygen reduction reaction. Journal of Materials Chemistry A, 2022, 10, 10408-10416.	5.2	13

#	Article	IF	Citations
65970	Mechanistic Insights into Copper Oxides Catalyzed Bio-Based Furfural Hydrogenation Using Methanol as In-Situ Hydrogen Donor. SSRN Electronic Journal, 0, , .	0.4	0
65971	Hybrid density functional study on band structure engineering of ZnS(110) surface by anionâ€“cation codoping for overall water splitting. New Journal of Chemistry, 0, , .	1.4	2
65972	Enhancing Propane Direct Dehydrogenation Performances Through Temperature Induced Vox Dispersion and Alumina Support Phase Transformation. SSRN Electronic Journal, 0, , .	0.4	0
65973	Unveiling the roles of halogen ions in the surface passivation of CsPbI₃ perovskite solar cells. Physical Chemistry Chemical Physics, 2022, 24, 10184-10192.	1.3	21
65974	Rationally integrated nickel sulfides for lithium storage: S/N co-doped carbon encapsulated NiS/Cu₂S with greatly enhanced kinetic property and structural stability. Inorganic Chemistry Frontiers, 2022, 9, 2023-2035.	3.0	15
65975	Structural and electronic properties for Be-doped Pt_n (n = 1â€“12) clusters obtained by DFT calculations. Physical Chemistry Chemical Physics, 2022, 24, 7856-7861.	1.3	4
65976	A Pt/SnO₂/rGO interface more capable of converting ethanol to CO₂ in ethanol electro-oxidation: a detailed experimental/DFT study. Journal of Materials Chemistry A, 2022, 10, 10150-10161.	5.2	11
65977	Prediction of high Curie-temperature intrinsic ferromagnetic semiconductors and quantum anomalous Hall states in XBr₃ (X = Cu, Ag, Au) monolayers. Journal of Materials Chemistry C, 2022, 10, 6497-6507.	2.7	7
65978	Favorable photocatalytic properties of a GeS/GeS heterostructure by combining parallel and vertical electric fields: a theoretical study. Journal of Materials Chemistry C, 0, , .	2.7	0
65979	Molecular Dopant Induced Growth of Black Phase Cs _xFA _(1-x)PbI ₃ for Highly Efficient and Stable Perovskite Solar Cells. SSRN Electronic Journal, 0, , .	0.4	0
65980	Charge density wave in a SnSe₂ layer on and the effect of surface hydrogenation. Physical Chemistry Chemical Physics, 2022, 24, 6820-6827.	1.3	0
65981	On the Nature of Planar Defects in Transition Metal Diboride Line Compounds. SSRN Electronic Journal, 0, , .	0.4	0
65982	A predicted new catalyst to replace noble metal Pd for CO oxidative coupling to DMO. Catalysis Science and Technology, 2022, 12, 2542-2554.	2.1	3
65983	Intrinsic Ferromagnetic Janus Cr2pas Monolayer with High Curie Temperature and Controllable Magnetic Anisotropy. SSRN Electronic Journal, 0, , .	0.4	0
65984	Flame Normalizing-Induced Robust and Oriented Metallic Layer for Stable Zn Anode. SSRN Electronic Journal, 0, , .	0.4	0
65985	Shifting and Breaking Scaling Relations at Transition Metal Telluride Edges for Selective Electrochemical CO₂ Reduction. Journal of Materials Chemistry A, 0, , .	5.2	4
65986	The origin of anomalous hydrogen occupation in high entropy alloys. Journal of Materials Chemistry A, 2022, 10, 7228-7237.	5.2	11
65987	Manipulating Interfacial Atomic Structure of Pt/Ce1â^'Xyxo2â^'Î" to Improve Charge Transfer Capacity and Catalytic Activity in Aerobic Oxidation of Hmf. SSRN Electronic Journal, 0, , .	0.4	0

#	Article	IF	Citations
65988	High Water and Oxygen Reactivity Inducing Excellent Anti-Corrosive Performance in Waterborne Ti2ctx/Epoxy Composite Coating. SSRN Electronic Journal, 0, , .	0.4	0
65989	Tin/Tic Heterostructures Embedded with Single Tungsten Atoms Enhance Polysulfide Entrapment and Conversion for High-Capacity Lithium-Sulfur Battery Applications. SSRN Electronic Journal, 0, , .	0.4	0
65990	The hybridizaiton of iodoplumbate with xanthene dye: white emission and high photocurrent response driven by strong organic/inorganic interactions. Inorganic and Nano-Metal Chemistry, 0, , 1-8.	0.9	0
65991	The effect of different energy portions on the 2D/3D stability swapping for 13-atom metal clusters. Physical Chemistry Chemical Physics, 2022, 24, 6515-6524.	1.3	1
65992	Origin of multiple voltage plateaus in P2-type sodium layered oxides. Materials Horizons, 2022, 9, 1460-1467.	6.4	5
65993	Synthesis of Ultrathin Aupt Alloy Porous Nanowires with AbundantÂ Electrocatalytic Active Sites for Excellent Electrocatalysts. SSRN Electronic Journal, 0, , .	0.4	0
65994	Highly efficient flexible Liâ€“S full batteries with hollow Ruâ€“RuO_{2â^’x}nanofibers as robust polysulfide anchoring-catalysts and lithium dendrite inhibitors. Journal of Materials Chemistry A, 2022, 10, 8826-8836.	5.2	19
65995	Reductive Depolymerization of Lignin by Bifunctional Ru-Based Catalysts Supported on Tungstated-Zirconia. SSRN Electronic Journal, 0, , .	0.4	0
65996	Correlated organicâ€“inorganic motion enhances stability and charge carrier lifetime in mixed halide perovskites. Nanoscale, 2022, 14, 4644-4653.	2.8	18
65997	An efficient screening strategy towards multifunctional catalysts for the simultaneous electroreduction of NO₃^{â^’}, NO₂^{â^’} and NO to NH₃. Journal of Materials Chemistry A, 2022, 10, 9707-9716.	5.2	52
65998	Nanoconfined Sns2 in Robust Sno2 Nanocrystals Building Heterostructures for Stable Sodium Ion Storage. SSRN Electronic Journal, 0, , .	0.4	0
65999	Peroxymonosulfate Activation by Black Tio2 Nanotube Arrays Under Solar Light: Switching the Activation Mechanism and Enhancing Catalytic Activity and Stability. SSRN Electronic Journal, 0, , .	0.4	0
66000	Catalytic properties of the ferryl ion in the solid state: a computational review. Catalysis Science and Technology, 2022, 12, 3069-3087.	2.1	1
66001	Structural Diversity and Unusual Valence States in Compressed Na-Hg System. SSRN Electronic Journal, 0, , .	0.4	0
66002	Unveiling a Three Phase Mixed Heterojunction via Phaseâ€Selective Anchoring of Polymer for Efficient Photocatalysis. Advanced Energy Materials, 2022, 12, .	10.2	11
66003	Anharmonic GrÃ¼neisen theory based on self-consistent phonon theory: Impact of phonon-phonon interactions neglected in the quasiharmonic theory. Physical Review B, 2022, 105, .	1.1	11
66004	Pressure-induced transition from pure electronic to mixed ionic-electronic conduction in strontium hydride. Applied Physics Letters, 2022, 120, 073904.	1.5	2
66005	Ab initio molecular-dynamics simulations of electronic structures and characteristics of Cu/SiO2/Pt memristive stack. , 2022, 18, 83-92.		0

#	Article	IF	Citations
66006	First-principles mobility prediction for amorphous semiconductors. Physical Review B, 2022, 105, .	1.1	3
66007	Spin-Peierls Distortion of TiPO₄ Causing a Transition from a Magnetic to a Nonmagnetic Insulating State and Its Effect on the Thermoelectric Properties: Density Functional Theory Analysis. Inorganic Chemistry, 2022, 61, 3843-3850.	1.9	1
66008	Engineering of Band Structure of Bismuth Selenide Ultrathin Nanosheets as Multifunctional Material for Photocatalytic Application. Advanced Materials Interfaces, 2022, 9, .	1.9	8
66009	Unveiling the Bonding Nature of C3 Intermediates in the CO₂ Reduction Reaction through the Oxygen-Deficient Cu₂O(110) Surfaceâ”€A DFT Study. Journal of Physical Chemistry C, 2022, 126, 5502-5512.	1.5	11
66010	High-Field Magnetoelectric and Spin-Phonon Coupling in Multiferroic (NH₄)₂[FeCl₅Â·(H₂O)]. Inorganic Chemistry, 2022, 61, 3434-3442.	1.9	3
66011	Real-Time Modulation of Hydrogen Evolution Activity of Graphene Electrodes Using Mechanical Strain. ACS Applied Materials & Interfaces, 2022, 14, 10691-10700.	4.0	2
66012	Binding and Exchange Reactions of Hydrogen Isotopes on Surfaces of Dispersed Pt Nanoparticles. Journal of Physical Chemistry C, 2022, 126, 3923-3938.	1.5	3
66013	Reaction Pathway of Photocatalytic Water Splitting on Two-Dimensional TiO₂ Nanosheets. Journal of Physical Chemistry C, 2022, 126, 3915-3922.	1.5	10
66014	Transformation of Metal Halides to Facet-Modulated Lead Halide Perovskite Platelet Nanostructures on A-Site Cs-Sublattice Platform. Nano Letters, 2022, 22, 1633-1640.	4.5	8
66015	Importance of Chemical Distortion on the Hysteretic Oxygen Capacity in Li-Excess Layered Oxides. ACS Applied Materials & Interfaces, 2022, 14, 9057-9065.	4.0	5
66016	Phonon spectrum of <mml:math xmlns:mml="http://www.w3.org/1998/Math/MathML"><mml:mrow><mml:msub><mml:mi>Pr</mml:mi><mml:mn>2</mml:mn></mml:n mathvariant="normal">O</mml:mi><mml:mn>7</mml:mn></mml:msub></mml:mrow></mml:math> and <mml:math xmlns:mml="http://www.w3.org/1998/Math/MathML"><mml:mrow><mml:msub><mml:mi>Pr</mml:mi><mml:mn>2</mml:mn></mml:n m. Physical Review B, 2022, 105, .	1.1	5
66017	Computational Design of Gas Sensors Based on V3S4 Monolayer. Nanomaterials, 2022, 12, 774.	1.9	7
66018	gâ€€ ₃ N ₄ â€Supported Metalâ€Pair Catalysts toward Efficient Electrocatalytic Nitrogen Reduction: A Computational Evaluation. Advanced Theory and Simulations, 0, , 2100579.	1.3	2
66019	Redox-mediated electrosynthesis of ethylene oxide from CO2 and water. Nature Catalysis, 2022, 5, 185-192.	16.1	40
66020	Adsorption Behavior of Environmental Gas Molecules on Pristine and Defective MoSi₂N₄: Possible Application as Highly Sensitive and Reusable Gas Sensors. ACS Omega, 2022, 7, 8706-8716.	1.6	20
66021	Electronic phase transition, spin filtering effect, and spin Seebeck effect in 2D high-spin-polarized VSi2X4 (X = N, P, As). Applied Physics Letters, 2022, 120, .	1.5	31
66022	Thermodynamic Stability and Intrinsic Activity of La1â^'xSrxMnO3 (LSM) as an Efficient Bifunctional OER/ORR Electrocatalysts: A Theoretical Study. Catalysts, 2022, 12, 260.	1.6	3
66023	Evidence for a single-layer van der Waals multiferroic. Nature, 2022, 602, 601-605.	13.7	104

#	Article	IF	Citations
66024	Study of Substitutional Adsorption of an Iron Film on a Silver Surface. Bulletin of the Russian Academy of Sciences: Physics, 2022, 86, 124-129.	0.1	0
66025	Thermodynamic Modeling of the Ge-X (X = As, Se, S, P) Systems. Journal of Electronic Materials, 2022, 51, 2114-2130.	1.0	3
66026	Photoluminescence spectrum of divacancy in porous and nanocrystalline cubic silicon carbide. Journal of Applied Physics, 2022, 131, .	1.1	8
66027	Photoluminescence Lightening: Extraordinary Oxygen Modulated Dynamics in WS₂ Monolayers. Nano Letters, 2022, 22, 2112-2119.	4.5	16
66028	Assessing the Accuracy of Machine Learning Thermodynamic Perturbation Theory: Density Functional Theory and Beyond. Journal of Chemical Theory and Computation, 2022, 18, 1382-1394.	2.3	9
66029	Robust growth of two-dimensional metal dichalcogenides and their alloys by active chalcogen monomer supply. Nature Communications, 2022, 13, 1007.	5.8	42
66030	Six-dimensional state-to-state quantum dynamics of H₂/D₂ scattering from Cu(100): Validity of site-averaging model. Chinese Journal of Chemical Physics, 2022, 35, 143-152.	0.6	1
66031	Modulating the dynamics of BrÃ¸nsted acid sites on PtWOx inverse catalyst. Nature Catalysis, 2022, 5, 144-153.	16.1	35
66032	Filament Engineering of Twoâ€Dimensional hâ€BN for a Selfâ€Power Mechanoâ€Nociceptor System. Small, 2022, 18, e2200185.	5.2	25
66033	Dual topology in van der Waals-type superconductor Nb2S2C. Tungsten, 2023, 5, 357-363.	2.0	6
66034	Designing light-element materials with large effective spin-orbit coupling. Nature Communications, 2022, 13, 919.	5.8	26
66035	Optoelectronic properties of Ag2S/graphene and FeS2/graphene nanostructures and interfaces: A density functional study including dispersion forces. Journal of Materials Research, 2022, 37, 1047-1058.	1.2	2
66036	Bridge role of weak chemical bonding in photocatalytic performance of asymmetric 2H-MoS₂/BiOCl Janus heterostructure. Materials Research Express, 2022, 9, 025902.	0.8	2
66037	Layered MoSi₂N₄ as Electrode Material of Znâ€“Air Battery. Physica Status Solidi - Rapid Research Letters, 2022, 16, .	1.2	8
66038	Hydrogenated Amorphous Titania with Engineered Surface Oxygen Vacancy for Efficient Formaldehyde and Dye Removals under Visible-Light Irradiation. Nanomaterials, 2022, 12, 742.	1.9	4
66039	Understanding Contact Electrification at Water/Polymer Interface. Research, 2022, 2022, 9861463.	2.8	30
66040	Temperature-Resolved Anisotropic Displacement Parameters from Theory and Experiment: A Case Study. Crystals, 2022, 12, 283.	1.0	0
66041	Non-Abelian braiding of Weyl nodes via symmetry-constrained phase transitions. Physical Review B, 2022, 105, .	1.1	14

#	Article	IF	Citations
66042	Eu²⁺ Doping Concentration-Induced Site-Selective Occupation and Photoluminescence Tuning in KSrScSi₂O₇:Eu²⁺ Phosphor. ACS Materials Au, 2022, 2, 374-380.	2.6	24
66043	Ferroelectric Properties of KNbO3 Doped with Na : First-Principles Calculations. Journal of Physics: Conference Series, 2022, 2209, 012003.	0.3	2
66044	Pressure-Induced Dimensional Crossover in a Kagome Superconductor. Physical Review Letters, 2022, 128, 077001.	2.9	27
66045	Mechanical properties, thermal conductivity and defect formation energies of samarium immobilization in Gd2Zr2O7: First-principles study and irradiation experiment. Journal of Rare Earths, 2023, 41, 422-433.	2.5	3
66046	Application of Materials Genome Methods in Thermoelectrics. Frontiers in Materials, 2022, 9, .	1.2	4
66047	Strainâ€Plasmonic Coupled Broadband Photodetector Based on Monolayer MoS₂. Small, 2022, 18, e2107104.	5.2	25
66048	Stacking-Dependent Interlayer Ferroelectric Coupling and MoirÃ© Domains in a Twisted AgBiP₂Se₆ Bilayer. Journal of Physical Chemistry Letters, 2022, 13, 2027-2032.	2.1	6
66049	Trends in Formic Acid Electro-Oxidation on Transition Metals Alloyed with Platinum and Palladium. Journal of Physical Chemistry C, 2022, 126, 4374-4390.	1.5	8
66050	Low-temperature acanthite-like phase of <mml:math xmlns:mml="http://www.w3.org/1998/Math/MathML"><mml:mrow><mml:msub><mml:mi>Cu</mml:mi><mml:mn>2</mml:mn></mml: mathvariant="normal">S</mml:mi></mml:mrow></mml:math> : Electronic and transport properties. Physical Review B, 2022, 105, .	1.1	8
66051	Catalyzed Decomposition of Methanol-d₄ on Vanadium Nanoclusters Supported on an Ultrathin Film of Al₂O₃/NiAl(100). Journal of Physical Chemistry C, 2022, 126, 3903-3914.	1.5	9
66052	Planar Heterojunction of Ultrathin CrTe₃ and CrTe₂ van der Waals Magnet. ACS Nano, 2022, 16, 4348-4356.	7.3	10
66053	Electrospun V₂O₃@Carbon Nanofibers as a Flexible and Binder-Free Cathode for Highly Stable Aqueous Zn-Ion Full Batteries. ACS Applied Energy Materials, 2022, 5, 3525-3535.	2.5	27
66054	Pressure-Induced Stabilization of Sodium Halide Perovskites. Journal of Physical Chemistry C, 2022, 126, 4248-4254.	1.5	0
66055	Regulating Electronic Descriptors for the Enhanced ORR Activity of FePc-Functionalized Graphene via Substrate Doping and/or Ligand Exchange: A Theoretical Study. Journal of Physical Chemistry C, 2022, 126, 4458-4471.	1.5	8
66056	Giant effective magnetic fields from optically driven chiral phonons in <mml:math xmlns:mml="http://www.w3.org/1998/Math/MathML"><mml:mrow><mml:mn>4</mml:mn><mml:mi>f</mml:mi><mml:mrow></mml:m paramagnets. Physical Review Research, 2022, 4, .	1.3	28
66057	Simultaneous stiffening and strengthening of nanodiamond by fivefold twins. MRS Bulletin, 2022, 47, 219-230.	1.7	5
66058	Pressureâ€induced enhancement of mechanical performance in ZrC system. International Journal of Quantum Chemistry, 0, , .	1.0	0
66059	Interfacial Effect on Photo-Modulated Magnetic Properties of Core/Shell-Structured NiFe/NiFe2O4 Nanoparticles. Materials, 2022, 15, 1347.	1.3	0

#	Article	IF	Citations
66060	Boosting the potassium-ion storage performance enabled by engineering of hierarchical MoSSe nanosheets modified with carbon on porous carbon sphere. Science Bulletin, 2022, 67, 933-945.	4.3	96
66061	Observation of a Novel Lattice Instability in Ultrafast Photoexcited SnSe. Physical Review X, 2022, 12, .	2.8	10
66062	Selfâ€Healing Mechanism of Lithium in Lithium Metal. Advanced Science, 2022, 9, e2105574.	5.6	25
66063	Pressure-induced dimerization and collapse of antiferromagnetism in the Kitaev material <mml:math xmlns:mml="http://www.w3.org/1998/Math/MathML"><mml:mrow><mml:mi>Î±</mml:mi><mml:mtext>â^'</mml:mtext><mml:msub Physical Review B, 2022, 105, .	1.1	3
66064	Anisotropic electrical properties of aligned PtSe2 nanoribbon arrays grown by a pre-patterned selective selenization process. Nano Research, 0, , 1.	5.8	1
66065	Acid anion electrolyte effects on platinum for oxygen and hydrogen electrocatalysis. Communications Chemistry, 2022, 5, .	2.0	48
66066	Sparse Gaussian Process Regression-Based Machine Learned First-Principles Force-Fields for Saturated, Olefinic, and Aromatic Hydrocarbons. ACS Physical Chemistry Au, 2022, 2, 260-264.	1.9	5
66067	In Situ Characterization of Corrosion Processes of As-Extruded Pure Magnesium Using X-Ray Computed Microtomography. Corrosion, 2022, 78, 350-358.	0.5	0
66068	Ultrahigh reversible hydrogen storage in K and Ca decorated 4-6-8 biphenylene sheet. International Journal of Hydrogen Energy, 2022, 47, 41833-41847.	3.8	41
66069	Interfacial engineering manipulation of magnetic anisotropy evolution via orbital reconstruction in low-dimensional manganite superlattices. Science China Materials, 2022, 65, 1902-1911.	3.5	3
66070	Ultrasensitive Boronâ€“Nitrogen-Codoped CVD Graphene-Derived NO₂ Gas Sensor. ACS Materials Au, 2022, 2, 356-366.	2.6	15
66071	Microscopic Mechanism of the Heatâ€Induced Blueshift in Phosphors and a Logarithmic Energy Dependence on the Nearest Dopantâ€“Vacancy Distance. Angewandte Chemie - International Edition, 2022, 61, .	7.2	12
66072	Reversible Hydrogen-Induced Phase Transformations in La_{0.7}Sr_{0.3}MnO₃ Thin Films Characterized by In Situ Neutron Reflectometry. ACS Applied Materials & Interfaces, 2022, 14, 10898-10906.	4.0	10
66073	Conformational, Reactivity Analysis, Wavefunction-Based Properties, Molecular Docking and Simulations of a Benzamide Derivative with Potential Antitumor Activity-DFT and MD Simulations. Polycyclic Aromatic Compounds, 2023, 43, 2015-2031.	1.4	3
66074	The Energetics and Topology of Grain Boundaries in Magnesium: An Ab Initio Study. , 2022, 1, 15-30.		0
66075	Anomalous valley Hall effect in antiferromagnetic monolayers. Npj 2D Materials and Applications, 2022, 6, .	3.9	18
66076	Thermoelastic Martensitic Transformation and Shape Memory Effect in Nanoplates Based on Tiâ€“Ni Alloys: Experiment, Modeling by Density Functional Theory and Molecular Dynamics. Journal of Surface Investigation, 2022, 16, 128-133.	0.1	0
66077	Theoretical Investigation on the Hydrogen Evolution, Oxygen Evolution, and Oxygen Reduction Reactions Performances of Two-Dimensional Metal-Organic Frameworks Fe3(C2X)12 (X = NH, O, S). Molecules, 2022, 27, 1528.	1.7	10

#	Article	IF	Citations
66078	Cation disorder engineering yields AgBiS2 nanocrystals with enhanced optical absorption for efficient ultrathin solar cells. Nature Photonics, 2022, 16, 235-241.	15.6	100
66079	Correlating the Voltage Hysteresis in Li- and Mn-Rich Layered Oxides to Reversible Structural Changes by Using X-ray and Neutron Powder Diffraction. Journal of the Electrochemical Society, 2022, 169, 020554.	1.3	3
66080	Enhanced localized dipole of Pt-Au single-site catalyst for solar water splitting. Proceedings of the National Academy of Sciences of the United States of America, 2022, 119, .	3.3	17
66081	Origin of insulating and nonferromagnetic <mml:math xmlns:mml="http://www.w3.org/1998/Math/MathML"><mml:msub><mml:mi>SrRuO</mml:mi><mml:mn>3</mml:mn></mml:msub> monolayers. Physical Review B, 2022, 105, .	1.1	12
66082	Structural and energetic properties of vacancy defects in MXene surfaces. Physical Review Materials, 2022, 6, .	0.9	5
66083	High Stability of Methanol to Aromatic Conversion over Bimetallic Ca,Ga-Modified ZSM-5. ACS Catalysis, 2022, 12, 3189-3200.	5.5	28
66084	Negative thermal expansion of two-dimensional magnets. Applied Physics Letters, 2022, 120, .	1.5	6
66085	On a high photocatalytic activity of high-noble alloys Auâ€“Ag/TiO2 catalysts during oxygen evolution reaction of water oxidation. Scientific Reports, 2022, 12, 2604.	1.6	15
66086	Heusler-based synthetic antiferrimagnets. Science Advances, 2022, 8, eabg2469.	4.7	6
66087	Giant tunneling magnetoresistance and electroresistance in <mml:math xmlns:mml="http://www.w3.org/1998/Math/MathML"><mml:mrow><mml:mi>Î±</mml:mi><mml:mtext>â€”</mml:mtext><mml:msub> -based van der Waals multiferroic tunnel junctions. Physical Review B, 2022, 105, .	1.1	20
66088	Large scale dataset of real space electronic charge density of cubic inorganic materials from density functional theory (DFT) calculations. Scientific Data, 2022, 9, 59.	2.4	1
66089	Phononic real Chern insulator with protected corner modes in graphynes. Physical Review B, 2022, 105, .	1.1	16
66090	Equation of State Determination for Rhenium Using First-Principles Molecular Dynamics Calculations and High-Pressure Experiments. Advances in Condensed Matter Physics, 2022, 2022, 1-6.	0.4	0
66091	Significantly enhanced interlayer ferromagnetic coupling in van der Waals Fe3GeTe2 bilayer by Be-ion intercalation. Applied Physics Letters, 2022, 120, .	1.5	5
66092	Dissolution of Portlandite in Pure Water: Part 2 Atomistic Kinetic Monte Carlo (KMC) Approach. Materials, 2022, 15, 1442.	1.3	19
66093	Charge ordering mechanism in silver difluoride. Physical Review B, 2022, 105, .	1.1	4
66094	Exploring the Effects of Ionic Defects on the Stability of CsPbI₃ with a Deep Learning Potential. ChemPhysChem, 2022, 23, e202100841.	1.0	8
66095	Novel Trends in MXene/Conducting Polymeric Hybrid Nanoclusters. Journal of Cluster Science, 2023, 34, 45-76.	1.7	23

#	Article	IF	Citations
66096	Triphasic Metal Oxide Photocatalyst for Reaction Siteâ€Specific Production of Hydrogen Peroxide from Oxygen Reduction and Water Oxidation. Advanced Energy Materials, 2022, 12, .	10.2	17
66097	Pressure-Induced Phase Transition and Band Gap Decrease in Semiconducting Î²-Cu₂V₂O₇. Inorganic Chemistry, 2022, 61, 3697-3707.	1.9	7
66098	Structural, electronic, and transport properties of 1D Ta2Ni3Se8 semiconducting material. Applied Physics Letters, 2022, 120, .	1.5	6
66099	DFT investigation of physical properties and electronic structure of metastable cubic CrC partially substituted with transitional metals. Journal of Applied Physics, 2022, 131, 085108.	1.1	1
66100	Evidence for multiple liquidâ€“liquid phase transitions in carbon, and the Friedel ordering of its liquid state. Physics of Plasmas, 2022, 29, 022108.	0.7	2
66101	Strain-mediated ferromagnetism and low-field magnetic reversal in Co doped monolayer $$WS_2$$. Scientific Reports, 2022, 12, 2593.	1.6	10
66102	Extremely Anisotropic Thermoelectric Properties of SnSe Under Pressure. Energy and Environmental Materials, 2023, 6, .	7.3	8
66103	Towards an universal artificial synapse using MXene-PZT based ferroelectric memristor. Ceramics International, 2022, 48, 16263-16272.	2.3	15
66104	Polarity-Tunable Photocurrent through Band Alignment Engineering in a High-Speed WSe₂/SnSe₂ Diode with Large Negative Responsivity. ACS Nano, 2022, 16, 4578-4587.	7.3	23
66105	Engineering Pore Walls of Mesoporous Tungsten Oxides via Ce Doping for the Development of High-Performance Smart Gas Sensors. Chemistry of Materials, 2022, 34, 2321-2332.	3.2	18
66106	Activity Origin of Antimony Nanosheets toward Selective Electroreduction of CO₂ to Formic Acid. Journal of Physical Chemistry C, 2022, 126, 4015-4023.	1.5	7
66107	Influence of Metal Identity on Light-Induced Switchable Adsorption in Azobenzene-Based Metalâ€“Organic Frameworks. ACS Applied Materials & Interfaces, 2022, 14, 11192-11199.	4.0	14
66108	Unusual Properties of Hydrogen-Bonded Ferroelectrics: The Case of Cobalt Formate. Physical Review Letters, 2022, 128, 077601.	2.9	6
66109	Potassium Storage Performance of UiO-66 Derivatives from First Principles Calculations. Journal of Physical Chemistry C, 2022, 126, 4286-4295.	1.5	5
66110	Metal-Coordinating Single-Boron Sites Confined in Antiperovskite Borides for N₂-to-NH₃ Catalytic Conversion. ACS Catalysis, 2022, 12, 2967-2978.	5.5	11
66111	Direct Growth of Magnetic Non-van der Waals Cr₂X₃ (X = S, Se, and Te) on SiO₂/Si Substrates through the Promotion of KOH. Chemistry of Materials, 2022, 34, 2342-2351.	3.2	11
66112	Thermal conductivity of two stable bilayer phosphorene stackings: A computation study. Journal of Applied Physics, 2022, 131, 075101.	1.1	0
66113	Short-range order controlling atomic dynamics in Y-based metallic glasses. Physical Review B, 2022, 105, .	1.1	3

#	Article	IF	Citations
66114	Two-Dimensional Layered Green Phosphorus as an Anode Material for Li-Ion Batteries. ACS Applied Energy Materials, 2022, 5, 2184-2191.	2.5	6
66115	Hydrogen trapping and embrittlement in high-strength Al alloys. Nature, 2022, 602, 437-441.	13.7	109
66116	Effect of Doped Metals Rh, Pd, and Cu over the IrO₂(110) Surface: Improving C₂ Selectivity during Oxidative Coupling of Methane. Journal of Physical Chemistry C, 2022, 126, 4306-4318.	1.5	7
66117	Reduced Fermi Level Pinning at Physisorptive Sites of Moire-MoS₂/Metal Schottky Barriers. ACS Applied Materials & Interfaces, 2022, 14, 11903-11909.	4.0	17
66118	A Stable Cu(I)-Based Ultramicroporous NKMOF-8-Br with High CH₄ Uptake for Efficient Separation of CH₄/N₂ Mixtures. Journal of Chemical & Engineering Data, 2022, 67, 1654-1662.	1.0	6
66119	Understanding Lithium Local Environments in LiMn_{0.5}Ni_{0.5}O₂ Cathodes: A DFT-Supported ⁶Li Solid-State NMR Study. Journal of Physical Chemistry C, 2022, 126, 4276-4285.	1.5	2
66120	Gas-Phase Synthesis of Metal Olefins: Plasma-Assisted Methane Dehydrogenation and Câ•C Bond Formation. Journal of Physical Chemistry A, 2022, 126, 1123-1131.	1.1	1
66121	Schottky and Ohmic Contacts at Î±-Tellurene/2D Metal Interfaces. ACS Applied Electronic Materials, 2022, 4, 1082-1088.	2.0	12
66122	Atomic Correlation between Bilayer Graphene and Double-Walled Carbon Nanotubes. Journal of Physical Chemistry C, 2022, 126, 4030-4036.	1.5	1
66123	Two-Dimensional Bismuthene Nanosheets for Selective Detection of Toxic Gases. ACS Applied Nano Materials, 2022, 5, 2984-2993.	2.4	29
66124	Sound velocities, and mechanical and electronic properties of the intermetallic compound <mml:math xmlns:mml="http://www.w3.org/1998/Math/MathML"><mml:mrow><mml:mi>Ce</mml:mi><mml:msub><mml:mi>Al</mml:mi><mml:m at high pressure. Physical Review B, 2022, 105, .	1.1	5
66125	Persistent Room-Temperature Photodarkening in Cu-Doped <mml:math xmlns:mml="http://www.w3.org/1998/Math/MathML" display="inline"><mml:mrow><mml:mi>Î²</mml:mi><mml:mtext>â˜’</mml:mtext><mml:msub><mml:mrow><mml:mi>Ga</mml:mi><mml:mathvariant="normal">O</mml:mi></mml:mrow><mml:mrow><mml:mn>3</mml:mn></mml:mrow></mml:msub></mml:mrow></mml: Physical Review Letters, 2022, 128, 077402.	2.9	7
66126	Two-nodal surface phonons in solid-state materials. Physical Review B, 2022, 105, .	1.1	37
66127	N-doped MoS2 via assembly transfer on an elastomeric substrate for high-photoresponsivity, air-stable and stretchable photodetector. Nano Research, 2022, 15, 9866-9874.	5.8	8
66128	Revealing the quasiparticle electronic and excitonic nature in cubic, tetragonal, and hexagonal phases of FAPbI₃. AIP Advances, 2022, 12, 025330.	0.6	2
66129	Critical point and supercritical regime of MgO. Physical Review B, 2022, 105, .	1.1	6
66130	Tunable band gaps and optical absorption properties of bent MoS2 nanoribbons. Scientific Reports, 2022, 12, 3008.	1.6	14
66131	é”'ç¢²åˆ•é‡'Sb2Te3ä¸ç©ºä½æ—åºåŒ–çš„åŽŸä½ç”µæ˜¾å¾®å¦ç©¶. Chinese Science Bulletin, 2022, , .	0.4	1

#	Article	IF	Citations
66132	Design of Hierarchical Porosity Via Manipulating Chemical and Microstructural Complexities in Highâ€Entropy Alloys for Efficient Water Electrolysis. Advanced Science, 2022, 9, e2105808.	5.6	22
66133	Structures and properties of ionic crystals and condensed phase ionic liquids predicted with the generalized energyâ€based fragmentation method. Journal of Computational Chemistry, 2022, 43, 704-716.	1.5	6
66134	Large Dzyaloshinskii-Moriya interaction and atomic layer thickness dependence in a ferromagnet-<mml:math xmlns:mml="http://www.w3.org/1998/Math/MathML"><mml:msub><mml:mrow><mml:mi>WS</mml:mi></mml:mrow><mml:mn>2</m heterostructure. Physical Review B, 2022, 105, .	1.1	14
66135	Notable effect of magnetic order on the phonon transport in semi-hydrogenated graphene. Applied Physics Letters, 2022, 120, .	1.5	8
66136	Highâ€Performance Monolayer SiMeâ€Graphene nâ€Type Fieldâ€Effect Transistors with Low Supply Voltage and High Onâ€State Current in Subâ€5 nm Gate Length. Advanced Electronic Materials, 0, , 2101359.	2.6	0
66137	Highly active Fe36Co44 bimetallic nanoclusters catalysts for hydrolysis of ammonia borane: The first-principles study. Chinese Chemical Letters, 2023, 34, 107261.	4.8	46
66138	Strain-tuned mechanical, electronic, and optoelectronic properties of two-dimensional transition metal sulfides ZrS2: a first-principles study. Journal of Molecular Modeling, 2022, 28, 63.	0.8	5
66139	Surface modification of ZnIn2S4 layers to realize energy-transfer-mediated photocatalysis. National Science Review, 2022, 9, .	4.6	18
66140	Ferromagnetism in armchair graphene nanoribbon heterostructures. Physical Review B, 2022, 105, .	1.1	3
66141	Local Coordination Environment of 3d and 4d Transition Metal Ions in LiCl-KCl Eutectic Mixture. Materials, 2022, 15, 1478.	1.3	0
66142	Effects of local bonding between solute atoms and vacancy on formation of nanoclusters in Al-Mg-Si alloys. Keikinzoku/Journal of Japan Institute of Light Metals, 2022, 72, 47-53.	0.1	0
66143	Prospect of DFT Utilization in Polymer-Graphene Composites for Electromagnetic Interference Shielding Application: A Review. Polymers, 2022, 14, 704.	2.0	8
66144	Graph-based discovery and analysis of atomic-scale one-dimensional materials. National Science Review, 2022, 9, .	4.6	5
66145	Pressure-induced phase transition and increase of oxygen-iodine coordination in magnesium iodate. Physical Review B, 2022, 105, .	1.1	9
66146	Structural Changes in Monolayer Cobalt Oxides under Ambient Pressure CO and O₂ Studied by In Situ Grazing-Incidence X-ray Absorption Fine Structure Spectroscopy. Journal of Physical Chemistry C, 2022, 126, 3411-3418.	1.5	9
66147	Large-scale epitaxy of two-dimensional van der Waals room-temperature ferromagnet Fe5GeTe2. Npj 2D Materials and Applications, 2022, 6, .	3.9	37
66148	Improving the transferability of density functional theory predictions through correlation analysis: Structural and energetic properties of <mml:math xmlns:mml="http://www.w3.org/1998/Math/MathML"><mml:mrow><mml:mi>Ni</mml:mi><mml:mi>X</mml:mi></mml:mrow></mml:m alloys <mml:math		

#	Article	IF	Citations
66150	Ab initio calculation of the magnetic Gibbs free energy of materials using magnetically constrained supercells. Physical Review B, 2022, 105, .	1.1	2
66151	Tailoring Sr2Fe1.5Mo0.5O6â^Î´ with Sc as a new single-phase cathode for proton-conducting solid oxide fuel cells. Science China Materials, 2022, 65, 1485-1494.	3.5	66
66152	Self-assembled monolayers direct a LiF-rich interphase toward long-life lithium metal batteries. Science, 2022, 375, 739-745.	6.0	368
66153	Tuning Nitrate Electroreduction Activity via an Equilibrium Adsorption Strategy: A Computational Study. Journal of Physical Chemistry Letters, 2022, 13, 1726-1733.	2.1	25
66154	Laser-Patterned Submicrometer Bi₂Se₃â€“WS₂ Pixels with Tunable Circular Polarization at Room Temperature. ACS Applied Materials & Interfaces, 2022, 14, 9504-9514.	4.0	2
66155	Screening LiMn₂O₄ Surface Modification Schemes under Theoretical Guidance. ACS Applied Materials & Interfaces, 2022, 14, 10353-10362.	4.0	14
66156	Probing the Thermodynamics of MoirÃ© Patterns in Molecular Self-Assembly at the Liquidâ€“Solid Interface. Chemistry of Materials, 2022, 34, 2449-2457.	3.2	3
66157	High Energy Density Polymeric Nitrogen Nanotubes inside Carbon Nanotubes. Chinese Physics Letters, 2022, 39, 036101.	1.3	8
66158	Manipulation of spin orientation via ferroelectric switching in Fe-doped <mml:math xmlns:mml="http://www.w3.org/1998/Math/MathML"><mml:msub><mml:mi mathvariant="normal">Bi</mml:mi><mml:mn>2</mml:mn></mml:msub><mml:msub><mml:mi mathvariant="normal">WO</mml:mi><mml:mn>6</mml:mn></mml:msub></mml:math> from first principles. Physical Review B, 2022, 105, .	1.1	4
66159	Absence of Spin Frustration in the KagomÃ© Layers of Cu2+ Ions in Volborthite Cu3V2O7(OH)2Â·2H2O and Observation of the Suppression and Re-Entrance of Specific Heat Anomalies in Volborthite under an External Magnetic Field. Condensed Matter, 2022, 7, 24.	0.8	1
66160	Hidden breathing kagome topology in hexagonal transition metal dichalcogenides. Physical Review B, 2022, 105, .	1.1	12
66161	Intermetallic disordered magnet<mml:math xmlns:mml="http://www.w3.org/1998/Math/MathML"><mml:mrow><mml:msub><mml:mi>Gd</mml:mi><mml:mn>2</mml:mn></mml:msub></mml:mrow></mml:math> its relation to other<mml:math xmlns:mml="http://www.w3.org/1998/Math/MathML"><mml:mrow><mml:msub><mml:mi>AlB</mml:mi><mml:mn>2</mml:mn></mml:msub></mml:mrow></mml:math> Physical Review B, 2022, 105, .	1.1	4
66162	Hirshfeld atom refinement based on projector augmented wave densities with periodic boundary conditions. IUCrJ, 2022, 9, 286-297.	1.0	9
66163	From simple to complex crystal chemistry in the REâ€“Auâ€“Tt systems (RE = La, Ce, Pr, Nd; Tt = Ge, Pb). ACS Organic & Inorganic Au, 2022, 2, 318-326.	1.9	5
66164	Type-II Band Alignment and Tunable Optical Absorption in MoSSe/InS van der Waals Heterostructure. Frontiers in Chemistry, 2022, 10, 861838.	1.8	2
66165	Bending strain effects on the optical and optoelectric properties of GaN nanowires. Nano Research, 2022, 15, 4575-4581.	5.8	7
66166	RE ₃Rh₂Sn₄ (REÂ=ÂY, Gdâ€“Tm, Lu) â€“ first stannides with Lu₃Co₂In₄ type structure. Zeitschrift Fur Kristallographie - Crystalline Materials, 2022, 237, 51-59.	0.4	2
66167	Microstructure of Methylammonium Lead Iodide Perovskite Thin Films: A Comprehensive Study of the Strain and Texture. Advanced Energy Materials, 0, , 2103627.	10.2	7

#	Article	IF	Citations
66168	Hierarchically Porous and Defective Carbon Fiber Cathode for Efficient Zn-Air Batteries and Microbial Fuel Cells. Advanced Fiber Materials, 2022, 4, 795-806.	7.9	26
66169	Monolayer <mml:math xmlns:mml="http://www.w3.org/1998/Math/MathML"><mml:msub><mml:mi>CeI</mml:mi><mml:mn>2</mml:mn></mml:msub></m : An intrinsic room-temperature ferrovalley semiconductor. Physical Review B, 2022, 105, .	1.1	50
66170	Origin of observed narrow bandgap of mica nanosheets. Scientific Reports, 2022, 12, 2868.	1.6	9
66171	In-plane magnetization and electronic structures in BiFeO3/graphene superlattice. Applied Physics Letters, 2022, 120, .	1.5	3
66172	Crystallographic Calculations and First-Principles Calculations of Heterogeneous Nucleation Potency of Î³-Fe on La2O2S Particles. Materials, 2022, 15, 1374.	1.3	4
66173	Microscopic Mechanism of the Heatâ€Induced Blueshift in Phosphors and a Logarithmic Energy Dependence on the Nearest Dopantâ€“Vacancy Distance. Angewandte Chemie, 2022, 134, .	1.6	0
66174	Screening for new thermoelectric material: A semiconducting TaS3 with nanoporous structure. Journal of Materiomics, 2022, 8, 1031-1037.	2.8	1
66175	The core structure and the Peierls stress of the 90Â° dislocation and the 60Â° dislocation in aluminum investigated by the fully discrete Peierls model. Chinese Physics B, 0, , .	0.7	0
66176	Flat-Band-Induced Anomalous Anisotropic Charge Transport and Orbital Magnetism in Kagome Metal CoSn. Physical Review Letters, 2022, 128, 096601.	2.9	22
66177	Reliable Lattice Dynamics from an Efficient Density Functional Approximation. Chemistry of Materials, 2022, 34, 2562-2568.	3.2	12
66178	Reaction product-driven restructuring and assisted stabilization of a highly dispersed Rh-on-ceria catalyst. Nature Catalysis, 2022, 5, 119-127.	16.1	46
66179	Comparative Study of Proton Exchange in Tri- and Hexatitanates: Correlations between Stability and Electronic Properties. Inorganic Chemistry, 2022, 61, 3918-3930.	1.9	6
66180	Two-Dimensional PtS2/MoTe2 van der Waals Heterostructure: An Efficient Potential Photocatalyst for Water Splitting. Frontiers in Chemistry, 2022, 10, 847319.	1.8	12
66181	Synthesis of Fluorine-Doped Lithium Argyrodite Solid Electrolytes for Solid-State Lithium Metal Batteries. ACS Applied Materials & Interfaces, 2022, 14, 11483-11492.	4.0	11
66182	High Entropy Oxide Relaxor Ferroelectrics. ACS Applied Materials & Interfaces, 2022, 14, 11962-11970.	4.0	26
66183	Dissolving Diamond: Kinetics of the Dissolution of (100) and (110) Single Crystals in Nickel and Cobalt Films. Chemistry of Materials, 2022, 34, 2599-2611.	3.2	3
66184	Theoretical Investigation of the Active Sites in N-Doped Graphene Bilayer for the Oxygen Reduction Reaction in Alkaline Media in PEMFCs. Journal of Physical Chemistry C, 2022, 126, 5863-5872.	1.5	8
66185	Elucidating Synergistic Mechanisms of Adsorption and Electrocatalysis of Polysulfides on Double-Transition Metal MXenes for Naâ€“S Batteries. ACS Applied Materials & Interfaces, 2022, 14, 10298-10307.	4.0	18

#	Article	IF	Citations
66186	Oxygen-Terminated Nb₂CO₂ MXene with Interfacial Self-Assembled COF as a Bifunctional Catalyst for Durable Zincâ€“Air Batteries. ACS Applied Materials & Interfaces, 2022, 14, 10738-10746.	4.0	22
66187	Density Functional Theory Calculations of the Stability, Electronic Structure, and Magnetism of ReS₂ Nanoribbons: An Emerging Material for Electrocatalytic Reactions. ACS Applied Nano Materials, 2022, 5, 2385-2394.	2.4	4
66188	Tunable Ti³⁺-Mediated Charge Carrier Dynamics of Atomic Layer Deposition-Grown Amorphous TiO₂. Journal of Physical Chemistry C, 2022, 126, 4542-4554.	1.5	25
66189	Conformational Gap Control in CsTaS₃. Journal of the American Chemical Society, 2022, 144, 3398-3410.	6.6	1
66190	From n-alkane to polyacetylene on Cu (110): Linkage modulation in chain growth. Science China Chemistry, 2022, 65, 733-739.	4.2	1
66191	Design Elements for Enhanced Hydrogen Isotope Separations in Barely Porous Organic Cages. ACS Omega, 2022, 7, 7963-7972.	1.6	7
66192	Threefold Fermions, Weyl Points, and Superconductivity in the Mirror Symmetry Lacking Semiconductor TlCd2Te4. Nanomaterials, 2022, 12, 679.	1.9	1
66193	Nature of the bonded-to-atomic transition in liquid silica to TPa pressures. Journal of Applied Physics, 2022, 131, .	1.1	4
66194	Flame Spray Pyrolysis as a Synthesis Platform to Assess Metal Promotion in In₂O₃â€Catalyzed CO₂ Hydrogenation. Advanced Energy Materials, 2022, 12, .	10.2	34
66195	Spiral effect of helical carbon nanorods boosting electrocatalysis of oxygen reduction reaction. Science China Materials, 2022, 65, 1531-1538.	3.5	6
66196	Basicity Contributions to Interfacial Structure and Oxygen Potential of CaOâ€“MnOâ€“SiO2 slag. Metallurgical and Materials Transactions B: Process Metallurgy and Materials Processing Science, 0, , 1.	1.0	2
66197	nergy, metastability, and optical properties of anion-disordered <mml:math xmlns:mml="http://www.w3.org/1998/Math/MathML"><mml:mrow><mml:mi>R</mml:mi><mml:msub><mml:mi mathvariant="normal">O</mml:mi><mml:mi>x</mml:mi></mml:msub><mml:msub><mml:mi mathvariant="normal">H</mml:mi><mml:mrow><mml:mn>3</mml:mn><mml:mo>â^’</mml:mo><mml:mn>2</mml:mn><mml:mi>x</mml:mi></mml:mrow></mml:msub></mml:mrow></mml:math>		

#	Article	IF	Citations
66204	Role of electronic excitation on the anomalous magnetism of elemental copper. Physical Review B, 2022, 105, .	1.1	2
66205	Field-induced reagent concentration and sulfur adsorption enable efficient electrocatalytic semihydrogenation of alkynes. Science Advances, 2022, 8, eabm9477.	4.7	40
66206	Tuning the band gap and effective mass of black arsenic phosphide monolayer by in-plane strain. Materials Research Express, 2022, 9, 025009.	0.8	4
66207	The half-metallity induced by out-of-plane electric field on phosphorene nanoribbons. Chinese Physics B, 0, , .	0.7	1
66208	Electronic properties and stability of M₂O₃ (MÂ=ÂAl, Ga, In) and alloy (M_xGa_{1â€x})₂O₃ in Î± and Î² phases: A theoretical study. Journal of the American Ceramic Society, 2022, 105, 4554-4563.	1.9	3
66209	Anisotropic Growth of Copper Nanorods Mediated by Cl^{â€“} Ions. ACS Omega, 2022, 7, 7414-7420.	1.6	0
66210	First principles study on sodium de-intercalation from NaMnPO4. Materials Today: Proceedings, 2022, 62, S7-S11.	0.9	3
66211	Ab initio investigations of point and complex defect structures in B2-FeAl. Physical Review Materials, 2022, 6, .	0.9	3
66212	Regulation of phase transition temperature and preparation for doping-VO2 smart thermal control films. Journal of Applied Physics, 2022, 131, .	1.1	12
66213	Precise Control over Local Atomic Structures in Niâ€“Mo Bimetallic Alloys for the Hydrodeoxygenation Reaction: A Combination between Density Functional Theory and Microkinetic Modeling. Journal of Physical Chemistry C, 2022, 126, 4319-4328.	1.5	5
66214	Polarization-Enhanced Photovoltaic Effects in a High-Temperature Molecular Ferroelectric [C₆N₂H₁₈][SbI₅]-Based Solar Device. ACS Applied Energy Materials, 2022, 5, 2738-2746.	2.5	4
66215	Sub-Angstrom Imaging of Nondegenerate KekulÃ© Structures in a Two-Dimensional Halogen-Bonded Supramolecular Network. Journal of Physical Chemistry C, 2022, 126, 4241-4247.	1.5	5
66216	Wide-Bandgap Perovskite Quantum Dots in Perovskite Matrix for Sky-Blue Light-Emitting Diodes. Journal of the American Chemical Society, 2022, 144, 4009-4016.	6.6	92
66217	Controllable Synthesis of Narrow-Gap van der Waals Semiconductor Nb₂GeTe₄ with Asymmetric Architecture for Ultrafast Photonics. ACS Nano, 2022, 16, 4239-4250.	7.3	15
66218	Structure, Stability, and Photocatalytic Activity of a Layered Perovskite Niobate after Flux-Mediated Sn(II) Exchange. Inorganic Chemistry, 2022, 61, 4062-4070.	1.9	7
66219	The Role of the Bi³⁺ Lone Pair Effect in Bi(H₃O)(SO₄)₂, Bi(HSO₄)₃, and Bi₂(SO₄)₃. Inorganic Chemistry, 2022, 61, 4102-4113.	1.9	3
66220	Molecular-Scale Manipulation of Layer Sequence in Heteroassembled Nanosheet Films toward Oxygen Evolution Electrocatalysts. ACS Nano, 2022, 16, 4028-4040.	7.3	29
66221	Anderson-Type Polyoxometalate-Assisted Synthesis of Defect-Rich Doped 1T/2H-MoSe₂ Nanosheets for Efficient Seawater Splitting and Mg/Seawater Batteries. ACS Applied Materials & Interfaces, 2022, 14, 10246-10256.	4.0	45

#	Article	IF	Citations
66222	Coexistence of Semiconducting Ferromagnetics and Piezoelectrics down 2D Limit from Non van der Waals Antiferromagnetic LiNbO₃-Type FeTiO₃. Journal of Physical Chemistry Letters, 2022, 13, 1991-1999.	2.1	4
66223	Origin of Asymmetric Splitting of Kondo Peak in Spin-Polarized Scanning Tunneling Spectroscopy: Insights from First-Principles-Based Simulations. Journal of Physical Chemistry Letters, 2022, 13, 2094-2100.	2.1	6
66224	Optimization of Energy Storage Properties in Lead-Free Barium Titanate-Based Ceramics via B-Site Defect Dipole Engineering. ACS Sustainable Chemistry and Engineering, 2022, 10, 2930-2937.	3.2	21
66225	First-Principles Surface Characterization and Water Adsorption of Fe₃P Schreibersite. ACS Earth and Space Chemistry, 2022, 6, 512-520.	1.2	2
66226	Computational Search and Stability Analysis of Two-Dimensional Tin Oxides. Journal of Physical Chemistry C, 2022, 126, 4647-4654.	1.5	0
66227	Theoretical Analysis of Electronic Structure and Optical Properties of Potassium Dihydrogen Phosphate Crystal Affected by [011] Screw Dislocation. Crystal Growth and Design, 2022, 22, 1764-1769.	1.4	1
66228	Cr_xPt_{1â€“x}Te₂ (x â‰ˆ 0.45): A Family of Air-Stable and Exfoliatable van der Waals Ferromagnets. ACS Nano, 2022, 16, 3852-3860.	7.3	9
66229	Magnetic properties and promising magnetocaloric performances in the antiferromagnetic GdFe2Si2 compound. Science China Materials, 2022, 65, 1345-1352.	3.5	116
66230	Computational design of BC3N2 based single atom catalyst for dramatic activation of inert CO2 and CH4 gasses into CH3COOH with ultralow CH4 dissociation barrier. Chinese Chemical Letters, 2023, 34, 107213.	4.8	61
66231	Pressure-Induced Phase Transition and Compression Properties of HfO₂ Nanocrystals. Inorganic Chemistry, 2022, 61, 3498-3507.	1.9	4
66232	Substantial Improvement of Operating Stability by Strengthening Metalâ€Halogen Bonds in Halide Perovskites. Advanced Functional Materials, 2022, 32, .	7.8	16
66233	Metal-insulator transition in monolayer MoS₂ via contactless chemical doping. 2D Materials, 2022, 9, 025026.	2.0	8
66234	Unraveling the Role of Nitrogenâ€Doped Carbon Nanowires Incorporated with <scp>MnO₂</scp> Nanosheets as High Performance Cathode for Zincâ€Ion Batteries. Energy and Environmental Materials, 2023, 6, .	7.3	27
66235	Stability and formation of hydroxylated <mml:math xmlns:mml="http://www.w3.org/1998/Math/MathML"><mml:mrow><mml:mi>Î±</mml:mi><mml:mtext>â€“</mml:mtext><mml:msub><mml:mi mathvariant="normal">O</mml:mi><mml:mn>3</mml:mn></mml:msub><mml:mrow><mml:mo>(</mml:mo><mml:mn>0001</mml:mn> surfaces at high temperatures. Physical Review Research, 2022, 4, .		
66236	Optical Properties of OLED Materials by TDDFT. Journal of Physics: Conference Series, 2022, 2207, 012039.	0.3	1
66237	Pressure-tuned one- to quasi-two-dimensional structural phase transition and superconductivity in <mml:math xmlns:mml="http://www.w3.org/1998/Math/MathML"><mml:msub><mml:mi mathvariant="normal">LiP</mml:mi><mml:mn>15</mml:mn></mml:msub></mml:math>. Physical Review B, 2022, 105, .	1.1	4
66238	High-Throughput Calculation of Interlayer van der Waals Forces Validated with Experimental Measurements. Research, 2022, 2022, 9765121.	2.8	10
66239	A deep potential model with long-range electrostatic interactions. Journal of Chemical Physics, 2022, 156, 124107.	1.2	57

#	Article	IF	Citations
66240	Elucidate interfacial disorder effects on the perpendicular magnetic anisotropy at Fe/MgO heterostructure from first-principles calculations. Journal of Physics Condensed Matter, 2022, 34, 214009.	0.7	2
66241	First-principles study of two-dimensional HfS2/GaS van der Waals heterostructure for photocatalytic action. Physica E: Low-Dimensional Systems and Nanostructures, 2022, 142, 115257.	1.3	10
66242	The diamond NV-center transition energies in the vicinity of an intrinsic stacking fault. AIP Advances, 2022, 12, 035009.	0.6	3
66243	Structure transformation and electronic properties of m-aminobenzoic acid under different pressures. International Journal of Modern Physics C, 2022, 33, .	0.8	3
66244	Electronic and Lattice Thermal Conductivity Switching by 3Dâ”2D Crystal Structure Transition in Nonequilibrium (Pb_{1â”}_xSn_x)Se. Advanced Electronic Materials, 2022, 8, .	2.6	6
66245	Amorphous black phosphorus: wet-chemical synthesis and atomic disordering-dependent electrocatalytic performance. 2D Materials, 2022, 9, 025019.	2.0	2
66246	Theoretical study of decomposition of formic acid over <scp>Pd</scp> catalyst anchored on <scp>N</scp> â€doped graphene. International Journal of Quantum Chemistry, 0, , .	1.0	1
66247	Modeling surface spin polarization on ceria-supported Pt nanoparticles. Journal of Physics Condensed Matter, 2022, , .	0.7	0
66248	A Strong Two-Dimensional Semiconductor I-B₄C with High Carrier Mobility. Journal of Physical Chemistry C, 2022, 126, 6036-6046.	1.5	2
66249	Laserâ€Engraved Boronâ€Doped Diamond for Copper Catalyzed Nonâ€Enzymatic Glucose Sensing. Advanced Materials Interfaces, 0, , 2200034.	1.9	3
66250	Revealing the Potential of Ternary Medium-Entropy Alloys as Exceptional Electrocatalysts toward Nitrogen Reduction: An Example of Heusler Alloys. ACS Applied Materials & Interfaces, 2022, 14, 15235-15242.	4.0	15
66251	Highly Luminescent and Multifunctional Zeroâ€Dimensional Cesium Lanthanide Chloride (Cs₃LnCl₆) Colloidal Nanocrystals. Advanced Optical Materials, 2022, 10, .	3.6	8
66252	A Synergetic Codoping Strategy Enabling Performance Improvement of Pureâ€Blue Perovskite Quantum Dots Lightâ€Emitting Diodes. Advanced Optical Materials, 2022, 10, .	3.6	11
66253	First-Principles Study of Tritium Trapping in Î³-LiAlO₂ Nanovoids. Journal of Physical Chemistry C, 2022, 126, 5767-5776.	1.5	3
66254	Anisotropic mechanical response, high negative thermal expansion, and outstanding dynamical stability of biphenylene monolayer revealed by machine-learning interatomic potentials. FlatChem, 2022, 32, 100347.	2.8	24
66255	Exploring the Effect of Pd on the Oxygen Reduction Performance of Pt by In Situ Raman Spectroscopy. Analytical Chemistry, 2022, 94, 4779-4786.	3.2	18
66256	Rational Design of Two-Dimensional Porous Boron Phosphide as Efficient Cathode Material for Li and Na Ion Batteries: A First-Principles Study. Journal of Physical Chemistry C, 2022, 126, 5092-5100.	1.5	24
66257	Insight into Subsurface Adsorption Derived from a Lattice-Gas Model and Monte Carlo Simulations. Journal of Physical Chemistry C, 2022, 126, 5343-5353.	1.5	2

#	Article	IF	Citations
66258	Photochemical Fluorination of TiO₂(110) Produces an Atomically Thin Passivating Layer. Journal of Physical Chemistry C, 2022, 126, 4899-4906.	1.5	1
66259	Interplay between Charge-Density-Wave, Superconductivity, and Ferromagnetism in CuIr_{2â€“x}Cr_xTe₄ Chalcogenides. Journal of Physical Chemistry Letters, 2022, 13, 2442-2451.	2.1	12
66260	Time-reversal symmetry breaking in frustrated superconductor <mml:math xmlns:mml="http://www.w3.org/1998/Math/MathML"><mml:msub><mml:mrow><mml:mi>Re</mml:mi></mml:mrow><mml:mn>2</mml:mn> Physical Review B, 2022, 105, .	3.7	5
66261	Dual-gated single-molecule field-effect transistors beyond Mooreâ€™s law. Nature Communications, 2022, 13, 1410.	5.8	38
66262	Dynamic chemical processes on ZnO surfaces tuned by physisorption under ambient conditions. Journal of Energy Chemistry, 2022, , .	7.1	3
66263	Influence of inter- and intra-valley carrier dynamics on the optical properties of monolayer TMDCs. , 2022, , .		0
66264	First-Principles Study of Electronic Properties of Substitutionally Doped Monolayer SnP3. Materials, 2022, 15, 2462.	1.3	1
66265	Hybrid nodal-ring phonons with hourglass dispersion in <mml:math xmlns:mml="http://www.w3.org/1998/Math/MathML"><mml:msub><mml:mi>AgAlO</mml:mi><mml:mn>2</mml:mn></mml:msub> Physical Review Materials, 2022, 6, .	3.1	17
66266	Electronic Properties of the Weyl Semimetals Co₂MnX (X=Si, Ge, Sn). Physica Status Solidi - Rapid Research Letters, 2022, 16, .	1.2	2
66267	A High-Throughput Computational Study on the Stability of Ni- and Ti-Doped Zr2Fe Alloys. Energies, 2022, 15, 2310.	1.6	2
66268	First-principles study of hydrogen storage on Li, Na and K-decorated defective boron nitride nanosheets. European Physical Journal B, 2022, 95, 1.	0.6	9
66269	Macroscale Robust Superlubricity on Metallic NbB₂. Advanced Science, 2022, 9, e2103815.	5.6	8
66270	Two-band superconductivity through structural and electronic reconstruction on interface: YBa₂Cu₃O₇/LaAlO₃(001). Journal of Applied Physics, 2022, 131, 125303.	1.1	0
66271	Effect of cation configuration and solvation on the band positions of zinc ferrite (100). Photochemical and Photobiological Sciences, 2022, , 1.	1.6	0
66272	Metalâ€“Support Interactions within a Dual-Site Pd/YMn₂O₅ Catalyst during CH₄ Combustion. ACS Catalysis, 2022, 12, 4430-4439.	5.5	16
66273	Ab Initio Evaluation of Solid-State Transformation Pathways from Ferrihydrite to Goethite. ACS Earth and Space Chemistry, 2022, 6, 800-809.	1.2	4
66274	Short- to Intermediate-Range Structure, Transport, and Thermophysical Properties of LiFâ€“NaFâ€“ZrF4 Molten Salts. Frontiers in Physics, 2022, 10, .	1.0	5
66275	Borophene and Pristine Graphene 2D Sheets as Potential Surfaces for the Adsorption of Electron-Rich and Electron-Deficient Ï€-Systems: A Comparative DFT Study. Nanomaterials, 2022, 12, 1028.	1.9	7

#	Article	IF	Citations
66276	Prediction of freestanding semiconducting bilayer borophenes. Nano Research, 2022, 15, 5752-5757.	5.8	15
66277	Screening transition metal-based polar pentagonal monolayers with large piezoelectricity and shift current. Npj Computational Materials, 2022, 8, .	3.5	13
66278	Exploring Mechanisms of Hydration and Carbonation of MgO and Mg(OH)₂ in Reactive Magnesium Oxide-Based Cements. Journal of Physical Chemistry C, 2022, 126, 6196-6206.	1.5	18
66279	Heterogeneous manganese-oxide-catalyzed successive cleavage and functionalization of alcohols to access amides and nitriles. CheM, 2022, 8, 1906-1927.	5.8	18
66280	Spinâ€“Phonon Coupling in Ferromagnetic Monolayer Chromium Tribromide. Advanced Materials, 2022, 34, e2108506.	11.1	8
66281	Diradical Characters of s-Indaceno[1,2,3-cd;5,6,7-câ€™dâ€™]Diphenalene with and without Interaction with MgO(001). E-Journal of Surface Science and Nanotechnology, 2022, 20, 59-67.	0.1	4
66282	Ferroelectric control of pseudospin texture in CuInP₂S₆ monolayer. Journal of Physics Condensed Matter, 2022, 34, 204001.	0.7	3
66283	Relation between Reactive Surface Sites and Precursor Choice for Area-Selective Atomic Layer Deposition Using Small Molecule Inhibitors. Journal of Physical Chemistry C, 2022, 126, 4845-4853.	1.5	15
66284	Local positional and spin symmetry breaking as a source of magnetism and insulation in paramagnetic <mml:math xmlns:mml="http://www.w3.org/1998/Math/MathML"><mml:mrow><mml:mi>EuTi</mml:mi><mml:msub><mml:mo mathvariant="normal">O</mml:mi><mml:mn>3</mml:mn></mml:msub></mml:mrow></mml:math>. Physical Review Materials, 2022, 6, .	0.9	8
66285	Experimental and Theoretical Investigation of Metalâ€“Support Interactions in Metal-Oxide-Supported Rhenium Materials. Journal of Physical Chemistry C, 2022, 126, 4472-4482.	1.5	5
66286	Exploring the Effect of the Number of Hydrogen Atoms on the Properties of Lanthanide Hydrides by DMFT. Applied Sciences (Switzerland), 2022, 12, 3498.	1.3	0
66287	First-Principles Calculations on Semiconducting Îµ-GeS and Îµ-SnS Monolayer Nanosheets with Photocatalytic Activity for Sunlight-Driven Water Splitting. ACS Applied Nano Materials, 2022, 5, 3900-3912.	2.4	18
66288	Molecular modelling and computational studies of peptide diphenylalanine nanotubes, containing waters: structural and interactions analysis. Journal of Molecular Modeling, 2022, 28, 81.	0.8	7
66289	Designing Selfâ€Adaptive Donorâ€Switchâ€Acceptor Systems for Molecular Optoâ€Electronic Conversion Based on Dimethyldihydropyrene/Cyclophanediene. Chemistry - an Asian Journal, 2022, , .	1.7	0
66290	Charged Lithium adsorption on pristine and defective silicene: A theoretical study. Journal of Physics Condensed Matter, 2022, , .	0.7	1
66291	Crystal structure evolution and superconductivity of the ternary hydride <mml:math xmlns:mml="http://www.w3.org/1998/Math/MathML"><mml:msub><mml:mi>CSH</mml:mi><mml:mn>3</mml:mn></mml:msub></mml:math> under pressure. Physical Review B, 2022, 105, .	1.1	2
66292	Taâ€“TiOx nanoparticles as radical scavengers to improve the durability of Feâ€“Nâ€“C oxygen reduction catalysts. Nature Energy, 2022, 7, 281-289.	19.8	93
66293	Kâ€Functionalized Carbon Quantum Dotsâ€Induced Interface Assembly of Carbon Nanocages for Ultrastable Potassium Storage Performance. Small Methods, 2022, 6, e2101627.	4.6	12

#	Article	IF	Citations
66294	Modeling polarons in density functional theory: lessons learned from TiO₂. Journal of Physics Condensed Matter, 2022, 34, 204006.	0.7	6
66295	Structural phase transition of monochalcogenides investigated with machine learning. Physical Review B, 2022, 105, .	1.1	7
66296	Intrinsic Ultralow Lattice Thermal Conductivity in the Full-Heusler Compound <mml:math xmlns:mml="http://www.w3.org/1998/Math/MathML" display="inline" overflow="scroll"><mml:msub><mml:mi>Ba</mml:mi><mml:mn>2</mml:mn></mml:msub><mml:mrow><mml:mi>Ag</mml:mi><mml:m Physical Review Applied, 2022, 17, .	1.5	17
66297	Atomic Model of Gold Adsorption onto the Pyrite Surface with DFT Study. Minerals (Basel,) Tj ETQq1 1 0.784314 rgBT /Overlock 10 T	0.8	4
66298	Selfâ€Coâ€Electrolysis for Coâ€Production of Phosphate and Hydrogen in Neutral Phosphate Buffer Electrolyte. Advanced Materials, 2022, 34, e2200058.	11.1	17
66299	Hybridization-driven strong anharmonicity in Yb-filled skutterudites. Physical Review B, 2022, 105, .	1.1	4
66300	Binary dopant segregation enables hematite-based heterostructures for highly efficient solar H2O2 synthesis. Nature Communications, 2022, 13, 1499.	5.8	24
66301	Monolayer Sc₂CF₂ as a Potential Selective and Sensitive NO₂ Sensor: Insight from First-Principles Calculations. ACS Omega, 2022, 7, 9267-9275.	1.6	3
66302	Phase transitions and properties of lanthanum under high pressures. Journal of Physics Condensed Matter, 2022, 34, 204005.	0.7	2
66303	First-principles study of defect formation energies in <mml:math xmlns:mml="http://www.w3.org/1998/Math/MathML"><mml:mi>LaO</mml:mi><mml:mi>X</mml:mi><mml:msub><mml:mi mathvariant="normal">S</mml:mi><mml:mn>2</mml:mn></mml:msub></mml:math> <mml:math xmlns:mml="http://www.w3.org/1998/Math/MathML"><mml:mrow><mml:mo>(</mml:mo><mml:mi>X</mml:mi><mml:mo>= Review B, 2022, 105, .	1.1	2
66304	Discovery of a Slaterâ€“Pauling Semiconductor ZrRu_{1.5}Sb with Promising Thermoelectric Properties. Advanced Functional Materials, 2022, 32, .	7.8	12
66305	Room Temperature Fabrication of SnO₂ Electrodes Enabling Barrierâ€Free Electron Extraction for Efficient Flexible Perovskite Photovoltaics. Advanced Functional Materials, 2022, 32, .	7.8	42
66306	Constructing Interfacial Nanolayer Stabilizes 4.3 V Highâ€Voltage Allâ€Solidâ€State Lithium Batteries with PEOâ€Based Solidâ€State Electrolyte. Advanced Functional Materials, 2022, 32, .	7.8	23
66307	A Computational Framework to Accelerate the Discovery of Perovskites for Solar Thermochemical Hydrogen Production: Identification of Gd Perovskite Oxide Redox Mediators. Advanced Functional Materials, 2022, 32, .	7.8	7
66308	Structural and electronic properties of Pt modified Au(100) surface. Scientific Reports, 2022, 12, 3859.	1.6	1
66309	Evaporating potential. Joule, 2022, 6, 690-701.	11.7	60
66310	Accelerated screening of functional atomic impurities in halide perovskites using high-throughput computations and machine learning. Journal of Materials Science, 2022, 57, 10736-10754.	1.7	10
66311	Hidden phases with neuromorphic responses and highly enhanced piezoelectricity in an antiferroelectric prototype. Physical Review B, 2022, 105, .	1.1	8

#	Article	IF	Citations
66312	Highly efficient and selective electrocatalytic hydrogen peroxide production on Co-O-C active centers on graphene oxide. Communications Chemistry, 2022, 5, .	2.0	33
66313	Efficient Electrochemical Reduction of CO₂ to CO by Ag-Decorated B-Doped g-C₃N₄: A Combined Theoretical and Experimental Study. Industrial & Engineering Chemistry Research, 2022, 61, 10400-10408.	1.8	11
66314	Cluster- and energy-separated extreme states in a synthesized superatomic solid. Physical Review B, 2022, 105, .	1.1	1
66315	Lithium superionic conductors with corner-sharing frameworks. Nature Materials, 2022, 21, 924-931.	13.3	67
66316	Pressure-induced creation and annihilation of Weyl points in <mml:math xmlns:mml="http://www.w3.org/1998/Math/MathML"><mml:msub><mml:mi>T</mml:mi><mml:mi>d</mml:mi></mml:msub><mml:mte mathvariant="normal">W</mml:mi></mml:mrow><mml:mrow><mml:mn>0.5</mml:mn></mml:mrow></mml:msub><mml:msub><mml Physical Review B, 2022, 105, .	1.1	2
66317	Spin-lattice couplings in two-dimensional <mml:math xmlns:mml="http://www.w3.org/1998/Math/MathML"><mml:msub><mml:mrow><mml:mi>CrI</mml:mi></mml:mrow><mml:mn>3</ from first-principles computations. Physical Review B, 2022, 105, .	1.1	20
66318	Half-integer anomalous currents in 2D materials from a QFT viewpoint. Scientific Reports, 2022, 12, 5439.	1.6	4
66319	Co-segregation behavior and weakening effect of the major elements in Al-Zn-Mg-Cu series alloys on Al Î£3(111)[110] symmetrical tilt grain boundary: a first-principles study. Journal of Materials Research and Technology, 2022, 18, 3158-3172.	2.6	6
66320	Revealing the interplay between â€œintelligent behaviorâ€•and surface reconstruction of non-precious metal doped SrTiO3 catalysts during methane combustion. Catalysis Today, 2022, , .	2.2	5
66321	Dual storage and release of molecular oxygen in comet 67P/Churyumovâ€“Gerasimenko. Nature Astronomy, 2022, 6, 724-730.	4.2	8
66322	Effect of YRu-VO complex on the OER activity of V-shaped RuO2 Î£103 nanotwin. Physica B: Condensed Matter, 2022, 637, 413884.	1.3	2
66323	Superconductivity in Heusler compound ScAu₂Al. Journal of Physics Condensed Matter, 2022, 34, 195403.	0.7	1
66324	Tungsten-oxide frameworks with visible light absorption: An ab initio study. Applied Physics Letters, 2022, 120, 121901.	1.5	0
66325	Phase transitions and pâ€“T phase diagram of the multiferroic TbFe ₃ (BO ₃) ₄ crystal. Journal of Raman Spectroscopy, 0, , .	1.2	2
66326	Functional Groups Assisted Tunable Dielectric Permittivity of Guestâ€Free Znâ€Based Coordination Polymers for Gate Dielectrics. Chemistry - A European Journal, 2022, 28, .	1.7	2
66327	Photo-magnetization in two-dimensional sliding ferroelectrics. Npj 2D Materials and Applications, 2022, 6, .	3.9	8
66328	Improved adhesion of TiN coatings on Al₂O₃â€“carbide composites by DFT calculations and experimental arcâ€PVD synthesis. Journal of the American Ceramic Society, 2022, 105, 4859-4869.	1.9	2
66329	A direct Z-scheme MoSi₂N₄/BlueP vdW heterostructure for photocatalytic overall water splitting. Journal Physics D: Applied Physics, 2022, 55, 215502.	1.3	29

#	Article	IF	Citations
66330	Influence of local structural distortion on the magnetism of <mml:math xmlns:mml="http://www.w3.org/1998/Math/MathML"><mml:msub><mml:mrow><mml:mi>Na</mml:mi></mml:mrow><mml:mrow><mml:mn>2</mn> compounds. Physical Review B, 2022, 105, .	1.1	4
66331	Insights into Interaction of CO(_2) with N and B-doped Graphenes. Communications in Physics, 2022, 32, .	0.0	0
66332	Surface Structures from NH₃ Chemisorption in CVD and ALD of AlN, GaN, and InN Films. Journal of Physical Chemistry C, 2022, 126, 5885-5895.	1.5	6
66333	Quantifying Force and Energy in Single-Molecule Metalation. Journal of the American Chemical Society, 2022, , .	6.6	3
66334	Governing Interlayer Strain in Bismuth Nanocrystals for Efficient Ammonia Electrosynthesis from Nitrate Reduction. ACS Nano, 2022, 16, 4795-4804.	7.3	76
66335	Mechanism for Acetone and Crotonaldehyde Production during Steam Reforming of Ethanol over La_{0.7}Sr_{0.3}MnO_{3â€“x} Perovskite: Evidence for a Shared C4 Aldol Addition Intermediate. ACS Catalysis, 2022, 12, 4358-4374.	5.5	3
66336	Charting the Lattice Thermal Conductivities of Iâ€“IIIâ€“VI₂ Chalcopyrite Semiconductors. Chemistry of Materials, 2022, 34, 2833-2841.	3.2	22
66337	Synergistic Effects of V and Ni Catalysts on Hydrogen Sorption Kinetics of Mg-Based Hydrogen Storage Materials: A Computational Study. Journal of Physical Chemistry C, 2022, 126, 5483-5492.	1.5	5
66338	Decoding the Gate Opening Mechanism of the Flexible Framework RPM3â€“Zn upon Hydrocarbon Inclusion. Chemistry of Materials, 2022, 34, 3246-3252.	3.2	3
66339	M_xLa_{1â€“x}SiO_{2â€“y}N_z (M = Ca/Sr/Ba): Elucidating and Tuning the Structure and Eu²⁺ Local Environments to Develop Full-Visible Spectrum Phosphors. Chemistry of Materials, 2022, 34, 4039-4049.	3.2	14
66340	Ligand Control of Structural Diversity in Luminescent Hybrid Copper(I) Iodides. Chemistry of Materials, 2022, 34, 3206-3216.	3.2	23
66341	Catalytic Performance and Near-Surface X-ray Characterization of Titanium Hydride Electrodes for the Electrochemical Nitrate Reduction Reaction. Journal of the American Chemical Society, 2022, 144, 5739-5744.	6.6	31
66342	MoSe₂/SnS Nanoheterostructures for Water Splitting. ACS Applied Nano Materials, 2022, 5, 4293-4304.	2.4	22
66343	Surface Reconstruction with a Sandwich-like C/Cu/C Catalyst for Selective and Stable CO₂ Electroreduction. ACS Applied Materials & Interfaces, 2022, 14, 13261-13270.	4.0	14
66344	Spinâ€Glass State above Room Temperature in a Layered Nickelate La_n₊₁Ni_nO₃_n₊₁. Advanced Electronic Materials, 2022, 8, .	2.6	0
66345	Electronic Effect or Underpotentially Deposited Hydrogen? Insights into the effect of Pb on formic acid electroâ€oxidation on Pt. ChemCatChem, 0, , .	1.8	1
66346	The Universal Growth of Ultrathin Perovskite Single Crystals. Advanced Materials, 2022, 34, e2108396.	11.1	11
66347	Topological properties of Sb(111) surface: A first-principles study. Chinese Physics B, 2022, 31, 047105.	0.7	0

#	Article	IF	Citations
66348	Explaining the structure sensitivity of Pt and Rh for aqueous-phase hydrogenation of phenol. Journal of Chemical Physics, 2022, 156, 104703.	1.2	7
66349	Screening Promising CsV₃Sb₅-Like Kagome Materials from Systematic First-Principles Evaluation. Chinese Physics Letters, 2022, 39, 047402.	1.3	21
66350	Chlorobenzenesulfonic Potassium Salts as the Efficient Multifunctional Passivator for the Buried Interface in Regular Perovskite Solar Cells. Advanced Energy Materials, 2022, 12, .	10.2	119
66351	Tetragonal-structure germanene van der Waals 2D crystal and its Raman spectra. Applied Physics A: Materials Science and Processing, 2022, 128, 1.	1.1	0
66352	Toward accurate and efficient dynamic computational strategy for heterogeneous catalysis: Temperature-dependent thermodynamics and kinetics for the chemisorbed on-surface CO. Chinese Chemical Letters, 2022, 33, 4936-4942.	4.8	7
66353	Strong magnetoelectric coupling at an atomic nonmagnetic electromagnetic probe in bismuth ferrite. Physical Review B, 2022, 105, .	1.1	4
66354	Carboxylated carbon quantum dot-induced binary metalâ€“organic framework nanosheet synthesis to boost the electrocatalytic performance. Materials Today, 2022, 54, 42-51.	8.3	76
66355	General Synthetic Strategy to Ordered Mesoporous Carbon Catalysts with Singleâ€Atom Metal Sites for Electrochemical CO₂ Reduction. Small, 2022, 18, e2107799.	5.2	13
66356	A Unique Nanoflakeâ€Shape Bimetallic Tiâ€“Nb Oxide of Superior Catalytic Effect for Hydrogen Storage of MgH₂. Small, 2022, 18, e2107013.	5.2	44
66357	Magnetoelectric Effect in Hydrogen Harvesting: Magnetic Field as a Trigger of Catalytic Reactions. Advanced Materials, 2022, 34, e2110612.	11.1	18
66358	Highly anisotropic mechanical and optical properties of 2D NbOX2 (XÂ=ÂCl, Br, I) revealed by first-principle. Nanotechnology, 2022, 33, 275701.	1.3	7
66359	Fe binuclear sites convert methane to acetic acid with ultrahigh selectivity. CheM, 2022, 8, 1658-1672.	5.8	40
66360	Alloying Effect on the Stability of Ti₅Si₃ from Firstâ€Principles Study. Physica Status Solidi (B): Basic Research, 2022, 259, .	0.7	2
66361	Temperature effect on charge-state transition levels of defects in semiconductors. Physical Review B, 2022, 105, .	1.1	7
66362	Tunable band gap in twisted bilayer graphene. Physical Review B, 2022, 105, .	1.1	4
66363	Macro-superlubric triboelectric nanogenerator based on tribovoltaic effect. Matter, 2022, 5, 1532-1546.	5.0	40
66364	In Situ Growth Mechanism for Highâ€Quality Hybrid Perovskite Singleâ€Crystal Thin Films with High Area to Thickness Ratio: Looking for the Sweet Spot. Advanced Science, 2022, 9, e2104788.	5.6	16
66365	Typeâ€II van der Waals Heterostructures Based on AsP and Transition Metal Dichalcogenides: Great Promise for Applications in Solar Cell. Physica Status Solidi - Rapid Research Letters, 2022, 16, .	1.2	9

#	Article	IF	Citations
66366	Carbon defect qubit in two-dimensional WS2. Nature Communications, 2022, 13, 1210.	5.8	12
66367	Prediction of the crystal structure and properties of energetic <scp>LLM</scp> â€105:oxidant cocrystals: A theoretical study. Journal of the Chinese Chemical Society, 0, , .	0.8	0
66368	Dynamical tuning of the thermal conductivity via magnetophononic effects. Physical Review B, 2022, 105, .	1.1	7
66369	First-Principle Study of CsPbBr₃ and CsPbI₃ Perovskite Solar Cells. ECS Journal of Solid State Science and Technology, 2022, 11, 035012.	0.9	5
66370	Pressure-induced structural transition, metallization, and topological superconductivity in PdSSe. Physical Review B, 2022, 105, .	1.1	9
66371	Universal machine learning framework for defect predictions in zinc blende semiconductors. Patterns, 2022, 3, 100450.	3.1	22
66372	The speed limit of optoelectronics. Nature Communications, 2022, 13, 1620.	5.8	18
66373	Stable CsPbX3 mixed halide alloyed epitaxial films prepared by pulsed laser deposition. Applied Physics Letters, 2022, 120, .	1.5	13
66374	Band transport by large FrÃ¶hlich polarons in MXenes. Nature Physics, 2022, 18, 544-550.	6.5	40
66375	Catalytic Activity Enhancement on Alcohol Dehydrogenation via Directing Reaction Pathways from Single- to Double-Atom Catalysis. Journal of the American Chemical Society, 2022, 144, 4913-4924.	6.6	68
66376	Composition-dependent ordering transformations in Ptâ€“Fe nanoalloys. Proceedings of the National Academy of Sciences of the United States of America, 2022, 119, e2117899119.	3.3	10
66377	Development of a force field for modeling lithium borosilicate glasses. International Journal of Applied Glass Science, 2022, 13, 444-456.	1.0	7
66378	A New Superconductor Parent Compound NaMn₆Bi₅ with Quasi-One-Dimensional Structure and Lower Antiferromagnetic-Like Transition Temperatures. Chinese Physics Letters, 2022, 39, 047401.	1.3	10
66379	Electronic and topological properties of Bi(110) ultrathin films grown on a Cu(111) substrate. Physical Review B, 2022, 105, .	1.1	5
66380	Band Structure Engineering and Defect Passivation of Cu_xAg_{1â€“x}InS₂/ZnS Quantum Dots to Enhance Photoelectrochemical Hydrogen Evolution. ACS Omega, 2022, 7, 9642-9651.	1.6	4
66381	The Nexus between ASAT and Density Functional Theory. , 2022, , 201-221.		0
66382	Migration Barrier Estimation of Carbon in Lead for Leadâ€“Acid Battery Applications: A Density Functional Theory Approach. Solids, 2022, 3, 177-187.	1.1	2
66383	Tetrahedral W₄ cluster confined in graphene-like C₂N enables electrocatalytic nitrogen reduction from theoretical perspective. Nanotechnology, 2022, 33, 245706.	1.3	8

#	Article	IF	Citations
66384	Orthorhombic <mml:math xmlns:mml="http://www.w3.org/1998/Math/MathML"><mml:msub><mml:mi>ScB</mml:mi><mml:mn>3</mml:mn></mml:msub></mm and hexagonal <mml:math xmlns:mml="http://www.w3.org/1998/Math/MathML"><mml:msub><mml:mi>ScB</mml:mi><mml:mn>6</mml:mn></mml:msub></mm with high hardness. Physical Review B, 2022, 105, .	1.1	10
66385	Magnetization reversal driven by electron localization-delocalization crossover in the inverse spinel <mml:math xmlns:mml="http://www.w3.org/1998/Math/MathML"><mml:mrow><mml:msub><mml:mi>Co</mml:mi><mml:mn>2</mml:mn></mml:mn></mml: Physical Review B, 2022, 105, .	1.1	5
66386	Interplay Between Electronic States and Structural Stability in Cation-Deficient VCoSb, NbCoSb, and TaCoSb Half-Heuslers. Journal of Electronic Materials, 2022, 51, 2043-2053.	1.0	5
66387	Tunable electronic properties and band alignments of MoSi2N4/GaN and MoSi2N4/ZnO van der Waals heterostructures. Applied Physics Letters, 2022, 120, .	1.5	33
66388	Dynamics of Hydrogen in Silicon at Finite Temperatures from First Principles. Physica Status Solidi (B): Basic Research, 2022, 259, .	0.7	7
66389	Resonant inelastic X-ray scattering as a probe of Jeffâ€‰=â€‰1/2 state in 3d transition-metal oxide. Npj Quantum Materials, 2022, 7, .	1.8	1
66390	Gradient Doping in Snâ€“Pb Perovskites by Barium Ions for Efficient Singleâ€Junction and Tandem Solar Cells. Advanced Materials, 2022, 34, e2110351.	11.1	62
66391	Regimented Charge Transport Phenomena in Semiconductive Self-Assembled Rhenium Nanotubes. ACS Applied Materials & Interfaces, 2022, 14, 12423-12433.	4.0	1
66392	Effect of Single-Atom Defects on Metal Surfaces on Porphycene Tautomerization. Journal of Physical Chemistry C, 2022, 126, 4871-4878.	1.5	1
66393	Disclosing the Nature of Asymmetric Interface Magnetism in Co/Pt Multilayers. ACS Applied Materials & Interfaces, 2022, 14, 12766-12776.	4.0	8
66394	Gadolinium Changes the Local Electron Densities of Nickel 3d Orbitals for Efficient Electrocatalytic CO ₂ Reduction. Angewandte Chemie, 0, , .	1.6	1
66395	Chemically Stable Low-Dimensional Electrides in Transition Metal-Rich Monochalcogenides: Theoretical and Experimental Explorations. Journal of the American Chemical Society, 2022, 144, 4496-4506.	6.6	8
66396	Role of Fluoride Doping in Low-Temperature Combustion-Synthesized ZrO_x Dielectric Films. ACS Applied Materials & Interfaces, 2022, 14, 12340-12349.	4.0	7
66397	QUAM-AFM: A Free Database for Molecular Identification by Atomic Force Microscopy. Journal of Chemical Information and Modeling, 2022, 62, 1214-1223.	2.5	8
66398	Ultralow-Resistivity Molybdenum-Carbide Thin Films Deposited by Plasma-Enhanced Atomic Layer Deposition Using a Cyclopentadienyl-Based Precursor. Chemistry of Materials, 2022, 34, 2576-2584.	3.2	9
66399	Palladium (Pd⁰) Loading-Controlled Catalytic Activity and Selectivity for Chlorophenol Hydrodechlorination and Hydrosaturation. Environmental Science & Technology, 2022, 56, 4447-4456.	4.6	22
66400	Adsorption of Oxygen to High Entropy Alloy Surfaces for up to 2 ML Coverage Using Density Functional Theory and Monte Carlo Calculations. Langmuir, 2022, 38, 3158-3169.	1.6	9
66401	Computational Mechanism of Methyl Levulinate Conversion to Î³-Valerolactone on UiO-66 Metal Organic Frameworks. ACS Sustainable Chemistry and Engineering, 2022, 10, 3567-3573.	3.2	8

#	Article	IF	Citations
66402	Selfâ€Regulated Chemical Substitution in a Highly Strained Perovskite Oxide. Advanced Functional Materials, 2022, 32, .	7.8	3
66403	Realization of Coexisting Charge Density Wave and Quantum Spin/Anomalous Hall State in Monolayer NbTe₂. Advanced Functional Materials, 2022, 32, .	7.8	11
66404	Phase Modulation Enabled High Thermoelectric Performance in Polycrystalline GeSe_{0.75}Te_{0.25}. Advanced Functional Materials, 2022, 32, .	7.8	7
66405	[LiCl₂]^{â^'} Superhalide: A New Charge Carrier for Graphite Cathode of Dualâ€Ion Batteries. Advanced Functional Materials, 2022, 32, .	7.8	14
66406	Catalytic Potential of Postâ€Transition Metal Doped Grapheneâ€Based Singleâ€Atom Catalysts for the CO₂ Electroreduction Reaction. ChemPhysChem, 2022, 23, .	1.0	6
66407	Pollution to solution: A universal electrocatalyst for reduction of all NOx-based species to NH3. Chem Catalysis, 2022, 2, 622-638.	2.9	27
66408	Controlling the Formation of Two Concomitant Polymorphs in Hg(II) Coordination Polymers. Inorganic Chemistry, 2022, 61, 4965-4979.	1.9	7
66409	Magnetic anisotropy and orbital magnetic moment in Co films and <mml:math xmlns:mml="http://www.w3.org/1998/Math/MathML"><mml:mi>Co</mml:mi><mml:mo>/</mml:mo><mml:mi>X</mml:mi></mml:ma bilayers (<mml:math) Tj ETQq1 1 0.784314 rgBT /Overlock 10 Tf 50 457 Td (xmlns:mml="http://www.w3.org/1998/Math/MathML"><m	1.1	8
66410	Insight into the underlying competitive mechanism for the shift of the charge neutrality point in a trilayer-graphene field-effect transistor. EScience, 2022, 2, 319-328.	25.0	14
66411	Wide-spectrum polarization-sensitive and fast-response photodetector based on 2D group IV-VI semiconductor tin selenide. Fundamental Research, 2022, 2, 985-992.	1.6	8
66412	Carbon Material With Ordered Sub-Nanometer Hole Defects. Frontiers in Chemistry, 2022, 10, 858154.	1.8	0
66413	Molecular Inclusion of Small Aging Products into the Hexanitrohexaazaisowurtzitane (CLâ€20) Lattice: Part I, Infrared Spectra. Propellants, Explosives, Pyrotechnics, 2022, 47, .	1.0	2
66414	Boosting Support Reducibility and Metal Dispersion by Exposed Surface Atom Control for Highly Active Supported Metal Catalysts. ACS Catalysis, 2022, 12, 4402-4414.	5.5	19
66415	Evaluation of performance of machine learning methods in mining structureâ€“property data of halide perovskite materials. Chinese Physics B, 2022, 31, 056302.	0.7	8
66416	Nonmetallic Active Sites on Nickel Phosphide in Oxygen Evolution Reaction. Nanomaterials, 2022, 12, 1130.	1.9	3
66417	Sound velocity softening in body-centered cubic niobium under shock compression. Physical Review B, 2022, 105, .	1.1	2
66418	Bridge-bond formation in aluminum and its alloys under high pressure. Physical Review Materials, 2022, 6, .	0.9	3
66419	Mesophase Transitions in [(C₂H₅)₄N][FeBrCl₃] and [(CH₃)₄N][FeBrCl₃] Ferroic Plastic Crystals. Chemistry of Materials, 2022, 34, 2585-2598.	3.2	5

#	Article	IF	Citations
66420	An assessment of density functionals for predicting CO2 adsorption in diamine-functionalized metalâ€“organic frameworks. Journal of Chemical Physics, 2022, 156, 154113.	1.2	7
66421	Coexistence of the hourglass and nodal-line dispersions in Nb3SiTe6 revealed by ARPES. IScience, 2022, 25, 103952.	1.9	0
66422	Continuous Kubo-Greenwood formula: Theory and numerical implementation. Physical Review E, 2022, 105, 035307.	0.8	1
66423	Phase stability of the argon crystal: first-principles study based on random phase approximation plus renormalized single excitation corrections. New Journal of Physics, 2022, 24, 033049.	1.2	4
66424	Sodium and potassium ion rich ferroelectric solid electrolytes for traditional and electrode-less structural batteries. APL Materials, 2022, 10, .	2.2	7
66425	Remarkable decrease in lattice thermal conductivity of transition metals borides TiB₂ by dimensional reduction. Nanotechnology, 2022, 33, 235706.	1.3	3
66426	Origin of enhanced thermal atomic layer etching of amorphous HfO₂. Journal of Vacuum Science and Technology A: Vacuum, Surfaces and Films, 2022, 40, 022604.	0.9	5
66427	First-Principles Study of Methanol Adsorption and Dissociation Reactivity on the Anatase TiO2(101) Surface: The Effect of Co doping and Oxygen Vacancy. Catalysis Letters, 0, , 1.	1.4	5
66428	Atomistic insights into highly active reconstructed edges of monolayer 2H-WSe2 photocatalyst. Nature Communications, 2022, 13, 1256.	5.8	35
66429	Liquid-phase sintering enabling mixed ionic-electronic interphases and free-standing composite cathode architecture toward high energy solid-state battery. Nano Research, 2022, 15, 6156-6167.	5.8	10
66430	Thermodynamic Study of Er-Bi and Er-Te Systems by Combination of First-Principles Calculations and the CALPHAD Method. Journal of Phase Equilibria and Diffusion, 2022, 43, 126-138.	0.5	2
66431	<scp>BSSEâ€corrected</scp> consistent Gaussian basis sets of <scp>tripleâ€zeta</scp> valence with polarization quality of the fifth period for <scp>solidâ€state</scp> calculations. Journal of Computational Chemistry, 2022, 43, 839-846.	1.5	20
66432	Multiâ€Center Magnon Excitations Open the Entire Brillouin Zone to Terahertz Magnetometry of Quantum Magnets. Advanced Quantum Technologies, 0, , 2200023.	1.8	2
66433	Atomically dispersed quintuple nitrogen and oxygen co-coordinated zirconium on graphene-type substrate for highly efficient oxygen reduction reaction. Cell Reports Physical Science, 2022, 3, 100773.	2.8	4
66434	Graph-based machine learning beyond stable materials and relaxed crystal structures. Physical Review Materials, 2022, 6, .	0.9	1
66435	Computational analysis of the optical response of ZnSe with d-orbital defects. Journal of Physics Condensed Matter, 2022, 34, 205402.	0.7	3
66436	Modulating the Electronic Structure of FeCo Nanoparticles in Nâ€Doped Mesoporous Carbon for Efficient Oxygen Reduction Reaction. Advanced Science, 2022, 9, e2200394.	5.6	52
66437	Using Featureâ€Assisted Machine Learning Algorithms to Boost Polarity in Leadâ€Free Multicomponent Niobate Alloys for Highâ€Performance Ferroelectrics. Advanced Science, 2022, 9, e2104569.	5.6	11

#	Article	IF	Citations
66438	Vibrational fingerprints of ferroelectric HfO2. Npj Quantum Materials, 2022, 7, .	1.8	24
66439	Geometries, electronic structures, and bonding properties of endohedral Groupâ€14 Zintl clusters <scp>TM</scp>@<scp>E₁₀</scp> (<scp>TM</scp> = Fe, Co, Ni; E = Ge, Sn, Pb). Journal of Path to high <mml:math xmlns:mml="http://www.w3.org/1998/Math/MathML"><mml:msub><mml:mi>T</mml:mi><mml:mi mathvariant="normal">c</mml:mi></mml:msub></mml:math> superconductivity via Rb substitution of guest metal atoms in the <mml:math xmlns:mml="http://www.w3.org/1998/Math/MathML"><mml:mrow><mml:mi>Sr</mml:mi><mml:msub><mml:mi mathvariant="normal">B</mml:mi><mml:mn>3</mml:mn></mml:msub><mml:msub><mml:mi mathvariant	1.5	3
66440		1.1	17
66441	In-situ STS studies and first principles calculations on bare and Sn adsorbed UHV exfoliated WS₂ layers. IOP Conference Series: Materials Science and Engineering, 2022, 1221, 012046.	0.3	2
66442	Performance Enhancement of APW+lo Calculations by Simplest Separation of Concerns. Computation, 2022, 10, 43.	1.0	4
66443	Two-Dimensional Oxide Alloys Probed at the Atomic Level: (V,Fe)₂O₃ Honeycomb Monolayers on Pt(111). Journal of Physical Chemistry C, 2022, 126, 5070-5078.	1.5	2
66444	The Influence of Alloying Segregation on Zinc-Induced Embrittlement at the Î±/Î³-Fe Interface. Metallurgical and Materials Transactions A: Physical Metallurgy and Materials Science, 2022, 53, 1604-1612.	1.1	2
66445	Structures and Electromagnetic Properties of Boron Nitride Nanoribbons Doped with Transition Metals. ChemPhysChem, 2022, , .	1.0	1
66446	Deeper insights into the photoluminescence properties and (photo)chemical reactivity of cadmium red (CdS1â^'xSex) paints in renowned twentieth century paintings by state-of-the-art investigations at multiple length scales. European Physical Journal Plus, 2022, 137, 1.	1.2	5
66447	Stepwise Dopant Selection Process for Highâ€Nickel Layered Oxide Cathodes. Advanced Energy Materials, 2022, 12, .	10.2	35
66448	Machine learning for impurity charge-state transition levels in semiconductors from elemental properties using multi-fidelity datasets. Journal of Chemical Physics, 2022, 156, 114110.	1.2	5
66449	Strong coupling between a topological insulator and a III-V heterostructure at terahertz frequency. Physical Review Materials, 2022, 6, .	0.9	7
66450	Study of the Temperature- and Pressure-Dependent Structural Properties of Alkali Hydrido-closo-borate Compounds. Inorganic Chemistry, 2022, 61, 5224-5233.	1.9	5
66451	Theoretical study of the interfacial properties of carbon nanotube/epoxy resin nanocomposites. Japanese Journal of Applied Physics, 0, , .	0.8	0
66452	A comparative study on the stability of the furfural molecule on the low index Ni, Pd and Pt surfaces. Royal Society Open Science, 2022, 9, 211516.	1.1	4
66453	Self-doping behavior and cation disorder in <mml:math xmlns:mml="http://www.w3.org/1998/Math/MathML"><mml:msub><mml:mi>MgSnN</mml:mi><mml:mn>2</mml:mn></mml:msub></mml:math> Physical Review B, 2022, 105, .	1.1	10
66454	Efficient and universal characterization of atomic structures through a topological graph order parameter. Npj Computational Materials, 2022, 8, .	3.5	11
66455	Stacking-Mediated Type-I/Type-II Transition in Two-Dimensional MoTe2/PtS2 Heterostructure: A First-Principles Simulation. Crystals, 2022, 12, 425.	1.0	17

#	Article	IF	Citations
66456	Deep UV transparent conductive oxide thin films realized through degenerately doped wide-bandgap gallium oxide. Cell Reports Physical Science, 2022, 3, 100801.	2.8	15
66457	Kohn anomaly and elastic softening in body-centered cubic molybdenum at high pressure. Physical Review B, 2022, 105, .	1.1	1
66458	Electronic and Near-Infrared-II Optical Properties of I-Doped Monolayer MoTe₂: A First-Principles Study. ACS Omega, 2022, 7, 11956-11963.	1.6	7
66459	Ferroelectric control of band structures in the two-dimensional Janus WSSe/In2Se3 van der Waals heterostructures. Physica E: Low-Dimensional Systems and Nanostructures, 2022, 142, 115256.	1.3	6
66460	Elaborated Reaction Pathway of Photothermal Catalytic CO ₂ Conversion with H ₂ O on Gallium Oxideâ€Đecorated and â€Đefective Surfaces. Chemistry - A European Journal, 2022, , .	1.7	1
66461	Ultralow thermal conductivity and anharmonic rattling in two-dimensional WB4 monolayer. Applied Physics Letters, 2022, 120, .	1.5	5
66462	Charge carrier nonadiabatic dynamics in non-metal doped graphitic carbon nitride. Journal of Chemical Physics, 2022, 156, 094702.	1.2	22
66463	Highly Asymmetric Graphene Layer Doping and Band Structure Manipulation in Rare Earthâ€“Graphene Heterostructure by Targeted Bonding of the Intercalated Gadolinium. Journal of Physical Chemistry C, 2022, 126, 6863-6873.	1.5	10
66464	Insight into the Mechanism and Effect of H₂O on CaO Sulfation by Density Functional Theory. Energy & Fuels, 2022, 36, 3749-3759.	2.5	0
66465	Fluoride Doping in Crystalline and Amorphous Indium Oxide Semiconductors. Chemistry of Materials, 0, , .	3.2	1
66466	Electron Correlation Enhances Orbital Polarization at a Ferromagnetic Metal/Insulator Interface: Depth-Resolved X-ray Magnetic Circular Dichroism and First-Principles Study. ACS Applied Electronic Materials, 2022, 4, 1794-1799.	2.0	5
66467	Optically Controlled Polarization Switching in an Organic Ferroelectric with Light- and Temperature-Triggered Phase Transitions. Chemistry of Materials, 2022, 34, 3067-3075.	3.2	8
66468	Tuning the Metalâ€“Insulator Transition in TiO₂/VO₂ Superlattices by Modifying the Layer Thickness or Inducing Defects. Journal of Physical Chemistry C, 2022, 126, 6016-6027.	1.5	4
66469	Photocatalytic Reduction of CO₂ with H₂O Mediated by Ce-Tailored Bismuth Oxybromide Surface Frustrated Lewis Pairs. ACS Catalysis, 2022, 12, 4016-4025.	5.5	95
66470	Tracking Electrochemical-Cycle-Induced Surface Structure Evolutions of Cathode Material LiMn₂O₄ with Improved Operando Raman Spectroscopy. Langmuir, 2022, 38, 3887-3895.	1.6	7
66471	Two-Dimensional Metal/Semiconductor Contact in a Janus MoSH/MoSi₂N₄ van der Waals Heterostructure. Journal of Physical Chemistry Letters, 2022, 13, 2576-2582.	2.1	36
66472	A first-principles study on the electrochemical reaction activity of 3d transition metal single-atom catalysts in nitrogen-doped graphene: Trends and hints. EScience, 2022, 2, 219-226.	25.0	51
66473	Anisotropic Dzyaloshinskiiâ€“Moriya Interaction and Topological Magnetism in Two-Dimensional Magnets Protected by P4ì…m2 Crystal Symmetry. Nano Letters, 2022, 22, 2334-2341.	4.5	26

#	Article	IF	Citations
66474	High-Throughput Screening of Rattling-Induced Ultralow Lattice Thermal Conductivity in Semiconductors. Journal of the American Chemical Society, 2022, 144, 4448-4456.	6.6	26
66475	Toward Rational Design of Dual-Metal-Site Catalysts: Catalytic Descriptor Exploration. ACS Catalysis, 2022, 12, 3420-3429.	5.5	40
66476	Chemical Control of Magnetic Ordering in Hybrid Feâ€“Cl Layered Double Perovskites. Chemistry of Materials, 2022, 34, 2813-2823.	3.2	27
66477	Synthesis of Mg Alkoxide Nanowires from Mg Alkoxide Nanoparticles upon Ligand Exchange. ACS Applied Materials & Interfaces, 2022, 14, 13820-13827.	4.0	0
66478	Using Hyperoptimized Tensor Networks and First-Principles Electronic Structure to Simulate the Experimental Properties of the Giant {Mn₈₄} Torus. Journal of Physical Chemistry Letters, 2022, 13, 2365-2370.	2.1	3
66479	Mechanical strength and band alignment of BAs/GaN heterojunction polar interfaces: A first-principles calculation study. Physical Review Materials, 2022, 6, .	0.9	2
66480	Spin-polarized topological phases in a ferromagnetic <mml:math xmlns:mml="http://www.w3.org/1998/Math/MathML"><mml:mrow><mml:msub><mml:mi>Bi</mml:mi><mml:mn>2</mml:mn></mml:m bilayer tuned by electric and magnetic fields. Physical Review B, 2022, 105, .	2.1	2
66481	Single-site Pt-doped RuO ₂ hollow nanospheres with interstitial C for high-performance acidic overall water splitting. Science Advances, 2022, 8, eabl9271.	4.7	117
66482	Ab Initio Study of Chiral Phonons in Ternary YAlSi Compound. Crystals, 2022, 12, 436.	1.0	4
66483	A single-Pt-atom-on-Ru-nanoparticle electrocatalyst for CO-resilient methanol oxidation. Nature Catalysis, 2022, 5, 231-237.	16.1	133
66484	Ternary pentagonal BNSi monolayer: Two-dimensional structure with potentially high carrier mobility and strong excitonic effects for photocatalytic applications. Physical Review Materials, 2022, 6, .	0.9	15
66485	Pressure-Induced Structural Phase Transition and Metallization of CrCl₃ under Different Hydrostatic Environments up to 50.0 GPa. Inorganic Chemistry, 2022, 61, 4852-4864.	1.9	14
66486	A Theoretical Discussion on the Stability of (O₂)^{â^'} and (S₂)^{â^'} Species in KCl and KBr Salts: Luminescence Spectra and Defect Energy Formation. Journal of Physical Chemistry C, 2022, 126, 6060-6064.	1.5	0
66487	Hydrogen Storage Performance of Preferentially Oriented Mg/rGO Hybrids. Chemistry of Materials, 2022, 34, 2963-2971.	3.2	8
66488	Ruthenium Icosahedra and Ultrathin Platelets: The Role of Surface Chemistry on the Nanoparticle Structure. Chemistry of Materials, 2022, 34, 2931-2944.	3.2	5
66489	Adsorption Geometries and Electronic Properties of a Dipolar Phosphonate-Based Monolayer on the NiO Surface. Journal of Physical Chemistry C, 2022, 126, 5793-5804.	1.5	1
66490	First-Principles Analysis of the Oxide-Ion Conduction Mechanism in Si-Deficient Lanthanum Silicate Apatite. Journal of Physical Chemistry C, 2022, 126, 5805-5812.	1.5	3
66491	Collective Motion Improves the Stability and Charge Carrier Lifetime of Metal Halide Perovskites: A Phonon-Resolved Nonadiabatic Molecular Dynamics Study. Journal of Physical Chemistry Letters, 2022, 13, 3016-3022.	2.1	12

#	Article	IF	Citations
66492	Nearâ€Infrared and Visibleâ€Range Optoelectronics in 2D Hybrid Perovskite/Transition Metal Dichalcogenide Heterostructures. Advanced Materials Interfaces, 2022, 9, .	1.9	6
66493	Metalâ€“Metal Bonding as an Electrode Design Principle in the Low-Strain Cluster Compound LiScMo₃O₈. Journal of the American Chemical Society, 2022, 144, 5841-5854.	6.6	11
66494	Insights into the Hydrogen Evolution Reaction on 2D Transition-Metal Dichalcogenides. Journal of Physical Chemistry C, 2022, 126, 5151-5158.	1.5	32
66495	Formation of Graphene Nanoscrolls and Their Electronic Structures Based on Ab Initio Calculations. Journal of Physical Chemistry Letters, 2022, 13, 2500-2506.	2.1	3
66496	A Liquidâ€Metal Electrocatalyst as a Selfâ€Healing Anchor to Suppress Polysulfide Shuttling in Lithiumâ€Sulfur Batteries. Batteries and Supercaps, 2022, 5, .	2.4	1
66497	Strain and electric field tuning the electronic properties of two-dimensional MoS2/ScCl3 van der Waals heterostructure. Journal of Materials Science: Materials in Electronics, 2022, 33, 10461-10470.	1.1	1
66498	Thermal Properties of 2D Dirac Materials MN₄ (M = Be and Mg): A First-Principles Study. ACS Omega, 2022, 7, 10812-10819.	1.6	13
66499	First-principles calculations of high-pressure physical properties anisotropy for magnesite. Scientific Reports, 2022, 12, 3691.	1.6	3
66500	Activation of CO2 on the Surfaces of Bare, Ti-Adsorbed and Ti-Doped C60. Fuels, 2022, 3, 176-183.	1.3	1
66501	Computational Insight into TMâ€“N_x Embedded Graphene Bifunctional Electrocatalysts for Oxygen Evolution and Reduction Reactions. ACS Physical Chemistry Au, 2022, 2, 305-315.	1.9	10
66502	<mml:math xmlns:mml="http://www.w3.org/1998/Math/MathML"><mml:mi>p</mml:mi></mml:math> -type behavior of CrN thin films via control of point defects. Physical Review B, 2022, 105, .	1.1	4
66503	Pt Atom on the Wall of Atomic Layer Deposition (ALD)â€Made MoS₂ Nanotubes for Efficient Hydrogen Evolution. Small, 2022, 18, e2105129.	5.2	29
66504	Measurement of electronic structure in van der Waals ferromagnet Fe_{5-x}GeTe₂. Chinese Physics B, 0, , .	0.7	1
66505	Interfacial triferroicity in monolayer chromium dihalide. Physical Review B, 2022, 105, .	1.1	5
66506	Tuning the Bandgap of Topological Edge States by Inclinedâ€Electric Field. Physica Status Solidi - Rapid Research Letters, 2022, 16, .	1.2	3
66507	Controlling transition metal atomic ordering in two-dimensional Mo_{1â^'x}W _x S₂ alloys. 2D Materials, 2022, 9, 025016.	2.0	9
66508	High-surface-area titanium nitride nanosheets as zinc anode coating for dendrite-free rechargeable aqueous batteries. Science China Materials, 2022, 65, 1771-1778.	3.5	21
66509	Stackingâ€Fault Enhanced Oxygen Redox in Li₂MnO₃. Advanced Energy Materials, 2022, 12, .	10.2	17

#	Article	IF	Citations
66510	A DFT-Based Descriptor to Predict the Water Vapor Corrosion Resistance of Rare-Earth Monosilicates. Materials, 2022, 15, 2414.	1.3	0
66511	Observation of multiple nodal lines in SmSbTe. Physical Review Materials, 2022, 6, .	0.9	14
66512	The Theoretical Study of Unexpected Magnetism in 2D Si-Doped AlN. Frontiers in Physics, 2022, 10, .	1.0	1
66513	The interplay of intra- and intermolecular errors in modeling conformational polymorphs. Journal of Chemical Physics, 2022, 156, 104112.	1.2	14
66514	Electrocatalytic Reduction of N₂ to NH₃ Over Defective 1Tâ€²â€WX₂ (X=S, Se, Te) Monolayers. ChemSusChem, 2022, 15, .	3.6	6
66515	Insights into catalytic behavior of TiMgn (n=1â€“12) nanoclusters in hydrogen storage and dissociation process: A DFT investigation. International Journal of Hydrogen Energy, 2022, 47, 13418-13429.	3.8	15
66516	Electronic and Optical Properties of the Typeâ€II GaN/SiH van der Waals Heterostructure: A Firstâ€Principles Study. Physica Status Solidi (B): Basic Research, 2022, 259, .	0.7	3
66517	Niobium-doped cobalt phosphide nanowires realizing enhanced electrocatalytic activity for overall water splitting. International Journal of Hydrogen Energy, 2022, 47, 13251-13260.	3.8	17
66518	Interstitial boron-triggered electron-deficient Os aerogels for enhanced pH-universal hydrogen evolution. Nature Communications, 2022, 13, 1143.	5.8	152
66519	Epitaxial growth of an atom-thin layer on a LiNi0.5Mn1.5O4 cathode for stable Li-ion battery cycling. Nature Communications, 2022, 13, 1565.	5.8	32
66520	Dynamical structural instability and its implications for the physical properties of infinite-layer nickelates. Physical Review B, 2022, 105, .	1.1	9
66521	First-principles core energies of isolated basal and prism screw dislocations in magnesium. Materials Research Letters, 2022, 10, 360-368.	4.1	4
66522	Atomically Precise Delineation of As Antisite Defect States from Undoped Gallium Arsenide Host Lattice by Scanning Tunneling Microscopy and Spectroscopy Measurements and Density Functional Theory Calculations. Physica Status Solidi (B): Basic Research, 0, , 2100652.	0.7	1
66523	Computation-guided design and preparation of durable and efficient WC-Mo2C heterojunction for hydrogen evolution reaction. Cell Reports Physical Science, 2022, 3, 100784.	2.8	6
66524	General embedded cluster protocol for accurate modeling of oxygen vacancies in metal-oxides. Journal of Chemical Physics, 2022, 156, 124704.	1.2	9
66525	Light-emitting field-effect transistors with EQE over 20% enabled by a dielectric-quantum dots-dielectric sandwich structure. Science Bulletin, 2022, 67, 529-536.	4.3	23
66526	Intrinsic electrochemical activity of Ni in Ni3Sn4 anode accommodating high capacity and mechanical stability for fast-charging lithium-ion batteries. Journal of Energy Chemistry, 2022, 71, 470-477.	7.1	7
66527	Combined first-principles-Monte Carlo analysis to evaluate the effect of surface hydrogen on the secondary electron yield of nickel. Journal of Applied Physics, 2022, 131, .	1.1	6

#	Article	IF	Citations
66528	Giant Chern number of a Weyl nodal surface without upper limit. Physical Review B, 2022, 105, .	1.1	4
66529	Heterointerface Created on Auâ€Clusterâ€Loaded Unilamellar Hydroxide Electrocatalysts as a Highly Active Site for the Oxygen Evolution Reaction. Advanced Materials, 2022, 34, e2110552.	11.1	36
66530	Excited electron and spin dynamics in topological insulator: A perspective from ab initio non-adiabatic molecular dynamics. Fundamental Research, 2022, 2, 506-510.	1.6	2
66531	Structural phase transitions and Raman identifications of the layered van der Waals magnet <mml:math xmlns:mml="http://www.w3.org/1998/Math/MathML"><mml:msub><mml:mi>CrI</mml:mi><mml:mn>2</mml:mn></mml:msub></m Physical Review B, 2022, 105, .	1.1	2
66532	Photoluminescence of Cis-Polyacetylene Semiconductor Material. Applied Sciences (Switzerland), 2022, 12, 2830.	1.3	3
66533	Addressing Dynamics at Catalytic Heterogeneous Interfaces with DFT-MD: Anomalous Temperature Distributions from Commonly Used Thermostats. Journal of Physical Chemistry Letters, 2022, 13, 2644-2652.	2.1	12
66534	Probing borophene oxidation at the atomic scale. Nanotechnology, 2022, 33, 235702.	1.3	7
66535	Influence of heat treatments in H2 and Ar on the E1 center in Î²-Ga2O3. Journal of Applied Physics, 2022, 131, .	1.1	11
66536	Ru/NC heterointerfaces boost energy-efficient production of green H2 over a wide pH range. Nano Research, 2022, 15, 5134-5142.	5.8	21
66537	Synthesis of a magnetic Ï€-extended carbon nanosolenoid with Riemann surfaces. Nature Communications, 2022, 13, 1239.	5.8	20
66538	Mechanism of Oxygen Reduction Reaction in Alkaline Medium on Nitrogenâ€Doped Graphyne and Graphdiyne Families: A First Principles Study. ChemPhysChem, 2022, 23, e202100900.	1.0	2
66539	Heterogeneous relational message passing networks for molecular dynamics simulations. Npj Computational Materials, 2022, 8, .	3.5	14
66540	The equation of state and shock-driven decomposition of polymethylmethacrylate (PMMA). Journal of Applied Physics, 2022, 131, .	1.1	5
66541	Good performance of Sc (0001) surface adsorbing CO molecule. Journal of the Korean Physical Society, 0, , 1.	0.3	0
66542	Native Vacancy Defects in MXenes at Etching Conditions. Chemistry of Materials, 2022, 34, 2896-2906.	3.2	23
66543	Disproportionation of <mml:math xmlns:mml="http://www.w3.org/1998/Math/MathML" display="inline"><mml:mrow><mml:msub><mml:mrow><mml:mi>SO</mml:mi></mml:mrow><mml:mrow><mml:mn>2</mml:mn></mml:mrow></mml:msub></mml:mrow></mml:math> at High Pressure and Temperature. Physical Review Letters, 2022, 128, 106001.	2.9	13
66544	Impact of band-bending on the k-resolved electronic structure of Si-doped GaN. Physical Review Research, 2022, 4, .	1.3	3
66545	Deep ultra-violet plasmonics: exploiting momentum-resolved electron energy loss spectroscopy to probe germanium. Optics Express, 2022, 30, 12630.	1.7	2

#	Article	IF	Citations
66546	Electronic and optical properties of fully fluorinated Janus MoSSe monolayer. , 2022, , 207199.		0
66547	Strong four-phonon scattering in monolayer and hydrogenated bilayer BAs with horizontal mirror symmetry. Applied Physics Letters, 2022, 120, .	1.5	30
66548	Formation and local structure of framework Al Lewis sites in beta zeolites. Journal of Chemical Physics, 2022, 156, 104702.	1.2	2
66549	Breakdown of atomic spin-orbit coupling picture in an apparently isolated pseudo-one-dimensional iridate: <mml:math xmlns:mml="http://www.w3.org/1998/Math/MathML"><mml:mrow><mml:msub><mml:mi>Sr</mml:mi><mml:mn>3</mml:mn></mml:msub></mml:mrow></mml:math> Physical Review B, 2022, 105, .	1.1	2
66550	Origin of Efficiency Enhancement by Lattice Expansion in Hybrid-Perovskite Solar Cells. Physical Review Letters, 2022, 128, 136401.	2.9	28
66551	Superconducting ScP4 with a novel phosphorus framework. Applied Physics A: Materials Science and Processing, 2022, 128, 1.	1.1	2
66552	Two-Dimensional Palladium Phosphoronitride for Oxygen Reduction. ACS Applied Materials & Interfaces, 2022, 14, 12156-12167.	4.0	10
66553	A Local Atomic Mechanism for Monoclinic-Tetragonal Phase Boundary Creation in Li-Doped Na_{0.5}K_{0.5}NbO₃ Ferroelectric Solid Solution. Inorganic Chemistry, 2022, 61, 4335-4349.	1.9	9
66554	Molten Salt Thermal Treatment Synthesis of S-Doped V₂CT_x and Its Performance as a Cathode in Aqueous Zn-Ion Batteries. ACS Applied Materials & Interfaces, 2022, 14, 14482-14491.	4.0	11
66555	Ab Initio Exploration of Energetically and Kinetically Favorable ORR Activity on a 1T-ZrO₂ Monolayer for a Nonaqueous Lithiumâ€“Oxygen Battery. ACS Applied Materials & Interfaces, 2022, 14, 13410-13418.	4.0	0
66556	Self-replicating Biophotoelectrochemistry System for Sustainable CO Methanation. Environmental Science & Technology, 2022, 56, 4587-4596.	4.6	9
66557	Superionic Conduction in the Plastic Crystal Polymorph of Na₄P₂S₆. ACS Energy Letters, 2022, 7, 1403-1411.	8.8	9
66558	Gadolinium Changes the Local Electron Densities of Nickel 3d Orbitals for Efficient Electrocatalytic CO₂ Reduction. Angewandte Chemie - International Edition, 2022, 61, .	7.2	32
66559	The Influence of Surface Chemistry on Critical Current Density for Garnet Electrolyte. Advanced Functional Materials, 2022, 32, .	7.8	22
66560	The Role of Undercoordinated Sites on Zinc Electrodes for CO₂ Reduction to CO. Advanced Functional Materials, 2022, 32, .	7.8	30
66561	Thicknessâ€Driven Morphotropic Phase Transition in Metastable Ferroelectric CaTiO ₃ Films. Advanced Electronic Materials, 0, , 2101398.	2.6	2
66562	Coexistence of Ferroelectriclike Polarization and Dirac-like Surface State in <mml:math xmlns:mml="http://www.w3.org/1998/Math/MathML" display="inline"><mml:mrow><mml:msub><mml:mrow><mml:mi>TaNiTe</mml:mi></mml:mrow><mml:mrow><mml:mn>5</mml:mn></mml:mrow> Physical Review Letters, 2022, 128, 106802.	2.9	7
66563	Boosting Zn||I2 Batteryâ€™s Performance by Coating a Zeolite-Based Cation-Exchange Protecting Layer. Nano-Micro Letters, 2022, 14, 82.	14.4	62

#	Article	IF	Citations
66564	Uncovering the Mechanism of the Hydrogen Poisoning on Ru Nanoparticles via Density Functional Theory Calculations. Catalysts, 2022, 12, 331.	1.6	7
66565	Potassium hydride-intercalated graphite as an efficient heterogeneous catalyst for ammonia synthesis. Nature Catalysis, 2022, 5, 222-230.	16.1	37
66566	Chemical Potential Diagram Guided Rational Tuning of Electrical Properties: A Case Study of CsPbBr₃ for Xâ€ray Detection. Advanced Materials, 2022, 34, e2110252.	11.1	24
66567	Magnetization-driven Lifshitz transition and charge-spin coupling in the kagome metal YMn6Sn6. Communications Physics, 2022, 5, .	2.0	10
66568	Atomic Molybdenum for Synthesis of Ammonia with 50% Faradic Efficiency. Small, 2022, 18, e2106327.	5.2	20
66569	Firstâ€principles design of Naâ€ion superionic conductors: Interstitialâ€based Na diffusion in NaCuZrS3. Chemistry - A European Journal, 2022, , .	1.7	0
66570	Firstâ€Principles Studies on the Atomistic Properties of Metallic Magnesium as Anode Material in Magnesiumâ€ion Batteries. ChemSusChem, 2022, 15, .	3.6	9
66571	Single Atoms Anchored in Hexagonal Boron Nitride for Propane Dehydrogenation from First Principles. ChemCatChem, 2022, 14, .	1.8	6
66572	Oxygen vacancies confined in porous Co3V2O8 sheets for durable and high-energy aqueous sodium-ion capacitors. Nano Research, 2022, 15, 5123-5133.	5.8	14
66573	Linear magnetoresistance induced by mobility fluctuations in iodine-intercalated tungsten ditelluride. Physical Review B, 2022, 105, .	1.1	5
66574	Excellently balanced water-intercalation-type heat-storage oxide. Nature Communications, 2022, 13, 1452.	5.8	5
66575	Direct observation of ferroelectricity in two-dimensional MoS2. Npj 2D Materials and Applications, 2022, 6, .	3.9	30
66576	3â€Dimensional Scanning of Entire Unit Cells in Single Nanoparticles.. ChemNanoMat, 2022, 8, .	1.5	0
66577	High-temperature superconductivity below 100 GPa in ternary C-based hydride <mml:math xmlns:mml="http://www.w3.org/1998/Math/MathML"><mml:mrow><mml:mi>M</mml:mi><mml:msub><mml:mi mathvariant="normal">C</mml:mi><mml:mn>2</mml:mn></mml:msub><mml:msub><mml:mi mathvariant="normal">H</mml:mi><mml:mn>8</mml:mn></mml:msub></mml:mrow></mml:math> with		

#	Article	IF	Citations
66582	Effects of LiCl template amount on structure, morphology, and electrochemical performance of porous Si@C anodes. Ionics, 0, , 1.	1.2	0
66583	Microscopic EDL structures and chargeâ€“potential relation on stepped platinum surface: Insights from the ab initio molecular dynamics simulations. Journal of Chemical Physics, 2022, 156, 104701.	1.2	12
66584	Tetrahedral Alignment and Covalent Bonding Enable Fast Sodium Conduction in Na₃XS₄ (X = P, V). Journal of Physical Chemistry C, 2022, 126, 6161-6170.	1.5	3
66585	Periodic DFTB for Supported Clusters: Implementation and Application on Benzene Dimers Deposited on Graphene. Computation, 2022, 10, 39.	1.0	6
66586	Understanding the piezoelectric origin of bismuth layer-structured ferroelectric polycrystal using first-principle method. Journal of the European Ceramic Society, 2022, 42, 3865-3876.	2.8	7
66587	Large Magnetic Gap in a Designer Ferromagnetâ€“Topological Insulatorâ€“Ferromagnet Heterostructure. Advanced Materials, 2022, 34, e2107520.	11.1	17
66588	Hydrodynamically enhanced thermal transport due to strong interlayer interactions: A case study of strained bilayer graphene. Physical Review B, 2022, 105, .	1.1	15
66589	Selective CO-to-acetate electroreduction via intermediate adsorption tuning on ordered Cuâ€“Pd sites. Nature Catalysis, 2022, 5, 251-258.	16.1	118
66590	Direct imaging and mechanism study of C6 Î±-olefin adsorption on faujasite and Linde Type A zeolites. Nano Research, 2022, 15, 5322-5330.	5.8	6
66591	First principles study of 2D half-metallic ferromagnetism in Janus Mn2XSb (X = As, P) monolayers. Applied Physics Letters, 2022, 120, .	1.5	10
66592	The Speciation and Coordination of a Deep Earth Carbonateâ€Silicateâ€Metal Melt. Journal of Geophysical Research: Solid Earth, 2022, 127, .	1.4	4
66593	Experimental Observations versus Firstâ€Principles Calculations for Niâ€“Mnâ€“Ga Ferromagnetic Shape Memory Alloys: A Review. Physica Status Solidi - Rapid Research Letters, 2022, 16, .	1.2	5
66594	Chemical environment dependent Stabilities, electronic properties and diffusions behaviors of intrinsic point defects in novel Two-Dimensional MoSi2N4 monolayer. Applied Surface Science, 2022, 592, 153214.	3.1	6
66595	Comparison and theoretical analysis of the photocatalytic performance of Ni2+-Fe3+-CO32â^'-LDHs and Ni2+-Al3+-CO32â^'-LDHs. Journal of Molecular Structure, 2022, 1262, 132969.	1.8	1
66596	Exploring far-from-equilibrium ultrafast polarization control in ferroelectric oxides with excited-state neural network quantum molecular dynamics. Science Advances, 2022, 8, eabk2625.	4.7	8
66597	Experimental and first-principles studies of superconductivity in topological nodal line semimetal SnTaS₂. Superconductor Science and Technology, 2022, 35, 064001.	1.8	2
66598	Three-dimensional hierarchical nanoporous (Mn,Ni)-Doped Cu2S architecture towards high-efficiency overall water splitting. International Journal of Hydrogen Energy, 2022, 47, 11827-11840.	3.8	7
66599	Atomic reconfiguration among tri-state transition at ferroelectric/antiferroelectric phase boundaries in Pb(Zr,Ti)O3. Nature Communications, 2022, 13, 1390.	5.8	17

#	Article	IF	Citations
66600	Exceptionally active and stable RuO2 with interstitial carbon for water oxidation in acid. CheM, 2022, 8, 1673-1687.	5.8	52
66601	Spin Properties and Metal-Semiconductor Transition of Nitrogen-Containing Zigzag Graphyne Nanoribbon Caused by Magnetic Atom Doping. Frontiers in Materials, 2022, 9, .	1.2	1
66602	Achieving complete electrooxidation of ethanol by single atomic Rh decoration of Pt nanocubes. Proceedings of the National Academy of Sciences of the United States of America, 2022, 119, e2112109119.	3.3	40
66603	Threshold potentials for fast kinetics during mediated redox catalysis of insulators in Liâ€“O2 and Liâ€“S batteries. Nature Catalysis, 2022, 5, 193-201.	16.1	51
66604	Effect of residual strain on magnetic properties and Hall effect in chiral antiferromagnet Mn₃Sn. Journal Physics D: Applied Physics, 2022, 55, 275001.	1.3	6
66605	High Mixing Entropy Enhanced Energy States in Metallic Glasses. Chinese Physics Letters, 2022, 39, 046401.	1.3	5
66606	First-principles prediction of magnetic properties in Fe(Co,Ni)(C,N)_{0.5} alloys. Applied Physics Letters, 2022, 120, 132405.	1.5	10
66607	Spatially controlled graphene- <mml:math xmlns:mml="http://www.w3.org/1998/Math/MathML"><mml:msub><mml:mrow><mml:mi>MoSe</mml:mi></mml:mrow><mml:mn> lateral heterostructure for sensing applications: Insights from first-principles calculations. Physical Review B, 2022, 105, .	1.1	2
66608	Detailed Characterization of a Fully Additive Covalent Bonded PCB Manufacturing Process (SBU-CBM) Tj ETQq0 0 0 rgBT /Overlock 10 T	1.3	1
66609	Geometricalâ€, Electronicâ€•and Optical Properties of Vanadium Dioxide: A Theoretical Perspective from Metaâ€GGA SCAN. ChemistrySelect, 2022, 7, .	0.7	4
66610	Localized Phonon Densities of States at Grain Boundaries in Silicon. Microscopy and Microanalysis, 2022, 28, 672-679.	0.2	2
66611	Electronegativity and chemical hardness of elements under pressure. Proceedings of the National Academy of Sciences of the United States of America, 2022, 119, e2117416119.	3.3	25
66612	Degenerated Hole Doping and Ultraâ€Low Lattice Thermal Conductivity in Polycrystalline SnSe by Nonequilibrium Isovalent Te Substitution. Advanced Science, 2022, 9, e2105958.	5.6	7
66613	Quasi-Freestanding Bilayer Borophene on Ag(111). Nano Letters, 2022, 22, 3488-3494.	4.5	31
66614	Supramolecular Tiling of a Conformationally Flexible Precursor. Journal of Physical Chemistry Letters, 2022, 13, 2180-2186.	2.1	9
66615	LiAlTt (Tt = Si, Ge): Experimental and Theoretical Reinvestigation on the Thermoelectric Properties of 8-Valence-Electron Half-Heusler Compounds. ACS Applied Energy Materials, 2022, 5, 3793-3799.	2.5	5
66616	Construction and Sensing Amplification of Raspberry-Shaped MOF@MOF. Inorganic Chemistry, 2022, 61, 4705-4713.	1.9	13
66617	Electrical Regulation of CO₂ Adsorption in the Metalâ€“Organic Framework MIL-53. ACS Applied Materials & Interfaces, 2022, 14, 13904-13913.	4.0	6

#	Article	IF	Citations
66618	Existence of BeCN₂ and Its First-Principles Phase Diagram: Be and C Introducing Structural Diversity. Journal of the American Chemical Society, 2022, 144, 5155-5162.	6.6	12
66619	Synergetic Nanoarchitectonics of Defects and Cocatalysts in Oxygen-Vacancy-Rich BiVO₄/reduced graphene oxide Mottâ€“Schottky Heterostructures for Photocatalytic Water Oxidation. ACS Applied Materials & Interfaces, 2022, 14, 12180-12192.	4.0	9
66620	Accelerated Ionic and Charge Transfer through Atomic Interfacial Electric Fields for Superior Sodium Storage. ACS Nano, 2022, 16, 4775-4785.	7.3	28
66621	Fully Optical Modulation of the Two-Dimensional Electron Gas at the Î³-Al₂O₃/SrTiO₃ Interface. Journal of Physical Chemistry Letters, 2022, 13, 2976-2985.	2.1	9
66622	Revealing Elusive Intermediates of Platinum Cathodic Corrosion through DFT Simulations. Journal of Physical Chemistry Letters, 2022, 13, 3047-3052.	2.1	8
66623	Reactivity of Surface Lewis and BrÃ¸nsted Acid Sites in Zeolite Catalysis: A Computational Case Study of DME Synthesis Using H-SSZ-13. Journal of Physical Chemistry C, 2022, 126, 5896-5905.	1.5	16
66624	Size-Dependent Effects in Fullerene-Based Catalysts for Nonaqueous Liâ€“Air Battery Applications. ACS Applied Energy Materials, 2022, 5, 3380-3391.	2.5	10
66625	Improving Lattice Rigidity and Charge Carrier Lifetime by Engineering Spacer Cation of Ruddlesdenâ€“Popper Perovskites: A Time-Domain Ab Initio Study. Journal of Physical Chemistry Letters, 2022, 13, 2718-2724.	2.1	11
66626	Intrinsic Ferromagnetism of Two-Dimensional (2D) MnO₂ Revisited: A Many-Body Quantum Monte Carlo and DFT+U Study. Journal of Physical Chemistry C, 2022, 126, 5813-5821.	1.5	6
66627	Adsorption of Transition-Metal Clusters on Graphene and N-Doped Graphene: A DFT Study. Langmuir, 2022, 38, 3694-3710.	1.6	23
66628	Proximity Effect on the Reactivity of Dioxygen Activated over Distant Binuclear Fe Sites in Zeolite Matrices. Journal of Physical Chemistry C, 2022, 126, 4854-4861.	1.5	0
66629	Computational Investigation of Orderly Doped Transition Metal Dichalcogenides: Implications for Nanoscale Optoelectronic Devices. ACS Applied Nano Materials, 2022, 5, 3824-3831.	2.4	5
66630	Strategy for Fabricating Ultrathin Au Film Electrodes with Ultralow Optoelectrical Losses and High Stability. ACS Applied Materials & Interfaces, 2022, 14, 12797-12811.	4.0	9
66631	Enhanced Gas Sensing Performance of rGO Wrapped Crystal Facet-Controlled Co₃O₄ Nanocomposite Heterostructures. Journal of Physical Chemistry C, 2022, 126, 4879-4888.	1.5	9
66632	Searching for Band-Dispersive and Defect-Tolerant Semiconductors from Element Substitution in Topological Materials. Journal of the American Chemical Society, 2022, 144, 4685-4694.	6.6	4
66633	A comparison of waterâ€“gas shift reaction on ZnO $$left(10overline{1 }0ight)$$ surface and 6Cu cluster deposited over ZnO $$left(10overline{1 }0ight)$$ surface using density functional theory studies. Journal of Molecular Modeling, 2022, 28, 84.	0.8	4
66634	Suppressing Oxygen-Induced Deterioration of Metal Halide Perovskites by Alkaline Earth Metal Doping: A Quantum Dynamics Study. Journal of the American Chemical Society, 2022, 144, 5543-5551.	6.6	29
66635	Orally Fast-Disintegrating Resveratrol/Cyclodextrin Nanofibrous Films as a Potential Antioxidant Dietary Supplement. ACS Food Science & Technology, 2022, 2, 568-580.	1.3	10

#	Article	IF	Citations
66636	A first principles investigation of ternary and quaternary IIâ€“VI zincblende semiconductor alloys. Modelling and Simulation in Materials Science and Engineering, 2022, 30, 044001.	0.8	1
66637	Theoretical Calculation and Performance Analysis of Four-Element Metal Nitride Coatings Based on First Principles. Journal of Materials Engineering and Performance, 2022, 31, 8084-8093.	1.2	2
66638	Organic frameworks confined Cu single atoms and nanoclusters for tandem electrocatalytic CO₂ reduction to methane. SmartMat, 2022, 3, 183-193.	6.4	35
66639	Interface and M³⁺/M²⁺ Valence Dualâ€Engineering on Nickel Cobalt Sulfoselenide/Black Phosphorus Heterostructure for Efficient Water Splitting Electrocatalysis. Energy and Environmental Materials, 2023, 6, .	7.3	23
66640	The Sensitivity of Metal Oxide Electrocatalysis to Bulk Hydrogen Intercalation: Hydrogen Evolution on Tungsten Oxide. Journal of the American Chemical Society, 2022, 144, 6420-6433.	6.6	32
66641	Single-molecule field effect and conductance switching driven by electric field and proton transfer. Science Advances, 2022, 8, eabm3541.	4.7	22
66642	Nontrivial Doping Evolution of Electronic Properties in Isingâ€Superconducting Alloys. Advanced Materials, 2022, , 2200492.	11.1	9
66643	Phase Transitions and Amorphization of M2AgF4 (M = Na, K, Rb) Compounds at High Pressure. Crystals, 2022, 12, 458.	1.0	1
66644	Enhancing the performance of traditional La2NiO4+x cathode for proton-conducting solid oxide fuel cells with Zn-doping. Ceramics International, 2022, 48, 19626-19632.	2.3	30
66645	A dataset of 175k stable and metastable materials calculated with the PBEsol and SCAN functionals. Scientific Data, 2022, 9, 64.	2.4	8
66646	Magnetic Properties of A2Ni2TeO6 (A = K, Li): Zigzag Order in the Honeycomb Layers of Ni2+ Ions Induced by First and Third Nearest-Neighbor Spin Exchanges. Materials, 2022, 15, 2563.	1.3	8
66647	Band offset trends in IVâ€“VI layered semiconductor heterojunctions. Journal of Physics Condensed Matter, 2022, 34, 195003.	0.7	3
66648	Biotemplate Fabrication of Hollow Tubular Ce_xSr_{1â€“x}TiO₃ with Regulable Surface Acidity and Oxygen Mobility for Efficient Destruction of Chlorobenzene: Intrinsic Synergy Effect and Reaction Mechanism. Environmental Science & Technology, 2022, 56, 5796-5807.	4.6	45
66649	Homologous Alkali Metal Copper Rare-Earth Chalcogenides A₂Cu_{2n}Ln₄Q_{7+n} (n = 1, 2, 3). Chemistry of Materials, 2022, 34, 3409-3422.	3.2	6
66650	Reduction of Transition-Metal Columbite-Tantalite as a Highly Efficient Electrocatalyst for Water Splitting. ACS Applied Materials & Interfaces, 2022, 14, 15090-15102.	4.0	3
66651	Revealing the Origin of Nitrogen Electroreduction Activity of Molybdenum Disulfide Supported Iron Atoms. Journal of Physical Chemistry C, 2022, 126, 5180-5188.	1.5	22
66652	Short-Range to Long-Range Ni/Mn Order in LiMn_{2â€“x}Ni_xO₄ (0.38 â‰¤ x â‰¤ 0.50) Positive Electrode Materials: A Gradual Temperature-Driven Sublattice Disorder through Antiphase Boundary Defects. Chemistry of Materials, 2022, 34, 3152-3167.	3.2	4
66653	Metal Halide Double Perovskite Fast Lithium Ion Conductors with a Unique Octahedral B-Site Vacancy Migration Mechanism. ACS Applied Energy Materials, 2022, 5, 4926-4933.	2.5	1

#	Article	IF	Citations
66654	Structural Features and the Li-Ion Diffusion Mechanism in Tantalum-Doped Li₇La₃Zr₂O₁₂ Solid Electrolytes. ACS Applied Energy Materials, 2022, 5, 2959-2967.	2.5	9
66655	Electronic Tuning in WSe₂/Au via van der Waals Interface Twisting and Intercalation. ACS Nano, 2022, 16, 6541-6551.	7.3	17
66656	Oxygen Vacancies Promoted Piezoelectricity toward Piezo-Photocatalytic Decomposition of Tetracycline over SrBi₄Ti₄O₁₅. ACS ES&T Engineering, 2022, 2, 1365-1375.	3.7	50
66657	Polymer Structure Predictor (PSP): A Python Toolkit for Predicting Atomic-Level Structural Models for a Range of Polymer Geometries. Journal of Chemical Theory and Computation, 2022, 18, 2737-2748.	2.3	7
66658	Enhanced Thermoelectric Performance in Ternary Skutterudite Co(Ge_{0.5}Te_{0.5})₃ via Band Engineering. Inorganic Chemistry, 2022, 61, 4442-4452.	1.9	9
66659	Lattice dynamics and its effects on magnetocrystalline anisotropy energy of pristine and hole-doped <mml:math xmlns:mml="http://www.w3.org/1998/Math/MathML"><mml:msub><mml:mi>YCo</mml:mi><mml:mn>5</mml:mn></mml:msub></mml:math> from first principles. Physical Review B, 2022, 105, .	1.1	4
66660	First-principles Study of a New BP₂ Two-dimensional Material. Chinese Physics B, 0, , .	0.7	0
66661	Hubbard-corrected oxide formation enthalpies without adjustable parameters. Journal of Physics Communications, 2022, 6, 035009.	0.5	5
66662	Role of intrinsic defects in cubic NaNbO₃: A computational study based on hybrid density-functional theory. Journal of Applied Physics, 2022, 131, 124106.	1.1	4
66663	Toward ferromagnetic semimetal ground state with multiple Weyl nodes in van der Waals crystal MnSb₄Te₇. New Journal of Physics, 2022, 24, 043033.	1.2	7
66664	Simultaneous switching of supramolecular chirality and organizational chirality driven by Coulomb expansion. Nano Research, 0, , 1.	5.8	2
66665	First-principles based study of magnetic states and high-pressure enthalpy landscape of manganese sulfide polymorphs. Journal of Applied Physics, 2022, 131, 115904.	1.1	1
66666	Crystalline structures of l-cysteine and l-cystine: a combined theoretical and experimental characterization. Amino Acids, 2022, 54, 1123-1133.	1.2	17
66667	Ultrathin (In, Mg) films on Si(111): A nearly freestanding double-layer metal. Physical Review B, 2022, 105, .	1.1	3
66668	Electronic and magnetic properties of honeycomb arsenicâ€“phosphorus nanoribbons via a first-principles study. Canadian Journal of Physics, 2022, 100, 277-283.	0.4	2
66669	Gating Orbital Memory with an Atomic Donor. Physical Review Letters, 2022, 128, 106801.	2.9	2
66670	Toward Addressing the Challenge to Predict the Heat Capacities of RDX and HMX Energetic Materials. Propellants, Explosives, Pyrotechnics, 0, , .	1.0	1
66671	The Intrinsic Thermodynamic Difficulty and a Stepâ€Guided Mechanism for the Epitaxial Growth of Uniform Multilayer MoS₂ with Controllable Thickness. Advanced Materials, 2022, 34, e2201402.	11.1	27

#	Article	IF	Citations
66672	First-principles study on the strain-modulated structure and electronic properties of janus tin oxide selenide monolayer. , 2022, 166, 207212.		6
66673	Multiscale simulation approach to investigate the binder distribution in catalyst layers of high-temperature polymer electrolyte membrane fuel cells. Scientific Reports, 2022, 12, 3810.	1.6	3
66674	Gapless excitations inside the fully gapped kagome superconductors <mml:math xmlns:mml="http://www.w3.org/1998/Math/MathML"><mml:mrow><mml:mi>A</mml:mi><mml:msub><mml:mi mathvariant="normal">V</mml:mi><mml:mn>3</mml:mn></mml:msub><mml:msub><mml:mi>Sb</mml:mi><mml:mn>5</mml:mn></mml:msub></mml:mrow></mml:math> Physical Review B, 2022, 105, .	1.1	20
66675	Family of Two-Dimensional Transition Metal Dichlorides: Fundamental Properties, Structural Defects, and Environmental Stability. Journal of Physical Chemistry Letters, 2022, 13, 2165-2172.	2.1	19
66676	Direct Synthesis of Stable 1Tâ€MoS₂ Doped with Ni Single Atoms for Water Splitting in Alkaline Media. Small, 2022, 18, e2107238.	5.2	58
66677	Adsorbateâ€induced modifications in the optical response of Si(553)â€Au nanowires. Physica Status Solidi - Rapid Research Letters, 0, , .	1.2	0
66678	Morphology and Growth Habit of the New Flux-Grown Layered Semiconductor KBiS₂ Revealed by Diffraction Contrast Tomography. Crystal Growth and Design, 2022, 22, 3228-3234.	1.4	2
66679	Strain Adjustment Realizes the Photocatalytic Overall Water Splitting on Tetragonal Zircon BiVO₄. Advanced Science, 2022, 9, e2105299.	5.6	37
66680	First-principles study on the electronic properties of GeC/BSe van der Waals heterostructure: A direct Z-scheme photocatalyst for overall water splitting. Physical Review Materials, 2022, 6, .	0.9	12
66681	Cost effective modification of SmCo5-type alloys. AIP Advances, 2022, 12, .	0.6	1
66682	Catalytic Reduction of Carbon Dioxide on the (001), (011), and (111) Surfaces of TiC and ZrC: A Computational Study. Journal of Physical Chemistry C, 2022, 126, 5138-5150.	1.5	7
66683	Construction of Al-Mg-Zn Interatomic Potential and the Prediction of Favored Glass Formation Compositions and Associated Driving Forces. Materials, 2022, 15, 2062.	1.3	3
66684	Improved Thermoelectric Performance of p-Type Argyrodite Cu₈GeSe₆ via the Simultaneous Engineering of the Electronic and Phonon Transports. ACS Applied Materials & Interfaces, 2022, 14, 16330-16337.	4.0	8
66685	Fermi surface topology and anisotropic superconducting gap in electron-doped hydride compounds at high pressure. Physical Review Materials, 2022, 6, .	0.9	2
66686	Emergence of a Two-Dimensional Topological Dirac Semimetal Phase in a Phthalocyanine-Based Covalent Organic Framework. Chemistry of Materials, 2022, 34, 3178-3184.	3.2	9
66687	Self-healing Growth of LaNiO₃ on a Mixed-Terminated Perovskite Surface. ACS Applied Materials & Interfaces, 2022, 14, 16928-16938.	4.0	4
66688	Modulation of the B4N monolayer as an efficient electrocatalyst for hydrogen evolution reaction. International Journal of Hydrogen Energy, 2022, 47, 11511-11519.	3.8	1
66689	Magnetocrystalline anisotropy in Vâ€“ and Cuâ€“doped Fe16N2. AIP Advances, 2022, 12, .	0.6	2

#	Article	IF	Citations
66690	Lattice strain suppresses point defect formation in halide perovskites. Nano Research, 2022, 15, 5746-5751.	5.8	21
66691	Breaking the activity limitation of iridium single-atom catalyst in hydrogenation of quinoline with synergistic nanoparticles catalysis. Nano Research, 2022, 15, 5024-5031.	5.8	41
66692	Dielectric response of rock-salt crystals at finite temperatures from first principles. Physical Review Materials, 2022, 6, .	0.9	5
66693	A Theoretical Study of Fe Adsorbed on Pure and Nonmetal (N, F, P, S, Cl)-Doped Ti3C2O2 for Electrocatalytic Nitrogen Reduction. Nanomaterials, 2022, 12, 1081.	1.9	6
66694	Ionic contribution to van der Waals interaction of polar compounds. Physical Review B, 2022, 105, .	1.1	0
66695	Transition metal anchored on C₉N₄ as a single-atom catalyst for CO₂ hydrogenation: A first-principles study. Chinese Physics B, 2022, 31, 107306.	0.7	3
66696	Characterization of Zr-Nb-Fe(-Cr) precipitates in Zr-based alloys using density functional theory. Materials Today Communications, 2022, 31, 103381.	0.9	2
66697	High-Throughput Computational Screening for Bipolar Magnetic Semiconductors. Research, 2022, 2022, 9857631.	2.8	4
66698	Coexistence of antiferromagnetism and superconductivity in Mn/Nb(110). Physical Review B, 2022, 105, .	1.1	12
66699	Structural stability and optical properties of tin-based iodide perovskite. Japanese Journal of Applied Physics, 2022, 61, 031003.	0.8	4
66700	Why is it so difficult to realize Dy⁴⁺ in asâ€synthesized BaZrO₃?. Journal of the American Ceramic Society, 2022, 105, 4242-4249.	1.9	4
66701	Slaterâ€“Koster parametrization for the phonons of monolayer MoX₂(X = S, Se or Te). Journal of Physics Condensed Matter, 2022, 34, 195702.	0.7	1
66702	Synergy between Palladium Single Atoms and Nanoparticles via Hydrogen Spillover for Enhancing CO₂ Photoreduction to CH₄. Advanced Materials, 2022, 34, e2200057.	11.1	162
66703	Subnanometric alkaline-earth oxide clusters for sustainable nitrate to ammonia photosynthesis. Nature Communications, 2022, 13, 1098.	5.8	60
66704	Nonlocal pseudopotential energy density functional for orbital-free density functional theory. Nature Communications, 2022, 13, 1385.	5.8	10
66705	A promising thermoelectrics In4SnSe4 with a wide bandgap and cubic structure composited by layered SnSe and In4Se3. Journal of Materiomics, 2022, 8, 982-991.	2.8	5
66706	Pressure-driven symmetry transitions in dense <mml:math xmlns:mml="http://www.w3.org/1998/Math/MathML"><mml:msub><mml:mi mathvariant="normal">H</mml:mi><mml:mn>2</mml:mn></mml:msub><mml:mi mathvariant="normal">O</mml:mi></mml:math> ice. Physical Review B, 2022, 105, .	1.1	9
66707	Comment on â€œWideâ€Rangeâ€Tunable pâ€Type Conductivity of Transparent CuI_{1â€x}Br_x Alloyâ€• Advanced Functional Materials, 2022, 32, .	7.8	4

#	Article	IF	Citations
66708	Deciphering the lithium storage chemistry in flexible carbon fiberâ€based selfâ€supportive electrodes. , 2022, 4, 820-832.		87
66709	pHâ€Controlled Switch over Coadsorption and Separation for Mixed Cs⁺ and Sr²⁺ by an Acidâ€Resistant Potassium Thioantimonate. Advanced Functional Materials, 2022, 32, .	7.8	18
66710	High thermoelectric performance realized through manipulating layered phonon-electron decoupling. Science, 2022, 375, 1385-1389.	6.0	194
66711	Large piezoelectricity response in Li and Ti (or Zr) co-alloyed w-AlN. Journal of Applied Physics, 2022, 131, .	1.1	1
66712	Unravelling the functional complexity of oxygen-containing groups on carbon for the reduction of NO with NH3. Journal of the Taiwan Institute of Chemical Engineers, 2022, 133, 104261.	2.7	4
66713	A high-performance MnO2 cathode doped with group â…§ metal for aqueous Zn-ion batteries: In-situ X-Ray diffraction study on Zn2+ storage mechanism. Journal of Power Sources, 2022, 527, 231198.	4.0	14
66714	The effect of Cr content on intragranular Îº-carbide precipitation in Fe-Mn-Al-(Cr)-C low-density steels: A multiscale investigation. Materials Characterization, 2022, 186, 111801.	1.9	13
66715	Evidence of a 2D Electron Gas in a Singleâ€Unitâ€Cell of Anatase TiO₂ (001). Advanced Science, 2022, 9, e2105114.	5.6	7
66716	Ingrained: An Automated Framework for Fusing Atomicâ€Scale Image Simulations into Experiments. Small, 2022, 18, e2102960.	5.2	12
66717	Solid solution of CaSiO3 and MgSiO3 perovskites in the lower mantle: The role of ferrous iron. American Mineralogist, 2023, 108, 439-446.	0.9	1
66718	Oxygen vacancy-rich amorphous FeNi hydroxide nanoclusters as an efficient electrocatalyst for water oxidation. Journal of Energy Chemistry, 2022, 71, 167-173.	7.1	42
66719	Computational Screening of Single-Metal-Atom Embedded Graphene-Based Electrocatalysts Stabilized by Heteroatoms. Frontiers in Chemistry, 2022, 10, 873609.	1.8	6
66720	Multiferroic van der Waals heterostructure <mml:math xmlns:mml="http://www.w3.org/1998/Math/MathML"><mml:mrow><mml:msub><mml:mi>FeCl</mml:mi><mml:mn>2</mml:mn></mm : Nonvolatile electrically switchable electronic and spintronic properties. Physical Review B, 2022, 105, .	1.1	23
66721	Two-dimensional g-C6N6/SiP-GaS van der Waals heterojunction for overall water splitting under visible light. International Journal of Hydrogen Energy, 2022, 47, 16014-16024.	3.8	11
66722	Fault-tolerant resource estimate for quantum chemical simulations: Case study on Li-ion battery electrolyte molecules. Physical Review Research, 2022, 4, .	1.3	22
66723	Topological nodal line semimetal in an all-sp ² monoclinic carbon. New Journal of Physics, 2022, 24, 043007.	1.2	4
66724	Crystal growth engineering and origin of the weak ferromagnetism in antiferromagnetic matrix of orthochromates from t-e orbital hybridization. IScience, 2022, 25, 104111.	1.9	10
66725	Giant Bandgap Engineering in Two-Dimensional Ferroelectric Îµ-In₂Se₃. Journal of Physical Chemistry Letters, 2022, 13, 3261-3268.	2.1	7

#	Article	IF	Citations
66726	Regulating MoS2 edge site for photocatalytic nitrogen fixation: A theoretical and experimental study. Chemical Engineering Journal, 2022, 442, 136211.	6.6	27
66727	Photothermal Catalytic Water Splitting at Diverse Two-Phase Interfaces Based on Cuâ€“TiO₂. ACS Applied Energy Materials, 2022, 5, 4564-4576.	2.5	12
66728	First-Row Transition Metal Antimonates for the Oxygen Reduction Reaction. ACS Nano, 2022, 16, 6334-6348.	7.3	23
66729	Chemically Stable Guanidinium Covalent Organic Framework for the Efficient Capture of Low-Concentration Iodine at High Temperatures. Journal of the American Chemical Society, 2022, 144, 6821-6829.	6.6	89
66730	Electronic bandstructure modulation of MoX2/ZnO(X:S,Se) heterostructure by applying external electric field. Surfaces and Interfaces, 2022, 29, 101817.	1.5	8
66731	The Contrasting Impacts of the Al₂O₃ and Y₂O₃ Insertion Layers on the Crystallization of ZrO₂ Films for Dynamic Random Access Memory Capacitors. Advanced Electronic Materials, 2022, 8, .	2.6	4
66732	Ab initio screening of two-dimensional CuQ _x and AgQ _x chalcogenides. Journal of Physics Condensed Matter, 2022, 34, 305703.	0.7	2
66733	Switchable quantum anomalous Hall effect in a ferromagnetic topological crystalline insulating NpSb monolayer. Journal Physics D: Applied Physics, 2022, 55, 305301.	1.3	1
66734	Influence of the Preparation Method of Au, Pd, Pt, and Rh/TiO2 Nanostructures and Their Catalytic Activity on the CO Oxidation at Low Temperature. Topics in Catalysis, 2022, 65, 798-816.	1.3	8
66735	Assessment of micropore accessibility for hydrocarbon oxidation in manganese oxide sieves. Applied Catalysis A: General, 2022, 635, 118557.	2.2	5
66736	Precise and controllable tandem strategy triggering boosted oxygen reduction activity. Chinese Journal of Catalysis, 2022, 43, 1042-1048.	6.9	10
66737	Formation energies, electronic properties and elemental diffusion of Cuâ€“Crâ€“Nb (GRCop) alloys. Physica B: Condensed Matter, 2022, 637, 413909.	1.3	5
66738	M₄B₆X₆ as a New Family of Highâ€Efficient Electrocatalysts: The Role of Surface Reconstruction in Water Oxidization. ChemSusChem, 2022, 15, .	3.6	4
66739	Electrochemical CO2 reduction to ethylene by ultrathin CuO nanoplate arrays. Nature Communications, 2022, 13, 1877.	5.8	172
66740	Understanding of Layer-Dependent Stability and Rashba Spin Splitting of Two-Dimensional Organicâ€“Inorganic Halide Perovskites Î±-FABX₃ (B = Ge, Sn, and Pb; X = Cl, Br, and I). Journal of Physical Chemistry C, 2022, 126, 6448-6455.	1.5	1
66741	Structural Modularization of Cu₂Te Leading to High Thermoelectric Performance near the Mottâ€“Ioffeâ€“Regel Limit. Advanced Materials, 2022, 34, e2108573.	11.1	20
66742	Investigation of double perovskites Sr2SmNbO6 and X2CoNbO6 (X=Sr,Ba) with SCAN functional and plus U correction. , 2022, 1, 100019.		9
66743	Growth and characterization of (Ga1 â^' xGdx)2O3 by pulsed laser deposition for wide bandgap applications. Applied Physics A: Materials Science and Processing, 2022, 128, 1.	1.1	2

#	Article	IF	Citations
66744	Mechanisms of Ionic Diffusion and Stability of the Na₄MnCr(PO₄)₃ Cathode. , 2022, 4, 860-867.		13
66745	Inducing a deep impurity level in Li2SnO3 by ionic Biâ€“O bonding to enhance light absorption in photocatalysis. International Journal of Hydrogen Energy, 2022, 47, 13683-13692.	3.8	5
66746	Improvement of look ahead based on quadratic approximation for crystal structure prediction. Science and Technology of Advanced Materials Methods, 0, , 0-0.	0.4	0
66747	Catalytic activity of nickel and cobalt for amination of ethylene glycol: Which is better?. Molecular Catalysis, 2022, 522, 112243.	1.0	2
66748	Element segregation and thermal stability of Niâ€“Pd nanoparticles. Journal of Materials Science, 2022, 57, 7384-7399.	1.7	7
66749	Spin transport properties of highly lattice-matched all-Heusler-alloy magnetic tunnel junction. Journal of Applied Physics, 2022, 131, .	1.1	12
66750	Valley-dependent properties in two-dimensional <mml:math xmlns:mml="http://www.w3.org/1998/Math/MathML"><mml:mrow><mml:msub><mml:mi>Cr</mml:mi><mml:mn>2</mml:mn></mml:msub><mml:mi>N</mml:mi></mml:mrow></mml:math> MXene predicted from first principles. Physical Review Materials, 2022, 6, .	2.9	14
66751	Mechanisms of Photoluminescence in Copper-Containing Fluoride Borate Crystals. Journal of Physical Chemistry C, 0, , .	1.5	4
66752	CoFeVSb: A promising candidate for spin valve and thermoelectric applications. Physical Review B, 2022, 105, .	1.1	17
66753	Atomistic insights on hydrogen plasma treatment for stabilizing High-k/Si interface. Applied Surface Science, 2022, 593, 153297.	3.1	3
66754	The exclusive surface and electronic effects of Ni on promoting the activity of Pt towards alkaline hydrogen oxidation. Nano Research, 2022, 15, 5865-5872.	5.8	12
66755	Adsorption-induced chemical reaction for in situ immobilization of radioactive anions on pristine Î²-Bi2O3 microflowers. Separation and Purification Technology, 2022, 292, 121045.	3.9	3
66756	Temperature and pressure driven spin transitions and piezochromism in a Mn-based hybrid perovskite. Physical Review Materials, 2022, 6, .	0.9	3
66757	Effect of intentional chemical doping on crystallographic and electric properties of the pyrochlore Bi2Sn2O7. Materials and Design, 2022, 216, 110549.	3.3	7
66758	Strain Effects in Wurtzite Boron Nitride: Elastic Constants, Internal Strain, and Deformation Potentials from Hybrid Functional Density Functional Theory. Physica Status Solidi - Rapid Research Letters, 2022, 16, .	1.2	4
66759	Flexoelectricity in hexagonal boron nitride monolayers. Extreme Mechanics Letters, 2022, 52, 101669.	2.0	12
66760	Charge density wave order in the kagome metal <mml:math xmlns:mml="http://www.w3.org/1998/Math/MathML"><mml:mi>A</mml:mi><mml:mrow><mml:msub><mml:mi mathvariant="normal">V</mml:mi><mml:mn>3</mml:mn></mml:msub><mml:msub><mml:mi>Sb</mml:mi><mml:mn>5</mml:mn></mml:r <mml:math		

#	Article	IF	Citations
66762	Large Area Ultrathin InN and Tin Doped InN Nanosheets Featuring 2D Electron Gases. ACS Nano, 2022, 16, 5476-5486.	7.3	8
66763	Interrelationship of bonding strength with structural stability of ternary oxide phases of MgSnO3: A first-principles study. Physica B: Condensed Matter, 2022, 637, 413896.	1.3	7
66764	Topological band transition between hexagonal and triangular lattices with (px, py) orbitals. Journal of Physics Condensed Matter, 2022, , .	0.7	5
66765	An Endotenon Sheath-Inspired Double-Network Binder Enables Superior Cycling Performance of Silicon Electrodes. Nano-Micro Letters, 2022, 14, 87.	14.4	31
66766	A new Pr0.25Nd0.25Sr0.5MnO3-Î´ cathode for proton-conducting solid oxide fuel cells. Ceramics International, 2022, 48, 11872-11878.	2.3	9
66767	First-principles investigation of the significant anisotropy and ultrahigh thermoelectric efficiency of a novel two-dimensional Ga₂I₂S₂ at room temperature. International Journal of Extreme Manufacturing, 2022, 4, 025001.	6.3	13
66768	A first-principles study on the electrical conductivity of Ag2S1â^'xSex (xâ€‰=â€‰0, 0.25,) Tj ETQq0 0 0 rgBT /Ove	1.5	11
66769	Metal-organic framework derived dual-metal sites for electroreduction of carbon dioxide to HCOOH. Applied Catalysis B: Environmental, 2022, 311, 121377.	10.8	40
66770	Effect of P modification on the structure and catalytic performance of Ti-MWW zeolite. Microporous and Mesoporous Materials, 2022, , 111887.	2.2	1
66771	Investigation of the electrocatalytic mechanisms of urea oxidation reaction on the surface of transition metal oxides. Journal of Colloid and Interface Science, 2022, 620, 442-453.	5.0	22
66772	A first-principles prediction on the structural, electronic, elastic, phonon, and transport properties of BaSiN2. Indian Journal of Physics, 0, , 1.	0.9	1
66773	Investigation of Rare Earth-Containing Double Phosphates of the Type A₃Ln(PO₄)₂ (Ln = Y, La, Pr, Nd, and Smâ€“Lu) as Potential Nuclear Waste Forms. Chemistry of Materials, 2022, 34, 3819-3830.	3.2	9
66774	Mo2CS2-MXene supported single-atom catalysts for efficient and selective CO2 electrochemical reduction. Applied Surface Science, 2022, 592, 153339.	3.1	20
66775	Understanding the Trend in Coreâ€“Shell Preferences for Bimetallic Nanoclusters: A Machine Learning Approach. Journal of Physical Chemistry C, 2022, 126, 6847-6853.	1.5	4
66776	Octahedral rotation induced spin state and metalâ€“insulator transition in LaCoO<mml:math xmlns:mml="http://www.w3.org/1998/Math/MathML" display="inline" id="d1e389" altimg="si83.svg"><mml:msub><mml:mrow /><mml:mrow><mml:mn>3</mml:mn></mml:mrow></mml:msub></mml:math> films. Journal of Magnetism and Magnetic Materials, 2022, 555, 169318.	1.0	1
66777	Spin-Polarized Band Structure at MoTe₂/Bi₂Se₃ Interface Designed from First Principles. Journal of the Physical Society of Japan, 2022, 91, .	0.7	0
66778	Symmetry-protected Dirac nodal lines and large spin Hall effect in a <mml:math xmlns:mml="http://www.w3.org/1998/Math/MathML"><mml:mrow><mml:msub><mml:mi mathvariant="normal">V</mml:mi><mml:mn>6</mml:mn></mml:msub><mml:msub><mml:mi>Sb</mml:mi><mml:mn>4</mml:mn></ kagome bilayer. Physical Review B, 2022, 105, .	1.1	3
66779	Genesis of MoS2 from model-Mo-oxide precursors supported on Î³-alumina. Journal of Catalysis, 2022, 408, 303-315.	3.1	4

#	Article	IF	Citations
66780	Transversal Halide Motion Intensifies Bandâ€Toâ€Band Transitions in Halide Perovskites. Advanced Science, 2022, 9, e2200706.	5.6	12
66781	Reconstructed covalent organic frameworks. Nature, 2022, 604, 72-79.	13.7	190
66782	Semiconducting Paddle-Wheel Metalâ€“Organic Complex with a Compact Cuâ€“S Cage. Journal of Physical Chemistry C, 2022, 126, 6300-6307.	1.5	0
66783	Friction of Ti₃C₂T_x MXenes. Nano Letters, 2022, 22, 3356-3363.	4.5	46
66784	Fermi level tuning and double-dome superconductivity in the kagome metal <mml:math xmlns:mml="http://www.w3.org/1998/Math/MathML"><mml:msub><mml:mi mathvariant="normal">CsV</mml:mi><mml:mn>3</mml:mn></mml:msub><mml:msub><mml:mi mathvariant="normal">Sb</mml:mi><mml:mrow><mml:mn>5</mml:mn><mml:mo>â^’</mml:mo><mml:mi>x</mml:mi></mml:mrow><mml:mi mathvariant="normal">Sn</mml:mi><mml:mi>x</mml:mi></mml:msub></mml:math>. Physical Review Materials, 2022, 6, .	0.9	74
66785	Nanotwin-induced ductile mechanism in thermoelectric semiconductor PbTe. Matter, 2022, 5, 1839-1852.	5.0	10
66786	Strain and external electric field modulation of the electronic and optical properties of GaN/WSe2 vdWHs. Physica E: Low-Dimensional Systems and Nanostructures, 2022, 142, 115258.	1.3	16
66787	Li plating on alloy with superior electro-mechanical stability for high energy density anode-free batteries. Energy Storage Materials, 2022, 49, 135-143.	9.5	23
66788	Deep dive into machine learning density functional theory for materials science and chemistry. Physical Review Materials, 2022, 6, .	0.9	28
66789	Collective plasmonic modes in the chiral multifold fermionic material CoSi. Physical Review B, 2022, 105, .	1.1	9
66790	Crystal structures and superconductivity of carbonaceous sulfur hydrides at pressures up to 300 GPa. Physical Review B, 2022, 105, .	1.1	3
66791	Activated metal-organic frameworks (a-MIL-100 (Fe)) as fillers in polymer electrolyte for high-performance all-solid-state lithium metal batteries. Materials Today Communications, 2022, 31, 103518.	0.9	23
66792	Regulating Interfacial Spin Hall Conductivity with Ferroelectricity. Journal of Physical Chemistry Letters, 2022, 13, 3310-3316.	2.1	1
66793	Catalytic cycloaddition of CO2 to epoxides by the synergistic effect of acidity and alkalinity in a functionalized biochar. Chemical Engineering Journal, 2022, 442, 136265.	6.6	27
66794	Polarization-dependent H2O adsorption on polar surfaces of BiAlO3 (0001). Materials Today Communications, 2022, , 103511.	0.9	0
66795	Effects of oxygen concentration and irradiation defects on the oxidation corrosion of body-centered-cubic iron surfaces: A first-principles study. Chinese Physics B, 0, , .	0.7	2
66796	Role of carbon and hydrogen in limiting <mml:math xmlns:mml="http://www.w3.org/1998/Math/MathML"><mml:mi>n</mml:mi></mml:math> -type doping of monoclinic <mml:math xmlns:mml="http://www.w3.org/1998/Math/MathML"><mml:mrow><mml:mo>(</mml:mo><mml:msub><mml:mi>Al</mml:mi><mml:mi>ma. Physical Review B, 2022, 105, .	1.1	18
66797	Synergistic Effect of 3D Flexible Framework with Sodiophilic Mesoporous SnO₂ Nanosheet Arrays on Dendrite-Free Sodium Metal Batteries. ACS Applied Materials & Interfaces, 2022, 14, 16394-16403.	4.0	9

#	Article	IF	Citations
66798	A new transition metal diphosphide Î±-MoP₂ synthesized by a high-temperature and high-pressure technique. Chinese Physics B, 2023, 32, 018102.	0.7	3
66799	Rapid Self-Decomposition of g-C₃N₄ During Gasâ€“Solid Photocatalytic CO₂ Reduction and Its Effects on Performance Assessment. ACS Catalysis, 2022, 12, 4560-4570.	5.5	86
66800	Synergistic regulation of hydrogen adsorption/desorption via dual interfaces of Cu/Ni/Ni(OH)2 toward efficient hydrogen evolution reaction. International Journal of Hydrogen Energy, 2022, 47, 14053-14062.	3.8	4
66801	Properties of Mo-based TMDCs/Ti2CT2ï¼ˆT = O, F, OHï¼‰vdWs heterostructures for full spectrum electromagnetic absorption. Solid State Communications, 2022, 346, 114720.	0.9	2
66803	Hydrogen evolution reaction catalyst with high catalytic activity by interplay between organic molecules and transition metal dichalcogenide monolayers. Materials Today Energy, 2022, 25, 100976.	2.5	4
66804	Development of neural network potential for MD simulation and its application to TiN. Computational Materials Science, 2022, 206, 111303.	1.4	2
66805	Mg,Ti-base surface integrated layer and bulk doping to suppress lattice oxygen evolution of Ni-rich cathode material at a high cut-off voltage. Journal of Energy Chemistry, 2022, 71, 434-444.	7.1	23
66806	A Series of Ternary Metal Chloride Superionic Conductors for Highâ€Performance Allâ€Solidâ€State Lithium Batteries. Advanced Energy Materials, 2022, 12, .	10.2	42
66807	Boosting acidic water oxidation performance by constructing arrays-like nanoporous IrxRu1â^'xO2 with abundant atomic steps. Nano Research, 2022, 15, 5933-5939.	5.8	25
66808	Orderly disorder in magic-angle twisted trilayer graphene. Science, 2022, 376, 193-199.	6.0	63
66809	Adsorption of molecular iodine on the Ag(111) surface: Phase transitions, silver reconstruction, and iodide growth. Journal of Chemical Physics, 2022, 156, 164702.	1.2	4
66810	Fluorescence spectrum and charge state control of divacancy qubits via illumination at elevated temperatures in <mml:math xmlns:mml="http://www.w3.org/1998/Math/MathML"><mml:mrow><mml:mn>4</mml:mn><mml:mi>H</mml:mi></mml:mrow></mml:m silicon carbide. Physical Review B, 2022, 105, .	1.1	5
66811	A Firstâ€Principles Study of the Structural, Magnetic, Optical Properties and Doping Effect in Chromium Arsenide. Physica Status Solidi (B): Basic Research, 0, , 2200062.	0.7	0
66812	Adsorption Characteristics of Gas Molecules Adsorbed on Graphene Doped with Mn: A First Principle Study. Molecules, 2022, 27, 2315.	1.7	6
66813	Oxygen Vacancy Formation and Migration within the Antiphase Boundaries in Lanthanum Scandate-Based Oxides: Computational Study. Materials, 2022, 15, 2695.	1.3	0
66814	The first principle research of CaO and MgO particulate heterogeneous nucleation in Mg alloys. Applied Surface Science, 2022, 593, 153224.	3.1	10
66815	Sampling lattices in semi-grand canonical ensemble with autoregressive machine learning. Npj Computational Materials, 2022, 8, .	3.5	3
66816	First-principles study of the (001) and (110) surfaces of CrCoIrGa Heusler alloy. Physica Scripta, 2022, 97, 055809.	1.2	2

#	Article	IF	Citations
66817	Metalâ€Doped PdH(111) Catalysts for CO₂ Reduction. ChemSusChem, 2022, 15, .	3.6	7
66818	Theoretical study of M ₆ X ₂ and M ₆ XXâ€² structure (M = Au, Ag;) Tj ETQq1 1 0.784314 rgB properties under biaxial strain. Chinese Physics B, 2022, 31, 097101.	0.7	2
66819	Unsupervised machine learning to classify crystal structures according to their structural distortion: A case study on Li-argyrodite solid-state electrolytes. Energy and AI, 2022, 9, 100159.	5.8	3
66820	Bio-inspired synthesis of transition-metal oxide hybrid ultrathin nanosheets for enhancing the cycling stability in lithium-ion batteries. Nano Research, 2022, 15, 5064-5071.	5.8	8
66821	Theoretical insight on dopamine, ascorbic acid and uric acid adsorption on graphene as material for biosensors. Computational and Theoretical Chemistry, 2022, 1212, 113705.	1.1	1
66822	Quantum capacitance of supercapacitor electrodes based on the F-functionalized M2C MXenes: A first-principles study. Vacuum, 2022, 201, 111094.	1.6	12
66823	Facilitating Hot Electron Injection from Graphene to Semiconductor by Rectifying Contact for Visâ€“NIRâ€Driven H₂O₂ Production. Small, 2022, 18, e2200885.	5.2	14
66824	Bonding character of intermediates in onâ€surface Ullmann reactions revealed with energy decomposition analysis. Journal of Computational Chemistry, 2023, 44, 179-189.	1.5	2
66825	Interfacial properties of two-dimensional CdS/GO from DFT. Surfaces and Interfaces, 2022, 30, 101960.	1.5	4
66826	Atomic scale simulation of the strain rate and temperature dependence of crack growth and stacking faults in zirconium. Computational Materials Science, 2022, 206, 111220.	1.4	5
66827	Nanoimaging of the Edge-Dependent Optical Polarization Anisotropy of Black Phosphorus. Nano Letters, 2022, 22, 3180-3186.	4.5	6
66828	Identification of potential metal oxides for NO₂ capture: A density functional theory study. Journal of the American Ceramic Society, 2022, 105, 5299-5308.	1.9	3
66829	Intrinsically Low Thermal Conductivity in the n-Type Vacancy-Ordered Double Perovskite Cs₂SnI₆: Octahedral Rotation and Anharmonic Rattling. Chemistry of Materials, 2022, 34, 3301-3310.	3.2	32
66830	Vanishing Electronic Band Gap in Two-Dimensional Hydrogen-Bonded Organic Frameworks. Chemistry of Materials, 2022, 34, 3461-3467.	3.2	6
66831	Understanding the Origin of the Particularly Small and Anisotropic Thermal Expansion of MOFâ€74. Advanced Theory and Simulations, 2022, 5, .	1.3	5
66832	On-Surface Debromination of C₆Br₆: C₆ Ring versus C₆ Chain. ACS Nano, 2022, 16, 6578-6584.	7.3	14
66833	Hydrogen adsorption behavior on AXenes Na₂N and K₂N: a first-principles study. Materials Research Express, 2022, 9, 045501.	0.8	4
66834	Atomically sharp domain walls in an antiferromagnet. Science Advances, 2022, 8, eabn3535.	4.7	12

#	Article	IF	Citations
66835	Magnetic properties in a IIIA-nitride monolayer doped with Ag: A density functional theory investigation. Results in Physics, 2022, 35, 105396.	2.0	5
66836	Pseudo-adsorption and long-range redox coupling during oxygen reduction reaction on single atom electrocatalyst. Nature Communications, 2022, 13, 1734.	5.8	56
66837	Negative differential friction coefficients of two-dimensional commensurate contacts dominated by electronic phase transition. Nano Research, 2022, 15, 5758-5766.	5.8	5
66838	Large Transverse and Longitudinal Magnetoâ€Thermoelectric Effect in Polycrystalline Nodalâ€Line Semimetal Mg₃Bi₂. Advanced Materials, 2022, 34, e2200931.	11.1	28
66839	Chemically identifying single adatoms with single-bond sensitivity during oxidation reactions of borophene. Nature Communications, 2022, 13, 1796.	5.8	18
66840	Atomistic Insight into the Hydration States of Layered Double Hydroxides. ACS Omega, 2022, 7, 12412-12423.	1.6	9
66841	Spontaneous Magnetic Skyrmions in Single-Layer CrInX₃ (X = Te, Se). Nano Letters, 2022, 22, 3440-3446.	4.5	34
66842	Chalcogen Atom-Doped Graphene and Its Performance in N2 Activation. Surfaces, 2022, 5, 228-237.	1.0	0
66843	Correlation of mechanical properties and electronic structures for NdFeB permanent magnet under hydrostatic pressure based on first-principle calculation. Journal of Materials Research and Technology, 2022, 18, 3410-3427.	2.6	5
66844	Dislocation loop evolution in Krâ€irradiated ThO₂. Journal of the American Ceramic Society, 2022, 105, 5419-5435.	1.9	11
66845	Electronic Structure Study of Various Transition Metal Oxide Spinels Reveals a Possible Design Strategy for Charge Transport Pathways. Journal of the Electrochemical Society, 2022, 169, 040542.	1.3	3
66846	Tailoring BaCe0.8Y0.2O3 proton-conducting oxide with Li ions for an enhanced stability. Ceramics International, 2022, 48, 17987-17993.	2.3	8
66847	Data-Driven Multi-Scale Modeling and Optimization for Elastic Properties of Cubic Microstructures. Integrating Materials and Manufacturing Innovation, 2022, 11, 230-240.	1.2	6
66848	Data-driven discovery of high performance layered van der Waals piezoelectric NbOI2. Nature Communications, 2022, 13, 1884.	5.8	22
66849	Coverage-Induced Chiral Transition of Co(II)-5,15-Diphenylporphyrin Self-Assemblies on Cu(111). Journal of Physical Chemistry C, 2022, 126, 6745-6752.	1.5	4
66850	Elucidating electrocatalytic mechanism for large-scale cycloalkanol oxidation integrated with hydrogen evolution. Chemical Engineering Journal, 2022, 442, 136264.	6.6	16
66851	Origin of the type-II Weyl state in topological antiferromagnetic <mml:math xmlns:mml="http://www.w3.org/1998/Math/MathML"><mml:msub><mml:mi>YbMnBi</mml:mi><mml:mn>2</mml:mn></mml:msub></ Physical Review B, 2022, 105, .	1.1	6
66852	First-Principles Calculations of Two-Dimensional CdO/HfS2 Van der Waals Heterostructure: Direct Z-Scheme Photocatalytic Water Splitting. Frontiers in Chemistry, 2022, 10, 879402.	1.8	4

#	Article	IF	Citations
66853	First-Principles Calculations on Lateral Heterostructures of Armchair Graphene Antidot Nanoribbons for Band Alignment. ACS Applied Nano Materials, 2022, 5, 5699-5708.	2.4	1
66854	Evolution of ultraflat band in the van der Waals kagome semiconductor <mml:math xmlns:mml="http://www.w3.org/1998/Math/MathML"><mml:mrow><mml:msub><mml:mi>Pd</mml:mi><mml:mn>3</mml:mn></mml:mr		

#	Article	IF	Citations
66871	Quantum Tunnelling Driven H₂ Formation on Graphene. Journal of Physical Chemistry Letters, 2022, 13, 3173-3181.	2.1	10
66872	Second nearest-neighbor modified embedded atom method interatomic potentials for Na-Mâ''Sn (MÂ=ÂCu,) Tj ETQq1 1 0.784314 rgBT	1.4	3
66873	Atomically Dispersed Cu Sites on Dualâ€Mesoporous Nâ€Doped Carbon for Efficient Ammonia Electrosynthesis from Nitrate. ChemSusChem, 2022, 15, .	3.6	21
66874	Chiral structures of electric polarization vectors quantified by X-ray resonant scattering. Nature Communications, 2022, 13, 1769.	5.8	6
66875	Flat phonon modes driven ultralow thermal conductivities in Sr3AlSb3 and Ba3AlSb3 Zintl compounds. Applied Physics Letters, 2022, 120, .	1.5	6
66876	Structural Phase Transitions in closo-Dicarbadodecaboranes C₂B₁₀H₁₂. Inorganic Chemistry, 2022, 61, 5813-5823.	1.9	4
66877	Role of sintering temperature on electronic and mechanical properties of thermoelectric material: A theoretical and experimental study of TiCoSb half-Heusler alloy. Materials Chemistry and Physics, 2022, 281, 125854.	2.0	11
66878	Charge self-consistent electronic structure calculations with dynamical mean-field theory using Quantum ESPRESSO, Wannier 90 and TRIQS. Journal of Physics Condensed Matter, 2022, 34, 235601.	0.7	4
66879	Giant anomalous Hall and anomalous Nernst conductivities in antiperovskites and their tunability via magnetic fields. Physical Review Materials, 2022, 6, .	0.9	8
66880	Modification of LiMn2O4 surfaces by controlling the Acidâ€"Base surface chemistry of atomic layer deposition. Applied Surface Science, 2022, 599, 153329.	3.1	5
66881	Role of Ferroelectric In₂Se₃ in Polysulfide Shuttling and Charging/Discharging Kinetics in Lithium/Sodiumâ€"Sulfur Batteries. ACS Applied Materials & Interfaces, 2022, 14, 16178-16184.	4.0	17
66882	Single-crystal graphene on Ir(110). Physical Review B, 2022, 105, .	1.1	7
66883	Electrochemical Stability of Zinc and Copper Surfaces in Protic Ionic Liquids. Langmuir, 2022, 38, 4633-4644.	1.6	4
66884	Predicted superior hydrogen evolution activities of MoC via surface dopant. International Journal of Hydrogen Energy, 2022, 47, 13664-13673.	3.8	7
66885	Strain-tunable metamagnetic critical endpoint in Mott insulating rare-earth titanates. Physical Review B, 2022, 105, .	1.1	6
66886	Accurate and efficient approximate quasiparticle DFTâ€1/2 band structure calculations of transition metal oxide perovskites. Physica Status Solidi (B): Basic Research, 0, , .	0.7	0
66887	Binding and energetics of oxygen at the CuInSe₂ chalcopyrite and the CuInSe₂/CdS interface. Physica Scripta, 0, , .	1.2	1
66888	Order parameters for antiferromagnetic structures: A first-principles study of iridium manganese. Physical Review Materials, 2022, 6, .	0.9	0

#	Article	IF	Citations
66889	Novel polymerization of nitrogen in zinc nitrides at high pressures. Journal of Physics Condensed Matter, 2022, 34, 235702.	0.7	3
66890	Tuning the Phase Transition of SrFeO_{3â^'Î´} by Mn toward Enhanced Catalytic Activity and CO₂ Resistance for the Oxygen Reduction Reaction. ACS Applied Materials & Interfaces, 2022, 14, 17358-17368.	4.0	11
66891	Improving Results by Improving Densities: Density-Corrected Density Functional Theory. Journal of the American Chemical Society, 2022, 144, 6625-6639.	6.6	45
66892	Electron delocalization enhances the thermoelectric performance of misfit layer compound (Sn_{1â^'x}Bi_xS)_{1.2}(TiS₂)₂. Chinese Physics B, 2022, 31, 117202.	0.7	1
66893	Ferroelectricity coexisted with p-orbital ferromagnetism and metallicity in two-dimensional metal oxynitrides. Npj Computational Materials, 2022, 8, .	3.5	20
66894	Enhanced afterglow performance of Zn2SiO4:Mn2+ by Pr3+ doping and mechanism. Ceramics International, 2022, 48, 19358-19366.	2.3	11
66895	Linear dichroism and polarization controllable persistent spin helix in two-dimensional ferroelectric ZrOI2 monolayer. Nano Research, 2022, 15, 6779-6789.	5.8	7
66896	Modifying magnetic properties of MnBi with carbon: an experimental and theoretical study. Journal Physics D: Applied Physics, 2022, 55, 265003.	1.3	4
66897	Equilibrium phase diagrams of isostructural and heterostructural two-dimensional alloys from first principles. IScience, 2022, 25, 104161.	1.9	1
66898	First-principles study of direct band gap semiconductors XS2 (X= Zr and Hf) with orthorhombic symmetry. Journal Physics D: Applied Physics, 0, , .	1.3	0
66899	Enabling fast-charging selenium-based aqueous batteries via conversion reaction with copper ions. Nature Communications, 2022, 13, 1863.	5.8	27
66900	Origin of the Enhanced Hydrogen Evolution Reaction Activity of Grain Boundaries in MoS₂ Monolayers. Journal of Physical Chemistry C, 2022, 126, 6215-6222.	1.5	5
66901	Overlapping electron density and the global delocalization of Ï€â€aromatic fragments as the reason of conductivity of the biphenylene network. Journal of Computational Chemistry, 2023, 44, 168-178.	1.5	8
66902	Tuning the carrier scattering mechanism to improve the thermoelectric performance of p-type Mg3Sb1.5Bi0.5-based material by Ge doping. Materials Today Energy, 2022, 25, 100977.	2.5	3
66903	Nitrogen-vacancy defects in germanium. AIP Advances, 2022, 12, 045110.	0.6	2
66904	Theoretical study on the influence of Cr, Mo, and W alloying additions on the helium behavior in nickel. Journal of Nuclear Materials, 2022, 565, 153720.	1.3	5
66905	Effects of Y2O3 on the microstructure evolution and electromagnetic interference shielding mechanism of soft magnetic FeCoSiMoNiBCu alloys by laser cladding. Additive Manufacturing, 2022, 55, 102811.	1.7	2
66906	Unprotected quadratic band crossing points and quantum anomalous Hall effect in FeB2 monolayer. Science China: Physics, Mechanics and Astronomy, 2022, 65, 1.	2.0	4

#	Article	IF	Citations
66907	Interlayer magnetophononic coupling in MnBi2Te4. Nature Communications, 2022, 13, 1929.	5.8	22
66908	Defect-Induced Decomposition of Energetic Nitro Compounds at MgO Surface. Surface Science, 2022, , 122085.	0.8	2
66909	Chemical Potential Switching of the Anomalous Hall Effect in an Ultrathin Noncollinear Antiferromagnetic Metal. Advanced Materials, 2022, 34, e2200487.	11.1	7
66910	High-temperature phonon-mediated superconductivity in monolayer Mg2B4C2. Npj Quantum Materials, 2022, 7, .	1.8	11
66911	Molecular Bending: An Important Factor Affecting the Packing of Self-Assembled Monolayers of Triptycene-Based Molecular Rods on a (111) Gold Surface. Journal of Physical Chemistry C, 2022, 126, 7193-7207.	1.5	2
66912	Robust kagome electronic structure in the topological quantum magnets <mml:math xmlns:mml="http://www.w3.org/1998/Math/MathML"><mml:mrow><mml:mi>X</mml:mi><mml:msub><mml:mi>Mn</mml:mi><mml:mi><mml:math		

#	Article	IF	Citations
66925	Redox-active Hexaazatriphenylene@MXene composite for high-performance flexible proton batteries. Composites Part B: Engineering, 2022, 235, 109750.	5.9	21
66926	Role of the Metal Atom in a Carbonâ€Based Singleâ€Atom Electrocatalyst for Liï£¿S Redox Reactions. Small, 2022, 18, e2200395.	5.2	33
66927	Ultraviolet Quantum Emitters in Hexagonal Boron Nitride from Carbon Clusters. Journal of Physical Chemistry Letters, 2022, 13, 3150-3157.	2.1	11
66928	Atomistic simulations of the deformation behavior of an Nb nanowire embedded in a NiTi shape memory alloy. Acta Materialia, 2022, 228, 117764.	3.8	5
66929	Surface pourbaix plots of M@N4-graphene single-atom electrocatalysts from density functional theory thermodynamic modeling. Electrochimica Acta, 2022, 412, 140155.	2.6	29
66930	The electronic structures and p-type performance of group IA and VA atoms in NiO: A first principles study. Journal of Applied Physics, 2022, 131, .	1.1	8
66931	Hydrazine Hydrate Intercalated 1T-Dominant MoS₂ with Superior Ambient Stability for Highly Efficient Electrocatalytic Applications. ACS Applied Materials & Interfaces, 2022, 14, 16338-16347.	4.0	17
66932	Exploring a high-carrier-mobility black phosphorus/MoSe2 heterostructure for high-efficiency thin film solar cells. Solar Energy, 2022, 236, 576-585.	2.9	13
66933	Adding MgCl₂ to Molten NaClâ^'UCl_n (n=3, 4): Insights from Firstâ€Principles Molecular Dynamics. ChemPhysChem, 2022, 23, .	1.0	2
66934	Sensitive and Reliable Fluorescent Thermometer Based on a Red-Emitting Li₂MgHfO₄:Mn⁴⁺ Phosphor. Inorganic Chemistry, 2022, 61, 8126-8134.	1.9	12
66935	Recyclable regeneration of NiO/NaF catalyst: Hydrogen evolution via steam reforming of oxygen-containing volatile organic compounds. Energy Conversion and Management, 2022, 258, 115456.	4.4	12
66936	Comprehensive Modulation of Conductance Anisotropy in Low-Symmetry <mml:math xmlns:mml="http://www.w3.org/1998/Math/MathML" display="inline" overflow="scroll"><mml:msub><mml:mrow><mml:mi>Re</mml:mi><mml:mi mathvariant="normal">S</mml:mi></mml:mrow><mml:mn>2</mml:mn></mml:msub></mml:math> Transistors. Physical Review Applied, 2022, 17, .	1.5	2
66937	Interface Engineering of Co(OH)₂ Nanosheets Growing on the KNbO₃ Perovskite Based on Electronic Structure Modulation for Enhanced Peroxymonosulfate Activation. Environmental Science & Technology, 2022, 56, 5200-5212.	4.6	136
66938	Promoting Water Activation by Photogenerated Holes in Monolayer C₂N. Journal of Physical Chemistry Letters, 2022, 13, 3332-3337.	2.1	7
66939	Carbon-free high-performance cathode for solid-state Li-O ₂ battery. Science Advances, 2022, 8, eabm8584.	4.7	15
66940	A first-principles study on crystal structures and metallization of sodium-rich sulfides under high pressure. Journal of Physics Condensed Matter, 2022, , .	0.7	0
66941	Enhanced dissociation activation of CO2 on the Bi/Cu(1 1 1) interface by the synergistic effect. Journal of Catalysis, 2022, 410, 1-9.	3.1	8
66942	Modulation of the metal-insulator transition in VO2 nanoparticles with nRu+W (n=1â€“4) codoping: Implications for energy-saving smart windows. Vacuum, 2022, 201, 111079.	1.6	2

#	Article	IF	Citations
66943	Silver boosts ultra-long cycle life for metal sulfide lithium-ion battery anodes: Taking AgSbS2 nanowires as an example. Journal of Colloid and Interface Science, 2022, 621, 416-430.	5.0	7
66944	Dislocation evolution in copper in the absence and presence of hydrogen. Materials Science & Engineering A: Structural Materials: Properties, Microstructure and Processing, 2022, 842, 143082.	2.6	1
66945	Hydrogen diffusion on and into the hydrogen-covered Pd(1 0 0) surfaces from first-principles. Chemical Physics Letters, 2022, 794, 139509.	1.2	2
66946	Improving the electrochemical performances of Li-rich Li1.2Ni0.13Co0.13Mn0.54O2 through cooperative doping of Na+ and Mg2+. Electrochimica Acta, 2022, 414, 140169.	2.6	12
66947	A novel square planar N42â^' ring with aromaticity in BeN4. Matter and Radiation at Extremes, 2022, 7, .	1.5	19
66948	On the origin of the high-temperature desorption of subsurface hydrogen from Ni (1 1 0). Chemical Physics Letters, 2022, 794, 139479.	1.2	0
66949	Enhanced thermoelectric performance of Hafnium free n-type ZrNiSn half-Heusler alloys by isoelectronic Si substitution. Materials Today Physics, 2022, 24, 100648.	2.9	9
66950	CO2 reduction on a nanostructured La0.5Ba0.5CoO3 perovskite: Electrochemical characterization and DFT calculations. Journal of CO2 Utilization, 2022, 59, 101973.	3.3	3
66951	Structures of boundaries and corners of fully-closed hexagonal domains in HVPE-AlN film. Acta Materialia, 2022, 229, 117838.	3.8	0
66952	Revealing the impact of acceptor dopant type on the electrical conductivity of sodium bismuth titanate. Acta Materialia, 2022, 229, 117808.	3.8	7
66953	First-principles study of radiation defects in silicon. Computational Materials Science, 2022, 207, 111273.	1.4	9
66954	L12-strengthened multicomponent Co-Al-Nb-based alloys with high strength and matrix-confined stacking-fault-mediated plasticity. Acta Materialia, 2022, 229, 117763.	3.8	36
66955	Unveiling the effect of vacancy defects on structural, mechanical, electronic and diffusion properties of copper (I) iodide. Scripta Materialia, 2022, 213, 114634.	2.6	4
66956	Optical response, lithiation and charge transfer in Sn-based 211 MAX phases with electron localization function. Journal of Materials Research and Technology, 2022, 18, 2470-2479.	2.6	13
66957	Influence of titanium on the clustering of vacancy, rhenium and osmium in tungsten-titanium alloys: First-principles study. Fusion Engineering and Design, 2022, 178, 113098.	1.0	1
66958	Anisotropic large magnetoresistance and Fermi surface topology of terbium monoantimonide. Materials Today Physics, 2022, 24, 100657.	2.9	3
66959	Mechanism of complete dehydrogenation of ammonia borane in electrochemical alkaline environment. Computational Materials Science, 2022, 207, 111306.	1.4	7
66960	Characteristic mechanism for fast <mml:math xmlns:mml="http://www.w3.org/1998/Math/MathML" altimg="si1.svg"><mml:msup><mml:mi mathvariant="normal">H</mml:mi><mml:mo>â^'</mml:mo></mml:msup></mml:math> conduction in <mml:math xmlns:mml="http://www.w3.org/1998/Math/MathML" altimg="si15.svg"><mml:mrow><mml:msub><mml:mtext>LaH</mml:mtext><mml:mrow><mml:mn>2.5</mml:mn></mml:mrow></mml:msub><mml:mi mathvariant="normal">O</mml:mi><mml:mrow><mml:mn>0.25</mml:mn></mml:mrow></mml:msub></mml:mrow></mml:math>.	3.8	8

#	Article	IF	Citations
66961	Ab initio-guided X-ray photoelectron spectroscopy quantification of Ti vacancies in Ti<mml:math xmlns:mml="http://www.w3.org/1998/Math/MathML" altimg="si1.svg"><mml:msub><mml:mrow /><mml:mrow><mml:mn>1</mml:mn><mml:mo>â^'</mml:mo><mml:mi>Î´</mml:mi></mml:mrow></mml:msub></mml:math>O<mml:math xmlns:mml="http://www.w3.org/1998/Math/MathML" altimg="si2.svg"><mml:msub><mml:mrow /><mml:mi>x</mml:mi></mml:msub></mml:math>N<mml:math xmlns:mml="http://www.w3.org/1998/Math/MathML" altimg="si3.svg"><mml:msub><mml:mrow /. Acta M	3.8	2
66962	Hydrogen accommodation in the TiZrNbHfTa high entropy alloy. Acta Materialia, 2022, 229, 117832.	3.8	11
66963	Enhancement of hydrogen evolution reaction kinetics in alkaline media by fast galvanic displacement of nickel with rhodium â€“ From smooth surfaces to electrodeposited nickel foams. Electrochimica Acta, 2022, 414, 140214.	2.6	10
66964	Correlation-assisted Peierls gap in divalent metal ion (Zn+2, Cd+2, Mg+2, Ca+2, Sr+2 and Ba+2) doped M-VO2: First principle analysis. Solid State Communications, 2022, 347, 114710.	0.9	2
66965	Computational synthesis of 2D materials: A high-throughput approach to materials design. Computational Materials Science, 2022, 207, 111238.	1.4	7
66966	First Principles Study on the Dissolution Corrosion Behavior of RAFM Steel in the Liquid PbLi. Journal of Nuclear Materials, 2022, 563, 153634.	1.3	5
66967	Interaction of transmutation products with precipitates, dislocations and grain boundaries in neutron irradiated W. Materialia, 2022, 22, 101370.	1.3	17
66968	Assessing Mgâ€“Scâ€“(rare earth) ternary phase stability via constituent binary cluster expansions. Computational Materials Science, 2022, 207, 111240.	1.4	1
66969	Structure, mechanical and thermo-physical properties of lanthanide fission product doped UO2 in U(V) state: A density functional study. Solid State Communications, 2022, 347, 114739.	0.9	2
66970	Carbon driven oxygen retention in uranium oxycarbide (UCO) fluorite phase. Journal of Nuclear Materials, 2022, 563, 153662.	1.3	0
66971	Exploring monolayer Janus MoSSe as potential gas sensor for Cl2, H2S and SO2. Computational and Theoretical Chemistry, 2022, 1211, 113665.	1.1	8
66972	Crystal structure and octahedral deformation of orthorhombic perovskite ABO3: Case study of SrRuO3. Journal of Solid State Chemistry, 2022, 309, 122998.	1.4	3
66973	Operando electrochemical TEM, ex-situ SEM and atomistic modeling studies of MnS dissolution and its role in triggering pitting corrosion in 304L stainless steel. Corrosion Science, 2022, 199, 110184.	3.0	22
66974	Irradiation damage versus lattice distortion in AlNbTiVCrx (xÂ=Â0, 0.5, 1) high-entropy alloys from first-principles calculations and irradiation experiments. Journal of Nuclear Materials, 2022, 563, 153630.	1.3	7
66975	Molecular dynamics study of fission gas behaviour and solubility in molten FLiNaK salt. Journal of Nuclear Materials, 2022, 563, 153633.	1.3	3
66976	Understanding and controlling inversion boundaries in ZnO. Acta Materialia, 2022, 229, 117804.	3.8	5
66977	Unusual structure and properties of germanium under pressure. Computational Materials Science, 2022, 207, 111310.	1.4	2
66978	Lithiation MAX derivative electrodes with low overpotential and long-term cyclability in a wide-temperature range. Energy Storage Materials, 2022, 47, 611-619.	9.5	3

#	Article	IF	Citations
66979	Wigner energy in irradiated graphite: A first-principles study. Journal of Nuclear Materials, 2022, 563, 153663.	1.3	2
66980	High-throughput generation of potential energy surfaces for solid interfaces. Computational Materials Science, 2022, 207, 111302.	1.4	4
66981	Matrix controlled structural phase transformations in embedded metallic nanoparticles. Scripta Materialia, 2022, 213, 114632.	2.6	1
66982	Improvement of thermoelectric properties for silicene by the hydrogenation effect. Results in Physics, 2022, 36, 105422.	2.0	4
66983	Bromate incorporation in calcite and aragonite. Geochimica Et Cosmochimica Acta, 2022, 324, 17-25.	1.6	2
66984	Atomistic mechanisms underlying plasticity and crack growth in ceramics: a case study of AlN/TiN superlattices. Acta Materialia, 2022, 229, 117809.	3.8	29
66985	Ab initio investigations of electronic structure, mechanical properties, phonon stability, and thermodynamics of the Mgâ€“Er system. Vacuum, 2022, 199, 110968.	1.6	8
66986	NiCo-layered double hydroxide with cation vacancy defects for high-performance supercapacitors. Electrochimica Acta, 2022, 413, 140143.	2.6	18
66987	Transport behavior and thermoelectric properties of SnSe/SnS heterostructure modulated with asymmetric strain engineering. Computational Materials Science, 2022, 207, 111271.	1.4	5
66988	Effects of interatomic potential on fracture behaviour in single- and bicrystalline tungsten. Computational Materials Science, 2022, 207, 111283.	1.4	16
66989	Study on the structural properties of refining slags by molecular dynamics with deep learning potential. Journal of Molecular Liquids, 2022, 353, 118787.	2.3	7
66990	First principles calculations to investigate magnetic tetranuclear ferrous complexes. Journal of Materials Research and Technology, 2022, 18, 2546-2551.	2.6	2
66991	Passivation effect of NTCDA nanofilm on black phosphorus. Results in Physics, 2022, 36, 105466.	2.0	0
66992	Stability of phase boundary between L12-Ni3Al phases: A phase field study. Intermetallics, 2022, 144, 107528.	1.8	46
66993	Effect of the local chemical environment on oxidation resistance mechanisms in AlNbTiZr refractory high entropy alloys: A first-principles study. Scripta Materialia, 2022, 213, 114624.	2.6	4
66994	One-step facile fabrication of N, S co-doped carbon modified NiS/MoS2 heterostructure microspheres with improved sodium storage performance. Journal of Power Sources, 2022, 529, 231282.	4.0	12
66995	Ab initio screening of refractory nitrides and carbides for high temperature hydrogen permeation barriers. Journal of Nuclear Materials, 2022, 563, 153611.	1.3	3
66996	Mapping relationships between cation-F bonds and the heat capacity, thermal conductivity, viscosity of molten NaF-BeF2. Journal of Molecular Liquids, 2022, 354, 118915.	2.3	2

#	Article	IF	Citations
66997	High-performance lithium metal battery realized by regulating Li+ flux distribution on artificial-solid-electrolyte-interphase functionalized 3D carbon framework-Li anode. Materials Today Physics, 2022, 24, 100672.	2.9	3
66998	First-principles study on the solute-induced low diffusion and self-trapping of helium in fcc iron. Journal of Nuclear Materials, 2022, 563, 153613.	1.3	1
66999	Fundamental invariant-neural network potential energy surface and dissociative chemisorption dynamics of N2 on rigid Ni(1 1 1). Computational and Theoretical Chemistry, 2022, 1211, 113679.	1.1	1
67000	The adsorption properties and stable configurations of hydroxyl groups at Mo edge of MoS2 (100) surface. Materials Chemistry and Physics, 2022, 283, 126051.	2.0	4
67001	Carbon ene-yne working in oxygenator: A theoretical study. Diamond and Related Materials, 2022, 125, 108991.	1.8	4
67002	The deposition of Cu2O and Cu by photochemical reduction method promotes the efficient degradation of organic pollutants by Sn-TiO2 under visible light. Applied Catalysis A: General, 2022, 637, 118602.	2.2	1
67003	High-energy-density metal nitrides with armchair chains. Matter and Radiation at Extremes, 2022, 7, .	1.5	10
67004	First-principles investigations on the interface structure, stability and electronic properties of UN/ZrC for dispersion nuclear fuel. Journal of Nuclear Materials, 2022, 563, 153622.	1.3	1
67005	Prediction the photocatalytic water splitting of bismuth vanady1 oxyhalide BiVO3F based on density functional theory. Molecular Catalysis, 2022, 524, 112244.	1.0	0
67006	Exploration of perfluorooctane sulfonate degradation properties and mechanism via electron-transfer dominated radical process. Water Research, 2022, 215, 118259.	5.3	26
67007	Implications of coordination chemistry to cationic interactions in honeycomb layered nickel tellurates. Computational Materials Science, 2022, 207, 111322.	1.4	9
67008	Atomic-scale structure clarification of the planar Z phase and its influence on the magnetic properties in Sm(CoFeCuZr) permanent magnets. Acta Materialia, 2022, 230, 117846.	3.8	8
67009	A reasonable approach to describe the atom distributions and configurational entropy in high entropy alloys based on site preference. Intermetallics, 2022, 144, 107489.	1.8	9
67010	Pairwise dilatational strain as a parametric model describing potential secondary phase formation and high-angle grain misorientation in as-cast high-entropy alloys. Intermetallics, 2022, 144, 107462.	1.8	0
67011	Ab initio study of mechanical properties of hexagonal high-entropy ceramic (Mo0.25Nb0.25Ta0.25V0.25)(Al0.5Si0.5)2 with dual mixing of cation and anion sublattice. Journal of Physics and Chemistry of Solids, 2022, 165, 110701.	1.9	3
67012	Monoclinic mC28 carbon: A sp2-sp3 hybridized carbon allotrope with superhard and metallic properties. Chemical Physics, 2022, 558, 111503.	0.9	0
67013	Delithiation-induced oxygen vacancy formation increases microcracking of LiCoO2 cathodes. Journal of Power Sources, 2022, 533, 231316.	4.0	6
67014	Design principles of low-activation high entropy alloys. Journal of Alloys and Compounds, 2022, 907, 164526.	2.8	12

#	Article	IF	Citations
67015	V2C MXene enriched with -O termination as high-efficiency electrocatalyst for lithium-oxygen battery. Applied Materials Today, 2022, 27, 101464.	2.3	6
67016	A robust and efficient line search for self-consistent field iterations. Journal of Computational Physics, 2022, 459, 111127.	1.9	2
67017	An in-plane S-scheme heterostructure drives H2 production with water and solar energy. Chemical Engineering Journal, 2022, 437, 135280.	6.6	17
67018	Flexoelectricity and electronic properties of monolayer GaSe under shear strain gradient. Physics Letters, Section A: General, Atomic and Solid State Physics, 2022, 436, 128090.	0.9	4
67019	Study of vacancy, voids, atom adsorption and domain substitution in hexagonal gallium nitride monolayer. Surfaces and Interfaces, 2022, 30, 101898.	1.5	1
67020	Anchoring of phthalic acid on MgO(100). Surface Science, 2022, 720, 122007.	0.8	1
67021	3D hierarchical local heterojunction as ultra-highly efficient Fenton-like catalyst: Mechanism of coupling the proton-coupled electron transfer under nanoconfinement effect. Journal of Environmental Chemical Engineering, 2022, 10, 107604.	3.3	9
67022	Correlation between redox active sites and sodium storage behavior in dye/graphene nanohybrids. Applied Surface Science, 2022, 587, 152859.	3.1	2
67023	Determination of thermodynamic growth conditions for a high-efficiency Cu<mml:math xmlns:mml="http://www.w3.org/1998/Math/MathML" display="inline" id="d1e1705" altimg="si10.svg"><mml:msub><mml:mrow		

#	Article	IF	Citations
67033	Integrated carbon capture and utilization: Synergistic catalysis between highly dispersed Ni clusters and ceria oxygen vacancies. Chemical Engineering Journal, 2022, 437, 135394.	6.6	33
67034	Thermodynamic re-modelling of the Cuâ€“Nbâ€“Sn system: Integrating the nausite phase. Calphad: Computer Coupling of Phase Diagrams and Thermochemistry, 2022, 77, 102409.	0.7	4
67035	Revealing the superlative electrochemical properties of o-B2N2 monolayer in Lithium/Sodium-ion batteries. Nano Energy, 2022, 96, 107066.	8.2	29
67036	Atomistic prediction on the composition- and configuration-dependent bandgap of Ga(As,Sb) using cluster expansion and ab initio thermodynamics. Materials Science and Engineering B: Solid-State Materials for Advanced Technology, 2022, 280, 115713.	1.7	1
67037	A facile approach to tailor electrocatalytic properties of MnO2 through tuning phase transition, surface morphology and band structure. Chemical Engineering Journal, 2022, 438, 135561.	6.6	21
67038	Magnetic properties of amorphous silicon carbonitride-based magnetoceramics synthesized using phenyl-substituted polysilazane as a precursor. Journal of Alloys and Compounds, 2022, 905, 164282.	2.8	2
67039	Local atomic ordering strategy for high strength Mg alloy design by first-principle calculations. Journal of Alloys and Compounds, 2022, 907, 164491.	2.8	10
67040	Self-supported Co9S8-Ni3S2-CNTs/NF electrode with superwetting multistage micro-nano structure for efficient bifunctional overall water splitting. Journal of Colloid and Interface Science, 2022, 616, 287-297.	5.0	33
67041	The SiPb monolayer with high thermoelectric performance at room temperature. Surfaces and Interfaces, 2022, 30, 101831.	1.5	1
67042	Zirconium-enhanced segregation tendency of solutes X and Zr-X co-segregation induced synergistic/antagonistic effects on Ni Î£5 [001](210) grain boundary. Materials Today Communications, 2022, 31, 103319.	0.9	1
67043	Exploring the stable structures and photovoltaic properties of an ideal pseudo-binary alloy: Indium gallium phosphide. Computational Materials Science, 2022, 209, 111351.	1.4	1
67044	xmlns:mml="http://www.w3.org/1998/Math/MathML" display="inline" id="d1e809" altimg="si132.svg"><mml:msub><mml:mrow /><mml:mrow><mml:mn>3</mml:mn></mml:mrow></mml:msub></mml:math>AlC<mml:math xmlns:mml="http://www.w3.org/1998/Math/MathML" display="inline" id="d1e817"	1.4	3
67045	The segregation of transition metals to iron grain boundaries and their effects on cohesion. Acta Materialia, 2022, 231, 117902.	3.8	26
67046	Carbon-rehybridization-induced templated growth of metal nanoclusters on graphene moirÃ© patterns. Carbon, 2022, 192, 295-300.	5.4	6
67047	Investigating the role of ultrasound in improving the photocatalytic ability of CQD decorated boron-doped g-C3N4 for tetracycline degradation and first-principles study of nitrogen-vacancy formation. Carbon, 2022, 192, 405-417.	5.4	68
67048	Cu vacancy engineering of cage-compound BaCu2Se2: Realization of temperature-dependent hole concentration for high average thermoelectric figure-of-merit. Chemical Engineering Journal, 2022, 437, 135302.	6.6	6
67049	Property changes in two-dimensional electride bilayers through compression, sliding, and twisting. Applied Surface Science, 2022, 586, 152596.	3.1	4
67050	Controllable carrier polarity in 2D HfS2(1â^'x)Te2x for short-wave infrared photodiodes. Infrared Physics and Technology, 2022, 123, 104139.	1.3	2

#	Article	IF	Citations
67051	Semi-metallic PC5 monolayer as a superior anode material for potassium ion batteries: A first principles study. Colloids and Surfaces A: Physicochemical and Engineering Aspects, 2022, 643, 128756.	2.3	25
67052	Surface-engineered Mo2C: an ideal electrode for 2D semiconductor-based complementary circuit with Schottky-barrier-free contacts. Materials Today Chemistry, 2022, 24, 100790.	1.7	1
67053	TiO2 nanoarrays modification by a novel Cobalt-heteroatom doped graphene complex for photoelectrochemical water splitting: An experimental and theoretical study. Journal of Molecular Liquids, 2022, 356, 118960.	2.3	9
67054	Thermally-induced spin transition in Fe(4,4â€²-Azopyridine)[Fe(CN)5NO]. Journal of Solid State Chemistry, 2022, 310, 123054.	1.4	12
67055	Hot atom chemistry: Oxygen at stepped platinum surfaces. Applied Surface Science Advances, 2022, 9, 100240.	2.9	1
67056	Regulating interfacial desolvation via a weakly coordinating solvent molecule enhances Li-ion storage at subzero temperatures. Chemical Engineering Science, 2022, 254, 117633.	1.9	3
67057	Nitrogen and sulfur co-doped graphene nanoribbons with well-ordered stepped edges for high-performance potassium-ion battery anodes. Energy Storage Materials, 2022, 48, 325-334.	9.5	16
67058	Hydrogen solubility in Zrâ€“Nb alloys. Scripta Materialia, 2022, 214, 114652.	2.6	6
67059	Effect of hybridization in PdAlY-(Ni/Au/Ir) metallic glasses thin films on electrical resistivity. Scripta Materialia, 2022, 214, 114681.	2.6	0
67060	Boosting high voltage cycling of LiCoO2 cathode via triisopropanolamine cyclic borate electrolyte additive. Journal of Power Sources, 2022, 532, 231372.	4.0	14
67061	Composition-controlled ultrathin holey TiO1â^'xNx nanosheets as powerful hybridization matrices for highly mass-efficient electrocatalysts. Chemical Engineering Journal, 2022, 437, 135415.	6.6	7
67062	Batch active learning for accelerating the development of interatomic potentials. Computational Materials Science, 2022, 208, 111330.	1.4	8
67063	Structure and electronic properties of LnScO3 compounds: A GGAÂ+ÂU calculation. Computational Materials Science, 2022, 208, 111350.	1.4	1
67064	Computational screening of single transition metal atom embedded in nitrogen doped graphene for CH4 detection. Materials Today Communications, 2022, 31, 103383.	0.9	0
67065	Single-Walled Black Phosphorus Nanotube as a NO2 Gas Sensor. Materials Today Communications, 2022, 31, 103434.	0.9	3
67066	Interface transition from Ohmic to Schottky contact in Ti3X2/MoS2 (X= B, C, N): Insights from first-principles. Surfaces and Interfaces, 2022, 30, 101823.	1.5	4
67067	Microstructure and electrical properties of new high-entropy rare-earth zirconates. Journal of Alloys and Compounds, 2022, 906, 164331.	2.8	16
67068	Synthesis, structure, and electrical conductivity of Sr2LiH2N nitride hydride. Journal of Solid State Chemistry, 2022, 310, 123051.	1.4	5

#	Article	IF	Citations
67069	Investigation of swelling behaviors of U-10Zr metallic fuel in the low temperature regime via a cavitational void swelling model. Journal of Nuclear Materials, 2022, 564, 153665.	1.3	2
67070	Fast and extensive intercalation chemistry in Wadsley-Roth phase based high-capacity electrodes. Journal of Energy Chemistry, 2022, 69, 601-611.	7.1	6
67071	Electric field controlled CO2 capture and activation on BC6N monolayers: A first-principles study. Surfaces and Interfaces, 2022, 30, 101885.	1.5	6
67072	Atomic site occupancy of alloying elements and Laves phase stability in Î³-Î³â€² Co-base superalloys. Journal of Alloys and Compounds, 2022, 906, 164261.	2.8	4
67073	2D Janus and non-Janus diamanes with an in-plane negative Poisson's ratio for energy applications. Materials Today Advances, 2022, 14, 100225.	2.5	10
67074	Electronic structure properties of boronâ€“doped and carbonâ€“boronâ€“codoped TiO2(B) for photocatalytic applications. Journal of Physics and Chemistry of Solids, 2022, 165, 110685.	1.9	3
67075	Upcycling of electroplating sludge into Fe3C-decorated N,P dual-doped porous carbon via microalgae as efficient sulfur host for lithiumâ€“sulfur batteries. Surfaces and Interfaces, 2022, 30, 101869.	1.5	6
67076	Investigation on the local structure and properties of molten Li2CO3-K2CO3 binary salts by machine learning potentials. Journal of Molecular Liquids, 2022, 356, 118979.	2.3	7
67077	Room temperature ferromagnetism in Gd-doped AlN hierarchical microstructures: Experimental and theoretical insights. Journal of Alloys and Compounds, 2022, 907, 164461.	2.8	3
67078	Single noble metals (Pd, Pt and Ir) anchored Janus MoSSe monolayers: Efficient oxygen reduction/evolution reaction bifunctional electrocatalysts and harmful gas detectors. Journal of Colloid and Interface Science, 2022, 616, 177-188.	5.0	10
67079	Interface bonding and failure mechanism of Ti(001)/Si(001) and TiO2(001)/Si(001) interfaces: A firstâ€“principles study. Surfaces and Interfaces, 2022, 30, 101833.	1.5	3
67080	Effect of selected dopants on conductivity and moisture stability of Li3PS4 sulfide solid electrolyte: a first-principles study. Materials Today Chemistry, 2022, 24, 100837.	1.7	4
67081	Could Î»-Ti3O5 with lamellar and channel microstructure characteristics determine the excellent properties of LIBs? The first-principles study of Î»-Ti3O5 lithiation mechanism. Materials Today Communications, 2022, 31, 103332.	0.9	1
67082	Study of phase-pure TiO2 for the removal of fluorides in water. Materials Today Communications, 2022, 31, 103389.	0.9	2
67083	Highly selective formaldehyde sensor using silicon doped graphene: A theoretical study. Materials Today Communications, 2022, 31, 103452.	0.9	2
67084	Intrinsic defect-related thermoluminescence in Li1âˆ’xNaxMgPO4 (0Ââ‰¤xÂâ‰¤Â0.20). Materials Today Communications, 2022, 31, 103346.	0.9	2
67085	Transverse electronic transport through nucleobase-pairs of a DNA wire. Materials Today Chemistry, 2022, 24, 100834.	1.7	2
67086	Feâ€“Nâ€“C single-atom nanozymes based sensor array for dual signal selective determination of antioxidants. Biosensors and Bioelectronics, 2022, 205, 114097.	5.3	45

#	Article	IF	Citations
67087	Outstanding thermal conductivity and mechanical properties in the direct gap semiconducting penta-NiN2 monolayer confirmed by first-principles. Physica E: Low-Dimensional Systems and Nanostructures, 2022, 140, 115221.	1.3	10
67088	Surface stability of WN ultrathin films under O2 and H2O exposure: A first-principles study. Applied Surface Science, 2022, 588, 152940.	3.1	5
67089	Thermodynamically driven Al migration across ultrathin Ag layered electrodes without thermal loading. Applied Surface Science, 2022, 588, 152907.	3.1	3
67090	Polyether sulfone and Li6.4La3Zr1.4Ta0.6O12 based polymer-in-ceramic electrolyte with enhanced conductivity at low temperature for solid state lithium batteries. Applied Materials Today, 2022, 27, 101447.	2.3	4
67091	Understanding the surface structure evolution and electron emission behaviors during the activation of Ir-coated dispenser cathodes. Vacuum, 2022, 200, 111016.	1.6	3
67092	Design and tailoring of carbon-Al2O3 double coated nickel-based cation-disordered cathodes towards high-performance Li-ion batteries. Nano Energy, 2022, 96, 107071.	8.2	26
67093	Nitrobenzene inarched carbon nitride nanotube drives efficient directional carriers separation for superior photocatalytic hydrogen production. Journal of Colloid and Interface Science, 2022, 616, 691-700.	5.0	15
67094	Persistent luminescence ratiometric thermometry. Chemical Engineering Journal, 2022, 438, 135573.	6.6	24
67095	Chirality distribution of single-walled carbon nanotubes grown from gold nanoparticles. Carbon, 2022, 192, 259-264.	5.4	10
67096	Possible topological states in two dimensional Kagome ferromagnet MnGe. Journal of Alloys and Compounds, 2022, 907, 164389.	2.8	5
67097	Tuning the magnetic properties of FeTe2 monolayer doped by (TM: V, Mn, and Co). Journal of Magnetism and Magnetic Materials, 2022, 552, 169204.	1.0	6
67098	Enhancing cycling stability in Li-rich Mn-based cathode materials by solid-liquid-gas integrated interface engineering. Nano Energy, 2022, 97, 107201.	8.2	17
67099	Honeycomb-like puckered PbTe monolayer: A promising n-type thermoelectric material with ultralow lattice thermal conductivity. Journal of Alloys and Compounds, 2022, 907, 164439.	2.8	25
67100	The spin-state transition in ACo2O4 spinels (AÂ=ÂBe, Mg, Ca, Cd, Zn). Journal of Magnetism and Magnetic Materials, 2022, 552, 169206.	1.0	1
67101	Predicted crystal structures of AlN4 at high pressure. Solid State Communications, 2022, 348-349, 114745.	0.9	0
67102	Tailoring the structural stability, electrochemical performance and CO2 tolerance of aluminum doped SrFeO3. Separation and Purification Technology, 2022, 290, 120843.	3.9	10
67103	Sustainable Fe3+ reduction by Fe3O4@tourmaline in Fenton-like system. Chemical Engineering Journal, 2022, 437, 135480.	6.6	23
67104	Computational insights into structural, electronic and optical properties of Al0.5Ga0.5N nanowire with different diameters. Chemical Physics Letters, 2022, 797, 139597.	1.2	0

#	Article	IF	Citations
67105	Flame normalizing-induced robust and oriented metallic layer for stable Zn anode. Chemical Engineering Journal, 2022, 437, 135246.	6.6	18
67106	First-principles study of CO gas adsorption on pristine and Fe-doped H<mml:math xmlns:mml="http://www.w3.org/1998/Math/MathML" display="inline" id="d1e1723" altimg="si98.svg"><mml:msub><mml:mrow /><mml:mrow><mml:mn>4</mml:mn><mml:mo>,</mml:mo><mml:mn>4</mml:mn><mml:mo>,</mml:mo><mml:mn>4</mml:mn><mml:mn> Applied Surface Science, 2022, 586, 152749.	3.1	5
67107	Quantitative calculations of thermal-expansion coefficient in Feâ€“Ni alloys: First-principles approach. Current Applied Physics, 2022, 38, 76-80.	1.1	3
67108	Extreme structure and spontaneous lift of spin degeneracy in doped perforated bilayer graphenes. Carbon, 2022, 192, 61-70.	5.4	6
67109	A graphdiyne analogue for dendrite-free lithium metal anode. Electrochimica Acta, 2022, 416, 140286.	2.6	2
67110	Using tetramethylammonium hydroxide electrolyte to inhibit corrosion of Mg-based amorphous alloy anodes: A route for promotion energy density of Ni-MH battery. Journal of Alloys and Compounds, 2022, 907, 164293.	2.8	5
67111	Li- and Na-doped bismuth titanate pyrochlores: From the point of view ab initio calculation and experiment. Solid State Ionics, 2022, 379, 115904.	1.3	0
67112	Trade-off effect of 3d transition metal doped boron nitride on anchoring polysulfides towards application in lithium-sulfur battery. Journal of Colloid and Interface Science, 2022, 616, 886-894.	5.0	4
67113	Theoretical study the influence of partial substitute noble metal Pd/Ag of PdAg-based catalyst by non-noble metal Ni/Cu for 1,3-Butadiene hydrogenation. Applied Surface Science, 2022, 588, 152897.	3.1	2
67114	Vapor pressure-controllable molecular inorganic precursors for growth of monolayer WS2: Influence of precursor-substrate interaction on growth thermodynamics. Applied Surface Science, 2022, 587, 152829.	3.1	4
67115	CoP/Cu3P heterostructured nanoplates for high-rate supercapacitor electrodes. Chemical Engineering Journal, 2022, 437, 135352.	6.6	66
67116	Hydrogen absorption and diffusion behaviors in cube-shaped palladium nanoparticles revealed by ambient-pressure X-ray photoelectron spectroscopy. Applied Surface Science, 2022, 587, 152797.	3.1	7
67117	An ab initio simulation and experimental studies of the glass-forming ability and properties of Al86Ni(14-x)Zrx (xÂ=Â1âˆ¼7) alloys. Journal of Non-Crystalline Solids, 2022, 586, 121566.	1.5	8
67118	Hydrogen localization and cluster formation in Î±-Zr from first-principles investigations. Computational Materials Science, 2022, 209, 111384.	1.4	3
67119	First principles study of the structural, electronic, magnetic and optical properties of the Fe doped CoS2 thin films. Thin Solid Films, 2022, 751, 139228.	0.8	1
67120	Ordered and disordered two-dimensional tellurium-selenium binary compounds from swarm intelligence and first principles. Materials Today Communications, 2022, 31, 103409.	0.9	0
67121	First-principles study of the effect of aluminum content on the elastic properties of Cu-Al alloys. Materials Today Communications, 2022, 31, 103399.	0.9	5
67122	Micro-mechanism of multi-pathway activation peroxymonosulfate by copper-doped cobalt silicate: The dual role of copper. Applied Catalysis B: Environmental, 2022, 309, 121276.	10.8	45

#	Article	IF	Citations
67123	In-situ growing polyaniline nano-spine array on FeVO4 nanobelts as high-performance rechargeable aluminum-ion battery cathode. Applied Surface Science, 2022, 591, 153157.	3.1	11
67124	One-pot synthesis of novel porous carbon adsorbents derived from poly vinyl chloride for high methane adsorption uptake. Chemical Engineering Journal, 2022, 440, 135867.	6.6	9
67125	Au decorated Pd nanowires for methane oxidation to liquid C1 products. Applied Catalysis B: Environmental, 2022, 308, 121223.	10.8	20
67126	NO adsorption on the Os, Ir, and Pt embedded tri-s-triazine based graphitic carbon nitride: A DFT study. Applied Surface Science, 2022, 590, 153104.	3.1	14
67127	Nano gold coupled black titania composites with enhanced surface plasma properties for efficient photocatalytic alkyne reduction. Applied Catalysis B: Environmental, 2022, 309, 121222.	10.8	11
67128	The flexible Janus X2PAs (XÂ=ÂSi, Ge and Sn) monolayers with in-plane and out-of-plane piezoelectricity. Applied Surface Science, 2022, 589, 152999.	3.1	23
67129	Electrochemical reforming of ethanol with acetate Co-Production on nickel cobalt selenide nanoparticles. Chemical Engineering Journal, 2022, 440, 135817.	6.6	19
67130	Two-dimensional Sc2CCl2/SiS2 van der Waals heterostructure with high solar power conversion efficiency. Applied Surface Science, 2022, 591, 153232.	3.1	8
67131	Type-II CdS/PtSSe heterostructures used as highly efficient water-splitting photocatalysts. Applied Surface Science, 2022, 589, 152931.	3.1	59
67132	Influence of Co and Co-F co-doping on defect-induced intrinsic ferromagnetic properties of PbPdO2 nanoparticles. Journal of Magnetism and Magnetic Materials, 2022, 553, 169240.	1.0	2
67133	Electron redistribution of ruthenium-tungsten oxides Mott-Schottky heterojunction for enhanced hydrogen evolution. Applied Catalysis B: Environmental, 2022, 308, 121229.	10.8	69
67134	A new Sc-doped La0.5Sr0.5MnO3-Î´ cathode allows high performance for proton-conducting solid oxide fuel cells. Sustainable Materials and Technologies, 2022, 32, e00409.	1.7	13
67135	CdS/ethylenediamine nanowires 3D photocatalyst with rich sulfur vacancies for efficient syngas production from CO2 photoreduction. Applied Catalysis B: Environmental, 2022, 308, 121227.	10.8	59
67136	How do the products in methane dehydroaromatization impact the distinct stages of the reaction?. Applied Catalysis B: Environmental, 2022, 309, 121274.	10.8	15
67137	Amorphous NiSb2O6â€“ nanofiber: A d-/p-block Janus electrocatalyst toward efficient NH3 synthesis through boosted N2 adsorption and activation. Applied Catalysis B: Environmental, 2022, 308, 121225.	10.8	12
67138	Outstanding stability of Gd-doped UO2 against surface oxidation: First-principles study. Applied Surface Science, 2022, 589, 152955.	3.1	1
67139	Large enhancement of thermoelectric properties of CoSb3 tuned by uniaxial strain. Journal of Alloys and Compounds, 2022, 908, 164404.	2.8	1
67140	Exploring the structural stability, electronic and thermal attributes of synthetic 2D materials and their heterostructures. Applied Surface Science, 2022, 590, 153131.	3.1	15

#	Article	IF	Citations
67141	Vacancy-engineered half-metallicity and magnetic anisotropy in CrSI semiconductor monolayer. Journal of Alloys and Compounds, 2022, 909, 164797.	2.8	63
67142	Electric field tunable electronic properties of antimonene/graphyne van der Waals heterostructure. Journal of Alloys and Compounds, 2022, 909, 164653.	2.8	7
67143	Growth and Electrical Properties of Polymorphs of Mo-Te Crystals. Materials Research Bulletin, 2022, 151, 111796.	2.7	1
67144	Construction of dual active sites on diatomic metal (FeCoâˆ’N/C-x) catalysts for enhanced Fenton-like catalysis. Applied Catalysis B: Environmental, 2022, 309, 121256.	10.8	40
67145	Density functional theory screening of thiophene adsorbents and study of adsorption mechanism. Surface Science, 2022, 721, 122069.	0.8	3
67146	Subtle modulation on electronic properties of platinum by Cu-Nx containing carbon support for highly efficient electrocatalytic hydrogen evolution. Applied Surface Science, 2022, 591, 153057.	3.1	7
67147	An emerging direct monolayer Î´-AlP3: High stability, desirable carrier mobility, NO2-sensitive sensing performance, and superior catalytic properties toward the nitrogen reduction reaction. Applied Surface Science, 2022, 591, 153191.	3.1	11
67148	Element segregation and thermal stability of Niâ€“Rh nanoparticles. Journal of Solid State Chemistry, 2022, 311, 123096.	1.4	8
67149	Insights into enhanced O3 adsorption on Ti/ anatase TiO2 (1 0 1) surfaces by positive electric Fields: A theoretical exploration. Chemical Engineering Journal, 2022, 440, 135665.	6.6	8
67150	A combined first-principles and machine-learning investigation on the stability, electronic, optical, and mechanical properties of novel C6N7-based nanoporous carbon nitrides. Carbon, 2022, 194, 230-239.	5.4	24
67151	Heterogeneous interface in hollow ferroferric oxide/ iron phosphide@carbon spheres towards enhanced Li storage. Journal of Colloid and Interface Science, 2022, 617, 442-453.	5.0	15
67152	Optimal surface/diffusion-controlled kinetics of bimetallic selenide nanotubes for hybrid supercapacitors. Journal of Colloid and Interface Science, 2022, 617, 304-314.	5.0	18
67153	Theoretical insights into the CO/NO oxidation mechanisms on single-atom catalysts anchored H4,4,4-graphyne and H4,4,4-graphyne/graphene sheets. Fuel, 2022, 319, 123810.	3.4	8
67154	Density functional theory study of CH4 dissociation and C C coupling on W-terminated WC(0001) surface. Applied Surface Science, 2022, 591, 153128.	3.1	5
67155	Unveiling the promotion of intermediates transport kinetics on the N/S co-doping 3D structure titanium carbide aerogel for high-performance supercapacitors. Journal of Colloid and Interface Science, 2022, 618, 161-172.	5.0	8
67156	Peroxymonosulfate activation by black TiO2 nanotube arrays under solar light: Switching the activation mechanism and enhancing catalytic activity and stability. Journal of Hazardous Materials, 2022, 433, 128796.	6.5	24
67157	Design strategy of bifunctional catalysts for CO oxidation. Fuel, 2022, 320, 123909.	3.4	10
67158	Anomalous elasticity of talc at high pressures: Implications for subduction systems. Geoscience Frontiers, 2022, 13, 101381.	4.3	4

#	Article	IF	Citations
67159	Impact of ultrathin coating layer on lithium-ion intercalation into particles for lithium-ion batteries. Chemical Engineering Journal, 2022, 440, 135565.	6.6	7
67160	Tandem catalysis on adjacent active motifs of copper grain boundary for efficient CO2 electroreduction toward C2 products. Journal of Energy Chemistry, 2022, 70, 219-223.	7.1	29
67161	Dangling bonds on the Cl- and Br-terminated Si(100) surfaces. Applied Surface Science, 2022, 591, 153080.	3.1	7
67162	2D-Mo3S4 phase as promising contact for MoS2. Applied Surface Science, 2022, 589, 152971.	3.1	6
67163	Screening of transition metal single-atom catalysts doped on Î³-graphyne-like BN sheet for efficient nitrogen reduction reaction. Journal of Alloys and Compounds, 2022, 908, 164675.	2.8	13
67164	Titanium and fluorine co-modification strengthens high-voltage electrochemical performance of LiCoO2. Journal of Alloys and Compounds, 2022, 909, 164787.	2.8	5
67165	Clathrate structure of polymerized fullerite C60. Carbon, 2022, 194, 297-302.	5.4	3
67166	Asymmetric surfaces endow Janus bismuth oxyhalides with enhanced electronic and catalytic properties for the hydrogen evolution reaction. Journal of Colloid and Interface Science, 2022, 617, 204-213.	5.0	12
67167	A biocompatible bismuth based metal-organic framework as efficient light-sensitive drug carrier. Journal of Colloid and Interface Science, 2022, 617, 578-584.	5.0	12
67168	Cobalt phosphosulfide nanoparticles encapsulated into heteroatom-doped carbon as bifunctional electrocatalyst for Znâ^'air battery. , 2022, 1, 100027.		51
67169	Solvent evaporation induced preferential crystal orientation BiI3 films for the high efficiency MA3Bi2I9 perovskite solar cells. Journal of Alloys and Compounds, 2022, 909, 164725.	2.8	7
67170	Janus Aluminum Oxysulfide Al2OS: A promising 2D direct semiconductor photocatalyst with strong visible light harvesting. Applied Surface Science, 2022, 589, 152997.	3.1	21
67171	Strain adjustment Pt-doped Ti2CO2 as an efficient bifunctional catalyst for oxygen reduction reactions and oxygen evolution reactions by first-principles calculations. Applied Surface Science, 2022, 590, 153149.	3.1	16
67172	Nonlinear optical and detonation properties of semiorganic nitrate crystal C6H14N2(NO3)3Â·H3O. Journal of Alloys and Compounds, 2022, 908, 164632.	2.8	1
67173	Formation of carbonate and oxalate species on a Cobalt-modified Fe3O4(111) surface: Comparison of DFT+U, hybrid functionals, and the random phase approximation. Surface Science, 2022, 721, 122068.	0.8	2
67174	A strategic high throughput search for identifying stable Li based half Heusler alloys for spintronics applications. Journal of Magnetism and Magnetic Materials, 2022, 553, 169244.	1.0	2
67175	Highly efficient, field-assisted water splitting enabled by a bifunctional Ni3Fe magnetized wood carbon. Chemical Engineering Journal, 2022, 439, 135722.	6.6	17
67176	Nitrogen-stabilized oxygen vacancies in TiO2 for site-selective loading of Pt and CoOx cocatalysts toward enhanced photoreduction of CO2 to CH4. Chemical Engineering Journal, 2022, 439, 135744.	6.6	24

#	Article	IF	Citations
67177	N-doped carbon nanosheets supported-single Fe atom for p-nitrophenol degradation via peroxymonosulfate activation. Applied Surface Science, 2022, 591, 153124.	3.1	21
67178	Surface water H-bonding network is key controller of selenate adsorption on [0 1 2] Î±-alumina: An Ab-initio study. Journal of Colloid and Interface Science, 2022, 617, 136-146.	5.0	14
67179	Probing the structural evolution and its impact on magnetic properties of FeCoNi(AlMn)x high-entropy alloy at the nanoscale. Journal of Alloys and Compounds, 2022, 910, 164724.	2.8	6
67180	Superoxide anion and singlet oxygen dominated faster photocatalytic elimination of nitric oxide over defective bismuth molybdates heterojunctions. Journal of Colloid and Interface Science, 2022, 618, 248-258.	5.0	4
67181	Enhanced water splitting photocatalyst enabled by two-dimensional GaP/GaAs van der Waals heterostructure. Applied Surface Science, 2022, 591, 153198.	3.1	12
67182	Activation or passivation: Influence of halogen dopant (F, Cl, Br) on photothermal activity of Mn2O3 in degrading toluene. Applied Catalysis B: Environmental, 2022, 309, 121236.	10.8	34
67183	Doping level and environment dependence of structural stability and magnetic properties in Mn-doped WS2 bilayer in first principles. Current Applied Physics, 2022, 39, 1-7.	1.1	1
67184	Controlling the metal work function through atomic-scale surface engineering. Applied Surface Science, 2022, 589, 152932.	3.1	2
67185	Global instability index as a crystallographic stability descriptor of halide and chalcogenide perovskites. Journal of Energy Chemistry, 2022, 70, 1-8.	7.1	13
67186	From high temperature phase formation to transition metal substitution in the Fe/Al9Co2(001) system. Applied Surface Science, 2022, 591, 153100.	3.1	0
67187	Understanding the anchoring effect on Li plating with Indium Tin oxide layer functionalized hosts for Li metal anodes. Chemical Engineering Journal, 2022, 440, 135827.	6.6	10
67188	Effect of reduction on NOÂ+ÂCO reaction performance of CuO-Co3O4 symbiotic oxide porous nanosheet and DFT calculation. Applied Surface Science, 2022, 589, 153052.	3.1	5
67189	Adsorption of NO2 and CO molecules on Ni (1 1 1) supported defective Graphene: A DFT study. Applied Surface Science, 2022, 590, 153027.	3.1	7
67190	Quantum studies of methane-metal inelastic diffraction and trapping: The variation with molecular orientation and phonon coupling. Chemical Physics, 2022, 559, 111516.	0.9	6
67191	Enhanced magnetic anisotropy in two-dimensional <mml:math xmlns:mml="http://www.w3.org/1998/Math/MathML" display="inline" id="d1e370" altimg="si3.svg"><mml:mrow><mml:mn>2</mml:mn><mml:mi>H</mml:mi><mml:mo linebreak="goodbreak" linebreakstyle="after">â^’</mml:mo><mml:mi>T</mml:mi><mml:mi>a</mml:mi><mml:msub><mml:mrow><mml:mi>S</mml:mi></mml	1.0	5
67192	by self-intercalation: A DFT study. Journal of Magnetism and Magnetic Materials, 2022, 553, 168988. Rational design of two dimensional single crystalline Na3V2(PO4)2F3 nanosheets for boosting Na+ migration and mitigating grain pulverization. Chemical Engineering Journal, 2022, 439, 135533.	6.6	22
67193	Leveraging doping and defect engineering to modulate exciton dissociation in graphitic carbon nitride for photocatalytic elimination of marine oil spill. Chemical Engineering Journal, 2022, 439, 135668.	6.6	31
67194	Dual-Conductive Li alloy composite anode constructed by a synergetic Conversion-Alloying reaction with LiMgPO4. Chemical Engineering Journal, 2022, 439, 135705.	6.6	10

#	Article	IF	Citations
67195	Understanding the effect of transition metals and vacancy boron nitride catalysts on activity and selectivity for CO2 reduction reaction to valuable products: A DFT-D3 study. Fuel, 2022, 319, 123808.	3.4	13
67196	Theoretical investigation of HER/OER/ORR catalytic activity of single atom-decorated graphyne by DFT and comparative DOS analyses. Applied Surface Science, 2022, 592, 153237.	3.1	46
67197	A key role of soft and refractory coke in the deactivation of Î³â€“Al2O3 catalysts during low-temperature methyl oleate epoxidation: An experiment and DFT study. Fuel, 2022, 321, 124064.	3.4	2
67198	MOF etching-induced Co-doped hollow carbon nitride catalyst for efficient removal of antibiotic contaminants by enhanced perxymonosulfate activation. Chemical Engineering Journal, 2022, 441, 136074.	6.6	45
67199	Tuning single metal atoms anchored on graphdiyne for highly efficient and selective nitrate electroreduction to ammonia under aqueous environments: A computational study. Applied Surface Science, 2022, 592, 153213.	3.1	27
67200	Insights into in-situ TiB/dual-phase Ti alloy interface and its high load-bearing capacity. Journal of Materials Science and Technology, 2022, 119, 156-166.	5.6	24
67201	Regioselectivity regulation of styrene hydroformylation over Rh-based Phosphides: Combination of DFT calculations and kinetic studies. Chemical Engineering Journal, 2022, 441, 136101.	6.6	9
67202	Lithium dendrite suppression with Li3N-rich protection layer formation on 3D anode via ultra-low temperature nitriding. Chemical Engineering Journal, 2022, 441, 136067.	6.6	14
67203	Enabling efficient electrocatalytic conversion of N2 to NH3 by Ti3C2 MXene loaded with semi-metallic 1Tâ€²-MoS2 nanosheets. Applied Catalysis B: Environmental, 2022, 310, 121277.	10.8	54
67204	Shape-shifting nanoparticles on a perovskite oxide for highly stable and active heterogeneous catalysis. Chemical Engineering Journal, 2022, 441, 136025.	6.6	13
67205	Photocatalytic applications of 2D surface decorated boron phosphides: A density functional theory investigation. Applied Surface Science, 2022, 592, 153236.	3.1	3
67206	Hydrogen storage by spillover on Ni4 cluster embedded in three vacancy graphene. A DFT and dynamics study. Journal of Physics and Chemistry of Solids, 2022, 167, 110706.	1.9	6
67207	Nanoconfined SnS2 in robust SnO2 nanocrystals building heterostructures for stable sodium ion storage. Chemical Engineering Journal, 2022, 442, 136222.	6.6	28
67208	Precise regulation of CO2 packing pattern in s-block metal doped single-layer covalent organic frameworks for high-performance CO2 capture and separation. Chemical Engineering Journal, 2022, 441, 135903.	6.6	7
67209	Single-atomic iron-nitrogen 2D MOF-originated hierarchically porous carbon catalysts for enhanced oxygen reduction reaction. Chemical Engineering Journal, 2022, 441, 135849.	6.6	31
67210	Surface self-reconstruction of telluride induced by in-situ cathodic electrochemical activation for enhanced water oxidation performance. Applied Catalysis B: Environmental, 2022, 310, 121355.	10.8	16
67211	Integrating band engineering with point defect scattering for high thermoelectric performance in Bi2Si2Te6. Chemical Engineering Journal, 2022, 441, 135968.	6.6	15
67212	Directional utilization disorder charge via In-plane driving force of functionalized graphite carbon nitride for the robust photocatalytic degradation of fluoroquinolone. Chemical Engineering Journal, 2022, 442, 135943.	6.6	14

#	Article	IF	Citations
67213	Bandgap engineering of strained S-terminated MXene and its promising application as NOx gas sensor. Applied Surface Science, 2022, 592, 153296.	3.1	14
67214	Electronic modulation and vacancy engineering of Ni9S8 to synergistically boost efficient water splitting: Active vacancy-metal pairs. Applied Catalysis B: Environmental, 2022, 310, 121356.	10.8	41
67215	Single-atom Ir and Ru anchored on graphitic carbon nitride for efficient and stable electrocatalytic/photocatalytic hydrogen evolution. Applied Catalysis B: Environmental, 2022, 310, 121318.	10.8	72
67216	Electrocatalytic nitrate reduction to ammonia on defective Au1Cu (111) single-atom alloys. Applied Catalysis B: Environmental, 2022, 310, 121346.	10.8	113
67217	Surface-layer bromine doping enhanced generation of surface oxygen vacancies in bismuth molybdate for efficient photocatalytic nitrogen fixation. Applied Catalysis B: Environmental, 2022, 310, 121319.	10.8	51
67218	Investigation of mechanical, lattice dynamical, electronic and thermoelectric properties of half Heusler chalcogenides: A DFT study. Journal of Physics and Chemistry of Solids, 2022, 167, 110704.	1.9	5
67219	Significance of gallium doping for high Ni, low Co/Mn layered oxide cathode material. Chemical Engineering Journal, 2022, 441, 135821.	6.6	34
67220	Edge engineering of platinum nanoparticles via porphyrin-based ultrathin 2D metalâ€“organic frameworks for enhanced photocatalytic hydrogen generation. Chemical Engineering Journal, 2022, 442, 136144.	6.6	31
67221	Insights into the synergistic effect of catalyst acidity and solvent basicity for effective production of pentose from glucose. Chemical Engineering Journal, 2022, 442, 136224.	6.6	9
67222	A novel Ï€-d conjugated cobalt tetraaza[14]annulene based atomically dispersed electrocatalyst for efficient CO2 reduction. Chemical Engineering Journal, 2022, 442, 136129.	6.6	16
67223	The in-depth description of phonon transport mechanisms for XC (X=Si, Ge) under hydrostatic pressure: Considering pressure-induced phase transitions. International Journal of Heat and Mass Transfer, 2022, 191, 122851.	2.5	4
67224	Unraveling the active sites of Cs-promoted Ru/Î³-Al2O3 catalysts for ammonia synthesis. Applied Catalysis B: Environmental, 2022, 310, 121269.	10.8	12
67225	Electric resonance-induced hydrate dissociation acceleration to extract methane gas. Fuel, 2022, 321, 124014.	3.4	4
67226	Desirable bonding interactions between organo-functional triazinedithiol groups and heavy metal ions for significantly improved adsorption or dispersion property. Chemical Engineering Journal, 2022, 442, 136220.	6.6	10
67227	Accurate structural descriptor enabled screening for nitrogen and oxygen vacancy codoped TiO2 with a large bandgap narrowing. Journal of Materials Science and Technology, 2022, 122, 84-90.	5.6	8
67228	Modulation of photocatalytic activity of SrBi2Ta2O9 nanosheets in NO removal by tuning facets exposure. Journal of Materials Science and Technology, 2022, 122, 91-100.	5.6	12
67229	New design concept for stable Î±-silicon nitride based on the initial oxidation evolution at the atomic and molecular levels. Journal of Materials Science and Technology, 2022, 122, 156-164.	5.6	7
67230	Ab initio Simulation of Dissolution Energy and Bond Energy of Hydrogen with 3sp, 3d, and 4d Impurities in bcc Iron. Physics of the Solid State, 2021, 63, 1065-1068.	0.2	0

#	Article	IF	Citations
67231	Why the Magnetiteâ€“Gold Coreâ€“Shell Nanoparticles Are Not Quite Good and How to Improve Them. Physics of the Solid State, 2021, 63, 1536-1540.	0.2	5
67232	Theoretical Investigations on Interfacial Behavior of Agâ€“Cuâ€“Ti/Si₃N₄ Wetting System. Journal of Nanoelectronics and Optoelectronics, 2021, 16, 1780-1790.	0.1	5
67233	The Effect of Compressive and Tensile Strains on the Electron Structure of Phosphorene. Physics of the Solid State, 2021, 63, 1690-1694.	0.2	0
67234	Substitutional oxygen activated photoluminescence enhancement in monolayer transition metal dichalcogenides. Science China Materials, 2022, 65, 1034-1041.	3.5	6
67235	Strain tunable intrinsic ferromagnetic in 2D square CrBr₂. AIP Advances, 2021, 11, 115220.	0.6	4
67236	MnæŽºæ¡MoSe2åš¸å…³å¼,è¯¨ç»“çš„åš‡å±žé“¸æ€§. Scientia Sinica: Physica, Mechanica Et Astronomica, 2021,	0.2	0
67237	Boron and Nitrogen Codoped Multilayer Graphene as a Counter Electrode: A Combined Theoretical and Experimental Study on Dye-Sensitized Solar Cells under Ambient Light Conditions. Journal of Physical Chemistry C, 2021, 125, 24894-24901.	1.5	9
67238	Spin-Orbit-Entangled Nature of Magnetic Moments and Kitaev Magnetism in Layered Halides. Applied Science and Convergence Technology, 2021, 30, 191-194.	0.3	8
67239	First Principal Simulation of Palladium Nanocatalysts Surfaces. Journal of Surface Investigation, 2021, 15, 1270-1277.	0.1	0
67240	Ionic Rectification across Ionic and Mixed Conductor Interfaces. Nano Letters, 2021, 21, 10086-10091.	4.5	1
67241	Structural, Electronic and Magnetic Properties of Mn2Co1-xVxZ (Z = Ga, Al) Heusler Alloys: An Insight from DFT Study. Magnetochemistry, 2021, 7, 159.	1.0	3
67242	Thermal transport in beta-gallium oxide thin-films using non-gray Boltzmann transport equation. Journal of Physics Condensed Matter, 2022, 34, 105603.	0.7	3
67243	Modulation of strain on electronic structure and contact type of BP/SnS van der waals heterostructure. Journal Physics D: Applied Physics, 2022, 55, 125102.	1.3	4
67244	Evolution of the conductive filament system in HfO2-based memristors observed by direct atomic-scale imaging. Nature Communications, 2021, 12, 7232.	5.8	85
67245	Coupled Current Jumps and Domain Wall Creeps in a Defectâ€Engineered Ferroelectric Resistive Memory. Advanced Electronic Materials, 0, , 2101059.	2.6	5
67246	Structural stabilities, electronic structures, photocatalysis and optical properties of Î³-GeN and Î±-SnP monolayers: a first-principles study. Materials Research Express, 2021, 8, 125010.	0.8	1
67247	Probabilistic deep learning approach for targeted hybrid organic-inorganic perovskites. Physical Review Materials, 2021, 5, .	0.9	5
67248	Proton Transferâ€Driven Modification of 3D Hybrid Perovskites to Form Oriented 2D Ruddlesdenâ€“Popper Phases. Small Science, 2022, 2, .	5.8	6

#	Article	IF	Citations
67249	Giant Biquadratic Exchange in 2D Magnets and Its Role in Stabilizing Ferromagnetism of <mml:math xmlns:mml="http://www.w3.org/1998/Math/MathML" display="inline"><mml:mrow><mml:msub><mml:mrow><mml:mi>NiCl</mml:mi></mml:mrow><mml:mrow><mml:mn>2</mml:mn></m Monolayers. Physical Review Letters, 2021, 127, 247204.	2.9	31
67250	Giant nonlinear Hall effect in twisted bilayer WTe2. Npj Quantum Materials, 2021, 6, .	1.8	22
67251	Accurate Simulations of the Reaction of H₂on a Curved Pt Crystal through Machine Learning. Journal of Physical Chemistry Letters, 2021, 12, 12157-12164.	2.1	5
67252	Dislocationâ€Mediated Hydride Precipitation in Zirconium. Small, 2022, 18, e2105881.	5.2	4
67253	Effect of a Support on the Properties of Zinc Oxide Based Sorbents. Nanomaterials, 2022, 12, 89.	1.9	1
67254	Accelerating cathode material discovery through ab initio random structure searching. APL Materials, 2021, 9, 121111.	2.2	13
67255	Expanding the Supramolecular Toolkit: Computed Molecular and Crystal Properties for Supporting the Crystal Engineering of Higher-Order Molecular Ionic Cocrystals. Crystal Growth and Design, 2022, 22, 485-496.	1.4	10
67256	The Deep Eutectic Solvent Precipitation Synthesis of Metastable Zn₄V₂O₉. Inorganic Chemistry, 2022, 61, 154-169.	1.9	9
67257	Rational Crystal Structure Design and Nonlinear-Optical Properties of Noncentrosymmetric RbCu₂NbS₄. Inorganic Chemistry, 2022, 61, 657-663.	1.9	2
67258	Orientation-Dependent Electronic and Mechanical Properties of Tungsten Nitride Nanosheets: Implications for Flexible Devices. ACS Applied Nano Materials, 2021, 4, 13771-13777.	2.4	7
67259	Irradiation-Induced Defects and Their Effects on the Electronic Structures in T-Carbon. Journal of Physical Chemistry C, 2021, 125, 28067-28074.	1.5	1
67260	Enhanced Photovoltaic Performance via a Bifunctional Additive in Tin-Based Perovskite Solar Cells. ACS Applied Energy Materials, 2022, 5, 108-115.	2.5	12
67261	Bottom-up, scalable synthesis of anatase nanofilament-based two-dimensional titanium carbo-oxide flakes. Materials Today, 2022, 54, 8-17.	8.3	24
67262	Realizing topological states in type-II Dirac semimetal PdTe2: an angle-resolved photoemission and quantum oscillations study. Bulletin of Materials Science, 2022, 45, 1.	0.8	4
67263	Density Functional Theory Study of CO Adsorption on the CaFe₂O₄ (001) Surface. ISIJ International, 2021, 61, 2937-2943.	0.6	0
67264	Chemical passivation of methylammonium fragments eliminates traps, extends charge lifetimes, and restores structural stability of CH3NH3PbI3 perovskite. Nano Research, 2022, 15, 4765-4772.	5.8	12
67265	Toward an Understanding of the Reversible Li-CO₂ Batteries over Metalâ€“N₄-Functionalized Graphene Electrocatalysts. ACS Nano, 2022, 16, 1523-1532.	7.3	52
67266	Two-Dimensional Conductive Metalâ€“Organic Frameworks as Highly Efficient Electrocatalysts for Lithiumâ€“Sulfur Batteries. ACS Applied Materials & Interfaces, 2021, 13, 61205-61214.	4.0	15

#	Article	IF	Citations
67267	Accessing High-Power Near-Infrared Spectroscopy Using Cr³⁺-Substituted Metal Phosphate Phosphors. Chemistry of Materials, 2022, 34, 337-344.	3.2	52
67268	A Low-Temperature Structural Transition in Canfieldite, Ag₈SnS₆, Single Crystals. Inorganic Chemistry, 2021, 60, 19345-19355.	1.9	3
67269	Computational prediction of Mo2@g-C6N6 monolayer as an efficient electrocatalyst for N2 reduction. Chinese Chemical Letters, 2022, 33, 4623-4627.	4.8	24
67270	Vibrational Spectroscopy Signatures of Catalytically Relevant Configurations for N₂ Reduction to NH₃ on Fe Surfaces via Density Functional Theory. Journal of Physical Chemistry C, 2021, 125, 27919-27930.	1.5	1
67271	2D Nb₃SBr₇ and Ta₃SBr₇: Experimentally Achievable Janus Photocatalysts with Robust Coexistence of Strong Optical Absorption, Intrinsic Charge Separation, and Ultrahigh Solar-to-Hydrogen Efficiency. ACS Applied Materials & Interfaces, 2022, 14, 1643-1651.	4.0	7
67272	Controllable anisotropic thermoelectric properties in 2D covalent organic radical frameworks. Applied Physics Letters, 2021, 119, .	1.5	16
67273	Bias-dependent tunneling anisotropic magnetoresistance in antiferromagnetic Pd-doped FeRh-based junctions. Applied Physics Letters, 2021, 119, .	1.5	2
67274	Interfaceâ€Structureâ€Modulated CuF₂/CF_x Composites for Highâ€Performance Lithium Primary Batteries. Energy and Environmental Materials, 2023, 6, .	7.3	14
67275	Discovery of Robust Ferroelectricity in 2D Defective Semiconductor Î±â€˜Ga₂Se₃. Small, 2022, 18, e2105599.	5.2	21
67276	Effect of vacancy defects on electronic and magnetic properties of zigzag silicon nanoribbons. , 2021, , .		0
67277	Extending Absorption of Cs₂AgBiBr₆ to Nearâ€Infrared Region (â‰ˆ1350Ânm) with Intermediate Band. Advanced Functional Materials, 2022, 32, .	7.8	30
67278	Thermoelectric performance of XI₂ (X = Ge, Sn, Pb) bilayers. Chinese Physics B, 0, , .	0.7	1
67279	Full-zone valley polarization landscape of finite-momentum exciton in transition metal dichalcogenide monolayers. Physical Review Research, 2021, 3, .	1.3	8
67280	Ligand Fieldâ€Induced Exotic Dopant for Infrared Transparent Electrode: W in Rutile SnO₂. Advanced Functional Materials, 2022, 32, .	7.8	8
67281	Armchair Janus MoSSe Nanoribbon with Spontaneous Curling: A First-Principles Study. Nanomaterials, 2021, 11, 3442.	1.9	3
67282	First-Principles Study on Adsorption and Decomposition of NOx on Mo (110) Surface. Advances in Condensed Matter Physics, 2021, 2021, 1-10.	0.4	0
67283	The Potential of Phosphorus Nitride Monolayer for Liâ€“S Battery from the Anchoring and Diffusing Perspective: A Firstâ€Principles Study. Advanced Theory and Simulations, 2022, 5, .	1.3	4
67284	Water Gas Shift Reaction Activity on Fe (110): A DFT Study. Catalysts, 2022, 12, 27.	1.6	3

#	Article	IF	Citations
67285	Structural phase transition and electronic structure of binary CaO and SrO under high pressure. Materials Today: Proceedings, 2022, 62, 2744-2747.	0.9	1
67286	Inverse design of two-dimensional materials with invertible neural networks. Npj Computational Materials, 2021, 7, .	3.5	15
67287	Common microscopic origin of the phase transitions in Ta2NiS5 and the excitonic insulator candidate Ta2NiSe5. Npj Computational Materials, 2021, 7, .	3.5	19
67288	Symmetry-enforced topological band crossings in orthorhombic crystals: Classification and materials discovery. Physical Review Materials, 2021, 5, .	0.9	15
67289	Interfacial-engineering-enabled practical low-temperature sodium metal battery. Nature Nanotechnology, 2022, 17, 269-277.	15.6	69
67290	Ternary Mg-Nb-H polyhydrides under high pressure. Physical Review B, 2021, 104, .	1.1	23
67291	A DFT study of the effect of stacking on the quantum capacitance of bilayer graphene materials. New Carbon Materials, 2021, 36, 1062-1070.	2.9	10
67292	Prediction of coexistence of anomalous valley Hall and quantum anomalous Hall effects in breathing kagome-honeycomb lattices. Physical Review B, 2021, 104, .	1.1	6
67293	Interface engineering of ferroelectricity in thin films of thiophosphate <mml:math xmlns:mml="http://www.w3.org/1998/Math/MathML"><mml:mrow><mml:mi>A</mml:mi><mml:mi>B</mml:mi></mml:mrow><mml:mr		

#	Article	IF	Citations
67303	Effect of off-stoichiometry on the thermal conductivity of amorphous GeTe. Physica Scripta, 2021, 96, 125730.	1.2	0
67304	Surface-Functionalized Hafnia with Bespoke Ferroelectric Properties for Memory and Logic Applications. , 2021, , .		1
67305	Selfâ€Limiting Synthesis of Ultrathin Ge(110) Single Crystal via Liquid Metal. Small, 2022, 18, e2106341.	5.2	6
67306	Pressure-induced isostructural clustering and semiconductor-to-semimetal transition in <mml:math xmlns:mml="http://www.w3.org/1998/Math/MathML"><mml:mrow><mml:mn>2</mml:mn><mml:mi>H</mml:mi></mml:mrow><mml:mn mathvariant="normal">W</mml:mi><mml:msub><mml:mrow><mml:mo>(</mml:mo><mml:msub><mml:mi>Se</mml:mi><mml:mrow> Physical Review B, 2021, 104, .	1.1	2
67307	Observation of a New Polyhalide Phase in Ag-Cl2 System at High Pressure. Crystals, 2021, 11, 1565.	1.0	0
67308	Dynamics at Polarized Carbon Dioxideâ€“Iron Oxyhydroxide Interfaces Unveil the Origin of Multicarbon Product Formation. ACS Catalysis, 2022, 12, 411-430.	5.5	19
67309	Local Spatial Polarization Induced Efficient Charge Separation of Squaraineâ€Linked COF for Enhanced Photocatalytic Performance. Advanced Functional Materials, 2022, 32, .	7.8	56
67310	Chemically and electrically tunable spin polarization in ferroelectric Cd-based hybrid organic-inorganic perovskites. Physical Review B, 2021, 104, .	1.1	5
67311	Activation of two dopants, Bi and Er in Î´-doped layer in Si crystal. Nano Futures, 2021, 5, 045005.	1.0	0
67312	Colossal angular magnetoresistance in the antiferromagnetic semiconductor <mml:math xmlns:mml="http://www.w3.org/1998/Math/MathML"><mml:msub><mml:mi>EuTe</mml:mi><mml:mn>2</mml:mn></mml:msub></mml:mi> Physical Review B, 2021, 104, .	1.1	15
67313	Novel polymorphs and polytypes of lithium chloride from structure predictions based on charge equilibration via neural network technique. Physical Review Materials, 2021, 5, .	0.9	2
67314	Quantifying Effects of Active Site Proximity on Rates of Methanol Dehydration to Dimethyl Ether over Chabazite Zeolites through Microkinetic Modeling. ACS Materials Au, 2022, 2, 163-175.	2.6	7
67315	Superconductivity in the Layered Cage Compound Ba₃Rh₄Ge₁₆. Chinese Physics Letters, 2021, 38, 127402.	1.3	2
67316	Large magnetic anisotropy in Coâ€“Feâ€“Niâ€“N ordered structures: a first-principles study. Journal of Physics Condensed Matter, 2022, 34, 095503.	0.7	2
67317	On the liquidâ€“liquid phase transition of dense hydrogen. Nature, 2021, 600, E12-E14.	13.7	12
67318	Stabilizing the Exotic Carbonic Acid by Bisulfate Ion. Molecules, 2022, 27, 8.	1.7	4
67319	Creation and annihilation of mobile fractional solitons in atomic chains. Nature Nanotechnology, 2022, 17, 244-249.	15.6	12
67320	Impact of the Structural Modification of Diamondoid Cd(II) MOFs on the Nonlinear Optical Properties. ACS Applied Materials & Interfaces, 2021, 13, 60163-60172.	4.0	13

#	Article	IF	Citations
67321	Decreasing Structural Dimensionality of Double Perovskites for Phase Stabilization toward Efficient X-ray Detection. ACS Applied Materials & Interfaces, 2021, 13, 61447-61453.	4.0	11
67322	Phaseâ€Control of Singleâ€Crystalline Inorganic Halide Perovskites via Molecular Coordination Engineering. Advanced Functional Materials, 2022, 32, .	7.8	14
67323	Realizing Kagome Band Structure in Two-Dimensional Kagome Surface States of <mml:math xmlns:mml="http://www.w3.org/1998/Math/MathML" display="inline"><mml:mrow><mml:mi>R</mml:mi><mml:msub><mml:mrow><mml:mi mathvariant="normal">V</mml:mi></mml:mrow><mml:mrow><mml:mn>6</mml:mn></mml:mrow></mml:msub><mml:msub><mml:m		

#	Article	IF	Citations
67339	DyOCl: A rare-earth based two-dimensional van der Waals material with strong magnetic anisotropy. Physical Review B, 2021, 104, .	1.1	13
67340	Cyclized Polyacrylonitrile as a Promising Support for Single Atom Metal Catalyst with Synergistic Active Site. Small, 2022, 18, e2104142.	5.2	8
67341	Lithium Diffusion in Silicon Encapsulated with Graphene. Nanomaterials, 2021, 11, 3397.	1.9	3
67342	Commensurate Stacking Phase Transitions in an Intercalated Transition Metal Dichalcogenide. Advanced Materials, 2022, 34, e2108550.	11.1	5
67343	Candidate structure for the <mml:math xmlns:mml="http://www.w3.org/1998/Math/MathML"><mml:msub><mml:mrow><mml:mi mathvariant="normal">H</mml:mi></mml:mrow><mml:mn>2</mml:mn></mml:msub></mml:math> -PRE phase of solid hydrogen. Physical Review B, 2021, 104, .	1.1	5
67344	Magnetic Structure and Origin of Insulating Behavior in the Ba2CuOsO6 System, and the Role of A-Site Ionic Size in Its Bandgap Opening: Density Functional Theory Approaches. Nanomaterials, 2022, 12, 144.	1.9	3
67345	Electronic properties and reactivity of oxidized graphene nanoribbons and their interaction with phenol. Journal of Molecular Modeling, 2022, 28, 23.	0.8	1
67346	Investigations of the Effect of H2 in CO Oxidation over Ceria Catalysts. Catalysts, 2021, 11, 1556.	1.6	3
67347	Spin Seebeck effect driven by thermal flux in two-dimensional ferromagnets. Journal of Applied Physics, 2021, 130, 223902.	1.1	4
67348	Identifying an Alternative Hydride Transfer Pathway for CO ₂ Reduction on CdTe(111) and CuInS ₂ (112) Surfaces. Advanced Theory and Simulations, 2022, 5, 2100413.	1.3	5
67349	CO Adsorbate Promotes Polaron Photoactivity on the Reduced Rutile TiO₂(110) Surface. Jacs Au, 2022, 2, 234-245.	3.6	22
67350	Pentagraphite <mml:math xmlns:mml="http://www.w3.org/1998/Math/MathML"><mml:msub><mml:mi mathvariant="normal">C</mml:mi><mml:mn>8</mml:mn></mml:msub></mml:math> : An all- <mml:math xmlns:mml="http://www.w3.org/1998/Math/MathML"><mml:mrow><mml:mi>s</mml:mi><mml:msup><mml:mi>p</mml:mi><mml:m topological nodal-line semimetal. Physical Review B, 2021, 104, .	1.1	6
67351	Pressure-densified new rhombohedral phase of <mml:math xmlns:mml="http://www.w3.org/1998/Math/MathML"><mml:mrow><mml:msub><mml:mi>EuSn</mml:mi><mml:mn>2</mml:mn></mml:m Physical Review B, 2021, 104, .	1.1	4
67352	Theoretical Insight Into Diamond Doping and Its Possible Effect on Diamond Tool Wear During Cutting of Steel. Frontiers in Materials, 2021, 8, .	1.2	2
67353	Topological states in the noncentrosymmetric superconductors LaPtSi and LaPtGe. Physical Review B, 2021, 104, .	1.1	2
67354	Chemical mechanism of formation of two-dimensional electron gas at the Al2O3/TiO2 interface by atomic layer deposition. Materials Today Advances, 2021, 12, 100195.	2.5	4
67355	Antiferromagnetic Order and Linear Magnetoresistance in Fe-Substituted Shandite Co₃In₂S₂. Chemistry of Materials, 2021, 33, 9741-9749.	3.2	14
67356	Twist-to-Untwist Evolution and Cation Polarization Behavior of Hybrid Halide Perovskite Nanoplatelets Revealed by Cryogenic Transmission Electron Microscopy. Journal of Physical Chemistry Letters, 2021, 12, 12187-12195.	2.1	4

#	Article	IF	Citations
67357	Unveiling the Nature of Light-Triggered Hole Traps in Lead Halide Perovskites: A Study with Time-Dependent Density Functional Theory. Journal of Physical Chemistry Letters, 2021, 12, 12075-12083.	2.1	3
67358	Role of A-Site Molecular Ions in the Polar Functionality of Metalâ€“Organic Framework Perovskites. Chemistry of Materials, 2021, 33, 9666-9676.	3.2	3
67359	Alteration of Electronic Band Structure via a Metalâ€“Semiconductor Interfacial Effect Enables High Faradaic Efficiency for Electrochemical Nitrogen Fixation. ACS Nano, 2021, 15, 20364-20376.	7.3	32
67360	Screening of Transition-Metal Single-Atom Catalysts Anchored on Covalentâ€“Organic Frameworks for Efficient Nitrogen Fixation. ACS Applied Materials & Interfaces, 2022, 14, 1024-1033.	4.0	32
67361	Mo₂C-MoO₂ Heterostructure Quantum Dots for Enhanced Electrocatalytic Nitrogen Reduction to Ammonia. ACS Nano, 2022, 16, 643-654.	7.3	55
67362	SiCP₄ Monolayer with a Direct Band Gap and High Carrier Mobility for Photocatalytic Water Splitting. Journal of Physical Chemistry Letters, 2022, 13, 190-197.	2.1	16
67363	Spin Polarization-Assisted Dopant Segregation at a Coherent Phase Boundary. ACS Nano, 2021, 15, 19938-19944.	7.3	6
67364	3D V₂CT_xâ€“rGO Architectures with Optimized Ion Transport Channels toward Fast Lithium-Ion Storage. ACS Applied Materials & Interfaces, 2021, 13, 61258-61266.	4.0	9
67365	Evaluating the Electronic Structure of Coexisting Excitonic and Multiexcitonic States in Periodic Systems: Significance for Singlet Fission. Journal of Chemical Theory and Computation, 2022, 18, 394-405.	2.3	4
67366	Au with sp³ Hybridization in Li₅AuP₂. Journal of Physical Chemistry Letters, 2022, 13, 236-242.	2.1	2
67367	Chiroptically Active 1D Ultrathin AuAg Nanostructures. Journal of Physical Chemistry C, 2022, 126, 434-443.	1.5	3
67368	Design Principles of Bifunctional Electrocatalysts for Engineered Interfaces in Naâ€“S Batteries. ACS Catalysis, 2021, 11, 15149-15161.	5.5	24
67369	Large Gap Two-Dimensional Topological Insulators with the Significant Rashba Effect in Ethynyl and Methyl Functionalized PbSn Monolayers. Journal of Physical Chemistry Letters, 2021, 12, 12202-12209.	2.1	3
67370	Strong MoirÃ© Excitons in High-Angle Twisted Transition Metal Dichalcogenide Homobilayers with Robust Commensuration. Nano Letters, 2022, 22, 203-210.	4.5	12
67371	Rational Design of Main Group Metal-Embedded Nitrogen-Doped Carbon Materials as Frustrated Lewis Pair Catalysts for CO₂ Hydrogenation to Formic Acid. ACS Applied Materials & Interfaces, 2022, 14, 1002-1014.	4.0	21
67372	Role of Low-Coordinated Ce in Hydride Formation and Selective Hydrogenation Reactions on CeO₂ Surfaces. ACS Catalysis, 2022, 12, 624-632.	5.5	20
67373	Adjustable Dimensionality of Microaggregates of Silicon in Hollow Carbon Nanospheres: An Efficient Pathway for High-Performance Lithium-Ion Batteries. ACS Nano, 2022, 16, 1119-1133.	7.3	25
67374	Thermodynamic and Electronic Properties of Two-Dimensional SrTiO₃. Journal of Physical Chemistry C, 2022, 126, 517-524.	1.5	9

#	Article	IF	Citations
67375	First-Principles Study of the Structural, Electronic, and Enhanced Optical Properties of SnS/TaS₂ Heterojunction. ACS Applied Materials & Interfaces, 2022, 14, 2177-2184.	4.0	5
67376	Biphasic Î±/Î²-Type NaMn_{0.89}Fe_{0.11}O₂ as a Cathode for Sodium-Ion Batteries: Structural Insight and High-Performance Relation. ACS Applied Energy Materials, 2022, 5, 116-125.	2.5	5
67377	Sublayer Stable Fe Dopant in Porous Pd Metallene Boosts Oxygen Reduction Reaction. ACS Nano, 2022, 16, 522-532.	7.3	52
67378	Atomistic Observation of Temperature-Dependent Defect Evolution within Sub-stoichiometric WO_{3â€“x} Catalysts. ACS Applied Materials & Interfaces, 2022, 14, 2194-2201.	4.0	14
67379	Computational Investigation of the Interfacial Stability of Lithium Chloride Solid Electrolytes in All-Solid-State Lithium Batteries. ACS Applied Materials & Interfaces, 2022, 14, 1241-1248.	4.0	20
67380	The growth of Î² phase in Mg-Gd-Y-Ni alloy by experimental and first-principles study. Journal of Magnesium and Alloys, 2021, , .	5.5	4
67381	Stabilizing a Nickel-Rich (LiNi_{0.89}Co_{0.055}Mn_{0.055}O₂) Cathode Material by Doping Zirconium or Molybdenum: A First-Principles Study. Journal of Physical Chemistry C, 2021, 125, 27543-27555.	1.5	17
67382	Thermally Averaged Magnetic Anisotropy Tensors via Machine Learning Based on Gaussian Moments. Journal of Chemical Theory and Computation, 2022, 18, 1-12.	2.3	10
67383	NaSb₃O₂(SO₄)₃Â·H₂O: A New Alkali-Metal Antimony(III) Sulfate with a Unique Sb₆O₂₀H₄ Unit and Moderate Birefringence. Crystal Growth and Design, 2022, 22, 478-484.	1.4	11
67384	Architecting a Hydrated Ca_{0.24}V₂O₅ Cathode with a Facile Desolvation Interface for Superior-Performance Aqueous Zinc Ion Batteries. ACS Applied Materials & Interfaces, 2021, 13, 60035-60045.	4.0	26
67385	Structure and Oxygen Evolution Activity of Î²-NiOOH: Where Are the Protons?. ACS Catalysis, 2022, 12, 295-304.	5.5	28
67386	First principles study on the structures and properties of aluminum under high pressures. , 2021, , .		0
67387	Regulating the Electron Localization of Metallic Bismuth for Boosting CO2 Electroreduction. Nano-Micro Letters, 2022, 14, 38.	14.4	21
67388	Field controllable electronic properties of MnPSe3/WS2 heterojunction for photocatalysis. Journal of Central South University, 2021, 28, 3728-3736.	1.2	11
67389	Pressure-induced superconductivity and structure phase transition in Pt2HgSe3. Npj Quantum Materials, 2021, 6, .	1.8	10
67390	Nitrogen diffusion in zinc oxide. Journal of Applied Physics, 2021, 130, 245702.	1.1	0
67391	Biaxial Tensile Strain-Induced Enhancement of Thermoelectric Efficiency of Î±-Phase Se2Te and SeTe2 Monolayers. Nanomaterials, 2022, 12, 40.	1.9	2
67392	5f Covalency Synergistically Boosting Oxygen Evolution of UCoO₄ Catalyst. Journal of the American Chemical Society, 2022, 144, 416-423.	6.6	48

#	Article	IF	Citations
67393	Magnetic Weyl Semimetallic Phase in Thin Films of <mml:math xmlns:mml="http://www.w3.org/1998/Math/MathML" display="inline"><mml:mrow><mml:msub><mml:mrow><mml:mi>Eu</mml:mi></mml:mrow><mml:mrow><mml:mn>2</mml:mn></mml:mrow></mml:msub><mml:msub><mml:mrow><mml:mi mathvariant="normal">O</mml:mi></mml:mrow><mml:mrow><mml:mn>7</mml:mn></mml:mrow></mml:msub></mml:mrow></mml:math>. Physical Review Letters, 2021, 127, 277204.	2.9	17
67394	Comparative Study on the Flame Retardancy and Retarding Mechanism of Rare Earth (La, Ce, and) Tj ETQq1 1 0.784314 rgBT /Overlock	1.6	14
67395	Band gap opening in the <mml:math xmlns:mml="http://www.w3.org/1998/Math/MathML"><mml:msub><mml:mi>BiSbTeSe</mml:mi><mml:mn>2</mml:mn></mml:msub></mml:math> topological surface state induced by ferromagnetic surface reordering. Physical Review Materials, 2021, 5, .	0.9	3
67396	Puffing Up Hollow Carbon Nanofibers with Highâ€Energy Metalâ€Organic Frameworks for Capacitiveâ€Dominated Potassiumâ€Ion Storage. Small, 2022, 18, e2105767.	5.2	13
67397	SOME PHYSICAL PROPERTIES OF HALF-HEUSLER COMPOUND NaYSi : FIRST-PRINCIPLES STUDY. , 0, , .		0
67398	Graphene Acid for Lithiumâ€Ion Batteriesâ€”Carboxylation Boosts Storage Capacity in Graphene. Advanced Energy Materials, 2022, 12, .	10.2	25
67399	Importance of surface oxygen vacancies for ultrafast hot carrier relaxation and transport in <mml:math xmlns:mml="http://www.w3.org/1998/Math/MathML"><mml:msub><mml:mi>Cu</mml:mi><mml:mn>2</mml:mn></mml:msub></mml:math>O. Physical Review Research, 2021, 3, .	1.3	9
67400	Quantum Buckling in Metalâ€“Organic Framework Materials. Nano Letters, 2021, 21, 10341-10345.	4.5	1
67401	Insight into Composition and Intermediate Evolutions of Copper-Based Catalysts during Gas-Phase CO2 Electroreduction to Multicarbon Oxygenates. Catalysts, 2021, 11, 1502.	1.6	4
67402	Lattice thermal conductivity including phonon frequency shifts and scattering rates induced by quartic anharmonicity in cubic oxide and fluoride perovskites. Physical Review B, 2021, 104, .	1.1	40
67403	Ultrasound elasticity of diamond at gigapascal pressures. Proceedings of the National Academy of Sciences of the United States of America, 2021, 118, .	3.3	6
67404	Realizing n-type gete through suppressing the formation of cation vacancies and bi-doping*. Chinese Physics Letters, 2021, 38, 127201.	1.3	5
67405	Visualizing band selective enhancement of quasiparticle lifetime in a metallic ferromagnet. Nature Communications, 2021, 12, 7169.	5.8	4
67406	Magnetization of silicene via coverage with gadolinium: Effects of thickness, symmetry, strain, and coverage. Physical Review B, 2021, 104, .	1.1	5
67407	Light-driven permanent transition from insulator to conductor. Physical Review B, 2021, 104, .	1.1	6
67408	Structural Transition of Vacancyâ€“Solute Complexes in Alâ€“Mgâ€“Si Alloys. Metals, 2022, 12, 2.	1.0	3
67409	Design of nanoscale capacitors based on metallic borophene and insulating boron nitride layers. Physical Review Materials, 2021, 5, .	0.9	1
67410	Ultraintense Zero-Phonon Line from a Mn⁴⁺ Red-Emitting Phosphor for High-Quality Backlight Display Applications. Inorganic Chemistry, 2021, 60, 19197-19205.	1.9	12

#	Article	IF	Citations
67411	Boron in Ni-Rich NCM811 Cathode Material: Impact on Atomic and Microscale Properties. ACS Applied Energy Materials, 2022, 5, 524-538.	2.5	22
67412	Unveiling White Light Emission of a One-Dimensional Cu(I)-Based Organometallic Halide toward Single-Phase Light-Emitting Diode Applications. Journal of Physical Chemistry Letters, 2021, 12, 12345-12351.	2.1	17
67413	Reaction Mechanism of Li₂MnO₃ Electrodes in an All-Solid-State Thin-Film Battery Analyzed by Operando Hard X-ray Photoelectron Spectroscopy. Journal of the American Chemical Society, 2022, 144, 236-247.	6.6	16
67414	Surface Functionalization of WS₂ Nanosheets with Alkyl Chains for Enhancement of Dispersion Stability and Tribological Properties. ACS Applied Materials & Interfaces, 2022, 14, 1334-1346.	4.0	10
67415	Solid-State Calcium-Ion Diffusion in Ca_{1.5}Ba_{0.5}Si₅O₃N₆. Chemistry of Materials, 2022, 34, 128-139.	3.2	7
67416	Computational Screening of Bimetallic Catalysts: Application to Ammonia Decomposition. Journal of Physical Chemistry C, 2022, 126, 192-202.	1.5	1
67417	Coal-Derived Graphene/MoS₂ Heterostructure Electrodes for Li-Ion Batteries: Experiment and Simulation Study. ACS Applied Materials & Interfaces, 2021, 13, 59950-59961.	4.0	15
67418	Rapid Water Diffusion at Cryogenic Temperatures through an Inchworm-like Mechanism. Nano Letters, 2022, 22, 340-346.	4.5	5
67419	Enhanced Light Emission through Symmetry Engineering of Halide Perovskites. Journal of the American Chemical Society, 2022, 144, 297-305.	6.6	5
67420	Unveiling charge dynamics of visible light absorbing oxysulfide for efficient overall water splitting. Nature Communications, 2021, 12, 7055.	5.8	31
67421	Self-Etherification of 5-Hydroxymethylfurfural to 5,5â€²(Oxy-bis(methylene))bis-2-furfural over Hierarchically Micromesoporous ZSM-5: The Role of BrÃ¸nsted- and Lewis-Acid Sites. Industrial & Engineering Chemistry Research, 2022, 61, 987-994.	1.8	3
67422	Revisiting phonon transport in perovskite <mml:math xmlns:mml="http://www.w3.org/1998/Math/MathML"><mml:msub><mml:mi>SrTiO</mml:mi><mml:mn>3</mml:mn></mml:msub><mml:mi></mml:mi></mml:math> : Anharmonic phonon renormalization and four-phonon scattering. Physical Review B, 2021, 104, .	1.1	19
67423	Electrochemical Performance of Iron-Doped Cobalt Oxide Hierarchical Nanostructure. Processes, 2021, 9, 2176.	1.3	9
67424	Riemannian geometry of resonant optical responses. Nature Physics, 2022, 18, 290-295.	6.5	58
67425	Enhanced ferroelectric and piezoelectric properties of BCT-BZT at the morphotropic phase boundary driven by the coexistence of phases with different symmetries. Physical Review B, 2021, 104, .	1.1	26
67426	Highly efficient ethylene production via electrocatalytic hydrogenation of acetylene under mild conditions. Nature Communications, 2021, 12, 7072.	5.8	51
67427	Superconducting hydrogen tubes in hafnium hydrides at high pressure. Physical Review B, 2021, 104, .	1.1	11
67428	A first-principles study of hydrogen surface coverage on Î´-Pu (100), (111), and (110) surfaces. Journal of Chemical Physics, 2021, 155, 234702.	1.2	2

#	Article	IF	Citations
67429	Ordering in liquid and its heredity impact on phase transformation of Mg-Al-Ca alloys. Journal of Magnesium and Alloys, 2023, 11, 2006-2017.	5.5	12
67430	Rh2CoX (X=Al, Ga ve In) BileÅŸiklerinin YapÄ±sal, Elastik, Elektronik ve Manyetik Ã–zellikleri. Gazi University Journal of Science Part A:engineering and Innovation, 0, , 505-514.	0.2	0
67431	Nickel particleâ€“enabled width-controlled growth of bilayer molybdenum disulfide nanoribbons. Science Advances, 2021, 7, eabk1892.	4.7	19
67432	Ultralow thermal conductivity of thermoelectric compound Ag₂BaGeSe₄. AIP Advances, 2021, 11, 125320.	0.6	1
67433	CO2 coordination-driven top-down synthesis of a 2D non-layered metalâ€“organic framework. Fundamental Research, 2022, 2, 674-681.	1.6	11
67434	Cooperative catalysis coupling photo-/photothermal effect to drive Sabatier reaction with unprecedented conversion and selectivity. Joule, 2021, 5, 3235-3251.	11.7	91
67435	Structural, electronic and dielectric properties of Tellurium 1-D nanostructures : a DFT study. Applied Physics A: Materials Science and Processing, 2022, 128, 1.	1.1	1
67436	Understanding the flat band in <mml:math xmlns:mml="http://www.w3.org/1998/Math/MathML"><mml:mn>1</mml:mn><mml:mi>T</mml:mi><mml:mtext>â€‘</mml:mtext><mml:mtext><m using a rotated basis. Physical Review B, 2021, 104, .	1.1	4
67437	Implicit Solvation Methods for Catalysis at Electrified Interfaces. Chemical Reviews, 2022, 122, 10777-10820.	23.0	82
67438	A DFT+U look into experimentally synthesized monoclinic scheelite BiVO₄. Journal of Applied Physics, 2021, 130, 235107.	1.1	7
67439	Specialising neural network potentials for accurate properties and application to the mechanical response of titanium. Npj Computational Materials, 2021, 7, .	3.5	26
67440	Line defects in monolayer TiSe2 with adsorption of Pt atoms potentially enable excellent catalytic activity. Nano Research, 2022, 15, 4687-4692.	5.8	9
67441	CoS₂ Nanoparticles Anchored on MoS₂ Nanorods As a Superior Bifunctional Electrocatalyst Boosting Li₂O₂ Heteroepitaxial Growth for Rechargeable Liâ€“O₂ Batteries. Small, 2022, 18, e2105752.	5.2	20
67442	Waterâ€“Solid Interface Engineering Stabilizes Kâ€“Birnessite Cathode. Advanced Functional Materials, 2022, 32, 2108267.	7.8	2
67443	<mml:math xmlns:mml="http://www.w3.org/1998/Math/MathML"><mml:msub><mml:mi>CrSbSe</mml:mi><mml:mn>3</mml:mn></mml:msub></ : A pseudo one-dimensional ferromagnetic semiconductor. Physical Review Materials, 2021, 5, .	3.1	1
67444	Momentum-resolved electronic structure and band offsets in an epitaxial NbN/GaN superconductor/semiconductor heterojunction. Science Advances, 2021, 7, eabi5833.	4.7	5
67445	Density functional theory study of graphene adhesion on WX₂ (Xâ€‰=â€‰S and Se) monolayer: Role of atom vacancy and atomic reorganization defects. International Journal of Quantum Chemistry, 2022, 122, .	1.0	6
67446	Unconventional Stoichiometries of Naâ€“O Compounds at High Pressures. Materials, 2021, 14, 7650.	1.3	0

#	Article	IF	Citations
67447	A shortcut to the thermodynamic limit for quantum many-body calculations of metals. Nature Computational Science, 2021, 1, 801-808.	3.8	14
67448	Two-dimensional oxides assembled by <mml:math xmlns:mml="http://www.w3.org/1998/Math/MathML"><mml:msub><mml:mi>M</mml:mi><mml:mn>4</mml:mn></mml:msub></mml clusters (<mml:math) Tj ETQq1 1 0.784314 rgBT /Overlock 10 Tf 50 702 Td (xmlns:mml="http://www.w3.org/1998/Math/MathML"><m Review Research, 2021, 3, .	1.3	5
67449	Relationship between ferroelectric polarization and stoichiometry of <mml:math xmlns:mml="http://www.w3.org/1998/Math/MathML"><mml:msub><mml:mi>HfO</mml:mi><mml:mn>2</mml:mn></mml:msub></mm surfaces. Physical Review Materials, 2021, 5, .	0.9	4
67450	Highâ€Performance Pâ€Channel Tin Halide Perovskite Thin Film Transistor Utilizing a 2Dâ€"3D Coreâ€"Shell Structure. Advanced Science, 2022, 9, e2104993.	5.6	21
67451	Observation of topological edge states in the quantum spin Hall insulator <mml:math xmlns:mml="http://www.w3.org/1998/Math/MathML"><mml:msub><mml:mrow><mml:mi>Ta</mml:mi></mml:mrow><mml:mn>2</mn Physical Review B, 2021, 104, .	1.2	10
67452	Photochromism of UV-annealed Fe-doped SrTiO3. Applied Physics Letters, 2021, 119, .	1.5	2
67453	The Characteristic of Fe as a Î²-Ti Stabilizer in Ti Alloys. Materials, 2021, 14, 7516.	1.3	8
67454	Lattice siteâ€"dependent metal leaching in perovskites toward a honeycomb-like water oxidation catalyst. Science Advances, 2021, 7, eabk1788.	4.7	41
67455	Topological surface states in superconducting <mml:math xmlns:mml="http://www.w3.org/1998/Math/MathML"><mml:msub><mml:mi>CaBi</mml:mi><mml:mn>2</mml:mn></mml:msub></mn Physical Review B, 2021, 104, .	1.1	3
67456	First-Principle Investigations of (Ti1Ââ€"ÂxVx)2FeGa Ðlloys. A Study on Structural, Ðœagnetic, Ð•lectronic, and Ð•lastic Ðroperties. Russian Journal of Physical Chemistry A, 2021, 95, 2592-2599.	0.1	4
67457	Isolated-Mn²⁺-like Luminescent Behavior in CsMnF₃ Caused by Competing Magnetic Interactions at Cryogenic Temperature. Journal of Physical Chemistry C, 2021, 125, 27800-27809.	1.5	5
67458	Data-Driven Studies of the Magnetic Anisotropy of Two-Dimensional Magnetic Materials. Journal of Physical Chemistry Letters, 2021, 12, 12048-12054.	2.1	15
67459	Significance of the Chemical Environment of an Element in Nonadiabatic Molecular Dynamics: Feature Selection and Dimensionality Reduction with Machine Learning. Journal of Physical Chemistry Letters, 2021, 12, 12026-12032.	2.1	11
67460	Amphiphilic Carborane-Based Covalent Organic Frameworks as Efficient Polysulfide Nano-Trappers for Lithiumâ€"Sulfur Batteries. ACS Applied Materials & Interfaces, 2021, 13, 60373-60383.	4.0	22
67461	Transition Metal-Free Half-Metallicity in Two-Dimensional Gallium Nitride with a Quasi-Flat Band. Journal of Physical Chemistry Letters, 2021, 12, 12150-12156.	2.1	3
67462	Tailoring of Visible Light Driven Photocatalytic Activities of Flowerâ€Like BiOBr Microparticles Towards Wastewater Purification Application. Advanced Materials Interfaces, 2022, 9, .	1.9	6
67463	Ab Initio Molecular Dynamics Assessment on the Mixed Ionicâ€"Electronic Transport for Crystalline Poly(3-Hexylthiophene) Using Full Explicit Lithium-Based Dopants and Additives. Macromolecules, 2022, 55, 113-124.	2.2	6
67464	Paramagnetic ⁷Li NMR Shifts and Magnetic Properties of Divalent Transition Metal Silylamide Ate Complexes [LiM{N(SiMe₃)₂}₃] (M²⁺ =) Tj ETQq1 1 0.784314 rgBT /	1.9	2

#	Article	IF	Citations
67465	Ironâ€“Cobalt-Based Materials: An Efficient Bimetallic Catalyst for Ammonia Synthesis at Low Temperatures. ACS Catalysis, 2022, 12, 587-599.	5.5	17
67466	Anomalous Hall signatures of nonsymmorphic nodal lines in the doped chromium chalcospinel <mml:math xmlns:mml="http://www.w3.org/1998/Math/MathML"><mml:msub><mml:mrow><mml:mi>CuCr</mml:mi></mml:mrow><mml:mn>2</mml:mn> Physical Review B, 2021, 104, .	1.1	2
67467	Stabilized tilted-octahedra halide perovskites inhibit local formation of performance-limiting phases. Science, 2021, 374, 1598-1605.	6.0	115
67468	Density Functional Theory Study of Monoclinic FeNbO₄: Bulk Properties and Water Dissociation at the (010), (011), (110), and (111) Surfaces. Journal of Physical Chemistry C, 2021, 125, 27566-27577.	1.5	6
67469	Atomic and Electronic Structure of Pt/TiO₂ Catalysts and Their Relationship to Catalytic Activity. Nano Letters, 2022, 22, 145-150.	4.5	16
67470	Octahedral Symmetry Modification Induced Orbital Occupancy Variation in VO₂. Journal of Physical Chemistry Letters, 2022, 13, 75-82.	2.1	3
67471	A Phosphonated Poly(ethylenedioxythiophene) Derivative with Low Oxidation Potential for Energy-Efficient Bioelectronic Devices. Chemistry of Materials, 2022, 34, 140-151.	3.2	7
67472	Ligand-Assisted Charge-Transfer Mechanism: The Case of CdSe/Cysteine/MoS₂ Heterostructures. Journal of Physical Chemistry Letters, 2021, 12, 12329-12335.	2.1	4
67473	Highly Stable Germanium Microparticle Anodes with a Hybrid Conductive Shell for High Volumetric and Fast Lithium Storage. ACS Applied Materials & Interfaces, 2022, 14, 750-760.	4.0	2
67474	Role of the A-Element in the Structural, Mechanical, and Electronic Properties of Ti₃AC₂ MAX Phases. Inorganic Chemistry, 2022, 61, 2129-2140.	1.9	4
67475	Understanding Crystal Structures to Guide Form Selection of Active Pharmaceutical Ingredients: A Case Study of AZD9567. Crystal Growth and Design, 2022, 22, 535-546.	1.4	3
67476	Coexisting Charge-Ordered States with Distinct Driving Mechanisms in Monolayer VSe₂. ACS Nano, 2022, 16, 783-791.	7.3	11
67477	Localized Orbital Excitation Drives Bond Formation in Plasmonic Catalysis. ACS Applied Materials & Interfaces, 2021, 13, 60115-60124.	4.0	2
67478	Monitoring oxygen production on mass-selected iridiumâ€“tantalum oxide electrocatalysts. Nature Energy, 2022, 7, 55-64.	19.8	108
67479	Cerium-based lead-free chalcogenide perovskites for photovoltaics. Physical Review B, 2021, 104, .	1.1	6
67480	Soft-mode anisotropy in the negative thermal expansion material <mml:math xmlns:mml="http://www.w3.org/1998/Math/MathML"><mml:msub><mml:mrow><mml:mi>ReO</mml:mi></mml:mrow><mml:mn>3</mml:mn> Physical Review B, 2021, 104, .	1.1	0
67481	Understanding the phase transformation mechanisms that affect the dynamic response of Fe-based microstructures at the atomic scales. Journal of Applied Physics, 2021, 130, .	1.1	8
67482	COMPARISON OF PBE AND SCAN FUNCTIONALS ON WATER-SILICA SURFACE INTERACTION. , 0, , .		0

#	Article	IF	Citations
67483	Iron-rich talc as air-stable platform for magnetic two-dimensional materials. Npj 2D Materials and Applications, 2021, 5, .	3.9	7
67484	Forming mechanism of equilibrium and non-equilibrium metallurgical phases in dissimilar aluminum/steel (Alâ€“Fe) joints. Scientific Reports, 2021, 11, 24251.	1.6	8
67485	A generalizable machine learning potential of Agâ€“Au nanoalloys and its application to surface reconstruction, segregation and diffusion. Modelling and Simulation in Materials Science and Engineering, 2022, 30, 025003.	0.8	8
67486	Decoupling between Shockley partials and stacking faults strengthens multiprincipal element alloys. Proceedings of the National Academy of Sciences of the United States of America, 2021, 118, .	3.3	11
67487	Understanding the Role of Electronic Effects in CO on the Ptâ€“Sn Alloy Surface via Band Structure Measurements. ACS Catalysis, 2022, 12, 219-225.	5.5	14
67488	Epitaxial growth of black phosphorene enabled on black-phosphorene-like group IV-VI substrates. Physical Review B, 2021, 104, .	1.1	3
67489	Induction of large magnetic anisotropy energy and formation of multiple Dirac states in SrIrO₃ films: Role of correlation and spinâ€“orbit coupling. Applied Physics Letters, 2021, 119, 261906.	1.5	2
67490	Assessing the effect of H on the electronic properties of 4H-SiC. Chinese Physics B, 0, , .	0.7	2
67491	Proton dynamics in water confined at the interface of the grapheneâ€“MXene heterostructure. Journal of Chemical Physics, 2021, 155, 234707.	1.2	5
67492	Spin qubit based on the nitrogen-vacancy center analog in a diamond-like compound C3BN. Journal of Applied Physics, 2021, 130, .	1.1	2
67493	Improvement of Interfacial Properties of 4H-SiC/SiO₂ by Nitrogen Plasma Treatment. , 2021, , .		0
67494	Mixing ReaxFF parameters for transition metal oxides using force-matching method. Journal of Molecular Modeling, 2022, 28, 8.	0.8	4
67495	Increasing Silicon Concentration and Doping Heteroatom to Successfully Realize High HER Catalytic Activity in 2D Metal-Free BSi_n (n = 1â€“4) Structures: A First-Principles Study. Journal of the Electrochemical Society, 2021, 168, 126527.	1.3	3
67496	Oxygen Diffusion in Platinum Electrodes: A Molecular Dynamics Study of the Role of Extended Defects. Advanced Materials Interfaces, 2022, 9, .	1.9	7
67497	MOFâ€Derived MnV₂O₄/C Microparticles with Graphene Coating Anchored on Graphite Sheets: Oxygen Defect Engaged High Performance Aqueous Zincâ€ion Battery. Advanced Materials Interfaces, 2022, 9, .	1.9	6
67498	Effect of Ni Doping on the Embrittlement of Liquid Zinc at Î£5 Fe Austenite Grain Boundary. Metals, 2022, 12, 27.	1.0	1
67499	First-principles study of the impact of chemical doping and functional groups on the absorption spectra of graphene. Semiconductor Science and Technology, 2022, 37, 025013.	1.0	4
67500	Incubation of the Kane-Mele model in <mml:math xmlns:mml="http://www.w3.org/1998/Math/MathML"><mml:mrow><mml:msub><mml:mrow><mml:mi>X</mml:mi><mml:mi mathvariant="normal">N</mml:mi></mml:mrow><mml:mn>4</mml:mn></mml:msub></mml:mrow></mml:math> -embedded graphene <mml:math		

#	Article	IF	Citations
67501	2D multifunctional SiAs2/GeAs2 van der waals heterostructure. Nanotechnology, 2021, , .	1.3	1
67502	Highâ€Performance Zincâ€Air Batteries Based on Bifunctional Hierarchically Porous Nitrogenâ€Doped Carbon. Small, 2022, 18, e2105928.	5.2	23
67503	Unusual ferrimagnetic ground state in rhenium ferrite. European Physical Journal Plus, 2022, 137, 1.	1.2	1
67504	Ultrastable Orthorhombic Na₂TiSiO₅ Anode for Lithiumâ€Ion Battery. Advanced Energy Materials, 2022, 12, .	10.2	18
67505	Topological Properties in Strained Monolayer Antimony Iodide. Chinese Physics Letters, 2021, 38, 117301.	1.3	4
67506	Activation of <c> dislocations in Mg with solute Y. Journal of Magnesium and Alloys, 2021, , .	5.5	13
67507	Broadband Optical Constants and Nonlinear Properties of SnS2 and SnSe2. Nanomaterials, 2022, 12, 141.	1.9	11
67508	Non-PGM Electrocatalysts for PEM Fuel Cells: A DFT Study on the Effects of Fluorination of FeNx-Doped and N-Doped Carbon Catalysts. Molecules, 2021, 26, 7370.	1.7	7
67509	The Third-Order Elastic Constants and Mechanical Properties of 30Â° Partial Dislocation in Germanium: A Study from the First-Principles Calculations and the Improved Peierlsâ€“Nabarro Model. Crystals, 2022, 12, 4.	1.0	0
67510	The critical role of synthesis conditions on small polaron carrier concentrations in hematiteâ€”A first-principles study. Journal of Applied Physics, 2021, 130, .	1.1	4
67511	Challenges of Overcoming Defects in Wide Bandgap Semiconductor Power Electronics. Electronics (Switzerland), 2022, 11, 10.	1.8	11
67512	Tuning the magnetic anisotropy of ferromagnetic <mml:math xmlns:mml="http://www.w3.org/1998/Math/MathML"><mml:msub><mml:mi>MnS</mml:mi><mml:mn>2</mml:mn></mml:msub></mm monolayers via electron occupation of Mn <mml:math xmlns:mml="http://www.w3.org/1998/Math/MathML"><mml:mi>d</mml:mi></mml:math> orbitals. Physical Review B, 2021, 104, .	1.1	6
67513	Elastic Properties and Deformation Mechanisms in the van der Waals Singleâ€Crystalline Indium Selenide. Physica Status Solidi - Rapid Research Letters, 2022, 16, 2100418.	1.2	1
67514	Giant thermoelectric figure of merit in multivalley high-complexity-factor LaSO. Physical Review Materials, 2021, 5, .	0.9	3
67515	Prediction of NbXGe (Xâ€‰=â€‰Rh, Ir) half-Heusler semiconducting compounds with promising thermoelectric property using 18-electron rule. Applied Physics A: Materials Science and Processing, 2022, 128, 1.	1.1	1
67516	Experimental and Theoretical Study on the Substitution Patterns in Lithium Germanides: The Case of Li₁₅Ge₄vs Li₁₄ZnGe₄. European Journal of Inorganic Chemistry, 2022, 2022, .	1.0	2
67517	Magnetic anisotropy and stability of Fe3Ga compounds. Eurasian Journal of Physics and Functional Materials, 2021, 5, 229-235.	0.2	0
67518	Exceptional Photocatalytic Activities of rGO Modified (B,N) Coâ€Doped WO₃, Coupled with CdSe QDs for One Photon Zâ€Scheme System: A Joint Experimental and DFT Study. Advanced Science, 2022, 9, e2102530.	5.6	52

#	Article	IF	Citations
67519	Polarizationâ€Induced Bandâ€Alignment Transition and Nonvolatile pâ€n Junctions in 2D Van der Waals Heterostructures. Advanced Electronic Materials, 2022, 8, .	2.6	9
67520	Transition Metal and N Doping on AlP Monolayers for Bifunctional Oxygen Electrocatalysts: Density Functional Theory Study Assisted by Machine Learning Description. ACS Applied Materials & Interfaces, 2022, 14, 1249-1259.	4.0	48
67521	A Mo5N6 electrocatalyst for efficient Na2S electrodeposition in room-temperature sodium-sulfur batteries. Nature Communications, 2021, 12, 7195.	5.8	80
67522	Boosting O₂ Reduction and H₂O Dehydrogenation Kinetics: Surface Nâ€Hydroxymethylation of gâ€C₃N₄ Photocatalysts for the Efficient Production of H₂O₂. Advanced Functional Materials, 2022, 32, .	7.8	76
67523	Point defect induced incommensurate dipole moments in the <mml:math xmlns:mml="http://www.w3.org/1998/Math/MathML"><mml:mrow><mml:mi mathvariant="normal">K</mml:mi><mml:msub><mml:mi>Ca</mml:mi><mml:mn>2</mml:mn></mml:msub><mml:msub><mml:mi>Nb</mml:mi> <mml:mi mathvariant="normal">O</mml:mi><mml:mn>10</mml:mn></mml:msub></mml:mrow></mml:math> Dion-Jacobson layered perovskite. Physical Review B, 2021, 104, .	1.1	1
67524	Monoelemental two-dimensional iodinene nanosheets: a first-principles study of the electronic and optical properties. Journal Physics D: Applied Physics, 2022, 55, 135104.	1.3	5
67525	PdZn intermetallic compound stabilized on ZnO/nitrogen-decorated carbon hollow spheres for catalytic semihydrogenation of alkynols. Nano Research, 2022, 15, 3090-3098.	5.8	14
67526	Direct evidence of two-dimensional electron gas-like band structures in hafnene. Nano Research, 2022, 15, 3770-3774.	5.8	0
67527	Screening Topological Quantum Materials for Na-Ion Battery Cathode. , 2022, 4, 175-180.		12
67528	Effect of the Configuration of Copper Oxideâ€“Ceria Catalysts in NO Reduction with CO: Superior Performance of a Copperâ€“Ceria Solid Solution. ACS Applied Materials & Interfaces, 2021, 13, 61078-61087.	4.0	37
67529	Charge-Compensated Doping Extends Carrier Lifetimes in SrTiO₃ by Passivating Oxygen Vacancy Defects. Journal of Physical Chemistry Letters, 2021, 12, 12040-12047.	2.1	20
67530	Heterogeneous Interface-Derived Engineered Electronic Structure of SiO with Enhanced Lithium Storage. ACS Applied Energy Materials, 2022, 5, 750-759.	2.5	2
67531	Defects and Phase Formation in Non-Stoichiometric LaFeO₃: a Combined Theoretical and Experimental Study. Chemistry of Materials, 2021, 33, 9473-9485.	3.2	9
67532	Unveiling 2D Ferroelectricity and Ferromagnetism Interaction in van der Waals Heterobilayers. Journal of Physical Chemistry C, 2021, 125, 27837-27843.	1.5	2
67533	Water in an External Electric Field: Comparing Charge Distribution Methods Using ReaxFF Simulations. Journal of Chemical Theory and Computation, 2022, 18, 580-594.	2.3	7
67534	Nb-Implanted BaO as a Support for Gold Single Atoms. Journal of Physical Chemistry C, 2021, 125, 28059-28066.	1.5	3
67535	Boron-Functionalized Organic Framework as a High-Performance Metal-Free Catalyst for N₂ Fixation. Journal of Physical Chemistry Letters, 2021, 12, 12142-12149.	2.1	9
67536	Effects of co-doping in semiconductors: CdTe. Physical Review B, 2021, 104, .	1.1	5

#	Article	IF	Citations
67537	Oxygen Vacancy Engineering of Molybdenum Oxide Nanobelts by Fe Ion Intercalation for Aerobic Oxidative Desulfurization. ACS Applied Nano Materials, 2021, 4, 13379-13387.	2.4	10
67538	Photoactive Control of Surface-Enhanced Raman Scattering with Reduced Graphene Oxide in Gas Atmosphere. ACS Nano, 2022, 16, 577-587.	7.3	10
67539	Nonstoichiometric Molybdenum Trioxide Adjustable Energy Barrier Enabling Ultralong-Life All-Solid-State Lithium Batteries. ACS Applied Materials & Interfaces, 2021, 13, 60907-60920.	4.0	11
67540	Tunable Electrical Conductivity of Flexible Metalâ€“Organic Frameworks. Chemistry of Materials, 2022, 34, 254-265.	3.2	7
67541	Large-Size Superlattices Synthesized by Sequential Sulfur Substitution-Induced Transformation of Metastable MoTe₂. Chemistry of Materials, 2021, 33, 9760-9768.	3.2	5
67542	KCs₂Pb₂(HCOO)₂Cl₅: A Lead Formate with Strong Second-Harmonic-Generation Response Obtained by an Anionic Substitution. Inorganic Chemistry, 2022, 61, 1130-1135.	1.9	1
67543	Anomalous Lattice Thermal Conductivity in Rocksalt IIAâ€“VIA Compounds. ACS Applied Energy Materials, 2022, 5, 882-896.	2.5	8
67544	Insights into the Activity Screening and Hydroformylation Kinetics of Rh-Based Bimetallic Phosphides. ACS Catalysis, 2021, 11, 15235-15243.	5.5	16
67545	Stabilities of Isomers of Phosphorus on Transition Metal Substrates. Chemistry of Materials, 2021, 33, 9447-9453.	3.2	7
67546	Oxidation Dynamics of Supported Catalytic Cu Clusters: Coupling to Fluxionality. ACS Catalysis, 2022, 12, 818-827.	5.5	7
67547	Comment on â€œExperimental Evidence for a New Two-Dimensional Honeycomb Phase of Silicon: A Missing Link in the Chemistry and Physics of Silicon Surfaces?â€• Journal of Physical Chemistry C, 2022, 126, 866-867.	1.5	1
67548	Bioactive Metalâ€“Organic Frameworks with Specific Metalâ€“Nitrogen (Mâ€“N) Active Sites for Efficient Sonodynamic Tumor Therapy. ACS Nano, 2021, 15, 20003-20012.	7.3	53
67549	Discovery of Leadâ€Free Perovskites for Highâ€Performance Solar Cells via Machine Learning: Ultrabroadband Absorption, Low Radiative Combination, and Enhanced Thermal Conductivities. Advanced Science, 2022, 9, e2103648.	5.6	35
67550	An Ensemble Learning Platform for the Large-Scale Exploration of New Double Perovskites. ACS Applied Materials & Interfaces, 2022, 14, 717-725.	4.0	16
67551	Manipulation on active electronic states of metastable phase Î²-NiMoO4 for large current density hydrogen evolution. Nature Communications, 2021, 12, 5960.	5.8	86
67552	Self-powered perovskite CH3NH3PbBr3 field effect transistor with fast response and high sensitivity in sensing. Materials Today Advances, 2021, 12, 100185.	2.5	2
67553	Structural investigation of the efficient capture of Cs⁺ and Sr²⁺ by a microporous Cdâ€“Snâ€“Se ion exchanger constructed from mono-lacunary supertetrahedral clusters. Inorganic Chemistry Frontiers, 2022, 9, 2880-2894.	3.0	8
67554	Nucleation and growth mechanism in the early stages of nickel coating in jet electrodeposition: a coarse-grained molecular simulation and experimental study. RSC Advances, 2022, 12, 11052-11059.	1.7	4

#	Article	IF	Citations
67555	First-Principles Study of the Structural, Electronic, Dynamical, and Mechanical Properties of Pd-Nb Binary Systems. SSRN Electronic Journal, 0, , .	0.4	0
67556	A Mn single atom catalyst with Mnâ€“N₂O₂ sites integrated into carbon nanosheets for efficient electrocatalytic CO₂ reduction. Journal of Materials Chemistry A, 2022, 10, 10892-10901.	5.2	28
67557	Mechanistic insights into the pseudocapacitive performance of bronze-type vanadium dioxide with mono/multi-valent cations intercalation. Journal of Materials Chemistry A, 2022, 10, 10439-10451.	5.2	14
67558	Intermetallic YIr₂ nanoparticles with negatively charged Ir active sites for catalytic hydrogenation of cyclohexanone to cyclohexanol. Catalysis Science and Technology, 2022, 12, 3088-3093.	2.1	2
67559	Thermally induced spin-crossover in the Fe(3-ethynylpyridine)₂[M(CN)₄] series with M = Ni, Pd, and Pt. The role of the electron density found at the CN 5Ïƒ orbital. New Journal of Chemistry, 2022, 46, 9618-9628.	1.4	8
67560	An atlas of room-temperature stability and vibrational anharmonicity of cubic perovskites. Materials Horizons, 2022, 9, 1896-1910.	6.4	8
67561	Anchoring boron on a covalent organic framework as an efficient single atom metal-free photo-electrocatalyst for nitrogen fixation: a first-principles analysis. Physical Chemistry Chemical Physics, 2022, 24, 10765-10774.	1.3	12
67562	Tunable structural and electronic properties of C₄XY (X â‰ Y = H, Cl and F) monolayers by functionalization, electric field and strain engineering. New Journal of Chemistry, 2022, 46, 9383-9388.	1.4	2
67563	Challenges of modeling nanostructured materials for photocatalytic water splitting. Chemical Society Reviews, 2022, 51, 3794-3818.	18.7	64
67564	Unravelling the key factors in the chlorine-promoted epoxidation of ethylene over a silverâ€“copper oxide nanocatalyst. Nanoscale, 2022, 14, 7332-7340.	2.8	3
67565	Probing the presence and absence of metal-fullerene electron transfer reactions in helium nanodroplets by deflection measurements. Physical Chemistry Chemical Physics, 2022, 24, 10378-10383.	1.3	1
67566	A critical evaluation of the catalytic role of CO₂ in propane dehydrogenation catalyzed by chromium oxide from a DFT-based microkinetic simulation. Physical Chemistry Chemical Physics, 2022, 24, 11030-11038.	1.3	3
67567	Cooperative coupling of anisotropic phonon modes intensifies visible thermochromism in layered Î±-MoO₃. Materials Horizons, 2022, 9, 1631-1640.	6.4	7
67568	Tuning the magnetic anisotropy energy by external electric fields of CoPt dimers deposited on graphene. Physical Chemistry Chemical Physics, 2022, 24, 9576-9588.	1.3	4
67569	In situ phosphating of Zn-doped bimetallic skeletons as a versatile electrocatalyst for water splitting. Energy and Environmental Science, 2022, 15, 2425-2434.	15.6	50
67570	A DFT Calculation: Gas Sensitivity of Defect GeSe to Air Decomposition Products (CO, No and) Tj ETQq1 1 0.784314 rgBT /Overlock 1	2.4	14
67571	Anisotropic thermal and electrical transport properties induced high thermoelectric performance in an Ir₂Cl₂O₂ monolayer. Physical Chemistry Chemical Physics, 2022, 24, 11268-11277.	1.3	17
67572	Biphenylene monolayer: a novel nonbenzenoid carbon allotrope with potential application as an anode material for high-performance sodium-ion batteries. Physical Chemistry Chemical Physics, 2022, 24, 10712-10716.	1.3	22

#	Article	IF	Citations
67573	The crystal structures, phase stabilities, electronic structures and bonding features of iridium borides from first-principles calculations. RSC Advances, 2022, 12, 11722-11731.	1.7	7
67574	Maximizing the peroxidase-like activity of Pd@Pt_xRu_{4â^'x} nanocubes by precisely controlling the shell thickness and their application in colorimetric biosensors. Nanoscale, 2022, 14, 7596-7606.	2.8	2
67575	Stable freestanding two-dimensional anionic electrons in YCl with extremely weak interlayer interaction. Journal of Materials Chemistry C, 0, , .	2.7	2
67576	Uncovering the multifaceted roles of nitrogen defects in graphitic carbon nitride for selective photocatalytic carbon dioxide reduction: a density functional theory study. Physical Chemistry Chemical Physics, 2022, 24, 11124-11130.	1.3	4
67577	Modification of Mgf(2-X)B(X) (X=0.0 and 1.0) and Mgf1 (F-Defected) for Anti-Reflective Material Commonly Used in Opticianry Lenses and Coatings with Boron Dopant: The First-Principles Study. SSRN Electronic Journal, 0, , .	0.4	0
67578	Directed exfoliating and ordered stacking of transition-metal-dichalcogenides. Nanoscale, 2022, 14, 7484-7492.	2.8	2
67579	A bifunctional GeC/SnSSe heterostructure for highly efficient photocatalysts and photovoltaic devices. Nanoscale, 2022, 14, 7292-7302.	2.8	24
67580	Effect of stress regulation on electronic structure and optical properties of TiOCl₂ monolayer. Wuli Xuebao/Acta Physica Sinica, 2022, 71, 077101.	0.2	2
67581	Acetylene hydrogenation catalyzed by bare and Ni doped CeO₂(110): the role of frustrated Lewis pairs. Physical Chemistry Chemical Physics, 2022, 24, 11295-11304.	1.3	12
67582	CSPTH: A Crystal Structure Prediction Framework on Tianhe-2 Supercomputer. Computer Science and Application, 2022, 12, 866-878.	0.0	0
67583	Phase transitions of dense liquid nitrogen and equation of state. Wuli Xuebao/Acta Physica Sinica, 2022, .	0.2	0
67584	First principles study of optoelectronic and photocatalytic performance of novel transition metal dipnictide XP₂ (X = Ti, Zr, Hf) monolayers. RSC Advances, 2022, 12, 11202-11206.	1.7	2
67585	Potential energy barrier for proton transfer in compressed benzoic acid. RSC Advances, 2022, 12, 11436-11441.	1.7	1
67586	Modulation of the coordination environment enhances the electrocatalytic efficiency of Mo single atoms toward water splitting. Journal of Materials Chemistry A, 2022, 10, 8784-8797.	5.2	17
67587	Structural dynamics of Ru clusters during nitrogen dissociation in ammonia synthesis. Physical Chemistry Chemical Physics, 2022, 24, 10820-10825.	1.3	6
67588	Self-Assembled Molecular Nanowires on Prepatterned Ge(001) Surfaces. Chemical Science, 0, , .	3.7	0
67589	Theoretical predictions of phase stability for orthorhombic and hexagonal ternary MAB phases. Physical Chemistry Chemical Physics, 2022, 24, 11249-11258.	1.3	18
67590	A Novel Sulfide Phosphor, Banaals3:Eu2+, Discovered Via Particle Swarm Optimization. SSRN Electronic Journal, 0, , .	0.4	0

#	Article	IF	Citations
67591	Theoretical investigation of the olefin cycle in H-SSZ-13 for the ethanol-to-olefins process using ab initio calculations and kinetic modeling. Catalysis Science and Technology, 2022, 12, 3311-3321.	2.1	2
67592	Billiard Catalysis at Ti3c2 Mxene/Max Heterostructure for Efficient Nitrogen Fixation. SSRN Electronic Journal, 0, , .	0.4	1
67593	Rational Development of Coâ€Doped Mesoporous Ceria with High Peroxidaseâ€Mimicking Activity at Neutral pH for Paperâ€Based Colorimetric Detection of Multiple Biomarkers. Advanced Functional Materials, 2022, 32, .	7.8	39
67594	Diamond-Like Films from Twisted Few-Layer Graphene. JETP Letters, 2022, 115, 161-166.	0.4	4
67595	Insight into the effect of alkali treatment on enhancing adsorptivity of activated carbon for HCl removal in H2 feedstock. Chemical Papers, 0, , 1.	1.0	0
67596	Data-driven approach to parameterize <mml:math xmlns:mml="http://www.w3.org/1998/Math/MathML"><mml:mi>SCAN</mml:mi><mml:mo>+</mml:mo><mml:mi>U</mml:mi></mml:m for an accurate description of <mml:math xmlns:mml="http://www.w3.org/1998/Math/MathML"><mml:mrow><mml:mn>3</mml:mn><mml:mi>d</mml:mi></mml:mrow></mml: transition metal oxide thermochemistry. Physical Review Materials, 2022, 6, .	0.9	6
67597	Local Density of States Modulated by Strain in Marginally Twisted Bilayer Graphene. Chinese Physics Letters, 2022, 39, 047403.	1.3	2
67598	Effect of pressure on anisotropy in elasticity, sound velocity, and thermal conductivity of vanadium borides. Advanced Composites and Hybrid Materials, 2022, 5, 2297-2305.	9.9	23
67599	Electron-Level Mechanistic Insights into Ce Doping for Enhanced Efficiency Degradation of Bisphenol A under Visible Light Irradiation. Nanomaterials, 2022, 12, 1382.	1.9	6
67600	Unravelling Charge Carrier Mobility in d₀â€Metalâ€based Spinels. Batteries and Supercaps, 2022, 5, .	2.4	5
67601	TCSP: a Template-Based Crystal Structure Prediction Algorithm for Materials Discovery. Inorganic Chemistry, 2022, 61, 8431-8439.	1.9	10
67602	Electronic, Magnetic, and Optical Performances of Non-Metals Doped Silicon Carbide. Frontiers in Chemistry, 2022, 10, 898174.	1.8	20
67603	Delicately Tailored Ternary Phosphate Electrolyte Promotes Ultrastable Cycling of Na₃V₂(PO₄)₂F₃-Based Sodium Metal Batteries. ACS Applied Materials & Interfaces, 2022, 14, 17444-17453.	4.0	20
67604	High-T_C Two-Dimensional Ferroelectric CuCrS₂ Grown via Chemical Vapor Deposition. ACS Nano, 2022, 16, 8141-8149.	7.3	23
67605	From atomic semimetal to topological nontrivial insulator. Physical Review B, 2022, 105, .	1.1	5
67606	Waferâ€Scale 2Hâ€MoS₂ Monolayer for High Surfaceâ€enhanced Raman Scattering Performance: Chargeâ€Transfer Coupled with Molecule Resonance. Advanced Materials Technologies, 2022, 7, .	3.0	14
67607	Theoretical Screening of Transition Metalâ€“N₄-Doped Graphene for Electroreduction of Nitrate. ACS Catalysis, 2022, 12, 5407-5415.	5.5	43
67608	Scalable Lithiophilic/Sodiophilic Porous Buffer Layer Fabrication Enables Uniform Nucleation and Growth for Lithium/Sodium Metal Batteries. Advanced Functional Materials, 2022, 32, .	7.8	21

#	Article	IF	Citations
67609	Congregated-electrons-strengthened anchoring and mineralization of gaseous formaldehyde on a novel self-supporting Cu2-xSe/Cu2O heterojunction photocatalyst under visible lights: A viable mesh for designing air purifier. Applied Catalysis B: Environmental, 2022, 312, 121427.	10.8	21
67610	Structural Stability and Optoelectronic Properties of Lead-Free Halide Perovskite CsSnBr3 by Introducing Transition-Metal Dopants. Journal of Electronic Materials, 0, , 1.	1.0	2
67611	Enhanced room-temperature NO2 sensing performance of SnO2/Ti3C2 composite with double heterojunctions by controlling co-exposed {221} and {110} facets of SnO2. Sensors and Actuators B: Chemical, 2022, 365, 131919.	4.0	19
67612	Numerical quality control for DFT-based materials databases. Npj Computational Materials, 2022, 8, .	3.5	6
67613	Bond-Valence Parameterization for the Accurate Description of DFT Energetics. Journal of Chemical Theory and Computation, 2022, 18, 3257-3267.	2.3	3
67614	Peel-and-Stick Integration of Atomically Thin Nonlayered PtS Semiconductors for Multidimensionally Stretchable Electronic Devices. ACS Applied Materials & Interfaces, 2022, 14, 20268-20279.	4.0	5
67615	In situ dual doping for constructing efficient CO2-to-methanol electrocatalysts. Nature Communications, 2022, 13, 1965.	5.8	84
67616	Bond formation at polycarbonate | X interfaces (X = Ti, Al, TiAl) probed by X-ray photoelectron spectroscopy and density functional theory molecular dynamics simulations. Applied Surface Science, 2022, , 153363.	3.1	2
67617	High thermoelectric performance in metastable phase of silicon: A first-principles study. Applied Physics Letters, 2022, 120, .	1.5	5
67618	High-Mobility Metastable Rock-Salt Type (Sn,Ca)Se Thin Film Stabilized by Direct Epitaxial Growth on a YSZ (111) Single-Crystal Substrate. ACS Applied Materials & Interfaces, 2022, 14, 18682-18689.	4.0	1
67619	Structures, stabilities, optoelectronic and photocatalytic properties of Janus aluminium mono-chalcogenides Al(Ga, In)STe monolayers. Physica E: Low-Dimensional Systems and Nanostructures, 2022, 142, 115229.	1.3	2
67620	NaClO-induced sodium-doped cyano-rich graphitic carbon nitride nanosheets with nitrogen vacancies to boost photocatalytic hydrogen peroxide production. Chemical Engineering Journal, 2022, 443, 136501.	6.6	22
67621	Graphene Quantum Dots Pinned on Nanosheetsâ€Assembled NiCoâ€LDH Hollow Microâ€Tunnels: Toward Highâ€Performance Pouchâ€Type Supercapacitor via the Regulated Electron Localization. Small, 2022, 18, e2201286.	5.2	48
67622	Ti-modification enhanced the activity of flexible mesh-type Mn/Î³-Al2O3/Al catalyst for indoor HCHO removal under humid conditions. Applied Catalysis A: General, 2022, , 118638.	2.2	2
67623	Asymmetrical Câ€“C Coupling for Electroreduction of CO on Bimetallic Cuâ€“Pd Catalysts. ACS Catalysis, 2022, 12, 5275-5283.	5.5	35
67624	Photoinduced evolution of lattice orthorhombicity and conceivably enhanced ferromagnetism in LaMnO3 membranes. Npj Quantum Materials, 2022, 7, .	1.8	8
67625	Microstructure, optical and magnetic properties of Zr-doped SnO synthesized by the hydrothermal method. Ceramics International, 2022, 48, 22827-22835.	2.3	3
67626	Z₃ Charge Density Wave of Silicon Atomic Chains on a Vicinal Silicon Surface. ACS Nano, 2022, 16, 6598-6604.	7.3	5

#	Article	IF	Citations
67627	First-Principles Analysis of Ethylene Oligomerization on Single-Site Ga³⁺ Catalysts Supported on Amorphous Silica. ACS Catalysis, 2022, 12, 5416-5424.	5.5	4
67628	Modeling atomic layer deposition of alumina using reactive force field molecular dynamics. MRS Advances, 2022, 7, 185-189.	0.5	1
67629	Does the composition in PtGe clusters play any role in fighting CO poisoning?. Journal of Chemical Physics, 2022, 156, 174301.	1.2	3
67630	Efficient humidity sensor based on surfactant free Cu2ZnSnS4 nanoparticles. Ceramics International, 2022, 48, 28898-28905.	2.3	3
67631	Zeroâ€Dimensional Organic Copper(I) Iodide Hybrid with High Antiâ€Water Stability for Blueâ€Lightâ€Excitable Solidâ€State Lighting. Advanced Optical Materials, 2022, 10, .	3.6	48
67632	Ferroelectric polarization tailored interfacial charge distribution to modify magnetic properties of two-dimensional Janus FeBrI/In2S3 heterostructures. Applied Physics Letters, 2022, 120, .	1.5	10
67633	Effect of MnO₂ Polymorphsâ€™ Structure on Low-Temperature Catalytic Oxidation: Crystalline Controlled Oxygen Vacancy Formation. ACS Applied Materials & Interfaces, 2022, 14, 18525-18538.	4.0	27
67634	Insights into Fe Species Structureâ€Performance Relationship for Direct Methane Conversion toward Oxygenates over Feâ€MOR Catalysts. ChemCatChem, 2022, 14, .	1.8	4
67635	Influence of hydrogen and helium nucleation on the mechanical properties of beryllium by first-principles calculations. Nuclear Materials and Energy, 2022, 31, 101181.	0.6	2
67636	Valley-symmetry-broken magnetic topological responses in <mml:math xmlns:mml="http://www.w3.org/1998/Math/MathML"><mml:mrow><mml:msub><mml:mrow><mml:mo>(</mml:mo><mml:mi>Pt</mml:mi> and <mml:math xmlns:mml="http://www.w3.org/1998/Math/MathML"><mml:mrow. Physical Review B, 2022, 105, .	1.1	8
67637	Deep machine learning unravels the structural origin of midâ€gap states in chalcogenide glass for highâ€density memory integration. InformaÄnÃ-MateriÃ¡ly, 2022, 4, .	8.5	34
67638	Adsorption and Sensing Properties of Formaldehyde on Chemically Modified Graphene Surfaces. Crystals, 2022, 12, 553.	1.0	9
67639	Electronic and Optical Properties of Twin T-Graphene Co-Doped with Boron and Phosphorus. Materials, 2022, 15, 2876.	1.3	5
67640	Tuning the activation of O2 on Pt single-atom catalyst using external-electric field: A first-principles study. Physica B: Condensed Matter, 2022, 638, 413934.	1.3	2
67641	Boosting hydrogen and oxygen evolution of porous CoP nanosheet arrays through electronic modulating with oxygen-anion-incorporation. Journal of Colloid and Interface Science, 2022, 622, 239-249.	5.0	11
67642	NbCX (X=F, Cl, Br, I) with Highly Anisotropic Fermi Velocity, Optical, Mechanical and Electric Transport Properties. Chemical Physics, 2022, , 111551.	0.9	1
67643	Quasi Solidâ€state Electrolytes of Li₂Sn₂(bdc)₃(H₂O)_x Metalâ€organic Frameworks for Lithium Metal Battery. Electroanalysis, 2022, 34, 1667-1672.	1.5	2
67644	Effective peroxymonosulfate activation by natural molybdenite for enhanced atrazine degradation: Role of sulfur vacancy, degradation pathways and mechanism. Journal of Hazardous Materials, 2022, 435, 128899.	6.5	35

#	Article	IF	Citations
67645	Ferroelectricity and Piezoelectric Response of (Sc,Y)N/(Al,Ga,In)N Monolayer Alternating Stacked Structures by Firstâ€Principles Calculations. Physica Status Solidi (B): Basic Research, 2022, 259, .	0.7	6
67646	Synergic Reaction Kinetics over Adjacent Ruthenium Sites for Superb Hydrogen Generation in Alkaline Media. Advanced Materials, 2022, 34, e2110604.	11.1	108
67647	Enhanced tunneling electroresistance effect by designing interfacial ferroelectric polarization in multiferroic tunnel junctions. Physical Review B, 2022, 105, .	1.1	1
67648	Layer-by-Layer Assembly of CeO_{2â€“x}@C-rGO Nanocomposites and CNTs as a Multifunctional Separator Coating for Highly Stable Lithiumâ€“Sulfur Batteries. ACS Applied Materials & Interfaces, 2022, 14, 18634-18645.	4.0	24
67649	A potential-driven switch of activity promotion mode for the oxygen evolution reaction at Co3O4/NiOxHy interface. EScience, 2022, 2, 438-444.	25.0	103
67650	Participation of nitrogen impurities in the growth of grown-in oxide precipitates in nitrogen-doped Czochralski silicon. Journal of Applied Physics, 2022, 131, 155703.	1.1	0
67651	Oxidation Catalysis over Solid-State Keggin-Type Phosphomolybdic Acid with Oxygen Defects. Journal of the American Chemical Society, 2022, 144, 7693-7708.	6.6	30
67652	One-Step Facile Synthesis of High-Activity Nitrogen-Doped PtNiN Oxygen Reduction Catalyst. ACS Applied Energy Materials, 2022, 5, 5245-5255.	2.5	11
67653	Ordering Degree-Dependent Activity of Pt₃M (M = Fe, Mn) Intermetallic Nanoparticles for Electrocatalytic Methanol Oxidation. Journal of Physical Chemistry Letters, 2022, 13, 3549-3555.	2.1	7
67654	Design, Synthesis, and Optoelectronic Properties of the High-Purity Phase in Layered AETMN₂ (AE = Sr, Ba; TM = Ti, Zr, Hf) Semiconductors. Inorganic Chemistry, 2022, 61, 6650-6659.	1.9	4
67655	Improving Rare-Earth Mineral Separation with Insights from Molecular Recognition: Functionalized Hydroxamic Acid Adsorption onto BastnÃsite and Calcite. Langmuir, 2022, 38, 5439-5453.	1.6	6
67656	Unlocking bimetallic active sites via a desalination strategy for photocatalytic reduction of atmospheric carbon dioxide. Nature Communications, 2022, 13, 2146.	5.8	60
67657	Prediction of quantum anomalous Hall effect in CrI₃/ScCl₂ bilayer heterostructure. Chinese Physics B, 2022, 31, 107304.	0.7	1
67658	Structural Design and Physical Properties of Gallium Nitrides under High Pressures. Journal of Physical Chemistry C, 2022, 126, 7773-7777.	1.5	2
67659	Precise control of surface oxygen vacancies in ZnO nanoparticles for extremely high acetone sensing response. Journal of Advanced Ceramics, 2022, 11, 769-783.	8.9	33
67660	Argyrodite-type advanced lithium conductors and transport mechanisms beyond paddle-wheel effect. Nature Communications, 2022, 13, 2078.	5.8	27
67661	Synergistic Geometric and Electronic Effects in Biâ€“Cu Bimetallic Catalysts for CO₂ Electroreduction to Formate over a Wide Potential Window. ACS Sustainable Chemistry and Engineering, 2022, 10, 5693-5701.	3.2	9
67662	Cu₂I₂[NH(CH₃)₂]₂: synthesis, structure, characterizations and theoretical studies. Molecular Crystals and Liquid Crystals, 0, , 1-9.	0.4	0

#	Article	IF	Citations
67663	Interfacial Engineering of a Phase-Controlled Heterojunction for High-Efficiency HER, OER, and ORR Trifunctional Electrocatalysis. ACS Omega, 2022, 7, 13687-13696.	1.6	13
67664	Pressure dependent magnetic properties on bulk CrBr3 single crystals. Journal of Alloys and Compounds, 2022, 911, 165034.	2.8	5
67665	First-principles study of the monolayer MoSeTe for gas sensing applications. Chemical Physics, 2022, , 111548.	0.9	3
67667	Engineering multiphasic MoSe2/NiSe heterostructure interfaces for superior hydrogen production electrocatalysis. Applied Catalysis B: Environmental, 2022, 312, 121434.	10.8	50
67668	Probing the role of grain boundaries in single Cu nanoparticle oxidation by in situ plasmonic scattering. Physical Review Materials, 2022, 6, .	0.9	4
67669	Remarkable Thermoelectric Performance in K₂CdPb Crystals with 1D Building Blocks via Structure Particularity and Bond Heterogeneity. ACS Applied Energy Materials, 2022, 5, 5146-5158.	2.5	6
67670	Minority report: Structure and bonding of YbNi3Ga9 and YbCu3Ga8 obtained in gallium flux. Journal of Solid State Chemistry, 2022, , 123157.	1.4	0
67671	2D spontaneous valley polarization from inversion symmetric single-layer lattices. Npj Computational Materials, 2022, 8, .	3.5	31
67672	Surface hydroxyl dependent adsorption of ruthenium on SiO2(0 0 1) â€“ Understanding metalâ€“support interaction. Applied Surface Science, 2022, 593, 153396.	3.1	3
67673	Experimental and Computational Studies of Compression and Deformation Behavior of Hafnium Diboride to 208 GPa. Materials, 2022, 15, 2762.	1.3	2
67674	Exploring the sensing ability of <scp>B</scp> â€•and <scp>Si</scp> â€•doped <scp> WS ₂ </scp> monolayer toward <scp>CO</scp> and <scp>NO</scp> gas. International Journal of Quantum Chemistry, 0, , .	1.0	2
67675	Substrate effect on hydrogen evolution reaction in two-dimensional Mo2C monolayers. Scientific Reports, 2022, 12, 6076.	1.6	3
67676	Li₅Sn, the Most Lithium-Rich Binary Stannide: A Combined Experimental and Computational Study. Journal of the American Chemical Society, 2022, 144, 7096-7110.	6.6	7
67677	2D SnSe Cathode Catalyst Featuring an Efficient Facetâ€Dependent Selective Li₂O₂ Growth/Decomposition for Liâ€“Oxygen Batteries. Advanced Energy Materials, 2022, 12, .	10.2	45
67678	Firstâ€principles insights on anion redox activity in Na_xFe_{1/8}Ni_{1/8}Mn_{3/4}O₂: Toward efficient highâ€energy cathodes for Naâ€ion batteries. Journal of the American Ceramic Society, 2023, 106, 109-119.	1.9	5
67679	Instability of the Li₇SiPS₈ Solid Electrolyte at the Lithium Metal Anode and Interphase Formation. Chemistry of Materials, 2022, 34, 3659-3669.	3.2	12
67680	Observation of mid-gap states emerging in the O-terminated interface of Cr2O3/graphene: A combined study of ab initio prediction and photoemission analysis. Applied Surface Science, 2022, , 153416.	3.1	1
67681	Graphene on silicon: Effects of the silicon surface orientation on the work function and carrier density of graphene. Physical Review B, 2022, 105, .	1.1	2

#	Article	IF	Citations
67682	First-principles study of substitutional solute and carbon interactions in tungsten. Tungsten, 2022, 4, 231-238.	2.0	3
67683	DFT Study of the BH₄^{â”} Hydrolysis on Au(111) Surface. ChemPhysChem, 2022, 23, .	1.0	3
67684	Insights into the Reaction of 1-Butene Catalytic Cracking in HZSM-5 from First-Principles: Reaction Mechanism and Microkinetics Research. Industrial & Engineering Chemistry Research, 2022, 61, 5429-5441.	1.8	4
67685	Local Stability to Periodicity in the EuMg _{5+ x} Type: Chemical Pressure, Disordered Channels, and Predicted Superstructure in YZn _{5.225}. Zeitschrift Fur Anorganische Und Allgemeine Chemie, 0, , .	0.6	2
67686	High-Pressure Synthesis, Electronic Properties, and Raman Spectroscopy of Barium Tetraborate BaB₄O₇ Polymorphs. Crystal Growth and Design, 2022, 22, 3405-3412.	1.4	2
67687	Synergetic Charge Transfer and Spin Selection in CO Oxidation at Neighboring Magnetic Single-Atom Catalyst Sites. Nano Letters, 2022, 22, 3744-3750.	4.5	27
67688	Partially charged single-atom Ru supported on ZrO2 nanocrystals for highly efficient ethylene hydrosilylation with triethoxysilane. Nano Research, 2022, 15, 5857-5864.	5.8	9
67689	ZnSe/Ta2O5 heterojunction with high carrier separation efficiency: Experimental and theoretical calculations. Applied Surface Science, 2022, 593, 153456.	3.1	2
67690	An activity descriptor for perovskite oxides in catalysis. Chem Catalysis, 2022, 2, 1163-1176.	2.9	7
67691	Interplay between structural, magnetic, and electronic states in the pyrochlore iridate <mml:math xmlns:mml="http://www.w3.org/1998/Math/MathML"><mml:msub><mml:mrow><mml:mi>Eu</mml:mi></mml:mrow><mml:mn>2</mml:mn></mml:msub><mml:mrow><mml:mi mathvariant="normal">O</mml:mi></mml:mrow><mml:mn>7</mml:mn></mml:msub></mml:math>. Physical Review B, 2022, 105, .	1.1	6
67692	Surface Ligand Tuning of Coordination Geometry and Pb 6s² Electronic Pair Stereochemical Activity in MAPbBr₃ Perovskite Nanoparticles: A Joint Experimental and Theoretical Insight. Journal of Physical Chemistry C, 2022, 126, 7500-7509.	1.5	4
67693	Giant Stokes shift for charged vacancies in monolayer SnS. Physical Review Materials, 2022, 6, .	0.9	2
67694	Enhanced ferromagnetic ordering of Mn trimer symmetrically and fully exposed on iridium-doped graphene. Journal of Physics B: Atomic, Molecular and Optical Physics, 0, , .	0.6	0
67695	Electronic and optical properties of TMDs/Hg0.33Cd0.66Te. Journal of Materials Science: Materials in Electronics, 2022, 33, 11542.	1.1	0
67696	Two-Dimensional Cs3Sb2I9â^'xClx Film with (201) Preferred Orientation for Efficient Perovskite Solar Cells. Materials, 2022, 15, 2883.	1.3	9
67697	Eu₂Mg₃Bi₄: Competing Magnetic Orders on a Buckled Honeycomb Lattice. Chemistry of Materials, 2022, 34, 3902-3909.	3.2	0
67698	High-performance artificial neurons based on Ag/MXene/GST/Pt threshold switching memristors. Chinese Physics B, 2023, 32, 017304.	0.7	4
67699	Charge Compensation Mechanisms and Oxygen Vacancy Formations in LiNi_{1/3}Co_{1/3}Mn_{1/3}O₂: First-Principles Calculations. ACS Omega, 2022, 7, 14875-14886.	1.6	6

#	Article	IF	Citations
67700	Perovskite synthesizability using graph neural networks. Npj Computational Materials, 2022, 8, .	3.5	16
67701	Charge density wave states in phase-engineered monolayer VTe₂. Chinese Physics B, 2022, 31, 077101.	0.7	4
67702	Crystalline C ₃ N ₃ H ₃ tube (3,0) nanothreads. Proceedings of the National Academy of Sciences of the United States of America, 2022, 119, e2201165119.	3.3	13
67703	Tuning Spin Texture and Spectroscopic Limited Maximum Efficiency through Chemical Composition Space in Double Halide Perovskites. ACS Applied Energy Materials, 2022, 5, 5579-5588.	2.5	5
67704	Confinementâ€Enhanced Selective Oxidation of Lignin Derivatives to Formic Acid Over Feâ€Cu/ZSMâ€5 Catalysts Under Mild Conditions. ChemSusChem, 2022, 15, .	3.6	1
67705	Synthesis, crystal structure, optical bandgap, and electronic structure of Cs2FeP2S6. Solid State Sciences, 2022, , 106891.	1.5	1
67706	First-principles design and experimental validation of Î²-Ti alloys with high solid-solution strengthening and low elasticities. Materials Science & Engineering A: Structural Materials: Properties, Microstructure and Processing, 2022, 843, 143053.	2.6	9
67707	Prediction of Large Second Harmonic Generation in the Metal-Oxide/Organic Hybrid Compound CuMoO3(p2c). Symmetry, 2022, 14, 824.	1.1	0
67708	Effect of co-doping and defects on electronic, magnetic, and optical properties in SnO<mml:math xmlns:mml="http://www.w3.org/1998/Math/MathML" display="inline" id="d1e617" altimg="si29.svg"><mml:msub><mml:mrow /><mml:mrow><mml:mn>2</mml:mn></mml:mrow></mml:msub></mml:math>: A first-principles study. Physica B: Condensed Matter, 2022, 639, 413924.	1.3	5
67709	Hidden Local Symmetry Breaking in Silver Diamondoid Compounds is Root Cause of Ultralow Thermal Conductivity. Advanced Materials, 2022, 34, e2202255.	11.1	20
67710	Thickness-dependent neutralization of low-energy alkali-metal ions scattering on graphene. Physical Review A, 2022, 105, .	1.0	2
67711	Uniaxial Strain Control of Bulk Ferromagnetism in Rare-Earth Titanates. Physical Review Letters, 2022, 128, 167201.	2.9	5
67712	In Situ Evolution of Secondary Metallic Phases in Off-Stoichiometric ZrNiSn for Enhanced Thermoelectric Performance. ACS Applied Materials & Interfaces, 2022, 14, 19579-19593.	4.0	18
67713	Experimental and theoretical study on enhanced electrochemistry of aluminum substitution LLZO garnet solid electrolytes. Materials Research Express, 0, , .	0.8	1
67714	First-Principles Study of Honeycomb Borophene on the Mo₂C Substrate. Journal of Physical Chemistry C, 2022, 126, 7288-7293.	1.5	1
67715	First-Principles Prediction of Superconductivity in High-Buckled Two-Dimensional Tin. ACS Applied Electronic Materials, 2022, 4, 2062-2069.	2.0	4
67716	First-principles study of interface stability and behaviors of He at the W/Y2O3 interface. Materials Today Communications, 2022, , 103520.	0.9	0
67717	The influences of atom relaxation on the DFT-calculated friction properties of theÂh-BN/h-BN and Gr/Gr interfaces. Tribology International, 2022, 173, 107586.	3.0	6

#	Article	IF	Citations
67718	Concomitant appearance of conductivity and superconductivity in (111) <mml:math xmlns:mml="http://www.w3.org/1998/Math/MathML"><mml:mrow><mml:msub><mml:mi>LaAlO</mml:mi><mml:mn>3</mml:mn></m interface with metal capping. Physical Review Materials, 2022, 6, .	0.9	3
67719	<scp>Hydrogenâ€Bonded</scp> Engineering Enhancing Phase Transition Temperature in Molecular Perovskite Ferroelastic. Chinese Journal of Chemistry, 2022, 40, 1559-1565.	2.6	24
67720	Theoretical Investigation of the Role of Anion and Trivalent Cation Substitution in the Physical Properties of Lead-Free Zero-Dimensional Perovskites. Journal of Physical Chemistry C, 2022, 126, 7245-7255.	1.5	8
67721	Dataâ€Driven Approach to Designing Twoâ€dimensional Van der Waals Heterostructures: Misjudgment of Band Alignment Type and its mechanism. Physica Status Solidi - Rapid Research Letters, 0, , .	1.2	2
67722	Diamond formation mechanism in chemical vapor deposition. Proceedings of the National Academy of Sciences of the United States of America, 2022, 119, e2201451119.	3.3	17
67723	Agâ€“Bi Charge Redistribution Creates Deep Traps in Defective Cs₂AgBiBr₆: Machine Learning Analysis of Density Functional Theory. Journal of Physical Chemistry Letters, 2022, 13, 3645-3651.	2.1	18
67724	Rare-earth defects in GaN: A systematic investigation of the lanthanide series. Physical Review Materials, 2022, 6, .	0.9	6
67725	NiS/MoS2 Mott-Schottky heterojunction-induced local charge redistribution for high-efficiency urea-assisted energy-saving hydrogen production. Chemical Engineering Journal, 2022, 443, 136321.	6.6	58
67726	Hybrid algorithm of Bayesian optimization and evolutionary algorithm in crystal structure prediction. Science and Technology of Advanced Materials Methods, 2022, 2, 67-74.	0.4	1
67727	Experimental and theoretical investigations of a multiwalled carbon nanotubes/SnO2/polyaniline ternary nanohybrid electrode for energy storage. Surfaces and Interfaces, 2022, 30, 101978.	1.5	5
67728	Access to Ru(IV)â€“Ru(V) and Ru(V)â€“Ru(VI) Redox in Layered Li₇RuO₆ via Intercalation Reactions. Chemistry of Materials, 2022, 34, 3724-3735.	3.2	3
67729	Structural Phase Transitions between Layered Indium Selenide for Integrated Photonic Memory. Advanced Materials, 2022, 34, e2108261.	11.1	16
67730	Plasmonic Carbon Nitride Polymers to Boost Hydrogen Generation. Advanced Sustainable Systems, 2022, 6, .	2.7	6
67731	Modelling magnesium surfaces and their dissolution in an aqueous environment using an implicit solvent model.. Journal of Chemical Physics, 2022, 156, 174702.	1.2	1
67732	Greatly Enhanced Methanol Oxidation Reaction of <scp>CoPt</scp> Truncated Octahedral Nanoparticles by External Magnetic Fields. Energy and Environmental Materials, 2023, 6, .	7.3	6
67733	Effect of cobalt doping on the enhanced energy storage performance of 2D vanadium diselenide: experimental and theoretical investigations. Nanotechnology, 2022, 33, 295703.	1.3	7
67734	Electron Doping and Physical Properties in the Ferromagnetic Semimetal Co₃Sn_{2â€“x}Sb_xS₂. Journal of Physical Chemistry C, 2022, 126, 7230-7237.	1.5	1
67735	Revealing the Nature of Active Sites on Ptâ€“Gd and Ptâ€“Pr Alloys during the Oxygen Reduction Reaction. ACS Applied Materials & Interfaces, 2022, 14, 19604-19613.	4.0	16

#	Article	IF	Citations
67736	Abnormal Evolution of a Layered Structure and Band Gap in AgInP₂S₆ under Compression. Journal of Physical Chemistry C, 0, , .	1.5	1
67737	Atomic Layer Deposition of Co_xO_y Films: Oxidants versus Composition. Advanced Materials Interfaces, 2022, 9, .	1.9	2
67738	CO₂ Reduction to C₁ and C₂ Compounds on Sulfur-Deficient Mackinawite (FeS): A Density Functional Theory Study. Journal of Physical Chemistry C, 2022, 126, 7012-7021.	1.5	7
67739	Epitaxial ScxAl1â^'xN on GaN exhibits attractive high-K dielectric properties. Applied Physics Letters, 2022, 120, . XGT <mml:math	1.5	17
67740			

#	Article	IF	Citations
67754	Superconducting proximity effect in <mml:math xmlns:mml="http://www.w3.org/1998/Math/MathML"><mml:mrow><mml:mrow><mml:mo>(</mml:mo><mml:mrow><mml:msqrt><mml:mn>3</mml:mn></mml:msqrt><mml:mo>×</mml:mo><mml:mn>3</mml:mn></mml:mrow><mml:mo>)</mml:mo></mml:mrow><mml:mi>R</mml:mi><mml:mn>30</mml:mn><mml:mo>°</mml:mo></mml:mrow></mml:math> Ni nanoislands on Pb(111). Physical Review Materials, 2022, 6, .	3.1	1
67755	Firstâ€principles analysis of proton conduction mechanism in perovskiteâ€structured sodium tantalate. Journal of the American Ceramic Society, 0, , .	1.9	2
67756	Flexoelectric effect induced pâ€“n homojunction in monolayer GeSe. 2D Materials, 2022, 9, 035005.	2.0	11
67757	Revisiting the Chevrel Phase: Impact of Dispersion Corrections on the Properties of Mo6S8 for Cathode Applications**. Batteries and Supercaps, 2022, 5, .	2.4	3
67758	Heavy 2D VSi2N4: High capacity and full battery open-circuit voltage as Li/Na-ion batteries anode. Applied Surface Science, 2022, 593, 153354.	3.1	12
67759	CoP@C with chemisorption-catalysis effect toward lithium polysulfides as multifunctional interlayer for high-performance lithium-sulfur batteries. Electrochimica Acta, 2022, 419, 140391.	2.6	4
67760	Enhanced Catalytic Performance of N-Doped Carbon Sphere-Supported Pd Nanoparticles by Secondary Nitrogen Source Regulation for Formic Acid Dehydrogenation. ACS Applied Materials & Interfaces, 2022, 14, 18550-18560.	4.0	16
67761	First-Principles Calculations of Thermoelectric Transport Properties of Quaternary and Ternary Bulk Chalcogenide Crystals. Materials, 2022, 15, 2843.	1.3	14
67762	Electroreduction of nitrogen to ammonia by single-atom catalysis with synergistic boron-carbon nitrogen nanotubes. Journal of Environmental Chemical Engineering, 2022, 10, 107752.	3.3	5
67763	Effects of Bond Strength on the Electronic Structure and Thermoelectric Properties of Î²â€VA Monolayers (Sb, As, and P). ChemNanoMat, 2022, 8, .	1.5	3
67764	Characteristic Resistive Switching of Rare-Earth Oxyhydrides by Hydride Ion Insertion and Extraction. ACS Applied Materials & Interfaces, 2022, 14, 19766-19773.	4.0	3
67765	Mechanistic Investigation and Free Energies of the Reactive Adsorption of Ethanol at the Alumina/Water Interface. Journal of Physical Chemistry C, 2022, 126, 7446-7455.	1.5	8
67766	Density Functional Theoryâ€Based Calculations for 2D Hexagonal Lanthanide Metals. Advanced Theory and Simulations, 0, , 2200057.	1.3	5
67767	First-principles study of magnetic properties of the cobalt doped silver copper sulfides. Computational Condensed Matter, 2022, , e00680.	0.9	1
67768	Re-examining the role of subsurface oxygen vacancies in the dissociation of H2O molecules on anatase TiO2. Applied Surface Science, 2022, 594, 153452.	3.1	3
67769	Combining Organic Plastic Salts with a Bicontinuous Electrospun PVDFâ€“HFP/Li₇La₃Zr₂O₁₂ Membrane: LiF-Rich Solid-Electrolyte Interphase Enabling Stable Solid-State Lithium Metal Batteries. ACS Applied Materials & Interfaces, 2022, 14, 18922-18934.	4.0	15
67770	Effects of fabrication atmosphere conditions on the physico-chemical properties of garnet electrolyte. Ionics, 2022, 28, 2673-2683.	1.2	1
67771	A high-entropy spinel ceramic oxide as the cathode for proton-conducting solid oxide fuel cells. Journal of Advanced Ceramics, 2022, 11, 794-804.	8.9	102

#	Article	IF	Citations
67772	Deep potentials for materials science. Materials Futures, 2022, 1, 022601.	3.1	61
67773	Machine learning approach for longitudinal spin fluctuation effects in bcc Fe at<mml:math xmlns:mml="http://www.w3.org/1998/Math/MathML"><mml:msub><mml:mi>T</mml:mi><mml:mi>c</mml:mi></mml:msub></mml:ma under Earth-core conditions. Physical Review B, 2022, 105, .	1.1	4
67774	Cyclohexanedodecol-Assisted Interfacial Engineering for Robust and High-Performance Zinc Metal Anode. Nano-Micro Letters, 2022, 14, 110.	14.4	42
67775	Interplay between anisotropic spin texture and large gap topological insulating phases in functionalized MXenes. Chinese Journal of Physics, 2022, 77, 2346-2354.	2.0	7
67776	Structural stability and electronic properties of Er nanowire on Si(001). Physica E: Low-Dimensional Systems and Nanostructures, 2022, , 115233.	1.3	0
67777	Assessing the Long-Term Reactivity to Achieve Compatible Electrolyteâ€“Electrode Interfaces for Solid-State Rechargeable Lithium Batteries Using First-Principles Calculations. Journal of Physical Chemistry C, 2022, 126, 8227-8237.	1.5	3
67778	Cu(C₂N₄H₄)₂Br₂Â·2H₂O: an antiferromagnetic cyanoguanidine coordination compound and its characterization. Zeitschrift Fur Naturforschung - Section B Journal of Chemical Sciences, 2022, .	0.3	1
67779	Electronically Activated Fe₅C₂ via N-Doped Carbon to Enhance Photothermal Syngas Conversion to Light Olefins. ACS Catalysis, 2022, 12, 5316-5326.	5.5	19
67780	First-principles calculations of AlAs/CdS heterostructure with tunable electronic properties. Scientia Sinica: Physica, Mechanica Et Astronomica, 2022, 52, 297303.	0.2	3
67781	The Magnetic Genome of Two-Dimensional van der Waals Materials. ACS Nano, 2022, 16, 6960-7079.	7.3	149
67782	Computational Investigation of Two-Dimensional Vanadium Boride Compounds for Na-Ion Batteries. ACS Omega, 2022, 7, 14765-14771.	1.6	9
67783	Chlorine-Infused Wide-Band Gap p-CuSCN/n-GaN Heterojunction Ultraviolet-Light Photodetectors. ACS Applied Materials & Interfaces, 2022, 14, 17889-17898.	4.0	8
67784	Tunable electronic structure in twisted WTe2/WSe2 heterojunction bilayer. AIP Advances, 2022, 12, .	0.6	4
67785	Insight into the Active Sites of N,P-Codoped Carbon Materials for Electrocatalytic CO₂ Reduction. Inorganic Chemistry, 2022, 61, 6073-6082.	1.9	13
67786	Salt-Assisted MoS₂ Growth: Molecular Mechanisms from the First Principles. Journal of the American Chemical Society, 2022, 144, 7497-7503.	6.6	30
67787	Complex structure due to As bonding and interplay with electronic structure in superconducting <mml:math xmlns:mml="http://www.w3.org/1998/Math/MathML"><mml:mrow><mml:msub><mml:mi>BaNi</mml:mi><mml:mn>2</mml:mn></ Physical Review B, 2022, 105, .	1.1	5
67788	High Chern number quantum anomalous Hall effect tunable by stacking order in van der Waals topological insulators. Physical Review B, 2022, 105, .	1.1	16
67789	Anisotropy of the magnetic and transport properties of <mml:math xmlns:mml="http://www.w3.org/1998/Math/MathML"><mml:mrow><mml:msub><mml:mi mathvariant="normal">EuZn</mml:mi><mml:mn>2</mml:mn></mml:msub><mml:msub><mml:mi mathvariant="normal">As</mml:mi><mml:mn>2</mml:mn></mml:msub></mml:mrow></mml:math>. Physical Review B, 2022, 105, .	1.1	9

#	Article	IF	Citations
67790	Anomalous valley Hall effect in<mml:math xmlns:mml="http://www.w3.org/1998/Math/MathML"><mml:mi>A</mml:mi></mml:math>-type antiferromagnetic van der Waals heterostructures. Physical Review B, 2022, 105, .	1.1	11
67791	Bridging microscopy with molecular dynamics and quantum simulations: an atomAI based pipeline. Npj Computational Materials, 2022, 8, .	3.5	10
67792	Mn2+-activated dual-wavelength emitting materials toward wearable optical fibre temperature sensor. Nature Communications, 2022, 13, 2166.	5.8	70
67793	Taming Electrons in Pt/C Catalysts to Boost the Mesokinetics of Hydrogen Production. Engineering, 2022, 14, 124-133.	3.2	1
67794	Multimodal Gas Sensor Detecting Hydroxyl Groups with Phase Transition Based on Ecoâ€Friendly Leadâ€Free Metal Halides. Advanced Functional Materials, 2022, 32, .	7.8	8
67795	Elementary mechanism for the electrocatalytic reduction of nitrobenzene on late-transition-metal surfaces from density functional theory. Chem Catalysis, 2022, 2, 1362-1379.	2.9	7
67796	First-Principle Study on Electronic Structure and Magnetism in Doped MgO Materials. Journal of Superconductivity and Novel Magnetism, 2022, 35, 2037-2045.	0.8	5
67797	Transition Metal Carboâ€Chalcogenide â€œTMCC:â€•A New Family of 2D Materials. Advanced Materials, 2022, 34, e2200574.	11.1	18
67798	Sulfur Engineering on NiFe Layered Double Hydroxide at Ambient Temperature for High Current Density Oxygen Evolution Reaction. ACS Applied Energy Materials, 2022, 5, 4603-4612.	2.5	17
67799	Understanding the dopability of p-type Mg₂(Si,Sn) by relating hybrid-density functional calculation results to experimental data. JPhys Energy, 2022, 4, 035001.	2.3	3
67800	An integrated computational and experimental method for predicting hydrogen plateau pressures of TiFe1-xMx-based room temperature hydrides. International Journal of Hydrogen Energy, 2022, 47, 17673-17682.	3.8	15
67801	Exploring the Stability of Single-Atom Catalysts Using the Density Functional Theory-Based Global Optimization Method: H₂ Formation on VO_x/Î³-Al₂O₃(100). Journal of Physical Chemistry C, 2022, 126, 6973-6981.	1.5	7
67802	Topological Ordering of Memory Glass on Extended Length Scales. Journal of the American Chemical Society, 2022, 144, 7414-7421.	6.6	8
67803	Assessing the role of surface carbon on the surface stability and reactivity of Î²-Mo2C catalysts. Applied Surface Science, 2022, , 153415.	3.1	3
67804	Multidimensional <scp>Co₃O₄</scp>/<scp>NiO</scp> heterojunctions with richâ€boundaries incorporated into reduced graphene oxide network for expanding the range of lithiophilic host. InformaÄnÃ-MateriÃ¡ly, 2022, 4, .	8.5	19
67805	First-Principles Insights into Lithium-Rich Ternary Phosphide Superionic Conductors: Solid Electrolytes or Active Electrodes. ACS Applied Materials & Interfaces, 2022, 14, 18373-18382.	4.0	0
67806	Sensing properties of nonmetal doped blue phosphorene toward <scp>NO</scp> and <scp>NO₂</scp> molecules: A firstâ€principles study. International Journal of Quantum Chemistry, 2022, 122, .	1.0	4
67807	Effect of Surface [Cu₄O] Moieties on the Activity of Cu-Based Catalysts. ACS Catalysis, 2022, 12, 5162-5173.	5.5	10

#	Article	IF	Citations
67808	Anomalies at the Dirac Point in Graphene and Its Hole-Doped Compositions. Physical Review Letters, 2022, 128, 166401.	2.9	3
67809	Single pair of Weyl nodes in the spin-canted structure of <mml:math xmlns:mml="http://www.w3.org/1998/Math/MathML"><mml:mrow><mml:msub><mml:mi>EuCd</mml:mi><mml:mn>2</mml:mn></ Physical Review B, 2022, 105, .	1.1	13
67810	Oxygen activation on Ba-containing perovskite materials. Science Advances, 2022, 8, eabn4072.	4.7	29
67811	The Combination of Structure Prediction and Experiment for the Exploration of Alkaliâ€Earth Metalâ€Contained Chalcopyriteâ€Like IR Nonlinear Optical Material. Advanced Science, 2022, 9, e2106120.	5.6	44
67812	Defect physics of the quasi-two-dimensional photovoltaic semiconductor GeSe. Chinese Physics B, 2022, 31, 116103.	0.7	2
67813	Stabilization of Black Phosphorene by Edge-Selective Adsorption of C₆₀ Molecules. Journal of Physical Chemistry C, 2022, 126, 6874-6879.	1.5	2
67814	Magnetic phase transition induced ferroelectric polarization in <mml:math xmlns:mml="http://www.w3.org/1998/Math/MathML"><mml:msub><mml:mi>BaFeF</mml:mi><mml:mn>4</mml:mn></mml:msub></m with room-temperature weak ferromagnetism. Physical Review Materials, 2022, 6, .	0.9	1
67815	Nearâ€Infrared Lightâ€Emitting Diodes utilizing a Europiumâ€Activated Calcium Oxide Phosphor with External Quantum Efficiency of up to 54.7%. Advanced Materials, 2022, 34, e2201887.	11.1	132
67816	Beyond Simple Structureâ€“Function Relationships: The Interplay of Geometry, Electronic Structure, and Molecule/Electrode Coupling in Single-Molecule Junctions. Journal of Physical Chemistry C, 2022, 126, 6653-6661.	1.5	3
67817	Quantifying the Dzyaloshinskii-Moriya Interaction Induced by the Bulk Magnetic Asymmetry. Physical Review Letters, 2022, 128, 167202.	2.9	25
67818	Extended Shear Deformation of the Immiscible Cuâ€“Nb Alloy Resulting in Nanostructuring and Oxygen Ingress with Enhancement in Mechanical Properties. ACS Omega, 2022, 7, 13721-13736.	1.6	3
67819	Unveiling the Role of the Ti Dopant and Viable Si Doping of Hematite for Practically Efficient Solar Water Splitting. ACS Catalysis, 2022, 12, 5112-5122.	5.5	28
67820	Directed Energy Deposition of Multi-Principal Element Alloys. Frontiers in Materials, 2022, 9, .	1.2	4
67821	NiFe2O4/Ketjen Black Composites as Efficient Membrane Separators to Suppress the Shuttle Effect for Long-Life Lithium-Sulfur Batteries. Nanomaterials, 2022, 12, 1347.	1.9	7
67822	Electrolyte-free graphite electrode with enhanced interfacial conduction using Li+-conductive binder for high-performance all-solid-state batteries. Energy Storage Materials, 2022, 49, 481-492.	9.5	10
67823	Facet dependent surface energy gap on magnetic topological insulators. Physical Review B, 2022, 105, .	1.1	6
67824	Highly selective transfer hydrogenation of furfural into furfuryl alcohol by interfacial frustrated Lewis pairs on CeO2. Journal of Catalysis, 2022, 410, 54-62.	3.1	26
67825	Hard Xâ€ray Photoemission Study of Heuslerâ€type Fe _{2â€•x} Re _x VAl Thermoelectric Compounds. Physica Status Solidi (B): Basic Research, 0, , .	0.7	1

#	Article	IF	Citations
67826	Segregation and diffusion behaviours of helium at grain boundaries in silicon carbide ceramics: first-principles calculations and experimental investigations. Journal of the European Ceramic Society, 2022, 42, 4066-4075.	2.8	11
67827	Photochemical anisotropy and direction-dependent optical absorption in semiconductors. Journal of Chemical Physics, 2022, 156, 154703.	1.2	1
67828	Out-of-plane magnetic anisotropy in bulk ilmenite<mml:math xmlns:mml="http://www.w3.org/1998/Math/MathML"><mml:msub><mml:mi mathvariant="normal">CoTiO</mml:mi><mml:mn>3</mml:mn></mml:msub></mml:math>. Physical Review B, 2022, 105, .	1.1	2
67829	Field-tunable toroidal moment and anomalous Hall effect in noncollinear antiferromagnetic Weyl semimetal Co1/3TaS2. Npj Quantum Materials, 2022, 7, .	1.8	13
67830	Optical absorption and stability enhancement in mixed lead, tin, and germanium hybrid halide perovskites for photovoltaic applications. Vacuum, 2022, 201, 111106.	1.6	8
67831	Effect of Al content on the structural stability of Î£3 (111) twin boundary in Ti1-xAlxN hard coatings: A first-principles study. Surface and Coatings Technology, 2022, 439, 128454.	2.2	2
67832	Impurity Combination Effect on Oxygen Absorption in Î±2-Ti3Al. Metals, 2022, 12, 650.	1.0	2
67833	Configurational entropy-induced phase transition in spinel LiMn₂O₄. Chinese Physics B, 2022, 31, 098202.	0.7	3
67834	Two-dimensional auxetic pentagonal materials as water splitting photocatalysts with excellent performances. Journal of Materials Science, 2022, 57, 7667-7679.	1.7	3
67835	Investigation of veryintenseD3-band emission in multi-crystalline silicon wafers using electron microscopy and hyperspectral photoluminescence imaging. Journal of Applied Physics, 2022, 131, 145703.	1.1	0
67836	First-principles calculations and experimental study of Al-doped Fe1-xAlxF3Â·0.33H2O/C cathodes for Li-ion batteries. Ionics, 0, , 1.	1.2	2
67837	Tuning the surface states of TiO2 using Cu5 atomic clusters. Applied Surface Science, 2022, 594, 153455.	3.1	7
67838	Persistent half-metallic ferromagnetism in a (111)-oriented manganite superlattice. Npj Computational Materials, 2022, 8, .	3.5	4
67839	The physical properties of a semi-hard magnetic Fe3Pd alloy with negative enthalpy of formation. Journal of Magnetism and Magnetic Materials, 2022, , 169395.	1.0	0
67840	A Generic Sacrificial Layer for Wideâ€Range Freestanding Oxides with Modulated Magnetic Anisotropy. Advanced Functional Materials, 2022, 32, .	7.8	24
67841	Predicting the lattice thermal conductivity of alloyed compounds from the perspective of configurational entropy. Npj Computational Materials, 2022, 8, .	3.5	7
67842	Density Functional Theory Approach to the Vibrational Properties and Magnetic Specific Heat of the Covalent Chain Antiferromagnet KFeS2. Molecules, 2022, 27, 2663.	1.7	3
67843	Adsorption Structure and Reactivity of a Putative Asymmetric Molecular Conductor; 4-Isocyanophenyl Disulfide on Au(111). Journal of Physical Chemistry C, 2022, 126, 6601-6611.	1.5	3

#	Article	IF	Citations
67844	Developing a Double Protection Strategy for High-Performance Spinel LiNi_{0.5}Mn_{1.5}O₄ Cathodes. ACS Applied Energy Materials, 2022, 5, 6401-6409.	2.5	6
67845	Porous aza-doped graphene-analogous 2D material a unique catalyst for CO2 conversion to formic-acid by hydrogenation and electroreduction approaches. Molecular Catalysis, 2022, 524, 112285.	1.0	23
67846	Relationship between local coordinates and thermal conductivity in amorphous carbon. Journal of Vacuum Science and Technology A: Vacuum, Surfaces and Films, 2022, 40, .	0.9	4
67847	Oxygen point defect stabilized metastable M3â€phase VO2 films. Applied Materials Today, 2022, 27, 101474.	2.3	2
67848	Insights into the sulfite activation by cobalt(II) sulfide for acetaminophen removal: A synergistic catalysis and DFT calculations. Journal of Environmental Chemical Engineering, 2022, 10, 107709.	3.3	5
67849	Excellent catalytic performance of Cu+ modified HZSM-5 to produce para-xylene via the toluene methylation reaction: High catalytic active site combining with channel shape selectivity. Microporous and Mesoporous Materials, 2022, 337, 111910.	2.2	3
67850	Study of band alignment type in Janus HfSe2/Ga2SeS and HfSeS/GaSe heterostructures. Computational Materials Science, 2022, 209, 111432.	1.4	2
67851	Electronic and magnetic properties of the superhalogen Fe(NO3)3 absorbed monolayer MoS2: The regulating performance. Materials Today Communications, 2022, 31, 103569.	0.9	1
67852	Oriented external electric fields act as a â€œswitchâ€•of Pt-M/BC3N2 diatomic catalysts activate pristine ammonia borane dehydrogenation: A DFT study. Materials Today Communications, 2022, 31, 103544.	0.9	2
67853	Revealing trace Si effect on precipitation behavior and properties of Cu-Cr-Zr alloy: Experiments and first-principles calculations. Journal of Alloys and Compounds, 2022, 910, 164945.	2.8	3
67854	Abnormal in-plane thermal conductivity anisotropy in bilayer Î±-phase tellurene. International Journal of Heat and Mass Transfer, 2022, 192, 122908.	2.5	2
67855	Theoretical investigation on electrocatalytic reduction of CO2 to methanol and methane by bimetallic atoms TM1/TM2-N@Gra (TMÂ=ÂFe, Co, Ni, Cu). Applied Surface Science, 2022, 593, 153377.	3.1	27
67856	Neural network approach to diffusion of B and N adatoms on the Pt(111) surface. Current Applied Physics, 2022, 39, 62-69.	1.1	2
67857	Bifunctional integrated electrode for high-efficient hydrogen production coupled with 5-hydroxymethylfurfural oxidation. Applied Catalysis B: Environmental, 2022, 312, 121400.	10.8	63
67858	Metal-organic framework-derived three-dimensional CoSe2/Cd0.8Zn0.2S Schottky junction for highly efficient photocatalytic H2 evolution. Applied Surface Science, 2022, 593, 153420.	3.1	14
67859	Investigation of structural, magnetic and electronic properties of CoMnSb superstructure: A DFT study. Computational Materials Science, 2022, 210, 111441.	1.4	3
67860	Theoretical investigations of Janus WSeTe monolayer and related van der Waals heterostructures with promising thermoelectric performance. Applied Surface Science, 2022, 593, 153402.	3.1	14
67861	Quasi-two-dimensional topological Co3Sn2S2 composite toward high rate sodium ion storage. Chemical Engineering Journal, 2022, 443, 136420.	6.6	4

#	Article	IF	Citations
67862	In-situ construction of Cuâ€“Co4N@CC hierarchical binder-free cathode for advanced and flexible Liâ€“CO2 batteries: Electron structure and mass transfer modulation. Journal of Power Sources, 2022, 535, 231446.	4.0	9
67863	Electronic and magnetic properties of sub-unit cell Î±-Fe2O3 films on the Î±-Al2O3 (0001) substrate. Computational Materials Science, 2022, 210, 111442.	1.4	2
67864	First-principles study of two-dimensional MoN2X2Y2 (X=B<mml:math) Tj ETQq0 0 0 rgBT /Overlock 10 Tf 50 682 Td (xmlns:mml="http://www.w3.org/1998/Math/MathML" display="inline" id="d1e488" altimg="si38.svg"><mml:msub><mml:mrow /><mml:mrow><mml:mn>2</mml:mn></mml:mrow></mml:msub></mml:math> adsorption properties. Computational Materials Science, 2022, 210, 111388.	3.1	9
67865	Tailoring the coordination environment of cobalt in a single-atom catalyst through phosphorus doping for enhanced activation of peroxymonosulfate and thus efficient degradation of sulfadiazine. Applied Catalysis B: Environmental, 2022, 312, 121408.	10.8	80
67866	Graph neural network predictions of metal organic framework CO<mml:math xmlns:mml="http://www.w3.org/1998/Math/MathML" display="inline" id="d1e488" altimg="si38.svg"><mml:msub><mml:mrow /><mml:mrow><mml:mn>2</mml:mn></mml:mrow></mml:msub></mml:math> adsorption properties. Computational Materials Science, 2022, 210, 111388.	1.4	19
67867	BiOBr/Bi2S3 heterojunction with S-scheme structureand oxygen defects: In-situ construction and photocatalytic behavior for reduction of CO2 with H2O. Journal of Colloid and Interface Science, 2022, 620, 407-418.	5.0	56
67868	Rational design of highly efficient electrocatalytic single-atom catalysts for nitrogen reduction on nitrogen-doped graphene and g-C2N supports. Journal of Power Sources, 2022, 535, 231449.	4.0	12
67869	Creating low coordination atoms on MoS2/NiS2 heterostructure toward modulating the adsorption of oxygenated intermediates in lithium-oxygen batteries. Chemical Engineering Journal, 2022, 442, 136311.	6.6	21
67870	Building dual active sites Co3O4/Cu electrode to break scaling relations for enhancement of electrochemical reduction of nitrate to high-value ammonia. Journal of Hazardous Materials, 2022, 434, 128887.	6.5	25
67871	Deep-blue emissive Cs3Cu2I5 perovskites nanocrystals with 96.6% quantum yield via InI3-assisted synthesis for light-emitting device and fluorescent ink applications. Nano Energy, 2022, 98, 107270.	8.2	35
67872	Bis-ammonium salts with strong chemisorption to halide ions for fast and durable aqueous redox Zn ion batteries. Nano Energy, 2022, 98, 107278.	8.2	17
67873	Cost-effective calculation of defects in Si using hybrid density functional with downsampled reciprocal grids. Current Applied Physics, 2022, 39, 51-55.	1.1	1
67874	Scanning tunneling microscopy and spectroscopy of NiTe2. Surface Science, 2022, 722, 122099.	0.8	1
67875	Intensity-modulated carbon monoxide gas sensor based on cerium dioxide-coated thin-core-fiber Mach-Zehnder interferometer. Optics and Laser Technology, 2022, 152, 108183.	2.2	12
67876	High performance of non-enzymatic glucose biosensors based on the design of microstructure of Ni2P/Cu3P nanocomposites. Applied Surface Science, 2022, 593, 153395.	3.1	10
67877	Electronic structure, magnetism and disorder effect in double half-Heusler alloy Mn2FeCoSi2. Journal of Magnetism and Magnetic Materials, 2022, 555, 169367.	1.0	10
67878	Atomically dispersed ruthenium in carbon aerogels as effective catalysts for pH-universal hydrogen evolution reaction. Chemical Engineering Journal, 2022, 442, 136337.	6.6	27
67879	Atomic structures of ordered monolayer GP zones in Mg-Zn-X (X= Ca, Nd) systems. Scripta Materialia, 2022, 216, 114744.	2.6	8

#	Article	IF	Citations
67880	Atomically-dispersed Mn-(N-C2)2(O-C2)2 sites on carbon for efficient oxygen reduction reaction. Energy Storage Materials, 2022, 49, 209-218.	9.5	26
67881	Klein tunneling and ballistic transport in graphene and related materials. , 0, , 118-142.		0
67882	Quantum transport in disordered graphene-based materials. , 0, , 143-218.		0
67883	Ab initio and multiscale quantum transport in graphene-based materials. , 0, , 232-299.		0
67884	Electronic structure calculations: the density functional theory (DFT). , 0, , 314-331.		0
67885	Electronic structure calculations: the many-body perturbation theory (MBPT). , 0, , 332-337.		0
67886	Green's functions and ab initio quantum transport in the Landauerâ€“BÃ¼ttiker formalism. , 0, , 338-357.		0
67887	Chapter 4. Computer Modelling. RSC Materials Monographs, 0, , 148-179.	0.2	0
67888	Ab Initio Study of Mechanical Deformation. , 2005, , 439-448.		0
67889	Quantum Theory of Reactive Scattering and Adsorption at Surfaces. , 2005, , 1713-1733.		0
67928	Transport Processes in Polymer Electrolyte Fuel Cells: Insights from Multiscale Molecular Simulations. , 0, , 321-339.		1
67929	Dilute carbon in H3S under pressure. Npj Computational Materials, 2022, 8, .	3.5	9
67930	Defect formation in Yb-doped <mml:math xmlns:mml="http://www.w3.org/1998/Math/MathML"><mml:msub><mml:mi>CsPbCl</mml:mi><mml:mn>3</mml:mn></mml:msub></mml:math> from first principles with implications for quantum cutting. Physical Review Materials, 2022, 6, .	3.1	8
67931	Srâ€Doped Superionic Hydrogen Glass: Synthesis and Properties of SrH₂₂. Advanced Materials, 2022, 34, e2200924.	11.1	10
67932	Realâ€Space Crystal Structure Analysis by Lowâ€Dose Focalâ€Series TEM Imaging of Organic Materials with Nearâ€Atomic Resolution. Advanced Materials, 2022, 34, e2202088.	11.1	4
67933	Insights and Activation Energy Surface of the Dehydrogenation of C₂H_xO Species in Ethanol Oxidation Reaction on Ir(100). ChemPhysChem, 2022, 23, .	1.0	3
67934	2D Homogeneous Holey Carbon Nitride: An Efficient Anode Material for Liâ€ion Batteries With Ultrahigh Capacity. ChemPhysChem, 2022, 23, .	1.0	12
67935	Interactions between glucosides of the tip of the S1 subunit of SARS-CoV-2 spike protein and dry and wet surfaces of CuO and Cuâ€”A model for the surfaces of coinage metals. Colloids and Surfaces B: Biointerfaces, 2022, 214, 112465.	2.5	2

#	Article	IF	Citations
67936	(C₅H₆N)Pb₂X₅ (X = Cl, Br): Hybrid Lead Halides Based on Seven-Coordinate Pb(II). Inorganic Chemistry, 2022, 61, 6530-6538.	1.9	7
67937	Sequential Pressure-Induced B1â€“B2 Transitions in the Anion-Ordered Oxyhydride Ba₂YHO₃. Inorganic Chemistry, 2022, 61, 7043-7050.	1.9	1
67938	Two-Dimensional Quaternary Transition Metal Sulfide CrMoA₂S₆ (A = C, Si, or) Tj ETQq0 0 0 rgBT /Overlock 1 Chemistry Letters, 2022, 13, 3850-3856.	2.1	6
67939	Chemomechanical Interactions Dictate Lithium Surface Diffusion Kinetics in the Solid Electrolyte Interphase. Langmuir, 2022, 38, 5472-5480.	1.6	8
67940	Probing the Disorder Inside the Cubic Unit Cell of Halide Perovskites from First-Principles. ACS Applied Materials & Interfaces, 2022, 14, 22973-22981.	4.0	12
67941	Unusual High Hardness and Load-Dependent Mechanical Characteristics of Hydrogenated Carbonâ€“Nitrogen Hybrid Films. ACS Applied Materials & Interfaces, 2022, 14, 20220-20229.	4.0	3
67942	Syngas Conversion to C₂ Species over WC and M/WC (M = Cu or Rh) Catalysts: Identifying the Function of Surface Termination and Supported Metal Type. ACS Applied Materials & Interfaces, 2022, 14, 19491-19504.	4.0	2
67943	Ultrafast Carbothermal Shock Constructing Ni₃Fe_{1â€“x}Cr_x Intermetallic Integrated Electrodes for Efficient and Durable Overall Water Splitting. ACS Applied Materials & Interfaces, 2022, 14, 19524-19533.	4.0	10
67944	Tuning Phase Transition and Thermochromic Properties of Vanadium Dioxide Thin Films via Cobalt Doping. ACS Applied Materials & Interfaces, 2022, 14, 19736-19746.	4.0	16
67945	Engineering Magnetic Anisotropy and Emergent Multidirectional Soft Ferromagnetism in Ultrathin Freestanding LaMnO₃ Films. ACS Nano, 2022, 16, 7580-7588.	7.3	14
67946	Electronic Band Tuning and Multivalley Raman Scattering in Monolayer Transition Metal Dichalcogenides at High Pressures. ACS Nano, 2022, 16, 8064-8075.	7.3	13
67947	Anisotropic Infrared Response and Orientation-Dependent Strain-Tuning of the Electronic Structure in Nb₂SiTe₄. ACS Nano, 2022, 16, 8107-8115.	7.3	7
67948	Low Temperature Nano Mechano-electrocatalytic CH₄ Conversion. ACS Nano, 2022, 16, 8684-8693.	7.3	19
67949	Unveiling the charge transfer dynamics steered by built-in electric fields in BiOBr photocatalysts. Nature Communications, 2022, 13, 2230.	5.8	117
67950	Surface restructuring of a perovskite-type air electrode for reversible protonic ceramic electrochemical cells. Nature Communications, 2022, 13, 2207.	5.8	65
67951	Stabilization of hexazine rings in potassium polynitride at high pressure. Nature Chemistry, 2022, 14, 794-800.	6.6	22
67952	Stabilizing superconductivity of ternary metal pentahydride $$hbox {CaCH}_{{5}}$$ via electronic topological transitions under high pressure from first principles evolutionary algorithm. Scientific Reports, 2022, 12, 6700.	1.6	3
67953	Effect of chemical substitution and external strain on phase stability and ferroelectricity in two dimensional M₂CT₂ MXenes. Nanoscale, 2022, , .	2.8	4

#	Article	IF	Citations
67954	DFT and MD investigations of the biomolecules of phenothiazine derivatives: interactions with gold and water molecules and investigations in search of effective drug for SARS-CoV-2. Journal of Biomolecular Structure and Dynamics, 2023, 41, 4522-4533.	2.0	5
67955	Spin-state transition of Co ion (S = 2 â†' S = 5/2) in hole substituted 1D chain of Ca₃Co₂O₆. Journal of Physics Condensed Matter, 2022, 34, 285803.	0.7	2
67956	On the importance of electronâ€“electron and electronâ€“phonon scatterings and energy renormalizations during carrier relaxation in monolayer transition-metal dichalcogenides. Journal of Physics Condensed Matter, 2022, 34, 285601.	0.7	2
67957	Ferroelectricity in a semiconducting all-inorganic halide perovskite. Science Advances, 2022, 8, eabj5881.	4.7	37
67958	Enhancing ionic conductivity in solid electrolyte by relocating diffusion ions to under-coordination sites. Science Advances, 2022, 8, eabj7698.	4.7	37
67961	Dft+U Study on the Magnetic Properties of 3d Transition Metal Doped Î'12 Borophene. SSRN Electronic Journal, 0, , .	0.4	0
67962	Boost the large driving photovoltages for overall water splitting in direct Z-scheme heterojunctions by interfacial polarization. Catalysis Science and Technology, 2022, 12, 3614-3621.	2.1	10
67963	Cooperative Catalytic Mo-S-Co Heterojunctions with Sulfur Vacancies for Kinetically Boosted Lithium-Sulfur Battery. SSRN Electronic Journal, 0, , .	0.4	0
67964	W exsolution promotes the in situ reconstruction of a NiW electrode with rich active sites for the electrocatalytic oxidation of 5-hydroxymethylfurfural (HMF). Catalysis Science and Technology, 2022, 12, 3363-3371.	2.1	8
67965	Dual Doping with Cation and Anion for Enhancing the Structural Stability of Sodium-Ion Layered Cathode. Physical Chemistry Chemical Physics, 2022, , .	1.3	3
67966	Benchmarking the Two-Dimensional Conductive Y3(C6x6)2 (Y= Co, Cu, Pd, Pt; X= Nh, NHS, S) Metal-Organic Framework Nanosheets for Co2 Reduction Reaction with Tunable Performance. SSRN Electronic Journal, 0, , .	0.4	0
67967	Conduction band-edge valley splitting in two-dimensional ferroelectric AgBiP₂S₆ by magnetic doping: towards electron valley-polarized transport. RSC Advances, 2022, 12, 13765-13773.	1.7	4
67968	Epitaxially Grown Porous Heterostructure of Hexagonal Boron Nitride/Graphene as Efficient Electrocatalyst for H2o2ÂGeneration. SSRN Electronic Journal, 0, , .	0.4	0
67969	Predicted stable electrides in Mgâ€“Al systems under high pressure. Physical Chemistry Chemical Physics, 2022, , .	1.3	0
67970	Hybrid-metal hydroxyl fluoride nanosheet arrays as a bifunctional electrocatalyst for efficient overall water splitting. Journal of Materials Chemistry A, 2022, 10, 11774-11783.	5.2	11
67971	Enhancing the remarkable adsorption of Pb²⁺ in a series of sulfonic-functionalized Zr-based MOFs: a combined theoretical and experimental study for elucidating the adsorption mechanism. Dalton Transactions, 2022, 51, 7503-7516.	1.6	10
67972	Bi Vacancy Simultaneous Manipulation of Bulk Adsorption and Carrier Utilization to Replenish the Mechanism of Cr(Vi) Photoreduction at Universal Ph. SSRN Electronic Journal, 0, , .	0.4	0
67973	A single-atom vanadium-doped 2D semiconductor platform for attomolar-level molecular sensing. Journal of Materials Chemistry A, 2022, 10, 13298-13304.	5.2	12

#	Article	IF	Citations
67974	Computational vibrational spectroscopy of moleculeâ€“surface interactions: what is still difficult and what can be done about it. Physical Chemistry Chemical Physics, 2022, 24, 15158-15172.	1.3	12
67975	Strain-induced spin-gapless semiconductors and pure thermal spin-current in magnetic black arsenic-phosphorus monolayers. Physical Chemistry Chemical Physics, 2022, 24, 13897-13904.	1.3	2
67976	Quantum spin Hall effect in tilted penta silicene and its isoelectronic substitutions. Physical Chemistry Chemical Physics, 2022, 24, 15201-15207.	1.3	6
67977	Water on porous, nitrogen-containing layered carbon materials: the performance of computational model chemistries. Physical Chemistry Chemical Physics, 2022, , .	1.3	0
67978	Quantum Anomalous Hall Effect in Monolayer Ferromagnetic Crc with Extremly High Curie Temperature. SSRN Electronic Journal, 0, , .	0.4	0
67979	Two Dimensional Pts2/Bn Heterostructure as an S-Scheme Photocatalyst with Enhanced Activity for Overall Water Decomposition. SSRN Electronic Journal, 0, , .	0.4	0
67981	Theoretical understanding of oxygen stability in Mnâ€“Fe binary layered oxides for sodium-ion batteries. Journal of Materials Chemistry A, 2022, 10, 11101-11109.	5.2	2
67982	Ultralow Lattice Thermal Conductivity and Promising Thermoelectric Properties of New 2d Mow3te8 Membrane. SSRN Electronic Journal, 0, , .	0.4	0
67983	Out-of-plane dipole-modulated photogenerated carrier separation and recombination at Janus-MoSSe/MoS₂ van der Waals heterostructure interfaces: an ab initio time-domain study. Physical Chemistry Chemical Physics, 2022, 24, 11743-11757.	1.3	2
67984	NiCoPâ€“CeO₂ composites for efficient electrochemical oxygen evolution. RSC Advances, 2022, 12, 13639-13644.	1.7	2
67985	Investigations on the thermoelectric and thermodynamic properties of Y₂CT₂ (T = O, F, OH). RSC Advances, 2022, 12, 14377-14383.	1.7	3
67986	Alkali Metal Doping in B-C3n4 Extends Carrier Lifetime and Increases the Co2 Adsorption: Dft Study and Time-Domain Ab Initio Analysis. SSRN Electronic Journal, 0, , .	0.4	0
67987	Direct Evidence for the Decisive Role of OH* Activation in CO Electro-Oxidation Reaction. SSRN Electronic Journal, 0, , .	0.4	0
67988	First-Principles Insights into Complex Interplays Among Nano-Phases in an Al-Cu-Li-Zr Alloy. SSRN Electronic Journal, 0, , .	0.4	0
67989	Screening of transition metal single-atom catalysts supported by a WS₂ monolayer for electrocatalytic nitrogen reduction reaction: insights from activity trend and descriptor. Physical Chemistry Chemical Physics, 2022, 24, 13384-13398.	1.3	10
67990	Enhanced No2-Sensing Performances of Ceo2 Nanoparticles on Mos2 at Room Temperature. SSRN Electronic Journal, 0, , .	0.4	0
67991	Magnetic Complexity, Magnetodielectric Effect and Dft Calculations on Correlation Driven Gd2comno6 Insulator. SSRN Electronic Journal, 0, , .	0.4	0
67992	Super high-performance 7-atomic-layer thermoelectric material ZrGe₂N₄. Nanoscale, 2022, 14, 8797-8805.	2.8	5

#	Article	IF	Citations
67993	The Structural, Electronic and Thermal Transport Properties of Pentagonal Ms2 (M = Zn, Cd) Monolayers: A First-Principles Studyâ€. SSRN Electronic Journal, 0, , .	0.4	0
67994	Local Phase Transformation Strengthening at Microtwin Boundaries in Nickel Based Superalloys. SSRN Electronic Journal, 0, , .	0.4	0
67995	Unraveling the relationships between chemical bonding and thermoelectric properties: n-type ABO₃ perovskites. Journal of Materials Chemistry A, 2022, 10, 11039-11045.	5.2	10
67996	Single Transition Metal Atom Anchored in C3b a Efficient and Selective Electrocatalyst for Nitrogen Reduction Reaction. SSRN Electronic Journal, 0, , .	0.4	0
67997	Excellent Optoelectronic and Thermoelectric Properties of Two-Dimensional Transition Metal Dinitride Hfn2. SSRN Electronic Journal, 0, , .	0.4	0
67998	Pressure-driven thermoelectric properties of defect chalcopyrite structured ZnGa₂Te₄:ab initiostudy. RSC Advances, 2022, 12, 12573-12582.	1.7	8
67999	Physical Properties and Radiation Tolerance of High-Entropy Pyrochlores Gd ₂(Ti _{0.25}Zr _{0.25}Sn) Tj ETQq0 0 0 rgBT /Overlock 10 Tf 50 512 Td ₇ and Individual Pyrochlores Gd ₂X ₂O ₇ (X= Ti, Zr, Sn, Hf) from First Principles Calculations. SSRN Electronic Journal, 0, , .	0.4	0
68000	Modulation of the Interfacial Charge Density on Fe2pâ€“Cop by Coupling Ceo2 for Accelerating Alkaline Electrocatalytic Hydrogen Evolution Reaction and Overall Water Splitting. SSRN Electronic Journal, 0, , .	0.4	0
68001	Tuning phase compositions of MoS₂ nanomaterials for enhanced heavy metal removal: performance and mechanism. Physical Chemistry Chemical Physics, 2022, 24, 13305-13316.	1.3	6
68002	First principles study on structural, electronic and optical properties of HfS_{2(1â^'x)}Se_{2x} and ZrS_{2(1â^'x)}Se_{2x} ternary alloys. RSC Advances, 2022, 12, 14061-14068.	1.7	6
68004	MoWS₂ nanosheets incorporated nanocarbons for high-energy-density pseudocapacitive negatrode material and hydrogen evolution reaction. Sustainable Energy and Fuels, 2022, 6, 2941-2954.	2.5	10
68005	FeP2 monolayer: Isoelectronic analogue of MoS2 with excellent electronic and optical properties. Physical Chemistry Chemical Physics, 0, , .	1.3	1
68006	Depolarization of Few-Layer III-V and II-VI Materials through Symmetric Rumpling. Physical Chemistry Chemical Physics, 2022, , .	1.3	0
68007	pH dependent reactivity of boehmite surfaces from first principles molecular dynamics. Physical Chemistry Chemical Physics, 2022, 24, 14177-14186.	1.3	4
68008	An All-in-One Zeolite@Ru-Al2o3 Nanoplatform Towards Highly Efficient, Anticoking, and Recyclable Hydrocarbon Cracking Catalysis. SSRN Electronic Journal, 0, , .	0.4	0
68009	MgH₂/single-atom heterojunctions: effective hydrogen storage materials with facile dehydrogenation. Journal of Materials Chemistry A, 2022, 10, 19839-19851.	5.2	23
68010	Reaction surfaces and interfaces of metal sulfides: cryo-XPS meets HAXPES and DFT. Faraday Discussions, 2022, , .	1.6	3
68011	Cyclobis(Paraquat-P-Phenylene) â€“ Mediated Electrosynthesis of New-Type Nanocomposite of Palladium Nanoparticles with Designated Macrocyclic Organic Compound. SSRN Electronic Journal, 0, , .	0.4	0

#	Article	IF	Citations
68012	Evaluation of the Electrochemical Stability, Interfacial Reaction, and Molecular Behavior of Ether-Functionalized Pyrrolidinium as Novel Electrolyte for Lithium Metal Battery by Quantum and Molecular Dynamics Simulations. SSRN Electronic Journal, 0, , .	0.4	0
68013	Electrical and magneto-transport in the 2D semiconducting MXene Ti₂CO₂. Journal of Materials Chemistry C, 2022, 10, 9062-9072.	2.7	5
68014	Concurrent In-Situ Oxidation State Engineering of Heterostructured Catalyst Toward Near-Optimal Water Oxidation. SSRN Electronic Journal, 0, , .	0.4	0
68015	Polarization Induced Self-Doping Effects and P-N Junctions in Heterostructures Based on F-Gan-H Stacking. SSRN Electronic Journal, 0, , .	0.4	0
68016	Electrocatalytic CO₂ reduction reaction on dual-metal- and nitrogen-doped graphene: coordination environment effect of active sites. Materials Advances, 2022, 3, 4566-4577.	2.6	10
68017	Incorporating Au₁₁ nanoclusters on MoS₂ nanosheet edges for promoting the hydrogen evolution reaction at the interface. Nanoscale, 2022, 14, 7919-7926.	2.8	9
68019	Significant enhancement of lattice thermal conductivity of monolayer AlN under bi-axial strain: a first principles study. Physical Chemistry Chemical Physics, 2022, 24, 16065-16074.	1.3	5
68020	Evolution of Metastable Thin Film with High-Hardness Wear Resistance for Advanced Cutting Tool Application. SSRN Electronic Journal, 0, , .	0.4	0
68021	A new mechanistic proposal for the aromatic cycle of the MTO process based on a computational investigation for H-SSZ-13. Catalysis Science and Technology, 2022, 12, 3516-3523.	2.1	7
68022	Towards the rational design of Pt-based alloy catalysts for the low-temperature water-gas shift reaction: from extended surfaces to single atom alloys. Chemical Science, 2022, 13, 6385-6396.	3.7	9
68023	Experimental and Theoretical Identifications of Durable Feâ€“Nx Configurations Embedded in Graphitic Carbon Nitride for Uranium Photoreduction. SSRN Electronic Journal, 0, , .	0.4	0
68024	First-Principles Study of the Stability and Migration of Xe and Cs in U3si. SSRN Electronic Journal, 0, , .	0.4	0
68025	Building up the â€œGenomeâ€•of bi-atom catalysts toward efficient HER/OER/ORR. Journal of Materials Chemistry A, 2022, 10, 11600-11612.	5.2	40
68026	Theoretical Proposal of a Revolutionary Water-Splitting Photocatalyst: The Monolayer of Boron Phosphide. SSRN Electronic Journal, 0, , .	0.4	0
68027	Structural Stabilization of Cation Disordered Rock-Salt Cathode Materials: Coupling between High-Ratio Inactive Ti4+ Cation and Mn2+/Mn4+ Two-Electron Redox Pair. SSRN Electronic Journal, 0, , .	0.4	0
68028	Strain-Tunable Zeeman Splitting and Optical Properties of Crbr3/Gec Van Der Waals Heterostructure. SSRN Electronic Journal, 0, , .	0.4	0
68029	Towards a new packing pattern of Li adsorption in two-dimensional pentagonal BCN. Physical Chemistry Chemical Physics, 2022, 24, 13194-13200.	1.3	8
68030	In situ Raman spectroscopy reveals the structure evolution and lattice oxygen reaction pathway induced by the crystallineâ€“amorphous heterojunction for water oxidation. Chemical Science, 2022, 13, 5639-5649.	3.7	14

#	Article	IF	Citations
68031	Atomistic Calculation of the Melting Point of the High-Entropy Cantor Alloy CoCrFeMnNi. Doklady Physical Chemistry, 2022, 502, 11-17.	0.2	2
68032	Theoretical Exploration of Site Selective PerovskitesÂ for the Application of Flexible Optoresponsive MemoryÂ Devices. SSRN Electronic Journal, 0, , .	0.4	0
68033	H2o2 Activation by Two-Dimensional Metal-Organic Frameworks with Different Metal Nodes for Micropollutants Degradation: Metal Dependence of Boosting Reactive Oxygen Species Generation. SSRN Electronic Journal, 0, , .	0.4	0
68034	Unraveling the Effects of Fe and Mn Promoters on the Tungstated Zirconia Catalyst: A Dft Study. SSRN Electronic Journal, 0, , .	0.4	0
68035	Tailoring Î± ₂/Î³ And Î³/Î³ Interfaces in TiAl Alloys Via Segregation: A Multiscale QM/MM Study. SSRN Electronic Journal, 0, , .	0.4	0
68036	Bifunctional Al2o3/Polyacrylonitrile Membrane to Suppress the Shuttling of Polysulfides in Lithium-Sulfur Batteries. SSRN Electronic Journal, 0, , .	0.4	0
68037	4-Nitrophenylacetylene-modified Cu₂O cubes and rhombic dodecahedra showing superior photocatalytic activity through surface band structure modulation. Journal of Materials Chemistry C, 2022, 10, 8422-8431.	2.7	11
68038	Why heterogeneous single-atom catalysts preferentially produce CO in the electrochemical CO₂ reduction reaction. Chemical Science, 2022, 13, 6366-6372.	3.7	35
68039	Superior energy storage properties in NaNbO₃-based ceramics via synergistically optimizing domain and band structures. Journal of Materials Chemistry A, 2022, 10, 11613-11624.	5.2	40
68040	Robust route to photocatalytic nitrogen fixation mediated by capitalizing on defect-tailored InVO₄ nanosheets. Environmental Science: Nano, 2022, 9, 1996-2005.	2.2	13
68041	Electronic Properties and Magnetostriction in Fe-Ga Alloy of D03 Structure. SSRN Electronic Journal, 0, , .	0.4	0
68042	Rational design of Mâ€“N₄â€“Gr/V₂C heterostructures as highly active ORR catalysts: a density functional theory study. RSC Advances, 2022, 12, 14368-14376.	1.7	6
68043	Synergetic effect between Pd²⁺ and Ir⁴⁺ species promoting direct ethane dehydrogenation into ethylene over bimetallic PdIr/AC catalysts. Catalysis Science and Technology, 0, , .	2.1	1
68044	A Novel Tetrahedral Spectral Element Method for Kohn-Sham Model. SSRN Electronic Journal, 0, , .	0.4	0
68045	Regulating the electronic and magnetic properties of 1Tâ€²-ReS₂ by fabricating nanoribbons and transition-metal doping: a theoretical study. Nanoscale, 2022, 14, 8454-8462.	2.8	16
68046	Unraveling the modified regulation of ternary substitution on Na₃V₂(PO₄)₃ for sodium ion batteries. Journal of Materials Chemistry A, 2022, 10, 11340-11353.	5.2	21
68047	Mechanochemical Synthesis of Heterophase Molybdenum Carbides for All-Ph Hydrogen Evolution Reactions. SSRN Electronic Journal, 0, , .	0.4	0
68048	Interfacial Electronic Rearrangement and Synergistic Catalysis for Alkaline Water Splitting in Carbon Encapsulated Ni (111)/Ni3c (113) Heterostructure. SSRN Electronic Journal, 0, , .	0.4	0

#	Article	IF	Citations
68049	Li-ion conductivity in Li₂OHCl_{1â^'x}Br_x solid electrolytes: grains, grain boundaries and interfaces. Journal of Materials Chemistry A, 2022, 10, 11574-11586.	5.2	24
68050	Tailoring magnetic anisotropy by graphene-induced selective skyhook effect on 4f-metals. Nanoscale, 2022, 14, 7682-7691.	2.8	4
68051	Interpenetrated N-rich MOF derived vesicular N-doped carbon for high performance lithium ion battery. Dalton Transactions, 2022, 51, 7817-7827.	1.6	2
68052	Prediction and realisation of high mobility and degenerate p-type conductivity in CaCuP thin films. Chemical Science, 2022, 13, 5872-5883.	3.7	12
68053	Significant Two-Step Potential-Induced Surface Reconstruction Observed on Au(111) in Aqueous Sulfuric Acid. SSRN Electronic Journal, 0, , .	0.4	0
68054	Sn4+ Doped Biobr1-Xclx with Improved Photocatalytic Performance for Degrading High Concentration Organic Dyes and Antibiotics. SSRN Electronic Journal, 0, , .	0.4	0
68055	Alloying two-dimensional NbSi₂N₄: a new strategy to realize half-metallic antiferromagnets. Nanoscale, 2022, 14, 8078-8084.	2.8	5
68056	Enhanced Photoluminescence in Cd _xZn _(1-x)S _y Solid Solution Through Defect Activation Strategy to Suppress the Non-Radiative Recombination. SSRN Electronic Journal, 0, , .	0.4	0
68057	Inverse design of stable spinel compounds with high optical absorption via materials genome engineering. Journal of Materials Chemistry A, 2022, 10, 12503-12509.	5.2	3
68058	Influence of Intercalated Gd Atoms on Graphene-4h-Sic(0001) Properties. SSRN Electronic Journal, 0, , .	0.4	0
68059	Activation of Basal-Plane Sulfur Sites on Mos2@Ni3s2 Nanorods by Zr Plasma Ion Implantation for Bifunctional Electrocatalysts. SSRN Electronic Journal, 0, , .	0.4	0
68060	Tuning the enzyme-like activities of cerium oxide nanoparticles using a triethyl phosphite ligand. Biomaterials Science, 2022, 10, 3245-3258.	2.6	6
68061	Prediction of SiS₂ and SiSe₂ as promising anode materials for sodium-ion batteries. Physical Chemistry Chemical Physics, 2022, 24, 13189-13193.	1.3	7
68062	The design and synthesis of spinel one-dimensional multi-shelled nanostructures for Li-ion batteries. Nanoscale, 2022, 14, 7692-7701.	2.8	2
68063	Topological transformation construction of a CoSe₂/N-doped carbon heterojunction with a three-dimensional porous structure for high-performance sodium-ion half/full batteries. Inorganic Chemistry Frontiers, 2022, 9, 3176-3186.	3.0	9
68064	Anisotropy of thermal transport in phosphorene: A comparative first-principles study using different exchange-correlation functional. Materials Advances, 0, , .	2.6	0
68065	Structures, properties, and applications of nitrogen-doped graphene. Theoretical and Computational Chemistry, 2022, , 211-248.	0.2	3
68066	Understanding the role of anharmonic phonons in diffusion of bcc metals. Physical Review Materials, 2022, 6, .	0.9	1

#	Article	IF	Citations
68067	Analysis of the Structural, Electronic and Magnetic Properties of Pd2FeTl. Gazi University Journal of Science, 2023, 36, 441-449.	0.6	0
68068	Vibrational properties of <mml:math xmlns:mml="http://www.w3.org/1998/Math/MathML"><mml:mrow><mml:msub><mml:mi>SrVO</mml:mi><mml:mn>2</mml:mn></ mathvariant="normal">H</mml:mi></mml:mrow></mml:math> with large spin-phonon coupling. Physical Review Materials, 2022, 6, .	0.9	0
68069	Floquet valley-polarized quantum anomalous Hall state in nonmagnetic heterobilayers. Physical Review B, 2022, 105, .	1.1	16
68070	Vibrational properties of <mml:math xmlns:mml="http://www.w3.org/1998/Math/MathML"><mml:mrow><mml:msub><mml:mi>CuInP</mml:mi><mml:mn>2</mml:mn><mml:m mathvariant="normal">S</mml:mi><mml:mn>6</mml:mn></mml:msub></mml:mrow></mml:math> across the ferroelectric transition. Physical Review B, 2022, 105, .	1.1	14
68071	Engineering Low-Coordination Single-Atom Cobalt on Graphitic Carbon Nitride Catalyst for Hydrogen Evolution. ACS Catalysis, 2022, 12, 5517-5526.	5.5	67
68072	Spin-Group Symmetry in Magnetic Materials with Negligible Spin-Orbit Coupling. Physical Review X, 2022, 12, .	2.8	26
68073	Bipolar semiconductor in two-dimensional covalent organic frameworks. Physical Review B, 2022, 105, .	1.1	5
68074	Shear band formation during nanoindentation of EuB6 rare-earth hexaboride. Communications Materials, 2022, 3, .	2.9	3
68075	Atomic Intercalation Induced Spin-Flip Transition in Bilayer CrI3. Nanomaterials, 2022, 12, 1420.	1.9	3
68076	Electronic structure and resonant inelastic x-ray scattering in osmates. I. Perovskite <mml:math xmlns:mml="http://www.w3.org/1998/Math/MathML"><mml:msub><mml:mi>NaOsO</mml:mi><mml:mn>3</mml:mn></mml:msub></ Physical Review B, 2022, 105, .	1.1	21
68077	Theoretical Prediction and Experimental Validation of the Glass-Forming Ability and Magnetic Properties of Fe-Si-B Metallic Glasses from Atomic Structures. Materials, 2022, 15, 3149.	1.3	6
68078	Composite NiCo₂O₄@CeO₂ Microsphere as Cathode Catalyst for Highâ€Performance Lithiumâ€“Oxygen Battery. Advanced Science, 2022, 9, e2200523.	5.6	26
68079	Weyl semimetal in the rare-earth hexaboride family supporting a pseudonodal surface and a giant anomalous Hall effect. Physical Review B, 2022, 105, .	1.1	4
68080	Antiferromagnetic second-order topological insulator with fractional mass-kink. Npj Computational Materials, 2022, 8, .	3.5	19
68081	Thermodynamic Modelling of the Te-X (X = Cu, Ga, Li, Sr) Systems. Journal of Phase Equilibria and Diffusion, 2022, 43, 193-213.	0.5	5
68082	Modeling antiphase boundary energies of Ni3Al-based alloys using automated density functional theory and machine learning. Npj Computational Materials, 2022, 8, .	3.5	15
68083	Protonic Conduction in La₂NiO₄₊_{Î´} and La<sub>2â€_xA_xNiO₄₊_{Î´} (AÂ= Ca,) Tj ET Q q 0.0 0 rgBT /O		
68084	Robust Ruddlesdenâ€Popper phase Sr₃Fe_{1.3}Mo_{0.5}N_{i0.2}O_{7â€Î´} decorated with inâ€situ exsolved Ni nanoparticles as an efficient anode for hydrocarbon fueled solid oxide fuel cells. SusMat, 2022, 2, 487-501.	7.8	18

#	Article	IF	Citations
68085	Structure and motifs of iron oxides from 1 to 3 TPa. Physical Review Materials, 2022, 6, .	0.9	1
68086	New Insights into Phase Separation of Cerium Hydrides under Pressure. ACS Omega, 2022, 7, 15681-15687.	1.6	0
68087	Efficient Lithium Storage of Siâ€Based Anode Enabled by a Dualâ€Component Protection Strategy. Advanced Energy and Sustainability Research, 2022, 3, .	2.8	6
68088	Monolayer SnI2: An Excellent p-Type Thermoelectric Material with Ultralow Lattice Thermal Conductivity. Materials, 2022, 15, 3147.	1.3	11
68089	Discovery of Pb-free hybrid organicâ€“inorganic 2D perovskites using a stepwise optimization strategy. Npj Computational Materials, 2022, 8, .	3.5	9
68090	An extended computational approach for point-defect equilibria in semiconductor materials. Npj Computational Materials, 2022, 8, .	3.5	3
68091	Adsorption and Migration of Silver on Group IV Semiconductor (001) Surfaces by Density Functional Theory. Journal of Physical Chemistry C, 2022, 126, 8134-8142.	1.5	1
68092	Direct Electron Transfer between Aromatic Molecules inside and outside the ZSM-5 Zeolite Channels: An Identification of the EPR Spectra of 1,3,5-Trimethylbenzene Radical Cations. Journal of Physical Chemistry C, 2022, 126, 7421-7430.	1.5	0
68093	Molecular Design of Two-Dimensional Covalent Heptazine Frameworks for Photocatalytic Overall Water Splitting under Visible Light. Journal of Physical Chemistry Letters, 2022, 13, 3949-3956.	2.1	17
68094	Optimization of segmented thermoelectric devices composed of high-temperature thermoelectric material La2Te3. Advanced Composites and Hybrid Materials, 2022, 5, 2884-2895.	9.9	27
68095	Oxygen Reduction Reaction and Electronic Properties of LnO-Terminated Surfaces of Pr₂NiO₄ and La₂NiO₄. Journal of Physical Chemistry C, 2022, 126, 7390-7399.	1.5	5
68096	Interface Stability-Controlled Growth of Fe_xGe on Ge (100), (110), and (111) Substrates. Journal of Physical Chemistry C, 2022, 126, 7674-7679.	1.5	1
68097	Insight into Luminescence Enhancement of Alkaline-Earth Metal Ion-Doped CsPbBr₃ Perovskite Nanocrystals. Journal of Physical Chemistry C, 2022, 126, 7588-7595.	1.5	7
68098	Electronic structure of the homologous series of Ruddlesdenâ€“Popper phases SrO(SrTiO₃)_n, (n = 0â€“3, â^ž). Zeitschrift Fur Kristallographie - Crystalline Materials, 2022, 237, 201-214.	0.4	1
68099	Tunable Surface Chemistry in Heterogeneous Bilayer Singleâ€Atom Catalysts for Electrocatalytic NO_x Reduction to Ammonia. Advanced Functional Materials, 2022, 32, .	7.8	30
68100	Cellulose nanofiberâ€derived carbon aerogel for advanced roomâ€temperature sodiumâ€“sulfur batteries. , 2023, 5, .		15
68101	Two-dimensional ordering governs the overpotential of Li intercalation and plating on graphene and its variants. Journal of Applied Physics, 2022, 131, .	1.1	1
68102	Pressure-induced evolution of structure and electronic property of GeP. Journal of Applied Physics, 2022, 131, .	1.1	3

#	Article	IF	Citations
68103	High-temperature fractional quantum Hall state in the Floquet kagome flat band. Physical Review B, 2022, 105, .	1.1	7
68104	Origin of layer-dependent electrical conductivity of transition metal dichalcogenides. Physical Review B, 2022, 105, .	1.1	5
68105	Actual pseudocapacity for Li ion storage in tunable coreâ€shell electrode architectures. EcoMat, 2022, 4, .	6.8	8
68106	SnS₂ Monolayer-Supported Transition Metal Atoms as Efficient Bifunctional Oxygen Electrocatalysts: A Theoretical Investigation. Energy & Fuels, 2022, 36, 4992-4998.	2.5	9
68107	Dataâ€driven and constrained optimization of semiâ€local exchange and nonlocal correlation functionals for materials and surface chemistry. Journal of Computational Chemistry, 2022, 43, 1104-1112.	1.5	3
68108	Boosting the Performance Gain of Ru/C for Hydrogen Evolution Reaction Via Surface Engineering. Energy and Environmental Materials, 2023, 6, .	7.3	7
68109	Dependency of sliding friction for two-dimensional systems on electronegativity. Physical Review B, 2022, 105, .	1.1	3
68110	Lithiumâ€ion Battery Technology for Voltage Control of Perpendicular Magnetization. Advanced Functional Materials, 2022, 32, .	7.8	11
68111	Automated exploitation of the big configuration space of large adsorbates on transition metals reveals chemistry feasibility. Nature Communications, 2022, 13, 2087.	5.8	8
68112	Experimental and first-principles study on TiB/TiC interface in hybrid (TiB+TiC)/Ti6Al4V composite. Ceramics International, 2022, 48, 22554-22559.	2.3	12
68113	Regulating multiscale structures of nickel-iron-based electrocatalysts for efficient water oxidation. Cell Reports Physical Science, 2022, 3, 100870.	2.8	4
68114	Modulating AgIn@In2O3 coreâ€shell catalysts for amplified electrochemical reduction of CO2 to formate. ChemElectroChem, 0, , .	1.7	1
68115	Insights Into the Electronic Properties of PbBi Atomic Layers on Ge(111) and Si(111) Surfaces. Frontiers in Materials, 2022, 9, .	1.2	5
68116	Near Room-Temperature Synthesis of Vertical Graphene Nanowalls on Dielectrics. ACS Applied Materials & Interfaces, 2022, 14, 21348-21355.	4.0	5
68117	Effect of vertical strain and in-plane biaxial strain on type-II MoSi2N4/Cs3Bi2I9 van der Waals heterostructure. Journal of Applied Physics, 2022, 131, .	1.1	11
68118	Silver(II) route to unconventional superconductivity. Physical Review B, 2022, 105, .	1.1	2
68119	Computational Study of the C₂P₄ Monolayer as a Stable Two-Dimensional Material with High Carrier Mobility: Implications for Nanoelectronic Devices. ACS Applied Nano Materials, 2022, 5, 6972-6979.	2.4	4
68120	Tailoring the Interface in High Performance Planar Perovskite Solar Cell by ZnOS Thin Film. ACS Applied Energy Materials, 2022, 5, 5680-5690.	2.5	9

#	Article	IF	Citations
68121	Transport in Lithium Garnet Oxides as Revealed by Atomistic Simulations. Annual Review of Materials Research, 2022, 52, 305-330.	4.3	2
68122	Controllable Acceleration and Deceleration of Charge Carrier Transport in Metalâ€Halide Perovskite Singleâ€Crystal by Csâ€Cation Induced Bandgap Engineering. Small, 2022, 18, e2107680.	5.2	3
68123	Phase engineering of Cr5Te8 with colossal anomalous Hall effect. Nature Electronics, 2022, 5, 224-232.	13.1	68
68124	Chemical Characterization of a Three-Dimensional Double-Decker Molecule on a Surface via Scanning-Tunneling-Microscopy-Based Tip-Enhanced Raman Spectroscopy. Journal of Physical Chemistry C, 0, , .	1.5	4
68125	Dimensional crossover and symmetry transformation of charge density waves in <mml:math xmlns:mml="http://www.w3.org/1998/Math/MathML"><mml:msub><mml:mi>VSe</mml:mi><mml:mn>2</mml:mn></mml:msub></mm Physical Review B, 2022, 105, .	1.1	7
68126	<mml:math xmlns:mml="http://www.w3.org/1998/Math/MathML"><mml:mrow><mml:mi>B</mml:mi><mml:mn>1</mml:mn><mml:mtext>â†’</mml:mtext>â†’</mm phase transition of ferropericlase at planetary interior conditions. Physical Review B, 2022, 105, .	1.1	2
68127	Sacrificial Dopant to Enhance the Activity and Durability of Electrochemical N₂ Reduction Catalysis. ACS Catalysis, 2022, 12, 5684-5697.	5.5	12
68128	Modeling temperature, frequency, and strain effects on the linear electro-optic coefficients of ferroelectric oxides. Journal of Applied Physics, 2022, 131, .	1.1	4
68129	High-Entropy Borides under Extreme Environment of Pressures and Temperatures. Materials, 2022, 15, 3239.	1.3	7
68130	Tunable Electronic Properties of MoS2/SiC Heterostructures: A First-Principles Study. Journal of Electronic Materials, 2022, 51, 3714-3726.	1.0	3
68131	Effects of local compositional and structural disorder on vacancy formation in entropy-stabilized oxides from first-principles. Npj Computational Materials, 2022, 8, .	3.5	7
68132	Exsolution of CoFe(Ru) nanoparticles in Ru-doped (La0.8Sr0.2)0.9Co0.1Fe0.8Ru0.1O3â^'Î´ for efficient oxygen evolution reaction. Nano Research, 2022, 15, 6977-6986.	5.8	34
68133	Pressure-induced structural transformation of clathrate <mml:math xmlns:mml="http://www.w3.org/1998/Math/MathML"><mml:msub><mml:mi>Ge</mml:mi><mml:mn>136</mml:mn></mml:msub></m via ultrafast recrystallization of an amorphous intermediate. Physical Review B, 2022, 105, .	1.1	1
68134	High pressure nanoarchitectonics and metallization of barium chloride and barium bromide. Journal of Physics Condensed Matter, 2022, 34, 294002.	0.7	1
68135	Role of disorder in the synthesis of metastable zinc zirconium nitrides. Physical Review Materials, 2022, 6, .	0.9	14
68136	Electronic Structure Calculation of Cr3+ and Fe3+ in Phosphor Host Materials Based on Relaxed Structures by Molecular Dynamics Simulation. Technologies, 2022, 10, 56.	3.0	2
68137	Structure-Performance Descriptors and the Role of the Axial Oxygen Atom on Mâ€“N₄â€“C Single-Atom Catalysts for Electrochemical CO₂ Reduction. ACS Catalysis, 2022, 12, 5441-5454.	5.5	50
68138	Titania Nanomaterials for Sarin Decomposition: Understanding Fundamentals. ACS Applied Nano Materials, 2022, 5, 6659-6670.	2.4	2

#	Article	IF	Citations
68139	Breaking adsorption-energy scaling limitations of electrocatalytic nitrate reduction on intermetallic CuPd nanocubes by machine-learned insights. Nature Communications, 2022, 13, 2338.	5.8	119
68140	Generalized universal equation of states for magnetic materials: A novel formulation for an interatomic potential in Fe. Physical Review Materials, 2022, 6, .	0.9	0
68141	Ca Solubility in a BiFeO₃-Based System with a Secondary Bi₂O₃ Phase on a Nanoscale. Journal of Physical Chemistry C, 2022, 126, 7696-7703.	1.5	1
68142	New stable structures of OsN₄ predicted using first-principles calculations. Phase Transitions, 0, , 1-11.	0.6	0
68143	Magnetic Weyl Semimetal in <mml:math xmlns:mml="http://www.w3.org/1998/Math/MathML" display="inline"><mml:mrow><mml:msub><mml:mrow><mml:mi mathvariant="normal">K</mml:mi></mml:mrow><mml:mrow><mml:mn>2</mml:mn></mml:mrow></mml:msub><mml:msub><mml:m		

#	Article	IF	Citations
68157	Effect of carbon atoms on the reliability of potassium-ion electrets used in vibration-powered generators. Japanese Journal of Applied Physics, 2022, 61, SH1013.	0.8	4
68158	Temperature-Induced Structure Transformation from Co_{0.85}Se to Orthorhombic Phase CoSe₂ Realizing Enhanced Hydrogen Evolution Catalysis. ACS Omega, 2022, 7, 15901-15908.	1.6	4
68159	Reversely trapping atoms from a perovskite surface for high-performance and durable fuel cell cathodes. Nature Catalysis, 2022, 5, 300-310.	16.1	175
68160	Spin-lattice-charge coupling in quasi-one-dimensional spin-chain <mml:math xmlns:mml="http://www.w3.org/1998/Math/MathML"><mml:mrow><mml:msub><mml:mi>NiTe</mml:mi><mml:mn>2</mml:mn></mml:msub><mml:msub><mml:mi mathvariant="normal">O</mml:mi><mml:mn>5</mml:mn></mml:msub></mml:mrow></mml:math>. Physical Review Materials, 2022, 6, .	0.9	5
68161	Layered double hydroxide nanosheets activate CsPbBr3 nanocrystals for enhanced photocatalytic CO2 reduction. Nano Research, 2022, 15, 5953-5961.	5.8	22
68162	Momentum-Space Spin Antivortex and Spin Transport in Monolayer Pb. Physical Review Letters, 2022, 128, 166601.	2.9	6
68163	Structureâ"Reactivity Relationship of $$hbox {Pt}_n$$ (nÂ=Â1,3,7) Nanoparticles Supported on (5,5) CNT: An Ab Initio Study. Topics in Catalysis, 0, , 1.	1.3	0
68164	Effects of Support and CO₂ on the Performances of Vanadium Oxide-Based Catalysts in Propane Dehydrogenation. ACS Catalysis, 2022, 12, 5736-5749.	5.5	14
68165	Novel Functionality in Switchable Polar Materials. Advanced Electronic Materials, 0, , 2200146.	2.6	0
68166	Manipulating the metal-to-insulator transition and magnetic properties in manganite thin films via epitaxial strain. Physical Review B, 2022, 105, .	1.1	2
68167	Unraveling Molecular Fingerprints of Catalytic Sulfur Poisoning at the Nanometer Scale with Near-Field Infrared Spectroscopy. Journal of the American Chemical Society, 2022, 144, 8848-8860.	6.6	8
68168	Concurrent Pressure-Induced Spin-State Transitions and Jahnâ€"Teller Distortions in MnTe. Chemistry of Materials, 2022, 34, 3931-3940.	3.2	6
68169	A Mechanistic Study of Oxygen Replenishment of Reduced Perovskites in Chemical Looping Redox Reactions. Journal of Physical Chemistry C, 2022, 126, 7431-7445.	1.5	3
68170	Conflicting Role of Inversion of the LiMn₂O₄ Spinel on Lithium-Ion Battery Capacity from First-Principles Calculations. Journal of Physical Chemistry C, 2022, 126, 7374-7382.	1.5	5
68171	Hydrogen Adsorption on the Vertical Heterostructures of Graphene and Two-Dimensional Electrides: A First-Principles Study. ACS Omega, 2022, 7, 16063-16069.	1.6	2
68172	Hydrogen Activation and Spillover on Anatase TiO₂-Supported Ag Single-Atom Catalysts. Journal of Physical Chemistry C, 2022, 126, 7482-7491.	1.5	13
68173	Filling Octahedral Interstices by Building Geometrical Defects to Construct Active Sites for Boosting the Oxygen Evolution Reaction on NiFe₂O₄. Advanced Functional Materials, 2022, 32, .	7.8	27
68174	Covalent Organic Frameworks-based Nanocomposites for Oxygen reduction reaction. Journal of Inclusion Phenomena and Macrocyclic Chemistry, 2022, 102, 477-485.	0.9	2

#	Article	IF	Citations
68175	Magnetism engineering of nanographene: An enrichment strategy by co-depositing diverse precursors on Au(111). Chinese Chemical Letters, 2023, 34, 107450.	4.8	4
68176	Nano-faceted stabilization of polar-oxide thin films: The case of MgO(111) and NiO(111) surfaces. Applied Surface Science, 2022, 596, 153490.	3.1	5
68177	Efficient Yellow Self-Trapped Exciton Emission in Sb³⁺-Doped RbCdCl₃ Metal Halides. Inorganic Chemistry, 2022, 61, 7143-7152.	1.9	34
68178	Unraveling Electronic Trends in O* and OH* Surface Adsorption in the MO₂ Transition-Metal Oxide Series. Journal of Physical Chemistry C, 2022, 126, 7903-7909.	1.5	8
68179	Triplet Superconductivity from Nonlocal Coulomb Repulsion in an Atomic Sn Layer Deposited onto a Si(111) Substrate. Physical Review Letters, 2022, 128, 167002.	2.9	23
68180	First principles study of hafnium intercalation between graphene and Ir(111) substrate. Chinese Physics B, 2022, 31, 106801.	0.7	1
68181	Stabilizing zinc anode for high-performance aqueous zinc ion batteries via employing a novel inositol additive. Journal of Alloys and Compounds, 2022, 914, 165231.	2.8	15
68182	CO Oxidation Catalytic Effects of Intrinsic Surface Defects in Rhombohedral LaMnO₃. ChemPhysChem, 2022, 23, e202200152.	1.0	1
68183	Machine learning for a finite size correction in periodic coupled cluster theory calculations. Journal of Chemical Physics, 2022, 156, .	1.2	4
68184	Fully exposed palladium cluster catalysts enable hydrogen production from nitrogen heterocycles. Nature Catalysis, 2022, 5, 485-493.	16.1	118
68185	Modulation Doping Enables Ultrahigh Power Factor and Thermoelectric ZT in nâ€Type Bi₂Te_{2.7}Se_{0.3}. Advanced Science, 2022, 9, e2201353.	5.6	19
68186	Enhanced supercapacitor performance of Bi2O3 by Mn doping. Journal of Alloys and Compounds, 2022, 914, 165258.	2.8	20
68187	Origami-controlled strain engineering of tunable flat bands and correlated states in folded graphene. Physical Review Materials, 2022, 6, .	0.9	9
68188	Unified theory of second sound in two-dimensional materials. Physical Review B, 2022, 105, .	1.1	7
68189	Janus VXY monolayers with tunable large Berry curvature. Journal of Semiconductors, 2022, 43, 042501.	2.0	4
68190	Observation of a linked-loop quantum state in a topological magnet. Nature, 2022, 604, 647-652.	13.7	18
68191	Boron Incorporation in Silicate Melt: Pressure-induced Coordination Changes and Implications for B Isotope Fractionation. Frontiers in Earth Science, 2022, 10, .	0.8	0
68192	Novel Amorphous Carbons for the Adsorption of Phosphate: Part I. Elucidation of Chemical Structure of N-Metal-Doped Chars. ACS Omega, 2022, 7, 14490-14504.	1.6	1

#	Article	IF	Citations
68193	Efficient Synthesis of WB_{5â€“x}â€“WB₂ Powders with Selectivity for WB_{5â€“x} Content. Inorganic Chemistry, 2022, 61, 6773-6784.	1.9	3
68194	Stress and Defect Effects on Electron Transport Properties at SnO₂/Perovskite Interfaces: A First-Principles Insight. ACS Omega, 2022, 7, 16187-16196.	1.6	4
68195	Peroxymonosulfate Activation on Synergistically Enhanced Single-Atom Co/Co@C for Boosted Chemiluminescence of Tris(bipyridine) Ruthenium(II) Derivative. Analytical Chemistry, 2022, 94, 6866-6873.	3.2	21
68196	Optoelectronic Properties Prediction of Lead-Free Methylammonium Alkaline-Earth Perovskite Based on DFT Calculations. ACS Omega, 2022, 7, 16204-16210.	1.6	6
68197	Ion Migration Mechanisms in the Sodium Sulfide Solid Electrolyte Na_{3â€“x}Sb_{1â€“x}W_xS₄. Chemistry of Materials, 2022, 34, 4166-4171.	3.2	6
68198	Mechanical, optical, and thermoelectric properties of semiconducting <mml:math xmlns:mml="http://www.w3.org/1998/Math/MathML"><mml:mrow><mml:msub><mml:mi>ZnIn</mml:mi><mml:mn>2</mml:mn></mml:msub></mml:mrow><mml:math		

#	Article	IF	Citations
68211	Contributions of bulk and surface energies in stabilizing metastable polymorphs: A comparative study of group 3 sesquioxides <mml:math xmlns:mml="http://www.w3.org/1998/Math/MathML"><mml:mrow><mml:msub><mml:mi>La</mml:mi><mml:mn>2</mml:mn></mml:msub><mml:msub><mml:mi mathvariant="normal">O</mml:mi><mml:mn>3</mml:mn></mml:msub></mml:mrow><mml:mo>,</mml:mo><mml:mo>Â</mml:mo><mml:msub><mml:mi mathvariant="normal">O</mml:mi><mml:mn>3</mml:mn></mml:msub><. Physical Review Materials, 2022, 6, .	2.9	2
68212	Formation, doping, and lithium incorporation in LiFePO4. AIP Advances, 2022, 12, .	0.6	4
68213	Robust Tunable Large-Gap Quantum Spin Hall States in Monolayer Cu₂S on Insulating Substrates. ACS Omega, 2022, 7, 15760-15768.	1.6	4
68214	Vibrational Entropy of Crystalline Solids from Covariance of Atomic Displacements. Entropy, 2022, 24, 618.	1.1	4
68215	Structure Determination, Mechanical Properties, Thermal Stability of Co2MoB4 and Fe2MoB4. Materials, 2022, 15, 3031.	1.3	0
68216	Band structure of molybdenum disulfide: from first principle to analytical band model. Journal of Computational Electronics, 0, , 1.	1.3	1
68217	Electronic and Optical Properties of Eu²⁺-Activated Narrow-Band Phosphors for Phosphor-Converted Light-Emitting Diode Applications: Insights from a Theoretical Spectroscopy Perspective. Journal of the American Chemical Society, 2022, 144, 8038-8053.	6.6	28
68218	Rationalizing hydrogen evolution mechanism on the slab of Zn-reduced 2Hâ€“MoS2 monolayer by density functional theory calculations. International Journal of Hydrogen Energy, 2022, 47, 19005-19015.	3.8	6
68219	Influence of doping Sn direction and concentration on vanadium pentoxide based on density functional theory. Functional Materials Letters, 2022, 15, .	0.7	0
68220	Investigating the Elusive Nature of Atomic O from CO₂ Dissociation on Pd(111): The Role of Surface Hydrogen. Journal of Physical Chemistry C, 2022, 126, 7870-7879.	1.5	1
68221	Hexagonal boron phosphide and boron arsenide van der Waals heterostructure as high-efficiency solar cell. Chinese Physics B, 2022, 31, 097301.	0.7	2
68222	Coordination of Ethylamine on Small Silver Clusters: Structural and Topological (ELF, QTAIM) Analyses. Inorganic Chemistry, 2022, 61, 7274-7285.	1.9	6
68223	A machine-learned interatomic potential for silica and its relation to empirical models. Npj Computational Materials, 2022, 8, .	3.5	36
68224	Tetravalent doping in hafnium-zirconium oxides to lower polarization switching voltage. , 2022, , .		0
68225	Efficient and stable noble-metal-free catalyst for acidic water oxidation. Nature Communications, 2022, 13, 2294.	5.8	89
68226	The quest for a bidirectional auxetic, elastic, and enhanced fracture toughness material: Revisiting the mechanical properties of the <scp>BeH₂</scp> monolayers. Journal of Computational Chemistry, 2023, 44, 248-255.	1.5	3
68227	Exploring Stability of Transition-Metal Single Atoms on Cu₂O Surfaces. Journal of Physical Chemistry C, 2022, 126, 8065-8078.	1.5	5
68228	Multifunctional Cr Substitution Modulates Electrochemical Activity of Mn_{1â€“x}Cr_xO for High-Performance Lithium-Ion Battery Anodes. ACS Applied Materials & Interfaces, 2022, 14, 21028-21037.	4.0	8

#	Article	IF	Citations
68229	Enabling high energy lithium metal batteries via single-crystal Ni-rich cathode material co-doping strategy. Nature Communications, 2022, 13, 2319.	5.8	143
68230	First-Principles Investigation of Electronic Properties and Phase Transition of Ti₃O₅. Journal of Physical Chemistry C, 2022, 126, 7809-7817.	1.5	8
68231	Insulating antiferromagnetism in VTe. Physical Review B, 2022, 105, .	1.1	2
68232	Structural and Electronic Effect Driven Distortions in Visible Light Absorbing Polar Materials ATa₂V₂O₁₁ (A = Sr, Pb). Journal of Physical Chemistry C, 2022, 126, 8047-8055.	1.5	0
68233	First-Principles Study of Oxygen-Induced Disintegration and Ripening of Late Transition Metal Nanoparticles on Rutile-TiO₂(110). Journal of Physical Chemistry C, 2022, 126, 8056-8064.	1.5	1
68234	Influence of the Chemical Pressure on the Magnetic Properties of the Mixed Anion Cuprates Cu2OX2 (X = Cl, Br, I). Computation, 2022, 10, 73.	1.0	1
68235	Theoretical Insights on the Two-Dimensional Transitional Metal Trihydroxytriaminophenalenyl for Highly Efficient Carbon Dioxide Electroreduction. Journal of the Electrochemical Society, 2022, 169, 056512.	1.3	0
68236	Accurate firstâ€principles treatment of the highâ€temperature cubic phase of hafnia. Physica Status Solidi - Rapid Research Letters, 0, , .	1.2	4
68237	Anisotropic terahertz optostriction in group-IV monochalcogenide compounds. Physical Review B, 2022, 105, .	1.1	1
68238	Water-stable metalâ€“organic framework (UiO-66) supported on zirconia nanofibers membrane for the dynamic removal of tetracycline and arsenic from water. Applied Surface Science, 2022, 596, 153559.	3.1	19
68239	Orthorhombic charge density wave on the tetragonal lattice of EuAl₄. IUCrJ, 2022, 9, 378-385.	1.0	10
68240	A CeO2-Doped Copper Matrix Self-Lubricating Composite With Well-Balanced Mechanical and Lubricating Properties Fabricated by Spark Plasma Sintering. Metallurgical and Materials Transactions A: Physical Metallurgy and Materials Science, 0, , 1.	1.1	2
68241	Motivating Ru-bri site of RuO2 by boron doping toward high performance acidic and neutral oxygen evolution. Nano Research, 2022, 15, 7008-7015.	5.8	20
68242	A Submicrosecond-Response Ultravioletâ€“Visibleâ€“Near-Infrared Broadband Photodetector Based on 2D Tellurosilicate InSiTe₃. ACS Nano, 2022, 16, 7745-7754.	7.3	32
68243	Slipâ€Lineâ€Guided Growth of Graphene. Advanced Materials, 2022, 34, e2201188.	11.1	7
68244	Effect of low-frequency optical phonons on the thermal conductivity of <mml:math xmlns:mml="http://www.w3.org/1998/Math/MathML"><mml:mrow><mml:mn>2</mml:mn><mml:mi>H</mml:mi></mml:mrow></mml molybdenum disulfide. Physical Review B, 2022, 105, .	1.1	6
68245	Mechanical properties of Li2MoO4 single crystals. Journal of Applied Physics, 2022, 131, .	1.1	3
68246	Single-atom metal tuned sulfur vacancy for efficient H2 activation and hydrogen evolution reaction on MoS2 basal plane. Applied Surface Science, 2022, 597, 153614.	3.1	9

#	Article	IF	Citations
68247	The Growth of High-Quality Hexagonal GaTe Nanosheets Induced by ZnO Nanocrystals. Crystals, 2022, 12, 627.	1.0	0
68248	First-principles investigation of the role of Cr in the electronic properties of the two-dimensional <mml:math xmlns:mml="http://www.w3.org/1998/Math/MathML"><mml:mrow><mml:msub><mml:mi>Mo</mml:mi><mml:mi>x</mml:mi></mml:msub></mml:mr and <mml:math xmlns:mml="http://www.w3.org/1998/Math/MathML"><mml:mrow><mml:msub><mml:m. Physical Review Materials, 2022, 6, .	3.1	6
68249	Ternary antimonide NaCd4Sb3: Hydride synthesis, crystal structure and transport properties. Zeitschrift Fur Anorganische Und Allgemeine Chemie, 0, , .	0.6	2
68250	Crystalline and Electronic Structures of Ultrathin Cadmium Sulfide Films. Physica Status Solidi - Rapid Research Letters, 0, , .	1.2	0
68251	First-Principles Study on the Impact of Stress on Depassivation of Defects at a-SiO2/Si Interfaces. Frontiers in Materials, 2022, 9, .	1.2	1
68252	First principles study of SnX₂ (XÂ=ÂS, Se) and Janus SnSSe monolayer for thermoelectric applications. Nanotechnology, 2022, 33, 325402.	1.3	10
68253	Charge density waves in monolayer and few-layer <mml:math xmlns:mml="http://www.w3.org/1998/Math/MathML"><mml:msub><mml:mi>NbS</mml:mi><mml:mn>2</mml:mn></mml:msub></mm and phase modulation by doping, thickness, and temperature. Physical Review B, 2022, 105, .	1.1	2
68254	Cl-Doped Li₁₀SnP₂S₁₂ with Enhanced Ionic Conductivity and Lower Li-Ion Migration Barrier. ACS Applied Materials & Interfaces, 2022, 14, 22225-22232.	4.0	9
68255	Ultralow diffusion barrier of double transition metal MoWC monolayer as Li-ion battery anode. Journal of Materials Science, 2022, 57, 10702-10713.	1.7	8
68256	Emergent multiferroism with magnetodielectric coupling in EuTiO3 created by a negative pressure control of strong spin-phonon coupling. Nature Communications, 2022, 13, 2364.	5.8	23
68257	Gauche Effect on 2D Phosphorus Allotropesâ€™ Energetics. Journal of Physical Chemistry C, 2022, 126, 8883-8888.	1.5	1
68258	Bambooâ€Based Biomaterials for Cell Transportation and Bone Integration. Advanced Healthcare Materials, 2022, 11, e2200287.	3.9	8
68259	Impact of band structure on wave function dissipation in field emission resonance. Physical Review B, 2022, 105, .	1.1	1
68260	Molecular modeling of lactoferrin for food and nutraceutical applications: insights from in silico techniques. Critical Reviews in Food Science and Nutrition, 2023, 63, 9074-9097.	5.4	2
68261	Cu atoms induce a new reconstruction in the MnGa(001) surface: An ab-initio study. Applied Surface Science, 2022, 597, 153514.	3.1	3
68262	Theoretical study of topological properties of ferromagnetic pyrite CoS₂. Journal Physics D: Applied Physics, 2022, 55, 304004.	1.3	4
68263	Ordered Sn distribution adjacent to the precipitate-matrix interface in a Mgâ€“9.8wt.%Sn alloy. Journal of Magnesium and Alloys, 2022, , .	5.5	1
68264	Controlling the Cathodic Potential of KVPO₄F through Oxygen Substitution. Chemistry of Materials, 2022, 34, 4523-4535.	3.2	18

#	Article	IF	Citations
68265	Nitrogen Decoration of Basal-Plane Dislocations in <mml:math xmlns:mml="http://www.w3.org/1998/Math/MathML" display="inline" overflow="scroll"><mml:mn>4</mml:mn><mml:mrow><mml:mrow><mml:mi mathvariant="normal">H</mml:mi></mml:mrow></mml:mrow></mml:math> - <mml:math xmlns:mml="http://www.w3.org/1998/Math/MathML" display="inline" overflow="scroll"><mml:mi>SiC</mml:mi></mml:math>. Physical Review Applied, 2022, 17, .	1.5	5
68266	Probing direct bandgap of double perovskites Rb2LiTlX6 (X = Cl, Br) and optoelectronic characteristics for Solar cell applications: DFT calculations. Journal of Materials Research and Technology, 2022, 18, 4775-4785.	2.6	20
68267	Understanding Large Negative Thermal Expansion of NdFe(CN)₆ through the Electronic Structure and Lattice Dynamics. Inorganic Chemistry, 2022, 61, 7813-7819.	1.9	2
68268	Ostwald Ripening in an Oxideâ€onâ€Metal System. Advanced Materials Interfaces, 0, , 2200222.	1.9	3
68269	Adsorption of Noble Gases on Hydrogenated Group IV Monolayers: Stability and Electronic Properties. Journal of Electronic Materials, 2022, 51, 4073-4078.	1.0	1
68270	Understanding the Onset of Surface Degradation in LiNiO₂ Cathodes. ACS Applied Energy Materials, 2022, 5, 5730-5741.	2.5	10
68271	Prussian Blue decorated g-C3N4 â€“ From novel synthesis to insight study on charge transfer strategy for improving visible-light driven photo-Fenton catalytic activity. Journal of Alloys and Compounds, 2022, 916, 165331.	2.8	10
68272	Heteroanionic Melilite Oxysulfide: A Promising Infrared Nonlinear Optical Candidate with a Strong Second-Harmonic Generation Response, Sufficient Birefringence, and Wide Bandgap. ACS Applied Materials & Interfaces, 2022, 14, 23645-23652.	4.0	33
68273	First-principles study of the adsorption and dissociation of NO on the Be(0001) surface. European Physical Journal B, 2022, 95, .	0.6	0
68274	Improved performances of Cr2N monolayer as electrode of lithium ion battery through surface termination: A first-principles calculation. Journal of Physics and Chemistry of Solids, 2022, 168, 110794.	1.9	5
68275	Hydrogenation-induced high-temperature superconductivity in two-dimensional molybdenum carbide Mo₂C₃. Europhysics Letters, 2022, 138, 46002.	0.7	8
68276	Pyrrolidinium-Based Organic Cation (BMP)-Intercalated Organic (Coronene) Anode for High-Voltage Dual-Ion Batteries: A Comparative Study with Graphite. Journal of Physical Chemistry C, 2022, 126, 9264-9274.	1.5	5
68277	Molecular Dynamics Study of the Photodegradation of Polymeric Chains. Journal of Physical Chemistry Letters, 2022, 13, 4374-4380.	2.1	2
68278	Polar magneto-optical Kerr effect in antiferromagnetic <mml:math xmlns:mml="http://www.w3.org/1998/Math/MathML"><mml:msub><mml:mi>M</mml:mi><mml:mn>2</mml:mn></mml:msub><mml:mi mathvariant="normal">As</mml:mi><mml:mo>Â</mml:mo><mml:mrow><mml:mo>(</mml:mo><mml:mi>M</mml:mi><mml:mo>=	1.1	2
68279	Self-supporting copper electrode prepared by ultrasonic impact for hydrogen evolution reaction. Journal of Alloys and Compounds, 2022, 916, 165283.	2.8	5
68280	Magnetic ordering and topology in <mml:math xmlns:mml="http://www.w3.org/1998/Math/MathML"><mml:mrow><mml:msub><mml:mi>Mn</mml:mi><mml:mn>2</mml:mn></mml:msub> and <mml:math xmlns:mml="http://www.w3.org/1998/Math/MathML"><mml:mrow><mml:msub><mml:mi>Mn</mml:mi><mml:mn>2</mml:mn></mml:msub> Physical Review B, 2022, 105, .	1.1	6
68281	2D spin transport through graphene-MnBi2Te4 heterojunction. Nanotechnology, 2022, , .	1.3	2
68282	Near-zero Poissonâ€™s ratio and suppressed mechanical anisotropy in strained black phosphorene/SnSe van der Waals heterostructure: a first-principles study. Applied Mathematics and Mechanics (English) Tj ETQq1 1 0.784314 rgBT /Ove	2.8	7

#	Article	IF	Citations
68283	Low-energy electronic structure of perovskite and Ruddlesden-Popper semiconductors in the Ba-Zr-S system probed by bond-selective polarized x-ray absorption spectroscopy, infrared reflectivity, and Raman scattering. Physical Review B, 2022, 105, .	1.1	5
68284	Complex transport and magnetism of the ternary boride <mml:math xmlns:mml="http://www.w3.org/1998/Math/MathML"><mml:mrow><mml:msub><mml:mi>YbPt</mml:mi><mml:mn>5</mml:mn></mml:msub><mml:msub><mml:mi mathvariant="normal">B</mml:mi><mml:mn>2</mml:mn></mml:msub></mml:mrow></mml:math>. Physical Review B, 2022, 105, .	1.1	3
68285	First-principles calculations on the magnetism of Ti-defected lepidocrocite-related TiO2 nanosheet. Solid State Sciences, 2022, , 106907.	1.5	0
68286	In-plane optical and electrical anisotropy in low-symmetry layered GeS microribbons. NPG Asia Materials, 2022, 14, .	3.8	5
68287	Valence fluctuation driven superconductivity in orthorhombic lead telluride. Physical Review B, 2022, 105, .	1.1	1
68288	Perspective of the electronâ€“phonon interaction on the electrical transport in thermoelectric/electronic materials. Applied Physics Letters, 2022, 120, .	1.5	5
68289	Uniform nucleation and epitaxy of bilayer molybdenum disulfide on sapphire. Nature, 2022, 605, 69-75.	13.7	174
68290	Establishing a theoretical insight for penta-coordinated iron-nitrogen-carbon catalysts toward oxygen reaction. Nano Research, 2022, 15, 6067-6075.	5.8	28
68291	Titanium Monoxide with in Situ Grown Rutile TiO₂ Nanothorns as a Heterostructured Job-Sharing Anode Material for Lithium-Ion Storage. ACS Applied Energy Materials, 2022, 5, 5691-5703.	2.5	5
68292	3D Analogs of Square-Net Nodal Line Semimetals: Band Topology of Cubic LaIn₃. Chemistry of Materials, 2022, 34, 4446-4455.	3.2	5
68293	Resolving Activation Entropy of CO Oxidation under the Solidâ€“Gas and Solidâ€“Liquid Conditions from Machine Learning Simulation. ACS Catalysis, 2022, 12, 6265-6275.	5.5	7
68294	Role of Rotation Angle and Grain Boundary in Tuning the Li Intercalation Concentration to Induce Phase Transition in Bilayer MoS₂. Journal of Physical Chemistry C, 2022, 126, 8539-8544.	1.5	1
68295	Theoretical insights on the influence of Au core in Au<mml:math xmlns:mml="http://www.w3.org/1998/Math/MathML" display="inline" id="d1e1248" altimg="si35.svg"><mml:msub><mml:mrow /><mml:mrow><mml:mi mathvariant="normal">x</mml:mi></mml:mrow></mml:msub></mml:math>@Pd<mml:math xmlns:mml="http://www.w3.org/1998/Math/MathML" display="inline" id="d1e1256" altimg="si36.svg"><mml:msub><mml:mrow /><mml:mrow><mml:mi mathvariant="normal">x</mml:mi></mml:mrow></mml:msub></mml:math> alloy nanoparticles for CO oxidation: A DFT study. Applied Surface Science, 2022, 600, 154102.	1.0	1
68296	Selectively anchoring single atoms on specific sites of supports for improved oxygen evolution. Nature Communications, 2022, 13, 2473.	5.8	73
68297	Effect of solute atom adsorption on heterogeneous nucleation by in-situ MgO particles: Experimental and theoretical studies. Journal of Magnesium and Alloys, 2023, 11, 3642-3656.	5.5	2
68298	SF6 and SOF2 interaction studies on novel Tricycle Red Phosphorene sheets based on first-principles studies. Chemical Physics Letters, 2022, 800, 139674.	1.2	20
68299	Orbital Trap of Xenon: Driving Force Distinguishing between Xe and Kr Found at a Single Ag(I) Site in MFI Zeolite at Room Temperature. Journal of Physical Chemistry C, 2022, 126, 8312-8326.	1.5	5
68300	E(3)-equivariant graph neural networks for data-efficient and accurate interatomic potentials. Nature Communications, 2022, 13, 2453.	5.8	336

#	Article	IF	Citations
68301	Negative Second Harmonic Response of Sn⁴⁺ in the Fresnoite Oxysulfide Ba₂SnSSi₂O₇. Chemistry of Materials, 2022, 34, 4375-4383.	3.2	9
68302	Density-Dependent Microstructures and Electromechanical Properties of Amorphous InGaZnO₄ Semiconductors: An Ab Initio Study. ACS Applied Electronic Materials, 2022, 4, 2545-2551.	2.0	3
68303	Integrated Highâ€Throughput and Machine Learning Methods to Accelerate Discovery of Molten Salt Corrosionâ€Resistant Alloys. Advanced Science, 2022, 9, e2200370.	5.6	15
68304	Structural, Electronic, and Transport Properties of Phosphoreneâ€“Graphene Lateral Heterostructure Anodes: Insights from First-Principles Calculations. Journal of Physical Chemistry C, 2022, 126, 8928-8937.	1.5	7
68305	Observation of Ultrastrong Coupling between Substrate and the Magnetic Topological Insulator MnBi₂Te₄. Nano Letters, 2022, 22, 3856-3864.	4.5	6
68306	Direct Detection of V-V Atom Dimerization and Rotation Dynamic Pathways upon Ultrafast Photoexcitation in <mml:math xmlns:mml="http://www.w3.org/1998/Math/MathML" display="inline"><mml:mrow><mml:msub><mml:mrow><mml:mi>VO</mml:mi></mml:mrow><mml:mrow><mml:mn>2</mml:mn></ Physical Review X, 2022, 12, .	2.8	6
68307	Size-limited high-density nanopore formation in two-dimensional moirÃ© materials. Physical Review B, 2022, 105, .	1.1	0
68308	A Stacked Plasmonic Metamaterial with Strong Localized Electric Field Enables Highly Efficient Broadband Lightâ€Driven CO₂ Hydrogenation. Advanced Materials, 2022, 34, e2202367.	11.1	40
68309	Interface Engineering of Transition Metal Dichalcogenide/GaN heterostructures: Modified Broadband for Photoelectronic Performance. Chinese Physics B, 0, , .	0.7	0
68310	Interplay between quantum anomalous Hall effect and magnetic skyrmions. Proceedings of the National Academy of Sciences of the United States of America, 2022, 119, e2122952119.	3.3	5
68311	p-orbital multiferroics in single-layer SiN. Applied Physics Letters, 2022, 120, .	1.5	6
68312	Prediction of novel two-dimensional room-temperature ferromagnetic rare-earth material - GdB2N2 with large perpendicular magnetic anisotropy. Materials Today Physics, 2022, 24, 100700.	2.9	2
68313	Unique Catalytic Mechanism for Ru-Loaded Ternary Intermetallic Electrides for Ammonia Synthesis. Journal of the American Chemical Society, 2022, 144, 8683-8692.	6.6	38
68314	Tuning Molecular Inhibitors and Aluminum Precursors for the Area-Selective Atomic Layer Deposition of Al₂O₃. Chemistry of Materials, 2022, 34, 4646-4659.	3.2	15
68315	Intrinsic defects in primary halide perovskites: A first-principles study of the thermodynamic trends. Physical Review Materials, 2022, 6, .	0.9	15
68316	Selective Hydrogenation of 1,3-Butadiene over Ceria Catalyst: A Molecular Insight. Molecular Catalysis, 2022, 524, 112331.	1.0	3
68317	Combined Experimental and Computational Study of Molybdenum and Niobium for Nuclear Sensor Application. Jom, 2022, 74, 2676-2685.	0.9	1
68318	Controlling the nucleation of multiple precipitates in precipitation-strengthened steel through Mo partitioning. Materials Science and Technology, 2022, 38, 876-881.	0.8	0

#	Article	IF	Citations
68319	Robust half-metallicities of alkali-metal-based half-Heusler compounds. Physical Review Materials, 2022, 6, .	0.9	9
68320	Electrochemically induced amorphous-to-rock-salt phase transformation in niobium oxide electrode for Li-ion batteries. Nature Materials, 2022, 21, 795-803.	13.3	69
68321	Theoretical investigation on the electronic structure of new InSe/CrS2 van der Waals heterostructure. Journal of Materials Research, 2022, 37, 2157-2164.	1.2	3
68322	Multiple Anion Chemistry for Ionic Layer Thickness Tailoring in Bi_{2+2n}O_{2+2n}Se_nX₂ (X = Cl, Br) van der Waals Semiconductors with Low Thermal Conductivities. Chemistry of Materials, 2022, 34, 4751-4764.	3.2	3
68323	Observation of Hole Transfer in MoS₂/WS₂ Van der Waals Heterostructures. ACS Photonics, 2022, 9, 1709-1716.	3.2	10
68324	Indirect mechanism of Au adatom diffusion on the Si(100) surface. Physical Review B, 2022, 105, .	1.1	4
68325	Alumina Graphene Catalytic Condenser for Programmable Solid Acids. Jacs Au, 2022, 2, 1123-1133.	3.6	9
68326	Induction and Maintenance of Local Structural Durability for Highâ€Energy Nickelâ€Rich Layered Oxides. Small Methods, 2022, 6, e2200255.	4.6	9
68327	Effect of interlayer Dzyaloshinskii-Moriya interaction on spin structure in synthetic antiferromagnetic multilayers. Physical Review B, 2022, 105, .	1.1	9
68328	Quantum plasmonics of few electrons in strongly confined doped semiconducting oxide: A DFTâ€‰+â€‰U study of ZnGaO. Journal of Applied Physics, 2022, 131, 173101.	1.1	0
68329	Enhanced Mechanical, Thermal and Electrical Properties of Highâ€Entropy HfMoNbTaTiVWZr Thin Film Metallic Glass and its Nitrides. Advanced Engineering Materials, 2022, 24, .	1.6	16
68330	Synthesis and Stabilization of Cubic Gauche Polynitrogen under Radio-Frequency Plasma. Chemistry of Materials, 2022, 34, 4712-4720.	3.2	5
68331	A Monodisperse Îµâ€²-(Co_xFe_{1â€“x})_{2.2}C Bimetallic Carbide Catalyst for Direct Conversion of Syngas to Higher Alcohols. ACS Catalysis, 2022, 12, 6016-6028.	5.5	13
68332	Heterostructured Co3O4/VO2 nanosheet array catalysts on carbon cloth for hydrogen evolution reaction. International Journal of Hydrogen Energy, 2022, 47, 18983-18991.	3.8	5
68333	In-situ self-templating synthesis of 3D hierarchical porous carbons from oxygen-bridged porous organic polymers for high-performance supercapacitors. Nano Research, 2022, 15, 7759-7768.	5.8	25
68334	Anchored SnS nanorods based on a carbon-enhanced Nb2CTx three-dimensional nanoflower framework achieve stable, high capacity Na-ion storage. Applied Surface Science, 2022, 597, 153598.	3.1	7
68335	Reversible hydrogen storage for NLi4-Decorated honeycomb borophene oxide. International Journal of Hydrogen Energy, 2022, 47, 19168-19174.	3.8	8
68336	Intrinsically patterned corrals in monolayer Ag5Se2 and selective molecular co-adsorption. Nano Research, 2022, 15, 6730-6735.	5.8	3

#	Article	IF	Citations
68337	Nano-crumples induced Sn-Bi bimetallic interface pattern with moderate electron bank for highly efficient CO2 electroreduction. Nature Communications, 2022, 13, 2486.	5.8	99
68338	Structural stability, mechanical and optoelectronic properties of strain-tuned mixed-halide perovskites CsPbX3-aYa. Physica B: Condensed Matter, 2022, 639, 414016.	1.3	3
68339	Surface functionalization of Linde F (K) nano-zeolite and its application for photocatalytic wastewater treatment and hydrogen production. Applied Physics A: Materials Science and Processing, 2022, 128, 1.	1.1	7
68340	Symmetry-enforced nodal chain phonons. Npj Quantum Materials, 2022, 7, .	1.8	19
68341	High Energy Storage Performance in Ba_{0.85}Ca_{0.15}Zr_{0.1}Ti_{0.9}O₃â€ZnO Hybrid Perovskite Solid Solution Thin Films. Advanced Electronic Materials, 2022, 8, .	2.6	4
68342	Buckled Honeycomb Lattice Compound Sr₃CaOs₂O₉ Exhibiting Antiferromagnetism above Room Temperature. Chemistry of Materials, 2022, 34, 4741-4750.	3.2	3
68343	First principles study of electronic structure of cerium carbonate unit cell to explain its crystal morphology. Emergent Materials, 2022, 5, 1915-1924.	3.2	2
68344	Controlled Doping of Electrocatalysts through Engineering Impurities. Advanced Materials, 2022, 34, e2203030.	11.1	12
68345	Kinetic and Thermodynamic Factors Influencing Palladium Nanoparticle Redispersion into Mononuclear Pd(II) Cations in Zeolite Supports. Journal of Physical Chemistry C, 2022, 126, 8337-8353.	1.5	12
68346	Catalytically efficient Ni-NiOx-Y2O3 interface for medium temperature water-gas shift reaction. Nature Communications, 2022, 13, 2443.	5.8	25
68347	Synthesis, structure and transport properties of high-pressure modification VO2(S). Materialia, 2022, 23, 101456.	1.3	1
68348	Magnetic skyrmion manipulation in CrTe2/WTe2 2D van der Waals heterostructure. Applied Physics Letters, 2022, 120, .	1.5	10
68349	Quantitative Analysis of Nanorough Hydrogenated Si(111) Surfaces through Vibrational Spectral Assignment by Periodic DFT Calculations. Journal of Physical Chemistry C, 2022, 126, 8278-8286.	1.5	0
68350	Monoatomic tantalum induces ordinary-pressure phase transition from graphite to n-type diamond. Carbon, 2022, 196, 466-473.	5.4	8
68351	Efficient conversion of low-concentration nitrate sources into ammonia on a Ru-dispersed Cu nanowire electrocatalyst. Nature Nanotechnology, 2022, 17, 759-767.	15.6	318
68352	Rational Design of Coordination Bond Connected Metal Organic Frameworks/MXene Hybrids for Efficient Solar Water Splitting. Advanced Functional Materials, 2022, 32, .	7.8	56
68353	Global Minima Search for Sodium- and Magnesium-Adsorbed Polymorphic Borophene. Journal of Physical Chemistry C, 2022, 126, 8605-8614.	1.5	5
68354	Valley-dependent topological phase transition and quantum anomalous valley Hall effect in single-layer RuClBr. Physical Review B, 2022, 105, .	1.1	61

#	Article	IF	Citations
68355	Atomic overlayer of permeable microporous cuprous oxide on palladium promotes hydrogenation catalysis. Nature Communications, 2022, 13, 2597.	5.8	22
68356	Super Longâ€Cycling Allâ€Solidâ€State Battery with Thin Li₆PS₅Clâ€Based Electrolyte. Advanced Energy Materials, 2022, 12, .	10.2	58
68357	Computational design of ternary NiO/MPt interface active sites for H2O dissociation. International Journal of Hydrogen Energy, 2022, 47, 20040-20048.	3.8	2
68358	Structure and Magnetic Properties of Ni₄V₃O₁₀, an Antiferromagnet with Three Types of Vanadiumâ€“Oxygen Polyhedra. Chemistry of Materials, 2022, 34, 4721-4731.	3.2	0
68359	Strongly anisotropic electronic and magnetic structures in oxide dichlorides <mml:math xmlns:mml="http://www.w3.org/1998/Math/MathML"><mml:msub><mml:mi mathvariant="normal">RuOCl</mml:mi><mml:mn>2</mml:mn></mml:msub></mml:math> and <mml:math xmlns:mml="http://www.w3.org/1998/Math/MathML"><mml:msub><mml:mi mathvariant="normal">OsOCl</mml:mi><mml:mn>2</mml:mn></mml:msub></mml:math>. Physical Review B, 2022, 105, .	1.1	6
68360	High-entropy perovskite oxides: A versatile class of materials for nitrogen reduction reactions. Science China Materials, 2022, 65, 2711-2720.	3.5	13
68361	Defective NiO as a Stabilizer for Au Single-Atom Catalysts. ACS Catalysis, 2022, 12, 6149-6158.	5.5	30
68362	Electrochemical reduction of CO2 at the earth-abundant transition metal-oxides/copper interfaces. Catalysis Today, 2023, 409, 53-62.	2.2	7
68363	First-principles computational tensile test of Î³-Fe grain boundaries considering the effect of magnetism: Electronic origin of grain boundary embrittlement due to Zn segregation. Physical Review Materials, 2022, 6, .	0.9	4
68364	Precisely controlled Pd nanoclusters confined in porous organic cages for size-dependent catalytic hydrogenation. Applied Catalysis B: Environmental, 2022, 315, 121487.	10.8	20
68365	Emergence of topological and trivial interface states in <mml:math xmlns:mml="http://www.w3.org/1998/Math/MathML"><mml:mrow><mml:mi mathvariant="normal">V</mml:mi><mml:msub><mml:mi>Se</mml:mi><mml:mn>2</mml:mn></mml:msub></mml:mrow></mml:math> films coupled to <mml:math xmlns:mml="http://www.w3.org/1998/Math/MathML"><mml:mrow><mml:msub><mml:mi>Bi</mml:mi><mml:mn>2</mml:mn></mml:m Physical Review B, 2022, 105, .	1.1	0
68366	Possible Control of Earth's Boron Budget by Metallic Iron. Geophysical Research Letters, 2022, 49, .	1.5	3
68367	Spin Polarization of Mn Could Enhance Grain Boundary Sliding in Mg. Materials, 2022, 15, 3483.	1.3	0
68368	Allowable stretching bond force constants on carbon nanomaterials: A DFT study. Diamond and Related Materials, 2022, 126, 109083.	1.8	2
68369	Microspherical copper tetrathiovanadate with stable binding site as ultra-rate and extended longevity anode for sodium-ion half/full batteries. Chemical Engineering Journal, 2022, 446, 136772.	6.6	14
68370	Toward rational design of supported vanadia catalysts of lignin conversion to phenol. Chemical Engineering Journal, 2022, 446, 136965.	6.6	4
68371	Activationâ€Induced Surface Modulation of Biowasteâ€Derived Hierarchical Porous Carbon for Supercapacitors. ChemPlusChem, 2022, 87, .	1.3	18
68372	Volatile Products of the Autoxidation of Poly(ethylenimine) in CO₂ Sorbents. Journal of Physical Chemistry C, 2022, 126, 8807-8816.	1.5	9

#	Article	IF	Citations
68373	Single-Atom Mo Anchored on a Poly(heptazine imide) Nanosheet as a Novel Electrocatalyst Showing Excellent Behavior toward Nitrogen Reduction Reaction. Journal of Physical Chemistry C, 2022, 126, 7859-7869.	1.5	5
68374	Two-dimensional TeX(X=C, Si, Ge) monolayers with strong intrinsic electric field for efficiency hydrogen evolution reaction. Surfaces and Interfaces, 2022, 31, 102011.	1.5	4
68375	Unique Photoelectric Properties and Defect Tolerance of Lead-Free Perovskite Cs₃Cu₂I₅ with Highly Efficient Blue Emission. Journal of Physical Chemistry Letters, 2022, 13, 4177-4183.	2.1	12
68376	Unveiling the Stressâ€Buffering Mechanism of Deep Lithiated Ag Nanowires: A Polymer Segmental Motion Strategy toward Ultraâ€Robust Li Metal Anodes. Advanced Functional Materials, 2022, 32, .	7.8	13
68377	Electronic structure of <mml:math xmlns:mml="http://www.w3.org/1998/Math/MathML"><mml:mi>Î²</mml:mi><mml:mo>â€²</mml:mo><mml:msub><mml:mi mathvariant="normal">Al</mml:mi><mml:mn>3</mml:mn></mml:msub><mml:msub><mml:mi mathvariant="normal">Mg</mml:mi><mml:mn>2</mml:mn></mml:msub></mml:math> and <mml:math xmlns:mml="http://www.w3.org/1998/Math/MathML"><mml:msub><mml:mi mathvariant="normal">Al</mml:mi><mml:mn>13</mml:mn></mml:msub><mml:msub><mml:mi mathvaria	1.1	3
68378	Application of atomic simulation for studying hydrogen embrittlement phenomena and mechanism in iron-based alloys. International Journal of Hydrogen Energy, 2022, 47, 20288-20309.	3.8	24
68379	Effects of Fluorination and Molybdenum Codoping on Monoclinic BiVO₄ Photocatalyst by HSE Calculations. ACS Omega, 0, , .	1.6	2
68380	Giant Effects of Interlayer Interaction on Valence-Band Splitting in Transition Metal Dichalcogenides. Journal of Physical Chemistry C, 2022, 126, 8667-8675.	1.5	2
68381	High-Throughput Experimentation for Selective Growth of Small-Diameter Single-Wall Carbon Nanotubes Using Ru-Promoted Co Catalysts. Chemistry of Materials, 2022, 34, 4548-4559.	3.2	2
68382	Two-dimensional germanene-based Janus material Ge8HnX8â^'n (nâ€¯=â€¯0â€“8, Xâ€¯=â€¯F, Cl, Br, I) for photovoltaic and photocatalytic applications. Applied Surface Science, 2022, 598, 153633.	3.1	6
68383	Performance and mechanism of FeS₂/FeS_xO_y as highly effective Fenton-like catalyst for phenol degradation. Environmental Technology (United Kingdom), 2023, 44, 3731-3740.	1.2	1
68384	Charging/discharging mechanism in Mg3Bi2 anode for Mg-ion batteries; The role of the spin-orbit coupling. Chemical Physics Letters, 2022, 801, 139694.	1.2	6
68385	Exploration of potassium silicide compounds under high pressure. Physica B: Condensed Matter, 2022, , 414013.	1.3	0
68386	A theoretical study on tetragonal BaTiO3 modified by surface co-doping for photocatalytic overall water splitting. International Journal of Hydrogen Energy, 2022, 47, 19073-19085.	3.8	4
68387	The Importance of Stacking and Coordination for Li, Na, and Mg Diffusion and Intercalation in Ti₃C₂T₂ MXene. Advanced Materials Interfaces, 2022, 9, .	1.9	5
68388	First-Principles Study on Possible Half-Metallic Ferrimagnetism in Double Perovskites Pb2XXâ€²O6 (X = Ti,) Tj ETQq1 1 0.784314 rgBT	1.3	6
68389	Superconducting Li10Se electride under pressure. Journal of Chemical Physics, 2022, 156, .	1.2	8
68390	Electrically tunable magnetism and unique intralayer charge transfer in Janus monolayer MnSSe for spintronics applications. Physical Review B, 2022, 105, .	1.1	14

#	Article	IF	Citations
68391	Anionic and Cationic Co-Substitutions of S into Vertically Aligned WTe₂ Nanosheets as Catalysis for Hydrogen Evolution under Alkaline Conditions. ACS Applied Nano Materials, 2022, 5, 7123-7131.	2.4	3
68392	Ferroelectric <mml:math xmlns:mml="http://www.w3.org/1998/Math/MathML"><mml:msub><mml:mi>HfO</mml:mi><mml:mn>2</mml:mn></mml:msub></m and the importance of strain. Physical Review Materials, 2022, 6, .	0.9	5
68393	Electron count dictates phase separation in Heusler alloys. Physical Review Materials, 2022, 6, .	0.9	2
68394	Synthesis, characterization, and DFT Raman study of pure and Mnâ€doped LiTaO₃ nanofibers. Journal of the American Ceramic Society, 2022, 105, 5956-5965.	1.9	1
68395	Role of Defects and Radiation Damage on He Diffusion in Magnetite: Implication for (U-Th)/He Thermochronology. Minerals (Basel, Switzerland), 2022, 12, 590.	0.8	6
68396	Tuning the electronic structure and inverse degree of inverse spinel ferrites by integrating samarium orthoferrite for efficient water oxidation. Applied Catalysis B: Environmental, 2022, 315, 121504.	10.8	15
68397	Compositional Variation in FAPb_{1â€“x}Sn_xI₃ and Its Impact on the Electronic Structure: A Combined Density Functional Theory and Experimental Study. ACS Applied Materials & Interfaces, 2022, 14, 34253-34261.	4.0	5
68398	Revealing the Nature of Câ€“C Coupling Sites on a Cu Surface for CO₂ Reduction. Journal of Physical Chemistry Letters, 2022, 13, 4434-4440.	2.1	10
68399	Maximizing intrinsic anomalous Hall effect by controlling the Fermi level in simple Weyl semimetal films. Physical Review B, 2022, 105, .	1.1	4
68400	A plasma bombing strategy to synthesize high-loading single-atom catalysts for oxygen reduction reaction. Cell Reports Physical Science, 2022, 3, 100880.	2.8	31
68401	Scaling and Confinement in Ultrathin Chalcogenide Films as Exemplified by GeTe. Small, 2022, 18, e2201753.	5.2	13
68402	Metallic Carbonitride MXene Based Photonic Hyperthermia for Tumor Therapy. Small, 2022, 18, e2200646.	5.2	16
68403	Universal Principles for the Rational Design of Single Atom Electrocatalysts? Handle with Care. ACS Catalysis, 2022, 12, 5846-5856.	5.5	60
68404	Impact of Surface Faceting on Gas Sensing Selectivity of NiO: Revealing the Adsorption Sites of Organic Vapors on the {111} Facet. Journal of Physical Chemistry C, 2022, 126, 8037-8046.	1.5	9
68405	How to Make Personal Protective Equipment Spontaneously and Continuously Antimicrobial (Incorporating Oxidase-like Catalysts). ACS Nano, 2022, 16, 7755-7771.	7.3	27
68406	Unravelling the Nature of the Intrinsic Complex Structure of Binaryâ€Phase Naâ€Layered Oxides. Advanced Materials, 2022, 34, e2202137.	11.1	21
68407	Experimental and theoretical insight into DSSCs mechanism influenced by different doping metal ions. Applied Surface Science, 2022, 597, 153607.	3.1	4
68408	Improving the Electrochemical Activity of PdSe2 by Constructing P/T Structural Interfaces. Applied Surface Science, 2022, , 153626.	3.1	1

#	Article	IF	Citations
68409	Enhanced catalytic performance of transition metal-doped Cr2O3 catalysts for propane dehydrogenation: A microkinetic modeling study. Chemical Engineering Journal, 2022, 446, 136913.	6.6	4
68410	Surprising Chemistry of 6-Azidotetrazolo[5,1-a]phthalazine: What a Purported Natural Product Reveals about the Polymorphism of Explosives. Journal of Organic Chemistry, 2022, 87, 6680-6694.	1.7	5
68411	High-Throughput Discovery and Investigation of Auxetic Two-Dimensional Crystals. Chemistry of Materials, 2022, 34, 4344-4354.	3.2	6
68412	High Dielectric Permittivity of Î±-NaFeO₂-Type Layered Nitrides. Chemistry of Materials, 2022, 34, 4505-4513.	3.2	4
68413	Nitriding behavior and mechanical properties of AerMet100 steel and first-principles calculations of phase interfaces. Journal of Materials Research and Technology, 2022, 19, 46-60.	2.6	3
68414	First-principles study of electronic, cohesive and elastic properties of silica polymorphs. Materials Today Communications, 2022, 31, 103607.	0.9	2
68415	Alternative Cu3Zn catalysts for enhanced reduction of CO2 to CH4: A density functional theory-based approach. Surfaces and Interfaces, 2022, 31, 102030.	1.5	2
68416	Facet-Dependent Bactericidal Activity of Ag₃PO₄ Nanostructures against Gram-Positive/Negative Bacteria. ACS Omega, 2022, 7, 16616-16628.	1.6	5
68417	Fishâ€scaleâ€like nanoâ€porous membrane based on zeolite nanosheets for long stable zincâ€based flow battery. AICHE Journal, 2022, 68, .	1.8	10
68418	Selective Enhancement of Methane Formation in Electrochemical CO₂ Reduction Enabled by a Raman-Inactive Oxygen-Containing Species on Cu. ACS Catalysis, 2022, 12, 6036-6046.	5.5	22
68419	Exploring the Origin of Anionic Redox Activity in Super Li-Rich Iron Oxide-Based High-Energy-Density Cathode Materials. Chemistry of Materials, 2022, 34, 4536-4547.	3.2	10
68420	A Vanadiumâ€Based Fluoroxide Cathode Material for Lithiumâ€Ion Storage with High Energy Density. Advanced Sustainable Systems, 2022, 6, .	2.7	22
68421	Metal Hydrides with In Situ Built Electron/Ion Dual-Conductive Framework for Stable All-Solid-State Li-Ion Batteries. ACS Nano, 2022, 16, 8040-8050.	7.3	5
68422	Modulating Pt-O-Pt atomic clusters with isolated cobalt atoms for enhanced hydrogen evolution catalysis. Nature Communications, 2022, 13, 2430.	5.8	98
68423	Effect of non-magnetic doping on magnetic state and Li/Na adsorption and diffusion of black phosphorene. Journal of Physics Condensed Matter, 2022, 34, 285704.	0.7	3
68424	Atomic structure of an FeCrMoCBY metallic glass revealed by high energy x-ray diffraction. Journal of Physics Condensed Matter, 2022, 34, 285301.	0.7	2
68425	Effects of the Cationic Structure on the Adsorption Performance of Ionic Polymers toward Au(III): an Experimental and DFT Study. Langmuir, 2022, 38, 6116-6127.	1.6	6
68426	Tunability of the bandgap of SnS by variation of the cell volume by alloying with A.E. elements. Scientific Reports, 2022, 12, 7434.	1.6	9

#	Article	IF	Citations
68427	Extra contribution to the crystal stability of insensitive explosive TATB: The cooperativity of intermolecular interactions. Defence Technology, 2023, 25, 88-98.	2.1	4
68428	Rational design of carbon nitride for remarkable photocatalytic H2O2 production. Chem Catalysis, 2022, 2, 1720-1733.	2.9	31
68429	Multiferroic materials based on transition-metal dichalcogenides: Potential platform for reversible control of Dzyaloshinskii-Moriya interaction and skyrmion via electric field. Physical Review B, 2022, 105, .	1.1	17
68430	London Dispersionâ€Corrected Density Functionals Applied to van der Waals Stacked Layered Materials: Validation of Structure, Energy, and Electronic Properties. Advanced Theory and Simulations, 0, , 2200055.	1.3	5
68431	Tetragonal polymorph of <mml:math xmlns:mml="http://www.w3.org/1998/Math/MathML"><mml:msub><mml:mrow><mml:mi>BaFe</mml:mi></mml:mrow><mml:mn>2</mml:mn></mml:msub><mml:mi mathvariant="normal">S</mml:mi></mml:mrow><mml:mn>2</mml:mn></mml:msub><mml:mi mathvariant="normal">O</mml:mi></mml:math> as an antiferromagnetic Mott insulator. Physical Review Materials, 2022, 6, .	0.9	2
68432	A powerful approach to develop nitrogen-doped graphene sheets: theoretical and experimental framework. Journal of Materials Science, 0, , .	1.7	3
68433	Cesium Manganese Bromide Nanocrystal Sensitizers for Broadband Vis-to-NIR Downshifting. ACS Energy Letters, 2022, 7, 1850-1858.	8.8	30
68434	Triangular Arrangement of Ferromagnetic Iron Chains in the Highâ€T_C Ferromagnet TiFe_{1â^'x}Os_{2+x}B₂. Chemistry - A European Journal, 2022, 28, .	1.7	2
68435	Screening promising TM-doped CeO2 monolayer for formaldehyde sensor with high sensitivity and selectivity. Chinese Chemical Letters, 2023, 34, 107476.	4.8	8
68436	Non-metallic carbon-based catalysts for acetylene hydrochlorination: The effect of graphitization degree of carbonaceous material. Catalysis Communications, 2022, 167, 106458.	1.6	3
68437	Recycling spent LiNi _{1-x-y} Mn _x Co _y O ₂ cathodes to bifunctional NiMnCo catalysts for zinc-air batteries. Proceedings of the National Academy of Sciences of the United States of America, 2022, 119, e2202202119.	3.3	89
68438	Lowering the Water Oxidation Overpotential by Spin-Crossover in Cobalt Hexacyanoferrate. Journal of Physical Chemistry Letters, 2022, 13, 4104-4110.	2.1	14
68439	Synthesis of distorted octahedral C-doped nickel nanocrystals encapsulated in CNTs: A highly active and stable catalyst for water pollutions treatment. Chemical Engineering Journal, 2022, 446, 136805.	6.6	4
68440	Modulated Ferromagnetism and Electric Polarization Induced by Surface Vacancy in MX₂ Monolayers. Journal of Physical Chemistry C, 0, , .	1.5	4
68441	Giant nonlinear anomalous Hall effect induced by spin-dependent band structure evolution. Physical Review Research, 2022, 4, .	1.3	14
68442	Effect of alloying in monolayer niobium dichalcogenide superconductors. Nature Communications, 2022, 13, 2376.	5.8	5
68443	Triggering the Direct Câ€“C Coupling of Gaseous CO into C₂ Oxygenates by Synergizing Interfacial Interactions and Reversible Spatial Dynamic Confinement. Journal of Physical Chemistry C, 2022, 126, 8645-8654.	1.5	5
68444	Indium doped bismuth subcarbonate nanosheets for efficient electrochemical reduction of carbon dioxide to formate in a wide potential window. Journal of Colloid and Interface Science, 2022, 624, 261-269.	5.0	14

#	Article	IF	Citations
68445	H2O2 formation mechanisms on the (1 1 2) and (3 1 0) facets of SnO2 via water oxidation reaction with the participation of Bicarbonate: DFT and experimental Investigations. Applied Surface Science, 2022, 596, 153634.	3.1	4
68446	Designing vacancy-filled Heusler thermoelectric semiconductors by the Slater-Pauling rule. Materials Today Energy, 2022, 27, 101035.	2.5	8
68447	SO2 adsorption and conversion on pristine and defected calcite {1 0 4} surface: A density functional theory study. Applied Surface Science, 2022, 596, 153575.	3.1	11
68448	Highly efficient two-dimensional Ag2Te cathode catalyst featuring a layer structure derived catalytic anisotropy in lithium-oxygen batteries. Energy Storage Materials, 2022, 50, 96-104.	9.5	27
68449	Coherent Heterostructure Mesh Grown by Gap-Filling Epitaxial Chemical Vapor Deposition. Chemistry of Materials, 0, , .	3.2	2
68450	Tuning the Electronic Structure of Layered Co-based Serpentine Nanosheets for Efficient Oxygen Evolution Reaction. Journal Physics D: Applied Physics, 0, , .	1.3	2
68451	Chemical Reactions and Phase Stabilities in the Siâ€“Te System at High Pressures and High Temperatures. Inorganic Chemistry, 2022, 61, 7349-7357.	1.9	0
68452	Synthesis and Growth of Rare Earth Borates NaSrR(BO₃)₂ (R = Hoâ€“Lu, Y, Sc). Inorganic Chemistry, 2022, 61, 7497-7505.	1.9	6
68453	Unveiling the Valence State of Interstitial Bromine on Charge Carrier Lifetime in CH₃NH₃PbBr₃ by Quantum Dynamics Simulation. Journal of Physical Chemistry Letters, 2022, 13, 4193-4199.	2.1	2
68454	Promotional Effect of Pt-Doping on the Catalytic Performance of Ptâ^'CeO2 Catalyst for CO Oxidation. Catalysts, 2022, 12, 529.	1.6	3
68455	Metallic Phase Transition Metal Dichalcogenide Quantum Dots as Promising Bio-Imaging Materials. Nanomaterials, 2022, 12, 1645.	1.9	7
68456	Topological states in superlattices of HgTe class of materials for engineering three-dimensional flat bands. Physical Review Research, 2022, 4, .	1.3	11
68457	Cubic-spinel AgIn5S8-based thermoelectric materials: synthesis, phonon transport and defect chemistry. Materials Today Energy, 2022, 27, 101029.	2.5	4
68458	Nonlinear Optical and Photocurrent Responses in Janus MoSSe Monolayer and MoS₂â€“MoSSe van der Waals Heterostructure. Nano Letters, 2022, 22, 4145-4152.	4.5	25
68459	Evidence for H₂-Induced Ductility in a Pt/Al₂O₃ Catalyst. ACS Catalysis, 2022, 12, 5979-5989.	5.5	9
68460	Atomistic mechanism of phase transformation between topologically close-packed complex intermetallics. Nature Communications, 2022, 13, 2487.	5.8	15
68461	Secondâ€Order Nonlinear Optical Responses of AlN Twoâ€Dimensional Monolayer: A Realâ€Time Firstâ€Principles Study. ChemPhysChem, 2022, , e202100901.	1.0	0
68462	Dipole Engineering Strategy for Regulating the Electronic Contact of a Two-Dimensional <mml:math xmlns:mml="http://www.w3.org/1998/Math/MathML" display="inline"		

#	Article	IF	Citations
68463	Structural and electronic properties of the random alloy <mml:math xmlns:mml="http://www.w3.org/1998/Math/MathML"><mml:mrow><mml:msub><mml:mi>ZnSe</mml:mi><mml:mi>x</mml:mi></mml:msub><mml:mo>(</mml:mo><mml:mi mathvariant="normal">S</mml:mi><mml:mrow><mml:mn>1</mml:mn><mml:mo>â^’</mml:mo><mml:mi>x</mml:mi></mml:mrow></mml:mrow></mml:math> Physical Review B, 2022, 105, .	1.1	2
68464	Spacer Cation Engineering of Two-Dimensional Hybrid Perovskites with Tunable Band Alignment and Optoelectronic Properties. Journal of Physical Chemistry C, 2022, 126, 8408-8416.	1.5	10
68465	Efficient near-infrared phosphors discovered by parametrizing the Eu(II) 5d-to-4f energy gap. Matter, 2022, 5, 1924-1936.	5.0	31
68466	Characterization and simulation of graphite edge surfaces for the analysis of carbonaceous material separation from sulfide ores by flotation. Minerals Engineering, 2022, 182, 107590.	1.8	7
68467	Highly tunable and strongly bound exciton in <mml:math xmlns:mml="http://www.w3.org/1998/Math/MathML"><mml:mrow><mml:msub><mml:mi>MoSi</mml:mi><mml:mn>2</mml:mn></mml:msub><mml:mo>(</mml:mo><mml:mi mathvariant="normal">N</mml:mi><mml:mn>4</mml:mn></mml:msub></mml:mrow></mml:math> via strain engineering. Physical Review B, 2022, 105, .	1.1	11
68468	Interface Coordination Stabilizing Reversible Redox of Zinc for Highâ€Performance Zincâ€Iodine Batteries. Small, 2022, 18, e2200168.	5.2	35
68469	Effects of Conjugated Structure on Electronic and Transport Properties in Organic-inorganic Hybrid Superlattices Cd₂Se₂(C₂H₄N₂)_{1/2}. Journal of Physics Condensed Matter, 2022, 34, .	0.7	2
68470	Probing the charge transfer and electronâ€“hole asymmetry in grapheneâ€“graphene quantum dot heterostructure. Nanotechnology, 2022, 33, 325704.	1.3	2
68471	Strongly Quantum-Confined Perovskite Nanowire Arrays for Color-Tunable Blue-Light-Emitting Diodes. ACS Nano, 2022, 16, 8388-8398.	7.3	19
68472	First Principle Investigation of the Incorporation of Trivalent Lanthanides and Actinides in Hydroxycarbonate and Hydroxychloride Green Rust. Journal of Physical Chemistry C, 2022, 126, 8016-8028.	1.5	2
68473	Machine Learning Interatomic Potential for High-Throughput Screening of High-Entropy Alloys. Jom, 2022, 74, 2908-2920.	0.9	2
68474	Observation of nontrivial topological electronic structure of orthorhombic SnSe. Physical Review Materials, 2022, 6, .	0.9	0
68475	Waterâ€Resistant Leadâ€Free Perovskitoid Single Crystal for Efficient Xâ€Ray Detection. Advanced Functional Materials, 2022, 32, .	7.8	18
68476	Topography inversion in scanning tunneling microscopy of single-atom-thick materials from penetrating substrate states. Scientific Reports, 2022, 12, 7321.	1.6	2
68477	Tilted spin current generated by the collinear antiferromagnet ruthenium dioxide. Nature Electronics, 2022, 5, 267-274.	13.1	64
68478	Investigation of the Redox Potential of Lithium and Its Dissolution in the LiClâ€“KCl Eutectic. Journal of the Electrochemical Society, 2022, 169, 056517.	1.3	2
68479	Fabrication of Celluloseâ€“Graphite Foam via Ion Cross-linking and Ambient-Drying. Nano Letters, 2022, 22, 3931-3938.	4.5	21
68480	Strain-tunable self-passivated porous phosphorene for high-efficiency helium separation. Journal Physics D: Applied Physics, 2022, 55, 315501.	1.3	1

#	Article	IF	Citations
68481	Activation of Raman modes in monolayer transition metal dichalcogenides through strong interaction with gold. Physical Review B, 2022, 105, .	1.1	9
68482	Multiscale machine-learning interatomic potentials for ferromagnetic and liquid iron. Journal of Physics Condensed Matter, 2022, 34, 305402.	0.7	5
68483	Adaptive semi-empirical model for non-contact atomic force microscopy. Chinese Physics B, 0, , .	0.7	0
68484	Observation of Topological Flat Bands in the Kagome Semiconductor Nb₃Cl₈. Nano Letters, 2022, 22, 4596-4602.	4.5	37
68485	Recent advances in the tuning of the organic framework materials â€“ The selections of ligands, reaction conditions, and post-synthesis approaches. Journal of Colloid and Interface Science, 2022, 623, 378-404.	5.0	7
68486	Alloying driven multifold fermionâ€toâ€Weyl semimetal transition in CoSi _{1â€•x} A _x (A= Ge, Sn). Physica Status Solidi - Rapid Research Letters, 0, , .	1.2	0
68487	Electric control of valley polarization in monolayer WSe2 using a van der Waals magnet. Nature Nanotechnology, 2022, 17, 721-728.	15.6	28
68488	Regulating local charges of atomically dispersed Mo+ sites by nitrogen coordination on cobalt nanosheets to trigger water dissociation for boosted hydrogen evolution in alkaline media. Journal of Energy Chemistry, 2022, 72, 125-132.	7.1	17
68489	Charge-Transfer and <mml:math xmlns:mml="http://www.w3.org/1998/Math/MathML"><mml:mrow><mml:mi>d</mml:mi><mml:mi>d</mml:mi></mml:mrow></mml:ma excitations in <mml:math xmlns:mml="http://www.w3.org/1998/Math/MathML"><mml:msub><mml:mi>AgF</mml:mi><mml:mn>2</mml:mn></mml:msub></mm Physical Review Research, 2022, 4, .	1.3	7
68490	Design of novel dilute magnetic semiconductors by exhaustive first-principles calculations and scale-bridging simulations. Materials Today Communications, 2022, 31, 103604.	0.9	3
68491	<mml:math xmlns:mml="http://www.w3.org/1998/Math/MathML"><mml:mrow><mml:msub><mml:mi>Cr</mml:mi><mml:mn>2</mml:mn></mml: mathvariant="normal">S</mml:mi><mml:mn>3</mml:mn></mml:msub></mml:mrow></mml:math> a bipolar semiconducting fully compensated ferrimagnet. Physical Review Materials, 2022, 6, .	0.9	1
68492	Tailoring Photoinduced Nonequilibrium Magnetizations in In₂Se₃ Bilayers. Advanced Optical Materials, 2022, 10, .	3.6	5
68493	Anisotropic giant magnetoresistance and Fermi surface topology in the layered compound <mml:math xmlns:mml="http://www.w3.org/1998/Math/MathML"><mml:msub><mml:mi>YbBi</mml:mi><mml:mn>2</mml:mn></mml:msub></mm Physical Review B, 2022, 105, .	1.1	3
68494	Scattering lifetime and High figure of merit in CsAgO predicted by methods beyond relaxation time approximation. Journal of Physics Condensed Matter, 2022, , .	0.7	0
68495	Dataâ€Driven Investigation of the Synthesizability and Bandgap of Double Perovskite Halides. Advanced Theory and Simulations, 2022, 5, .	1.3	7
68496	Selective Reduction of Carboxylic Acids to Aldehydes with Promoted MoO₃ Catalysts. ACS Catalysis, 2022, 12, 6313-6324.	5.5	8
68497	Unusual re-entrant spin-glass-behavior and enhanced diamagnetism in sp3-rich sulfur/oxygen doped highly oriented pyrolytic graphite. Diamond and Related Materials, 2022, 126, 109074.	1.8	0
68498	Promoting Oxygen Evolution Reaction Induced by Synergetic Geometric and Electronic Effects of IrCo Thin-Film Electrocatalysts. ACS Catalysis, 2022, 12, 6334-6344.	5.5	12

#	Article	IF	Citations
68499	Pyridinic-N doping carbon layers coupled with tensile strain of FeNi alloy for activating water and urea oxidation. Green Energy and Environment, 2024, 9, 684-694.	4.7	6
68500	The stable behavior of low thermal conductivity in 1T-sandwich structure with different components. Journal of Applied Physics, 2022, 131, .	1.1	2
68501	Insight into the mechanism of the key step for the production of 1,4-butanediol on Ni(111) surface: A DFT study. Molecular Catalysis, 2022, 524, 112335.	1.0	1
68502	Fast Transformation of CO₂ into CO Via a Hydrogen Bond Network on the Cu Electrocatalysts. Journal of Physical Chemistry C, 2022, 126, 7841-7848.	1.5	8
68503	Ab initio systematic description of thermodynamic and mechanical properties of binary bcc Ti-based alloys. Materials Today Communications, 2022, 31, 103583.	0.9	1
68504	Scalable synthesis of hcp ruthenium-molybdenum nanoalloy as a robust bifunctional electrocatalyst for hydrogen evolution/oxidation. Journal of Energy Chemistry, 2022, 72, 176-185.	7.1	24
68505	First principles calculations investigation of optoelectronic properties and photocatalytic CO2 reduction of (MoSi2N4)5-n/(MoSiGeN4)n in-plane heterostructures. Results in Physics, 2022, 37, 105549.	2.0	19
68506	Synthesis of monolayer carbon-coated TiO2 as visible-light-responsive photocatalysts. Applied Materials Today, 2022, 27, 101498.	2.3	12
68507	Electronic structure of chabazite zeolites H-SSZ-13 and H-SAPO-34. Microporous and Mesoporous Materials, 2022, 338, 111957.	2.2	3
68508	New phase of lead chalcogenide alloy: Ternary alloy PbSrSe<mml:math xmlns:mml="http://www.w3.org/1998/Math/MathML" altimg="si3.svg"><mml:msub><mml:mrow /><mml:mn>2</mml:mn></mml:msub></mml:math> for future thermoelectric application. Materialia, 2022, 23, 101443.	1.3	0
68509	High-entropy alloy inspired development of compositionally complex superhard (Hf,Ta,Ti,V,Zr)-B-N coatings. Materials and Design, 2022, 218, 110695.	3.3	4
68510	Experimental study and thermodynamic modeling of the Tiâ€“Cuâ€“B system. Calphad: Computer Coupling of Phase Diagrams and Thermochemistry, 2022, 77, 102431.	0.7	0
68511	First-principles study of local structure and optical properties of Yb/F co-doped silica glass for optical fiber applications. Optical Materials, 2022, 128, 112388.	1.7	1
68512	Strain-tunable Zeeman splitting and optical properties of CrBr3/GeC van der Waals heterostructure. Results in Physics, 2022, 37, 105559.	2.0	2
68513	Interaction between helium and transition metals in vanadium: A first-principles investigation. Nuclear Materials and Energy, 2022, 31, 101189.	0.6	2
68514	Structural, electronic, mechanical and thermodynamic properties of Uâ€“Si intermetallic compounds: A comprehensive first principles calculations. Progress in Nuclear Energy, 2022, 148, 104229.	1.3	5
68515	Interface robust magnetoelectric coupling effect in ferromagnetic/ferroelectric BiFeO3/KNbO3 heterostructure: First-principles calculations. Results in Physics, 2022, 37, 105538.	2.0	4
68516	First-principles calculations of (0 0 1)-Al//(0 0 1) interface in Al-Cu alloys: Atomic structure, bonding strength, stability and electronic properties. Computational Materials Science, 2022, 210, 111485.	1.4	4

#	Article	IF	Citations
68517	Computational insight into the grain boundary structure and atomic mobility in metallic lithium. Acta Materialia, 2022, 233, 117988.	3.8	4
68518	Defect-independent migration of Li on C3B for Li-ion battery anode material. Solid State Ionics, 2022, 380, 115939.	1.3	5
68519	Achieving enhanced high-temperature mechanical properties in Mg-Nd-Sm-Zn-Ca-Zr alloy by Ag addition. Materials Today Communications, 2022, 31, 103666.	0.9	5
68520	Correlation governs the impurity (Ti, Zr, Hf) diffusion in faceâ^'centered cubic iridium through firstâ^'principles calculation. Calphad: Computer Coupling of Phase Diagrams and Thermochemistry, 2022, 77, 102433.	0.7	1
68521	Suppressing disorder-order phase transition of Gd2Zr2O7 pyrochlore by Dy3+ doping and their impact on luminescence. Materials Today Chemistry, 2022, 24, 100931.	1.7	3
68522	The influence of atomic delocalization on dynamic behavior in Ce-Ni metallic melts. Computational Materials Science, 2022, 210, 111473.	1.4	0
68523	Enhancement in thermoelectric properties of ZrNiSn-based alloys by Ta doping and Hf substitution. Acta Materialia, 2022, 233, 117976.	3.8	13
68524	First principles study of the lattice thermal conductivity of alkaline earth oxides. Computational Materials Science, 2022, 210, 111446.	1.4	4
68525	Revisiting the mechanism of highly efficient CO oxidation by single iron atom catalysis on Pt(100). Materials Today Communications, 2022, 31, 103609.	0.9	0
68526	Experimental and first-principles study on amorphous aluminum nitride induced island-like nucleation and planar growth of lithium metal anode. Electrochimica Acta, 2022, 421, 140520.	2.6	1
68527	A quantification study of hydrogen-induced cohesion reduction at the atomic scale. Materials and Design, 2022, 218, 110702.	3.3	5
68528	A study of 2H and 1T phases of Janus monolayers and their van der Waals heterostructure with black phosphorene for optoelectronic and thermoelectric applications. Journal of Solid State Chemistry, 2022, 311, 123159.	1.4	3
68529	Temperature quenching of Cr3+ in ASc(Si1-xGex)2O6 (A=Li/Na) solid solutions. Optical Materials, 2022, 128, 112433.	1.7	9
68530	The role of entropy and enthalpy in high entropy carbides. Computational Materials Science, 2022, 210, 111474.	1.4	8
68531	Genetic structural phase evolution from Li-containing S-like phase precipitates towards S-phase in AlCuLiMg alloys. Acta Materialia, 2022, 233, 117997.	3.8	8
68532	Perfect dual spin filtering effect and large magnetoresistance in all-carbon devices based on C18 cyclo molecule from first principles. Physics Letters, Section A: General, Atomic and Solid State Physics, 2022, 441, 128166.	0.9	4
68533	Graphdiyne@MoS2/WS2 heterostructures for infrared and visible photodetectors: A first-principles study. Computational Materials Science, 2022, 210, 111459.	1.4	4
68534	Molecular dynamics simulations on AlCl3-LiCl molten salt with deep learning potential. Computational Materials Science, 2022, 210, 111494.	1.4	7

#	Article	IF	Citations
68535	Molecular dynamics and density functional theory study on the potassium distribution and lattice thermal conductivity of K RhO2. Physics Letters, Section A: General, Atomic and Solid State Physics, 2022, 441, 128151.	0.9	0
68536	Improving Tc in sodalite-like boron-nitrogen compound M2(BN)6. Materials Today Physics, 2022, 25, 100699.	2.9	7
68537	The predictability of the ground state of 3d transition metal ion as luminescent centers in the tetrahedral sites in inorganic compounds. Journal of Luminescence, 2022, 247, 118919.	1.5	1
68538	Pressure-induced metallization and robust superconductivity in pristine 1T-HfSe2. Materials Today Physics, 2022, 25, 100698.	2.9	11
68539	CoSe2 nanodots confined in multidimensional porous nanoarchitecture towards efficient sodium ion storage. Nano Energy, 2022, 98, 107326.	8.2	46
68540	High-efficient yellow-green emission in (TDMP)MnBr4 single crystal with modulation of spin-phonon-charge interactions. Materials Today Physics, 2022, 25, 100703.	2.9	23
68541	Flexible 3D porous boron nitride interconnected network as a high-performance Li-and Na-ion battery electrodes. Electrochimica Acta, 2022, 421, 140491.	2.6	9
68542	Investigation of W/Mo co-doping with multiple concentrations in photocatalyst BiVO4 by first-principles calculations. Solid State Communications, 2022, 351, 114794.	0.9	2
68543	A high-pressure study of EuN using XRD and DFT. Solid State Communications, 2022, 351, 114811.	0.9	0
68544	Low coverage disordered decanethiol monolayers on Au(001): A conjecture regarding the formation of Au-adatom-molecule complexes. Applied Surface Science, 2022, 594, 153364.	3.1	2
68545	Ag rearrangement induced metal-insulator phase transition in thermoelectric MgAgSb. Materials Today Physics, 2022, 25, 100702.	2.9	0
68546	Ab initio calculations on thermal conductivity of Fe-Ni-O fluid: Constraints on the thermal evolution of Earth's core. Earth and Planetary Science Letters, 2022, 589, 117581.	1.8	0
68547	Charge compensation and solid-state lighting application for dysprosium-activated Ba2TeP2O9 phosphor. Journal of Alloys and Compounds, 2022, 912, 165188.	2.8	11
68548	Strain and electric field dependent spin polarization in two-dimensional arsenene/CrI3 heterostructure. Journal of Alloys and Compounds, 2022, 912, 165093.	2.8	1
68549	Suppressing oxygen vacancies on the surface of Li-rich material as a high-energy cathode via high oxygen affinity Ca0.95Bi0.05MnO3 coating. Electrochimica Acta, 2022, 421, 140465.	2.6	3
68550	Novel atomic-scale graphene metamaterials with broadband electromagnetic wave absorption and ultra-high elastic modulus. Carbon, 2022, 196, 146-153.	5.4	9
68551	The intrinsic mechanical properties of NbTaTiZr and the influence of alloying elements Mo and W: A first-principles study. Journal of Alloys and Compounds, 2022, 911, 165109.	2.8	3
68552	Three-dimensional Langevin dynamics of N atom scattering from N-covered Ag(1 1 1). Chemical Physics, 2022, 560, 111557.	0.9	0

#	Article	IF	Citations
68553	Structural degradation behavior of Mg2-Pr Ni4 upon hydrogenation. Journal of Alloys and Compounds, 2022, 912, 165272.	2.8	4
68554	Ground-state structure, orbital ordering and metal-insulator transition in double-perovskite PrBaMn2O6. Journal of Alloys and Compounds, 2022, 912, 165150.	2.8	5
68555	Fabrication and characterisation of ZnO@TiO2 core/shell nanowires using a versatile kinetics-controlled coating growth method. Applied Surface Science, 2022, 594, 153463.	3.1	2
68556	Understanding of photocatalytic partial oxidation of methanol to methyl formate on surface doped La(Ce) TiO2: Experiment and DFT calculation. Journal of Catalysis, 2022, 411, 31-40.	3.1	10
68557	Modulation of electronic and magnetic properties of monolayer 1T-VSe2 by ferroelectric LiNbO3 (0001) surface. Journal of Physics and Chemistry of Solids, 2022, 167, 110745.	1.9	1
68558	Segregation tendency and properties of FeRh1-Pt alloys. Journal of Magnetism and Magnetic Materials, 2022, 556, 169403.	1.0	1
68559	Atomic structure and electrical/ionic activity of antiphase boundary in CH3NH3PbI3. Acta Materialia, 2022, 234, 118010.	3.8	6
68560	The trapping effects of silicon and phosphorus on point defects in Î³-Fe. Computational Materials Science, 2022, 210, 111488.	1.4	1
68561	Ba3(ZnB5O10)PO4:Tb3+ green phosphor: Microwave-assisted sintering synthesis and thermally stable photoluminescence. Journal of Alloys and Compounds, 2022, 911, 165087.	2.8	15
68562	In-situ phase transformation and corrosion behavior of TiNi via LPBF. Corrosion Science, 2022, 203, 110348.	3.0	11
68563	Modification of surface electronic structure via Ru-doping: Porous Ruâ€“CoFeP nanocubes to boost the oxygen evolution reaction. Journal of Power Sources, 2022, 537, 231506.	4.0	5
68564	Cu-induced enhancement of interfacial bonding for brazed diamond grits with Ni Cr filler alloys. International Journal of Refractory Metals and Hard Materials, 2022, 106, 105874.	1.7	8
68565	Hybridization of iron phthalocyanine and MoS2 for high-efficiency and durable oxygen reduction reaction. Journal of Energy Chemistry, 2022, 71, 528-538.	7.1	10
68566	A Combined Machine Learning and High-Energy X-ray Diffraction Approach to Understanding Liquid and Amorphous Metal Oxides. Journal of the Physical Society of Japan, 2022, 91, .	0.7	7
68567	Mass transfer effect to electrochemical reduction of CO2: Electrode, electrocatalyst and electrolyte. Journal of Energy Storage, 2022, 52, 104764.	3.9	39
68568	Electronic structures and magnetic properties of 3d transition metal doped monolayer RhI3. Chemical Physics Letters, 2022, 799, 139643.	1.2	1
68569	Hierarchical WMoC nano array with optimal crystal facet as a non-noble metal cathode for proton exchange membrane water electrolyser. Journal of Power Sources, 2022, 538, 231557.	4.0	9
68570	Unraveling the roles of Al, Mn and Co in the Ni-rich cathode material for Li-ion batteries. Colloids and Surfaces A: Physicochemical and Engineering Aspects, 2022, 648, 129185.	2.3	7

#	Article	IF	Citations
68571	Determining the diffusion behavior of point defects in zirconium by a multiscale modelling approach. Journal of Nuclear Materials, 2022, 566, 153772.	1.3	5
68572	In situ co-doping strategy for achieving long-term cycle stability of single-crystal Ni-rich cathodes at high voltage. Chemical Engineering Journal, 2022, 445, 136825.	6.6	31
68573	Hole-mediated ferromagnetic coupling in two-dimensional CrI3/VSe2 van der Waals heterostructures. Surface Science, 2022, 723, 122121.	0.8	0
68574	Tailoring surface carboxyl groups of mesoporous carbon boosts electrochemical H2O2 production. Journal of Colloid and Interface Science, 2022, 622, 849-859.	5.0	12
68575	Highly active platinum single-atom catalyst grafted onto 3D carbon cloth support for the electrocatalytic hydrogen evolution reaction. Applied Surface Science, 2022, 595, 153480.	3.1	10
68576	Nonmetallic surface plasmon resonance coupling with pyroelectric effect for enhanced near-infrared-driven CO2 reduction. Chemical Engineering Journal, 2022, 445, 136739.	6.6	14
68577	Bottom-up strategy for precisely designing and fabricating direct Z-scheme photocatalyst with wedge-type heterointerface bridged by chemical bond. Chemical Engineering Journal, 2022, 445, 136785.	6.6	10
68578	Escape inhibition of unsymmetrical dimethylhydrazine in aqueous solution by carboxyl-rich graphene oxide. Journal of Molecular Liquids, 2022, 359, 119197.	2.3	2
68579	Highly selective electrocatalytic hydrogenation of benzoic acid over Pt/C catalyst supported on carbon fiber. Chemical Engineering Journal, 2022, 445, 136719.	6.6	13
68580	Chemical looping combustion of sulfur paste to SO2 by phosphogypsum oxygen carrier for sulfur acid production. Fuel, 2022, 323, 124386.	3.4	13
68581	Generation of positively charged nanoparticles by fracto-emission and their deposition into films during aerosol deposition. Applied Surface Science, 2022, 593, 153466.	3.1	3
68582	First-principles screening of Pt doped Ti2CNL (Nâ€¯=â€¯O, S and Se, Lâ€¯=â€¯F, Cl, Br and I) as high-performance catalysts for ORR/OER. Applied Surface Science, 2022, 596, 153574.	3.1	31
68583	Rashba states localized to InSe layer in InSe/GaTe(InTe) heterostructure. Applied Surface Science, 2022, 595, 153528.	3.1	5
68584	Laser fabrication of Pt anchored Mo2C micropillars as integrated gas diffusion and catalytic electrode for proton exchange membrane water electrolyzer. Applied Catalysis B: Environmental, 2022, 314, 121455.	10.8	18
68585	Intermolecular hydrogen bond modulating the selective coupling of protons and CO2 to CH4 over nitrogen-doped carbon layers modified cobalt. Chemical Engineering Journal, 2022, 444, 136585.	6.6	12
68586	Tuning the activity and selectivity of nitrogen reduction reaction on double-atom catalysts by B doping: A density functional theory study. Nano Energy, 2022, 99, 107363.	8.2	21
68587	Efficient activation of peroxymonosulfate mediated by Co(II)-CeO2 as a novel heterogeneous catalyst for the degradation of refractory organic contaminants: Degradation pathway, mechanism and toxicity assessment. Journal of Hazardous Materials, 2022, 435, 129013.	6.5	41
68588	Two-dimensional ZnO/BlueP van der Waals heterostructure used for visible-light driven water splitting: A first-principles study. Spectrochimica Acta - Part A: Molecular and Biomolecular Spectroscopy, 2022, 278, 121359.	2.0	9

#	Article	IF	Citations
68589	Direct Z-scheme MoSe2/TiO2 heterostructure with improved piezoelectric and piezo-photocatalytic performance. Journal of Colloid and Interface Science, 2022, 622, 637-651.	5.0	15
68590	The dynamical stability, electronic, elastic properties and ideal strength of diamond-like cubic B2CN: A first-principles study. Solid State Communications, 2022, 352, 114805.	0.9	3
68591	Strain-tuning of transport gaps and semiconductor-to-conductor phase transition in twinned graphene. Acta Materialia, 2022, 234, 117987.	3.8	0
68592	Environmentally benign methane-regulated catalytic desulfurization. Applied Catalysis B: Environmental, 2022, 312, 121436.	10.8	7
68593	DensityTool: A post-processing tool for space- and spin-resolved density of states from VASP. Computer Physics Communications, 2022, 277, 108384.	3.0	9
68594	Bilateral phonon transport modulation of Bi-layer TMDCs (MX2, M=Mo, W; X=S). International Journal of Thermal Sciences, 2022, 179, 107669.	2.6	1
68595	Performance optimization of Ca and Y co-doped CeO2-based electrolyte for intermediate-temperature solid oxide fuel cells. Journal of Alloys and Compounds, 2022, 913, 165317.	2.8	13
68596	Which kind of nitrogen chemical states doped carbon dots loaded by g-C3N4 is the best for photocatalytic hydrogen production. Journal of Colloid and Interface Science, 2022, 622, 662-674.	5.0	43
68597	Molecular engineering to introduce carbonyl between nickel salophen active sites to enhance electrochemical CO2 reduction to methanol. Applied Catalysis B: Environmental, 2022, 314, 121451.	10.8	32
68598	Unveiling the origin of alkali metal promotion in CO2 methanation over Ru/ZrO2. Applied Catalysis B: Environmental, 2022, 314, 121476.	10.8	27
68599	In-situ exfoliation and assembly of 2D/2D g-C3N4/TiO2(B) hierarchical microflower: Enhanced photo-oxidation of benzyl alcohol under visible light. Carbon, 2022, 196, 401-409.	5.4	38
68600	Triptycene incorporated carbon nitride based donor-acceptor conjugated polymers with superior visible-light photocatalytic activities. Journal of Colloid and Interface Science, 2022, 622, 675-689.	5.0	8
68601	Heterogeneous interface-boosted zinc storage of H2V3O8 nanowire/Ti3C2Tx MXene composite toward high-rate and long cycle lifespan aqueous zinc-ion batteries. Energy Storage Materials, 2022, 50, 63-74.	9.5	37
68602	F-GDY and F-GDY/Graphene as anodes in lithium-ion batteries: A first-principle investigation. Applied Surface Science, 2022, 595, 153543.	3.1	6
68603	Helium interaction with solutes and impurities in neutron-irradiated nanostructured ferritic alloys: A first principles study. Journal of Nuclear Materials, 2022, 566, 153771.	1.3	2
68604	Adsorption and dissociation of water molecules on the <mml:math xmlns:mml="http://www.w3.org/1998/Math/MathML" altimg="si2.svg"><mml:mi>î±</mml:mi></mml:math>-Pu<mml:math xmlns:mml="http://www.w3.org/1998/Math/MathML" altimg="si3.svg"><mml:msub><mml:mrow /><mml:mn>2</mml:mn></mml:msub></mml:math>O<mml:math xmlns:mml="http://www.w3.org/1998/Math/MathML" altimg="si4.svg"><mml:msub><mml:mrow />	1.3	1
68605	Ammonia decomposition over iron-based catalyst: Exploring the hidden active phase. Applied Catalysis B: Environmental, 2022, 314, 121475.	10.8	17
68606	Theoretical study of the initial stages of Ba growth on Si(100) substrate. Surface Science, 2022, 723, 122107.	0.8	0

#	Article	IF	Citations
68607	Synergistic effect of Cu+ single atoms and Cu nanoparticles supported on alumina boosting water-gas shift reaction. Applied Catalysis B: Environmental, 2022, 313, 121468.	10.8	25
68608	Embedding indium nitride at the interface of indium-oxide/indium-zinc-sulfide heterostructure with enhanced interfacial charge transfer for high photocatalytic hydrogen evolution. Journal of Colloid and Interface Science, 2022, 622, 539-548.	5.0	11
68609	Biaxial strain tuned electronic structure, lattice thermal conductivity and thermoelectric properties of MgI2 monolayer. Materials Science in Semiconductor Processing, 2022, 148, 106791.	1.9	3
68610	Electroreduction of N₂ to NH₃ catalyzed by a Mn/Re(111) single-atom alloy catalyst with high activity and selectivity: a new insight from a first-principles study. Catalysis Science and Technology, 2022, 12, 4074-4085.	2.1	6
68611	Importance of the many-body effects on the structural properties of the novel iron oxide Fe₂O. Physical Chemistry Chemical Physics, 2022, , .	1.3	0
68612	Formation of oxygen vacancies in the Li-rich Mn-based cathode material Li_{1.167}Ni_{0.167}Co_{0.167}Mn_{0.5}O<sub&g calculations. Wuli Xuebao/Acta Physica Sinica, 2022, .		
68613	Strain engineering of lateral heterostructures based on group-V enes (As, Sb, Bi) for infrared optoelectronic applications calculated by first principles. RSC Advances, 2022, 12, 14578-14585.	1.7	2
68614	Structural phase transitions in <mml:math xmlns:mml="http://www.w3.org/1998/Math/MathML"><mml:mrow><mml:mi>SrTi</mml:mi><mml:msub><mml:mi mathvariant="normal">O</mml:mi><mml:mn>3</mml:mn></mml:msub></mml:mrow></mml:math> from deep potential molecular dynamics. Physical Review B, 2022, 105, .	1.1	25
68615	Map of Two-Dimensional Tungsten Chalcogenide Compounds (Wâ€“S, Wâ€“Se, Wâ€“Te) Based on USPEX Evolutionary Search. JETP Letters, 2022, 115, 292-296.	0.4	3
68616	General relationship between the band-gap energy and iodine-oxygen bond distance in metal iodates. Physical Review Materials, 2022, 6, .	0.9	7
68617	Oxygenate Reactions over PdCu and PdAg Catalysts: Distinguishing Electronic and Geometric Effects on Reactivity and Selectivity. ACS Catalysis, 2022, 12, 5766-5775.	5.5	4
68618	Investigation of the W/Y₂O₃ heterogeneous interface properties and its effect on hydrogen behavior using first-principles calculations. Nuclear Fusion, 2022, 62, 086015.	1.6	2
68619	Magnetically tunable Dirac and Weyl fermions in the Zintl materials family. Physical Review Materials, 2022, 6, .	0.9	9
68620	Switchable quantum anomalous and spin Hall effects in honeycomb magnet EuCd₂As₂. New Journal of Physics, 2022, 24, 053038.	1.2	5
68621	Organic self-assembled monolayers on superconducting NbSe₂: interfacial electronic structure and energetics*. Journal of Physics Condensed Matter, 2022, 34, 294003.	0.7	2
68622	CO2/carbonate-mediated electrochemical water oxidation to hydrogen peroxide. Nature Communications, 2022, 13, 2668.	5.8	44
68623	Freeâ€Standing Nanoarrays with Energetic Electrons and Active Sites for Efficient Plasmonâ€Driven Ammonia Synthesis. Small, 2022, 18, e2201269.	5.2	6
68624	Plastic deformation of bulk and micropillar single crystals of Mo5Si3 with the tetragonal D8 structure. International Journal of Plasticity, 2022, , 103339.	4.1	1

#	Article	IF	Citations
68625	Boosting electrocatalytic hydrogen evolution over the wide pH range for CoP3 nanowire arrays via Ni doping. Journal of Alloys and Compounds, 2022, 915, 165440.	2.8	4
68626	Structural and phase evolution in U3Si2 during steam corrosion. Corrosion Science, 2022, 204, 110373.	3.0	3
68627	Tuning electronic, magnetic and catalytic behaviors of biphenylene network by atomic doping. Nanotechnology, 2022, 33, 345701.	1.3	34
68628	The topological nodal lines and drum-head-like surface states in semimetals CrSi2, MoSi2 and WSi2. Physica B: Condensed Matter, 2022, 639, 413928.	1.3	3
68629	Revealing the Structure of Single Cobalt Sites in Carbon Nitride for Photocatalytic CO₂ Reduction. Journal of Physical Chemistry C, 2022, 126, 8596-8604.	1.5	11
68630	Interactions of Hydrogen Atoms with Acceptorâ€“Dioxygen Complexes in Czochralskiâ€Grown Silicon. Physica Status Solidi (A) Applications and Materials Science, 2022, 219, .	0.8	2
68631	Modeling Fission Spikes in Nuclear Fuel using a Multigroup Model of Electronic Energy Transport. Journal of Nuclear Materials, 2022, , 153797.	1.3	0
68632	Prediction of SEI Formation in Allâ€Solidâ€State Batteries: Computational Insights from PCLâ€based Polymer Electrolyte Decomposition on Lithiumâ€Metal. Batteries and Supercaps, 2022, 5, .	2.4	11
68633	Observation of in-plane excitonâ€“polaritons in monolayer WSe₂ driven by plasmonic nanofingers. Nanophotonics, 2022, 11, 3149-3157.	2.9	4
68634	Control of perpendicular magnetic anisotropy at the Fe/MgO interface by phthalocyanine insertion. Physical Review B, 2022, 105, .	1.1	6
68635	Gasâ€Phase Errors Affect DFTâ€Based Electrocatalysis Models of Oxygen Reduction to Hydrogen Peroxide. ChemElectroChem, 2022, 9, .	1.7	2
68636	Mechanism of ozone-assisted catalytic oxidation of isopropanol over single-atom platinum catalysts at ambient temperature. Chemical Engineering Journal, 2022, 446, 136989.	6.6	11
68637	Unraveling the electronegativity-dominated intermediate adsorption on high-entropy alloy electrocatalysts. Nature Communications, 2022, 13, 2662.	5.8	196
68638	Critical phonon frequency renormalization and dual phonon coexistence in layered Ruddlesden-Popper inorganic perovskites. Physical Review B, 2022, 105, .	1.1	16
68639	The structural, electronic and thermal transport properties of pentagonal MS2 (M = Zn, Cd) monolayers: A first-principles study. Journal of Physics and Chemistry of Solids, 2022, 167, 110792.	1.9	4
68640	Pressure-Driven Ne-Bearing Polynitrides with Ultrahigh Energy Density. Chinese Physics Letters, 2022, 39, 056102.	1.3	7
68641	Exploring the potential of Ti2BT2 (TÂ=ÂF, Cl, Br, I, O, S, Se and Te) monolayers as anode materials for lithium and sodium ion batteries. Applied Surface Science, 2022, 596, 153619.	3.1	18
68642	Ambiguous structure determination from powder data: four different structural models of 4,11-difluoroquinacridone with similar X-ray powder patterns, fit to the PDF, SSNMR and DFT-D. IUCrJ, 2022, 9, 406-424.	1.0	8

#	Article	IF	Citations
68643	Photoelectronic properties for heteroatom derivatives of graphdiyne monolayer sheet. Journal of Physics and Chemistry of Solids, 2022, 167, 110793.	1.9	0
68644	Manganese promotion of a cobalt Fischer-Tropsch catalyst to improve operation at high conversion. Journal of Catalysis, 2022, 411, 97-108.	3.1	12
68645	Accelerated computation of lattice thermal conductivity using neural network interatomic potentials. Computational Materials Science, 2022, 211, 111472.	1.4	5
68646	New mechanistic insights into direct ethylene glycol synthesis from syngas over modified Rh carbonyl catalysts. Fuel, 2022, 324, 124500.	3.4	0
68647	Experimental modeling of antimony sulfides-rich geothermal deposits and their solubility in the presence of polymeric antiscalants. Geothermics, 2022, 104, 102452.	1.5	3
68648	Performance improvement of dye-sensitized double perovskite solar cells by adding Ti3C2T MXene. Chemical Engineering Journal, 2022, 446, 136963.	6.6	37
68649	Site preference, thermodynamic, and magnetic properties of the ternary Laves phase Ti(Fe<sub>1 â€“) Tj ETQq0 0 0 rgBT /Overlock 10 T MgZn₂-type. International Journal of Materials Research, 2022, 97, 450-460.	0.1	0
68650	The Naâ€“H system: from first-principles calculations to thermodynamic modeling. International Journal of Materials Research, 2022, 97, 845-853.	0.1	5
68651	Reconstruction and structural transition at metal/diamond interfaces. International Journal of Materials Research, 2022, 97, 768-771.	0.1	0
68652	Thermodynamic modeling of the sodium alanates and the Naâ€“Alâ€“H system. International Journal of Materials Research, 2022, 97, 1484-1494.	0.1	4
68653	Experimental and theoretical characterization of Al₃Sc precipitates in Alâ€“Mgâ€“Siâ€“Cuâ€“Scâ€“Zr alloys. International Journal of Materials Research, 2022, 97, 321-324.	0.1	0
68654	Charge doping to flat AgF₂ monolayers in a chemical capacitor setup. Physical Chemistry Chemical Physics, 2022, 24, 15705-15717.	1.3	3
68655	Enhanced Câ€“H bond activation by tuning the local environment of surface lattice oxygen of MoO₃. Chemical Science, 2022, 13, 7468-7474.	3.7	3
68656	Superior mechanical flexibility, lattice thermal conductivity and electron mobility of the hexagonal honeycomb carbon nitride monolayer. Physical Chemistry Chemical Physics, 2022, 24, 13951-13964.	1.3	2
68657	First-principles calculations of the structural, energetic, electronic, optical, and photocatalytic properties of BaTaO₂N low-index surfaces. New Journal of Chemistry, 2022, 46, 11540-11552.	1.4	1
68658	Metal nanoparticles at grain boundaries of titanate toward efficient carbon dioxide electrolysis. Journal of Materials Chemistry A, 0, , .	5.2	3
68659	Analyzing the TiO₂ surface reactivity based on oxygen vacancies computed by DFT and DFTB methods. Journal of Physics Condensed Matter, 2022, 34, 314004.	0.7	3
68660	Revealing superstructure ordering in <mml:math xmlns:mml="http://www.w3.org/1998/Math/MathML"><mml:mrow><mml:msub><mml:mi>Co</mml:mi><mml:mrow><mml:mn>1</mml:mn> Heusler alloys and its effect on structural, magnetic, and electronic properties. Physical Review B, 2022, 105, .	1.1	2

#	Article	IF	Citations
68661	Electric field- and strain-induced bandgap modulation in bilayer C2N. Applied Physics Letters, 2022, 120, .	1.5	4
68662	Strain dependent magnetic properties of 1T-VSe2 monolayer. Journal of the Korean Physical Society, 2022, 81, 133-138.	0.3	3
68663	Quantitative analysis of diffraction by liquids using a pink-spectrum X-ray source. Journal of Synchrotron Radiation, 2022, 29, 1033-1042.	1.0	4
68664	Tensile deformation behavior and generalized stacking fault energy surface of Î³-Fe23C6 by atomistic modelling. Vacuum, 2022, 202, 111180.	1.6	1
68665	Near-Infrared Absorption Properties of Neutral Bis(1,2-dithiolene) Platinum(II) Complexes Using Density Functional Theory. Nanomaterials, 2022, 12, 1704.	1.9	4
68666	Dependence of cuprous oxide conductivity on metal doping: a hybrid density functional simulation. European Physical Journal B, 2022, 95, .	0.6	0
68667	Identifying of Pure and Defected Ti2C Materials Using Gas Probe Molecules: First Principles Calculations. Chemistry - an Asian Journal, 2022, , .	1.7	0
68668	Effects of rare earth element Ce on structural, electronic, magnetic and optical properties of CeYFeO (xÂâ€‹=Ââ€‹0.0625, 0.125): ab initio study. Journal of Solid State Chemistry, 2022, 312, 123226.	1.4	1
68669	Evidence of carbon-supported porphyrins pyrolyzed for the oxygen reduction reaction keeping integrity. Scientific Reports, 2022, 12, 8072.	1.6	13
68670	Understanding edge effect for Li atom insertion: nano layered transition metal dichalcogenides. Applied Surface Science, 2022, , 153723.	3.1	0
68671	Atomically chemically graded Ti/TiN interface. Applied Surface Science, 2022, 597, 153637.	3.1	6
68672	Work function of the oxygen functionalized graphenic surfaces â€“ integral experimental and theoretical approach. Applied Surface Science, 2022, , 153671.	3.1	3
68673	Efficient passivation on halide perovskite by tailoring the organic molecular functional groups: First-principles investigation. Applied Surface Science, 2022, 597, 153716.	3.1	6
68674	Mechanism and Dynamics of CO₂ Formation in Formic Acid Decomposition on Pt Surfaces. ACS Catalysis, 2022, 12, 6486-6494.	5.5	2
68675	Two-Dimensional V₂N MXene Monolayer as a High-Capacity Anode Material for Lithium-Ion Batteries and Beyond: First-Principles Calculations. ACS Omega, 2022, 7, 17756-17764.	1.6	18
68676	High-Voltage Redox Mediator of an Organic Electrolyte for Supercapacitors by Lewis Base Electrocatalysis. ACS Applied Materials & Interfaces, 2022, 14, 24497-24508.	4.0	9
68677	Evidence for spin swapping in an antiferromagnet. Nature Physics, 2022, 18, 800-805.	6.5	12
68678	Lattice Oxygen of PbO₂ (101) Consuming and Refilling via Electrochemical Ozone Production and H₂O Dissociation. Journal of Physical Chemistry C, 2022, 126, 8627-8636.	1.5	7

#	Article	IF	Citations
68679	D-band frontier: A new hydrogen evolution reaction activity descriptor of Pt single-atom catalysts. Journal of Energy Chemistry, 2022, 72, 203-209.	7.1	16
68680	<mml:math xmlns:mml="http://www.w3.org/1998/Math/MathML"><mml:mrow><mml:msub><mml:mi>Ta</mml:mi><mml:mn>14</mml:mn></mml:msub></mml:mrow></mml:math> : A possible one-dimensional topological insulator. Physical Review B, 2022, 105, .	1.1	20
68681	Improving the HCHO Sensing Selectivity on Ag-Doped Graphene by Oxygen Functionalization: A First-Principles Study. ACS Omega, 0, , .	1.6	1
68682	Stability, electronic and magnetic properties of half-metallic alloy CrLaCoAl (100) surface. Physica B: Condensed Matter, 2022, , 414015.	1.3	0
68683	Coexistence of Robust Edge States and Superconductivity in Few-Layer Stanene. Physical Review Letters, 2022, 128, .	2.9	11
68684	2D Homologous Series SrFM_nBiS_{n+2} (M = Pb,) Tj ETQq1 1 0.784314 rgBT /Overlock 10 Tf 50 5 Sr₂F₂Bi_{2/3}S₂. Inorganic Chemistry, 2022, 61, 8233-8240.	1.9	2
68685	Anisotropic interface characteristics of bilayer GeSe based field effect transistors. Physica E: Low-Dimensional Systems and Nanostructures, 2022, , 115317.	1.3	0
68686	<mml:math xmlns:mml="http://www.w3.org/1998/Math/MathML"><mml:mrow><mml:mi>A</mml:mi><mml:mi>b</mml:mi></mml:mrow></mml:ma <mml:math xmlns:mml="http://www.w3.org/1998/Math/MathML"><mml:mrow><mml:mi>i</mml:mi><mml:mi>n</mml:mi><mml:mi>i</mml:mi> point defect calculations for structural properties of a model austenitic steel alloy. Physical Review Materials, 2022, 6, .	0.9	1
68687	High-throughput predictions of metalâ€“organic framework electronic properties: theoretical challenges, graph neural networks, and data exploration. Npj Computational Materials, 2022, 8, .	3.5	43
68688	Coreâ€“Shell Three-Dimensional Perovskite Nanocrystals with Chiral-Induced Spin Selectivity for Room-Temperature Spin Light-Emitting Diodes. Journal of the American Chemical Society, 2022, 144, 9707-9714.	6.6	47
68689	Galvanic Corrosion and Electric Field in Lithium Anode Passivation Films: Effects on Self-Discharge. Journal of Physical Chemistry C, 2022, 126, 8565-8580.	1.5	13
68690	Abnormal nonlinear optical responses on the surface of topological materials. Npj Computational Materials, 2022, 8, .	3.5	6
68691	Multiple optimization strategies for improving photocatalytic performance of the h-BN/flower-ring g-C3N4 heterostructures: Morphology engineering and internal electric field effect. Chemical Engineering Journal, 2022, 446, 137027.	6.6	51
68692	Itinerant magnetism, electronic properties and half-metallicity of Co2ZrSn and Co2HfSn Heusler alloys. Journal of Alloys and Compounds, 2022, 918, 165464.	2.8	3
68693	Organic phosphoric acid induced coral-like palladium network nanostructures for superior polyhydric alcohols electrocatalysis. Journal of Colloid and Interface Science, 2022, 623, 1122-1131.	5.0	3
68694	Effects of substitutional Ga on the phonons of <mml:math xmlns:mml="http://www.w3.org/1998/Math/MathML"><mml:mi>Î´</mml:mi></mml:math> -phase Pu based on density functional theory calculations. Physical Review B, 2022, 105, .	1.1	0
68695	Radio-frequency magnetron sputtered thin-film La0.5Sr0.5Co0.95Nb0.05O3-Î´ perovskite electrodes for intermediate temperature symmetric solid oxide fuel cell (IT-SSOFC). Materials Reports Energy, 2022, 2, 100095.	1.7	3
68696	Understanding of the Band Gap Transition in Cs₃Sb₂Cl_{9â€“x}Br_x: Anion Site Preference-Induced Structural Distortion. ACS Applied Energy Materials, 2022, 5, 6952-6961.	2.5	14

#	Article	IF	Citations
68697	Surface reconstruction in core@shell nanoalloys: interplay between size and strain. Acta Materialia, 2022, , 118038.	3.8	4
68698	Prediction of new topological superconductor candidate <mml:math xmlns:mml="http://www.w3.org/1998/Math/MathML"><mml:mn>1</mml:mn><mml:mi>T</mml:mi><mml:mtext>â€“</mml:mtext><mml:mn> Physical Review Research, 2022, 4, .	1.3	2
68699	Ultralowâ€k Amorphous Boron Nitride Based on Hexagonal Ring Stacking Framework for 300 mm Silicon Technology Platform. Advanced Materials Technologies, 2022, 7, .	3.0	7
68700	Theory-guided design of hydrogen-bonded cobaltoporphyrin frameworks for highly selective electrochemical H2O2 production in acid. Nature Communications, 2022, 13, 2721.	5.8	38
68701	Plasmon-induced super-semiconductor at room temperature in nanostructured bimetallic arrays. Applied Physics Reviews, 2022, 9, 021412.	5.5	1
68702	Giant Negative Magnetoresistance beyond Chiral Anomaly in Topological Material YCuAs₂. Advanced Materials, 2022, 34, e2201597.	11.1	6
68703	Buffering Octahedra in Mo₄Zr₉P: Intergrowth as a Solution to the Frustrated Packing of Tricapped Trigonal Prisms and Icosahedra. Inorganic Chemistry, 2022, 61, 8298-8308.	1.9	2
68704	Large Spectral Shift of Mn²⁺ Emission Due to the Shrinkage of the Crystalline Host Lattice of the Hexagonal CsCdCl₃ Crystals and Phase Transition. Inorganic Chemistry, 2022, 61, 8356-8365.	1.9	15
68705	Manipulation of Band Alignment in Two-Dimensional Vertical WSe₂/BA₂Pbl₄ Ruddlesdenâ€“Popper Perovskite Heterojunctions via Defect Engineering. Journal of Physical Chemistry Letters, 2022, 13, 4579-4588.	2.1	10
68706	Stabilization and Self-Passivation of Grain Boundaries in Halide Perovskite by Rigid Body Translation. Journal of Physical Chemistry Letters, 2022, 13, 4628-4633.	2.1	5
68707	Theoretical Study on the Contribution of Interfacial Functional Groups to the Adhesive Interaction between Epoxy Resins and Aluminum Surfaces. Langmuir, 2022, 38, 6653-6664.	1.6	19
68708	A High-Performance Electrode Based on van der Waals Heterostructure for Neural Recording. Nano Letters, 2022, 22, 4400-4409.	4.5	8
68709	High CO-Tolerant Ru-Based Catalysts by Constructing an Oxide Blocking Layer. Journal of the American Chemical Society, 2022, 144, 9292-9301.	6.6	29
68710	Defect-gradient-induced Rashba effect in van der Waals PtSe2 layers. Nature Communications, 2022, 13, 2759.	5.8	13
68711	A new class of bilayer kagome lattice compounds with Dirac nodal lines and pressure-induced superconductivity. Nature Communications, 2022, 13, 2773.	5.8	19
68712	Zeolite-confined subnanometric PtSn mimicking mortise-and-tenon joinery for catalytic propane dehydrogenation. Nature Communications, 2022, 13, 2716.	5.8	33
68713	High-performance photocatalytic nonoxidative conversion of methane to ethane and hydrogen by heteroatoms-engineered TiO2. Nature Communications, 2022, 13, 2806.	5.8	89
68714	Breaking scaling relationships in alkynol semi-hydrogenation by manipulating interstitial atoms in Pd with d-electron gain. Nature Communications, 2022, 13, 2754.	5.8	36

#	Article	IF	Citations
68715	Atomic-scale understanding of the Na and Cl trapping on the Mo1.33C(OH)2-MXene. Scientific Reports, 2022, 12, 8340.	1.6	4
68716	Active sites and deactivation of room temperature CO oxidation on Co₃O₄ catalysts: combined experimental and computational investigations. Journal of Physics Condensed Matter, 2022, 34, 354001.	0.7	4
68717	Interfacial electronic properties of metal/CsSnBr3 heterojunctions. Nanotechnology, 2022, , .	1.3	1
68718	The quantum confinement effects on the electronic properties of monolayer GeS nanoribbon with tube-edged reconstruction. Nanotechnology, 2022, 33, 345202.	1.3	2
68719	All topological bands of all nonmagnetic stoichiometric materials. Science, 2022, 376, eabg9094.	6.0	84
68720	BA₂XBr₄ (X = Pb, Cu, Sn): from lead to lead-free halide perovskite scintillators. Materials Advances, 2022, 3, 5087-5095.	2.6	16
68721	Electron paramagnetic resonance spectroscopy and first-principles calculations of Cr³⁺ doped KDP crystals. CrystEngComm, 2022, 24, 4948-4954.	1.3	7
68722	Theoretical study on the effect of Ge-S/F co-doping on the crystal structure and properties of Li₂MSiO₄(M=Mn,Fe). Wuli Xuebao/Acta Physica Sinica, 2022, .	0.2	0
68723	In situ reconstruction enhanced dual-site catalysis towards nitrate electroreduction to ammonia. Journal of Materials Chemistry A, 2022, 10, 12669-12678.	5.2	20
68724	Sodium tungsten bronze-supported Pt electrocatalysts for the high-performance hydrogen evolution reaction. Catalysis Science and Technology, 2022, 12, 4498-4510.	2.1	11
68725	Enhanced acetylene semi-hydrogenation on a subsurface carbon tailored Niâ€“Ga intermetallic catalyst. Journal of Materials Chemistry A, 2022, 10, 19722-19731.	5.2	17
68726	Manipulating the electronic structure and physical properties in monolayer Mo₂I₃Br₃via strain and doping. Nanoscale, 2022, 14, 8934-8943.	2.8	3
68727	Iridium-decorated carbon nanotubes as cathode catalysts for Li-CO2 batteries with a highly efficient direct Li2CO3 formation/decomposition capability. , 0, 1, .		1
68728	Theoretical insight into the anion vacancy healing process during the oxygen evolution reaction on TaON and Ta₃N₅. Physical Chemistry Chemical Physics, 2022, 24, 13999-14006.	1.3	4
68729	Optical and defect properties of mid-IR laser crystal Dy³⁺: PbGa₂S₄: a DFT and XPS study. CrystEngComm, 2022, 24, 5149-5155.	1.3	2
68730	Using the site-knockout strategy to understand the low activity of the nitrate electroreduction reaction on Pt(111). New Journal of Chemistry, 0, , .	1.4	0
68731	Formation Mechanism of CsPbBr3/Cs4PbBr6 Microscale Composites Assisted by Imidazolium Cations and Their Device Application. Dalton Transactions, 0, , .	1.6	2
68732	Two-dimensional metalâ€“organic frameworks as efficient electrocatalysts for bifunctional oxygen evolution/reduction reactions. Journal of Materials Chemistry A, 2022, 10, 13005-13012.	5.2	21

#	Article	IF	Citations
68733	Computational discovery of spin-polarized semimetals in spinel materials. Materials Advances, 0, , .	2.6	0
68734	Silver modified copper foam electrodes for enhanced reduction of CO₂ to C₂₊ products. Materials Advances, 2022, 3, 4964-4972.	2.6	11
68735	Compression-induced crimping of boron nanotubes from borophenes: a DFT study. Physical Chemistry Chemical Physics, 2022, 24, 14566-14572.	1.3	2
68736	Tuning the metal-insulator transition and magnetic properties of (SrVO₃)₅/(SrTiO₃)₁ (111) heterostructures. Wuli Xuebao/Acta Physica Sinica, 2022, .	0.2	0
68737	Electronic structures of hydroxylated low index surfaces of rutile and anatase-type titanium dioxide. Physical Chemistry Chemical Physics, 2022, 24, 15091-15102.	1.3	9
68738	First-principles study on structural, electronic, magnetic and thermodynamic properties of lithium ferrite LiFe₅O₈. RSC Advances, 2022, 12, 15973-15979.	1.7	2
68739	Enhancing the catalytic activity of CdX and ZnX (X = S, Se and Te) nanostructures for the hydrogen evolution reaction via transition metal doping. Materials Advances, 2022, 3, 5772-5777.	2.6	2
68740	Phthalo-carbonitride nanosheets as excellent N₂ reduction reaction electrocatalysts: a first-principles study. Physical Chemistry Chemical Physics, 2022, 24, 14472-14478.	1.3	5
68741	Kinetic square scheme in oxygen-redox battery electrodes. Energy and Environmental Science, 2022, 15, 2591-2600.	15.6	21
68742	Bilayer-favored intercalation induced efficient and selective liquid phase production of bilayer graphene. Journal of Materials Chemistry A, 2022, 10, 14381-14391.	5.2	2
68743	Insight into the inclusion of heteroatom impurities in Silicon structures. Physical Chemistry Chemical Physics, 0, , .	1.3	0
68744	Effect of strain on the formation of Guinierâ€"Preston zone in Alâ€"Cu alloys from first-principles. Materials Express, 2022, 12, 369-372.	0.2	0
68745	Exchange Correlation Effects in Modulated Martensitic Structures of the Mn2NiGa Alloy. Physics of Metals and Metallography, 2022, 123, 375-380.	0.3	3
68746	Role of hydrogen in stability and mobility of vacancy clusters in tungsten. Tungsten, 2022, 4, 219-230.	2.0	7
68747	Influence of Th, Zr, and Ti Dopants on Solution Property of Xe in Uranium Dioxide with Defects: A DFT + U Study. Metals, 2022, 12, 879.	1.0	3
68748	ÐÐ ÑÐ¾Ñ€Ð±Ñ†Ð¸Ð•Ð¿ÐµÑ€Ð¾Ð´Ð°Ñ Ð²Ð¾Ð´Ð¾Ñ€Ð¾Ð´Ð° Ð½Ð° Ð²Ñƒ Ð¼Ñ€Ð½Ñ‹Ñ… Ñ…Ð»ÐŒÐºÐ¾Ð¾ÐµÐ½		
68749	Electronic and vibrational properties of bulk <mml:math xmlns:mml="http://www.w3.org/1998/Math/MathML"><mml:mrow><mml:msub><mml:mi>Cr</mml:mi><mml:mn>2</mml:mn></mml:m from first-principles calculations. Physical Review B, 2022, 105, .	1.1	0
68750	Phonon Symphony of Stacked Multilayers and Weak Bonds Lowers Lattice Thermal Conductivity. Advanced Materials, 2022, 34, .	11.1	6

#	Article	IF	Citations
68751	Heatâ€Triggered Ferriâ€toâ€Paramagnetic Transition Accelerates Redox Coupleâ€Mediated Electrocatalytic Water Oxidation. Advanced Functional Materials, 2022, 32, .	7.8	8
68752	Resolving the Role of Configurational Entropy in Improving Cycling Performance of Multicomponent Hexacyanoferrate Cathodes for Sodiumâ€Ion Batteries. Advanced Functional Materials, 2022, 32, .	7.8	37
68753	Manipulating interfacial atomic structure of Pt/Ce1â^'xYxO2â^'Î´ to improve charge transfer capacity and catalytic activity in aerobic oxidation of HMF. Applied Surface Science, 2022, 598, 153769.	3.1	5
68754	The ultra-low lattice thermal conductivity dominated by the quartic anharmonicity in Bi-based binary compounds A₃Bi (AÂ=ÂK, Rb). Europhysics Letters, 2022, 138, 56001.	0.7	3
68755	Surface Structures and Their Relative Stabilities of Orthorhombic YAlO3: A First-Principles Study. Acta Metallurgica Sinica (English Letters), 0, , .	1.5	0
68756	Multifunctional two-dimensional van der Waals Janus magnet Cr-based dichalcogenide halides. Npj Computational Materials, 2022, 8, .	3.5	17
68757	Effective decoupling of ferromagnetic sublattices by frustration in Heusler alloys. Physical Review B, 2022, 105, .	1.1	9
68758	Insights into the Adsorption, Alloy Formation, and Poisoning Effects of Hg on Monometallic and Bimetallic Adsorbents. Langmuir, 0, , .	1.6	2
68759	High-pressure behavior of tetragonal barium carbodiimide, BaNCN. Journal of Alloys and Compounds, 2022, 918, 165632.	2.8	3
68760	Photoluminescence Properties and Energy Transfers in the Novel LiYMgWO₆: Dy³⁺, Tm³⁺. , 2022, 1, 025001.		3
68761	Deep potential development of transition-metal-rich carbides. MRS Advances, 0, , .	0.5	0
68762	Rational Design of Endohedral Superhalogens without Using Metal Cations and Electron Counting Rules. Journal of Physical Chemistry A, 0, , .	1.1	3
68763	Layer-independent ferromagnetic insulators in a new structural phase of <mml:math xmlns:mml="http://www.w3.org/1998/Math/MathML"><mml:mrow><mml:msub><mml:mi>Cr</mml:mi><mml:mn>2</mml:mn></mml:r mathvariant="normal">S</mml:mi><mml:mn>3</mml:mn></mml:msub></mml:mrow></mml:math>. Physical Review Materials, 2022, 6, .	0.9	3
68764	A global design principle for polysulfide electrocatalysis in lithiumâ€“sulfur batteriesâ€”A computational perspective. , 2022, 1, .		13
68765	Theoretical Study on Electronic, Magnetic and Optical Properties of Non-Metal Atoms Adsorbed onto Germanium Carbide. Nanomaterials, 2022, 12, 1712.	1.9	19
68766	Fast Intercalation of Lithium in Semiâ€Metallic Î³â€GeSe Nanosheet: A New Groupâ€IV Monochalcogenide for Lithiumâ€Ion Battery Application. ChemSusChem, 2022, 15, .	3.6	13
68767	Pressure-induced electronic transitions in samarium monochalcogenides. Physical Review B, 2022, 105, .	1.1	2
68768	Theoretical Investigation of Effects of Transition Elements on Phase Stabilities and Elastic Properties of the Î³â€² Phase in Coâ€“Vâ€“Ta Superalloys. Frontiers in Materials, 2022, 9, .	1.2	0

#	Article	IF	Citations
68769	Trends in Surface Oxygen Formation Energy in Perovskite Oxides. ACS Omega, 2022, 7, 18427-18433.	1.6	2
68770	A strategy to address the challenge of electrochemical CO2 and N2 coupling to synthesis urea on two-dimensional metal borides (MBenes) by computational screening. Materials Today Physics, 2022, 26, 100726.	2.9	15
68771	Vibrational Entropy Contribution to Mixing Free Energy of Ni-Rich LiNi1-yCoyO2. Journal of the Electrochemical Society, 0, , .	1.3	0
68772	Complex spin Hamiltonian represented by an artificial neural network. Physical Review B, 2022, 105, .	1.1	8
68773	Onâ€purpose Ethylene Production via CO₂â€assisted Ethane Oxidative Dehydrogenation: Selectivity Control of Iron Oxide Catalysts. ChemCatChem, 2022, 14, .	1.8	6
68774	Trimethoxyboroxine as an electrolyte additive to enhance the 4.5Ââ€‹V cycling performance of a Ni-rich layered oxide cathode. EScience, 2022, 2, 486-493.	25.0	21
68775	Exceptionally high work density of a ferroelectric dynamic organic crystal around room temperature. Nature Communications, 2022, 13, .	5.8	15
68776	Helical spin ordering in room-temperature metallic antiferromagnet Fe3Ga4. Journal of Alloys and Compounds, 2022, 917, 165532.	2.8	2
68777	Theoretical Studies on the Role of Guest in Î±-CL-20/Guest Crystals. Molecules, 2022, 27, 3266.	1.7	1
68778	Electricâ€Fieldâ€Tunable Bandgaps in the Inverseâ€Designed Nanoporous Graphene/Graphene Heterobilayers. Advanced Electronic Materials, 2022, 8, .	2.6	3
68779	Optoelectronic and mechanical properties of the orthogonal and tetragonal Cu2CdGe(SxSe1â^'x)4 semiconducting system via first principles methods. Journal of Applied Physics, 2022, 131, .	1.1	7
68780	Extrinsic Localized Excitons in Patterned 2D Semiconductors. Advanced Functional Materials, 0, , 2203060.	7.8	8
68781	Interlayer Engineering of Band Gap and Hole Mobility in p-Type Oxide SnO. ACS Applied Materials & Interfaces, 2022, 14, 25670-25679.	4.0	8
68782	Magnetic Anisotropy and Jahnâ€“Teller Effect in Ferromagnetic Two-Dimensional CrGa₂Te₄. ACS Applied Electronic Materials, 2022, 4, 3220-3225.	2.0	2
68783	Coexisting charge density wave and ferromagnetic instabilities in monolayer InSe. Npj Computational Materials, 2022, 8, .	3.5	18
68784	Effect of urea on arrangement of novel Mg(II) perrhenate crystal structures and their optical properties: Experimental and theoretical insight. Journal of Solid State Chemistry, 2022, 312, 123263.	1.4	2
68785	Effect of Mg(II), Mn(II), and Fe(II) doping on the mechanical properties and electronic structure of calcite. Materials Today Communications, 2022, , 103725.	0.9	2
68786	Mechanistic Insight into the Photo-Oxidation of Perfluorocarboxylic Acid over Boron Nitride. Environmental Science & Technology, 2022, 56, 8942-8952.	4.6	13

#	Article	IF	Citations
68787	New Reactive Force Field for Simulations of MoS₂ Crystallization. Journal of Physical Chemistry C, 2022, 126, 9475-9481.	1.5	9
68788	How Do A-Site Cations Regulate Trap States at Defective Surfaces of Lead Iodide Perovskites?. Journal of Physical Chemistry Letters, 2022, 13, 4831-4839.	2.1	7
68789	Optimal alloying in hydrides: Reaching room-temperature superconductivity in <mml:math xmlns:mml="http://www.w3.org/1998/Math/MathML"><mml:msub><mml:mi>LaH</mml:mi><mml:mn>10</mml:mn></mml:msub></mml:math> Physical Review B, 2022, 105, .	1.1	8
68790	In-Situ and controllable construction of Mo2N embedded Mo2C nanobelts as robust electrocatalyst for superior pH-universal hydrogen evolution reaction. Journal of Alloys and Compounds, 2022, 918, 165611.	2.8	11
68791	A Nonstoichiometric Niobium Oxide/Graphite Composite for Fastâ€Charge Lithiumâ€Ion Batteries. Small, 2022, 18, .	5.2	13
68792	Bipolar Magnetic Molecules for Spinâ€Polarized Electric Current in Molecular Junctions. Angewandte Chemie - International Edition, 2022, 61, .	7.2	9
68793	Effect of off-stoichiometric composition on half-metallic character of Co₂Fe(Ga,Ge) investigated using saturation magnetization and giant magnetoresistance effect. Journal Physics D: Applied Physics, 2022, 55, 345003.	1.3	1
68794	Tunable electronic and magnetic properties of Cr₂Ge₂Te₆ monolayer by organic molecular adsorption. Nanotechnology, 2022, 33, 345705.	1.3	8
68795	Critical role of magnetic moments in heavy-fermion materials: Revisiting <mml:math xmlns:mml="http://www.w3.org/1998/Math/MathML"><mml:msub><mml:mrow><mml:mi>SmB</mml:mi></mml:mrow><mml:mn>6</mml:mn></mml:msub></mml:math> Physical Review B, 2022, 105, .	1.1	6
68796	High-Throughput Computational Exploration of MOFs with Open Cu Sites for Adsorptive Separation of Hydrogen Isotopes. ACS Applied Materials & Interfaces, 2022, 14, 24980-24991.	4.0	10
68797	Transport and optical properties of the chiral semiconductor Ag ₃ AuSe ₂. Zeitschrift Fur Anorganische Und Allgemeine Chemie, 0, , .	0.6	0
68798	Theory of liquid-mediated strain release in two-dimensional materials. Physical Review Materials, 2022, 6, .	0.9	1
68799	Interstitial proton transport through defective MXenes. Applied Physics Letters, 2022, 120, 211601.	1.5	1
68800	Ba₂MAsQ₅ (Q = S and Se) Family of Polar Structures with Large Second Harmonic Generation and Phase Matchability. Chemistry of Materials, 2022, 34, 5283-5293.	3.2	7
68801	Diamond (111) surface reconstruction and epitaxial graphene interface. Physical Review B, 2022, 105, .	1.1	3
68802	First-principles investigations to evaluate Mo₂B monolayers as promising two-dimensional anode materials for Mg-ion batteries. JPhys Energy, 2022, 4, 035002.	2.3	3
68803	Insights into controllable electronic properties of 2D type-II Twin-Graphene/g-C3N4 and type-I Twin-Graphene/hBN vertical heterojunctions via external electric field and strain engineering. Physics Letters, Section A: General, Atomic and Solid State Physics, 2022, 443, 128216.	0.9	0
68804	Configuration stability and electronic properties of diamane with boron and nitrogen dopants. Physical Review B, 2022, 105, .	1.1	4

#	Article	IF	Citations
68805	Direct Synthesis and Delamination of Swollen Layered Ferrierite for the Reductive Etherification of Furfural. ChemCatChem, 2022, 14, .	1.8	3
68806	Construction of the Largest Metal-Centered Double-Ring Tubular Boron Clusters Based on Actinide Metal Doping. Journal of Physical Chemistry A, 0, , .	1.1	3
68807	Facile Microwave Synthesis of a Narrow-Band Green-Emitting Phosphor Cs₃MnBr₅ and the Effect of Anion Substitution on Its Luminescence Properties. Inorganic Chemistry, 2022, 61, 8782-8787.	1.9	8
68808	Strain-promoted conductive metal-benzenhexathiolate frameworks for overall water splitting. Journal of Colloid and Interface Science, 2022, 624, 160-167.	5.0	10
68809	Crystallographic dependence of CO2 hydrogenation pathways over HCP-Co and FCC-Co catalysts. Applied Catalysis B: Environmental, 2022, 315, 121529.	10.8	24
68810	Bipolar Magnetic Molecules for Spinâ€Polarized Electric Current in Molecular Junctions. Angewandte Chemie, 2022, 134, .	1.6	2
68811	Bi₃TeBO₉: A Promising Mid-Infrared Nonlinear Optical Crystal with a Large Laser Damage Threshold. Inorganic Chemistry, 2022, 61, 8870-8878.	1.9	4
68812	Surface Resonant Raman Scattering from Cu(110). Physical Review Letters, 2022, 128, .	2.9	1
68813	Toward Recyclable Polymers: Ring-Opening Polymerization Enthalpy from First-Principles. Journal of Physical Chemistry Letters, 2022, 13, 4778-4785.	2.1	12
68814	Tailored design of well-defined hierarchical nitrogen-doped carbon via salt-confined strategy for selective Cd(â…¡) adsorption. Chemical Engineering Journal, 2022, 446, 137222.	6.6	2
68815	Unconventional Highly Active and Stable Oxygen Reduction Catalysts Informed by Computational Design Strategies. Advanced Energy Materials, 2022, 12, .	10.2	4
68816	Solidlike to liquidlike behavior of Cu diffusion in superionic <mml:math xmlns:mml="http://www.w3.org/1998/Math/MathML"><mml:mrow><mml:msub><mml:mi>Cu</mml:mi><mml:mn>2</mml:mn></mml:mathvariant="normal">X</mml:mi></mml:mrow></mml:math> <mml:math xmlns:mml="http://www.w3.org/1998/Math/MathML"><mml:mrow><mml:mo>(</mml:mo><mml:mi>X</mml:mi><mml:mo>=</mml:mo>: A. Physical Review Materials, 2022, 6, .	0.9	7
68817	Displacement of hydrogen position in di-hydride of V-Ti-Cr solid solution alloys. Acta Materialia, 2022, 234, 118055.	3.8	11
68818	Reconstructing the coordination environment of single atomic Fe-catalysts for boosting the Fenton-like degradation activities. Applied Catalysis B: Environmental, 2022, 315, 121536.	10.8	39
68819	Machine learning sparse tight-binding parameters for defects. Npj Computational Materials, 2022, 8, .	3.5	6
68820	H₂ Activation on Pristine and Substitutional ZnO(101Ì…0) and Cr₂O₃(001) Surfaces by Density Functional Theory Calculations. Journal of Physical Chemistry C, 2022, 126, 9059-9068.	1.5	13
68821	Synergistic introduction of oxygen vacancy and silver/silver iodide: Realizing deep structure regulation on bismuth oxybromide for robust carbon dioxide reduction and pollutant oxidation. Journal of Colloid and Interface Science, 2022, 624, 181-195.	5.0	5
68822	A Class of Magnetic Topological Material Candidates with Hypervalent Bi Chains. Journal of the American Chemical Society, 2022, 144, 9785-9796.	6.6	9

#	Article	IF	Citations
68823	Multifunctional surface modification with Co-free spinel structure on Ni-rich cathode material for improved electrochemical performance. Journal of Alloys and Compounds, 2022, 918, 165454.	2.8	6
68824	Surface Chemistry of the Molecular Solar Thermal Energy Storage System 2,3â€Dicyanoâ€Norbornadiene/Quadricyclane on Ni(111). ChemPhysChem, 2022, 23, .	1.0	7
68825	Glucose electrooxidation modelling studies on carbon nanotube supported Pd catalyst with response surface methodology and density functional theory. Journal of Physics and Chemistry of Solids, 2022, 168, 110810.	1.9	6
68826	Cl-induced passivity breakdown in Î±-Fe2O3 (0001), Î±-Cr2O3 (0001), and their interface: A DFT study. Journal of Materials Science and Technology, 2022, 129, 70-78.	5.6	13
68827	Volumes and spin states of FeHx: Implication for the density and temperature of the Earthâ€™s core. American Mineralogist, 2023, 108, 667-674.	0.9	2
68829	The effect of Zr doping on the structural property and helium behavior of Ti3SiC2 by first-principles study. Materials Today Communications, 2022, 31, 103701.	0.9	1
68830	Insight into the stacking fault energy, dislocation, and thermodynamic properties of L12-Al3X(X Sc, Ti,) Tj ETQq0 0 0 rgBT /Overlock 10 T	0.9	1
68831	Modeling the thermodynamics of the FeTi hydrogenation under para-equilibrium: An ab-initio and experimental study. Calphad: Computer Coupling of Phase Diagrams and Thermochemistry, 2022, 77, 102426.	0.7	3
68832	Surface defects engineered Bi4Ti3O12 nanosheets for photocatalytic degradation of antibiotic levofloxacin. Applied Catalysis A: General, 2022, 640, 118675.	2.2	11
68833	Possibility of N-type Doping in CaAl₂Si₂-type Zintl Phase Compound CaZn₂X₂ (X = As, P). Journal of the Physical Society of Japan, 2022, 91, .	0.7	2
68834	Chemical Pressure Effect on Structural and Physical Properties of 15R-SrVO_{2.2}N_{0.6} with Anion-Vacancy Order. Journal of the Physical Society of Japan, 2022, 91, .	0.7	0
68835	Computational screening of O-functional MXenes for electrocatalytic ammonia synthesis. Chinese Journal of Catalysis, 2022, 43, 1860-1869.	6.9	9
68836	Highly dispersed nickel species on iron-based perovskite for CO2 electrolysis in solid oxide electrolysis cell. Chinese Journal of Catalysis, 2022, 43, 1710-1718.	6.9	10
68837	Metal organic framework-ionic liquid hybrid catalysts for the selective electrochemical reduction of CO2 to CH4. Chinese Journal of Catalysis, 2022, 43, 1687-1696.	6.9	14
68838	Ammonium cobalt phosphate with asymmetric coordination sites for enhanced electrocatalytic water oxidation. Chinese Journal of Catalysis, 2022, 43, 1955-1962.	6.9	7
68839	Diffusion of krypton and xenon in uranium mononitride; a Density Functional Theory Study. Journal of Nuclear Materials, 2022, 566, 153803.	1.3	2
68840	Understanding the unusual-caged dynamics from the microstructure and interatomic interactions in binary metallic glass-forming liquids. Journal of Non-Crystalline Solids, 2022, 590, 121699.	1.5	7
68841	<mml:math xmlns:mml="http://www.w3.org/1998/Math/MathML" display="inline" id="d1e3544" altimg="si14.svg"><mml:mrow><mml:mi>A</mml:mi><mml:mi>b</mml:mi></mml:mrow></mml:math> <mml:math xmlns:mml="http://www.w3.org/1998/Math/MathML" display="inline" id="d1e3552" altimg="si15.svg"><mml:mrow><mml:mi>i</mml:mi><mml:mi>n</mml:mi><mml:mi>i</mml:mi><mml:mi>t</mml:mi><mml:mi>i</mml:mi> morphology prediction of Zr hydride precipitates using atomistically informed Eshelbyâ€™s ell. Computational Materials Science, 2022, 211, 111500.	1.4	11

#	Article	IF	Citations
68842	Crystal structure prediction with machine learning-based element substitution. Computational Materials Science, 2022, 211, 111496.	1.4	13
68843	Diffusion in A15 Nb3Sn: An atomistic study. Acta Materialia, 2022, 234, 118050.	3.8	7
68844	Spin-related bimetallic-hybridization induced by asymmetric super-nearest exchange interaction in single-atom dimer for hydrogen evolution reaction. Materials Chemistry and Physics, 2022, 287, 126291.	2.0	3
68845	Coordination Li diffusion chemistry in NASICON Li1.5Al0.5Ge1.5(PO4)3 solid electrolyte. Solid State Ionics, 2022, 381, 115947.	1.3	3
68846	The effects of solutes on precipitated phase/matrix interface stability and their distribution tendencies between the two phases in Co-based superalloys. Computational Materials Science, 2022, 211, 111547.	1.4	3
68847	Insights into the function of semi-metallic 1Tâ€™ phase ReS2 as cocatalyst decorated g-C3N4 nanotubes for enhanced photocatalytic hydrogen production activity. Materials Today Advances, 2022, 15, 100257.	2.5	9
68848	Monte-Carlo modeling of phonon thermal transport using DFT-based anisotropic dispersion relations over the full Brillouin zone. Computational Materials Science, 2022, 211, 111528.	1.4	2
68849	Construction of a 3D/2D plasmonic Z-scheme heterojunction with electrostatic self-assembly for full-spectrum solar-light driven photocatalytic protons reduction. Materials Today Advances, 2022, 15, 100249.	2.5	3
68850	Chlorine in NiO promotes electroreduction of CO2 to formate. Applied Materials Today, 2022, 28, 101528.	2.3	4
68851	Structural, elastic, dynamical and thermophysical characteristics of rare-earth dihydrides XH2 (X =) Tj ETQq1 1 0.784314 rgBT /Overlo	1.6	4
68852	Synthesis, characterization, and electronic structure of SrBi2S4. Journal of Solid State Chemistry, 2022, 312, 123250.	1.4	1
68853	Density functional theory study of N2 adsorption and dissociation on 3d transition metal atoms doped Ir(1 0 0) surface. Applied Surface Science, 2022, 597, 153678.	3.1	7
68854	Atomically dispersed non-noble Cu dimer anchored on a novel graphitic carbon nitride as a promising catalyst for the conversion of CO to CH2CH2. Applied Surface Science, 2022, 597, 153761.	3.1	3
68855	How arsenic makes amorphous GeSe a robust chalcogenide glass for advanced memory integration. Scripta Materialia, 2022, 218, 114834.	2.6	17
68856	In-situ growth of MoO2@N doped carbon on Mo2C-MXene for superior lithium storage. Applied Surface Science, 2022, 597, 153688.	3.1	31
68857	Catalytic elemental sulfur-assisted methane activation at low temperature. Applied Catalysis B: Environmental, 2022, 315, 121518.	10.8	7
68858	Two-dimensional semiconducting Ag2X (XÂ=ÂS, Se) with Janus-induced built-in electric fields and moderate band edges for overall water splitting. Applied Surface Science, 2022, 597, 153707.	3.1	9
68859	Revisit the VEC criterion in high entropy alloys (HEAs) with high-throughput ab initio calculations: A case study with Al-Co-Cr-Fe-Ni system. Journal of Alloys and Compounds, 2022, 916, 165477.	2.8	14

#	Article	IF	Citations
68860	Atomic-scale unveiling of strengthening in interstitial solid soluted Nb-rich TiAl alloys. Journal of Alloys and Compounds, 2022, 917, 165484.	2.8	8
68861	LiXO2(XÂ=ÂCo, Rh, Ir) and solar light photocatalytic water splitting for hydrogen generation. Spectrochimica Acta - Part A: Molecular and Biomolecular Spectroscopy, 2022, 279, 121410.	2.0	1
68863	Molecular dynamics simulations of proton conducting media containing phosphoric acid. Physical Chemistry Chemical Physics, 2022, 24, 15522-15531.	1.3	7
68864	Unusual Ordering Behavior of Co3al-Based Î“â€² Phase with L12 Structure Predicted by the Thermodynamic Model with Support of First-Principles Calculations. SSRN Electronic Journal, 0, , .	0.4	0
68865	Metal Monovacancy-Induced Spin Polarization for Simultaneous Energy Recovery and Wastewater Purification. SSRN Electronic Journal, 0, , .	0.4	0
68866	Cation-Assisted Lithium Ion Diffusion in a Lithium Oxythioborate Halide Glass Solid Electrolyte. SSRN Electronic Journal, 0, , .	0.4	0
68867	Unravelling the Co2 Methanation Mechanisms on a Ni-Batio3 Catalyst: A Theoretical Investigation. SSRN Electronic Journal, 0, , .	0.4	0
68868	Sulfur-Dopant-Promoted Electrocatalytic Reduction of Nitrate by a Self-Supported Iron Cathode: Selectivity, Stability, and Underlying Mechanism. SSRN Electronic Journal, 0, , .	0.4	0
68869	Ultra-High Capacity of Li1.6-Xmn0.4tixo2 as a Cathode Material. SSRN Electronic Journal, 0, , .	0.4	0
68870	Complex Segregation and Fracture Mechanisms at Interfaces in Liquid Metal Embrittlement and Corrosion. SSRN Electronic Journal, 0, , .	0.4	1
68871	Understanding the effect of lattice polarisability on the electrochemical properties of lithium tetrahaloaluminates, LiAlX₄ (X = Cl, Br, I). Journal of Materials Chemistry A, 0, , .	5.2	3
68872	Modeling Ni Redistribution in the Fuel Electrode of Solid Oxide Cells Through Ni(Oh)2 Diffusion and Ni-Ysz Wettability Change. SSRN Electronic Journal, 0, , .	0.4	0
68873	Study of diffusion and conduction in lithium garnet oxides Li_xLa₃Zr_{xâ^'5}Ta_{7â^'x}O₁₂ by machine learning interatomic potentials. Physical Chemistry Chemical Physics, 2022, 24, 15025-15033.	1.3	7
68874	A two-dimensional Î±-As/Î±-AsP van der Waals heterostructure for photovoltaic applications. Physical Chemistry Chemical Physics, 2022, 24, 16058-16064.	1.3	3
68875	Predicting Mechanical Properties of High Entropy Alloys with Face Centered Cubic Structure from First Principles Calculations. SSRN Electronic Journal, 0, , .	0.4	0
68876	Bimetallic Mmos4 (M = Ni, Co, Cu) Cocatalysts Architected CDS Nanoflowers for Synergistically Boosting Visible-Light-Driven Photocatalytic H2 Evolution from Water and Benzyl Alcohol. SSRN Electronic Journal, 0, , .	0.4	0
68877	Cuncn Derived Cu-Based/Cxny Catalysts for Highly Selective Co2 Electroreduction to Hydrocarbons. SSRN Electronic Journal, 0, , .	0.4	0
68878	High Performance Carbon Dioxide Electroreduction in Ionic Liquids with in Situ Shell-Isolated Nanoparticle-Enhanced Raman Spectroscopy. SSRN Electronic Journal, 0, , .	0.4	0

#	Article	IF	Citations
68879	Chemical Templates That Assemble the Metal Superhydrides. SSRN Electronic Journal, 0, , .	0.4	1
68880	Chemical Interaction, Self-Ordering and Corrosion Inhibition Properties of 2-Mercaptobenzothiazole Monolayers: Dft Atomistic Modelling on Metallic Copper. SSRN Electronic Journal, 0, , .	0.4	0
68881	Off-stoichiometry in Iâ€“IIIâ€“VI₂ chalcopyrite absorbers: a comparative analysis of structures and stabilities. Faraday Discussions, 0, 239, 357-374.	1.6	2
68882	Structural dimension modulation in a new oxysulfide system of Ae₂Sb₂O₂S₃ (Ae = Ca and Ba). Inorganic Chemistry Frontiers, 2022, 9, 3552-3558.	3.0	4
68883	Thermodynamic Modeling of the Pd-Zn System with Uncertainty Quantification and its Implication to Tailor Catalysts. SSRN Electronic Journal, 0, , .	0.4	0
68884	Fast Identification, and Construction of Adsorbate-Adsorbent Geometries for High Throughput Computational Applications: The Automatic Surface Adsorbate Structure Provider (Asap) Algorithm. SSRN Electronic Journal, 0, , .	0.4	0
68885	Two-dimensional heterotriangulene-based manganese organic frameworks: bipolar magnetic and half semiconductors with perpendicular magnetocrystalline anisotropy. Nanoscale, 2022, 14, 8865-8874.	2.8	4
68886	Efficient Co-Production of Hydrogen and Value-Added Formate Over Bifunctional Nicomo Alloy Electrocatalyst with Nanosheet/Nanotube Architecture and Versatile Mo Modulation. SSRN Electronic Journal, 0, , .	0.4	0
68887	Formic Acid Dehydrogenation Over Pd Single Atom or Cluster Supported on Nitrogen-Doped Graphene: A Dft Study. SSRN Electronic Journal, 0, , .	0.4	0
68888	Data-Driven Design of a High-Performance, Two-Dimensional Graphene-Based Seawater Desalination Membrane. SSRN Electronic Journal, 0, , .	0.4	0
68889	General Strategy for Enhanced Ch4 Selectivity in Photocatalytic Co2 Reduction Reactions by Surface Oxophilicity Engineering. SSRN Electronic Journal, 0, , .	0.4	0
68890	Adsorption of NO, NO₂ and H₂O in divalent cation faujasite type zeolites: a density functional theory screening approach. Physical Chemistry Chemical Physics, 2022, 24, 15565-15578.	1.3	6
68891	Hydrogen Atoms in Tungsten Nitride Compounds Promoting the Formation of Atomic Vacancies in Nuclear Fusion Reactors. SSRN Electronic Journal, 0, , .	0.4	0
68892	Experimental and theoretical investigation on the ORR activity of AgVO₃. Materials Chemistry Frontiers, 2022, 6, 2042-2050.	3.2	2
68893	Pressure-Driven Ferroelectric Phase Transition for the Pnma-Cspbbr3: Mechanical and Dynamical Stability Study. SSRN Electronic Journal, 0, , .	0.4	0
68894	High-Pressure Stability and Superconductivity of Vanadium Hydrides. SSRN Electronic Journal, 0, , .	0.4	0
68895	Effect of Solution Soaking on the Electrochemical Properties of Li6.5la3zr1.5ta0.5o12/Polyethylene Oxide Composite Electrolyte. SSRN Electronic Journal, 0, , .	0.4	0
68896	High-performance potassium poly(heptazine imide) films for photoelectrochemical water splitting. Chemical Science, 2022, 13, 7541-7551.	3.7	24

#	Article	IF	Citations
68897	Five coordinated Mn in Ba₄Mn₂Si₂Te₉: synthesis, crystal structure, physical properties, and electronic structure. Dalton Transactions, 2022, 51, 9265-9277.	1.6	4
68898	Inserted Effects of MXene on Switching Mechanisms and Characteristics of SiO₂-Based Memristor: Experimental and First-Principles Investigations. IEEE Transactions on Electron Devices, 2022, 69, 3688-3693.	1.6	3
68899	Ultrathin Znti-Ldh Nanosheet: A Bifunctional Lewis and Bronsted Acid Photocatalyst for Synthesis of N-Benzylideneanilline Via a Tandem Reaction. SSRN Electronic Journal, 0, , .	0.4	0
68900	Synergetic catalysis of pâ€“d hybridized single-atom catalysts: first-principles investigations. Journal of Materials Chemistry A, 2022, 10, 13066-13073.	5.2	3
68901	Temperature-Dependant Active Sites for Methane Continuous Conversion to Methanol Over Cu-Zeolite Catalysts Using Water as the Oxidant. SSRN Electronic Journal, 0, , .	0.4	1
68902	Boosting Elementary Steps Kinetics Towards Energetic Alkaline Hydrogen Evolution Via Dual Sites on Phase-Separated Niâ€“Cuâ€“Mn/Hydroxide. SSRN Electronic Journal, 0, , .	0.4	0
68903	Insights into the Removal Paths of Adsorbed Oxygen in the Synthesis of Light Olefins from Syngas on Îş-Fe5c2(510) Surface. SSRN Electronic Journal, 0, , .	0.4	0
68904	Layered Zn-Based Semiconductors K2zn3s4 and Rb2zn3se4: Crystal Growth, Structure and Potential P-Type Transparent Conductivity. SSRN Electronic Journal, 0, , .	0.4	0
68905	Construction of Cos-Encapsulated in Ultrahigh Nitrogen Doped Carbon Nanofibers from Energetic Metal-Organic Frameworks for Superior Sodium Storage. SSRN Electronic Journal, 0, , .	0.4	0
68906	First-Principles Study of the Behaviors of He Atoms at Tic(110)/V(110) Interface. SSRN Electronic Journal, 0, , .	0.4	0
68907	Quantum theory of electronic excitation and sputtering by transmission electron microscopy. Nanoscale, 2023, 15, 1053-1067.	2.8	5
68908	Construction of multidimensional CdS@MoS2 heterojunction for enhancing the activity and transfer efficiency of photogenerated carriers. New Journal of Chemistry, 0, , .	1.4	0
68909	First-principles design of hetero CoM (M = 3d, 4d, 5d block metals) double-atom catalysts for oxygen evolution reaction under alkaline conditions. Nanoscale Advances, 2022, 4, 2913-2921.	2.2	3
68910	Unraveling the Adhesive Properties, Thermal Stability, and Initial Diffusion Mechanisms of Al/Nio Nanothermites with Various Dominant Surfaces: A First-Principles Study. SSRN Electronic Journal, 0, , .	0.4	0
68911	Revisiting the Origin of Orr and Her Activities of N-Doped Î“-Graphdiyne from the Perspective of Edge Effects. SSRN Electronic Journal, 0, , .	0.4	0
68912	NVIDIAâ€™s Quantum InfiniBand Network Congestion Control Technology andÂIts Impact onÂApplication Performance. Lecture Notes in Computer Science, 2022, , 26-43.	1.0	0
68913	Dual Functional Effect of Oxygen Vacancies and Depolarity Shield Embedded Nico2o4 Cathode in Lithium Sulfur Battery. SSRN Electronic Journal, 0, , .	0.4	0
68914	Maximizing the Energy Density and Stability of Ni-Rich Layered Cathode Materials with Multivalent Dopants Via Machine Learning. SSRN Electronic Journal, 0, , .	0.4	0

#	Article	IF	Citations
68915	A Van Der Waals Cacl Semiconducting Electrene and Ferromagnetic Half-Metallicity Induced by Superhalogen Decoration. SSRN Electronic Journal, 0, , .	0.4	0
68916	Multi-interfacial engineering of a coil-like NiSâ€“Ni₂P/Ni hybrid to efficiently boost electrocatalytic hydrogen generation in alkaline and neutral electrolyte. Journal of Materials Chemistry A, 2022, 10, 13410-13417.	5.2	16
68917	Insights into Cation-Disorder Effect on Stability, Electronic Structure and Defect Properties of Zn-Iv-Nitrides: The Case of Zngen2. SSRN Electronic Journal, 0, , .	0.4	0
68918	Hydrogen Dissociation in Li-Decorated 2d Boron Hydride AndÂBorophene: An Ab-Initio Study. SSRN Electronic Journal, 0, , .	0.4	0
68919	Role of Copper in the Formation of Carbon during Direct Synthesis of Methylchlorosilanes. SSRN Electronic Journal, 0, , .	0.4	3
68920	The Strengthening Effects of Re-X (X=Mo, W, Cr Ta, Re) Mediated by Their Local Partitioning Behaviors at Î“/Î“' Interface InÂNi-Based Single Crystal Superalloys. SSRN Electronic Journal, 0, , .	0.4	0
68921	Deep Dive into Lattice Dynamics and Phonon Anharmonicity for Intrinsically Low Thermal Expansion Coefficient in Cus. SSRN Electronic Journal, 0, , .	0.4	0
68922	Surface Functionalization of Two-Dimensional Boridene Family: Enhanced Stability, Tunable Electronic Property, and High Catalytic Activity. SSRN Electronic Journal, 0, , .	0.4	0
68923	Electronic structure of oxide and halide perovskites. , 2022, , .		0
68924	A family of superconducting boron crystals made of stacked bilayer borophenes. Nanoscale, 2022, 14, 9754-9761.	2.8	5
68925	Boosting the Interfacial Hydrogen Migration for Efficient Alkaline Hydrogen Evolution on Pt-Based Nanowires. SSRN Electronic Journal, 0, , .	0.4	0
68926	Oxygen Vacancies in Cu/Tio2 Boost Strong Metalâ€“Support Interaction and Improve the Catalyst's Activity, Selectivity, and Stability in Co2 Hydrogenation to Methanol. SSRN Electronic Journal, 0, , .	0.4	0
68927	Significant reduction in lattice thermal conductivity in a p-type filled skutterudite due to strong electronâ€“phonon interactions. Journal of Materials Chemistry A, 2022, 10, 13484-13491.	5.2	8
68928	First-Principles Investigation of Tib3 ÂUnder High Pressure. SSRN Electronic Journal, 0, , .	0.4	0
68929	Calculation of charge density wave phase diagram by interacting eigenmodes method. Journal of Physics Condensed Matter, 0, , .	0.7	0
68930	Effect of Doping on Rutile TiO ₂ Surface Stability and Crystal Shapes. ChemistryOpen, 2022, 11, .	0.9	2
68931	Modeling Metallic Halide Local Structures in Salt Melts Using a Genetic Algorithm. Journal of Physical Chemistry C, 0, , .	1.5	0
68932	Adsorption of Hydrogen Peroxide on Two-Dimensional Transition Metal Chalcogenides. Journal of Contemporary Physics, 2022, 57, 170-173.	0.1	1

#	Article	IF	Citations
68933	Aqueous phase reforming of xylose using bimetallic <scp> Pt ₃ â€Re _x </scp> / <scp> SiO ₂ </scp> catalysts for <scp> H ₂ </scp> production: Experimental and computational study. International Journal of Energy Research, 0, , .	2.2	0
68934	Evaluate dimensionless figure of merit for thermoelectric materials based on the intrinsic carrier concentration and bipolar effect. Materials Today Communications, 2022, , 103760.	0.9	0
68935	Fixture-free omnidirectional prestretching fabrication and integration of crumpled in-plane micro-supercapacitors. Science Advances, 2022, 8, .	4.7	22
68936	Surface facet dependence of Ru and Ru-based alloy oxidation resistance using ab initio thermodynamics calculation. Surface Science, 2022, 724, 122129.	0.8	1
68937	The behaviors of dislocation loops punched by helium interstitials accumulation under the temperature gradient field in tungsten. Journal of Nuclear Science and Technology, 0, , 1-8.	0.7	0
68938	Kinetic Control of Anion Stoichiometry in Hexagonal BaTiO3. Inorganics, 2022, 10, 73.	1.2	0
68939	Symmetry-enforced nodal cage phonons in <mml:math xmlns:mml="http://www.w3.org/1998/Math/MathML"><mml:mrow><mml:msub><mml:mi>Th</mml:mi><mml:mn>12</mml:mn></mml: Physical Review B, 2022, 105, .	1.1	0
68940	Crystal structure, electronic structure and phase stability of the Cu2-xMxCd (M=Zn, Ga, Ge, Sn) pseudo-binary Laves phases: effect of valence electron concentration. Journal of Solid State Chemistry, 2022, 313, 123283.	1.4	3
68941	Strain-engineered topological phase transitions in ferrovalley <mml:math xmlns:mml="http://www.w3.org/1998/Math/MathML"><mml:mrow><mml:mn>2</mml:mn><mml:mi>H</mml:mi><mml:mtext> monolayer. Physical Review B, 2022, 105, .	1.1	24
68942	Imaging defects in two-dimensional crystals by convergent-beam electron diffraction. Physical Review B, 2022, 105, .	1.1	1
68943	Emergent plasmonic excitations in Mexican-hat and bell-shaped bands of hybridized Dirac electrons in graphene/topological insulator heterostructures. Physical Review B, 2022, 105, .	1.1	0
68944	The corrosion behavior of CVD SiC coatings on SiCf/SiC composites in a simulated molten salt reactors environment. Corrosion Science, 2022, 204, 110411.	3.0	5
68945	Thermal expansion and phonon anharmonicity of cuprite studied by inelastic neutron scattering and ab initio calculations. Physical Review B, 2022, 105, .	1.1	5
68946	First-principles study of the T center in silicon. Physical Review Materials, 2022, 6, .	0.9	12
68947	Experimental and theoretical investigations on fullerene (C₆₀) induced compact CH₃NH₃PbI₃ perovskite thin films. Physica Scripta, 0, , .	1.2	2
68948	Comparative Study of Cold Electron Emission from 2D Ti₃C₂T_X MXene Nanosheets with Respect to Its Precursor Ti₃SiC₂ MAX Phase. ACS Applied Electronic Materials, 2022, 4, 2656-2666.	2.0	32
68949	A theoretical framework for oxygen redox chemistry for sustainable batteries. Nature Sustainability, 2022, 5, 708-716.	11.5	23
68950	Two-Dimensional ZnS/SnS2 Heterojunction as a Direct Z-Scheme Photocatalyst for Overall Water Splitting: A DFT Study. Materials, 2022, 15, 3786.	1.3	5

#	Article	IF	Citations
68951	Emergent Topological Hall Effect from Exchange Coupling in Ferromagnetic Cr₂Te₃/Noncoplanar Antiferromagnetic Cr₂Se₃ Bilayers. ACS Nano, 2022, 16, 8974-8982.	7.3	14
68952	Strain Tunable Electronic Band Structure and Magnetic Anisotropy of CrI₃ Bilayer. ECS Journal of Solid State Science and Technology, 2022, 11, 063008.	0.9	3
68953	Al₄Ir: An Alâ€“Ir Binary-Phase Superstructure of the Ni₂Al₃ Type. Inorganic Chemistry, 2022, 61, 8823-8833.	1.9	0
68954	Electronâ€“Hole Excitation Induced Softening in Boron Carbide-Based Superhard Materials. ACS Applied Materials & Interfaces, 0, , .	4.0	1
68955	Cu-mediated grain boundary engineering in Ndâ€“Ceâ€“Feâ€“B nanostructured permanent magnets. Materials Today Nano, 2022, 19, 100230.	2.3	1
68956	First-principles study on the magnetic and electronic properties of quadruple perovskite CeCu3Co4O12. Chemical Physics Letters, 2022, , 139736.	1.2	0
68957	Understanding the structure of Cu-doped MgAl2O4 for CO2 hydrogenation catalyst precursor using experimental and computational approaches. International Journal of Hydrogen Energy, 2022, 47, 21369-21374.	3.8	2
68958	Physically Informed Machine Learning Prediction of Electronic Density of States. Chemistry of Materials, 2022, 34, 4848-4855.	3.2	23
68959	Optimization and inference of bin widths for histogramming inelastic neutron scattering spectra. Journal of Applied Crystallography, 2022, 55, 533-543.	1.9	0
68960	Fundamental mechanisms of hexagonal boron nitride sensing of dopamine, tryptophan, ascorbic acid, and uric acid by first-principles study. Journal of Molecular Modeling, 2022, 28, .	0.8	6
68961	HfO_x/AlO_y Superlatticeâ€Like Memristive Synapse. Advanced Science, 2022, 9, .	5.6	17
68962	Crystallization of Ge-Rich GeSbTe Alloys: The Riddle Is Solved. ACS Applied Electronic Materials, 2022, 4, 2682-2688.	2.0	11
68963	Melting curve of magnesium up to 460â€‰GPa from ab initio molecular dynamics simulations. Journal of Applied Physics, 2022, 131, .	1.1	2
68964	Single-crystalline transition metal phosphide superconductor WP studied by Raman spectroscopy and first-principles calculations. Physical Review B, 2022, 105, .	1.1	1
68965	Fe[4-(3-Phenylpropyl)Pyridine]2[Fe(CN)5NO]: A 2D Coordination Polymer with Thermally-Induced Spin Transition and Nature of Its Asymmetric Hysteresis Loop. Journal of Inorganic and Organometallic Polymers and Materials, 2022, 32, 3677-3690.	1.9	5
68966	Tailoring Excitonic and Optoelectronic Properties of Transition Metal Dichalcogenide Bilayers. Journal of Physical Chemistry C, 2022, 126, 9173-9184.	1.5	10
68967	Intrinsic defects and the influences on electrical transport properties in quaternary diamond-like compounds: Cd2Cu3In3Te8 as an example. Journal of Materiomics, 2022, 8, 1222-1229.	2.8	4
68968	Visualizing discrete Fermi surfaces and possible nodal-line to Weyl state evolution in ZrSiTe. Npj Quantum Materials, 2022, 7, .	1.8	2

#	Article	IF	Citations
68969	Revisiting Activity Tuning Using Lattice Strain: CO Decomposition in Terrace Ru(0001) and Stepped Ru(1015) Surfaces. Journal of Physical Chemistry C, 0, , .	1.5	1
68970	A comparative investigation of different exchangeâ€correlation functionals oriented prediction of structural, electronic, optical, and transport properties of the novel quaternary <scp>LiTiCoSn</scp>. International Journal of Energy Research, 0, , .	2.2	1
68971	Borates as a new direction in the design of oxide ion conductors. Science China Materials, 2022, 65, 2737-2745.	3.5	8
68972	Predicting Van der Waals Heterostructures by a Combined Machine Learning and Density Functional Theory Approach. ACS Applied Materials & Interfaces, 2022, 14, 25907-25919.	4.0	8
68973	Strain-Driven Bimetallic-Interface Orbital Hybridization for Hydrogen Evolution Reaction. ACS Omega, 0, , .	1.6	2
68974	Near-infrared-driven photoelectrocatalytic oxidation of urea on La-Ni-based perovskites. Chemical Engineering Journal, 2022, 446, 137240.	6.6	13
68975	First-principles Calculations of Magnetic Anisotropy of Fe and Co Films, Separated by Nonmagnetic Metallic Interlayers. Physics of the Solid State, 2022, 64, 56-63.	0.2	1
68976	Quantum and temperature effects on the crystal structure of superhydride <mml:math xmlns:mml="http://www.w3.org/1998/Math/MathML"><mml:msub><mml:mi>LaH</mml:mi><mml:mn>10</mml:mn></mml:msub></mml:math>: A path integral molecular dynamics study. Physical Review B, 2022, 105, .	1.1	4
68977	Electronic and topological properties of the van der Waals layered superconductor PtTe. Physical Review B, 2022, 105, .	1.1	0
68978	Microstructure Evolution and Its Correlation with Performance in Nitrogen-Containing Porous Carbon Prepared by Polypyrrole Carbonization: Insights from Hybrid Calculations. Materials, 2022, 15, 3705.	1.3	1
68979	Pressure-induced topological phase transition in XMR material YbAs: a first-principles study. European Physical Journal Plus, 2022, 137, .	1.2	1
68980	Multiscale numerical tool for studying nonlinear dynamics in solids induced by strong laser pulses. Physical Review E, 2022, 105, .	0.8	6
68981	Extending ab initio simulations for the ion-ion structure factor of warm dense aluminum to the hydrodynamic limit using neural network potentials. Physical Review B, 2022, 105, .	1.1	6
68982	On the question of the applicability of the principle of thermodynamic similarity in liquid alkali metals. Journal of Physics: Conference Series, 2022, 2270, 012033.	0.3	0
68983	A highly sulfur resistant and stable heterogeneous catalyst for liquid-phase hydrogenation. Applied Catalysis B: Environmental, 2022, 315, 121566.	10.8	18
68984	N, P co-doped pitch derived soft carbon nanoboxes as high-performance anodes for sodium-ion batteries. Journal of Alloys and Compounds, 2022, 918, 165691.	2.8	15
68985	Fluxionality of Subnano Clusters Reshapes the Activity Volcano of Electrocatalysis. ChemCatChem, 2022, 14, .	1.8	10
68986	Design of Catalysts for Selective Hydrogenation of Acrylonitrile via Confining Single Metal Atoms within a C₂N Framework. Journal of Physical Chemistry C, 2022, 126, 10053-10060.	1.5	7

#	Article	IF	Citations
68987	Low lattice thermal conductivity of hydrideâ€based cubic antiperovskites <scp> A ₃ HB </scp> (aÂ=ÂLi, Na; BÂ=ÂS, se, Te) with higherâ€order anharmonicity correction. International Journal of Energy Research, 2022, 46, 13687-13697.	2.2	6
68988	Accurate Band Offset Prediction of Sc₂O₃/GaN and Î¸-Al₂O₃/GaN Heterojunctions Using a Dielectric-Dependent Hybrid Functional. ACS Applied Electronic Materials, 2022, 4, 2747-2752.	2.0	2
68989	Giant converse magnetoelectric effect in a multiferroic heterostructure with polycrystalline Co2FeSi. NPG Asia Materials, 2022, 14, .	3.8	13
68990	Toluene Adsorption on CeO2 (111) Studied by FTIR and DFT. Topics in Catalysis, 2022, 65, 934-943.	1.3	3
68991	Dipole-regulated bandgap and high electron mobility for bilayer Janus MoSiGeN4. Applied Physics Letters, 2022, 120, .	1.5	6
68992	Investigation of Carbon Dioxide Interaction with Transition Metal Dichalcogenides by First Principles. Journal of Contemporary Physics, 2022, 57, 166-169.	0.1	3
68993	Occupation preferences and impacts of interstitial H, C, N, and O on magnetism and phase stability of Ni₂MnGa magnetic shape memory alloys by first-principles calculations. Journal of Applied Physics, 2022, 131, 205101.	1.1	0
68994	NiCu Anchored on a Specific TiO₂ Face Tunes Electron Density for Selective Hydrogenation of Fatty Acids into Alkanes or Alcohols. ACS Sustainable Chemistry and Engineering, 2022, 10, 7349-7361.	3.2	8
68995	Two-Dimensional Multifunctional Metalâ€“Organic Framework with Intrinsic Bipolar Magnetic Semiconductivity and Negative Poissonâ€™s Ratio. ACS Applied Electronic Materials, 2022, 4, 3198-3204.	2.0	6
68996	Ð˜ÑÐ»ÐµÐ´Ð¾Ð²Ð°Ð½Ð¸Ðµ Ð²Ð»Ð¸ÑÐ½Ð¸Ñ Ð¾Ð±Ð¾Ð³Ð°Ñ‰ÐµÐ½Ð¸Ñ Ð¾Ð´Ð½Ð¾ÑÑ‚ÐµÐ½Ð¾Ñ‡Ð½Ð¾Ð¹ Ñ‚Ð²ÐµÑ€Ð´Ð¾Ð¹ Ñ€Ð°ÑÑ‚Ð²Ð¾Ñ€Ð° Ñ‚Ð¸Ñ‚Ð°Ð½Ð° Ð½Ð°		
68997	Which Is Better for Hydrogen Evolution on Metal@MoS₂ Heterostructures from a Theoretical Perspective: Single Atom or Monolayer?. ACS Applied Materials & Interfaces, 2022, 14, 25592-25600.	4.0	2
68998	Machine-Learning-Assisted Catalytic Performance Predictions of Single-Atom Alloys for Acetylene Semihydrogenation. ACS Applied Materials & Interfaces, 2022, 14, 25288-25296.	4.0	9
68999	Dramatically Enhanced Second Harmonic Generation in Janus Groupâ€III Chalcogenide Monolayers. Advanced Optical Materials, 2022, 10, .	3.6	8
69000	Orbital and electronic responses in the GaN/AlN quantum structures constructed on different crystal planes. Applied Physics Express, 2022, 15, 071002.	1.1	1
69001	Fe₂ Dimers for Nonâ€Polar Diatomic O₂ Electroreduction. ChemSusChem, 2022, 15, .	3.6	2
69003	Two-dimensional magnetoelectric multiferroics in a <mml:math xmlns:mml="http://www.w3.org/1998/Math/MathML"><mml:mrow><mml:mi>MnSTe</mml:mi><mml:mo>/</mml:mo><mml:mi>In</mml:mi><mml:msub><mml:mi></mml:mi> heterobilayer with ferroelectrically controllable skyrmions. Physical Review B, 2022, 105, .	3.7	21
69004	Grain Boundaryâ€Derived Cu⁺/Cu⁰ Interfaces in CuO Nanosheets for Low Overpotential Carbon Dioxide Electroreduction to Ethylene. Advanced Science, 2022, 9, .	5.6	51
69005	Self-extinguishing Janus separator with high safety for flexible lithium-sulfur batteries. Science China Materials, 2022, 65, 2169-2178.	3.5	23

#	Article	IF	Citations
69006	Dominant Effects of Epitaxial Strain on the Phase Control of Heterostructural (In_xGa_{1â€“x})₂O₃ Alloys. ACS Applied Electronic Materials, 2022, 4, 2711-2717.	2.0	4
69007	Unexpectedly Large Contribution of Oxygen to Charge Compensation Triggered by Structural Disordering: Detailed Experimental and Theoretical Study on a Li₃NbO₄â€“NiO Binary System. ACS Central Science, 2022, 8, 775-794.	5.3	10
69008	Jacutingaite family: An efficient platform for coexistence of spin valley Hall effects, valley spin-valve realization, and layer spin crossover. Physical Review B, 2022, 105, .	1.1	8
69009	Prediction of high- <mml:math xmlns:mml="http://www.w3.org/1998/Math/MathML"><mml:msub><mml:mi>T</mml:mi><mml:mi>c</mml:mi></mml:msub></mml:ma superconductivity in <mml:math xmlns:mml="http://www.w3.org/1998/Math/MathML"><mml:mrow><mml:msub><mml:mi mathvariant="normal">H</mml:mi><mml:mn>6</mml:mn></mml:msub><mml:mi		

#	Article	IF	Citations
69024	Catalytically active atomically thin cuprate with periodic Cu single sites. National Science Review, 2023, 10, .	4.6	2
69025	New structure and insight on the phase transition within the Cu-Pd-Sn system with 25 at. % Sn. Materialia, 2022, 24, 101461.	1.3	0
69026	Periodic corner holes on the Si(111)-7Ã—7 surface can trap silver atoms. Nature Communications, 2022, 13, .	5.8	4
69027	Mn3O4/MnS heterostructure for electrode and asymmetric supercapacitor under high charge/discharge current. Electrochimica Acta, 2022, 424, 140630.	2.6	13
69028	Ab Initio Calculation of Surface-Controlled Photocatalysis in Multiple-Phase BiVO₄. Journal of Physical Chemistry C, 2022, 126, 9541-9550.	1.5	6
69029	The Key Role of Competition between Orbital and Electrostatic Interactions in the Adsorption on Transition Metal Singleâ€Atom Catalysts Anchored by Nâ€doped Graphene. ChemCatChem, 2022, 14, .	1.8	12
69030	Towards universal neural network potential for material discovery applicable to arbitrary combination of 45 elements. Nature Communications, 2022, 13, .	5.8	71
69031	Highly heterogeneous epitaxy of flexoelectric BaTiO3-Î´ membrane on Ge. Nature Communications, 2022, 13, .	5.8	22
69032	Impact of interstitial elements on the stacking fault energy of an equiatomic CoCrNi medium entropy alloy: theory and experiments. Science and Technology of Advanced Materials, 2022, 23, 376-392.	2.8	7
69033	The Impact of Nanoscale Percolation in Yttriumâ€Doped BaZrO₃ on the Oxygen Ion and Proton Conductivities: A Density Functional Theory and Kinetic Monte Carlo Study. Advanced Energy and Sustainability Research, 2022, 3, .	2.8	5
69034	Unraveling the Structural Instability of Li(Ni _{0.80} Co _{0.15} Al _{0.05}) Tj ETQq0 0 0 rgBT /Overlock 10	5.2	3
69035	Surface conversion derived core-shell nanostructures of Co particles@RuCo alloy for superior hydrogen evolution in alkali and seawater. Applied Catalysis B: Environmental, 2022, 315, 121554.	10.8	29
69036	Unveiling the role of C60-supported vanadium single atoms for catalytic overall water splitting. Cell Reports Physical Science, 2022, 3, 100910.	2.8	7
69037	Atomistic Simulation of the Lattice Properties of SnSe. Semiconductors, 0, , .	0.2	0
69038	Strong Hydrogen Bonds in Acetylenedicarboxylic Acid Dihydrate. International Journal of Molecular Sciences, 2022, 23, 6164.	1.8	0
69039	Constructing two-dimensional holey graphyne with unusual annulative Ï€-extension. Matter, 2022, 5, 2306-2318.	5.0	34
69040	Shear strain alters the structure and migration mechanism of self-interstitial atoms in copper. Physical Review Materials, 2022, 6, .	0.9	1
69041	Dynamic transformation between bilayer islands and dinuclear clusters of Cr oxide on Au(111) through environment and interface effects. Proceedings of the National Academy of Sciences of the United States of America, 2022, 119, .	3.3	9

#	Article	IF	Citations
69042	PdAg/Ag(111) Surface Alloys: A Highly Efficient Catalyst of Oxygen Reduction Reaction. Nanomaterials, 2022, 12, 1802.	1.9	3
69043	Unveiling Temperature-Dependence Mechanisms of Perpendicular Magnetic Anisotropy at <mml:math xmlns:mml="http://www.w3.org/1998/Math/MathML" display="inline" overflow="scroll"><mml:mi>Fe</mml:mi></mml:math> / <mml:math xmlns:mml="http://www.w3.org/1998/Math/MathML" display="inline" overflow="scroll"><mml:mrow><mml:mi>Mg</mml:mi><mml:mi mathvariant="normal">O</mml:mi></mml:mrow></mml:math> Interfaces. Physical Review Applied, 2022,	1.5	5
69044	Insights into the influence of functional groups on the properties of graphene from firstâ€principles calculations. Journal of Physical Organic Chemistry, 2022, 35, .	0.9	2
69045	Abrupt Negative Thermal Expansion and Magnetic Structure of V₃O₅. Chemistry of Materials, 2022, 34, 5294-5300.	3.2	2
69046	Implementation of self-consistent MGGA functionals in augmented plane wave based methods. Physical Review B, 2022, 105, .	1.1	4
69047	Interfacially Enhanced Stability and Electrochemical Properties of C/SiO_x Nanocomposite Lithiumâ€ion Battery Anodes. Advanced Materials Interfaces, 2022, 9, .	1.9	12
69048	Magnetic tuning in a novel half-metallic Ir₂TeI₂ monolayer. Journal of Semiconductors, 2022, 43, 052001.	2.0	2
69049	Achieving High Thermoelectric Performance of Eco-Friendly SnTe-Based Materials by Selective Alloying and Defect Modulation. ACS Applied Materials & Interfaces, 2022, 14, 25802-25811.	4.0	9
69050	Understanding Competitive Photo-Induced Molecular Oxygen Dissociation and Desorption Dynamics atop a Reduced Rutile TiO₂(110) Surface: A Time-Domain Ab Initio Study. ACS Catalysis, 2022, 12, 6702-6711.	5.5	13
69051	Breaking the Linear Relation in the Dissociation of Nitrogen on Iron Surfaces. ChemPhysChem, 2022, 23, .	1.0	4
69052	Monolayer Sc₂I₂S₂: An Excellent n-Type Thermoelectric Material with Significant Anisotropy. ACS Applied Energy Materials, 2022, 5, 7230-7239.	2.5	9
69053	Atomic study of hydrogen behaviors at â^3(111) grain boundary in equiatomic CoCrNi and CoCrNiFe alloys. Tungsten, 2022, 4, 239-247.	2.0	4
69054	Direct <mml:math xmlns:mml="http://www.w3.org/1998/Math/MathML"><mml:mrow><mml:mi>d</mml:mi><mml:mtext>â^’</mml:mtext><mml:mi>d</m hybridization mechanism for strong anisotropic carrier transport in layered <mml:math xmlns:mml="http://www.w3.org/1998/Math/MathML"><mml:mrow><mml:msub><mml:mi>Mo</mml:mi><mml:mn>2</mml:mn></mml Physical Review B, 2022, 105, .	1.1	3
69055	Enhanced Photogenerated Hole Oxidation Capability of Li2SnO3 by Sb Incorporation in Photocatalysis Through Band Structure Modification. Catalysis Letters, 2023, 153, 1109-1119.	1.4	1
69056	Impact of Coordination Environment on Single-Atom-Embedded C₃N for Oxygen Electrocatalysis. ACS Sustainable Chemistry and Engineering, 2022, 10, 7692-7701.	3.2	14
69057	Facile Dissolutionâ€“Crystallization Strategy to Achieve Rapid and Uniform Distribution of Sulfur on Porous Carbon for Lithiumâ€–Sulfur Batteries. ACS Omega, 0, , .	1.6	1
69058	Simultaneous nanocatalytic surface activation of pollutants and oxidants for highly efficient water decontamination. Nature Communications, 2022, 13, .	5.8	117
69059	Pressure-Enhanced Photocurrent in One-Dimensional SbSI via Lone-Pair Electron Reconfiguration. Materials, 2022, 15, 3845.	1.3	6

#	Article	IF	Citations
69060	Protected valley states and generation of valley- and spin-polarized current in monolayer <mml:math xmlns:mml="http://www.w3.org/1998/Math/MathML"><mml:mrow><mml:msub><mml:mrow><mml:mi>M</mml:mi> Physical Review B, 2022, 105, .	1.1	21
69061	Modulation electronic structure of NiS nanoarray induced by Fe, V doping for high efficiency water and urea electrolysis. Journal of Industrial and Engineering Chemistry, 2022, 113, 170-180.	2.9	12
69062	Band Modulation and Strain Fluctuation for Realizing High Average zT in GeTe. Advanced Energy Materials, 2022, 12, .	10.2	13
69063	Influence of deuterium-induced volume changes on optical transmission in Fe/V (001) and Cr/V (001) superlattices. Physical Review B, 2022, 105, .	1.1	1
69064	Visualizing the Anomalous Catalysis in Two-Dimensional Confined Space. Nano Letters, 2022, 22, 4661-4668.	4.5	3
69065	Bimetallic hydroxyl fluoride with highâ€rate lithium storage performance: Co _{0.} <scp> ₆ Zn ₀ </scp> _{.4} (<scp>OH</scp>)F material. International Journal of Energy Research, 0, , .	2.2	0
69066	First-principles investigations of structural, elastic and electronic properties of hydrous fayalite. Arabian Journal of Geosciences, 2022, 15, .	0.6	0
69067	Adamantanes as White-Light Emitters: Controlling the Arrangement and Functionality by External Coulomb Forces. Journal of Physical Chemistry C, 0, , .	1.5	2
69068	KSSOLV 2.0: An efficient MATLAB toolbox for solving the Kohn-Sham equations with plane-wave basis set. Computer Physics Communications, 2022, 279, 108424.	3.0	9
69069	Dynamics of Proton Transfer on Boehmite (010) Surface in Anhydrous and Hydrous Environments. Physica Status Solidi (B): Basic Research, 0, , 2200058.	0.7	0
69070	Oxidation of two-dimensional electrides: Structural transition and the formation of half-metallic channels protected by oxide layers. Physical Review B, 2022, 105, .	1.1	1
69071	Enhanced ferroelectricity by strain gradient in few-layer HfO₂thin films. Europhysics Letters, 2022, 139, 46003.	0.7	1
69072	Transport properties and phase diagrams of FeSe1â^'S (0â‰¤xâ‰¤1) single crystals. Journal of Alloys and Compounds, 2022, , 165760.	2.8	1
69073	Efficient photocatalytic hydrogen evolution coupled with benzaldehyde production over 0D Cd0.5Zn0.5S/2D Ti3C2 Schottky heterojunction. Journal of Advanced Ceramics, 2022, 11, 1117-1130.	8.9	48
69074	Remarkable Structural Modifications of Tialite Solid Solutions Obtained by Different Methods. Materials, 2022, 15, 3981.	1.3	2
69075	Tracing the Anharmonicity and Superionic Phase Transition of Hydrous FeO2H. Frontiers in Earth Science, 2022, 10, .	0.8	1
69076	Wafer-scale solution-processed 2D material analog resistive memory array for memory-based computing. Nature Communications, 2022, 13, .	5.8	60
69077	Metal coordination determines the catalytic activity of IrO2 nanoparticles for the oxygen evolution reaction. Journal of Catalysis, 2022, 412, 78-86.	3.1	13

#	Article	IF	Citations
69078	Controlling Stoichiometry in Ultrathin van der Waals Films: PtTe₂, Pt₂Te₃, Pt₃Te₄, and Pt₂Te₂. ACS Nano, 2022, 16, 9908-9919.	7.3	8
69079	Cationâ€Alloyingâ€Induced Blueâ€Shifted and Wideâ€Spectrum Polarizationâ€Sensitive Photodetection in Quasiâ€1D SbBiS₃. Small Structures, 2022, 3, .	6.9	10
69080	Phase equilibria in the Y2O3-Nb2O5 system up to 2500Âà„ƒ: New high-temperature experiments and thermodynamic modeling. Journal of Alloys and Compounds, 2022, 918, 165714.	2.8	3
69081	Stability, metallicity, and magnetism in niobium silicide nanofilms. Physical Review Materials, 2022, 6, .	0.9	1
69082	Mixed Anion Semiconductor In₈S_{2.82}Te_{6.18}(Te₂)₃. Inorganic Chemistry, 2022, 61, 9040-9046.	1.9	1
69083	Smallest Stable <mml:math xmlns:mml="http://www.w3.org/1998/Math/MathML" display="inline"><mml:mrow><mml:mi>Si</mml:mi><mml:mo>/</mml:mo><mml:msub><mml:mi>SiO</mml:mi><mml:mn>2</mml:mn> Interface that Suppresses Quantum Tunneling from Machine-Learning-Based Global Search. Physical Review Letters, 2022, 128, .	2.9	18
69084	Tuning intrinsic defects in ZnO films by controlling the vacuum annealing temperature: an experimental and theoretical approach. Physica Scripta, 2022, 97, 075811.	1.2	1
69085	Rational design of copper-based single-atom alloy catalysts for electrochemical CO2 reduction. Nano Research, 2022, 15, 7116-7123.	5.8	43
69086	Explore the underlying mechanism of graphitic C3N5-hosted single-atom catalyst for electrocatalytic nitrogen fixation. International Journal of Hydrogen Energy, 2022, 47, 22035-22044.	3.8	15
69087	Allotropes selection apropos of photocatalytic CO2 reduction from first principles studies. Materials Today Physics, 2022, , 100751.	2.9	3
69088	Role of Optical Phonons and Anharmonicity in the Appearance of the Heat Capacity Boson Peak-like Anomaly in Fully Ordered Molecular Crystals. Journal of Physical Chemistry Letters, 2022, 13, 5061-5067.	2.1	7
69089	Ab initio molecular dynamics (AIMD) simulations of NaCl, UCl<mml:math xmlns:mml="http://www.w3.org/1998/Math/MathML" altimg="si1.svg"><mml:msub><mml:mrow /><mml:mn>3</mml:mn></mml:msub></mml:math> and NaCl-UCl<mml:math xmlns:mml="http://www.w3.org/1998/Math/MathML" altimg="si1.svg"><mml:msub><mml:mrow /><mml:mn>3</mml:mn></mml:msub></mml:math> molten salts. Journal of Nuclear Materials, 2022,	1.3	13
69090	Theoretical prediction of superconductivity in monolayer <mml:math xmlns:mml="http://www.w3.org/1998/Math/MathML"><mml:msub><mml:mi mathvariant="normal">B</mml:mi><mml:mn>3</mml:mn></mml:msub><mml:mi mathvariant="normal">N</mml:mi></mml:math>. Physical Review B, 2022, 105, .	1.1	6
69091	Exploring the correlation between the spin-state configuration and the magnetic order in Co-substituted <mml:math xmlns:mml="http://www.w3.org/1998/Math/MathML"><mml:msub><mml:mi>BiFeO</mml:mi><mml:mn>3</mml:mn></mml:msub> Physical Review Materials, 2022, 6, .	0.9	1
69092	Design of Ru-Ni diatomic sites for efficient alkaline hydrogen oxidation. Science Advances, 2022, 8, .	4.7	89
69093	The surface of metal boride tinted by oxygen evolution reaction for enhanced water electrolysis. Journal of Energy Chemistry, 2022, 72, 509-515.	7.1	19
69094	Phase diagrams and critical temperatures for coherent and incoherent mixtures of InAs_{1â^'x}Sb_x alloys using first-principles calculations. Journal of Applied Physics, 2022, 131, 215102.	1.1	1
69095	Self-assembly of magnetic Co atoms on stanene. Physical Review Materials, 2022, 6, .	0.9	1

#	Article	IF	Citations
69096	Highly active Ni/Co-metal organic framework bifunctional electrocatalyst for water splitting reaction. International Journal of Hydrogen Energy, 2022, 47, 22787-22795.	3.8	20
69097	A first-principles investigation of nitrogen reduction to ammonia on zirconium nitride and oxynitride surfaces. Journal of Materials Science, 2022, 57, 10213-10224.	1.7	8
69098	Boosting the performance of single-atom catalysts via external electric field polarization. Nature Communications, 2022, 13, .	5.8	52
69099	Unfolding the structural stability of nanoalloys via symmetry-constrained genetic algorithm and neural network potential. Npj Computational Materials, 2022, 8, .	3.5	9
69100	Controlled growth of two-dimensional InAs single crystals via van der Waals epitaxy. Nano Research, 0, , .	5.8	4
69101	Competing dynamical and lattice instabilities in <mml:math xmlns:mml="http://www.w3.org/1998/Math/MathML"><mml:mrow><mml:msub><mml:mrow><mml:mi>R</mml:mi><mml:mj mathvariant="normal">VO</mml:mi></mml:mrow><mml:mn>4</mml:mn></mml:msub></mml:mrow></mml:math> rare-earth vanadium oxides under high pressure. Physical Review Materials, 2022, 6, .	0.9	2
69102	Stimulating the Pre-Catalyst Redox Reaction and the Protonâ€“Electron Transfer Process of Cobalt Phthalocyanine for CO₂ Electroreduction. Journal of Physical Chemistry C, 2022, 126, 9665-9672.	1.5	7
69103	Predicting the optimal chemical composition of functionalized carbon catalysts towards oxidative dehydrogenation of ethanol to acetaldehyde. Nano Today, 2022, 44, 101508.	6.2	4
69104	Reliable crystal structure predictions from first principles. Nature Communications, 2022, 13, .	5.8	17
69105	Constructing highly active alloy-perovskite interfaces for efficient electrochemical CO2 reduction reaction. Separation and Purification Technology, 2022, 296, 121411.	3.9	15
69106	Electrons and phonons in uranium hydrides - effects of polar bonding. Journal of Nuclear Materials, 2022, 567, 153817.	1.3	5
69107	In-situ neutron-transmutation for substitutional doping in 2D layered indium selenide based phototransistor. ELight, 2022, 2, .	11.9	18
69108	Comment on â€œA novel two-dimensional boron-carbon-nitride (BCN) monolayer: A first-principles insightâ€•[J. Appl. Phys. 130, 114301 (2021)]. Journal of Applied Physics, 2022, 131, 216101.	1.1	0
69109	Rational design of mixed-matrix metal-organic framework membranes for molecular separations. Science, 2022, 376, 1080-1087.	6.0	160
69110	Nitrogen reduction reaction (NRR) modelling: A case that illustrates the challenges of DFT studies in electrocatalysis. Current Opinion in Electrochemistry, 2022, 35, 101073.	2.5	10
69111	Mechanism of Conductivity in the Rare Earth Layered Ln₂MoO₆ (Ln = La, Pr,) Tj ETQq1 1 0.784314 rgBT /Ov 2022, 126, 9623-9633.	1.5	7
69112	Ultrafast Preparation of Nonequilibrium FeNi Spinels by Magnetic Induction Heating for Unprecedented Oxygen Evolution Electrocatalysis. Research, 2022, 2022, .	2.8	7
69113	Nanotubes from Ternary WS_{2(1â€“x)}Se_{2x} Alloys: Stoichiometry Modulated Tunable Optical Properties. Journal of the American Chemical Society, 2022, 144, 10530-10542.	6.6	15

#	Article	IF	Citations
69114	First-principle study on the effects of hydrogen in combination with alloy solutes on local mechanical properties of steels. International Journal of Hydrogen Energy, 2022, 47, 22243-22260.	3.8	3
69115	Origin and regulation of oxygen redox instability in high-voltage battery cathodes. Nature Energy, 2022, 7, 808-817.	19.8	55
69116	Structure and Interactions at the Mg(0001)/Water Interface: An ab initio Study. Journal of Chemical Physics, 0, , .	1.2	2
69117	First-principles prediction of anomalously strong phase dependence of transport and mechanical properties of lithium fluoride. Acta Materialia, 2022, 235, 118077.	3.8	10
69118	Dual-Metal Active Sites Mediated by p-Block Elements: Knowledge-Driven Design of Oxygen Reduction Reaction Catalysts. ACS Omega, 2022, 7, 19676-19686.	1.6	2
69119	Re Modulation of Metallic Ultrathin 2M-WS₂ for Highly Efficient Hydrogen Evolution in Both Acidic and Alkaline Media. ACS Applied Energy Materials, 2022, 5, 7674-7680.	2.5	0
69120	A DFT study of two-dimensional P2Si monolayer modified by single transition metal (Sc-Cu) atoms for efficient electrocatalytic CO2 reduction. Chinese Chemical Letters, 2023, 34, 107579.	4.8	5
69121	Dependence of local atomic structure on piezoelectric properties of PbZr_{1â^'x}Ti_xO₃ materials. Journal of Asian Ceramic Societies, 0, , 1-6.	1.0	0
69122	First-principles study on Î´-Pu surface stability. AIP Advances, 2022, 12, 065001.	0.6	1
69123	Bi doping of Sb2S3 light-harvesting films: Toward suitable energy level alignment and broad absorption for solar cells. Chemical Engineering Journal, 2022, 446, 137400.	6.6	22
69124	Strain-tunable carrier mobility of Fe-doped GaN: A first-principles study. , 2022, 168, 207300.		2
69125	Exploring the Interfacial Reaction of Nano Al/CuO Energetic Films through Thermal Analysis and Ab Initio Molecular Dynamics Simulation. Molecules, 2022, 27, 3586.	1.7	4
69126	Monolayer and bilayer siligraphenes as high-performance anode materials for potassium ion batteries: A first principles study. Journal of Molecular Liquids, 2022, 360, 119523.	2.3	19
69127	How Water Attacks MXene. Chemistry of Materials, 2022, 34, 4975-4982.	3.2	44
69128	Structural phase transition and superconductivity of ytterbium under high pressure. Physical Review B, 2022, 105, .	1.1	25
69129	Search of chalcopyrite materials based on hybrid density functional theory calculation. Journal of Physics Communications, 2022, 6, 065001.	0.5	1
69130	In Situ TEM Studies of the Oxidation of Li Dendrites at High Temperatures. Advanced Functional Materials, 2022, 32, .	7.8	13
69131	Exploring the electronic and optical anisotropy of quasi-one-dimensional ternary chalcogenide CrSbSe3: a DFT study. Solid State Sciences, 2022, 130, 106926.	1.5	6

#	Article	IF	Citations
69132	Intercalation-driven ferroelectric-to-ferroelastic conversion in a layered hybrid perovskite crystal. Nature Communications, 2022, 13, .	5.8	27
69133	Elastic Lattice Enabling Reversible Tetrahedral Li Storage Sites in a Highâ€Capacity Manganese Oxide Cathode. Advanced Materials, 2022, 34, .	11.1	15
69134	Charge-to-spin conversion in the quasi-two-dimensional electron gas emerging at the hydrogen-doped interface between <mml:math xmlns:mml="http://www.w3.org/1998/Math/MathML"><mml:msub><mml:mi>LiNbO</mml:mi><mml:mn>3</mml:mn></mml:msub></m and <mml:math xmlns:mml="http://www.w3.org/1998/Math/MathML"><mml:msub><mml:mi>LaAlO</mml:mi><mml:mn>3</mml:mn></mml:msub></m Physical Review Materials, 2022, 6, .	0.9	3
69135	Machine Learning Force Field Aided Cluster Expansion Approach to Configurationally Disordered Materials: Critical Assessment of Training Set Selection and Size Convergence. Journal of Chemical Theory and Computation, 2022, 18, 3795-3804.	2.3	6
69136	Spinâ€Transport through Van der Waals Heterojunctions Based on 2Dâ€Ferromagnet and Transition Metal Dichalcogenides: A Study from Firstâ€Principles Calculations. Advanced Theory and Simulations, 2022, 5, .	1.3	2
69137	Hydrogenation/Hydrodeoxygenation Selectivity Modulation by Cometal Addition to Palladium on Carbon-Coated Supports. ACS Sustainable Chemistry and Engineering, 2022, 10, 7759-7771.	3.2	4
69138	Tailoring the electronic and optical properties of ZrS2/ZrSe2 vdW heterostructure by strain engineering. Thin Solid Films, 2022, 755, 139332.	0.8	6
69139	Regulating *OCHO Intermediate as Rateâ€Determining Step of Defective Oxynitride Nanosheets Enabling Robust CO₂ Electroreduction. Advanced Energy Materials, 2022, 12, .	10.2	32
69140	Oxide-Derived Coreâ€“Shell Cu@Zn Nanowires for Urea Electrosynthesis from Carbon Dioxide and Nitrate in Water. ACS Nano, 2022, 16, 9095-9104.	7.3	86
69141	Band gap modulation of penta-BCN through different ways. Diamond and Related Materials, 2022, 126, 109114.	1.8	1
69142	Influence of Bi Substitution with Rare-Earth Elements on the Transport Properties of BiCuSeO Oxyselenides. ACS Applied Energy Materials, 2022, 5, 7830-7841.	2.5	2
69143	Kineticsâ€Controlled Interfacial Synthesis of Janus and Patchy Heterostructures Based on Perovskite Nanocrystals. Advanced Optical Materials, 2022, 10, .	3.6	4
69144	Selenium vacancies enable efficient immobilization and bidirectional conversion acceleration of lithium polysulfides for advanced Li-S batteries. Nano Research, 2022, 15, 7234-7246.	5.8	19
69145	Combined Deep Learning and Classical Potential Approach for Modeling Diffusion in UiO-66. Journal of Chemical Theory and Computation, 2022, 18, 3593-3606.	2.3	19
69146	Intrinsic ferromagnetic Janus Cr2PAs monolayer with controllable magnetic anisotropy. Physics Letters, Section A: General, Atomic and Solid State Physics, 2022, 444, 128239.	0.9	4
69147	Structural, Optical, Luminescence, and Electrical Properties of Eu/Li- and Eu/Na-Codoped Magnesium Bismuth Niobate Pyrochlores. Inorganic Chemistry, 0, , .	1.9	6
69148	Atomic Interactions and Orderâ€“Disorder Transition in FCC-Type FeCoNiAl1-xTix High-Entropy Alloys. Materials, 2022, 15, 3992.	1.3	2
69149	Weyl semimetal states in transition metal monochalcogenide superlattices AX/BX (A, B = Cr, Mo, W, A â‰) Tj ETQq1 1 0.784314 rgB	1.3	1

#	Article	IF	Citations
69150	Theory of superconductivity mediated by Rashba coupling in incipient ferroelectrics. Physical Review B, 2022, 105, .	1.1	12
69151	Separation of<scp>CH₄</scp>/<scp>N₂</scp>by an ultraâ€stable metalâ€“organic framework with the highest breakthrough selectivity. AICHE Journal, 2022, 68, .	1.8	26
69152	Decomposition Kinetics of H₂O₂ on Pd Nanocrystals with Different Shapes and Surface Strains. ChemCatChem, 2022, 14, .	1.8	5
69153	High-throughput first-principles study of physical properties of L12-Al3M particles. Materials Today Communications, 2022, , 103748.	0.9	0
69154	Revealing the weak Fermi level pinning effect of 2D semiconductor/2D metal contact: A case of monolayer In2Ge2Te6 and its Janus structure In2Ge2Te3Se3. Materials Today Physics, 2022, 26, 100749.	2.9	18
69155	Simultaneously Enhancing Catalytic Performance and Increasing Density of Bifunctional CuN₃ Active Sites in Dopant-Free 2D C₃N₃Cu for Oxygen Reduction/Evolution Reactions. ACS Omega, 2022, 7, 19794-19803.	1.6	4
69156	Diffusion behavior of gas molecules in the one-dimensional channel of AlPO4-5 molecular sieves. Microporous and Mesoporous Materials, 2022, 340, 112024.	2.2	4
69157	Density functional theory study of hydrogen as reducing agent of hematite (Î±-Fe2O3) in ironmaking process. Thin Solid Films, 2022, 754, 139321.	0.8	0
69158	Sulfide-modified zero-valent iron activated periodate for sulfadiazine removal: Performance and dominant routine of reactive species production. Water Research, 2022, 220, 118676.	5.3	87
69159	Anticorrosion mechanism of Al-modified phosphate ceramic coating in the high-temperature marine atmosphere. Surface and Coatings Technology, 2022, 441, 128572.	2.2	6
69160	Methoxy-substituted naphthothiophenes â€“ Single molecules' vs. condensed phase properties and prospects for organic electronics applications. Synthetic Metals, 2022, 287, 117094.	2.1	2
69161	Design rules for defect-free 3D perovskite-perovskite interfaces. Surfaces and Interfaces, 2022, 31, 102073.	1.5	0
69162	Ab initio random structure searching and catalytic properties of copper-based nanocluster with Earth-abundant metals for the electrocatalytic CO2-to-CO conversion. Molecular Catalysis, 2022, 527, 112406.	1.0	3
69163	2D lead free Ruddlesden-Popper phase perovskites as efficient photovoltaic materials: A first-principles investigation. Computational Materials Science, 2022, 211, 111545.	1.4	6
69164	In-situ forming lithiophilic-lithiophobic gradient interphases for dendrite-free all-solid-state Li metal batteries. Nano Energy, 2022, 99, 107395.	8.2	10
69165	EAPOTc: An integrated empirical interatomic potential optimization platform for compound solids. Computational Materials Science, 2022, 211, 111551.	1.4	1
69166	First-principle study on the stability, mechanical, electronic, and optical properties of two-dimensional scandium oxyhalides. Materials Chemistry and Physics, 2022, 287, 126306.	2.0	3
69167	On the stability of MOPO4 structure types with M: V, Mo, Nb, W, Ta, Sb. Journal of Solid State Chemistry, 2022, 312, 123221.	1.4	0

#	Article	IF	Citations
69168	Ab initio investigation of the screw dislocation-hydrogen interaction in bcc tungsten and iron. Acta Materialia, 2022, 234, 118048.	3.8	13
69169	Optoelectronic and photocatalytic properties of stable pentagonal B2S and B2Se monolayers. Computational Materials Science, 2022, 211, 111524.	1.4	1
69170	Solute-induced near-isotropic performance of laser powder bed fusion manufactured pure titanium. Additive Manufacturing, 2022, 56, 102907.	1.7	5
69171	The inhibition efficiencies of some organic corrosion inhibitors of iron: An insight from density functional theory study. Computational and Theoretical Chemistry, 2022, 1214, 113759.	1.1	5
69172	Thermodynamics of point defect disorder and off-stoichiometry in ThO2 and Th1-U O2. Journal of Nuclear Materials, 2022, 567, 153804.	1.3	4
69173	Theoretical and experimental approaches for the determination of functional properties of MgSnN2 thin films. Solar Energy Materials and Solar Cells, 2022, 244, 111797.	3.0	6
69174	Two-dimensional VSi2P4 as an anode material for Li-ion batteries. Materials Chemistry and Physics, 2022, 287, 126323.	2.0	6
69175	Modifying electronic and magnetic properties of the <mml:math xmlns:mml="http://www.w3.org/1998/Math/MathML" display="inline" id="d1e536" altimg="si31.svg"><mml:mi>Î²</mml:mi></mml:math>-Sb monolayer by doping with III-, IV-, and V-group atoms. Physica E: Low-Dimensional Systems and Nanostructures, 2022, 142, 115315.	1.3	3
69176	Lithium inserted ZnSnN2 thin films for solar absorber: n to p-type conversion. Materials Today Chemistry, 2022, 25, 100957.	1.7	5
69177	Robust ferroelectric-gating-dependent electronic and magnetic properties in a 1T-VSe2/BiAlO3(0001) multiferroic heterostructure. Materials Today Physics, 2022, 26, 100743.	2.9	2
69178	Blue-emitting 0D Cs3ZnX5 (X = Cl, Br) perovskite nanocrystals based on self-trapped excitons. Journal of Luminescence, 2022, 249, 119048.	1.5	6
69179	Quantum spin Hall effect in two-dimensional transition-metal chalcogenides MX<mml:math xmlns:mml="http://www.w3.org/1998/Math/MathML" display="inline" id="d1e813" altimg="si33.svg"><mml:msub><mml:mrow /><mml:mrow><mml:mn>5</mml:mn></mml:mrow></mml:msub></mml:math> (M = Zr, Hf and X = S, Se,) Tj ETQq1 1 0.784314 rgBT /(	1.3	2
69180	In situ electronic redistribution tuning of ZnIn2S4 nanosheets on NiCo2S4 hollow tube for boosted photocatalytic hydrogen evolution. Applied Surface Science, 2022, 598, 153801.	3.1	12
69181	Room temperature ferromagnetism and transport properties in InN/VTe2 van der Waals heterostructures. Applied Surface Science, 2022, 598, 153781.	3.1	3
69182	Accelerating CO2 reduction on novel double perovskite oxide with sulfur, carbon incorporation: Synergistic electronic and chemical engineering. Chemical Engineering Journal, 2022, 446, 137161.	6.6	34
69183	Preparation of ultra-thin porous carbon nitride and its photocatalytic H2O2 production and photodegradation of RhB. Applied Surface Science, 2022, 598, 153866.	3.1	8
69184	Understanding catalytic activity trends of atomic pairs in single-atom catalysts towards oxygen reduction reactions. Applied Surface Science, 2022, 598, 153873.	3.1	3
69185	Ab initio phase stabilities of rare-earth lean Nd-based hard magnets. Journal of Magnetism and Magnetic Materials, 2022, 559, 169529.	1.0	3

#	Article	IF	Citations
69186	First-principles study on the vertical heterostructure of the BSe and AlN monolayers. Applied Surface Science, 2022, 598, 153830.	3.1	7
69187	Defect thermodynamics in spinel oxides leading to plasmonic behavior. Journal of Physics and Chemistry of Solids, 2022, 168, 110822.	1.9	1
69188	Theoretical proposal of a revolutionary water-splitting photocatalyst: The monolayer of boron phosphide. Applied Surface Science, 2022, 598, 153844.	3.1	6
69189	Realizing robust and efficient acidic oxygen evolution by electronic modulation of 0D/2D CeO2 quantum dots decorated SrIrO3 nanosheets. Applied Catalysis B: Environmental, 2022, 315, 121579.	10.8	28
69190	Investigation on bifunctional catalytic performance of Anti-Perovskite Ni3ZnC, Co3ZnC and Ni3FeN for Hydrogen/Oxygen evolution reactions. Applied Surface Science, 2022, 598, 153814.	3.1	7
69191	B N counterpart of biphenylene network: A theoretical investigation. Applied Surface Science, 2022, 598, 153674.	3.1	18
69192	Effect of Cr-substitution on vanadium dioxide thin films studied by soft X-ray magnetic circular dichroism. Journal of Alloys and Compounds, 2022, 918, 165515.	2.8	12
69193	Atomically dispersed Fe-Cu dual-site catalysts synergistically boosting oxygen reduction for hydrogen fuel cells. Chemical Engineering Journal, 2022, 446, 137112.	6.6	43
69194	Ab initio investigations of Fe(110)/graphene interfaces. Applied Surface Science, 2022, 598, 153714.	3.1	4
69195	Photocatalysis/enzymolysis-based biomimetic Schottky junction reduces tumor interstitial solid and fluid phases for deep-penetrating tumor therapy. Chemical Engineering Journal, 2022, 446, 137196.	6.6	3
69196	The homojunction formed by h-In2O3(1 1 0) and c-In2O3(4 4 0) promotes carbon dioxide hydrogenation to methanol on graphene oxide modified In2O3. Journal of Colloid and Interface Science, 2022, 623, 1048-1062.	5.0	12
69197	Thermodynamic stability of niobium-doped ceria surfaces. Journal of Molecular Structure, 2022, 1265, 133416.	1.8	2
69202	Tailored Computational Approaches to Interrogate Heavy Element Chemistry and Structure in Condensed Phase. ACS Symposium Series, 0, , 219-245.	0.5	0
69203	Advances in Structure Prediction of Lanthanides and Actinides with Genetic Algorithms. ACS Symposium Series, 0, , 157-171.	0.5	0
69204	Molecular Dynamics Simulations of U(III) and U(IV) in Molten Chlorides. ACS Symposium Series, 0, , 365-386.	0.5	1
69205	Rashba effect and flat band in one-dimensional helical Se atomic chain. Wuli Xuebao/Acta Physica Sinica, 2022, .	0.2	0
69206	A Systematic Theoretical Study the Active Sites of Potassium Promoter on the Activity of Water Gas Shift Reaction Over Pt(111). SSRN Electronic Journal, 0, , .	0.4	0
69207	Single boron modulated graphdiyne nanosheets for efficient electrochemical nitrogen fixation: a first-principles study. Physical Chemistry Chemical Physics, 2022, 24, 19817-19826.	1.3	2

#	Article	IF	Citations
69208	Mode selective chemistry for the dissociation of methane on efficient Ni/Pt-bimetallic alloy catalysts. Physical Chemistry Chemical Physics, 2022, 24, 16596-16610.	1.3	3
69209	Adsorption of CO over the Heusler alloy CrCoIrGa(001) surface: first-principles insights. RSC Advances, 2022, 12, 17853-17863.	1.7	1
69210	Rationally Designed Ws2/C2n Layered Heterostructures for Enhanced Photocatalytic Hydrogen Evolution: Interface and Bandgap Engineering. SSRN Electronic Journal, 0, , .	0.4	0
69211	Magnetic nature and hyperfine interactions of transition metal atoms adsorbed on ultrathin insulating films: a challenge for DFT. Physical Chemistry Chemical Physics, 2022, 24, 15891-15903.	1.3	5
69212	Ba₃(BO₃)₂: the first example of the dynamic disordering in borate crystal. Physical Chemistry Chemical Physics, 0, , .	1.3	0
69213	Displacement Vorticity as Origin of MoirÃ© Potentials in Twisted WSe ₂/MoSe ₂ Bilayers. SSRN Electronic Journal, 0, , .	0.4	0
69214	Submicron Ti₂CT_xMXene particulates as high-rate intercalation anode materials for Li-ion batteries. Journal of Materials Chemistry A, 2022, 10, 15474-15484.	5.2	7
69215	Liquid exfoliation of five-coordinate layered titanate K₂Ti₂O₅ single crystals in water. CrystEngComm, 2022, 24, 5112-5119.	1.3	1
69216	Improved photocatalytic activity of TiO₂ nanoparticles through nitrogen and phosphorus co-doped carbon quantum dots: an experimental and theoretical study. Physical Chemistry Chemical Physics, 2022, 24, 15271-15279.	1.3	15
69217	Theoretical investigation on structure and optoelectronic performance of two-dimensional fluorbenzidine perovskites. Wuli Xuebao/Acta Physica Sinica, 2022, 71, 208801.	0.2	2
69218	3d Carbonaceous Nanostructured Transition Metal Nitride, Carbonitride and Carbide as Polysulfide Regulators for Lithium-Sulfur Batteries. SSRN Electronic Journal, 0, , .	0.4	0
69219	Bright tunable luminescence of Sb³⁺ doping in zero-dimensional lead-free halide Cs₃ZnCl₅ perovskite crystals. Dalton Transactions, 2022, 51, 10029-10035.	1.6	9
69220	Atmospheric atomic layer deposition of SnO₂ thin films with tin(<scp>ii</scp>) acetylacetonate and water. Dalton Transactions, 2022, 51, 9278-9290.	1.6	15
69221	Biphenylene Network as Sodium Ion Battery Anode Material. SSRN Electronic Journal, 0, , .	0.4	0
69222	Thermodynamic Modeling of the Pd-Zn System with Uncertainty Quantification and its Implication to Tailor Catalysts. SSRN Electronic Journal, 0, , .	0.4	1
69223	Structural and electronic properties of pristine and hydrogen-terminated c-BN(100) surfaces. Physical Chemistry Chemical Physics, 2022, 24, 16237-16243.	1.3	4
69224	Sn4+ Doped Biobr1-Xclx with Improved Photocatalytic Performance for Degrading High Concentration Organic Dyes and Antibiotics. SSRN Electronic Journal, 0, , .	0.4	0
69225	Low-coordinated cobalt arrays for efficient hydrazine electrooxidation. Energy and Environmental Science, 2022, 15, 3246-3256.	15.6	36

#	Article	IF	Citations
69226	Sonochemical synthesis of ZnCo₂O₄/Ag₃PO₄ heterojunction photocatalysts for the degradation of organic pollutants and pathogens: a combined experimental and computational study. New Journal of Chemistry, 2022, 46, 14030-14042.	1.4	6
69227	Strain engineering and the hidden role of magnetism in monolayer VTe₂. Nanoscale, 2022, 14, 10009-10015.	2.8	2
69228	Investigating the Electrochemical Properties of Sno Monolayer in Sodium Ion Batteries. SSRN Electronic Journal, 0, , .	0.4	0
69229	Photogalvanic Effect in Spin-Polarized Zigzag Antimonene Nanoribbon with Cr and Co Edge-Modification. SSRN Electronic Journal, 0, , .	0.4	0
69230	New Approach to the Compound Energy Formalism (Nacef)Part Ii. Thermodynamic Modelling of the Alâ€“Nb System Supported by First-Principles Calculations. SSRN Electronic Journal, 0, , .	0.4	0
69231	Highly efficient and thermally stable broadband near-infrared emitting fluoride Cs₂KGaF₆:Cr³⁺ for multiple LED applications. Journal of Materials Chemistry C, 2022, 10, 10292-10301.	2.7	15
69232	DFT study of N,S co-doped graphene anodes for Na-ion storage and diffusion. New Journal of Chemistry, 2022, 46, 13866-13873.	1.4	3
69233	Putting xenon and nitrogen under pressure: towards new layered and two-dimensional nitrogen allotropes with crown ether-like nanopores. Journal of Materials Chemistry C, 2022, 10, 10374-10381.	2.7	6
69234	Antiferromagnetic ordering in the TM-adsorbed AlN monolayer (TM = V and Cr). RSC Advances, 2022, 12, 16677-16683.	1.7	2
69235	Effective High-throughput Screening of Two-Dimensional Layered Materials for Potential Lithium-ion battery Anodes. Dalton Transactions, 0, , .	1.6	0
69236	Ultra-Fast and Ultra-Efficient Removal of Cr (Vi) by the Aqueous Solutions of Monolayer Mxene (Ti3c2tx). SSRN Electronic Journal, 0, , .	0.4	0
69237	Self-Supported Graphene Oxide Encapsulated Chalcopyrite Electrode for High-Performance Li-Ion Capacitor. SSRN Electronic Journal, 0, , .	0.4	0
69238	Oxidation at the sub-nanoscale: oxygen adsorption on graphene-supported size-selected Ag clusters. Journal of Materials Chemistry A, 0, , .	5.2	3
69239	Novel boron nitride MXenes as promising energy storage materials. Nanoscale, 2022, 14, 9086-9096.	2.8	4
69240	Stitching Electron Localized Heptazine Units with â€œCarbon Patchesâ€•to Regulate Exciton Dissociation Behavior of Carbon Nitride for Photocatalytic Elimination of Petroleum Hydrocarbons. SSRN Electronic Journal, 0, , .	0.4	0
69241	A new direct band gap Siâ€“Ge allotrope with advanced electronic and optical properties. Physical Chemistry Chemical Physics, 2022, 24, 16310-16316.	1.3	2
69242	Nanostructure engineering of two-dimensional diamonds toward high thermal conductivity and approaching zero Poisson's ratio. Physical Chemistry Chemical Physics, 2022, 24, 15340-15348.	1.3	5
69243	Theoretical study on Y-doped Na₂ZrO₃ as a high-capacity Na-rich cathode material based on anionic redox. Physical Chemistry Chemical Physics, 2022, 24, 16183-16192.	1.3	7

#	Article	IF	Citations
69244	Reaction-driven selective CO₂ hydrogenation to formic acid on Pd(111). Physical Chemistry Chemical Physics, 2022, 24, 16997-17003.	1.3	5
69245	Antifluorite-type Na₅FeO₄ as a low-cost, environment-friendly cathode with combined cationic/anionic redox activity for sodium ion batteries: a first-principles investigation. RSC Advances, 2022, 12, 17410-17421.	1.7	3
69246	Investigation of Interfacial Interaction of Graphene Oxide and Ti3c2tx (Mxene) Via Atomic Force Microscopy. SSRN Electronic Journal, 0, , .	0.4	0
69247	Unraveling the role of chemical composition in the lattice thermal conductivity of oxychalcogenides as thermoelectric materials. Journal of Materials Chemistry A, 2022, 10, 19941-19952.	5.2	6
69248	Efficient Alcoholysis Reaction from Furfuryl Alcohol to Ethyl Levulinate Using Simple Nickel-Titanium Dioxide. SSRN Electronic Journal, 0, , .	0.4	0
69249	Pressure induced phase diagram of double-layer ice under confinement: A first-principles study. Physical Chemistry Chemical Physics, 0, , .	1.3	2
69250	In situ imaging the dynamics of sodium metal deposition and stripping. Journal of Materials Chemistry A, 2022, 10, 14875-14883.	5.2	6
69251	Efficient Synthesis of the Liquid Fuel 2,5-Dimethylfuran from Biomass Derived 5-(Chloromethyl)Furfural at Room Temperature. SSRN Electronic Journal, 0, , .	0.4	0
69252	Unraveling the Effects of P and S Doping Over G-C3n4 in Strengthening Lewis Basicity for Co2/Glycerol Conversion: A Theoretical and Experimental Study. SSRN Electronic Journal, 0, , .	0.4	0
69253	The impacts of molecular adsorption on antiferromagnetic MnPS₃ monolayers: enhanced magnetic anisotropy and intralayer Dzyaloshinskiiâ€“Moriya interaction. Materials Horizons, 2022, 9, 2384-2392.	6.4	11
69254	Temperature-dependence of the band gap in the all-inorganic perovskite CsPbI₃ from room to high temperatures. Physical Chemistry Chemical Physics, 2022, 24, 16003-16010.	1.3	17
69255	Extremely Low Thermal Conductivity in Basb2se4: Synthesis, Characterization, and Dft Studies. SSRN Electronic Journal, 0, , .	0.4	0
69256	Charge Carrier Management in Semiconductors: Modeling Charge Transport and Recombination. Springer Handbooks, 2022, , 365-398.	0.3	2
69257	Dual promotional effect of Cu_xO clusters grown with atomic layer deposition on TiO₂ for photocatalytic hydrogen production. Catalysis Science and Technology, 2022, 12, 4511-4523.	2.1	8
69258	Piezoelectricity and related properties in orthorhombic cadmium diiodate. Journal of Materials Chemistry C, 2022, 10, 9499-9511.	2.7	2
69259	Dynamics in the O(2 Ã— 1) adlayer on Ru(0001): bridging timescales from milliseconds to minutes by scanning tunneling microscopy. Physical Chemistry Chemical Physics, 2022, 24, 15265-15270.	1.3	3
69260	Photocatalytic hydrogen production and storage in carbon nanotubes: a first-principles study. RSC Advances, 2022, 12, 17029-17035.	1.7	6
69261	Doping-engineered biphenylene as a metal-free electrocatalyst for the hydrogen evolution reaction. Sustainable Energy and Fuels, 2022, 6, 3446-3452.	2.5	8

#	Article	IF	Citations
69262	Ru@Ni₃S₂ nanorod arrays as highly efficient electrocatalysts for the alkaline hydrogen evolution reaction. Inorganic Chemistry Frontiers, 2022, 9, 3885-3897.	3.0	9
69263	Synergistic Catalysis Induced Reaction Pathway for Facile Synthesis of Long Chain 1,2-Diol from Xylose in Acid-Metal Dual Catalyst System. SSRN Electronic Journal, 0, , .	0.4	0
69264	Ab initio high-throughput screening of transition metal double chalcogenide monolayers as highly efficient bifunctional catalysts for photochemical and photoelectrochemical water splitting. Journal of Materials Chemistry A, 2022, 10, 14060-14069.	5.2	7
69265	Mechanisms of temperature-dependent oxygen absorption/release and appearance of intermediate phase in Î²-Ce₂Zr₂O₈: study based on oxygen vacancy formation energy computations. RSC Advances, 2022, 12, 16717-16722.	1.7	0
69266	Thermodynamic stability of Pdâ€“Ru alloy nanoparticles: combination of density functional theory calculations, supervised learning, and Wangâ€“Landau sampling. Physical Chemistry Chemical Physics, 2022, 24, 15452-15461.	1.3	3
69267	Discovery of Superconductivity in K-Doped 2,2'-Bipyridine. SSRN Electronic Journal, 0, , .	0.4	0
69268	Au Catalysis for the Reduction of Metal Ions Towards Universal Core-Shell Nanostructures With Shells at Sub-Nanometer Scale. SSRN Electronic Journal, 0, , .	0.4	0
69269	Boosting the Efficient Urea Synthesis Via Cooperative Electroreduction of N2 and Co2 on Mop. SSRN Electronic Journal, 0, , .	0.4	0
69270	The resistive nature of decomposing interfaces of solid electrolytes with alkali metal electrodes. Journal of Materials Chemistry A, 2022, 10, 19732-19742.	5.2	14
69271	Revisiting the Origin of Orr and Her Activities of N-Doped Î“-Graphdiyne from the Perspective of Edge Effects. SSRN Electronic Journal, 0, , .	0.4	0
69272	Relation between Cation Distribution and Chemical Bonds in Spinel Nife2o4. SSRN Electronic Journal, 0, , .	0.4	0
69273	Magnetic and Structural Properties of the Fe5si1-Xgexb2 System. SSRN Electronic Journal, 0, , .	0.4	0
69274	Angle-resolved photoemission spectroscopy of electronic structure of 1<i>T</i>-NbSeTe. Wuli Xuebao/Acta Physica Sinica, 2022, 71, 127901.	0.2	1
69275	A new concept of atomically thin pâ€“n junction based on Ca₂N/Na₂N donorâ€“acceptor heterostructure: a first-principles study. Nanoscale, 0, , .	2.8	4
69276	Facile synthesis and phase stability of Cu-based Na₂Cu(SO₄)₂Â·xH₂O (x = 0â€“2) sulfate minerals as conversion type battery electrodes. Dalton Transactions, 2022, 51, 11169-11179.	1.6	2
69277	Delamination of MoS₂/SiO₂ interfaces under nanoindentation. Physical Chemistry Chemical Physics, 2022, 24, 15991-16002.	1.3	7
69278	Exploration of Stable Novel Al2o3 by High-Throughput Calculation Screening and Density Functional Theory. SSRN Electronic Journal, 0, , .	0.4	0
69279	Ultra-Dilute High-Entropy Alloy Catalyst with Core-Shell Structure for High-Active Hydrogenation of Furfural to Furfuryl Alcohol at Mild Temperature. SSRN Electronic Journal, 0, , .	0.4	0

#	Article	IF	Citations
69280	Predicting spinel solid solutions using a random atom substitution method. Physical Chemistry Chemical Physics, 0, , .	1.3	2
69281	Electro-elastic properties of a piezoelectric Te₂O(PO₄)₂crystal. CrystEngComm, 2022, 24, 5128-5134.	1.3	4
69282	Split of the Magnetic and Crystallographic States in Fe1-Xrhxge. SSRN Electronic Journal, 0, , .	0.4	0
69283	Unveiling Composition Dependent Electronic Behaviors of Tunnel Na3-Xhxti4o9:ÂStability and Oscillatory Band Gap. SSRN Electronic Journal, 0, , .	0.4	0
69284	High Catalytic Activity of Mbenes-Supported Single Atom Catalysts for Oxygen Reduction and Oxygen Evolution Reaction. SSRN Electronic Journal, 0, , .	0.4	0
69285	A first-principles study on environmental stability and optoelectronic properties of bismuth oxychloride/cesium lead chloride van der Waals heterojunctions. Wuli Xuebao/Acta Physica Sinica, 2022, .	0.2	0
69286	Reassignment of magic numbers for icosahedral Au clusters: 310, 564, 928 and 1426. Nanoscale, 2022, 14, 9053-9060.	2.8	3
69287	Eg Obital Occupancy-Dependent Intrinsic Catalytic Activity of Zn-Co-Mn Spinel Oxides for Peroxymonosulfate Activation. SSRN Electronic Journal, 0, , .	0.4	0
69288	Effect of nanostructuring on the activation of CO₂ on molybdenum carbide nanoparticles. Physical Chemistry Chemical Physics, 0, , .	1.3	7
69289	Thermal Transport and Thermoelectric Properties of Alkali-Metal Telluride Na2te from First-Principles Study. SSRN Electronic Journal, 0, , .	0.4	0
69290	A novel porous graphitic carbon nitride (g-C₇N₃) substrate: prediction of metal-based Ï€â€“d conjugated nanosheets toward the highly active and selective electrocatalytic nitrogen reduction reaction. Journal of Materials Chemistry A, 2022, 10, 15036-15050.	5.2	20
69291	The role of permanent and induced electrostatic dipole moments for Schottky barriers in Janus MXY/graphene heterostructures: a first-principles study. Dalton Transactions, 0, , .	1.6	11
69292	Prediction of novel two-dimensional Dirac nodal line semimetals in Al₂B₂ and AlB₄ monolayers. Nanoscale, 2022, 14, 11270-11283.	2.8	5
69293	Electronic and Optical Properties of C₁₆S₈ and C₁₆S₄Se₄ Molecules and Crystals. New Journal of Chemistry, 0, , .	1.4	1
69294	Eu²⁺ doped halide perovskite KCaCl₃ with high-efficiency blue emission and scintillation application. Journal of Materials Chemistry C, 2022, 10, 9636-9643.	2.7	21
69295	Understanding the electrochemical reaction mechanisms of precious metals Au and Ru as cathode catalysts in Liâ€“CO₂ batteries. Journal of Materials Chemistry A, 2022, 10, 14028-14040.	5.2	10
69296	Density-Functional Theory Study of Point Defect Formation and Diffusion in Î'-Alumina and Effects of Applied Strain and Alloy Doping. SSRN Electronic Journal, 0, , .	0.4	0
69297	A machine learning protocol for revealing ion transport mechanisms from dynamic NMR shifts in paramagnetic battery materials. Chemical Science, 2022, 13, 7863-7872.	3.7	10

#	Article	IF	Citations
69298	Synthesis of size-controlled boehmite sols: application in high-performance hydrogen-selective ceramic membranes. Journal of Materials Chemistry A, 2022, 10, 12869-12881.	5.2	10
69299	Combined Density Functional Theory Calculation and Non-Equilibrium Green's Function Approach to Predict the Sensitivity of Nitrogen-Containing Gases Over Pttens2-N Monolayers (N =0 - 2). SSRN Electronic Journal, 0, , .	0.4	0
69300	Revealing intrinsic spin coupling in transition metal-doped graphene. Physical Chemistry Chemical Physics, 2022, 24, 16300-16309.	1.3	7
69301	Stable Nitrogen-Rich Yttrium Nitrides Under High Pressure. SSRN Electronic Journal, 0, , .	0.4	0
69302	Phase transition and electronic properties of Coâ€“As binary compounds at high pressure. RSC Advances, 2022, 12, 18102-18106.	1.7	0
69303	Control of electric properties of silicene heterostructure by reversal of ferroelectric polarization. Wuli Xuebao/Acta Physica Sinica, 2022, 71, 177303.	0.2	1
69304	Prediction of two-dimensional monolayer C₂O₂Fe with chiral magnetic and ferroelectric orders. Physical Chemistry Chemical Physics, 2022, 24, 16827-16835.	1.3	2
69305	Pressure enhanced negative thermal expansion in 2H CuScO₂ from first-principles calculations. Physical Chemistry Chemical Physics, 2022, 24, 16622-16627.	1.3	2
69306	Synergistic Catalysis Induced Reaction Pathway for Facile Synthesis of Long Chain 1,2-Diol from Xylose in Acid-Metal Dual Catalyst System. SSRN Electronic Journal, 0, , .	0.4	0
69307	First-Principles Assessment of Chemical Lithiation of Sulfide Electrolytes and its Impact on Their Transport, Electronic and Mechanical Properties. SSRN Electronic Journal, 0, , .	0.4	0
69308	Antimony doping to enhance luminescence of tin(<scp>iv</scp>)-based hybrid metal halides. Inorganic Chemistry Frontiers, 2022, 9, 3865-3873.	3.0	9
69309	A penta-BCP sheet with strong piezoelectricity and a record high positive Poisson's ratio. Journal of Materials Chemistry C, 2022, 10, 10302-10309.	2.7	6
69310	Computational screening of single transition-metal atoms anchored to g-C₉N₄ as catalysts for N₂ reduction to NH₃. Physical Chemistry Chemical Physics, 2022, 24, 17155-17162.	1.3	5
69311	Cs₂AgBiBr₆-Tellurium heterojunction-based high-performance X-ray detectors. , 2022, , .		1
69312	Structural and physical properties of Sr/Ca and Mg/Ca substituted hydroxyapatite: modeling and experiments. Ferroelectrics, 2022, 590, 41-48.	0.3	5
69313	Ab initio investigation of structural and electronic properties of BaTiO₃/Si heterostructure. Ferroelectrics, 2022, 590, 66-72.	0.3	0
69314	Origin of the low formation energy of oxygen vacancies in CeO₂. Chinese Physics B, 2022, 31, 107102.	0.7	1
69315	Theoretical prediction of mechanics, transport, and thermoelectric properties of full Heusler compounds <mml:math xmlns:mml="http://www.w3.org/1998/Math/MathML"><mml:mrow><mml:msub><mml:mi>Na</mml:mi><mml:mn>2</mml:mn></mml:msub></mml:mrow></mml:math> and <mml:math		

#	Article	IF	Citations
69316	Dielectric-dependent hybrid functional calculations on the electronic band gap of <mml:math xmlns:mml="http://www.w3.org/1998/Math/MathML"><mml:mn>3</mml:mn><mml:mi>d</mml:mi></mml:math> transition metal doped <mml:math xmlns:mml="http://www.w3.org/1998/Math/MathML"><mml:msub><mml:mi>SnS</mml:mi><mml:mn>2</mml:mn></mml:msub></mm and their optical properties. Physical Review B, 2022, 105, .	1.1	5
69317	Phase transition of a MoS2 monolayer through top layer desulfurization by He+ ion irradiation. Journal of Applied Physics, 2022, 131, .	1.1	4
69318	In-situ embedding CoTe catalyst into 1Dâ€“2D nitrogen-doped carbon to didirectionally regulate lithium-sulfur batteries. Nano Research, 2022, 15, 8972-8982.	5.8	31
69319	Role of vacancies in tuning the electronic and magnetic properties of BiCoO₃. Physica Scripta, 2022, 97, 075819.	1.2	1
69320	Manipulation of Spin Polarization in Boron-Substituted Graphene Nanoribbons. ACS Nano, 2022, 16, 11244-11250.	7.3	12
69321	Practicality assessment: Temperature-governed performance of CO2-containing Liâ€“O2 batteries. Chemical Engineering Journal, 2022, 449, 137744.	6.6	1
69322	Anharmonicity-induced phonon hardening and phonon transport enhancement in crystalline perovskite <mml:math xmlns:mml="http://www.w3.org/1998/Math/MathML"><mml:msub><mml:mi>BaZrO</mml:mi><mml:mn>3</mml:mn></mml:msub></m Physical Review B, 2022, 105, .	1.1	26
69323	Natural Stibnite for Lithium-/Sodium-Ion Batteries: Carbon Dots Evoked High Initial Coulombic Efficiency. Nano-Micro Letters, 2022, 14, .	14.4	42
69324	On the nature of planar defects in transition metal diboride line compounds. Materialia, 2022, 24, 101478.	1.3	4
69325	Ab Initio Studies of Work Function Changes of CO Adsorption on Clean and Pd-Doped ZnGa2O4(111) Surfaces for Gas Sensors. Applied Sciences (Switzerland), 2022, 12, 5978.	1.3	3
69326	Developing Potential Energy Surfaces for Graphene-Based 2Dâ€“3D Interfaces From Modified High-Dimensional Neural Networks for Applications in Energy Storage. Journal of Electrochemical Energy Conversion and Storage, 2022, 19, .	1.1	4
69327	Intrinsic Valley Splitting and Direct-to-Indirect Band Gap Transition in Monolayer HfZrSiCO₂. Journal of Physical Chemistry Letters, 2022, 13, 5204-5212.	2.1	11
69328	The Diffusion Mechanism of Ge During Oxidation of Si/SiGe Nanofins. ACS Applied Materials & Interfaces, 2022, 14, 29422-29430.	4.0	3
69329	Manipulating Spin Polarization of Defected Co3O4 for Highly Efficient Electrocatalysis. Transactions of Tianjin University, 2022, 28, 163-173.	3.3	19
69330	First-principles prediction of the half-metallicity in quaternary Heusler CoRhCrAl thin films. Physica Scripta, 2022, 97, 075812.	1.2	1
69331	Immobilizing U cations in Sr2Fe2O6-Î´ as a new cathode for proton-conducting solid oxide fuel cells. Ceramics International, 2022, 48, 28751-28758.	2.3	2
69332	Physicochemical Screen Effect of Li Ions in Oxygen Redox Cathodes for Advanced Sodium-Ion Batteries. Chemistry of Materials, 2022, 34, 5971-5979.	3.2	6
69333	Optical and electronic anisotropy of a 2D semiconductor SiP. Nano Research, 2022, 15, 8579-8586.	5.8	8

#	Article	IF	Citations
69334	Nonthermal melting of charge density wave order via nucleation in <mml:math xmlns:mml="http://www.w3.org/1998/Math/MathML"><mml:msub><mml:mi>VTe</mml:mi><mml:mn>2</mml:mn></mml:msub></mml Physical Review B, 2022, 105, .	1.1	6
69335	Superconducting and structural properties of the noncentrosymmetric <mml:math xmlns:mml="http://www.w3.org/1998/Math/MathML"><mml:mrow><mml:msub><mml:mi>Re</mml:mi><mml:mn>6</mml:mn></mml:m superconductor under high pressure. Physical Review B, 2022, 105, .	1.1	2
69336	Deep machine learning potential for atomistic simulation of Fe-Si-O systems under Earth's outer core conditions. Physical Review Materials, 2022, 6, .	0.9	8
69337	Toward machine learning for microscopic mechanisms: A formula search for crystal structure stability based on atomic properties. Journal of Applied Physics, 2022, 131, .	1.1	2
69338	First-principles predictions of qubits in defective MgS. Physical Review B, 2022, 105, .	1.1	1
69339	T-Phase and H-Phase Coupled TMD van der Waals Heterostructure ZrS₂/MoTe₂ with Both Rashba Spin Splitting and Type-III Band Alignment. Journal of Physical Chemistry C, 2022, 126, 10601-10609.	1.5	5
69340	Formation of <mml:math xmlns:mml="http://www.w3.org/1998/Math/MathML"><mml:mrow><mml:mi mathvariant="normal">N</mml:mi><mml:msub><mml:mi mathvariant="normal">H</mml:mi><mml:mn>3</mml:mn></mml:msub><mml:mtext>â‹…</mml:mtext><mml:mi>Xe</mml:mi></mml:m compound at the extreme condition of planetary interiors. Physical Review B, 2022, 105, .	1.1	5
69341	Engineering magnetic topological insulators in <mml:math xmlns:mml="http://www.w3.org/1998/Math/MathML"><mml:mrow><mml:msub><mml:mrow><mml:mi>Eu</mml:mi></mml:mrow></mml:mrow><mml Zintl compounds. Physical Review B, 2022, 105, .	1.1	11
69342	Magnetotransport Study of van der Waals <mml:math xmlns:mml="http://www.w3.org/1998/Math/MathML" display="inline" overflow="scroll"><mml:msub><mml:mrow><mml:mi>Cr</mml:mi><mml:mi>PS</mml:mi></mml:mrow><mml:mn>4</mml:mn></mml: stretchy="false">(</mml:mo><mml:mi>Pt</mml:mi><mml:mo>,</mml:mo><mml:mi>Pd</mml:mi><mml:mo) Tj ETQq0 0 0 rgBT /Overlo </mml:math Room-Temperature Anomalous Hall Effect. Physical Review Applied, 2022, 17, .	1.5	6
69343	xmlns:mml="http://www.w3.org/1998/Math/MathML"><mml:msub><mml:mi>T</mml:mi><mml:mi>c</mml:mi></mml:msub></mml: up to 23.6ÂK and robust superconductivity in the transition metal <mml:math xmlns:mml="http://www.w3.org/1998/Math/MathML"><mml:mi>Î´</mml:mi><mml:mtext>â‹…</mml:mtext><mml:mi>Ti</mml:mi></m phase at megabar pressure. Physical Review B, 2022, 105, .	1.1	13
69344	Dual-metal atoms embedded into two-dimensional covalent organic framework as efficient electrocatalysts for oxygen evolution reaction: A DFT study. Nano Research, 2022, 15, 7994-8000.	5.8	25
69345	Computational Insight into Metallated Graphynes as Single Atom Electrocatalysts for Nitrogen Fixation. ACS Applied Materials & Interfaces, 2022, 14, 27861-27872.	4.0	22
69346	Theoretical Studies of a Silica Functionalized Acrylamide for Calcium Scale Inhibition. Polymers, 2022, 14, 2333.	2.0	2
69347	Tension-induced phase transformation and anomalous Poisson effect in violet phosphorene. Materials Today Physics, 2022, 27, 100755.	2.9	3
69348	First-Principles Calculations of the Exchange Interaction of the CrGeTe3/NiO Interface. Frontiers in Materials, 0, 9, .	1.2	0
69349	Tensileâ€Strained RuO₂ Loaded on Antimonyâ€Tin Oxide by Fast Quenching for Protonâ€Exchange Membrane Water Electrolyzer. Advanced Science, 2022, 9, .	5.6	28
69350	All-Solid-State Li Batteries with NCMâ€“Garnet-Based Composite Cathodes: The Impact of NCM Composition on Material Compatibility. ACS Applied Energy Materials, 2022, 5, 6913-6926.	2.5	25
69351	The stability and electronic structures of Li2MnO3 in highly charged states. Journal of Materials Research, 0, , .	1.2	0

#	Article	IF	Citations
69352	Ab initio investigation on preferred orientation at the Al/Al3(Zr,Y) interface in Alâ€“Zrâ€“Y alloy. Journal of Applied Physics, 2022, 131, .	1.1	4
69353	CdS/CuCo2S4 dots-on-rods boosting charge separation and hydrogen evolution. International Journal of Hydrogen Energy, 2022, 47, 23632-23643.	3.8	4
69354	Two-dimensional <mml:math xmlns:mml="http://www.w3.org/1998/Math/MathML"><mml:mrow><mml:mi>M</mml:mi><mml:msub><mml:mi>Si</mml:mi><mml:mr mathvariant="normal">N</mml:mi><mml:mn>4</mml:mn></mml:msub></mml:mrow></mml:math> monolayers and van der Waals heterostructures: Promising spintronic properties and band alignments. Physical Review Materials, 2022, 6, .	0.9	15
69355	Phase-Dependent Epitaxy for Antimonene Growth on Silver Substrate. Frontiers in Physics, 0, 10, .	1.0	4
69356	Accelerated Mining of 2D Van der Waals Heterojunctions by Integrating Supervised and Unsupervised Learning. Chemistry of Materials, 2022, 34, 5571-5583.	3.2	7
69357	Leveraging Nitrogen Linkages in the Formation of a Porous Thoriumâ€“Organic Nanotube Suitable for Iodine Capture. Inorganic Chemistry, 2022, 61, 9480-9492.	1.9	14
69358	High Thermoelectric Performance in 2D Technetium Dichalcogenides TcX₂ (X = S, Se, or) Tj ETQq0 0 0 rgBT /Overlock 10 Tf	2.5	11
69359	Influence of Hexagonal Boron Nitride on Electronic Structure of Graphene. Molecules, 2022, 27, 3740.	1.7	2
69360	Synthesis of adjustable {312}/{004} facet heterojunction MWCNTs/Bi5O7I photocatalyst for ofloxacin degradation: Novel insights into the charge carriers transport. Journal of Hazardous Materials, 2022, 437, 129374.	6.5	12
69361	Bright Green Emission from Self-Trapped Excitons Triggered by Sb³⁺ Doping in Rb₄CdCl₆. Chemistry of Materials, 2022, 34, 5717-5725.	3.2	72
69362	Allotropy in ultra high strength materials. Nature Communications, 2022, 13, .	5.8	3
69363	Pressure-induced superconductivity and nontrivial band topology in compressed Î³-InSe. Physical Review B, 2022, 105, .	1.1	7
69364	Electronic transport coefficients from density functional theory across the plasma plane. Physical Review E, 2022, 105, .	0.8	7
69365	Symmetry progression and possible polar metallicity in NiPS3 under pressure. Npj 2D Materials and Applications, 2022, 6, .	3.9	4
69366	Insight into the Fergusoniteâ€“Scheelite Phase Transition of ABO₄-Type Oxides by Density Functional Theory: A Case Study of the Subtleties of the Ground State of BiVO₄. Chemistry of Materials, 2022, 34, 5334-5343.	3.2	6
69367	How to Change the Reaction Chemistry on Nonprecious Metal Oxide Nanostructure Materials for Electrocatalytic Oxidation of Biomassâ€Derived Glycerol to Renewable Chemicals. Advanced Materials, 2023, 35, .	11.1	17
69368	Controllable electrodeposition of ordered carbon nanowalls on Cu(111) substrates. Materials Today, 2022, 57, 75-83.	8.3	3
69369	In Situ Structural Reconstruction to Generate the Active Sites for CO₂ Electroreduction on Bismuth Ultrathin Nanosheets. Advanced Energy Materials, 2022, 12, .	10.2	40

#	Article	IF	Citations
69370	Theoretical Study on the Structural, Elastic, Electronic and Thermodynamic Properties of Long-Period Superstructures h- and r-Al2Ti under High Pressure. Materials, 2022, 15, 4236.	1.3	1
69371	Room-temperature liquid metal synthesis of nanoporous copper-indium heterostructures for efficient carbon dioxide reduction to syngas. Science China Materials, 2022, 65, 3504-3512.	3.5	8
69372	Growth mechanism and self-polarization of bilayer InSb (111) on Bi (001) substrate. Journal of Physics Condensed Matter, 2022, 34, 335001.	0.7	0
69373	Effect of hydrogen on magnetic properties in MgO studied by first-principles calculations and experiments. Scientific Reports, 2022, 12, .	1.6	2
69374	Determining the Hyperfine Structure and Clock Transitions for Kramers Rare-Earth Ions in a Crystal under a Magnetic Field: Beyond Spin Hamiltonian. Journal of Physical Chemistry C, 2022, 126, 9926-9936.	1.5	5
69375	Spontaneous Formate Oxidation on the 2D Surface Metal Fluoride Interface Reconstructed from the AgPdF Surface. Journal of Physical Chemistry C, 2022, 126, 9683-9695.	1.5	6
69376	Strong, tough, ionic conductive, and freezing-tolerant all-natural hydrogel enabled by cellulose-bentonite coordination interactions. Nature Communications, 2022, 13, .	5.8	108
69377	Freezing solute atoms in nanograined aluminum alloys via high-density vacancies. Nature Communications, 2022, 13, .	5.8	18
69378	Observation of anomalous amplitude modes in the kagome metal CsV3Sb5. Nature Communications, 2022, 13, .	5.8	34
69379	Designing doping strategy in arsenene monolayer for spintronic and optoelectronic applications: a case study of germanium and nitrogen as dopants. Journal of Physics Condensed Matter, 2022, 34, 355301.	0.7	2
69380	Experimental and Theoretical Study of Stable and Metastable Phases in Sputtered CuInS₂. Advanced Science, 2022, 9, .	5.6	8
69381	Elucidation of Structureâ€“Activity Relations in Proton Electroreduction at Pd Surfaces: Theoretical and Experimental Study. Small, 2022, 18, .	5.2	7
69382	Carrier control in Snâ€“Pb perovskites via 2D cation engineering for all-perovskite tandem solar cells with improved efficiency and stability. Nature Energy, 2022, 7, 642-651.	19.8	121
69383	Elasticity, mechanical and thermal properties of polycrystalline hafnium carbide and tantalum carbide at high pressure. Journal of the European Ceramic Society, 2022, 42, 5220-5228.	2.8	6
69384	Highâ€Performance Thermoelectric Material and Module Driven by Mediumâ€Entropy Engineering in SnTe. Advanced Functional Materials, 2022, 32, .	7.8	30
69385	Bismuth oxyhalide quantum dots modified sodium titanate necklaces with exceptional population of oxygen vacancies and photocatalytic activity. Journal of Colloid and Interface Science, 2022, 625, 750-760.	5.0	23
69386	Machine Learning and First-Principles Discovery of Ternary Superhard Materials. ACS Symposium Series, 0, , 211-238.	0.5	0
69387	Physically driven enhancement of the stability of Bi2O3-based ionic conductors via grain boundary engineering. NPG Asia Materials, 2022, 14, .	3.8	7

#	Article	IF	Citations
69388	Dirac Fermions in the Boron Nitride Monolayer with a Tetragon. Journal of Physical Chemistry Letters, 2022, 13, 5508-5513.	2.1	14
69389	Atomic-Level Modulation-Induced Electron Redistribution in Co Coordination Polymers Elucidates the Oxygen Reduction Mechanism. ACS Catalysis, 2022, 12, 7531-7540.	5.5	36
69390	Multi-Level Resistive Switching in SnSe/SrTiO3 Heterostructure Based Memristor Device. Nanomaterials, 2022, 12, 2128.	1.9	8
69391	Proximity Effects in 2D VSe₂ Magnets via Interface Coupling with a BiFeO₃(0001) Ferromagnetic Surface. Journal of Physical Chemistry C, 0, , .	1.5	3
69392	Molecule bridged graphene/Ag for highly conductive ink. Science China Materials, 2022, 65, 2771-2778.	3.5	5
69393	Constructing Ni-VN interfaces with superior electrocatalytic activity for alkaline hydrogen evolution reaction. Journal of Colloid and Interface Science, 2022, 626, 486-493.	5.0	3
69394	Enhanced electrical transport properties of PbTe single crystal through Ga substitution synthesized by a Pb-flux method. Journal of Alloys and Compounds, 2022, 920, 165953.	2.8	3
69395	Interlayerâ€Incorporation of MoS₂ (TMâ€MoS₂) to Achieve Unique Magnetic and Electronic Properties for Spintronics. Advanced Electronic Materials, 2022, 8, .	2.6	4
69396	Mechanistic Differences between Electrochemical Hydrogenation and Hydrogenolysis of 5â€Hydroxymethylfurfural and Their pH Dependence. ChemSusChem, 2022, 15, .	3.6	18
69397	Mechanistic and Experimental Study of the CuxO@C Nanocomposite Derived from Cu3(BTC)2 for SO2 Removal. Catalysts, 2022, 12, 689.	1.6	0
69398	A Hybrid Functional Study on Perovskite-Based Compounds CsPb_{1â^'Î±}Zn_{Î±}I_{3â^'Î²}X_{Î²} (X = Cl or Br). Journal of Physical Chemistry Letters, 2022, 13, 5900-5909.	2.1	8
69399	Recent advances in density functional theory and molecular dynamics simulation of mechanical, interfacial, and thermal properties of natural gas hydrates in Canada. Canadian Journal of Chemical Engineering, 2022, 100, 2557-2571.	0.9	2
69400	An analysis of point defects in ZnTe using density functional theory calculations. Journal of Alloys and Compounds, 2022, 921, 166017.	2.8	2
69401	Hydroxyl vacancies triggered high methanol oxidation activity of monolayered layered double hydroxides for energy-saving hydrogen production. Materials Today Energy, 2022, 28, 101082.	2.5	10
69402	First-Principles Study of n*AlN/n*ScN Superlattices with High Dielectric Capacity for Energy Storage. Nanomaterials, 2022, 12, 1966.	1.9	3
69403	Magnetic proximity induced valley-contrasting quantum anomalous Hall effect in a graphene-<mml:math xmlns:mml="http://www.w3.org/1998/Math/MathML"><mml:msub><mml:mrow><mml:mi>CrBr</mml:mi></mml:mrow><mml:mn>3</mml:mn></	1.1	11
69404	Dynamical study of the origin of the charge density wave in <mml:math xmlns:mml="http://www.w3.org/1998/Math/MathML"><mml:mrow><mml:mi>A</mml:mi><mml:msub><mml:mi mathvariant="normal">V</mml:mi><mml:mn>3</mml:mn></mml:msub><mml:msub><mml:mi>Sb</mml:mi><mml:mn>5</mml:mn></ (<mml:math) Tj ETQq0 0 0 rgBT /Overlock 10 Tf 50 97 Td (xmlns:mml="http://www.w3.org/1998/Math/MathML"><mml:mrow><mml:m	1.1	17
69405	Effect of iron vacancies on magnetic order and spin dynamics of the spin-ladder <mml:math xmlns:mml="http://www.w3.org/1998/Math/MathML"><mml:msub><mml:mi mathvariant="normal">BaFe</mml:mi><mml:mrow><mml:mn>2</mml:mn><mml:mo>â^'</mml:mo><mml:mi>Î´</mml:mi></mml:mrow></ mathvariant="normal">S</mml:mi><mml:mrow><mml:mn>1.5</mml:mn></mml:mrow></mml:msub><mml:msub><mml:mi mathvariant="normal">Se</mml:mi><mml:mrow><mml:mn>1.5</mml:mn></mml:mrow></mml:msub></mml:math>. Physical Review B, 2022, 105, .	1.1	3

#	Article	IF	Citations
69406	New Type of Anticommutative Dynamical Magnetoelectric Response. Physical Review Letters, 2022, 128, .	2.9	1
69407	AbÂInitio Simulation of Amorphous Graphite. Physical Review Letters, 2022, 128, .	2.9	25
69408	Generalized Wilson loop method for nonlinear light-matter interaction. Npj Quantum Materials, 2022, 7, .	1.8	10
69409	Sr-Based Sub/Surface Integrated Layer and Bulk Doping to Enhance High-Voltage Cycling of a Ni-Rich Cathode Material. ACS Sustainable Chemistry and Engineering, 2022, 10, 7883-7895.	3.2	11
69410	Selective formation of ultrathin PbSe on Ag(111). Chinese Physics B, 2022, 31, 096801.	0.7	2
69411	Examination of a Structural Preference in Quaternary Alkali-Metal (A) Rare-Earth (R) Copper Tellurides by Combining Experimental and Quantum-chemical Means. Inorganic Chemistry, 2022, 61, 9269-9282.	1.9	6
69412	Microscopic functionality of FeN4 sites in polymeric carbon nitride for efficient H2S oxidation. Applied Surface Science, 2022, 600, 154011.	3.1	6
69413	Machine learning the metastable phase diagram of covalently bonded carbon. Nature Communications, 2022, 13, .	5.8	9
69414	Anisotropic carrier dynamics in a laser-excited <mml:math xmlns:mml="http://www.w3.org/1998/Math/MathML"><mml:msub><mml:mi>Fe</mml:mi><mml:mn>1</mml:mn></mml:msub><mml:r heterostructure from real-time time-dependent density functional theory. Physical Review B, 2022, 105, .	1.1	2
69415	Chemical Interpretation of Charged Point Defects in Semiconductors: A Case Study of Mg₂Si. ChemNanoMat, 2022, 8, .	1.5	2
69416	Direct investigation of the atomic structure and decreased magnetism of antiphase boundaries in garnet. Nature Communications, 2022, 13, .	5.8	1
69417	Properties of high entropy borides synthesized via microwave-induced plasma. APL Materials, 2022, 10, .	2.2	13
69418	Stability of high-temperature salty ice suggests electrolyte permeability in water-rich exoplanet icy mantles. Nature Communications, 2022, 13, .	5.8	13
69419	Suppressing the Excitonic Effect in Covalent Organic Frameworks for Metal-Free Hydrogen Generation. Jacs Au, 2022, 2, 1848-1856.	3.6	9
69420	Weak electronic correlations in the kagome superconductor <mml:math xmlns:mml="http://www.w3.org/1998/Math/MathML"><mml:mrow><mml:mi>A</mml:mi><mml:msub><mml:mi mathvariant="normal">V</mml:mi><mml:mn>3</mml:mn></mml:msub><mml:msub><mml:mi>Sb</mml:mi><mml:mn>5</mml:mn></ (<mml:math) Tj ETQq0 0 0 rgBT /Overlock 10 Tf 50 172 Td (xmlns:mml="http://www.w3.org/1998/Math/MathML"><mml:mrow><mml:r	1.1	2
69421	Uncovering the Nature of Band Gap Engineering of Adsorption Energy by Elucidating an Adsorbate Bonding Mechanism on Two-Dimensional TiO₂(110). Journal of Physical Chemistry C, 2022, 126, 10677-10685.	1.5	3
69422	NMR Crystallography of Monovalent Cations in Inorganic Matrices: Na⁺ Siting and the Local Structure of Na⁺ Sites in Ferrierites. Journal of Physical Chemistry C, 0, , .	1.5	0
69423	Transition-metal single atom catalyst embedded in C2N for toxic-gas reduction reaction and selective gas-sensing application: Atomic-scale study. Applied Surface Science, 2022, 599, 154037.	3.1	13

#	Article	IF	Citations
69424	Partially Diffusive Helium-Silica Compound under High Pressure. Chinese Physics Letters, 0, , .	1.3	3
69425	Enhancing the bifunctional activity of CoSe2 nanocubes by surface decoration of CeO2 for advanced zinc-air batteries. Journal of Colloid and Interface Science, 2022, 625, 839-849.	5.0	14
69426	Mechanical and electronic properties of <mml:math xmlns:mml="http://www.w3.org/1998/Math/MathML"><mml:mi>Î±</mml:mi><mml:mtext>â€™</mml:mtext><mml:mrow><mml:msub><(<mml:math xmlns:mml="http://www.w3.org/1998/Math/MathML"><mml:mi>M</mml:mi></mml:math>) Tj ETQq0 0 0 rgBT /Overlock 1	1.1	17
69427	monolayers. Physical Review B, 2022, 105, . First-principles study of sodium adsorption and diffusion on vacancies, N, S, and NS-codoped graphene. Materials Today Communications, 2022, 32, 103817.	0.9	2
69428	A first principle study of electronic structure and magnetic properties of TlFe2Se2. Materials Today: Proceedings, 2022, , .	0.9	0
69429	Synergistic Effects in the Activity of Nanoâ€Transitionâ€Metal Clusters Pt12M (M = Ir, Ru or Rh) for NO Dissociation. ChemPhysChem, 0, , .	1.0	0
69430	Evaluation of crystalline quality of traveling heater method (THM) grown Cd0.9Zn0.1Te0.98Se0.02 crystals. Applied Physics Letters, 2022, 120, .	1.5	4
69431	Successive Deprotonation Steering the Structural Evolution of Supramolecular Assemblies on Ag(111). Molecules, 2022, 27, 3876.	1.7	2
69432	Effect of High Order Phonon Scattering on the Thermal Conductivity and Its Response to Strain of a Penta-NiN₂ Sheet. Journal of Physical Chemistry Letters, 2022, 13, 5734-5741.	2.1	16
69433	Effects of Subsurface Oxide on Cu₁/CeO₂ Single-Atom Catalysts for CO Oxidation: A Theoretical Investigation. Inorganic Chemistry, 2022, 61, 10006-10014.	1.9	5
69434	La2Ti2O7 nanosheets synthesized under magnetic field for ofloxacin ferrophotocatalytic degradation. Journal of Environmental Chemical Engineering, 2022, 10, 108088.	3.3	6
69435	Bi₃TeBO₉: A Borate Piezoelectric Crystal with a High Piezoelectric Coefficient. Crystal Growth and Design, 0, , .	1.4	2
69436	Activated chemical bonds in nanoporous and amorphous iridium oxides favor low overpotential for oxygen evolution reaction. Nature Communications, 2022, 13, .	5.8	31
69437	Electrochemical Sodiation and Desodiation of Gallium. Journal of the Electrochemical Society, 2022, 169, 060525.	1.3	3
69438	Platinum equationÂof state to greater than two terapascals: Experimental data and analytical models. Physical Review B, 2022, 105, .	1.1	8
69439	Thickness-Dependent Magnetism and Topological Properties of EuSn₂As₂. ACS Applied Electronic Materials, 2022, 4, 3212-3219.	2.0	5
69440	New families of quantum spin Hall insulators with rashba effect in functionalized InBi monolayers. , 2022, 168, 207320.		1
69441	In-plane anisotropic charge dynamics in the layered polar Dirac semimetal <mml:math xmlns:mml="http://www.w3.org/1998/Math/MathML"><mml:msub><mml:mi>BaMnSb</mml:mi><mml:mn>2</mml:mn></mml:msub> Physical Review B, 2022, 105, .	1.1	0

#	Article	IF	Citations
69442	Structure, Diffusion, and Stability of Lithium Salts in Aprotic Dimethyl Sulfoxide and Acetonitrile Electrolytes. Journal of Physical Chemistry C, 2022, 126, 10266-10272.	1.5	7
69443	Scalable, inexpensive, one-pot, facile synthesis of crystalline two-dimensional birnessite flakes. Matter, 2022, 5, 2365-2381.	5.0	11
69444	Revealing the Electrochemistry in a Voltaic Cell by In Situ Electron Microscopy. ChemElectroChem, 2022, 9, .	1.7	0
69445	Femtomolarâ€Level Molecular Sensing of Monolayer Tungsten Diselenide Induced by Heteroatom Doping with Longâ€Term Stability. Advanced Functional Materials, 2022, 32, .	7.8	21
69446	Multi-defects engineering of NiCo2O4 for catalytic propane oxidation. Applied Surface Science, 2022, 600, 154040.	3.1	45
69447	Characterization of the ferroelectric phase transition in monolayer In<mml:math xmlns:mml="http://www.w3.org/1998/Math/MathML" display="inline" id="d1e975" altimg="si51.svg"><mml:msub><mml:mrow /><mml:mrow><mml:mn>2</mml:mn></mml:mrow></mml:msub></mml:math>Se<mml:math xmlns:mml="http://www.w3.org/1998/Math/MathML" display="inline" id="d1e983" altimg="si52.svg"><mml:msub><mml:mrow />	3.1	1
69448	Elucidating the origin of chiroptical activity in chiral 2D perovskites through nano-confined growth. Nature Communications, 2022, 13, .	5.8	41
69449	Electronic states dressed by an out-of-plane supermodulation in the quasi-two-dimensional kagome superconductor <mml:math xmlns:mml="http://www.w3.org/1998/Math/MathML"><mml:mrow><mml:msub><mml:mi>CsV</mml:mi><mml:mn>3</mml:mn></mml:msub></mml:mrow> Physical Review B, 2022, 105, .	1.1	13
69450	pH Dependence of MgO, TiO₂, and Î³-Al₂O₃ Surface Chemistry from First Principles. Journal of Physical Chemistry C, 2022, 126, 10216-10223.	1.5	21
69451	Regulation of Electronic Structures to Boost Efficient Nitrogen Fixation: Synergistic Effects between Transition Metals and Boron Nanotubes. ACS Applied Materials & Interfaces, 0, , .	4.0	1
69452	Capturing Polysulfides with a Functional Anhydride Compound for Lithiumâ€“Sulfur Batteries. ACS Applied Energy Materials, 2022, 5, 7719-7727.	2.5	10
69453	Decoupling the electronic and geometric effects of Pt catalysts in selective hydrogenation reaction. Nature Communications, 2022, 13, .	5.8	39
69454	On-Surface Synthesis of C144 Hexagonal Coronoid with Zigzag Edges. ACS Nano, 2022, 16, 10600-10607.	7.3	16
69455	Novel design of single transition metal atoms anchored on C6N6 nanosheet for electrochemical and photochemical N2 reduction to Ammonia. Catalysis Today, 2023, 424, 113804.	2.2	6
69456	Gallium-Doped Zinc Oxide Nanostructures for Tunable Transparent Thermoelectric Films. ACS Applied Nano Materials, 2022, 5, 8631-8639.	2.4	13
69457	Oxygen vacancies in Cu/TiO2 boost strong metal-support interaction and CO2 hydrogenation to methanol. Journal of Catalysis, 2022, 413, 284-296.	3.1	54
69458	Phase formation behavior and electronic transport properties of HfSe2-HfTe2 solid solution system. Journal of Alloys and Compounds, 2022, 920, 166028.	2.8	7
69459	Anderson transition in stoichiometric Fe2VAl: high thermoelectric performance from impurity bands. Nature Communications, 2022, 13, .	5.8	15

#	Article	IF	Citations
69460	Gapless Dirac magnons in CrCl3. Npj Quantum Materials, 2022, 7, .	1.8	11
69461	A Peculiar Binding Characterization of DNA (RNA) Nucleobases at MoOS-Based Janus Biosensor: Dissimilar Facets Role on Selectivity and Sensitivity. Biosensors, 2022, 12, 442.	2.3	2
69462	Adsorption mechanism and performance analysis of alkaloids as green corrosion inhibitors on mild steel. Theoretical Chemistry Accounts, 2022, 141, .	0.5	1
69463	Machine learning for metallurgy V: A neural-network potential for zirconium. Physical Review Materials, 2022, 6, .	0.9	9
69464	Distinct nitriding behaviors of Î³ and Î³â€² phases in Ni-based superalloys: A first-principles study. Journal of Alloys and Compounds, 2022, 920, 165996.	2.8	3
69465	Density functional theory study of rare earth Y, Ce and La-catalyzed oxidation mechanism of Ta(1 0 0) and Ta(1 1 0) surfaces. Applied Surface Science, 2022, 599, 154061.	3.1	4
69466	Electronic â€œBridgeâ€•Construction via Ag Intercalation to Diminish Catalytic Anisotropy for 2D Tin Diselenide Cathode Catalyst in Lithiumâ€“Oxygen Batteries. Advanced Energy Materials, 2022, 12, .	10.2	33
69467	Spatially composition-graded monolayer tungsten selenium telluride. Applied Physics Letters, 2022, 120, 231903.	1.5	0
69468	Tin-Substituted Chalcopyrite: An n-Type Sulfide with Enhanced Thermoelectric Performance. Chemistry of Materials, 2022, 34, 5860-5873.	3.2	12
69469	Electronic structure, magnetic properties, and pairing tendencies of the copper-based honeycomb lattice <mml:math xmlns:mml="http://www.w3.org/1998/Math/MathML"><mml:mrow><mml:msub><mml:mi>Na</mml:mi><mml:mn>2</mml:mn></mml:msub></mml:mrow></mml:math> Physical Review B, 2022, 105, .	1.1	0
69470	MnTa₂N₄: A Ternary Nitride Spinel with a Strong Magnetic Frustration. Chemistry of Materials, 2022, 34, 6098-6107.	3.2	2
69471	In situ formation of lithiophilic Li22Sn5 alloy and high Li-ion conductive Li2S/Li2Se via metal chalcogenide SnSSe for dendrite-free Li metal anodes. Journal of Energy Chemistry, 2022, 73, 339-347.	7.1	20
69472	Two [Co(bipy)₃]³⁺-Templated Silver Halobismuthate Hybrids: Syntheses, Structures, Photocurrent Responses, and Theoretical Studies. Inorganic Chemistry, 2022, 61, 9808-9815.	1.9	13
69473	Giant Rashba Spin Splitting in Sb/Bi2Se3/Sb and Sb/Sb2Te3 /Sb Heterojunctions. Journal of Electronic Materials, 0, , .	1.0	0
69474	Epitaxial growth of inch-scale single-crystal transition metal dichalcogenides through the patching of unidirectionally orientated ribbons. Nature Communications, 2022, 13, .	5.8	34
69475	Quantum confinement effect on defect level of hydrogen doped rutile VO2 nanowires. Journal of Applied Physics, 2022, 131, .	1.1	4
69476	Electronic phase transitions in quasi-one-dimensional atomic chains: Au wires on Si(553). Physical Review B, 2022, 105, .	1.1	0
69477	Functional Carbon and Silicon Monolayers in Biphenylene Network. ACS Applied Electronic Materials, 2022, 4, 3056-3070.	2.0	9

#	Article	IF	Citations
69478	Molecular modulating of cobalt phthalocyanines on amino-functionalized carbon nanotubes for enhanced electrocatalytic CO2 conversion. Nano Research, 2023, 16, 3649-3657.	5.8	14
69479	First-Principles Calculations on Janus MoSSe/Graphene van der Waals Heterostructures: Implications for Electronic Devices. ACS Applied Nano Materials, 2022, 5, 8371-8381.	2.4	20
69480	Removing Fluoride-Terminations from Multilayered V₂CT_x MXene by Gas Hydrolyzation. ACS Omega, 2022, 7, 23790-23799.	1.6	5
69481	Oriented Organization of Poly(3â€Hexylthiophene) for Efficient and Stable Antimony Sulfide Solar Cells. Energy and Environmental Materials, 2023, 6, .	7.3	2
69482	Enhanced Polyaniline Composites for Supercapacitor Applications. Journal of Electronic Materials, 0, , .	1.0	0
69483	On native point defects in ZnSe. Applied Physics Letters, 2022, 120, .	1.5	3
69484	Quantum embedding methods for correlated excited states of point defects: Case studies and challenges. Physical Review B, 2022, 105, .	1.1	18
69485	High-entropy hydrides for fast and reversible hydrogen storage at room temperature: Binding-energy engineering via first-principles calculations and experiments. Acta Materialia, 2022, 236, 118117.	3.8	30
69486	Manipulating the Resistive Switching in Epitaxial SrCoO_{2.5} Thin-Film-Based Memristors by Strain Engineering. ACS Applied Electronic Materials, 2022, 4, 2729-2738.	2.0	5
69487	Spin-Orbit Coupling Electronic Structures of Organic-Group Functionalized Sb and Bi Topological Monolayers. Nanomaterials, 2022, 12, 2041.	1.9	4
69488	Synthesis of 2D Î±â€GeTe Single Crystals and Î±â€GeTe/WSe₂ Heterostructures with Enhanced Electronic Performance. Advanced Functional Materials, 2022, 32, .	7.8	6
69489	Tailoring electric dipole of hole-transporting material p-dopants for perovskite solar cells. Joule, 2022, 6, 1689-1709.	11.7	38
69490	First-Principles Study of the Enhanced Magnetic Anisotropy and Transition Temperature in a CrSe₂ Monolayer via Hydrogenation. ACS Applied Electronic Materials, 2022, 4, 3240-3245.	2.0	18
69491	Fast atomic structure optimization with on-the-fly sparse Gaussian process potentials [*]. Journal of Physics Condensed Matter, 2022, 34, 344007.	0.7	2
69492	Structural instability and charge modulations in the kagome superconductor <mml:math xmlns:mml="http://www.w3.org/1998/Math/MathML"><mml:mi>A</mml:mi><mml:msub><mml:mi mathvariant="normal">V</mml:mi><mml:mn>3</mml:mn></mml:msub><mml:msub><mml:mi mathvariant="normal">Sb</mml:mi><mml:mn>5</mml:mn></mml:msub></mml:math>. Physical Review B, 2022, 105, .	1.1	11
69493	Crucial role of vibrational entropy in the <mml:math xmlns:mml="http://www.w3.org/1998/Math/MathML"><mml:mrow><mml:mi>Si</mml:mi><mml:mo>(</mml:mo><mml:mn>111</mml:mn> surface structure stability. Physical Review B, 2022, 105, .	1.1	1
69494	Homogeneous nitrogen-doped (111)-type layered Sr5Nb4O15â^'xNx as a visible-light-responsive photocatalyst for water oxidation. Nano Research, 2022, 15, 9976-9984.	5.8	8
69495	2D Higherâ€Metal Nitride Nanosheets for Solar Steam Generation. Small, 2022, 18, .	5.2	21

#	Article	IF	Citations
69496	Subâ€Nanometer Electron Beam Phase Patterning in 2D Materials. Advanced Science, 2022, 9, .	5.6	11
69497	Towards Solidâ€State Magnesium Batteries: Ligandâ€Assisted Superionic Conductivity. Batteries and Supercaps, 2022, 5, .	2.4	16
69498	Electronic and topological band evolution of VB-group transitionmetal monocarbides M2C (M=V, Nb,) Tj ETQq0 0 0 rgBT /Overlock 10 Tf	0.9	4
69499	Capturing dynamic ligand-to-metal charge transfer with a long-lived cationic intermediate for anionic redox. Nature Materials, 2022, 21, 1165-1174.	13.3	34
69500	A first-principle study of electronic, thermoelectric, and optical properties of sulfur doped c-HfO₂. Physica Scripta, 2022, 97, 075813.	1.2	3
69501	Surfaceâ€toâ€Bulk Synergistic Modification of Single Crystal Cathode Enables Stable Cycling of Sulfideâ€Based Allâ€Solidâ€State Batteries at 4.4 V. Advanced Energy Materials, 2022, 12, .	10.2	30
69502	Oxidation behaviour of sperrylite and platarsite (100) surfaces: A DFT study. Materials Today Communications, 2022, 32, 103868.	0.9	1
69503	W⁵⁺â€“W⁵⁺ Pair Induced LSPR of W₁₈O₄₉ to Sensitize ZnIn₂S₄ for Fullâ€Spectrum Solarâ€Lightâ€Driven Photocatalytic Hydrogen Evolution. Advanced Functional Materials, 2022, 32, .	7.8	48
69504	Nontrivial Topological States in BaSn₅ Superconductor Probed by de Haasâ€“van Alphen Quantum Oscillations. Chinese Physics Letters, 2022, 39, 067101.	1.3	1
69505	Strain Engineering the Ferroelectric Polarization and Optical Absorption in the FEÎ²-In₂Se₃ Monolayer. Journal of Physical Chemistry C, 2022, 126, 10181-10189.	1.5	9
69506	Spin-Valley Depolarization in van der Waals Heterostructures. Journal of Physical Chemistry Letters, 2022, 13, 5501-5507.	2.1	4
69507	Discovering Superhard Bâ€“Nâ€“O Compounds by Iterative Machine Learning and Evolutionary Structure Predictions. ACS Omega, 2022, 7, 21035-21042.	1.6	5
69508	Depleted Oxygen Defect State Enhancing Tungsten Trioxide Photocatalysis: A Quantum Dynamics Perspective. Journal of Physical Chemistry Letters, 2022, 13, 5571-5580.	2.1	15
69509	Ab Initio Investigation of Covalently Immobilized Cobalt-Centered Metalâ€“Organic Catalysts for CO₂ Reduction: The Effect of the Substrate on the Reaction Energetics. Journal of Physical Chemistry C, 2022, 126, 10081-10100.	1.5	2
69510	Ga₃Te₃I: novel 1D and 2D semiconductor materials with promising electronic and optical properties. Journal Physics D: Applied Physics, 2022, 55, 374005.	1.3	6
69511	Robust Pt/TiO2/Ni(OH)2 nanosheet arrays enable outstanding performance for high current density alkaline water electrolysis. Applied Catalysis B: Environmental, 2022, 316, 121654.	10.8	24
69512	Finite Temperature Ultraviolet-Visible Dielectric Functions of Tantalum Pentoxide: A Combined Spectroscopic Ellipsometry and First-Principles Study. Photonics, 2022, 9, 440.	0.9	2
69513	Selecting the Reaction Path in On-Surface Synthesis through the Electron Chemical Potential in Graphene. Journal of the American Chemical Society, 2022, 144, 11003-11009.	6.6	2

#	Article	IF	Citations
69514	Simple Chemical Rules for Predicting Band Structures of Kagome Materials. Journal of the American Chemical Society, 2022, 144, 10978-10991.	6.6	20
69515	The Fe₂O₃ (0001) Surface Under Electroreduction Conditions: A DFT Study of L-Cysteine Adsorption. Journal of the Electrochemical Society, 2022, 169, 064513.	1.3	1
69516	Improvement of the Interface between the Lithium Anode and a Garnet-Type Solid Electrolyte of Lithium Batteries Using an Aluminum-Nitride Layer. Nanomaterials, 2022, 12, 2023.	1.9	10
69517	Van der Waals Templateâ€Assisted Lowâ€Temperature Epitaxial Growth of 2D Atomic Crystals. Advanced Functional Materials, 2022, 32, .	7.8	4
69518	Understanding proton transfer in nonâ€aqueous biopolymers based on helical peptides: A quantum mechanical study. International Journal of Quantum Chemistry, 0, , .	1.0	0
69519	Probing the structure sensitivity of dimethyl oxalate partial hydrogenation over Ag nanoparticles: A combined experimental and microkinetic study. Chemical Engineering Science, 2022, 259, 117830.	1.9	9
69520	Near-ideal electromechanical coupling in textured piezoelectric ceramics. Nature Communications, 2022, 13, .	5.8	41
69521	Nonlinear optical response of ferroelectric oxides: First-principles calculations within the time and frequency domains. Physical Review Materials, 2022, 6, .	0.9	5
69522	Boosting Lightâ€Driven Photocatalytic Water Splitting of Bi₄NbO₈Br by Polarization Field. Solar Rrl, 2022, 6, .	3.1	4
69523	Optimum excitation wavelength and photon energy threshold for spintronic terahertz emission from Fe/Pt bilayer. IScience, 2022, 25, 104615.	1.9	8
69524	Nodeless time-reversal symmetry breaking in the centrosymmetric superconductor <mml:math xmlns:mml="http://www.w3.org/1998/Math/MathML"><mml:mrow><mml:msub><mml:mi>Sc</mml:mi><mml:mn>0.9</mml:mn></mml:r probed by muon-spin spectroscopy. Physical Review Materials, 2022, 6, .	3.1	3
69525	Theoretical Investigation of Switch Effect on the Efficiency and Adaptivity of Molecular Optoelectronic Conversion Devices. Chemistry - an Asian Journal, 0, , .	1.7	0
69526	Optical study of <mml:math xmlns:mml="http://www.w3.org/1998/Math/MathML"><mml:mrow><mml:msub><mml:mi>RbV</mml:mi><mml:mn>3</mml:mn></mml:msub></mml:mrow></mml:math> : Multiple density-wave gaps and phonon anomalies. Physical Review B, 2022, 105, .	1.1	15
69527	Synergistic Manipulation of Interdependent Thermoelectric Parameters in SnTeâ€“AgBiTe₂ Alloys by Mn Doping. ACS Applied Materials & Interfaces, 2022, 14, 29032-29038.	4.0	8
69528	Anisotropic Dzyaloshinskii-Moriya interaction protected by D2d crystal symmetry in two-dimensional ternary compounds. Npj Computational Materials, 2022, 8, .	3.5	17
69529	Enhanced reversible hydrogen storage efficiency of zirconiumâ€decorated biphenylene monolayer: A computational study. Energy Storage, 2022, 4, .	2.3	13
69530	Monolayer MSi₂P₄ (M = V, Nb, and Ta) as Highly Efficient Sulfur Host Materials for Lithiumâ€“Sulfur Batteries. ACS Applied Materials & Interfaces, 2022, 14, 27833-27841.	4.0	13
69531	Theoretical Prediction of the Monolayer Hf2Br4 as Promising Thermoelectric Material. Materials, 2022, 15, 4120.	1.3	2

#	Article	IF	Citations
69532	First-Principles Study of Siliconâ€“Tin Alloys as a High-Temperature Thermoelectric Material. Materials, 2022, 15, 4107.	1.3	3
69533	MoirÃ© band structures of twisted phosphorene bilayers. Physical Review B, 2022, 105, .	1.1	3
69534	Defective UiO-66-NH₂ Functionalized with Stable Superoxide Radicals toward Electrocatalytic Nitrogen Reduction with High Faradaic Efficiency. ACS Applied Materials & Interfaces, 2022, 14, 26571-26586.	4.0	15
69535	S₂P₂C₁₂: A two-dimensional anisotropic Janus material with tunable Dirac cone. Journal of Applied Physics, 2022, 131, 224303.	1.1	1
69536	Dynamical properties of the magnetic topological insulator <mml:math xmlns:mml="http://www.w3.org/1998/Math/MathML"><mml:mrow><mml:mi>T</mml:mi><mml:msub><mml:mi>Bi</mml:mi> : Phonons dispersion, Raman active modes, and chiral phonons study. Physical Review B, 2022, 105, .	1.1	7
69537	Decoupled atomic contribution boosted high thermoelectric performance in mixed cation spinel oxides ACo2O4. Applied Physics Letters, 2022, 120, .	1.5	4
69538	Atomic-Scale Insights into Comparative Mechanisms and Kinetics of Naâ€“S and Liâ€“S Batteries. ACS Catalysis, 2022, 12, 7664-7676.	5.5	23
69539	Lithiating magneto-ionics in a rechargeable battery. Proceedings of the National Academy of Sciences of the United States of America, 2022, 119, .	3.3	5
69540	Theoretical study of potential n-type and p-type dopants in GaN from data mining and first-principles calculation. Semiconductor Science and Technology, 2022, 37, 085004.	1.0	1
69541	Influence of Cu Doping on the Hydration of Dicalcium Silicate: A First-Principles Study. ACS Sustainable Chemistry and Engineering, 2022, 10, 8094-8104.	3.2	9
69542	Strong Neel Ordering and Luminescence Correlation in a Twoâ€Dimensional Antiferromagnet. Laser and Photonics Reviews, 0, , 2100431.	4.4	3
69543	Evolution of magnetic phase in two dimensional van der Waals Mn1-xNixPS3 single crystals. Journal of Physics Condensed Matter, 0, , .	0.7	5
69544	Strain engineering on the thermoelectric performance of monolayer AlP3: A first-principles study. Physica E: Low-Dimensional Systems and Nanostructures, 2022, , 115365.	1.3	1
69545	Site selective 5f electronic correlations in Î²-uranium. Chinese Physics B, 0, , .	0.7	0
69546	Machine learning for exploring small polaron configurational space. Npj Computational Materials, 2022, 8, .	3.5	8
69547	Band Edge Engineering of 2D Perovskite Structures through Spacer Cation Engineering for Solar Cell Applications. Journal of Physical Chemistry C, 2022, 126, 9937-9947.	1.5	6
69548	Mechanical properties and their sensitivity to point defects: <mml:math xmlns:mml="http://www.w3.org/1998/Math/MathML"><mml:mrow><mml:mo>(</mml:mo><mml:mi>HfNbTaTiZr</mml:mi><mml:mo>) mathvariant="normal">C</mml:mi></mml:mrow></mml:math> high-entropy carbide. Physical Review B, 2022, 105, .	1.1	3
69549	Structural Diversity in Oxoiridates with 1D Ir_nO_{3(n+1)} Chain Fragments and Flat Bands. Inorganic Chemistry, 0, , .	1.9	1

#	Article	IF	Citations
69550	Atomistic Mechanisms of Binary Alloy Surface Segregation from Nanoseconds to Seconds Using Accelerated Dynamics. Journal of Chemical Theory and Computation, 2022, 18, 4447-4455.	2.3	3
69551	Thermodynamics up to the melting point in a TaVCrW high entropy alloy: Systematic <mml:math xmlns:mml="http://www.w3.org/1998/Math/MathML"><mml:mrow><mml:mi>a</mml:mi><mml:mi>b</mml:mi></mml:mrow><mml:mo study aided by machine learning potentials. Physical Review B, 2022, 105, .	1.1	16
69552	Novel inorganic crystal structures predicted using autonomous simulation agents. Scientific Data, 2022, 9, .	2.4	7
69553	Cobalt Anti-MXenes as Promising Anode Materials for Sodium-Ion Batteries. Journal of Physical Chemistry C, 2022, 126, 10298-10308.	1.5	8
69554	Intrinsic local symmetry breaking in nominally cubic paraelectric <mml:math xmlns:mml="http://www.w3.org/1998/Math/MathML"><mml:mrow><mml:mi>BaTi</mml:mi><mml:msub><mml:mi mathvariant="normal">O</mml:mi><mml:mn>3</mml:mn></mml:msub></mml:mrow></mml:math>. Physical Review B, 2022, 105, .	1.1	10
69555	Effects of order-disorder transition on phase relationship, elastic strength, and mechanical anisotropy of Al-Li alloys. Materialia, 2022, 24, 101483.	1.3	0
69556	Origin of supertetragonality in <mml:math xmlns:mml="http://www.w3.org/1998/Math/MathML"><mml:msub><mml:mi>BaTiO</mml:mi><mml:mn>3</mml:mn></mml:msub></m Physical Review Materials, 2022, 6, .	0.9	4
69557	Electric field induced spin resolved graphene pâ€“n junctions on magnetic Janus VSeTe monolayer. Journal Physics D: Applied Physics, 2022, 55, 365303.	1.3	7
69558	Deep-learning density functional theory Hamiltonian for efficient ab initio electronic-structure calculation. Nature Computational Science, 2022, 2, 367-377.	3.8	38
69559	Regulating iron species compositions by Fe-Al interaction in CO2 hydrogenation. Journal of Catalysis, 2022, 413, 331-341.	3.1	17
69560	Leucine on Silica: A Combined Experimental and Modeling Study of a System Relevant for Origins of Life, and the Role of Water Coadsorption. Langmuir, 2022, 38, 8038-8053.	1.6	4
69561	Oxygen-containing surface functional groups, mesoporous structure and photothermal effect co-modulated highly-efficient H2O2 production and pollutant degradation. Electrochimica Acta, 2022, 426, 140755.	2.6	5
69562	Anharmonic Lattice Dynamics in Sodium Ion Conductors. Journal of Physical Chemistry Letters, 2022, 13, 5938-5945.	2.1	9
69563	Lowâ€temperature synthesis of highâ€entropy (Hf_{0.2}Ti_{0.2}Mo_{0.2}Ta_{0.2}Nb_{0.2})B₂ powders combined with theoretical forecast of its elastic and thermal properties. Journal of the American Ceramic Society, 2022, 105, 6370-6383.	1.9	7
69564	Li₈MnO₆: A Novel Cathode Material with Only Anionic Redox. ACS Applied Materials & Interfaces, 2022, 14, 29832-29843.	4.0	2
69565	Exploring the Impact of the Linker Length on Heat Transport in Metalâ€“Organic Frameworks. Nanomaterials, 2022, 12, 2142.	1.9	5
69566	Origin of uniaxial magnetic anisotropy in MnAlC_x: A first-principles study. AIP Advances, 2022, 12, 065221.	0.6	1
69567	Long-chain hydrocarbons by CO2 electroreduction using polarized nickel catalysts. Nature Catalysis, 2022, 5, 545-554.	16.1	107

#	Article	IF	Citations
69568	Thermodynamic modeling of Cr and Crâ€“H systems up to high temperatures and high pressures. International Journal of Hydrogen Energy, 2022, , .	3.8	2
69569	Stability, electronic, and mechanical properties of Si/Ge substitutionally doped T2CO2 (TÂ=ÂZr and Hf). Solid State Communications, 2022, 353, 114856.	0.9	3
69570	Role of an Interface for Hydrogen Production Reaction over Size-Controlled Supported Metal Catalysts. ACS Catalysis, 2022, 12, 8082-8093.	5.5	9
69571	Large Vertical Piezoelectricity in a Janus Cr2I3F3 Monolayer. Materials, 2022, 15, 4418.	1.3	4
69572	Achieving High-Temperature Ferromagnetism by Means of Magnetic Ion Dimerization in the Graphene-like Mn₂N₆C₆ Monolayer. Journal of Physical Chemistry C, 2022, 126, 10139-10144.	1.5	7
69573	Synergistically Enhanced Single-Atom Nickel Catalysis for Alkaline Hydrogen Evolution Reaction. ACS Applied Materials & Interfaces, 2022, 14, 29822-29831.	4.0	9
69574	Insights of the Ionic Transport in Intercalated Two-Dimensional Materials Leveraging Lattice Dynamics. Journal of Physical Chemistry C, 2022, 126, 10209-10215.	1.5	3
69575	Observation of <mml:math xmlns:mml="http://www.w3.org/1998/Math/MathML" display="inline"><mml:mrow><mml:mi mathvariant="normal">Î“</mml:mi></mml:mrow></mml:math> -Valley MoirÃ© Bands and Emergent Hexagonal Lattice in Twisted Transition Metal Dichalcogenides. Physical Review X, 2022, 12, .	2.8	18
69576	Automated Bonding Analysis with Crystal Orbital Hamilton Populations. ChemPlusChem, 2022, 87, .	1.3	15
69577	Phase Stability, Elastic and Electronic Properties of Ni₃Ti Intermetallic Doped with Mn and Fe: Firstâ€Principles Calculations. Physica Status Solidi (B): Basic Research, 2022, 259, .	0.7	2
69578	SrAgAsS₄: A Noncentrosymmetric Sulfide with Good Infrared Nonlinear Optical Performance Induced by Aliovalent Substitution from Centrosymmetric SrGa₂S₄. Inorganic Chemistry, 2022, 61, 9205-9212.	1.9	6
69579	AA-stacked borophene-graphene bilayer as an anode material for alkali-metal ion batteries with a superhigh capacity. Chinese Physics B, 2022, 31, 116302.	0.7	2
69580	Hydrogenation of CO and CO₂ Catalyzed by Potassium Chloride F Centers. Journal of Physical Chemistry C, 2022, 126, 9713-9723.	1.5	3
69581	Improve the tribo-corrosion behavior of oil-in-water emulsion-based drilling fluids by new derivatives of fatty acid-based green inhibitors. Tribology International, 2022, 174, 107723.	3.0	11
69582	Tetravalent Doping in Fluorite-Based Ferroelectric Oxides for Reduced Voltage Operations. ACS Applied Materials & Interfaces, 0, , .	4.0	3
69583	Particle Swarm Predictions of a SrB₈ Monolayer with 12-Fold Metal Coordination. Journal of the American Chemical Society, 2022, 144, 11120-11128.	6.6	12
69584	Strong Spin-Phonon Coupling in Two-Dimensional Magnetic Semiconductor CrSBr. Journal of Physical Chemistry C, 2022, 126, 10574-10583.	1.5	12
69585	Inâ€“Bi Electrocatalyst for the Reduction of CO₂ to Formate in a Wide Potential Window. ACS Applied Materials & Interfaces, 2022, 14, 28890-28899.	4.0	16

#	Article	IF	Citations
69586	Machine Learning Approaches for Accelerating the Discovery of Thermoelectric Materials. ACS Symposium Series, 0, , 1-32.	0.5	5
69587	Mechanistic Study on Enhanced Electrocatalytic Nitrogen Reduction Reaction by Mo Single Clusters Supported on MoS₂. ACS Applied Materials & Interfaces, 2022, 14, 28900-28910.	4.0	8
69588	Design of Novel Transition-Metal-Doped C₆N₂ with High-Efficiency Polysulfide Anchoring and Catalytic Performances toward Application in Lithiumâ€“Sulfur Batteries. ACS Applied Materials & Interfaces, 2022, 14, 29120-29130.	4.0	32
69589	Methane decomposition to high-quality carbon nanotubes: well-distributed NiCo alloy catalysts derived from layered double hydroxide. Journal of Materials Science, 0, , .	1.7	0
69590	Adsorption properties of radionuclides on BC3: the first principles study. Molecular Physics, 2022, 120, .	0.8	1
69591	Magnetic octupole tensor decomposition and second-order magnetoelectric effect. Annals of Physics, 2022, 447, 168964.	1.0	6
69592	Inorganic Crystal Structure Prototype Database Based on Unsupervised Learning of Local Atomic Environments. Journal of Physical Chemistry A, 0, , .	1.1	1
69593	Superconductive materials with <mml:math xmlns:mml="http://www.w3.org/1998/Math/MathML"><mml:msub><mml:mi>MgB</mml:mi><mml:mn>2</mml:mn></mml:msub></mml:math>-like structures from data-driven screening. Physical Review B, 2022, 105, .	1.1	10
69594	Direct electro-synthesis of valuable C=N compound from NO. Chem Catalysis, 2022, 2, 1807-1818.	2.9	21
69595	Understanding the mechanism of shockwave induced graphite-to-diamond phase transition. Materialia, 2022, 24, 101487.	1.3	0
69596	Microscopic origin of room-temperature ferromagnetism in the double perovskite <mml:math xmlns:mml="http://www.w3.org/1998/Math/MathML"><mml:mrow><mml:msub><mml:mi>Sr</mml:mi><mml:mn>2</mml:mn></mml:msub></mml:mrow></mml:math> Physical Review B, 2022, 105, .	1.1	0
69597	<mml:math xmlns:mml="http://www.w3.org/1998/Math/MathML"><mml:msub><mml:mi>NaNO</mml:mi><mml:mn>3</mml:mn></mml:msub></mml:math> monolayer: A stable graphenelike supersalt with strong four-phonon scattering and low lattice thermal conductivity insensitive to temperature. Physical Review Materials, 2022, 6, .	0.9	8
69598	Not a Mere Decoration: Impact of Submonolayer Coverages of Nickel on Fundamental Properties of Platinum. Journal of Physical Chemistry C, 2022, 126, 10167-10180.	1.5	3
69599	Theoretical validation of inhibition mechanisms of benzotriazole with copper and cobalt for CMP and post-CMP cleaning applications. Microelectronic Engineering, 2022, 262, 111833.	1.1	7
69600	Properties of AgBiI4 using high through-put DFT and machine learning methods. Journal of Applied Physics, 2022, 131, .	1.1	8
69601	Excited quantum anomalous and spin Hall effect: dissociation of flat-bands-enabled excitonic insulator state. Nanotechnology, 2022, 33, 415001.	1.3	12
69602	Functional group contributions for azo derivatives as anode materials for KIBs: A first-principles study. Materials Chemistry and Physics, 2022, 289, 126430.	2.0	1
69603	Solid-state performance of a meta-GGA screened hybrid density functional constructed from Pauli kinetic enhancement factor dependent semilocal exchange hole. Journal of Chemical Physics, 0, , .	1.2	4

#	Article	IF	Citations
69604	Thermodynamics and phase stability of Li₈XO₆ octalithium ceramic breeder materials (X = Pb, Ce, Ge, Zr, Sn). Journal of Physics Condensed Matter, 0, , .	0.7	1
69605	Mechanism of Catalytic Transfer Hydrogenation for Furfural Using Single Ni Atom Catalysts Anchored to Nitrogen-Doped Graphene Sheets. Inorganic Chemistry, 2022, 61, 9138-9146.	1.9	10
69606	Phosphorescence in Mn⁴⁺-Doped R⁺/R²⁺ Germanates (R⁺ = Na⁺ or K⁺, R²⁺ = Sr²⁺). Inorganic Chemistry, 2022, 61, 9364-9374.	1.9	0
69607	Structural And Electronic Properties of PtSe2/GaP Heterostructure. Materials Today: Proceedings, 2022, 67, 161-164.	0.9	13
69608	The effects of defects on the defect formation energy, electronic band structure, and electron mobility in 4Hâ€“SiC. AIP Advances, 2022, 12, .	0.6	2
69609	Al₂O₃/ZnO Heterostructure-Based Sensors for Volatile Organic Compounds in Safety Applications. ACS Applied Materials & Interfaces, 2022, 14, 29331-29344.	4.0	15
69610	Theoretical investigation on twoâ€dimensional monofluorinated phenylethylammonium perovskite. International Journal of Quantum Chemistry, 2022, 122, .	1.0	2
69611	Tunable green syngas generation from CO ₂ and H ₂ O with sunlight as the only energy input. Proceedings of the National Academy of Sciences of the United States of America, 2022, 119, .	3.3	16
69612	Electronic structure, magnetic properties and magnetocaloric performance in rare earths (RE) based RE2BaZnO5 (REÂ=ÂGd, Dy, Ho, and Er) compounds. Acta Materialia, 2022, 236, 118114.	3.8	68
69613	Optimizing thermoelectric performance of CoSbS0.85Se0.15 by doping 3d transition metal ions M (M =) Tj ETQq1 1 0.784314 rgBT /Ov	1.4	2
69614	A modified elastic constant calculation method for triclinic-like special quasi-random structures: Application to Pd-M (M=Cu, Ag) solid solutions. Materials Today Communications, 2022, , 103795.	0.9	0
69615	Metal-phosphorus network on Pt(111). 2D Materials, 2022, 9, 045002.	2.0	6
69616	Measuring and directing charge transfer in heterogenous catalysts. Nature Communications, 2022, 13, .	5.8	19
69617	Improved proton-transfer barriers with van der Waals density functionals: Role of repulsive non-local correlation. Journal of Chemical Physics, 2022, 156, .	1.2	3
69618	Revisiting Oxygen Adsorption on Ir(100). Journal of Physical Chemistry C, 2022, 126, 10035-10044.	1.5	7
69619	Mechanism of Pressure-Driven Band Gap Evolutions in Lead-Free Halide Double Perovskites. Journal of Physical Chemistry C, 2022, 126, 10230-10236.	1.5	5
69620	Realizing nearly isotropic thermoelectric properties in 2D-layered SnS nanomaterials through highly symmetric metastable-phase powder precursors. Nano Research, 2022, 15, 7713-7722.	5.8	2
69621	Structural defects in compounds <mml:math xmlns:mml="http://www.w3.org/1998/Math/MathML"><mml:mrow><mml:mi>Zn</mml:mi><mml:mi>X</mml:mi><mml:mi>Sb</mml:m <mml:math xmlns:mml="http://www.w3.org/1998/Math/MathML"><mml:mo>(</mml:mo><mml:mi>X</mml:mi><mml:mo>=</mml:mo><mml:mi>C : Origin of disorder and its relationship with electronic pro. Physical Review Materials, 2022, 6, .	0.9	2

#	Article	IF	Citations
69622	CO2 chemisorption and dissociation on flat and stepped transition metal surfaces. Applied Surface Science, 2022, 599, 154024.	3.1	11
69623	Thermoelectric performance in a Si allotrope with ultralow thermal conductivity: a first-principles study combining phonon-limited electronic transport calculations. Materials Today Physics, 2022, 27, 100756.	2.9	3
69624	Tuning magnetic anisotropy and Dzyaloshinskii-Moriya interaction via interface engineering in nonisostructural <mml:math xmlns:mml="http://www.w3.org/1998/Math/MathML"><mml:mrow><mml:msub><mml:mi>SrCuO</mml:mi><mml:mn>2</mml:mn></m heterostructures. Physical Review B, 2022, 105, .	1.1	2
69625	Combining Ni3P and Lewis Acidâ€“Base Pair as a High-Performance Catalyst for Amination of 1-Octanol. Catalysis Letters, 2023, 153, 1215-1226.	1.4	1
69626	Tunable Ferromagnetism in LaCoO₃ Epitaxial Thin Films. Advanced Materials Interfaces, 2022, 9, .	1.9	4
69627	Hydrogenated Cs2AgBiBr6 for significantly improved efficiency of lead-free inorganic double perovskite solar cell. Nature Communications, 2022, 13, .	5.8	109
69628	Signature of Kondo hybridisation with an orbital-selective Mott phase in 4d Ca2â^'xSrxRuO4. Npj Quantum Materials, 2022, 7, .	1.8	4
69629	Magnetoresistance of Ni/WSe₂/Ni junctions: robustness against the thickness of WSe₂. Nanotechnology, 2022, 33, 385001.	1.3	3
69630	Hybrid DFT/Data-Driven Approach for Searching for New Quasicrystal Approximants in Sc-X (X = Rh, Pd,) Tj ETQq0 0 0 rgBT /Overlock 10	1.4	4
69631	Machine learning molecular dynamics simulations toward exploration of high-temperature properties of nuclear fuel materials: case study of thorium dioxide. Scientific Reports, 2022, 12, .	1.6	10
69632	Steering surface reconstruction of copper with electrolyte additives for CO2 electroreduction. Nature Communications, 2022, 13, .	5.8	47
69633	Feâ€VS₂ Electrocatalyst with Organic Matrixâ€Mediated Electron Transfer for Highly Efficient Nitrogen Fixation. ChemSusChem, 2022, 15, .	3.6	8
69634	In Situ Surface-Sensitive Investigation of Multiple Carbon Phases on Fe(110) in the Fischerâ€“Tropsch Synthesis. ACS Catalysis, 2022, 12, 7609-7621.	5.5	13
69635	Dual-functional hosts derived from metal-organic frameworks reduce dissolution of polyselenides and inhibit dendrite growth in a sodium-selenium battery. Energy Storage Materials, 2022, 51, 249-258.	9.5	22
69636	Elucidation of Metal Local Environments in Singleâ€Atom Catalysts Based on Carbon Nitrides. Small, 2022, 18, .	5.2	15
69637	Niobium-doped layered cathode material for high-power and low-temperature sodium-ion batteries. Nature Communications, 2022, 13, .	5.8	85
69638	Strong bulk-surface interaction dominated in-plane anisotropy of electronic structure in GaTe. Communications Physics, 2022, 5, .	2.0	10
69639	Crystal Prediction and Design of Tunable Light Emission in BTBâ€Based Metalâ€Organic Frameworks. Advanced Optical Materials, 2022, 10, .	3.6	3

#	Article	IF	Citations
69640	Superconductivity in S-rich phases of lanthanum sulfide under high pressure. Physical Review Materials, 2022, 6, .	0.9	3
69641	CO₂â€Induced Twoâ€Dimensional Amorphous TiO₂ and Its Excellent Filmâ€Forming Properties. ChemNanoMat, 2022, 8, .	1.5	2
69642	High Anisotropic Optoelectronics in Monolayer Binary M₈X₁₂ (M = Mo, W; X =) Tj ETQq0 0 0 rgBT /Overlock	4.0	5
69643	Harnessing Optimized Surface Reconstruction of Single-Atom Ni-Doped Ni-NiO/NC Precatalysts toward Robust H₂O₂ Production. ACS Applied Materials & Interfaces, 2022, 14, 26803-26813.	4.0	5
69644	Deciphering the phase transition-induced ultrahigh piezoresponse in (K,Na)NbO3-based piezoceramics. Nature Communications, 2022, 13, .	5.8	39
69645	Hole conductivity through a defect band in <mml:math xmlns:mml="http://www.w3.org/1998/Math/MathML"><mml:msub><mml:mrow><mml:mi>ZnGa</mml:mi></mml:mrow><mml:mn>2</ mathvariant="normal">O</mml:mi></mml:mrow><mml:mn>4</mml:mn></mml:msub></mml:math>. Physical Review Materials, 2022, 6, .	0.9	4
69647	Superconductivity in compressed ternary alkaline boron hydrides. Physical Review B, 2022, 105, .	1.1	24
69648	First-principles calculations on CO2 hydrogenation to formic acid over a metal-doped boron phosphide. Molecular Catalysis, 2022, 527, 112412.	1.0	2
69649	Multi-scale Design and Synthesis Strategy of Ni-doped SnO2 Hollow Spheres as Anode Material for Lithium-ion Batteries. International Journal of Electrochemical Science, 0, , ArticleID:220737.	0.5	1
69650	Theoretical study of the effect of coordination environment on the activity of metal macrocyclic complexes as electrocatalysts for oxygen reduction. IScience, 2022, 25, 104557.	1.9	6
69651	A comparative study the structural, mechanical, and electronic properties of medium-entropy MAX phase (TiZrHf)2SC with Ti2SC, Zr2SC, Hf2SC via first-principles. Journal of Materials Research and Technology, 2022, 19, 2717-2729.	2.6	10
69652	Spin engineering of single-site metal catalysts. Innovation(China), 2022, 3, 100268.	5.2	6
69653	Adsorption and sensing of CO on VS2 monolayer decorated with transition metals (Cr, Mn, Fe, Co, Ni): A first-principles study. FlatChem, 2022, 34, 100389.	2.8	2
69654	Ondansetron/Cyclodextrin inclusion complex nanofibrous webs for potential orally fast-disintegrating antiemetic drug delivery. International Journal of Pharmaceutics, 2022, 623, 121921.	2.6	10
69655	Elastic behavior of binary and ternary refractory multi-principal-element alloys. Materials and Design, 2022, 219, 110820.	3.3	9
69656	Water oxidation sites located at the interface of Pt/SrTiO3 for photocatalytic overall water splitting. Chinese Journal of Catalysis, 2022, 43, 2223-2230.	6.9	18
69657	Reversible transformation between terrace and step sites of Pt nanoparticles on titanium under CO and O2 environments. Chinese Journal of Catalysis, 2022, 43, 2026-2033.	6.9	2
69658	Structural diversity and unusual valence states in compressed Na-Hg system. Computational Materials Science, 2022, 211, 111561.	1.4	0

#	Article	IF	Citations
69659	Electronic and magnetic properties of the WSO Janus monolayer engineered by intrinsic defects. Surfaces and Interfaces, 2022, 32, 102114.	1.5	2
69660	Cotton-derived carbon fiber-supported Ni nanoparticles as nanoislands to anchor single-atom Pt for efficient catalytic reduction of 4-nitrophenol. Applied Catalysis A: General, 2022, 643, 118734.	2.2	11
69661	Magnetic properties of FePc sheet modified by the adsorption of gas molecules. Computational and Theoretical Chemistry, 2022, 1214, 113793.	1.1	0
69662	Dependence of mobility and Lorenz number on electronic structure and scattering in wurtzite ZnO. Materials Chemistry and Physics, 2022, 287, 126382.	2.0	0
69663	Physical insights on the ultralow thermal conductivity of Ag8XSe6 (XÂ=ÂSi, Ge, and Sn). Inorganic Chemistry Communication, 2022, 142, 109689.	1.8	3
69664	Iron promoted MOF-derived carbon encapsulated NiFe alloy nanoparticles core-shell catalyst for CO2 methanation. Journal of CO2 Utilization, 2022, 62, 102093.	3.3	17
69665	Defect recovery processes in Cr-B binary and Cr-Al-B MAB phases: structure-dependent radiation tolerance. Acta Materialia, 2022, 235, 118099.	3.8	10
69666	Effects of the in-plane uniaxial and biaxial strains on the structural and electronic properties of the monolayer ZrS2: A first-principles investigation. Thin Solid Films, 2022, 755, 139343.	0.8	5
69667	In situ-transition nanozyme triggered by tumor microenvironment boosts synergistic cancer radio-/chemotherapy through disrupting redox homeostasis. Biomaterials, 2022, 287, 121620.	5.7	32
69668	Atomistic simulations of AuTi high-temperature shape memory alloys. International Journal of Mechanical Sciences, 2022, 227, 107467.	3.6	2
69669	Breaking the scaling relations for efficient N2-to-NH3 conversion by a bowl active site design: Insight from LaRuSi and isostructural electrides. Chinese Journal of Catalysis, 2022, 43, 2183-2192.	6.9	9
69670	First-principles calculations of the cleavage energy in random solid solutions: A case study for TiZrNbHf high-entropy alloy. Computational Materials Science, 2022, 212, 111575.	1.4	0
69671	Theoretical insights into electronic structure and NRR catalytic mechanism based on halide perovskites CsPbBr3-xIx. Computational Materials Science, 2022, 212, 111576.	1.4	5
69672	Adsorption of residual gas on the (001) surface of Cs/O co-sensitized In0.53Ga0.47As photocathode. Vacuum, 2022, 203, 111242.	1.6	2
69673	Prediction of new stable phases of FePd2 crystal alloy. Journal of Solid State Chemistry, 2022, 313, 123328.	1.4	0
69674	Remove the â€“F Terminal Groups on Ti3C2Tx by Reaction with Sodium Metal to Enhance Pseudocapacitance. Energy Storage Materials, 2022, 50, 802-809.	9.5	14
69675	In-situ formation of Are-MXY(M = Mo, W; (X â‰ Y) = S, Se, Te) van der Waals heterostructure. Journal of Solid State Chemistry, 2022, 313, 123284.	1.4	2
69676	A novel carbonate nitrogen triacetemetal C<mml:math xmlns:mml="http://www.w3.org/1998/Math/MathML" display="inline" id="d1e709" altimg="si31.svg"><mml:msub><mml:mrow /><mml:mrow><mml:mn>5</mml:mn></mml:mrow></mml:msub></mml:math>N<mml:math xmlns:mml="http://www.w3.org/1998/Math/MathML" display="inline" id="d1e717" altimg="si32.svg"><mml:msub><mml:mrow /><mml:mrow><mml:mn>4</mml:mn></mml:mrow></mml:ms	1.3	1

#	Article	IF	Citations
69677	Intrinsic anion vacancy of Mo6X6 (XÂ=ÂS, Se, Te) nanowires as a promising nitrogen fixation catalysis: A first-principles study. Chemical Physics Letters, 2022, 802, 139752.	1.2	0
69678	First-principles investigation of V2CSe2 MXene as a potential anode material for non-lithium metal ion batteries. Current Applied Physics, 2022, 41, 7-13.	1.1	7
69679	Preferential growth of HT-LiCo1-xAlxO2 cathode micro-bricks via an intermediate-facilitated solid-solid-gas reaction. Journal of Power Sources, 2022, 542, 231700.	4.0	2
69680	Enhancing kinetic and electrochemical performance of layered MoS2 cathodes with interlayer expansion for Mg-ion batteries. Journal of Power Sources, 2022, 542, 231722.	4.0	6
69681	Potential accident tolerant fuel candidate: Investigation of physical properties of the ternary phase U2CrN3. Journal of Nuclear Materials, 2022, 568, 153851.	1.3	5
69682	X-ray induced coloration behavior of Lu2O3:Eu transparent ceramics and the impact of ZrO2 and HfO2 sintering additives. Optical Materials, 2022, 131, 112641.	1.7	4
69683	Delicate surface vacancies engineering of Ru doped MOF-derived Ni-NiO@C hollow microsphere superstructure to achieve outstanding hydrogen oxidation performance. Journal of Energy Chemistry, 2022, 72, 395-404.	7.1	29
69684	The spatially separated active sites for holes and electrons boost the radicals generation for toluene degradation. Journal of Hazardous Materials, 2022, 437, 129329.	6.5	9
69685	Theoretical design of Janus-In2STe/InSe lateral heterostructure: A DFT investigation. Physica E: Low-Dimensional Systems and Nanostructures, 2022, 143, 115359.	1.3	5
69686	A stable "rocking-chair" zinc-ion battery boosted by low-strain Zn3V4(PO4)6 cathode. Nano Energy, 2022, 100, 107520.	8.2	24
69687	Enhanced thermoelectric performance of the AlN/GaN bilayer. Physica E: Low-Dimensional Systems and Nanostructures, 2022, 143, 115333.	1.3	2
69688	First-principles study of surface segregation in bimetallic Cu3M(1 1 1) (MÂ=ÂAu, Ag, and Zn) alloys in presence of adsorbed CO. Computational Materials Science, 2022, 212, 111550.	1.4	2
69689	Pumpkin-like MoP-MoS2@Aspergillus niger spore-derived N-doped carbon heterostructure for enhanced potassium storage. Journal of Energy Chemistry, 2022, 72, 479-486.	7.1	14
69690	New method of atomistic modeling of <mml:math xmlns:mml="http://www.w3.org/1998/Math/MathML" display="inline" id="d1e340" altimg="si168.svg"><mml:mrow><mml:mi>Î±</mml:mi><mml:mo linebreak="goodbreak" linebreakstyle="after">â^'</mml:mo><mml:mi>Î±</mml:mi><mml:mo>â€²</mml:mo></mml:mrow></mml:math> phase transition in Feâ€“Cr alloy with effective accounting for vibrational entropy. Computational Materials Science, 2022, 212, 111563.	1.4	1
69691	Insight into ideal shear strength of Ni-based dilute alloys using first-principles calculations and correlational analysis. Computational Materials Science, 2022, 212, 111564.	1.4	1
69692	Ab-initio calculations of corundum structured Î±-(Al0.75Cr0.22Me0.03)2O3 compounds (MeÂ=ÂSi, Fe, Mn, Ti,) Tj ETQq1 1 0.784314 rgB	1.4	3
69693	Enabling deep conversion reactions by weakening molybdenum-oxygen bonds through K+ pre-intercalation. Electrochimica Acta, 2022, 425, 140694.	2.6	0
69694	Ultrahigh elasticity and anomalous softening of Î±-Ag2S under pressure. Chemical Physics Letters, 2022, 802, 139801.	1.2	2

#	Article	IF	Citations
69695	Synthesis of Co-NC catalysts from spent lithium-ion batteries for fenton-like reaction: Generation of singlet oxygen with â¯¼100% selectivity. Carbon, 2022, 197, 76-86.	5.4	15
69696	Mechanical and thermal properties of zirconium claddings after doping niobium: Understanding from first-principles calculations. Journal of Nuclear Materials, 2022, 568, 153876.	1.3	3
69697	Effect of Ag cocatalyst on highly selective photocatalytic CO2 reduction to HCOOH over CuO/Ag/UiO-66 Z-scheme heterojunction. Journal of Catalysis, 2022, 413, 31-47.	3.1	24
69698	MSSe-N2CO2 (MÂ=ÂMo, W and NÂ=ÂZr, Hf) van der Waals heterostructures; A first principles study. Chemical Physics, 2022, 561, 111607.	0.9	1
69699	Theoretical study on the hydrogen capture and damage mechanisms of PuO2 nanograin boundary. Journal of Solid State Chemistry, 2022, 313, 123314.	1.4	2
69700	Ferromagnetism and valley polarization in Janus single-layer VSCl. Physica E: Low-Dimensional Systems and Nanostructures, 2022, 143, 115341.	1.3	6
69701	Green corrosion inhibitors for drilling operation: New derivatives of fatty acid-based inhibitors in drilling fluids for 1018 carbon steel in CO2-saturated KCl environments. Materials Chemistry and Physics, 2022, 288, 126406.	2.0	10
69702	Evolution of the structure and properties of (Zr1-xHfx)B2 solid solution ceramics from first-principle theory. Vacuum, 2022, 203, 111283.	1.6	4
69703	An effective activation method for industrially produced TiFeMn powder for hydrogen storage. Journal of Alloys and Compounds, 2022, 919, 165847.	2.8	6
69704	Composition and property optimization of rare-earth-free Mn-Al-C magnet by phase stability and magnetic behavior analysis. Journal of Alloys and Compounds, 2022, 919, 165773.	2.8	4
69705	Promoting low-temperature methanol production over mixed oxide supported Cu catalysts: Coupling ceria-promotion and photo-activation. Applied Catalysis B: Environmental, 2022, 315, 121599.	10.8	8
69706	Unraveling the effects of Fe and Mn promoters on the tungstated zirconia catalyst: A DFT study. Applied Surface Science, 2022, 599, 154052.	3.1	2
69707	Spin polarized STM imaging of nanoscale NÃ©el skyrmions in an SrIrO3/SrRuO3 perovskite bilayer. Applied Surface Science, 2022, 599, 153766.	3.1	2
69708	Exploring two-dimensional carbides as highly active catalysts for the oxygen reduction reaction: A density functional theory approach. Applied Surface Science, 2022, 599, 153907.	3.1	1
69709	Factors influencing the structure of the complex-defects in AF2: RE3+ (A= Ca, Sr and Ba): A first-principles study. Journal of Luminescence, 2022, 250, 119058.	1.5	4
69710	Low-temperature selective production of propylene from non-oxidative dehydrogenation of propane over unconventional Zr/ZK-5 catalysts. Fuel Processing Technology, 2022, 235, 107362.	3.7	7
69711	Highly efficient propane dehydrogenation promoted by reverse waterâ€“gas shift reaction on Pt-Zn alloy surfaces. Fuel, 2022, 325, 124833.	3.4	14
69712	Inverse design and high-throughput screening of TM-A (TM: Transition metal; A: O, S, Se) cathodes for chloride-ion batteries. Energy Storage Materials, 2022, 51, 80-87.	9.5	7

#	Article	IF	Citations
69713	Gap switching in metal-organic coordination chains. Journal of Magnetism and Magnetic Materials, 2022, 560, 169561.	1.0	1
69714	Doping and defect engineering induced extremely high magnetization and large coercivity in Co doped MoTe2. Journal of Alloys and Compounds, 2022, 918, 165750.	2.8	7
69715	Defective and doped MgO monolayer as promising 2D materials for optoelectronic and spintronic applications. Materials Science in Semiconductor Processing, 2022, 149, 106876.	1.9	10
69716	Computational screening and catalytic origin of transition metal supported on g-t-C3N4 as single-atom catalysts for nitrogen reduction reaction. Applied Surface Science, 2022, 599, 153880.	3.1	19
69717	Interrupted anion-network enhanced Li+-ion conduction in Li3+yPO4Iy. Energy Storage Materials, 2022, 51, 88-96.	9.5	6
69718	Tuning the selectivity of cerium oxide for ethanol dehydration to ethylene. Applied Surface Science, 2022, 599, 153963.	3.1	7
69719	First-principles study on the electronic, mechanical and optical properties for silicon allotropes in hexagonal 2â€“7 stacking orders. Scripta Materialia, 2022, 219, 114843.	2.6	7
69720	Mechanism of high magnetic field effect on the D03-L12 phase transition in Fe-Ga alloys. Journal of Alloys and Compounds, 2022, 919, 165818.	2.8	2
69721	In situ reconstruction of defect-rich SnO2 through an analogous disproportionation process for CO2 electroreduction. Chemical Engineering Journal, 2022, 446, 137444.	6.6	7
69722	Extending nonhysteretic oxygen capacity in P2-type Ni-Mn binary Na oxides. Chemical Engineering Journal, 2022, 446, 137429.	6.6	6
69723	N-functionalized Ti2B MBene as high-performance anode materials for sodium-ion batteries: A DFT study. Applied Surface Science, 2022, 599, 153927.	3.1	18
69724	Lanthanum Oxyfluoride modifications boost the electrochemical performance of Nickel-rich cathode. Applied Surface Science, 2022, 599, 153928.	3.1	4
69725	Synthesis of Dual-Active-Sites Ni-Ni2In catalysts for selective hydrogenation of furfural to furfuryl alcohol. Fuel, 2022, 325, 124898.	3.4	16
69726	Role of spin-resolved anti-bonding states filling for enhanced HER performance in 3d transition metals doped monolayer WSe2. Applied Surface Science, 2022, 599, 153979.	3.1	12
69727	Equiatomic quaternary CoXCrAl (XÂ=ÂV, Nb, and Ta) Heusler compounds: Insights from DFT calculations. Journal of Magnetism and Magnetic Materials, 2022, 560, 169620.	1.0	3
69728	Multistage charge redistribution constructing heterostructured WO3@RuSe2 on Si for enhanced photoelectrochemical hydrogen evolution. Chemical Engineering Journal, 2022, 446, 137462.	6.6	12
69729	Optimizing the thermoelectric transmission of monolayer HfSe2 by strain engineering. Journal of Physics and Chemistry of Solids, 2022, 169, 110834.	1.9	6
69730	Mechanism of photocatalytic water splitting of 2D WSeTe/XS2 (XÂ=ÂHf, Sn, Zr) van der Waals heterojunctions under the interaction of vertical intrinsic electric and built-in electric field. Applied Surface Science, 2022, 599, 154012.	3.1	23

#	Article	IF	Citations
69731	First principles modeling of CO2 adsorption on (100), (010), and (001) surfaces of wollastonite for applications in enhanced rock weathering. Surface Science, 2022, 724, 122143.	0.8	2
69732	Accelerated oxygen evolution kinetics on hematite by Zn2+ for boosting the photoelectrochemical water oxidation. Journal of Alloys and Compounds, 2022, 919, 165853.	2.8	2
69733	Hexavalent chromium adsorption by tetrahexylphosphonium modified beidellite clay. Applied Clay Science, 2022, 228, 106623.	2.6	8
69734	Machine learning potentials of kaolinite based on the potential energy surfaces of GGA and meta-GGA density functional theory. Applied Clay Science, 2022, 228, 106596.	2.6	6
69735	Unidirectional charge transport originated from defect boundary on two-dimensional heterostructure. Applied Surface Science, 2022, 599, 153940.	3.1	0
69736	Assembling Ti3C2 MXene into ZnIn2S4-NiSe2 S-scheme heterojunction with multiple charge transfer channels for accelerated photocatalytic H2 generation. Chemical Engineering Journal, 2022, 447, 137488.	6.6	62
69737	Two-dimensional CdO/PtSSe heterojunctions used for Z-scheme photocatalytic water-splitting. Applied Surface Science, 2022, 599, 153960.	3.1	23
69738	Single vacancies at Î£5, Î£9 and Î£11 grain boundaries of copper and the geometrical factors that affect their site preference. Journal of Physics and Chemistry of Solids, 2022, 169, 110833.	1.9	4
69739	Hybrid heterostructure of transition metal dichalcogenides as potential photocatalyst for hydrogen evolution. Applied Surface Science, 2022, 599, 154057.	3.1	7
69740	CO conversion over LaFeO3 perovskite during chemical looping processes: Influences of Ca-doping and oxygen species. Applied Catalysis B: Environmental, 2022, 316, 121598.	10.8	20
69741	Unveiling the nanoalloying modulation on hydrogen evolution activity of ruthenium-based electrocatalysts encapsulated by B/N co-doped graphitic nanotubes. Applied Catalysis B: Environmental, 2022, 316, 121626.	10.8	13
69742	Reconfiguring the interface charge of Co@Carbon polyhedron for enhanced capacitive deionization. Chemical Engineering Journal, 2022, 447, 137438.	6.6	22
69743	Phase crossover in transition metal dichalcogenide monolayers on metal substrates. Applied Surface Science, 2022, 599, 153949.	3.1	1
69744	Activating inert antimony for selective CO2 electroreduction to formate via bimetallic interactions. Applied Catalysis B: Environmental, 2022, 316, 121619.	10.8	17
69745	Engineering asymmetric Fe coordination centers with hydroxyl adsorption for efficient and durable oxygen reduction catalysis. Applied Catalysis B: Environmental, 2022, 316, 121607.	10.8	23
69746	Exploiting the trade-offs of electron transfer in MOF-derived single Zn/Co atomic couples for performance-enhanced zinc-air battery. Applied Catalysis B: Environmental, 2022, 316, 121591.	10.8	51
69747	Durable and eco-friendly peroxymonosulfate activation over cobalt/tin oxides-based heterostructures for antibiotics removal: Insight to mechanism, degradation pathway. Journal of Colloid and Interface Science, 2022, 625, 479-492.	5.0	8
69748	Understanding targeted modulation mechanism in SrTiO3 using K+ for solar water splitting. Applied Catalysis B: Environmental, 2022, 316, 121613.	10.8	18

#	Article	IF	Citations
69749	In-situ crosslinked Zn2+-conducting polymer complex interphase with synergistic anion shielding and cation regulation for high-rate and dendrite-free zinc metal anodes. Chemical Engineering Journal, 2022, 448, 137653.	6.6	18
69750	Crystal chemistry and thermodynamic modelling of the Al13(Fe,TM)4 solid solutions (TM = Co, Cr, Ni,) Tj ETQq1 1 0.784314 rgBT /Ov	2.8	6
69751	DFT study on hydrogen storage of Be or V modified boron-doped porous graphene. Materials Science in Semiconductor Processing, 2022, 150, 106884.	1.9	4
69752	Oriented construction Cu3P and Ni2P heterojunction to boost overall water splitting. Chemical Engineering Journal, 2022, 448, 137706.	6.6	51
69753	Metal organic framework derived perovskite/spinel heterojunction as efficient bifunctional oxygen electrocatalyst for rechargeable and flexible Zn-air batteries. Journal of Colloid and Interface Science, 2022, 625, 502-511.	5.0	21
69754	Reduction of charge carrier recombination by Ce gradient doping and surface polarization for solar water splitting. Chemical Engineering Journal, 2022, 448, 137602.	6.6	22
69755	Multiscale modeling of hydrogenolysis of ethane and propane on Ru(0001): Implications for plastics recycling. Applied Catalysis B: Environmental, 2022, 316, 121597.	10.8	14
69756	Tetrakis(4-sulphophenyl) porphyrin cross-linked polypyrrole network with enhanced bulk conductivity and polysulfide regulation for improved Li-S battery performances. Chemical Engineering Journal, 2022, 447, 137428.	6.6	10
69757	Fabrication of hetero-metal oxide NiCo2V2O8 hollow nanospheres for efficient visible light-driven CO2 photoreduction. Applied Catalysis B: Environmental, 2022, 316, 121663.	10.8	17
69758	High Solar-to-Hydrogen Efficiency Photocatalytic Hydrogen Evolution Reaction with the Hfse2/Inse Van Der Waals Heterostructure and Solar Light. SSRN Electronic Journal, 0, , .	0.4	0
69759	Blue Luminescence of Lead-Free Cs2cucl4ÂGlass Ceramics with Long-Term Water-Resistance Stability. SSRN Electronic Journal, 0, , .	0.4	0
69760	Tunable Band Gap of Diamond Twin Boundaries by Strain Engineering. SSRN Electronic Journal, 0, , .	0.4	0
69761	The Impact of Disorder on the 4o-Martensite of Ni-Mn-Sn Heusler Alloy. SSRN Electronic Journal, 0, , .	0.4	0
69762	Flux Crystal Growth of Rubidium-Iron Silicates and Germanates and Their Ion-Exchange Using Alkali Nitrate Salts. SSRN Electronic Journal, 0, , .	0.4	0
69763	Predict Low Energy Structures of Bsi Monolayer as High-Performance Li/Na/K Ion Battery Anode. SSRN Electronic Journal, 0, , .	0.4	0
69764	Electrocatalytic activity of a Î²-Sb two-dimensional surface for the hydrogen evolution reaction. Physical Chemistry Chemical Physics, 2022, 24, 17832-17840.	1.3	2
69765	A nitrogen- and carbonyl-rich conjugated small-molecule organic cathode for high-performance sodium-ion batteries. Journal of Materials Chemistry A, 2022, 10, 16249-16257.	5.2	6
69766	Polymorphic Ga₂S₃ nanowires: phase-controlled growth and crystal structure calculations. Nanoscale Advances, 2022, 4, 3218-3225.	2.2	1

#	Article	IF	Citations
69767	Single Zn Atom Catalyst on Ti2cn2 Mxenes for Efficient Co. SSRN Electronic Journal, 0, , .	0.4	0
69768	Density Functional Theory Study on the Electronic, Optical and Adsorption Properties of Ti-, Fe- and Ni- Doped Graphene. SSRN Electronic Journal, 0, , .	0.4	0
69769	Experimental and Computational Insights into the Anomalous Thermal Expansion of (Nh4)Reo4,. SSRN Electronic Journal, 0, , .	0.4	0
69770	Double Synergetic Feco-Nanoparticles and Single Atoms Embedded in N-Doped Carbon Nanotube Arrays as Efficient Bifunctional Catalyst for High-Performance Zinc-Air Batteries. SSRN Electronic Journal, 0, , .	0.4	0
69771	High-throughput computational evaluation of lattice thermal conductivity using an optimized Slack model. Materials Advances, 2022, 3, 6826-6830.	2.6	17
69772	An excellent lead oxyiodide with a strong second-harmonic generation response and a large birefringence induced by the oriented arrangement of highly distorted [PbO₄I₂] polyhedra. Inorganic Chemistry Frontiers, 2022, 9, 4464-4469.	3.0	3
69773	Strain tunable nanoporous r-N-GDY membrane for efficient seawater desalination. Journal of Materials Chemistry A, 2022, 10, 16533-16540.	5.2	7
69774	Coordination/cation exchangeable dual sites intercalated multilayered T₃C₂T_x MXene for selective and ultrafast removal of thallium(<scp>i</scp>) from water. Environmental Science: Nano, 2022, 9, 3385-3396.	2.2	1
69775	Interface-assisted phase transition in MOF-derived MoS₂/CoS₂ heterostructures for highly efficient dual-pH hydrogen evolution and overall water splitting. Journal of Materials Chemistry A, 2022, 10, 16115-16126.	5.2	18
69776	Electrochemical Partial Reduction of Ni(Oh)2 to Ni(Oh)2/Ni Via Coupled Oxidation of an Interfacing Nial Intermetallic Compound for Robust Hydrogen Evolution. SSRN Electronic Journal, 0, , .	0.4	0
69777	Lattice Dynamics and Spin-Phonon Coupling in the Noncollinear Antiferromagnetic Antiperovskite Mn3nin. SSRN Electronic Journal, 0, , .	0.4	0
69778	Dual-Electric-Polarity Augmented Cyanoethyl Cellulose-Based Triboelectric Nanogenerator with Ultra-High Triboelectric Charge Density and Enhanced Moisture Resistance Performance. SSRN Electronic Journal, 0, , .	0.4	0
69779	Cr(Vi) Adsorption and Reduction by Magnetite-Humic Acid Adsorption Complexes: Synergistic/Antagonistic Mechanism and Multi-Step Reaction Model. SSRN Electronic Journal, 0, , .	0.4	0
69780	The rise of MAX phase alloys â€“ large-scale theoretical screening for the prediction of chemical order and disorder. Nanoscale, 2022, 14, 10958-10971.	2.8	15
69781	Electric field and strain engineering tuning Rashba spin splitting in quasi-one-dimensional organicâ€“inorganic hybrid perovskites (MV)AI₃Cl₂ (MV = methylviologen, A =) Tj ETQq0 0 0 rgBT /Overlock 1	0.0	0
69782	Green chemistry and first-principles theory enhance catalysis: synthesis and 6-fold catalytic activity increase of sub-5 nm Pd and Pt@Pd nanocubes. Nanoscale, 2022, 14, 10155-10168.	2.8	4
69783	Magnetic and Structural Properties of the Fe5si1-Xgexb2 System. SSRN Electronic Journal, 0, , .	0.4	0
69784	A Modified Slater-Pauling Rule for the Heusler Compounds Alloyed with Late Transition Metals Via Compressed Sensing and Density Functional Theory. SSRN Electronic Journal, 0, , .	0.4	0

#	Article	IF	Citations
69785	Effects of Tungsten on Vacancy Aggregation Behavior and its Induction for Interstitial and Vacancy Migration in Tantalumâ€“Tungsten Alloys: A First-Principles Study. SSRN Electronic Journal, 0, , .	0.4	0
69786	Catalyst Dependent Single-Walled Carbon Nanotube Formation from Polyaromatic Hydrocarbon Molecule: Pt(111) Surface Versus Pt Nanoparticle. SSRN Electronic Journal, 0, , .	0.4	0
69787	First-Principles Kinetic Monte Carlo Modeling of Propylene Epoxidation on the Ti2cuo6/Cu(111) and Cu2o(111) Surfaces. SSRN Electronic Journal, 0, , .	0.4	0
69788	Overall direct photocatalytic water-splitting on C2mm-graphyne: a novel two-dimensional carbon allotrope. Journal of Materials Chemistry C, 2022, 10, 10843-10852.	2.7	13
69789	Halide sublattice dynamics drive Li-ion transport in antiperovskites. Journal of Materials Chemistry A, 2022, 10, 15731-15742.	5.2	3
69790	Computational Simulation Study on Adsorption and Separation of Ch4/H2 in Five Higher-Valency Covalent Organic Frameworks. SSRN Electronic Journal, 0, , .	0.4	0
69791	Large Vertical Piezoelectricity and High-Temperature Ferromagnetism in 2d Ferromagnetic Semiconductors Mnasx (X = I,Br,Cl). SSRN Electronic Journal, 0, , .	0.4	0
69792	Preparation of an interpenetrating bimetal metalâ€“organic framework via metal metathesis used for promoting gas adsorption. Inorganic Chemistry Frontiers, 2022, 9, 5434-5443.	3.0	3
69793	Lateral transition-metal dichalcogenide heterostructures for high efficiency thermoelectric devices. Nanoscale, 2022, 14, 11750-11759.	2.8	10
69794	A First-Principles Study: Three Novel N-Rich Bariumâ"Nitrogen Compounds at High Pressures. SSRN Electronic Journal, 0, , .	0.4	0
69795	Epitaxial growth and electronic properties of an antiferromagnetic semiconducting VI₂ monolayer. Nanoscale, 2022, 14, 10559-10565.	2.8	5
69796	Giant tunable Rashba spin splitting in two-dimensional polar perovskites TlSnX₃ (X = Cl,) Tj ETQq1 1 0.784314 rgBT /Ove	1.3	9
69797	Investigations on electron beam irradiated rare-earth doped SrF₂ for application as low fading dosimeter material: evidence for and DFT simulation of a radiation-induced phase. Journal of Materials Chemistry C, 2022, 10, 11579-11587.	2.7	4
69798	Electronâ€“phonon relaxation at the Au/WSe₂ interface is significantly accelerated by a Ti adhesion layer: time-domain ab initio analysis. Nanoscale, 2022, 14, 10514-10523.	2.8	7
69799	Dynamic simulation on surface hydration and dehydration of monoclinic zirconia. Chinese Journal of Chemical Physics, 2022, 35, 629-638.	0.6	4
69800	Single-Crystalline Î'-Mno2 Catalysts with Tailored Exposed Crystal Facets for Boosting Catalytic Soot Oxidation: The Crystal Facet-Dependent Activity. SSRN Electronic Journal, 0, , .	0.4	0
69801	The Interface between Long-Period Stacking-Ordered (Lpso) Structure and Î" Phase in Mg-Gd-Al Alloys. SSRN Electronic Journal, 0, , .	0.4	0
69802	Explicating the irreversible electric-field-assisted ferroelectric phase transition in the otherwise antiferroelectric sodium niobate for energy storage systems. Journal of Materials Chemistry C, 2022, 10, 10500-10510.	2.7	7

#	Article	IF	Citations
69803	Methane plasma-mediated phase engineering of Ni nanosheets for alkaline hydrogen evolution. Nanoscale, 2022, 14, 12275-12280.	2.8	2
69804	Symmetry breaking in Ge_{1â^'x}Mn_xTe and the impact on thermoelectric transport. Journal of Materials Chemistry A, 2022, 10, 16468-16477.	5.2	11
69805	Two dimensional Janus Ti-trihalide monolayers with half-metallic characteristics, Mott insulator properties and tunable magnetic anisotropy. Journal of Materials Chemistry C, 2022, 10, 10616-10626.	2.7	6
69806	Eldfellite-type cathode material, NaV(SO₄)₂, for Na-ion batteries. Materials Advances, 2022, 3, 6993-7001.	2.6	1
69807	A first principles study of a van der Waals heterostructure based on MS₂ (M = Mo, W) and Janus CrSSe monolayers. Nanoscale Advances, 2022, 4, 3557-3565.	2.2	5
69808	Unveiling the hybridization between the Cr-impurity-mediated flat band and the Rashba-split state of the Î±-Au/Si(111) surface. Nanoscale, 2022, 14, 11227-11234.	2.8	4
69809	An environment-friendly and acid-degradable polymer templated synthesis of single-crystal hierarchical zeolites. Journal of Materials Chemistry A, 2022, 10, 15698-15707.	5.2	6
69810	Large Magnetoresistance in Phosphorus-Sulfur Compounds (Tmps4) Based Temperature Regulated Spin-Caloritronic Devices. SSRN Electronic Journal, 0, , .	0.4	0
69811	Excellent Optoelectronic and Thermoelectric Properties of Two-Dimensional Transition Metal Dinitride Hfn2. SSRN Electronic Journal, 0, , .	0.4	0
69812	Density functional theory analysis for H₂S adsorption on pyridinic N- and oxidized N-doped graphenes. RSC Advances, 2022, 12, 19955-19964.	1.7	1
69813	Effective regulation of the electronic properties of a biphenylene network by hydrogenation and halogenation. RSC Advances, 2022, 12, 20088-20095.	1.7	7
69814	Remarkably enhanced dynamic oxygen migration on graphene oxide supported by copper substrate. Nanoscale Horizons, 2022, 7, 1082-1086.	4.1	5
69815	Modulation of intrinsic defect in vertically grown ZnO nanorods by ion implantation. Physical Chemistry Chemical Physics, 0, , .	1.3	1
69816	Dual Experimental and Computational Approach to Elucidate the Effect of Ga on Cu/Ceo2â€“Zro2 Catalyst for Co2 Hydrogenation. SSRN Electronic Journal, 0, , .	0.4	0
69817	Insights into Cation-Disorder Effect on Stability, Electronic Structure and Defect Properties of Zn-Iv-Nitrides: The Case of Zngen2. SSRN Electronic Journal, 0, , .	0.4	0
69818	Computational Investigation of Li Anchored Graphene as a Catalyst for Nitrogen Fixation. SSRN Electronic Journal, 0, , .	0.4	0
69819	Photodetection and scintillation characterizations of novel lead-bismuth double perovskite halides. Journal of Materials Chemistry C, 2022, 10, 11266-11275.	2.7	7
69820	Temperature-driven phase transition of Ti₂CN from first-principles calculations. Physical Chemistry Chemical Physics, 2022, 24, 20848-20855.	1.3	3

#	Article	IF	Citations
69821	Theoretical insights into the electroreduction of nitrate to ammonia on graphene-based single-atom catalysts. Nanoscale, 2022, 14, 10862-10872.	2.8	57
69822	Lithiation Mechanism and Performance of Monoclinic ZnP₂ Anode Materials. Acta Chimica Sinica, 2022, 80, 756.	0.5	3
69823	The Zintl phase compounds AEIn₂As₂ (AE = Ca, Sr, Ba): topological phase transition under pressure. Physical Chemistry Chemical Physics, 2022, 24, 17337-17347.	1.3	8
69824	Large piezoelectric response in ferroelectric/multiferroelectric metal oxyhalide MOX₂ (M = Ti, V and X = F, Cl and Br) monolayers. Nanoscale, 2022, 14, 11676-11683.	2.8	7
69825	Work function regulation of surface-engineered Ti₂CT₂MXenes for efficient electrochemical nitrogen reduction reaction. Nanoscale, 2022, 14, 12610-12619.	2.8	14
69826	Deep potential for a face-centered cubic Cu system at finite temperatures. Physical Chemistry Chemical Physics, 2022, 24, 18361-18369.	1.3	5
69827	Exploring the air stability of all-inorganic halide perovskites in the presence of photogenerated electrons by DFT and AIMD studies. Sustainable Energy and Fuels, 2022, 6, 3778-3787.	2.5	3
69828	Understanding the effect of the exchange-correlation functionals on methane and ethane formation over ruthenium catalysts. Chinese Journal of Chemical Physics, 0, , .	0.6	1
69829	Mo-Embedded Ir-Based Electrocatalyst for Nitrogen Reduction Reaction: A Computational Study. SSRN Electronic Journal, 0, , .	0.4	0
69830	Performance of the nitrogen reduction reaction on metal bound g-C₆N₆: a combined approach of machine learning and DFT. Physical Chemistry Chemical Physics, 2022, 24, 17050-17058.	1.3	15
69831	Rationally Designed Metal-N-C/Mos2 Heterostructures as Bifunctional Oxygen Electrocatalysts: A Computational Study. SSRN Electronic Journal, 0, , .	0.4	0
69832	Functional Properties of A-Site Cation Ordered La2mnnio6 Double Perovskites. SSRN Electronic Journal, 0, , .	0.4	0
69833	The structural and electronic richness of buckled honeycomb AsP bilayers. Nanoscale, 2022, 14, 10136-10142.	2.8	3
69834	An All-Heusler Alloy Magnetic Tunneling Junction with Low Resistance Area Product and High Magnetocrystalline Anisotropy: A Dft Study. SSRN Electronic Journal, 0, , .	0.4	0
69835	Synergetic Mechanism of B, N Co-Doping for Boosting Carbon Materials Catalytic Performance. SSRN Electronic Journal, 0, , .	0.4	0
69836	Density Functional Theory Study of Ni Segregation in Cuni(111) Alloy with Chemisorbed Co, O, or H. SSRN Electronic Journal, 0, , .	0.4	0
69837	The flexoelectric effect of perovskite superlattice based on first principles. Wuli Xuebao/Acta Physica Sinica, 2022, .	0.2	0
69838	Trace Pt Atoms as Electronic Promoters in Pd Clusters for Direct Synthesis of Hydrogen Peroxide. SSRN Electronic Journal, 0, , .	0.4	0

#	Article	IF	Citations
69839	Reactions between Sicl4 and H2o on Rutile Tio2 Surfaces in Atomic Layer Deposition of Sio2 by First-Principles Calculations. SSRN Electronic Journal, 0, , .	0.4	0
69840	Synergistic Effects of Oxygen Vacancies and Heterostructures for Visible-Light-Driven Photoreduction of Uranium. SSRN Electronic Journal, 0, , .	0.4	0
69841	A first-principles study of exciton self-trapping and electric polarization in one-dimensional organic lead halide perovskites. Physical Chemistry Chemical Physics, 2022, 24, 17323-17328.	1.3	9
69842	Redispersion of Exsolved Cu Nanoparticles on Lafeo3 Photocatalyst for Tunable Photocatalytic Co2 Reduction. SSRN Electronic Journal, 0, , .	0.4	0
69843	Composition Stability of Single Fcc Phase in Cr-Fe-Mn-Ni Alloys: First-Principles Prediction and Experimental Validation. SSRN Electronic Journal, 0, , .	0.4	0
69844	Rational design of highly efficient MXene-based catalysts for the water-gas-shift reaction. Physical Chemistry Chemical Physics, 2022, 24, 18265-18271.	1.3	4
69845	Surface potential-determined performance of Ti₃C₂T₂ (T = O, F,) Tj ETQq0 0 0 rgBT /Overlock 10 sodium ion batteries. Nanoscale, 2022, 14, 10549-10558.	2.8	9
69846	Robust pure spin current induced by the photogalvanic effect in half-silicane with spatial inversion symmetry. Nanoscale, 2022, 14, 11316-11322.	2.8	8
69847	A First-Principles Study: Three Novel N-Rich Bariumâ€'Nitrogen Compounds at High Pressures. SSRN Electronic Journal, 0, , .	0.4	0
69848	Dft+U Study on the Magnetic Properties of 3d Transition Metal Doped Î'12 Borophene. SSRN Electronic Journal, 0, , .	0.4	0
69849	Monolayer GaOCl: a novel wide-bandgap 2D material with hole-doping-induced ferromagnetism and multidirectional piezoelectricity. Nanoscale, 2022, 14, 11369-11377.	2.8	3
69850	Re-examining the giant magnetization density in Î±â€²â€²-Fe₁₆N₂ with the SCAN+U method. Physical Chemistry Chemical Physics, 2022, 24, 17879-17884.	1.3	3
69851	Multi-Component Alloying Effects on the Stability and Mechanical Properties of Nb and Nb-Si Alloys: A First-Principles Study. SSRN Electronic Journal, 0, , .	0.4	1
69852	Experimental and computational approaches to study the chlorination mechanism of pentlandite with ammonium chloride. RSC Advances, 2022, 12, 19232-19239.	1.7	0
69853	Opto-Electronic Properties of Carbon Doped Nio. SSRN Electronic Journal, 0, , .	0.4	0
69854	Selective Hydrogenation of Furfural to Furfuryl Alcohol Over Oxygen Vacancies Enriched Layered Double Hydroxide Supported Ru Nanoparticles Catalyst. SSRN Electronic Journal, 0, , .	0.4	0
69855	N-Bridged Ni and Mn Single-Atom Pair Sites: A Highly Efficient Electrocatalyst for Co2 Conversion to Co. SSRN Electronic Journal, 0, , .	0.4	0
69856	Orthorhombic C32: A Topological Semimetal with Nodal Ring. SSRN Electronic Journal, 0, , .	0.4	0

#	Article	IF	Citations
69857	A vapochromic dye/graphene coated long-period fiber grating for benzene vapor sensing. Materials Chemistry Frontiers, 2022, 6, 2438-2446.	3.2	3
69858	MÃ¶bius-aromatic interlocked Mn₂B₁₀H₁₀ wheel to metal-doped boranaphthalene M₂@B₁₀H₈ and M₂B₅ 2D-sheets (M = Mn and Fe): A Molecules to Materials continuum using DFT Study. Chemical Science, 0, , .	3.7	1
69859	Insights into syngas to methanol conversion on Cr₂O₃ oxide from first-principles-based microkinetic simulations. Chinese Journal of Chemical Physics, 0, , .	0.6	2
69860	Insight into the effects of coverage, water, and defects on the properties of the catechol/TiO₂ interface. Chinese Journal of Chemical Physics, 0, , .	0.6	0
69861	Strain engineering in single-atom catalysts: GaPS₄ for bifunctional oxygen reduction and evolution. Inorganic Chemistry Frontiers, 2022, 9, 4272-4280.	3.0	15
69862	Tunable mono- and di-methylation of amines with methanol over bimetallic CuCo nanoparticle catalysts. Green Chemistry, 2022, 24, 5965-5977.	4.6	7
69863	New approaches to high-energy-density cathode and anode architectures for lithium-sulfur batteries. , 2022, , 353-439.		0
69864	Topological Defect and Sp3/Sp2 Carbon Interface Derived from Zif-8 with Linker Vacancies for Oxygen Reduction Reaction. SSRN Electronic Journal, 0, , .	0.4	0
69865	Amine Functionalization Derived Lattice Engineered and Electron Deficient Palladium CatalystÂFor Selective Production of Hydrogen Peroxide. SSRN Electronic Journal, 0, , .	0.4	0
69866	Enhancing Electrocatalytic Nitrogen Fixation Beyond Coherent Heterointerfacial Boundaries. SSRN Electronic Journal, 0, , .	0.4	0
69867	Cu segregation in Auâ€“Cu nanoparticles exposed to hydrogen atmospheric pressure: how is fcc symmetry maintained?. Faraday Discussions, 0, 242, 375-388.	1.6	4
69868	Surface phosphorization for the enhanced photoelectrochemical performance of an Fe₂O₃/Si photocathode. Nanoscale, 2022, 14, 11261-11269.	2.8	4
69869	Alleviating the Self-Discharge and Enhancing the Polysulphides Conversion Kinetics with Laco3oh Nanocrystals Decorated Hierarchical Porous Carbon. SSRN Electronic Journal, 0, , .	0.4	0
69870	In situgrowth of 2D ZnIn₂S₄nanosheets on sulfur-doped porous Ti₃C₂T_xMXene 3D multi-functional architectures for photocatalytic H₂evolution. Journal of Materials Chemistry C, 2022, 10, 10636-10644.	2.7	7
69871	Deducing Surface Chemistry and Annealing Conditions from Observed Nanoparticle Shapes: A Study of Scandate Cathodes. SSRN Electronic Journal, 0, , .	0.4	0
69872	Oriented design of triple atom catalysts for electrocatalytic nitrogen reduction with the genetic-algorithm-based global optimization method driven by first principles calculations. Journal of Materials Chemistry A, 0, , .	5.2	5
69873	Nanoconfining red phosphorus within MOF-derived hierarchically porous carbon networks for high performance potassium storage. Materials Chemistry Frontiers, 2022, 6, 2184-2189.	3.2	2
69874	Neighboring Site Synergies in Co Defective Ru-Co Spinel Oxide Towards Oxygen Evolution Reaction. SSRN Electronic Journal, 0, , .	0.4	0

#	Article	IF	Citations
69875	2d Boron-Nitride Featuring B4 Tetrahedros: an Efficient Photocatalyst for Water Splitting. SSRN Electronic Journal, 0, , .	0.4	0
69876	Understanding the role of Cu⁺/Cu⁰sites at Cu₂O based catalysts in ethanol production from CO₂electroreduction -A DFT study. RSC Advances, 2022, 12, 19394-19401.	1.7	9
69877	A Unique Ternary Ce(III)-Quercetin-Phenanthroline Assembly with Antioxidant and Anti-Inflammatory Properties. SSRN Electronic Journal, 0, , .	0.4	0
69878	Strain-tunable charge carrier transport properties and optical properties of CrI₃> monolayer using first-principles. Wuli Xuebao/Acta Physica Sinica, 2022, .	0.2	0
69879	FIRST-PRINCIPLES CALCULATIONS FOR Ni-Al-Cr ALLOYS USING CLUSTER-PLUS-GLUE-ATOM MODEL. Wuli Xuebao/Acta Physica Sinica, 2022, .	0.2	0
69880	Screening of Two Dimensional Cd-Chalcogenides Few Layer Structures as Potential Candidates for Photocatalysis. SSRN Electronic Journal, 0, , .	0.4	0
69881	Role of Î±-MoC(100) in Methanol Steam Reforming: A Mechanistic Study of DFT. Chinese Journal of Chemical Physics, 0, , .	0.6	1
69882	Electrochemical CO₂ reduction on Cu single atom catalyst and Cu nanoclusters: an ab initio approach. Physical Chemistry Chemical Physics, 2022, 24, 15767-15775.	1.3	4
69883	The origins of segregation behaviors of solute atoms and their effect on the strength of Î±-Al//Î¸â€²-Al₂Cu interfaces in Alâ€“Cu alloys. Physical Chemistry Chemical Physics, 2022, 24, 18370-18392.	1.3	6
69884	Structural engineering brings new electronic properties to Janus ZrSSe and HfSSe monolayers. Physical Chemistry Chemical Physics, 2022, 24, 17824-17831.	1.3	1
69885	Solidification Paths and Thermodynamic Assessment of the Alâ€“Agâ€“Sc System. SSRN Electronic Journal, 0, , .	0.4	0
69886	Monolayer NaW₂O₂Br₆: a gate tunable near-infrared hyperbolic plasmonic surface. Nanoscale Advances, 2022, 4, 3282-3290.	2.2	2
69887	Changing charge transfer mode with cobaltâ€“molybdenum bimetallic atomic pairs for enhanced nitrogen fixation. Journal of Materials Chemistry A, 2022, 10, 15595-15604.	5.2	3
69888	High-Performance Thermoelectric Î“-Gese and its Group-Iv Monochalcogenide Isostructural Family. SSRN Electronic Journal, 0, , .	0.4	0
69889	Increasing the Adhesion of W to Si Substrates Using Cr/Ti Interlayers. SSRN Electronic Journal, 0, , .	0.4	0
69890	Superconductivity and topological states in hexagonal TaC and NbC. Physical Chemistry Chemical Physics, 2022, 24, 18419-18426.	1.3	2
69891	Comparative density functional studies of BiMO₃ polymorphs (M = Al, Ga, In) based on LDA, GGA, and meta-GGA functionals. New Journal of Chemistry, 0, , .	1.4	1
69892	Ultrafast dynamics of spin relaxation in monolayer WSe₂ and the WSe₂/graphene heterojunction. Physical Chemistry Chemical Physics, 2022, 24, 16538-16544.	1.3	3

#	Article	IF	Citations
69893	Electrically-driven robust tuning of lattice thermal conductivity. Physical Chemistry Chemical Physics, 2022, 24, 17479-17484.	1.3	5
69894	Unravelling the origin of long-term stability for Cs⁺ and Sr²⁺ solidification inside sodalite. Physical Chemistry Chemical Physics, 2022, 24, 18083-18093.	1.3	3
69895	Structural transition and interconversion between the 2D self-assembled structures of pentacene. Physical Chemistry Chemical Physics, 0, , .	1.3	0
69896	Versatile van der Waals heterostructures of Î³-GeSe with h-BN/graphene/MoS₂. Journal of Materials Chemistry C, 2022, 10, 10995-11004.	2.7	9
69897	Enhanced Ionic Conductivity and Air Stability of Bi2se3-Doped 80li2s-20p2s5 Solid-State Electrolytes. SSRN Electronic Journal, 0, , .	0.4	0
69898	First-principles prediction on antimony-doping effects on the cyclic stability of tin anodes for lithium-ion batteries. Physical Chemistry Chemical Physics, 2022, 24, 17542-17546.	1.3	1
69899	Study on cation-tuned performance of halide solid electrolyte. Wuli Xuebao/Acta Physica Sinica, 2022, .	0.2	0
69900	Studies on Structural, Electronic and Optical Properties of Nonlinear Optical Material Li-in-Se and Li-in-Te Under High Pressure. SSRN Electronic Journal, 0, , .	0.4	0
69901	Ab Initio Study of the Structural Properties of the Coâ€“Niâ€“Sn Heusler Alloys. Physics of the Solid State, 2022, 64, 129-134.	0.2	0
69902	Effects of B segregation on Mo-rich phase precipitation in S31254 super-austenitic stainless steels: Experimental and first-principles study. Chinese Physics B, 2022, 31, 116402.	0.7	6
69903	Influence of Î³ Radiation on the Crystal Structure of BiFeO3. Russian Journal of Inorganic Chemistry, 2022, 67, 588-597.	0.3	5
69904	Strain engineering and hydrogen effect for two-dimensional ferroelectricity in monolayer group-IV monochalcogenides MX (M = Sn, Ge; X = Se, Te, S). Chinese Physics B, 2023, 32, 036802.	0.7	1
69905	Switchable Electric Dipole from Polaron Localization in Dielectric Crystals. Physical Review Letters, 2022, 129, .	2.9	3
69906	Ultralowâ€Expansion Lithium Metal Composite Anode via Gradient Framework Design. Advanced Functional Materials, 2022, 32, .	7.8	18
69907	Cationic-potential tuned biphasic layered cathodes for stable desodiation/sodiation. Science Bulletin, 2022, 67, 1589-1602.	4.3	31
69908	Realistic computer models of amorphous <mml:math xmlns:mml="http://www.w3.org/1998/Math/MathML"><mml:msub><mml:mi>ZrO</mml:mi><mml:mn>2</mml:mn></mml:msub></m : <mml:math xmlns:mml="http://www.w3.org/1998/Math/MathML"><mml:mrow><mml:msub><mml:mi>Ta</mml:mi><mml:mn>2</mml:mn></mml mathvariant="normal">O</mml:mi><mml:mn>5</mml:mn></mml:msub></mml:mrow></mml:math> : Structural, optical, and vibrational properties. Physical Review B, 2022, 105, .	1.1	3
69909	Novel Valence Transition in Elemental Metal Europium around 80ÂGPa. Physical Review Letters, 2022, 129, .	2.9	5
69910	First principles investigation on the hydrogen adsorption on planar aluminene with boron, carbon, and nitrogen as impurities. Molecular Physics, 0, , .	0.8	0

#	Article	IF	Citations
69911	Ab initio molecular dynamics free energy study of enhanced copper (II) dimerization on mineral surfaces. Communications Chemistry, 2022, 5, .	2.0	3
69912	Quasi-solid-state Zn-air batteries with an atomically dispersed cobalt electrocatalyst and organohydrogel electrolyte. Nature Communications, 2022, 13, .	5.8	127
69913	A Seawaterâ€Corrosionâ€Resistant and Isotropic Zero Thermal Expansion (Zr,Ta)(Fe,Co)₂ Alloy. Advanced Materials, 2022, 34, .	11.1	12
69914	Theoretical calculation guided materials design and capture mechanism for Znâ€“Se batteries via heteroatomâ€doped carbon. , 2022, 1, 59-67.		19
69915	Phase transition behavior of heterostructural alloys: Effects of size mismatch and site preference. Physical Review B, 2022, 105, .	1.1	0
69916	Interfacial interaction of parallel carbon nanotubes under external electric field: A first-principles study. Modern Physics Letters B, 0, , .	1.0	0
69917	Energy Harvesting from Atomically Thin Co₂Te₃. Journal of Physical Chemistry C, 2022, 126, 12545-12553.	1.5	4
69918	Structural Characterization and Influence of Defects on the Optical Properties of the Oxygen-Deficient Perovskite Ba₃LiNb₂O_{8.5}â–¡_{0.5}. Inorganic Chemistry, 2022, 61, 10272-10282.	1.9	0
69919	Insights into the Hydrogenolysis Mechanism of Diphenyl Ether over Cl-Modified Pt/Î³-Al₂O₃ Catalysts by Experimental and Theoretical Studies. ACS Sustainable Chemistry and Engineering, 2022, 10, 8897-8907.	3.2	7
69920	Addressing solar photochemistry durability with an amorphous nickel antimonate photoanode. Cell Reports Physical Science, 2022, 3, 100959.	2.8	6
69921	Approaches for handling high-dimensional cluster expansions of ionic systems. Npj Computational Materials, 2022, 8, .	3.5	10
69922	Discovering Surface Structure and the Mechanism of Graphene Oxide-Triggered CeO₂â€“WO₃/TiO₂ Catalysts for NO Abatement with NH₃. ACS Catalysis, 2022, 12, 8386-8403.	5.5	24
69923	Prediction of the electronic structure, optical and vibrational properties of ScXCo2Sb2 (Xâ€‰=â€‰V, Nb and) Tj ETQq0 0 0 rgBT /Over	0.9	3
69924	Pressure engineering of intertwined phase transitions in lanthanide monopnictide NdSb. Science China: Physics, Mechanics and Astronomy, 2022, 65, .	2.0	2
69925	Switchable topological phase transition and nonlinear optical properties in a <mml:math xmlns:mml="http://www.w3.org/1998/Math/MathML"><mml:mrow><mml:msub><mml:mi>ReC</mml:mi><mml:mn>2</mml:mn></mml:msub><mml:mathvariant="normal">H</mml:mi></mml:mrow></mml:math> monolayer. Physical Review B, 2022, 105, .	1.1	6
69926	Quasi-bonding-induced gap states in metal/two-dimensional semiconductor junctions: Route for Schottky barrier height reduction. Physical Review B, 2022, 105, .	1.1	11
69927	Reactive Oxygen Species Sequestration Induced Synthesis of Î²-PbO and Its Polymorphic Transformation to Î±-PbO at Atomically Thin Regimes. ACS Nano, 2022, 16, 10679-10691.	7.3	3
69928	Phase evolution and thermal stability of novel high-entropy (Mo0.2Nb0.2Ta0.2V0.2W0.2)Si2 ceramics. Journal of the European Ceramic Society, 2022, 42, 5314-5322.	2.8	12

#	Article	IF	Citations
69929	Elucidating CO Oxidation Pathways on Rh Atoms and Clusters on the â€œ29â€•Cu₂O/Cu(111) Surface. Journal of Physical Chemistry C, 2022, 126, 11091-11102.	1.5	1
69930	Electrochemical Stability of ZnMn₂O₄: Understanding Zn-Ion Rechargeable Battery Capacity and Degradation. Journal of Physical Chemistry C, 2022, 126, 10957-10967.	1.5	4
69931	C/H/O/F/Al ReaxFF Force Field Development and Application to Study the Condensed-Phase Poly(vinylidene fluoride) and Reaction Mechanisms with Aluminum. Journal of Physical Chemistry C, 2022, 126, 11058-11074.	1.5	7
69932	Effect of Multiple Oxygen Vacancies on the Optical and Thermodynamic Properties of La_{0.75}Sr_{0.25}Co_{0.25}Fe_{0.75}O_{3â^Î´} Perovskite. Journal of Physical Chemistry C, 2022, 126, 11421-11425.	1.5	1
69933	Ab-initio calculations of shallow dopant qubits in silicon from pseudopotential and all-electron mixed approach. Communications Physics, 2022, 5, .	2.0	1
69934	Chiral phonons entangled with multiple Hall effects and unified convention for pseudoangular momentum in two-dimensional materials. Physical Review B, 2022, 105, .	1.1	4
69935	Structural, electronics, magnetic, optical, mechanical and hydrogen storage properties of <scp>Gaâ€based hydrideâ€perovskites</scp> X <scp> GaH ₃ </scp> (X Â=ÂK, Li). International Journal of Energy Research, 2022, 46, 15617-15626.	2.2	34
69936	In Situ Induced Latticeâ€Matched Interfacial Oxygenâ€Passivationâ€Layer Endowing Liâ€Rich and Mnâ€Based Cathodes with Ultralong Life. Small, 2022, 18, .	5.2	10
69937	Highly efficient and selective H2/CH4 separation by graphene membranes with embedded crown ethers. International Journal of Hydrogen Energy, 2022, 47, 24835-24842.	3.8	6
69938	Elucidating the Reaction Mechanism of Atomic Layer Deposition of Al₂O₃ with a Series of Al(CH₃)_xCl_{3â€“x} and Al(C_yH_{2y+1})₃ Precursors. Journal of the American Chemical Society, 2022, 144, 11757-11766.	6.6	8
69939	Alâ€Doping Driven Suppression of Capacity and Voltage Fadings in 4dâ€Element Containing Liâ€Ionâ€Battery Cathode Materials: Machine Learning and Density Functional Theory. Advanced Energy Materials, 2022, 12, .	10.2	42
69940	Topological Crystalline Insulator Candidate ErAsS with Hourglass Fermion and Magneticâ€Tuned Topological Phase Transition. Advanced Materials, 2022, 34, .	11.1	6
69941	Diffusion of oxygen in Mg-doped <mml:math xmlns:mml="http://www.w3.org/1998/Math/MathML"><mml:mrow><mml:mi>Î±</mml:mi><mml:mtext>â^’</mml:mtext><mml:msub><mml:mathvariant="normal">O</mml:mi><mml:mn>3</mml:mn></mml:msub></mml:mrow></mml:math> : The corundum conundrum explained. Physical Review Materials, 2022, 6, .	0.9	1
69942	Substrate-Selective Intermolecular Interaction and the Molecular Self-Assemblies: 1,3,5-Tris(4-bromophenyl)benzene Molecules on the Ag(111) and Si(111) (â^š3 Ã— â^š3)-Ag Surfaces. Langmuir, 2022, 38, 8881-8889.	1.6	2
69943	Magnetic structure of oxygen-deficient perovskite nickelates with ordered vacancies. Physical Review Research, 2022, 4, .	1.3	6
69944	Critical-Element-Free Permanent-Magnet Materials Based on <mml:math xmlns:mml="http://www.w3.org/1998/Math/MathML" display="inline" overflow="scroll"><mml:msub><mml:mi>Ce</mml:mi><mml:mn>2</mml:mn></mml:msub><mml:msub><mml:mi>Fe</mml:mi><mml:mathvariant="normal">B</mml:mi></mml:mrow></mml:math>. Physical Review Applied,	1.5	1
69945	13â€2: Modification of ZnMgO NPs for Improving Device Performance of Allâ€Inkjetâ€Printed Quantumâ€Dot Lightâ€Emitting Diodes. Digest of Technical Papers SID International Symposium, 2022, 53, 136-140.	0.1	0
69946	Extraordinary Mechanical Performance in Charged Carbyne. Chinese Physics B, 0, , .	0.7	0

#	Article	IF	Citations
69947	Materials informatics for dielectric loss tangent in the millimeter wave region. Japanese Journal of Applied Physics, 0, , .	0.8	1
69948	Computational Study of Zn Single-Atom Catalysts on In₂O₃ Nanomaterials for Direct Synthesis of Acetic Acid from CH₄ and CO₂. ACS Applied Nano Materials, 0, , .	2.4	5
69949	Dual-metal precursors for the universal growth of non-layered 2D transition metal chalcogenides with ordered cation vacancies. Science Bulletin, 2022, 67, 1649-1658.	4.3	10
69950	Understanding Electronâ€“Phonon Interactions in 3D Lead Halide Perovskites from the Stereochemical Expression of 6s² Lone Pairs. Journal of the American Chemical Society, 2022, 144, 12247-12260.	6.6	38
69951	Effects of <mml:math xmlns:mml="http://www.w3.org/1998/Math/MathML"><mml:msup><mml:mrow><mml:mi>Ca</mml:mi></mml:mrow><mml:mrow><m substitution on the properties of cementitious tobermorite. Physical Review Materials, 2022, 6, .	3.2	2
69952	<mml:math xmlns:mml="http://www.w3.org/1998/Math/MathML"><mml:msub><mml:mi mathvariant="normal">Er</mml:mi><mml:mrow><mml:mn>0.5</mml:mn></mml:mrow></mml:msub><mml:msub><mml:mi mathvariant="normal">Dy</mml:mi><mml:mrow><mml:mn>0.5</mml:mn></mml:mrow></mml:msub><mml:msub><mml:mi mathvariant="normal">FeO</mml:mi><mml:mn>3</mml:mn></mml:msub></mml:math> : Bulk magnetization, neutron scattering, specific heat, and density functional theory studies. Physical Re	1.1	2
69953	A Deep Neural Network Potential for Water Confined in Graphene Nanocapillaries. Journal of Physical Chemistry C, 2022, 126, 10546-10553.	1.5	7
69954	Temperature-dependent phonon anharmonicity and thermal transport in <mml:math xmlns:mml="http://www.w3.org/1998/Math/MathML"><mml:msub><mml:mi mathvariant="normal">CuInTe</mml:mi><mml:mn>2</mml:mn></mml:msub></mml:math>. Physical Review B, 2022, 105, .	1.1	16
69955	Catalytic Tandem CO₂â€“Ethane Reactions and Hydroformylation for C3 Oxygenate Production. ACS Catalysis, 2022, 12, 8279-8290.	5.5	8
69956	High-Throughput Screening of Stable Single-Atom Catalysts in CO₂ Reduction Reactions. ACS Catalysis, 2022, 12, 8269-8278.	5.5	32
69957	Effect of mixing the low-valence transition metal atoms <mml:math xmlns:mml="http://www.w3.org/1998/Math/MathML"><mml:mi>Y</mml:mi></mml:math> = Co, Fe, Mn, Cr, V, Ti, or Sc on the properties of quaternary Heusler compounds <mml:math xmlns:mml="http://www.w3.org/1998/Math/MathML"><mml:mrow><mml:msub><mml:mi mathvariant="normal">Co</mml:mi><mml:mrow><mml:mn>2</mml:mn><mml:mo>â^’</mml:mo><mml:mi>x</mml:mi></mml:mrow><mml:mrow><mathvariant="norm. Physical Review Materials, 2022, 6, .	0.9	4
69958	Maximizing the mechanical performance of Ti3AlC2-based MAX phases with aid of machine learning. Journal of Advanced Ceramics, 2022, 11, 1307-1318.	8.9	43
69959	First-Principles Calculations on the HER Performance of TiO2 Nanosheet with Passivated Codoping. Catalysis Letters, 0, , .	1.4	1
69960	Converting Brownmillerite to Alternate Layers of Oxygenâ€Deficient and Conductive Nanoâ€Sheets with Enhanced Thermoelectric Properties. Advanced Energy Materials, 2022, 12, .	10.2	5
69961	Metal-Organic Frameworks Offering Tunable Binary Active Sites toward Highly Efficient Urea Oxidation Electrolysis. Research, 2022, 2022, .	2.8	18
69962	Unique Conduction Band Minimum of Semiconductors Possessing a Zincblende-Type Framework. Inorganic Chemistry, 2022, 61, 10359-10364.	1.9	3
69963	Phonon-Assisted Nonradiative Recombination Tuned by Organic Cations in Ruddlesden-Popper Hybrid Perovskites. Physical Review Applied, 2022, 17, .	1.5	4
69964	Role of spin-orbit coupling in canted ferromagnetism and spin-wave dynamics of <mml:math xmlns:mml="http://www.w3.org/1998/Math/MathML"><mml:msub><mml:mi>SrRuO</mml:mi><mml:mn>3</mml:mn></mml:msub></m Physical Review B, 2022, 105, .	1.1	11

#	Article	IF	Citations
69965	Photo-assisted decoration of Ag-Pt nanoparticles on Si photocathodes for reducing overpotential toward enhanced photoelectrochemical water splitting. Science China Materials, 2022, 65, 3033-3042.	3.5	4
69966	Insights Into to the KX (X = Cl, Br, I) Adsorptionâ€Assisted Stabilization of CsPbI ₂ Br Surface. Small, 0, , 2202623.	5.2	5
69967	A Zero-Dimensional Organic Lead Bromide of (TPA)2PbBr4 Single Crystal with Bright Blue Emission. Nanomaterials, 2022, 12, 2222.	1.9	6
69968	Polarization-Resolved and Helicity-Resolved Raman Intensity of Monolayer and Bilayer Î²-InSe. Journal of Physical Chemistry C, 2022, 126, 11219-11228.	1.5	0
69969	K⁺ Single Cation Ionic Liquids Electrolytes with Low Melting Asymmetric Salt. Journal of Physical Chemistry C, 2022, 126, 11407-11413.	1.5	8
69970	The structure, electronic, and magnetic properties of PbRuO₃ under hydrostatic pressure: A first-principles study. Journal of Applied Physics, 2022, 131, 243902.	1.1	0
69971	Planar Ï€-extended cycloparaphenylenes featuring an all-armchair edge topology. Nature Chemistry, 2022, 14, 871-876.	6.6	19
69972	A unique Co@CoO catalyst for hydrogenolysis of biomass-derived 5-hydroxymethylfurfural to 2,5-dimethylfuran. Nature Communications, 2022, 13, .	5.8	66
69973	Molecular Structure and Phase Equilibria of Molten Fluoride Salt with and without Dissolved Cesium: FLiNaKâ€“CsF (5 mol %). ACS Applied Energy Materials, 2022, 5, 8067-8074.	2.5	4
69974	Giant bipolar unidirectional photomagnetoresistance. Proceedings of the National Academy of Sciences of the United States of America, 2022, 119, .	3.3	4
69975	Prediction of stable Li-Sn compounds: boosting ab initio searches with neural network potentials. Npj Computational Materials, 2022, 8, .	3.5	7
69976	Unraveling the role of tungsten as a minor alloying element in the oxidation NiCr alloys. Npj Materials Degradation, 2022, 6, .	2.6	5
69977	Elastic deformation and elastic wave velocity of iron and its binary interstitial alloys: Temperature, pressure and interstitial atom concentration dependences. Physica B: Condensed Matter, 2022, 644, 414134.	1.3	4
69978	First-principles study of optical properties of monolayer h-BN and its defect structures under equibiaxial strain. Applied Physics A: Materials Science and Processing, 2022, 128, .	1.1	9
69979	Single-atom catalysts modified by molecular groups for electrochemical nitrogen reduction. Nano Research, 2022, 15, 9663-9669.	5.8	11
69980	Straightforward strategy for selecting and tuning substrates for two-dimensional material epitaxy. Physical Review Materials, 2022, 6, .	0.9	3
69981	Strengthening Engineered Nanocrystal Three-Dimensional Superlattices via Ligand Conformation and Reactivity. ACS Nano, 2022, 16, 11692-11707.	7.3	8
69982	Unraveling the Unique Role of Methyl Position on the Ring-Opening Barrier in Photocatalytic Decomposition of Xylene Isomers. ACS Catalysis, 2022, 12, 8363-8371.	5.5	8

#	Article	IF	Citations
69983	Ultralow Lattice Thermal Conductivity and High Thermoelectric Figure of Merit in Dually Substituted Cu₁₂Sb₄S₁₃ Tetrahedrites. Advanced Electronic Materials, 2022, 8, .	2.6	4
69984	Promoting biomass electrooxidation via modulating proton and oxygen anion deintercalation in hydroxide. Nature Communications, 2022, 13, .	5.8	60
69985	Two-dimensional Ruddlesden-Popper halide perovskite solar absorbers with short-chain interlayer spacers. Physical Review Materials, 2022, 6, .	0.9	5
69986	Magnetic Collapse in Fe3Se4 under High Pressure. Materials, 2022, 15, 4583.	1.3	1
69987	X-ray diffraction study and molecular dynamic simulation of liquid Al-Cu alloys: a new data and interatomic potentials comparison. Journal of Molecular Modeling, 2022, 28, .	0.8	0
69988	The factors affecting the diffusion properties of hydrogen in palladium copper alloys: Ab initio study. International Journal of Hydrogen Energy, 2022, 47, 27579-27589.	3.8	6
69989	Large piezoelectric and elastic properties in B and Sc codoped wurtzite AlN. Journal of Applied Physics, 2022, 131, .	1.1	6
69990	Effect of geometry on magnetism of Hund's metals: Case study of <mml:math xmlns:mml="http://www.w3.org/1998/Math/MathML"><mml:msub><mml:mi>BaRuO</mml:mi><mml:mn>3</mml:mn></mml:msub>-/t Physical Review B, 2022, 105, .	1.1	1
69991	Improving carrier mobility in two-dimensional semiconductors with rippled materials. Nature Electronics, 2022, 5, 489-496.	13.1	52
69992	Ultrafast self-heating synthesis of robust heterogeneous nanocarbides for high current density hydrogen evolution reaction. Nature Communications, 2022, 13, .	5.8	62
69993	Giant magnetic anisotropy in single-molecule magnet with transition-metal adatom. International Journal of Modern Physics C, 0, , .	0.8	0
69994	Pressure-induced phase transitions in weak interlayer coupling CdPS3. Applied Physics Letters, 2022, 120, .	1.5	3
69995	Deep-Level Defects Induced Degradation of Negative Differential Resistance in GaN-Based Resonant Tunneling Diodes. ACS Applied Electronic Materials, 2022, 4, 3535-3542.	2.0	2
69996	RKKY-type in-plane ferromagnetism in layered <mml:math xmlns:mml="http://www.w3.org/1998/Math/MathML"><mml:msub><mml:mi mathvariant="normal">Mn</mml:mi><mml:mrow><mml:mn>1</mml:mn><mml:mo>/</mml:mo><mml:mn>4</mml:mn></mml:mrow mathvariant="normal">NbS</mml:mi><mml:mn>2</mml:mn></mml:msub></mml:math> single crystals. Physical Review B, 2022, 105, .	1.1	3
69997	Theoretical Study of a Novel WSi₂N₄/MoSi₂N₄ Heterostructure with Ultrafast Carrier Transport. Journal of Physical Chemistry C, 2022, 126, 11380-11388.	1.5	20
69998	Connecting Thermodynamics of Alkali Ion Exchange on the Quartz (101) Surface with Density Functional Theory Calculations. Journal of Physical Chemistry A, 2022, 126, 4286-4294.	1.1	2
69999	The Thermodynamic Stability of InxGa1Ââ€“ xN Solid Solutions. Technical Physics Letters, 0, , .	0.2	0
70000	Chemical trends in the high thermoelectric performance of the pyrite-type dichalcogenides <mml:math xmlns:mml="http://www.w3.org/1998/Math/MathML"><mml:msub><mml:mi>ZnS</mml:mi><mml:mn>2</mml:mn></mml:msub><mml , and <mml:math xmlns:mml="http://www.w3.org/1998/Math/MathML"><mml:msub><mml:mi>CdSe</mml:mi><mml:mn>2</mml:mn></mml:msub></ Physical Review B, 2022, 105, .	1.1	6

#	Article	IF	Citations
70001	Low-dimensional Magnetism in Compounds with Different Dimensions of Magnetic Interaction. Doklady BGUIR, 2022, 20, 62-70.	0.1	0
70002	Interlayer Hopping Kinetics of Vacancies in CrI ₃ Layers Leading to Monolayer/Bilayer Heterostructures. Advanced Materials Interfaces, 0, , 2200626.	1.9	0
70003	Topological nodal surface semimetal states in <mml:math xmlns:mml="http://www.w3.org/1998/Math/MathML"><mml:mrow><mml:msub><mml:mi>Sr</mml:mi><mml:mn>5</mml:mn></<mml:r compounds <mml:math		

#	Article	IF	Citations
70019	Autonomous synthesis system integrating theoretical, informatics, and experimental approaches for large-magnetic-anisotropy materials. Science and Technology of Advanced Materials Methods, 2022, 2, 280-293.	0.4	3
70020	Visualizing Eigen/Zundel cations and their interconversion in monolayer water on metal surfaces. Science, 2022, 377, 315-319.	6.0	47
70021	Photo-Induced Charge Transfer of Fullerene and Non-Fullerene Conjugated Polymer Blends via Ab Initio Excited-State Dynamics. Journal of Physical Chemistry C, 2022, 126, 12015-12024.	1.5	1
70022	DFT + U Study of Uranium Dioxide and Plutonium Dioxide with Occupation Matrix Control. Journal of Physical Chemistry C, 2022, 126, 11426-11435.	1.5	13
70023	Hole Concentration Reduction in CuI by Zn Substitution and its Mechanism: Toward Device Applications. ACS Applied Materials & Interfaces, 2022, 14, 33463-33471.	4.0	9
70024	High Tc superconductivity in layered hydrides XH15 (X = Ca, Sr, Y, La) under high pressures. Frontiers of Physics, 2022, 17, .	2.4	3
70025	Effect of Magnetic Impurities on Superconductivity in LaH₁₀. Advanced Materials, 2022, 34, .	11.1	24
70026	Magnetic phase transition of monolayer chromium trihalides investigated with machine learning: toward a universal magnetic Hamiltonian. Journal of Physics Condensed Matter, 2022, 34, 395901.	0.7	1
70027	Combined surface x-ray diffraction and density functional theory study of the germanene/Al(111)-<mml:math xmlns:mml="http://www.w3.org/1998/Math/MathML"><mml:mrow><mml:mrow><mml:mo>(</mml:mo><mml:mrow><mml:msqrt><mr structure. Physical Review B, 2022, 106, .	1.1	4
70028	Theoretical inspection of TM-P4C single-atom electrocatalysts: High performance for oxygen reduction and evolution reactions. Electrochimica Acta, 2022, 427, 140853.	2.6	4
70029	Inducing Dzyaloshinskiiâ€“Moriya interaction in symmetrical multilayers using post annealing. Scientific Reports, 2022, 12, .	1.6	4
70030	Few-cycle optical field breakdown and damage of gallium oxide and gallium nitride. APL Materials, 2022, 10, .	2.2	3
70031	Surfaceâ€Confined Synthesis of Ultrafine Ptâ€Rare Earth Nanoalloys on Nâ€Functionalized Supports. Advanced Functional Materials, 2022, 32, .	7.8	10
70032	Intrinsic electronic property and adsorption of organic molecules on specific iron surface: an ab initio DFT and DFTB study. Journal of Adhesion Science and Technology, 2023, 37, 1837-1855.	1.4	9
70033	MoSi2N4/CrS2 van der Waals heterostructure with high solar-to-hydrogen efficiency. Physica E: Low-Dimensional Systems and Nanostructures, 2022, 144, 115443.	1.3	4
70034	Modeling magnetic multipolar phases in density functional theory. Physical Review B, 2022, 106, .	1.1	7
70035	Engineering Electronic Platinumâ€“Carbon Support Interaction to Tame Carbon Monoxide Activation. Fundamental Research, 2022, , .	1.6	2
70036	Robustness of Bilayer Hexagonal Ice against Surface Symmetry and Corrugation. Physical Review Letters, 2022, 129, .	2.9	14

#	Article	IF	Citations
70037	Surface Passivation and Detrimental Heat-Induced Diffusion Effects in RbF-Treated Cu(In,Ga)Se₂ Solar Cell Absorbers. ACS Applied Materials & Interfaces, 2022, 14, 34101-34112.	4.0	3
70038	Third-order topological insulators with wallpaper fermions in Tl4PbTe3 and Tl4SnTe3. Npj Computational Materials, 2022, 8, .	3.5	1
70039	Optoelectronic properties of 2D van der Waals heterostructure As/PtS2 by first-principles calculations. Materials Today: Proceedings, 2022, 67, 250-253.	0.9	1
70040	Colossal piezoresistance in narrow-gap <mml:math xmlns:mml="http://www.w3.org/1998/Math/MathML"><mml:mrow><mml:msub><mml:mi>Eu</mml:mi><mml:mn>1</mml:mn></mml:msub></mml:mrow></mml:math> Physical Review B, 2022, 106, .	3.7	2
70041	Selective removal of radioactive iodine from water using reusable Fe@Pt adsorbents. Water Research, 2022, 222, 118864.	5.3	17
70042	Vibrational Relaxation of Highly Vibrationally Excited Molecules Scattered from Au(111): Role of the Dissociation Barrier. Journal of Physical Chemistry C, 2022, 126, 12003-12008.	1.5	2
70043	Cooperative Interactions between Surface Terminations Explain Photocatalytic Water Splitting Activity on <mml:math xmlns:mml="http://www.w3.org/1998/Math/MathML" display="inline" overflow="scroll"><mml:msub><mml:mrow><mml:mi>Sr</mml:mi><mml:mi>Ti</mml:mi><mml:mi mathvariant="normal">O</mml:mi></mml:mrow><mml:mn>3</mml:mn></mml:msub></mml:math>. , 2022, 1, .		4
70044	Interstitial Atomic Bi Chargeâ€Alternating Processor Boosts Twofold Molecular Oxygen Activation Enabling Rapid Catalytic Oxidation Reactions at Room Temperature. Advanced Functional Materials, 2022, 32, .	7.8	16
70045	Interstitial Li⁺ Occupancy Enabling Radiative/Nonradiative Transition Control toward Highly Efficient Cr³⁺-Based Near-Infrared Luminescence. ACS Applied Materials & Interfaces, 2022, 14, 31035-31043.	4.0	32
70046	Ultimate mechanical properties of enstatite. Physics and Chemistry of Minerals, 2022, 49, .	0.3	1
70047	First-principles calculations of the optical properties of Phagraphene. Modern Physics Letters B, 2022, 36, .	1.0	1
70048	Thermodynamic investigation of phase transformation in Sn anode for magnesium batteries. APL Materials, 2022, 10, .	2.2	3
70049	Exploration of glassy state in Prussian blue analogues. Nature Communications, 2022, 13, .	5.8	21
70050	Ultranarrow Bandgap Seâ€Deficient Bimetallic Selenides for High Performance Alkali Metalâ€Ion Batteries. Advanced Functional Materials, 2022, 32, .	7.8	30
70051	Soft-mode-phonon-mediated insulatorâ€“superconductor transition in doped two-dimensional topological insulator RuC. Applied Physics Letters, 2022, 121, 013102.	1.5	0
70052	Band-Structure Engineering of Copper Benzenehexathiol for Reversible Mechanochromism: A First-Principles Study. Journal of Physical Chemistry C, 2022, 126, 11642-11651.	1.5	0
70053	Hierarchical Doping Engineering with Active/Inert Dual Elements Stabilizes LiCoO₂ to 4.6ÂV. Advanced Energy Materials, 2022, 12, .	10.2	39
70054	Visible-Light Photocatalytic Chlorite Activation Mediated by Oxygen Vacancy Abundant Nd-Doped BiVO₄ for Efficient Chlorine Dioxide Generation and Pollutant Degradation. ACS Applied Materials & Interfaces, 2022, 14, 31920-31932.	4.0	12

#	Article	IF	Citations
70055	Crystallization of A₃Ln(BO₃)₂ (A = Na, K; Ln = Lanthanide) from a Boric Acid Containing Hydroxide Melt: Synthesis and Investigation of Lanthanide Borates as Potential Nuclear Waste Forms. Inorganic Chemistry, 2022, 61, 11232-11242.	1.9	7
70056	Advanced and Functional Structured Ceramics: MgF2 and ZnS. Materials, 2022, 15, 4780.	1.3	4
70057	Regulation of Dendrite-Free Li Plating via Lithiophilic Sites on Lithium-Alloy Surface. ACS Applied Materials & Interfaces, 2022, 14, 33952-33959.	4.0	15
70058	Theoretical and Experimental Studies of Gallate Melilite Electrides from Topotactic Reduction of Interstitial Oxide Ion Conductors. Inorganic Chemistry, 2022, 61, 10915-10924.	1.9	2
70059	2D MXenes for Hotâ€Carrier Photodetection. Advanced Optical Materials, 2022, 10, .	3.6	7
70060	Stacking-dependent exciton multiplicity in <mml:math xmlns:mml="http://www.w3.org/1998/Math/MathML"><mml:msub><mml:mi>WSe</mml:mi><mml:mn>2</mml:mn></mml:msub></mr bilayers. Physical Review B, 2022, 106, .	1.1	14
70061	On-Site Synthesis and Characterizations of Atomically-Thin Nickel Tellurides with Versatile Stoichiometric Phases through Self-Intercalation. ACS Nano, 2022, 16, 11444-11454.	7.3	10
70062	The New High-Pressure Phases of Nitrogen-Rich Agâ€“N Compounds. Materials, 2022, 15, 4986.	1.3	5
70063	Construction of CoS-encapsulated in ultrahigh nitrogen doped carbon nanofibers from energetic metal-organic frameworks for superior sodium storage. Carbon, 2022, 198, 353-363.	5.4	19
70064	Predicting Elastic Constants of Refractory Complex Concentrated Alloys Using Machine Learning Approach. Materials, 2022, 15, 4997.	1.3	6
70065	Anhydrous Fast Proton Transport Boosted by the Hydrogen Bond Network in a Dense Oxideâ€Ion Array of Î±â€MoO₃. Advanced Materials, 2022, 34, .	11.1	23
70066	Intrinsic valley-related multiple Hall effect in the two-dimensional organometallic lattice of NbTa-benzene. Physical Review B, 2022, 106, .	1.1	3
70067	Atomic-scale insights on hydrogen trapping and exclusion at incoherent interfaces of nanoprecipitates in martensitic steels. Nature Communications, 2022, 13, .	5.8	27
70068	Suppression and compensation effect of oxygen on the behavior of heavily boron-doped diamond films. Chinese Physics B, 2023, 32, 038101.	0.7	2
70069	Subnanometric Ru clusters with upshifted D band center improve performance for alkaline hydrogen evolution reaction. Nature Communications, 2022, 13, .	5.8	262
70070	Ferric oxide nanoclusters with low-spin FeIII anchored g-C3N4 rod for boosting photocatalytic activity and degradation of diclofenac in water under solar light. Applied Catalysis B: Environmental, 2022, 317, 121725.	10.8	35
70071	NiFe Layered Double Hydroxide Electrocatalysts for an Efficient Oxygen Evolution Reaction. ACS Applied Energy Materials, 2022, 5, 8592-8600.	2.5	23
70072	High performance of hot-carrier generation, transport and injection in TiN/TiO2 junction. Frontiers of Physics, 2022, 17, .	2.4	1

#	Article	IF	Citations
70073	Nanopore-Patterned CuSe Drives the Realization of the PbSeâ€“CuSe Lateral Heterostructure. ACS Applied Materials & Interfaces, 2022, 14, 32738-32746.	4.0	6
70074	Synthesis, characterization and thermoluminescence based high dose neutron and gamma dosimetry study of Al ₅ BO ₉ : Mn, Li nanophosphor. Journal of the American Ceramic Society, 0, , .	1.9	5
70075	Fundamental Properties of Transition-Metals-Adsorbed Germanene: A DFT Study. Coatings, 2022, 12, 948.	1.2	2
70076	Lithiation Pathway Mechanism of Si-C Composite Anode Revealed by the Role of Nanopore usingIn SituLithiation. ACS Energy Letters, 2022, 7, 2469-2476.	8.8	8
70077	Study of Metalâ€“Dielectric Interface for Improving Electrical Properties and Reliability of DRAM Capacitor. Advanced Materials Technologies, 2023, 8, .	3.0	2
70078	Influence of ion irradiation-induced defects on phase formation and thermal stability of Ti0.27Al0.21N0.52 coatings. Acta Materialia, 2022, 237, 118160.	3.8	7
70079	Enhanced Emission from Defect Levels in Multilayer MoS₂. Advanced Optical Materials, 2022, 10, .	3.6	9
70080	Between Elemental Match and Mismatch: From K12Ge3.5Sb6 to Salts of (Ge2Sb2)2â^', (Ge4Sb12)4â^', and (Ge4Sb14)4â^'. Angewandte Chemie, 0, , .	1.6	0
70081	Tuning charge density wave order and superconductivity in the kagome metals <mml:math xmlns:mml="http://www.w3.org/1998/Math/MathML"><mml:mrow><mml:msub><mml:mi>KV</mml:mi><mml:mn>3</mml:mn></mml: width="0.16em" /><mml:msub><mml:mi>Sn</mml:mi><mml:mi>x</mml:mi></mml:msub></mml:mrow></mml:math> and <mml:math xmlns:mml="http://www.w3.org/1998/Math/MathML"><mml:mrow><mml:msub><m. Physical Review Materials, 2022, 6, .	0.9	13
70082	Charge transfer and metal-insulator transition in (CrO₂)_m/(TaO₂)_n superlattices. Journal of Physics Condensed Matter, 0, , .	0.7	1
70083	3D Hierarchical Grapheneâ€CNT Anode for Sodiumâ€Ion Batteries: a Firstâ€Principles Assessment. Advanced Theory and Simulations, 2022, 5, .	1.3	1
70084	Non-stoichiometry of (TiZrHfVNbTa)C and its significance to the microstructure and mechanical properties. Journal of the European Ceramic Society, 2022, 42, 6347-6355.	2.8	13
70085	A simple descriptor for magnetic classification of 2D MXene materials. AIP Advances, 2022, 12, .	0.6	4
70086	Lithography-free, high-density MoTe2 nanoribbon arrays. Materials Today, 2022, 58, 8-17.	8.3	4
70087	Magnetic Moment Preservation and Emergent Kondo Resonance of Co-Phthalocyanine on Semimetallic Sb(111). Physical Review Letters, 2022, 129, .	2.9	3
70088	Superb storage and energy saving separation of hydrocarbon gases in boron nitride nanosheets via a mechanochemical process. Materials Today, 2022, 57, 26-34.	8.3	6
70089	Metal element doping in Cs(Pb1Ââ^'ÂDE)Br3 for solar cell materials. Chemical Engineering Journal Advances, 2022, 12, 100364.	2.4	1
70090	An Ab-initio study of the Y decorated 2D holey graphyne for hydrogen storage application. Nanotechnology, 2022, 33, 405406.	1.3	11

#	Article	IF	Citations
70091	In Situ Growth of Strained Matrix on CsPbI₃ Perovskite Quantum Dots for Balanced Conductivity and Stability. ACS Nano, 2022, 16, 10534-10544.	7.3	16
70092	Density Functional Theory Studies on Dimension-Controlled Self-Assemblies from Cadmium Telluride Nanoclusters: Implications for Solar Cell Applications. ACS Applied Nano Materials, 0, , .	2.4	1
70093	<scp>Ultralowâ€Energyâ€Barrier H₂O₂</scp> Dissociation on Coordinatively Unsaturated Metal Centers in Binary <scp>Ceâ€Fe</scp> Prussian Blue Analogue for Efficient and Stable <scp>Photoâ€Fenton</scp> Catalysis. Energy and Environmental Materials, 2023, 6, .	7.3	3
70094	Reconstructing the Linear Relations by Designing Bi-Atom Sites on NbS₂ for the Efficient Nitrogen Reduction Reaction. Journal of the Electrochemical Society, 2022, 169, 076506.	1.3	0
70095	High figure-of-merit and power generation in high-entropy GeTe-based thermoelectrics. Science, 2022, 377, 208-213.	6.0	233
70096	Unraveling the Anchoring Effect of MXene-Supported Single Atoms as Cathodes for Aluminumâ€“Sulfur Batteries. , 2022, 4, 1436-1445.		11
70097	Anisotropic Chalcogenide Perovskite CaZrS₃: A Promising Thermoelectric Material. Journal of Physical Chemistry C, 2022, 126, 11751-11760.	1.5	13
70098	Artificial neural network-based path integral simulations of hydrogen isotope diffusion in palladium. JPhys Energy, 2022, 4, 034004.	2.3	10
70099	Surface Transformation Enables a Dendriteâ€Free Zincâ€Metal Anode in Nonaqueous Electrolyte. Advanced Materials, 2022, 34, .	11.1	34
70100	Controlled photoinduced electron transfer from g-C3N4 to CuCdCe-LDH for efficient visible light hydrogen evolution reaction. International Journal of Hydrogen Energy, 2022, 47, 40227-40241.	3.8	13
70101	Angstrom-confined catalytic water purification within Co-TiOx laminar membrane nanochannels. Nature Communications, 2022, 13, .	5.8	97
70102	Machine-learning prediction of Vegard's law factor and volume size factor for binary substitutional metallic solid solutions. Acta Materialia, 2022, 237, 118166.	3.8	5
70103	Effect of Zr addition on the local structure and mechanical properties of Tiâ€“Taâ€“Nbâ€“Zr refractory high-entropy alloys. Journal of Materials Research and Technology, 2022, 19, 4428-4438.	2.6	12
70104	Achieving a High-Rate and Stable Li₄Ti₅O₁₂ Anode via a â€œThree-in-Oneâ€•Strategy. Journal of Physical Chemistry C, 2022, 126, 12283-12293.	1.5	4
70105	Phase change in GeTe/Sb2Te3 superlattices: Formation of the vacancy-ordered metastable cubic structure via Ge migration. Applied Surface Science, 2022, 602, 154274.	3.1	3
70106	Silica-assisted pyro-hydrolysis of CaCl2 waste for the recovery of hydrochloric acid (HCl): Reaction pathways with the evolution of Ca(OH)Cl intermediate by experimental investigation and DFT modelling. Journal of Hazardous Materials, 2022, 439, 129620.	6.5	7
70107	Magnetoâ€Optical Properties of Oxidized Co Nanowires on Pt Substrate. Physica Status Solidi (B): Basic Research, 2022, 259, .	0.7	4
70108	V4C3TX MXene: First-principles computational and separator modification study on immobilization and catalytic conversion of polysulfide in Li-S batteries. Journal of Colloid and Interface Science, 2022, 627, 992-1002.	5.0	9

#	Article	IF	Citations
70109	Controllable Valley Polarization and Strain Modulation in 2D 2Hâ€“VS2/CuInP2Se6 Heterostructures. Nanomaterials, 2022, 12, 2461.	1.9	3
70110	Coordination Symmetry Breaking of Singleâ€Atom Catalysts for Robust and Efficient Nitrate Electroreduction to Ammonia. Advanced Materials, 2022, 34, .	11.1	83
70111	Atomistic weak interaction criterion for the specificity of liquid metal embrittlement. Scientific Reports, 2022, 12, .	1.6	4
70112	Cation-selective two-dimensional polyimine membranes for high-performance osmotic energy conversion. Nature Communications, 2022, 13, .	5.8	49
70113	Synergistic effect of atomic layer deposition-assisted cocatalyst and crystal facet engineering in SnS2 nanosheet for solar water oxidation. Science Bulletin, 2022, 67, 1562-1571.	4.3	14
70114	The phonon transport properties in a new ferroelectric carbonâ€“boron framework with hostâ€“guest clathrate structure. European Physical Journal B, 2022, 95, .	0.6	2
70115	Platinumâ€“Dysprosium Alloys as Oxygen Electrodes in Alkaline Media: An Experimental and Theoretical Study. Nanomaterials, 2022, 12, 2318.	1.9	1
70116	Octave-spanning emission across the visible spectrum from single crystalline 1,3,5,7-tetrakis-(p-methoxyphenyl)adamantane. Optical Materials Express, 2022, 12, 3517.	1.6	1
70117	High-Throughput Prediction of the Band Gaps of van der Waals Heterostructures via Machine Learning. Nanomaterials, 2022, 12, 2301.	1.9	3
70118	Hydrogen-induced enhancement of thermal stability in VZr(H) metallic glasses. Materialia, 2022, 24, 101496.	1.3	2
70119	Coalescence dynamics of platinum group metal nanoparticles revealed by liquid-phase transmission electron microscopy. IScience, 2022, 25, 104699.	1.9	1
70120	Anharmonic phonon renormalization and thermal transport in the type-I <mml:math xmlns:mml="http://www.w3.org/1998/Math/MathML"><mml:mrow><mml:msub><mml:mi>Ba</mml:mi><mml:mn>8</mml:mn></mml:msub> clathrate from first principles. Physical Review B, 2022, 106, .	1.1	9
70121	Magnetochemical effects on phase stability and vacancy formation in fcc Fe-Ni alloys. Physical Review B, 2022, 106, .	1.1	7
70122	Controlled Synthesis of Transition Metal Phosphide Nanoparticles to Establish Composition-Dependent Trends in Electrocatalytic Activity. Chemistry of Materials, 2022, 34, 6255-6267.	3.2	17
70123	Two pairs of topological Shockley surface bands in the ternary compound <mml:math xmlns:mml="http://www.w3.org/1998/Math/MathML"><mml:mrow><mml:msub><mml:mi>SnSb</mml:mi><mml:mn>2</mml:mn></mml:msub></mml:mrow></mml:math>. Physical Review B, 2022, 106, .	1.1	0
70124	18â€Crownâ€6 Additive to Enhance Performance and Durability in Solutionâ€Processed Halide Perovskite Electronics. Small, 2022, 18, .	5.2	4
70125	Antiferromagnetic ordering of organic Mott insulator <mml:math xmlns:mml="http://www.w3.org/1998/Math/MathML"><mml:mi>Î»</mml:mi><mml:mtext>â€²</mml:mtext><mml:msub><mml:mrow><mml:mathvariant="normal">GaCl</mml:mi><mml:mn>4</mml:mn></mml:msub></mml:math>. Physical Review B, 2022, 106, .	1.1	2
70126	Prediction of New Structures of the Naâ€“Sb Alloy Anode for Na-Ion Batteries. Journal of Physical Chemistry C, 2022, 126, 11468-11474.	1.5	2

#	Article	IF	Citations
70127	Pressure engineering of colossal magnetoresistance in the ferrimagnetic nodal-line semiconductor <mml:math xmlns:mml="http://www.w3.org/1998/Math/MathML"><mml:mrow><mml:msub><mml:mi>Mn</mml:mi><mml:mn>3</mml:mn></mml: Physical Review B, 2022, 106, .	1.1	13
70128	Bi vacancy simultaneous manipulation of bulk adsorption and carrier utilization to replenish the mechanism of Cr(VI) photoreduction at universal pH. Chemical Engineering Journal, 2022, 450, 138106.	6.6	4
70129	Metal-insulator transition and robust thermoelectricity via strain-tuned interplay between structural and electronic properties in <mml:math xmlns:mml="http://www.w3.org/1998/Math/MathML"><mml:mrow><mml:msub><mml:mrow><mml:mo>(</mml:mo><mml:msub><mml:mm Physical Review Research, 2022, 4, .	1.3	3
70130	From the gas phase to the solid state: The chemical bonding in the superheavy element flerovium. Journal of Chemical Physics, 2022, 157, .	1.2	6
70131	Effects of biaxial strain on thermal conductivity of novel puckered C2N2 monolayer: A first-principles study. Solid State Communications, 2022, , 114881.	0.9	0
70132	Spin-Sensitive Epitaxial In₂Se₃ Tunnel Barrier in In₂Se₃/Bi₂Se₃ Topological van der Waals Heterostructure. ACS Applied Materials & Interfaces, 2022, 14, 34093-34100.	4.0	2
70133	Fast constructing polarity-switchable zinc-bromine microbatteries with high areal energy density. Science Advances, 2022, 8, .	4.7	19
70134	Benchmarking structural evolution methods for training of machine learned interatomic potentials. Journal of Physics Condensed Matter, 2022, 34, 385901.	0.7	2
70135	Sub-Nanometer Resolved Tip-Enhanced Raman Spectroscopy of a Single Molecule on the Si(111) Substrate. Journal of Physical Chemistry C, 2022, 126, 12121-12128.	1.5	5
70136	Accurate Computational Prediction of Core-Electron Binding Energies in Carbon-Based Materials: A Machine-Learning Model Combining Density-Functional Theory and GW. Chemistry of Materials, 2022, 34, 6240-6254.	3.2	22
70137	First-Principles Study of Metal Impurities in Silicon Carbide: Structural, Magnetic, and Electronic Properties. Frontiers in Materials, 0, 9, .	1.2	6
70138	Rational Design of Synergistic Structure Between Single-Atoms and Nanoparticles for CO2 Hydrogenation to Formate Under Ambient Conditions. Frontiers in Chemistry, 0, 10, .	1.8	3
70139	Observation of polarity-switchable photoconductivity in III-nitride/MoSx core-shell nanowires. Light: Science and Applications, 2022, 11, .	7.7	38
70140	Local dipole enhancement of space-charge piezophototronic catalysts of core-shell polytetrafluoroethylene@TiO2 nanospheres. Nano Energy, 2022, 102, 107619.	8.2	16
70141	Rashbaâ€“Edelstein Effect in the hâ€BN Van Der Waals Interface for Magnetization Switching. Advanced Materials, 2022, 34, .	11.1	9
70142	Kinetic energy-free Hartreeâ€“Fock equations: an integral formulation. Journal of Mathematical Chemistry, 2023, 61, 343-361.	0.7	1
70143	Excellent magnetocaloric performance in the carbide compounds RE2Cr2C3 (RE = Er, Ho, and Dy) and their composites. Materials Today Physics, 2022, 27, 100786.	2.9	35
70144	Iridiumâ€“Iron Diatomic Active Sites for Efficient Bifunctional Oxygen Electrocatalysis. ACS Catalysis, 2022, 12, 9397-9409.	5.5	47

#	Article	IF	Citations
70145	Interfacial engineering of Co-doped 1T-MoS2 coupled with V2C MXene for efficient electrocatalytic hydrogen evolution. Chemical Engineering Journal, 2022, 450, 138157.	6.6	30
70146	Experimental and DFT studies of flower-like Ni-doped Mo2C on carbon fiber paper: A highly efficient and robust HER electrocatalyst modulated by Ni(NO3)2 concentration. Journal of Advanced Ceramics, 2022, 11, 1294-1306.	8.9	75
70147	Prediction of Above-Room-Temperature Superconductivity in Lanthanide/Actinide Extreme Superhydrides. Journal of the American Chemical Society, 2022, 144, 13394-13400.	6.6	33
70148	A â€œlocalâ€•stacking fault energy model for concentrated alloys. Acta Materialia, 2022, 238, 118165.	3.8	13
70149	Rational Design of Smart Metalâ€“Organic Frameworks for Light-Modulated Gas Transport. ACS Applied Materials & Interfaces, 2022, 14, 32009-32017.	4.0	5
70150	Sandwich-Polarized Heterojunction: Efficient Charge Separation and Redox Capability Protection for Photocatalytic Overall Water Splitting. ACS Applied Materials & Interfaces, 2022, 14, 32018-32025.	4.0	4
70151	Robust Quantum Anomalous Hall States in Monolayer and Few-Layer TiTe. Nano Letters, 2022, 22, 5379-5384.	4.5	15
70152	Identification of the phosphorus-doping defect in MgS as a potential qubit. Chinese Physics B, 0, , .	0.7	0
70153	Ab initio machine learning of phase space averages. Journal of Chemical Physics, 2022, 157, .	1.2	4
70154	Transition-Metal Interlink Neural Network: Machine Learning of 2D Metalâ€“Organic Frameworks with High Magnetic Anisotropy. ACS Applied Materials & Interfaces, 2022, 14, 33726-33733.	4.0	9
70155	Roomâ€Temperature Printing of Ultrathin Quasiâ€2D GaN Semiconductor via Liquid Metal Gallium Surface Confined Nitridation Reaction. Advanced Materials Technologies, 2022, 7, .	3.0	6
70156	RuO2 electronic structure and lattice strain dual engineering for enhanced acidic oxygen evolution reaction performance. Nature Communications, 2022, 13, .	5.8	145
70157	Cu/Fe dual atoms catalysts derived from Cu-MOF for Zn-air batteries. Materials Today Energy, 2022, 28, 101086.	2.5	1
70158	Anisotropy of the Electric Field Gradient in Two-Dimensional Î±-MoO3 Investigated by 57Mn(57Fe) Emission MÃ¶ssbauer Spectroscopy. Crystals, 2022, 12, 942.	1.0	2
70159	Single Atom Catalysts: What Matters Most, the Active Site or The Surrounding?. ChemCatChem, 2022, 14, .	1.8	18
70160	Strain Effects on the Electronic and Optical Properties of Blue Phosphorene. Frontiers in Chemistry, 0, 10, .	1.8	0
70161	Sulfur-Functionalized Titanium Carbide Ti₃C₂T_x (MXene) Nanosheets Modified Light Absorbers for Ambient Fabrication of Sb₂S₃ Solar Cells. ACS Applied Nano Materials, 2022, 5, 12107-12116.	2.4	7
70162	Electron-phonon coupling strength from ab initio frozen-phonon approach. Physical Review Materials, 2022, 6, .	0.9	10

#	Article	IF	Citations
70163	Identification of high-dielectric constant compounds from statistical design. Npj Computational Materials, 2022, 8, .	3.5	4
70164	Experimental Realization and Computational Investigations of B₂S₂ as a New 2D Material with Potential Applications. ACS Applied Materials & Interfaces, 2022, 14, 32330-32340.	4.0	8
70165	Microscopic theory of superconducting phase diagram in infinite-layer nickelates. Physical Review B, 2022, 106, .	1.1	11
70166	Formation of solid <mml:math xmlns:mml="http://www.w3.org/1998/Math/MathML"><mml:mrow><mml:msub><mml:mi>SiO</mml:mi><mml:mn>2</mml:mn></ compound at high pressure and high temperature. Physical Review B, 2022, 106, .	1.1	1
70167	Enhanced thermoelectric ZT in the tails of the Fermi distribution via electron filtering by nanoinclusions: Model electron transport in nanocomposites. Physical Review Materials, 2022, 6, .	0.9	1
70168	Revealing the Role of d-Orbital Occupation in Edge Reconstruction of 1T-Transition-Metal Dichalcogenides. Journal of Physical Chemistry C, 2022, 126, 11389-11399.	1.5	3
70169	Evaluation of the local structure and electrochemical behavior in the LiCl-KCl-SmCl3 melt. Journal of Molecular Liquids, 2022, 363, 119818.	2.3	5
70170	Floating Particles in the Melt during the Growth of Î²-Ga2O3 Single Crystals Using the Czochralski Method. Metals, 2022, 12, 1171.	1.0	2
70171	Growth, characterization, and photovoltaic application of copper oxide thin films. Thin Solid Films, 2022, 757, 139381.	0.8	6
70172	Dualâ€Band Perovskite Bulk Heterojunction Selfâ€Powered Photodetector for Encrypted Communication and Imaging. Advanced Optical Materials, 2022, 10, .	3.6	33
70173	Heterovalent Doping Enabled Efficient and Stable Extrinsic Selfâ€Trapped Exciton Emission in Zeroâ€Dimensional Cesium Zinc Halides. Advanced Optical Materials, 2022, 10, .	3.6	9
70174	Novel one- and two-dimensional InSbS3 semiconductors for photocatalytic water splitting: The role of edge electron states. International Journal of Hydrogen Energy, 2022, 47, 27481-27492.	3.8	3
70175	Largeâ€Scale Synthesis and Applications of Hafniumâ€“Tantalum Carbides. Advanced Functional Materials, 2022, 32, .	7.8	8
70176	High performance IEICO-4F/WSe2 heterojunction photodetector based on photoluminescence quenching behavior. Nano Research, 2022, 15, 8595-8602.	5.8	5
70177	Synthesis of the Two-Dimensional Robust Kagome Lattice on Au(111) via the Introduction of Fe Atoms. Journal of Physical Chemistry C, 2022, 126, 12009-12014.	1.5	3
70178	Sodiumâ€Coordinated Polymeric Phthalocyanines as Stable Highâ€Capacity Organic Anodes for Sodiumâ€Ion Batteries. Energy and Environmental Materials, 2023, 6, .	7.3	1
70179	Interplay between Oxygen Octahedral Rotation and Deformation in the Acentric ARTiO₄ Series toward Negative Thermal Expansion. Chemistry of Materials, 2022, 34, 6492-6504.	3.2	5
70180	Heterogeneous catalyst design by generative adversarial network and first-principles based microkinetics. Scientific Reports, 2022, 12, .	1.6	3

#	Article	IF	Citations
70181	ZIFâ€Mg(OH)₂ Dual Template Assisted Selfâ€Confinement of Small PtCo NPs as Promising Oxygen Reduction Reaction in PEM Fuel Cell. Advanced Energy Materials, 2022, 12, .	10.2	24
70182	Tunable Schottky barrier in Janus-XGa₂ Y/Graphene (X/YÂ=ÂS, Se, Te; X â‰ Y) van der Waals heterostructures. Nanotechnology, 2022, 33, 425704.	1.3	8
70183	Metal-free boron doped g-C3N5 catalyst: Efficient doping regulatory strategy for photocatalytic water splitting. Applied Surface Science, 2022, 601, 154186.	3.1	9
70184	Bonding-unsaturation-dependent superconductivity in P-rich sulfides. Matter and Radiation at Extremes, 2022, 7, .	1.5	10
70185	Reaction Mechanism of Deoxydehydration by Ceria-Supported Monomeric Rhenium Catalysts: A Computational Study. Journal of Physical Chemistry C, 2022, 126, 11566-11573.	1.5	6
70186	Room-temperature logic-in-memory operations in single-metallofullerene devices. Nature Materials, 2022, 21, 917-923.	13.3	47
70187	Evidence of a room-temperature quantum spin Hall edge state in a higher-order topological insulator. Nature Materials, 2022, 21, 1111-1115.	13.3	32
70188	Near-Infrared Broadband ZnTa₂O₆:Cr³⁺ Phosphor for pc-LEDs and Its Application to Nondestructive Testing. Inorganic Chemistry, 2022, 61, 11284-11292.	1.9	17
70189	Revisiting the Iodine Vacancy Surface Defects to Rationalize Passivation Strategies in Perovskite Solar Cells. Journal of Physical Chemistry Letters, 2022, 13, 6694-6700.	2.1	15
70190	Spaceâ€Confined Oneâ€Step Growth of 2D MoO₂/MoS₂ Vertical Heterostructures for Superior Hydrogen Evolution in Alkaline Electrolytes. Small, 2022, 18, .	5.2	20
70191	Photocatalytic Câ€“H Bond Activation of Toluene on Rutile TiO₂(110). Journal of Physical Chemistry C, 2022, 126, 11963-11970.	1.5	9
70192	Methanol Synthesis from CO₂/CO Mixture on Cuâ€“Zn Catalysts from Microkinetics-Guided Machine Learning Pathway Search. Journal of the American Chemical Society, 2022, 144, 13401-13414.	6.6	36
70193	Nâ€“p-Conductor Transition of Gas Sensing Behaviors in Mo₂CT_x MXene. ACS Sensors, 2022, 7, 2225-2234.	4.0	20
70194	Theoretical Understanding of thermoelectric energy conversion efficiency in Lead-Free halide double perovskites showing intrinsic defect tolerance. Applied Thermal Engineering, 2022, 215, 119024.	3.0	9
70195	Nitrogen doping of indium oxide for enhanced photocatalytic reduction of CO2 to methanol. Nano Energy, 2022, 101, 107613.	8.2	47
70196	MXene-mediated regulation of local electric field surrounding polyoxometalate nanoparticles for improved lithium storage. Science China Materials, 2022, 65, 2958-2966.	3.5	8
70197	In-situ construction of Li4Ti5O12/rutile TiO2 heterostructured nanorods for robust and high-power lithium storage. Nano Research, 2023, 16, 1513-1521.	5.8	11
70198	Surface and Optoelectronic Properties of Ultrathin Trigonal Selenium: A Density Functional Theory Study with van der Waals Correction. Langmuir, 2022, 38, 8485-8494.	1.6	4

#	Article	IF	Citations
70199	Toward Complete Exfoliation of the Chemisorbed Two-Dimensional Iron Silicates on Ru(0001) via Hydrogenation. Journal of Physical Chemistry C, 2022, 126, 11769-11778.	1.5	2
70200	Spin Polarized Electronic Transport and Photocurrent in Chiral Methionine Molecule via Magnetic Tunnel Junction Model from First Principles. Advanced Quantum Technologies, 2022, 5, .	1.8	2
70201	Chalcogenide MAX phases Zr2Se(B1-xSex) (x=0â€“0.97) and their conduction behaviors. Acta Materialia, 2022, 237, 118183.	3.8	6
70202	Uncovering strong Ï€-metal interactions on Ag and Au nanosurfaces under ambient conditions via in-situ surface-enhanced Raman spectroscopy. CheM, 2022, 8, 2514-2528.	5.8	13
70203	Mechanism of local lattice distortion effects on vacancy migration barriers in fcc alloys. Physical Review Materials, 2022, 6, .	0.9	0
70204	Synthesis, Characterization, and First-Principles Analysis of the MAB-Like Ternary Transition-Metal Boride Fe(MoB)₂. Inorganic Chemistry, 2022, 61, 11046-11056.	1.9	6
70205	Enhanced acidic gas adsorption performance of arsenene by Pt mediation. AIP Advances, 2022, 12, 075108.	0.6	0
70206	An All-in-One Zeolite@Ru-Al2O3 Nanoplatform towards Highly Efficient, Anticoking, and Recyclable Hydrocarbon Cracking Catalysis. Materials Today Nano, 2022, , 100244.	2.3	1
70207	Surface Coverage as an Important Parameter for Predicting Selectivity Trends in Electrochemical CO₂ Reduction. Journal of Physical Chemistry C, 2022, 126, 11927-11936.	1.5	9
70208	Robust route to H2O2 and H2 via intermediate water splitting enabled by capitalizing on minimum vanadium-doped piezocatalysts. Nano Research, 2022, 15, 7986-7993.	5.8	24
70209	Computational analysis of the enhancement of photoelectrolysis using transition metal dichalcogenide heterostructures. Journal of Physics Condensed Matter, 2022, 34, 375001.	0.7	3
70210	First-principles indicators of ferroic parameters in epitaxial BiFeO3 and BiCrO3. Journal of Applied Physics, 2022, 132, .	1.1	0
70211	Deep Dive into Lattice Dynamics and Phonon Anharmonicity for Intrinsically Low Thermal Expansion Coefficient in CuS. ChemNanoMat, 2022, 8, .	1.5	3
70212	Construction of Pd nanoparticles/two-dimensional Co-MOF nanosheets heterojunction for enhanced electrocatalytic hydrodechlorination. Applied Catalysis B: Environmental, 2022, 317, 121730.	10.8	26
70213	Experimental Realization of Atomic Monolayer Si₉C₁₅. Advanced Materials, 2022, 34, .	11.1	11
70214	Design of Three-Dimensional Metallic Biphenylene Networks for Na-Ion Battery Anodes with a Record High Capacity. ACS Applied Materials & Interfaces, 2022, 14, 32043-32055.	4.0	7
70215	Boosted ammonium production by single cobalt atom catalysts with high Faradic efficiencies. Proceedings of the National Academy of Sciences of the United States of America, 2022, 119, .	3.3	43
70216	Identifying Substrate-Dependent Chemical Bonding Nature at Molecule/Metal Interfaces Using Vibrational Sum Frequency Generation Spectroscopy and Theoretical Calculations. Journal of Physical Chemistry C, 2022, 126, 11298-11309.	1.5	3

#	Article	IF	Citations
70217	Scalable Production of Ultrathin Boron Nanosheets from a Lowâ€€Cost Precursor. Advanced Materials Interfaces, 2022, 9, .	1.9	14
70218	Photocatalytic Reduction of Carbon Dioxide to Methane at the Pd-Supported TiO₂ Interface: Mechanistic Insights from Theoretical Studies. ACS Catalysis, 2022, 12, 8558-8571.	5.5	23
70219	Alkali metal doping in Bâ€“C3N4 extends carrier lifetime and increases the CO2 adsorption: DFT study and time-domain Ab initio analysis. Journal of Physics and Chemistry of Solids, 2022, , 110905.	1.9	2
70220	Zero-Dimensional Hybrid Indium Halides with Efficient and Tunable White-Light Emissions. Journal of Physical Chemistry Letters, 2022, 13, 6635-6643.	2.1	19
70221	Benzenehexol-based 2D MOF as high-performance electrocatalyst for oxygen reduction reaction. Applied Surface Science, 2022, 601, 154187.	3.1	10
70222	Role of macrocyclic salen-type Schiff base ligands in one-dimensional Co(II) complexes for superior activities toward oxygen reduction/evolution reactions. International Journal of Hydrogen Energy, 2022, 47, 27000-27011.	3.8	5
70223	Hydrated Anions: From Clusters to Bulk Solution with Quasi-Chemical Theory. Accounts of Chemical Research, 2022, 55, 2201-2212.	7.6	9
70224	Between Elemental Match and Mismatch: From K₁₂Ge_{3.5}Sb₆ to Salts of (Ge₂Sb₂)^{2â^'}, (Ge₄Sb₁₂)^{4â^'}, and (Ge₄Sb₁₄)^{4â^'}. Angewandte Chemie - International Edition, 2022, 61, .	7.2	3
70225	Band Structure Engineering of Bi₄O₄SeCl₂ for Thermoelectric Applications. ACS Organic & Inorganic Au, 2022, 2, 405-414.	1.9	7
70226	Role of Functional Thiolated Molecules on the Enhanced Electronic Transport of Interconnected MoS₂ Nanostructures. Journal of Physical Chemistry C, 2022, 126, 12159-12167.	1.5	0
70227	Effects of intrinsic point defects on antiphase boundary energy of Î³'-Ni3Al from first-principles calculations. Journal of Materials Science, 2022, 57, 12916-12928.	1.7	4
70228	Acoustic phonon dispersion of <mml:math xmlns:mml="http://www.w3.org/1998/Math/MathML"><mml:mi>Î±</mml:mi><mml:mtext>â^'</mml:mtext><mml:msub><mml:mi mathvariant="normal">RuCl</mml:mi><mml:mn>3</mml:mn></mml:msub></mml:math>. Physical Review B, 2022, 106, .	1.1	7
70229	Solid and Hollow Poly(p-xylylene) Particles Synthesis via Metalâ€“Organic Framework-Templated Chemical Vapor Polymerization. Chemistry of Materials, 0, , .	3.2	4
70230	Ferroelectric Domain Engineering Using Structural Defect Ordering. Chemistry of Materials, 2022, 34, 6468-6475.	3.2	7
70231	Lecithin Capping Ligands Enable Ultrastable Perovskite-Phase CsPbI₃ Quantum Dots for Rec. 2020 Bright-Red Light-Emitting Diodes. Journal of the American Chemical Society, 2022, 144, 13302-13310.	6.6	59
70232	Discrimination of xylene isomers in a stacked coordination polymer. Science, 2022, 377, 335-339.	6.0	94
70233	Synergetic Catalysis of Magnetic Single-Atom Catalysts Confined in Graphitic-C₃N₄/CeO₂(111) Heterojunction for CO Oxidization. Journal of Physical Chemistry Letters, 2022, 13, 6367-6375.	2.1	16
70234	Structure-Dependent Electrical Double-Layer Capacitances of the Basal Plane Pd(hkl) Electrodes in HClO₄. Journal of Physical Chemistry C, 2022, 126, 11414-11420.	1.5	5

#	Article	IF	Citations
70235	Size-effect on Ni electrocatalyst: The case of electrochemical benzyl alcohol oxidation. Nano Research, 2023, 16, 202-208.	5.8	7
70236	General Synthesis of Tube-like Nanostructured Perovskite Oxides with Tunable Transition Metalâ€“Oxygen Covalency for Efficient Water Electrooxidation in Neutral Media. Journal of the American Chemical Society, 2022, 144, 13163-13173.	6.6	39
70237	Surface-Based Post-synthesis Manipulation of Point Defects in Metal Oxides Using Liquid Water. ACS Applied Materials & Interfaces, 2022, 14, 34059-34068.	4.0	3
70238	Highly Efficient and Stable Saline Water Electrolysis Enabled by Selfâ€Supported Nickelâ€Iron Phosphosulfide Nanotubes With Heterointerfaces and Underâ€Coordinated Metal Active Sites. Advanced Functional Materials, 2022, 32, .	7.8	60
70239	Chern Number Tunable Quantum Anomalous Hall Effect in Monolayer Transitional Metal Oxides via Manipulating Magnetization Orientation. Physical Review Letters, 2022, 129, .	2.9	36
70240	Unravelling the Catalytic Activity of MnO₂, TiO₂, and VO₂ (110) Surfaces by Oxygen Coadsorption on Sodium-Adsorbed MO₂ {M = Mn, Ti, V}. ACS Omega, 0, , .	1.6	5
70241	Predicted Pressure-Induced High-Energy-Density Iron Pentazolate Salts. Chinese Physics Letters, 2022, 39, 087101.	1.3	4
70242	Extended X-ray absorption fine structure spectroscopy measurements and ab initio molecular dynamics simulations reveal the hydration structure of the radium(II) ion. IScience, 2022, 25, 104763.	1.9	9
70243	A Bismuth-Based Metalâ€“Organic Framework for Visible-Light-Driven Photocatalytic Decolorization of Dyes and Oxidation of Phenylboronic Acids. Inorganic Chemistry, 2022, 61, 11110-11117.	1.9	6
70244	Interstitial B-Doping in Pt Lattice to Upgrade Oxygen Electroreduction Performance. ACS Catalysis, 2022, 12, 8848-8856.	5.5	17
70245	Bixbyite-type Ln2O3 as promoters of metallic Ni for alkaline electrocatalytic hydrogen evolution. Nature Communications, 2022, 13, .	5.8	62
70246	Magnetism in doped infinite-layer <mml:math xmlns:mml="http://www.w3.org/1998/Math/MathML"><mml:msub><mml:mi>NdNiO</mml:mi><mml:mn>2</mml:mn></mml:msub> studied by combined density functional theory and dynamical mean-field theory. Physical Review B, 2022, 106, .	1.1	7
70247	Ab initio analysis of MxLa1â^'xB6 as a solar radiation shielding material. AIP Advances, 2022, 12, .	0.6	1
70248	Cubic Stuffed-Diamond Semiconductors LiCu₃TiQ₄ (Q = S, Se, and Te). Journal of the American Chemical Society, 2022, 144, 12789-12799.	6.6	5
70249	Tailoring Nitrogen Species in Diskâ€Like Carbon Anode Towards Superior Potassium Ion Storage. Small, 2022, 18, .	5.2	11
70250	Computational Pourbaix Diagrams for MXenes: A Key Ingredient toward Proper Theoretical Electrocatalytic Studies. Advanced Theory and Simulations, 2023, 6, .	1.3	16
70251	Vibronic Excitonâ€“Phonon States in Stack-Engineered van der Waals Heterojunction Photodiodes. Nano Letters, 2022, 22, 5751-5758.	4.5	6
70252	Thermoelectric properties of composition-controlled Fe₂TiSi-based full-Heusler thin films. Applied Physics Express, 2022, 15, 085502.	1.1	2

#	Article	IF	Citations
70253	Intermolecular forces at ice and water interfaces: Premelting, surface freezing, and regelation. Journal of Chemical Physics, 2022, 157, .	1.2	10
70254	Decoupling the Chemical and Mechanical Strain Effect on Steering the CO₂ Activation over CeO₂-Based Oxides: An Experimental and DFT Approach. ACS Applied Materials & Interfaces, 2022, 14, 33094-33119.	4.0	17
70255	Mutual spin-phonon driving effects and phonon eigenvector renormalization in nickel (II) oxide. Proceedings of the National Academy of Sciences of the United States of America, 2022, 119, .	3.3	1
70256	Anisotropic magnon damping by zero-temperature quantum fluctuations in ferromagnetic CrGeTe3. Nature Communications, 2022, 13, .	5.8	10
70257	Activating lattice oxygen of two-dimensional MnXnâ^'1O2 MXenes via zero-dimensional graphene quantum dots for water oxidation. Science China Materials, 2022, 65, 3053-3061.	3.5	12
70258	Atomic imaging of zeolite-confined single molecules by electron microscopy. Nature, 2022, 607, 703-707.	13.7	49
70259	Improved Durability of High-Performance Intermediate-Temperature Solid Oxide Fuel Cells with a Ba-Doped La_{0.6}Sr_{0.4}Co_{0.2}Fe_{0.8}O_{3â^'Î´} Cathode. ACS Applied Materials & Interfaces, 2022, 14, 33052-33063.	4.0	7
70260	Identifying the Correlation between Structural Parameters and Anisotropic Magnetic Properties in Ïɛ¿Mnïɛ¿V Semiconductors: A Possible Roomâ€Temperature Magnetism. Advanced Materials, 0, , 2200074.	11.1	0
70261	Oxygen Vacancy Formation and Interface Charge Transfer at Misfit Dislocations in Gd-Doped CeO₂/MgO Heterostructures. Journal of Physical Chemistry C, 2022, 126, 11735-11750.	1.5	2
70262	First-Principles Study of Irn (n = 3â€“5) Clusters Adsorbed on Graphene and Hexagonal Boron Nitride: Structural and Magnetic Properties. Nanomaterials, 2022, 12, 2436.	1.9	0
70263	Metastable skyrmion phase stabilized in wider Tâ€“H region of Î²-Mn type Co₇Zn₇Mn₆ chiral magnet. Journal of Physics Condensed Matter, 2022, 34, 365801.	0.7	1
70264	Photoinduced small electron polarons generation and recombination in hematite. Npj Computational Materials, 2022, 8, .	3.5	10
70265	Variation in spin contamination and diradical character with distance between a singlet biradical molecule and surface. Surfaces and Interfaces, 2022, 33, 102206.	1.5	3
70266	Theoretical understanding on all-solid frustrated Lewis pair sites of C₂N anchored by single metal atom. Journal of Chemical Physics, 0, , .	1.2	2
70267	Ab Initio Investigation of CH₄ Dehydrogenation on a (CeO₂)₁₀ Cluster. Journal of Physical Chemistry C, 2022, 126, 11937-11948.	1.5	1
70268	Understanding and Modifying the Scaling Relations for Ammonia Synthesis on Dilute Metal Alloys: From Single-Atom Alloys to Dimer Alloys. ACS Catalysis, 2022, 12, 9201-9212.	5.5	18
70269	The interface between long-period stacking-ordered (LPSO) structure and Î²' phase in Mg-Gd-Al alloys. Journal of Alloys and Compounds, 2022, 923, 166267.	2.8	6
70270	The simplest dense carbon allotrope: Ultra-hard body-centered tetragonal C4. Journal of Solid State Chemistry, 2022, 314, 123424.	1.4	5

#	Article	IF	Citations
70271	Polarization Electric Field in 2D Polar Monolayer Silicon Monochalcogenides SiX (Xâ€‰=â€‰S, Se) as Potential Photocatalysts for Water Splitting. Physica Status Solidi - Rapid Research Letters, 2023, 17, .	1.2	1
70272	Unraveling the capacitive effect in the vacancy-heterostructure WTe2/MoTe2 for hydrogen evolution reaction by the grand canonical potential kinetics. International Journal of Hydrogen Energy, 2022, , .	3.8	0
70273	Influences of multicenter bonding and interstitial elements on pseudo-twinned Î³-TiAl crystal. Physica Scripta, 0, , .	1.2	0
70274	Universal Principle for Large-Scale Production of a High-Quality Two-Dimensional Monolayer via Positive Charge-Driven Exfoliation. Journal of Physical Chemistry Letters, 2022, 13, 6597-6603.	2.1	6
70275	From molecular adsorption to decomposition of methanol on various ZnO facets: A periodic DFT study. Applied Surface Science, 2022, 602, 154150.	3.1	6
70276	Trapping Capability of Small Vacancy Clusters in the Î±-Zr Doped with Alloying Elements: A First-Principles Study. Crystals, 2022, 12, 997.	1.0	0
70277	Enhancement of the Catalytic Activity of Double Metal Cyanides for the Oxidation of Styrene by the Presence of Included Alcohols. Langmuir, 2022, 38, 8696-8707.	1.6	2
70278	Effect of functional groups on tribological properties of lubricants and mechanism investigation. Friction, 2023, 11, 911-926.	3.4	18
70279	Zeeman-type energy level splittings controlled by an electric field. Physical Review B, 2022, 106, .	1.1	1
70280	Billiard Catalysis at Ti3C2 MXene/MAX Heterostructure for Efficient Nitrogen Fixation. Applied Catalysis B: Environmental, 2022, 317, 121755.	10.8	17
70281	Elastically induced magnetization at ultrafast time scales in a chiral helimagnet. Physical Review B, 2022, 106, .	1.1	4
70282	Highly efficient blue emissive copper halide Cs5Cu3Cl6I2 scintillators for X-ray detection and imaging. Ceramics International, 2022, 48, 30788-30796.	2.3	16
70283	Cr₂XTe₄ (X = Si, Ge) monolayers: a new type of two-dimensional high-T _C Ising ferromagnetic semiconductors with a large magnetic anisotropy. Journal of Physics Condensed Matter, 2022, 34, 384001.	0.7	18
70284	Effect of Ag substitution on ferroelectricity in KNbSi₂O₇. Journal of the Ceramic Society of Japan, 2022, 130, 410-415.	0.5	2
70285	2D Multiferroicity with Ferroelectric Switching Induced Spin-Constrained Photoelectricity. ACS Nano, 2022, 16, 11174-11181.	7.3	13
70286	Significant variation of structural, electronic, magnetic, and polarized properties induced by strain in armchair MoSTe nanoribbon. Journal of Applied Physics, 2022, 132, 015101.	1.1	0
70287	Electronic structure of the highly conductive perovskite oxide <mml:math xmlns:mml="http://www.w3.org/1998/Math/MathML"><mml:mrow><mml:msub><mml:mi>SrMoO</mml:mi><mml:mn>3</mml:mn></mml:msub></mml:mrow></mml:math>. Physical Review Materials, 2022, 6, .	3.9	3
70288	F-Type Pseudo-Halide Anions for High-Efficiency and Stable Wide-Band-Gap Inverted Perovskite Solar Cells with Fill Factor Exceeding 84%. ACS Nano, 2022, 16, 10798-10810.	7.3	45

#	Article	IF	Citations
70289	Mn environment in doped SrTiO3 revealed by first-principles calculation of hyperfine splittings. Applied Physics Letters, 2022, 121, .	1.5	4
70290	Symmetry-Breaking-Induced Multifunctionalities of Two-Dimensional Chromium-Based Materials for Nanoelectronics and Clean Energy Conversion. Physical Review Applied, 2022, 18, .	1.5	18
70291	Enhancing hydrogen evolution reaction performance of transition metal doped two-dimensional electride Ca2N. Chinese Chemical Letters, 2023, 34, 107643.	4.8	5
70292	Enhanced Photocatalytic Hydrogen Evolution from Water Splitting on Ta₂O₅/SrZrO₃ Heterostructures Decorated with Cu_xO/RuO₂ Cocatalysts. ACS Applied Materials & Interfaces, 2022, 14, 31767-31781.	4.0	15
70293	Tuning the electronic and magnetic properties of O Vacancy and nonmetallic atoms doped monolayer SnO: A first-principles study. Solid State Communications, 2022, 354, 114884.	0.9	1
70294	Rashba Splitting and Electronic Valley Characteristics of Janus Sb and Bi Topological Monolayers. International Journal of Molecular Sciences, 2022, 23, 7629.	1.8	2
70295	Surface Vacancy Generation by STM Tunneling Electrons in the Presence of Indigo Molecules on Cu(111). Journal of Physical Chemistry C, 2022, 126, 14103-14115.	1.5	3
70296	Tetrahalidometallate(II) Ionic Liquids with More than One Metal: The Effect of Bromide versus Chloride. Chemistry - A European Journal, 2022, 28, .	1.7	5
70297	Modifying the Magnetic and Electronic Properties of Monolayer 2Hâ€VS₂ via Ferroelectric Substrate with Different Surface Terminations. Physica Status Solidi (B): Basic Research, 2022, 259, .	0.7	0
70298	Brittle and ductile behavior in monolayer MoS2. Materials Today Nano, 2022, 20, 100245.	2.3	2
70299	Highly Efficient and Ultraâ€Broadband Yellow Emission of Leadâ€Free Antimony Halide toward White Lightâ€Emitting Diodes and Visible Light Communication. Laser and Photonics Reviews, 2022, 16, .	4.4	36
70300	Electrochemical reduction of CO2 on single-atom catalysts anchored on N-terminated TiN (1 1 1): Low overpotential and high selectivity. Applied Surface Science, 2022, 602, 154239.	3.1	5
70301	Light-matter interactions in van der Waals photodiodes from first principles. Physical Review B, 2022, 106, .	1.1	5
70302	Defect and interstitial B synergistically promote the stability and H2 dissociation of Pd6 supported by graphene. International Journal of Hydrogen Energy, 2022, 47, 28423-28433.	3.8	1
70303	Clusterâ€Glass for Lowâ€Cost Whiteâ€Light Emission. Advanced Materials, 2022, 34, .	11.1	8
70304	Insight into highly catalytic performance of Co/Î³-Al2O3 for ethylene glycol amination: Promotion of catalytic activity of Co by acid sites and base sites. Molecular Catalysis, 2022, 528, 112492.	1.0	1
70305	Calculation screening of Janus WSSe monolayer modified with single platinum group metal atom as efficient bifunctional oxygen electrocatalysts. Applied Catalysis A: General, 2022, 643, 118777.	2.2	6
70306	High resolution solid state NMR in paramagnetic metal-organic frameworks. Solid State Nuclear Magnetic Resonance, 2022, 120, 101811.	1.5	3

#	Article	IF	Citations
70307	A triatomic carbon and derived pentacarbides with superstrong mechanical properties. IScience, 2022, 25, 104712.	1.9	6
70308	Microstructure and properties of Cuâ€“Niâ€“Coâ€“Siâ€“Crâ€“Mg alloys with different Si contents after multi-step thermo-mechanical treatment. Materials Science & Engineering A: Structural Materials: Properties, Microstructure and Processing, 2022, 850, 143532.	2.6	15
70309	The effect of Ta, W, and Re additions on the tensile-deformation behavior of model Ni-based single-crystal superalloys at intermediate temperature. Materials Science & Engineering A: Structural Materials: Properties, Microstructure and Processing, 2022, 850, 143594.	2.6	2
70310	A DFT+U study on the structural, electronic, magnetic, and optical properties of Fe and Co co-doped CuO. Materials Today Communications, 2022, 32, 103923.	0.9	4
70311	Kinetics investigation of the oxygen evolution reaction on the characteristic facets of Î³-Cu3V2O8. Molecular Catalysis, 2022, 528, 112493.	1.0	1
70312	Elucidating facet dependent electronic and electrochemical properties of Cu2O nanocrystals using AFM/SCEM and DFT. Nano Today, 2022, 45, 101538.	6.2	6
70313	Ternary molybdenum sulfo-selenides alloy DS-MoSSe anode for high performance metal-ion batteries from first principles calculations. Materials Today Communications, 2022, 32, 103974.	0.9	0
70314	Thermal stability of the magnetic moment in amorphous carbon thin film - An experimental and ab-initio study. Diamond and Related Materials, 2022, 127, 109200.	1.8	0
70315	Effects of the Tc, Ru, Rh and Cd substitution doping on the structural, electronic, magnetic and optical properties of blue P monolayer. Thin Solid Films, 2022, 756, 139386.	0.8	2
70316	Synergetic effects of Sn and Ti incorporated in MWW zeolites on promoting the oxidative hydration of ethylene with H2O2 to ethylene glycol. Journal of Catalysis, 2022, 413, 554-564.	3.1	7
70317	On the shifting peak of volcano plots for oxygen reduction and evolution. Electrochimica Acta, 2022, 426, 140799.	2.6	11
70318	The electronic structure, elastic properties, dynamical stability and thermoelectric properties of rock-salt and orthorhombic phases of CdS: First-principles calculations. Solid State Communications, 2022, 353, 114779.	0.9	4
70319	Revealing structural, mechanical, and electronic properties of M<mml:math xmlns:mml="http://www.w3.org/1998/Math/MathML" altimg="si87.svg" display="inline" id="d1e1055"><mml:msub><mml:mrow /><mml:mrow><mml:mn>4</mml:mn></mml:mrow></mml:msub></mml:math>C<mml:math xmlns:mml="http://www.w3.org/1998/Math/MathML" altimg="si88.svg" display="inline" id="d1e1063"><mml:msub><mml:mrow /><mml:mrow><mml:mn>3</mml:mn></mml:mrow></mml:msub></	0.9	7
70320	Key roles of formyl insertion mechanism and C-O scission of oxygenates on cobalt carbide in syngas Conversion: A detailed reaction network analysis. Journal of Catalysis, 2022, 413, 455-466.	3.1	6
70321	Influence of the monovalent bismuth on optical properties in Bi-doped silica optical fiber. Optical Materials, 2022, 131, 112720.	1.7	0
70322	Seed-assisted epitaxy of intermetallic compounds with interface-determined orientation: Incommensurate Nowotny chimney-ladder FeGe epitaxial film. Acta Materialia, 2022, 236, 118130.	3.8	2
70323	Interface chemistry effects in nanofluids: Experimental and computational study of oil-based nanofluids with gold nanoplates. Journal of Molecular Liquids, 2022, 362, 119762.	2.3	3
70324	Precipitation-based grain boundary design alters Inter- to Trans-granular Fracture in AlCrN Thin Films. Acta Materialia, 2022, 237, 118156.	3.8	10

#	Article	IF	Citations
70325	Multi-objective materials bayesian optimization with active learning of design constraints: Design of ductile refractory multi-principal-element alloys. Acta Materialia, 2022, 236, 118133.	3.8	22
70326	Spin reorientation in CoV2O4 thin film: A first principles study. Computational Materials Science, 2022, 212, 111603.	1.4	1
70327	Umbrella sampling with machine learning potentials applied for solid phase transition of GeSbTe. Chemical Physics Letters, 2022, 803, 139813.	1.2	2
70328	Insights into the photocatalytic mechanism of S-scheme g-C3N4/BiOBr heterojunction. Inorganic Chemistry Communication, 2022, 143, 109732.	1.8	6
70329	First-principles study on magnetocrystalline anisotropy of cobalt films: hcp vs fcc. Current Applied Physics, 2022, 41, 148-155.	1.1	2
70330	Water accelerated activity of Ru NPs in sequential hydrogenation of nitrobenzene to cyclohexylamine. Journal of Catalysis, 2022, 413, 546-553.	3.1	8
70331	On the affected strength of Al grain boundaries by Zn segregation: A first-principles interpretation. Computational Materials Science, 2022, 212, 111604.	1.4	5
70332	Origin of high piezoelectricity in CBT-based Aurivillius ferroelectrics: Glide of (Bi2O2)2+ blocks and suppressed internal bias field. Acta Materialia, 2022, 237, 118146.	3.8	4
70333	Nonthermal effects in H-doped tungsten at high electronic temperatures. Journal of Nuclear Materials, 2022, 568, 153896.	1.3	1
70334	Cation-assisted lithium ion diffusion in a lithium oxythioborate halide glass solid electrolyte. Electrochimica Acta, 2022, 426, 140806.	2.6	1
70335	Thermoelectric power generation in the core of a nuclear reactor. Energy Conversion and Management, 2022, 268, 115949.	4.4	9
70336	Synergetic enhancement of activity and selectivity for reverse water gas shift reaction on Pt-Re/SiO2 catalysts. Journal of CO2 Utilization, 2022, 63, 102128.	3.3	12
70337	Bistructural Pseudocontinuous Solid Solution with Hierarchical Microstructures from Ab initio Study: Application to the Mg2Snâ^'Mg3Sb2 System. Acta Materialia, 2022, 236, 118139.	3.8	3
70338	True colours shining through: Determining site distributions in coloured Li-containing quaternary Heusler compounds. Journal of Solid State Chemistry, 2022, 314, 123372.	1.4	1
70339	Micro mechanism of latent heat enhancement of polyethylene glycol/aminated modified palygorskite composite phase change materials. Applied Clay Science, 2022, 228, 106641.	2.6	5
70340	Metal-to-semiconductor transitions in constituent-tunable layered two-dimensional Nb W1-Se2 based on first principles calculations. Physica E: Low-Dimensional Systems and Nanostructures, 2022, 144, 115388.	1.3	2
70341	Transition metal substituted MoS2/WS2 van der Waals heterostructure for realization of dilute magnetic semiconductors. Journal of Magnetism and Magnetic Materials, 2022, 560, 169567.	1.0	6
70342	Anomalous transverse effects and Magneto-Optical properties of Co-based Heusler Compounds. Computational Materials Science, 2022, 213, 111625.	1.4	1

#	Article	IF	Citations
70343	Boosting the epoxidation of long-chain linear Î±-olefins via bimetallic CoIr composite. Fuel, 2022, 326, 125050.	3.4	2
70344	Band engineering and improved thermoelectric performance in p-type SmMg2Sb2: A first-principles study. Materials Today Physics, 2022, 27, 100779.	2.9	1
70345	Insight into catalyst of tetramethylguanidine decorated palygorskite for CO2 conversion assisted with zinc halides. Applied Clay Science, 2022, 228, 106626.	2.6	5
70346	Enhancing glass forming ability and magnetic properties of Coâ€“Feâ€“Siâ€“B metallic glasses by similar element substitution: Experimental and theoretical investigations. Computational Materials Science, 2022, 213, 111639.	1.4	4
70347	An ultrahigh rate dendrite-free Zn metal deposition/striping enabled by silver nanowire aerogel with optimal atomic affinity with Zn. Energy Storage Materials, 2022, 51, 453-464.	9.5	22
70348	In-situ X-ray studies of high-entropy layered oxide cathode for sodium-ion batteries. Energy Storage Materials, 2022, 51, 159-171.	9.5	26
70349	Effect of chemical composition and atomic configuration on thermodynamic stability and elastic properties of AlB<mml:math xmlns:mml="http://www.w3.org/1998/Math/MathML" display="inline" id="d1e2304" altimg="si41.svg"><mml:msub><mml:mrow /><mml:mrow><mml:mn>2</mml:mn></mml:mrow></mml:msub></mml:math>-type Sc<mml:math xmlns:mml="http://www.w3.org/1998/Math/MathML" display="inline" id="d1e2312" altimg="si158.svg"><mml:msub><mml:mrow /><mml:mrow><mml:mn>1</mml:mn><mml:mo>â^’	1.4	2
70350	Janus MoSSe/C3N heterostructures: A flexible anode for lithium/sodium-ion batteries. Physica E: Low-Dimensional Systems and Nanostructures, 2022, 144, 115402.	1.3	1
70351	Rashba spin splitting in two-dimensional electron gas in polar-polar perovskite oxide heterostructure LaVO3/KTaO3: A DFT investigation. Physica E: Low-Dimensional Systems and Nanostructures, 2022, 144, 115394.	1.3	4
70352	Tuning bandgap and energy stability of Organic-Inorganic halide perovskites through surface engineering. Computational Materials Science, 2022, 213, 111649.	1.4	1
70353	An ab-initio study on two-dimensional semiconductor alloys: Monolayer Mo1-xCrxS2. Journal of Physics and Chemistry of Solids, 2022, 169, 110877.	1.9	0
70354	First-principles study on the electronic, magnetic, and Li-ion mobility properties of N-doped Ti2CO2. Solid State Ionics, 2022, 383, 115983.	1.3	1
70355	Solution processed edge activated Ni-MoS2 nanosheets for highly sensitive room temperature NO2 gas sensor applications. Applied Surface Science, 2022, 600, 154086.	3.1	26
70356	Three-dimensional nitrogen-doped MXene as support to form high-performance platinum catalysts for water-electrolysis to produce hydrogen. Chemical Engineering Journal, 2022, 446, 137443.	6.6	18
70357	In situ oxygen doped Ti3C2T MXene flexible film as supercapacitor electrode. Chemical Engineering Journal, 2022, 446, 137451.	6.6	22
70358	Mechanical characterisation of V-4Cr-4Ti alloy: Tensile tests under high energy synchrotron diffraction. Journal of Nuclear Materials, 2022, 569, 153911.	1.3	3
70359	Evolution of in-plane heat transport in tellurium from 2D to 3D. Materials Today Physics, 2022, 27, 100776.	2.9	1
70360	Atomistic kinetic Monte Carlo simulation on atomic layer deposition of TiN thin film. Computational Materials Science, 2022, 213, 111620.	1.4	4

#	Article	IF	Citations
70361	Differentiating the dominant intrinsic kinetics for lithium dendrite growth under different circumstances by computational study. Computational Materials Science, 2022, 213, 111637.	1.4	0
70362	Adsorption mechanism of yttrium ions onto ion-adsorption type rare earths ore. Separation and Purification Technology, 2022, 299, 121641.	3.9	13
70363	Evaluation of the electrochemical stability, interfacial reaction, and molecular behavior of ether-functionalized pyrrolidinium as novel electrolyte for lithium metal battery by quantum and molecular dynamics simulations. Applied Surface Science, 2022, 600, 154077.	3.1	1
70364	Regulating anionic redox activity of lithium-rich layered oxides via LiNbO3 integrated modification. Nano Energy, 2022, 101, 107555.	8.2	26
70365	Enhanced NO2-sensing performances of CeO2 nanoparticles on MoS2 at room temperature. Applied Surface Science, 2022, 600, 154157.	3.1	7
70366	The nanocopper interface induces the formation of a new ultrastable glass phase. Journal of Non-Crystalline Solids, 2022, 593, 121764.	1.5	0
70367	Electron-Deficient Pd clusters induced by spontaneous reduction of support defect for selective phenol hydrogenation. Chemical Engineering Science, 2022, 260, 117867.	1.9	2
70368	Metal-cation-mixed lead-less two-dimensional hybrid perovskites with high carrier mobility and promoted light adsorption. Materials Today Physics, 2022, 27, 100769.	2.9	3
70369	Intrinsic multiferroic MnOF monolayer with room-temperature ferromagnetism. Materials Today Physics, 2022, 27, 100775.	2.9	6
70370	Unveiling passivation roles of PEA+ in CsPbI2Br surface. Chemical Physics, 2022, 562, 111651.	0.9	2
70371	First principles study of the effect of uniaxial strain on monolayer MoS2. Physica E: Low-Dimensional Systems and Nanostructures, 2022, 144, 115401.	1.3	7
70372	Novel plate-on-plate hollow structured BiOBr/Bi2MoO6 p-n heterojunctions: In-situ chemical etching preparation and highly improved photocatalytic antibacterial activity. Separation and Purification Technology, 2022, 298, 121666.	3.9	19
70373	Thermal transport properties of anisotropic materials RbCaX (X = As, Sb) with strong anharmonicity. Computational Materials Science, 2022, 213, 111618.	1.4	8
70374	Facile fabrication of a novel spindlelike MoS2/BiVO4 Z-scheme heterostructure with superior visible-light-driven photocatalytic disinfection performance. Separation and Purification Technology, 2022, 299, 121706.	3.9	13
70375	Structural, electronic, and optical properties of rare-earth-doped SrTiO3 perovskite: A first-principles study. Physica B: Condensed Matter, 2022, 643, 414160.	1.3	8
70376	Thermal stability and protective properties of phenylphosphonic acid on Cu(111). Applied Surface Science, 2022, 600, 154036.	3.1	1
70377	Probing the charged defects in single-layer WS2 at atomic level. Materials Today Physics, 2022, 27, 100773.	2.9	1
70378	Examining the thermodynamic stability of mixed principal element oxides in AlCoCrFeNi high-entropy alloy by first-principles. Computational Materials Science, 2022, 213, 111619.	1.4	9

#	Article	IF	Citations
70379	Three non-metallic carbon materials with comparable electrical conductivity to metals. Diamond and Related Materials, 2022, 128, 109230.	1.8	4
70380	Experimental and DFT investigations on enhanced stability found on Re-, Rh-, and Nb-promoted Pt/WOx/Î³-Al2O3 catalyst during aqueous-phase glycerol hydrogenolysis. Fuel, 2022, 326, 125019.	3.4	6
70381	Two-dimensional conductive Ï€-conjugated metal-organic frameworks as promising electrocatalysts for highly efficient hydrogen evolution reaction. Applied Surface Science, 2022, 601, 154241.	3.1	7
70382	Helium bubble facetation in tungsten thin films. Scripta Materialia, 2022, 220, 114918.	2.6	2
70383	A novel sulfide phosphor, BaNaAlS3:Eu2+, discovered via particle swarm optimization. Journal of Alloys and Compounds, 2022, 922, 166187.	2.8	8
70384	Borate narrowed band gap of nickel-iron layer double hydroxide to mediate rapid reconstruction kinetics for water oxidation. Applied Catalysis B: Environmental, 2022, 317, 121713.	10.8	42
70385	Interface engineering of GeP/Graphene/BiVO4 heterostructure for photocatalytic Application: A computational study. Applied Surface Science, 2022, 601, 154243.	3.1	5
70386	Interlayer intercalation of Li/Al-LDHs responsible for high-efficiency boron extraction. Desalination, 2022, 539, 115966.	4.0	12
70387	Effects of oxidizing molecules on the thermal decomposition of TTDO by ab initio molecular dynamics simulations. Journal of Molecular Graphics and Modelling, 2022, 116, 108270.	1.3	1
70388	DFT combined with XANES to investigate the sulfur fixation mechanisms of H2S on different CaO surfaces. Fuel, 2022, 327, 125204.	3.4	3
70389	Tin-based metal organic framework catalysts for high-efficiency electrocatalytic CO2 conversion into formate. Journal of Colloid and Interface Science, 2022, 626, 836-847.	5.0	26
70390	Non-equilibrium synthesis of stacking faults-abundant Ru nanoparticles towards electrocatalytic water splitting. Applied Catalysis B: Environmental, 2022, 316, 121682.	10.8	16
70391	Opposite surface stress induced the distinctly different contact behaviors of monolayer and bilayer borophene on Ag(1 1 1). Applied Surface Science, 2022, 601, 154093.	3.1	4
70392	Do two-dimensional group IV-VI M4X9 monolayers have photocatalytic activity toward overall water splitting? A comprehensive theoretical investigation. Applied Surface Science, 2022, 601, 154225.	3.1	1
70393	Anchoring Ni/NiO heterojunction on freestanding carbon nanofibers for efficient electrochemical water oxidation. Journal of Colloid and Interface Science, 2022, 626, 995-1002.	5.0	4
70394	Anchored Fe atoms for N O bond activation to boost electrocatalytic nitrate reduction at low concentrations. Applied Catalysis B: Environmental, 2022, 317, 121721.	10.8	27
70395	Bi/BiFe(oxy)hydroxide for sustainable lattice oxygen-boosted electrocatalysis at a practical high current density. Applied Catalysis B: Environmental, 2022, 317, 121685.	10.8	7
70396	CeO2 nanosheets with anion-induced oxygen vacancies for promoting photocatalytic toluene mineralization: Toluene adsorption and reactive oxygen species. Applied Catalysis B: Environmental, 2022, 317, 121694.	10.8	46

#	Article	IF	Citations
70397	Edge electron-rich carbon nitride via Ï€-acceptor frame with high-efficient charge separation for photocatalytic hydrogen evolution and environmental remediation. Journal of Colloid and Interface Science, 2022, 626, 889-898.	5.0	7
70398	Atomistic investigation on the impact of substitutional Al and Si atoms on the carbon kinetics in ferrite. Journal of Alloys and Compounds, 2022, 921, 166031.	2.8	2
70399	Physical properties and radiation tolerance of high-entropy pyrochlores Gd2(Ti0.25Zr0.25Sn0.25Hf0.25)2O7 and individual pyrochlores Gd2X2O7 (X= Ti, Zr, Sn, Hf) from first principles calculations. Scripta Materialia, 2022, 220, 114898.	2.6	5
70400	Band structure, photoluminescent properties, and energy transfer behavior of a multicolor tunable phosphor K3Lu(PO4)2: Tb3+, Eu3+ for warm white light-emitting diodes. Journal of Luminescence, 2022, 251, 119133.	1.5	12
70401	First-principles study on the electric control of ferromagnetic behaviour of two-dimensional BaTiO3 (0Â0Â1) ultrathin film doped with Cr. Applied Surface Science, 2022, 601, 154240.	3.1	0
70402	Br-induced P-poor defective nickel phosphide for highly efficient overall water splitting. Applied Catalysis B: Environmental, 2022, 316, 121686.	10.8	44
70403	Analysis of the adsorption characteristics of gasification pollutants (HCl, COS, H2S, NH3 and HCN) on Ti-anchored graphene substrates. Surface Science, 2022, 725, 122148.	0.8	7
70404	Modified Co electronic states in double-anionic CoPS nanocrystals induce highly efficient electrocatalytic hydrogen evolution. Journal of Alloys and Compounds, 2022, 922, 166114.	2.8	0
70405	Phase stability, phonon, electronic, and optical properties of not-yet-synthesized CsScS2, CsYS2, and APmS2 (A= Li, Na, K, Rb, Cs) materials: Insights from first-principles calculations. Materials Science in Semiconductor Processing, 2022, 150, 106936.	1.9	4
70406	Chemical functionalization of low-buckled SiGe monolayer: Effects on the electronic and magnetic properties. Materials Science in Semiconductor Processing, 2022, 150, 106949.	1.9	1
70407	Electronic properties and defect levels induced by <mml:math xmlns:mml="http://www.w3.org/1998/Math/MathML" display="inline" id="d1e1065" altimg="si112.svg"><mml:mrow><mml:mi>n</mml:mi><mml:mo>/</mml:mo><mml:mi>p</mml:mi></mml:mrow></mml:math>-type defect-complexes in Ge. Materials Science in Semiconductor Processing, 2022, 150, 106906.	1.9	4
70408	Two-dimensional V-shaped PdI2: Auxetic semiconductor with ultralow lattice thermal conductivity and ultrafast alkali ion mobility. Applied Surface Science, 2022, 601, 154176.	3.1	10
70409	Enhanced perpendicular magnetic anisotropy in single Ir doped WSe2 monolayer by the application of small strain: first-principles study. Journal of Magnetism and Magnetic Materials, 2022, 561, 169690.	1.0	0
70410	Surficial amide-enabled integrated organic anodeâ€“binder electrode for electrochemical reversibility and fast redox kinetics in lithiumâ€“ion batteries. Applied Surface Science, 2022, 601, 154220.	3.1	5
70411	The removal mechanism of Cr(VI) by calcium titanate: Insight into the role of surface reduced Cr(III) in removal process. Applied Surface Science, 2022, 601, 154235.	3.1	10
70412	NiCo5S8 structure with unique morphology as a cathode active material for All-Solid-State Lithium-Sulfur batteries. Chemical Engineering Journal, 2022, 450, 138050.	6.6	11
70413	Quasi-metallic lithium encapsulated in the subnanopores of hard carbon for hybrid lithiumâ€“ion/lithium metal batteries. Chemical Engineering Journal, 2022, 450, 138049.	6.6	8
70414	Surface lattice oxygen mobility inspired peroxymonosulfate activation over Mn2O3 exposing different crystal faces toward bisphenol A degradation. Chemical Engineering Journal, 2022, 450, 138147.	6.6	8

#	Article	IF	Citations
70415	Mn-doped FeS with larger lattice spacing as advance anode for sodium ion half/full battery. Chemical Engineering Journal, 2022, 450, 137960.	6.6	15
70416	Enhanced electrocatalytic full water-splitting reaction by interfacial electric field in 2D/2D heterojunction. Chemical Engineering Journal, 2022, 450, 137789.	6.6	27
70417	Superior indicative and regulative function of Fe doping amount for MnO2 catalyst with an oxygen vacancy in NH3-SCR reaction: A DFTÂ+ÂU study. Applied Surface Science, 2022, 601, 154162.	3.1	7
70418	Significantly improved thermoelectric properties of Nb-doped ZrNiSn half-Heusler compounds. Chemical Engineering Journal, 2022, 449, 137898.	6.6	11
70419	Enhancing propane direct dehydrogenation performances through temperature induced VOx dispersion and alumina support phase transformation. Chemical Engineering Journal, 2022, 450, 137969.	6.6	6
70420	Cooperative catalytic Mo-S-Co heterojunctions with sulfur vacancies for kinetically boosted lithium-sulfur battery. Chemical Engineering Journal, 2022, 450, 138115.	6.6	23
70421	Insight into the elemental mercury immobilization mechanism with carbon and sulfur over the mackinawite (FeS) surface via density functional theory. Chemical Engineering Journal, 2022, 450, 137934.	6.6	6
70422	Facile synthesis of hierarchical Ti3C2@FeOOH nanocomposites for antimony contaminated wastewater treatment: Performance, mechanisms, reutilization, and sustainability. Chemical Engineering Journal, 2022, 450, 138038.	6.6	14
70423	Facet-Selective hydrogen evolution on Rh2P electrocatalysts in pH-Universal media. Chemical Engineering Journal, 2022, 449, 137790.	6.6	13
70425	Doping Asymmetry and Layer-Selective Metal-Insulator Transition in Trilayer <mml:math xmlns:mml="http://www.w3.org/1998/Math/MathML" display="inline"><mml:mrow><mml:msub><mml:mrow><mml:mi mathvariant="normal">K</mml:mi></mml:mrow><mml:mrow><mml:mn>3</mml:mn><mml:mo>+</mml:mo><mml:mi>x</mml:mi></mml:mrow></mml:msub><mml:msub><mml:mrow><mml:mi mathvariant="normal">C</mml:mi></mml:mrow><mml:mrow><mml:mn>60</mml:mn></mml:mrow></mml:msub></mml:mrow></mml:math>. Physical Review Letters, 2022, 129, .	2.9	3
70426	Identifying the crystal structure of T1 precipitates in Al-Li-Cu alloys by ab initio calculations and HAADF-STEM imaging. Journal of Materials Science and Technology, 2023, 133, 41-57.	5.6	17
70427	Synthesis, formation mechanism, and intrinsic physical properties of several As/P-containing MAX phases. Journal of Materials Science and Technology, 2023, 133, 23-31.	5.6	1
70428	High-capacity, high-rate, and dendrite-free lithium metal anodes based on a 3D mixed electronic-ionic conductive and lithiophilic scaffold. Science China Materials, 2022, 65, 2989-2996.	3.5	1
70429	Feasible Structure Manipulation of Vanadium Selenide into VSe2 on Au(111). Nanomaterials, 2022, 12, 2518.	1.9	2
70430	Atomicâ€Łevel Pt Electrocatalyst Synthesized via Iced Photochemical Method for Hydrogen Evolution Reaction with High Efficiency. Small, 2022, 18, .	5.2	13
70431	The determining role of T species in the catalytic potential of MXenes: Water adsorption and dissociation on Mo2CT. Catalysis Today, 2023, 424, 113848.	2.2	8
70432	The First-Principles Study of External Strain Tuning the Electronic and Optical Properties of the 2D MoTe2/PtS2 van der Waals Heterostructure. Frontiers in Chemistry, 0, 10, .	1.8	4
70433	Cobalt Quaterpyridine Complexes for Highly Efficient Heterogeneous CO₂ Reduction in Aqueous Media. Advanced Energy Materials, 2022, 12, .	10.2	11

#	Article	IF	Citations
70434	Machineâ€Learningâ€Based Exploration of Bending Flexoelectricity in Novel 2D Van der Waals Bilayers. Advanced Energy Materials, 2022, 12, .	10.2	10
70435	Nanosheet-Engineered NH₂-MIL-125 with Highly Active Facets for Enhanced Solar CO₂ Reduction. ACS Catalysis, 2022, 12, 9486-9493.	5.5	42
70436	Altering the Arrangement of Framework Al Atoms in MEL Zeolites Using Mixtures of Tetrabutylammonium and Sodium Structure-Directing Agents. Chemistry of Materials, 2022, 34, 6835-6852.	3.2	3
70437	High performance solid-state thermoelectric energy conversion via inorganic metal halide perovskites under tailored mechanical deformation. Frontiers in Energy, 2022, 16, 581-594.	1.2	6
70438	Metal Cation Pre-Intercalated Ti₃C₂T_x MXene as Ultra-High Areal Capacitance Electrodes for Aqueous Supercapacitors. ACS Applied Energy Materials, 2022, 5, 9373-9382.	2.5	20
70439	Study on Stability and Elastic Properties of Î²-TiX (X=Nb, Ta) Alloys From First-Principles Calculations. Frontiers in Materials, 0, 9, .	1.2	0
70440	Strain-tunable pure Hâ^' conduction in one-atom-thick hexagonal boron nitride for high-energyâ€"density fuel cells. Chemical Engineering Journal, 2022, 450, 138223.	6.6	3
70441	Ion-Permselective Polyphenylene Sulfide-Based Solid-State Separator for High Voltage LiNi_{0.5}Mn_{1.5}O₄ Battery. Journal of the Electrochemical Society, 2022, 169, 070532.	1.3	1
70442	First-Principles Study on the Adsorption Behavior of O2 on the Surface of Plutonium Gallium System. Materials, 2022, 15, 5035.	1.3	2
70443	Dislocation-induced stop-and-go kinetics of interfacial transformations. Nature, 2022, 607, 708-713.	13.7	38
70444	K-point longitudinal acoustic phonons are responsible for ultrafast intervalley scattering in monolayer MoSe2. Nature Communications, 2022, 13, .	5.8	13
70445	Density functional theory screening of some fundamental physical properties of Cs2InSbCl6 and Cs2InBiCl6 double perovskites. European Physical Journal B, 2022, 95, .	0.6	34
70446	Prediction of Core Electron Reactivity and High Oxidation States in Radium under High Pressure. Journal of Physical Chemistry C, 0, , .	1.5	2
70447	A Highly Stable Allâ€Solidâ€State Naâ€"O₂/H₂O Battery with Low Overpotential Based on Sodium Hydroxide. Advanced Functional Materials, 2022, 32, .	7.8	9
70448	Selective Hydrogenation of Crotonaldehyde on SiO₂â€Supported Pt Clusters: A DFT Study. Advanced Theory and Simulations, 2022, 5, .	1.3	1
70449	High-temperature superconducting ternary <mml:math xmlns:mml="http://www.w3.org/1998/Math/MathML"><mml:mi>Li</mml:mi><mml:mtext>â^'</mml:mtext><mml:mi>R</mml:mi><mml:mi mathvariant="normal">H</mml:mi></mml:math> superhydrides at high pressures <mml:math xmlns:mml="http://www.w3.org/1998/Math/MathML"><mml:mo>(</mml:mo><mml:mi>R</mml:mi><mml:mo>=</mml:mo><mml:mi>Sc</mml:mi> Physical Review B, 2022, 106, .	1.1	4
70450	A comparable study of defect diffusion and recombination in Si and GaN. Journal of Applied Physics, 2022, 132, .	1.1	0
70451	Ethyl Viologen as a Superoxide Quencher to Enhance the Oxygen Reduction Reaction in Liâ€"O₂ Batteries. ACS Applied Energy Materials, 2022, 5, 9040-9048.	2.5	2

#	Article	IF	Citations
70452	Theoretical and experimental insights into CO2 formation on Co2C catalysts in syngas conversion to Value-Added chemicals. Applied Surface Science, 2022, 602, 154379.	3.1	3
70453	Molecular Dynamics Simulations of PtTi High-Temperature Shape Memory Alloys Based on a Modified Embedded-Atom Method Interatomic Potential. Materials, 2022, 15, 5104.	1.3	0
70454	Identifying Redox Orbitals and Defects in Lithium-Ion Cathodes with Compton Scattering and Positron Annihilation Spectroscopies: A Review. Condensed Matter, 2022, 7, 47.	0.8	3
70455	Microscopic identification of stepped SiC(0001) and the reaction site of hydrogen-rich epitaxial growth. Physical Review B, 2022, 106, .	1.1	0
70456	Monodisperse polar NiCo2O4 nanoparticles decorated porous graphene aerogel for high-performance lithium sulfur battery. Journal of Energy Chemistry, 2022, 74, 239-251.	7.1	19
70457	First-Principles Study on the Adsorption and Dissociation Behavior of H2 on the Surface of a Plutoniumâ€“Gallium System. Coatings, 2022, 12, 1019.	1.2	1
70458	Competing electronic states emerging on polar surfaces. Nature Communications, 2022, 13, .	5.8	7
70459	Chemically Induced Surface Potential Modulation at Pd|Al₂O₃|Graphene Field Effect Transistors: Implications for Enhanced H₂ Sensing. ACS Applied Nano Materials, 2022, 5, 10941-10950.	2.4	2
70460	Computational screening of materials with extreme gap deformation potentials. Npj Computational Materials, 2022, 8, .	3.5	1
70461	Ferroelectric control of band alignments and magnetic properties in the two-dimensional multiferroic VSe₂/In₂Se₃. Journal of Physics Condensed Matter, 2022, 34, 425801.	0.7	2
70462	Unlocking Interfacial Electron Transfer of Ruthenium Phosphides by Homologous Coreâ€“Shell Design toward Efficient Hydrogen Evolution and Oxidation. Advanced Materials, 2022, 34, .	11.1	51
70463	Elucidating the Initial Steps in Î±-Uranium Hydriding Using First-Principles Calculations. Langmuir, 2022, 38, 9335-9346.	1.6	2
70464	Ferroelasticity in Two-Dimensional Tetragonal Materials. Physical Review Letters, 2022, 129, .	2.9	14
70465	Unveiling the atomic position of C in <mml:math xmlns:mml="http://www.w3.org/1998/Math/MathML"><mml:mrow><mml:msub><mml:mi>Mn</mml:mi><mml:mn>5</mml:mn></mml:msub><mml:mi mathvariant="normal">C</mml:mi><mml:mi>x</mml:mi></mml:mrow></mml:math> thin films. Physical Review Materials, 2022, 6, .	0.9	1
70466	Determining the interlayer shearing in twisted bilayer MoS2 by nanoindentation. Nature Communications, 2022, 13, .	5.8	12
70467	Magnetism between magnetic adatoms on monolayer NbSe₂. 2D Materials, 2022, 9, 045012.	2.0	1
70468	Probing Copper and Copperâ€“Gold Alloy Surfaces with Space-Quantized Oxygen Molecular Beam. Jacs Au, 0, , .	3.6	2
70469	Photo-assisted reductive cleavage and catalytic hydrolysis-mediated persulfate activation by mixed redox-couple-involved CuFeS2 for efficient trichloroethylene oxidation in groundwater. Water Research, 2022, 222, 118885.	5.3	10

#	Article	IF	Citations
70470	First-principles studies of monolayers MoSi2N4 decorated with transition metal single-atom for visible light-driven high-efficient CO2 reduction by strain and electronic engineering. Chemical Engineering Journal, 2022, 450, 138198.	6.6	11
70471	Effect of alloying elements on liquid metal embrittlement of pure BCC Fe in contact with liquid lead-bismuth eutectic: Experiments and first principles calculation. Corrosion Science, 2022, 208, 110522.	3.0	6
70472	Effect of exchange-correlation functionals on the estimation of migration barriers in battery materials. Npj Computational Materials, 2022, 8, .	3.5	18
70473	Fully Exposed Platinum Clusters on a Nanodiamond/Graphene Hybrid for Efficient Low-Temperature CO Oxidation. ACS Catalysis, 2022, 12, 9602-9610.	5.5	25
70474	Electronic Structure Modulation of RuO₂ by TiO₂ Enriched with Oxygen Vacancies to Boost Acidic O₂ Evolution. ACS Catalysis, 2022, 12, 9437-9445.	5.5	60
70475	Pressure-induced photoconductivity enhancement and positiveâ€“negative switch in bulk silicon. Applied Physics Letters, 2022, 121, .	1.5	6
70476	Transuranium Sulfide via the Boron Chalcogen Mixture Method and Reversible Water Uptake in the NaCuTS₃ Family. Journal of the American Chemical Society, 2022, 144, 13773-13786.	6.6	7
70477	Penta-BeP₂ Monolayer: A Superior Sensor for Detecting Toxic Gases in the Air with Excellent Sensitivity, Selectivity, and Reversibility. ACS Applied Materials & Interfaces, 2022, 14, 35229-35236.	4.0	16
70478	First-Principles Calculations of the Spin-Dependent Electronic Structure and Strain Tunability in 2D Non-van der Waals Chromium Chalcogenides Cr₂X₃ (X = S, Se, Te): Implications for Spintronics Applications. ACS Applied Nano Materials, 0, , .	2.4	5
70479	Effects of transition metal doping on CsGeBr3 perovskite: First-principles study. AIP Advances, 2022, 12, .	0.6	1
70480	Structural, electronic, mechanical and thermodynamic properties of antiperovskites Ti3InX (X=C and) Tj ETQq0 0 0 rgBT /Overlock 10 Tf	1.6	5
70481	Highly modulated dual semimetal and semiconducting Î³-GeSe with strain engineering. 2D Materials, 2022, 9, 045014.	2.0	11
70482	Signature of lattice dynamics in twisted 2D homo/hetero-bilayers. 2D Materials, 2022, 9, 045018.	2.0	9
70483	Microstructure control and strengthening mechanism of fine-grained cast Mg alloys based on grain boundary segregation of Al solute. Materials Science & Engineering A: Structural Materials: Properties, Microstructure and Processing, 2022, 851, 143665.	2.6	10
70484	Towards targeted electronic properties of two-dimensional BaTiO3 films by tailoring surface structures: A first-principles study. Applied Surface Science, 2022, 602, 154377.	3.1	2
70485	Polar methylammonium organic cations detune state coupling and extend hot-carrier lifetime in lead halide perovskites. CheM, 2022, 8, 3051-3063.	5.8	4
70486	First-principles calculations to investigate structural, elastic, electronic, and thermoelectric properties of monolayer and bulk beryllium chalcogenides. Chemical Physics, 2022, 562, 111660.	0.9	7
70487	Dynamic strain and switchable polarization: A pathway to enhance the oxygen evolution reaction on InSnO2N. Journal of Catalysis, 2022, 413, 720-727.	3.1	3

#	Article	IF	Citations
70488	High-Temperature Thermodynamics Modeling of Graphite. Applied Sciences (Switzerland), 2022, 12, 7556.	1.3	1
70489	Thermal transport and thermoelectric properties of alkali-metal telluride Na2Te from first-principles study. Solid State Communications, 2022, 354, 114890.	0.9	0
70490	Thickness and defect dependent electronic, optical and thermoelectric features of $$hbox {WTe}_2$$. Scientific Reports, 2022, 12, .	1.6	6
70491	Simmate: a framework for materials science. Journal of Open Source Software, 2022, 7, 4364.	2.0	2
70492	Novel polymeric phases proposed by cold-pressing SiC tubes. Journal of Physics Condensed Matter, 0, , .	0.7	1
70493	A DFT-based microkinetic theory for Fe2O3 reduction by CO in chemical looping. Proceedings of the Combustion Institute, 2023, 39, 4447-4455.	2.4	4
70494	Three-dimensional quasiquantized Hall insulator phase in <mml:math xmlns:mml="http://www.w3.org/1998/Math/MathML"><mml:mrow><mml:mi>Sr</mml:mi><mml:msub><mml:mi>Si</mml:mi><mml:mn>2</mml:mn></mml:msub><mml:mr Physical Review B, 2022, 106, .	1.1	1
70495	Predicting Lattice Vibrational Frequencies Using Deep Graph Neural Networks. ACS Omega, 2022, 7, 26641-26649.	1.6	2
70496	Melting curve and transport properties of ammonia ice up to the deep mantle conditions of Uranus and Neptune. Physical Review B, 2022, 106, .	1.1	2
70497	Study of Thermoelectric Performance and Intrinsic Defect of Promising n- type half-Heusler FeGeW. Journal Physics D: Applied Physics, 0, , .	1.3	0
70498	Vaporâ€“liquid assisted chemical vapor deposition of Cu₂X materials. 2D Materials, 2022, 9, 045013.	2.0	3
70499	Câ€“Doping Induced Oxygen-Vacancy in WO₃ Nanosheets for CO₂ Activation and Photoreduction. ACS Catalysis, 2022, 12, 9670-9678.	5.5	71
70500	Exploring the Impact of Lone Pairs on the Structural Features of Alkalineâ€Earth (A) Transitionâ€Metal (M,Mâ€™) Chalcogenides (Q) AMM'Q₃. European Journal of Inorganic Chemistry, 2022, 2022, .	1.0	13
70501	Topological states in Chevrel phase materials from first principles calculations. Physical Review B, 2022, 106, .	1.1	1
70502	Single-phase bimetal sulfide or metal sulfide heterojunction: Which one is better for reversible oxygen electrocatalyst?. Journal of Energy Chemistry, 2022, 74, 420-428.	7.1	27
70503	First-principle studies of twisted bilayer black phosphorus. Journal of the Korean Physical Society, 0, , .	0.3	1
70504	Topochemical Synthesis of LiCoF₃ with a High-Temperature LiNbO₃-Type Structure. Inorganic Chemistry, 2022, 61, 11746-11756.	1.9	0
70505	Ab-initio calculations of substitutional co-segregation interactions at coherent bcc Fe-Cu interfaces. Journal of Nuclear Materials, 2022, , 153923.	1.3	0

#	Article	IF	Citations
70506	Strain Sensitivity of<mml:math xmlns:mml="http://www.w3.org/1998/Math/MathML" display="inline" overflow="scroll"><mml:mi>Li</mml:mi></mml:math>-ion Conductivity inÎ²-<mml:math xmlns:mml="http://www.w3.org/1998/Math/MathML" display="inline" overflow="scroll"><mml:msub><mml:mi>Li</mml:mi><mml:mn>3</mml:mn></mml:msub><mml:msub><mml:mi>PS</mml:mi><mml:m Electrolyte. , 2022, 1, .		4
70507	Sub-nanometer Copper Clusters as Alternative Catalysts for the Selective Oxidation of Methane to Methanol with Molecular O₂. Journal of Physical Chemistry A, 2022, 126, 4941-4951.	1.1	6
70508	Zinc Titanium Nitride Semiconductor toward Durable Photoelectrochemical Applications. Journal of the American Chemical Society, 2022, 144, 13673-13687.	6.6	15
70509	Sc-B₂₄N₂₄: A New Low-Density Allotrope of BN. Journal of Physical Chemistry C, 0, , .	1.5	3
70510	Ru Single-Atom Decorated Black TiO₂ Nanosheets for Efficient Solar-Driven Hydrogen Production. ACS Sustainable Chemistry and Engineering, 2022, 10, 10311-10317.	3.2	11
70511	Impact of surface-active site heterogeneity and surface hydroxylation in Ni doped ceria catalysts on oxidative dehydrogenation of propane. Journal of Catalysis, 2022, 413, 681-691.	3.1	6
70512	Selective hydrodeoxygenation of 5-hydroxymethylfurfural (HMF) to 2,5-dimethylfuran (DMF) over carbon supported copper catalysts using isopropyl alcohol as a hydrogen donor. Applied Catalysis B: Environmental, 2022, 317, 121790.	10.8	23
70513	Direct Band Gap in Multilayer Transition Metal Dichalcogenide Nanoscrolls with Enhanced Photoluminescence. , 2022, 4, 1547-1555.		4
70514	Ultrasensitive Chemiresistive Gas Sensor Can Diagnose Asthma and Monitor Its Severity by Analyzing Its Biomarker H₂S: An Experimental, Clinical, and Theoretical Study. ACS Sensors, 2022, 7, 2243-2252.	4.0	11
70515	Transition Metals Embedded Siloxene as Singleâ€Atom Catalyst for Advanced Sulfur Host in Lithiumâ€“Sulfur Batteries: A Theoretical Study. Advanced Energy Materials, 2022, 12, .	10.2	10
70516	Role Of Orbital Bond and Local Magnetism In Fe₃GeTe₂ and Fe₄GeTe₂: Implication For Ultrathin Nano Devices. ACS Applied Nano Materials, 0, , .	2.4	4
70517	High-density Fe single atoms anchored on 2D-Fe2C12 monolayer materials for N2 reduction to NH3 with high activity and selectivity. Applied Surface Science, 2022, 602, 154380.	3.1	4
70518	Insight into stepwise dealumination in acid-treatment of IM-5 for catalytic cracking of n-heptane and Fischer-Tropsch naphtha. Microporous and Mesoporous Materials, 2022, 342, 112117.	2.2	2
70519	1,1-Dimethylhydrazine adsorption on intrinsic, vacancy, and N-doped graphene: a first-principle study. Journal of Molecular Modeling, 2022, 28, .	0.8	1
70520	Mass transport in a highly immiscible alloy on extended shear deformation. Journal of Materials Science and Technology, 2023, 134, 197-208.	5.6	3
70521	Comparative study on potassium poisoning of Cu-CHA catalysts for NH3-SCR: Stability and transformation of Cu2+ ions. Journal of Environmental Chemical Engineering, 2022, 10, 108305.	3.3	3
70522	Efficient Strategy for Investigating the Third-Order Nonlinear Optical (NLO) Properties of Solid-State Coordination Polymers. Inorganic Chemistry, 2022, 61, 12386-12395.	1.9	13
70523	An optoelectronic heterostructure for neuromorphic computing: CdS/V3O5. Applied Physics Letters, 2022, 121, .	1.5	6

#	Article	IF	Citations
70524	Structure, magnetic and adsorption properties of novel FePt/h-BN heteromaterials. Nano Research, 0, , .	5.8	2
70525	Ion and Particle Size Effects on the Surface Reactivity of Anatase Nanoparticleâ€“Aqueous Electrolyte Interfaces: Experimental, Density Functional Theory, and Surface Complexation Modeling Studies. Minerals (Basel, Switzerland), 2022, 12, 907.	0.8	1
70526	Investigation of the Stability and Hydrogen Evolution Activity of Dual-Atom Catalysts on Nitrogen-Doped Graphene. Nanomaterials, 2022, 12, 2557.	1.9	6
70527	First-Principles Survey of Acceptor Dopants for p-Type Cesium Lead Bromide. Journal of Physical Chemistry C, 2022, 126, 12294-12300.	1.5	4
70528	Magnetic ground state of supported monatomic Fe chains from first principles. Journal of Physics Condensed Matter, 2022, 34, 395803.	0.7	1
70529	Free Energy and Solvation Structure Analysis for Adsorption of Aromatic Molecules at Pt(111)/Water Interface by 3D-RISM Theory. Chemistry Letters, 2022, 51, 791-795.	0.7	1
70530	MoS₂ and WS₂ Nanosheets Decorated on Metalâ€“Organic Framework-Derived Cobalt/Carbon Nanostructures as Electrocatalysts for Hydrogen Evolution. ACS Applied Nano Materials, 2022, 5, 10696-10703.	2.4	10
70531	An integrated Si photocathode with lithiation-activated molybdenum oxide nanosheets for efficient ammonia synthesis. Nano Energy, 2022, 102, 107639.	8.2	11
70532	Rational design of a topological polymeric solid electrolyte for high-performance all-solid-state alkali metal batteries. Nature Communications, 2022, 13, .	5.8	99
70533	Surface Diffusion-Limited Growth of Large and High-Quality Monolayer Transition Metal Dichalcogenides in Confined Space of Microreactor. ACS Nano, 2022, 16, 11360-11373.	7.3	7
70534	Direct photo-curing 3D printing of nickel-based electrocatalysts for highly-efficient hydrogen evolution. Nano Energy, 2022, 102, 107615.	8.2	17
70535	Room-temperature deposited fluorine-doped tantalum pentoxide for stable organic solar cells. Organic Electronics, 2022, , 106607.	1.4	0
70536	A novel electrochemical sensor based on CuO-CeO2/MXene nanocomposite for quantitative and continuous detection of H2O2. Journal of Electroanalytical Chemistry, 2022, 921, 116655.	1.9	14
70537	Fast identification, and construction of adsorbate-adsorbent geometries for high throughput computational applications: The Automatic Surface Adsorbate Structure Provider (ASAP) algorithm. Computational and Theoretical Chemistry, 2022, 1216, 113830.	1.1	2
70538	Bonding Heterogeneity Inducing Low Lattice Thermal Conductivity and High Thermoelectric Performance in 2D CdTe₂. ACS Applied Energy Materials, 2022, 5, 9549-9558.	2.5	11
70539	An ab initio molecular dynamics investigation of the thermophysical properties of molten NaCl-MgCl<mml:math xmlns:mml="http://www.w3.org/1998/Math/MathML" altimg="si1.svg"><mml:msub><mml:mrow /><mml:mn>2</mml:mn></mml:msub></mml:math>. Journal of Nuclear Materials, 2022, 570, 153916.	1.3	9
70540	Coherent interfaces govern direct transformation from graphite to diamond. Nature, 2022, 607, 486-491.	13.7	60
70541	Enhanced superconductivity in <mml:math xmlns:mml="http://www.w3.org/1998/Math/MathML"><mml:msub><mml:mi>CuH</mml:mi><mml:mn>2</mml:mn></mml:msub></mml:math> monolayers. Physical Review B, 2022, 106, .	1.1	7

#	Article	IF	Citations
70542	Energy and mechanical properties predictions in Fe-Ni binary system by ab initio calculations. Materials Today Communications, 2022, 33, 104118.	0.9	1
70543	First-principles perspective on full-spectrum infrared photodetectors from doping an excitonic insulator. Physical Review B, 2022, 106, .	1.1	1
70544	Machine Learning for Designing Mixed Metal Halides for Efficient Ammonia Separation and Storage. Journal of Physical Chemistry C, 2022, 126, 12184-12196.	1.5	5
70545	Role of External Stimuli in Engineering Magnetic Phases and Real-Time Spin Dynamics of Co/Mn Oxides. Journal of Physical Chemistry Letters, 2022, 13, 6755-6761.	2.1	2
70546	A-type antiferromagnetic order in semiconducting <mml:math xmlns:mml="http://www.w3.org/1998/Math/MathML"><mml:msub><mml:mi mathvariant="normal">EuMg</mml:mi><mml:mn>2</mml:mn></mml:msub><mml:msub><mml:mi mathvariant="normal">Sb</mml:mi><mml:mn>2</mml:mn></mml:msub></mml:math> single crystals. Physical Review B, 2022, 106, .	1.1	12
70547	High hydrogen storage ability of a decorated g-C3N4 monolayer decorated with both Mg and Li: A density functional theory (DFT) study. International Journal of Hydrogen Energy, 2022, 47, 28548-28555.	3.8	15
70548	Stability of oxidized states of freestanding and ceria-supported PtOx particles. Journal of Chemical Physics, 2022, 157, .	1.2	4
70549	A first-principle assisted framework for designing high elastocaloric Niâ€“Mn-based magnetic shape memory alloy. Journal of Materials Science and Technology, 2023, 134, 151-162.	5.6	10
70550	An Excellent and Fast Anodes for Lithium-Ion Batteries Based on the 1Tâ€²-MoTe₂ Phase Material. ACS Applied Energy Materials, 2022, 5, 9625-9640.	2.5	5
70551	Monomolecular mechanisms of isobutanol conversion to butenes catalyzed by acidic zeolites: Alcohol isomerization as a key to the production of linear butenes. Journal of Catalysis, 2022, 413, 786-802.	3.1	4
70552	Phonon properties of biphenylene monolayer by first-principles calculations. Applied Physics Letters, 2022, 121, .	1.5	19
70553	Sr-substitution-guided Eu2+ site engineering of Ca9Nd(PO4)7:Eu2+ for high-efficiency white light-emitting diodes. Optik, 2022, 267, 169699.	1.4	2
70554	Exploration of electrical contact type in two-dimensional WS2/Nb2CX2 (XÂ=ÂH, F, Cl) heterostructures. Applied Surface Science, 2022, 602, 154390.	3.1	6
70555	Electron delocalization triggers nonradical Fenton-like catalysis over spinel oxides. Proceedings of the National Academy of Sciences of the United States of America, 2022, 119, .	3.3	99
70556	Expanded graphite supported TiO2 composites using polyaniline as the anchor: Improved catalytic performance for the electro-Fenton-like reaction. Electrochimica Acta, 2022, 428, 140910.	2.6	0
70557	Electron mediation enhanced magnetocrystalline anisotropy and Curie temperature of FeCl2 monolayer by an electride substrate. Applied Physics Letters, 2022, 121, .	1.5	2
70558	Rapid discovery of stable materials by coordinate-free coarse graining. Science Advances, 2022, 8, .	4.7	15
70559	Cooperative Reaction of Hydrogen-Networked Water Molecules at the SiCâ€“H₂O₂ Solution Interface: Microscopic Insights from Ab Initio Molecular Dynamics. Journal of Physical Chemistry C, 0, , .	1.5	3

#	Article	IF	Citations
70560	Tri-MX: New group-IV monochalcogenide monolayers with excellent piezoelectricity and special optical properties. Applied Surface Science, 2022, 602, 154391.	3.1	4
70561	Novel (Super)Hard SiCN from Crystal Chemistry and First Principles. Silicon, 2023, 15, 511-520.	1.8	4
70562	Molecular Electrides: An In Silico Perspective. ChemPhysChem, 2022, 23, .	1.0	4
70563	<tt>DMC-ICE13</tt>: Ambient and high pressure polymorphs of ice from diffusion Monte Carlo and density functional theory. Journal of Chemical Physics, 2022, 157, .	1.2	7
70564	Synergetic Effects of Zn Alloying and Defect Engineering on Improving the CdS Buffer Layer of Cu₂ZnSnS₄ Solar Cells. Inorganic Chemistry, 2022, 61, 12293-12300.	1.9	4
70565	Hydrogen dissociation in Li-decorated borophene and borophene hydride: An ab-initio study. Applied Surface Science, 2022, 603, 154323.	3.1	8
70566	Favorable Role of the Metalâ€“Support Perimeter Region in Electrochemical NH₃ Synthesis: A Density Functional Theory Study on Ru/BaCeO₃. ACS Omega, 0, , .	1.6	0
70567	Releasing the limited catalytic activity of CeO2-supported noble metal catalysts via UV-induced deep dechlorination. Journal of Catalysis, 2022, 413, 703-712.	3.1	2
70568	From an atomistic study of olivine under pressure to the understanding of the macroscopic energy release in earthquakes. Geosystems and Geoenvironment, 2023, 2, 100108.	1.7	1
70569	Heterogeneous formation of EPFRs from aromatic adsorbates on the carbonaceous particulate matter. Applied Surface Science, 2022, 602, 154316.	3.1	1
70570	Single atom microscopy in wideâ€bandgap nitrides. International Journal of Applied Ceramic Technology, 0, , .	1.1	0
70571	Defect structure in quantum-cutting <mml:math xmlns:mml="http://www.w3.org/1998/Math/MathML"><mml:msup><mml:mrow><mml:mi>Yb</mml:mi></mml:mrow><mml:mrow><m -doped <mml:math xmlns:mml="http://www.w3.org/1998/Math/MathML"><mml:mrow><mml:mi>CsPb</mml:mi><mml:msub><mml:mi>Cl</mml:mi><m perovskites probed by x-ray absorption and atomic pair distribution function analysis. Physical Review Materials, 2022, 6, .	0.9	4
70572	Surface Doping in Poly(3,4-ethylenedioxythiophene)-Based Nanoscale Films: Insights for Polymer Electronics. ACS Applied Nano Materials, 2022, 5, 12143-12153.	2.4	7
70573	Predicting mechanical properties of high entropy alloys with face centered cubic structure from first principles calculations. Materials Today Communications, 2022, 32, 104059.	0.9	1
70575	Effects of Excess Cu Atoms on Hydrogen Permeability, Solubility, and Diffusivity in Pd-Cu Alloys with B2-Type Crystal Structures. Nippon Kinzoku Gakkaishi/Journal of the Japan Institute of Metals, 2022, 86, 140-148.	0.2	1
70576	Investigation of water gas shift reactivity on Fe5C2 (111): A DFT study. Molecular Catalysis, 2022, 529, 112538.	1.0	1
70577	Existence of yttrium allotrope with incommensurate hostâ€“guest structure at moderate pressure: First evidence from computational approach. Computational Materials Science, 2022, 213, 111652.	1.4	2
70578	Planar carbon allotrope B-graphyne as lithium-ion battery anode materials. Chemical Physics Letters, 2022, 804, 139897.	1.2	1

#	Article	IF	Citations
70579	Constructing Cu-CuO heterostructured skin on Cu cubes to promote electrocatalytic ammonia production from nitrate wastewater. Journal of Hazardous Materials, 2022, 439, 129653.	6.5	32
70580	Enhanced charge storage performance of MXene based all-solid-state supercapacitor with vertical graphene arrays as the current collector. Journal of Energy Storage, 2022, 54, 105355.	3.9	19
70581	Polyethylene oxide-intercalated nanoporous graphene membranes for ultrafast H2/CO2 separation: Role of graphene confinement effect on gas molecule binding. Journal of Membrane Science, 2022, 660, 120821.	4.1	7
70582	Temperature-dependent bandgap of (In,Ga)As via : A ython ackage for roperty rediction of seudobinary systems using canonical ensemble. Chemical Physics Letters, 2022, 804, 139887.	1.2	0
70583	Magnetic field and strain effects in Janus-like Weyl semimetals MoTeSe with four Weyl points. Computational Materials Science, 2022, 213, 111617.	1.4	1
70584	Electrical transport and magnetic properties of the triangular-lattice compound Zr<mml:math xmlns:mml="http://www.w3.org/1998/Math/MathML" altimg="si73.svg" display="inline" id="d1e934"><mml:msub><mml:mrow /><mml:mrow><mml:mn>2</mml:mn></mml:mrow></mml:msub></mml:math>NiP<mml:math xmlns:mml="http://www.w3.org/1998/Math/MathML" altimg="si73.svg" display="inline" id="d1e942"><mml:msub><mml:mrow />	1.2	0
70585	The strain induced synergistic catalysis of FeN4 and MnN3 dual-site catalysts for oxygen reduction in proton- /anion- exchange membrane fuel cells. Applied Catalysis B: Environmental, 2022, 317, 121770.	10.8	53
70586	Coupling ceria with dual-phased molybdenum carbides for efficient and stable hydrogen evolution electrocatalysis at large-current-density in freshwater and seawater. Applied Catalysis B: Environmental, 2022, 317, 121774.	10.8	21
70587	Boosting photocatalytic nitrogen reduction to ammonia by dual defective -C N and K-doping sites on graphitic carbon nitride nanorod arrays. Applied Catalysis B: Environmental, 2022, 317, 121752.	10.8	22
70588	Energy conversion performance of porous ZrTe hybrid derived from chemical transformation of Zr(OH)4. Fuel, 2022, 328, 125264.	3.4	18
70589	Utilizing fast ion conductor for single-crystal Ni-rich cathodes to achieve dual-functional modification of conductor network constructing and near-surface doping. Energy Storage Materials, 2022, 52, 19-28.	9.5	25
70590	Pressure-induced YSe3 and Y3Se with charming structures and properties. Journal of Alloys and Compounds, 2022, 923, 166465.	2.8	0
70591	Insight into reactive species-dependent photocatalytic toluene mineralization and deactivation pathways via modifying hydroxyl groups and oxygen vacancies on BiOCl. Applied Catalysis B: Environmental, 2022, 317, 121761.	10.8	45
70592	Synergistic effect of interstitial C doping and oxygen vacancies on the photoreactivity of TiO2 nanofibers towards CO2 reduction. Applied Catalysis B: Environmental, 2022, 317, 121773.	10.8	38
70593	Facile in-situ construction of plate-on-plate structured Bi2MoO6/BiOI Z-scheme heterojunctions enriched with oxygen vacancies for highly efficient photocatalytic performances. Applied Surface Science, 2022, 602, 154319.	3.1	9
70594	Ultra-high capacity of Li1.6â˜xMn0.4TixO2 as a cathode material. Journal of Alloys and Compounds, 2022, 923, 166356.	2.8	2
70595	The strengthening effects of Re-X (X Mo, W, Cr Ta, Re) mediated by their local partitioning behaviors at Î³/Î³â€² interface in Ni-based single crystal superalloys. Journal of Alloys and Compounds, 2022, 923, 166367.	2.8	6
70596	Interface reconstruction via lithium thermal reduction to realize a long life all-solid-state battery. Energy Storage Materials, 2022, 52, 1-9.	9.5	12

#	Article	IF	Citations
70597	Computational insights into electronic, magnetic and optical properties of Mn(II)-doped ZnTe with and without vacancy defects. Materials Science in Semiconductor Processing, 2022, 150, 106965.	1.9	5
70598	Unveiling the origin of enhanced catalytic performance of NiCu alloy for semi-hydrogenation of acetylene. Chemical Engineering Journal, 2022, 450, 138244.	6.6	17
70599	Oriented interlayered charge transfer in NiCoFe layered double hydroxide/MoO3 stacked heterostructure promoting the oxygen-evolving behavior. Journal of Colloid and Interface Science, 2022, 627, 891-899.	5.0	21
70600	Synthesis of noble metal chalcogenides via cation exchange reactions. , 2022, 1, 626-634.		17
70601	A first-principles study on the effect of ideal tensile/shear strain on the chemical bond length and charge density distribution of U₃Si₂. Wuli Xuebao/Acta Physica Sinica, 2022, .	0.2	0
70602	Theoretical Simulation and Experimental Verification of the Competition between Different Recombination Channels in GaN Semiconductor. Journal of Materials Chemistry C, 0, , .	2.7	2
70603	Tunable Schottky and ohmic contacts in the Ti₂NF₂/Î±-Te van der Waals heterostructure. Physical Chemistry Chemical Physics, 2022, 24, 21388-21395.	1.3	1
70604	Sustainable solid form screening: mechanochemical control over nucleobase hydrogen-bonded organic framework polymorphism. CrystEngComm, 2022, 24, 6505-6511.	1.3	2
70605	Stretched three-dimensional white graphene with a tremendous lattice thermal conductivity increase rate. RSC Advances, 2022, 12, 22581-22589.	1.7	2
70606	Effect of Spin-Orbit Coupling on the Electronic and Magnetic Properties of Heusler Alloy Pt2mnga. SSRN Electronic Journal, 0, , .	0.4	0
70607	High-Efficiency ResistiveÂSwitchÂAnd Artificial Synaptic Simulation InÂAntimony-Based Perovskite Devices. SSRN Electronic Journal, 0, , .	0.4	0
70608	Temperature-Dependent Impact of Antiphase Boundaries on Properties of Fe3al. SSRN Electronic Journal, 0, , .	0.4	0
70609	First-principles high-throughput screening of bulk piezo-photocatalytic materials for sunlight-driven hydrogen production. Journal of Materials Chemistry A, 2022, 10, 18132-18146.	5.2	14
70610	Selectivity of volatile organic compounds on the surface of zinc oxide nanosheets for gas sensors. Physical Chemistry Chemical Physics, 2022, 24, 20491-20505.	1.3	2
70611	Topologic Transition-Induced Abundant Undercoordinated Fe Active Sites in Nifeooh for Superior Oxygen Evolution. SSRN Electronic Journal, 0, , .	0.4	0
70612	First-Principles Study on the Temperature Dependent Elasticity and Thermodynamical Properties of Thermoelectric Material Nisbs. SSRN Electronic Journal, 0, , .	0.4	0
70613	The Preparation of Pani-Doped Co-Ni-Zif Carbonized Derivatives and the Exploration of Eet Process by the Dft Calculation and the Prediction of Related Functional Genes. SSRN Electronic Journal, 0, , .	0.4	0
70615	Achieving Highly Sensitive and Room-Temperature No2 Detection of Nanoflower-Like Ws2 by In-Situ Constructing Wo3/Ws2 Heterojunction. SSRN Electronic Journal, 0, , .	0.4	0

#	Article	IF	Citations
70616	Determination of Highly Active and Selective Surface for the Oxidative Dehydrogenation of Ethane Over Phase-Pure M1 Movnbteox Catalyst. SSRN Electronic Journal, 0, , .	0.4	0
70617	First-Principles Calculation of Kh2po4ÂAnharmonic Force Constants Phonon Dispersion Curves. SSRN Electronic Journal, 0, , .	0.4	0
70618	Significant Difference of Lanthanide Fission Products Diffusion in Cr and Î±-Fe: An Atomic-Level Study. SSRN Electronic Journal, 0, , .	0.4	0
70619	A Multifunctional Separator Based on Dilithium Tetraaminophthalocyanine Self-Assembled on Rgo with Improved Cathode and Anode Performance in Li-S Batteries. SSRN Electronic Journal, 0, , .	0.4	0
70620	Noble-Metal-Free Chalcogenide Nanotwins for Efficient and Stable Photocatalytic Pure Water Splitting by Surface Phosphorization and Cocatalyst Modification. SSRN Electronic Journal, 0, , .	0.4	0
70621	Efficient Predictions of Formation Energies and Convex Hulls from Density Functional Tight Binding Calculations. SSRN Electronic Journal, 0, , .	0.4	0
70622	Predicted crystal structures of xenon and alkali metals under high pressures. Physical Chemistry Chemical Physics, 2022, 24, 18119-18123.	1.3	2
70623	Lead-free perovskite Rb₂Sn_{1â^'x}Te_xCl₆ with bright luminescence for optical thermometry and tunable white light emitting diodes. Journal of Materials Chemistry C, 2022, 10, 13217-13224.	2.7	8
70624	Role of Oxygen Vacancies on Surface Reaction of Water Oxidation in Wo3 Studied by Density Functional Theory (Dft) and Experiment. SSRN Electronic Journal, 0, , .	0.4	0
70625	Highly Durable Fuel Cell Electrocatalyst with Low-Loading Pt-Co Nanoparticles Dispersed Over Single-Atom Pt-Co-N-Graphene Nanofiber. SSRN Electronic Journal, 0, , .	0.4	0
70626	Selective olefin production on silica based iron catalysts in Fischerâ€“Tropsch synthesis. Catalysis Science and Technology, 2022, 12, 5814-5828.	2.1	9
70627	Exploring the effect of partial B-site Al³⁺â€“Mg²⁺ dual substitution on optoelectronic, surface, and photocatalytic properties of BaTaO₂N. Materials Advances, 2022, 3, 7348-7359.	2.6	3
70628	Structure-dependent high-T_C ferromagnetism in Mn-doped GeSe. Nanoscale, 2022, 14, 13343-13351.	2.8	5
70629	High electron mobility and wide-bandgap properties in a novel 1D PdGeS₃ nanochain. Physical Chemistry Chemical Physics, 2022, 24, 18868-18876.	1.3	3
70630	Size-dependence of fullerene-like confinement in catalytic methanol cracking. New Journal of Chemistry, 0, , .	1.4	0
70631	The mechanism of a PVDF/CsPbBr₃ perovskite composite fiber as a self-polarization piezoelectric nanogenerator with ultra-high output voltage. Journal of Materials Chemistry A, 2022, 10, 21893-21904.	5.2	45
70632	Enhanced photoluminescence stability and internal defect evolution of the all-inorganic lead-free CsEuCl₃ perovskite nanocrystals. Physical Chemistry Chemical Physics, 2022, 24, 18860-18867.	1.3	2
70633	Selective CO₂ reduction on topological Chern magnet TbMn₆Sn₆. Physical Chemistry Chemical Physics, 2022, 24, 18600-18607.	1.3	4

#	Article	IF	Citations
70634	First-principles study on the structure prediction and electronic properties of two-dimensional SiP₂ allotropes. Wuli Xuebao/Acta Physica Sinica, 2022, .	0.2	0
70635	Strengthening and High-Temperature Softening Resistance of Low Si-Added Cu-Cr-Zr Alloy for Fusion Reactor Application. SSRN Electronic Journal, 0, , .	0.4	0
70636	Spray Coated Few-Layer Graphene as Aluminium Battery Cathode. Sustainable Energy and Fuels, 0, , .	2.5	1
70637	A bottom-up approach from medium-sized bilayer boron nanoclusters to bilayer borophene nanomaterials. Nanoscale, 2022, 14, 11443-11451.	2.8	12
70638	Stereodynamics effects in grazing-incidence fast-molecule diffraction. Physical Chemistry Chemical Physics, 2022, 24, 19541-19551.	1.3	0
70639	Determining the origin of poor electronic conductivity and ultrafast ionic conductivity in Na₃V₂(PO₄)₂FO₂ based on first principles and ab initio molecular dynamics methods. Physical Chemistry Chemical Physics, 2022, 24, 19362-19370.	1.3	1
70640	Auxetic ographene: a new 2D Dirac nodal-ring semimetal carbon-based material with a high negative Poisson's ratio. Physical Chemistry Chemical Physics, 2022, 24, 21806-21811.	1.3	1
70641	Synthesis, structural evolution and optical properties of a new family of oxychalcogenides [Sr₃VO₄][MQ₃] (M = Ga, In, Q = S, Se). Inorganic Chemistry Frontiers, 2022, 9, 4768-4775.	3.0	7
70642	Competition between reverse water gas shift reaction and methanol synthesis from CO₂: influence of copper particle size. Nanoscale, 2022, 14, 13551-13560.	2.8	11
70643	Zn Single Atom on N-Doped Carbon: Highly Active and Selective Catalyst for Electrochemical Reduction of Nitrate to Ammonia. SSRN Electronic Journal, 0, , .	0.4	0
70644	Physical insights into the Au growth on the surface of a LaAlO₃/SrTiO₃ heterointerface. RSC Advances, 2022, 12, 24146-24155.	1.7	1
70645	High thermoelectric performance in metal phosphides MP₂ (M = Co, Rh and Ir): a theoretical prediction from first-principles calculations. RSC Advances, 2022, 12, 23829-23838.	1.7	1
70646	Macroporous perovskite nanocrystal composites for ultrasensitive copper ion detection. Nanoscale, 2022, 14, 11953-11962.	2.8	5
70647	Highly dispersed Co-N-RGO electrocatalyst based on an interconnected hierarchical pore framework for proton exchange membrane fuel cells. Catalysis Science and Technology, 2022, 12, 6285-6293.	2.1	3
70648	Semiconductors with a chiral crystal structure in group IVB transition metal pernitrides. Physical Chemistry Chemical Physics, 2022, 24, 22046-22056.	1.3	2
70649	Diffusion Mechanism and Electrochemical Investigation of 1~T Phase Al-Mos$_{2}$@Rgo Nano-Composite as a High-Performance Anode for Sodium-Ion Batteries. SSRN Electronic Journal, 0, , .	0.4	0
70650	On-purpose design of dual active sites in single V atom anchored C₂N nanosheets for propane dehydrogenation catalysis. Inorganic Chemistry Frontiers, 2022, 9, 5517-5526.	3.0	2
70651	Axial ligand engineering for highly efficient oxygen reduction catalysts in transition metalâ€“N₄ doped graphene. New Journal of Chemistry, 2022, 46, 16138-16150.	1.4	9

#	Article	IF	Citations
70652	Formation of the quasi-planar B₅₆ boron cluster: topological path from B₁₂ and disk aromaticity. Physical Chemistry Chemical Physics, 0, , .	1.3	1
70653	Impurity Ferromagnetism of Pd-Fe and Pd-Co Alloys: Ab Initio vs. Experiment. , 0, , .		0
70654	The effect of co-alloying elements on site preference and shear deformation resistance of Î³â€²-Ni₃Al. Ferroelectrics, 2022, 593, 166-173.	0.3	1
70655	Elastic response of monolayer <mml:math xmlns:mml="http://www.w3.org/1998/Math/MathML"><mml:mrow><mml:msub><mml:mi>Si</mml:mi><mml:mrow><mml:mn>1</mml:mn><mml:mn>1</mml:mn><mml:mn>1</mml:mn></mml:mrow></mml:msub></mml:mrow></mml:math> Physical Review B, 2022, 106, .	1.1	1
70656	Miscibility of rock and ice in the interiors of water worlds. Scientific Reports, 2022, 12, .	1.6	9
70657	Physical Properties and Structural Stability of Cobalt Pyrovanadate Co₂V₂O₇ under High-Pressure Conditions. Journal of Physical Chemistry C, 2022, 126, 13416-13426.	1.5	5
70658	Interatomic Potential to Predict the Favored Glass-Formation Compositions and Local Atomic Arrangements of Ternary Al-Ni-Ti Metallic Glasses. Crystals, 2022, 12, 1065.	1.0	2
70659	Data-Driven Investigation of Tellurium-Containing Semiconductors for CO₂ Reduction: Trends in Adsorption and Scaling Relations. Journal of Physical Chemistry C, 2022, 126, 13224-13236.	1.5	1
70660	Dynamic Response of Oxygen Vacancies in the Deacon Reaction over Reduced Single Crystalline CeO_{2â€“x}(111) Surfaces. Journal of Physical Chemistry C, 2022, 126, 13202-13212.	1.5	4
70661	Screening and Investigation of a Single Transition Metal Atom Dispersed on 2D WS₂ as an Effective Electrocatalyst for Nitrogen Fixation: A Computational Study. Journal of Physical Chemistry C, 2022, 126, 13147-13156.	1.5	6
70662	Addressing the origin of highly catalytic activity of A-site Sr-doped perovskite cathodes for intermediate-temperature solid oxide fuel cells. Electrochemistry Communications, 2022, 140, 107341.	2.3	10
70663	Unoccupied topological surface state in <mml:math xmlns:mml="http://www.w3.org/1998/Math/MathML"><mml:mrow><mml:msub><mml:mi>MnBi</mml:mi><mml:mn>2</mml:mn></mml:msub></mml:mrow></mml:math> Physical Review B, 2022, 106, .	1.1	1
70664	A theoretical investigation of the effect of Ga alloying on thermodynamic stability, electronic-structure, and oxidation resistance of Ti2AlC MAX phase. Scientific Reports, 2022, 12, .	1.6	2
70665	Self-consistent calculations of charge self-trapping energies: A comparative study of polaron formation and migration in <mml:math xmlns:mml="http://www.w3.org/1998/Math/MathML"><mml:msub><mml:mrow><mml:mi>PbTiO</mml:mi></mml:mrow><mml:mn> Physical Review Materials, 2022, 6, .	0.9	2
70666	Superconductivity in a two monolayer thick indium film on Si(111) <mml:math xmlns:mml="http://www.w3.org/1998/Math/MathML"><mml:mrow><mml:msqrt><mml:mn>3</mml:mn></mml:msqrt><mml:mo>Ã—</mml:mo> -B. Physical Review B, 2022, 106, .	1.1	2
70667	Doping-stabilized Au-N compounds via lithium atoms at high pressure. Physical Review Research, 2022, 4, .	1.3	0
70668	Hidden Local Symmetry Breaking in a Kagome-Lattice Magnetic Weyl Semimetal. Journal of the American Chemical Society, 2022, 144, 14339-14350.	6.6	8
70669	Phase Transformation-Induced Quantum Dot States on the Bi/Si(111) Surface. ACS Applied Materials & Interfaces, 2022, 14, 36217-36226.	4.0	2

#	Article	IF	Citations
70670	Electronic Structure of Conventional Slater Type Antiferromagnetic Insulators: AIrO₃ (A=Sr, Ba) Perovskites. Journal of Physics: Conference Series, 2022, 2315, 012033.	0.3	0
70671	Tailoring cobaltâ€free La_{0.5}Sr_{0.5}FeO_{3â€Î´} cathode with a nonmetal cationâ€doping strategy for highâ€performance protonâ€conducting solid oxide fuel cells. SusMat, 2022, 2, 607-616.	7.8	42
70672	Tunable dâ€Band Centers of Ni₅P₄ Ultraâ€Thin Nanosheets for Highlyâ€Efficient Hydrogen Evolution Reaction. Advanced Materials Interfaces, 2022, 9, .	1.9	7
70673	Donor doping of corundum (AlxGa1â^'x)2O3. Applied Physics Letters, 2022, 121, .	1.5	7
70674	Evolution of the Electronic Structure of Ultrathin MnBi₂Te₄ Films. Nano Letters, 2022, 22, 6320-6327.	4.5	10
70675	Unraveling the Key Atomic Interactions in Determining the Varying Li/Na/K Storage Mechanism of Hard Carbon Anodes. Advanced Energy Materials, 2022, 12, .	10.2	18
70676	New QSPR model for prediction of corrosion inhibition using conceptual density functional theory. Journal of Molecular Modeling, 2022, 28, .	0.8	8
70677	Laser Irradiation Effect on the p-GaSe/n-HfS₂ PN-Heterojunction for High-Performance Phototransistors. ACS Applied Materials & Interfaces, 2022, 14, 35927-35939.	4.0	6
70678	Localization Mechanism of Interstitial Electronic States in Electride Mayenite. Journal of Physical Chemistry Letters, 2022, 13, 7155-7160.	2.1	6
70679	Computational Evaluation of Al-Decorated g-CN Nanostructures as High-Performance Hydrogen-Storage Media. Nanomaterials, 2022, 12, 2580.	1.9	2
70680	Magnetic and electronic transitions in monolayer electride <mml:math xmlns:mml="http://www.w3.org/1998/Math/MathML"><mml:msub><mml:mi mathvariant="normal">Gd</mml:mi><mml:mn>2</mml:mn></mml:msub><mml:mi mathvariant="normal">C</mml:mi></mml:math> induced by hydrogenation: A first-principles study. Physical Review B, 2022, 106, .	1.1	5
70681	Irreversible phase transitions of the multiferroic oxide Mn₃TeO₆ at high pressures. Applied Physics Letters, 2022, 121, 044102.	1.5	0
70682	Measurements and numerical calculations of thermal conductivity to evaluate the quality of Î²-gallium oxide thin films grown on sapphire and silicon carbide by molecular beam epitaxy. Applied Physics Letters, 2022, 121, .	1.5	4
70683	Fully auxetic and multifunctional of two-dimensional <mml:math xmlns:mml="http://www.w3.org/1998/Math/MathML"><mml:mi>Î´</mml:mi></mml:math> -GeS and <mml:math xmlns:mml="http://www.w3.org/1998/Math/MathML"><mml:mi>Î´</mml:mi></mml:math> -GeSe. Physical Review B, 2022, 106, .	1.1	5
70684	Tracking single adatoms in liquid in a transmission electron microscope. Nature, 2022, 609, 942-947.	13.7	30
70685	Density Functional Theory Study on Magnetic character and Mn Crystal Field Split Levels in Mn-doped SnO Monolayer. Journal of Superconductivity and Novel Magnetism, 2022, 35, 2975-2986.	0.8	1
70686	Highâ€Voltage Aluminiumâ€Sulfur Batteries with Functional Polymer Membrane. Advanced Functional Materials, 2022, 32, .	7.8	4
70687	Large Dzyaloshinskii-Moriya interaction and field-free topological chiral spin states in two-dimensional alkali-based chromium chalcogenides. Physical Review B, 2022, 106, .	1.1	13

#	Article	IF	Citations
70688	Multiple valence bands convergence and strong phonon scattering lead to high thermoelectric performance in p-type PbSe. Nature Communications, 2022, 13, .	5.8	37
70689	Constructing a Micrometer-Sized Structure through an Initial Electrochemical Process for Ultrahigh-Performance Li⁺ Storage. ACS Applied Materials & Interfaces, 2022, 14, 35522-35533.	4.0	4
70690	Adsorption Site Preference Determined by Triangular Topology: Application of the Method of Moments to Transition Metal Surfaces. Journal of Physical Chemistry C, 2022, 126, 13505-13519.	1.5	4
70691	Novel Prediction Model of Band Gap in Organicâ€“Inorganic Hybrid Perovskites Based on a Simple Cluster Model Database. Journal of Physical Chemistry C, 2022, 126, 13409-13415.	1.5	6
70692	Structure stabilization effect of vacancies and entropy in hexagonal WN. Acta Crystallographica Section B: Structural Science, Crystal Engineering and Materials, 2022, 78, 678-684.	0.5	0
70693	Tailoring magnetism in silicon-doped zigzag graphene edges. Scientific Reports, 2022, 12, .	1.6	2
70694	Microscopic origin of magnetism in monolayer <mml:math xmlns:mml="http://www.w3.org/1998/Math/MathML"><mml:mrow><mml:mn>3</mml:mn><mml:mi>d</mml:mi><mml:mrow><mml:mn transition metal dihalides. Physical Review B, 2022, 106, .	1.1	18
70695	Endless Dirac nodal lines in kagome-metal Ni3In2S2. Npj Computational Materials, 2022, 8, .	3.5	8
70696	Molecular simulation on hydrogen storage properties of five novel covalent organic frameworks with the higher valency. International Journal of Hydrogen Energy, 2022, 47, 29390-29398.	3.8	4
70697	Electric field and strain-induced band-gap engineering and manipulation of the Rashba spin splitting in Janus van der Waals heterostructures. Physical Review B, 2022, 106, .	1.1	16
70698	Persistent exchange splitting in the chiral helimagnet <mml:math xmlns:mml="http://www.w3.org/1998/Math/MathML"><mml:mrow><mml:msub><mml:mi>Cr</mml:mi><mml:mrow><mml:mn>1</mml:mn> Physical Review B, 2022, 106, .	1.1	2
70699	Toward Computational Screening of Bimetallic Alloys for Methane Activation: A Case Study of MgPt Alloy. ACS Catalysis, 2022, 12, 9458-9472.	5.5	9
70700	Lewis Acid Site Assisted Bifunctional Activity of Tin Doped Gallium Oxide and Its Application in Rechargeable Znâ€Air Batteries. Small, 2022, 18, .	5.2	9
70701	Electronic and Microscopic Properties of Spin Â½ System, CuInO(VO₄). International Journal of Innovative Research in Physics, 2022, 3, 32-38.	0.1	0
70702	Electronic Structure and External Electric Field Modulation of Polyethylene/Graphene Interface. Polymers, 2022, 14, 2949.	2.0	0
70703	Carrier-induced metal-insulator transition in trirutile <mml:math xmlns:mml="http://www.w3.org/1998/Math/MathML"><mml:mrow><mml:msub><mml:mi>MgTa</mml:mi><mml:mn>2</mml:mn></ mathvariant="normal">O</mml:mi><mml:mn>6</mml:mn></mml:msub></mml:mrow></mml:math>. Physical Review Materials, 2022, 6, .	0.9	1
70704	Pressure Induced Disorder-Order Phase Transitions in the Al4Cr Phases. Crystals, 2022, 12, 1008.	1.0	1
70705	Enhanced High-Temperature Thermoelectric Performance by Strain Engineering in BiOCl. Physical Review Applied, 2022, 18, .	1.5	29

#	Article	IF	Citations
70706	Hot-Carrier Physics of Transition-Metal Carbides and Nitrides: Insight from Electronic Structure. Physical Review Applied, 2022, 18, .	1.5	0
70707	High-throughput screening of stable and efficient double inorganic halide perovskite materials by DFT. Scientific Reports, 2022, 12, .	1.6	17
70708	Soft-phonon anharmonicity, floppy modes, and Na diffusion in <mml:math xmlns:mml="http://www.w3.org/1998/Math/MathML"><mml:mrow><mml:msub><mml:mi>Na</mml:mi><mml:mn>3</mml:mn></mml: mathvariant="normal">F</mml:mi><mml:mi>Y</mml:mi></mml:mrow><mml:mo>Â</mml:mo><mml:mrow><mml:mo>(</mml:mo><mr : Ab initio. Physical Review B, 2022, 106, .	1.1	9
70709	Molecular-level insight into photocatalytic CO2 reduction with H2O over Au nanoparticles by interband transitions. Nature Communications, 2022, 13, .	5.8	100
70710	LaBr2 bilayer multiferroic moirÃ© superlattice with robust magnetoelectric coupling and magnetic bimerons. Npj Computational Materials, 2022, 8, .	3.5	12
70711	Strength of correlations in a silver-based cuprate analog. Physical Review B, 2022, 106, .	1.1	2
70712	Momentum space imaging of Ïƒ orbitals for chemical analysis. Science Advances, 2022, 8, .	4.7	5
70713	A Theoretical Investigation on the Physical Properties of Zirconium Trichalcogenides, ZrS3, ZrSe3 and ZrTe3 Monolayers. Energies, 2022, 15, 5479.	1.6	4
70714	Unexpected Chemical Activity of a Mineral Surface: The Role of Crystal Water in Tobermorite. Journal of Physical Chemistry C, 2022, 126, 12405-12412.	1.5	13
70715	The Orbital Nature of Electron Holes in BaFeO₃ and Implications for Defect Chemistry. Journal of Physical Chemistry C, 2022, 126, 12809-12819.	1.5	4
70716	Theoretical Study of Ba₂X₆ (X = S, Se, Te) for Thermoelectric Applications Based on First-Principles Calculations and Machine Learning. Journal of Physical Chemistry C, 2022, 126, 12735-12741.	1.5	1
70717	First principles DFT analysis on the diffusion kinetics of hydrogen isotopes through bcc iron (Fe): Role of temperature and surface coverage. International Journal of Hydrogen Energy, 2022, 47, 31481-31498.	3.8	6
70718	First-principles study of magnetic properties of the transition metal ion-doped methylamonium lead bromide. International Journal of Modern Physics B, 0, , .	1.0	1
70719	Structural, Electronic, Mechanical, and Thermodynamic Properties of Na Deintercalation from Olivine NaMnPO4: First-Principles Study. Materials, 2022, 15, 5280.	1.3	2
70720	Honeycomb-Kagome lattice Na3Te2: Dirac half-metal with quantum anomalous Hall effect. Chemical Physics, 2022, 562, 111658.	0.9	0
70721	Mo₂N Quantum Dots Decorated Nâ€Doped Graphene Nanosheets as Dualâ€Functional Interlayer for Dendriteâ€Free and Shuttleâ€Free Lithiumâ€Sulfur Batteries. Advanced Functional Materials, 2022, 32, .	7.8	77
70722	Photoluminescent Properties of Two-Dimensional Manganese(II)-Based Perovskites with Different-Length Arylamine Cations. Inorganic Chemistry, 2022, 61, 11973-11980.	1.9	10
70723	High thermoelectric performance induced by strong anharmonic effects in monolayer (PbX)2 (X) Tj ETQq1 1 0.784314 rgBT /Overlock	1.5	35

#	Article	IF	Citations
70724	Theoretical Understanding of Polar Topological Phase Transitions in Functional Oxide Heterostructures: A Review. Small Methods, 2022, 6, .	4.6	9
70725	Artificial Intelligence-Aided Mapping of the Structureâ€“Compositionâ€“Conductivity Relationships of Glassâ€“Ceramic Lithium Thiophosphate Electrolytes. Chemistry of Materials, 2022, 34, 6702-6712.	3.2	12
70726	Trapping Hydrogen Atoms in Vacancies of Li₂TiO₃ Crystal: A First-Principles Study. ACS Omega, 2022, 7, 27149-27156.	1.6	1
70727	Nanocatalytic Interface to Decode the Phytovolatile Language for Latent Crop Diagnosis in Future Farms. Analytical Chemistry, 2022, 94, 11081-11088.	3.2	3
70728	Direct Z-Scheme Photocatalytic System: Insights into the Formative Factors of Photogenerated Carriers Transfer Channel from Ultrafast Dynamics. ACS Catalysis, 2022, 12, 9570-9578.	5.5	32
70729	Dry reforming of methane on doped Ni nanoparticles: Feature-assisted optimizations and ranking of doping metals for direct activations of CH4 and CO2. Nano Research, 2022, 15, 9670-9682.	5.8	6
70730	Second-order and real Chern topological insulator in twisted bilayer <mml:math xmlns:mml="http://www.w3.org/1998/Math/MathML"><mml:mi>Î±</mml:mi></mml:math> -graphyne. Physical Review B, 2022, 106, .	1.1	6
70731	Redâ€Emitting Perovskite Variant Cs₂PtCl₆ Phosphor: Material Design, Luminous Mechanism, and Application in Highâ€Colorâ€Rendering White Lightâ€Emitting Diodes. Advanced Optical Materials, 2022, 10, .	3.6	15
70732	Stepâ€Climbing Epitaxy of Layered Materials with Giant Outâ€ofâ€Plane Lattice Mismatch. Advanced Materials, 2022, 34, .	11.1	8
70733	Carrier dynamics in (Ga,In)(Sb,Bi)/GaSb quantum wells for laser applications in the mid-infrared spectral range. Scientific Reports, 2022, 12, .	1.6	3
70734	Significant two-step potential-induced surface reconstruction observed on Au(1 1 1) in aqueous sulfuric acid. Electrochemistry Communications, 2022, 140, 107332.	2.3	1
70735	Generalized quasiharmonic approximation via space group irreducible derivatives. Physical Review B, 2022, 106, .	1.1	8
70736	Anomalous Crystal Shapes of Topological Crystalline Insulators. Physical Review Letters, 2022, 129, .	2.9	3
70737	Probing Dynamic Selfâ€Reconstruction on Perovskite Fluorides toward Ultrafast Oxygen Evolution. Advanced Science, 2022, 9, .	5.6	19
70738	Stability and Rupture of an Ultrathin Ionic Wire. Physical Review Letters, 2022, 129, .	2.9	1
70739	Composition-transferable machine learning potential for LiCl-KCl molten salts validated by high-energy x-ray diffraction. Physical Review B, 2022, 106, .	1.1	3
70740	Mode-selective ballistic pathway to a metastable electronic phase. Structural Dynamics, 2022, 9, 045102.	0.9	2
70741	Orbital memory from individual Fe atoms on black phosphorus. Physical Review Research, 2022, 4, .	1.3	1

#	Article	IF	Citations
70742	Bandgap Engineering of Cesium Lead Halide Perovskite CsPbBr₃ through Cu Doping. Advanced Theory and Simulations, 2022, 5, .	1.3	5
70743	Structure and electronic properties of amorphous strontium titanate. Physical Review Materials, 2022, 6, .	0.9	2
70744	First-principles study on the magnetic and electronic properties of the high-pressure orthorhombic phase of MnSe. Physical Review B, 2022, 106, .	1.1	1
70745	Tunnel-structured willemite Zn2SiO4: Electronic structure, elastic, and thermal properties. Journal of Advanced Ceramics, 2022, 11, 1249-1262.	8.9	6
70746	Surface Stability Analysis with H Adsorption Affected the Magnetic Fluctuation of Brownmillerite SrCoO_{2.5} Based on the Electron Counting Model by Layers. Journal of Physical Chemistry C, 2022, 126, 12251-12263.	1.5	3
70747	Diversity of structural phases in <mml:math xmlns:mml="http://www.w3.org/1998/Math/MathML"><mml:mrow><mml:mi>A</mml:mi><mml:mi>Ge</mml:mi><mml:msub><mml:mi> halides. Physical Review B, 2022, 106, .	1.1	9
70748	Evidence for electronic signature of a magnetic transition in the topological magnet HoSbTe. Physical Review B, 2022, 106, .	1.1	2
70749	On the choice of shape and size for truncated cluster-based x-ray spectral simulations of 2D materials. Journal of Chemical Physics, 2022, 157, .	1.2	3
70750	Data-Driven Enhancement of ZT in SnSe-Based Thermoelectric Systems. Journal of the American Chemical Society, 2022, 144, 13748-13763.	6.6	16
70751	Ultrahigh Lithium Storage Capacity of Al₂C Monolayer in a Restricted Multilayered Growth Mechanism. ACS Applied Materials & Interfaces, 2022, 14, 35663-35672.	4.0	4
70752	Mechanical Insights into the Electrochemical Properties of Thornlike Micro-/Nanostructures of PDA@MnO₂@NMC Composites in Aqueous Zn Ion Batteries. ACS Applied Materials & Interfaces, 2022, 14, 36079-36091.	4.0	12
70753	Unraveling the Catalytic Performance of the Nonprecious Metal Single-Atom-Embedded Graphitic s-Triazine-Based C₃N₄ for CO₂ Hydrogenation. ACS Applied Materials & Interfaces, 2022, 14, 35844-35853.	4.0	11
70754	Quantum effects in thermal reaction rates at metal surfaces. Science, 2022, 377, 394-398.	6.0	11
70755	Na₃H(ZnH₄) Antiperovskite: A Large Octahedral Distortion with an Off-Centering Hydride Anion Coupled to Molecular Hydride. Chemistry of Materials, 2022, 34, 6815-6823.	3.2	8
70756	Wafer-Scale Anion Exchange Conversion of Nonlayered PtS Films to van der Waals Two-Dimensional PtTe₂ Layers with Negative Photoresponsiveness. Chemistry of Materials, 2022, 34, 6996-7005.	3.2	3
70757	Rich Indiumâ€Vacancies In₂S₃ with Atomic pâ€“n Homojunction for Boosting Photocatalytic Multifunctional Properties. Small, 2022, 18, .	5.2	28
70758	Room-temperature epitaxial welding of 3D and 2D perovskites. Nature Materials, 2022, 21, 1042-1049.	13.3	32
70759	FeNi LDH/V2CTx/NF as Self-Supported Bifunctional Electrocatalyst for Highly Effective Overall Water Splitting. Nanomaterials, 2022, 12, 2640.	1.9	20

#	Article	IF	Citations
70760	Advanced Spectroscopic and Computational Studies of a Cobalt(II) Coordination Polymer with Single-Ion-Magnet Properties. Journal of Physical Chemistry C, 2022, 126, 13268-13283.	1.5	1
70761	Interaction between solute atoms and vacancies in Al-Mg-X (X¼Si, Ge) alloys. Keikinzoku/Journal of Japan Institute of Light Metals, 2022, 72, 427-429.	0.1	1
70762	Inactive (PbI ₂) ₂ RbCl stabilizes perovskite films for efficient solar cells. Science, 2022, 377, 531-534.	6.0	623
70763	Atomically Sharp, Closed Bilayer Phosphorene Edges by Self-Passivation. ACS Nano, 2022, 16, 12822-12830.	7.3	8
70764	An Integrated Experimental and Computational Platform to Explore Gas Hydrate Promotion, Inhibition, Rheology, and Mechanical Properties at McGill University: A Review. Energies, 2022, 15, 5532.	1.6	4
70765	Nonradical-dominated peroxymonosulfate activation through bimetallic Fe/Mn-loaded hydroxyl-rich biochar for efficient degradation of tetracycline. Nano Research, 2023, 16, 155-165.	5.8	22
70766	Ultrafast laser matter interactions: modeling approaches, challenges, and prospects. Modelling and Simulation in Materials Science and Engineering, 2022, 30, 083001.	0.8	4
70767	Coherent helicity-dependent spin-phonon oscillations in the ferromagnetic van der Waals crystal CrI3. Nature Communications, 2022, 13, .	5.8	15
70768	Giant and Controllable Photoplasticity and Photoelasticity in Compound Semiconductors. Physical Review Letters, 2022, 129, .	2.9	4
70769	Spin State as a Participator for Demetalation Durability and Activity of Feâ€“Nâ€“C Electrocatalysts. Journal of Physical Chemistry C, 2022, 126, 13168-13181.	1.5	15
70770	Theoretical Study on the High HER/OER Electrocatalytic Activities of 2D GeSi, SnSi, and SnGe Monolayers and Further Improvement by Imposing Biaxial Strain or Doping Heteroatoms. Molecules, 2022, 27, 5092.	1.7	6
70771	Probing the structure of vanadium tetracyanoethylene using electron energy-loss spectroscopy. APL Materials, 2022, 10, .	2.2	1
70772	Hierarchical Thiospinel NiCo₂S₄/Polyaniline Hybrid Nanostructures as a Bifunctional Electrocatalyst for Highly Efficient and Durable Overall Water Splitting. Advanced Materials Interfaces, 2022, 9, .	1.9	6
70773	Simulation calculation of the influence of interstitial atoms on the desorption behavior of tritium in nuclear graphite. Chemical Physics, 2022, , 111683.	0.9	0
70774	Band versus Polaron: Charge Transport in Antimony Chalcogenides. ACS Energy Letters, 2022, 7, 2954-2960.	8.8	13
70775	Unveiling the interplay of deformation mechanism in wrought Mgâ€“Sc alloy with different content of manganese. Journal of Materials Research and Technology, 2022, 20, 3522-3536.	2.6	7
70776	Dynamic Evolution of Methane Oxidation on Pd-Based Catalysts: A Reactive Force Field Molecular Dynamics Study. Journal of Physical Chemistry C, 2022, 126, 14201-14210.	1.5	5
70777	Heteroepitaxy of semiconducting 2H-MoTe2 thin films on arbitrary surfaces for large-scale heterogeneous integration. , 2022, 1, 701-708.		15

#	Article	IF	Citations
70778	Thermoelectric properties of the Janus PtSTe monolayer compared with its parent structures. Physical Review Materials, 2022, 6, .	0.9	3
70779	Giant and reversible electronic structure evolution in a magnetic topological material <mml:math xmlns:mml="http://www.w3.org/1998/Math/MathML"><mml:msub><mml:mi mathvariant="normal">EuCd</mml:mi><mml:mn>2</mml:mn></mml:msub><mml:msub><mml:mi mathvariant="normal">As</mml:mi><mml:mn>2</mml:mn></mml:msub></mml:math>. Physical Review B, 2022, 106, .	1.1	8
70780	Electric fields and strains effect on the electronic and optical properties of Zr2CO2/MoSSe van der Waals heterostructure. Materials Today Communications, 2022, 33, 104295.	0.9	5
70781	Computational Modeling of Physical Surface Reactions of Precursors in Atomic Layer Deposition by Monte Carlo Simulations on a Home Desktop Computer. Chemistry of Materials, 2022, 34, 7635-7649.	3.2	7
70782	Mechanistic insights into hydrogen evolution reaction on Ni2B(001) facet using first-principle calculations. International Journal of Hydrogen Energy, 2022, 47, 29622-29635.	3.8	6
70783	P-type ohmic contacts of MBenes with MoS₂ for nanodevices and logic circuits. 2D Materials, 2022, 9, 045022.	2.0	5
70784	Defectâ€Decorated NiFe Bimetallic Nanocatalysts for the Enhanced Hydrodeoxygenation of Guaiacol. ChemCatChem, 2022, 14, .	1.8	8
70785	24.8%-efficient planar perovskite solar cells via ligand-engineered TiO2 deposition. Joule, 2022, 6, 2186-2202.	11.7	44
70786	Nanoscale MXene Interlayer and Substrate Adhesion for Lubrication: A Density Functional Theory Study. ACS Applied Nano Materials, 2022, 5, 10516-10527.	2.4	28
70787	Zeolite-like molecules: Promising dielectrics for two-dimensional semiconductors. Science China Materials, 2023, 66, 233-240.	3.5	2
70788	The effect of antisite disorder on magnetic and exchange bias properties of Gd-substituted Y₂CoMnO₆ double perovskite. Journal of Physics Condensed Matter, 2022, 34, 435801.	0.7	3
70789	Low electronic conductivity of <mml:math xmlns:mml="http://www.w3.org/1998/Math/MathML"><mml:mrow><mml:msub><mml:mi>Li</mml:mi><mml:mn>7</mml:mn></mml:msub><mml:msub><mml:mi mathvariant="normal">O</mml:mi><mml:mn>12</mml:mn></mml:msub></mml:mrow></mml:math> solid electrolytes from first principles. Physical Review Materials, 2022, 6, .	0.9	8
70790	Highly efficient water splitting in step-scheme PtS2/GaSe van der Waals heterojunction. Journal of Applied Physics, 2022, 132, .	1.1	5
70791	I4/mcm-Si₄₈: An Ideal Topological Nodal-Line Semimetal. , 2022, 4, 1726-1733.		4
70792	Rigid Body Approximation for the Anharmonic Description of Moleculeâ€“Surface Vibrations. Journal of Chemical Theory and Computation, 2022, 18, 5618-5635.	2.3	6
70793	Back Contact Engineering to Improve CZTSSe Solar Cell Performance by Inserting MoO3 Sacrificial Nanolayers. Sustainability, 2022, 14, 9511.	1.6	4
70794	First-principle prediction of structural and mechanical properties in NbMoTaWRex refractory high-entropy alloys with experimental validation. Rare Metals, 2022, 41, 3343-3350.	3.6	6
70795	Modulation of Redox Chemistry of Na₂Mn₃O₇ by Selective Boron Doping Prompted by Na Vacancies. ACS Applied Materials & Interfaces, 2022, 14, 38769-38777.	4.0	7

#	Article	IF	Citations
70796	Firstâ€Principles Study of the 30Â° and 90Â° Partial Dislocations in HgTe, CdTe, and Hg_{0.7}Cd₀_{.3}Te. Physica Status Solidi (B): Basic Research, 2022, 259, .	0.7	2
70797	An Investigation of Monolayer As_{1â^'}_xP_x Solid Solutions: From a Theoretical Perspective. Advanced Materials Interfaces, 2022, 9, .	1.9	0
70798	MyElas: An automatized tool-kit for high-throughput calculation, post-processing and visualization of elasticity and related properties of solids. Computer Physics Communications, 2022, 281, 108495.	3.0	8
70799	Local Epitaxial Templating Effects in Ferroelectric and Antiferroelectric ZrO₂. ACS Applied Materials & Interfaces, 2022, 14, 36771-36780.	4.0	7
70800	Physics-Guided Descriptors for Prediction of Structural Polymorphs. Journal of Physical Chemistry Letters, 2022, 13, 7342-7349.	2.1	4
70801	The role of central heteroatom in electrochemical nitrogen reduction catalyzed by polyoxometalate-supported single-atom catalyst. Nano Research, 2023, 16, 309-317.	5.8	20
70802	Electric field tuning of magnetic states in single magnetic molecules. Physical Review B, 2022, 106, .	1.1	1
70803	Screening of bimetallic electrocatalysts for water purification with machine learning. Journal of Chemical Physics, 2022, 157, .	1.2	3
70804	Dirac nodal lines and nodal loops in the topological kagome superconductor <mml:math xmlns:mml="http://www.w3.org/1998/Math/MathML"><mml:mrow><mml:msub><mml:mi>CsV</mml:mi><mml:mn>3</mml:mn></mml:msub></mml:mrow></mml:math>Sb₅. Physical Review B, 2022, 106, .	1.1	8
70805	Amplified Local Strain Signal in Strain-Plasmonic Coupled van der Waals Heterostructures. Physical Review Applied, 2022, 18, .	1.5	1
70806	Kinetic Origins of High Selectivity of Metal Phosphides for Ethane Dehydrogenation. Industrial & Engineering Chemistry Research, 2022, 61, 12083-12091.	1.8	3
70807	Mechanistic Insight into Hydrocarbon Synthesis via CO₂ Hydrogenation on Ï‡-Fe₅C₂ Catalysts. ACS Applied Materials & Interfaces, 2022, 14, 37637-37651.	4.0	14
70808	Van der Waals Epitaxy of c-Oriented Wurtzite AlGaN on Polycrystalline Mo Substrates for Enhanced Heat Dissipation. ACS Applied Materials & Interfaces, 2022, 14, 37947-37957.	4.0	4
70809	Laplacian-level meta-generalized gradient approximation for solid and liquid metals. Physical Review Materials, 2022, 6, .	0.9	10
70810	Competitive Adsorption of NH₃ and H₂O in Metalâ€“Organic Framework Materials: MOF-74. Chemistry of Materials, 2022, 34, 7906-7915.	3.2	4
70811	Stable Liquid-Sulfur Generation on Transition-Metal Dichalcogenides toward Low-Temperature Lithiumâ€“Sulfur Batteries. ACS Nano, 2022, 16, 14412-14421.	7.3	10
70812	Superalkali functionalized two-dimensional haeckelite monolayers: A novel hydrogen storage architecture. International Journal of Hydrogen Energy, 2022, 47, 33391-33402.	3.8	10
70813	Graphene frameworks-confined synthesis of 2D-layered NiCoP for the electrochemical sensing of H2O2 at lower overpotential. Mikrochimica Acta, 2022, 189, .	2.5	5

#	Article	IF	Citations
70814	Critical current density and vortex phase diagram in the superconductor <mml:math xmlns:mml="http://www.w3.org/1998/Math/MathML"><mml:msub><mml:mrow><mml:mi>Sn</mml:mi></mml:mrow><mml:mrow><mml:mn>3</mml:mn></mml:mrow><mml:m Physical Review B, 2022, 106, .	1.1	3
70815	Atomic transistors based on seamless lateral metal-semiconductor junctions with a sub-1-nm transfer length. Nature Communications, 2022, 13, .	5.8	22
70816	Effects of Ga Substitution on the Local Structure of Na₂Zn₂TeO₆. Inorganic Chemistry, 2022, 61, 13067-13076.	1.9	3
70817	Pressure-stabilized structures of water-neon system under high pressure. Physical Review B, 2022, 106, .	1.1	1
70818	Role of Electronic Passivation in Stabilizing the Lithium- <mml:math xmlns:mml="http://www.w3.org/1998/Math/MathML" display="inline" overflow="scroll"><mml:msub><mml:mi>Li</mml:mi><mml:mi>x</mml:mi></mml:msub><mml:msub><mml:mi>PO</mml:mi><mml:mi mathvariant="normal">N</mml:mi></mml:mrow><mml:mi>z</mml:mi></mml:msub></mml:math> Solid-Electrolyte Interphase. , 2022, 1, .	3	3
70819	Dzyaloshinskii-Moriya interaction and magnetic skyrmions induced by curvature. Physical Review B, 2022, 106, .	1.1	8
70820	Discovery of New Plasmonic Metals via Highâ€Throughput Machine Learning. Advanced Optical Materials, 2022, 10, .	3.6	2
70821	Effects of thermal, elastic, and surface properties on the stability of SiC polytypes. Physical Review B, 2022, 106, .	1.1	6
70822	Defect levels of <mml:math xmlns:mml="http://www.w3.org/1998/Math/MathML"><mml:mrow><mml:mn>3</mml:mn><mml:msup><mml:mi>d</mml:mi><mml:mi transition-metal series in wide-gap oxide and fluoride insulators: A first-principles study. Physical Review B, 2022, 106, .	1.1	3
70823	Broadband BiOCl Nonlinear Saturable Absorber for Wattâ€Level Passively Qâ€Switched Yb:LuAG Single Crystal Fiber Laser. Advanced Optical Materials, 2022, 10, .	3.6	14
70824	Plastic/Ductile Bulk 2D van der Waals Singleâ€Crystalline SnSe₂ for Flexible Thermoelectrics. Advanced Science, 2022, 9, .	5.6	20
70825	Theoretical prediction of Curie temperature in two-dimensional ferromagnetic monolayer. Journal of Applied Physics, 2022, 132, .	1.1	8
70826	Two-dimensional <mml:math xmlns:mml="http://www.w3.org/1998/Math/MathML"><mml:mrow><mml:mi>Mo</mml:mi><mml:msub><mml:mi>Te</mml:mi></mml:mi><mml:mi van der Waals heterostructures for tunnel-FET applications. Physical Review Materials, 2022, 6, .	3.1	8
70827	Pressure-induced structural phase transition of vanadium: a revisit from the perspective of ensemble theory. Journal of Physics Condensed Matter, 2022, 34, 425404.	0.7	4
70828	Factors influencing halide vacancy transport in perovskite solar cells. Discover Materials, 2022, 2, .	1.0	7
70829	Theoretical prediction of high entropy intermetallic compound phase via first principles calculations, artificial neuron network and empirical models: A case of equimolar AlTiCuCo. Physica B: Condensed Matter, 2022, 646, 414275.	1.3	2
70831	Multi-scale simulations and phase stability prediction of mixed Li₂S_{1-x}Se_x system. Journal of Physics: Conference Series, 2022, 2298, 012003.	0.3	0
70832	Optimization of Yolkâ€“Shell NiCo₂S₄ Spheres as Catalysts for High-Performance Rechargeable Liâ€“O₂ Batteries. ACS Applied Energy Materials, 2022, 5, 10415-10426.	2.5	3

#	Article	IF	Citations
70833	Potential hydrogen storage materials from Li decorated Nâ€doped Meâ€graphene. International Journal of Energy Research, 2022, 46, 24554-24564.	2.2	3
70834	Nonsymmorphic P21/mâ€MoTe ₂ : Novel 2D Topological Materials. Physica Status Solidi - Rapid Research Letters, 0, , 2200188.	1.2	1
70835	Hydrogen Behavior at Crystalline/Amorphous Interface of Transparent Oxide Semiconductor and Its Effects on Carrier Transport and Crystallization. ACS Applied Materials & Interfaces, 2022, 14, 39535-39547.	4.0	5
70836	Linear paired electrochemical valorization of glycerol enabled by the electro-Fenton process using a stable NiSe2 cathode. Nature Catalysis, 2022, 5, 716-725.	16.1	48
70837	Ultra-flat and long-lived plasmons in a strongly correlated oxide. Nature Communications, 2022, 13, .	5.8	4
70838	Crystal structure solution of a high-pressure polymorph of scintillating <mml:math xmlns:mml="http://www.w3.org/1998/Math/MathML"><mml:msub><mml:mi>MgMoO</mml:mi><mml:mn>4</mml:mn></mml:msub> and its electronic structure. Physical Review B, 2022, 106, .	1.1	2
70839	Origin of the unusual property contrast in K₂Bi₈Se₁₃ phase-change material. Applied Physics Letters, 2022, 121, 061901.	1.5	0
70840	Concurrence of auxetic effect and topological phase transition in a 2D phosphorous nitride. Applied Physics Letters, 2022, 121, 063101.	1.5	0
70841	Structural transformation of methyl urotropine perchlorate under high pressure. Journal of Molecular Modeling, 2022, 28, .	0.8	0
70842	<scp>Mo₂P</scp> Monolayer as a Superior Electrocatalyst for Urea Synthesis from Nitrogen and Carbon Dioxide Fixation: A Computational Study. Energy and Environmental Materials, 2024, 7, .	7.3	7
70843	Influence of chemical disorder on mechanical and thermal properties of multi-component rare earth zirconate pyrochlores (nRE1/n)2Zr2O7. Journal of Applied Physics, 2022, 132, .	1.1	3
70844	Triple nodal points characterized by their nodal-line structure in all magnetic space groups. Physical Review B, 2022, 106, .	1.1	6
70845	Universal higher-order bulk-boundary correspondence of triple nodal points. Physical Review B, 2022, 106, .	1.1	10
70846	A paradigm shift in CO tolerant catalyst design for fuel cells via introducing defect-controlled carbon molecular sieve layers. Materials Today Energy, 2022, , 101124.	2.5	5
70847	Theoretical research into low-voltage Na2TiSiO5 anode for lithium-ion battery. Rare Metals, 0, , .	3.6	1
70848	Electrocatalyst with Dynamic Formation of the Dual-Active Site from the Dual Pathway Observed by In Situ Raman Spectroscopy. ACS Catalysis, 2022, 12, 10276-10284.	5.5	40
70849	Shape-Controlled Pathways in the Hydrogen Production from Ethanol Steam Reforming over Ceria Nanoparticles. ACS Catalysis, 2022, 12, 10482-10498.	5.5	10
70850	Hydrolysis of Acetamide on Low-Index CeO₂ Surfaces: Ceria as a Deamidation and General De-esterification Catalyst. ACS Catalysis, 2022, 12, 10222-10234.	5.5	5

#	Article	IF	Citations
70851	Enhancing Electrocatalytic Nitrogen Reduction on Few-Layer Antimonene in an Aqueous Potassium Sulfate Electrolyte. Journal of Physical Chemistry C, 2022, 126, 13629-13639.	1.5	8
70852	First-Principles Study of Ferroelectric and Optical Properties in Derivatives of Thiourea. Journal of Physical Chemistry C, 2022, 126, 13920-13928.	1.5	1
70853	Intrinsic Regularity of Catalytic Cobalt Chalcogenides in Lithiumâ€Sulfur Battery: Theoretical Study Delivers New Insights. Chemistry - A European Journal, 2022, 28, .	1.7	0
70854	Synthesis of perovskite-type LaWN3 by high-pressure solid-state metathesis reaction. Journal of Solid State Chemistry, 2022, 315, 123508.	1.4	5
70855	Structural transformations and thermal stability of RhGe synthesized under high temperature and pressure. Journal of Physics Condensed Matter, 2022, 34, 424001.	0.7	0
70856	Luminescence Enhancement of a Gold Nanocluster Hydrogel Facilitated by Water for Erasable Water Writing and Visual Solvent Differentiation. ACS Sustainable Chemistry and Engineering, 2022, 10, 11406-11414.	3.2	4
70857	Boosting Nitrogen Reduction Activity by Defect Engineering in 2D Iron Monochalcogenides FeX (X=S,) Tj ETQq0 0 0 rgBT /Overlock 10 T	6.9	6
70858	Single-layer intrinsic 2H-phase LuX ₂ (X = Cl, Br, I) with large valley polarization and anomalous valley Hall effect. Chinese Physics B, 2023, 32, 037306.	0.7	2
70859	Formic Acid Generation from CO2 Reduction by MOF-253 Coordinated Transition Metal Complexes: A Computational Chemistry Perspective. Catalysts, 2022, 12, 890.	1.6	1
70860	Anomalous ferroelectricity and double-negative effects in bilayer hexagonal boron nitride. Physical Review B, 2022, 106, .	1.1	7
70861	Excitation-Dependent Anisotropic Raman Response of Atomically Thin Pentagonal PdSe₂. ACS Physical Chemistry Au, 2022, 2, 482-489.	1.9	3
70862	A Dual Functional Artificial SEI Layer Based on a Facile Surface Chemistry for Stable Lithium Metal Anode. Molecules, 2022, 27, 5199.	1.7	2
70863	Catalytic hosts with strong adsorption strength for long shelf-life lithium-sulfur batteries under lean electrolyte. Nano Research, 2023, 16, 427-438.	5.8	3
70864	Role of water structure in alkaline water electrolysis. IScience, 2022, 25, 104835.	1.9	8
70865	Zigzag magnetic order in a novel tellurate compound Na4â”ÎNiTeO6 with S = 1 chains. Science China: Physics, Mechanics and Astronomy, 2022, 65, .	2.0	1
70866	Porously Reduced 2â€Dimensional <scp>Bi₂O₂CO₃</scp> Petals for Strainâ€Mediated Electrochemical <scp>CO₂</scp> Reduction to <scp>HCOOH</scp>. Energy and Environmental Materials, 2024, 7, .	7.3	4
70867	Competing magnetic and nonmagnetic states in monolayer <mml:math xmlns:mml="http://www.w3.org/1998/Math/MathML"><mml:msub><mml:mi>VSe</mml:mi><mml:mn>2</mml:mn></mml:msub></mml:math> with charge density wave. Physical Review B, 2022, 106, .	1.1	8
70868	Adjustable Mixed Conductive Interphase for Dendrite-Free Lithium Metal Batteries. ACS Nano, 2022, 16, 13101-13110.	7.3	19

#	Article	IF	Citations
70869	Strain-tunable magnetic transition in few-layer 1T-VSe2. Applied Physics Letters, 2022, 121, .	1.5	4
70870	Nearly Ideal Two-Dimensional Electron Gas Hosted by Multiple Quantized Kronigâ€“Penney States Observed in Few-Layer InSe. ACS Nano, 2022, 16, 13014-13021.	7.3	1
70871	Prediction of super hardness in transition metal hexa-nitrides from density functional theory computations. Materialia, 2022, 25, 101550.	1.3	3
70872	Dual-function oxygen vacancy of BiOBr intensifies pollutant adsorption and molecular oxygen activation to remove tetracycline hydrochloride. Chemical Engineering Journal, 2023, 451, 138731.	6.6	21
70873	Workhorse minimally empirical dispersion-corrected density functional with tests for weakly bound systems: <mml:math xmlns:mml="http://www.w3.org/1998/Math/MathML"><mml:mrow><mml:msup><mml:mrow><mml:mi mathvariant="normal">r</mml:mi></mml:mrow><mml:mn>2</mml:mn></mml:msup><mml:mi>SCAN</mml:mi><mml:mo>+</mml:mo> Physical Review B, 2022, 106, .	1.1	18
70874	Solution-Mediated Inversion of SnSe to Sb2Se3 Thin-Films. Nanomaterials, 2022, 12, 2898.	1.9	0
70875	Prediction of phonon-mediated superconductivity and topological surface states in NbRu<mml:math xmlns:mml="http://www.w3.org/1998/Math/MathML" altimg="si66.svg" display="inline" id="d1e232"><mml:msub><mml:mrow /><mml:mrow><mml:mn>3</mml:mn></mml:mrow></mml:msub></mml:math>C. Physica B: Condensed Matter, 2022, 646, 414255.	1.3	2
70876	Morphological Control of Nanoporous Copper Formed from Conversion Reaction Synthesis. Journal of Physical Chemistry C, 2022, 126, 14878-14885.	1.5	2
70877	Localized phase transformation at stacking faults and mechanism-based alloy design. Acta Materialia, 2022, 240, 118287.	3.8	6
70878	Structural and electronic effects boosting Ni-doped Mo2C catalyst toward high-efficiency C O/C C bonds cleavage. Journal of Energy Chemistry, 2022, 75, 109-116.	7.1	10
70879	Controlled Growth of Wafer-Scale Transition Metal Dichalcogenides with a Vertical Composition Gradient for Artificial Synapses with High Linearity. ACS Nano, 2022, 16, 12318-12327.	7.3	6
70880	Direct 3D Printing of Binder-Free Bimetallic Nanomaterials as Integrated Electrodes for Glycerol Oxidation with High Selectivity for Valuable C₃ Products. ACS Nano, 2022, 16, 12202-12213.	7.3	11
70881	Nanoscale Valley Modulation by Surface Plasmon Interference. Nano Letters, 2022, 22, 6923-6929.	4.5	8
70882	Highly Efficient Aggregation-Induced Electrochemiluminescence of Al(III)-Cbatpy Metalâ€“Organic Gels Obtained by Ultrarapid Self-Assembly for a Biosensing Application. Analytical Chemistry, 2022, 94, 12196-12203.	3.2	19
70883	Gate-mediated transition between antiferromagnetic topological and Chern insulators in honeycomb <mml:math xmlns:mml="http://www.w3.org/1998/Math/MathML"><mml:msub><mml:mi>X</mml:mi><mml:mn>3</mml:mn></mml:msub><mml:m mathvariant="normal">MnN</mml:mi><mml:mn>3</mml:mn></mml:msub></mml:math> <mml:math xmlns:mml="http://www.w3.org/1998/Math/MathML"><mml:mo>(</mml:mo><mml:mi>X</mml:mi><mml:mo>=</mml:mo><mml:mi>S Physical Review B, 2022, 106, .	1.1	3
70884	Coexistence of the Piezoelectricity and Intrinsic Quantum-Spin Hall Effect in GaTeS and InTeS Monolayers: Implications for Spintronic Devices. ACS Applied Nano Materials, 2022, 5, 11037-11044.	2.4	2
70885	Functional Group Effects on the Electrochemical Properties of Carboranethiol Monolayers on Au(111) As Studied by Density Functional Theory: Implications for Organic Electronics. ACS Applied Nano Materials, 2022, 5, 11185-11193.	2.4	0
70886	Solution-Grown Ternary Semiconductors: Nanostructuring and Stereoelectronic Lone Pair Distortions in Iâ€“Vâ€“VI₂ Materials. Chemistry of Materials, 2022, 34, 7357-7368.	3.2	5

#	Article	IF	Citations
70887	High-surface-area corundum nanoparticles by resistive hotspot-induced phase transformation. Nature Communications, 2022, 13, .	5.8	16
70888	Tuning the Structural and Magnetic Properties in Mixed Cation Mn_xCo_{2â€“x}P₂S₆. Inorganic Chemistry, 2022, 61, 13719-13727.	1.9	1
70889	Ti Sn O2 phase separation modulated electronic structure and kinetic behaviors for high-rate and long-cycle anodes. Composites Part B: Engineering, 2022, 243, 110151.	5.9	5
70890	First-Principles Calculations of Two-Dimensional Monolayer PdSe₂ for Selective Sensing of Nitrogen-Containing Gases. ACS Applied Nano Materials, 2022, 5, 11519-11528.	2.4	9
70891	Selfâ€Derivation and Surface Reconstruction of Feâ€Doped Ni₃S₂ Electrode Realizing Highâ€Efficient and Stable Overall Water and Urea Electrolysis. Advanced Energy Materials, 2022, 12, .	10.2	84
70892	2D solar cell with record high power conversion efficiency based on low-symmetry IV-V₂ bilayer heterostructure. Journal Physics D: Applied Physics, 2022, 55, 435501.	1.3	0
70893	Mechanism of CO2 adsorption on point-defective MgO surfaces: First-principles study. Applied Surface Science, 2022, 604, 154647.	3.1	12
70894	Density functional theory assessment of the lithiation thermodynamics and phase evolution in si-based amorphous binary alloys. Energy Storage Materials, 2022, 53, 42-50.	9.5	2
70895	Au Nanoparticles Loaded Bi5Ti3FeO15 Ferroelectric Nanosheets with Enhanced Photocatalytic Activity for NO Removal. Catalysis Letters, 0, , .	1.4	0
70896	Cobalt-Dimer Nitrides: A Potential Novel Family of High-Temperature Superconductors. Chinese Physics Letters, 2022, 39, 097401.	1.3	2
70897	A Deep Neural Network Interface Potential for Liâ€Cu Systems. Advanced Materials Interfaces, 0, , 2201346.	1.9	4
70898	A High Airâ€Stability and Liâ€Metalâ€Compatible Li_{3+2x}P_{1âˆ’x}Bi_xS_{4âˆ’1.5x}O_{1.5x} Sulfide Electrolyte for Allâ€Solidâ€State Liâ€“Metal Batteries. Advanced Functional Materials, 2022, 32, .	7.8	17
70899	Mo-embedded Ir-based electrocatalyst for nitrogen reduction reaction: A computational study. Materials Today Communications, 2022, 33, 104318.	0.9	1
70900	The electronic, structural, ferroelectric and optical properties of strontium and zirconium co-doped BaTiO<mml:math xmlns:mml="http://www.w3.org/1998/Math/MathML" altimg="si54.svg" display="inline" id="d1e364"><mml:msub><mml:mrow /><mml:mrow><mml:mn>3</mml:mn></mml:mrow></mml:msub></mml:math>: First-principles calculations. Solid State Communications, 2022, 355, 114939.	0.9	9
70901	Computationally accelerated discovery of functional and structural Heusler materials. MRS Bulletin, 2022, 47, 559-572.	1.7	4
70902	Dipole Switching by Intramolecular Electron Transfer in Single-Molecule Magnetic Complex [Mn₁₂O₁₂(O₂CR)₁₆(H₂O)₄]. Journal of Physical Chemistry A, 2022, 126, 5265-5272.	1.1	0
70903	Anomalous enhancement of thermoelectric performance in GeTe with specific interaxial angle and atomic displacement synergy. Cell Reports Physical Science, 2022, 3, 101009.	2.8	1
70904	Ultralow Melting Temperature of High-Pressure Face-Centered Cubic Superionic Ice. Journal of Physical Chemistry Letters, 2022, 13, 7448-7453.	2.1	2

#	Article	IF	Citations
70905	Photoinduced Small Hole Polarons Formation and Recombination in All-Inorganic Perovskite from Quantum Dynamics Simulation. Journal of Physical Chemistry Letters, 2022, 13, 7532-7540.	2.1	8
70906	Charge Transfer-Triggered Bi³⁺Near-Infrared Emission in Y₂Ti₂O₇for Dual-Mode Temperature Sensing. ACS Applied Materials & Interfaces, 2022, 14, 36834-36844.	4.0	26
70907	Ferroelectric domain wall in two-dimensional GeS. Journal of Applied Physics, 2022, 132, 074302.	1.1	2
70908	Ferroelectricity Induced by Oxygen Vacancies in Rhombohedral <scp>ZrO₂</scp> Thin Films. Energy and Environmental Materials, 2024, 7, .	7.3	8
70909	Defect chemistry of p-type perovskite oxide La0.2Sr0.8FeO3-Î´: a combined experimental and computational study. Journal of the Korean Ceramic Society, 2022, 59, 876-888.	1.1	6
70910	Cascade of pressure-driven phase transitions in the topological nodal-line superconductor <mml:math xmlns:mml="http://www.w3.org/1998/Math/MathML"><mml:msub><mml:mi mathvariant="normal">PbTaSe</mml:mi><mml:mn>2</mml:mn></mml:msub></mml:math>. Physical Review B, 2022, 106, .	1.1	3
70911	Multiple dimensions of spin-gapless semiconducting states in tetragonal <mml:math xmlns:mml="http://www.w3.org/1998/Math/MathML"><mml:mrow><mml:msub><mml:mi>Sr</mml:mi><mml:mn>2</mml:mn></mml:msub></mml:mrow></mml:math> Physical Review B, 2022, 106, .	1.1	24
70912	Electrochemical reduction of CO2 on Cu doped titanium nanotubesâ€”An insight on ethylene selectivity. Electrochimica Acta, 2022, 431, 141078.	2.6	4
70913	Enabling Ab Initio Material Design of <mml:math xmlns:mml="http://www.w3.org/1998/Math/MathML" display="inline" overflow="scroll"><mml:mrow><mml:mi>In</mml:mi><mml:mi>As</mml:mi></mml:mrow><mml:mo>/</mml:mo><mml:mrow><mml:m Superlattices for Infrared Detection. Physical Review Applied, 2022, 18, .	1.5	1
70914	How Hydrodynamic Phonon Transport Determines the Convergence of Thermal Conductivity in Two-Dimensional Materials. Nanomaterials, 2022, 12, 2854.	1.9	5
70915	Electrosynthesis of ammonia with high selectivity and high rates via engineering of the solid-electrolyte interphase. Joule, 2022, 6, 2083-2101.	11.7	71
70916	First-principles calculations of Schottky barrier height at barium titanate/metal interface. Japanese Journal of Applied Physics, 2022, 61, SN1029.	0.8	0
70917	Equilibrium Particle Shape and Surface Chemistry of Disordered Li-Excess, Mn-Rich Li-ion Cathodes through First-Principles Modeling. Chemistry of Materials, 2022, 34, 7210-7219.	3.2	6
70918	Dehydrochlorination of PCDDs on SWCN-Supported Ni10 and Ni13 Clusters, a DFT Study. Molecules, 2022, 27, 5074.	1.7	1
70919	Partial Palladium Oxidation over Various Oxide Supports for a Higher Reactivity of PdO with Respect to CH₄. Journal of Physical Chemistry C, 2022, 126, 13132-13146.	1.5	0
70920	Rational design of non-noble-metal-based alloy catalysts for hydrogen activation: a density functional theory study. Molecular Simulation, 0, , 1-7.	0.9	0
70921	Band alignment of monolayer MoS2/4H-SiC heterojunction via first-principles calculations and x-ray photoelectron spectroscopy. Applied Physics Letters, 2022, 121, .	1.5	2
70922	Twoâ€Dimensional Perovskite Single Crystals for Highâ€Performance Xâ€ray Imaging and Exploring <scp>MeV</scp> Xâ€ray Detection. Energy and Environmental Materials, 2024, 7, .	7.3	7

#	Article	IF	Citations
70923	Computational Biomaterials: Computational Simulations for Biomedicine. Advanced Materials, 2023, 35, .	11.1	10
70924	Demonstration of Low Work Function Perovskite SrVO₃ Using Thermionic Electron Emission. Advanced Functional Materials, 2022, 32, .	7.8	11
70925	Ionic forces and stress tensor in all-electron density functional theory calculations using an enriched finite-element basis. Physical Review B, 2022, 106, .	1.1	3
70926	Spontaneous Hybrid Crossâ€Linked Network Induced by Multifunctional Copolymer toward Mechanically Resilient Perovskite Solar Cells. Advanced Functional Materials, 2022, 32, .	7.8	28
70927	Screening 0D Materials for 2D Nanoelectronics Applications. Advanced Electronic Materials, 0, , 2200393.	2.6	2
70928	Highly efficient blue InGaN nanoscale light-emitting diodes. Nature, 2022, 608, 56-61.	13.7	57
70929	Generative design of stable semiconductor materials using deep learning and density functional theory. Npj Computational Materials, 2022, 8, .	3.5	7
70930	Low lattice thermal conductivity in Zintl phases <mml:math xmlns:mml="http://www.w3.org/1998/Math/MathML"><mml:mrow><mml:msub><mml:mi>Na</mml:mi><mml:mn>2</mml:mn></mml:msub></mml:mrow></mml:math> and <mml:math xmlns:mml="http://www.w3.org/1998/Math/MathML"><mml:mrow><mml:msub><mml:mi>Na</mml:mi><mml:mn>2</mml:mn></mml:msub></mml:mrow></mml:math> : An ab initio study. Physical Review Materials, 2022, 6, .	0.9	2
70931	Phonon-mediated Migdal effect in semiconductor detectors. Physical Review D, 2022, 106, .	1.6	8
70932	Monolayer <mml:math xmlns:mml="http://www.w3.org/1998/Math/MathML"><mml:mrow><mml:mi>Mn</mml:mi><mml:mi>X</mml:mi></mml:mrow></mml:math> and Janus <mml:math xmlns:mml="http://www.w3.org/1998/Math/MathML"><mml:mrow><mml:mi>X</mml:mi><mml:mi>Mn</mml:mi><mml:mi>Y</mml:mi></mml:mrow></mml:math>		

#	Article	IF	Citations
70941	Enhancing carbon dioxide reduction electrocatalysis by tuning metal-support interactions: A first principles study. Green Chemical Engineering, 2022, , .	3.3	1
70942	Kinetic pathway of Î³-to-Î´ phase transition in CsPbI3. CheM, 2022, 8, 3120-3129.	5.8	23
70943	Iron doping of NiSe2 nanosheets to accelerate reaction kinetics in sodium-ion half/full batteries. Science China Materials, 2023, 66, 69-78.	3.5	20
70944	Computational exploration of dual atom catalysts loaded on defective graphene for oxygen reduction reaction. Applied Surface Science, 2022, 605, 154534.	3.1	5
70945	Mn-incorporated Co3O4 bifunctional electrocatalysts for zinc-air battery application: An experimental and DFT study. Applied Catalysis B: Environmental, 2022, 319, 121909.	10.8	45
70946	New evaluation of the thermodynamics stability for bcc-Fe. Journal of Physics Condensed Matter, 0, , .	0.7	0
70947	Piezoelectricity across 2D Phase Boundaries. Advanced Materials, 2022, 34, .	11.1	11
70948	Cu²⁺â€Chelatable and ROSâ€Scavenging MXenzyme as NIRâ€IIâ€Triggered Bloodâ€“Brain Barrierâ€Crossing Nanocatalyst against Alzheimer's Disease. Small, 2022, 18, .	5.2	25
70949	Theoretical Evaluation of Electrochemical Nitrate Reduction Reaction on Graphdiyne-Supported Transition Metal Single-Atom Catalysts. ACS Omega, 2022, 7, 31309-31317.	1.6	5
70950	Distribution of multiple Al substitution in HY zeolite and BrÃ¸nsted acid strength - A periodic DFT study. Microporous and Mesoporous Materials, 2022, 344, 112184.	2.2	3
70951	Hafnia for analog memristor: Influence of stoichiometry and crystalline structure. Physical Review Materials, 2022, 6, .	0.9	6
70952	Combined Cornerâ€Sharing and Edgeâ€Sharing Networks in Hybrid Nanocomposite with Unusual Latticeâ€Oxygen Activation for Efficient Water Oxidation. Advanced Functional Materials, 2022, 32, .	7.8	26
70953	Coordination Engineering of Ultraâ€Uniform Ruthenium Nanoclusters as Efficient Multifunctional Catalysts for Zincâ€“Air Batteries. Small Science, 2022, 2, .	5.8	5
70954	Understanding intercalation chemistry for sustainable aqueous zincâ€“manganese dioxide batteries. Nature Sustainability, 2022, 5, 890-898.	11.5	111
70955	Ab-Initio Study of Calcium Fluoride Doped with Heavy Isotopes. Crystals, 2022, 12, 1128.	1.0	1
70956	Efficient Crystal Structure Prediction for Structurally Related Molecules with Accurate and Transferable Tailor-Made Force Fields. Journal of Chemical Theory and Computation, 2022, 18, 5725-5738.	2.3	7
70957	First-principles study on electronic and optical properties of van der Waals heterostructures stacked by g-ZnO and Janus-WSSe monolayers. Applied Surface Science, 2022, 604, 154620.	3.1	10
70958	Ferromagnetic Order in Semiconducting Crâ€Doped Î±â€MnTe Nanosheets Grown by Chemical Vapor Deposition. Advanced Electronic Materials, 2022, 8, .	2.6	2

#	Article	IF	Citations
70959	The structural, elastic, electronic, magnetic and optical properties of SrNiO3 perovskite: A DFT and DFT+U study. Results in Physics, 2022, 41, 105920.	2.0	4
70960	Accurate large-scale simulations of siliceous zeolites by neural network potentials. Npj Computational Materials, 2022, 8, .	3.5	12
70961	Topological properties of CsCl type superconducting materials. Physics Letters, Section A: General, Atomic and Solid State Physics, 2022, , 128385.	0.9	1
70962	Lattice instability, anharmonicity and Raman spectra of BaO under high pressure: A first principles study. Journal of Physics and Chemistry of Solids, 2022, 170, 110967.	1.9	2
70963	Transition metal impurities in silicon: computational search for a semiconductor qubit. Npj Computational Materials, 2022, 8, .	3.5	3
70964	First-principles study on the ultralow lattice thermal conductivity of BiSeI. Physica B: Condensed Matter, 2022, , 414278.	1.3	4
70965	Electronic and Magnetic Properties of the BaTiO$$_{3}$$/LaMnO$$_{3}$$ Interface: a DFT Study. Journal of Superconductivity and Novel Magnetism, 2022, 35, 2225-2229.	0.8	2
70966	A single tiny Ti (O2) cluster decorated an ultra-small boron nitride nanotube for hydrogen storage material: A density functional theory study. International Journal of Hydrogen Energy, 2022, 47, 29907-29914.	3.8	8
70967	Strategies for Modulating the Catalytic Activity and Selectivity of Manganese Antimonates for the Oxygen Reduction Reaction. ACS Catalysis, 2022, 12, 10826-10840.	5.5	4
70968	Unveiling the interaction of nanopatterned void superlattices with irradiation cascades. Acta Materialia, 2022, 239, 118282.	3.8	6
70969	Intrinsic Nonlinear Electric Spin Generation in Centrosymmetric Magnets. Physical Review Letters, 2022, 129, .	2.9	10
70970	Fast Ion Transport Mechanism and Electrochemical Stability of Trivalent Metal Iodide-based Na Superionic Conductors Na₃XI₆ (X = Sc, Y, La, and In). ACS Applied Materials & Interfaces, 2022, 14, 36864-36874.	4.0	6
70971	Step-Assisted On-Surface Synthesis of Graphene Nanoribbons Embedded with Periodic Divacancies. Journal of the American Chemical Society, 2022, 144, 14798-14808.	6.6	16
70972	CO₂ Hydrogenation to Methanol over Inverse ZrO₂/Cu(111) Catalysts: The Fate of Methoxy under Dry and Wet Conditions. Journal of Physical Chemistry C, 2022, 126, 14479-14486.	1.5	8
70973	Compositional Dependence of Magnetocrystalline Anisotropy, Magnetic Moments, and Energetic and Electronic Properties on Fe-Pt Alloys. Materials, 2022, 15, 5679.	1.3	2
70974	Large Room Temperature Anomalous Transverse Thermoelectric Effect in Kagome Antiferromagnet YMn₆Sn₆. Advanced Materials, 2022, 34, .	11.1	20
70975	Partially Ordered Lanthanide Carboxylates with a Highly Adaptable 1D Polymeric Structure. Polymers, 2022, 14, 3328.	2.0	1
70976	Mg2+ doping into Li sites to improve anionic redox reversibility and thermal stability of lithium-rich manganese-based oxides cathode. Materials Today Energy, 2022, 29, 101116.	2.5	12

#	Article	IF	Citations
70977	Mechanisms of the carbon deposition at the Ni/YSZ interface: A combination study of microscopic observation and first-principles calculation. International Journal of Hydrogen Energy, 2022, 47, 29027-29036.	3.8	3
70978	Pressure-dependent photoluminescence of Eu-activated aluminate hydride Sr3â^'xAxAlO4H:Eu2+ (Aâ€‰=â€‰Ca, Ba; xâ€‰=â€‰0, 1): Application of advanced U-determination technique for luminescence wavelength prediction. Journal of Applied Physics, 2022, 132, .	2.5	3
70979	The Effect of Cr Substitution on the Anomalous Hall Effect of Co3â^'xCrxAl (x = 0, 1, 2, 3) Heusler Compounds: An Ab Initio Study. Applied Sciences (Switzerland), 2022, 12, 8303.	1.3	0
70980	Ultratough Hydrogenâ€Bondâ€Bridged Phosphorene Films. Advanced Materials, 2022, 34, .	11.1	9
70981	Mechanism Controlling Elevated Temperature Deformation in Additively Manufactured Eutectic High-Entropy Alloy. Metallurgical and Materials Transactions A: Physical Metallurgy and Materials Science, 0, , .	1.1	1
70982	Characterization of cordierite based hâ€BN doped ceramics as an electronic substrate/circuit board material. International Journal of Applied Ceramic Technology, 2022, 19, 3461-3479.	1.1	2
70983	Tuning the Catalytic Activity of Bifunctional Cobalt Boride Nanoflakes for Overall Water Splitting over a Wide pH Range. Journal of the Electrochemical Society, 2022, 169, 096507.	1.3	4
70984	Hole doping in a negative charge transfer insulator. Communications Physics, 2022, 5, .	2.0	3
70985	A van der Waals CaCl semiconducting electrene and ferromagnetic half-metallicity induced by superhalogen decoration. Materials Today Communications, 2022, 32, 104176.	0.9	0
70986	A-site deficiency in La0.5Ca0.5MnO3-Î´ cathode allows high performance for proton-conducting solid oxide fuel cells. Ceramics International, 2022, 48, 35586-35592.	2.3	2
70987	Intrinsic dipole-induced self-doping in Janus MXY-based (M = Mo, W; X = S; Y = Se, Te) pâ€“n junctions. Journal Physics D: Applied Physics, 2022, 55, 435303.	1.3	7
70988	Catalytic Hydrogenolysis of Lignin into Phenolics by Internal Hydrogen over Ru Catalyst. ChemCatChem, 2022, 14, .	1.8	5
70989	Polymerization of nitrogen in two theoretically predicted high-energy compounds ScN₆ and ScN₇ under modest pressure. New Journal of Physics, 2022, 24, 083015.	1.2	3
70990	Coexistence of charge-2 Dirac and Weyl phonons in chiral space groups. Physical Review B, 2022, 106, .	1.1	7
70991	High-capacity hydrogen storage in yttrium-decorated Î¨-graphene: Acumen from density functional theory. Journal of Applied Physics, 2022, 132, .	1.1	7
70992	DFT-assisted rational design of CoMxP/CC (M = Fe, Mn, and Ni) as efficient electrocatalyst for wide pH range hydrogen evolution and oxygen evolution. Nano Research, 2022, 15, 8897-8907.	5.8	41
70993	DFT simulation of conductivity of the p-type doped and charge-injected cis-polyacetylene. Molecular Physics, 0, , .	0.8	1
70994	Magnetization tunable Weyl states in <mml:math xmlns:mml="http://www.w3.org/1998/Math/MathML"><mml:mrow><mml:mi>Eu</mml:mi><mml:msub><mml:mi mathvariant="normal">B</mml:mi><mml:mn>6</mml:mn></mml:msub></mml:mrow></mml:math>. Physical Review B, 2022, 106, .	1.1	9

#	Article	IF	Citations
70995	Phonon study of Jahnâ€“Teller distortion and phase stability in NaMnO2 for sodium-ion batteries. Journal of Applied Physics, 2022, 132, .	1.1	3
70996	Metal contacts with Moire interfaces on WSe2 for ambipolar applications. Applied Physics Letters, 2022, 121, .	1.5	7
70997	Stable ferromagnetism and high Curie temperature in VGe₂N₄. New Journal of Physics, 2022, 24, 083008.	1.2	4
70998	Twoâ€Dimensional Organometallic Frameworks with Pyridinic Singleâ€Metalâ€Atom Sites for Bifunctional ORR/OER. Advanced Functional Materials, 2022, 32, .	7.8	32
70999	Adsorption and Reactivity of Chiral Modifiers in Heterogeneous Catalysis: 1-(1-Naphthyl)ethylamine on Pt Surfaces. ACS Catalysis, 2022, 12, 10514-10521.	5.5	2
71000	Computational Investigation of the Stability of Di-p-Tolyl Disulfide â€œHiddenâ€•and â€œConventionalâ€• Polymorphs at High Pressures. Crystals, 2022, 12, 1157.	1.0	3
71001	DFT study of TiO₂ brookite (210) surface doped with silver and molybdenum. Materials Research Express, 0, , .	0.8	1
71002	Low Thermal Conductivity and High Thermoelectric Performance of Kagomeâ€Like As and Sb Monolayers: A Firstâ€Principles Study. Physica Status Solidi - Rapid Research Letters, 2022, 16, .	1.2	2
71003	Tuning the Electronic, Ion Transport, and Stability Properties of Li-rich Manganese-based Oxide Materials with Oxide Perovskite Coatings: A First-Principles Computational Study. ACS Applied Materials & Interfaces, 2022, 14, 37009-37018.	4.0	2
71004	Introducing BrÃ¸nsted acid sites to accelerate the bridging-oxygen-assisted deprotonation in acidic water oxidation. Nature Communications, 2022, 13, .	5.8	42
71005	Manipulation of Intrinsic Quantum Anomalous Hall Effect in 2D MoYN₂CSCl Mxene. Chinese Physics B, 0, , .	0.7	0
71006	Laser-induced enhancement of vertical polarization in ferroelectric bilayer WTe₂. Journal of Physics Condensed Matter, 2022, 34, 424003.	0.7	1
71007	Inverse spin crossover in fluorinated Fe(1,10-phenanthroline)<mml:math xmlns:mml="http://www.w3.org/1998/Math/MathML" display="inline" id="d1e331" altimg="si4.svg"><mml:msub><mml:mrow /><mml:mrow><mml:mn>2</mml:mn></mml:mrow></mml:msub></mml:math>(NCS)<mml:math xmlns:mml="http://www.w3.org/1998/Math/MathML" display="inline" id="d1e339" altimg="si4.svg"><mml:msub><mml:mrow /><mml:mrow><mml:mn>2</mml:mn></mml:mrow></mml:msu	0.9	3
71008	A large anomalous Hall conductivity induced by Weyl nodal lines in Fe70Al30. Applied Physics Letters, 2022, 121, .	1.5	2
71009	Band Gap Calculations for Thoriumâ€Doped LiCAF. Advanced Theory and Simulations, 2022, 5, .	1.3	3
71010	A stable low-symmetry T-phase of MSi₂Z₄ (M = Mo, W; Z = P, As) nanosheets with promising electronic and photovoltaic properties: Insight from first-principles calculations. Applied Physics Letters, 2022, 121, 073101.	1.5	1
71011	Role of exact exchange in the structural and electronic properties of the Î± and Î³ phases of cerium: a density functional theory study. New Journal of Physics, 2022, 24, 093032.	1.2	2
71012	<mml:math xmlns:mml="http://www.w3.org/1998/Math/MathML"><mml:mi>A</mml:mi></mml:math> -type antiferromagnetic order in the Zintl-phase insulator <mml:math xmlns:mml="http://www.w3.org/1998/Math/MathML"><mml:mrow><mml:msub><mml:mi>EuZn</mml:mi><mml:mn>2</mml:mn></mml:msub><mml:msub><mml:mi mathvariant="normal">P</mml:mi><mml:mn>2</mml:mn></mml:msub></mml:mrow></mml:math>. Physical Review B, 2022, 106, .	1.1	1

#	Article	IF	Citations
71013	Friedel Oscillations Induce Hydrogen Accumulation near theÎ£3 (111) Twin Boundaries in Î³â€²-Fe. Steel Research International, 2022, 93, .	1.0	1
71014	Improving Material Property Prediction by Leveraging the Large-Scale Computational Database and Deep Learning. Journal of Physical Chemistry C, 2022, 126, 16297-16305.	1.5	4
71015	Bi₁₂O₁₇Cl₂ with a Sextuple Bïï£¿O Layer Composed of Rockâ€Salt and Fluorite Units and its Structural Conversion through Fluorination to Enhance Photocatalytic Activity. Advanced Functional Materials, 2022, 32, .	7.8	13
71016	The stability and properties of the PtFe2 Laves phases. Physica B: Condensed Matter, 2022, , 414268.	1.3	0
71017	Unraveling the Structure and Surface Chemistry of the Phosphosulfide Phase Formed on Ni₂P under Hydrodesulfurization Reaction Conditions: A DFT Study. Journal of Physical Chemistry C, 2022, 126, 14187-14200.	1.5	5
71018	Two-dimensional antiferromagnetic semiconductor Tâ€™-MoTeI from first principles. Journal of Physics Condensed Matter, 2022, 34, 415801.	0.7	1
71019	First-principles study of (Ni, Pd, Au)-embedded VS2 monolayers for adsorption of CO, H2S, NO, NO2 and SO2. FlatChem, 2022, 36, 100421.	2.8	5
71020	DFT-1/2 and shell DFT-1/2 methods: electronic structure calculation for semiconductors at LDA complexity. Journal of Physics Condensed Matter, 2022, 34, 403001.	0.7	17
71022	On the energetics of the cubicâ€toâ€hexagonal transformations in TiAl+Mo alloys. Acta Materialia, 2022, 240, 118268.	3.8	1
71023	Stability Design Principles of Manganese-Based Oxides in Acid. Chemistry of Materials, 2022, 34, 7774-7787.	3.2	17
71024	Selective electronic excitations in nearly half-metallic Heusler alloy NiFeMnSnâ€”A Raman spectroscopic study. Applied Physics Letters, 2022, 121, .	1.5	2
71025	Interfacial Charge-Transfer Excitons Help the Photoreduction of CO₂ on TiO₂. ACS Catalysis, 2022, 12, 11024-11035.	5.5	6
71026	Metalâ€“Organic Framework Accelerated One-Step Capture and Reduction of Palladium to Catalytically Active Nanoparticles. ACS Applied Materials & Interfaces, 2022, 14, 40408-40417.	4.0	8
71027	Photocatalytic degradation of tetracycline wastewater through heterojunction based on 2D rhombic ZrMo2O8 nanosheet and nano-TiO2. Journal of Nanoparticle Research, 2022, 24, .	0.8	5
71028	Structural Stabilization of Cation-Disordered Rock-Salt Cathode Materials: Coupling between a High-Ratio Inactive Ti⁴⁺ Cation and a Mn²⁺/Mn⁴⁺ Two-Electron Redox Pair. ACS Applied Materials & Interfaces, 2022, 14, 38865-38874.	4.0	7
71029	Density functional theory study on hydrogen storage capacity of metal-embedded penta-octa-graphene. International Journal of Hydrogen Energy, 2022, 47, 32552-32564.	3.8	15
71030	Unsaturated coordination Cu-doped Ni3S2 enhanced OER activity by promoting in situ surface electro-oxidation. Journal of Materials Research, 2022, 37, 2417-2427.	1.2	2
71031	Tuning skyrmions in B20 compounds by <mml:math xmlns:mml="http://www.w3.org/1998/Math/MathML"><mml:mn>4</mml:mn><mml:mi>d</mml:mi></mml:math> and <mml:math xmlns:mml="http://www.w3.org/1998/Math/MathML"><mml:mn>5</mml:mn><mml:mi>d</mml:mi></mml:math> doping. Physical Review Materials, 2022, 6, .	0.9	2

#	Article	IF	Citations
71032	Structure and Magnetic Properties of a Nanosized Iron-Doped Bismuth Titanate Pyrochlore. Inorganic Chemistry, 2022, 61, 13369-13378.	1.9	4
71033	Raman spectrum of MXene Ti ₂ C under planar symmetrical strain: Firstâ€principles calculations. Journal of Raman Spectroscopy, 0, , .	1.2	0
71034	Suppression of Pressure-Induced Phase Transitions in a Monoclinically Distorted LiNbO₃-Type CuNbO₃ by Preference for a CuO₃ Triangular Coordination Environment. Inorganic Chemistry, 2022, 61, 12719-12725.	1.9	0
71035	Anomalous bond softening mediated by strain-induced Friedel-like oscillations in a <mml:math xmlns:mml="http://www.w3.org/1998/Math/MathML"><mml:mrow><mml:msub><mml:mi>BC</mml:mi><mml:mn>2</mml:mn></mml:mathvariant="normal">N</mml:mi></mml:mrow></mml:math> superlattice. Physical Review B, 2022, 106, .	1.1	2
71036	Luminescence from Selfâ€Trapped Excitons and Energy Transfers in Vacancyâ€Ordered Hexagonal Halide Perovskite Cs₂HfF₆ Doped with Rare Earths for Radiation Detection. Advanced Optical Materials, 2022, 10, .	3.6	5
71037	Atomic-scale 3D imaging of individual dopant atoms in an oxide semiconductor. Nature Communications, 2022, 13, .	5.8	2
71038	Platform for probing radiation transport properties of hydrogen at conditions found in the deep interiors of red dwarfs. Physics of Plasmas, 2022, 29, .	0.7	5
71039	Mixed-Functionalized <mml:math xmlns:mml="http://www.w3.org/1998/Math/MathML" display="inline" overflow="scroll"><mml:msub><mml:mi>Sc</mml:mi><mml:mn>2</mml:mn></mml:msub><mml:mi mathvariant="normal">C</mml:mi><mml:msub><mml:mi>T</mml:mi><mml:mi>x</mml:mi></mml:msub></mml:math> (<mml:math xmlns:mml="http://www.w3.org/1998/Math/MathML" display="inline") Tj ETQq1 1 0.784314 rgBT /Overlock 10 Tf 50 457	2.5	7
71040	Firstâ€Principles Exploration of 2D Benzenehexathiolate Coordination Nanosheets for Broadband Electrochromic Devices. Advanced Functional Materials, 2022, 32, .	7.8	7
71041	Coupling Intracompound Charge Transfer and Clusterâ€Centered Excited States in Cu(I) Halide Hybrids for Â Efficient White Light Emission. Advanced Optical Materials, 2022, 10, .	3.6	15
71042	Octylamineâ€Supporting Interlayer Expanded Molybdenum Diselenide as a Highâ€Power Cathode for Rechargeable Mg Batteries. Energy and Environmental Materials, 2023, 6, .	7.3	4
71043	GPU Acceleration of Large-Scale Full-Frequency GW Calculations. Journal of Chemical Theory and Computation, 2022, 18, 4690-4707.	2.3	17
71044	High-Throughput Selection and Experimental Realization of Two New Ce-Based Nitride Perovskites: CeMoN₃ and CeWN₃. Chemistry of Materials, 2022, 34, 6883-6893.	3.2	10
71045	Unveiling the mechanism for selective cleavage of C-C bonds in sugar reactions on tungsten trioxideâ€“based catalysts. Proceedings of the National Academy of Sciences of the United States of America, 2022, 119, .	3.3	12
71046	Insight into Pyroelectricity and Phase Transitions in Ferroelectrics from Nonequilibrium Approach: The Case of PbTiO₃. Advanced Theory and Simulations, 2022, 5, .	1.3	1
71047	Temperature induced modulation of resonant Raman scattering in bilayer 2H-MoS2. Scientific Reports, 2022, 12, .	1.6	7
71048	The High Photoresponse of Stressâ€Tuned MoTe₂ Optoelectronic Devices in the Telecommunication Band. Physica Status Solidi - Rapid Research Letters, 2022, 16, .	1.2	2
71049	Development of high-energy non-aqueous lithium-sulfur batteries via redox-active interlayer strategy. Nature Communications, 2022, 13, .	5.8	33

#	Article	IF	Citations
71050	Exploring CO₂ electrochemical reduction mechanism on two-dimensional metal 2,3,6,7,10,11-triphenylenehexathiolate frameworks using density functional theory. Molecular Physics, 2022, 120, .	0.8	2
71051	Dimensional Control of Chiral Antimony Halide Compounds for Enhanced Circular Dichroism. Crystal Growth and Design, 2022, 22, 5552-5558.	1.4	3
71052	Tuning the workfunction of ZnO through surface doping with Mn from first-principles simulations. Surface Science, 2022, 726, 122175.	0.8	3
71053	Theoretical Investigation of Cuâ€“Au Alloy for Carbon Dioxide Electroreduction: Cu/Au Ratio Determining C₁/C₂ Selectivity. Journal of Physical Chemistry Letters, 2022, 13, 8002-8009.	2.1	7
71054	Achieving weak anisotropy in N-type I-doped SnSe polycrystalline thermoelectric materials. Journal of the European Ceramic Society, 2022, 42, 7027-7035.	2.8	4
71055	Computational modelling on the stability of solid electrolytes in magnesium-ion batteries. Journal of Physics: Conference Series, 2022, 2298, 012009.	0.3	0
71056	Graphene/biphenylene heterostructure: Interfacial thermal conduction and thermal rectification. Applied Physics Letters, 2022, 121, .	1.5	16
71057	Highly efficient overall urea electrolysis via single-atomically active centers on layered double hydroxide. Science Bulletin, 2022, 67, 1763-1775.	4.3	63
71058	High capacity hydrogen storage on zirconium decorated Î³-graphyne: A systematic first-principles study. International Journal of Hydrogen Energy, 2023, 48, 37834-37846.	3.8	6
71059	Cation configuration in transition-metal layered oxides. Matter, 2022, 5, 3869-3882.	5.0	16
71060	Investigation on photocatalytic property of SiH/GaSe and SiH/InSe heterojunctions for photocatalytic water splitting. International Journal of Hydrogen Energy, 2022, 47, 31295-31308.	3.8	15
71061	Insights into Cation Ordering of Double Perovskite Oxides from Machine Learning and Causal Relations. Chemistry of Materials, 2022, 34, 7563-7578.	3.2	12
71062	Alkene-Catalyzed Rapid Layer-by-Layer Thinning of Black Phosphorus for Precise Nanomanufacturing. ACS Nano, 2022, 16, 13111-13122.	7.3	8
71063	Concentration Optimization of Localized Cu0 and Cu+ on Cu-Based Electrodes for Improving Electrochemical Generation of Ethanol from Carbon Dioxide. International Journal of Molecular Sciences, 2022, 23, 9373.	1.8	3
71064	Improving Alkaline Hydrogen Oxidation Activity of Palladium through Interactions with Transition-Metal Oxides. ACS Catalysis, 2022, 12, 10894-10904.	5.5	13
71065	Theoretical Design of Highly Efficient 2D Thermoelectric Device Based on Janus MoSSe and Graphene Heterostructure. ACS Applied Energy Materials, 2022, 5, 9581-9586.	2.5	7
71066	Symmetry of ferroelectric switching and domain walls in hafnium dioxide. Physical Review B, 2022, 106, .	1.1	3
71067	Suppressing Polysulfides Shuttling and Promoting Sulfur Utilization via Transition Metal and Nitrogen Co-Doping on Graphdiyne Cathodes of Lithium-Sulfur Batteries: A First-Principles Modeling. ACS Applied Energy Materials, 2022, 5, 9722-9732.	2.5	3

#	Article	IF	Citations
71068	Relativistic Effects Stabilize Unusual Gold(II) Sulfate Structure via Aurophilic Interactions. Inorganic Chemistry, 2022, 61, 13077-13084.	1.9	2
71069	Tuning the local electronic structure of oxygen vacancies over copper-doped zinc oxide for efficient CO2 electroreduction. EScience, 2022, 2, 518-528.	25.0	47
71070	In-situ doping nickel single atoms in two-dimensional MXenes analogue support for room temperature NO2 sensing. Nano Research, 2022, 15, 9544-9553.	5.8	6
71071	Highâ€Pressure Crystal Structures of Pb₂CO₄ and PbC₂O₅ with Tetrahedral [CO₄] and Pyrocarbonate [C₂O₅] atomic groups. ChemistrySelect, 2022, 7, .	0.7	4
71072	Two-dimensional <mml:math xmlns:mml="http://www.w3.org/1998/Math/MathML"><mml:msub><mml:mi>CP</mml:mi><mml:mn>2</mml:mn></mml:msub></mml: and <mml:math xmlns:mml="http://www.w3.org/1998/Math/MathML"><mml:mrow><mml:msub><mml:mi>Li</mml:mi><mml:mi>x</mml:mi></mml:ms		

#	Article	IF	Citations
71088	Sulfur Vacancy-Enriched Rhombohedral ZnIn₂S₄ Nanosheets for Highly Efficient Photocatalytic Overall Water Splitting under Visible Light Irradiation. ACS Applied Energy Materials, 2022, 5, 10187-10195.	2.5	23
71089	Mechanistic Insights and Rational Design of Ca-Doped CeO₂ Catalyst for Acetic Acid Ketonization. ACS Sustainable Chemistry and Engineering, 2022, 10, 11068-11077.	3.2	3
71090	Direct Determination of Band Gap of Defects in a Wide Band Gap Semiconductor. ACS Applied Materials & Interfaces, 2022, 14, 36875-36881.	4.0	7
71091	Alginateâ€“Sodium Sulfate Decahydrate Phase Change Composite with Extended Stability. ACS Applied Polymer Materials, 2022, 4, 6563-6571.	2.0	8
71092	Prediction of the ferroelastic and negative Poissonâ€™s ratio of a two-dimensional Î±-CaX (Xâ€‰=â€‰S, Se) monolayer. European Physical Journal Plus, 2022, 137, .	1.2	1
71093	Room-temperature ferromagnetism in two-dimensional <mml:math xmlns:mml="http://www.w3.org/1998/Math/MathML"><mml:msub><mml:mi>CrBr</mml:mi><mml:mn>3</mml:mn></mml:msub></mml Physical Review Materials, 2022, 6, .	0.9	1
71094	Interfacial Embedding for Highâ€Efficiency and Stable Methylammoniumâ€Free Perovskite Solar Cells with Fluoroarene Hydrazine. Advanced Energy Materials, 2022, 12, .	10.2	30
71095	Electrically tunable two-dimensional heterojunctions for miniaturized near-infrared spectrometers. Nature Communications, 2022, 13, .	5.8	36
71096	Evolution of Weyl nodes in Ni-doped thallium niobate pyrochlore Tl2â^'xNixNb2O7. Science China: Physics, Mechanics and Astronomy, 2022, 65, .	2.0	3
71097	Realization of unpinned two-dimensional dirac states in antimony atomic layers. Nature Communications, 2022, 13, .	5.8	12
71098	Strong Optical Excitation and High Thermoelectric Performance in 2D Holeyâ€Phosphorene Monolayer. Energy Technology, 0, , 2200400.	1.8	2
71099	Liquid-Phase Effects on Adsorption Processes in Heterogeneous Catalysis. Jacs Au, 2022, 2, 2119-2134.	3.6	10
71100	Dzyaloshinskii-Moriya interaction induced magnetoelectric coupling in a tetrahedral molecular spin-frustrated system. Physical Review B, 2022, 106, .	1.1	2
71101	First Principles Determination of the Potential-of-Zero-Charge in an Alumina-Coated Aluminum/Water Interface Model for Corrosion Applications. Journal of the Electrochemical Society, 2022, 169, 081502.	1.3	1
71102	Deducing surface chemistry and annealing conditions from observed nanoparticle shapes: A study of scandate cathodes. Applied Surface Science, 2022, 605, 154541.	3.1	1
71103	Simple machine-learned interatomic potentials for complex alloys. Physical Review Materials, 2022, 6, .	0.9	7
71104	First- and second-order magneto-optical effects and intrinsically anomalous transport in the two-dimensional van der Waals layered magnets <mml:math		

#	Article	IF	Citations
71107	Deep reaction network exploration at a heterogeneous catalytic interface. Nature Communications, 2022, 13, .	5.8	12
71108	Prediction of surface termination preference of out-of-plane ordered double-transition metal MXenes (o-MXenes) from first-principles calculations. Journal of Physics: Conference Series, 2022, 2321, 012012.	0.3	1
71110	Interfacial Space Charge Enhanced Sodium Storage in a Zeroâ€Strain Cerium Niobite Perovskite Anode. Advanced Functional Materials, 2022, 32, .	7.8	11
71111	Oxygen Healing and CO₂/H₂/Anisole Dissociation on Reduced Molybdenum Oxide Surfaces Studied by Density Functional Theory. ChemPhysChem, 2022, 23, .	1.0	1
71112	Effective hamiltonian of crystal field method for periodic systems containing transition metals. Molecular Physics, 0, , .	0.8	2
71113	Dimensional Transformation of Molecular Magnetic Materials. ACS Nano, 2022, 16, 13232-13240.	7.3	0
71114	WSe₂â€“VSe₂ Alloyed Nanosheets to Enhance the Catalytic Performance of Hydrogen Evolution Reaction. ACS Nano, 2022, 16, 12569-12579.	7.3	19
71115	Electron-Injection and Atomic-Interface Engineering toward Stabilized Defected 1T-Rich MoS₂ as High Rate Anode for Sodium Storage. ACS Nano, 2022, 16, 12425-12436.	7.3	34
71116	Theoretical Insights on the Comparison of Li-Ion Conductivity in Halide Superionic Conductors Li₃MCl₆, Li₂M_{2/3}Cl₄, and LiMCl₄ (M = Y, Sc, Al, and Sm). Journal of Physical Chemistry C, 2022, 126, 13105-13113.	1.5	10
71117	Tetrathiafulvalene Derivatives as Hole-Transporting Materials in Perovskite Solar Cell. Journal of Physical Chemistry A, 2022, 126, 5079-5088.	1.1	5
71118	Heusler alloy catalysts for electrochemical CO2 reduction. Journal of Chemical Physics, 2022, 157, .	1.2	6
71119	Nitrogen Electroreduction on Boropheneâ€Supported Atomic and Diatomic Transition Metals: Stability, Activity and Selectivity Improvements via Defectâ€Engineering. ChemSusChem, 2022, 15, .	3.6	3
71120	Role of coordination site in governing the structural, electronic and optical properties of Ca-doped strontium barium niobate. Physica Scripta, 2022, 97, 095814.	1.2	0
71121	Effect of ReÂand Ta on self-trapping of helium in tungsten: a first-principles calculation. Nuclear Fusion, 2022, 62, 096017.	1.6	1
71122	Band lineup at hexagonal<mml:math xmlns:mml="http://www.w3.org/1998/Math/MathML"><mml:msub><mml:mrow><mml:mi>Si</mml:mi></mml:mrow><mml:mi>x</mml:mi></mml:msub></mml:math>/3C-SiC(111) heterojunction. Physical Review B, 2022, 106, .	1.1	1
71123	Spin-Filter Magnetic Tunnel Junctions Based on A-Type Antiferromagnetic CrSBr with Giant Tunnel Magnetoresistance. Magnetochemistry, 2022, 8, 89.	1.0	4
71125	Changes in electronic and optical characteristics of halogenâ€“alkali adsorbed WSe2 monolayer. Journal of Materials Science: Materials in Electronics, 0, , .	1.1	0
71126	Large Memory Window of van der Waals Heterostructure Devices Based on MOCVDâ€Grown 2D Layered Ge₄Se₉. Advanced Materials, 2022, 34, .	11.1	16

#	Article	IF	Citations
71127	â€œMagicâ€•Molecules and a New Look at Chemical Diversity of Hydrocarbons. Journal of Physical Chemistry Letters, 2022, 13, 7600-7606.	2.1	5
71128	Probing Heterodimer and Multiadsorbate Hydrocarbon Adsorption Trends in the MFI Framework. Journal of Physical Chemistry C, 2022, 126, 13894-13904.	1.5	1
71129	Unveiling Interstitial Anionic Electron-Driven Ultrahigh K-Ion Storage Capacity in a Novel Two-Dimensional Electride Exemplified by Sc₃Si₂. Journal of Physical Chemistry Letters, 2022, 13, 7439-7447.	2.1	14
71130	Enabling robust structural and interfacial stability of micron-Si anode toward high-performance liquid and solid-state lithium-ion batteries. Energy Storage Materials, 2022, 52, 547-561.	9.5	80
71131	New insights into the mechanical and thermal properties of UN1-C from first-principles calculations. Journal of Nuclear Materials, 2022, 571, 153991.	1.3	3
71132	Biomass-derived carbon fiber with atomic Mn-N4 sites for efficient electrocatalytic oxygen reduction reaction. Journal of Materials Science, 2022, 57, 15943-15953.	1.7	2
71133	High-Pressure Structural Transformation Pathway and Electronic Properties of AgGaTe₂: Ab Initio Evolutionary Structural Searching. Journal of Physical Chemistry C, 2022, 126, 14236-14244.	1.5	1
71134	Metalâ€“Support Interaction and Charge Distribution in Ceria-Supported Au Particles Exposed to CO. Chemistry of Materials, 0, , .	3.2	6
71135	Point Defects Control Guest Molecule Diffusion in the 1D Pores of Zn(tbip). Journal of Physical Chemistry C, 2022, 126, 14321-14328.	1.5	6
71136	The Piezoelectricity and Dopingâ€Induced Ferromagnetism of Janus XYP ₂ (X/Y = Si, Ge, Sn,) Tj ETQq1 1 0.784314 rgBT /	0.7	0
71137	Effect of Co and Cr on the Stability of Strengthening Phases in Nickelbase Superalloys. Crystals, 2022, 12, 1084.	1.0	2
71138	Controlled growth of 2D structured Cu2WS4 nanoflakes for high-performance all-solid-state supercapacitors. Journal of Electroanalytical Chemistry, 2022, 922, 116718.	1.9	9
71139	Surface and Trapping Energies as Predictors for the Photocatalytic Degradation of Aromatic Organic Pollutants. Journal of Physical Chemistry C, 2022, 126, 14859-14877.	1.5	6
71140	Intermetallic compounds RE ₂Ga₂Mg (REÂ=ÂTbâ€“Tm, Lu) with Mo₂B₂Fe-type structure. Zeitschrift Fur Naturforschung - Section B Journal of Chemical Sciences, 2022, 77, 693-702.	0.3	3
71141	Strain modulated electronic and optical properties of laterally stitched MoSi2N4/XSi2N4 (X=W, Ti) 2D heterostructures. Physica E: Low-Dimensional Systems and Nanostructures, 2022, 144, 115471.	1.3	12
71142	Tuning the electronic and optical properties of SrTiO3 for optoelectronic and photocatalytic applications by plasmonic-metal doping: a DFT-computation. Optical and Quantum Electronics, 2022, 54, .	1.5	4
71143	Singleâ€Step Synthesis of Feâ€"Fe₃O₄ Catalyst for Highly Efficient and Selective Electrochemical Nitrogen Reduction. ChemSusChem, 2022, 15, .	3.6	6
71144	First-principles studies of the mixed-dimensional van der Waals heterostructures of graphene/MnF4. Journal of Applied Physics, 2022, 132, .	1.1	0

#	Article	IF	Citations
71145	Vacancy localization effects on <mml:math xmlns:mml="http://www.w3.org/1998/Math/MathML"><mml:msub><mml:mi mathvariant="normal">MX</mml:mi><mml:mn>2</mml:mn></mml:msub></mml:math> transition-metal dichalcogenides: A systematic ab initio study. Physical Review Materials, 2022, 6, .	0.9	5
71146	Ab initio inspection of thermophysical experiments for zirconium near melting. Journal of Applied Physics, 2022, 132, .	1.1	6
71147	Ultrawideband and High-Resolution Terahertz Spectroscopy: Structural Identification of Glucose. Photonics, 2022, 9, 602.	0.9	4
71148	Computation-accelerated discovery of the K2NiF4-type oxyhydrides combing density functional theory and machine learning approach. Frontiers in Chemistry, 0, 10, .	1.8	0
71149	A computational study of electrical contacts to all-inorganic perovskite CsPbBr₃. Nanotechnology, 2022, 33, 475701.	1.3	3
71150	Possible coexistence of short-range resonating valence bond and long-range stripe correlations in the spatially anisotropic triangular-lattice quantum magnet <mml:math xmlns:mml="http://www.w3.org/1998/Math/MathML"><mml:msub><mml:mi mathvariant="normal">Cu</mml:mi><mml:mn>2</mml:mn></mml:msub></mml:math> (OH) <mml:math xmlns:mml="http://www.w3.org/1998/Math/MathML"><mml:msub><mml:mrow /><mml:mn>3</mml:mn></mml:msub><mml:msub><mml:mi mathvariant="normal">NO</mml:mi><mml:m	1.1	3
71151	Ab initio study of shock-compressed copper. Physical Review B, 2022, 106, .	1.1	9
71152	A polymer electrolyte design enables ultralow-work-function electrode for high-performance optoelectronics. Nature Communications, 2022, 13, .	5.8	7
71153	CO₂ Laserâ€Induced Graphene with an Appropriate Oxygen Species as an Efficient Electrocatalyst for Hydrogen Peroxide Synthesis. Chemistry - A European Journal, 2022, 28, .	1.7	11
71154	Grand Canonical Monte Carlo simulation study hydrogen storage by Li-decorated pha-graphene. Chinese Physics B, 0, , .	0.7	0
71155	Correct and Accurate Polymorphic Energy Ordering of Transition-Metal Monoxides Obtained from Semilocal and Onsite-Hybrid Exchange-Correlation Approximations. Journal of Physical Chemistry C, 2022, 126, 14650-14660.	1.5	4
71156	Hydrogen Activation by C ₂ H ₂ Acting as a Substrate Molecule on Atomically Dispersed Catalysts for the Semiâ€hydrogenation of C ₂ H ₂. ChemistrySelect, 2022, 7, .	0.7	0
71157	First-Principles Calculations of the Structural, Electronic, Optical, and Mechanical Properties of 21 Pyrophosphate Crystals. Crystals, 2022, 12, 1139.	1.0	3
71158	In-situ construction of a thermodynamically stabilized interface on the surface of single crystalline Ni-rich cathode materials via a one-step molten-salt route. Nano Research, 2023, 16, 6771-6779.	5.8	6
71159	Electrochemical Conversion of Alcohols into Acidic Commodities on Nickel Sulfide Nanoparticles. Inorganic Chemistry, 2022, 61, 13433-13441.	1.9	9
71160	Structural, electronic, and magnetic properties of <mml:math xmlns:mml="http://www.w3.org/1998/Math/MathML"><mml:msub><mml:mi>CrTe</mml:mi><mml:mn>2</mml:mn></mml:msub></mml:math> Physical Review Materials, 2022, 6, .	3.1	11
71161	Effect of O-Vacancy Concentration and Proximity on Electronic Metalâ€“Support Interactions: Ru/ZrO₂ Catalysts. ACS Catalysis, 2022, 12, 10065-10079.	5.5	5
71162	ZnO with Controllable Oxygen Vacancies for Photocatalytic Nitrogen Oxide Removal. ACS Catalysis, 2022, 12, 10004-10017.	5.5	45

#	Article	IF	Citations
71163	Clarifying the zeolitic imidazolate framework effect on superior electrochemical properties of hydrogen storage alloys. Electrochimica Acta, 2022, 430, 141054.	2.6	0
71164	Biphenylene: A Twoâ^'Dimensional Grapheneâ^'Based Coating with Superior Antiâ^'Corrosion Performance. Materials, 2022, 15, 5675.	1.3	4
71165	Interactions of Water with Pristine and Defective MoS₂. Langmuir, 2022, 38, 10419-10429.	1.6	4
71166	Ab Initio Study of Structure and Transport Properties of Warm Dense Nitric Oxide. Inorganics, 2022, 10, 120.	1.2	0
71167	Revealing the role of Î£3{112} Si grain boundary local structures in impurity segregation. Journal of Applied Physics, 2022, 132, 085102.	1.1	0
71168	Sulfur-dopant-promoted electrocatalytic reduction of nitrate by a self-supported iron cathode: Selectivity, stability, and underlying mechanism. Applied Catalysis B: Environmental, 2022, 319, 121862.	10.8	19
71169	Single transition metal atom stabilized on double metal carbide MXenes for hydrogen evolution reaction: a density functional theory study. Journal Physics D: Applied Physics, 0, , .	1.3	2
71170	Facilitating ab initio configurational sampling of multicomponent solids using an on-lattice neural network model and active learning. Journal of Chemical Physics, 2022, 157, .	1.2	5
71171	Pressure-induced superconductivity in quasi-one-dimensional semimetal <mml:math xmlns:mml="http://www.w3.org/1998/Math/MathML"><mml:mrow><mml:msub><mml:mi>Ta</mml:mi><mml:mn>2</mml:mn></mml:msub><mml:mi>P</mml:mi><mml:mn></mml:mn></mml:mrow></mml:math>. Physical Review Materials, 2022, 6, .	2.4	5
71172	Entropy and heterogeneous interface engineering promote the low thermal conductivity in SnTe-based thermoelectric materials. Applied Physics A: Materials Science and Processing, 2022, 128, .	1.1	2
71173	Fe₂O₃/MoO₃@NG Heterostructure Enables High Pseudocapacitance and Fast Electrochemical Reaction Kinetics for Lithium-Ion Batteries. ACS Applied Materials & Interfaces, 2022, 14, 37747-37758.	4.0	11
71174	Hardness of molecules and bandgap of solids from a generalized gradient approximation exchange energy functional. Journal of Chemical Physics, 2022, 157, .	1.2	0
71175	Role of bimetallic Auâ€“Ir subnanometer clusters mediating O₂ adsorption and dissociation on anatase TiO₂ (101). Journal of Chemical Physics, 2022, 157, 084309.	1.2	0
71176	Semiconductive vertical graphene nanoribbons self-assembled on diamond (100) surface by oxidation: a DFT study. Applied Surface Science, 2022, , 154646.	3.1	1
71177	Regulating Niâ€“Oâ€“V bond in nickel doped vanadium catalysts for propane dehydrogenation. Applied Catalysis A: General, 2022, 644, 118819.	2.2	0
71178	Effect of oxidation on mechanical properties of Ni/Cu interface: A density functional theory study. Materials Today Communications, 2022, 33, 104307.	0.9	3
71179	Coherent Picture on the Pure Spin Transport between <mml:math xmlns:mml="http://www.w3.org/1998/Math/MathML" display="inline"><mml:mrow><mml:mi>Ag</mml:mi><mml:mo>/</mml:mo><mml:mi>Bi</mml:mi></mml:mrow></mml:math> and Ferromagnets. Physical Review Letters, 2022, 129, .	2.9	2
71180	Diverse Functions of Oxygen Vacancies for Oxygen Ion Conduction. ACS Applied Energy Materials, 2022, 5, 11122-11132.	2.5	7

#	Article	IF	Citations
71181	Chemical stability and degradation mechanism of Mg3Sb2-Bi thermoelectrics towards room-temperature applications. Acta Materialia, 2022, 239, 118301.	3.8	12
71182	Effects of charging, strain, and doping on the interaction between H2 and nitrogen-rich Penta-CN2 sheet. International Journal of Hydrogen Energy, 2022, 47, 34183-34194.	3.8	5
71183	Broad Elastic Softening of (Mg,Fe)O Ferropericlase Across the Iron Spin Crossover and a Mixedâ€Spin Lower Mantle. Journal of Geophysical Research: Solid Earth, 2022, 127, .	1.4	3
71184	Self-Enhancing Photoelectrochemical Properties in van der Waals Ferroelectric CuInP₂S₆ by Photoassisted Acid Hydrolysis. ACS Applied Materials & Interfaces, 2022, 14, 40126-40135.	4.0	5
71185	As-Li electrides under high pressure: Superconductivity, plastic, and superionic states. Physical Review B, 2022, 106, .	1.1	10
71186	The structure of sc16â€‰GaP obtained at 17.5â€‰GPa and 1400â€‰K. High Pressure Research, 0, , 1-9.	0.4	0
71187	Nitrogen-tailored quasiparticle energy gaps of polyynes. Chinese Physics B, 0, , .	0.7	0
71188	Self-energy corrected DFT-NEGF for conductance in molecular junctions: an accurate and efficient implementation for TRANSIESTA package applied to Au electrodes. Journal of Physics Condensed Matter, 2022, 34, 435901.	0.7	2
71189	Interband Transitions and Critical Points of Singleâ€Crystal Thoria Compared with Urania. Physica Status Solidi (B): Basic Research, 0, , 2200238.	0.7	1
71190	Boosting Electrical Response toward Trace Volatile Organic Compounds Molecules via Pulsed Temperature Modulation of Pt Anchored WO₃ Chemiresistor. Small Methods, 2022, 6, .	4.6	11
71191	Electronic State Coupling Between Structural Deformation and Surficial Defects in Coâ€Layered LaCoSi for Hydrogen Evolution Reaction. Physica Status Solidi - Rapid Research Letters, 0, , 2200287.	1.2	1
71192	Facile preparation and efficient MnxCoy porous nanosheets for the sustainable catalytic process of soot. Green Energy and Environment, 2024, 9, 516-528.	4.7	2
71193	Efficient Control of the Shuttle Effect in Sodiumâ€“Sulfur Batteries with Functionalized Nanoporous Graphenes. ACS Applied Nano Materials, 0, , .	2.4	5
71194	Noncentrosymmetric characteristics of defects on <mml:math xmlns:mml="http://www.w3.org/1998/Math/MathML"><mml:msub><mml:mi>WTe</mml:mi><mml:mn>2</mml:mn></mml:msub></mml:math> Physical Review B, 2022, 106, .	1.1	1
71195	Facet-Controlled LiMn2O4/C as Deionization Electrode with Enhanced Stability and High Desalination Performance. Nano-Micro Letters, 2022, 14, .	14.4	20
71196	N-Doped Carbon as a Promoted Substrate for Ir Nanoclusters toward Hydrogen Oxidation in Alkaline Electrolytes. Inorganic Chemistry, 2022, 61, 14187-14194.	1.9	4
71197	Noble-Nanoparticle-Decorated Ti₃C₂T_x MXenes for Highly Sensitive Volatile Organic Compound Detection. ACS Omega, 2022, 7, 29195-29203.	1.6	13
71198	Boosting Electrochemical CO₂ Reduction to Methane via Tuning Oxygen Vacancy Concentration and Surface Termination on a Copper/Ceria Catalyst. ACS Catalysis, 2022, 12, 10973-10983.	5.5	34

#	Article	IF	Citations
71199	Dynamical Study of Adsorbate-Induced Restructuring Kinetics in Bimetallic Catalysts Using the PdAu(111) Model System. Journal of the American Chemical Society, 2022, 144, 15132-15142.	6.6	13
71200	Interfacial electronic interaction enabling exposed Pt(110) facets with high specific activity in hydrogen evolution reaction. Nano Research, 2023, 16, 174-180.	5.8	12
71201	Study on the magnetic origin in p-type ferromagnetic semiconductor (Ga,Fe)Sb: ab initio calculations. Physica Scripta, 2022, 97, 095813.	1.2	3
71202	Self-Assembled Decanethiolate Monolayers on Au(001): Expanding the Family of Known Phases. Langmuir, 2022, 38, 10202-10215.	1.6	1
71203	Revealing Phosphorus Nitrides up to the Megabar Regime: Synthesis of Î±â€²â€²P₃N_{5,} Î˜â€²P₃N₅ and PN₂. Chemistry - A European Journal, 2022, 28, .	1.7	6
71204	Activating multisite high-entropy alloy nanocrystals via enriching Mâ€“pyridinic Nâ€“C bonds for superior electrocatalytic hydrogen evolution. Science Bulletin, 2022, 67, 1890-1897.	4.3	20
71205	Heterostructured Bi₂S₃/MoS₂ Nanoarrays for Efficient Electrocatalytic Nitrate Reduction to Ammonia Under Ambient Conditions. ACS Applied Materials & Interfaces, 2022, 14, 38835-38843.	4.0	17
71206	Trinuclear Magnesium Imidazolate Borohydride Complex. Inorganic Chemistry, 2022, 61, 12708-12718.	1.9	0
71207	Nâ€stabilized metal single atoms enabled rich defects for nobleâ€metal alloy toward superior water reduction. EcoMat, 2023, 5, .	6.8	3
71208	Pressure-induced metallization in the absence of a structural transition in the layered ferromagnetic insulator <mml:math xmlns:mml="http://www.w3.org/1998/Math/MathML"><mml:mrow><mml:msub><mml:mi>Cr</mml:mi><mml:mn>2</mml:mn></mml:m Physical Review B, 2022, 106, .	1.1	3
71209	Ab initio study of Li-Mg-B superconductors. Physical Review Materials, 2022, 6, .	0.9	6
71210	Functional Pyromellitic Diimide as a Corrosion Inhibitor for Galvanized Steel: An Atomic-Scale Engineering. ACS Omega, 2022, 7, 27116-27125.	1.6	1
71211	Enhancing the thermionic electron emission performance of hafnium with nanocluster doping. Applied Physics Letters, 2022, 121, 061603.	1.5	0
71212	Bromo- and iodo-bridged building units in metal-organic frameworks for enhanced carrier transport and CO2 photoreduction by water vapor. Nature Communications, 2022, 13, .	5.8	42
71213	Hydrothermally decorated robust bimetallic sulfides with heterojunction interfaces for efficient hydrogen generation. International Journal of Hydrogen Energy, 2022, 47, 40254-40263.	3.8	3
71214	Unraveling the Electronic Effect of Transition-Metal Dopants (M = Fe, Co, Ni, and Cu) and Graphene Substrate on Platinumâ€“Transition Metal Dimers for Hydrogen Evolution Reaction. Inorganic Chemistry, 2022, 61, 13210-13217.	1.9	8
71215	Band structural and absorption characteristics of antimonene/bismuthene monolayer heterojunction calculated by first-principles. Frontiers in Chemistry, 0, 10, .	1.8	0
71216	Temperature- and Field-Induced Transformation of the Magnetic State in Co_{2.5}Ge_{0.5}BO₅. Inorganic Chemistry, 2022, 61, 13034-13046.	1.9	0

#	Article	IF	Citations
71217	Dramatic Enhancement of Rare-Earth Metalâ€“Organic Framework Stability Via Metal Cluster Fluorination. Jacs Au, 2022, 2, 1889-1898.	3.6	10
71218	Suppressing Charged Cation Antisites via Se Vapor Annealing Enables pâ€Type Dopability in AgBiSe₂â€“SnSe Thermoelectrics. Advanced Materials, 2022, 34, .	11.1	7
71219	Bond-order potential for the surface-terminated titanium carbide MXene monolayers <mml:math xmlns:mml="http://www.w3.org/1998/Math/MathML"><mml:msub><mml:mi mathvariant="normal">Ti</mml:mi><mml:mrow><mml:mi>n</mml:mi><mml:mo>+</mml:mo><mml:mn>1</mml:mn></mml:mrow></m mathvariant="normal">C</mml:mi><mml:mi>n</mml:mi></mml:msub><mml:msub><mml:mi>T</mml:mi><mml:mi>x</mml:mi></mml:m		

#	Article	IF	Citations
71235	Yttrium doped covalent triazine frameworks as promising reversible hydrogen storage material: DFT investigations. International Journal of Hydrogen Energy, 2022, 47, 30567-30579.	3.8	17
71236	Structural evolution and strain generation of derived-Cu catalysts during CO2 electroreduction. Nature Communications, 2022, 13, .	5.8	55
71237	HSH-carbon: A novel sp2â€“sp3 carbon allotrope with an ultrawide energy gap. Frontiers of Physics, 2022, 17, .	2.4	5
71238	Low and Anisotropic Tensile Strength and Thermal Conductivity in the Single-Layer Fullerene Network Predicted by Machine-Learning Interatomic Potentials. Coatings, 2022, 12, 1171.	1.2	13
71239	Metal-oxygen bonding nanoarchitectonics for regulation of oxygen evolution reaction performance in FeNi-codoped CoOOH. International Journal of Hydrogen Energy, 2022, 47, 29762-29770.	3.8	8
71240	Orthogonal antiferromagnetism to canted ferromagnetism in CaCo3Ti4O12 quadruple perovskite driven by underlying kagome lattices. Communications Materials, 2022, 3, .	2.9	2
71241	Anharmonic thermodynamic properties and phase boundary across the postperovskite transition in <mml:math xmlns:mml="http://www.w3.org/1998/Math/MathML"><mml:mrow><mml:mi>MgSi</mml:mi><mml:msub><mml:mi mathvariant="normal">O</mml:mi><mml:mn>3</mml:mn></mml:msub></mml:mrow></mml:math>. Physical Review B, 2022, 106, .	3.1	6
71242	Ab initio investigation of the magnetic and ferroelectric properties of <mml:math xmlns:mml="http://www.w3.org/1998/Math/MathML"><mml:msub><mml:mi>BaCuF</mml:mi><mml:mn>4</mml:mn></mml:msub></mml:math> under hydrostatic pressure. Physical Review B, 2022, 106, .	3.2	0
71243	Toward Computing Accurate Free Energies in Heterogeneous Catalysis: a Case Study for Adsorbed Isobutene in H-ZSM-5. ACS Physical Chemistry Au, 2022, 2, 399-406.	1.9	11
71244	Dopant-driven Interlayer Electronic State Coupling in Layered Bi2SeO2 Surface for Accelerating CO2 Reduction to HCOOH. Catalysis Letters, 2023, 153, 1839-1846.	1.4	1
71245	Direct observation of geometric and sliding ferroelectricity in an amphidynamic crystal. Nature Materials, 2022, 21, 1158-1164.	13.3	71
71246	Magnetic and Electronic Properties of <mml:math xmlns:mml="http://www.w3.org/1998/Math/MathML" display="inline" overflow="scroll"><mml:mrow><mml:mi>Al</mml:mi><mml:mi mathvariant="normal">N</mml:mi></mml:mrow><mml:mo>/</mml:mo><mml:msub><mml:mi>VSe</mml:mi><mml:mn>2</mml:mn></mml:msub></mml:math> van der Waals Heterostructures from Combined First-Principles and SchrÃ¶dinger-Poisson Simulations. Physical Review Applied, 2022, 18, .	4.5	5
71247	Unraveling the Co(IV)-Mediated Oxidation Mechanism in a Co₃O₄/PMS-Based Hierarchical Reactor: Toward Efficient Catalytic Degradation of Aromatic Pollutants. ACS ES&T Engineering, 2022, 2, 1836-1846.	3.7	23
71248	Role of Sr doping and external strain on relieving bottleneck of oxygen diffusion in La2â^'xSrxCuO4â^'Î´. Scientific Reports, 2022, 12, .	1.6	1
71249	First-principles Analysis of Stearic Acid Adsorption on Calcite (104) Surface. E-Journal of Surface Science and Nanotechnology, 2022, , .	0.1	0
71250	Fundamental investigations on the sodium-ion transport properties of mixed polyanion solid-state battery electrolytes. Nature Communications, 2022, 13, .	5.8	26
71251	Hydrogen Bond-Driven Orderâ€“Disorder Phase Transition in the Near-Room-Temperature Nonlinear Optical Switch [Ag(NH₃)₂]₂SO₄. Jacs Au, 2022, 2, 2059-2067.	3.6	13
71252	Defective Boron Nitride Inducing the Lithiumâ€ion Migration on the Subâ€Surface of LiBH₄. Advanced Functional Materials, 2022, 32, .	7.8	5

#	Article	IF	Citations
71253	Improving the Energetic Stability and Electrocatalytic Performance of Au/WSSe Single-Atom Catalyst with Tensile Strain. Nanomaterials, 2022, 12, 2793.	1.9	8
71254	Accurate and Efficient Calculation of the Solution Enthalpy and Diffusivity of Solutes in Liquid Metals Using Machine Learning Potential. Journal of Chemical Theory and Computation, 2022, 18, 5568-5576.	2.3	2
71255	A tungsten deep neural-network potential for simulating mechanical property degradation under fusion service environment. Nuclear Fusion, 2022, 62, 126013.	1.6	13
71256	Porous lanthanide metalâ€“organic frameworks with metallic conductivity. Proceedings of the National Academy of Sciences of the United States of America, 2022, 119, .	3.3	24
71257	Critical Evaluation and Thermodynamic Modeling of the Li-Se and Na-Se Binary Systems Using Combined CALPHAD and First-Principles Calculations Method. Metals, 2022, 12, 1349.	1.0	1
71258	Tuning Electronic Structures of Transition Metal Carbides to Boost Oxygen Evolution Reactions in Acidic Medium. ACS Nano, 2022, 16, 13834-13844.	7.3	31
71259	Evidence for Topological Features in the Electronic and Phononic Bands of ZGeSb (Z = Hf, Zr, Ti) Class of Compounds. Journal of Physics Condensed Matter, 0, , .	0.7	0
71260	Understanding the Effect of Ni-Substitution on the Oxygen Evolution Reaction of (100) IrO₂ Surfaces. ACS Catalysis, 2022, 12, 10961-10972.	5.5	3
71261	Boosting electrochemical nitrate-ammonia conversion via organic ligands-tuned proton transfer. Nano Energy, 2022, 103, 107705.	8.2	16
71262	Perovskite superlattices with efficient carrier dynamics. Nature, 2022, 608, 317-323.	13.7	66
71263	Fast-charging aluminiumâ€“chalcogen batteries resistant to dendritic shorting. Nature, 2022, 608, 704-711.	13.7	77
71264	Auger Processes and Excited State Dynamics in WS₂/Graphene Heterostructures: A First-Principles Perspective. Journal of Physical Chemistry Letters, 2022, 13, 7371-7379.	2.1	5
71265	Doping Effect and Li-Ion Conduction Mechanism of ALi₆XO₆ (A = K or Rb and X = Pentavalent): A First-Principles Study. Journal of Physical Chemistry C, 2022, 126, 13548-13559.	1.5	0
71266	Phase Stability and Electronic Properties of Hybrid Organicâ€“Inorganic Perovskite Solid Solution (CH(NH₂)₂)_x(CH₃NH₃)_{1â€“x}Pb(Br<sub> as a Function of Composition. Journal of Physical Chemistry C, 2022, 126, 13640-13648.	1.5	
71267	Deep Insights into Complicated Superdislocation Dissociation and Core Properties of Dislocation in L1 ₂ â€Al ₃ RE Compounds: A Comprehensive Firstâ€Principles Study. Physica Status Solidi (B): Basic Research, 0, , 2200211.	0.7	0
71268	The First-Principle Study on Tuning Optical Properties of MA2Z4 by Cr Replacement of Mo Atoms in MoSi2N4. Nanomaterials, 2022, 12, 2822.	1.9	4
71269	Electrochemical nitrogen reduction reaction on the precise number of Mo atoms anchored biphenylene. Molecular Catalysis, 2022, 530, 112579.	1.0	4
71270	Pressure-induced phase transitions and mechanical properties of ternary nanolaminated carbide Mo2Ga2C from first-principles calculations. Journal of Materials Research and Technology, 2022, 20, 1699-1707.	2.6	0

#	Article	IF	Citations
71271	First-principles study on the electronic structure transition of Î²-UH3 under high pressure. Matter and Radiation at Extremes, 2022, 7, .	1.5	4
71272	Interstitial hydrogen atoms in W-nitride compounds promoting the formation of atomic vacancies in nuclear fusion reactors. Nuclear Materials and Energy, 2022, 32, 101229.	0.6	3
71273	DFT study on the electrochemical synthesis of ammonia over Mo2C(121) with N-doping. Molecular Catalysis, 2022, 530, 112637.	1.0	1
71274	The role of water in the catalytic CO2 binding by alkaline earth Y faujasitÐµs. Microporous and Mesoporous Materials, 2022, 343, 112125.	2.2	2
71275	First-principles study of the structural, electronic, dynamical, and mechanical properties of Pdâ€“Nb binary systems. Calphad: Computer Coupling of Phase Diagrams and Thermochemistry, 2022, 78, 102457.	0.7	0
71276	Three-dimensional reduction graphene oxide (rGO) supported ScFeO3 for enhancing microwave absorption properties. Materials Characterization, 2022, 191, 112168.	1.9	8
71277	Structure and stability of van der Waals layered group-IV monochalcogenides. Journal of Vacuum Science and Technology A: Vacuum, Surfaces and Films, 2022, 40, .	0.9	3
71278	Surface functionalization effect on physical properties and quantum capacitance of Ca2C MXenes. FlatChem, 2022, 35, 100414.	2.8	9
71279	Species transformation and removal mechanism of various iodine species at the Bi2O3@MnO2 interface. Water Research, 2022, 223, 118965.	5.3	4
71280	Revealing the effects of Nb micro-alloying on microstructure and mechanical properties of FeCrAl thin films: Experimental and computational investigations. Surface and Coatings Technology, 2022, 446, 128774.	2.2	4
71281	Influence of element substitution on structural stability and hydrogen storage performance: A theoretical and experimental study on TiCr2-xMnx alloy. Renewable Energy, 2022, 197, 564-573.	4.3	14
71282	Highly active nitrogen â€“ doped carbon nanostructures as electrocatalysts for bromine evolution reaction: A combined experimental and DFT study. Journal of Catalysis, 2022, 413, 1005-1016.	3.1	0
71283	Combined density functional theory calculation and non-equilibrium Green's function approach to predict the sensitivity of nitrogen-containing gases over PtTenS2-n monolayers (nÂ=Â0â€“2). FlatChem, 2022, 35, 100418.	2.8	5
71284	Time-varying electrochemically heterogeneous entities during the micro-galvanic corrosion associated with nanoscale precipitates in an Al-Cu-Li alloy. Corrosion Science, 2022, 206, 110542.	3.0	8
71285	Large-Scale DFT Methods for Calculations of Materials with Complex Structures. Journal of the Physical Society of Japan, 2022, 91, .	0.7	3
71286	Adsorption of ionic liquids forming species on Ti3C2T MXenes surfaces by first-principle calculations. FlatChem, 2022, 35, 100413.	2.8	6
71287	Single Ni atom embedded Janus WSSe monolayer as a cost-effective electrocatalyst for oxygen evolution reaction. Molecular Catalysis, 2022, 530, 112625.	1.0	3
71288	Non-bonding electronic reconfiguration by surface engineering in shandite A3M2S2 (A=Fe, Co; M=In,) Tj ETQq1 1 0.784314 rgBT /Ove	2.0	P

#	Article	IF	Citations
71289	High accuracy neural network interatomic potential for NiTi shape memory alloy. Acta Materialia, 2022, 238, 118217.	3.8	9
71290	Modeling Ni redistribution in the hydrogen electrode of solid oxide cells through Ni(OH)2 diffusion and Ni-YSZ wettability change. Journal of Power Sources, 2022, 545, 231924.	4.0	4
71291	Highly efficient unitized regenerative hydrogen peroxide cycle cell with ultralow overpotential for renewable energy storage. Journal of Power Sources, 2022, 545, 231948.	4.0	5
71292	Experimental and theoretical identifications of durable Feâ€“Nx configurations embedded in graphitic carbon nitride for uranium photoreduction. Journal of Environmental Chemical Engineering, 2022, 10, 108374.	3.3	2
71293	Co-Nx-enriched porous carbon nanofibers as efficient oxygen electrocatalyst for flexible Zn-air batteries. Journal of Power Sources, 2022, 544, 231865.	4.0	10
71294	Variation of the critical temperature with the lattice parameter in K3C60. Carbon, 2022, 199, 181-188.	5.4	3
71295	Gadolinium oxyorthogermanate Gd2GeO5: An efficient solid refrigerant material for magnetic cryocoolers. Materials Today Physics, 2022, 27, 100810.	2.9	6
71296	TMP/Pd complex immobilized on graphene oxide for efficient pseudocapacitive energy storage with combined experimental and DFT study. Journal of Molecular Liquids, 2022, 364, 120008.	2.3	0
71297	Insights into strain dependent lattice thermal conductivity of tin oxide. Acta Materialia, 2022, 239, 118289.	3.8	1
71298	First-principles study on electronic properties and lattice configurations of Ni3S2/LiAlO2 interface towards lithium ions storage. Solid State Ionics, 2022, 384, 115995.	1.3	0
71299	Unravelling the CO2 methanation mechanisms on a Ni-BaTiO3 catalyst: A theoretical investigation. Journal of CO2 Utilization, 2022, 64, 102170.	3.3	1
71300	Hydrogen uptake induced by CO2 enhances hydrogen embrittlement of iron in hydrogen blended natural gas. Corrosion Science, 2022, 207, 110594.	3.0	7
71301	Global structure search for new 2D PtSSe allotropes and their potential for thermoelectirc and piezoelectric applications. Chemical Physics Letters, 2022, 805, 139913.	1.2	3
71302	First-principles study on the effect of atomic swap on the electronic properties and quantum capacitance of Sc2CF2 monolayer. Vacuum, 2022, 204, 111371.	1.6	4
71303	Critical issues on coherent interface energy calculations revisited: The case of Al/TiB<mml:math xmlns:mml="http://www.w3.org/1998/Math/MathML" altimg="si5.svg" display="inline" id="d1e6011"><mml:msub><mml:mrow /><mml:mrow><mml:mn>2</mml:mn></mml:mrow></mml:msub></mml:math>. Surfaces and Interfaces, 2022, 33, 102272.	1.5	0
71304	Tuning of surface morphology in Li layered oxide cathode materials. Acta Materialia, 2022, 238, 118229.	3.8	16
71305	Investigating the transformation and capacitive performance of Al-induced NiCoP nanosheets as an advanced electrode material for supercapacitors. Surfaces and Interfaces, 2022, 33, 102290.	1.5	2
71306	Pressure-driven ferroelectric phase transition for the Pnma-CsPbBr3: Mechanical and dynamical stability study. Journal of Solid State Chemistry, 2022, 314, 123402.	1.4	1

#	Article	IF	Citations
71307	Boosting room temperature response of Pd-based hydrogen sensor by constructing in situ nanoparticles. Physica E: Low-Dimensional Systems and Nanostructures, 2022, 144, 115464.	1.3	1
71308	Systematic search of the rotation-compatible polar phases in perovskite oxides: A first-principles study. Current Applied Physics, 2022, 42, 43-49.	1.1	1
71309	Bifunctional Al2O3/polyacrylonitrile membrane to suppress the growth of lithium dendrites and shuttling of polysulfides in lithium-sulfur batteries. Electrochimica Acta, 2022, 428, 140955.	2.6	7
71310	Carbon dioxide adsorption of two-dimensional Mo2C MXene. Diamond and Related Materials, 2022, 128, 109277.	1.8	16
71311	The structural, elastic, electronic, and optical properties of Janus Zr2COT (T = S, Se, and Te) MXenes. Solid State Communications, 2022, 354, 114893.	0.9	5
71312	Two-dimensional AuSe/SnSe heterostructure for solar photocatalytic hydrogen evolution reaction with Z-scheme. Solar Energy Materials and Solar Cells, 2022, 247, 111940.	3.0	8
71313	Periodic DFT calculation for the formation of EPFRs from phenol on Î³-Al2O3 (110): Site-dependent mechanism and the role of ambient water. Journal of Environmental Chemical Engineering, 2022, 10, 108386.	3.3	4
71314	Development of novel ferritic steels strengthened by the Co16X6Si7-G phase: A theoretical and experimental study. Materials and Design, 2022, 222, 111021.	3.3	1
71315	Tunable magnetic behavior, conductivity and valley polarization in two-dimensional YMnO3/2H-VS2 multiferroic heterostructures. Physica E: Low-Dimensional Systems and Nanostructures, 2022, 144, 115459.	1.3	1
71316	Polytypic omega/omega-like transformation in a refractory high-entropy alloy. Acta Materialia, 2022, 238, 118207.	3.8	8
71317	H2O2 activation by two-dimensional metal-organic frameworks with different metal nodes for micropollutants degradation: Metal dependence of boosting reactive oxygen species generation. Journal of Hazardous Materials, 2022, 440, 129757.	6.5	14
71318	Synthesis, properties, and applications of carbyne nanocrystals. Materials Science and Engineering Reports, 2022, 151, 100692.	14.8	12
71319	Green corrosion inhibition for carbon steel reinforcement in chloride-polluted simulated concrete pore solution using Urtica Dioica extract. Journal of Building Engineering, 2022, 58, 105055.	1.6	7
71320	Density functional theory study on the electronic, optical and adsorption properties of Ti-, Fe- and Ni-doped graphene. Diamond and Related Materials, 2022, 128, 109290.	1.8	6
71321	Assessment of the structural and electronic properties of Ga<mml:math xmlns:mml="http://www.w3.org/1998/Math/MathML" altimg="si119.svg" display="inline" id="d1e469"><mml:msub><mml:mrow /><mml:mrow><mml:mi>x</mml:mi></mml:mrow></mml:msub></mml:math>In<mml:math xmlns:mml="http://www.w3.org/1998/Math/MathML" altimg="si120.svg" display="inline" id="d1e477"><mml:msub><mml:mrow /><mml:mrow><mml:mn>1</mml:mn><mml:mo>â^’</mml:mo><mml:m	0.6	0
71322	Atomistic mechanism for whole-field distortion of the substitutional solid solutions. Materials and Design, 2022, 222, 111057.	3.3	2
71323	ZW-21: A novel two-dimensional graphene-based anode material for the lithium-ion battery. Diamond and Related Materials, 2022, 128, 109298.	1.8	4
71324	Graphdiyne supported single-atom cobalt catalyst for oxygen reduction reaction: The role of the co-adsorbates. Chemical Physics Letters, 2022, 804, 139805.	1.2	2

#	Article	IF	Citations
71325	Atomic and electronic properties of different types of SiC/SiO2 interfaces: First-principles calculations. Surfaces and Interfaces, 2022, 33, 102273.	1.5	1
71326	A DFT study of H2 adsorption on Li-decorated C-doped BN nanochains. Diamond and Related Materials, 2022, 128, 109248.	1.8	4
71327	Interactions between irradiation defects and nitrogen in <mml:math xmlns:mml="http://www.w3.org/1998/Math/MathML" altimg="si72.svg"><mml:mi>Î±</mml:mi></mml:math>â€Fe: an integrated experimental and theoretical study. Acta Materialia, 2022, 239, 118227.	3.8	3
71328	Tunning magnetism and anisotropy by ferroelectric polarization in 2D van der Waals multiferroic heterostructures. Materials Today Physics, 2022, 27, 100803.	2.9	6
71329	Local Phase Transformation Strengthening at Microtwin Boundaries in Nickel-Based Superalloys. Acta Materialia, 2022, 238, 118206.	3.8	10
71330	N-based single and double transition metal V2N/CrVN monolayers as high capacity anode materials for Li-ion batteries. Materials Chemistry and Physics, 2022, 290, 126531.	2.0	4
71331	Stacking faults in a mechanically strong Al(Mg)â€“Al3Mg2 composite. Composites Part B: Engineering, 2022, 245, 110211.	5.9	14
71332	Adsorption and dissociation of high-pressure hydrogen on Fe (100) and Fe2O3 (001) surfaces: Combining DFT calculation and statistical thermodynamics. Acta Materialia, 2022, 239, 118267.	3.8	15
71333	Strain-tunable optical properties of the promising infrared detector AsP monolayer: A first-principles study. Solid State Communications, 2022, 354, 114898.	0.9	3
71334	Improved photoresponse of graphitic carbon nitride films via pressure engineering. Carbon, 2022, 199, 453-461.	5.4	5
71335	Adsorption of the prototypical organic corrosion inhibitor benzotriazole on the Cu(100) surface. Corrosion Science, 2022, 207, 110589.	3.0	6
71336	Atomic scale insight into the mechanisms of chloride induced steel corrosion in concrete. Construction and Building Materials, 2022, 351, 128811.	3.2	4
71337	Comparatively study of the electronic structure, thermal expansivity and lattice thermal conductivity of CaOn (n = 1, 2, 3). Physica B: Condensed Matter, 2022, 644, 414216.	1.3	2
71338	Electronic structure and effective mass analysis of doped TiO<mml:math xmlns:mml="http://www.w3.org/1998/Math/MathML" altimg="si38.svg" display="inline" id="d1e1187"><mml:msub><mml:mrow /><mml:mrow><mml:mn>2</mml:mn></mml:mrow></mml:msub></mml:math> (anatase) systems using DFT+<mml:math xmlns:mml="http://www.w3.org/1998/Math/MathML" altimg="si149.svg" display="inline" id="d1e1195"><mml:mi>U</mml:mi></mml:math>. Computational Materials Science, 2022, 214, 111714.	1.4	3
71339	A unique ternary Ce(III)-quercetin-phenanthroline assembly with antioxidant and anti-inflammatory properties. Journal of Inorganic Biochemistry, 2022, 235, 111947.	1.5	5
71340	Shell DFT-1/2 method towards engineering accuracy for semiconductors: GGA versus LDA. Computational Materials Science, 2022, 213, 111669.	1.4	5
71341	Electrochemical and structural investigation of copper phthalocyanine: Application in the analysis of kidney disease biomarker. Electrochimica Acta, 2022, 428, 140951.	2.6	6
71342	Strain-induced enhancement of carrier transport and optical absorption in Cs3Bi2Br9 perovskite. Solid State Communications, 2022, 354, 114918.	0.9	2

#	Article	IF	Citations
71343	Multilayer graphene sunk growth on Cu(111) surface. Carbon, 2022, 199, 233-240.	5.4	10
71344	Energy band engineering of hydroxyethyl group grafted on the edge of 3D g-C3N4 nanotubes for enhanced photocatalytic H2 production. Materials Today Physics, 2022, 27, 100806.	2.9	17
71345	Stability and electronic properties of five new ternary tantalum carbonitrides. Computational Materials Science, 2022, 214, 111728.	1.4	2
71346	Mechanistic and thermodynamic insights into the SO2 oxidation on MnO2 catalysts: A combined theoretical and experimental study. Chemosphere, 2022, 307, 135885.	4.2	5
71347	First-principles investigation of lead-free trigonal CsGeI3-xBrx mixed-halide perovskite system for optoelectronic applications: Electronic and optical properties. Materials Science in Semiconductor Processing, 2022, 151, 107017.	1.9	3
71348	Benchmarking the two-dimensional conductive Y3(C6X6)2 (YÂ=ÂCo, Cu, Pd, Pt; XÂ=ÂNH, NHS, S) metal-organic framework nanosheets for CO2 reduction reaction with tunable performance. Fuel Processing Technology, 2022, 236, 107427.	3.7	21
71349	Theoretical study on the clusterâ€“surface interaction: The case of subnanometer Ptâ€“Re clusters supported on MgO(100). Computational Materials Science, 2022, 214, 111697.	1.4	0
71350	The surface double-coupling on single-crystal LiNi0.8Co0.1Mn0.1O2 for inhibiting the formation of intragranular cracks and oxygen vacancies. Energy Storage Materials, 2022, 52, 534-546.	9.5	83
71351	Lewis acid Fe3+ in TiO2 ultra-thin nanosheet boosts oxygen species activation. Applied Surface Science, 2022, 603, 154433.	3.1	2
71352	First-principles study of a stable anode interface based on the electron tunneling effect to suppress transition metal reduction in lithium halide solid-state electrolytes. Chemical Engineering Journal Advances, 2022, 12, 100377.	2.4	4
71353	Lattice dynamics and spinâ€“phonon coupling in the noncollinear antiferromagnetic antiperovskite Mn<mml:math xmlns:mml="http://www.w3.org/1998/Math/MathML" altimg="si49.svg" display="inline" id="d1e1524"><mml:msub><mml:mrow /><mml:mrow><mml:mn>3</mml:mn></mml:mrow></mml:msub></mml:math>NiN. Journal of Magnetism and Magnetic Materials, 2022, 562, 169813.	1.0	8
71354	Exploring the structural stability and optical properties of rare-earth doped K3LuSi2O7 phosphor from first-principles calculations. Journal of Luminescence, 2022, 251, 119224.	1.5	2
71355	Anomalous transverse effects in nodal line compounds Co<mml:math xmlns:mml="http://www.w3.org/1998/Math/MathML" altimg="si84.svg" display="inline" id="d1e1114"><mml:msub><mml:mrow /><mml:mrow><mml:mn>2</mml:mn></mml:mrow></mml:msub></mml:math>TaX (X = Al, Ga). Journal of Magnetism and Magnetic Materials, 2022, 562, 169766.	1.0	1
71356	First-principles study on the electronic properties of layered Ga2O3/TeO2 heterolayers for high-performance electronic devices. Applied Surface Science, 2022, 602, 154382.	3.1	4
71357	Unveiling composition dependent electronic behaviors of tunnel Na3-xHxTi4O9: Stability and oscillatory band gap. Journal of Solid State Chemistry, 2022, 315, 123480.	1.4	0
71358	Superhard high-entropy dodecaboride with high electrical conductivity. Scripta Materialia, 2022, 220, 114938.	2.6	5
71359	Surface Cu+ modified ZnIn2S4 for promoted visible-light photocatalytic hydrogen evolution. Journal of Energy Chemistry, 2022, 74, 341-348.	7.1	18
71360	Crystal and magnetic structures of the Ir(V) JeffIr = 0 double perovskite LaSrNiIrO6. Journal of Solid State Chemistry, 2022, 315, 123477.	1.4	1

#	Article	IF	Citations
71361	Ordered double transition metal MBene: the hexagonal ScTiB2 monolayer as a superior anode material for lithium-ion batteries. Computational Materials Science, 2022, 214, 111736.	1.4	2
71362	Thermoelectric properties of monolayer MoSi2N4 and MoGe2N4 with large Seebeck coefficient and high carrier mobility: A first principles study. Journal of Solid State Chemistry, 2022, 315, 123447.	1.4	13
71363	Vacancy-based diffusion mechanisms in B2-FeAl: DFT study. Computational Materials Science, 2022, 214, 111712.	1.4	2
71364	Theoretical investigation of chemical reaction kinetics of CO catalytic combustion over NiNx-Gr. Colloids and Surfaces A: Physicochemical and Engineering Aspects, 2022, 653, 129962.	2.3	3
71365	A DFT+U approach to doped SrTiO3 for solar harvesting applications. Computational Materials Science, 2022, 214, 111743.	1.4	6
71366	A strain-engineered self-intercalation Ta9Se12 based bifunctional single atom catalyst for oxygen evolution and reduction reactions. Applied Surface Science, 2022, 602, 154378.	3.1	3
71367	Surface functionalization of two-dimensional boridene family: Enhanced stability, tunable electronic property, and high catalytic activity. Applied Surface Science, 2022, 602, 154374.	3.1	3
71368	Engineering the pin effect through selective doping and architecture design towards high-rate sodium storage performance. Energy Storage Materials, 2022, 52, 189-200.	9.5	12
71369	Guidelines for the synthesis of molybdenum nitride: Understanding the mechanism and the control of crystallographic phase and nitrogen content. Journal of Alloys and Compounds, 2022, 924, 166576.	2.8	3
71370	Investigations on ion irradiation induced modifications in Th 5f occupancy in thoria. Journal of Nuclear Materials, 2022, 570, 153961.	1.3	1
71371	Unraveling the adhesive properties, thermal stability, and initial diffusion mechanisms of Al/NiO nanothermites with various dominant surfaces: A first-principles study. Applied Surface Science, 2022, 603, 154399.	3.1	5
71372	Metallic three-dimensional porous siligraphene as a superior anode material for Li/Na/K-ion batteries. Colloids and Surfaces A: Physicochemical and Engineering Aspects, 2022, 652, 129894.	2.3	8
71373	Unveiling the mechanism of liquid-liquid extraction separation of Li+/Mg2+ using tributyl phosphate/ionic liquid mixed solvents. Journal of Molecular Liquids, 2022, 365, 120080.	2.3	7
71374	3D artificial electron and ion conductive pathway enabled by MgH2 nanoparticles supported on g-C3N4 towards dendrite-free Li metal anode. Energy Storage Materials, 2022, 52, 220-229.	9.5	6
71375	Towards Ni-rich layered oxides cathodes with low Li/Ni intermixing by mild molten-salt ion exchange for lithium-ion batteries. Nano Energy, 2022, 102, 107626.	8.2	29
71376	3D carbonaceous nanostructured transition metal nitride, carbonitride and carbide as polysulfide regulators for lithium-sulfur batteries. Nano Energy, 2022, 102, 107659.	8.2	14
71377	DFT-FE 1.0: A massively parallel hybrid CPU-GPU density functional theory code using finite-element discretization. Computer Physics Communications, 2022, 280, 108473.	3.0	24
71378	Investigation on luminescence behavior of Mg4Ta2O9 through experimental and first-principles calculation methods. Journal of Luminescence, 2022, 251, 119221.	1.5	0

#	Article	IF	Citations
71379	Room-temperature half-metallicity in rich Ti-alloyed <mml:math xmlns:mml="http://www.w3.org/1998/Math/MathML" altimg="si20.svg" display="inline" id="d1e1077"><mml:mrow><mml:msub><mml:mrow><mml:mi mathvariant="normal">CrSi</mml:mi></mml:mrow><mml:mrow><mml:mn>2</mml:mn></mml:mrow></mml:msub><mml:msub><mml:mrow><mml:mi mathvariant="normal">N</mml:mi></mml:mrow><mml:mrow><mml:mn>4</mml:mn></mml:mrow></mml:msub></mml:mrow> monolayer. Journal of Magnetism and Magnetic Materials, 2022, 562, 169742.	1.0	3
71380	Pyridazine doped g-C3N4 with nitrogen defects and spongy structure for efficient tetracycline photodegradation and photocatalytic H2 evolution. Chemosphere, 2022, 307, 136087.	4.2	14
71381	First-principles and machine-learning study of electronic and phonon transport in carbon-based AA-stacked bilayer biphenylene nanosheets. Journal of Physics and Chemistry of Solids, 2022, 170, 110909.	1.9	7
71382	Design ambipolar conductivity on wide-gap semiconductors: The case of Al- and Na-doped CaS. Materials Science in Semiconductor Processing, 2022, 151, 107024.	1.9	7
71383	Bayesian calibration of interatomic potentials for binary alloys. Computational Materials Science, 2022, 214, 111660.	1.4	2
71384	Structure characterization and steam oxidation performance of U3Si2 with Zr alloying additions. Journal of Nuclear Materials, 2022, 570, 153951.	1.3	3
71385	Improving photoelectric perfomance with hydrogen on Al-doped ZnO. Materials Chemistry and Physics, 2022, 291, 126680.	2.0	10
71386	Bimetallic MMoS4 (M = Ni, Co, Cu) cocatalysts architected CdS nanoflowers for synergistically boosting visible-light-driven photocatalytic H2 evolution from water and benzyl alcohol. Journal of Alloys and Compounds, 2022, 924, 166645.	2.8	6
71387	Symmetry-correct bonding in density functional theory calculations for delta phase Pu. Journal of Nuclear Materials, 2022, 570, 153954.	1.3	4
71388	Polymerâ€“assisted preparation of porous woodâ€“based metallic composites for efficient catalytic reduction of organic pollutants. Industrial Crops and Products, 2022, 187, 115387.	2.5	6
71389	MuFinder: A program to determine and analyse muon stopping sites. Computer Physics Communications, 2022, 280, 108488.	3.0	7
71390	Synergistic effects of oxygen vacancies and heterostructures for visible-light-driven photoreduction of uranium. Separation and Purification Technology, 2022, 301, 121966.	3.9	10
71391	Synthesis of enriched oxygen vacancy TiO2 microsphere with rapid response to isopropylamine and its application in herbicide detection. Sensors and Actuators B: Chemical, 2022, 370, 132423.	4.0	2
71392	Moisture-enabled hydrovoltaic power generation with milk protein nanofibrils. Nano Energy, 2022, 102, 107709.	8.2	14
71393	High-throughput screening of protective layers to stabilize the electrolyte-anode interface in solid-state Li-metal batteries. Nano Energy, 2022, 102, 107640.	8.2	12
71394	New room-temperature 2D hexagonal topological insulator OsC: First Principle Calculations. Materials Science in Semiconductor Processing, 2022, 151, 107009.	1.9	8
71395	Structural and nano-mechanical characteristics of a novel mixture of natural hydroxyapatite materials: Insights from ab-initio calculations and experiments. Materials Letters, 2022, 326, 132977.	1.3	8
71396	Stable single layer structures of aluminum oxide: Vibrational and electronic characterization of magnetic phases. Computational Materials Science, 2022, 214, 111745.	1.4	1

#	Article	IF	Citations
71397	Vinyl chloride catalytic combustion on Pt/CeO2: Tuning Pt chemical state to promote Cl removing. Chemosphere, 2022, 307, 135861.	4.2	8
71398	Easy fabrication of performant and broadband response SnS/Si photodetector. Materials Science in Semiconductor Processing, 2022, 151, 106991.	1.9	5
71399	MEAM interatomic potential for thermodynamic and mechanical properties of lithium allotropes. Computational Materials Science, 2022, 214, 111706.	1.4	3
71400	The effect of Ru-Ru coordination numbers on CO2 methanation over Ru supported catalyst. Applied Surface Science, 2022, 603, 154398.	3.1	6
71401	Solid solution softening of Ti2AlC induced by alloying of boron. Journal of Alloys and Compounds, 2022, 925, 166712.	2.8	0
71402	Impurity properties in phosphorene: First-principles calculations and comparisons. Materials Science in Semiconductor Processing, 2022, 151, 107006.	1.9	0
71403	The design of the highly active NH3-SCR catalyst Ce-W/UiO-66: Close coupling of active sites and acidic sites. Separation and Purification Technology, 2022, 300, 121864.	3.9	9
71404	Alkali ions pre-intercalated 3D crinkled Ti3C2Tx MXene architectures for advanced sodium storage. Chemical Engineering Journal, 2022, 450, 138453.	6.6	12
71405	Selective regulation of Pt clusters inside KY zeolite using atomic layer deposition for n-octane reforming. Fuel, 2022, 330, 125671.	3.4	3
71406	Metallic 3D porous borophosphene: A high rate-capacity and ultra-stable anode material for alkali metal ion batteries. Vacuum, 2022, 205, 111418.	1.6	7
71407	Stacking surface derived catalytic capability and by-product prevention for high efficient two dimensional Bi2Te3 cathode catalyst in Li-oxygen batteries. Applied Catalysis B: Environmental, 2022, 318, 121844.	10.8	11
71408	Transition metal decorated ZnO monolayer for CO and NO sensing: A DFTÂ+ÂU study with vdW correction. Applied Surface Science, 2022, 604, 154570.	3.1	6
71409	Tuning the selective sensing properties of transition metal dichalcogenides (MoX2: X= Se, Te) toward sulfurrich gases. Materials Today Chemistry, 2022, 26, 101069.	1.7	7
71410	Anomalous pressure-responsive emission enhancement of FCO-CzS due to molecular configuration and electronic structure changes. Spectrochimica Acta - Part A: Molecular and Biomolecular Spectroscopy, 2022, 283, 121723.	2.0	2
71411	Engineering d-band center of iron single atom site through boron incorporation to trigger the efficient bifunctional oxygen electrocatalysis. Journal of Colloid and Interface Science, 2022, 628, 331-342.	5.0	29
71412	Graphene, phosphorene and silicene coatings on the (0001) surfaces of hcp metals: Structural stability and hydrophobicity. Materials Today Communications, 2022, 33, 104281.	0.9	0
71413	Synergistic effects of zeolite and oxygen vacancies in SnO2 for formaldehyde sensing: Molecular simulation insights & experimental verification. Applied Surface Science, 2022, 604, 154511.	3.1	11
71414	Iodide and charge migration at defective surfaces of methylammonium lead triiodide perovskites: The role of hydrogen bonding. Applied Surface Science, 2022, 604, 154501.	3.1	2

#	Article	IF	Citations
71415	Improved NO2 gas sensing performance of 2D MoS2/Ti3C2Tx MXene nanocomposite. Applied Surface Science, 2022, 604, 154624.	3.1	11
71416	Construction of rGO-coupled C3N4/C3N5 2D/2D Z-scheme heterojunction to accelerate charge separation for efficient visible light H2 evolution. Applied Catalysis B: Environmental, 2022, 318, 121822.	10.8	65
71417	Ab initio study of the effects of Cr on helium behaviors in Feâ€“YCr (Y = 9.38, 12.50Âat%) austenitic binary alloys. Materials Today Communications, 2022, 33, 104207.	0.9	0
71418	Amine functionalization derived lattice engineered and electron deficient palladium catalyst for selective production of hydrogen peroxide. Applied Surface Science, 2022, 604, 154464.	3.1	2
71419	In-situ N-defect and single-metal atom synergetic engineering of high-efficiency Agâ€“Nâ€“C electrocatalysts for CO2 reduction. Applied Catalysis B: Environmental, 2022, 318, 121826.	10.8	16
71420	Junction of ZnmIn2S3+m and bismuth vanadate as Z-scheme photocatalyst for enhanced hydrogen evolution activity: The role of interfacial interactions. Journal of Colloid and Interface Science, 2022, 628, 488-499.	5.0	16
71421	Efficient purification of auto-exhaust carbon particles over non-noble metals (Fe, Co, Cu) decorated hexagonal NiO nanosheets. Fuel, 2022, 330, 125662.	3.4	7
71422	Temperature-dependant active sites for methane continuous conversion to methanol over Cu-zeolite catalysts using water as the oxidant. Fuel, 2022, 329, 125483.	3.4	8
71423	Tuning electronic behaviors of WS2 by molecular doping. Materials Today Communications, 2022, 33, 104226.	0.9	2
71424	Sb-doped Li10GeP2S12-type electrolyte Li10SnP2-xSbxS12 with enhanced ionic conductivity and lower lithium-ion migration barrier. Journal of Colloid and Interface Science, 2022, 627, 1039-1046.	5.0	6
71425	Different passivation behavior between Î± and Î² phases of Ti-6Al-4V in HCl solutions under oxygenated/deoxygenated conditions. Applied Surface Science, 2022, 604, 154539.	3.1	8
71426	A family of Li B monolayers with a wide spectrum of potential applications. Applied Surface Science, 2022, 604, 154317.	3.1	31
71427	Ab initio investigation of the interface between <mml:math xmlns:mml="http://www.w3.org/1998/Math/MathML" altimg="si11.svg" display="inline" id="d1e785"><mml:mrow><mml:mtext>Mo10S24</mml:mtext></mml:mrow></mml:math> nanoflakes and the <mml:math xmlns:mml="http://www.w3.org/1998/Math/MathML" altimg="si12.svg" display="inline" id="d1e791"><mml:mrow><mml:mtext>Au(111)</mml:mtext></mml:mrow></mml:math> surface: Interplay between interaction energy and morphology. Applied Surface Science, 2022, 604, 154413.	3.1	2
71428	Hydrogenation and hydrogenolysis of 5-hydroxymethylfurfural to 2,5-dimethylfuran via synergistic catalysis of Ni2In and acid-base sites. Applied Surface Science, 2022, 604, 154579.	3.1	12
71429	Formic acid dehydrogenation over Pd single atom or cluster supported on nitrogen-doped graphene: A DFT study. Applied Surface Science, 2022, 604, 154510.	3.1	7
71430	Realizing efficient C-N coupling via electrochemical co-reduction of CO2 and NO3- on AuPd nanoalloy to form urea: Key C-N coupling intermediates. Applied Catalysis B: Environmental, 2022, 318, 121819.	10.8	36
71431	Synergistic Pt-CeO2 interface boosting low temperature dry reforming of methane. Applied Catalysis B: Environmental, 2022, 318, 121809.	10.8	46
71432	Comparative study of hydrodeoxygenation performance over Ni and Ni2P catalysts for upgrading of lignin-derived phenolic compound. Fuel, 2023, 331, 125663.	3.4	8

#	Article	IF	Citations
71433	Carbon matrix with atomic dispersion of binary cobalt/iron-N sites as efficient peroxymonosulfate activator for organic pollutant oxidation. Chemical Engineering Journal, 2023, 451, 138574.	6.6	2
71434	Cr(VI) adsorption and reduction by magnetite-humic acid adsorption complexes under mildly acidic conditions: Synergistic/antagonistic mechanism and multi-step reaction model. Chemical Engineering Journal, 2023, 451, 138648.	6.6	14
71435	Metal monovacancy-induced spin polarization for simultaneous energy recovery and wastewater purification. Chemical Engineering Journal, 2023, 451, 138537.	6.6	30
71436	Modulation of the interfacial charge density on Fe2Pâ€“CoP by coupling CeO2 for accelerating alkaline electrocatalytic hydrogen evolution reaction and overall water splitting. Chemical Engineering Journal, 2023, 451, 138550.	6.6	44
71437	Prediction of HER electrocatalyst with enhanced performance based on atoms-doped black phosphorene: A first-principles study. Applied Surface Science, 2022, 604, 154508.	3.1	5
71438	A new 2D metallic K3Cl2 nanosheet as a promising candidate of NO2 gas sensor and capturer. Applied Surface Science, 2022, 604, 154554.	3.1	0
71439	High catalytic activity of MBenes-supported single atom catalysts for oxygen reduction and oxygen evolution reaction. Applied Surface Science, 2022, 604, 154522.	3.1	18
71440	Boosting elementary steps kinetics towards energetic alkaline hydrogen evolution via dual sites on phase-separated Niâ€“Cuâ€“Mn/hydroxide. Chemical Engineering Journal, 2023, 451, 138540.	6.6	11
71441	In-situ topotactic construction of novel rod-like Bi2S3/Bi5O7I p-n heterojunctions with highly enhanced photocatalytic activities. Journal of Materials Science and Technology, 2023, 135, 126-141.	5.6	25
71442	Lamellar-structured anodes based on lithiophilic gradient enable dendrite-free lithium metal batteries with high capacity loading and fast-charging capability. Chemical Engineering Journal, 2023, 451, 138570.	6.6	7
71443	Mechanism for the promotional formation of NH4+ by SO2 on different mineral dust surfaces. Particuology, 2023, 75, 109-118.	2.0	2
71444	Caterpillar-like 3D graphene nanoscrolls@CNTs hybrids decorated with Co-doped MoSe2 nanosheets for electrocatalytic hydrogen evolution. Journal of Materials Science and Technology, 2023, 136, 43-53.	5.6	16
71445	High-capacity and ultrastable lithium storage in SnSe₂â€“SnO₂@NC microbelts enabled by heterostructures. Dalton Transactions, 2022, 51, 12071-12079.	1.6	1
71448	Gold Decorated Hydroxyapatiteâ€“CeO₂ Enabled Surface Frustrated Lewis Pairs for CO Oxidation. Advanced Energy and Sustainability Research, 2022, 3, .	2.8	3
71449	Growth of bilayer MoTe2 single crystals with strong non-linear Hall effect. Nature Communications, 2022, 13, .	5.8	18
71450	Building Metalâ€Molecule Interface towards Stable and Reversible Zn Metal Anodes for Aqueous Rechargeable Zinc Batteries. Advanced Functional Materials, 2022, 32, .	7.8	87
71451	Pressureâ€induced latticeâ€dynamical stability and superconductivity of ternary pentahydride <scp> MgNiH ₅ </scp>. International Journal of Energy Research, 2022, 46, 24064-24073.	2.2	2
71452	First-principles study on high-pressure phases and compression properties of gold-bearing intermetallic compounds. Journal of Physics Condensed Matter, 2022, 34, 464001.	0.7	3

#	Article	IF	Citations
71453	Low temperature CVD growth of WSe₂ enabled by moisture-assisted defects in the precursor powder. 2D Materials, 2022, 9, 045026.	2.0	2
71454	Local structure and its implications for the relaxor ferroelectric <mml:math xmlns:mml="http://www.w3.org/1998/Math/MathML"><mml:mrow><mml:msub><mml:mi>Cd</mml:mi><mml:mn>2</mml:mn></mml:msub><mml:msub><mml:mi mathvariant="normal">O</mml:mi><mml:mn>7</mml:mn></mml:msub></mml:mrow></mml:math>. Physical Review Research, 2022, 4, .	1.3	0
71455	Polarons free from many-body self-interaction in density functional theory. Physical Review B, 2022, 106, .	1.1	9
71456	Ruâ€Dopingâ€Induced Spin Frustration and Enhancement of the Roomâ€Temperature Anomalous Hall Effect in La_{2/3}Sr_{1/3}MnO₃ Films. Advanced Materials, 2022, 34, .	11.1	6
71457	Moâ€Incorporated Magnetite Fe₃O₄ Featuring Cationic Vacancies Enabling Fast Lithium Intercalation for Batteries. Small, 2022, 18, .	5.2	7
71458	Insights into LiMXO₄F (Mâ€“X = Alâ€“P and Mgâ€“S) as Cathode Coatings for High-Performance Lithium-Ion Batteries. ACS Applied Materials & Interfaces, 2022, 14, 44859-44868.	4.0	1
71459	Cobalt-Molybdenum Oxides for Effective Coupling of Ethane Activation and Carbon Dioxide Reduction Catalysis. ACS Catalysis, 2022, 12, 12227-12245.	5.5	4
71460	Bismuth Complex Controlled Morphology Evolution and CuSCN-Induced Transport Improvement Enable Efficient BiI3 Solar Cells. Nanomaterials, 2022, 12, 3121.	1.9	1
71461	Computational Investigation of a NASICON-Type Solid Electrolyte Material LiGe2(PO4)3. Sustainable Chemistry, 2022, 3, 404-414.	2.2	1
71462	Low-power phase-change memory cell based on a doped GeTe/InP heterostructure: a first-principles study. Journal of Computational Electronics, 0, , .	1.3	0
71463	Systematic electronic structure in the cuprate parent state from quantum many-body simulations. Science, 2022, 377, 1192-1198.	6.0	13
71464	DFT-1/2 method applied to 3D topological insulators. Journal of Physics Condensed Matter, 2022, 34, 465501.	0.7	2
71465	Coexistence and Coupling of Spin-Induced Ferroelectricity and Ferromagnetism in Perovskites. Physical Review Letters, 2022, 129, .	2.9	9
71466	Methanol Synthesis Over PdIn, In₂O₃, and CuZn From First-Principles Microkinetics: Similarities and Differences. Journal of Physical Chemistry C, 2022, 126, 15235-15246.	1.5	5
71467	H2O in situ induced active site structure dynamics for efficient methane direct oxidation to methanol over Fe-BEA zeolite. Journal of Catalysis, 2022, 414, 302-312.	3.1	6
71468	Fabrication of Lithium Indolide and Derivates for Ion Conduction. ACS Applied Materials & Interfaces, 2022, 14, 41095-41102.	4.0	3
71469	Prospective on the Doping Engineering of Vacancy-Ordered Halide Double Perovskites for Enhanced Optoelectronic Properties. Journal of Physical Chemistry C, 2022, 126, 15501-15508.	1.5	5
71470	Grain boundary structural transformation induced by co-segregation of aliovalent dopants. Nature Communications, 2022, 13, .	5.8	6

#	Article	IF	Citations
71471	Hole-Doping to a Cu(I)-Based Semiconductor with an Isovalent Cation: Utilizing a Complex Defect as a Shallow Acceptor. Journal of the American Chemical Society, 2022, 144, 16572-16578.	6.6	15
71472	Preparation, Supramolecular Organization, and On-Surface Reactivity of Enantiopure Subphthalocyanines: From Bulk to 2D-Polymerization. Journal of the American Chemical Society, 2022, 144, 16579-16587.	6.6	10
71473	Indium Epitaxy on SiC(0001): A Roadmap to Large Scale Growth of the Quantum Spin Hall Insulator Indenene. Journal of Physical Chemistry C, 2022, 126, 16289-16296.	1.5	4
71474	Disclosing the Biocide Activity of Î±-Ag2â''2xCuxWO4 (0 â‰ x â‰ 0.16) Solid Solutions. International Journal of Molecular Sciences, 2022, 23, 10589.	1.8	2
71475	Effects of high-order anharmonicity on anomalous lattice dynamics and thermal transport in fully filled skutterudite <mml:math xmlns:mml="http://www.w3.org/1998/Math/MathML"><mml:mrow><mml:msub><mml:mi>YbFe</mml:mi><mml:mn>4</mml:mn></mml:msub></mml:mrow></mml:math>Sb₁₂. Physical Review Materials, 2022, 6, .	0.9	8
71476	Electronic Modulation of the Interaction between Fe Single Atoms and WO_{2.72â€“x} for Photocatalytic N₂ Reduction. ACS Catalysis, 2022, 12, 11860-11869.	5.5	15
71477	High-resolution diffraction reveals magnetoelastic coupling and coherent phase separation in tetragonal CuMnAs. Physical Review Materials, 2022, 6, .	0.9	0
71478	Interface Reactions Dominate Low-Temperature CO Oxidation Activity over Pt/CeO₂. Journal of Physical Chemistry C, 2022, 126, 16164-16171.	1.5	9
71479	Pressure-driven tunable properties of the small-gap chalcopyrite topological quantum material <mml:math xmlns:mml="http://www.w3.org/1998/Math/MathML"><mml:msub><mml:mrow><mml:mi>ZnGeSb</mml:mi></mml:mrow><mml:mn>2</mml:mn></mml:msub></mml:math>: A first-principles study. Physical Review B, 2022, 106, .	1.1	2
71480	Allâ€Electric Nonassociative Learning in Nickel Oxide. Advanced Intelligent Systems, 2022, 4, .	3.3	17
71481	Towards Ge-based electronic devices: Increased longevity of alkanethiol-passivated Ge(100) in low humidity environments. Thin Solid Films, 2022, 759, 139466.	0.8	3
71482	Phase transformation and amorphization resistance in high-entropy MAX phase M2SnC (MÂ=ÂTi, V, Nb, Zr,) Tj ETQq1 1 0.784314 rgBT	3.8	17
71483	High hydrogen isotopes permeation resistance in (TiVAlCrZr)O multi-component metal oxide glass coating. Acta Materialia, 2022, 238, 118204.	3.8	5
71484	Pronounced inhibitory mechanism of Cr on vacancy-like defects in Fe9Cr alloy irradiation with helium ions. Nuclear Materials and Energy, 2022, 33, 101235.	0.6	0
71485	Flux crystal growth of rubidiumâ€“iron silicates and germanates and their ion-exchange using alkali nitrate salts. Solid State Sciences, 2022, 132, 106995.	1.5	0
71486	Prediction of single-boron anchored on MXene catalysts for high-efficient electrocatalytic nitrogen reduction reaction. Molecular Catalysis, 2022, 531, 112658.	1.0	4
71487	First-principles study of divacancy defect in arsenene nanoribbon. , 2022, 170, 207376.		0
71488	Atomic structure, electronic structure and optical absorption of inorganic perovskite compounds Cs2SnI6-nXn (XÂ=ÂF, Cl, br; nÂ=ÂOÂâ¼Â6): A first-principles study. Solar Energy, 2022, 245, 25-36.	2.9	5

#	Article	IF	Citations
71489	Porous silica coating with excellent atomic oxygen protection performance and flexibility. Surface and Coatings Technology, 2022, 447, 128840.	2.2	9
71490	First-principles insights into complex interplays among nano-phases in an Al-Cu-Li-Zr alloy. Acta Materialia, 2022, 239, 118304.	3.8	11
71491	Fast proton and water transport in ceramic membrane-based magic-angle graphene. Water Research, 2022, 225, 119076.	5.3	1
71492	Reversible Lithium-Ion Storage in h-Bi2Ge3O9-Based Anode: Experimental and Theoretical Studies. Journal of Electroanalytical Chemistry, 2022, 923, 116804.	1.9	3
71493	Synergize curvature and confinement effects for Fe-, Co-, Ni- N2 sites on graphene nanobuds towards eNRR. Molecular Catalysis, 2022, 531, 112656.	1.0	0
71494	Adsorption, thermal conversion, and catalytic hydrogenation of acrolein on Cu surfaces. Journal of Catalysis, 2022, 414, 257-266.	3.1	5
71495	2D boron-nitride featuring B4 tetrahedros: An efficient photocatalyst for water splitting. Molecular Catalysis, 2022, 531, 112662.	1.0	0
71496	The separation performance of two-dimensional ZnPP-grid molecular sieve for C6 alkane molecules:A first-principles calculation. Journal of Membrane Science, 2022, 662, 121030.	4.1	0
71497	Enabling the fast sodium ions diffusion by constructing reduced graphene oxide/TiO2/MXenes tandem architecture for durable sodium ions battery. Journal of Electroanalytical Chemistry, 2022, 922, 116771.	1.9	1
71498	Nitrogen doping effects on the physical and chemical properties of bilayer graphdiyne: A density functional theory approach. Applied Surface Science Advances, 2022, 11, 100301.	2.9	1
71499	Transition metal atom anchored by defective WSSe monolayer as bifunctional single atom catalyst for ORR and OER. Journal of Electroanalytical Chemistry, 2022, 922, 116731.	1.9	5
71500	Theoretical analysis of Polyethylene terephthalate (PET) adsorption on Co and Mn-doped ZnO (000-1). Molecular Catalysis, 2022, 531, 112688.	1.0	3
71501	An ambient ductile TiHfVNbTa refractory high-entropy alloy: Cold rolling, mechanical properties, lattice distortion, and first-principles prediction. Materials Science & Engineering A: Structural Materials: Properties, Microstructure and Processing, 2022, 856, 144046.	2.6	25
71502	Orthorhombic C32: A topological semimetal with nodal ring. Physics Letters, Section A: General, Atomic and Solid State Physics, 2022, 451, 128397.	0.9	0
71503	Synergistic reinforcement effect of Fe and in-situ synthesized MgAlB4 whiskers in Al matrix composites. Composites Part B: Engineering, 2022, 246, 110267.	5.9	3
71504	Suitability and performance of NaNi1-x(VO)xPO4 mixed polyanion glass and Glass-Ceramic cathodes for Na-ion battery. Materials Science and Engineering B: Solid-State Materials for Advanced Technology, 2022, 285, 115938.	1.7	2
71505	Interfacial structures and decomposition reactions of hybrid anion-based ionic liquids at lithium metal surface from first-principles and ab initio molecular dynamics. Journal of Molecular Liquids, 2022, 366, 120232.	2.3	2
71506	Extremely low thermal conductivity in BaSb2Se4: Synthesis, characterization, and DFT studies. Journal of Solid State Chemistry, 2022, 315, 123524.	1.4	3

#	Article	IF	Citations
71507	Two-dimensional penta-siligraphene with high performance for nonâ€'lithium metal ions batteries anode materials. Solid State Ionics, 2022, 385, 116020.	1.3	3
71508	Chemical domain structure and its formation kinetics in CrCoNi medium-entropy alloy. Acta Materialia, 2022, 240, 118314.	3.8	25
71509	The effect of spacer cations on optoelectronic properties of two-dimensional perovskite based on first-principles calculations. Surfaces and Interfaces, 2022, 34, 102343.	1.5	3
71510	Ion-exchange-induced high-performance of inverse spinel Mg2VO4 for aqueous zinc-ion batteries. Journal of Power Sources, 2022, 549, 232075.	4.0	13
71511	Pressure induced phase transition in heavy fermion metal UTe2: A first-principles study. Physics Letters, Section A: General, Atomic and Solid State Physics, 2022, 451, 128401.	0.9	1
71512	Tunable electronic properties of diamond (100) surface via boron-nitrogen co-termination: A first-principles study. Diamond and Related Materials, 2022, 129, 109387.	1.8	1
71513	Structural features of heavily boron-doped graphite and diamond microcrystals synthesized at high pressures. Diamond and Related Materials, 2022, 129, 109383.	1.8	1
71514	Tuning charge transfer of Pt cluster by support defects in Pt/TiO2 for photocatalytic conversion of fatty acid into diesel-like alkane. Journal of Cleaner Production, 2022, 375, 133975.	4.6	9
71515	First-principles study on optoelectronic properties of lead-free inorganic iodide double perovskite Cs2AgSb1-xGaxI6. Solid State Communications, 2022, 356, 114936.	0.9	1
71516	Bulk photovoltaic effect in partial overlap MoSe2/mmath:math xmlns:mml="http://www.w3.org/1998/Math/MathML" altimg="si55.svg" display="inline" id="d1e421"><mml:msub><mml:mrow /><mml:mrow><mml:mn>2</mml:mn></mml:mrow></mml:msub></mml:math>-WSe<mml:math xmlns:mml="http://www.w3.org/1998/Math/MathML" altimg="si55.svg" display="inline" id="d1e429"><mml:msub><mml:mrow /><mml:mrow><mml:mn>2</mml:mn></mml:mrow></mml:msub></	0.8	0
71517	Janus B2XY (X, YÂ=ÂS, Se, Te) monolayers as piezoelectric Materials: A First-Principle study. Chemical Physics Letters, 2022, 806, 140007.	1.2	3
71518	Anisotropic and outstanding mechanical, thermal conduction, optical, and piezoelectric responses in a novel semiconducting BCN monolayer confirmed by first-principles and machine learning. Carbon, 2022, 200, 500-509.	5.4	16
71519	Mechanical behaviors of equiatomic and near-equiatomic face-centered-cubic phase high-entropy alloys probed using in situ neutron diffraction. International Journal of Plasticity, 2022, 158, 103417.	4.1	24
71520	Mechanism of high- and low-valence doping on adsorbed oxygen of SnO2-based gas sensors and a strategy to combine the advantages of both dopants. Sensors and Actuators B: Chemical, 2022, 371, 132603.	4.0	5
71521	Impact of hydrogen coverage on silane adsorption during Si epitaxy from ab initio simulations. Solid-State Electronics, 2022, 197, 108441.	0.8	1
71522	Experimental and computational insights into the anomalous thermal expansion of (NH4)ReO4. Journal of Solid State Chemistry, 2022, 315, 123531.	1.4	0
71523	First-principles study of 3sp impurity (S, P, Si, Al) effects on vacancy-mediated diffusion in Ni and Ni-33Cr alloys. Computational Materials Science, 2022, 214, 111768.	1.4	4
71524	High pressure synthesis, physical properties and electronic structure of monovalent iron compound LaFePH. Journal of Solid State Chemistry, 2022, 315, 123546.	1.4	0

#	Article	IF	Citations
71525	The site preference and doping effect on mechanical properties of Ni3Al-based Î³â€² phase in superalloys by combing first-principles calculations and thermodynamic model. Arabian Journal of Chemistry, 2022, 15, 104278.	2.3	9
71526	Stabilization of superconductive Laâ€“Y alloy superhydride with Tc above 90ÂK at megabar pressure. Materials Today Physics, 2022, 28, 100840.	2.9	4
71527	High Curie temperature and large perpendicular magnetic anisotropy in two-dimensional half metallic OsI3 monolayer with quantum anomalous Hall effect. Materials Today Physics, 2022, 28, 100847.	2.9	9
71528	A thermochemical database from high-throughput first-principles calculations and its application to analyzing phase evolution in AM-fabricated IN718. Acta Materialia, 2022, 240, 118331.	3.8	2
71529	Tunable band gap of diamond twin boundaries by strain engineering. Carbon, 2022, 200, 483-490.	5.4	2
71530	Ab initio investigation of the structural and electronic properties of tantalum thallium chalcogenides TaTlX3 (X = S,Se). Journal of Solid State Chemistry, 2022, 315, 123534.	1.4	5
71531	Theoretical insights into the oxygen supply performance of Î±-Fe2O3 in the chemical-looping reforming of methane. Chemical Engineering Science, 2022, 262, 118041.	1.9	6
71532	Ultrahigh yield strength and large uniform elongation achieved in ultrafine-grained titanium containing nitrogen. Acta Materialia, 2022, 240, 118356.	3.8	18
71533	Ionic covalent organic frameworks triggered efficient synergy: Li+ de-solvation and the formation of LiF-rich interphase. Journal of Power Sources, 2022, 548, 232001.	4.0	3
71534	Effects of rare-earth elements on twinning deformation of Al alloys from first-principles calculations. Solid State Communications, 2022, 356, 114946.	0.9	2
71535	A metallic CP3 monolayer with very high absorption coefficients for visible light and as the CO2 absorbent. Chemical Physics Letters, 2022, 806, 140041.	1.2	0
71536	A high-throughput ab-initio study of diverse glasses: Accuracy of the atomic structure and refractive index. Computational Materials Science, 2022, 214, 111765.	1.4	2
71537	High solar-to-hydrogen efficiency photocatalytic hydrogen evolution reaction with the HfSe2/InSe heterostructure. Journal of Power Sources, 2022, 547, 232008.	4.0	38
71538	Supported Ni0@C N catalyst with dual-reaction surfaces: Structure-performance relation in the selective hydrogenation of p-chloronitrobenzene. Applied Surface Science, 2022, 606, 154786.	3.1	4
71539	Thermodynamic assessment of the Gaâ€“Lu system by the combination of ab-initio calculations and the CALPHAD approach. Calphad: Computer Coupling of Phase Diagrams and Thermochemistry, 2022, 79, 102464.	0.7	2
71540	Magnetic and structural properties of the Fe5Si1-xGexB2 system. Journal of Solid State Chemistry, 2022, 316, 123576.	1.4	1
71541	Super-exchange interaction induced by neighboring bimetallic hybridization in bismuthene for hydrogen evolution reaction. Chemical Physics Letters, 2022, 806, 140012.	1.2	3
71542	Li-decorated Î²1-graphyne for high-performance CO2 capture and separation over N2. Applied Surface Science, 2022, 605, 154724.	3.1	4

#	Article	IF	Citations
71543	Enhanced mechanisms of oxygen reduction on Pr0.4Sr0.6Co0.2Fe0.8O3-Î´ impregnated La1â^'xSrxCo1â^'yFeyO3-Î´ cathodes for solid oxide fuel cells. Journal of Alloys and Compounds, 2022, 927, 167033.	2.8	2
71544	Point defect properties of the VCrMnFe0.33 multi-principal alloy from first-principles calculations. Materials Today Communications, 2022, 33, 104485.	0.9	1
71545	Study on lattice discreteness effect on superdislocation core properties of Ni3Al by improved semi-discrete variational Peierls-Nabarro model. Intermetallics, 2022, 151, 107695.	1.8	1
71546	High-throughput screening of highly active and selective single-atom catalysts for ammonia synthesis on WB2 (0 0 1) surface. Applied Surface Science, 2022, 606, 154935.	3.1	2
71547	Two-Dimensional metal-free compounds of BC4N and BC6N2 with boron atoms as highly efficient catalytic centers toward sulfur redox in lithium-sulfur batteries. Applied Surface Science, 2022, 606, 154773.	3.1	3
71548	Recognition of water-dissociation effect toward lattice oxygen activation on single-atom Co catalyst in toluene oxidation. Applied Catalysis B: Environmental, 2022, 319, 121962.	10.8	16
71549	First-principles kinetic Monte Carlo modeling of propylene epoxidation on the Ti2CuO6/Cu(111) and Cu2O(111) surfaces. Applied Surface Science, 2022, 605, 154683.	3.1	1
71550	Effect of substitution of Mn and Ga atoms by Fe atom in the Mn2GaC MAX phase. Journal of Magnetism and Magnetic Materials, 2022, 563, 169860.	1.0	1
71551	Activation energy of homogeneous nucleation of Zr hydride: Density functional theory calculation. Computational Materials Science, 2022, 215, 111769.	1.4	1
71552	Effects of vacancies on the electronic structures and photocatalytic properties of g-C3N4. Vacuum, 2022, 206, 111483.	1.6	4
71553	Computational simulation study on adsorption and separation of CH4/H2 in five higher-valency covalent organic frameworks. Materials Today Communications, 2022, 33, 104374.	0.9	3
71554	Magnetic complexity, magnetodielectric effect and DFT calculations on correlation driven Gd2CoMnO6 insulator. Journal of Magnetism and Magnetic Materials, 2022, 563, 169880.	1.0	4
71555	Thermodynamic properties of Na2MgSiO4: DFT calculation and experimental validation. Calphad: Computer Coupling of Phase Diagrams and Thermochemistry, 2022, 79, 102480.	0.7	4
71556	Implications of electron and hole doping on the magnetic properties of spinâ€“orbit entangled Ca4IrO6 from DFT calculations. Journal of Magnetism and Magnetic Materials, 2022, 563, 169861.	1.0	0
71557	Surface modification of MCr2O4 (MÂ=ÂMg and Zn) by Cu-Doping: Theoretical prediction and experimental observation of enhanced catalysis for CO oxidation. Applied Surface Science, 2022, 605, 154681.	3.1	1
71558	Mineralize complex organic contaminants using only oxygen on dense copper atoms embedded in the walls of carbon nanotubes. Applied Surface Science, 2022, 605, 154760.	3.1	1
71559	Realization of transition metal selenide active facets via synergistic sulfur doping for bifunctional alkaline water splitting applications: A comparative study. Applied Surface Science, 2022, 605, 154804.	3.1	9
71560	Rational design synergistic metal-free dual-atom electrocatalyst for N2 to NH3 reaction on g-CN: A first principle study. Applied Surface Science, 2022, 605, 154831.	3.1	8

#	Article	IF	Citations
71561	Emergence of Rashba splitting and spin-valley properties in Janus MoGeSiP2As2 and WGeSiP2As2 monolayers. Journal of Magnetism and Magnetic Materials, 2022, 563, 169897.	1.0	12
71562	An embedded-atom method potential for studying the properties of Fe-Pb solid-liquid interface. Journal of Nuclear Materials, 2022, 572, 154041.	1.3	1
71563	Electrochemical formic acid oxidation catalyzed by graphene supported bimetallic Pd-Ni clusters: The role of Ni content and the hydrogen coverage effect. Applied Surface Science, 2022, 606, 154944.	3.1	4
71564	The impact of disorder on the 4O-martensite of Niâ€“Mnâ€“Sn Heusler alloy. Intermetallics, 2022, 151, 107708.	1.8	4
71565	First-principles investigation on electronic structures and energetic characteristics of Î³/Î³ tilt grain boundaries in Î³-TiAl intermetallic. Intermetallics, 2022, 151, 107723.	1.8	5
71566	Temperature and thickness dependent dielectric functions of MoTe2 thin films investigated by spectroscopic ellipsometry. Applied Surface Science, 2022, 605, 154813.	3.1	6
71567	Optically transparent ferromagnetic 2D WSe2/VSe2 heterostructure with high Curie temperature and high refractive index. Applied Surface Science, 2022, 605, 154754.	3.1	6
71568	Two-dimensional GaS/MoTe2 van der Waals heterostructures with tunable electronic and optical properties. Materials Science in Semiconductor Processing, 2022, 152, 107103.	1.9	4
71569	Viscosity of liquid gallium: Neural network potential molecular dynamics and experimental study. Computational Materials Science, 2022, 215, 111802.	1.4	8
71570	A potential C-S-H nucleation mechanism: atomistic simulations of the portlandite to C-S-H transformation. Cement and Concrete Research, 2022, 162, 106965.	4.6	11
71571	Prediction of van Hove singularities, excellent thermoelectric performance, and non-trivial topology in monolayer rhenium dichalcogenides. Materials Today Communications, 2022, 33, 104468.	0.9	5
71572	Structural and optoelectronic properties of Ge- and Si -based inorganic two dimensional Ruddlesden Popper halide perovskites. Materials Today Communications, 2022, 33, 104368.	0.9	1
71573	Interaction mechanism between cadmium species and Fe/Mn-doped carbon materials in municipal solid waste incineration flue gas: A density functional theory study. Applied Surface Science, 2022, 605, 154824.	3.1	3
71574	Transition metal embedded graphynes as advanced bifunctional single atom catalysts for oxygen reduction and evolution reactions. Applied Surface Science, 2022, 605, 154828.	3.1	11
71575	The ordering behavior of Co3Al-based Î³â€² phase with L12 structure predicted by the thermodynamic model with support of first-principles calculations. Materials Today Communications, 2022, 33, 104447.	0.9	1
71576	Relation between cation distribution and chemical bonds in spinel NiFe2O4. Materials Today Communications, 2022, 33, 104436.	0.9	5
71577	New superhard tetragonal BCN from crystal chemistry and first principles. Materialia, 2022, 26, 101581.	1.3	8
71578	Site-dependent mechanical properties of 3d transition metal-doped MnV intrinsic ductile intermetallic: First-principles and data mining study. Computational Materials Science, 2022, 215, 111801.	1.4	1

#	Article	IF	Citations
71579	Rationally designed metal-N-C/MoS2 heterostructures as bifunctional oxygen electrocatalysts: A computational study. Applied Surface Science, 2022, 606, 154969.	3.1	7
71580	In situ mitigating cation mixing of Ni-rich cathode at high voltage via Li2MnO3 injection. Energy Storage Materials, 2022, 53, 212-221.	9.5	13
71581	Passivation of surface defects in FAPbI3 perovskite by methimazole molecule: A first-principles investigation. Applied Surface Science, 2022, 605, 154829.	3.1	3
71582	DFT investigations of pressure effect on lead-free double perovskites Cs2ZrCl6 and Cs2ZrBr6: Structural stability and band gap evolution. Materials Today Communications, 2022, 33, 104366.	0.9	0
71583	A combined experimental and theoretical study of small and large vacancy clusters in tungsten. Journal of Nuclear Materials, 2022, 571, 154019.	1.3	9
71584	A in-plane biaxial strain tunable electronic structures and magnetic properties of Fe2C monolayer. Journal of Magnetism and Magnetic Materials, 2022, 563, 169959.	1.0	5
71585	Effect of vacancy defects and co-doping on the quantum capacitance of silicene-based electrode materials. Applied Surface Science, 2022, 605, 154673.	3.1	9
71586	Investigating the electrochemical properties of SnO monolayer in sodium-ion batteries. Journal of Physics and Chemistry of Solids, 2022, 171, 110975.	1.9	6
71587	Effect of molecular impurities on properties of clean and cesiated Mo(001) surface: A DFT study of the low coverage limit. Applied Surface Science, 2022, 605, 154706.	3.1	2
71588	In-situ induced sulfur vacancy from phosphorus doping in FeS2 microflowers for high-efficiency lithium storage. Materials Today Nano, 2022, 20, 100261.	2.3	8
71589	Dual-site passivation of tin-related defects enabling efficient lead-free tin perovskite solar cells. Nano Energy, 2022, 103, 107818.	8.2	37
71590	Low power consumed PV-electrolysis with CoFeP nanowires for hydrazine-assisted hydrogen production. Applied Surface Science, 2022, 606, 154951.	3.1	7
71591	A DFT study of H2S, H2O, SO2 and CH4 Adsorption Behavior on Graphene Surface Decorated with Alkaline Earth Metals. Surface Science, 2022, 726, 122178.	0.8	2
71592	Adjustable electronic properties of PtSe2/HfS2 heterostructures via strain engineering. Applied Surface Science, 2022, 606, 154838.	3.1	4
71593	Hydrogen delaying the formation of Guinier-Preston zones in aluminium alloys. Acta Materialia, 2022, 241, 118373.	3.8	5
71594	Elucidation of formation and transformation mechanisms of Ca-rich Laves phase in Mg-Al-Ca-Mn alloys. Journal of Alloys and Compounds, 2022, 928, 167177.	2.8	2
71595	Species identification of phosphate at the ZrO2/water interface: A combined ATR-FTIR and DFT study. Applied Surface Science, 2022, 606, 154946.	3.1	1
71596	Heterogeneous nucleation interface between LaAlO3 and niobium carbide: First-principles calculation. Applied Surface Science, 2022, 606, 154731.	3.1	4

#	Article	IF	Citations
71597	Layered Zn-based semiconductors K2Zn3S4 and Rb2Zn3Se4: Crystal growth, structure and potential p-type transparent conductivity. Journal of Alloys and Compounds, 2022, 927, 167098.	2.8	0
71598	Effects of short-range order on phase equilibria and opto-electronic properties of ternary alloy ZnxCd1-xTe. Solar Energy Materials and Solar Cells, 2022, 248, 111971.	3.0	1
71599	Exploring the effect of partial RE (Nd, Eu, Tm) substitution on Sn sites on the electronic and physical properties of BaSnO3. Physica B: Condensed Matter, 2022, 646, 414306.	1.3	1
71600	Blue luminescence of Cs2CuCl4 glass ceramics with long-term water-resistance stability. Journal of Non-Crystalline Solids, 2022, 597, 121867.	1.5	5
71601	Rational design of the first and second coordination spheres for copper single-atom catalyst to boost highly efficient oxygen reduction. Applied Surface Science, 2022, 605, 154832.	3.1	6
71602	Bi3Se4 nanodots in porous carbon: A new anode candidate for fast lithium/sodium storage. Energy Storage Materials, 2022, 53, 1-12.	9.5	19
71603	Size, electronic and magnetic effects on the deviation of Retgersâ€™ law in binary FCC alloys. Journal of Solid State Chemistry, 2022, 316, 123569.	1.4	2
71604	Two-dimensional MgAl2S4 as potential photocatalyst for water splitting and strategies to boost its performance. Applied Surface Science, 2022, 605, 154826.	3.1	3
71605	A general rule for predicting the magnetic moment of Cobalt-based Heusler compounds using compressed sensing and density functional theory. Journal of Magnetism and Magnetic Materials, 2022, 563, 169818.	1.0	1
71606	Morphology engineering of Co-MOF nanostructures to tune their electrochemical performances for electrocatalyst and energy-storage applications supported by DFT studies. Applied Surface Science, 2022, 605, 154691.	3.1	9
71607	Insights into Cation-disorder effect on stability, electronic structure and defect properties of Zn-IV-nitrides: The case of ZnGeN2. Materials Today Communications, 2022, 33, 104385.	0.9	0
71608	The influence of different functional groups on quantum capacitance, electronic and optical properties of Hf2C MXene. Applied Surface Science, 2022, 605, 154830.	3.1	10
71609	Metal-coordination and surface adhesion-assisted molding enabled strong, water-resistant carboxymethyl cellulose films. Carbohydrate Polymers, 2022, 298, 120084.	5.1	12
71610	First-principles calculation on effects of oxygen vacancy on Î±-MnO2 and Î²-MnO2 during oxygen reduction reaction for rechargeable metal-air batteries. Journal of Alloys and Compounds, 2022, 926, 166924.	2.8	9
71611	Rationally designed WS<mml:math xmlns:mml="http://www.w3.org/1998/Math/MathML" altimg="si186.svg" display="inline" id="d1e919"><mml:msub><mml:mrow /><mml:mrow><mml:mn>2</mml:mn></mml:mrow></mml:msub></mml:math>/C<mml:math xmlns:mml="http://www.w3.org/1998/Math/MathML" altimg="si186.svg" display="inline" id="d1e927"><mml:msub><mml:mrow /><mml:mrow><mml:mn>2</mml:mn></mml:mrow></mml:msub></mml:math>N layered heterostructures	3.1	6
71612	Theoretical insights into multi-metal atoms embedded nitrogen-doped graphene as efficient bifunctional catalysts for oxygen reduction and evolution reactions. Applied Surface Science, 2022, 605, 154714.	3.1	10
71613	Square lattice antiferromagnets (NO)M(NO3)3 (M = Co, Ni): Effects of anisotropy. Journal of Alloys and Compounds, 2022, 929, 167197.	2.8	0
71614	Adsorption of metal atoms on MoSi2N4 monolayer: A first principles study. Materials Science in Semiconductor Processing, 2022, 152, 107072.	1.9	61

#	Article	IF	Citations
71615	Dual-electric-polarity augmented cyanoethyl cellulose-based triboelectric nanogenerator with ultra-high triboelectric charge density and enhanced electrical output property at high humidity. Nano Energy, 2022, 103, 107748.	8.2	23
71616	Etching-assisted synthesis of single atom Ni-tailored Pt nanocatalyst enclosed by high-index facets for active and stable oxygen reduction catalysis. Nano Energy, 2022, 103, 107800.	8.2	13
71617	Sensing applications of GeBi nanosheet for environmentally toxic/non-toxic gases: Insights from density functional theory calculations. Applied Surface Science, 2022, 606, 154741.	3.1	5
71618	Shortening the screening process towards high-performance 2D-MOF NRR electrocatalysts with <mml:math xmlns:mml="http://www.w3.org/1998/Math/MathML" altimg="si7.svg"><mml:mrow><mml:mi mathvariant="normal">Î”</mml:mi><mml:mfenced open="(") Tj ETQq1 1 0.784314 rgBT /Overlock 10 Tf 50 622 Td (close=")"><mml:mr width="0.333333em" /><mml:msub><mml:mi>Î¼</mml:mi><mml:mrow><mml:mtext>B</mml:mtext><mml:mi>_<. Applied Surface	3.1	11
71619	Porous silicon particles embedded in N-doped graphene and carbon nanotube framework for high-performance lithium-ion batteries. Journal of Alloys and Compounds, 2022, 927, 167055.	2.8	8
71620	First-principles calculations study of TiS2/Ti2CS2 heterostructure as an anode material for Li/Na/K-ion batteries. Computational Materials Science, 2022, 215, 111784.	1.4	6
71621	Multi-methodological study of temperature trends in MÃ¶ssbauer effect in Sn. Computational Materials Science, 2022, 215, 111780.	1.4	2
71622	Magnetocaloric response with significant mechanical efficiency in frustrated intermetallic compound Pr2Co0.86Si2.88. Intermetallics, 2022, 151, 107730.	1.8	1
71623	Exploration of new direct gap semiconductor Na2X (X = S and Se) monolayers. Applied Surface Science, 2022, 606, 154809.	3.1	4
71624	CALPHAD modeling of uranium nitride (UN) fabrication routes enabled by first-principles calculations. Calphad: Computer Coupling of Phase Diagrams and Thermochemistry, 2022, 79, 102463.	0.7	0
71625	Role of quantum well in Pd(111) thin film magnetism. Journal of Magnetism and Magnetic Materials, 2022, 563, 169891.	1.0	1
71626	Perforated nitrogen-rich graphene-like carbon nanolayers supported Cu-In catalyst for boosting CO2 electroreduction to CO. Journal of Energy Chemistry, 2022, 75, 383-390.	7.1	16
71627	Tuning the size and chemisorption of FeP4 by trace Ru doping for hydrazine-assisted hydrogen evolution in seawater at largeâ€ƈurrentâ€ƌensity. Applied Catalysis B: Environmental, 2022, 319, 121950.	10.8	29
71628	Molecular levels unveil the membrane fouling mitigation mechanism of a superpotent N-rGO catalytic ozonation membrane: Interfacial catalytic reaction pathway and induced EfOM transformation reactions. Applied Catalysis B: Environmental, 2022, 319, 121943.	10.8	11
71629	A general strategy and a consolidated mechanism for low-methane hydrogenolysis of polyethylene over ruthenium. Applied Catalysis B: Environmental, 2022, 319, 121899.	10.8	25
71630	Insights to electronic structures, elastic properties, fracture toughness, and thermal properties of M23C6 carbides. International Journal of Refractory Metals and Hard Materials, 2022, 109, 105985.	1.7	17
71631	Lattice dynamics and elastic properties of Î±-U at high-temperature and high-pressure by machine learning potential simulations. Journal of Nuclear Materials, 2022, 572, 154029.	1.3	6
71632	Thermoelectric power factor of MnSb2X4 (XÂ=ÂS, Se) spinel chalcogenides â€“ A DFT study. Computational Materials Science, 2022, 215, 111758.	1.4	2

#	Article	IF	Citations
71633	Unravelling the regulating role of graphene coating on improving the electrochemical performance of pyrophosphate cathode material: A first-principles study. Applied Surface Science, 2022, 605, 154814.	3.1	3
71634	K+ and CeO2 nanoparticles modified OMS-2 nanorods for enhanced activity and stability of photocatalytic toluene oxidation: K+ charge modulation and mechanistic investigation. Chemical Engineering Journal, 2023, 451, 138943.	6.6	13
71635	High-throughput informed machine learning models for ultrastrong B-N solids. Computational Materials Science, 2022, 215, 111789.	1.4	3
71636	Constructing machine learning potentials with active learning. , 2023, , 313-327.		1
71637	Optical properties and simulated x-ray near edge spectra for Y2O2S and Er doped Y2O2S. Materials Today Communications, 2022, 33, 104328.	0.9	1
71638	To define nonradiative defects in semiconductors: An accurate DLTS simulation based on first-principle. Computational Materials Science, 2022, 215, 111760.	1.4	4
71639	First-principles study of <mml:math xmlns:mml="http://www.w3.org/1998/Math/MathML" altimg="si71.svg" display="inline" id="d1e3448"><mml:mi>A</mml:mi></mml:math>TcO<mml:math xmlns:mml="http://www.w3.org/1998/Math/MathML" altimg="si72.svg" display="inline" id="d1e3453"><mml:msub><mml:mrow /><mml:mrow><mml:mn>4</mml:mn></mml:mrow></mml:msub></mml:math> pertechnetates. Journal of Physics and Chemistry of Solids, 2022, 171, 110979.	1.9	4
71640	Strain tailored electronic structure and magnetic properties of Fe-doped Zr8C4T8 (TÂ=ÂF, O) monolayers. Physica E: Low-Dimensional Systems and Nanostructures, 2023, 145, 115488.	1.3	2
71641	Stitching electron localized heptazine units with â€œcarbon patchesâ€•to regulate exciton dissociation behavior of carbon nitride for photocatalytic elimination of petroleum hydrocarbons. Chemical Engineering Journal, 2023, 452, 139092.	6.6	7
71642	Towards an ultra-long lifespan Li-CO2: electron structure and charge transfer pathway regulation on hierarchical architecture. Chemical Engineering Journal, 2023, 451, 138953.	6.6	2
71643	Pt/C as a bifunctional ORR/iodide oxidation reaction (IOR) catalyst for Zn-air batteries with unprecedentedly high energy efficiency of 76.5%. Applied Catalysis B: Environmental, 2023, 320, 121992.	10.8	31
71644	Basics of dynamics. , 2023, , 117-133.		1
71645	In situ growth of ZnO nanosheets on Ti3C2Tx MXene for Superior-Performance Zinc-Nickel secondary battery. Chemical Engineering Journal, 2023, 451, 139073.	6.6	15
71646	TTDFT: A GPU accelerated Tucker tensor DFT code for large-scale Kohn-Sham DFT calculations. Computer Physics Communications, 2023, 282, 108516.	3.0	1
71647	Temperature dependence of solute segregation energies at W GBs from first principles. Scripta Materialia, 2023, 222, 115059.	2.6	4
71648	Interface design for the transport properties in asymmetric two-dimensional van der Waals multiferroic tunnel junctions. Physica E: Low-Dimensional Systems and Nanostructures, 2023, 145, 115501.	1.3	5
71649	2D RhTe Monolayer: A highly efficient electrocatalyst for oxygen reduction reaction. Journal of Colloid and Interface Science, 2023, 629, 971-980.	5.0	2
71650	Rationally designed oxygen vacancy for achieving effective and kinetically boosted Na-Se batteries. Chemical Engineering Journal, 2023, 451, 139062.	6.6	5

#	Article	IF	Citations
71651	Trace Pt atoms as electronic promoters in Pd clusters for direct synthesis of hydrogen peroxide. Chemical Engineering Journal, 2023, 451, 138867.	6.6	18
71652	Oxidation of iodide by PbO2, the major lead pipe corrosion product: Kinetics, mechanism and formation of toxic iodinated disinfection by-products. Chemical Engineering Journal, 2023, 451, 139033.	6.6	4
71653	Extraordinary deactivation offset effect of zinc and arsenic on V2O5 â^'WO3/TiO2 catalysts: Like cures like. Journal of Hazardous Materials, 2023, 441, 129894.	6.5	7
71654	Quasicrystal stability in complex aluminum alloys: Insights from first principles models on structural motifs in crystalline approximants. Scripta Materialia, 2023, 222, 115046.	2.6	5
71655	Bringing the promises of microreactors and gold catalysis to lignocellulosic biomass valorization: A study on oxidative transformation of furfural. Chemical Engineering Journal, 2023, 452, 138903.	6.6	5
71656	A bifunctional nitrogen doped carbon network as the interlayer for dendrite-free Zn anode. Chemical Engineering Journal, 2023, 452, 139264.	6.6	9
71657	Construction of Co/Ni-Free P2-layered metal oxide cathode with high reversible oxygen redox for sodium ion batteries. Chemical Engineering Journal, 2023, 452, 138912.	6.6	13
71658	Unravelling the regulation mechanism of nanoflower shaped Na3V2(PO4)3 in methanolâ€“water system for high performance sodium ion batteries. Chemical Engineering Journal, 2023, 451, 138780.	6.6	14
71659	Radical-promoted room-temperature terminal alkyne activation on Au(111). Surface Science, 2023, 727, 122180.	0.8	1
71660	Low temperature mechano-catalytic biofuel conversion using liquid metals. Chemical Engineering Journal, 2023, 452, 139350.	6.6	6
71661	Iron nitride nanoparticles for rapid dechlorination of mixed chlorinated ethene contamination. Journal of Hazardous Materials, 2023, 442, 129988.	6.5	10
71662	Catalyst geometry dependent single-walled carbon nanotube formation from polyaromatic hydrocarbon molecule: Pt(111) surface versus Pt nanoparticle. Carbon, 2023, 201, 483-490.	5.4	2
71663	Synergistic effect of CoOx and Ni-Co alloy in Ni-Co/SAPO-11 catalysts for the deoxygenation of stearic acids. Chemical Engineering Journal, 2023, 451, 138929.	6.6	12
71664	On the structure of rare-earth sesquioxide Sm2O3 in Sm2Co17-type magnets. Scripta Materialia, 2023, 222, 115018.	2.6	3
71665	A mechanism in boosting H2 generation: nanotip-enhanced local temperature and electric field with the boundary layer. Journal of Colloid and Interface Science, 2023, 629, 755-765.	5.0	6
71666	Alleviating the self-discharge and enhancing the polysulphides conversion kinetics with LaCO3OH nanocrystals decorated hierarchical porous carbon. Chemical Engineering Journal, 2023, 452, 139091.	6.6	16
71667	Tuned layered double hydroxide-based catalysts inducing singlet oxygen evolution: Reactive oxygen species evolution mechanism exploration, norfloxacin degradation and catalysts screen based on machine learning. Applied Catalysis B: Environmental, 2023, 320, 121880.	10.8	19
71668	N-bridged Ni and Mn single-atom pair sites: A highly efficient electrocatalyst for CO2 conversion to CO. Applied Catalysis B: Environmental, 2023, 320, 121953.	10.8	13

#	Article	IF	Citations
71669	Insights into highly efficient piezocatalytic molecule oxygen activation over Bi2Fe4O9: Active sites and mechanism. Chemical Engineering Journal, 2023, 452, 139300.	6.6	19
71670	On the role of Zr to facilitate the synthesis of diesel and jet fuel range intermediates from biomass-derived carbonyl compounds over aluminum phosphate. Applied Catalysis B: Environmental, 2023, 320, 121936.	10.8	5
71671	A multifunctional separator based on dilithium tetraaminophthalocyanine self-assembled on rGO with improved cathode and anode performance in Liâ€“S batteries. Carbon, 2023, 201, 307-317.	5.4	6
71672	The new role of pivotal intermediate CH in CO activation and conversion to hydrocarbons on the transition metal catalysts. Fuel, 2023, 331, 125788.	3.4	1
71673	High performance carbon dioxide electroreduction in ionic liquids with in situ shell-isolated nanoparticle-enhanced Raman spectroscopy. Chemical Engineering Journal, 2023, 451, 138975.	6.6	9
71674	Density-functional theory. , 2023, , 27-65.		0
71675	CuNCN derived Cu-based/CxNy catalysts for highly selective CO2 electroreduction to hydrocarbons. Applied Catalysis B: Environmental, 2023, 320, 121948.	10.8	10
71676	Nitrogen-doped cobalt-iron oxide cocatalyst boosting photoelectrochemical water splitting of BiVO4 photoanodes. Applied Catalysis B: Environmental, 2023, 320, 121947.	10.8	30
71677	Transient absorption study on Red Vermilion darkening in presence of chlorine ions and after UV exposure. Journal of Photochemistry and Photobiology A: Chemistry, 2023, 435, 114291.	2.0	2
71678	Theoretical study of the M7X6 type of vacancy ordered phases in nonstoichiometric hafnium and tantalum carbides. International Journal of Refractory Metals and Hard Materials, 2023, 110, 106005.	1.7	0
71679	Atomic-structure and charge redistribution modified by intrinsic strain in Î±-fe/TMN (TM=Ti/Zr/Hf/V/Nb/Ta) interfaces. Physica E: Low-Dimensional Systems and Nanostructures, 2023, 145, 115495.	1.3	3
71680	Single metal atom anchored on porous boron nitride nanosheet for efficient collaborative urea electrosynthesis: A computational study. Chemical Engineering Journal, 2023, 451, 138885.	6.6	18
71681	Properties and self-adsorptions for ZrC low-index surfaces: A first-principles study. Surface Science, 2023, 727, 122188.	0.8	1
71682	The role of repulsive and attractive forces in low-energy (3â€“15 eV) electron stimulated desorption of anions from molecular layers grown on clean and contaminated metallic substrates. Chemical Physics, 2023, 564, 111661.	0.9	1
71683	A novel approach for the prevention of ionizing radiation-induced bone loss using a designer multifunctional cerium oxide nanozyme. Bioactive Materials, 2023, 21, 547-565.	8.6	15
71684	Engineering the interface of porous CoMoO3 nanosheets with Co3Mo nanoparticles for high-performance electrochemical overall water splitting. Journal of Materials Science and Technology, 2023, 137, 184-192.	5.6	9
71685	The real-time dynamic holographic display of LN:Bi,Mg crystals and defect-related electron mobility. Opto-Electronic Advances, 2022, 5, 210135-210135.	6.4	8
71686	Understanding the role of Cl doping in the oxygen evolution reaction on cuprous oxide by DFT. Physical Chemistry Chemical Physics, 2022, 24, 25347-25355.	1.3	2

#	Article	IF	Citations
71687	Activation of Peroxymonosulfate for Degrading Ibuprofen Via Single Atom Cu Anchored by Carbon Skeleton and Chlorine Atom: The Radical and Non-Radical Pathways. SSRN Electronic Journal, 0, , .	0.4	0
71688	Identification of Hydrogen Trapping in Aluminum Alloys Via Muon Spin Relaxation Method and First-Principles Calculations. SSRN Electronic Journal, 0, , .	0.4	0
71689	Spinel nitride solid solutions: charting properties in the configurational space with explainable machine learning. , 2022, 1, 665-678.		1
71690	First-Principles Study on Thermodynamic Stability, Mechanical Properties, and Low Lattice Thermal Conductivity of Mg-Zn-Y and Mg-Al-Y Alloys with Long-Period Stacking Ordered (Lpso) Structures. SSRN Electronic Journal, 0, , .	0.4	0
71691	Electric field tunability of the electronic properties and contact types in the MoS₂/SiH heterostructure. RSC Advances, 2022, 12, 24172-24177.	1.7	3
71692	Doping atom improves photocatalytic performance in a new metal-free organic photocatalyst for water splitting. Physical Chemistry Chemical Physics, 2022, 24, 29350-29356.	1.3	12
71693	The structure and electronic properties of the MoSe₂/PtS₂ van der Waals heterostructure. Physical Chemistry Chemical Physics, 2022, 24, 19853-19864.	1.3	2
71694	First-principles study of CO₂ hydrogenation to formic acid on single-atom catalysts supported on SiO₂. Physical Chemistry Chemical Physics, 2022, 24, 19938-19947.	1.3	2
71695	Morphology and carrier mobility of high-B-content B_xAl_{1â^'x}N ternary alloys from an ab initio global search. Nanoscale, 2022, 14, 11335-11342.	2.8	1
71696	Upconversion and multiexciton generation in organic Mn(<scp>ii</scp>) complex boost the quantum yield to > 100%. Materials Chemistry Frontiers, 2022, 6, 3102-3114.	3.2	10
71697	Synergistic Effect ÂOf Mn 3+ ÂAnd Oxygen Vacancy OnÂTheÂBifunctional Oxygen Electrocatalytic Performance of Mnox/CntsÂComposites. SSRN Electronic Journal, 0, , .	0.4	0
71698	Computational screen of M₂P metal phosphides for catalytic ethane dehydrogenation. Catalysis Science and Technology, 2022, 12, 5629-5639.	2.1	1
71699	Defective Lithium Titanate Oxide with Stable Cycling Over a Wide Voltage Window. SSRN Electronic Journal, 0, , .	0.4	0
71700	Regulating the electronic structure of MoO₂/Mo₂C/C by heterostructure and oxygen vacancies for boosting lithium storage kinetics. Dalton Transactions, 2022, 51, 12620-12629.	1.6	3
71701	Theoretical design of platinumâ€“sliver single atom alloy catalysts with CO adsorbate-induced surface structures. Physical Chemistry Chemical Physics, 2022, 24, 19488-19501.	1.3	0
71702	Unraveling the Improved Co2 Adsorption and Cooh* Formation Over Cu-Decorated Zno Nanosheets for Co2 Reduction Toward C O. SSRN Electronic Journal, 0, , .	0.4	2
71703	Capacity prediction of K-ion batteries: a machine learning based approach for high throughput screening of electrode materials. Materials Advances, 2022, 3, 7833-7845.	2.6	7
71704	Phosphorus Doping and Phosphate Coating Enhance the Performance OfÂÂLini0.8co0.1mn0.1o2. SSRN Electronic Journal, 0, , .	0.4	0

#	Article	IF	Citations
71705	Heating-Induced Exfoliation and Thermal Reduction of Moo3 Particles Monitored by In-Situ Transmission Electron Microscopy. SSRN Electronic Journal, 0, , .	0.4	0
71706	Metal-Organic Framework-Induced Edge-Riched Growth of Layered Bi2se3 Towards Ultrafast Na-Ion Storage. SSRN Electronic Journal, 0, , .	0.4	0
71707	Surface Modification of Mcr2o4 (M = Mg and Zn) by Cu-Doping: Theoretical Prediction and Experimental Observation of Enhanced Catalysis for Co Oxidation. SSRN Electronic Journal, 0, , .	0.4	0
71708	Switching of Co2 Hydrogenation Selectivity Via Chlorine Poisoning Over Ru/Tio2 Catalyst. SSRN Electronic Journal, 0, , .	0.4	0
71709	Multi-scale simulation of proton diffusion in dislocation cores in BaZrO₃. Physical Chemistry Chemical Physics, 2022, 24, 21440-21451.	1.3	2
71710	Lanthanide/actinide boride nanoclusters and nanomaterials based on boron frameworks consisting of conjoined B_n rings (n = 7â€“9). Physical Chemistry Chemical Physics, 2022, 24, 21078-21084.	1.3	1
71711	Modulating the Schottky barrier of MXenes/2D SiC contacts via functional groups and biaxial strain: a first-principles study. Physical Chemistry Chemical Physics, 2022, 24, 20837-20847.	1.3	7
71712	Mechanism of the two-dimensional WSeTe/Zr₂CO₂ direct Z-scheme van der Waals heterojunction as a photocatalyst for water splitting. Physical Chemistry Chemical Physics, 2022, 24, 21030-21039.	1.3	4
71713	Comprehensive Mechanism of Co Electroreduction on Dacs Anchored on N-Doped Graphene. SSRN Electronic Journal, 0, , .	0.4	0
71714	Carbonate Dimorphism, and the Reinterpretation of Rates of (Non)-Stoichiometric Oxygen-Driven Catalytic Cycles. SSRN Electronic Journal, 0, , .	0.4	0
71715	Two-Dimensional Mgal2s4 as Potential Photocatalyst for Water Splitting and Strategies to Boost its Performance. SSRN Electronic Journal, 0, , .	0.4	0
71716	Sustainable production of gluconic acid and glucuronic acid via microwave-assisted glucose oxidation over low-cost Cu-biochar catalysts. Green Chemistry, 2022, 24, 6657-6670.	4.6	20
71717	Novel mixed H⁺/e^{â^'}/O^{2â^'} conducting cathode material PrBa_{0.9}K_{0.1}Fe_{1.9}Zn_{0.1}O_{5+Î´} for proton-conducting solid oxide fuel cells. Journal of Materials Chemistry A, 2022, 10, 17425-17433.	5.2	15
71718	Different interfacial reactivity of lithium metal chloride electrolytes with high voltage cathodes determines solid-state battery performance. Energy and Environmental Science, 2022, 15, 3933-3944.	15.6	28
71719	A new metal complex-templated silver iodobismuthate exhibiting photocurrent response and photocatalytic property. Dalton Transactions, 2022, 51, 13361-13367.	1.6	8
71720	Lattice distortion derived catalytic degradation in multi-oxide cathode catalyst for Liâ€“oxygen batteries. Journal of Materials Chemistry A, 2022, 10, 18078-18086.	5.2	2
71721	First principles prediction of two-dimensional Janus XMoGeN₂ (X = S, Se and Te) materials. Dalton Transactions, 2022, 51, 14338-14344.	1.6	10
71722	The effect of doping and strain on superconductivity of T-graphene. Physical Chemistry Chemical Physics, 0, , .	1.3	2

#	Article	IF	Citations
71723	bcc superstructures: RE₂RuIn with RE = Sc, Y, Dy-Tm and Lu. Dalton Transactions, 2022, 51, 14156-14164.	1.6	5
71724	Tailoring the optoelectronic properties and dielectric profiles of few-layer S-doped MoO₃ and O-doped MoS₂ nanosheets: a first-principles study. Physical Chemistry Chemical Physics, 2022, 24, 25440-25451.	1.3	6
71725	A smeltingâ€“rolling strategy for ZnIn bulk phase alloy anodes. Chemical Science, 2022, 13, 11656-11665.	3.7	30
71726	Fast charge transfer between iodide ions and a delocalized electron system on the graphite surface for boosting hydrogen production. Journal of Materials Chemistry A, 2022, 10, 23982-23989.	5.2	3
71727	Interfacial Biâ€“S bonds modulate band alignment for efficient solar water oxidation. Nanoscale, 2022, 14, 14520-14528.	2.8	6
71728	Achieving high-rate and high-capacity Zn metal anodesviaa three-in-one carbon protective layer. Journal of Materials Chemistry A, 2022, 10, 17440-17451.	5.2	27
71729	A new phosphorene allotrope: the assembly of phosphorene nanoribbons and chains. Physical Chemistry Chemical Physics, 2022, 24, 22572-22579.	1.3	4
71730	Twist-stacked 2D bilayer Fe₃GeTe₂ with tunable magnetism. Journal of Materials Chemistry C, 2022, 10, 12741-12750.	2.7	8
71731	Tripletâ€“triplet energy transfer from Bi³⁺to Sb³⁺in zero-dimensional indium hybridsviaa B-site co-doping strategy toward white-light emission. Inorganic Chemistry Frontiers, 2022, 9, 5960-5968.	3.0	7
71732	Two-dimensional antiferromagnetic topological insulator in KCuSe/NaMnBi van der Waals heterobilayers. Physical Chemistry Chemical Physics, 0, , .	1.3	0
71733	Metal center regulation of the porphyrin unit in covalent organic polymers for boosting the photocatalytic CO₂ reduction activity. Catalysis Science and Technology, 2022, 12, 6527-6539.	2.1	2
71734	The structure of methanol at 5.09 GPa: the fortuitous formation of a new high-pressure phase. CrystEngComm, 0, , .	1.3	0
71735	Lower thermal conductivity of body centered cubic carbon (C14): a comparative study with diamond. Physical Chemistry Chemical Physics, 2022, 24, 23817-23824.	1.3	2
71736	Oxidative decomposition of dimethyl methylphosphonate on rutile TiO₂(110): the role of oxygen vacancies. Physical Chemistry Chemical Physics, 2022, 24, 23402-23419.	1.3	3
71737	Isomeric dibenzooctazethrene diradicals for high-performance air-stable organic field-effect transistors. Chemical Science, 2022, 13, 11442-11447.	3.7	7
71738	Nitrogen stabilizes the wurtzite polymorph in ZnSe_{1â^'x}Te_x thin films. Journal of Materials Chemistry C, 2022, 10, 15806-15815.	2.7	1
71739	Two-dimensional AlXY (X = S, Se, and Y = Cl, Br, I) monolayers: promising photocatalysts for water splitting with high-anisotropic carrier mobilities. Journal of Materials Chemistry A, 2022, 10, 22676-22685.	5.2	9
71740	Two-dimensional type-II XSi₂P₄/MoTe₂ (X = Mo, W) van der Waals heterostructures with tunable electronic and optical properties. New Journal of Chemistry, 0, , .	1.4	3

#	Article	IF	Citations
71741	Mercurial possibilities: determining site distributions in Cu₂HgSnS₄ using ^{63/65}Cu, ¹¹⁹Sn, and ¹⁹⁹Hg solid-state NMR spectroscopy. Physical Chemistry Chemical Physics, 2022, 24, 24306-24316.	1.3	5
71742	All-organic covalent organic frameworks/perylene diimide urea polymer S-scheme photocatalyst for boosted H2 generation. Chinese Journal of Catalysis, 2022, 43, 2581-2591.	6.9	53
71743	Density functional theory based computational investigations on the stability of highly active trimetallic PtPdCu nanoalloys for electrochemical oxygen reduction. Faraday Discussions, 0, , .	1.6	1
71744	First-principles molecular dynamics simulations of UCl_nâ€“MgCl₂ (n = 3, 4) molten salts. Physical Chemistry Chemical Physics, 2022, 24, 24281-24289.	1.3	1
71745	High throughput exploration of the oxidation landscape in high entropy alloys. Materials Horizons, 2022, 9, 2644-2663.	6.4	5
71746	A DFT prediction of two-dimensional MB₃ (M = V, Nb, and Ta) monolayers as excellent anode materials for lithium-ion batteries. RSC Advances, 2022, 12, 28525-28532.	1.7	6
71747	The atomic defects on the (104) and (110) surfaces of the MgCl₂-supported Zieglerâ€“Natta catalyst: a periodic DFT study. Catalysis Science and Technology, 2022, 12, 6761-6770.	2.1	3
71748	Structural evolution, photoelectron spectra and vibrational properties of anionic GdGe_n^{â^’} (n = 5â€“18) nanoalloy clusters: a DFT insight. RSC Advances, 2022, 12, 22020-22030.	1.7	5
71749	Tuning photoelectron dynamic behavior of thiolate-protected MAu₂₄ nanoclusters via heteroatom substitution. Nanoscale Horizons, 2022, 7, 1192-1200.	4.1	17
71750	The mechanism of alkali promoting water splitting on g-C₃N₄. New Journal of Chemistry, 2022, 46, 17713-17719.	1.4	0
71751	The Effect of Chemical Disorder on Magnetic Properties of Feni and Fe2ni2n Alloy. SSRN Electronic Journal, 0, , .	0.4	0
71752	Niobium tellurium as a novel broadband saturable absorber for pulsed fiber lasers. Journal of Materials Chemistry C, 2022, 10, 13201-13209.	2.7	8
71753	Spall Strength and Equation of States of 2050-T84 Al-Li Alloy Under Shock Compression Up to 120 GPA. SSRN Electronic Journal, 0, , .	0.4	0
71754	Borophene-Based Mixed-Dimensional Van Der Waals Heterojunctions for High-Performance Self-Powered Photodetector. SSRN Electronic Journal, 0, , .	0.4	0
71755	Passivation of PEA+ to CsPbI3 (110) Surface States: From the First Principles Calculations. Journal of Renewable Materials, 2022, .	1.1	2
71756	Effect of Bulk and Surface Composition on Control of Surface Reactivity Towards C, O, and H Over Ni+Ga Intermetallic Compounds in Propane Steam Reforming Reaction. SSRN Electronic Journal, 0, , .	0.4	0
71757	Penta-OsP₂ and penta-RhS₂ sheets derived from marcasite and pyrite with low lattice thermal conductivity. Journal of Materials Chemistry A, 2022, 10, 21356-21367.	5.2	3
71758	Liquid metal-based electrosynthesis of stratified zincâ€“organic frameworks. Journal of Materials Chemistry C, 0, , .	2.7	2

#	Article	IF	Citations
71759	Monolayer H-MoS₂ with high ion mobility as a promising anode for rubidium (cesium)-ion batteries. Nanoscale Advances, 2022, 4, 3756-3763.	2.2	3
71760	Exchange interactions in the 1T-VSe₂ monolayer and their modulation via electron doping using alkali metal adsorption and the electride substrate. Materials Horizons, 2022, 9, 2785-2796.	6.4	10
71761	Interface Modulation of Perovskite Oxides to Simultaneously Enhance the Activity and Stability Toward Oxygen Evolution Reaction. SSRN Electronic Journal, 0, , .	0.4	0
71762	Crystal structure prediction of N-halide phthalimide compounds: halogen bonding synthons as a touchstone. CrystEngComm, 2022, 24, 6066-6075.	1.3	3
71763	Mechanical, electronic and catalytic properties of 2H-1T' MoS2 heterointerfaces. Physical Chemistry Chemical Physics, 0, , .	1.3	0
71764	Catalytic formation of oxalic acid on the partially oxidised greigite Fe₃S₄(001) surface. Physical Chemistry Chemical Physics, 2022, 24, 20104-20124.	1.3	2
71765	A carbon capture and storage technique using gold nanoparticles coupled with Cu-based composited thin film catalysts. Sustainable Energy and Fuels, 2022, 6, 4765-4778.	2.5	1
71766	Elucidating electrochemical CO₂ reduction reaction processes on Cu(hkl) single-crystal surfaces by in situ Raman spectroscopy. Energy and Environmental Science, 2022, 15, 3968-3977.	15.6	58
71767	Novel Ptni Nanoflowers Regulated by a Third Element (Rh, Ru, Pd) as Efficient Multifunctional Electrocatalysts for Orr, Mor and Her. SSRN Electronic Journal, 0, , .	0.4	0
71768	A symmetric direct ammonia fuel cell using ternary NiCuFe alloy embedded in a carbon network as electrodes. Journal of Materials Chemistry A, 2022, 10, 18701-18713.	5.2	11
71769	Theoretical prediction of alkali oxide M₂O (M = Na and K) monolayers and formation of their Janus structure. New Journal of Chemistry, 2022, 46, 17386-17393.	1.4	1
71770	Crystal habit analysis of LiFePO₄ microparticles by AFM and first-principles calculations. CrystEngComm, 2022, 24, 6891-6901.	1.3	4
71771	Lattice dynamic stability and electronic structures of ternary hydrides La_{1â^'x}Y_xH₃via first-principles cluster expansion. RSC Advances, 2022, 12, 26808-26814.	1.7	2
71772	High-loading Fe₁ sites on vanadium disulfides: a scalable and non-defect-stabilized single atom catalyst for electrochemical nitrogen reduction. Journal of Materials Chemistry A, 2022, 10, 21142-21148.	5.2	3
71773	Photocatalytic properties of anisotropic Î²-PtX₂ (X = S, Se) and Janus Î²-PtSSe monolayers. Physical Chemistry Chemical Physics, 2022, 24, 22289-22297.	1.3	16
71774	A coordination environment effect of single-atom catalysts on their nitrogen reduction reaction performance. Physical Chemistry Chemical Physics, 2022, 24, 18854-18859.	1.3	6
71775	Influence of Main Group Elements on Structural, Electronic, Magnetic and Half-Metallic Properties of Do3-Type Mn3z (Z = Al, Ga, in, Si, Ge, Sn, P, as and Sb) Compounds - a Dft Study. SSRN Electronic Journal, 0, , .	0.4	0
71776	Vapor-phase hydrothermal construction of defective MoS₂ for highly selective electrocatalytic hydrogenation of cinnamaldehyde. Materials Advances, 2022, 3, 8250-8259.	2.6	0

#	Article	IF	Citations
71777	An ab initio investigation of the temperature-dependent energetic barriers towards CrAlB and (Mo,Cr)AlB formation in a metastable synthesis scenario. Nanoscale, 2022, 14, 12866-12874.	2.8	3
71778	Lithium stabilizes square-two-dimensional metal sheets: a computational exploration. Nanoscale, 2022, 14, 11770-11778.	2.8	0
71779	Heterogenization of molecular cobalt catalysts in robust metalâ€“organic frameworks for efficient photocatalytic CO₂ reduction. Catalysis Science and Technology, 2022, 12, 5418-5424.	2.1	3
71780	Anomalous Behavior of Strain Modulated Lattice Thermal Transport in Piezoelectric Crystals and the Effect of Polarization. SSRN Electronic Journal, 0, , .	0.4	0
71781	Unveiling the Enhancement Essence on Li2s Deposition by the Polarized Topological Î’-Polyvinylidene Fluoride: More than Built-In Electric Field Effect. SSRN Electronic Journal, 0, , .	0.4	0
71782	Phase Selection in Al90ce10ÂVerses Al90tb10ÂBy Molecular Dynamics Simulations Using Machine Leaning Interatomic Potentials. SSRN Electronic Journal, 0, , .	0.4	0
71783	Morphology Controlling of Oxygen Vacancy-Rich Biocl Nanoflowers for Photocatalytic Co2 Reduction. SSRN Electronic Journal, 0, , .	0.4	0
71785	Effect of 4d Transition Metals on the Electronic and Magnetic Properties of Twin Graphene. SSRN Electronic Journal, 0, , .	0.4	0
71786	Phase Stability, Ultrafine Microstructure, and Mechanical Properties of High-Pressure Phase of Mg ₈₅Zn ₆Y ₉. SSRN Electronic Journal, 0, , .	0.4	0
71787	Understanding the facet effects of heterogeneous Rh₂P catalysts for styrene hydroformylation. Catalysis Science and Technology, 2022, 12, 6112-6119.	2.1	4
71788	Hybrid Density Functional Theory Study of Substitutional Gd in ÃŸ-Ga2O3. SSRN Electronic Journal, 0, , .	0.4	0
71789	Simulation of Multi-Shell Fullerenes Using Machine-Learning Gaussian Approximation Potential. SSRN Electronic Journal, 0, , .	0.4	0
71790	Novel insights into lattice thermal transport in nanocrystalline Mg₃Sb₂ from first principles: the crucial role of higher-order phonon scattering. Physical Chemistry Chemical Physics, 2022, 24, 20891-20900.	1.3	5
71791	Room-temperature spin valve effect in the TiCr₂N₄ monolayer. Journal of Materials Chemistry C, 2022, 10, 12422-12427.	2.7	3
71792	Lead-free double perovskites: how divalent cations tune the electronic structure for photovoltaic applications. Journal of Materials Chemistry C, 2022, 10, 12276-12285.	2.7	6
71793	Radical-Friedelâ€“Crafts benzylation of arenes with benzyl ethers over 2H-MoS₂: ether cleavage into carbon- and oxygen-centered radicals. Dalton Transactions, 2022, 51, 15322-15329.	1.6	2
71794	Oxygen vacancy regulated selective hydrogenation of Î±,Î²-unsaturated aldehydes over LDH surface group coordinated transition metal photocatalysts. Catalysis Science and Technology, 2022, 12, 6163-6173.	2.1	5
71795	Tuning the structural stability and electrochemical properties in graphene anode materials by B doping: a first-principles study. Physical Chemistry Chemical Physics, 2022, 24, 21452-21460.	1.3	7

#	Article	IF	Citations
71796	Intrinsic type-II van der Waals heterostructures based on graphdiyne and XSSe (X = Mo, W): a first-principles study. Physical Chemistry Chemical Physics, 2022, 24, 21331-21336.	1.3	1
71797	Designing SnS/MoS₂ van der Waals heterojunction for direct Z-scheme photocatalytic overall water-splitting by DFT investigation. Physical Chemistry Chemical Physics, 2022, 24, 21321-21330.	1.3	3
71798	A promising type-II Î²-AsP/g-C₆N₆ van der Waals heterostructure photocatalyst for water splitting: a first-principles study. Physical Chemistry Chemical Physics, 2022, 24, 24939-24949.	1.3	6
71799	The influence of adsorption geometry on the reduction affinity of nitroaromatics on Au(111). Physical Chemistry Chemical Physics, 2022, 24, 22960-22970.	1.3	3
71800	Design principles of nitrogen-doped graphene nanoribbons as highly effective bifunctional catalysts for Liâ€“O₂ batteries. Physical Chemistry Chemical Physics, 2022, 24, 22589-22598.	1.3	3
71801	Density functional theoretical study of the tungsten-doped In₂O₃ catalyst for CO₂ hydrogenation to methanol. Physical Chemistry Chemical Physics, 2022, 24, 25522-25529.	1.3	8
71802	Layer-polarized anomalous Hall effects in valleytronic van der Waals bilayers. Materials Horizons, 2023, 10, 483-490.	6.4	16
71803	Effects of pâ€“d orbital mixings on magnetocrystalline anisotropy for D_{3d}-symmetric ferromagnetic semiconducting monolayers. Physical Chemistry Chemical Physics, 2022, 24, 24553-24561.	1.3	1
71804	Enhanced Electroreduction of CO₂ by Niâ^'Nâ^'C Catalysts from the Interplay Between Valency and Local Coordination Symmetry. Journal of Materials Chemistry A, 0, , .	5.2	0
71805	Activated layered double hydroxides: assessing the surface anion basicity and its connection with the catalytic activity in the cyanoethylation of alcohols. Physical Chemistry Chemical Physics, 2022, 24, 23507-23516.	1.3	2
71806	A high-throughput screening permeability separator with high catalytic conversion kinetics for Liâ€“S batteries. Journal of Materials Chemistry A, 2022, 10, 22080-22092.	5.2	20
71807	Hydrogenation of CO₂ to methanol over In-doped m-ZrO₂: a DFT investigation into the oxygen vacancy size-dependent reaction mechanism. Physical Chemistry Chemical Physics, 2022, 24, 23182-23194.	1.3	4
71808	Studies on the photoelectronic properties of a manganese (Mn)-doped lead-free double perovskite. Physical Chemistry Chemical Physics, 2022, 24, 25648-25655.	1.3	5
71809	Improving the DFT Computational Accuracy for CO Activation on Fe Surfaces by Bayesian Error Estimation Functional With Van der Waals Correlation. SSRN Electronic Journal, 0, , .	0.4	0
71810	Enhanced Photoactivity and Anti-Photocorrosion of Z-Scheme Zr2co2/Wse2ÂHeterostructure for Overall Water Splitting. SSRN Electronic Journal, 0, , .	0.4	0
71811	Experimental Study of Covalent Cr ₃C ₂ with High Ionicity: Sound Velocities, Elasticity and Mechanical Properties Under High Pressure. SSRN Electronic Journal, 0, , .	0.4	0
71812	Quantitative prediction of CeO₂ and LaAlO₃ infrared spectra based on first-principles calculations. RSC Advances, 2022, 12, 24055-24062.	1.7	0
71813	High-pressure transformations of CaC₂O₅â€“ a full structural trend from double [CO₃] triangles through the isolated group of [CO₄] tetrahedra to framework and layered structures. Physical Chemistry Chemical Physics, 2022, 24, 23578-23586.	1.3	8

#	Article	IF	Citations
71814	Exploring the photocatalytic properties and carrier dynamics of 2D Janus XMMXâ€² (X = S, Se; M = Ga, In;) Tj ETQq0 0 0 rgBT /Overlock	1.3	6
71815	The potential thermoelectric material Tl₃XSe₄ (X = V, Ta, Nb): a first-principles study. Physical Chemistry Chemical Physics, 2022, 24, 24447-24456.	1.3	4
71816	Modulation of electronic bandgaps and subsequent implications on SQ efficiencies via strain engineering in ultrathin SnX (X = S, Se) nanowires. Journal of Materials Chemistry C, 0, , .	2.7	0
71817	Aggregation and support effects in the oxidation of fluxional atomic metal clusters. The paradigmatic Cu₅ case. Physical Chemistry Chemical Physics, 2022, 24, 24810-24822.	1.3	5
71818	Anisotropy-induced phase transitions in an intrinsic half-Chern insulator Ni₂I₂. Nanoscale, 2022, 14, 13378-13388.	2.8	5
71819	Theoretical insights into graphenylene-based triple-atom catalysts for efficient nitrogen fixation. Physical Chemistry Chemical Physics, 2022, 24, 25041-25050.	1.3	5
71820	Theoretical design of high-performance halogen anion batteries with MXene electrodes: influence of functional groups, metals, and anions. Journal of Materials Chemistry A, 2022, 10, 21611-21621.	5.2	9
71821	A theoretical roadmap for the best oxygen reduction activity in two-dimensional transition metal tellurides. Chemical Science, 2022, 13, 11048-11057.	3.7	2
71822	Electric field-induced switching of anomalous Nernst conductivity in the 2D MoTe₂/VSe₂ heterostructure. Physical Chemistry Chemical Physics, 2022, 24, 22523-22530.	1.3	3
71823	Demonstration of 10+ hour energy storage with Ï•1â€²â€² laboratory size solid oxide ironâ€“air batteries. Energy and Environmental Science, 2022, 15, 4659-4671.	15.6	2
71824	Inhibiting the decomposition of methylammonium using cations with low deprotonation energy. Journal of Materials Chemistry A, 2022, 10, 22742-22749.	5.2	3
71825	Efficient direct conversion of methane into methanol on CuZn hetero-diatomic catalysts with certain coordination spheres: a DFT study. Physical Chemistry Chemical Physics, 2022, 24, 24264-24270.	1.3	3
71826	Hierarchical S-modified Cu porous nanoflakes for efficient CO₂electroreduction to formate. Nanoscale, 2022, 14, 13679-13688.	2.8	7
71827	Rhombohedral trilayer graphene is more stable than its Bernal counterpart. Nanoscale, 2022, 14, 16295-16302.	2.8	8
71828	Spontaneous magnetic merons in a half-metallic Mn₂I₃Br₃ monolayer with easy-plane anisotropy. Physical Chemistry Chemical Physics, 2022, 24, 27612-27618.	1.3	6
71829	Intrinsic spin, valley and piezoelectric polarizations in room-temperature ferrovalley Janus TiXY (XY = SCl and SeBr) monolayers. Nanoscale, 2022, 14, 15156-15164.	2.8	7
71830	2d Titanium Carbonitride Ti3cntx Mxene with Attractive Microwave Absorption Properties in X and Ku Bands. SSRN Electronic Journal, 0, , .	0.4	0
71831	Pressure-induced phase transition in Î±- and Î²-BiNbO₄. Physical Chemistry Chemical Physics, 2022, 24, 20546-20552.	1.3	5

#	Article	IF	Citations
71832	Doping and heterojunction strategies for constructing V-doped Ni₃FeN/Ni anchored on N-doped graphene tubes as an efficient overall water splitting electrocatalyst. Journal of Materials Chemistry A, 2022, 10, 18877-18888.	5.2	17
71833	Promotion of the selective catalytic reduction of NO_x with NH₃ over microporous Cu-SSZ-13 by H₂O and OH groups at low temperatures: a density functional theory study. Catalysis Science and Technology, 2022, 12, 5524-5532.	2.1	6
71834	Capture and detection of SO₂ using a chemically stable Mg(<scp>ii</scp>)â€“MOF. Journal of Materials Chemistry A, 2022, 10, 18636-18643.	5.2	7
71835	Ab initio determination of a simultaneous dual-ion charging mechanism for Ni_{0.25}Mn_{0.75}O₂ through redox reactions of Ni²⁺/Ni⁴⁺ and O^{2â^’}/O^{â^’}. Journal of Materials Chemistry A, 2022, 10, 18916-18927.	5.2	1
71836	The structural, electronic and optical properties of four Î±-Se-based heterostructures with hyperbolic characteristics. Physical Chemistry Chemical Physics, 2022, 24, 21674-21687.	1.3	1
71837	Enhanced emission efficiency in doped CsPbBr₃ perovskite nanocrystals: the role of ion valence. Journal of Materials Chemistry C, 2022, 10, 14737-14745.	2.7	2
71838	Constructing Interstitial Pillar to Manipulating Interlamination Interaction Force: Towards High Sodium-Content P2/O3 Intergrowth Cathodes. SSRN Electronic Journal, 0, , .	0.4	0
71839	N, P co-doping triggered phase transition of MoS₂ with enlarged interlayer spacing for efficient hydrogen evolution. New Journal of Chemistry, 2022, 46, 15693-15700.	1.4	5
71840	Coexistence of In- and Out-of-Plane Piezoelectricity in Janus Xssin2 (X=Cr, Mo, W) Monolayers. SSRN Electronic Journal, 0, , .	0.4	0
71841	Dominant role of OH^{â^’} and Ti³⁺ defects on the electronic structure of TiO₂ thin films for water splitting. Dalton Transactions, 2022, 51, 15300-15311.	1.6	6
71842	Elucidating Reaction Pathways in Co2 Electroreduction: Case Study of Ag and Cu2o@Ag Catalysts. SSRN Electronic Journal, 0, , .	0.4	0
71843	Modulating Electronic Structure of Ternary Transition MetalÂPhosphide for Enhanced Hydrogen Evolution Activity. SSRN Electronic Journal, 0, , .	0.4	0
71844	Few-layered V₂C MXene derived 3D V₃S₄nanocrystal functionalized carbon flakes boosting polysulfide adsorption and catalytic conversion towards Liâ€“S batteries. Journal of Materials Chemistry A, 2022, 10, 18679-18689.	5.2	17
71845	Anomalous thermal transport behavior in graphene-like carbon nitride (C₃N). Journal of Materials Chemistry C, 2022, 10, 12080-12090.	2.7	2
71846	Tunable type-II lateral MoSi₂N₄/WSi₂N₄ heterostructures for photocatalytic applications. Physical Chemistry Chemical Physics, 2022, 24, 26307-26315.	1.3	4
71847	Controlling the speciation and selectivity of Si₃N₄ supported palladium nanostructures for catalysed acetylene selective hydrogenation. Inorganic Chemistry Frontiers, 2022, 9, 5969-5981.	3.0	3
71848	Thermal activation significantly improves the organic pollutant removal rate of low-grade manganese ore in a peroxymonosulfate system. RSC Advances, 2022, 12, 20735-20745.	1.7	0
71849	Tuning the optical band gap and electrical properties of NiO thin films by nitrogen doping: a joint experimental and theoretical study. RSC Advances, 2022, 12, 21940-21945.	1.7	5

#	Article	IF	Citations
71850	Remarkable ferroelectricity-modulated electronic and magnetic properties in a 2H-VS₂/BiAlO₃(0001) hybrid system. Physical Chemistry Chemical Physics, 2022, 24, 18966-18977.	1.3	2
71851	Charge transfer modulation in charge transfer co-crystals driven by crystal structure morphology. Physical Chemistry Chemical Physics, 2022, 24, 18816-18823.	1.3	3
71852	Rational design of 2D ferroelectric heterogeneous catalysts for controllable hydrogen evolution reaction. Journal of Materials Chemistry A, 2022, 10, 22228-22235.	5.2	7
71853	Modeling of the cathodic and anodic polarization curves of metals and alloys at an electronic level. Journal of Materials Chemistry A, 2022, 10, 17652-17658.	5.2	0
71854	Effects of Aluminum Diffusion on the Oxide of the Fecral Alloys Surface: A Firstâ€“Principles Study. SSRN Electronic Journal, 0, , .	0.4	0
71855	Doping P atom with a lone pair: an effective strategy to realize high HER catalytic activity and avoid deactivation under wide H* coverage on 2D silicene and germanene by increasing the structural rigidity. Nanoscale, 2022, 14, 10918-10928.	2.8	4
71856	In-Depth Insight into the Mechanism on Photocatalytic Selective Co2 Reduction Coupled with Tetracycline Oxidation Over Bio1- X Br/G-C3n4. SSRN Electronic Journal, 0, , .	0.4	0
71857	New monoclinic ruthenium dioxide with highly selective hydrogenation activity. Catalysis Science and Technology, 2022, 12, 6556-6565.	2.1	4
71858	Unfolding the terahertz spectrum of soft porous crystals: rigid unit modes and their impact on phase transitions. Journal of Materials Chemistry A, 2022, 10, 17254-17266.	5.2	10
71859	A predicted orthogonal semimetallic carbon with negative thermal expansion and compressibility. Physical Chemistry Chemical Physics, 2022, 24, 23497-23506.	1.3	2
71860	Tailoring interlayer magnetic coupling to modify the magnetic properties of FeCl₂ bilayers by self-intercalation. Journal of Materials Chemistry C, 2022, 10, 14955-14962.	2.7	9
71861	Reactivity of anatase (001) surface from first-principles many-body Green's function theory. RSC Advances, 2022, 12, 28178-28184.	1.7	1
71862	A phase field model combined with a genetic algorithm for polycrystalline hafnium zirconium oxide ferroelectrics. Nanoscale, 2022, 14, 14997-15009.	2.8	3
71863	Revealing the promotion of carbonyl groups on vacancy stabilized Pt₄/nanocarbons for propane dehydrogenation. Physical Chemistry Chemical Physics, 2022, 24, 23236-23244.	1.3	2
71864	Synthesis of poly(2,6-diaminopyridine) using a rotating packed bed toward efficient production of polypyrrole-derived electrocatalysts. Reaction Chemistry and Engineering, 0, , .	1.9	0
71865	High-throughput screening of transition metal doping and defect engineering on single layer SnS₂ for the water splitting hydrogen evolution reaction. Journal of Materials Chemistry A, 2022, 10, 21315-21326.	5.2	9
71866	Doping of the Mn vacancy of Mn₂B₂ with a single different transition metal atom as the dual-function electrocatalyst. Physical Chemistry Chemical Physics, 2022, 24, 20988-20997.	1.3	6
71867	Two-dimensional IVâ€“VA₃ monolayers with enhanced charge mobility for high-performance solar cells. Physical Chemistry Chemical Physics, 2022, 24, 20694-20700.	1.3	2

#	Article	IF	Citations
71868	Effect of manganese substitution of ferrite nanoparticles on particle grain structure. Nanoscale Advances, 2022, 4, 3957-3965.	2.2	3
71869	Elemental (im-)miscibility determines phase formation of multinary nanoparticles co-sputtered in ionic liquids. Nanoscale Advances, 2022, 4, 3855-3869.	2.2	3
71870	NiCoP nanoparticle-decorated carbon nanosheet arrays assembled on nickel nanowires for volumetric energy-dense supercapacitors. Journal of Materials Chemistry A, 2022, 10, 18000-18013.	5.2	8
71871	The surface reconstruction induced enhancement of the oxygen evolution reaction on Î±-SnWO₄ (010) based on a density functional theory study. Physical Chemistry Chemical Physics, 2022, 24, 19382-19392.	1.3	1
71872	Hybrid Dense Carbon Allotropes from Crystal Chemistry and First Principles: 'Glitter' C6, 'Isoglitter' C8 and 'Metaglitter' C8. SSRN Electronic Journal, 0, , .	0.4	0
71873	Construction of Group Iii Nitride Van Der Waals Heterostructures for Highly Efficient Photocatalyst. SSRN Electronic Journal, 0, , .	0.4	0
71874	Hydrogen Production from H2s on Metal-Doped Fes Mackinawite Monolayer Via Dft Calculations. SSRN Electronic Journal, 0, , .	0.4	0
71875	Improved Electrochemical Behaviors and Mechanism of Ni0.9mn0.1wo4 Electrode for Supercapacitor Applications. SSRN Electronic Journal, 0, , .	0.4	0
71876	Oxidation behavior of layered Fe_nGeTe₂ (n = 3, 4, 5) and Cr₂Ge₂Te₆ governed by interlayer coupling. Nanoscale, 2022, 14, 11452-11460.	2.8	1
71877	Novel Phase Transition for Xsnn$_2$ (X=Mg,Zn) Under Uniaxial Compression. SSRN Electronic Journal, 0, , .	0.4	0
71879	Prediction of a novel 2D porous boron nitride material with excellent electronic, optical and catalytic properties. Physical Chemistry Chemical Physics, 2022, 24, 21009-21019.	1.3	5
71880	2D NbIrTe₄ and TaRhTe₄ monolayers: two fascinating topological insulators as electrocatalysts for oxygen reduction. Inorganic Chemistry Frontiers, 2022, 9, 6133-6146.	3.0	2
71881	Synthetic control of structure and conduction properties in Naâ€“Yâ€“Zrâ€“Cl solid electrolytes. Journal of Materials Chemistry A, 2022, 10, 21565-21578.	5.2	10
71882	A generic dual d-band model for interlayer ferromagnetic coupling in a transition-metal doped MnBi₂Te₄ family of materials. Nanoscale, 2022, 14, 13689-13695.	2.8	5
71883	Polaron formation and transport in Bi₂WO₆ studied by DFT+U and hybrid PBE0 functional approaches. Physical Chemistry Chemical Physics, 2022, 24, 22918-22927.	1.3	5
71884	First principles investigation of anionic redox in bisulfate lithium battery cathodes. Physical Chemistry Chemical Physics, 2022, 24, 22756-22767.	1.3	1
71885	Integrating ferromagnetism and ferroelectricity in an iron chalcogenide monolayer: a first-principles study. Nanoscale, 2022, 14, 14231-14239.	2.8	2
71886	Electronic Descriptors for Vacancy Formation and Hydrogen Solution in Be-Rich Intermetallics. SSRN Electronic Journal, 0, , .	0.4	0

#	Article	IF	Citations
71887	Raising the solubility of Gd yields superior thermoelectric performance in n-type PbSe. Journal of Materials Chemistry A, 2022, 10, 20386-20395.	5.2	8
71888	Carbon-incorporated bimetallic phosphide nanospheres derived from MOFs as superior electrocatalysts for hydrogen evolution. Dalton Transactions, 2022, 51, 14517-14525.	1.6	2
71889	Origin of the exceptional selectivity of NaA zeolite for the radioactive isotope ⁹⁰Sr²⁺. Inorganic Chemistry Frontiers, 2022, 9, 6258-6270.	3.0	5
71890	Prediction of highly stable two-dimensional materials of boron and phosphorus: structural and electronic properties. Physical Chemistry Chemical Physics, 0, , .	1.3	0
71891	Biaxial stress and functional groups (T = O, F, and Cl) tuning the structural, mechanical, and electronic properties of monolayer molybdenum carbide. Physical Chemistry Chemical Physics, 2022, 24, 17862-17869.	1.3	7
71892	Wide-Ph-Range Adaptable Ammonia Electrosynthesis from Nitrate on Cu-Pd Interfaces. SSRN Electronic Journal, 0, , .	0.4	0
71893	Anodic Role of Mg12nd in the Micro-Galvanic Corrosion of Binary Mgâ€'Nd Alloys. SSRN Electronic Journal, 0, , .	0.4	1
71894	Co2 Coverage Accelerates Oxygen Removal in Oxy-Combustion Systems. SSRN Electronic Journal, 0, , .	0.4	0
71895	â€œBreathingâ€•organic cation to stabilize multiple structures in low-dimensional Ge-, Sn-, and Pb-based hybrid iodide perovskites. Inorganic Chemistry Frontiers, 2022, 9, 4892-4898.	3.0	3
71896	Constructing trifunctional MoTe₂/As van der Waals heterostructures for versatile energy applications. New Journal of Chemistry, 2022, 46, 20172-20181.	1.4	9
71897	Alkali metal-mediated interfacial charge redistribution toward near-optimal water oxidation. Journal of Materials Chemistry A, 0, , .	5.2	0
71898	Axial coordination modification of Mâ€"N₄single-atom catalysts to regulate the electrocatalytic CO₂reduction reaction. Journal of Materials Chemistry C, 2022, 10, 15948-15956.	2.7	14
71899	Reaction-intermediate-induced atomic mobility in heterogeneous metal catalysts for electrochemical reduction of CO₂. Physical Chemistry Chemical Physics, 2022, 24, 19432-19442.	1.3	3
71900	The adsorption behaviors of N₂O on penta-graphene and Ni-doped penta-graphene. RSC Advances, 2022, 12, 23937-23945.	1.7	4
71901	Self-passivated edges of ZnO nanoribbons: a global search. Nanoscale, 2022, 14, 15468-15474.	2.8	1
71902	Emergent superconductivity in K₂ReH₉ under pressure. Journal of Materials Chemistry C, 2022, 10, 14626-14632.	2.7	2
71903	Engineering Co and Ru dual-metal atoms on nitrogen-doped carbon as highly efficient bifunctional oxygen electrocatalysts. Catalysis Science and Technology, 2022, 12, 5435-5441.	2.1	6
71904	Unexpected low thermal expansion coefficients of pentadiamond. Physical Chemistry Chemical Physics, 2022, 24, 23561-23569.	1.3	3

#	Article	IF	Citations
71905	Exploring room-temperature ferromagnetism in WXBC (X = W, Mn, Fe) monolayers. RSC Advances, 2022, 12, 28433-28440.	1.7	6
71906	Radical defects modulate the photocatalytic response in 2D-graphitic carbon nitride. Chemical Science, 2022, 13, 9927-9939.	3.7	20
71907	Ultrahigh anisotropic carrier mobility in ZnSb monolayers functionalized with halogen atoms. RSC Advances, 2022, 12, 26994-27001.	1.7	2
71908	Above-room Curie temperature and barrier-layer-dependent tunneling magnetoresistance in 1T-CrO₂ monolayer based magnetic tunnel junctions. Physical Chemistry Chemical Physics, 2022, 24, 22007-22015.	1.3	0
71909	Spin and valence variation in cobalt doped barium strontium titanate ceramics. Physical Chemistry Chemical Physics, 2022, 24, 19865-19881.	1.3	2
71910	Transparent fluoride glass-ceramics with phase-selective crystallization for middle IR photonics. Journal of Materials Chemistry C, 2022, 10, 12947-12956.	2.7	5
71911	Diverse Electronic Structures Governed by N-Substitution in Stable Two-Dimensional Dumbbell Carbonitrides. SSRN Electronic Journal, 0, , .	0.4	0
71912	The origin of high Na⁺ ion conductivity in Na_{1+x}Zr₂Si_xP_{3â^'x}O₁₂ NASICON materials. Physical Chemistry Chemical Physics, 2022, 24, 22154-22167.	1.3	6
71913	A two-dimensional Sb/InS van der Waals heterostructure for electronic and optical related applications. Physical Chemistry Chemical Physics, 2022, 24, 22000-22006.	1.3	0
71914	Adenine-based bio-MOFs with high water and acidâ€“base stability for ammonia capture. CrystEngComm, 2022, 24, 7420-7426.	1.3	5
71915	Effectively Enhanced Oxygen Reduction Activity and Stability of Triple-Conducting Composite Cathodes by Strongly Interacting Interfaces for Protonic Ceramic Fuel Cells. SSRN Electronic Journal, 0, , .	0.4	0
71916	Ultralow thermal conductivity and anisotropic thermoelectric performance in layered materials LaMOCh (M = Cu, Ag; Ch = S, Se). Physical Chemistry Chemical Physics, 2022, 24, 21261-21269.	1.3	6
71917	Comparative study of Janus B₂XY (X, Y = S, Se, Te) and F-BNBN-H monolayers for water splitting: revealing the positive and negative roles of the intrinsic dipole. Physical Chemistry Chemical Physics, 2022, 24, 20980-20987.	1.3	1
71918	Ba₃Zr₂Cu₄S₉: the first quaternary phase of the Baâ€“Zrâ€“Cuâ€“S system. New Journal of Chemistry, 2022, 46, 15976-15986.	1.4	3
71919	Theoretical Insights into the Removal Pathways of Adsorbed Oxygen on the Surface of Î§-Fe5c2(510). SSRN Electronic Journal, 0, , .	0.4	0
71920	High Throughput Theoretical Prediction of the Low Friction at the Interfaces of Homo- and Heterojunction Composed of C3n. SSRN Electronic Journal, 0, , .	0.4	0
71921	Probing the Structural, Electronic and Optical Properties of Pure and B, N, or Li Substituted Cyclo-18 Ring: Density Functional Theory Investigations. SSRN Electronic Journal, 0, , .	0.4	0
71922	Transition Metal Dualâ€“Atom Ni2/Tio2 Catalysts for Photoelectrocatalytic Hydrogen Evolution: A Density Functional Theory Study. SSRN Electronic Journal, 0, , .	0.4	0

#	Article	IF	Citations
71923	Excellent Optoelectronic and Thermoelectric Properties of Two-Dimensional Transition Metal Dinitride Hfn2. SSRN Electronic Journal, 0, , .	0.4	0
71924	Heterointerface and Oxygen Vacancy of Co(Oh)2/Con to Synergistically Boost Alkaline Water Splitting. SSRN Electronic Journal, 0, , .	0.4	0
71925	Strain-mediated oxygen evolution reaction on magnetic two-dimensional monolayers. Nanoscale Horizons, 2022, 7, 1404-1410.	4.1	6
71926	First-principles calculations for determining the mechanism of the photocatalytic selective oxidation of toluene to benzaldehyde on the g-C₃N₄ catalyst. New Journal of Chemistry, 2022, 46, 16922-16931.	1.4	3
71927	Hydrothermal liquefaction of lignin to aromatics over the perovskite catalysts. Journal of Fuel Chemistry and Technology, 2022, 50, 984-992.	0.9	2
71928	Exploring the Impact of the Nitrogen Layer on a Cu(001) Substrate on the Spin Crossover Properties of [Fe(Saleen-I)2]Br: A Dft Study. SSRN Electronic Journal, 0, , .	0.4	0
71929	Unveiling the HER and ORR activity origin of isolated Co sites supported on N-doped carbon. MATEC Web of Conferences, 2022, 363, 01001.	0.1	0
71930	Pressure-induced non-radiative losses in halide perovskite light-emitting diodes. Journal of Materials Chemistry C, 2022, 10, 12560-12568.	2.7	6
71931	Electric field-controlled reversible high-temperature perpendicular magnetic anisotropy in cobaltateâ€“manganite heterostructures. Journal of Materials Chemistry C, 2022, 10, 12844-12852.	2.7	4
71932	Neural-network-backed evolutionary search for SrTiO₃(110) surface reconstructions. , 2022, 1, 703-710.		7
71933	Pt nanoparticles under oxidizing conditions â€“ implications of particle size, adsorption sites and oxygen coverage on stability. Nanoscale Advances, 0, , .	2.2	1
71934	Tunability of the electronic properties and contact types of the silicane/MoSi₂N₄ heterostructure under an electric field. New Journal of Chemistry, 2022, 46, 18076-18082.	1.4	1
71935	The role of Mo species in Niâ€“Mo catalysts for dry reforming of methane. Physical Chemistry Chemical Physics, 2022, 24, 21461-21469.	1.3	4
71936	Cos2 Enhanced Sno2@Rgo Heterostructure Quantum Dots for Advanced Lithium-Ion Battery Anode. SSRN Electronic Journal, 0, , .	0.4	0
71937	Intrinsic ferromagnetism and the quantum anomalous Hall effect in two-dimensional MnOCl₂ monolayers. Physical Chemistry Chemical Physics, 2022, 24, 20530-20537.	1.3	1
71938	Computational investigation of van der Waals corrections in the adsorption properties of molecules on the Cu(111) surface. Physical Chemistry Chemical Physics, 2022, 24, 20294-20302.	1.3	3
71939	Lattice dynamics across the ferroelastic phase transition in Ba₂ZnTeO₆: a Raman and first-principles study. Physical Chemistry Chemical Physics, 2022, 24, 20152-20163.	1.3	2
71940	First-principles study of two-dimensional C-silicyne nanosheet as a promising anode material for rechargeable Li-ion batteries. Physical Chemistry Chemical Physics, 2022, 24, 20274-20281.	1.3	4

#	Article	IF	Citations
71941	Robust ferromagnetism and Weyl half-semimetal in a two-dimensional vanadium boride monolayer. Nanoscale, 2022, 14, 12491-12497.	2.8	1
71942	W₄PCl₁₁monolayer: an unexplored 2D material with moderate direct bandgap and strong visible-light absorption for highly efficient solar cells. Nanoscale, 2022, 14, 12386-12394.	2.8	4
71943	Synergy of non-lithium cation doping and the lithium concentration affecting lithium ion transport in solid electrolytes. Journal of Materials Chemistry A, 2022, 10, 18087-18094.	5.2	1
71944	Tunable magnetocrystalline anisotropy of two-dimensional Fe₃GeTe₂ with adsorbed 5d-transition metal. Physical Chemistry Chemical Physics, 2022, 24, 21470-21476.	1.3	5
71945	Two-dimensional carbon materials with an anisotropic Dirac cone: high stability and tunable Fermi velocity. Physical Chemistry Chemical Physics, 2022, 24, 19263-19268.	1.3	2
71946	Interplay of structural fluctuations and charge carrier dynamics is key for high performance of hybrid lead halide perovskites. Inorganic Chemistry Frontiers, 2022, 9, 5549-5561.	3.0	5
71947	Oxygen defect engineering endows Co₃O₄ nanosheets with advanced aluminum ion storage. Journal of Materials Chemistry A, 2022, 10, 18322-18332.	5.2	4
71948	Structural and compositional properties of 2D CH₃NH₃PbI₃ hybrid halide perovskite: a DFT study. RSC Advances, 2022, 12, 25924-25931.	1.7	11
71949	Tunable uniaxial, area, and volume negative thermal expansion in quartz-like and diamond-like metalâ€“organic frameworks. RSC Advances, 2022, 12, 21770-21779.	1.7	1
71950	Highly tailored gap-like structure for excellent thermoelectric performance. Energy and Environmental Science, 2022, 15, 4058-4068.	15.6	11
71951	Single atom functionalization in vanadium dichalcogenide monolayers: towards enhanced electrocatalytic activity. Sustainable Energy and Fuels, 2022, 6, 5337-5344.	2.5	3
71952	Tunability of the electronic properties and electrical contact in Graphene/SiH heterostructure. Physical Chemistry Chemical Physics, 0, , .	1.3	2
71953	Structural, Electronic, Optical, and Potassium Anodic Electrochemical Characteristics of 2-Dimensional Silicane: A Density Functional Theory Investigation. SSRN Electronic Journal, 0, , .	0.4	0
71954	First-Principles Study of Oxygen Evolution on Co3o4 with Short-Range Ordered IR Doping. SSRN Electronic Journal, 0, , .	0.4	0
71955	Phase transition from a nonmagnetic to a ferromagnetic state in a twisted bilayer graphene nanoflake: the role of electronic pressure on the magic-twist. Nanoscale, 2022, 14, 11945-11952.	2.8	4
71956	Mechanistic insight into electrocatalytic glyoxal reduction on copper and its relation to CO₂ reduction. Chemical Science, 2022, 13, 11205-11214.	3.7	3
71957	Morphology-Controlled Synthesis of Cu2o Encapsulated Phase Change Materials: Superior Photothermal Conversion and Storage Performance in Visible Light Regime. SSRN Electronic Journal, 0, , .	0.4	0
71958	Li-Decorated Î'1-Graphyne for High-Performance Co2 Capture and Separation Over N2. SSRN Electronic Journal, 0, , .	0.4	0

#	Article	IF	Citations
71959	High-Throughput Screening of Half-Antiperovskites with a Stacked Kagome Lattice. SSRN Electronic Journal, 0, , .	0.4	0
71960	Computational Screening of Bimetallene for the Composite Lithium Metal Anode. SSRN Electronic Journal, 0, , .	0.4	0
71961	Interface engineering of hierarchical P-doped NiSe/2H-MoSe₂nanorod arrays for efficient hydrogen evolution. Inorganic Chemistry Frontiers, 2022, 9, 5507-5516.	3.0	11
71962	Spall Strength and Equation of States of 2050-T84 Al-Li Alloy Under Shock Compression Up to 120 GPA. SSRN Electronic Journal, 0, , .	0.4	0
71963	A Deep Learning-Based Potential Developed for Calcium Silicate Hydrates with Both High Accuracy and Efficiency. SSRN Electronic Journal, 0, , .	0.4	0
71964	First-Principles Study of the Effect of Non-StoichiometryÂOn Sensing MechanismÂOf NoxÂOn Wo3(001) Surfaces. SSRN Electronic Journal, 0, , .	0.4	0
71965	Influence of Interfacial Configuration on Bonding Properties and Thermal Conductivity of Heterogeneous Interface in Al/Graphite Composite Used for Electronic Packaging. SSRN Electronic Journal, 0, , .	0.4	0
71966	Atomic mechanism of lithium intercalation induced phase transition in layered MoS₂. Physical Chemistry Chemical Physics, 2022, 24, 18777-18782.	1.3	3
71967	Theory and Computation in Photo-Electro-Chemical Catalysis: Highlights, Challenges, and Prospects. Engineering Materials, 2022, , 3-43.	0.3	0
71968	Mo-Embedded Ir-Based Electrocatalyst for Nitrogen Reduction Reaction: A Computational Study. SSRN Electronic Journal, 0, , .	0.4	0
71969	Modulating Vacancies Concentration Ratio of Cationic and Anionic in Wo3 for Driving High Performance Magnesium Ions Storage. SSRN Electronic Journal, 0, , .	0.4	0
71970	Accelerating the reaction kinetics of lithiumâ€“oxygen chemistry by modulating electron acceptanceâ€“donation interaction in electrocatalysts. Journal of Materials Chemistry A, 2022, 10, 17267-17278.	5.2	18
71971	Biphenylene Network as Sodium Ion Battery Anode Material. SSRN Electronic Journal, 0, , .	0.4	0
71972	In silico design of single transition metal atom anchored defective boron carbide monolayers as high-performance electrocatalysts for the nitrogen reduction reaction. Nanoscale, 2022, 14, 12823-12829.	2.8	6
71973	Stereodynamics of adiabatic and non-adiabatic energy transfer in a molecule surface encounter. Physical Chemistry Chemical Physics, 2022, 24, 19753-19760.	1.3	4
71974	Ni activated Mo₂C by regulating the interfacial electronic structure for highly efficient lithium-ion storage. Nanoscale, 2022, 14, 14575-14584.	2.8	2
71975	Data-driven design of dual-metal-site catalysts for the electrochemical carbon dioxide reduction reaction. Journal of Materials Chemistry A, 2022, 10, 18803-18811.	5.2	14
71976	Confinement catalysis of a single atomic vacancy assisted by aliovalent ion doping enabled efficient NO electroreduction to NH₃. Journal of Materials Chemistry A, 2022, 10, 18690-18700.	5.2	42

#	Article	IF	Citations
71977	Significant enhancement of piezoelectricity induced by oxygen adsorption in monolayer and multilayer MoS₂. Journal of Materials Chemistry C, 0, , .	2.7	0
71978	Quantum anomalous Hall effect in germanene by proximity coupling to a semiconducting ferromagnetic substrate NiI₂. Physical Chemistry Chemical Physics, 2022, 24, 21631-21637.	1.3	5
71979	LiMn₂O₄ cathodes with F anion doping for superior performance of lithium-ion batteries. Physical Chemistry Chemical Physics, 2022, 24, 21638-21644.	1.3	3
71980	Eldfellite NaV(SO₄)₂ as a versatile cathode insertion host for Li-ion and Na-ion batteries. Journal of Materials Chemistry A, 0, , .	5.2	1
71981	The magnetic properties of pressurized CsV₃Sb₅ calculated by using a hybrid functional. Physical Chemistry Chemical Physics, 2022, 24, 18179-18184.	1.3	3
71982	Investigating the role of structural water on the electrochemical properties of Î±-V₂O₅ through density functional theory. Physical Chemistry Chemical Physics, 2022, 24, 24271-24280.	1.3	1
71983	In-plane CrI₂/CrI₃ 2D superlattices: novel electronic properties and strain induced phase transition. Physical Chemistry Chemical Physics, 2022, 24, 25530-25536.	1.3	1
71984	The â€œburst effectâ€•of hydrogen desorption in MgH₂ dehydrogenation. Journal of Materials Chemistry A, 2022, 10, 22363-22372.	5.2	18
71985	Possibility of regulating valley-contrasting physics and topological properties by ferroelectricity in functionalized arsenene. Physical Chemistry Chemical Physics, 2022, 24, 23910-23918.	1.3	1
71986	Antibonding induced anharmonicity leading to ultralow lattice thermal conductivity and extraordinary thermoelectric performance in CsK₂X (X = Sb, Bi). Journal of Materials Chemistry C, 2022, 10, 15822-15832.	2.7	10
71987	A high-rate capability and energy density sodium ion full cell enabled by F-doped Na₂Ti₃O₇ hollow spheres. Journal of Materials Chemistry A, 2022, 10, 23232-23243.	5.2	5
71988	A strain-induced considerable decrease of lattice thermal conductivity in 2D KAgSe with Coulomb interaction. Physical Chemistry Chemical Physics, 2022, 24, 24917-24923.	1.3	4
71989	Defective Ultrathin ZnIn2S4 Nanosheets Boosting CO2 Photoreduction Property. Springer Theses, 2022, , 47-64.	0.0	0
71990	Feasibility study of Mg storage in a bilayer silicene anode via application of an external electric field. RSC Advances, 2022, 12, 20583-20598.	1.7	0
71991	Magnesium Storage Enhancement of Molybdenum Dioxide in Hybrid Magnesium Lithium Batteries. SSRN Electronic Journal, 0, , .	0.4	0
71992	Anchoring Highly Distributed Pt Species with a Strong Metal-Support Interaction Over Chemically Oxidized Graphitic Carbon Nitride for Photocatalytic Hydrogen Evolution: The Effect of Reducing Agents on Photocatalytic Properties. SSRN Electronic Journal, 0, , .	0.4	0
71993	First principles predictionÂofÂstructural,ÂmechanicalÂandÂoptoelectronicÂpropertiesÂofÂlead-freeÂdoubleÂperovskites A2SeX6Â(A=Rb,ÂK;ÂX=Cl,ÂBr,ÂI). SSRN Electronic Journal, 0, , .	0.4	1
71994	Concentric Spherical Neural Network for 3D Representation Learning. , 2022, , .		0

#	Article	IF	Citations
71995	Zn single atom on N-doped carbon: Highly active and selective catalyst for electrochemical reduction of nitrate to ammonia. Chemical Engineering Journal, 2023, 452, 139533.	6.6	18
71996	A synergistic route of heterointerface and metal single-atom configurations towards enhancing microwave absorption. Chemical Engineering Journal, 2023, 452, 139430.	6.6	13
71997	Transition metal Dualâ€“Atom Ni2/TiO2 catalysts for photoelectrocatalytic hydrogen Evolution: A density functional theory study. Applied Surface Science, 2023, 608, 155132.	3.1	7
71998	Zinc deposition characteristics on different substrates for aqueous zinc ion battery. Applied Surface Science, 2023, 607, 155111.	3.1	15
71999	One-pot solvothermal synthesis of flower-like Fe-doped In2S3/Fe3S4 S-scheme hetero-microspheres with enhanced interfacial electric field and boosted visible-light-driven CO2 reduction. Journal of Colloid and Interface Science, 2023, 629, 1027-1038.	5.0	21
72000	Maximizing the energy density and stability of Ni-rich layered cathode materials with multivalent dopants via machine learning. Chemical Engineering Journal, 2023, 452, 139254.	6.6	11
72001	Single-crystalline Î±-MnO2 catalysts with tailored exposed crystal facets for boosting catalytic soot oxidation: The crystal facet-dependent activity. Applied Surface Science, 2023, 608, 155116.	3.1	12
72002	Ultra-Dilute high-entropy alloy catalyst with core-shell structure for high-active hydrogenation of furfural to furfuryl alcohol at mild temperature. Chemical Engineering Journal, 2023, 452, 139526.	6.6	17
72003	Tuning oxygen vacancy in SnO2 inhibits Pt migration and agglomeration towards high-performing fuel cells. Applied Catalysis B: Environmental, 2023, 320, 122017.	10.8	19
72004	First-principles design of an ultralow frictional interface of a black phosphorus and graphene heterostructure with oxide functionalization and high-pressure conditions. Applied Surface Science, 2023, 608, 155092.	3.1	9
72005	Modulating lattice oxygen activity of Ca2Fe2O5 brownmillerite for the co-production of syngas and high purity hydrogen via chemical looping steam reforming of toluene. Applied Catalysis B: Environmental, 2023, 320, 122010.	10.8	22
72006	Photogalvanic effect in spin-polarized zigzag antimonene nanoribbon with Cr and Co edge-modification. Physica E: Low-Dimensional Systems and Nanostructures, 2023, 145, 115508.	1.3	0
72007	Theoretical expolartion of site selective Perovskites for the application of electronic and optoresponsive memory devices. Physica E: Low-Dimensional Systems and Nanostructures, 2023, 145, 115514.	1.3	2
72008	Homogeneously distributed heterostructured interfaces in rice panicle-like SbBi-Bi2Se3-Sb2Se3 nanowalls for robust sodium storage. Chemical Engineering Journal, 2023, 452, 139363.	6.6	5
72009	Formic acid formation via direct hydration reaction (COÂ+ÂH2OÂâ†'ÂHCOOH) on magnesia-silver composite. Applied Surface Science, 2023, 607, 155067.	3.1	54
72010	Valence engineering at the interface of MoS2/Mo2C heterostructure for bionic nitrogen reduction. Chemical Engineering Journal, 2023, 452, 139515.	6.6	9
72011	A first-principles study the effects of nitrogen on the lattice distortion, mechanical, and electronic properties of (ZrHfNbTa)C1-N high entropy carbonitrides. Journal of Alloys and Compounds, 2023, 930, 167378.	2.8	10
72012	Effects of manganese-doping on the enhanced solar photocatalytic properties of AgBr catalyst: Mechanism and DFT modeling. Applied Surface Science, 2023, 607, 154993.	3.1	6

#	Article	IF	Citations
72013	Electronic changes at the platinum interface induced by bismuth and tellurium adatom adsorption. Applied Surface Science, 2023, 608, 155137.	3.1	2
72014	Rh promotional effects on Ptâ€“Rh alloy catalysts for chemoselective hydrogenation of nitrobenzene to p-aminophenol. Chemical Engineering Journal, 2023, 452, 139448.	6.6	16
72015	Using first-principles modeling to investigate dehydrogenation of perhydro-dibenzyltoluene on Pt/M surface alloys (MÂ=ÂFe, Ni, and Cu). Fuel, 2023, 331, 125779.	3.4	7
72016	Redispersion of exsolved Cu nanoparticles on LaFeO3 photocatalyst for tunable photocatalytic CO2 reduction. Chemical Engineering Journal, 2023, 452, 139273.	6.6	14
72017	Boosted photocatalytic hydrogen production over two-dimensional/two-dimensional Ta3N5/ReS2 van der Waals heterojunctions. Journal of Colloid and Interface Science, 2023, 629, 455-466.	5.0	18
72018	Investigation of electronic and photocatalytic properties of AgTi2(PO4)3 NASICON-type phosphate: Combining experimental data and DFT calculations. Journal of Photochemistry and Photobiology A: Chemistry, 2023, 435, 114289.	2.0	9
72019	Unraveling the effects of P and S doping over g-C3N4 in strengthening Lewis basicity for CO2/glycerol conversion: A theoretical and experimental study. Carbon, 2023, 201, 129-140.	5.4	18
72020	Cohesion properties and hydrogen permeation at PdCu/TiAl interface. Surface Science, 2023, 727, 122190.	0.8	1
72021	The direct Z-scheme g-C6N6/WTe2 van der Waals heterojunction as photocatalyst over water splitting in the visible light: Designing strategy from first principles. Journal of Photochemistry and Photobiology A: Chemistry, 2023, 435, 114263.	2.0	2
72022	A computational finding on the effect of Ï€-conjugated acceptors in thiophene-linked coumarin dyes for potential suitability in DSSC application. Journal of Photochemistry and Photobiology A: Chemistry, 2023, 435, 114300.	2.0	3
72023	Direct activation of PMS by highly dispersed amorphous CoOx clusters in anatase TiO2 nanosheets for efficient oxidation of biomass-derived alcohols. Applied Surface Science, 2023, 607, 154997.	3.1	8
72024	Theoretical realization of fully spin-polarized nodal box with traversing Brillouin zone surface state. Physical Review B, 2022, 106, .	1.1	5
72025	Enhancing first-principles simulations of complex solid-state ion conductors using topological analysis of procrystal electron density. Npj Computational Materials, 2022, 8, .	3.5	2
72026	Magneto-optical Kerr effect and magnetoelasticity in a weakly ferromagnetic <mml:math xmlns:mml="http://www.w3.org/1998/Math/MathML"><mml:msub><mml:mrow><mml:mi>RuF</mml:mi></mml:mrow><mml:mn>4</mml:mn> monolayer. Physical Review B, 2022, 106, .	1.1	2
72027	Enhanced cycling stability of La0.2Sr0.8CoO3â^'Î´ for oxygen evolution reaction via trace doping of Nb. Ceramics International, 2022, 48, 36992-36999.	2.3	3
72028	Strong Influence of the Anion Radius on the Passivation of Selenium Vacancy in Monolayer InSe: Insights from Time-Domain Ab Initio Analysis. Journal of Physical Chemistry C, 2022, 126, 15072-15079.	1.5	0
72029	Selective Reduction of CO₂ on Ti₂C(OH)₂ MXene through Spontaneous Crossing of Transition States. ACS Applied Materials & Interfaces, 2022, 14, 40913-40920.	4.0	8
72030	Adjusting oxygen vacancies in perovskite LaCoO3 by electrochemical activation to enhance the hydrogen evolution reaction activity in alkaline condition. Journal of Energy Chemistry, 2023, 76, 226-232.	7.1	13

#	Article	IF	Citations
72031	Electrocatalytic CO2 reduction to alcohols by modulating the molecular geometry and Cu coordination in bicentric copper complexes. Nature Communications, 2022, 13, .	5.8	52
72032	Dynamic stabilization of perovskites at elevated temperatures: A comparison between cubic <mml:math xmlns:mml="http://www.w3.org/1998/Math/MathML"><mml:msub><mml:mi>BaFeO</mml:mi><mml:mn>3</mml:mn></mml:msub> and vacancy-ordered monoclinic <mml:math xmlns:mml="http://www.w3.org/1998/Math/MathML"><mml:msub><mml:mi>BaFeO</mml:mi><mml:mrow><mml:mn>2.67</mml:mn> Physical Review B, 2022, 106, .	1.1	0
72033	Prediction of Stable Silver Fluorides. Journal of Physical Chemistry C, 2022, 126, 15057-15063.	1.5	1
72034	Hydride Generation on the Cu-Doped CeO2(111) Surface and Its Role in CO2 Hydrogenation Reactions. Catalysts, 2022, 12, 963.	1.6	8
72036	First-Principles Study on the Stability, Site Preference, Electronic Structure and Magnetism of Alloyed Fe3B with Ni3P-Type Structure. Materials, 2022, 15, 5990.	1.3	0
72037	Cuâ€“S Bonds as an Atomic-Level Transfer Channel to Achieve Photocatalytic CO₂ Reduction to CO on Cu-Substituted ZnIn₂S₄. ACS Sustainable Chemistry and Engineering, 2022, 10, 11902-11912.	3.2	21
72038	Li2TiO3 Dopant and Phosphate Coating Improve the Electrochemical Performance of LiCoO2 at 3.0â€“4.6ÂV. Transactions of Tianjin University, 2023, 29, 46-61.	3.3	4
72039	Revealing *OOH key intermediates and regulating H ₂ O ₂ photoactivation by surface relaxation of Fenton-like catalysts. Proceedings of the National Academy of Sciences of the United States of America, 2022, 119, .	3.3	33
72041	Monolayer TiNI with Anisotropic Optical and Mechanical Properties. Crystals, 2022, 12, 1202.	1.0	0
72042	Importance of Edge and Corner Sites on CeO₂ Nanoparticles for Direct Conversion of Methane to Methanol. ACS Applied Nano Materials, 2022, 5, 12600-12606.	2.4	5
72043	Simulation and Calculation for Predicting Structures and Properties of High-Entropy Alloys. , 0, , .		2
72044	What Happens at Surfaces and Grain Boundaries of Halide Perovskites: Insights from Reactive Molecular Dynamics Simulations of CsPbI₃. ACS Applied Materials & Interfaces, 2022, 14, 40841-40850.	4.0	19
72045	High-Spin Orbital Interactions Across van der Waals Gaps Controlling the Interlayer Ferromagnetism in van der Waals Ferromagnets. Journal of the American Chemical Society, 2022, 144, 16272-16275.	6.6	3
72046	Cd0.9Co0.1S Nanorods with an Internal Electric Field and Photothermal Effect Synergistically for Boosting Photocatalytic H2 Evolution. International Journal of Molecular Sciences, 2022, 23, 9756.	1.8	3
72047	Protonic SOFCs with a novel La0.4K0.1Ca0.5MnO3-Î´ cathode. Ceramics International, 2022, 48, 35599-35605.	2.3	3
72048	Tip-Mediated Bandgap Tuning for Monolayer Transition Metal Dichalcogenides. ACS Nano, 2022, 16, 14918-14924.	7.3	7
72049	Solid-State Synthesis of ZnO/ZnS Photocatalyst with Efficient Organic Pollutant Degradation Performance. Catalysts, 2022, 12, 981.	1.6	9
72050	Electronic Structures and Photoelectric Properties in Cs3Sb2X9 (X = Cl, Br, or I) under High Pressure: A First Principles Study. Nanomaterials, 2022, 12, 2982.	1.9	3

#	Article	IF	Citations
72051	Scale-Dependent Optimized Homoepitaxy of InAs(111)A. Crystal Growth and Design, 2022, 22, 5958-5965.	1.4	1
72052	Trends in the Behavior of Point Defects in MB and MAB Phases. Chemistry of Materials, 2022, 34, 7807-7816.	3.2	1
72053	Reproducibility of Hybrid Density Functional Calculations for Equation-of-State Properties and Band Gaps. Journal of Physical Chemistry A, 2022, 126, 5924-5931.	1.1	7
72054	Inverted-design for highly-active hydrogen evolution electrocatalyst of MoS2@Ni3S2 core-shell via unlocking the potential of Mo. Particuology, 2023, 77, 56-61.	2.0	1
72055	Analytical Model of CVD Growth of Graphene on Cu(111) Surface. Nanomaterials, 2022, 12, 2963.	1.9	3
72056	Discovery of Efficient Visibleâ€light Driven Oxygen Evolution Photocatalysts: Automated Highâ€Throughput Computational Screening of MA₂Z₄. Advanced Functional Materials, 2022, 32, .	7.8	19
72057	Exceptional strain strengthening and tuning of mechanical properties of TiN. Physical Review B, 2022, 106, .	1.1	3
72058	Phase transition of potassium atoms on silicene- <mml:math xmlns:mml="http://www.w3.org/1998/Math/MathML"><mml:mrow><mml:mo>(</mml:mo><mml:mrow><mml:mn>1 Physical Review B, 2022, 106, .	1.1	1
72059	Hydrogenated Carbon Monolayer in Biphenylene Network Offers a Potential Paradigm for Nanoelectronic Devices. Journal of Physical Chemistry C, 2022, 126, 15491-15500.	1.5	8
72060	Multireference Study of Optically Addressable Vanadium-Based Molecular Qubit Candidates. Journal of Physical Chemistry A, 2022, 126, 6329-6335.	1.1	4
72061	Tailoring the Time-Averaged Structure for Polarization-Sensitive Chiral Perovskites. Journal of the American Chemical Society, 2022, 144, 16020-16033.	6.6	13
72062	Photoemission Spectroscopy Using Virtual Photons Emitted by Positron Sticking: A Complementary Probe for Top-Layer Surface Electronic Structures. Physical Review Letters, 2022, 129, .	2.9	5
72063	Three-dimensional Au nanoparticles-decorated Î³-Fe2O3@reduced graphene oxide core-shell heterojunctions for highly sensitive room-temperature gas sensors. Ceramics International, 2022, 48, 37064-37074.	2.3	6
72064	Acetaldehyde binding energies: a coupled experimental and theoretical study. Monthly Notices of the Royal Astronomical Society, 2022, 516, 2586-2596.	1.6	8
72065	Thickness Dependent Ultrafast Charge Transfer in BP/MoS₂ Heterostructure. Advanced Functional Materials, 2022, 32, .	7.8	14
72066	Uniform In Situ Grown ZIF-L Layer for Suppressing Hydrogen Evolution and Homogenizing Zn Deposition in Aqueous Zn-Ion Batteries. ACS Applied Materials & Interfaces, 2022, 14, 40031-40042.	4.0	18
72067	Humble planar defects in SiGe nanopillars. Physical Review B, 2022, 106, .	1.1	1
72068	Structural and magnetic phase transitions in quasi-two-dimensional <mml:math xmlns:mml="http://www.w3.org/1998/Math/MathML"><mml:msub><mml:mi>VBr</mml:mi><mml:mn>3</mml:mn></mml:msub></m Physical Review B, 2022, 106, .	1.1	4

#	Article	IF	Citations
72069	Forced Disorder in the Solid Solution Li₃Pâ€“Li₂S: A New Class of Fully Reduced Solid Electrolytes for Lithium Metal Anodes. Journal of the American Chemical Society, 2022, 144, 16350-16365.	6.6	13
72070	Prediction and Characterization of Graphitic Structures at Diamond Grain Boundaries. Journal of Physical Chemistry C, 2022, 126, 15019-15029.	1.5	2
72071	Pressure-stabilized superconducting electride <mml:math xmlns:mml="http://www.w3.org/1998/Math/MathML"><mml:msub><mml:mrow><mml:mi>Li</mml:mi></mml:mrow><mml:mn>5</mml:mn></mml:msub><mml:mrow><mml:mi mathvariant="normal">C</mml:mi></mml:math>. Physical Review B, 2022, 106, .	1.1	10
72072	Enhanced carbon solubility in solvent for SiC rapid solution growth: Thermodynamic evaluation of Crâ€“Ceâ€“Siâ€“C system. Journal of Rare Earths, 2023, 41, 1272-1278.	2.5	2
72073	Heterostrain-enabled ultrahigh electrostrain in lead-free piezoelectric. Nature Communications, 2022, 13, .	5.8	39
72074	Van der Waals imprinting of black-phosphorus-like binary alloyed monolayers with tunable band gaps and moirÃ© superstructures. Physical Review B, 2022, 106, .	1.1	3
72075	First-Principles Insights on Intrinsic Stability and Electronic Properties of Cu2ZnGeS4 Surface. Journal of Electronic Materials, 2022, 51, 6196-6203.	1.0	0
72076	Quantum transport evidence of boundary states and Lifshitz transition in <mml:math xmlns:mml="http://www.w3.org/1998/Math/MathML"><mml:mrow><mml:msub><mml:mi>Bi</mml:mi><mml:mn>11</mml:mn></mml:msub></mml:mrow></mml:math> Physical Review B, 2022, 106, .	1.1	1
72077	First-Principles Study on the Nanofriction Properties of Diamane: The Thinnest Diamond Film. Nanomaterials, 2022, 12, 2939.	1.9	5
72078	Metallic Aluminum Suboxides with Ultrahigh Electrical Conductivity at High Pressure. Research, 2022, 2022, .	2.8	3
72079	Above-room-temperature strong intrinsic ferromagnetism in 2D van der Waals Fe3GaTe2 with large perpendicular magnetic anisotropy. Nature Communications, 2022, 13, .	5.8	87
72080	Strain Engineering in Ni-Co-Mn-Sn Magnetic Shape Memory Alloys: Influence on the Magnetic Properties and Martensitic Transformation. Materials, 2022, 15, 5889.	1.3	2
72082	Acetate formation on metals via CH4 carboxylation by CO2: A DFT study. Catalysis Today, 2022, , .	2.2	0
72083	In Silico Band-Gap Engineering of Cr₂C MXenes as Efficient Photocatalysts for Water-Splitting Reactions. Journal of Physical Chemistry C, 2022, 126, 14886-14896.	1.5	7
72084	Ion Conductivity in a Magnesium Borohydride Ammonia Borane Solid-State Electrolyte. Journal of Physical Chemistry C, 2022, 126, 15118-15127.	1.5	6
72085	Enhancing Ionic Conductivity by in Situ Formation of Li₇SiPS₈/Argyrodite Hybrid Solid Electrolytes. Chemistry of Materials, 2022, 34, 7666-7677.	3.2	2
72086	High-efficiency photocatalyst based on a MoSiGeN4/SiC heterojunction. Journal of Materials Science, 2022, 57, 16404-16417.	1.7	7
72087	First-Principles Study of Cu-Based Inorganic Hole Transport Materials for Solar Cell Applications. Materials, 2022, 15, 5703.	1.3	1

#	Article	IF	Citations
72088	On Agreement of Experimental Data and Calculated Results in Grain Boundary Segregation. Metals, 2022, 12, 1389.	1.0	5
72089	N-Doped CrS2 Monolayer as a Highly-Efficient Catalyst for Oxygen Reduction Reaction: A Computational Study. Nanomaterials, 2022, 12, 3012.	1.9	1
72090	Titanium-Decorated Planar Aluminene for Hydrogen Storage Using Density Functional Theory. Materials Science Forum, 0, 1069, 79-85.	0.3	1
72091	Favorable optical response for non-ferromagnetic (La2/3Sr1/3MnO3)n/SrTiO3 (001) ultrathin heterojunction: a potential photomagnetoelectric device. European Physical Journal Plus, 2022, 137, .	1.2	0
72092	Effect of chemical disorder on the magnetic anisotropy in <mml:math xmlns:mml="http://www.w3.org/1998/Math/MathML"><mml:mrow><mml:mi>L</mml:mi><mml:msub><mml:mn>1</mml:mn> FeNi from first-principles calculations. Physical Review Research, 2022, 4, .	1.3	5
72093	Assembling Au₄ Tetrahedra to 2D and 3D Superatomic Crystals Based on Superatomic-Network Model. ACS Omega, 2022, 7, 32708-32716.	1.6	0
72094	First-principles study on ultralow lattice thermal conductivity in HfGeTe₄. Modern Physics Letters B, 0, , .	1.0	1
72095	High Formability Bromide Solid Electrolyte with Improved Ionic Conductivity for Bulk-Type All-Solid-State Lithiumâ€“Metal Batteries. ACS Applied Energy Materials, 2022, 5, 10604-10610.	2.5	2
72096	Computational design of non-equiatomic CoCrFeNi alloys towards optimized mechanical and surface properties. Journal of Materials Research, 2022, 37, 2738-2748.	1.2	3
72097	Crystal structure and electronic properties of BrF under high-pressure. Chinese Journal of Physics, 2022, , .	2.0	1
72098	¹⁷O Labeling Reveals Paired Active Sites in Zeolite Catalysts. Journal of the American Chemical Society, 2022, 144, 16916-16929.	6.6	10
72099	Spin-dependent tunneling in 2D MnBi2Te4-based magnetic tunnel junctions. MRS Bulletin, 2022, 47, 1177-1184.	1.7	5
72100	Hydrophenazine-linked two-dimensional ladder-type crystalline fused aromatic network with high charge transport. CheM, 2022, 8, 3130-3144.	5.8	7
72101	Enhanced polarization and abnormal flexural deformation in bent freestanding perovskite oxides. Nature Communications, 2022, 13, .	5.8	28
72102	Dark matter direct detection from the single phonon to the nuclear recoil regime. Physical Review D, 2022, 106, .	1.6	9
72103	Design of Organicâ€“Inorganic Hybrid Heterostructured Semiconductors via High-Throughput Materials Screening for Optoelectronic Applications. Journal of the American Chemical Society, 2022, 144, 16656-16666.	6.6	13
72104	Influence of Orbital Character on the Ground State Electronic Properties in the van Der Waals Transition Metal Iodides VI₃ and CrI₃. Nano Letters, 2022, 22, 7034-7041.	4.5	11
72105	Bitumenâ€Derived Onionâ€Like Soft Carbon as Highâ€Performance Potassiumâ€Ion Battery Anode. Small, 2022, 18, .	5.2	23

#	Article	IF	Citations
72106	Co-Operative Influence of O₂ and H₂O in the Degradation of Layered Black Arsenic. Journal of Physical Chemistry C, 2022, 126, 15222-15228.	1.5	1
72107	Cl₂-Doped CuSCN Hole Transport Layer for Organic and Perovskite Solar Cells with Improved Stability. ACS Energy Letters, 2022, 7, 3139-3148.	8.8	20
72108	Heterostructure-based 3D-CdS/TiO2 nanotubes/Ti: Photoelectrochemical performances and interface simulation investigation. Ceramics International, 2022, 48, 36731-36738.	2.3	3
72109	Tracking the Interaction between a CO-Functionalized Probe and Two Ag-Phthalocyanine Conformers by Local Vertical Force Spectroscopy. Journal of Physical Chemistry A, 2022, 126, 6890-6897.	1.1	0
72110	Rational design of perovskite ferrites as high-performance proton-conducting fuel cell cathodes. Nature Catalysis, 2022, 5, 777-787.	16.1	73
72111	Nature and Dynamic Evolution of Rh Single Atoms Trapped by CeO₂ in CO Hydrogenation. ACS Catalysis, 2022, 12, 12253-12267.	5.5	8
72112	Quasiâ€Continuous Tuning of Carrier Polarity in Monolayered Molybdenum Dichalcogenides through Substitutional Vanadium Doping. Advanced Functional Materials, 0, , 2204760.	7.8	6
72113	Selective adsorption of liquid long-chain Î±-olefin/paraffin on Mg-MOF-74: Adsorption behavior and interaction mechanism. Nano Research, 2023, 16, 1595-1605.	5.8	4
72114	Effect of Alloying Elements and Low Temperature Plasma Nitriding on Corrosion Resistance of Stainless Steel. Materials, 2022, 15, 6575.	1.3	4
72115	Efficient Sensing of Selected Amino Acids as Biomarker by Green Phosphorene Monolayers: Smart Diagnosis of Viruses. Advanced Theory and Simulations, 2022, 5, .	1.3	6
72116	Tuning Fe Spin Moment in Feâ€“Nâ€“C Catalysts to Climb the Activity Volcano via a Local Geometric Distortion Strategy. Advanced Science, 2022, 9, .	5.6	23
72117	Accurately Determining the Phase Transition Temperature of CsPbI₃ via Random-Phase Approximation Calculations and Phase-Transferable Machine Learning Potentials. Chemistry of Materials, 2022, 34, 8561-8576.	3.2	8
72118	Electronâ€“phonon calculations using a Wannier-based supercell approach: Applications to the monolayer MoS<mml:math xmlns:mml="http://www.w3.org/1998/Math/MathML" display="inline" id="d1e132" altimg="si69.svg"><mml:msub><mml:mrow /><mml:mrow><mml:mn>2</mml:mn></mml:mrow></mml:msub></mml:math> mobility. Solid-State Electronics, 2022, , 108461.	0.8	0
72119	Topological electronic structure evolution with symmetry-breaking spin reorientation in <mml:math xmlns:mml="http://www.w3.org/1998/Math/MathML"><mml:mrow><mml:mo>(</mml:mo><mml:msub><mml:mi>Fe</mml:mi><mml:mi>m</mml:mi> Physical Review B, 2022, 106, .	3.2	2
72120	Density Functional Theory Calculations of the Stacking-Dependent Optoelectronic Properties of 2D GeSe/SnS Heterobilayers: Implications for Photovoltaics. ACS Applied Nano Materials, 2022, 5, 12217-12223.	2.4	2
72121	Nb12+â€”niobespherene: a full-metal hollow-cage cluster with superatomic stability and resistance to CO attack. National Science Review, 2023, 10, .	4.6	4
72122	Nail-like Î±-SnWO₄ Array Film with Increased Reactive Facets for Photoelectrochemical Water Splitting. Journal of Physical Chemistry C, 2022, 126, 15596-15605.	1.5	5
72123	Cr₂Ge₂Te₆ nanoribbons with perpendicular magnetic anisotropy and half metallicity: a DFT study. Journal Physics D: Applied Physics, 2022, 55, 485003.	1.3	1

#	Article	IF	Citations
72124	Intrinsic Ferromagnetism in 2D Fe₂H with a High Curie Temperature. ACS Applied Materials & Interfaces, 2022, 14, 44745-44752.	4.0	4
72125	Urea Production on Metalâ€Free Dual Silicon Doped C9N4 Nanosheet Under Ambient Conditions by Electrocatalysis: A First Principles Study. ChemPhysChem, 0, , .	1.0	3
72126	Ambient-pressure high- <mml:math xmlns:mml="http://www.w3.org/1998/Math/MathML"><mml:msub><mml:mi>T</mml:mi><mml:mi>c</mml:mi></mml:msub></mml:ma superconductivity in doped boron-nitrogen clathrates <mml:math xmlns:mml="http://www.w3.org/1998/Math/MathML"><mml:mrow><mml:mi>La</mml:mi><mml:msub><mml:mrow><mml:mo>(</mml and <mml:math xmlns:mml="http://www.w3.org/1998/Math/MathML"><mml:mrow><mml:mi mat. Physical Review B, 2022, 106, .	1.1	7
72127	[Cs6Cl][Ga5GeQ12] (Q = S, Se): two novel porous layered chalcohalides exhibiting two-band emission and ion exchange properties. Science China Chemistry, 2022, 65, 1903-1910.	4.2	2
72128	Evolution of Framework Al Arrangements in CHA Zeolites during Crystallization in the Presence of Organic and Inorganic Structure-Directing Agents. Crystal Growth and Design, 2022, 22, 6275-6295.	1.4	10
72129	Density Functional Theory Study of Controllable Optical Absorptions and Magneto-Optical Properties of Magnetic CrI₃ Nanoribbons: Implications for Compact 2D Magnetic Devices. ACS Applied Nano Materials, 2022, 5, 14388-14399.	2.4	2
72130	Extraction of Chemical Reactivity and Structural Relaxations of an Organic Dye from the Short-Range Interaction with a Molecular Probe. Journal of Physical Chemistry Letters, 2022, 13, 8660-8665.	2.1	2
72131	Quantitative determination of interlayer electronic coupling at various critical points in bilayer <mml:math xmlns:mml="http://www.w3.org/1998/Math/MathML"><mml:mrow><mml:mi>Mo</mml:mi><mml:msub><mml:mi mathvariant="normal">S</mml:mi><mml:mn>2</mml:mn></mml:msub></mml:mrow></mml:math>. Physical Review B, 2022, 106, .	1.1	4
72132	Overlaying Monolayer Metalâ€“Organic Framework on PtSe₂â€Based Gas Sensor for Tuning Selectivity. Advanced Functional Materials, 2022, 32, .	7.8	25
72133	Suppression of Methane Formation by Regulating the Hydrogenation Capability of Metal Oxides in Alkylation of Benzene with Syngas. Industrial & Engineering Chemistry Research, 2022, 61, 13354-13363.	1.8	1
72134	Sr-doped BaZr0.5Fe0.5O3-Î´ cathode with improved chemical stability and higher performance for proton-conducting solid oxide fuel cells. Ceramics International, 2022, 48, 35642-35648.	2.3	3
72135	Crystal structure from laboratory X-ray powder diffraction data, DFT-D calculations, and Hirshfeld surface analysis of (S)-dapoxetine hydrochloride. Powder Diffraction, 2022, 37, 216-224.	0.4	1
72136	Thermoelectric transport properties of XAgP (X = Sr and Ba) from first principles. Journal of Physics Condensed Matter, 2022, 34, 455501.	0.7	1
72137	Experimental and Theoretical Study of Sorption Capacity of Hexagonal Boron Nitride Nanoparticles: Implication for Wastewater Purification from Antibiotics. Nanomaterials, 2022, 12, 3157.	1.9	5
72138	Comparison of magnetic anisotropy and structural properties in chemically ordered CoPt and FePt nanoparticles. Physical Review B, 2022, 106, .	1.1	0
72139	A first-principles and mesoscopic model analysis for pair, trio, and quarto interactions of Au adatoms on Ag(100). Surface Science, 2023, 727, 122191.	0.8	1
72140	Insights into the high-pressure behavior of solid bromine from hybrid density functional theory calculations. Physical Review B, 2022, 106, .	1.1	1
72141	Ab initio Interfacial Chemical Stability of Argyrodite Sulfide Electrolytes and Layered-Structure Cathodes in Solid-State Lithium Batteries. Jom, 2022, 74, 4664-4671.	0.9	3

#	Article	IF	Citations
72142	Mechanistic insights into propylene oxidation to acrolein over gold catalysts. Chinese Journal of Chemical Engineering, 2023, 57, 39-49.	1.7	3
72143	Theoretical Study on the Electrochemical Water Splitting of Two-Dimensional Metalâ€“Organic Frameworks TM3C12O12 (TM = Mn, Fe, Co, Ni). Crystals, 2022, 12, 1289.	1.0	5
72144	The GaSe/g-C6N6 type-II van der Waals heterostructure: A prospective water-splitting photocatalyst under acidic, alkaline and neutral conditions. Thin Solid Films, 2022, 758, 139419.	0.8	4
72145	Enhancing the Photoinduced Interlayer Charge Transfer and Spatial Separation in Type-II Heterostructure of WS₂ and Asymmetric Janus-MoSSe with Intrinsic Self-Build Electric Field. Journal of Physical Chemistry Letters, 2022, 13, 8484-8494.	2.1	13
72146	Origin of the High Selectivity of the Ptâ€“Rh Thin-Film H₂ Gas Sensor Studied by Operando Ambient-Pressure X-ray Photoelectron Spectroscopy at Working Conditions. Journal of Physical Chemistry Letters, 2022, 13, 8546-8552.	2.1	3
72147	Enabling structural and interfacial stability of 5ÂV spinel LiNi0.5Mn1.5O4 cathode by a coherent interface. Journal of Energy Chemistry, 2023, 76, 266-276.	7.1	11
72148	Hard antiphase domain boundaries in strontium titanate unravelled using machine-learned force fields. Physical Review Materials, 2022, 6, .	0.9	4
72149	Modulating the microscopic lattice distortions through the Al-rich layers for boosting the ferroelectricity in Al:HfO₂ nanofilms. Journal Physics D: Applied Physics, 2022, 55, 455501.	1.3	3
72150	Why Ultrafast Photoinduced CO Desorption Dominates over Oxidation on Ru(0001). Journal of Physical Chemistry Letters, 2022, 13, 8516-8521.	2.1	5
72151	Electronâ€Transport Layers Employing Strongly Bound Ligands Enhance Stability in Colloidal Quantum Dot Infrared Photodetectors. Advanced Materials, 2022, 34, .	11.1	16
72152	Controllable N Doped in Carbon Nanolayers@Mo ₂ C Nanodots as Electrocatalyst Boosts Highâ€efficient Hydrogen Production. Particle and Particle Systems Characterization, 0, , 2200142.	1.2	2
72153	Ru-Doping of P2-Na_xMn_{0.75}Ni_{0.25}O₂-Layered Oxides for High-Energy Na-Ion Battery Cathodes: First-Principles Insights on Activation and Control of Reversible Oxide Redox Chemistry. ACS Applied Energy Materials, 2022, 5, 10721-10730.	2.5	6
72154	Elastic properties of disordered binary hcp-Fe alloys under high pressure: Effects of light elements. ChemPhysMater, 2023, 2, 155-163.	1.4	2
72155	CO2-free high-purity ethylene from electroreduction of CO2 with 4% solar-to-ethylene and 10% solar-to-carbon efficiencies. Cell Reports Physical Science, 2022, 3, 101053.	2.8	8
72156	Unraveling the Effect of A-Site Sr-Doping in Double Perovskites Ca_{2â€“x}Sr_xScRuO₆ (x = 0 and 1): Structural Interpretation and Mechanistic Investigations of Trifunctional Electrocatalytic Effects. ACS Applied Energy Materials, 2022, 5, 11632-11645.	2.5	7
72157	Revelation of the transitionâ€metal doping mechanism in lithium manganese phosphate for high performance of lithiumâ€ion batteries. , 2022, 1, .		16
72158	High-capacity hydrogen storage in zirconium decorated zeolite templated carbon: Predictions from DFT simulations. International Journal of Hydrogen Energy, 2022, 47, 38671-38681.	3.8	7
72159	Amorphous CeO₂â€“Cu Heterostructure Enhances CO₂ Electroreduction to Multicarbon Alcohols. , 2022, 4, 1999-2008.		6

#	Article	IF	Citations
72160	Nanophotonic control of thermal emission under extreme temperatures in air. Nature Nanotechnology, 2022, 17, 1104-1110.	15.6	12
72161	Enhanced Magnetism in Heterostructures with Transition-Metal Dichalcogenide Monolayers. Journal of Physical Chemistry Letters, 2022, 13, 8879-8887.	2.1	6
72162	P-type conductivity in Sn-doped Sb₂Se₃. JPhys Energy, 2022, 4, 045006.	2.3	9
72163	Spontaneous Seed Formation during Electrodeposition Drives Epitaxial Growth of Metastable Bismuth Selenide Microcrystals. Journal of the American Chemical Society, 2022, 144, 18272-18285.	6.6	7
72164	Role of Graphene on Ni/NiO for the Hydrogen Evolution Reaction. Journal of Physical Chemistry C, 2022, 126, 16158-16163.	1.5	4
72165	Synergistically Promoting Coking Resistance of a La_{0.4}Sr_{0.4}Ti_{0.85}Ni_{0.15}O_{3â^'Î´} Anode by Ru-Doping-Induced Active Twin Defects and Highly Dispersed Ni Nanoparticles. ACS Applied Materials & Interfaces, 2022, 14, 44002-44014.	4.0	4
72166	Ab initio study of electron mobility in V<mml:math xmlns:mml="http://www.w3.org/1998/Math/MathML" altimg="si1.svg" display="inline" id="d1e1129"><mml:msub><mml:mrow /><mml:mrow><mml:mn>2</mml:mn></mml:mrow></mml:msub></mml:math>O<mml:math xmlns:mml="http://www.w3.org/1998/Math/MathML" altimg="si2.svg" display="inline" id="d1e1137"><mml:msub><mml:mrow /><mml:mrow><mml:mn>5</mml:mn></mml:mrow></mml:msub></	0.8	3
72167	Performance of a Solid Cell with a Solidâ€Liquid Electrolyte Prepared by a Microwaveâ€Assisted Sintering Technique fromÂMCMâ€41â€‰and Ionic Liquids. ChemistrySelect, 2022, 7, .	0.7	1
72168	Black Phosphorous Mediates Surface Charge Redistribution of CoSe₂ for Electrochemical H₂O₂ Production in Acidic Electrolytes. Advanced Materials, 2022, 34, .	11.1	25
72169	On the Role of Interfacial Water Dynamics for Electrochemical Stability of RuO₂ and IrO₂. ChemCatChem, 2022, 14, .	1.8	9
72170	Ultra-Low Thermal Conductivity of MoirÃ© Diamanes. Membranes, 2022, 12, 925.	1.4	5
72171	ACuZrQ₃ (A = Rb, Cs; Q = S, Se, Te): Direct Bandgap Semiconductors and Metals with Ultralow Thermal Conductivity. Chemistry of Materials, 2022, 34, 8389-8402.	3.2	11
72172	Hybrid improper ferroelectricity in A-cation ordered perovskite BaSrBi$$_2$$O$$_6$$. Journal of the Korean Physical Society, 0, , .	0.3	1
72173	Stability and electronic properties of layered NaMnO2 using the SCAN(+U). Journal of the Korean Physical Society, 0, , .	0.3	0
72174	Ultrathin Niobate Nanosheet Assembly with Au NPs and CdS QDs as a Highly Efficient Photocatalyst. Chemistry - A European Journal, 0, , .	1.7	0
72175	Immobilization of AgCl/Pd Heterojunctions on Nitrogenâ€Doped Carbon Nanotubes: Interfacial Designâ€Induced Electronic Regulation Enhances Photocatalytic Activity. Chemistry - A European Journal, 2022, 28, .	1.7	3
72176	Computational exploration and screening of novel Janus MA2Z4 (M = Sc-Zn, Y-Ag, Hf-Au; A=Si, Ge; Z=N,) Tj ETQq0 0 0 rgBT /Overlock 10	2.4	17
72177	Strong Dzyaloshinskii-Moriya interaction in monolayer <mml:math xmlns:mml="http://www.w3.org/1998/Math/MathML"><mml:msub><mml:mi>CrI</mml:mi><mml:mn>3</mml:mn></mml:msub></m on metal substrates. Physical Review B, 2022, 106, .	1.1	6

#	Article	IF	Citations
72178	Quantum-Chemical Simulation of Molecular Hydrogen Abstraction from Magnesium Borohydride Triammoniate. Russian Journal of Inorganic Chemistry, 2022, 67, 1591-1605.	0.3	0
72179	CO hydrogenation on stepped Cu and CuZn alloy surfaces: Competition between methanol synthesis and methanation pathways. Chinese Chemical Letters, 2023, 34, 107809.	4.8	2
72180	Novel Class of Rhenium Borides Based on Hexagonal Boron Networks Interconnected by Short B₂ Dumbbells. Chemistry of Materials, 2022, 34, 8138-8152.	3.2	2
72181	Evolution of a metastable thin film with highâ€hardness wear resistance for advanced cutting tool application. Journal of the American Ceramic Society, 0, , .	1.9	0
72182	Efficient and improved prediction of the band offsets at semiconductor heterojunctions from meta-GGA density functionals: A benchmark study. Journal of Chemical Physics, 2022, 157, .	1.2	5
72183	Tuning Electronic Structure and Composition of FeNi Nanoalloys for Enhanced Oxygen Evolution Electrocatalysis via a General Synthesis Strategy. Small, 2022, 18, .	5.2	9
72184	Two-dimensional ternary chalcogenides <mml:math xmlns:mml="http://www.w3.org/1998/Math/MathML"><mml:mrow><mml:mi>Fe</mml:mi><mml:msub><mml:mi>X</mml:mi><mml:mr <mml:math		

#	Article	IF	Citations
72196	The role of Cu1â€“O3 species in single-atom Cu/ZrO2 catalyst for CO2 hydrogenation. Nature Catalysis, 2022, 5, 818-831.	16.1	165
72197	Oxidative Addition of Methane and Reductive Elimination of Ethane and Hydrogen on Surfaces: From Pure Metals to Single Atom Alloys. Journal of the American Chemical Society, 2022, 144, 18650-18671.	6.6	5
72198	Improving the catalytic activity of two-dimensional Mo2C for hydrogen evolution reaction by doping and vacancy defects. International Journal of Hydrogen Energy, 2022, 47, 38517-38523.	3.8	4
72199	Quantum electron liquid and its possible phase transition. Nature Materials, 2022, 21, 1269-1274.	13.3	9
72200	Multiple polarization phases and strong magnetoelectric coupling in the layered transition metal phosphorus chalcogenides <mml:math xmlns:mml="http://www.w3.org/1998/Math/MathML"><mml:mrow><mml:mi>T</mml:mi><mml:mi>M</mml:mi><mml:msub><mml:mi		

#	Article	IF	Citations
72214	Theory-Guided Exploration of the Sr₂Nb₂O₇ System for Increased Dielectric and Piezoelectric Properties and Synthesis of Vanadium-Alloyed Sr₂Nb₂O₇. Chemistry of Materials, 2022, 34, 8536-8543.	3.2	2
72215	Superatom Molecular Orbitals of Li@C₆₀: Effects of the Li Position and the Substrate. Journal of Physical Chemistry C, 2022, 126, 15891-15898.	1.5	4
72216	Tuning the Thermoelectric Performance of CaMnO₃-Based Ceramics by Controlled Exsolution and Microstructuring. ACS Applied Energy Materials, 2022, 5, 12396-12407.	2.5	3
72217	Accelerating syngas-to-aromatic conversion via spontaneously monodispersed Fe in ZnCr2O4 spinel. Nature Communications, 2022, 13, .	5.8	15
72218	Evolution of precipitate and precipitate/matrix interface in Al-Zn-Mg-Cu (-Ag) alloys. Journal of Materials Science and Technology, 2023, 138, 157-170.	5.6	15
72219	Influence of water contamination on the sputtering of silicon with low-energy argon ions investigated by molecular dynamics simulations. Beilstein Journal of Nanotechnology, 0, 13, 986-1003.	1.5	1
72220	The Crystal Structure of Carbonic Acid. Inorganics, 2022, 10, 132.	1.2	1
72221	Critical topology and pressure-induced superconductivity in the van der Waals compound AuTe2Br. Npj Quantum Materials, 2022, 7, .	1.8	3
72222	Modified HSE06 functional applied to anatase TiO₂: influence of exchange fraction on the quasiparticle electronic structure and optical response. Electronic Structure, 2022, 4, 045001.	1.0	4
72223	Similarity of materials and data-quality assessment by fingerprinting. MRS Bulletin, 2022, 47, 991-999.	1.7	3
72224	CoSe₂ Subnanometer Belts with Se Vacancies and Ni Substitutions for the Efficient Electrosynthesis of High-Value-Added Nitriles Coupled with Hydrogen Generation. ACS Catalysis, 2022, 12, 11391-11401.	5.5	19
72225	Effects of thin metal contacts on few-layer van der Waals ferrielectric CuInP2S6. Journal of Applied Physics, 2022, 132, .	1.1	1
72226	A Universal Machine Learning Framework for Electrocatalyst Innovation: A Case Study of Discovering Alloys for Hydrogen Evolution Reaction. Advanced Functional Materials, 2022, 32, .	7.8	30
72227	Mechanism of C-N bonds formation in electrocatalytic urea production revealed by ab initio molecular dynamics simulation. Nature Communications, 2022, 13, .	5.8	50
72228	Improving Catalytic Activity of â€œJanusâ€•MoSSe Based on Surface Interface Regulation. Molecules, 2022, 27, 6038.	1.7	2
72229	High-Throughput Predictions of the Stabilities of Multi-Type Long-Period Stacking Ordered Structures in High-Performance Mg Alloys. Nanomaterials, 2022, 12, 3240.	1.9	1
72230	Thermodynamic and electrical transport properties of <mml:math xmlns:mml="http://www.w3.org/1998/Math/MathML"><mml:mrow><mml:msub><mml:mi mathvariant="normal">UTe</mml:mi><mml:mn>2</mml:mn></mml:msub></mml:mrow></mml:math> under uniaxial stress. Physical Review B, 2022, 106, .	1.1	8
72231	Electronic structure of <mml:math xmlns:mml="http://www.w3.org/1998/Math/MathML"><mml:mrow><mml:mi>Î±</mml:mi><mml:mo>â^’</mml:mo><mml:msub><mml:mi mathvariant="normal">O</mml:mi><mml:mn>3</mml:mn></mml:msub></mml:mrow></mml:math> grain boundaries containing reactive element segregants. Physical Review Materials, 2022, 6, .	0.9	1

#	Article	IF	Citations
72232	Green and Energy-Saving Recycling of LiCoO₂ by Synergetic Pyrolysis with Polyvinyl Chloride Plastics. ACS Sustainable Chemistry and Engineering, 2022, 10, 12329-12341.	3.2	7
72233	A flexible and scalable scheme for mixing computed formation energies from different levels of theory. Npj Computational Materials, 2022, 8, .	3.5	8
72234	BaCO3 Nanoparticles-Modified Composite Cathode with Improved Electrochemical Oxygen Reduction Kinetics for High-Performing Ceramic Fuel Cells. Catalysts, 2022, 12, 1046.	1.6	4
72235	Linear-in-frequency optical conductivity over a broad range in the three-dimensional Dirac semimetal candidate <mml:math xmlns:mml="http://www.w3.org/1998/Math/MathML"><mml:msub><mml:mi mathvariant="normal">Ir</mml:mi><mml:mn>2</mml:mn></mml:msub><mml:msub><mml:mi mathvariant="normal">In</mml:mi><mml:mn>8</mml:mn></mml:msub><mml:mi>Se</mml:mi></mml:math>.	1.1	1
72236	Reconfigurable band alignment of <mml:math xmlns:mml="http://www.w3.org/1998/Math/MathML"><mml:mrow><mml:mi>m</mml:mi><mml:mtext>â^'</mml:mtext><mml:mi>GaS (<mml:math) Tj ETQq0 0 0 rgBT /Overlock 10 Tf 50 577 Td (xmlns:mml="http://www.w3.org/1998/MathML"><mml:mrow><mml:m	1.1	8
72237	Shapeâ€Controlled NaTaO ₃ by Fluxâ€Mediated Synthesis. Advanced Functional Materials, 0, , 2206641.	7.8	2
72238	Spinor <mml:math xmlns:mml="http://www.w3.org/1998/Math/MathML"><mml:mrow><mml:mi>G</mml:mi><mml:mi>W</mml:mi></mml:mrow></mml:m /Bethe-Salpeter calculations in BerkeleyGW: Implementation, symmetries, benchmarking, and performance. Physical Review B, 2022, 106, .	1.1	7
72239	Theoretical Insight into Tuning CO₂ Methanation and Reverse Water Gas Shift Reactions on MoO_x-Modified Ni Catalysts. Journal of Physical Chemistry C, 2022, 126, 18078-18089.	1.5	6
72240	Designing high-efficiency metal and semimetal contacts to two-dimensional semiconductor Î³-GeSe. Applied Physics Letters, 2022, 121, .	1.5	11
72241	Sr Doping and Oxygen Vacancy Formation in La1â^'xSrxScO3â^'Î´ Solid Solutions: Computational Modelling. Crystals, 2022, 12, 1300.	1.0	2
72242	Two-dimensional semimetal states in transition metal trichlorides: A first-principles study. Applied Physics Letters, 2022, 121, .	1.5	1
72243	Softened <mml:math xmlns:mml="http://www.w3.org/1998/Math/MathML"><mml:mrow><mml:mi>s</mml:mi><mml:msup><mml:mrow><mml:mi>p</mml bonding network leads to strong anharmonicity and weak hydrodynamics in graphene+. Physical Review B, 2022, 106, .	1.1	12
72244	Ca₃Mn₂O₇â€layered perovskites: Effects of Laâ€and Yâ€doping on phase stability, microstructure, and thermoelectric transport. Journal of the American Ceramic Society, 2023, 106, 213-226.	1.9	5
72245	Observation of anisotropic Dirac cones in the topological material <mml:math xmlns:mml="http://www.w3.org/1998/Math/MathML"><mml:msub><mml:mrow><mml:mi>Ti</mml:mi></mml:mrow><mml:mn>2</mml mathvariant="normal">P</mml:mi></mml:math>. Physical Review B, 2022, 106, .	1.1	4
72246	First-principles prediction of the lattice thermal conductivity of two-dimensional (2D) h-BX (Xâ€‰=â€‰P, As,) Tj ETQq0 0 0 rgBT /Overl 132, .	1.1	10
72247	Ultrafast Suppression of the Ferroelectric Instability in <mml:math xmlns:mml="http://www.w3.org/1998/Math/MathML" display="inline"><mml:mrow><mml:msub><mml:mrow><mml:mi>KTaO</mml:mi></mml:mrow><mml:mrow><mml:mn>3</mml:mn> Physical Review Letters, 2022, 129, .	2.9	8
72248	VELAS: An open-source toolbox for visualization and analysis of elastic anisotropy. Computer Physics Communications, 2023, 283, 108540.	3.0	9
72249	Revisiting the Role of Physical Confinement and Chemical Regulation of 3D Hosts for Dendrite-Free Li Metal Anode. Nano-Micro Letters, 2022, 14, .	14.4	23

#	Article	IF	Citations
72250	Tunable magnetocrystalline anisotropy and valley polarization in an intrinsic ferromagnetic Janus <mml:math xmlns:mml="http://www.w3.org/1998/Math/MathML"><mml:mn>2</mml:mn><mml:mi>H</mml:mi></mml:math> -VTeSe monolayer. Physical Review B, 2022, 106, .	1.1	8
72251	Machine learning prediction on intermetallic compounds with implemented virtual-center-atom structural descriptor. Science and Technology of Advanced Materials Methods, 2022, 2, 334-344.	0.4	0
72252	2D electrene LaH₂ monolayer: an ideal ferrovalley direct semiconductor with room-temperature ferromagnetic stability. Journal of Physics Condensed Matter, 2022, 34, 475303.	0.7	2
72253	Type-II Heterojunction CdIn₂S₄/BiVO₄ Coupling with CQDs to Improve PEC Water Splitting Performance Synergistically. ACS Applied Materials & Interfaces, 2022, 14, 45392-45402.	4.0	32
72254	Tailorable magnetocrystalline anisotropy at the <mml:math xmlns:mml="http://www.w3.org/1998/Math/MathML"><mml:msub><mml:mi>MnPt</mml:mi><mml:mn>3</mml:mn></mml:msub><mr surface. Physical Review B, 2022, 106, .	1.1	0
72255	Construction of novel PG/GeP2 and PG/SiP2 vdW heterostructures for high-efficiency photocatalytic water splitting. Applied Surface Science, 2023, 608, 155106.	3.1	34
72256	Symmetry relation database and its application to ferroelectric materials discovery. MRS Communications, 0, , .	0.8	0
72257	Computational prediction of new magnetic materials. Journal of Chemical Physics, 2022, 157, 124704.	1.2	2
72258	Short- and Long-Time Dynamics of Hydrogen Spillover from a Single Atom Platinum Active Site to the Cu(111) Host Surface. Journal of Physical Chemistry C, 2022, 126, 17093-17101.	1.5	9
72259	Enabling stable 4.6ÂV LiCoO2 cathode through oxygen charge regulation strategy. Journal of Energy Chemistry, 2023, 76, 557-565.	7.1	9
72260	Interface engineering breaks both stability and activity limits of RuO2 for sustainable water oxidation. Nature Communications, 2022, 13, .	5.8	77
72261	Zero-point renormalization of the band gap of semiconductors and insulators using the projector augmented wave method. Physical Review B, 2022, 106, .	1.1	13
72262	Chiral 2D Cu(I) Halide Frameworks. Chemistry of Materials, 2022, 34, 8262-8270.	3.2	16
72263	Defective g-C3N4 supported Ru3 single-cluster catalyst for ammonia synthesis through parallel reaction pathways. Nano Research, 2023, 16, 3580-3587.	5.8	8
72264	Predicting solid state material platforms for quantum technologies. Npj Computational Materials, 2022, 8, .	3.5	3
72265	Theory of Borazine-Derived Nanothreads: Enumeration, Reaction Pathways, and Piezoelectricity. ACS Nano, 2022, 16, 15884-15893.	7.3	2
72266	Computational Screening of Na₃MBr₆ Compounds as Sodium Solid Electrolytes. Chemistry of Materials, 2022, 34, 8356-8365.	3.2	7
72267	Jahnâ^'Teller Distortion-Stabilized Halide Double Perovskites with Unusual Rock-Salt-type Ordering of Divalent B-Site Cations. Chemistry of Materials, 2022, 34, 8207-8212.	3.2	5

#	Article	IF	Citations
72268	Molecular understanding of interphase formation via operando polymerization on lithium metal anode. Cell Reports Physical Science, 2022, 3, 101057.	2.8	6
72269	Spontaneous Polarization and Polarization-Induced Electron Sheet Charge of YbAlN on GaN: A First-Principles Study. ACS Applied Electronic Materials, 2022, 4, 4772-4780.	2.0	1
72270	Real-Space Identification of Non-Noble Single Atomic Catalytic Sites within Metal-Coordinated Supramolecular Networks. ACS Nano, 2022, 16, 14284-14296.	7.3	6
72271	The HEALED SBU Library of Chemically Realistic Building Blocks for Construction of Hypothetical Metalâ€“Organic Frameworks. ACS Applied Materials & Interfaces, 2022, 14, 43372-43386.	4.0	5
72272	Orbital-selective band hybridisation at the charge density wave transition in monolayer TiTe2. Npj Quantum Materials, 2022, 7, .	1.8	8
72273	First-principles comparative study of Cr migration in O3 and O/P hybrid-phased <mml:math xmlns:mml="http://www.w3.org/1998/Math/MathML"><mml:msub><mml:mi>NaCrO</mml:mi><mml:mn>2</mml:mn></mml:msub> Physical Review Materials, 2022, 6, .	3.1	0
72274	Adsorption of atomic and molecular monolayers on Pt-supported graphene. Chemical Physics, 2023, 564, 111713.	0.9	3
72275	Stabilization of Lithium Metal Interfaces by Constructing Composite Artificial Solid Electrolyte Interface with Mesoporous TiO₂ and Perfluoropolymers. Small, 2022, 18, .	5.2	7
72276	Activating basal plane of Janus VSSe for efficient hydrogen evolution reaction by non-noble metal element doping: A first-principal study. International Journal of Hydrogen Energy, 2022, 47, 34924-34931.	3.8	5
72277	Highly Stable Singleâ€Atom Modified MXenes as Cathodeâ€Active Bifunctional Catalysts in Liâ€“CO₂ Battery. Advanced Functional Materials, 2022, 32, .	7.8	15
72279	Self-templating synthesis and structural regulation of nanoporous rhodium-nickel alloy nanowires efficiently catalyzing hydrogen evolution reaction in both acidic and alkaline electrolytes. Nano Research, 2023, 16, 2026-2034.	5.8	4
72280	Oxynitride-surface engineering of rhodium-decorated gallium nitride for efficient thermocatalytic hydrogenation of carbon dioxide to carbon monoxide. Communications Chemistry, 2022, 5, .	2.0	5
72281	Selective production of ethylene from CO2 over CuAg tandem electrocatalysts. Journal of Industrial and Engineering Chemistry, 2022, 116, 191-198.	2.9	14
72282	Probing the Optical Dynamics of Quantum Emitters in Hexagonal Boron Nitride. PRX Quantum, 2022, 3, .	3.5	8
72283	Experimental and Theoretical Characterization of Rh Single Atoms Supported on Î³-Al₂O₃ with Varying Hydroxyl Contents during NO Reduction by CO. ACS Catalysis, 2022, 12, 11697-11715.	5.5	14
72284	Lattice Oxygen-Induced d-Band Shifting for Enhanced Hydrogen Oxidation Reaction on Nickel. ACS Catalysis, 2022, 12, 11830-11837.	5.5	19
72285	Coexistence of two types of short-range order in Siâ€“Geâ€“Sn medium-entropy alloys. Communications Materials, 2022, 3, .	2.9	3
72286	Passivation of Mid-Gap Electronic States at Calcium Aluminosilicate Glass Surfaces upon Water Exposure: An Ab Initio Study. Journal of Physical Chemistry B, 2022, 126, 7709-7719.	1.2	1

#	Article	IF	Citations
72287	High Thermoelectric Performance and Low Lattice Thermal Conductivity in Lattice-Distorted High-Entropy Semiconductors AgMnSn_{1â€“x}Pb_xSbTe₄. Chemistry of Materials, 2022, 34, 8959-8967.	3.2	9
72288	Uniaxial strain induced anisotropic bandgap engineering in freestanding BiFeO3 films. APL Materials, 2022, 10, .	2.2	2
72289	Lattice Dynamics of BCC Titanium and Its Nonlinear Response to High Temperature Deformations in Ab Initio Molecular Dynamics. Physics of the Solid State, 0, , .	0.2	0
72290	Highly tunable band inversion in <mml:math xmlns:mml="http://www.w3.org/1998/Math/MathML"><mml:mrow><mml:mi>A</mml:mi><mml:msub><mml:mi>B</mml:mi><mml:m		

#	Article	IF	Citations
72306	First-principles studies of defect behaviour in bismuth germanate. Scientific Reports, 2022, 12, .	1.6	1
72307	Bi₂Se₃ Growth on (001) GaAs Substrates for Terahertz Integrated Systems. ACS Applied Materials & Interfaces, 2022, 14, 42683-42691.	4.0	4
72308	Trifunctional electrocatalysts based on feather-like NiCoP 3D architecture for hydrogen evolution, oxygen evolution, and urea oxidation reactions. Ceramics International, 2023, 49, 659-668.	2.3	21
72309	Heterointerface effects of lithium intercalation and diffusion in van der Waals heterostructures. Physical Review Materials, 2022, 6, .	0.9	4
72310	An ab initio investigation on the mechanism of formaldehyde oxidation: A case of heterogeneous catalytic reaction over graphene-like MnO2 monolayer anchored different single atoms (Fe, Co, and) Tj ETQq0 0 0 rgBT /Overlock 10 Tf 5	3.3	6
72311	Effect of B and Ce on the grain boundary segregation of Mo-rich phases in super-austenitic stainless steels. Applied Physics A: Materials Science and Processing, 2022, 128, .	1.1	2
72312	Strain-tunable Dzyaloshinskii-Moriya interaction and skyrmions in two-dimensional Janus <mml:math xmlns:mml="http://www.w3.org/1998/Math/MathML"><mml:mrow><mml:msub><mml:mi>Cr</mml:mi><mml:mn>2</mml:mn></mml:r		

#	Article	IF	Citations
72325	Bonding Inhomogeneity and Strong Anharmonicity Induce Ultralow Lattice Thermal Conductivity in Calcium Pyrovanadate. Journal of Physical Chemistry C, 2022, 126, 16492-16498.	1.5	2
72326	Regulation and Stabilization of the Zinc Metal Anode Interface by Electroless Plating of a Multifunctionalized Polydopamine Layer. ACS Applied Materials & Interfaces, 2022, 14, 43215-43225.	4.0	11
72327	Strain-induced two-dimensional topological insulators in monolayer 1Tâ€²-RuO₂. Journal of Physics Condensed Matter, 2022, 34, 475502.	0.7	2
72328	Two growth modes of nanostructures near Cu(111) step edges in CoCu and PtCu surface alloys. European Physical Journal B, 2022, 95, .	0.6	0
72329	A Cost-Effective Long-Wave Infrared Detector Material Based on Graphene@PtSe2/HfSe2 Bidirectional Heterostructure: A First-Principles Study. Crystals, 2022, 12, 1244.	1.0	0
72330	Evolution of ground state in <mml:math xmlns:mml="http://www.w3.org/1998/Math/MathML"><mml:msub><mml:mi mathvariant="normal">Cr</mml:mi><mml:mn>2</mml:mn></mml:msub><mml:msub><mml:mi mathvariant="normal">Te</mml:mi><mml:mn>3</mml:mn></mml:msub></mml:math> single crystal under applied magnetic field. Physical Review B, 2022, 106, .	1.1	1
72331	Metallic B2C3P Monolayer as Li-Ion Battery Materials: A First-Principles Study. Processes, 2022, 10, 1809.	1.3	7
72332	Pressure-induced decomposition of cadmium iodide. Europhysics Letters, 2022, 140, 16003.	0.7	4
72333	Tunable Mott Dirac and Kagome Bands Engineered on 1T-TaS₂. Nano Letters, 2022, 22, 7902-7909.	4.5	6
72334	Graphyne supported Co13, Fe13 and Ni13 nano-cluster as efficient electrocatalysts for nitrogen reduction reaction: A first principles study. Catalysis Today, 2023, 423, 113906.	2.2	1
72335	Atomic and Electronic Structure of the Al₂O₃/Al Interface during Oxide Propagation Probed by Ab Initio Grand Canonical Monte Carlo. ACS Applied Materials & Interfaces, 2022, 14, 42613-42627.	4.0	2
72336	Adsorption of <mml:math xmlns:mml="http://www.w3.org/1998/Math/MathML" display="inline" overflow="scroll"><mml:mi>Na</mml:mi></mml:math> Atoms on Electron-Deficient Doped <mml:math xmlns:mml="http://www.w3.org/1998/Math/MathML" display="inline" overflow="scroll"><mml:msub><mml:mrow><mml:mi>Mo</mml:mi><mml:mi mathvariant="normal">S</mml:mi></mml:mrow><mml:mn>2</mml:mn></mml:msub></mml:math> for Battery Electrodes. Physical Review Applied, 2022, 18, .	1.5	3
72337	Automated versus Chemically Intuitive Deconvolution of Density Functional Theory (DFT)-Based Gas-Phase Errors in Nitrogen Compounds. Industrial & Engineering Chemistry Research, 2022, 61, 13375-13382.	1.8	3
72338	Surface Organometallic Chemistry on Zeolites: Synthesis of Group IV Metal Alkyls and Metal Hydrides on Hierarchical Mesoporous H-ZSM-5. Chemistry of Materials, 2022, 34, 8777-8789.	3.2	1
72339	The SrS doped with Cl and K: a promising ambipolar semiconductor for transparent electronics application. Journal Physics D: Applied Physics, 2022, 55, 455108.	1.3	4
72340	Hard x-ray angle-resolved photoemission from a buried high-mobility electron system. Physical Review B, 2022, 106, .	1.1	1
72341	Aligning Fe2O3 photo-sheets on TiO2 nanofibers with hydrophilic and aerophobic surface for boosting photoelectrochemical performance. Nano Research, 2023, 16, 4178-4187.	5.8	3
72342	Prediction of stability and lifetime of carbyne, carbyneâ€“graphene and similar low-dimensional nanostructures. Applied Nanoscience (Switzerland), 0, , .	1.6	1

#	Article	IF	Citations
72343	Roles of Anion Sites in Highâ€Performance GeTe Thermoelectrics. Advanced Functional Materials, 2022, 32, .	7.8	11
72344	Rapid Hierarchical Screening for Promising Ternary and Quaternary Inorganic Solid-State Electrolytes. Journal of Physical Chemistry C, 2022, 126, 15996-16005.	1.5	2
72345	High Stability and Inoxidizability of Monolayer Topological Insulator ZrTe₅. Journal of Physical Chemistry C, 2022, 126, 16069-16074.	1.5	0
72346	Spontaneous Valley Polarization and Electrical Control of Valley Physics in Single-Layer TcIrGe₂S₆. Journal of Physical Chemistry Letters, 2022, 13, 8749-8754.	2.1	5
72347	A quest to high-capacity hydrogen storage in zirconium decorated pentagraphene: DFT perspectives. International Journal of Hydrogen Energy, 2022, 47, 36190-36203.	3.8	15
72348	Lattice Instability and Ultralow Lattice Thermal Conductivity of Layered PbIF. ACS Applied Materials & Interfaces, 2022, 14, 40738-40748.	4.0	9
72349	Direct observation of coexisting Kondo hybridization and antiferromagnetic state in <mml:math xmlns:mml="http://www.w3.org/1998/Math/MathML"><mml:msub><mml:mi>UAs</mml:mi><mml:mn>2</mml:mn></mml:msub></mm Physical Review B, 2022, 106, .	1.1	2
72350	Structural, elastic, phononic, optical and electronic properties investigation of two-dimensional XIS (X=Al, Ga, In) for photocatalytic water splitting. International Journal of Hydrogen Energy, 2022, 47, 41640-41647.	3.8	7
72351	Following Adsorbed Intermediates on a Platinum Gas Diffusion Electrode in H₃PO₃-Containing Electrolytes Using In Situ X-ray Absorption Spectroscopy. ACS Catalysis, 2022, 12, 11472-11484.	5.5	6
72352	High-throughput screening of room temperature active Peltier cooling materials in Heusler compounds. Npj Computational Materials, 2022, 8, .	3.5	8
72353	Green Triplet Self-Trapped Exciton Emission in Layered Rb₃Cd₂Cl₇:Sb³⁺ Perovskite: Comparison with RbCdCl₃:Sb³⁺. Journal of Physical Chemistry Letters, 2022, 13, 8436-8446.	2.1	19
72354	Critical Role of Explicit Inclusion of Solvent and Electrode Potential in the Electrochemical Description of Nitrogen Reduction. ACS Catalysis, 2022, 12, 11530-11540.	5.5	22
72355	Control of Hot Carrier Cooling in Lead Halide Perovskites by Point Defects. Journal of the American Chemical Society, 2022, 144, 18126-18134.	6.6	15
72356	What is the Real Origin of the Activity of Feâ€“Nâ€“C Electrocatalysts in the O₂ Reduction Reaction? Critical Roles of Coordinating Pyrrolic N and Axially Adsorbing Species. Journal of the American Chemical Society, 2022, 144, 18144-18152.	6.6	105
72357	The electron transfer mechanism between metal and silicon oxide composites for triboelectric nanogenerators. Advanced Composites and Hybrid Materials, 2022, 5, 3223-3231.	9.9	5
72358	Phonons in complex twisted crystals: Angular momenta, interactions, and topology. Physical Review B, 2022, 106, .	1.1	4
72359	Orbital-selective Mott and Peierls transition in HxVO2. Npj Quantum Materials, 2022, 7, .	1.8	5
72360	Ultrasensitive Formaldehyde Sensor Based on SnO₂ with Rich Adsorbed Oxygen Derived from a Metal Organic Framework. ACS Sensors, 2022, 7, 2577-2588.	4.0	17

#	Article	IF	Citations
72361	Highly efficient electrocatalytic nitrogen fixation enabled by the bridging effect of Ru in plasmonic nanoparticles. Nano Research, 2023, 16, 360-370.	5.8	11
72362	<mml:math xmlns:mml="http://www.w3.org/1998/Math/MathML"><mml:mrow><mml:mi>Î±</mml:mi><mml:mo>â^'</mml:mo><mml:msub><mml:m as a platform for the exploration of the electronic band structure of single layer <mml:math xmlns:mml="http://www.w3.org/1998/Math/MathML"><mml:mrow><mml:mi>Î²</mml:mi><mml:mrow><mml:mo>â^'</mml:mo><mml:m Physical Review B, 2022, 106, .	1.1	1
72363	Pauling-type adsorption of O2 induced electrocatalytic singlet oxygen production on Nâ€“CuO for organic pollutants degradation. Nature Communications, 2022, 13, .	5.8	45
72364	Data-augmentation for graph neural network learning of the relaxed energies of unrelaxed structures. Npj Computational Materials, 2022, 8, .	3.5	15
72365	Carbon-oxygen surface formation enhances secondary electron yield in Cu, Ag and Au. Scientific Reports, 2022, 12, .	1.6	5
72366	Density Functional Theory-Based Thermodynamic Model for Stable Scale Formation in Lead-Water Systems. Journal of Physical Chemistry C, 2022, 126, 16841-16850.	1.5	2
72367	From Binary to Ternary Transition-Metal Nitrides: A Boost toward Nitrogen Magneto-Ionics. ACS Applied Materials & Interfaces, 2022, 14, 44581-44590.	4.0	6
72368	Pressure Engineering Promising Transparent Oxides with Large Conductivity Enhancement and Strong Thermal Stability. Advanced Science, 0, , 2202973.	5.6	1
72369	Prediction of Two-Dimensional Group IV Nitrides A_xN_y (A = Sn,) Tj ETQq0 0 0 rgBT /Overlock 10 Physical Chemistry Letters, 2022, 13, 9316-9325.	2.1	6
72370	Visible-light-driven non-oxidative dehydrogenation of alkanes at ambient conditions. Nature Energy, 2022, 7, 1042-1051.	19.8	31
72371	First-principles study of charge-ordered insulating phases in Ruddlesden-Popper LaSr2V2O7. Current Applied Physics, 2022, , .	1.1	0
72372	Interface regulation of Cu2Se via Cu-Se-C bonding for superior lithium-ion batteries. Nano Research, 2023, 16, 2421-2427.	5.8	10
72373	A highly efficient high-entropy metal hydroxymethylate electrocatalyst for oxygen evolution reaction. Chemical Engineering Journal, 2023, 453, 139510.	6.6	4
72374	Self-repairing interphase reconstructed in each cycle for highly reversible aqueous zinc batteries. Nature Communications, 2022, 13, .	5.8	71
72375	Selfâ€Passivated Metal Klein Edge of 1Tâ€Phase Transition Metal Dichalcogenides and the Induced Highâ€Efficient Hydrogen Evolution Reaction Activity. Advanced Functional Materials, 2022, 32, .	7.8	2
72376	Copper Nanoparticle/N-Doped Ti₃C₂T_x MXene Hybrids with Enhanced Peroxidase-like Activity for Colorimetric Glucose Sensing. ACS Applied Nano Materials, 2022, 5, 15531-15538.	2.4	5
72377	Skin-Deep Aspect of Thermopower in Bi₂Q₃, PbQ, and BiCuQO (Q = Se, Te): Hidden One-Dimensional Character of Their Band Edges Leading to High Thermopower. Accounts of Chemical Research, 2022, 55, 2811-2820.	7.6	1
72378	A combined ionic Lewis acid descriptor and machine-learning approach to prediction of efficient oxygen reduction electrodes for ceramic fuel cells. Nature Energy, 2022, 7, 866-875.	19.8	64

#	Article	IF	Citations
72379	CH₄ Activation over Perovskite Catalysts: True Density and Reactivity of Active Sites. ACS Catalysis, 2022, 12, 11845-11853.	5.5	7
72380	A Machine Learning Model To Predict CO₂ Reduction Reactivity and Products Transferred from Metal-Zeolites. ACS Catalysis, 2022, 12, 12336-12348.	5.5	18
72381	Flexible and High-Throughput Photothermal Biosensors for Rapid Screening of Acute Myocardial Infarction Using Thermochromic Paper-Based Image Analysis. Analytical Chemistry, 2022, 94, 13233-13242.	3.2	47
72382	Highâ€Capacity Splitting of Monoâ€and Dibranched Hexane Isomers by a Robust Zincâ€Based Metalâ€“Organic Framework. Angewandte Chemie, 2022, 134, .	1.6	7
72383	Low-lying electronic states with giant linear dichroic ratio observed in <mml:math xmlns:mml="http://www.w3.org/1998/Math/MathML"><mml:msub><mml:mi>PdSe</mml:mi><mml:mn>2</mml:mn></mml:msub></mml:math> Physical Review B, 2022, 106, .	1.1	2
72384	Regulating the Oxygen Affinity of Single Atom Catalysts by Dual-atom Design for Enhanced Oxygen Reduction Reaction Activity. Chemical Research in Chinese Universities, 2022, 38, 1275-1281.	1.3	6
72385	MISPR: an open-source package for high-throughput multiscale molecular simulations. Scientific Reports, 2022, 12, .	1.6	5
72386	Two-dimensional Janus like scandium-based MXenes as photocatalysts for overall water splitting: A first-principles study. Sustainable Materials and Technologies, 2022, 34, e00502.	1.7	3
72387	Two types of charge order with distinct interplay with superconductivity in the kagome material CsV3Sb5. Communications Physics, 2022, 5, .	2.0	19
72388	Capacitively and Inductively Coupled Excitons in Bilayer <mml:math xmlns:mml="http://www.w3.org/1998/Math/MathML" display="inline"><mml:mrow><mml:msub><mml:mrow><mml:mi>MoS</mml:mi></mml:mrow><mml:mrow><mml:mn>2</mml:mn></mml:mrow> Physical Review Letters, 2022, 129, .	2.9	2
72389	Selfâ€Modulationâ€Guided Growth of 2D Tellurides with Ultralow Thermal Conductivity. Small, 2022, 18, .	5.2	4
72390	Edge states of topological acoustic phonons in graphene zigzag nanoribbons. Physical Review B, 2022, 106, .	1.1	25
72391	Momentum-selective orbital hybridisation. Nature Communications, 2022, 13, .	5.8	1
72392	Confinement of volatile fission products in the crystalline organic electride Cs+(15C5)2â€¢eâ^'. Journal of Applied Physics, 2022, 132, .	1.1	2
72393	Highâ€Throughput Dataâ€Driven Prediction of Stable Highâ€Performance Naâ€Ion Sulfide Solid Electrolytes. Advanced Functional Materials, 2022, 32, .	7.8	4
72394	Design of superior electrostriction in BaTiO₃â€based leadâ€free relaxors via the formation of polarization nanoclusters. InformaÄnÂ-MateriÃ¡ly, 2023, 5, .	8.5	9
72395	Electronic and Optical Properties of BP, InSe Monolayer and BP/InSe Heterojunction with Promising Photoelectronic Performance. Materials, 2022, 15, 6214.	1.3	4
72396	Highly Selective Methane to Methanol Conversion on Inverse SnO₂/Cu₂O/Cu(111) Catalysts: Unique Properties of SnO₂ Nanostructures and the Inhibition of the Direct Oxidative Combustion of Methane. ACS Catalysis, 2022, 12, 11253-11262.	5.5	10

#	Article	IF	Citations
72397	Electrical switching of spin-polarized current in multiferroic tunneling junctions. Npj Computational Materials, 2022, 8, .	3.5	3
72398	Controlling selective nucleation and growth of dysprosium islands on graphene by metal intercalation. Physical Review Materials, 2022, 6, .	0.9	1
72399	Flexoelectricity-Driven Mechanical Switching of Polarization in Metastable Ferroelectrics. Physical Review Letters, 2022, 129, .	2.9	2
72400	Phonon-mediated Superconductivity in Two-dimensional MBP (M=Li, Na, Ti). Journal of Low Temperature Physics, 0, , .	0.6	0
72401	Sign-reversed anomalous Nernst effect in the ferromagnetic Weyl-semimetal Fe3â˜Î´GeTe2: the role of Fe vacancies. Science China: Physics, Mechanics and Astronomy, 2022, 65, .	2.0	3
72402	Tunable Weyl half-semimetals in two-dimensional iron-based materials <mml:math xmlns:mml="http://www.w3.org/1998/Math/MathML"><mml:mrow><mml:mi>M</mml:mi><mml:mi>FeSe</mml:mi></mml:mrow><m Physical Review B, 2022, 106, .	1.1	6
72403	Symmetryâ€Protected Twoâ€Level System in the H ₃ Center Enabled by a Spinâ€“Photon Interface: A Competitive Qubit Candidate for the NISQ Technology. Advanced Quantum Technologies, 0, , 2200044.	1.8	1
72404	DFT Modelling of Li6SiO4Cl2 Electrolyte Material for Li-Ion Batteries. Batteries, 2022, 8, 137.	2.1	1
72405	Rhodium nanocrystals on porous graphdiyne for electrocatalytic hydrogen evolution from saline water. Nature Communications, 2022, 13, .	5.8	101
72406	Mott transition and superexchange mechanism in magnetically doped <mml:math xmlns:mml="http://www.w3.org/1998/Math/MathML"><mml:mrow><mml:mi>X</mml:mi><mml:msub><mml:mi>Si</mml:mi><mml:mn mathvariant="normal">N</mml:mi><mml:mn>4</mml:mn></mml:msub></mml:mrow></mml:math> caused by large <mml:math xmlns:mml="http://www.w3.org/1998/Math/MathML"><mml:mrow><mml:mn>3</mml:mn><mml:mi>d</mml:mi></mml:mrow></mml: orbital onsite Coulomb interaction. Physical Review B, 2022, 106, .	1.1	3
72407	Scanning tunneling microscopy study of natural black arsenic. Physical Review B, 2022, 106, .	1.1	0
72408	Boosting Electrocatalytic Reduction of CO₂ to HCOOH on Ni Single Atom Anchored WTe₂ Monolayer. Small, 2022, 18, .	5.2	37
72409	Functional-Unit-Based Material Design: Ultralow Thermal Conductivity in Thermoelectrics with Linear Triatomic Resonant Bonds. Journal of the American Chemical Society, 2022, 144, 18552-18561.	6.6	14
72410	solid_dmft: gray-boxing DFT+DMFT materials simulations with TRIQS. Journal of Open Source Software, 2022, 7, 4623.	2.0	2
72411	Cuâ€“Au nanoparticles produced by the aggregation of gasâ€phase metal atoms for CO oxidation. Aggregate, 2022, 3, .	5.2	9
72412	Achieving Narrowed Bandgaps and Blueâ€Light Excitabilityâ€‰in Zeroâ€Dimensional Hybrid Metal Halide Phosphors via Introducing Cationâ€“Cation Bonding. Energy and Environmental Materials, 2024, 7, .	7.3	9
72413	High Quantum Efficiency of Stable Sbâ€Based Perovskiteâ€Like Halides toward White Light Emission and Flexible Xâ€Ray Imaging. Advanced Optical Materials, 2022, 10, .	3.6	31
72414	Selective Photocatalytic Dehydrogenation of Formic Acid by an In Situ-Restructured Copper-Postmetalated Metalâ€“Organic Framework under Visible Light. Journal of the American Chemical Society, 2022, 144, 16433-16446.	6.6	26

#	Article	IF	Citations
72415	Tuning the magnetic anisotropy and topological phase with electronic correlation in single-layer <mml:math xmlns:mml="http://www.w3.org/1998/Math/MathML"><mml:mrow><mml:mi>H</mml:mi><mml:mtext>â^'</mml:mtext><mml:msub><r Physical Review B, 2022, 106, .	1.1	19
72416	Oneâ€Step Exfoliation Method for Plasmonic Activation of Largeâ€Area 2D Crystals. Advanced Science, 2022, 9, .	5.6	10
72417	First-Principles Study of Electronic Properties of Cesium Chloride Double Perovskites Using a DFT-1/2 Approach. Journal of Physical Chemistry C, 2022, 126, 15065-15071.	1.5	2
72418	Vacancy Hardening and Ordering in Rhenium Tungsten Carbides. Journal of Physical Chemistry C, 2022, 126, 15215-15221.	1.5	1
72419	Accelerated Development of High Voltage Liâ€Ion Cathodes. Advanced Energy Materials, 2022, 12, .	10.2	7
72420	Effects of the pH Value on the Electrodeposition of Feâ€“P Alloy as a Magnetic Film Material. Journal of Physical Chemistry C, 2022, 126, 15472-15484.	1.5	6
72421	The Magnetic Properties of Fe4BO7 and Mn4BO7 Tetraborates in Three Structural Types. JETP Letters, 0, , .	0.4	0
72422	First-principles investigation of spin-orbit coupling driven magnetism of the <mml:math xmlns:mml="http://www.w3.org/1998/Math/MathML"><mml:mn>3</mml:mn><mml:mi>d</mml:mi><mml:mtext>â^'</mml:mtext><m double-perovskite <mml:math xmlns:mml="http://www.w3.org/1998/Math/MathML"><mml:msub><mml:mrow><mml:mo>(</mml:mo><mml:mi) Tj ETQq1 1 0.784314 mathvariant="normal">FeIr</mml:mi> Physical Review B, 2022, 106, .	1.1	4
72423	Lattice strain and band overlap of the thermoelectric composite <mml:math xmlns:mml="http://www.w3.org/1998/Math/MathML"><mml:mrow><mml:msub><mml:mi>Mg</mml:mi><mml:mn>2</mml:mn></mml Physical Review B, 2022, 106, .	1.1	8
72424	First-principles investigation of ferroelectric and piezoelectric properties in one-dimensional transition metal oxytetrahalides. Physical Review B, 2022, 106, .	1.1	0
72425	Nitrogen and Sulfur Coâ€Doped Hierarchically Porous Carbon Nanotubes for Fast Potassium Ion Storage. Small, 2022, 18, .	5.2	53
72426	Searching for Circular Photo Galvanic Effect in Oxyhalide Perovskite Bi₄NbO₈Cl. Advanced Functional Materials, 2022, 32, .	7.8	5
72427	Pyrophosphate Na₂CoP₂O₇ Polymorphs as Efficient Bifunctional Oxygen Electrocatalysts for Zincâ€“Air Batteries. ACS Applied Materials & Interfaces, 2022, 14, 40761-40770.	4.0	4
72428	Graphdiyne oxide nanosheets display selective anti-leukemia efficacy against DNMT3A-mutant AML cells. Nature Communications, 2022, 13, .	5.8	20
72429	Improvement of Openâ€Circuit Voltage Deficit via Preâ€Treated NH₄⁺ Ion Modification of Interface between SnO₂ and Perovskite Solar Cells. Small, 2022, 18, .	5.2	8
72430	Mott Insulator Ca2RuO4 under External Electric Field. Materials, 2022, 15, 6657.	1.3	1
72431	Borohydride Ammoniate Solid Electrolyte Design for Allâ€Solidâ€State Mg Batteries. Energy and Environmental Materials, 2024, 7, .	7.3	6
72432	Synthesis, properties and thermal decomposition particularities of magnesium borohydride ammoniates. International Journal of Hydrogen Energy, 2022, 47, 35320-35328.	3.8	1

#	Article	IF	Citations
72433	Towards Ï€ â€wires on a semiconductor surface: Benzyne on Si(001). ChemPhysChem, 0, , .	1.0	1
72434	Ambient-Pressure Recoverable Polynitrogen Solids Assembled by Pentazolate Rings with High Energy Density. Inorganic Chemistry, 2022, 61, 15532-15539.	1.9	1
72435	Orientation dependence of electronic properties of antimony selenide nanowires. Nano Express, 2022, 3, 035008.	1.2	1
72436	Topological and quantum stability of low-dimensional crystalline lattices with multiple nonequivalent sublattices*. New Journal of Physics, 2022, 24, 103015.	1.2	8
72437	Thermodynamics and Kinetics of the Cathodeâ€“Electrolyte Interface in All-Solid-State Liâ€“S Batteries. Journal of the American Chemical Society, 2022, 144, 18009-18022.	6.6	24
72438	Characterizations of AlGaN/GaN Membrane-type Photodetectors. , 2023, 1, 314-320.		0
72439	Structural, Electronic, and Magnetic Characteristics of Graphitic Carbon Nitride Nanoribbons and Their Applications in Spintronics. Journal of Physical Chemistry C, 2022, 126, 16429-16436.	1.5	3
72440	Effect of Co-Substitution on Hydrogen Absorption and Desorption Reactions of YMgNi₄-Based Alloys. Journal of Physical Chemistry C, 2022, 126, 16943-16951.	1.5	6
72441	Effect of Strain on the Lattice Thermal Conductivity in SrTiO ₃ from Firstâ€Principles Calculations. Physica Status Solidi - Rapid Research Letters, 0, , 2200207.	1.2	0
72442	Large-gap quantum anomalous Hall states induced by functionalizing buckled Bi-III monolayer/ <mml:math xmlns:mml="http://www.w3.org/1998/Math/MathML"><mml:mrow><mml:msub><mml:mi>Al</mml:mi><mml:mn>2</mml:mn></mml:msub><mml:mi mathvariant="normal">O</mml:mi><mml:mn>3</mml:mn></mml:mrow></mml:math>. Physical Review B, 2022, 106, .	3.7	2
72443	Water Uptake in an Anion Exchange Membrane Based on Polyamine: A First-Principles Study. Journal of Physical Chemistry B, 2022, 126, 7418-7428.	1.2	5
72444	Method to Determine the Distribution of Substituted or Intercalated Ions in Transition-Metal Dichalcogenides: Fe_xVSe₂ and Fe_{1â€“x}V_xSe₂. Chemistry of Materials, 2022, 34, 8528-8535.	3.2	2
72445	Direct Observation of Solventâ€“Reaction Intermediate Interactions in Heterogeneously Catalyzed Alcohol Coupling. Journal of the American Chemical Society, 2022, 144, 17387-17398.	6.6	1
72446	Theoretical investigation on yttrium clustering in tungsten grain boundary region and strengthening effect. Journal of Applied Physics, 2022, 132, .	1.1	2
72447	High-capacity hydrogen storage in zirconium decorated psi-graphene: acumen from density functional theory and molecular dynamics simulations. International Journal of Hydrogen Energy, 2023, 48, 37860-37871.	3.8	15
72448	Phosphorus-doped iron-nitrogen-carbon catalyst with penta-coordinated single atom sites for efficient oxygen reduction. Nano Research, 2023, 16, 1810-1819.	5.8	20
72449	First Principles Study of Photocatalytic Reduction of CO₂ to CH₄ on WS₂-Supported Pt Clusters. Journal of Physical Chemistry C, 2022, 126, 16702-16709.	1.5	4
72450	Chemoselective Hydrogenation of Nitro Compounds by MoS₂ via Introduction of Independent Active Hydrogen-Donating Sites. ACS Catalysis, 2022, 12, 12170-12178.	5.5	7

#	Article	IF	Citations
72451	Bond engineering of molecular ferroelectrics renders soft and high-performance piezoelectric energy harvesting materials. Nature Communications, 2022, 13, .	5.8	26
72452	Study on the color mechanism of amethyst after heat treatment and first-principle calculation. Applied Physics A: Materials Science and Processing, 2022, 128, .	1.1	0
72453	Bistable H₂Pc Molecular Conductance Switch on Ag(100). Journal of Physical Chemistry C, 2022, 126, 16767-16776.	1.5	1
72454	Large tunable Rashba spin splitting and piezoelectric response in Janus chromium dichalcogenide monolayers. Physical Review B, 2022, 106, .	1.1	16
72455	Single Iron-dimer Catalysts on MoS2 Nanosheet for Potential Nitrogen Activation. Chemical Research in Chinese Universities, 2022, 38, 1226-1231.	1.3	1
72456	Mg₂Fe₂O₅ Nanoparticle-Decorated Ca₂Fe₂O₅â€“CaFe₂O₄ Heterostructure for Efficient Photocatalytic CO₂ Conversion. ACS Sustainable Chemistry and Engineering, 2022, 10, 12651-12658.	3.2	8
72457	Ionic Dynamics of the Charge Carrier in Layered Solid Materials for Mg Rechargeable Batteries. Chemistry of Materials, 2022, 34, 8769-8776.	3.2	3
72458	Giant tunnel magnetoresistance in two-dimensional van der Waals magnetic tunnel junctions. <mml:math xmlns:mml="http://www.w3.org/1998/Math/MathML"><mml:mrow><mml:mi>Ag</mml:mi><mml:mtext>/</mml:mtext><mml:mi>Cr</mml:mi><mml:msub><mml:mi mathvariant="normal">I</mml:mi><mml:mn>3</mml:mn></mml:msub><mml:mtext>/</mml:mtext><mml:mi>Mo</mml:mi><mml:msub><mml:mi mathvariant="normal">N</mml:mi><mml:mn>4</mml:mn></mml:msub><mml:mtext>/</mml:mtext><mml:mi>Cr</mml:mi> Physical Review B, 2022, 106, .	1.1	2
72459	Assessing the Drawbacks and Benefits of Ion Migration in Lead Halide Perovskites. ACS Energy Letters, 2022, 7, 3401-3414.	8.8	46
72460	Exploring Structure-Sensitive Relations for Small Species Adsorption Using Machine Learning. Journal of Chemical Information and Modeling, 2022, 62, 4361-4368.	2.5	13
72461	Synthesis of superconducting two-dimensional non-layered PdTe by interfacial reactions. , 2022, 1, 908-914.		6
72462	Quadrupole topological insulators in Ta2M3Te5 (Mâ€‰=â€‰Ni, Pd) monolayers. Npj Quantum Materials, 2022, 7, .	1.8	18
72463	Comprehensive study of band structure driven thermoelectric response of <mml:math xmlns:mml="http://www.w3.org/1998/Math/MathML"><mml:msub><mml:mi>ZrTe</mml:mi><mml:mn>5</mml:mn></mml:msub></mml: Physical Review B, 2022, 106, .	1.1	4
72464	Light Absorption and Emission by Defects in Doped Nickel Oxide. Advanced Photonics Research, 0, , 2200138.	1.7	0
72465	Activity Self-Optimization Steered by Dynamically Evolved Fe³⁺@Fe²⁺ Double-Center on Fe₂O₃ Catalyst for NH₃-SCR. Jacs Au, 2022, 2, 2352-2358.	3.6	7
72466	Capture Mechanism of Cadmium in Agricultural Soil Via Iron-Modified Graphene. Inorganics, 2022, 10, 150.	1.2	1
72468	Biased self-diffusion on Cu surface due to electric field gradients. Journal Physics D: Applied Physics, 2022, 55, 465302.	1.3	3
72469	The C-H Bond Activation Triggered by Subsurface Mo Dopant on MgO Catalyst in Oxidative Coupling of Methane. Catalysts, 2022, 12, 1083.	1.6	1

#	Article	IF	Citations
72470	Efficient microwave absorption with Vn+1CnT MXenes. Cell Reports Physical Science, 2022, 3, 101073.	2.8	29
72471	Theoretical Investigation of the Oxygen Reduction Reaction over Platinum Catalysts Supported by Multiâ€Edged Vertically Aligned Carbon Nanofiber for Electrocatalyst Preparation. ChemElectroChem, 0, , .	1.7	2
72472	Atomic Adsorption-Controlled Magnetic Properties of a Two-Dimensional (2D) Janus Monolayer. ACS Applied Electronic Materials, 2022, 4, 4507-4513.	2.0	10
72473	Ionâ€Migration Mechanism: An Overall Understanding of Anionic Redox Activity in Metal Oxide Cathodes of Li/Naâ€Ion Batteries. Advanced Materials, 2022, 34, .	11.1	35
72474	The Effect of La3+ on the Methylene Blue Dye Removal Capacity of the La/ZnTiO3 Photocatalyst, a DFT Study. Nanomaterials, 2022, 12, 3137.	1.9	11
72475	A first-principles study on the physical properties of two-dimensional Nb3Cl8, Nb3Br8 and Nb3I8. Applied Physics A: Materials Science and Processing, 2022, 128, .	1.1	4
72476	A Simultaneous Materialâ€Device Optimization for Plasmonic Devices: A Combined Ab Initio and Electromagnetic Simulation for Photothermal Transducers. Advanced Optical Materials, 2022, 10, .	3.6	2
72477	Grapheneâ€Assisted Epitaxy of Highâ€Quality GaN Films on GaN Templates. Advanced Optical Materials, 2022, 10, .	3.6	8
72478	Prediction of electronic work function of the second phase in binary magnesium alloy based on machine learning method. Journal of Materials Research, 2022, 37, 3792-3802.	1.2	2
72479	Strain-induced stacking transition in bilayer graphene. Journal of Physics Condensed Matter, 2022, 34, 475302.	0.7	3
72480	Frenkel pair formation energy for cubic Fe₃O₄ in DFTâ€‰+â€‰U calculations. Journal of Physics Condensed Matter, 2022, 34, 475701.	0.7	5
72481	Facile Electroless Plating Method to Fabricate a Nickelâ€“Phosphorus-Modified Copper Current Collector for a Lean Lithium-Metal Anode. ACS Applied Materials & Interfaces, 2022, 14, 45433-45443.	4.0	9
72482	Feature of the Endohedral Metallofullerene Y@C₈₂ and Gd@C₈₂ Polymerization under High Pressure. Journal of Physical Chemistry C, 2022, 126, 17366-17373.	1.5	2
72483	Symmetry-enforced electronic nodal straight lines in CsNb₃SBr₇. New Journal of Physics, 2022, 24, 093033.	1.2	0
72484	Effect of Halide Anions on the Electroreduction of CO 2 Âto C 2 H 4 : A Density Functional Theory Study. ChemPhysChem, 0, , .	1.0	3
72485	Tuning lattice strain in biphenylene for enhanced electrocatalytic oxygen reduction reaction in proton exchange membrane fuel cells. International Journal of Hydrogen Energy, 2022, 47, 36294-36305.	3.8	4
72486	Robust Metalâ€“Organic Frameworks with High Industrial Applicability in Efficient Recovery of C3H8 and C2H6 from Natural Gas Upgrading. Engineering, 2023, 23, 56-63.	3.2	11
72487	Electronic Properties and Electrocatalytic Water Splitting Activity for Precious-Metal-Adsorbed Silicene with Nonmetal Doping. ACS Omega, 2022, 7, 33156-33166.	1.6	2

#	Article	IF	Citations
72488	Prediction of single-atom-thick transition metal nitride <mml:math xmlns:mml="http://www.w3.org/1998/Math/MathML"><mml:msub><mml:mi>CrN</mml:mi><mml:mn>4</mml:mn></mml:msub></mml with a square-planar network and high-temperature ferromagnetism. Physical Review B, 2022, 106, .	1.1	8
72489	High-Efficiency and Wavelength-Tunable Near-Infrared Emission of Lanthanide Ions Doped Lead-Free Halide Double Perovskite Nanocrystals toward Fluorescence Imaging. ACS Applied Materials & Interfaces, 2022, 14, 42215-42222.	4.0	16
72490	Hierarchal Porous Graphene-Structured Electrocatalysts with Feâ€“N₅ Active Sites Modified with Fe Clusters for Enhanced Performance Toward Oxygen Reduction Reaction. ACS Applied Materials & Interfaces, 2022, 14, 42038-42047.	4.0	8
72491	Analysis of grain boundary embrittlement by Cu and Sn in paramagnetic <mml:math xmlns:mml="http://www.w3.org/1998/Math/MathML"><mml:mrow><mml:mi>Î³</mml:mi><mml:mtext>â^'</mml:mtext><mml:mi>Fe by first-principles computational tensile test. Physical Review Materials, 2022, 6, .	2.0	2
72492	Overchargeâ€Induced Phase Heterogeneity and Resultant Twinâ€Like Layer Deformation in Lithium Cobalt Oxide Cathode for Lithiumâ€Ion Batteries. Advanced Science, 2022, 9, .	5.6	13
72493	Revealing the Impact of Cl Substitution on the Crystallization Behavior and Interfacial Stability of Superionic Lithium Argyrodites. Advanced Functional Materials, 2022, 32, .	7.8	18
72494	Abâ€‰Initio Study of Alloying Impact on the Stability of Cementite in Transformationâ€Induced Plasticityâ€Assisted Advanced Steels. Advanced Engineering Materials, 0, , 2200532.	1.6	0
72496	New insights into the interfacial interactions of O2 and H2O molecules with PuH2 (110) and (111) surfaces from first-principles calculations. International Journal of Hydrogen Energy, 2022, 47, 36593-36604.	3.8	5
72497	Strain propagation in layered two-dimensional halide perovskites. Science Advances, 2022, 8, .	4.7	8
72498	Modeling the Potential-Dependent Kinetics of CO₂ Electroreduction on Single-Nickel Atom Catalysts with Explicit Solvation. ACS Catalysis, 2022, 12, 11380-11390.	5.5	19
72499	Ordering Transitions of Liquid Crystals Triggered by Metal Oxide-catalyzed Reactions of Sulfur Oxide Species. Journal of the American Chemical Society, 2022, 144, 16378-16388.	6.6	4
72500	Layer-dependent electronic structure, dynamic stability, and phonon properties of few-layer SnSe. Physical Review B, 2022, 106, .	1.1	3
72501	Catalytic Synergies in Bimetallic Ruï£¿Pt Singleâ€“Atom Catalysts via Speciation Control. Advanced Functional Materials, 2022, 32, .	7.8	12
72502	Highly Reversible Lithium Host Materials for Highâ€Energyâ€Density Anodeâ€Free Lithium Metal Batteries. Advanced Functional Materials, 2022, 32, .	7.8	23
72503	Vibrational Characteristics of Au-Doped Si Nanowires: A Molecular Dynamics Study with a Modified Embedded Atom Method Potential Developed for Si-H-Au Systems. Journal of Nanomaterials, 2022, 2022, 1-15.	1.5	0
72504	Correlation-corrected band topology and topological surface states in iron-based superconductors. Physical Review B, 2022, 106, .	1.1	7
72505	Formation of dimethoxy bridged dinuclear iron(III) complex of pyridoxal Schiff base with iron-catalyzed oxidative Câ^'N bond cleavage â€“ Structure, magnetic properties, and DFT calculations. Polyhedron, 2022, , 116156.	1.0	0
72506	Discovery of orthorhombic perovskite oxides with low thermal conductivity by first-principles calculations. Journal of Advanced Ceramics, 2022, 11, 1596-1603.	8.9	15

#	Article	IF	Citations
72507	Electrocatalytic hydrogenation of quinolines with water over a fluorine-modified cobalt catalyst. Nature Communications, 2022, 13, .	5.8	18
72508	Ultraâ€Stable Titanium Carbide MXene Functionalized with Heterocyclic Aromatic Amines. Advanced Functional Materials, 2022, 32, .	7.8	9
72509	Making and breaking of chemical bonds in single nanoconfined molecules. Science Advances, 2022, 8, .	4.7	1
72510	Orbital Hall effect in crystals: Interatomic versus intra-atomic contributions. Physical Review B, 2022, 106, .	1.1	8
72511	Role of Additives in Solid Electrolyte Interphase Formation in Al Anode Dual-Ion Batteries. ACS Applied Energy Materials, 2022, 5, 13398-13409.	2.5	6
72512	Great Influence of Organic Cation Motion on Charge Carrier Dynamics in Metal Halide Perovskite Unraveled by Unsupervised Machine Learning. Journal of Physical Chemistry Letters, 2022, 13, 8537-8545.	2.1	10
72513	X-ray Photoelectron Spectroscopic Study of Reduced Alkali Tungsten Oxides with Localized and Delocalized Electrons. Journal of Physical Chemistry C, 2022, 126, 15436-15445.	1.5	5
72514	Rashba-like spin-orbit interaction and spin texture at the <mml:math xmlns:mml="http://www.w3.org/1998/Math/MathML"><mml:mrow><mml:msub><mml:mi>KTaO</mml:mi><mml:mn>3</mml:mn></ surface from DFT calculations. Physical Review B, 2022, 106, .	1.1	4
72515	Pressure-induced novel structure with graphene-like boron-layer in titanium monoboride. Chinese Physics B, 0, , .	0.7	3
72516	Structural and Chemical Modifications of Few-Layer Transition Metal Phosphorous Trisulfides by Electron Irradiation. Journal of Physical Chemistry C, 2022, 126, 15446-15455.	1.5	2
72517	High Thermoelectric Properties of Janus WSeS Bilayer Membranes with Different Stacking Modes. Journal of Electronic Materials, 2022, 51, 6320-6332.	1.0	1
72518	Chemical interaction, self-ordering and corrosion inhibition properties of 2-mercaptobenzothiazole monolayers: DFT atomistic modeling on metallic copper. Corrosion Science, 2022, 209, 110658.	3.0	8
72519	MgCr₂O₄-Modified CuO/Cu₂O for High-Temperature Thermochemical Energy Storage with High Redox Activity and Sintering Resistance. ACS Applied Materials & Interfaces, 2022, 14, 43151-43162.	4.0	7
72520	Pressure-Engineered Ti₃C₂T_x MXene with Enhanced Conductivity and Accelerated Reaction Kinetics of Lithium Storage. ACS Applied Materials & Interfaces, 2022, 14, 46056-46067.	4.0	2
72521	Coexistence of Strong and Weak Topological Orders in a Quasi-One-Dimensional Material. Physical Review Letters, 2022, 129, .	2.9	3
72522	Remote Oxygen Scavenging of the Interfacial Oxide Layer in Ferroelectric Hafniumâ€“Zirconium Oxide-Based Metalâ€“Oxideâ€“Semiconductor Structures. ACS Applied Materials & Interfaces, 2022, 14, 43897-43906.	4.0	4
72523	Prediction of Carbon Dioxide Reduction Catalyst Using Machine Learning with a Few-Feature Model: WLEDZ. Journal of Physical Chemistry C, 2022, 126, 17025-17035.	1.5	7
72524	Adsorption of imidazolium-based ionic liquids on the Fe(1 0 0) surface for corrosion inhibition: Physisorption or chemisorption?. Journal of Molecular Liquids, 2022, 367, 120489.	2.3	12

#	Article	IF	Citations
72525	A Unified Understanding of Diverse Spin Textures of Kramersâ€“Weyl Fermions in Nonmagnetic Chiral Crystals. Advanced Functional Materials, 2022, 32, .	7.8	8
72526	Phase Transformation Temperatures, Î³â€“Î³â€² Lattice Parameter Misfit, and Î³â€² Precipitate Morphology in Coâ€“Tiâ€“V Alloys. Metallurgical and Materials Transactions A: Physical Metallurgy and Materials Science, 2022, 53, 4011-4022.	1.1	2
72527	Strain-induced strengthening in superconducting Î²-Mo2C through high pressure and high temperature. Journal of the European Ceramic Society, 2023, 43, 88-98.	2.8	6
72528	Hydrogen diffusion coefficient in monoclinic zirconia in presence of oxygen vacancies. International Journal of Hydrogen Energy, 2022, 47, 33517-33529.	3.8	3
72529	First-principles study of water incorporation in Fe-containing wadsleyite. Physics of the Earth and Planetary Interiors, 2022, 333, 106940.	0.7	1
72530	Direct Characterization of Typeâ€I Band Alignment in 2D Ruddlesdenâ€“Popper Perovskites. Advanced Energy Materials, 2022, 12, .	10.2	12
72531	Tantalum Diboride: The Superhard and Metallic Boride. Crystal Growth and Design, 2022, 22, 6201-6206.	1.4	5
72532	Surface-Mounted Dipolar Molecular Rotors Driven by External Electric Field, As Revealed by Torque Analyses. ACS Omega, 2022, 7, 35159-35169.	1.6	2
72533	OH spectator at IrMo intermetallic narrowing activity gap between alkaline and acidic hydrogen evolution reaction. Nature Communications, 2022, 13, .	5.8	48
72534	A Systematic First-Principles Study of Computational Parameters Affecting Self-diffusion Coefficients in FCC Ag, Cu, and Ni. Journal of Phase Equilibria and Diffusion, 0, , .	0.5	0
72535	Bistable carbon-vacancy defects in h-BN. , 0, 1, .		4
72536	Van der Waals Interaction-Driven Self-Assembly of V₂O₅Nanoplates and MXene for High-Performing Zinc-Ion Batteries by Suppressing Vanadium Dissolution. ACS Nano, 2022, 16, 14539-14548.	7.3	100
72537	Insights into the Effect of the Adsorption Preference of Additives on the Anisotropic Growth of ZSMâ€5 Zeolite. Chemistry - A European Journal, 2022, 28, .	1.7	2
72538	Highly Efficient Broadband Near-Infrared Luminescence with Zero-Thermal-Quenching in Garnet Y₃In₂Ga₃O₁₂:Cr³⁺ Phosphors. Chemistry of Materials, 2022, 34, 8418-8426.	3.2	61
72539	CO₂ Electroreduction in Water with a Heterogenized C-Substituted Nickel Cyclam Catalyst. Inorganic Chemistry, 2022, 61, 15841-15852.	1.9	5
72540	Electride Formation in Baâ€“P System and the Unexpected Structure Transition of Electrides under Pressure. Journal of Physical Chemistry C, 2022, 126, 16815-16824.	1.5	5
72541	New CrOX (XÂ=ÂCl, Br, I) monolayer with ultra-wide single spin states. Europhysics Letters, 2022, 140, 16002.	0.7	0
72542	Strain Effects on the Two-Dimensional Cr₂N MXene: An Ab Initio Study. ACS Omega, 2022, 7, 33884-33894.	1.6	6

#	Article	IF	Citations
72543	First Experimental Synthesis of Mg Orthocarbonate by the MgCO3 + MgO = Mg2CO4 Reaction at Pressures of the Earthâ€™s Lower Mantle. JETP Letters, 2022, 116, 477-484.	0.4	7
72544	Establishing Substoichiometric Ag Oxidation and Its Physicochemical, Optoelectrical, and Structural Consequences for Ag Electrodes. ACS Applied Electronic Materials, 2022, 4, 4683-4693.	2.0	7
72545	Ti₂CT₂ MXene as Anodes for Metal Ion Batteries: From Monolayer to Bilayer to Pillar Structure. Langmuir, 2022, 38, 11732-11742.	1.6	9
72546	Crystal Structure and Thermoelectric Properties of Layered Van der Waals Semimetal ZrTiSe₄. Chemistry of Materials, 2022, 34, 8858-8867.	3.2	5
72547	DFT calculation of structures and electronic characteristic of VOPO₄ polymorphs. Physica Scripta, 2022, 97, 105805.	1.2	1
72548	Differing pressure response of lattice structure in LaTMSb2 (TM = Au or Ag) ternary antimonides. Bulletin of Materials Science, 2022, 45, .	0.8	0
72549	Vacancy dynamics in niobium and its native oxides and their potential implications for quantum computing and superconducting accelerators. Physical Review B, 2022, 106, .	1.1	7
72550	Single-atom rhodium anchored on S-doped black phosphorene as a promising bifunctional electrocatalyst for overall water splitting. Chinese Chemical Letters, 2023, 34, 107812.	4.8	2
72551	Engineering Thermoelectric Performance of <scp>Î±â€GeTe</scp> by Ferroelectric Distortion. Energy and Environmental Materials, 0, , .	7.3	3
72552	MoirÃ© Phonons in Magic-Angle Twisted Bilayer Graphene. Nano Letters, 2022, 22, 7791-7797.	4.5	14
72553	Hydrogen-induced volume changes, dipole tensor, and elastic hydrogen-hydrogen interaction in a metallic glass. Physical Review B, 2022, 106, .	1.1	0
72554	Emergent topological states via digital (001) oxide superlattices. Npj Computational Materials, 2022, 8, .	3.5	1
72555	Dynamics of non-metal-regulated FeCo bimetal microenvironment on oxygen reduction reaction activity and intrinsic mechanism. Nano Research, 2023, 16, 2199-2208.	5.8	5
72556	Identification of a nitrogen vacancy in GaN by scanning probe microscopy. Physical Review B, 2022, 106, .	1.1	3
72557	Two-dimensional intrinsic ferrovalley Janus 2H-VSeS monolayer with high Curie temperature and robust valley polarization. Physical Review Materials, 2022, 6, .	0.9	2
72558	Controllable synthesis and crystal facet, composition and temperature dependent gas sensing properties of Sn1â^'xS-CdS superlattice nanowires with ultrafast response. Sensors and Actuators B: Chemical, 2023, 377, 132762.	4.0	2
72559	Tunable Solid Acid Catalyst Thin Films Prepared by Atomic Layer Deposition. ACS Applied Materials & Interfaces, 2022, 14, 43171-43179.	4.0	1
72560	First-Principles Study of Enhanced Absorption in Van der Waals Heterostructure of MoS2/Cd0.90Zn0.10Te0.93Se0.07 in the Visible Region. Journal of Electronic Materials, 2022, 51, 6595-6602.	1.0	1

#	Article	IF	Citations
72561	Enhanced Intralayer Ferromagnetism in CrI₃ by Interfacial Super-Superexchange Interaction. Journal of Physical Chemistry C, 2022, 126, 17306-17312.	1.5	2
72562	Exhaustive characterization of modified Si vacancies in 4H-SiC. Nanophotonics, 2022, 11, 4565-4580.	2.9	3
72563	Nonclassical Nucleation of Zinc Oxide from a Physically Motivated Machine-Learning Approach. Journal of Physical Chemistry C, 0, , .	1.5	5
72564	Defect effect on the stability, electronic and magnetic properties equal-atomic CrLaCoAl alloy by the first-principles calculations. Applied Physics A: Materials Science and Processing, 2022, 128, .	1.1	1
72565	A first-principles study of Janus monolayer MXY (Mâ€‰=â€‰Mo, W; X, Yâ€‰=â€‰S, Se, Te)/SiO2 van der Waals heterojunctions for integrated optical fibers. Advanced Composites and Hybrid Materials, 2022, 5, 3232-3244.	9.9	10
72566	Novel two-dimensional PdSe phase: A puckered material with excellent electronic and optical properties. Frontiers of Physics, 2022, 17, .	2.4	4
72569	Nano-scale collinear multi-Q states driven by higher-order interactions. Nature Communications, 2022, 13, .	5.8	5
72570	Tuning the Coordination Microenvironment to Boost the Electrocatalytic HER Activity of M₃(C₆O₃S₃)₂. Journal of Physical Chemistry C, 2022, 126, 16606-16614.	1.5	1
72571	Emergent Negative Differential Resistance with an Undisturbed Topological Surface State. Journal of Physical Chemistry C, 2022, 126, 16744-16750.	1.5	1
72572	Orbital Orientation-based Theoretical Design of Single-Atom Catalysts for the Hydrogen Evolution Reaction. Journal of Physical Chemistry C, 2022, 126, 16656-16662.	1.5	1
72573	Trends of earthâ€abundant transition metalâ€doped in <scp> CoSe ₂ </scp> microstructures towards improved water splitting and supercapacitor applications. International Journal of Energy Research, 2022, 46, 24588-24601.	2.2	6
72574	Role of defects in ultra-high gain in fast planar tin gallium oxide UV-C photodetector by MBE. Applied Physics Letters, 2022, 121, .	1.5	6
72575	Oxygen Vacancies Enhanced Ozonation toward Phenol Derivatives Removal over O_v-Bi₂O₃. ACS ES&T Water, 2022, 2, 1725-1733.	2.3	11
72576	Constructing fast-ion-conductive disordered interphase for high-performance zinc-ion and zinc-iodine batteries. Matter, 2022, 5, 4363-4378.	5.0	48
72577	Constructing Three-Dimensional Flexible Lithiophilic Scaffolds with Bi₂O₃ Nanosheets toward Stable Li Metal Anodes. ACS Applied Energy Materials, 2022, 5, 12874-12883.	2.5	3
72578	FINETUNA: fine-tuning accelerated molecular simulations. Machine Learning: Science and Technology, 2022, 3, 03LT01.	2.4	11
72579	Mechanism driven design of trimer Ni1Sb2 site delivering superior hydrogenation selectivity to ethylene. Nature Communications, 2022, 13, .	5.8	19
72580	High-throughput design of functional-engineered MXene transistors with low-resistive contacts. Npj Computational Materials, 2022, 8, .	3.5	16

#	Article	IF	Citations
72581	Time-reversal symmetry broken quantum spin Hall phase in the van der Waals heterostructure ZrTe₅/Cr₂Ge₂Te₆. New Journal of Physics, 2022, 24, 093029.	1.2	1
72582	Understanding the switching mechanism of oxygen-doped Sb phase-change material: Insights from first principles. Journal of Applied Physics, 2022, 132, 115110.	1.1	1
72583	Sodiumâ€Intercalated Manganese Oxides for Achieving Ultraâ€Stable and Fast Charge Storage Kinetics in Wideâ€Voltage Aqueous Supercapacitors. Advanced Functional Materials, 2022, 32, .	7.8	17
72584	Highâ€Capacity Splitting of Monoâ€and Dibranched Hexane Isomers by a Robust Zincâ€Based Metalâ€“Organic Framework. Angewandte Chemie - International Edition, 2022, 61, .	7.2	20
72585	Molecular intercalation of transition metal dichalcogenide nanosheets to enhance electrocatalytic activity toward hydrogen evolution reaction. Bulletin of the Korean Chemical Society, 2022, 43, 1352-1363.	1.0	4
72586	Capturing the ground state of uranium dioxide from first principles: Crystal distortion, magnetic structure, and phonons. Physical Review B, 2022, 106, .	1.1	7
72587	Enhanced Activity of Oxygen Reduction Reaction on Pr₆O₁₁-Assisted PtPr Alloy Electrocatalysts. ACS Applied Materials & Interfaces, 2022, 14, 41861-41869.	4.0	6
72588	Restructuring and Reshaping of CsPbX₃ Perovskites by Lithium Salts. Advanced Materials Interfaces, 2022, 9, .	1.9	3
72589	Spin-related electronic pathway through single molecule on Au(111). Chinese Chemical Letters, 2023, 34, 107813.	4.8	4
72590	Negative Thermal Expansion Induced in Tri-graphene and T-graphene by the Rigid-Unit Modes. Journal of the American Chemical Society, 2022, 144, 16703-16707.	6.6	5
72591	A DFT + U-D3 Study of the Adsorption of Hydrogen Fluoride and Ethylene Carbonate on the Niobium-Doped (001), (011), and (111) Surfaces of Lithium Manganese Oxide. Journal of the Electrochemical Society, 2022, 169, 090507.	1.3	2
72592	First-principles study on remote van der Waals epitaxy through graphene monolayer on semiconductor substrates. Chinese Physics B, 0, , .	0.7	0
72593	Theoretical investigation of high coverage water adsorption on Co and Ni doped Î³-Al2O3 surface. Journal of Materials Science, 2022, 57, 16710-16724.	1.7	2
72594	Vacancy diffusion on a brominated Si(100) surface: Critical effect of the dangling bond charge state. Journal of Chemical Physics, 2022, 157, 124705.	1.2	1
72595	Critical ionic transport across an oxygen-vacancy ordering transition. Nature Communications, 2022, 13, .	5.8	6
72596	Control of Surface Chemical Reactions through Solid Stiffness. Physical Review Letters, 2022, 129, .	2.9	3
72597	Atomically dispersed chromium coordinated with hydroxyl clusters enabling efficient hydrogen oxidation on ruthenium. Nature Communications, 2022, 13, .	5.8	35
72598	Identification of the Intrinsic Active Site in Phase-Pure M1 Catalysts for Oxidation Dehydrogenation of Ethane by Density Functional Theory Calculations. Journal of Physical Chemistry C, 2022, 126, 17536-17543.	1.5	1

#	Article	IF	Citations
72599	Oxidase-like ZnCoFe Three-Atom Nanozyme as a Colorimetric Platform for Ascorbic Acid Sensing. Analytical Chemistry, 2022, 94, 14308-14316.	3.2	31
72600	Experimental and theoretical studies on two-dimensional vanadium carbide hybrid nanomaterials derived from V4AlC3 as excellent catalyst for MgH2. Journal of Magnesium and Alloys, 2023, 11, 3790-3799.	5.5	11
72601	Strain-Modulated Interlayer Charge and Energy Transfers in MoS₂/WS₂ Heterobilayer. ACS Applied Materials & Interfaces, 2022, 14, 46841-46849.	4.0	4
72602	The effect of zirconium on the Ti-(42-46 at.%)Al system. Acta Materialia, 2022, 241, 118414.	3.8	6
72603	Chern insulators and high Curie temperature Dirac half-metal in two-dimensional metalâ€“organic frameworks. Applied Physics Letters, 2022, 121, .	1.5	4
72604	Catalytic mechanism and activity of N₂ reduction on boron-decorated crystalline carbon nitride. 2D Materials, 2022, 9, 045035.	2.0	2
72605	Modeling interfaces of fluorite-structure compounds using slab charge distribution. Science and Technology of Advanced Materials Methods, 2022, 2, 392-401.	0.4	1
72606	Interface engineering of snow-like Ru/RuO2 nanosheets for boosting hydrogen electrocatalysis. Science Bulletin, 2022, 67, 2103-2111.	4.3	18
72607	Double synergetic FeCo-nanoparticles and single atoms embedded in N-doped carbon nanotube arrays as efficient bifunctional catalyst for high-performance zinc-air batteries. Materials Today Energy, 2022, 29, 101138.	2.5	6
72608	Atomic and Superatomic Orbital Interactions in In8FeNan Clusters. Journal of Cluster Science, 2023, 34, 1953-1964.	1.7	1
72609	Microstructure, microhardness and work function of in-situ Al-Cu composite processed by mechanical alloying by means of high-pressure torsion. Continuum Mechanics and Thermodynamics, 2023, 35, 1433-1444.	1.4	2
72610	Hot-Carrier Transfer across a Nanoparticleâ€“Molecule Junction: The Importance of Orbital Hybridization and Level Alignment. Nano Letters, 2022, 22, 8786-8792.	4.5	15
72611	Novel two-dimensional SiC2 monolayer with potential as a superior anode for sodium-ion batteries. Journal of Materials Science, 2022, 57, 18406-18416.	1.7	1
72612	Evolutionary Search for Novel Thorium Borides toward Advanced Nuclear Fuels. Journal of Physical Chemistry C, 2022, 126, 17759-17768.	1.5	6
72613	Manipulating Hubbard-type Coulomb blockade effect of metallic wires embedded in an insulator. National Science Review, 2023, 10, .	4.6	6
72614	Bimetallic Alloys b-As_xP_{1â€“x} at High Concentration Differences: Ideal for Photonic Devices. Journal of Physical Chemistry Letters, 2022, 13, 9501-9509.	2.1	3
72615	2D Dumbbell Silicene as a High Storage Capacity and Fast Ion Diffusion Anode for Li-Ion Batteries. ACS Applied Materials & Interfaces, 2022, 14, 47262-47271.	4.0	23
72616	Electron-phonon interaction and point contact enhanced superconductivity in trigonal PtBi₂. Low Temperature Physics, 2022, 48, 747-754.	0.2	2

#	Article	IF	Citations
72617	Continuously tunable ferroelectric domain width down to the single-atomic limit in bismuth tellurite. Nature Communications, 2022, 13, .	5.8	13
72618	Atomistic Insight into the Epitaxial Growth Mechanism of Single-Crystal Two-Dimensional Transition-Metal Dichalcogenides on Au(111) Substrate. ACS Nano, 2022, 16, 17356-17364.	7.3	11
72619	Catalytic Reduction of 4-Nitrophenol to 4-Aminophenol Using Ag@Iâ±-Ti(HPO₄)₂Â·H₂O: Experimental and Computational Studies. Industrial & Engineering Chemistry Research, 2022, 61, 15181-15194.	1.8	1
72620	Random forest incorporating ab-initio calculations for corrosion rate prediction with small sample Al alloys data. Npj Materials Degradation, 2022, 6, .	2.6	8
72621	Tuning moirÃ© excitons in Janus heterobilayers for high-temperature Bose-Einstein condensation. Science Advances, 2022, 8, .	4.7	17
72622	Structural Disorder in Higher-Temperature Phases Increases Charge Carrier Lifetimes in Metal Halide Perovskites. Journal of the American Chemical Society, 2022, 144, 19137-19149.	6.6	46
72623	Effect of Structural Morphology and Material Factors on Radiative Properties of Hybrid Perovskite/Nanoporous GaN Hierarchical Composite Structure. , 2023, 1, 261-273.		1
72624	Real-space measurement of orbital electron populations for Li1-xCoO2. Nature Communications, 2022, 13, .	5.8	8
72625	Pâ€Induced Permeation of Nickel into WO₃ Octahedra to Form a Synergistic Catalyst for Urea Oxidation**. ChemSusChem, 2022, 15, .	3.6	1
72626	Charge Separation in Monolayer WSe₂ by Strain Engineering: Implications for Strain-Induced Diode Action. ACS Applied Nano Materials, 2022, 5, 15095-15101.	2.4	3
72627	Reaction Mechanism of Na-Ion Deintercalation in Na₂CoSiO₄. Journal of Physical Chemistry C, 2022, 126, 16983-16992.	1.5	3
72628	Defect structures and dopant solution states of Hfâ€doped Si ₃ N ₄ ceramics. International Journal of Applied Ceramic Technology, 0, , .	1.1	0
72629	Slippery Paraelectric Transition-Metal Dichalcogenide Bilayers. Nano Letters, 2022, 22, 7984-7991.	4.5	8
72630	Electronic and transport properties of semimetal ZrBeSi crystal: a firstâ€principles study. Journal of Physics Condensed Matter, 0, , .	0.7	1
72631	Electronic structure and magnetic properties of <mml:math xmlns:mml="http://www.w3.org/1998/Math/MathML"><mml:mrow><mml:mn>3</mml:mn><mml:mi>d</mml:mi></mml:mrow><mml:m double perovskite material. Physical Review Materials, 2022, 6, .	3.1	3
72632	Twist Angle Effects on the Absorbance, Carrier Lifetime, and Diffusion Properties in Low Dimension Typeâ€II MoS₂/WS₂ Heterobilayers. Advanced Materials Interfaces, 2022, 9, .	1.9	2
72633	Construction of a sandwich-like Gr/Ni composite coating on AZ91D magnesium alloy to achieve excellent corrosion and wear resistances in the seawater. Diamond and Related Materials, 2022, 130, 109400.	1.8	3
72634	Lowâ€Energy Hydrogen Ions Enable Efficient Roomâ€Temperature and Rapid Plasma Hydrogenation of TiO₂ Nanorods for Enhanced Photoelectrochemical Activity. Small, 2022, 18, .	5.2	1

#	Article	IF	Citations
72635	Role of Si in the Oxide Nucleation and Growth Mechanisms of 60Si2Mn Spring Steel: Experimental and First-Principles Study. Oxidation of Metals, 0, , .	1.0	2
72636	Non-Negligible Role of Multifunctional MXene Hosts for Liâ€“S Batteries: Anchoring and Electrocatalysis. Journal of Physical Chemistry C, 2022, 126, 17066-17075.	1.5	5
72637	Computational studies on defect chemistry and Li-ion conductivity of spinel-type LiAl5O8 as coating material for Li-metal electrode. Scientific Reports, 2022, 12, .	1.6	3
72638	Enhanced Electrocatalytic CO₂ Conversion to CH₄ via Molecular Engineering on Copper Salphen Complexes. Journal of Physical Chemistry C, 2022, 126, 17502-17509.	1.5	5
72639	New CuSO₄â€related highâ€temperature polymorph of Ag^{II}SO₄**. Zeitschrift Fur Anorganische Und Allgemeine Chemie, 2022, 648, .	0.6	2
72640	Firstâ€Principles Calculations of Physical Properties and Stability of Orthorhombic FeN₂ under High Pressure. Physica Status Solidi (B): Basic Research, 2023, 260, .	0.7	0
72641	Promoted Thermal Reduction of Copper Oxide Surfaces by N-Heterocyclic Carbenes. Journal of Physical Chemistry C, 0, , .	1.5	1
72642	Single-layer and bilayer MoSTe for photocatalytic water splitting: Role of optical absorption correction and band edge distribution. Results in Physics, 2022, 42, 106033.	2.0	6
72643	Novel Bi2Sn2O7 quantum dots/TiO2 nanotube arrays S-scheme heterojunction for enhanced photoelectrocatalytic degradation of sulfamethazine. Applied Catalysis B: Environmental, 2023, 321, 122053.	10.8	31
72644	Activating dislocation mediated plasticity in boron carbide through Al-doping. Acta Materialia, 2022, 241, 118412.	3.8	15
72645	Negative Longitudinal Piezoelectricity Coexisting with both Negative and Positive Transverse Piezoelectricity in a Hybrid Formate Perovskite. ACS Applied Materials & Interfaces, 2022, 14, 46449-46456.	4.0	3
72646	Efficient electrochemical CO2 reduction reaction on a robust perovskite type cathode with in-situ exsolved Fe-Ru alloy nanocatalysts. Separation and Purification Technology, 2023, 304, 122287.	3.9	17
72647	A Combined XPS and Computational Study of the Chemical Reduction of BMPâ€TFSI by Lithium**. Batteries and Supercaps, 2022, 5, .	2.4	4
72648	Engineering Sn doping Ni/chitosan to boost higher alcohols synthesis from direct coupling of aqueous ethanol: Modifying adsorption of aldehyde intermediates for C-C bond cleavage suppressing. Applied Catalysis B: Environmental, 2023, 321, 122048.	10.8	5
72649	Pressure-induced superconductivity extending across the topological phase transition in thallium-based topological materials. Cell Reports Physical Science, 2022, 3, 101094.	2.8	5
72650	Defective hBN-Supported Fe₂N Single Cluster Catalyst for Active and Selective Electro-Reduction of Multiple CO to Propane: Theoretical Elucidation of Metalâ€“Nonmetal Synergic Effects. ACS Applied Materials & Interfaces, 2022, 14, 46657-46664.	4.0	2
72651	Application of Machine Learning Methods to Approximate the Binding Energy of CO Molecules on the Surface of Pd Nanoparticles. Journal of Surface Investigation, 2022, 16, 901-908.	0.1	0
72652	Effect of layered-coupling in twisted WSe2 moirÃ© superlattices. Nano Research, 2023, 16, 3435-3442.	5.8	6

#	Article	IF	Citations
72653	A First-principles Study: Three Novel N-Rich Bariumâ€“Nitrogen Compounds at High Pressures. Results in Physics, 2022, 42, 106030.	2.0	4
72654	Origin of the herringbone reconstruction of Au(111) surface at the atomic scale. Science Advances, 2022, 8, .	4.7	12
72655	Role of Coatings as Artificial Solid Electrolyte Interphases on Lithium Metal Self-Discharge. Journal of Physical Chemistry C, 2022, 126, 17490-17501.	1.5	5
72656	Understanding magnetocrystalline anisotropy based on orbital and quadrupole moments. Journal of Physics Condensed Matter, 2022, 34, 473001.	0.7	5
72657	First principles study of Mo, W doped CrBr3 alloy compounds. Materials Today Communications, 2022, 33, 104592.	0.9	0
72658	Role of Morphology of Platinum-Based Nanoclusters in ORR/OER Activity for Nonaqueous Liâ€“Air Battery Applications. ACS Applied Energy Materials, 2022, 5, 12561-12570.	2.5	6
72659	High-performance electron mobility and photoabsorption in Bi2O2Se nanoribbons. Applied Physics Letters, 2022, 121, .	1.5	3
72660	Identification of an Oxygen Defect in Hexagonal Boron Nitride. Journal of Physical Chemistry Letters, 2022, 13, 9544-9551.	2.1	11
72661	The role of the surface passivation in the mechanical properties of wurtzite InAs and InP nanowires: first-principles calculations. European Physical Journal Plus, 2022, 137, .	1.2	0
72662	Adsorbate chemical environment-based machine learning framework for heterogeneous catalysis. Nature Communications, 2022, 13, .	5.8	30
72663	Effect of Silicon Element on the Solid Solubility of Carbon in Î±-Fe. Materials Performance and Characterization, 2022, 11, 324-334.	0.2	0
72664	Firstâ€Principles Design of a Highly Active and Selective V₂CO₂â€Based Doubleâ€Atom Catalyst for Ethane Dehydrogenation to Ethylene. ChemCatChem, 2022, 14, .	1.8	2
72665	Electronic structure of Humble defects in Ge and <mml:math xmlns:mml="http://www.w3.org/1998/Math/MathML"><mml:mrow><mml:msub><mml:mi>Ge</mml:mi><mml:mrow><mml:mn>1−</mml:mn><mml:mi>x</mml:mi></mml:mrow></mml:msub><mml:msub><mml:mi>Mn</mml:mi><mml:mn>0.8</mml:mn></m Physical Review B, 2022, 106, .	1.1	0
72666	Pressure-induced phase transitions of CsSnBr₃ perovskite from first-principles calculations. Physica Scripta, 2022, 97, 115811.	1.2	1
72667	Coordination Effect-Promoted Durable Ni(OH)2 for Energy-Saving Hydrogen Evolution from Water/Methanol Co-Electrocatalysis. Nano-Micro Letters, 2022, 14, .	14.4	35
72668	Elucidating the Chemical Order and Disorder in High-Entropy MXenes: A High-Throughput Survey of the Atomic Configurations in Ti₃ and TiVCrMoC₃. Chemistry of Materials, 2022, 34, 9062-9071.	3.2	13
72669	Ni-Doped Ti₃CNT_x-Coated Nanoporous Covalent Organic Frameworks to Accelerate Hydrogen Diffusion for Enhanced Hydrogen Evolution. ACS Applied Nano Materials, 2022, 5, 15042-15052.	2.4	4
72670	Role of doping and defect quenching in antiferroelectric <mml:math xmlns:mml="http://www.w3.org/1998/Math/MathML"><mml:msub><mml:mi>NaNbO</mml:mi><mml:mn>3</mml:mn></mml:msub> from first principles. Physical Review B, 2022, 106, .	1.1	3

#	Article	IF	Citations
72671	Prediction of Room-Temperature Ferromagnetic Semiconductors in CrMoA₂B₂ (A = Se and Te; B = Br and I) Monolayers. Journal of Physical Chemistry C, 2022, 126, 17390-17397.	1.5	6
72672	D-band center optimization of iron carbide via Cr substitution for enhanced alkaline hydrogen evolution. Materials Today Energy, 2022, 29, 101133.	2.5	9
72673	Aluminum-Doped Mesoporous Copper Oxide Nanofibers Enabling High-Efficiency CO₂ Electroreduction to Multicarbon Products. Chemistry of Materials, 2022, 34, 9023-9030.	3.2	8
72674	Coupling of nanocrystal hexagonal array and two-dimensional metastable substrate boosts H2-production. Nature Communications, 2022, 13, .	5.8	22
72675	Density Functional Theory Study on the Enhancement Mechanism of the Photocatalytic Properties of the g-C₃N₄/BiOBr(001) Heterostructure. ACS Omega, 2022, 7, 36479-36488.	1.6	5
72676	Unraveling the electrocatalytic reduction mechanism of enols on copper in aqueous media. Nature Communications, 2022, 13, .	5.8	3
72677	Janus structures of SMoSe and SVSe compositions with low enthalpy and unusual crystal chemistry. Journal of Applied Crystallography, 2022, 55, 1324-1335.	1.9	3
72678	Band Structure and Phonon Transport Engineering Realizing Remarkable Improvement in Thermoelectric Performance of Cu₂SnSe₄ Incorporated with In₂Te₃. ACS Applied Materials & Interfaces, 2022, 14, 45628-45635.	4.0	3
72679	Effect of the interfacial electronic coupling of nickel-iron sulfide nanosheets with layer Ti3C2 MXenes as efficient bifunctional electrocatalysts for anion-exchange membrane water electrolysis. Applied Catalysis B: Environmental, 2023, 321, 122039.	10.8	27
72680	A Fast and Robust Method for Predicting the Phase Stability of Refractory Complex Concentrated Alloys using Pairwise Mixing Enthalpy. Acta Materialia, 2022, 241, 118389.	3.8	2
72681	<mml:math xmlns:mml="http://www.w3.org/1998/Math/MathML"><mml:mrow><mml:msub><mml:mi>Ta</mml:mi><mml:mn>14</mml:mn></mml:m : A tantalum-rich superconductor with a honeycomb network structure. Physical Review B, 2022, 106, .	3.7	8
72682	CO₂ Hydrogenation to Methanol on Indium Oxide-Supported Rhenium Catalysts: The Effects of Size. ACS Catalysis, 2022, 12, 12658-12669.	5.5	36
72683	NiMn-based metal-organic framework with optimized eg orbital occupancy as efficient bifunctional electrocatalyst for lithium-oxygen batteries. Chemical Engineering Journal, 2023, 452, 139524.	6.6	10
72685	Helicity-tunable spin Hall and spin Nernst effects in unconventional chiral fermion semimetals <mml:math xmlns:mml="http://www.w3.org/1998/Math/MathML"><mml:mrow><mml:mi>X</mml:mi><mml:mi>Y</mml:mi></mml:mrow></mml:		

#	Article	IF	Citations
72690	From Heterostructures to Solidâ€Solutions: Structural Tunability in Mixed Halide Perovskites. Advanced Materials, 2023, 35, .	11.1	5
72691	Low-Temperature Methanol Synthesis by a Cu-Loaded LaH_{2+x} Electride. ACS Catalysis, 2022, 12, 12572-12581.	5.5	4
72692	Mapping the Room-Temperature Dynamic Stabilities of Inorganic Halide Double Perovskites. Chemistry of Materials, 2022, 34, 9072-9085.	3.2	2
72693	Mapping the Porous and Chemical Structureâ€“Function Relationships of Trace CH₃I Capture by Metalâ€“Organic Frameworks using Machine Learning. ACS Applied Materials & Interfaces, 2022, 14, 47209-47221.	4.0	7
72694	Schiff-Base Covalent Organic Framework/Carbon Nanotubes Composite for Advanced Potassium-Ion Batteries. ACS Applied Nano Materials, 2022, 5, 15592-15599.	2.4	19
72695	High Selective Direct Synthesis of H₂O₂ over Pd₁@Î³â€Al₂O₃ Singleâ€Atom Catalyst. ChemCatChem, 2022, 14, .	1.8	0
72696	Band alignment and interlayer hybridisation in transition metal dichalcogenide/hexagonal boron nitride heterostructures. 2D Materials, 2022, 9, 045036.	2.0	2
72697	Potential high-Tc superconductivity in YCeH and LaCeH under pressure. Materials Today Physics, 2022, 28, 100873.	2.9	13
72698	Volcano-type relationship between oxidation states and catalytic activity of single-atom catalysts towards hydrogen evolution. Nature Communications, 2022, 13, .	5.8	48
72699	Phase stability of (<mml:math) Tj ETQq1 1 0.784314 rgBT /Overlock 10 Tf 50 402 Td (xmlns:mml="http://www.w3.org/1998/Math/Math mathvariant="normal">O</mml:mi><mml:mn>3</mml:mn></mml:msub></mml:math> polymorphs: A first-principle. Physical Review Materials, 2022, 6, .	0.9	11
72700	Monolayer-like lattice dynamics in bulk WSe2. Materials Today Physics, 2022, 28, 100856.	2.9	4
72701	First-Principles Investigation of the Electrocatalytic Reduction of CO₂ on Zirconium-Based Single-, Double-, and Triple-Atom Catalysts Anchored on a Graphitic Carbon Nitride Monolayer. ACS Applied Nano Materials, 2022, 5, 15409-15417.	2.4	12
72702	Role of van der Waals interactions on the binding energies of 2D transition-metal dichalcogenides. Applied Surface Science, 2023, 608, 155163.	3.1	13
72703	Unifying the Nitrogen Reduction Activity of Anatase and Rutile TiO₂ Surfaces. ChemPhysChem, 2023, 24, .	1.0	3
72704	Stability trend, weak bonding, and magnetic properties of the Alâ€•and Siâ€•containing ternaryâ€•layered borides MAB phases. Journal of the American Ceramic Society, 2023, 106, 1513-1530.	1.9	10
72705	Interfacial Stability of Layered LiNi_xMn_yCo_{1â€“xâ€“y}O₂ Cathodes with Sulfide Solid Electrolytes in All-Solid-State Rechargeable Lithium-Ion Batteries from First-Principles Calculations. Journal of Physical Chemistry C, 2022, 126, 17482-17489.	1.5	6
72706	Template Driven Self-Assembly of the Pentacene Structure on the Si(553)-Pb Surface. Journal of Physical Chemistry C, 0, , .	1.5	0
72707	Ab Initio Study of Electronic and Lattice Dynamical Properties of Monolayer ZnO Under Strain. Journal of Electronic Materials, 0, , .	1.0	1

#	Article	IF	Citations
72708	Electron-doping induced tunable magnetisms in 2D Janus TiXO (X = S, Se). Physica E: Low-Dimensional Systems and Nanostructures, 2023, 145, 115518.	1.3	3
72709	High-mobility two-dimensional carriers from surface Fermi arcs in magnetic Weyl semimetal films. Npj Quantum Materials, 2022, 7, .	1.8	12
72710	Identification of Highly Selective Surface Pathways for Methane Dry Reforming Using Mechanochemical Synthesis of Pdâ€“CeO₂. ACS Catalysis, 2022, 12, 12809-12822.	5.5	19
72711	Metal-organic coordination polymers-derived ultra-small MoC nanodot/N-doped carbon combined with CdS: A hollow Z-type catalyst for stable and efficient H2 production/CO2 reduction. Applied Surface Science, 2023, 608, 155176.	3.1	5
72712	Experimental Realization of Spinâ€Polarized States on Mg ₃ Bi ₂ Surface. Physica Status Solidi - Rapid Research Letters, 0, , 2200250.	1.2	0
72713	Role of the Magnetic Anisotropy in Atomic-Spin Sensing of 1D Molecular Chains. ACS Nano, 2022, 16, 16402-16413.	7.3	13
72714	Modeling of ultrafast X-ray induced magnetization dynamics in magnetic multilayer systems. Npj Computational Materials, 2022, 8, .	3.5	4
72715	Large Exchange Coupling Between Localized Spins and Topological Bands in MnBi₂Te₄. Advanced Materials, 2022, 34, .	11.1	5
72716	Thickness-dependent electronic band structure in MBE-grown hexagonal InTe films. Physical Review B, 2022, 106, .	1.1	4
72717	Unconventional Ferroelectricity with Quantized Polarizations in Ionic Conductors: High-Throughput Screening. Journal of Physical Chemistry Letters, 2022, 13, 9552-9557.	2.1	7
72718	Pressure-Induced Electride States in Intermetallic BaMg₂ Compounds. Journal of Physical Chemistry C, 2022, 126, 17374-17380.	1.5	5
72719	Rapid Plasma Exsolution from an Aâ€site Deficient Perovskite Oxide at Room Temperature. Advanced Energy Materials, 2022, 12, .	10.2	13
72720	Plasmonic Photocatalysis with Chemically and Spatially Specific Antennaâ€“Dual Reactor Complexes. ACS Nano, 2022, 16, 17365-17375.	7.3	18
72721	Rational Design of Black Phosphorus-Based Direct Z-Scheme Photocatalysts for Overall Water Splitting: The Role of Defects. Journal of Physical Chemistry Letters, 2022, 13, 9363-9371.	2.1	17
72722	Plasma Postâ€Treatment Processâ€Induced Grain Coalescence to Improve the Electron Fieldâ€Emission Properties of Ultrananocrystalline Diamond Films. Physica Status Solidi (A) Applications and Materials Science, 2022, 219, .	0.8	2
72723	Boosting the solar conversion efficiency of MoSe₂/PtX₂ (XÂ=ÂO, S) vdW heterostructure by strain and electric field engineering. Physica Scripta, 2022, 97, 115801.	1.2	5
72724	Effects of aluminum diffusion on the oxide of the FeCrAl alloys surface: A firstâ€“principles study. Materials Today Communications, 2022, 33, 104594.	0.9	1
72725	Hybrid molecular beam epitaxy of germanium-based oxides. Communications Materials, 2022, 3, .	2.9	3

#	Article	IF	Citations
72726	Charge dynamics of a noncentrosymmetric magnetic Weyl semimetal. Npj Quantum Materials, 2022, 7, .	1.8	6
72727	The kagomÃ© metals RbTi₃Bi₅ and CsTi₃Bi₅. Zeitschrift Fur Naturforschung - Section B Journal of Chemical Sciences, 2022, 77, 757-764.	0.3	14
72728	Facet-dependent catalytic activity of CeO2 toward methanol synthesis from methane. Journal of Rare Earths, 2023, 41, 1938-1944.	2.5	2
72729	Computational analysis on native and extrinsic point defects in YAG using the metaGGA SCAN method. Theoretical Chemistry Accounts, 2022, 141, .	0.5	2
72730	Tuning the electrocatalytic CO reduction on bilayer C3N via rotation, translation and metal intercalation. Applied Surface Science, 2022, , 155204.	3.1	0
72731	Effect of solutes on the performance of Zn-coating and Zn-inducing transgranular cracking in steel based on DFT calculations. Journal of Materials Research and Technology, 2022, , .	2.6	0
72732	Explorations on properties of Îµâ€² phase and new crystalline phase of Fe3Ge alloy under high pressures. Physics Letters, Section A: General, Atomic and Solid State Physics, 2022, 452, 128450.	0.9	0
72733	Mechanistic insights into copper oxides catalyzed bio-based furfural hydrogenation using methanol as in-situ hydrogen donor. Renewable Energy, 2022, 200, 88-97.	4.3	11
72734	Investigations on molybdenum phosphide surfaces for CO2 adsorption and activation. Journal of CO2 Utilization, 2022, 65, 102246.	3.3	0
72735	Selective incorporation of Fe and Co into the Ni2MnGa (001) surfaces: a DFT analysis. Surfaces and Interfaces, 2022, 34, 102367.	1.5	4
72736	Self-supported graphene oxide encapsulated chalcopyrite electrode for high-performance Li-ion capacitor. Journal of Energy Storage, 2022, 55, 105791.	3.9	8
72737	Density functional theory study on the adsorption properties of SO2 gas on graphene, N, Ti, and Nâ€“Ti doped graphene. , 2022, 171, 207401.		4
72738	Quantum capacitance of vacancy-defected and co-doped stanene for supercapacitor electrodes: A theoretical study. Electrochimica Acta, 2022, 433, 141261.	2.6	10
72739	Dual experimental and computational approach to elucidate the effect of Ga on Cu/CeO2â€“ZrO2 catalyst for CO2 hydrogenation. Journal of CO2 Utilization, 2022, 65, 102251.	3.3	3
72740	Theoretical SERS study of the strength and suitability of Cu12 nanostar for SERS: Complete theoretical studies, coinage metal SM12 comparisons, benzothiazole (BTH) adsorbent. Computational and Theoretical Chemistry, 2022, 1217, 113889.	1.1	8
72741	Crystalline aluminum silicides with electride state and superconductivity under high pressure. Materials Today Physics, 2022, 28, 100853.	2.9	4
72742	Mechanical performance of doped Wâ€“Cu nanocomposites. Materials Science & Engineering A: Structural Materials: Properties, Microstructure and Processing, 2022, 857, 144102.	2.6	3
72743	Constructing interstitial pillar to manipulating interlamination interaction force: Towards high sodium-content P2/O3 intergrowth cathodes. Electrochimica Acta, 2022, 433, 141253.	2.6	3

#	Article	IF	Citations
72744	Gas sensing properties of alkali metal decorated pristine and defect Î±-AsP monolayer toward acid SO2 and alkaline NH3 molecules. Solid State Communications, 2022, 356, 114962.	0.9	1
72745	Zero-dimensional rubidium zinc halide blue-emitting quantum dots for X-ray imaging. Journal of Luminescence, 2022, 252, 119374.	1.5	3
72746	Two new BN polymorphs with wide-bandgap. Diamond and Related Materials, 2022, 130, 109410.	1.8	3
72747	Highly distorted Cr3+-doped fluoroantimonate with high absorption efficiency for multifunctional near-infrared spectroscopy applications. Materials Today Chemistry, 2022, 26, 101194.	1.7	7
72748	Comparative characteristics of various solvents of the Na, Ba, B//O, F system for the growth of Î²-BaB2O4 crystals and PT-diagram of BaB2O4 polymorphs. Journal of Crystal Growth, 2022, 599, 126895.	0.7	0
72749	Intrinsic ultra-low lattice thermal conductivity in orthorhombic BiSI: An excellent thermoelectric material. Journal of Alloys and Compounds, 2022, 929, 167347.	2.8	5
72750	Density functional theory study of Ni segregation in CuNi(111) alloy with chemisorbed CO, O, or H. Journal of Physics and Chemistry of Solids, 2022, 171, 111021.	1.9	2
72751	Rapid electrochemical detection of levodopa using polyaniline-modified screen-printed electrodes for the improved management of Parkinson's disease. Physics in Medicine, 2022, 14, 100052.	0.6	4
72752	Investigation of hardness in transition metal hexa-nitrides in cubic structure: A first-principles study. Journal of Physics and Chemistry of Solids, 2022, 171, 111022.	1.9	4
72753	Cyclobis(paraquat-p-phenylene) â€“ mediated electrosynthesis of new-type nanocomposite of palladium nanoparticles with designated macrocyclic organic compound. Electrochimica Acta, 2022, 434, 141271.	2.6	1
72754	Mn diffusion in the ferritic Fe-25Â%Cr Alloy: A First-principles study. Materials Science and Engineering B: Solid-State Materials for Advanced Technology, 2022, 286, 116042.	1.7	4
72755	First-principles study on the temperature dependent elasticity and thermodynamical properties of thermoelectric material NiSbS. Materials Today Communications, 2022, 33, 104504.	0.9	0
72756	DFT+U study and in-situ TEM investigation of high-entropy titanate pyrochlore (Lu0.25Y0.25Eu0.25Gd0.25)2Ti2O7. Journal of the European Ceramic Society, 2022, 42, 7546-7552.	2.8	2
72757	Atomic Ti-Nx sites with switchable coordination number for enhanced visible-light photocatalytic water disinfection. Journal of Cleaner Production, 2022, 377, 134423.	4.6	8
72758	Enhanced photoactivity and anti-photocorrosion of Z-scheme Zr2CO2/WSe2 heterostructure for overall water splitting. Journal of Physics and Chemistry of Solids, 2022, 171, 111014.	1.9	12
72759	Insights on the proton mechanism in carbonyl-based organic electrode of neutral aqueous battery. Journal of Power Sources, 2022, 550, 232110.	4.0	4
72760	Alloying effects on inhibiting hydrogen evolution of Zn metal anode in rechargeable aqueous batteries. Materials Today Communications, 2022, 33, 104576.	0.9	2
72761	Ultra-fast and ultra-efficient removal of Cr (VI) by the aqueous solutions of monolayer MXene (Ti3C2Tx). Chemosphere, 2022, 308, 136573.	4.2	6

#	Article	IF	Citations
72762	Charge analysis in (RE)CrO4 scheelites by combined Raman spectroscopy and computer simulations. Journal of Solid State Chemistry, 2022, 316, 123624.	1.4	3
72763	Anisotropic spin Hall and spin Nernst effects in bismuth semimetal. Journal of Magnetism and Magnetic Materials, 2022, 563, 169949.	1.0	4
72764	High-throughput screening to predict highly active dual-atom catalysts for electrocatalytic reduction of nitrate to ammonia. Nano Energy, 2022, 103, 107866.	8.2	33
72765	Efficient electrocatalysts with strong core-shell interaction for water splitting: The modulation of selectivity and activity. Journal of Alloys and Compounds, 2022, 929, 167247.	2.8	3
72766	First-principles investigation of mechanical properties, elastic anisotropy, and ultralow lattice thermal conductivities of ductile Mgâ€“Bi alloys. Vacuum, 2022, 206, 111535.	1.6	3
72767	Si-addition contributes to overcoming the strength-ductility trade-off in high-entropy alloys. International Journal of Plasticity, 2022, 159, 103443.	4.1	37
72768	Tuning the coordination environment of Fe atoms enables 3D porous Fe/N-doped carbons as bifunctional electrocatalyst for rechargeable zinc-air battery. Journal of Colloid and Interface Science, 2022, 628, 1067-1076.	5.0	4
72769	Effect of the mechanical strength on the ion transport in a transition metal lithium halide electrolyte: first-principle calculations. Materials Today Communications, 2022, 33, 104570.	0.9	4
72770	Adhesion, tensile and shear properties of a-C/TiC interface: A first-principles study. Diamond and Related Materials, 2022, 130, 109416.	1.8	5
72771	Enhanced activity and stability of Ce-doped PrCrO3-supported nickel catalyst for dry reforming of methane. Separation and Purification Technology, 2022, 303, 122245.	3.9	12
72772	In-situ surface patch-passivation via phosphorus oxygen bond for efficient PbS colloidal quantum dot infrared solar cells. Solar Energy Materials and Solar Cells, 2022, 248, 112040.	3.0	2
72773	Ab-initio modeling of chloride binding at hydrocalumite/sodium chloride solution interfaces. Cement and Concrete Research, 2022, 162, 106996.	4.6	3
72774	The origin of the P-type conductivity for Cu and Ag-doped NiO: Density functional theory study. Materials Today Communications, 2022, 33, 104552.	0.9	2
72775	Rare earth metal element doped g-GaN monolayer : Study of structural, electronic, magnetic, and optical properties by first-principle calculations. Physica B: Condensed Matter, 2022, 647, 414367.	1.3	7
72776	Theoretical simulation structural, elastic, electronic, optical, vibrational and thermal properties of AgGaxIn1-xS2 (x = 0, 0.25, 0.5, 0.75, 1). Vacuum, 2022, 206, 111505.	1.6	4
72777	Experimental and DFT studies on spinel NiMn2O4 flower derived from bimetallic MOF as an efficient electrode for next-generation supercapacitor. Colloids and Surfaces A: Physicochemical and Engineering Aspects, 2022, 655, 130244.	2.3	5
72778	Interface induced transition from Schottky-to-Ohmic contacts in single-walled carbon nanotube-based van der Waals Schottky heterostructures. Materials Today Nano, 2022, 20, 100267.	2.3	0
72779	Anomalous behavior of strain modulated lattice thermal transport in piezoelectric crystals and the effect of polarization. Acta Materialia, 2022, 241, 118406.	3.8	0

#	Article	IF	Citations
72781	One-pot construction of CoSe nanoparticles anchored on single-atomic-Co doped carbon for pH-universal hydrogen evolution. Materials Chemistry Frontiers, 2022, 6, 3577-3588.	3.2	6
72782	A high-performance Na-storage cathode enabled by layered P2-type K_xMnO₂ with enlarged interlayer spacing and fast diffusion channels for sodium-ion batteries. Journal of Materials Chemistry A, 2022, 10, 25168-25177.	5.2	7
72783	Theoretical Screening of Lead-Free Hybrid Organicâ€“Inorganic Halide Double Perovskites for Solar Cells. Journal of Materials Chemistry C, 0, , .	2.7	1
72784	SnSe₂ monolayer with square lattice structure: a promising p-type thermoelectric material with an indirect bandgap and low lattice thermal conductivity. Journal of Materials Chemistry C, 2022, 10, 16116-16125.	2.7	11
72785	Local chemical origin of ferroelectric behavior in wurtzite nitrides. Journal of Materials Chemistry C, 2022, 10, 17557-17566.	2.7	12
72786	Computational Techniques for Nanostructured Materials. , 2022, , 459-480.		0
72787	Theoretical study on the stability, ferroelectricity and photocatalytic properties of CaBiO₃. RSC Advances, 2022, 12, 30764-30770.	1.7	2
72788	High-temperature magnetic skyrmions in BiCrX₃ (X = Se and Te) monolayers. Physical Chemistry Chemical Physics, 2022, 24, 26477-26484.	1.3	1
72789	Effect of Na-ion intercalation on the thermal conductivity of carbon honeycomb nanostructure. Physical Chemistry Chemical Physics, 2022, 24, 25537-25546.	1.3	0
72790	A trade-off between ligand and strain effects optimizes the oxygen reduction activity of Pt alloys. Energy and Environmental Science, 2022, 15, 5181-5191.	15.6	21
72791	Theoretically revealing the activity origin of the hydrogen evolution reaction on carbon-based single-atom catalysts and finding ideal catalysts for water splitting. Journal of Materials Chemistry A, 2022, 10, 24362-24372.	5.2	5
72792	Metallic WN plasmonic fabricated g-C₃N₄ significantly steered photocatalytic hydrogen evolution under visible and near-infrared light. Catalysis Science and Technology, 2022, 12, 7369-7378.	2.1	2
72793	Thermoelectric performance of novel single-layer ZrTeSe₄. Physical Chemistry Chemical Physics, 2022, 24, 28250-28256.	1.3	2
72794	Formulating electronic descriptors to rationally design graphene-supported single-atom catalysts for oxygen electrocatalysis. Journal of Materials Chemistry A, 2022, 10, 25098-25105.	5.2	1
72795	Unveiling the uncommon blue-excitable broadband yellow emission from self-trapped excitons in a zero-dimensional hybrid tellurium halide. Journal of Materials Chemistry C, 0, , .	2.7	2
72796	Co-doping of tellurium with bismuth enhances stability and photoluminescence quantum yield of Cs₂AgInCl₆ double perovskite nanocrystals. Nanoscale, 2022, 14, 15691-15700.	2.8	7
72797	A novel red-emitting phosphor with an unusual concentration quenching effect for near-UV-based WLEDs. Inorganic Chemistry Frontiers, 2022, 9, 6358-6368.	3.0	14
72798	Covalent surface modification of bifunctional two-dimensional metal carbide MXenes as sulfur hosts for sodiumâ€“sulfur batteries. Nanoscale, 2022, 14, 17027-17035.	2.8	8

#	Article	IF	Citations
72799	Two dimensional monolayers TetraHex-CX₂ (X = N, P, As, and Sb) with superior electronic, mechanical and optical properties. Physical Chemistry Chemical Physics, 2022, 24, 29601-29608.	1.3	3
72800	Insights into the effect of oxygen vacancies on the epoxidation of 1-hexene with hydrogen peroxide over WO_{3â^'x}/SBA-15. Catalysis Science and Technology, 2022, 12, 6827-6837.	2.1	5
72801	Syntheses and Characterization of Two New Layered Ternary Chalcogenides NaScQ₂ (Q = Se and Te). New Journal of Chemistry, 0, , .	1.4	0
72802	A theoretical study of H2S adsorption and dissociation mechanism on defected graphene doped with Pt. Journal of Fuel Chemistry and Technology, 2022, 50, 1211-1219.	0.9	3
72803	Ru/Rh catalyzed selective hydrogenation of CO₂ to formic acid: a first principles microkinetics analysis. Catalysis Science and Technology, 2022, 12, 7219-7232.	2.1	7
72804	Hybrid density functional theory calculations for the electronic and optical properties of Fe³⁺-doped KDP crystals. CrystEngComm, 2022, 24, 8082-8088.	1.3	5
72805	Lithium Selenometallates of Triel Elements, Li5MSe4 (M = Al and Ga), Aliovalent Doping and Their Ionic Conductivity. Dalton Transactions, 0, , .	1.6	0
72806	Vacancy defect engineered BiVO₄ with low-index surfaces for photocatalytic application: a first principles study. RSC Advances, 2022, 12, 31317-31325.	1.7	1
72807	Ultrahigh thermoelectric performance of Janus Î±-STe₂ and Î±-SeTe₂ monolayers. Physical Chemistry Chemical Physics, 0, , .	1.3	0
72808	Insights into reaction mechanisms of ethanol electrooxidation at the Pt/Au(111) interfaces using density functional theory. Physical Chemistry Chemical Physics, 2022, 24, 27277-27288.	1.3	2
72809	Atomic-scale insight into the lattice volume plunge of Li_xCoO₂ upon deep delithiation. Energy Advances, 2023, 2, 103-112.	1.4	2
72810	Electronic and thermoelectric properties of semiconducting Bi₂SSe₂ and Bi₂S₂Se monolayers with high optical absorption. Physical Chemistry Chemical Physics, 2022, 24, 26753-26763.	1.3	4
72811	Promoting the mechanism of OMS-2 for gas adsorption in different K⁺ concentrations. RSC Advances, 2022, 12, 30549-30556.	1.7	0
72812	The GaPS₂Se₂ monolayer: a novel stable 2D Janus semiconductor with anisotropic properties for spontaneous water splitting under the irradiation of solar light. Journal of Materials Chemistry C, 2022, 10, 17135-17144.	2.7	9
72813	Prediction of stable silver selenide-based energy materials sustained by rubidium selenide alloying. New Journal of Chemistry, 2022, 46, 22050-22063.	1.4	3
72814	Giant tunneling magnetoresistance in two-dimensional magnetic tunnel junctions based on double transition metal MXene ScCr2C2F2. Nanoscale Advances, 0, , .	2.2	0
72815	Two dimensional twin T-graphene: monolayer for visible-light photocatalytic water splitting and bulk for anode material of magnesium batteries. RSC Advances, 2022, 12, 30349-30358.	1.7	3
72816	Si₅-pentagonal rings and Y-shaped Si₄ building blocks in Li₃₂Si₁₈ system: similarities with the crystalline Zintl phase Li₁₂Si₇. Molecular Systems Design and Engineering, 0, , .	1.7	0

#	Article	IF	Citations
72817	Reaction mechanism and kinetics for N₂ reduction to ammonia on the Feâ€“Ru based dual-atom catalyst. Journal of Materials Chemistry A, 2022, 10, 23323-23331.	5.2	6
72818	A penta-silicene nanoribbon-based 3D silicon allotrope with high carrier mobility and thermoelectric performance. Physical Chemistry Chemical Physics, 2022, 24, 27413-27422.	1.3	2
72819	Interlayer spacing in pillared and grafted MCM-22 type silicas: density functional theory analysis versus experiment. Physical Chemistry Chemical Physics, 2023, 25, 4680-4689.	1.3	3
72820	Argyrodite configuration determination for DFT and AIMD calculations using an integrated optimization strategy. RSC Advances, 2022, 12, 31156-31166.	1.7	2
72821	Novel two-dimensional ferromagnetic materials CrX₂ (X = O, S, Se) with high Curie temperature. Journal of Materials Chemistry C, 2022, 10, 17665-17674.	2.7	13
72822	A two-dimensional PtS₂/BN heterostructure as an S-scheme photocatalyst with enhanced activity for overall water splitting. Physical Chemistry Chemical Physics, 2022, 24, 26908-26914.	1.3	4
72823	Electronic structure of strain-tunable Janus WSSeâ€“ZnO heterostructures from first-principles. RSC Advances, 2022, 12, 31303-31316.	1.7	5
72824	Lithium-ion diffusion in the grain boundary of polycrystalline solid electrolyte Li_{6.75}La₃Zr_{1.5}Ta_{0.5}O₁₂ (LLZTO): a computer simulation and theoretical study. Physical Chemistry Chemical Physics, 2022, 24, 27355-27361.	1.3	4
72825	Transition-metal decorated graphdiyne monolayer as an efficient sensor toward phosphide (PH₃) and arsine (AsH₃). Physical Chemistry Chemical Physics, 2022, 24, 26622-26630.	1.3	3
72826	Easy-axis rotation in ferromagnetic monolayer CrN induced by fluorine and chlorine functionalization. Physical Chemistry Chemical Physics, 2022, 24, 25426-25433.	1.3	7
72827	MoSSe/Hf(Zr)S₂ heterostructures used for efficient Z-scheme photocatalytic water-splitting. Physical Chemistry Chemical Physics, 2022, 24, 25287-25297.	1.3	13
72828	Modulation of the kinetics of outer-sphere electron transfer at graphene by a metal substrate. Physical Chemistry Chemical Physics, 2022, 24, 25203-25213.	1.3	1
72829	P-block atom modified Sn(200) surface as a promising electrocatalyst for two-electron CO₂ reduction: a first-principles study. Physical Chemistry Chemical Physics, 2022, 24, 26556-26563.	1.3	2
72830	The Rashba effect in two-dimensional hybrid perovskites: the impacts of halogens and surface ligands. Physical Chemistry Chemical Physics, 2022, 24, 27827-27835.	1.3	1
72831	Breaking scaling relations in nitric oxide reduction by surface functionalization of MXenes. Journal of Materials Chemistry A, 2022, 10, 25201-25211.	5.2	8
72832	Effect of fullerene on the anisotropy, domain size and relaxation of a perpendicularly magnetized Pt/Co/C₆₀/Pt system. Journal of Materials Chemistry C, 2022, 10, 17236-17244.	2.7	1
72833	Incorporated O-CoP nanosheets with an Oâ€“P interpenetrated interface as electrocatalytic cathodes for rechargeable Liâ€“CO₂ batteries. New Journal of Chemistry, 0, , .	1.4	0
72834	Study of spacer-layer-tunable ferromagnetic half-metalâ€”ferromagnetic insulator transition in SrVO₃/SrTiO₃ superlattice<. Wuli Xuebao/Acta Physica Sinica, 2022, .	0.2	0

#	Article	IF	Citations
72835	Bismuthâ€“nickel bimetal nanosheets with a porous structure for efficient hydrogen production in neutral and alkaline media. Nanoscale, 2022, 14, 17210-17221.	2.8	3
72836	Transition metal dichalcogenide magnetic atomic chains. Nanoscale Advances, 2022, 4, 4905-4912.	2.2	3
72837	Anisotropic photoresponse behavior of a LaAlO₃ single-crystal-based vacuum-ultraviolet photodetector. Nanoscale, 2022, 14, 16829-16836.	2.8	1
72838	Tuning CO₂ hydrogenation selectivity on Ni/TiO₂ catalysts via sulfur addition. Catalysis Science and Technology, 0, , .	2.1	0
72839	Theoretically evaluating two-dimensional tetragonal Si₂Se₂ and SiSe₂ nanosheets as anode materials for alkali metal-ion batteries. Physical Chemistry Chemical Physics, 2022, 24, 26241-26253.	1.3	6
72840	Direct tuning of large-gap quantum spin Hall effect in mono transition metal carbide MXenes. Journal of Materials Chemistry A, 2022, 10, 24238-24246.	5.2	1
72841	Insights into the multifunctional applications of strategically Co doped MoS₂ nanoflakes. Materials Advances, 2022, 3, 8740-8759.	2.6	1
72842	Transition metal single atom embedded GaN monolayer surface for efficient and selective CO₂ electroreduction. Journal of Materials Chemistry A, 2022, 10, 24280-24289.	5.2	5
72843	Electronic structure manipulation via composition tuning for the development of highly conductive and acid-stable oxides. Journal of Materials Chemistry A, 2022, 10, 23155-23164.	5.2	1
72844	Chemical Bonding With Plane Waves. , 2022, , .		2
72845	Enhancing the catalytic OER performance of MoS₂ via Fe and Co doping. Nanoscale, 2022, 14, 16148-16155.	2.8	24
72846	Local structural distortions and reduced thermal conductivity in Ge-substituted chalcopyrite. Journal of Materials Chemistry A, 2022, 10, 23874-23885.	5.2	7
72847	Theoretical investigation of selective CO₂ capture and desorption controlled by an electric field. Physical Chemistry Chemical Physics, 2022, 24, 28141-28149.	1.3	2
72848	Critical stresses in mechanochemical reactions. Chemical Science, 2022, 13, 12651-12658.	3.7	7
72849	DFT based microkinetic modeling of confinement driven [4 + 2] Dielsâ€“Alder reactions between ethene and isoprene in H-ZSM5. Catalysis Science and Technology, 2022, 12, 7389-7407.	2.1	1
72850	Toward highly efficient bifunctional electrocatalysts for zincâ€“air batteries: from theoretical prediction to a ternary FeCoNi design. Nanoscale, 2022, 14, 17447-17459.	2.8	2
72851	Defect-type AlO_xnanointerface boosting layered Mn-based oxide cathode for wide-temperature sodium-ion battery. Journal of Materials Chemistry A, 2022, 10, 24216-24225.	5.2	7
72852	Materials design principles of amorphous cathode coatings for lithium-ion battery applications. Journal of Materials Chemistry A, 2022, 10, 22245-22256.	5.2	10

#	Article	IF	Citations
72853	Defect formation and carrier compensation in the layered oxychalcogenide La₂CdO₂Se₂: an insight from first principles. Journal of Materials Chemistry C, 0, , .	2.7	0
72854	The electronic structure and interfacial contact with metallic borophene of monolayer ScSX (X = I,) Tj ETQq1 1 0.784314 rgBT /Overlo	1.3	3
72855	Introducing the 1H-Na₂S monolayer as a new direct gap semiconductor with feature-rich electronic and magnetic properties. Physical Chemistry Chemical Physics, 2022, 24, 27505-27514.	1.3	2
72856	Role of heteroatom-doping in enhancing catalytic activities and the stability of single-atom catalysts for oxygen reduction and oxygen evolution reactions. Nanoscale, 2022, 14, 16286-16294.	2.8	13
72857	A Paradigm for Systematic Screening and Evaluation of Artificial Solid-Electrolyte Interfaces for Lithium Metal Anodes: A Computational Study of Binary Selenides. Journal of Materials Chemistry A, 0, , .	5.2	0
72858	KMnCuTe₂: a layered antiferromagnetic semiconductor with long metalâ€“metal distance. RSC Advances, 2022, 12, 29003-29009.	1.7	0
72859	Structural, electronic phase transitions and thermal spin transport properties in 2D NbSe₂ and NbS₂: a first-principles study. Physical Chemistry Chemical Physics, 2023, 25, 1632-1641.	1.3	5
72860	Strong electronâ€“phonon coupling driven charge density wave states in stoichiometric 1T-VS₂ crystals. Journal of Materials Chemistry C, 2022, 10, 16657-16665.	2.7	1
72861	Properties of spinel-type Ti-Li-M composite oxides (M = Li, Na, Cu, and Ag) predicted by density functional theory. Physical Chemistry Chemical Physics, 0, , .	1.3	0
72862	A first-principles study on atomic-scale pore design of microporous carbon electrodes for lithium-ion batteries. Nanoscale Advances, 2022, 4, 5378-5391.	2.2	4
72863	One-dimensional metal thiophosphate nanowires by cluster assembly. Nanoscale, 0, , .	2.8	0
72864	Establishment of a BaTiO3-based Computational Science Platform to Predict Multi-component Properties. Journal of Sensor Science and Technology, 2022, 31, 318-323.	0.1	0
72865	Schottky barrier heights and mechanism of charge transfer at metal-Bi2OS2 interfaces. Science China Materials, 2023, 66, 811-818.	3.5	6
72866	Tunable Band Alignment in the Arsenene/WS2 Heterostructure by Applying Electric Field and Strain. Crystals, 2022, 12, 1390.	1.0	4
72867	On the Possible Magnetic Properties of Ultrathin Mn2GaC Films on Al2O3 Substrates. JETP Letters, 2022, 116, 323-328.	0.4	2
72868	Gap opening at the Dirac point of graphene on Cu(111): Hybridization versus sublattice symmetry breaking. Surface Science, 2022, , 122196.	0.8	0
72869	Assembly-induced spin transfer and distance-dependent spin coupling in atomically precise AgCu nanoclusters. Nature Communications, 2022, 13, .	5.8	18
72870	Pressure-induced structural phase transitions of zirconium: an ab initio study based on statistical ensemble theory. Journal of Physics Condensed Matter, 2022, 34, 505402.	0.7	1

#	Article	IF	Citations
72871	Structure Effect on the Response of ZnGa2O4 Gas Sensor for Nitric Oxide Applications. Nanomaterials, 2022, 12, 3759.	1.9	4
72872	Computational study of CO2 methanation over two-dimensional molybdenum carbide catalysts. International Journal of Hydrogen Energy, 2023, 48, 24826-24832.	3.8	1
72873	Theoretical Study of ZnS Monolayer Adsorption Behavior for CO and HF Gas Molecules. ACS Omega, 2022, 7, 40176-40183.	1.6	2
72874	Manipulating the Microenvironment of Surfactant-Encapsulated Pt Nanoparticles to Promote Activity and Selectivity. ACS Catalysis, 2022, 12, 13930-13940.	5.5	7
72875	Photocatalytic hydrogen generation from overall water splitting with direct Z-scheme driven by two-dimensional InTe/Bismuthene heterostructure. International Journal of Hydrogen Energy, 2023, 48, 138-146.	3.8	20
72877	Compositional effects in the liquid Feâ€“Niâ€“C system at high pressure. Physics and Chemistry of Minerals, 2022, 49, .	0.3	0
72878	Sulfur-induced dynamic reconstruction of iron-nitrogen species for highly active neutral oxygen reduction reactions. Science China Chemistry, 2022, 65, 2476-2486.	4.2	3
72879	Achieving Low Lattice Thermal Conductivity in Halfâ€Heusler Compound LiCdSb via Zintl Chemistry. Small Science, 0, , 2200065.	5.8	4
72880	Stability of Pt₁₀Sn₃ Clusters Supported on Î³â€Al₂O₃ in Oxidizing Environment: a DFT Comparison of Alloying and Size Effects. ChemCatChem, 2022, 14, .	1.8	2
72881	A Novel Insight into the Strain Effect of T _{2g} Mode Splitting and Bandgap in Diamond. Physica Status Solidi - Rapid Research Letters, 0, , 2200344.	1.2	0
72882	In operandoâ€formed interface between silver and perovskite oxide for efficient electroreduction of carbon dioxide to carbon monoxide. , 2023, 5, .		2
72883	Electronic Band Structure and Surface States in Dirac Semimetal LaAgSb2. Materials, 2022, 15, 7168.	1.3	4
72884	Chemical Vapor Transport Synthesis of Cu(VO)₂(AsO₄)₂ With Two Distinct Spin-1/2 Magnetic Ions. Inorganic Chemistry, 2022, 61, 16539-16548.	1.9	3
72885	Zinc doping induced WS2 accelerating the HER and ORR kinetics: A theoretical and experimental validation. Catalysis Today, 2023, 423, 113921.	2.2	2
72886	Quasiplastic deformation in shocked nanocrystalline boron carbide: Grain boundary sliding and local amorphization. Journal of the European Ceramic Society, 2023, 43, 208-216.	2.8	12
72887	Niâ€Doped CuO Nanoarrays Activate Urea Adsorption and Stabilizes Reaction Intermediates to Achieve Highâ€Performance Urea Oxidation Catalysts. Advanced Science, 2022, 9, .	5.6	24
72888	Ab Initio Investigation of Planar Defects in Immm-Ni2(Cr,Mo,W) Strengthened HAYNES 244 Alloy. Metallurgical and Materials Transactions A: Physical Metallurgy and Materials Science, 2022, 53, 4188-4206.	1.1	2
72889	Magnetotransport around the Morin transition in Î±-Fe₂O₃ single crystals. Journal of Applied Physics, 2022, 132, 163903.	1.1	0

#	Article	IF	Citations
72890	Large Distortion of Fused Aromatics on Dielectric Interlayers Quantified by Photoemission Orbital Tomography. ACS Nano, 2022, 16, 17435-17443.	7.3	5
72891	A unified superatomic-molecule theory for local aromaticity in Ï€-conjugated systems. National Science Review, 2023, 10, .	4.6	4
72892	The SWSe-BP vdW Heterostructure as a Promising Photocatalyst for Water Splitting with Power Conversion Efficiency of 19.4%. ACS Omega, 2022, 7, 37061-37069.	1.6	4
72893	Investigations on the structural, electrical, magnetic and 57Fe MÃ¶ssbauer studies of YFeO3. Ceramics International, 2023, 49, 7500-7505.	2.3	1
72894	Potential dependence of OER/EOP performance on heteroatom-doped carbon materials by grand canonical density functional theory. Journal of Chemical Physics, 2022, 157, .	1.2	4
72895	Br Vacancy Defects Healed Perovskite Indoor Photovoltaic Modules with Certified Power Conversion Efficiency Exceeding 36%. Advanced Science, 2022, 9, .	5.6	18
72896	Electronic Properties and Chemical Bonding in V2FeSi and Fe2VSi Heusler Alloys. Crystals, 2022, 12, 1546.	1.0	3
72897	Photocatalytic Oxidative Dehydrogenation of Propane for Selective Propene Production with TiO₂. Jacs Au, 2022, 2, 2607-2616.	3.6	3
72898	Crossover from Ising- to Rashba-type superconductivity in epitaxial Bi2Se3/monolayer NbSe2 heterostructures. Nature Materials, 2022, 21, 1366-1372.	13.3	16
72899	The effects of point defect type, location, and density on the Schottky barrier height of Au/MoS2 heterojunction: a first-principles study. Scientific Reports, 2022, 12, .	1.6	6
72900	A novel two-dimensional C36 fullerene network; an isotropic, auxetic semiconductor with low thermal conductivity and remarkable stiffness. Materials Today Nano, 2023, 21, 100280.	2.3	11
72901	High thermoelectric performance of intrinsic few-layers T-HfSe2. Materials Today Communications, 2022, 33, 104789.	0.9	0
72902	Momentum-inversion symmetry breaking on the Fermi surface of magnetic topological insulators. Physical Review Materials, 2022, 6, .	0.9	3
72903	Generating two-dimensional ferromagnetic charge density waves via external fields. Physical Review B, 2022, 106, .	1.1	0
72904	Theoretical investigation of phase transitions in the shape memory alloy NiTi. Physical Review B, 2022, 106, .	1.1	7
72905	A study of anisotropic thermoelectric properties of bulk Germanium Sulfide in its Pnma phase: a combined first-principles and machine-learning approach. Physica Scripta, 2022, 97, 125804.	1.2	6
72906	Energy-Level Alignment of Zn-Phthalocyanine-Physisorbed Graphitic Carbon Nitride: Effects of Corrugation. Journal of Physical Chemistry C, 2022, 126, 18208-18215.	1.5	2
72907	Solid solution softening and hardening in binary BCC alloys. Acta Materialia, 2023, 243, 118440.	3.8	12

#	Article	IF	Citations
72908	Multiscale Structural Gel Polymer Electrolytes with Fast Li⁺ Transport for Longâ€Life Li Metal Batteries. Advanced Functional Materials, 2023, 33, .	7.8	37
72909	Structural and electrical properties of Mgâ€“Cu- and Mgâ€“Cuâ€“Li-doped bismuth niobate semiconductors with the pyrochlore structure. Ceramics International, 2022, , .	2.3	3
72910	EXPERIMENTAL AND COMPUTATIONAL STUDY OF THE STRUCTURE AND BONDING INTERACTIONS IN LAYERED COMPOUNDS OF MOLYBDENUM DISULFIDE WITH GUANIDINE DERIVATIVES. Journal of Structural Chemistry, 2022, 63, 1558-1567.	0.3	1
72911	Facile phase transition to Î²- from Î±-SnSe by uniaxial strain. Current Applied Physics, 2022, , .	1.1	0
72912	Tuning the Nonradiative Electronâ€“Hole Recombination with Defects in Monolayer Black Phosphorus. Journal of Physical Chemistry Letters, 2022, 13, 10162-10168.	2.1	7
72913	Charge self-regulation in 1T'''-MoS2 structure with rich S vacancies for enhanced hydrogen evolution activity. Nature Communications, 2022, 13, .	5.8	56
72914	Structural and Electronic Effects at the Interface between Transition Metal Dichalcogenide Monolayers (MoS2, WSe2, and Their Lateral Heterojunctions) and Liquid Water. International Journal of Molecular Sciences, 2022, 23, 11926.	1.8	0
72915	3D Sodiophilic Ti₃C₂ MXene@g-C₃N₄ Hetero-Interphase Raises the Stability of Sodium Metal Anodes. ACS Nano, 2022, 16, 17197-17209.	7.3	26
72916	Simultaneous enhancement of hardness and wear and corrosion resistance of highâ€entropy transitionâ€metal nitride. Journal of the American Ceramic Society, 2023, 106, 1356-1368.	1.9	1
72917	Theoretical Study of Oxygen Reduction Reaction Mechanism in Metal-Free Carbon Materials: Defects, Structural Flexibility, and Chemical Reaction. ACS Nano, 2022, 16, 16394-16401.	7.3	13
72918	Graphene/Cs₂PbI₂Cl₂ van der Waals heterostructure with tunable Schottky barriers and contact types. Journal of Applied Physics, 2022, 132, 165101.	1.1	0
72919	Decentering the Symmetry via Docking B and F in the KBe₂BO₃F₂-Family Structure. Inorganic Chemistry, 2022, 61, 17855-17863.	1.9	0
72920	Directing the Surface Atomic Geometry on Copper Sulfide for Enhanced Electrochemical Nitrogen Reduction. ACS Catalysis, 2022, 12, 13638-13648.	5.5	5
72921	Optoelectronics of Atomic Metalâ€“Semiconductor Interfaces in Tin-Intercalated MoS₂. ACS Nano, 2022, 16, 17080-17086.	7.3	5
72922	Facet-Dependent Gas Adsorption Selectivity on ZnO: A DFT Study. Chemosensors, 2022, 10, 436.	1.8	4
72923	A data-driven and topological mapping approach for the a priori prediction of stable molecular crystalline hydrates. Proceedings of the National Academy of Sciences of the United States of America, 2022, 119, .	3.3	3
72924	Computational Insights into Ru, Pd and Pt fcc Nano-Catalysts from Density Functional Theory Calculations: The Influence of Long-Range Dispersion Corrections. Catalysts, 2022, 12, 1287.	1.6	2
72925	Dynamic Polarization Behaviors of Equimolar CoCrFeNi High-Entropy Alloy Compared with 304 Stainless Steel in 0.5 M H2SO4 Aerated Aqueous Solution. Materials, 2022, 15, 6976.	1.3	1

#	Article	IF	Citations
72926	Ionicity and hydrogen affinity of water layers on metals. , 0, , .		0
72927	Creating two-dimensional solid helium via diamond lattice confinement. Nature Communications, 2022, 13, .	5.8	2
72928	Influence of compressive strain on the hydrogen storage capabilities of graphene: a density functional theory study. Bulletin of Materials Science, 2022, 45, .	0.8	6
72930	Two-dimensional heterostructures formed by graphenelike ZnO and MgO monolayers for optoelectronic applications. Physical Review Materials, 2022, 6, .	0.9	2
72931	<mml:math xmlns:mml="http://www.w3.org/1998/Math/MathML"><mml:mrow><mml:mi>J</mml:mi><mml:mo>=</mml:mo><mml:mn>0</mml:mn> nonmagnetic insulating state in <mml:math xmlns:mml="http://www.w3.org/1998/Math/MathML"><mml:mrow><mml:msub><mml:mi		

#	Article	IF	Citations
72945	Pair vacancy defects in Î²-Ga2O3 crystal: Ab initio study. Optical Materials: X, 2022, 16, 100200.	0.3	2
72946	Tunable magnetic anisotropy in two-dimensional <mml:math xmlns:mml="http://www.w3.org/1998/Math/MathML"><mml:mrow><mml:mi>Cr</mml:mi><mml:msub><mml:mi>X</mml:mi></mml:msub></mml:mrow></mml:math> heterostructures. Physical Review B, 2022, 106, .	1.1	5
72947	Multi-twinned gold nanoparticles with tensile surface steps for efficient electrocatalytic CO2 reduction. Science China Chemistry, 0, , .	4.2	1
72948	Simultaneous electrical and thermal rectification in a monolayer lateral heterojunction. Science, 2022, 378, 169-175.	6.0	46
72949	Van der Waals lattice-induced colossal magnetoresistance in Cr2Ge2Te6 thin flakes. Nature Communications, 2022, 13, .	5.8	5
72950	AI-accelerated materials informatics method for the discovery of ductile alloys. Journal of Materials Research, 2022, 37, 3491-3504.	1.2	4
72951	Comparative Study of the Compressibility of M3V2O8 (M = Cd, Zn, Mg, Ni) Orthovanadates. Crystals, 2022, 12, 1544.	1.0	7
72952	Morphology-controlled synthesis of Cu2O encapsulated phase change materials: Photothermal conversion and storage performance in visible light regime. Chemical Engineering Journal, 2023, 454, 140089.	6.6	13
72953	Electron and configuration engineering of atomic Cu and multi-oxidated Cu2+1O centers via gasifiable reductant strategy for efficient oxygen reduction toward Zn-air battery. Nano Research, 2023, 16, 2383-2391.	5.8	2
72954	Attenuating metal-substrate conjugation in atomically dispersed nickel catalysts for electroreduction of CO2 to CO. Nature Communications, 2022, 13, .	5.8	71
72955	Transition metal atom adsorption on the titanium carbide MXene: Trends across the periodic table for the bare and O-terminated surfaces. Physical Review Materials, 2022, 6, .	0.9	2
72956	Nanoscale coherent phonon spectroscopy. Science Advances, 2022, 8, .	4.7	12
72957	26.2: Invited Paper: Computational chemistry study of an aggregationâ€induced delayed fluorescence material: synthesis and properties. Digest of Technical Papers SID International Symposium, 2022, 53, 286-299.	0.1	0
72958	First-Principles Investigation of Morphological Evolution of Tungsten Growth on Alumina Surfaces: Implications for Thin-Film Growth. ACS Applied Nano Materials, 2022, 5, 16365-16375.	2.4	2
72959	Half-integer Wannier diagram and Brown-Zak fermions of graphene on hexagonal boron nitride. Physical Review B, 2022, 106, .	1.1	3
72960	Theoretical calculation and experimental research for structural stability and electronic properties induced by certain cluster defects in ADP crystal. Optical Materials Express, 2022, 12, 4422.	1.6	1
72961	Efficient hydrogen evolution reaction due to topological polarization. Physical Review B, 2022, 106, .	1.1	4
72962	Berry curvature induced anomalous Hall conductivity in the magnetic topological oxide double perovskite <mml:math xmlns:mml="http://www.w3.org/1998/Math/MathML"><mml:mrow><mml:msub><mml:mi>Sr</mml:mi><mml:mn>2</mml:mn></mml:msub></mml:mrow></mml:math> Physical Review B, 2022, 106, .	1.1	6

#	Article	IF	Citations
72963	Unexpected Redispersion Effect of Au Nanoclusters for Enormous Enhancement of Electrocatalytic Stability and Activity. Advanced Functional Materials, 2022, 32, .	7.8	9
72964	Dual Metalâ€Assisted Defect Engineering towards Highâ€Performance Perovskite Solar Cells. Advanced Functional Materials, 2022, 32, .	7.8	16
72965	Wide Bandgap Nanocoatings for Polymer Dielectric with Outstanding Electrical Strength. Advanced Materials Interfaces, 2022, 9, .	1.9	10
72966	Enhanced superconductivity and electron correlations in intercalated <mml:math xmlns:mml="http://www.w3.org/1998/Math/MathML"><mml:msub><mml:mi>ZrTe</mml:mi><mml:mn>3</mml:mn></mml:msub></mml:math> Physical Review B, 2022, 106, .	1.1	0
72967	Recommender system for discovery of inorganic compounds. Npj Computational Materials, 2022, 8, .	3.5	2
72968	Two-Dimensional Nanosheets of Titanium Carbonitride Ti₃CNT_x MXene for Microwave Absorption in the X and Ku Bands. ACS Applied Nano Materials, 2022, 5, 17133-17141.	2.4	4
72969	Constitutional isomerism of the linkages in donorâ€“acceptor covalent organic frameworks and its impact on photocatalysis. Nature Communications, 2022, 13, .	5.8	63
72970	Spontaneous Ferromagnetism Induced Topological Transition in <mml:math xmlns:mml="http://www.w3.org/1998/Math/MathML" display="inline"><mml:mrow><mml:msub><mml:mrow><mml:mi>EuB</mml:mi></mml:mrow><mml:mrow><mml:mn>6</mml:mn></mml:mrow> Physical Review Letters, 2022, 129, .	2.9	8
72971	Theoretical study on photocatalytic performance of ZnO/C2N heterostructure towards high efficiency water splitting. Frontiers in Chemistry, 0, 10, .	1.8	0
72972	Spatiotemporal imaging of charge transfer in photocatalyst particles. Nature, 2022, 610, 296-301.	13.7	170
72973	Magnetotransport in Graphene/Pb_{0.24}Sn_{0.76}Te Heterostructures: Finding a Way to Avoid Catastrophe. ACS Nano, 2022, 16, 19346-19353.	7.3	1
72974	Density functional theory investigations into the magnetic ordering of <mml:math xmlns:mml="http://www.w3.org/1998/Math/MathML"><mml:mrow><mml:msub><mml:mi mathvariant="normal">U</mml:mi><mml:mn>3</mml:mn></mml:msub><mml:msub><mml:mi mathvariant="normal">O</mml:mi><mml:mn>8</mml:mn></mml:msub></mml:mrow></mml:math>. Physical Review Materials, 2022, 6, .	0.9	3
72975	Highly flexible and superhydrophobic MOF nanosheet membrane for ultrafast alcohol-water separation. Science, 2022, 378, 308-313.	6.0	97
72976	NO Degradation on the Anatase TiO₂ (001) Surface in the Presence of Water. Journal of Physical Chemistry C, 2022, 126, 17544-17553.	1.5	2
72977	Waterâ€“Gas Shift Reaction over Au(111): The Effect of Potassium from a First-Principles-Based Microkinetic Model Analysis. Journal of Physical Chemistry C, 2022, 126, 17579-17588.	1.5	6
72978	Band Alignment Engineering in ns² Electrons Doped Metal Halide Perovskites. Laser and Photonics Reviews, 2023, 17, .	4.4	26
72979	Doping an Oxophilic Metal into a Metal Carbide: Unravelling the Synergy between the Microstructure of the Catalyst and Its Activity and Selectivity for Hydrodeoxygenation. ACS Catalysis, 2022, 12, 13980-13998.	5.5	5
72980	Excitons at the Phase Transition of 2D Hybrid Perovskites. ACS Photonics, 2022, 9, 3609-3616.	3.2	16

#	Article	IF	Citations
72981	Structural and electronic properties of rare-earth chromites: A computational and experimental study. Physical Review B, 2022, 106, .	1.1	2
72982	Compositionâ€Controllable Syntheses and Property Modulations from 2D Ferromagnetic Fe₅Se₈ to Metallic Fe₃Se₄ Nanosheets. Advanced Materials, 2023, 35, .	11.1	16
72983	Thickness- and Twist-Angle-Dependent Interlayer Excitons in Metal Monochalcogenide Heterostructures. ACS Nano, 2022, 16, 18695-18707.	7.3	3
72984	Templated encapsulation of platinum-based catalysts promotes high-temperature stability to 1,100â€‰Â°C. Nature Materials, 2022, 21, 1290-1297.	13.3	44
72985	A Brand-New Hybrid Structure with Advantageous Electron State for Ultrahigh Energy Density Asymmetric Supercapacitors. ACS Energy Letters, 2022, 7, 4204-4214.	8.8	9
72986	A Novel Two-Dimensional ZnSiP2 Monolayer as an Anode Material for K-Ion Batteries and NO2 Gas Sensing. Molecules, 2022, 27, 6726.	1.7	2
72987	Thermal Percolation of Antiperovskite Superionic Conductor into Porous MXene Scaffold for Highâ€Capacity and Stable Lithium Metal Battery. Small Methods, 2022, 6, .	4.6	1
72988	Temperatureâ€dependent elastic and thermodynamic properties of ZrC, HfC, and their solid solutions (Zr_{0.5}Hf_{0.5})C. Journal of the American Ceramic Society, 2023, 106, 2024-2036.	1.9	2
72989	Effect of temperature on CO oxidation over Pt(111) in two-dimensional confinement. Journal of Chemical Physics, 2022, 157, 144701.	1.2	1
72990	Strain-induced enhancement of carrier mobility and optoelectronic properties in antimonene/germanane vdW heterostructure. Applied Physics A: Materials Science and Processing, 2022, 128, .	1.1	1
72991	Coordination Engineering of Singleâ€Atom Iron Catalysts for Oxygen Evolution Reaction. ChemCatChem, 2022, 14, .	1.8	9
72992	Anchoring Metalâ€Organic Frameworkâ€Derived ZnTe@C onto Elastic Ti₃C₂T_x MXene with 0D/2D Dual Confinement for Ultrastable Potassiumâ€Ion Storage. Advanced Energy Materials, 2022, 12, .	10.2	18
72993	Roomâ€Temperature Solidâ€State Transformation of Na4SnS4Â·14H2O into Na4Sn2S6Â·5H2O: an Unusual Epitaxial Reaction Including Bond Formation, Mass Transport, and Ionic Conductivity. Chemistry - A European Journal, 0, , .	1.7	2
72994	Evolution of defect structures leading to high ZT in GeTe-based thermoelectric materials. Nature Communications, 2022, 13, .	5.8	59
72995	Prediction on local structure and properties of LiCl-KCl-AlCl3 ternary molten salt with deep learning potential. Journal of Molecular Liquids, 2023, 375, 120689.	2.3	4
72996	New Ion Substitution Method to Enhance Electrochemical Reversibility of Coâ€Rich Layered Materials for Liâ€Ion Batteries. Advanced Energy Materials, 2023, 13, .	10.2	11
72997	Penta-graphene and phagraphene: thermal expansion, linear compressibility, and Poissonâ€™s ratio. Journal of Physics Condensed Matter, 2022, 34, 505301.	0.7	3
72998	CAT: A Compound Attachment Tool for the Construction of Composite Chemical Compounds. Journal of Chemical Information and Modeling, 0, , .	2.5	0

#	Article	IF	Citations
72999	Band-folding-driven high tunnel magnetoresistance ratios in (111)-oriented junctions with <mml:math xmlns:mml="http://www.w3.org/1998/Math/MathML"><mml:msub><mml:mi>SrTiO</mml:mi><mml:mn>3</mml:mn></mml:msub></m barriers. Physical Review B, 2022, 106, .	3.7	3
73000	ZnMn₂O₄/Carbon Composite Recycled from Spent Zinc-Carbon Batteries for Zn-Air Battery Applications. Journal of the Electrochemical Society, 2022, 169, 100544.	1.3	3
73001	Reversal of anomalous Hall conductivity by perpendicular electric field in 2D WSe2/VSe2 heterostructure. Communications Physics, 2022, 5, .	2.0	7
73002	Caâ€vacancy effect on the stability of substitutional divalent cations in calciumâ€deficient hydroxyapatite. Journal of the American Ceramic Society, 2023, 106, 1587-1596.	1.9	1
73003	Selfâ€Intercalated Magnetic Heterostructures in 2D Chromium Telluride. Advanced Functional Materials, 2023, 33, .	7.8	12
73004	Revealing the effect of Ni NPs on the ignition characteristics of Al/ethanol nanofluid fuel: Experimental and DFT insights. Applied Surface Science, 2022, , 155508.	3.1	0
73005	Hydrogenation of carbon dioxide to formic acid over Pd doped thermally activated Ni/Al layered double hydroxide. Reaction Kinetics, Mechanisms and Catalysis, 2022, 135, 3007-3019.	0.8	1
73006	Hydrolysis mechanism of Li-argyrodite Li6PS5Cl in air. Rare Metals, 2023, 42, 47-55.	3.6	6
73007	Dehydrogenation versus deprotonation of disaccharide molecules in vacuum: a thorough theoretical investigation. Royal Society Open Science, 2022, 9, .	1.1	0
73008	Hydrogen-Induced Restructuring of a Cu(100) Electrode in Electroreduction Conditions. Journal of the American Chemical Society, 2022, 144, 19284-19293.	6.6	20
73009	Atomic and electronic structures of nitrogen vacancies in silicon nitride: Emergence of floating gap states. Physical Review B, 2022, 106, .	1.1	3
73010	Emergent MoirÃ© Phonons Due to Zone Folding in WSe₂â€“WS₂ Van der Waals Heterostructures. ACS Nano, 2022, 16, 16260-16270.	7.3	10
73011	Feâ€“Nâ€“C Boosts the Stability of Supported Platinum Nanoparticles for Fuel Cells. Journal of the American Chemical Society, 2022, 144, 20372-20384.	6.6	50
73012	First-Principles Investigation of Structural, Thermoelectric, and Optical Properties of Half-Heusler Compound ScRhTe under Varied Pressure. Crystals, 2022, 12, 1472.	1.0	3
73013	Observation of Surface Superconductivity in a 3D Dirac Material. Advanced Functional Materials, 2022, 32, .	7.8	3
73014	A Review on the Molecular Modeling of Argyrodite Electrolytes for All-Solid-State Lithium Batteries. Energies, 2022, 15, 7288.	1.6	7
73015	A Mechanistic Study of Methanol Steam Reforming on Ni2P Catalyst. Catalysts, 2022, 12, 1174.	1.6	7
73016	Synthesis, Crystal Structures, Mechanical Properties, and Formation Mechanisms of Cubic Tungsten Nitrides. Chemistry of Materials, 2022, 34, 9261-9269.	3.2	3

#	Article	IF	Citations
73017	Rock-Salt-Ordered Nitrohalide Double Antiperovskites: Theoretical Design and Experimental Verification. Chemistry of Materials, 2022, 34, 9098-9103.	3.2	2
73018	High-pressure II-III phase transition in solid hydrogen: Insights from state-of-the-art ab initio calculations. Physical Review Research, 2022, 4, .	1.3	1
73019	Highly Dispersed Ruâ€“Co Nanoparticles Interfaced With Nitrogenâ€Doped Carbon Polyhedron for High Efficiency Reversible Liâ€“O₂ Battery. Small, 2022, 18, .	5.2	4
73020	Effects of ferromagnetism in ab initio calculations of basic structural parameters of Fe-A (A = Mo, Nb,) Tj ETQq1 1 0.784314 rgBT /Over	0.6	3
73021	Recent progress of iron-based electrocatalysts for nitrogen reduction reaction. Journal of Materials Science and Technology, 2023, 140, 121-134.	5.6	13
73022	Hydrogen Bonding Promotes Alcohol Câ€“C Coupling. Journal of the American Chemical Society, 2022, 144, 18986-18994.	6.6	16
73023	Carrier-driven magnetic and topological phase transitions in two-dimensional IIIâ€“V semiconductors. Nano Research, 0, , .	5.8	2
73024	Nonunique fraction of Fock exchange for defects in two-dimensional materials. Physical Review B, 2022, 106, .	1.1	3
73025	Quinary, Senary, and Septenary High Entropy Alloy Nanoparticle Catalysts from Core@Shell Nanoparticles and the Significance of Intraparticle Heterogeneity. ACS Nano, 2022, 16, 18873-18885.	7.3	32
73026	Itinerant antiferromagnetism in <mml:math xmlns:mml="http://www.w3.org/1998/Math/MathML"><mml:mrow><mml:msub><mml:mi>Co</mml:mi><mml:mn>3</mml:mn></mml mathvariant="normal">S</mml:mi><mml:mrow><mml:mn>4</mml:mn><mml:mo>â^’</mml:mo><mml:mi>Î´</mml:mi></mml:mrow> Physical Review B, 2022, 106, .	1.1	4
73027	Robust UV Plasmonic Properties of Co-Doped Ag2Te. Crystals, 2022, 12, 1469.	1.0	0
73028	Low-energy moirÃ© phonons in twisted bilayer van der Waals heterostructures. Physical Review B, 2022, 106, .	1.1	5
73029	Temperatureâ€Programmed Separation of Hexane Isomers by a Porous Calcium Chloranilate Metalâ€Organic Framework. Angewandte Chemie, 2022, 134, .	1.6	4
73030	First-principles equationÂof state of CHON resin for inertial confinement fusion applications. Physical Review E, 2022, 106, .	0.8	5
73031	Tailoring the superposition of finite-momentum valley exciton states in transition-metal dichalcogenide monolayers by using polarized twisted light. Physical Review B, 2022, 106, .	1.1	4
73032	Topological defect and sp3/sp2 carbon interface derived from ZIF-8 with linker vacancies for oxygen reduction reaction. Carbon, 2023, 203, 76-87.	5.4	10
73033	An unconstrained approach to systematic structural and energetic screening of materials interfaces. Nature Communications, 2022, 13, .	5.8	8
73034	Quantum spin Hall effect from multiscale band inversion in twisted bilayer <mml:math xmlns:mml="http://www.w3.org/1998/Math/MathML"><mml:mrow><mml:msub><mml:mi>Bi</mml:mi><mml:mn>23</mml:mn></mml:msub><mml:mn> Physical Review Research, 2022, 4, .	2.3	5

#	Article	IF	Citations
73035	Direct production of olefins from syngas with ultrahigh carbon efficiency. Nature Communications, 2022, 13, .	5.8	18
73036	Enhanced Crystallinity of Covalent Organic Frameworks Formed Under Physical Confinement by Exfoliated Graphene. Small, 2022, 18, .	5.2	1
73037	A Novel Monoclinic Phase and Electrically Tunable Magnetism of van der Waals Layered Magnet CrTe₂. Chinese Physics B, 0, , .	0.7	1
73038	Transient electron scavengers modulate carrier density at a polar/nonpolar perovskite oxide heterojunction. Physical Review Materials, 2022, 6, .	0.9	1
73039	Polymeric Hydronitrogen N₄H: A Promising High-Energy-Density Material and High-Temperature Superconductor. ACS Applied Materials & Interfaces, 2022, 14, 49986-49994.	4.0	2
73040	Electro-Design of Bimetallic PdTe Electrocatalyst for Ethanol Oxidation: Combined Experimental Approach and Ab Initio Density Functional Theory (DFT)â€"Based Study. Nanomaterials, 2022, 12, 3607.	1.9	2
73041	Singleâ€Atomic Pd Embedded 2D gâ€C₃N₄ Homogeneous Catalyst Analogues for Efficient LMCT Induced Fullâ€Visibleâ€Light Photocatalytic Suzuki Coupling**. ChemistrySelect, 2022, 7, .	0.7	4
73042	Continuous epitaxy of single-crystal graphite films by isothermal carbon diffusion through nickel. Nature Nanotechnology, 2022, 17, 1258-1264.	15.6	25
73043	Dynamics of CO₂ Dissociative Chemisorption on W(110). Journal of Physical Chemistry C, 2022, 126, 17935-17941.	1.5	0
73044	Partial breakdown of translation symmetry at a structural quantum critical point associated with a ferroelectric soft mode. Physical Review B, 2022, 106, .	1.1	1
73045	Two-dimensional obstructed atomic insulators with fractional corner charge in the <mml:math xmlns:mml="http://www.w3.org/1998/Math/MathML"><mml:mrow><mml:msub><mml:mrow><mml:mi>M</mml:mi>	1.1	8
73046	Crystal Structures and Electronic Properties of BaAu Compound under High Pressure. Materials, 2022, 15, 7381.	1.3	0
73048	Quantum nanomagnets in on-surface metal-free porphyrin chains. Nature Chemistry, 2023, 15, 53-60.	6.6	28
73049	Al³⁺ Introduction Hydrated Vanadium Oxide Induced High Performance for Aqueous Zincâ€Ion Batteries. Small, 2022, 18, .	5.2	20
73050	Regulating nitrogen vacancies within graphitic carbon nitride to boost photocatalytic hydrogen peroxide production. SusMat, 2022, 2, 617-629.	7.8	17
73051	Temperature-dependent structural, mechanical, and thermodynamic properties of B2-phase Ti2AlNb for aerospace applications. Journal of Materials Science, 2022, 57, 19553-19570.	1.7	4
73052	Computational Design of a Strain-Induced 2D/2D g-C₃N₄/ZnO S-Scheme Heterostructured Photocatalyst for Water Splitting. ACS Applied Energy Materials, 2022, 5, 13997-14007.	2.5	16
73053	Designing TiO2/Au/Prussian blue heterostructures nanorod arrays for ultra-stable cycle and ultra-fast response electrochromism. Nano Research, 2023, 16, 3294-3303.	5.8	7

#	Article	IF	Citations
73054	Effect of stacking type and magnetic moment in spin-valley polarized MoS₂â€“MoSe₂ heterobilayers. AIP Advances, 2022, 12, 105214.	0.6	0
73055	Looking beyond Adsorption Energies to Understand Interactions at Surface using Machine Learning. ChemistrySelect, 2022, 7, .	0.7	1
73056	Prediction for high superconducting ternary hydrides below megabar pressure. Journal of Physics Condensed Matter, 2022, 34, 505404.	0.7	7
73057	Effect of hexagonality on the pressure-dependent lattice dynamics of 4H-SiC. New Journal of Physics, 2022, 24, 113015.	1.2	4
73058	Cyclo[18]carbon Formation from C₁₈Br₆ and C₁₈(CO)₆ Precursors. Journal of Physical Chemistry Letters, 2022, 13, 10318-10325.	2.1	7
73059	Exploring the Metalâ€“Insulator Transition in (Ga,Mn)As by Molecular Absorption. Nano Letters, 2022, 22, 9190-9197.	4.5	0
73060	Strongly Modulated Exfoliation and Functionalization of MXenes with Rationally Designed Groups in Polymer: A Theoretical Study. Chemistry of Materials, 2022, 34, 9414-9424.	3.2	8
73061	Active cation-integration high-entropy Prussian blue analogues cathodes for efficient Zn storage. Nano Research, 2023, 16, 2486-2494.	5.8	16
73062	Modulating the optical and electrical properties of MoSe2 (Molybdenum diselenide) and WS2 (Tungsten disulfide) monolayer by the adsorption of halogen (F, Cl, Br, I and At) atoms. Optical and Quantum Electronics, 2022, 54, .	1.5	1
73063	Phonon Inelastic Scattering in Ultrathin HfO2-Based Layer-by-Layer Nanostructure. International Journal of Thermophysics, 2022, 43, .	1.0	0
73064	Comprehensive Study of Electronic, Optical, and Thermophysical Properties of Metavanadates CaV₂O₆ and MgV₂O₆. Inorganic Chemistry, 2022, 61, 17623-17633.	1.9	1
73065	First-Principles Study of the Phonon Lifetime and Low Lattice Thermal Conductivity of Monolayer Î³-GeSe: A Comparative Study. ACS Applied Nano Materials, 2022, 5, 15441-15448.	2.4	4
73066	Effect of Electrolyte Media on the Catalysis of Fe Phthalocyanine toward the Oxygen Reduction Reaction: Ab Initio Molecular Dynamics Simulations and Experimental Analyses. ACS Catalysis, 2022, 12, 12786-12799.	5.5	14
73067	On mechanical twinning in tetragonal lattice. Philosophical Magazine, 2023, 103, 119-136.	0.7	1
73068	First-principles determination of high thermal conductivity of PCF-graphene: A comparison with graphene. Applied Physics Letters, 2022, 121, .	1.5	8
73069	Attractive Electron Delocalization Behavior of FeCoMoPB Amorphous Nanoplates for Highly Efficient Alkaline Water Oxidation. Small, 2022, 18, .	5.2	11
73070	Magnetic anisotropy energies and metal-insulator transitions in monolayers of <mml:math xmlns:mml="http://www.w3.org/1998/Math/MathML"><mml:mrow><mml:mi>Î±</mml:mi><mml:mtext>â^’</mml:mtext><mml:msub><mml:mi>OsCl</mml:mi><mml:mn>3</mml:mn></mml:msub></mml:mrow></mml:math> and <mml:math xmlns:mml="http://www.w3.org/1998/Math/MathML"><mml:msub><mml:mi>OsCl</mml:mi><mml:mn>3</mml:mn></mml:msub></mml:math> on graphene. Physical Review B, 2022, 106, .	1.1	2
73071	Lithiation of a Silicon Oxide Cluster Adsorbed onto Graphene Oxide: Quantum-Chemical Simulation. Russian Journal of Inorganic Chemistry, 2022, 67, 1785-1793.	0.3	1

#	Article	IF	Citations
73072	Enhanced Oxide Reduction by Hydrogen at Cuprous Oxideâ€“Copper Interfaces near Ascending Step Edges. Journal of Physical Chemistry C, 2022, 126, 18645-18651.	1.5	1
73073	Computational insights into the energy storage of ultraporous MOFs NU-1501-M (M = Al or Fe): Protonization revealing and performance improving by decoration of superalkali clusters. International Journal of Hydrogen Energy, 2022, 47, 41034-41045.	3.8	5
73074	Efficient reduction of hexavalent chromium with microscale Fe/Cu bimetals: Efficiency and the role of Cu. Chinese Chemical Letters, 2023, 34, 107932.	4.8	3
73075	Photo-controllable Ion-Gated Metalâ€“Organic Framework MIL-53 Sub-nanochannels for Efficient Osmotic Energy Generation. ACS Nano, 2022, 16, 16343-16352.	7.3	12
73076	The spontaneous polarization of In-doped Î²-Ga₂O₃ by first-principles calculation. AIP Advances, 2022, 12, 105115.	0.6	1
73077	Tuning Dehalogenative Coupling of Br₂Py on Bimetallic Templates. Langmuir, 2022, 38, 13392-13400.	1.6	1
73078	Insight into the Stability and Properties of Znâ€Đoped KH ₂ PO ₄ Crystal by Hybrid Density Functional Theory. Crystal Research and Technology, 0, , 2200107.	0.6	0
73079	Unusual precipitation induced by solute segregation in coherent twin boundary in titanium alloys. Acta Materialia, 2023, 242, 118466.	3.8	5
73080	Emergent Behavior in Oxidation Catalysis over Single-Atom Pd on a Reducible CeO₂ Support via Mixed Redox Cycles. ACS Catalysis, 2022, 12, 12927-12941.	5.5	12
73081	Studies on the local structure of the Fâ€‰â‹…â€‰OH site in topaz by magic angle spinning nuclear magnetic resonance and Raman spectroscopy. European Journal of Mineralogy, 2022, 34, 507-521.	0.4	0
73082	Phase and polarization modulation in two-dimensional In ₂ Se ₃ via in situ transmission electron microscopy. Science Advances, 2022, 8, .	4.7	18
73083	Molecular Engineering of Quinone-Based Nickel Complexes and Polymers for All-Organic Li-Ion Batteries. Molecules, 2022, 27, 6805.	1.7	1
73084	Highly insulating phase of Bi2O2Se thin films with high electronic performance. Nano Research, 2023, 16, 3224-3230.	5.8	4
73085	Photocatalytic CO ₂ â€“toâ€“Ethylene Conversion over Bi ₂ S ₃ /CdS Heterostructures Constructed via Facile Cation Exchange. Research, 2022, 2022, .	2.8	4
73086	Understanding the lithiation limits of high-capacity organic battery anodes by atomic charge derivative analysis. Journal of Chemical Physics, 2022, 157, .	1.2	4
73087	Screening of the Transition Metal Single Atom Anchored on Î±-Borophene Catalysts as a Feasible Strategy for Electrosynthesis of Urea. Chemistry of Materials, 2022, 34, 9402-9413.	3.2	12
73088	Effect of localization on photoluminescence and zero-field splitting of silicon color centers. Physical Review B, 2022, 106, .	1.1	7
73089	Strain effects on high-harmonic generation in monolayer hexagonal boron nitride. Frontiers in Physics, 0, 10, .	1.0	1

#	Article	IF	Citations
73090	Simplified Kinetic Model for $$hbox {NH}_3$$-SCR Over Cu-CHA Based on First-Principles Calculations. Topics in Catalysis, 2023, 66, 743-749.	1.3	2
73091	First-Principles Insights on the Formation Mechanism of Innermost Layers of Solid Electrolyte Interphases on Carbon Anodes for Lithium-Ion Batteries. Nanomaterials, 2022, 12, 3654.	1.9	0
73092	Passivating {100} Facets of PbS Colloidal Quantum Dots via Perovskite Bridges for Sensitive and Stable Infrared Photodiodes. Advanced Functional Materials, 2023, 33, .	7.8	15
73093	High- versus Low-Spin Ni²⁺ in Elongated Octahedral Environments: Sr₂NiO₂Cu₂Se₂, Sr₂NiO₂Cu₂S₂, and Sr₂NiO₂Cu₂(Se_{1â€“x}S_x)₂. Chemistry of Materials, 2022, 34, 9503-9516.	3.2	1
73094	Competition of Iodide/Bromide Ions in the Formation of Methylammonium Lead Halide in Different Solvents. Journal of Physical Chemistry C, 2022, 126, 17656-17662.	1.5	1
73095	Strong Metalâ€“Sulfur Hybridization in the Conduction Band of the Quasi-One-Dimensional Transition-Metal Trichalcogenides: TiS₃ and ZrS₃. Journal of Physical Chemistry C, 2022, 126, 17647-17655.	1.5	4
73096	Discrete scale invariance of the quasi-bound states at atomic vacancies in a topological material. Proceedings of the National Academy of Sciences of the United States of America, 2022, 119, .	3.3	0
73097	Stable configurations and electronic properties of hydrogenated 10-18-6 graphyne. Applied Physics A: Materials Science and Processing, 2022, 128, .	1.1	0
73098	The mechanism of phase transition induced by oxygen doping in zirconium nitride thin films. Journal of Materials Science, 2022, 57, 18456-18467.	1.7	0
73099	New Spin-Polarized Electron Source Based on Alkali Antimonide Photocathode. Physical Review Letters, 2022, 129, .	2.9	12
73100	Unusual electric polarization behavior in elemental quasi-two-dimensional allotropes of selenium. Physical Review Materials, 2022, 6, .	0.9	1
73101	Heterostructures Stimulate Electricâ€Field to Facilitate Optimal Zn²⁺ Intercalation in MoS₂ Cathode. Small, 2022, 18, .	5.2	24
73102	First-principles calculations for the effect of energetic point defect formation on electronic properties of the Weyl MX family (Mâ€¯=â€¯Nb, Ta; Xâ€¯=â€¯P, As). Chinese Journal of Physics, 2023, 82, 15-30.	2.0	2
73103	Direct identification of the charge state in a single platinum nanoparticle on titanium oxide. Science, 2022, 378, 202-206.	6.0	24
73104	Direct strain correlations at the single-atom level in three-dimensional core-shell interface structures. Nature Communications, 2022, 13, .	5.8	10
73105	Magnetic and charge instabilities in vanadium-based topological kagome metals. Physical Review B, 2022, 106, .	1.1	1
73106	Promoting nickel oxidation state transitions in single-layer NiFeB hydroxide nanosheets for efficient oxygen evolution. Nature Communications, 2022, 13, .	5.8	101
73107	First-principles electronic structure investigation of HgBa₂Ca_{nâ^'1}Cu_nO_{2n+2+x} with the SCAN density functional. AIP Advances, 2022, 12, 105308.	0.6	0

#	Article	IF	Citations
73108	Prediction of structural, electronic, and lattice dynamical properties of ABO3 [A = K, Rb, Cs; B = Sn, Sb] perovskite compounds. Physica B: Condensed Matter, 2023, 649, 414355.	1.3	9
73109	Screening and design of 2D metalâ€“organic frameworks for hydrogen evolution reaction through controlling transition metals and heteroligands. Materials Today Nano, 2022, 20, 100278.	2.3	2
73110	Atomically engineered cobaltite layers for robust ferromagnetism. Science Advances, 2022, 8, .	4.7	5
73111	Atomistic Simulations of Defects Production under Ion Irradiation in Epitaxial Graphene on SiC. Physica Status Solidi - Rapid Research Letters, 2023, 17, .	1.2	1
73112	Accelerating equilibration in first-principles molecular dynamics with orbital-free density functional theory. Physical Review Research, 2022, 4, .	1.3	12
73113	V (Nb) Single Atoms Anchored by the Edge of a Graphene Armchair Nanoribbon for Efficient Electrocatalytic Nitrogen Reduction: A Theoretical Study. Inorganic Chemistry, 2022, 61, 17864-17872.	1.9	9
73114	Investigating the elastic, mechanical, and thermal properties of polycrystalline Mo2C under high pressure and high temperature. Ceramics International, 2023, 49, 7341-7349.	2.3	3
73115	Ferrate-Modified Biochar for Greenhouse Gas Mitigation: First-Principles Calculation and Paddy Field Trails. Agronomy, 2022, 12, 2661.	1.3	5
73116	Turning Electrocatalytic Activity Sites for the Oxygen Evolution Reaction on Brownmillerite to Oxyhydroxide. ACS Applied Materials & Interfaces, 2022, 14, 47560-47567.	4.0	10
73117	Experimental Study of Diamond-like Carbon Film on Aermet100 Steel and First-Principles Calculation of Interfacial Adhesion. ACS Applied Materials & Interfaces, 2022, 14, 48262-48275.	4.0	4
73118	Synthesis, structure, characterizations and theoretical research of a chain-like iodoplumbate hybrid. Molecular Crystals and Liquid Crystals, 2023, 757, 85-94.	0.4	0
73119	Niâ€“O₄ as Active Sites for Efficient Oxygen Evolution Reaction with Electronic Metalâ€“Support Interactions. ACS Applied Materials & Interfaces, 2022, 14, 47542-47548.	4.0	3
73120	Promoting the Oxygen Evolution Reaction via Morphological Manipulation of a Lamellar Nanorod-Assembled Ni(II)-Pyrazolate Superstructure. ACS Applied Materials & Interfaces, 2022, 14, 47775-47787.	4.0	3
73121	Deep learning interatomic potential for Ca-O system at high pressure. Physical Review Materials, 2022, 6, .	0.9	1
73122	Construction of Longâ€Range Magnetic Sequences on Different Surfaces of BaTiO3. ChemPhysChem, 0, , .	1.0	0
73123	Enhanced Thermoelectric Performance in Black Phosphorene via Tunable Interlayer Twist. Small, 2022, 18, .	5.2	11
73124	Exploring the Morphotropic Phase Boundary in Epitaxial PbHf_{1â€“x}Ti_xO₃ Thin Films. Chemistry of Materials, 2022, 34, 9613-9623.	3.2	3
73125	Enhanced Pd/aâ€WO₃/VO₂ Hydrogen Gas Sensor Based on VO₂ Phase Transition Layer. Small Methods, 2022, 6, .	4.6	5

#	Article	IF	Citations
73126	Role of Al additions in secondary phase formation in CoCrFeNi high entropy alloys. APL Materials, 2022, 10, 101108.	2.2	4
73127	Comprehensive Studies of Magnetic Transitions and Spinâ€“Phonon Couplings in the Tetrahedral Cobalt Complex Co(AsPh₃)₂I₂. Inorganic Chemistry, 2022, 61, 17123-17136.	1.9	5
73128	Tunable Photocatalytic Water Splitting Performance of Armchair MoSSe Nanotubes Realized by Polarization Engineering. Inorganic Chemistry, 2022, 61, 17353-17361.	1.9	7
73129	A Codoping Strategy for Efficient Planar Heterojunction Sb₂S₃ Solar Cells. Advanced Energy Materials, 2022, 12, .	10.2	22
73130	Stable CsPbBr₃ Achieved by Porphyrinâ€“Thiol Surface Management and Their Dualâ€Stimuli Responsive for Optical Encoding. Advanced Materials Interfaces, 2023, 10, .	1.9	5
73131	Unexpected features in the optical vibrational spectra of Î´-UO3. , 0, 1, .		0
73132	Gold-catalyzed reduction of metal ions for core-shell structures with subnanometer shells. Cell Reports Physical Science, 2022, 3, 101105.	2.8	3
73133	Entangled polarizations in ferroelectrics: A focused review of polar topologies. Acta Materialia, 2023, 243, 118485.	3.8	8
73134	Active Motif Change of Niâ€Fe Spinel Oxide by Ir Doping for Highly Durable and Facile Oxygen Evolution Reaction. Advanced Functional Materials, 2023, 33, .	7.8	17
73135	Cu-Doping-Modified Order State, Ferroelectric Property, Multiscale Inhomogeneities, and Local Structure in the Relaxor KTa_{1â€“x}Nb_xO₃ Crystal. Crystal Growth and Design, 2022, 22, 6766-6774.	1.4	1
73136	Multiple Dirac points including potential spin-orbit Dirac points in nonsymmorphic HfGe0.92Te. Science China: Physics, Mechanics and Astronomy, 2023, 66, .	2.0	6
73137	Theoretical and Comparative Analysis of Graphdiyne and Confined Flexible Nitrogen-Doped Graphdiyne-Supported Single-Atom Catalysts for Electrochemical Nitrogen Reduction. Journal of Physical Chemistry C, 2022, 126, 18282-18291.	1.5	4
73138	Theoretical Prediction of Two-Dimensional Metal Boride Mg₄B₆ as a High-Capacity Electrode Material for Lithium-Ion Batteries. Journal of Physical Chemistry C, 2022, 126, 17474-17481.	1.5	3
73140	Selective activation of four quasi-equivalent Câ€“H bonds yields N-doped graphene nanoribbons with partial corannulene motifs. Nature Communications, 2022, 13, .	5.8	5
73141	Monolayer Fullerene Networks as Photocatalysts for Overall Water Splitting. Journal of the American Chemical Society, 2022, 144, 19921-19931.	6.6	35
73142	Ising-like Magnetism in Quasi-Two-Dimensional Co(NO3)2Â·2H2O. Materials, 2022, 15, 7066.	1.3	0
73143	Stacking dependent ferroelectricity and antiferroelectricity in quasi-one-dimensional oxyhalides <mml:math xmlns:mml="http://www.w3.org/1998/Math/MathML"><mml:mrow><mml:mi>NbO</mml:mi><mml:msub><mml:mi>X</mml:mi><mml:mi><mml:n Physical Review Materials, 2022, 6, .	0.9	2
73144	Uncovering mechanism of photocatalytic performance enhancement induced by multivariate defects on SnS2. Nano Research, 2023, 16, 2102-2110.	5.8	4

#	Article	IF	Citations
73145	Three-Dimensional Activity Volcano Plot under an External Electric Field. ACS Catalysis, 2022, 12, 13542-13548.	5.5	2
73146	Switchable single-molecule electronic and thermoelectric device induced by light in a designed diarylethene molecule. Physical Review B, 2022, 106, .	1.1	4
73147	Non-Covalent Interactions in the Crystal Structures of Perbrominated Sulfonium Derivatives of the closo-Decaborate Anion. International Journal of Molecular Sciences, 2022, 23, 12022.	1.8	0
73148	A Defectâ€Engineered NanozymeÂfor Targeted NIRâ€II Photothermal Immunotherapy of Cancer. Advanced Materials, 2024, 36, .	11.1	27
73149	Tunable Energy-Level Alignment in Multilayers of Carboxylic Acids on Silver. Physical Review Applied, 2022, 18, .	1.5	1
73150	Multiscale Isomerization of Magic-Sized Inorganic Clusters Chemically Driven by Atomic-Bond Exchanges. Chemistry of Materials, 2022, 34, 9527-9535.	3.2	6
73151	Density functional description of spin, lattice, and spin-lattice dynamics in antiferromagnetic and paramagnetic phases at finite temperatures. Physical Review B, 2022, 106, .	1.1	10
73152	Surface Characterization of the Solutionâ€Processed Organicâ€“Inorganic Hybrid Perovskite Thin Films. Small, 0, , 2204271.	5.2	1
73153	Optical properties of polar and nonpolar GaN/AlN multiquantum well systemsâ€”DFT study. Journal of Applied Physics, 2022, 132, 164306.	1.1	1
73154	Single Transition Metal Atoms Anchored on Defective MoS₂ Monolayers for the Electrocatalytic Reduction of Nitric Oxide into Ammonia and Hydroxylamine. Inorganic Chemistry, 2022, 61, 17448-17458.	1.9	9
73155	Arsenic Monolayers Formed by Zero-Dimensional Tetrahedral Clusters and One-Dimensional Armchair Nanochains. ACS Nano, 2022, 16, 17087-17096.	7.3	2
73156	Highly efficient photocatalytic overall water splitting in two-dimensional van der Waals MoS₂/Hf₂CO₂ heterostructure. Journal Physics D: Applied Physics, 2023, 56, 035501.	1.3	5
73157	Two-Dimensional Electron Gas in MoSi₂N₄/VSi₂N₄ Heterojunction by First Principles Calculation. Chinese Physics Letters, 2022, 39, 127301.	1.3	1
73158	Ab-Initio Studies of the Micromechanics and Interfacial Behavior of Al3Y|fcc-Al. Metals, 2022, 12, 1680.	1.0	1
73159	Planar MN₄ (Mâ€‰=â€‰Zn, Cd) Monolayers: 2D Anisotropic Dirac Semimetals of Ultrahigh Fermi Velocities. Physica Status Solidi - Rapid Research Letters, 2023, 17, .	1.2	1
73160	Band inversion induced large-gap quantum spin Hall states in III-Bi-monolayer/ <mml:math xmlns:mml="http://www.w3.org/1998/Math/MathML"><mml:msub><mml:mi mathvariant="normal">SiO</mml:mi><mml:mn>2</mml:mn></mml:msub></mml:math>. Physical Review B, 2022, 106, .	1.1	1
73161	Structures, Scaling Relations, and Selectivities of the Copper-Based Binary Catalysts for CO₂ Reduction Reactions. Journal of Physical Chemistry C, 2022, 126, 17966-17974.	1.5	1
73162	Photon and Phonon Coherence to Enhance Photoluminescence by Magnetic Polarons in Mn-Doped Rb₃Cd₂Cl₇ Perovskites. Journal of Physical Chemistry C, 2022, 126, 18855-18866.	1.5	1

#	Article	IF	Citations
73163	Insight into stabilities and magnetism of EuGen (nâ€‰=â€‰1â€“20) nanoclusters: an assessment of electronic aromaticity. Journal of Materials Science, 2022, 57, 19338-19355.	1.7	5
73164	Tuning optical bandgap of crystalline MgO by MeV Co ion beam induced defects. Applied Physics A: Materials Science and Processing, 2022, 128, .	1.1	5
73165	A High-Rate, Durable Cathode for Sodium-Ion Batteries: Sb-Doped O3-Type Ni/Mn-Based Layered Oxides. ACS Nano, 2022, 16, 18058-18070.	7.3	38
73166	Plasmonic high-entropy carbides. Nature Communications, 2022, 13, .	5.8	18
73167	The role of alkali metal cations and platinum-surface hydroxyl in the alkaline hydrogen evolution reaction. Nature Catalysis, 2022, 5, 923-933.	16.1	79
73168	Detailed Structural and Electrochemical Comparison between High Potential Layered P2-NaMnNi and Doped P2-NaMnNiMg Oxides. ACS Applied Energy Materials, 2022, 5, 13735-13750.	2.5	5
73169	Tin Nanoclusters Confined in Nitrogenated Carbon for the Oxygen Reduction Reaction. ACS Nano, 2022, 16, 18830-18837.	7.3	11
73170	A Nearly Zero-Strain Li-Rich Rock-Salt Oxide with Multielectron Redox Reactions as a Cathode for Li-Ion Batteries. Chemistry of Materials, 2022, 34, 9711-9721.	3.2	7
73171	Tuning Ironâ€“Oxygen Covalency in Perovskite Oxides for Efficient Electrochemical Sensing. Journal of Physical Chemistry C, 2022, 126, 17618-17626.	1.5	0
73172	Favorable Electrocatalytic Ammonia Oxidation Reaction Thermodynamics on the Î²-NiOOH(0001) Surface Computed by Density Functional Theory. Journal of Physical Chemistry C, 2022, 126, 17952-17965.	1.5	6
73173	Electronic, Optical, Mechanical and Li-Ion Storage Properties of Novel Benzotrithiophene-Based Graphdiyne Monolayers Explored by First Principles and Machine Learning. Batteries, 2022, 8, 194.	2.1	3
73174	Defect Thermodynamics and Transport Properties of Proton Conducting Oxide BaZr1âˆ’xYxO3âˆ’Î´ (xâ€‰=â€‰0.1) Guided by Density Functional Theory Modeling. Jom, 2022, 74, 4506-4526.	0.9	5
73176	Synthetic Engineering in Na₂MSn₂(NCN)₆ (M = Mn, Fe, Co, and Ni) Based on Electronic Structure Theory. Inorganic Chemistry, 2022, 61, 18221-18228.	1.9	3
73177	Atomically precise control of rotational dynamics in charged rare-earth complexes on a metal surface. Nature Communications, 2022, 13, .	5.8	6
73178	High-Frequency Sheet Conductance of Nanolayered WS₂ Crystals for Two-Dimensional Nanodevices. ACS Applied Nano Materials, 2022, 5, 15557-15562.	2.4	2
73179	Charting Câ€“C coupling pathways in electrochemical CO ₂ reduction on Cu(111) using embedded correlated wavefunction theory. Proceedings of the National Academy of Sciences of the United States of America, 2022, 119, .	3.3	21
73180	Interfacial water engineering boosts neutral water reduction. Nature Communications, 2022, 13, .	5.8	56
73181	Discovery of YbNiSb-Based Half-Heusler Alloys as Promising Thermoelectric Materials. ACS Applied Energy Materials, 2022, 5, 12630-12639.	2.5	2

#	Article	IF	Citations
73182	Switchable half-metallicity in A-type antiferromagnetic NiI2 bilayer coupled with ferroelectric In2Se3. Npj Computational Materials, 2022, 8, .	3.5	21
73183	Breaking the scaling relationship in selective oxidation of methane via dynamic Metal-Intermediate Coordination-Induced modulation of reactivity descriptors on an atomically dispersed Rh/ZrO2 catalyst. Journal of Catalysis, 2022, 416, 68-84.	3.1	3
73184	Antiferromagnetic insulating state in layered nickelates at half filling. Scientific Reports, 2022, 12, .	1.6	2
73185	Impact of radiation-induced point defects on thermal carrier decay processes in GaAs. Acta Materialia, 2023, 242, 118480.	3.8	1
73186	First-principles study of vacancy defects in TiVTa and TiVTaNb concentrated solid-solution alloys. Journal of Nuclear Materials, 2023, 573, 154096.	1.3	4
73187	Monolayer <mml:math xmlns:mml="http://www.w3.org/1998/Math/MathML"><mml:mrow><mml:mi>C</mml:mi><mml:mn>2</mml:mn><mml:mo></mml:mo></mml:mrow></mml:math> (<mml:math) Tj ETQq1 1 0.784314 rgBT /Overlock 10 Tf 50 542 Td (xmlns:mml="http://www.w3.org/1998/Math/MathML"><mml:mrow> ideal IR-VIS light tran. Physical Review Materials, 2022, 6, .	0.9	2
73188	Effect of vacancies on photogalvanic effect in two-dimensional WSe2 photodetector. Applied Surface Science, 2023, 610, 155401.	3.1	5
73189	Intrinsic bitunable magnetism/polarity behavior in 2D Janus Cr2I3Y3 (Yâ€‰=â€‰F, Cl, or Br) systems. Npj 2D Materials and Applications, 2022, 6, .	3.9	4
73190	Deposition of Horizontally Stacked Zn Crystals on Single Layer 1Tâ€VSe₂ for Dendriteâ€Free Zn Metal Anodes. Advanced Energy Materials, 2022, 12, .	10.2	11
73191	Effect of vacancy concentration on the production selectivity of Janus In2S2X (X=Se, Te) monolayer heterojunction photocatalytic reduction of CO2. Physica E: Low-Dimensional Systems and Nanostructures, 2023, 146, 115549.	1.3	2
73192	Synthesis of Epitaxial MoS₂/MoO₂ Coreâ€“Shell Nanowires by Two-Step Chemical Vapor Deposition with Turbulent Flow and Their Physical Properties. ACS Omega, 2022, 7, 39362-39369.	1.6	1
73193	Dicarbon nitride and Janus transition metal chalcogenides van der Waals heterojunctions for photocatalytic water splitting. Journal of Physics Condensed Matter, 2023, 35, 014003.	0.7	2
73194	Atomically Dispersed Dualâ€Site Cathode with a Record High Sulfur Mass Loading for Highâ€Performance Roomâ€Temperature Sodiumâ€“Sulfur Batteries. Advanced Materials, 2023, 35, .	11.1	46
73195	Mo₃ReRuC: A Noncentrosymmetric Superconductor Formed in the MoReRuâ€“Mo₂C System. Inorganic Chemistry, 2022, 61, 17115-17122.	1.9	0
73196	Ultraâ€Narrow Linewidth Photoâ€Emitters in Polymorphic Selenium Nanoflakes. Small, 0, , 2204302.	5.2	0
73197	Insights into the effect of cobalt substitution into copper-manganese oxides on enhanced benzene oxidation activity. Applied Catalysis B: Environmental, 2023, 323, 122099.	10.8	10
73198	Estimates of Quantum Tunneling Effects for Hydrogen Diffusion in PuO2. Applied Sciences (Switzerland), 2022, 12, 11005.	1.3	1
73199	Plastic deformation in silicon nitride ceramics via bond switching at coherent interfaces. Science, 2022, 378, 371-376.	6.0	40

#	Article	IF	Citations
73200	Ab initio guided minimal model for the â€œKitaevâ€•material <mml:math xmlns:mml="http://www.w3.org/1998/Math/MathML"><mml:msub><mml:mi mathvariant="normal">BaCo</mml:mi><mml:mn>2</mml:mn></mml:msub></mml:math> (<mml:math) Tj ETQq0 0 0 rgBT /Overlock 10	1.1	17
73201	: Importance of direct hopping, third-neighbor. Physical Review B, 2022, 106, . Spin-orbital Yu-Shiba-Rusinov states in single Kondo molecular magnet. Nature Communications, 2022, 13, .	5.8	4
73202	Enhanced Optoelectronic Performance Induced by Ion Migration in Lead-Free CsCu₂I₃ Single-Crystal Microrods. ACS Applied Materials & Interfaces, 2022, 14, 49975-49985.	4.0	5
73203	Reconstruction of Zigzag Graphene Edges: Energetics, Kinetics, and Residual Defects. Journal of Physical Chemistry Letters, 2022, 13, 10326-10330.	2.1	1
73204	Antiphase boundaries in III-V semiconductors: Atomic configurations, band structures, and Fermi levels. Physical Review B, 2022, 106, .	1.1	3
73205	Reconstruction of Thiospinel to Active Sites and Spin Channels for Water Oxidation. Advanced Materials, 2023, 35, .	11.1	27
73206	Scalable Production of Biodegradable, Recyclable, Sustainable Celluloseâ€“Mineral Foams via Coordination Interaction Assisted Ambient Drying. ACS Nano, 2022, 16, 16414-16425.	7.3	24
73207	Synthesis and Characterization of Catalytically Active Au Coreâ”€Pd Shell Nanoparticles Supported on Alumina. Langmuir, 2022, 38, 12859-12870.	1.6	2
73208	Toward Understanding the Effect of Fluoride Ions on the Solvation Structure in Lithium Metal Batteries: Insights from First-Principles Simulations. ACS Applied Materials & Interfaces, 2022, 14, 48762-48769.	4.0	3
73209	Significant regulation of stress on the contribution of optical phonons to thermal conductivity in layered Li2ZrCl6: First-principles calculations combined with the machine-learning potential approach. Applied Physics Letters, 2022, 121, .	1.5	11
73210	Ab-initio investigation on the phase stabilities of Au-M Alloys (M= Na, K, Rb and Cs). Physica Scripta, 0, , .	1.2	0
73211	Polaronic defects in monolayer CeO₂: Quantum confinement effect and strain engineering. Journal of Chemical Physics, 0, , .	1.2	1
73212	Unravelling the Interfacial Dynamics of Bandgap Funneling in Bismuthâ€Based Halide Perovskites. Advanced Materials, 2023, 35, .	11.1	7
73213	Stochastic atomic modeling and optimization with fullrmc. Journal of Applied Crystallography, 2022, 55, 1664-1676.	1.9	7
73214	Nonreciprocal charge transport in topological superconductor candidate Bi2Te3/PdTe2 heterostructure. Npj Quantum Materials, 2022, 7, .	1.8	10
73215	Carbon Quantum Dots Bridged TiO2/CdIn2S4 toward Photocatalytic Upgrading of Polycyclic Aromatic Hydrocarbons to Benzaldehyde. Molecules, 2022, 27, 7292.	1.7	1
73216	Critical role of water structure around interlayer ions for ion storage in layered double hydroxides. Nature Communications, 2022, 13, .	5.8	11
73217	Experimental and theoretical studies of native deep-level defects in transition metal dichalcogenides. Npj 2D Materials and Applications, 2022, 6, .	3.9	10

#	Article	IF	Citations
73218	Band gaps of halide perovskites from a Wannier-localized optimally tuned screened range-separated hybrid functional. Physical Review Materials, 2022, 6, .	0.9	9
73219	Mo-Doped Metalâ€“Organic Frameworks for Efficient Nitrogen Reduction Reaction: A Density Functional Theory Study. ACS Sustainable Chemistry and Engineering, 2022, 10, 14064-14072.	3.2	10
73220	Thermoelectric Efficiency of Two-Dimensional Pentagonal-PdSe₂ at High Temperatures and the Role of Strain. ACS Applied Energy Materials, 2022, 5, 14522-14530.	2.5	6
73221	Zeeman Effect in Centrosymmetric Antiferromagnetic Semiconductors Controlled by an Electric Field. Physical Review Letters, 2022, 129, .	2.9	9
73222	The Nature of Ferromagnetism in a System of Self-Ordered Î±-FeSi2 Nanorods on a Si(111)-4Â° Vicinal Surface: Experiment and Theory. Nanomaterials, 2022, 12, 3707.	1.9	0
73223	Extremely Suppressed Energetic Disorder in a Chemically Doped Conjugated Polymer. Advanced Materials, 2023, 35, .	11.1	5
73224	Understanding Activity Trends in Furfural Hydrogenation on Transition Metal Surfaces. ACS Catalysis, 2022, 12, 12902-12910.	5.5	21
73225	Structure and Properties of Cubic PuH2 and PuH3: A Density Functional Theory Study. Crystals, 2022, 12, 1499.	1.0	1
73226	Interface sites on vanadia-based catalysts are highly active for NO removal under realistic conditions. Journal of Environmental Sciences, 2024, 136, 523-536.	3.2	3
73227	Characterization of Lanthanum Monazite Surface Chemistry and Crystal Morphology through Density Functional Theory and Experimental Approaches. Journal of Physical Chemistry C, 2022, 126, 18952-18962.	1.5	3
73228	Mechanical Amorphization of Chitosan with Different Molecular Weights. Polymers, 2022, 14, 4438.	2.0	12
73229	First-principles Landau-like potential for <mml:math xmlns:mml="http://www.w3.org/1998/Math/MathML"><mml:msub><mml:mi>BiFeO</mml:mi><mml:mn>3</mml:mn></mml:msub><mml:msub><mml:mi></mml:mi><mml:mn></mml:mn></mml:msub> and related materials. Physical Review B, 2022, 106, .	3.7	2
73230	High-Throughput Inverse Design for 2D Ferroelectric Rashba Semiconductors. Journal of the American Chemical Society, 2022, 144, 20035-20046.	6.6	5
73231	High-throughput screening of half-antiperovskites with a stacked kagome lattice. Acta Materialia, 2023, 242, 118474.	3.8	7
73232	Two Silver Halobismuthate Hybrids Decorated by Photosensitive Metal Complexes: Syntheses, Structures, Photoelectric Properties, and Theoretical Studies. Crystal Growth and Design, 2022, 22, 7434-7442.	1.4	8
73233	Transition Metal dâ€band Center Tuning by Interfacial Engineering to Accelerate Polysulfides Conversion for Robust Lithiumâ€“Sulfur Batteries. Small, 2022, 18, .	5.2	14
73234	Synergistic electronic and geometric effects of Au/<scp>CeO₂</scp> catalyst for oxidative esterification of methacrolein. AICHE Journal, 2023, 69, .	1.8	3
73235	Phase Stability, Strong Four-Phonon Scattering, and Low Lattice Thermal Conductivity in Superatom-Based Superionic Conductor Na₃OBH₄. ACS Applied Materials & Interfaces, 2022, 14, 47882-47891.	4.0	7

#	Article	IF	Citations
73236	Polar Magnetism Above 600 K with High Adaptability in Perovskite Oxides. ACS Applied Materials & Interfaces, 2022, 14, 48052-48060.	4.0	3
73237	Size-Dependent Nucleation in Crystal Phase Transition from Machine Learning Metadynamics. Physical Review Letters, 2022, 129, .	2.9	6
73238	Phonon-Fostered Valley Polarization of Interlayer Excitons in van der Waals Heterostructures. Journal of Physical Chemistry C, 2022, 126, 18128-18138.	1.5	3
73239	Theoretical Study on the Vapochromic Ni(II)â€“Quinonoid Complex: One-Dimensional Stacking Structure-Based Color Switching. Journal of Physical Chemistry A, 2022, 126, 7687-7694.	1.1	1
73240	Point Defects Stability, Hydrogen Diffusion, Electronic Structure, and Mechanical Properties of Defected Equiatomic Î³(U,Zr) from First-Principles. Materials, 2022, 15, 7452.	1.3	2
73241	Computational insights into the lattice dynamics of Pu(IV) oxalates. Journal of Nuclear Materials, 2023, 573, 154106.	1.3	3
73242	Energetic and Kinetic Coupling between the Intercalated Atom and Intrinsic S Vacancy in the MoS₂ Bilayer. Journal of Physical Chemistry C, 2022, 126, 18560-18570.	1.5	1
73243	Stability of Magnesium Binary and Ternary Compounds for Batteries Determined from First Principles. Journal of Physical Chemistry Letters, 2022, 13, 10092-10100.	2.1	4
73244	Anharmonic Interaction in Negative Thermal Expansion Material CaTiF₆. Inorganic Chemistry, 2022, 61, 17378-17386.	1.9	5
73245	A solid-to-solid metallic conversion electrochemistry toward 91% zinc utilization for sustainable aqueous batteries. Science Advances, 2022, 8, .	4.7	80
73246	Magnetic ground state of plutonium dioxide: DFT+U calculations. Chinese Physics B, 0, , .	0.7	0
73247	Theoretical exploration of mechanical and superconducting properties of two-dimensional Cairo penta- <mml:math xmlns:mml="http://www.w3.org/1998/Math/MathML"><mml:msub><mml:mi>BP</mml:mi><mml:mn>2</mml:mn></mml:msub></mml: : A first-principles study. Physical Review Materials, 2022, 6, .	0.9	0
73248	Dependence of the electronic structure of Î² â€Si 6â€z Al z O z N 8â^' z on the (Al,O) concentration z and on the temperature. Zeitschrift Fur Anorganische Und Allgemeine Chemie, 0, , .	0.6	1
73249	Physical Insights on the Thermoelectric Performance of Cs₂SnBr₆ with Ultralow Lattice Thermal Conductivity. Journal of Physical Chemistry Letters, 2022, 13, 9736-9744.	2.1	2
73250	Nucleation and Growth of Dendritic Islands during Platinum Oxidation-Reduction Cycling. Journal of the Electrochemical Society, 2022, 169, 112506.	1.3	3
73251	Surface Chemistry of Ketones and Diketones on Lewis Acidic Î³-Al₂O₃ Probed by Infrared Spectroscopy. Journal of Physical Chemistry C, 2022, 126, 17554-17568.	1.5	1
73252	Influence of Al-O and Al-C Clusters on Defects in Graphene Nanosheets Derived from Coal-Tar Pitch via Al4C3 Precursor. Materials, 2022, 15, 7312.	1.3	1
73253	Li-Ion Diffusion Correlations in LiAlGeO₄: Quasielastic Neutron Scattering and Ab Initio Simulation. ACS Applied Energy Materials, 2022, 5, 14119-14126.	2.5	1

#	Article	IF	Citations
73254	Temperatureâ€Programmed Separation of Hexane Isomers by a Porous Calcium Chloranilate Metalâ€Organic Framework. Angewandte Chemie - International Edition, 2022, 61, .	7.2	23
73255	A Wide Bandgap Halide Perovskite Based Selfâ€Powered Blue Photodetector with 84.9% of External Quantum Efficiency. Advanced Materials, 2022, 34, .	11.1	6
73256	Rashba effects in lead-free ferroelectric semiconductor <mml:math xmlns:mml="http://www.w3.org/1998/Math/MathML"><mml:mrow><mml:mo>[</mml:mo><mml:msub><mml:mi>Cs</mml:mi><mml:n Physical Review Materials, 2022, 6, .	3.1	3
73257	Charge-to-spin conversion in twisted <mml:math xmlns:mml="http://www.w3.org/1998/Math/MathML"><mml:mi>graphene</mml:mi><mml:mo>/</mml:mo><mml:msub><mml:mi>W heterostructures. Physical Review B, 2022, 106, .	3.2	20
73258	Piezoelectric ferromagnetism in two-dimensional materials via materials screening. Physical Review B, 2022, 106, .	1.1	8
73259	Electronic structures and stability investigation of large band gap topological insulators <mml:math xmlns:mml="http://www.w3.org/1998/Math/MathML"><mml:mi>M</mml:mi><mml:msub><mml:mi mathvariant="normal">Tl</mml:mi><mml:mn>4</mml:mn></mml:msub><mml:msub><mml:mi mathvariant="normal">Te</mml:mi><mml:mn>3</mml:mn></mml:msub></mml:math> (<mml:math) Tj ETQq1 1 0.784314 rgBT /Ov Physical Review Materials, 2022, 6, .	0.9	1
73260	Mesoscopic fluctuating domains in strontium titanate. Physical Review B, 2022, 106, .	1.1	9
73261	Unconventional magnetoresistive behavior near magnetic compensation temperature in ferrimagnetic Mn_{2.21}Ru_{0.86}Ga films. Applied Physics Letters, 2022, 121, 182403.	1.5	0
73262	Elucidating the Role of Ni(Pd) in Ni(Pd)-Mo₂C/Carbon Catalysts for the Hydrodeoxygenation of Dibenzofuran and Bio-Oil. Industrial & Engineering Chemistry Research, 0, , .	1.8	1
73263	Tunable Interstitial Anionic Electrons in Layered MXenes. Journal of Physics Condensed Matter, 0, , .	0.7	0
73264	Aluminum formate, Al(HCOO) ₃ : An earth-abundant, scalable, and highly selective material for CO ₂ capture. Science Advances, 2022, 8, .	4.7	39
73265	Proposal of a novel two-dimensional ZnCS3 monolayer as an efficient hydrogen evolution electro-catalyst. Journal of Electroanalytical Chemistry, 2022, 925, 116907.	1.9	1
73266	Predicting Diamond-like Nitrides as Infrared Nonlinear Optical Materials with High Thermal Conductivity. Chemistry of Materials, 2022, 34, 10059-10067.	3.2	8
73267	Polymer-like Inorganic Double Helical van der Waals Semiconductor. Nano Letters, 2022, 22, 9054-9061.	4.5	4
73268	Si/Al Ratio Determines the SCR Performance of Cu-SSZ-13 Catalysts in the Presence of NO₂. Environmental Science & Technology, 2022, 56, 17946-17954.	4.6	10
73269	Magnetic and Spinâ€Polarized Optical Properties of Co and Mn Adsorbed Î³â€GeSe. Physica Status Solidi - Rapid Research Letters, 2023, 17, .	1.2	0
73270	Enhanced strength-ductility synergy via high dislocation density-induced strain hardening in nitrogen interstitial CrMnFeCoNi high-entropy alloy. Journal of Materials Science and Technology, 2023, 141, 184-192.	5.6	40
73271	The influence of leveler Brilliant Green on copper superconformal electroplating based on electrochemical and theoretical study. Journal of Industrial and Engineering Chemistry, 2023, 118, 78-90.	2.9	9

#	Article	IF	Citations
73272	On the structure of one-dimensional TiO2 lepidocrocite. Matter, 2023, 6, 128-141.	5.0	12
73273	High-Throughput Screening of Strong Electronâ€“Phonon Couplings in Ternary Metal Diborides. Inorganic Chemistry, 2022, 61, 18154-18161.	1.9	5
73274	Facile fabrication of nanoflower-like WO3/WS2 heterojunction for highly sensitive NO2 detection at room temperature. Journal of Hazardous Materials, 2023, 443, 130316.	6.5	30
73275	Determination of single-crystal elastic moduli of LiREF4 (REâ€‰=â€‰Y, Gd, and Tb) by resonant ultrasound spectroscopy. Journal of Applied Physics, 2022, 132, .	1.1	0
73276	High Cationic Dispersity Boosted Oxygen Reduction Reactivity in Multiâ€Element Doped Perovskites. Advanced Functional Materials, 2023, 33, .	7.8	4
73277	Significant boosting effect of single atom Pt towards the ultrasonic generation of H2O2: A two-way catalytic mechanism. Applied Catalysis B: Environmental, 2023, 323, 122143.	10.8	9
73278	Role of titanium and organic precursors in molecular layer deposition of â€œtitaniconeâ€•hybrid materials. Beilstein Journal of Nanotechnology, 0, 13, 1240-1255.	1.5	1
73279	Interfacial reactions of catalytic ozone membranes resulting in the release and degradation of irreversible foulants. Water Research, 2022, 226, 119244.	5.3	9
73280	Indium-doped Î²-MnO2 catalyst for activation of peroxymonosulfate to generate singlet oxygen with complete selectivity. Journal of Cleaner Production, 2022, 380, 134953.	4.6	8
73281	Transformation of long-period stacking ordered structures in Mg-Gd-Y-Zn alloys upon synergistic characterization of first-principles calculation and experiment and its effects on mechanical properties. Journal of Magnesium and Alloys, 2022, , .	5.5	2
73282	Doped Ru to enable next generation barrier-less interconnect. Journal of Applied Physics, 2022, 132, .	1.1	3
73283	Atomic Layer Deposition of Sb₂Te₃/GeTe Superlattice Film and Its Meltâ€Quenchingâ€Free Phaseâ€Transition Mechanism for Phaseâ€Change Memory. Advanced Materials, 2022, 34, .	11.1	9
73284	Highly Active and Stable Ni/La-Doped Ceria Material for Catalytic CO₂ Reduction by Reverse Water-Gas Shift Reaction. ACS Applied Materials & Interfaces, 2022, 14, 50739-50750.	4.0	9
73285	Synergy of in-situ heterogeneous interphases tailored lithium deposition. Nano Research, 2023, 16, 8304-8312.	5.8	16
73286	Scaling of Berry-curvature monopole dominated large linear positive magnetoresistance. Proceedings of the National Academy of Sciences of the United States of America, 2022, 119, .	3.3	7
73287	Chemical-Potential-Dependent Thermodynamic Study of Electrochemical Nitric Oxide Reduction to Ammonia on Single-Cluster Catalysts. Journal of Physical Chemistry C, 2022, 126, 19209-19218.	1.5	2
73288	Electronic topological transitions and mechanical properties of hafnium dioxide allotrope at high pressure: Evolutionary first-principles techniques. Physica B: Condensed Matter, 2022, , 414456.	1.3	0
73289	First-principles study of two-dimensional half-metallic ferromagnetism in NiXCl (X = S and Se) monolayer. AIP Advances, 2022, 12, 115105.	0.6	1

#	Article	IF	Citations
73290	Effect of surface Se concentration on stability and electronic structure of monolayer Bi2O2Se. Applied Surface Science, 2023, 611, 155528.	3.1	4
73291	Ultralow Lattice Thermal Conductivity in the Aikinite Structure Family, Cu_xPb_xBi_{2â€“x}S₃, and Thermoelectric Properties of Cu_{0.14}Pb_{0.14}Bi_{1.86}S₃. ACS Applied Energy Materials, 2022, 5, 14222-14230.	2.5	4
73292	Accurate and Efficient Prediction of Highly Disordered Bi₂O₃ with Optimum Structure Pool: Combined Approach of the Special Quasirandom Structure Method and Structure Sampling. Journal of Physical Chemistry C, 2022, 126, 18885-18892.	1.5	3
73293	Two-dimensional antiferromagnetic nodal-line semimetal and quantum anomalous Hall state in the van der Waals heterostructure germanene/Mn₂S₂. Journal of Physics Condensed Matter, 2022, 34, 505702.	0.7	1
73294	Efficient predictions of formation energies and convex hulls from density functional tight binding calculations. Journal of Materials Science and Technology, 2023, 141, 236-244.	5.6	8
73295	Correlated electronic structure of the kagome metal <mml:math xmlns:mml="http://www.w3.org/1998/Math/MathML"><mml:mrow><mml:msub><mml:mi>Mn</mml:mi><mml:mn>3</mml:mn></m Physical Review B, 2022, 106, .	1.1	3
73296	DFT study on decomposition of hydrazine nitrate on Ir(1 0 0) surface. Computational and Theoretical Chemistry, 2022, 1217, 113917.	1.1	4
73297	Why mercury is a superconductor. Physical Review B, 2022, 106, .	1.1	4
73298	Synthesis and Crystal Structure of a New Orthorhombic Polytype of Potassium Ferricyanide. Zeitschrift Fur Anorganische Und Allgemeine Chemie, 0, , .	0.6	0
73299	Fine structure of the charge density wave in bulk VTe2. APL Materials, 2022, 10, .	2.2	4
73300	The negative thermal expansion behavior in Prussian blue analogue Zn3[Fe(CN)6]2: A first-principles study. Physics Letters, Section A: General, Atomic and Solid State Physics, 2022, 453, 128493.	0.9	1
73301	A reference-free MEAM potential for Î±-Fe and Î³-Fe. Journal of Physics Condensed Matter, 2022, 34, 505901.	0.7	0
73302	Two dimensional Zr₂CO₂/H-FeCl₂ van der Waals heterostructures with tunable band gap, potential difference and magnetic anisotropy. Journal of Physics Condensed Matter, 2023, 35, 024001.	0.7	1
73303	Unraveling the structure and composition sensitivity of transition metal phosphide toward catalytic performance of C2H2 semi-hydrogenation. Journal of Catalysis, 2022, 416, 112-128.	3.1	3
73304	Stochastic path-integral approach for predicting the superconducting temperatures of anharmonic solids. Physical Review B, 2022, 106, .	1.1	0
73305	First-principles study of the structural and electronic properties of BN-ring doped graphene. Physical Review Materials, 2022, 6, .	0.9	1
73306	Macroscale superdurable superlubricity achieved in lubricant oil via operando tribochemical formation of fullerene-like carbon. Cell Reports Physical Science, 2022, 3, 101130.	2.8	3
73307	Stable nitrogen-rich yttrium nitrides under high pressure. Solid State Communications, 2022, 358, 115001.	0.9	3

#	Article	IF	Citations
73308	Spontaneous formation of carbon dots helps to distinguish molecular fluorophores species. Applied Surface Science, 2023, 610, 155536.	3.1	3
73309	Diffusion mechanism and electrochemical investigation of 1T phase Alâ€“MoS2@rGO nano-composite as a high-performance anode for sodium-ion batteries. Chemical Engineering Journal, 2023, 454, 140140.	6.6	14
73310	General strategy for enhanced CH4 selectivity in photocatalytic CO2 reduction reactions by surface oxophilicity engineering. Journal of Catalysis, 2022, 415, 77-86.	3.1	8
73311	Monte Carlo simulations of surface segregation to discover new hydrogen separation membranes. International Journal of Hydrogen Energy, 2023, 48, 2221-2230.	3.8	2
73312	Stability of and conduction in single-walled <mml:math xmlns:mml="http://www.w3.org/1998/Math/MathML"><mml:msub><mml:mrow><mml:mi>Si</mml:mi></mml:mrow><mml:mn>2</mml:mn></mml:msub></mml:math> nanotubes. Physical Review Materials, 2022, 6, .	3.1	1
73313	Enhancing the thermoelectric performance of Î²-Zn4Sb3 via progressive incorporation of Zn interstitials. Nano Energy, 2022, 104, 107967.	8.2	3
73314	Lifshitz transitions and hybrid Weyl points in RbAg5Se3. New Journal of Physics, 0, , .	1.2	0
73315	Insight into the Effect of Cu Species and Its Origin in Pt-Based Catalysts on Reaction Pathways of Glycerol Oxidation. ACS Catalysis, 2022, 12, 14140-14151.	5.5	9
73316	Robust Second-Order Topological Insulators with Giant Valley Polarization in Two-Dimensional Honeycomb Ferromagnets. Nano Letters, 2023, 23, 91-97.	4.5	20
73317	Unraveling Electroreductive Mechanisms of Biomass-Derived Aldehydes via Tailoring Interfacial Environments. ACS Catalysis, 2022, 12, 14072-14085.	5.5	15
73318	First-Principles Investigation of Interfacial Reconstruction in Epitaxial SrTiO₃/Si Photocathodes. Journal of Physical Chemistry C, 2022, 126, 18813-18821.	1.5	1
73319	Coupling Cobalt Phthalocyanine Molecules on 3D Nitrogenâ€Doped Vertical Graphene Arrays for Highly Efficient and Robust CO₂ Electroreduction. Small, 2022, 18, .	5.2	9
73320	Chiral Dirac-like fermion in spin-orbit-free antiferromagnetic semimetals. Innovation(China), 2022, 3, 100343.	5.2	4
73321	Catalytic oxidation of propane over Pt-Pd bimetallic nanoparticles supported on TiO2. Molecular Catalysis, 2022, 532, 112738.	1.0	2
73322	Understanding the difference in bulk modulus between Y-doped SrCeO3 and Y-doped SrZrO3 by ultrasonic transmission method and density functional theory. Materialia, 2022, 26, 101616.	1.3	0
73323	Unique Atomic and Electronic Structures of Oxygen Vacancies in Amorphous SnO₂ from First Principles and Informatics. Journal of Physical Chemistry C, 0, , .	1.5	1
73324	Purcell-induced suppression of superradiance for molecular overlayers on noble atom surfaces. Journal of Chemical Physics, 2022, 157, 194111.	1.2	0
73325	Novel PtNi nanoflowers regulated by a third element (Rh, Ru, Pd) as efficient multifunctional electrocatalysts for ORR, MOR and HER. Chemical Engineering Journal, 2023, 454, 140131.	6.6	14

#	Article	IF	Citations
73326	Solvation structure and dynamics of Li and LiO2 and their transformation in non-aqueous organic electrolyte solvents from first-principles simulations. Chinese Journal of Catalysis, 2022, 43, 2850-2857.	6.9	2
73327	Atomic-Scale Pentagraphene Ribbons Stabilized with Alkali Metals under Moderate Pressures. Inorganic Chemistry, 0, , .	1.9	1
73328	Electronic properties of graphene/CdX (X=S, Se, and Te) semiconductor heterostructure and a proposal of all-optical injection and detection of electron spins in graphene. Physica E: Low-Dimensional Systems and Nanostructures, 2023, 146, 115559.	1.3	0
73329	Red shift in optical excitations on layered copper perovskites under pressure: role of the orthorhombic instability. Chemistry - A European Journal, 0, , .	1.7	2
73330	In-situ constructed Cu/CuNC interfaces for low-overpotential reduction of CO2 to ethanol. National Science Review, 2023, 10, .	4.6	15
73331	Multifunctional PbS₂ Monolayer with an In-Plane Negative Poisson Ratio and Photocatalytic Water Splitting Properties. Journal of Physical Chemistry Letters, 2022, 13, 10494-10499.	2.1	10
73332	Raman spectroscopy of lithium niobite (LiNbO2). Chemical Physics Letters, 2022, 807, 140111.	1.2	0
73333	Mechanism of mixed conductivity in crystalline and amorphous lithium lanthanum titanate. Solid State Ionics, 2022, 386, 116029.	1.3	1
73334	Tunable activity of electrocatalytic CO dimerization on strained Cu surfaces: Insights from ab initio molecular dynamics simulations. Chinese Journal of Catalysis, 2022, 43, 2898-2905.	6.9	4
73335	Molecular interaction with defected h-BN. Computational and Theoretical Chemistry, 2022, 1217, 113911.	1.1	1
73336	Strain-induced tunable electronic properties in graphite-diamond hybrids. Materials Today Physics, 2022, 28, 100879.	2.9	1
73337	Tuning Metalâ€“Organic Framework (MOF) Topology by Regulating Ligand and Secondary Building Unit (SBU) Geometry: Structures Built on 8-Connected M₆ (M = Zr, Y) Clusters and a Flexible Tetracarboxylate for Propane-Selective Propane/Propylene Separation. Journal of the American Chemical Society, 2022, 144, 21702-21709.	6.6	31
73338	Enhancement of tunneling currents by isoelectronic nitrogen-atom doping at semiconductor pn junctions; comparison of indirect and direct band-gap systems. Japanese Journal of Applied Physics, 2022, 61, 124002.	0.8	1
73339	Directional growth of quasi-2D Cu2O monocrystals on rGO membranes in aqueous environments. IScience, 2022, 25, 105472.	1.9	0
73340	MNBr (M = Mo, Cr, V) monolayer: two-dimensional ferromagnetic half-metallic materials with high Curie temperature. Journal Physics D: Applied Physics, 2022, 55, 505002.	1.3	3
73341	Native point defects and polaron transport in zirconium pyrovanadate. Solid State Ionics, 2022, 386, 116033.	1.3	1
73342	Synergy of yolk-shelled structure and tunable oxygen defect over CdS/CdCO3-CoS2: Wide band-gap semiconductors assist in efficient visible-light-driven H2 production and CO2 reduction. Chemical Engineering Journal, 2023, 454, 140113.	6.6	8
73343	Ni<mml:math xmlns:mml="http://www.w3.org/1998/Math/MathML" altimg="si23.svg" display="inline" id="d1e1503"><mml:mi>Î±</mml:mi></mml:math>-Al<mml:math xmlns:mml="http://www.w3.org/1998/Math/MathML" altimg="si224.svg" display="inline" id="d1e1508"><mml:msub><mml:mrow /><mml:mrow><mml:mn>2</mml:mn></mml:mrow></mml:msub></mml:math>O<mml:math xmlns:mml="	3.1	2

#	Article	IF	Citations
73344	Interlayer Coupling Induced Phonon-Glassâ€“Electron-Crystal Behavior in van der Waals Heterostructure PtSe₂/Î³-GeSe. ACS Applied Energy Materials, 2022, 5, 13610-13616.	2.5	7
73345	Facet-dependent electronic state of Pt single atoms anchoring on CeO2 nanocrystal for CO (preferential) oxidation. Journal of Catalysis, 2022, 415, 174-185.	3.1	24
73346	Beyond single-crystal surfaces: The GAL21 water/metal force field. Journal of Chemical Physics, 2022, 157, .	1.2	2
73347	Computational Investigation of Metal Oxides as Candidate Hydrogen Storage Materials. Journal of Physical Chemistry C, 2022, 126, 18661-18669.	1.5	3
73348	Effective synthesis of ethyl levulinate via alcoholysis of furfuryl alcohol over simple nickel-titanium dioxide. Applied Catalysis A: General, 2022, 648, 118921.	2.2	1
73349	Strong band renormalization and emergent ferromagnetism induced by electron-antiferromagnetic-magnon coupling. Nature Communications, 2022, 13, .	5.8	4
73350	Transparency and p-Type Conductivity of BeSe Doped with Group VA Atoms: A Hybrid Functional Study. Journal of Physical Chemistry C, 2022, 126, 19446-19454.	1.5	4
73351	Oxygen Deficiency and Migration-Mediated Electric Polarization in Magnetic Fe,Co-Substituted SrTiO3â^Î´. Magnetochemistry, 2022, 8, 144.	1.0	1
73352	Graphitic-nitrogen-enriched carbon skeleton with embedment of Fe3C for superior performance air cathode in zinc-air battery. Materials Today Energy, 2023, 31, 101194.	2.5	2
73353	Anharmonic lattice dynamics and structural phase transition of SnTe monolayer from first principles. Journal of Physics Condensed Matter, 2023, 35, 035401.	0.7	1
73354	First principle studies of TiO₂-ZnO alloys under high pressure. Journal of Physics Condensed Matter, 2023, 35, 024003.	0.7	1
73355	Effect of cationic chemical disorder on defect formation energies in uraniumâ€“plutonium mixed oxides. Journal of Applied Physics, 2022, 132, .	1.1	5
73356	Revealing the hydrogenated structure of silicene- <mml:math xmlns:mml="http://www.w3.org/1998/Math/MathML"><mml:mrow><mml:mrow><mml:mo>(</mml:mo><mml:mrow><mml:mi>â^š</mml:mi></mml:mrow></mml:mr by tip-induced dehydrogenation. Physical Review B, 2022, 106, .	1.1	1
73357	Interstitial-driven local chemical order enables ultrastrong face-centered cubic multicomponent alloys. Acta Materialia, 2023, 243, 118495.	3.8	17
73358	Charge order landscape and competition with superconductivity in kagome metals. Nature Materials, 0, , .	13.3	22
73359	Squarate-Based Metal-Organic Frameworks for Highly Selective and Sensitive Electrochemical Sensing of Dopamine. Journal of the Electrochemical Society, 2022, 169, 116504.	1.3	2
73360	Enhanced thermoelectric performance of skutterudite Co1â^'Ni Sn1.5Te1.5â^' with switchable conduction behavior. Materials Today Physics, 2022, 28, 100889.	2.9	3
73361	First-principles study of the stability and migration of Xe and Cs in U₃Si. Journal of Physics Condensed Matter, 2022, 34, 505502.	0.7	0

#	Article	IF	Citations
73362	First-principles study of non-radiative carrier capture by defects at amorphous-SiO₂/Si(100) interface. Chinese Physics B, 0, , .	0.7	0
73363	Electronically phase separated nano-network in antiferromagnetic insulating LaMnO3/PrMnO3/CaMnO3 tricolor superlattice. Nature Communications, 2022, 13, .	5.8	5
73364	First-principles investigation of phase stability in layered <mml:math xmlns:mml="http://www.w3.org/1998/Math/MathML"><mml:mrow><mml:msub><mml:mi>Na</mml:mi><mml:mi>x</mml:mi></mml:msub></mml:mrow></mml:m Physical Review Materials, 2022, 6, .	3.1	1
73365	Synergy of Platinum Single Atoms and Platinum Atomic Clusters on Sulfurâ€Doped Titanium Nitride Nanotubes for Enhanced Hydrogen Evolution Reaction. Small, 2022, 18, .	5.2	13
73366	Synthesis and characterization of the ceramic refractory metal high entropy nitride thin films from Cr-Hf-Mo-Ta-W system. Surface and Coatings Technology, 2022, 449, 128987.	2.2	6
73367	Theoretical insight into hydrogen production from methanol steam reforming on Pt(111). Molecular Catalysis, 2022, 532, 112745.	1.0	1
73368	Temperature-dependent impact of antiphase boundaries on properties of Fe3Al. Intermetallics, 2022, 151, 107746.	1.8	2
73369	The Limits of Proxy-Guided Superhard Materials Screening. Chemistry of Materials, 2022, 34, 10003-10010.	3.2	3
73370	Engineering electronic structures of Janus monolayer group-III monochalcogenides via biaxial strain. Physics Letters, Section A: General, Atomic and Solid State Physics, 2022, 455, 128504.	0.9	2
73371	Tuning the half-metallicity in reconstructed CrN (111) surfaces. Surfaces and Interfaces, 2022, 35, 102420.	1.5	4
73372	Exploring high pressure structural transformations, electronic properties and superconducting properties of MH2 (MÂ=ÂNb, Ta). Arabian Journal of Chemistry, 2022, 15, 104347.	2.3	1
73373	Helium electron beam rf plasma for low-k surface functionalization. Journal of Vacuum Science and Technology B:Nanotechnology and Microelectronics, 2022, 40, 062203.	0.6	0
73374	Development of a sustainable nitrogen-doped biochar desulfurizer for solid oxide fuel cell systems. Biomass and Bioenergy, 2022, 167, 106631.	2.9	0
73375	Lignin-derived carbon quantum dots/Ni-MOL heterojunction from red phosphorus-assisted ball milling pretreatment and their application in photocatalysis: An insight from experiment and DFT calculation. Industrial Crops and Products, 2022, 189, 115829.	2.5	4
73376	Electronic descriptors for vacancy formation and hydrogen solution in Be-rich intermetallics. Acta Materialia, 2022, 241, 118428.	3.8	6
73377	A universal approach for predicting electrolyte decomposition in carbon materials: On the basis of thermodynamics. Energy Storage Materials, 2022, 53, 946-957.	9.5	1
73378	Effect of 4d transition metals on the electronic and magnetic properties of twin graphene. Journal of Magnetism and Magnetic Materials, 2022, 564, 170127.	1.0	4
73379	Cu-Nx active sites derived from copper phthalocyanine in porous carbon promoting oxygen reduction reaction. Synthetic Metals, 2022, 291, 117204.	2.1	2

#	Article	IF	Citations
73380	Non-trivial band topology in Bi doped Lanthanum monopnictides (LaX; X = As and Sb). Solid State Communications, 2022, 358, 114976.	0.9	0
73381	First-principles investigation of TiB3 under high pressure. Solid State Communications, 2022, 358, 114989.	0.9	1
73382	Non-metal doping in triple perovskite Ba2K2Te2O9 for enhanced photovoltaic properties: A first-principles study. Optik, 2022, 271, 170098.	1.4	0
73383	Regulating on photocatalytic overall water splitting performance of gallium thiophosphate based on transition metal doping: A first-principles study. Molecular Catalysis, 2022, 533, 112765.	1.0	0
73384	First-principles calculations on brazed diamond with FeCoCrNi high entropy alloys doped with strong carbide-forming elements. Solid State Communications, 2022, 357, 114980.	0.9	8
73385	Mitigating interfacial instability of high-voltage sodium layered oxide cathodes with coordinative polymeric structure. Journal of Power Sources, 2022, 552, 232235.	4.0	6
73386	Synergistic effect of BrÃ¸nsted/Lewis acid in olefin aromatization during MTO over Zn modified H-SAPO-34 zeolite: A periodic DFT study. Molecular Catalysis, 2022, 533, 112755.	1.0	2
73387	Synchronized integration of iron/cobalt dual-metal in nitrogen-doped carbon hollow spheres for enriched supercapacitive and oxygen reduction reaction performances. Journal of Energy Storage, 2022, 56, 105895.	3.9	5
73388	Transition Metalâ^'N/Graphene for advanced Lithiumâ€“Sulfur Batteries: A first principles study. Chemical Physics Letters, 2022, 808, 140118.	1.2	2
73389	Thermodynamic stability reversal of iron sulfides at the nanoscale: Insights into the iron sulfide formation in low-temperature aqueous solution. Geochimica Et Cosmochimica Acta, 2022, 338, 220-228.	1.6	6
73390	Surface protrusion induced by inter-diffusion on Cu-Sn micro-pillars. Materials and Design, 2022, 224, 111318.	3.3	0
73391	A novel low-temperature Fe-Fe double-atom catalyst for a â€œfast SCRâ€•reaction. Molecular Catalysis, 2022, 533, 112769.	1.0	5
73392	Electronic-level deciphering of the desalination mechanism of high-performance graphenylene membranes. Journal of Membrane Science, 2022, 664, 121068.	4.1	9
73393	Adsorption, sensing, electronic and magnetic properties of phosgene (COCl2) molecule adsorbed on Nb-doped arsenene: First-principles study. Solid State Communications, 2022, 357, 114975.	0.9	3
73394	Electronic properties and magnetism of CrCl3 nanoribbons. Journal of Magnetism and Magnetic Materials, 2022, 564, 170105.	1.0	4
73395	Enhancement mechanism of P dopant on atomically distributed FeN4P-C electrocatalyst over a wide pH range. Electrochimica Acta, 2022, 436, 141452.	2.6	4
73396	Exploring site-selective photoluminescence of Eu3+ and Tb3+ ions in Sr10(PO4)6F2 and the development of different phosphor materials. Optical Materials, 2022, 134, 113077.	1.7	5
73397	Influence of the co-doping and line-doping on the quantum capacitance of stanene for supercapacitor electrodes. Chemical Physics Letters, 2022, 808, 140123.	1.2	2

#	Article	IF	Citations
73398	Dataset for electronic and optical properties of Y2O2S and Er dopped Y2O2S calculated using density functional theory and simulated x-ray near edge spectra. Data in Brief, 2022, 45, 108671.	0.5	0
73399	CoFe2O4-APTES nanocomposite for the selective determination of tacrolimus in dosage forms: Perspectives from computational studies. Surfaces and Interfaces, 2022, 35, 102406.	1.5	1
73400	Improving thermoelectric properties of Cu2O powder via interface modification. Solid State Communications, 2022, 357, 114982.	0.9	1
73401	Self-supported Mo-doped TiO2 electrode for ambient electrocatalytic nitrogen oxidation. Electrochimica Acta, 2022, 435, 141333.	2.6	6
73402	Thermodynamic modeling of the Pdâ€“Zn system with uncertainty quantification and its implication to tailor catalysts. Calphad: Computer Coupling of Phase Diagrams and Thermochemistry, 2022, 79, 102491.	0.7	3
73403	The lattice distortion, mechanical and thermodynamic properties of A(Zr0.2Sn0.2Ti0.2Hf0.2Nb0.2)O3 (AÂ=ÂSr, Ba) high-entropy perovskite with B-site disorder: First principles prediction. Materials and Design, 2022, 224, 111308.	3.3	9
73404	Experimental and density functional theory studies of laminar double-oxidized graphene oxide nanofiltration membranes. Chemical Engineering Research and Design, 2022, 188, 590-606.	2.7	5
73405	Effect of hydrogen content on superconductivity in Laâ€“H compounds. Results in Physics, 2022, 43, 106060.	2.0	0
73406	SEI formation mechanisms and Li+ dissolution in lithium metal anodes: Impact of the electrolyte composition and the electrolyte-to-anode ratio. Journal of Power Sources, 2022, 551, 232203.	4.0	9
73407	Quadruple perovskite CaCu3Fe2Re2O12: A potential actuator based on a multiscale model. Materials Today Communications, 2022, 33, 104811.	0.9	0
73408	First-principles study on selenium-doped Li10GeP2S12 solid electrolyte: Effects of doping on moisture stability and Li-ion transport properties. Materials Today Chemistry, 2022, 26, 101223.	1.7	3
73409	Y2Mo3O12â€“Ba0.5Sr0.5Co0.8Fe0.2O3-Î´ cathode catalyst for proton-conducting solid oxide fuel cells. Journal of Power Sources, 2022, 551, 232073.	4.0	11
73410	Application of graphdiyne oxide in photoelectrochemical-type photodetectors and ultrafast fiber lasers. Nano Today, 2022, 47, 101653.	6.2	10
73411	Distribution of the mechanical properties of Tiâ€“Cu combinatorial thin film evaluated using nanoindentation experiments and molecular dynamics with a neural network potential. Materials Today Communications, 2022, 33, 104750.	0.9	1
73412	Thermodynamic properties and hydration behavior of ye'elimite. Cement and Concrete Research, 2022, 162, 106995.	4.6	10
73413	Hot corrosion behavior and mechanism of cryo-rolled MP159 superalloy with long rod-like Î³â€² phase. Corrosion Science, 2022, 209, 110706.	3.0	3
73414	Computational screening of bimetallene for the composite lithium metal anode. Applied Surface Science, 2023, 609, 155403.	3.1	1
73415	First-principles studies of the two-dimensional 1H-BeP2 as an electrode material for rechargeable metal ion (Li+, Na+, K+) batteries. Computational Materials Science, 2023, 216, 111868.	1.4	5

#	Article	IF	Citations
73416	Comprehensive understanding of local lattice distortion in dilute and equiatomic FCC alloys. Materials Chemistry and Physics, 2023, 293, 126928.	2.0	0
73417	Evidence of molecular clicking on self-assembled monolayers on Au (111) and their properties. Computational Materials Science, 2023, 216, 111809.	1.4	0
73418	Role of vibrational entropy in impurity segregation at grain boundaries in bcc iron. Computational Materials Science, 2023, 216, 111858.	1.4	3
73419	First principle studies on electronic and thermoelectric properties of Fe2TiSn based multinary Heusler alloys. Computational Materials Science, 2023, 216, 111856.	1.4	3
73420	One-pot synthesis of 2,5-bis(hydroxymethyl)furan from biomass derived 5-(chloromethyl)furfural in high yield. Journal of Energy Chemistry, 2023, 76, 421-428.	7.1	6
73421	CeO2 modified carbon nanotube electrified membrane for the removal of antibiotics. Chemosphere, 2023, 310, 136771.	4.2	5
73422	Enhanced spinâ€“orbit torque efficiency with low resistivity in perpendicularly magnetized heterostructures consisting of Si-alloyed Î²-W layers. Applied Surface Science, 2023, 609, 155352.	3.1	4
73423	The half-metallicity induced by non-magnetic adatoms on phosphorene nanoribbons. Physica B: Condensed Matter, 2023, 648, 414406.	1.3	1
73424	aflow.org: A web ecosystem of databases, software and tools. Computational Materials Science, 2023, 216, 111808.	1.4	17
73425	Unraveling the improved CO2 adsorption and COOH* formation over Cu-decorated ZnO nanosheets for CO2 reduction toward CO. Chemical Engineering Journal, 2023, 452, 139701.	6.6	23
73426	Î¸â€²â€²â€² precipitate phase, GP zone clusters and their origin in Al-Cu alloys. Journal of Alloys and Compounds, 2023, 930, 167396.	2.8	1
73427	Investigation of interfacial interaction of graphene oxide and Ti3C2Tx (MXene) via atomic force microscopy. Applied Surface Science, 2023, 609, 155303.	3.1	4
73428	The hydrogen-resistant surface of steels designed by alloy elements doping: First-principles calculations. Computational Materials Science, 2023, 216, 111854.	1.4	4
73429	First-principles prediction of the missed Pmmn phase for a GaTe monolayer as a new two-dimensional semiconductor. Scripta Materialia, 2023, 223, 115073.	2.6	10
73430	Deciphering the electronic-level mechanism of Na+ transport in a graphdiyne desalination membrane with periodic nanopores. Desalination, 2023, 546, 116183.	4.0	6
73431	First-principles study on SrSnO₃ as a transparent conductive oxide. Wuli Xuebao/Acta Physica Sinica, 2023, .	0.2	0
73432	Highly efficient SWCNT/GaAs van der Waals heterojunction solar cells enhanced by Nafion doping. Journal of Alloys and Compounds, 2023, 932, 167624.	2.8	3
73433	Large magnetoresistance in phosphorus-sulfur compounds (TMPS4) based temperature regulated spin-caloritronic devices. Physica E: Low-Dimensional Systems and Nanostructures, 2023, 146, 115529.	1.3	2

#	Article	IF	Citations
73434	Effects of Li contents on the stability, electronic and Li-ion diffusion properties of Li_{3x}La_{(2/3)-x}<teshuzifu>Â†_{(1/3)-2x}TiO₃ surface. Wuli Xuebao/Acta Physica Sinica, 2023, .		
73435	Tunable electronic and optical properties of 2D SiGe/SnI2 vdW heterostructures for high-performance ultraviolet photodetectors. Computational Materials Science, 2023, 216, 111845.	1.4	4
73436	First-principles calculations on O-atom diffusion on fluorinated graphene. Wuli Xuebao/Acta Physica Sinica, 2023, .	0.2	0
73437	Copper-based Ruddlesden-Popper perovskite oxides activated hydrogen peroxide for coal pyrolysis wastewater (CPW) degradation: Performance and mechanism. Environmental Research, 2023, 216, 114591.	3.7	6
73438	Photo-electric properties of preferred orientation of tin oxide studied by first-principles. Materials Science and Engineering B: Solid-State Materials for Advanced Technology, 2023, 287, 116080.	1.7	4
73439	Relay photo/thermal catalysis enables efficient cascade upgrading of sugars to lactic acid: Mechanism study and life cycle assessment. Chemical Engineering Journal, 2023, 452, 139687.	6.6	15
73440	Encapsulate lithium sulfide cathodes with carbon-doped MoS2 for fast kinetics in lithium-sulfur batteries, a theoretical study. Acta Materialia, 2023, 242, 118441.	3.8	7
73441	Identification and evolution of ultrafine precipitates in Fe-Cu alloys by first-principles modeling of positron annihilation. Acta Materialia, 2023, 242, 118429.	3.8	5
73442	Encapsulating Pd/g-C3N4 with acrylic acid to enhance the catalytic partial hydrogenation performance of isoprene. Carbon, 2023, 201, 1174-1183.	5.4	2
73443	Influence of intercalated Gd atoms on graphene-4H-SiC(0001) properties. Applied Surface Science, 2023, 609, 155365.	3.1	1
73444	Unraveling the substitution and strain-induced hydrogen diffusion performance of ZrCo-based intermetallics. Computational Materials Science, 2023, 216, 111849.	1.4	2
73445	Numerical investigation of dislocation climb under stress and irradiation. Acta Materialia, 2023, 242, 118431.	3.8	4
73446	Multiatom activation of single-atom electrocatalysts via remote coordination for ultrahigh-rate two-electron oxygen reduction. Journal of Energy Chemistry, 2023, 76, 622-630.	7.1	14
73447	Insights into impact interaction between graphene and High-speed atomic oxygen for aerospace protection application. Applied Surface Science, 2023, 609, 155274.	3.1	4
73448	Effects of N-doping and oxygen vacancies on electronic structure of LiFePO4. Physica B: Condensed Matter, 2023, 648, 414437.	1.3	1
73449	Large vertical piezoelectricity and high-temperature ferromagnetism in 2D ferromagnetic semiconductors MnAsX (X = I,Br,Cl). Physica E: Low-Dimensional Systems and Nanostructures, 2023, 146, 115544.	1.3	2
73450	Constructing efficient ternary PtTeCu nano-catalysts with 2D ultrathin-sheet structures for oxidation reaction of alcohols. Applied Surface Science, 2023, 609, 155301.	3.1	3
73451	Nickel-iron layered silicate nanomembrane as efficient electrocatalyst for oxygen evolution reaction in alkaline media. Fuel, 2023, 332, 126209.	3.4	5

#	Article	IF	Citations
73452	Theoretical prediction on stability, electronic and activity properties of single-atom catalysts anchored graphene and boron phosphide heterostructures. Fuel, 2023, 332, 126213.	3.4	10
73453	Effects of strain and Al doping on monolayer h-BN: First-principles calculations. Physica E: Low-Dimensional Systems and Nanostructures, 2023, 146, 115546.	1.3	4
73454	Electronic structure modulation of Ru/W20O58 catalyst via interfacial Ruâ€“Oâ€“W bridging bond for high-performance Liâ€“O2 batteries. Applied Surface Science, 2023, 609, 155453.	3.1	9
73455	Phase regulation of WO3 for highly selective oxygen reduction to hydrogen peroxide. Chemical Engineering Journal, 2023, 452, 139449.	6.6	11
73456	CoS2 enhanced SnO2@rGO heterostructure quantum dots for advanced lithium-ion battery anode. Journal of Power Sources, 2023, 553, 232265.	4.0	13
73457	Enhancing Znâ€“CO2 battery with a facile Pd doped perovskite cathode for efficient CO2 to CO conversion. Energy, 2023, 263, 125688.	4.5	4
73458	A perspective LDHs/Ti3C2O2 design by DFT calculation for photocatalytic reduction of CO2 to C2 organics. Applied Surface Science, 2023, 609, 155445.	3.1	5
73459	Diverse electronic structures governed by N-substitution in stable two-dimensional dumbbell carbonitrides. Applied Surface Science, 2023, 609, 155463.	3.1	0
73460	Crystal structure and stability of phases in Mg-Zn alloys: A comprehensive first-principles study. Acta Materialia, 2023, 242, 118443.	3.8	9
73461	Insight into the effect of surface coverage of carbon support on selective CO2 electroreduction to C2H4 over copper-based catalyst. Applied Surface Science, 2023, 609, 155394.	3.1	6
73462	Metallic bismuth nanoclusters confined in micropores for efficient electrocatalytic reduction of carbon dioxide with long-term stability. Journal of Colloid and Interface Science, 2023, 630, 81-90.	5.0	8
73463	Catalytic debromination of waste brominated resin by co-pyrolysis with Pd-containing spent automotive catalysts. Resources, Conservation and Recycling, 2023, 188, 106721.	5.3	6
73464	Roles of hydrogen in structural stability and electronic property of bulk hydrogenated amorphous silicon. Computational Materials Science, 2023, 216, 111846.	1.4	4
73465	Group IIIâ€“V hexagonal pnictide clusters and their promise for graphene-like materials. , 2023, , 139-155.		0
73466	Amphiphilic ligand in situ assembly of uranyl active sites and selective interactions of molybdenum disulfide. Journal of Hazardous Materials, 2023, 442, 130089.	6.5	0
73467	Innovative strategy to optimize the temperature-dependent lattice misfit and coherency of iridium-based Î³/Î³â€™ interfaces. Applied Surface Science, 2023, 609, 155369.	3.1	0
73468	Predict low energy structures of BSi monolayer as high-performance Li/Na/K ion battery anode. Applied Surface Science, 2023, 609, 155222.	3.1	8
73469	Identification of oxidation states in <mml:math xmlns:mml="http://www.w3.org/1998/Math/MathML" altimg="si20.svg" display="inline" id="d1e1095"><mml:mi>Î³</mml:mi></mml:math>-graphyne by computational XPS and NEXAFS spectra. Applied Surface Science, 2023, 609, 155134.	3.1	5

#	Article	IF	Citations
73470	TM-N4C (TMÂ=ÂCo, Pd, Pt and Ru) as OER electrocatalysts in lithium-oxygen batteries: First-principles study. Applied Surface Science, 2023, 609, 155331.	3.1	4
73471	Anchoring highly distributed Pt species over oxidized graphitic carbon nitride for photocatalytic hydrogen evolution: The effect of reducing agents. Applied Surface Science, 2023, 609, 155305.	3.1	6
73472	Optimal doping elements for inhibiting surface-diffusion of adatoms on Cu3Sn. Applied Surface Science, 2023, 609, 155003.	3.1	4
73473	Pd doping Au(1 1 1) surfaces enhancing formaldehyde adsorption: A first-principle study. Computational Materials Science, 2023, 216, 111885.	1.4	5
73474	Artificial visible light-induced H2O2 production using polymeric K/O-doped carbon nitride as a catalyst. Applied Surface Science, 2023, 609, 155432.	3.1	8
73475	Hydrogen production from H2S on metal-doped FeS Mackinawite monolayer via DFT calculations. Applied Surface Science, 2023, 609, 155322.	3.1	1
73476	Precipitation and hydrolysis of water-soluble ammonium polyphosphate on calcite surface depend on the number of P species. Colloids and Surfaces A: Physicochemical and Engineering Aspects, 2023, 656, 130331.	2.3	1
73477	The electronic, mechanical properties and in-plane negative Poissonâ€™s ratio in novel pentagonal NiX2 (XÂ=ÂS, Se, Te) monolayers with strong anisotropy: A first-principles prediction. Computational Materials Science, 2023, 216, 111873.	1.4	8
73478	TiN/TiC heterostructures embedded with single tungsten atoms enhance polysulfide entrapment and conversion for high-capacity lithium-sulfur battery applications. Energy Storage Materials, 2023, 54, 410-420.	9.5	23
73479	Hydrogen trapping, desorption and clustering in heterophase interfaces of W-ZrC alloy. Acta Materialia, 2023, 242, 118469.	3.8	7
73480	Easily exfoliable monolayer of GdTe<mml:math xmlns:mml="http://www.w3.org/1998/Math/MathML" altimg="si40.svg" display="inline" id="d1e691"><mml:msub><mml:mrow /><mml:mrow><mml:mn>3</mml:mn></mml:mrow></mml:msub></mml:math>: ab initio study. Computational Materials Science, 2023, 216, 111869.	1.4	0
73481	Accurate interatomic potential for the nucleation in liquid Ti-Al binary alloy developed by deep neural network learning method. Computational Materials Science, 2023, 216, 111843.	1.4	6
73482	Electronic and transport properties of Heusler alloy based magnetic tunneling junctions: A first principles study. Computational Materials Science, 2023, 216, 111852.	1.4	3
73483	Defects study in zinc blende ZnS utilizing optimized hybrid functional. Computational Materials Science, 2023, 216, 111827.	1.4	4
73484	Break through the strength-ductility trade-off dilemma in aluminum matrix composites via precipitation-assisted interface tailoring. Acta Materialia, 2023, 242, 118470.	3.8	34
73485	High thermoelectric power factor in <mml:math xmlns:mml="http://www.w3.org/1998/Math/MathML" altimg="si10.svg" display="inline" id="d1e211"><mml:mrow><mml:mi>L</mml:mi><mml:mi>a</mml:mi><mml:mi>V</mml:mi><mml:msub><mml:mrow><mml:mi>O</mml:mi> heterostructure. Physica E: Low-Dimensional Systems and Nanostructures, 2023, 146, 115525.	1.3	1
73486	Influence of oxygen and nitrogen doping on the structure and magnetic properties of CoNi alloy: First principle calculations. Journal of Physics and Chemistry of Solids, 2023, 172, 111082.	1.9	10
73487	Interfacial properties of polyethylene/Ti3C2Tx mxene nanocomposites investigated by first-principles calculations. Applied Surface Science, 2023, 609, 155344.	3.1	7

#	Article	IF	Citations
73488	Interface engineering of Ni/NiO heterostructures with abundant catalytic active sites for enhanced methanol oxidation electrocatalysis. Journal of Colloid and Interface Science, 2023, 630, 570-579.	5.0	20
73489	Tailoring the sensing capability of 2H-MoSe2 via 3d transition metal decoration. Applied Surface Science, 2023, 610, 155399.	3.1	6
73490	Fermi surface of LaSb2 and direct observation of a CDW transition. Applied Surface Science, 2023, 610, 155477.	3.1	2
73491	Facile and rapid synthesis of hierarchical LDHs array by universal molten salt with bound water toward efficient oxygen evolution electrocatalysis. Chemical Engineering Journal, 2023, 452, 139686.	6.6	3
73492	NaOH-modified biochar supported Fe/Mn bimetallic composites as efficient peroxymonosulfate activator for enhance tetracycline removal. Chemical Engineering Journal, 2023, 454, 139949.	6.6	35
73493	Influence of oxygen addition on the oxidation resistance of TiAlN. Scripta Materialia, 2023, 224, 115148.	2.6	3
73494	Bimetallic Zn3Sn2 electrocatalyst derived from mixed oxides enhances formate production towards CO2 electroreduction reaction. Applied Surface Science, 2023, 608, 155110.	3.1	3
73495	Experimental study of covalent Cr3C2 with high ionicity: Sound velocities, elasticity, and mechanical properties under high pressure. Scripta Materialia, 2023, 224, 115146.	2.6	2
73496	Theoretical insight into the electronic, optical, and photocatalytic properties and quantum capacitance of Sc2CT2 (T = F, P, Cl, Se, Br, O, Si, S, OH) MXenes. Vacuum, 2023, 207, 111615.	1.6	15
73497	Unveiling the enhancement essence on Li2S deposition by the polarized topological Î²-polyvinylidene fluoride: Beyond built-in electric field effect. Chemical Engineering Journal, 2023, 453, 139752.	6.6	2
73498	PHP-graphene nanoribbon-assembled porous metallic carbon for sodium-ion battery anode with high specific capacity. Carbon, 2023, 202, 112-118.	5.4	5
73499	Deep-red to NIR mechanoluminescence in centrosymmetric perovskite MgGeO3: Mn2+ for potential dynamic signature anti-counterfeiting. Chemical Engineering Journal, 2023, 453, 139671.	6.6	28
73500	Intermetallic niobium boride toward efficient adsorption and catalysis of polysulfides in Lithium-Sulfur batteries. Chemical Engineering Journal, 2023, 453, 139566.	6.6	5
73501	Simultaneous catalytic oxidation mechanism of NO and Hg0 over single-atom iron catalyst. Applied Surface Science, 2023, 609, 155298.	3.1	9
73502	Predicting single-phase solid solutions in as-sputtered high entropy alloys: High-throughput screening with machine-learning model. Journal of Materials Science and Technology, 2023, 138, 70-79.	5.6	10
73503	In situ formation of a lithiophilic surface on 3D current collectors to regulate lithium nucleation and growth for dendrite-free lithium metal anodes. Chemical Engineering Journal, 2023, 453, 139903.	6.6	18
73504	First-principles calculations of the temperature dependence of stacking fault energies in Mg. Scripta Materialia, 2023, 224, 115075.	2.6	2
73505	Photocatalytic degradation of organic pollutants over MoS2/Ag-ZnFe2O4 Z-scheme heterojunction: Revealing the synergistic effects of exposed crystal facets, defect engineering, and Z-scheme mechanism. Chemical Engineering Journal, 2023, 453, 139775.	6.6	47

#	Article	IF	Citations
73506	Short range ordering improves elastic properties of Mo additive W-Re solid solution: A first principles investigation. Scripta Materialia, 2023, 224, 115132.	2.6	4
73507	Efficient Pd on carbon catalyst for ammonium formate dehydrogenation: Effect of surface oxygen functional groups. Applied Catalysis B: Environmental, 2023, 321, 122015.	10.8	8
73508	Membrane-free pure H2 production over single dispersed Ru-anchored Pt3Ni alloys via coupling ethanol selective electrooxidation. Applied Catalysis B: Environmental, 2023, 321, 122065.	10.8	15
73509	Hydrogen trapping potential of a few novel molecular clusters and ions. , 2023, , 297-312.		0
73510	Stable nanoparticles dispersion induced an unprecedented high strength in a bulk W-TiC alloy. Scripta Materialia, 2023, 224, 115136.	2.6	2
73511	Interfacial coupled engineering of plasmonic amorphous MoO3-x nanodots/g-C3N4 nanosheets for photocatalytic water splitting and photothermal conversion. Chemical Engineering Journal, 2023, 453, 139875.	6.6	16
73512	High-throughput calculation of interfacial friction of two-dimensional materials. Wuli Xuebao/Acta Physica Sinica, 2023, .	0.2	0
73513	Activating well-defined Î±-Fe2O3 nanocatalysts by near-surface Mn atom functionality for auto-exhaust soot purification. Applied Catalysis B: Environmental, 2023, 321, 122077.	10.8	13
73514	Selective hydrogenation of acetylene to ethylene: Performance of a Pt monolayer over an Î±-WC(0001) surface for binding and hydroconversion of acetylene. Surface Science, 2023, 728, 122197.	0.8	1
73515	Adsorption structures of catechol on the ZnO(10-10) surface. Applied Surface Science, 2023, 610, 155504.	3.1	1
73516	Defect-engineered plasmonic Z-scheme heterostructures for superior photoelectrochemical water oxidation. Applied Surface Science, 2023, 610, 155454.	3.1	1
73517	Synergistic effect of Mn3+ and oxygen vacancy on the bifunctional oxygen electrocatalytic performance of MnOX/CNTs composites. Journal of Alloys and Compounds, 2023, 933, 167728.	2.8	13
73518	Electrochemical hydroxidation of sulfide for preparing sulfur-doped NiFe (oxy) hydroxide towards efficient oxygen evolution reaction. Chemical Engineering Journal, 2023, 454, 140030.	6.6	7
73519	Universal construction of sulfur doped molybdenum-based nanosheets for enhanced hydrogen evolution in a wide pH range. Applied Catalysis B: Environmental, 2023, 322, 122131.	10.8	6
73520	Efficient catalytic ozonation over Co-ZFO@Mn-CN for oxalic acid degradation: Synergistic effect of oxygen vacancies and HOO-Mn-NX bonds. Applied Catalysis B: Environmental, 2023, 322, 122085.	10.8	14
73521	A first-principles study on the electronic, piezoelectric, and optical properties and strain-dependent carrier mobility of Janus TiXY (X â‰ Y, X/Y = Cl, Br, I) monolayers. Physical Chemistry Chemical Physics, 2022, 25, 274-285.	1.3	4
73522	Lewis acid Sn-Beta catalysts for the cycloaddition of isoprene and methyl acrylate: a greener route to bio-derived monomers. Catalysis Science and Technology, 2022, 12, 7439-7447.	2.1	4
73523	Fluoride-assisted detection of glutathione by surface Ce³⁺/Ce⁴⁺ engineered nanoceria. Journal of Materials Chemistry B, 2022, 10, 9855-9868.	2.9	11

#	Article	IF	Citations
73524	Stack-dependent ion diffusion behavior in two-dimensional bilayer C₃B. Dalton Transactions, 2022, 51, 17902-17910.	1.6	2
73525	Storage of Na in 2D SnS for Na ion batteries: a DFT prediction. Physical Chemistry Chemical Physics, 2022, 24, 29609-29615.	1.3	12
73526	Spin evolution and flip in the oxygen reduction reaction: a theoretical study of Cu(Ni)XP₂S₆(X = In, Bi and Cr). Journal of Materials Chemistry A, 2022, 10, 25262-25271.	5.2	3
73527	¹H chemical shift anisotropy: a high sensitivity solid-state NMR dynamics probe for surface studies?. Physical Chemistry Chemical Physics, 2023, 25, 5348-5360.	1.3	4
73528	Study on the electronic and optical properties of van der Waals heterostructures of blue phosphorene and Janus-WSeS monolayers for photocatalytic water splitting. Materials Advances, 2022, 3, 9063-9070.	2.6	4
73529	First principles prediction of electronic, mechanical, transport and optical properties of the silicane/Ga₂SSe heterostructure. RSC Advances, 2022, 12, 31935-31942.	1.7	5
73530	Structural, electronic, optical and photocatalytic properties of KTaO₃ with NiO cocatalyst modification. RSC Advances, 2022, 12, 32270-32279.	1.7	0
73531	Precise and scalable fabrication of metal pair-site catalysts enabled by intramolecular integrated donor atoms. Journal of Materials Chemistry A, 2022, 10, 25307-25318.	5.2	4
73532	Designing Ferrimagnetic-Ferroelastic Multiferroic Semiconductor in FeMoClO₄ Nanosheet via Element Substitution. Nanoscale, 0, , .	2.8	1
73533	Investigation of the effect of point defects on the Li-ion conductivity of Li3InCl6. Dalton Transactions, 0, , .	1.6	1
73534	The reducibility and oxidation states of oxide-supported rhenium: Experimental and theoretical investigations. Physical Chemistry Chemical Physics, 0, , .	1.3	0
73535	Synergistic defect engineering for improving n-type NbFeSb thermoelectric performance through high-throughput computations. Journal of Materials Chemistry A, 2022, 10, 24598-24610.	5.2	3
73536	Water interaction with B-site (B = Al, Zr, Nb, and W) doped SrFeO_{3â^'Î´}-based perovskite surfaces for thermochemical water splitting applications. Physical Chemistry Chemical Physics, 2022, 24, 28975-28983.	1.3	2
73537	Insights into photoinduced carrier dynamics and hydrogen evolution reaction of organic PM6/PCBM heterojunctions. Journal of Materials Chemistry A, 2022, 10, 24529-24537.	5.2	3
73538	Decoration of defective graphene with MoS2 enabling enhanced anchoring and catalytic conversion of polysulfides for lithium-sulfur batteries: A first-principles study. Physical Chemistry Chemical Physics, 0, , .	1.3	2
73539	Effect of the water coverage on the interaction of O₂ and H₂ with the Na-LTA zeolite by first-principles simulations. Inorganic Chemistry Frontiers, 2023, 10, 383-395.	3.0	1
73540	Charge transfer modulated heterointerfaces for hydrogen production at all pH values. Journal of Materials Chemistry A, 2022, 10, 24927-24937.	5.2	6
73541	Effect of temperature on structural, dynamical, and electronic properties of Sc₂Te₃ from first-principles calculations. RSC Advances, 2022, 12, 32796-32802.	1.7	1

#	Article	IF	Citations
73542	Catalytic Activity of 1D Chains of Gold Oxide on a Stepped Gold Surface from Density Functional Theory. Physical Chemistry Chemical Physics, 0, , .	1.3	0
73543	Tuning of hole carrier density in p-type Î±-SnWO₄ by exploiting oxygen defects. Materials Advances, 2022, 3, 9111-9116.	2.6	3
73544	Actinide-doped boron clusters: from borophenes to borospherenes. Physical Chemistry Chemical Physics, 2022, 24, 29705-29711.	1.3	2
73545	Revealing the anisotropic phonon behaviours of layered SnS by angle/temperature-dependent Raman spectroscopy. RSC Advances, 2022, 12, 32262-32269.	1.7	1
73546	Prediction of the ferrovalley property with sizable valley splitting in Janus monolayer GdBrI. Physical Chemistry Chemical Physics, 2022, 24, 28457-28464.	1.3	5
73547	Facile synthesis of a high-efficiency NiFe bimetallic catalyst without pre-reduction for the selective hydrogenation reaction of furfural. Catalysis Science and Technology, 2023, 13, 457-467.	2.1	3
73548	Effect of oxygen coordination on the electrocatalytic nitrogen fixation of a vanadium single-atom catalyst embedded in graphene. New Journal of Chemistry, 2022, 46, 22936-22943.	1.4	5
73549	Enhanced photoelectric performance of MoSSe/MoS₂ van der Waals heterostructures with tunable multiple band alignment. Physical Chemistry Chemical Physics, 2022, 24, 29882-29890.	1.3	4
73550	The active ruthenium (101) crystal plane selectively exposed byin situmetal hyperaccumulation on a living plant for overall water splitting. Green Chemistry, 2022, 24, 9668-9676.	4.6	4
73551	Theoretical study on the ferroelectric and light absorption properties of Li₂SbBiO₆ for harvesting visible light. RSC Advances, 2022, 12, 32027-32034.	1.7	3
73552	Electronic state evolution of oxygen-doped monolayer WSe₂ assisted by femtosecond laser irradiation. Physical Chemistry Chemical Physics, 2023, 25, 2043-2049.	1.3	2
73553	Structural design strategies for superionic sodium halide solid electrolytes. Journal of Materials Chemistry A, 2022, 10, 24301-24309.	5.2	9
73554	Transition Metals Trimers on C₂N as Electrochemical Catalysts for CO₂ Reduction to CH₄: A First-Principles Study. Hans Journal of Nanotechnology, 2022, 12, 330-339.	0.1	0
73555	Defect engineering in the MA₂Z₄ monolayer family for enhancing the hydrogen evolution reaction: first-principles calculations. Sustainable Energy and Fuels, 2022, 7, 164-171.	2.5	7
73556	Theoretical investigation of single-atom catalysts anchored on pure carbon substrate for electroreduction of NO to NH₃. Physical Chemistry Chemical Physics, 2022, 24, 29112-29119.	1.3	1
73557	Modulating the water gas shift reaction via strong interfacial interaction between a defective oxide matrix and exsolved metal nanoparticles. Journal of Materials Chemistry A, 2022, 10, 24995-25008.	5.2	1
73558	A glutamate anion boosted zinc anode for deep cycling aqueous zinc ion batteries. Journal of Materials Chemistry A, 2022, 10, 25029-25038.	5.2	19
73559	Ga and Zn increase the oxygen affinity of Cu-based catalysts for the CO_x hydrogenation according to ab initio atomistic thermodynamics. Chemical Science, 2022, 13, 13442-13458.	3.7	6

#	Article	IF	Citations
73560	Structure andÂElectronic Properties ofÂUltrathin (In, Mg) Films onÂSi(111). Springer Theses, 2022, , 53-69.	0.0	0
73561	Visible-light driven H₂ evolution over a precious metal-free hybrid photocatalyst constructed from CuO and NiFe layered double hydroxide. Catalysis Science and Technology, 2023, 13, 675-683.	2.1	3
73562	Potassium clusters in tungsten grain boundaries: Formation mechanism and strengthening effect. Journal of Nuclear Materials, 2023, 573, 154135.	1.3	2
73563	Disordering in Fe3Ga alloy of D03 structure: Effect on stability and magnetostriction. Computational Materials Science, 2023, 216, 111878.	1.4	0
73564	Trends in opto-electronic properties of MgxZn1-xSnN2 using first principles methods. Materials Chemistry and Physics, 2023, 294, 126995.	2.0	1
73565	Single-crystal Li-rich layered cathodes with suppressed voltage decay by double-layer interface engineering. Energy Storage Materials, 2023, 54, 651-660.	9.5	22
73566	First-principles study of chalcogen-bonded self-assembly structures on silicene: Some insight into the fabrication of molecular architectures on surfaces through chalcogen bonding. Chemical Physics, 2023, 565, 111763.	0.9	0
73567	Magnesium storage enhancement of molybdenum dioxide in hybrid magnesium lithium batteries. Electrochimica Acta, 2023, 437, 141498.	2.6	0
73568	Microstates and defects of incoherent Î£3 [111] twin boundaries in aluminum. Acta Materialia, 2023, 243, 118499.	3.8	7
73569	N doped porous carbon nanosheets with enhanced zinc ion storage capability. Journal of Power Sources, 2023, 554, 232348.	4.0	12
73570	Effect of biaxial [110] strain on monolayer MoS2 and its vacancy defect system: A first-principles study. Journal of Solid State Chemistry, 2023, 317, 123711.	1.4	2
73571	Ball milling enhanced Cr(VI) removal of zero-valent iron biochar composites: Functional groups response and dominant reduction species. Chemosphere, 2023, 311, 137174.	4.2	23
73572	Hollandite-type potassium titanium oxide with exceptionally stable cycling performance as a new cathode material for potassium-ion batteries. Energy Storage Materials, 2023, 54, 680-688.	9.5	3
73573	Local lattice distortions, phase stability, and mechanical properties of NbMoTaWHfx alloys: A combined theoretical and experimental study. Computational Materials Science, 2023, 217, 111891.	1.4	3
73574	Excellent optoelectronic and thermoelectric properties of two-dimensional transition metal dinitride HfN2. Physica B: Condensed Matter, 2023, 649, 414505.	1.3	2
73575	The effects of solutes like ruthenium on precipitation of Ïƒ phase and Ïƒ/Î³ interface stability in Ni-based superalloys. Intermetallics, 2023, 152, 107768.	1.8	4
73576	Ab-initio molecular dynamics study of heterogeneous nucleation at the liquid-Y/Î±-Al2O3 interface. Computational Materials Science, 2023, 217, 111899.	1.4	2
73577	On the atomic structure of the <mml:math xmlns:mml="http://www.w3.org/1998/Math/MathML" altimg="si35.svg" display="inline" id="d1e627"><mml:msup><mml:mrow><mml:mi>Î²</mml:mi></mml:mrow><mml:mrow><mml:mo>â€²</mml:mo><mml:mo>â€²</mml:mo> precipitate by density functional theory. Computational Materials Science, 2023, 217, 111871.	1.4	0

#	Article	IF	Citations
73578	Adsorption of NO gas molecule on the vacancy defected and transition metal doped antimonene: A first-principles study. Vacuum, 2023, 207, 111654.	1.6	7
73579	First-principles predictions of stable structure of AuAl2 under high pressure. Solid State Communications, 2023, 359, 115009.	0.9	0
73580	Revisiting the structure, interaction, and dynamical property of ionic liquid from the deep learning force field. Journal of Power Sources, 2023, 555, 232350.	4.0	3
73581	First-principles study of Al/Al3Ni interfaces. Computational Materials Science, 2023, 217, 111896.	1.4	1
73582	First-principles study of point defect diffusion in CoMn2O4 crystal. Electrochimica Acta, 2023, 437, 141520.	2.6	3
73583	Metal-organic framework-induced edge-riched growth of layered Bi2Se3 towards ultrafast Na-ion storage. Journal of Power Sources, 2023, 555, 232387.	4.0	18
73584	Trash to treasure: Green synthesis of novel Ag2O/Ag2CO3 Z-scheme heterojunctions with highly efficient photocatalytic activities derived from waste mussel shells. Chemical Engineering Journal, 2023, 454, 140259.	6.6	11
73585	Achieving fast ion diffusion in aqueous zinc-ion batteries by cathode reconstruction design. Chemical Engineering Journal, 2023, 454, 140260.	6.6	8
73586	Electronic structure and magnetocaloric properties of Ce2Fe17â^'xCox compounds upon Co substitution. Journal of Alloys and Compounds, 2023, 935, 168060.	2.8	4
73587	Helium bubbles diffusion in aluminum: Influence of gas pressure. Journal of Nuclear Materials, 2023, 573, 154123.	1.3	5
73588	Automag: An automatic workflow software for calculating the ground magnetic state of a given structure and estimating its critical temperature. Computer Physics Communications, 2023, 283, 108571.	3.0	1
73589	Cr-promoted formation of B2+L21 composite nanoprecipitates and enhanced mechanical properties in ferritic alloy. Acta Materialia, 2023, 243, 118506.	3.8	10
73590	High-performance thermoelectric monolayer Î³-GeSe and its group-IV monochalcogenide isostructural family. Chemical Engineering Journal, 2023, 454, 140242.	6.6	16
73591	â€˜Anti-sluggishâ€™ Ti diffusion in HCP high-entropy alloys: Chemical complexity vs. lattice distortions. Scripta Materialia, 2023, 224, 115117.	2.6	13
73592	Hollow ppy@Ti2Nb10O29-x@NC bowls: A stressâ€“release structure with vacancy defects and coating interface for Li capacitor. Chemical Engineering Journal, 2023, 454, 140287.	6.6	12
73593	Oxygen vacancyâ€“rich Cu2O@Cu with a hydrophobic microenvironment for highly selective C C coupling to generate C2H4. Chemical Engineering Journal, 2023, 454, 140321.	6.6	11
73594	A systematic theoretical study the active sites of potassium promoter on the activity of water-gas shift reaction over Pt(1 1 1). Applied Surface Science, 2023, 611, 155638.	3.1	5
73595	DFT crystal and electronic structure of the direct bandgap Cu(1-x)NaxPF6: (x = 0.125n, n = 1â€“7). Journal of Physics and Chemistry of Solids, 2023, 173, 111116.	1.9	0

#	Article	IF	Citations
73596	Are olefin aromatization reactions structure sensitive over Al pairs and single Al in H-ZSM-5 Zeolite?. Fuel, 2023, 333, 126541.	3.4	3
73597	Influence of uncoordinated N content on Ni N C electrocatalyst for CO2 reduction: Combining first principle with machine learning. Fuel, 2023, 333, 126563.	3.4	3
73598	Effects of alloying elementsÂXÂ(Cr, Fe and Mo) on the interfacial properties of Î³-Ni(110)/TiC(110) in TiC-particles reinforced NMCs: First-principles study. Optics and Laser Technology, 2023, 158, 108870.	2.2	0
73599	Formation mechanism of stacking faults within Î±â€²â€² martensite in Ti-7Âwt%Mo alloy. Journal of Alloys and Compounds, 2023, 934, 168039.	2.8	3
73600	Semiconductor-metal transition caused by increased surface charge in two-dimensional quintuple-layers Al2O3 materials. Applied Surface Science, 2023, 610, 155614.	3.1	3
73601	Rapid discovery of inorganic-organic solid composite electrolytes by unsupervised learning. Chemical Engineering Journal, 2023, 454, 140151.	6.6	8
73602	Atomically precise Ni6(SC2H4Ph)12 nanoclusters on graphitic carbon nitride nanosheets for boosting photocatalytic hydrogen evolution. Journal of Colloid and Interface Science, 2023, 631, 212-221.	5.0	9
73603	AuPd nanoporous dendrites: High electrocatalytic activity and surface plasmon-enhanced stability for ethanol electrooxidation. Chemical Engineering Journal, 2023, 453, 139962.	6.6	9
73604	Atomic modification of Mo(1 0 0) surface for corrosion resistance. Applied Surface Science, 2023, 610, 155509.	3.1	1
73605	The adsorption and diffusion behaviors of nitrogen impurities in <mml:math xmlns:mml="http://www.w3.org/1998/Math/MathML" altimg="si80.svg" display="inline" id="d1e548"><mml:mi>h</mml:mi></mml:math>-BN by first-principles study. Materials Science in Semiconductor Processing, 2023, 154, 107175.	1.9	1
73606	A new perspective on the initial hydrogenation of TiFe0.9M0.1 (MÂ=ÂV, Cr, Fe, Co, Ni) alloys gained from surface oxide analyses and nucleation energetics. Applied Surface Science, 2023, 610, 155443.	3.1	3
73607	Activation of peroxymonosulfate for degrading ibuprofen via single atom Cu anchored by carbon skeleton and chlorine atom: The radical and non-radical pathways. Science of the Total Environment, 2023, 858, 160097.	3.9	7
73608	Origin of synergistic effect between Fe/Mn minerals and biochar for peroxymonosulfate activation. Chemical Engineering Journal, 2023, 453, 139899.	6.6	29
73609	Theoretical exploration of high-pressure crystal structures and valence states in the Liâ€“Cl system. Journal of Alloys and Compounds, 2023, 933, 167818.	2.8	1
73610	Coordination engineering of single-atom copper embedded graphene-like borocarbonitrides for hydrogen production. Applied Surface Science, 2023, 610, 155506.	3.1	5
73611	Evolutional solid phase and solid-liquid interface uranium immobilization mechanisms by nanoscale zero-valent iron and enhanced uranium stability control strategy. Chemical Engineering Journal, 2023, 453, 139924.	6.6	15
73612	A dealloyed bulk FeNi pattern with exposed highly active facets for cost-effective oxygen evolution. Applied Catalysis B: Environmental, 2023, 323, 122171.	10.8	15
73613	Coexistence of in- and out-of-plane piezoelectricity in Janus XSSiN2 (XÂ=ÂCr, Mo, W) monolayers. Applied Surface Science, 2023, 610, 155586.	3.1	13

#	Article	IF	Citations
73614	Synergistic surface activation during photocatalysis on perovskite derivative sites in heterojunction. Applied Catalysis B: Environmental, 2023, 323, 122146.	10.8	15
73615	Thinnest npn homojunction for inspired photoelectrochemical water splitting. Applied Catalysis B: Environmental, 2023, 323, 122182.	10.8	8
73616	Electrocatalysis in Liâ€“O2 battery over single-atom catalyst based on g-C3N4 substrate. Applied Surface Science, 2023, 610, 155481.	3.1	5
73617	The formation of high energy density fuel via the hydrogenation of naphthalene over Ni catalyst: The combined DFT and microkinetic analysis. Fuel, 2023, 333, 126307.	3.4	2
73618	Comparative analysis of NOx reduction on Pt, Pd, and Rh catalysts by DFT calculation and microkinetic modeling. Applied Surface Science, 2023, 611, 155572.	3.1	4
73619	Experimental investigation and thermodynamic assessment of the Alâ€“Agâ€“Sc system. Journal of Alloys and Compounds, 2023, 934, 167980.	2.8	8
73620	Ab initio Methods for Electronic Transport in Semiconductors and Nanostructures. Springer Handbooks, 2023, , 1515-1558.	0.3	0
73621	Hybrid Functional Calculations for Antimony Doping in CdTe. , 2022, , .		0
73622	Effect of Pressure on Electronic, Mechanical and Dynamic Properties for Orthorhombic WP. Gazi University Journal of Science, 2023, 36, 1759-1773.	0.6	1
73623	La0.75Sr0.25MnO3-based perovskite oxides as efficient and durable bifunctional oxygen electrocatalysts in rechargeable Zn-air batteries. Science China Materials, 2023, 66, 1002-1012.	3.5	4
73624	Janus V₂AsP monolayer : a ferromagnetic semiconductor with a narrow band gap, a high Curie temperature and controllable magnetic anisotropy. Journal of Physics Condensed Matter, 0, , .	0.7	0
73625	Structure and Stoichiometry Self-Organization in a Mixed Vanadiumâ€“Iron Oxide Honeycomb Film on Ru(0001). Journal of Physical Chemistry C, 2022, 126, 19947-19955.	1.5	1
73626	Accelerating NADH oxidation and hydrogen production with mid-gap states of nitrogen-rich carbon nitride photocatalyst. IScience, 2022, 25, 105567.	1.9	7
73627	Flexible 2D Boron Imidazolate Framework for Polysulfide Adsorption in Lithiumâ€“Sulfur Batteries. Chemistry of Materials, 2022, 34, 10451-10458.	3.2	8
73628	Theoretical studies of non-noble metal single-atom catalyst Ni1/MoS2: Electronic structure and electrocatalytic CO2 reduction. Science China Materials, 2023, 66, 1079-1088.	3.5	27
73629	What Differentiates Dielectric Oxides and Solid Electrolytes on the Pathway toward More Efficient Energy Storage?. Batteries, 2022, 8, 232.	2.1	7
73630	Thermal Transport and Thermoelectric Properties of Rb₂PdX₆ (X=Cl, Br) from Firstâ€principles Study. ChemNanoMat, 2023, 9, .	1.5	1
73631	Ultralow Loss and High Tunability in a Nonâ€perovskite Relaxor Ferroelectric. Advanced Functional Materials, 2023, 33, .	7.8	4

#	Article	IF	Citations
73632	Ti_nO_{2nâ€“1}/MXene Hierarchical Bifunctional Catalyst Anchored on Graphene Aerogel toward Flexible and High-Energy Liâ€“S Batteries. ACS Nano, 2022, 16, 19133-19144.	7.3	22
73633	Segregation of Re at the Î³/Î³â€² boundary of Ni-based single crystal superalloys revealed by first-principles calculations based Monte-Carlo simulations. Journal of Materials Science and Technology, 2023, 143, 54-61.	5.6	5
73634	Revealing the dynamics of the alloying and segregation of Pt-Co nanoparticles via in-situ environmental transmission electron microscopy. Nano Research, 2023, 16, 3055-3062.	5.8	4
73635	Structural and magnetic properties of LaVO3 - Absence of anomalous diamagnetism. Ceramics International, 2022, , .	2.3	0
73636	Mg-doped CaCO3 nanoarchitectures assembled by ($$4overline{41}$$) high-index facets for efficient trace removal of Pb(II). Rare Metals, 2023, 42, 525-535.	3.6	3
73637	Insights into the Mechanism and Reactivity of Zeolite-Catalyzed Alkylphenol Dealkylation. ACS Catalysis, 2022, 12, 14227-14242.	5.5	4
73638	A pragmatic protocol for determining charge transfer states of molecules at metal surfaces by constrained density functional theory. Journal of Chemical Physics, 2022, 157, .	1.2	6
73639	Crystal and electronic structures of <mml:math xmlns:mml="http://www.w3.org/1998/Math/MathML"><mml:msub><mml:mi>BiS</mml:mi><mml:mn>2</mml:mn></mml:msub></mml -based compounds <mml:math		

#	Article	IF	Citations
73650	Valence-skipping and quasi-two-dimensionality of superconductivity in a van der Waals insulator. Nature Communications, 2022, 13, .	5.8	5
73651	Selective sensing properties and enhanced ferromagnetism in CrI₃ monolayer via gas adsorption. Nanotechnology, 0, , .	1.3	0
73652	Cobalt as a promising dopant for producing semi-insulating Î²-Ga2O3 crystals: Charge state transition levels from experiment and theory. APL Materials, 2022, 10, .	2.2	6
73653	Structure and electronic properties of domain walls and stacking fault defects in prospective photoferroic materials bournonite and enargite. Journal of Applied Physics, 2022, 132, .	1.1	2
73654	Producing Tunable Broadband Near-Infrared Emission through Co-Substitution in (Ga_{1â€“x}Mg_x)(Ga_{1â€“x}Ge_x)O₄:Cr<sup>3 ACS Applied Materials & Interfaces, 2022, 14, 51157-51164.	8.3	28
73655	Critical role of hydrogen sorption kinetics in electrocatalytic CO2 reduction revealed by on-chip in situ transport investigations. Nature Communications, 2022, 13, .	5.8	14
73656	Single pair of multi-Weyl points in nonmagnetic crystals. Physical Review B, 2022, 106, .	1.1	20
73657	Phonon Thermal Transport in <mml:math xmlns:mml="http://www.w3.org/1998/Math/MathML" display="inline" overflow="scroll"><mml:msub><mml:mi>Bi</mml:mi><mml:mn>2</mml:mn></mml:msub><mml:msub><mml:mi>Te</mml:mi><mml:mn from a Deep-Neural-Network Interatomic Potential. Physical Review Applied, 2022, 18, .	4.6	9
73658	Accurate and efficient band-gap predictions for metal halide perovskites at finite temperature. Npj Computational Materials, 2022, 8, .	3.5	15
73659	A theoretical study of the atomic layer deposition of HfO2 on Si(100) surfaces using tetrakis(ethylmethylamino) hafnium and water. Applied Surface Science, 2022, , 155702.	3.1	3
73660	Palm Sugar-Induced Formation of Hexagonal Tungsten Oxide with Nanorod-Assembled Three-Dimensional Hierarchical Frameworks for Nitrogen Dioxide Sensing. ACS Sustainable Chemistry and Engineering, 2022, 10, 15035-15045.	3.2	3
73661	Blue TiO2 with tunable oxygen-vacancy defects for enhanced photocatalytic diesel oil degradation. Applied Surface Science, 2023, 611, 155716.	3.1	5
73662	First-principles calculations on superconductivity and H-diffusion kinetics in Mgâ€“Bâ€“H phases under pressures. International Journal of Hydrogen Energy, 2023, 48, 4006-4015.	3.8	5
73663	Role of large Rashba spin-orbit coupling in second-order nonlinear optical effects of polar <mml:math xmlns:mml="http://www.w3.org/1998/Math/MathML"><mml:mrow><mml:msub><mml:mi>BiB</mml:mi><mml:mn>3</mml:mn></mml:msub><mml:msub><mml:mi>O</mml:mi><mml:mn>6</mml:mn></mml:msub></mml:mrow></mml:math>. Physical Review B, 2022, 106, .	1.1	8
73664	Reconstructing the Semiconductor Band Structure by Deep Learning. Mathematics, 2022, 10, 4268.	1.1	0
73665	Super-resolved timeâ€“frequency measurements of coupled phonon dynamics in a 2D quantum material. Scientific Reports, 2022, 12, .	1.6	1
73666	Control of Electrolyte Decomposition by Mixing Transition Metal Ions in Spinel Oxides as Positive Electrode Active Materials for Mg Rechargeable Batteries. Journal of Physical Chemistry C, 2022, 126, 19074-19083.	1.5	2
73667	Effects of a single vacancy on electronic properties of a Ca2N electride bilayer. Applied Surface Science, 2023, 612, 155721.	3.1	1

#	Article	IF	Citations
73668	Detection of nonpolar n-dodecane at room temperature using multiphase MoS2 chemiresistive sensor: Investigation of charge transfer on nonpolar VOC molecule. Sensors and Actuators B: Chemical, 2023, 376, 132994.	4.0	3
73669	<scp>DFT</scp>Â+â€‰U calculations of structural, magnetic, and electrochemical properties and Na⁺ diffusion barrier in the <scp>O3</scp>â€phase of <scp>NaTm₀</scp>_.<scp>₅Ni₀</scp>_.<scp>₅O<sub> (TmÂ=ÂTi, Mn). International Journal of Quantum Chemistry, 2023, 123, .	1.9	2
73670	A general strategy to synthesize single-atom metal-oxygen doped polymeric carbon nitride with highly enhanced photocatalytic water splitting activity. Applied Catalysis B: Environmental, 2023, 323, 122180.	10.8	28
73671	Topologically protected surface states in TaPdTe5. , 2022, 1, .		0
73672	One-step hydrothermal synthesis of hierarchically structured MoS2 nanorods via reaction intermediates as self-templates for chemoselective hydrogenation. Chemical Engineering Journal, 2023, 454, 140330.	6.6	7
73673	Dislocation Networkâ€Boosted PtNi Nanocatalysts Welded on Nickel Foam for Efficient and Durable Hydrogen Evolution at Ultrahigh Current Densities. Advanced Energy Materials, 2023, 13, .	10.2	18
73674	Computational evaluation of 2D metal-organic frameworks with TMX4-centers (X = O, S and Se) for CO2 electroreduction. International Journal of Hydrogen Energy, 2023, 48, 3486-3494.	3.8	10
73675	Anisotropic mechanical response of a 2D covalently bound fullerene lattice. Carbon, 2023, 202, 118-124.	5.4	12
73676	Chloride-Promoted High-Rate Ambient Electrooxidation of Methane to Methanol on Patterned Cuâ€“Ti Bimetallic Oxides. ACS Catalysis, 2022, 12, 14321-14329.	5.5	7
73677	Multifunctional 2D g-C₄N₃/MoS₂ vdW Heterostructure-Based Nanodevices: Spin Filtering and Gas Sensing Properties. ACS Sensors, 2022, 7, 3450-3460.	4.0	37
73678	Metallization of hydrogen by intercalating ammonium ions in metal fcc lattices at lower pressure. Applied Physics Letters, 2022, 121, 192601.	1.5	3
73679	Carbonate dimorphism, and the reinterpretation of rates of lattice and excess oxygen-driven catalytic cycles. Journal of Catalysis, 2022, 416, 423-438.	3.1	0
73680	Thermally Driven Point Defect Transformation in Antimony Selenosulfide Photovoltaic Materials. Advanced Materials, 2023, 35, .	11.1	11
73681	Interfacial Electronic Rearrangement and Synergistic Catalysis for Alkaline Water Splitting in Carbon-Encapsulated Ni (111)/Ni3C (113) Heterostructures. Catalysts, 2022, 12, 1367.	1.6	2
73682	Oxygenâ€Chlorine Chemisorption Scaling for Seawater Electrolysis on Transition Metals: The Role of Redox. Advanced Theory and Simulations, 2023, 6, .	1.3	1
73683	Accelerating the discovery of novel magnetic materials using machine learningâ€“guided adaptive feedback. Proceedings of the National Academy of Sciences of the United States of America, 2022, 119, .	3.3	7
73684	Fundamental Principles toward Designing High Na-Containing P2-Structured â€œLayeredâ€•Na-Transition Metal Oxides as High-Performance Cathode Materials for Na-Ion Batteries. Chemistry of Materials, 2022, 34, 10470-10483.	3.2	8
73685	Tunable optoelectronic and photocatalytic properties of BAs-BSe van der Waals heterostructures by strain engineering. Chemical Physics, 2022, , 111769.	0.9	0

#	Article	IF	Citations
73686	First-principles study on the lattice thermal conductivity of layered Dirac semimetal BeN<mml:math xmlns:mml="http://www.w3.org/1998/Math/MathML" altimg="si29.svg" display="inline" id="d1e625"><mml:msub><mml:mrow /><mml:mrow><mml:mn>4</mml:mn></mml:mrow></mml:msub></mml:math>. Physica E: Low-Dimensional Systems and Nanostructures, 2023, 147, 115571.	1.3	4
73687	The first-principles study of structural and electronic properties of two-dimensional SiC/GeC lateral polar heterostructures. Journal of Applied Physics, 2022, 132, 184301.	1.1	0
73688	Defective Nanoporous Zinc Cobaltite as a Potential Bifunctional Oxygen Electrocatalyst. ACS Applied Energy Materials, 2022, 5, 13635-13644.	2.5	1
73689	Single-Atom Low-Valent Alkaline-Earth-Metal Catalysts for Electrochemical Nitrogen Reduction with an Acceptanceâ€“Backdonation Mechanism. ACS Applied Materials & Interfaces, 2022, 14, 52079-52086.	4.0	8
73690	Design and synthesis of dispersed Ni2P/Co nano heterojunction as bifunctional electrocatalysis for boosting overall water splitting. International Journal of Hydrogen Energy, 2023, 48, 3355-3363.	3.8	8
73691	Fortnet, a software package for training Behler-Parrinello neural networks. Computer Physics Communications, 2023, 284, 108580.	3.0	2
73692	Machine learning prediction of the mechanical properties of refractory multicomponent alloys based on a dataset of phase and first principles simulation. , 0, 1, .		0
73693	Effects of F and Cl Doping in Cubic Li₇La₃Zr₂O₁₂ Solid Electrolyte: A First-Principles Investigation. ACS Applied Energy Materials, 2022, 5, 15086-15092.	2.5	8
73694	Ultrathin Feâ€“ReS₂ Nanosheets as Electrocatalysts for Accelerating Sulfur Reduction in Liâ€“S Batteries. ACS Applied Materials & Interfaces, 2022, 14, 50870-50879.	4.0	6
73695	Ball-Milled Processed, Selective Fe/h-BN Nanocatalysts for CO₂ Hydrogenation. ACS Applied Nano Materials, 2022, 5, 16475-16488.	2.4	6
73696	Development of a ReaxFF potential for Auâ€“Pd. Journal of Physics Condensed Matter, 2023, 35, 065901.	0.7	1
73697	Unveiling a Surface Electronic Descriptor for Feâ€“Co Mixing Enhanced the Stability and Efficiency of Perovskite Oxygen Evolution Electrocatalysts. ACS Catalysis, 2022, 12, 14698-14707.	5.5	3
73698	Quasi-one-dimensional characters in topological semimetal TaNiTe₅. Chinese Physics B, 2023, 32, 056801.	0.7	1
73699	Structural, magnetic, and transport properties of epitaxial thin films of equiatomic quaternary CoFeCrGa Heusler alloy. Journal of Applied Physics, 2022, 132.	1.1	2
73700	Tunable electronic properties and negative differential resistance effect of the intrinsic type-III ZrS<mml:math xmlns:mml="http://www.w3.org/1998/Math/MathML" altimg="si13.svg" display="inline" id="d1e711"><mml:msub><mml:mrow /><mml:mrow><mml:mn>2</mml:mn></mml:mrow></mml:msub></mml:math>/WTe<mml:math xmlns:mml="http://www.w3.org/1998/Math/MathML" altimg="si13.svg" display="inline" id="d1e719"><mml:msub><mml:mrow /><mml:mrow><mml:mn>2</mml:mn></mml:mrow></mml:msub></	3.1	6
73701	Quasi-One-Dimensional Linarite-Type PbCu(SeO4)(OH)2 with Competing Nearest-Neighbor and Next-Nearest-Neighbor Intrachain Exchange Interactions. Materials, 2022, 15, 7860.	1.3	0
73702	Diffusion-Mediated Morphological Transformation in Bifunctional Mn₂O₃/CuOâ€“(VO)₃(PO₄)₂·6H₂O for Enhanced Electrochemical Water Splitting. ACS Applied Materials & Interfaces, 2022, 14, 52204-52215.	4.0	6
73703	Theoretical analysis of the thermoelectric properties of penta-PdX2 (X = Se, Te) monolayer. Frontiers in Chemistry, 0, 10, .	1.8	1

#	Article	IF	Citations
73704	Fe-N4/Co-N4 active sites engineered porous carbon with encapsulated FeCo alloy as an efficient bifunctional catalyst for rechargeable zinc-air battery. Journal of Alloys and Compounds, 2023, 935, 168107.	2.8	7
73705	Feature-Rich Electronic Properties of Sliding Bilayer Germanene. ACS Omega, 0, , .	1.6	0
73706	Anti-Jahn-Teller effect induced ultrafast insulator to metal transition in perovskite BaBiO3. Npj Computational Materials, 2022, 8, .	3.5	3
73707	Iron-rich Feâ€“O compounds at Earthâ€™s core pressures. Innovation(China), 2023, 4, 100354.	5.2	4
73708	Phase transition and properties of ternary MgGeN₂ under pressure: a first principles investigation. Physica Scripta, 2022, 97, 125826.	1.2	5
73709	Second-order topological insulator in van der Waals heterostructures of <mml:math xmlns:mml="http://www.w3.org/1998/Math/MathML"><mml:msub><mml:mrow><mml:mi>CoBr</mml:mi></mml:mrow><mml:mn>2</mml:mn> Physical Review B, 2022, 106, .	3.7	4
73710	Interfacial charge transfer induced antiferromagnetic metals and magnetic phase transition in (CrO$_2$)$_m$/(TaO$_2$)$_n$ superlattices. Journal of Physics Condensed Matter, 0, , .	0.7	0
73711	Low-Temperature Production of Glyceric Acid from Biomass-Based Sugar via the Cooperative Roles of MgO and NaBF₄. Industrial & Engineering Chemistry Research, 2022, 61, 16689-16701.	1.8	2
73712	Activating magnetoelectric optical properties by twisting antiferromagnetic bilayers. Physical Review B, 2022, 106, .	1.1	3
73713	A Two-Dimensional van der Waals Heterostructure with Isolated Electron-Deficient Cobalt Sites toward High-Efficiency CO₂ Electroreduction. Journal of the American Chemical Society, 2022, 144, 21502-21511.	6.6	24
73714	Simultaneously improving Rashba-type and Zeeman effects in two-dimensional multiferroics. Physical Review B, 2022, 106, .	1.1	0
73715	Pressureâ€Tailored Selfâ€Driven and Broadband Photoresponse in PbI₂. Small Methods, 2022, 6, .	4.6	4
73716	Ca silicide films - promising materials for silicon optoelectronics. Japanese Journal of Applied Physics, 0, , .	0.8	1
73717	Electronic and magnetic properties of CrI3 grain boundary. Applied Surface Science, 2023, 612, 155705.	3.1	1
73718	How the Facet Edge Controls the Overall CO Oxidation in Nanoporous Gold: Combined Atomistic Characterization/DFT Study of Residual Ag Distribution and Catalytic Activity. ACS Catalysis, 2022, 12, 14445-14458.	5.5	1
73719	High-Throughput Estimation of Phonon Thermal Conductivity from First-Principles Calculations of Elasticity. Journal of Physical Chemistry A, 2022, 126, 8771-8780.	1.1	4
73720	Observation of gapped Dirac cones in a two-dimensional Su-Schrieffer-Heeger lattice. Nature Communications, 2022, 13, .	5.8	4
73721	Reductive Dehalogenation of Herbicides Catalyzed by Pd⁰NPs in a H₂-Based Membrane Catalyst-Film Reactor. Environmental Science & Technology, 2022, 56, 18030-18040.	4.6	7

#	Article	IF	Citations
73722	Incorporating 2D Î³-Al2O3 nanosheets into the flexible PEO-based solid electrolyte for lithium metal batteries. Electrochimica Acta, 2023, 437, 141504.	2.6	9
73723	Full Temperature-Dependent Potential and Anharmonicity in Metallic Hydrogen: Colossal NQE and the Consequences. Journal of Physical Chemistry C, 2022, 126, 19355-19366.	1.5	2
73724	Ground-state structures, electronic structure, transport properties and optical properties of Ca-based anti-Ruddlesden-Popper phase oxide perovskites. Physical Review Materials, 2022, 6, .	0.9	3
73725	Tailoring Interfacial Charge Transfer of Epitaxially Grown Ir Clusters for Boosting Hydrogen Oxidation Reaction. Advanced Energy Materials, 2023, 13, .	10.2	11
73726	Understanding Your Support System: The Design of a Stable Metalâ€“Organic Framework/Polyazoamine Support for Biomass Conversion. Chemistry of Materials, 2022, 34, 9854-9864.	3.2	4
73727	Two-dimensional half Chern-Weyl semimetal with multiple screw axes. Physical Review B, 2022, 106, .	1.1	3
73728	Pt2 Dimer Anchored Vertically in Defective BN Monolayer as an Efficient Catalyst for N2 Reduction: A DFT Study. Catalysts, 2022, 12, 1387.	1.6	6
73729	Excellent spin-filtering and giant tunneling magnetoresistance in a dual-electrode van der Waals magnetic tunnel junction based on ferromagnetic CrSe2. Applied Surface Science, 2023, 611, 155588.	3.1	7
73730	Atomic structure generation from reconstructing structural fingerprints. Machine Learning: Science and Technology, 2022, 3, 045018.	2.4	3
73731	Aluminum-based microporous metalâ€“organic framework for noble gas separation. Journal of Industrial and Engineering Chemistry, 2023, 118, 181-186.	2.9	7
73732	Ferroelectric van der Waals heterostructures of CuInP₂S₆ for non-volatile memory device applications. Nanotechnology, 2023, 34, 065701.	1.3	5
73733	Ultrahigh Mass Activity for the Hydrogen Evolution Reaction by Anchoring Platinum Single Atoms on Active {100} Facets of TiC via Cation Defect Engineering. Advanced Functional Materials, 2023, 33, .	7.8	11
73734	Photoinduced Rippling of Two-Dimensional Hexagonal Nitride Monolayers. Nano Letters, 2022, 22, 9006-9012.	4.5	5
73735	Autocatalytic reduction-assisted synthesis of segmented porous PtTe nanochains for enhancing methanol oxidation reaction. , 2023, 2, e9120041.		20
73736	Electrochemical Reduction of Carbon Dioxide at TiO₂/Au Nanocomposites. ACS Applied Materials & Interfaces, 2022, 14, 51889-51899.	4.0	9
73737	Origin of negative thermal expansion and pressure-induced amorphization in zirconium tungstate from a machine-learning potential. Physical Review B, 2022, 106, .	1.1	9
73738	Signature of topological band crossing in ferromagnetic <mml:math xmlns:mml="http://www.w3.org/1998/Math/MathML"><mml:msub><mml:mrow><mml:mi>Cr</mml:mi></mml:mrow><mml:mrow><mml:mn>3</mml:mn></mml:mrow><mml:mr epitaxial thin film. Physical Review Research, 2022, 4, .	1.0	
73739	Arsenic Adsorption on Nanoscale Zerovalent Iron Immobilized on Reduced Graphene Oxide (nZVI/rGO): Experimental and Theoretical Approaches. Journal of Physical Chemistry C, 2022, 126, 19916-19925.	1.5	4

#	Article	IF	Citations
73740	Role of Cuâ€doping in <scp>CdTe</scp> thin films: Experiments and simulations. Surface and Interface Analysis, 2023, 55, 151-161.	0.8	1
73741	Theoretical Study on Gas Sensing of SO₂ on TH-Si_xC_y. Journal of Physics: Conference Series, 2022, 2370, 012030.	0.3	0
73742	Atomically dispersed bimetallic Feâ€“Co electrocatalysts for green production of ammonia. Nature Sustainability, 2023, 6, 169-179.	11.5	30
73743	Strain-regulated Electronic Properties of Helical Polymer with Phenylacetylene Monomers â€“ A First Principle Study. Modelling and Simulation in Materials Science and Engineering, 0, , .	0.8	0
73744	Correlating the perovskite/polymer multi-mode reactions with deep-level traps in perovskite solar cells. Joule, 2022, 6, 2849-2868.	11.7	29
73745	Predicted superconductivity and superionic state in the electride Li₅N under high pressure. New Journal of Physics, 2022, 24, 113012.	1.2	8
73746	Ab initio study on fcc Pr with correlation matrix renormalization theory. Physical Review B, 2022, 106, .	1.1	1
73747	Bulk structure of Si2BN predicted by computational approaches. Diamond and Related Materials, 2022, , 109530.	1.8	1
73748	Charge carrier mobilities of organic semiconductors: ab initio simulations with mode-specific treatment of molecular vibrations. Npj Computational Materials, 2022, 8, .	3.5	8
73749	Iron and silicon isotope fractionation in silicate melts using first-principles molecular dynamics. Geochimica Et Cosmochimica Acta, 2023, 343, 212-233.	1.6	1
73750	A density functional theory study of thiophene and pyridine adsorption on Pt/Rh-doped Cu (100) surface. Surface Science, 2023, 729, 122212.	0.8	2
73751	Low-temperature crystallization of LaFeO3 perovskite with inherent catalytically surface for the enhanced oxygen evolution reaction. Nano Energy, 2023, 105, 108003.	8.2	4
73752	Atomically Smooth Defect-Free III-As Heterostructures on InP(111) Substrate for Next-Generation Electronic Devices. ACS Applied Nano Materials, 2022, 5, 17033-17041.	2.4	0
73753	Blue Light-Excitable Broadband Yellow Emission in a Zero-Dimensional Hybrid Bismuth Halide with Type-II Band Alignment. Inorganic Chemistry, 2022, 61, 19483-19491.	1.9	7
73754	Atomic-Layer-Deposited Aluminum Oxide Thin Films Probed with X-ray Scattering and Compared to Molecular Dynamics and Density Functional Theory Models. ACS Omega, 2022, 7, 41033-41043.	1.6	4
73755	Ultrahigh strength and negative thermal expansion and low thermal conductivity in graphyne nanosheets confirmed by machine-learning interatomic potentials. FlatChem, 2022, 36, 100446.	2.8	11
73756	Self-Discharge Mechanism of High-Voltage KVPO₄F for K-Ion Batteries. ACS Applied Energy Materials, 2022, 5, 14913-14921.	2.5	6
73757	Metal Halides for Highâ€Capacity Energy Storage. Small, 2023, 19, .	5.2	2

#	Article	IF	Citations
73758	Theoretical insights into the Peierls plasticity in SrTiO3 ceramics via dislocation remodelling. Nature Communications, 2022, 13, .	5.8	7
73759	Tuning the electron transport behavior at Li/LATP interface for enhanced cyclability of solid-state Li batteries. Nano Research, 2023, 16, 1634-1641.	5.8	12
73760	Extremely strong four-phonon scattering and ultra-low lattice thermal conductivity due to quartic anharmonicity in fluoride perovskites XHgF3 (X = K, Rb). Physics Letters, Section A: General, Atomic and Solid State Physics, 2022, 456, 128550.	0.9	3
73761	Enhanced Curie temperature and skyrmion stability by strain in room temperature ferromagnetic semiconductor CrISe monolayer. Applied Physics Letters, 2022, 121, .	1.5	7
73762	Opto-electronic properties of carbon doped NiO. Journal of Physics and Chemistry of Solids, 2023, 174, 111110.	1.9	1
73763	Nature of support plays vital roles in H2O promoted CO oxidation over Pt catalysts. Journal of Catalysis, 2022, 416, 364-374.	3.1	4
73764	Intrinsic carrier losses in tellurium due to radiative and Auger recombinations. Applied Physics Letters, 2022, 121, .	1.5	2
73765	Pressure-induced ferroelectric transition in LiBC. Physical Review B, 2022, 106, .	1.1	0
73766	Parallel-Self-Assembling Stack, Center-Capture Effect, and Reactivity-Enhancing Effect of N-Layer (N = 1, 2, 3) Cyclo[18]carbon. ACS Nano, 2022, 16, 21345-21355.	7.3	3
73767	Cobalt atom sites anchored on sulfhydryl decorated UiO-66 to activate peroxymonosulfate for norfloxacin degradation. Journal of Environmental Chemical Engineering, 2023, 11, 108972.	3.3	3
73768	Platinum Graphene Catalytic Condenser for Millisecond Programmable Metal Surfaces. Journal of the American Chemical Society, 2022, 144, 22113-22127.	6.6	12
73769	Planar defectâ€“free pure red perovskite light-emitting diodes via metastable phase crystallization. Science Advances, 2022, 8, .	4.7	23
73770	Two-Dimensional Half-Metallic and Semiconducting Lanthanide-Based MXenes. ACS Omega, 2022, 7, 40929-40940.	1.6	2
73771	Prediction of a superhard high-pressure phase for CN: First-principles. Modern Physics Letters B, 2022, 36, .	1.0	1
73772	High-performance self-powered integrated system of pressure sensor and supercapacitor based on Cu@Cu2O/graphitic carbon layered porous structure. Journal of Colloid and Interface Science, 2023, 632, 140-150.	5.0	4
73773	2D SnO/MoO3 van der Waals heterojunction with tunable electronic behavior for multifunctional applications: DFT calculations. Applied Surface Science, 2023, 611, 155719.	3.1	4
73774	Cloning the Dirac cones of bilayer graphene to the zone center by selenium adsorption. Npj 2D Materials and Applications, 2022, 6, .	3.9	2
73775	Spin interaction and magnetism in cobaltate Kitaev candidate materials: An ab initio and model Hamiltonian approach. Physical Review B, 2022, 106, .	1.1	5

#	Article	IF	Citations
73776	Thermal conductivity of group-III phosphides: The special case of GaP. Physical Review B, 2022, 106, .	1.1	2
73777	Elastic properties of moirÃ© lattices in epitaxial two-dimensional materials. Physical Review B, 2022, 106, .	1.1	2
73778	Ab Initio Investigation of the Adsorption and Dissociation of O2 on Cu-Skin Cu3Au(111) Surface. Catalysts, 2022, 12, 1407.	1.6	2
73779	First-Principles Insights into the Thermocatalytic Cracking of Ammonia-Hydrogen Blends on Fe(110): 1. Thermodynamics. Journal of Physical Chemistry C, 2022, 126, 19733-19744.	1.5	2
73780	Constructing a Composite Structure by a Gradient Mg²⁺ Doping Strategy for High-Performance Sodium-Ion Batteries. ACS Applied Materials & Interfaces, 2022, 14, 51846-51854.	4.0	6
73781	Red-Emitting SrGa₂O₄:Cu²⁺ Phosphor with Super-Long Persistent Luminescence. Chemistry of Materials, 2022, 34, 10068-10076.	3.2	10
73783	Simultaneously tuning interlayer spacing and termination of MXenes by Lewis-basic halides. Nature Communications, 2022, 13, .	5.8	36
73784	Discovery of chalcogenides structures and compositions using mixed fluxes. Nature, 2022, 612, 72-77.	13.7	20
73785	Boosted photocatalytic efficiency of GQDs sensitized (BiO)2CO3/Î²-Bi2O3 heterojunction via enhanced interfacial charge transfer. Chinese Chemical Letters, 2023, 34, 107967.	4.8	1
73786	Mechanism of carrier doping induced magnetic phase transitions in two-dimensional materials. Physical Review B, 2022, 106, .	1.1	3
73787	Singleâ€Atom Catalysts with Ultrahigh Catalaseâ€Like Activity Through Electron Filling and Orbital Energy Regulation. Advanced Functional Materials, 2023, 33, .	7.8	19
73788	Pressure, Directional Dependent Mechanical Anisotropies and Phase Transition Studies ofÎ²-5-nitro-2,4-dihydro-3H-1,2,4-triazol-3-one (NTO) and 2,4,6-triamino-1,3,5-trinitrobenzene (TATB). Journal of Physics Condensed Matter, 0, , .	0.7	0
73789	Photovoltaic-Driven Flexible Single-Walled Carbon Nanotubes for Self-Powered and Polarization-Sensitive Infrared Photodetection. ACS Applied Electronic Materials, 2022, 4, 5602-5607.	2.0	3
73790	Scandium wetting of tungsten surfaces in â€œscandateâ€•thermionic cathodes. Surfaces and Interfaces, 2022, , 102476.	1.5	0
73791	A Tour of Soft Atomic Motions: Chemical Pressure Quadrupoles Across Transition Metalâ€“Main Group 1:2 Structure Types. Chemistry of Materials, 2022, 34, 10011-10024.	3.2	8
73792	A new mode of luminescence in lanthanide oxalates metalâ€“organic frameworks. Scientific Reports, 2022, 12, .	1.6	5
73793	Decrease in Tumor Interstitial Pressure for Enhanced Drug Intratumoral Delivery and Synergistic Tumor Therapy. ACS Nano, 2022, 16, 18376-18389.	7.3	17
73794	Exploring two-dimensional van der Waals heavy-fermion material: Data mining theoretical approach. Npj 2D Materials and Applications, 2022, 6, .	3.9	7

#	Article	IF	Citations
73795	Molecular oxygen enhances H2O2 utilization for the photocatalytic conversion of methane to liquid-phase oxygenates. Nature Communications, 2022, 13, .	5.8	30
73796	First-Principles Study on Mechanical and Optical Behavior of Plutonium Oxide under Typical Structural Phases and Vacancy Defects. Materials, 2022, 15, 7785.	1.3	0
73797	Electronically Nonadiabatic H Atom Scattering from Low Miller Index Surfaces of Silver. Langmuir, 2022, 38, 14162-14171.	1.6	0
73798	Prediction of 2D ferromagnetic metal VNI monolayer with tunable topological properties. Journal of Applied Physics, 2022, 132, 183913.	1.1	3
73799	Adsorption energies on transition metal surfaces: towards an accurate and balanced description. Nature Communications, 2022, 13, .	5.8	24
73800	Surface metal-EDTA coordination layer activates NixFe3-xO4 spinel as an outstanding electrocatalyst for oxygen evolution reaction. Journal of Colloid and Interface Science, 2023, 632, 44-53.	5.0	6
73801	Multifunctional catalytic activity of Cu3N (001) surface: A first-principles study. ChemPhysMater, 2022, , .	1.4	2
73802	Topological hinge modes in Dirac semimetals. Frontiers of Physics, 2023, 18, .	2.4	8
73803	Massive Monte Carlo simulations-guided interpretable learning of two-dimensional Curie temperature. Patterns, 2022, 3, 100625.	3.1	7
73804	Epitaxial Growth of Single-Layer Kagome Nanoflakes with Topological Band Inversion. ACS Nano, 2022, 16, 21079-21086.	7.3	2
73805	Effect of Al₂O₃ addition on the thermal expansion of sodium alkalineâ€earth silicate glasses: A molecular dynamics study. Journal of the American Ceramic Society, 2023, 106, 1809-1822.	1.9	2
73806	Mott Schottky CoSx-MoOx@NF heterojunctions electrode for H2 production and urea-rich wastewater purification. Science of the Total Environment, 2023, 858, 160170.	3.9	10
73807	Surfacial proton conducting CeO2 nanosheets. Ceramics International, 2023, 49, 9138-9146.	2.3	4
73808	Determination of highly active and selective surface for the oxidative dehydrogenation of ethane over phase-pure M1 MoVNbTeOx catalyst. Journal of Catalysis, 2022, 416, 277-288.	3.1	3
73809	Exploration of NaSICON Frameworks as Calcium-Ion Battery Electrodes. Chemistry of Materials, 2022, 34, 10133-10143.	3.2	5
73810	Charge Recombination Dynamics in a Metal Halide Perovskite Simulated by Nonadiabatic Molecular Dynamics Combined with Machine Learning. Journal of Physical Chemistry Letters, 2022, 13, 10734-10740.	2.1	7
73811	Dynamic Structural Evolution of [Rh(NO)₂]⁺ Complex/Rh Metal Cluster in Zeolite during de-NOx via in Situ Formed NH₃ under Lean/Rich Periodic Conditions. Journal of Physical Chemistry C, 2022, 126, 19147-19158.	1.5	3
73812	Impenetrable Barrier at the Metalâ€“Mott Insulator Junction in Polymorphic 1H and 1T NbSe₂ Lateral Heterostructure. Journal of Physical Chemistry Letters, 2022, 13, 10713-10721.	2.1	1

#	Article	IF	Citations
73813	Photooxidation browning mechanism of small Î±-dicarbonyl compounds on natural mineral particle in the presence of methylamine/ammonia. Chemical Physics Letters, 2022, , 140187.	1.2	0
73814	Hole-doping induced ferromagnetism in 2D materials. Npj Computational Materials, 2022, 8, .	3.5	20
73815	Reactions between SiCl4 and H2O on rutile TiO2 surfaces in atomic layer deposition of SiO2 by first-principles calculations. Surfaces and Interfaces, 2023, 36, 102454.	1.5	2
73816	Magnetoresistance relaxation steps originating from dynamic spin-orbital interactions in <mml:math xmlns:mml="http://www.w3.org/1998/Math/MathML"><mml:mrow><mml:msub><mml:mi>Ca</mml:mi><mml:mn>3</mml:mn></mml:mathvariant="normal">O</mml:mi><mml:mn>7</mml:mn></mml:msub></mml:mrow></mml:math>. Physical Review B, 2022, 106, .	1.1	1
73817	Tailoring electronic structure of Ni-Fe oxide by V incorporation for effective electrocatalytic water oxidation. Applied Surface Science, 2023, 611, 155732.	3.1	6
73818	Electrochemical assessment of highly reversible SnO2â€“coated Zn metal anodes prepared via atomic layer deposition for aqueous Zn-ion batteries. Applied Surface Science, 2023, 611, 155633.	3.1	13
73819	Stacked Si2BN monolayers as ultra-high-capacity anode material for divalent Mg-ion batteries. FlatChem, 2022, 36, 100444.	2.8	2
73820	Pressure-induced first-order antiferromagnetic to ferromagnetic transition in MnN. Journal of Alloys and Compounds, 2022, , 168120.	2.8	0
73821	Hybrid Artificial Solid Electrolyte Interphase with Dendrite-Free Lithium Deposition and High Ion Transport Kinetics. ACS Applied Materials & Interfaces, 2022, 14, 52993-53006.	4.0	4
73822	Revealing the synergy between zinc and aluminum in Cu/ZnO/Al2O3 industrial catalyst. Journal of Chemical Physics, 2022, 157, .	1.2	1
73823	A Novel Membrane-like 2D Aâ€™-MoS2 as Anode for Lithium- and Sodium-Ion Batteries. Membranes, 2022, 12, 1156.	1.4	4
73824	Dependency of Ag wetting on the oxygen nonstoichiometry of oxide surfaces. Applied Surface Science, 2023, 611, 155699.	3.1	8
73825	Realization of high-quality Sr4Fe6O13 epitaxial film and its phase competition with SrFeO2.5. Ceramics International, 2022, , .	2.3	1
73826	Boosting the lithium-ion storage performance of perovskite Sr VO3â^' via Sr cation and O anion deficient engineering. Science Bulletin, 2022, , .	4.3	4
73828	Stabilized Nitrogen Framework Anions in the Gaâ€“N System. Journal of the American Chemical Society, 2022, 144, 21640-21647.	6.6	7
73829	Origin of Enhanced Photocatalytic Activity in Direct Band Gap g-C₃N₄ Nanoribbons with Tunable Electronic Properties for Water-Splitting Reaction: A First-Principles Study. Journal of Physical Chemistry C, 2022, 126, 19627-19636.	1.5	6
73830	DFT study on TiO2 facet-dependent As(III) oxidation process: Importance of As(IV) species. Surface Science, 2023, 729, 122219.	0.8	3
73831	A generalizable, uncertainty-aware neural network potential for GeSbTe with Monte Carlo dropout. Solid-State Electronics, 2023, 199, 108508.	0.8	2

#	Article	IF	Citations
73832	Investigation and understanding of the mechanical properties of MXene by high-throughput computations and interpretable machine learning. Extreme Mechanics Letters, 2022, 57, 101921.	2.0	10
73833	Construction of group III nitride van der Waals heterostructures for highly efficient photocatalyst. Applied Surface Science, 2022, , 155679.	3.1	2
73834	Edge magnetism of triangular graphene nanoflakes embedded in hexagonal boron nitride. Carbon, 2023, 203, 59-67.	5.4	5
73835	Thermal expansion of plasma-exposed tungsten. Journal of Applied Physics, 2022, 132, .	1.1	1
73836	Highly efficient VOC gas sensors based on Li-doped diamane. Applied Surface Science, 2023, 611, 155694.	3.1	13
73837	Topological Superconductivity Based on Antisymmetric Spinâ€“Orbit Coupling. Nano Letters, 2022, 22, 9000-9005.	4.5	8
73838	Interaction between peptides and an MoS2 monolayer containing a nanopore: First-principles calculations. Chinese Journal of Physics, 2023, 84, 486-499.	2.0	0
73839	Comparative study on high-pressure physical properties of monoclinic MgCO3 and Mg2CO4. Scientific Reports, 2022, 12, .	1.6	1
73840	TaIrTe₄ Monolayer with Topological Insulator Characteristic: A New and Highly Efficient Electrocatalyst toward Oxygen Reduction Reaction. Journal of Physical Chemistry C, 2022, 126, 19685-19692.	1.5	2
73841	Origin of room temperature ferromagnetism in optically transparent 2D graphene/Co-doped ZnO/graphene. Applied Surface Science, 2023, 611, 155746.	3.1	0
73842	MgXN₂ (X = Hf/Zr) Monolayers: Auxetic Semiconductor with Highly Anisotropic Optical/Mechanical Properties and Carrier Mobility. Journal of Physical Chemistry Letters, 2022, 13, 10534-10542.	2.1	2
73843	Sub-volt switching of nanoscale voltage-controlled perpendicular magnetic tunnel junctions. Communications Materials, 2022, 3, .	2.9	13
73844	Compressive strain-induced enhancement in valley polarization in Î²-phosphorene like SnS monolayers. Applied Surface Science, 2023, 611, 155675.	3.1	4
73845	Raman scattering investigation of structural phase transition in compressed EuSn2As2. Applied Physics Letters, 2022, 121, .	1.5	2
73846	First-principles study of the interaction between H/He impurities and vacancy in tetragonal Be$$_{12}$$Ti. Journal of Materials Science, 2022, 57, 20631-20640.	1.7	1
73847	On the Formation and Multiplicity of Si [001] Small Angle Symmetric Tilt Grain Boundaries: Atomistic Simulation of Directional Growth. Crystal Growth and Design, 2022, 22, 7491-7500.	1.4	2
73848	Stabilization of Dinuclear Rhodium and Iridium Clusters on Layered Titanate and Niobate Supports. Inorganic Chemistry, 2023, 62, 1113-1121.	1.9	0
73849	2D WSe2/MoSi2N4 type-II heterojunction with improved carrier separation and recombination for photocatalytic water splitting. Applied Surface Science, 2023, 611, 155674.	3.1	21

#	Article	IF	Citations
73850	Firstâ€principles study of the magnetic exchange forces between the RuO2(110) surface and a Fe tip. ChemPhysChem, 0, , .	1.0	0
73851	Vacancy-Stabilized Superionic State in Na_{3â€“x}Sb_{1â€“x}W_xS₄. ACS Applied Energy Materials, 2022, 5, 14053-14058.	2.5	3
73852	A Machine Learningâ€Assisted Approach to a Rapid and Reliable Screening for Mechanically Stable Perovskiteâ€Based Materials. Advanced Functional Materials, 2023, 33, .	7.8	6
73853	Effect of Composition and Local Environment on CO₂ Adsorption on Nickel and Magnesium Oxide Solid Solutions. Journal of Physical Chemistry C, 2022, 126, 19705-19714.	1.5	0
73854	A Systematic Theoretical Study on Electronic Interaction in Cu-based Single-Atom Alloys. ACS Omega, 2022, 7, 41586-41593.	1.6	2
73855	Boosting the Transesterification Reaction by Adding a Single Na Atom into g-C3N4 Catalyst for Biodiesel Production: A First-Principles Study. Energies, 2022, 15, 8432.	1.6	2
73856	Transport characteristics and lattice dynamics with phonon topology accentuation in layered CuTlX (X: S, Se). Physica Scripta, 2022, 97, 125820.	1.2	1
73857	Predictions of structural stability, elastic anisotropy, and thermodynamic properties of TM5Si3C (TM) Tj ETQq1 1 0.784314 rgBT /Ove	1.6	5
73859	On-surface synthesis of disilabenzene-bridged covalent organic frameworks. Nature Chemistry, 2023, 15, 136-142.	6.6	15
73860	Surface Chemistry Determined Electrochemical Sensing Performance of Red Phosphorus and Single Walled Carbon Nanotube Composites. Advanced Functional Materials, 2023, 33, .	7.8	4
73861	Hydrogenation of CO₂ to Methane over a Ru/RuTiO₂ Surface: A DFT Investigation into the Significant Role of the RuO₂ Overlayer. ACS Catalysis, 2022, 12, 14654-14666.	5.5	3
73862	Fully-exposed Pt-Fe cluster for efficient preferential oxidation of CO towards hydrogen purification. Nature Communications, 2022, 13, .	5.8	34
73863	Halide-sodalites: thermal behavior at low temperatures and local deviations from the average structure. Zeitschrift Fur Kristallographie - Crystalline Materials, 2023, 238, 27-38.	0.4	0
73864	Emergent ferromagnetism and insulator-metal transition in Î´-doped ultrathin ruthenates. Npj Quantum Materials, 2022, 7, .	1.8	9
73865	Evaluation of Machine Learning Interatomic Potentials for the Properties of Gold Nanoparticles. Nanomaterials, 2022, 12, 3891.	1.9	7
73866	Weak Electronâ€“Phonon Coupling and Enhanced Thermoelectric Performance in nâ€type PbTeâ€“Cu₂Se via Dynamic Phase Conversion. Advanced Energy Materials, 2023, 13, .	10.2	18
73867	Breaking the Volcano-Shaped Relationship for Highly Efficient Electrocatalytic Nitrogen Reduction: A Computational Guideline. ACS Applied Materials & Interfaces, 2022, 14, 52806-52814.	4.0	10
73868	Thermal Conductivity of Hydrous Wadsleyite Determined by Nonâ€Equilibrium Molecular Dynamics Based on Machine Learning. Geophysical Research Letters, 2022, 49, .	1.5	2

#	Article	IF	Citations
73869	Training biases in machine learning for the analytic continuation of quantum many-body Green's functions. Physical Review Research, 2022, 4, .	1.3	2
73870	Strong CO₂ Chemisorption in a Metalâ€“Organic Framework with Proximate Znâ€“OH Groups. Inorganic Chemistry, 2022, 61, 18710-18718.	1.9	1
73871	Anomalous Hall conductivity control in <mml:math xmlns:mml="http://www.w3.org/1998/Math/MathML"><mml:msub><mml:mrow><mml:mi>Mn</mml:mi></mml:mrow><mml:mn>3</mml:mn></mml:msub></mml:math> antiperovskite by epitaxial strain along the kagome plane. Physical Review B, 2022, 106, .	1.1	1
73872	Computational Insight into Defective Boron Nitride Supported Double-Atom Catalysts for Electrochemical Nitrogen Reduction. Catalysts, 2022, 12, 1404.	1.6	0
73873	Interaction of elements in dilute Mg alloys: a DFT and machine learning study. Journal of Materials Research and Technology, 2022, 21, 4512-4525.	2.6	10
73874	Influence of Group-IVA Doping on Electronic and Optical Properties of ZnS Monolayer: A First-Principles Study. Nanomaterials, 2022, 12, 3898.	1.9	3
73875	Polarizable Force Field for Acetonitrile Based on the Single-Center Multipole Expansion. Journal of Physical Chemistry B, 2022, 126, 9339-9348.	1.2	0
73876	Vacancy-Regulated Charge Carrier Dynamics and Suppressed Nonradiative Recombination in Two-Dimensional ReX₂ (X = S, Se). Journal of Physical Chemistry Letters, 2022, 13, 10656-10665.	2.1	5
73877	Interlayer Coupling Induced Sharp Increase of the Curie Temperature in a Two-Dimensional MnSn Multilayer. ACS Omega, 2022, 7, 43316-43320.	1.6	3
73878	Experimental X-ray Charge-Density Studiesâ”€A Suitable Probe for Superconductivity? A Case Study on MgB₂. Journal of Physical Chemistry A, 2022, 126, 8494-8507.	1.1	4
73879	Boronâ€“nitrogen co-terminated diamond (110) surface for nitrogen-vacancy quantum sensors from first-principles calculations. Journal of Physics Condensed Matter, 2023, 51, 025001.	0.7	0
73880	Resta-like preconditioning for self-consistent field iterations in the linearized augmented planewave method. Electronic Structure, 0, , .	1.0	0
73881	Anti-phase boundary accelerated exsolution of nanoparticles in non-stoichiometric perovskite thin films. Nature Communications, 2022, 13, .	5.8	12
73882	Atomic-scale observation of strain-dependent reversible topotactic transition in La0.7Sr0.3MnOx films under an ultra-high vacuum environment. Materials Today Physics, 2022, 29, 100922.	2.9	6
73883	Physics of phonons in systems with approximate screw symmetry. Physical Review B, 2022, 106, .	1.1	1
73884	Individually-atomic governing dâ€”Ï€* orbital interactions via Cu-promoted optimization of Fe-d band centers for high-efficiency zinc-air battery. Nano Research, 2023, 16, 4634-4642.	5.8	8
73885	Photo-Induced Displacive Phase Transition in Two-dimensional MoTe₂ from First-Principle Calculations. , 0, , .		0
73886	Electric Resonance-Based Depressurization and Augmented Injection in Low-Permeability Reservoirs. Energy & Fuels, 0, , .	2.5	1

#	Article	IF	Citations
73887	Two-Dimensional Penta-NiPS Sheets: Two Stable Polymorphs. Journal of Physical Chemistry C, 2022, 126, 19455-19461.	1.5	3
73888	Self-standing hollow porous Co/a-WOx nanowire with maximum Mott-Schottky effect for boosting alkaline hydrogen evolution reaction. Nano Research, 2023, 16, 4603-4611.	5.8	7
73889	Facile Synthesis of Mediumâ€Entropy Metal Sulfides as Highâ€Efficiency Electrocatalysts toward Oxygen Evolution Reaction. Advanced Functional Materials, 2023, 33, .	7.8	33
73890	Amorphous iron fluorosulfate as a high-capacity cathode utilizing combined intercalation and conversion reactions with unexpectedly high reversibility. Nature Energy, 2023, 8, 30-39.	19.8	18
73891	Mixed-Domain Charge Transport in the Sâ€“Se System from First-Principles. , 2022, 4, 2579-2589.		0
73892	Quantum water desalination: Water generation through separate pathways for protons and hydroxide ions in membranes. Journal of Applied Physics, 2022, 132, 194302.	1.1	1
73893	Ferromagnetic impurity induced Majorana zero mode in iron-based superconductors. Physical Review B, 2022, 106, .	1.1	2
73894	Short hydrogen-bond network confined on COF surfaces enables ultrahigh proton conductivity. Nature Communications, 2022, 13, .	5.8	49
73895	Modeling Luminescence Spectrum of BaZrO₃:Ti Including Vibronic Coupling from First Principles Calculations. Journal of Chemical Theory and Computation, 2022, 18, 7714-7721.	2.3	4
73896	Flat-Band-Induced Many-Body Interactions and Exciton Complexes in a Layered Semiconductor. Nano Letters, 2022, 22, 8883-8891.	4.5	1
73897	Structural and electronic properties of Na-B-H compounds at high pressure. Physical Review B, 2022, 106, .	1.1	2
73898	Li₂NiSe₂: a new type intrinsic two dimensional ferromagnetic semiconductor above 200 K. Chinese Physics B, 0, , .	0.7	0
73899	Ideal simple shear strengths of two HfNbTaTi-based quinary refractory multi-principal element alloys. APL Materials, 2022, 10, .	2.2	7
73900	Exploring the subtle factors that control the structural preferences in Cu₇Te₄. Journal of Physics Condensed Matter, 0, , .	0.7	1
73901	Effects of B and In on the band structure of BGa(In)As alloys. Journal of Applied Physics, 2022, 132, .	1.1	1
73902	Customized development of promising Cu-Cr-Ni-Co-Si alloys enabled by integrated machine learning and characterization. Acta Materialia, 2023, 243, 118484.	3.8	6
73903	Vanadium Dioxide-Based Miniaturized Thermal Sensors: Humidity Effects on Phase Change and Sensitivity. ACS Applied Electronic Materials, 2022, 4, 5456-5467.	2.0	2
73904	Large Gap Topological Insulating Phase and Anisotropic Rashba and Chiral Spin Textures in Monolayer Zintl A₂MX₂. ACS Applied Electronic Materials, 2022, 4, 5308-5316.	2.0	1

#	Article	IF	Citations
73905	Black Arsenicâ€“Phosphorus Nanosheets for Highly Responsive Photodetection and Dual-Wavelength Ultrafast Pulse Generation at Telecommunication Bands. ACS Applied Materials & Interfaces, 2022, 14, 52270-52278.	4.0	2
73906	An Original Empirical Method for Simulating V L_{2,3} Edges: The Example of KVPO₄F and KVOPO₄ Cathode Materials. Journal of Physical Chemistry C, 2022, 126, 19782-19791.	1.5	2
73907	Split of the magnetic and crystallographic states in Fe1â^'Rh Ge. Journal of Alloys and Compounds, 2022, , 167943.	2.8	0
73908	Electron Counting and High-Pressure Phase Transformations in Metal Hexaborides. Inorganic Chemistry, 2022, 61, 18701-18709.	1.9	2
73909	Fabrication of honeycomb AuTe monolayer with Dirac nodal line fermions. Chinese Physics B, 2023, 32, 016102.	0.7	2
73910	Development of a Mg/O ReaxFF Potential to describe the Passivation Processes in Magnesiumâ€ion Batteries**. ChemSusChem, 2023, 16, .	3.6	5
73911	Ab initio study of RaWO4: Comparison with isoelectronic tungstates. Journal of Solid State Chemistry, 2023, 317, 123709.	1.4	2
73912	Evolution of Low-Dimensional Phosphorus Allotropes on Ag(111). Chemistry of Materials, 2022, 34, 10651-10658.	3.2	3
73913	Testing the r²SCAN Density Functional for the Thermodynamic Stability of Solids with and without a van der Waals Correction. ACS Materials Au, 2023, 3, 102-111.	2.6	8
73914	Cumulative polarization in conductive interfacial ferroelectrics. Nature, 2022, 612, 465-469.	13.7	43
73915	Pressure stabilized polymeric nitrogen in N2F and N10F compounds. Results in Physics, 2022, 43, 106093.	2.0	1
73916	Dual-site collaboration boosts electrochemical nitrogen reduction on Ru-S-C single-atom catalyst. Chinese Journal of Catalysis, 2022, 43, 3177-3186.	6.9	6
73917	Tunable electronic, magnetic, and optical properties of carbon-nanomaterial/Î±-Fe2O3 interface: A first-principles study. Materials Today Communications, 2022, 33, 104890.	0.9	0
73918	Strengthening and high-temperature softening resistance of low Si-added Cuâ€“Crâ€“Zr alloy for fusion reactor application. Materials Science & Engineering A: Structural Materials: Properties, Microstructure and Processing, 2022, 861, 144328.	2.6	4
73919	QPHT graphene as a high-performance lithium ion battery anode materials with low diffusion barrier and high capacity. Physics Letters, Section A: General, Atomic and Solid State Physics, 2022, 456, 128549.	0.9	2
73920	Tunable magnetoresistance in Li2BaSi. Physics Letters, Section A: General, Atomic and Solid State Physics, 2022, 456, 128541.	0.9	0
73921	Thermodynamic modeling of the Ni-Ti-Cr system and the B2/B19â€² martensitic transformation. Calphad: Computer Coupling of Phase Diagrams and Thermochemistry, 2022, 79, 102505.	0.7	2
73923	Novel phase transition for XSnN<mml:math xmlns:mml="http://www.w3.org/1998/Math/MathML" altimg="si35.svg" display="inline" id="d1e406"><mml:msub><mml:mrow /><mml:mrow><mml:mn>2</mml:mn></mml:mrow></mml:msub></mml:math> (X = Mg, Zn) under uniaxial compression. Materials Today Communications, 2022, 33, 104753.	0.9	5

#	Article	IF	Citations
73924	Magnetic properties of transition-metal atomic monolayer in nickel supercell: Density functional theory and Monte Carlo simulation. Journal of Magnetism and Magnetic Materials, 2022, 564, 170173.	1.0	12
73925	First-principles study of the effect of non-stoichiometry on sensing mechanism of NO on WO3 (001) surfaces. Materials Today Communications, 2022, 33, 104926.	0.9	0
73926	Solute clustering governed elastic properties in aluminum. Calphad: Computer Coupling of Phase Diagrams and Thermochemistry, 2022, 79, 102494.	0.7	1
73927	Density functional theory study of active sites and reaction mechanism of ORR on Pt surfaces under anhydrous conditions. Chinese Journal of Catalysis, 2022, 43, 3126-3133.	6.9	4
73928	Realizing a strong visible-light absorption band in piezoelectric 2D carbon nitride sheets for enhanced piezocatalysis. Nano Energy, 2022, 104, 107983.	8.2	14
73929	Growth mechanism and characteristics of Î²-Ga2O3 heteroepitaxailly grown on sapphire by metalorganic chemical vapor deposition. Materials Today Advances, 2022, 16, 100320.	2.5	4
73930	First-principles study of TM supported SnSe2 monolayer as an efficient electrocatalyst for NOER. Molecular Catalysis, 2022, 533, 112789.	1.0	0
73931	Influence of interfacial configuration on bonding properties and thermal conductivity of heterogeneous interface in Al/Graphite composite used for electronic packaging. Surfaces and Interfaces, 2022, 35, 102452.	1.5	2
73932	Luminescent thermal behavior of Eu3+ in K5Bi(Mo W1-O4)4 phosphors. Optical Materials, 2022, 134, 113211.	1.7	3
73933	Packing of inhibitor molecules during area-selective atomic layer deposition studied using random sequential adsorption simulations. Journal of Vacuum Science and Technology A: Vacuum, Surfaces and Films, 2022, 40, .	0.9	8
73934	Investigation of superconductivity in ultrahigh pressure phases of yttrium. Solid State Communications, 2022, 358, 115004.	0.9	0
73935	Effects of surface Chemistry, particle morphology and pretreatment on zircon flotation. Minerals Engineering, 2022, 190, 107904.	1.8	3
73936	pH-Induced selective electrocatalytic hydrogenation of furfural on Cu electrodes. Chinese Journal of Catalysis, 2022, 43, 3142-3153.	6.9	20
73937	Boosting the efficiency of urea synthesis via cooperative electroreduction of N₂ and CO₂ on MoP. Journal of Materials Chemistry A, 2022, 11, 232-240.	5.2	30
73938	First-principles study on bilayer SnP₃ as a promising thermoelectric material. Physical Chemistry Chemical Physics, 2022, 24, 29693-29699.	1.3	2
73939	Experimental absence of the non-perovskite ground state phases of MaPbI₃ explained by a Funnel Hopping Monte Carlo study based on a neural network potential. Materials Advances, 2023, 4, 184-194.	2.6	4
73940	Investigation of the Structure of Atomically Dispersed NiN_x Sites in Ni and N-Doped Carbon Electrocatalysts by ⁶¹Ni MÃ¶ssbauer Spectroscopy and Simulations. Journal of the American Chemical Society, 2022, 144, 21741-21750.	6.6	2
73941	Electronic properties and storage capability of two-dimensional nitridosilicate MnSi₂N₄ from first-principles. AIP Advances, 2022, 12, 115127.	0.6	0

#	Article	IF	Citations
73942	Negative-positive oscillation in interfacial friction of a <mml:math xmlns:mml="http://www.w3.org/1998/Math/MathML"><mml:mrow><mml:msub><mml:mi>In</mml:mi><mml:mn>21</mml:mn></mml:m -graphene heterojunction. Physical Review B, 2022, 106, .	2.1	5
73943	Improvement mechanism of thermal conductivity in T6/T7â€treated Alâ€Siâ€Mg cast alloy: Experimental studies and DFT calculations. Advanced Engineering Materials, 0, , .	1.6	0
73944	Ceramic Wafer Scintillation Screen by Utilizing Nearâ€Unity Blueâ€Emitting Leadâ€Free Metal Halide (C₈H₂₀N)₂Cu₂Br₄. Advanced Functional Materials, 2023, 33, .	7.8	48
73945	Ferroelectric and antiferroelectric distortions coupling of nitride perovskite LaWN₃ under epitaxial strain using first-principles calculations. Europhysics Letters, 2022, 140, 56001.	0.7	1
73946	Hydrogen at symmetric tilt grain boundaries in aluminum: segregation energies and structural features. Scientific Reports, 2022, 12, .	1.6	3
73947	Amorphous SnO2 decorated ZnSn(OH)6 promotes interfacial hydroxyl polarization for deep photocatalytic toluene mineralization. Journal of Hazardous Materials, 2023, 444, 130436.	6.5	10
73948	Machine-learning-based prediction of first-principles XANES spectra for amorphous materials. Physical Review Materials, 2022, 6, .	0.9	1
73949	Theoretical studies on internal strain of face-centered-cubic metal nanoparticles. Physical Review B, 2022, 106, .	1.1	1
73950	Single crystal growth and properties of the polar ferromagnet <mml:math xmlns:mml="http://www.w3.org/1998/Math/MathML"><mml:mrow><mml:msub><mml:mi>Mn</mml:mi><mml:mrow><mml:mn>1.05< with Kagome layers, huge magnetic anisotropy and slow spin dynamics. Physical Review Materials, 2022, 6, .	0.9	0
73951	First-principles study of He retention and clustering in Al-Ga alloy. International Journal of Modern Physics C, 0, , .	0.8	0
73952	Sulfur Vacancy-Rich Carbonaceous Co₉S₈-ZnS Nanotubes for the Oxygen Evolution Reaction. ACS Applied Energy Materials, 2022, 5, 14869-14880.	2.5	1
73953	Native defects in monolayer GaS and GaSe: Electrical properties and thermodynamic stability. Physical Review Materials, 2022, 6, .	0.9	2
73954	Interfacial Coupling SnSe₂/SnSe Heterostructures as Long Cyclic Anodes of Lithiumâ€Ion Battery. Advanced Science, 2023, 10, .	5.6	13
73955	Machine learning of carbon vacancy formation energy in high-entropy carbides. Journal of the European Ceramic Society, 2023, 43, 1315-1321.	2.8	6
73956	Unveiling Chemically Robust Bimetallic Squarateâ€Based Metalâ€“Organic Frameworks for Electrocatalytic Oxygen Evolution Reaction. Advanced Energy Materials, 2023, 13, .	10.2	22
73957	High-entropy alloy catalysts: Fundamental aspects, promises towards electrochemical NH3 production, and lessons to learn from deep neural networks. Nano Energy, 2023, 105, 108027.	8.2	10
73958	A New Insight into the Mechanisms Underlying the Discoloration, Sorption, and Photodegradation of Methylene Blue Solutions with and without BNOx Nanocatalysts. Materials, 2022, 15, 8169.	1.3	3
73959	Two-dimensional hourglass Weyl nodal loop in monolayer Pb(ClO2)2 and Sr(ClO2)2. New Journal of Physics, 0, , .	1.2	0

#	Article	IF	Citations
73960	Understanding the Reactivity of Supported Late Transition Metals on a Bare Anatase (101) Surface: A Periodic Conceptual DFT Investigation. ChemPhysChem, 2023, 24, .	1.0	4
73961	Composition-dependent photocatalytic activity and high-mobility carrier gas in NaTaO3/BaBiO3 heterojunctions. Surfaces and Interfaces, 2023, 36, 102486.	1.5	2
73962	Discovery of Salt Hydrates for Thermal Energy Storage. Journal of the American Chemical Society, 2022, 144, 21617-21627.	6.6	6
73963	2D transitional-metal nickel compounds monolayer: Highly efficient multifunctional electrocatalysts for the HER, OER and ORR. International Journal of Hydrogen Energy, 2023, 48, 4242-4252.	3.8	17
73964	Cesium-mediated electron redistribution and electron-electron interaction in high-pressure metallic CsPbI3. Nature Communications, 2022, 13, .	5.8	10
73965	Lattice dynamics of <mml:math xmlns:mml="http://www.w3.org/1998/Math/MathML"><mml:mi>Î²</mml:mi><mml:mo>â^'</mml:mo><mml:msub><mml:mi mathvariant="normal">FeSi</mml:mi><mml:mn>2</mml:mn></mml:msub></mml:math> nanorods. Physical Review B, 2022, 106, .	1.1	0
73966	Exciton Nature of Plasma Phase Transition in Warm Dense Fluid Hydrogen: ROKS Simulation. ChemPhysChem, 0, , .	1.0	0
73967	Band Edges Engineering of 2D/2D Heterostructures: The C₃N₄/Phosphorene Interface. ChemPhysChem, 2023, 24, .	1.0	2
73968	Thermal properties of the metallic delafossite <mml:math xmlns:mml="http://www.w3.org/1998/Math/MathML"><mml:mrow><mml:mi>PdCo</mml:mi><mml:msub><mml:mi mathvariant="normal">O</mml:mi><mml:mn>2</mml:mn></mml:msub></mml:mrow></mml:math> : A combined experimental and first-principles study. Physical Review Materials, 2022, 6, .	0.9	2
73969	Lattice distortion optimized hybridization and superlubricity of MoS2/MoSe2 heterointerfaces via MoirÃ© patterns. Applied Surface Science, 2023, 613, 155760.	3.1	4
73970	Improved Hydrogen Generation of Al-H2O Reaction by BiOX (X = Halogen) and Influence Rule. Materials, 2022, 15, 8199.	1.3	0
73971	Towards the ionizing radiation induced bond dissociation mechanism in oxygen, water, guanine and DNA fragmentation: a density functional theory simulation. Scientific Reports, 2022, 12, .	1.6	4
73972	First-principles study to probe the effect of substitution at X and Z sites on the electronic, magnetic and transport properties of Co2X(V, Nb, Ta)Z(Al, Ga, In, Si, Ge, Sn) Heusler alloys. Solid State Communications, 2023, 359, 115022.	0.9	1
73973	The experimental and theoretical research on the near infrared luminescent property of KAL11O17:Fe3ï¼‹ and RbAl11O17:Fe3ï¼‹. Optical Materials: X, 2022, , 100212.	0.3	0
73974	Breaking structure sensitivity in CO2 hydrogenation by tuning metalâ€“oxide interfaces in supported cobalt nanoparticles. Nature Catalysis, 2022, 5, 1051-1060.	16.1	39
73975	Hydrogen Adsorption on Pdâ€“In Intermetallic Surfaces. Topics in Catalysis, 2023, 66, 1457-1464.	1.3	1
73976	Discontinuous Galerkin method with Voronoi partitioning for quantum simulation of chemistry. Research in Mathematical Sciences, 2022, 9, .	0.5	1
73977	Costâ€Effective H₂O₂â€Regeneration of Powdered Activated Carbon by Isolated Fe Sites. Advanced Science, 2023, 10, .	5.6	5

#	Article	IF	Citations
73978	Influence of carbon on hydrogen retention in molybdenum for nuclear material application: A first-principles investigation. Nuclear Materials and Energy, 2022, 33, 101311.	0.6	0
73979	Controllable ferroelectricity and bulk photovoltaic effect in elemental group-V monolayers through strain engineering. Physical Review B, 2022, 106, .	1.1	4
73980	Coâ€Substituted BiFeO₃: Electronic, Ferroelectric, and Thermodynamic Properties from First Principles. Advanced Theory and Simulations, 2023, 6, .	1.3	2
73981	A^IB₃^{II}C₃^{III}Q₈^{VI}: A New Family for the Design of Infrared Nonlinear Optical Materials by Coupling Octahedra and Tetrahedra Units. Journal of the American Chemical Society, 2022, 144, 21916-21925.	6.6	54
73982	Revealing the Origin of Heterogeneous Phase Transition and Deformation Behavior in Au-Ag-Cu-Based Multicomponent Alloys. Metals, 2022, 12, 1966.	1.0	1
73983	Interactions of alloying Cr/Ti with substitutional solutes and self-interstitial atoms in vanadium. Journal of Nuclear Materials, 2023, 574, 154160.	1.3	3
73984	Active orbital degree of freedom and potential spin-orbit-entangled moments in the Kitaev magnet candidate <mml:math xmlns:mml="http://www.w3.org/1998/Math/MathML"><mml:msub><mml:mi>BaCo</mml:mi><mml:mn>2</mml:mn></mml:msub><mn Physical Review B, 2022, 106, .	1.1	2
73985	NiAl-layered double hydroxides stabilized Pt clusters with enhanced metal-support interaction: Boosting hydrogen isotope separation. Applied Surface Science, 2023, 611, 155780.	3.1	5
73986	Bowing-alleviated continuous bandgap engineering of wafer-scale WS2xSe2(1-x) monolayer alloys and their assembly into hetero-multilayers. NPG Asia Materials, 2022, 14, .	3.8	5
73987	Boron-doped g-CN monolayer as a promising anode for Na/K-ion batteries. Surfaces and Interfaces, 2023, 36, 102479.	1.5	10
73988	Band valley modification under strain in monolayer WSe2. AIP Advances, 2022, 12, .	0.6	4
73989	Suppressing ion migration in metal halide perovskite via interstitial doping with a trace amount of multivalent cations. Nature Materials, 2022, 21, 1396-1402.	13.3	74
73990	Impact of vacancies on structure, stability and properties of hexagonal transition metal diborides, MB2 (MÂ=ÂSc, Y, Ti, Zr, Hf, V, Nb, Ta, Cr, Mo, W, Mn, and Fe). Materialia, 2022, 26, 101629.	1.3	6
73991	On the Stability of Potential Photovoltaic Absorber In₅S₄. Journal of Physical Chemistry C, 2022, 126, 19971-19977.	1.5	1
73992	Steric Hindrance of NH₃ Diffusion on Pt(111) by Co-Adsorbed O-Atoms. Journal of the American Chemical Society, 2022, 144, 21791-21799.	6.6	6
73993	Dilution of a polar magnet: Structure and magnetism of Zn-substituted <mml:math xmlns:mml="http://www.w3.org/1998/Math/MathML"><mml:mrow><mml:msub><mml:mi>Co</mml:mi><mml:mn>2</mml:mn></mml:mr mathvariant="normal">O</mml:mi><mml:mn>8</mml:mn></mml:msub></mml:mrow></mml:math>. Physical Review B, 2022, 106, .	1.1	4
73994	Self-layering of (Ti,Al)N by interface-directed spinodal decomposition of (Ti,Al)N/TiN multilayers: First-principles and experimental investigations. Materials and Design, 2022, 224, 111392.	3.3	5
73995	Integrated DFT and experimental study on Co3O4/CeO2 catalyst for direct synthesis of dimethyl carbonate from CO2. Journal of CO2 Utilization, 2023, 67, 102323.	3.3	6

#	Article	IF	Citations
73996	A cocklebur-like sulfur host with the TiO2-VOx heterostructure efficiently implementing one-step adsorption-diffusion-conversion towards long-life Liâ€“S batteries. Composites Part B: Engineering, 2023, 249, 110410.	5.9	52
73997	aflow++: A C++ framework for autonomous materials design. Computational Materials Science, 2023, 217, 111889.	1.4	14
73998	Improved electrochemical behavior and mechanism of Ni0.90Mn0.10WO4 electrode for supercapacitor applications. Journal of Alloys and Compounds, 2023, 934, 167977.	2.8	1
73999	Synergized N, P dual-doped 3D carbon host derived from filter paper for durable lithium metal anodes. Journal of Colloid and Interface Science, 2023, 632, 1-10.	5.0	5
74000	1D Bi2S3 nanorods modified 2D BiOI nanoplates for highly efficient photocatalytic activity: Pivotal roles of oxygen vacancies and Z-scheme heterojunction. Journal of Materials Science and Technology, 2023, 142, 45-59.	5.6	17
74001	Large in-plane and out-of-plane piezoelectricity in 2D Î³-LiMX2 (M=Al, Ga and In; X=S, Se and Te) monolayers. Materials Science in Semiconductor Processing, 2023, 154, 107222.	1.9	5
74002	Single-layer MoS2 with adjacent Mo sites for efficient electrocatalytic nitrogen fixation via spin-delocalized electrons effect. Applied Catalysis B: Environmental, 2023, 323, 122186.	10.8	5
74003	The enhanced effect of magnetism on the thermoelectric performance of a CrI₃ monolayer. Nanoscale, 2023, 15, 1032-1041.	2.8	3
74004	Mechanistic assessment of NO oxidative activation on tungsten-promoted ceria catalysts and its consequence for low-temperature NH3-SCR. Applied Energy, 2023, 330, 120306.	5.1	3
74005	A general approach to simulate the atom distribution, lattice distortion, and mechanical properties of multi-principal element alloys based on site preference: Using FCC_CoNiV and CoCrNi to demonstrate and compare. Journal of Alloys and Compounds, 2023, 935, 168016.	2.8	4
74006	The dual-active-site tandem catalyst containing Ru single atoms and Ni nanoparticles boosts CO2 methanation. Applied Catalysis B: Environmental, 2023, 323, 122190.	10.8	32
74007	Entrapped Moleculeâ€Like Europiumâ€Oxide Clusters in Zinc Oxide with Nearly Unaffected Host Structure. Small, 2023, 19, .	5.2	4
74008	Density Functional Evaluation of Catechol Adsorption on Pristine and Reduced TiO₂(B)(100) Ultrathin Sheets for Dye-Sensitized Solar Cell Applications. Inorganic Chemistry, 0, , .	1.9	1
74009	Heterogeneous Fe(IV) O mediated fenton-like process on Fe-Zr heterojunction for selective oxidation of organic pollutants at near neutral pH. Chemical Engineering Journal, 2023, 454, 140516.	6.6	4
74010	DFT+U study on the magnetic properties of 3d transition metal doped Î² borophene. Physica E: Low-Dimensional Systems and Nanostructures, 2023, 147, 115576.	1.3	2
74011	A Class of Auxiliary Passivators for Polymer Dielectrics. Advanced Electronic Materials, 2023, 9, .	2.6	5
74012	Effect of point defect-induced surface active sites of MoSi2N4 on performance of photocatalytic CO2 reduction. Applied Catalysis A: General, 2023, 650, 118975.	2.2	3
74013	Role of solute atoms and vacancy in hydrogen embrittlement mechanism of aluminum: A first-principles study. International Journal of Hydrogen Energy, 2023, 48, 4516-4528.	3.8	4

#	Article	IF	Citations
74014	Spin Selectivity in Chiral Hybrid Cobalt Halide Films with Ultrasmooth Surface. Small Methods, 2022, 6, .	4.6	5
74015	Phosphorus nanoclusters and insight into the formation of phosphorus allotropes. Nanoscale, 2023, 15, 1338-1346.	2.8	4
74016	Amorphous structures for enhancing the electrochemical activity of nickel disulfide for efficient methanol oxidation. New Journal of Chemistry, 2023, 47, 875-881.	1.4	2
74017	Oxygen vacancies assist a facet effect to modulate the microstructure of TiO₂ for efficient photocatalytic O₂ activation. Nanoscale, 2023, 15, 768-778.	2.8	7
74018	Hydrogenated V2O5 with fast Zn-ion migration kinetics as high-performance cathode material for aqueous zinc-ion batteries. Electrochimica Acta, 2023, 439, 141717.	2.6	11
74019	New horizons of MBenes: highly active catalysts for the CO oxidation reaction. Nanoscale, 2023, 15, 483-489.	2.8	2
74020	Programming a triple-shelled CuS@Ni(OH)2@CuS heterogeneous nanocage as robust electrocatalysts enabling long-term highly sensitive glucose detection. Electrochimica Acta, 2023, 438, 141588.	2.6	2
74021	Toward a new definition of surface energy for late transition metals. Physical Chemistry Chemical Physics, 2023, 25, 1977-1986.	1.3	2
74022	On the stability of peptide secondary structures on the TiO₂ (101) anatase surface: a computational insight. Physical Chemistry Chemical Physics, 2022, 25, 392-401.	1.3	0
74023	A density functional theory study of a water gas shift reaction on Ag(111): potassium effect. Physical Chemistry Chemical Physics, 2022, 25, 768-777.	1.3	1
74024	Pressure-induced phase transition and band-gap decrease in semiconducting Na3Bi(IO3)6. Results in Physics, 2023, 44, 106156.	2.0	4
74025	High-pressure equation of state of cesium fluoride to 120â€…GPa. , 2017, 6, 011101-011101.		0
74026	Defect related room temperature ferromagnetism in N-implanted ZnO film. , 2018, 7, 011104-011104.		0
74027	Condensability sieving porous coordination polymer membranes for preferential permeation of C1â€“C4 alkanes over H2. , 2022, 2, 100044.		0
74028	A graphene-like semiconducting BC₂P monolayer as a promising material for a Li-ion battery and CO₂ adsorbent. Physical Chemistry Chemical Physics, 2023, 25, 2430-2438.	1.3	11
74029	In the search for the bottlenecks of ammonia synthesis over Ru/Vulcan under ambient conditions. Faraday Discussions, 0, , .	1.6	0
74030	Structure and registry of the silica bilayer film on Ru(0001) as viewed by LEED and DFT. Physical Chemistry Chemical Physics, 2022, 24, 29721-29730.	1.3	1
74031	High thermoelectric performance of two-dimensional layered AB₂Te₄ (A = Sn,) Tj ETQq1 1 0.784314 rgBT /O	1.3	6

#	Article	IF	Citations
74032	Concentration dependent alloying behaviour of liquid GaAu. Chemical Communications, 2022, 58, 13771-13774.	2.2	1
74033	Exploring the direction-dependency of conductive filament formation and oxygen vacancy migration behaviors in HfO₂-based RRAM. Physical Chemistry Chemical Physics, 2023, 25, 3521-3534.	1.3	2
74034	Computational study of bulk and surface properties on ruthenium oxide (RuO₂). MATEC Web of Conferences, 2022, 370, 02003.	0.1	0
74035	Electron passivation in CaF₂ on calcium metal anodes. Physical Chemistry Chemical Physics, 2022, 24, 29579-29585.	1.3	1
74036	Theoretical insights into interfacial stability and ionic transport of Li₂OHBr solid electrolyte for all-solid-state batteries. RSC Advances, 2022, 12, 34627-34633.	1.7	0
74037	A study of the Rashba effect in two-dimensional ternary compounds ABC monolayers (A = Sb, Bi; B = Se,) Tj ETQq1 1 0.784314 rgBT /Ov	1.3	0
74038	Photoabsorbance of supported metal clusters: ab initio density matrix and model studies of large Ag clusters on Si surfaces. Physical Chemistry Chemical Physics, 2023, 25, 14757-14765.	1.3	1
74039	High-throughput analysis of tetragonal transition metal Xenes. Physical Chemistry Chemical Physics, 2022, 24, 29406-29412.	1.3	1
74040	Influence of the zeolite support on the catalytic properties of confined metal clusters: a periodic DFT study of O₂ dissociation on Cu_n clusters in CHA. Physical Chemistry Chemical Physics, 2022, 24, 30044-30050.	1.3	2
74041	Alleviation of Self-Heating Effect in Top-Gated Ultrathin In₂O₃ FETs Using a Thermal Adhesion Layer. IEEE Transactions on Electron Devices, 2023, 70, 113-120.	1.6	3
74042	Identification of distinctive structural and optoelectronic properties of Bi₂O₃ polymorphs controlled by tantalum addition. Journal of Materials Chemistry C, 2022, 10, 17925-17935.	2.7	1
74043	New family of layered N-based cathode materials for sodium-ion batteries. RSC Advances, 2022, 12, 34200-34207.	1.7	2
74044	Insight into charge transfer between graphene and palladium nanosheets investigated by Raman spectroscopy. New Journal of Chemistry, 0, , .	1.4	0
74045	Low temperature ammonia synthesis by surface protonics over metal supported catalysts. Faraday Discussions, 0, 243, 179-197.	1.6	2
74046	First-principles based deep neural network force field for molecular dynamics simulation of Nâ€“Gaâ€“Al semiconductors. Physical Chemistry Chemical Physics, 2023, 25, 2349-2358.	1.3	5
74047	Charge and adsorption height dependence of the self-metalation of porphyrins on ultrathin MgO(001) films. Physical Chemistry Chemical Physics, 2022, 24, 28540-28547.	1.3	0
74048	Two -dimensional semimetal AlSb monolayer with multiple nodal-loops and extraordinary transport properties under uniaxial strain. Nanoscale, 0, , .	2.8	0
74049	Identifying the effect of Ni solubility on the thermoelectric properties of HfNiSn-based half-Heuslers. Acta Materialia, 2023, 244, 118591.	3.8	3

#	Article	IF	Citations
74050	Effect of bulk and surface composition of NiÂ+ÂGa intermetallic compound catalysts in propane steam/wet reforming: Origins of nearly ideal experimental product selectivity. Journal of Catalysis, 2023, 417, 260-273.	3.1	0
74051	Mechanism and adjustability of negative differential resistance of 2-phenylpyridine molecular devices by graphene electrode bending. Wuli Xuebao/Acta Physica Sinica, 2023, .	0.2	0
74052	Atomistic insights into the mechanical anisotropy and fragility of monolayer fullerene networks using quantum mechanical calculations and machine-learning molecular dynamics simulations. Extreme Mechanics Letters, 2023, 58, 101929.	2.0	25
74053	Magnetic-field-regulated Ni-Fe-Mo ternary alloy electrocatalysts with enduring spin polarization enhanced oxygen evolution reaction. Chemical Engineering Journal, 2023, 455, 140821.	6.6	16
74054	Selective furfural hydrogenolysis towards 2-methylfuran by controlled poisoning of Cuâ€“Co catalysts with chlorine. Reaction Chemistry and Engineering, 2023, 8, 687-698.	1.9	4
74055	2D MoS₂/BiOBr van der Waals heterojunctions by liquid-phase exfoliation as photoelectrocatalysts for hydrogen evolution. Nanoscale, 0, , .	2.8	6
74056	Tailored modifications of the electronic properties of g-C₃N₄/C₂N-h2D nanoribbons by first-principles calculations. Physical Chemistry Chemical Physics, 2023, 25, 1153-1160.	1.3	11
74057	Twisted grain boundary leads to high thermoelectric performance in tellurium crystals. Energy and Environmental Science, 2023, 16, 125-137.	15.6	5
74058	Enhanced stability of sub-nanometric iridium decorated graphitic carbon nitride for H₂ production upon hydrous hydrazine decomposition. Physical Chemistry Chemical Physics, 2023, 25, 1081-1095.	1.3	2
74059	Fast electrochemical redox kinetics of two-dimensional TiO2/Ti3C2T (MXene) heterostructure for high-performance lithium-ion capacitor. Journal of Electroanalytical Chemistry, 2023, 928, 117034.	1.9	5
74060	Tuning electronic and optical properties of BlueP/MoSe2 van der Waals heterostructures by strain and external electric field. Results in Physics, 2023, 44, 106135.	2.0	4
74061	Effect of alkali metal adsorption over pristine Ga2STe janus monolayer in enhancing the visible region absorption. , 2023, 173, 207463.		0
74062	First principles investigation on Na-ion storage in two-dimensional boron-rich B₂N, B₃N, and B₅N. Physical Chemistry Chemical Physics, 2023, 25, 1123-1132.	1.3	3
74063	Soft anharmonic coupled vibrations of Li and SiO₄ enable Li-ion diffusion in amorphous Li₂Si₂O₅. Journal of Materials Chemistry A, 2023, 11, 1712-1722.	5.2	2
74064	Ultrasonically-assisted synthesis of CeO2 within WS2 interlayers forming type II heterojunction for a VOC photocatalytic oxidation. Ultrasonics Sonochemistry, 2023, 92, 106245.	3.8	11
74065	Highly efficient extraction of uranium from seawater by polyamide and amidoxime co-functionalized MXene. Environmental Pollution, 2023, 317, 120826.	3.7	15
74066	Effects of Cl/Br substitution of antimony octahedra on photoluminescence and a new engineering strategy for performance optimization. Materials Today Chemistry, 2023, 27, 101275.	1.7	0
74067	Optimizing the microstructures and enhancing the mechanical properties of AZ81 alloy by adding TC4 particles. Materials Science & Engineering A: Structural Materials: Properties, Microstructure and Processing, 2023, 863, 144518.	2.6	10

#	Article	IF	Citations
74068	A novel highly stable two-dimensional boron phase with promising potentials in energy fields. Journal of Materials Chemistry A, 2023, 11, 828-837.	5.2	2
74069	Rb₂CdSi₄S₁₀: novel [Si₄S₁₀] T2-supertetrahedra-contained infrared nonlinear optical material with large band gap. Materials Horizons, 2023, 10, 619-624.	6.4	33
74070	Large second harmonic generation in a penta-CdO₂ sheet exfoliated from its bulk phase. Journal of Materials Chemistry A, 2022, 11, 167-177.	5.2	3
74071	Stability and electronic structures of Cmmm-Pt3M alloys. Physics Letters, Section A: General, Atomic and Solid State Physics, 2023, 457, 128540.	0.9	12
74072	Ba₄FeAgS₆: a new antiferromagnetic and semiconducting quaternary sulfide. Dalton Transactions, 2023, 52, 621-634.	1.6	2
74073	Phase-structure design for sodium chloride solid electrolytes with outstanding performance: a first-principles approach. Journal of Materials Chemistry A, 2023, 11, 1906-1919.	5.2	5
74074	Phase stability and electronic structure of CsPbCl₃ under hydrostatic stress and anion substitution. Physical Chemistry Chemical Physics, 2023, 25, 1279-1289.	1.3	3
74075	Theoretical design of two-dimensional AMInP₂X₃Y₃ (AM = Li, Na,) Tj ETQq1 1 0.784314 rgBT /O 570-577.	2.6	2
74076	Giant spin-dependent Seebeck effect from fully spin-polarized carriers in n-doped EuTiO₃: a prototype material for spin-caloritronic applications. Journal of Materials Chemistry A, 2023, 11, 6842-6853.	5.2	1
74077	Boosting photocatalytic H₂O₂ production in pure water over a plasmonic photocatalyst with polyethylenimine modification. Journal of Materials Chemistry A, 2023, 11, 1503-1510.	5.2	15
74078	Electromechanical response of group-IV monochalcogenide monolayers. Journal of Materials Chemistry C, 0, , .	2.7	1
74079	Highly anisotropic 1/3-magnetization plateau in a ferrimagnet Cs₂Cu₃(SeO₃)₄Â·2H₂O: topology of magnetic bonding necessary for magnetization plateau. Dalton Transactions, 2022, 52, 118-127.	1.6	0
74080	Evidence of direct Z-scheme triazine-based g-C₃N₄/BiOI (001) heterostructures: a hybrid density functional investigation. Physical Chemistry Chemical Physics, 2022, 25, 847-856.	1.3	3
74081	Fully coupled segregation and precipitation kinetics model with ab initio input for the Fe-Au system. Acta Materialia, 2023, 244, 118577.	3.8	4
74082	Cooperative stabilization by highly efficient nanoseeds and reinforced interphase toward practical Li metal batteries. Energy Storage Materials, 2023, 55, 517-526.	9.5	10
74083	Correlation of phase (in)stability and lattice misfits for high-power-density Na cathodes. Journal of Materials Chemistry A, 2023, 11, 5104-5111.	5.2	2
74084	Si regulation of hydrogen adsorption on nanoporous PdSi hybrids towards enhancing electrochemical hydrogen evolution activity. Inorganic Chemistry Frontiers, 2023, 10, 1101-1111.	3.0	3
74085	Na2Mn(CO3)2: A carbonate based prototype cathode material for Na-ion batteries with high rate capability â€" An ab-initio study. Electrochimica Acta, 2023, 439, 141687.	2.6	1

#	Article	IF	Citations
74086	Creating metal-carbide interactions to boost ammonia oxidation activity for low-temperature direct ammonia fuel cells. Journal of Catalysis, 2023, 417, 129-139.	3.1	5
74087	Surface oxidation protection strategy of CoS₂ by V₂O₅ for electrocatalytic hydrogen evolution reaction. Nanoscale Horizons, 2023, 8, 338-345.	4.1	6
74088	High photocatalytic solar-to-hydrogen efficiency by the edge-passivated antimonene nanoribbons with anisotropic vacuum levels. Applied Catalysis A: General, 2023, 650, 119004.	2.2	3
74089	Curvature effects on the bifunctional oxygen catalytic performance of single atom metalâ€“Nâ€“C. Nanoscale, 2023, 15, 2276-2284.	2.8	8
74090	Boosting zinc-ion storage in hydrated vanadium oxides via migration regulation. Energy Storage Materials, 2023, 55, 279-288.	9.5	25
74091	In situ generated oxygen vacancy on Nb2O5 for boosted catalytic activities of M/Nb2O5 in photothermal CO2 reforming of CH4. Journal of CO2 Utilization, 2023, 67, 102330.	3.3	2
74092	Quantum manifestations in electronic properties of bilayer phosphorene nanoribbons. Physical Chemistry Chemical Physics, 0, , .	1.3	0
74093	In-plane graphene incorporated borocarbonitride: Directional utilization of disorder charge via micro Ï€-conjugated heterointerface for photocatalytic CO2 reduction. Carbon, 2023, 203, 847-855.	5.4	3
74094	Catalytic active centers beyond transition metals: atomically dispersed alkaline-earth metals for the electroreduction of nitrate to ammonia. Journal of Materials Chemistry A, 2023, 11, 1817-1828.	5.2	51
74095	Tautomerization of single asymmetric oxahemiporphycene molecules on Cu(111). Physical Chemistry Chemical Physics, 0, , .	1.3	0
74096	Theoretical insight into the relevance between the oxidation states of CeO₂ supported Pt^{4+/2+/1+/0/2â^'} and their HER performance. CrystEngComm, 2022, 25, 40-47.	1.3	2
74097	Computational screening of transition metal atom doped C3N as electrocatalysts for nitrogen fixation. Molecular Catalysis, 2023, 535, 112888.	1.0	3
74098	CASM â€" A software package for first-principles based study of multicomponent crystalline solids. Computational Materials Science, 2023, 217, 111897.	1.4	9
74099	Steering selectivity in the detection of exhaled biomarkers over oxide nanofibers dispersed with noble metals. Journal of Materials Chemistry A, 2023, 11, 3535-3545.	5.2	5
74100	Diamond-XII: a new type of exotic cubic carbon allotrope. Materials Advances, 2023, 4, 709-714.	2.6	4
74101	Strain-induced magnetic phase transition, magnetic anisotropy switching and bilayer antiferromagnetic skyrmions in van der Waals magnet CrTe₂. Nanoscale, 2023, 15, 1561-1567.	2.8	9
74102	Ir/Niâ€“NiO/CNT composites as effective electrocatalysts for hydrogen oxidation. Journal of Materials Chemistry A, 2023, 11, 5076-5082.	5.2	7
74103	Theoretical insight into electrocatalytic nitrogen fixation on transition-metal decorated melon-based carbon nitride. Molecular Catalysis, 2023, 535, 112862.	1.0	1

#	Article	IF	Citations
74104	Aluminum functionalized few-layer silicene as anode material for alkali metal ion batteries. Molecular Systems Design and Engineering, 2023, 8, 379-387.	1.7	5
74105	Heterogeneous molecular Coâ€“Nâ€“C catalysts for efficient electrochemical H₂O₂ synthesis. Energy and Environmental Science, 2023, 16, 446-459.	15.6	27
74106	Nonvolatile electrical control of valley splitting by ferroelectric polarization switching in a two-dimensional AgBiP₂S₆/CrBr₃ multiferroic heterostructure. Nanoscale, 2023, 15, 1718-1729.	2.8	2
74107	Improved CO2 electrolysis by a Fe nanoparticle-decorated (Ce, La, Sr)(CrFe)O3-Î´ perovskite using a combined strategy of lattice defect-building. Electrochimica Acta, 2023, 439, 141699.	2.6	4
74108	Heterogeneous crystallineâ€“amorphous interface for boosted electrocatalytic nitrogen reduction to ammonia. Journal of Materials Chemistry A, 2023, 11, 818-827.	5.2	9
74109	Li⁺ storage and transport in high-voltage spinel-type LiNi_{0.5}Mn_{1.5}O₄ codoped with F^{â^'} and Cu²⁺. Journal of Materials Chemistry A, 2023, 11, 838-848.	5.2	4
74110	Role of dose optimization in Ru atomic layer deposition for low resistivity films. Journal of Vacuum Science and Technology B:Nanotechnology and Microelectronics, 2023, 41, .	0.6	2
74111	Boriding of tungsten by the powder-pack process: Phase formation, growth kinetics and enhanced neutron shielding. International Journal of Refractory Metals and Hard Materials, 2023, 110, 106049.	1.7	4
74112	First-principles study of oxygen evolution on Co3O4 with short-range ordered Ir doping. Molecular Catalysis, 2023, 535, 112852.	1.0	2
74113	New lead-iodide formates with a strong second-harmonic generation response and suitable birefringence obtained by the substitution strategy. Chemical Science, 2022, 14, 136-142.	3.7	3
74114	Experimentally informed structure optimization of amorphous TiO₂ films grown by atomic layer deposition. Nanoscale, 0, , .	2.8	1
74115	Theoretical investigation of the role of hydrogenation-induced strain in single-layer h10-Si. Physical Chemistry Chemical Physics, 2022, 25, 203-208.	1.3	0
74116	Few-layer Î´-MnO2 nanosheets grown on three-dimensional N-doped hierarchically porous carbon networks for long-life aqueous zinc ion batteries. Carbon, 2023, 203, 326-336.	5.4	10
74117	Laser induced trace doping of Pd on Ru nanoparticles for an efficient hydrogen evolution electrocatalyst. Nanoscale, 2023, 15, 1554-1560.	2.8	1
74118	Modelling amorphous materials via a joint solid-state NMR and X-ray absorption spectroscopy and DFT approach: application to alumina. Chemical Science, 2023, 14, 1155-1167.	3.7	5
74119	Effects of M cations on crystal structure and optical properties of MTe3O8 tellurites. Solid State Sciences, 2023, 135, 107067.	1.5	0
74120	Scalable synthesis of MIL-88A(Fe) for efficient aerobic oxidation of cyclohexene to 2-cyclohexene-1-ol. Molecular Catalysis, 2023, 535, 112899.	1.0	3
74121	Tunable Schottky barrier in van der Waals heterojunction composed of graphene and SiCP4 from first principle calculations. Results in Physics, 2023, 44, 106189.	2.0	0

#	Article	IF	Citations
74122	Exploring a novel class of Janus MXenes by first principles calculations: structural, electronic and magnetic properties of Sc₂CXT, X = O, F, OH; T = C, S, N. Physical Chemistry Chemical Physics, 2023, 25, 1881-1888.	1.3	5
74123	Thermodynamic mechanism of controllable growth of two-dimensional uniformly ordered boron-doped graphene. Nanoscale Horizons, 2023, 8, 346-352.	4.1	2
74124	Novel high-pressure phases of nitrogen-rich Yâ€“N compounds. Dalton Transactions, 2023, 52, 1000-1008.	1.6	2
74125	Metastable properties of a garnet type Li₅La₃Bi₂O₁₂ solid electrolyte towards low temperature pressure driven densification. Journal of Materials Chemistry A, 2022, 11, 364-373.	5.2	3
74126	Atom-dispersed Au combined with nano-Au on halloysite nanotubes with closo-dodecaborate promotes synergistic effects for enhanced photocatalysis. Journal of Materials Chemistry A, 2023, 11, 809-817.	5.2	17
74127	Extracellular polymeric substances enhance dissolution and microbial methylation of mercury sulfide minerals. Environmental Sciences: Processes and Impacts, 2023, 25, 44-55.	1.7	5
74128	A simple descriptor for the nitrogen reduction reaction over single atom catalysts. Materials Horizons, 2023, 10, 852-858.	6.4	13
74129	Constructing asymmetrical dual catalytic sites in manganese oxides enables fast and stable lithiumâ€“oxygen catalysis. Journal of Materials Chemistry A, 2023, 11, 1188-1198.	5.2	3
74130	Interface modulation of perovskite oxides to simultaneously enhance the activity and stability toward oxygen evolution reaction. Chemical Engineering Journal, 2023, 455, 140829.	6.6	2
74131	Vacancy-fused multiple layers of copper sulfoselenide superstructures: a propitious HER electrocatalyst in acidic medium. Catalysis Science and Technology, 2023, 13, 694-704.	2.1	2
74132	Catalysis of dinitrogen activation and reduction by a single Fe₁₃ cluster and its doped systems. Physical Chemistry Chemical Physics, 2023, 25, 1196-1204.	1.3	1
74133	Understanding the role of quaternary ammonium cations on the interaction of bitumen with clay:A molecular modeling study. Construction and Building Materials, 2023, 364, 129970.	3.2	2
74134	Effect of different oxygen species on the oxidative coupling of methane over TiO2 catalysts. Applied Catalysis A: General, 2023, 650, 118998.	2.2	4
74135	Insights into the mechanistic CO2 conversion to methanol on single Ru atom anchored on MoS2 monolayer. Molecular Catalysis, 2023, 535, 112878.	1.0	6
74136	Hydroperoxyl-mediated C-H bond activation on Cr single atom catalyst: An alternative to the Fenton mechanism. Journal of Catalysis, 2023, 417, 323-333.	3.1	4
74137	Enhancing the stability of the polymeric Lewis-base-assisted dual-phase 3D CsPbBr₃â€“Cs₄PbBr₆ perovskite by molecular engineering and self-passivation. Journal of Materials Chemistry C, 2022, 11, 307-320.	2.7	2
74138	Targeted leveling of the undercoordinated high field density sites renders effective zinc dendrite inhibition. Energy Storage Materials, 2023, 55, 117-129.	9.5	15
74139	Emerging homogeneous superlattices in CaTiO₃ bulk thermoelectric materials. Materials Horizons, 2023, 10, 454-465.	6.4	5

#	Article	IF	Citations
74140	Effects of Fe Doping on Martensitic Transformation and Magnetic Properties of Ni-Mn-Ti All-d-metal Heusler Alloy. Wuli Xuebao/Acta Physica Sinica, 2023, .	0.2	0
74141	Topological phase transition and skyrmions in a Janus MnSbBiSe₂Te₂ monolayer. Physical Chemistry Chemical Physics, 2022, 25, 96-105.	1.3	3
74142	Elucidating reaction pathways in CO2 electroreduction: Case study of Ag and Cu2O@Ag catalysts. Journal of Catalysis, 2023, 417, 1-13.	3.1	8
74143	Raman spectra of 2D titanium carbide MXene from machine-learning force field molecular dynamics. Journal of Materials Chemistry C, 2023, 11, 1311-1319.	2.7	17
74144	High-performance oxide thin-film diode and its conduction mechanism based on ALD-assisted interface engineering. Journal of Materials Chemistry C, 2023, 11, 1336-1345.	2.7	2
74145	Molecular polysulfide-scavenging sulfurizedâ€“triazine polymer enable high energy density Li-S battery under lean electrolyte. Energy Storage Materials, 2023, 55, 225-235.	9.5	6
74146	Improving the DFT computational accuracy for CO activation on Fe surfaces by Bayesian error estimation functional with van der Waals correlation. Computational and Theoretical Chemistry, 2023, 1219, 113968.	1.1	0
74147	High-valence Zr-incorporated nickel phosphide boosting reaction kinetics for highly efficient and robust overall water splitting. Chemical Engineering Journal, 2023, 455, 140908.	6.6	16
74148	Nanoscale structural and electronic properties of cellulose/graphene interfaces. Physical Chemistry Chemical Physics, 0, , .	1.3	1
74149	Tri-coordinated Au dopant induced out-of-plane ferroelectricity and enhanced ferromagnetism in chromium triiodide. Journal of Materials Chemistry C, 2023, 11, 1111-1118.	2.7	4
74150	Mixed mismatch model predicted interfacial thermal conductance of metal/semiconductor interface. Wuli Xuebao/Acta Physica Sinica, 2023, 72, 034401.	0.2	6
74151	High capacity and stability induced by sandwich-like structure and metalâ€“O configuration for CoNi2S4/Ti3C2Tx heterostructure electrode. Electrochimica Acta, 2023, 439, 141643.	2.6	2
74152	<i>Ab Initio</i> Local-Energy and Local-Stress Calculations for Materials Science and Engineering. Nippon Kinzoku Gakkaishi/Journal of the Japan Institute of Metals, 2023, 87, 1-17.	0.2	0
74153	Unexpected spontaneous symmetry breaking and diverse ferroicity in two-dimensional mono-metal phosphorus chalcogenides. Nanoscale, 0, , .	2.8	0
74154	Axially coordinated Coâ€“N₄ sites for the electroreduction of nitrobenzene. Journal of Materials Chemistry A, 2023, 11, 5095-5103.	5.2	4
74155	Adsorption and sensing of formaldehyde on pristine and noble metal doped tellurene: A first-principles investigation. Chemical Physics Letters, 2023, 811, 140244.	1.2	4
74156	Rhenium anchored Ti₃C₂T_x (MXene) nanosheets for electrocatalytic hydrogen production. Nanoscale Advances, 2023, 5, 349-355.	2.2	5
74157	Adjusting OH tolerance of Ni4 clusters supported on ultra-small carbon nanotube with lattice vacancies for hydrogen oxidation catalysts. Materials Today Chemistry, 2023, 27, 101262.	1.7	0

#	Article	IF	Citations
74158	Heterointerface engineering constructs microenvironment enhancing catalytic kinetics of Fe/Ni oxyhydroxide@FeNi alloy for overall water splitting. New Journal of Chemistry, 2023, 47, 708-718.	1.4	4
74159	Lithium-rich diamond-like solid electrolytes for lithium batteries. Electrochimica Acta, 2023, 439, 141637.	2.6	2
74160	Accelerating the evaluation of crucial descriptors for catalyst screening via message passing neural network. , 2023, 2, 59-68.		1
74161	FeS₂intercalated montmorillonite as a multifunctional separator coating for high-performance lithiumâ€“sulfur batteries. Inorganic Chemistry Frontiers, 2023, 10, 651-665.	3.0	5
74162	Synthesis and high-temperature ferromagnetism of Fe-doped SiGe diluted magnetic semiconductor thin films. Nanoscale, 2023, 15, 2206-2213.	2.8	6
74163	A new high capacity cathode material for Li/Na-ion batteries: dihafnium sulfide (Hf₂S). Physical Chemistry Chemical Physics, 2023, 25, 1114-1122.	1.3	1
74164	Strain engineering the electronic properties of the type-II CdO/MoS2 van der Waals heterostructure. Thin Solid Films, 2023, 764, 139626.	0.8	7
74165	Ultralow lattice thermal conductivity and promising thermoelectric properties of a new 2D MoW3Te8 membrane. Results in Physics, 2023, 44, 106136.	2.0	2
74166	Exploring coverage-dependent chain-growth mechanisms on Ru(111) for Fischerâ€“Tropsch synthesis. Catalysis Science and Technology, 2023, 13, 437-456.	2.1	2
74167	Tweezer-like magnetic tip control of the local spin state in the FeOEP/Pb(111) adsorption system: a preliminary exploration based on first-principles calculations. Nanoscale, 2023, 15, 2369-2376.	2.8	2
74168	In situconstruction of an Î±-MoC/g-C₃N₄Mottâ€“Schottky heterojunction with high-speed electron transfer channel for efficient photocatalytic H₂evolution. Inorganic Chemistry Frontiers, 2023, 10, 832-840.	3.0	4
74169	Electron density and thermal motion of diamond at elevated temperatures. Acta Crystallographica Section A: Foundations and Advances, 2023, 79, 41-50.	0.0	2
74170	Thermophysical properties in the Al-Cu-Ag system: A combined CALPHAD and first-principles study. Journal of Molecular Liquids, 2023, 370, 121001.	2.3	1
74171	Bandgap widening through doping for improving the photocatalytic oxidation ability of narrow-bandgap semiconductors. Physical Chemistry Chemical Physics, 2022, 25, 255-261.	1.3	2
74172	3D all boron based porous topological metal for Mg- and Al-ion batteries anode material: A first principle study. Chemical Physics Letters, 2023, 812, 140267.	1.2	5
74173	A computational study on CO₂ electrochemical reduction on two dimensional metal-1,2,3,4,5,6,7,8,9,10,11,12-perthiolated coronene frameworks. New Journal of Chemistry, 0, , .	1.4	0
74174	Thermoelectric properties and lattice dynamics of tetragonal topological semimetal Ba₃Si₄. Physical Chemistry Chemical Physics, 2023, 25, 1987-1997.	1.3	1
74175	Advanced materials based on montmorillonite modified with poly(ethylenimine) and poly(2-methyl-2-oxazoline): Experimental and DFT study. Colloids and Surfaces A: Physicochemical and Engineering Aspects, 2023, 659, 130784.	2.3	3

#	Article	IF	Citations
74176	Topologic transition-induced abundant undercoordinated Fe active sites in NiFeOOH for superior oxygen evolution. Nano Energy, 2023, 106, 108044.	8.2	10
74177	Designing Mg alloys with high strength and ductility by reducing the strength difference between the basal and non-basal slips. Materials and Design, 2023, 225, 111476.	3.3	12
74178	Crumpled graphene oxide for enhanced room temperature gas sensing: understanding the critical roles of surface morphology and functionalization. Journal of Materials Chemistry A, 2022, 11, 447-459.	5.2	5
74179	Enhancing magneto-ionic effects in cobalt oxide films by electrolyte engineering. Nanoscale Horizons, 2022, 8, 118-126.	4.1	3
74180	Spin-crossover in the Fe(4X-pyridine)₂[Fe(CN)₅NO] series with X = Cl, Br, and I. Role of the distortion for the iron atom coordination environment. New Journal of Chemistry, 2022, 47, 238-249.	1.4	6
74181	A new adsorption energy-barrier relation and its application to CO₂ hydrogenation to methanol over In₂O₃-supported metal catalysts. Chemical Communications, 2023, 59, 940-943.	2.2	3
74182	High-performance zincâ€“air batteries enabled by hybridizing atomically dispersed FeN₂ with Co₃O₄ nanoparticles. Journal of Materials Chemistry A, 2023, 11, 1312-1323.	5.2	6
74183	On the product and transition-state shape selectivities in 2-heptene isomerization. Chemical Physics Letters, 2023, 812, 140263.	1.2	0
74184	Grain boundary sliding and distortion on a nanosecond timescale induce trap states in CsPbBr₃: ab initio investigation with machine learning force field. Nanoscale, 2022, 15, 285-293.	2.8	14
74185	Pressure dependence of the bulk modulus and Debye temperature in δ-MH₂ (M = Y, Sc, Lu) and ε-YH₃ from ultrasonic measurements of elasticity at <mml:math xmlns:mml="http://www.w3.org/1998/Math/MathML" altimg="si39.svg" display="inline" id="d1e1073"><mml:mi>T</mml:mi></mml:math>=<mml:math xmlns:mml="http://www.w3.org/1998/Math/MathML" altimg="si7.svg" display="inline" id="d1e1078"><mml:msub><mml:mrow		

#	Article	IF	Citations
74194	Computational screening of single-atom catalysts for direct electrochemical NH3 synthesis from NO on defective boron phosphide monolayer. Applied Surface Science, 2023, 611, 155764.	3.1	10
74195	Strain-enhanced properties of Janus Si2PAs monolayer as a promising photocatalyst for the splitting of water: Insights from first-principles calculations. Colloids and Surfaces A: Physicochemical and Engineering Aspects, 2023, 659, 130782.	2.3	10
74196	Hydrogen induced structural phase transformation in ScNiSn-based intermetallic hydride characterized by experimental and computational studies. Acta Materialia, 2023, 244, 118549.	3.8	2
74197	Strain effect on the defect formation and diffusion in Ti2AlC and Ti3AlC2: A first-principles study. Computational Materials Science, 2023, 218, 111946.	1.4	1
74198	The origin of selective electro-adsorption of cations by few-layered 2D MXene electrode. Desalination, 2023, 548, 116295.	4.0	5
74199	A phase-field study of stainless-steel oxidation from high-temperature carbon dioxide exposure. Computational Materials Science, 2023, 218, 111996.	1.4	1
74200	Coupled effect of Cr and Al on interactions between a prismatic interstitial dislocation loop and an edge dislocation line in Fe-Cr-Al alloy. Acta Materialia, 2023, 245, 118651.	3.8	7
74201	An ab initio study of structural phase transitions of crystalline aluminium under ultrahigh pressures based on ensemble theory. Computational Materials Science, 2023, 218, 111960.	1.4	1
74202	MgO promoted by Fe2O3 and nitrate molten salt for fast and enhanced CO2 capture: Experimental and DFT investigation. Separation and Purification Technology, 2023, 307, 122766.	3.9	7
74203	Effect of Mo addition on hydrogen segregation at Î±-Fe grain boundaries: A first-principles investigation of the mechanism by which Mo addition improves hydrogen embrittlement resistance in high-strength steels. Computational Materials Science, 2023, 218, 111951.	1.4	10
74204	Hybrid density functional theory study of substitutional Gd in <mml:math xmlns:mml="http://www.w3.org/1998/Math/MathML" altimg="si1.svg"><mml:mrow><mml:mi>Î²</mml:mi></mml:mrow></mml:math>-Ga2O3. Physica B: Condensed Matter, 2023, 651, 414558.	1.3	4
74205	Topological properties and strain effects of binary monoclinic superconductors RhX2 (X=Sb,Bi). Physica B: Condensed Matter, 2023, 650, 414569.	1.3	2
74206	The structure and mechanical properties of NbHfTaW refractory high-entropy alloy: A combined theoretical and experimental study. International Journal of Refractory Metals and Hard Materials, 2023, 111, 106067.	1.7	3
74207	A dispersion-corrected DFT method for zeolite-based CO2/N2 separation: Assessment and application. Journal of Environmental Chemical Engineering, 2023, 11, 109052.	3.3	2
74208	Effect of transition metals on the crystal field in CeCo0.4Fe0.6Ge3. Intermetallics, 2023, 153, 107776.	1.8	1
74209	Exploring the relationship between the accelerated austenite reversion and two-steps solution treatment in a Cr-Ni-Mo cryogenic maraging stainless steel. Materials Characterization, 2023, 196, 112581.	1.9	3
74210	Molecular dynamics of electric-field driven ionic systems using a universal neural-network potential. Computational Materials Science, 2023, 218, 111955.	1.4	2
74211	Enhancing the thermal stability of n-type Mg3+xSb1.5Bi0.49Te0.01 by defect manipulation. Nano Energy, 2023, 106, 108036.	8.2	7

#	Article	IF	Citations
74212	High-pressure stability and superconductivity of vanadium hydrides*. Physica B: Condensed Matter, 2023, 651, 414603.	1.3	1
74213	Density functional theory study of formation and diffusion of hydrogen, deuterium, and tritium in Pd-V intermetallic compounds. Computational Materials Science, 2023, 218, 111976.	1.4	2
74214	A novel tetrahedral spectral element method for Kohn-Sham model. Journal of Computational Physics, 2023, 474, 111831.	1.9	0
74215	Influence of oxygen and nitrogen doping on the structure and magnetic properties of FePt alloy: First principles calculations. Computational Materials Science, 2023, 218, 111963.	1.4	11
74216	Accurate Feâ€“He machine learning potential for studying He effects in BCC-Fe. Journal of Nuclear Materials, 2023, 574, 154183.	1.3	1
74217	Pressure-induced dynamically stable HeK2S under moderate conditions. Solid State Communications, 2023, 360, 115054.	0.9	0
74218	Hydroxyl-functionalized ZnO monolayers for optoelectronic devices: Atomic structures and electronic properties. Vacuum, 2023, 208, 111721.	1.6	1
74219	High local oxygen coverage causes initial oxidation of UN(001) surface. Journal of Nuclear Materials, 2023, 574, 154171.	1.3	0
74220	<mml:math xmlns:mml="http://www.w3.org/1998/Math/MathML" altimg="si38.svg" display="inline" id="d1e522"><mml:msub><mml:mrow><mml:mi>Î±</mml:mi></mml:mrow><mml:mrow><mml:mn>1</mml:mn></mml:mrow></mml:r xmlns:mml="http://www.w3.org/1998/Math/MathML" altimg="si36.svg" display="inline" id="d1e532"><mml:msub><mml:mrow /><mml:mrow><mml:mn>2</mml:mn></mml:mrow></mml:msub></mml:math> layered materials as auspicious anodes for Lithium batteries. Materials Chemistry and Physics, 2023, 295, 127146.	2.0	4
74221	Evolution of microstructure, mechanical and thermal properties with varied oxygen contents in TiAlON coatings. International Journal of Refractory Metals and Hard Materials, 2023, 111, 106074.	1.7	1
74222	Nanosized LaInO3 perovskite for efficient electrocatalytic reduction of CO2 to formate. Journal of CO2 Utilization, 2023, 68, 102342.	3.3	6
74223	Preparation and irradiation stability of A2B2O7 pyrochlore high-entropy ceramic for immobilization of high-level nuclear waste. Journal of Nuclear Materials, 2023, 574, 154212.	1.3	10
74224	Elastic investigation for the existence of B33 phase in TiNi shape memory alloys using atomistically informed Eshelbyâ€™s ellipsoidal inclusion. Computational Materials Science, 2023, 218, 111954.	1.4	7
74225	Atomic structures of grain boundaries for Si and Ge: A simulated annealing method with artificial-neural-network interatomic potentials. Journal of Physics and Chemistry of Solids, 2023, 173, 111114.	1.9	3
74226	A novel black-P/blue-P heterostructure for the photovoltaic applications. Chemical Physics Letters, 2023, 812, 140242.	1.2	1
74227	Enhancement strategies for ZnSe based photocatalysts: Application to environmental remediation and energy conversion. Chemical Engineering Research and Design, 2023, 170, 415-435.	2.7	14
74228	A novel Co1.29Ni1.71O4/glycerolate-derived oxygen-vacancies-containing TiO2 composite for highly efficient photocatalytic hydrogen evolution. Journal of Environmental Chemical Engineering, 2023, 11, 109142.	3.3	4
74229	Development of GD-containing austenitic stainless steel. Journal of Nuclear Materials, 2023, 574, 154197.	1.3	3

#	Article	IF	Citations
74230	Adhesion, bonding and tensile properties of Ti doped WC (001)/diamond (111) interface: A first-principles calculation. International Journal of Refractory Metals and Hard Materials, 2023, 111, 106075.	1.7	5
74231	Ab-initio study of vacancy-defective aluminium nitride nanosheets as trifluoroacetonitrile gas sensor. Applied Surface Science, 2023, 612, 155803.	3.1	2
74232	Role of lattice thermal conductivity in thermoelectric properties of chalcopyrite-type antimonides XSiSb2 (X = Mg, Be): A DFT insight. Materials Chemistry and Physics, 2023, 295, 127190.	2.0	3
74233	Theoretical study on the photocatalytic behavior of isoelectronic S/Se-doped BiVO4: DFT+U approach. Physica B: Condensed Matter, 2023, 650, 414535.	1.3	4
74234	Molecular insight into structural and mechanical properties of Halloysite structure. Computational Materials Science, 2023, 218, 111948.	1.4	5
74235	Reconstruction of interfacial thermal transport mediated by hotspot in silicon-based nano-transistors. International Journal of Heat and Mass Transfer, 2023, 202, 123676.	2.5	0
74236	Study on microstructure, mechanical properties and thermal performance of single-phase (Ti,Zr,Hf)B2 solid solution. Materials Today Communications, 2023, 34, 105228.	0.9	0
74237	Discovery of superconductivity in K-doped 2,2<mml:math xmlns:mml="http://www.w3.org/1998/Math/MathML" altimg="si134.svg" display="inline" id="d1e516"><mml:msup><mml:mrow /><mml:mrow><mml:mo>â€²</mml:mo></mml:mrow></mml:msup></mml:math>-bipyridine. Materials Science and Engineering B: Solid-State Materials for Advanced Technology, 2023, 288, 116155.	1.7	2
74238	Modeling assisted synthesis of Zr-doped Li3-xIn1-xZrxCl6 with ultrahigh ionic conductivity for lithium-ion batteries. Journal of Power Sources, 2023, 556, 232465.	4.0	4
74239	Adsorption and infrared spectra simulations of acrylic acid over (001) surface of molybdenum carbide. Chemical Physics, 2023, 566, 111798.	0.9	0
74240	Structural and thermal-mechanical properties of Ln3Ta5O15 (LnÂ=ÂCe, Pr, Nd, Sm, Eu, Gd, Tb) for thermal barrier coatings. Computational Materials Science, 2023, 218, 111938.	1.4	4
74241	A DFT study of site-dependent energetics of hexagonal MoS<mml:math xmlns:mml="http://www.w3.org/1998/Math/MathML" altimg="si86.svg" display="inline" id="d1e488"><mml:msub><mml:mrow /><mml:mrow><mml:mn>2</mml:mn></mml:mrow></mml:msub></mml:math> nanoparticles under varying reaction conditions. Surface Science, 2023, 729, 122231.	0.8	1
74242	Single Zn atom catalyst on Ti2CN2 MXenes for efficient CO oxidation. Physica E: Low-Dimensional Systems and Nanostructures, 2023, 147, 115595.	1.3	3
74243	Integration of amorphous CoSnO3 onto wrinkled MXene nanosheets as efficient electrocatalysts for alkaline hydrogen evolution. Separation and Purification Technology, 2023, 308, 122947.	3.9	14
74244	An investigation on the stability, electronic, and optical properties of new MoSOâ€“WSO lateral heterostructures. Applied Surface Science, 2023, 613, 155980.	3.1	1
74245	Computational studies of Ag5 atomic quantum clusters deposited on anatase and rutile TiO2 surfaces. Applied Surface Science, 2023, 613, 156054.	3.1	4
74246	Citric acid-modified MIL-88A(Fe) for enhanced photo-Fenton oxidation in water decontamination. Separation and Purification Technology, 2023, 308, 122945.	3.9	5
74247	A machine-learning interatomic potential to understand primary radiation damage of silicon. Computational Materials Science, 2023, 218, 111970.	1.4	3

#	Article	IF	Citations
74248	Effect of strain on the band structure and optical properties of Na2Bi2(SeO3)3F2. Computational Materials Science, 2023, 218, 111962.	1.4	0
74249	Electron and ion transport behavior of Vanadium based MXene induced by pressure for Lithium ion intercalated electrodes. Journal of Colloid and Interface Science, 2023, 633, 207-217.	5.0	3
74250	Large-scale atomistic simulation of dislocation core structure in face-centered cubic metal with Deep Potential method. Computational Materials Science, 2023, 218, 111941.	1.4	0
74251	Improved mobility and photovoltaic performance of two-dimensional Ruddlesdenâ^'Popper (ThMA)2(MA)2M3I10 perovskites applied in perovskite solar cells. Journal of Alloys and Compounds, 2023, 937, 168464.	2.8	3
74252	High anisotropy in titanium trisulfide monolayer: Ultrahigh carrier mobilities and large excitonic absorption. Chemical Physics, 2023, 566, 111796.	0.9	1
74253	Selective spin injection of g-SiC6 monolayer for dioxygen activation. Applied Surface Science, 2023, 613, 155911.	3.1	0
74254	Modulating the electron structure of Co-3d in Co3O4â^'x/WO2.72 for boosting peroxymonosulfate activation and degradation of sulfamerazine: Roles of high-valence W and rich oxygen vacancies. Journal of Hazardous Materials, 2023, 445, 130576.	6.5	26
74255	Lead-free Dionâ€"Jacobson halide perovskites CsMX2Y2 (M = Sb, Bi and X, Y = Cl, Br, I) used for optoelectronic applications via first principle calculations. Journal of Physics and Chemistry of Solids, 2023, 174, 111157.	1.9	8
74256	A novel (CaO/CeO2)@CeO2 composite adsorbent based on microinjection titration-calcination strategy for CO2 adsorption. Chemical Engineering Journal, 2023, 454, 140485.	6.6	6
74257	Synergy between nitrogen, phosphorus co-doped carbon quantum dots and ZnO nanorods for enhanced hydrogen production. Journal of Alloys and Compounds, 2023, 937, 168397.	2.8	12
74258	Spall strength and equation of states for 2050-T84 Alâ€"Li alloy under shock compression up to 120ÂGPa. Journal of Physics and Chemistry of Solids, 2023, 174, 111138.	1.9	3
74259	DFT exploring mechanism of graphene to preserve metallic copper in the marine. Materials Today Communications, 2023, 34, 105015.	0.9	0
74260	Î±-In2O3 monolayer: A promising material as field-effect phototransistor and out-of-plane piezoelectric device. Applied Surface Science, 2023, 614, 156198.	3.1	10
74261	Design, fabrication, and characterization of high-temperature piezoelectric vibration sensor based on the Ho: CNGS crystal. Journal of Alloys and Compounds, 2023, 937, 168449.	2.8	1
74262	Enhanced electrochemical chlorination of anisole in Fe2O3 nanoparticles integrating with crystal facet effect. Applied Surface Science, 2023, 612, 155802.	3.1	1
74263	Simulation of multi-shell fullerenes using Machine-Learning Gaussian Approximation Potential. Carbon Trends, 2023, 10, 100239.	1.4	8
74264	Symbiotic Ni3Se4/Ni heterostructure induced by unstable NiSe2 for enhanced hydrogen generation. Chemical Engineering Journal, 2023, 454, 140488.	6.6	10
74265	Ferroelectric control of magnetic coupling of monolayer MnBr<mml:math xmlns:mml="http://www.w3.org/1998/Math/MathML" altimg="si5.svg" display="inline" id="d1e318"><mml:msub><mml:mrow /><mml:mrow><mml:mn>2</mml:mn></mml:mrow></mml:msub></mml:math> in semiconducting multiferroic van der Waals heterostructure. Applied Surface Science, 2023, 614, 156201.	3.1	6

#	Article	IF	Citations
74266	Tuning the atomic structures and electronic properties of two-dimensional C60/ZnO materials via external impacts. Applied Surface Science, 2023, 612, 155857.	3.1	2
74267	Theoretical studies on thermodynamic stabilities and luminescent mechanisms of defects and lanthanide ions in BaZrSi3O9. Journal of Luminescence, 2023, 255, 119579.	1.5	0
74268	Adsorption behavior of small molecule on monolayered SiAs and sensing application for NO2 toxic gas. Applied Surface Science, 2023, 613, 156010.	3.1	7
74269	Exploration of threshold and resistive-switching behaviors in MXene/BaFe12O19 ferroelectric memristors. Applied Surface Science, 2023, 613, 155956.	3.1	13
74270	Understanding the origins of low lattice thermal conductivity in a novel two-dimensional monolayer NaCuS for achieving medium-temperature thermoelectric applications. Applied Surface Science, 2023, 614, 156167.	3.1	4
74271	Enhanced electrocatalytic water splitting by adjusting the local reaction environment with nickel coordination regulation. Journal of Alloys and Compounds, 2023, 938, 168557.	2.8	1
74272	Structural properties of FemCun (m+nÂ=Â13) clusters and their interaction with CO and H2: A DFT study. Materials Today Communications, 2023, 34, 105036.	0.9	0
74273	Electronic structure, magnetic and thermodynamic properties of yttrium based half Heusler alloys YXZ (X = Fe, Co, Cr; Z = As, Sb): A first principles study. Computational Condensed Matter, 2023, 34, e00776.	0.9	1
74274	Interfacial charge transfer and electronic structure of diamond/c-BN heterointerface. Computational Materials Science, 2023, 218, 111947.	1.4	2
74275	Phase stability and optoelectronic properties of lead-free CsSn1â^'Ge I3 mixed halide perovskites: A first-principles study. Journal of Physics and Chemistry of Solids, 2023, 174, 111183.	1.9	0
74276	The intrinsic high ductility in B2 intermetallic compound YAg: Causality clarified by ab initio study. Materials Today Communications, 2023, 34, 105177.	0.9	0
74277	First-principles study of the behaviors of He atoms at TiC(110)/V(110) interface. Journal of Physics and Chemistry of Solids, 2023, 174, 111141.	1.9	4
74278	Computational prediction of stable semiconducting Zn-C binary compounds. Materials Science in Semiconductor Processing, 2023, 155, 107237.	1.9	1
74279	Performance and mechanisms of Cr(VI) removal by nano-MnO2 with different lattices. Journal of Molecular Structure, 2023, 1275, 134624.	1.8	3
74280	High throughput theoretical prediction of the low friction at the interfaces of homo- and heterojunction composed of C3N. Applied Surface Science, 2023, 612, 155718.	3.1	2
74281	Oxidic structures on copper-gold alloy nanofacets. Applied Surface Science, 2023, 613, 155913.	3.1	1
74282	Suppressed charge-density-wave, robust ferromagnetism and Lifshitz transition in Sm2Ru3Ge5 crystal under high pressure. Journal of Alloys and Compounds, 2023, 937, 168337.	2.8	4
74283	A unified framework of slip controlled bending and rippled superlattice design of few-layer graphene. Applied Surface Science, 2023, 613, 155979.	3.1	2

#	Article	IF	Citations
74284	Nanotwinning-induced pseudoplastic deformation in boron carbide under low temperature. International Journal of Mechanical Sciences, 2023, 242, 107998.	3.6	5
74285	Large vacancy-defective graphene for enhanced lithium storage. Carbon Trends, 2023, 10, 100237.	1.4	4
74286	Oxygen dissociation on the C3N monolayer: A first-principles study. Applied Surface Science, 2023, 613, 155912.	3.1	3
74287	Synthesis, crystal structure and 19F NMR parameters modelling of CaTiF6(H2O)2 yielding to a revision of the bond-valence parameters for the Ti4+/Fâ¯ ion pair. Journal of Solid State Chemistry, 2023, 319, 123793.	1.4	1
74288	Hydrogen sorption kinetics and mechanism of Mg2Fe(1â¯x)NixH6. Journal of Alloys and Compounds, 2023, 937, 168212.	2.8	2
74289	Revisiting the origin of ORR and HER activities of N-doped Î³-graphdiyne from the perspective of edge effects. Applied Surface Science, 2023, 613, 156084.	3.1	4
74290	Correlation of conductivity enhancement and Al-site defects in nanocolumnar ZnO films under vacuum annealing by experimental and calculations. Applied Surface Science, 2023, 613, 155985.	3.1	1
74291	Strain-regulated magnetic phase transition and perpendicular magnetic anisotropy in CrSBr monolayer. Physica E: Low-Dimensional Systems and Nanostructures, 2023, 147, 115590.	1.3	1
74292	A DFT study of Mn3O4 Hausmannite thin films supported on coinage metals. Applied Surface Science, 2023, 612, 155920.	3.1	4
74293	Two novel phases of germa-graphene: Prediction, electronic and transport applications. Applied Surface Science, 2023, 614, 156107.	3.1	5
74294	Optical and thermoelectric properties of square lattice phases of alkali halide compounds. Journal of Physics and Chemistry of Solids, 2023, 174, 111142.	1.9	1
74295	First-principles study of impurity diffusion coefficients in Niobium. Vacuum, 2023, 209, 111739.	1.6	0
74296	Expounding lemonal terpenoids as corrosion inhibitors for copper using DFT based calculations. Applied Surface Science, 2023, 614, 156066.	3.1	3
74297	Two-dimensional interface superstructures assembled by well-ordered solute atoms. Journal of Materials Science and Technology, 2023, 142, 253-259.	5.6	2
74298	C2H2 selective hydrogenation over transition metal carbide (MxCy): Probing into the influences of crystal facet, M type and M: C ratio on C2H4 activity, selectivity and catalyst stability. Fuel, 2023, 336, 127131.	3.4	1
74299	Water dopant control of structural stability and charge recombination of perovskite solar cells: A first-principles study. Applied Surface Science, 2023, 612, 155794.	3.1	1
74300	Precise preparation of Î±-Fe2O3/SnO2 core-shell nanowires via atomic layer deposition for selective MEMS-based H2S gas sensor. Sensors and Actuators B: Chemical, 2023, 378, 133111.	4.0	14
74301	The initial oxidation of the 4H-SiC (0001) surface with C-related point defects: Insight by first-principles calculations. Applied Surface Science, 2023, 614, 156161.	3.1	1

#	Article	IF	Citations
74302	Defective lithium titanate oxide with stable cycling over a wide voltage window. Applied Surface Science, 2023, 614, 156134.	3.1	2
74303	Dynamic re-construction of sulfur tailored Cu2O for efficient electrochemical CO2 reduction to formate over a wide potential window. Applied Surface Science, 2023, 613, 156130.	3.1	5
74304	Theoretical exploration of the structural evolution of sodium sulfide clusters in Na-S batteries. Applied Surface Science, 2023, 613, 155906.	3.1	4
74305	Electronic structures of defects in bottom-up N-doped graphene nanoribbons: Experiment and theory. Applied Surface Science, 2023, 612, 155874.	3.1	0
74306	Doping induced asymmetry adjacent structure in h-VN nanoribbon for the promotion of N2 fixation. Applied Surface Science, 2023, 612, 155839.	3.1	3
74307	Insights into crystal structure, elasticity, lattice dynamics, and thermodynamics of ternary magnesium alloy MgZn2Ce. Vacuum, 2023, 209, 111755.	1.6	1
74308	Dense dislocations induced ductile SnTe thermoelectric semiconductor over a wide range of temperatures. Journal of Materials Science and Technology, 2023, 144, 213-218.	5.6	13
74309	Tailored Pd/C bifunctional catalysts for styrene production under an ethylbenzene oxidative dehydrogenation assisted direct dehydrogenation scheme. Applied Catalysis B: Environmental, 2023, 324, 122205.	10.8	6
74310	Mechanochemical localization of vanadia on titania to prepare a highly sulfur-resistant catalyst for low-temperature NH3-SCR. Applied Catalysis B: Environmental, 2023, 324, 122290.	10.8	4
74311	Atomically dispersed cerium sites in carbon-doped boron nitride for photodriven CO2 reduction: Local polarization and mechanism insight. Applied Catalysis B: Environmental, 2023, 324, 122235.	10.8	9
74312	Highly selective nitrate reduction to ammonia on CoO/Cu foam via constructing interfacial electric field to tune adsorption of reactants. Applied Catalysis B: Environmental, 2023, 324, 122201.	10.8	21
74313	Adjustable heterointerface-vacancy enhancement effect in RuO2@Co3O4 electrocatalysts for efficient overall water splitting. Applied Catalysis B: Environmental, 2023, 324, 122294.	10.8	38
74314	Stabilizing the interfacial Cu0-Cu+ dual sites toward furfural hydrodeoxygenation to 2-methylfuran via fabricating nest-like copper phyllosilicate precursor. Fuel, 2023, 337, 127212.	3.4	7
74315	Augmented thermoelectric performance of LiCaX (X = As, Sb) Half Heusler compounds via carrier concentration optimization. Journal of Physics and Chemistry of Solids, 2023, 174, 111182.	1.9	3
74316	Achieving highest Young's modulus in Al-Li by tracing the size and bonding evolution of Li-rich precipitates. Journal of Materials Science and Technology, 2023, 145, 125-135.	5.6	8
74317	Efficient carbon monoxide electroreduction on two-dimensional transition metal phosphides: A computational study. Applied Surface Science, 2023, 613, 156025.	3.1	2
74318	A comparative analysis of different van der Waals treatments for molecular adsorption on the basal plane of 2H-MoS2. Surface Science, 2023, 729, 122226.	0.8	5
74319	Regulating potassium state to enable the high performance of Co3O4 for catalytic oxidation. Fuel, 2023, 335, 126968.	3.4	5

#	Article	IF	Citations
74320	Rational design of trimetallic AgPtâ€“Fe3O4 nanozyme for catalyst poisoning-mediated CO colorimetric detection. Biosensors and Bioelectronics, 2023, 223, 115022.	5.3	11
74321	Atom-scale understanding the adsorption mechanism of uranyl in the interlayer of montmorillonite: Insight from DFTÂ+ÂU calculation. Applied Surface Science, 2023, 612, 155910.	3.1	3
74322	Strengthening the Ti/TiN interface against shear failure with Al dopants: A molecular dynamics study. Applied Surface Science, 2023, 613, 156024.	3.1	1
74323	Density functional theory investigation of Pr adsorption on the anatase TiO<mml:math xmlns:mml="http://www.w3.org/1998/Math/MathML" altimg="si13.svg" display="inline" id="d1e2774"><mml:msub><mml:mrow /><mml:mrow><mml:mn>2</mml:mn></mml:mrow></mml:msub></mml:math>(101) surface for photovoltaic applications. Applied Surface Science, 2023, 613, 156042.	3.1	2
74324	Transport and thermoelectric properties of strongly anharmonic Full-Heusler compounds CsK2M (M=As, Bi). Materials Today Communications, 2023, 34, 105134.	0.9	1
74325	Scaffold-regulation buffered MoS2 anode kinetics for high-performance Na-/K-ion storage. Journal of Materials Science and Technology, 2023, 145, 14-24.	5.6	19
74326	Highly selective production of singlet oxygen by manipulating the spin state of single-atom Coâ€“N moieties and electron localization. Applied Catalysis B: Environmental, 2023, 324, 122248.	10.8	15
74327	Two-dimensional alloying MNS4 (M, NÂ=ÂMn, Fe, Co, Ni, Pd) materials with pentagonal pucker for highly efficient electrocatalytic hydrogen reaction. Applied Surface Science, 2023, 612, 155897.	3.1	2
74328	A dual defect co-modified S-scheme heterojunction for boosting photocatalytic CO2 reduction coupled with tetracycline oxidation. Applied Catalysis B: Environmental, 2023, 324, 122232.	10.8	25
74329	Piezo-photocatalysts based on a ferroelectric high-entropy oxide. Applied Catalysis B: Environmental, 2023, 324, 122204.	10.8	16
74330	Properties of typical non-metallic inclusions in steel: First-principles calculations. Materials Today Communications, 2023, 34, 105118.	0.9	0
74331	Predicting the adsorption and reduction of NO2 on Sr-doped CeO2(1 1 1) using first-principles calculations. Applied Surface Science, 2023, 612, 155896.	3.1	0
74332	Understanding the temperature-dependent H2O promotion effect on SO2 resistance of MnO -CeO2 catalyst for SCR denitration. Applied Catalysis B: Environmental, 2023, 324, 122263.	10.8	26
74333	Iterative machine learning method for screening high-performance catalysts for H2O2 production. Chemical Engineering Science, 2023, 267, 118368.	1.9	2
74334	Heat capacity and thermal conductivity of CdCr2Se4 ferromagnet: Magnetic field dependence, experiment and calculations. Journal of Physics and Chemistry of Solids, 2023, 174, 111139.	1.9	1
74335	Unique CO2-modified VO2(B) nanosheets for lithium batteries with high electrochemical performance. Journal of Alloys and Compounds, 2023, 936, 168215.	2.8	2
74336	Design of elevated temperature phase change materials of carbonate-villiaumite eutectic mixtures: Method, validation, and application. Solar Energy Materials and Solar Cells, 2023, 251, 112155.	3.0	1
74337	Variable thermal transport in black, blue, and violet phosphorene from extensive atomistic simulations with a neuroevolution potential. International Journal of Heat and Mass Transfer, 2023, 202, 123681.	2.5	5

#	Article	IF	Citations
74338	Single-atom Co-N-C catalysts for high-efficiency reverse water-gas shift reaction. Applied Catalysis B: Environmental, 2023, 324, 122298.	10.8	11
74339	Heterogeneous nucleation of T1 precipitates in solid solution of Al-Cu-Li alloys from Ag-rich structures: An ab initio study. Scripta Materialia, 2023, 225, 115191.	2.6	11
74340	SPIN: [S]imple [P]ython [I]pywidgets [N]otebook interface to obtain the optoelectronic properties of materials employing DFT. Computer Physics Communications, 2023, 284, 108614.	3.0	0
74341	Realizing n-type CdSb with promising thermoelectric performance. Journal of Materials Science and Technology, 2023, 144, 54-61.	5.6	2
74342	Density functional investigation of the interaction of H2O with spinel Li1-xMn2O4 surfaces: Implications for aqueous Li-ion batteries. Applied Surface Science, 2023, 612, 155822.	3.1	3
74343	Synergistic adsorption effect on Co3O4(1 1 0) surface to promote the ethanol sensing properties: Experiment and theory. Applied Surface Science, 2023, 612, 155776.	3.1	8
74344	Natural halloysite nanotubes supported Ru as highly active catalyst for photothermal catalytic CO2 reduction. Applied Catalysis B: Environmental, 2023, 324, 122262.	10.8	21
74345	Density-functional theory study of point defect formation and diffusion in Î±-alumina and effects of applied strain and alloy doping. Materials Today Communications, 2023, 34, 105068.	0.9	2
74346	Experimental determination of the Hâ€“Hf phase diagram using in situ neutron diffraction. Journal of Alloys and Compounds, 2023, 937, 168353.	2.8	3
74347	Se-doped Li₆PS₅Cl and Li_{5.5}PS_{4.5}Cl_{1.5} with improved ionic conductivity and interfacial compatibility: a high-throughput DFT study. Journal of Materials Chemistry C, 2022, 10, 18294-18302.	2.7	2
74348	Insight into the solvent effects on ethanol oxidation on Ir(100). Physical Chemistry Chemical Physics, 2023, 25, 2190-2202.	1.3	2
74349	Experimental and theoretical investigations on the anti-perovskite nitrides Co₃CuN, Ni₃CuN and Co₃MoN for ammonia synthesis. Faraday Discussions, 0, 243, 97-125.	1.6	2
74350	First-principles calculations of local structure and electronic properties of Er³⁺-doped TiO₂. Wuli Xuebao/Acta Physica Sinica, 2022, 71, 246102.	0.2	0
74351	Spatial charge separation on the (110)/(102) facets of cocatalyst-free ZnIn₂S₄for the selective conversion of 5-hydroxymethylfurfural to 2,5-diformylfuran. Green Chemistry, 2023, 25, 692-699.	4.6	13
74352	Untangling product selectivity on clean low index rutile TiO₂ surfaces using first-principles calculations. Physical Chemistry Chemical Physics, 2023, 25, 2203-2211.	1.3	1
74353	Mechanism of Ammonia Synthesis on Fe₃Mo₃N. Faraday Discussions, 0, , .	1.6	1
74354	Theoretical exploration of the structural, electronic and optical properties of g-C₃N₄/C₃N heterostructures. Physical Chemistry Chemical Physics, 2023, 25, 4081-4092.	1.3	5
74355	Structure and dissolution of silicophosphate glass. RSC Advances, 2022, 12, 34882-34889.	1.7	1

#	Article	IF	Citations
74356	Edge engineering on layered WS₂ toward the electrocatalytic reduction of CO₂: a first principles study. Physical Chemistry Chemical Physics, 2022, 24, 30027-30034.	1.3	3
74357	Strain and thickness effects on the electronic structures of low-energy two-dimensional Cd_xTe_y phases. Physical Chemistry Chemical Physics, 2022, 24, 29772-29780.	1.3	2
74358	Tuning low-temperature CO oxidation activities via N-doping on graphene-supported three-coordinated nickle single-atom catalysts. Physical Chemistry Chemical Physics, 2022, 24, 29586-29593.	1.3	1
74359	Superconductivity of monolayer functionalized biphenylene with Dirac cones. Physical Chemistry Chemical Physics, 2023, 25, 2875-2881.	1.3	3
74360	Complementary effects of functionalization, vacancy defects and strain engineering in activating the basal plane of monolayer FePS₃ for HER. Sustainable Energy and Fuels, 2022, 6, 5621-5630.	2.5	1
74361	Thermodynamic and magnetic properties of Pt₅₀Mn_{50-x}M_x (M=) Tj ETQq1 1 0.784314 rgBT /Ov	0.1	2
74362	Ab-initio techniques, VASP and CASTEP, are used to investigate the electronic properties of B2 compounds formed between Ti and group VIII elements - a comparative study. MATEC Web of Conferences, 2022, 370, 02005.	0.1	0
74363	Experimental and Computational Studies of Sulfided NiMo Supported on Pillared Clay: Catalyst Activation and Guaiacol Adsorption Sites. Physical Chemistry Chemical Physics, 0, , .	1.3	0
74364	Multielectron reaction of AlCl _n in borophene for rechargeable aluminum batteries. Energy Material Advances, 2022, 2022, .	4.7	10
74365	Accelerated discovery of defect tolerant organo-halide perovskites. Journal of Materials Chemistry C, 2022, 10, 18385-18392.	2.7	1
74366	Hydrogen-induced phase stability and phonon mediated-superconductivity in two-dimensional van der Waals Ti₂C MXene monolayer. Physical Chemistry Chemical Physics, 2023, 25, 2227-2233.	1.3	1
74367	Anomalously Supercooled H2-D2 Mixtures Flowing inside a Carbon Nano Tube. Physical Chemistry Chemical Physics, 0, , .	1.3	0
74368	Polarization-resolved and helicity-resolved Raman spectra of monolayer XP3 (X=Ge and In). Physical Chemistry Chemical Physics, 0, , .	1.3	0
74369	Modulating the electronic structure of ternary transition metal phosphide for enhanced hydrogen evolution activity. Dalton Transactions, 2022, 51, 18722-18733.	1.6	2
74370	Piezo-Phototronic Enhancement of Vertical Structure Photodetectors Based on 2D CsPbBr₃ Nanosheets. Journal of Nanoelectronics and Optoelectronics, 2022, 17, 769-774.	0.1	0
74371	DFT mechanistic study of Pt Sub-monolayer adsorption on BiAlO₃ (0001) polar surfaces. Ferroelectrics, 2022, 599, 95-111.	0.3	0
74372	Formation of monolayer <mml:math xmlns:mml="http://www.w3.org/1998/Math/MathML"><mml:mrow><mml:msub><mml:mi mathvariant="normal">V</mml:mi><mml:mn>5</mml:mn></mml:msub><mml:msub><mml:mi>Se</mml:mi><mml:mn>8</mml:mn></ from multilayer <mml:math xmlns:mml="http://www.w3.org/1998/Math/MathML"><mml:msub><mml:mi>VSe</mml:mi><mml:mn>2</mml:mn></mml:msub></mm films via V- and Se-desorption. Physical Review B, 2022, 106, .	1.1	0
74373	Intrinsic Ferroelectric Quantum Spin Hall Insulator in Monolayer Na₃Bi with Surface Trimerization. Journal of Physical Chemistry Letters, 2022, 13, 11059-11064.	2.1	3

#	Article	IF	Citations
74374	Hydrogen atom collisions with a semiconductor efficiently promote electrons to the conduction band. Nature Chemistry, 2023, 15, 326-331.	6.6	9
74375	HfSe₂/GaSe Heterostructure as a Promising Near-Room-Temperature Thermoelectric Material. Journal of Physical Chemistry C, 2022, 126, 20326-20331.	1.5	3
74376	Clarification of underneath capacity loss for O3-type Ni, co free layered cathodes at high voltage for sodium ion batteries. Journal of Energy Chemistry, 2023, 77, 479-486.	7.1	11
74377	Theoretical antiferromagnetism of ordered face-centered cubic Cr-Ni alloys. Physical Review Materials, 2022, 6, .	0.9	3
74378	strucscan: A lightweight Python-based framework for high-throughput material simulation. Journal of Open Source Software, 2022, 7, 4719.	2.0	0
74379	Antiferromagnetic fluctuations and orbital-selective Mott transition in the van der Waals ferromagnet <mml:math xmlns:mml="http://www.w3.org/1998/Math/MathML"><mml:mrow><mml:msub><mml:mtext>Fe</mml:mtext><mml:mrow><mml:m Physical Review B, 2022, 106, .	1.1	3
74380	Chiral nanocrystals grown from MoS2 nanosheets enable photothermally modulated enantioselective release of antimicrobial drugs. Nature Communications, 2022, 13, .	5.8	20
74381	A generic designing rule for realizing quantum anomalous Hall phase in a transition-metal trichalcogenide family. Science China Materials, 0, , .	3.5	4
74382	First-principles study of quantum defect candidates in beryllium oxide. Physical Review B, 2022, 106, .	1.1	1
74383	InBi: A Ferroelastic Monolayer with Strain Tunable Spinâ€“Orbit Dirac Points and Carrier Self-Doping Effect. ACS Nano, 2022, 16, 21546-21554.	7.3	7
74384	The thermodynamically directed dendrite-free lithium metal batteries on LiZn alloy surface. Nano Research, 2023, 16, 8354-8359.	5.8	2
74385	High critical field superconductivity at ambient pressure in <mml:math xmlns:mml="http://www.w3.org/1998/Math/MathML"><mml:msub><mml:mi mathvariant="normal">MoB</mml:mi><mml:mn>2</mml:mn></mml:msub></mml:math> stabilized in the P6/mmm structure via Nb substitution. Physical Review B, 2022, 106, .	1.1	3
74386	On the Sorption Mode of U(IV) at Calcium Silicate Hydrate: A Comparison of Adsorption, Absorption in the Interlayer, and Incorporation by Means of Density Functional Calculations. Minerals (Basel,) Tj ETQq0 0 0 rgBT /Overlock 10 Tf 50 25	0.8	5
74387	Instability of the magnetic state of <mml:math xmlns:mml="http://www.w3.org/1998/Math/MathML"><mml:mrow><mml:mi>M</mml:mi><mml:mi mathvariant="normal">P</mml:mi><mml:msub><mml:mi>X</mml:mi><mml:mn>3</mml:mn></mml:msub></mml:mrow><mml:mspa width="4pt"		

#	Article	IF	Citations
74392	Nitrogen-Doped Carbon-Encapsulated FeCo Alloy Nanostructures with Surface-Dangling Fe(Co)-N_x Active Sites for Oxygen Reduction in Alkaline and Acid Media. ACS Applied Nano Materials, 2022, 5, 18035-18047.	2.4	3
74393	Improved opto-electro-mechanical properties of Cs2TeBr6 double perovskite by Ge doping. Journal of Applied Physics, 2022, 132, .	1.1	1
74394	Simulation of BCC dissolution in Feâ€“Crâ€“Ni system by ICME. Journal of Iron and Steel Research International, 2023, 30, 660-676.	1.4	4
74395	Ab initio construction of full phase diagram of MgO-CaO eutectic system using neural network interatomic potentials. Physical Review Materials, 2022, 6, .	0.9	3
74396	Direct determination of band-gap renormalization in degenerately doped ultrawide band gap Î²-<mml:math xmlns:mml="http://www.w3.org/1998/Math/MathML"><mml:mrow><mml:msub><mml:mi>Ga</mml:mi><mml:mn>2</mml:mn></mml:msub><mml:msub><mml:mi mathvariant="normal">O</mml:mi><mml:mn>3</mml:mn></mml:msub></mml:mrow></mml:math> semiconductor. Physical Review B, 2022, 106, .	1.1	5
74397	Rational Design of Fe/Co-based Diatomic Catalysts for Li-S Batteries by First-principles Calculations. Chinese Physics B, 0, , .	0.7	0
74398	Uncovering the Electrolyte-Dependent Transport Mechanism of LiO₂ in Lithium-Oxygen Batteries. Journal of the American Chemical Society, 2022, 144, 22150-22158.	6.6	8
74399	rGOç©ºé—´å™ŸÿÇ”Ÿé•¿è¶…è–„In2S3çº³ç±³ç‰‡ç”¨äºŽæž„å»ºé«˜æ•ˆå‡† ä¸€ç»´Sb2Se3åŸºå¼‚è´¨ç»“å…‰é˜´æž Science China Materials	6.5	8
74400	Improving the interfacial stability, conductivity, and electrochemical performance of Li2MoO3@g-C3N4 composite as a promising cathode for lithium-ion battery. Journal of Industrial and Engineering Chemistry, 2022, , .	2.9	0
74401	Defining shapes of two-dimensional crystals with undefinable edge energies. Nature Computational Science, 2022, 2, 729-735.	3.8	2
74402	Manipulating Selectivity of Hydroxyl Radical Generation by Single-Atom Catalysts in Catalytic Ozonation: Surface or Solution. Environmental Science & Technology, 2022, 56, 17753-17762.	4.6	23
74403	Acid-stable antimonate based catalysts for the electrocatalytic oxygen evolution reaction. Nano Research, 2023, 16, 4691-4697.	5.8	4
74404	Two dimensional GeO2/MoSi2N4 van der Waals heterostructures with robust type-II band alignment. Frontiers of Physics, 2023, 18, .	2.4	3
74405	Response of Raman-active modes in monolayer <mml:math xmlns:mml="http://www.w3.org/1998/Math/MathML"><mml:mrow><mml:mn>1</mml:mn><mml:msup><mml:mi>T</mml:mi></mml:msup></mml:mrow></mml:math> to charge doping. Physical Review B, 2022, 106, .	1.1	1
74406	Mechanical anisotropy and multiple direction-dependent Dirac states in a synthesized <mml:math xmlns:mml="http://www.w3.org/1998/Math/MathML"><mml:mrow><mml:msub><mml:mi>Ag</mml:mi><mml:mn>3</mml:mn></mml:msub><mml:msub><mml:mi mathvariant="normal">C</mml:mi><mml:mn>20</mml:mn></mml:msub></mml:mrow></mml:math> monolayer. Physical Review B, 2022, 106, .	1.1	1
74407	Argon equationÂof state data to 1 TPa: Shock compression experiments and simulations. Physical Review B, 2022, 106, .	1.1	2
74408	First-principle calculations of sulfur dioxide adsorption on the Ca-montmorillonite. Scientific Reports, 2022, 12, .	1.6	2
74409	Two-dimensional superconducting MoSi2N4(MoN)4n homologous compounds. National Science Review, 0, , .	4.6	3

#	Article	IF	Citations
74410	Stability and electronic structure of NV centers at dislocation cores in diamond. Physical Review B, 2022, 106, .	1.1	0
74411	Polycations inclusion to simultaneously boost permeation and selectivity of two-dimensional TaS2 membranes for acid recovery. Separation and Purification Technology, 2023, 309, 122759.	3.9	2
74412	Ferromagnetism with Strong Perpendicular Magnetic Anisotropy in Epitaxial <mml:math xmlns:mml="http://www.w3.org/1998/Math/MathML" display="inline" overflow="scroll"><mml:msub><mml:mrow><mml:mi>Sr</mml:mi><mml:mi>Mn</mml:mi></mml:mrow><mml:mrow><mml:mn>0.3</mml:mn></mml:mrow></mml:msub><mml:msub><mml:mi mathvariant="normal">O</mml:mi></mml:mrow></mml:mrow><mml:mn>3</mml:mn></mml:msub></mml:math> Perovskite. Physical Review Applied, 2022, 18, .	4.6	2
74413	Effect of W Addition on Fe-P-C-B Soft-Magnetic Amorphous Alloy. Materials, 2022, 15, 8416.	1.3	1
74414	When Molecular Dimerization Induces Magnetic Biâ€Stability at the Metalâ€“Organic Interface. , 0, , 2200005.		1
74415	Dualâ€Site Functionalization on Supported Metal Monolayer Electrocatalysts for Selective CO₂ Reduction. Advanced Energy Materials, 2023, 13, .	10.2	17
74416	Grain Boundary Complexions Enable a Simultaneous Optimization of Electron and Phonon Transport Leading to Highâ€Performance GeTe Thermoelectric Devices. Advanced Energy Materials, 2023, 13, .	10.2	22
74417	Pulse High Temperature Sintering to Prepare Singleâ€Crystal High Nickel Oxide Cathodes with Enhanced Electrochemical Performance. Advanced Energy Materials, 2023, 13, .	10.2	17
74418	Nonâ€Trivial Topological States in Spinâ€Polarized 2D Electron Gas at EuOâ€“KTO Interface with the Rashba Spin Texture. , 0, , 2200026.		0
74419	Highly Conductive p-Type Transparent Conducting Electrode with Sulfur-Doped Copper Iodide. Chemistry of Materials, 2022, 34, 10517-10527.	3.2	11
74420	Synthesis and Calculations of Wurtzite Al_{1â€“x}Gd_xN Heterostructural Alloys. Chemistry of Materials, 2022, 34, 10639-10650.	3.2	1
74421	Hydrogen Evolution Volcano(es)â€”From Acidic to Neutral and Alkaline Solutions. Catalysts, 2022, 12, 1541.	1.6	3
74422	Theoretical Prediction of Antiferromagnetic Skyrmion Crystal in Janus Monolayer CrSi₂N₂As₂. ACS Nano, 2023, 17, 1144-1152.	7.3	10
74423	Gluing Ba0.5Sr0.5Co0.8Fe0.2O3âˆ'Î´ with Co3O4 as a cathode for proton-conducting solid oxide fuel cells. Science China Materials, 2023, 66, 955-963.	3.5	27
74424	Efficient and selective gold recovery from e-waste by simple and easily synthesized covalent organic framework. Chemical Engineering Journal, 2023, 455, 140523.	6.6	12
74425	Pressure-induced ferroelectric and anti-ferroelectric phase transitions in LaN. Science China: Physics, Mechanics and Astronomy, 2023, 66, .	2.0	3
74426	Mo doping provokes two electron reaction in MnO2 with ultrahigh capacity for aqueous zinc ion batteries. Nano Research, 2023, 16, 2511-2518.	5.8	22
74427	Experimental and Theoretical Correlation of Modulated Architectures of Î²-Ag2MoO4 Microcrystals: Effect of Different Synthesis Routes on the Morphology, Optical, Colorimetric, and Photocatalytic Properties. Journal of Inorganic and Organometallic Polymers and Materials, 2023, 33, 424-450.	1.9	9

#	Article	IF	Citations
74428	Reconfiguration toward Selfâ€Assembled Monolayer Passivation for Highâ€Performance Perovskite Solar Cells. Advanced Energy Materials, 2023, 13, .	10.2	13
74429	Antiferromagnetic nodal loop and strain-controllable magnetic phase transition in monolayer MnAl. Applied Physics Letters, 2022, 121, .	1.5	2
74430	Theoretical study of the interface engineering for H-diamond field effect transistors with h-BN gate dielectric and graphite gate. Applied Physics Letters, 2022, 121, 211601.	1.5	3
74431	Unconventional Superconductivity at LaVO₃/SrTiO₃ Interfaces. ACS Applied Electronic Materials, 2022, 4, 5859-5866.	2.0	4
74432	Density functional theory study of the enhancement of quantum capacitance of graphene by phosphorous doping. International Journal of Quantum Chemistry, 2023, 123, .	1.0	2
74433	Sulfur-Mediated Synthesis of Spherical Nickel Nanoparticles in a Chemical Vapor Reactor. ACS Omega, 2022, 7, 43958-43964.	1.6	1
74434	Phase Transitions and Electric Properties of PbBr2 under High Pressure: A First-Principles Study. Materials, 2022, 15, 8222.	1.3	0
74435	Topological charge-2 Dirac phonons in three dimensions: Theory and realization. Physical Review B, 2022, 106, .	1.1	9
74436	Propelling polysulfide redox by Fe3C-FeN heterostructure@nitrogen-doped carbon framework towards high-efficiency Li-S batteries. Journal of Energy Chemistry, 2023, 78, 105-114.	7.1	31
74437	1Tâ€™ Re_xMo_{1â^'}_xS₂â€“2H MoS₂ Lateral Heterojunction for Enhanced Hydrogen Evolution Reaction Performance. Advanced Functional Materials, 2023, 33, .	7.8	12
74438	Classical and machine learning interatomic potentials for BCC vanadium. Physical Review Materials, 2022, 6, .	0.9	3
74439	The Effect of Yttrium on the Solution and Diffusion Behaviors of Helium in Tungsten: First-Principles Simulations. Materials, 2022, 15, 8468.	1.3	0
74440	Axion insulators protected by <mml:math xmlns:mml="http://www.w3.org/1998/Math/MathML"><mml:mrow><mml:msub><mml:mi>C</mml:mi><mml:mn>2</mml:mn></mml:m mathvariant="double-struck">T</mml:mi></mml:mrow></mml:math> symmetry, their <mml:math xmlns:mml="http://www.w3.org/1998/Math/MathML"><mml:mi>K</mml:mi></mml:math> -theory invariants, and material realizations. Physical Review B, 2022, 106, .	1.1	1
74441	First-Principles Study of B Segregation at Austenite Grain Boundary and Its Effect on the Hardenability of Low-Alloy Steels. Metals, 2022, 12, 2006.	1.0	2
74442	Superior electrocatalytic negative electrode with tailored nitrogen functional group for vanadium redox flow battery. Journal of Energy Chemistry, 2023, 78, 148-157.	7.1	11
74443	Phase-Controllable Chemical Vapor Deposition Synthesis of Atomically Thin MoTe2. Nanomaterials, 2022, 12, 4133.	1.9	2
74444	Earth-abundant photocatalyst for H ₂ generation from NH ₃ with light-emitting diode illumination. Science, 2022, 378, 889-893.	6.0	62
74445	The First-Principles Study On The Investigation of Magnetic and Electronic Properties of Ga4X3Mn (X =) Tj ETQq1 1 0.784314 rgBT /O	0.1	0

#	Article	IF	Citations
74446	Behavior of Hydrogarnetâ€Type Defects in Hydrous Stishovite at Various Temperatures and Pressures. Journal of Geophysical Research: Solid Earth, 2023, 128, .	1.4	1
74447	Interaction Mechanism of RGD Tripeptide on Different Surfaces of Mg and Mg Alloys: A First-Principles Study. Coatings, 2022, 12, 1814.	1.2	1
74448	Entangling free electrons and optical excitations. Science Advances, 2022, 8, .	4.7	11
74449	Effects of fluorination on crystal structure and electrochemical performance of antiperovskite solid electrolytes. Journal of Energy Chemistry, 2023, 77, 521-528.	7.1	11
74450	Relationship between elements migration of Î±-AlFeMnSi phase and micro-galvanic corrosion sensitivity of Alâ€”Znâ€”Mg alloy. International Journal of Minerals, Metallurgy and Materials, 2023, 30, 112-121.	2.4	4
74451	Super-exchange effect induced by early 3d metal doping on NiFe2O4(0 0 1) surface for oxygen evolution reaction. Journal of Energy Chemistry, 2023, 78, 21-29.	7.1	5
74452	Strain-induced antipolar phase in hafnia stabilizes robust thin-film ferroelectricity. Science Advances, 2022, 8, .	4.7	17
74453	Fingerprints of carbon defects in vibrational spectra of GaN considering the isotope effect. Physical Review B, 2022, 106, .	1.1	0
74454	<mml:math xmlns:mml="http://www.w3.org/1998/Math/MathML"><mml:mrow><mml:mi>S</mml:mi><mml:mo>=</mml:mo><mml:mn>1</mml:mn><mml:mr dimer system <mml:math xmlns:mml="http://www.w3.org/1998/Math/MathML"><mml:mrow><mml:msub><mml:mi mathvariant="normal">K</mml:mi><mml:mn>2</mml:mn></mml:msub><mml:mi>Ni</mml:mi><mml:msub><mml:mrow><mml:mo>(</mml:mo> : A candida. Physical Review B, 2022, 106, .	1.1	1
74455	Effect of N Doping on the Electronic and Optical Properties of Narrow Tellurene Nanoribbons: First-Principles Study. Journal of Electronic Materials, 0, , .	1.0	0
74456	Ground-State Surface of All-Inorganic Halide Perovskites. Journal of Physical Chemistry C, 2022, 126, 21155-21161.	1.5	4
74457	Enhanced Photocatalytic Benzene Oxidation to Phenol over Monoclinic WO₃ Nanorods under Visible Light. ACS Catalysis, 2022, 12, 14976-14989.	5.5	16
74458	Intrinsic properties and dopability effects on the thermoelectric performance of binary Sn chalcogenides from first principles. Frontiers in Electronic Materials, 0, 2, .	1.6	0
74459	Emergent charge order in pressurized kagome superconductor CsV3Sb5. Nature, 2022, 611, 682-687.	13.7	55
74460	Correlation of adsorbent cavity structure with adsorption behavior and interaction of long-chain Î±-olefin/paraffin on microporous adsorbents. Nano Research, 2023, 16, 5721-5732.	5.8	2
74461	Ni-Based Janus Pentagonal Monolayers as Promising Water-Splitting Photocatalysts. Journal of Physical Chemistry C, 2022, 126, 20354-20363.	1.5	6
74462	Unveiling the Decisive Factor for the Sharp Transition in the Scanning Tunneling Spectroscopy of a Single Nickelocene Molecule. Journal of Physical Chemistry Letters, 2022, 13, 11262-11270.	2.1	2
74463	Two-dimensional SiC/AlN based type-II van der Waals heterobilayer as a promising photocatalyst for overall water disassociation. Scientific Reports, 2022, 12, .	1.6	7

#	Article	IF	Citations
74464	Uncovering the Fundamental Role of Interlayer Water in Charge Storage for Bilayered V₂O₅â€¢Â·â€†nH₂O Xerogel Cathode Materials. Advanced Energy Materials, 2023, 13, .	10.2	32
74465	Insights into CO Oxidation in Cu/CeO₂ Catalysts: O₂ Activation at the Dualâ€Interfacial Sites. European Journal of Inorganic Chemistry, 2023, 26, .	1.0	1
74467	Alkali Metals and Cerium-Modified Laâ€“Co-Based Perovskite Catalysts: Facile Synthesis, Excellent Catalytic Performance, and Reaction Mechanisms for Soot Combustion. ACS Catalysis, 2022, 12, 15056-15075.	5.5	22
74468	Spectroscopic study of nitrogen incorporation in Ge, Sb, and Te elemental systems: A step toward the understanding of nitrogen effect in phase-change materials. Journal of Applied Physics, 2022, 132, .	1.1	2
74469	Sifting for substitutional elements that decrease thermal conductivity of a thermal barrier material. European Physical Journal Plus, 2022, 137, .	1.2	4
74470	Theoretical and experimental investigations on Mn doped <mml:math xmlns:mml="http://www.w3.org/1998/Math/MathML"><mml:mrow><mml:msub><mml:mi>Bi</mml:mi><mml:mn>2</mml:mn></mml:msub></mml:mrow></mml:math> topological insulator. Physical Review Materials, 2022, 6, .	2.9	0
74471	Engineering coexistence between free and trapped carriers via extrinsic polarons. Physical Review Materials, 2022, 6, .	0.9	1
74472	Real-space obstruction in quantum spin Hall insulators. Physical Review B, 2022, 106, .	1.1	4
74473	Nitrogen-Doped Bismuth Nanosheet as an Efficient Electrocatalyst to CO2 Reduction for Production of Formate. International Journal of Molecular Sciences, 2022, 23, 14485.	1.8	5
74474	Electric-field switching of the antiferromagnetic topological state in a multiferroic heterobilayer. Physical Review B, 2022, 106, .	1.1	4
74475	Role of electronic correlations in room-temperature ferromagnetism of monolayer <mml:math xmlns:mml="http://www.w3.org/1998/Math/MathML"><mml:mrow><mml:mi>Mn</mml:mi><mml:msub><mml:mi>Se</mml:mi></mml:msub></mml:mrow></mml:math>. Physical Review B, 2022, 106, .	1.1	3
74476	Resolving the Chemical Formula of Nesquehonite via NMR Crystallography, DFT Computation, and Complementary Neutron Diffraction. Chemistry - A European Journal, 2023, 29, .	1.7	0
74477	2D rare-earth metal carbides (MXenes) Mo₂NdC₂T₂ electronic structure and magnetic properties: A DFTâ€‰+â€‰U study. Journal of Applied Physics, 2022, 132, 204301.	1.1	2
74478	Unraveling the origin of the peculiar transition in the magnetically ordered phase of the Weyl semimetal <mml:math xmlns:mml="http://www.w3.org/1998/Math/MathML"><mml:mrow><mml:msub><mml:mi>Co</mml:mi><mml:mn>3</mml:mn><mml:mi mathvariant="normal">S</mml:mi><mml:mn>2</mml:mn></mml:msub></mml:mrow></mml:math>. Physical Review B, 2022, 106, .	1.1	3
74479	Fast Exchange with Gaussian Basis Set Using Robust Pseudospectral Method. Journal of Chemical Theory and Computation, 2022, 18, 7306-7320.	2.3	6
74480	Iron(II) Phthalocyanine Adsorbed on Defective Graphenes: A Density Functional Study. ACS Omega, 2022, 7, 43915-43922.	1.6	4
74481	Topological corner states in graphene by bulk and edge engineering. Physical Review B, 2022, 106, .	1.1	4
74482	Tunable intrinsic spin Hall conductivity in BiTeI by applying hydrostatic pressure. Journal of Applied Physics, 2022, 132, 203903.	1.1	0

#	Article	IF	Citations
74483	Tailoring Bulk Photovoltaic Effects in Magnetic Sliding Ferroelectric Materials. Nano Letters, 2022, 22, 9297-9305.	4.5	11
74484	Multi-component Alloying Effects on the Stability and Mechanical Properties of Nb and Nbâ€“Si Alloys: A First-Principles Study. Metallurgical and Materials Transactions A: Physical Metallurgy and Materials Science, 2023, 54, 450-472.	1.1	3
74485	Dual Pt-Ni atoms dispersed on N-doped carbon nanostructure with novel (NiPt)-N4C2 configurations for synergistic electrocatalytic hydrogen evolution reaction. Science China Materials, 2023, 66, 1389-1397.	3.5	14
74486	Comparing the accuracy of melting temperature prediction methods for high entropy alloys. Journal of Applied Physics, 2022, 132, .	1.1	2
74487	Stacking Fault Induced Symmetry Breaking in van der Waals Nanowires. ACS Nano, 2022, 16, 21199-21207.	7.3	5
74488	A New Zero-Dimensional (CsK2)BiCl6 Metal Halide: Boosting Emission via B-Site Mn-Doping. Crystals, 2022, 12, 1681.	1.0	2
74489	Superconductivity in the high-entropy alloy <mml:math xmlns:mml="http://www.w3.org/1998/Math/MathML"><mml:mrow><mml:msub><mml:mrow><mml:mo>(</mml:mo></mml:mrow><mml:mn>1</mml:mn> Physical Review B, 2022, 106, .	1.1	10
74490	Ultrathin NiPt Single-Atom Alloy for Synergistically Accelerating Alkaline Hydrogen Evolution. ACS Applied Energy Materials, 2022, 5, 15136-15145.	2.5	6
74491	Theoretical Study of Superhigh-Efficiency Janus WSSe/Î²-Te Non-Perovskite Heterojunction Solar Cells. ACS Applied Energy Materials, 2022, 5, 15316-15325.	2.5	4
74492	Mechanistic Study of CrS2/BP as a Direct Z-Scheme Heterojunction for Photocatalyst of Splitting Water Under Biaxial Strain. Catalysis Letters, 2024, 154, 60-70.	1.4	1
74493	Designing high-TC superconductors with BCS-inspired screening, density functional theory, and deep-learning. Npj Computational Materials, 2022, 8, .	3.5	16
74494	Structural and electronic properties of hydrogen - functionalized armchair germanene nanoribbons: A first-principles study. Can Tho University Journal of Science, 2022, 14, 25-31.	0.1	0
74495	Multiferroic nitride perovskites with giant polarizations and large magnetic moments. Physical Review B, 2022, 106, .	1.1	4
74496	Comprehensive investigation of the extremely low lattice thermal conductivity and thermoelectric properties of <mml:math xmlns:mml="http://www.w3.org/1998/Math/MathML"><mml:mrow><mml:msub><mml:mtext>BaIn</mml:mtext><mml:mn>2</mml:mn> Physical Review B, 2022, 106, .	1.1	1
74497	Supramolecular Anisotropy in a Surface-Confined Bicomponent System. Journal of Physical Chemistry C, 2022, 126, 20739-20746.	1.5	0
74498	Magnetic field induced <mml:math xmlns:mml="http://www.w3.org/1998/Math/MathML"><mml:mrow><mml:mi>a</mml:mi><mml:mi>b</mml:mi></mml:mrow></mml: -plane rotation of the Eu magnetic moments in trigonal <mml:math xmlns:mml="http://www.w3.org/1998/Math/MathML"><mml:mrow><mml:msub><mml:mi mathvariant="normal">EuMg</mml:mi><mml:mn>2</mml:mn></mml:msub><mml:msub><mml:mi mathvariant="normal">	1.1	5
74499	Ti₃C₂â€MXene Partially Derived Hierarchical 1D/2D TiO₂/Ti₃C₂ Heterostructure Electrode for Highâ€Performance Capacitive Deionization. Advanced Science, 2023, 10, .	5.6	32
74500	Discovery of LaAlO3 as an efficient catalyst for two-electron water electrolysis towards hydrogen peroxide. Nature Communications, 2022, 13, .	5.8	21

#	Article	IF	Citations
74501	Ab â€“ initio study on the stability and electronic property of graphene nanosheets: Applications to batteries. International Journal of Quantum Chemistry, 2023, 123, .	1.0	2
74502	Theory of thermal properties of magnetic materials with unknown entropy. Physical Review Materials, 2022, 6, .	0.9	3
74504	Tuning UV Absorption in Imine-Linked Covalent Organic Frameworks via Methylation. Journal of Physical Chemistry C, 2022, 126, 21338-21347.	1.5	6
74505	Extrinsic to intrinsic mechanism crossover of anomalous Hall effect in the Ir-doped MnPtSn Heusler system. Physical Review B, 2022, 106, .	1.1	1
74506	High-refractive index and mechanically cleavable non-van der Waals InGaS3. Npj 2D Materials and Applications, 2022, 6, .	3.9	9
74507	The structural, mechanical, electronic, and optical properties of Janus Hf2CXY (X, Y = O, S, Se or Te, X â‰) Tj ETQq1 1 0.784314 rgBT /C		2
74508	2D Oxides Realized via Confinement Heteroepitaxy. Advanced Functional Materials, 2023, 33, .	7.8	4
74509	The thermoelectric properties of XTe (X = Ge, Sn and Pb) monolayers from first-principles calculations. Physica Scripta, 2022, 97, 125709.	1.2	1
74510	Interface Engineering of Oxygen Vacancy Ordering in an Oxide Superlattice. Journal of Physical Chemistry C, 2022, 126, 20627-20635.	1.5	2
74511	DFT Insight into Conductive and Magnetic Properties of Heterostructures with BaTiO3 Overlayer. Materials, 2022, 15, 8334.	1.3	0
74512	Density Functional Theory Study of Deoxydehydration Reaction by TiO₂-Supported Monomeric and Dimeric Molybdenum Oxide Catalysts. Journal of Physical Chemistry C, 2022, 126, 20375-20387.	1.5	3
74513	Bonding Heterogeneity Leads to Hierarchical and Ultralow Lattice Thermal Conductivity in Sodium Metavanadate. Journal of Physical Chemistry Letters, 2022, 13, 11160-11168.	2.1	2
74514	Sulfur-Vacancy Passivation via Selenium Doping in Sb₂S₃ Solar Cells: Density Functional Theory Analysis. Journal of Physical Chemistry C, 2022, 126, 20786-20792.	1.5	4
74515	Controlled Synthesis of Palladium Phosphides with Tunable Crystal Phases and Their Sulfur-Tolerant Performance. ACS Catalysis, 2022, 12, 15193-15206.	5.5	13
74516	Rational Design of Dynamic Bimetallic NiCoSe₂/2D Ti₃C₂T_x MXene Hybrids for a High-Performance Flexible Supercapacitor and Hydrogen Evolution Reaction. Energy & Fuels, 2022, 36, 15066-15079.	2.5	8
74517	Dynamics of Co/Co2C redox cycle and their catalytic consequences in Fischerâ€“Tropsch synthesis on cobaltâ€“manganese catalysts. Chemical Engineering Journal, 2023, 455, 140577.	6.6	4
74518	Toward the ferroelectric field-effect transistor on BaTiO3/LaMnO3 heterostructure: DFT investigation. Journal of Materials Science, 2022, 57, 21620-21629.	1.7	3
74519	Surface-Clean Au₂₅ Nanoclusters in Modulated Microenvironment Enabled by Metalâ€“Organic Frameworks for Enhanced Catalysis. Journal of the American Chemical Society, 2022, 144, 22008-22017.	6.6	50

#	Article	IF	Citations
74520	Quantum Hall phase in graphene engineered by interfacial charge coupling. Nature Nanotechnology, 2022, 17, 1272-1279.	15.6	17
74521	Understanding Structural Incorporation of Oxygen Vacancies in Perovskite Cobaltite Films and Potential Consequences for Electrocatalysis. Chemistry of Materials, 2022, 34, 10373-10381.	3.2	4
74522	New Alloy of an Al-Chalcogen System: AlSe Surface Alloys on Al(111). ACS Omega, 2022, 7, 45174-45180.	1.6	0
74523	Atomistic Insights into the Oxidation of Flat and Stepped Platinum Surfaces Using Large-Scale Machine Learning Potential-Based Grand-Canonical Monte Carlo. ACS Catalysis, 2022, 12, 14812-14824.	5.5	7
74524	N-donating and water-resistant Zn-carboxylate frameworks for humid carbon dioxide capture from flue gas. Fuel, 2023, 336, 126793.	3.4	5
74525	On the Nature of Three-Atom Metal Cluster Catalysis for N₂ Reduction to Ammonia. ACS Catalysis, 2022, 12, 14964-14975.	5.5	21
74526	Electronic, Tensile, and Sliding Characteristics of the C/Ti Interface: A First-Principles Study. Langmuir, 2022, 38, 15113-15120.	1.6	2
74527	Design Guidelines for Two-Dimensional Transition Metal Dichalcogenide Alloys. Chemistry of Materials, 2022, 34, 10279-10290.	3.2	5
74528	Electronic structures and strengthening mechanisms of superhard high-entropy diborides. Rare Metals, 2023, 42, 614-628.	3.6	10
74529	Carbon-supported CoS4-C single-atom nanozyme for dramatic improvement in CO2 electroreduction to HCOOH: A DFT study combined with hybrid solvation model. Chinese Chemical Letters, 2023, 34, 108018.	4.8	3
74530	Intercalation of argon in honeycomb structures towards promising strategy for rechargeable Li-ion batteries. Journal of Physics Condensed Matter, 2023, 35, 085301.	0.7	0
74531	Origin of Near-Zero Thermal Expansion in A₂O(PO₄)₂ Oxides over an Ultrawide Temperature Range. Journal of Physical Chemistry C, 2022, 126, 21871-21881.	1.5	1
74532	Antibacterial, UV-Protective, Hydrophobic, Washable, and Heat-Resistant BN-Based Nanoparticle-Coated Textile Fabrics: Experimental and Theoretical Insight. ACS Applied Bio Materials, 2022, 5, 5595-5607.	2.3	2
74533	Effect of magnetism and phonons on localized carriers in the ferrimagnetic kagome metals <mml:math xmlns:mml="http://www.w3.org/1998/Math/MathML"><mml:mrow><mml:msub><mml:mtext>GdMn</mml:mtext><mml:mn>6</mml:mn> and <mml:math xmlns:mml="http://www.w3.org/1998/Math/MathML"><mml:mrow><mml:msub><mml:mtext>TbMn</mml:mtext><mml:mn>6</mml:mn> Physical Review B, 2022, 106,	1.1	8
74534	Switching of CO2 hydrogenation selectivity via chlorine poisoning over Ru/TiO2 catalyst. Nano Research, 2023, 16, 4786-4792.	5.8	4
74535	Ni optimizes Ir reaction pathway through IrNi alloy synergistic effect to improve overall water splitting efficiency. International Journal of Hydrogen Energy, 2023, 48, 8440-8449.	3.8	7
74536	First-principles study of energy transport in tin oxynitride lattice. Journal of the Korean Physical Society, 0, , .	0.3	0
74537	Euphonic: inelastic neutron scattering simulations from force constants and visualization tools for phonon properties. Journal of Applied Crystallography, 2022, 55, 1689-1703.	1.9	5

#	Article	IF	Citations
74538	Effect of Mn doping and charge transfer on LaTi_{1â^'x}Mn _x O₃. Journal of Physics Condensed Matter, 2023, 35, 055601.	0.7	1
74539	The encapsulation of atomically-thin MgB₂-based superconductors in two-dimensional material bilayers. Superconductor Science and Technology, 2023, 36, 015012.	1.8	1
74540	Atomic-size dependence of the cohesive energy, bandgap, Young's modulus, and Raman frequency in different MA2Z4: A bond relaxation investigation. Applied Physics Letters, 2022, 121, .	1.5	13
74541	Optical properties of SiV and GeV color centers in nanodiamonds under hydrostatic pressures up to 180 GPa. Physical Review B, 2022, 106, .	1.1	6
74542	Hourglass charge-three Weyl phonons. Physical Review B, 2022, 106, .	1.1	21
74543	Investigation on electronic properties modulation of vdW GaN/WSe₂ heterostructure by electric field. Modern Physics Letters B, 0, , .	1.0	0
74544	Using Machine Learning Potentials to Explore Interdiffusion at Metalâ€“Chalcogenide Interfaces. ACS Applied Materials & Interfaces, 2022, 14, 56963-56974.	4.0	4
74545	Non-volatile electric-field control of inversion symmetry. Nature Materials, 2023, 22, 207-215.	13.3	12
74546	Machineâ€learning predictions of caffeine coâ€crystal formation accompanying experimental and molecular validations. Journal of Food Process Engineering, 2023, 46, .	1.5	5
74547	Ga and Zn Atom-Doped CuAl₂O₄(111) Surface-Catalyzed CO₂ Conversion to Dimethyl Ether: Importance of Acidic Sites. Journal of Physical Chemistry C, 2022, 126, 21628-21637.	1.5	6
74548	Breaking of Inversion Symmetry and Interlayer Electronic Coupling in Bilayer Graphene Heterostructure by Structural Implementation of High Electric Displacement Fields. Journal of Physical Chemistry Letters, 2022, 13, 11571-11580.	2.1	5
74549	Synergistic Effect of Surface pâ€Doping and Passivation Improves the Efficiency, Stability, and Reduces Lead Leakage in Allâ€Inorganic CsPbIBr₂â€Based Perovskite Solar Cells. Small, 2023, 19, .	5.2	7
74550	Exploring the Ti₂CO₂â€“WSe₂ Heterostructure as a Direct Z-Scheme Photocatalyst for Water Splitting: A Non-Adiabatic Study. Journal of Physical Chemistry C, 2022, 126, 20852-20863.	1.5	14
74551	2D/2D Transitionâ€Metalâ€Sulfide Selfâ€Assembly Enables a Huge Tolerance to High Concentration Cr(VI) and Prominent Photocatalytic Reduction Performance. ChemCatChem, 0, , .	1.8	0
74552	Electronic properties of Î± -Mn-type non-centrosymmetric superconductor Re_{5.5}Ta under hydrostatic pressure. Superconductor Science and Technology, 2023, 36, 025002.	1.8	1
74553	Interlayer Registry Dictates Interfacial 2D Material Ferroelectricity. ACS Applied Materials & Interfaces, 2022, 14, 57492-57499.	4.0	2
74554	Atomic and Electronic Structures of the Interfaces between Perovskite La_{0.75}Sr_{0.25}MnO₃ and Brownmillerite SrCoO_{2.}₅. Physica Status Solidi (B): Basic Research, 2023, 260, .	0.7	1
74556	Low lattice thermal conductivity in alkali metal based Heusler alloys. Physical Review Materials, 2022, 6, .	0.9	3

#	Article	IF	Citations
74557	Selfâ€Reconstruction of Singleâ€Atomâ€Thick A Layers in Nanolaminated MAX Phases for Enhanced Oxygen Evolution. Advanced Functional Materials, 2023, 33, .	7.8	5
74559	Cataloguing MoSi₂N₄ and WSi₂N₄ van der Waals Heterostructures: An Exceptional Material Platform for Excitonic Solar Cell Applications. Advanced Materials Interfaces, 2023, 10, .	1.9	24
74560	Large bilinear magnetoresistance from Rashba spin-splitting on the surface of a topological insulator. Physical Review B, 2022, 106, .	1.1	3
74561	Predicting the Stability and Loading for Electrochemical Preparation of Single-Atom Catalysts. ACS Catalysis, 2023, 13, 79-86.	5.5	5
74562	Band parameters of group IIIâ€“V semiconductors in wurtzite structure. Journal of Applied Physics, 2022, 132, .	1.1	1
74563	Strain-induced ultrahigh power conversion efficiency in BP-MoSe₂ vdW heterostructure. Nanotechnology, 2023, 34, 085403.	1.3	1
74564	Plasma Oxidation of Copper: Molecular Dynamics Study with Neural Network Potentials. ACS Nano, 2022, 16, 20680-20692.	7.3	4
74565	Tuning the Magnetic Properties of Cr2TiC2Tx through Surface Terminations: A Theoretical Study. Nanomaterials, 2022, 12, 4364.	1.9	1
74566	Unraveling the roles of single transition metal atom anchored on equivalent stoichiometry graphitic carbon nitride (gC₆N₆) for carbon dioxide reduction: a density functional theory study. Journal Physics D: Applied Physics, 2022, 56, 024004.	1.3	0
74567	Density Functional Calculations of the Sequential Adsorption of Hydrogen on Single Atom and Small Clusters of Pd and Pt Supported on Au(111). Electrocatalysis, 0, , .	1.5	0
74568	Effect of nonâ€covalent interactions in 2, <scp>5â€diâ€Meâ€pyrazineâ€diâ€N</scp> â€oxide â€•methanol â€“ Carbon nanotube electrocatalytic system. Journal of the Chinese Chemical Society, 0, , .	0.8	0
74569	Stress effect on lattice thermal conductivity of anode material NiNb₂O₆ for lithium-ion batteries. Chinese Physics B, 2023, 32, 058201.	0.7	1
74570	Towards B-doped p-BaSi₂ films on Si substrates by co-sputtering of BaSi₂, Ba, and B-doped Si targets. Japanese Journal of Applied Physics, 2023, 62, SD1010.	0.8	4
74571	Topological superconductivity and large spin Hall effect in the kagome family Ti6X4 (XÂ= Bi, Sb, Pb, Tl,) Tj ETQq1 1 0.784314 rgBT /Ov	1.9	6
74572	Pressure Stabilized Lithium-Aluminum Compounds with Both Superconducting and Superionic Behaviors. Physical Review Letters, 2022, 129, .	2.9	13
74573	Thermodynamics and Kinetics Accounting for Antithermal Quenching of Luminescence in Sc₂(MoO₄)₃: Yb/Er: Perspective beyond Negative Thermal Expansion. Journal of Physical Chemistry Letters, 2022, 13, 12032-12040.	2.1	3
74574	Anisotropic linear and nonlinear charge-spin conversion in topological semimetal <mml:math xmlns:mml="http://www.w3.org/1998/Math/MathML"><mml:mrow><mml:msub><mml:mi>SrIrO</mml:mi><mml:mn>3</mml:mn></mml:msub></mml:mrow></mml:math> Physical Review B, 2022, 106, .	1.1	4
74575	Exploring the Zr X O (X â€‰=â€‰S and Se) Janus Monolayers for Optoelectronic and Spintronic Applications. Physica Status Solidi - Rapid Research Letters, 0, , 2200427.	1.2	0

#	Article	IF	Citations
74576	Reduced Potential Barrier of Sodium-Substituted Disordered Rocksalt Cathode for Oxygen Evolution Electrocatalysts. Nanomaterials, 2023, 13, 10.	1.9	6
74577	AlGaN UV Detector with Largely Enhanced Heat Dissipation on Mo Substrate Enabled by van der Waals Epitaxy. Crystal Growth and Design, 0, , .	1.4	2
74578	Hydrogen Atom Adsorption-Induced Spin Reversal and Vacancies Boosting Hydrogen Evolution Reaction in Defective H-VS₂ Monolayers. Journal of Physical Chemistry C, 2022, 126, 21272-21280.	1.5	0
74579	Elemental segregation inhibits hydrogen embrittlement in aluminium alloys. , 2023, 2, 100099.		2
74580	Single â€œSwiss-rollâ€•microelectrode elucidates the critical role of iron substitution in conversion-type oxides. Science Advances, 2022, 8, .	4.7	3
74581	Quantum dynamics reveal different ligand effects by vibrational excitation in the dissociative chemisorption of HCl on the Au/Ag(111) surface. Journal of Chemical Physics, 2022, 157, .	1.2	3
74582	First-principles prediction of 1H-Na₂Se monolayer: effects of external strain and point defects associated with constituent atoms. Physica Scripta, 2023, 98, 025805.	1.2	1
74583	Bilayer MN4-O-MN4 by bridge-bonded oxygen ligands: Machine learning to accelerate the design of bifunctional electrocatalysts. Renewable Energy, 2023, 203, 445-454.	4.3	8
74584	Isomerism effects in relaxation dynamics of Au₂₄(SR)₁₆ thiolate-protected gold nanoclusters. Nanotechnology, 2023, 34, 105701.	1.3	3
74585	Origin of the nucleation preference of coherent and semicoherent nanoprecipitates in Al–Cu alloys based on atomistically informed classical nucleation theory. Journal of Alloys and Compounds, 2022, , 168559.	2.8	0
74586	Prediction of erbiumâ€“nitrogen compounds as high-performance high-energy-density materials. Journal of Physics Condensed Matter, 2023, 35, 085701.	0.7	3
74587	Effects of Multiple Local Environments on Electron Energy Loss Spectra of Epitaxial Perovskite Interfaces. Journal of Physical Chemistry C, 2022, 126, 21453-21466.	1.5	0
74588	Tailoring the Optical and Electronic Properties of 2D Hybrid Dionâ€“Jacobson Copper Chloride Perovskites. Journal of Physical Chemistry C, 2022, 126, 21297-21307.	1.5	2
74589	Tunable Intervalence Charge Transfer in Ruthenium Prussian Blue Analog Enables Stable and Efficient Biocompatible Artificial Synapses. Advanced Materials, 2023, 35, .	11.1	3
74590	Enhanced Second-Harmonic Generation of van der Waals CuInP₂S₆ via Pressure-Regulated Cationic Displacement. Chemistry of Materials, 2023, 35, 242-250.	3.2	10
74591	Modeling Short-Range and Three-Membered Ring Structures in Lithium Borosilicate Glasses Using a Machine-Learning Potential. Journal of Physical Chemistry C, 2022, 126, 21507-21517.	1.5	7
74592	Creating superconductivity in WB2 through pressure-induced metastable planar defects. Nature Communications, 2022, 13, .	5.8	13
74593	Peripheral-nitrogen effects on the Ru1 centre for highly efficient propane dehydrogenation. Nature Catalysis, 2022, 5, 1145-1156.	16.1	42

#	Article	IF	Citations
74594	Yttrium incorporation in Cr₂AlC: On the metastable phase formation and decomposition of (Cr,Y)₂AlC MAX phase thin films. Journal of the American Ceramic Society, 2023, 106, 2652-2665.	1.9	1
74595	Collective dynamics in liquid Si under high pressure above the melting line minimum. Journal of Molecular Liquids, 2023, 371, 121116.	2.3	0
74596	Magnetization-induced phase transition from a semimetal to a Chern insulator in monolayer <mml:math xmlns:mml="http://www.w3.org/1998/Math/MathML"><mml:mrow><mml:msub><mml:mi>VGa</mml:mi><mml:mn>2</mml:mn></mml:msub></mml:mrow></mml:math> Physical Review B, 2022, 106, .	1.1	4
74597	Enhancement of Electronic and Optoelectronic Performance of the InSe Multilayer by Surface Transfer Engineering. ACS Applied Electronic Materials, 2022, 4, 5867-5874.	2.0	0
74598	Regulating the metal-support interactions by tuning the ratios between N and B based on the C2N motif to develop efficient Pd-based catalysts for CO oxidative coupling to DMO: A DFT study. Applied Surface Science, 2023, 614, 156205.	3.1	7
74599	Quenchingâ€Induced Defects Liberate the Latent Reversible Capacity of Lithium Titanate Anode. Advanced Materials, 2023, 35, .	11.1	7
74600	Uncovering the CO₂ Capture Mechanism of NaNO₃-Promoted MgO by ¹⁸O Isotope Labeling. Jacs Au, 2022, 2, 2731-2741.	3.6	7
74601	Rational Design of PdAg Catalysts for Acetylene Selective Hydrogenation via Structural Descriptor-based Screening Strategy. ACS Catalysis, 2023, 13, 433-444.	5.5	8
74602	Active hydrogen boosts electrochemical nitrate reduction to ammonia. Nature Communications, 2022, 13, .	5.8	127
74603	Strain Engineering of Two-Dimensional Piezophotocatalytic Materials for Improved Hydrogen Evolution Reaction. ACS Sustainable Chemistry and Engineering, 2022, 10, 16924-16934.	3.2	7
74604	Cooperative Electronic Structure Modulator of Fe Singleâ€Atom Electrocatalyst for High Energy and Long Cycle Liâ€“S Pouch Cell. Advanced Materials, 2023, 35, .	11.1	27
74605	Anion Exchange Reaction of CsPbBr₃ Perovskite Nanocrystals: Affinity of Halide Ion Matters. ChemistrySelect, 2022, 7, .	0.7	4
74606	Onâ€Surface Synthesis of Chiral Graphene Nanoribbon Segments via the Quarterâ€Anthryl on Au(111) Surface. Advanced Materials Interfaces, 2023, 10, .	1.9	4
74607	Three-in-one organic-inorganic heterostructures: From scalable ball-milling synthesis to freestanding cathodes with high areal capacity for aqueous zinc-ion batteries. Chemical Engineering Journal, 2023, 457, 141140.	6.6	11
74608	Developing Waste Forms for Transuranic Elements: Quaternary Neptunium Fluorides of the Type Na_xMNp₆F₃₀ (M = Ti, V, Cr, Mn, Fe, Co, Ni, Al, Ga). Journal of the American Chemical Society, 2023, 145, 465-475.	6.6	1
74609	Alkali Metal Cations as Chargeâ€Transfer Bridge for Polarization Promoted Solarâ€toâ€H₂ Conversion. Advanced Functional Materials, 2023, 33, .	7.8	9
74610	Effect of fluorine ion irradiation on the properties of monolayer molybdenum disulfide. Journal of Applied Physics, 2022, 132, 225107.	1.1	1
74611	First Principles Study of Double Boron Atoms Supported on Graphitic Carbon Nitride (g-C3N4) for Nitrogen Electroreduction. Crystals, 2022, 12, 1744.	1.0	0

#	Article	IF	Citations
74612	Design principles for transition metal nitride stability and ammonia generation in acid. Joule, 2023, 7, 150-167.	11.7	7
74613	Half-Metallic Heusler Alloy/MoS₂ Based Magnetic Tunnel Junction. ACS Applied Materials & Interfaces, 2022, 14, 55167-55173.	4.0	1
74614	Element-wise representations with ECNet for material property prediction and applications in high-entropy alloys. Npj Computational Materials, 2022, 8, .	3.5	3
74615	Improvement of the reliability of potassium-ion electrets thorough an additional oxidation process. Applied Physics Letters, 2022, 121, 243903.	1.5	0
74616	The chemical states and electronic states of layered carbide superconductor ThMo₂Si₂C. Physica Scripta, 2023, 98, 015818.	1.2	1
74617	Sulfurâ€Doped rGO Aerogel Enables the Anchoring of 1T/2H MoS₂ for Durable Oxygen Reduction Reaction Catalyst Support. ChemSusChem, 2023, 16, .	3.6	2
74618	Ammonia synthesis by enhanced photocatalysis of N2 over oxygen-sulfur co-doped semi-crystalline g-C3N4. Journal of Materials Science, 2022, 57, 21869-21884.	1.7	2
74619	Structure, half-metallic and magnetic properties of bulk and (001) surface of Rb₂XMoO₆ (X = Cr, Sc) double perovskites: a DFT + U study. Physica Scripta, 2023, 98, 015807.	1.2	10
74620	Anomalous circularly polarized light emission in organic light-emitting diodes caused by orbitalâ€“momentum locking. Nature Photonics, 2023, 17, 193-199.	15.6	38
74621	The Local Coordination Effects on the Reactivity and Speciation of Active Sites in Graphene-Embedded Single-Atom Catalysts over Wide pH and Potential Range. Nanomaterials, 2022, 12, 4309.	1.9	3
74622	Enhanced Adsorption Selectivity of Carbon Dioxide and Ethane on Porous Metalâ€“Organic Framework Functionalized by a Sulfur-Rich Heterocycle. Nanomaterials, 2022, 12, 4281.	1.9	4
74623	Towards extreme fast charging of 4.6ÂV LiCoO2 via mitigating high-voltage kinetic hindrance. Journal of Energy Chemistry, 2023, 78, 13-20.	7.1	6
74624	Triple hourglass Weyl phonons. Physical Review B, 2022, 106, .	1.1	12
74625	Interaction-driven topological phase transition in monolayer <mml:math xmlns:mml="http://www.w3.org/1998/Math/MathML"><mml:msub><mml:mi mathvariant="normal">CrCl</mml:mi><mml:mn>2</mml:mn></mml:msub></mml:math> (pyrazine) <mml:math xmlns:mml="http://www.w3.org/1998/Math/MathML"><mml:msub><mml:mrow /><mml:mn>2</mml:mn></mml:msub></mml:math>. Physical Review B, 2022, 106, .	1.1	1
74626	Regulating the Electronic Structure of Freestanding Graphene on SiC by Ge/Sn Intercalation: A Theoretical Study. Molecules, 2022, 27, 9004.	1.7	1
74627	SBH17: Benchmark Database of Barrier Heights for Dissociative Chemisorption on Transition Metal Surfaces. Journal of Chemical Theory and Computation, 2023, 19, 245-270.	2.3	8
74628	Mechanistic exploration of furfural hydrogenation on copper surface in aqueous phase by DFT and AIMD simulations. Journal of Catalysis, 2023, 418, 1-12.	3.1	7
74629	On the mechanism of dehalogenation of methyl halides (Br and Cl) on Ag(111) and Au(111) surfaces: A DFT study. Applied Surface Science, 2023, 615, 156059.	3.1	3

#	Article	IF	Citations
74630	Symmetry-enforced planar nodal chain phonons in non-symmorphic materials. Journal of Applied Physics, 2022, 132, .	1.1	4
74631	Density Functional Theory Analysis Identifying the Mechanism for Ignition Sensitivity of Ammonium Periodate Compared with Ammonium Perchlorate. Journal of Physical Chemistry C, 2022, 126, 21723-21733.	1.5	1
74632	Quantitative Evidence to Challenge the Traditional Model in Heterogeneous Catalysis: Kinetic Modeling for Ethane Dehydrogenation over Fe/SAPO-34. Jacs Au, 2023, 3, 165-175.	3.6	5
74633	Quasi-One-Dimensional Metallicity in Compressed CsSnI₃. Journal of the American Chemical Society, 2022, 144, 23595-23602.	6.6	2
74634	Local structure transformations promoting high lithium diffusion in defect perovskite type structures. Electrochimica Acta, 2023, 441, 141759.	2.6	1
74635	Cold Nanozyme for Precise Enzymatic Antitumor Immunity. ACS Nano, 2022, 16, 21491-21504.	7.3	16
74636	First principles of Si-doped BC2N single layer for hydrogen evolution reaction (HER). International Journal of Hydrogen Energy, 2023, 48, 7294-7304.	3.8	5
74637	Diameter-dependent ultrafast lithium-ion transport in carbon nanotubes. Journal of Chemical Physics, 2023, 158, .	1.2	2
74638	Electric-controlled tunable thermal switch based on Janus monolayer MoSSe. Npj Computational Materials, 2022, 8, .	3.5	3
74639	Extremely Shallow Valence Band in Lanthanum Trihydride. Journal of the American Chemical Society, 2023, 145, 560-566.	6.6	0
74640	Theoretical Studies on Layered Perovskite Photocatalysts Sr₂M₂O₇ (M = Nb and Ta) Modified by NiO Cocatalysts. Journal of Physical Chemistry C, 2023, 127, 319-327.	1.5	1
74641	Layer-stacking of chalcogenide-terminated MXenes Ti₂CT₂(T = O, S, Se, Te) and their applications in metal-ion batteries. Nanotechnology, 2023, 34, 105704.	1.3	0
74642	Computational discovery of two-dimensional rare-earth iodides: promising ferrovalley materials for valleytronics. 2D Materials, 2023, 10, 015021.	2.0	7
74643	Band valley flattening and exciton appearance/disappearance under isotropic strain in monolayer WS2. European Physical Journal Plus, 2022, 137, .	1.2	0
74644	Electric field induced tunable half-metallicity in an <mml:math xmlns:mml="http://www.w3.org/1998/Math/MathML"><mml:mi>A</mml:mi></mml:math> -type antiferromagnetic bilayer <mml:math xmlns:mml="http://www.w3.org/1998/Math/MathML"><mml:msub><mml:mi mathvariant="normal">LaBr</mml:mi><mml:mn>2</mml:mn></mml:msub></mml:math>. Physical Review B, 2022, 106, .	1.1	15
74645	Facile synthesis of Ru nanoclusters embedded in carbonaceous shells for hydrogen evolution reaction in alkaline and acidic media. Journal of Electroanalytical Chemistry, 2022, , 117116.	1.9	1
74647	Enhanced Hydrogen Evolution Performance of Carbon Nitride Using Transition Metal and Boron Coâ€Đopants. Small Structures, 2023, 4, .	6.9	8
74648	Material transformers: deep learning language models for generative materials design. Machine Learning: Science and Technology, 2023, 4, 015001.	2.4	2

#	Article	IF	Citations
74649	Characterization and modeling studies towards Al3Ti/Mg interfaces in Ti reinforced AZ31 alloys. Journal of Materials Science and Technology, 2023, 147, 197-206.	5.6	4
74650	Ferroelectricity in HfO₂ from a Coordination Number Perspective. Chemistry of Materials, 2023, 35, 94-103.	3.2	11
74651	Hexagonal boron nitride nanoribbon as a novel metal-free catalyst for high-efficiency NO reduction to NH3. Fuel, 2023, 339, 126943.	3.4	7
74652	Resolving the Oxygen Species on Ozone Activated AgAu Alloy Catalysts for Oxidative Methanol Coupling. Journal of Physical Chemistry C, 2022, 126, 21568-21575.	1.5	1
74653	Pressure-induced band-gap energy increase in a metal iodate. Physical Review B, 2022, 106, .	1.1	4
74654	Fluctuations at Metal Halide Perovskite Grain Boundaries Create Transient Trap States: Machine Learning Assisted Ab Initio Analysis. ACS Applied Materials & Interfaces, 2022, 14, 55753-55761.	4.0	13
74655	Indoor photovoltaics awaken the worldâ€™s first solar cells. Science Advances, 2022, 8, .	4.7	26
74656	Na₂Ba[Na₂Sn₂S₇]: Structural Tolerance Factorâ€Guided NLO Performance Improvement. Angewandte Chemie, 2023, 135, .	1.6	0
74657	Spin-defect qubits in two-dimensional transition metal dichalcogenides operating at telecom wavelengths. Nature Communications, 2022, 13, .	5.8	6
74658	The effect mechanism of Si on the cementite growth behavior in Feâ€“Crâ€“C steel: first-principles calculations and experiments. Journal of Materials Science, 2022, 57, 22067-22081.	1.7	1
74659	Exchange-mediated magnon-phonon scattering in monolayer <mml:math xmlns:mml="http://www.w3.org/1998/Math/MathML"><mml:msub><mml:mi mathvariant="normal">CrI</mml:mi><mml:mn>3</mml:mn></mml:msub></mml:math>. Physical Review B, 2022, 106, .	1.1	8
74660	Activating Singleâ€Atom Ni Site via Firstâ€Shell Si Modulation Boosts Oxygen Reduction Reaction. Small, 2023, 19, .	5.2	7
74661	Adjusting the 3d Orbital Occupation of Ti in Ti₃C₂ MXene via Nitrogen Doping to Boost Oxygen Electrode Reactions in Liâ€“O₂ Battery. Small, 2023, 19, .	5.2	9
74662	Computational Identification of Ternary Wide-Band-Gap Oxides for High-Power Electronics. , 2022, 1, .		3
74663	Effect of h-BN Support on Photoluminescence of ZnO Nanoparticles: Experimental and Theoretical Insight. Materials, 2022, 15, 8759.	1.3	1
74664	An evaluation for geometries, formation enthalpies, and dissociation energies of diatomic and triatomic (C, H, N, O), NO3, and HNO3 molecules from the PAW DFT method with PBE and optB88-vdW functionals. AIP Advances, 2022, 12, .	0.6	2
74665	An EAM potential for Î±-brass copperâ€“zinc alloys: application to plasticity and fracture. Modelling and Simulation in Materials Science and Engineering, 2023, 31, 015004.	0.8	1
74666	Electric Field and Strain Tuning of 2D Semiconductor van der Waals Heterostructures for Tunnel Field-Effect Transistors. ACS Applied Materials & Interfaces, 2023, 15, 1762-1771.	4.0	7

#	Article	IF	Citations
74667	A Firstâ€Principles Investigation of MgGeN2 Under Uniaxial Compression. Physica Status Solidi (B): Basic Research, 2023, 260, .	0.7	3
74668	Theoretical study of Cr₂X₃S₃ (X = Br, I) monolayers for thermoelectric and spin caloritronics properties. Nanotechnology, 2023, 34, 095704.	1.3	3
74669	Two-dimensional ABC3 (A = Sc, Y; B = Al, Ga, In; C = S, Se, Te) with intrinsic electric field for photocatalytic water splitting. International Journal of Hydrogen Energy, 2023, 48, 5929-5939.	3.8	6
74670	Accessible active sites activated by nano cobalt antimony oxide @ carbon nanotube composite electrocatalyst for highly enhanced hydrogen evolution reaction. International Journal of Hydrogen Energy, 2023, 48, 7719-7736.	3.8	8
74671	Electronic Structure and Hardness of Mn3N2 Synthesized under High Temperature and High Pressure. Metals, 2022, 12, 2164.	1.0	0
74672	Band Alignments, Electronic Structure, and Core-Level Spectra of Bulk Molybdenum Dichalcogenides (MoS₂, MoSe₂, and MoTe₂). Journal of Physical Chemistry C, 2022, 126, 21022-21033.	1.5	4
74673	Bifunctional synergistic CoP/Coral-like g-C3N4 catalyst: Boosting the photocatalytic water splitting hydrogen evolution and appreciation of anisalcohol at same time. Applied Surface Science, 2023, 614, 156187.	3.1	4
74674	Diamane Oxide. Two-Dimensional Film with Mixed Coverage and a Variety of Electronic Properties. Journal of Physical Chemistry Letters, 2022, 13, 11383-11390.	2.1	3
74675	Localized d-Electron Effect on Spin Polarization of Vertical Heterostructures of Nanoporous Bilayer Graphene. Russian Physics Journal, 0, , .	0.2	0
74676	Assessment of Acid Gas Adsorption Selectivities in MIL-125-NH₂. Journal of Physical Chemistry C, 2022, 126, 21414-21425.	1.5	0
74677	WanTiBEXOS: A Wannier based Tight Binding code for electronic band structure, excitonic and optoelectronic properties of solids. Computer Physics Communications, 2023, 285, 108636.	3.0	4
74678	Theoretical Modeling of Oxide Ion Conductivity in Doped LaSrGa₃O₇ Melilites. Journal of Physical Chemistry C, 2022, 126, 21375-21380.	1.5	0
74679	High Temperature Polymer Electrolyte Membrane Fuel Cells with High Phosphoric Acid Retention. ACS Energy Letters, 2023, 8, 529-536.	8.8	6
74680	A Novel Two-Dimensional Allotrope of Silicon Grown on Al(111): A Case Study of the Interface Effect. Journal of Physical Chemistry C, 2022, 126, 21482-21495.	1.5	3
74681	A Universal Perovskite Nanocrystal Ink for Highâ€Performance Optoelectronic Devices. Advanced Materials, 2023, 35, .	11.1	14
74682	Interfacial Energy Level Modulation by Tuning the Electronic Character of Covalent Organic Frameworks: A Linker Functionalization Strategy. Journal of Physical Chemistry C, 2022, 126, 21496-21506.	1.5	2
74683	Potential and support-dependent hydrogen evolution reaction activation energies on sulfur vacancies of MoS2 from GC-DFT. International Journal of Hydrogen Energy, 2023, 48, 8478-8488.	3.8	9
74684	Photoluminescence studies of non-toxic monoclinic yttrium oxide quantum dots synthesized at low temperature for live cell imaging applications. Ceramics International, 2023, 49, 13200-13207.	2.3	3

#	Article	IF	Citations
74685	Molecular Mechanism and Microkinetic Analysis of the Reverse Water Gas Shift Reaction Heterogeneously Catalyzed by the Mo₂C MXene. ACS Catalysis, 2022, 12, 15658-15667.	5.5	5
74686	Ab Initio Microkinetics of H₂S Interactions with Clean and Sulfided Au(110) at Low Temperature: A Strong Assistance in Partial Dissociation from Single Sulfur Atoms. Journal of Physical Chemistry C, 2022, 126, 21585-21595.	1.5	0
74687	Understanding X-ray Photoelectron Spectra of Ionic Liquids: Experiments and Simulations of 1-Butyl-3-methylimidazolium Thiocyanate. Journal of Physical Chemistry B, 2022, 126, 10500-10509.	1.2	2
74688	Synthetic diamond identification under X-ray excitation. Cell Reports Physical Science, 2023, 4, 101208.	2.8	5
74689	Single-Crystal Growth, Structure, and Transport Properties of a New Dirac Semimetal LaMg_{0.83}Sb₂. Chemistry of Materials, 2023, 35, 304-312.	3.2	0
74690	Effect of Charge Non-Uniformity on the Lithium Dendrites and Improvement by the LiF Interfacial Layer. ACS Applied Energy Materials, 2022, 5, 15078-15085.	2.5	5
74691	Modulation of Structure and Optical Property of Nitrogen-Incorporated VO2 (M1) Thin Films by Polyvinyl Pyrrolidone. Materials, 2023, 16, 208.	1.3	1
74692	Spectroscopic evidence of flat bands in breathing kagome semiconductor Nb3I8. Communications Materials, 2022, 3, .	2.9	13
74693	Lutetium-Doped ZnO to Improve Photovoltaic Performance: A First-Principles Study. ACS Applied Electronic Materials, 2022, 4, 6253-6260.	2.0	10
74694	Simulated Superlattice and Electronic Properties of Cation-Disordered <mml:math xmlns:mml="http://www.w3.org/1998/Math/MathML" display="inline" overflow="scroll"><mml:mrow><mml:mi>Zn</mml:mi><mml:mi>Ge</mml:mi><mml:mi mathvariant="normal">N</mml:mi></mml:mrow></mml:math> <mml:math xmlns:mml="http://www.w3.org/1998/Math/MathML" display="inline" overflow="scroll"><mml:msub><mml:mi /><mml:mn>2</mml:mn></mml:msub></mml:math> and its Inte	1.5	3
74695	Improving Electrochemical Activity of P2â€type Na _{2/3} Mn _{2/3} Ni _{1/3} O ₂ by Controlling its Crystallinity. Batteries and Supercaps, 0, , .	2.4	0
74696	Tailoring of Photoluminescence Properties in Allâ€Vacuum Deposited Perovskite via Ruddlesdenâ€“Popper Faults. Advanced Functional Materials, 2023, 33, .	7.8	1
74697	In Quest of Lowâ€Leakage Dynamic Random Access Memory Enabled by Doped TiO₂ Dielectrics. Advanced Theory and Simulations, 2023, 6, .	1.3	1
74698	Robust architecture of 2D nano Mg-based borohydride on graphene with superior reversible hydrogen storage performance. Journal of Materials Science and Technology, 2023, 146, 121-130.	5.6	9
74699	Highâ€temperature oxidation of 60Si2Mn spring steel in dry air and wet air: Insights from an experimental and firstâ€principles study. Steel Research International, 0, , .	1.0	1
74700	Probing the Kinetic Origin of Varying Oxidative Stability of Ethylâ€vs. Propylâ€spaced Amines for Direct Air Capture. ChemSusChem, 2023, 16, .	3.6	7
74701	Electronic level modelling of graphene-borophene lateral heterostructures as anodes in Li-ion batteries. Applied Surface Science, 2023, 614, 156227.	3.1	2
74702	Ab initio calculation of hafnium and zirconium melting curves via the Lindemann criterion. Physical Review B, 2022, 106, .	1.1	4

#	Article	IF	Citations
74703	Ab initio structural optimization at finite temperatures based on anharmonic phonon theory: Application to the structural phase transitions of <mml:math xmlns:mml="http://www.w3.org/1998/Math/MathML"><mml:msub><mml:mi>BaTiO</mml:mi><mml:mn>3</mml:mn></mml:msub></m Physical Review B, 2022, 106, .	1.1	5
74704	Coexistence of trihexagonal and star-of-David pattern in the charge density wave of the kagome superconductor <mml:math xmlns:mml="http://www.w3.org/1998/Math/MathML"><mml:mrow><mml:mi>A</mml:mi><mml:msub><mml:mi mathvariant="normal">V</mml:mi><mml:mn>3</mml:mn></mml:msub><mml:msub><mml:mi>Sb</mml:mi><mml:mn>5</mml:mn> Physical Review B, 2022, 106, .	1.1	31
74705	Stability of FeVO4-II under Pressure: A First-Principles Study. Crystals, 2022, 12, 1835.	1.0	4
74706	Gas-liquid two-phase flow-based triboelectric nanogenerator with ultrahigh output power. Science Advances, 2022, 8, .	4.7	34
74707	Iridium single atoms incorporated in Co3O4 efficiently catalyze the oxygen evolution in acidic conditions. Nature Communications, 2022, 13, .	5.8	72
74708	Phase stability of double perovskite in Pr[Ba1Ââ^'ÂxSrx][Co1 â^' yFey]2O5.5 using genetic algorithm and density functional theory. Journal of the Korean Ceramic Society, 2023, 60, 434-439.	1.1	1
74709	Defect induced ambipolar conductivity in wide-bandgap semiconductor SrS: Theoretical perspectives. Applied Physics Letters, 2022, 121, .	1.5	4
74710	Coupled Co-Doped MoS₂ and CoS₂ as the Dual-Active Site Catalyst for Chemoselective Hydrogenation. ACS Applied Materials & Interfaces, 2023, 15, 1317-1325.	4.0	7
74711	In Situ Raman Spectroscopy and DFT Studies of the Phase Transition from Zircon to Reidite at High Pâ€“T Conditions. Minerals (Basel, Switzerland), 2022, 12, 1618.	0.8	2
74712	Development of a semi-empirical interatomic potential appropriate for the radiation defects in V-Ti-Ta-Nb high-entropy alloy. Journal of Physics Condensed Matter, 2023, 35, 055701.	0.7	3
74713	Mechanism and Kinetics-Guided Discovery of Nanometal Scissors to Cut Phosphoester Bonds. ACS Catalysis, 2023, 13, 504-514.	5.5	9
74714	Porous-Induced Performance Enhancement of Flat Boron Sheets for Lithium-Ion Batteries. Journal of Physical Chemistry C, 2022, 126, 21542-21549.	1.5	1
74715	Completely Anisotropic Ultrafast Optical Switching and Directionâ€Dependent Photocarrier Diffusion in Layered ZrTe₅. Advanced Optical Materials, 2023, 11, .	3.6	3
74716	Remarkable thermoelectric performance of carbon-based schwarzites. Advanced Composites and Hybrid Materials, 2023, 6, .	9.9	16
74717	Anchoring Ru active sites on Nâ€CNTs for an improved oneâ€pot cellobiose conversion. ChemNanoMat, 0, , .	1.5	0
74718	Giant Polarization in Quasiâ€Adiabatic Ferroelectric Na⁺ Electrolyte for Solidâ€State Energy Harvesting and Storage. Advanced Functional Materials, 2023, 33, .	7.8	2
74719	Structure sensitivity of ethanol steam reforming over the Rh catalyst: Reaction kinetics and deactivation mechanisms. Applied Surface Science, 2023, 614, 156116.	3.1	5
74720	Efficient and Reusable Sorbents Based on Nanostructured BN Coatings for Water Treatment from Antibiotics. International Journal of Molecular Sciences, 2022, 23, 16097.	1.8	1

#	Article	IF	Citations
74721	Precisely Constructed Metal Sulfides with Localized Singleâ€Atom Rhodium for Photocatalytic Câ^'H Activation and Direct Methanol Coupling to Ethylene Glycol. Advanced Materials, 2023, 35, .	11.1	15
74722	Mechanistic Insights on the Low-Temperature Oxidation of CO Catalyzed by Isolated Co Ions in N-Doped Carbon. ACS Catalysis, 2022, 12, 15529-15540.	5.5	1
74724	Metalâ€Free Carbonâ€Based Covalent Organic Frameworks with Heteroatomâ€Free Units Boost Efficient Oxygen Reduction. Advanced Materials, 2023, 35, .	11.1	41
74725	Efficient electrolytic conversion of nitrogen oxyanion and oxides to gaseous ammonia in molten alkali. Chemical Engineering Journal, 2023, 456, 141060.	6.6	2
74726	Design Novel Chalcone Crystals for Enhancement of Nonlinear Optical Activity and Higher Molecular Structural Stability. Crystal Growth and Design, 2023, 23, 592-601.	1.4	2
74727	Defectâ€Induced Atomic Arrangement in CoFe Bimetallic Heterostructures with Boosted Oxygen Evolution Activity. Small, 2023, 19, .	5.2	11
74728	Tuning the Electronic and Mechanical Properties of Kagome Graphene via Hydrogenation. Journal of Physical Chemistry C, 2022, 126, 21426-21437.	1.5	1
74729	Enhanced Selectivity in the Electroproduction of H₂O₂ via F/S Dualâ€Doping in Metalâ€Free Nanofibers. Advanced Materials, 2023, 35, .	11.1	30
74730	First-principle prediction of one-dimensional silicon allotropes: Promising new candidate for chemical and electrochemical hydrogen storage. International Journal of Hydrogen Energy, 2022, , .	3.8	2
74731	Graphene/MoSi2X4: A class of van der Waals heterojunctions with unique mechanical and optical properties and controllable electrical contacts. Applied Surface Science, 2023, 614, 156095.	3.1	5
74732	Multiple Open and Closed Nodalâ€Line Phonons in Solids with a 1 Space Group. , 0, , 2200085.		0
74733	Unlocking the hidden chemical space in cubic-phase garnet solid electrolyte for efficient quasi-all-solid-state lithium batteries. Nature Communications, 2022, 13, .	5.8	27
74734	Strain-engineering in two-dimensional transition metal dichalcogenide alloys. Journal of Applied Physics, 2022, 132, .	1.1	3
74735	Liquid metal synthesis solvents for metallic crystals. Science, 2022, 378, 1118-1124.	6.0	52
74736	Structural Analysis of Amorphous GeO₂ under High Pressure Using Reverse Monte Carlo Simulations. Journal of the Physical Society of Japan, 2022, 91, .	0.7	2
74737	First-Principles Molecular Dynamics Simulations on Waterâ€“Solid Interface Behavior of H2O-Based Atomic Layer Deposition of Zirconium Dioxide. Nanomaterials, 2022, 12, 4362.	1.9	1
74738	Computational assessment of solute segregation at twin boundaries in magnesium: A two-factor model and solute effect on strengthening. Journal of Applied Physics, 2022, 132, 225102.	1.1	1
74739	Band Alignment in Black Phosphorus/Transition Metal Dichalcogenide Heterolayers: Impact of Charge Redistribution, Electric Field, Strain, and Layer Engineering. Journal of Electronic Materials, 2023, 52, 1474-1483.	1.0	2

#	Article	IF	Citations
74740	Ru tailored hydrous cobalt phosphate as a rational approach for high-performance alkaline oxygen evolution reaction. Materials Today Chemistry, 2022, 26, 101267.	1.7	2
74741	Quantum phase transitions driven by sliding in bilayer <mml:math xmlns:mml="http://www.w3.org/1998/Math/MathML"><mml:mrow><mml:msub><mml:mi>MnBi</mml:mi><mml:mn>2</mml:mn></ Physical Review B, 2022, 106, .	3.7	8
74742	Coexistence of giant Rashba spin splitting and quantum spin Hall effect in H-Pb-F. Chinese Physics B, 0, , .	0.7	0
74743	H2 physisorption in fluorinated MOF-74: The role of fluorine from the perspective of electronic structure calculations. International Journal of Hydrogen Energy, 2023, 48, 8997-9007.	3.8	4
74744	Ab Initio Study of High-Capacity Hydrogen Storage in Lithium-Shrouded Honeycomb Borophene Oxide Nanosheet. Journal of Physical Chemistry C, 2022, 126, 20762-20772.	1.5	2
74745	The ability of <scp>BC₃</scp> to remove <scp>Cs</scp> from nuclear wastewater. International Journal of Quantum Chemistry, 2023, 123, .	1.0	4
74746	Crystalline Phases Regulate Electronic Trap States at Defective Surfaces of Lead Halide Perovskites. Journal of Physical Chemistry Letters, 2022, 13, 11473-11480.	2.1	1
74747	Crystal Phase Sensitivity of 5-Hydroxymethylfurfural Hydrodeoxygenation over a Pt₁Co Single-Atom Alloy Catalyst. Journal of Physical Chemistry C, 2022, 126, 20807-20815.	1.5	5
74748	Room-temperature valence transition in a strain-tuned perovskite oxide. Nature Communications, 2022, 13, .	5.8	5
74749	Anion Doping Delays Nonradiative Electronâ€“Hole Recombination in Cs-Based All-Inorganic Perovskites: Time Domain ab Initio Analysis. Journal of Physical Chemistry Letters, 2022, 13, 11375-11382.	2.1	10
74750	All hourglass bosonic excitations in the 1651 magnetic space groups and 528 magnetic layer groups. Physical Review Materials, 2022, 6, .	0.9	0
74751	Research on novel quantum phenomena of transition metal-doped ZrO2 nanosheets. Journal of Chemical Physics, 2022, 157, .	1.2	2
74752	Evolution of multiple spillover hydrogen species on anatase titanium dioxide. Cell Reports Physical Science, 2022, 3, 101190.	2.8	3
74753	Machine learning guided discovery of ternary compounds involving La and immiscible Co and Pb elements. Npj Computational Materials, 2022, 8, .	3.5	4
74754	Mechanical Stabilities and Properties of Graphene-like 2D III-Nitrides: A Review. Crystals, 2023, 13, 12.	1.0	2
74755	Pd single atom supported on N-doped egg tray graphene as formic acid dehydrogenation catalysts. 2D Materials, 0, , .	2.0	1
74756	Formation of Diamane Nanostructures in Bilayer Graphene on Langasite under Irradiation with a Focused Electron Beam. Nanomaterials, 2022, 12, 4408.	1.9	5
74757	Boron-doped armchair germanene nanoribbons with a width of six atoms in an external field: a DFT study. Journal of Molecular Modeling, 2023, 29, .	0.8	0

#	Article	IF	Citations
74758	Room-Temperature CO Oxidative Coupling for Oxamide Production over Interfacial Au/ZnO Catalysts. ACS Catalysis, 2023, 13, 735-743.	5.5	7
74759	Ï€-Stacks of radical-anionic naphthalenediimides in a metal-organic framework. Science Advances, 2022, 8, .	4.7	8
74760	Near-Infrared-Induced Photothermal Enhanced Photocatalytic H₂ Production for 3D/2D Heterojunctions of Snowflake-like CuS/g-C₃N₄ Nanosheets. Inorganic Chemistry, 2023, 62, 624-635.	1.9	12
74761	High-throughput theoretical optimization of the selective reduction reaction of NO with NH3 on metal-organic frameworks. Surface Science, 2022, , 122238.	0.8	0
74762	Origin of negative electrocaloric effect in Pnma -type antiferroelectric perovskites. Physical Review B, 2022, 106, .	1.1	2
74763	Superlattices of Gadolinium and Bismuth Based Thallium Dichalcogenides as Potential Magnetic Topological Insulators. Nanomaterials, 2023, 13, 38.	1.9	1
74764	A short review on diffusion coefficients in magnesium alloys and related applications. Journal of Magnesium and Alloys, 2022, 10, 3289-3305.	5.5	9
74765	Li and group-III impurity doping in <mml:math xmlns:mml="http://www.w3.org/1998/Math/MathML"><mml:msub><mml:mi>ZnSnN</mml:mi><mml:mn>2</mml:mn></mml:msub> : Potential and limitations. Physical Review Materials, 2022, 6, .	3.1	1
74766	Spontaneous Hetero-attachment of Single-Component Colloidal Precursors for the Synthesis of Asymmetric Auâ€“Ag₂X (X = S, Se) Heterodimers. Chemistry of Materials, 2022, 34, 10849-10860.	3.2	1
74767	Highly stable coherent nanoprecipitates via diffusion-dominated solute uptake and interstitial ordering. Nature Materials, 2023, 22, 434-441.	13.3	28
74768	Adsorption of the hydrophobic organic pollutant hexachlorobenzene to phyllosilicate minerals. Environmental Science and Pollution Research, 2023, 30, 36824-36837.	2.7	6
74769	Charge Balanced Vacancy Engineering to Enhance the Thermoelectric Properties of GeMnTe₂. Physica Status Solidi (B): Basic Research, 2023, 260, .	0.7	1
74770	Enhancing thermoelectric properties of MCoSb-based alloys by entropy-driven energy-filtering effects and band engineering. Materials Today Physics, 2023, 30, 100957.	2.9	1
74771	A scheme to fabricate magnetic graphene-like cobalt nitride CoN₄ monolayer proposed by first-principles calculations. Applied Physics Express, 2023, 16, 015505.	1.1	0
74772	Are Janus MoSSe/Ti3C2-MXene heterostructures excellent anode materials for Na-ion batteries? A computational insight combined experiment. Applied Surface Science, 2023, 614, 156196.	3.1	4
74773	Selective Hydrogenation of CO₂ to CH₃OH on a Dynamically Magic Single-Cluster Catalyst: Cu₃/MoS₂/Ag(111). ACS Catalysis, 2023, 13, 714-724.	5.5	9
74774	Enhanced magnetism in Ruâ€doped hybrid improper perovskite Ca₃Mn₂O₇ via experimental and firstâ€principles study. Journal of the American Ceramic Society, 2023, 106, 2455-2465.	1.9	3
74775	Interweaving Polar Charge Orders in a Layered Metallic Superatomic Crystal. Physical Review X, 2022, 12, .	2.8	0

#	Article	IF	Citations
74776	A chiral SrSi2 (srs) superstructure constructed by a dual interaction system showing isotropic electrical conductivity. Chinese Chemical Letters, 2023, 34, 108100.	4.8	1
74777	Artificial heterointerfaces of defect-rich Ni and amorphous/crystalline MoN enable efficient hydrogen evolution reaction. Chemical Engineering Journal, 2023, 457, 141173.	6.6	16
74778	Selective Conversion of Glycerol to Valueâ€Added C₃ Products: Effect of Catalyst Surface Structure. ChemCatChem, 2023, 15, .	1.8	2
74779	Nitrogen-doped carbon for selective pseudo-metal-free hydrodeoxygenation of 5-hydroxymethylfurfural to 2,5-dimethylfuran: Importance of trace iron impurity. Journal of Catalysis, 2023, 417, 396-407.	3.1	7
74780	Asymmetric magnetic proximity interactions in MoSe2/CrBr3 van der Waals heterostructures. Nature Materials, 2023, 22, 305-310.	13.3	16
74781	Atomic Insights of Selfâ€Healing in Silicon Nanowires. Advanced Functional Materials, 2023, 33, .	7.8	3
74782	Photolysis versus Photothermolysis of N₂O on a Semiconductor Surface Revealed by Nonadiabatic Molecular Dynamics. Journal of the American Chemical Society, 2023, 145, 476-486.	6.6	14
74783	Probing Spin Dynamics on Diamond Surfaces Using a Single Quantum Sensor. PRX Quantum, 2022, 3, .	3.5	19
74784	Phonon transport mechanism of HfO2 Ultrathin Film with Temperature-Correction Full-Band Monte Carlo Simulation. Journal of Physics Condensed Matter, 0, , .	0.7	0
74785	First principles-based study of the influence of pressure on the gas adsorption performance of coal. Materials Today Communications, 2023, 34, 105269.	0.9	0
74786	Influence of the cation distribution, atomic substitution, and atomic vacancies on the physical properties of <mml:math xmlns:mml="http://www.w3.org/1998/Math/MathML"><mml:mrow><mml:msub><mml:mrow><mml:mi>C</mml:mi><mml:mi>o</mml:mi> and <mml:math xmlns:mml="http://www.w3.org/1998/Math/MathML"><mml:mrow><mml:msub><mml:mrow><mml:mi>N</mml:mi><mml:mi>i</. Physical Review Materials, 2022, 6, .	0.9	3
74787	First-principles study of N and S co-doping in diamond. Diamond and Related Materials, 2023, 132, 109651.	1.8	3
74788	Identification of a Magnetic Phase via a Raman Spectrum in Single-Layer MnSe: An ab Initio Study. Journal of Physical Chemistry C, 2022, 126, 21891-21898.	1.5	1
74789	Structural, electronic, and magnetic properties of X3Pt and XPt3 (X=Fe, Co, or Ni) alloys: Density functional theory and Monte Carlo simulation. Physica B: Condensed Matter, 2023, 651, 414615.	1.3	8
74790	Enhanced Electronâ€“Hole Separation in Phosphorus-Coordinated Co Atom on g-C₃N₄ toward Photocatalytic Overall Water Splitting. Journal of Physical Chemistry Letters, 2022, 13, 11961-11967.	2.1	5
74791	An examination of phononâ€“inelastic moleculeâ€“metal scattering using reduced density matrix and stochastic wave packet methods. Journal of Chemical Physics, 2023, 158, 024701.	1.2	0
74792	Hydrogen-Sensing Properties of Ultrathin Pt-Co Alloy Films. Chemosensors, 2022, 10, 512.	1.8	2
74793	Airâ€condition process for scalable fabrication of CdS/ZnS 1D/2D heterojunctions toward efficient and stable photocatalytic hydrogen production. , 2023, 5, .		15

#	Article	IF	Citations
74794	Lithium Superionic Conduction in BH₄â€Substituted Thiophosphate Solid Electrolytes. Advanced Science, 2023, 10, .	5.6	4
74795	Chiral magnetism, lattice dynamics, and anomalous Hall conductivity in <mml:math xmlns:mml="http://www.w3.org/1998/Math/MathML"><mml:mrow><mml:msub><mml:mi mathvariant="normal">V</mml:mi><mml:mn>3</mml:mn></mml:msub><mml:mi>AuN</mml:mi></mml:mrow></mml:math> antiferromagnetic antiperovskite. Physical Review Materials, 2022, 6, .	2.9	2
74796	Cation ordering induced two-dimensional vertical ferroelectricity in tungsten and molybdenum trioxides. Physical Review B, 2022, 106, .	1.1	0
74797	Fast, Multiâ€Bit, and Visâ€Infrared Broadband Nonvolatile Optoelectronic Memory with MoS₂/2Dâ€Perovskite Van der Waals Heterojunction. Advanced Materials, 2023, 35, .	11.1	22
74798	First-principles calculations to investigate doping effects on electrical conductivity and interfacial contact resistance of TiO2. Applied Surface Science, 2023, 614, 156202.	3.1	5
74799	Architecture Design and Catalytic Activity: Nonâ€Noble Bimetallic CoFe/fe₃O₄ Coreâ€“Shell Structures for CO₂ Hydrogenation. Advanced Science, 2023, 10, .	5.6	6
74800	Superconductivity in Thâ€“H and Puâ€“H Compounds under Highâ€Pressure Conditions: A Firstâ€Principles Study. Physica Status Solidi (B): Basic Research, 2023, 260, .	0.7	1
74801	Structure, Stability, and Electronic Properties of Hydrogenated Monolayer 2D Silicon Allotropes by Firstâ€Principles Calculation. Physica Status Solidi (B): Basic Research, 2023, 260, .	0.7	0
74802	ShakeNBreak: Navigating the defect configurational landscape. Journal of Open Source Software, 2022, 7, 4817.	2.0	11
74803	Effects of Aâ€site replacement (Sm, Y, and Pr) on catalytic performances of mullite catalysts for NO oxidation. Fuel, 2023, 337, 126838.	3.4	2
74804	Ultrafast X-ray imaging of the light-induced phase transition in VO2. Nature Physics, 0, , .	6.5	11
74806	Effects of Selenium Doping in Zinc Telluride from First Principles. Journal of Physical Chemistry C, 2022, 126, 21348-21355.	1.5	0
74807	Vacancy-Ordered Double Perovskites Cs₂BI₆ (B = Pt, Pd, Te, Sn): An Emerging Class of Thermoelectric Materials. Journal of Physical Chemistry Letters, 2022, 13, 11655-11662.	2.1	14
74808	Slight compositional variation-induced structural disorder-to-order transition enables fast Na+ storage in layered transition metal oxides. Nature Communications, 2022, 13, .	5.8	12
74809	Strain control of hybridization between dark and localized excitons in a 2D semiconductor. Nature Communications, 2022, 13, .	5.8	16
74810	Influence of High Pressure on the Pedal-like Motion and Photoreactivity in the Cocrystals of 1,2-Di(4-pyridyl)ethylene with trans-2-(4-Fluorophenyl)vinylboronic Acid. Crystal Growth and Design, 2023, 23, 246-255.	1.4	0
74811	Mean-field approach for Anderson-type off-diagonal disorder. Physical Review B, 2022, 106, .	1.1	2
74812	Geometrical configuration modulation via iron doping and defect engineering in spinel oxides for enhanced oxygen revolution activity. Chemical Engineering Journal, 2023, 456, 140975.	6.6	5

#	Article	IF	Citations
74813	Efficient and Thermally Robust Broadband Nearâ€Infrared Emission in a Garnet Ca₃MgHfGe₃O₁₂:Cr³⁺ Phosphor. Advanced Optical Materials, 2023, 11, .	3.6	12
74814	Insights into nonvolatile resistive switching in monolayer hexagonal boron nitride. Journal of Applied Physics, 2022, 132, .	1.1	3
74815	Electrical and magnetic properties of antiferromagnetic semiconductor MnSi2N4 monolayer. Frontiers in Chemistry, 0, 10, .	1.8	2
74816	Hyperbolic Behavior and Antiferromagnetic Order in Rare-Earth Tellurides. Crystals, 2022, 12, 1839.	1.0	0
74817	Collective Atomic Motion in Crystals Under Shear Stress by First Principles Phonon Calculations. Materia Japan, 2022, 61, 841-843.	0.1	0
74818	Unraveling the Broadband Emission in Mixed Tinâ€Lead Layered Perovskites. Advanced Optical Materials, 2023, 11, .	3.6	6
74819	Electrocatalytic Biomass Upgrading of Furfural using Transitionâ€Metal Borides via Density Functional Theory Investigation. Small, 2023, 19, .	5.2	8
74820	Computational description of surface hydride phases on Pt(111) electrodes. Journal of Chemical Physics, 2023, 158, .	1.2	8
74821	Ab initio determination on diffusion coefficient and viscosity of FeNi fluid under Earthâ€™s core condition. Scientific Reports, 2022, 12, .	1.6	2
74822	Electronic and optical properties of the buckled and puckered phases of phosphorene and arsenene. Scientific Reports, 2022, 12, .	1.6	4
74823	Constructing metal-free heterophotocatalyst using two-dimensional carbon nitride sheets and violet phosphorene for highly efficient visible-light photocatalysis. Journal of Materials Science and Technology, 2023, 146, 113-120.	5.6	4
74824	Gradient area-selective deposition for seamless gap-filling in 3D nanostructures through surface chemical reactivity control. Nature Communications, 2022, 13, .	5.8	11
74825	Free radicals induced ultra-rapid synthesis of N-doped carbon sphere catalyst with boosted pyrrolic N active sites for efficient acetylene hydrochlorination. Nano Research, 0, , .	5.8	0
74826	Sliding induced multiple polarization states in two-dimensional ferroelectrics. Nature Communications, 2022, 13, .	5.8	39
74827	Tuning the C₁/C₂ Selectivity of Electrochemical CO₂ Reduction on Cuâ€“CeO₂ Nanorods by Oxidation State Control. Advanced Materials, 2023, 35, .	11.1	17
74828	Metal Singleâ€Site Molecular Complexâ€“MXene Heteroelectrocatalysts Interspersed Graphene Nanonetwork for Efficient Dualâ€Task of Water Splitting and Metalâ€“Air Batteries. Advanced Functional Materials, 2023, 33, .	7.8	16
74829	Toward Sabatier Optimal for Ammonia Synthesis with Paramagnetic Phase of Ferromagnetic Transition Metal Catalysts. Journal of the American Chemical Society, 2022, 144, 23089-23095.	6.6	26
74830	WI3 Monolayer: Electronic Band Structure and Magnetic Anisotropy Under an External Electric Field. Journal of Electronic Materials, 0, , .	1.0	0

#	Article	IF	Citations
74831	Effects of lattice strain on hydrogen diffusion, trapping and escape in bcc iron from ab-initio calculations. International Journal of Hydrogen Energy, 2023, 48, 8198-8215.	3.8	6
74832	Probing the antiferromagnetic structure of bilayer <mml:math xmlns:mml="http://www.w3.org/1998/Math/MathML"><mml:msub><mml:mrow><mml:mi>CrI</mml:mi></mml:mrow><mml:mn>3</mml:mn> by second harmonic generation: A first-principles study. Physical Review B, 2022, 106, .	1.1	0
74833	Atomic and electronic structures of the interface and twin boundaries in epitaxial CuO films on a ZnO substrate. Materials Today Communications, 2022, 33, 105022.	0.9	0
74834	Achieving highly selective electrochemical CO2 reduction to C2H4 on Cu nanosheets. Journal of Energy Chemistry, 2023, 79, 312-320.	7.1	11
74835	First-Principles Study on the Structural, Elastic and Thermodynamic Properties of Binary Pd-Sn Compounds. Journal of Electronic Materials, 2023, 52, 1875-1887.	1.0	2
74836	Ternary magnesium gallides â€“ synthesis, crystal chemistry and properties of CaMgGa, SrMgGa, BaMgGa and YbMgGa. Zeitschrift Fur Anorganische Und Allgemeine Chemie, 0, , .	0.6	1
74837	The effective spin-splitting manipulation of monolayer WSe₂ and Janus WSSe on SrIrO₃(111) surface: A DFT study. AIP Advances, 2022, 12, 125308.	0.6	0
74838	Thermal-inert and ohmic-contact interface for high performance half-Heusler based thermoelectric generator. Nature Communications, 2022, 13, .	5.8	18
74839	Electronic band engineering of Mg₂Si by isoelectronic impurity doping: a first-principles study for enhancing thermoelectric properties. Japanese Journal of Applied Physics, 2023, 62, SD1007.	0.8	0
74840	Determining the contribution of Mo single atoms components in MoO2 nanocatalyst in transfer hydrogenation. Nano Research, 2023, 16, 2302-2310.	5.8	4
74841	Predicting Frequency from the External Chemical Environment: OH Vibrations on Hydrated and Hydroxylated Surfaces. Journal of Chemical Theory and Computation, 2022, 18, 7683-7694.	2.3	3
74842	Blue phosphorene/graphdiyne heterostructure as a potential anode for advanced lithium-ion batteries: First-principle investigation. Applied Surface Science, 2023, 614, 156169.	3.1	3
74843	High-temperature superconductivity in two-dimensional hydrogenated titanium diboride: Ti2B2H4. Materials Today Physics, 2023, 30, 100954.	2.9	5
74844	A noise-robust data assimilation method for crystal structure determination using powder diffraction intensity. Journal of Chemical Physics, 2022, 157, 224112.	1.2	1
74845	Interfacial role of Ionic liquids in CO2 electrocatalytic Reduction: A mechanistic investigation. Chemical Engineering Journal, 2023, 457, 141076.	6.6	1
74846	Ultra-strong Mg alloy with nano-grain structures produced by a high-throughput magnetron co-sputtering method for the full chemistry spectra. Journal of Materials Science, 2022, 57, 21813-21827.	1.7	1
74847	Single atom catalysts supported on metallic C5N monolayers for oxygen reduction/evolution reactions with more active sites than loaded metal atoms. Applied Surface Science, 2023, 614, 156048.	3.1	4
74848	Evolution of the Fe-Co magnetism and magnetic proximity effects in alternate Fe/Co monolayers on nonmagnetic <mml:math xmlns:mml="http://www.w3.org/1998/Math/MathML"><mml:msub><mml:mrow><mml:mi>Cu</mml:mi></mml:mrow><mml:mn>3</mml:mn> Physical Review B, 2022, 106, .	1.1	0

#	Article	IF	Citations
74849	In-depth insight into the mechanism on photocatalytic selective CO2 reduction coupled with tetracycline oxidation over BiO1-Br/g-C3N4. Applied Surface Science, 2023, 614, 156017.	3.1	5
74850	(<mml:math xmlns:mml="http://www.w3.org/1998/Math/MathML"><mml:msub><mml:mi) Tj ETQq1 1 0.784314 rgBT /Overlock 10 T mathvariant="normal">GeTe</mml:mi><mml:mn>2</mml:mn></mml:msub></mml:math> : An antiferromagnetic triangular Ising lattic. Physical Review B, 2022, 106, .	1.1	3
74851	Orderâ€“disorder competition in equiatomic 3dâ€“transitionâ€“metal quaternary alloys: phase stability and electronic structure. Science and Technology of Advanced Materials Methods, 2023, 3, .	0.4	0
74852	2D honeycomb transformation into dodecagonal quasicrystals driven by electrostatic forces. Nature Communications, 2022, 13, .	5.8	5
74853	Cobalt diselenide nanotetrapod: An efficient electrocatalyst for hydrogen evolution reaction. Catalysis Today, 2023, 423, 113978.	2.2	0
74854	Cu⁺@Sb³⁺-Codoped All-Inorganic Metal Halide of Cs₂ZnCl₄ with Tunable Dual Emission for Fluorescence Anticounterfeiting and Information Encryption. Journal of Physical Chemistry C, 2023, 127, 807-815.	1.5	6
74855	Computational study of adsorption of magnesium polysulfides on VS4 magnesium sulfur batteries. Materials Today: Proceedings, 2023, 76, 352-358.	0.9	1
74856	Hotspots and Tendencies of Energy Optimization Based on Bibliometric Review. Energies, 2023, 16, 158.	1.6	1
74857	Influence of an N,N,N-Trimethyl-1-adamantyl Ammonium (TMAda⁺) Structure Directing Agent on Al Distributions and Pair Features in Chabazite Zeolite. Chemistry of Materials, 2022, 34, 10811-10822.	3.2	4
74858	Atomically Precise Integration of Multiple Functional Motifs in Catalytic Metalâ€“Organic Frameworks for Highly Efficient Nitrate Electroreduction. Jacs Au, 2022, 2, 2765-2777.	3.6	8
74859	Prediction of bipolar <mml:math xmlns:mml="http://www.w3.org/1998/Math/MathML"><mml:mrow><mml:msub><mml:mi>VSi</mml:mi><mml:mn>2</mml:mn></mml: and <mml:math xmlns:mml="http://www.w3.org/1998/Math/MathML"><mml:mrow><mml:msub><mml:mi>VGe</mml:mi><mml:mn>2</mml:mn></mml monolayers with high Curie temperature and strong magnetocrystalline. Physical Review B, 2022, 106, .	1.1	4
74860	Overcoming the doping limit in semiconductors via illumination. Physical Review B, 2022, 106, .	1.1	5
74861	Two-dimensional binary transition metal nitride <mml:math xmlns:mml="http://www.w3.org/1998/Math/MathML"><mml:mi>M</mml:mi><mml:msub><mml:mi mathvariant="normal">N</mml:mi><mml:mn>4</mml:mn></mml:msub></mml:math> (<mml:math) Tj ETQq0 0 0 rgBT /Overlock 10 Tf	1	6
74862	Chern numbers of topological phonon band crossing determined with inelastic neutron scattering. Physical Review B, 2022, 106, .	1.1	7
74863	Displacement vorticity as the origin of moirÃ© potentials in twisted WSe2/MoSe2 bilayers. Matter, 2023, 6, 493-505.	5.0	0
74864	Triggering Fast Lithium Ion Conduction in LiPS₄I. , 0, , 144-154.		0
74865	Tailoring the magnetic exchange interaction in MnBi2Te4 superlattices via the intercalation of ferromagnetic layers. Nature Electronics, 0, , .	13.1	2
74866	Theoretical insights into electronic structures and durability of single-atom Pd/TiN catalysts. International Journal of Hydrogen Energy, 2022, , .	3.8	1

#	Article	IF	Citations
74867	Lecture Notes on First-Principles Methods Using a Plane-Wave Basis Set (Part 4). Materia Japan, 2022, 61, 878-886.	0.1	0
74868	Formation of Monolayer Charge Density Waves and Anomalous Edge Doping in Na Doped Bulk VSe₂. Advanced Materials Interfaces, 2023, 10, .	1.9	1
74869	Understanding effect of distortions and vacancies in wurtzite AlScN ferroelectric memory materials: Vacancy-induced multiple defect state types and relaxation dependence in transition energy levels. AIP Advances, 2022, 12, .	0.6	2
74870	Study the application of nitrogenated holey graphene (C2N) nanosheets as a high-performance anode material for magnesium ion battery (MIB): DFT study. Inorganic Chemistry Communication, 2023, 148, 110296.	1.8	3
74871	Modeling polar order in compressively strained <mml:math xmlns:mml="http://www.w3.org/1998/Math/MathML"><mml:msub><mml:mi>SrTiO</mml:mi><mml:mn>3</mml:mn></mml:msub></m Physical Review B, 2022, 106, .	1.1	0
74872	Thruâ€Hole Epitaxy: A Highway for Controllable and Transferable Epitaxial Growth. Advanced Materials Interfaces, 2023, 10, .	1.9	5
74873	Phenylâ€Free Polynorbornenes for Potential Anion Exchange Ionomers for Fuel Cells and Electrolyzers. Advanced Energy Materials, 2023, 13, .	10.2	16
74874	Tl-based TlAgX (Xâ€‰=â€‰S, Se) monolayers with ultra-low lattice thermal conductivity and high ZT: a first-principles study. Journal of Materials Science, 2022, 57, 21607-21619.	1.7	1
74875	Strong synergy between single atoms and single-atom alloys enables active and selective H2O2 synthesis. Chem Catalysis, 2022, 2, 3607-3620.	2.9	8
74876	Enhanced optical properties and mechanisms of Ba-doped LaMnO3 perovskite ceramic coating. Ceramics International, 2023, 49, 11696-11704.	2.3	3
74877	First-principles study on the electronic structures and topological properties of Bi(110)/IV-VI and Bi(110)/V-V van der Waals heterostructures. Applied Surface Science, 2023, 614, 156027.	3.1	2
74878	Aerosol Spray Drying Guided Synthesis of Ultrasmall Alloyed Bimetallic Nanoparticles Supported on Silica for Catalytic Semihydrogenation. Small, 2023, 19, .	5.2	6
74879	Large magnetostriction of heavy-metal-element doped Fe-based alloys. Journal of Applied Physics, 2022, 132, 215105.	1.1	0
74880	Spin-momentum locking from topological quantum chemistry: Applications to multifold fermions. Physical Review B, 2022, 106, .	1.1	4
74881	Lanthanide Contraction Builds Better Highâ€Voltage LiCoO₂ Batteries. Advanced Functional Materials, 2023, 33, .	7.8	23
74882	Suppressing the filament formation by aluminum doping in anatase titanium oxide. AIP Advances, 2022, 12, 125212.	0.6	0
74883	Interplay of defect levels and rare earth emission centers in multimode luminescent phosphors. Nature Communications, 2022, 13, .	5.8	63
74884	Construction of Cobalt Molybdenum Diselenide Threeâ€phase Heterojunctions for Electrocatalytic Hydrogen Evolution in Acid Medium. Chemistry - an Asian Journal, 2023, 18, .	1.7	3

#	Article	IF	Citations
74885	Stability and Acidity of Sites at the External Surface and at Point Defects of Faujasite. ChemCatChem, 2023, 15, .	1.8	3
74886	Unique low-energy line defects and lateral heterostructures in phosphorene. Physica Scripta, 2023, 98, 015815.	1.2	1
74887	Methylidyne Adsorption on Pt(211) Probed by Reflection Absorption Infrared Spectroscopy (RAIRS). Journal of Physical Chemistry C, 2022, 126, 20886-20891.	1.5	0
74888	Arsenic doping and diffusion in CdTe: a DFT study of bulk and grain boundaries. Journal of Physics Condensed Matter, 2023, 35, 075702.	0.7	0
74889	Advantageous Role of N-doping on K@Al in COS/CS2 Hydrolysis: Diminished Oxygen Mobility and Rich basic sites. Fuel, 2023, 337, 126882.	3.4	7
74890	Long-Range Magnetic Order in Nickel Hydroxide-Functionalized Graphene Quantum Dots. Journal of Physical Chemistry Letters, 2022, 13, 11536-11542.	2.1	0
74891	Activity Enhancement of PtIr Catalysts for Complete Ethanol Oxidation Reaction by Tuning Câ€“O Coupling Abilities. Journal of Physical Chemistry C, 2022, 126, 21650-21666.	1.5	2
74892	Squishing Skyrmions: Symmetry-Guided Dynamic Transformation of Polar Topologies Under Compression. Journal of Physical Chemistry Letters, 2022, 13, 11335-11345.	2.1	1
74893	Special quasirandom structures description of the local structure of disordered Bi0.5K0.5TiO3. Journal of Applied Physics, 2022, 132, .	1.1	1
74894	Origin of Structural Anomaly in Cuprous Halides. Journal of Physical Chemistry Letters, 2022, 13, 11438-11443.	2.1	7
74895	Step pinning and hillock formation in (Al,Ga)N films on native AlN substrates. Journal of Applied Physics, 2022, 132, .	1.1	3
74896	CO2 electroreduction to multicarbon products in strongly acidic electrolyte via synergistically modulating the local microenvironment. Nature Communications, 2022, 13, .	5.8	68
74897	Classical Density Functional Theory Approach to Vibrational Properties and Lattice Specific Heat of a Quasi-one-dimensional Antiferromagnet KFeSe2. JETP Letters, 0, , .	0.4	0
74898	Anisotropic phonon and magnon vibration and gate-tunable optoelectronic properties of nickel thiophosphite. 2D Materials, 2023, 10, 025001.	2.0	2
74899	Ethane dehydrogenation over the g-C3N4 supported metal single-atom catalysts to enhance reactivity and coking-resistance ability. Nano Research, 2023, 16, 6142-6152.	5.8	4
74901	Trinitroaromatic Salts as High-Energy-Density Organic Cathode Materials for Li-Ion Batteries. ACS Applied Materials & Interfaces, 2023, 15, 1129-1137.	4.0	3
74902	Efficient electrocatalytic valorization of chlorinated organic water pollutant to ethylene. Nature Nanotechnology, 2023, 18, 160-167.	15.6	31
74903	Spin-State Regulation of Nickel Cobalt Spinel toward Enhancing the Electron Transfer Process of Oxygen Redox Reactions in Lithiumâ€“Oxygen Batteries. Energy & Fuels, 2023, 37, 735-745.	2.5	3

#	Article	IF	Citations
74904	Inhomogeneous Defect Distribution in Mixed-Polytype Metal Halide Perovskites. ACS Energy Letters, 2023, 8, 356-360.	8.8	5
74905	Mechanism for SO2 poisoning of Cu-CHA during low temperature NH3-SCR. Journal of Catalysis, 2023, 417, 497-506.	3.1	2
74906	Data-driven methods for discovery of next-generation electrostrictive materials. Npj Computational Materials, 2022, 8, .	3.5	2
74907	Strain tunable quantum emission from atomic defects in hexagonal boron nitride for telecom-bands. Scientific Reports, 2022, 12, .	1.6	3
74908	Grain Refinement via Changing the Shuffling Motion of the Grain Boundary by Traces of Ce and Lu in Gold Alloys. Journal of Physical Chemistry C, 2022, 126, 21864-21870.	1.5	0
74909	Valley-polarized quantum anomalous Hall effect in van der Waals heterostructures based on monolayer jacutingaite family materials. Frontiers of Physics, 2023, 18, .	2.4	5
74910	Highâ€Performance Solutionâ€Processed 2D Pâ€Type WSe₂ Transistors and Circuits through Molecular Doping. Advanced Materials, 2023, 35, .	11.1	13
74911	Orderâ^'disorder interfaces in a graphitic carbon nitride-nanoclay composite for improved photodynamic antibiotics. Communications Materials, 2022, 3, .	2.9	2
74912	Ce_xZr_{1â€“x}O₂-Supported CrO_x Catalysts for CO₂-Assisted Oxidative Dehydrogenation of Propaneâ"€Probing the Active Sites and Strategies for Enhanced Stability. ACS Catalysis, 2023, 13, 213-223.	5.5	7
74913	PdCu Electrocatalysts for Selective Nitrate and Nitrite Reduction to Nitrogen. ACS Catalysis, 2023, 13, 87-98.	5.5	15
74914	Density Functional Theory Study of the Point Defects on KDP (100) and (101) Surfaces. Molecules, 2022, 27, 9014.	1.7	2
74916	Phase evolution for oxidizing bismuth selenide. Journal of Physics Condensed Matter, 2023, 35, 075401.	0.7	0
74917	Effect of titanium, antimony, and ruthenium doping on tin dioxide adsorption properties. Quantumâ€chemical modeling. Journal of the Chinese Chemical Society, 0, , .	0.8	0
74918	Phase-controllable large-area two-dimensional In2Se3 and ferroelectric heterophase junction. Nature Nanotechnology, 2023, 18, 55-63.	15.6	45
74919	Periodic Density Functional Theory Calculations of Uranyl Tetrachloride Compounds Engaged in Uranylâ€"Cation and Uranylâ€"Hydrogen Interactions: Electronic Structure, Vibrational, and Thermodynamic Analyses. Inorganic Chemistry, 2023, 62, 372-380.	1.9	11
74920	Diamond/c-BN van der Waals heterostructure with modulated electronic structures. Chinese Physics B, 0, , .	0.7	0
74921	Toward a Consistent Prediction of Defect Chemistry in CeO₂. Chemistry of Materials, 2023, 35, 207-227.	3.2	16
74922	Giant anomalous thermal Hall effect in tilted type-I magnetic Weyl semimetal <mml:math xmlns:mml="http://www.w3.org/1998/Math/MathML"><mml:mrow><mml:msub><mml:mtext>Co</mml:mtext><mml:mn>3</mml:mn> Physical Review B, 2022, 106, .	3.5	5

#	Article	IF	Citations
74923	Highly Efficient Hydrosilylation of Ethyne over Pt/ZrO₂ Catalysts with Size-Dependent Metalâ€“Support Interactions. Industrial & Engineering Chemistry Research, 2022, 61, 18703-18711.	1.8	1
74924	Thermoelectric Figure of Merit of a Superatomic Crystal <mml:math xmlns:mml="http://www.w3.org/1998/Math/MathML" display="inline" overflow="scroll"><mml:msub><mml:mi>Re</mml:mi><mml:mn>6</mml:mn></mml:msub><mml:msub><mml:mi>Se</mml:mi><mml:mi><mml:mrow><mml:mrow><mml:mi mathvariant="normal">I</mml:mi></mml:mrow></mml:mrow><mml:mn>2</mml:mn></mml:msub></mml:math> Monolayer. Physical Review Applied, 2022, 18, .	4.6	3
74925	Na₂Ba[Na₂Sn₂S₇]: Structural Tolerance Factorâ€Guided NLO Performance Improvement. Angewandte Chemie - International Edition, 2023, 62, .	7.2	15
74926	Ordered Mesopore Confined Pt Nanoclusters Enable Unusual Self-Enhancing Catalysis. ACS Central Science, 2022, 8, 1633-1645.	5.3	7
74927	Uncovering compounds with promising piezoresistive properties via high-throughput first-principles survey. Materials Today Communications, 2023, 34, 105240.	0.9	0
74928	Controllable Chirality and Band Gap of Quantum Anomalous Hall Insulators. Nano Letters, 2023, 23, 305-311.	4.5	9
74929	Experimental and Computational Approaches to Sulfonated Poly(arylene ether sulfone) Synthesis Using Different Halogen Atoms at the Reactive Site. Membranes, 2022, 12, 1286.	1.4	0
74930	Harvesting the Gas Molecules by Bioinspired Design of 1D/2D Hybrids Toward Sensitive Acetone Detecting. Small Structures, 2023, 4, .	6.9	3
74931	High-Gain MoS₂/Ta₂NiSe₅ Heterojunction Photodetectors with Charge Transfer and Suppressing Dark Current. ACS Applied Materials & Interfaces, 2022, 14, 56384-56394.	4.0	14
74932	Mean Value Ensemble Hubbard-U Correction for Spin-Crossover Molecules. Journal of Physical Chemistry Letters, 2022, 13, 12049-12054.	2.1	3
74933	Magnetic Surface on Nonmagnetic Bulk of Electride Hf₂S. Journal of Physical Chemistry C, 2023, 127, 696-701.	1.5	2
74934	Realizing Metastable Cobaltite Perovskite via Proton-Induced Filling of Oxygen Vacancy Channels. ACS Applied Materials & Interfaces, 2023, 15, 1574-1582.	4.0	5
74935	Theoretical prediction of two-dimensional BC2X (XÂ=ÂN, P, As) monolayers: ab initio investigations. Scientific Reports, 2022, 12, .	1.6	40
74936	Visualizing the atomic defects by scanning tunneling microscopy in the type-II Dirac semimetal NiTe₂. Physica Scripta, 2023, 98, 015020.	1.2	1
74937	First principles investigation of electronic structure, elasticity, thermodynamic properties and lattice thermal conductivity of Mg2V2O7. Computational and Theoretical Chemistry, 2023, 1220, 113988.	1.1	0
74938	Tailoring the Sb₂Se₃/rGO Heterointerfaces for Modulation of Electrocatalytic Hydrogen Evolution Performances in Acidic Media. ACS Applied Energy Materials, 2023, 6, 58-67.	2.5	5
74939	Ampere-level current density ammonia electrochemical synthesis using CuCo nanosheets simulating nitrite reductase bifunctional nature. Nature Communications, 2022, 13, .	5.8	119
74940	Finite-temperature investigation of homovalent and heterovalent substituted <mml:math xmlns:mml="http://www.w3.org/1998/Math/MathML"><mml:msub><mml:mi>BaTiO</mml:mi><mml:mn>3</mml:mn></mml:msub></mml:math> from first principles. Physical Review B, 2022, 106, .	1.1	2

#	Article	IF	Citations
74941	Cooperative Effects of Active Sites in the MTO Process: A Computational Study of the Aromatic Cycle in H-SSZ-13. ACS Catalysis, 2023, 13, 624-632.	5.5	4
74942	Significant Zero Thermal Expansion Via Enhanced Magnetoelastic Coupling in Kagome Magnets. Advanced Materials, 2023, 35, .	11.1	6
74943	Printable high-efficiency organic ionic photovoltaic materials discovered by high-throughput first-principle calculations. IScience, 2022, 25, 105639.	1.9	0
74944	Synthesis-on-substrate of quantum dot solids. Nature, 2022, 612, 679-684.	13.7	167
74945	Exploring strong and weak topological states on isostructural substitutions in TlBiSe$$_2$$. Scientific Reports, 2022, 12, .	1.6	2
74946	Selectivity of Electrochemical Ion Insertion into Manganese Dioxide Polymorphs. ACS Applied Materials & Interfaces, 2023, 15, 1513-1524.	4.0	1
74947	Defect Chemistry in Zn3V4(PO4)6. Batteries, 2023, 9, 5.	2.1	0
74948	Thermoelectric transport properties of orthorhombic RbBaX (X = Sb, Bi) with strong anharmonicity. Journal of Chemical Physics, 2023, 158, .	1.2	4
74949	Structural and electronic properties of two-dimensional titanium carbo-oxides. 2D Materials, 2023, 10, 015019.	2.0	1
74950	Modular divergent creation of dual-cocatalysts integrated semiconducting sulfide nanotriads for enhanced photocatalytic hydrogen evolution. Nano Research, 0, , .	5.8	0
74951	Facet-Dependent SERS Activity of Co3O4. International Journal of Molecular Sciences, 2022, 23, 15930.	1.8	4
74952	Three-dimensional Zn-based alloys for dendrite-free aqueous Zn battery in dual-cation electrolytes. Nature Communications, 2022, 13, .	5.8	47
74953	Effect of oxygen defects on microstructure, optical and vibrational properties of ScN films deposited on MgO substrate from experiment and first principles. Applied Surface Science, 2023, 615, 156203.	3.1	0
74954	Orbitalâ€Hybridizationâ€Driven Charge Density Wave Transition in CsV₃Sb₅ Kagome Superconductor. Advanced Materials, 2023, 35, .	11.1	11
74955	The Atomic Structure and Mechanical Properties of ZIF-4 under High Pressure: Ab Initio Calculations. Molecules, 2023, 28, 22.	1.7	5
74956	Impact of gadolinium doping into the frustrated antiferromagnetic lithium manganese oxide spinel. IScience, 2023, 26, 105869.	1.9	0
74957	Suppressed Internal Intrinsic Stress Engineering in Highâ€Performance Niâ€Rich Cathode Via Multilayered In Situ Coating Structure. Energy and Environmental Materials, 0, , .	7.3	1
74958	Theoretical Study of Dynamical and Electronic Properties of Noncentrosymmetric Superconductor NbReSi. Materials, 2023, 16, 78.	1.3	2

#	Article	IF	Citations
74959	Influence of the surface states on the nonlinear Hall effect in Weyl semimetals. Physical Review B, 2022, 106, .	1.1	4
74960	Self-assembled wide bandgap nanocoatings enabled outstanding dielectric characteristics in the sandwich-like structure polymer composites. Nano Convergence, 2022, 9, .	6.3	9
74961	Influence of interaction between organic cation and inorganic unit in bi-based hybrid perovskites for photoelectronic properties. Heliyon, 2022, 8, e12528.	1.4	0
74962	High-donor electrolyte endows graphite with anion-derived interphase to achieve stable K-storage. Science China Materials, 2023, 66, 932-943.	3.5	1
74963	Antibonding p-d and s-p Hybridization Induce the Optimization of Thermal and Thermoelectric Performance of MGeTe₃ (M = In and Sb). ACS Applied Energy Materials, 2022, 5, 15566-15577.	2.5	4
74964	Spatial Modulation and Thermal-Induced Spin Phase Transition on the Negative Thermal Expansion of ScF₃ with Metal Dopants. Chemistry of Materials, 2022, 34, 11039-11046.	3.2	0
74965	Spinâ€“Spin Interaction in Îµ-VOPO₄ through Doping Light Elements. Journal of Physical Chemistry C, 2022, 126, 21034-21039.	1.5	1
74966	Enhanced room-temperature NO2 sensing performance of mulberry-like Cu2O/CuO composites. Sensors and Actuators A: Physical, 2023, 350, 114136.	2.0	7
74967	Efficient Visibleâ€Lightâ€Initiated Dehydrogenative Coupling of Amines for Coproduction of Imines and Hydrogen over NiS/ZnIn₂S₄. Solar Rrl, 2023, 7, .	3.1	2
74968	Bulk generalized Dzyaloshinskii-Moriya interaction in <mml:math xmlns:mml="http://www.w3.org/1998/Math/MathML"><mml:mi mathvariant="script">PT</mml:mi></mml:math> -symmetric antiferromagnets. Physical Review B, 2022, 106, .	1.1	0
74969	Charge-transfer interface of insulating metal-organic frameworks with metallic conduction. Nature Communications, 2022, 13, .	5.8	5
74970	Engineering the Near-Surface Structure of WO₃ by an Amorphous Layer with Trivalent Ni and Self-Adapting Oxygen Vacancies for Efficient Photocatalytic and Photoelectrochemical Acidic Oxygen Evolution Reaction. ACS Applied Materials & Interfaces, 2022, 14, 54769-54780.	4.0	6
74971	Patterning the consecutive Pd ₃ to Pd ₁ on Pd ₂ Ga surface via temperature-promoted reactive metal-support interaction. Science Advances, 2022, 8, .	4.7	8
74972	Fusing 2D and 3D molecular graphs as unambiguous molecular descriptors for conformational and chiral stereoisomers. Briefings in Bioinformatics, 2023, 24, .	3.2	2
74973	Entropy-stabilized silicides: Expanding the B20 single-phase region from mono-silicide to high-entropy silicide. APL Materials, 2022, 10, .	2.2	4
74974	Photoelectric current generation in a monolayer MoSe₂â€“WS₂ lateral heterojunction. Journal Physics D: Applied Physics, 2023, 56, 065304.	1.3	2
74975	Deciphering phase evolution in complex metal oxide thin films via high-throughput materials synthesis and characterization. Nanotechnology, 2023, 34, 125701.	1.3	1
74976	Atomically dispersed golds on degradable zero-valent copper nanocubes augment oxygen driven Fenton-like reaction for effective orthotopic tumor therapy. Nature Communications, 2022, 13, .	5.8	11

#	Article	IF	Citations
74977	The super-exchange interaction between single-atom dimers and clusters increases reactive activity for hydrogen evolution reaction. Molecular Physics, 0, , .	0.8	0
74978	Multiferroic monolayers VOX (X = Cl, Br, I): tunable ferromagnetism via charge doping and ferroelastic switching. Chinese Physics B, 0, , .	0.7	0
74979	Effective six-band model and unconventional spin-singlet pairing in Kagome superconductor CsV₃Sb₅. New Journal of Physics, 2022, 24, 123016.	1.2	5
74980	Highly sensitive and self powered ultraviolet photo detector based on ZnO nanorods coated with TiO2. Sensors and Actuators A: Physical, 2023, 350, 114112.	2.0	9
74981	Correlated Rattling of Sodiumâ€Chains Suppressing Thermal Conduction in Thermoelectric Stannides. Advanced Materials, 0, , 2207646.	11.1	0
74982	Fast monitoring of organic dye degradation coupled with a colorimetric approach in a Ag-modified TiO2 nanotube photocatalytic system. Ceramics International, 2022, , .	2.3	6
74983	Electrocatalytic Reduction of CO2 to C1 Compounds by Zn-Based Monatomic Alloys: A DFT Calculation. Catalysts, 2022, 12, 1617.	1.6	6
74984	Interstitialâ€Electronâ€Induced Topological Molecular Crystals. , 2023, 2, .		1
74985	Entropy-driven multiscale defects enhance the thermoelectric properties of ZrCoSb-based half-Heusler alloys. Chemical Engineering Journal, 2023, 455, 140676.	6.6	10
74986	Helium-bearing superconductor at high pressure. Physical Review B, 2022, 106, .	1.1	3
74987	Giant and strain-tunable interfacial magnetic anisotropy in MgO-based magnetic heterostructures with heavy atoms insertion. Physica Scripta, 2023, 98, 015022.	1.2	0
74988	Integrating Interactive Noble Metal Single-Atom Catalysts into Transition Metal Oxide Lattices. Journal of the American Chemical Society, 2022, 144, 23214-23222.	6.6	55
74989	Tunable Schottky contact at the graphene/Janus SMoSiN₂ interface for high-efficiency electronic devices. Journal Physics D: Applied Physics, 2023, 56, 045306.	1.3	3
74990	Mechanisms and Kinetics of the Dehydrogenation of C₆â€“C₈ Cycloalkanes, Cycloalkenes, and Cyclodienes to Aromatics in H-MFI Zeolite Framework. ACS Catalysis, 2023, 13, 99-112.	5.5	5
74991	Atomic-Scale Insights into the Interfacial Polarization Effect in the InGaN/GaN Heterostructure for Solar Cells. ACS Applied Materials & Interfaces, 2022, 14, 55762-55769.	4.0	5
74992	Conductive C₃NS Monolayer with Superior Properties for K Ion Batteries. Journal of Physical Chemistry Letters, 2022, 13, 12055-12060.	2.1	4
74993	Porous heterostructure of graphene/hexagonal boron nitride as an efficient electrocatalyst for hydrogen peroxide generation. , 2023, 5, .		12
74994	Temperature-dependent mechanical properties of TaC and HfC. Journal of Materials Science, 2023, 58, 157-169.	1.7	4

#	Article	IF	Citations
74995	Impact of MeV Ni Ion-Implanted Defects in Band Modification of MgO. Journal of Electronic Materials, 2023, 52, 1937-1947.	1.0	3
74996	High-Throughput Computational Screening of Two-Dimensional Semiconductors. Journal of Physical Chemistry Letters, 2022, 13, 11581-11594.	2.1	51
74997	Manifesting Epoxide and Hydroxyl Groups in XPS Spectra and Valence Band of Graphene Derivatives. Nanomaterials, 2023, 13, 23.	1.9	3
74998	Unraveling the Defect-Dominated Broadband Emission Mechanisms in (001)-Preferred Two-Dimensional Layered Antimony-Halide Perovskite Film. Journal of Physical Chemistry Letters, 2022, 13, 11736-11744.	2.1	4
74999	Ternary superconducting hydrides stabilized via Th and Ce elements at mild pressures. Fundamental Research, 2022, , .	1.6	5
75000	Degradation of bisphenol A in an oxidation system constructed from Mo2C MXene and peroxymonosulfate. Npj Clean Water, 2022, 5, .	3.1	9
75001	Sugar moiety driven adsorption of nucleic acid on graphene quantum dots: Photophysical, thermodynamic and theoretical evidence. Journal of Molecular Liquids, 2023, 371, 121148.	2.3	1
75002	Impact of magnetic and antisite disorder on the vibrational densities of states in <mml:math xmlns:mml="http://www.w3.org/1998/Math/MathML"><mml:msub><mml:mi mathvariant="normal">Ni</mml:mi><mml:mn>2</mml:mn></mml:msub><mml:mi>MnSn</mml:mi></mml:math> Heusler alloys. Physical Review B, 2022, 106, .	1.1	7
75003	Hydrogen Storage in Partially Exfoliated Magnesium Diboride Multilayers. Small, 2023, 19, .	5.2	9
75004	Thermodynamic assessment within the Zrâ€“Bâ€“Câ€“O quaternary system. Journal of the American Ceramic Society, 2023, 106, 3127-3140.	1.9	1
75005	Unveiling surface stability and oxygen diffusion of rareâ€earth zirconate pyrochlores by density functional theory. Journal of the American Ceramic Society, 2023, 106, 2589-2600.	1.9	2
75006	Yukawa-Friedel-tail pair potentials for warm dense matter applications. Physical Review E, 2022, 106, .	0.8	4
75007	Insights into the formation of environmentally persistent free radicals during photocatalytic degradation processes of ceftriaxone sodium by ZnO/ZnIn2S4. Chemosphere, 2023, 314, 137618.	4.2	7
75008	Spectra stable deep-blue light-emitting diodes based on cryolite-like cerium(III) halides with nanosecond d-f emission. Science Advances, 2022, 8, .	4.7	11
75009	Dramatic Tuning of the Topological Hall Effect in A _x RhO ₂ (AÂ=ÂK, Rb, and Cs) Crystals by Electron Concentration or Cation. Advanced Functional Materials, 0, , 2211214.	7.8	0
75010	Effects of cesium addition on the properties of Na+-Î²/Î²"-alumina solid electrolyte. Journal of the European Ceramic Society, 2022, , .	2.8	0
75011	Enhanced Photoluminescence in Cd_xZn_{1â€“x}S Solid Solution by Suppressing Non-Radiative Recombination for White Light-Emitting Diodes. ACS Applied Nano Materials, 2023, 6, 61-75.	2.4	3
75012	Electronic and magnetic structure of ultrathin Co₉Se₈ nanosheets and Co₉Se₈ bulk from density functional theory calculations. Journal of Applied Physics, 2022, 132, 234303.	1.1	1

#	Article	IF	Citations
75013	Flipping of antiferromagnetic to superconducting states in pressurized quasi-one-dimensional manganese-based compounds. Physical Review B, 2022, 106, .	1.1	6
75014	Neighboring Site Synergies in Co-Defective Ruâ€“Co Spinel Oxide toward Oxygen Evolution Reaction. ACS Sustainable Chemistry and Engineering, 2023, 11, 290-299.	3.2	4
75015	Electronic properties and tunability in graphene/3D-InP mixed-dimensional van der Waals heterostructure. Frontiers of Physics, 2023, 18, .	2.4	1
75016	Fe Substitutions Improve Spectral Response of Bi₂WO₆-Based Photoanodes. ACS Applied Energy Materials, 2022, 5, 15333-15344.	2.5	5
75017	Highly Sensitive Tinâ€Lead Perovskite Photodetectors with Over 450 Days Stability Enabled by Synergistic Engineering for Pulse Oximetry System. Advanced Materials, 2023, 35, .	11.1	22
75018	CdSe_xS_{1â€“x} Alloyed Nanoplatelets with Continuously Tunable Blue-Green Emission. Chemistry of Materials, 2022, 34, 10361-10372.	3.2	3
75019	Phonon-limited mobility and quantum transport in fluorinated diamane MOSFETs from the first-principles calculations. Carbon, 2023, 204, 295-304.	5.4	1
75020	Magnetic proximity controlled Rashba and valley splittings in monolayer Janus ZrNX/VTe2 (X = Br, I) heterostructure. Physica E: Low-Dimensional Systems and Nanostructures, 2023, 148, 115616.	1.3	4
75021	Density Functional Theory Calculations of Equilibrium Mo Isotope Fractionation Factors among MoO_xS_{4â€“x}^{2â€“} Species in the Aqueous Phase by the ONIOM Method. ACS Earth and Space Chemistry, 2023, 7, 142-155.	1.2	0
75022	Nanoscale probing of surface potential landscape at MoS₂/BP van der Waals pâ€“n heterojunction. Nanotechnology, 2023, 34, 095702.	1.3	1
75023	Hydrogen-Doping-Enabled Boosting of the Carrier Mobility and Stability in Amorphous IGZTO Transistors. ACS Applied Materials & Interfaces, 2022, 14, 57016-57027.	4.0	7
75024	Unraveling the Mechanism of Structural Stability and Electrochemical Performance of N/Fâ€Modified Li ₂ FeSiO ₄ : A Firstâ€Principles Study. Advanced Theory and Simulations, 0, , 2200610.	1.3	0
75025	Computational Investigation of Site-Dependent Activation Barriers of Zeolite-Catalyzed Protolytic Cracking Reactions. ACS Catalysis, 2023, 13, 179-190.	5.5	2
75026	First Principles Investigation of the Effects of Chemical Short-Range Ordering Clusters on the Ideal Tensile Strength and Ductility of Aluminum Alloys. Metals, 2022, 12, 2143.	1.0	1
75029	Cluster Formation Effect of Water on Pristine and Defective MoS2 Monolayers. Nanomaterials, 2023, 13, 229.	1.9	1
75030	Strain-Enabled Control of Chiral Magnetic Structures in MnSeTe Monolayer. Chinese Physics Letters, 2023, 40, 017501.	1.3	3
75031	The bio-inspired heterogeneous single-cluster catalyst Ni100â€“Fe₄S₄ for enhanced electrochemical CO₂ reduction to CH₄. Nanoscale, 2023, 15, 2756-2766.	2.8	17
75032	Strong in-plane optical anisotropy in 2D van der Waals antiferromagnet VOCl. Nano Research, 2023, 16, 7481-7488.	5.8	1

#	Article	IF	Citations
75033	Fabrication of 3D hollow acorn-shell-like PtBi intermetallics via a surfactant-free pathway for efficient ethylene glycol electrooxidation. Nano Research, 2023, 16, 6560-6567.	5.8	8
75034	Coupled ferroelectricity and superconductivity in bilayer Td-MoTe2. Nature, 2023, 613, 48-52.	13.7	50
75035	In situ electrochemical Raman spectroscopy and ab initio molecular dynamics study of interfacial water on a single-crystal surface. Nature Protocols, 2023, 18, 883-901.	5.5	16
75036	Microscopic origin of the abnormal elastic behavior accompanying the superconducting transition in Nb3Sn crystals: An extended ab initio study. Journal of Alloys and Compounds, 2023, 941, 168891.	2.8	2
75037	Isolated Metalloid Tellurium Atomic Cluster on Nitrogenâ€Doped Carbon Nanosheet for Highâ€Capacity Rechargeable Lithiumâ€CO₂ Battery. Advanced Science, 2023, 10, .	5.6	8
75038	Neutron diffraction study on anomalous thermal expansion of CrB2. , 2023, 42, 100009.		3
75039	Effects of sintering condition on giant dielectric and nonlinear current-voltage properties of Na1/2Y1/2Cu3Ti3.975Ta0.025O12 ceramics. Heliyon, 2023, 9, e12946.	1.4	5
75040	Bonding states of hydrogen for supported Ti clusters on pristine and defective graphene. International Journal of Hydrogen Energy, 2023, , .	3.8	1
75041	Magnetocaloric Effect in Lightlyâ€Doped Fe₅Si₃ Single Crystals. , 2023, 2, .		0
75042	Delafossite as hole transport layer a new pathway for efficient perovskite-based solar sells: Insight from experimental, DFT and numerical analysis. Solar Energy, 2023, 250, 18-32.	2.9	29
75043	Strain data augmentation enables machine learning of inorganic crystal geometry optimization. Patterns, 2023, 4, 100663.	3.1	0
75044	Novel Janus 2D structures of XMoY (X, Y = O, S, Se, Te) composition for solar hydrogen production. International Journal of Hydrogen Energy, 2023, 48, 14226-14237.	3.8	5
75045	Defect Engineering of Green Phosphorene Nanosheets for Detecting Volatile Organic Compounds: A Computational Approach. ACS Applied Nano Materials, 2023, 6, 1496-1506.	2.4	5
75046	Suppressing non-radiative recombination in metal halide perovskite solar cells by synergistic effect of ferroelasticity. Nature Communications, 2023, 14, .	5.8	9
75047	Unusual isostructural Br/I substitution effect on the crystal structure and optical properties of hybrid halobismuthates. New Journal of Chemistry, 0, , .	1.4	0
75048	Pt nanoclusters on GaN nanowires for solar-asssisted seawater hydrogen evolution. Nature Communications, 2023, 14, .	5.8	23
75049	Biphenylene network as sodium ion battery anode material. Physical Chemistry Chemical Physics, 2023, 25, 4340-4348.	1.3	5
75050	Thiosemicarbazonecopper/Halido Systems: Structure and DFT Analysis of the Magnetic Coupling. Inorganics, 2023, 11, 31.	1.2	1

#	Article	IF	Citations
75051	Van der Waals Black Phosphorus/Bi₁₀O₆S₉ Heterojunction Harvesting Ambient Electric Field Energy for Enhanced Photoelectrochemical Sense. Journal of Physical Chemistry C, 2023, 127, 1229-1243.	1.5	2
75052	Development and Validation of Versatile Deep Atomistic Potentials for Metal Oxides. Journal of Physical Chemistry Letters, 2023, 14, 468-475.	2.1	8
75053	Thermoelectric properties of layered oxyselenides with 3d transition metal ions. Journal of the American Ceramic Society, 2023, 106, 2918-2929.	1.9	7
75054	2D Ladder Polyborane: An Ideal Dirac Semimetal with a Multi-Field-Tunable Band Gap. ACS Nano, 2023, 17, 1638-1645.	7.3	3
75055	Electronic and optical properties of Janus-like hexagonal monolayer materials of group IV-VI. Physical Review Materials, 2023, 7, .	0.9	2
75056	Supercritical fluid-assisted fabrication of C-doped Co3O4 nanoparticles based on polymer-coated metal salt nanoreactors for efficient enzyme-mimicking and glucose sensor properties. Nano Research, 2023, 16, 7431-7442.	5.8	7
75057	Aerophilic Triphase Interface Tuned by Carbon Dots Driving Durable and Flexible Rechargeable Zn-Air Batteries. Nano-Micro Letters, 2023, 15, .	14.4	26
75058	Altering Ligand Microenvironment of Atomically Dispersed CrN₄ by Axial Ligand Sulfur for Enhanced Oxygen Reduction Reaction in Alkaline and Acidic Medium. Small, 2023, 19, .	5.2	6
75059	Interface formation and Schottky barrier height for Y, Nb, Au, and Pt on Ge as determined by hard x-ray photoelectron spectroscopy. AIP Advances, 2023, 13, 015305.	0.6	0
75060	Preparation of Al Zn1-O resistive switching film by solâ€“gel method and its corrosion behavior in 3.5Âwt% NaCl solution. Applied Surface Science, 2023, 615, 156279.	3.1	1
75061	Self-diffusion coefficient and sound velocity of Fe-Ni-O fluid: Implications for the stratification of Earth's outer core. Physics of the Earth and Planetary Interiors, 2023, 335, 106983.	0.7	4
75062	Structural, magnetic and magnetocaloric properties in distorted RE ₂NiTiO₆ double perovskite compounds. JPhys Energy, 2023, 5, 014017.	2.3	6
75063	Effects of Alloying on the Interface Energy of the $$gamma ''$$-Phase in Nickel-Based Superalloys. Metallurgical and Materials Transactions A: Physical Metallurgy and Materials Science, 0, , .	1.1	0
75064	Combined Photoredox Catalysis for Value-Added Conversion of Contaminants at Spatially Separated Dual Active Sites. Research, 2023, 6, .	2.8	6
75065	Role of Water on Zeolite-Catalyzed Dehydration of Polyalcohols and EVOH Polymer. ACS Catalysis, 2023, 13, 1503-1512.	5.5	7
75066	Effective Interfaces between Fullerene Derivatives and CH₃NH₃PbI₃ to Improve Perovskite Solar Cell Performance. Journal of Physical Chemistry C, 2023, 127, 41-51.	1.5	0
75067	Effect of MoSe₂ nanoribbons with NW30 edge reconstructions on the electronic and catalytic properties by strain engineering. Physical Chemistry Chemical Physics, 2023, 25, 4297-4304.	1.3	5
75068	The role of single-atom Rh-dopants in the adsorption properties of OH and CO on stepped Ag(211) surfaces. Physical Chemistry Chemical Physics, 2023, 25, 4939-4949.	1.3	1

#	Article	IF	Citations
75069	CO ₂ adsorption on the (111) surface of fcc-structure high entropy alloys. Science and Technology of Advanced Materials Methods, 2023, 3, .	0.4	1
75070	The effect of dissolved chlorides on the photocatalytic degradation properties of titania in wastewater treatment. Physical Chemistry Chemical Physics, 2023, 25, 4161-4176.	1.3	4
75071	Mn₂P₂S₃Se₃: a two-dimensional Janus room-temperature antiferromagnetic semiconductor with a large out-of-plane piezoelectricity. Journal of Materials Chemistry C, 2023, 11, 2703-2711.	2.7	4
75072	Doubled strength and ductility via maraging effect and dynamic precipitate transformation in ultrastrong medium-entropy alloy. Nature Communications, 2023, 14, .	5.8	13
75073	Bicontinuous oxide heteroepitaxy with enhanced photoconductivity. Nature Communications, 2023, 14, .	5.8	0
75074	Thermodynamic Origin of the Photostability of the Two-Dimensional Perovskite PEA₂Pb(I_{1â€“x}Br_x)₄. ACS Energy Letters, 2023, 8, 943-949.	8.8	9
75075	Breathing Behaviour Modification of Gallium MILâ€53 Metalâ€“Organic Frameworks Induced by the Bridging Framework Inorganic Anion. Chemistry - A European Journal, 2023, 29, .	1.7	1
75076	Machine learning-driven synthesis of TiZrNbHfTaC5 high-entropy carbide. Npj Computational Materials, 2023, 9, .	3.5	8
75077	Changing the Interaction of a Single-Molecule Magnetic Moment with a Superconductor. Nano Letters, 2023, 23, 1622-1628.	4.5	1
75078	Nucleation of zeolitic imidazolate frameworks: from molecules to nanoparticles. Nanoscale, 2023, 15, 3504-3519.	2.8	2
75079	First-principles study on GeC/Î²-AsP heterostructure with type-II band alignment for photocatalytic water splitting. Applied Surface Science, 2023, 617, 156298.	3.1	7
75080	Magnetic molecular orbitals in MnSi. Science Advances, 2023, 9, .	4.7	2
75081	Toward an efficient f-in-core/f-in-valence switchable description for DFTB calculations of Ce 4f states in ceria. Journal of Chemical Physics, 2023, 158, .	1.2	1
75082	The pressure and temperature evolution of the Ca₃V₂O₈ crystal structure using powder X-ray diffraction. CrystEngComm, 2023, 25, 1240-1251.	1.3	5
75083	Nitrogen-Doped Carbon Sponge Derived from the Self-Assembly of a Poly(amic acid) for High Performance Oxygen Reduction Reaction. New Journal of Chemistry, 0, , .	1.4	2
75084	Heteroatom-Doped Nickel Sulfide for Efficient Electrochemical Oxygen Evolution Reaction. Energies, 2023, 16, 881.	1.6	13
75085	Synergistic Catalytic Effect of Ag and MgO Nanoparticles Supported on Defective BN Surface in CO Oxidation Reaction. Materials, 2023, 16, 470.	1.3	0
75086	Prediction of monolayer <mml:math xmlns:mml="http://www.w3.org/1998/Math/MathML"><mml:mrow><mml:mi>Fe</mml:mi><mml:msub><mml:mi mathvariant="normal">P</mml:mi><mml:mn>4</mml:mn></mml:msub></mml:mrow></mml:math> with intrinsic half-metal ferrimagnetism above room temperature. Physical Review B, 2023, 107, .	1.1	10

#	Article	IF	Citations
75087	Reversible doping polarity and ultrahigh carrier density in two-dimensional van der Waals ferroelectric heterostructures. Frontiers of Physics, 2023, 18, .	2.4	4
75088	Rational Design of a Super-Alkali Compound with Reversible Photoluminescence. Inorganic Chemistry, 2023, 62, 1054-1061.	1.9	0
75089	Substitutional effect of Ti-based AB2 hydrogen storage alloys: A density functional theory study. International Journal of Hydrogen Energy, 2023, 48, 13227-13235.	3.8	5
75090	Equilibrium Shapes of Ag, Ni, and Ir Nanoparticles under CO Conditions. Catalysts, 2023, 13, 146.	1.6	0
75091	Direct Visualization of Localized Vibrations at Complex Grain Boundaries. Advanced Materials, 2023, 35, .	11.1	7
75092	Prediction of one-dimensional CrN nanostructure as a promising ferromagnetic half-metal. Chinese Physics B, 0, , .	0.7	0
75093	Computational Studies of Auto-Active van der Waals Interaction Molecules on Ultra-Thin Black-Phosphorus Film. Molecules, 2023, 28, 681.	1.7	2
75094	First principles study on stability of base and precious metals pentlandite-like compounds. Theoretical Chemistry Accounts, 2023, 142, .	0.5	0
75095	Evolution of Weyl-like semi-metallicity in an all-sp2 carbon allotrope. Journal of Physics and Chemistry of Solids, 2023, 176, 111229.	1.9	0
75096	Ab Initio Theoretical Study of DyScO3 at High Pressure. Crystals, 2023, 13, 165.	1.0	0
75097	Investigating the factors that influence sacrificial hydrogen evolution activity for three structurally-related molecular photocatalysts: thermodynamic driving force, excited-state dynamics, and surface interaction with cocatalysts. Physical Chemistry Chemical Physics, 0, , .	1.3	1
75098	Unexpected Enhanced Thermal Conductivity of Ga_xIn_{1â€“x}Sb Ternary Alloys. Journal of Physical Chemistry C, 2023, 127, 3246-3255.	1.5	2
75099	Large enhancement of thermal conductivity of aluminum-reduced graphene oxide composites prepared by a single-step method. Oxford Open Materials Science, 2023, 3, .	0.5	1
75100	Intrinsic Defects and the Inducing Conduction Mechanism of Langasite-Type High-Temperature Piezoelectric Crystals. ACS Applied Materials & Interfaces, 2023, 15, 3152-3162.	4.0	1
75101	Screening chloride Liâ€ion conductors using highâ€throughput forceâ€field molecular dynamics. Journal of the American Ceramic Society, 2023, 106, 3035-3044.	1.9	3
75102	Bonding iron chalcogenides in a hierarchical structure for high-stability sodium storage. Journal of Colloid and Interface Science, 2023, 637, 251-261.	5.0	5
75103	Excess <mml:math xmlns:mml="http://www.w3.org/1998/Math/MathML" display="inline" overflow="scroll"><mml:msub><mml:mrow><mml:mi>Pb</mml:mi><mml:mi>Br</mml:mi></mml:mrow><mml:mn>2</mml:mn></mml: Passivation of Large <mml:math xmlns:mml="http://www.w3.org/1998/Math/MathML" display="inline" overflow="scroll"><mml:mrow><mml:mi>Pb</mml:mi><mml:mi mathvariant="normal">S</mml:mi></mml:mrow></mml:math> Colloidal Quantum Dots to Reduce Dark-Current Density for Near-Infrared Detection. Physical Review Applied, 2023, 19, .	1.5	7
75104	Firstâ€principles Density Functional Theory Elucidation of the Hydrogen Evolution Reaction on TMâ€promoted TiC₂ (TM=Fe, Co, Ni, Cu, Ru, Rh, Pd, Ag, Os, Ir, Pt, and Au). ChemPhysChem, 2023, 24, .	1.0	2

#	Article	IF	Citations
75105	Structural and Luminescence Properties of Cu(I)X-Quinoxaline under High Pressure (X = Br, I). Crystals, 2023, 13, 100.	1.0	0
75106	Role of Local Structural Distortions on the Origin of j = 1/2 Pseudo-Spin State in Sodium Iridate. ACS Applied Electronic Materials, 0, , .	2.0	0
75107	Superior Performances of Selfâ€Driven Nearâ€Infrared Photodetectors Based on the SnTe:Si/Si Heterostructure Boosted by Bulk Photovoltaic Effect. Small, 2023, 19, .	5.2	1
75108	Large Magnetoresistance and Perfect Spin-Injection Efficiency in Two-Dimensional Strained <mml:math xmlns:mml="http://www.w3.org/1998/Math/MathML" display="inline" overflow="scroll"><mml:msub><mml:mi>VSi</mml:mi><mml:mn>2</mml:mn></mml:msub><mml:msub><mml:mi mathvariant="normal">N</mml:mi><mml:mn>4</mml:mn></mml:msub></mml:math> -Based Room-Temperature Magnetic-Tunnel-Junction Devices. Physical Review Applied, 2023, 19, .	1.5	3
75109	Multi-functional application potential of Ruddlesden-Popper perovskite-based heterostructure PtSe2/Cs2PbI4 with tunable electronic properties. Journal of Physics Condensed Matter, 0, , .	0.7	0
75110	Eutectic Mixture Formation and Relaxation Dynamics of Coamorphous Mixtures of Two Benzodiazepine Drugs. Pharmaceutics, 2023, 15, 196.	2.0	1
75111	Dodecagonal Zinc Oxide (<mml:math xmlns:mml="http://www.w3.org/1998/Math/MathML") Tj ETQq0 0 0 rgBT /Overlock 10 Tf 50 522	1.5	5
75112	Detection of Toxic Gases. Physical Review Applied, 2023, 19, . Two-Dimensional Ferroelasticity and Domain-Wall Flexoelectricity in HgX₂ (X = Br or I) Monolayers. Journal of Physical Chemistry Letters, 2023, 14, 420-429.	2.1	2
75113	Amide cluster induced and hydrogen bonding regulated luminescence of linear aliphatic polyamide 1212 with a long alkane chain. Polymer Chemistry, 2023, 14, 573-586.	1.9	3
75114	Theoretical study on an oxygen-modified phosphorene autogenous Z-scheme heterojunction for hydrogen evolution. Chemical Communications, 2023, 59, 1517-1520.	2.2	2
75115	Magnon corner states in twisted bilayer honeycomb magnets. Physical Review B, 2023, 107, .	1.1	11
75116	Giant and tunable Rashba spin splitting and Quantum Spin Hall Effect in H-Pb-Cl. Wuli Xuebao/Acta Physica Sinica, 2023, .	0.2	0
75117	Design of SA-FLP Dual Active Sites for Nonoxidative Coupling of Methane. ACS Catalysis, 2023, 13, 1299-1309.	5.5	10
75118	Advancing Electrode Properties through Functionalization for Solid Oxide Cells Application: A Review. Chemistry - an Asian Journal, 2023, 18, .	1.7	3
75119	Enhanced Reactivity of Magic-Sized Inorganic Clusters by Engineering the Surface Ligand Networks. Chemistry of Materials, 2023, 35, 700-708.	3.2	4
75120	Piezoelectric Response of Plastic Ionic Molecular Crystals: Role of Molecular Rotation. Crystal Growth and Design, 2023, 23, 729-740.	1.4	6
75121	Van der Waals Engineering of Ultrafast Carrier Dynamics in Magnetic Heterostructures. Nano Letters, 2023, 23, 414-421.	4.5	5
75122	Electron magnetic moment of transient chiral phonons in <mml:math xmlns:mml="http://www.w3.org/1998/Math/MathML"><mml:msub><mml:mi>KTaO</mml:mi><mml:mn>3</mml:mn></mml:msub> Physical Review B, 2023, 107, .	1.1	9

#	Article	IF	Citations
75123	Non-epitaxial single-crystal 2D material growth by geometric confinement. Nature, 2023, 614, 88-94.	13.7	36
75124	Investigation on adsorption of sodium fluoro-aluminates on graphite by density functional theory. Journal of Molecular Liquids, 2023, 373, 121252.	2.3	0
75125	The role of alloying carbon on thermodynamic properties of ZrN: A first principle study. Solid State Communications, 2023, 361, 115076.	0.9	4
75126	Theoretical Study of the Dissolution Mechanism at the FeCr2O4-Slag Interface: Density Functional Theory and Molecular Dynamics Simulations. Jom, 2023, 75, 1460-1470.	0.9	1
75127	Heptacoordinate transition-metal-decorated metallo-borospherenes and multiple-helix metallo-boronanotubes. Nanoscale, 0, , .	2.8	1
75128	High-temperature oxidation mechanism of ZrCoSb-based half-Heusler thermoelectric compounds. Journal of Materials Science and Technology, 2023, 148, 242-249.	5.6	4
75129	Impact of single Pt atom adsorption on fundamental properties of blue phosphorene and its activity toward hydrogen evolution reaction. International Journal of Hydrogen Energy, 2023, 48, 12321-12332.	3.8	5
75130	Size Effect of Electrical and Optical Properties in Cr2+:ZnSe Nanowires. Nanomaterials, 2023, 13, 369.	1.9	0
75131	Effects of Al and La elements on mechanical properties of CoNiFe0.6Cr0.6 high-entropy alloys: a first-principles study. Journal of Materials Research and Technology, 2023, 23, 1130-1140.	2.6	25
75132	Wide-Temperature Tunable Phonon Thermal Switch Based on Ferroelectric Domain Walls of Tetragonal KTN Single Crystal. Nanomaterials, 2023, 13, 376.	1.9	0
75133	Cuâ€Ðoped MoSi₂N₄ Monolayer as a Potential NH₃ Sensor. ChemPhysChem, 2023, 24, .	1.0	5
75134	Controlled-Release Mechanism Regulates Rhodium Migration and Size Redistribution Boosting Catalytic Methane Conversion. ACS Catalysis, 2023, 13, 1197-1206.	5.5	6
75135	A Novel Diamagnetic Insulating Quadruple Perovskite Oxide YCu₃Rh₄O₁₂. Materials Transactions, 2023, , .	0.4	1
75136	Interaction Energy and Isosteric Heat of Adsorption between Hydrogen and Magnesium Diboride. Physical Chemistry Chemical Physics, 0, , .	1.3	1
75137	On Structural and Magnetic Properties of Substituted SmCo5 Materials. Materials, 2023, 16, 547.	1.3	6
75138	Prediction of Novel Ultrahard Phases in the Bâ€“Câ€“N System from First Principles: Progress and Problems. Materials, 2023, 16, 886.	1.3	11
75139	Halogen-Doped Chevrel Phase Janus Monolayers for Photocatalytic Water Splitting. Nanomaterials, 2023, 13, 368.	1.9	1
75140	Ferroelectric higher-order topological insulator in two dimensions. Physical Review B, 2023, 107, .	1.1	5

#	Article	IF	Citations
75141	Synthesis of metal cation doped nanoparticles for single atom alloy catalysts using spontaneous cation exchange. Journal of Materials Chemistry A, 0, , .	5.2	1
75142	Compound Defects in Halide Perovskites: A First-Principles Study of CsPbI₃. Journal of Physical Chemistry C, 2023, 127, 1189-1197.	1.5	5
75143	Got Coke? Self-Limiting Poisoning Makes an Ultra Stable and Selective Sub-Nano Cluster Catalyst. ACS Catalysis, 2023, 13, 1533-1544.	5.5	5
75144	Experimental and theoretical studies of effective piezoelectric coefficients of 2-2 connectivity AlN/AlScN composite piezoelectric films. Composites Communications, 2023, 38, 101502.	3.3	1
75145	Spin-dependent plasma frequency from all-electron ab initio calculations including spin-orbit coupling. Physical Review B, 2023, 107, .	1.1	0
75146	Layered Metal Oxide Nanosheets with Enhanced Interlayer Space for Electrochemical Deionization. Advanced Materials, 0, , 2210871.	11.1	15
75147	Coherent Phononâ€Induced Gigahertz Optical Birefringence and Its Manipulation in SrTiO₃. Advanced Science, 2023, 10, .	5.6	3
75148	Metastable Cubic Structure Exceeds Capacity Limit of Antifluorite Li₅FeO₄ Cathode Using Small Polarized Oxygen Redox. Advanced Energy Materials, 2023, 13, .	10.2	6
75149	Long distance bimetallic site in crystal with relay metal-N-N-metal mechanism and new descriptors for electrocatalytic nitrogen reduction reaction. Applied Catalysis A: General, 2023, 652, 119030.	2.2	5
75150	Non-equilibrium kinetics for improving ionic conductivity in garnet solid electrolyte. Materials Horizons, 2023, 10, 1324-1331.	6.4	1
75151	N-doped carbon nanotubes with high amount of graphitic nitrogen as an excellent electrocatalyst for water splitting in alkaline solution. Journal of Electroanalytical Chemistry, 2023, 931, 117160.	1.9	3
75152	Probing how Ti- and Nb-substitution affect the stability and improve the electrochemical performance of Î²- and Îµ-LiVOPO₄. Journal of Materials Chemistry A, 0, , .	5.2	0
75153	Unraveling the Surface State Evolution of IrO₂ in Ethane Chemical Looping Oxidative Dehydrogenation. ACS Catalysis, 2023, 13, 1381-1399.	5.5	8
75154	Systematic DFT+U and Quantum Monte Carlo Benchmark of Magnetic Two-Dimensional (2D) CrX₃ (X = I, Br, Cl, F). Journal of Physical Chemistry C, 2023, 127, 1176-1188.	1.5	10
75155	Large Spin Hall Conductivity and Excellent Hydrogen Evolution Reaction Activity in Unconventional PtTe _{1.75} Monolayer. Research, 2023, 6, .	2.8	1
75156	Tunable magnetic and electronic properties of armchair BeN₄ nanoribbons. Physical Chemistry Chemical Physics, 2023, 25, 5029-5036.	1.3	2
75157	Co and Ni single sites on the (111)_n surface of Î³-Al₂O₃ â€“ a periodic boundary DFT study. , 2023, 1, 117-128.		2
75158	Insight into Nitrogen Doped Waste-Tire Carbon for Radical and Nonradical Oxidation via a Probe-Based Kinetic Model. ACS ES&T Water, 2023, 3, 129-138.	2.3	1

#	Article	IF	Citations
75159	Two-dimensional ruthenium boride: a Dirac nodal loop quantum electrocatalyst for efficient hydrogen evolution reaction. Journal of Materials Chemistry A, 2023, 11, 3717-3724.	5.2	4
75160	Optical activity of solids from first principles. Physical Review B, 2023, 107, .	1.1	13
75161	The structure and optical properties of semiconductor nitrides MgSiN₂, MgGeN₂, ZnSiN₂, ZnGeN₂. Proceedings of the National Academy of Sciences of Belarus Physics and Mathematics Series, 2023, 58, 424-430.	0.1	0
75162	Blocking the reverse reactions of overall water splitting on a Rh/GaNâ€“ZnO photocatalyst modified with Al2O3. Nature Catalysis, 2023, 6, 80-88.	16.1	41
75163	Moisture-Induced reversible structure conversion of Zero-Dimensional organic cuprous bromide hybrids for multiple photoluminescent anti-Counterfeiting, information encryption and rewritable luminescent paper. Chemical Engineering Journal, 2023, 458, 141436.	6.6	26
75164	Remote control of spin polarization of topological corner states. Physical Review B, 2023, 107, .	1.1	1
75165	The interplay of organic spacer and small cation for efficient Dionâ€Jacobson perovskite solar cells. Solar Rrl, 0, , .	3.1	4
75166	Fully Flexible MXene-based Gas Sensor on Paper for Highly Sensitive Room-Temperature Nitrogen Dioxide Detection. ACS Sensors, 2023, 8, 103-113.	4.0	40
75167	Electronic and topological properties of kagome lattice LaV3Si2. Tungsten, 0, , .	2.0	0
75168	Pressure-induced charge orders and their postulated coupling to magnetism in hexagonal multiferroic LuFe2O4. Npj Quantum Materials, 2023, 8, .	1.8	5
75169	Vibrational properties of TiVC-based Mxenes by first-principles calculation and experiments. Materials Today Communications, 2023, 34, 105396.	0.9	0
75170	Formation of Amorphous Carbon Multiâ€Walled Nanotubes from Random Initial Configurations. Physica Status Solidi (B): Basic Research, 2023, 260, .	0.7	8
75171	Critical Role of Surface Termination of Sapphire Substrates in Crystallographic Epitaxial Growth of MoS₂ Using Inorganic Molecular Precursors. ACS Nano, 2023, 17, 1196-1205.	7.3	10
75172	Energy- and carbon-efficient CO2/CO electrolysis to multicarbon products via asymmetric ion migrationâ€“adsorption. Nature Energy, 2023, 8, 179-190.	19.8	41
75173	CO₂electroreduction performance of PtS₂supported single transition metal atoms: a theoretical study. Physical Chemistry Chemical Physics, 2023, 25, 4773-4779.	1.3	5
75174	Screening rareâ€earth aluminates as promising thermal barrier coatings by highâ€throughput firstâ€principles calculations. Journal of the American Ceramic Society, 2023, 106, 3089-3102.	1.9	1
75175	A semiconductor Sc₂S₃ monolayer with ultrahigh carrier mobility for UV blocking filter application. Physical Chemistry Chemical Physics, 2023, 25, 5550-5558.	1.3	1
75176	Widely Tunable Berry Curvature in the Magnetic Semimetal Cr₁₊_{Î´}Te₂. Advanced Materials, 2023, 35, .	11.1	11

#	Article	IF	Citations
75177	Anharmonicity in bcc refractory elements: A detailed ab initio analysis. Physical Review B, 2023, 107, .	1.1	7
75178	Discovery of Clustered-P1 Borophene and Its Application as the Lightest High-Performance Transistor. ACS Applied Materials & Interfaces, 2023, 15, 3182-3191.	4.0	8
75179	ZIF-derived non-bonding Co/Zn coordinated hollow carbon nitride for enhanced removal of antibiotic contaminants by peroxymonosulfate activation: Performance and mechanism. Applied Catalysis B: Environmental, 2023, 325, 122401.	10.8	29
75180	Ultrabroadband plasmon driving selective photoreforming of methanol under ambient conditions. Proceedings of the National Academy of Sciences of the United States of America, 2023, 120, .	3.3	2
75181	Oxygen vacancy-engineered titanium-based perovskite for boosting H ₂ O activation and lower-temperature hydrolysis of organic sulfur. Proceedings of the National Academy of Sciences of the United States of America, 2023, 120, .	3.3	12
75182	Znâ€“Y dual atomic site catalyst featuring metalâ€“metal interactions as a nanozyme with peroxidase-like activity. Journal of Materials Chemistry A, 2023, 11, 2326-2333.	5.2	5
75183	Coupled oxygen desorption and structural reconstruction accompanying reduction of copper oxide. Journal of Chemical Physics, 2023, 158, .	1.2	2
75184	Impact of H₂O on the Microscopic Oxidation Mechanism of Lollingite: Experimental and Theoretical Analyses. Langmuir, 0, , .	1.6	0
75185	Sintering temperatureâ€“induced structural transition in LaCrO₃â€based conducting oxides synthesized from nanoâ€powders. Journal of the American Ceramic Society, 2023, 106, 3209-3219.	1.9	1
75186	Ultrathin quantum light source with van der Waals NbOCl2 crystal. Nature, 2023, 613, 53-59.	13.7	56
75187	Amino-tethering synthesis strategy toward highly accessible sub-3-nm L10-PtM catalysts for high-power fuel cells. Matter, 2023, 6, 963-982.	5.0	12
75188	Adsorption of water and organic solvents on the calcite <mml:math xmlns:mml="http://www.w3.org/1998/Math/MathML" altimg="si1.svg"><mml:mrow><mml:mo stretchy="false">[</mml:mo><mml:mn>10</mml:mn><mml:mover accent="true"><mml:mrow><mml:mn>1</mml:mn></mml:mrow><mml:mrow><mml:mo stretchy="false">Â¯</mml:mo></mml:mrow></mml:mover><mml:mn>4</mml:mn><mml:mo stretchy="false">]</mml:mo></mml:mrow></mml:math> surface: Implications for marble conservation	3.1	2
75189	Cytotoxicity and First-principles Calculations of ZnS:6.25%Br Quantum Dots and Their Effect on the Growth of Aspergillus oryzae. Nano, 2023, 18, .	0.5	1
75190	Superconductivity in the Li-B-C system at 100 GPa. Physical Review B, 2023, 107, .	1.1	4
75191	Enhancing the interfacial stability of all-solid-state high-energy sodium-ion batteries by coating materials: First principles calculations. Applied Surface Science, 2023, 616, 156479.	3.1	2
75192	White Light Emission from Single-Component Cs₇Cd₃Br₁₃:Pb²⁺,Mn²⁺ Crystals with High Quantum Efficiency and Enhanced Thermodynamic Stability. Chemistry of Materials, 2023, 35, 773-782.	3.2	14
75193	Approaching the quantum limit in two-dimensional semiconductor contacts. Nature, 2023, 613, 274-279.	13.7	100
75194	Perspective on ultrathin layered Ni-doped MoS2 hybrid nanostructures for the enhancement of electrochemical properties in supercapacitors. Journal of Energy Chemistry, 2023, 80, 335-349.	7.1	21

#	Article	IF	Citations
75195	Energetics and Kinetics of Hydrogen Electrosorption on a Graphene-Covered Pt(111) Electrode. Jacs Au, 2023, 3, 526-535.	3.6	5
75196	Periodic plane-wave electronic structure calculations on quantum computers. Materials Theory, 2023, 7, .	2.2	1
75197	In-plane charged domain walls with memristive behaviour in a ferroelectric film. Nature, 2023, 613, 656-661.	13.7	33
75198	Differences in solvation thermodynamics of oxygenates at Pt/Al2O3 perimeter versus Pt(111) terrace sites. IScience, 2023, 26, 105980.	1.9	1
75199	Octahedral rotations and defect-driven metallicity at the (001) surface of <mml:math xmlns:mml="http://www.w3.org/1998/Math/MathML"><mml:msub><mml:mrow><mml:mi>CaTiO</mml:mi></mml:mrow><mml:mn>3< Physical Review B, 2023, 107, .	1.1	1
75200	Origin of Vanadium Site Sequential Oxidation in K_xVPO₄F_{1â€“y}O_y. Chemistry of Materials, 2023, 35, 617-627.	3.2	2
75201	Emergent Transitions: Discord between Electronic and Chemical Pressure Effects in the REAl₃ (RE = Sc, Y, Lanthanides) Series. Inorganic Chemistry, 2023, 62, 4405-4416.	1.9	2
75202	Flattening bent Janus nanodiscs expands lattice parameters. CheM, 2023, 9, 948-962.	5.8	3
75203	Enhancement of CO adsorption energy on defective graphene-supported Cu13 cluster and prediction with an induction energy model. Applied Surface Science, 2023, 615, 156368.	3.1	6
75204	Intercalation on Transition Metal Trichalcogenides via a Quasiâ€Amorphous Phase with 1D Order. Advanced Functional Materials, 0, , 2208702.	7.8	1
75205	A class of Ga-Al-P-based compounds with disordered lattice as advanced anode materials for Li-ion batteries. Journal of Energy Chemistry, 2023, 79, 12-21.	7.1	4
75206	Renormalizing Antiferroelectric Nanostripes in Î²â€²-In₂Se₃ via Optomechanics. Journal of Physical Chemistry Letters, 2023, 14, 677-684.	2.1	4
75207	The Atomic Drill Bit: Precision Controlled Atomic Fabrication of 2D Materials. Advanced Materials, 2023, 35, .	11.1	4
75208	Novel electronic and magnetic features in XC (X = Si and Ge) monolayers induced by doping with group-VA atoms. New Journal of Chemistry, 2023, 47, 2787-2796.	1.4	3
75209	Superior Limit of Light-Absorption Improvement in Two-Dimensional Haeckelite GaN-ZnO by Nonadiabatic Molecular Dynamics Simulation. Journal of Physical Chemistry Letters, 2023, 14, 663-669.	2.1	3
75210	Corrosive Influence of Carbon Dioxide on Crack Initiation in Quartz: Comparison with Liquid Water and Vacuum Environments. Journal of Geophysical Research: Solid Earth, 0, , .	1.4	1
75211	Evolution of static charge density wave order, amplitude mode dynamics, and suppression of Kohn anomalies at the hysteretic transition in <mml:math xmlns:mml="http://www.w3.org/1998/Math/MathML"><mml:msub><mml:mrow><mml:mi>EuTe</mml:mi></mml:mrow><mml:mn>4</ Physical Review B, 2023, 107, .	1.1	3
75212	Control over Berry Curvature Dipole with Electric Field in <mml:math xmlns:mml="http://www.w3.org/1998/Math/MathML" display="inline"><mml:mrow><mml:msub><mml:mrow><mml:mi>WTe</mml:mi></mml:mrow><mml:mrow><mml:mn>2</mml:mn> Physical Review Letters, 2023, 130, .	2.9	11

#	Article	IF	Citations
75213	Highly efficient hydrogen storage of a Sc decorated biphenylene monolayer near ambient temperature: ab initio simulations. Sustainable Energy and Fuels, 2023, 7, 996-1010.	2.5	7
75214	Phase-controlled van der Waals growth of wafer-scale 2D MoTe2 layers for integrated high-sensitivity broadband infrared photodetection. Light: Science and Applications, 2023, 12, .	7.7	69
75215	Effect of osmium substitution on structural, electronic, mechanical, and thermodynamic properties of Wâ€“Os alloys: A first-principles study. Journal of Materials Research, 2023, 38, 883-893.	1.2	1
75216	Dynamic semiconductor-electrolyte interface for sustainable solar water splitting over 600 hours under neutral conditions. Science Advances, 2023, 9, .	4.7	54
75217	First-principles calculations of monolayered Al₂Te₅: a promising 2D donor semiconductor with ultrahigh visible light harvesting. Nanoscale, 2023, 15, 2578-2585.	2.8	3
75218	Subnanometric Pt clusters supported on MgO-incorporated porous carbon as efficient metalâ€“base bifunctional catalysts for reductive heterocyclization reactions. Green Chemistry, 2023, 25, 1107-1119.	4.6	4
75219	Defect physics in 2D monolayer I-VII semiconductor AgI. Materials Today Nano, 2023, 22, 100304.	2.3	3
75220	Three-Dimensional Silicene-Based Materials: A Universal Anode for Monovalent and Divalent Ion Batteries. Journal of Physical Chemistry C, 2023, 127, 1198-1208.	1.5	8
75221	Post cobalt doping and defect engineering of NbSSe for efficient hydrogen evolution reaction. Journal of Materials Chemistry A, 2023, 11, 2690-2697.	5.2	7
75222	A customized strategy to design intercalation-type Li-free cathodes for all-solid-state batteries. National Science Review, 2023, 10, .	4.6	6
75223	Exploring the Potential Energy Surface of Pt6 Sub-Nano Clusters Deposited over Graphene. International Journal of Molecular Sciences, 2023, 24, 870.	1.8	1
75224	Optoelectronic and magnetic properties of transition metals-adsorbed GeC monolayer. Modern Physics Letters B, 0, , .	1.0	0
75225	High-pressure <mml:math xmlns:mml="http://www.w3.org/1998/Math/MathML"><mml:mrow><mml:mi>h</mml:mi><mml:mi>P</mml:mi><mml:mn>3</mml:mn> yttrium allotrope with <mml:math xmlns:mml="http://www.w3.org/1998/Math/MathML"><mml:mrow><mml:mi>Ca</mml:mi><mml:msub><mml:mi>Hg</mml:mi><mml:mi><mml:n -type structure as a prototype of the <mml:math xmlns:mml="http://www.w3.org/1998/Math/MathML"><mml:mrow><mml:mi>h</mml:mi><mml:mi>P</mml:mi><mml:mn>3</mml:mn>	1.1	1
75226	Extraordinary Acceleration of an Electrophilic Reaction Driven by the Polar Surface of 2D Aluminosilicate Nanosheets. Small, 2023, 19, .	5.2	3
75227	Observation of spin-momentum locked surface states in amorphous Bi2Se3. Nature Materials, 2023, 22, 200-206.	13.3	25
75228	First-Principles Prediction of Structure and Properties of the Cu2TeO6 Monolayer. Applied Sciences (Switzerland), 2023, 13, 815.	1.3	1
75229	The kinetics and potential dependence of the hydrogen evolution reaction optimized for the basal-plane Te vacancy site of MoTe2. Chem Catalysis, 2023, 3, 100489.	2.9	4
75230	Synergistically boosting the anchoring effect and catalytic activity of MXenes as bifunctional electrocatalysts for sodiumâ€“sulfur batteries by single-atom catalyst engineering. Nanoscale, 2023, 15, 2747-2755.	2.8	7

#	Article	IF	Citations
75231	Toward the design of ultrahigh-entropy alloys via mining six million texts. Nature Communications, 2023, 14, .	5.8	18
75232	Stabile fluoro-benzene-based spacer for lead-free Dionâ€“Jacobson perovskites. RSC Advances, 2023, 13, 1185-1193.	1.7	3
75233	Effective electronic band structure of monoclinic Î²â^'(AlxGa1â^'x)2O3 alloy semiconductor. AIP Advances, 2023, 13, 015101.	0.6	1
75234	Atomic-displacement threshold energies and defect generation in irradiated Î²-Ga2O3: A first-principles investigation. Journal of Applied Physics, 2023, 133, .	1.1	10
75235	On the atomistic origin of the polymorphism and the dielectric physical properties of beryllium oxide. Journal of Computational Chemistry, 0, , .	1.5	2
75236	Improving the Catalytic Performance of the Hydrogen Evolution Reaction of Î±â€MoB₂ via Rational Doping by Transition Metal Elements. ChemPhysChem, 2023, 24, .	1.0	1
75237	Improved Defect Tolerance and Charge Carrier Lifetime in Tinâ€“Lead Mixed Perovskites: Ab Initio Quantum Dynamics. Journal of Physical Chemistry Letters, 2023, 14, 499-507.	2.1	6
75238	Heterointerface and Tensile Strain Effects Synergistically Enhances Overall Waterâ€Splitting in Ru/RuO₂ Aerogels. Small, 2023, 19, .	5.2	36
75239	A First-principles investigation of the structural and electronic properties of Two-dimensional Hf2CSe2. Materials Today: Proceedings, 2023, , .	0.9	0
75240	A novel S-type CsxWO3/BiOI heterojunction photocatalyst constructed in graphene aerogel with high degradation efficiency for enrofloxacin: Degradation mechanism and DFT calculation. Journal of Environmental Chemical Engineering, 2023, , 109301.	3.3	2
75241	A DFT Study of Alkaline Earth Metal-Doped FAPbI3 (111) and (100) Surfaces. Molecules, 2023, 28, 372.	1.7	0
75242	Origin of anomalously stabilizing ice layers on methane gas hydrates near rock surface. Physical Chemistry Chemical Physics, 2023, 25, 6636-6652.	1.3	3
75243	Half-metallic antiferromagnets induced by non-magnetic adatoms on bilayer silicene. RSC Advances, 2023, 13, 2404-2410.	1.7	1
75244	Edge reconstruction of 2D-Xene (X=Si, Ge, Sn) zigzag nanoribbons. Physica E: Low-Dimensional Systems and Nanostructures, 2023, , 115655.	1.3	0
75245	Structural characteristics and thermal stability of Pt-Ni nanoparticles. Applied Physics A: Materials Science and Processing, 2023, 129, .	1.1	0
75246	Fast Surface Oxygen Release Kinetics Accelerate Nanoparticle Exsolution in Perovskite Oxides. Journal of the American Chemical Society, 2023, 145, 1714-1727.	6.6	12
75247	Effect of Rare-Earth Element Doping on NiFe-Layered Double Hydroxides for Water Oxidation at Ultrahigh Current Densities. ACS Sustainable Chemistry and Engineering, 2023, 11, 1333-1343.	3.2	13
75248	Stability and electronic properties of two-dimensional Ga2O3 and (MxGa1-x)2O3 (MÂ=ÂAl, Ga) alloys. Applied Surface Science, 2023, 616, 156439.	3.1	1

#	Article	IF	Citations
75249	Ultrathin high-temperature ferromagnetic rare-earth films: GdScGe and GdScSi monolayers. Frontiers in Physics, 0, 10, .	1.0	1
75250	DFT computations combined with semiempirical modeling of variations with temperature of spectroscopic and magnetic properties of Gd³⁺-doped PbTiO₃. Physical Chemistry Chemical Physics, 0, , .	1.3	0
75252	Preparation of Agâ€“Fe2O3-Based black and electrically insulating coatings by magnetron sputtering from metal targets. Vacuum, 2023, 210, 111839.	1.6	2
75253	Influence of transition metal defects on electronic and magnetic properties of bulk silicon: Ab-initio simulation. Materials Today Communications, 2023, 34, 105415.	0.9	5
75254	Metastable-phase platinum oxide for clarifying the Ptâ€“O active site for the hydrogen evolution reaction. Energy and Environmental Science, 2023, 16, 574-583.	15.6	27
75255	Controlling the electrochemical activity of dahlia-like Î²-NiS@rGO by interface polarization. Dalton Transactions, 0, , .	1.6	2
75256	Filling the Gap between Heteroatom Doping and Edge Enrichment of 2D Electrocatalysts for Enhanced Hydrogen Evolution. ACS Nano, 2023, 17, 1287-1297.	7.3	9
75257	Engineering Multiple Microstructural Defects for Recordâ€Breaking Thermoelectric Properties of Chalcopyrite Cu_{1â€}_xAg_xGaTe₂. Small, 2023, 19, .	5.2	7
75258	DFTâ€based Machine Learning for Ensemble Effect of Pd@Au Electrocatalysts on CO₂ Reduction Reaction. ChemPhysChem, 2023, 24, .	1.0	3
75259	Unraveling the Mechanism for H2O2 Photogeneration on Polymeric Carbon Nitride with Alkali Metal Modification. Catalysts, 2023, 13, 218.	1.6	2
75260	Direct analysis at temporal and molecular level of deactivating coke species formed on zeolite catalysts with diverse pore topologies. Catalysis Science and Technology, 2023, 13, 1288-1300.	2.1	6
75261	An Atomistic View of Platinum Cluster Growth on Pristine and Defective Graphene Supports. Small, 0, , 2207484.	5.2	3
75262	Understanding the doping mechanism of Sn in TiO2 nanorods toward efficient photoelectrochemical performance. Journal of Materials Science, 2023, 58, 2156-2169.	1.7	4
75263	Computational Exploration of Ultralow Lattice Thermal Conductivity and High Figure of Merit in p-Type Bulk RbX₂Sb (X = K, Na). ACS Applied Energy Materials, 2023, 6, 939-949.	2.5	5
75264	Monolayer group-V binary compounds <mml:math xmlns:mml="http://www.w3.org/1998/Math/MathML"><mml:mi>Ï</mml:mi></mml:math> -BiP and <mml:math xmlns:mml="http://www.w3.org/1998/Math/MathML"><mml:mi>Ï</mml:mi></mml:math> -SbP with ultrahigh piezoelectricity and stability. Physical Review Materials, 2023, 7, .	0.9	4
75265	Monte Carlo studies of noncollinear magnetic phases in multiferroic <mml:math xmlns:mml="http://www.w3.org/1998/Math/MathML"><mml:mrow><mml:msub><mml:mi>Cu</mml:mi><mml:mn>2</mml:mn></mml:msub></mml:mrow></mml:math> Physical Review B, 2023, 107, .	1.2	2
75266	Experimental evidence for the significance of optical phonons in thermal transport of tin monosulfide. New Journal of Physics, 0, , .	1.2	0
75267	Tuning the electronic and magnetic properties of MgO monolayer by nonmetal doping: A first-principles investigation. Materials Today Communications, 2023, 34, 105422.	0.9	1

#	Article	IF	Citations
75268	Superconducting and structural properties of the phosphorus-rich Nb2P5 superconductor under high pressure. Tungsten, 2023, 5, 364-369.	2.0	3
75269	Oxygen diffusion in the orthorhombic FeNbO₄ material: a computational study. Physical Chemistry Chemical Physics, 2023, 25, 6797-6807.	1.3	4
75270	Control of Explosive Chemical Reactions by Optical Excitations: Defect-Induced Decomposition of Trinitrotoluene at Metal Oxide Surfaces. Molecules, 2023, 28, 953.	1.7	0
75271	Effects of monolayer and bilayer silica films on Fe-Phthalocyanine adsorption properties. EPJ Applied Physics, 2023, 98, 7.	0.3	0
75272	Anisotropic Rashba coupling to polar modes in KTaO₃. JPhys Materials, 2023, 6, 014007.	1.8	4
75273	Resolving Atomistic Structure and Oxygen Evolution Activity in Nickel Antimonates. Journal of Materials Chemistry A, 0, , .	5.2	3
75274	Electrical spectroscopy of defect states and their hybridization in monolayer MoS2. Nature Communications, 2023, 14, .	5.8	13
75275	Tutorial: Systematic development of polynomial machine learning potentials for elemental and alloy systems. Journal of Applied Physics, 2023, 133, .	1.1	4
75276	Pressure-Induced Structural Transformations and Electronic Transitions in TeO₂ Glass by Raman Spectroscopy. Journal of Physical Chemistry Letters, 2023, 14, 387-394.	2.1	2
75277	A Double-Functional Additive Containing Nucleophilic Groups for High-Performance Zn-Ion Batteries. ACS Nano, 2023, 17, 1610-1621.	7.3	107
75278	Bimolecular Reaction Mechanism in the Amido Complex-Based Atomic Layer Deposition of HfO₂. Chemistry of Materials, 2023, 35, 529-538.	3.2	5
75279	Atomically Dispersed Alkalineâ€Earth Metals as Active Centers for CO₂ Electroreduction to Exclusively Produce Formate. Small Structures, 2023, 4, .	6.9	23
75280	Superconductivity of graphenelike hydrogen in <mml:math xmlns:mml="http://www.w3.org/1998/Math/MathML"><mml:mrow><mml:msub><mml:mi mathvariant="normal">H</mml:mi><mml:mn>2</mml:mn></mml:msub><mml:mi>He</mml:mi></mml:mrow></mml:math> at high pressure. Physical Review B, 2023, 107, .	1.1	1
75281	The effect of chemical disorder on magnetic properties of FeNi and Fe2Ni2N alloys. Journal of Magnetism and Magnetic Materials, 2023, 568, 170362.	1.0	2
75282	Ab initio study on structural, magnetic phase and helium migration behaviour of FCC Fe 6.25 at.% Cr binary alloys. Philosophical Magazine, 0, , 1-24.	0.7	0
75283	Synergistic Au passivation and prolonged aging optimization enhance the long-term catalytic stability of porous YSZ/Pt electrodes. Journal of Alloys and Compounds, 2023, 940, 168812.	2.8	1
75284	Size and near-surface engineering in weak-oxidative confined space to fabricate 4 nm L10-PtCo@Pt nanoparticles for oxygen reduction reaction. Nano Research, 2023, 16, 6622-6631.	5.8	7
75285	Arsenene as a promising sensor for the detection of H₂S: a first-principles study. RSC Advances, 2023, 13, 2234-2247.	1.7	6

#	Article	IF	Citations
75286	Microscopic mechanism of low lattice thermal conductivity in natural superlattice materials <mml:math xmlns:mml="http://www.w3.org/1998/Math/MathML"><mml:mrow><mml:mi>Ba</mml:mi><mml:mi>X</mml:mi><mml:mi>Y</mml:mi>		

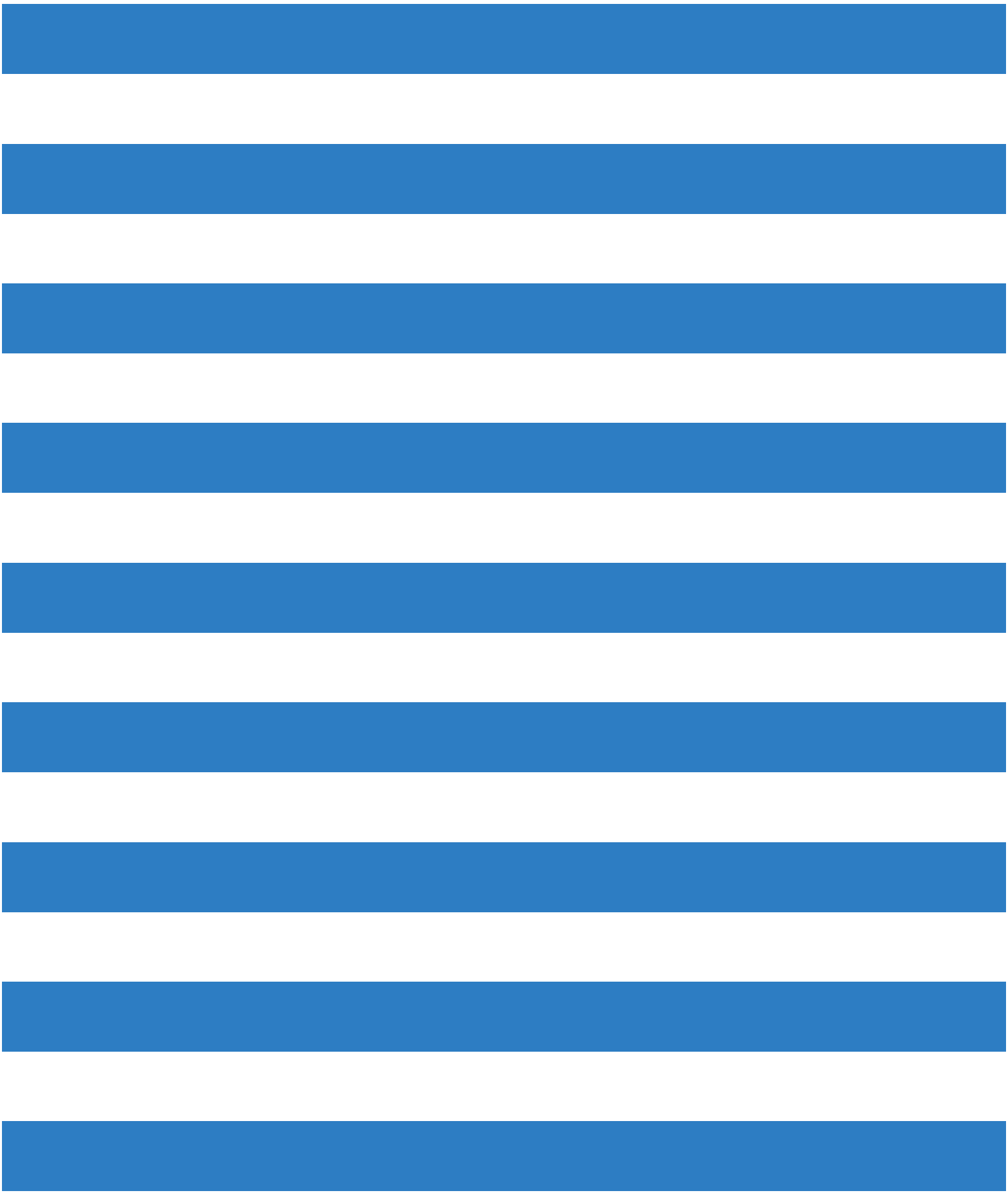

#	Article	IF	Citations
75304	S-functionalized 2D V₂B as a promising anode material for rechargeable lithium ion batteries. Physical Chemistry Chemical Physics, 0, , .	1.3	0
75305	An ab initio approach to anisotropic alloying into the Si(001) surface. Physical Chemistry Chemical Physics, 0, , .	1.3	0
75306	Preparation of Sulfur and Nitrogen Co-doped Carbon-Based Porous Nanomaterials for Efficient Electrocatalytic N2 Reduction. Journal of Electronic Materials, 2023, 52, 2227-2235.	1.0	1
75307	Machine-learning atomic simulation for heterogeneous catalysis. Npj Computational Materials, 2023, 9, .	3.5	11
75308	A general approach to 3D-printed single-atom catalysts. , 2023, 2, 129-139.		39
75309	Enumerating Stable Nanopores in Graphene and Their Geometrical Properties Using the Combinatorics of Hexagonal Lattices. Journal of Chemical Information and Modeling, 2023, 63, 870-881.	2.5	1
75310	Monolayer and bilayer lanthanide compound Gd2C with large magnetic anisotropy energy and high Curie temperature. Journal of Materials Science, 2023, 58, 268-280.	1.7	1
75311	The surface charge induced high activity of oxygen reduction reaction on the PdTe₂ bilayer. Physical Chemistry Chemical Physics, 2023, 25, 4105-4112.	1.3	2
75312	Theoretical determination of superior high-temperature thermoelectricity in an n-type doped 2H-ZrI₂ monolayer. Nanoscale, 2023, 15, 4397-4407.	2.8	5
75313	Material Effects on Electron-Capture Decay in Cryogenic Sensors. Physical Review Applied, 2023, 19, .	1.5	1
75314	Magnetism and unconventional topology in LaCoO3/SrIrO3 heterostructure. Applied Physics Letters, 2023, 122, .	1.5	3
75315	Revisiting two thiophosphate compounds constituting d⁰transition metal HfP₂S₆and d¹⁰transition metal Î±-Ag₄P₂S₆as multifunctional materials for combining second harmonic generation response and photocurrent response. CrystEngComm, 2023, 25, 1175-1185.	1.3	4
75316	First Principles Calculations of Hydrogen Evolution Reaction and Proton Migration on Stepped Surfaces of SrTiO ₃. Advanced Theory and Simulations, 0, , 2200619.	1.3	0
75317	Suppressed Fluctuations as the Origin of the Static Magnetic Order in Strained <mml:math xmlns:mml="http://www.w3.org/1998/Math/MathML" display="inline"><mml:mrow><mml:msub><mml:mrow><mml:mi>Sr</mml:mi></mml:mrow><mml:mrow><mml:mn>2</mml:mn></ Physical Review Letters, 2023, 130, .	2.9	3
75318	Thermodynamics and kinetics of Pb intercalation under graphene on SiC(0001). Carbon, 2023, 205, 336-344.	5.4	6
75319	Critical role of magnetic moments in the lattice dynamics of <mml:math xmlns:mml="http://www.w3.org/1998/Math/MathML"><mml:msub><mml:mrow><mml:mi>YBa</mml:mi></mml:mrow><mml:mrow><mml:mn>2< mathvariant="normal">O</mml:mi></mml:mrow><mml:mn>6</mml:mn></mml:msub></mml:math>. Physical Review B, 2023, 107, .	1.1	2
75321	Enhanced reversibility of fluorine substituted bis-BN cyclohexane for hydrogen storage: A first-principles approach. International Journal of Hydrogen Energy, 2023, 48, 13503-13515.	3.8	3
75322	Exciton dispersion and excitonâ€“phonon interaction in solids by time-dependent density functional theory. Journal of Chemical Physics, 2023, 158, .	1.2	0

#	Article	IF	Citations
75323	Kirigami-Inspired Thermal Regulator. Physical Review Applied, 2023, 19, .	1.5	2
75324	Self-Powered Broadband Photodetector Based on a Monolayer <mml:math xmlns:mml="http://www.w3.org/1998/Math/MathML" display="inline" overflow="scroll"><mml:mrow><mml:mi>In</mml:mi><mml:mi>Se</mml:mi></mml:mrow></mml:math> p - i - n Homojunction. Physical Review Applied, 2023, 19, .	1.5	8
75325	A synergetic model for implementing single-component white-light emission: a case study of zero-dimensional cadmium halides. Materials Chemistry Frontiers, 2023, 7, 705-712.	3.2	8
75326	Comparative studies of interatomic potentials for modeling point defects in wurtzite GaN. AIP Advances, 2023, 13, 015015.	0.6	1
75327	Hole polarons in <mml:math xmlns:mml="http://www.w3.org/1998/Math/MathML"><mml:msub><mml:mi>LaFeO</mml:mi><mml:mn>3</mml:mn></mml:msub></m and <mml:math xmlns:mml="http://www.w3.org/1998/Math/MathML"><mml:mrow><mml:msub><mml:mi>La</mml:mi><mml:mrow><mml:mn>1</mml:mm Physical Review B, 2023, 107, .	1.1	2
75328	Tailoring the nucleation and growth routes of discharge products for lithium-oxygen batteries through the facet engineering of Ni2P catalysts. Energy Storage Materials, 2023, 56, 506-514.	9.5	9
75329	Mechanochemical Synthesis of Sustainable Ternary and Quaternary Nanostructured Cu2SnS3, Cu2ZnSnS4, and Cu2ZnSnSe4 Chalcogenides for Thermoelectric Applications. Nanomaterials, 2023, 13, 366.	1.9	13
75330	Carbon intercalated MoS2 cocatalyst on g-C3N4 photo-absorber for enhanced photocatalytic H2 evolution under the simulated solar light. International Journal of Hydrogen Energy, 2023, 48, 13827-13842.	3.8	7
75331	Roomâ€Temperatureâ€Processable Highly Reliable Resistive Switching Memory with Reconfigurability for Neuromorphic Computing and Ultrasonic Tissue Classification. Advanced Functional Materials, 2023, 33, .	7.8	9
75332	A new high voltage alluaudite sodium battery insertion material. Materials Today Chemistry, 2023, 27, 101316.	1.7	1
75333	Reaction Mechanisms and Kinetics of Nanozymes: Insights from Theory and Computation. Advanced Materials, 2024, 36, .	11.1	28
75334	A high voltage aqueous proton battery using an optimized operation of a MoO₃ positive electrode. Journal of Materials Chemistry A, 2023, 11, 2360-2366.	5.2	7
75335	Unstable stacking fault energy and peierls stress for evaluating slip system competition in body-centered cubic metals. Journal of Materials Research and Technology, 2023, 22, 3413-3422.	2.6	7
75336	Effects of Si Substrates with Variable Initial Orientations on the Growth and Thermoelectric Properties of Bi-Sb-Te Thin Films. Nanomaterials, 2023, 13, 257.	1.9	2
75337	The Transfer Hydrogenation of Cinnamaldehyde Using Homogeneous Cobalt(II) and Nickel(II) (E)-1-(Pyridin-2-yl)-N-(3-(triethoxysilyl)propyl)methanimine and the Complexes Anchored on Fe3O4 Support as Pre-Catalysts: An Experimental and In Silico Approach. Molecules, 2023, 28, 659.	1.7	1
75338	Theoretical proposal and material realization of ferromagnetic negative charge-transfer energy insulator. Physical Review B, 2023, 107, .	1.1	0
75339	Predicting and accessing metastable phases. Materials Advances, 2023, 4, 1101-1112.	2.6	0
75340	Rational design of artificial interphase buffer layer with 3D porous channel for uniform deposition in magnesium metal anodes. Energy Storage Materials, 2023, 55, 816-825.	9.5	21

#	Article	IF	Citations
75341	An iron-base oxygen-evolution electrode for high-temperature electrolyzers. Nature Communications, 2023, 14, .	5.8	15
75342	Valley physics and anomalous valley Hall effect in single-layer <mml:math xmlns:mml="http://www.w3.org/1998/Math/MathML"><mml:mrow><mml:mi>h</mml:mi><mml:mtext>â^’</mml:mtext><mml:mi>M</mml:mi>		

#	Article	IF	Citations
75359	The high magnetoresistance performance of epitaxial half-metallic CrO₂-based magnetic junctions. Physical Chemistry Chemical Physics, 2023, 25, 1848-1857.	1.3	2
75360	Ab Initio Simulation of Structure and Properties in Ni-Based Superalloys: Haynes282 and Inconel740. Materials, 2023, 16, 887.	1.3	2
75361	Demonstrating the source of inherent instability in NiFe LDH-based OER electrocatalysts. Journal of Materials Chemistry A, 2023, 11, 4067-4077.	5.2	34
75362	Improved corrosion resistance of super austenite stainless steel by B-induced nucleation of Laves phase. Corrosion Science, 2023, 213, 110974.	3.0	11
75363	Mechanochemistry and the Evolution of Ionic Bonds in Dense Silver Iodide. Jacs Au, 2023, 3, 402-408.	3.6	4
75364	Generation of magnetic skyrmions in two-dimensional magnets via interfacial proximity. Physical Review B, 2023, 107, .	1.1	3
75365	Theoretical exploration of structural, mechanical and thermodynamic properties of Cr5SiB2 under pressure. Indian Journal of Physics, 0, , .	0.9	0
75366	Highâ€pressureâ€induced multiple phase transitions of parabanic acid. Journal of Raman Spectroscopy, 2023, 54, 404-413.	1.2	2
75367	Screening of Alkali Metal-Exchanged Zeolites for Nitrogen/Methane Separation. Langmuir, 2023, 39, 1277-1287.	1.6	4
75368	Steering from electrochemical denitrification to ammonia synthesis. Nature Communications, 2023, 14, .	5.8	14
75369	Finite temperature properties of uranium mononitride. Journal of Nuclear Materials, 2023, 576, 154241.	1.3	2
75370	Insight at the atomic scale of corrosion inhibition: DFT study of 8-hydroxyquinoline on oxidized aluminum surfaces. Physical Chemistry Chemical Physics, 2023, 25, 4284-4296.	1.3	4
75371	Effective strategies toward imine-linked cationic covalent organic frameworks for rapid and selective removal of ⁹⁹TcO₄^â from water: insights from DFT and MD calculations. Environmental Science: Nano, 2023, 10, 611-624.	2.2	2
75372	Lattice Mismatchâ€Induced Formation of Copper Nanoplates with Embedded Ultrasmall Platinum or Palladium Cores for Tunable Optical Properties. Small, 2023, 19, .	5.2	1
75373	Semimetallic Orbital Hybridization by Particular Surface Engineering in Ternary Cobalt Silicide to Accelerate Oxygen Evolution Reaction. Physica Status Solidi - Rapid Research Letters, 0, , 2200445.	1.2	1
75374	Pdâ€PdO Nanodomains on Amorphous Ru Metallene Oxide for Highâ€Performance Multifunctional Electrocatalysis. Advanced Materials, 2023, 35, .	11.1	51
75375	Critical Influence of Organic Aâ€²â€Site Ligand Structure on 2D Perovskite Crystallization. Small, 2023, 19, .	5.2	9
75376	Deep eutectic solvothermal NiS₂/CdS synthesis for the visible-light-driven valorization of the biomass intermediate 5-hydroxymethylfurfural (HMF) integrated with H₂ production. Green Chemistry, 2023, 25, 2620-2628.	4.6	13

#	Article	IF	Citations
75377	Interface modifications for RuO₂-decorated MoS₂nanosheets as excellent electrocatalysts for alkaline hydrogen evolution reactions. New Journal of Chemistry, 2023, 47, 2899-2906.	1.4	2
75378	Effects of State Filling and Localization on Chemical Expansion in Praseodymium-Oxide Perovskites. Journal of Materials Chemistry A, 0, , .	5.2	0
75379	Interface, vacancy, and morphology engineering synergistically improve In₂S₃@Cu₂S electrocatalytic performance for pH-universal HER. Journal of Materials Chemistry A, 2023, 11, 2262-2272.	5.2	10
75380	Anomalous change of electronic properties for uniaxial-strained LaAlO3/SrTiO3 (001) heterostructure. Journal of Applied Physics, 2023, 133, .	1.1	2
75381	Tuning Discharge Behavior of Hollandite Î±-MnO₂ in Hydrated Zinc Ion Battery by Transition Metal Substitution. Journal of Physical Chemistry C, 2023, 127, 907-918.	1.5	2
75382	Direct prediction of inelastic neutron scattering spectra from the crystal structure. Machine Learning: Science and Technology, 0, , .	2.4	1
75383	Two-dimensional Hâ€“ and Fâ€“BX (X = O, S, Se, and Te) photocatalysts with ultrawide bandgap and enhanced photocatalytic performance for water splitting. RSC Advances, 2023, 13, 2301-2310.	1.7	0
75384	First-principles investigation of defective graphene anchored with small silicon clusters as a potential anode material for lithium-ion batteries. Surface Science, 2023, , 122250.	0.8	2
75385	High temperature phases of borophene: borophene glass and liquid. Nanoscale Horizons, 2023, 8, 353-360.	4.1	3
75386	Highâ€Throughput Screening Assisted Discovery of a Stable Layered Antiâ€Ferromagnetic Semiconductor: CdFeP₂Se₆. Advanced Functional Materials, 2023, 33, .	7.8	1
75387	One-pot synthesized nano-heterostructure with dual-modal catalytic ROS generation ability for high-metastatic orthotopic osteosarcoma therapy. Carbon, 2023, 204, 196-210.	5.4	5
75388	Stability and Strength of Monolayer Polymeric C₆₀. Nano Letters, 2023, 23, 652-658.	4.5	14
75389	Machine Learning Interatomic Potential to Investigate Fundamentals of Electrolytes for Li-ion Solid-State Batteries. , 2023, 1, 83-91.		2
75390	Ferroaxial Transitions in Glaserite-type Compounds: Database Screening, Phonon Calculations, and Experimental Verification. Chemistry of Materials, 0, , .	3.2	5
75391	Metal halide HgI2 monolayer with auxetic property and photocatalysis application. Computational Materials Science, 2023, 219, 112007.	1.4	1
75392	Coupling between improper ferroelectricity and ferrimagnetism in the hexagonal ferrite <mml:math xmlns:mml="http://www.w3.org/1998/Math/MathML"><mml:msub><mml:mi>LuFeO</mml:mi><mml:mn>3</mml:mn></mml:msub></mml:math> Physical Review Research, 2023, 5, .	1.3	0
75393	Intrinsic electron mobility and lattice thermal conductivity of Î²-Si3N4 from first-principles. Solid State Communications, 2023, 361, 115066.	0.9	1
75394	Self-generated Schottky barriers in niobium carbide MXene nanocatalysts for theory-oriented sonocatalytic and NIR-II photonic hyperthermia tumor therapy. Nano Today, 2023, 48, 101750.	6.2	13

#	Article	IF	Citations
75395	Blocking effect in Nb-engineered high-entropy oxides with strengthened grain boundary corrosion resistance. Chemical Engineering Journal, 2023, 457, 141346.	6.6	8
75396	Influence of group IV element on basic mechanical properties of BCC medium-entropy alloys using machine-learning potentials. Computational Materials Science, 2023, 219, 112010.	1.4	1
75397	Active metal dependent side reactions for the reductive amination of furfural. Molecular Catalysis, 2023, 536, 112914.	1.0	1
75398	Mechanical and electronic properties of MX/YTe (MÂ=ÂGe, Sn; XÂ=ÂS, Se, Te) van der Waals heterostructures. Surfaces and Interfaces, 2023, 36, 102604.	1.5	2
75399	Effect of preadsorbing gas molecules on the adsorption of SO2 molecule on Hf2CO2 MXene by first-principles study. Surfaces and Interfaces, 2023, 36, 102639.	1.5	2
75400	Single-atom solutions promote carbon dioxide capture. Applied Energy, 2023, 332, 120570.	5.1	9
75401	Self-intercepting interference of hydrogen-bond induced flexible hybrid film to facilitate lithium extraction. Chemical Engineering Journal, 2023, 458, 141403.	6.6	11
75402	Defect engineering enabling p-type Mo(S,Se)2:TM (TMÂ=ÂV, Nb, Ta) towards high-efficiency kesterite solar cells. Chemical Engineering Journal, 2023, 457, 141348.	6.6	12
75403	Single transition metal atoms anchored on a two-dimensional polyimide covalent-organic framework as single-atom catalysts for photocatalytic CO2 reduction: A first-principles study. Catalysis Communications, 2023, 175, 106604.	1.6	0
75404	Biphenylene with doping B/N as promising metal-free single-atom catalysts for electrochemical oxygen reduction reaction. Journal of Power Sources, 2023, 558, 232613.	4.0	14
75405	Microkinetic modeling with machine learning predicted binding energies of reaction intermediates of ethanol steam reforming: The limitations. Molecular Catalysis, 2023, 537, 112940.	1.0	1
75406	Fourth order Heisenberg models with minimal number of parameters for two-dimensional magnetic crystals. Journal of Magnetism and Magnetic Materials, 2023, 568, 170385.	1.0	0
75407	Effect of doping concentration on the antiferromagnetic transition temperature of multiferroic YMnO3: A first-principles study. Computational Materials Science, 2023, 218, 111999.	1.4	0
75408	Regulation of magnetism on Fe- and Ni-doped SnO2 (1 1 0) surfaces by oxygen vacancy and adsorbed O2 molecule. Journal of Magnetism and Magnetic Materials, 2023, 567, 170356.	1.0	1
75409	Rapid electron transfer-promoted tetracycline hydrochloride degradation: Enhanced activity in visible light-coupled peroxymonosulfate with PdO/g-C3N4/kaolinite catalyst. Chemical Engineering Journal, 2023, 457, 141191.	6.6	16
75410	Atomistic investigation of the impact of phosphorus impurities on the tungsten grain boundary decohesion. Computational Materials Science, 2023, 219, 112017.	1.4	3
75411	Effect of Sn oxides on the thermal conductivity of polycrystalline SnSe. Materials Today Physics, 2023, 31, 100967.	2.9	3
75412	Facile fabrication of atomically dispersed Ru-P-Ru ensembles for efficient hydrogenations beyond isolated single atoms. Chinese Journal of Catalysis, 2023, 45, 107-119.	6.9	3

#	Article	IF	Citations
75413	The Importance of Mgâ€“Sb Interactions in Achieving High Conduction Band Degeneracy in Mg3Sb2 for High n-Type Thermoelectric Performance. Materials Today Physics, 2023, 31, 100959.	2.9	4
75414	Construction of two-dimensional lateral heterostructures by graphenelike ZnO and GaN monolayers for potential optoelectronic applications. Surfaces and Interfaces, 2023, 36, 102635.	1.5	1
75415	Overcoming significant challenges in extracting off-stoichiometric thermodynamics using the compound energy formalism through complementary use of experimental and first principles data: A case study of Ba1-xSrxFeO3-Î´. Solid State Ionics, 2023, 390, 116115.	1.3	0
75416	Defect Engineering of TlPt₂S₃ for Highly Polarization-Sensitive Photodetector. IEEE Photonics Journal, 2023, 15, 1-6.	1.0	1
75417	Enhancing topological Weyl Semimetals by Janus transition-metal dichalcogenides structures. Computational Materials Science, 2023, 218, 112004.	1.4	3
75418	Cellulose filter papers derived separator featuring effective ion transferring channels for sodium-ion batteries. Journal of Power Sources, 2023, 558, 232649.	4.0	8
75419	Highly active and stable Cu Fe /AC-H catalysts with CuFe2O4 for NO reduction by CO in the presence of H2O and SO2 under regeneration gas. Chemical Engineering Journal, 2023, 458, 141304.	6.6	3
75420	Topological properties of half Heusler compounds: Tuned by the spin-orbit coupling and p-d hybridization. Physics Letters, Section A: General, Atomic and Solid State Physics, 2023, 460, 128612.	0.9	0
75421	Superhard orthorhombic BCN allotropes: oIm12-BCN and oPm12-BCN. Diamond and Related Materials, 2023, 132, 109689.	1.8	4
75422	Suppressing zinc dendrite growth in aqueous battery via Znâ€“Al alloying with spatially confined zinc reservoirs. Journal of Power Sources, 2023, 558, 232628.	4.0	12
75423	Effects of edge type and reconstruction on the electronic properties and magnetism of 1Tâ€²-ReS2 nanoribbons: A study based on DFT calculations. Journal of Magnetism and Magnetic Materials, 2023, 567, 170351.	1.0	13
75424	Computational study of electronic, magnetic, and optical properties of Fe(II) mono-doped and (Fe(II),) Tj ETQq1 1 0.784314 rgBT /Ove	1.0	2
75425	Calculation of tunable electronic and optical properties of AlSb/CdSe heterojunction based on first principles. Applied Surface Science, 2023, 614, 156261.	3.1	4
75426	Interface engineering of NiTe/NiCo-LDH core-shell structure to enhance oxygen evolution electrocatalysis performance. Journal of Alloys and Compounds, 2023, 938, 168673.	2.8	9
75427	Controlling the reactions of free radicals with metal-radical interaction. Chinese Journal of Catalysis, 2023, 45, 120-131.	6.9	7
75428	Realizing high reversibility and safety of Zn anode via binary mixture of organic solvents. Nano Energy, 2023, 107, 108175.	8.2	20
75429	Simulation study on uniaxial tensile mechanical and thermal properties of rhenium tungsten alloys. Nuclear Instruments & Methods in Physics Research B, 2023, 535, 247-254.	0.6	2
75430	Microwave-accelerated hydrolysis for hydrogen production over a cobalt-loaded multi-walled carbon nanotube-magnetite composite catalyst. Applied Energy, 2023, 333, 120538.	5.1	8

#	Article	IF	Citations
75431	An unexpectedly stable Y2B5 compound with the fractional stoichiometry under ambient pressure. Arabian Journal of Chemistry, 2023, 16, 104546.	2.3	5
75432	The rendering from the periodic system of elements on the stability, elastic, and electronic properties of M2AC phases. Materialia, 2023, 27, 101676.	1.3	2
75433	Atomic scale simulations of <mml:math xmlns:mml="http://www.w3.org/1998/Math/MathML" altimg="si12.svg" display="inline" id="d1e2335"><mml:mrow><mml:mo>{</mml:mo><mml:mn>112</mml:mn><mml:mo>}</mml:mo></mml:mrow></mml:math> symmetric incoherent twin boundaries in gold. Materialia, 2023, 27, 101678.	1.3	0
75434	Manipulating the electronic, magnetic, and optical properties of single-walled armchair phosphorus nanotubes by encapsulating transition metal nanowires. Materials Today Communications, 2023, 34, 105253.	0.9	1
75435	Synthesis and characterization of narrow band emitting phosphors for plant growth and display applications. Optik, 2023, 274, 170570.	1.4	1
75436	Heteroatom bay-annulated perylene imides/g-C3N4 heterojunctions for efficient photocatalytic H2O2 evolution. Journal of Alloys and Compounds, 2023, 938, 168500.	2.8	9
75437	Catalytic active interfacial Bâ€“C bonds of boron nanosheet/reduced graphene oxide heterostructures for efficient oxygen reduction reaction. Composites Part B: Engineering, 2023, 252, 110496.	5.9	3
75438	Sb and O dual doping of Chlorine-rich lithium argyrodite to improve air stability and lithium compatibility for all-solid-state batteries. Journal of Power Sources, 2023, 559, 232659.	4.0	48
75439	Bulk and monolayer thermoelectric and optical properties of anisotropic NbS<mml:math xmlns:mml="http://www.w3.org/1998/Math/MathML" altimg="si61.svg" display="inline" id="d1e859"><mml:msub><mml:mrow /><mml:mn>2</mml:mn></mml:msub></mml:math>Cl<mml:math xmlns:mml="http://www.w3.org/1998/Math/MathML" altimg="si61.svg" display="inline" id="d1e867"><mml:msub><mml:mrow /><mml:mn>2</mml:mn></mml:msub></mml:math>	0.9	0
75440	Remarkable reactivity of Fe modified Cu(100) surface towards CO2 decomposition: A DFT study. Materials Today Communications, 2023, 34, 105395.	0.9	3
75441	First-principles study on physical properties of actinide-based ternary (UC)mAl3C2 (m = 1, 2, 3) carbides. Vacuum, 2023, 209, 111810.	1.6	5
75442	Porous CoFe2O4 nanorods: VOC gas-sensing characteristics and DFT calculation. Sensors and Actuators B: Chemical, 2023, 379, 133286.	4.0	10
75443	Highly efficient detection of ofloxacin in water by samarium oxide and Î²-cyclodextrin-modified laser-induced graphene electrode. Microchemical Journal, 2023, 186, 108353.	2.3	10
75444	Correlation between radiation resistance and structural factors of ABO3-type perovskites. Nuclear Instruments & Methods in Physics Research B, 2023, 536, 88-96.	0.6	1
75445	Coating lithium titanate anodes with a mixed ionic-electronic conductor for high-rate lithium-ion batteries. Journal of Power Sources, 2023, 559, 232657.	4.0	7
75446	Electronic, mechanical, and optical properties of BP nanotubes: A first-principles study. Computational Condensed Matter, 2023, 34, e00785.	0.9	1
75447	Strain effect on the phonon transport properties of hydrogenated 2D GaN. Vacuum, 2023, 209, 111808.	1.6	5
75448	Contaction of atoms for outstanding dielectric characteristics in KX-passivated polymer dielectrics. Nano Energy, 2023, 107, 108152.	8.2	4

#	Article	IF	Citations
75449	Enabling molecular dynamics simulations of helium bubble formation in tritium-containing austenitic stainless steels: An Fe-Ni-Cr-H-He potential. Journal of Nuclear Materials, 2023, 575, 154232.	1.3	1
75450	Computational design of two-dimensional GeP based flexible strain sensor: Distinct J-V response. Sensors and Actuators A: Physical, 2023, 351, 114155.	2.0	4
75451	Highly efficient and tunable broadband UV excitable Ba9Lu2Si6O24:Eu2+, Mn2+ single-phase white-light-emitting phosphors. Journal of Alloys and Compounds, 2023, 938, 168650.	2.8	9
75452	Thermodynamic reassessment of Feâ€“Nbâ€“V system. Calphad: Computer Coupling of Phase Diagrams and Thermochemistry, 2023, 80, 102529.	0.7	1
75453	The suppression of He bubble growth in Ni-Mo-Cr alloy by yttrium doping: Irradiation experiment combined with the first-principles calculation. Scripta Materialia, 2023, 226, 115270.	2.6	3
75454	Cmc21-CdO: Emerging direct band gap semiconductor with ultrahigh mobility and enhanced visible-light optical absorptions. Physica B: Condensed Matter, 2023, 652, 414645.	1.3	1
75455	Interaction mechanism of transition metal phthalocyanines on transition metal nitride supports. Applied Surface Science, 2023, 614, 156204.	3.1	3
75456	New approach to the compound energy formalism (NACEF) Part II. Thermodynamic modelling of the Alâ€“Nb system supported by first-principles calculations. Calphad: Computer Coupling of Phase Diagrams and Thermochemistry, 2023, 80, 102522.	0.7	0
75457	Exceptionally strong boron nitride nanotube aluminum composite interfaces. Extreme Mechanics Letters, 2023, 59, 101952.	2.0	3
75458	Investigations of the Mnâ€“Niâ€“Sm ternary system by means of anomalous X-ray diffraction, X-ray absorption and DFT calculations. Journal of Alloys and Compounds, 2023, 939, 168682.	2.8	0
75459	Growth of high-density horizontal SWNT arrays by pre-cracking of carbon source. Carbon, 2023, 205, 27-32.	5.4	1
75460	Improved mechanical properties of Co-free high-entropy Cantor alloy: A first-principles study. Results in Materials, 2023, 17, 100364.	0.9	2
75461	First-principle studies of monolayer and bulk InSe1â^'xSx. Applied Surface Science, 2023, 615, 156389.	3.1	0
75462	Interdiffusion and atomic mobility of the Mgâ€“Snâ€“Zn system. Calphad: Computer Coupling of Phase Diagrams and Thermochemistry, 2023, 80, 102524.	0.7	4
75463	Twinning mediated plasticity in high entropy CoCr1.3FeNi0.7MnNb (xâ€¯=â€¯0.3, 0.367, 0.4) ultrafine lamellar eutectic by tuning stacking fault energy. Scripta Materialia, 2023, 227, 115271.	2.6	7
75464	Dopant-based modulation of structural, electronic, and electrochemical properties of Li-excessive Li2NiO2 cathodes. Current Applied Physics, 2023, 48, 1-10.	1.1	0
75465	Theoretical study on adsorption structures and electrical properties of Cu (110) with [Cu(Î¼-HCOO)(OH)2]2. Physica B: Condensed Matter, 2023, 652, 414632.	1.3	2
75466	Excellent high temperature elasticity and thermodynamic properties of W-Cr alloys: A first-principles study. Nuclear Materials and Energy, 2023, 34, 101367.	0.6	1

#	Article	IF	Citations
75467	Exploring of the quantum capacitance of MoS2/graphene heterostructures for supercapacitor electrodes. FlatChem, 2023, 38, 100471.	2.8	6
75468	A first-principles study of the heterogeneous nucleation of Mg on AlN reinforcement particles. Materials Today Communications, 2023, 34, 105277.	0.9	0
75469	Influence of N-doped concentration on the electronic properties and quantum capacitance of Hf2CO2 MXene. Vacuum, 2023, 210, 111826.	1.6	7
75470	Influence of vacancy defects on the electronic and optical properties of graphene/MoS2 heterostructures: A first principles study. Materials Today Communications, 2023, 34, 105313.	0.9	3
75471	Optical absorption of defect chalcopyrite and defect stannite ZnGa2Se4 under high pressure. Journal of Alloys and Compounds, 2023, 939, 168733.	2.8	2
75472	Comparative research of hierarchical CoS2@C and Co3S4@C nanosheet as advanced supercapacitor electrodes. Journal of Energy Storage, 2023, 60, 106551.	3.9	9
75473	Hydrogenated Si-doped g-C3N4: Promising electrocatalyst for CO2 capture and conversion. Applied Surface Science, 2023, 614, 156195.	3.1	2
75474	Two-dimensional valleytronic semiconductor with spontaneous spin and huge valley polarization in monolayer MnCoO6Bi2. Physica E: Low-Dimensional Systems and Nanostructures, 2023, 148, 115654.	1.3	1
75475	Self-assembly CuO surface decorated with NiAl2O4 for high-temperature thermochemical energy storage: Excellent performance and strong interaction mechanism. Journal of Energy Storage, 2023, 59, 106370.	3.9	2
75476	Plasma-assisted synthesis of Ni4Mo/MoO2 @carbon nanotubes with multiphase-interface for high-performance overall water splitting electrocatalysis. Journal of Alloys and Compounds, 2023, 939, 168755.	2.8	10
75477	Curvature effect on graphene-based Co/Ni single-atom catalysts. Applied Surface Science, 2023, 615, 156357.	3.1	17
75478	Enhanced secondary electron emission properties of Zn doped MgO thin films prepared by aerosol assisted chemical vapor deposition. Materials Science in Semiconductor Processing, 2023, 157, 107323.	1.9	1
75479	SnS2/AuNPs surface-enhanced Raman scattering sensor for rapid and selective quantification of methimazole in serum and meat samples. Sensors and Actuators B: Chemical, 2023, 380, 133325.	4.0	8
75480	Mechanism of photocatalytic reduction of CO2 to CH4 on F-doped defective anatase TiO2(101) surface: A density functional theory study. Surface Science, 2023, 730, 122247.	0.8	1
75481	Bulk substitution of F-terminations from Ti3C2Tx MXene by cation pillaring and gas hydrolysation. FlatChem, 2023, 38, 100470.	2.8	0
75482	Ab-initio study of Schottky barrier heights at metal-diamond (1 1 1) interfaces. Applied Surface Science, 2023, 615, 156329.	3.1	3
75483	An ultrastable sodium-ion battery anode enabled by carbon-coated porous NaTi2(PO4)3 olive-like nanospheres. Journal of Colloid and Interface Science, 2023, 635, 417-426.	5.0	22
75484	Incorporation of volatile fission products in UN and PuN and comparison to oxides. Journal of Nuclear Materials, 2023, 576, 154267.	1.3	3

#	Article	IF	Citations
75485	Investigation of novel leveler Rhodamine B on copper superconformal electrodeposition of microvias by theoretical and experimental studies. Applied Surface Science, 2023, 615, 156266.	3.1	9
75486	â€œSniffâ€•lung cancer biomarkers in breath using N-doped monolayer WS2: A theoretical feasibility. Applied Surface Science, 2023, 614, 156257.	3.1	4
75487	The role of vacancy in alloyed (001)-Al//(001) interface. Materials Today Communications, 2023, 34, 105260.	0.9	0
75488	Unveiling adsorption characteristics of BC5 monolayer: High electronic anisotropy and gas sensing performance. Applied Surface Science, 2023, 615, 156226.	3.1	8
75489	Hexagonal and tetragonal ScX (XÂ=ÂP, As, Sb) nanosheets for optoelectronics and straintronics. Applied Surface Science, 2023, 615, 156306.	3.1	17
75490	High carrier mobilities and tunable band structures in two-dimensional <mml:math xmlns:mml="http://www.w3.org/1998/Math/MathML" altimg="si112.svg" display="inline" id="d1e917"><mml:mrow><mml:mi>M</mml:mi><mml:mi>N</mml:mi></mml:mrow></mml:math>H<mml:math xmlns:mml="http://www.w3.org/1998/Math/MathML" altimg="si65.svg" display="inline" id="d1e925"><mml:msub><mml:mrow		

#	Article	IF	Citations
75503	Giant band gap bowing in two dimensional Pb<mml:math xmlns:mml="http://www.w3.org/1998/Math/MathML" altimg="si65.svg" display="inline" id="d1e531"><mml:msub><mml:mrow /><mml:mrow><mml:mn>1</mml:mn><mml:mo>â^’</mml:mo><mml:mi>x</mml:mi></mml:mrow></mml:msub></mml:math>Sn<mml:math xmlns:mml="http://www.w3.org/1998/Math/MathML" altimg="si66.svg" display="inline" id="d1e543"><mml:msub><mml:mrow /><mml:mrow><mml:mi>x</mml:mi></mml:mrow></mml:msub></m	1.9	6
75504	COF-C4N Nanosheets with uniformly anchored single metal sites for electrocatalytic OER: From theoretical screening to target synthesis. Applied Catalysis B: Environmental, 2023, 325, 122366.	10.8	22
75505	Atomic-level understanding on progressive lithiation of few-layer MoS2 with surface vacancies. Journal of Alloys and Compounds, 2023, 939, 168663.	2.8	1
75506	Differentiation on crystallographic orientation dependence of hydrogen diffusion in Î±-Fe and Î³-Fe: DFT calculation combined with SKPFM analysis. Applied Surface Science, 2023, 615, 156395.	3.1	2
75507	Computational screening of two-dimensional substrates for stabilizing honeycomb borophene. Applied Surface Science, 2023, 615, 156388.	3.1	3
75508	Effects of Sc on the vacancy and solute behaviours in aluminium. Journal of Materials Science and Technology, 2023, 148, 41-51.	5.6	9
75509	Band modulation and optoelectronic properties of 2D Janus Ge2SeTe/Sn2SSe van der Waals heterostructures. Journal of Luminescence, 2023, 257, 119682.	1.5	2
75510	Designing a thermodynamically stable and intrinsically ductile refractory alloy. Journal of Alloys and Compounds, 2023, 939, 168597.	2.8	5
75511	Temperature versus type: Which is the determining factor in biomass-based electrocatalyst performance?. Applied Catalysis B: Environmental, 2023, 325, 122391.	10.8	7
75512	Magnetic coupling for highly efficient and tunable emission in CsCdX3:Mn perovskites. Journal of Luminescence, 2023, 257, 119657.	1.5	2
75513	Reduction-tolerant SnO2 assisted by surface hydroxyls for selective CO2 electroreduction to formate over wide potential range. Nano Energy, 2023, 108, 108193.	8.2	8
75514	Novel ternary compound transition metal dichalcogenide TiNbS4 as promising anodes materials for Li-ion batteries: A DFT study. Applied Surface Science, 2023, 615, 156322.	3.1	5
75515	Boosting ethanol oxidation by NiOOH-CuO nano-heterostructure for energy-saving hydrogen production and biomass upgrading. Applied Catalysis B: Environmental, 2023, 325, 122388.	10.8	49
75516	Thermoelectric properties of two-dimensional double transition metal MXenes: ScYC<mml:math xmlns:mml="http://www.w3.org/1998/Math/MathML" altimg="si100.svg" display="inline" id="d1e1224"><mml:msub><mml:mrow><mml:mi>T</mml:mi></mml:mrow><mml:mrow><mml:mn>2</mml:mn></mml:mrow></mml	1.9	7
75517	Journal of Physics and Chemistry of Solids, 2023, 176, 111210. Unveiling the role of defects in iron oxyhydroxide for oxygen evolution. Journal of Colloid and Interface Science, 2023, 635, 167-175.	5.0	12
75518	The S-Fe(Ni) sub-surface active sites for efficient and stable overall water splitting. Applied Catalysis B: Environmental, 2023, 325, 122365.	10.8	16
75519	Sequential active-site switches in integrated Cu/Fe-TiO2 for efficient electroreduction from nitrate into ammonia. Applied Catalysis B: Environmental, 2023, 325, 122360.	10.8	27
75520	Cobalt clusters decorated CoxMn1â^’xO nanocomposites for improving the efficiency of syngas to lower olefins with lower CO2 emission. Applied Catalysis B: Environmental, 2023, 325, 122347.	10.8	1

#	Article	IF	Citations
75521	MIL-101(CuFe) Nanozymes with Excellent Peroxidase-like Activity for Simple, Accurate, and Visual Naked-Eye Detection of SARS-CoV-2. Analytical Chemistry, 0, , .	3.2	7
75522	Activated Lone-Pair Electrons Lead to Low Lattice Thermal Conductivity: A Case Study of Boron Arsenide. Journal of Physical Chemistry Letters, 2023, 14, 139-147.	2.1	2
75523	The changeable coordination of structural and bonding characteristics in amorphous Cu₂Te from ab initio molecular dynamics simulations. Journal of Applied Physics, 2022, 132, 244302.	1.1	0
75524	Vickers hardness prediction from machine learning methods. Scientific Reports, 2022, 12, .	1.6	1
75525	ELECTRONIC STRUCTURE, CHEMICAL BONDING, AND PHASE STABILITY OF THORIUM BORIDES ThB4, ThB6 AND ThB12. Journal of Structural Chemistry, 2022, 63, 1943-1948.	0.3	0
75526	Phosphine-Stabilized Hidden Ground States in Gold Clusters Investigated via a Au_n(PH₃)_m Database. ACS Nano, 2023, 17, 1012-1021.	7.3	3
75527	Honeycombâ€Layered Oxides With Silver Atom Bilayers and Emergence of Nonâ€Abelian SU(2) Interactions. Advanced Science, 2023, 10, .	5.6	3
75528	Tunable Electronic and Magnetic Properties of T-CrTe₂ Monolayer by Li Adsorption. Integrated Ferroelectrics, 2023, 231, 133-141.	0.3	0
75529	Reinforced Photogenerated Electrons in Few-Layer C₃N₅ for Enhanced Catalytic NO Oxidation and CO₂ Reduction. ACS Catalysis, 2023, 13, 785-795.	5.5	27
75530	Theoretical Investigations on the Structure, Elastic and Thermal Conductivities of Li₂MO₃ (Mâ€‰=â€‰Sn, Zr and Ti) Ceramics. Integrated Ferroelectrics, 2023, 231, 153-162.	0.3	5
75531	Discriminating and understanding molecular crystal polymorphism. Journal of Computational Chemistry, 0, , .	1.5	0
75532	Investigation of PbSnTeSe High-Entropy Thermoelectric Alloy: A DFT Approach. Materials, 2023, 16, 235.	1.3	2
75533	Enhanced Thermoelectric Performance in GeTe by Synergy of Midgap state and Band Convergence. Advanced Functional Materials, 2023, 33, .	7.8	7
75534	Engineering oxygen vacancy to accelerate proton conduction in Y-doped BaZrO3. Ceramics International, 2023, 49, 13321-13329.	2.3	2
75535	Toward High-Performance Mg-S Batteries via a Copper Phosphide Modified Separator. ACS Nano, 2023, 17, 1255-1267.	7.3	16
75536	Controlled Synthesis of Subâ€Millimeter Nonlayered WO₂ Nanoplates via a WSe₂â€Assisted Method. Advanced Materials, 2023, 35, .	11.1	8
75537	Superconductivity and topological properties in the kagome metals <mml:math xmlns:mml="http://www.w3.org/1998/Math/MathML"><mml:mi mathvariant="normal">Cs</mml:mi><mml:msub><mml:mi>M</mml:mi><mml:mn>3</mml:mn></mml:msub><mml:msub><mml:mi mathvariant="normal">Te</mml:mi><mml:mn>5</mml:mn></mml:msub></mml:math> (<mml:math) Tj ETQq0 0 0 rgBT /Overlock 10 Tf	1.1	5
75538	first-principles investigation. Physical Review B, 2022, 106, . Theory of shallow and deep boron defects in <mml:math xmlns:mml="http://www.w3.org/1998/Math/MathML"><mml:mrow><mml:mn>4</mml:mn><mml:mi mathvariant="normal">H</mml:mi></mml:mrow></mml:math> -SiC. Physical Review B, 2022, 106, .	1.1	4

#	Article	IF	Citations
75539	An L-band emitter with quantum memory in silicon. Npj Computational Materials, 2022, 8, .	3.5	6
75540	Comparison of long-range corrected kernels and range-separated hybrids for excitons in solids. Physical Review B, 2022, 106, .	1.1	2
75541	High-Pressure X-ray Diffraction and DFT Studies on Spinel FeV2O4. Crystals, 2023, 13, 53.	1.0	0
75543	Solute atom segregation to I1 stacking fault and its bounding partial dislocations in a Mgâ€“Bi alloy. Journal of Magnesium and Alloys, 2022, , .	5.5	1
75544	Multidentate Molecule Anchoring Halide Perovskite Surface and Regulating Crystallization Kinetics toward Efficient Lightâ€Emitting Diodes. Small, 2023, 19, .	5.2	10
75545	Regulating Surface Oxygen Activity by Perovskiteâ€Coatingâ€Stabilized Ultrahighâ€Nickel Layered Oxide Cathodes. Advanced Materials, 2023, 35, .	11.1	15
75546	Prediction of novel tetravalent metal pentazolate salts with anharmonic effect. Fundamental Research, 2022, , .	1.6	1
75547	Suppressing interfacial side reactions of zinc metal anode via isolation effect toward high-performance aqueous zinc-ion batteries. Nano Research, 2023, 16, 6789-6797.	5.8	13
75548	Anomalous stability of non-van der Waals bonded B4C nanosheets through surface reconstruction. Journal of Applied Physics, 2022, 132, .	1.1	1
75549	Facile Synthesis of Gram-Scale Mesoporous Ag/TiO₂ Photocatalysts for Pharmaceutical Water Pollutant Removal and Green Hydrogen Generation. ACS Omega, 2023, 8, 1249-1261.	1.6	5
75550	Multiple Topological Magnetism in van der Waals Heterostructure of MnTe₂/ZrS₂. Nano Letters, 2023, 23, 312-318.	4.5	9
75551	Atomic-Layer-Deposition Derived Pt subnano Clusters on the (110) Facet of Hexagonal Al₂O₃ Plates: Efficient for Formic Acid Decomposition and Water Gas Shift. ACS Catalysis, 2023, 13, 887-901.	5.5	4
75552	Atomic-Scale Determination of Cation and Magnetic Order in the Triple Perovskite Sr3Fe2ReO9. Microscopy and Microanalysis, 0, , .	0.2	0
75553	Development of Porous Crystalline Materials for Selective Binding of O₂ from Air. Journal of Physical Chemistry C, 2023, 127, 776-787.	1.5	2
75554	Mixed Sulfur/Selenium Anions Weaken Electron-Vibrational Interaction in Cu₂ZnSn(S,Se)₄ Photoabsorber. Journal of Physical Chemistry Letters, 2023, 14, 107-115.	2.1	1
75555	Î³-BaFe2O4: a fresh playground for room temperature multiferroicity. Nature Communications, 2022, 13, .	5.8	4
75556	Revisiting Competitive Adsorption of Small Molecules in the Metalâ€“Organic Framework Ni-MOF-74. Inorganic Chemistry, 2023, 62, 950-956.	1.9	5
75557	Designing orbital and charge ordering multiferroics by superlattice strategy and strain engineering. Physical Review B, 2022, 106, .	1.1	2

#	Article	IF	Citations
75558	A carbon mixed selenium sulfide separator coating for lithiumâ€sulfur battery life enhancement. ChemElectroChem, 2023, 10, .	1.7	1
75559	Accelerated formation of iodine vacancies in <scp> CH ₃ NH ₃ PbI ₃ </scp> perovskites: The impact of oxygen and charges. EcoMat, 0, , .	6.8	2
75560	The Ultrahigh Adsorption Capacity and Excellent Photocatalytic Degradation Activity of Mesoporous CuO with Novel Architecture. Nanomaterials, 2023, 13, 142.	1.9	3
75561	Magnocolumbites Mg_{1â€“x}M</sub>x</sub>Nb₂O_{6â^Î´} (x = 0, 0.1, and 0.2; M = Li and Cu) as New Oxygen Ion Conductors: Theoretical Assessment and Experiment. Journal of Physical Chemistry C, 2023, 127, 52-58.	1.5	4
75562	Efficient n-Type Surface Doping in Diamond. Journal of Physical Chemistry C, 2023, 127, 642-648.	1.5	2
75563	High-temperature ferromagnetism and strong Ï€-conjugation feature in two-dimensional manganese tetranitride. Chinese Physics B, 0, , .	0.7	0
75564	Optimizing density-functional simulations for two-dimensional metals. Physical Review Materials, 2022, 6, .	0.9	1
75565	Facile Synthesis of Nb-Doped CoTiO3 Hexagonal Microprisms as Promising Anode Materials for Lithium-Ion Batteries. Inorganics, 2023, 11, 10.	1.2	0
75566	High-throughput first-principle prediction of collinear magnetic topological materials. Npj Computational Materials, 2022, 8, .	3.5	2
75567	Fabrication of Stepâ€Scheme Heterojunction between Layered MoO₃/TiO₂ for Photocatalytic H₂ Evolution and Study on the Mechanism. Advanced Sustainable Systems, 2023, 7, .	2.7	9
75568	A machine-learned spin-lattice potential for dynamic simulations of defective magnetic iron. Scientific Reports, 2022, 12, .	1.6	4
75569	Optimal Icosahedral Copper-Based Bimetallic Clusters for the Selective Electrocatalytic CO2 Conversion to One Carbon Products. Nanomaterials, 2023, 13, 87.	1.9	4
75570	Double Paddleâ€Wheel Enhanced Sodium Ion Conduction in an Antiperovskite Solid Electrolyte. Advanced Energy Materials, 2023, 13, .	10.2	11
75571	Switchable large-gap quantum spin Hall state in the two-dimensional <mml:math xmlns:mml="http://www.w3.org/1998/Math/MathML"><mml:mi>M</mml:mi><mml:mrow><mml:msub><mml:mi mathvariant="normal">Si</mml:mi><mml:mn>2</mml:mn></mml:msub><mml:msub><mml:mi>Z</mml:mi><mml:mn>4</mml:mn></mml:msub></mml:mrow></mml:math> class of materials. Physical Review B, 2022, 106, .	1.1	8
75572	Strongly correlated itinerant magnetism near superconductivity in <mml:math xmlns:mml="http://www.w3.org/1998/Math/MathML"><mml:msub><mml:mrow><mml:mi>NiTa</mml:mi></mml:mrow><mml:mn>4</mml:mn></mml:msub></mml:math> Physical Review B, 2022, 106, .	1.1	1
75573	Atom-Specific Probing of Electron Dynamics in an Atomic Adsorbate by Time-Resolved X-Ray Spectroscopy. Physical Review Letters, 2022, 129, .	2.9	1
75574	â€œO-Sâ€•Charge Transfer Mechanism Guiding Design of a ZnIn₂S₄/SnSe₂/In₂Se₃ Heterostructure Photocatalyst for Efficient Hydrogen Production. ACS Catalysis, 2023, 13, 1020-1032.	5.5	13
75575	Binding Energy and Diffusion Barrier of Formic Acid on Pd(111). Journal of Physical Chemistry A, 2023, 127, 142-152.	1.1	0

#	Article	IF	Citations
75576	Planar Gliding and Vacancy Condensation: The Role of Dislocations in the Chemomechanical Degradation of Layered Transition-Metal Oxides. Chemistry of Materials, 2023, 35, 584-594.	3.2	7
75577	Pressureâ€Tuning Photothermal Synergy to Optimize the Photoelectronic Properties in Amorphous Halide Perovskite Cs₃Bi₂I₉. Advanced Science, 2023, 10, .	5.6	13
75578	Systematic Theoretical Study of CO Activation over Clean and Potassium-Modified Transition Metals. Journal of Physical Chemistry C, 2023, 127, 265-278.	1.5	1
75579	Upper-Bound Energy Minimization to Search for Stable Functional Materials with Graph Neural Networks. Jacs Au, 2023, 3, 113-123.	3.6	2
75580	Preparation and Characterization of Francisite Solid Solutions Cu₃Bi(Se_{1â€“x}Te_xO₃)₂O₂Br (x = 0â€“1): Possibility for Francisites as Starting Materials for Oxide van der Waals Ferromagnets. Chemistry of Materials, 0, , .	3.2	2
75581	First-Principle Study of Ca3Y2Ge3O12 Garnet: Dynamical, Elastic Properties and Stability under Pressure. Crystals, 2023, 13, 29.	1.0	0
75582	First Ultrathin Pure Polyoxometalate 2D Material as a Peroxidase-Mimicking Catalyst for Detecting Oxidative Stress Biomarkers. ACS Applied Materials & Interfaces, 2023, 15, 1486-1494.	4.0	14
75583	Hybrid-Density Functional Calculations of Structural, Electronic, Magnetic, and Thermodynamic Properties of Î±-Cu2P2O7. Applied Sciences (Switzerland), 2023, 13, 498.	1.3	2
75584	Dye-sensitized Bi2MoO6 for highly efficient photocatalytic degradation of levofloxacin under LED light irradiation. Materials Today Sustainability, 2023, 21, 100311.	1.9	8
75585	Vacancy Manipulation Induced Optimal Carrier Concentration, Band Convergence and Low Lattice Thermal Conductivity in Nanoâ€Crystalline SnTe Yielding Superior Thermoelectric Performance. Advanced Functional Materials, 2023, 33, .	7.8	10
75586	Electronic properties of 3dtransition metal dihalide monolayers predicted by<scp>DFT</scp>methods: Is there a pattern or are the results random?. Journal of the Chinese Chemical Society, 2023, 70, 359-371.	0.8	1
75587	Photocatalytic NO_x Oxidation of BiOCl Nanostructure-Based Films Grown Using Aerosol-Assisted Chemical Vapor Deposition. ACS Applied Nano Materials, 2023, 6, 738-749.	2.4	2
75588	Role of morphology in defect formation and photo-induced carrier instabilities in amorphous indium oxide. Applied Physics Letters, 2022, 121, .	1.5	0
75589	Activation of metal-free porous basal plane of biphenylene through defects engineering for hydrogen evolution reaction. International Journal of Hydrogen Energy, 2023, 48, 10545-10554.	3.8	8
75590	Crystal and Electronic Structures of New Two Dimensional 3-NH3-PyPbX4 Haloplumbate Materials. Materials, 2023, 16, 353.	1.3	1
75591	Magneto-volume effect in Fe_nTi_{13-n} clusters during thermal expansion. Chinese Physics B, 0, , .	0.7	0
75592	Adsorption of NH₃ on Monolayer SiC Doped with Noble Metals: A First-Principles Study. Integrated Ferroelectrics, 2023, 231, 89-97.	0.3	2
75593	Nanolaminated <mml:math xmlns:mml="http://www.w3.org/1998/Math/MathML"><mml:mrow><mml:msub><mml:mi mathvariant="normal">Fe</mml:mi><mml:mn>2</mml:mn></mml:msub><mml:mi>A</mml:mi></mml:mrow><mml:msub><mml:mi mathvariant="normal">B</mml:mi><mml:mn>2</mml:mn></mml:msub></mml:math> and <mml:math xmlns:mml="http://www.w3.org/1998/Math/MathML"><mml:mrow><mml:msub><mml:mi mathvariant="normal">Mn</mml:mi><mml:mn>2</mml:mn></mml:msub><mml:mi>A</mml:mi></mml:mrow><mml:msub><mml:mi	0.9	4

#	Article	IF	Citations
75594	Molecular adsorption on coinage metal subnanoclusters: A <scp>DFT</scp> + <scp>D3</scp> investigation. Journal of Computational Chemistry, 0, , .	1.5	1
75595	General Synthesis of 2D Magnetic Transition Metal Dihalides via Trihalide Reduction. ACS Nano, 2023, 17, 363-371.	7.3	10
75596	Electric-Field-Tunable Spin Polarization and Carrier-Transport Anisotropy in an A-Type Antiferromagnetic van der Waals Bilayer. Physical Review Applied, 2022, 18, .	1.5	6
75597	Oxygen vacancies at the origin of pinned moments in oxide interfaces: The example of tetragonal <mml:math xmlns:mml="http://www.w3.org/1998/Math/MathML"><mml:mi>CuO</mml:mi><mml:mo>/</mml:mo><mml:msub><mml:mrow><m Physical Review B, 2022, 106, .	1.1	0
75598	Biaxial Hard Compression, Anisotropic Elastic Property, and Pressure-Induced Isosymmetric Phase Transition in Ammonium Bicarbonate. Journal of Physical Chemistry C, 2023, 127, 831-841.	1.5	1
75599	Pressure-Induced Phase Transition in Multilayered Vanadium Diselenide Nanosheets. Journal of Physical Chemistry C, 2023, 127, 368-380.	1.5	1
75600	High-efficiency hydrogen evolution reaction photocatalyst for water splitting of Type-II Î²-AsP/g-C3N4 van der Waals heterostructure. International Journal of Hydrogen Energy, 2023, 48, 10051-10061.	3.8	10
75601	Enhanced Intrinsic Anomalous Valley Hall Effect Induced by Spinâ€“Orbit Coupling in MXene Monolayer M₃N₂O₂ (M = Y, La). Journal of Physical Chemistry Letters, 2023, 14, 132-138.	2.1	9
75602	Role of Hidden Spin Polarization in Nonreciprocal Transport of Antiferromagnets. Physical Review Letters, 2022, 129, .	2.9	9
75603	Microscopic physical origin of charge traps in 3D NAND flash memories. Japanese Journal of Applied Physics, 0, , .	0.8	0
75604	Large kagome family candidates with topological superconductivity and charge density waves. Physical Review B, 2022, 106, .	1.1	18
75605	Ab Initio Calculations of Transport and Optical Properties of Dense Zr Plasma Near Melting. Symmetry, 2023, 15, 48.	1.1	2
75606	Algorithms for Predicting the Physical Properties of Nanocrystals and Large Clusters. , 2011, , 1-25.		0
75607	First Principles Study on the Features of CaxSr2â^'xTa2O7 (x = 0, 1) as a Photocatalytic Material. , 0, , .		0
75608	Tunable electronic properties of GeC/BAs van der Waals heterostructure under external electric field and strain. Physica E: Low-Dimensional Systems and Nanostructures, 2023, 149, 115628.	1.3	3
75609	Stress and defects cooperatively regulate the photocatalytic performance of AlN bulk phase materials. International Journal of Hydrogen Energy, 2023, 48, 14707-14716.	3.8	2
75610	Unconventional Charge-to-Spin Conversion in Graphene/ <mml:math xmlns:mml="http://www.w3.org/1998/Math/MathML" display="inline" overflow="scroll"><mml:msub><mml:mrow><mml:mi>Mo</mml:mi><mml:mi>Te</mml:mi></mml:mrow><mml:mn>2</mml:mn></mml van der Waals Heterostructures. Physical Review Applied, 2023, 19, .	1.5	10
75611	Simple and accurate estimation of metal, semiconductor, and insulator work functions. Physical Review Materials, 2023, 7, .	0.9	1

#	Article	IF	Citations
75612	Atomistic simulations of diffusion in <mml:math xmlns:mml="http://www.w3.org/1998/Math/MathML"><mml:msup><mml:mi>Î³</mml:mi><mml:mo>â€²</mml:mo></mml:msup></mm -strengthened Co-based superalloys and its connection to selective alumina formation in early-stage oxidation. Physical Review Materials, 2023, 7, .	0.9	1
75613	Regulating Eu²⁺ Multisite Occupation through Structural Disorder toward Broadband Near-Infrared Emission. Chemistry of Materials, 2023, 35, 1432-1439.	3.2	26
75614	Density Functional Theory Studies on Magnetic Manipulation in NiI₂ Layers. ACS Applied Electronic Materials, 2023, 5, 920-927.	2.0	6
75615	Enhanced Catalytic Activity of Bimetallic Ordered Catalysts for Nitrogen Reduction Reaction by Perturbation of Scaling Relations. ACS Catalysis, 2023, 13, 2190-2201.	5.5	15
75616	A semiconductive copper iodobismuthate hybrid: structure, optical properties and photocurrent response. Dalton Transactions, 2023, 52, 2999-3005.	1.6	3
75617	Interface engineering for substantial performance enhancement in epitaxial all-perovskite oxide capacitors. NPG Asia Materials, 2023, 15, .	3.8	1
75618	Ab initio study of fundamental properties of XInO₃ (X = K, Rb, Cs) perovskites. Open Chemistry, 2023, 21, .	1.0	1
75619	First-Principles Calculations Study of Small Polarons Around Oxygen Vacancies in SrMoO4. Journal of Electronic Materials, 0, , .	1.0	0
75620	Ensemble Effects in Adsorbateâ€“Adsorbate Interactions in Microkinetic Modeling. Journal of Chemical Theory and Computation, 0, , .	2.3	1
75621	Intrinsic defects at the interface of the FAPbI₃/MAPbI₃ superlattice: insight from first-principles calculations. Physical Chemistry Chemical Physics, 2023, 25, 6369-6379.	1.3	3
75622	Revealing the crystal facet effect on N₂O formation during the NH₃-SCR over Î±-MnO₂ catalysts. RSC Advances, 2023, 13, 4032-4039.	1.7	6
75623	High-Pressure X-ray Diffraction Study of Orthorhombic Ca₂Zr₅Ti₂O₁₆. Journal of Physical Chemistry C, 2023, 127, 2069-2077.	1.5	0
75624	Orbital contribution to the regulation of the spin-valley coupling in antiferromagnetic monolayer <mml:math xmlns:mml="http://www.w3.org/1998/Math/MathML"><mml:msub><mml:mi>MnPTe</mml:mi><mml:mn>3</mml:mn></mml:msub></r Physical Review B, 2023, 107, .	1.1	6
75625	Reversible bipolar thermopower of ionic thermoelectric polymer composite for cyclic energy generation. Nature Communications, 2023, 14, .	5.8	13
75626	p-Type ohmic contact to MoS₂via binary compound electrodes. Journal of Materials Chemistry C, 2023, 11, 3119-3126.	2.7	1
75627	Stable Multifunctional Aluminum Phosphides at High Pressures. Physical Chemistry Chemical Physics, 0, , .	1.3	0
75628	Direct bandgaps, Weyl fermions, and strong light absorption ability in Janus Ti2OFCl MOene. Applied Physics Letters, 2023, 122, .	1.5	3
75629	A New 3D Carbon Allotrope Composed of Penta-graphene Nanotubes with Low Lattice Thermal Conductivity. Journal of Physical Chemistry Letters, 2023, 14, 1082-1087.	2.1	1

#	Article	IF	Citations
75630	Dual hydrogen production from electrocatalytic water reduction coupled with formaldehyde oxidation via a copper-silver electrocatalyst. Nature Communications, 2023, 14, .	5.8	38
75631	Collective Magnetic Behavior in Vanadium Telluride Induced by Self-Intercalation. ACS Nano, 2023, 17, 2450-2459.	7.3	5
75632	Single-crystalline Mg-substituted Na₄Mn₃(PO₄)₂P₂O₇ nanoparticles as a high capacity and superior cycling cathode for sodium-ion batteries. Nanoscale, 2023, 15, 4830-4838.	2.8	1
75633	Effects of different amounts of N heteroatoms on the structural and electronic properties of graphene and the adsorption behavior of Li atoms. Modern Physics Letters B, 0, , .	1.0	0
75634	Unveiling Electronic Behaviors in Heterochiral Charge-Density-Wave Twisted Stacking Materials with 1.25 nm Unit Dependence. ACS Nano, 2023, 17, 2702-2710.	7.3	5
75635	First principles insights into the relative stability, electronic and catalytic properties of coreâ€“shell, Janus and mixed structural patterns for bimetallic Pdâ€“X nano-alloys (X = Co, Ni, Cu, Rh, Ag, Ir, Pt, Au). Physical Chemistry Chemical Physics, 2023, 25, 4667-4679.	1.3	0
75636	Phase field modeling microstructural evolution of Fe-Cr-Al systems at thermal treatment. Frontiers in Energy Research, 0, 11, .	1.2	0
75637	Suppressing the initial capacity fade in Li-rich Li₅FeO₄with anionic redox by partial Co substitution â€“ a first-principles study. Sustainable Energy and Fuels, 2023, 7, 1502-1521.	2.5	2
75638	Ligand-Engineered Spin Crossover in Fe(II)-Based Molecular and Metalâ€“Organic Framework Systems. Journal of Physical Chemistry C, 2023, 127, 2735-2740.	1.5	3
75639	Segregation and Oxidation Behavior in Be {101Ì…1} Grain Boundary by First-Principles Calculations. Journal of Physical Chemistry C, 2023, 127, 2648-2656.	1.5	1
75640	Adsorption properties of a paracyclophane molecule on NaCl/Au surfaces: a first-principles study. Physical Chemistry Chemical Physics, 2023, 25, 6060-6066.	1.3	1
75641	Efficient computational design of two-dimensional van der Waals heterostructures: Band alignment, lattice mismatch, and machine learning. Physical Review Materials, 2023, 7, .	0.9	9
75642	Dielectric Properties of Nanoconfined Water from Ab Initio Thermopotentiostat Molecular Dynamics. Journal of Chemical Theory and Computation, 2023, 19, 1035-1043.	2.3	11
75643	Large spontaneous valley polarization and high magnetic transition temperature in stable two-dimensional ferrovalley <mml:math xmlns:mml="http://www.w3.org/1998/Math/MathML"><mml:mrow><mml:mi		

#	Article	IF	Citations
75648	The synergistic effect of Ti and Nb in TiNbC leads to enhanced anode performance for Na-ion batteries - first-principles calculations. Physica Scripta, 2023, 98, 025710.	1.2	2
75649	Dimension-dependent magnetic anisotropy for tunable anomalous Hall effect in transition metal dichalcogenides. Physical Review B, 2023, 107, .	1.1	4
75650	General approach for atomically dispersed precious metal catalysts toward hydrogen reaction. , 2023, 5, .		6
75651	Effect of Mo Content on Hydrogen Evolution Reaction of 1400 MPa-Grade High-Strength Bolt Steel. Materials, 2023, 16, 1020.	1.3	1
75652	Validity of DFT-based spin-orbit torque calculation for perpendicular magnetic anisotropy in iron thin films. AIP Advances, 2023, 13, 015034.	0.6	0
75653	Tetragonal SnOFeSe: A possible parent compound of the FeSe-based superconductor. Physical Review B, 2023, 107, .	1.1	0
75654	Selectively converting CO2 to HCOOH on Cu-alloys integrated in hematite-driven artificial photosynthetic cells. Journal of Energy Chemistry, 2023, 79, 601-610.	7.1	8
75655	Synthesis of Î±-Borylmethyl-(E)-allylborons via Cu-Catalyzed Diboration of 1-Substituted Allenols and Their Application in Stereoselective Aldehyde Allylation. ACS Catalysis, 0, , 2351-2358.	5.5	2
75656	Structure effects of Pt₁₅ clusters for the oxygen reduction reaction: first-principles calculations. Physical Chemistry Chemical Physics, 2023, 25, 4764-4772.	1.3	2
75657	1D group Vâ€“Vlâ€“VII ternary nanowires: moderate band gaps, easy to exfoliate from bulk, and unexpected ferroelectricity. Physical Chemistry Chemical Physics, 2023, 25, 6112-6120.	1.3	3
75658	Electronic and electromechanical properties of vertical and lateral 2D heterostructures. , 2023, , 51-71.		0
75659	High conductivity enabled by concerted Li ion diffusion in Li₃Y(Br₃Cl₃) solid electrolytes for all-solid-state batteries. Journal of Materials Chemistry A, 2023, 11, 4334-4344.	5.2	5
75660	The Snâ€“red Pâ€“Feâ€“based alloy materials for efficient Liâ€“ion battery anodes. Journal of Industrial and Engineering Chemistry, 2023, 121, 299-311.	2.9	10
75661	Iron Vacancy Accelerates Fe(II)-Induced Anoxic As(III) Oxidation Coupled to Iron Reduction. Environmental Science & Technology, 2023, 57, 2175-2185.	4.6	15
75662	Two-Dimensional Î±-SiX (X = N, P) Monolayers as Efficient Anode Material for Li-Ion Batteries: A First-Principles Study. ACS Applied Nano Materials, 2023, 6, 2103-2115.	2.4	14
75663	Coordination-Dependent Chemical Reactivity of TFSI Anions at a Mg Metal Interface. ACS Applied Materials & Interfaces, 2023, 15, 7518-7528.	4.0	10
75664	Effective chemisorption of polysulfides through organic molecules for high-performance lithiumâ€“sulfur batteries. Chemical Engineering Journal, 2023, 459, 141556.	6.6	6
75665	Polarons and electrical leakage in <mml:math xmlns:mml="http://www.w3.org/1998/Math/MathML"><mml:msub><mml:mi>BaZrO</mml:mi><mml:mn>3</mml:mn></mml:msub> and <mml:math xmlns:mml="http://www.w3.org/1998/Math/MathML"><mml:msub><mml:mi>BaCeO</mml:mi><mml:mn>3</mml:mn></mml:msub> Physical Review Materials, 2023, 7, .	0.9	3

#	Article	IF	Citations
75666	Computational determination of a graphene-like TiB₄ monolayer for metal-ion batteries and a nitrogen reduction electrocatalyst. Physical Chemistry Chemical Physics, 2023, 25, 7436-7444.	1.3	3
75667	Investigation of adsorption behaviors, and electronic and magnetic properties for small gas molecules adsorbed on Pt-doped arsenene by density functional calculations. RSC Advances, 2023, 13, 3807-3817.	1.7	6
75668	The Evolution of Band Topology in Two-Dimensional Weyl Half-Metals. Journal of Physical Chemistry Letters, 2023, 14, 825-831.	2.1	3
75669	Ultrabroadband Emission from CsCu₂I₃/Cs₃Cu₂I₅ Dual-Phase Glass-Ceramics with Long-Term Stability. , 2023, 1, 481-490.		4
75670	Crystal and Electronic Structure of Oxygen Vacancy Stabilized Rhombohedral Hafnium Oxide. ACS Applied Electronic Materials, 2023, 5, 754-763.	2.0	11
75671	Spin-selective contact type and strong Fermi level pinning at a CrI3/metal interface. Materials Today Nano, 2023, 22, 100309.	2.3	3
75672	Phase Competition and Strong SHG Responses of the Li₂M^{II}M^{IV}Se₄ Family: Atom Response Theory Predictions versus Experimental Results. Chemistry of Materials, 2023, 35, 1159-1167.	3.2	2
75673	Resolving Diverse Oxygen Transport Pathways Across Srâ€Doped Lanthanum Ferrite and Metalâ€Perovskite Heterostructures. Advanced Materials Interfaces, 2023, 10, .	1.9	2
75674	Bismuth antiphase domain wall: A three-dimensional manifestation of the Su-Schrieffer-Heeger model. Physical Review B, 2023, 107, .	1.1	2
75675	Heterogeneous Structure of Sn/SnO₂ Constructed via Phase Engineering for Efficient and Stable CO₂ Reduction. ACS Applied Materials & Interfaces, 2023, 15, 7529-7537.	4.0	6
75676	Optimizing the electronic structures of Ca Sr1-Co0.7Fe0.3O3-Î´ anodes for high-temperature oxygen evolution reaction. Chem Catalysis, 2023, 3, 100504.	2.9	5
75677	Heat transport properties of novel carbon monolayer (net-Y): a comparative study with graphene. Physical Chemistry Chemical Physics, 2023, 25, 4915-4922.	1.3	1
75678	High-Throughput DFT-Based Discovery of Next Generation Two-Dimensional (2D) Superconductors. Nano Letters, 2023, 23, 969-978.	4.5	12
75679	One-dimensional semimetal contacts to two-dimensional semiconductors. Nature Communications, 2023, 14, .	5.8	13
75680	Altering the Alkaline Metal Ions in Lepidocrocite-Type Layered Titanate for Sodium-Ion Batteries. ACS Applied Materials & Interfaces, 2023, 15, 5028-5037.	4.0	4
75681	Promoting Molecular Exchange on Rare-Earth Oxycarbonate Surfaces to Catalyze the Waterâ€“Gas Shift Reaction. Journal of the American Chemical Society, 2023, 145, 2252-2263.	6.6	8
75682	Solâ€Gelâ€Derived Ordered Mesoporous High Entropy Spinel Ferrites and Assessment of Their Photoelectrochemical and Electrocatalytic Water Splitting Performance. Small, 2023, 19, .	5.2	15
75683	Enabling Room-Temperature Triferroic Coupling in Dual Transition-Metal Dichalcogenide Monolayers Via Electronic Asymmetry. Journal of the American Chemical Society, 2023, 145, 2485-2491.	6.6	14

#	Article	IF	Citations
75684	Growth of Mesoscale Ordered Two-Dimensional Hydrogen-Bond Organic Framework with the Observation of Flat Band. Physical Review Letters, 2023, 130, .	2.9	12
75685	Unveiling the synergistic effect of multi-valence Cu species to promote formaldehyde oxidation for anodic hydrogen production. CheM, 2023, 9, 963-977.	5.8	14
75686	Effects of the surface termination and the oxygen vacancy position on <mml:math xmlns:mml="http://www.w3.org/1998/Math/MathML"><mml:msub><mml:mi>LaNiO</mml:mi><mml:mn>3</mml:mn></mml:msub></m ultra-thin films: First-principles study. Physical Review Materials, 2023, 7, .	0.9	0
75687	Engineering ZnO with Cu doping to lower the transition pressure: Experimental and theoretical investigations. AIP Advances, 2023, 13, .	0.6	3
75688	Interface contact and modulated electronic properties by in-plain strains in a grapheneâ€“MoS₂ heterostructure. RSC Advances, 2023, 13, 2903-2911.	1.7	1
75689	Mixed-domain Charge Transport in the S-Se System from First Principles. , 2023, , .		0
75690	An hydrogen adsorption study on graphene-based surfaces with coreâ€“shell type catalysts. Carbon Letters, 0, , .	3.3	1
75691	Ultralow contact resistance in organic transistors via orbital hybridization. Nature Communications, 2023, 14, .	5.8	22
75692	Proposal of Low-Loss Non-Volatile Mid-Infrared Optical Phase Shifter Based on Ge₂Sb₂Te₃S₂. IEEE Transactions on Electron Devices, 2023, 70, 2106-2112.	1.6	5
75693	Half-Metallicity and Magnetic Anisotropy in Double-Perovskite GdBaCo₂O₆ Films Prepared via Topotactic Oxidation. Chemistry of Materials, 2023, 35, 1295-1300.	3.2	4
75694	Enhancement of Perpendicular Magnetic Anisotropy and Curie Temperature in V-Doped Two-Dimensional CrSI Janus Semiconductor Monolayer. Journal of Physical Chemistry C, 2023, 127, 2003-2011.	1.5	6
75695	Hydrogen Trapping and Precipitation of Alloy Carbides in Molybdenum Added Steels and Vanadium Added Steels. Tetsu-To-Hagane/Journal of the Iron and Steel Institute of Japan, 2023, 109, 438-449.	0.1	2
75696	NaBeAs and NaBeSb: Novel Ternary Pnictides with Enhanced Thermoelectric Performance. Journal of Physical Chemistry C, 2023, 127, 1733-1743.	1.5	5
75697	Large gap two-dimensional topological insulators with the coexistence of a significant Rashba effect and piezoelectricity in functionalized PbGe monolayers. Nanoscale, 2023, 15, 4045-4052.	2.8	0
75698	Lattice Dynamics and Electronâ€“Phonon Coupling in Double Perovskite Cs₂NaFeCl₆. Journal of Physical Chemistry C, 2023, 127, 1908-1916.	1.5	9
75699	Single Unitâ€Cell Layered Bi₂Fe₄O₉ Nanosheets: Synthesis, Formation Mechanism, and Anisotropic Thermal Expansion. Small, 2023, 19, .	5.2	1
75700	Unified graph neural network force-field for the periodic table: solid state applications. , 2023, 2, 346-355.		11
75701	DFT Study on the Enhancement of Isobaric Specific Heat of GaN and InN Nanosheets for Use as Nanofluids in Solar Energy Plants. Materials, 2023, 16, 915.	1.3	2

#	Article	IF	Citations
75702	Facet-Dependent Ba Dissolution of Tetragonal BaTiO₃ Single Crystal Surfaces. Journal of Physical Chemistry C, 2023, 127, 1848-1854.	1.5	0
75703	Significant enhancement of ferromagnetism above room temperature in epitaxial 2D van der Waals ferromagnet Fe_{5â^'Î´}GeTe₂/Bi₂Te₃ heterostructures. Nanoscale, 2023, 15, 2223-2233.	2.8	3
75704	Photoinduced Carrier Transfer Dynamics in MoSSe/WSSe Vertical and Lateral Heterostructures. Journal of Physical Chemistry C, 2023, 127, 2078-2087.	1.5	3
75705	Passivation of Hematite by a Semiconducting Overlayer Reduces Charge Recombination: An Insight from Nonadiabatic Molecular Dynamics. Journal of Physical Chemistry Letters, 2023, 14, 879-887.	2.1	12
75706	Role of Hollow Defects in Lattice Phase Separation and Electronic Features in Quasi-One-Dimensional Bi₄I₄ Crystals. Journal of Physical Chemistry C, 2023, 127, 2098-2103.	1.5	1
75707	Migration of Ga vacancies and interstitials in <mml:math xmlns:mml="http://www.w3.org/1998/Math/MathML"><mml:mrow><mml:mi>Î²</mml:mi><mml:mtext>â^'</mml:mtext><mml:msub><mathvariant="normal">O</mml:mi><mml:mn>3</mml:mn></mml:msub></mml:mrow></mml:math>. Physical Review B, 2023, 107, .	1.1	13
75708	First Theoretical Realization of a Stable Two-Dimensional Boron Fullerene Network. Applied Sciences (Switzerland), 2023, 13, 1672.	1.3	1
75709	Band Structure, Phonon Spectrum and Thermoelectric Properties of Ag3CuS2. Materials, 2023, 16, 1130.	1.3	1
75710	Pushing the Performance Limit of Cu/CeO₂ Catalyst in CO₂ Electroreduction: A Cluster Model Study for Loading Single Atoms. ACS Nano, 2023, 17, 2620-2628.	7.3	11
75711	Band Engineering of Valleytronics WSe₂-MoS₂ Heterostructures via Stacking form, Magnetic moment and Thickness. Chinese Physics B, 0, , .	0.7	0
75712	Oriented Conversion of a LA/HMF Mixture to GVL and FDCA in a Biphasic Solvent over a Ru Single-Atom/Nanoparticle Dual-Site Catalyst. ACS Catalysis, 2023, 13, 2268-2276.	5.5	11
75713	Effect of nano-CaO particle on the microstructure, mechanical properties and corrosion behavior of lean Mg-1Zn alloy. Journal of Magnesium and Alloys, 2024, 12, 794-814.	5.5	5
75714	Exploring the Interdependence between Electronically Unfavorable Situations and Pressure in a Chalcogenide Superconductor. Inorganics, 2023, 11, 61.	1.2	0
75715	Hardness and Mechanical Properties of Wurtzite Bâ€“Câ€“N Compounds. Journal of Physical Chemistry C, 2023, 127, 2581-2588.	1.5	0
75716	Theoretical study of single-nonmetal-modified V2CO2 MXene as an efficient electrocatalyst for overall water splitting. International Journal of Hydrogen Energy, 2023, 48, 15473-15482.	3.8	4
75717	Photo-controllable heterostructured crystals of metalâ€“organic frameworksviareversible photocycloaddition. Chemical Science, 2023, 14, 1852-1860.	3.7	5
75719	Proton transfer in layered hydrogen-bonded system Î³-MOOH (M = Al, Sc): Robust bi-mode ferroelectricity and 1D superionic conductivity. Applied Physics Letters, 2023, 122, 042901.	1.5	2
75720	High Thermoelectric Performance in Earthâ€Abundant Cu₃SbS₄ by Promoting Doping Efficiency via Rational Vacancy Design. Advanced Functional Materials, 2023, 33, .	7.8	21

#	Article	IF	Citations
75721	Unravelling intrinsic descriptors based on a two-stage activity regulation of bimetallic 2D c-MOFs for CO₂RR. Nanoscale, 2023, 15, 4991-5000.	2.8	6
75722	Janus Ga2SeTe and In2SeTe nanosheets: Excellent photocatalysts for hydrogen production under neutral pH. International Journal of Hydrogen Energy, 2023, 48, 16358-16369.	3.8	7
75723	NiFeP Anchored on rGO as a Multifunctional Interlayer To Promote the Redox Kinetics for Liâ€“S Batteries via Regulating d-Bands of Ni-Based Phosphides. ACS Sustainable Chemistry and Engineering, 2023, 11, 1742-1751.	3.2	15
75724	Screening High-Entropy Alloys for Carbon Dioxide Reduction Reaction Using Alchemical Perturbation Density Functional Theory. Minerals, Metals and Materials Series, 2023, , 119-126.	0.3	0
75725	Application of First Principles Computations Based on Density Functional Theory (DFT) in Cathode Materials of Sodium-Ion Batteries. Batteries, 2023, 9, 86.	2.1	3
75726	Properties of carbon up to 10 million kelvin from Kohn-Sham density functional theory molecular dynamics. Physical Review E, 2023, 107, .	0.8	6
75727	Influence of the charge compensating agent on tunable emission of the Ba2MgWO6:Eu3+ double perovskite. Ceramics International, 2023, 49, 16038-16043.	2.3	3
75728	MoS₂@C with S vacancies vertically anchored on V₂C-MXene for efficient lithium and sodium storage. Inorganic Chemistry Frontiers, 2023, 10, 1587-1602.	3.0	25
75729	Efficient synthesis of diethyl oxalate from transesterification of dimethyl oxalate and ethanol using alkaline catalysts and kinetic studies of transesterification. New Journal of Chemistry, 2023, 47, 5510-5518.	1.4	1
75730	Multiple Chelation-Assisted Lithiation Improves the Performance of Phosphate-Modified LiNi_{0.8}Co_{0.1}Mn_{0.1}O₂. Journal of the Electrochemical Society, 2023, 170, 010525.	1.3	1
75731	Phase stability of Fe from first principles: Atomistic spin dynamics coupled with ab initio molecular dynamics simulations and thermodynamic integration. Physical Review B, 2023, 107, .	1.1	3
75732	Thermodynamic and Kinetic Investigation on Electrogeneration of Hydroxyl Radicals for Water Purification. ACS ES&T Engineering, 2023, 3, 2161-2170.	3.7	3
75733	Evidence of Symmetry Breaking in a Gd₂ di-nuclear molecular polymer. Physical Chemistry Chemical Physics, 0, , .	1.3	0
75734	DFT modeling of atomic layer deposition of Ru interconnect metal for EUV scaling. MRS Advances, 2023, 8, 768-772.	0.5	0
75735	Novel Geometric Ferroelectric EuInO₃ Single Crystals with Topological Vortex Domains. Crystal Growth and Design, 2023, 23, 1980-1986.	1.4	5
75736	Excitonic luminescence of iodine-intercalated HfS₂. Applied Physics Letters, 2023, 122, 042102.	1.5	2
75737	Shape-Dependent CO₂ Hydrogenation to Methanol over Cu₂O Nanocubes Supported on ZnO. Journal of the American Chemical Society, 2023, 145, 3016-3030.	6.6	19
75738	Dynamic rhenium dopant boosts ruthenium oxide for durable oxygen evolution. Nature Communications, 2023, 14, .	5.8	77

#	Article	IF	Citations
75739	Accessing the thermal conductivities of Sb₂Te₃ and Bi₂Te₃/Sb₂Te₃ superlattices by molecular dynamics simulations with a deep neural network potential. Physical Chemistry Chemical Physics, 2023, 25, 6164-6174.	1.3	4
75740	Two-dimensional MX₂Y₄ systems: ultrahigh carrier transport and excellent hydrogen evolution reaction performances. Physical Chemistry Chemical Physics, 2023, 25, 4519-4527.	1.3	17
75741	Two-Dimensional Ordered Double-Transition Metal Carbides for the Electrochemical Nitrogen Reduction Reaction. ACS Applied Materials & Interfaces, 2023, 15, 6797-6806.	4.0	14
75742	Single-atom catalysis enabled by high-energy metastable structures. Chemical Science, 2023, 14, 2631-2639.	3.7	5
75743	COx hydrogenation to methanol and other hydrocarbons under mild conditions with Mo3S4@ZSM-5. Nature Communications, 2023, 14, .	5.8	11
75744	Tracking the Role of Defect Types in Co₃O₄ Structural Evolution and Active Motifs during Oxygen Evolution Reaction. Journal of the American Chemical Society, 2023, 145, 2271-2281.	6.6	77
75745	The MoirÃ© pattern rule of the twisted bilayer graphene and its electronic property under a strain. European Physical Journal Plus, 2023, 138, .	1.2	1
75746	Insights into Photoinduced Carrier Dynamics and Overall Water Splitting of Z-Scheme van der Waals Heterostructures with Intrinsic Electric Polarization. Journal of Physical Chemistry Letters, 2023, 14, 798-808.	2.1	15
75747	Electronâ€“phonon effects and temperature-dependence of the electronic structure of monoclinic Î²-Ga2O3. APL Materials, 2023, 11, .	2.2	5
75748	High-Throughput Experimentation, Theoretical Modeling, and Human Intuition: Lessons Learned in Metalâ€“Organic-Framework-Supported Catalyst Design. ACS Central Science, 2023, 9, 266-276.	5.3	5
75749	Selective hydrogenation via precise hydrogen bond interactions on catalytic scaffolds. Nature Communications, 2023, 14, .	5.8	5
75750	Graphene Induced High Thermoelectric Performance in ZnO/Graphene Heterostructure. Advanced Materials Interfaces, 2023, 10, .	1.9	4
75751	Investigation of CdSe and ZnSe as Potential Back Surface Field Layers for CdTeâ€Based Solar Cells: A Study from First Principles Calculations. Advanced Theory and Simulations, 2023, 6, .	1.3	3
75752	Nanoalloys and catalytic applications. , 2023, , 401-436.		0
75753	Spontaneous Anomalous Hall Effect Arising from an Unconventional Compensated Magnetic Phase in a Semiconductor. Physical Review Letters, 2023, 130, .	2.9	37
75754	Pressure driven rotational isomerism in 2D hybrid perovskites. Nature Communications, 2023, 14, .	5.8	14
75755	Anisotropic Rashba effect in two-dimensional non-Janus transition-metal dichalcogenide, <mml:math xmlns:mml="http://www.w3.org/1998/Math/MathML"><mml:mrow><mml:mi>M</mml:mi><mml:mi>SSe</mml:mi></mml:mrow><mml: Review B, 2023, 107, .	1.1	4
75756	Electronic correlations and universal long-range scaling in kagome metals. Physical Review Research, 2023, 5, .	1.3	2

#	Article	IF	Citations
75757	Funnel-shaped electronic structure and enhanced thermoelectric performance in ultralight <mml:math xmlns:mml="http://www.w3.org/1998/Math/MathML"><mml:mrow><mml:msub><mml:mi mathvariant="normal">C</mml:mi><mml:mi>x</mml:mi></mml:msub><mml:msub><mml:mrow><mml:mo>(</mml:mo><mml:mi>BN</mml: biphenylene networks. Physical Review B, 2023, 107, .	1.1	7
75758	Compression of gaseous hydrogen into warm dense states up to 95ÂGPa using multishock compression technique. Physical Review B, 2023, 107, .	1.1	1
75759	Ensemble averages of ab initio optical, transport, and thermoelectric properties of hexagonal <mml:math xmlns:mml="http://www.w3.org/1998/Math/MathML"><mml:mrow><mml:msub><mml:mi>Si</mml:mi><mml:mi>x</mml:mi></mml:ms alloys. Physical Review Materials, 2023, 7, .	0.9	1
75760	Integrating Photoluminescence and Ferromagnetism in Carbon Quantum Dot/ZnO by Interfacial Orbital Hybridization for Multifunctional Bioprobes. ChemPhysChem, 0, , .	1.0	1
75761	Tracking and Understanding Dynamics of Atoms and Clusters of Late Transition Metals with In-Situ DRIFT and XAS Spectroscopy Assisted by DFT. Journal of Physical Chemistry C, 2023, 127, 3032-3046.	1.5	6
75762	Adsorbed CO₂-Mediated CO₂ Photoconversion Cycle into Solar Fuel at the O Vacancy Site of Zirconium Oxide. Journal of Physical Chemistry C, 2023, 127, 1776-1788.	1.5	4
75763	Highâ€Efficiency Reactive Oxygen Species Generation by Multiphase and TiO₆ Distortionâ€Mediated Superior Piezocatalysis in Perovskite Ferroelectrics. Advanced Functional Materials, 2023, 33, .	7.8	13
75764	Interfacial effects on lithium-ion diffusion in two-dimensional lateral black phosphorusâ€“graphene heterostructures. Physical Chemistry Chemical Physics, 2023, 25, 6830-6837.	1.3	1
75765	First-principles study on ultrafast Li-ion diffusion in halospinel Li₂Sc_{2/3}Cl₄ through multichannels designed by aliovalent doping. Journal of Materials Chemistry A, 2023, 11, 4272-4279.	5.2	2
75766	Anion regulating endows core@shell structured hollow carbon spheres@MoSxSe2â^'x with tunable and boosted microwave absorption performance. Nano Research, 2023, 16, 5756-5766.	5.8	21
75767	pâ€d Orbital Hybridization Engineered Singleâ€Atom Catalyst for Electrocatalytic Ammonia Synthesis. Energy and Environmental Materials, 0, , .	7.3	7
75768	Engineering Chemo-Mechanical Properties of Zn Surfaces via Alucone Coating. Journal of Physical Chemistry C, 2023, 127, 2481-2492.	1.5	0
75770	Seven-photon absorption from Na⁺/Bi³⁺-alloyed Cs₂AgInCl₆perovskites. Materials Horizons, 2023, 10, 1406-1415.	6.4	8
75771	Hydrodeoxygenation of acetic acid over Ni-promoted Cu-based catalysts: a theoretical mechanism and kinetic study. Catalysis Science and Technology, 2023, 13, 1345-1357.	2.1	1
75772	Ab initio study of changing the oxygen reduction activity of Coâ€“Fe-based perovskites by tuning the B-site composition. Physical Chemistry Chemical Physics, 2023, 25, 4236-4242.	1.3	0
75773	Molecular layer-by-layer re-stacking of MoS₂â€“In₂Se₃ by electrostatic means: assembly of a new layered photocatalyst. Materials Chemistry Frontiers, 2023, 7, 937-945.	3.2	0
75774	Grain Refinement Mechanisms of TiC0.5N0.5 Nanoparticles in Aluminum. Materials, 2023, 16, 1214.	1.3	2
75775	Machine learning assisted investigation of the barocaloric performance in ammonium iodide. Applied Physics Letters, 2023, 122, .	1.5	6

#	Article	IF	Citations
75776	Spatial confinement of sliver nanoparticles in nitrogen-doped carbon framework with high catalytic activity and long-term cycling. Frontiers in Energy Research, 0, 10, .	1.2	1
75777	Sustainable upcycling of post-consumer waste to metal-graphene catalysts for green chemicals and clean water. Cell Reports Physical Science, 2023, , 101256.	2.8	0
75778	Energy-overlap of the Dirac surface state with bulk bands in <mml:math xmlns:mml="http://www.w3.org/1998/Math/MathML"><mml:mrow><mml:msub><mml:mi>SnBi</mml:mi><mml:mn>2</mml:mn></mml:msub></mml:mrow></mml:math> Physical Review Materials, 2023, 7, .	2.4	0
75779	Chemical heterogeneity modulated zero thermal expansion alloy over super-wide temperature range. Cell Reports Physical Science, 2023, , 101254.	2.8	0
75780	Dual-plasmon-enhanced nitrophenol hydrogenation over W₁₈O₄₉â€“Au heterostructures studied at the single-particle level. Catalysis Science and Technology, 0, , .	2.1	1
75781	Charge multipole correlations and order in <mml:math xmlns:mml="http://www.w3.org/1998/Math/MathML"><mml:mrow><mml:msub><mml:mi>Cs</mml:mi><mml:mn>2</mml:mn></mml:msub></mml:mrow></mml:math> Physical Review Research, 2023, 5, .	4.2	5
75782	Abnormal behavior of preferred formation of the cationic vacancies from the interior in a Î³-GeSe monolayer with the stereo-chemical antibonding lone-pair state. Nanoscale Horizons, 2023, 8, 404-411.	4.1	6
75783	Interfacial bonding between iron and Mo- and Cr-doped tungsten carbides. Journal of Applied Physics, 2023, 133, .	1.1	8
75784	Giant valley-Zeeman coupling in the surface layer of an intercalated transition metal dichalcogenide. Nature Materials, 2023, 22, 459-465.	13.3	9
75785	Structural insight into the magnesium borohydride â€“ ethylenediamine solid-state Mg-ion electrolyte system. Dalton Transactions, 2023, 52, 2404-2411.	1.6	3
75786	Insight into the Anchoring Effect of Twoâ€Dimensional TiX₂ (X = S, Se) Materials for Sodiumâ€“Sulfur Batteries: A Firstâ€Principles Study. Advanced Theory and Simulations, 2023, 6, .	1.3	1
75787	In-gap states and strain-tuned band convergence in layered structure trivalent iridate K0.75Na0.25IrO2. Physical Chemistry Chemical Physics, 0, , .	1.3	1
75788	Strain engineering a persistent spin helix with infinite spin lifetime. Physical Review B, 2023, 107, .	1.1	1
75789	Room-temperature magnetism in two-dimensional metalâ€“organic frameworks enabled by electrostatic gating. Journal of Materials Chemistry A, 2023, 11, 5548-5558.	5.2	10
75790	Highly NH₃ Sensitive and Selective Ti₃C₂O₂-Based Gas Sensors: A Density Functional Theory-NEGF Study. ACS Omega, 2023, 8, 4261-4269.	1.6	12
75791	Chirality variation from self-assembly on Ullmann coupling for the DBCh adsorbate on Au(111) and Ag(111). Nanoscale Advances, 2023, 5, 1368-1377.	2.2	5
75792	High-performance Ce doped three-dimensional ordered macroporous Co-based catalysts on CO oxidation. Catalysis Science and Technology, 2023, 13, 2015-2025.	2.1	4
75793	Grape bunches of novel conjugated chain bonded fullerene oligomers: design of a potential electron trap carbonaceous molecular material. Physical Chemistry Chemical Physics, 0, , .	1.3	0

#	Article	IF	Citations
75794	In situ quantitative single-molecule study of site-specific photocatalytic activity and dynamics on ultrathin g-C₃N₄ nanosheets. Nanoscale, 2023, 15, 3449-3460.	2.8	5
75795	First-principles screening of transition metal doped anatase TiO₂(101) surfaces for the electrocatalytic nitrogen reduction. Physical Chemistry Chemical Physics, 2023, 25, 5827-5835.	1.3	2
75796	Real-Space Observation of Ripple-Induced Symmetry Crossover in Ultrathin MnPS₃. ACS Nano, 2023, 17, 1916-1924.	7.3	1
75797	Stability and Physical Properties of the L12-Î³â€² Phase in the CoNiAlTi-System. Metallurgical and Materials Transactions A: Physical Metallurgy and Materials Science, 0, , .	1.1	0
75798	Tuning of Second-Harmonic Generation in Zn-Based Metalâ€“Organic Frameworks by Controlling the Structural Interpenetrations: A First-Principles Investigation. Journal of Physical Chemistry C, 2023, 127, 2058-2068.	1.5	3
75799	The Role of M³⁺ Substitutional Doping (M = In, Sb, Bi) in the Passivation of the Î±-CsPbI₃(100) Surface. Journal of Physical Chemistry C, 2023, 127, 1713-1721.	1.5	7
75800	Radical polymeric p-doping and grain modulation for stable, efficient perovskite solar modules. Science, 2023, 379, 288-294.	6.0	59
75801	Combined ab initio and experimental screening of phase stabilities in the Co-Fe-Ti- <mml:math		

#	Article	IF	Citations
75812	Prediction and Characterization of Two-Dimensional Zn₂VN₃. Journal of Physical Chemistry Letters, 2023, 14, 1148-1155.	2.1	5
75813	DFT-D3 study of two-dimensional polymerization of C₆₀ crystal under high pressure. Japanese Journal of Applied Physics, 0, , .	0.8	0
75814	Synthesis, crystal structure, DFT, and photovoltaic studies of BaCeCuS₃. New Journal of Chemistry, 2023, 47, 5378-5389.	1.4	9
75815	Materials synthesizability and stability prediction using a semi-supervised teacher-student dual neural network. , 0, , .		1
75816	Mechanisms of Degradation of Na₂Ni[Fe(CN)₆] Functional Electrodes in Aqueous Media: A Combined Theoretical and Experimental Study. Journal of Physical Chemistry C, 2023, 127, 2204-2214.	1.5	3
75817	Role of electron localisation in H adsorption and hydride formation in the Mg basal plane under aqueous corrosion: a first-principles study. Physical Chemistry Chemical Physics, 2023, 25, 5989-6001.	1.3	4
75818	Doping and pretreatment optimized the adsorption of *OCHO on bismuth for the electrocatalytic reduction of CO₂to formate. Nanoscale, 2023, 15, 4477-4487.	2.8	4
75819	Firstâ€principles study on stability, <scp>Debye</scp> temperature, mechanical, electronic and magnetic properties of <scp>Fe₂B</scp> compounds. International Journal of Quantum Chemistry, 2023, 123, .	1.0	1
75820	Covalent-like bondings and abnormal formation of ferroelectric structures in binary ionic salts. Science Advances, 2023, 9, .	4.7	2
75821	Thermodynamic and Kinetic Barriers Limiting Solid-State Reactions Resolved through In Situ Synchrotron Studies of Lithium Halide Salts. Chemistry of Materials, 2023, 35, 917-926.	3.2	1
75822	Ultraporous, Ultrasmall MgMn₂O₄ Spinel Cathode for a Room-Temperature Magnesium Rechargeable Battery. ACS Nano, 2023, 17, 3135-3142.	7.3	6
75823	General low-temperature growth of two-dimensional nanosheets from layered and nonlayered materials. Nature Communications, 2023, 14, .	5.8	39
75824	Sliding ferroelectricity in bilayer honeycomb structures: A first-principles study. Physical Review B, 2023, 107, .	1.1	11
75825	Trends in CO₂ Reduction on Transition Metal Dichalcogenide Edges. ACS Catalysis, 2023, 13, 2341-2350.	5.5	8
75826	2D coordination sheets based on tetranuclear cuprofullerene pentafluorobenzoate and their electronic properties. Inorganic Chemistry Frontiers, 2023, 10, 1731-1738.	3.0	3
75827	Molecular-Dynamics Analysis of the Mechanical Behavior of Plasma-Facing Tungsten. ACS Applied Materials & Interfaces, 2023, 15, 8709-8722.	4.0	2
75828	DFT calculations of structural, magnetic, and stability of FeNiCo-based and FeNiCr-based quaternary alloys. Journal of Applied Physics, 2023, 133, .	1.1	3
75829	Valley Hall effect in graphene-like <mml:math xmlns:mml="http://www.w3.org/1998/Math/MathML"><mml:mrow><mml:mi>Sn</mml:mi><mml:mi>X</mml:mi></mml:mrow></mml:math> (<mml:math) Tj ETQq1 1 0.784314 rgBT /Overlock 10 Tf 50 62 Td (xmlns:mml="http://www.w3.org/1998/Math/MathML"><mml:mrow> Physical Review B, 2023, 107, .	1.1	4

#	Article	IF	Citations
75830	Tuning the interplay of spin-orbit coupling and trigonal crystal-field effect in the Ising-like spin system <mml:math xmlns:mml="http://www.w3.org/1998/Math/MathML"><mml:msub><mml:mi mathvariant="normal">Ca</mml:mi><mml:mn>3</mml:mn></mml:msub><mml:msub><mml:mi mathvariant="normal">Co</mml:mi><mml:mn>2</mml:mn></mml:msub><mml:msub><mml:mi mathvariant="normal">O</mml:mi><mml:mn>6</mml:mn></mml:msub></mml:math>. Physical Review B, 2023, 107, .	1.1	0
75831	Tunable Salt-Inclusion Chalcogenides for Ion Exchange, Photoluminescence, and Scintillation. Chemistry of Materials, 2023, 35, 1417-1431.	3.2	3
75832	Synthesis of Thermally Stable and Highly Luminescent Cs₅Cu₃Cl₆I₂ Nanocrystals with Nonlinear Optical Response. Small, 2023, 19, .	5.2	3
75833	Growth mechanism of metal iron particles with sulfur additives in direct reduction: First-principles calculations and experiments. Powder Technology, 2023, 419, 118287.	2.1	1
75834	Click and Detect: Versatile Ampicillin Aptasensor Enabled by Click Chemistry on a Grapheneâ€“Alkyne Derivative. Small, 2023, 19, .	5.2	1
75835	Correlation of the crystal features, magnetic parameters, and electronic structure of Bi-substituted BaFe12-xBixO19 hexaferrites: Theoretical background. Ceramics International, 2023, 49, 15492-15499.	2.3	5
75836	Emergent magnetic-nonmagnetic transition in strain-tuned zigzag-edged <mml:math xmlns:mml="http://www.w3.org/1998/Math/MathML"><mml:msub><mml:mi>PtSe</mml:mi><mml:mn>2</mml:mn></mml:msub></mml:math> nanoribbon. Physical Review Research, 2023, 5, .	1.3	1
75837	Modular electrochemical production of hydrogen using Mottâ€“Schottky Co9S8/Ni3S2 heterojunction as a redox mediator. International Journal of Hydrogen Energy, 2023, 48, 16184-16197.	3.8	4
75838	Unconventional Anisotropy in Excitonic Properties and Carrier Mobility in Iodine-Based XTeI (X = Ga,) Tj ETQq0 0 0 rgBT /Overlock 10 Tf 5 127, 1992-2002.	1.5	10
75839	The kinetics of carbon pair formation in silicon prohibits reaching thermal equilibrium. Nature Communications, 2023, 14, .	5.8	2
75840	Defect and strain engineered MoS₂/graphene catalyst for an enhanced hydrogen evolution reaction. RSC Advances, 2023, 13, 4056-4064.	1.7	5
75841	Raman Spectroscopy Signatures of Boron-Rich Superhard Materials from Density Functional Theory. Journal of Physical Chemistry C, 2023, 127, 2104-2115.	1.5	6
75842	Influence of Element Doping and Surface Oxidation on CoP for Overall Water Splitting: A First-Principles Study. Journal of Physical Chemistry C, 2023, 127, 1808-1821.	1.5	4
75843	Ordered vacancy compounds: the case of the MangÃ©li phases of TiO2. , 2023, , 533-565.		0
75844	Modeling metamaterials: Planar heterostructures based on graphene, silicene, and germanene. , 2023, , 27-50.		0
75845	Theoretical prediction of two-dimensional II-V compounds. Physical Review Materials, 2023, 7, .	0.9	0
75846	Charged species redistribution at electrochemical interfaces: a model system of the zirconium oxide/water interface. Physical Chemistry Chemical Physics, 2023, 25, 6380-6391.	1.3	1
75847	Density functional theory study of adsorption of H2O on Î³-U(110) surface. Indian Journal of Physics, 0, , .	0.9	0

#	Article	IF	Citations
75848	The Physics of Twin Boundary Termination in Cu(In, Ga)Se₂ Absorbers. Solar Rrl, 2023, 7, .	3.1	2
75849	Molecular Dynamics with Chemical Accuracyâ”€Alkane Adsorption in Acidic Zeolites. ACS Catalysis, 2023, 13, 2011-2024.	5.5	5
75850	Catching the Killer: Dynamic Disorder Design Rules for Smallâ€Molecule Organic Semiconductors. Advanced Functional Materials, 2023, 33, .	7.8	5
75851	Tuning of the electronic and photocatalytic properties of Janus WSiGeZ₄ (Z = N, P, and As) monolayers via strain engineering. Physical Chemistry Chemical Physics, 2023, 25, 7278-7288.	1.3	12
75852	Theoretical design of porous dodecagonal germanium carbide (d-GeC) monolayer. RSC Advances, 2023, 13, 3290-3294.	1.7	7
75853	Sc2CX (X=N2, ON, O2) MXenes as a promising anode material: A first-principles study. Journal of Applied Physics, 2023, 133, .	1.1	5
75854	Influence of Quantum Oscillations in the Thermal Scattering Law of Zirconium Carbide on Neutron Thermalization and Criticality. Nuclear Science and Engineering, 2023, 197, 1800-1813.	0.5	0
75855	Vinylene carbonate reactivity at lithium metal surface: first-principles insights into the early steps of SEI formation. Journal of Materials Chemistry A, 2023, 11, 5660-5669.	5.2	6
75856	Understanding the electronic pi-system of 2D covalent organic frameworks with Wannier functions. Scientific Reports, 2023, 13, .	1.6	4
75857	Aligning Metal Coordination Sites in Metalâ€“Organic Framework-Enabled Metallaphotoredox Catalysis. ACS Applied Materials & Interfaces, 2023, 15, 5139-5147.	4.0	2
75858	Imparting Metal Oxides with High Sensitivity Toward Lightâ€Activated NO₂ Detection Via Tailored Interfacial Chemistry. Advanced Functional Materials, 2023, 33, .	7.8	2
75859	Mechanisms of interlayer exciton emission and giant valley polarization in van der Waals heterostructures. Physical Review B, 2023, 107, .	1.1	5
75860	Formation of surface states on Pb(111) by Au adsorption. Scientific Reports, 2023, 13, .	1.6	0
75861	Modulation of CO₂ adsorption thermodynamics and selectivity in alkali-carbonate activated N-rich porous carbons. Journal of Materials Chemistry A, 2023, 11, 12811-12826.	5.2	2
75862	Efficient fabrication of single-wall carbon nanotube nanoreactors by defect-induced cutting. Nanoscale, 2023, 15, 3931-3939.	2.8	1
75863	Stability and Elasticity of Quasi-Hexagonal Fullerene Monolayer from First-Principles Study. Crystals, 2023, 13, 224.	1.0	7
75864	Automated Graph Neural Networks Accelerate the Screening of Optoelectronic Properties of Metalâ€“Organic Frameworks. Journal of Physical Chemistry Letters, 2023, 14, 1239-1245.	2.1	2
75865	Chlorine Adsorption on the Ag(110) Surface: STM and DFT Study. Journal of Physical Chemistry C, 2023, 127, 2266-2273.	1.5	1

#	Article	IF	Citations
75866	Partially Reversible Anionic Redox for Lithium-Excess Cobalt Oxides with Cation-Disordered Rocksalt Structure. Journal of Physical Chemistry C, 2023, 127, 2194-2203.	1.5	4
75867	Accelerated Discovery of Novel Garnet-Type Solid-State Electrolyte Candidates via Machine Learning. ACS Applied Materials & Interfaces, 2023, 15, 5049-5057.	4.0	7
75868	Strong anharmonicity and high thermoelectric performance of cubic thallium-based fluoride perovskites TlXF₃ (X = Hg, Sn, Pb). Physical Chemistry Chemical Physics, 2023, 25, 5776-5784.	1.3	6
75869	First-principles study of the ferrielectric of X-doped KNbO₃ (Xâ€‰=â€‰Na, Rb, and Cs). Ferroelectrics, 2023, 603, 267-275.	0.3	1
75873	Charge transport in mixed metal halide perovskite semiconductors. Nature Materials, 2023, 22, 216-224.	13.3	32
75874	Greatly recovered electrochemical performances of regenerated graphite anode enabled by an artificial PMMA solid electrolyte interphase layer. Energy Storage Materials, 2023, 56, 457-467.	9.5	11
75875	Learning local equivariant representations for large-scale atomistic dynamics. Nature Communications, 2023, 14, .	5.8	86
75876	Electronic structure characteristics of two-dimensional ferroelectric heterostructures Î±-In₂Se₃/ZnSe. Journal of Physics Condensed Matter, 2023, 35, 145501.	0.7	4
75877	Allâ€Transfer Electrode Interface Engineering Toward Harshâ€Environmentâ€Resistant MoS₂ Fieldâ€Effect Transistors. Advanced Materials, 2023, 35, .	11.1	7
75878	Nanotwinned Copper Foil for â€œZero Excessâ€•Lithiumâ€“Metal Batteries. ACS Applied Energy Materials, 2023, 6, 2140-2150.	2.5	5
75879	The Stability of a Mixed-Phase Barium Cerium Iron Oxide under Reducing Conditions in the Presence of Hydrogen. Molecules, 2023, 28, 1429.	1.7	0
75881	A comprehensive study on the thermodynamics of the Al13Fe4 solid solution in the Al-Fe-Mn ternary system. Journal of Alloys and Compounds, 2023, 944, 169054.	2.8	4
75882	The formation of O vacancy on ZrO2/Pd and its effect on methane dry reforming: Insights from DFT and microkinetic modeling. Applied Surface Science, 2023, 619, 156679.	3.1	14
75883	Sign change of anomalous Hall effect and anomalous Nernst effect in the Weyl semimetal CeAlSi. Physical Review B, 2023, 107, .	1.1	11
75884	Monolayer chromium dichloride: An anti-ferromagnetic semiconductor with a high NÃ©el temperature above room temperature. Physica E: Low-Dimensional Systems and Nanostructures, 2023, 149, 115666.	1.3	1
75885	Dipolar effects on the work function of an alkali-iodide overlayer (XI, X= Li, Na, K, Rb, and Cs) on tungsten surfaces. Physica Scripta, 0, , .	1.2	1
75886	In-situ constructed SnO2 gradient buffer layer as a tight and robust interphase toward Li metal anodes in LATP solid state batteries. Journal of Energy Chemistry, 2023, 80, 89-98.	7.1	12
75887	Improving MgO/Fe insulator-metal interface structure through oxygen-precoating of Fe(0 0 1). Applied Surface Science, 2023, 618, 156628.	3.1	0

#	Article	IF	Citations
75888	Synergetic optimization of thermoelectric properties in SnSe film via manipulating Se vacancies. Journal of Alloys and Compounds, 2023, 943, 169115.	2.8	1
75889	Biaxial strain tunable quantum capacitance and photocatalytic properties of Hf2CO2 monolayer. Applied Surface Science, 2023, 616, 156579.	3.1	9
75890	Selective semi-hydrogenation of alkynes on palladium-selenium nanocrystals. Journal of Catalysis, 2023, 418, 247-255.	3.1	5
75891	Effects of transition metal intercalation on the electronic and magnetic properties of CrI3/WSe2 heterostructure. Materials Science in Semiconductor Processing, 2023, 158, 107361.	1.9	1
75892	Noble-metal single atom with non-metal co-doped graphene: First-principles investigation of structures, electronic and magnetic properties. Journal of Magnetism and Magnetic Materials, 2023, 568, 170418.	1.0	1
75893	Orbital polarization change and magnetic enhancement in rutile MnO2-Î´ epitaxial films. Applied Surface Science, 2023, 618, 156654.	3.1	0
75894	Assembly and electrocatalytic CO2 reduction of two-dimensional bimetallic porphyrin-based conjugated cobalt metal-organic framework. Electrochimica Acta, 2023, 443, 141896.	2.6	4
75895	A 3D nanocomposite of NiCo2S4/CuCo2S4 heterostructure synthesized by chemical precipitation for asymmetric supercapacitors. Journal of Alloys and Compounds, 2023, 943, 169170.	2.8	9
75896	Coherent twin-oriented Al3Sc-based precipitates in Al matrix. Scripta Materialia, 2023, 229, 115351.	2.6	1
75897	Facile synthesis of flexible and scalable Cu/Cu2O/CuO nanoleaves photoelectrodes with oxidation-induced self-initiated charge-transporting platform for photoelectrochemical water splitting enhancement. Journal of Alloys and Compounds, 2023, 942, 169094.	2.8	11
75898	Cubic structured silver antimony sulfide-selenide solid solution thin films for sustainable photodetection and photovoltaic application. Journal of Alloys and Compounds, 2023, 942, 169072.	2.8	4
75899	Interplay of magnetic and electric coupling across the spin density wave to conical magnetic ordering in a BaHoFeO4 spin-cluster chain compound. Journal of Alloys and Compounds, 2023, 942, 169017.	2.8	5
75900	Competition between Li2Se2Sx conversion and Li Ion transport on graphene surface coordination doped with transition metal and N. Chemical Engineering Journal Advances, 2023, 14, 100468.	2.4	0
75901	Influence of C-vacancy-line defect on electronic and optical properties and quantum capacitance of Ti2CO2 MXene: A first-principles study. Journal of Physics and Chemistry of Solids, 2023, 176, 111254.	1.9	3
75902	Dual-optimization strategy engineered Ti-based metal-organic framework with Fe active sites for highly-selective CO2 photoreduction to formic acid. Applied Catalysis B: Environmental, 2023, 327, 122418.	10.8	19
75903	Controllable contact types of Janus MoSH and WSi2N4 van der Waals heterostructures via biaxial strain and external electric field. Physica E: Low-Dimensional Systems and Nanostructures, 2023, 149, 115668.	1.3	3
75904	A type-II GaP/GaSe van der Waals heterostructure with high carrier mobility and promising photovoltaic properties. Applied Surface Science, 2023, 618, 156544.	3.1	8
75905	Understanding the influence of bending on OER activity in metal phthalocyanines: A first-principles study. Applied Surface Science, 2023, 618, 156582.	3.1	6

#	Article	IF	Citations
75906	Atom-passivated GeC nanosheets for photocatalytic overall water splitting with high solar-to-hydrogen conversion efficiency. Surfaces and Interfaces, 2023, 37, 102667.	1.5	0
75907	Role of Si segregation in the structural, mechanical, and compositional evolution of high-temperature oxidation resistant Cr-Si-B2Â±z thin films. Journal of Alloys and Compounds, 2023, 944, 169203.	2.8	6
75908	Energy spectrum and light absorption of arsenene quantum dots. Materials Today Communications, 2023, 35, 105542.	0.9	0
75909	Preparation of high-quality alkylated gasoline with low alkane-to-alkene ratio catalyzed by polyether-based BrÃ¸nsted-Lewis acidic deep eutectic solvent. Fuel, 2023, 340, 127565.	3.4	4
75910	Phase-field study of elastic effects on precipitate evolution in (Al)0.05CrFeNi. International Journal of Mechanical Sciences, 2023, 247, 108163.	3.6	1
75911	Efficient CO2 utilization and sustainable energy conversion via aqueous Zn-CO2 batteries. Nano Energy, 2023, 109, 108242.	8.2	9
75912	Reaching the initial coulombic efficiency and structural stability limit of P2/O3 biphasic layered cathode for sodium-ion batteries. Journal of Colloid and Interface Science, 2023, 638, 758-767.	5.0	9
75913	Rational design of one inorganic-organic hybrid Z-scheme heterojunction for high-performance photocatalytic water splitting. Fuel, 2023, 341, 127682.	3.4	2
75914	Theoretical study the electrocatalytic performance and mechanism of novel designed electrocatalyst Ru@2DMs for CO2RR. Fuel, 2023, 340, 127541.	3.4	5
75915	Regulation of the electronic structure and ferromagnetism by implanting topological defects in a bismuth monolayer. Materials Research Bulletin, 2023, 161, 112174.	2.7	0
75916	First-principles study of different oxidation process on Al(111) and Cu(111): Metal pulled-off effect. Surface Science, 2023, 731, 122260.	0.8	0
75917	Revealing the activity origin of ultrathin nickel metalâ€“organic framework nanosheet catalysts for selective electrochemical nitrate reduction to ammonia: Experimental and density functional theory investigations. Journal of Colloid and Interface Science, 2023, 638, 26-38.	5.0	9
75918	Design of PtM (MÂ=ÂRu, Au, or Sn) bimetallic particles supported on TS-1 for the direct dehydrogenation of n-butane. Fuel, 2023, 341, 127630.	3.4	3
75919	SrCuP and SrCuSb Zintl phases as potential thermoelectric materials. Journal of Alloys and Compounds, 2023, 942, 169123.	2.8	3
75920	The electronic and optical properties of multi-layer Bi2O2X (XÂ=ÂS, Se, Te) by first-principles calculations. Applied Surface Science, 2023, 618, 156541.	3.1	7
75921	Self-organized hetero-nanodomains actuating super Li+ conduction in glass ceramics. Nature Communications, 2023, 14, .	5.8	6
75922	Ab Initio Simulation of Dielectric and Optical Properties of Ices Ih and III and Lattice Frameworks of Hydrates sI and sH. Physics of the Solid State, 2022, 64, 576-586.	0.2	0
75923	Effect of Ni-Doping on the Hydrogen Storage Properties of Nanoscale MgH2. Russian Journal of Physical Chemistry A, 2022, 96, 3220-3231.	0.1	0

#	Article	IF	Citations
75924	Synergistic Effect between Fe⁴⁺ and Co⁴⁺ on Oxygen Evolution Reaction Catalysis for CaFe_{1â€“}<i>_x</i>Co<i>_x</i>O<sub>3 Materials Transactions, 2023, , .	0.4	0
75925	Evolution of the valence state of Ru metal ions in correlation with the structural and electronic properties of double perovskite ruthenates; A₂SmRuO₆ (where A = Ba &) Tj ETQq1 1 0.784314 rgBT /Ov	2.0	14
75926	Combined piezoelectricity, valley splitting and Dzyaloshinskiiâ€“Moriya interaction in Janus GdXY (X, Y =) Tj ETQq0 0 0 rgBT /Overlock 1	1.3	2
75927	The regulating effect of boron doping and its concentration on the photocatalytic overall water splitting of a polarized g-C₃N₅ material. Physical Chemistry Chemical Physics, 2023, 25, 8592-8599.	1.3	3
75928	Transition-state correlations for predicting thermochemistry of adsorbates and surface reactions. Physical Chemistry Chemical Physics, 2023, 25, 8412-8423.	1.3	0
75929	Tuning a small electron polaron in FePO₄ by P-site or O-site doping based on DFT+U and KMC simulation. Physical Chemistry Chemical Physics, 2023, 25, 8734-8742.	1.3	2
75930	Inverse â€˜intra-latticeâ€™ charge transfer in nickelâ€“molybdenum dual electrocatalysts regulated by under-coordinating the molybdenum center. Chemical Science, 2023, 14, 3056-3069.	3.7	0
75931	Low temperature molten salt synthesis of noncentrosymmetric (NH₄)₃SbF₃(NO₃)₃and centrosymmetric (NH₄)₃SbF₄(NO₃)₂. Inorganic Chemistry Frontiers, 2023, 10, 2107-2114.	3.0	6
75932	Ag-doped Pd nano-dendritic for promoting the electrocatalytic oxidation of ethylene to ethylene glycol. Materials Chemistry Frontiers, 2023, 7, 1437-1445.	3.2	2
75933	In situ Growth of Co3O4 Nanoparticles on Nitrogen-doped Reduced Graphene Oxide for High-Efficiency Oxygen Reduction Catalysis. New Journal of Chemistry, 0, , .	1.4	1
75934	Alkylammonium bis(trifluoromethylsulfonyl)imide as a dopant in the hole-transporting layer for efficient and stable perovskite solar cells. Energy and Environmental Science, 2023, 16, 2226-2238.	15.6	12
75935	Transport and thermoelectric properties of penta-Sb₂X monolayers. Journal of Materials Chemistry C, 2023, 11, 5156-5166.	2.7	0
75936	Searching for d⁰ spintronic materials: bismuthene monolayer doped with IVA-group atoms. RSC Advances, 2023, 13, 5885-5892.	1.7	7
75937	Janus Î²-PdXY (X/Y = S, Se, Te) materials with high anisotropic thermoelectric performance. Nanoscale, 2023, 15, 5964-5975.	2.8	5
75938	Discovery of a metastable van der Waals semiconductor via polymorphic crystallization of an amorphous film. Materials Horizons, 2023, 10, 2254-2261.	6.4	2
75939	Spin-polarization anisotropy controlled by bending in tungsten diselenide nanoribbons and tunable excitonic states. Journal of Materials Chemistry C, 2023, 11, 4711-4727.	2.7	2
75940	Ternary pentagonal BXN (X = C, Si, Ge, and Sn) sheets with high piezoelectricity. RSC Advances, 2023, 13, 9636-9641.	1.7	3
75941	Achieving real Ohmic contact by the dual protection of outer layer atoms and surface functionalization in 2D metal Mxenes/MoSi₂N₄ heterostructures. Journal of Materials Chemistry C, 2023, 11, 4728-4741.	2.7	9

#	Article	IF	Citations
75942	Activating dual atomic electrocatalysts for the nitric oxide reduction reaction through the P/S element. Materials Horizons, 2023, 10, 2160-2168.	6.4	8
75943	Design, synthesis, and application of covalent organic frameworks as catalysts. New Journal of Chemistry, 2023, 47, 6765-6788.	1.4	4
75944	Can magnetotransport properties provide insight into the functional groups in semiconducting MXenes?. Nanoscale, 2023, 15, 10254-10263.	2.8	1
75945	Vacancy impacts on electronic and mechanical properties of MX2 (M = Mo, W and X = S, Se) monolayers. RSC Advances, 2023, 13, 6498-6506.	1.7	3
75946	First principles calculation of the ZnV₂O₆(001) surface terminations: the thermodynamic stability and electronic structure study. Physical Chemistry Chemical Physics, 2023, 25, 12352-12362.	1.3	1
75947	Deciphering the photocatalytic hydrogen generation process of Fresnoite Ba₂TiGe₂O₈ by electronic structure and bond analyses. Dalton Transactions, 2023, 52, 3769-3776.	1.6	1
75948	Oxygen migration performance of LaFeO₃ perovskite-type oxygen carriers with Sr doping. Physical Chemistry Chemical Physics, 2023, 25, 9216-9224.	1.3	0
75949	Ga₄C-family crystals, a new generation of star thermoelectric materials, achieved by band degeneracies, valley anisotropy, and strong phonon scattering among others. Journal of Materials Chemistry A, 2023, 11, 8013-8023.	5.2	3
75950	Tuning the water-splitting mechanism on titanium dioxide surfaces through hydroxylation. Physical Chemistry Chemical Physics, 2023, 25, 9264-9272.	1.3	0
75951	A ï¬rst-principle study of bilayer black phosphorene as a potential anode material in sodium-ion batteries. Physical Chemistry Chemical Physics, 0, , .	1.3	0
75952	The Î²-PdBi₂monolayer for efficient electrocatalytic NO reduction to NH₃: a computational study. Inorganic Chemistry Frontiers, 2023, 10, 2677-2688.	3.0	6
75953	The effect of magnetic order on the thermal transport properties of the intrinsic two-dimensional magnet 2H-VSe₂. Physical Chemistry Chemical Physics, 2023, 25, 9817-9823.	1.3	2
75954	Lead-free 2D MASnBr₃ and Ruddlesdenâ€“Popper BA₂MASn₂Br₇ as light harvesting materials. RSC Advances, 2023, 13, 7939-7951.	1.7	1
75955	N₂ adsorption on high-entropy alloy surfaces: unveiling the role of local environments. Journal of Materials Chemistry A, 2023, 11, 12973-12983.	5.2	1
75956	New mechanistic insights into the role of water in the dehydration of ethanol into ethylene over ZSM-5 catalysts at low temperature. Green Chemistry, 2023, 25, 3644-3659.	4.6	6
75957	Shapes of phases in isothermal phase diagrams: what is wrong with the Thermo-Calc logo. Materials Horizons, 0, , .	6.4	0
75958	Combined experimental and DFT approach to BiNbO₄polymorphs. RSC Advances, 2023, 13, 5576-5589.	1.7	5
75959	Electron-phonon coupling, bipolar effect, and thermoelectric performance of the CuSbS₂ monolayer. Physical Chemistry Chemical Physics, 0, , .	1.3	2

#	Article	IF	Citations
75960	Charting Ba-Based Double Perovskite Oxides for Visible-Light-Driven Photocatalytic Water Splitting. Journal of Physical Chemistry C, 2023, 127, 3968-3976.	1.5	5
75961	Ni-Intercalation-Induced Topological Nodal Line States and Superconductivity in NiTe. Journal of Physical Chemistry C, 2023, 127, 4303-4309.	1.5	4
75962	Quantum Oscillation and Electronic Structure of Sn₄As₃ and Sn₄P₃. Journal of Physical Chemistry C, 2023, 127, 4319-4325.	1.5	1
75963	A novel lithium decorated N-doped 4,6,8-biphenylene for reversible hydrogen storage: Insights from density functional theory. International Journal of Hydrogen Energy, 2023, 48, 17216-17229.	3.8	15
75964	Unfolding the band structure of van der Waals heterostructures. Physical Review Materials, 2023, 7, .	0.9	4
75966	Al and Ti location in the MFI orthorhombic HZSM-5 framework. DFT calculation and neutron diffraction experiment. Journal of Materials Science, 2023, 58, 3934-3946.	1.7	3
75967	Metal-to-Insulating Transition in the Perovskite System YSr₂Cu₂FeO_{8â^Î´}(0 < Î´ < 1) Modeled by DFT Methods. Inorganic Chemistry, 2023, 62, 3445-3456.	1.9	3
75968	Surface-Dependent Hydrogen Evolution Activity of Copper Foil. Materials, 2023, 16, 1777.	1.3	0
75970	Vibrational properties of <mml:math xmlns:mml="http://www.w3.org/1998/Math/MathML"><mml:msub><mml:mi>LiNbO</mml:mi><mml:mn>3</mml:mn></mml:msub></m and <mml:math xmlns:mml="http://www.w3.org/1998/Math/MathML"><mml:msub><mml:mi>LiTaO</mml:mi><mml:mn>3</mml:mn></mml:msub></m under uniaxial stress. Physical Review Materials, 2023, 7, .	0.9	3
75971	Inter-quintuple layer coupling and topological phase transitions in the chalcogenide topological insulators. Electronic Structure, 2023, 5, 015001.	1.0	1
75972	Evidence for intrinsic defects and nanopores as hotspots in 2D PdSe2 dendrites for plasmon-free SERS substrate with a high enhancement factor. Npj 2D Materials and Applications, 2023, 7, .	3.9	6
75973	Customized reaction route for ruthenium oxide towards stabilized water oxidation in high-performance PEM electrolyzers. Nature Communications, 2023, 14, .	5.8	66
75974	Band structure, superconductivity, and polytypism in <mml:math xmlns:mml="http://www.w3.org/1998/Math/MathML"><mml:msub><mml:mi>AuSn</mml:mi><mml:mn>4</mml:mn></mml:msub></m Physical Review Materials, 2023, 7, .	0.9	3
75975	Active Learning Accelerating to Screen Dual-Metal-Site Catalysts for Electrochemical Carbon Dioxide Reduction Reaction. ACS Applied Materials & Interfaces, 2023, 15, 12986-12997.	4.0	4
75976	X-ray free electron laser studies of electron and phonon dynamics of graphene adsorbed on copper. Physical Review Materials, 2023, 7, .	0.9	1
75977	Nonharmonic contributions to the high-temperature phonon thermodynamics of Cr. Physical Review B, 2023, 107, .	1.1	0
75978	Direct Mechanochemical Synthesis, Phase Stability, and Electrochemical Performance of Î±-NaFeO₂. Inorganic Chemistry, 2023, 62, 3358-3367.	1.9	3
75979	Enabling the transition to ductile MAX phases and the exfoliation to MXenes via tuning the A element. Journal of the American Ceramic Society, 2023, 106, 3765-3776.	1.9	4

#	Article	IF	Citations
75980	Tailoring WB morphology enables d-band centers to be highly active for high-performance lithium-sulfur battery. Chinese Chemical Letters, 2023, 34, 108189.	4.8	4
75981	Co₂P-Assisted Atomic Coâ€“N₄ Active Sites with a Tailored Electronic Structure Enabling Efficient ORR/OER for Rechargeable Znâ€“Air Batteries. ACS Applied Materials & Interfaces, 2023, 15, 9240-9249.	4.0	13
75982	Charge quenching at defect states in transition metal dichalcogenideâ€“graphene van der Waals heterobilayers. Physical Review B, 2023, 107, .	1.1	1
75983	Structure and Optical Properties of Polymeric Carbon Nitrides from Atomistic Simulations. Chemistry of Materials, 2023, 35, 1547-1559.	3.2	9
75984	Microstructural Manipulation for Enhanced Average Thermoelectric Performance: A Case Study of Tin Telluride. ACS Applied Materials & Interfaces, 2023, 15, 9656-9664.	4.0	8
75985	Defect-Engineering of 2D Dichalcogenide VSe2 to Enhance Ammonia Sensing: Acumens from DFT Calculations. Biosensors, 2023, 13, 257.	2.3	6
75986	Sandwich Structured Metal oxide/Reduced Graphene Oxide/Metal Oxideâ€Based Polymer Electrolyte Enables Continuous Inorganicâ€“Organic Interphase for Fast Lithiumâ€ion Transportation. Small, 2023, 19, .	5.2	8
75987	Catalytic performance of binary transition metal sulfide FeCoS2/rGO for lithiumâ€“sulfur batteries. Journal of Solid State Electrochemistry, 2023, 27, 1045-1053.	1.2	2
75988	Electronic properties and hydrogen evolution reaction performance of silicene with precious metal-doped nonmetal ring: first-principles calculations. Journal of Materials Science, 2023, 58, 4487-4498.	1.7	0
75989	Lattice Distorted Rhodium Nanocrystals in Porous Nanofiber toward Aqueous Zinc-CO₂ System. , 2023, 5, 1271-1280.		2
75990	Rational Design of Molybdenumâ€Doped Cobalt Nitride Nanowire Arrays for Robust Overall Water Splitting. ChemSusChem, 2023, 16, .	3.6	10
75991	Structures and properties of uraniumâ€“niobium intermetallic compounds under high pressure: A first principles study. Journal of Applied Physics, 2023, 133, .	1.1	1
75992	Work Function-Tailored Nitrogenase-like Fe Double-Atom Catalysts on Transition Metal Dichalcogenides for Nitrogen Fixation. ACS Sustainable Chemistry and Engineering, 2023, 11, 4990-4997.	3.2	6
75993	Theoretical prediction of novel two-dimensional MA₂Z₄ family for Li/Na battery anodes. 2D Materials, 2023, 10, 025020.	2.0	2
75994	Ab initio Boltzmann approach to coupled magnon-phonon thermal transport in ferromagnetic crystals. Physical Review B, 2023, 107, .	1.1	14
75995	Porous Organic Polymer with Hierarchical Structure and Limited Volume Expansion for Ultrafast and Highly Durable Sodium Storage. Advanced Materials, 2023, 35, .	11.1	27
75996	Direct observation of oxygen vacancy formation and migration over ceria surface by in situ environmental transmission electron microscopy. Journal of Rare Earths, 2024, 42, 676-682.	2.5	2
75998	On the limitations of thermal atomic layer deposition of InN using ammonia. Journal of Vacuum Science and Technology A: Vacuum, Surfaces and Films, 2023, 41, .	0.9	4

#	Article	IF	Citations
75999	First-principles phonon calculations of neodymium-magnet compounds. Journal of Applied Physics, 2023, 133, .	1.1	1
76000	Computational Design of a Two-Dimensional Copper Carbide Monolayer as a Highly Efficient Catalyst for Carbon Monoxide Electroreduction to Ethanol. ACS Applied Materials & Interfaces, 2023, 15, 13033-13041.	4.0	3
76001	Suppressed Fermi Level Pinning and Wide-Range Tunable Schottky Barrier in CrX₃ (X = I,) Tj ETQq0 0 0 rgBT /Overlock 10 T	2.1	3
76002	Simulation studies of secondary electron yield with electron transport from Cu (110) surfaces containing C2, N2, CO2, or NO2 adsorbates. Frontiers in Materials, 0, 10, .	1.2	0
76003	Oxidation State Engineering in Octahedral Ni by Anchored Sulfate to Boost Intrinsic Oxygen Evolution Activity. ACS Nano, 2023, 17, 6770-6780.	7.3	17
76004	Oxygenated Triazineâ€Heptazine Heterostructure Creates an Enormous Ascension to the Visible Light Photocatalytic Hydrogen Evolution Performance of Porous C₃N₄ Nanosheets. Small, 2023, 19, .	5.2	13
76005	First-principles theory of the pressure-induced invar effect in FeNi alloys. Physical Review B, 2023, 107, .	1.1	2
76006	Activating Mobile Dislocation in Boron Carbide at Room Temperature via Al Doping. Physical Review Letters, 2023, 130, .	2.9	6
76007	Single-Phase Ternary Compounds with a Disordered Lattice and Liquid Metal Phase for High-Performance Li-Ion Battery Anodes. Nano-Micro Letters, 2023, 15, .	14.4	7
76008	Synergistic effects of Nb and Mo on hydrogen-induced cracking of pipeline steels: A combined experimental and numerical study. Journal of Materials Science and Technology, 2023, 158, 156-170.	5.6	6
76009	Topological states of thermoelectric Yb-filled skutterudites. Physical Review B, 2023, 107, .	1.1	3
76010	Nano FeSb₂S₄ Anchored on Exfoliated Graphite for Sodium-Ion Battery Anode via a Two-Step Fabrication. Energy & Fuels, 2023, 37, 5577-5585.	2.5	2
76011	Impact of Polarization Effect on Exciton Binding Energies and Charge Transport for the Crystals of Chlorinated ITIC Derivatives. Journal of Physical Chemistry C, 2023, 127, 5597-5603.	1.5	13
76012	Wideâ€Bandgap Rareâ€Earth Iodate Single Crystals for Superior Xâ€Ray Detection and Imaging. Advanced Science, 2023, 10, .	5.6	7
76013	Study of digital and analog resistive switching memories based on methylammonium lead iodide (MAPbI₃) perovskite by experiments and DFT calculations. Journal Physics D: Applied Physics, 2023, 56, 215301.	1.3	3
76014	Role of Lifshitz transition stabilized carbon hexagon structure from biaxial strain: A case of sodium carbide with superconducting condition. Ceramics International, 2023, 49, 20088-20095.	2.3	3
76015	First-Principles Investigation on Phase Stability, Mechanical Properties, Bonding Characteristic and Slip Properties of Ti-Co Binary Intermetallic Compounds. Metals, 2023, 13, 628.	1.0	0
76016	Prediction of Ta₂Câ€Type Vacancyâ€Layered Structures in the Ternary Hfâ€“Taâ€“C System. Physica Status Solidi (B): Basic Research, 2023, 260, .	0.7	0

#	Article	IF	Citations
76017	Incorporation and migration of xenon in uranium-plutonium mixed nitride; A density functional theory study. Journal of Nuclear Materials, 2023, 577, 154330.	1.3	1
76018	Singleâ€Atom and Hierarchicalâ€Pore Aerogel Confinement Strategy for Lowâ€Platinum Fuel Cells. Advanced Materials, 2023, 35, .	11.1	7
76019	Magnetoresistance anomaly in Fe5GeTe2 homo-junctions induced by its intrinsic transition. Nano Research, 2023, 16, 10443-10450.	5.8	3
76020	Metalâ€“Support Interactions in Heterogeneous Catalysis: DFT Calculations on the Interaction of Copper Nanoparticles with Magnesium Oxide. ACS Omega, 2023, 8, 10591-10599.	1.6	3
76021	Roomâ€Temperature Intrinsic Ferromagnetic Chromium Tellurium Compounds with Thicknessâ€Tunable Magnetic Texture. Advanced Materials, 2023, 35, .	11.1	4
76022	Ultraâ€fast Piezocatalysts Enabled By Interfacial Interaction of Reduced Graphene Oxide/MoS₂ Heterostructures. Advanced Materials, 2023, 35, .	11.1	26
76023	Double resonant tunable second harmonic generation in two-dimensional layered materials through band nesting. Physical Review B, 2023, 107, .	1.1	1
76024	Mechanistic Insight into Solution-Based Atomic Layer Deposition of CuSCN Provided by In Situ and Ex Situ Methods. ACS Applied Materials & Interfaces, 2023, 15, 19536-19544.	4.0	2
76025	Adsorption and sensing properties of SF6 decomposed gases on Mg-MOF-74. Solid State Communications, 2023, 363, 115120.	0.9	7
76026	Crystallinity engineering for overcoming the activityâ€“stability tradeoff of spinel oxide in Fenton-like catalysis. Proceedings of the National Academy of Sciences of the United States of America, 2023, 120, .	3.3	23
76027	Optical Properties and Metalâ€Dependent Charge Transfer in Iodido Pentelates. ChemPlusChem, 2023, 88, .	1.3	1
76028	Synthesis of core/shell nanocrystals with ordered intermetallic single-atom alloy layers for nitrate electroreduction to ammonia. , 2023, 2, 624-634.		37
76029	Graph Neural Network Guided Evolutionary Search of Grain Boundaries in 2D Materials. ACS Applied Materials & Interfaces, 2023, 15, 20520-20530.	4.0	1
76030	Active and durable R2MnRuO7 pyrochlores with low Ru content for acidic oxygen evolution. Nature Communications, 2023, 14, .	5.8	9
76031	Modulating the electronic structure of MoS3 catalyst via heteroatom doping for Electrocatalytic nitrogen reduction reaction: A theoretical study. Molecular Catalysis, 2023, 541, 113117.	1.0	0
76032	Synergy of VN and Fe₂O₃ Enables High Performance Anodes for Asymmetric Supercapacitors. ACS Applied Materials & Interfaces, 2023, 15, 18819-18827.	4.0	13
76033	Strain engineering of type-II C2N/WS2 van der Waals heterojunction for highly enhanced photocatalytic hydrogen evolution. International Journal of Hydrogen Energy, 2023, 48, 26119-26132.	3.8	2
76034	Stable CuIn alloy for electrochemical CO2 reduction to CO with high-selectivity. Materials Today Physics, 2023, 33, 101050.	2.9	6

#	Article	IF	Citations
76035	Metal Vacancies in CoAl-Layered Double Hydroxide Nanosheets Enabling Boosted Visible Light Driven CO₂ Photoreduction. Journal of Physical Chemistry C, 0, , .	1.5	0
76036	Effects of native and H related defects on magnetic properties of SrCoO_{2.5} and HSrCoO_{2.5}. Journal of Applied Physics, 2023, 133, 135702.	1.1	1
76037	Engineering two-dimensional SnC/HfSSe heterojunction as a direct Z-scheme photocatalyst for water splitting hydrogen evolution. Applied Surface Science, 2023, 626, 157247.	3.1	17
76038	Deducing subnanometer cluster size and shape distributions of heterogeneous supported catalysts. Nature Communications, 2023, 14, .	5.8	5
76039	Theoretical study on the reaction kinetics of CO oxidation by nitrogen-doped graphene catalysts with different ligand structures. Molecular Catalysis, 2023, 541, 113103.	1.0	1
76040	Insight into the Electrochemical CO₂-to-Ethanol Conversion Catalyzed by Cu₂S Nanocrystal-Decorated Cu Nanosheets. ACS Applied Materials & Interfaces, 2023, 15, 18857-18866.	4.0	7
76041	Atomic structure, stability, and dissociation of dislocations in cadmium telluride. International Journal of Plasticity, 2023, 163, 103552.	4.1	7
76042	High symmetry structure and large strain field fluctuation lead enhancement of thermoelectric performance of quaternary alloys by tuning configurational entropy. Chemical Engineering Journal, 2023, 462, 142185.	6.6	2
76043	Assessing factors that determine adatom migration and clustering on a thin film oxide; Pt1 and Rh1 on the â€œ29â€•CuxO/Cu(1 1 1) surface. Applied Surface Science, 2023, 628, 157145.	3.1	2
76044	Moistureâ€Tailored 2D Dionâ€“Jacobson Perovskites for Reconfigurable Optoelectronics. Advanced Materials, 2023, 35, .	11.1	10
76045	Effect of doping IVB, VB and VIB elements on structure, stability, elastic and electronic properties of the O and B2 of Ti2AlNb intermetallic: A first principles study. Journal of Physics and Chemistry of Solids, 2023, 179, 111362.	1.9	1
76046	Efficient atomistic simulations of radiation damage in W and Wâ€“Mo using machine-learning potentials. Journal of Nuclear Materials, 2023, 577, 154325.	1.3	5
76047	Band Positionâ€Independent Piezoâ€Electrocatalysis for Ultrahigh CO₂ Conversion. Advanced Materials, 2023, 35, .	11.1	31
76048	An experimental and theoretical approach to organic functionalization of carbon nanofibers using fresh neem leaves. International Journal of Hydrogen Energy, 2023, 48, 27242-27258.	3.8	0
76049	Effect of Complex Modifier on Properties of Heat-Hardened Sodium Silicate-Bonded Sand for Castings Production. International Journal of Metalcasting, 2024, 18, 269-277.	1.5	1
76050	Ag@Pt core-shell icosahedral nanocrystals with solid solution interface improve pH-Universal hydrogen evolution at large current densities. Composites Part B: Engineering, 2023, 254, 110600.	5.9	5
76051	Pressure-induced enhancement of thermoelectric performance of CoP3 by the structural phase transition. Acta Materialia, 2023, 248, 118773.	3.8	4
76052	Monovacancy-hydrogen interaction in pure aluminum: Experimental and ab-initio theoretical positron annihilation study. Acta Materialia, 2023, 248, 118770.	3.8	6

#	Article	IF	Citations
76053	Efficient Synthesis of 2D Mica Nanosheets by Solvothermal and Microwave-Assisted Techniques for CO2 Capture Applications. Materials, 2023, 16, 2921.	1.3	2
76054	Computational Insights into Alloying and Confinement Effects on Promoted Activity and Selectivity of C₂ Oxygenate over Rh-Based Catalysts. Journal of Physical Chemistry C, 0, , .	1.5	0
76055	Electronic and surface engineering of Mo doped Ni@C nanocomposite boosting catalytic upgrading of aqueous bio-ethanol to bio-jet fuel precursors. Chemical Engineering Journal, 2023, 461, 141888.	6.6	8
76056	MXene-based single atom catalysts for efficient CO2RR towards CO: A novel strategy for high-throughput catalyst design and screening. Chemical Engineering Journal, 2023, 461, 141936.	6.6	9
76057	Effectively enhanced oxygen reduction activity and stability of triple-conducting composite cathodes by strongly interacting interfaces for protonic ceramic fuel cells. Chemical Engineering Journal, 2023, 461, 142056.	6.6	8
76058	Strained induced metallic to semiconductor transitions in 2D Ruddlesden Popper perovskites: A GGAÂ+ÂSOC approach. Applied Surface Science, 2023, 627, 157244.	3.1	0
76059	First-principles study of the bandgap renormalization and optical property of Î²-LiGaO₂. Chinese Physics B, 2023, 32, 047101.	0.7	0
76060	Regulation of the spin orbit coupling by changing the doping ratio x in the surface of monolayer (SxSe1-x)MSe. Physica E: Low-Dimensional Systems and Nanostructures, 2023, 151, 115734.	1.3	0
76061	Interfacial Chemistry in the Electrocatalytic Hydrogenation of CO₂ over C-Supported Cu-Based Systems. ACS Catalysis, 2023, 13, 5876-5895.	5.5	3
76062	Highly active cobalt-free perovskites with Bi doping as bifunctional oxygen electrodes for solid oxide cells. Chemical Engineering Journal, 2023, 461, 142051.	6.6	8
76063	Designing Nâ€Confused Metalloporphyrinâ€Based Covalent Organic Frameworks for Enhanced Electrocatalytic Carbon Dioxide Reduction. Small, 2023, 19, .	5.2	5
76064	Spin and current transport in the robust half-metallic magnet c-CoFeGe. Journal of Physics Condensed Matter, 2023, 35, 285502.	0.7	2
76065	Inhibiting polysulfide shuttling with a flexible â€œskinâ€•for highly stable Lithium-Sulfur batteries. Materials Letters, 2023, 343, 134378.	1.3	3
76066	Trends in high-temperature H2 production on CeO2 Co-doped with trivalent cations in solid oxide electrolysis cells. Journal of Catalysis, 2023, 420, 1-8.	3.1	5
76067	Vertical strain engineering of Van der Waals heterostructures. Nanotechnology, 0, , .	1.3	0
76068	Two-Dimensional Ultrahigh Unconventional Piezoelectricity Driven by Charge Screening. Journal of Physical Chemistry Letters, 2023, 14, 3430-3435.	2.1	0
76069	Sulfolane-containing aqueous electrolyte solutions for producing efficient ampere-hour-level zinc metal battery pouch cells. Nature Communications, 2023, 14, .	5.8	53
76070	Adsorption Tuning of Polarity and Magnetism in AgCr2S4 Monolayer. Materials, 2023, 16, 3058.	1.3	1

#	Article	IF	Citations
76071	Characterization of Planar Defect in Layered Perovskite Photocatalyst Y₂Ti₂O₅S₂ by Electron Microscopy and First-Principles Calculations. Journal of Physical Chemistry C, 2023, 127, 7887-7893.	1.5	3
76072	Binuclear spin-crossover [Fe(bt)(NCS)2]2(bpm) complex: A study using first principles calculations. Journal of Chemical Physics, 2023, 158, .	1.2	1
76073	The effects of electric field and strain on the BP/GeTe van der Waals heterojunction. Journal Physics D: Applied Physics, 2023, 56, 315102.	1.3	1
76074	Cooperative roles of water and metal-support interfaces in the selective hydrogenation of cinnamaldehyde over cobalt boride catalysts. Cell Reports Physical Science, 2023, 4, 101367.	2.8	1
76075	A pressure-induced high-pressure metallic GeTe phase. Journal of Chemical Physics, 2023, 158, .	1.2	1
76076	Electrodeposited copper oxides with a suppressed interfacial amorphous phase using mixed-crystalline ITO and their enhanced photoelectrochemical performances. Journal of Energy Chemistry, 2023, 82, 277-286.	7.1	3
76077	The Facet Dependence of CO2 Electroreduction Selectivity on a Pd3Au Bimetallic Catalyst: A DFT Study. Molecules, 2023, 28, 3169.	1.7	1
76078	Magnetic field effects and excitonic selection rules in monolayer palladium diselenide as a large-gap quantum spin Hall insulator. Physical Review B, 2023, 107, .	1.1	0
76079	Influence of Mo Doping on Electronic and Magnetic Properties of Monolayer CrX₃: A First-Principles Study. ECS Journal of Solid State Science and Technology, 2023, 12, 043001.	0.9	0
76080	Enhancing the accuracy of density functional tight binding models through ChIMES many-body interaction potentials. Journal of Chemical Physics, 2023, 158, .	1.2	3
76081	DFT Study of CO2 Reduction Reaction to CH3OH on Low-Index Cu Surfaces. Catalysts, 2023, 13, 722.	1.6	3
76082	Predicted the structural diversity and electronic properties of Ptâ^'N compounds under high pressure. Journal of Physics Condensed Matter, 2023, 35, 285501.	0.7	0
76083	Photo-carrier induced composition separation in mixed-halide CsPb(I _x Br<sub>1â^'x) Tj ETQq0 0 0 rgBT /Overlock 10 Tf 50 2023, 16, 041002.	1.1	0
76084	Effect of Surface Termination on Carrier Dynamics of Metal Halide Perovskites: Ab Initio Quantum Dynamics Study. Electronic Materials Letters, 0, , .	1.0	0
76085	Electron deficiency modulates hydrogen adsorption strength of Ru single-atomic catalyst for efficient hydrogen evolution. Renewable Energy, 2023, 210, 258-268.	4.3	3
76087	Regulating the Anion Redox and Suppressing the Structural Distortion of Cation-Disordered Rock-Salt Cathode Materials to Improve Cycling Durability through Chlorine Substitution. ACS Applied Materials & Interfaces, 2023, 15, 17938-17946.	4.0	3
76088	Electronic Modulation of Metalâ€Organic Frameworks Caused by Atomically Dispersed Ru for Efficient Hydrogen Evolution. Small, 2023, 19, .	5.2	8
76089	Dynamic catalysis of sub-nanometer metal clusters in oxygen dissociation. , 2023, , 100002.		0

#	Article	IF	Citations
76090	CoTe₂: A Quantum Critical Dirac Metal with Strong Spin Fluctuations. Advanced Materials, 2023, 35, .	11.1	3
76091	High-density nanoprecipitates and phase reversion via maraging enable ultrastrong yet strain-hardenable medium-entropy alloy. Acta Materialia, 2023, 248, 118810.	3.8	17
76092	Characterizing and Overcoming Surface Paramagnetism in Magnetoelectric Antiferromagnets. Physical Review Letters, 2023, 130, .	2.9	2
76093	Insights into the interfacial speciation of Ni in the corrosion layer of high burnup Zircaloy-2 cladding: A combined XRD, XAS, and LFDFT study. Corrosion Science, 2023, 215, 111024.	3.0	0
76094	Furfural hydrogenation into tetrahydrofurfuryl alcohol under ambient conditions: Role of Ni-supported catalysts and hydrogen source. Industrial Crops and Products, 2023, 195, 116390.	2.5	2
76095	Interface alloying design to improve the stability and cohesion of W/HfC interface by first-principles study. Journal of Nuclear Materials, 2023, 577, 154320.	1.3	3
76096	Atomic structure and bonding in fluorinated graphite intercalated with a strong fluoroxidant. Diamond and Related Materials, 2023, 135, 109851.	1.8	2
76097	Gas sensing potential of monolayer MoB: A first principles study. Vacuum, 2023, 210, 111883.	1.6	5
76098	Competing spin fluctuations in <mml:math xmlns:mml="http://www.w3.org/1998/Math/MathML"><mml:msub><mml:mi mathvariant="normal">Sr</mml:mi><mml:mn>2</mml:mn></mml:msub><mml:msub><mml:mi mathvariant="normal">RuO</mml:mi><mml:mn>4</mml:mn></mml:msub></mml:math> and their tuning through epitaxial strain. Physical Review B, 2023, 107, .	1.1	0
76099	Surface engineering of carbon fiber via upcycling of waste gases generated during carbon fiber production: A sustainable approach towards high-performance composites. Composites Part B: Engineering, 2023, 255, 110624.	5.9	2
76100	Optimization of Ti with modified SiC ceramics for electromagnetic absorption properties. Materials Characterization, 2023, 198, 112761.	1.9	10
76101	In-situ construction of hierarchical 2D MoS2/1D Te hybrid for supercapacitor applications. Journal of Energy Storage, 2023, 60, 106703.	3.9	9
76102	First-principles design of highly active and durable Ti55Cx@Pt92 nanocatalyst for oxygen reduction reaction through charge control at nanointerfaces. Applied Surface Science, 2023, 618, 156685.	3.1	1
76103	Hollow macroporous CeO2/Î²-Bi2O3 heterostructure sphere via one-step spray solution combustion synthesis for efficient photocatalysis. Applied Surface Science, 2023, 619, 156718.	3.1	8
76104	Facet effects on bimetallic ZnSn hydroxide microcrystals for selective electrochemical CO2 reduction. Green Energy and Environment, 2023, , .	4.7	1
76105	Concentration Phase Separation of Substitutionâ€Doped Atoms in TMDCs Monolayer. Small, 2023, 19, .	5.2	5
76106	Thermal atomic layer etching of cobalt using plasma chlorination and chelation with hexafluoroacetylacetone. Applied Surface Science, 2023, 619, 156751.	3.1	1
76107	Single-atom Pt supported on non-metal doped WS2 for photocatalytic CO2 reduction: A first-principles study. Applied Surface Science, 2023, 626, 157252.	3.1	8

#	Article	IF	Citations
76108	The effect of alkyl chain length on imidazole chloroaluminate ionic liquid/Pt(1 1 1) interface and aluminum deposition: A DFT-D3 study. Chemical Physics, 2023, 568, 111842.	0.9	1
76109	Promoter not inhibitor: The antidotal effects of arsenic on lead-poisoning V2O5â^'WO3/TiO2 catalyst for selective catalytic reduction of NO with NH3. Journal of Cleaner Production, 2023, 397, 136621.	4.6	3
76110	A theoretical study of 0D Ti2CO2/2D g-C3N4 Schottky-junction for photocatalytic hydrogen evolution. Applied Surface Science, 2023, 616, 156562.	3.1	7
76111	P-doped biochar regulates nZVI nanocracks formation for superefficient persulfate activation. Journal of Hazardous Materials, 2023, 450, 130999.	6.5	23
76112	Investigation of the effect of F-doping on the solid-electrolyte property of Li3InCl6. Journal of Power Sources, 2023, 567, 232962.	4.0	6
76113	Effect of alloying elements on elastic properties, generalized stacking fault energy, and critical resolved shear stress of Pd metal: A first principle study. Vacuum, 2023, 211, 111898.	1.6	3
76114	Boosting photocatalytic ammonia synthesis performance over OVs-Rich Ru/W18O49: Insights into the roles of oxygen vacancies in enhanced hydrogen spillover effect. Chemical Engineering Journal, 2023, 461, 141892.	6.6	12
76115	Role of phosphorous in transition metal phosphides for selective hydrogenolysis of hindered Câ€“O bonds. Journal of Catalysis, 2023, 421, 403-418.	3.1	1
76116	Energetic and configurational mechanisms to facilitate mica nanosheets synthesis by organo-ammonium cation intercalation. Computational Materials Science, 2023, 224, 112162.	1.4	1
76117	Cluster structure of doped atoms and elastic properties in Î³-Ni by first-principles calculations. Computational Materials Science, 2023, 224, 112183.	1.4	0
76118	Promising high temperature thermoelectric performance of layered oxypnictide YZnAsO. Physica B: Condensed Matter, 2023, 657, 414811.	1.3	0
76119	Theoretical study of the mechanism of the hydrogen evolution reaction on the V2C MXene: Thermodynamic and kinetic aspects. Journal of Catalysis, 2023, 421, 252-263.	3.1	11
76120	Strain induced effects on the electronic and phononic properties of 2H and 1T<mml:math xmlns:mml="http://www.w3.org/1998/Math/MathML" altimg="si11.svg" display="inline" id="d1e274"><mml:msup><mml:mrow /><mml:mrow><mml:mo>â€²</mml:mo></mml:mrow></mml:msup></mml:math> monolayer MoS2. Physica B: Condensed Matter, 2023, 655, 414701.	1.3	3
76121	Vacancy defects in nitrogen doped diamond. Physica B: Condensed Matter, 2023, 655, 414769.	1.3	0
76122	Anomalous temperature dependence of self-interstitial diffusivity in metallic lithium and sodium. Materialia, 2023, 28, 101718.	1.3	0
76123	First-principle studies of oxidation effects on grain boundary strength in nickel. Materialia, 2023, 28, 101745.	1.3	2
76124	Insight into B S ratio model and surface atom interactions of co-doping diamond: First-principles studies. Diamond and Related Materials, 2023, 135, 109824.	1.8	2
76125	Enhanced strength and plasticity in a Nb2MoWC0.5 alloy via eutectic dilute carbide. Materials Science & Engineering A: Structural Materials: Properties, Microstructure and Processing, 2023, 872, 144920.	2.6	1

#	Article	IF	Citations
76126	Magnetic, optoelectronic, and rietveld refined structural properties of Al3+ substituted nanocrystalline Ni-Cu spinel ferrites: An experimental and DFT based study. Journal of Magnetism and Magnetic Materials, 2023, 573, 170675.	1.0	7
76127	Directed synthesis of nylon 5X key monomer cadaverine with alkaline metal modified Ru@FAU catalysts. Applied Catalysis A: General, 2023, 658, 119172.	2.2	2
76128	Micro-kinetics of ethylene and methane oxidation on platinum. Chemical Engineering Journal, 2023, 464, 142608.	6.6	3
76129	Realization of multifunction in perovskite-based van der Waals heterostructure by interface engineering strategy: The case of CsPbBr3/Janus MoSSe. Applied Surface Science, 2023, 618, 156626.	3.1	5
76130	Room-temperature deformation of single crystals of the sigma-phase compound FeCr with the tetragonal D8b structure investigated by micropillar compression. Acta Materialia, 2023, 249, 118829.	3.8	5
76131	The interplay between solute atoms and vacancy clusters in magnesium alloys. Acta Materialia, 2023, 249, 118805.	3.8	4
76132	L21-strengthened face-centered cubic high-entropy alloy with well pitting resistance. Corrosion Science, 2023, 215, 111043.	3.0	9
76133	Geometric and electronic effects of Co@NPC catalyst in chemoselective hydrogenation: Tunable activity and selectivity via N,P co-doping. Journal of Catalysis, 2023, 421, 65-76.	3.1	7
76134	Transfer learning aided high-throughput computational design of oxygen evolution reaction catalysts in acid conditions. Journal of Energy Chemistry, 2023, 80, 744-757.	7.1	7
76135	A novel core-shell structured Fe@CeO2-ZIF-8 catalyst for the reduction of NO by CO. Journal of Catalysis, 2023, 421, 240-251.	3.1	4
76136	First-principles calculation and experimental study of mixed crystal Tm:(LuxY1-x)3AG. Infrared Physics and Technology, 2023, 130, 104588.	1.3	2
76137	First-principles study of the native defects with charge states in ZrSe<mml:math xmlns:mml="http://www.w3.org/1998/Math/MathML" altimg="si10.svg" display="inline" id="d1e937"><mml:msub><mml:mrow /><mml:mrow><mml:mn>2</mml:mn></mml:mrow></mml:msub></mml:math>. Solid State Communications, 2023, 365, 115138.	0.9	2
76138	Magnetic nano-size normal spinel-ZnFe2O4 and inverse spinel-MnFe2O4 for catalytic ozonation: Performance and mechanism. Separation and Purification Technology, 2023, 313, 123535.	3.9	1
76139	Phase transformation and radiation resistance of B-site high entropy pyrochlores. Scripta Materialia, 2023, 229, 115367.	2.6	6
76140	Electron-rich platinum single sites anchored on sulfur-doped covalent organic frameworks for boosting anti-Markovnikov hydrosilylation of alkenes. Chemical Engineering Journal, 2023, 463, 142255.	6.6	6
76141	Effects of magnetic ordering on structural stability and phonon transport in monolayer Td-VX2 (X=Se, I). Physics Letters, Section A: General, Atomic and Solid State Physics, 2023, 469, 128746.	0.9	2
76142	Reduced MgFe hydrotalcite efficiently catalyzes the aerobic oxidation of alkylarenes. Applied Catalysis A: General, 2023, 657, 119143.	2.2	2
76143	Adjacent diatomic Cu1N3/Mo1S2 entities decorated carbon nitride for markedly enhanced photocatalytic hydrogen generation. Chemical Engineering Journal, 2023, 463, 142470.	6.6	2

#	Article	IF	Citations
76144	Theory-guided doping of LaCoO3 nanoparticles for enhanced antimicrobial performance. Chemical Engineering Journal, 2023, 464, 142710.	6.6	6
76145	Carbon-confined Cu-Pd alloy nanoparticles as high-performance catalysts for acetylene selective hydrogenation. Chemical Engineering Journal, 2023, 464, 142609.	6.6	7
76146	Prediction of superior thermoelectric performance in unexplored doped-BiCuSeO via machine learning. Materials and Design, 2023, 229, 111868.	3.3	3
76147	First-principles study of electronic and optical properties of NH3-adsorbed Sc2CO2 monolayer and its application in gas sensors. Journal of Materials Research and Technology, 2023, 24, 173-184.	2.6	4
76148	Screening and activating small-molecule Se in microporous S-decorated/N-doped carbon spheres for an enhanced rate performance. Applied Surface Science, 2023, 619, 156724.	3.1	1
76149	Sizeâ^'selected Cu4 cluster anchored on C2N monolayer for efficient nitrite electroreduction to ammonia: a computational study. Applied Surface Science, 2023, 620, 156825.	3.1	2
76150	Enhanced dehalogenation of brominated DBPs by catalyzed electrolysis using Vitamin B12 modified electrodes: Kinetics, mechanisms, and mass balances. Journal of Hazardous Materials, 2023, 449, 131052.	6.5	6
76151	Prediction of mechanical properties of AlTiCrVNb high entropy alloys with B2 ordered structure. Journal of Materials Research and Technology, 2023, 24, 440-448.	2.6	2
76152	Carbon nanotubes rolled from Me-graphene. Diamond and Related Materials, 2023, 135, 109845.	1.8	4
76153	S and N coordinated single-atom catalysts for electrochemical CO2 reduction with superior activity and selectivity. Applied Surface Science, 2023, 619, 156747.	3.1	8
76154	Ga-doped AlN monolayer nano-sheets as promising materials for environmental sensing applications. Computational and Theoretical Chemistry, 2023, 1223, 114086.	1.1	6
76155	One-dimensional 3d-TMâ€"solophene polymers as high-activity singleâ€atom catalysts for CO oxidation. Applied Surface Science, 2023, 618, 156680.	3.1	1
76156	Transition metal doped pyrrole-NC for high-performance CO2 reduction reaction to C1 products. Applied Surface Science, 2023, 618, 156678.	3.1	12
76157	Oxygen Reduction and Hydrogen Evolution Reactions on Zigzag ReS2 Nanoribbons. Applied Surface Science, 2023, 618, 156677.	3.1	1
76158	Synergistic effects of Ta and Mo on the hydrogen embrittlement resistance in ultra-high strength hot stamping steel. Materials Science & Engineering A: Structural Materials: Properties, Microstructure and Processing, 2023, 872, 144956.	2.6	5
76159	Al2O3/ZnO composite-based sensors for battery safety applications: An experimental and theoretical investigation. Nano Energy, 2023, 109, 108301.	8.2	8
76160	Phonon thermal transport in two-dimensional PbTe monolayers via extensive molecular dynamics simulations with a neuroevolution potential. Materials Today Physics, 2023, 34, 101066.	2.9	2
76161	States of Pt/CeO2 catalysts for CO oxidation below room temperature. Journal of Catalysis, 2023, 421, 285-299.	3.1	9

#	Article	IF	Citations
76162	A chloride-free electrolyte to suppress the anodic hydrogen evolution corrosion of magnesium anode in aqueous magnesium air batteries. Chemical Engineering Journal, 2023, 464, 142655.	6.6	4
76163	Tunable broadband near-infrared emission in LiScO2:Cr3+ phosphor induced by the variation of chromium ion concentration. Journal of Luminescence, 2023, 257, 119758.	1.5	8
76164	Enhancement in the thermoelectric performance of ZrNiSn-based alloys through extra Zr-rich nanoprecipitates with superstructures. Chemical Engineering Journal, 2023, 464, 142531.	6.6	2
76165	Theoretical studies of sliding ferroelectricity, magnetoelectric couplings, and piezo-multiferroicity in two-dimensional magnetic materials. Chemical Physics Letters, 2023, 818, 140430.	1.2	8
76166	Selective oxidation of vanadium from vanadium slag by CO2 during CaCO3 roasting treatment. Separation and Purification Technology, 2023, 312, 123407.	3.9	7
76167	Charge localization induced by Fe doping in porous Bi5O7I Micro-flower for enhanced photoreduction of CO2 to CO. Separation and Purification Technology, 2023, 312, 123379.	3.9	16
76168	Revealing active edge sites induced by oriented lattice bending of Co-CeO2 nanosheets for boosting auto-exhaust soot oxidation. Journal of Catalysis, 2023, 421, 351-364.	3.1	11
76169	Prediction of new stable crystal structures for ternary ErAgTe2 and YAgTe2 semiconductors: Ab initio study. Solid State Sciences, 2023, 139, 107160.	1.5	1
76170	First-principles study on the electronic and magnetic properties of BN/CrOBr heterostructures. Physics Letters, Section A: General, Atomic and Solid State Physics, 2023, 471, 128789.	0.9	0
76171	Thermal resistance from non-equilibrium phonons at Siâ€“Ge interface. Materials Today Physics, 2023, 34, 101063.	2.9	4
76172	DFT-guided flux synthesis of a family of layered titanates crystallizing in the lepidocrocite structure type. Solid State Sciences, 2023, 139, 107161.	1.5	0
76173	Controlling of Localization by Elemental-substitution Effect in Layered BiCh₂-based Compounds LaO_{1â^'}_xF_xBiS_{2â^'}_ySe_y. Journal of the Physical Society of Japan, 2023, 92, .	1.7	1
76174	Improving photocatalytic performance of defective titania for carbon dioxide photoreduction by Cu cocatalyst with SCN- ion modification. Chemical Engineering Journal, 2023, 463, 142358.	6.6	7
76175	Dependence of predicted bulk properties of hexagonal hydroxyapatite on exchangeâ€“correlation functional. Computational Materials Science, 2023, 224, 112153.	1.4	5
76176	Enhanced tunneling electroresistance effect in Pt/BiAlO3/Pt ferroelectric tunnel junctions by a graphene interlayer. Applied Surface Science, 2023, 619, 156726.	3.1	4
76177	Compatibility of DFT+U with non-collinear magnetism and spin-orbit coupling within a framework of numerical atomic orbitals. Computer Physics Communications, 2023, 286, 108684.	3.0	1
76178	First principles study of oxygen diffusion in plutonium dioxide, sesquioxide, and their interface under activated conditions. Journal of Nuclear Materials, 2023, 578, 154348.	1.3	4
76179	Atomic and electronic structure of grain boundaries in a-Al2O3: A combination of machine learning, first-principles calculation and electron microscopy. Scripta Materialia, 2023, 229, 115368.	2.6	3

#	Article	IF	Citations
76180	Oxygen-vacancy-rich MoO2 supported nickel as electrocatalysts to promote alkaline hydrogen evolution and oxidation reactions. Chemical Engineering Journal, 2023, 464, 142671.	6.6	8
76181	Syngas-to-C2 oxygenates over the inverse Mo6C4/Cu catalyst: Identifying the role of synergistic effect. Applied Surface Science, 2023, 619, 156746.	3.1	0
76182	Prediction of photogalvanic effect enhancement in Janus transition metal dichalcogenide monolayers induced by spontaneous curling. Applied Surface Science, 2023, 619, 156730.	3.1	8
76183	Theoretical insights into the removal pathways of adsorbed oxygen on the surface of Ï‡-Fe5C2(5 1 0). Chemical Engineering Science, 2023, 271, 118576.	1.9	4
76184	Origin and regulation of interfacial instability for nickel-rich cathodes and NASICON-type Li1+xAlxTi2â^'x(PO4)3 solid electrolytes in solid-state lithium batteries. Applied Surface Science, 2023, 619, 156741.	3.1	3
76185	An exceptionally strong, ductile and impurity-tolerant austenitic stainless steel prepared by laser additive manufacturing. Acta Materialia, 2023, 250, 118868.	3.8	4
76186	Strongly enhanced infrared absorption of HfSe2 monolayer by lanthanide doping: A first-principles study. Results in Physics, 2023, 48, 106415.	2.0	3
76187	Mechanistic and kinetics insights into structure sensitivity of 2,6-Diamino-3,5-Dinitropiridine hydrogenation over Ni catalysts. Journal of Catalysis, 2023, 421, 162-171.	3.1	1
76188	The effect of B/P/S doping on Li+ charge transfer during ion transport along the H-diamond surface: A first-principles calculation. Diamond and Related Materials, 2023, 135, 109846.	1.8	1
76189	Phosphorus and transition metal co-segregation in ferritic iron grain boundaries and its effects on cohesion. Acta Materialia, 2023, 250, 118850.	3.8	5
76190	Regulating the d-p band center of FeP/Fe2P heterostructure host with built-in electric field enabled efficient bidirectional electrocatalyst toward advanced lithium-sulfur batteries. Chemical Engineering Journal, 2023, 463, 142397.	6.6	20
76191	Density functional theory studies of Pt2Ga and Pd2Ga monolayers as multifunctional electrocatalytic materials. Computational Materials Science, 2023, 224, 112164.	1.4	0
76192	Earth-abundant Co nanoparticles encapsulated in N-doped hollow carbon sphere for highly selective hydrodeoxygenation of biomass-derived vanillin. Chemical Engineering Journal, 2023, 463, 142472.	6.6	9
76193	Exploring the basal/prismatic slip transfer at grain boundaries in magnesium: A molecular dynamic simulation. Vacuum, 2023, 212, 111995.	1.6	2
76194	Tuning the UV absorbing ability of CeO2 nanoparticles with Fâ^' doping. FlatChem, 2023, 39, 100494.	2.8	6
76195	Design rules for the thermal and elastic properties of rare-earth disilicates. Materialia, 2023, 28, 101729.	1.3	0
76196	Unraveling the ferroelectric switching mechanisms in ferroelectric pure and La doped HfO2 epitaxial thin films. Materials Today Physics, 2023, 34, 101064.	2.9	6
76197	Automated calculations of exchange magnetostriction. Computational Materials Science, 2023, 224, 112158.	1.4	1

#	Article	IF	Citations
76198	Surface alloy with sulfur leading piezoelectricity from non-piezoelectricity of pentagonal-PdPSe. Journal of Alloys and Compounds, 2023, 947, 169640.	2.8	3
76199	CO oxidation mechanism on surfaces of B-site doped SrFeO3--based perovskite materials for thermochemical water splitting. Computational and Theoretical Chemistry, 2023, 1224, 114109.	1.1	0
76200	Insight into the effect of Li/P co-doping on the electronic structure and photocatalytic performance of g-C3N4 by the first principle. Applied Surface Science, 2023, 623, 157031.	3.1	13
76201	Indirect interactions between the ionic liquid and Cu surface in 0.5ÂM HCl: a novel mechanism explaining cathodic corrosion inhibition. Corrosion Science, 2023, 216, 111100.	3.0	12
76202	Dual MOF-derived Fe/N/P-tridoped carbon nanotube as high-performance oxygen reduction catalysts for zinc-air batteries. Applied Catalysis B: Environmental, 2023, 327, 122469.	10.8	58
76203	Structural construction of Bi-anchored honeycomb N-doped porous carbon catalyst for efficient CO2 conversion. Chemical Engineering Journal, 2023, 464, 142672.	6.6	5
76204	Anisotropic and high thermal conductivity in monolayer quasi-hexagonal fullerene: A comparative study against bulk phase fullerene. International Journal of Heat and Mass Transfer, 2023, 206, 123943.	2.5	18
76205	On the enhanced performance of Pt-based high-entropy alloys catalyst during waterâ€“gas shift reaction: A density functional theory study. Applied Surface Science, 2023, 623, 157023.	3.1	3
76206	Periodic DFT study on heavy metals Cu(II) and Pb(II) atoms adsorption on Na-montmorillonite (010) edge surface. Solid State Communications, 2023, 366-367, 115171.	0.9	1
76207	An anti Si/Zr-poisoning strategy of Al grain refinement by the evolving effect of doped complex. Acta Materialia, 2023, 249, 118812.	3.8	14
76208	Symmetry-breaking of LiMn6 hexatomic-ring in grain surface of Li2MnO3. Journal of Energy Chemistry, 2023, 81, 110-117.	7.1	1
76209	A dual-halogen electrolyte for protective-layer-free all-solid-state lithium batteries. Journal of Power Sources, 2023, 568, 232992.	4.0	7
76210	Phase equilibria and non-transformable tetragonal zirconia in ZrO2-RETaO4 systems and their stabilization mechanism: Experiments and calculations. Ceramics International, 2023, 49, 15969-15978.	2.3	2
76211	Breakdown of the correlation between oxidation states and core electron binding energies at the sub-nanoscale. Applied Surface Science, 2023, 619, 156755.	3.1	1
76212	Structure and stability investigation of oxygen interaction with Fe in bcc-Fe. Vacuum, 2023, 212, 112005.	1.6	1
76213	Defective 1TËŠ-MoX2 (XÂ=ÂS, Se, Te) monolayers for electrocatalytic ammonia synthesis: Steric and electronic effects on the catalytic activity. Fuel, 2023, 342, 127779.	3.4	1
76214	Phase transformation induced transitional twin boundary in body-centered cubic metals. Acta Materialia, 2023, 249, 118815.	3.8	10
76215	Development of TaC-based transition metal carbide superlattices via compound target magnetron sputtering. International Journal of Refractory Metals and Hard Materials, 2023, 113, 106165.	1.7	4

#	Article	IF	Citations
76216	Activation of Co-O bond in (110) facet exposed Co3O4 by Cu doping for the boost of propane catalytic oxidation. Journal of Hazardous Materials, 2023, 452, 131319.	6.5	35
76217	High temperature elastic properties of sub-stoichiometric yttrium dihydrides. Materials Today Communications, 2023, 35, 105879.	0.9	0
76218	Unveiling reactive origin through the in situ 2D coreâ€“shell formation, Ni(CN)2@Ni2P, derived from Hofmann-type MOF for water oxidation. Chemical Engineering Journal, 2023, 465, 142705.	6.6	2
76219	Predicting formation of chemically graded metal/ceramic interfaces. Computational Materials Science, 2023, 224, 112155.	1.4	0
76220	Tunable magnetic phase transition and magnetocaloric effect in the rare-earth-free Al-Mn-Fe-Co-Cr high-entropy alloys. Materials and Design, 2023, 229, 111894.	3.3	17
76221	Machine learning insight into h-BN growth on Pt(111) from atomic states. Applied Surface Science, 2023, 621, 156893.	3.1	4
76222	Molecular dynamics simulations of CaCl2â€“NaCl molten salt based on the machine learning potentials. Solar Energy Materials and Solar Cells, 2023, 254, 112275.	3.0	3
76223	Structural and mechanical properties of Al/TiC interface with vacancies: First-principles study. Physics Letters, Section A: General, Atomic and Solid State Physics, 2023, 471, 128786.	0.9	1
76224	Atomic-scale de-passivation mechanisms of anatase TiO2 induced by corrosive halides based on density-functional theory. Applied Surface Science, 2023, 621, 156859.	3.1	1
76225	2D Mg2M2X5 (MÂ=ÂB, Al, Ga, In, Tl; XÂ=ÂS, Se, Te) monolayers: Novel stable semiconductors for water splitting photocatalysts. Applied Surface Science, 2023, 621, 156892.	3.1	6
76226	Interfacial properties of In-plane monolayer 2H-MoTe2/1T'-WTe2 heterostructures. Applied Surface Science, 2023, 623, 157022.	3.1	1
76227	Correlation between stabilizing and strengthening effects due to grain boundary segregation in iron-based alloys: Theoretical models and first-principles calculations. Acta Materialia, 2023, 251, 118899.	3.8	6
76228	The effect of defects for the ion transport of Li3ScCl6 and Li3InCl6 with the interface of lithium metal anode: A first-principles study. Materials Today Communications, 2023, 35, 105764.	0.9	0
76229	Unraveling the role of defect types in Fe3O4 for efficient NIR-driven photocatalytic inactivation. Applied Surface Science, 2023, 622, 156860.	3.1	4
76230	Datasets on the elastic and mechanical properties of hydroxyapatite: A first principle investigation, experiments, and pedagogical perspective. Data in Brief, 2023, 48, 109075.	0.5	3
76231	Record volumetric activities of oxygen electroreduction in partly packing graphene/AgTCNQ electrodes. Carbon Trends, 2023, 11, 100254.	1.4	0
76232	Nitrogen-doped or boron-doped twin T-graphene as advanced and reversible hydrogen storage media. Applied Surface Science, 2023, 622, 156895.	3.1	11
76233	Theoretical study on surface stability, distortion and oxygen adsorption behavior of TiZrHfNb high entropy alloys. Surface Science, 2023, 732, 122273.	0.8	0

#	Article	IF	Citations
76234	Controlling diffusion in gold bonding materials for high reliability via microalloying of trace rare earth metals. Scripta Materialia, 2023, 230, 115395.	2.6	3
76235	Effect of four-phonon scattering on anisotropic thermal transport in bulk hexagonal boron nitride by machine learning interatomic potential. International Journal of Heat and Mass Transfer, 2023, 207, 124011.	2.5	5
76236	Structural, electronic, elastic and thermal properties of Cr-doped U3Si2: A DFT study. Journal of Nuclear Materials, 2023, 579, 154388.	1.3	1
76237	Microstructural and magnetic properties of Mn2FeSi and Mn2FeAl alloys prepared in bulk form. Journal of Alloys and Compounds, 2023, 947, 169672.	2.8	6
76238	A comparative study of cubic methylammonium lead iodide (CH3NH3PbI3) perovskite by using density functional theory. Materials Today Communications, 2023, 35, 105814.	0.9	1
76239	New insights into thermal processes of metal deposits on h-BN/Rh(1 1 1): A comparison of Au and Rh. Applied Surface Science, 2023, 623, 157041.	3.1	0
76240	Small-data-based machine learning interatomic potentials for graphene grain boundaries enabled by structural unit model. Carbon Trends, 2023, 11, 100260.	1.4	1
76241	Efficient electrocatalysts of single metal atom supported on defective graphene for oxygen reduction reaction (ORR): A first principles study. Chemical Physics, 2023, 570, 111888.	0.9	2
76242	Synthesis of large-size bulk hierarchically graphene-structured porous carbon and its versatile applications as hosts of sulfur and lithium for Li-S full cells and electrocatalyst for water splitting. Journal of Alloys and Compounds, 2023, 947, 169587.	2.8	0
76243	Theoretical design toward highly efficient single-atom catalysts for nitrogen reduction by regulating the â€œacceptance-donationâ€•mechanism. Applied Surface Science, 2023, 623, 156827.	3.1	9
76244	(002) oriented ZnO and ZnO:S thin films by direct ultrasonic spray pyrolysis: A comparative analysis of structure, morphology and physical properties. Materials Today Communications, 2023, 35, 105909.	0.9	2
76245	Insight into the interfacial interactions of CO2 with PuH2 (100), (110), and (111) surfaces from first-principles calculations. Vacuum, 2023, 212, 112026.	1.6	0
76246	Construction of strong built-in electric field in binary metal sulfide heterojunction to propel high-loading lithium-sulfur batteries. Journal of Energy Chemistry, 2023, 81, 492-501.	7.1	10
76247	Calculation of tunable electronic and optical properties of AlP/InSe heterostructure based on first principles. Materials Science in Semiconductor Processing, 2023, 160, 107443.	1.9	0
76248	Discerning the crystal structure and engineering the optoelectronic properties through substitution of divalent cations (M= Zn, N = Ge) in C3H3MNI3 for solar cell applications. Materials Science in Semiconductor Processing, 2023, 160, 107449.	1.9	3
76249	Fabrication of L10-ordered FeNi films by denitriding FeNiN(001) and FeNiN(110) films. Journal of Alloys and Compounds, 2023, 946, 169450.	2.8	2
76250	One-dimensional Î³-Al2O3 growth from the oxidation of NiAl. Corrosion Science, 2023, 216, 111069.	3.0	5
76251	First principles investigation on electronic structure, elasticity, thermodynamic properties of Î±-Cu2As2O7. Materials Science and Engineering B: Solid-State Materials for Advanced Technology, 2023, 292, 116371.	1.7	0

#	Article	IF	Citations
76252	Enhanced piezoelectric response of AlN via alloying of transitional metals, and influence of type and distribution of transition metals. Nano Energy, 2023, 111, 108390.	8.2	5
76253	Red anatase TiO2 microspheres with exposed major {0 0 1} facets and boron-stabilized hydrogen-occupied oxygen vacancies for visible-light-responsive water oxidation. Journal of Colloid and Interface Science, 2023, 640, 211-219.	5.0	2
76254	Strain tuning of the electronic structure and optical properties of novel Janus MgBrI monolayer: Insights from first-principles calculations. Computational Condensed Matter, 2023, 35, e00802.	0.9	1
76255	Construction of diluted magnetic semiconductor to endow nonmagnetic semiconductor with spin-regulated photocatalytic performance. Nano Energy, 2023, 110, 108381.	8.2	14
76256	VTAnDeM: A python toolkit for simultaneously visualizing phase stability, defect energetics, and carrier concentrations of materials. Computer Physics Communications, 2023, 287, 108691.	3.0	1
76257	First-principles calculations integrated with experimental optical and electronic properties for MoS2-graphene heterostructures and MoS2-graphene-Au heterointerfaces. Applied Surface Science, 2023, 623, 156948.	3.1	3
76258	Theoretical study on mechanical and electronic properties of ternary diborides Sc0.5V0.5B2, Sc0.5Nb0.5B2 and Sc0.5Ta0.5B2. Materials Today Communications, 2023, 35, 105760.	0.9	1
76259	Single 1:7H solid-solution phase achieving in iron-rich Sm-Co-Fe-Cu-Zr magnets. Journal of Alloys and Compounds, 2023, 945, 169373.	2.8	3
76260	Design of molecular M N C dual-atom catalysts for nitrogen reduction starting from surface state analysis. Journal of Colloid and Interface Science, 2023, 640, 983-989.	5.0	3
76261	Ab initio prediction of temperature-dependent stability of heterogeneous B19â€² phase in TiNi alloy using atomistically informed Eshelbyâ€™s ellipsoidal inclusion. Materials Today Communications, 2023, 35, 105861.	0.9	1
76262	Surface Gibbs free energy analyses of Sr segregation in lanthanum strontium iron oxide. Surface Science, 2023, 732, 122268.	0.8	0
76263	Design and development of low density, high strength ZrNbAlVTi high entropy alloy for high temperature applications. International Journal of Refractory Metals and Hard Materials, 2023, 113, 106222.	1.7	7
76264	The effects of mixing non-metal atoms in the B1 structured transition metal carbo-nitrides on their structure and mechanical properties: HfC1-N. Open Ceramics, 2023, 14, 100356.	1.0	0
76265	Zr4+ and Bi3+ codoped Cs2Ag0.3Na0.7InCl6 double perovskite for single-composition white-light emitting phosphors and multimodal optical anti-counterfeiting. Journal of Luminescence, 2023, 258, 119783.	1.5	9
76266	Transforming the electronic properties of phosphorene through charge transfer superatomic doping. Surface Science, 2023, 732, 122269.	0.8	2
76267	Enhanced catalytic performance of CuFeS2 chalcogenides for activation of persulfate towards decolorization and disinfection of pollutant in water. Materials Chemistry and Physics, 2023, 301, 127564.	2.0	5
76268	Efficiently electrochemical CO2 reduction on molybdenum-nitrogen-carbon catalysts with optimized p-block axial ligands. Chemical Engineering Science, 2023, 273, 118638.	1.9	2
76269	Designing layered V2O3@C with stable oxygen defects via UV-curing technology for highâ€‘performance Zn-ion hybrid supercapacitors. Applied Surface Science, 2023, 622, 156951.	3.1	7

#	Article	IF	Citations
76270	Integration of multiple advantages into one catalyst: non-CO pathway of methanol oxidation electrocatalysis on surface Ir-modulated PtFeIr jagged nanowires. Journal of Colloid and Interface Science, 2023, 640, 348-358.	5.0	6
76271	Machine Learning for the edge energies of high symmetry Au nanoparticles. Surface Science, 2023, 732, 122265.	0.8	2
76272	Room-temperature efficient NO2 sensors based on Cr-modiï¬ed ZnO@graphene-like UC composites. Journal of Alloys and Compounds, 2023, 945, 169306.	2.8	0
76273	Phonon hardening and the effect of phonon transport in cubic antiperovskites <mml:math xmlns:mml="http://www.w3.org/1998/Math/MathML" altimg="si5.svg" display="inline" id="d1e2134"><mml:mrow><mml:msub><mml:mrow><mml:mi>A</mml:mi></mml:mrow><mml:mrow><mml:mn>3</mml:mn></mml:mrow></mml:msub></mml:mrow></mml:math> (A = Li, Na; B = Se, Te) induced by quartic anharmonicity. Materials Today Communications, 2023, 35, 105450.	3.9	2
76274	High solar-to-hydrogen efficiency in AsP/GaSe heterojunction for photocatalytic water splitting: A DFT study. Materials Science in Semiconductor Processing, 2023, 159, 107393.	1.9	7
76275	Oxidative desulfurization of thiophene derivatives with L-proline/benzene sulfonic acid deep eutectic solvent and their interaction: An experimental and computational study. Journal of Cleaner Production, 2023, 406, 136878.	4.6	4
76276	First-principles investigation of structural, electronic, and energetic properties of BaSnO3 (001) surfaces. Vacuum, 2023, 212, 111977.	1.6	5
76277	Biochar doped carbon nitride to enhance the photocatalytic hydrogen evolution through synergy of nitrogen vacancies and bridging carbon structure: Nanoarchitectonics and first-principles calculation. Carbon, 2023, 209, 117988.	5.4	8
76278	Liquid-solid contact electrification and its effect on the formation of electric double layer: An atomic-level investigation. Nano Energy, 2023, 111, 108442.	8.2	3
76279	First-principles studies on the structural, electronic and thermal transport characteristics of half-Heusler compounds LiXN (X=Mg, Zn). Solid State Communications, 2023, 366-367, 115156.	0.9	0
76280	Phase behavior of metastable water based on fully ab initio simulations. Journal of Non-Crystalline Solids, 2023, 610, 122307.	1.5	0
76281	Probing temperature effects on the stacking fault energy of GH3536 superalloy using first-principles theory. Intermetallics, 2023, 157, 107882.	1.8	3
76282	First-principles studies the optical properties of defective-GQDs and -fullerene. Computational Condensed Matter, 2023, 35, e00793.	0.9	0
76283	Spontaneous post-growth oxygen dissipation and electrical improvement of silver electrodes in substoichiometric oxidation states. Applied Surface Science, 2023, 623, 156998.	3.1	5
76284	The CrBr3 monolayer: Two dimension sodium ion battery anode material to characterize state-of-charge by magnetism. Applied Surface Science, 2023, 623, 157074.	3.1	1
76285	A novel smart framework for sustainable nanocomposite electrolytes based on ionic liquids of dye-sensitized solar cells by a covalently multifunctional graphene oxide-vinyl imidazole/4-tert-butylpyridine cobalt complex. Journal of Alloys and Compounds, 2023, 945, 169241.	2.8	2
76286	Architecture design of novel carbon family: Polyhedra as building blocks. Carbon Trends, 2023, 11, 100256.	1.4	3
76287	Full-scale simulation and experimental verification of the phase-transition temperature of a VO2 nanofilm as smart window materials. Materials Today Communications, 2023, 35, 105758.	0.9	0

#	Article	IF	Citations
76288	Surface states modulation of topological insulator Bi2Se3 by noble metal decoration for gas sensing kinetic engineering. Sensors and Actuators B: Chemical, 2023, 385, 133662.	4.0	1
76289	Enabling high ionic conductivity in yttrium-based lithium halide electrolytes by composition modulation for all-solid-state batteries. Materials Today Chemistry, 2023, 30, 101510.	1.7	4
76290	Computational screening of Ï‡3 borophene based single-atom catalysts for N2 reduction. Catalysis Today, 2023, 418, 114079.	2.2	4
76291	DFT+U calculations on <mml:math xmlns:mml="http://www.w3.org/1998/Math/MathML" altimg="si85.svg" display="inline" id="d1e768"><mml:mrow><mml:msub><mml:mrow><mml:mi mathvariant="normal">U</mml:mi></mml:mrow><mml:mrow><mml:mn>3</mml:mn></mml:mrow></mml:msub><mml:msub><mml:mrow><mml:mi mathvariant="normal">O</mml:mi></mml:mrow><mml:mrow><mml:mn>8</mml:mn></mml:mrow></mml:msub></mml:mrow></mml: surface: thermodynamic stability and polarity compensation. Surface Science, 2023, 732, 122266.	1.8	0
76292	Superior efficiency hydrogen peroxide production in acidic media through epoxy group adjacent to Co-O/C active centers on carbon black. Chemical Engineering Journal, 2023, 465, 142691.	6.6	3
76293	Manipulation of contact type in MoSSe/Ti3C2 heterostructures via the functionalization of chalcogens and halogens. Surfaces and Interfaces, 2023, 38, 102855.	1.5	0
76294	The optical properties of In2S3 films in the far-infrared spectral range. Infrared Physics and Technology, 2023, 131, 104662.	1.3	0
76295	Effects of uniaxial strain on elastic and electronic properties of hydrogenated XC (X=Si, Ge, and Sn) monolayers by first-principles calculations. Physics Letters, Section A: General, Atomic and Solid State Physics, 2023, 472, 128808.	0.9	1
76296	Oscillating local minimum energy site and its effect on the spinodal decomposition of TiAlN: A first-principles study. Vacuum, 2023, 212, 112069.	1.6	0
76297	A BP3-AlP3 heterobilayer for the bifunctional photocatalysis of CO2 reduction. Applied Surface Science, 2023, 621, 156890.	3.1	5
76298	Two-dimensional PtI2/Bi2S3 and PtI2/Bi2Se3 heterostructures with high solar-to-hydrogen efficiency. Colloids and Surfaces A: Physicochemical and Engineering Aspects, 2023, 666, 131286.	2.3	1
76299	Epitaxially strained ultrathin LaNiO3/LaAlO3 and LaNiO3/SrTiO3 superlattices: A density functional theory + U study. Current Applied Physics, 2023, 50, 53-60.	1.1	2
76300	Metronidazole photodegradation under solar light with UiO-66-NH2 photocatalyst: Mechanisms, pathway, and toxicity assessment. Journal of Environmental Chemical Engineering, 2023, 11, 109744.	3.3	0
76301	Electronic structure and carrier mobility of BC6N/BN van der Waals heterostructure induced by in-plane strains. Applied Surface Science, 2023, 623, 157007.	3.1	11
76302	Thermodynamic re-modeling of the Yb-Sb system aided by first-principles calculations. Calphad: Computer Coupling of Phase Diagrams and Thermochemistry, 2023, 81, 102541.	0.7	1
76303	First-principles investigations of the crystal and electronic structures, dynamical and mechanical stabilities, Born effective charges and dielectric permittivities of a novel tetragonal zirconia. Physica B: Condensed Matter, 2023, 659, 414862.	1.3	0
76304	Crucial role of alkali metal ions and Si/Al ratio in selective adsorption of 1-octene using faujasite zeolites. Separation and Purification Technology, 2023, 314, 123531.	3.9	1
76305	Structural, Electronic, Optical, and potassium anodic electrochemical characteristics of 2-Dimensional Silicane: A density functional theory investigation. Journal of Electroanalytical Chemistry, 2023, 938, 117442.	1.9	0

#	Article	IF	Citations
76306	Copper decorated graphyne as a promising nanocarrier for cisplatin anti-cancer drug: A DFT study. Applied Surface Science, 2023, 622, 156885.	3.1	4
76307	Thermodynamic assessment of the ternary Niâ€“Ti-Hf system. Calphad: Computer Coupling of Phase Diagrams and Thermochemistry, 2023, 81, 102546.	0.7	0
76308	Insights into the enhanced performance of NiCo-LDH modified Pd/NF cathode for electrocatalytic hydrodechlorination. Fuel, 2023, 341, 127689.	3.4	9
76309	Unrevealing the phase transition of high-performing high-nitrogen energetic material 1,5-diaminotetrazole-4: N-oxide via first-principles studies. Materials Today Communications, 2023, 35, 105940.	0.9	0
76310	Revealing the nature of dinuclear active sites on CenTiOx catalysts for the selective catalytic reduction NOx with NH3. Journal of Environmental Chemical Engineering, 2023, 11, 109685.	3.3	1
76311	Hydrogen-surface interaction from first-principles calculations and its implication to hydrogen embrittlement mechanisms of titanium. Applied Surface Science, 2023, 621, 156871.	3.1	4
76312	Anchored Coâ€“oxo generated by cobalt single atoms outperformed aqueous species from the counterparts in peroxymonosulfate treatment. Applied Catalysis B: Environmental, 2023, 328, 122483.	10.8	6
76313	The nature of a low angle grain boundary in a Si bi-crystal with added Fe impurities. Acta Materialia, 2023, 252, 118917.	3.8	2
76314	Formation of ReS2/ReO3 semiconductor-metal heterostructure boosts electrocatalytic performance of pristine ReS2 nanoparticles in hydrogen evolution reaction. Applied Materials Today, 2023, 32, 101781.	2.3	4
76315	Crystal structure modulation of SnSe thermoelectric material by AgBiSe2 solid solution. Journal of the European Ceramic Society, 2023, 43, 3383-3389.	2.8	6
76316	Doping strategy on properties and chemical mechanical polishing performance of CeO2 Abrasives: A DFT assisted experimental study. Applied Surface Science, 2023, 623, 156997.	3.1	5
76317	Insight into the oxidation mechanisms of vanadium slag and its application in the separation of V and Cr. Journal of Cleaner Production, 2023, 405, 136981.	4.6	4
76318	First-principles investigation of two-dimensional magnesium chloride: Environmental stability and fundamental properties. Physica E: Low-Dimensional Systems and Nanostructures, 2023, 151, 115715.	1.3	1
76319	Effect of strain on the effective mass of GaN and the mobility of AlGaN/GaN two-dimensional electron gas. Materials Today Communications, 2023, 35, 105788.	0.9	3
76320	Chiral phonons in binary compounds <mml:math xmlns:mml="http://www.w3.org/1998/Math/MathML" altimg="si17.svg" display="inline" id="d1e1274"><mml:mi>A</mml:mi></mml:math>Bi (<mml:math xmlns:mml="http://www.w3.org/1998/Math/MathML" altimg="si12.svg" display="inline" id="d1e1285"><mml:msub><mml:mrow	0.9	3
76321	Short bandgap of porphyrin molecules (Py) filled in a semiconducting single-walled carbon nanotube (Py@NT17) for highly efficient organic photovoltaic cells. Materials Science and Engineering B: Solid-State Materials for Advanced Technology, 2023, 293, 116456.	1.7	2
76322	Boosted Z-scheme photocatalytic overall water splitting with faceted Bi4TaO8Cl crystals as water oxidation photocatalyst. Applied Catalysis B: Environmental, 2023, 328, 122541.	10.8	6
76323	Metalloids (B, Si) and non-metal (N, P, S) doped graphene nanosheet as a supercapacitor electrode: A density functional theory study. Materials Today Communications, 2023, 35, 105905.	0.9	1

#	Article	IF	Citations
76324	Theoretical approach to the one-step versus two-step spin transitions in Hofmann-like FeII SCO metal-organic frameworks. Materials Today Chemistry, 2023, 30, 101489.	1.7	1
76325	Unraveling the role of Fe5C2 in CH4 formation during CO2 hydrogenation over hydrophobic iron catalysts. Applied Catalysis B: Environmental, 2023, 327, 122449.	10.8	7
76326	Theoretical study of the influence of H-SAPO-34 modified with Zn2+ on the formation of butadiene. Chemical Engineering Science, 2023, 273, 118652.	1.9	0
76327	Ti-decorated nitrogen-rich BeN4 monolayer for reversible hydrogen storage: DFT investigations. Applied Surface Science, 2023, 622, 156806.	3.1	6
76328	New insights into the co-adsorption behavior of H2O and H2 on defective PuH2 (100), (110), and (111) surfaces from first-principles study. Vacuum, 2023, 212, 112044.	1.6	1
76329	Ir-trimer anchored on the Co-supported Pd nanocrystals Opens the Ultra-efficient Channel on oxygen reduction reaction. Applied Surface Science, 2023, 622, 156857.	3.1	2
76330	Zn-doped nickel iron (oxy)hydroxide nanocubes passivated by polyanions with high catalytic activity and corrosion resistance for seawater oxidation. Journal of Energy Chemistry, 2023, 81, 82-92.	7.1	6
76331	The hinge morphology of SnO2 as multifunctional semiconductor: What we can learn from simulations, theory, and experiments. Applied Surface Science, 2023, 622, 156904.	3.1	3
76332	Structure, vibrations and electronic transport in silicon suboxides: Application to physical unclonable functions. Journal of Non-Crystalline Solids: X, 2023, 18, 100179.	0.5	1
76333	Theoretical study on structural transformation and mechanical properties of Ni3Ti1-xNbx. Results in Materials, 2023, 18, 100387.	0.9	0
76334	First-principles study of Xe behavior in Î´-UZr2. Journal of Nuclear Materials, 2023, 579, 154387.	1.3	1
76335	First-principles calculations to investigate structural, electronics, optical, and mechanical properties of Bi-based novel fluoroperovskites TBiF3 (T = Hg, Xe) for optoelectronic applications. Materials Science in Semiconductor Processing, 2023, 160, 107399.	1.9	13
76336	Activation of basal-plane sulfur sites on MoS2 @Ni3S2 nanorods by Zr plasma ion implantation for bifunctional electrocatalysts. Journal of Alloys and Compounds, 2023, 947, 169448.	2.8	5
76337	Electronegative diversity induced localized built-in electric field in a single phased MoSxSeyNz for selectivity-enhanced visible photocatalytic CO2 reduction. Applied Catalysis B: Environmental, 2023, 330, 122625.	10.8	10
76338	CALPHAD aided mechanical properties screening in full composition space of NbC-TiC-VC-ZrC ultra-high temperature ceramics. International Journal of Refractory Metals and Hard Materials, 2023, 113, 106191.	1.7	3
76339	Surpassing Pt hydrogen production from {200} facet-riched polyhedral Rh2P nanoparticles by one-step synthesis. Applied Catalysis B: Environmental, 2023, 330, 122645.	10.8	4
76340	Two-dimensional van der Waals layered VSi2N4 as anode materials for alkali metal (Li, Na and K) ion batteries. Journal of Physics and Chemistry of Solids, 2023, 178, 111339.	1.9	3
76341	Uncertainty quantification of predicting stable structures for high-entropy alloys using Bayesian neural networks. Journal of Energy Chemistry, 2023, 81, 118-124.	7.1	2

#	Article	IF	Citations
76342	2D/2D Z-scheme-based Î±-Fe2O3 @NGr heterojunction implanted with Pt single-atoms for remarkable photocatalytic hydrogen evolution. Applied Catalysis B: Environmental, 2023, 330, 122586.	10.8	15
76343	Atomistic mechanism of Î·â€™-to-Î· transformation in Al-Zn-Mg-Cu alloys. Scripta Materialia, 2023, 231, 115474.	2.6	6
76344	CO2 electroreduction on single atom catalysts: Is water just a solvent?. Journal of Catalysis, 2023, 422, 1-11.	3.1	10
76345	Significance of different dopamine species as reducing agents of graphene oxide: Fundamental aspects. Surface Science, 2023, 732, 122285.	0.8	1
76346	Defect engineered Janus MoSiGeN4 as highly efficient electrocatalyst for hydrogen evolution reaction. Applied Surface Science, 2023, 622, 156894.	3.1	9
76347	DFT study of superlight ambient temperature reversible H2 storage media based on Li decorated on new planar BCN. Applied Surface Science, 2023, 622, 156947.	3.1	9
76348	Efficient biobased carboxylic acids synthesis by synergistic electrocatalysis of multi-active sites on bimetallic Cu-Co oxide/oxyhydroxide. Applied Catalysis B: Environmental, 2023, 331, 122709.	10.8	8
76349	Amorphous quantum dots co-catalyst: Defect level induced solar-to-hydrogen production. Applied Catalysis B: Environmental, 2023, 330, 122583.	10.8	8
76350	Dual functional effect of oxygen vacancies and depolarity shield embedded NiCo2O4 cathode in lithium sulfur battery. Applied Surface Science, 2023, 622, 156939.	3.1	3
76351	Novel dual-photoelectrode photoelectrocatalytic system based on TiO2 nanoneedle arrays photoanode and nitrogen-doped carbon dots/Co3O4 photocathode for efficient water purification at low/no applied voltage. Applied Catalysis B: Environmental, 2023, 331, 122676.	10.8	6
76352	Ion diffusion, and hysteresis of magnesium hydride conversion electrode materials. Journal of Materials Science and Technology, 2023, 155, 47-53.	5.6	2
76353	Freeâ€“templated synthesis of Nâ€“doped PtCu porous hollow nanospheres for efficient ethanol oxidation and oxygen reduction reactions. Applied Catalysis B: Environmental, 2023, 330, 122602.	10.8	8
76354	Effect of flue gas components on the removal of cadmium pollutants by transition metal-modified activated carbon: Density functional theory and thermodynamic study. Fuel, 2023, 343, 128011.	3.4	7
76355	Precisely optimizing polysulfides adsorption and conversion by local coordination engineering for high-performance Li-S batteries. Nano Energy, 2023, 110, 108353.	8.2	20
76356	Micro-alloying effects of Ni on the microstructure and mechanical properties of an Al-Zn-Mg-Cu-Sc-Zr alloy. Journal of Alloys and Compounds, 2023, 947, 169667.	2.8	6
76357	Design of bifunctional TiO2-SSZ-13 mixed supports for potassium-resistant vanadia catalysts for NH3-SCR. Fuel, 2023, 342, 127804.	3.4	3
76358	Atomic-scale engineering of cation vacancies in two-dimensional unilamellar metal oxide nanosheets for electricity generation from water evaporation. Nano Energy, 2023, 110, 108348.	8.2	8
76359	Ab initio study of pressure-dependent phonon heat conduction in cubic boron nitride. International Journal of Heat and Mass Transfer, 2023, 208, 124092.	2.5	3

#	Article	IF	Citations
76360	Intrinsic ferromagnetic half-metal: Non-equivalent alloying compounds CrMnI6 monolayer. Applied Surface Science, 2023, 623, 157084.	3.1	3
76361	Unraveling reactive oxygen species-dependent toluene mineralization routes via construction of TixSn1â^'xO2 infinite solid solution photocatalysts. Applied Catalysis B: Environmental, 2023, 330, 122628.	10.8	6
76362	A revisit to the role of Mo in an MP35N superalloy: An experimental and theoretical study. Journal of Materials Science and Technology, 2023, 157, 60-70.	5.6	2
76363	Systemic analysis to reveal the improved stability of LiNi0.6Co0.2Mn0.2O2 electrodeâ€“electrolyte interface modulated by N-methylpyrrolidone. Chinese Journal of Analytical Chemistry, 2023, 51, 100250.	0.9	1
76364	Simultaneous polarization engineering and selectivity regulation achieved using polymeric carbon nitride for promoting NOx photo-oxidation. Applied Catalysis B: Environmental, 2023, 330, 122582.	10.8	5
76365	Unravelling the role of metal-metal oxide interfaces of Cu/ZnO/ZrO2/Al2O3 catalyst for methanol synthesis from CO2: Insights from experiments and DFT-based microkinetic modeling. Applied Catalysis B: Environmental, 2023, 332, 122743.	10.8	8
76366	Stable Li deposition of 3D highstrength-lithiophilicity-porous CuZn current collector with gradient structure. Journal of Alloys and Compounds, 2023, 951, 169953.	2.8	4
76367	Nonlinear optical crystals KPb3(3-C5H4NCOO)2Br5 and KPb3(3-C5H4NCOO)2Cl3Br2 with new Pb-centered nitrogen-halide polyhedrons obtained by the halide anionic substitution. Journal of Alloys and Compounds, 2023, 951, 169945.	2.8	0
76368	Penta nitrogen coordinated cobalt single atom catalysts with oxygenated carbon black for electrochemical H2O2 production. Applied Catalysis B: Environmental, 2023, 331, 122712.	10.8	8
76369	Boron pretreatment promotes phosphorization of FeNi catalysts for oxygen evolution. Applied Catalysis B: Environmental, 2023, 330, 122598.	10.8	20
76370	Subphase exploration for SmFe12-based permanent magnets by Gibbs energies obtained with first-principles cluster-expansion method. Journal of Alloys and Compounds, 2023, 950, 169849.	2.8	0
76371	Novel CoFeAlMn high-entropy alloys with excellentsoft magnetic properties and high thermal stability. Journal of Materials Science and Technology, 2023, 153, 22-31.	5.6	12
76372	Observation of low thermal expansion behavior and weak thermal anisotropy in M3A2C phases. Journal of Materials Science and Technology, 2023, 154, 210-216.	5.6	2
76373	Enabling extraordinary oxygen reduction reaction activity of dual alkaline earth-substituted perovskite cathodes for intermediate-temperature solid oxide fuel cells. Materials Research Bulletin, 2023, 164, 112245.	2.7	3
76374	Highly conductive S-doped FeSe2-xSx microsphere with high tap density for practical sodium storage. , 2023, 2, 100120.		8
76375	Activating the Î²-Ga2O3 surface for epitaxy growth and dopant incorporation using low chemical-hardness metal overlayers. Journal of Alloys and Compounds, 2023, 951, 169793.	2.8	0
76376	Electronic structure and oxygen vacancy tuning of Co & Ni co-doped W18O49 nanourchins for efficient TEA gas sensing. Chemical Engineering Journal, 2023, 465, 142815.	6.6	16
76377	MSGCorep: A package for corepresentations of magnetic space groups. Computer Physics Communications, 2023, 288, 108722.	3.0	7

#	Article	IF	Citations
76378	Noble metal single-atoms for lithium-ion batteries: A booster for ultrafast charging/discharging in carbon electrodes. Applied Surface Science, 2023, 624, 157161.	3.1	3
76379	Interaction between bilayer borophene and metal or inert substrates. Applied Surface Science, 2023, 626, 157157.	3.1	4
76380	Influence of solution-hardening on the mechanical properties and wear resistance of copper alloys. Wear, 2023, 523, 204869.	1.5	0
76381	Semi-metallic bilayer borophene for lithium-ion batteries anode material: A first-principles study. Chemical Physics, 2023, 571, 111911.	0.9	4
76382	Cu4@C2N for effective electrochemical CO2 reduction and intermediates dependent adsorption behaviours: A computational study. Applied Surface Science, 2023, 626, 157126.	3.1	4
76383	Design, synthesis and investigating the interaction of novel s-triazine collector with pyrite surface: A DFT-D3+U and experimental studies. Surfaces and Interfaces, 2023, 38, 102820.	1.5	1
76384	Synergetic effect of the interface electric field and the plasmon electromagnetic field in Au-Ag alloy mediated Z-type heterostructure for photocatalytic hydrogen production and CO2 reduction. Applied Catalysis B: Environmental, 2023, 331, 122700.	10.8	5
76385	Crystal structure, magnetic and electronic features of Nd<mml:math xmlns:mml="http://www.w3.org/1998/Math/MathML" altimg="si56.svg" display="inline" id="d1e245"><mml:msub><mml:mrow /><mml:mrow><mml:mi>x</mml:mi></mml:mrow></mml:msub></mml:math>Y<mml:math xmlns:mml="http://www.w3.org/1998/Math/MathML" altimg="si57.svg" display="inline" id="d1e259"><mml:msub><mml:mrow /><mml:mrow><mml:mn>3</mml:mn></mml:mrow></mml:msub></mml:math>Fe<mml:math xmlns:mml="http://www.w3.org/1998/Math/MathML" altimg="si58.svg" display="inline" id="d1e273"><mml:msub><mml:mrow /><mml:mrow><mml:mn>5</mml:mn></mml:mrow></mml:msub></mml:math>O<mml:math xmlns:mml="http://www.w3.org/1998/Math/MathML" altimg="si59.svg" display="inline" id="d1e287"><mml:msub><mml:mrow /><mml:mrow><mml:mn>12</mml:mn></mml:mrow></mml:msub></mml:math> garnet ceramics. Journal of Alloys and Compounds, 2023, 952, 169987.	1.4	1
76386	Sr and Fe co-doped Ba2In2O5 as a new proton-conductor-derived cathode for proton-conducting solid oxide fuel cells. Journal of the European Ceramic Society, 2023, 43, 4573-4579.	2.8	21
76387	Mechanistic insight into electron orientation by tailoring Niâ€“Cu atom-pairs for high-performance CO2 electroreduction. Applied Catalysis B: Environmental, 2023, 330, 122654.	10.8	16
76388	Impurity-related defect complexes-mediated ferromagnetism and impurity band hopping conduction in a highly compensated Zn-doped SnO2. Materials Science in Semiconductor Processing, 2023, 162, 107518.	1.9	1
76389	Lattice softness regulates recombination and lifetime of carrier in Germanium doped CsPbI2Br perovskite: First principles DFT and NAMD simulations. Journal of Solid State Chemistry, 2023, 322, 123981.	1.4	0
76390	Enhanced electrocatalytic cathodic degradation of 2,4-dichlorophenoxyacetic acid based on a synergistic effect obtained from Co single atoms and Cu nanoclusters. Applied Catalysis B: Environmental, 2023, 332, 122748.	10.8	7
76391	Electronic excitation induced non-thermal phase transition of tungsten. Journal of Alloys and Compounds, 2023, 952, 170087.	2.8	1
76392	ARPES studies of the ground state electronic properties of the van der Waals transition metal trichalcogenide CoPS<mml:math xmlns:mml="http://www.w3.org/1998/Math/MathML" altimg="si7.svg" display="inline" id="d1e439"><mml:msub><mml:mrow /><mml:mrow><mml:mn>3</mml:mn></mml:mrow></mml:msub></mml:math>. Chemical Physics Letters, 2023, 823, 140511.	1.2	3
76393	Facilitating interface charge transfer via constructing NiO/NiCo2O4 heterostructure for oxygen evolution reaction under alkaline conditions. Journal of Colloid and Interface Science, 2023, 643, 214-222.	5.0	10
76394	Efficacy of pyrostilpnite (Ag3SbS3) mineral as thermoelectric material: A first principles study. Materials Science in Semiconductor Processing, 2023, 162, 107513.	1.9	3
76395	Reaction-driven evolutions of Pt states over Pt-CeO2 catalysts during CO oxidation. Applied Catalysis B: Environmental, 2023, 330, 122662.	10.8	3

#	Article	IF	Citations
76396	Nanoscale Periodic Trapping Sites for Interlayer Excitons Built by Deformable Molecular Crystal on 2D Crystal. ACS Nano, 2023, 17, 7775-7786.	7.3	2
76397	Rational design of heterogenized molecular phthalocyanine hybrid single-atom electrocatalyst towards two-electron oxygen reduction. Nature Communications, 2023, 14, .	5.8	36
76398	Selfâ€Formed Fluorinated Interphase with Fe Valence Gradient for Dendriteâ€Free Solidâ€State Sodiumâ€Metal Batteries. Advanced Functional Materials, 2024, 34, .	7.8	5
76399	Influence of phosphorus-doped bilayer graphene configuration on the oxygen reduction reaction in acidic solution. Carbon, 2023, 210, 118012.	5.4	0
76400	Structural arrangement and improved thermoelectric figure of merit in hexagonal SiX(X=N,P,As,Sb,Bi) monolayers: understanding from first-principles calculations. Journal Physics D: Applied Physics, 0, , .	1.3	0
76401	Screening Multiâ€layered Twoâ€dimensional Cdâ€chalcogenide Structures as Potential Candidates for Photocatalysis. ChemPhysChem, 0, , .	1.0	0
76402	Adsorption effects and mechanisms of phosphorus by nanosized laponite. Chemosphere, 2023, 331, 138684.	4.2	7
76403	Hydrogen Absorption Performance and O2 Poisoning Resistance of Pd/ZrCo Composite Film. Materials, 2023, 16, 3159.	1.3	0
76404	Study of structural, electronic, and magnetic properties of L10-ordered CoPt and NiPt: An ab initio calculations and Monte Carlo simulation. Solid State Communications, 2023, 363, 115112.	0.9	9
76405	Localized magnetic moment induced by boron adatoms chemisorbed on graphene. Journal of Physics Condensed Matter, 0, , .	0.7	0
76406	3D microstructure evolution in Na<mml:math xmlns:mml="http://www.w3.org/1998/Math/MathML" altimg="si13.svg" display="inline" id="d1e2248"><mml:msub><mml:mrow /><mml:mrow><mml:mi>x</mml:mi></mml:mrow></mml:msub></mml:math>FePO<mml:math xmlns:mml="http://www.w3.org/1998/Math/MathML" altimg="si156.svg" display="inline" id="d1e2256"><mml:msub><mml:mrow /> of monolayer X<mml:math xmlns:mml="http://www.w3.org/1998/Math/MathML" altimg="si86.svg" display="inline" id="d1e657"><mml:msub><mml:mrow /><mml:mrow><mml:mn>3</mml:mn></mml:mrow></mml:msub></mml:math>YZ<mml:math xmlns:mml="http://www.w3.org/1998/Math/MathML" altimg="si87.svg" display="inline" id="d1e665"><mml:msub><mml:mrow />	4.0	3
76407	Combining Theoretical and Experimental Methods to Probe Confinement within Microporous Solid Acid Catalysts for Alcohol Dehydration. ACS Catalysis, 2023, 13, 5955-5968.	1.3	0
76408	Large optical anisotropy in quasi-one-dimensional tantalum thallium chalcogenides TaTlX3 (X = S, Se): A first-principles investigation. Materials Chemistry and Physics, 2023, 303, 127754.	5.5	4
76409	Theoretical insights into nonmetal-doped graphyne-supported noble metal electrocatalysts for NH3 synthesis via nitrogen reduction. Applied Surface Science, 2023, 617, 156550.	2.0	2
76410	A theoretical study of the functionalized carbon dots surfaces binding with silver nanostructures. Computational and Theoretical Chemistry, 2023, 1223, 114087.	3.1	11
76411	Density Functional Theory Studies of the Direct Conversion of Methane to Methanol Using O₂ on Graphitic MN₄G-BN (M = Fe, Co, Cu) and CuN₄G-PN Single-Atom Catalysts. ACS Applied Nano Materials, 0, , .	1.1	1
76412	Electronic structure of the magnetic halide double perovskites <mml:math xmlns:mml="http://www.w3.org/1998/Math/MathML"><mml:mrow><mml:msub><mml:mi>Cs</mml:mi><mml:mn>2</mml:mn> from first principles. Physical Review Materials, 2023, 7, .	2.4	3
76413		2.9	4

#	Article	IF	Citations
76414	Synergistic double-atom catalysts of metal-boron anchored on g-C2N for electrochemical nitrogen reduction: Mechanistic insight and catalyst screening. Journal of Energy Chemistry, 2023, 80, 350-360.	7.1	13
76415	Formation mechanism of mirror twin grain boundaries in molecular beam epitaxy grown monolayer WSe₂â€“MoSe₂ lateral heterojunctions. 2D Materials, 2023, 10, 035010.	2.0	2
76416	First-principles calculations to investigate Structural, Electronic, optical and mechanical properties of Cu-based fluoroperovskite XCuF3 (XÂ=ÂK, Ru). Computational and Theoretical Chemistry, 2023, 1224, 114115.	1.1	6
76417	Chemical ordering effects on martensitic transformations in Mg-Sc alloys. Acta Materialia, 2023, 249, 118854.	3.8	2
76418	Structural incorporation of iron influences biomethylation potential of mercury sulfide. Geochimica Et Cosmochimica Acta, 2023, 349, 115-125.	1.6	1
76419	Understanding the hydrogen evolution reaction activity of doped single-atom catalysts on two-dimensional GaPS4 by DFT and machine learning. Journal of Energy Chemistry, 2023, 81, 93-100.	7.1	17
76420	An advanced organic cathode for non-aqueous and aqueous calcium-based dual ion batteries. Journal of Power Sources, 2023, 569, 232995.	4.0	8
76421	Zn-enriched cathode layer interface via atomic surface reduction of LiNi0.5Mn1.5O4: Computational and experimental insights. Journal of Power Sources, 2023, 569, 233017.	4.0	1
76422	Self-supported copper selenide nanosheets for electrochemical carbon dioxide conversion to syngas with a broad H2-to-CO ratio. Electrochimica Acta, 2023, 449, 142213.	2.6	5
76423	Achieving high energy storage performance by LaMg0.5Ti0.5O3 modification of multiphase engineered Bi0.5Na0.5TiO3â€“based ceramics. Ceramics International, 2023, 49, 16225-16234.	2.3	6
76424	Computational design of one FeCoNiCuZn high-entropy alloy for high-performance electrocatalytic nitrate reduction. Applied Surface Science, 2023, 626, 157246.	3.1	2
76425	Tunable valley characteristics of WSe2 and WSe2/VSe2 heterostructure. Applied Surface Science, 2023, 624, 157111.	3.1	3
76426	Ba3GeTeS4: A new quaternary heteroanionic chalcogenide semiconductor. Journal of Solid State Chemistry, 2023, 323, 124028.	1.4	2
76427	Strain driven anomalous anisotropic enhancement in the thermoelectric performance of monolayer MoS2. Applied Surface Science, 2023, 626, 157139.	3.1	12
76428	Theoretical design of buckled honeycomb binary ZrX (X=S, Se, Te) monolayers and valley splitting of heterostructures constructed with MoTe2. Physica B: Condensed Matter, 2023, 660, 414899.	1.3	0
76429	CeO2 promotes electrocatalytic formic acid oxidation of Pd-based alloys. Journal of Alloys and Compounds, 2023, 948, 169665.	2.8	2
76430	Construction of hollow binary oxide heterostructures by Ostwald ripening for superior photoelectrochemical removal of reactive brilliant blue KNR dye. , 2023, 2, 100117.		14
76431	Heterojunction material BiYO3/g-C3N4 modified with cellulose nanofibers for photocatalytic degradation of tetracycline. Carbohydrate Polymers, 2023, 312, 120829.	5.1	16

#	Article	IF	Citations
76432	Syngas-to-Hydrocarbons on the transition metal catalysts: Revealing the function of surface hydroxyl intermediate served as co-adsorbed promoter or hydrogenating species. Fuel, 2023, 343, 127967.	3.4	0
76433	A computational study of adsorption of H2S and SO2 on the activated carbon surfaces. Journal of Molecular Graphics and Modelling, 2023, 122, 108463.	1.3	2
76434	Chemical and interfacial design in the visible-light-absorbing ferroelectric thin films. Journal of the European Ceramic Society, 2023, 43, 3275-3288.	2.8	1
76435	Revealing the effects of transition metal doping on CoSe cocatalyst for enhancing photocatalytic H2 production. Applied Catalysis B: Environmental, 2023, 328, 122503.	10.8	24
76436	Discovery of two-dimensional Ga2S3 monolayers for efficient photocatalytic overall water splitting to produce hydrogen. Applied Surface Science, 2023, 626, 157215.	3.1	4
76437	Efficient simultaneous removal of NOx and CO at low temperatures over integrated Mn2Co1Ox/iron mesh monolithic catalyst via NH3-SCR coupling with CO oxidation reactions. Chemical Engineering Journal, 2023, 465, 142611.	6.6	13
76438	Al-modified environmental barrier coatings for protection against water vapor corrosion. Corrosion Science, 2023, 217, 111123.	3.0	7
76439	Cobalt-doped molybdenum disulfide for efficient sulfite activation to remove As(III): Preparation, efficacy, and mechanisms. Journal of Hazardous Materials, 2023, 452, 131311.	6.5	8
76440	Preventing H2S poisoning of dense Pd membranes for H2 purification using an electric-field: An Ab initio study. Surface Science, 2023, 733, 122303.	0.8	2
76441	Modification mechanisms of hypereutectic Al-Fe alloys treated by Sm/Yb addition: Experiments and first-principles calculations. Journal of Alloys and Compounds, 2023, 948, 169786.	2.8	5
76442	Unconventional s-p-d hybridization in modulating frontier orbitals of carbonaceous radicals on PdBi nanosheets for efficient ethanol electrooxidation. Applied Catalysis B: Environmental, 2023, 328, 122521.	10.8	9
76443	Atomistic insight into impact of solute segregation on Î±-Mg/FCC-Al2Ca interface stability. Journal of Alloys and Compounds, 2023, 948, 169766.	2.8	0
76444	The effect of rutile TiO<mml:math xmlns:mml="http://www.w3.org/1998/Math/MathML" altimg="si35.svg" display="inline" id="d1e1312"><mml:msub><mml:mrow /><mml:mrow><mml:mn>2</mml:mn></mml:mrow></mml:msub></mml:math>(110) surface on the physicochemical properties of subnanometer Auâ€“Pd clusters: A DFT study. Surface Science, 2023, 733, 122287.	0.8	1
76445	Transport properties of refractory high-entropy alloys with single-phase body-centered cubic structure. Scripta Materialia, 2023, 231, 115464.	2.6	5
76446	N, S codoped carbon matrix-encapsulated CoFe/Co0.2Fe0.8S heterostructure as a highly efficient and durable bifunctional oxygen electrocatalyst for rechargeable zinc-air batteries. Journal of Colloid and Interface Science, 2023, 642, 1-12.	5.0	4
76447	Stable and robust single transition metal atom catalyst for CO2 reduction supported on defective WS2. Applied Surface Science, 2023, 624, 157073.	3.1	9
76448	High-density electron transfer in Ni-metalâ€“organic framework@FeNi-layered double hydroxide for efficient electrocatalytic oxygen evolution. Journal of Colloid and Interface Science, 2023, 642, 505-512.	5.0	6
76449	Metal/CeO2â^'x with regulated heterointerface, interfacial oxygen vacancy and electronic structure for highly efficient hydrogen evolution reaction. Applied Surface Science, 2023, 626, 157248.	3.1	2

#	Article	IF	Citations
76450	Modulation of the magnetic, electronic, and optical behaviors of WS2 after metals adsorption: A first-principles study. Chemical Physics, 2023, 571, 111903.	0.9	39
76451	Similarities and trends in adsorbate induced reconstruction â€“ Structure and stability of FCC iron and cobalt surface carbides. Applied Surface Science, 2023, 626, 157245.	3.1	3
76452	Electrocatalytic hydrogen evolution on the MoS2/C60 heterostructure: Reaction mechanism and activity improvement. Applied Surface Science, 2023, 624, 157163.	3.1	1
76453	First-principles study on effects of X (Ta, Ti, and W) on the nitriding behavior of Î³â€²-Ni3Al in Ni-based superalloys: From the surface adsorption and diffusion of nitrogen. Applied Surface Science, 2023, 626, 157249.	3.1	0
76454	High-pressure hydrogen adsorption in clay minerals: Insights on natural hydrogen exploration. Fuel, 2023, 344, 127919.	3.4	21
76455	Fabrication of three-dimensional hollow nanocassette photocatalysts RE-TiO2 (REÂ=ÂLa, Ce, Sm, Yb, and) Tj ETQq1 1 0.784314 rgBT /O Surface Science, 2023, 626, 157239.	3.1	3
76457	Electronic structure and magnetic properties of YXâ€²CrZ (Xâ€²â€‰=â€‰Fe, Co, Ni; Zâ€‰=â€‰Al,Ga, In) quaternary Heusler alloys. Indian Journal of Physics, 2023, 97, 733-749.	0.9	4
76459	Quantum transport of sub-5 nm InSe and In₂SSe monolayers and their heterostructure transistors. Nanoscale, 2023, 15, 3496-3503.	2.8	3
76460	Hydrogen diffusion on the tin-covered tungsten surface: A first-principles study. Journal of Nuclear Materials, 2023, 577, 154282.	1.3	3
76461	Revealing the bifunction mechanism of LaCoO3 as electrocatalyst: Oxygen vacancies effect and synergistic reaction process. Journal of Alloys and Compounds, 2023, 941, 168918.	2.8	3
76462	Unveiling the synergistic effects of Re-Mo alloying on diffusion behaviors in Î³-Ni: From a theoretical perspective. Journal of Materials Research and Technology, 2023, 23, 1214-1224.	2.6	3
76463	C60 surface-supported TM@Si16 (TMÂ=ÂTi, Zr, Hf) superatoms as self-assembled photocatalysts. Applied Surface Science, 2023, 616, 156465.	3.1	3
76464	Two-dimensional conductive covalent organic framework for efficient electrocatalytic nitrogen reduction reaction. Vacuum, 2023, 210, 111852.	1.6	2
76465	Remarkable formaldehyde photo-oxidation efficiency of Zn2SnO4 co-modified by Mo doping and oxygen vacancies. Separation and Purification Technology, 2023, 310, 123202.	3.9	10
76466	Novel two-dimensional C6B4 monolayer as an anode for Li-/Na-ion batteries with high theoretical capacity. Applied Surface Science, 2023, 616, 156468.	3.1	7
76467	Cobalt single atom induced catalytic active site shift in carbon-doped BN for efficient photodriven CO2 reduction. Applied Surface Science, 2023, 616, 156451.	3.1	3
76468	Decreasing the W-Cr solid solution decomposition rate: Theory, modelling and experimental verification. Journal of Nuclear Materials, 2023, 576, 154288.	1.3	3
76469	Ultra-high oxygen evolution potential of CuO5-Zn1 active sites on SnO2(1 1 0) surface and its origin: DFT theoretical study. Applied Surface Science, 2023, 616, 156469.	3.1	0

#	Article	IF	Citations
76470	Theoretical calculation of hydrogen evolution reaction in two-dimensional As2X3(X=S, Se, Te) doped with transition metal atoms. Applied Surface Science, 2023, 616, 156475.	3.1	6
76471	First-principles assessment of chemical lithiation of sulfide solid electrolytes and its impact on their transport, electronic and mechanical properties. Journal of Power Sources, 2023, 560, 232689.	4.0	4
76472	Mechanistic understanding of N₂ activation: a comparison of unsupported and supported Ru catalysts. Faraday Discussions, 0, , .	1.6	0
76473	Planar buckling controlled optical conductivity of SiC monolayer from Deep-UV to visible light region: A first-principles study. Materials Chemistry and Physics, 2023, 297, 127395.	2.0	1
76474	Highly stabilized single-crystal P2-type layered oxides obtained via rational crystal orientation modulation for sodium-ion batteries. Chemical Engineering Journal, 2023, 458, 141515.	6.6	10
76475	Two-dimensional dual topological insulator in hexagonal IrO. New Journal of Physics, 2023, 25, 023010.	1.2	0
76476	Direct Growth of Uniform Bimetallic Coreâ€Shell or Intermetallic Nanoparticles on Carbon via a Surfaceâ€Confinement Strategy for Electrochemical Hydrogen Evolution Reaction. Advanced Functional Materials, 2023, 33, .	7.8	10
76477	Thickness dependent properties of quasi-layered MgGeN2 thin films. Materials Letters, 2023, 337, 133860.	1.3	4
76478	Kinetically versus thermodynamically controlled factors governing elementary pathways of GaP(111) surface oxidation. Journal of Power Sources, 2023, 560, 232663.	4.0	1
76479	First principles investigations of structural and electronic properties of Ga-doped ZnZrO solid solutions for catalytic reduction of CO2. Molecular Catalysis, 2023, 537, 112941.	1.0	1
76480	First-principles study of noble metal atom doped Fe(100) as electrocatalysts for nitrogen reduction reaction. Materials Chemistry and Physics, 2023, 297, 127396.	2.0	1
76481	Passivation effect of theophylline on the surface defects of MAPbI3 perovskite. Computational Materials Science, 2023, 219, 112028.	1.4	5
76482	Electronic, magnetic and optical properties of zigzag ZnO nanoribbons under the coupling action of electric field and strains. Thin Solid Films, 2023, 768, 139698.	0.8	2
76483	Dynamic investigations on hydrogenâ€“helium interaction around the vacancy in BCC iron from ab-initio calculations. Nuclear Fusion, 2023, 63, 046005.	1.6	2
76484	Unidirectional domain growth of hexagonal boron nitride thin films. Applied Materials Today, 2023, 30, 101734.	2.3	5
76485	Reaction mechanisms and activities of dual-metal sites for Li-CO2 batteries: The first-principle investigation. Applied Surface Science, 2023, 616, 156493.	3.1	4
76486	DFT-study supported synergistic electrochemical supercapacitor performance of Bi2MoS6 nanosheets. Journal of Energy Storage, 2023, 60, 106661.	3.9	1
76487	Theoretical study on the influence of the extra N in transition metal-N4 embedded graphene as efficient CO2 reduction catalysts. Applied Surface Science, 2023, 616, 156494.	3.1	1

#	Article	IF	Citations
76488	Development of a novel sensor based on Bi2O3 and carbonized UIO-66-NH2 nanocomposite for efficient detection of Pb(â...¡) ion in water environment. Applied Surface Science, 2023, 616, 156510.	3.1	6
76489	Tuning gas-sensitive properties of the twin graphene decorated with transition metal via small electrical field: A viewpoint of first principle. Diamond and Related Materials, 2023, 133, 109707.	1.8	6
76490	Electronic properties and photon scattering of buckled and planar few-layer 2D GaN. Vacuum, 2023, 210, 111861.	1.6	10
76491	Ca-driven stable regulatory of alkalinity within desilication products: Experimental, modeling, transformation mechanism and DFT study. Science of the Total Environment, 2023, 868, 161708.	3.9	11
76492	Interplay of dopant and polarons in trifunctional semimagnetic semiconductor for supercapacitor applications: Local structure and electronic structure investigations. Journal of Energy Storage, 2023, 60, 106655.	3.9	1
76493	A carbon allotrope with twisted Dirac cones induced by grain boundaries composed of pentagons and octagons. Physical Chemistry Chemical Physics, 2023, 25, 4230-4235.	1.3	0
76494	Strategies for fitting accurate machine-learned inter-atomic potentials for solid electrolytes. Materials Futures, 2023, 2, 015101.	3.1	3
76495	Electronic structures and photovoltaic applications of vdW heterostructures based on Janus group-IV monochalcogenides: insights from first-principles calculations. Physical Chemistry Chemical Physics, 2023, 25, 5663-5672.	1.3	3
76496	Bi5O7Br-nanotube@Au-nanoparticle core-shell assembly for high signal-to-noise ratio SERS detection of adenine. Materials Today Communications, 2023, 34, 105471.	0.9	2
76497	Metal-organic framework derived functional MnO2 via an in-situ oxidation strategy for advanced quasi-solid-state supercapacitors. Journal of Power Sources, 2023, 560, 232705.	4.0	9
76498	Identifying active sites at the Cu/Ce interface for hydrogen borrowing reactions. Journal of Catalysis, 2023, 418, 163-177.	3.1	9
76499	First principle calculation of structural, electronic, magnetic, and elastic properties of ferromagnetic Cu2MnZ (Z = Pb, P, As, Bi, S, Se, and Te) Heusler alloys. Physica B: Condensed Matter, 2023, 653, 414673.	1.3	3
76500	Efficient electrocatalytic CO2 reduction on Ti3C2O2 surfaces: The effect of single-atom TM anchoring on product selectivity. Applied Surface Science, 2023, 616, 156492.	3.1	5
76501	Theoretical screening of synergistic transition metal dual-atom catalysts for overall water splitting. Computational Materials Science, 2023, 220, 112034.	1.4	1
76502	Electronic and magnetic properties of mono and bimetallic subnanometer clusters. A DFT research. Materials Today Communications, 2023, 34, 105483.	0.9	0
76503	Enhancement of the magnetic and mechanical properties by introducing element carbon for Ti-based alloy. Journal of Magnetism and Magnetic Materials, 2023, 568, 170438.	1.0	2
76504	Enhanced free-exciton luminescence in Cs2SnBr6â^'I : A first-principles study. Chemical Engineering Journal, 2023, 458, 141533.	6.6	3
76505	Segregation of solute elements and strengthening effects of CoCrNiCux medium-entropy alloys: A combined experimental and simulation study. Journal of Alloys and Compounds, 2023, 941, 169015.	2.8	4

#	Article	IF	Citations
76506	Structural features, thermal stability and catalytic implication of Feâ€“Ni nanoparticles. Journal of Solid State Chemistry, 2023, 320, 123863.	1.4	1
76507	Theoretical and Empirical Insight into Dopant, Mobility and Defect States in W Doped Amorphous In₂ O₃ for High-Performance Enhancement Mode BEOL Transistors. , 2022, , .		0
76508	Deterioration of irradiation resistance of ODS-F/M steel under high concentration of helium. Journal of Nuclear Materials, 2023, 577, 154293.	1.3	0
76509	Constructing highly active surface-nanostructured core/bi-shell La1.2Sr0.8Ni0.5Mn0.5O4+Î´ cathode for protonic ceramic fuel cells. Chemical Engineering Journal, 2023, 459, 141459.	6.6	9
76510	Efficient Hydrogenation of Methyl Palmitate to Hexadecanol over Cu/m-ZrO₂ Catalysts: Synergistic Effect of Cu Species and Oxygen Vacancies. ACS Catalysis, 2023, 13, 2047-2060.	5.5	18
76511	Uniaxial compressions induced complementarity and anisotropic behaviors in CuVP₂S₆. Journal of Physics Condensed Matter, 2023, 35, 135501.	0.7	1
76512	Metallic 1H-BeP2 monolayer as a potential anode material for Li-ion/Na-ion batteries: A first principles study. Colloids and Surfaces A: Physicochemical and Engineering Aspects, 2023, 662, 131037.	2.3	3
76513	Revealing the decisive factors of the lattice thermal conductivity reduction by electron-phonon interactions in half-Heusler semiconductors. Materials Today Physics, 2023, 31, 100993.	2.9	1
76514	In situ generation of H2O2 over Ce-doped BaTiO3 catalysts for enhanced piezo-photocatalytic degradation of pollutants in aqueous solution. Colloids and Surfaces A: Physicochemical and Engineering Aspects, 2023, 663, 131030.	2.3	7
76515	Metal Ion-Incorporated Lead-Free Perovskites toward Broadband Photodetectors. ACS Applied Electronic Materials, 2023, 5, 5291-5302.	2.0	5
76516	Lanthanum Oxyhalide Monolayers: An Exceptional Dielectric Companion to 2-D Semiconductors. IEEE Transactions on Electron Devices, 2023, 70, 1509-1519.	1.6	3
76517	Strong anharmonic phonon scattering and superior thermoelectric properties of Li2NaBi. Materials Today Physics, 2023, 31, 100990.	2.9	11
76518	Mobility of carbon-decorated screw dislocations in bcc iron. Acta Materialia, 2023, 247, 118716.	3.8	1
76519	Van der Waals stacking of multilayer In2Se3 with 2D metals induces transition from Schottky to Ohmic contact. Applied Surface Science, 2023, 617, 156557.	3.1	4
76520	Coexistence of Bulk-Nodal and Surface-Nodeless Cooper Pairings in a Superconducting Dirac Semimetal. Physical Review Letters, 2023, 130, .	2.9	6
76521	Wave-layered dendrite-free lithium deposition with unprecedented long-term cyclability. Journal of Power Sources, 2023, 560, 232697.	4.0	0
76522	The combined effects of Mg2+ and Sr2+ incorporation during CaCO3 precipitation and crystal growth. Geochimica Et Cosmochimica Acta, 2023, 345, 16-33.	1.6	1
76523	Oxygen vacancy engineering of zinc oxide for boosting piezo-electrocatalytic hydrogen evolution. Applied Surface Science, 2023, 616, 156556.	3.1	25

#	Article	IF	Citations
76524	Stochastic algorithms for self-consistent calculations of electronic structures. Mathematics of Computation, 2023, 92, 1693-1728.	1.1	0
76525	Emergence of metallic surface states and negative differential conductance in thin Î²-FeSi₂ films on Si(001). Journal of Physics Condensed Matter, 2023, 35, 135001.	0.7	0
76526	Access and Capture of Layered Double Perovskite Polytypic Phase through High-Pressure Engineering. Journal of Physical Chemistry C, 2023, 127, 2407-2415.	1.5	5
76527	First-principles study of origin of perpendicular magnetic anisotropy in MgO|CoFeB|Ta structures. Results in Physics, 2023, 45, 106239.	2.0	0
76528	The OER/ORR activities of copper oxyhydroxide series electrocatalysts. Molecular Catalysis, 2023, 537, 112942.	1.0	4
76529	Theoretical study of M2CO2 MXenes stability and adsorption properties for heavy metals ions removal from water. Computational Materials Science, 2023, 220, 112042.	1.4	2
76530	Nonrelativistic Spin-Momentum Coupling in Antiferromagnetic Twisted Bilayers. Physical Review Letters, 2023, 130, .	2.9	19
76531	H2O2 mediated oxidation mechanism of pyrite (0 0 1) surface in the presence of oxygen and water. Applied Surface Science, 2023, 617, 156568.	3.1	2
76532	Realizing spontaneous valley polarization and topological phase transitions in monolayer ScX2 (XÂ=ÂCl,) Tj ETQq0 0 0 rgBT /Overlock 10	3.8	17
76533	Optoelectronic, mechanical, and thermoelectric properties of Na/I co-doped SnSe via ab initio calculations. Journal of Solid State Chemistry, 2023, 320, 123858.	1.4	1
76534	Non-leaded, KSnI3 based perovskite solar cell: A DFT study along with SCAPS simulation. Materials Chemistry and Physics, 2023, 297, 127426.	2.0	22
76535	Analysis of the structural, elastic constants, electronic, optical, dynamical, and thermodynamic in dicalcium silicate with various pressures. Vacuum, 2023, 210, 111869.	1.6	6
76536	Biâ€“C monolayer as a promising 2D anode material for Li, Na, and K-ion batteries. Physical Chemistry Chemical Physics, 2023, 25, 4980-4986.	1.3	5
76537	Exploring efficient hydrogen evolution electrocatalysts of nonmetal atom doped Mo₂CO₂ MXenes by first-principles screening. Physical Chemistry Chemical Physics, 2023, 25, 5056-5065.	1.3	5
76538	Adsorption of 3d transition-metal atoms on two-dimensional penta-graphene: A first-principles study. Journal of Saudi Chemical Society, 2023, 27, 101611.	2.4	3
76539	Cooperative effect of strain and electric field on Schottky barriers in van der Waals heterostructure of graphene and hydrogenated phosphorus carbide. Physica E: Low-Dimensional Systems and Nanostructures, 2023, 148, 115665.	1.3	2
76540	Screening of single-atom catalysts of transition metal supported on MoSe2 for high-efficiency nitrogen reduction reaction. Molecular Catalysis, 2023, 537, 112967.	1.0	4
76541	Experimental and first-principles study on the interfacial interactions between vertically aligned carbon nanotubes and growth substrates: Prospects for better substrate adhesion. Diamond and Related Materials, 2023, 133, 109734.	1.8	0

#	Article	IF	Citations
76542	Strong phonon mode induced by carbon vacancy accelerating hole transfer in SiC/MoS2 heterostructure. Applied Surface Science, 2023, 617, 156554.	3.1	5
76543	Dynamic structural and microstructural responses of a metalâ€“organic framework type material to carbon dioxide under dual gas flow and supercritical conditions. Journal of Applied Crystallography, 2023, 56, 222-236.	1.9	2
76544	Monoclinic C12: A new superhard carbon allotrope. Physica B: Condensed Matter, 2023, 653, 414696.	1.3	0
76545	Insights into the synergy of platinum and nickel carbonate hydroxide for efficient methanol electro-oxidation. Applied Surface Science, 2023, 616, 156587.	3.1	3
76546	Voltage induced lattice contraction enabling superior cycling stability of MnO2 cathode in aqueous zinc batteries. Energy Storage Materials, 2023, 56, 524-531.	9.5	11
76547	Electronic reconfiguration induced by anchoring orbital interaction onto asymmetric FeIn2S4 surface for hydrogen evolution reaction. Physica B: Condensed Matter, 2023, 654, 414704.	1.3	0
76548	First principle study on high-entropy perovskites Ca(Ti0.25Zr0.25Hf0.25Sn0.25)O3 and Ca(Ti0.25Zr0.25Hf0.25Ce0.25)O3 as thermal barrier coatings. Materials Chemistry and Physics, 2023, 297, 127460.	2.0	1
76549	Electrocatalytic nitrogen fixation performance of two-dimensional Metal-Organic Frameworks Cu3(C6O6) and TM/Cu3(C6O6) from first-principle study. Chemical Physics, 2023, 568, 111837.	0.9	1
76550	Atomic structure and large magnetic anisotropy in air-sensitive layered ferromagnetic VI₃. Nanoscale, 2023, 15, 4628-4635.	2.8	1
76551	Room temperature d ⁰ ferromagnetism in carbon doped LaH₃: insights from density functional theory simulations. Journal Physics D: Applied Physics, 2023, 56, 095001.	1.3	0
76552	The local structure and electronic properties of Ho3+-doped BaY2F8: A first-principles method. Materials Chemistry and Physics, 2023, 298, 127459.	2.0	0
76553	Recent advances in theab initiotheory of solid-state defect qubits. Nanophotonics, 2023, 12, 359-397.	2.9	12
76554	Effects of carbon defects on interfacial anchoring of NiFe-LDH for seawater electro-oxidation. Journal of Materials Chemistry A, 2023, 11, 10277-10286.	5.2	5
76555	The giant tunneling electroresistance effect in monolayer In₂SSeTe-based lateral ferroelectric tunnel junctions. Materials Advances, 2023, 4, 1572-1582.	2.6	2
76556	Theoretical study the catalytic performance and mechanism of novel designed single atom catalysts M1/2DMs for 1,3-butadiene hydrogenation. Applied Surface Science, 2023, 617, 156585.	3.1	0
76557	Sulfideâ€Bridged Covalent Quinoxaline Frameworks for Lithiumâ€“Organosulfide Batteries. Advanced Materials, 2023, 35, .	11.1	12
76558	Toward the Speed Limit of Phaseâ€Change Memory. Advanced Materials, 2023, 35, .	11.1	14
76559	Superconducting state of the van der Waals layered PdH2 structure at high pressure. International Journal of Hydrogen Energy, 2023, 48, 16769-16778.	3.8	3

#	Article	IF	Citations
76560	Static and Dynamic Disorder in Formamidinium Lead Bromide Single Crystals. Journal of Physical Chemistry Letters, 2023, 14, 1288-1293.	2.1	10
76561	Predicting chemical exfoliation: fundamental insights into the synthesis of MXenes. Npj 2D Materials and Applications, 2023, 7, .	3.9	10
76562	Novel ultrahard sp2/sp3 hybrid carbon allotrope from crystal chemistry and first principles: Body-centered tetragonal C6 (â€˜neoglitterâ€™). Diamond and Related Materials, 2023, 133, 109747.	1.8	3
76563	Pseudospin-selective Floquet band engineering in black phosphorus. Nature, 2023, 614, 75-80.	13.7	51
76564	Activating MoS₂ Basal Plane via Nonâ€noble Metal Doping For Enhanced Hydrogen Production. ChemistrySelect, 2023, 8, .	0.7	4
76565	Covalent organic frameworks with Ni-Bis(dithiolene) and Co-porphyrin units as bifunctional catalysts for Li-O ₂ batteries. Science Advances, 2023, 9, .	4.7	24
76566	Enhancing dehydrogenation performance of MgH2/graphene heterojunctions via noble metal intercalation. International Journal of Hydrogen Energy, 2023, 48, 16733-16744.	3.8	6
76567	Novel Boron-rich Phosphides with High Hardness, Large Strain, and Magnetism. Journal of Physical Chemistry Letters, 2023, 14, 1310-1317.	2.1	3
76568	Grain refinement in titanium prevents low temperature oxygen embrittlement. Nature Communications, 2023, 14, .	5.8	8
76569	Conjugated dual size effect of core-shell particles synergizes bimetallic catalysis. Nature Communications, 2023, 14, .	5.8	18
76570	Theoretical Calculations on Metal Catalysts Toward Waterâ€Gas Shift Reaction: a Review. Chemistry - A European Journal, 2023, 29, .	1.7	3
76571	Al Coordination and Ga Interstitial Stability in a Î²-(Al_{0.2}Ga_{0.8})₂O₃ Thin Film. ACS Applied Materials & Interfaces, 2023, 15, 8601-8608.	4.0	0
76572	Probing the Structure and Dynamics of Na⁺ Ionic Doped LiF Crystals in Fluoride Eutectic Salt by Solid-State NMR. Journal of Physical Chemistry C, 2023, 127, 3093-3098.	1.5	0
76573	Effects of chemical complexity on the initial oxidation resistance of HfC1â^’N ceramics. Computational Materials Science, 2023, 220, 112037.	1.4	2
76574	Fast ion-conductive electrolyte based on a doped LaAlO3 with an amorphous surface layer for low-temperature solid oxide fuel cells. Journal of Power Sources, 2023, 561, 232723.	4.0	6
76575	MOF-derived ultrasmall Ru@RuO2 heterostructures as bifunctional and pH-universal electrocatalysts for 0.79ÂV asymmetric amphoteric overall water splitting. Chemical Engineering Journal, 2023, 460, 141672.	6.6	17
76576	Chiral Magnetic Interactions in Small Fe Clusters Triggered by Symmetry-Breaking Adatoms. Symmetry, 2023, 15, 397.	1.1	0
76577	Coupling a Main-Group Metal with a Transition Metal to Create Biatom Catalysts for Nitric Oxide Reduction. Physical Review Applied, 2023, 19, .	1.5	4

#	Article	IF	Citations
76578	Mo₂CF₂/WS₂: Two-Dimensional Van Der Waals Heterostructure for Overall Water Splitting Photocatalyst from Five-Step Screening. Journal of Physical Chemistry Letters, 2023, 14, 1363-1370.	2.1	3
76579	Metal borohydrides as ambient-pressure high-<mml:math xmlns:mml="http://www.w3.org/1998/Math/MathML"><mml:msub><mml:mi>T</mml:mi><mml:mi>c</mml:mi></mml:msub> Physical Review B, 2023, 107, .	3.7	9
76580	Oxygen Adsorption on Polar and Non-Polar Zn:ZnO Heterostructures from First Principles. Materials, 2023, 16, 1275.	1.3	0
76581	In-Depth Insight into a Passive Film through Hydrogen-Bonding Network in an Aqueous Zinc Battery. ACS Applied Materials & Interfaces, 2023, 15, 7949-7958.	4.0	4
76582	Pressure and temperature effects on (TiZrTa)C medium-entropy carbide from first-principles. Journal of Materials Research and Technology, 2023, 23, 2288-2300.	2.6	5
76583	Modular calcination strategy to construct defect-rich nitrogen-doped Nb2O5 for boosting photocatalytic oxidation of cyclohexane to cyclohexanone in solvent-free conditions. Applied Surface Science, 2023, 617, 156600.	3.1	7
76584	Topologically Frustrated Graphene Antidot Lattice Semiconductors with Room-Temperature Magnetism. Journal of Physical Chemistry C, 2023, 127, 3276-3284.	1.5	1
76585	Size and Quality of Quantum Mechanical Data Set for Training Neural Network Force Fields for Liquid Water. Journal of Physical Chemistry B, 2023, 127, 1422-1428.	1.2	0
76586	Perovskite super-particles for commercial displays. Cell Reports Physical Science, 2023, 4, 101275.	2.8	2
76587	Manganese Local Environment Modulation via SiO₄ Substitution to Boost Sodium Storage Performance of Na₄MnCr(PO₄)₃. Small, 2023, 19, .	5.2	8
76588	Negative piezoelectricity and enhanced electrical conductivity at the interfaces of two-dimensional dialkali oxide and chalcogenide monolayers. Physical Review B, 2023, 107, .	1.1	7
76589	Voltage-Controlled Dzyaloshinskii-Moriya Interaction Torque Switching of Perpendicular Magnetization. Physical Review Letters, 2023, 130, .	2.9	9
76590	Tunable topologically driven Fermi arc van Hove singularities. Nature Physics, 2023, 19, 682-688.	6.5	4
76591	Electronic properties and surface states of RbNi<mml:math xmlns:mml="http://www.w3.org/1998/Math/MathML" altimg="si2.svg" display="inline" id="d1e205"><mml:msub><mml:mrow /><mml:mrow><mml:mn>2</mml:mn></mml:mrow></mml:msub></mml:math>Se<mml:math xmlns:mml="http://www.w3.org/1998/Math/MathML" altimg="si2.svg" display="inline"	1.3	2
76592	Atomically Dispersed Cu Catalysts on Sulfide-Derived Defective Ag Nanowires for Electrochemical CO₂ Reduction. ACS Nano, 2023, 17, 2387-2398.	7.3	17
76593	Systematic Search for Stabilizing Dopants in ZrO₂ and HfO₂ Using First-Principles Calculations. , 2022, , .		1
76594	Phase transition enhanced thermoelectric performance for perovskites: The case of AgTaO3. Current Applied Physics, 2023, 48, 84-89.	1.1	2
76595	Microscopic Mechanism of Enhanced Catalytic Activity for Ammonia Synthesis in Y₅M₃(M = Si/Ge) Electrides. Journal of Physical Chemistry C, 2023, 127, 2953-2962.	1.5	1

#	Article	IF	Citations
76596	Electric-field-tunable thermal conductivity in anti-ferroelectric materials. Materials Today Physics, 2023, 32, 100998.	2.9	1
76597	DFTÂ+ÂU study of electronic and optical properties of Cu3TMTe4: TMÂ=ÂV, Nb, Ta with incorporation of SOC. Materials Today: Proceedings, 2023, , .	0.9	2
76598	Doping Copper Selenide for Tuning the Crystal Structure and Thermoelectric Performance of Germanium Telluride-Based Materials. ACS Applied Materials & Interfaces, 2023, 15, 8327-8335.	4.0	3
76599	Thermodynamics modeling of ZrCo-H systems with biaxial compressive strain during desorption. Journal of Nuclear Materials, 2023, 577, 154301.	1.3	1
76600	Highly Stable Electrochemical Supercapacitor Performance of Self-Assembled Ferromagnetic Q-Carbon. ACS Applied Materials & Interfaces, 2023, 15, 8305-8318.	4.0	11
76601	Giant electrophotonic response in two-dimensional halide perovskite <mml:math xmlns:mml="http://www.w3.org/1998/Math/MathML"><mml:msub><mml:mrow><mml:mi>Cs</mml:mi></mml:mrow><mml:mn>3</mml:mn> mathvariant="normal">I</mml:mi></mml:mrow><mml:mn>9</mml:mn></mml:msub></mml:math> by strain engineering. Physical Review Materials, 2023, 7, .	0.9	1
76603	First-Principles Study of Structural and Electronic Properties of Monolayer PtX₂ and Janus PtXY (X, Y = S, Se, and Te) via Strain Engineering. ACS Omega, 2023, 8, 5715-5721.	1.6	3
76604	Machine learning method to predict the interlayer sliding energy barrier of polarized MoS2 layers. Computational Materials Science, 2023, 220, 112062.	1.4	3
76605	Fluorination-Induced Asymmetry in Vacancy-Ordered Brownmillerite: Route to Multiferroic Behavior. Chemistry of Materials, 2023, 35, 991-998.	3.2	1
76606	Accurate description of hydrogen diffusivity in bcc metals using machine-learning moment tensor potentials and path-integral methods. Acta Materialia, 2023, 247, 118739.	3.8	6
76607	Unraveling the Water Oxidation Mechanism on a Stoichiometric and Reduced Rutile TiO₂ (100) Surface Using First-Principles Calculations. Journal of Physical Chemistry C, 2023, 127, 3444-3451.	1.5	2
76608	Calculation of dislocation binding to helium-vacancy defects in tungsten using hybrid ab initio-machine learning methods. Acta Materialia, 2023, 247, 118734.	3.8	10
76609	Monolayer Kagome metals AV3Sb5. Nature Communications, 2023, 14, .	5.8	7
76610	First-principles study of SrTe and BaTe: Promising wide-band-gap semiconductors with ambipolar doping. Current Applied Physics, 2023, 48, 90-96.	1.1	1
76611	Atomically Unveiling an Atlas of Polytypes in Transition-Metal Trihalides. Journal of the American Chemical Society, 2023, 145, 3624-3635.	6.6	6
76613	Cobalt doping of Mg3Sb2 monolayer: Improved thermoelectric performance. Physics Letters, Section A: General, Atomic and Solid State Physics, 2023, 463, 128684.	0.9	0
76614	Insights into the Fischerâ€“Tropsch mechanism on Ï‡-Fe5C2(510) based on the hydrogen coverage effect. Molecular Catalysis, 2023, 538, 112990.	1.0	1
76615	First-Principles Study of the Effect of Ni-Doped on the Spinel-Type Mn-Based Cathode Discharge. ACS Applied Materials & Interfaces, 2023, 15, 8208-8216.	4.0	3

#	Article	IF	Citations
76616	Nearly-freestanding supramolecular assembly with tunable structural properties. Scientific Reports, 2023, 13, .	1.6	2
76617	Heteroepitaxial Control of Fermi Liquid, Hund Metal, and Mott Insulator Phases in Singleâ€Atomicâ€Layer Ruthenates. Advanced Materials, 0, , 2208833.	11.1	4
76618	Atomically dispersed iridium catalysts on silicon photoanode for efficient photoelectrochemical water splitting. Nature Communications, 2023, 14, .	5.8	32
76619	Mechanisms of the preferential cleavage of Ti2AlNb-based alloy: The influence of grain size and local plasticity. Materials Science & Engineering A: Structural Materials: Properties, Microstructure and Processing, 2023, 867, 144741.	2.6	3
76620	Intrinsic thermal stability enhancement in n-type Mg3Sb2 thermoelectrics toward practical applications. Acta Materialia, 2023, 247, 118752.	3.8	6
76621	In situ formation of stable solid electrolyte interphase with high ionic conductivity for long lifespan all-solid-state lithium metal batteries. Energy Storage Materials, 2023, 57, 1-13.	9.5	17
76622	Sizeâ€Induced Ferroelectricity in Antiferroelectric Oxide Membranes. Advanced Materials, 2023, 35, .	11.1	5
76623	Strong quartic anharmonicity, ultralow thermal conductivity, high band degeneracy and good thermoelectric performance in Na2TlSb. Npj Computational Materials, 2023, 9, .	3.5	18
76624	Novel theoretical insight on CO2 electroreduction mechanism induced by aromatic ester-functionalized ionic liquids: A bulk-phase reaction pathway. Journal of Molecular Liquids, 2023, 375, 121392.	2.3	2
76625	Coupled Spin-Valley, Rashba Effect, and Hidden Spin Polarization in WSi₂N₄ Family. Journal of Physical Chemistry Letters, 2023, 14, 1494-1503.	2.1	17
76626	Pressure tuning of structure, magnetic frustration, and carrier conduction in the Kitaev spin liquid candidate <mml:math xmlns:mml="http://www.w3.org/1998/Math/MathML"><mml:mrow><mml:msub><mml:mi>Cu</mml:mi><mml:mn>2</mml:mn></mml: Physical Review B, 2023, 107, .	1.1	3
76627	Giant Rashba effect and nonlinear anomalous Hall conductivity in a two-dimensional molybdenum-based Janus structure. Physical Review B, 2023, 107, .	1.1	1
76628	Million-scale data integrated deep neural network for phonon properties of heuslers spanning the periodic table. Npj Computational Materials, 2023, 9, .	3.5	7
76629	Electronic, Thermal, and Thermoelectric Transport Properties of ReSe2 and Re2Te5. International Journal of Energy Research, 2023, 2023, 1-10.	2.2	2
76630	Universal properties of metal-supported oxide films from linear scaling relationships: elucidation of mechanistic origins of strong metalâ€“support interactions. Chemical Science, 2023, 14, 3206-3214.	3.7	6
76631	First-principles calculations of the high pressure and temperature properties of Fe₇C₃. Chinese Physics B, 0, , .	0.7	0
76632	How Adsorption Affects the Energy Release in an Azothiophene-Based Molecular Solarâ€“Thermal System. Journal of Physical Chemistry Letters, 2023, 14, 1470-1477.	2.1	3
76633	(2Ã—1) Reconstruction Mechanism of Rutile TiO₂(011) Surface. ACS Nano, 2023, 17, 3549-3556.	7.3	1

#	Article	IF	Citations
76634	First-principles study of thermoelectric performance of monolayer Ge₂<i>X</i>₄S₂ (<i>X </i>= P, As). Wuli Xuebao/Acta Physica Sinica, 2023, 72, 077201.	0.2	0
76635	Thermochromic composite film of VO2 nanoparticles and [(C2H5)2NH2]2NiBr4@SiO2 nanospheres for smart window applications. Chemical Engineering Journal, 2023, 460, 141715.	6.6	3
76636	Effects on the glassy phase and electronic structure of <mml:math xmlns:mml="http://www.w3.org/1998/Math/MathML" altimg="si5.svg" display="inline" id="d1e1296"><mml:mrow><mml:msub><mml:mrow><mml:mi mathvariant="normal">Ca</mml:mi></mml:mrow><mml:mrow><mml:mn>3</mml:mn></mml:mrow></mml:msub><mml:msub><mml:mi mathvariant="normal">Co</mml:mi></mml:mrow><mml:mrow><mml:mn>2</mml:mn></mml:mrow></mml:msub><mml:msub><mml:mi mathvariant="normal">O</mml:mi></mml:mrow><mml:mrow><mml:mn>6</mml:mn></mml:mrow></. Physica B: Cond	1.3	1
76637	Phonon transport in <mml:math xmlns:mml="http://www.w3.org/1998/Math/MathML"><mml:mrow><mml:msub><mml:mi>Cu</mml:mi><mml:mn>2</mml:mn></ : Effects of spin-orbit coupling and higher-order phonon-phonon scattering. Physical Review B, 2023, 107, .	1.1	8
76638	Effects of cation and anion substitution in KVPO4F for K-ion batteries. Energy Storage Materials, 2023, 57, 81-91.	9.5	5
76639	Mechanical Behavior of Austenitic Steel under Multi-Axial Cyclic Loading. Materials, 2023, 16, 1367.	1.3	1
76640	Synthesis of technetium hydride <mml:math xmlns:mml="http://www.w3.org/1998/Math/MathML"><mml:mrow><mml:mi>Tc</mml:mi><mml:msub><mml:mi mathvariant="normal">H</mml:mi><mml:mrow><mml:mn>1.3</mml:mn></mml:mrow></mml:msub></mml:mrow></mml:math> at 27 GPa. Physical Review B, 2023, 107, .	1.1	1
76641	In Situ Photo-Fenton-Like Tandem Reaction for Selective Gluconic Acid Production from Glucose Photo-Oxidation. ACS Catalysis, 2023, 13, 2637-2646.	5.5	13
76642	Suppressing Hydrogen Evolution via Anticatalytic Interfaces toward Highly Efficient Aqueous Zn-Ion Batteries. ACS Nano, 2023, 17, 3948-3957.	7.3	34
76643	New High-Pressure Structures of Transition Metal Carbonates with O3Câ€“CO3 Orthooxalate Groups. Symmetry, 2023, 15, 421.	1.1	2
76644	Enhanced reversible hydrogen storage performance of Mg-decorated g-C2N: First principles calculations. Computational Materials Science, 2023, 220, 112046.	1.4	4
76645	The role of electronâ€“phonon scattering on thermoelectric properties of intermetallic compounds XSi (X = Co, Rh). Japanese Journal of Applied Physics, 2023, 62, 020904.	0.8	3
76646	Phase-engineered cathode for super-stable potassium storage. Nature Communications, 2023, 14, .	5.8	57
76647	Role of electronic correlations in the kagome-lattice superconductor <mml:math xmlns:mml="http://www.w3.org/1998/Math/MathML"><mml:mrow><mml:msub><mml:mi>LaRh</mml:mi><mml:mn>3</mml:mn></ mathvariant="normal">B</mml:mi><mml:mn>2</mml:mn></mml:msub></mml:mrow></mml:math>. Physical Review B, 2023, 107, .	1.1	4
76648	Role of solvation model on the stability of oxygenates on Pt(111): A comparison between microsolvation, extended bilayer, and extended metal/water interface. Electrochemical Science Advances, 2024, 4, .	1.2	10
76649	Possible structural quantum criticality tuned by rare-earth ion substitution in infinite-layer nickelates. Physical Review Materials, 2023, 7, .	0.9	5
76650	Band Structure and Exciton Dynamics in Quasiâ€2D Dodecylammonium Halide Perovskites. Advanced Optical Materials, 2023, 11, .	3.6	3
76651	Study of Optoelectronic Features in Polar and Nonpolar Polymorphs of the Oxynitride Tin-Based Semiconductor InSnO₂N. Journal of Physical Chemistry Letters, 2023, 14, 1548-1555.	2.1	2

#	Article	IF	Citations
76652	The effect of Si addition on the structure and mechanical properties of equiatomic CoCrFeMnNi high entropy alloy by experiment and simulation. Materialia, 2023, 27, 101707.	1.3	5
76654	Electronic origin of Suzuki segregation of transition metal elements in face-centered cubic Co and Ni alloys. Computational Materials Science, 2023, 220, 112033.	1.4	0
76655	Hidden Zeeman-type spin polarization in bulk crystals. Physical Review B, 2023, 107, .	1.1	0
76656	Synchrotron-based operando X-ray diffraction and X-ray absorption spectroscopy study of LiCo0.5Fe0.5PO4 mixed d-metal olivine cathode. Scientific Reports, 2023, 13, .	1.6	3
76657	Strain enhanced magnetism of V-implanted CrI3 monolayer. Applied Physics Letters, 2023, 122, .	1.5	2
76658	Local ordering in Ge/Geâ€“Sn semiconductor alloy core/shell nanowires revealed by extended x-ray absorption fine structure (EXAFS). Applied Physics Letters, 2023, 122, .	1.5	4
76659	First principles characterization of C-doped magnetically-enhanced D022-Mn<mml:math xmlns:mml="http://www.w3.org/1998/Math/MathML" altimg="si19.svg" display="inline" id="d1e226"><mml:msub><mml:mrow /><mml:mrow><mml:mn>3</mml:mn></mml:mrow></mml:msub></mml:math>Ga surfaces. Computational Materials Science, 2023, 220, 112027.	1.4	1
76660	Supercapacitor Performance of Magnetite Nanoparticles Enhanced by a Catecholate Dispersant: Experiment and Theory. Molecules, 2023, 28, 1562.	1.7	1
76661	In Silico High-Throughput Design and Prediction of Structural and Electronic Properties of Low-Dimensional Metalâ€“Organic Frameworks. ACS Applied Materials & Interfaces, 2023, 15, 9494-9507.	4.0	6
76662	Interfacial interaction of monolayer MX2 (M=Mo, W; X=S, Se, Te)/SiO2 interfaces for composite optical fibers. Surfaces and Interfaces, 2023, 37, 102739.	1.5	1
76663	Computational mining of GeH-based Janus IIIâ€“VI van der Waals heterostructures for solar cell applications. Physical Chemistry Chemical Physics, 2023, 25, 6674-6683.	1.3	0
76664	Enhanced Thermoelectric Performance of Mg-Doped AgSbTe₂ by Inhibiting the Formation of Ag₂Te. ACS Applied Materials & Interfaces, 2023, 15, 9508-9516.	4.0	2
76665	Insight into the structural and magnetic properties of RECo12B6 (REÂ=ÂCe, Pr, Nd) compounds: A combined experimental and theoretical investigation. Acta Materialia, 2023, 247, 118757.	3.8	55
76666	Directional Migration and Rapid Coalescence of Au Nanoparticles on Anisotropic ReS₂. Nano Letters, 2023, 23, 1211-1218.	4.5	6
76667	Comparative study of first-principles approaches for effective Coulomb interaction strength Ueff between localized f-electrons: Lanthanide metals as an example. Journal of Chemical Physics, 2023, 158, .	1.2	3
76668	Reversible Hydrogen Storage Media by g-CN Monolayer Decorated with NLi4: A First-Principles Study. Nanomaterials, 2023, 13, 647.	1.9	2
76669	Reconstruction and stability of Fe₃O₄(001) surface: an investigation based on PSO and machine learning. Chinese Physics B, 0, , .	0.7	0
76670	Delocalized Bi-tetrahedral cluster induced ultralow lattice thermal conductivity in Bi3Ir3O11. Materials Today Physics, 2023, 32, 101005.	2.9	2

#	Article	IF	Citations
76671	[2,1,3]-Benzothiadiazole-Spaced Co-Porphyrin-Based Covalent Organic Frameworks for O₂ Reduction. ACS Nano, 2023, 17, 3492-3505.	7.3	13
76672	Singleâ€atomic tungstenâ€doped Co₃O₄ nanosheets for enhanced electrochemical kinetics in lithiumâ€“sulfur batteries. , 2023, 5, .		15
76673	Coordination Tailoring of Epitaxial Perovskite-Derived Iron Oxide Films for Efficient Water Oxidation Electrocatalysis. ACS Catalysis, 2023, 13, 2751-2760.	5.5	10
76674	High-Temperature Thermodynamics of Uranium from Ab Initio Modeling. Applied Sciences (Switzerland), 2023, 13, 2123.	1.3	1
76675	Exact first-principles calculation reveals universal moirÃ© potential in twisted two-dimensional materials. Physical Review B, 2023, 107, .	1.1	2
76676	Two-dimensional Janus AsXY (Xâ€‰=â€‰Se, Te; Yâ€‰=â€‰Br, I) monolayers for photocatalytic water splitting. European Physical Journal B, 2023, 96, .	0.6	4
76677	Atomic Scaled Depth Correlation to the Oxygen Reduction Reaction Performance of Single Atom Ni Alloy to the NiO₂ Supported Pd Nanocrystal. Advanced Science, 2023, 10, .	5.6	4
76678	Machine learning based modeling of disordered elemental semiconductors: understanding the atomic structure of a-Si and a-C. Semiconductor Science and Technology, 2023, 38, 043001.	1.0	1
76679	N-doped and sulfur vacancy-rich TiO2@SnS2 nanoporous arrays for the plasmonic photocatalytic H2 evolution. International Journal of Hydrogen Energy, 2023, , .	3.8	0
76680	Influence of f Electrons on the Electronic Band Structure of Rare-Earth Nickelates. Condensed Matter, 2023, 8, 19.	0.8	3
76681	Solvothermal Synthesis of LaF3:Ce Nanoparticles for Use in Medicine: Luminescence, Morphology and Surface Properties. Ceramics, 2023, 6, 492-503.	1.0	2
76682	Atomic and electronic structures of interfaces between amorphous (Al2O3)1â^'x(SiO2)x and GaN polar surfaces revealed by first-principles simulated annealing technique. Journal of Applied Physics, 2023, 133, .	1.1	1
76683	Effect of Hydrostatic Pressure on Lone Pair Activity and Phonon Transport in Bi₂O₂S. ACS Applied Energy Materials, 2023, 6, 2401-2411.	2.5	4
76684	Predicting lattice thermal conductivity from fundamental material properties using machine learning techniques. Journal of Materials Chemistry A, 2023, 11, 5801-5810.	5.2	9
76685	Hydroformylation over polyoxometalates supported single-atom Rh catalysts. , 2023, 2, 20220064.		3
76686	Thermal transport properties of two-dimensional boron dichalcogenides from a first-principles and machine learning approach. Chinese Physics B, 2023, 32, 054402.	0.7	0
76687	Visualizing Higher-Fold Topology in Chiral Crystals. Physical Review Letters, 2023, 130, .	2.9	3
76688	High-throughput computation of Raman spectra from first principles. Scientific Data, 2023, 10, .	2.4	8

#	Article	IF	Citations
76689	Cooperative diffusion in body-centered cubic iron in Earth and super-Earthsâ€™ inner core conditions. Journal of Physics Condensed Matter, 2023, 35, 154002.	0.7	4
76690	Luminescence and Mechanism of Mn²⁺ Substitution in Cs₇Cd₃Br₁₃ with Two Types of Coordination Number. Inorganic Chemistry, 2023, 62, 3075-3083.	1.9	4
76691	A direction-sensitive photodetector based on the two-dimensional WSe2/MoSe2 lateral heterostructure with enhanced photoresponse. Results in Physics, 2023, 46, 106271.	2.0	2
76692	Scalable manufacturing of quantum light emitters in silicon under rapid thermal annealing. Optics Express, 2023, 31, 8352.	1.7	8
76693	First-Principles-Based Insight into Electrochemical Reactivity in a Cobalt-Carbonate-Hydroxide Pseudocapacitor. ACS Omega, 2023, 8, 6743-6752.	1.6	0
76694	Magnetic-field switching of second-harmonic generation in noncentrosymmetric magnet <mml:math xmlns:mml="http://www.w3.org/1998/Math/MathML"><mml:mrow><mml:msub><mml:mi>Eu</mml:mi><mml:mn>2</mml:mn></mml:mathvariant="normal">O</mml:mi><mml:mn>7</mml:mn></mml:msub></mml:mrow></mml:math>. Physical Review Materials, 2023, 7, .	0.9	2
76695	A simple Pb-doping to achieve bonding evolution, VSn and resonant level shifting for regulating thermoelectric transport behavior of SnTe. Journal of Materials Science and Technology, 2023, 151, 66-72.	5.6	6
76696	Chelator-Free Radiolabeling with Theoretical Insights and Preclinical Evaluation of Citrate-Functionalized Hydroxyapatite Nanospheres for Potential Use as Radionanomedicine. Industrial & Engineering Chemistry Research, 2023, 62, 3194-3205.	1.8	2
76697	<mml:math xmlns:mml="http://www.w3.org/1998/Math/MathML"><mml:msub><mml:mi mathvariant="normal">Si</mml:mi><mml:mn>9</mml:mn></mml:msub><mml:msub><mml:mi mathvariant="normal">C</mml:mi><mml:mn>15</mml:mn></mml:msub></mml:math> monolayer: A silicon carbide allotrope with remarkable physical properties. Physical Review B, 2023, 107, .	1.1	7
76699	Boosting sodium storage performance of hard carbons by regulating oxygen functionalities of the cross-linked asphalt precursor. Carbon, 2023, 206, 94-104.	5.4	26
76700	On the self-consistency of DFT-1/2. Journal of Chemical Physics, 2023, 158, .	1.2	0
76701	Quasi-One-Dimensional Transition-Metal Chalcogenide Semiconductor (Nb₄Se₁₅I₂)I₂. Inorganic Chemistry, 2023, 62, 3067-3074.	1.9	1
76702	Enhanced gaseous acetone adsorption on montmorillonite by ball milling generated Siâ€“OH and interlayer under synergistic modification with H2O2 and tetramethylammonium bromide. Chemosphere, 2023, 321, 138114.	4.2	4
76703	Observation of highly anisotropic bulk dispersion and spin-polarized topological surface states in <mml:math xmlns:mml="http://www.w3.org/1998/Math/MathML"><mml:msub><mml:mi>CoTe</mml:mi><mml:mn>2</mml:mn></mml:msub></mml:math>. Physical Review B, 2023, 107, .	1.1	5
76704	Interfacial reinforcement of core-shell HMX@energetic polymer composites featuring enhanced thermal and safety performance. Defence Technology, 2024, 31, 387-399.	2.1	1
76705	Strengthening the Hydrogen Spillover Effect via the Phase Transformation of W₁₈O₄₉ for Boosted Hydrogen Oxidation Reaction. ACS Catalysis, 2023, 13, 2834-2846.	5.5	9
76706	Two-Dimensional Octuple-Atomic-Layer M2Si2N4 (M = Al, Ga and In) with Long Carrier Lifetime. Micromachines, 2023, 14, 405.	1.4	0
76707	Propane Dehydrogenation on Pt_xSn_y (x, y â‰ 4) Clusters on Al₂O₃(110). ACS Catalysis, 2023, 13, 2802-2812.	5.5	13

#	Article	IF	Citations
76708	Thin lamellar Li7La3Zr2O12 solid electrolyte with g-C3N4 as grain boundary modifier for high-performance all-solid-state lithium battery. Journal of Power Sources, 2023, 562, 232784.	4.0	5
76709	A comparative ab initio study of acetylene activation over Au9 cluster and Au9 supported over ZnO monolayer. Computational and Theoretical Chemistry, 2023, 1222, 114072.	1.1	0
76710	Universal ion-transport descriptors and classes of inorganic solid-state electrolytes. Materials Horizons, 2023, 10, 1757-1768.	6.4	4
76711	Fluorinated MXenes accelerate the hydrogen evolution activity of in situ induced snowflake-like nano-Pt. Journal of Materials Chemistry A, 2023, 11, 5830-5840.	5.2	9
76712	Potential rules for stable transition metal hexafluorides with high oxidation states under high pressures. Physical Chemistry Chemical Physics, 2023, 25, 6726-6732.	1.3	0
76713	Monolayer group IV monochalcogenides T-MX (M = Sn, Ge; X = S, Se) with fine piezoelectric performance and stability. Applied Physics Letters, 2023, 122, .	1.5	5
76714	Theoretical study of phonon and electron transport in low band gap Janus MXene monolayer MoWCO2 for thermoelectric application. Applied Physics Letters, 2023, 122, .	1.5	5
76715	Kineticâ€Modulated Crystal Phase of Ru for Hydrogen Oxidation. Small, 2023, 19, .	5.2	2
76716	Topological spin textures in <mml:math xmlns:mml="http://www.w3.org/1998/Math/MathML"><mml:mrow><mml:mn>1</mml:mn><mml:mi>T</mml:mi></mml:mrow></mml:m -phase Janus magnets: Interplay between Dzyaloshinskii-Moriya interaction, magnetic frustration, and isotropic higher-order interactions. Physical Review B, 2023, 107, .	1.1	9
76717	Copper content effects on passive film of modified 00Cr20Ni18Mo6CuN super austenitic stainless steels in acidic environment. Heliyon, 2023, 9, e13652.	1.4	0
76718	Synthesis of Phase Junction Cadmium Sulfide Photocatalyst under Sulfurâ€Rich Solution System for Efficient Photocatalytic Hydrogen Evolution. Small, 2023, 19, .	5.2	14
76719	Intrinsic layer-polarized anomalous Hall effect in bilayer <mml:math xmlns:mml="http://www.w3.org/1998/Math/MathML"><mml:mrow><mml:mi>Mn</mml:mi><mml:msub><mml:mi>Bi</mml:mi> Physical Review B, 2023, 107, .	1.1	11
76720	Ultrathin positively charged electrode skin for durable anion-intercalation battery chemistries. Nature Communications, 2023, 14, .	5.8	9
76721	Interfacial interaction between graphene and ferromagnets: First principles study. Physica B: Condensed Matter, 2023, 655, 414740.	1.3	1
76722	Local structural investigation of non-crystalline materials at high pressure: the case of GeO₂ glass. Journal of Physics Condensed Matter, 2023, 35, 164001.	0.7	1
76723	Amorphous nickel tungstate nanocatalyst boosts urea electrooxidation. Chemical Engineering Journal, 2023, 460, 141826.	6.6	9
76724	X-ray Absorption Spectroscopy Studies of a Molecular CO₂-Reduction Catalyst Deposited on Graphitic Carbon Nitride. Journal of Physical Chemistry C, 2023, 127, 3626-3633.	1.5	1
76725	Adsorption of 2-hydroxynaphthalene, naphthalene, phenanthrene, and pyrene by polyvinyl chloride microplastics in water and their bioaccessibility under in vitro human gastrointestinal system. Science of the Total Environment, 2023, 871, 162157.	3.9	7

#	Article	IF	Citations
76726	Antiferromagnetic insulating state in quasi-one-dimensional K2Cr3As3H. Science China: Physics, Mechanics and Astronomy, 2023, 66, .	2.0	2
76727	Designed Concave Octahedron Heterostructures Decode Distinct Metabolic Patterns of Epithelial Ovarian Tumors. Advanced Materials, 2023, 35, .	11.1	13
76728	First-Principles Calculation and Kink-Dislocation Dynamics Simulation on Dislocation Plasticity in TiZr-Based Concentrated Solid-Solution Alloys. Metals, 2023, 13, 351.	1.0	0
76729	First-principles study of the effect of the local coordination environment on the electrochemical activity of Pd1-CxNy single atom catalysts. Chemical Engineering Science, 2023, 270, 118551.	1.9	2
76730	Structural dynamics of Schottky and Frenkel defects in CeO₂: a density-functional theory study. JPhys Energy, 2023, 5, 025004.	2.3	1
76731	Enhanced low-temperature behavior of selective catalytic reduction of NOx by CO on Fe-based catalyst with looping oxygen vacancy. Chemical Engineering Journal, 2023, 461, 141814.	6.6	9
76732	Synergizing lattice strain and electron transfer in TMSs@Â1ÂT-MoS2 in-plane heterostructures for efficient hydrogen evolution reaction. Applied Catalysis B: Environmental, 2023, 328, 122445.	10.8	10
76734	Atomistic Origins of Reversible Noncatalytic Gasâ€“Solid Interfacial Reactions. Journal of the American Chemical Society, 0, , .	6.6	1
76735	Bimetallic Synergy in Single-Atom Alloy Nanocatalysts for CO₂ Reduction to Ethylene. ACS Applied Nano Materials, 2023, 6, 2394-2402.	2.4	5
76736	CO₂ Reduction Mechanism on the Cu₂O(110) Surface: A Firstâ€Principles Study. ChemPhysChem, 2023, 24, .	1.0	2
76737	Phonon, electron, and magnon excitations in antiferromagnetic <mml:math xmlns:mml="http://www.w3.org/1998/Math/MathML"><mml:mrow><mml:mi>L</mml:mi><mml:msub><mml:mn>1</mml:mn> -type MnPt. Physical Review B, 2023, 107, .	3.7	2
76738	Combined experimental and DFT investigation of temozolomide sensing properties of 2Dâ^Â2D interface of rich oxygen vacancies of WO3â^'x and sulfur-doped g-C3N4 nanosheets hybrids composites. Journal of Environmental Chemical Engineering, 2023, 11, 109459.	3.3	0
76739	An ab initio study of catechol sensing in pristine and transition metal decorated Î³-graphyne. Nanotechnology, 2023, 34, 175503.	1.3	2
76740	Structural Significance of Hydrophobic and Hydrogen Bonding Interaction for Nanoscale Hybridization of Antiseptic Miramistin Molecules with Molybdenum Disulfide Monolayers. Molecules, 2023, 28, 1702.	1.7	0
76741	Decay processes of long-lived phonons in 6H-SiC. Journal of Physics Condensed Matter, 2023, 35, 175701.	0.7	0
76742	Origins of Electrical Compensation in Siâ€Doped HVPE GaN. Physica Status Solidi (B): Basic Research, 2023, 260, .	0.7	3
76743	Reasonable Design of MXene-Supported Dual-Atom Catalysts with High Catalytic Activity for Hydrogen Evolution and Oxygen Evolution Reaction: A First-Principles Investigation. Materials, 2023, 16, 1457.	1.3	9
76744	Intercalation Chemistry of the Disordered Rocksalt Li₃V₂O₅ Anode from Cluster Expansions and Machine Learning Interatomic Potentials. Chemistry of Materials, 2023, 35, 1537-1546.	3.2	9

#	Article	IF	Citations
76745	First-principles study of the structural and electronic properties of tetragonal ZrOX (X = S, Se, and) Tj ETQq0 0 0 rgBT /Overlock 10 Tf 50 photocatalysis. Journal of Chemical Physics, 2023, 158, 094708.	1.2	2
76746	Biosynthetic modulation of carbon-doped ZnO for rapid photocatalytic endocrine disruptive remediation and hydrogen evolution. Journal of Cleaner Production, 2023, 394, 136393.	4.6	9
76747	Morphology effects in MnCeOx solid solution-catalyzed NO reduction with CO: Active sites, water tolerance, and reaction pathway. Nano Research, 2023, 16, 6951-6959.	5.8	18
76748	A metallic La₃C₂ monolayer with remarkable activity for the hydrogen evolution reaction: a first-principles study. Journal of Materials Chemistry A, 2023, 11, 6394-6402.	5.2	4
76749	Laser-ablated violet phosphorus/graphene heterojunction as ultrasensitive ppb-level room-temperature NO sensor. Chinese Chemical Letters, 2023, 34, 108199.	4.8	5
76750	Origin of the Universal Potential-Dependent Organic Oxidation on Nickel Oxyhydroxide. ACS Catalysis, 2023, 13, 2916-2927.	5.5	7
76751	First-Principles Calculation of Ligand Field Parameters for L-Edge Spectra of Transition Metal Sites of Arbitrary Symmetry. Symmetry, 2023, 15, 472.	1.1	2
76752	Effect of strain on the thermoelectric properties of threeâ€dimensional <scp>PtS₂</scp>: A firstâ€principles study. International Journal of Quantum Chemistry, 2023, 123, .	1.0	1
76753	Interpretable design of Ir-free trimetallic electrocatalysts for ammonia oxidation with graph neural networks. Nature Communications, 2023, 14, .	5.8	17
76754	Ferromagnetism Induced by Magnetic Dilution in Van der Waals Material Metal Thiophosphates. Advanced Quantum Technologies, 2023, 6, .	1.8	3
76755	A Two-in-one host for High-loading cathode and Dendrite-free anode realized by activating metallic nitrides heterostructures toward Li-S full batteries. Chemical Engineering Journal, 2023, 460, 141862.	6.6	6
76756	Electronic and Excitonic Properties of MSi₂Z₄ Monolayers. Small, 2023, 19, .	5.2	10
76757	Exploration and investigation of stable novel Al2O3 by high-throughput screening and density functional theory. Journal of Materials Research and Technology, 2023, 23, 4244-4257.	2.6	8
76758	Pyridinic-nitrogen on ordered mesoporous carbon: A versatile NAD(P)H mimic for borrowing-hydrogen reactions. Journal of Catalysis, 2023, 419, 80-98.	3.1	5
76759	Thermodynamics of native defects in V2O5 crystal: A first-principles method. Computational Materials Science, 2023, 220, 112071.	1.4	2
76760	Band Engineering of the Second Phase to Reach High Thermoelectric Performance in Cu₂Seâ€Based Composite Material. Advanced Materials, 2023, 35, .	11.1	11
76761	Fabrication of supported Pt/CeO₂ nanocatalysts doped with different elements for CO oxidation: theoretical and experimental studies. Dalton Transactions, 2023, 52, 3661-3670.	1.6	1
76762	Two-Dimensional Ferroelectricity in a Single-Atom Adsorbed BiI₃ Monolayer. Journal of Physical Chemistry C, 2023, 127, 3898-3903.	1.5	1

#	Article	IF	Citations
76763	Surface engineering of inorganic solid-state electrolytes via interlayers strategy for developing long-cycling quasi-all-solid-state lithium batteries. Nature Communications, 2023, 14, .	5.8	31
76764	Construction of twisted graphene-silicene heterostructures. Nano Research, 2023, 16, 7926-7930.	5.8	1
76765	Enhanced Magnetization in CoFe₂O₄ Through Hydrogen Doping. Advanced Functional Materials, 2023, 33, .	7.8	7
76766	Modulating vacancies concentration ratio of cationic and anionic in WO3 for driving high performance magnesium ions storage. Energy Storage Materials, 2023, 57, 125-135.	9.5	9
76767	Ferroelectricity and High Curie Temperature in a 2D Janus Magnet. ACS Applied Materials & Interfaces, 2023, 15, 10133-10140.	4.0	6
76768	Point vacancy defects in hexagonal boron nitride studied by first-principles. , 2023, 9, 011104-011104.		0
76769	Positron trapping at the effective open volume in FeCr alloy containing hydrogen/helium atoms. , 2023, 9, 011001-011001.		0
76770	High pseudocapacitive lithium-storage behaviors of amorphous titanium oxides with titanium vacancies and open channels. Electrochimica Acta, 2023, 444, 142021.	2.6	4
76771	Quantum Anomalous Hall Effects Controlled by Chiral Domain Walls. Chinese Physics Letters, 2023, 40, 037502.	1.3	2
76772	Highâ€throughput screening of phaseâ€engineered atomically thin transitionâ€metal dichalcogenides for van der Waals contacts at the <scp>Schottkyâ€“Mott</scp> limit. InformaÄnÃ-MateriÃ¡ly, 2023, 5, .	8.5	11
76773	Defect Mo_S Misidentified as Mo_{S2} in Monolayer MoS₂ by Scanning Transmission Electron Microscopy: A First-Principles Prediction. Journal of Physical Chemistry Letters, 2023, 14, 1840-1847.	2.1	3
76774	Unraveling the bond structure, porosity, and mechanical properties amorphous ZIF-4 and its topological equivalents: Large scale ab initio calculations. APL Materials, 2023, 11, .	2.2	3
76775	Raman and NMR spectroscopic and theoretical investigations of the cubic laves-phases REAl₂ (RE = Sc, Y, La, Yb, Lu). Dalton Transactions, 2023, 52, 3391-3402.	1.6	3
76776	Anharmonic thermo-elasticity of tungsten from accelerated Bayesian adaptive biasing force calculations with data-driven force fields. Physical Review Materials, 2023, 7, .	0.9	1
76777	Tuning charge carrier dynamics through spacer cation functionalization in layered halide perovskites: an ab initio quantum dynamics study. Journal of Materials Chemistry C, 2023, 11, 3521-3532.	2.7	0
76778	Effects of intermixing and oxygen vacancies on a two-dimensional electron gas at the polar <mml:math xmlns:mml="http://www.w3.org/1998/Math/MathML"><mml:mrow><mml:mrow><mml:mo>(</mml:mo><mml:mrow><mml:mi>TbSc		

#	Article	IF	Citations
76781	Ab Initio Study of Adsorption of Polymers on Metalâ€“Organic Framework Surfaces. Journal of Physical Chemistry C, 2023, 127, 3715-3725.	1.5	2
76782	First-principles study on the thermoelectric properties of Sr2Si and Sr2Ge. Materials Today Physics, 2023, 32, 101015.	2.9	5
76783	Assessing the Surface Chemistry of 2D Transition Metal Carbides (MXenes): A Combined Experimental/Theoretical ¹³C Solid State NMR Approach. Journal of the American Chemical Society, 2023, 145, 4003-4014.	6.6	6
76784	Surface Tamm States of 2â€“5 nm Nanodiamond via Raman Spectroscopy. Nanomaterials, 2023, 13, 696.	1.9	2
76785	Effects of hydrostatic pressure on the thermoelectric performance of BaZrS3. European Physical Journal Plus, 2023, 138, .	1.2	0
76786	Simultaneous Optical Trapping and Electromagnetic Micromanipulation of Ferromagnetically Doped NaYF₄ Microparticles. , 2023, 1, 615-622.		6
76787	Ptâ€‰:â€‰Ge Ratio as a Lever of Activity and Selectivity Control of Supported PtGe Clusters in Thermal Dehydrogenation**. ChemCatChem, 2023, 15, .	1.8	1
76788	Tuning of magnetic, electronic and electrolytic water properties of silicene supported precious-metal by non-metal doping and vacancy defect. FlatChem, 2023, 38, 100486.	2.8	2
76789	Humidity-Tolerant Moisture-Driven Energy Generator with MXene Aerogelâ€“Organohydrogel Bilayer. ACS Nano, 2023, 17, 5472-5485.	7.3	30
76790	Tuneable physical properties of ReI3 through ferroelectric polarization switching in 2D van der Waals multiferroic heterostructures. Physics Letters, Section A: General, Atomic and Solid State Physics, 2023, 464, 128699.	0.9	0
76791	Dislocations as natural quantum wires in diamond. Physical Review Materials, 2023, 7, .	0.9	1
76792	High Curie temperature Chern insulator and spin-gapless semiconducting ferromagnetic h-CrC monolayer: A first-principles study. Computational Materials Science, 2023, 220, 112070.	1.4	2
76793	Engineering nanoscale H supply chain to accelerate methanol synthesis on ZnZrOx. Nature Communications, 2023, 14, .	5.8	19
76794	Targeted synthesis of predicted metastable compounds using modulated elemental reactants. Journal of Vacuum Science and Technology A: Vacuum, Surfaces and Films, 2023, 41, .	0.9	2
76795	An ab initio method on large sized molecular aggregate system: Predicting absorption spectra of crystalline organic semiconducting films. Journal of Chemical Physics, 2023, 158, .	1.2	4
76796	Possible Origin of Low-Frequency Magnetic Flux Noise in Superconducting Devices. Journal of Physical Chemistry Letters, 2023, 14, 1854-1861.	2.1	1
76797	Ultra-high thermal conductivity of two-dimensional C₂₃. Nanotechnology, 2023, 34, 175704.	1.3	1
76798	Organic Eutectic Mixture Incorporated with Graphene Oxide Sheets as Lithiophilic Artificial Protective Layer for Dendriteâ€Free Lithium Metal Batteries. Advanced Energy Materials, 2023, 13, .	10.2	8

#	Article	IF	Citations
76799	Anisotropic Permittivities and Transmittance of Double Layer Graphene. , 2017, , .		0
76800	Optical method for quantifying the potential of zero charge at the platinumâ€“water electrochemical interface. Nature Materials, 2023, 22, 503-510.	13.3	18
76801	Firstâ€Principles Density Functional Theory and Machine Learning Technique for the Prediction of Water Adsorption Site on PtPdâ€Based Highâ€Entropyâ€Alloy Catalysts. Advanced Theory and Simulations, 2023, 6, .	1.3	3
76802	First-principles study on tuning electronic and optical properties in graphene rotation on h-BN. Chemical Physics Letters, 2023, 815, 140366.	1.2	0
76803	Electrochemical Conversion of Cu Nanowire Arrays into Metal-Organic Frameworks HKUST-1. Journal of the Electrochemical Society, 2023, 170, 022506.	1.3	1
76804	Regulating Na Occupation in P2â€Type Layered Oxide Cathode for Allâ€Climate Sodiumâ€Ion Batteries. Advanced Energy Materials, 2023, 13, .	10.2	18
76805	Mn²⁺-Activated Photostimulable Persistent Nanophosphors by Pr³⁺ Codoping for Rewritable Information Storage. ACS Applied Nano Materials, 2023, 6, 3054-3064.	2.4	5
76806	Metal-Free Carbon Nitride Nanosheet Supported the Pentacoordinated Silicon Intermediates for Photocatalytic Overall Water Splitting. Journal of Physical Chemistry Letters, 2023, 14, 1918-1927.	2.1	5
76807	Effect of substitution of 3d, 4d and 5d elements on structural, electronic, magnetic properties and XMCD spectra of Co-based full Heusler alloys: A DFT study. AIP Advances, 2023, 13, 025152.	0.6	0
76808	Effects of impurities on the cooling of photoexcited carriers in La_{1â^'x}Sr_xCoO_{3â^'Î´}: A DFT and nonadiabatic molecular dynamics study. Journal of Applied Physics, 2023, 133, 065107.	1.1	1
76809	Structure and Dynamics in Liquid Iron at High Pressure and Temperature. A First Principles Study. Journal of Geophysical Research: Solid Earth, 2023, 128, .	1.4	3
76810	First-Principles Study of the Doping Effect in Half Delithiated LiNiO₂ Cathodes. ACS Applied Energy Materials, 2023, 6, 2134-2139.	2.5	1
76811	Hexamethylenetetramine additive with zincophilic head and hydrophobic tail for realizing ultra-stable Zn anode. Chemical Engineering Journal, 2023, 460, 141902.	6.6	22
76812	Fermi-Level Instability as a Way to Tailor the Properties of La₃Te₄. Journal of Physical Chemistry Letters, 2023, 14, 1962-1967.	2.1	3
76813	Electron doping of a double-perovskite flat-band system. Proceedings of the National Academy of Sciences of the United States of America, 2023, 120, .	3.3	1
76814	Machine learning-aided Genetic algorithm in investigating the structureâ€“property relationship of SmFe12-based structures. Journal of Applied Physics, 2023, 133, .	1.1	2
76815	Theoretical Analysis of Magnetic Coupling in the Ti₂C Bare MXene. Journal of Physical Chemistry C, 2023, 127, 3706-3714.	1.5	6
76816	CO₂ coverage on Pd catalysts accelerates oxygen removal in oxy-combustion systems. Physical Chemistry Chemical Physics, 2023, 25, 6527-6536.	1.3	0

#	Article	IF	Citations
76817	Enhanced stability of two-dimensional halide perovskites under an electric field for photocatalytic HI splitting. Journal of Materials Chemistry A, 2023, 11, 6311-6320.	5.2	2
76818	Proton migration barriers in BaFeO_{3â^'Î´} â€“ insights from DFT calculations. Journal of Materials Chemistry A, 2023, 11, 6336-6348.	5.2	4
76819	Simulations with machine learning potentials identify the ion conduction mechanism mediating non-Arrhenius behavior in LGPS. JPhys Energy, 2023, 5, 024004.	2.3	7
76820	Polaron-assisted electronic transport in ZnP₂ nanowires. Journal of Materials Chemistry C, 2023, 11, 4243-4253.	2.7	0
76821	Realizing Wideâ€Gamut Humanâ€Centric Display Lighting with K₃AlP₃O₉N:Eu²⁺. Advanced Optical Materials, 2023, 11, .	3.6	8
76822	Unlocking the electronic, optical and transport properties of semiconductor coupled quantum dots using first principles methods. International Journal of Quantum Chemistry, 0, , .	1.0	0
76823	Triggering superconductivity, semiconducting states, and ternary valley structure in graphene via functionalization with Si-N layers. Physical Review B, 2023, 107, .	1.1	2
76825	Probing single-chain conformation and its impact on the optoelectronic properties of donorâ€“accepter conjugated polymers. Journal of Materials Chemistry A, 2023, 11, 12928-12940.	5.2	4
76826	Synthesis of Graphene Quantum Dots Enhanced Nano Ca(OH)2 from Ammoniated CaCl2. Materials, 2023, 16, 1568.	1.3	2
76828	Coupling nitrate capture with ammonia production through bifunctional redox-electrodes. Nature Communications, 2023, 14, .	5.8	37
76829	pH- and Facet-Dependent Surface Chemistry of TiO₂ in Aqueous Environment from First Principles. ACS Applied Materials & Interfaces, 2023, 15, 11216-11224.	4.0	13
76830	Indirect Z-scheme hydrogen production photocatalyst based on two-dimensional GeC/MoSi2N4 van der Waals heterostructures. International Journal of Hydrogen Energy, 2023, 48, 18301-18314.	3.8	9
76831	High-Pressure Pulsing of Ammonia Results in Carbamate as Strongly Inhibiting Adsorbate of Methanol Synthesis over Cu/ZnO/Al₂O₃. Journal of Physical Chemistry C, 2023, 127, 3497-3505.	1.5	0
76832	Increasing the Strain Resistance of Si/SiO₂ Interfaces for Flexible Electronics. ACS Omega, 2023, 8, 7555-7565.	1.6	1
76833	Few-Layered Hexagonal Boron Nitrides as Highly Effective and Stable Solid Adsorbents for Ammonia Separation. Industrial & Engineering Chemistry Research, 2023, 62, 3705-3715.	1.8	6
76834	Chemical interactions that govern the structures of metals. Proceedings of the National Academy of Sciences of the United States of America, 2023, 120, .	3.3	2
76835	Experimental Data Confirm Carrier-Cascade Model for Solid-State Conductance across Proteins. Journal of Physical Chemistry B, 2023, 127, 1728-1734.	1.2	1
76836	Surface specific adsorption of glucose to ZnO. Physical Chemistry Chemical Physics, 2023, 25, 7805-7814.	1.3	1

#	Article	IF	Citations
76837	Improving lithium polysulfides adsorption by oxygen-vacancy defects: By first-principles calculation. Computational Materials Science, 2023, 220, 112038.	1.4	0
76838	Two-Dimensional Dielectrics for Future Electronics: Hexagonal Boron Nitride, Oxyhalides, Transition-Metal Nitride Halides, and Beyond. ACS Applied Electronic Materials, 2023, 5, 623-631.	2.0	8
76839	Double-perovskite van der Waals heterostructure Cs2NaInCl6-XS2 (X=Cr, Mo, W) as great potential material in photovoltaic devices. Surfaces and Interfaces, 2023, 37, 102734.	1.5	0
76840	Effect of Lithium Substitution Ratio of Polymeric Binders on Interfacial Conduction within All-Solid-State Battery Anodes. ACS Applied Materials & Interfaces, 2023, 15, 13131-13143.	4.0	3
76841	Alloying engineering for thermoelectric performance enhancement in p-type skutterudites with synergistic carrier concentration optimization and thermal conductivity reduction. Journal of Advanced Ceramics, 2023, 12, 539-552.	8.9	1
76842	A combined experimental and theoretical study on the structural, optical and electronic properties of hetero interface-functionalized MoS2 /Co3O4 nanocomposite. Surfaces and Interfaces, 2023, 37, 102750.	1.5	6
76843	First-principles study for discovery of novel synthesizable 2D high-entropy transition metal carbides (MXenes). Journal of Materials Chemistry A, 2023, 11, 5681-5695.	5.2	6
76844	A New Group of 2D Nonâ€van der Waals Materials with Ultra Low Exfoliation Energies. Advanced Electronic Materials, 2023, 9, .	2.6	5
76845	Origin of performance degradation in high-delithiation Li_xCoO₂: insights from direct atomic simulations using global neural network potentials. Journal of Materials Chemistry A, 2023, 11, 5370-5379.	5.2	2
76846	Ultraâ€low singleâ€atom Pt on gâ€C₃N₄ for electrochemical hydrogen peroxide production. , 2023, 5, .		8
76847	The Open Catalyst 2022 (OC22) Dataset and Challenges for Oxide Electrocatalysts. ACS Catalysis, 2023, 13, 3066-3084.	5.5	32
76848	A Facile Synthesis of BiO(ClBr) _{0.5â^'x/2} I _x Microsphere Assembly as Highâ€efficiency Visibleâ€light Driven Photocatalyst. ChemistrySelect, 2023, 8, .	0.7	0
76849	Facile Synthesis of Palladiumâ€Silver Dilute Alloy Catalyst for Acetylene Hydrogenation. ChemCatChem, 2023, 15, .	1.8	4
76850	Electric field manipulation of spin chirality and skyrmion dynamic. Science Advances, 2023, 9, .	4.7	12
76851	Dual Metal Site Fe Single Atom Catalyst with Improved Stability in Acidic Conditions. Catalysts, 2023, 13, 418.	1.6	0
76852	A first-principles study on the multiferroicity of semi-modified X₂M (X = C, Si; M = F, Cl) monolayers. Physical Chemistry Chemical Physics, 2023, 25, 7965-7973.	1.3	0
76853	Strategies to Improve the Oxygen Reduction Reaction Activity on Ptâ€“Bi Bimetallic Catalysts: A Density Functional Theory Study. Journal of Physical Chemistry Letters, 2023, 14, 1990-1998.	2.1	4
76854	Ultrahigh Nitrogen Content Carbon Nanosheets for High Stable Sodium Metal Anodes. Advanced Science, 2023, 10, .	5.6	11

#	Article	IF	Citations
76855	Tailoring alloy compositions by glucose towards superior Niâ€“Cuâ€“C electrocatalysts for hydrogen evolution reaction. International Journal of Hydrogen Energy, 2024, 52, 334-342.	3.8	2
76856	Hysteresis and training effect in the electric control of spin current in <mml:math xmlns:mml="http://www.w3.org/1998/Math/MathML"><mml:mi>Pt</mml:mi><mml:mo>/</mml:mo><mml:msub><mml:mrow><mml:mi mathvariant="normal">Y</mml:mi></mml:mrow><mml:mn>3</mml:mn></mml:msub><mml:msub><mml:mrow><mml:mi mathvariant="normal">O</mml:mi></mml:mrow><mml:mn>12</mml:mn></mml:msub></mml:math> heterostructures. Physical Review B, 2023, 107, .	3.7	2
76857	Continuous-flow electrosynthesis of ammonia by nitrogen reduction and hydrogen oxidation. Science, 2023, 379, 707-712.	6.0	107
76858	Design of Flameâ€Made ZnZrO_x Catalysts for Sustainable Methanol Synthesis from CO₂. Advanced Energy Materials, 2023, 13, .	10.2	7
76859	Correlation-Driven Topological Transition in Janus Two-Dimensional Vanadates. Materials, 2023, 16, 1649.	1.3	5
76860	Achieving type-II SnSSe/as van der waals heterostructure with satisfactory oxygen tolerance for optoelectronic and photovoltaic applications. Journal of Solid State Chemistry, 2023, 321, 123925.	1.4	3
76861	Theoretical study of hydrogen adsorption kinetics: Mg17Al12 vs pure Mg. International Journal of Hydrogen Energy, 2023, , .	3.8	0
76862	Self-Assembly of Glutamic Acid and Serine on Au(111). Langmuir, 2023, 39, 3168-3172.	1.6	1
76863	Rational design of Lewis base molecules for stable and efficient inverted perovskite solar cells. Science, 2023, 379, 690-694.	6.0	147
76864	Layered Semiconductor Cr_{0.32}Ga_{0.68}Te_{2.33} with Concurrent Broken Inversion Symmetry and Ferromagnetism: A Bulk Ferrovalley Material Candidate. Journal of the American Chemical Society, 2023, 145, 4683-4690.	6.6	3
76865	First principles study of optical properties of Ni- and Pd-doped TiO2 as visible light catalyst. Materials for Renewable and Sustainable Energy, 2023, 12, 47-52.	1.5	0
76866	Highly anisotropic and ultra-diffusive vacancies in Î±-antimonene. Nanoscale, 2023, 15, 4821-4829.	2.8	1
76867	Analogy and dissimilarity of excitons in monolayer and bilayer of MoSe₂. 2D Materials, 0, , .	2.0	4
76869	Designing for dopability in semiconducting AgInTe₂. Journal of Materials Chemistry C, 2023, 11, 3832-3840.	2.7	3
76870	The highest melting point material: Searched by Bayesian global optimization with deep potential molecular dynamics. Journal of Advanced Ceramics, 2023, 12, 803-814.	8.9	3
76871	Fast carrier diffusion via synergistic effects between lithium-ions and polarons in rutile TiO₂. Physical Chemistry Chemical Physics, 2023, 25, 7519-7526.	1.3	1
76872	Nanoscale-mixed ZnNiCu hydroxide composite catalyst for improved photocatalytic hydrogen evolution. International Journal of Hydrogen Energy, 2023, 48, 18657-18669.	3.8	0
76873	A Novel Electrocatalyst Pd(II)@Ni ₃ (HITP) ₂ for Ultrasensitive Detection of Chloramphenicol: Experimental and Computational Investigation. Chemistry - A European Journal, 0, , .	1.7	1

#	Article	IF	Citations
76874	Earthâ€™s volatile depletion trend is consistent with a high-energy Moon-forming impact. Communications Earth & Environment, 2023, 4, .	2.6	3
76875	Post-dissociation Dynamics of N₂ on Ru(0001): How Far Can the â€œHotâ€•N Atoms Travel?. Journal of Physical Chemistry C, 2023, 127, 4079-4086.	1.5	2
76876	Study of the Bandgap and Crystal Structure of Cu4TiSe4: Theory vs. Experiment. Crystals, 2023, 13, 331.	1.0	1
76877	Thermal batteries based on inverse barocaloric effects. Science Advances, 2023, 9, .	4.7	7
76878	Emergence of Rashba-/Dresselhaus effects in Ruddlesdenâ€“Popper halide perovskites with octahedral rotations. Journal of Physics Condensed Matter, 2023, 35, 174001.	0.7	6
76879	Interface catalytic regulation via electron rearrangement and hydroxyl radicals triggered by oxygen vacancies and heavy metal ions. Chemical Science, 2023, 14, 2960-2970.	3.7	2
76880	First principles approach for promising oxide ion conducting ABGa₃O₇ melilite structures. Physical Chemistry Chemical Physics, 2023, 25, 7028-7031.	1.3	0
76881	Phase selection in aluminum rare-earth metallic alloys by molecular dynamics simulations using machine learning interatomic potentials. Physical Review Materials, 2023, 7, .	0.9	0
76882	Multi-peak emission of In2O3 induced by oxygen vacancy aggregation. Journal of Applied Physics, 2023, 133, .	1.1	2
76883	Chiral and Catalytic Effects of Site-Specific Molecular Adsorption. Journal of Physical Chemistry Letters, 2023, 14, 2072-2077.	2.1	1
76884	Role of oxygen vacancies on surface reaction of water oxidation in WO3 studied by density functional theory (DFT) and experiment. Molecular Catalysis, 2023, 539, 113005.	1.0	3
76885	Structure-controlled valley splitting and anomalous valley Hall effect in Janus VSe₂/VSeX (X = S, Te) heterojunctions. Journal Physics D: Applied Physics, 2023, 56, 135301.	1.3	1
76886	Ultra-Wide bandgap Quasi Two-Dimensional Î²-Ga2O3 with highly In-Plane anisotropy for power electronics. Applied Surface Science, 2023, 619, 156771.	3.1	0
76887	Thermoelectric Properties of Zintl Arsenide EuCuAs. Journal of Electronic Materials, 2023, 52, 3121-3131.	1.0	1
76888	Uniaxial Strain-Induced Tunable Mid-infrared Light Emission from Thin Film Black Phosphorus. Journal of Physical Chemistry Letters, 2023, 14, 2092-2098.	2.1	3
76889	Electrocatalytic methane direct conversion to methanol in electrolyte of ionic liquid. Electrochimica Acta, 2023, 445, 142065.	2.6	5
76890	Density functional theory-based quantum-computational analysis on the strain-assisted electronic and photocatalytic properties of BX-MSSe (Xâ€‰=â€‰P, As and Mâ€‰=â€‰Mo, W) heterostructures. Applied Physics A: Materials Science and Processing, 2023, 129, .	1.1	1
76891	Chlorine-promoted copper catalysts for CO2 electroreduction into highly reduced products. Cell Reports Physical Science, 2023, 4, 101294.	2.8	2

#	Article	IF	Citations
76892	On the Nature of Hydrophobic Organic Compound Adsorption to Smectite Minerals Using the Example of Hexachlorobenzene-Montmorillonite Interactions. Minerals (Basel, Switzerland), 2023, 13, 280.	0.8	2
76893	Electronic and Optical Properties of Alkaline Earth Metal Fluoride Crystals with the Inclusion of Many-Body Effects: A Comparative Study on Rutile MgF2 and Cubic SrF2. Symmetry, 2023, 15, 539.	1.1	2
76894	Water-favored reaction mechanism for selective catalytic conversion of 2-methylfuran to 1,4-pentanediol. Chemical Engineering Journal, 2023, 461, 141944.	6.6	4
76895	Bamboo-derived hydrophobic porous graphitized carbon for adsorption of volatile organic compounds. Chemical Engineering Journal, 2023, 461, 141979.	6.6	15
76896	Photocatalytic Composite Sr₂MgSi₂O₇:(Eu,) Tj ETQq0 0 0 rgBT /Overlock 10 Tf 50 592 Td (Dy)/g Phosphors and Photocatalysts on Round-the-Clock Photocatalytic Degradation of Methylene Blue. , 2023, 1, 688-700.		7
76898	[illegible] Values of A-Site Cation Ordered phases derived from La<mml:math xmlns:mml="http://www.w3.org/1998/Math/MathML" altimg="si102.svg" display="inline" id="d1e1428"><mml:msub><mml:mrow /><mml:mrow><mml:mn>2</mml:mn></mml:mrow></mml:msub></mml:math>MnNiO<mml:math xmlns:mml="http://www.w3.org/1998/Math/MathML" altimg="si103.svg" display="inline" id="d1e1436"><mml:msub><mml:mrow /><mml:mrow><mml:mn>6</mml:mn></mml:mrow></mml:msub></mml:math>	1.3	0
76899	Combining Machine Learning and Many-Body Calculations: Coverage-Dependent Adsorption of CO on Rh(111). Physical Review Letters, 2023, 130, .	2.9	11
76900	Successful preparation of BaCo _{0.5}Fe _{0.5}O _{3â€“ Î´} cathode oxide by rapidly cooling allowing for high-performance proton-conducting solid oxide fuel cells. Journal of Advanced Ceramics, 2023, 12, 587-597.	8.9	35
76901	Interlayer Charge Transfer Regulates Single-Atom Catalytic Activity on Electride/Graphene 2D Heterojunctions. Journal of the American Chemical Society, 2023, 145, 4774-4783.	6.6	34
76902	Two new barium phosphides predicted by first-principles evolutionary algorithm. International Journal of Modern Physics C, 0, , .	0.8	0
76903	Enhanced electrocatalytic nitrate reduction to ammonia on cobalt oxide nanosheets via multiscale defect modulation. Chemical Engineering Journal, 2023, 461, 141960.	6.6	25
76904	Lifting surface reconstruction of Au (100) by tellurium adsorption. Nano Research, 0, , .	5.8	0
76905	Atomic Structural Origin of the High Methanol Selectivity over In₂O₃â€“Metal Interfaces: Metalâ€“Support Interactions and the Formation of a InO_x Overlayer in Ru/In₂O₃ Catalysts during CO₂ Hydrogenation. ACS Catalysis, 2023, 13, 3187-3200.	5.5	26
76906	MoS2/NiSe2/rGO Multiple-Interfaced Sandwich-like Nanostructures as Efficient Electrocatalysts for Overall Water Splitting. Nanomaterials, 2023, 13, 752.	1.9	2
76907	Prediction of stable radon fluoride molecules and geometry optimization using first-principles calculations. Scientific Reports, 2023, 13, .	1.6	4
76908	Decoding Li⁺/Na⁺ Exchange Route Toward Highâ€Performance Mnâ€Based Layered Cathodes for Liâ€Ion Batteries. Advanced Functional Materials, 2023, 33, .	7.8	6
76909	A significantly improved hydrogen storage performance of nanocrystalline Tiâ€“Feâ€“Mnâ€“Pr alloy. Journal of Materials Research and Technology, 2023, 23, 4566-4575.	2.6	3
76910	Self-reduction of Mn⁴⁺ to Mn²⁺: NaY₉Si₆O₂₆:Mn²⁺ red phosphors with excellent thermal stability for NUV LEDs. Journal of Materials Chemistry C, 2023, 11, 3865-3874.	2.7	6

#	Article	IF	Citations
76911	Why can cobalt(III) corrole form more stable metal/organic interfaces than cobalt(II) porphyrin?. Journal of Porphyrins and Phthalocyanines, 0, , A-L.	0.4	0
76912	Lowâ€Temperature Carbonized Nitrogenâ€Doped Hard Carbon Nanofiber Toward Highâ€Performance Sodiumâ€Ion Capacitors. Energy and Environmental Materials, 2023, 6, .	7.3	11
76913	First-principle insights of initial hydration behavior affected by copper impurity in alite phase based on static and molecular dynamics calculations. Journal of Cleaner Production, 2023, 398, 136478.	4.6	2
76914	Accurate descriptions of molecule-surface interactions in electrocatalytic CO2 reduction on the copper surfaces. Nature Communications, 2023, 14, .	5.8	12
76915	Mechanical and electronic properties of transition metal hexa-nitrides in hexagonal structure from density functional theory calculations. Computational Materials Science, 2023, 221, 112084.	1.4	2
76916	Highly Stable Garnet Fe₂Mo₃O₁₂ Cathode Boosts the Lithiumâ€“Air Battery Performance Featuring a Polyhedral Framework and Cationic Vacancy Concentrated Surface. Advanced Science, 2023, 10, .	5.6	20
76917	Composition-dependent structural characteristics and mechanical properties of amorphous SiBCN ceramics by ab-initio calculations. Journal of Advanced Ceramics, 2023, 12, 984-1000.	8.9	2
76918	Theoretical study on the reduction mechanism of CO₂ to HCOOH on Pd₃Au: an explicit solvent model is essential. Journal of Materials Chemistry A, 2023, 11, 6591-6602.	5.2	4
76919	Thermal transport across copperâ€“water interfaces according to deep potential molecular dynamics. Physical Chemistry Chemical Physics, 2023, 25, 6746-6756.	1.3	3
76920	Abnormal thermal expansion coefficients in (Nd_{1â^'x}Dy_x)₂Zr₂O₇pyrochlore: The effect of low-lying optical phonons. Journal of Advanced Ceramics, 2023, 12, 1001-1014.	8.9	2
76921	NaGaSe₂: A Water-Loving Multifunctional Non-van der Waals Layered Selenogallate. Inorganic Chemistry, 2023, 62, 3886-3895.	1.9	2
76922	Structural ordering governs stiffness and ductile-to-brittle transition in Alâ€“Li alloys. Journal of Chemical Physics, 2023, 158, .	1.2	2
76923	Computational design of a new palladium alloy with efficient hydrogen storage capacity and hydrogenation-dehydrogenation kinetics. International Journal of Hydrogen Energy, 2023, 48, 18795-18803.	3.8	1
76924	Ullmann-Like Covalent Bond Coupling without Participation of Metal Atoms. ACS Nano, 2023, 17, 4387-4395.	7.3	0
76925	Magnetic-field modulation of topological electronic state and emergent magneto-transport in a magnetic Weyl semimetal. Innovation(China), 2023, 4, 100399.	5.2	4
76926	High-throughput screening of hybrid quaternary halide perovskites for optoelectronics. Journal of Materials Chemistry A, 2023, 11, 6465-6473.	5.2	2
76927	Van der Waals Epitaxy Growth of 2D Singleâ€Element Roomâ€Temperature Ferromagnet. Advanced Materials, 2023, 35, .	11.1	3
76928	Point defect properties in high entropy MAX phases from first-principles calculations. Acta Materialia, 2023, 248, 118783.	3.8	6

#	Article	IF	Citations
76929	Evidences of Topological Surface States in the Nodal-Line Semimetal SnTaS₂ Nanoflakes. ACS Nano, 2023, 17, 4913-4921.	7.3	1
76930	Electron-Beam- and Thermal-Annealing-Induced Structural Transformations in Few-Layer MnPS₃. ACS Nano, 2023, 17, 4250-4260.	7.3	4
76931	Toward Perfect Surfaces of Transition Metal Dichalcogenides with Ion Bombardment and Annealing Treatment. ACS Applied Materials & Interfaces, 2023, 15, 16153-16161.	4.0	1
76932	Unveiling a high capacity multi-redox (Nb⁵⁺/Nb⁴⁺/Nb³⁺) NASICON-Nb₂(PO₄)₃ anode for Li- and Na-ion batteries. Journal of Materials Chemistry A, 2023, 11, 8173-8183.	5.2	7
76933	Tuning the Mottness in Sr₃Ir₂O₇ via Bridging Oxygen Vacancies. Chinese Physics Letters, 2023, 40, 037101.	1.3	1
76934	Voltage-controlled magnetic anisotropy in heterostructures with a two-dimensional magnetic material. Physical Review B, 2023, 107, .	1.1	3
76935	Molecular dynamics simulations of displacement cascades in vanadium: Generation and types of dislocation loops. Nuclear Materials and Energy, 2023, 34, 101394.	0.6	1
76936	Synthesis of five-layered chiral perovskite nanowires and enacting chiroptical activity regulation. Cell Reports Physical Science, 2023, 4, 101299.	2.8	4
76937	Rh-doped ultrathin NiFeLDH nanosheets drive efficient photocatalytic water splitting. International Journal of Hydrogen Energy, 2024, 52, 371-384.	3.8	4
76938	Enhanced Magnetism and Anomalous Hall Transport through Two-Dimensional Tungsten Disulfide Interfaces. Nanomaterials, 2023, 13, 771.	1.9	3
76939	Understanding the piezocatalytic properties of the BaTiO₃(001) surfaceviadensity functional theory. Physical Chemistry Chemical Physics, 2023, 25, 8631-8640.	1.3	2
76940	Electronic structure, magnetic properties, spin orientation, and doping effect in <mml:math xmlns:mml="http://www.w3.org/1998/Math/MathML"><mml:mrow><mml:msub><mml:mi>Mn</mml:mi><mml:mn>3</mml:mn></mml:msub><mml:msub><mml:mi>Sn</mml:mi><mml:mn></mml:mn></mml:msub></mml:mrow></mml:math> Physical Review B, 2023, 107, .	1.1	3
76941	Supercritical CO ₂ â€induced New Chemical Bond of Câ‹¯Oâ‹¯Si in Graphdiyne to Achieve Robust Roomâ€Temperature Ferromagnetism. ChemPhysChem, 0, , .	1.0	1
76942	DFT-Based Study for the Enhancement of CO₂ Adsorption on Metal-Doped Nitrogen-Enriched Polytriazines. ACS Omega, 2023, 8, 8876-8884.	1.6	7
76943	Charge fluctuation drives anion rotation to enhance the conductivity of Na₁₁M₂PS₁₂ (M = Si, Ge, Sn) superionic conductors. Physical Chemistry Chemical Physics, 2023, 25, 7634-7641.	1.3	2
76944	Insights into SO₂ Poisoning Mechanisms of Fresh and Hydrothermally Aged Cu-KFI Catalysts for NH₃-SCR Reaction. Environmental Science & Technology, 2023, 57, 4308-4317.	4.6	9
76945	Solution-Phase Synthesis and Photoluminescence of Quaternary Chalcohalide Semiconductors. Chemistry of Materials, 2023, 35, 2165-2172.	3.2	7
76946	First-principles theoretical analysis of magnetically tunable topological semimetallic states in antiferromagnetic DyPdBi. Physical Review B, 2023, 107, .	1.1	3

#	Article	IF	Citations
76947	A general thermodynamics-triggered competitive growth model to guide the synthesis of two-dimensional nonlayered materials. Nature Communications, 2023, 14, .	5.8	10
76948	Antiferromagnetic topological magnetism in synthetic van der Waals antiferromagnets. Physical Review B, 2023, 107, .	1.1	6
76949	Superconducting H₇ chain in gallium hydrides at high pressure. Physical Chemistry Chemical Physics, 2023, 25, 7223-7228.	1.3	2
76950	Mixed Germaniaâ€Silica Films on Ru(0001): A combined experimental and theoretical study. Israel Journal of Chemistry, 0, , .	1.0	0
76951	Electrical and magnetic anisotropies in van der Waals multiferroic CuCrP2S6. Nature Communications, 2023, 14, .	5.8	19
76952	How cation nature controls the bandgap and bulk Rashba splitting of halide perovskites. Journal of Computational Chemistry, 2023, 44, 1395-1403.	1.5	1
76953	Two-dimensional XY ferromagnetism above room temperature in Janus monolayer V₂XN (X) Tj ETQq0 0 0 rgBT /Overlock 10	1.3	7
76954	High-temperature ferromagnetism in <mml:math xmlns:mml="http://www.w3.org/1998/Math/MathML"><mml:msub><mml:mrow><mml:mi>Cr</mml:mi></mml:mrow><mml:mrow><mml:mi mathvariant="normal">P</mml:mi></mml:mrow></mml:msub></mml:math>. Physical Review Materials, 2023, 7, .	2.4	2
76955	Identifying magic-number structures of supported sub-nano Ni clusters and the influence of hydrogen coverage: a density functional theory based particle swarm optimization investigation. Catalysis Science and Technology, 2023, 13, 2080-2091.	2.1	0
76956	All-pH Hydrogen Evolution by Heterophase Molybdenum Carbides Prepared via Mechanochemical Synthesis. ACS Sustainable Chemistry and Engineering, 2023, 11, 3585-3593.	3.2	9
76957	Chemical Trends of Surface Reconstruction and Band Positions of Nonmetallic Perovskite Oxides from First Principles. Chemistry of Materials, 2023, 35, 2047-2057.	3.2	3
76958	Effects of NH4+ doping on the hydrogen storage properties of metal hydrides. International Journal of Hydrogen Energy, 2023, , .	3.8	1
76959	Surface Density of Cobalt Single Atoms Manipulating Hydroxyl Radical Generation Via Dual Pathways: Electrons Supply and Active sites. Advanced Functional Materials, 2023, 33, .	7.8	4
76960	Optical Effect Modulation in Polarized Raman Spectroscopy of Transparent Layered Î±â€MoO₃. Small, 2023, 19, .	5.2	5
76961	A High-Throughput Screening toward Efficient Nitrogen Fixation: Transition Metal Single-Atom Catalysts Anchored on an Emerging Ï€â€“Ï€ Conjugated Graphitic Carbon Nitride (g-C₁₀N₃) Substrate with Dirac Dispersion. ACS Applied Materials & Interfaces, 2023, 15, 11812-11826.	4.0	18
76962	Unraveling the Strong Fluorescence Enhancement of HPBI Molecules by ZIF-8 Colloidal Suspensions via Adsorption Analysis. Langmuir, 2023, 39, 3312-3319.	1.6	1
76963	Stable Rb-B compounds under high pressure. Physical Review Research, 2023, 5, .	1.3	5
76964	A Sâ€Scheme MOFâ€onâ€MOF Heterostructure. Advanced Functional Materials, 2023, 33, .	7.8	40

#	Article	IF	Citations
76965	Cu2Oâˆ’Cuç•Œé¢ä¸Šçš„Cu+å’ŒCu0åœ¨ä¿ƒè¿›çˆ”µå,¬åŒ–CO2è¿˜åŽŸé«˜æ•ˆå’Œé«˜é€‰æ‹©æ€§åœ°çˆ”Ÿæˆ C2+äº§ç‰© ©. Science China		13
76966	Electronic structure and physical properties of the candidate topological material GdAgGe. Physical Review B, 2023, 107, .	1.1	2
76967	Tuning magnetism by electric field in MnPS3/Sc2CO2 van der Waals heterostructure. Applied Physics Letters, 2023, 122, .	1.5	11
76968	First-principles study of crystal structure search, stability and mechanical property of magnesium-lithium binary system. Physica Scripta, 2023, 98, 045801.	1.2	0
76969	Synergistic promotions between CO2 capture and in-situ conversion on Ni-CaO composite catalyst. Nature Communications, 2023, 14, .	5.8	41
76970	Modulation of Local Charge Distribution Stabilized the Anionic Redox Process in Mn-Based P2-Type Layered Oxides. ACS Applied Materials & Interfaces, 2023, 15, 11691-11702.	4.0	9
76971	Origin of oxygen-redox and transition metals dissolution in Ni-rich LixNi0.8Co0.1Mn0.1O2 cathode. Journal of Chemical Physics, 2023, 158, .	1.2	3
76972	A deep learning approach to predict thermophysical properties of metastable liquid Ti-Ni-Cr-Al alloy. Journal of Applied Physics, 2023, 133, .	1.1	4
76973	Algorithms and Software. Theoretical Chemistry and Computational Modelling, 2023, , 301-315.	0.2	0
76974	Synthesizability of transition-metal dichalcogenides: a systematic first-principles evaluation. Materials Futures, 2023, 2, 015001.	3.1	5
76975	In Situ Synchrotron XRD Characterization of Piezoelectric Al1âˆ’xScxN Thin Films for MEMS Applications. Materials, 2023, 16, 1781.	1.3	1
76976	Charge Density Evolution Governing Interfacial Friction. Journal of the American Chemical Society, 2023, 145, 5536-5544.	6.6	12
76977	Structure and magnetism of rhodium particles as a size effect. Europhysics Letters, 2023, 141, 66002.	0.7	0
76978	Determining surface-specific Hubbard-U corrections and identifying key adsorbates on nickel and cobalt oxide catalyst surfaces. Physical Chemistry Chemical Physics, 2023, 25, 8903-8912.	1.3	1
76979	Magnetic tuning of band topology evidenced by exotic quantum oscillations in the Dirac semimetal <mml:math xmlns:mml="http://www.w3.org/1998/Math/MathML"><mml:msub><mml:mi>EuMnSb</mml:mi><mml:mn>2</mml:mn></mml:msub> Physical Review B, 2023, 107, .	1.1	3
76980	Y3Fe0.5SiSe7: A new cation-deficient quaternary mixed transition metal chalcogenide with extremely low thermal conductivity. Solid State Sciences, 2023, 138, 107133.	1.5	0
76981	The Role of Glyoxal as an Intermediate in the Electrochemical CO₂ Reduction Reaction on Copper. Journal of Physical Chemistry C, 2023, 127, 4496-4510.	1.5	2
76983	Semicrystalline IrO_x with Abundant Boundaries for Overall Water Splitting. Inorganic Chemistry, 2023, 62, 4011-4019.	1.9	2

#	Article	IF	Citations
76984	Orthogonal luminescence lifetime encoding by intermetallic energy transfer in heterometallic rare-earth MOFs. Nature Communications, 2023, 14, .	5.8	12
76985	Effect of stacking configuration on high harmonic generation from bilayer hexagonal boron nitride. Optics Express, 2023, 31, 9817.	1.7	2
76986	Evidence of high-temperature exciton condensation in a two-dimensional semimetal. Nature Communications, 2023, 14, .	5.8	7
76987	Ion Irradiation Effects on Two-Dimensional MXene Ti₂C for Applications in Extreme Conditions: Combined Ab Initio and Monte Carlo Simulations. ACS Applied Nano Materials, 2023, 6, 3463-3471.	2.4	2
76988	Controllable p-type doping of 2D MoS₂via Sodium intercalation for optoelectronics. Journal of Materials Chemistry C, 2023, 11, 3386-3394.	2.7	0
76989	Comprehensive study on electronic structures of SiGe/Ga$$_{2}$$SeTe vdW heterobilayer. Journal of Materials Science, 2023, 58, 4020-4030.	1.7	4
76990	Doping Engineering for Optimizing Piezoelectric and Elastic Performance of AlN. Materials, 2023, 16, 1778.	1.3	0
76991	Active sampling for neural network potentials: Accelerated simulations of shear-induced deformation in Cuâ€“Ni multilayers. Journal of Chemical Physics, 2023, 158, 114103.	1.2	0
76992	One-dimensional magnetism and Rashba-like effects in zigzag bismuth nanoribbons. Physical Review Materials, 2023, 7, .	0.9	1
76993	One dimensional wormhole corrosion in metals. Nature Communications, 2023, 14, .	5.8	14
76994	Effect of Diffusion Constraints and ZnO_x Speciation on Nonoxidative Dehydrogenation of Propane and Isobutane over ZnO-Containing Catalysts. ACS Catalysis, 2023, 13, 3356-3369.	5.5	7
76995	Understanding element solution energies in nickelbase alloys using machine learning. Materials Research Express, 2023, 10, 036503.	0.8	1
76996	Boron vacancy-driven thermodynamic stabilization and improved mechanical properties of AlB₂-type tantalum diborides as revealed by first-principles calculations. JPhys Materials, 2023, 6, 025002.	1.8	3
76997	Towards an accurate description of one-dimensional pnictogen allotropes in nano-confinements. Physical Chemistry Chemical Physics, 2023, 25, 9256-9263.	1.3	0
76999	Theoretical design and discovery of twoâ€dimensional materials for nextâ€generation flexible piezotronics and energy conversion. , 2023, 2, .		2
77000	Atomic coordination structural dynamic evolution of single-atom Mo catalyst for promoting H2 activation in slurry phase hydrocracking. Science Bulletin, 2023, 68, 503-515.	4.3	13
77001	Role of MoO_x/Ni(111) interfacial sites in direct deoxygenation of phenol toward benzene. Catalysis Science and Technology, 2023, 13, 2201-2211.	2.1	2
77002	2D carbon nitride as a support with single Cu, Ag, and Au atoms for carbon dioxide reduction reaction. Physical Chemistry Chemical Physics, 2023, 25, 8574-8582.	1.3	11

#	Article	IF	Citations
77003	Twisted bilayer zigzag-graphene nanoribbon junctions with tunable edge states. Nature Communications, 2023, 14, .	5.8	11
77004	Anharmonic lattice dynamics and the origin of intrinsic ultralow thermal conductivity in AgI materials. Physical Review B, 2023, 107, .	1.1	6
77005	Expanding the low-dimensional interface engineering toolbox for efficient perovskite solar cells. Nature Energy, 2023, 8, 284-293.	19.8	23
77006	ANi₅Bi_{5.6+Î´} (A = K, Rb, and Cs): Quasi-One-Dimensional Metals Featuring [Ni₅Bi_{5.6+Î´}]^{â^'} Double-Walled Column with Strong Diamagnetism. Inorganic Chemistry, 2023, 62, 3788-3798.	1.9	2
77007	Coordination Inversion of the Tetrahedrally Coordinated Ru_{4f} Surface Complex on RuO₂(100) and Its Decisive Role in the Anodic Corrosion Process. ACS Catalysis, 2023, 13, 3433-3443.	5.5	8
77008	Broadband and Persistent Luminescence in <mml:math xmlns:mml="http://www.w3.org/1998/Math/MathML" display="inline" overflow="scroll"><mml:mi>Eu</mml:mi></mml:math> -Doped <mml:math xmlns:mml="http://www.w3.org/1998/Math/MathML" display="inline" overflow="scroll"><mml:mrow><mml:mi>Sr</mml:mi><mml:mi>Al</mml:mi></mml:mrow></mml:math> <mml:math xmlns:mml="http://www.w3.org/1998/Math/MathML" display="inline" overflow="scroll"><mml:mn	1.5	4
77009	Rationalizing Functionalized MXenes as Effective Anchor Materials for Lithiumâ€“Sulfur Batteries via First-Principles Calculations. Journal of Physical Chemistry Letters, 2023, 14, 2215-2221.	2.1	4
77010	Construction of charge transfer chain in Bi12TiO20-Bi4Ti3O12/Î±-Bi2O3 composites to accelerate photogenerated charge separation. Nano Research, 2023, 16, 3730-3740.	5.8	3
77011	Toward Atomistic Understanding of Materials with the Conversionâ€“Alloying Mechanism in Li-Ion Batteries. Chemistry of Materials, 2023, 35, 2835-2845.	3.2	2
77012	Metal-decorated Î³-graphyne as a drug transporting agent for the mercaptopurine chemotherapy drug: a DFT study. Physical Chemistry Chemical Physics, 2023, 25, 9461-9471.	1.3	4
77013	Emergence of flat bands in twisted bilayer <mml:math xmlns:mml="http://www.w3.org/1998/Math/MathML"><mml:mrow><mml:msub><mml:mi mathvariant="normal">C</mml:mi><mml:mn>3</mml:mn></mml:msub><mml:mi mathvariant="normal">N</mml:mi></mml:mrow></mml:math> induced by simple localization and	1.1	1
77014	xmlns:mml="http://www.w3.org/1998/Math/MathML"><mml:mrow><mml:msub><mml:mi mathvariant="normal">MgCr</mml:mi><mml:mn>2</mml:mn></mml:msub><mml:mi>X</mml:mi></mml:mrow><mml:msub><mml:m /><mml:mn>4</mml:mn></mml:msub><mml:mo>Â</mml:mo><mml:mo>(</mml:mo><mml:mi>X</mml:mi><mml:mo>=</mml:mo>	0.9	0
77015	Physic Tunable Electronic Properties of Two-Dimensional GaSe1â^'xTex Alloys. Nanomaterials, 2023, 13, 818.	1.9	0
77016	Grain-boundary segregation and superior mechanical properties in a multicomponent L12 Ni46.5Co24Fe8Al12.5Ti9 superlattice alloy. Frontiers in Materials, 0, 10, .	1.2	0
77017	Abnormal strain-dependent thermal conductivity in biphenylene monolayer using machine learning interatomic potential. Applied Physics Letters, 2023, 122, .	1.5	7
77018	Surface-enriched ultrafine Pt nanoparticles coupled with defective CoP as efficient trifunctional electrocatalyst for overall water splitting and flexible Zn-air battery. Chinese Journal of Catalysis, 2023, 46, 36-47.	6.9	33
77019	Achieving high Li+ diffusion in reduced graphene oxide/NaTi2(PO4)3 heterostructures for enhanced lithium ions storage. Journal of Materials Science, 2023, 58, 4541-4551.	1.7	3
77020	Electronic, Optical, Mechanical, and Electronic Transport Properties of SrCu2O2: A First-Principles Study. Materials, 2023, 16, 1829.	1.3	1

#	Article	IF	Citations
77021	Theoretical Study on the Role of Solvents in Lithium Polysulfide Anchoring on Vanadium Disulfide Facets for Lithiumâ€“Sulfur Batteries. Journal of Physical Chemistry C, 2023, 127, 4416-4424.	1.5	3
77022	Prediction of LiCrTe$_2$ monolayer as a half-metallic ferromagnet with a high Curie temperature. Chinese Physics B, 0, , .	0.7	0
77023	Oxygen Vacancies-Rich S-Cheme BiOBr/CdS Heterojunction with Synergetic Effect for Highly Efficient Light Emitting Diode-Driven Pollutants Degradation. Nanomaterials, 2023, 13, 830.	1.9	3
77024	Thermodynamic stability of Liâ€“Bâ€“C compounds from first principles. Physical Chemistry Chemical Physics, 2023, 25, 7344-7353.	1.3	2
77025	Rapid Interlayer Charge Separation and Extended Carrier Lifetimes due to Spontaneous Symmetry Breaking in Organic and Mixed Organicâ€“Inorganic Dionâ€“Jacobson Perovskites. Journal of the American Chemical Society, 2023, 145, 5297-5309.	6.6	24
77026	Engineering Magnetic Anisotropy of Rhenium Atom in Nitrogenized Divacancy of Graphene. Nanomaterials, 2023, 13, 829.	1.9	1
77027	Defect-Induced Efficient Heteroepitaxial Growth of Single-Wall Carbon Nanotubes @ Hexagonal Boron Nitride Films. Materials, 2023, 16, 1864.	1.3	0
77028	Quasi-one-dimensional Mn6Bi5 and its electronic structure. Applied Physics Letters, 2023, 122, .	1.5	1
77029	Screening of electrode materials for ammonium ion batteries by high throughput calculation. RSC Advances, 2023, 13, 6548-6556.	1.7	0
77030	Carbon Dioxide Reduction on Transition Metal Dichalcogenides with Ni and Cu Edge Doping: A Densityâ€Functional Theory Study. ChemPhysChem, 2023, 24, .	1.0	1
77031	Rapid prediction of phonon structure and properties using the atomistic line graph neural network (ALIGNN). Physical Review Materials, 2023, 7, .	0.9	6
77032	Coupling between Charge Density Wave Ordering and Magnetism in Ho₂Ir₃Si₅. Chemistry of Materials, 2023, 35, 1980-1990.	3.2	6
77033	Mechanistic Insight into the Promotion of the Low-Temperature NH₃-Selective Catalytic Reduction Activity over Mn_xCe_{1â€“x}O_y Catalysts: A Combined Experimental and Density Functional Theory Study. Environmental Science & Technology, 2023, 57, 3875-3882.	4.6	22
77034	A well-fabricated Ru@C material derived from Ru/Zn-MOF with high activity and stability in the hydrogenation of 4-chloronitrobenzene. Physical Chemistry Chemical Physics, 2023, 25, 8556-8563.	1.3	2
77035	Modeling and simulation of coverage and film properties in deposition process on large-scale pattern using statistical ensemble method. Japanese Journal of Applied Physics, 2023, 62, SI1006.	0.8	1
77036	Understanding the direct methane conversion to oxygenates on graphene-supported single 3d metal atom catalysts. Chemical Papers, 0, , .	1.0	0
77037	Drastic Gas Sensing Selectivity in 2-Dimensional MoS₂ Nanoflakes by Noble Metal Decoration. ACS Nano, 2023, 17, 4404-4413.	7.3	27
77038	Hybrid nodal-chain semimetal with emergent flat band in MgCaN₂. New Journal of Physics, 2023, 25, 033005.	1.2	2

#	Article	IF	Citations
77039	A search for new back contacts for CdTe solar cells. Science Advances, 2023, 9, .	4.7	7
77040	Diamane-like Films Based on Twisted G/BN Bilayers: DFT Modelling of Atomic Structures and Electronic Properties. Nanomaterials, 2023, 13, 841.	1.9	2
77041	Anionic S-doping of a ZnMn2O4/CNTs cathode material enhances its Zn2+ storage performance in aqueous zinc-ion batteries. Journal of Power Sources, 2023, 564, 232863.	4.0	9
77042	First-principles study on the stability and mechanical properties of TiC$$_x$$N$$_{1-x}$$. Journal of Materials Science, 2023, 58, 4474-4486.	1.7	0
77043	In search of Pca2₁ phase ferroelectrics. JPhys Materials, 2023, 6, 024001.	1.8	1
77044	Electronic and magnetic properties of charged point defects in monolayer CrI₃. Physical Chemistry Chemical Physics, 2023, 25, 8809-8815.	1.3	0
77045	High thermoelectric performance of layered <mml:math xmlns:mml="http://www.w3.org/1998/Math/MathML"><mml:mi>LaAg</mml:mi><mml:mi>X</mml:mi><mml:mi mathvariant="normal">O</mml:mi><mml:mo>Â</mml:mo><mml:mo>(</mml:mo><mml:mi>X</mml:mi><mml:mo>=</mml:mo><mml:m from electrical and thermal transport calculations. Physical Review Materials, 2023, 7, .	0.9	3
77046	Physical Insights on the Phonon Dispersion of TiS₂. Advanced Theory and Simulations, 2023, 6, .	1.3	3
77047	Tunable band-structures of MSe₂/C₃N (M = Mo and W) van der Waals Heterojunctions. Materials Research Express, 2023, 10, 035004.	0.8	0
77048	Pseudoâ€Elasticity and Variable Electroâ€Conductivity Mediated by Sizeâ€Dependent Deformation Twinning in Molybdenum Nanocrystals. Small, 2023, 19, .	5.2	1
77049	Theoretical investigation of the MXene precursors MoxV4-xAlC3 (0â€‰â‰â€‰xâ€‰â‰â€‰4). Scientific Reports, 2023, 13, .	1.6	3
77050	Optical Absorption and Secondâ€Harmonic Generation in VioletÂPhosphorene: Experimental and Theoretical Aspects. Advanced Optical Materials, 2023, 11, .	3.6	5
77051	The pivotal role of Ag species on porous nanosheets in the significant reduction of soot ignition temperature. Chemical Engineering Journal, 2023, 461, 142107.	6.6	2
77052	Anomalous Hall Conductivity and Nernst Effect of the Ideal Weyl Semimetallic Ferromagnet EuCd₂As₂. Advanced Science, 2023, 10, .	5.6	6
77053	Effect of Co substitution on ferrimagnetic Heusler compound Mn3Ga. Current Applied Physics, 2023, 49, 78-82.	1.1	0
77054	Selective catalytic hydrodeoxygenation of vanillin to 2-Methoxy-4-methyl phenol and 4-Methyl cyclohexanol over Pd/CuFe2O4 and PdNi/CuFe2O4 catalysts. Chemical Engineering Journal, 2023, 462, 142110.	6.6	4
77055	Drastic oscillation of peierls stress from peierls-nabarro model calculation and its remedy. Journal of Materials Research and Technology, 2023, 23, 5502-5519.	2.6	2
77056	Synthesis, crystal structures and semiconducting properties of new hexacyanidometallates. Dalton Transactions, 2023, 52, 3971-3980.	1.6	0

#	Article	IF	Citations
77057	DFT-aided machine learning-based discovery of magnetism in Fe-based bimetallic chalcogenides. Scientific Reports, 2023, 13, .	1.6	2
77058	Mixed Microscopic Eu²⁺ Occupancies in the Nextâ€Generation Red LED Phosphor Sr[Li₂Al₂O₂N₂]:Eu²⁺ (SALON:Eu²⁺). Advanced Optical Materials, 2023, 11, .	3.6	9
77059	Tiny (ZnO) clusters supported on graphene for solar energy trapping: A density functional theory study. Journal of the Taiwan Institute of Chemical Engineers, 2023, 144, 104769.	2.7	2
77060	Anomalous doping effects on stabilizing unusual phases of lithium fluoride for enhanced rechargeable battery interfaces. Acta Materialia, 2023, 248, 118813.	3.8	4
77061	Bifunctional catalyst of CuMn-HZSM-5 for selective catalytic reduction of NO and CO oxidation under oxygen atmosphere. Chemical Engineering Journal, 2023, 462, 142113.	6.6	9
77062	Exploring the relationship between lattice distortion and phase stability in a multi-principal element alloy system based on machine learning method. Computational Materials Science, 2023, 221, 112089.	1.4	9
77063	Constructing atomic surface concaves on Bi5O7Br nanotube for efficient photocatalytic CO2 reduction. Nano Energy, 2023, 109, 108305.	8.2	22
77064	Large magnetoresistance and spin-polarized photocurrent in Mn2.25Co0.75Ga0.5Sn0.5/MgO/Mn2.25Co0.75Ga0.5Sn0.5 magnetic tunnel junctions. Computational Materials Science, 2023, 221, 112086.	1.4	0
77065	Theoretical and Experimental Assessments of Elementary Steps and Bound Intermediates in Catalytic H₂â€“O₂ Reactions on Dispersed Pt Nanoparticles. Journal of Physical Chemistry C, 2023, 127, 4553-4569.	1.5	1
77066	Theoretical and ²⁷Al NMR Spectroscopic Investigations of Binary Intermetallic Alkaline-Earth Aluminides. Inorganic Chemistry, 2023, 62, 4260-4271.	1.9	4
77067	Regulation of Interfacial Lattice Oxygen Activity by Fullâ€Surface Modification Engineering towards Long Cycling Stability for Coâ€Free Liâ€Rich Mnâ€Based Cathode. Small, 2023, 19, .	5.2	4
77068	Analytical Forces for the Optimized Effective Potential Calculations. Journal of Chemical Theory and Computation, 2023, 19, 1744-1752.	2.3	0
77069	Tuning scintillation properties of <mml:math xmlns:mml="http://www.w3.org/1998/Math/MathML"><mml:mrow><mml:msub><mml:mi>Lu</mml:mi><mml:mn>2</mml:mn></mml:r mathvariant="normal">O</mml:mi><mml:mn>5</mml:mn></mml:msub></mml:mrow></mml:math> by Ce and Ca codoping. Physical Review B, 2023, 107, .	1.1	3
77070	Regulating Hollow Carbon Cage Supported NiCo Alloy Nanoparticles for Efficient Electrocatalytic Hydrogen Evolution Reaction. ACS Applied Materials & Interfaces, 2023, 15, 12078-12087.	4.0	14
77071	Density functional theory study of Br doped CsPbI₃ perovskite for photovoltaic and optoelectronic applications. Physica Scripta, 2023, 98, 045505.	1.2	7
77072	Understanding photoluminescence of bismuth-doped ternary alkaline earth <mml:math xmlns:mml="http://www.w3.org/1998/Math/MathML"><mml:msup><mml:mi>d</mml:mi><mml:mn>10</mml:mn></mml:msup></mml metal oxides via first-principles calculations. Physical Review B, 2023, 107, .	1.1	2
77073	Fabrication of stable multi-level resistance states in a Nb-doped Ge₂Sb₂Te₅ device. Journal of Materials Chemistry C, 2023, 11, 3770-3777.	2.7	5
77074	Synthesizing Crâ€Based Twoâ€Dimensional Conjugated Metalâ€Organic Framework Through Onâ€Surface Substitution Reaction. Small, 2023, 19, .	5.2	6

#	Article	IF	Citations
77075	Tailored Band Edge Positions by Fractional Ligand Replacement of Nonconductive Colloidal Quantum Dot Films. Journal of Physical Chemistry C, 2023, 127, 4825-4832.	1.5	4
77076	High-Performance Colloidal Quantum Dot Photodiodes via Suppressing Interface Defects. ACS Applied Materials & Interfaces, 2023, 15, 12061-12069.	4.0	7
77077	Effect of terminations on the hydrogen evolution reaction mechanism on Ti₃C₂ MXene. Journal of Materials Chemistry A, 2023, 11, 6886-6900.	5.2	15
77078	Thermodynamics of diamond formation from hydrocarbon mixtures in planets. Nature Communications, 2023, 14, .	5.8	12
77079	A Strong Magnetic Field Alters the Activity and Selectivity of the CO2RR by Restraining Câ€“C Coupling. Magnetochemistry, 2023, 9, 65.	1.0	5
77080	First-Principles Investigation on Phonon Mode Conversion of Thermal Transport in Silicene Under Tensile Strain. International Journal of Thermophysics, 2023, 44, .	1.0	0
77081	Ultrahighâ€Voltage LiCoO₂ at 4.7ÂV by Interface Stabilization and Band Structure Modification. Advanced Materials, 2023, 35, .	11.1	34
77082	Multilayered Atomic Relaxation in van der Waals Heterostructures. Physical Review X, 2023, 13, .	2.8	4
77083	Moâ€Modified ZnIn₂S₄@NiTiO₃ Sâ€Scheme Heterojunction with Enhanced Interfacial Electric Field for Efficient Visibleâ€Lightâ€Driven Hydrogen Evolution. Advanced Functional Materials, 2023, 33, .	7.8	31
77084	Ultralow Fe instigated defect engineering of hierarchical Nâ€“Porous carbon for highly efficient electrocatalysis. Materials and Design, 2023, 227, 111782.	3.3	3
77085	Structural properties of Bi/Au(110). Nanotechnology, 2023, 34, 235601.	1.3	0
77086	The Atomistic Understanding of the Ice Recrystallization Inhibition Activity of Antifreeze Glycoproteins. Crystals, 2023, 13, 405.	1.0	1
77087	Monolayer and bilayer <mml:math xmlns:mml="http://www.w3.org/1998/Math/MathML"><mml:msub><mml:mi>PtCl</mml:mi><mml:mn>3</mml:mn></mml:msub></mm : Energetics, magnetism, and band topology. Physical Review B, 2023, 107, .	1.1	4
77088	Electrical and thermal conductivity of fcc and hcp iron under conditions of the Earth's core from ab initio simulations. Physical Review B, 2023, 107, .	1.1	4
77089	A computational method to estimate spinâ€“orbital interaction strength in solid state systems. Computational Materials Science, 2023, 221, 112090.	1.4	1
77090	Efficient catalysts of surface hydrophobic Cu-BTC with coordinatively unsaturated Cu(I) sites for the direct oxidation of methane. Proceedings of the National Academy of Sciences of the United States of America, 2023, 120, .	3.3	8
77091	Exceptional Photocatalytic Hydrogen Peroxide Production from Sandwichâ€Structured Graphene Interlayered Phenolic Resins Nanosheets with Mesoporous Channels. Advanced Functional Materials, 2023, 33, .	7.8	20
77092	Theoretical analysis of electrochromism of Ni-deficient nickel oxide â€“ from bulk to surfaces. Physical Chemistry Chemical Physics, 2023, 25, 7974-7985.	1.3	1

#	Article	IF	Citations
77093	Hole doping dependent electronic instability and electron-phonon coupling in infinite-layer nickelates. Physical Review B, 2023, 107, .	1.1	4
77094	Chemical bonding engineering for high-symmetry Cu2S-based materials with high thermoelectric performance. Materials Today Physics, 2023, 32, 101028.	2.9	3
77095	Catalytic CO Oxidation by Single Atom Catalysts of Transition Metal-doped Ï‡₃-Borophene: A First Principles Study. Chemistry Letters, 2023, 52, 249-253.	0.7	1
77096	Electronic Structure Calculations of Static Hyper(Polarizabilities) of Substrate-Supported Group-IV and -V Elemental Monolayers. ACS Omega, 2023, 8, 9614-9620.	1.6	0
77097	Flexo-Ferroelectricity and a Work Cycle of a Two-Dimensional-Monolayer Actuator. ACS Nano, 2023, 17, 5121-5128.	7.3	1
77098	Electrolyte Solvation Structure Regulation Promotes Aluminumâ€“Air Batteries to Approach Theoretical Discharge Capacity. Journal of Physical Chemistry C, 2023, 127, 4439-4450.	1.5	1
77099	Highly Efficient CO Oxidation on Atomically Thin Pt Plates Supported on Irreducible Si 7 Ã— 7. Journal of Physical Chemistry C, 2023, 127, 4527-4534.	1.5	0
77100	Strain effect on the high T _c superconductor YBa₂Cu₃O₇: an ab initio study comparing bulk and monolayer models. Electronic Structure, 2023, 5, 015002.	1.0	0
77101	Extended calculation of electronic excitations for direct detection of dark matter. Physical Review D, 2023, 107, .	1.6	7
77102	Comprehensive Mechanism for CO Electroreduction on Dualâ€Atomâ€Catalystâ€Anchored Nâ€Doped Graphene. ChemPhysChem, 0, , .	1.0	0
77103	Floquet engineering of magnetic topological insulator <mml:math xmlns:mml="http://www.w3.org/1998/Math/MathML"><mml:mrow><mml:msub><mml:mi>MnBi</mml:mi><mml:mn>2</mml:mn></mml:msub></mml:mrow></mml:math> films. Physical Review B, 2023, 107, .	1.1	4
77104	Accurate prediction of oxygen vacancy concentration with disordered A-site cations in high-entropy perovskite oxides. Npj Computational Materials, 2023, 9, .	3.5	6
77105	Creating and Stabilizing an Oxidized Pd Surface under Reductive Conditions for Photocatalytic Hydrogenation of Aromatic Carbonyls. Journal of the American Chemical Society, 2023, 145, 5353-5362.	6.6	6
77106	Machine Learning Molecular Dynamics Simulations for Evaluation of High-Temperature Properties of Nuclear Fuel Materials. Materia Japan, 2023, 62, 175-181.	0.1	0
77107	Iridium Incorporation into MnO₂ for an Enhanced Electrocatalytic Oxygen Evolution Reaction. ChemCatChem, 2023, 15, .	1.8	3
77108	New C_{2h} phase of group III monochalcogenide monolayers AlX (X = S, Se, and Te) with anisotropic crystal structure: first-principles study. RSC Advances, 2023, 13, 6838-6846.	1.7	1
77109	Stacking-dependent topological magnons in bilayer <mml:math xmlns:mml="http://www.w3.org/1998/Math/MathML"><mml:msub><mml:mi>CrI</mml:mi><mml:mn>3</mml:mn></mml:msub></mml:math> Physical Review Materials, 2023, 7, .	0.9	3
77110	The first-principle study on certain structural, band-structural, elastic, optical and piezoelectric properties of the Ca, Zr and Ca/Zr-doped BaTiO3. Modern Physics Letters B, 2023, 37, .	1.0	4

#	Article	IF	Citations
77111	BiOCl Nanoflowers with High Levels of Oxygen Vacancy for Photocatalytic CO₂ Reduction. ACS Applied Nano Materials, 2023, 6, 3608-3617.	2.4	17
77112	Enhanced Thermoelectric Properties of Zr_{0.85â€“x}Hf_xNb_{0.15â€“y}Ta_yCoSb Medium-Entropy Alloys: Tradeoff between â€œWhat to Alloyâ€•and â€œHow Much to Alloyâ€• Chemistry of Materials, 2023, 35, 2202-2212.	3.2	3
77113	The electronic and interfacial properties of a vdW heterostructure composed of penta-PdSe₂and biphenylene monolayers. Materials Advances, 2023, 4, 1566-1571.	2.6	2
77114	First principles study on stacking-dependent electronic structure of CrI₃/Î±- In2Se3 heterostructures. Journal of Applied Physics, 2023, 133, 085703.	1.1	1
77115	Amorphous As2S3 Doped with Transition Metals: An Ab Initio Study of Electronic Structure and Magnetic Properties. Nanomaterials, 2023, 13, 896.	1.9	1
77116	Electric-Field Emission Mechanism in Q-Carbon Field Emitters. ACS Omega, 2023, 8, 9307-9318.	1.6	5
77117	Synchrotron X-ray Study for Defect Structure in MgAl₂O₄ Spinel Induced by Swift Heavy Ions. Materia Japan, 2023, 62, 169-174.	0.1	0
77118	First-principle calculations of stable configurations and electronic structures of pristine and discharged spinel Mg1.31V1.67-xNixO4 (xÂ=Â0, 0.13) as cathode materials for magnesium secondary batteries. Computational Materials Science, 2023, 221, 112087.	1.4	1
77119	Pressure-Induced Reversible Local Structural Disorder in Superconducting AuAgTe4. Inorganics, 2023, 11, 99.	1.2	1
77120	Designing polar textures with ultrafast neuromorphic features from atomistic simulations. Neuromorphic Computing and Engineering, 2023, 3, 012002.	2.8	3
77121	Ferromagnetic GdX (X = Cl, Br) Monolayers with Large Perpendicular Magnetic Anisotropy and High Curie Temperature. Journal of Physical Chemistry C, 2023, 127, 4643-4650.	1.5	3
77122	Phase diagram and thermoelastic property of iron oxyhydroxide across the spin crossover under extreme conditions. Physical Review B, 2023, 107, .	1.1	1
77123	Critical role of hydrogen for superconductivity in nickelates. Nature, 2023, 615, 50-55.	13.7	31
77124	Two-dimensional rectangular bismuth bilayer: A novel dual topological insulator. Frontiers of Physics, 2023, 18, .	2.4	2
77125	The single-atom catalytic activity of the hydrogen evolution reaction of the experimentally synthesized boridene 2D material: a density functional theory study. Journal of Molecular Modeling, 2023, 29, .	0.8	0
77126	Coherent Control of a Nuclear Spin via Interactions with a Rare-Earth Ion in the Solid State. PRX Quantum, 2023, 4, .	3.5	9
77127	Important roles of surface functionalized groups of MXenes on adsorption capacities of Sr and Cs: A theoretical study. Journal of Molecular Structure, 2023, 1283, 135261.	1.8	1
77128	Electrocatalytic reduction of N2 on FeRu dual-atom catalyst anchored in N-doped phosphorene. Molecular Catalysis, 2023, 539, 113032.	1.0	1

#	Article	IF	Citations
77129	First‐Principles Calculations and a Theoretical Model for Predicting Stacking Fault Energies in Binary Magnesium Alloys. Advanced Engineering Materials, 2023, 25, .	1.6	0
77131	xmlns:mml="http://www.w3.org/1998/Math/MathML" altimg="si37.svg" display="inline" id="d1e96"><mml:msub><mml:mrow /><mml:mrow><mml:mn>2</mml:mn></mml:mrow></mml:msub></mml:math> and Mg<mml:math xmlns:mml="http://www.w3.org/1998/Math/MathML" altimg="si65.svg" display="inline"	2.3	2
77132	AtomVision: A Machine Vision Library for Atomistic Images. Journal of Chemical Information and Modeling, 2023, 63, 1708-1722.	2.5	6
77133	Disorder-tuned conductivity in amorphous monolayer carbon. Nature, 2023, 615, 56-61.	13.7	24
77134	Magnesium oxide-water compounds at megabar pressure and implications on planetary interiors. Nature Communications, 2023, 14, .	5.8	7
77135	Water-Induced Structural Evolution of LaTMSi Ternary Intermetallic Electrides. Chemistry of Materials, 2023, 35, 1972-1979.	3.2	0
77136	Topological Nodal Surface and Quadratic Dirac Semimetal States and van Hove Singularities in ScH₃ and LuH₃ Superconductors. ACS Omega, 2023, 8, 9607-9613.	1.6	4
77137	The Microzone Structure Regulation of Diamond/Cu-B Composites for High Thermal Conductivity: Combining Experiments and First-Principles Calculations. Materials, 2023, 16, 2021.	1.3	1
77138	Reconstruction of Low Dimensional Electronic States by Altering the Chemical Arrangement at the SrTiO₃ Surface. Advanced Functional Materials, 2023, 33, .	7.8	2
77139	Theoretical Evaluation of Highly Efficient Nitrate Reduction to Ammonia on InBi. Journal of Physical Chemistry Letters, 2023, 14, 2410-2415.	2.1	4
77140	Analysis of diffuse scattering in electron diffraction data for the crystal structure determination of Pigment Orange 13, C₃₂H₂₄Cl₂N₈O₂. Acta Crystallographica Section B: Structural Science, Crystal Engineering and Materials, 2023, 79, 122-137.	0.5	2
77141	Dzyaloshinskii-Moriya interaction and skyrmions in antiferromagnetic-based heterostructures. Journal of Magnetism and Magnetic Materials, 2023, 572, 170594.	1.0	0
77142	Mechanism of CO₂ photoreduction by selenium-doped carbon nitride with cobalt clusters as cocatalysts. Physical Chemistry Chemical Physics, 2023, 25, 8705-8713.	1.3	1
77143	Experimental and theoretical study of synthesis and properties of Cu2O/TiO2 heterojunction for photoelectrochemical purposes. Surfaces and Interfaces, 2023, 37, 102751.	1.5	3
77144	Anharmonic phonon renormalization and two-channel thermal transport in SrTiO3 using full temperature-dependent interatomic force constant. Physics Letters, Section A: General, Atomic and Solid State Physics, 2023, 467, 128727.	0.9	0
77145	Engineering axion insulator and other topological phases in superlattices without inversion symmetry. Physical Review B, 2023, 107, .	1.1	4
77146	Regioselective Reduction of NAD⁺ to 1,4‐NADH with a Bioinspired Metal Sulfide Electrocatalyst. ChemCatChem, 2023, 15, .	1.8	0
77147	Ti-6Al-4V to over 1.2 TPa: Shock Hugoniot experiments, <mml:math xmlns:mml="http://www.w3.org/1998/Math/MathML"><mml:mrow><mml:mi>a</mml:mi><mml:mi>b</mml:mi></mml:mrow><mml:mo calculations, and a broad-range multiphase equation of state. Physical Review B, 2023, 107, .	1.1	1

#	Article	IF	Citations
77148	The emergence of considerable room temperature magnetocaloric performances in the transition metal high-entropy alloys. Materials Today Physics, 2023, 32, 101031.	2.9	28
77149	Electronic Structure of the Weak Topological Insulator Candidate Zintl Ba₃Cd₂Sb₄. Chinese Physics Letters, 2023, 40, 047101.	1.3	1
77150	Influence of Nitrogen Substitution on the Electronic Structure of Ti₂O₃: Insights into the Dopingâ€Induced Insulatorâ€toâ€Metal Transition. Physica Status Solidi (B): Basic Research, 2023, 260, .	0.7	0
77151	Change in the Electronic Environment of the VO_x Active Center via Support Modification to Enhance Hg Oxidation Activity. ACS Catalysis, 2023, 13, 3775-3787.	5.5	4
77152	Structures of Smâ€“Cu intermetallics with Fe as subphase candidates in SmFe₁₂-based permanent magnets studied by first-principles thermodynamics. Japanese Journal of Applied Physics, 2023, 62, 030902.	0.8	1
77153	Spin filters based on two-dimensional materials Co₂Si and Cu₂Si. Journal of Physics Condensed Matter, 2023, 35, 195001.	0.7	0
77154	New stable ultrawide bandgap As₂O₃ semiconductor materials. JPhys Materials, 2023, 6, 025003.	1.8	7
77155	Spinel-Anchored Iridium Single Atoms Enable Efficient Acidic Water Oxidation via Intermediate Stabilization Effect. ACS Catalysis, 2023, 13, 3757-3767.	5.5	21
77156	Efficient Voltage-Driven Oxidation of Water and Alcohols by an Organic Molecular Catalyst Directly Attached to a Carbon Electrode. Journal of the American Chemical Society, 2023, 145, 5786-5794.	6.6	4
77157	CuSe₂ Nanocubes Enabling Efficient Sodium Storage. ACS Applied Materials & Interfaces, 2023, 15, 12976-12985.	4.0	7
77158	Relay catalysis of Pt single atoms and nanoclusters enables alkyl/aryl C-O bond scission for oriented lignin upgrading and N-functionalization. Chemical Engineering Journal, 2023, 462, 142225.	6.6	6
77159	Unexpected Piezoresistive Effect, Roomâ€Temperature Ferromagnetism, and Thermal Stability of 2D Î²â€CuI Crystals in Reduced Graphene Oxide Membrane. Advanced Electronic Materials, 2023, 9, .	2.6	3
77160	Electromagnetic evolution in proton-containing spinel <mml:math xmlns:mml="http://www.w3.org/1998/Math/MathML"><mml:mrow><mml:msub><mml:mi>NiCo</mml:mi><mml:mn>2</mml:mn></mml:msub><mml:msub><mml:mi mathvariant="normal">O</mml:mi><mml:mn>4</mml:mn></mml:msub></mml:mrow></mml:math> thin films via ionic liquid gating. Physical Review B, 2023, 107, .	1.1	2
77161	Highâ€Performance Industrialâ€Grade pâ€Type (Bi,Sb)₂Te₃ Thermoelectric Enabled by a Stepwise Optimization Strategy. Advanced Materials, 2023, 35, .	11.1	23
77162	Strain induced metal-semiconductor transition in two-dimensional topological half metals. IScience, 2023, 26, 106312.	1.9	4
77163	Ligand vacancy channels in pillared inorganic-organic hybrids for electrocatalytic organic oxidation with enzyme-like activities. Nature Communications, 2023, 14, .	5.8	1
77164	Redoxâ€Stabilized Sn/SnO₂ Nanostructures for Efficient and Stable CO₂ Electroreduction to Formate. ChemElectroChem, 2023, 10, .	1.7	1
77165	Lithium Ion Transport Environment by Molecular Vibrations in Ionâ€Conducting Glasses. Energy and Environmental Materials, 0, , .	7.3	2

#	Article	IF	Citations
77166	Structural, electronic, and Li-ion mobility properties of garnet-type Li₇La₃Zr₂O₁₂ surface: An insight from first-principles calculations. Chinese Physics B, 2023, 32, 068201.	0.7	1
77167	Efficient Inorganic Vaporâ€Assisted Defects Passivation for Perovskite Solar Module. Advanced Materials, 2023, 35, .	11.1	10
77168	Kinetic Understanding of Catalytic Selectivity and Product Distribution of Electrochemical Carbon Dioxide Reduction Reaction. Jacs Au, 2023, 3, 905-918.	3.6	8
77169	Chlorine-induced mixed valence of CuOx/C to promote the electroreduction of carbon dioxide to ethylene. Nano Research, 2023, 16, 8827-8835.	5.8	2
77170	Effect of Magnetic Coupling on the Optical Properties of Oxide Co Nanowires on Vicinal Pt Surfaces. Magnetochemistry, 2023, 9, 72.	1.0	0
77171	Extremely promising monolayer materials with robust ferroelectricity and extraordinary piezoelectricity: Î´-AsN, Î´-SbN, and Î´-BiN. Nanoscale, 2023, 15, 6363-6370.	2.8	7
77172	Vertically Aligned Bismuthene Nanosheets on MXene for High-Performance Capacitive Deionization. ACS Nano, 2023, 17, 4843-4853.	7.3	53
77173	Directing and Understanding the Translation of a Single Molecule Dipole. Journal of Physical Chemistry Letters, 2023, 14, 2487-2492.	2.1	1
77174	Hole doping induced ferromagnetism and Dzyaloshinskiiâ€“Moriya interaction in the two-dimensional group-IVA oxides. Journal of Physics Condensed Matter, 2023, 35, 204003.	0.7	0
77175	A comprehensive investigation of the plasmonic-photocatalytic properties of gold nanoparticles for CO₂ conversion to chemicals. Nanoscale, 2023, 15, 7051-7067.	2.8	2
77176	Pressure-Induced Transition from Wurtzite and Epitaxial Stabilization for Thin Films of Rocksalt MgSnN₂. Chemistry of Materials, 2023, 35, 2095-2106.	3.2	3
77177	Onâ€line Optimization of Integrated Carbon Capture and Conversion Process via the Ratings Concept: A Combined DFT and Microkinetic Modeling Approach. ChemCatChem, 0, , .	1.8	0
77178	Computational and experimental investigations on the effect of crystallinity and crystal size on Na-transport in nanoscaled Si: implications for Si-based anodes for Na-ion batteries. Journal of Solid State Electrochemistry, 2023, 27, 1227-1240.	1.2	0
77179	Efficient N₂ electroreduction to ammonia in an isopropanolâ€“PBS electrolyte using NiFe₂O₄in situ grown on nickel foam. Energy Advances, 2023, 2, 547-555.	1.4	1
77180	Site-specific anisotropic assembly of amorphous mesoporous subunits on crystalline metalâ€“organic framework. Nature Communications, 2023, 14, .	5.8	12
77181	Polarization and built-in electric field improve the photocatalytic overall water splitting efficiency of C2N/ZnSe heterostructures. International Journal of Hydrogen Energy, 2023, 48, 19554-19563.	3.8	12
77182	Two-Dimensional AMgB (A = Na, K; B = P, As, Sb, Bi) with Promising Optoelectronic and Thermoelectric Performances. ACS Applied Electronic Materials, 2023, 5, 1405-1419.	2.0	4
77183	Magnetism and <mml:math xmlns:mml="http://www.w3.org/1998/Math/MathML"><mml:mrow><mml:mi>T</mml:mi><mml:mtext>a</mml:mtext><mml:mi>x</mml:mi> phase diagrams of Na- and Ag-substituted <mml:math xmlns:mml="http://www.w3.org/1998/Math/MathML"><mml:msub><mml:mi mathvariant="normal">EuCd</mml:mi><mml:mn>2</mml:mn></mml:msub><mml:msub><mml:mi mathvariant="normal">As</mml:mi><mml:mn>2</mml:mn></mml:msub></mml:math>. Physical Review M	0.9	2

#	Article	IF	Citations
77184	Single atomic Ru in TiO2 boost efficient electrocatalytic water oxidation to hydrogen peroxide. Science Bulletin, 2023, 68, 613-621.	4.3	6
77185	Electrocatalytic Hydrogen Evolution at Full Atomic Utilization over ITO-Supported Sub-nano-Pt_n Clusters: High, Size-Dependent Activity Controlled by Fluxional Pt Hydride Species. Journal of the American Chemical Society, 2023, 145, 5834-5845.	6.6	15
77186	Prediction of topological phases in metastable ferromagnetic <mml:math xmlns:mml="http://www.w3.org/1998/Math/MathML"><mml:mrow><mml:mi>M</mml:mi><mml:mi mathvariant="normal">P</mml:mi><mml:msub><mml:mi>X</mml:mi><mml:mn>3</mml:mn></mml:msub></mml:mrow></mml:math> monolayers. Physical Review B, 2023, 107, .	1.1	3
77187	Single-Crystalline Bi₂YO₄Cl with Facet-Aided Photocarrier Separation for Robust Solar Water Splitting. ACS Catalysis, 2023, 13, 3854-3863.	5.5	8
77188	Molybdenum based 2D conductive Metalâ€“Organic frameworks as efficient single-atom electrocatalysts for N2 reduction: A density functional theory study. International Journal of Hydrogen Energy, 2023, 48, 19972-19983.	3.8	8
77189	First-principles-based simulation of the electrocaloric effect. , 2023, , 63-91.		0
77190	In-situ growth of low-dimensional perovskite-based insular nanocrystals for highly efficient light emitting diodes. Light: Science and Applications, 2023, 12, .	7.7	17
77191	Hydrogen spillover effects in the Fischerâ€“Tropsch reaction over carbon nanotube supported cobalt catalysts. Catalysis Science and Technology, 2023, 13, 1888-1904.	2.1	3
77192	Multiscale theoretical tools for in silico macromolecular chemistry and engineering. , 2023, , 17-69.		2
77193	Labâ€onâ€Fiber Based on Optimized Gallium Selenide for Femtosecond Modeâ€Locked Lasers and Fiberâ€Compatible Photodetectors. Advanced Photonics Research, 2023, 4, .	1.7	2
77194	Interfacial oxygen coordination environment regulation towards high-performance Li-rich layered oxide cathode. Chemical Engineering Journal, 2023, 462, 142194.	6.6	1
77195	Reducing the refractive index by replacing an [AlPO₄]Â° unit with [BPO₄]Â° in fused silica. Optical Materials Express, 2023, 13, 935.	1.6	2
77196	Excitation-Wavelength-Dependent Charge-Carrier Lifetime in Hematite: An Insight from Nonadiabatic Molecular Dynamics. Journal of Physical Chemistry Letters, 2023, 14, 2448-2454.	2.1	1
77197	Upcycling natural Limestone waste for thermochemical energy storage by utilising tailored CaZrO₃ nanoadditives. Materials Advances, 2023, 4, 1905-1915.	2.6	6
77198	Superstoichiometric Alloying of H and Closeâ€Packed Feâ€Ni Metal Under High Pressures: Implications for Hydrogen Storage in Planetary Core. Geophysical Research Letters, 2023, 50, .	1.5	3
77199	Electronic processes occurring during ultrafast demagnetization of cobalt triggered by x-ray photons tuned to the Co <mml:math xmlns:mml="http://www.w3.org/1998/Math/MathML"><mml:msub><mml:mi>L</mml:mi><mml:mn>3</mml:mn></mml:msub></mml:m resonance. Physical Review B, 2023, 107, .	1.1	2
77200	Theoretical study on the magnetic properties of cathode materials in the lithiumâ€“ion battery. Journal of Chemical Physics, 2023, 158, .	1.2	2
77201	MOFs-alginate/polyacrylic acid/poly (ethylene imine) heparin-mimicking beads as a novel hemoadsorbent for bilirubin removal in vitro and vivo models. International Journal of Biological Macromolecules, 2023, 235, 123868.	3.6	2

#	Article	IF	Citations
77202	Surfaceâ€Dependent Electrocatalytic Activity of CoSe₂ for Lithium Sulfur Battery. Advanced Materials Interfaces, 2023, 10, .	1.9	2
77203	Electronic structural and lattice thermodynamic properties of MAlO2 and M5AlO4 (Mâ€‰=â€‰Li, Na, K) sorbents for CO2 capture applications. Discover Chemical Engineering, 2023, 3, .	1.1	3
77204	Single-Atom-Anchored Two-Dimensional MoSi₂N₄ Monolayers for Efficient Electroreduction of CO₂ to Formic Acid and Methane. ACS Applied Energy Materials, 2023, 6, 3236-3243.	2.5	5
77205	Reversible Thermal Conductivity Modulation of Non-equilibrium (Sn_{1â€“x}Pb_x)S by 2Dâ€“3D Structural Phase Transition above Room Temperature. ACS Applied Energy Materials, 2023, 6, 3504-3513.	2.5	1
77206	Pt overlayer for direct oxidation of CH4 to CH3OH. Chinese Chemical Letters, 2023, 34, 108292.	4.8	4
77207	Strainâ€Driven Superlubricity of Graphene/Graphene in Commensurate Contact. Advanced Materials Interfaces, 2023, 10, .	1.9	5
77208	Topology Hierarchy of Transition Metal Dichalcogenides Built from Quantum Spin Hall Layers. Advanced Materials, 2023, 35, .	11.1	2
77209	Openâ€Shell Diradicalâ€Sensitized Electron Transport Layer for Highâ€Performance Colloidal Quantum Dot Solar Cells. Advanced Materials, 2023, 35, .	11.1	15
77210	Ab Initio Melting Temperatures of Bcc and Hcp Iron Under the Earthâ€™s Inner Core Condition. Geophysical Research Letters, 2023, 50, .	1.5	10
77211	Enabling an Intrinsically Safe and Highâ€Energyâ€Density 4.5ÂVâ€Class Lithiumâ€Ion Battery with Synergistically Incorporated Fast Ion Conductors. Advanced Energy Materials, 2023, 13, .	10.2	11
77212	Nanowires exfoliated from one-dimensional van der Waals transition metal trihalides and quadrihalides. Nanoscale Advances, 2023, 5, 2096-2101.	2.2	1
77213	Efficient and Stable Perovskite Solar Cells by Tailoring of Interfaces. Advanced Materials, 2023, 35, .	11.1	21
77214	Machine learning and density functional theory simulation of the electronic structural properties for novel quaternary semiconductors. Physical Chemistry Chemical Physics, 2023, 25, 9123-9130.	1.3	4
77215	Insights into the Role of Graphitic Carbon Nitride as a Photobase in Protonâ€Coupled Electron Transfer in (sp³)Câ€“H Oxygenation of Oxazolidinones. Angewandte Chemie - International Edition, 2023, 62, .	7.2	18
77216	Structural Phase Transition of Quinone-Containing PAH Derivatives on Au(111) at High Coverage. Journal of Physical Chemistry C, 2023, 127, 5039-5043.	1.5	0
77217	Iridium oxide nanoribbons with metastable monoclinic phase for highly efficient electrocatalytic oxygen evolution. Nature Communications, 2023, 14, .	5.8	31
77218	Generation of Helical States â€“ Breaking of Symmetries, Curie's Principle, and Excited States**. ChemPhysChem, 0, , .	1.0	0
77219	First-principles study on the interfacial bonding strength and segregation at Mg/MgZn2 matrix interface. Journal of Magnesium and Alloys, 2023, , .	5.5	1

#	Article	IF	Citations
77220	Einblicke in die Rolle von Graphitkohlenstoffnitrid als Photobase beim protonengekoppelten Elektronentransfer bei der (sp³)Câ^'Hâ€Oxygenierung von Oxazolidinonen. Angewandte Chemie, 2023, 135, .	1.6	2
77221	Two-phase transition induced cation-disordered Li-reactive bi-metallic phosphides enabling high-performance Li-storage. Chemical Engineering Journal, 2023, 462, 142208.	6.6	0
77222	Ab-initio predictions of mechanical, electronic, magnetic, and transport properties of bulk and heterostructure of a novel Fe-Cr based full Heusler chalcogenide. Journal of Physics and Chemistry of Solids, 2023, 178, 111307.	1.9	0
77223	Alloying of Cu with Ru Enabling the Relay Catalysis for Reduction of Nitrate to Ammonia. Advanced Materials, 2023, 35, .	11.1	83
77224	Revealing the mechanisms of lithium-ion transport and conduction in composite solid polymer electrolytes. Cell Reports Physical Science, 2023, 4, 101321.	2.8	6
77225	Crotonaldehyde Adsorption on Cu-Pt Surface Alloys: A Quantum Mechanics Study. Chemistry, 2023, 5, 463-478.	0.9	2
77226	Achieving sustainability of greenhouses by integrating stable semi-transparent organic photovoltaics. Nature Sustainability, 2023, 6, 539-548.	11.5	25
77227	Nanoscaling and Heterojunction for Photocatalytic Hydrogen Evolution by Bimetallic Metalâ€Organic Frameworks. Advanced Functional Materials, 2023, 33, .	7.8	4
77228	Photoinduced Dynamics at the <mml:math xmlns:mml="http://www.w3.org/1998/Math/MathML" display="inline"><mml:mrow><mml:mtext>Water</mml:mtext><mml:mo>/</mml:mo><mml:msub><mml:mrow><mml:mi>TiO</mml:mi></mml:m stretchy="false">(</mml:mo><mml:mn>101</mml:mn><mml:mo) Tj ETQq0 0 0 rgBT /Overlock 10 Tf 50 412 Td (stretchy="false">)</mml:mo>	2.9	2
77229	Effect of steric hindrance on the interfacial connection of MOF-on-MOF architectures. Nanoscale Advances, 2023, 5, 2111-2117.	2.2	2
77230	Enhancing spin splitting by symmetry and molecular orbital hybridization in VO2. Computational Materials Science, 2023, 222, 112100.	1.4	2
77231	Reactant conversionâ€"intercalation strategy toward interlayer-expanded MoS₂ microflowers with superior supercapacitor performance. Dalton Transactions, 2023, 52, 4537-4547.	1.6	4
77232	Gold Nanoparticles Enriched Graphene System for Therapeutics: A Novel Combination of Experimental and Theoretical Studies. Journal of Inorganic and Organometallic Polymers and Materials, 2023, 33, 1331-1338.	1.9	5
77233	Charge Redistribution of Co9S8/MoS2 Heterojunction Microsphere Enhances Electrocatalytic Hydrogen Evolution. Biomimetics, 2023, 8, 104.	1.5	6
77234	In Situ Neutron Scattering Study of the Structure Dynamics of the Ru/Ca₂N:e^{â€"} Catalyst in Ammonia Synthesis. Chemistry of Materials, 2023, 35, 2456-2462.	3.2	3
77235	Atomistic Evolution of Hf2S/Î³â€² Interfaces in a Hf-containing Ni-based Single-Crystal Superalloy. Acta Metallurgica Sinica (English Letters), 2023, 36, 1038-1046.	1.5	1
77236	Low thermal conductivity mechanism of co-doped ceramics for thermal barrier coatings applications. Journal of Materials Science, 2023, 58, 4695-4706.	1.7	2
77237	Steering CO ₂ electroreduction pathway toward ethanol via surface-bounded hydroxyl species-induced noncovalent interaction. Proceedings of the National Academy of Sciences of the United States of America, 2023, 120, .	3.3	9

#	Article	IF	Citations
77238	A New Organic Conductor of Tetramethyltetraselenafulvalene (TMTSF) with a Magnetic Dy(III) Complex. Magnetochemistry, 2023, 9, 77.	1.0	1
77239	Revealing the promising near-room-temperature thermoelectric performance in Ag2Se single crystals. Journal of Materiomics, 2023, 9, 754-761.	2.8	7
77240	Petroleum-Pitch-Based Carbon Nanocages Encapsulated Few-Layer MoS₂ with S Vacancies for a High-Performance Sodium-Ion Battery. Energy & Fuels, 2023, 37, 4641-4649.	2.5	7
77241	Methane Activation and Coupling Pathways on Ni2P Catalyst. Catalysts, 2023, 13, 531.	1.6	3
77242	On-surface synthesis of enetriynes. Nature Communications, 2023, 14, .	5.8	1
77243	Engineering high-spin state cobalt cations in spinel ZnCo2O4 for spin channel propagation and electrocatalytic activity enhancement in Li-O2 battery. Chemical Engineering Journal, 2023, 462, 142288.	6.6	10
77244	InN/XS₂ (X = Zr, Hf) vdW heterojunctions: promising Z-scheme systems with high hydrogen evolution activity for photocatalytic water splitting. Physical Chemistry Chemical Physics, 2023, 25, 8144-8152.	1.3	3
77245	Efficient conversion of lignin to alkylphenols over highly stable inverse spinel MnFe2O4 catalysts. Frontiers of Chemical Science and Engineering, 2023, 17, 1085-1095.	2.3	2
77246	Manipulating the ordered oxygen complexes to achieve high strength and ductility in medium-entropy alloys. Nature Communications, 2023, 14, .	5.8	7
77247	Ambipolar Electrochemistry of Preâ€Intercalated Ti₃C₂T_x MXene in Ionic Liquid Electrolyte. Batteries and Supercaps, 2023, 6, .	2.4	2
77248	A computational investigation of the decomposition of acetic acid in H-SSZ-13 and its role in the initiation of the MTO process. Catalysis Science and Technology, 2023, 13, 1905-1917.	2.1	3
77249	Topological tailoring-induced Dirac cone in ultrathin niobium diboride nanosheets for electrocatalytic sulfur reduction reaction. Materials Today Physics, 2023, 32, 101029.	2.9	1
77250	Effect of the surface termination on the adsorption of flue gas by the titanium carbide MXene. Materials Today Chemistry, 2023, 29, 101441.	1.7	5
77251	Ambient light stimulation enabling intense and long-lasting ultraviolet-C persistent luminescence from Pr³⁺-doped YBO₃ in bright environments. Journal of Materials Chemistry C, 2023, 11, 4492-4499.	2.7	6
77252	Aromatic hexazine [N6]4â^' anion featured in the complex structure of the high-pressure potassium nitrogen compound K9N56. Nature Chemistry, 2023, 15, 641-646.	6.6	9
77253	The enhanced photocatalytic and photothermal effects of Ti3C2 Mxene quantum dot/macroscopic porous graphitic carbon nitride heterojunction for Hydrogen Production. Journal of Colloid and Interface Science, 2023, 641, 309-318.	5.0	11
77254	Study on the Half-Auxetic Behavior of Layered Nitrogen-Doped Graphdiyne. Advances in Condensed Matter Physics, 2023, 12, 1-8.	0.1	0
77255	Dynamical Screening of Local Spin Moments at Metalâ€“Molecule Interfaces. ACS Nano, 2023, 17, 5974-5983.	7.3	2

#	Article	IF	Citations
77256	C₃N₂: the missing part of highly stable porous graphitic carbon nitride semiconductors. Nanoscale Horizons, 2023, 8, 662-673.	4.1	5
77257	Plurality of excitons in Ruddlesdenâ€“Popper metal halides and the role of the B-site metal cation. Materials Advances, 2023, 4, 1720-1730.	2.6	1
77258	Selective and effective oxidation of 5-hydroxymethylfurfural by tuning the intermediates adsorption on Co-Cu-CNx. Nano Research, 2023, 16, 6670-6678.	5.8	5
77259	Influence of Sr doping on the photoelectronic properties of CsPbX₃ (X = Cl, Br, or I): a DFT investigation. Physical Chemistry Chemical Physics, 2023, 25, 9592-9598.	1.3	3
77260	A New Spinel Chloride Solid Electrolyte with High Ionic Conductivity and Stability for Na-Ion Batteries. , 2023, 5, 1009-1017.		6
77261	Thickness-dependent catalytic activity of hydrogen evolution based on single atomic catalyst of Pt above MXene. Journal of Physics Condensed Matter, 2023, 35, 204001.	0.7	1
77262	Theoretical prediction of the electronic structure, optical properties and photocatalytic performance of type-I SiS/GeC and type-II SiS/ZnO heterostructures. RSC Advances, 2023, 13, 7436-7442.	1.7	4
77263	Firstâ€Principles Modeling of the Adsorption Mechanism of Carboxylic and Phosphonic Acids onto Pristine and Defective Delafossite CuAlO₂ Surfaces. Physica Status Solidi (B): Basic Research, 2023, 260, .	0.7	0
77264	Improved ductility of Mgâ€“3Gdâ€“0.6Zr alloy by cuboid-shaped phase: Experiments and first-principle calculations. Materials Science and Technology, 2023, 39, 1816-1826.	0.8	0
77265	Anomalous Photoluminescence Enhancement and Resonant Charge Transfer in Type-II 2D Lateral Heterostructures. Chinese Physics B, 0, , .	0.7	0
77266	Ruthenium doping in the MoS₂/AB heterostructure for the hydrogen evolution reaction in acidic media. Dalton Transactions, 2023, 52, 4891-4899.	1.6	2
77267	Electrically tunable Gilbert damping in van der Waals heterostructures of two-dimensional ferromagnetic metals and ferroelectrics. Applied Physics Letters, 2023, 122, .	1.5	3
77268	Development of Deep Potentials of Molten MgCl₂â€“NaCl and MgCl₂â€“KCl Salts Driven by Machine Learning. ACS Applied Materials & Interfaces, 0, , .	4.0	4
77269	Anharmonic phonon behavior via irreducible derivatives: Self-consistent perturbation theory and molecular dynamics. Physical Review B, 2023, 107, .	1.1	1
77270	High reactivity of mesoporous CeO₂ to dissociate chemical warfare agent sarin. Materials Chemistry Frontiers, 0, , .	3.2	0
77271	Quantum-mechanics-based molecular dynamics simulations of the structure and performance of sulfur-enriched Li3PS4 cathodes. Cell Reports Physical Science, 2023, 4, 101326.	2.8	1
77272	Tin Metal Improves the Lithiation Kinetics of High-Capacity Silicon Anodes. Chemistry of Materials, 2023, 35, 2281-2288.	3.2	3
77273	A New Anti-Alias Model of Ab Initio Calculations of the Generalized Stacking Fault Energy in Face-Centered Cubic Crystals. Crystals, 2023, 13, 461.	1.0	0

#	Article	IF	Citations
77274	First-Principles Examination of Multiple Criteria of Organic Solvent Oxidative Stability in Batteries. Chemistry of Materials, 2023, 35, 2518-2530.	3.2	4
77275	Data Mining and Graph Network Deep Learning for Band Gap Prediction in Crystalline Borate Materials. Inorganic Chemistry, 2023, 62, 4716-4726.	1.9	2
77276	In Situ Reaction Fabrication of a Mixedâ€Ion/Electronâ€Conducting Skeleton Toward Stable Lithium Metal Anodes. Energy and Environmental Materials, 2023, 6, .	7.3	2
77277	Universal Solid-Phase Seed-Mediated Synthesis of Monodisperse and Ultrasmall L1₀-PtM Intermetallic Nanocrystals. Chemistry of Materials, 2023, 35, 2559-2568.	3.2	6
77278	(n, m) Distribution of Single-Walled Carbon Nanotubes Grown from a Non-Magnetic Palladium Catalyst. Molecules, 2023, 28, 2453.	1.7	1
77279	Floquet Engineering of Nonequilibrium Valley-Polarized Quantum Anomalous Hall Effect with Tunable Chern Number. Nano Letters, 2023, 23, 2166-2172.	4.5	8
77280	Phase-Controllable Growth of Air-Stable SnS Nanostructures for High-Performance Photodetectors with Ultralow Dark Current. ACS Applied Materials & Interfaces, 0, , .	4.0	2
77282	Phase formation capability and compositional design of Î²-phase multiple rare-earth principal component disilicates. Nature Communications, 2023, 14, .	5.8	3
77283	Tungsten Oxide Mediated Quasi-van der Waals Epitaxy of WS₂ on Sapphire. ACS Nano, 2023, 17, 5399-5411.	7.3	8
77284	An automated reaction route mapping for the reaction of NO and active species on Ag₄ clusters in zeolites. Physical Chemistry Chemical Physics, 2023, 25, 8524-8531.	1.3	1
77285	Hydration at Highly Crowded Interfaces. Physical Review Letters, 2023, 130, .	2.9	1
77287	Ultrasound-triggered interfacial engineering-based microneedle for bacterial infection acne treatment. Science Advances, 2023, 9, .	4.7	23
77288	Computational studies on functionalized Janus MXenes MMâ€²CT₂, (M, Mâ€² = Zr, Ti, Hf, M â‰ Mâ€²; T) Tj ETQq0 0 0 rgB 2023, 13, 7972-7979.	1.7	3
77289	Coupling interface constructions of FeOOH/NiCo2S4 by microwave-assisted method for efficient oxygen evolution reaction. Rare Metals, 2023, 42, 1847-1857.	3.6	8
77290	WS₂ Transistors with Sulfur Atoms Being Replaced at the Interface: First-Principles Quantum-Transport Study. ACS Omega, 2023, 8, 10419-10425.	1.6	2
77291	Water Oxidation-Induced Surface Reconstruction and Dissolution at the RuO₂(110) Surface Revealed by First-Principles Simulation. Journal of Physical Chemistry C, 2023, 127, 5334-5342.	1.5	7
77292	Profiling the off-center atomic displacements in CuCl at finite temperatures with a deep-learning potential. Physical Review Materials, 2023, 7, .	0.9	0
77293	Tuning the mechanical anisotropy of biphenylene by boron and nitrogen doping. Computational Materials Science, 2023, 222, 112119.	1.4	5

#	Article	IF	Citations
77294	Stability of sulfur molecules and insights into sulfur allotropy. Physical Chemistry Chemical Physics, 2023, 25, 9294-9299.	1.3	4
77295	Red Emission from Copper-Vacancy Color Centers in Zinc Sulfide Colloidal Nanocrystals. ACS Nano, 2023, 17, 5963-5973.	7.3	3
77296	First-Principles Study of the Effects of Ti Content on Mechanical Properties and Microscopic Mechanism in Cu2AlMn1â€“xTix Alloys. Crystals, 2023, 13, 466.	1.0	0
77297	Economically viable electrocatalytic ethylene production with high yield and selectivity. Nature Sustainability, 2023, 6, 827-837.	11.5	13
77298	Molecular switching on surfaces. Surface Science Reports, 2023, 78, 100596.	3.8	6
77299	â€œOne Stone Five Birdsâ€•Plasma Activation Strategy Synergistic with Ru Single Atoms Doping Boosting the Hydrogen Evolution Performance of Metal Hydroxide. Advanced Functional Materials, 2023, 33, .	7.8	22
77300	Hybrid Functional-Based Scissors Operator for Perovskite Oxide Nanostructures: A NaTaO₃ Case Study. Journal of Physical Chemistry C, 2023, 127, 5604-5612.	1.5	0
77301	SiCO Ceramics as Storage Materials for Alkali Metals/Ions: Insights on Structure Moieties from Solidâ€State NMR and DFT Calculations. ChemSusChem, 2023, 16, .	3.6	0
77302	Crystalline phase transformation of Co-MOF derivatives on ordered mesoporous carbons for high-performance supercapacitor applications. CrystEngComm, 2023, 25, 1941-1950.	1.3	2
77303	Spinâ€“Orbit Coupling Notably Retards Non-radiative Electronâ€“Hole Recombination in Methylammonium Lead Triiodide Perovskites. Journal of Physical Chemistry Letters, 2023, 14, 2715-2721.	2.1	8
77304	Efficient discovery of multiple minimum action pathways using Gaussian process. Journal of Physics Communications, 2023, 7, 025004.	0.5	0
77305	The structural and thermodynamic properties of CaLi₂ at high pressure. International Journal of Modern Physics C, 0, , .	0.8	0
77306	Asymmetric Janus functionalization induced magnetization and switchable out-of-plane polarization in 2D MXene Mo₂CXXâ€². Physical Chemistry Chemical Physics, 2023, 25, 8676-8683.	1.3	3
77307	Experimental and ab initio Investigation on the Effect of CO and CO₂ during Hydrodeoxygenation of mâ€Cresol over Co/SBAâ€15. ChemCatChem, 2023, 15, .	1.8	0
77308	Strain-induced dark exciton generation in rippled monolayer MoS₂. Physical Chemistry Chemical Physics, 2023, 25, 9894-9900.	1.3	1
77309	A two-dimensional tetragonal structure of vanadium telluride. Nano Research, 0, , .	5.8	0
77310	Pentagonal C_mX_nY_{6â€“mâ€“n} (m =) Tj ETQq0 0 0 rgBT /Over Poisson Ratios with Giant Piezoelectric Effects. Journal of Physical Chemistry Letters, 2023, 14, 2692-2701.	2.1	2
77311	Nanoscale Hydrophobicity and Electrochemical Mapping Provides Insights into Facet Dependent Silver Nanoparticle Dissolution. Journal of Physical Chemistry Letters, 2023, 14, 2665-2673.	2.1	0

#	Article	IF	Citations
77312	Single-crystalline van der Waals layered dielectric with high dielectric constant. Nature Materials, 2023, 22, 832-837.	13.3	26
77313	Investigation of Rechargeable Calcium Metal-Selenium Batteries Enabled by Borate-Based Electrolytes. Chemistry of Materials, 2023, 35, 2363-2370.	3.2	5
77314	Insights into the Origin of High Activity of Ni₅P₄(0001) for Hydrogen Evolution Reaction. Journal of Physical Chemistry C, 2023, 127, 5385-5394.	1.5	8
77315	Valence Band Structure Degeneracy Enhanced Thermoelectric Performance in Î²-Cu₂Se. Journal of Physical Chemistry C, 2023, 127, 5576-5583.	1.5	3
77316	Copper Cobalt Selenide as a Bifunctional Electrocatalyst for the Selective Reduction of CO₂ to Carbon-Rich Products and Alcohol Oxidation. ACS Applied Materials & Interfaces, 0, , .	4.0	4
77317	Native point defects in antiperovskite Ba₃SbN: a promising semiconductor for photovoltaics. Physical Chemistry Chemical Physics, 2023, 25, 9800-9806.	1.3	2
77318	Emergence of bond-dependent highly anisotropic magnetic interactions in <mml:math xmlns:mml="http://www.w3.org/1998/Math/MathML"><mml:mrow><mml:msub><mml:mi>Sr</mml:mi><mml:mn>1</mml:mn> : A theoretical study. Physical Review B, 2023, 107, .	1.1	0
77319	The Inducement and â€œRejuvenationâ€•of Li Dendrites by Space Confinement and Positive Fe/Coâ€Sites. Small, 2023, 19, .	5.2	4
77320	Highly in-plane anisotropic optical properties of fullerene monolayers. Science China: Physics, Mechanics and Astronomy, 2023, 66, .	2.0	5
77321	Mechanochemical synthesis and structural evaluation of a metastable polymorph of Ti₃Sn. Zeitschrift Fur Naturforschung - Section B Journal of Chemical Sciences, 2023, 78, 209-214.	0.3	0
77322	Theoretical exploration on the activity of copper single-atom catalysts for electrocatalytic reduction of CO₂. Journal of Materials Chemistry A, 2023, 11, 7735-7745.	5.2	8
77323	Distilling universal activity descriptors for perovskite catalysts from multiple data sources via multi-task symbolic regression. Materials Horizons, 2023, 10, 1651-1660.	6.4	4
77324	Boosting Pseudocapacitive Behavior of Supercapattery Electrodes by Incorporating a Schottky Junction for Ultrahigh Energy Density. Nano-Micro Letters, 2023, 15, .	14.4	21
77325	Strongly Correlated Electronic Properties of FeO Studied by the SCAN+U Functional. Journal of Physical Chemistry C, 2023, 127, 5513-5518.	1.5	1
77327	A general-purpose machine learning Pt interatomic potential for an accurate description of bulk, surfaces, and nanoparticles. Journal of Chemical Physics, 2023, 158, .	1.2	6
77328	A DFT study of structural and electronic properties of some B₁₂-based compounds under hydrostatic pressure. Physica Scripta, 2023, 98, 045907.	1.2	0
77329	First-principles density functional calculations for non-lead perovskites. , 2023, , .		0
77330	Engineering the catalytic properties of CeO2 catalyst in HCl-assisted propane dehydrogenation by effective doping: A first-principles-based microkinetic simulation. Frontiers in Chemistry, 0, 11, .	1.8	0

#	Article	IF	Citations
77331	Roomâ€Temperature Magnetism in 2D MnGa₄â€H Induced by Hydrogen Insertion. Advanced Materials, 2023, 35, .	11.1	5
77332	AisNet: A Universal Interatomic Potential Neural Network with Encoded Local Environment Features. Journal of Chemical Information and Modeling, 2023, 63, 1756-1765.	2.5	1
77334	Superconductivity in <mml:math xmlns:mml="http://www.w3.org/1998/Math/MathML"><mml:mrow><mml:msub><mml:mi>Li</mml:mi><mml:mn>x</mml:mn></mml:msub><mml:mi>Mo</mml:mi><mml:mn>6</mml:mn></mml:mrow></mml:math> electride. Physical Review B, 2023, 107, .	3.1	8
77335	The Significance of an In Situ ALD Al₂O₃ Stacked Structure for pâ€Type SnO TFT Performance and Monolithic Allâ€ALDâ€Channel CMOS Inverter Applications. Advanced Electronic Materials, 2023, 9, .	2.6	3
77336	Depolarization induced IIIâ€“V triatomic layers with tristable polarization states. Nanoscale Horizons, 2023, 8, 616-623.	4.1	1
77337	Bottom-Up Synthesis of Metalated Carbyne Ribbons via Elimination Reactions. Journal of the American Chemical Society, 2023, 145, 6203-6209.	6.6	0
77338	Multiphoton excited singlet/triplet mixed self-trapped exciton emission. Nature Communications, 2023, 14, .	5.8	10
77339	Band Structure Engineering of MXenes for Lowâ€Loss Visible Epsilonâ€Nearâ€Zero Properties by Firstâ€Principles Calculation. Advanced Electronic Materials, 2023, 9, .	2.6	0
77340	Smoothing Energy Transfer Enabling Efficient Largeâ€Area Quasiâ€2D Perovskite Lightâ€Emitting Diodes. Laser and Photonics Reviews, 2023, 17, .	4.4	1
77341	A multi-layered graphene based gas sensor platform for discrimination of volatile organic compounds via differential intercalation. Journal of Materials Chemistry C, 2023, 11, 4703-4710.	2.7	0
77342	BSSEâ€corrected consistent Gaussian basis sets of tripleâ€zeta valence quality of the lanthanides <scp>Laâ€Lu</scp> for solidâ€state calculations. Journal of Computational Chemistry, 2023, 44, 1418-1425.	1.5	1
77343	Acetyleneâ€Mediated Borophosphene Dirac Materials as Efficient Anode Materials for Lithiumâ€Ion Batteries. ChemPhysChem, 2023, 24, .	1.0	2
77344	Electrochemical Reduction of Nitrates on CoO Nanoclustersâ€Functionalized Graphene with Highest Mass Activity and Nearly 100% Selectivity to Ammonia. Advanced Energy Materials, 2023, 13, .	10.2	22
77345	Topological insulator Bi2Se3 for highly sensitive, selective and anti-humidity gas sensors. IScience, 2023, 26, 106387.	1.9	3
77346	Single transition metal atom centered clusters activating semiconductor surface lattice atoms for efficient solar fuel production. Journal of Materials Chemistry A, 2023, 11, 7746-7755.	5.2	2
77347	Controlled synthesis of monodispersed ZnSe microspheres for enhanced photo-catalytic application and its corroboration using density functional theory. Physical Chemistry Chemical Physics, 2023, 25, 10567-10582.	1.3	1
77348	From high-entropy alloys to high-entropy ceramics: The radiation-resistant highly concentrated refractory carbide (CrNbTaTiW)C. Acta Materialia, 2023, 250, 118856.	3.8	16
77349	Degradation of Methylene Blue by Hot Electrons Transfer in SnSe. Advanced Materials Interfaces, 2023, 10, .	1.9	1

#	Article	IF	Citations
77350	Ensemble Effect of Ruthenium Single-Atom and Nanoparticle Catalysts for Efficient Hydrogen Evolution in Neutral Media. ACS Applied Materials & Interfaces, 0, , .	4.0	0
77351	Nontrivial role of polar optical phonons in limiting electron mobility of two-dimensional Ga₂O₃ from first-principles. Physical Chemistry Chemical Physics, 2023, 25, 10175-10183.	1.3	1
77352	Symbolic Regression in Materials Science: Discovering Interatomic Potentials from Data. Genetic and Evolutionary Computation, 2023, , 1-30.	1.0	1
77353	Symmetry-dependent antiferromagnetic proximity effects on valley splitting. Physical Review B, 2023, 107, .	1.1	0
77354	Theoretical investigation of charge transfer between two defects in a wide band gap semiconductor. Physical Review B, 2023, 107, .	1.1	1
77355	Decreased spin-resolved anti-bonding states filling to accelerate CHO conversion into CH₂O in transitional metal-doped Mo₂C monolayers during CO₂ reduction. Journal of Materials Chemistry A, 0, , .	5.2	0
77356	Search for semiconducting materials among 18-electron half-Heusler alloys. Solid State Communications, 2023, 364, 115133.	0.9	4
77357	Ultralow diffusion barrier induced by intercalation in layered N-based cathode materials for sodium-ion batteries. RSC Advances, 2023, 13, 8182-8189.	1.7	1
77358	Neural network potentials for accelerated metadynamics of oxygen reduction kinetics at Auâ€“water interfaces. Chemical Science, 2023, 14, 3913-3922.	3.7	8
77359	Charge Trapping and Emission Properties in CAAC-IGZO Transistor: A First-Principles Calculations. Materials, 2023, 16, 2282.	1.3	2
77360	Supramolecular tuning of supported metal phthalocyanine catalysts for hydrogen peroxide electrosynthesis. Nature Catalysis, 2023, 6, 234-243.	16.1	51
77361	Divalent organic cations as a novel protective layer for perovskite materials. Journal of Materials Chemistry A, 2023, 11, 11684-11695.	5.2	3
77362	Theoretical insights into the support effect on the NO activation over platinum-group metal catalysts. Journal of Chemical Physics, 2023, 158, .	1.2	2
77363	Promoterâ€“Poison Partnership Protects Platinum Performance in Coked Cluster Catalysts. Journal of Physical Chemistry C, 2023, 127, 5376-5384.	1.5	0
77364	Nucleation Stage for the Oriented Growth of Tantalum Sulfide Monolayers on Au(111). Journal of Physical Chemistry C, 2023, 127, 5622-5630.	1.5	0
77365	Mechanisms of adsorbing hydrogen gas on metal decorated graphene. Physical Review Materials, 2023, 7, .	0.9	2
77366	Unraveling the Detailed Interactions between the Surface Species and Nanoparticle Catalyst by a Temperature-Programed Desorption Spectrum at the Molecular Level via a Multi-Scale Simulation and Modeling Experiment. Journal of Physical Chemistry C, 2023, 127, 5299-5307.	1.5	0
77367	Systematic atomic structure datasets for machine learning potentials: Application to defects in magnesium. Physical Review B, 2023, 107, .	1.1	6

#	Article	IF	Citations
77368	Visibleâ€lightâ€responsive Photocatalyst Based on Nitrogenâ€doped Bulk Oxide YTaO_{4â^’x}N_y for Zâ€scheme Overall Water Splitting. Chemistry - an Asian Journal, 2023, 18, .	1.7	4
77369	Computational Modelling of Pyrrolic MN4 Motifs Embedded in Graphene for Catalyst Design. Catalysts, 2023, 13, 566.	1.6	1
77370	High temperature ferromagnetic metal: a Janus CrSSe monolayer. Physical Chemistry Chemical Physics, 2023, 25, 9958-9964.	1.3	6
77371	PEA2PbI4: fast two-dimensional lead iodide perovskite scintillator with green and red emission. Materials Today Chemistry, 2023, 29, 101455.	1.7	6
77372	Ferroelectric polarization and interface engineering coupling of Z-scheme ZnIn2S4/Î±-In2Se3 heterostructure for efficient photocatalytic water splitting. Journal of Applied Physics, 2023, 133, .	1.1	1
77373	Topological band inversion in HgTe(001): Surface and bulk signatures from photoemission. Physical Review B, 2023, 107, .	1.1	0
77374	Stable Mo/1T-MoS₂ Monolith Catalyst with a Metallic Interface for Large Current Water Splitting. ACS Applied Materials & Interfaces, 0, , .	4.0	0
77375	Theoretical study on hydrogen evolution reaction in transition metal borides. Rare Metals, 2023, 42, 1808-1812.	3.6	2
77376	The Effect of Cr Additive on the Mechanical Properties of Ti-Al Intermetallics by First-Principles Calculations. Crystals, 2023, 13, 488.	1.0	1
77377	Quantum Catalytic Performance for the Hydrogen Evolution Reaction and the Ethanol Oxidation Reaction in Topological Edge States of SrPd and BaPd Semimetal Monolayers: A Theoretical Study. Journal of Physical Chemistry C, 2023, 127, 5271-5280.	1.5	2
77378	Fluence dependent dynamics of excitons in monolayer MoSi₂Z₄ (Z =) Tj ETQq0 0 0 rgBT /Overlock 10 Tf 50 34	0.7	4
77379	Two-dimensional layered Dionâ€“Jacobson phase organicâ€“inorganic tin iodide perovskite field-effect transistors. Journal of Materials Chemistry A, 2023, 11, 7767-7779.	5.2	11
77380	Subsurface Li Monolayer on Cu(111) Surfaces for Upgrading Ethanol to n-Butanol: A Computational Study. ACS Applied Nano Materials, 2023, 6, 7156-7165.	2.4	0
77381	Unraveling oxygen vacancy site mechanism of Rh-doped RuO2 catalyst for long-lasting acidic water oxidation. Nature Communications, 2023, 14, .	5.8	63
77382	The Temperature Dependence of the Hexagonal Boron Nitride Oxidation Resistance, Insights from Firstâ^’Principle Computations. Nanomaterials, 2023, 13, 1041.	1.9	1
77383	Probing Local Environments of Oxygen Vacancies Responsible for Hydration in Sc-Doped Barium Zirconates at Elevated Temperatures: In Situ X-ray Absorption Spectroscopy, Thermogravimetry, and Active Learning Ab Initio Replica Exchange Monte Carlo Simulations. Chemistry of Materials, 2023, 35, 2289-2301.	3.2	3
77384	Theoretical Assessment of the Mechanism and Active Sites in Alkene Dimerization on Ni Monomers Grafted onto Aluminosilicates: (Niâ€“OH)⁺ Centers and Câ€“C Coupling Mediated by Lewis Acidâ€“Base Pairs. Journal of the American Chemical Society, 2023, 145, 6349-6361.	6.6	8
77385	Highâ€rate Decoupled Water Electrolysis System Integrated with Î±â€MoO₃ as a Redox Mediator with Fast Anhydrous Proton Kinetics. Advanced Functional Materials, 2023, 33, .	7.8	4

#	Article	IF	Citations
77386	Structure and Growth Mechanism of the 2D Ice on the Hydrophobic Metal Surface. Springer Theses, 2023, , 45-72.	0.0	0
77387	Magnetic proximity effect in LaO/EuO heterostructures: A first-principles study. Physical Review B, 2023, 107, .	1.1	0
77388	Simulating Highly Activated Sticking of H₂ on Al(110): Quantum versus Quasi-Classical Dynamics. Journal of Physical Chemistry C, 2023, 127, 5395-5407.	1.5	1
77389	A DFT study on how vanadium affects hydrogen storage kinetics in magnesium nickel hydride. International Journal of Hydrogen Energy, 2023, 48, 20378-20387.	3.8	2
77390	Electrical conductivity of iron in Earth's core from microscopic Ohm's law. Physical Review B, 2023, 107, .	1.1	8
77391	A theoretical study of the NbS₂ monolayer as a promising anchoring material for lithiumâ€“sulfur batteries. Physical Chemistry Chemical Physics, 2023, 25, 10097-10102.	1.3	4
77392	Understanding the activity of single atom catalysts for CO₂ reduction to C₂ products: A high throughput computational screening. New Journal of Chemistry, 2023, 47, 7225-7231.	1.4	4
77393	Structure and Dynamics of Ion Hydrates on NaClÂsurface. Springer Theses, 2023, , 107-135.	0.0	0
77394	Predicted bismuthâ€“tellurium under high pressures. Phase Transitions, 2023, 96, 328-336.	0.6	1
77395	Recipe for higher order topology on the triangular lattice. Physical Review B, 2023, 107, .	1.1	0
77396	Structure and Bonding in Amorphous Red Phosphorus**. Angewandte Chemie - International Edition, 2023, 62, .	7.2	3
77397	Band alignment at the strontium germanate interface with silicon. Physical Review B, 2023, 107, .	1.1	0
77398	Interconversion of the Eigen/Zundel Cations on Metal Surfaces. Springer Theses, 2023, , 73-106.	0.0	0
77399	Magnetism in curved VSe₂ monolayers. RSC Advances, 2023, 13, 8307-8316.	1.7	0
77400	Synthesis and Characterization of the Orthorhombic Sn₃O₄ Polymorph. Angewandte Chemie, 2023, 135, .	1.6	0
77401	Synthesis and Characterization of the Orthorhombic Sn₃O₄ Polymorph. Angewandte Chemie - International Edition, 2023, 62, .	7.2	7
77402	Structural and thermodynamic properties of quasi-2D Mo_(1â€“x)W_x(S, Se,) Tj ETQq0 0 0 rgBT /Overlock 10	1.3	1
77403	Struktur und Bindung im amorphen roten Phosphor**. Angewandte Chemie, 2023, 135, .	1.6	0

#	Article	IF	Citations
77404	Graphene Capping of Cu Back-End-of-Line Interconnects Reduces Resistance and Improves Electromigration Lifetime. ACS Applied Nano Materials, 2023, 6, 4170-4177.	2.4	3
77405	Sustainable methane utilization technology via photocatalytic halogenation with alkali halides. Nature Communications, 2023, 14, .	5.8	7
77406	Computational Design and Theoretical Properties of WC₃N₆, an H-Free Melaminate and Potential Multifunctional Material. Journal of the American Chemical Society, 2023, 145, 6986-6993.	6.6	6
77407	Rationally Integrating 2D Confinement and High Sodiophilicity toward SnO₂/Ti₃C₂T_x Composites for Highâ€Performance Sodiumâ€Metal Anodes. Small, 2023, 19, .	5.2	5
77408	Computational Investigation of Precursor Blocking during Area-Selective Atomic Layer Deposition Using Aniline as a Small-Molecule Inhibitor. Langmuir, 2023, 39, 4265-4273.	1.6	2
77409	Tensile strain and finite size modulation of low lattice thermal conductivity in monolayer TMDCs (HfSe₂ and ZrS₂) from first-principles: a comparative study. Physical Chemistry Chemical Physics, 2023, 25, 9225-9237.	1.3	6
77410	Ab Initio Siteâ€Selective Occupancy and Luminescence Enhancement in Broadband NIR Emitting Phosphor Mg₇Ga₂GeO₁₂:Cr³⁺. Laser and Photonics Reviews, 2023, 17, .	4.4	37
77411	Improvement of carbon dioxide electroreduction by crystal surface modification of ZIF-8. Dalton Transactions, 2023, 52, 5234-5242.	1.6	2
77412	Emergent second-harmonic generation in van der Waals heterostructure of bilayer MoS ₂ and monolayer graphene. Science Advances, 2023, 9, .	4.7	6
77413	Selective Photochromic Response to Low-Dose X-ray Radiation Detection in One-Dimensional Cadmium-Viologen Complexes. Inorganic Chemistry, 2023, 62, 4990-4998.	1.9	9
77414	An effective strategy for CO₂ reduction to C1 products using Cu-embedded MoS₂ electrocatalyst: DFT study. New Journal of Chemistry, 2023, 47, 6932-6942.	1.4	2
77415	Temperature dependence of carrier mobility in hydrogenated germanane field-effect transistor with various electrode materials. Japanese Journal of Applied Physics, 2023, 62, 030905.	0.8	0
77416	Metal-organic frameworks for nanoconfinement of chlorine in rechargeable lithium-chlorine batteries. Joule, 2023, 7, 515-528.	11.7	21
77417	Predicting thermoelectric transport properties from composition with attention-based deep learning. Machine Learning: Science and Technology, 2023, 4, 015037.	2.4	2
77418	Electronic density response of warm dense matter. Physics of Plasmas, 2023, 30, .	0.7	23
77419	In-plane anisotropy in van der Waals epitaxial MoS2 on MoO2(010). Applied Physics Letters, 2023, 122, .	1.5	1
77420	Extended phase homogeneity and improved out-of-plane charge transfer in Sb and Te co-alloyed n-type BiSe layered compound with extraordinary thermoelectric performance. Materials Today Physics, 2023, 33, 101047.	2.9	2
77421	Methanol Synthesis on Copper-Doped F Centers. Journal of Physical Chemistry C, 2023, 127, 5321-5333.	1.5	0

#	Article	IF	Citations
77422	Single atom modified two-dimensional bismuthenes for toxic gas detection. Physical Chemistry Chemical Physics, 2023, 25, 9249-9255.	1.3	4
77423	Study of pnictides for photovoltaic applications. Physical Chemistry Chemical Physics, 2023, 25, 9626-9635.	1.3	1
77424	Atomically Sharp Internal Interface in a Chiral Weyl Semimetal Nanowire. Nano Letters, 2023, 23, 2695-2702.	4.5	6
77425	Polytypism of Ln(SeO₃)(HSeO₃)·2H₂O compounds: synthesis and crystal structure of the first monoclinic modification of Nd(SeO₃)(HSeO₃)·2H₂O, DFT calculations and order/disorder description. Acta Crystallographica Section B: Structural Science, Crystal Engineering and Materials, 2023, 79, 176-183.	0.5	2
77426	Efficient magnetization reversal by self-generated spin–orbit torque in magnetic bulk Rashba materials. Applied Physics Letters, 2023, 122, .	1.5	1
77427	Ab initio investigation of Bi/BaTiO₃ and Bi/PbTiO₃ heterostructures for spintronic applications. Ferroelectrics, 2023, 605, 27-35.	0.3	1
77428	Machine learned interatomic potential for dispersion strengthened plasma facing components. Journal of Chemical Physics, 2023, 158, .	1.2	7
77429	The ion equation of state of plasmas in the warm dense matter regime. AIP Advances, 2023, 13, 035223.	0.6	0
77430	Lead-Free Solid State Mechanochemical Synthesis of Cs₂NaBi_{1–x}Fe_xCl₆ Double Perovskite: Reduces Band Gap and Enhances Optical Properties. Inorganic Chemistry, 2023, 62, 4861-4871.	1.9	8
77431	Investigating the role of phonons in the phase stability of uranium-based Laves phases. RSC Advances, 2023, 13, 8646-8656.	1.7	2
77432	Structural and physical properties of hydroxyapatite modified by Sr/Ca substitutions. Ferroelectrics, 2023, 605, 117-128.	0.3	2
77433	Coupling Ternary Selenide SnSb₂Se₄ with Graphene Nanosheets for High‐Performance Potassium‐Ion Batteries. Energy and Environmental Materials, 2023, 6, .	7.3	9
77434	Thermodynamic analysis of the interaction between metal vacancies and hydrogen in bulk Cu. Physical Chemistry Chemical Physics, 2023, 25, 9168-9175.	1.3	5
77435	Hot carrier relaxation dynamics in non-stoichiometric CdSe quantum dots: computational insights. Journal of Materials Chemistry A, 2023, 11, 8256-8264.	5.2	4
77436	Cd implantation in <mml:math xmlns:mml="http://www.w3.org/1998/Math/MathML"><mml:mrow><mml:mi>Î±</mml:mi><mml:mtext>â^'</mml:mtext><mml:msub><: An atomic scale study. Physical Review Materials, 2023, 7, .	0.0	0
77437	Theoretical design of a photodetector based on a two-dimensional SnSe₂/GaP type-II heterostructure. CrystEngComm, 2023, 25, 2326-2338.	1.3	0
77438	Accelerating self-consistent field iterations in Kohn-Sham density functional theory using a low-rank approximation of the dielectric matrix. Physical Review B, 2023, 107, .	1.1	2
77439	In Situ Structure of a Mo-Doped Pt–Ni Catalyst during Electrochemical Oxygen Reduction Resolved from Machine Learning-Based Grand Canonical Global Optimization. Jacs Au, 2023, 3, 1162-1175.	3.6	7

#	Article	IF	Citations
77440	Biâ€Deficiency Leading to Highâ€Performance in Mg₃(Sb,Bi)₂â€Based Thermoelectric Materials. Advanced Materials, 2023, 35, .	11.1	6
77441	First-principles simulations of liquid iron-heavy element alloys at high pressure. Physics of the Earth and Planetary Interiors, 2023, 337, 107008.	0.7	0
77443	Intercalation of p-Aminopyridine and p-Ethylenediamine Molecules into Orthorhombic In1.2Ga0.8S3 Single Crystals. Materials, 2023, 16, 2368.	1.3	1
77444	One-Dimensional Periodic Buckling at a Symmetry-Incompatible Heterointerface of the NaCl(001) Monolayer on Ir(111). Journal of Physical Chemistry C, 2023, 127, 6109-6114.	1.5	1
77445	Thermoelectric response of single quintuple layer sodium copper chalcogenides persisting at high temperature. Physical Chemistry Chemical Physics, 2023, 25, 10082-10089.	1.3	1
77446	Low-rank approximations for accelerating plane-wave hybrid functional calculations in unrestricted and noncollinear spin density functional theory. Journal of Chemical Physics, 2023, 158, .	1.2	4
77447	Quintuple Function Integration in Two-Dimensional Cr(II) Five-Membered Heterocyclic Metal Organic Frameworks via Tuning Ligand Spin and Lattice Symmetry. Journal of the American Chemical Society, 2023, 145, 7869-7878.	6.6	14
77448	Heterogeneous intercalated metal-organic framework active materials for fast-charging non-aqueous Li-ion capacitors. Nature Communications, 2023, 14, .	5.8	8
77449	Novel tungsten nitride crystal providing nanochannels for hydrogen removal and recycling in PFMs. Journal of Chemical Physics, 2023, 158, 124125.	1.2	0
77450	New Insights on the Tensile Strength and Fracture Mechanism of c-ZrO2/Î±-Al2O3 Interfaces. Applied Sciences (Switzerland), 2023, 13, 3742.	1.3	0
77452	Engineering electrode/electrolyte interface charge transfer of a TiO_{2â^'x} photoanode with enriched surface oxygen vacancies for efficient water splitting. Reaction Chemistry and Engineering, 0, , .	1.9	0
77453	Controlled Surface Modification to Revive Shallow NV^{â€“} Centers. Nano Letters, 2023, 23, 2563-2569.	4.5	4
77454	Sustainable upcycling of spent LiCoO2 to an ultra-stable battery cathode at high voltage. Nature Sustainability, 2023, 6, 797-805.	11.5	52
77455	Phase transition, optical, and elastic properties of a new hybrid organicâ€“inorganic perovskite: [(R)-(+)-3-aminoquinuclidine]KI3. APL Materials, 2023, 11, .	2.2	2
77456	Quantum paraelectricity and structural phase transitions in strontium titanate beyond density functional theory. Physical Review Materials, 2023, 7, .	0.9	11
77457	Matrix transformation of lunar regolith and its use as a feedstock for additive manufacturing. IScience, 2023, 26, 106382.	1.9	2
77458	Lattice dynamics and in-plane antiferromagnetism in <mml:math xmlns:mml="http://www.w3.org/1998/Math/MathML"><mml:mrow><mml:msub><mml:mi>Mn</mml:mi><mml:mi>x</mml:mi></mml:m across the entire composition range. Physical Review B, 2023, 107, .	1.1	1
77459	Critical interphase overpotential as a lithium dendrite-suppression criterion for all-solid-state lithium battery design. Nature Energy, 2023, 8, 473-481.	19.8	38

#	Article	IF	Citations
77460	Spin-phonon interaction and short-range order in <mml:math xmlns:mml="http://www.w3.org/1998/Math/MathML"><mml:mrow><mml:msub><mml:mi>Mn</mml:mi><mml:mn>3</mml:mn></mml:msub></mml:mrow></mml:math>. Physical Review B, 2023, 107, .	1.3	2
77461	Absorption Modulation and Anomalous Thermal Transport in Two-dimensional X-AlN(X=C,Si,TC) Semiconductor. Wuli Xuebao/Acta Physica Sinica, 2023, .	0.2	0
77462	Unveiling positive impacts of fluorine anion doping on extraordinary catalytic activity of bifunctional-layered double perovskite electrodes for solid oxide fuel cells and electrolysis cells. Materials Today Chemistry, 2023, 29, 101469.	1.7	3
77463	Single-atom vibrational spectroscopy with chemical-bonding sensitivity. Nature Materials, 2023, 22, 612-618.	13.3	10
77464	Bridging Synthesis and Controllable Doping of Monolayer 4 in. Length Transitionâ€Metal Dichalcogenides Single Crystals with High Electron Mobility. Advanced Materials, 2023, 35, .	11.1	8
77465	Quantitative Evaluation of the Carrier Separation Performance of Heterojunction Photocatalysts: The Case of g-C₃N₄/SrTiO₃. Journal of Physical Chemistry Letters, 2023, 14, 2927-2932.	2.1	1
77466	Co-deposition of hole-selective contact and absorber for improving the processability of perovskite solar cells. Nature Energy, 2023, 8, 462-472.	19.8	43
77467	First-principles study of ferroelectricity, antiferroelectricity, and ferroelasticity in two-dimensional <mml:math xmlns:mml="http://www.w3.org/1998/Math/MathML"><mml:mi>Î³</mml:mi></mml:math>-AlOOH. Physical Review B, 2023, 107, .	1.1	6
77468	The axial ligands optimized activity of CO2 electroreduction to CO over penta-coordinated single atom ironâ€“nitrogenâ€“carbon catalysts. Materials Today Chemistry, 2023, 29, 101461.	1.7	3
77469	Enhanced Curie temperature in partially decorated CrSnSe₃ monolayer with alkali metals (Li, Na, and K). Physical Chemistry Chemical Physics, 2023, 25, 9437-9444.	1.3	0
77470	Frequency Splitting of Chiral Phonons from Broken Time-Reversal Symmetry in <mml:math xmlns:mml="http://www.w3.org/1998/Math/MathML" display="inline"><mml:mrow><mml:msub><mml:mrow><mml:mi>CrI</mml:mi></mml:mrow><mml:mrow><mml:mn>3</mml:mn></mml:mrow></mml:msub></mml:mrow></mml:math>. Physical Review Letters, 2023, 130, .	2.9	7
77471	Antiferromagnetic <mml:math xmlns:mml="http://www.w3.org/1998/Math/MathML"><mml:mrow><mml:mi>Fe</mml:mi><mml:msub><mml:mi>Te</mml:mi><mml:mi>m</mml:mi></mml:msub></mml:mrow></mml:math> formation at the <mml:math xmlns:mml="http://www.w3.org/1998/Math/MathML"><mml:mrow><mml:msub><mml:mi>Sb</mml:mi><mml:mn>2</mml:mn></mml:msub></mml:mrow></mml:math>. Physical Review Materials, 2023, 7, .	0.9	0
77472	Water adsorption on lead dioxide from abÂinitio molecular dynamics simulations. Journal of Chemical Physics, 2023, 158, .	1.2	1
77473	Phosphorus Optimized Metastable Hexagonalâ€Closeâ€Packed Phase Nickel for Efficient Hydrogen Peroxide Production in Neutral Media. Advanced Functional Materials, 2023, 33, .	7.8	6
77474	A van der Waals Heterostructure with an Electronically Textured MoirÃ© Pattern: PtSe₂/PtTe₂. ACS Nano, 2023, 17, 5913-5920.	7.3	1
77475	Trap-limited diffusion of Zn in <mml:math xmlns:mml="http://www.w3.org/1998/Math/MathML"><mml:mrow><mml:mi>Î²</mml:mi><mml:mtext>â€²</mml:mtext><mml:msub><mathvariant="normal">O</mml:mi><mml:mn>3</mml:mn></mml:msub></mml:math>. Physical Review Materials, 2023, 7, .	0.9	1
77476	Early melting of tantalum carbide under anisotropic stresses: An <mml:math xmlns:mml="http://www.w3.org/1998/Math/MathML"><mml:mrow><mml:mi>a</mml:mi><mml:mi>b</mml:mi></mml:mrow></mml:math> <mml:math xmlns:mml="http://www.w3.org/1998/Math/MathML"><mml:mrow><mml:mi>i</mml:mi><mml:mi>n</mml:mi><mml:mi>i</mml:mi></mml:math> molecular dynamics study. Physical Review B, 2023, 107, .	1.1	4
77477	Investigation of the Interaction Between Au and Brookite TiO2 Using Transmission Electron Microscopy and Density Functional Theory. Bulletin of the Chemical Society of Japan, 2023, 96, 373-380.	2.0	3

#	Article	IF	Citations
77478	Computational Discovery of Active and Selective Metalâ€Nitrogenâ€Graphene Catalysts for Electrooxidation of Water to H₂O₂. ChemCatChem, 2023, 15, .	1.8	0
77479	The effects of point defects on thermal-mechanical properties of BiCuOTe: a first-principles study. Physical Chemistry Chemical Physics, 2023, 25, 10715-10725.	1.3	1
77480	Nitrogen and sulfur co-doped Ti₃C₂T_x MXenes for high-rate lithium-ion batteries. Physical Chemistry Chemical Physics, 2023, 25, 10635-10646.	1.3	2
77481	The charge effects on the hydrogen evolution reaction activity of the defected monolayer MoS₂. Physical Chemistry Chemical Physics, 2023, 25, 10956-10965.	1.3	5
77482	Tunable Electronic Properties of Substitutionally Doped CSb Monolayer. Physica Status Solidi - Rapid Research Letters, 0, , .	1.2	0
77483	Revealing the impact of organic spacers and cavity cations on quasi-2D perovskites via computational simulations. Scientific Reports, 2023, 13, .	1.6	0
77484	Approaching the free-ion limit in magnetically isotropic gadolinium(<scp>iii</scp>) via borohydride ligands. Physical Chemistry Chemical Physics, 2023, 25, 10689-10696.	1.3	1
77485	Doping- and strain-tuned high Curie temperature half-metallicity and quantum anomalous Hall effect in monolayer <mml:math xmlns:mml="http://www.w3.org/1998/Math/MathML"><mml:mrow><mml:msub><mml:mi>NiAl</mml:mi><mml:mn>2</mml:mn></mml:msub><mml:msub><mml:mi mathvariant="normal">S</mml:mi><mml:mn>4</mml:mn></mml:msub></mml:mrow></mml:math> with non-Dirac and Dirac states. Physical Review B, 2023, 107, .	1.1	2
77486	Dynamic Zinc in Liquid Metal Media as a Metal Ion Source for Highly Porous ZIFâ€8 Synthesis. Advanced Functional Materials, 0, , .	7.8	4
77487	Influence of Capping Ligands, Solvent, and Thermal Effects on CdSe Quantum Dot Optical Properties by DFT Calculations. ACS Omega, 2023, 8, 11467-11478.	1.6	3
77488	Wavelength engineerable porous organic polymer photosensitizers with protonation triggered ROS generation. Nature Communications, 2023, 14, .	5.8	12
77489	Identification of Hydrogen Trapping in Aluminum Alloys Via Muon Spin Relaxation Method and First-Principles Calculations. Metallurgical and Materials Transactions A: Physical Metallurgy and Materials Science, 2023, 54, 2374-2383.	1.1	1
77490	A Liâ€“Li₄Ti₅O₁₂ Composite Anode for Reducing Interfacial Resistance of Solidâ€State Batteries. Small Structures, 2023, 4, .	6.9	4
77491	Orbital distortion and electric field control of sliding ferroelectricity in a boron nitride bilayer. Journal of Physics Condensed Matter, 2023, 35, 235001.	0.7	2
77492	A systematic computational investigation of lithiation-induced structural phase transitions of O-functionalized MXenes. Physical Chemistry Chemical Physics, 2023, 25, 9428-9436.	1.3	2
77493	Enhancement of spin-orbit torque in <mml:math xmlns:mml="http://www.w3.org/1998/Math/MathML"><mml:mrow><mml:msub><mml:mi>WS</mml:mi><mml:mn>2</mml:mn></mml:msub></mml:mrow></mml:math> trilayers via spin-orbit proximity effect. Physical Review B, 2023, 107, .	1.1	2
77494	Origin of the variation in lattice thermal conductivities in pyrite-type dichalcogenides. Physical Review B, 2023, 107, .	1.1	2
77495	RKKY interactions mediated by topological states in transition metal doped bismuthene. Journal of Applied Physics, 2023, 133, .	1.1	2

#	Article	IF	Citations
77496	Tetracarbonates in silicate melts may be at the origin of a deep carbon reservoir in the deep Earth. Communications Earth & Environment, 2023, 4, .	2.6	1
77497	Unfolding the structure-property relationships of Li2S anchoring on two-dimensional materials with high-throughput calculations and machine learning. Journal of Energy Chemistry, 2023, 82, 31-39.	7.1	5
77498	2D MoSi2N4 as electrode material of Li-air battery â€" A DFT study. Journal of Nanoparticle Research, 2023, 25, .	0.8	5
77499	Mesoporous Pt@Pt-skin Pt3Ni core-shell framework nanowire electrocatalyst for efficient oxygen reduction. Nature Communications, 2023, 14, .	5.8	38
77500	Crystal graph convolution neural networks for fast and accurate prediction of adsorption ability of Nb₂CT_x towards Pb(<scp>ii</scp>) and Cd(<scp>ii</scp>) ions. Journal of Materials Chemistry A, 2023, 11, 9009-9018.	5.2	8
77501	Amorphized Defective Fullerene with a Singleâ€Atom Platinum for Roomâ€Temperature Hydrogen Storage. Advanced Energy Materials, 2023, 13, .	10.2	3
77502	A family of robust Dirac cone materials: two-dimensional hexagonal M₃X₂ (M) Tj ETQq0 0 0 rgBT /Overlock 10	1.3	2
77503	Isolated Rh atoms in dehydrogenation catalysis. Scientific Reports, 2023, 13, .	1.6	1
77504	Inhibition Mechanism of MgO Addition on Highâ€Temperature Oxidation of Magnetite: Density Functional Theory and Ab Initio Molecular Dynamics Methods Joint Research and Experimental Verification. Steel Research International, 2023, 94, .	1.0	2
77505	Residual Molecular Groupsâ€™ Adsorption in Tuning the Transport Properties of Carbon Nanotubes. ACS Applied Electronic Materials, 2023, 5, 1853-1858.	2.0	0
77506	DFT characterization of a new possible two-dimensional BN allotrope with a biphenylene network structure. Physical Chemistry Chemical Physics, 2023, 25, 11613-11619.	1.3	4
77507	The role of interstitial Cu on thermoelectric properties of ZrNiSn half-Heusler compounds. Materials Today Physics, 2023, 33, 101049.	2.9	3
77508	Regulating the Coordination Environment of Single-Atom Catalysts Anchored on Thiophene Linked Porphyrin for an Efficient Nitrogen Reduction Reaction. ACS Applied Materials & Interfaces, 2023, 15, 15545-15560.	4.0	15
77509	Tailoring high-energyÂstorage NaNbO3-based materials from antiferroelectric to relaxor states. Nature Communications, 2023, 14, .	5.8	28
77510	Selective Oxidation of CH₄ to CH₃OH by Transition-Metal Single-Atom-Embedded N-Doped Graphene Catalysts with Oxidants N₂O and O₂: Oxygen Adsorption Energy as an Activity Descriptor. Journal of Physical Chemistry C, 2023, 127, 5800-5809.	1.5	2
77511	Surface energy and surface stability of cesium tin halide perovskites: a theoretical investigation. Physical Chemistry Chemical Physics, 2023, 25, 10583-10590.	1.3	4
77512	Magnetic properties of rare-earth-lean ThMn12-type (Nd,X)Fe11Ti (X: Y and Ce) compounds: A DFT study. Journal of Magnetism and Magnetic Materials, 2023, 572, 170645.	1.0	1
77513	BrÃ¸nsted Acid Strength Does Not Change for Bulk and External Sites of MFI Except for Al Substitution Where Silanol Groups Form. ACS Catalysis, 2023, 13, 4470-4487.	5.5	0

#	Article	IF	Citations
77514	Higher-order Rayleigh-quotient gradient effect on electron correlations. Journal of Chemical Physics, 2023, 158, .	1.2	2
77515	The Study of Nickel Impurity Segregation on LSNT Perovskite Open Surfaces by Ab Initio Molecular Dynamics. Russian Microelectronics, 2022, 51, 654-658.	0.1	0
77516	Synergistic Functionality of Dopants and Defects in Coâ€Phthalocyanine/Bâ€CN Zâ€Scheme Photocatalysts for Promoting Photocatalytic CO₂ Reduction Reactions. Small, 2023, 19, .	5.2	10
77517	Theoretical study on structural and mechanical properties of Si-containing ternary transition metal nitrides M_{0.5}Si_{0.5}N (M = Ti, Zr, Hf). RSC Advances, 2023, 13, 9109-9118.	1.7	0
77518	Unveiling Strong Ionâ€“Electronâ€“Lattice Coupling and Electronic Antidoping in Hydrogenated Perovskite Nickelate. Advanced Materials, 2023, 35, .	11.1	4
77519	Structural, electronic and optical properties of graphene/C₂P₄ van der Waals heterostructures with direct bandgap and high absorption coefficient. International Journal of Modern Physics B, 2024, 38, .	1.0	0
77520	Addressing the Conflict between Mobility and Stability in Oxide Thinâ€film Transistors. Advanced Science, 2023, 10, .	5.6	7
77522	Acid Catalysis over Crystalline Zr₃SO₉: Role of the Local Structure in Generating Acidity. ACS Catalysis, 2023, 13, 4517-4532.	5.5	0
77523	Doping effects on the ferroelectric properties of wurtzite nitrides. Applied Physics Letters, 2023, 122, .	1.5	6
77524	Fast rate lithium metal batteries with long lifespan enabled by graphene oxide confinement. Energy Advances, 2023, 2, 712-724.	1.4	3
77525	Thermodynamic Origin of High Efficiency in Long-Wavelength InGaN-Based LEDs on Si Substrates. Journal of Physical Chemistry C, 2023, 127, 7520-7527.	1.5	2
77526	Mechanistic Understanding of Alkaliâ€Metalâ€Ion Effect on Defect State in SrTiO₃ During the Defect Engineering for Boosting Solar Water Splitting. Advanced Functional Materials, 2023, 33, .	7.8	9
77527	Promoting Effect of Nitride as Support for Pd Hydrodechlorination Catalyst. Langmuir, 2023, 39, 4692-4700.	1.6	1
77528	Structural mapping and tuning of mixed halide ions in amorphous sulfides for fast Li-ion conduction and high deformability. Journal of Materials Chemistry A, 2023, 11, 7457-7467.	5.2	2
77529	Transferability of Zr-Zr interatomic potentials. Journal of Nuclear Materials, 2023, 584, 154391.	1.3	6
77530	Layer-dependent electronic structures and optical properties of two-dimensional PdSSe. Physical Chemistry Chemical Physics, 2023, 25, 11827-11838.	1.3	4
77531	Theoretical study of the catalytic performance of Fe and Cu single-atom catalysts supported on Mo2C toward the reverse waterâ€“gas shift reaction. Frontiers in Chemistry, 0, 11, .	1.8	4
77532	Oxygen isotope effect in <mml:math xmlns:mml="http://www.w3.org/1998/Math/MathML"><mml:mrow><mml:msub><mml:mi mathvariant="normal">VO</mml:mi><mml:mn>2</mml:mn></mml:msub></mml:mrow></mml:math>. Physical Review B, 2023, 107, .	1.1	1

#	Article	IF	Citations
77533	Selective Interstitial Hydration Explains Anomalous Structural Distortions and Ionic Conductivity in 6H-Ba₄Ta₂O₉Â·1/2H₂O. Chemistry of Materials, 2023, 35, 2740-2751.	3.2	0
77534	A Biocompatible Supercapacitor Diode with Enhanced Rectification Capability toward Ion/Electronâ€Coupling Logic Operations. Advanced Materials, 2023, 35, .	11.1	8
77535	Acceptor and compensating donor doping of single crystalline SnO (001) films grown by molecular beam epitaxy and its perspectives for optoelectronics and gas-sensing. Applied Physics Letters, 2023, 122, 122101.	1.5	0
77536	Aromatic Clusters and Hydrogen Storage. Energies, 2023, 16, 2833.	1.6	0
77537	Optimizing Electromagnetic Interference Shielding of Ultrathin Nanoheterostructure Textiles through Interfacial Engineering. ACS Applied Materials & Interfaces, 2023, 15, 15965-15975.	4.0	5
77538	Computational Screening of p -Type Transparent Conducting Oxides Using the Optical Absorption Spectra and Oxygen-Vacancy Formation Energies. Physical Review Applied, 2023, 19, .	1.5	5
77539	Acetic Acid Production from CH₄ and CO₂ via Synergistic Catalysis between Pd Particles and Oxygen Vacancies Generated in ZrO₂. Journal of Physical Chemistry C, 2023, 127, 5841-5854.	1.5	3
77540	Near-Field Radiative Heat Transfer between $eta-$GeSe monolayers: An ab initio study. Nanoscale and Microscale Thermophysical Engineering, 2023, 27, 95-109.	1.4	1
77541	Highly-conductive Cu-substituted brownmillerite with emergent 3-dimensional oxygen vacancy channels. Journal of Materials Chemistry C, 2023, 11, 5147-5155.	2.7	1
77542	Engineering Catalytically Active Sites by Sculpting Artificial Edges on MoS₂ Basal Plane for Dinitrogen Reduction at a Low Overpotential. Small, 2023, 19, .	5.2	3
77543	Investigating magnetic van der Waals materials using data-driven approaches. Journal of Materials Chemistry C, 2023, 11, 5601-5610.	2.7	5
77544	Strong Magnetocaloric Coupling in Oxyorthosilicate with Dense Gd³⁺ Spins. Inorganic Chemistry, 2023, 62, 5282-5291.	1.9	6
77545	Metallic WO2-decorated g-C3N4 nanosheets as noble-metal-free photocatalysts for efficient photocatalysis. Chinese Journal of Catalysis, 2023, 47, 161-170.	6.9	20
77546	Post-plasma catalysis: charge effect on product selectivity in conversion of methane and nitrogen plasma to ethylene and ammonia. Catalysis Science and Technology, 2023, 13, 2966-2981.	2.1	3
77547	A DFT Study of Ruthenium fcc Nano-Dots: Size-Dependent Induced Magnetic Moments. Nanomaterials, 2023, 13, 1118.	1.9	2
77548	Highly Oxidized Oxide Surface toward Optimum Oxygen Evolution Reaction by Termination Engineering. ACS Nano, 2023, 17, 6811-6821.	7.3	8
77549	Hexagonal warping effect in the Janus group-VIA binary monolayers with large Rashba spin splitting and piezoelectricity. Physical Chemistry Chemical Physics, 2023, 25, 10827-10835.	1.3	0
77550	Co@CoO-catalyzed reductive amination driven by hydride-like NH2â€“ species. Chinese Journal of Catalysis, 2023, 47, 181-190.	6.9	3

#	Article	IF	Citations
77551	Photoelectrocatalytic reduction of CO2 catalyzed by TiO2/TiN nanotube heterojunction: Nitrogen assisted active hydrogen mechanism. Chinese Journal of Catalysis, 2023, 47, 243-253.	6.9	8
77552	Electronic signatures of successive itinerant, antiferromagnetic transitions in hexagonal La₂Ni₇. Journal of Physics Condensed Matter, 2023, 35, 245501.	0.7	1
77553	High-Pressure Diffusion Control: Na Extraction from NaAlB₁₄. Chemistry of Materials, 2023, 35, 3008-3014.	3.2	3
77554	First-principles structure prediction of two-dimensional HCN polymorphs obtained via formal molecular polymerization. Nanoscale, 0, , .	2.8	0
77555	First-principles study of square chalcogen bond interactions and its adsorption behavior on silver surface. Physical Chemistry Chemical Physics, 2023, 25, 10836-10844.	1.3	0
77556	Computational Study of the Adsorption of Small Gas Molecules on Pillar[5]arenes. ChemistrySelect, 2023, 8, .	0.7	1
77557	Electrochemical Oxidation of Methane to Methanol on Electrodeposited Transition Metal Oxides. Journal of the American Chemical Society, 2023, 145, 6927-6943.	6.6	10
77558	Ab Initio Study of the Electronic Structure and Lattice Dynamics of Scheelite Type AgTcO₄. Physica Status Solidi (B): Basic Research, 2023, 260, .	0.7	0
77559	First-principles analysis of electrochemical hydrogen storage behavior for hydrogenated amorphous silicon thin film in high-capacity proton battery. International Journal of Hydrogen Energy, 2023, 48, 20238-20252.	3.8	2
77560	Stable Sulfuric Vapor Transport and Liquid Sulfur Growth on Transition Metal Dichalcogenides. Crystal Growth and Design, 2023, 23, 2287-2294.	1.4	0
77561	Atomistic mechanisms for catalytic transformations of NO to NH₃, N₂O, and N₂ by Pd. Chinese Journal of Chemical Physics, 2023, 36, 94-102.	0.6	0
77562	Prominent Size Effects without a Depolarization Field Observed in Ultrathin Ferroelectric Oxide Membranes. Physical Review Letters, 2023, 130, .	2.9	11
77563	Ni nanoparticle coupled surface oxygen vacancies for efficient synergistic conversion of palmitic acid into alkanes. Chinese Journal of Catalysis, 2023, 47, 229-242.	6.9	7
77564	Effect of pressure of vanadium nitride using XRD and DFT. High Pressure Research, 2023, 43, 58-67.	0.4	0
77565	Visualizing the Atomic Configuration of Carbonate GroupsÂ in a (Cu,C)Ba₂Ca₃Cu₄O_{11+Î´} Superconductor. Advanced Materials, 2023, 35, .	11.1	2
77566	Thermodynamics of phase stability and disorder in Inter-Lanthanide ternary ABO3 oxides from first principles. Materials and Design, 2023, 228, 111830.	3.3	1
77567	Hybrid sp³/sp² Two-Dimensional Nanodiamonds for Electrochemical Ozone Production. ACS ES&T Engineering, 2023, 3, 894-905.	3.7	3
77568	Ru-based catalysts for efficient CO2 methanation: Synergistic catalysis between oxygen vacancies and basic sites. Nano Research, 2023, 16, 12153-12164.	5.8	9

#	Article	IF	Citations
77569	Intrinsic ferroelectrics and carrier doping-induced metallic multiferroics in an atomic wire. Journal of Materiomics, 2023, 9, 892-898.	2.8	3
77570	Theoretical insights into the epitaxial growth of black arsenene enabled on GeS(001). Journal of Physics Condensed Matter, 2023, 35, 244001.	0.7	0
77571	Genesis of Active Pt/CeO₂ Catalyst for Dry Reforming of Methane by Reduction and Aggregation of Isolated Platinum Atoms into Clusters. Small, 2023, 19, .	5.2	6
77572	Experimental and theoretical thermodynamic studies in Ba₂MgReO₆â€"the ground state in the context of Jahn-Teller effect. Journal of Physics Condensed Matter, 2023, 35, 245603.	0.7	1
77573	Tetragonal Mexican-hat dispersion and switchable half-metal state with multiple anisotropic Weyl fermions in penta-graphene. New Journal of Physics, 2023, 25, 033033.	1.2	0
77574	Crystal structures of two phases of Pigment Yellow 110 from X-ray powder diffraction data. Zeitschrift Fur Kristallographie - Crystalline Materials, 2023, .	0.4	0
77575	Density Functional Theory Study of CO2 Hydrogenation on Transition-Metal-Doped Cu(211) Surfaces. Molecules, 2023, 28, 2852.	1.7	1
77576	Giant tunneling magnetoresistance in in-plane double-barrier magnetic tunnel junctions based on MXene Cr₂C. Physical Chemistry Chemical Physics, 2023, 25, 10991-10997.	1.3	2
77577	Structural Bistability in RbI Monolayers on Ag(111). Journal of Physical Chemistry Letters, 2023, 14, 3023-3030.	2.1	2
77578	Improving the optoelectronic properties of single-crystalline antimony sulfide rods through simultaneous defect suppression and surface cleaning. Journal of Materials Chemistry A, 2023, 11, 8826-8835.	5.2	2
77579	Effect of Linker Structure and Functionalization on Secondary Gas Formation in Metalâ€"Organic Frameworks. Journal of Physical Chemistry A, 2023, 127, 2881-2888.	1.1	0
77580	CrPS4 Nanoflakes as Stable Direct-Band-Gap 2D Materials for Ultrafast Pulse Laser Applications. Nanomaterials, 2023, 13, 1128.	1.9	2
77581	Enhanced Thermoelectric Performance of Nanostructured Cu₂SnS₃ (CTS) via Ag Doping. ACS Applied Nano Materials, 2023, 6, 6323-6333.	2.4	4
77582	A defect formation mechanism induced by structural reconstruction of a well-known silicon grain boundary.. Acta Materialia, 2023, 250, 118827.	3.8	1
77583	Engineering Morphology and Ni Substitution of Ni_xCo_{3â€“x}O₄ Spinel Oxides to Promote Catalytic Combustion of Ethane: Elucidating the Influence of Oxygen Defects. ACS Catalysis, 2023, 13, 4683-4699.	5.5	18
77584	Theoretical screening of single atom doping on Î²-Ga₂O₃ (100) for photoelectrochemical water splitting with high activity and low limiting potential. Nanoscale, 2023, 15, 6913-6919.	2.8	1
77585	Ternary NASICON-typed Na3.8MnV0.8Zr0.2(PO4)3 cathode with stable Mn2+/Mn3+ redox and fast sodiation/desodiation kinetics for Na-ion batteries. Energy Storage Materials, 2023, 58, 271-278.	9.5	14
77586	Precise electronic structure modulation on MXene-based single atom catalysts for high-performance electrocatalytic CO2 reduction reaction: A first-principle study. Journal of Colloid and Interface Science, 2023, 642, 273-282.	5.0	9

#	Article	IF	Citations
77587	Quasi-One-Dimensional ZrS₃ Nanoflakes for Broadband and Polarized Photodetection with High Tuning Flexibility. ACS Applied Materials & Interfaces, 2023, 15, 16999-17008.	4.0	6
77588	SuperConga: An open-source framework for mesoscopic superconductivity. Applied Physics Reviews, 2023, 10, 011317.	5.5	3
77589	Strong Scattering from Low-Frequency Rattling Modes Results in Low Thermal Conductivity in Antimonide Clathrate Compounds. Chemistry of Materials, 2023, 35, 2918-2935.	3.2	3
77590	Transition-Metal-Free, Pure p-Block Alloy Electrocatalysts for the Highly Efficient Nitrate Reduction to Ammonia. Chemistry of Materials, 2023, 35, 2884-2891.	3.2	3
77591	How fast do defects migrate in halide perovskites: insights from on-the-fly machine-learned force fields. Chemical Communications, 2023, 59, 4660-4663.	2.2	6
77592	Single crystal synthesis and low-lying electronic structure of V3S4. Journal of Alloys and Compounds, 2023, 949, 169776.	2.8	0
77593	Selective Self-Assembly and Modification of Herringbone Reconstructions at a Solidâ€“Liquid Interface of Au(111). Journal of Physical Chemistry Letters, 2023, 14, 3057-3062.	2.1	2
77594	Fine electron and phonon transports manipulation by Mn compensation for high thermoelectric performance of Sb2Te3(SnTe)n materials. Materials Today Physics, 2023, 33, 101055.	2.9	2
77595	Efficient Yellow Emission and Near-Unified Photoluminescence Quantum Yield of Sb³⁺ in a One-Dimensional Confinement Cadmium Chloride Lattice. ACS Applied Electronic Materials, 2023, 5, 2365-2374.	2.0	4
77596	Materials design of edge-modified polymeric carbon nitride nanoribbons for the photocatalytic CO₂ reduction reaction. Physical Chemistry Chemical Physics, 2023, 25, 9901-9908.	1.3	3
77597	Structural and Composition Evolution of Palladium Catalyst for CO Oxidation under Steady-State Reaction Conditions. Journal of Physical Chemistry C, 2023, 127, 6262-6270.	1.5	4
77598	PtTe₂/Sb₂S₃ Nanoscale Heterostructures for the Photocatalytic Direct Z-Scheme with High Solar-to-Hydrogen Efficiency: A Theoretical Investigation. ACS Applied Nano Materials, 2023, 6, 5591-5601.	2.4	11
77599	Selfâ€Reconstructed Spinel Surface Structure Enabling the Longâ€Term Stable Hydrogen Evolution Reaction/Oxygen Evolution Reaction Efficiency of FeCoNiRu Highâ€Entropy Alloyed Electrocatalyst. Advanced Science, 2023, 10, .	5.6	22
77600	Ferroelectricity in layered bismuth oxide down to 1 nanometer. Science, 2023, 379, 1218-1224.	6.0	18
77601	Selective Ethylene Glycol Oxidation to Formate on Nickel Selenide with Simultaneous Evolution of Hydrogen. Advanced Science, 2023, 10, .	5.6	28
77602	First-principles study of the initial stage of Pentacene adsorption on the twofold surface of the Ag-In-Yb quasicrystal. Journal of Physics: Conference Series, 2023, 2461, 012016.	0.3	0
77603	Excitation Wavelengthâ€Dependent Upconversion Luminescence Enhancement in Tm³⁺â€Doped LiErF₄@LiYF₄ System Under High Pressure. Advanced Optical Materials, 2023, 11, .	3.6	2
77604	Structure and Stability of Metalloporphyrin Networks on Au(111). Journal of Physical Chemistry C, 2023, 127, 6569-6577.	1.5	0

#	Article	IF	Citations
77605	Data-Driven Design of High-Performance Graphene-Based Seawater Desalination Membranes. ACS Applied Nano Materials, 2023, 6, 5889-5900.	2.4	8
77606	Growth of single-crystal black phosphorus and its alloy films through sustained feedstock release. Nature Materials, 2023, 22, 717-724.	13.3	24
77607	Topological Spin Textures in a Nonâ€Collinear Antiferromagnet System. Advanced Materials, 2023, 35, .	11.1	12
77608	Evaluation of DFT+U and HSE Frameworks for Strongly Correlated Iron Oxide. ChemistrySelect, 2023, 8, .	0.7	0
77609	Accelerated Perovskite Oxide Development for Thermochemical Energy Storage by a Highâ€Throughput Combinatorial Approach. Advanced Energy Materials, 2023, 13, .	10.2	2
77610	Structure engineering of CeO₂for boosting the Au/CeO₂nanocatalyst in the green and selective hydrogenation of nitrobenzene. Nanoscale Horizons, 2023, 8, 812-826.	4.1	5
77611	Effects of High Pressure on the Bandgap and the dâ€“d Crystal Field Transitions in Wolframite NiWO₄. Journal of Physical Chemistry C, 2023, 127, 6543-6551.	1.5	7
77612	Dynamics of Dissociative Chemisorption of NH₃ on Fe(111) on a Twelve-Dimensional Potential Energy Surface. Journal of Physical Chemistry C, 2023, 127, 6328-6336.	1.5	2
77613	Finite-Temperature Mechanical Properties of Organic Molecular Crystals from Classical Molecular Simulation. Crystal Growth and Design, 2023, 23, 2155-2168.	1.4	4
77614	Misorientation and Temperature Dependence of Small Angle Twist Grain Boundaries in Silicon: Atomistic Simulation of Directional Growth. Crystal Growth and Design, 2023, 23, 2893-2904.	1.4	1
77615	Intrinsic Nonlinear Planar Hall Effect. Physical Review Letters, 2023, 130, .	2.9	11
77616	Li self-diffusion and ion conductivity in congruent <mml:math xmlns:mml="http://www.w3.org/1998/Math/MathML"><mml:msub><mml:mi>LiNbO</mml:mi><mml:mn>3</mml:mn></mml:msub><m and <mml:math xmlns:mml="http://www.w3.org/1998/Math/MathML"><mml:msub><mml:mi>LiTaO</mml:mi><mml:mn>3</mml:mn></mml:msub><m single crystals. Physical Review Materials, 2023, 7, .	0.9	6
77617	Insights into selected 2D piezo Rashba semiconductors for self-powered flexible piezo spintronics: material to contact properties. Journal of Physics Condensed Matter, 2023, 35, 253001.	0.7	2
77618	Antimony doped tin(<scp>iv</scp>) hybrid metal halides with high-efficiency tunable emission, WLED and information encryption. Journal of Materials Chemistry C, 2023, 11, 5688-5700.	2.7	10
77619	Machineâ€Learningâ€Assisted Determination of the Global Zeroâ€Temperature Phase Diagram of Materials. Advanced Materials, 2023, 35, .	11.1	8
77620	First-principles study of the lattice thermal conductivity of the nitride perovskite <mml:math xmlns:mml="http://www.w3.org/1998/Math/MathML"><mml:msub><mml:mi>LaWN</mml:mi><mml:mn>3</mml:mn></mml:msub><m Physical Review B, 2023, 107, .	3.7	3
77621	Quasi-Two-Dimensional Intermetallic Electride CeRuSi for Efficient Alkaline Hydrogen Evolution. ACS Catalysis, 2023, 13, 4752-4759.	5.5	7
77623	Advances in bismuth-telluride-based thermoelectric devices: Progress and challenges. EScience, 2023, 3, 100122.	25.0	25

#	Article	IF	Citations
77624	Layer-by-layer disentanglement of Bloch states. Nature Physics, 2023, 19, 950-955.	6.5	4
77625	Quantum computation for periodic solids in second quantization. Physical Review Research, 2023, 5, .	1.3	7
77626	Effect of magnetic disorder on Cr interaction with 1/2âŸ¨111âŸ© screw dislocations in bcc iron. Journal of Applied Physics, 2023, 133, 125103.	1.1	0
77627	Structure, Magnetotransport, and Theoretical Study on the Layered Antiferromagnet Topological Phase EuCd₂As₂ under High Pressure. Advanced Quantum Technologies, 2023, 6, .	1.8	5
77628	Chemical Adsorption of HF, HCl, and H2O onto YF3 and Isostructural HoF3 Surfaces by First Principles. Crystals, 2023, 13, 555.	1.0	1
77630	Single-crystal growth and physical properties of <mml:math xmlns:mml="http://www.w3.org/1998/Math/MathML"><mml:mrow><mml:msub><mml:mi>LaMn</mml:mi><mml:mrow><mml:mn>0 Physical Review B, 2023, 107, .	1.1	1
77631	Abnormal phonon angular momentum due to off-diagonal elements in the density matrix induced by a temperature gradient. Physical Review B, 2023, 107, .	1.1	1
77632	Iodine Vacancies do not Cause Nonradiative Recombination in Halide Perovskites. , 2023, 2, .		6
77633	DFT Calculation of High-Angle Kink Boundary in 18R-LPSO Alloy. Materials Transactions, 2023, 64, 813-816.	0.4	2
77634	Valleytronics Candidate with Spontaneous Valley Polarization in A-Type Antiferromagnetic MoSi₂N₄/MnPS₃ Heterostructure. ACS Applied Electronic Materials, 2023, 5, 2046-2054.	2.0	6
77635	Explainable machine learning for predicting the band gaps of ABX3 perovskites. Materials Science in Semiconductor Processing, 2023, 161, 107427.	1.9	4
77636	Exceptional Sorption of Heavy Metals from Natural Water by Halloysite Particles: A New Prospect of Highly Efficient Water Remediation. Nanomaterials, 2023, 13, 1162.	1.9	4
77637	Electronic structure and optical properties of doped Î³-CuI scintillator: a first-principles study. RSC Advances, 2023, 13, 9615-9623.	1.7	3
77638	Enriching the Local Concentration of CO Intermediates on Cu Cavities for the Electrocatalytic Reduction of CO₂ to C₂₊ Products. ACS Applied Materials & Interfaces, 2023, 15, 16673-16679.	4.0	11
77639	Dynamics of photoinduced ferromagnetism in oxides with orbital degeneracy. Physical Review Research, 2023, 5, .	1.3	0
77640	A dendrite-free Ga-In-Sn-Zn solid-liquid composite anode for rechargeable zinc batteries. Energy Storage Materials, 2023, 58, 195-203.	9.5	12
77641	Spinâ€“Phonon Interactions and Anharmonic Lattice Dynamics in Fe ₃ GeTe ₂. , 0, , 2200089.		0
77642	Resistivity modulation of perovskite samarium nickelate with high-valence cations and the underlying mechanism. Applied Surface Science, 2023, 624, 157103.	3.1	1

#	Article	IF	Citations
77643	Highâ€rate electrochemical H₂O₂ production over multimetallic atom catalysts under acidicâ€“neutral conditions. , 2024, 6, .		2
77644	High photoactive black phase stability of CsPbI₃nanocrystals under damp-heat conditions of 85 Â°C and 85% relative humidity. Journal of Materials Chemistry A, 2023, 11, 10556-10564.	5.2	1
77645	Stable self-trapped broadband emission from an organolead halide coordination polymer with strong layer corrugation and high chemical robustness. Inorganic Chemistry Frontiers, 2023, 10, 2645-2652.	3.0	2
77646	Superionic effect and anisotropic texture in Earthâ€™s inner core driven by geomagnetic field. Nature Communications, 2023, 14, .	5.8	6
77647	Ferroelectricity in Low-Permittivity SrZrO₃ Epitaxial Films. Chemistry of Materials, 2023, 35, 2967-2974.	3.2	2
77648	Atomic-scale study clarifying the role of space-charge layers in a Li-ion-conducting solid electrolyte. Nature Communications, 2023, 14, .	5.8	16
77649	Distinct Magnetic Gaps between Antiferromagnetic and Ferromagnetic Orders Driven by Surface Defects in the Topological Magnet <mml:math xmlns:mml="http://www.w3.org/1998/Math/MathML" display="inline"><mml:mrow><mml:msub><mml:mrow><mml:mi>MnBi</mml:mi></mml:mrow><mml:mrow><mml:mn>2</mml:mn></ Physical Review Letters, 2023, 130, .	2.9	8
77650	First-principles screening of surface-charge-transfer molecular dopants for n-type diamond. Nanotechnology, 2023, 34, 265201.	1.3	0
77651	Tuning the metal valence state of Pd nanoparticles via codoping of Bâ€“N for chlorophenol hydrodechlorination. New Journal of Chemistry, 2023, 47, 8785-8796.	1.4	1
77652	Improving the intrinsic activity of ultrathin 2Dâ€“2D heterostructures by bridge-bonded Niâ€“Oâ€“Ti ligands for efficient oxygen evolution. Nanotechnology, 2023, 34, 255402.	1.3	1
77653	High-efficiency resistive switch and artificial synaptic simulation in antimony-based perovskite devices. Science China Technological Sciences, 2023, 66, 1141-1151.	2.0	4
77654	Carrier-Envelope Phase-Controlled Residual Current in Semiconductors. Symmetry, 2023, 15, 784.	1.1	0
77655	Enhancing efficiency of the ternary tri-chalcogenide MnPSe3 towards hydrogen evolution reaction by activating its basal plane. International Journal of Hydrogen Energy, 2023, 48, 21778-21787.	3.8	4
77656	Na⁺ Migration Mediated Phase Transitions Induced by Electric Field in the Framework Structured Tungsten Bronze. Journal of Physical Chemistry Letters, 2023, 14, 3152-3159.	2.1	2
77657	The evolution of structureâ€“property relationship of P2-type Na0.67Ni0.33Mn0.67O2 by vanadium substitution and organic electrolyte combinations for sodium-ion batteries. Journal of Solid State Electrochemistry, 2023, 27, 2067-2082.	1.2	3
77658	Modulation of oxygen-etching for generating nickel single atoms for efficient electroreduction of CO2 to syngas (CO/H2). Journal of Catalysis, 2023, 421, 332-341.	3.1	4
77659	Reactionâ€Induced Formation of Stable Mononuclear Cu(I)Cl Species on Carbon for Lowâ€Footprint Vinyl Chloride Production. Advanced Materials, 2023, 35, .	11.1	9
77660	High-performance non-Fermi-liquid metallic thermoelectric materials. Npj Computational Materials, 2023, 9, .	3.5	3

#	Article	IF	Citations
77661	First-principles study on the optoelectronic properties of the quasi-one-dimensional flexible semiconductor K2PdPS4I. Results in Physics, 2023, 47, 106396.	2.0	3
77662	ZrSe2-HfSe2 lateral heterostructures: stability, fundamental properties, and interline defects. Applied Physics A: Materials Science and Processing, 2023, 129, .	1.1	2
77663	Ti3CNT MXene/rGO scaffolds directing the formation of a robust, layered SEI toward high-rate and long-cycle lithium metal batteries. Energy Storage Materials, 2023, 58, 322-331.	9.5	10
77664	Quantum structural fluxion in superconducting lanthanum polyhydride. Nature Communications, 2023, 14, .	5.8	2
77665	Role of molecular modelling in the development of metal-organic framework for gas adsorption applications. Journal of Chemical Sciences, 2023, 135, .	0.7	4
77666	Highly selective electrocatalytic alkynol semi-hydrogenation for continuous production of alkenols. Nature Communications, 2023, 14, .	5.8	16
77667	Flexomagnetic noncollinear state with a plumb line shape spin configuration in edged two-dimensional magnetic CrI3. Npj Quantum Materials, 2023, 8, .	1.8	6
77668	The importance of the image forces and dielectric environment in modeling contacts to two-dimensional materials. Npj 2D Materials and Applications, 2023, 7, .	3.9	4
77669	High-throughput manufacturing of epitaxial membranes from a single wafer by 2D materials-based layer transfer process. Nature Nanotechnology, 2023, 18, 464-470.	15.6	12
77670	Vibrational signature of hydrated protons confined in MXene interlayers. Nature Communications, 2023, 14, .	5.8	14
77671	Regulated adsorption sites using atomically single cluster over biochar for efficient elemental mercury uptake. Biochar, 2023, 5, .	6.2	3
77672	Magnetism and charge density wave order in kagome FeGe. Nature Physics, 2023, 19, 814-822.	6.5	31
77673	Quantum oscillations in the centrosymmetric skyrmion-hosting magnet<mml:math xmlns:mml="http://www.w3.org/1998/Math/MathML"><mml:mrow><mml:msub><mml:mi>GdRu</mml:mi><mml:mn>2</mml:mn></mml:msub></mml:mrow></mml:math>. Physical Review B, 2023, 107, .	3.7	5
77674	Highâ€Activity Fe₃C as pHâ€Universal Electrocatalyst for Boosting Oxygen Reduction Reaction and Zincâ€Air Battery. Small, 2023, 19, .	5.2	15
77675	Interface-vacancy synergy of Co(OH)2/CoN to boost alkaline water splitting. Science China Materials, 2023, 66, 2246-2256.	3.5	4
77676	Competitive Trapping of Single Atoms onto a Metal Carbide Surface. ACS Nano, 2023, 17, 6955-6965.	7.3	30
77677	Unveiling the local structure of the amorphous metal $$ext {Fe}_{(1-x)}ext {Zr}_x$$ combining first-principles-based simulations and modelling of EXAFS spectra. Scientific Reports, 2023, 13, .	1.6	0
77678	Structural, mechanical and thermal properties of cubic bixbyite-structured high-entropy oxides. Chemical Engineering Journal, 2023, 464, 142649.	6.6	6

#	Article	IF	Citations
77679	Contrasting the Roles of Cu Interstitials and Sb Substitutions in Regulating Ferroelectric Distortions and Thermoelectric Properties of Î±-GeTe. ACS Applied Energy Materials, 2023, 6, 4065-4071.	2.5	4
77680	Enhanced Photocatalytic Activity of Two-Dimensional Polar Monolayer SiTe for Water-Splitting via Strain Engineering. Molecules, 2023, 28, 2971.	1.7	0
77681	Approach of Electronic Structure Calculations to Crystal. The Materials Research Society Series, 2023, , 209-255.	0.2	0
77682	Degradation of High Nickel Liâ€Ion Cathode Materials Induced by Exposure to Fullyâ€Charged State and Its Mitigation. Advanced Energy Materials, 2023, 13, .	10.2	7
77683	Hollow sphere of heterojunction (NiCu)S/NC as advanced anode for sodium-ion battery. Journal of Energy Chemistry, 2023, 82, 248-258.	7.1	9
77684	Deterministic Magnetic Switching in Perpendicular Magnetic Trilayers Through Sunlightâ€Induced Photoelectron Injection. Small, 2023, 19, .	5.2	5
77685	First-principles investigation of the effect of interfacial compositions on the formation energies of Î©â€² and T1 structures. Scripta Materialia, 2023, 231, 115435.	2.6	2
77686	Nitrogen adsorption via charge transfer on vacancies created during surfactant assisted exfoliation of TiB₂. Nanoscale, 2023, 15, 8204-8216.	2.8	7
77687	Prediction of two stable freestanding <mml:math xmlns:mml="http://www.w3.org/1998/Math/MathML"><mml:msub><mml:mi>Î²</mml:mi><mml:mn>12</mml:mn></mml:msub></mml borophanes: Structure, electronic properties, and superconductivity. Physical Review Materials, 2023, 7, .	0.9	5
77688	Facile synthesis of CuCo-CoO composite electrocatalyst for nitrate reduction to ammonia with high activity, selectivity and stability. Applied Surface Science, 2023, 624, 157118.	3.1	5
77689	An Efficient Continuous Flow Synthesis for the Preparation of N-Arylhydroxylamines: Via a DMAP-Mediated Hydrogenation Process. Molecules, 2023, 28, 2968.	1.7	2
77690	Predicting thermodynamic stability of magnesium alloys in machine learning. Computational Materials Science, 2023, 223, 112111.	1.4	5
77691	Computational investigation of MnIr and FeIr electrocatalyst for nitrogen reduction reaction. Electroanalysis, 0, , .	1.5	0
77692	Diversity of platinum-sites at platinum/fullerene interface accelerates alkaline hydrogen evolution. Nature Communications, 2023, 14, .	5.8	30
77693	Reconciling experimental catalytic data stemming from structure sensitivity. Chemical Science, 2023, 14, 4337-4345.	3.7	2
77694	Short-range ordering alters the dislocation nucleation and propagation in refractory high-entropy alloys. Materials Today, 2023, 65, 14-25.	8.3	16
77695	Step-guided epitaxial growth of blue phosphorene on vicinal Ag(111). Physical Review Materials, 2023, 7, .	0.9	3
77696	Ab Initio Prediction of Ultraâ€Wide Band Gap B _x Al _{1â^' x} N Materials. Advanced Electronic Materials, 0, , .	2.6	0

#	Article	IF	Citations
77697	Factors controlling heteroepitaxial phase formation at intermetallic-Al₃Sc/liquid interfaces. Journal of Applied Physics, 2023, 133, 124902.	1.1	0
77698	Classification of perovskite structural types with dynamical octahedral tilting. IUCrJ, 2023, 10, 309-320.	1.0	5
77699	Interface Analysis of LiCl as a Protective Layer of Li_{1.3}Al_{0.3}Ti_{1.7}(PO₄)₃ for Electrochemically Stabilized All-Solid-State Li-Metal Batteries. ACS Applied Materials & Interfaces, 2023, 15, 16562-16570.	4.0	8
77700	Role of Oxygen in Vacancy-Induced Phase Formation and Crystallization of Al₂TiO₅-Based Chemical Vapor-Deposited Coatings. Journal of Physical Chemistry C, 2023, 127, 6456-6465.	1.5	1
77701	Medium-Range Ordering in the Ionic Glass Electrolytes LiPON and LiSiPON. Chemistry of Materials, 2023, 35, 2730-2739.	3.2	1
77702	First-Principles Study of the Magnetic and Electronic Structure of NdB4. Materials, 2023, 16, 2627.	1.3	1
77703	Predicting the Na⁺ ion transport properties of NaSICON materials using density functional theory and Kinetic Monte Carlo. Journal of Materials Chemistry A, 2023, 11, 9160-9177.	5.2	2
77704	Stripe helical magnetism and two regimes of anomalous Hall effect in NdAlGe. Physical Review Materials, 2023, 7, .	0.9	4
77705	Attempted preparation of La _{0.5}Ba _{0.5}MnO _{3â^' Î´} leading to an in-situ formation of manganate nanocomposites as a cathode for proton-conducting solid oxide fuel cells. Journal of Advanced Ceramics, 2023, 12, 1189-1200.	8.9	24
77706	BinaryÂmolten salt in situ synthesis of sandwichâ€structure hybrids of hollow Î²â€Mo₂C nanotubes and Nâ€doped carbon nanosheets for hydrogen evolution reaction. , 2023, 5, .		11
77707	Top-down patterning of topological surface and edge states using a focused ion beam. Nature Communications, 2023, 14, .	5.8	3
77708	Designing single-site alloy catalysts using a degree-of-isolation descriptor. Nature Nanotechnology, 2023, 18, 611-616.	15.6	24
77709	Defect engineering of silicon with ion pulses from laser acceleration. Communications Materials, 2023, 4, .	2.9	2
77710	Prediction of a Reentrant Phase Transition Behavior of Cotunnite in Zirconia and Hafnia at High Pressures. Journal of Superhard Materials, 2023, 45, 10-19.	0.5	2
77711	Integrating surface and interface engineering to improve optoelectronic performance and environmental stability of MXene-based heterojunction towards broadband photodetection. Nano Research, 2023, 16, 10148-10155.	5.8	4
77712	Surface modification with lithium-ion conductor Li3PO4 to enhance the electrochemical performance of lithium-rich layered Li1.2Ni0.2Mn0.6O2. Ionics, 2023, 29, 2141-2152.	1.2	5
77713	Catalytic Activity Maps for Alloy Nanoparticles. Journal of the American Chemical Society, 2023, 145, 7352-7360.	6.6	10
77714	Pressure-induced electride phase formation in calcium: A key to its strange high-pressure behavior. Physical Review B, 2023, 107, .	1.1	2

#	Article	IF	Citations
77715	Electrochemical partial reduction of Ni(OH)2 to Ni(OH)2/Ni via coupled oxidation of an interfacing NiAl intermetallic compound for robust hydrogen evolution. Journal of Energy Chemistry, 2023, 82, 560-571.	7.1	7
77716	Two-dimensional C₆X (X = P₂, N₂, NP) with ultra-wide bandgap and high carrier mobility. Materials Research Express, 2023, 10, 045602.	0.8	0
77717	Unique (100) Surface Configuration Enables Promising Oxygen Reduction Performance for Pt₃Co Nanodendrite Catalysts. ACS Applied Materials & Interfaces, 2023, 15, 18217-18228.	4.0	3
77718	Large permittivity, low loss and defect structure in (Nb, Zn) co-doped SnO2 ceramics studied through a combined experimental and DFT calculational method. Ceramics International, 2023, , .	2.3	1
77719	Successive Short- and Long-Range Magnetic Ordering in Ba2Mn3(SeO3)6 with Honeycomb Layers of Mn3+ Ions Alternating with Triangular Layers of Mn2+ Ions. Materials, 2023, 16, 2685.	1.3	1
77720	Field-tunable Weyl points and large anomalous Hall effect in the degenerate magnetic semiconductor <mml:math xmlns:mml="http://www.w3.org/1998/Math/MathML"><mml:msub><mml:mi mathvariant="normal">EuMg</mml:mi><mml:mn>2</mml:mn></mml:msub><mml:msub><mml:mi mathvariant="normal">Bi</mml:mi><mml:mn>2</mml:mn></mml:msub></mml:math>. Physical Review B, 2023, 107, .	1.1	2
77721	Exploration of Photocatalytic Overall Water Splitting Mechanisms in the Z-Scheme SnS₂/Î²-As Heterostructure. Journal of Physical Chemistry C, 2023, 127, 6347-6355.	1.5	5
77722	Silicate Dissolution Mechanism from Metakaolinite Using Density Functional Theory. Nanomaterials, 2023, 13, 1196.	1.9	8
77723	Giant tunnel electroresistance in two-dimensional ferroelectric tunnel junctions constructed with a <mml:math xmlns:mml="http://www.w3.org/1998/Math/MathML"><mml:mrow><mml:msub><mml:mi>Sc</mml:mi><mml:mn>2</mml:mn></mml:msub></mml:mr van der Waals ferroelectric heterostructure. Physical Review B, 2023, 107, .	1.1	16
77724	Selective Uptake of Ethane/Ethylene Mixtures by UTSA-280 is Driven by Reversibly Coordinated Water Defects. Chemistry of Materials, 2023, 35, 2956-2966.	3.2	8
77725	Dirac Points in Two-Dimensional Semi-Metal B5ScNi Monolayer with Low Symmetry. Journal of Electronic Materials, 0, , .	1.0	0
77726	Boosting the broadband orange emission in organicâ€“inorganic hybrid (DPG)₃InBr₆viaantimony doping. New Journal of Chemistry, 2023, 47, 8249-8257.	1.4	4
77727	Theoretical insight into potential thermoelectric performance of ternary metal phosphide CaAgP. Applied Physics Letters, 2023, 122, 133905.	1.5	1
77728	The built-in electric field across FeN/Fe3N interface for efficient electrochemical reduction of CO2 to CO. Nature Communications, 2023, 14, .	5.8	33
77729	Machine-learning accelerated annealing with fitting-search style for multicomponent alloy structure predictions. Physical Review Materials, 2023, 7, .	0.9	0
77730	A first principles study of structural and optoelectronic properties and photocatalytic performance of GeCâ€“MX₂ (M = Mo and W; X = S and Se) van der Waals heterostructures. Physical Chemistry Chemical Physics, 2023, 25, 11169-11175.	1.3	3
77731	First-Principles Calculation of the Temperature-Dependent Transition Energies in Spin Defects. Journal of Physical Chemistry Letters, 2023, 14, 3266-3273.	2.1	10
77732	Atomic scale interfacial magnetism and origin of metal-insulator transition in (LaNiO$$_3$$)$$_n$$/(CaMnO$$_3$$)$$_m$$ superlattices: a first principles study. Scientific Reports, 2023, 13, .	1.6	3

#	Article	IF	Citations
77733	Electronegativity principle for hydrogen evolution activity using first-principles calculations. Physical Chemistry Chemical Physics, 2023, 25, 13289-13296.	1.3	1
77734	Immobilized triatomic CuB₂ clusters on 2D carbon nitride: highly selective conversion of CO to ethanol at low potentials. Physical Chemistry Chemical Physics, 2023, 25, 11501-11512.	1.3	1
77735	Highly Selective N2 Electroreduction to NH3 Using a Boronâ€Vacancyâ€Rich Diatomic Nbï¿¿B Catalyst. Small, 2023, 19, .	5.2	10
77736	Microwave-induced oxygen vacancy-rich surface boosts the cathode performance for proton-conducting solid oxide fuel cells. Ceramics International, 2023, 49, 22608-22616.	2.3	2
77737	Realization of 1.54â€Âµm Lightâ€Emitting Diodes Based on Er³⁺/Yb³⁺Coâ€Doped CsPbCl₃ Films. Advanced Materials, 2023, 35, .	11.1	13
77738	Alloyed triple half-Heuslers: a route toward high-performance thermoelectrics with intrinsically low lattice thermal conductivity. Journal of Materials Chemistry A, 0, , .	5.2	4
77739	Tuning magnetocrystalline anisotropy by controlling the orbital electronic configuration of two-dimensional magnetic materials. Nanoscale Advances, 0, , .	2.2	0
77740	Lattice dielectric properties of rutile <mml:math xmlns:mml="http://www.w3.org/1998/Math/MathML"><mml:msub><mml:mi>TiO</mml:mi><mml:mn>2</mml:mn></mml:msub></m : First-principles anharmonic self-consistent phonon study. Physical Review B, 2023, 107, .	1.1	3
77741	Experimental and Theoretical Investigations of Out-of-Plane Ordered Nanolaminate Transition Metal Borides: M₄CrSiB₂ (M = Mo, W, Nb). Inorganic Chemistry, 2023, 62, 5341-5347.	1.9	4
77742	Scanning Intrinsic Superconductivity and the Spin Hall Effect in Niobium Borides. Crystal Growth and Design, 2023, 23, 3562-3571.	1.4	2
77743	Straight and twisted open nodal-line phonon states in the CaI₂ family of materials. Physical Chemistry Chemical Physics, 2023, 25, 10561-10566.	1.3	1
77744	Weakened Crystalline SnNb ₂ O ₆ for Enhanced Performance in Photocatalytic H ₂ Production and CO ₂ Reduction. Chemistry - an Asian Journal, 0, , .	1.7	0
77745	Ammonia free catalytic reduction of nitric oxide on Ni-embedded graphene nanostructure: A density functional theory investigation. Molecular Catalysis, 2023, 541, 113119.	1.0	1
77746	Nanoscale fluctuation of stacking fault energy strengthens multi-principal element alloys. Journal of Materials Science and Technology, 2023, 158, 218-225.	5.6	0
77747	Chemical Aspect of Displacive-Type Ferroaxial Phase Transition from Perspective of Second-Order Jahnâ€“Teller Effect: NASICON Systems as an Example. Journal of the American Chemical Society, 2023, 145, 8090-8098.	6.6	7
77748	Interplay of structure and magnetism in <mml:math xmlns:mml="http://www.w3.org/1998/Math/MathML"><mml:mrow><mml:msub><mml:mi>LuFe</mml:mi><mml:mn>4</mml:mn></mml:msub></mml:mrow></ tuned by hydrostatic pressure. Physical Review B, 2023, 107, .	1.1	0
77749	Can Li Atoms Anchored on Boronâ€and Nitrogenâ€Doped Graphene Catalyze Dinitrogen Molecules to Ammonia? A DFT Study. ChemPhysChem, 2023, 24, .	1.0	1
77750	On-the-fly machine learning potential accelerated accurate prediction of lattice thermal conductivity of metastable silicon crystals. Physical Review Materials, 2023, 7, .	0.9	9

#	Article	IF	Citations
77751	Magnetic iron-cobalt silicides discovered using machine-learning. Physical Review Materials, 2023, 7, .	0.9	3
77752	Thousands of conductance levels in memristors integrated on CMOS. Nature, 2023, 615, 823-829.	13.7	66
77753	Two-dimensional rare-earth Janus <mml:math		

#	Article	IF	Citations
77769	Fast general two- and three-body interatomic potential. Physical Review B, 2023, 107, .	1.1	2
77770	New Transformation Pathway of cg-N from HeN₄ under Moderate Pressure. Journal of Physical Chemistry C, 2023, 127, 6655-6661.	1.5	2
77771	Evaluating metal oxide support effects on the RWGS activity of Mo₂C catalysts. Catalysis Science and Technology, 2023, 13, 2685-2695.	2.1	3
77772	Revisiting the Low-Index Surfaces of LaCoO₃ with a Passivation Strategy. Journal of Physical Chemistry C, 2023, 127, 6843-6851.	1.5	0
77773	Toward Understanding the Formation of Coke during the MCS Reaction: A Theoretical Approach. Journal of Physical Chemistry C, 2023, 127, 6680-6689.	1.5	2
77774	Role of Chemical Etching in the Nucleation of Nanopores in 2D MoS₂: Insights from First-Principles Calculations. Journal of Physical Chemistry C, 2023, 127, 6873-6883.	1.5	2
77775	Correlation of the spin state and catalytic property of Mâ€“N₄single-atom catalysts in oxygen reduction reactions. Physical Chemistry Chemical Physics, 2023, 25, 11673-11683.	1.3	6
77776	Silver Nanoparticle-Decorated Defective Zr-Based Metalâ€“Organic Frameworks for Efficient Electrocatalytic Carbon Dioxide Reduction with Ultrahigh Mass Activity. ACS Applied Energy Materials, 2023, 6, 4072-4078.	2.5	7
77777	Influences of C, Si and Mn on the wear resistance of coiled tubing steel. Wear, 2023, 524-525, 204854.	1.5	1
77778	Understanding Trends in Electrochemical Methanol Oxidation Reaction Activity on a Single Transition-Metal Atom Embedded in N-Coordinated Graphene Catalysts. Journal of Physical Chemistry Letters, 2023, 14, 3384-3390.	2.1	2
77779	Interplay among Hydrogen Chemisorption, Intercalation, and Bulk Diffusion at the Graphene-Covered Ni(111) Crystal. Journal of Physical Chemistry C, 2023, 127, 6938-6947.	1.5	0
77780	Polaron-induced metal-to-insulator transition in vanadium oxides from density functional theory calculations. Physical Review B, 2023, 107, .	1.1	1
77781	High-throughput screening of highly efficient Cu-based dual-atom catalysts to promote nitrate electroreduction for ammonia synthesis: A computational study. Molecular Catalysis, 2023, 541, 113095.	1.0	0
77782	On the Donor: Acceptor Features for Poly(3-hexylthiophene): TiO2 Quantum Dots Hybrid Materials Obtained via Water Vapor Flow Assisted Sol-Gel Growth. Polymers, 2023, 15, 1706.	2.0	0
77783	Hydrophobicity Tailoring of Ferric Covalent Organic Framework/MXene Nanosheets for Highâ€Efficiency Nitrogen Electroreduction to Ammonia. Advanced Science, 2023, 10, .	5.6	8
77784	Single-bonded nitrogen chain and porous nitrogen layer via Ceâ€“N compounds. Materials Advances, 2023, 4, 2162-2173.	2.6	1
77785	Nontrivial Topological Surface States in Ru₃Sn₇ toward Wide pHâ€Range Hydrogen Evolution Reaction. Advanced Materials, 2023, 35, .	11.1	56
77786	CH3I sensing using yttrium single atom-doped perovskite nanocrystals. Nano Research, 2023, 16, 10429-10435.	5.8	2

#	Article	IF	Citations
77787	Accelerated Workflow for Antiperovskiteâ€based Solid State Electrolytes. Batteries and Supercaps, 2023, 6, .	2.4	4
77788	Nitrogen-doped hollow carbon@tin disulfide as a bipolar dynamic host for lithium-sulfur batteries with enhanced kinetics and cyclability. Journal of Colloid and Interface Science, 2023, 644, 546-555.	5.0	9
77789	Comprehensive Study of Oxygen Vacancies on the Catalytic Performance of ZnO for CO/H₂ Activation Using Machine Learning-Accelerated First-Principles Simulations. ACS Catalysis, 2023, 13, 5104-5113.	5.5	6
77790	Hydrogen Isotope Separation Using Graphene-Based Membranes in Liquid Water. Langmuir, 2023, 39, 4975-4983.	1.6	1
77791	Understanding the Effect of Single Atom Cationic Defect Sites in an Al₂O₃ (012) Surface on Altering Selenate and Sulfate Adsorption: An Ab Initio Study. Journal of Physical Chemistry C, 2023, 127, 6925-6937.	1.5	0
77792	Interface-engineered ferroelectricity of epitaxial Hf0.5Zr0.5O2 thin films. Nature Communications, 2023, 14, .	5.8	5
77793	Well-defined double hysteresis loop in NaNbO3 antiferroelectrics. Nature Communications, 2023, 14, .	5.8	21
77794	Stoichiometric and Chiral Stacking Tailoring of Dibenzocarbazole Analogâ€“TCNB Chargeâ€Transfer Cocrystals via Supramolecular Assembly for Variable Optical Behaviors. Advanced Optical Materials, 2023, 11, .	3.6	4
77795	Versatility of infrared properties of MXenes. Materials Today, 2023, 64, 31-39.	8.3	21
77796	Structure transformation from SierpiÅ„ski triangles to chains assisted by gas molecules. National Science Review, 2023, 10, .	4.6	2
77797	Microstructure and Thermophysical Property Prediction for Chloride Composite Phase Change Materials: A Deep Potential Molecular Dynamics Study. Journal of Physical Chemistry C, 2023, 127, 6852-6860.	1.5	0
77798	Tailored BiVO₄ Photoanode Hydrophobic Microenvironment Enables Water Oxidative H₂O₂ Accumulation. Advanced Science, 2023, 10, .	5.6	7
77799	HfXO (Xâ€‰=â€‰S and Se) Janus monolayers as promising two-dimensional platforms for optoelectronic and spintronic applications. Journal of Materials Research, 0, , .	1.2	1
77800	A ten-fold coordinated high-pressure structure in hafnium dihydrogen with increasing superconducting transition temperature induced by enhancive pressure. Chinese Physics B, 2023, 32, 097402.	0.7	1
77801	Crystal growth, characterization and electronic band structure of TiSeS. Physical Review Materials, 2023, 7, .	0.9	1
77802	Vanadium-Containing Planar Heterostructures Based on Topological Insulators. JETP Letters, 2023, 117, 228-233.	0.4	0
77803	Cationâ€“Oxygen Bond Covalency: A Common Thread and a Major Influence toward Air/Waterâ€Stability and Electrochemical Behavior of â€œLayeredâ€•Naâ€“Transitionâ€Metalâ€Oxideâ€Based Cathode Materials. Advanced Energy Materials, 2023, 13, .	10.2	5
77804	High thermoelectric performance of two-dimensional SiPGaS/As heterostructures. Nanoscale, 2023, 15, 7302-7310.	2.8	3

#	Article	IF	Citations
77805	Progress of electrochemical synthesis of nitric acid: catalyst design, mechanistic insights, protocol and challenges. Journal of Materials Chemistry A, 2023, 11, 10125-10148.	5.2	12
77806	Sizeâ€Đependent Electrochemistry of Oxygenated Ti₃C₂T_x MXenes. Small Methods, 2023, 7, .	4.6	4
77807	Experimental and Ab-Initio Investigation of the Electrical Conductivity of Emeraldine Salt. Journal of Physical Chemistry C, 2023, 127, 6813-6824.	1.5	0
77808	Efficient seawater desalination in lamellar nanochannel-based boridene filtration membrane. Physical Chemistry Chemical Physics, 2023, 25, 11261-11267.	1.3	2
77809	Modulation of CO adsorption on 4,12,2-graphyne by Fe atom doping and applied electric field. Chinese Physics B, 2023, 32, 087101.	0.7	3
77810	DFTç”ç©¶ä¸‰å•åŽŸå¬åŒ–å‰‚ç”¨äºŽä¸€æ¥Nâ€“Câ€“Nå¶è•”æ˜•å°¿ç´. Science China Materials, 2023, 66, 2346-2353.	3.5	3
77811	Intermetallic alloy structureâ€“activity descriptors derived from inelastic X-ray scattering. Physical Chemistry Chemical Physics, 2023, 25, 11216-11226.	1.3	1
77812	Experimental and computational investigation on the charge storage performance of a novel Al2O3-reduced graphene oxide hybrid electrode. Scientific Reports, 2023, 13, .	1.6	10
77813	Stacking order and driving forces in the layered charge density wave phase of 1T-MX2 (M = Nb, Ta and X) Tj ETQq0 0 0 rgBT /Overlock 10	0.8	2
77814	Current-induced spin polarization in Janus WSSe monolayer. Physical Review B, 2023, 107, .	1.1	5
77815	Luâ€“Hâ€“N Phase Diagram from First-Principles Calculations. Chinese Physics Letters, 2023, 40, 057401.	1.3	29
77816	Electron transfer rules of minerals under pressure informed by machine learning. Nature Communications, 2023, 14, .	5.8	5
77817	In situ engineering 3D conductive core-shell nano-networks and electronic structure of bismuth alloy nanosheets for efficient electrocatalytic CO2 reduction. Science China Materials, 2023, 66, 2266-2273.	3.5	5
77818	Promising anode materials for alkali metal ion batteries: a case study on cobalt anti-MXenes. Physical Chemistry Chemical Physics, 2023, 25, 11789-11804.	1.3	1
77819	First-Principles Investigation on Electronic Properties and Surface Reactions of NaTaO₃ Adsorbed with Single-Metal Atoms. Journal of Physical Chemistry C, 2023, 127, 6702-6713.	1.5	0
77820	Insights into the Oxygen Evolution Reaction on Graphene-Based Single-Atom Catalysts from First-Principles-Informed Microkinetic Modeling. ACS Catalysis, 2023, 13, 5225-5235.	5.5	8
77821	Quasi-2D FCC lithium crystals inside defective bi-layer graphene: insights from first-principles calculations. Materials Today Energy, 2023, 34, 101293.	2.5	2
77822	Small bimetallic clusters Agn-1M (MÂ=ÂAu, Co, Cu, Ni, Pd, Pt; nÂ=Â3, 9, 15): Density functional theory and genetic algorithm. Surface Science, 2023, 733, 122290.	0.8	0

#	Article	IF	Citations
77823	Theoretical design of defects as a driving force for ion transport in <scp> Li ₃ OBr </scp> solid electrolyte. Energy and Environmental Materials, 0, , .	7.3	0
77824	Singleâ€Orientation Epitaxy of Quasiâ€1D Tellurium Nanowires on Mâ€Plane Sapphire for Highly Uniform Polarization Sensitive Shortâ€Wave Infrared Photodetection. Advanced Functional Materials, 2023, 33, .	7.8	12
77825	Impact of quartic anharmonicity on lattice thermal transport in EuTiO3: A comparative theoretical and experimental investigation. Materials Today Physics, 2023, 34, 101059.	2.9	2
77826	Large electrical strain in lead-free K0.5Na0.5NbO3-based ceramics by heterovalent doping. Journal of Materiomics, 2023, 9, 959-970.	2.8	2
77827	Synergistic marriage of CO2 reduction and sulfide oxidation towards a sustainable co-electrolysis process. Applied Catalysis B: Environmental, 2023, 332, 122718.	10.8	9
77828	Tracking Atomic Diffusion in Surface and Bulk CuO via Neural Network-Based Molecular Dynamics. Journal of Physical Chemistry C, 2023, 127, 6948-6958.	1.5	1
77829	Pressure-induced superconductivity in the photoelectric semiconductor BiSeI. Physical Review B, 2023, 107, .	1.1	1
77830	Modulating Electronic Structure with Copper Doping to Promote the Electrocatalytic Performance of Cobalt Disulfide in Liâ€“O₂ Batteries. Small, 2023, 19, .	5.2	14
77831	Theoretical Prediction of the Sublimation Behavior by Combining Ab Initio Calculations with Statistical Mechanics. Materials, 2023, 16, 2826.	1.3	1
77832	Bayesian optimization with active learning of design constraints using an entropy-based approach. Npj Computational Materials, 2023, 9, .	3.5	15
77833	First principles terahertz spectroscopy of molecular crystals: the crucial role of periodic boundary conditions benchmarked with experimental <scp>l</scp>-ascorbic acid spectra. Physical Chemistry Chemical Physics, 2023, 25, 12252-12258.	1.3	1
77834	Valley-Polarized Interlayer Excitons in 2D Chalcogenideâ€“Halide Perovskiteâ€“van der Waals Heterostructures. ACS Nano, 2023, 17, 7487-7497.	7.3	6
77835	Grazing-incidence diffraction reveals cellulose and pectin organization in hydrated plant primary cell wall. Scientific Reports, 2023, 13, .	1.6	5
77836	In situ growth of perovskite single-crystal thin films with low trap density. Cell Reports Physical Science, 2023, 4, 101363.	2.8	4
77837	Large piezoelectric response in a Jahn-Teller distorted molecular metal halide. Nature Communications, 2023, 14, .	5.8	11
77838	Selective synthesis of butane from carbon monoxide using cascade electrolysis and thermocatalysis at ambient conditions. Nature Catalysis, 2023, 6, 310-318.	16.1	17
77839	Thermodynamic UnderstandingÂof Impurity Phase Segregation in a PdCrO₂/CuCrO₂ Heterostructure. , 2023, 2, .		0
77840	Nanostructured Ni-MoCx: An efficient non-noble metal catalyst for the chemoselective hydrogenation of nitroaromatics. Nano Research, 2023, 16, 8919-8928.	5.8	11

#	Article	IF	Citations
77841	Superhard <mml:math xmlns:mml="http://www.w3.org/1998/Math/MathML"><mml:msub><mml:mi mathvariant="normal">BC</mml:mi><mml:mn>2</mml:mn></mml:msub><mml:mi mathvariant="normal">N</mml:mi></mml:math> in cubic diamondlike structure. Physical Review B, 2023, 107, .	1.1	5
77842	Molecular insights into the hydration of zwitterionic polymers. Molecular Systems Design and Engineering, 2023, 8, 1040-1048.	1.7	2
77843	Energy level alignments between organic and inorganic layers in 2D layered perovskites: conjugation vs. substituent. Nanoscale, 0, , .	2.8	0
77844	Absorption versus adsorption: high-throughput computation of impurities in 2D materials. Npj 2D Materials and Applications, 2023, 7, .	3.9	2
77845	Phosphorus diffusion and deactivation during SiGe oxidation. Journal of Applied Physics, 2023, 133, 135301.	1.1	0
77846	Semiconducting nonperovskite ferroelectric oxynitride designed ab initio. Applied Physics Letters, 2023, 122, 142902.	1.5	0
77847	Tuning Multiple Landau Quantization in Transition-Metal Dichalcogenide with Strain. Nano Letters, 0, , .	4.5	1
77848	High-entropy single-atom activated carbon catalysts for sustainable oxygen electrocatalysis. Nature Sustainability, 2023, 6, 816-826.	11.5	49
77849	C<mml:math xmlns:mml="http://www.w3.org/1998/Math/MathML" altimg="si34.svg" display="inline" id="d1e1137"><mml:msub><mml:mrow /><mml:mrow><mml:mn>4</mml:mn></mml:mrow></mml:msub></mml:math>N<mml:math xmlns:mml="http://www.w3.org/1998/Math/MathML" altimg="si34.svg" display="inline" id="d1e1145"><mml:msub><mml:mrow /><mml:mrow><mml:mn>4</mml:mn></mml:mrow></mml:msub></mml:math>: A symmetry-protected se	1.4	1
77850	Sr-Doped NASICON-Structured Cathode with Enhanced Conductivity for Ultrafast and High-Stability Sodium-Ion Storage. ACS Applied Energy Materials, 0, , .	2.5	1
77851	Effects of the antiferrodistortive instability on the structural behavior of <mml:math xmlns:mml="http://www.w3.org/1998/Math/MathML"><mml:msub><mml:mi>BaZrO</mml:mi><mml:mn>3</mml:mn></mml:msub></mml:math> by atomistic simulations. Physical Review B, 2023, 107, .	1.1	0
77852	Relative Stability of Pyrazinamide Polymorphs Revisited: A Computational Study of Bending and Brittle Forms Phase Transitions in a Broad Temperature Range. Crystals, 2023, 13, 617.	1.0	2
77853	High-Throughput First-Principles Prediction of Interfacial Adhesion Energies in Metal-on-Metal Contacts. ACS Applied Materials & Interfaces, 2023, 15, 19624-19633.	4.0	5
77854	Machine-learning-assisted discovery of boron-doped graphene with high work function as an anode material for Li/Na/K-ion batteries. Physical Chemistry Chemical Physics, 2023, 25, 12200-12206.	1.3	2
77855	Tailoring On-Surface Molecular Reactions and Assembly through Hydrogen-Modified Synthesis: From Triarylamine Monomer to 2D Covalent Organic Framework. ACS Nano, 2023, 17, 7366-7376.	7.3	2
77856	Structural and theoretical investigations on the â€œcoloringâ€•scheme of Î³-brass type phase Ag5Cd8. Journal of Solid State Chemistry, 2023, 323, 124019.	1.4	1
77857	Promotion Effect of Well-Defined Deposited Water Layer on Carbon Monoxide Oxidation Catalyzed by Single-Atom Alloys. Journal of Physical Chemistry Letters, 2023, 14, 3498-3505.	2.1	1
77858	Molecular orientation-dependent energetic shifts in solution-processed non-fullerene acceptors and their impact on organic photovoltaic performance. Nature Communications, 2023, 14, .	5.8	25

#	Article	IF	Citations
77859	Solution-Processed Hybrid Europium (II) Iodide Scintillator for Sensitive X-Ray Detection. Research, 2023, 6, .	2.8	1
77860	Friction properties of black phosphorus: a first-principles study. Nanotechnology, 2023, 34, 275703.	1.3	0
77861	Multiple surface states, nontrivial band topology, and antiferromagnetism in GdAuAl₄Ge₂. Chinese Physics B, 2023, 32, 077401.	0.7	2
77862	Computational Screening of Twoâ€Dimensional Metalâ€Organic Frameworks as Efficient Singleâ€Atom Catalysts for Oxygen Reduction Reaction. Chemistry - A European Journal, 2023, 29, .	1.7	2
77863	Elucidating the exceptional halide ion etching of bimetallic Agâ€“Cu oxides for efficient adsorption and porous nanostructure formation. Materials Horizons, 2023, 10, 2506-2515.	6.4	2
77864	Valley piezoelectricity promoted by spin-orbit coupling in quantum materials. Science China: Physics, Mechanics and Astronomy, 2023, 66, .	2.0	1
77865	A pyrolysis-free Ni/Fe bimetallic electrocatalyst for overall water splitting. Nature Communications, 2023, 14, .	5.8	56
77866	Selective sorption of oxygen and nitrous oxide by an electron donor-incorporated flexible coordination network. Communications Chemistry, 2023, 6, .	2.0	3
77867	Adsorption of NO_x (x = 1, 2) Molecules on the CoFeMnSi(001) Surface: First-Principles Insights. ACS Omega, 2023, 8, 14005-14012.	1.6	7
77868	Superior mechanical properties of multilayer covalent-organic frameworks enabled by rationally tuning molecular interlayer interactions. Proceedings of the National Academy of Sciences of the United States of America, 2023, 120, .	3.3	7
77869	Influence of defects on the valley polarization properties of monolayer <mml:math xmlns:mml="http://www.w3.org/1998/Math/MathML"><mml:msub><mml:mi>MoS</mml:mi><mml:mn>2</mml:mn></mml:msub></mm grown by chemical vapor deposition. Physical Review B, 2023, 107, .	1.1	3
77870	Substantial lifetime enhancement for Si-based photoanodes enabled by amorphous TiO2 coating with improved stoichiometry. Nature Communications, 2023, 14, .	5.8	5
77871	Efficient solar fuel production enabled by an iodide oxidation reaction on atomic layer deposited MoS₂. , 2023, 5, .		2
77872	Heterogeneous Integration of Freestanding Bilayer Oxide Membrane for Multiferroicity. Advanced Science, 2023, 10, .	5.6	4
77873	Self-Limited Embedding Alternating 585-Ringed Divacancies and Metal Atoms into Graphene Nanoribbons. Journal of the American Chemical Society, 0, , .	6.6	4
77874	Mining of lattice distortion, strength, and intrinsic ductility of refractory high entropy alloys. Npj Computational Materials, 2023, 9, .	3.5	10
77875	Revealing the Epitaxial Interface between Al₁₃Fe₄ and Al₅Fe₂ Enabling Atomic Al Interdiffusion. ACS Applied Materials & Interfaces, 2023, 15, 19593-19603.	4.0	5
77876	Room-temperature synthesis of lead-free copper(I)-antimony(III)-based double perovskite nanocrystals. APL Materials, 2023, 11, .	2.2	3

#	Article	IF	Citations
77877	A Quantum Monte Carlo Study of the Structural, Energetic, and Magnetic Properties of Two-Dimensional H and T Phase VSe₂. Journal of Physical Chemistry Letters, 2023, 14, 3553-3560.	2.1	3
77878	Hydrogen from catalytic non-thermal plasma-assisted steam methane reformingÂreaction. International Journal of Hydrogen Energy, 2023, 48, 24328-24341.	3.8	4
77879	Detailed Mechanical Characterization of LiCoO₂ and LiNi_{0.33}Co_{0.33}Mn_{0.33}O₂ Cathode Materials Using DFT Calculations. Chemistry Letters, 2023, 52, 317-321.	0.7	0
77880	Emergent charge density wave featuring quasi-one-dimensional chains in Ta-intercalated bilayer <mml:math xmlns:mml="http://www.w3.org/1998/Math/MathML"><mml:mrow><mml:mn>2</mml:mn><mml:mi>H</mml:mi></mml:mrow><mml:mrow><mml:mn mathvariant="normal">TaS</mml:mn><mml:mn>2</mml:mn></mml:msub></mml:math> with coexisting superconductivity. Physical Review B, 2023, 107, .	3.7	2
77881	A LaCl3-based lithium superionic conductor compatible with lithium metal. Nature, 2023, 616, 77-83.	13.7	84
77882	Synthesis, Characterization, and Modeling of a Chemically Ordered Quaternary Boride, Mo₄MnSiB₂. Crystal Growth and Design, 0, , .	1.4	0
77883	Bulk and surface electronic structure of <mml:math xmlns:mml="http://www.w3.org/1998/Math/MathML"><mml:msub><mml:mrow><mml:mi>NiBi</mml:mi></mml:mrow><mml:mn>3</mml:mn></m Physical Review B, 2023, 107, .	3.7	1
77884	Two-dimensional ferromagnetic semiconductors of rare-earth Janus 2H-GdIBr monolayers with large valley polarization. Nanoscale, 0, , .	2.8	3
77885	Magnetization reversal of perpendicular magnetic anisotropy regulated by ferroelectric polarization in CoFe₃N/BaTiO₃ heterostructures: first-principles calculations. RSC Advances, 2023, 13, 9924-9931.	1.7	1
77886	Proton Transport in Perfluorinated Ionomer Simulated by Machine-Learned Interatomic Potential. Journal of Physical Chemistry Letters, 2023, 14, 3581-3588.	2.1	5
77887	WhereWulff: A Semiautonomous Workflow for Systematic Catalyst Surface Reactivity under Reaction Conditions. Journal of Chemical Information and Modeling, 2023, 63, 2427-2437.	2.5	1
77888	Pressure-Induced Stability of Methane Hydrate from Machine Learning Force Field Simulations. Journal of Physical Chemistry C, 2023, 127, 7071-7077.	1.5	2
77889	Chirality Effects and Semiconductor versus Metallic Nature in Halide Nanotubes. Journal of Physical Chemistry C, 2023, 127, 7162-7171.	1.5	0
77890	TEXplorer.org: Thermoelectric material properties data platform for experimental and first-principles calculation results. APL Materials, 2023, 11, .	2.2	4
77891	First-Principles Insights into the Relative Stability, Physical Properties, and Chemical Properties of MoSe₂. ACS Omega, 2023, 8, 13799-13812.	1.6	3
77892	Large tunneling magnetoresistance in spin-filtering 1T-MnSe₂/h-BN van der Waals magnetic tunnel junction. Nanoscale, 2023, 15, 8447-8455.	2.8	2
77893	Realizing a Superconducting Square-Lattice Bismuth Monolayer. ACS Nano, 2023, 17, 7604-7610.	7.3	2
77894	Metal Encapsulation-Driven Strong Metalâ€“Support Interaction on Pt/Co₃O₄ during CO Oxidation. ACS Catalysis, 2023, 13, 5326-5335.	5.5	14

#	Article	IF	Citations
77895	Atomic-scale origin of the low grain-boundary resistance in perovskite solid electrolyte Li0.375Sr0.4375Ta0.75Zr0.25O3. Nature Communications, 2023, 14, .	5.8	12
77896	Non-volatile electric control of magnetic and topological properties of MnBi₂Te₄ thin films [*]. 2D Materials, 2023, 10, 035008.	2.0	2
77897	Efficient all-thermally evaporated perovskite light-emitting diodes for active-matrix displays. Nature Photonics, 2023, 17, 435-441.	15.6	25
77898	Effect of magnon-magnon interaction on ferromagnetism in hexagonal manganese pnictide monolayers. Physical Review B, 2023, 107, .	1.1	2
77899	Bulk Synthesis and Transport Properties of Rocksalt-Type Ti_{1â€“x}Mg_xN Solid Solution. Inorganic Chemistry, 2023, 62, 5951-5960.	1.9	2
77900	Density functional theory (DFT) simulation and approach to property-driven investigations in ceramic and composites materials. , 2023, , 461-490.		0
77901	First-principles surface reaction rates by ring polymer molecular dynamics and neural network potential: role of anharmonicity and lattice motion. Chemical Science, 2023, 14, 5087-5098.	3.7	3
77902	Crystal structure and electronic properties of low-dimensional hexamethylenediaminium lead halide perovskites. Dalton Transactions, 0, , .	1.6	1
77903	Continuous Roomâ€Temperature Spinâ€Injection Modulation Achieved by Spinâ€Filtering Competition in Molecular Spin Valves. Advanced Materials, 2023, 35, .	11.1	3
77904	Modulating interfacial charge redistribution of Ni2P/CuCo2S4 p-n nano-heterojunctions for efficient electrocatalytic overall water splitting. International Journal of Hydrogen Energy, 2023, 48, 25300-25314.	3.8	5
77905	Machine-learning-assisted rational design of 2D doped tellurene for fin field-effect transistor devices. Patterns, 2023, 4, 100722.	3.1	7
77906	Fluoroalkyl phosphonic acid radical scavengers for proton exchange membrane fuel cells. Journal of Materials Chemistry A, 2023, 11, 9748-9754.	5.2	6
77907	Insights to the fracture toughness, damage tolerance, electronic structure, and magnetic properties of carbides M₂C (M = Fe, Cr). Materials Research Express, 2023, 10, 046515.	0.8	0
77908	Diffusion of O Atoms on a CO-Covered Ru(0001) Surfaceâ”€A Combined High-Speed Scanning Tunneling Microscopy and Density Functional Theory Study at an Enhanced CO Coverage. Journal of Physical Chemistry C, 2023, 127, 7197-7210.	1.5	0
77909	Symmetryâ€Mismatchâ€Induced Ferromagnetism in the Interfacial Layers of CaRuO₃/SrTiO₃ Superlattices. Advanced Functional Materials, 2023, 33, .	7.8	6
77910	From Layered Antiferromagnet to 3D Ferromagnet: LiMnBi-to-MnBi Magneto-Structural Transformation. Chemistry of Materials, 0, , .	3.2	0
77911	Ceramic-based functional electrode materials for application in solid oxide cell-based electrochemical devices. , 2023, , 255-288.		0
77912	General and transferable tight binding model for two-dimensional Bismuth allotropes. Physica Scripta, 2023, 98, 055916.	1.2	0

#	Article	IF	Citations
77913	Acrossâ€Layer Sliding Ferroelectricity in 2D Heterolayers. Advanced Functional Materials, 2023, 33, .	7.8	14
77914	Hydrogen anion as a strong magnetic mediator for obtaining high-temperature ferromagnetic semiconductors: The case of hydride double perovskites. Physical Review B, 2023, 107, .	1.1	0
77915	Insight into the effects of S-vacancy and O-doping in monolayer VS2 as lithium-ion battery anodes from first-principles calculations. Surfaces and Interfaces, 2023, 38, 102851.	1.5	2
77916	Prediction of four Si₃N₄ compounds by first-principles calculations. AIP Advances, 2023, 13, 045310.	0.6	0
77917	Electrocatalytic reduction of CO₂ on size-selected nanoclusters of first-row transition metal nanoclusters: a comprehensive mechanistic investigation. Physical Chemistry Chemical Physics, 2023, 25, 11630-11652.	1.3	6
77918	Probing Anisotropic Deformation and Near-Infrared Emission Tuning in Thin-Layered InSe Crystal under High Pressure. Nano Letters, 2023, 23, 3493-3500.	4.5	6
77919	Role of Non-covalent Interaction toward Conductivity in a One-Dimensional Tube-like Silver-Thiolate Structure. Crystal Growth and Design, 2023, 23, 3164-3170.	1.4	1
77920	Formation of active sites on transition metals through reaction-driven migration of surface atoms. Science, 2023, 380, 70-76.	6.0	33
77921	Two-dimensional half-metallicity in transition metal atoms decorated Cr2Ge2Te6. Frontiers in Physics, 0, 11, .	1.0	3
77922	Surface redox pseudocapacitance-based vanadium nitride nanoparticles toward a long-cycling sodium-ion battery. Materials Today Energy, 2023, 34, 101300.	2.5	4
77923	Computational and experimental studies on band alignment of ZnO/In_xGa_{2â^'x}O₃/GaN heterojunctions. Journal of Chemical Physics, 2023, 158, 134720.	1.2	0
77924	Physical Review B, 2023, 107, . Nucleation interface of La2O3 <mml:math xmlns:mml="http://www.w3.org/1998/Math/MathML" altimg="si0032.svg"><mml:mrow><mml:mo stretchy="false">(</mml:mo><mml:mn>1</mml:mn><mml:mover) Tj ETQq1 1 0.784314 rgBT /Overlock 10 Tf 50 307 Td (accent="true"	0.9	0
77925	xmlns:mml="http://www.w3.org/1998/Math/MathML" altimg="si0033.svg"><mml:mrow><mml:mo stretch Liâ€"N₂ Battery for Ammonia Synthesis and Computational Insight. ACS Applied Materials & Interfaces, 2023, 15, 19032-19042.	4.0	1
77926	Pressure-induced ferroelectric-to-superconductor transition in <mml:math xmlns:mml="http://www.w3.org/1998/Math/MathML"><mml:msub><mml:mi mathvariant="normal">SnPS</mml:mi><mml:mn>3</mml:mn></mml:msub></mml:math>. Physical Review B, 2023, 107, .	1.1	0
77927	Enhancing the Understanding of the Oxygen Evolution Reaction on Bimetallic Two-Dimensional MOFs through Theoretical Investigation. Journal of Physical Chemistry C, 2023, 127, 7257-7267.	1.5	1
77928	Rapid and Scalable Transfer of Largeâ€Area Graphene Wafers. Advanced Materials, 2023, 35, .	11.1	8
77929	Robust half-metallicity and topological properties in square-net potassium manganese chalcogenides. Physical Review B, 2023, 107, .	1.1	2
77930	FeC6N monolayer with ideal properties for water splitting. Applied Surface Science, 2023, 626, 157203.	3.1	2

#	Article	IF	Citations
77931	Synergistic effect of phosphorus doping and MoS2 co-catalysts on g-C3N4 photocatalysts for enhanced solar water splitting. Journal of Materials Science and Technology, 2023, 158, 171-179.	5.6	21
77932	Ultrafine Fe₂C Iron Carbide Nanoclusters Trapped in Topological Carbon Defects for Efficient Electroreduction of Carbon Dioxide. Advanced Energy Materials, 2023, 13, .	10.2	4
77933	Oxygen Vacancy Boosts the V₂O₅ Performance for the Electrochemical H₂O₂ Product. Industrial & Engineering Chemistry Research, 0, , .	1.8	2
77934	Engineering d-p orbital hybridization through regulation of interband energy separation for durable aqueous Zn//VO2(B) batteries. Chemical Engineering Journal, 2023, 464, 142711.	6.6	6
77935	Constructing ion diffusion highway in strongly coupled WSe2-carbon hybrids enables superior energy storage performance. Matter, 2023, 6, 1604-1621.	5.0	5
77936	Fully Transparent Ultraviolet Photodetector with Ultrahigh Responsivity Enhanced by MXeneâ€Induced Photogating Effect. Advanced Optical Materials, 2023, 11, .	3.6	4
77937	Tailoring the Angular Mismatch in MoS₂ Homobilayers through Deformation Fields. Small, 2023, 19, .	5.2	2
77938	Insight into Catalytic Active Sites on TiO₂/RuO₂ and SnO₂/RuO₂ Alloys for Electrochemical CO₂ Reduction to CO and Formic Acid. ACS Catalysis, 2023, 13, 5491-5501.	5.5	5
77939	Template Based Synthesis of Porous Graphdiyne Nanosheet for Reversible and Fast NO₂ Detection by UV Irradiation. ChemPhysChem, 2023, 24, .	1.0	1
77940	High-mobility transport symmetry and effect of strain on electronic and optical properties in few-layer blue phosphorus. Computational Materials Science, 2023, 224, 112177.	1.4	2
77941	Interstitial Hydrogen Atom to Boost Intrinsic Catalytic Activity of Tungsten Oxide for Hydrogen Evolution Reaction. Small, 2023, 19, .	5.2	4
77942	Structural, vibrational, electronic, and elastic properties of 2D alkali carbide as a metallic material. Computational Condensed Matter, 2023, , e00805.	0.9	0
77943	Orbital degree of freedom induced multiple sets of second-order topological states in two-dimensional breathing Kagome crystals. Npj Quantum Materials, 2023, 8, .	1.8	6
77944	Unconventional Self-Reconstructed Trimer-like Metal Zigzag Edge of 1T-Phase Transition Metal Dichalcogenides. Journal of Physical Chemistry Letters, 2023, 14, 3651-3657.	2.1	0
77945	Order-disorder phase transition driven by interlayer sliding in lead iodides. Nature Communications, 2023, 14, .	5.8	2
77946	Fast and Durable Lithium Storage Enabled by Tuning Entropy in Wadsleyâ€"Roth Phase Titanium Niobium Oxides. Small, 2023, 19, .	5.2	9
77947	Contact Engineering of Halide Perovskites: Gold is Not Good Enough; Metalloid is Better. Small Methods, 0, , .	4.6	0
77948	Insights into the Electrochemical Production of Hydrogen Peroxide over Single-Atom Coâ€"Nâ€"C Catalysts with the Introduction of Carbon Vacancy Defect near the Coâ€"N₄ Site. Journal of Physical Chemistry Letters, 2023, 14, 3658-3668.	2.1	4

#	Article	IF	Citations
77949	Bi2S3/rGO nanocomposites with covalent heterojunctions as a high-performance aqueous zinc ion battery material. Ceramics International, 2023, 49, 22160-22169.	2.3	3
77950	Interfacial Electron Distribution of Co Nanoparticles Supported on Nâ€Doped Mesoporous Hollow Carbon Spheres Endows Highly Efficient ORR, OER, and HER. Advanced Materials Interfaces, 2023, 10, .	1.9	3
77951	Carbon-driven coherent nanoprecipitates enable ultrahigh yield strength in a high-entropy alloy. Materials Today Nano, 2023, 22, 100331.	2.3	0
77952	First principles investigation of cobalt-phthalocyanine active site tuning via atomic linker immobilization for CO2 electroreduction. Journal of Catalysis, 2023, 422, 43-55.	3.1	3
77953	Electronic structure and microscopic model of Cu$$_{2}$$(SeO$$_{3}$$)F$$_{2}$$: a 2-D AFM ladder compound. European Physical Journal B, 2023, 96, .	0.6	0
77954	Interstitial Segregation has the Potential to Mitigate Liquid Metal Embrittlement in Iron. Advanced Materials, 2023, 35, .	11.1	4
77955	Positive correlation of Nb/Cr doping with dehydrogenation performance of ZrCo-based hydrides. International Journal of Hydrogen Energy, 2023, , .	3.8	0
77956	Enhancing ferromagnetic coupling in CrXY (X = O, S, Se; Y = Cl, Br, I) monolayers by turning the covalent character of Cr-X bonds. Npj Computational Materials, 2023, 9, .	3.5	3
77957	Systematic search for stabilizing dopants in ZrO2 and HfO2 using first-principles calculations. IEEE Transactions on Semiconductor Manufacturing, 2023, , 1-1.	1.4	0
77958	Nanostructure-property relation of Î£5 grain boundary in HfNbZrTi high-entropy alloy under shear. Journal of Materials Science, 2023, 58, 6757-6774.	1.7	2
77959	Grapheneâ€Enhanced Metal Transfer Printing for Strong van der Waals Contacts between 3D Metals and 2D Semiconductors. Advanced Functional Materials, 2023, 33, .	7.8	5
77960	Uniform Longitudinal Zinc Growth beyond Interface Guided by Anionic Covalent Organic Framework for Dendriteâ€Free Aqueous Zinc Batteries. Batteries and Supercaps, 2023, 6, .	2.4	4
77961	Competition between phonon-vacancy and four-phonon scattering in cubic boron arsenide by machine learning interatomic potential. Physical Review Materials, 2023, 7, .	0.9	2
77962	High-Performances â€œFueledâ€•Photodetector Based on few-layered 2D Ternary Chalcogenide NiGa2S4. Journal of Materials Chemistry C, 0, , .	2.7	0
77963	A Ï€â€Bridge Spacer Embedded Electron Donorâ€“Acceptor Polymer for Flexible Electrochromic Znâ€ion Batteries. Advanced Materials, 2023, 35, .	11.1	7
77964	Origin of improved average power factor and mechanical properties of SnTe with high-dose Bi2Te3 alloying. Ceramics International, 2023, 49, 21916-21922.	2.3	3
77965	Hydrogen-bond-bridged intermediate for perovskite solar cells with enhanced efficiency and stability. Nature Photonics, 2023, 17, 478-484.	15.6	62
77966	Shock-induced metallization of polystyrene along the principal Hugoniot investigated by advanced thermal density functionals. Physical Review B, 2023, 107, .	1.1	1

#	Article	IF	Citations
77967	Nanoclayâ€Modulated Interfacial Chemical Bond and Internal Electric Field at the Co₃O₄/TiO₂ pâ€n Junction for Efficient Charge Separation. Small, 2023, 19, .	5.2	7
77968	Li-ion transport at the LiFePO4/Î³-Li3PO4 interface and its enhancement through surface nitrogen doping. Journal of Applied Physics, 2023, 133, .	1.1	2
77969	Ultra-low lattice thermal conductivity induces high-performance thermoelectricity in Janus group-VIA binary monolayers: A comparative investigation. Vacuum, 2023, 213, 112075.	1.6	5
77970	Optical spectroscopy and band structure calculations of the structural phase transition in the vanadium-based kagome metal <mml:math xmlns:mml="http://www.w3.org/1998/Math/MathML"><mml:mrow><mml:msub><mml:mi>ScV</mml:mi><mml:mn>6</mml:mn></ Physical Review B, 2023, 107, .	1.1	23
77971	Internal quantum efficiency higher than 100% achieved by combining doping and quantum effects for photocatalytic overall water splitting. Nature Energy, 2023, 8, 504-514.	19.8	38
77972	Exploring Proton Pair Motion Away from the Global Protonâ€“Tuple Energy Minimum in Yttrium-Doped Barium Zirconate. Inorganics, 2023, 11, 160.	1.2	1
77973	Magnetic Anisotropy of Single-Ion Magnet (PPh4)2 [ReF6]Â·2H2O. JETP Letters, 2023, 117, 606-611.	0.4	1
77974	Active site recovery and N-N bond breakage during hydrazine oxidation boosting the electrochemical hydrogen production. Nature Communications, 2023, 14, .	5.8	21
77975	Machine learning-assisted exploration of the intrinsic factors affecting the catalytic activity of ORR/OER bifunctional catalysts. Applied Surface Science, 2023, 628, 157225.	3.1	8
77976	Engineering Peculiar Cathode Electrolyte Interphase toward Sustainable and Highâ€Rate Liâ€“S Batteries. Advanced Energy Materials, 2023, 13, .	10.2	8
77977	Modulating the Protonâ€Conducting Lanes in Spinel ZnMn₂O₄through Offâ€Stoichiometry. Advanced Energy Materials, 2023, 13, .	10.2	7
77978	Comprehensive Mechanism and Microkinetic Model-Driven Rational Screening of 3N-Modulated Single-Atom Catalysts for Propane Dehydrogenation. ACS Catalysis, 2023, 13, 5529-5537.	5.5	6
77979	Uniform Zinc Deposition Regulated by a Nitrogenâ€Doped MXene Artificial Solid Electrolyte Interlayer. Small, 2023, 19, .	5.2	7
77980	Reversible hydrogen storage tendency of light-metal (Li/Na/K) decorated carbon nitride (C9N4) monolayer. International Journal of Hydrogen Energy, 2023, 48, 26301-26313.	3.8	11
77981	Direct Synthesis of Two-Dimensional SnSe and SnSe₂ through Molecular Scale Preorganization. Inorganic Chemistry, 2023, 62, 6274-6287.	1.9	2
77982	Calculated Outstanding Energy-Storage Media by Aluminum-Decorated Carbon Nitride (g-C3N4): Elucidating the Synergistic Effects of Electronic Structure Tuning and Localized Electron Redistribution. Crystals, 2023, 13, 655.	1.0	1
77983	Li ion diffusion behavior of Li₃OCl solid-state electrolytes with different defect structures: insights from the deep potential model. Physical Chemistry Chemical Physics, 2023, 25, 13297-13307.	1.3	2
77984	Quantum anomalous Hall effect with high Chern numbers in functionalized square-octagon Sb monolayers. 2D Materials, 0, , .	2.0	0

#	Article	IF	Citations
77985	Superconducting gap symmetry from Bogoliubov quasiparticle interference analysis on <mml:math xmlns:mml="http://www.w3.org/1998/Math/MathML"><mml:mrow><mml:msub><mml:mi>Sr</mml:mi><mml:mn>2</mml:mn></mml:r Physical Review B, 2023, 107, .	1.1	2
77986	An investigation for H2/N2 adsorptive separation in SIFSIX-2-Cu-i. International Journal of Hydrogen Energy, 2023, , .	3.8	1
77987	Electron-doping Ruddlesden-Popper nickelate. Europhysics Letters, 2023, 142, 26005.	0.7	1
77988	Effects of lithium intercalation in bilayer graphene. Physical Review B, 2023, 107, .	1.1	1
77989	Defect engineering mediated molecules coordination activation for one-pot synthesis of secondary amine over Bi2MoO6 hierarchical microspheres. Chemical Engineering Science, 2023, 275, 118747.	1.9	2
77990	Breakdown of the perfect crystal dynamics in dynamically disordered over-stoichiometric <mml:math xmlns:mml="http://www.w3.org/1998/Math/MathML"><mml:mrow><mml:msub><mml:mi>Nd</mml:mi><mml:mn>1.2</mml:mn></mml:mn></mml: Physical Review B, 2023, 107, .	1.1	1
77991	Accelerating the Discovery of Metastable IrO₂ for the Oxygen Evolution Reaction by the Self-Learning-Input Graph Neural Network. Jacs Au, 2023, 3, 1131-1140.	3.6	3
77992	Potential high-temperature superconductivity in the substitutional alloy of <mml:math xmlns:mml="http://www.w3.org/1998/Math/MathML"><mml:mrow><mml:mrow><mml:mo>(</mml:mo><mml:mi) Tj ETQq1 1 0.7843 mathvariant="normal">H</mml:mi><mml:mn>11</mml:mn></mml:msub></mml:mrow></mml:math> under High pressure. Physical Review B, 2023, 107, .	1.1	4
77993	R4N+ and Clâ¯ stabilized Î±-formamidinium lead triiodide and efficient bar-coated mini-modules. Joule, 2023, 7, 797-809.	11.7	6
77994	Strain-controllable high Curie temperature and magnetic anisotropy energy in two-dimensional Fe2Si and Fe2Ge. Physica E: Low-Dimensional Systems and Nanostructures, 2023, 151, 115732.	1.3	2
77995	Oxynitrides enabled photoelectrochemical water splitting with over 3,000 hrs stable operation in practical two-electrode configuration. Nature Communications, 2023, 14, .	5.8	8
77996	Boosting kinetics of tellurium redox reaction for high-performance aqueous zinc-tellurium batteries. Chemical Engineering Journal, 2023, 465, 142896.	6.6	14
77997	Comprehensive ab initio study of effects of alloying elements on generalized stacking fault energies of Ni and <mml:math xmlns:mml="http://www.w3.org/1998/Math/MathML"><mml:msub><mml:mi mathvariant="normal">Ni</mml:mi><mml:mn>3</mml:mn></mml:msub><mml:mi mathvariant="normal">Al</mml:mi></mml:math>. Physical Review Materials, 2023, 7, .	0.9	0
77998	Spinâ€“Orbit-Coupling-Induced Topological Transition and Anomalously Strong Intervalley Scattering in Two-Dimensional Bismuth Allotropes with Enhanced Thermoelectric Performances. ACS Applied Materials & Interfaces, 2023, 15, 19545-19559.	4.0	1
77999	Spontaneous valley polarization and valley-nonequilibrium quantum anomalous Hall effect in Janus monolayer ScBrI. Nanoscale, 2023, 15, 8395-8405.	2.8	18
78000	Structure and Reactivity of the Ionic Liquid [C1C1Im][Tf2N] on Cu(111). Topics in Catalysis, 0, , .	1.3	3
78001	Computational Design of Cation-Disordered Li₃Ta₂O₅ with Fast Ion Diffusion Dynamics and Rich Redox Chemistry for a High-Rate Li-Ion Battery Anode Material. Chemistry of Materials, 0, , .	3.2	0
78002	Nanomolding of metastable Mo4P3. Matter, 2023, 6, 1894-1902.	5.0	4

#	Article	IF	Citations
78003	Type-II MoSi₂N₄/MoS₂ van der Waals Heterostructure with Excellent Optoelectronic Performance and Tunable Electronic Properties. Journal of Physical Chemistry C, 2023, 127, 7878-7886.	1.5	6
78004	Morphological Sensitivity of Silver Nanoparticles to Environment. Environmental Science: Nano, 0, , .	2.2	0
78005	Selective nitric oxide electroreduction at monodispersed transition-metal sites with atomically precise coordination environment. Chem Catalysis, 2023, 3, 100598.	2.9	2
78006	An energy-saving support made of silver nanowire aerogel for hydrogen evolution reaction. Cell Reports Physical Science, 2023, 4, 101377.	2.8	2
78007	Designing ternary superconducting hydrides with A15-type structure at moderate pressures. Materials Today Physics, 2023, 34, 101086.	2.9	6
78008	The Effect of Hydrogen on Plastic Anisotropy of Mg and Î±-Ti/Zr from First-Principles Calculations. Materials, 2023, 16, 3016.	1.3	0
78009	Cation disorder dominates the defect chemistry of high-voltage LiMn_{1.5}Ni_{0.5}O₄ (LMNO) spinel cathodes. Journal of Materials Chemistry A, 2023, 11, 13353-13370.	5.2	7
78010	B2 to ordered omega transformation during isothermal annealing of refractory high entropy alloys: Implications for high temperature phase stability. Journal of Alloys and Compounds, 2023, 953, 170065.	2.8	4
78011	Understanding the wetting of transition metal dichalcogenides from an ab initio perspective. Physical Review Research, 2023, 5, .	1.3	0
78012	Ultralow lattice thermal conductivity of binary compounds A₂B (A = Cs, Rb & B = Se,) Tj ETQq1 1 0.784314 rgBT /Over 12157-12164.	1.3	5
78013	Ligand field tuning of d-orbital energies in metal-organic framework clusters. Communications Chemistry, 2023, 6, .	2.0	4
78014	Anharmonic Correction to Free Energy Barriers from DFT-Based Molecular Dynamics Using Constrained Thermodynamic Integration. Journal of Chemical Theory and Computation, 2023, 19, 2455-2468.	2.3	2
78015	Metalâ€“Organic-Framework-Derived 3D Hierarchical Matrixes for High-Performance Flexible Liâ€“S Batteries. ACS Applied Materials & Interfaces, 2023, 15, 20064-20074.	4.0	8
78016	Violet phosphorus transmission and photoconductance spectroscopy. Nanotechnology, 2023, 34, 285206.	1.3	6
78017	Bifunctional hierarchical NiCoP@FeNi LDH nanosheet array electrocatalyst for industrial-scale high-current-density water splitting. Journal of Materials Science and Technology, 2023, 159, 33-40.	5.6	21
78018	Directly Grow Ultrasmall Co₂P QDs on MoS₂ Nanosheets to Form Heterojunctions Greatly Boosting Electron Transfer toward Hydrogen Evolution. Journal of Physical Chemistry C, 2023, 127, 9681-9689.	1.5	2
78019	Symmetry-based computational search for novel binary and ternary 2D materials. 2D Materials, 2023, 10, 035007.	2.0	1
78020	Potential-Dependent Active Moiety of Feâ€“Nâ€“C Catalysts for the Oxygen Reduction Reaction. Journal of Physical Chemistry Letters, 2023, 14, 3749-3756.	2.1	10

#	Article	IF	Citations
78021	Synergistic effects of extrinsic photoconduction and photogating in a short-wavelength ZrS₃ infrared photodetector. Materials Horizons, 2023, 10, 2579-2586.	6.4	4
78022	Active learning strategies for atomic cluster expansion models. Physical Review Materials, 2023, 7, .	0.9	9
78023	Mechanism Regulating Self-Intercalation in Layered Materials. Nano Letters, 2023, 23, 3623-3629.	4.5	4
78024	Linker Aromaticity Reduces Band Dispersion in 2D Conductive Metalâ€“Organic Frameworks. , 2023, 5, 1476-1480.		3
78025	Modular development of deep potential for complex solid solutions. Physical Review B, 2023, 107, .	1.1	4
78026	Carbon-coating strengthens the solid electrolyte interphase to inhibit Si pulverization. Journal of Materials Chemistry A, 2023, 11, 9807-9815.	5.2	4
78027	Basal plane activation of two-dimensional transition metal dichalcogenides via alloying for the hydrogen evolution reaction: first-principles calculations and machine learning prediction. Journal of Materials Chemistry A, 2023, 11, 9964-9975.	5.2	4
78028	Morphology-dependent adsorption energetics of Ru nanoparticles on hcp-boron nitride (001) surface â€“ a first-principles study. Nanoscale Advances, 2023, 5, 2422-2426.	2.2	1
78029	Boron-Pnictogen Monolayers with Negative Poissonâ€™s ratio and Excellent Band Edge Positions for Photocatalytic Water Splitting. Physical Chemistry Chemical Physics, 0, , .	1.3	0
78030	NiO Matrix Decorated by Ru Single Atoms: Electron-Rich Ru-Induced High Activity and Selectivity toward Electrochemical N₂ Reduction. Journal of Physical Chemistry Letters, 2023, 14, 3785-3793.	2.1	4
78031	Extending the metal to insulator transitions of rareâ€earth nickelates towards low temperature ranges. Journal of the American Ceramic Society, 2023, 106, 5067-5077.	1.9	1
78032	Spectral Downshifting and Passivation Effects Using 2D Perovskite (OAm)₂SnBr₄ Films to Enhance the Properties of Si Nanowire Solar Cells. ACS Applied Energy Materials, 0, , .	2.5	1
78033	Yb doping effects on CMAS corrosion resistance of Yb-doped GdPO4 by first-principles calculation and experimental investigation. Corrosion Science, 2023, 218, 111175.	3.0	8
78034	Electronic properties and passivation mechanism of AlGaN/GaN heterojunction with vacancies: a DFT study. Physica Scripta, 2023, 98, 055405.	1.2	1
78035	Breaking BEP Relationship with Strong CO Binding and Low Câ€“C Coupling Barriers for Ethanol Synthesis on Boron-Doped Graphyne: Bond Order Conservation and Flexible Orbital Hybridization. Journal of Physical Chemistry C, 2023, 127, 7683-7694.	1.5	5
78036	Uncovering the Structural Evolution of Arsenene on SiC Substrate. Journal of Physical Chemistry C, 2023, 127, 7894-7899.	1.5	2
78037	Exploration of spatial confinement and ligand effects for oxygen reduction reaction on Fe-Nx embedded hole-graphene. Physical Chemistry Chemical Physics, 0, , .	1.3	0
78038	Ab initio prediction of anomalous Hall effect in antiferromagnetic <mml:math xmlns:mml="http://www.w3.org/1998/Math/MathML"><mml:msub><mml:mi>CaCrO</mml:mi><mml:mn>3</mml:mn></mml:msub> Physical Review B, 2023, 107, .	1.1	4

#	Article	IF	Citations
78039	Prediction of wide-gap topological insulating phase in metastable BiTeI. Applied Physics Express, 0, , .	1.1	0
78040	Theoretical investigation on NO reduction electro-catalyzed by transition-metal-anchored SnOSe nanotubes. Nano Research, 2023, 16, 8533-8541.	5.8	3
78041	Exploring the High-Temperature Stabilization of Cubic Zirconia from Anharmonic Lattice Dynamics. Crystal Growth and Design, 2023, 23, 3314-3319.	1.4	3
78042	A family of flexible two-dimensional semiconductors: MgMX₂Y₆(M = Ti/Zr/Hf;) Tj ETQq1 1 0.784314 rgBT /Ov	2.0	0
78043	DFT Simulation of a Gold Electrode Vapor-Deposition Growth Process and the Effect of Defects on the Electrode Work Function. Langmuir, 0, , .	1.6	0
78044	Electrochemistry-assisted selective butadiene hydrogenation with water. Nature Communications, 2023, 14, .	5.8	8
78045	Internal magnetic-field-enhanced photogenerated charge separation in ferromagnetic TiO2 surface heterojunctions. Journal of Materials Science and Technology, 2023, 160, 240-247.	5.6	1
78046	Impact of organicâ€“inorganic wavefunction delocalization on the electronic and optical properties of one-dimensional hybrid perovskites. Journal of Materials Chemistry C, 0, , .	2.7	0
78047	Pressure-Controlled Layer-by-Layer to Continuous Oxidation of ZrS₂(001) Surface. ACS Nano, 0, , .	7.3	0
78048	Ab initio calculation of the reflectivity of molecular fluids under shock compression. Physical Review B, 2023, 107, .	1.1	2
78049	High-Accuracy Neural Network Interatomic Potential for Silicon Nitride. Nanomaterials, 2023, 13, 1352.	1.9	1
78050	Diffusion of Sn donors in Î²-Ga₂O₃. APL Materials, 2023, 11, 041121.	2.2	2
78051	Peripheral Coordination-Dependent Descriptor for Selective Interactions between Near-Frontier Molecular Orbitals and Single-Atom Catalysts. , 2023, 1, 429-436.		1
78052	Condensation and asymmetric amplification of chirality in achiral molecules adsorbed on an achiral surface. Nature Communications, 2023, 14, .	5.8	3
78053	Band Gaps and Optical Properties of RENiO3 upon Strain: Combining First-Principles Calculations and Machine Learning. Materials, 2023, 16, 3070.	1.3	0
78055	Selectivity Control in Palladium-Catalyzed CH₂Br₂ Hydrodebromination on Carbon-Based Materials by Nuclearity and Support Engineering. ACS Catalysis, 2023, 13, 5828-5840.	5.5	2
78056	Mobile Kink Solitons in a Van der Waals Chargeâ€Densityâ€Wave Layer. Advanced Materials, 2023, 35, .	11.1	2
78057	Size of electron polarons in anatase <mml:math xmlns:mml="http://www.w3.org/1998/Math/MathML"><mml:msub><mml:mi>TiO</mml:mi><mml:mn>2</mml:mn></mml:msub></m and their role in photocatalysis. Physical Review B, 2023, 107, .	1.1	3

#	Article	IF	Citations
78058	Prediction of large magnetic moment materials with graph neural networks and random forests. Physical Review Materials, 2023, 7, .	0.9	4
78059	Determination of the absolute Raman crossâ€sections of Î±â€S₈ film at ultralow frequencies pumped by 488 and 785â€‰nm lasers. Bulletin of the Korean Chemical Society, 2023, 44, 629-633.	1.0	1
78060	Electrosynthesis of polymer-grade ethylene via acetylene semihydrogenation over undercoordinated Cu nanodots. Nature Communications, 2023, 14, .	5.8	11
78061	Exploring the role of 2D-C2N monolayers in potassium ion batteries. Journal of Molecular Modeling, 2023, 29, .	0.8	0
78062	Theoretical Comparison Study of Iodine and Astatine Adsorption on Au(111) Surface. E-Journal of Surface Science and Nanotechnology, 2023, 21, 318-323.	0.1	2
78063	1D Electronic Flat Bands in Untwisted MoirÃ© Superlattices. Advanced Materials, 2023, 35, .	11.1	6
78064	Insights into the mechanism of carboxylic acid hydrogenation into alcohols at the MnO/Cu (111) interface: a combined DFT and kinetic study. Catalysis Science and Technology, 2023, 13, 3158-3173.	2.1	1
78065	Quantitative Structural Description of Zeolites by Machine Learning Analysis of Infrared Spectra. Inorganic Chemistry, 2023, 62, 6608-6616.	1.9	1
78066	Localized Surface Plasmon Resonance in Metamaterials Composed of As1â^'zSbz Semimetal Nanoparticles in AlxGa1â^'xAs1â^'ySby Semiconductor Matrix. Nanomaterials, 2023, 13, 1355.	1.9	2
78067	Spin-induced Valley Polarization in Heterobilayer Janus Transition-metal Dichalcogenides. Journal Physics D: Applied Physics, 0, , .	1.3	0
78068	Charge transfer driving interfacial reconstructions in perovskite oxide heterostructures. Communications Physics, 2023, 6, .	2.0	2
78069	Surface modification of CuSe:a first-principles study. Wuli Xuebao/Acta Physica Sinica, 2023, .	0.2	0
78070	Single Atomâ€Engineered NIRâ€II Gold Clusters with Ultrahigh Brightness and Stability for Acute Kidney Injury. Small, 2023, 19, .	5.2	12
78071	Effect of local chemical environment on the point defects in AlNbTiZr refractory high entropy alloys. Journal of Nuclear Materials, 2023, 581, 154451.	1.3	2
78072	Development of a Niâ€“Al reactive force field for Ni-based superalloy: revealing electrostatic effects on mechanical deformation. Journal of Materials Research and Technology, 2023, 24, 4454-4467.	2.6	0
78073	Photoemission study of twisted monolayers and bilayers of <mml:math xmlns:mml="http://www.w3.org/1998/Math/MathML"><mml:msub><mml:mi>WSe</mml:mi><mml:mn>2</mml:mn></mml:msub></mml:math> on graphite substrates. Physical Review Materials, 2023, 7, .	3.1	1
78074	A quasi-one-dimensional bulk thermoelectrics with high performance near room temperature. Science Bulletin, 2023, 68, 920-927.	4.3	4
78075	Computational simulation of self-cleaning carbon-based membranes with zeolite porous structure for desalination. Diamond and Related Materials, 2023, 136, 109925.	1.8	1

#	Article	IF	Citations
78076	Paradoxical effects for a one-dimensional periodic potential embedded in a two-dimensional system. Physical Review B, 2023, 107, .	1.1	1
78077	Intrinsic point defects and the <mml:math xmlns:mml="http://www.w3.org/1998/Math/MathML"><mml:mi>n</mml:mi></mml:math> -type dopability of <mml:math xmlns:mml="http://www.w3.org/1998/Math/MathML"><mml:mrow><mml:msub><mml:mi>Bi</mml:mi><mml:mn>2</mml:mn></mml:msub><mml:msub><mml:mi mathvariant="normal">O</mml:mi><mml:mn>6</mml:mn></mml:msub></mml:mrow></mml:math> with higher photocatalytic performance: A hybrid functional study. Physical Review Materials, 2023, 7, .	2.9	2
78078	Controlling the carrier and phonon transport behavior of SnSe via stoichiometric adjustment. Current Applied Physics, 2023, 51, 13-21.	1.1	1
78079	Cryo-TEM studies of binder free high performance FeF2 cathode based full cells enabled by surface engineering. Energy Storage Materials, 2023, 59, 102779.	9.5	2
78080	The effect of spin-polarization, atomic ordering and charge transfer on the stability of CoCrNi medium entropy alloy. Materials Chemistry and Physics, 2023, 304, 127783.	2.0	2
78081	Monte Carlo Simulations of Water Adsorption in Aluminum Oxide Rod-Based Metalâ€“Organic Frameworks. Journal of Physical Chemistry C, 2023, 127, 7837-7851.	1.5	1
78082	Two-dimensional Pd₃(AsSe₄)₂ as a photocatalyst for the solar-driven oxygen evolution reaction: a first-principles study. RSC Advances, 2023, 13, 11742-11750.	1.7	1
78083	Ï‰â€Graphene: A Graphene Allotrope with Desirable Auxeticity and Dirac Cone. Advanced Theory and Simulations, 0, , .	1.3	0
78084	Ethylene Hydrogenation Molecular Mechanism on MoC_y Nanoparticles. Journal of Physical Chemistry C, 2023, 127, 7666-7673.	1.5	2
78085	Electronic Structure Engineering of Pt Species over Pt/WO₃ toward Highly Efficient Electrocatalytic Hydrogen Evolution. Small, 2023, 19, .	5.2	13
78086	Ferroelectric order in hybrid organic-inorganic perovskite NH4PbI3 with non-polar molecules and small tolerance factor. Npj Computational Materials, 2023, 9, .	3.5	2
78087	Designing dithiolene and bis(iminothiolato)-based 1D metal-organic-frameworks for electrocatalytic hydrogen evolution reaction. Theoretical Chemistry Accounts, 2023, 142, .	0.5	2
78088	Anodically designing of refreshable bi-metallic oxides for highly-efficient hydrogen evolution. Chemical Engineering Journal, 2023, 466, 143045.	6.6	4
78089	Enhanced Thermoelectric Efficiency in P-Type Mg₃Sb₂: Role of Monovalent Atoms Codoping at Mg sites. ACS Applied Materials & Interfaces, 2023, 15, 20175-20190.	4.0	4
78090	Work Function, Sputtering Yield and Microhardness of an Al-Mg Metal-Matrix Nanostructured Composite Obtained with High-Pressure Torsion. Applied Sciences (Switzerland), 2023, 13, 5007.	1.3	4
78091	Efficient calculation of derivatives of integrals in a basis of non-separable Gaussians. Journal of Chemical Physics, 2023, 158, .	1.2	2
78092	Structural and electronic properties and optical absorption of oxygen vacancy cluster defects in KDP crystals: hybrid density functional theory investigation. CrystEngComm, 2023, 25, 2959-2965.	1.3	5
78093	Interfacial configuration and interfacial regulation of electronic properties of MoS2 heterophase junctions. Materials Chemistry and Physics, 2023, 303, 127789.	2.0	0

#	Article	IF	Citations
78094	Adjustment of the Single Atom/Nanoparticle Ratio in Pd/CNT Catalysts for Phenylacetylene Selective Hydrogenation. ChemCatChem, 2023, 15, .	1.8	2
78095	Promising M2CO2/MoX2 (M = Hf, Zr; X = S, Se, Te) Heterostructures for Multifunctional Solar Energy Applications. Molecules, 2023, 28, 3525.	1.7	3
78096	Boosting the generation of key intermediate methyl radical (CH3â€¢) in OCM reaction on magnesium oxide catalysts by regulating the electronic state of the active site. Molecular Catalysis, 2023, 542, 113125.	1.0	1
78097	Insights into Interfacial Structure of Slagâ€“Metal Interface During Desulfurization Through XPS and DFT Simulations. Metallurgical and Materials Transactions B: Process Metallurgy and Materials Processing Science, 0, , .	1.0	0
78098	Stacking effect on the electronic structures of hexagonal GaTe. Journal Physics D: Applied Physics, 0, , .	1.3	1
78099	Halide Perovskite glues activate two-dimensional covalent organic framework crystallites for selective NO2 sensing. Nature Communications, 2023, 14, .	5.8	9
78100	Tunable spin and valley excitations of correlated insulators in Î“-valley moirÃ© bands. Nature Materials, 2023, 22, 731-736.	13.3	13
78101	Electrical tuning of robust layered antiferromagnetism in MXene monolayer. Applied Physics Letters, 2023, 122, .	1.5	5
78102	Regulating the Solvation Structure of Electrolyte via Dualâ€“Salt Combination for Stable Potassium Metal Batteries. Advanced Science, 2023, 10, .	5.6	7
78103	Effects of Alloying Elements on the Solution and Diffusion of Oxygen at Iron Grain Boundary Investigated by First-Principles Study. Metals, 2023, 13, 789.	1.0	0
78104	Selective furanyl ring hydrogenation of 5-hydroxymethylfurfural at sub-ambient temperature via steric effect on decorated Pd surfaces. International Journal of Hydrogen Energy, 2023, , .	3.8	0
78105	First-Principles Study of La2-xYxTi2O7 Solid Solution Antiferroelectrics for High-Efficiency Energy Storage. ECS Journal of Solid State Science and Technology, 0, , .	0.9	0
78106	Water-assisted sonochemically-induced demethylenation of benzyl alcohol to phenol over a structurally stable cupric oxide catalyst. Catalysis Science and Technology, 0, , .	2.1	0
78107	Synergy of Small Antiviral Molecules on a Black-Phosphorus Nanocarrier: Machine Learning and Quantum Chemical Simulation Insights. Molecules, 2023, 28, 3521.	1.7	0
78108	Coordinated Immobilization and Rapid Conversion of Polysulfide Enabled by a Hollow Metal Oxide/Sulfide/Nitrogenâ€Doped Carbon Heterostructure for Longâ€Cycleâ€Life Lithiumâ€Sulfur Batteries. Small, 2023, 19, .	5.2	10
78109	Dimensionality engineering dependence of vertical magnetization shift and magnetic anisotropy evolution in manganite superlattices. Journal of Magnetism and Magnetic Materials, 2023, 575, 170739.	1.0	0
78110	Unveiling deformation twin nucleation and growth mechanisms in BCC transition metals and alloys. Materials Today, 2023, 65, 90-99.	8.3	6
78111	Spinâ€Lattice Coupled Metamagnetism in Frustrated van der Waals Magnet CrOCl. Small, 0, , .	5.2	3

#	Article	IF	Citations
78112	Ab initio exploration of short-pitch skyrmion materials: Role of orbital frustration. Journal of Applied Physics, 2023, 133, .	1.1	5
78113	Direct Observation of Group-V Dopant Substitutional Defects in CdTe Single Crystals. Journal of the American Chemical Society, 0, , .	6.6	2
78114	A molecular understanding of citrate adsorption on calcium oxalate polyhydrates. Physical Chemistry Chemical Physics, 0, , .	1.3	0
78115	Enhancement of Bi-based niobate pyrochlores conductivity with Ru-doping. Structural, optical, and electrical properties. International Journal of Hydrogen Energy, 2023, , .	3.8	0
78116	Theoretical Study of Intercalation Effects: Graphene and hBN Layers in Metal and Monolayer Black Phosphorus Contacts. ACS Applied Electronic Materials, 0, , .	2.0	0
78117	Heat Sink Enhancement of Decalin by Symmetrical Imidazolium Ionic Liquid-Capped Metal Nanoparticles. Energy & Fuels, 2023, 37, 6545-6557.	2.5	2
78118	Hydride Anion Substitution Boosts Thermoelectric Performance of Polycrystalline SrTiO₃ via Simultaneous Realization of Reduced Thermal Conductivity and High Electronic Conductivity. Advanced Functional Materials, 2023, 33, .	7.8	3
78119	Superconducting Be₂SH₃ with kagome hydrogen at high pressure. Journal of Materials Chemistry C, 2023, 11, 6386-6392.	2.7	1
78120	Layeredâ€“Control Approach to Tune The Mobility of Perovskite SrTiO₃: A Density Functional Theory Prospects. ECS Journal of Solid State Science and Technology, 2023, 12, 054001.	0.9	1
78121	Highly Selective Electrochemical Reduction of CO₂ into Methane on Nanotwinned Cu. Journal of the American Chemical Society, 2023, 145, 9136-9143.	6.6	19
78122	Pt-stabilized electron-rich Ir structures for low temperature methane combustion with enhanced sulfur-resistance. Chemical Engineering Journal, 2023, 466, 143044.	6.6	6
78123	Superconductivity in the thorium nickel borocarbide ThNiBC. Europhysics Letters, 2023, 142, 36004.	0.7	1
78124	Reversible Pressureâ€Magnetic Modulation in a Tetrathiafulvaleneâ€Based Dyad Piezochromic Dysprosium Singleâ€Molecule Magnet**. Chemistry - A European Journal, 2023, 29, .	1.7	3
78125	A theoretical study of the effect and mechanism of FeN3-doped biochar for greenhouse gas mitigation. Biochar, 2023, 5, .	6.2	3
78126	A Deep Neural Network Potential to Study the Thermal Conductivity of MnBi2Te4 and Bi2Te3/MnBi2Te4 Superlattice. Journal of Electronic Materials, 0, , .	1.0	0
78127	Embedding atomic iron into C<mml:math xmlns:mml="http://www.w3.org/1998/Math/MathML" altimg="si23.svg" display="inline" id="d1e182"><mml:msub><mml:mrow /><mml:mrow><mml:mn>3</mml:mn></mml:mrow></mml:msub></mml:math>N nanoribbon to activate ferromagnetism. Journal of Magnetism and Magnetic Materials, 2023, 575, 170745.	1.0	0
78128	A topological approach to reconstructive solid-state transformations and its application for generation of new carbon allotropes. Acta Crystallographica Section B: Structural Science, Crystal Engineering and Materials, 2023, 79, 198-206.	0.5	0
78129	Temperature-dependent and magnetism-controlled Fermi surface changes in magnetic Weyl semimetals. Physical Review Research, 2023, 5, .	1.3	5

#	Article	IF	Citations
78130	Structural transitions at high pressure and metastable phase in Si0.8Ge0.2. Journal of Alloys and Compounds, 2023, 954, 170180.	2.8	0
78131	MatHub-2d: A database for transport in 2D materials and a demonstration of high-throughput computational screening for high-mobility 2D semiconducting materials. Science China Materials, 2023, 66, 2768-2776.	3.5	6
78132	Superior hydrogen storage capacity of Vanadium decorated biphenylene (Bi+V): A DFT study. International Journal of Hydrogen Energy, 2023, 48, 28076-28090.	3.8	10
78133	The effect of temperature and excitation energy on Raman scattering in bulk HfS₂. Journal of Physics Condensed Matter, 0, , .	0.7	0
78134	Oxygen-Driven Enhancement of the Electron Correlation in Hexagonal Iron at Earthâ€™s Inner Core Conditions. Journal of Physical Chemistry Letters, 0, , 3884-3890.	2.1	0
78135	Oxygen vacancies-enriched Fe-Cu bimetallic minerals-based magnetic biochar activated peroxydisulfate for durable sulfonamides degradation: pH-dependence adsorption and singlet oxygen evolution mechanism. Separation and Purification Technology, 2023, 317, 123866.	3.9	3
78136	A p-orbital honeycomb-Kagome lattice realized in a two-dimensional metal-organic framework. Communications Chemistry, 2023, 6, .	2.0	1
78137	Two-dimensional [<mml:math xmlns:mml="http://www.w3.org/1998/Math/MathML" altimg="si111.svg" display="inline" id="d1e2029"><mml:msup><mml:mrow /><mml:mrow><mml:mo>â€²</mml:mo></mml:mrow></mml:msup></mml:math>-phase MA<mml:math xmlns:mml="http://www.w3.org/1998/Math/MathML" altimg="si112.svg" display="inline" id="d1e2037"><mml:msub><mml:mrow /><mml:mrow><mml:mn>2</mml:mn></mml:mrow></mml:msub></mml:math>N<mml:math xmlns:mml=	3.1	1
78138	Influence of a Mo interlayer on the oxidation behavior of a Cr coating on a Zr alloy substrate. Corrosion Science, 2023, 218, 111192.	3.0	14
78139	Janus structures of the C_{2h} polymorph of gallium monochalcogenides: first-principles examination of Ga₂XY (X/Y = S, Se, Te) monolayers. RSC Advances, 2023, 13, 12153-12160.	1.7	1
78140	Rise and fall of Mott insulating gaps in <mml:math xmlns:mml="http://www.w3.org/1998/Math/MathML"><mml:msub><mml:mi>YNiO</mml:mi><mml:mn>3</mml:mn></mml:msub></mml:math> paramagnets as a reflection of symmetry breaking and remaking. Physical Review Materials, 2023, 7, .	2.9	5
78141	Models of Polaron Transport in Inorganic and Hybrid Organicâ€“Inorganic Titanium Oxides. Chemistry of Materials, 0, , .	3.2	1
78142	Self-reconstruction of (CoNiFeCuCr)Se high-entropy selenide for efficient oxygen evolution reaction. Applied Surface Science, 2023, 627, 157282.	3.1	4
78143	Rapid extraction of valuable metals from spent LiNixCoyMn1-x-yO2 cathodes based on synergistic effects between organic acids. Waste Management, 2023, 165, 19-26.	3.7	8
78144	Adsorption of sulfur on Au(111) surface: An extremely stable configuration. Journal of Molecular Graphics and Modelling, 2023, 122, 108494.	1.3	2
78145	Scalable synthesis of coordinatively unsaturated metal-nitrogen sites for large-scale CO2 electrolysis. Nature Communications, 2023, 14, .	5.8	9
78146	Alkali Metal Ion-Mediated Augmented Carrier Extraction in Iodobismuth Ternary Perovskite-Based Photovoltaic Device. ACS Applied Electronic Materials, 2023, 5, 5332-5342.	2.0	5
78147	Machine learning and DFT investigation of CO, CO₂ and CH₄ adsorption on pristine and defective two-dimensional magnesene. Physical Chemistry Chemical Physics, 2023, 25, 13170-13182.	1.3	3

#	Article	IF	Citations
78148	A facile and green synthesis of Mn and P functionalized graphitic carbon nitride nanosheets for spintronics devices and enhanced photocatalytic performance under visible-light. Journal of Colloid and Interface Science, 2023, 644, 397-414.	5.0	10
78149	Green hydrophobic deep eutectic solvents as low-viscosity and efficient lubricants. Tribology International, 2023, 185, 108531.	3.0	3
78150	Atomic-scale structural characterization and twin formation mechanisms of Î¼ phase within refractory Nb Ni alloy. Materials Characterization, 2023, 201, 112921.	1.9	0
78151	The Photochemical Stability of PbI2 and PbBr2: Optical and XPS and DFT Studies. Coatings, 2023, 13, 784.	1.2	2
78152	Mechanisms of Electronic and Ionic Transport during Mg Intercalation in Mgâ€“S Cathode Materials and Their Decomposition Products. Chemistry of Materials, 2023, 35, 3503-3512.	3.2	4
78153	Cs₂Ln₃CuS₈ (Ln = Laâ€“Nd, Smâ€“Tb): Synthesis, Crystal Structure, and Magnetic and Optical Properties. Inorganic Chemistry, 0, , .	1.9	2
78154	Elucidating the Effect of Ion Exchange Protocol on the Copper Exchange Efficacy, Copper Siting, and SCR activity in Cuâ€SSZâ€13. ChemPhysChem, 0, , .	1.0	0
78155	AuFe₃@Pd/Î³-Fe₂O₃ Nanosheets as an In Situ Regenerable and Highly Efficient Hydrogenation Catalyst. ACS Nano, 2023, 17, 8499-8510.	7.3	3
78156	Regulated Surface Electronic States of CuNi Nanoparticles through Metalâ€Support Interaction for Enhanced Electrocatalytic CO₂ Reduction to Ethanol. Small, 2023, 19, .	5.2	7
78157	Using a computationally driven screening to enhance magnetocaloric effect of metal monoborides. JPhys Energy, 0, , .	2.3	1
78158	Prediction of lattice distortion and mechanical behavior of tetragonal phase (Bi0.2Na0.2Ba0.2Sr0.2Ca0.2)TiO3 high-entropy perovskite with A-site disorder from first-principles calculations. Journal of Alloys and Compounds, 2023, 954, 170205.	2.8	3
78159	Cooperative multiple interactions of donor-Ï€-acceptor dyes enhance the efficiency and stability of perovskite solar cells. Physical Chemistry Chemical Physics, 0, , .	1.3	0
78160	Weak electron-phonon renormalization effect caused by the counteraction of the different phonon vibration modes in FeS₂. Physica Scripta, 2023, 98, 065902.	1.2	1
78161	Controllable and enormous spin splitting in antiferromagnetic MnPSe₃ through interfacial coupling with Janus MoSSe. Journal Physics D: Applied Physics, 0, , .	1.3	1
78162	â€œReduction-aggregationâ€•strategy to construct a low-cost and high-efficiency Ag/Al2O3 catalyst for NH3-SCO. Separation and Purification Technology, 2023, 317, 123881.	3.9	6
78163	Effect of aliovalent bismuth substitution on structure and optical properties of CsSnBr3. Communications Chemistry, 2023, 6, .	2.0	2
78164	Causal structure of interacting Weyl fermions in condensed matter systems. Nature Communications, 2023, 14, .	5.8	0
78165	Universal Maximum Strength of Solid Metals and Alloys. Physical Review Letters, 2023, 130, .	2.9	6

#	Article	IF	Citations
78166	Enhancing thermoelectric performance via relaxed spin polarization upon magnetic impurity doping. Journal of Materials Chemistry A, 0, , .	5.2	0
78167	Electron-irradiation-facilitated production of chemically homogenized nanotwins in nanolaminated carbides. Journal of Advanced Ceramics, 2023, , .	8.9	0
78168	Computational screening of effective g-C₃N₄ based single atom electrocatalysts for the selective conversion of CO₂. Nanoscale, 2023, 15, 8416-8423.	2.8	5
78169	Synergetic Câ€“H bond activation and Câ€“O formation on CuOx facilities facile conversion of methane to methanol. Applied Surface Science, 2023, 627, 157283.	3.1	1
78170	The influence of strong anharmonicity on high thermoelectric properties for the ternary compound NaMgX (X = As, Sb). Chemical Physics Letters, 2023, 823, 140521.	1.2	1
78171	Dehydrogenation behavior and mechanism of LiAlH4 adding nano-CeO2 with different morphologies. Nano Research, 2023, 16, 9426-9434.	5.8	13
78172	Highly efficient hydrogen production from methanol by single nickel atoms anchored on defective boron nitride nanosheet. Nano Research, 0, , .	5.8	0
78173	Superheterojunction covalent organic frameworks: Supramolecular synergetic charge transfer for highly efficient photocatalytic CO2 reduction. Applied Catalysis B: Environmental, 2023, 333, 122782.	10.8	12
78174	Strain-Induced Medium-Temperature Thermoelectric Performance of <mml:math xmlns:mml="http://www.w3.org/1998/Math/MathML" display="inline" overflow="scroll"><mml:msub><mml:mi>Cu</mml:mi><mml:mn>4</mml:mn></mml:msub><mml:msub><mml:mrow><mml:mi>Ti</mml:mi></mml:mrow></mml: : The Role of Four-Phonon Scattering. Physical Review Applied, 2023, 19, .	1.5	28
78175	Electronic properties and photocatalytic water splitting with high solar-to-hydrogen efficiency in a hBNC/Janus WSSe heterojunction: First-principles calculations. Physical Review B, 2023, 107, .	1.1	11
78176	Unconventional surface state pairs in a high-symmetry lattice with anti-ferromagnetic band-folding. Communications Physics, 2023, 6, .	2.0	3
78177	Metallization and superconductivity with Tc > 12ÂK in transition metal dichalcogenide HfS2 under pressure. Materials Today Physics, 2023, 34, 101091.	2.9	1
78178	Tunable Schottky contacts in graphene/XAu₄Y (X, Y = Se, Te) heterostructures. Physical Chemistry Chemical Physics, 2023, 25, 12245-12251.	1.3	3
78179	gâ€B₃C₂N₃: A Potential Two Dimensional Metalâ€free Photocatalyst for Overall Water Splitting**. ChemPhysChem, 2023, 24, .	1.0	2
78180	Defect Origin of the Light-Soaking Effects in Hybrid Perovskite Solar Cells. , 2023, , 239-263.		1
78181	Controlled electron transfer at the Ni-ZnO interface for ultra-fast and stable hydrogenation of N-propylcarbazole. Applied Catalysis B: Environmental, 2023, 334, 122792.	10.8	6
78182	Distinct ferrovalley characteristics of the Janus RuClX (X = F, Br) monolayer. Nanoscale, 2023, 15, 8278-8288.	2.8	13
78183	Structure phase engineering strategy through acetic acid coupling to boost hydrogen evolution reaction performance of 2H phase MoS2 at wide pH range. Fuel, 2023, 347, 128428.	3.4	8

#	Article	IF	Citations
78184	Liquidâ€“Crystal Structure Inheritance in Machine Learning Potentials for Network-Forming Systems. JETP Letters, 2023, 117, 370-376.	0.4	5
78185	Dzyaloshinskiiâ€“Moriya interactions in Nd2Fe14B as the origin of spin reorientation and the rotating magnetocaloric effect. Applied Materials Today, 2023, 32, 101825.	2.3	0
78186	How Do Surface Polar Molecules Contribute to High Openâ€Circuit Voltage in Perovskite Solar Cells?. Advanced Science, 2023, 10, .	5.6	9
78187	Strong ferromagnetism of g-C3N4 achieved by atomic manipulation. Nature Communications, 2023, 14, .	5.8	20
78188	Density functional theoretical assessment of titanium metal for adsorption of hydrogen, deuterium and tritium isotopes. Theoretical Chemistry Accounts, 2023, 142, .	0.5	0
78189	A highly active Pd clusters hosted by magnesium hydroxide nanosheets promoting hydrogen storage. Applied Catalysis B: Environmental, 2023, 333, 122793.	10.8	5
78190	Prediction of 2D IV-V semiconductors: Flexible monolayers with tunable bandgap and strong optical absorption as water-splitting photocatalysts. Nanoscale, 0, , .	2.8	1
78191	Critical behavior and exchange splitting in the two-dimensional antiferromagnet Mn on Re(0001). Physical Review B, 2023, 107, .	1.1	1
78192	Identification of Cu/Sc and Cu/Ti subsurface alloys for highly efficient CO electroreduction to C2 products. Applied Surface Science, 2023, , 157314.	3.1	1
78193	Fe4 cluster as the smallest 3D Fe cluster with unique quantum magnetic levitation effect on graphene. Applied Surface Science, 2023, 628, 157315.	3.1	1
78194	Topological Insulator Bi₂Se₃â€Assisted Heterostructure for Ultrafast Charging Sodiumâ€Ion Batteries. Small, 2023, 19, .	5.2	5
78195	Amorphous Zirconia-doped Tantala modeling and simulations using explicit multi-element spectral neighbor analysis machine learning potentials (EME-SNAP). Physical Review Materials, 2023, 7, .	0.9	1
78196	Magnetic order and magnetic anisotropy in two-dimensional ilmenenes. Nanoscale Advances, 2023, 5, 2813-2819.	2.2	2
78197	Parameter-free prediction of phase transition in PbTiO3 through combination of quantum mechanics and statistical mechanics. Scripta Materialia, 2023, 232, 115480.	2.6	4
78198	Pressure-induced transition from a Mott insulator to a ferromagnetic Weyl metal in La2O3Fe2Se2. Nature Communications, 2023, 14, .	5.8	2
78199	Quantum size effects in stacked multilayer graphene. Physica Scripta, 0, , .	1.2	0
78200	Optimizing Superconductivity: From Cuprates via Nickelates to Palladates. Physical Review Letters, 2023, 130, .	2.9	8
78201	The tunable interface charge transfer by polarization in two dimensional polar Al2O3/MoSO heterostructures. Journal of Materials Chemistry A, 0, , .	5.2	1

#	Article	IF	Citations
78202	Improved Mechanical Characterization of LiCoO2 Cathode Material by Ab-Initio Calculations Using Density Functional Theory. Bulletin of the Chemical Society of Japan, 2023, 96, 475-483.	2.0	0
78203	Observation of gapless nodal-line states in NdSbTe. Physical Review Materials, 2023, 7, .	0.9	2
78204	Effect of an electric field on ferroelectric and piezoelectric properties of brownmillerite <mml:math xmlns:mml="http://www.w3.org/1998/Math/MathML"><mml:mrow><mml:msub><mml:mi>Ca</mml:mi><mml:mn>2</mml:mn></mml:msub><mml:msub><mml:mi mathvariant="normal">O</mml:mi><mml:mn>5</mml:mn></mml:msub></mml:mrow></mml:math>. Physical Review B, 2023, 107, .	1.1	2
78205	Covalent bonding strategy to enable non-volatile organic cation perovskite for highly stable and efficient solar cells. Joule, 2023, 7, 1033-1050.	11.7	13
78206	Magneto-optical Kerr Effect in Ferroelectric Antiferromagnetic Two-Dimensional Heterostructures. ACS Applied Materials & Interfaces, 2023, 15, 22282-22290.	4.0	4
78207	Wâ€Doping Induced Efficient Tunnelâ€toâ€Layered Structure Transformation of Na_{0.44}Mn_{1â€}_xW_xO₂: Phase Evolution, Sodiumâ€Storage Properties, and Moisture Stability. Advanced Energy Materials, 2023, 13, .	10.2	19
78208	Reconstructing Oxygenâ€Deficient Zirconia with Ruthenium Catalyst on Atomicâ€Scale Interfaces toward Hydrogen Production. Advanced Functional Materials, 2023, 33, .	7.8	3
78209	In-situ formed hybrid phosphates coating layer enabling co-free Li-rich layered oxides with stable cycle performance. Materials Today Energy, 2023, 34, 101314.	2.5	1
78210	Tellurium filled carbon nanotubes cathodes for Li-Te batteries with high capacity and long-term cyclability. Nano Energy, 2023, 112, 108462.	8.2	4
78211	Spontaneous topological Hall effect induced by non-coplanar antiferromagnetic order in intercalated van der Waals materials. Nature Physics, 2023, 19, 961-968.	6.5	13
78212	Magnetoelectric coupling in multiferroics probed by optical second harmonic generation. Nature Communications, 2023, 14, .	5.8	5
78214	Equation of state, phase transitions, and band-gap closure in <mml:math xmlns:mml="http://www.w3.org/1998/Math/MathML"><mml:mrow><mml:mi>Pb</mml:mi><mml:msub><mml:mi>Cl</mml:mi><mml:mn and <mml:math xmlns:mml="http://www.w3.org/1998/Math/MathML"><mml:mrow><mml:mi>Sn</mml:mi><mml:msub><mml:mi>Cl</mml:mi><mml:mn Physical Review B, 2023, 107, .	1.1	0
78215	Experimental investigation and thermodynamic modeling of Cuâ€“Nbâ€“Si system. Transactions of Nonferrous Metals Society of China, 2023, 33, 824-838.	1.7	1
78216	The mechanical, thermodynamic and electronic properties of TM2CrB2 borides with TM = V, Nb, Ta: A first-principles predictions. Solid State Communications, 2023, 368, 115184.	0.9	7
78217	A combined theoretical and experimental investigation on the photocatalytic hydrogenation of CO₂ on Cu/ZnO polar surface. Nanoscale, 2023, 15, 9040-9048.	2.8	0
78218	Possible Extrinsic Ferroelectric-like Signals Originated from the Oxygen Vacancy Drift in HfO₂-Based Films. ACS Applied Electronic Materials, 2023, 5, 2718-2724.	2.0	1
78219	Mechanism of Stoichiometrically Governed Titanium Oxide Brownian Tree Formation on Stepped Au(111). Journal of Physical Chemistry C, 0, , .	1.5	1
78220	Investigating the Electromechanical Behavior of Unconventionally Ferroelectric Hf_{0.5}Zr_{0.5}O₂â€Based Capacitors Through Operando Nanobeam Xâ€Ray Diffraction. Advanced Electronic Materials, 2023, 9, .	2.6	0

#	Article	IF	Citations
78221	Stacking and layer dependence of magnetic properties in Ti₂C and Fe₂C. Journal Physics D: Applied Physics, 2023, 56, 345002.	1.3	2
78222	Single-Atom Anchored g-C3N4 Monolayer as Efficient Catalysts for Nitrogen Reduction Reaction. Nanomaterials, 2023, 13, 1433.	1.9	1
78223	Sb₄O₃(TeO₃)₂(HSO₄)(OH): An Antimony Tellurite Sulfate Exhibiting Large Optical Anisotropy Activated by Lone Pair Stereoactivity. Inorganic Chemistry, 2023, 62, 7123-7129.	1.9	13
78224	Breathable MOFs Layer on Atomically Grown 2D SnS₂ for Stable and Selective Surface Activation. Advanced Science, 2023, 10, .	5.6	4
78225	Time-Reversal-Even Nonlinear Current Induced Spin Polarization. Physical Review Letters, 2023, 130, .	2.9	5
78226	Large intrinsic anomalous Hall effect in both <mml:math xmlns:mml="http://www.w3.org/1998/Math/MathML"><mml:mrow><mml:msub><mml:mi>Nb</mml:mi><mml:mn>2</mml:mn></mml:msub></mml:mrow></mml:math> and <mml:math xmlns:mml="http://www.w3.org/1998/Math/MathML"><mml:mrow><mml:msub><mml:mi>Ta</mml:mi><mml:mn>2</mml:mn></mml:msub></mml:mrow></mml:math> with collinear antiferromagnetism. Physical Review B, 2023, 107, .	1.1	2
78227	Enabling enhanced lithium storage capacity of two-dimensional pentagonal BN₂ by aluminum doping. Journal of Materials Chemistry C, 0, , .	2.7	0
78228	Hydrogen and helium trapping in hcp beryllium. Communications Chemistry, 2023, 6, .	2.0	0
78229	DFT studies of the adsorption and decomposition of dimethyl ether on copper surface. Applied Surface Science, 2023, 627, 157310.	3.1	0
78230	<mml:math xmlns:mml="http://www.w3.org/1998/Math/MathML"><mml:mrow><mml:mi>Mn</mml:mi><mml:msub><mml:mrow><mml:mo>(</mml:mo><mml:mi mathvariant="normal">P</mml:mi></mml:mrow></mml:math> : Isovalent tuning of Mn-sublattice magnetic order. Physical Review B, 2023, 107, .	1.1	1
78231	A first-principles study on the early-stage corrosion of a NiWNb alloy in a chloride salt environment. Journal of Nuclear Materials, 2023, 582, 154457.	1.3	0
78232	Tribo-catalysis triggered the in-situ formation of amphiphilic molecules to reduce friction and wear. Tribology International, 2023, 185, 108541.	3.0	2
78233	Electron structure effects of S-doped In2O3 flowers on NO2 sensitivity. Materials Research Bulletin, 2023, 165, 112293.	2.7	4
78234	Study on the influence mechanism of mineral Ca on NO reduction in the high temperature oxygen-lean zone of ammonia-coal co-combustion. Fuel, 2023, 347, 128347.	3.4	5
78235	Magnetic properties of defect induced Î²-Ga2O3: A first principles study. Computational Condensed Matter, 2023, 35, e00810.	0.9	1
78236	Double Perovskite La₂MnNiO₆ as a Highâ€Performance Anode for Lithiumâ€Ion Batteries. Advanced Science, 2023, 10, .	5.6	4
78237	Tuning the reactivity of carbon surfaces with oxygen-containing functional groups. Nature Communications, 2023, 14, .	5.8	14
78238	Large current density for oxygen evolution from pyramidally-coordinated Co oxide. Applied Catalysis B: Environmental, 2023, 333, 122785.	10.8	6

#	Article	IF	Citations
78239	Construction of the Fast Potassiation Path in Sb_xBi_{1â€x}@NC Anode with Ultrahigh Cycling Stability for Potassiumâ€ion Batteries. Small, 2023, 19, .	5.2	7
78240	Monolithic Nickel Catalyst Featured with Highâ€Density Crystalline Steps for Stable Hydrogen Evolution at Large Current Density. Small, 2023, 19, .	5.2	4
78241	Thickness-dependent piezoelecticity of black arsenic from few-layer to monolayer. Solid State Communications, 2023, 368, 115175.	0.9	1
78242	Weak ferromagnetism at 48.5ÂK in rubidium-intercalated biphenyl. Results in Physics, 2023, 49, 106479.	2.0	0
78243	Irradiation damage reduces alloy corrosion rate via oxide space charge compensation effects. Acta Materialia, 2023, 253, 118956.	3.8	2
78244	Surface Ligand Engineering Ruthenium Nanozyme Superior to Horseradish Peroxidase for Enhanced Immunoassay. Advanced Materials, 2024, 36, .	11.1	29
78245	Electronic, Optical, piezoelectric properties and photocatalytic water splitting performance of Two-dimensional group IV-V compounds. Applied Surface Science, 2023, 627, 157317.	3.1	4
78246	Enhanced Cycling Stability of 4.6ÂV LiCoO₂ Cathodes by Inhibiting Catalytic Activity of its Interface Via MXene Modification. Advanced Functional Materials, 2023, 33, .	7.8	9
78247	Facile Control of Ferroelectricity Driven by Ingenious Interaction Engineering. Small, 2023, 19, .	5.2	15
78248	Construction of a robust solid electrolyte interphase on Ge anode to achieve a superior long-term cycle life of lithium-ion battery. Journal of Alloys and Compounds, 2023, 954, 170200.	2.8	3
78268	On the Dopant, Defect States, and Mobility in W Doped Amorphous In₂O₃ for BEOL Transistors. , 2023, , .		0
78295	Electrocatalytic Activation and Conversion of CO2 at Solidâ€“Liquid Model Interfaces: Computational Perspectives. Green Chemistry and Sustainable Technology, 2023, , 329-359.	0.4	0
78305	Relativistic Pseudopotentials. , 2024, , 35-64.		0
78356	Full Exclusion of Branched Hexanes from Their Linear Isomer by a Robust Aluminum Metalâ€“Organic Framework with Tailored Pore Structure. , 2023, 5, 1532-1536.		3
78445	Nonvolatile electro-mechanical coupling in two-dimensional lattices. Nanoscale Horizons, 0, , .	4.1	0
78621	Hexagonal boron nitride nanophotonics: a record-breaking material for the ultraviolet and visible spectral ranges. Materials Horizons, 2023, 10, 2427-2435.	6.4	9
78698	Design Principle for Tetrahedral Semiconductors and Their Functional Derivatives: Cation Stabilizing Charged Cluster Network. Nano Letters, 2023, 23, 4648-4653.	4.5	2
78853	Quasiparticle framework. , 2023, , 27-53.		0

#	Article	IF	Citations
78855	Substrate effects of two-dimensional materials on few-layer antimony. , 2023, , 449-463.		0
78866	Fundamental properties of transition-metal-adsorbed germanene. , 2023, , 235-248.		0
78868	BCN-adsorbed germanenes. , 2023, , 93-111.		0
78870	Chemical modification of Sb thin film. , 2023, , 437-448.		0
78871	Carbon-/boron-/nitrogen-substituted germaneness. , 2023, , 113-172.		0
79030	Structural dynamics in amorphous oxide semiconductors and its role in defect formation, electron transport and optical transparency. , 2023, , 97-114.		0
79031	Aspects of oxygen radical interactions with surfaces: effects of relative flux and kinetic energy. , 2023, , 185-206.		0
79061	Ultrafast Nucleation Reverses Dissolution of Transition Metal Ions for Robust Aqueous Batteries. Nano Letters, 2023, 23, 5307-5316.	4.5	8
79104	Interfacial Interaction in Colloidal Heteronanostructures of Tb³⁺-Complex and Eu³⁺-Doped Nanosheets: Implications for Bioprobes. ACS Applied Nano Materials, 2023, 6, 10023-10032.	2.4	0
79339	Realization of a Two-Dimensional Checkerboard Lattice in Monolayer Cu₂N. Nano Letters, 2023, 23, 5610-5616.	4.5	2
79420	Strain-Dependent Electronic and Optical Properties of Dirac-Semimetal Monolayer BeN₄. , 2022, , .		0
79435	Water Molecules, Small Clusters and Bulk Water. , 2023, , 95-114.		0
79447	Water Adsorption on Pt(111) Surfaces. , 2023, , 135-159.		0
79486	First-principles design of nanostructured electrode materials for Na-ion batteries: challenges and perspectives. Physical Chemistry Chemical Physics, 2023, 25, 18623-18641.	1.3	2
79519	Atomic-Resolution Mapping of Localized Phonon Modes at Grain Boundaries. Nano Letters, 0, , .	4.5	1
79579	Hydrogen bond network at the H2O/solid interface. , 2024, , 92-113.		0
79580	Crystal-liquid duality enhanced dynamical stability of hybrid perovskites. Physical Chemistry Chemical Physics, 2023, 25, 17787-17792.	1.3	1
79642	Integrating Machine Learning and Molecular Simulation for Material Design and Discovery. , 0, , .		0

#	Article	IF	Citations
79701	Enhanced thermal stability by short-range ordered ferroelectricity in K_{0.5}Na_{0.5}NbO₃-based piezoelectric oxides. Materials Horizons, 2023, 10, 2656-2666.	6.4	2
79748	Room-temperature stacking disorder in layered covalent-organic frameworks from machine-learning force fields. Materials Horizons, 2023, 10, 2883-2891.	6.4	4
79867	Adsorption Behaviors of Hydrogen on Equal Atomic Ratio TiZrV Film Applied in AB-BNCT by Density Functional Theory Study. Springer Proceedings in Physics, 2023, , 792-799.	0.1	0
79943	Cation-defect-induced self-reduction towards efficient mechanoluminescence in Mn²⁺-activated perovskites. Materials Horizons, 2023, 10, 3476-3487.	6.4	11
79977	Discovery of Novel Photocatalysts Using Machine Learning Approach. , 2023, , 233-261.		0
79989	Perovskite-Based Materials for Photovoltaic Applications: A Machine Learning Approach. , 2023, , 139-162.		0
80046	Ultra-thin magnetic film with giant phonon-drag for heat to spin current conversion. Materials Horizons, 0, , .	6.4	0
80083	Theoretical analysis of X-Ray Free-Electron-Laser Experimental Data Using Monte-Carlo and Molecular-Dynamics Based Computational Tools. , 2024, , 858-864.		1
80103	Bifunctionality of Zn dust in Ullmann Câ€“C cross-coupling by Ni/Pd dual catalysis: theoretical insight. Catalysis Science and Technology, 2023, 13, 4064-4068.	2.1	0
80163	Axis dependent conduction polarity in the air-stable semiconductor, PdSe₂. Materials Horizons, 2023, 10, 3740-3748.	6.4	4
80190	Enhancing anionic redox stability via oxygen coordination configurations. Materials Horizons, 0, , .	6.4	1
80197	Density functional theory to calculate accurate defect energy levels in silicon. AIP Conference Proceedings, 2023, , .	0.3	0
80306	Phonon-driven transient bandgap renormalization in perovskite single crystals. Materials Horizons, 0, , .	6.4	1
80550	The Effect of Aluminum Fraction on the Phonon Mean Free Path - Thermal Conductivity Relation of Al_xGa_{1-x}N Alloys. , 2023, , .		0
80662	Finite Element Methods for Density Functional Theory. , 2023, , 447-478.		0
80689	Pt single atoms meet metalâ€“organic frameworks to enhance electrocatalytic hydrogen evolution activity. Nanoscale Horizons, 0, , .	4.1	0
80927	Accurate Approximations of Density Functional Theory for Large Systems with Applications to Defects in Crystalline Solids. , 2023, , 525-578.		0
80929	Numerical Methods for Kohnâ€“Sham Models: Discretization, Algorithms, and Error Analysis. , 2023, , 333-400.		0

#	Article	IF	Citations
80958	VASP porting and parallel optimization on GPU like accelerator. , 2023, , .		0
81201	Material descriptors for thermoelectric performance of narrow-gap semiconductors and semimetals. Materials Horizons, 2023, 10, 4256-4269.	6.4	1
81309	Study on optical properties and photocatalytic properties of layered MoO3. , 2023, , .		0
81484	Methodology for Calculation of Elastic Constants of Diamane by Molecular Dynamics. , 2023, , .		0
81575	LaOMS₂ (M = Ti, V, and Cr): novel crystal spin valves without contact. Materials Horizons, 0, , .	6.4	0
81576	Bloch-type magnetic skyrmions in two-dimensional lattices. Materials Horizons, 2023, 10, 5071-5078.	6.4	1
81577	Zero-field-cooling exchange bias up to room temperature in the strained kagome antiferromagnet Mn_{3.1}Sn_{0.9}. Materials Horizons, 2023, 10, 4597-4608.	6.4	1
81579	A novel bifunctional thioarsenate based on unprecedented molecular [Cd₄As₈Se₁₆(Se₂)₂]^{8â¯} cluster anions. Chemical Communications, 2023, 59, 12124-12127.	2.2	2
81625	Mechanical instabilities in 2D-SiC with defects. AIP Conference Proceedings, 2023, , .	0.3	0
81692	Exploitation of mixed-valency chemistry for designing a monolayer with double ferroelectricity and triferroic couplings. Nanoscale, 2023, 15, 13567-13573.	2.8	0
81693	Electromechanical behaviour of violet phosphorene nanoflakes. Physical Chemistry Chemical Physics, 2023, 25, 24293-24297.	1.3	0
81726	Discovery of all-inorganic lead-free perovskites with high photovoltaic performance via ensemble machine learning. Materials Horizons, 0, , .	6.4	0
81752	Tools for overcoming reliance on energy-based measures in chemistry: a tutorial review. Chemical Society Reviews, 2023, 52, 5861-5874.	18.7	2
81800	Shared metadata for data-centric materials science. Scientific Data, 2023, 10, .	2.4	3
81860	SnIP-type atomic-scale inorganic double-helix semiconductors: Synthesis, properties, and applications. Nano Research, 2024, 17, 2111-2128.	5.8	0
82173	Recent Mechanistic Insights into Some Enzyme Mimetic Functions of Ceria. Challenges and Advances in Computational Chemistry and Physics, 2024, , 201-229.	0.6	0
82292	Solvent-induced local environment effect in plasmonic catalysis. Nanoscale Advances, 2023, 5, 5774-5779.	2.2	0
82387	Simulating excited states in metal organic frameworks: from light-absorption to photochemical CO₂ reduction. Materials Advances, 0, , .	2.6	0

#	Article	IF	Citations
82398	Modeling and Simulation of Electrochemical, Thermoelectric, and Magnetic Properties of MXenes. ACS Symposium Series, 0, , 143-168.	0.5	0
82495	Porting and optimization of VASP on domestic heterogeneous platform. , 2023, , .		0
82656	Experimental and Theoretical Investigation of Cation Site Occupation and Magnetic Ordering in Co-Ferrite Spinels. , 2023, , .		0
82664	Prediction of High Tunnel Magnetoresistance Ratios in (111)-Oriented Junctions with a SrTiO₃ Barrier. , 2023, , .		0
82667	Generation probability of point defects considering microscopic elastic scattering cross-sections in rare-earth permanent magnets via first-principles calculations. , 2023, , .		0
82702	Two-Dimensional Si2BNO4: A Potential Material for Optoelectronic Applicationsâ€"An Ab-Initio Study. Springer Proceedings in Materials, 2023, , 93-99.	0.1	0
82961	Short communication: Effect of Sn on the formation of <c>-component dislocation loops in Zr alloys: In situ ion irradiation studies and atomistic simulations. Journal of Nuclear Materials, 2023, 587, 154756.	1.3	1
82963	Molecular dynamics of high pressure tin phases: Empirical and machine learned interatomic potentials. AIP Conference Proceedings, 2023, , .	0.3	0
82964	DC electrical conductivity of platinum from ab initio simulations. AIP Conference Proceedings, 2023, , .	0.3	0
83035	First Principles Calculations of Cu Doped ZnO: a Potential Spintronic Material. , 2023, , .		0
83111	Machine Learning Interatomic Potentials: Keys to First-Principles Multiscale Modeling. Computational Methods in Engineering & the Sciences, 2023, , 427-451.	0.3	0
83142	Sublimation-based wafer-scale monolayer WS₂ formation via self-limited thinning of few-layer WS₂. Nanoscale Horizons, 2023, 9, 132-142.	4.1	1
83166	Horizontally Stacked Pristine and Li-Doped C₁₂ Carbyne Ring as Hydrogen Storage Materials: A DFT Study. , 2023, , .		0
83348	Deformation inÂMetals: Insights fromÂab-initio Calculations. , 2024, , 83-92.		0
83467	A covalency-aided electrochemical mechanism for CO₂ reduction: the synergistic effect of copper and boron dual active sites drives the formation of a high-efficiency ethanol product. Nanoscale, 2023, 15, 17776-17784.	2.8	1
83570	The CeO2 supported multi-nuclear NbxSy clusters for hydrogen evolution reaction. Sustainable Energy and Fuels, 0, , .	2.5	0
83627	Basic guidelines of first-principles calculations for suitable selection of electrochemical Li storage materials: a review. Journal of Materials Chemistry A, 2023, 11, 24482-24518.	5.2	4
83683	The role of oxygen defects in the electronic, optical and phonon dispersion of the LAGO perovskite: a density functional theory investigation. Dalton Transactions, 2023, 52, 16128-16139.	1.6	0

#	Article	IF	Citations
83709	Porous SnO₂ nanosheets for room temperature ammonia sensing in extreme humidity. Materials Horizons, 2024, 11, 184-195.	6.4	1
83737	Two-gap topological superconductor LaB₂ with high T_c = 30 K. Nanoscale Horizons, 2023, 9, 148-155.	4.1	0
83920	Tailoring ultrafast carrier dynamics in GeS and GeSe via Cu intercalation. , 2023, , .		0
84017	Prediction of 2D group-11 chalcogenides: insights into novel auxetic M₂X (M = Cu, Ag, Au;) Tj ETQq1 1 0.784314 rgBT /O	1.3	0
84045	Enriching 2D transition metal borides via MB XMenes (M = Fe, Co, Ir): Strong correlation and magnetism. Nanoscale Horizons, 0, , .	4.1	0
84371	Design and Development of B2 Ti50Pd50-xMx (M= Os, Ru, Co) as Potential High Temperature Shape Memory Alloys. , 0, , .		0
84426	A perspective on the building blocks of a solid-state battery: from solid electrolytes to quantum power harvesting and storage. Journal of Materials Chemistry A, 0, , .	5.2	0
84481	High activity and excellent durability of oxygen-vacancy-rich ruthenium manganese oxide solid-solution nanowires for the oxygen evolution reaction in acidic media. Journal of Materials Chemistry A, 2023, 11, 25252-25261.	5.2	1
84547	Large-Scale Materials Modeling at Quantum Accuracy: Ab Initio Simulations of Quasicrystals and Interacting Extended Defects in Metallic Alloys. , 2023, , .		0
84636	Catalytic Performance of Doped Ni2P Surfaces for Ammonia Synthesis â€. , 0, , .		0
84723	Accuracy of classical force fields for polyethylene structures away from equilibrium. MRS Communications, 2024, 14, 1-7.	0.8	0
84798	The design and optimization of heterogeneous catalysts using computational methods. Catalysis Science and Technology, 2024, 14, 515-532.	2.1	0
84934	Mica nanosheets synthesized via liquid Ga embrittlement: demonstrating enhanced CO₂ capture. Materials Advances, 0, , .	2.6	0
84966	Phonon vortices at heavy impurities in two-dimensional materials. Nanoscale Horizons, 0, , .	4.1	0
85032	High density electron doping in boron-doped twisted bilayer graphene: a ladder to extended flat-band. Materials Horizons, 2024, 11, 1046-1053.	6.4	0
85082	Topological phases in two-dimensional transition metal halides and oxides. , 2023, , .		0
85090	Single-atom catalysts supported on a hybrid structure of boron nitride/graphene for efficient nitrogen fixation via synergistic interfacial interactions. Nanoscale, 0, , .	2.8	0
85181	Automatic Identification of Abnormal Lung Sounds Using Time-Frequency Analysis and Convolutional Neural Network. , 2023, , .		0

#	Article	IF	Citations
85186	Improving the tight-binding description of spin-orbit interaction in a Si/Ge heterostructure for qubits applications. , 2023, , .		0
85187	Lateral Superlattice - A Possible Origin of the Large Leakage Current in Al_{1-x}Sc_xN. , 2023, , .		0
85190	Quantum Mechanical Modeling Techniques for High-Performance Low-k Amorphous Material Engineering: a Showcase for aBN. , 2023, , .		0
85199	Accommodation and Stability of Alloying Elements in Amorphous Grain Boundaries of Zirconia. , 2023, , 459-473.		0
85214	First Principles Characterization of $P_{n}V_{m}$ Clusters in Crystalline Silicon. , 2023, , .		0
85405	Deep-blue narrow-band emissive cesium europium bromide perovskite nanocrystals with record high emission efficiency for wide-color-gamut backlight displays. Materials Horizons, 2024, 11, 1294-1304.	6.4	0
85613	Nanoscale fabrication of heterostructures in thermoelectric SnTe. Nanoscale, 0, , .	2.8	0
85693	Review on mechanical and functional properties of refractory high-entropy alloy films by magnetron sputtering. Emergent Materials, 2024, 7, 77-101.	3.2	0
85810	Machine learning potential assisted exploration of complex defect potential energy surfaces. Npj Computational Materials, 2024, 10, .	3.5	0
86004	Thermal multiferroics in all-inorganic quasi-two-dimensional halide perovskites. Nature Materials, 2024, 23, 182-188.	13.3	1
86159	H-Mg Bond Weakening Mechanism of Graphene-Based Single-Atom Catalysts on MgH2(110) Surface. Springer Proceedings in Physics, 2024, , 485-496.	0.1	0
86214	Unravelling abnormal in-plane stretchability of two-dimensional metalâ€“organic frameworks by machine learning potential molecular dynamics. Nanoscale, 2024, 16, 3438-3447.	2.8	0
86218	First-principles investigation of the solid-solid interface energy of bcc Ti/hcp Ti. AIP Conference Proceedings, 2024, , .	0.3	0
86223	Ab-initio simulations of Ni and Ni0.5Cu0.5 generalized stacking fault energies. AIP Conference Proceedings, 2024, , .	0.3	0
86231	Impact of biaxial strain on optoelectronic properties of Janus monolayer PtSeTe. AIP Conference Proceedings, 2024, , .	0.3	1
86321	First principles study of helimagnetism in 1T-NiI2 monolayer. AIP Conference Proceedings, 2024, , .	0.3	0
86390	On the application of Marcusâ€“Hush theory to small polaron chemical dynamics in oxides: its relationship to the Holstein model and the importance of latticeâ€“orbital symmetries. Physical Chemistry Chemical Physics, 2024, 26, 4812-4827.	1.3	0
86392	Photoinduced Novel Lattice Instability in SnSe. Springer Theses, 2023, , 77-99.	0.0	0

#	Article	IF	Citations
86429	Modulating luminescence properties of CsMnBr₃-based lead-free single crystals by pseudohalide doping. Journal of Materials Chemistry C, 2024, 12, 2705-2713.	2.7	0
86561	Investigation of Bulk,ÂElectronicÂand Transport Properties of Armchair Silicene Nanoribbon as Liquefied Petroleum Gas Combustion Indicator: A DFT Study. Lecture Notes in Electrical Engineering, 2024, , 273-287.	0.3	0
86627	Engineering a hollow bowl-like porous carbon-confined Ruâ€“MgO hetero-structured nanopair as a high-performance catalyst for ammonia borane hydrolysis. Materials Horizons, 0, , .	6.4	1
86734	Synthesis of full spectrum responsive photocatalysts. , 2024, , 89-119.		0
86749	Characterization techniques for full-spectrum responsive photocatalysts. , 2024, , 121-155.		0
86785	Computational chemistry for water-splitting electrocatalysis. Chemical Society Reviews, 2024, 53, 2771-2807.	18.7	1
86820	Superalkali halide perovskites with suitable direct band gaps for photovoltaic applications. Nanoscale, 2024, 16, 5130-5136.	2.8	0
86831	First Principles Study onÂtheÂSegregation ofÂMetallic Solutes andÂNon-metallic Impurities inÂCu Grain Boundary. Minerals, Metals and Materials Series, 2024, , 989-999.	0.3	0
86860	Density functional theory methods applied to homogeneous and heterogeneous catalysis: a short review and a practical user guide. Physical Chemistry Chemical Physics, 2024, 26, 7950-7970.	1.3	0
86867	Ab initio quantum transport simulations of InAs avalanche photo-diodes within the GW approximation. , 2023, , .		0
86942	AFLOW for Alloys. Journal of Phase Equilibria and Diffusion, 0, , .	0.5	0
87174	Structure-driven tuning of catalytic properties of coreâ€“shell nanostructures. Nanoscale, 2024, 16, 5870-5892.	2.8	0
87680	Editorial: Theoretical study of two-dimensional materials for photocatalysis and photovoltaics. Frontiers in Chemistry, 0, 12, .	1.8	0
88169	Oxygen-induced SO2 formation and desorption on NiMoS (1Â¯010) edge surface on NiMoS2 catalyst. AIP Conference Proceedings, 2024, , .	0.3	0